JANUARY 1980
VOLUME 69 NUMBER 1

JOURNAL OF PHARMACEUTICAL SCIENCES

MARY H. FERGUSON
Editor

SHELLY ELLIOTT
Production Editor

MARCIA GARTRELL
Copy Editor

NICOLETTE TRIANTAFELLU
Copy Editor

EDWARD G. FELDMANN
Contributing Editor

SAMUEL W. GOLDSTEIN
Contributing Editor

BELLE R. BECK
Editorial Secretary

DAVID BOHARDT
Director of Publications

L. LUAN CORRIGAN
Assistant Director of Publications

EDITORIAL ADVISORY BOARD

JOHN AUTIAN
HERBERT A. LIEBERMAN
NORMAN R. FARNSWORTH
DAVID E. MANN, JR.
WILLIAM O. FOYE
GERALD J. PAPARIELLO
WILLIAM J. JUSKO
EDWARD G. RIPPIE

The *Journal of Pharmaceutical Sciences* (ISSN 0022-3549) is published monthly by the American Pharmaceutical Association (APhA) at 2215 Constitution Ave., N.W., Washington, DC 20037. Second-class postage paid at Washington, D.C., and at additional mailing office.

All expressions of opinion and statements of supposed fact appearing in articles or editorials carried in this journal are published on the authority of the writer over whose name they appear and are not to be regarded as necessarily expressing the policies or views of APhA.

Offices—Editorial, Advertising, and Subscription: 2215 Constitution Ave., N.W., Washington, DC 20037. Printing: 20th & Northampton Streets, Easton, PA 18042.

Annual Subscriptions—United States and foreign, industrial and government institutions $60, educational institutions $60, individuals *for personal use only* $30; single copies $5. All foreign subscriptions add $5 for postage. Subscription rates are subject to change without notice. Members of APhA may elect to receive the *Journal of Pharmaceutical Sciences* as a part of their annual $80 (foreign $85) APhA membership dues.

Claims—Missing numbers will not be supplied if dues or subscriptions are in arrears for more than 60 days or if claims are received more than 60 days after the date of the issue, or if loss was due to failure to give notice of change of address. APhA cannot accept responsibility for foreign delivery when its records indicate shipment was made.

Change of Address—Members and subscribers should notify at once both the Post Office and APhA of any change of address.

Photocopying—The code at the foot of the first page of an article indicates that APhA has granted permission for copying of the article beyond the limits permitted by Sections 107 and 108 of the U.S. Copyright Law provided that the copier sends the per copy fee stated in the code to the Copyright Clearance Center, Inc., P.O. Box 8891, Boston, MA 02114. Copies may be made for personal or internal use only and not for general distribution.

Microfilm—Available from University Microfilms International, 300 N. Zeeb Road, Ann Arbor, MI 48106.

© Copyright 1980, American Pharmaceutical Association, 2215 Constitution Ave., N.W., Washington, DC 20037; all rights reserved.

FDA: POLICEMAN OR TEACHER?

A few years ago, the big thing for the college age crowd was to dwell on the question, "who am I?"

Not only do persons undergo such identity crises but at times organizations and agencies also experience this type of traumatic soul-searching.

In a number of respects, the behavior of the Food and Drug Administration has appeared to this writer as suggesting that it is similarly uncertain as to its proper role or function. In particular, the Agency has often acted ambivalent and wavering as it has moved back and forth between at least two distinctly different roles: namely, that of a police officer and that of a teacher.

By law, the FDA has responsibility to oversee the purity, quality, identity, safety, usefulness, and related characteristics of the nation's food, drug, and cosmetic supply. With this legal mandate, the Agency is clearly a regulatory body and must operate in a manner to assure compliance.

But compliance itself can be achieved by at least two different routes. There is, of course, that of close supervision and monitoring combined with various enforcement measures. However, to rely solely on this approach would virtually necessitate one FDA agent for each person being monitored—clearly an unrealistic system.

This same problem is encountered in other aspects of day-to-day living; for example, adherence to traffic regulations and payment of income taxes. Both of these systems basically rely on voluntary compliance by the general public, coupled with spot checks of driving speed and sampling of tax returns for auditing. Similarly, the FDA must primarily rely on the voluntary compliance of those who operate within the professions and industries that are responsible for the products over which the FDA has jurisdiction. This voluntary compliance is encouraged by a parallel program of regulatory enforcement *via* product sampling, batch testing, marketplace surveys, plant inspections, and so on.

The relative emphasis which the Agency places on the voluntary route *versus* the enforcement route varies greatly from time-to-time depending upon a number of factors.

Among these is the "philosophic bent" of those persons who happen to be in the upper echelons of FDA at any given time. In particular, if the persons at the top are **enforcement oriented,** it can be expected that the general tenor of the Agency will reflect that leaning. Conversely, if they are **education oriented,** it is more likely that they will generally opt for policies that are persuasive toward voluntary compliance.

In Dr. Jere E. Goyan, the new Commissioner, we have someone with a long and distinguished background in health education. This is not to suggest that Dr. Goyan will be reluctant to use the regulatory enforcement approach if he feels it necessary; his past record shows that he can be forceful, decisive, and "hard-nosed" when he feels that such a manner is needed. However, we suspect that he will initially approach each problem with the perspective that education will frequently resolve such difficulties and make regulatory action unnecessary. Moreover, we are hopeful that this philosophy will permeate the entire Agency.

Again, there is an interesting corollary to be drawn from daily life. Society has learned that people's attitude regarding their police force is largely shaped when they are small children. It is far better if children can be taught that the policeman is there to help them and protect them than it is to make them fearful by scaring them with warnings that "the policeman is going to catch you!" By the same token, we expect that the police force will behave in a manner that warrants the trust and respect of both children and adults.

Similarly, if the FDA is to have both the trust and respect of those with whom it interfaces, then it too will need to conduct itself in a manner that encourages such an attitude.

Edward G. Feldmann

JOURNAL OF PHARMACEUTICAL SCIENCES

JANUARY 1980
VOLUME 69 NUMBER 1

RESEARCH ARTICLES

Role of Binders in Moisture-Induced Hardness Increase in Compressed Tablets and Its Effect on *In Vitro* Disintegration and Dissolution

Z. T. CHOWHAN

Received March 2, 1979, from the *Institute of Pharmaceutical Sciences, Syntex Research, Palo Alto, CA 94304.* Accepted for publication July 20, 1979.

Abstract □ The role of commonly used binders in the moisture-induced hardness increase in compressed tablets containing lactose as a major excipient was studied. Tablets compressed from granulations containing different binders at different moisture levels increased in hardness after overnight exposure to ambient room conditions. The results suggest that this hardness increase is related linearly to the amount of moisture loss from the tablets after compression. The magnitude of the hardness increase is related to the type and concentration of the binder used in wet granulation. The moisture-induced hardness increase in tablets prepared from granulations containing different binders had no effect on the tablet disintegration time and *in vitro* drug dissolution.

Keyphrases □ Binders—role in moisture-induced hardness increase in compressed tablets, disintegration, dissolution, *in vitro* □ Disintegration—of compressed tablets following moisture-induced hardness increase, role of binders, *in vitro* □ Dissolution—of compressed tablets following moisture-induced hardness increase, role of binders, *in vitro*

Recent studies (1, 2) discussed the hardness increase induced by partial moisture loss in compressed tablets prepared by wet granulation. Tablets compressed from granulations containing moisture levels above 2% increased in hardness during storage at ambient room conditions. When the granulation moisture levels during compression were below 2%, tablet hardness did not increase during storage at ambient room conditions. However, when these tablets were equilibrated under accelerated humidity and then exposed to ambient room conditions, tablet hardness increased due to partial moisture loss. Moisture-related hardness increases did not decrease *in vitro* drug dissolution.

The exact mechanism by which moisture affects tablet hardness is not understood fully. Previous results (1) suggested that a possible mechanism was the recrystallization of the soluble drug and/or soluble excipient in the void spaces caused by the moisture loss. Obviously, the physical properties of the drug–excipient combinations play a major role.

Since binders impart cohesiveness to the tablet and ensure tablet strength after compression, investigation of their role in the moisture-induced hardness increase is important. In this study, the tablets compressed from granulations containing the most commonly used binders at different moisture levels increased in hardness due to partial moisture loss during overnight exposure to ambient room conditions. The data suggest that the hardness increase is related linearly to the amount of moisture loss after compression. The magnitude of the hardness increase is related to the type and concentration of binder used in wet granulation. The moisture-related hardness increase in tablets prepared from granulations containing different binders did not affect the tablet disintegration time and *in vitro* drug dissolution.

EXPERIMENTAL

Materials—Acacia[1], povidone[2], starch[3], lactose[4], gelatin[5], and magnesium stearate[6] were USP grade, and salicylic acid[6] was analytical reagent grade. Methylcellulose[7], hydroxypropyl methylcellulose[8], hydroxypropylcellulose[9], and ethylcellulose[10] were used as received.

Granulation—The material was prepared by wet granulation. Lactose and salicylic acid were mixed in geometric proportions on a piece of glassine paper and then in a small planetary mixer[11] for 3 min. The granulating solution was added with mixing and was mixed for ~5 min. The wet granulation was passed through a No. 12 mesh screen and dried in trays in a forced-air drying oven at 50°. One-half of the granulation was dried to ~3% moisture, and the other half was dried until the moisture reached below 1%.

[1] J. T. Baker Chemical Co., Phillipsburg, NJ 08865.
[2] G.A.F. Corp., New York, N.Y.
[3] Staley Manufacturing Co., Decatur, Ill.
[4] Lactose regular, Foremost Food Co., San Francisco, CA 94104.
[5] Sigma Chemical Co., St. Louis, MO 63178.
[6] Mallinckrodt Chemical Works, St. Louis, MO 63160.
[7] Methocel, A-15 premium, Dow Chemical Co., Midland, Mich.
[8] Type 60 HG premium, Dow Chemical Co., Midland, Mich.
[9] Type HF, Hercules, Wilmington, Del.
[10] Ethocel, premium, Dow Chemical Co., Midland, Mich.
[11] Kitchen Aid model K5-A, Hobart Manufacturing Co., Troy, Ohio.

0022-3549/80/0100-0001$01.00/0
© 1980, American Pharmaceutical Association

Table I—Tablet Formulations (Milligrams of Ingredient per Tablet)

Ingredient	Formulation													
	A	B	C	D	E	F	G	H	I	J	K	L	M	N
Salicylic acid	19	19	19	19	19	19	19	19	19	19	19	19	19	19
Lactose	311.1	311.1	311.1	311.1	311.1	311.1	311.1	316.1	301.1	291.1	311.1	316.1	301.1	291.1
Starch	38	38	38	38	38	38	38	38	38	38	38	38	38	38
Magnesium stearate	1.9	1.9	1.9	1.9	1.9	1.9	1.9	1.9	1.9	1.9	1.9	1.9	1.9	1.9
Acacia	10	—	—	—	—	—	—	—	—	—	—	5	20	30
Ethylcellulose	—	10	—	—	—	—	—	—	—	—	—	—	—	—
Gelatin	—	—	10	—	—	—	—	—	—	—	—	—	—	—
Hydroxypropylcellulose	—	—	—	10	—	—	—	—	—	—	—	—	—	—
Hydroxypropyl methylcellulose	—	—	—	—	10	—	—	—	—	—	—	—	—	—
Methylcellulose	—	—	—	—	—	10	—	—	—	—	—	—	—	—
Povidone	—	—	—	—	—	—	10	5	20	30	—	—	—	—
Starch	—	—	—	—	—	—	—	—	—	—	10	—	—	—

These granulations then were screened separately through a No. 16 mesh screen, and appropriate proportions were mixed to obtain the desired moisture levels. Starch and magnesium stearate then were blended with the granulation. The granulation was stored in tightly closed jars; the moisture content was determined prior to compression.

The granulating solutions were prepared in the usual fashion. The solvent was water except for the ethylcellulose solution, in which 95% ethanol was used. Starch paste was prepared by boiling the water and mixing with starch.

Compression—Tablets were compressed with a single-punch machine[12] to a targeted hardness of 6 Strong–Cobb units. The punches and die were 0.95 cm in diameter and flat faced. The tablet weight was 380 mg.

Moisture Determination—The granulation moisture was determined with a moisture balance[13] by exposure to a 125-w IR lamp for 1 hr at the 70-v setting. The percent weight loss on drying was read directly from this instrument. The tablets were ground with a mortar and pestle, and the same procedure for moisture determination was followed.

Hardness Determination—Initial hardness was determined immediately after compression. The tablets were placed on open trays, exposed to ambient room conditions (23°, 25–50% relative humidity), and allowed to equilibrate and reach maximum hardness. For each hardness determination[14], 10 tablets were tested and the mean was calculated.

Disintegration Time—The disintegration apparatus consisted of a basket–rack assembly and a 1-liter beaker as described in the USP. The beaker containing 900 ml of distilled water was maintained at 37° in a constant-temperature water bath. The disintegration times of the individual tablets were noted, and the mean of six tablets was calculated.

***In Vitro* Dissolution**—The dissolution apparatus was the same as described previously (1). It consisted of a 1-liter beaker and a stirrer driven by a synchronous motor at 120 rpm. The beaker containing 600 ml of distilled water was maintained at 37° in a constant-temperature water bath. A stainless steel paddle, 2.5 × 7.6 cm, was centered at the end of a stainless steel shaft and was used as a stirrer. The distance between the bottom of the beaker and the bottom of the stirrer was maintained at 1.8 cm.

At zero time, a tablet was dropped into the stirred dissolution medium. Then, 5-ml samples were withdrawn at appropriate time intervals and filtered through a 0.80-μm pore size filter paper. The absorbance[15] of the salicylic acid in the solution was measured at 303 nm. Three tablets were run for each determination.

RESULTS AND DISCUSSION

To study the role of binders in the moisture-induced hardness increase

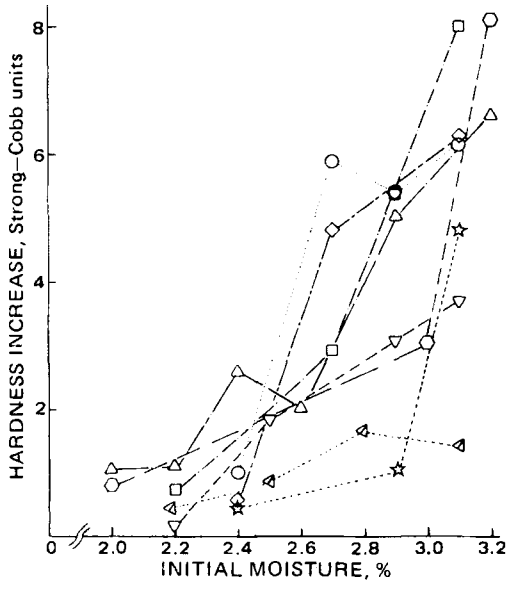

Figure 1—*Effect of binders on hardness increase induced by partial moisture loss in compressed tablets prepared by wet granulation. Key: ○, hydroxypropyl methylcellulose; △, ethylcellulose; ▽, hydroxypropylcellulose; □, povidone; ◇, methylcellulose; ○, gelatin; ☆, acacia; and ▲, starch.*

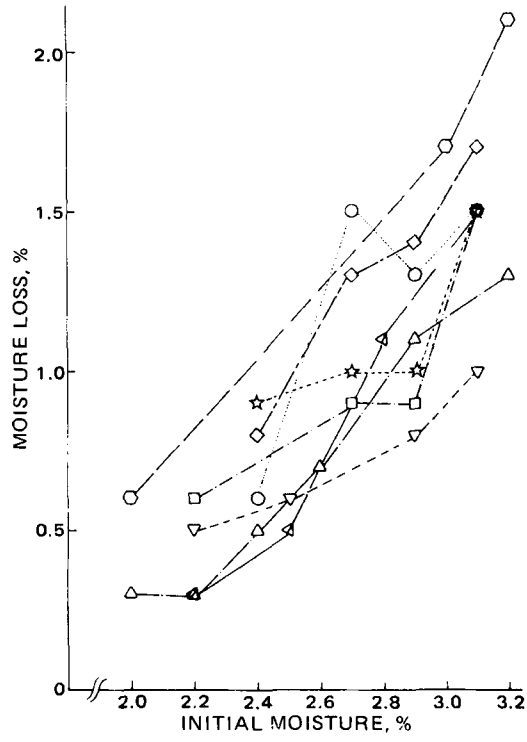

Figure 2—*Effect of binders on moisture loss inducing hardness increase in compressed tablets prepared by wet granulation. Key: ○, hydroxypropyl methylcellulose; △, ethylcellulose; ▽, hydroxypropylcellulose; □, povidone; ◇, methylcellulose; ○, gelatin; ☆, acacia; and ▲, starch.*

[12] Stokes model F4.
[13] Cenco, Central Scientific Co., Chicago, IL 60623.
[14] Heberlein hardness tester, Heberlein and Co., AG, Switzerland.
[15] Unicam recording spectrophotometer, SP 1800, Pye Unicam Ltd., Cambridge, England.

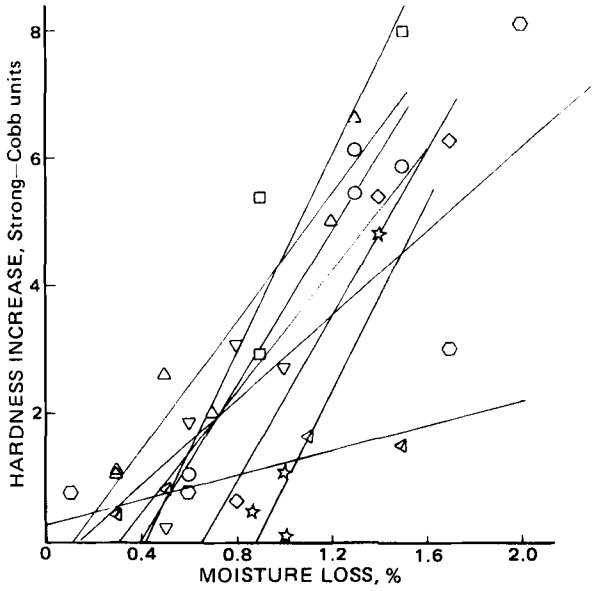

Figure 3—*Relationship between hardness increase and percent moisture loss in compressed tablets prepared by wet granulation using different binders. Equations of the regression lines and correlation coefficients (r) are: ○, hydroxypropyl methylcellulose, y = −2.348 + 5.932x, r = 0.968; △, ethylcellulose, y = −0.486 + 4.95x, r = 0.961; ▽, hydroxypropylcellulose, y = −1.49 + 4.74x, r = 0.819; □, povidone, y = −3.266 + 7.72x, r = 0.930; ◇, methylcellulose, y = −4.386 + 6.54x, r = 0.982; ☆, acacia, y = −6.45 + 7.236x, r = 0.970; ▲, starch, y = 0.32 + 0.9055x, r = 0.886; and ○, gelatin, y = −0.45 + 3.29x, r = 0.855.*

in compressed tablets, lactose was chosen as a major excipient since it is commonly used in tablets. The salicylic acid, starch, and magnesium stearate percentages were kept constant in the formulations studied (Table I).

The granulations containing 2–3.2% moisture and different binders at the 10-mg tablet level were compressed into tablets at a targeted initial hardness of 6 Strong-Cobb units. Above a 3.1% initial moisture level, it was not possible to compress the povidone, methylcellulose, hydroxypropyl methylcellulose, acacia, hydroxypropylcellulose, and starch granulations into tablets because of picking and sticking to the punches.

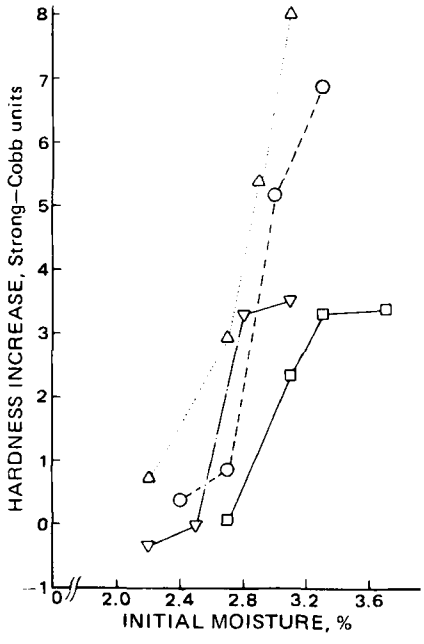

Figure 4—*Effect of the povidone concentration on the hardness increase induced by partial moisture loss in compressed tablets prepared by wet granulation. Key: ○, 5 mg/tablet; △, 10 mg/tablet; ▽, 20 mg/tablet; and □, 30 mg/tablet.*

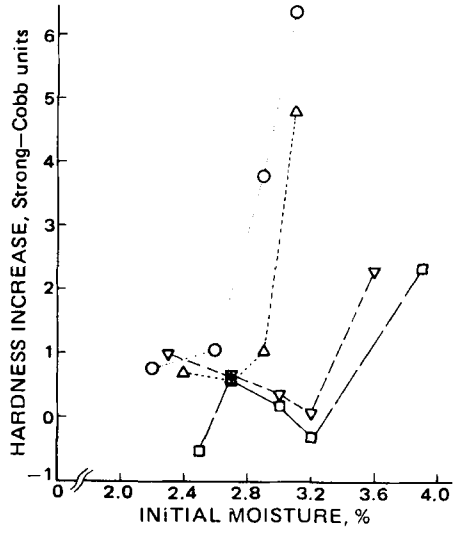

Figure 5—*Effect of the acacia concentration on the hardness increase induced by partial moisture loss in compressed tablets prepared by wet granulation. Key: ○, 5 mg/tablet; △, 10 mg/tablet; ▽, 20 mg/tablet; and □, 30 mg/tablet.*

Tablet hardness was determined again after overnight exposure to ambient room conditions.

The results of the hardness increase *versus* the percent initial moisture are given in Fig. 1. The tablets prepared with different binders that contained a higher moisture content showed large hardness increases, with the exception of starch, which showed a small hardness increase. The magnitude of the hardness increase at a given moisture content depended on the binder.

Plots of the percent moisture loss *versus* the initial moisture are shown in Fig. 2. The tablets prepared with different binders showed an increased moisture loss after overnight exposure to ambient room conditions as the moisture content during compression was increased. The differences in the moisture loss with the binders used in this study were due to the modification of the equilibrium moisture level in the tablets by the binder.

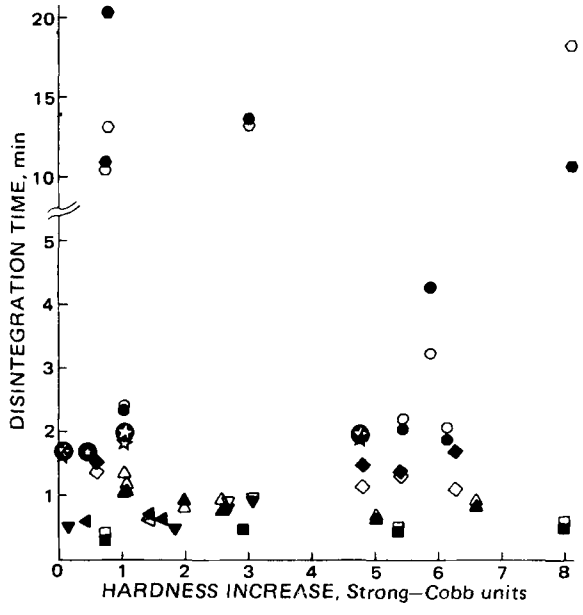

Figure 6—*Role of binders in tablet disintegration time as a function of hardness increase induced by partial moisture loss in compressed tablets prepared by wet granulation. Open symbols give the disintegration time before the hardness increase, and closed symbols give the disintegration time after the hardness increase. Key: ○, ●, hydroxypropyl methylcellulose; △, ▲, ethylcellulose; ▽, ▼, hydroxypropylcellulose; □, ■, povidone; ◇, ◆, methylcellulose; ☆, ✪, acacia; ○, ●, gelatin; and ◁, ◀, starch.*

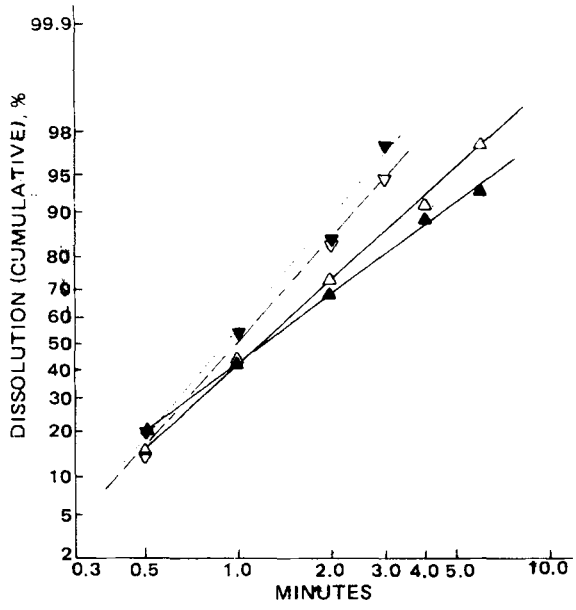

Figure 7—*Percent dissolution* versus *time plots on log probability paper showing the linear relationship. Open symbols give dissolution results before the hardness increase, and closed symbols give dissolution results after hardness increase. Key:* △, *ethylcellulose, initial moisture = 3.2%, and* ▽, *hydroxypropylcellulose, initial moisture = 3.1%.*

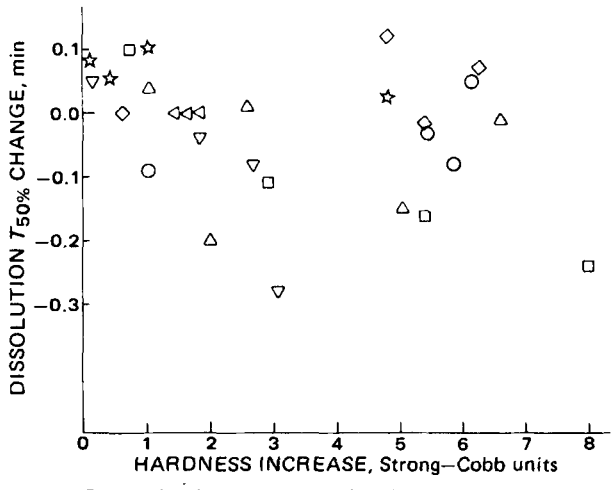

Figure 8—*Role of binders on* in vitro *dissolution as a function of the hardness increase induced by partial moisture loss in compressed tablets prepared by wet granulation. Key:* ○, *hydroxypropyl methylcellulose;* △, *ethylcellulose;* ▽, *hydroxypropylcellulose;* □, *povidone;* ◇, *methylcellulose;* ○, *gelatin;* ☆, *acacia; and* ◁, *starch.*

Figure 3 gives the relationship between the hardness increase and the percent moisture loss that occurred after the tablets were exposed to ambient room conditions. The tablets containing different binders had a reasonably linear relationship between the hardness increase and the percent moisture loss. These results indicate that the hardness increase in tablets mainly occurred due to the partial moisture loss after compression. Some of the solution of the soluble excipients and/or drug is forced into the void spaces between the compressed granules when the moisture in the granulation exceeds a certain level. Recrystallization of the excipients and/or drug from the saturated solution results in the formation of bridges at the point of contact, leading to a hardness increase.

The strength of the crystalline bridges depends not only on the amount of water-soluble excipient and/or drug deposited in the void spaces but also on the crystallization rate. Any change in the formulation such as the replacement of one binder with another would change the crystallization rate of the drug–excipient solution. This crystallization rate change would modify the size and number of crystalline bridges formed in the void spaces, resulting in different hardness increases.

Any change in the formulation would change the moisture sorption properties of the tablets and the magnitude of the hardness increase. For example, a formulation containing 66% water-insoluble drug, 18% lactose, 10% starch, 5% povidone, and 0.2% magnesium stearate (1) caused greater hardness increases compared to Formula G in this study, which contained about 82% lactose.

Changes in the binder concentrations in the tablet formulations also would change the moisture sorption properties. Two binders, povidone and acacia, were selected to investigate the influence of the binder concentration on the moisture-induced hardness increase. The amount of binder per tablet varied from 5 to 30 mg. The lactose amount was adjusted to keep the total weight per tablet constant. Figure 4 gives the effect of povidone concentration on the hardness increase induced by partial moisture loss. The maximum moisture-induced hardness increase was seen with 10 mg of povidone/tablet. With 20 and 30 mg of povidone/tablet, the hardness increase occurred at higher moisture levels and was less pronounced. With 5 mg of povidone/tablet, the hardness increase was slightly less pronounced compared to the 10-mg of povidone/tablet level at the same initial moisture content.

The effects of the acacia concentration on the hardness increase are shown in Fig. 5. As the amount of acacia in the formulation was increased, a higher initial moisture in the granulation was needed to increase hardness. In agreement with the povidone data (Fig. 4), the effect was less pronounced at higher acacia concentrations.

Physical properties of the drug–excipient combination were changed by changing the binder concentration. The granulations containing 10 mg of povidone/tablet could not be compressed at 3.5% moisture, while the formulation containing 30 mg of povidone/tablet were compressed easily at 3.7% moisture without picking or sticking. However, on equilibration at ambient room conditions, the moisture content of all povidone tablets essentially was the same. Similarly, the granulations containing lower acacia concentrations could not be compressed above 3.2% moisture; at 30 mg of acacia/tablet, the granulation containing 3.9% moisture easily was compressible.

The small hardness increases at higher binder concentrations due to the moisture-related effect could be explained by the crystallization rate decrease of the excipient–drug solution in the voids, which, in turn, results in the formation of fewer crystalline bonds, imparting lower additional strength to the tablet.

The role of binders in tablet disintegration time as a function of hardness increase induced by partial moisture loss is illustrated in Fig. 6. Tablets prepared from most binders did not show an increase in the disintegration time resulting from a moisture-induced hardness increase. However, tablets prepared by wet granulation with gelatin solution had an increased disintegration time in one case, when hardness increased only slightly, but the disintegration time decreased when the hardness increased by about 8 Strong–Cobb units. These results indicate that the hardness increase resulting from partial moisture loss in lactose-based tablets does not affect the tablet disintegration time.

Percent dissolved *versus* time profiles were generated for tablets prepared with different binders at 10 mg of binder/tablet and containing initial moisture levels of 2–3.2% before and after the hardness increase. The data from these tests were plotted on logarithmic probability graph paper (3), and the median ($T_{50\%}$) was obtained from the line. Figure 7 shows linear percent dissolved *versus* time plots. The dissolution median change was obtained by subtracting the dissolution median after the hardness increase from the dissolution median before the hardness increase (Fig. 8). The percent dissolved *versus* time profiles for tablets containing gelatin as a binder at 10 mg of gelatin/tablet and containing different initial moisture levels were not generated. It is obvious from the data given in Fig. 8 that the hardness increase induced by partial moisture loss from lactose-based tablets containing different binders had no effect on drug dissolution.

REFERENCES

(1) Z. T. Chowhan and L. Palagyi, *J. Pharm. Sci.*, **67**, 1385 (1978).
(2) Z. T. Chowhan, *Drug Dev. Ind. Pharm.*, **5**, 41 (1979).
(3) J. G. Wagner, *J. Pharm. Sci.*, **58**, 1253 (1969).

ACKNOWLEDGMENTS

The author thanks Ms. Maida Azadian and Ya Ping Lee for technical help.

Photodecomposition of Sulfonamides and Tetracyclines at Oil–Water Interfaces

W. H. K. SANNIEZ and N. PILPEL ˣ

Received December 12, 1978, from the *Department of Pharmacy, Chelsea College of Science, University of London, London SW3 6LX, England.* Accepted for publication July 13, 1979.

Abstract □ Changes that occur in the interfacial tension of hydrocarbon oils floated on dilute aqueous solutions of some sulfonamides and tetracyclines and irradiated with UV light were measured. Photodecomposition products in the oil and aqueous lyers were identified, and reaction mechanisms are proposed.

Keyphrases □ Sulfonamides—photodecomposition at oil-water interface □ Tetracyclines—photodecomposition at oil-water interface □ Photodecomposition—of sulfonamides and tetracyclines at oil-water interface

Many patients undergoing treatment with sulfonamides (1–3) or tetracyclines (4–6) become photosensitive; when subsequently exposed to strong sunlight, they develop skin rashes, fluid in the tissues (edema), and other symptoms.

Storck (7) suggested that sulfonamides in the body are converted into activated species, which combine with protein to form allergens. Alternative mechanisms were proposed to explain the photosensitizing action of the tetracyclines (5, 8). Because of the difficulty in identifying and measuring the reaction products *in vivo*, the processes involved in photosensitization are not well understood.

In vitro techniques recently were developed for studying the reactions of these drugs at air–water and oil–water interfaces under UV light (9–11). One convenient method involves floating a layer of a suitable oil on an aqueous drug solution, irradiating the system with UV light for various times, and analyzing the changes in the interfacial tension of the oil and in the chemical composition of the oil and aqueous layers.

This method was used to study the photochemical decomposition of three sulfonamides and four tetracyclines.

EXPERIMENTAL

Materials—Isopropylbenzene[1] (Puriss) and commercial dodecylbenzene[2] were purified further by passing them three times under slight pressure through a tightly packed bed of fuller's earth (2.5 cm thick), which was renewed after each passage. Sulfanilamide[3] (mp 165°), sulfathiazole[3] (mp 201°), and sulfapyridine[4] (mp 191°) were recrystallized three times from boiling water.

The best available grades of tetracycline[5], chlortetracycline[5], demeclocycline[5], oxytetracycline[6], and deoxytetracycline[7] were used without further purification. Reference standards of epitetracycline (quatrimycin), epichlortetracycline, epidemeclocycline, anhydrotetracycline, anhydrochlortetracycline, and anhydrodemeclocycline were obtained[8].

Triple-distilled water (surface tension 72.1 mN/m at 21°; specific conductivity $1.2 \times 10^{-6}\ \Omega^{-1}\ cm^{-1}$ at 21°; pH 5.7) was used.

Apparatus and Technique—The irradiation chamber is shown in Fig. 1. The UV-light source was a 125-w MB/U medium-pressure arc[9] equipped with a silica filter transmitting from 290 to 325 nm (9–11).

Twelve milliliters of isopropylbenzene or dodecylbenzene was floated on 20 ml of a dilute aqueous drug solution in a 6-cm diameter glass pot forming a 0.6-cm deep layer. Each system was placed in turn in the chamber and was irradiated for a predetermined time with its temperature maintained at 25 ± 2°.

After irradiation, the interfacial tension, γ, of the sample was measured *in situ* with a tensiometer[10] using a platinum ring. This technique required the floating hydrocarbon layer to be at least 0.5 cm deep. Wetting of the ring was achieved either by pulling it upward or pushing it downward through the interface, whichever gave the higher reading. The ring had a circumference of 3.86 cm and was made from 0.015-cm radius wire. The tensiometer readings, P, were converted to interfacial tension values, γ, by (12):

$$\gamma = P\left[0.725 + \left(\frac{0.0145P}{C^2(D-d)}\right)^{1/2}\right] \qquad \text{(Eq. 1)}$$

where D and d are the densities of water and the hydrocarbon oil at 20°, respectively. This equation incorporates correction terms for buoyancy and the weight of the liquid raised by the ring (13). The accuracy of the

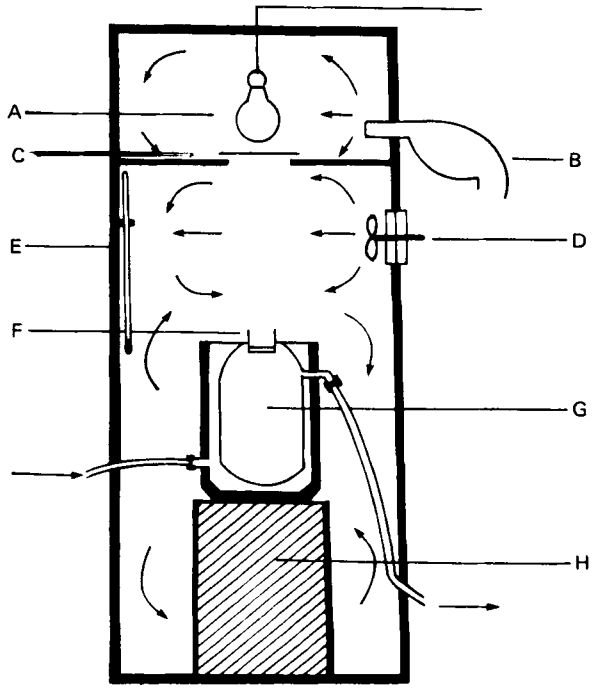

Figure 1—*UV irradiation chamber. Key: A, mercury lamp; B, cool air blower; C, silica filter; D, exhaust fan; E, thermometer; F, duNouy pot; G, glass thermostat (25 ± 2°); and H, support.*

[1] Aldrich Chemicals (surface tension 30.1 mN/m and interfacial tension 37.8 mN/m at 20°; n_D^{20} +1.4917; d_4^{20} +0.864; and UV transmission cutoff λ_{max} 287 nm).

[2] Dobane JN, Shell Chemicals (surface tension 32.2 mN/m and interfacial tension 45.9 mN/m at 20°; n_D^{20} +1.4865; d_4^{20} +0.878; and UV transmission cutoff λ_{max} 398 nm).

[3] British Drug Houses.

[4] May and Baker.

[5] Lederle Laboratories.

[6] Imperial Chemical Industries.

[7] Pfizer.

[8] World Health Organization.

[9] Phillips.

[10] DuNouy, Cambridge Instrument Co.

0022-3549/80/0100-0005$01.00/0
© 1980, American Pharmaceutical Association

Table I—Photosensitive Indexes

Additive	Isopropylbenzene	Dodecylbenzene
Sulfanilamide	0.36	0.37
Sulfathiazole	0.50	0.53
Sulfapyridine	0.58	0.62
Demeclocycline	1.4	1.1
Tetracycline	1.4	1.4
Chlortetracycline	2.0	2.0
Oxytetracycline	2.4	2.4

measurements was estimated at ±1%. Although higher accuracies can be achieved by drop weight or drop volume methods, these methods are unsuited to continuous *in situ* monitoring of samples. Since comparative rather than absolute values were required for this study, the accuracy was considered sufficient. It was confirmed by calibrating the instrument against pure benzene and isopropylbenzene[1] samples. If necessary, results were corrected to 20° by the factor of −0.04 mN/m/deg.

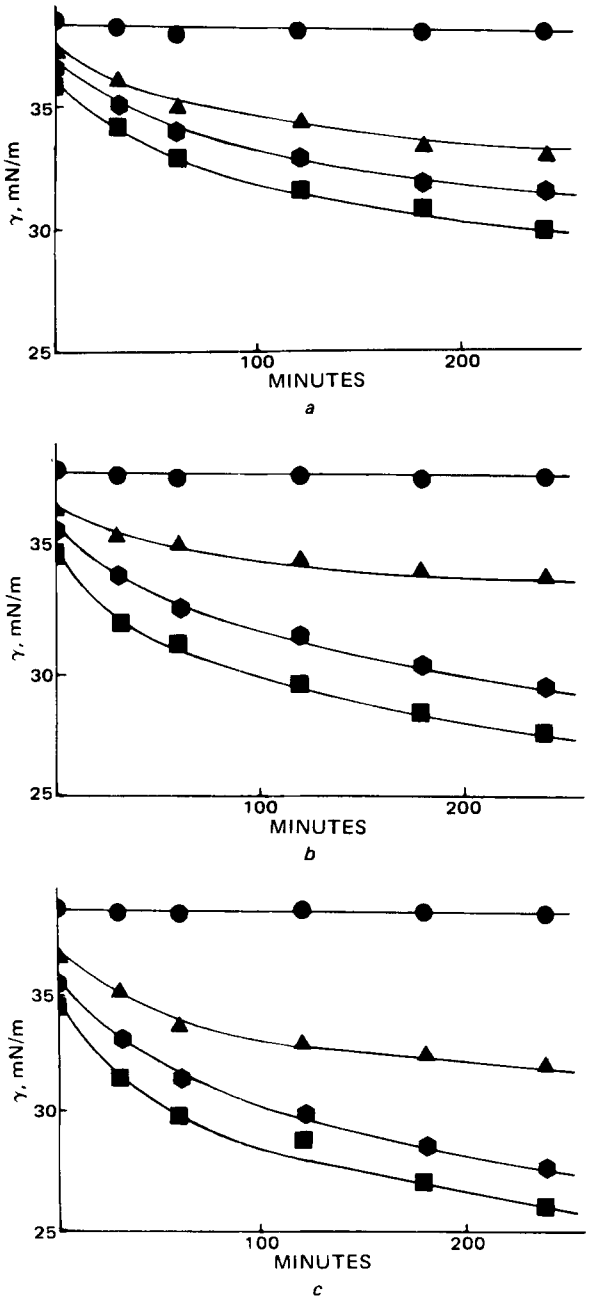

Figure 2—*Plots of interfacial tension* versus *irradiation time for isopropylbenzene systems with sulfapyridine* (a), *sulfathiazole* (b), *and sulfanilamide* (c). *Key (moles/dm³ of additive):* ●, *zero;* ▲, *1.5 × 10⁻⁵;* ●, *2.8 × 10⁻⁵; and* □, *1.0 × 10⁻⁴.*

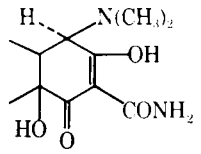

partial tetracycline structure

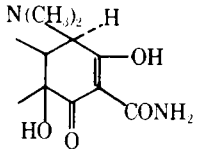

partial epimer structure

The reaction products that formed in the oil and aqueous layers after irradiation for 4 hr were analyzed by GLC and TLC combined with UV spectroscopy. Peroxides were determined in the oil phase by iodometric titration (14); the quantum efficiency of each additive was calculated from the amount of product and the light intensity, which was determined by an actinometric method using potassium ferrioxolate reagent (15).

RESULTS

The sulfonamides and tetracyclines were more soluble in water than in hydrocarbon oils and thus partitioned mainly in the aqueous phase. They also were adsorbed at the oil–water interface, causing the interfacial tension decreases with concentration that can be observed from the positions at which the various curves intersect the ordinates in Figs. 2 and 3 before irradiation was started.

Irradiation effects on the interfacial tensions of representative samples are shown in Figs. 2 and 3; all samples exhibited interfacial tension decreases with increasing irradiation time. The decrease, expressed as $-\delta\gamma/\delta t$ after 120 min of irradiation, depended on the nature and concentration of the additive but was nearly independent of the oil phase. For example, for a 1.6×10^{-4} mole/dm³ aqueous solution of sulfapyridine in contact with isopropylbenzene, $\delta\gamma/\delta t$ was −0.022; for the same solution in contact with dodecylbenzene, $\delta\gamma/\delta t$ was −0.023.

When the values of the moduli $|\delta\gamma/\delta t|$ were plotted against the square root of the additive concentration, $\sqrt{c}$ in $(\text{moles/dm}^3)^{1/2}$, straight lines were obtained (Figs. 4 and 5) (16). The slopes of these lines are given in Table I and are designated as the photosensitive indexes, X (*cf.*, Ref. 17).

Chemical analysis of the oil layers from systems containing tetracycline, chlortetracycline, and demeclocycline showed that irradiation caused peroxides–hydroperoxides to form fairly rapidly after induction for ~60 min. The peroxide buildup is shown in Figs. 6*a* and 6*b*, and it coincided with a gradual migration of the yellow color from the aqueous phase into the oil phase. Less peroxide was produced by oxytetracycline and by the sulfonamide additives (the latter produced a blue color), and the graphs for these systems approximately coincided with those for the isopropylbenzene and the dodecylbenzene alone, *i.e.*, with the bottom curves in Figs. 6*a* and 6*b*, respectively.

The other reaction products detected in the oil phases of the three tetracyclines (Fig. 6) were anhydrotetracycline, anhydrochlortetracycline, and anhydrodemeclocycline. They were identified by TLC combined with UV spectroscopy. Their R_f values were 0.88, 0.82, and 0.87, respectively. No other reaction products in the oil phases of the systems containing oxytetracycline or the three sulfonamides could be identified, except for the small peroxide amounts already mentioned.

Examination of the aqueous phases from all samples after irradiation for 240 min showed that the pH decreased from 5.4, 5.8, and 5.8 to 3.8, 4.1, and 4.4 in the systems containing sulfanilamide, sulfathiazole, and sulfapyridine, respectively. In the same period, between ~40 and 20% of each additive was converted into the corresponding 2,4-hydroxylaminebenzenesulfonamido derivative. These products were identified by comparing their UV spectra with those of authentic standards (7). Furthermore, the systems containing oxytetracycline produced β-deoxytetracycline, R_f 0.13, and the systems containing tetracycline, chlortetracycline, and demeclocycline produced the corresponding epimers (18) with R_f 0.21, 0.22, and 0.19, respectively.

The quantum efficiencies (moles of product per Einstein) of the additives were: sulfanilamide, 3.70; sulfathiazole, 2.90; sulfapyridine, 1.20; demeclocycline, 2.80; tetracycline, 2.00; and chlortetracycline, 1.60. The fact that the values were greater than unity indicates that the photochemical reactions proceeded by chain mechanisms (19).

DISCUSSION

The main decomposition products from the sulfonamides, *i.e.*, the 2,4-hydroxylaminobenzenesulfonamido derivatives, were soluble in water

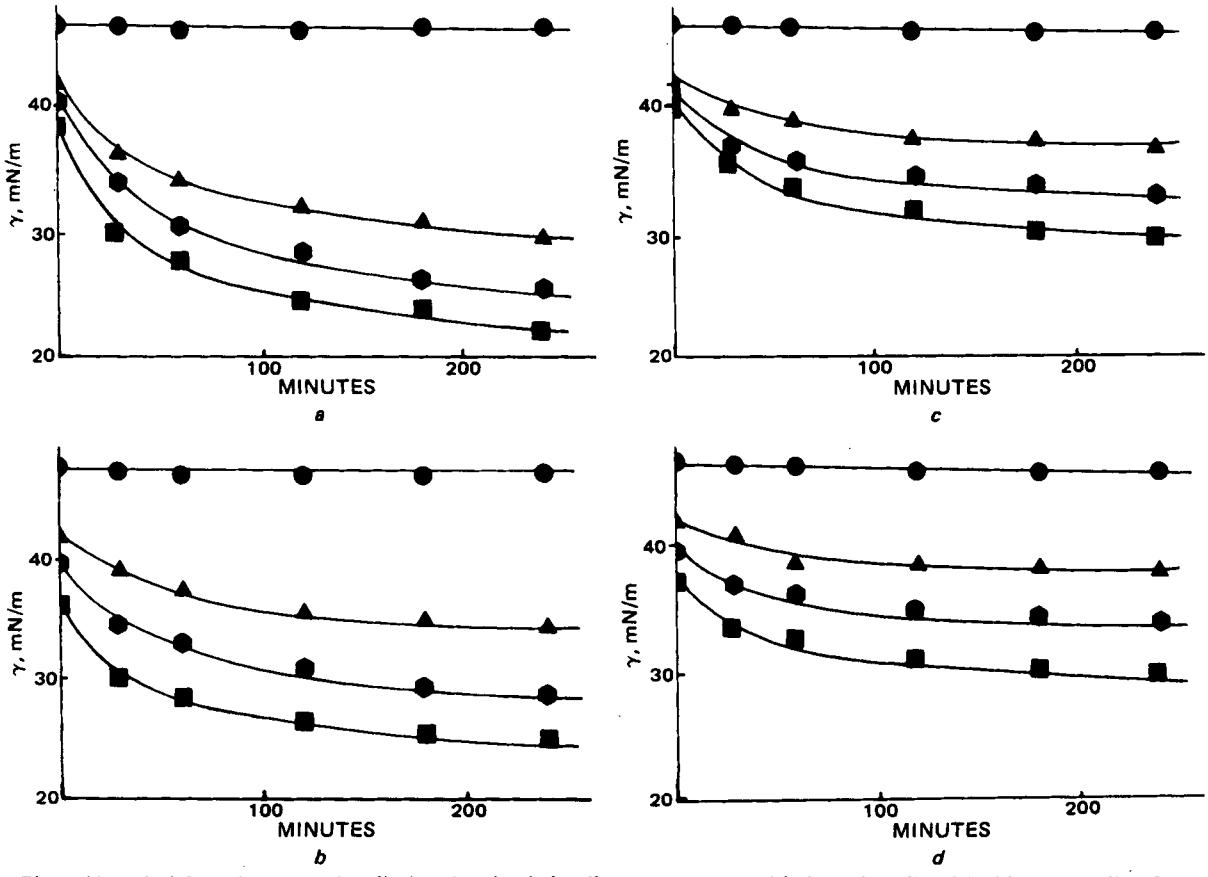

Figure 3—*Plots of interfacial tension* versus *irradiation time for dodecylbenzene systems with demeclocycline (a), chlortetracycline (b), tetracycline (c), and oxytetracycline (d). Key (moles/dm³ of additive): ●, zero; ▲, 1.5 × 10⁻⁴; ●, 5.2 × 10⁻⁴; and □, 1.0 × 10⁻³.*

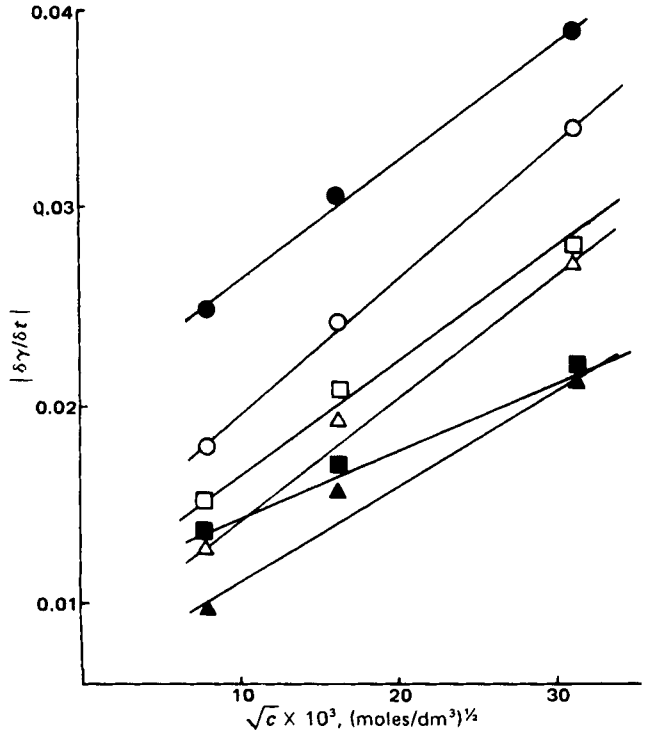

Figure 4—*Plots of* $|\delta\gamma/\delta t|$ versus $\sqrt{c}$. *Key: ●, sulfanilamide-dodecylbenzene; ▲, sulfathiazole-dodecylbenzene; ■, sulfapyridine-dodecylbenzene; ○, sulfanilamide-isopropylbenzene; △, sulfathiazole-isopropylbenzene; and □, sulfapyridine-isopropylbenzene.*

and probably were formed as shown in Scheme I in which the asterisk indicates an excited state (20).

$$RNHSO_2C_6H_4NH_2 \xrightarrow{h\nu} RNHSO_2C_6H_4NH_2^* \xrightarrow{H_2O} RNHSO_2C_6H_4NH^- + H_3O^+$$

$$RNHSO_2C_6H_4NH^- \xrightarrow{O_2,\ h\nu} RNHSO_2C_6H_4NHOH + H_2O_2$$

Scheme I

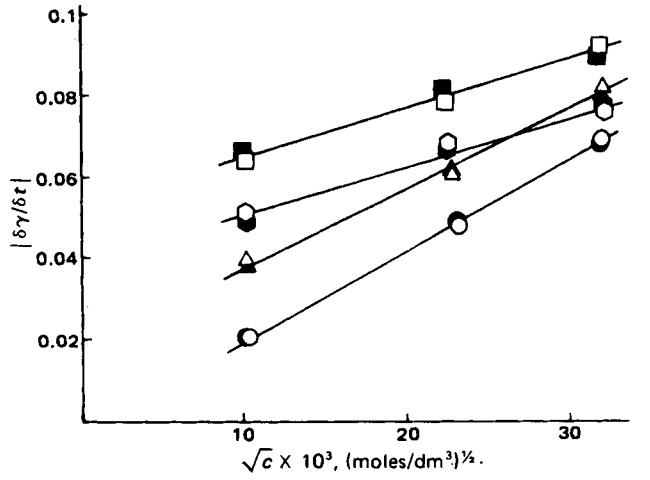

Figure 5—*Plots of* $|\delta\gamma/\delta t|$ versus $\sqrt{c}$. *Key: ●, oxytetracycline-dodecylbenzene; ▲, chlortetracycline-dodecylbenzene; ●, tetracycline-dodecylbenzene; ■, demeclocycline-dodecylbenzene; ○, oxytetracycline-isopropylbenzene; △, chlortetracycline-isopropylbenzene; ○, tetracycline-isopropylbenzene; and □, demeclocycline-isopropylbenzene.*

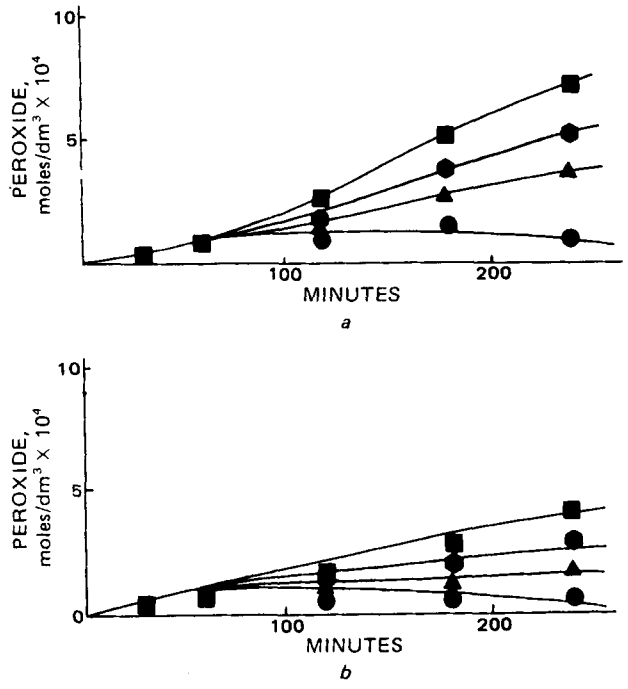

Figure 6—*Peroxide concentration* versus *UV irradiation time for isopropylbenzene systems (5 × 10^{-4} mole/dm³) (a) with isopropylbenzene alone (●), chlortetracycline (▲), tetracycline (●), and demeclocycline (■), and for dodecylbenzene systems (5 × 10^{-4} mole/dm³) (b) with dodecylbenzene alone (●), chlortetracycline (▲), tetracycline (●), and demeclocycline (■).*

This reaction scheme would account satisfactorily for the observed pH decreases in these systems.

The sulfonamides did not produce appreciable amounts of oil-soluble products. If they had, these products might have been expected to catalyze or sensitize the photodecomposition of the supernatant isopropylbenzene or dodecylbenzene (9, 10). In fact, the two oils yielded about the same amount of peroxide whether irradiated on their own or in the presence of the sulfonamides.

In contrast, when the same oils were irradiated in the presence of at least three of the tetracyclines, much larger amounts of peroxide were formed (Fig. 6). This increase presumably was due to the formation of the oil-soluble anhydrotetracycline (AT) derivatives (detected by analysis) as shown in Schemes II and III (8, 21):

$$AT \xrightarrow{h\nu} AT^*$$

Scheme II

$$AT^* + {}^3O_2 \rightarrow AT + {}^1O_2^*$$

Scheme III

The excited singlet molecular oxygen then could react with the hydrocarbon oil, *e.g.*, isopropylbenzene (Scheme IV):

$$C_6H_5CH(CH_3)_2 + {}^1O_2^* \xrightarrow{h\nu} \underset{\text{peroxide}}{C_6H_5C(CH_3)_2OO\cdot}$$

Scheme IV

thus producing the hydroperoxides. (A similar reaction would be expected to occur with dodecylbenzene, and this hypothesis is confirmed by the similarly shaped curves in Figs. 6*a* and 6*b*.)

The present work shows that the breakdown products from both drug classes considerably reduce the tension at an oil–water interface, and a measure of the effect is provided by the drug's photosensitive index, X (Table I) (*cf.*, Ref. 17). As defined, a small X implies a large reduction in interfacial tension during irradiation; on this basis, the sulfonamides (and sulfanilamide in particular) produce substantially larger effects than the tetracyclines.

Some connection eventually may be found between the photochemical decomposition of sulfonamides and tetracyclines at the oil–water interface *in vitro* and at the lipid–water interface of the cell wall (22). Such a connection might assist in elucidating the photosensitization mechanisms that occur *in vivo* and explain, for example, the observation that the ranking order of photosensitivity in Table I for the sulfonamides and oxytetracycline is the same as was obtained from *in vivo* experiments on patients (1, 3).

REFERENCES

(1) S. Epstein, *J. Invest. Dermatol.*, **2**, 43 (1939).
(2) W. M. Sams, *J. Am. Med. Assoc.*, **174**, 2043 (1960).
(3) R. L. Baer and L. C. Harber, *Arch. Dermatol.*, **83**, 61 (1961).
(4) M. S. Falk, *J. Am. Med. Assoc.*, **172**, 1156 (1960).
(5) W. F. Schorr and S. Monash, *Arch. Dermatol.*, **88**, 440 (1963).
(6) L. L. de Veder, *Can. Med. Assoc. J.*, **86**, 168 (1962).
(7) H. Storck, *Arch. Dermatol.*, **9**, 469 (1965).
(8) J. A. Wiebe and D. E. Moore, *J. Pharm. Sci.*, **66**, 186 (1977).
(9) A. E. Klein and N. Pilpel, *J. Chem. Soc. Farad. Trans. 1*, **69**, 1729 (1973).
(10) W. H. K. Sanniez and N. Pilpel, *ibid.*, **74**, 123 (1978).
(11) M. Nejmeh and N. Pilpel, *J. Pharm. Pharmacol.*, **30**, 74 (1978).
(12) H. H. Zuidema and G. W. Waters, *Ind. Eng. Chem. Anal. Ed.*, **13**, 312 (1941).
(13) W. D. Harkins and H. F. Jordan, *J. Am. Chem. Soc.*, **52**, 1751 (1930).
(14) D. K. Banjee and C. C. Budke, *Anal. Chem.*, **36**, 2367 (1964).
(15) C. G. Hatchard and C. A. Parker, *Proc. Roy. Soc. London*, **A235**, 518 (1956).
(16) H. W. Melville and S. Richards, *J. Chem. Soc.*, **1954**, 944.
(17) A. Felmeister and R. Schaubman, *J. Pharm. Sci.*, **58**, 64 (1969).
(18) "Textbook of Organic Medicinal and Pharmaceutical Chemistry," 5th ed., C. O. Wilson, O. Gisvold, and R. F. Doerge, Eds., Pitman Medical Publishing, London, England, 1965, chap. 16.
(19) J. G. Calvert and J. N. Pitts, "Photochemistry," Wiley, New York, N.Y., 1966, p. 589.
(20) N. J. Turro, G. S. Hammond, J. N. Pitts, Jr., *et al.*, "Annual Survey of Photochemistry," vol. 2, Interscience, New York, N.Y., 1968, p. 25.
(21) C. S. Foote, *Acc. Chem. Res.*, **1**, 104 (1963).
(22) A. C. Allison, I. A. Magnus, and M. R. Young, *Nature*, **209**, 874 (1966).

Comparative Pharmacokinetics of Coumarin Anticoagulants XLIV: Dose-Dependent Pharmacokinetics of Warfarin in Rats

KANJI TAKADA and GERHARD LEVY ˣ

Received June 4, 1979, from the *Department of Pharmaceutics, School of Pharmacy, State University of New York at Buffalo, Amherst, NY 14260.* Accepted for publication July 13, 1979.

Abstract □ The purpose of this investigation was to determine the effect of dose on warfarin pharmacokinetics in rats. First, in a crossover experiment, rats received ^{14}C-warfarin, 0.2 mg/kg iv, 12 hr after an injection of either nonradioactive warfarin (0.5 mg/kg) or saline solution. Warfarin concentrations in plasma declined triexponentially as a function of time. Pharmacokinetic analysis revealed that pretreatment with warfarin significantly decreased the apparent volume of distribution, total plasma clearance, and intrinsic plasma clearance of the drug. In the second part of the investigation, rats received single intravenous warfarin injections in the order of 0.1–1.0–0.1 or 1.0–0.1–1.0 mg/kg at 2-week intervals. The apparent volume of distribution, total plasma clearance, and intrinsic plasma clearance of the 1.0-mg/kg warfarin dose were appreciably lower than those of the 0.1-mg/kg dose. The decrease in the apparent volume of distribution of warfarin with increasing dose is consistent with the previously observed concentration dependence in hepatic uptake of the drug.

Keyphrases □ Coumarin anticoagulants—warfarin, dose-dependent pharmacokinetics, rats □ Warfarin—dose-dependent pharmacokinetics, rats □ Pharmacokinetics—warfarin, dose dependence, rats

Hepatic uptake of warfarin in rats, as reflected by the ratio of total warfarin concentration in the liver to the free warfarin concentration in serum during the postdistributive (β) phase, is highly dose or concentration dependent. A determination of warfarin concentrations in serum and liver of rats 6 hr after injection of either 0.1 or 1.0 mg/kg showed that concentrations in serum increased much more than proportionally and that concentrations in the liver increased much less than proportionally with dose (1). Therefore, the liver–serum concentration ratio decreased as the dose was increased from 0.1 to 1.0 mg/kg.

Since warfarin in the liver can account for a large fraction of the total drug in the body of rats (2), dose-dependent hepatic uptake may result in a dose-dependent change in the apparent volume of distribution of the drug. This possibility, as well as the possibility of other dose-dependent changes in warfarin pharmacokinetics in rats, was explored in this investigation. The nonlinear uptake or binding of warfarin by the liver in a concentration range in which serum protein binding of the drug is almost independent of concentration provides an opportunity to study a system that has been the subject of considerable theoretical interest and exploration (3, 4).

EXPERIMENTAL

The investigation was carried out in two parts. First, the pharmacokinetics of a small ^{14}C-warfarin dose were determined in a crossover study on rats that had been given either saline solution or a larger dose of nonradioactive warfarin 12 hr earlier. Second, in a triple crossover study, rats received either a high, then a low, and then again a high dose of warfarin or a low, then a high, and then again a low dose of the drug.

In the first part of the study, 10 male Sprague–Dawley rats, 360–505 g, were used. Rats 1a–4a were obtained from a supplier[1] who was unable to provide additional animals at that time; therefore, Rats 6a–10a were obtained from a different source[2]. A two-piece cannula of silicone rubber–polyethylene was implanted in the right jugular vein, under light ether anesthesia (5, 6), 2 days before the start of the experiment. The rats were placed in individual plastic metabolism cages with food[3] and water freely available.

Five rats received an intravenous injection of 0.9% sodium chloride solution while the other five animals received an intravenous injection of nonradioactive racemic warfarin, 0.5 mg/kg, through the cannula at 8 pm. The injection volume was ~2 ml/rat. Twelve hours later, all animals received an intravenous injection of racemic ^{14}C-warfarin[4] (158 μCi/mg), ~3.5 μCi/rat, together with enough nonradioactive racemic warfarin to constitute a total dose of 0.2 mg/kg. Mainstream blood samples (0.15–0.20 ml) were obtained at 5, 15, 30, 45, 60, 80, 100, 120, 150, and 200 min and then at less frequent intervals for ~50 hr by a technique described previously (6), except that saline solution rather than heparinized saline solution was used to displace blood from the external portion of the cannula.

The blood was transferred to heparinized capillary tubes[5], which were

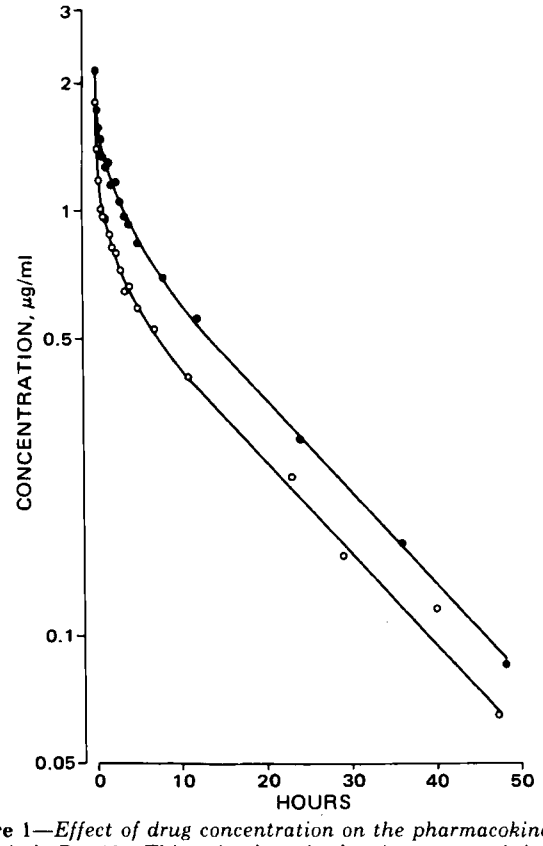

Figure 1—*Effect of drug concentration on the pharmacokinetics of warfarin in Rat 10a. This animal received an intravenous injection of ^{14}C-warfarin 12 hr after injection of saline solution (control experiment, open circles) and, 1 week later, the same dose of ^{14}C-warfarin 12 hr after intravenous injection of nonradioactive warfarin, 0.5 mg/kg (solid circles). The data points show the time course of ^{14}C-warfarin concentrations in serum. The lines were fitted to the data by computer.*

[1] Blue Spruce Farms, Altamont, N.Y.

[2] Holtzman Co., Madison, Wis.

[3] Charles River RMH 1000, Agway Inc., Syracuse, N.Y.

[4] Amersham Corp., Arlington Heights, Ill.

[5] Caraway, Sherwood Medical Industries, St. Louis, Mo.

0022-3549/80/0100-0009$01.00/0
© 1980, American Pharmaceutical Association

Table I—Effect of Drug Concentration on the Pharmacokinetics of Warfarin in Rats: Directly Determined Pharmacokinetic Constants and Serum Protein Binding [a]

Rat	Pre-treatment[b]	Body Weight, g	Constants of the Triexponential Equation[c]						Serum Free Fraction × 100[d]		Serum Protein Concentration, g/100 ml
			P	A	B	π	α	$\beta \times 100$	0.5 μg/ml	5 μg/ml	
1a	−	503	1.23	0.384	1.03	4.47	0.400	4.28	2.39	2.96	6.2
	+	505	2.36	0.127	1.39	9.75	0.867	4.72			
2a	−	487	0.956	0.150	1.02	3.10	0.519	3.47	1.20	1.42	7.1
	+	480	1.24	0.558	1.22	5.59	0.260	3.89			
3a	−	490	1.22	0.369	1.20	4.40	0.563	4.67	1.13	1.35	6.8
	+	482	1.38	0.512	0.995	5.61	0.572	3.77			
4a	−	486	1.74	0.771	0.896	5.11	0.400	2.00	1.02	1.22	6.2
	+	456	1.61	0.608	1.32	4.02	0.145	2.44			
5a	−	388	1.96	0.187	1.43	5.83	0.505	1.11	1.51	1.71	5.8
	+	373	2.03	0.316	1.29	3.63	0.441	1.19			
6a	−	360	1.42	0.402	0.805	6.71	0.622	4.08	—[e]	—[e]	—[e]
	+	361	0.460	0.483	0.876	5.46	0.786	2.54			
7a	−	418	1.19	0.337	0.900	5.01	0.216	4.86	2.81	3.18	7.1
	+	409	1.06	0.331	0.957	3.36	0.284	5.09			
8a	−	434	1.06	0.540	0.602	4.06	0.238	5.25	3.32	3.66	6.5
	+	431	1.03	0.270	1.07	3.52	0.372	6.87			
9a	−	462	1.08	0.300	0.902	3.54	0.247	5.38	2.50	2.98	7.6
	+	441	0.766	0.602	0.971	3.74	0.355	5.26			
10a	−	458	0.963	0.485	0.679	4.53	0.398	4.88	2.66	2.80	6.0
	+	485	0.760	0.599	0.919	3.23	0.276	4.83			
Mean	−	449	1.28	0.393	0.946	4.68	0.411	4.00	2.06 ± 0.80	2.36 ± 0.88[f]	6.6 ± 0.6
SD		46	0.33	0.178	0.242	1.06	0.142	1.42			
Mean	+	442	1.27	0.441	1.10	4.79	0.436	4.06			
SD		50	0.59	0.168	0.19	1.99	0.236	1.66			
Difference between + and −		NS	NS	NS	NS	NS	NS	NS			
Without Rat 5a											
Mean	−	455	1.21	0.415	0.893	4.55	0.400	4.32	2.13 ± 0.88	2.45 ± 0.96[f]	6.7 ± 0.6
SD		45	0.25	0.173	0.183	1.04	0.147	1.05			
Mean	+	450	1.19	0.454	1.08	4.92	0.435	4.38			
SD		45	0.56	0.172	0.185	2.06	0.250	1.40			
Difference between + and −		NS	NS	NS	$p < 0.05$	NS	NS	NS			

[a] The rats received an intravenous injection of ^{14}C-warfarin, 0.2 mg/kg 12 hr after an intravenous injection of either saline solution or nonradioactive warfarin, 0.5 mg/kg, in crossover fashion 1 week apart. [b] The − equals saline injection, and the + equals nonradioactive warfarin. Even-numbered rats received saline injection in the first experiment. [c] The P, A, and B values are in micrograms per milliliter based on a 0.2-mg/kg dose; π, α, and β values are in hours^{-1}. These constants describe the time course of warfarin concentrations: $C_t = Pe^{-\pi t} + Ae^{-\alpha t} + Be^{-\beta t}$, where C_t is the total drug concentration at time t. [d] Serum was collected 5 days after the end of the second experiment, and portions were spiked with ^{14}C-warfarin to yield total concentrations of about 0.5 and 5 μg/ml. [e] Rat 6 died 2 days after the second experiment, before serum for protein binding studies could be collected. [f] Significantly different from free fraction value at a total concentration of 0.5 μg/ml ($p < 0.001$ by paired t test).

centrifuged and cut at the erythrocyte–plasma interface after determination of the hematocrit. The plasma was removed, and warfarin was extracted, separated from its metabolites by TLC, and assayed by scintillation spectrometry as described previously (7). An aliquot of the injection solution was assayed in the same manner, and the plasma warfarin concentrations were normalized for small (9.5 ± 5.9%) interindividual variations from the designated dose. Crossover experiments were carried out 7 days later; animals that previously received saline pretreatment were pretreated with nonradioactive warfarin and *vice versa*. Cannula patency was maintained by replacing the saline solution in the cannula every day.

Five days after the end of the second experiment, blood was removed from the aorta of all animals under light ether anesthesia, and serum was separated. Portions of the serum were used to determine the free fraction of warfarin by equilibrium dialysis (2, 8) after addition of racemic ^{14}C-warfarin, ~0.5 and 5 μg/ml, respectively. The dialyses were done in duplicate. Total protein concentrations in serum were determined by the method of Gornall *et al.* (9) with rat albumin as the standard.

The second part of the study was carried out on adult male Sprague–Dawley rats[1] weighing 350–485 g at the beginning of the first experiment. They were cannulated and placed in metabolism cages as described in an earlier paragraph. The animals received intravenous injections of ^{14}C-warfarin, ~3.5 μCi, together with sufficient nonradioactive racemic warfarin to constitute a total dose of either 0.1 or 1.0 mg/kg. Two rats received the low, high, and low doses in that order, with a 14-day interval between each dose. Two other animals received the doses in the order high, low, and high dose.

Two additional rats received the high dose and then the low dose but expired due to apparent infection before the third (high) dose could be administered. These were the first two animals studied, and the infection problem was not encountered in the subsequently studied animals, apparently because the nonsterile saline solution previously used to fill the cannulas was replaced by sterile saline solution.

Blood sampling and analyses were carried out as in the first part of the investigation. Serum for protein binding determinations was obtained 14 days after the end of the third experiment.

The plasma warfarin concentration data obtained in the first and second parts of the investigation were fitted to a triexponential equation ($C_t = Pe^{-\pi t} + Ae^{-\alpha t} + Be^{-\beta t}$, where C_t is the drug concentration at time t) by a nonlinear least-squares regression procedure (10). Convergence was defined as a relative change in the residual sum of squares less than 10^{-4}. Data in all functions were weighted numerically equal. The apparent volume of the hypothetical central compartment was determined by dividing the injected dose by $P + A + B$. The area under the concentration–time curve (AUC) was calculated by the trapezoidal method to the last experimentally determined concentration, to which the area Ci/β was added, where Ci is the computer-estimated value of the last experimentally determined concentration. This AUC value was used to calculate total clearance (dose/AUC) and V_{area} (dose/$AUC \cdot \beta$). The AUC also was determined from the constants of the triexponential equation as the sum of P/π, A/α, and B/β. Intrinsic clearance was calculated by dividing the total clearance by the serum free fraction (f), using the average of the f values obtained at the 0.5- and 5-μg of warfarin/ml concentrations.

Statistical analyses were done by Student's t test (paired, two tailed).

RESULTS

Results of the first part of the investigation, in which 10 rats received an intravenous injection of ^{14}C-warfarin 12 hr after an injection of saline solution or of nonradioactive warfarin in a crossover experiment, are summarized in Tables I and II. Figure 1 shows the time course of ^{14}C-warfarin plasma concentrations in a typical animal; Fig. 2 shows the re-

Table II—Effect of Drug Concentration on the Pharmacokinetics of Warfarin in Rats: Derived Pharmacokinetic Constants [a]

Rat	Pre-treatment[b]	V_c, ml/kg	V_{area}, ml/kg	Total Clearance[c], ml/hr	Intrinsic Clearance[d], ml/hr	*AUC* by Trapezoidal Method, μg hr/ml	P/π, μg hr/ml	A/α, μg hr/ml	B/β, μg hr/ml	*AUC* from Constants[e], μg hr/ml
1a	−	75.8	177	3.81	142	26.4	0.275	0.960	24.1	25.3
	+	51.5	138	3.28	122	30.8	0.242	0.146	29.4	29.8
2a	−	93.9	190	3.21	245	30.3	0.308	0.289	29.4	30.0
	+	66.2	150	2.80	214	34.3	0.222	2.15	31.4	33.7
3a	−	71.7	157	3.60	290	27.2	0.277	0.655	25.7	26.6
	+	69.2	188	3.42	276	28.2	0.246	0.895	26.4	27.5
4a	−	58.7	214	2.07	185	46.9	0.341	1.93	44.8	47.1
	+	56.5	139	1.55	138	58.9	0.400	4.19	54.1	58.7
5a	−	55.9	140	0.602	37.4	129	0.336	0.370	129	130
	+	54.9	153	0.678	42.1	110	0.559	0.717	108	109
6a	−	76.0	236	3.46	—[f]	20.8	0.212	0.646	19.7	20.6
	+	11.0	220	2.02	—[f]	35.7	0.0842	0.615	34.5	35.2
7a	−	82.3	205	4.16	139	20.1	0.238	1.56	18.5	20.3
	+	85.1	189	3.93	131	20.8	0.315	1.17	18.8	20.3
8a	−	90.9	270	6.16	177	14.1	0.261	2.27	11.5	14.0
	+	84.4	171	5.07	145	17.0	0.293	0.726	15.6	16.6
9a	−	87.7	200	4.97	181	18.6	0.305	1.21	16.8	18.3
	+	85.5	168	3.89	142	22.7	0.205	1.70	18.5	20.4
10a	−	94.0	262	5.87	215	15.6	0.213	1.22	13.9	15.3
	+	87.7	189	4.43	162	21.9	0.235	2.17	19.0	21.4
Mean	−	78.7	205	3.79	179	34.9	0.277	1.11	33.3	34.8
SD		13.7	42	1.67	72	34.4	0.046	0.66	34.9	34.8
Mean	+	75.1	171	3.11	152	38.0	0.280	1.45	35.6	37.3
SD		18.5	26	1.36	64	27.9	0.127	1.17	27.8	27.9
Difference between + and −		NS	$p < 0.05$	$p < 0.01$	$p < 0.01$	NS[g]	NS	NS	NS	NS
Without Rat No. 5										
Mean	−	81.2	212	4.15	197	24.4	0.270	1.19	22.7	24.2
SD		11.8	38	1.31	51	10.0	0.042	0.64	10.1	10.1
Mean	+	77.3	172	3.37	166	30.0	0.249	1.53	27.5	29.3
SD		18.2	27	1.12	53	12.6	0.085	1.22	12.0	12.8
Difference between + and −		NS	$p < 0.02$	$p < 0.01$	$p < 0.01$	$p < 0.01$	NS	NS	NS	$p < 0.02$

[a] Based on P, A, B, π, α, and β values in Table I. [b] See footnote *b* in Table I. [c] Dose divided by *AUC* determined by the trapezoidal method. [d] Total clearance divided by the serum free fraction value obtained by averaging the two free fraction values for each animal listed in Table I. [e] Sum of P/π, A/α, and B/β. [f] Cannot be calculated due to lack of free fraction values. [g] $p < 0.01$ upon statistical analysis of $1/AUC$ values.

sults obtained in Rat 5a, which exhibited very much lower total and intrinsic clearances of warfarin than the rest of the group. The unusual animal is also noteworthy for its very long (≃ 60 hr) warfarin half-life (which showed excellent reproducibility in the crossover study) and its low serum protein concentration, suggestive of impaired liver function.

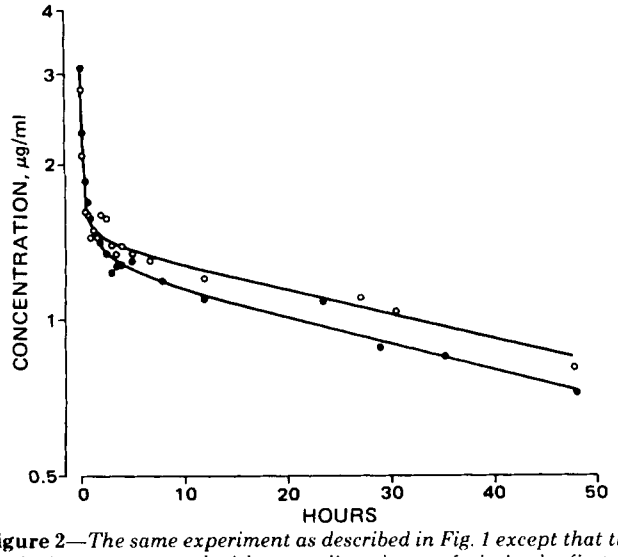

Figure 2—*The same experiment as described in Fig. 1 except that this rat (5a) was pretreated with nonradioactive warfarin in the first experiment and with saline solution in the second experiment. This rat had a much lower total clearance of warfarin and a lower serum protein concentration than the other nine animals, suggesting impaired liver function. The very long and reproducible half-life (60 hr compared to an average of 16 hr in the other rats) should be noted.*

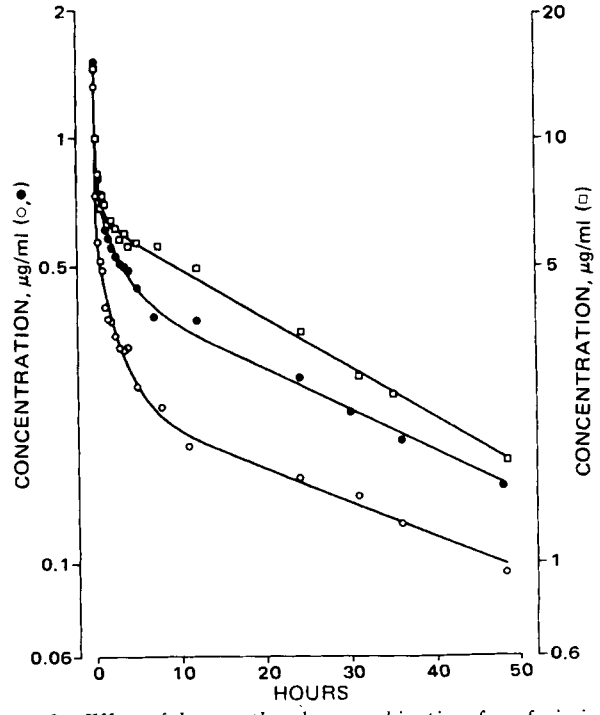

Figure 3—*Effect of dose on the pharmacokinetics of warfarin in Rat 1. This animal received intravenous injections of 0.1, 1.0, and 0.1 mg of ^{14}C-warfarin/kg at 2-week intervals. Key: ○, first dose (0.1 mg/kg); □, second dose (1.0 mg/kg); and ●, third dose (0.1 mg/kg). The data points show the time course of drug concentrations in plasma. The lines were fitted to the data by computer.*

Table III—Effect of Dose on the Pharmacokinetics of Warfarin in Rats: Directly Determined Pharmacokinetic Constants and Serum Protein Binding

Rat	Week	Dose, mg/kg	Body Weight, g	Constants of Triexponential Equation[a]						Serum Free Fraction × 100[b]	
				P	A	B	π	α	$\beta \times 100$	0.5 μg/ml	5 μg/ml
1	1	0.1	353	1.22	0.323	0.237	6.60	0.371	1.76	1.51	1.54
	3	1.0	374	10.8	2.19	6.48	6.66	1.18	2.68		
	5	0.1	393	1.11	0.341	0.446	5.41	0.409	2.18		
2	1	0.1	485	0.644	0.185	0.239	5.34	0.740	4.88	2.23	2.38
	3	1.0	452	4.27	1.10	5.99	4.71	0.471	5.87		
	5	0.1	509	0.634	0.154	0.356	4.26	0.556	4.76		
3	1	1.0	406	9.95	2.09	6.18	5.12	0.798	1.72	1.10	1.25
	3	0.1	421	1.12	0.221	0.453	4.05	0.422	2.41		
	5	1.0	442	8.99	3.85	6.97	10.3	1.51	1.57		
4	1	1.0	352	8.20	1.26	7.17	3.44	1.34	1.79	0.513	0.589
	3	0.1	380	1.01	0.316	0.525	3.94	0.567	2.22		
	5	1.0	401	9.15	1.64	7.45	5.90	0.791	1.69		
5[c]	1	1.0	457	7.60	3.21	5.36	6.84	0.685	2.51	—	—
	3	0.1	449	1.12	0.355	0.367	5.80	0.732	2.35		
	5	1.0	—	—	—	—	—	—	—		
6[c]	1	1.0	360	7.76	2.89	6.13	5.86	0.802	3.05	—	—
	3	0.1	391	1.01	0.407	0.425	5.87	0.495	2.81		
	5	1.0	—	—	—	—	—	—	—		

[a] The P, A, and B values are in micrograms per milliliter; the π, α, and β values are in hours^{-1}. These constants describe the time course of warfarin concentrations in serum; $C_t = Pe^{-\pi t} + Ae^{-\alpha t} + Be^{-\beta t}$, where C_t is the total drug concentration at time t. [b] Serum was collected 2 weeks after the end of the third experiment, and portions were spiked with ^{14}C-warfarin to yield total concentrations of about 0.5 and 5 μg/ml. [c] These animals died before the third experiment and before serum for free fraction determination could be obtained.

Therefore, the average results for the group and the statistical analyses in Tables I and II are presented not only for all 10 rats but also for the group without Rat 5a.

The time course of warfarin concentrations in plasma of all animals was best described by a triexponential equation, consistent with previous observations (11). The constants of that equation for each animal are listed in Table I. Pretreatment with 0.5 mg of warfarin/kg 12 hr earlier (a period somewhat shorter than the average biological half-life of the drug in this group of rats) had no apparent effect on the constants that characterize the so-called distribution phase of drug concentrations in plasma, *i.e.*, P, A, π, and α. There was also no apparent effect on β or, therefore, on the biological half-life of the drug. On the other hand, B was significantly increased by pretreatment with warfarin. The free fraction of warfarin in serum was almost constant over a 10-fold concentration range encompassing the maximum concentration of radioactive and nonradioactive drug in warfarin-pretreated animals and concentrations representing ≤20% of the initial warfarin concentration in these animals when they were pretreated with saline solution (Table I).

The apparent volume of the hypothetical central compartment (V_c) and the partial areas of the distribution phase, P/π and A/α, were not affected by warfarin pretreatment. However, V_{area} and total clearance were decreased significantly by that pretreatment (Table II). The intrinsic clearance of the drug decreased also. The excellent agreement of the AUC values determined by the trapezoidal method with those determined by summing the P/π, A/α, and B/β values reflects the good fit of the experimental data to the triexponential equation.

Consistent with theoretical considerations and previous observations (12), there was an essentially linear relationship between total clearance and serum free fraction of warfarin for the nine rats (*i.e.*, excluding Rat 5a), with a correlation coefficient of 0.87 ($p < 0.01$) for clearance values obtained in the control (saline pretreatment) experiments.

The second part of the study was a difficult three-way crossover experiment designed to confirm the effect of dose on V_{area} and total clearance and to examine the possible effect of dose on the distribution phase over a wider (10-fold) dose range. This experiment required measurements on each animal over 6 weeks and could be completed in only four rats during the time available. Figure 3 shows results obtained in one of two rats that received a 0.1-mg/kg dose first, a 1-mg/kg dose 2 weeks later, and another 0.1-mg/kg dose after 2 more weeks and that were sacrificed 2 weeks after the third dose to obtain serum for protein binding determinations. Figure 4 shows results obtained in one of two animals that received first the high dose, then the low dose, and then again the high dose of warfarin.

The results of the balanced three-way crossover experiment on four rats as well as results obtained from two rats that expired before the third dose are summarized in Tables III and IV. No averaging or statistical analyses were done because only two rats completed any one dosing sequence. It should be noted that P, A, and B will increase proportionally with dose if the pharmacokinetics are linear. In fact, P and A increased less than proportionally with only one exception (Rat 3, 5th week). On the other hand, B increased more than proportionally in all experiments (Table III). There were no apparently dose-dependent trends in π, α, and β. Serum free fraction values at warfarin concentrations of 0.5 and 5 μg/ml did not differ appreciably in any one animal (Table III).

The partial areas P/π and A/α did not increase proportionally with dose while B/β increased more than proportionally with dose (Table IV). There was no remarkable effect of dose on V_c, there occurred a consistent decrease of V_{area} at the higher dose, and there were consistent decreases of the total and intrinsic clearances at the higher dose. In all four rats receiving the three-dose sequence, V_c and V_{area} of the third dose were lower than those of the first (and equal) dose (Table IV).

DISCUSSION

The results of this investigation demonstrate a dose dependence in the pharmacokinetics of warfarin: V_{area}, intrinsic clearance, and, therefore, total clearance decreased with increasing dose in the dose range studied. The decrease in V_{area} is probably due, at least in part, to the previously demonstrated decreased uptake of warfarin by the liver with increasing dose (1) since the liver accounts for a major fraction of the total warfarin in the body following administration of a relatively small dose (2). Such a decrease in V_{area} is quite unusual; much more common is an increase in V_{area} with increasing dose due to decreased plasma protein binding of a drug at higher concentrations. However, O'Reilly *et al.* (13) reported a decrease in the apparent volume of distribution of dicumarol with increasing dose over the 150–600-mg dose range in adult humans. On the other hand, they did not observe such dose dependence with warfarin over the 50–200-mg dose range in the two humans studied (13). A limited study in this laboratory, carried out more than 10 years earlier when ^{14}C-warfarin was not available, revealed no apparent difference in the volume of distribution of warfarin in rats given injections of 4 and 12.5 mg/kg (14). Interestingly, the apparent volume of distribution of these very large doses (110–130 ml/kg) was slightly less than that of the 1-mg/kg dose in the present study.

Theoretical considerations suggest that, all else being equal, a reduction in liver uptake should cause an increase in β and, therefore, a decrease in the biological half-life of warfarin (15). However, the same considerations indicate that β will decrease if the intrinsic clearance is decreased. Thus, the lack of appreciable dose dependence of β in the present study may be rationalized by the opposing effects of decreased warfarin binding or uptake by the liver and decreased intrinsic clearance at the higher dose. It is possible that hepatic warfarin uptake may be due largely to specific binding of the drug to warfarin-metabolizing enzymes and that the decreased hepatic uptake and intrinsic clearance of warfarin at higher doses may be reflections of the same dose-dependent phenomenon.

Adequate blood volumes for serum protein binding studies were obtained only at the end of the crossover experiments to prevent premature exsanguination of the animals. It has been demonstrated previously in

Table IV—Effect of Dose on the Pharmacokinetics of Warfarin in Rats: Derived Pharmacokinetic Constants [a,b]

Rat	Week	Dose, mg/kg	V_c, ml/kg	V_{area}, ml/kg	Total Clearance, ml/hr	Intrinsic Clearance, ml/hr	*AUC* by Trapezoidal Method, μg hr/ml	P/π, μg hr/ml	A/α, μg hr/ml	B/β, μg hr/ml	*AUC* from Constants, μg hr/ml
1	1	0.1	56.1	390	2.43	159	14.5	0.185	0.871	13.5	14.6
	3	1.0	51.3	150	1.50	98.0	250	1.62	1.86	242	245
	5	0.1	52.7	211	1.81	118	21.7	0.205	0.834	20.5	21.5
2	1	0.1	93.4	365	8.64	374	5.61	0.121	0.250	4.90	5.27
	3	1.0	87.6	159	4.22	183	107	0.907	2.34	102	105
	5	0.1	87.6	263	6.37	276	7.99	0.149	0.277	7.48	7.91
3	1	1.0	54.9	159	1.11	61.7	365	1.94	2.62	359	364
	3	0.1	55.8	211	2.14	119	19.7	0.277	0.524	18.8	19.6
	5	1.0	50.5	144	1.00	55.6	442	0.873	2.55	444	447
4	1	1.0	60.2	139	0.873	158	403	2.38	0.940	401	404
	3	0.1	53.9	184	1.55	281	24.5	0.256	0.557	23.6	24.4
	5	1.0	54.9	134	0.905	164	443	1.55	2.07	441	445
5	1	1.0	61.7	181	2.07	—[c]	221	1.11	4.69	214	220
	3	0.1	54.3	261	2.74		16.4	0.193	0.485	15.6	16.3
	5	1.0	—	—	—		—	—	—	—	—
6	1	1.0	59.4	157	1.72	—[c]	209	1.32	3.60	201	206
	3	0.1	54.5	219	2.41		16.2	0.172	0.822	15.1	16.1
	5	1.0	—	—	—		—	—	—	—	—

[a] Based on P, A, B, π, α, and β values in Table III. [b] See footnotes *c*, *d*, and *e* in Table II for additional information. [c] Cannot be calculated due to lack of free fraction values.

this laboratory that serum free fraction values of warfarin in rats remain constant for at least 9 days (16). In another study, in which rats received a large single dose of warfarin, then daily smaller doses for 13 days, and then again a large dose, serum free fraction values were determined before and after this sequence (the time interval being ~35 days) and decreased by 18% on the average (17). We have no direct evidence that the free fraction values remained constant over 6 weeks of the present study. Therefore, there is some uncertainty concerning the *absolute* intrinsic clearance values in this study but not concerning the fact that intrinsic clearance did decrease with increasing dose (since the experiments were carried out in crossover fashion).

The three-way crossover experiments confirmed the results of the first part of the investigation in that they also demonstrated a decrease of V_{area} and intrinsic clearance with increasing dose. In addition, the three-way crossover experiments revealed a *relative* decrease in P and A and, therefore, in P/π and A/α with increasing dose. This result is probably due to an increased serum free fraction at the initial concentrations produced by the 1-mg/kg dose. It has been calculated that the free fraction of warfarin remains essentially constant at plasma warfarin concentrations up to 6 μg/ml and that it increases by 25 and >200% at concentrations of 96 and 282 μg/ml, respectively (18). Initial plasma warfarin concentrations following the 0.1- and 1-mg/kg doses in the present study were ~2 and 17 μg/ml, a difference large enough to expect some change in the free fraction. On the other hand, the first part of this study, in which V and A were not affected by pretreatment with warfarin, involved less than a twofold difference in initial concentration (considering the sum of the concentrations of ^{14}C-warfarin and nonradioactive drug) and these initial concentrations were well below 6 μg/ml.

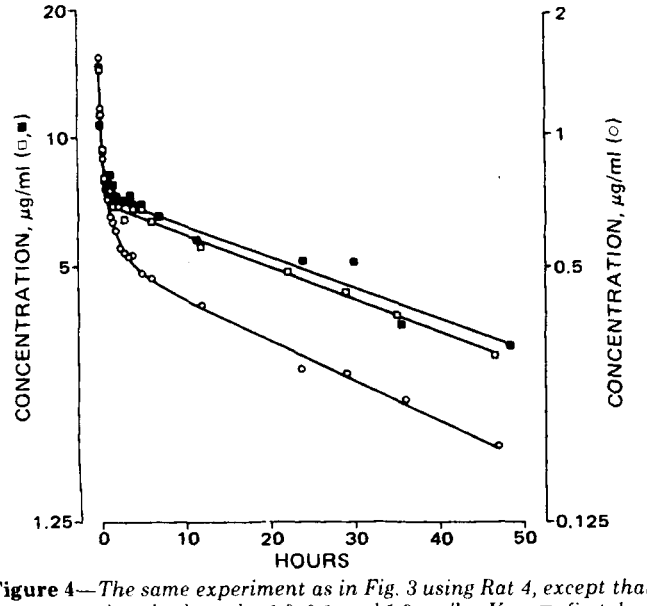

Figure 4—*The same experiment as in Fig. 3 using Rat 4, except that doses were given in the order 1.0, 0.1, and 1.0 mg/kg. Key:* □, *first dose (1.0 mg/kg);* ○, *second dose (0.1 mg/kg); and* ■, *third dose (1.0 mg/kg).*

The suggestion that the decrease in the P and A values after the 1-mg/kg dose (as compared to the corresponding values after the 0.1-mg/kg dose) is due to decreased plasma protein binding of warfarin finds support from results of a previous investigation (11). Studies of warfarin pharmacokinetics were carried out on 14 rats with widely different serum free fraction values (from 0.3×10^{-2} to 2.9×10^{-2}); all animals received a single 0.51-mg/kg injection. There was a statistically significant negative correlation between serum free fraction and P ($r = -0.873$, $p < 0.001$; the negative sign of the correlation coefficient was inadvertently omitted in the cited report).

In summary, warfarin pharmacokinetics in rats are dose dependent; the apparent volume of distribution of the drug, the intrinsic clearance, and the total clearance decrease with increasing dose in the 0.1–1-mg/kg dose range. At least one of these phenomena, *i.e.*, the decrease in the apparent volume of distribution, is probably due largely to decreased hepatic uptake of the drug. In addition, the apparent distribution phase of warfarin concentrations in plasma following intravenous injection of 1 mg/kg is less pronounced than that following a 0.1-mg/kg dose, probably due to decreased protein binding of the drug at the high initial plasma concentrations produced by the larger dose.

REFERENCES

(1) K. Takada and G. Levy, *J. Pharm. Sci.*, **68**, 1569 (1979).

(2) A. Yacobi and G. Levy, *ibid.*, **64**, 1660 (1975).

(3) P. J. McNamara, G. Levy, and M. Gibaldi, *J. Pharmacokinet. Biopharm.*, **7**, 195 (1979).

(4) J. G. Wagner, "Fundamentals of Clinical Pharmacokinetics," Drug Intelligence, Hamilton, Ill., 1971, pp. 270–283.

(5) J. R. Weeks and J. D. Davis, *J. Appl. Physiol.*, **19**, 540 (1964).

(6) J. J. Ashley and G. Levy, *Res. Commun. Chem. Pathol. Pharmacol.*, **4**, 297 (1972).

(7) A. Yacobi, L. B. Wingard, Jr., and G. Levy, *J. Pharm. Sci.*, **63**, 868 (1974).

(8) A. Yacobi and G. Levy, *J. Pharmacokinet. Biopharm.*, **3**, 439 (1975).

(9) A. G. Gornall, C. J. Bardawill, and M. M. David, *J. Biol. Chem.*, **177**, 751 (1949).

(10) C. M. Metzler, G. L. Elfring, and A. J. McEwen, "A Users Manual for NONLIN and Associated Programs," Upjohn, Kalamazoo, Mich., 1974.

(11) A. Yacobi and G. Levy, *J. Pharm. Sci.*, **66**, 567 (1977).

(12) G. Levy and A. Yacobi, *ibid.*, **63**, 805 (1974).

(13) R. A. O'Reilly, P. M. Aggeler, and L. S. Leong, *Thromb. Diath. Haemorrh.*, **11**, 1 (1964).
(14) R. Nagashima and G. Levy, *J. Pharm. Sci.*, **58**, 845 (1969).
(15) M. Gibaldi, G. Levy, and P. J. McNamara, *Clin. Pharmacol. Ther.*, **24**, 1 (1978).
(16) A. Yacobi, J. T. Slattery, and G. Levy, *J. Pharm. Sci.*, **66**, 941 (1977).
(17) A. Yacobi and G. Levy, *ibid.*, **66**, 1275 (1977).
(18) W. D. Wosilait, *Res. Commun. Chem. Pathol. Pharmacol.*, **6**, 943 (1973).

ACKNOWLEDGMENTS

Supported in part by Grant GM 20852 from the National Institute of General Medical Sciences, National Institutes of Health.

Previous paper in this series: K. Takada and G. Levy, *J. Pharm. Sci.*, **68**, 1569 (1979).

Comparative Pharmacokinetics of Coumarin Anticoagulants XLV: Pharmacokinetic and Pharmacodynamic Studies of Acute Interaction between Warfarin and Phenylbutazone in Rats

AVRAHAM YACOBI, CHII-MING LAI, and GERHARD LEVY ˣ

Received June 7, 1979, from the *Department of Pharmaceutics, School of Pharmacy, State University of New York at Buffalo, Amherst, NY 14260.* Accepted for publication July 6, 1979.

Abstract □ A comprehensive investigation of the effect of phenylbutazone on warfarin pharmacokinetics and anticoagulant activity was carried out in rats to identify and quantify various aspects of the interaction between these drugs. Adult male rats received intravenous racemic warfarin alone and together with phenylbutazone in a crossover experiment. Prothrombin complex activity and the plasma concentrations of phenylbutazone and of free and total (free plus protein-bound) warfarin were determined repeatedly for up to 60 hr. The total plasma clearance, the apparent volume of distribution, and the disposition rate constant (β) of warfarin were significantly increased and the intrinsic plasma warfarin clearance was significantly decreased during phenylbutazone administration. Phenylbutazone decreased the serum protein binding of warfarin both *in vitro* and *in vivo*, but the *in vivo* effect was much more pronounced, apparently due to the displacing effect of phenylbutazone metabolite(s). Phenylbutazone alone had no apparent effect on prothrombin complex activity *in vitro* but caused a modest, yet statistically significant, anticoagulant effect *in vivo*. The anticoagulant effect–plasma warfarin concentration curves for total and free warfarin were shifted to a considerably lower concentration range during phenylbutazone treatment. Thus, the interaction between phenylbutazone and warfarin involves at least three processes: an inhibition of warfarin biotransformation (decreased intrinsic clearance); displacement of warfarin from plasma protein binding sites (increased free fraction); and apparent potentiation of the anticoagulant action produced by a given plasma warfarin concentration. The latter may have been caused, at least in part, by a direct anticoagulant effect of phenylbutazone and/or its metabolite(s). The net effect of decreased protein binding and decreased intrinsic clearance was an increase in the total plasma warfarin clearance. The results of this investigation demonstrate that drug interactions can be complex and multifactorial.

Keyphrases □ Warfarin—interaction with phenylbutazone, pharmacokinetics, *in vitro* and *in vivo*, rats, prothrombin complex activity □ Phenylbutazone—interaction with warfarin, pharmacokinetics, *in vitro* and *in vivo*, rats, prothrombin complex activity □ Anticoagulants—warfarin, interaction with phenylbutazone, pharmacokinetics, *in vitro* and *in vivo*, rats, prothrombin complex activity

There is a tendency to attribute most drug interactions to only one of several theoretically possible mechanisms. This approach is probably unrealistic and reflects the limited scope and the relative lack of pharmacokinetic quantitation characteristic of most drug interaction studies. For example, one drug may displace another from plasma protein binding sites and cause the displaced drug to be eliminated more rapidly. Unless the increased clearance of the displaced drug is *quantitatively* consistent with the increase of its free fraction in plasma, additional interaction mechanisms must be sought. These additional mechanisms may operate in the same direction (*i.e.*, increased clearance) or in the opposite direction from that attributable to reduced plasma protein binding. Moreover, pharmacokinetic as well as pharmacodynamic interactions may occur so that an assessment of the therapeutic implications of the interacting system requires consideration of the net effect resulting from both types of interactions. These potential complexities suggest that comprehensive model drug interaction studies are needed for the development of more effective strategies for exploring potential or suspected interactions involving new drugs.

The interaction between the anticoagulant warfarin and the anti-inflammatory agent phenylbutazone is phenomenologically well established, and its potentially disastrous clinical consequences are generally appreciated (1–3). The interaction between these two drugs has been studied in humans (4–8) and in dogs (9). However, the recent development of clearance concepts (10, 11) and the availability of an animal model exhibiting wide interindividual differences in the plasma protein binding of warfarin under normal physiological conditions (12) have provided a more rational basis and a promising means for better exploration of the interaction.

The investigation described here consisted of a rigorous quantitative determination of the phenylbutazone effect on the elimination kinetics and anticoagulant action of warfarin in a crossover study on rats specially selected for wide interindividual differences in serum protein binding of warfarin and, therefore, in warfarin clearance. The phenylbutazone effect on serum protein binding of warfarin was determined *in vitro* and *in vivo*. The relationship between anticoagulant effect and warfarin concentration in plasma was determined for free and total (free plus bound) drug. The phenylbutazone effect *per se* on the coagulation process was examined *in vitro* and *in vivo*.

It is believed that the results of these studies will demonstrate the potential complexity and multifaceted characteristics of drug interactions, will illustrate the practical limitations of many drug interaction studies in humans,

0022-3549/80/0100-0014$01.00/0
© 1980, American Pharmaceutical Association

(13) R. A. O'Reilly, P. M. Aggeler, and L. S. Leong, *Thromb. Diath. Haemorrh.*, **11**, 1 (1964).
(14) R. Nagashima and G. Levy, *J. Pharm. Sci.*, **58**, 845 (1969).
(15) M. Gibaldi, G. Levy, and P. J. McNamara, *Clin. Pharmacol. Ther.*, **24**, 1 (1978).
(16) A. Yacobi, J. T. Slattery, and G. Levy, *J. Pharm. Sci.*, **66**, 941 (1977).
(17) A. Yacobi and G. Levy, *ibid.*, **66**, 1275 (1977).
(18) W. D. Wosilait, *Res. Commun. Chem. Pathol. Pharmacol.*, **6**, 943 (1973).

ACKNOWLEDGMENTS

Supported in part by Grant GM 20852 from the National Institute of General Medical Sciences, National Institutes of Health.

Previous paper in this series: K. Takada and G. Levy, *J. Pharm. Sci.*, **68**, 1569 (1979).

Comparative Pharmacokinetics of Coumarin Anticoagulants XLV: Pharmacokinetic and Pharmacodynamic Studies of Acute Interaction between Warfarin and Phenylbutazone in Rats

AVRAHAM YACOBI, CHII-MING LAI, and GERHARD LEVY ˣ

Received June 7, 1979, from the *Department of Pharmaceutics, School of Pharmacy, State University of New York at Buffalo, Amherst, NY 14260.* Accepted for publication July 6, 1979.

Abstract □ A comprehensive investigation of the effect of phenylbutazone on warfarin pharmacokinetics and anticoagulant activity was carried out in rats to identify and quantify various aspects of the interaction between these drugs. Adult male rats received intravenous racemic warfarin alone and together with phenylbutazone in a crossover experiment. Prothrombin complex activity and the plasma concentrations of phenylbutazone and of free and total (free plus protein-bound) warfarin were determined repeatedly for up to 60 hr. The total plasma clearance, the apparent volume of distribution, and the disposition rate constant (β) of warfarin were significantly increased and the intrinsic plasma warfarin clearance was significantly decreased during phenylbutazone administration. Phenylbutazone decreased the serum protein binding of warfarin both *in vitro* and *in vivo*, but the *in vivo* effect was much more pronounced, apparently due to the displacing effect of phenylbutazone metabolite(s). Phenylbutazone alone had no apparent effect on prothrombin complex activity *in vitro* but caused a modest, yet statistically significant, anticoagulant effect *in vivo*. The anticoagulant effect–plasma warfarin concentration curves for total and free warfarin were shifted to a considerably lower concentration range during phenylbutazone treatment. Thus, the interaction between phenylbutazone and warfarin involves at least three processes: an inhibition of warfarin biotransformation (decreased intrinsic clearance); displacement of warfarin from plasma protein binding sites (increased free fraction); and apparent potentiation of the anticoagulant action produced by a given plasma warfarin concentration. The latter may have been caused, at least in part, by a direct anticoagulant effect of phenylbutazone and/or its metabolite(s). The net effect of decreased protein binding and decreased intrinsic clearance was an increase in the total plasma warfarin clearance. The results of this investigation demonstrate that drug interactions can be complex and multifactorial.

Keyphrases □ Warfarin—interaction with phenylbutazone, pharmacokinetics, *in vitro* and *in vivo*, rats, prothrombin complex activity □ Phenylbutazone—interaction with warfarin, pharmacokinetics, *in vitro* and *in vivo*, rats, prothrombin complex activity □ Anticoagulants—warfarin, interaction with phenylbutazone, pharmacokinetics, *in vitro* and *in vivo*, rats, prothrombin complex activity

There is a tendency to attribute most drug interactions to only one of several theoretically possible mechanisms. This approach is probably unrealistic and reflects the limited scope and the relative lack of pharmacokinetic quantitation characteristic of most drug interaction studies. For example, one drug may displace another from plasma protein binding sites and cause the displaced drug to be eliminated more rapidly. Unless the increased clearance of the displaced drug is *quantitatively* consistent with the increase of its free fraction in plasma, additional interaction mechanisms must be sought. These additional mechanisms may operate in the same direction (*i.e.*, increased clearance) or in the opposite direction from that attributable to reduced plasma protein binding. Moreover, pharmacokinetic as well as pharmacodynamic interactions may occur so that an assessment of the therapeutic implications of the interacting system requires consideration of the net effect resulting from both types of interactions. These potential complexities suggest that comprehensive model drug interaction studies are needed for the development of more effective strategies for exploring potential or suspected interactions involving new drugs.

The interaction between the anticoagulant warfarin and the anti-inflammatory agent phenylbutazone is phenomenologically well established, and its potentially disastrous clinical consequences are generally appreciated (1–3). The interaction between these two drugs has been studied in humans (4–8) and in dogs (9). However, the recent development of clearance concepts (10, 11) and the availability of an animal model exhibiting wide interindividual differences in the plasma protein binding of warfarin under normal physiological conditions (12) have provided a more rational basis and a promising means for better exploration of the interaction.

The investigation described here consisted of a rigorous quantitative determination of the phenylbutazone effect on the elimination kinetics and anticoagulant action of warfarin in a crossover study on rats specially selected for wide interindividual differences in serum protein binding of warfarin and, therefore, in warfarin clearance. The phenylbutazone effect on serum protein binding of warfarin was determined *in vitro* and *in vivo*. The relationship between anticoagulant effect and warfarin concentration in plasma was determined for free and total (free plus bound) drug. The phenylbutazone effect *per se* on the coagulation process was examined *in vitro* and *in vivo*.

It is believed that the results of these studies will demonstrate the potential complexity and multifaceted characteristics of drug interactions, will illustrate the practical limitations of many drug interaction studies in humans,

0022-3549/80/0100-0014$01.00/0
© 1980, American Pharmaceutical Association

Table I—*In Vitro* Phenylbutazone Effect on Protein Binding of Warfarin in Rat Serum [a]

Phenylbutazone, μg/ml	Warfarin Concentration 0.43 μg/ml	0.70 μg/ml	1.43 μg/ml	2.90 μg/ml	Mean ± *SD*
0	0.586	0.569	0.553	0.645	0.588 ± 0.040
25	0.830	0.846	0.752	0.821	0.812 ± 0.041
50	1.02	0.914	0.893	0.893	0.930 ± 0.061
100	1.01	1.03	1.08	1.16	1.07 ± 0.067
200	2.27	2.21	2.29	2.45	2.30 ± 0.103

[a] Pooled serum from eight rats. Reported are values of free fraction × 100.

and will suggest the effort required for a comprehensive and quantitative exploration of drug interactions in general.

EXPERIMENTAL

***In Vitro* Phenylbutazone Effect on Serum Protein Binding of Warfarin**—Eight randomly selected adult male Sprague–Dawley rats[1] were sacrificed under ether anesthesia by withdrawal of all blood from the abdominal aorta. The blood was converted into serum, and the latter was pooled. Two-milliliter portions of serum were spiked with racemic ^{14}C-warfarin[2] and with phenylbutazone[3] to produce concentrations of 0.4–3 μg of warfarin/ml and 0–200 μg of phenylbutazone/ml. ^{14}C-Warfarin was dissolved in ethylene dichloride. A portion of this solution was transferred to a glass vial and evaporated under nitrogen flow. Ten microliters of phenylbutazone in 0.1 *N* NaOH was added to the warfarin, and the mixture was shaken thoroughly and mixed with the serum. The serum binding was determined by equilibrium dialysis at 37° (12).

***In Vivo* Phenylbutazone Effect on Serum Protein Binding of Warfarin**—Ten randomly selected rats, 340–415 g, received phenylbutazone, 40 mg/kg ip, initially followed by 20 mg/kg ip every 4 hr for 10 doses. Immediately before the first injection and 2 hr after the last one, 2.5–3.0 ml of blood was withdrawn from the tail artery. Serum was separated and spiked with ^{14}C-warfarin for protein binding determinations.

Assay of Warfarin and Phenylbutazone—The concentrations of warfarin in serum, plasma, and buffer solution were determined by extraction, TLC, and scintillation counting (13). Phenylbutazone in plasma and serum was assayed by the method of Jähnchen and Levy (14). That assay was modified slightly to increase the sensitivity. To 0.1 ml of plasma, 0.1 ml of 3 *N* HCl and 2 ml of *n*-heptane were added. After shaking for 30 min, the phases were separated by centrifugation at 1000×*g* for 3 min. To 1.8 ml of the *n*-heptane phase, 2 ml of 1 *N* NaOH was added. After shaking for 5 min and centrifuging for the same time, the heptane phase was discarded. To 1.8 ml of the sodium hydroxide phase, 3 ml of buffered

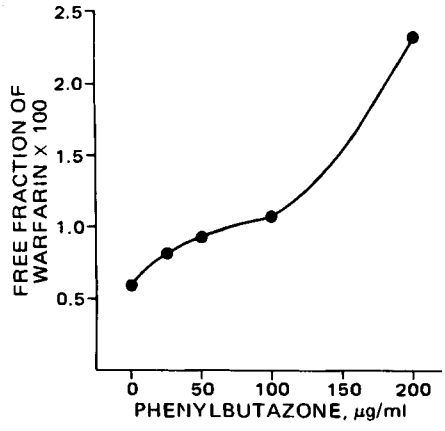

Figure 1—*Relationship between mean free fraction of warfarin in serum and phenylbutazone concentration. Both drugs were added to pooled rat serum* in vitro.

[1] Blue Spruce Farms, Altamont, N.Y.
[2] 3-[α-Acetonyl(benzyl-α-^{14}C)]-4-hydroxycoumarin, specific activity 71 μCi/mg, Amersham-Searle Corp., Arlington Heights, Ill.
[3] Geigy Pharmaceuticals, Ardsley, N.Y.

Table II—Phenylbutazone Effect on Warfarin Pharmacokinetics in Rats [a]

Pharmacokinetic Constant	Control	With Phenylbutazone
Total plasma clearance, ml/hr/kg	8.88 (2.92–24.0)	17.8[b] (6.74–41.2)
Half-life, hr	16.3 (6.31–31.6)	8.66[b] (4.55–14.6)
Volume of distribution, ml/kg	152 (117–219)	175[b] (128–271)
Serum free fraction × 100	0.908 (0.296–1.90)	2.92[b,c] (0.957–7.03)
Intrinsic plasma clearance, ml/hr/kg	985 ± 163 (764–1304)	651 ± 83[b] (497–796)

[a] Results are reported as mean values for 11 animals, with the range in parentheses. Standard deviations are omitted, with one exception, for reasons discussed in the text. [b] Statistically significantly different from the control value ($p < 0.01$) by paired *t* test. [c] The concentration of phenylbutazone in these serum samples was 67.1 ± 24.6 μg/ml.

permanganate solution (14) was added, and the mixture was incubated at 65° for 5 min. After cooling, 1 ml of *n*-heptane was added, and the procedure was continued as described previously (14). The assay was not affected by warfarin nor was the warfarin assay or recovery affected by phenylbutazone.

Warfarin–Phenylbutazone Interaction—Twelve dicumarol-screened (15, 16) male adult Sprague–Dawley rats, weighing 350–450 g and differing widely in dicumarol half-life, were selected from a group of 30 animals. They had unrestricted access to food[4] and water before and during the experiment. The rats were given intraperitoneal injections of phenylbutazone, 40 mg/kg, or saline solution at −2 hr and then 20 mg of phenylbutazone/kg or saline solution every 4 hr for 50–60 hr. The animals received warfarin, 0.6 mg/kg iv consisting of about 22 μCi of ^{14}C-warfarin[5]/kg and nonradioactive warfarin[6], except for three rats that received only 0.3 mg/kg in the experiment with phenylbutazone. Three weeks later, the rats that had received phenylbutazone received saline solution and *vice versa*. Blood samples were collected repeatedly from the tail artery for 40–60 hr after warfarin injection.

The warfarin injection solutions were prepared by separately dissolving the labeled and unlabeled drug in small volumes of 0.1 *N* NaOH. The

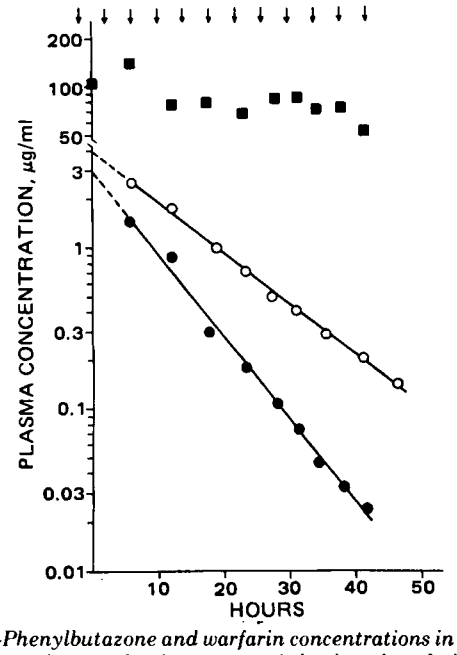

Figure 2—*Phenylbutazone and warfarin concentrations in the plasma of a representative rat after intravenous injection of warfarin alone* (○) *and with repeated intraperitoneal injections of phenylbutazone* (●). *The squares represent the phenylbutazone concentration in plasma, and the arrows indicate when phenylbutazone was injected.*

[4] Charles River Formula 4RF.
[5] About 8 μCi/rat, specific activity 71 μCi/mg.
[6] Endo Laboratories, Garden City, N.Y.

Table III—Phenylbutazone Effect on Serum Protein Binding of Warfarin in Rats Treated with Phenylbutazone Only [a]

	Warfarin[b], μg/ml		Phenylbutazone[b], μg/ml	Free Fraction of Warfarin in Serum × 100		
	Control	With Phenylbutazone		Control	With Phenylbutazone	Ratio[c]
Mean[d]	0.730	0.758	62	0.588	2.33[e]	4.0
SD	0.071	0.051	14	0.156	0.60	0.6
Range	0.630–0.861	0.665–0.846	37–78	0.260–0.767	1.32–3.26	3.3–5.1

[a] ^{14}C-Warfarin was added to the serum *in vitro*. [b] Measured after equilibrium dialysis. [c] Ratio of free fraction values, with phenylbutazone:control. [d] n = 10. [e] Statistically significantly different from the control value (paired t test, $p < 0.001$).

unlabeled drug solution was added to the labeled drug solution, and this mixture was diluted immediately with pH 7.4, 0.15 *M* phosphate buffer such that 1 ml of the final solution contained 0.29–0.34 mg of warfarin. Phenylbutazone was dissolved in 0.1 *N* NaOH, and the solution was diluted with saline; the pH was adjusted to ~8 with pH 7.4, 0.15 *M* phosphate buffer. The solutions were prepared just before injection.

Collection of multiple blood samples (0.45 ml) from rats, measurement of prothrombin time in 10-fold diluted plasma, conversion of prothrombin time to prothrombin complex activity (PCA), and calculation of prothrombin complex activity synthesis rates (R_{syn}) were carried out as described previously (16). Two 0.1-ml plasma samples were used for warfarin and phenylbutazone determinations, respectively. Two hours after the last phenylbutazone or saline injection, ~1.2 ml of blood was withdrawn, and the serum was separated. The latter was spiked with ~0.3 μg of ^{14}C-warfarin, and ~0.5 ml was used for serum protein binding determinations.

The apparent first-order elimination rate constant (β) and the warfarin biological half-life were determined from the least-squares slope of a plot of log plasma warfarin concentrations *versus* time. The apparent volume of distribution (V_d) was calculated by dividing the injected dose by the extrapolated zero-time plasma warfarin concentration. Total plasma clearance was calculated as the product of β and V_d, and intrinsic plasma clearance was calculated by dividing the total clearance by the serum free fraction of warfarin. The plasma warfarin concentrations at which the prothrombin complex activity R_{syn} was 0 and 50% of normal/day were determined from the linear portion of a plot of R_{syn} *versus* log plasma warfarin concentration.

RESULTS

Table I shows the *in vitro* effect of phenylbutazone (0–200 μg/ml) on the protein binding of warfarin (0.43–2.90 μg/ml) in rat serum. The warfarin concentrations were in the range of experimental interest. The free fraction of warfarin increased with increasing phenylbutazone concentration but was practically independent of warfarin concentration. A plot of mean free fraction value *versus* phenylbutazone concentration shows a shoulder in the 25–100-μg/ml range (Fig. 1). Therefore, the phenylbutazone dosage regimen was designed to maintain concentrations in this range to minimize fluctuations in the free fraction of warfarin in plasma during the *in vivo* experiments.

Figure 2 shows the effect of phenylbutazone administration on the warfarin concentrations in the plasma of a representative rat (Rat 3). Also shown are the plasma phenylbutazone concentrations. Blood samples were obtained at different times relative to the time of phenylbutazone injections (because blood sampling times were dictated primarily by the rate of the prothrombin complex activity change); this accounts for much of the fluctuation of the reported phenylbutazone concentrations in any one animal. The mean plasma phenylbutazone concentration of the 11 rats used in this study ranged from 45 to 90 μg/ml, with an average coefficient of variation of 29% in individual animals.

The phenylbutazone effects on warfarin pharmacokinetics in 11 rats are summarized in Table II. Phenylbutazone administration caused a significant increase in the total plasma clearance, apparent volume of distribution, and serum free fraction of warfarin and a significant decrease in the biological half-life and intrinsic plasma clearance of the drug. The animals used were selected by a screening test from a larger group of rats to obtain animals with widely different and relatively evenly distributed total clearance values. Consequently, all pharmacokinetic data in Table II, except those representing intrinsic clearance (which shows relatively small interindividual variation), are reported in terms of the mean and range of individual values rather than as the mean ± *SD*.

It is more informative to consider the ratio, phenylbutazone:control, than the absolute values of the pharmacokinetic constants. These ratios were determined individually for each animal and are reported as the mean ± *SD*, n = 11: total plasma clearance, 2.10 ± 0.40; intrinsic plasma clearance, 0.674 ± 0.120; and free fraction in serum, 3.16 ± 0.59. The relatively small coefficient of variation of these constants reflects a strong correlation between values obtained from individual rats in control experiments and during phenylbutazone administration. This correlation is shown in Fig. 3 for the biological half-life, in Fig. 4 for the apparent volume of distribution, and in Fig. 5 for the serum free fraction of warfarin.

There is no apparent relationship between the average plasma phenylbutazone concentration (indicative of the total clearance of that drug) in individual rats and the total or intrinsic warfarin clearance (alone or during phenylbutazone administration). On the other hand, there is some indication of a concentration–response relationship with respect to phenylbutazone inhibition of warfarin biotransformation. Specifically, there appears to be a negative correlation between average phenylbuta-

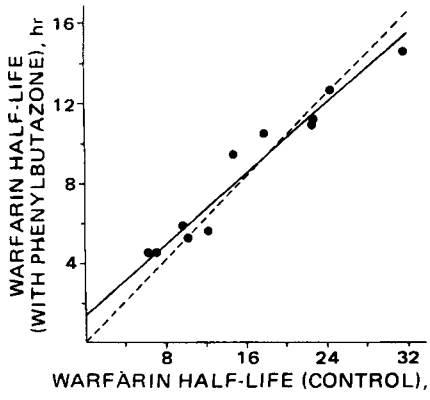

Figure 3—*Relationship between the warfarin biological half-life in control experiments and in the same rats during concomitant phenylbutazone administration. In this figure, as well as in Figs. 5 and 6, the continuous line was obtained by double-regression analysis and the stippled line was obtained by forcing the regression line through the origin. The correlation coefficient is 0.974, p < 0.001.*

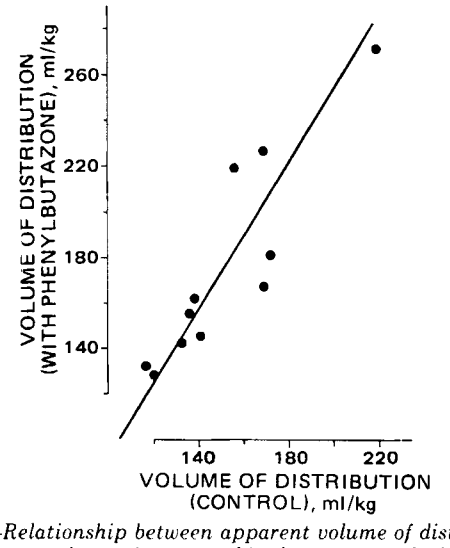

Figure 4—*Relationship between apparent volume of distribution of warfarin in control experiments and in the same rats during concomitant phenylbutazone administration. The correlation coefficient is 0.896, p < 0.001.*

Table IV—Effect of Phenylbutazone on Prothrombin Complex Activity (PCA) before Warfarin Administration and on the Maximum Anticoagulant Action of a Single Warfarin Dose in Individual Rats

Rat	PCA before Warfarin Administration, % of normal		Maximum Effect[a], PCA_{min}, % of normal	
	Control	With Phenylbutazone	Control	With Phenylbutazone
1	98.4	94.9	10.0	3.5
2	106.1	94.9	15.0	8.5
3	106.1	98.4	10.7	2.8
4	94.9	102.1	11.0	6.5
5	110.4	94.9	12.4	7.7
6	94.9	98.4	11.0	4.4
7[b]	102.1	96.6	13.8	12.2
8	102.1	100.2	12.8	2.3
9[b]	102.1	98.4	22.9	11.3
10	98.4	91.7	19.3	—[c]
11[b]	106.1	98.4	28.9	11.2
Mean	102.0	97.1[d]	11.8[e]	5.10[e,f]
SD	5.0	2.9	1.7	2.46

[a] Expressed as the lowest observed prothrombin complex activity value (PCA_{min}). [b] These rats received 0.3 mg of warfarin/kg with phenylbutazone (see text for explanation); the others received 0.6 mg of warfarin/kg with phenylbutazone. All rats received 0.6 mg of warfarin/kg in the control experiments. Even-numbered animals received phenylbutazone and warfarin in the first experiment; odd-numbered animals received only warfarin in the first experiment. [c] The experiment with this rat was discontinued because of severe bleeding. [d] Statistically significantly different from the control value (paired *t* test, $p < 0.05$). [e] Mean of the data for Rats 1–6 and 8 only. [f] Statistically significantly different from the control value (paired *t* test, $p < 0.001$).

zone concentration in plasma and the phenylbutazone:control ratio of the intrinsic warfarin clearances in individual animals (Fig. 6).

In view of the pronounced difference between the *in vitro* and *in vivo* effects of comparable phenylbutazone concentrations on serum protein binding of warfarin (free fraction values in Tables I and II), a group of rats was given a series of phenylbutazone injections (*i.e.*, no warfarin), and serum free fraction values were determined before and during phenylbutazone treatment. The results (Table III) show a magnitude of displacing effect similar to that observed in the *in vivo* warfarin–phenylbutazone interaction study and much greater than that observed in the *in vitro* experiments.

Theoretical considerations and previous experimental evidence (10) indicate that an essentially linear relationship between the total plasma clearance and the serum or plasma free fraction of warfarin should exist. Such correlations were obtained in the present study for warfarin in control experiments and during phenylbutazone administration (Fig. 7). The differences in the regression line slopes reflect the phenylbutazone effect on the intrinsic warfarin clearance. The shift of the free fraction values during phenylbutazone administration to a higher range than that observed without phenylbutazone is indicative of the displacing effect.

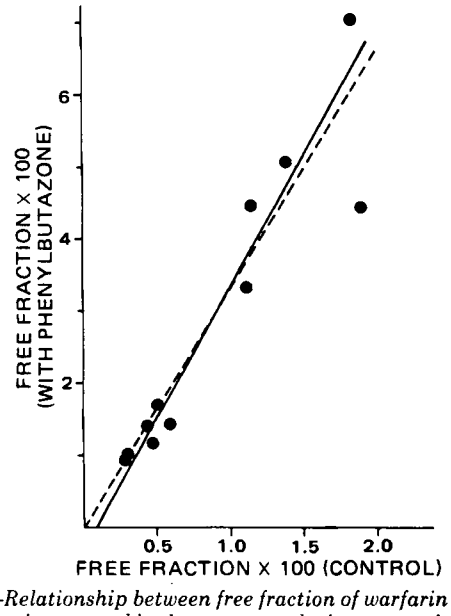

Figure 5—*Relationship between free fraction of warfarin in serum in control experiments and in the same rats during concomitant phenylbutazone administration. The correlation coefficient is 0.927,* $p < 0.001$.

Table V—Effect of Phenylbutazone on Relationship between Relative Prothrombin Complex Activity Synthesis Rate and Warfarin Concentration in Rat Plasma

Rat	$-m$[a], % of normal/day		C_{max}[b], μg/ml		Ratio, Control:With Phenylbutazone
	Control	With Phenylbutazone	Control	With Phenylbutazone	
1	1.16	1.32	0.298	0.0836	3.6
2	1.14	1.22	0.420	0.130	3.2
3	1.11	0.851	0.693	0.120	5.8
4	0.985	0.950	0.942	0.156	6.0
5	1.22	0.977	0.720	0.126	5.7
6	1.13	1.28	1.65	0.330	5.0
7	1.02	2.11	2.00	0.454	4.4
8	1.65	2.94	2.20	0.236	9.3
9	1.78	2.63	2.03	0.336	6.0
10	1.48	—[c]	2.72	—[c]	—[c]
11	2.72	1.58	3.14	0.754	4.2
Mean[d]	1.39	1.58[e]	1.41	0.272[f]	5.3
SD	0.535	0.731			1.7

[a] Slope of a plot of R_{syn}/R^0_{syn} *versus* log plasma warfarin concentration. [b] Intercept of the plot described in footnote *a* upon extrapolation to the concentration axis where $R_{syn}/R^0_{syn} = 0$. [c] The experiment with this rat was discontinued because of severe bleeding. [d] Without Rat 10. [e] No statistically significant difference between the two treatments. [f] Statistically significantly different from the control value (paired *t* test, $p < 0.001$).

Phenylbutazone, 100 μg/ml added *in vitro* to individual serum samples from 12 rats, had no effect on prothrombin complex activity. The prothrombin complex activity in serum (mean ± *SD*) was 98.2 ± 8.6% of normal without phenylbutazone and 98.4 ± 7.3% with added phenylbutazone. The ratio of prothrombin complex activity values, phenylbutazone:control, was 1.00 ± 0.03 (mean ± *SD*). On the other hand, phenylbutazone administered to rats caused a small but statistically significant prothrombin complex activity decrease (Table IV). This apparent anticoagulant effect was evident 2 hr after the first phenylbutazone dose, *i.e.*, at zero time relative to the time of warfarin injection when the first (before warfarin) blood sample was obtained (Fig. 2).

The maximum warfarin anticoagulant effect was significantly more pronounced during phenylbutazone administration than in the control experiments (Table IV). One animal (Rat 12), a slow eliminator given warfarin with phenylbutazone, was lost in the first part of the study due to hemorrhage. Therefore, the warfarin dosage in the second (crossover) part of the study was reduced to one-half in the three rats with the lowest total warfarin clearance. Even these three rats exhibited a more pronounced maximum anticoagulant effect during phenylbutazone administration, despite the reduced warfarin dose.

Repeated measurements of warfarin concentrations and prothrombin complex activity in the rats after warfarin administration permitted

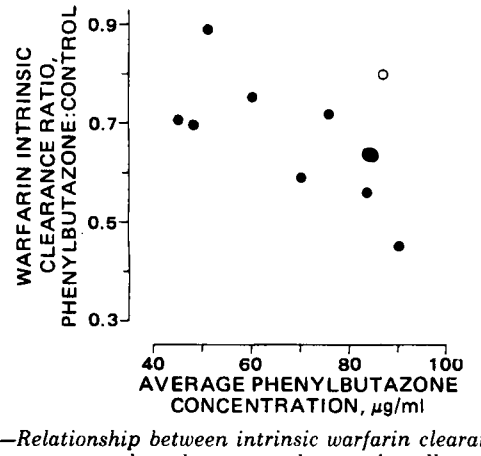

Figure 6—*Relationship between intrinsic warfarin clearance ratio, phenylbutazone:control, and average plasma phenylbutazone concentration. The correlation coefficient is −0.55* ($p < 0.1$) *for all 11 rats and −0.73* ($p < 0.02$) *for 10 rats (with O excluded).*

Table VI—Effect of Phenylbutazone on Total and Free Warfarin Concentrations in Plasma or Serum when the Anticoagulant Effect Is 50% of Maximum ($R_{syn} = 0.5\ R^0_{syn}$)

Rat	Total Concentration in Plasma, μg/ml		Control:With Phenylbutazone	Free Warfarin in Serum, μg/ml × 100		Control:With Phenylbutazone
	Control	With Phenylbutazone		Control	With Phenylbutazone	
1	0.110	0.0338	3.2	0.202	0.236	0.86
2	0.153	0.0507	3.0	0.291	0.222	1.3
3	0.246	0.0310	7.9	0.334	0.165	2.0
4	0.292	0.0463	6.3	0.330	0.154	2.1
5	0.280	0.0388	7.2	0.322	0.172	1.9
6	0.600	0.123	4.9	0.355	0.176	2.0
7	0.648	0.263	2.5	0.330	0.447	0.74
8	1.09	0.160	6.8	0.445	0.186	2.4
9	1.06	0.217	4.9	0.466	0.304	1.5
10	1.25			0.370		
11	2.06	0.364	5.7	0.612	0.348	1.8
Mean[a]	0.654	0.133[b]	5.2	0.369	0.241[b]	1.7[c]
SD			2.0			0.6

[a] Without Rat 10. [b] Statistically significantly different from the control value (paired *t* test, $p < 0.01$). [c] Statistically significantly different from the total concentration ratio (paired *t* test, $p < 0.001$).

determinations of the relationship between anticoagulant effect and drug concentration. Results obtained from a representative animal are shown in Fig. 8. The regression line of a plot of the relative prothrombin complex activity synthesis rate *versus* log plasma warfarin concentration can be characterized by its slope (m) and by the extrapolated intercept on the concentration axis at a synthesis rate of zero (C_{max}). The results obtained from all animals are summarized in Table V. The phenylbutazone effect is more readily apparent in Fig. 9, which is a schematic representation of the average results from all animals. There was a pronounced shift of the effect–log concentration regression line to a lower concentration range during phenylbutazone treatment, with no significant change in the slope.

A convenient index of anticoagulant effect is the warfarin concentration required to produce 50% inhibition of the prothrombin complex activity synthesis rate (referred to as the effective concentration). The effective concentrations of total as well as free warfarin were markedly reduced during phenylbutazone administration (Table VI). The average ratio of effective concentrations, control:phenylbutazone, was 5.2 for total drug and 1.8 for free drug. The difference in these ratios reflects the increased serum free fraction values of warfarin during phenylbutazone administration. There is no apparent correlation between the effective concentration ratios and the average phenylbutazone concentration in individual animals.

DISCUSSION

The results of this investigation demonstrate that the acute interaction between phenylbutazone and racemic warfarin in rats involves at least three mechanisms: displacement of warfarin from serum protein binding sites by phenylbutazone and its metabolites, inhibition of intrinsic warfarin clearance, and apparent potentiation of the anticoagulant action produced by a given plasma warfarin concentration. These effects were produced at average phenylbutazone concentrations in plasma (45–90 μg/ml) similar to those observed clinically. For example, 100 mg of the drug given three times a day to normal adult subjects resulted in plasma concentrations (mean ± *SD*) of 76 ± 7 μg/ml (7).

The phenylbutazone displacing effect on warfarin in serum was of similar magnitude in animals who received both drugs and in those who received only phenylbutazone (with warfarin added *in vitro*). On the other hand, *in vitro* phenylbutazone addition to serum from nonmedicated animals had a much less pronounced displacing effect at concentrations comparable to those obtained *in vivo*. These results indicate that the displacing effect is due not only to phenylbutazone but also to one or more of its metabolites. In fact, oxyphenbutazone, a major phenylbutazone metabolite, is strongly bound to albumin (17) and, therefore, may be a very effective displacer of warfarin from binding sites on the albumin molecule.

In theory, the more pronounced phenylbutazone displacing effect *in vivo* can be due also to accumulation of warfarin metabolites capable of competing with warfarin for albumin binding sites. There is indirect evidence that phenylbutazone inhibits the elimination of at least one warfarin metabolite in humans (7). However, the reduction of warfarin binding in serum from phenylbutazone-treated rats and from phenylbutazone- and warfarin-treated rats was comparable, indicating that warfarin metabolites contributed negligibly to the decreased protein binding of warfarin.

A recent report of a long-term multiple-dose study of the warfarin–phenylbutazone interaction in a single normal human subject stated that "changes in the degree of plasma binding of warfarin were the same as those found from *in vitro* experiments in which warfarin and phenylbutazone were added to control plasma samples" (8). Yet, the warfarin free fraction in that subject remained elevated after phenylbutazone

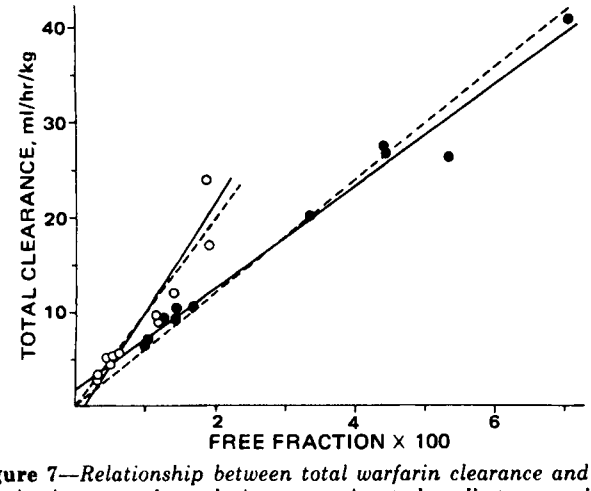

Figure 7—*Relationship between total warfarin clearance and free fraction in serum of rats during concomitant phenylbutazone administration (●) and in the same animals in control experiments (○). The correlation coefficient for the data with phenylbutazone is 0.997, p < 0.001, and that for the control data is 0.940, p < 0.001. There is a statistically significant difference (p < 0.001) in the slopes of the two regression lines.*

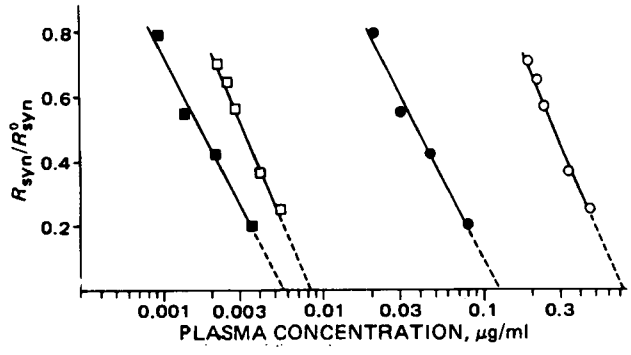

Figure 8—*Relationship between relative synthesis rate of prothrombin complex activity (R_{syn}/R^0_{syn}) and the total (free plus bound) concentration (circles) or the free concentration (squares) of warfarin in plasma of a representative rat. The closed symbols represent the relationship during phenylbutazone treatment, and the open symbols represent the relationship in the control experiment.*

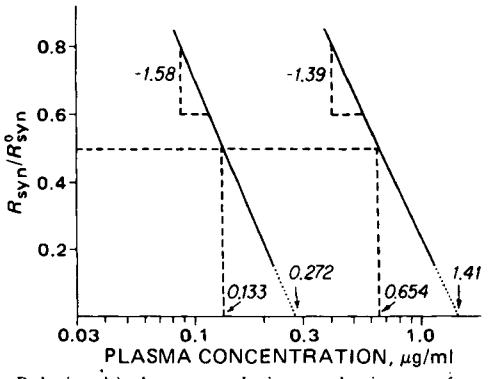

Figure 9—*Relationship between relative synthesis rate of prothrombin complex activity* (R_{syn}/R^0_{syn}) *and the total warfarin concentration in plasma of rats during treatment with phenylbutazone (left) and in control experiments (right) (based on the average data in Tables V and VI).*

administration was discontinued and plasma concentrations of this drug had decreased substantially, suggesting (as the authors acknowledged) that one or more phenylbutazone metabolites contributed to the displacing effect.

Phenylbutazone administration decreased the intrinsic warfarin clearance. This effect was less pronounced than the displacing effect, causing the total warfarin clearance to increase during phenylbutazone administration. Similar effects were observed in a chronic interaction study on one human subject (8). Whether chronic phenylbutazone administration would induce warfarin-metabolizing enzyme systems in rats remains to be determined. Since the total warfarin clearance is proportional to the drug's free fraction in plasma or serum, and since intrinsic drug clearance (*i.e.*, the proportionality constant in the relationship between total clearance and free fraction) differs relatively little between animals, a plot of total clearance *versus* free fraction in serum is essentially linear (10). If phenylbutazone treatment has a quantitatively similar effect on the intrinsic warfarin clearance in all animals, then the linear relationship between total clearance and the serum free fraction should remain. A decrease in intrinsic clearance and an increase in the serum free fraction should then cause the slope of the plot to decrease and the free fraction values to shift to a higher range. This is demonstrated strikingly by the present study (Fig. 7). The free fraction values were determined in serum rather than in plasma because we have found that addition of anticoagulants to blood affects the protein binding of warfarin.

The warfarin anticoagulant effect is a function of its free rather than of its total concentration in plasma (18). Consequently, decreased protein binding of warfarin due to phenylbutazone administration should shift the anticoagulant effect–plasma total warfarin concentration curve to the left, *i.e.*, to a lower concentration range. Such a shift is well demonstrated in this investigation (Fig. 9). However, a similar shift occurred in the anticoagulant effect–*free* warfarin concentration curve, albeit of considerably smaller magnitude. Such a shift may occur for at least two reasons. One is related to the fact that the phenylbutazone effect on warfarin pharmacokinetics is stereoselective. In humans, phenylbutazone decreases the total clearance of the more potent (*S*)-enantiomer and increases the total clearance of the (*R*)-enantiomer (7). The metabolic fate of the warfarin enantiomers in rats differs appreciably from that in humans (19), and there is no information about the possible stereoselectivity of the phenylbutazone interaction with warfarin in rats. A selective inhibition of the intrinsic clearance of (*S*)-warfarin would cause an increase in the (*S*)- to (*R*)-enantiomer concentration ratio in rat plasma after administration of racemic warfarin and a shift of the anticoagulant effect–free warfarin concentration curve to the left due to the higher potency of the (*S*)-enantiomer.

Another possible reason for such a shift is a direct effect of phenylbutazone (or its metabolites) on the blood-clotting process. Our studies have shown that phenylbutazone has no such effect when added *in vitro* to plasma but that even a single 40-mg/kg dose caused a small but statistically significant decrease of prothrombin complex activity 2 hr later (Table IV). It is possible that the effect was more pronounced during the interaction study, *i.e.*, following administration of several phenylbutazone doses.

The literature concerning the phenylbutazone effect on the blood-clotting process is conflicting. Some investigations in humans (6, 20) and a previous but very limited study on rats in our own laboratory (21) revealed no apparent effect. One investigator (22), however, reported observations concerning 44 patients on phenylbutazone of whom about one-third showed prolongation of the one-stage prothrombin time that was sometimes alarming. As explained by Koch-Weser and Sellers (2), a slight hypoprothrombinemic effect of a drug may escape detection in nonanticoagulated subjects but will be obvious in subjects whose prothrombin complex activity has already been depressed by coumarin anticoagulant therapy. Thus, technical difficulties of detection may account for the conflicting data concerning the effect of phenylbutazone administration on blood clotting.

This investigation, despite its relative comprehensiveness and the consequent technical difficulties and cost in time and effort, still falls far short of providing a complete picture of the phenylbutazone–warfarin interaction. The effect of warfarin on the disposition of phenylbutazone and its pharmacologically and physicochemically (with respect to displacing effect on warfarin) active metabolites has not been established; the dose or concentration dependence of the interaction is unknown (warfarin displacement from protein binding sites and warfarin metabolism inhibition may exhibit different effect–phenylbutazone concentration relationships, causing the net effect to be potentiation or reduction of anticoagulant response, depending on the doses used); time-dependent phenomena have not been explored; the mechanism of the increased anticoagulant effect of a given *free* warfarin concentration in plasma during phenylbutazone treatment has not been established. The latter effect could have been explored better if one warfarin enantiomer labeled with carbon 14 and the other labeled with tritium had been available. The alternative, separate interaction studies of phenylbutazone with (*R*)- and (*S*)-warfarin, could be helpful, but this would not reveal a possibly multifaceted interaction with results different from the sum of the interactions between phenylbutazone and each warfarin enantiomer separately.

The effort required to elucidate fully the mechanisms of a drug interaction can be enormous. If the drugs involved can produce potentially hazardous pharmacological effects (as is the case with phenylbutazone and warfarin), comprehensive studies in humans may be difficult or impossible. Cost–benefit and risk–benefit considerations rather than scientific curiosity will ultimately dictate how much we learn about many important drug interactions.

REFERENCES

(1) R. A. O'Reilly and P. M. Aggeler, *Pharmacol. Rev.*, **22**, 35 (1970).

(2) J. Koch-Weser and E. M. Sellers, *N. Engl. J. Med.*, **285**, 487 (1971).

(3) "Evaluations of Drug Interactions," 2nd ed., American Pharmaceutical Association, Washington, D.C., 1976, p. 295.

(4) P. M. Aggeler, R. A. O'Reilly, L. Leong, and P. E. Kowitz, *N. Engl. J. Med.*, **276**, 496 (1967).

(5) R. A. O'Reilly and P. M. Aggeler, *Proc. Soc. Exp. Biol. Med.*, **128**, 1080 (1968).

(6) R. A. O'Reilly and G. Levy, *J. Pharm. Sci.*, **59**, 1258 (1970).

(7) R. J. Lewis, W. F. Trager, K. K. Chan, A. Breckenridge, M. Orme, M. Rowland, and W. Schary, *J. Clin. Invest.*, **53**, 1607 (1974).

(8) W. L. Schary, R. J. Lewis, and M. Rowland, *Res. Commun. Chem. Pathol. Pharmacol.*, **10**, 663 (1975).

(9) K. A. Bachmann and A. M. Burkman, *J. Pharm. Pharmacol.*, **27**, 832 (1975).

(10) G. Levy and A. Yacobi, *J. Pharm. Sci.*, **63**, 805 (1974).

(11) G. R. Wilkinson and D. G. Shand, *Clin. Pharmacol. Ther.*, **18**, 377 (1975).

(12) A. Yacobi and G. Levy, *J. Pharm. Sci.*, **64**, 1660 (1975).

(13) A. Yacobi, L. B. Wingard, Jr., and G. Levy, *ibid.*, **63**, 868 (1974).

(14) E. Jähnchen and G. Levy, *Clin. Chem.*, **18**, 984 (1972).

(15) A. Yacobi and G. Levy, *J. Pharmacokinet. Biopharm.*, **2**, 239 (1974).

(16) L. B. Wingard, Jr., and G. Levy, *J. Pharmacol. Exp. Ther.*, **184**, 253 (1973).

(17) C. F. Chignell, *Life Sci.*, **7**, 1181 (1968).

(18) A. Yacobi and G. Levy, *Res. Commun. Chem. Pathol. Pharmacol.*, **12**, 405 (1975).

(19) L. R. Pohl, R. Bales, and W. F. Trager, *ibid.*, **15**, 233 (1976).

(20) B. B. Brodie, E. W. Lowman, J. J. Burns, P. R. Lee, T. Chenkin, A. Goldman, M. Weiner, and J. M. Steele, *Am. J. Med.*, **16**, 181

(1954).
(21) E. Jähnchen, L. B. Wingard, Jr., and G. Levy, *J. Pharmacol. Exp. Ther.*, **187**, 176 (1973).
(22) J. G. Humble, Empire Rheumatism Council Symposium on Butazolidin, 1953; through C. B. Hobbs, A. L. Miller, and J. H. Thornley, *Postgrad. Med. J.*, **41**, 563 (1965).

ACKNOWLEDGMENTS

Presented in part at the APhA Academy of Pharmaceutical Sciences, New Orleans meeting, November 1974.

Supported in part by Grant GM 20852 from the National Institute of General Medical Sciences, National Institutes of Health.

Simultaneous Solubilization of Steroid Hormones III: Thermodynamic Evaluation

B. LUNDBERG

Received December 5, 1978, from the *Department of Biochemistry and Pharmacy, Åbo Akademi, Porthansgatan 3, 20500 Åbo 50, Finland.* Accepted for publication July 11, 1979.

Abstract □ The temperature effect on the solubilization of some androgens, estrogens, and C_{21}-steroids in aqueous polysorbate 40 and in tetradecyltrimethylammonium bromide was studied. Dialysis studies showed a linear relationship between micellar and nonmicellar steroids, which indicates that solubilization is governed by a distribution coefficient. With known water solubilities and solubilization capacities for the steroids at different temperatures, the changes of free energy (ΔG_s°), enthalpy (ΔH_s°), and entropy (ΔS_s°) for solubilization were calculated. All steroids studied had negative ΔH_s° values in polysorbate 40, except progesterone and ethisterone. The ΔS_s° values were positive for all of the actual steroids except for estradiol in both association colloids and for 17α-hydroxyprogesterone in polysorbate 40. The highest values were obtained for progesterone and testosterone. The steroids showed lower ΔS_s° values when they were solubilized simultaneously than when they were solubilized separately. No clearcut correlation between the entropy change of solubilization and the simultaneous solubilization behavior could be derived. Obviously, the solubilization mechanism also must be considered. The thermodynamic solubilization parameters are discussed, and the need for temperature-solubilization studies is stressed.

Keyphrases □ Steroid hormones—solubilization, thermodynamics, temperature effect, micellar structure, androgens, estrogens, C_{21}-steroids, in polysorbate 40 and in tetradecyltrimethylammonium bromide □ Solubilization—steroid hormones in polysorbate 40 and in tetradecyltrimethylammonium bromide, thermodynamics □ Thermodynamics—steroid hormone solubilization in polysorbate 40 and in tetradecyltrimethylammonium bromide

Two previous reports from this laboratory dealt with the simultaneous solubilization of estrogens, C_{21}-steroids, and androgens in aqueous solutions of association colloids (1, 2). Estradiol is solubilized independently of the C_{21}-steroids and testosterone, while the solubilization of ethinyl estradiol with progesterone and with testosterone is dependent. A plausible mechanism for simultaneous solubilization was discussed (2). However, mere solubilization capacities at one temperature are not a good basis for thermodynamic discussion of the solubilization mechanism. In this study, the temperature effect on solubilization was investigated to elucidate the contributions of enthalpy and entropy to the free energy of solubilization.

The thermodynamic parameters controlling micellization have been studied and discussed (3–5), but the corresponding parameters for solubilization have been comparatively neglected. One difficult question is the choice of a model for thermodynamic parameter calculations. Humphreys and Rhodes (6) found that the micellar pseudophase model seemed applicable because solubilization was governed by a form of the distribution law. Plots for the determination of enthalpic and entropic values were complex.

More straightforward results were obtained by Simons and Rhodes (7) with a linear relationship between the free energy of solubilization and temperature, despite much scatter due to experimental difficulties. Their results favor the pseudophase model.

EXPERIMENTAL

Materials—The purification methods and purity tests for the association colloids and steroid hormones[1] were described previously (1), except that the steroid purity was checked by silica gel TLC. The labeled steroids[2], ^{3}H-estradiol, ^{3}H-progesterone, and ^{3}H-testosterone, had a radiochemical purity of 98% by TLC, and they were used without further purification. The association colloids were tetradecyltrimethylammonium bromide[3] and polysorbate 40[4].

Solubilization—Solubility studies were carried out as described previously (1), but samples were filtered through a 0.45-μm filter membrane[5] before steroid quantitation. The UV absorbance was used to calculate the amount of unlabeled steroid solubilized; liquid scintillation counting, with a toluene-based scintillation cocktail, was used for the labeled steroids.

The equilibration temperatures were controlled to ±0.2°. The equilibrium dialysis was performed using dialysis tubing[6]. Complete equilibration of the solutions was ensured. All of the experiments were done at least twice.

RESULTS AND DISCUSSION

Dialysis studies were done with the three ^{3}H-labeled steroids: estradiol, progesterone, and testosterone. Figure 1 shows typical results. The linearity of such plots confirms that the relationship between the micellar and nonmicellar steroid concentrations is linear in both saturated and nonsaturated systems. This linearity indicates that solubilization in these systems is governed by a distribution coefficient.

The solubilization capacities at different temperatures between 293 and 323 °K of the two surfactants (tetradecyltrimethylammonium bromide and polysorbate 40) for the sex steroids (estradiol, ethinyl estradiol, progestone, 17α-hydroxyprogesterone, testosterone, and ethisterone) were calculated from saturation solubilization experiments (Table I).

The temperature effect on simultaneous solubilization was studied with the following combinations: ethinyl estradiol–progesterone, ethinyl estradiol–17α-hydroxyprogesterone, and estradiol–testosterone, all in tetradecyltrimethylammonium bromide; and ethinyl estradiol–proges-

[1] Fluka AG. Schweiz.
[2] The Radiochemical Centre, England.
[3] K & K Laboratories.
[4] Atlas Chemical Industries.
[5] Millipore Corp.
[6] Med Cell International Ltd., England.

0022-3549/80/0100-0020$01.00/0
© 1980, American Pharmaceutical Association

(1954).
(21) E. Jähnchen, L. B. Wingard, Jr., and G. Levy, *J. Pharmacol. Exp. Ther.*, **187**, 176 (1973).
(22) J. G. Humble, Empire Rheumatism Council Symposium on Butazolidin, 1953; through C. B. Hobbs, A. L. Miller, and J. H. Thornley, *Postgrad. Med. J.*, **41**, 563 (1965).

ACKNOWLEDGMENTS

Presented in part at the APhA Academy of Pharmaceutical Sciences, New Orleans meeting, November 1974.

Supported in part by Grant GM 20852 from the National Institute of General Medical Sciences, National Institutes of Health.

Simultaneous Solubilization of Steroid Hormones III: Thermodynamic Evaluation

B. LUNDBERG

Received December 5, 1978, from the *Department of Biochemistry and Pharmacy, Åbo Akademi, Porthansgatan 3, 20500 Åbo 50, Finland.* Accepted for publication July 11, 1979.

Abstract □ The temperature effect on the solubilization of some androgens, estrogens, and C_{21}-steroids in aqueous polysorbate 40 and in tetradecyltrimethylammonium bromide was studied. Dialysis studies showed a linear relationship between micellar and nonmicellar steroids, which indicates that solubilization is governed by a distribution coefficient. With known water solubilities and solubilization capacities for the steroids at different temperatures, the changes of free energy (ΔG_s°), enthalpy (ΔH_s°), and entropy (ΔS_s°) for solubilization were calculated. All steroids studied had negative ΔH_s° values in polysorbate 40, except progesterone and ethisterone. The ΔS_s° values were positive for all of the actual steroids except for estradiol in both association colloids and for 17α-hydroxyprogesterone in polysorbate 40. The highest values were obtained for progesterone and testosterone. The steroids showed lower ΔS_s° values when they were solubilized simultaneously than when they were solubilized separately. No clearcut correlation between the entropy change of solubilization and the simultaneous solubilization behavior could be derived. Obviously, the solubilization mechanism also must be considered. The thermodynamic solubilization parameters are discussed, and the need for temperature-solubilization studies is stressed.

Keyphrases □ Steroid hormones—solubilization, thermodynamics, temperature effect, micellar structure, androgens, estrogens, C_{21}-steroids, in polysorbate 40 and in tetradecyltrimethylammonium bromide □ Solubilization—steroid hormones in polysorbate 40 and in tetradecyltrimethylammonium bromide, thermodynamics □ Thermodynamics—steroid hormone solubilization in polysorbate 40 and in tetradecyltrimethylammonium bromide

Two previous reports from this laboratory dealt with the simultaneous solubilization of estrogens, C_{21}-steroids, and androgens in aqueous solutions of association colloids (1, 2). Estradiol is solubilized independently of the C_{21}-steroids and testosterone, while the solubilization of ethinyl estradiol with progesterone and with testosterone is dependent. A plausible mechanism for simultaneous solubilization was discussed (2). However, mere solubilization capacities at one temperature are not a good basis for thermodynamic discussion of the solubilization mechanism. In this study, the temperature effect on solubilization was investigated to elucidate the contributions of enthalpy and entropy to the free energy of solubilization.

The thermodynamic parameters controlling micellization have been studied and discussed (3–5), but the corresponding parameters for solubilization have been comparatively neglected. One difficult question is the choice of a model for thermodynamic parameter calculations. Humphreys and Rhodes (6) found that the micellar pseudophase model seemed applicable because solubilization was governed by a form of the distribution law. Plots for the determination of enthalpic and entropic values were complex.

More straightforward results were obtained by Simons and Rhodes (7) with a linear relationship between the free energy of solubilization and temperature, despite much scatter due to experimental difficulties. Their results favor the pseudophase model.

EXPERIMENTAL

Materials—The purification methods and purity tests for the association colloids and steroid hormones[1] were described previously (1), except that the steroid purity was checked by silica gel TLC. The labeled steroids[2], ^{3}H-estradiol, ^{3}H-progesterone, and ^{3}H-testosterone, had a radiochemical purity of 98% by TLC, and they were used without further purification. The association colloids were tetradecyltrimethylammonium bromide[3] and polysorbate 40[4].

Solubilization—Solubility studies were carried out as described previously (1), but samples were filtered through a 0.45-μm filter membrane[5] before steroid quantitation. The UV absorbance was used to calculate the amount of unlabeled steroid solubilized; liquid scintillation counting, with a toluene-based scintillation cocktail, was used for the labeled steroids.

The equilibration temperatures were controlled to ±0.2°. The equilibrium dialysis was performed using dialysis tubing[6]. Complete equilibration of the solutions was ensured. All of the experiments were done at least twice.

RESULTS AND DISCUSSION

Dialysis studies were done with the three ^{3}H-labeled steroids: estradiol, progesterone, and testosterone. Figure 1 shows typical results. The linearity of such plots confirms that the relationship between the micellar and nonmicellar steroid concentrations is linear in both saturated and nonsaturated systems. This linearity indicates that solubilization in these systems is governed by a distribution coefficient.

The solubilization capacities at different temperatures between 293 and 323 °K of the two surfactants (tetradecyltrimethylammonium bromide and polysorbate 40) for the sex steroids (estradiol, ethinyl estradiol, progestone, 17α-hydroxyprogesterone, testosterone, and ethisterone) were calculated from saturation solubilization experiments (Table I).

The temperature effect on simultaneous solubilization was studied with the following combinations: ethinyl estradiol–progesterone, ethinyl estradiol–17α-hydroxyprogesterone, and estradiol–testosterone, all in tetradecyltrimethylammonium bromide; and ethinyl estradiol–proges-

[1] Fluka AG. Schweiz.
[2] The Radiochemical Centre, England.
[3] K & K Laboratories.
[4] Atlas Chemical Industries.
[5] Millipore Corp.
[6] Med Cell International Ltd., England.

0022-3549/80/0100-0020$01.00/0
© 1980, American Pharmaceutical Association

Table I—Solubilization Capacities of Surfactants for Hormonal Steroids as a Function of Temperature

Surfactant	Steroid	Moles of Steroid per Mole of Surfactant				
		293 °K	300.5 °K	308 °K	315.5 °K	323 °K
Polysorbate 40	Estradiol	0.013	0.016	0.019	0.022	0.026
	Ethinyl estradiol	0.18	0.23	0.27	0.32	0.37
	Testosterone	0.027	0.039	0.052	0.065	0.076
	Ethisterone	0.0007	0.0009	0.0012	0.0016	0.0018
	Progesterone	0.037	0.049	0.063	0.073	0.084
	17α-Hydroxyprogesterone	0.0072	0.0079	0.0085	0.0091	0.0091
Tetradecyltrimethylammonium bromide	Estradiol	0.068	0.080	0.092	0.105	0.118
	Ethinyl estradiol	0.27	0.34	0.43	0.51	0.57
	Testosterone	0.13	0.19	0.25	0.29	0.35
	Ethisterone	0.0046	0.0055	0.0066	0.0074	0.0083
	Progesterone	0.16	0.15	0.16	0.16	0.16
	17α-Hydroxyprogesterone	0.043	0.060	0.082	0.098	0.114

Table II—Solubilization Capacities of Surfactants for Simultaneous Solubilization of Hormonal Steroids as a Function of Temperature

Surfactant	Steroid Pair	Moles of Steroid per Mole of Surfactant				
		293 °K	300.5 °K	308 °K	315.5 °K	323 °K
Polysorbate 40	Ethinyl estradiol +	0.034	0.038	0.042	0.047	0.053
	progesterone	0.037	0.038	0.037	0.036	0.036
	Ethinyl estradiol +	0.063	0.070	0.075	0.082	0.087
	testosterone	0.027	0.031	0.036	0.041	0.045
	Estradiol +	0.013	0.014	0.016	0.018	0.020
	progesterone	0.037	0.041	0.046	0.051	0.056
Tetradecyltrimethylammonium bromide	Ethinyl estradiol +	0.037	0.043	0.049	0.055	0.060
	progesterone	0.16	0.20	0.23	0.27	0.30
	Ethinyl estradiol +	0.19	0.23	0.27	0.31	0.36
	17α-hydroxyprogesterone	0.0054	0.0072	0.0090	0.104	0.0120
	Estradiol +	0.013	0.016	0.018	0.021	0.023
	testosterone	0.027	0.036	0.047	0.058	0.068

terone, ethinyl estradiol–testosterone, and estradiol–progesterone, all in polysorbate 40 (Table II).

The linear relationship between the surfactant concentration and the amount of solubilized steroid (1, 2) as well as the linearity of the dialysis plots (Fig. 1) indicates that the solubilization is governed by a form of the distribution law. The equilibrium constant, K_s, between the micellar (mole fraction of the solute in the micelle, C_s^m) and the nonmicellar (aqueous solubility of the steroid in moles per liter, C_s^{aq}) steroid can be defined by (2, 6):

$$K_s = C_s^m/C_s^{aq} \qquad \text{(Eq. 1)}$$

Starting with the thermodynamic equilibrium constant for the solubilization, one can calculate the free energy change of solubilization, ΔG_s°:

$$\Delta G_s^\circ = -RT \ln K_s \qquad \text{(Eq. 2)}$$

Figures 2*a* and 2*b* show the variation of the free energy change of solubilization with temperature for steroid hormones in the two association colloids. The ΔG_s° values are calculated starting with the water solubility of the steroids at different temperatures (8) and the solubilization capacities at the corresponding temperatures. Most curves show a fairly linear relationship between ΔG_s° and temperature, which also was found for testosterone solubilization by *n*-alkyl polyoxyethylenes (7). The curves for estradiol and ethinyl estradiol in both surfactants show the greatest deviations from linearity. The most likely explanation for such curvature would be the variation of micellar structure with temperature (6). Estradiol and ethinyl estradiol also had the most negative ΔG_s° values, especially at lower temperatures. These facts may indicate a different solubilization mechanism for these steroids compared to the others.

The ΔG_s° values of testosterone and ethisterone differed only slightly. This finding is remarkable if one considers the much higher solubilization capacity for testosterone compared to ethisterone (2). Progesterone had more negative ΔG_s° values than 17α-hydroxyprogesterone, especially in polysorbate 40.

Estradiol and ethinyl estradiol also gave deviations from linearity in ΔG_s° *versus* T plots (Figs. 3*a* and 3*b*) when solubilized simultaneously with other steroids. Ethinyl estradiol gave more positive ΔG_s° values in combinations with progesterone, testosterone, and 17α-hydroxyprogesterone than when solubilized alone. 17α-Hydroxyprogesterone gave more positive values when solubilized with ethinyl estradiol. There was, however, no clearcut correlation between the ΔG_s° values of the steroids and their behaviors at simultaneous solubilization.

With the assumption that the standard molar enthalpy change is not temperature dependent in the range studied, Eq. 3 can be used:

$$\frac{d \ln K_s}{dT} = \frac{\Delta H_s^\circ}{RT^2} \qquad \text{(Eq. 3)}$$

The standard solubilization enthalpy change, ΔH_s°, may be obtained from the plot of $\ln K_s$ *versus* $1/T$. Such plots are found in Figs. 4 and 5 for steroids solubilized separately and simultaneously. The ΔH_s° values are summarized in Tables III and IV.

Testosterone had low negative ΔH_s° values when solubilized separately in both polysorbate 40 and tetradecyltrimethylammonium bromide. Testosterone had somewhat higher negative values when solubilized simultaneously with ethinyl estradiol in polysorbate 40 and with estradiol in tetradecyltrimethylammonium bromide. Ethinyl estradiol had moderately negative values when solubilized either separately or simultaneously and in both association colloids. Estradiol showed the largest negative values.

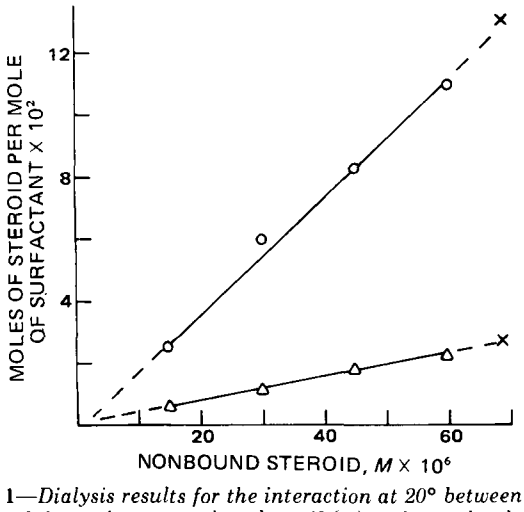

Figure 1—*Dialysis results for the interaction at 20° between testosterone and the surfactants polysorbate 40* (△) *and tetradecyltrimethylammonium bromide* (○) (× = *solubility points*).

Table III—Thermodynamic Changes [a] in Solubilization of Hormonal Steroids in Surfactants at 293°K

Surfactant	Steroid	$-\Delta G_s^\circ$, joules/mole	$-\Delta H_s^\circ$, joules/mole	ΔS_s°, joules/deg/mole
Polysorbate 40	Estradiol	18,631	28,018	−32
	Ethinyl estradiol	21,578	8,314	45
	Testosterone	14,552	1,081	46
	Ethisterone	14,816	−699	53
	Progesterone	17,174	−11,889	99
	17α-Hydroxyprogesterone	14,993	27,686	−43
Tetradecyltrimethylammonium bromide	Estradiol	22,661	32,674	−34
	Ethinyl estradiol	22,566	8,563	48
	Testosterone	20,740	2,744	61
	Ethisterone	19,344	5,570	47
	Progesterone	18,381	11,640	23
	17α-Hydroxyprogesterone	19,400	9,727	33

[a] ΔG_s°, ΔH_s°, and ΔS_s° refer to the unitary free energy, enthalpy, and entropy of solubilization, respectively.

17α-Hydroxyprogesterone had a large negative value in polysorbate 40 but had considerably lower values when alone and when together with ethinyl estradiol in tetradecyltrimethylammonium bromide. Progesterone showed the most ambivalent behavior. Solubilized separately and together with ethinyl estradiol in polysorbate 40, it gave positive ΔH_s° values. Alone in tetradecyltrimethylammonium bromide and together with estradiol and ethinyl estradiol in polysorbate 40, progesterone gave negative values.

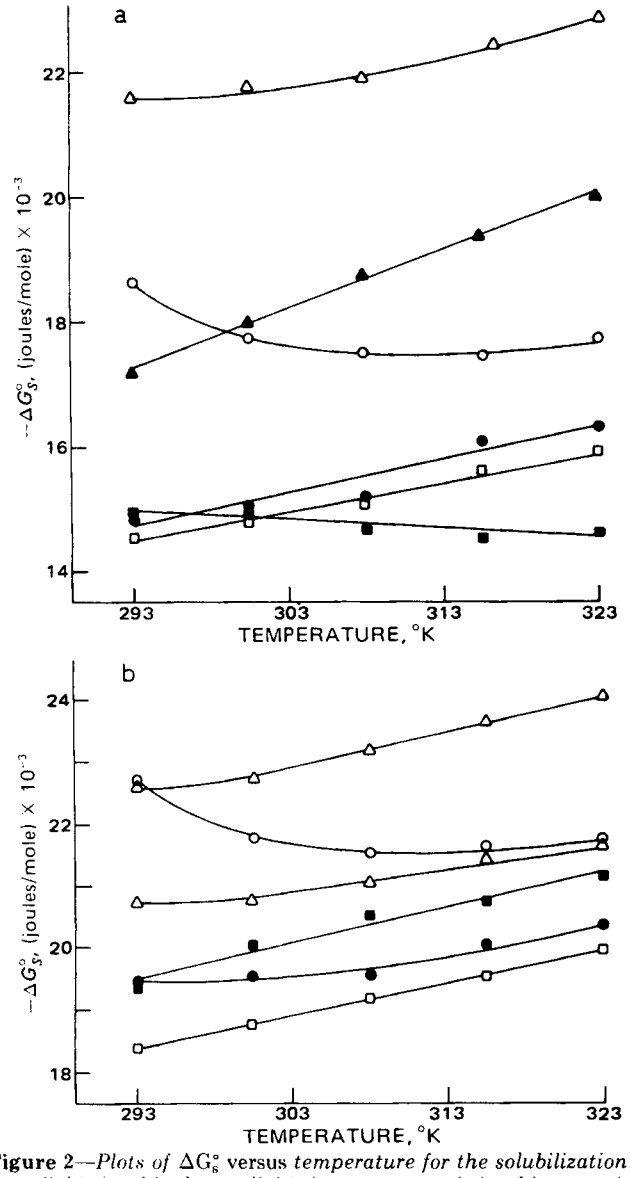

Figure 2—*Plots of* ΔG_s° versus *temperature for the solubilization of estradiol* (○), *ethinyl estradiol* (△), *testosterone* (□), *ethisterone* (●), *progesterone* (▲), *and 17α-hydroxyprogesterone* (■) *in polysorbate 40* (a) *and in tetradecyltrimethylammonium bromide* (b).

Starting with the ΔG_s° and ΔH_s° values, one can calculate the standard entropy change of solubilization, ΔS_s°:

$$\Delta G_s^\circ = \Delta H_s^\circ - T\Delta S_s^\circ \qquad \text{(Eq. 4)}$$

The ΔS_s° values for separate and simultaneous solubilization appear in Tables III and IV. The steroids showed large differences in entropy values. All of the steroids except estradiol and 17α-hydroxyprogesterone in polysorbate 40 had positive values. Progesterone in polysorbate 40 and testosterone in tetradecyltrimethylammonium bromide showed the highest values. At simultaneous solubilization, all steroids had lower entropy values than when solubilized individually, except progesterone in tetradecyltrimethylammonium bromide.

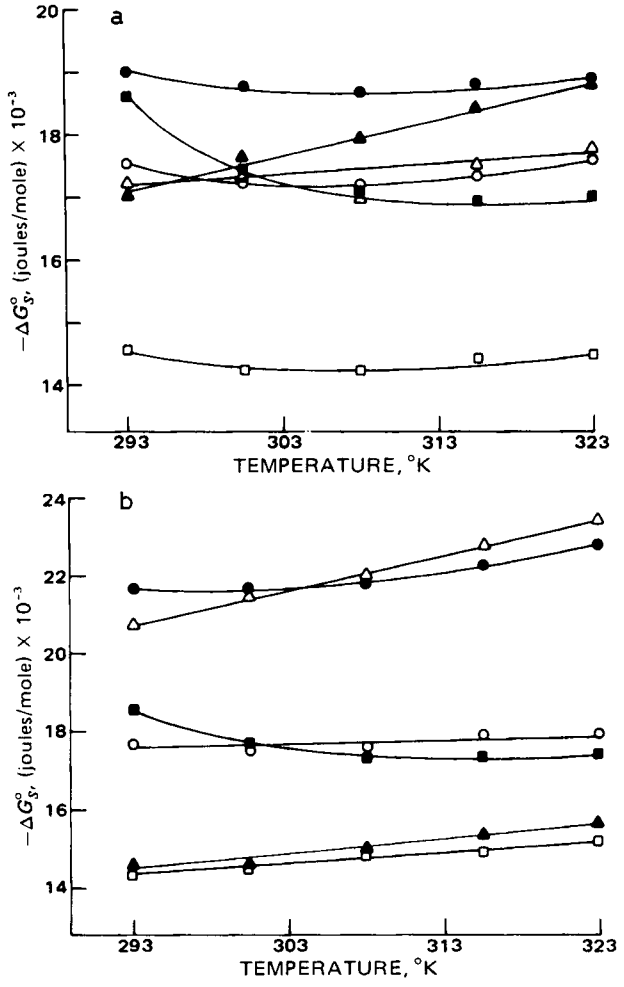

Figure 3—*Plots of* ΔG_s° versus *temperature for the simultaneous solubilization of* (a) *ethinyl estradiol* (○) *plus progesterone* (△), *ethinyl estradiol* (●) *plus testosterone* (□), *and estradiol* (■) *plus progesterone* (▲) *in polysorbate 40 and of* (b) *ethinyl estradiol* (○) *plus progesterone* (△), *ethinyl estradiol* (●) *plus 17α-hydroxyprogesterone* (□), *and estradiol* (■) *plus testosterone* (▲) *in tetradecyltrimethylammonium bromide.*

Table IV—Thermodynamic Changes[a] in Simultaneous Solubilization of Hormonal Steroids in Surfactants at 293°K

Surfactant	Steroid Pair	$-\Delta G_s^\circ$, joules/mole	$-\Delta H_s^\circ$, joules/mole	ΔS_s°, joules/deg/mole
Polysorbate 40	Ethinyl estradiol +	17,518	18,041	−2
	progesterone	17,174	11,058	21
	Ethinyl estradiol +	19,021	19,954	−3
	testosterone	14,552	15,797	−4
	Estradiol +	18,631	36,582	−61
	progesterone	17,174	−690	61
Tetradecyltrimethylammonium bromide	Ethinyl estradiol +	17,724	15,963	6
	progesterone	20,740	−5,570	90
	Ethinyl estradiol +	21,710	11,640	34
	17α-hydroxyprogesterone	14,291	6,901	25
	Estradiol +	18,631	32,591	−48
	testosterone	14,552	4,988	33

[a] ΔG_s°, ΔH_s°, and ΔS_s° refer to the unitary free energy, enthalpy, and entropy of solubilization, respectively.

A comparison of the contribution of the enthalpy and entropy changes to the free energy change of solubilization displayed large differences among the steroids. For estradiol in both surfactants, 17α-hydroxyprogesterone in polysorbate 40, and progesterone in tetradecyltrimethylammonium bromide, the enthalpy factor made the largest contribution to the negative free energy change. For the other steroids, the entropy was larger, and solubilization was thus essentially an entropy-driven process. The same situation generally applies to micelle formation from detergent molecules, which is accompanied by very small heat changes and is assumed to be controlled by a large ΔS.

The most popular explanation of the large unitary entropy change involved in the partitioning of hydrophobic molecules between aqueous and nonaqueous phases is the flickering cluster hypothesis (9). When organic compounds are placed in water, the water molecules arrange themselves around the apolar parts in flickering clusters. Stripping the water molecules from the apolar part of the solute results in large entropy and in the randomization of the water molecules. This treatment assumes that solubilization can be described as the transfer of a molecule from an aqueous to a nonaqueous phase. Application of this assumption to

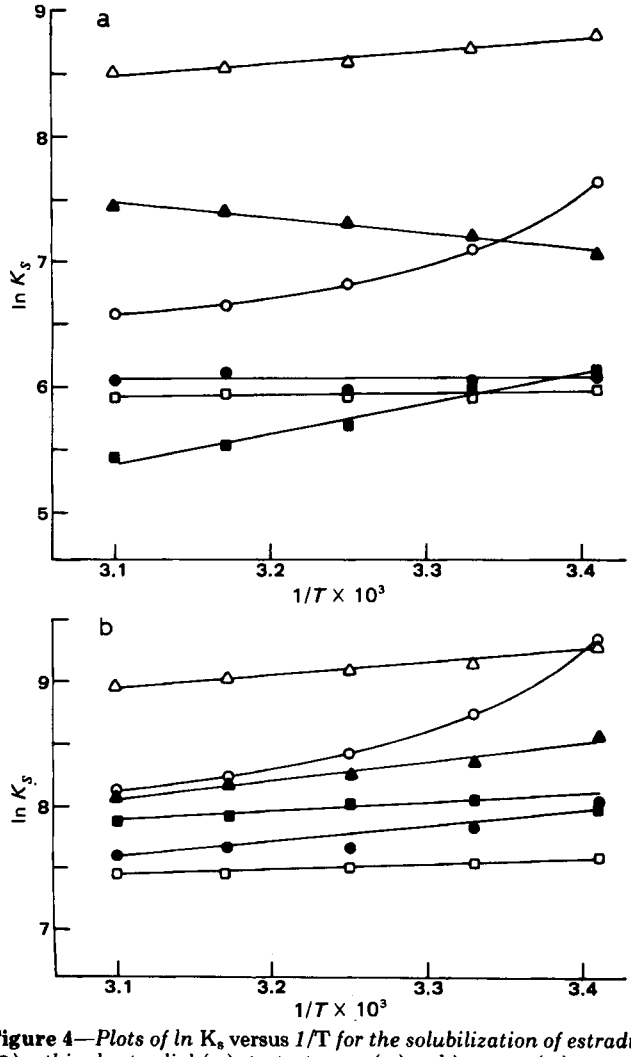

Figure 4—*Plots of ln* K_s versus *1/T for the solubilization of estradiol* (○), *ethinyl estradiol* (△), *testosterone* (□), *ethisterone* (●), *progesterone* (▲), *and 17α-hydroxyprogesterone* (■) *in polysorbate 40* (a) *and tetradecyltrimethylammonium bromide* (b).

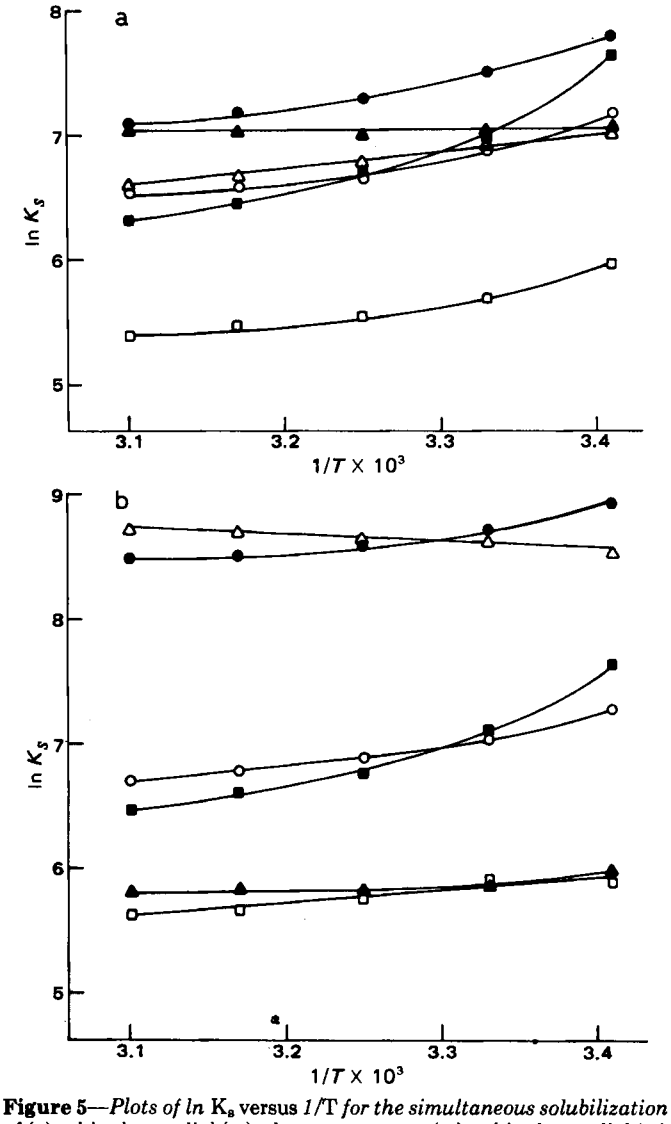

Figure 5—*Plots of ln* K_s versus *1/T for the simultaneous solubilization of* (a) *ethinyl estradiol* (○) *plus progesterone* (△), *ethinyl estradiol* (●) *plus testosterone* (□), *and estradiol* (■) *plus progesterone* (▲) *in polysorbate 40 and of* (b) *ethinyl estradiol* (○) *plus 17α-hydroxyprogesterone* (△) *and estradiol* (■) *plus testosterone* (▲) *in tetradecyltrimethylammonium bromide.*

steroid hormone solubilization is supported by the similarity between the thermodynamic parameters found in this study and those from octanol–water partitioning (8).

Although the flickering cluster hypothesis seems plausible, and the water ordering–disordering is important for the entropy change of solubilization, other factors may be significant. It was proposed (10) that the apolar solute molecule is held rigidly in a favored rotational configuration in the aqueous phase by the layer of water molecules surrounding it. In the micelle hydrocarbon core, its rotational oscillations are relatively unrestricted. This proposal is supported by the fact that there is no clearcut correlation between water solubility and ΔS_s°. Ethisterone has a much lower water solubility than testosterone [1.6 against 68.7 μmoles/liter at 20° (8)] and can be regarded as more hydrophobic. According to the flickering cluster hypothesis, ethisterone should have more structured water around it and should give a more positive ΔS_s° at the randomization of the water molecules. Thus, both the water and solute effects probably contribute to the effective ΔS_s°, but which is quantitatively the most important cannot be determined.

The contribution of the enthalpy change to the free energy change of solubilization is quantitatively minor for most steroids. Hence, there are interesting differences in their ΔH_s° values (Table III). The most notable difference is the rather large positive value of progesterone in polysorbate 40. Because similar ΔH_s° values can be expected for steroids solubilized by the same mechanism, the differences obtained indicate variations in that respect.

The simultaneous solubilization of steroids cannot be predicted by their free energies of solubilization (2). Testosterone and progesterone have less negative ΔH_s° values than ethinyl estradiol but are solubilized maximally in polysorbate 40, while the latter steroid has a lower solubility at simultaneous solubilization. These discrepancies may be explained by differences in the solubilization mechanism. If the solubilization loci of the steroids partly overlap, a steric hindrance to simultaneous solubilization will exist. When solubilized on its own in tetradecyltrimethylammonium bromide, ethinyl estradiol has a considerably larger ΔS_s° than progesterone, but the opposite is true at simultaneous solubilization (Tables III and IV).

On the contrary, progesterone and estradiol are solubilized independently of each other in polysorbate 40, and the ΔS_s° values of both decrease to about the same extent when the steroids are solubilized together. Also, the solubilizations of both testosterone and estradiol are changed at simultaneous solubilization in tetradecyltrimethylammonium bromide, and their ΔS_s° values are both lowered when the steroids are solubilized together. However, at this stage it is hard to rationalize these results in terms of the precise structure and ordering of the micelle and the solute in it.

Of course, the thermodynamic treatment in this study has limitations. Although the amount of solubilizate bound in a micellar system can be measured with accuracy, the calculation of C_s^m presents problems because it is a concentration term, and precise delineation of the micellar pseudophase boundary is difficult. Two other difficult aspects of the thermodynamic calculations regarding micellar binding are the selection of the standard state for the micellar cosolute and the incorporation of the appropriate activity corrections (11). For cosolutes with low water solubility such as steroid hormones, the C_s^{aq} term probably will approximate the activity value. However, the micellar solubilizate activity coefficients may differ significantly from unity. This deviation will introduce errors into the calculations of thermodynamic parameters derived from micellar binding equilibrium constants.

Although these limitations exist, data from studies of the temperature effect on solubilization processes can prove useful in expanding knowledge of this important branch of surface chemistry. Clearly, further studies of the effect of solutes on micelle structure are required before a theory rationalizing micellar solubilization can be formulated.

REFERENCES

(1) T. Lövgren, B. Heikius, B. Lundberg, and L. Sjöblom, *J. Pharm. Sci.*, **67**, 1419 (1978).

(2) B. Lundberg, T. Lövgren, and B. Heikius, *ibid.*, **68**, 542 (1979).

(3) D. Attwood and A. T. Florence, *Kolloid Z. Z. Polym.*, **246**, 580 (1971).

(4) C. Tanford, *J. Phys. Chem.*, **78**, 2469 (1974).

(5) D. Stigter, *J. Colloid Interface Sci.*, **47**, 473 (1974).

(6) K. J. Humphreys and C. T. Rhodes, *J. Pharm. Sci.*, **57**, 79 (1968).

(7) K. J. Simons and C. T. Rhodes, *Pharmazie*, **26**, 623 (1971).

(8) B. Lundberg, *Acta Pharm. Suec.*, **16**, 151 (1979).

(9) G. Nemethy, H. A. Scheraga, and W. Kauzmann, *J. Phys. Chem.*, **72**, 1842 (1968).

(10) R. H. Aranow and L. Witten, *ibid.*, **64**, 1643 (1960)

(11) P. Molyneux and C. T. Rhodes, *Kolloid Z. Z. Polym.*, **250**, 886 (1972).

Tetrazolium Salts in Pharmaceutical Analysis II: Direct Assay of Diethylstilbestrol and Diethylstilbestrol Dipropionate

NABIL M. OMAR ˣ and NAWAL A. EL-RABBAT

Received November 24, 1978, from the *Department of Pharmaceutical Chemistry, Faculty of Pharmacy, University of Assiut, Assiut, Egypt.* Accepted for publication July 10, 1979.

Abstract □ A convenient spectrophotometric determination of diethylstilbestrol and diethylstilbestrol dipropionate was developed involving their interaction with triphenyltetrazolium chloride at 50° for 45 min and subsequent measurement of the formazan formed. The significance of extended conjugation within the 4,4′-stilbenediol molecule to induce the color reaction is documented. Ideal adherence of color absorption to Beer's law permitted accurate and precise determination of diethylstilbestrol and diethylstilbestrol dipropionate pure forms over the range of 2–22 μg of diethylstilbestrol/ml. Application of the tetrazolium color reaction to the analysis of diethylstilbestrol dipropionate dosage forms was achieved without prior hydrolysis or extraction.

Keyphrases □ Diethylstilbestrol and diethylstilbestrol dipropionate—analysis, triphenyltetrazolium chloride colorimetry □ Colorimetry—analysis of diethylstilbestrol and diethylstilbestrol dipropionate with triphenyltetrazolium chloride □ Tetrazolium salts—colorimetric analysis of diethylstilbestrol and diethylstilbestrol dipropionate

The usual relatively small doses of diethylstilbestrol [(*E*)-α,α′-diethyl-4,4′-stilbenediol] require especially sensitive and precise pharmaceutical analysis. The phenolic hydroxyl group reactivity of this stilbene derivative has been used to develop diverse estimation procedures based on acetylation (1, 2), nitrosation (3), polarography of the nitrosation product (4), bromination (5), and UV irradiation (6).

Of the chromogenic reagents reported for interaction with phenols, interest has focused on the utility of phosphomolybdotungstate (7), iron (8), antimony (9), and vanadium (10) salts for diethylstilbestrol colorimetry. Some

0022-3549/80/0100-0024$01.00/0

© 1980, American Pharmaceutical Association

steroid hormone solubilization is supported by the similarity between the thermodynamic parameters found in this study and those from octanol–water partitioning (8).

Although the flickering cluster hypothesis seems plausible, and the water ordering–disordering is important for the entropy change of solubilization, other factors may be significant. It was proposed (10) that the apolar solute molecule is held rigidly in a favored rotational configuration in the aqueous phase by the layer of water molecules surrounding it. In the micelle hydrocarbon core, its rotational oscillations are relatively unrestricted. This proposal is supported by the fact that there is no clearcut correlation between water solubility and ΔS_s°. Ethisterone has a much lower water solubility than testosterone [1.6 against 68.7 μmoles/liter at 20° (8)] and can be regarded as more hydrophobic. According to the flickering cluster hypothesis, ethisterone should have more structured water around it and should give a more positive ΔS_s° at the randomization of the water molecules. Thus, both the water and solute effects probably contribute to the effective ΔS_s°, but which is quantitatively the most important cannot be determined.

The contribution of the enthalpy change to the free energy change of solubilization is quantitatively minor for most steroids. Hence, there are interesting differences in their ΔH_s° values (Table III). The most notable difference is the rather large positive value of progesterone in polysorbate 40. Because similar ΔH_s° values can be expected for steroids solubilized by the same mechanism, the differences obtained indicate variations in that respect.

The simultaneous solubilization of steroids cannot be predicted by their free energies of solubilization (2). Testosterone and progesterone have less negative ΔH_s° values than ethinyl estradiol but are solubilized maximally in polysorbate 40, while the latter steroid has a lower solubility at simultaneous solubilization. These discrepancies may be explained by differences in the solubilization mechanism. If the solubilization loci of the steroids partly overlap, a steric hindrance to simultaneous solubilization will exist. When solubilized on its own in tetradecyltrimethylammonium bromide, ethinyl estradiol has a considerably larger ΔS_s° than progesterone, but the opposite is true at simultaneous solubilization (Tables III and IV).

On the contrary, progesterone and estradiol are solubilized independently of each other in polysorbate 40, and the ΔS_s° values of both decrease to about the same extent when the steroids are solubilized together. Also, the solubilizations of both testosterone and estradiol are changed at simultaneous solubilization in tetradecyltrimethylammonium bromide, and their ΔS_s° values are both lowered when the steroids are solubilized together. However, at this stage it is hard to rationalize these results in terms of the precise structure and ordering of the micelle and the solute in it.

Of course, the thermodynamic treatment in this study has limitations. Although the amount of solubilizate bound in a micellar system can be measured with accuracy, the calculation of C_s^m presents problems because it is a concentration term, and precise delineation of the micellar pseudophase boundary is difficult. Two other difficult aspects of the thermodynamic calculations regarding micellar binding are the selection of the standard state for the micellar cosolute and the incorporation of the appropriate activity corrections (11). For cosolutes with low water solubility such as steroid hormones, the C_s^{aq} term probably will approximate the activity value. However, the micellar solubilizate activity coefficients may differ significantly from unity. This deviation will introduce errors into the calculations of thermodynamic parameters derived from micellar binding equilibrium constants.

Although these limitations exist, data from studies of the temperature effect on solubilization processes can prove useful in expanding knowledge of this important branch of surface chemistry. Clearly, further studies of the effect of solutes on micelle structure are required before a theory rationalizing micellar solubilization can be formulated.

REFERENCES

(1) T. Lövgren, B. Heikius, B. Lundberg, and L. Sjöblom, *J. Pharm. Sci.*, **67**, 1419 (1978).

(2) B. Lundberg, T. Lövgren, and B. Heikius, *ibid.*, **68**, 542 (1979).

(3) D. Attwood and A. T. Florence, *Kolloid Z. Z. Polym.*, **246**, 580 (1971).

(4) C. Tanford, *J. Phys. Chem.*, **78**, 2469 (1974).

(5) D. Stigter, *J. Colloid Interface Sci.*, **47**, 473 (1974).

(6) K. J. Humphreys and C. T. Rhodes, *J. Pharm. Sci.*, **57**, 79 (1968).

(7) K. J. Simons and C. T. Rhodes, *Pharmazie*, **26**, 623 (1971).

(8) B. Lundberg, *Acta Pharm. Suec.*, **16**, 151 (1979).

(9) G. Nemethy, H. A. Scheraga, and W. Kauzmann, *J. Phys. Chem.*, **72**, 1842 (1968).

(10) R. H. Aranow and L. Witten, *ibid.*, **64**, 1643 (1960)

(11) P. Molyneux and C. T. Rhodes, *Kolloid Z. Z. Polym.*, **250**, 886 (1972).

Tetrazolium Salts in Pharmaceutical Analysis II: Direct Assay of Diethylstilbestrol and Diethylstilbestrol Dipropionate

NABIL M. OMAR ˣ and NAWAL A. EL-RABBAT

Received November 24, 1978, from the *Department of Pharmaceutical Chemistry, Faculty of Pharmacy, University of Assiut, Assiut, Egypt.* Accepted for publication July 10, 1979.

Abstract □ A convenient spectrophotometric determination of diethylstilbestrol and diethylstilbestrol dipropionate was developed involving their interaction with triphenyltetrazolium chloride at 50° for 45 min and subsequent measurement of the formazan formed. The significance of extended conjugation within the 4,4′-stilbenediol molecule to induce the color reaction is documented. Ideal adherence of color absorption to Beer's law permitted accurate and precise determination of diethylstilbestrol and diethylstilbestrol dipropionate pure forms over the range of 2–22 μg of diethylstilbestrol/ml. Application of the tetrazolium color reaction to the analysis of diethylstilbestrol dipropionate dosage forms was achieved without prior hydrolysis or extraction.

Keyphrases □ Diethylstilbestrol and diethylstilbestrol dipropionate—analysis, triphenyltetrazolium chloride colorimetry □ Colorimetry—analysis of diethylstilbestrol and diethylstilbestrol dipropionate with triphenyltetrazolium chloride □ Tetrazolium salts—colorimetric analysis of diethylstilbestrol and diethylstilbestrol dipropionate

The usual relatively small doses of diethylstilbestrol [(*E*)-α,α′-diethyl-4,4′-stilbenediol] require especially sensitive and precise pharmaceutical analysis. The phenolic hydroxyl group reactivity of this stilbene derivative has been used to develop diverse estimation procedures based on acetylation (1, 2), nitrosation (3), polarography of the nitrosation product (4), bromination (5), and UV irradiation (6).

Of the chromogenic reagents reported for interaction with phenols, interest has focused on the utility of phosphomolybdotungstate (7), iron (8), antimony (9), and vanadium (10) salts for diethylstilbestrol colorimetry. Some

0022-3549/80/0100-0024$01.00/0

© 1980, American Pharmaceutical Association

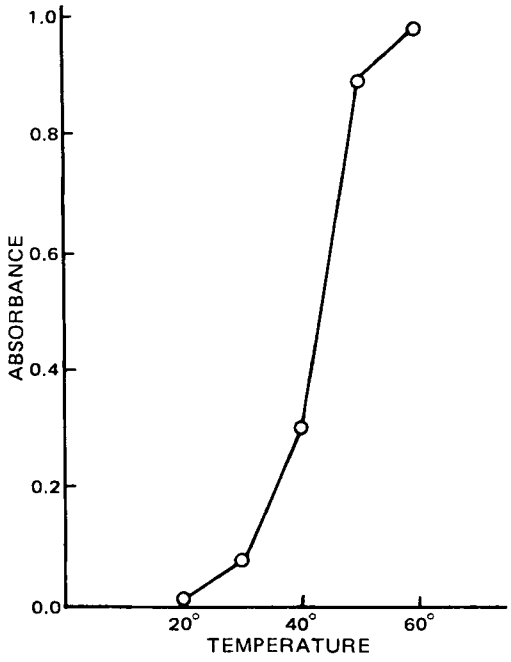

Figure 1—*Temperature effect on color development using 20 μg of diethylstilbestrol/ml, 45 min.*

of these methods lack specificity or sensitivity, and they often are subject to limitations. The compendial UV-irradiation procedures (11, 12), although apparently specific for diethylstilbestrol, may be tedious and time consuming, especially when oily formulations of diethylstilbestrol dipropionate are analyzed. Essential preliminary hydrolysis to diethylstilbestrol and its subsequent extraction might interfere with the accurate estimation of this ester.

Triphenyltetrazolium chloride (I) can be reduced to the corresponding highly colored formazan derivative by various dihydroxybenzene derivatives (13–15). This reduction offered a basis for investigating possible interactions of I with a different aromatic diol system such as 4,4′-stilbenediol, with the hope of introducing a new formazan-based colorimetric analysis of diethylstilbestrol and its dipropionate ester.

EXPERIMENTAL

Instrumentation—A double-beam spectrophotometer[1], a pH meter[2] fitted with calomel and glass electrodes, and a suitable thermostated[3] water bath were used.

Materials—Pharmaceutical grade diethylstilbestrol and diethylstilbestrol dipropionate were the working standards. Ethyl oleate, peanut oil, and sesame oil were chemically pure; other chemicals were analytically pure. As dosage forms, commercially marketed tablets[4,5] and parenteral solutions[6–9] of diethylstilbestrol and diethylstilbestrol dipropionate were analyzed.

[1] Spektromon-203, MOM, Budapest, Hungary.
[2] Radelkis OP-401/2, Budapest, Hungary.
[3] T-606.MTA, Budapest, Hungary.
[4] Stilbestrol (Misr Co. for Pharmaceuticals, Cairo, Egypt) contains 5.0 mg of diethylstilbestrol/tablet.
[5] Stilbestrol Dipropionate (G. Richter, Budapest, Hungary) contains 1.0 mg of diethylstilbestrol dipropionate/tablet.
[6] Stilbestrol (Misr Co. for Pharmaceuticals, Cairo, Egypt) contains 1.0 mg of diethylstilbestrol/1-ml ampul.
[7] Stilbestrol Dipropionate (G. Richter, Budapest, Hungary) contains 5.0 mg of diethylstilbestrol dipropionate/1-ml ampul.
[8] Stilbestrol Dipropionate (Evans, Bristol, England) contains 10.0 mg of diethylstilbestrol dipropionate/1-ml solution in ethyl oleate.
[9] Stilbestrol Dipropionate (Bayer, Liverkühsen, Germany) contains 5.0 mg of diethylstilbestrol dipropionate/1-ml solution in sesame oil.

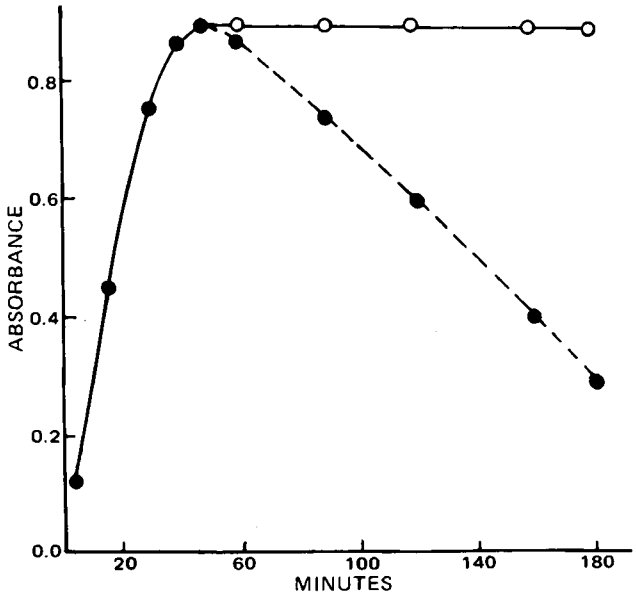

Figure 2—*Diethylstilbestrol–tetrazolium color–time curve using 20 μg of diethylstilbestrol/ml at 50° (●) and after cooling to room temperature (○).*

Reagents—*Tetrazolium Solution*—Compound I was diluted to 0.5% (w/v) in aldehyde-free ethanol[10]. This solution was kept in the dark.

Potassium Hydroxide Solution—Carbonate-free potassium hydroxide, 0.1 g, was dissolved in ~2 ml of distilled water and diluted to 100 ml with anhydrous ethanol. A fresh solution was prepared every 48 hr.

Standards—An accurately weighed amount of diethylstilbestrol or diethylstilbestrol dipropionate, previously dried at 80° *in vacuo* for 2 hr, was dissolved in anhydrous ethanol to a final concentration of 200 μg of diethylstilbestrol/ml.

Assay Samples—*Tablets*—Not less than 20 tablets were ground to a fine powder. An accurately weighed powder sample, equivalent to ~5 mg of diethylstilbestrol, was transferred to a 50-ml volumetric flask. Then 25 ml of anhydrous ethanol was added, and the solution was allowed to stand for 30 min with frequent shaking. The solution was diluted to volume with anhydrous ethanol, mixed well, and filtered through a dry filter into a dry flask. The first portions of the filtrate were discarded.

Injections and Solutions—A 1-ml precision syringe was used to transfer 1.0 ml of the injection solution into a suitable volumetric flask. The syringe was rinsed with 20% (v/v) *n*-heptane in ethanol; the rinses were collected in the flask and diluted quantitatively and stepwise with heptane–alcohol to obtain ~100–140 μg of the claimed diethylstilbestrol/ml.

Procedure—A 1.0-ml sample of the standard or of the sample was pipetted into a 10-ml volumetric flask containing 3.0 ml of the tetrazolium solution and 1.0 ml of the potassium hydroxide assay solution. The sample was mixed well, stoppered, and allowed to stand in the dark in a thermostated water bath at 50 ± 0.1° for 45 min. The red-orange reaction mixture was cooled and brought to volume with ethanol. The absorbance of this solution was measured in a 1-cm glass cell at 485 nm *versus* a blank prepared from 1.0 ml of ethanol (for tablets) or from *n*-heptane–ethanol (for injections) and treated as for the assay solution (heated at 50° for 45 min).

RESULTS AND DISCUSSION

Tetrazolium–Stilbenediol Interaction—Tetrazolium salts were considered for use in pharmaceutical colorimetric analysis because they yield highly colored formazans upon reduction (14–21). The tetrazolium cation may oxidize the enediol function with appreciable selectivity since only the 1,2- and 1,4-dihydroxybenzene derivatives induce blue tetrazolium reduction (13).

Reaction of the following phenols with I in 0.1% KOH at 20° for 30 min also gave no color with resorcinol and phloroglucinol, while a moderate to intense color was observed with pyrocatechol, pyrogallol, and hydroquinone. The 4,4′-stilbenediol reaction mixture became faint orange-red, but the color was augmented by the application of heat. Neither dihy-

[10] Aldehyde-free spectrograde (Prolabo, France).

Table I—Effect of Relative Reagent Concentrations on the Diethylstilbestrol–Tetrazolium Reaction Rate

Milliliters Added per 10 ml of Assay Solution[a]		
0.5% Tetrazolium Chloride	0.1% KOH	Absorbance, 485 nm
1.0	0.50	0.210
2.0	0.50	0.315
3.0	0.50	0.385
1.0	1.00	0.125
2.0	1.00	0.375
3.0	1.00	0.475[b]
4.0	1.00	0.470[c]
2.0	1.50	0.280
3.0	1.50	0.330
4.0	1.50	0.425

[a] Containing 10 μg of diethylstilbestrol/ml. [b] pH 10.50. [c] pH 9.35.

Table II—Replicate Analyses of Diethylstilbestrol Standard Solutions

Replication[a]	Absorbance, 485 nm
1	0.471
2	0.473
3	0.474
4	0.474
5	0.472
6	0.474
7	0.475
8	0.472
Average	0.473
SD	$\pm 1.3562 \times 10^{-3}$
RSD	2.867×10^{-3}

[a] Containing 10.0 μg of diethylstilbestrol/ml.

drostilbestrol[11] nor *trans*-stilbene induced formazan development under these conditions. These findings, although mostly qualitative, underline the possible reduction of tetrazolium salts by aromatic diols with widely separated enediol functions when the latter are conjugated properly with the carrier aromatic nuclei. This possibility encouraged further investigation of I for use in the photometric analysis of pharmaceutical 4,4′-stilbenediol derivatives.

Assay—Interaction of diethylstilbestrol with I proceeded analogously to 4,4′-stilbenediol; heating of the reaction mixture gradually intensified the color. The formazan absorbed with minimum and maximum extinctions at 408 and 485 nm, respectively, consistent with the absorption of triphenylformazan (17, 19, 22).

For the diethylstilbestrol concentration range studied, appropriate absorptivity readings were attained at 50–60° (Fig. 1). However, at >50°, blank solutions acquired a red tinge that could lower the sensitivity of the diethylstilbestrol–tetrazolium interaction. Accordingly, 50° was a convenient temperature because it combined a reasonable heating time with the production of only a faintly colored blank.

The color–time curve (Fig. 2) revealed maximum formazan formation when the reaction mixture was at 50° for 45–50 min; heating for longer periods seriously lowered color absorptivity. Interruption of the reaction after 45 min by efficient cooling to ambient temperature was sufficient to achieve good sensitivity. The formazan remained stable for >2 hr when kept in the dark. Under these conditions, maximum formazan development was effected by the addition of 1.0 ml of the working diethylstilbestrol solution to 3–4 ml of I in the presence of 1.0 ml of 0.1% KOH (Table I).

Quantitative Analysis—At fixed experimental conditions, the formazan absorption intensity was a function of the diethylstilbestrol concentration. Linear regression analysis of a Beer's plot at 485 nm revealed excellent adherence ($r = 0.9994$), with a slope (α) of 0.0465 ($\pm 1.08 \times 10^{-3}$) and an upper sensitivity limit of ~22 μg ($A = 1.02$) of diethylstilbestrol/ml. Replicate analyses of diethylstilbestrol working solutions (Table II) were fairly precise ($RSD = 2.811 \times 10^{-3}$). Recovery studies at different diethylstilbestrol concentrations (Table III) afforded a mean recovery of 99.45 ± 0.93%.

Since I could be used successfully for the photometric estimation of beclomethasone dipropionate[12] without prior hydrolysis (12, p. 44), a similar interaction for diethylstilbestrol dipropionate was considered.

[11] Hexestrol.
[12] Propaderm.

Table III—Recovery of Standard Diethylstilbestrol Solutions

Sample	Diethylstilbestrol, μg/ml Calculated[a]	Found[b]	Recovery, %
1	10.0	9.78	97.80
2	25.0	24.96	99.84
3	50.0	50.01	100.02
4	100.0	99.84	99.84
5	200.0	199.55	99.78
Mean			99.45
SD			±0.93
RSD			9.35×10^{-3}

[a] Initial concentration. [b] Average of five assays.

Table IV—Analysis of Diethylstilbestrol and Diethylstilbestrol Dipropionate Dosage Forms

Preparation[a]	Content, mg/unit Label Claim	Found[b]	Added	Recovered
Diethylstilbestrol				
Tablets	5.0	4.96	10.0	14.94
Injection	1.0	0.98	25.0	26.00
Diethylstilbestrol dipropionate				
Tablets	1.0	1.10	5.0	6.11
Injection[c]	5.0	4.98	5.0	9.95
	10.0	10.05	10.0	20.00
	10.0	9.75	10.0	19.80

[a] See *Experimental* for composition. [b] Average of three determinations. [c] Found 4.75, 9.89, and 9.64, respectively, as analyzed by the NF XIV procedure.

A direct estimation of this ester has not been reported. When reacted under the standard diethylstilbestrol assay, diethylstilbestrol dipropionate produced formazan with Beer's plot r and α values of 0.9992 and 0.0328 ($\pm 1.05 \times 10^{-3}$), respectively. Comparison of the diethylstilbestrol–diethylstilbestrol dipropionate molecular weight ratio to the respective Beer's plot slopes at 485 nm confirmed quantitative *in situ* diethylstilbestrol generation during the base-catalyzed interaction of I with diethylstilbestrol dipropionate.

The color reaction was applied successfully to the analysis of diethylstilbestrol and diethylstilbestrol dipropionate tablets (Table IV). Potential interference by reducing sugars in the tablets was eliminated by alcohol extraction prior to analysis. Interference studies of some common ingredients in diethylstilbestrol dipropionate formulations revealed no reduction of I. The compounds studied included phenobarbital, tetracaine, benzocaine, sulfathiazole, sulfathiourea, and nitroglycerin. Pharmaceutical catecholamines oxidized by I are not likely to be in diethylstilbestrol dosage forms.

Direct spectrophotometric determination of oily diethylstilbestrol dipropionate dosage forms is unreliable because of the high absorptivity of the oily vehicles (1, p. 475). However, neither sesame and olive oils nor ethyl oleate showed measurable absorptivity at 485 nm when tested as 0.8% (w/v) in heptane–alcohol. In addition, no formazan was observed when such solutions were reacted with I under the standard assay conditions. These results encouraged direct estimation of diethylstilbestrol dipropionate dosage forms by the proposed tetrazolium reaction (Table IV). Concordant results were obtained when the oily dipropionate formulations were analyzed directly by I or were preliminarily freed from their vehicles by the NF XIV procedure (10). However, relatively higher values than the claimed diethylstilbestrol dipropionate contents were shown by some intense yellow batches. Correction for intrinsic absorption of such samples was made by determining their initial absorptivity at 485 nm.

REFERENCES

(1) "The Qualitative Analysis of Drugs," D. C. Garrat, Chapman-Hall, London, England, 1964, p. 470.

(2) "The Egyptian Pharmacopoeia," University Press, Cairo, Egypt, 1953, p. 257.

(3) S. Gottleib, *J. Am. Pharm. Assoc., Sci. Ed.*, **37**, 147 (1948).

(4) D. Gry, *Dan. Tidsskr. Farm.*, **23**, 139 (1949).

(5) T. T. Cocking, *Analyst*, **68**, 144 (1943).

(6) D. Banes, *J. Assoc. Off. Agr. Chem.*, **44**, 323 (1961).

(7) M. Tubis and A. Bloom, *Ind. Eng. Chem., Anal. Ed.*, **14**, 309 (1942).

(8) J. D. Duerr and B. A. Pappas, *J. Am. Pharm. Assoc., Sci. Ed.*, **48**,

13 (1959).
(9) F. L. Warren, F. Goulden, and A. M. Robinson, *Biochem. J.*, **42**, 151 (1948).
(10) "The National Formulary," 14th ed., Mack Publishing Co., Easton, Pa., 1975, p. 205.
(11) "The United States Pharmacopeia," 19th rev., Mack Publishing Co., Easton, Pa., 1975, p. 142.
(12) "British Pharmacopoeia 1973," University Printing House, Cambridge, England, 1973, p. 443.
(13) J. E. Sinsheimer and E. F. Salim, *J. Anal. Chem.*, **37**, 566 (1965).
(14) E. F. Salim, P. E. Manni, and J. E. Sinsheimer, *J. Pharm. Sci.*, **53**, 391 (1964).
(15) N. M. Omar and N. A. El-Rabbat, *ibid.*, **67**, 779 (1978).
(16) R. Kuhn and D. Jerchel, *Ber.*, **74**, 949 (1941).
(17) W. J. Mader and R. R. Buck, *Anal. Chem.*, **24**, 666 (1952).
(18) D. Banes, *J. Am. Pharm. Assoc., Sci. Ed.*, **42**, 669 (1953).
(19) A. M. Mattson and C. O. Jensen, *Anal. Chem.*, **22**, 182 (1950).
(20) H. M. Hashmi, A. S. Adel, A. V. Viegas, and I. A. Ahmad, *Mikrochim. Acta*, **3**, 457 (1970).
(21) P. S. Vassileva-Alexandrova and P. S. Shismanor, *Anal. Chem.*, **47**, 1432 (1975).
(22) R. E. Graham, E. R. Biehl, and C. T. Kenner, *J. Pharm. Sci.*, **66**, 965 (1977).

Tissue Distribution and Metabolism of Drugs V: Effect of Secretin and Pancreozymin on Drug Transport in Rabbit Pancreas

MASATO ARAKAWA *§, KATSUHIKO OKUMURA *, and RYOHEI HORI‡x

Received April 10, 1979, from the **Institute of Pharmaceutical Sciences, Hiroshima University School of Medicine, Hiroshima 734, Japan,* and the ‡*Department of Pharmacy, Kyoto University Hospital, Sakyo-ku, Kyoto 606, Japan.* Accepted for publication July 16, 1979. §Present address: General Research Center, Wakunaga Pharmaceutical Co. Ltd., Kotachi, Hiroshima, Japan.

Abstract □ The effect of secretin and pancreozymin on the tissue distribution and penetration of drugs in the rabbit pancreas was studied to clarify hormonally regulated drug distribution. Drugs with high liquid solubility were distributed easily within the pancreas even during secretin or pancreozymin treatment, and these hormones had little effect on drug distribution from the blood to the pancreas. However, secretin increased the concentration ratio of dimethadione in the pancreatic juice (J) to plasma unbound dimethadione (Pf), probably because the pancreatic juice during secretin infusion is alkaline relative to the control. Secretin had no effect on the J/Pf of isonicotinamide and sulfanilamide. Secretin decreased the J/Pf of drugs with low lipophilicity or large molecular weight because the penetration rates of these drugs from cell water to pancreatic juice were not rapid enough to reach equilibrium. Pancreozymin was unable to change the J/Pf of any drug tested. These results suggest that the barrier between the blood and the pancreas or the barrier between the pancreas and the pancreatic juice is unchanged by secretin or pancreozymin.

Keyphrases □ Pancreas—drug transport, various drugs, effect of secretin, pancreozymin, pancreatic juice flow □ Pancreatic juice—effect of flow rate on pancreatic drug transport, various drugs □ Drug transport—pancreas, effect of secretin, pancreozymin, pancreatic juice flow, various drugs

Drug distribution has received increasing attention during recent years because such knowledge concerning the blood, organs, and tissues is needed to provide optimal treatment or protection from adverse reactions. Previous papers reported tissue distribution and penetration of drugs in the pancreas (1), lungs, (2, 3), and testes (4).

It was suggested that the lipid barrier in the pancreas plays a dominant role in drug distribution from the blood to the pancreas and that the lipid barrier and the molecular sieve barrier have independent roles in transport from the pancreas to the pancreatic juice. In these experiments, pancreatic juice secretion was stimulated by secretin infusion to maintain a constant juice flow. However, the pancreatic barriers could be changed by endogenous hormones that regulate pancreatic secretion during food digestion.

The purpose of this study was to determine experimentally whether secretin and pancreozymin, typical peptide hormones that stimulate pancreatic juice flow and bicarbonate or enzyme secretion, affect drug distribution and penetration in the pancreas. Some model drugs that exhibit remarkable lipophilicity, molecular size, and pKa were selected as discussed previously (1).

EXPERIMENTAL

Materials—Secretin[1], 3110 CHR U[2]/mg, was used. Pancreozymin[3], dimethadione, isonicotinamide, isonicotinic acid, sulfanilamide, sulfanilic acid, sulfisoxazole, and procainamide hydrochloride were obtained commercially. All other chemicals were analytical grade.

Animals—Male white rabbits, 2.0–3.0 kg, were housed in constant environment rooms and allowed free access to water and food.

Drug Permeation from Blood to Pancreatic Juice—The experimental procedures were almost identical to those described previously (1). Rabbits were anesthetized with pentobarbital sodium (27 mg/kg iv). Pancreatic juice was collected by cannulation into the pancreatic duct as described in the literature (5). Plasma drug concentrations were established and maintained by a suitable combination of priming injections and continuous intravenous infusion.

As the control, pancreatic juice was collected over 75 min prior to the administration of secretin or pancreozymin. The secretin effect was studied by a priming injection (1 CHR U/kg) and continuous intravenous infusion (2 CHR U/kg/hr), after which the pancreatic juice flow was stimulated from 14 (7–24 μl/min) to 39 (15–66 μl/min) μl/min. Pancreozymin also was studied using a priming injection (1 CHR U/kg) and continuous infusion (4 CHR U/kg/hr)[4]. In this experiment, secretin also was infused simultaneously to minimize the effect of secretin contamination in the pancreozymin preparation.

Drug Distribution—The pancreas was removed and homogenized at the end of each permeation experiment, and drug concentrations in the pancreas and blood were measured to determine the distribution ratio.

Analytical Methods—Drug concentrations in the plasma, plasma ultrafiltrate, pancreatic juice, and pancreas homogenate were determined

[1] Supplied by Eisai Co. Ltd., Tokyo, Japan.
[2] Crick, Harper and Raper Unit.
[3] Boots Pure Drug Co. Ltd., Nottingham, England.
[4] Since pancreozymin is less stable than secretin, a higher dose was used.

0022-3549/80/0100-0027$01.00/0
© 1980, American Pharmaceutical Association

13 (1959).
(9) F. L. Warren, F. Goulden, and A. M. Robinson, *Biochem. J.*, **42**, 151 (1948).
(10) "The National Formulary," 14th ed., Mack Publishing Co., Easton, Pa., 1975, p. 205.
(11) "The United States Pharmacopeia," 19th rev., Mack Publishing Co., Easton, Pa., 1975, p. 142.
(12) "British Pharmacopoeia 1973," University Printing House, Cambridge, England, 1973, p. 443.
(13) J. E. Sinsheimer and E. F. Salim, *J. Anal. Chem.*, **37**, 566 (1965).
(14) E. F. Salim, P. E. Manni, and J. E. Sinsheimer, *J. Pharm. Sci.*, **53**, 391 (1964).
(15) N. M. Omar and N. A. El-Rabbat, *ibid.*, **67**, 779 (1978).
(16) R. Kuhn and D. Jerchel, *Ber.*, **74**, 949 (1941).
(17) W. J. Mader and R. R. Buck, *Anal. Chem.*, **24**, 666 (1952).
(18) D. Banes, *J. Am. Pharm. Assoc., Sci. Ed.*, **42**, 669 (1953).
(19) A. M. Mattson and C. O. Jensen, *Anal. Chem.*, **22**, 182 (1950).
(20) H. M. Hashmi, A. S. Adel, A. V. Viegas, and I. A. Ahmad, *Mikrochim. Acta*, **3**, 457 (1970).
(21) P. S. Vassileva-Alexandrova and P. S. Shismanor, *Anal. Chem.*, **47**, 1432 (1975).
(22) R. E. Graham, E. R. Biehl, and C. T. Kenner, *J. Pharm. Sci.*, **66**, 965 (1977).

Tissue Distribution and Metabolism of Drugs V: Effect of Secretin and Pancreozymin on Drug Transport in Rabbit Pancreas

MASATO ARAKAWA *§, KATSUHIKO OKUMURA *, and RYOHEI HORI‡x

Received April 10, 1979, from the **Institute of Pharmaceutical Sciences, Hiroshima University School of Medicine, Hiroshima 734, Japan,* and the ‡*Department of Pharmacy, Kyoto University Hospital, Sakyo-ku, Kyoto 606, Japan.* Accepted for publication July 16, 1979. §Present address: General Research Center, Wakunaga Pharmaceutical Co. Ltd., Kotachi, Hiroshima, Japan.

Abstract □ The effect of secretin and pancreozymin on the tissue distribution and penetration of drugs in the rabbit pancreas was studied to clarify hormonally regulated drug distribution. Drugs with high liquid solubility were distributed easily within the pancreas even during secretin or pancreozymin treatment, and these hormones had little effect on drug distribution from the blood to the pancreas. However, secretin increased the concentration ratio of dimethadione in the pancreatic juice (J) to plasma unbound dimethadione (Pf), probably because the pancreatic juice during secretin infusion is alkaline relative to the control. Secretin had no effect on the J/Pf of isonicotinamide and sulfanilamide. Secretin decreased the J/Pf of drugs with low lipophilicity or large molecular weight because the penetration rates of these drugs from cell water to pancreatic juice were not rapid enough to reach equilibrium. Pancreozymin was unable to change the J/Pf of any drug tested. These results suggest that the barrier between the blood and the pancreas or the barrier between the pancreas and the pancreatic juice is unchanged by secretin or pancreozymin.

Keyphrases □ Pancreas—drug transport, various drugs, effect of secretin, pancreozymin, pancreatic juice flow □ Pancreatic juice—effect of flow rate on pancreatic drug transport, various drugs □ Drug transport—pancreas, effect of secretin, pancreozymin, pancreatic juice flow, various drugs

Drug distribution has received increasing attention during recent years because such knowledge concerning the blood, organs, and tissues is needed to provide optimal treatment or protection from adverse reactions. Previous papers reported tissue distribution and penetration of drugs in the pancreas (1), lungs, (2, 3), and testes (4).

It was suggested that the lipid barrier in the pancreas plays a dominant role in drug distribution from the blood to the pancreas and that the lipid barrier and the molecular sieve barrier have independent roles in transport from the pancreas to the pancreatic juice. In these experiments, pancreatic juice secretion was stimulated by secretin infusion to maintain a constant juice flow. However, the pancreatic barriers could be changed by endogenous hormones that regulate pancreatic secretion during food digestion.

The purpose of this study was to determine experimentally whether secretin and pancreozymin, typical peptide hormones that stimulate pancreatic juice flow and bicarbonate or enzyme secretion, affect drug distribution and penetration in the pancreas. Some model drugs that exhibit remarkable lipophilicity, molecular size, and pKa were selected as discussed previously (1).

EXPERIMENTAL

Materials—Secretin[1], 3110 CHR U[2]/mg, was used. Pancreozymin[3], dimethadione, isonicotinamide, isonicotinic acid, sulfanilamide, sulfanilic acid, sulfisoxazole, and procainamide hydrochloride were obtained commercially. All other chemicals were analytical grade.

Animals—Male white rabbits, 2.0–3.0 kg, were housed in constant environment rooms and allowed free access to water and food.

Drug Permeation from Blood to Pancreatic Juice—The experimental procedures were almost identical to those described previously (1). Rabbits were anesthetized with pentobarbital sodium (27 mg/kg iv). Pancreatic juice was collected by cannulation into the pancreatic duct as described in the literature (5). Plasma drug concentrations were established and maintained by a suitable combination of priming injections and continuous intravenous infusion.

As the control, pancreatic juice was collected over 75 min prior to the administration of secretin or pancreozymin. The secretin effect was studied by a priming injection (1 CHR U/kg) and continuous intravenous infusion (2 CHR U/kg/hr), after which the pancreatic juice flow was stimulated from 14 (7–24 μl/min) to 39 (15–66 μl/min) μl/min. Pancreozymin also was studied using a priming injection (1 CHR U/kg) and continuous infusion (4 CHR U/kg/hr)[4]. In this experiment, secretin also was infused simultaneously to minimize the effect of secretin contamination in the pancreozymin preparation.

Drug Distribution—The pancreas was removed and homogenized at the end of each permeation experiment, and drug concentrations in the pancreas and blood were measured to determine the distribution ratio.

Analytical Methods—Drug concentrations in the plasma, plasma ultrafiltrate, pancreatic juice, and pancreas homogenate were determined

[1] Supplied by Eisai Co. Ltd., Tokyo, Japan.
[2] Crick, Harper and Raper Unit.
[3] Boots Pure Drug Co. Ltd., Nottingham, England.
[4] Since pancreozymin is less stable than secretin, a higher dose was used.

0022-3549/80/0100-0027$01.00/0
© 1980, American Pharmaceutical Association

Table I—Effect of Secretin and Pancreozymin on Pancreatic Drug Distribution

Drug	$(Panc/Pf)_{control}$[a]	$(Panc/Pf)_{secretin}$	$(Panc/Pf)_{secretin\ pancreozymin}$
Procainamide	1.20 ± 0.32 (4)	1.18 ± 0.32 (4)	—
Sulfanilamide	0.99 ± 0.16 (3)	0.95 ± 0.12 (5)	0.89 ± 0.08 (3)
Dimethadione	0.50 ± 0.01 (3)	0.55 ± 0.05 (5)	0.53 ± 0.02 (5)
Sulfisoxazole	0.50 ± 0.03 (4)	0.58 ± 0.04 (7)	0.51 ± 0.02 (4)
Sulfanilic acid	0.21 ± 0.01 (3)	0.25 ± 0.02 (4)	—

[a] Panc/Pf indicates the concentration ratio of drug in the pancreas to unbound drug in the plasma. These data were obtained 2 hr after the constant drug infusion and represent the mean ± *SEM*, with the number of animals in parentheses.

according to the procedure described previously (1). The protein content of the pancreatic juice was measured by the Lowry method (6), and the calcium level in the biological fluids was analyzed by the *o*-cresolphthalein-edetate sodium method with a minor modification (7).

RESULTS AND DISCUSSION

Effect of Secretin and Pancreozymin on Drug Distribution in Pancreas—To ascertain the effect of secretin or pancreozymin on drug distribution in the pancreas, drug uptake was studied after constant infusion for 2 hr. Table I illustrates the concentration ratios of drugs in the pancreas to the plasma of unbound drugs, expressed as the distribution ratio (Panc/Pf) under various conditions. Acidic drugs did not distribute into the pancreas as easily as did the cationic or neutral drugs studied previously (1). However, there was no significant difference in distribution ratio between controls and secretin-infused animals or between secretin-infused animals and secretin–pancreozymin-coinfused animals.

Intracellular pH decreases following secretin infusion and ^{14}C-dimethadione (an acidic compound) in male rats and the decrease in the dimethadione distribution have been explained by the pH-partition theory (8). In the present study, no significant difference was detected in dimethadione distribution when the pancreas was stimulated by secretin. The pH change of the pancreatic juice during secretin infusion has been reported as 0.09, from pH 6.86 to 6.77 (8). When the values of 0.53 ml/g for the intracellular water space and 0.22 ml/g for the extracellular water space were adopted[5], the ratio of the secretin-stimulated pancreatic drug level to the control drug level was ≥0.93. This value is so low that it was difficult to detect by the methods used.

Secretin increased the pancreatic juice flow by 2.8 times, and pancreozymin increased the protein and calcium secretion by 6 times. Furthermore, significant decreases were detected in the physiological calcium

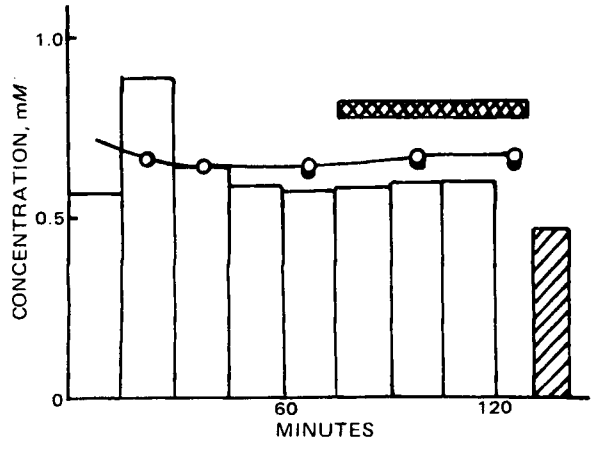

Figure 1—*Isonicotinamide concentration profile. Key: ○, total plasma drug concentration; ●, plasma free drug concentration; and ⊠, secretin infusion period. Open and hatched columns denote drug concentration in the pancreatic juice and in the pancreas, respectively.*

[5] Unpublished data.

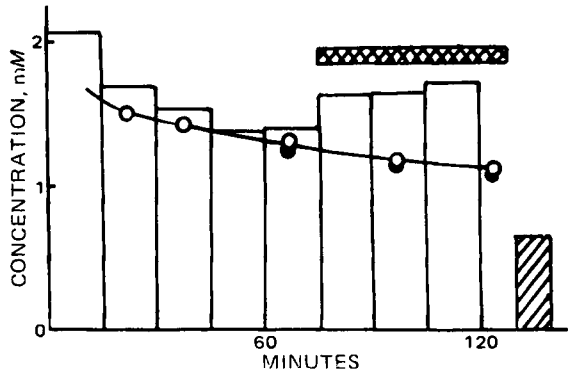

Figure 2—*Dimethadione concentration profile. Key: ○, total plasma drug concentration; ●, plasma free drug concentration; and ⊠, secretin infusion period. Open and hatched columns denote drug concentration in the pancreatic juice and in the pancreas, respectively.*

content of the rat pancreas during pancreozymin infusion (Panc/Pf of calcium content decreased from 1.41 ± 0.05 to 1.14 ± 0.08). This result probably was due to accelerated calcium secretion into the pancreatic juice during pancreozymin administration; the decreased pancreatic calcium could not be compensated fully by calcium from the blood. Thus, calcium apparently does not play a role in the distribution of these drugs in the pancreas. These results suggest that there is no correlation between drug distribution in the pancreas and pancreatic juice secretion or between the enzyme and calcium secretion.

Effect of Secretin and Pancreozymin on Drug Permeation from Blood to Pancreatic Juice—The effect of secretin on drug transport from the blood to the pancreatic juice was examined to clarify the transport barrier located in the luminal side of the pancreas. Drug levels in plasma and in the pancreatic juice following constant intravenous infusion of isonicotinamide, dimethadione, and isonicotinic acid with or without secretin are presented in Figs. 1–3 as a function of time. The ratios of pancreatic juice drug concentration to unbound plasma drug concentration (J/Pf) during the control period and during secretin infusion are listed in Table II, in which the percent change of J/Pf following secretin infusion also is indicated.

The values were calculated from the data obtained during the control period (45–75 min) and during secretin infusion (90–120 min). With isonicotinamide and sulfanilamide, whose molecular sizes are comparatively small, the J/Pf concentration ratios were almost unity and hardly were affected by secretin infusion (Fig. 1 and Table II). Dimethadione, whose molecular size and lipophilicity resemble those of isonicotinamide, exhibited significant concentration ratio increases (J/Pf) with secretin treatment (Fig. 2 and Table II).

Isonicotinic acid, which possesses structural units similar to isonicotinamide and has lower lipophilicity, showed smaller J/Pf ratios during secretin infusion than those of the controls (Fig. 3 and Table II). Almost the same results were obtained with sulfanilic acid, which has lower lipophilicity than sulfanilamide. Sulfisoxazole and procainamide, compounds with large molecular size compared with sulfanilamide and dimethadione, showed smaller J/Pf ratios during secretin infusion.

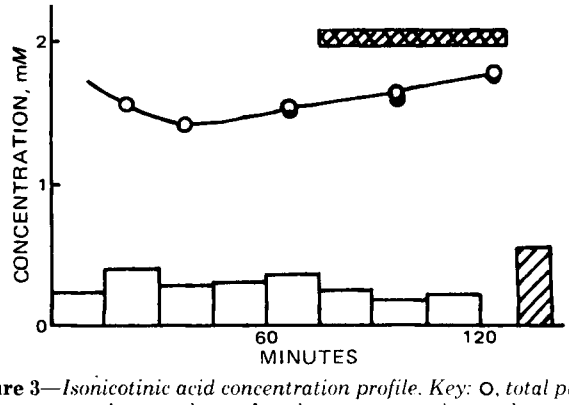

Figure 3—*Isonicotinic acid concentration profile. Key: ○, total plasma drug concentration; ●, plasma free drug concentration; and ⊠, secretin infusion period. Open and hatched columns denote drug concentration in the pancreatic juice and in the pancreas, respectively.*

Table II—Effect of Secretin on Drug Permeation into Pancreatic Juice

Drug	$(J/Pf)_{secretin}$[a]	$(J/Pf)_{control}$	Percent Change[b]	Statistics[c]
Dimethadione	1.83	1.41	+31 ± 6 (3)	$p < 0.05$
Isonicotinamide	0.91	0.92	−2 ± 2 (3)	NS
Sulfanilamide	1.08	1.23	−12 ± 2 (4)	$p < 0.05$
Isonicotinic acid	0.17	0.29	−40 ± 8 (3)	$p < 0.05$
Sulfanilic acid	0.03	0.08	−58 ± 6 (3)	$p < 0.01$
Sulfisoxazole	0.14	0.35	−57 ± 7 (3)	$p < 0.01$
Procainamide	0.09	0.19	−51 ± 6 (3)	$p < 0.01$

[a] J/Pf indicates the concentration ratio of drug in the pancreatic juice to unbound drug in the plasma. [b] Percent change was calculated from the individual data obtained during the control period and during the secretin infusion period. Data are presented with the standard error of the mean (*SEM*), and with the number of animals in parentheses. [c] The statistical test was the *t*-test of percent change.

These results suggest that drugs whose J/Pf ratios are almost unity easily penetrate the blood–pancreas barrier even during secretin treatment, unless there is a change in charge. Eventually, the pancreatic transport of drugs with high permeability would be independent of secretin treatment and of the pancreatic juice flow rate. However, with dimethadione, a weak acid with pKa 6.1, the high J/Pf ratios during secretin infusion could not be explained by its high permeability alone. One possible reason for this finding was the difference between the pancreatic juice pH during secretin treatment and that in the controls. According to the generally accepted view, increased pancreatic juice flow induced by secretin is linked with bicarbonate concentration increments (9).

If complete equilibrium were attained in the concentration ratio between the blood and the pancreatic juice, the transport ratio of acidic drugs would increase with the increase in juice alkalization by secretin infusion. Therefore, the increased transport ratio (J/Pf) of dimethadione caused by secretin infusion could be due to pancreatic juice alkalization and to the rapid partition. With acidic drugs such as isonicotinic acid, sulfanilic acid, and sulfisoxazole, the transport ratios decreased following secretin infusion. Since the transport ratio of acidic drugs theoretically would be greater than unity, as mentioned previously, the difference between the transport ratios of dimethadione and other acidic drugs might arise from differences in lipophilicity and molecular size. Procainamide was the model for basic drugs; the small J/Pf ratio and its decrease by secretin may be due to the alkaline state of pancreatic juice or to the bulky nature of the molecule.

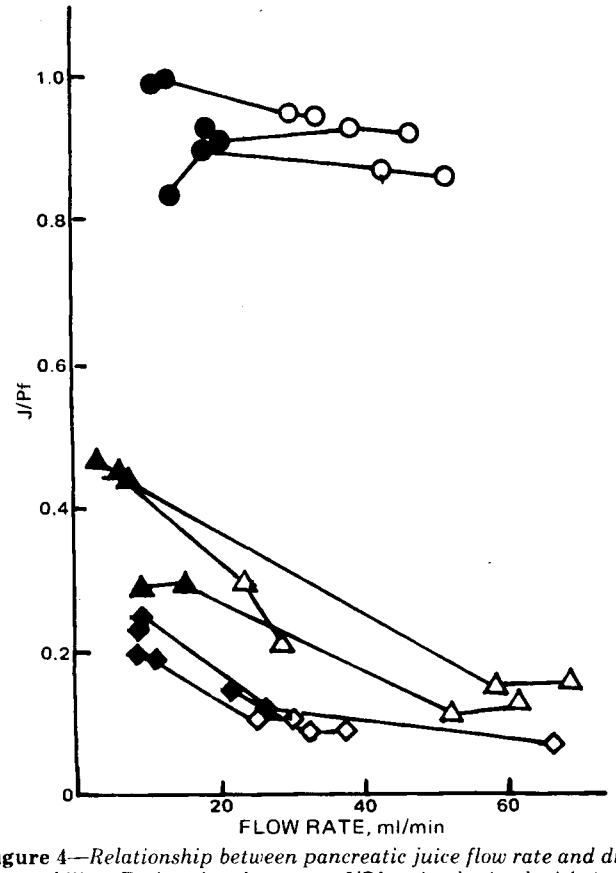

Figure 4—*Relationship between pancreatic juice flow rate and drug permeability. Each point denotes a J/Pf ratio obtained with (open symbol) or without (closed symbol) secretin. Key: ●—○, isonicotinamide; ▲—△, sulfisoxazole; and ♦—◇, procainamide.*

Table III—Effect[a] of Pancreozymin on Drug Permeation into Pancreatic Juice

Drug	$(J/Pf)_{secretin\ pancreozymin}$[b]	$(J/Pf)_{secretin}$	Percent Change[c]
Dimethadione	1.72	1.49	15 ± 4 (3)
Sulfanilamide	1.04	1.04	0 ± 4 (3)
Sulfisoxazole	0.09	0.10	−10 ± 9 (3)

[a] Data were not significant. The statistical test on the *t*-test of percent change. [b] See footnote *a* of Table II. [c] Percent change was calculated from the individual data obtained during secretin infusion period and during the secretin–pancreozymin coinfusion period. Data are presented with the standard error of the mean (*SEM*) and with the number of animals in parentheses.

To demonstrate the role of juice flow on drug movement from the blood to the pancreatic juice, the relationship between the transport ratio (J/Pf) and the pancreatic juice flow rate was examined (Fig. 4). The transport ratios (J/Pf) of procainamide and sulfisoxazole decreased as the juice flow increased, while the isonicotinamide J/Pf was unchanged. It was inferred that the transport ratios of drugs that cannot penetrate easily from the blood to the pancreatic juice due to their low lipophilicity and bulky molecular size decrease as pancreatic juice flow increases, probably because the penetration rates of these drugs are too slow to reach equilibrium before secretion.

A model of salicylic acid transfer from salivary gland cells into saliva by slower diffusion *via* lipid solvation was proposed (10, 11). Salicylic acid diffusion from cell water to saliva was not rapid enough to reach equilibrium, thus decreasing the salivary flow rate, which increased the saliva-to-plasma unbound salicylic acid concentration ratio by about one-third; dimethadione movement was rapid enough to reach equilibrium prior to excretion. In a study of the penetration of six water-soluble chemicals in bile, the permeation rate of small molecules was unchanged during bile flow stimulation while the penetration rate of large molecules decreased as bile flow increased (12). Based on these findings, it is speculated that the molecular sieve barrier and the lipid barrier exist independently even in secretin treatment. The effects of pancreozymin infusion on the permeation of dimethadione, sulfanilamide, and sulfisoxazole from the blood to the pancreatic juice are shown in Table III by the transport ratio (J/Pf) during pancreozymin treatment and during the control experiment.

The percent change of these transport ratios also is presented in Table III. During pancreozymin infusion, the protein and calcium contents of pancreatic juice increased 3.1- and 1.3-fold, respectively, while juice flow increased slightly. No significant difference was observed in the transport rate of these three drugs by pancreozymin infusion. Since no drug binding to enzyme protein in the pancreatic juice was detected by ultracentrifugation, these drugs must exist in the pancreatic juice as unbound molecules. Thus, the data given in Table III indicate that drug transport from the blood to the pancreatic juice is not changed by pancreozymin infusion. The data obtained using a limited number of model drugs support the suggested transport model of drug transfer from the blood to the pancreatic juice through a two-step barrier system: (*a*) a lipoidal barrier from the blood to the pancreas, and (*b*) a molecular sieve barrier and a lipoidal barrier from the cell to the pancreatic juice that coexist independently near the pancreatic duct surface. These barriers probably are rigid even during secretin or pancreozymin treatment.

REFERENCES

(1) R. Hori, M. Arakawa, and K. Okumura, *Chem. Pharm. Bull.*, **26**, 1135 (1978).

(2) K. Okumura, H. Yoshida, and R. Hori, *J. Pharm. Dyn.*, **1**, 230 (1978).

(3) R. Hori, H. Yoshida, and K. Okumura, *Chem. Pharm. Bull.*, **27**, 1321 (1979).

(4) K. Okumura, I. P. Lee, and R. L. Dixon, *J. Pharmacol. Exp. Ther.*, **194**, 89 (1975).

(5) T. Matsunaga, A. Yoshitani, T. Chin, H. Yazawa, M. Toh, M. Saiki, H. Kamogawa, and K. Egami, *Nihon. Univ. Dent. J.*, **45**, 575 (1971).

(6) E. Mizuno, T. Nishina, and M. Kitamura, *Rinsho Byori*, **19**, 427 (1971).
(7) H. V. Connerty and A. R. Broggs, *Am. J. Clin. Pathol.*, **45**, 290 (1966).
(8) C. D. Russell, R. J. Beschi, and R. H. Lindsay, *Int. J. Nucl. Med. Biol.*, **3**, 77 (1976).
(9) G. M. Makhlouf and A. L. Blum, *Gastroenterology*, **59**, 896 (1970).
(10) J. W. Putney, Jr., and J. F. Borzelleca, *J. Pharmacol. Exp. Ther.*, **182**, 515 (1972).
(11) J. F. Borzelleca and J. W. Putney, Jr., *ibid.*, **174**, 527 (1970).
(12) E. L. Forker, *Am. J. Physiol.*, **215**, 56 (1968).

Distribution Coefficients and *In Vitro* Human Serum Protein Binding of Spironolactone and Its 7α-Carboxymethyl Analog

ANTHONY S. NG *, RONALD B. KLUZA, and DAVID W. NEWTON ˣ

Received February 22, 1979, from the *Department of Pharmaceutics, Massachusetts College of Pharmacy, Boston, MA 02115.* Accepted for publication July 19, 1979. *Present address: Pharmacy Department, Children's Hospital of San Francisco, San Francisco, CA 94199.

Abstract □ The distribution coefficients of spironolactone (I) and its 7α-carboxymethyl analog (II) were determined at 22–25° in systems of *n*-octanol or chloroform and 0.1 *M* phosphate buffer at pH 7.4. The respective values for I in the two systems were 153.9 and 15.1, and those for II were 15.9 and 3.1. Protein binding studies of I and II were conducted with human serum albumin and human γ-globulin *via* equilibrium dialysis at 37°. The I fractions bound to 4% (w/v) albumin and to 1.16% (w/v) γ-globulin were 66 and 18%, respectively. The corresponding II fractions bound to the two proteins were 46 and 12%. The greater protein binding of I agrees with its superior lipophilicity to that of II. The binding of both I and II to albumin increased with increasing albumin concentration, whereas the binding of I and II to albumin did not change significantly as the concentrations of I or II were varied from 50 to 1300 ng/ml. Cooperativity and/or multiple classes of binding sites appear to be associated with the binding of I and II to albumin.

Keyphrases □ Spironolactone—distribution coefficients, *in vitro* human serum protein binding, 7α-carboxymethyl analog □ Protein binding—spironolactone, 7α-carboxymethyl analog, *in vitro* human serum □ Distribution coefficients—spironolactone, 7α-carboxymethyl analog, phosphate buffer with *n*-octanol or chloroform

The spirolactones are steroidal aldosterone antagonists clinically used to produce potassium-sparing diuresis. The spirolactones have been studied extensively because of their considerable biotransformation (1), potential carcinogenicity (2), and ability to induce hepatic detoxification of chemicals (3–5). The pharmacodynamic properties of spirolactones vary because of their differing structure–activity relationships and physicochemical properties (6). At least 19 spirolactones have been investigated (6, 7).

The purpose of this study was to determine the lipid–aqueous distribution coefficients and the extent of plasma protein binding of spironolactone and its 7α-carboxymethyl derivative.

EXPERIMENTAL

Materials—Spironolactone[1] (I) was tritiated[2] randomly and used without further purification. Tritiated 7α-carboxymethyl spirolactone[3] (II), human serum albumin[4], and human γ-globulin[5] were used as received. Other solvents and reagents were of analytical grade of purity.

Procedures—Ten solutions of I and II in the 50–500-ng/ml range were prepared in 0.1 *M* phosphate buffer at pH 7.4 and saturated previously with *n*-octanol or chloroform.

Three milliliters each of the sample solution and of the *n*-octanol or chloroform saturated previously with the phosphate buffer were placed in a glass tube with a polytef-lined screw cap, and the mixture was agitated on a horizontal shaker[6] for 30 min at room temperature (22–25°). The mixtures were allowed to stand for 2 hr, during which time the phases separated. An accurate volume from each phase then was mixed with 10 ml of Bray's solution (8), and the samples were analyzed for I or II by counting on a liquid scintillation spectrometer[7] for 5 min. Each experiment was conducted in triplicate. Distribution coefficient (*P*) values were calculated from (9):

$$P = (\text{counts in } n\text{-octanol phase}/\text{counts in aqueous phase}) \quad \text{(Eq. 1)}$$

$$\log P_{\text{chloroform}} = 1.12 \log P_{n\text{-octanol}} - 1.343 \quad \text{(Eq. 2)}$$

Eight solutions of I and II in the 50–1300-ng/ml range were prepared in 0.1 *M* phosphate buffer at pH 7.4. Human serum albumin solutions (1, 2, 3, 4, and 5% w/v) and a human γ-globulin solution (1.16% w/v) also were prepared in the phosphate buffer. Exactly 1.0 ml of the sample solution was introduced into one side of a dialysis cell[8] separated by a cellulose membrane[9], and 1.0 ml of protein solution was placed into the opposite half. After the cells were incubated for 24 hr at 37°, measured volumes of the sample and protein solutions were mixed with 10 ml of Bray's solution, and the mixtures were counted on a liquid scintillation spectrometer for 5 min. The percent of I or II bound to albumin or γ-globulin was determined from:

$$\text{percent bound} = \left[\frac{(\text{counts in protein}) - (\text{counts in sample solution})}{\text{counts in protein}}\right] \times 100 \quad \text{(Eq. 3)}$$

DISCUSSION

The distribution coefficients of I and II are reported in Table I. There is a considerable discrepancy between the values for I and II in this study and those determined previously (7). The I value determined in chloroform was 17% greater than the theoretical I value in chloroform calculated from Eq. 2 using the experimental value for the distribution coefficient of I in *n*-octanol. However, the reported value (7) for the distribution coefficient of I in *n*-octanol is 289% larger than the corresponding present study value. Similarly, the experimental value for the distribution coefficient of II in chloroform was 210% greater than the corresponding theoretical value, whereas the reported value (7) for the distribution coefficient of II in *n*-octanol is 449% greater than the value determined from this study.

The disagreement between the reported (7) and present study distribution coefficients of I and II in *n*-octanol is not readily discernible. The

[1] SC-9420, lot 308, mol. wt. 416.57, assay 100.44%, G. D. Searle & Co., Chicago, Ill.
[2] Catalytic exchange method, 95.5% assay by radiochromatogram, specific activity 4.27 mCi/mg, New England Nuclear, Boston, Mass.
[3] SC-25152, mol. wt. 400.53, tritiated in the 1- and 2-positions, 95.76% assay by radiochromatogram, specific activity 83.20 mCi/mg, G. D. Searle & Co., Chicago, Ill.
[4] Lot 34G-8120, mol. wt. 69,000, Sigma Chemical Co., St. Louis, Mo.
[5] Lot 113C-1010, Sigma Chemical Co., St. Louis, Mo.
[6] Precision Scientific Co., Ann Arbor, Mich.
[7] Model 3320, Packard Instrument Co., Downers Grove, Ill.
[8] Constructed of Plexiglas, Technilab Instrument Inc., Pequannock, N.J.
[9] Nominal pore size of 4.8 nm, impermeable to molecules with mol. wt. > 6000, Technilab Instrument Inc., Pequannock, N.J.

0022-3549/80/0100-0030$01.00/0
© 1980, American Pharmaceutical Association

(6) E. Mizuno, T. Nishina, and M. Kitamura, *Rinsho Byori*, **19**, 427 (1971).
(7) H. V. Connerty and A. R. Broggs, *Am. J. Clin. Pathol.*, **45**, 290 (1966).
(8) C. D. Russell, R. J. Beschi, and R. H. Lindsay, *Int. J. Nucl. Med. Biol.*, **3**, 77 (1976).
(9) G. M. Makhlouf and A. L. Blum, *Gastroenterology*, **59**, 896 (1970).
(10) J. W. Putney, Jr., and J. F. Borzelleca, *J. Pharmacol. Exp. Ther.*, **182**, 515 (1972).
(11) J. F. Borzelleca and J. W. Putney, Jr., *ibid.*, **174**, 527 (1970).
(12) E. L. Forker, *Am. J. Physiol.*, **215**, 56 (1968).

Distribution Coefficients and *In Vitro* Human Serum Protein Binding of Spironolactone and Its 7α-Carboxymethyl Analog

ANTHONY S. NG *, RONALD B. KLUZA, and DAVID W. NEWTON ˣ

Received February 22, 1979, from the *Department of Pharmaceutics, Massachusetts College of Pharmacy, Boston, MA 02115.* Accepted for publication July 19, 1979. *Present address: Pharmacy Department, Children's Hospital of San Francisco, San Francisco, CA 94199.

Abstract □ The distribution coefficients of spironolactone (I) and its 7α-carboxymethyl analog (II) were determined at 22–25° in systems of *n*-octanol or chloroform and 0.1 *M* phosphate buffer at pH 7.4. The respective values for I in the two systems were 153.9 and 15.1, and those for II were 15.9 and 3.1. Protein binding studies of I and II were conducted with human serum albumin and human γ-globulin *via* equilibrium dialysis at 37°. The I fractions bound to 4% (w/v) albumin and to 1.16% (w/v) γ-globulin were 66 and 18%, respectively. The corresponding II fractions bound to the two proteins were 46 and 12%. The greater protein binding of I agrees with its superior lipophilicity to that of II. The binding of both I and II to albumin increased with increasing albumin concentration, whereas the binding of I and II to albumin did not change significantly as the concentrations of I or II were varied from 50 to 1300 ng/ml. Cooperativity and/or multiple classes of binding sites appear to be associated with the binding of I and II to albumin.

Keyphrases □ Spironolactone—distribution coefficients, *in vitro* human serum protein binding, 7α-carboxymethyl analog □ Protein binding—spironolactone, 7α-carboxymethyl analog, *in vitro* human serum □ Distribution coefficients—spironolactone, 7α-carboxymethyl analog, phosphate buffer with *n*-octanol or chloroform

The spirolactones are steroidal aldosterone antagonists clinically used to produce potassium-sparing diuresis. The spirolactones have been studied extensively because of their considerable biotransformation (1), potential carcinogenicity (2), and ability to induce hepatic detoxification of chemicals (3–5). The pharmacodynamic properties of spirolactones vary because of their differing structure–activity relationships and physicochemical properties (6). At least 19 spirolactones have been investigated (6, 7).

The purpose of this study was to determine the lipid–aqueous distribution coefficients and the extent of plasma protein binding of spironolactone and its 7α-carboxymethyl derivative.

EXPERIMENTAL

Materials—Spironolactone[1] (I) was tritiated[2] randomly and used without further purification. Tritiated 7α-carboxymethyl spirolactone[3] (II), human serum albumin[4], and human γ-globulin[5] were used as received. Other solvents and reagents were of analytical grade of purity.

Procedures—Ten solutions of I and II in the 50–500-ng/ml range were prepared in 0.1 *M* phosphate buffer at pH 7.4 and saturated previously with *n*-octanol or chloroform.

Three milliliters each of the sample solution and of the *n*-octanol or chloroform saturated previously with the phosphate buffer were placed in a glass tube with a polytef-lined screw cap, and the mixture was agitated on a horizontal shaker[6] for 30 min at room temperature (22–25°). The mixtures were allowed to stand for 2 hr, during which time the phases separated. An accurate volume from each phase then was mixed with 10 ml of Bray's solution (8), and the samples were analyzed for I or II by counting on a liquid scintillation spectrometer[7] for 5 min. Each experiment was conducted in triplicate. Distribution coefficient (*P*) values were calculated from (9):

$$P = (\text{counts in } n\text{-octanol phase}/\text{counts in aqueous phase}) \quad \text{(Eq. 1)}$$

$$\log P_{\text{chloroform}} = 1.12 \log P_{n\text{-octanol}} - 1.343 \quad \text{(Eq. 2)}$$

Eight solutions of I and II in the 50–1300-ng/ml range were prepared in 0.1 *M* phosphate buffer at pH 7.4. Human serum albumin solutions (1, 2, 3, 4, and 5% w/v) and a human γ-globulin solution (1.16% w/v) also were prepared in the phosphate buffer. Exactly 1.0 ml of the sample solution was introduced into one side of a dialysis cell[8] separated by a cellulose membrane[9], and 1.0 ml of protein solution was placed into the opposite half. After the cells were incubated for 24 hr at 37°, measured volumes of the sample and protein solutions were mixed with 10 ml of Bray's solution, and the mixtures were counted on a liquid scintillation spectrometer for 5 min. The percent of I or II bound to albumin or γ-globulin was determined from:

$$\text{percent bound} = \left[\frac{(\text{counts in protein}) - (\text{counts in sample solution})}{\text{counts in protein}}\right] \times 100 \quad \text{(Eq. 3)}$$

DISCUSSION

The distribution coefficients of I and II are reported in Table I. There is a considerable discrepancy between the values for I and II in this study and those determined previously (7). The I value determined in chloroform was 17% greater than the theoretical I value in chloroform calculated from Eq. 2 using the experimental value for the distribution coefficient of I in *n*-octanol. However, the reported value (7) for the distribution coefficient of I in *n*-octanol is 289% larger than the corresponding present study value. Similarly, the experimental value for the distribution coefficient of II in chloroform was 210% greater than the corresponding theoretical value, whereas the reported value (7) for the distribution coefficient of II in *n*-octanol is 449% greater than the value determined from this study.

The disagreement between the reported (7) and present study distribution coefficients of I and II in *n*-octanol is not readily discernible. The

[1] SC-9420, lot 308, mol. wt. 416.57, assay 100.44%, G. D. Searle & Co., Chicago, Ill.
[2] Catalytic exchange method, 95.5% assay by radiochromatogram, specific activity 4.27 mCi/mg, New England Nuclear, Boston, Mass.
[3] SC-25152, mol. wt. 400.53, tritiated in the 1- and 2-positions, 95.76% assay by radiochromatogram, specific activity 83.20 mCi/mg, G. D. Searle & Co., Chicago, Ill.
[4] Lot 34G-8120, mol. wt. 69,000, Sigma Chemical Co., St. Louis, Mo.
[5] Lot 113C-1010, Sigma Chemical Co., St. Louis, Mo.
[6] Precision Scientific Co., Ann Arbor, Mich.
[7] Model 3320, Packard Instrument Co., Downers Grove, Ill.
[8] Constructed of Plexiglas, Technilab Instrument Inc., Pequannock, N.J.
[9] Nominal pore size of 4.8 nm, impermeable to molecules with mol. wt. > 6000, Technilab Instrument Inc., Pequannock, N.J.

0022-3549/80/0100-0030$01.00/0
© 1980, American Pharmaceutical Association

Table I—Distribution Coefficients of I and II Determined in 0.1 *M* Aqueous Phosphate Buffer at pH 7.4 *versus* *n*-Octanol and Chloroform

Compound	Experimental Values, mean ± *SEM*, %		Reported Values for	Calculated Values[a] for
	n-Octanol	Chloroform	*n*-Octanol	Chloroform
I	153.9 ± 15.3	15.1 ± 1.7	598.4[b]	12.9[c]
II	15.9 ± 0.7	3.1 ± 0.3	87.3[d]	1.0[e]

[a] From Eq. 2. [b] Antilog of log P = 2.777; Ref. 7. [c] Antilog of log P = 1.11, calculated from Eq. 2. [d] Antilog of log P = 1.941; Ref. 7. [e] Antilog of log P = 0.001, calculated from Eq. 2.

Table II—Binding of I and II to Human Serum Albumin and Human γ-Globulin.

Compound	Protein Binding, mean ± *SEM*, %			Binding Difference, %[a]		
	Albumin, 4%	Globulin, 1.16%	Total	Albumin, 4%	Globulin, 1.16%	Total
I	66.5 ± 0.4	18.3 ± 0.5	84.7 ± 0.4	—	—	—
II	45.7 ± 0.5	11.8 ± 0.5	57.5 ± 0.5	−31.2	−35.4	−32.1

[a] [(percent II − percent I)/percent I] × 100.

Table III—Comparison of Protein Binding Values for I and II

Compound	Present Study[a]	Protein Binding, %	
		Reference 7[b]	Reference 10[c]
I	84.7	94.2	91.1, 98.2
II	57.5	73.5	—

[a] Based on the sum of binding by 4% human serum albumin and 1.16% human γ-globulin. [b] Ultrafiltration method. [c] Lower value was obtained *via* equilibrium dialysis, and higher value was obtained *via* ultrafiltration; both were determined in human plasma at 550 ng of I/ml.

experimental distribution coefficients for I and II reported here are in closer agreement with the values predicted by Eq. 2. All distribution coefficient data determined in *n*-octanol indicate I to be 7–10 times more lipophilic than II. This difference may be attributed to the presence of a sulfur atom in the acetylthio substituent at the 7-position on I. The dominating contribution of the sulfur atom to lipophilicity is emphasized often *via* reference to the exemplary ninefold greater distribution coefficient of thiopental *versus* that of pentobarbital (9).

The values for percent protein binding determined in this study and those reported earlier (7, 10) are listed in Tables II and III. No binding of I or II to the dialysis membrane was demonstrated. The significant disagreement of the present results with those reported earlier may be attributed to at least the following factors:

1. The experimental conditions of Ref. 7 included using 20% (v/v) 1,3-butylene glycol and 4% (v/v) methanol to maintain drug solubility in the phosphate buffer as well as sample ultrafiltration *via* centrifugation at 4°. This low temperature could have influenced binding, resulting in values different from those found at 37°. The concentrations of human serum albumin utilized (7) are typical of clinical hypoalbuminemia (11). The previous investigators (7) did not study the binding of I or II to human γ-globulin.

2. The authors of Ref. 10 used fresh human plasma for I binding studies; however, serum protein concentrations and temperature conditions were not reported.

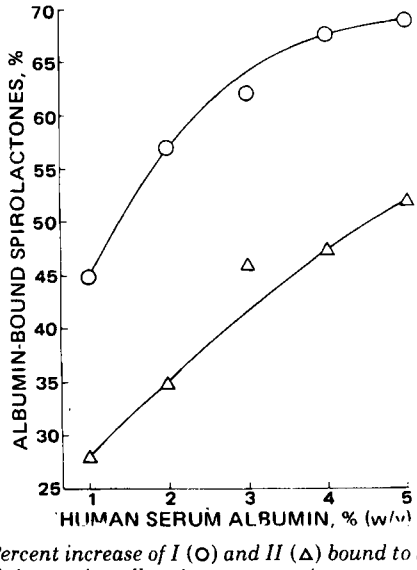

Figure 1—*Percent increase of I (○) and II (△) bound to human serum albumin with increasing albumin concentration.*

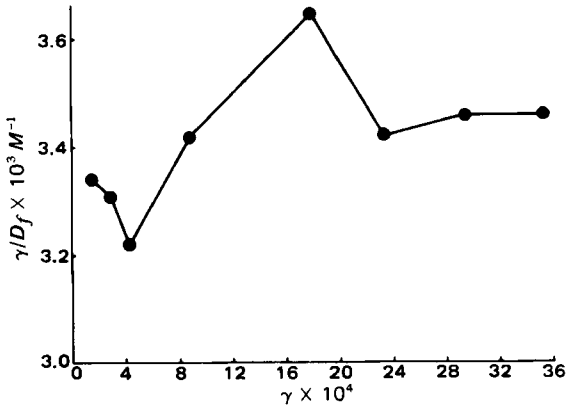

Figure 2—*Scatchard plot of* γ/D_f *versus* γ *for I over the 53.3–1278.0-ng/ml range (1.3–30.1 × 10⁻⁷ M) in 4.0% (w/v) (5.8 × 10⁻⁴ M) human serum albumin at pH 7.4 and 37°.*

Although several steroidal compounds, *e.g.*, corticosteroids, are bound extensively to human γ-globulins, albumin accounts for the greatest proportion of binding of these drugs to serum or plasma proteins (11–13). Furthermore, some steroids also are highly bound to serum lipoproteins (14). The present study results indicate 18% binding of I to human γ-globulin. Therefore, the comparative data in Table III suggest that the percent protein binding of I reported in Ref. 7 may be an overestimate resulting from the use of a mixed aqueous solvent system and albumin-only protein solutions. The low temperature centrifugation conditions used (7) also would increase the fraction of drug bound to albumin (11).

The present 85% value for the total binding of I in 4% (w/v) human serum albumin and 1.16% human γ-globulin (Table II) agrees with the 91% value determined in human plasma reported elsewhere (10). There was no significant variation in the percent binding of I or II to the serum proteins over the drug concentration range investigated. However, Fig. 1 shows that the binding of I and II increased proportionally with increasing albumin concentration.

A causal relationship between hydrophobicity (lipophilicity) and drug–protein binding was demonstrated for steroids (15) and other drugs (16, 17). The fact that the distribution coefficient of I is 7–10 times greater than that of II (Table I) correlates with the 32% superiority in protein binding of I over II (Table II). Scatchard plots (7, 18–20) of I and II in 4% (w/v) human serum albumin (Figs. 2 and 3) were prepared from:

$$\gamma/D_f = K(n - \gamma) \qquad \text{(Eq. 4)}$$

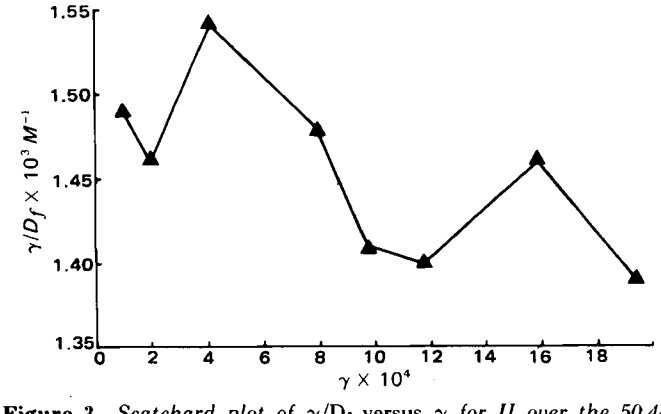

Figure 3—*Scatchard plot of* γ/D_f *versus* γ *for II over the 50.4–1006.0-ng/ml range (1.3–25.1 × 10⁻⁷ M) in 4% (w/v) (5.8 × 10⁻⁴ M) human serum albumin at pH 7.4 and 37°.*

where γ is the ratio of the concentration of albumin-bound spirolactone to that of albumin, D_f is the concentration of unbound spirolactone at dialysis equilibrium, K is the binding constant at equilibrium, and n is the number of a single type of binding sites. The previous investigators (7) apparently obtained linear plots of γ/D_f *versus* γ for several spirolactones. The concentrations of spirolactone used (7) appear to have been ~30–800 times higher than the peak serum concentrations of I and its metabolites detected in human males given a 200-mg oral dose (10).

The observed absence of linearity, together with the complexity of the Scatchard plots for I and II, strongly suggests diverse protein–ligand binding characteristics. Such deviations were reported to be due to cooperative ligand interaction, multiple-contact binding sites, or nonequivalent binding sites (20). Inspection of the Scatchard plots reveals several points of inflection, as well as both concave and convex curvatures at varying concentrations of bound I and II. Such patterns generally are the results of different types of binding sites, each exhibiting cooperative character. Furthermore, individual binding sites for I and II may overlap and also may contribute to the diverse binding pattern observed. Although no absolute conclusion can be drawn regarding which phenomenon dominates the binding pattern of I and II for human serum albumin, a single model of independent, equivalent binding is not applicable for the spirolactones studied.

REFERENCES

(1) A. Karim, J. Hribar, W. Aksamit, M. Doherty, and L. J. Chinn, *Drug Metab. Dispos.*, **3**, 467 (1975).

(2) D. J. Greenblatt and J. Koch-Weser, *J. Am. Med. Assoc.*, **225**, 40 (1973).

(3) C. D. Klaassen, *J. Pharmacol. Exp. Ther.*, **191**, 201 (1974).

(4) H. Selye, *Acta Hepato-Splenol.*, **17**, 394 (1970).

(5) H. Selye, *Science*, **169**, 775 (1970).

(6) R. M. Weier and L. M. Hofmann, *J. Med. Chem.*, **18**, 817 (1975).

(7) Y. M. Chien, L. M. Hofmann, H. J. Lambert, and L. C. Tao, *J. Pharm. Sci.*, **65**, 1337 (1976).

(8) G. Bray, *Anal. Biochem.*, **1**, 279 (1960).

(9) A. Leo, C. Hansch, and D. Elkins, *Chem. Rev.*, **71**, 525 (1971).

(10) A. Karim, B. A. Zagarella, J. Hribar, and M. Dooley, *Clin. Pharmacol. Ther.*, **19**, 158 (1976).

(11) J. J. Vallner, *J. Pharm. Sci.*, **66**, 447 (1977).

(12) J. C. Melby, *Rev. Pharmacol. Toxicol.*, **17**, 511 (1977).

(13) J. W. Bridges and A. G. E. Wilson, in "Progress in Drug Metabolism," vol. 1, J. W. Bridges and C. F. Chasseaud, Eds., Wiley, New York, N.Y., 1976, pp. 209–212.

(14) P. M. J. Hobbelen, A. Coert, J. A. A. Geelen, and J. vander Vies, *Biochem. Pharmacol.*, **24**, 165 (1975).

(15) W. Scholton, *Arzneim.-Forsch.*, **18**, 505 (1968).

(16) C. Hansch, in "Drug Design," vol. 1, E. J. Ariens, Ed., Academic, New York, N.Y., 1971, p. 271.

(17) J. Krieglstein, W. Meiler, and J. Staab, *Biochem. Pharmacol.*, **21**, 985 (1972).

(18) G. Scatchard, *Ann. N.Y. Acad. Sci.*, **51**, 660 (1949).

(19) H. G. Weder, J. Schildkneckt, R. A. Lutz, and P. Kesselring, *Eur. J. Biochem.*, **42**, 475 (1974).

(20) G. Schwarz, *Biophys. Struct. Mechanism*, **2**, 1 (1976).

ACKNOWLEDGMENTS

Abstracted in part from a thesis submitted by A. S. Ng to the Massachusetts College of Pharmacy in partial fulfillment of the Master of Science degree requirements.

The authors thank Searle Laboratories, Chicago, Ill., for donating samples of I and II. They also thank Ms. Dianne Copithorne for manuscript preparation.

Lidocaine Pharmacokinetics in Pregnant and Nonpregnant Sheep

DUANE C. BLOEDOW *x, DAVID H. RALSTON, and JOHN C. HARGROVE

Received November 6, 1978, from the *Department of Anesthesiology, University of Washington, Seattle, WA 98195.* Accepted for publication July 24, 1979.

*Present address: School of Pharmacy, University of Colorado, Boulder, CO 80309.

Abstract □ Lidocaine disposition kinetics were studied in the pregnant ewe following 0.5-, 1.0-, and 2.0-mg/kg iv bolus doses and in the nonpregnant ewe following a 1.0-mg/kg iv bolus dose. Arterial blood was assayed for lidocaine by GLC. The blood lidocaine concentration–time curves were computer fitted to a two-compartment open model. In the pregnant ewe, the total body clearance of lidocaine (38 ml/min/kg) remained constant with increasing dose and was correlated linearly with preinjection cardiac output. The apparent volume of distribution of the central compartment apparently increased with increasing dose. The half-life of the postdistributive phase and the volumes of distribution at steady state and during the postdistributive phase increased as the dose was increased from 0.5 to 1.0 mg/kg. These observations suggest dose-related distribution of lidocaine in the pregnant ewe. The total body clearance of lidocaine in the pregnant ewe was not different from that in the nonpregnant ewe after 1.0-mg/kg doses; however, the volumes of distribution of the central compartment at steady state and during the postdistributive phase and the half-life of the postdistributive phase were greater in the pregnant ewe. The greater total body clearance for lidocaine in sheep as compared to humans is consistent with the greater hepatic blood flow in sheep; calculated hepatic extraction ratios for sheep are similar to hepatic extraction ratios for humans.

Keyphrases □ Lidocaine—pharmacokinetics, pregnant and nonpregnant sheep □ Pharmacokinetics—lidocaine, pregnant and nonpregnant sheep □ Anesthetics—lidocaine, pharmacokinetics, pregnant and nonpregnant sheep

Few literature reports describe drug disposition kinetics in the pregnant individual, but drug pharmacokinetics during pregnant and nonpregnant states may differ markedly. Alterations in drug disposition kinetics could be related to maternal changes, including blood and/or tissue binding of the drug, changes in the rates or distribution of blood flow, and drug metabolism changes. More importantly, drug kinetics during pregnancy may be altered by the addition of the fetal–placental unit with its inherent abilities to distribute, bind, metabolize, and clear drugs.

Lidocaine disposition kinetics at three doses in the pregnant ewe are presented in this report, and a comparison is made with lidocaine disposition kinetics in the nonpregnant ewe.

EXPERIMENTAL

Pregnant and nonpregnant pure or crossbred Suffolk ewes, 64.6 ± 11.3 (mean ± *SD* on the day of surgery) and 66.7 ± 11.9 kg, respectively, were obtained locally. Pregnant ewes were studied from Day 137 to Day 143 of gestation (full term 147–150 days). The ewes were catheterized during sterile surgery under general endotracheal anesthesia, using halothane and oxygen with controlled mechanical ventilation.

Polyethylene catheters were placed into the femoral artery and femoral vein and advanced to the abdominal aorta and inferior vena cava, respectively. The femoral artery catheter was used for continuous blood pressure and heart rate monitoring, and the femoral vein catheter was used for lidocaine administration. A central venous catheter was inserted *via* percutaneous puncture into the external jugular vein and positioned in the right atrium. This catheter was used for the injection of indocya-

0022-3549/80/0100-0032$01.00/0

© 1980, American Pharmaceutical Association

where γ is the ratio of the concentration of albumin-bound spirolactone to that of albumin, D_f is the concentration of unbound spirolactone at dialysis equilibrium, K is the binding constant at equilibrium, and n is the number of a single type of binding sites. The previous investigators (7) apparently obtained linear plots of γ/D_f *versus* γ for several spirolactones. The concentrations of spirolactone used (7) appear to have been ~30–800 times higher than the peak serum concentrations of I and its metabolites detected in human males given a 200-mg oral dose (10).

The observed absence of linearity, together with the complexity of the Scatchard plots for I and II, strongly suggests diverse protein–ligand binding characteristics. Such deviations were reported to be due to cooperative ligand interaction, multiple-contact binding sites, or nonequivalent binding sites (20). Inspection of the Scatchard plots reveals several points of inflection, as well as both concave and convex curvatures at varying concentrations of bound I and II. Such patterns generally are the results of different types of binding sites, each exhibiting cooperative character. Furthermore, individual binding sites for I and II may overlap and also may contribute to the diverse binding pattern observed. Although no absolute conclusion can be drawn regarding which phenomenon dominates the binding pattern of I and II for human serum albumin, a single model of independent, equivalent binding is not applicable for the spirolactones studied.

REFERENCES

(1) A. Karim, J. Hribar, W. Aksamit, M. Doherty, and L. J. Chinn, *Drug Metab. Dispos.*, **3**, 467 (1975).

(2) D. J. Greenblatt and J. Koch-Weser, *J. Am. Med. Assoc.*, **225**, 40 (1973).

(3) C. D. Klaassen, *J. Pharmacol. Exp. Ther.*, **191**, 201 (1974).

(4) H. Selye, *Acta Hepato-Splenol.*, **17**, 394 (1970).

(5) H. Selye, *Science*, **169**, 775 (1970).

(6) R. M. Weier and L. M. Hofmann, *J. Med. Chem.*, **18**, 817 (1975).

(7) Y. M. Chien, L. M. Hofmann, H. J. Lambert, and L. C. Tao, *J. Pharm. Sci.*, **65**, 1337 (1976).

(8) G. Bray, *Anal. Biochem.*, **1**, 279 (1960).

(9) A. Leo, C. Hansch, and D. Elkins, *Chem. Rev.*, **71**, 525 (1971).

(10) A. Karim, B. A. Zagarella, J. Hribar, and M. Dooley, *Clin. Pharmacol. Ther.*, **19**, 158 (1976).

(11) J. J. Vallner, *J. Pharm. Sci.*, **66**, 447 (1977).

(12) J. C. Melby, *Rev. Pharmacol. Toxicol.*, **17**, 511 (1977).

(13) J. W. Bridges and A. G. E. Wilson, in "Progress in Drug Metabolism," vol. 1, J. W. Bridges and C. F. Chasseaud, Eds., Wiley, New York, N.Y., 1976, pp. 209–212.

(14) P. M. J. Hobbelen, A. Coert, J. A. A. Geelen, and J. vander Vies, *Biochem. Pharmacol.*, **24**, 165 (1975).

(15) W. Scholton, *Arzneim.-Forsch.*, **18**, 505 (1968).

(16) C. Hansch, in "Drug Design," vol. 1, E. J. Ariens, Ed., Academic, New York, N.Y., 1971, p. 271.

(17) J. Krieglstein, W. Meiler, and J. Staab, *Biochem. Pharmacol.*, **21**, 985 (1972).

(18) G. Scatchard, *Ann. N.Y. Acad. Sci.*, **51**, 660 (1949).

(19) H. G. Weder, J. Schildkneckt, R. A. Lutz, and P. Kesselring, *Eur. J. Biochem.*, **42**, 475 (1974).

(20) G. Schwarz, *Biophys. Struct. Mechanism*, **2**, 1 (1976).

ACKNOWLEDGMENTS

Abstracted in part from a thesis submitted by A. S. Ng to the Massachusetts College of Pharmacy in partial fulfillment of the Master of Science degree requirements.

The authors thank Searle Laboratories, Chicago, Ill., for donating samples of I and II. They also thank Ms. Dianne Copithorne for manuscript preparation.

Lidocaine Pharmacokinetics in Pregnant and Nonpregnant Sheep

DUANE C. BLOEDOW *x, DAVID H. RALSTON, and JOHN C. HARGROVE

Received November 6, 1978, from the *Department of Anesthesiology, University of Washington, Seattle, WA 98195.* Accepted for publication July 24, 1979.

*Present address: School of Pharmacy, University of Colorado, Boulder, CO 80309.

Abstract □ Lidocaine disposition kinetics were studied in the pregnant ewe following 0.5-, 1.0-, and 2.0-mg/kg iv bolus doses and in the nonpregnant ewe following a 1.0-mg/kg iv bolus dose. Arterial blood was assayed for lidocaine by GLC. The blood lidocaine concentration–time curves were computer fitted to a two-compartment open model. In the pregnant ewe, the total body clearance of lidocaine (38 ml/min/kg) remained constant with increasing dose and was correlated linearly with preinjection cardiac output. The apparent volume of distribution of the central compartment apparently increased with increasing dose. The half-life of the postdistributive phase and the volumes of distribution at steady state and during the postdistributive phase increased as the dose was increased from 0.5 to 1.0 mg/kg. These observations suggest dose-related distribution of lidocaine in the pregnant ewe. The total body clearance of lidocaine in the pregnant ewe was not different from that in the nonpregnant ewe after 1.0-mg/kg doses; however, the volumes of distribution of the central compartment at steady state and during the postdistributive phase and the half-life of the postdistributive phase were greater in the pregnant ewe. The greater total body clearance for lidocaine in sheep as compared to humans is consistent with the greater hepatic blood flow in sheep; calculated hepatic extraction ratios for sheep are similar to hepatic extraction ratios for humans.

Keyphrases □ Lidocaine—pharmacokinetics, pregnant and nonpregnant sheep □ Pharmacokinetics—lidocaine, pregnant and nonpregnant sheep □ Anesthetics—lidocaine, pharmacokinetics, pregnant and nonpregnant sheep

Few literature reports describe drug disposition kinetics in the pregnant individual, but drug pharmacokinetics during pregnant and nonpregnant states may differ markedly. Alterations in drug disposition kinetics could be related to maternal changes, including blood and/or tissue binding of the drug, changes in the rates or distribution of blood flow, and drug metabolism changes. More importantly, drug kinetics during pregnancy may be altered by the addition of the fetal–placental unit with its inherent abilities to distribute, bind, metabolize, and clear drugs.

Lidocaine disposition kinetics at three doses in the pregnant ewe are presented in this report, and a comparison is made with lidocaine disposition kinetics in the nonpregnant ewe.

EXPERIMENTAL

Pregnant and nonpregnant pure or crossbred Suffolk ewes, 64.6 ± 11.3 (mean ± *SD* on the day of surgery) and 66.7 ± 11.9 kg, respectively, were obtained locally. Pregnant ewes were studied from Day 137 to Day 143 of gestation (full term 147–150 days). The ewes were catheterized during sterile surgery under general endotracheal anesthesia, using halothane and oxygen with controlled mechanical ventilation.

Polyethylene catheters were placed into the femoral artery and femoral vein and advanced to the abdominal aorta and inferior vena cava, respectively. The femoral artery catheter was used for continuous blood pressure and heart rate monitoring, and the femoral vein catheter was used for lidocaine administration. A central venous catheter was inserted *via* percutaneous puncture into the external jugular vein and positioned in the right atrium. This catheter was used for the injection of indocya-

0022-3549/80/0100-0032$01.00/0

© 1980, American Pharmaceutical Association

Table I—Estimates of Pharmacokinetic Constants for Individual Pregnant Ewes

Dose, mg/kg	Subject	Estimated Constants and Coefficients of Variation[a] A, μg/ml	α, min^{-1}	B, μg/ml	β, min^{-1}	Measures of Fit r^2	Correlation Coefficient
0.5	1	1.21 (0.286)	0.553 (0.174)	0.190 (0.192)	0.0169 (0.154)	0.997	0.989
	2	1.71 (0.195)	0.549 (0.125)	0.130 (0.150)	0.0174 (0.109)	0.999	0.997
	3	0.993 (0.165)	0.445 (0.112)	0.161 (0.111)	0.0187 (0.118)	0.999	0.971
	4	1.42 (0.114)	0.331 (0.078)	0.166 (0.081)	0.0130 (0.092)	1.000	0.993
	5	1.24 (0.162)	0.385 (0.102)	0.111 (0.123)	0.0176 (0.108)	1.000	0.985
	Average	1.31 (0.183)	0.453 (0.124)	0.152 (0.133)	0.0167 (0.120)		
1.0	1	3.02 (0.225)	0.415 (0.174)	0.181 (0.166)	0.0128 (0.203)	0.999	0.994
	2	1.07 (0.197)	0.282 (0.140)	0.159 (0.127)	0.0125 (0.168)	0.999	0.987
	3	1.69 (0.113)	0.531 (0.072)	0.317 (0.061)	0.00954 (0.084)	0.998	0.993
	4	1.73 (0.294)	0.282 (0.221)	0.144 (0.208)	0.0107 (0.411)	0.998	0.993
	Average	1.88 (0.212)	0.378 (0.141)	0.201 (0.124)	0.0114 (0.217)		
2.0	1	4.31 (0.150)	0.368 (0.097)	0.616 (0.114)	0.0161 (0.093)	1.000	0.965
	2	1.80 (0.171)	0.131 (0.121)	0.329 (0.111)	0.00797 (0.163)	0.998	0.936
	3	2.44 (0.121)	0.199 (0.078)	0.566 (0.081)	0.0100 (0.095)	0.999	0.967
	4	4.49 (0.157)	0.337 (0.097)	0.435 (0.124)	0.0170 (0.106)	1.000	0.957
	5	2.45 (0.089)	0.205 (0.058)	0.443 (0.063)	0.0160 (0.049)	1.000	0.990
	Average	3.10 (0.140)	0.248 (0.090)	0.478 (0.098)	0.0134 (0.094)		

[a] Numbers in parentheses are coefficients of variation.

Table II—Estimates of Pharmacokinetic Constants for Individual Nonpregnant Ewes

Subject	Estimated Constants and Coefficients of Variation[a] A, μg/ml	α, min^{-1}	B, μg/ml	β, min^{-1}	Measures of Fit r^2	Correlation Coefficient
1	3.34 (0.208)	0.473 (0.146)	0.136 (0.174)	0.0200 (0.110)	1.000	0.907
2	7.20 (0.187)	0.625 (0.099)	0.330 (0.123)	0.0126 (0.143)	1.000	0.985
3	2.16 (0.100)	0.216 (0.058)	0.395 (0.076)	0.0199 (0.050)	1.000	0.994
Average	4.23 (0.177)	0.438 (0.109)	0.287 (0.109)	0.0175[b] (0.095)		

[a] Numbers in parentheses are coefficients of variation. [b] Statistically significant ($p < 0.05$) difference between nonpregnant and pregnant ewes (Table I) using the Student t test.

nine green[1] in the cardiac output determination by a dye dilution technique.

An arterial catheter was placed through a branch of the carotid artery and advanced centrally to obtain arterial blood for blood gas, cardiac output, and lidocaine determinations. Arterial rather than venous blood was chosen for lidocaine determination because of expected arterial–venous lidocaine concentration differences resulting from tissue drug uptake (1, 2). The arterial lidocaine concentration better reflects presentation of the drug to well-perfused vital organs, especially during drug distribution. A laparotomy was performed on the pregnant ewe for placement of a fetal arterial catheter for obtaining fetal blood samples for blood gas and lidocaine determinations and for monitoring fetal heart rate and blood pressure.

All catheterizers were filled with heparinized saline and either tunneled subcutaneously to the flank or wrapped securely around the neck or hindlimb. The animal was allowed a minimum of 24 hr to recover from anesthesia and surgery before studies were initiated. For all animals, the heart rate, blood pressure, and blood gases were used as measures of well-being during surgery and subsequent studies. The results of these physiological determinations and the fetal blood lidocaine levels will not be presented in this report.

On experimental days, the animal was placed in a sheep-restraining cage and measurements were taken during a 30-min control period to produce baseline blood gas[2], blood pressure, and heart rate[3] data. Cardiac output was measured three times during the control period. Following the control period, lidocaine hydrochloride[4] was injected intravenously over 10 sec at one of three doses (0.5, 1.0, or 2.0 mg/kg) to the pregnant ewe or at one dose (1.0 mg/kg) to the nonpregnant ewe. All lidocaine doses are expressed as amounts of lidocaine hydrochloride administered. In the pregnant animal, the lidocaine doses were administered randomly on consecutive days following surgery to quantitate possible lidocaine pharmacokinetic variations as a function of postsurgical time.

No systematic variations were apparent in lidocaine pharmacokinetics or in the heart rate, blood pressure, or blood gases measured on consecutive days following surgery. Arterial blood samples were collected at 1, 2, 5, 10, 15, 20, 30, 45, 60, 90, 120, and 150 min following lidocaine injection and were stored frozen in heparinized tubes until subsequent determination of whole blood lidocaine by a GLC method having a coefficient of variation of <5% over the concentration range studied (3). All lidocaine concentrations and pharmacokinetic data were expressed in terms of lidocaine base. Four of the 14 pregnant ewe studies were performed on ewes with twin fetuses. No significant pharmacokinetic differences were found between the pregnant ewes carrying one fetus and those carrying two fetuses.

Blood lidocaine concentration–time curves for each ewe were described adequately by the biexponential equation:

$$C = Ae^{-\alpha t} + Be^{-\beta t} \quad \text{(Eq. 1)}$$

where C is the blood lidocaine base concentration at time t and A, α, B, and β are constants. The blood concentration–time data were fitted[5] to Eq. 1 using the NONLIN nonlinear least-squares program (4). Each blood concentration data point was weighted with its squared reciprocal. This weighting factor was selected based on (5):

$$\ln \sigma^2 = \ln a + n \ln \bar{C} \quad \text{(Eq. 2)}$$

where σ^2 is the variance corresponding to the mean drug concentration, $\bar{C}$, for a group of subjects at a given time following injection and a and n are constants. If $n = 1$, an appropriate weighting factor is the reciprocal of the plasma drug concentration; if $n = 2$, the squared reciprocal of the plasma drug concentration may be used. Linear regression of $\ln \sigma^2$ as a function of $\ln \bar{C}$ for the data in this study resulted in n values of 1.39 ($r = 0.970$), 1.59 ($r = 0.923$), and 1.76 ($r = 0.890$) for the 0.5-, 1.0-, and 2.0-mg/kg doses in the pregnant ewes, respectively, and of 1.68 ($r = 0.986$) for the 1.0-mg/kg dose in the nonpregnant ewes. Because the n values approach two, each plasma concentration data point was weighted with its squared reciprocal.

Tables I and II contain estimates of the pharmacokinetic constants (A, α, B, and β) for each subject and values for the criteria used to assess the data fit from each subject to Eq. 1. The criteria were: the coefficient of variation of the estimated pharmacokinetic constants (standard deviation of the estimate/estimated constant), the coefficient of determination [$r^2 = \Sigma(\text{obs}^2 - \Sigma\text{dev}^2)/\Sigma\text{obs}^2$], and the correlation coefficient relating the equation-predicted and observed lidocaine concentrations. The coefficients of determination and correlation coefficients approached

[1] Cardio-Green, Hynson, Wescott and Dunning, Baltimore, Md.
[2] Radiometer BMS3 MK2 blood micro system with PHM71 MK2 acid-base analyzer, London Co., Cleveland, Ohio.
[3] Grass model 7 polygraph with Statham pressure transducers, Quincy, Mass.
[4] Xylocaine, Astra Pharmaceutical Products, Inc., Worcester, Mass.
[5] Using a CDC 6400 computer.

Table III—Pharmacokinetic Parameters in Pregnant Ewes following Intravenous Bolus Lidocaine Hydrochloride Administration (Means ± *SD*)

Dose, mg/kg	*n*	Weight, kg	Cardiac Output, liters/min	$t/2$ (α), min	$t/2$ (β), min	Total Body Clearance, ml/min/kg	V_c, liter/kg	V_{ss} liters/kg	V_B, liters/kg	k_{10}, min^{-1}	k_{12}, min^{-1}	k_{21}, min^{-1}
0.5	5	61.1	7.0	1.6[a]	42.2[b]	38	0.31[a]	1.69[b]	2.24[b]	0.124	0.282[a]	0.063
		±7.3	±1.5	±0.3	±6.5	±8	±0.06	±0.14	±0.24	±0.033	±0.075	±0.020
1.0	4	70.4	7.9[c]	2.0	61.8	42	0.48	2.73	3.63	0.094	0.244	0.052
		±13.4	±2.1	±0.6	±8.6	±13	±0.16	±0.45	±0.80	±0.041	±0.106	±0.028
2.0	5	65.9	6.1	3.2	59.2	34	0.54	2.16	2.83	0.074	0.142	0.044
		±14.3	±1.7	±1.4	±19.4	±7	±0.20	±0.55	±0.69	±0.039	±0.059	±0.012

[a] Statistically significant difference ($p < 0.05$) between the 0.5- and 2.0-mg/kg doses using the Student t test. [b] Statistically significant difference ($p < 0.01$) between the 0.5- and 1.0-mg/kg doses using the Student t test. [c] Three studies.

1.0, indicating that Eq. 1 adequately described the time course of the lidocaine concentration following bolus intravenous administration to pregnant and nonpregnant ewes.

The values for A, α, B, and β were used to calculate (6) pharmacokinetic parameters for the two-compartment open model (Scheme I):

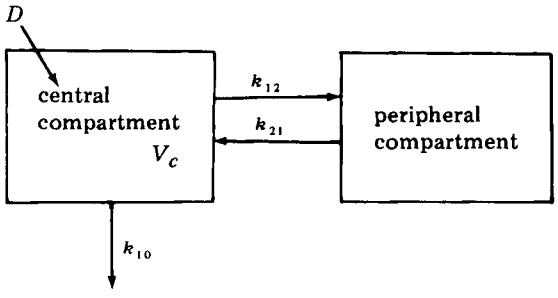

Scheme I

where D represents the intravenous bolus lidocaine hydrochloride dose, V_c is the apparent volume of distribution of the central compartment, k_{12} and k_{21} are the apparent first-order intercompartmental lidocaine distribution rate constants, and k_{10} is the apparent first-order lidocaine elimination rate constant.

RESULTS

The computer-determined estimates of A, α, B, and β for all pregnant animals within each dosage group were averaged and used to generate curves indicating the blood lidocaine concentration change with time following intravenous bolus dosing to pregnant ewes (Fig. 1). The equations in Fig. 1 indicate the average values of A, α, B, and β for each dosage group. Table III shows the means and standard deviations for physiological data and the pharmacokinetic parameters calculated from A, α, B, and β for the three doses in the pregnant ewes.

As the lidocaine dose increased, the slope of the α-phase (distributive phase) of the blood concentration–time curve increased (Fig. 1), as indicated by the increase in the α-phase half-life [$t/2$ (α), Table III]. Although the mean α-phase half-lives for the three doses did not all differ significantly from each other, the α-phase half-life following the 0.5-mg/kg dose differed significantly ($p < 0.05$) from that following the 2.0-mg/kg dose. The curves in Fig. 1 also indicate different slopes for the β-phases (postdistributive phase) of the blood concentration–time curves. These differences are reflected in the β-phase half-lives [$t/2$ (β)] in Table III. The β-phase half-life following the 0.5-mg/kg lidocaine dose differed significantly ($p < 0.01$) from that following the 1.0-mg/kg dose.

The correlation between the total body clearance (calculated by dividing the intravenous bolus dose by the area under the curve for each animal) and the body weight was positive ($r = 0.576$, $p < 0.05$). Therefore, the total body clearance values were normalized for weight prior to averaging within each group (Table III). Cardiac output (mean of the three control period determinations for each study) showed no significant statistical correlation with body weights. However, the correlation between total body clearance and cardiac output was positive ($r = 0.673$, $p < 0.02$, Fig. 2) for all studies performed with the pregnant ewes.

Each of the three volumes of distribution for lidocaine showed statistically significant ($p < 0.05$) positive correlations with body weight and, therefore, were weight normalized for inclusion in Table III. The mean apparent volume of distribution for the central compartment, V_c, following the 0.5-mg/kg dose differed significantly ($p < 0.05$) from that following the 2.0-mg/kg dose. The apparent volume of distribution of

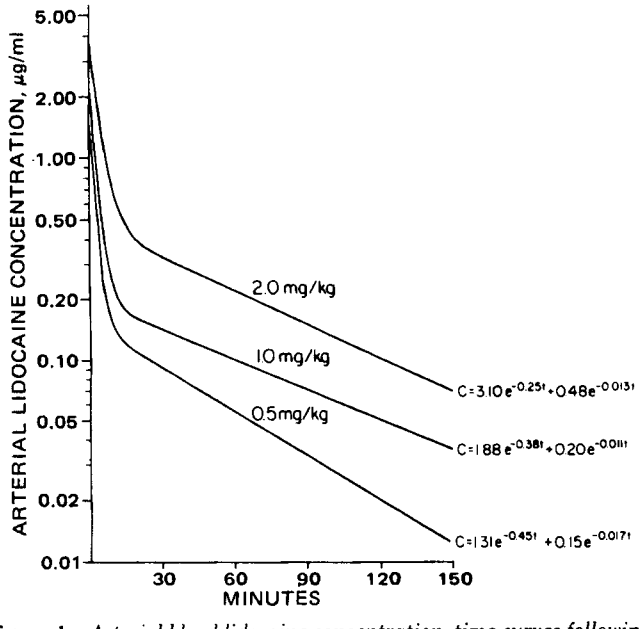

Figure 1—*Arterial blood lidocaine concentration–time curves following intravenous bolus lidocaine hydrochloride administration at three doses to pregnant ewes. The equations indicate the averaged computer estimates for* A, α, B, *and* β *used to generate each curve.*

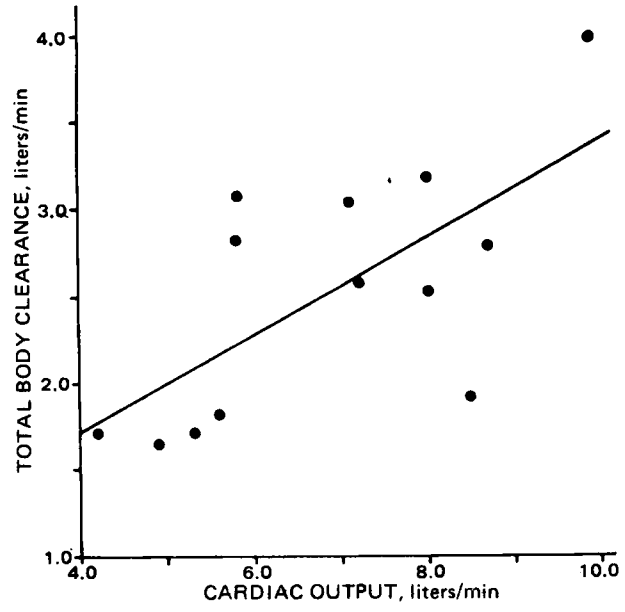

Figure 2—*Correlation between cardiac output and total body clearance of lidocaine following administration of 0.5, 1.0, and 2.0 mg of lidocaine hydrochloride/kg to pregnant sheep.*

Table IV—Individual Pharmacokinetic Parameters in Nonpregnant and Pregnant Ewes following a 1.0-mg/kg Intravenous Bolus Dose of Lidocaine Hydrochloride

Subject	Weight, kg	Cardiac Output, liters/min	$t_{1/2}$ (α), min	$t_{1/2}$ (β), min	Total Body Clearance, ml/min/kg	V_c, liter/kg	V_{ss}, liters/kg	V_B, liters/kg	k_{10}, min^{-1}	k_{12}, min^{-1}	k_{21}, min^{-1}
					Nonpregnant						
1	51.0	—[a]	1.5	34.7	63	0.25	1.60	3.12	0.251	0.204	0.038
2	75.6	6.5	1.1	55.0	23	0.12	1.28	1.83	0.200	0.398	0.039
3	80.2	10.2	3.2	34.8	29	0.34	1.01	1.45	0.085	0.100	0.050
Mean	68.9	8.4	1.9	41.5[b]	38	0.24[c]	1.30[d]	2.13[c]	0.179	0.234	0.042
SD	±15.7	±2.6	±1.1	±11.7	±22	±0.11	±0.30	±0.88	±0.085	±0.151	±0.007
					Pregnant						
1	60.2	5.8	1.7	54.2	47	0.32	2.47	3.68	0.149	0.243	0.036
2	60.9	8.0	2.5	55.5	52	0.71	3.28	4.19	0.074	0.173	0.048
3	71.6	—[a]	1.3	72.7	24	0.43	2.28	2.49	0.055	0.394	0.092
4	89.0	9.9	2.0	64.8	45	0.47	2.91	4.17	0.096	0.165	0.032
Mean	70.4	7.9	2.0	61.8	42	0.48	2.74	3.63	0.094	0.244	0.052
SD	±13.4	±2.1	±0.6	±8.7	±12	±0.16	±0.45	±0.80	±0.041	±0.106	±0.028

[a] Not determined. [b] Statistically significant ($p < 0.05$) difference between nonpregnant and pregnant ewes using the Student t test. [c] Statistically significant ($p < 0.10$) difference between nonpregnant and pregnant ewes using the Student t test. [d] Statistically significant ($p < 0.01$) difference between nonpregnant and pregnant ewes using the Student t test.

lidocaine at steady state, V_{ss}, relates the amount of lidocaine in the body to the blood lidocaine concentration at steady state; the apparent volume of distribution of lidocaine during the postdistributive phase, V_B, relates the amount of lidocaine in the body to the blood lidocaine concentration at any time during the postdistributive, β, phase (6). Mean values for these apparent volumes of distribution also are found in Table III. Both the apparent volume of distribution at steady state and the apparent volume of distribution during the postdistributive phase following the 0.5-mg/kg dose differed significantly ($p < 0.05$) from the corresponding volumes following the 1.0-mg/kg dose.

Table III shows that the lidocaine elimination rate constant, k_{10}, decreased as the dose increased; however, the mean elimination rate constants for each dose did not differ significantly from one another. The rate constants for lidocaine transfer between the central and peripheral compartments also are found in Table III. As the lidocaine dose was increased, both intercompartmental rate constants, k_{12} and k_{21}, decreased.

Figure 3 shows curves generated from averaged computer-determined estimates of A, α, B, and β from pregnant and nonpregnant ewes following 1.0 mg of lidocaine/kg. The Fig. 3 equations indicate the average values of A, α, B, and β. Table IV shows the means and standard deviations of physiological data and pharmacokinetic parameters for 1.0-mg of lidocaine/kg doses in nonpregnant ewes. Comparison of parameters

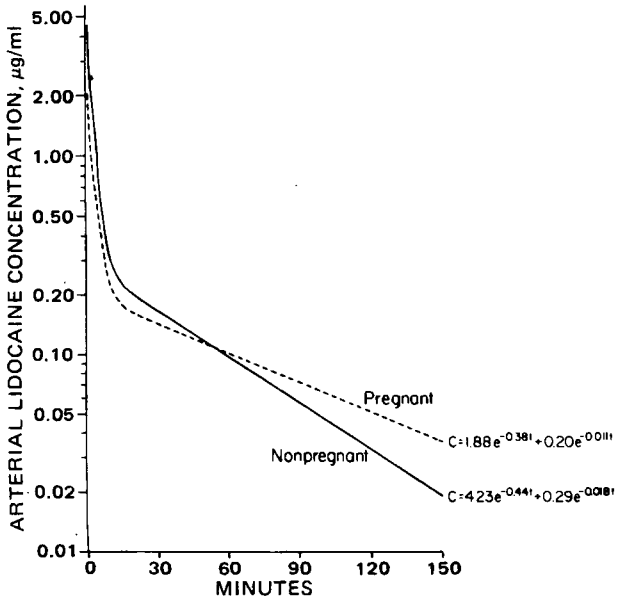

Figure 3—*Arterial blood lidocaine concentration–time curves following intravenous bolus administration of 1.0 mg of lidocaine hydrochloride/kg to pregnant and nonpregnant ewes. The equations indicate the averaged computer estimates for* A, α, B, *and* β *used to generate each curve.*

in the nonpregnant ewe with those in the pregnant ewe (Table IV) shows that the β-phase half-lives differed significantly ($p < 0.05$) between the two groups. Although the volumes of distribution and clearances in this limited sample of nonpregnant ewes did not correlate with weight, the values for these parameters were weight normalized for comparison with the pregnant animal group. The volume of distribution at steady state in the nonpregnant animal differed significantly ($p < 0.01$) from that in the pregnant animal. In addition, the apparent volume of distribution of the central compartment and during the postdistributive phase differed significantly between the two groups but at a lower level of significance ($p < 0.10$).

DISCUSSION

The use of the two-compartment open model (Scheme I) to describe lidocaine disposition in the pregnant ewe implies linearity of lidocaine disposition kinetics as a function of dose. The total body clearance for lidocaine (Table III) remained relatively constant as the intravenous bolus dose was increased from 0.5 to 2.0 mg/kg. Also, the area under the blood lidocaine concentration–time curve, AUC, showed a statistically significant ($r = 0.921$, $p < 0.001$, Fig. 4) linear correlation with the weight-normalized dose, D, according to:

$$AUC = \frac{1}{Cl_T}(D) \qquad \text{(Eq. 3)}$$

where Cl_T represents total body clearance. The regression line passed through the vertical axis near zero (−2.0 min × mg/liter), and the reciprocal of the slope (total body clearance) was 38 ml/min/kg.

Another linearity test in pharmacokinetics involves computer fitting of the blood drug concentration–time data for each animal to an appropriate linear pharmacokinetic model, computing and averaging the pharmacokinetic parameters for each dose, and comparing these averaged parameters among doses. The dose-related trends in the magnitudes of the pharmacokinetic parameters provide strong evidence of nonlinear kinetics (7). Comparisons of averaged pharmacokinetic parameters among different doses in pregnant ewes in this study can be made from the data in Table III. These data showed dose-related increases in the apparent volume of distribution of the central compartment and in the half-life of the α-phase and dose-related decreases in k_{10}, k_{12}, and k_{21} as the dose was increased from 0.5 to 2.0 mg/kg.

The dose-related increase in the apparent volume of distribution of the central compartment could be a result of the hemodynamic effects of lidocaine. Lidocaine is known to increase cardiac output in humans (at arterial lidocaine concentrations of 4–7 μg/ml) and in dogs (8–10), presumably by a central nervous system (CNS) effect evoked through the sympathetic nervous system. Following a bolus lidocaine injection, transient high lidocaine levels in the CNS could produce a brief, dose-related increase in cardiac output. Resulting tissue perfusion increases would promote more rapid tissue uptake of lidocaine and, therefore, an apparent dose-related increase in the volume of distribution of the central compartment. The effect of lidocaine on cardiac output and, hence, on tissue uptake would be brief and would not significantly alter lidocaine elimination; therefore, total body clearance of lidocaine remained un-

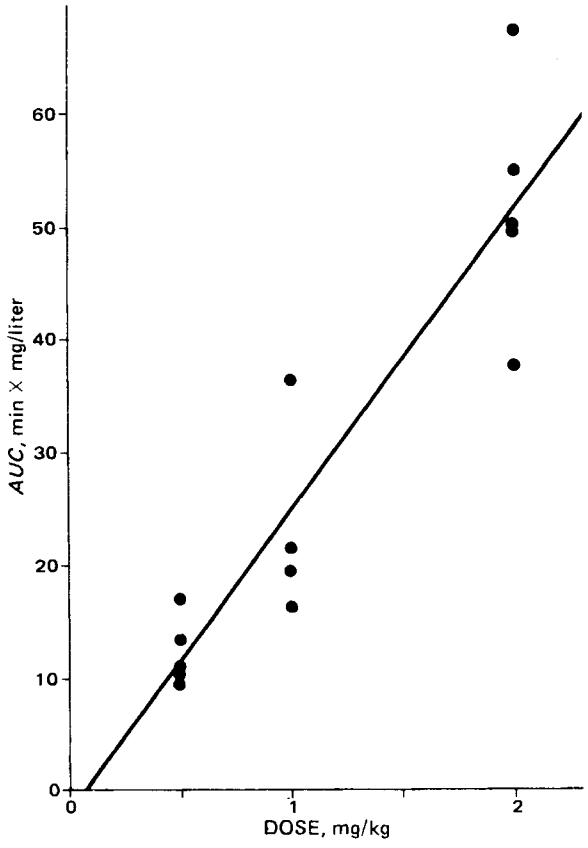

Figure 4—*Correlation between dose and area under the blood lidocaine concentration–time curve following administration of 0.5, 1.0, and 2.0 mg of lidocaine hydrochloride/kg to pregnant sheep.*

changed with dose (Table III). The brevity of the effect of lidocaine on cardiac output is supported by cardiac output measurements at 5 min following bolus lidocaine[6] injection; these cardiac output measurements were not different from the control values shown in Table III.

The dose-related increase in the apparent volume of distribution of the central compartment also is consistent with a probable decrease in the lidocaine fraction bound in plasma as blood lidocaine levels increase. A transient decrease in the lidocaine fraction bound at high blood lidocaine levels following a bolus dose may allow lidocaine to distribute more widely in the body, thus increasing the distribution volume.

The observation of a dose-related increase in the apparent volume of distribution of the central compartment (and a concomitant decrease in k_{10} and k_{12}) in pregnant sheep is consistent with trends reported describing lidocaine disposition kinetics in normal human volunteers (10). In that study, the apparent volume of distribution of the central compartment increased (0.44–0.48 liter/kg), the elimination rate constant k_{10} decreased (0.24–0.22 min^{-1}), and the intercompartmental rate constant k_{12} decreased (0.066–0.041 min^{-1}) as the intravenous bolus dose was increased (50–100 mg). An increase in the apparent volume of distribution of the central compartment in normal humans is consistent with a probable transient increase in cardiac output following a bolus lidocaine dose. In addition, this volume increase is consistent with a decrease in the percent of lidocaine bound in plasma as blood lidocaine levels increase. In humans, plasma lidocaine binding decreases from 75% at 0.4 μg/ml to 58% at 5 μg/ml (11). The mean extrapolated zero-time lidocaine concentrations in normal humans, 1.80 and 2.79 μg/ml following bolus doses of 50 and 100 mg, respectively (10), are in the concentration range where significant plasma binding changes occur. Thus, although pharmacokinetic parameters may not show statistically significant differences as the dose is increased, dose-related trends in pharmacokinetic parameters may offer increased insight into the drug disposition kinetics.

In addition to possible dose-related nonlinearities in the α-phase of lidocaine disposition, Table III shows evidence for dose-related kinetics during the β- or postdistributive phase in pregnant ewes. Following the 0.5-mg/kg dose, the β-phase half-life (42.2 min) differed significantly from that (61.8 min) following the 1.0-mg/kg dose. The β-phase half-life [$t/2(\beta)$] is related to the total body clearance, Cl_T, and to the apparent volume of distribution during the postdistributive phase, V_B, according to:

$$t/2(\beta) = \frac{0.693 V_B}{Cl_T} \qquad \text{(Eq. 4)}$$

Since the total body clearance of lidocaine in the pregnant ewe does not appear to change with dose, Eq. 4 indicates that an increase in the β-phase half-life of lidocaine may be a function of an increase in the apparent volume of distribution. This concept is consistent with the significant change in the volume of distribution during the postdistributive phase (2.24–3.63 liters/kg, Table III) as the lidocaine dose was increased from 0.5 to 1.0 mg/kg. A better indication of dose-related distribution changes is a comparison of the apparent volumes of distribution at steady state following different doses. This parameter is not dependent on elimination processes as is the apparent volume of distribution during the postdistributive phase. The change in the volume of distribution of lidocaine at steady state from 1.69 to 2.73 liters/kg as the dose was increased from 0.5 to 1.0 mg/kg was significant. Thus, the data indicate that dose-related changes in the apparent volume of distribution of lidocaine in the pregnant ewe may influence the biological half-life.

Lidocaine disposition kinetics in the nonpregnant ewe differed from the lidocaine disposition kinetics in the pregnant ewe (Table IV) at a 1.0-mg/kg dose. Figure 3 indicates that the initial lidocaine levels following a 1.0-mg/kg bolus dose were higher in the nonpregnant ewe, but that during the β-phase the blood levels in the nonpregnant ewe decreased more rapidly than in the pregnant ewe. These blood level changes are reflected in the pharmacokinetic parameters in Table IV. The lower apparent volume of distribution of the central compartment in the nonpregnant ewe resulted in higher initial blood lidocaine levels in the nonpregnant animal following a bolus dose based on body weight. In addition, the lower β-phase half-life in the nonpregnant ewe, 41.4 *versus* 61.8 min in the pregnant ewe, reflected the more rapid decline in blood lidocaine levels during the β-phase in the nonpregnant animal following a bolus dose.

Because total body clearances of lidocaine in the nonpregnant and pregnant animals were similar, the greater apparent volumes of distribution (V_c, V_{ss}, and V_B) in the pregnant animals indicated that differences between disposition kinetics in the nonpregnant and pregnant ewes probably were due to drug distribution changes. These changes may be due to differences between lidocaine binding in the plasma, blood, and/or peripheral tissues of the nonpregnant ewe as compared to binding in the corresponding maternal tissues of the pregnant ewe. In addition, fetal lidocaine uptake in the pregnant ewe undoubtedly influences distribution parameters as determined from maternal blood lidocaine levels.

The values for total body clearance of lidocaine in the pregnant sheep (38 ml/min/kg as determined by the method illustrated in Fig. 4) and in the nonpregnant sheep (38 ml/min/kg, Table IV) were considerably greater than the total body clearance reported for lidocaine in humans (9–14 ml/min/kg) (2, 10). In humans, the total body clearance of lidocaine increases as the cardiac output and, therefore, the hepatic blood flow increase (12, 13). In the pregnant sheep, the total body clearance also increased as the cardiac output (Fig. 2) and, presumably, the hepatic blood flow increased. Hepatic blood flow in normal humans is about 21 ml/min/kg (1.5 liters/min in a 70-kg human), and hepatic blood flow in pregnant and nonpregnant ewes is about 65 and 55 ml/min/kg, respectively (14). Thus, the hepatic blood flow in the ewe is sufficient to account for the comparatively higher total body clearance of lidocaine in sheep.

The proportion of the total drug entering the liver to that metabolized by the liver is the extraction ratio. The extraction ratio, E, may be calculated by (15):

$$E = \frac{Cl_T(1-f)}{Q} \qquad \text{(Eq. 5)}$$

where Cl_T is the total body clearance of drug, f is the drug fraction excreted unchanged from the body, and Q is the hepatic blood flow. Use of Eq. 5 for hepatic lidocaine extraction in the pregnant ewe is based on the assumptions that: (*a*) renal excretion is the only nonmetabolic excretory pathway for lidocaine, (*b*) the dose fraction excreted unchanged in the urine [0.014 (16)] in normal adult sheep is the same as that for pregnant ewes, (*c*) lidocaine metabolism occurs only in the liver, and (*d*) hepatic blood flow [65 ml/min/kg (14)] does not change significantly following the lidocaine injection. Cardiac output in the pregnant sheep measured 5 min following injection of 0.5, 1.0, or 2.0 mg of lidocaine/kg[6]

[6] D. C. Bloedow, D. H. Ralston, and J. C. Hargrove, unpublished results.

did not change significantly from control values; presumably, hepatic blood flow behaves similarly. The extraction ratio for lidocaine in the pregnant sheep was 0.57 using Eq. 5. Similar assumptions and calculations for the nonpregnant sheep [Q = 55 ml/min/kg (14)] yielded an extraction ratio of 0.69. These values are similar to the extraction ratio (~0.68) reported for lidocaine in humans (17).

The results of these studies provide evidence for subtle dose-related lidocaine kinetics in pregnant sheep. Further studies on lidocaine binding in ovine plasma and on cardiac output and blood flow distribution during the initial lidocaine distributive phase in sheep are necessary to substantiate the reasons for the apparent nonlinearity of lidocaine disposition.

REFERENCES

(1) G. T. Tucker and R. A. Boas, *Anesthesiology*, **34**, 538 (1971).

(2) G. T. Tucker and L. E. Mather, *Br. J. Anaesth. Suppl.*, **47**, 213 (1975).

(3) L. E. Mather and G. T. Tucker, *J. Pharm. Sci.*, **63**, 306 (1974).

(4) C. M. Metzler, G. L. Elfring, and A. J. McEwen, *Biometrics*, **30**, 562 (1974).

(5) K. S. Albert, A. J. Sedman, and J. G. Wagner, *J. Pharmacokinet. Biopharm.*, **2**, 381 (1974).

(6) M. Gibaldi and D. Perrier, "Pharmacokinetics," Dekker, New York, N.Y., 1975, pp. 48, 68, 177.

(7) J. G. Wagner, *J. Pharmacokinet. Biopharm.*, **1**, 363 (1973).

(8) J. J. Bonica, P. U. Berges, and K. Marokawa, *Anesthesiology*, **33**, 619 (1970).

(9) J. Thomsen, W. Terry, R. Stenlund, S. Queremit, and G. Rowe, *Arch. Int. Pharmacodyn. Ther.*, **194**, 83 (1971).

(10) M. Rowland, P. D. Thomson, A. Guichard, and K. L. Melmon, *Ann. N.Y. Acad. Sci.*, **179**, 383 (1971).

(11) G. T. Tucker, R. N. Boyes, P. O. Bridenbaugh, and D. C. Moore, *Anesthesiology*, **33**, 287 (1970).

(12) P. D. Thomson, K. L. Melmon, J. A. Richardson, K. Cohn, W. Steinbrunn, R. Cudihee, and M. Rowland, *Ann. Intern. Med.*, **78**, 499 (1973).

(13) K. A. Collinsworth, S. M. Kalman, and D. C. Harrison, *Circulation*, **50**, 1217 (1974).

(14) M. L. Katz and E. N. Bergman, *Am. J. Physiol.*, **216**, 946 (1969).

(15) G. R. Wilkinson and D. G. Shand, *Clin. Pharmacol. Ther.*, **18**, 377 (1975).

(16) H. O. Morishima, M. Finster, A. Fukunaga, H. Pedersen, R. N. Boyes, and B. G. Covino, "Abstracts of Scientific Papers," American Society of Anesthesiologists Annual Meeting, Chicago, Ill., 1975, pp. 85, 86.

(17) G. T. Tucker, L. Wiklund, A. Berlin-Wahlen, and L. E. Mather, *J. Pharmacokinet. Biopharm.*, **5**, 111 (1977).

ACKNOWLEDGMENTS

Presented at the Basic Pharmaceutics Section, APhA Academy of Pharmaceutical Sciences, Montreal meeting, May 1978.

Supported by National Institutes of Health Grants GM15991 and GM01160 and National Institute of Child Health and Human Development Grant 5P01-HD02274.

The authors thank Ms. L. Leanna Nielsen, Mr. David Wilbur, and Ms. Karen Powers for technical assistance and Ms. Barbara Armal for manuscript preparation.

False-Positive Alkaloid Reactions

ABDEL-AZIM M. HABIB

Received February 15, 1979, from the *Faculty of Pharmacy, Alexandria University, Alexandria, Egypt.* Accepted for publication July 20, 1979.

Abstract □ A variety of nonnitrogenous oxygenated compounds gave false-positive alkaloid reactions with Dragendorff's spray reagent. These compounds reacted positively if the oxygen function and the β-carbon bonded to the oxygen had high electron density. Thus, aldehydes, ketones, lactones, ethers, esters, epoxides, and peroxides with an ethylene bond or free alkyl groups at the β-carbon gave a positive reaction, provided that the availability of electrons at the oxygen and the β-carbon was not altered by electron withdrawal or hydrogen bonding. Carbonyl, ether, and ethylene functions were shown by IR evidence to be involved in coupling. Nitrogen-free, alkaloid-like acetone artifacts were obtained by interaction with fixed alkali and with acids. These compounds were postulated to be α,β-unsaturated aldol condensation products of acetone. Interaction with ammonia in addition yielded nitrogenous alkaloid-like artifacts.

Keyphrases □ Alkaloids—interference by nonnitrogenous alkaloid-like compounds, structural requirements for false-positive reaction □ Acetone artifacts—nonnitrogenous, alkaloid-like compounds, interference with alkaloid detection, structural requirements for false-positive reaction □ Dragendorff's reagent—false-positive alkaloid reaction with nonnitrogenous oxygenated compounds

Of the numerous reagents described for the detection of alkaloids (1), only a few have reliable sensitivity (2). All of these reagents suffer from nonspecificity. Many nitrogenous and nonnitrogenous plant constituents react with several of these reagents similarly to alkaloids (3–8). Some nonnitrogenous compounds react similarly to alkaloids in giving crystalline salts with acids (8).

BACKGROUND

TLC is the most versatile technique for alkaloid detection, separation, monitoring, identification, and quantitation. Dragendorff's spray, in its different modifications, is usually used for visualization of alkaloidal spots on paper and thin-layer chromatograms and in field tests with alkaloid test paper (9–11). Many reports have discussed its sensitivity and specificity (2), false reactions (3, 12), and modifications (13–20). However, many nonnitrogenous plant constituents react with this reagent in a manner typical of alkaloids (3, 12, 21). Such compounds may create difficulty, especially during alkaloid screening without sufficient partition purification steps (4). Complete elimination of these constituents cannot be accomplished through the one partition purification step required in many reported screening procedures (22–26). Moreover, significant amounts of such nonalkaloidal constituents may be detected even after further partition purification (12).

Farnsworth *et al.* (3) determined that any nonnitrogenous compound having conjugated carbonyl or lactone functions would react in a manner typical of alkaloids. The range of compounds that produce a false-positive reaction is greater than is generally realized (27), and compounds such as the common plant sterols and triterpenes are readily detected by Dragendorff's spray.

0022-3549/80/0100-0037$01.00/0

© 1980, American Pharmaceutical Association

did not change significantly from control values; presumably, hepatic blood flow behaves similarly. The extraction ratio for lidocaine in the pregnant sheep was 0.57 using Eq. 5. Similar assumptions and calculations for the nonpregnant sheep [Q = 55 ml/min/kg (14)] yielded an extraction ratio of 0.69. These values are similar to the extraction ratio (~0.68) reported for lidocaine in humans (17).

The results of these studies provide evidence for subtle dose-related lidocaine kinetics in pregnant sheep. Further studies on lidocaine binding in ovine plasma and on cardiac output and blood flow distribution during the initial lidocaine distributive phase in sheep are necessary to substantiate the reasons for the apparent nonlinearity of lidocaine disposition.

REFERENCES

(1) G. T. Tucker and R. A. Boas, *Anesthesiology*, **34**, 538 (1971).

(2) G. T. Tucker and L. E. Mather, *Br. J. Anaesth. Suppl.*, **47**, 213 (1975).

(3) L. E. Mather and G. T. Tucker, *J. Pharm. Sci.*, **63**, 306 (1974).

(4) C. M. Metzler, G. L. Elfring, and A. J. McEwen, *Biometrics*, **30**, 562 (1974).

(5) K. S. Albert, A. J. Sedman, and J. G. Wagner, *J. Pharmacokinet. Biopharm.*, **2**, 381 (1974).

(6) M. Gibaldi and D. Perrier, "Pharmacokinetics," Dekker, New York, N.Y., 1975, pp. 48, 68, 177.

(7) J. G. Wagner, *J. Pharmacokinet. Biopharm.*, **1**, 363 (1973).

(8) J. J. Bonica, P. U. Berges, and K. Marokawa, *Anesthesiology*, **33**, 619 (1970).

(9) J. Thomsen, W. Terry, R. Stenlund, S. Queremit, and G. Rowe, *Arch. Int. Pharmacodyn. Ther.*, **194**, 83 (1971).

(10) M. Rowland, P. D. Thomson, A. Guichard, and K. L. Melmon, *Ann. N.Y. Acad. Sci.*, **179**, 383 (1971).

(11) G. T. Tucker, R. N. Boyes, P. O. Bridenbaugh, and D. C. Moore, *Anesthesiology*, **33**, 287 (1970).

(12) P. D. Thomson, K. L. Melmon, J. A. Richardson, K. Cohn, W. Steinbrunn, R. Cudihee, and M. Rowland, *Ann. Intern. Med.*, **78**, 499 (1973).

(13) K. A. Collinsworth, S. M. Kalman, and D. C. Harrison, *Circulation*, **50**, 1217 (1974).

(14) M. L. Katz and E. N. Bergman, *Am. J. Physiol.*, **216**, 946 (1969).

(15) G. R. Wilkinson and D. G. Shand, *Clin. Pharmacol. Ther.*, **18**, 377 (1975).

(16) H. O. Morishima, M. Finster, A. Fukunaga, H. Pedersen, R. N. Boyes, and B. G. Covino, "Abstracts of Scientific Papers," American Society of Anesthesiologists Annual Meeting, Chicago, Ill., 1975, pp. 85, 86.

(17) G. T. Tucker, L. Wiklund, A. Berlin-Wahlen, and L. E. Mather, *J. Pharmacokinet. Biopharm.*, **5**, 111 (1977).

ACKNOWLEDGMENTS

Presented at the Basic Pharmaceutics Section, APhA Academy of Pharmaceutical Sciences, Montreal meeting, May 1978.

Supported by National Institutes of Health Grants GM15991 and GM01160 and National Institute of Child Health and Human Development Grant 5P01-HD02274.

The authors thank Ms. L. Leanna Nielsen, Mr. David Wilbur, and Ms. Karen Powers for technical assistance and Ms. Barbara Armal for manuscript preparation.

False-Positive Alkaloid Reactions

ABDEL-AZIM M. HABIB

Received February 15, 1979, from the *Faculty of Pharmacy, Alexandria University, Alexandria, Egypt.* Accepted for publication July 20, 1979.

Abstract □ A variety of nonnitrogenous oxygenated compounds gave false-positive alkaloid reactions with Dragendorff's spray reagent. These compounds reacted positively if the oxygen function and the β-carbon bonded to the oxygen had high electron density. Thus, aldehydes, ketones, lactones, ethers, esters, epoxides, and peroxides with an ethylene bond or free alkyl groups at the β-carbon gave a positive reaction, provided that the availability of electrons at the oxygen and the β-carbon was not altered by electron withdrawal or hydrogen bonding. Carbonyl, ether, and ethylene functions were shown by IR evidence to be involved in coupling. Nitrogen-free, alkaloid-like acetone artifacts were obtained by interaction with fixed alkali and with acids. These compounds were postulated to be α,β-unsaturated aldol condensation products of acetone. Interaction with ammonia in addition yielded nitrogenous alkaloid-like artifacts.

Keyphrases □ Alkaloids—interference by nonnitrogenous alkaloid-like compounds, structural requirements for false-positive reaction □ Acetone artifacts—nonnitrogenous, alkaloid-like compounds, interference with alkaloid detection, structural requirements for false-positive reaction □ Dragendorff's reagent—false-positive alkaloid reaction with nonnitrogenous oxygenated compounds

Of the numerous reagents described for the detection of alkaloids (1), only a few have reliable sensitivity (2). All of these reagents suffer from nonspecificity. Many nitrogenous and nonnitrogenous plant constituents react with several of these reagents similarly to alkaloids (3–8). Some nonnitrogenous compounds react similarly to alkaloids in giving crystalline salts with acids (8).

BACKGROUND

TLC is the most versatile technique for alkaloid detection, separation, monitoring, identification, and quantitation. Dragendorff's spray, in its different modifications, is usually used for visualization of alkaloidal spots on paper and thin-layer chromatograms and in field tests with alkaloid test paper (9–11). Many reports have discussed its sensitivity and specificity (2), false reactions (3, 12), and modifications (13–20). However, many nonnitrogenous plant constituents react with this reagent in a manner typical of alkaloids (3, 12, 21). Such compounds may create difficulty, especially during alkaloid screening without sufficient partition purification steps (4). Complete elimination of these constituents cannot be accomplished through the one partition purification step required in many reported screening procedures (22–26). Moreover, significant amounts of such nonalkaloidal constituents may be detected even after further partition purification (12).

Farnsworth *et al.* (3) determined that any nonnitrogenous compound having conjugated carbonyl or lactone functions would react in a manner typical of alkaloids. The range of compounds that produce a false-positive reaction is greater than is generally realized (27), and compounds such as the common plant sterols and triterpenes are readily detected by Dragendorff's spray.

0022-3549/80/0100-0037$01.00/0

© 1980, American Pharmaceutical Association

Table I—Compounds Tested in the Present Study that Reacted Positively with Dragendorff's Spray Reagent

Column A: Compounds with Conjugated Carbonyl or Lactone Functions		Column B: Compounds Lacking any Conjugated Carbonyl or Lactone Function	
Compound	Reaction[a]	Compound	Reaction[a]
With carbonyl or lactone as only reactive function		Nonconjugated aldehydes and ketones	
Conjugated aldehydes and ketones		Isobutyraldehyde	+++
Acrolein	+++	Menthone	++
Crotonaldehyde	+++	Camphor	++
Furfural	+++	Acetonylacetone	+
Cinnamic aldehyde	+++	Nonconjugated lactones	
Citral	++	Picrotoxin (picrotoxinin)	++
Carvone	+++	Arctiin	+++
3-Hydroxybenzaldehyde	+(±)	Isolipidiol	+
Acetophenone	+++	*Judeicin*	+
Benzophenone	++	α-β-Unsaturated alcohols (their ethers and esters)	
Chalcone	+++	Geraniol	+(±)
Benzil	++	Geranyl acetate	+
Progesterone	+	Linalyl acetate	+
Testosterone	+	Phenols, phenolic ethers, and esters	
Cortisone	++	Eugenol	+++
Conjugated lactones		Acetyleugenol	+++
Coumarin	+++	Anethole	+
Umbelliferone	+	Guaiacol	+(±)
Digitoxin	+++	Thymol	+(±)
Digoxin	+++	Acetylated thymol	+
Strophanthin	++	α,β-Unsaturated (or aromatic) acids and their esters	
Ouabain	+	Cinnamic acid	+(±)
Acovenosides[b]	+++	Ethyl cinnamate	+
Lactone *S.a.*[c]	+	Phenyl salicylate	+
With additional reactive ether or ester functions		Methyl salicylate	+
Piperonal	+++	Veratric acid	+++
Veratraldehyde	+++	Alcohols (their ethers and esters) with branching at β-carbon	
Anisaldehyde	++	Primary isobutanol	+
Vanillin	+(±)	Primary isobutyl acetate	+++
Acetylated vanillin	++	Isobutyl epoxide	+++
3-Butoxybenzaldehyde	++	Isoamyl alcohol	+
Khellin	+++	Isoamyl acetate	+++
Visnagin	+++	Isoamyl ether	++
Methoxsalen (xanthotoxin)	+++	Menthyl acetate	++
Bergapten	+++	Bornyl acetate	+
Imperatorin	+++	Isobornyl acetate	+
Santonin	+++	Acetylated β-amyrin	++
Xanthumin	++	Miscellaneous compounds	
Rotenone	(+++)[d]	Cineole	++
Total withanolides[e]	+++	*Ascaridole*	+++
Withaferin A	+++	Digitonin	++
A C_{28} steroid lactone from *Withania somnifera*[f]	(+)[f]	Diosgenin	+++
Acetylated rutin	+++	2,3-Dihydro-4-pyrone	+
Acetylated quercitin	++	Ethyl-2-cyclohexanone carboxylate	+++
Acetylated kaempferol glucoside	++	Cannabinoids[g]	+
Acetylated hyperoside	+		
Acetylated quercitin glucuronide	+(±)		
Acetylated quercitin pentoside	+		
Acetylated chrysophanic acid	+		
Acetylated sennidins A + B	+		
β-Glycyrrhetinic acid	+(±)		

[a] Key: +, faint reaction; ++, typical reaction; and +++, immediate typical reaction. [b] The total -olide fraction of *Acokanthera spectabilis*, isolated by a reported method (29), showed at least four Dragendorff-positive components on TLC. [c] A conjugated ketolactone isolated from *Senecio aegyptius* (38). [d] Some compounds that gave a typical orange-red color with the fresh reagent gave a typical bluish color with old reagent (*e.g.*, cortisone and rotenone). [e] The lactonic fraction of *Withania somnifera*, freed from any contaminating alkaloids, showed at least six Dragendorff-positive spots. [f] Isolated from the roots and reported to give a positive reaction with Dragendorff's reagent. [g] Extracted from *Cannabis* and chromatographed by reported methods (33, 34).

Farnsworth *et al.* (3) gave convincing explanations for certain confusing cases (7, 8) as well as certain claims about the detection and isolation of alkaloids (28) that were denied in a subsequent report (29). Nevertheless, the conclusion of these investigators did not apply to 19 of the 29 compounds listed as positively reacting miscellaneous compounds (Ref. 3, Table II, column B). Moreover, it gave no persuasive answer to observations by the present author; phytochemical screening of *Mentha microphylla* and *Lavandula dentata* of Saudi Arabia revealed two constituents in the former and one in the latter species that gave a positive reaction with Dragendorff's spray, and these compounds were identified as menthone, carvone, and camphor (30, 31). Arctiin, a nonconjugated lactonic lignan glycoside, also gave[1] a positive reaction with Dragendorff's reagent as well as with other alkaloid precipitants. The spray reagent was used for visualization of cineole and ascaridole on TLC. Menthone, camphor, cineole, ascaridole, and arctiin lack the minimal structural features determined by Farnsworth *et al.* (3).

This ambiguity prompted the present study to determine the minimal structural features for a false-positive alkaloid reaction with emphasis on the reaction with Dragendorff's spray.

EXPERIMENTAL

Test Compounds—The compounds were obtained from commercial sources. Some natural products were provided by investigators or separated by TLC from plant materials, crude drugs, or preparations. Localization of these compounds was achieved through reliance on reported R_f values in specified TLC systems and the use of specific chromogenic reagents (32–35), and no quantitation was attempted.

Acetylated Compounds—Acetylation of the test compounds was effected by pyridine–acetyl chloride or acetic anhydride–sulfuric acid. Chloroform extracts of the acetylated compounds were washed thoroughly with 2% HCl and water or with 2% $NaHCO_3$ and water, respectively.

[1] Dr. A. A. Omar, Department of Pharmacognosy, Faculty of Pharmacy, Alexandria University, Alexandria, Egypt, personal communication.

Table II—Compounds Reported by Farnsworth *et al.* (3) to React Positively with Dragendorff's Spray Reagent

Column A: Compounds with Conjugated Carbonyl or Lactone Structure		Column B: Compounds Lacking any Conjugated Carbonyl or Lactone Function	
Compound	Reaction[a]	Compound	Reaction[a]
Ten 4-methoxy-α-pyrones	++++	Eugenol	++++
Four coumarins	++++	Hydroxycitronellol	++++
Four furanocoumarins	++++	Menthyl salicylate	++++
Three γ-pyrones	++++	Phenyl salicylate	+++
Khellin	++++	Salicylic acid	++
Chalcone	++++	Benzyl acetate	++
β-Methoxychalcone	++++	Camphor	++
cis-1,4-Diphenyl-2-butene-1,4-dione	++++	Cineole (eucalyptol)	++
trans-1,4-Diphenyl-2-butene-1,4-dione	++++	Methyl salicylate	++
Acrolein	++++	Aspirin	+
Amyl cinnamate	++++	Anethole	+
Cinnamaldehyde	++++	Cinnamic acid	+
Digitoxin	++++	Geraniol	+
Menadione	++++	Guaiacol	+
Ouabain	++++	Hydroquinone	+
Triketohydrindene hydrate	++++	Phloroglucinol	+
Piperonal	++	Resorcinol	+
Quinone	+	Terpineol	+
Vanillin	+	Thymol	+

[a] Key: ++++, immediate persistent reaction with Dragendorff's reagent; +++, immediate, slight, persistent reaction; ++, immediate reaction, fading within 24 hr; and +, positive reaction only after 24 hr.

Table III—Reactions of Compounds with Alkaloidal Reagents

	Test Compounds[b]																					
	NACP		HACP		FACP		RuAc		QuAc		KmAc		ChAc		RhAc		Meth		Imp		Sant	
Reagent[a]	F1	F2	F1	F2	F1	F2	F1	F2	F1	F2	F1	F2	F1	F2	F1	F2	F1	F2	F1	F2	F1	F2
Drag. sp.	+	+	+	−	+	−	+	−	+	−	+	−	+	−	−	−	+	−	+	−	+	−
Drag. pt.	+	+	+	−	+	−	−	−	−	−	+	−	−	−	−	−	+	−	+	−	−	−
Mayer's	+	+	+	−	+	−	+	−	+	−	+	−	−	−	−	−	+	−	+	−	−	−
Wagner's	+	+	+	−	+	−	+	−	+	−	+	−	−	−	−	−	+	−	+	−	+	−
STA	+	+	+	−	+	−	+	−	+	−	+	−	−	−	−	−	+	−	+	−	−	−
Kraut's	+	+	+	−	+	−	−	−	+	−	+	−	−	−	−	−	+	−	+	−	−	−
R. salt	+	+	+	−	+	−	−	−	±	−	+	−	+	−	+	−	+	−	+	−	−	−

[a] Key: Drag. sp., Dragendorff's spray reagent (Munier–Macheboeuf modification) (13); Drag. pt., Dragendorff's precipitation reagent (16); STA, silicotungstic acid; and R. salt, Reinecke salt. [b] Key: NACP, ammonia-catalyzed acetone condensation products; HACP, acid-catalyzed acetone condensation products; FACP, fixed alkali-catalyzed acetone condensation products; RuAc, acetylated rutin; QuAc, acetylated quercitin; KmAc, acetylated kaempferol; ChAc, acetylated chrysophanic acid; RhAc, acetylated rhein; Meth, methoxsalen; Imp, imperatorin; Sant, santonin; F1, fraction 1 (initial chloroform extract from acid medium); and F2, fraction 2 (purified chloroform extract from alkaline medium), as described under *Experimental*.

Acetone Condensation Products—The products (if any) from the interaction of acetone with concentrated hydrochloric acid, acetone with sodium hydroxide pellets, or acetone with concentrated ammonium hydroxide solution were prepared by keeping each pair in a closed flask for 3 days with frequent agitation. The dark-brown residue obtained with acetone and concentrated hydrochloric acid contained acid-catalyzed acetone condensation products, the viscid brown residue obtained with acetone and sodium hydroxide pellets contained fixed alkali-catalyzed acetone condensation products, and the dark, brittle, glassy solid residue obtained with acetone and concentrated ammonium hydroxide solution contained ammonia-catalyzed acetone condensation products.

Preparation of Nonalkaloidal Coupled Compounds with Dragendorff's Reagent—For IR analysis, complexes of khellin, imperatorin (ammidin), veratric acid, and cineole were prepared by dissolving the test compounds in aqueous acetic acid (20–50%, according to solubility) and adding dropwise Dragendorff's precipitation reagent. Khellin gave a heavy reddish-brown precipitate instantaneously, imperatorin gave a dark-brown crystalline compound after several hours, veratric acid gave an amorphous dark-brown deposit after sitting overnight, and cineole yielded a deep blood-red oil.

Reagents—Munier–Macheboeuf Dragendorff's spray reagent (13), Dragendorff's precipitation reagent (36), Mayer's reagent (36), Wagner's reagent (23), Kraut's reagent (37), 12% aqueous silicotungstic acid solution, and saturated Reinecke salt solution were used.

Test Procedure—The test compounds were dissolved in chloroform, alcohol, acetone, or chlorofrom–alcohol to make 0.2% solutions when solubility permitted or lower concentrations otherwise. Dissolution of very volatile liquids was not attempted to guard against loss of the test compound during solvent evaporation.

Aliquots, 10 μl, of individual test compounds were applied to microchromatoplates prepared by the slurry technique (32). Without attempting development, the spotted areas were sprayed with Dragendorff's reagent. The reaction results were recorded immediately (11). Spots of some very volatile liquids were examined by viewing the chromatoplates from the back (*e.g.*, isobutyraldehyde and isobutyl epoxide).

When certain constituents were extracted from preparations, two initial spots of the crude extract were cochromatographed using specified TLC systems (32–35). In one chromatogram, the constituents were located using specific chromogenic reagents (32–35) and then were used to monitor the second chromatogram that was sprayed with Dragendorff's reagent.

Partition of Test Compounds and Preparations—The purified total cardenolide fraction of *Acokanthera spectabilis* (29), the alcoholic extract of *L. dentata*, certain acetylated flavonoids [rutin, quercitin, kaempferol, hyperoside (3-D-galactoside hemipentahydrate), and quercitin glucuronide], the fixed alkali-catalyzed acetone condensation products, the acid-catalyzed acetone condensation products, the ammonia-catalyzed acetone condensation products, santonin, methoxsalen (xanthotoxin), and imperatorin were subjected to partition between acid–base and organic solvents. A concentrated alcoholic solution of the material was taken in dilute hydrochloric acid, the acidic solution was extracted with two portions of chloroform (fraction 1), and the aqueous phase was alkalinized with ammonia solution and reextracted with two portions of chloroform (fraction 2). Both fractions were tested with Dragendorff's spray and precipitation reagents, Mayer's reagent, Wagner's reagent, silicotungstic acid solution, Reinecke salt solution, and Kraut's reagent.

Recording Results—If a very slight or no color was observed with the spray reagent, larger quantities of the test solution (20–50 μl) were retested. Test compounds and results are given in Tables I and II; Table III gives the results of the partition experiments.

RESULTS AND DISCUSSION

Of the many organic compounds tested, only positively reacting compounds are given in Table I. Compounds reported by Farnsworth *et*

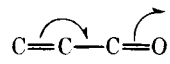

I

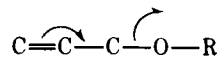

II

al. (3) to give a positive reaction are given in Table II after being categorized according to whether they conform to the structural requirements determined by these investigators.

The structures of 86 positively reacting compounds (Table I) and some of the 55 compounds reported by Farnsworth *et al.* (3) (Table II) were

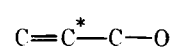

III

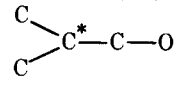

IV

studied. Many of the compounds were conjugated aldehydes, ketones, and lactones, thus fulfilling the minimal structural requirement indicated by Farnsworth *et al.* (3). These compounds are listed in column A of Tables I and II. Many other compounds lack these structural features (column B of Tables I and II).

Compounds of column B (Table I) have no common structural feature that correlate them to compounds of column A. While some have carbonyl or lactone functions (the first eight compounds), they lack conjugation to these functions. All other compounds of column B lack carbonyl or lactone functions. Thus, neither these features nor the conjugation is necessary for the reaction.

All of the positively reacting compounds are oxygenated, and the oxygen represents a site of high electron density—*viz.*, carbonyl, lactone,

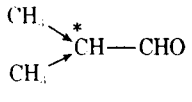

V

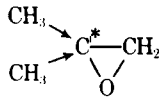

VI

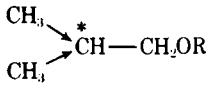

VII

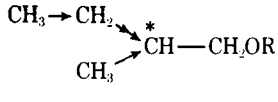

VIII

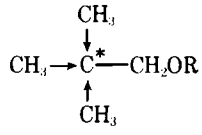

IX

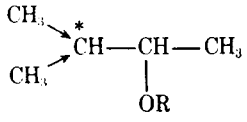

X

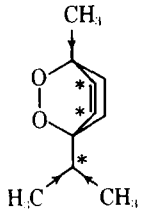

XI

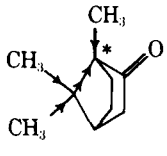

XII

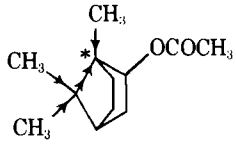

XIII

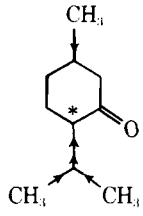

XIV

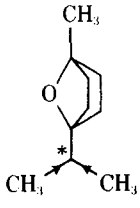

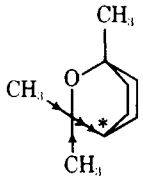

XVI

XVII

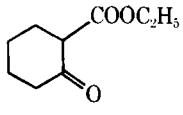

XVIII

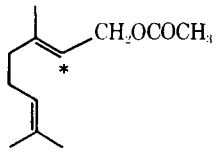

XIX

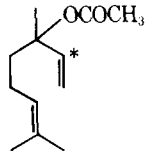

XX

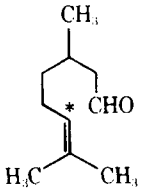

XXI

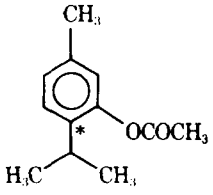

XXII

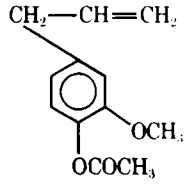

XXIII

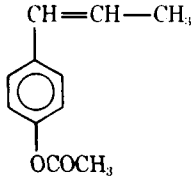

XXIV

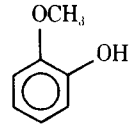

XXV

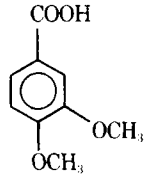

XXVI

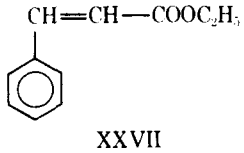

XXVII

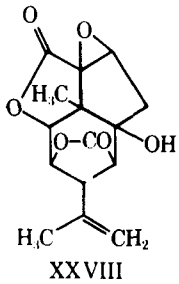

XXVIII

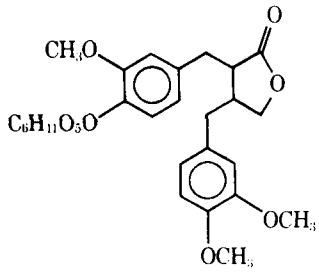

XXIX

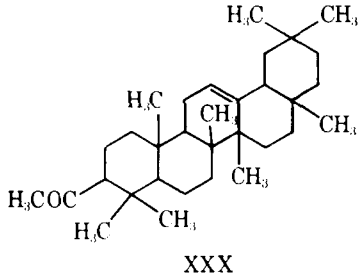

XXX

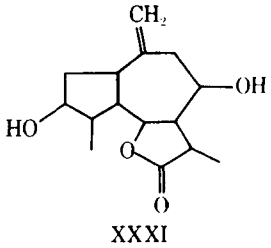

XXXI

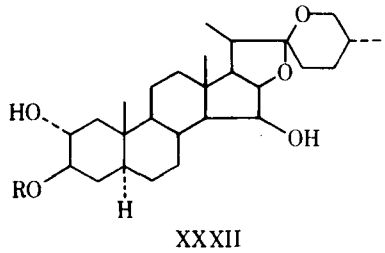

XXXII

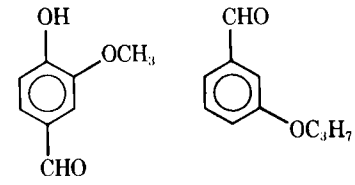

XXXIII

XXXIV

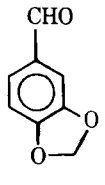

XXXV

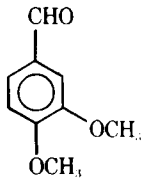

XXXVI

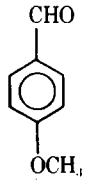

XXXVII

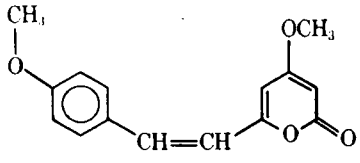

XXXVIII

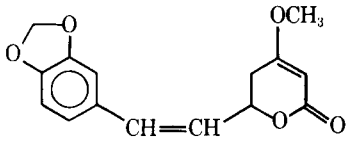

XXXIX

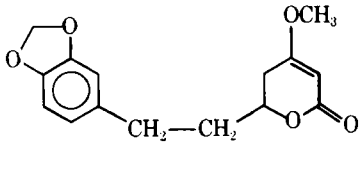

XL

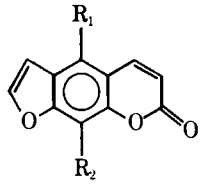

XLI

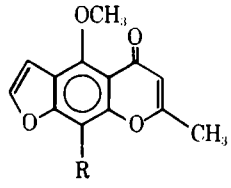

XLII

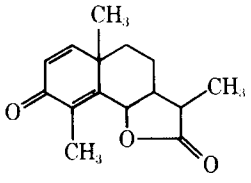

LXIII

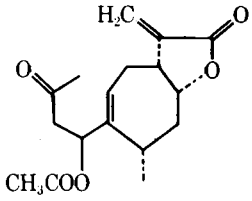

XLIV

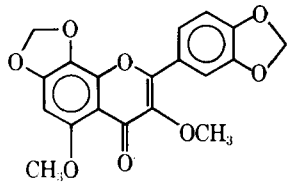

XLV

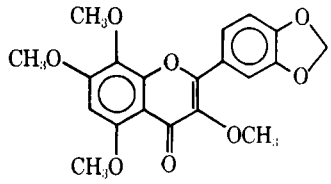

XLVI

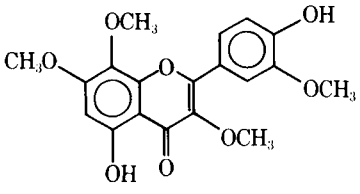

XLVII

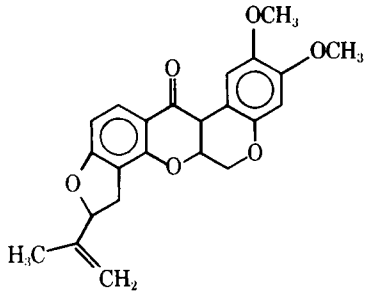

XLVIII

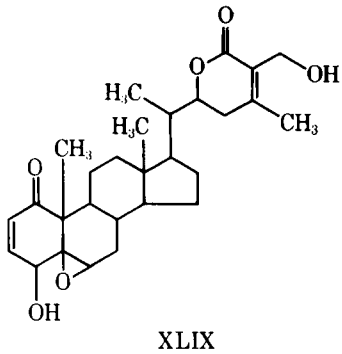

XLIX

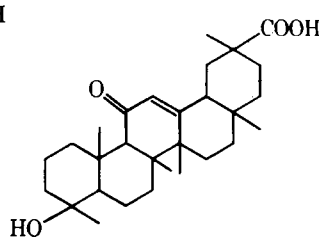

L

ether, ester, epoxide, and peroxide. This observation suggested that: (*a*) it may not be the carbonyl function *per se* but instead the high availability of its electrons that accounts for the reaction, and (*b*) other oxygen functions of comparably high electron density may react similarly. This suggestion has been realized by the strong positive reactions of some conjugated ethers and esters (Table I) and the positive reaction of some α,β-unsaturated alcohols and acids. The existence of the α,β-unsaturation in these compounds would increase substantially the electron density at the oxygen function (I and II), rendering it sufficiently basic to form coordinate complexes with Lewis acids (alkaloidal reagents).

The compounds studied lacking any conjugated carbonyl or lactone function were V, isobutyraldehyde; VI, isobutyl epoxide; VII, isobutyl ether (R = alkyl) or ester (R = acyl); VIII–X esters (R = acyl) or ethers (R = alkyl): VIII, active isopentyl ethers or esters; IX, neopentyl ethers or esters; and X, isopropylmethyl ethers or esters; XI, ascaridole; XII, camphor; XIII, bornyl acetate; XIV, menthone; XV, 1,4- and 1,8-cineoles; XVI, 2,3-dihydro-4-pyran; XVII, 5,6-dihydro-2-pyran; XVIII, ethyl-2-cyclohexanone carboxylate; XIX, geranyl acetate; XX, linalyl acetate; XXI, citronellal; XXII, thymol acetate; XXIII, acetyleugenol; XXIV, acetyl anethole; XXV, guaiacol; XXVI, veratric acid; XXVII, ethyl cinnamate; XXVIII, picrotoxinin; XXIX, arctiin; XXX, acetyl-β-amyrin; XXXI, lipidiol; and XXXII, digitonin (R = sugar moiety).

Many compounds that lack α,β-unsaturation (to the oxygen) react positively (Tables I and II). Nonetheless, in almost all of these compounds, the β-carbon (denoted by an asterisk) bears one or more free alkyl groups. The electron-repelling methyl groups increase the electron density at the β-carbon, resulting in the same effect as does α,β-unsaturation. In V–XV, the effect of the free alkyl groups is demonstrated; the arrowheads in the structural formulas of these compounds qualitatively represent the electron-repelling effect of these groups.

These observations were significant in establishing III or IV as the structural feature necessary for the false alkaloid reaction, provided that the high availability of electrons at the oxygen was not altered by other functions.

The β-carbon (denoted by an asterisk) of III may constitute a part of an aromatic structure. The oxygen function in III and IV may be an aldehyde, a ketone, a lactone, an alcoholic or phenolic ether, an ester, an oxide, or a peroxide.

Structures III and IV were demonstrated to fulfill the requirements of the test by the typical alkaloid-like reactions given by acrolein, crotonaldehyde, citral, carvone, XI, XIX, piperonal (XXXV), and veratraldehyde (XXXVI) (General Structure III) and by V–XV (General Structure IV).

If the oxygen of the essential structure is an alcohol, a phenol, or a hemiacetal, a negative or slight reaction is given, *e.g.*, geraniol, terpineol, linalool, borneol, isoborneol, primary isobutanol, pyrocatechol, resorcinol, pyrogallol, orcinol, hydroquinone, guaiacol, benzhydrol, thymol, α-amyrin, lanosterol, salicyl alcohol, isopentanol, and cinnamyl alcohol. Esterification of these alcohols and phenols in many instances gave positively reacting esters (Table I).

Carboxylic acids also were expected to react negatively due to their low availability of electrons at the carboxylic group or because acids tend to associate as cyclic dimers (39). Thus, crotonic, anisic, maleic, acrylic, benzoic, cinnamic, *p*-hydroxybenzoic, glycyrrhizic, glycyrrhetinic, and quillaic acids gave negative tests, despite the fulfillment of the structural requriement. Maleic anhydride, phthalic anhydride, and cantharidin also gave a negative reaction.

The reaction of compounds that fulfilled the essential requirement was affected by other functions that altered the electron density at the oxygen or the β-carbon. Thus, when the β-carbon was involved in an aromatic structure or a conjugated double bond system, electron-repelling substituents enhanced the reaction, *e.g.*, pyrocatechol (−) [*cf.*, guaiacol (±)

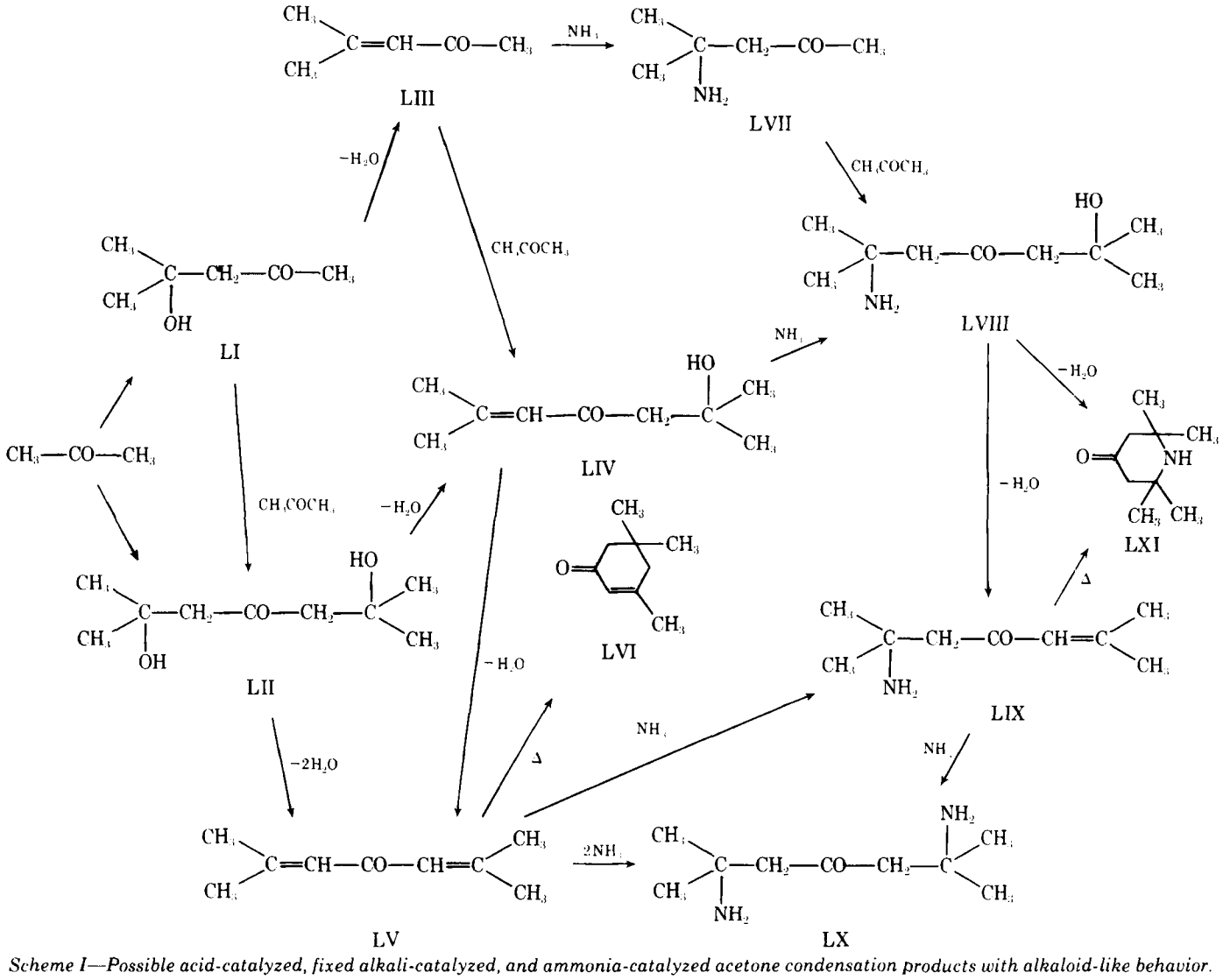

Scheme I—Possible acid-catalyzed, fixed alkali-catalyzed, and ammonia-catalyzed acetone condensation products with alkaloid-like behavior.

and eugenol (+++)], *m*-cresol (−) [*cf.*, thymol (+)], anisole (−) [*cf.*, anethole (+)], and benzaldehyde (−) and 3-hydroxybenzaldehyde (−) [*cf.*, anisaldehyde (++), veratraldehyde (+++), piperonal (+++), and 3-butoxybenzaldehyde (++)]. On the other hand, an electron-attracting substituent decreased or even eliminated the reaction, *e.g.*, acetophenone (+++) and *p*-aminoacetophenone (+++) [*cf.*, *p*-nitroacetophenone (−) and *p*-hydroxyacetophenone (−)].

The strong reactions given by 3-butoxybenzaldehyde, piperonal, veratraldehyde, eugenol, and acetyleugenol in contrast to the negative reactions given by benzaldehyde, 3-hydroxybenzaldehyde, and vanillin mean that the reaction of the former five compounds should not be attributed wholly to the conjugated carbonyl structure but should partially be attributed to their conjugated ether and/or ester functions. The same also applies to conjugated carbonyl compounds and lactones with additional reactive ether, ester, or carbonyl functions: XXXIII, vanillin; XXXIV, 3-butoxybenzaldehyde; XXXV, piperonal; XXXVI, veratraldehyde; XXXVII, anisaldehyde; XXXVIII, yangonin; XXXIX, methysticin; XL, dihydromethysticin; XLI, psoralen (furocoumarin) ($R_1 = R_2 = H$), bergapten ($R_1 = OCH_3$), methoxsalen ($R_2 = OCH_3$), imperatorin (R_2 = isoamyleneoxy), and isopimpinellin ($R_1 = R_2 = OCH_3$); XLII, furochromones khellin (R = OCH_3) and visnagin (R = H); XLIII, santonin; XLIV, xanthumin; XLV, meliternatin; XLVI, meliternin; XLVII, ternatin; XLVIII, rotenone; XLIX, withaferin A; and L, glycyrrhetinic acid.

The IR spectra of khellin, imperatorin, and veratric acid provided evidence that both the carbonyl and ether functions in these compounds are involved in the reaction. The strong band assigned to the carbonyl function (1655–1620 cm^{-1} in khellin, 1710–1650 cm^{-1} in imperatorin, and 1685–1655 cm^{-1} in veratric acid) were distorted and split in the spectra of the corresponding coupled compounds. More pronounced changes were observed in the region of the ether and aralkyl ether stretching vibration; thus, the strong bands at 1085 cm^{-1} in khellin and 1090 cm^{-1} in imperatorin were split into doublets of medium intensity in the spectra of the coupled compounds. The band at 1095 cm^{-1} with veratric acid appeared only as a shoulder in the spectrum of the coupled compound. The bands between 1000 and 979 cm^{-1} (–C=CH deformation) also were affected, *i.e.*, weakened and shifted toward a higher frequency in the spectra of the coupled compounds.

The reactivity of compounds with the essential structure was eliminated almost completely by hydroxyl groups in their structures. The hydroxyl groups competed for the oxygen function of the essential structure, through inter- and/or intramolecular hydrogen bonding. This competition may explain the contrast in the reaction of acetophenone (+++) *versus* *p*-hydroxyacetophenone (−), coumarin (+++) *versus* umbelliferone (±), anisaldehyde (+++) *versus* vanillin (±), digitoxin (+++) and strophanthin (++) *versus* ouabain (G-strophanthin) (+), menadione (++++) *versus* 3-hydroxymenadione (−), and santonin XLIII (+++) and xanthumin XLIV (+++) *versus* lipidiol XXXI (−) and isolipidiol (±).

Therefore, naturally occurring hydroxylated flavonoids and hydroxyanthracene derivatives were expected to react negatively. Acetylated derivatives of these compounds gave positive tests with Dragendorff's spray reagent (Table I) as well as with some other alkaloidal precipitants (Table III). Acetylation and alkylation not only eliminated the interfering action of the hydroxyls but also introduced additional conjugated ester or ether functions; thus, the alkaloid-like reaction was intensified.

Briggs and Locker (8) reported that XLV–XLVII, three alkylated hydroxyflavones, gave precipitates with the usual alkaloid reagents and gave crystalline salts with acids. This alkaloid-like behavior was attributed to the fact that each molecule was completely alkylated. However,

Farnsworth (4) stated that the reaction was due to the conjugated carbonyl function and that other flavonoids would react similarly. The present work shows both of these reports to be partially correct; despite the conjugated carbonyl nature, flavonoids do not show alkaloid-like behavior unless they are almost completely alkylated.

Being alkylated isoflavonoids, all rotenoids presumably give positive alkaloid reactions; *e.g.*, rotenone (+++).

Housholder and Camp (40) stated that treatment of plant material with acetone and ammonia solution can give rise to alkaloid-like artifacts. These investigators were unable to identify the condensation products of the reaction, but they reported that the reaction rate was enhanced by light and the atmosphere.

Upon wet packing a column of silica gel with benzene–acetone–ammonia and keeping it overnight prior to the application of any material, discoloration of the column was observed[2]. Draining and evaporating the brown solvent mixture yielded a brown residue, which gave typical alkaloid reactions with Dragendorff's spray reagent as well as with other alkaloid precipitants. Neither benzene nor the plant material but instead acetone and/or ammonia apparently were responsible for the production of the alkaloid-like artifacts because both were common factors.

These artifacts may be either nitrogenous condensation products of acetone and ammonia or nonnitrogenous, alkali-catalyzed aldol condensation products of acetone that fulfill the requirements of the false reaction.

Acid-catalyzed, fixed alkali-catalyzed, and ammonia-catalyzed acetone condensation products gave a strong positive reaction with Dragendorff's spray reagent. TLC revealed three main, qualitatively identical Dragendorff-positive spots in acid-catalyzed and fixed-alkali-catalyzed acetone condensation products at R_f 0.78, 0.67, and 0.55 on silica gel in chloroform–methanol (93:7) and at R_f 0.65, 0.53, and 0.42 on silica gel in chloroform–methanol–acetic acid (89:10:1), respectively. The ammonia-catalyzed acetone condensation products revealed at least seven spots, including three identical to those of the acid-catalyzed and fixed alkali-catalyzed condensation products. The additional four spots were at low R_f values: 0.32, 0.21, 0.11, and 0.00 in chloroform–methanol and 0.26, 0.45, 0.05, and 0.00 in chloroform–methanol–acetic acid. An eighth spot, R_f 0.50 in chloroform–methanol and 0.46 in chloroform–methanol–acetic acid, gave a typical pink color.

Obviously, the spots common in the acid-catalyzed, fixed alkali-catalyzed, and ammonia-catalyzed acetone condensation products were of nonnitrogenous compounds. This conclusion indicates the compounds to be aldol condensation products of acetone. Scheme I shows the possible reaction products of acetone with acids, fixed alkalis, and ammonia. Compounds LIII–LVI are α,β-unsaturated ketones that fulfill the structural requirement of the false reaction. The additional low R_f spots in the ammonia-catalyzed acetone condensation products were assumed to be amino compounds (LVII–LXI) that arise from the condensation of ammonia with the reactive α,β-unsaturated ketones LIII–LV. This assumption was favored by the positive nitrogen test given by the ammonia-catalyzed acetone condensation products. Further evidence for the postulated reaction sequence was the development of the additional low R_f spots, absent from the acid-catalyzed and fixed alkali-catalyzed condensation products, when the latter two were kept with concentrated ammonia solution overnight.

From the results of the partition experiments (Table III), nonnitrogenous Dragendorff-positive plant constituents apparently do not interfere with alkaloid detection and isolation if necessary partition purification steps are performed. The nitrogenous acetone–ammonia reaction products react typically as alkaloids and interfere seriously with alkaloid detection and/or isolation.

REFERENCES

(1) C. C. Fulton, *Am. J. Pharm.*, **104**, 244 (1932).

(2) R. Martello and N. R. Farnsworth, *Lloydia*, **25**, 176 (1962).

(3) N. R. Farnsworth, N. A. Pilwski, and F. J. Draus, *ibid.*, **25**, 312 (1962).

(4) N. R. Farnsworth, *J. Pharm. Sci.*, **55**, 225 (1966).

(5) L. Rosenthaler, "The Chemical Investigation of Plants," G. Bell and Sons Ltd., London, England, 1930, pp. 25, 26.

(6) C. O. Wilson and O. Gisvold, "Text Book of Organic Medicinal and Pharmaceutical Chemistry," 3rd ed., Lippincott, Philadelphia, Pa., 1956, p. 242.

(7) A. R. Furgiuele, Ph.D. dissertation, University of Pittsburgh, Pittsburgh, Pa., 1962, p. 100; through Ref. 3.

(8) L. H. Briggs and R. H. Locker, *J. Chem. Soc.*, **1949**, 2157.

(9) R. F. Raffauf, *Econ. Bot.*, **16**, 171 (1962).

(10) D. Kraft, *Pharmazie*, **8**, 170 (1956).

(11) G. K. Nikonov and A. I. Ban'Kovskii, *Tr. Vses. Nauchn-Issled. Inst. Lekarstv. Aromat. Rast.*, No. 11, 296 (1959); through *Chem. Abstr.*, **56**, 10490 (1962).

(12) N. R. Farnsworth and K. L. Euler, *Lloydia*, **25**, 186 (1962).

(13) R. Munier and M. Macheboeuf, *Bull. Soc. Chem. Biol.*, **33**, 846 (1951).

(14) E. Tyihak, *J. Chromatogr.*, **14**, 125 (1964).

(15) T. Thies and F. W. Reuther, *Naturwissenschaften*, **41**, 230 (1954).

(16) K. Thoma, R. Rombach, and E. Ulimann, *Sci. Pharm.*, **32**, 216 (1964).

(17) H. M. Bregoff, E. Roberts, and C. C. Delwiche, *J. Biol. Chem.*, **205**, 565 (1953).

(18) R. Munier, *Bull. Soc. Chem. Biol.*, **35**, 1225 (1953).

(19) H. Jatzkewitz and Z. Hoppe-Seylera, *Physiol. Chem.*, **292**, 99 (1953); through Ref 32.

(20) D. Vagujfalvi, *Planta Med.*, **8**, 34 (1960).

(21) V. H. C. Menben and G. Stopel, *ibid.*, **24**, 8 (1973).

(22) M. E. Wall, C. S. Fenske, J. W. Garvin, J. J. Willaman, Q. Jones, B. G. Schubert, and H. S. Gentry, *J. Am. Pharm. Assoc., Sci. Ed.*, **48**, 695 (1959).

(23) E. Abisch and T. Reichstein, *Helv. Chim. Acta*, **43**, 1844 (1960).

(24) X. A. Domingues, *Econ. Bot.*, **14**, 157 (1960).

(25) W. H. Tallent, V. L. Stromberg, and E. C. Horning, *J. Am. Chem. Soc.*, **77**, 6361 (1955).

(26) K. L. Euler and N. R. Farnsworth, *Lloydia*, **25**, 296 (1962).

(27) L. A. Anderson, N. S. Dogget, and M. S. F. Ross, *Planta Med.*, **32**, 2, 125 (1977).

(28) Y. A. Mohamed, "Proceedings of the 10th Science Week," Damascus, Syrian Arab Republic, part 1, 1969, p. 1.

(29) M. S. Karawya, S. M. Abdel-Wahab, and H. M. Niazi, *Planta Med.*, **24**, 234 (1973); M. S. Karawya, S. M. Abdel-Wahab, and H. M. Niazi, *Egypt. J. Pharm. Sci.*, **15**, 33 (1974).

(30) A. A. M. Habib and T. S. Sarg, *Bull. Fac. Sci., Riyadh Univ.*, **8**, 341 (1977).

(31) M. M. A. Hassan, A. A. M. Habib, and F. J. Muhtadi, *Pharmazie*, **31**, H9 (1976).

(32) E. Stahl, "Thin-Layer Chromatography," 2nd ed., Springer-Verlag, Berlin, Germany, 1969.

(33) K. Macek, "Pharmaceutical Application of Thin-Layer and Paper Chromatography," Elsevier, Amsterdam, The Netherlands, 1972.

(34) E. G. C. Clark, "The Isolation and Identification of Drugs," vols. I and II, Pharmaceutical Press, London, England, 1969 and 1975.

(35) "Official Methods of Analysis," 12th ed., Association of Official Analytical Chemists, Washington, D.C., 1975.

(36) A. K. Kiang and B. Douglas, Proc. Third Congress Pan Indian Ocean Scientific Association, Tananarive, Section G, 1957, p. 19; through Refs. 4 and 12.

(37) C. P. Stewart and A. Stolman, "Toxicology," vol. 2, Academic, New York, N.Y., 1961.

(38) A. A. M. Habib and A. M. Metwally, *Planta Med.*, **23**, 88 (1973).

(39) I. L. Finar, "Organic Chemistry," vol. I, 6th ed., Longman, London, England, 1973.

(40) D. E. Housholder and B. J. Camp, *J. Pharm. Sci.*, **54**, 1676 (1965).

[2] Dr. Nadia A. El-Sebakhy, Department of Pharmacognosy, Faculty of Pharmacy, Alexandria University, Alexandria, Egypt, personal communication.

ACKNOWLEDGMENTS

This work was carried out in part at the Faculty of Pharmacy, Riyadh University, Riyadh, Saudi Arabia.

The author thanks Dr. N. Abdel-Salam, Dr. A. A. Omar, and Dr. M. G. El-Ghazooly of the Department of Pharmacognosy, Alexandria University, for samples of isolated materials.

Prodrugs as Drug Delivery Systems IV: *N*-Mannich Bases as Potential Novel Prodrugs for Amides, Ureides, Amines, and Other NH-Acidic Compounds

HANS BUNDGAARD ˣ **and MARIANNE JOHANSEN**

Received May 21, 1979, from the *Department of Pharmaceutics, Royal Danish School of Pharmacy, 2 Universitetsparken, DK-2100 Copenhagen, Denmark.* Accepted for publication July 31, 1979.

Abstract □ The hydrolysis kinetics of a series of *N*-Mannich bases of carboxamides, thioamides, and other NH-acidic compounds were studied to assess their suitability as prodrugs for various drugs. The pH–rate profiles for the compounds were determined at 37° and were accounted for by assuming the spontaneous decomposition of both free and protonated Mannich bases. The reaction rate for the free base increased sharply with increasing steric effects of the amine component of the *N*-Mannich bases and also with increasing acidity of the amide component. *N*-Mannich bases may be potentially useful prodrugs for NH-acidic compounds such as various amides, imides, and ureides and for amines.

Keyphrases □ Prodrugs—*N*-Mannich bases of amides, ureides, amines, and imides, hydrolysis kinetics □ Hydrolysis kinetics—*N*-Mannich base prodrugs of amides, ureides, amines, and imides □ Amides—*N*-Mannich base derivatives as prodrugs, hydrolysis kinetics □ Amines—*N*-Mannich base derivatives as prodrugs, hydrolysis kinetics □ Imides—*N*-Mannich base derivatives as prodrugs, hydrolysis kinetics □ Ureides—*N*-Mannich base derivatives as prodrugs, hydrolysis kinetics □ *N*-Mannich bases—derivatives of amides, amines, imides, and ureides, potential as prodrugs, hydrolysis kinetics

Bioreversible derivatization of drug substances to produce prodrugs with altered physiochemical properties can improve substantially both drug efficacy and safety (1–3). Chemical transformation of active drug substances into inactive derivatives *per se*, which convert to the parent compounds within the body, may be relatively simple for drug substances possessing groups (*e.g.*, hydroxyl or carboxyl) that are bioreversibly esterifiable. However, for many drug molecules, no apparently readily derivatizable functional groups or entities are present.

BACKGROUND

As a part of studies (4–6) to identify potentially useful bioreversible derivatives of difficult-to-derive chemical entities and drug molecules, it was found that *N*-Mannich bases may be potentially useful prodrugs for NH-acidic compounds such as various amides, imides, and ureides and for amines.

N-Mannich bases of amides, imides, and various other NH-acidic compounds are known (7–10), and several drug substances bearing an NH-acidic group have been modified by *N*-aminomethylation and tested as potential medicinal agents, *e.g.*, hydantoins (11, 12), barbituric acids (13), sulfonamides (14), and succinimides (15, 16). However, almost no information on the stability and reactivity of such derivatives in aqueous solution is available. A recent study (17) of the degradation kinetics of rolitetracycline, a highly water-soluble *N*-Mannich base formed by condensation of the carboxamide group in tetracycline with formaldehyde and pyrrolidine (18), showed that the compound readily decomposed in aqueous solution to yield tetracycline, formaldehyde, and pyrrolidine quantitatively. The degradation half-life at pH 7.4 and 35° was 43 min, indicating the potential of *N*-Mannich bases as prodrugs, at least for carboxamides.

Based on this observation, numerous *N*-Mannich bases of various amides and other NH-acidic compounds were prepared. The decomposition kinetics of the compounds were studied in aqueous solution over a broad pH range to elucidate their stability and to assess their suitability as prodrugs for various drugs.

EXPERIMENTAL

The compounds (Table I) were prepared by heating formaldehyde, the amine (or the amine hydrochloride), and the amide in water–ethanol solutions according to standard literature procedures (7, 9, 10, 19). Several compounds were obtained as the hydrochloride (19).

All kinetic experiments were carried out in aqueous buffer solutions at 37.0 ± 0.1°. Hydrochloric acid, acetate, phosphate, borate, and carbonate buffers were used; the total buffer concentration was 0.1 *M* except in experiments where buffer effects were studied specifically. A constant ionic strength ($\mu = 0.5$) was maintained for each buffer by adding a calculated amount of potassium chloride. The initial concentration of the *N*-Mannich bases in the buffers was in the 10^{-4}–5×10^{-3} *M* range.

In rapid reactions, decomposition was followed spectrophotometrically[1] by recording absorbance changes at a wavelength where the absorptions of substrate and products differed maximally. Slower reactions were followed by measuring the amount of formaldehyde released using a colorimetric procedure described previously (20). The rate constants were determined from plots of log $(A_t - A_\infty)$ or log $(A_\infty - A_t)$ *versus* time, where A_t and A_∞ are the absorbance readings at time t and infinity, respectively.

RESULTS AND DISCUSSION

Decomposition Kinetics—At constant pH and temperature, the decomposition rates of the compounds studied followed strict first-order kinetics; the reactions went to completion in all kinetic runs, as revealed by the formation of formaldehyde and parent amide in stoichiometric amounts. Since the degradation rates were unaffected by variations (0.02–0.5 *M*) in the buffer concentrations used to maintain a constant pH, no general acid–base catalysis was apparent.

The influence of pH on the degradation rate for some compounds is shown in Fig. 1, where the logarithm of the observed apparent first-order rate constants, k_{obs}, was plotted against pH. The pH–rate profiles for the other compounds listed in Table I have a similar shape as those shown in Fig. 1. These pH dependences of k_{obs} can be accounted for by assuming spontaneous decomposition of the Mannich bases, B, and their conjugate acids, BH^+, as shown in Schemes I and II:

$$B \xrightarrow{k_1} \text{products}$$

Scheme I

$$BH^+ \xrightarrow{k_2} \text{products}$$

Scheme II

With $[B]_T$ as the total concentration of *N*-Mannich base (*i.e.*, $[B]_T = [B] + [BH^+]$), the overall rate equation is:

$$k_{obs}[B]_T = k_1[B] + k_2[BH^+] \qquad \text{(Eq. 1)}$$

where k_1 and k_2 are the apparent first-order rate constants for the spontaneous degradation of B and BH^+, respectively.

By introducing into Eq. 1 the identities:

$$[B] = \frac{K_a}{a_H + K_a}[B]_T \qquad \text{(Eq. 2)}$$

and:

$$[BH^+] = \frac{a_H}{a_H + K_a}[B]_T \qquad \text{(Eq. 3)}$$

[1] Zeiss PMQ II equipped with a thermostated cell compartment.

0022-3549/80/0100-0044$01.00/0
© 1980, American Pharmaceutical Association

Table I—Rate Data for Decomposition of Various *N*-Mannich Bases in Aqueous Solution (μ = 0.5; 37°) [a]

Compound	k_1, min^{-1}	$k_2 \times 10^4$, min^{-1}	pKa[b]	$t_{1/2}$[c], min
N-(Diethylaminomethyl)benzamide	0.52	1.1	7.7	4.0
N-(Ethylaminomethyl)benzamide	0.0084	0.9	7.5	190
N-(Methylaminomethyl)benzamide	0.0026	0.4	7.5	600
N-(Benzylaminomethyl)benzamide	0.0020	3.0	6.4	380
N-(Cyclohexylaminomethyl)benzamide	0.026	1.1	7.6	70
N-(Piperidinomethyl)benzamide	0.051	0.4	7.8	47
N-(Morpholinomethyl)benzamide	0.0005	6	5.6	1400
N-(Isobutylaminomethyl)benzamide	0.019	1.0	7.5	82
N-(Piperidinomethyl)niacinamide	0.17	1.0	7.5	8
N-(Morpholinomethyl)trichloroacetamide	0.72	ND	4.1	1.0
N-(Piperidinomethyl)trichloroacetamide	35	ND	6.5	0.02
N-(Piperidinomethyl)thiobenzamide	13	ND	6.6	0.06
N-(Morpholinomethyl)-*p*-toluenesulfonamide	ND[d]	1.5×10^4	ND[d]	<0.02
N-(Morpholinomethyl)-*N'*-acetylthiourea	0.91	ND	4.7	0.8
N-(Piperidinomethyl)methylurea	ND	ND	ND	5

[a] ND = not determined. [b] Kinetically determined values; for some compounds, pKa values also were determined titrimetrically and agreed with the kinetically obtained values. [c] Hydrolysis half-lives at pH 7.4 and 37°. [d] $k_1K_a = 1.9 \times 10^{-2}$ *M*/min.

where K_a is the apparent ionization constant of the protonated *N*-Mannich bases and a_H is the hydrogen-ion activity, the expression for k_{obs} is:

$$k_{obs} = \frac{k_1K_a}{a_H + K_a} + \frac{k_2a_H}{a_H + K_a} \qquad \text{(Eq. 4)}$$

The lines in Fig. 1 were constructed from Eq. 4 and the rate constants and pKa values given in Table I. Although Eq. 4 and, consequently, Schemes I and II adequately describe the observed degradation kinetics, other kinetically equivalent reactions can account for the observed k_{obs}–pH relationship.

Structural Effects on Reaction Rate—The rate data in Table I show that the structure of the amine component in the *N*-Mannich bases dramatically affected the rate constant, k_1 and, accordingly, the decomposition rate of the compounds in weakly acidic to basic aqueous solutions (*cf.*, the half-lives at pH 7.4). This result was predominantly a steric effect of the alkyl groups on the amine nitrogen. For some *N*-Mannich bases of benzamide, an excellent linear correlation existed between log k_1 and Charton's steric parameter, ν (21), for alkylamino groups (Fig. 2). The only deviation observed was for the benzylamine derivative and may have been due to the lower pKa value for the corresponding Mannich base as compared with the other compounds (Table I).

The data also show that for the same amine component, the *N*-Mannich base decomposition rate increased sharply with increasing acidity of the parent amide. The k_1 values of the piperidine derivatives increased in the order benzamide < niacinamide < thiobenzamide < trichloroacetamide, which is also the order of amide acidity. The difference in acidity among these amides was reflected in the pKa values for the Mannich bases with piperidine (Table I), and a linear correlation can be shown to exist between log k_1 and the pKa values for these *N*-Mannich base derivatives. For the most acidic amide of the compounds studied, *p*-toluenesulfonamide (pKa 10.3), k_1 was too high to be determined. A high k_1 value also was observed for morpholine derivatives of other acidic compounds such as succinimide, phenytoin, and barbital.

Structural factors other than steric effects and stability of leaving groups also may influence the reactivity of *N*-Mannich bases. Urea and thiourea Mannich bases were more reactive than expected on the basis of their acidity. Salicylamide derivatives degraded markedly faster in neutral solution than did the corresponding benzamide derivatives. The degradation half-lives of salicylamide *N*-Mannich bases with morpholine and α-alanine at pH 7.4 and 37° were 38 and 17 min, respectively [*cf.*, 1400 min for *N*-(morpholinomethyl)benzamide].

Reaction Mechanism—Although insufficient experimental evidence

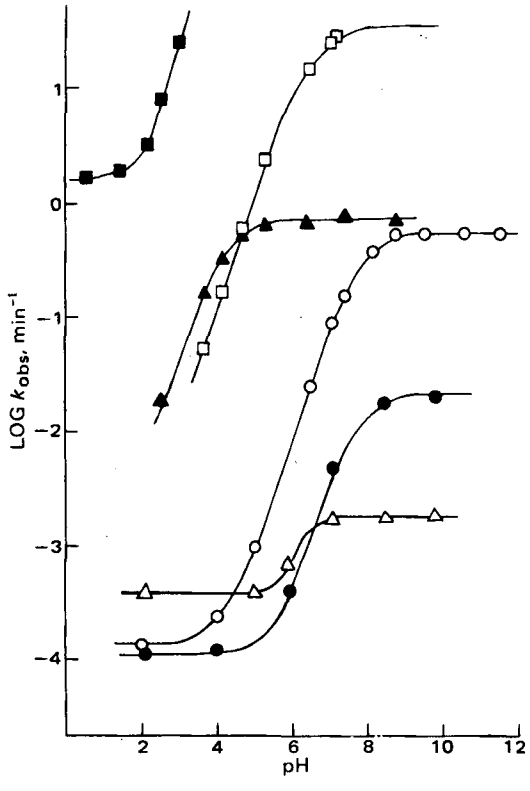

Figure 1—*The pH–rate profiles for the decomposition of various* N-*Mannich bases in aqueous solution at 37°. Key:* △, N-(*benzylaminomethyl*)*benzamide;* ●, N-(*isobutylaminomethyl*)*benzamide;* ○, N-(*diethylaminomethyl*)*benzamide;* ▲, N-(*morpholinomethyl*)*trichloroacetamide;* □, N-(*piperidinomethyl*)*trichloroacetamide; and* ■, N-(*morpholinomethyl*)-p-*toluenesulfonamide.*

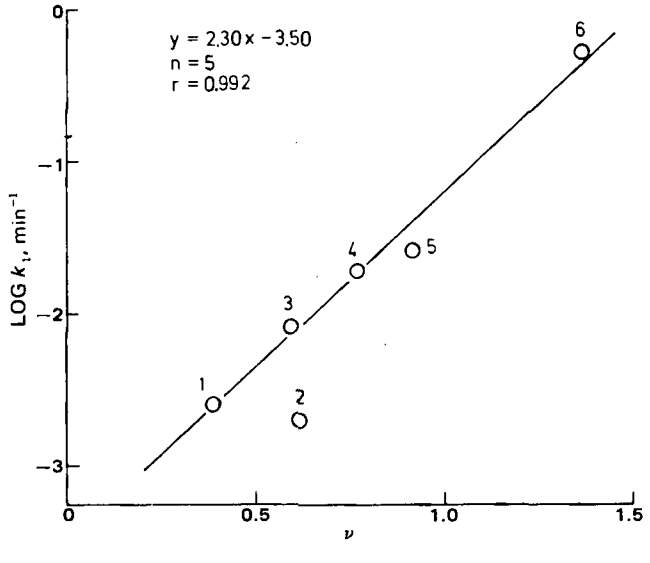

Figure 2—*Plot of log* k_1 *against Charton's steric substituent parameter for alkylamino groups for* N-*Mannich bases of benzamide* ($C_6H_5CONHCH_2R$). *Key: 1, R = methylamino; 2, R = benzylamino; 3, R = ethylamino; 4, R = isobutylamino; 5, R = cyclohexylamino; and 6, R = diethylamino. Compound 2 was excluded from the correlation plot.*

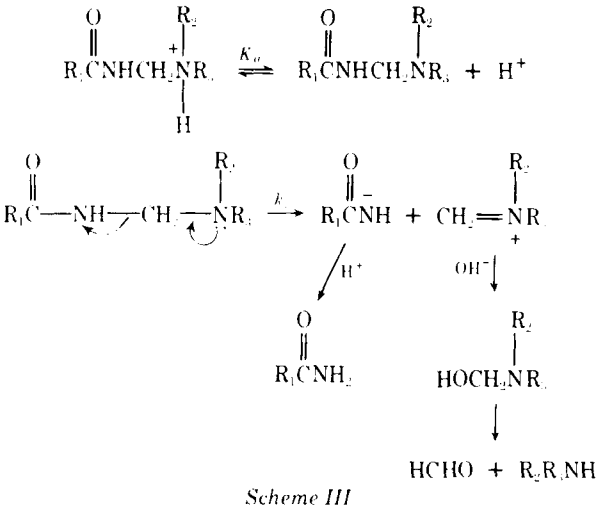

Scheme III

exists for a firm mechanistic scheme for the degradation, a plausible mechanism that agrees with the observed data is given in Scheme III. The rate-determining step involves unimolecular N–C bond cleavage with formation of an amide anion and an immonium cation. In subsequent fast steps, a solvent molecule transfers a proton to the amide anion and a hydroxide ion to the immonium ion, giving carbinolamine, which rapidly dissociates (22, 23) to formaldehyde and amine. In accord with this mechanism, the large steric effects exhibited by the amine alkyl groups may be explained as hindrance of amine solvation (*cf.*, 24), resulting in increasing nucleophilicity with increasing steric hindrance and, hence, increasing the lability of the N–C bond. The possible formation of *N*-(hydroxymethyl)amides in a rate-determining step does not seem likely since these compounds degraded much slower than the corresponding *N*-Mannich bases in separate experiments.

CONCLUSION

The present study shows that *N*-Mannich bases can be considered as potentially useful prodrugs of amides and various other compounds containing acidic NH-groups. By appropriate selection of the amine component, it should be feasible to obtain prodrugs with varying physicochemical properties such as the cleavage rate, aqueous solubility, and lipophilicity. Transformation of an amide into an *N*-Mannich base introduces a readily ionizable moiety, which may allow the preparation of derivatives with greatly increased aqueous solubilities at slightly acidic pH values where the stability is sufficiently high. For example, morpholine derivatives possess good aqueous solubility[2].

Finally, *N*-Mannich bases also can be considered as prodrug candidates for primary and secondary amines. The pKa of amines decreases considerably by *N*-amidomethylation. [With benzamide, the decrease is ~3 pKa units (*cf.*, Table I)]. Therefore, a potentially useful purpose for transforming amino compounds into *N*-Mannich base transport forms would be to increase the lipophilicity of the masked amines at physiological pH by depressing the ionization of the conjugate acid forms.

[2] H. Bundgaard and M. Johansen, unpublished results.

REFERENCES

(1) A. A. Sinkula and S. H. Yalkowsky, *J. Pharm. Sci.*, **64**, 181 (1975).

(2) V. Stella, in "Pro-drugs as Novel Drug Delivery Systems," T. Higuchi and V. Stella, Eds., American Chemical Society, Washington, D.C., 1975, p. 1.

(3) H. Bundgaard, *Arch. Pharm. Chem.*, **86**, 1 (1979).

(4) H. Bundgaard, A. Bagger Hansen, and C. Larsen, *Arch. Pharm. Chem., Sci. Ed.*, **6**, 231 (1978).

(5) H. Bundgaard and C. Larsen, *ibid.*, **7**, 41 (1979).

(6) H. Bundgaard, A. Bagger Hansen, and C. Larsen, *Int. J. Pharm.*, in press.

(7) A. Einhorn, *Justus Liebigs Ann. Chem.*, **343**, 207 (1905).

(8) *Ibid.*, **361**, 113 (1908).

(9) H. Hellmann and G. Opitz, "α-Aminoalkylierung," Verlag Chemie, Weinheim, West Germany, 1960, and references cited therein.

(10) M. Tramontini, *Synthesis*, **1973**, 703, and references cited therein.

(11) B. Lucka-Sobstel and A. Zejc, *Diss. Pharm. Pharmacol.*, **22**, 13 (1970).

(12) M. B. Winstead, D. E. Barr, C. R. Hamel, D. J. Renn, H. I. Parker, and R. M. Neumann, *J. Med. Chem.*, **8**, 117 (1965).

(13) M. Eckstein, A. Zejc, and J. Sulko, *Diss. Pharm. Pharmacol.*, **18**, 131 (1966).

(14) G. M. Sieger, W. C. Barringer, and J. E. Krueger, *J. Med. Chem.*, **14**, 458 (1971).

(15) B. Lucka-Sobstel and A. Zejc, *Diss. Pharm. Pharmacol.*, **23**, 135 (1971).

(16) J. Lange, S. Rump, E. Galecka, I. Ilczuk, M. Lechowska-Postek, T. Rabsztyn, T. Szymanska, and K. Walczyna, *Pharmazie*, **32**, 82 (1977).

(17) B. Vej-Hansen and H. Bundgaard, *Arch. Pharm. Chem., Sci. Ed.*, **7**, 65 (1979).

(18) W. J. Gottstein, W. F. Minor, and L. C. Cheney, *J. Am. Chem. Soc.*, **81**, 1198 (1959).

(19) Y. Watase, Y. Terao, and M. Sekiya, *Chem. Pharm. Bull.*, **21**, 2775 (1973).

(20) E. Sawicki, T. R. Hauser, T. W. Stanley, and W. Elbert, *Anal. Chem.*, **33**, 93 (1961).

(21) M. Charton, *J. Org. Chem.*, **43**, 3995 (1978).

(22) R. G. Kallen and W. P. Jencks, *J. Biol. Chem.*, **241**, 5864 (1966).

(23) W. R. Abrams and R. G. Kallen, *J. Am. Chem. Soc.*, **98**, 7777 (1976).

(24) V. M. Belikov, Y. N. Belokon, M. M. Dolgaya, and N. S. Martinkova, *Tetrahedron*, **26**, 1199 (1970).

Tocainide Conjugation in Humans: Novel Biotransformation Pathway for a Primary Amine

A. T. ELVIN *x, J. B. KEENAGHAN, E. W. BYRNES, P. A. TENTHOREY, P. D. McMASTER, B. H. TAKMAN, D. LALKA *, C. V. MANION, D. T. BAER, E. M. WOLSHIN, M. B. MEYER, and R. A. RONFELD

Received April 5, 1979, from *Astra Pharmaceutical Products, Inc., Framingham, MA 01701.* Accepted for publication July 26, 1979.
*Present address: Department of Pharmaceutics, School of Pharmacy, State University of New York at Buffalo, Amherst, NY 14260.

Abstract □ The metabolism of tocainide, an experimental antiarrhythmic drug, was studied in humans. Urinary excretion of unchanged drug was 28–55% in 24 hr after oral dosing. Urine hydrolysis with hydrochloric acid or β-glucuronidase increased tocainide recovery to 55–79%. Saccharo-1,4-lactone inhibited the β-glucuronidase-mediated tocainide recovery increase. Adjustment of urine to pH 13 produced a compound identified as 3-(2,6-xylyl)-5-methylhydantoin. Evidence suggests that it was derived from the same metabolite that formed the additional tocainide after acid or β-glucuronidase treatment. Tocainide carbamoyl *O*-β-D-glucuronide is the structure proposed for the metabolite. The suggested pathway for its formation involves the addition of carbon dioxide to the amino nitrogen of tocainide followed by uridine diphosphate glucuronic acid conjugation.

Keyphrases □ Tocainide—human metabolism, conjugation □ Antiarrhythmic agents—tocainide, human metabolism, conjugation □ Metabolism—tocainide in humans, conjugation

Tocainide, 2-amino-2′,6′-propionoxylidide (I), an analog of lidocaine (II), is an experimental antiarrhythmic drug undergoing clinical evaluation (1–6). Several studies of tocainide pharmacokinetics have been reported (2, 7, 8). In a human pharmacokinetic study, 90–100% bioavailability and 40% excretion of unchanged drug in the urine were reported (7). A novel metabolic pathway for the conjugation of this primary amine is described in this report.

EXPERIMENTAL

Chemicals—Tocainide (I), 3′,4′,5′-trideuterotocainide, and 2-aminobutyro-2′,6′-xylidide (III) were prepared as the hydrochloride salts by standard methods[1] (9).

Synthesis of 3-(2,6-xylyl)-5-methylhydantoin (IV) was carried out using a modification of a literature method (10). DL-Alanine ethyl ester hydrochloride was treated with phosgene in toluene to produce ethyl α-isocyanatopropionate, which then was treated with 2,6-xylidine. Cyclization was accomplished by treating the intermediate with 5 *N* NaOH. The crude product was purified by high-pressure liquid chromatography (HPLC). Compound IV was obtained as colorless crystals, mp 138.5–140.5°; NMR[2] ($CDCl_3$): δ 1.47 (d, J = 6.5 Hz, CH_3), 2.19, 2.17 (2s, 2 CH_3), 4.16 (q, J = 6.5 Hz, CH), and 7.16 (broad s, 3 aromatic, NH); electron-impact mass spectrometry[3]: 218 (M^+), 203 ($M - CH_3$), 157, 148, 147 (base peak), 132, 119, 113 (hydantoin ring), 105 (2,6-dimethylphenyl), 91, 77, 70, and 44; IR[4] (KBr): λ_{max} 3235 (NH), 1775 (C=O), 1703 (C=O), 1407, 1324, 1178, and 771 (3 adjacent H's) cm^{-1}.

Heptafluorobutyrylimidazole[5], mollusk β-glucuronidase (lyophilized; <0.7% arylsulfatase), and saccharo-1,4-lactone[6] were obtained from commercial sources. All other reagents were spectral or HPLC grade.

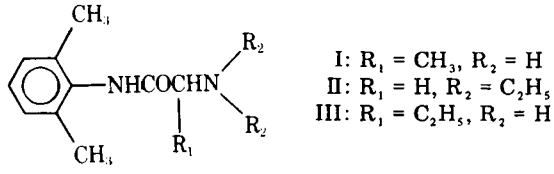

I: $R_1 = CH_3$, $R_2 = H$
II: $R_1 = H$, $R_2 = C_2H_5$
III: $R_1 = C_2H_5$, $R_2 = H$

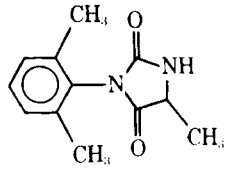

IV

Mass Spectrum[3]—GLC–mass spectrometry conditions were: glass column, 1.8 m × 2 mm i.d., 3% JXR on 100–120-mesh Gas Chrom Q[7]; carrier gas, helium at 30 ml/min; injector temperature, 250°; column temperature, programmed from 150 to 250° at 8°/min; separator temperature, 250°, transfer line temperature, 225°; ion source temperature 125°; vacuum, 5×10^{-6} torr; ionization energy, 70 ev; emission current, 0.3 mamp; and electron multiplier, 2.5 kv.

Determination of Tocainide in Biological Fluids—Samples were extracted using an aliquot of urine or plasma, 1 ml of the internal standard (III, 5 μg/ml), 1 ml of 1 *N* NaOH, distilled water to bring the solution to a total volume of 5 ml, and 5 ml of methylene chloride. The solution was mixed for 10 min and centrifuged at 2000 rpm, and the aqueous layer was discarded. The organic layer was transferred to a clean tube. Heptafluorobutyrylimidazole, 20 μl, was added for derivatization, and the sample was evaporated to dryness in a 45° water bath. The dry residue was washed with 2 ml of methylene chloride and 1 ml of 0.1 *N* NaOH. The aqueous layer was discarded, and the methylene chloride was evaporated. Ethyl acetate, 20 μl, was added, and 1 μl was injected into a gas–liquid chromatograph equipped with a flame-ionization detector[8].

An electron-capture detector[9] also was used, in which case ethyl acetate was substituted for the methylene chloride in the final wash without evaporation. Concentration was determined by measuring the peak height ratio of drug to internal standard and relating this ratio to a calibration curve (0.5–20 μg).

The monoheptafluorobutyryl derivative was stable for 24 hr. The GLC conditions were: glass column, 1.8 m × 2 mm i.d., 3% OV-17 on 80–100-mesh Gas Chrom Q[7] or 3% PC-3210 Ultraphase on 80–100-mesh Chromosorb WHP[5]; and carrier gas, helium at 30 ml/min. The injector, column, and detector temperatures were 250, 205, and 275°, respectively, for the OV-17 column and 220, 165, and 210° for the PC-3210 column.

In addition, tocainide and IV were assayed by HPLC. The liquid chromatograph consisted of a high-pressure pump[10], a valve and a 25-μl loop injector[11], a 30 × 0.39-cm octadecylsilane reversed-phase column[12], and a variable-wavelength detector[13] set at 205 nm. The mobile phase consisted of 25% acetonitrile in 0.05 *M* $NaClO_4$ at pH 4.0 with a 2-ml/min flow rate.

A single extraction was used as described except for the heptafluorobutyryl derivatization prior to evaporation. The dry sample was dis-

[1] E. W. Byrnes, P. D. McMaster, H. S. Feldman, G. H. Kronberg, B. H. Takman, and P. A. Tenthorey, to be published.
[2] NMR spectra were recorded on a Perkin-Elmer model R-20 with tetramethylsilane as the internal standard.
[3] Electron-impact mass spectra were obtained on a quadrupole Finnegan 1015-D.
[4] IR spectra were obtained on a Perkin-Elmer 25 grating IR spectrometer.
[5] Pierce Chemical Co., Rockford, Ill.
[6] Calbiochem, La Jolla, Calif.
[7] Applied Science Laboratories, State College, Pa.
[8] Varian 2700, Palo Alto, Calif.
[9] Varian 3700 with a ^{63}Ni-detector, Palo Alto, Calif.
[10] Model M6000A, Waters Associates, Milford, Mass.
[11] Model CV-6-μHPa-N60, Valco Valve, Houston, Tex.
[12] μBondapak C_{18}, Waters Associates, Milford, Mass.
[13] Model SF 770, Schoeffel, Westwood, N.J.

0022-3549/80/0100-0047$01.00/0
© 1980, American Pharmaceutical Association

Table I—Tocainide Recovery before and after Hydrolysis

Subject	Daily Tocainide Hydrochloride Dose, mg	Percent Tocainide Dose Excreted Unchanged	Released by Acid Hydrolysis	Released by β-Glucuronidase
PS[a]	3200	55	19	15
SK[a]	2400	48	31	30
MB[a]	2400	47	21	15
DL[b]	300	37	23	—
NL[a]	1800	28	30	27
WC[a]	2400	42	16	28

[a] Chronic administration, 24-hr urine collection. [b] Single dose, 24-hr urine collection.

solved in 200 μl of the mobile phase, and 25 μl was injected. Urine also was diluted 10-fold with distilled water and injected directly. Tocainide, III, and synthetic IV eluted at 4.3, 5.3, and 7.4 min, respectively.

Isolation of IV from Urine—A urine aliquot was adjusted to pH 9 with sodium hydroxide and extracted five times with equal volumes of methylene chloride to remove the tocainide. The pH was adjusted to 13 by the addition of sodium hydroxide, leading to the formation of IV. Hydrochloric acid was used to return the pH to 9, and the sample was extracted with methylene chloride. Preparative HPLC[14] was used to purify the crude IV. The other chromatographic conditions included a 1.0-ml injection loop[11], a 1.2-m × 0.95-cm porous silica column[15] (37–75-μm particles), and a 1% ethanol in chloroform mobile phase. The column was purged thoroughly with methanol each morning before use.

Drug Administration—Twenty-four-hour urine collections were obtained from five patients (two females and three males, ages 40–60) undergoing long-term treatment with tocainide hydrochloride. Individual oral doses ranged from 1.8 to 3.2 g/day in divided doses. A male volunteer received a single 300-mg oral dose of tocainide hydrochloride following an overnight fast. A second volunteer received a 300-mg dose as a 50:50 (w/w) mixture of tocainide and 3′,4′,5′-trideuterotocainide. Twenty-four-hour urine samples were collected from both volunteers.

Urine Hydrolysis—The acid hydrolysis involved mixing of 5.0 ml of urine with 5.0 ml of 4 *N* HCl, followed by incubation for 1 hr at 100°. An aliquot was taken for tocainide analysis by GLC and HPLC after cooling.

For the enzyme hydrolysis, a 1.0-ml urine aliquot adjusted to pH 4.0 with 0.5 *N* acetic acid was incubated with β-glucuronidase (pH 4, 25,000 Fishman units) in a water bath at 37°. After 12 hr, an additional 25,000 units of β-glucuronidase was added, and the incubation was continued for another 12 hr. Aliquots were assayed for tocainide as described. An identical set of samples was subjected to enzyme hydrolysis with 2 mg of saccharo-1,4-lactone, a specific inhibitor of β-glucuronidase, added with each addition of enzyme.

RESULTS AND DISCUSSION

Either acid hydrolysis or treatment with β-glucuronidase increased the tocainide amount recovered from the urine (Table I). Based on the five patients who received multiple tocainide doses, 44% of the oral dose was excreted as free tocainide. An acid or β-glucuronidase hydrolyzable metabolite accounted for an additional 23% of the dose. The excretion

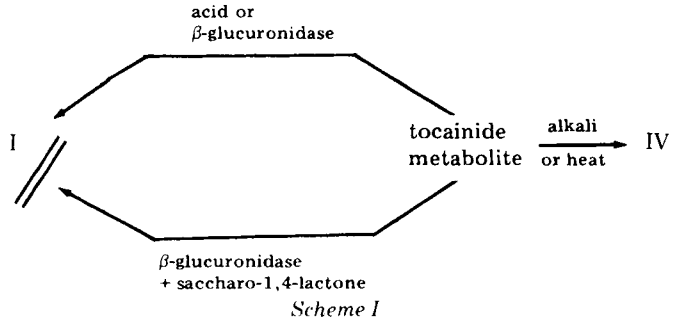

Scheme I

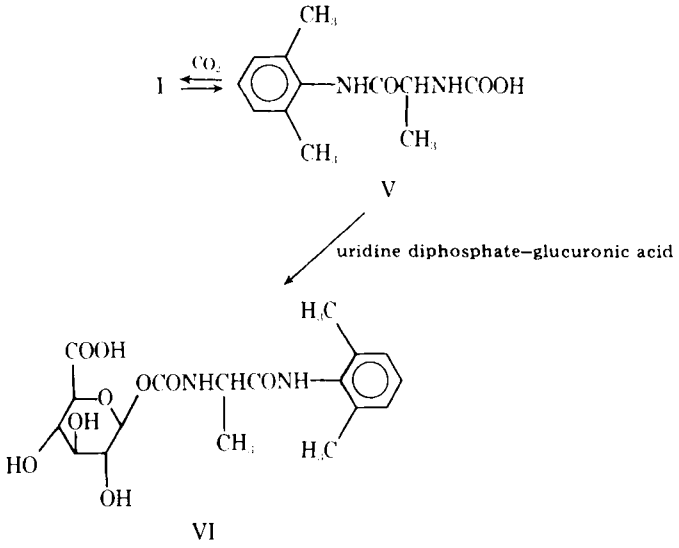

Scheme II—Metabolic pathway for tocainide uridine diphosphate–glucuronic acid conjugation.

pattern for the volunteer (Subject DL) who received a single dose was similar.

The basis for elucidating the metabolite structure is described in Scheme I. There was essentially complete recovery of the free tocainide with the five methylene chloride extractions at pH 9.0. These methylene chloride extracts did not contain IV. The remaining aqueous phase was adjusted to pH 13 and then readjusted to pH 9 prior to a methylene chloride extraction. This methylene chloride extract contained a significant amount of IV but not tocainide. Typically, the urine tocainide concentrations ranged from 200 to 600 μg/ml, and the IV concentrations were approximately half of that. These concentrations indicated that IV was formed at pH 13, that it could be extracted at pH 9, and that it was not derived directly from tocainide.

Direct injection of urine onto the HPLC column confirmed the absence of IV in the untreated urine. However, direct injection of urine, from which free tocainide had been removed, onto the GLC column resulted in a peak for IV, demonstrating its thermal formation. After acid hydrolysis or β-glucuronidase treatment of the urine, it was not possible to generate IV at pH 13. Furthermore, after extraction of IV from the alkaline urine, acid hydrolysis of the remaining urine did not yield additional tocainide.

The synthetic IV and the IV isolated from urine had identical retention times upon GLC analysis. Further confirmation of identity was obtained by IR, NMR, mass spectral, mixed melting-point, and elemental analyses. The mass spectrum of IV for the subject who had ingested tocainide with 3′,4′,5′-trideuterotocainide exhibited doublets with each ring fragment, confirming that IV arose from ingested tocainide.

The formation of tocainide upon acid- or β-glucuronidase-catalyzed hydrolysis suggested that the metabolite was a glucuronide conjugate of tocainide or of a labile compound that easily formed tocainide. The presence of a glucuronide conjugate was confirmed when simultaneous treatment with saccharo-1,4-lactone prevented enzyme-catalyzed tocainide release. For example, the tocainide concentrations in untreated urine, β-glucuronidase-treated urine, and urine treated with β-glucuronidase and saccharo-1,4-lactone were 199, 395, and 209 μg/ml, respectively. This specific inhibitor of β-glucuronidase was used since commercial β-glucuronidase preparations often contain other hydrolytic enzymes. Also, preliminary electrophoretic studies[16] indicated that the metabolite was negatively charged at pH 4.6 and neutral at pH 2.2. The metabolite on the electrophoretogram was identified by treatment with alkali, resulting in IV, and by acid hydrolysis, resulting in tocainide.

The simplest interpretation of these data was to hypothesize an *N*-glucuronide of tocainide for the metabolite structure. However, the formation of IV from the metabolite under strongly basic conditions or upon thermal decomposition could not be reconciled with the *N*-glucuronide structure.

An extra carbonyl group clearly was present in IV that was not present in tocainide. Compound IV definitely was a product of the metabolite

[14] Model ALC 202/401, Waters Associates, Milford, Mass.
[15] Porasil B, Waters Associates, Milford, Mass.
[16] Electrophoretic studies were conducted as described previously (11) using a HV-5000A power supply and FP-30S flat plate (Savant Instruments, Hicksville, N.Y.).

since tocainide did not produce IV when treated with alkali or heat. The explanation is that a carbonyl group is present in the metabolite between the amino nitrogen and the glucuronide moiety.

A proposed reaction for metabolite formation *in vivo* is presented in Scheme II. Based on the proposed metabolite structure, the data can be explained easily. Acid or enzyme hydrolysis initially would yield the carbamic acid (V), which would then easily generate tocainide. A carbamic acid is in a constant and rapid equilibrium with an amine. A change in the pH or the carbon dioxide–bicarbonate concentration can easily shift the equilibrium. Conjugation of V with glucuronic acid produces the proposed metabolite (VI), tocainide carbamoyl *O*-β-D-glucuronide. This structure also provides a reasonable explanation for the facile conversion to IV by attack of the amide nitrogen on the carbonyl carbon with displacement of the glucuronide moiety as a leaving group. The uncharged species at pH 2.2 found in the electrophoretic studies also can be explained since the inclusion of the carbonyl group would result in a loss of basicity of the nitrogen atom.

The reaction of tocainide with carbon dioxide has ample precedent in the transport mechanism for carbon dioxide by hemoglobin; hemoglobin carbamic acid accounts for ~12% of the carbon dioxide transported by the blood of resting humans (12). Glycine and glycylglycine with pKa values of ~8.0 often have been used as models for the reaction of hemoglobin with carbon dioxide (12); tocainide has a pKa of 7.8. Among other factors, the degree to which any amine combines with carbon dioxide will depend on its pKa, the pH, and the carbon dioxide concentration (12).

In summary, a pathway for the conjugation of an amine has been proposed. It was fortunate that tocainide carbamoyl *O*-β-D-glucuronide yielded a characteristic degradation product (IV). Whether this pathway applies to amines other than tocainide can be resolved only by further research.

REFERENCES

(1) D. J. Coltart, T. B. Berndt, R. Kernoff, and D. C. Harrison, *Am. J. Cardiol.*, **34**, 35 (1974).

(2) D. G. McDevitt, G. R. Wilkinson, R. F. Smith, R. L. Woosley, and J. A. Oates, *Clin. Pharmacol. Ther.*, **19**, 396 (1976).

(3) R. A. Winkle, P. J. Meffin, J. W. Fitzgerald, and D. C. Harrison, *Circulation*, **54**, 884 (1976).

(4) R. L. Woosley, D. G. McDevitt, A. S. Nies, R. F. Smith, G. R. Wilkinson, and J. A. Oates, *ibid.*, **56**, 980 (1977).

(5) R. A. Winkle, J. L. Anderson, F. Peters, P. J. Meffin, R. E. Fowles, and D. C. Harrison, *ibid.*, **57**, 787 (1978).

(6) R. A. Winkle, P. J. Meffin, and D. C. Harrison, *ibid.*, **57**, 1008 (1978).

(7) D. Lalka, M. B. Meyer, B. R. Duce, and A. T. Elvin, *Clin. Pharmacol. Ther.*, **19**, 757 (1976).

(8) A. Berlin-Wahlen, J. C. Barkus, J. B. Keenaghan, M. Lebeaux, and P. A. Tenthorey, *Acta Pharm. Suec.*, **14**, 417 (1977).

(9) N. Lofgren, "Studies on Local Anesthetics—Xylocaine," Ivar Haeggstroms, Stockholm, Sweden, 1948, p. 25.

(10) J. G. Lombardino and C. F. Gerber, *J. Med. Chem.*, **7**, 97 (1964).

(11) D. Lalka and N. Back, *Biochim. Biophys. Acta*, **236**, 47 (1971).

(12) J. V. Kilmartin and L. Rossi-Bernardi, *Physiol. Rev.*, **53**, 836 (1973).

ACKNOWLEDGMENTS

Presented in part at the American Society for Pharmacology and Experimental Therapeutics [*Pharmacologist*, **18**, 114 (1976)].

The authors thank Ms. L. Trahan for manuscript preparation.

Secondary Products of Itanoxone

JEAN-PIERRE RIEU *, GILBERT MOUZIN *, HENRI COUSSE *x, and ANDRÉ BOUCHERLE ‡

Received February 26, 1979, from the **P. Fabre S.A. Research Center, 17 avenue Jean Moulin, 81106 Castres, France*, and the ‡*U.E.R. of Pharmaceutical and Biological Sciences, 38240 Meylan, France.* Accepted for publication August 7, 1979.

Abstract □ Itanoxone synthesis by Friedel–Crafts reaction between itaconic anhydride and 2-chlorobiphenyl was studied. Five isomers corresponding to possible impurities were prepared and studied to perfect a reliable and practical method to detect these impurities in itanoxone.

Keyphrases □ Itanoxone—synthesis, synthesis and detection of impurities □ Hypolipidemic agents—itanoxone, synthesis, synthesis and detection of impurities □ Hypouricemic agents—itanoxone, synthesis, synthesis and detection of impurities

The Friedel–Crafts reaction between itaconic anhydride and an aromatic derivative was reported (1–3). This reaction was adapted to many aromatic substrates and led to the synthesis of a chemical series with interesting pharmacological properties (4, 5). Pharmacological and toxicological studies yielded a new compound, 4-[4′-(2-chlorophenyl)phenyl]-4-oxo-2-methylenebutanoic acid (F 1379) (I), whose International General Designation is itanoxone. Compound I is a powerful hypolipidemic and hypouricemic agent (6–8).

The impurities that might be found in I were defined, isolated, or synthesized. With both chemical and physicochemical data of secondary products and samples, a detection method for these impurities in the end-product was investigated.

BACKGROUND

The Friedel–Crafts reaction between itaconic anhydride and 2-chlorobiphenyl gave I as the main product as reported previously (4, 5) (Scheme I).

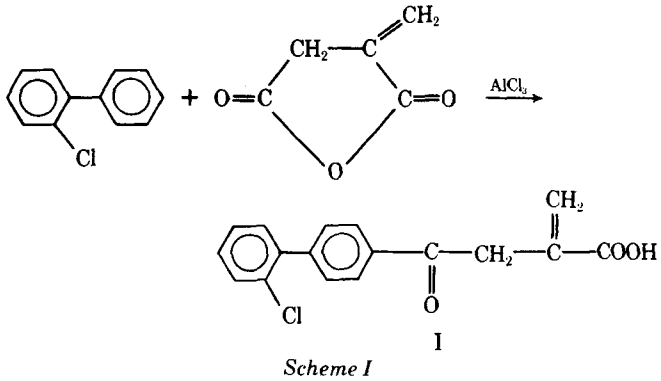

I

Scheme I

0022-3549/80/0100-0049$01.00/0

© 1980, American Pharmaceutical Association

since tocainide did not produce IV when treated with alkali or heat. The explanation is that a carbonyl group is present in the metabolite between the amino nitrogen and the glucuronide moiety.

A proposed reaction for metabolite formation *in vivo* is presented in Scheme II. Based on the proposed metabolite structure, the data can be explained easily. Acid or enzyme hydrolysis initially would yield the carbamic acid (V), which would then easily generate tocainide. A carbamic acid is in a constant and rapid equilibrium with an amine. A change in the pH or the carbon dioxide–bicarbonate concentration can easily shift the equilibrium. Conjugation of V with glucuronic acid produces the proposed metabolite (VI), tocainide carbamoyl *O*-β-D-glucuronide. This structure also provides a reasonable explanation for the facile conversion to IV by attack of the amide nitrogen on the carbonyl carbon with displacement of the glucuronide moiety as a leaving group. The uncharged species at pH 2.2 found in the electrophoretic studies also can be explained since the inclusion of the carbonyl group would result in a loss of basicity of the nitrogen atom.

The reaction of tocainide with carbon dioxide has ample precedent in the transport mechanism for carbon dioxide by hemoglobin; hemoglobin carbamic acid accounts for ~12% of the carbon dioxide transported by the blood of resting humans (12). Glycine and glycylglycine with pKa values of ~8.0 often have been used as models for the reaction of hemoglobin with carbon dioxide (12); tocainide has a pKa of 7.8. Among other factors, the degree to which any amine combines with carbon dioxide will depend on its pKa, the pH, and the carbon dioxide concentration (12).

In summary, a pathway for the conjugation of an amine has been proposed. It was fortunate that tocainide carbamoyl *O*-β-D-glucuronide yielded a characteristic degradation product (IV). Whether this pathway applies to amines other than tocainide can be resolved only by further research.

REFERENCES

(1) D. J. Coltart, T. B. Berndt, R. Kernoff, and D. C. Harrison, *Am. J. Cardiol.*, **34**, 35 (1974).

(2) D. G. McDevitt, G. R. Wilkinson, R. F. Smith, R. L. Woosley, and J. A. Oates, *Clin. Pharmacol. Ther.*, **19**, 396 (1976).

(3) R. A. Winkle, P. J. Meffin, J. W. Fitzgerald, and D. C. Harrison, *Circulation*, **54**, 884 (1976).

(4) R. L. Woosley, D. G. McDevitt, A. S. Nies, R. F. Smith, G. R. Wilkinson, and J. A. Oates, *ibid.*, **56**, 980 (1977).

(5) R. A. Winkle, J. L. Anderson, F. Peters, P. J. Meffin, R. E. Fowles, and D. C. Harrison, *ibid.*, **57**, 787 (1978).

(6) R. A. Winkle, P. J. Meffin, and D. C. Harrison, *ibid.*, **57**, 1008 (1978).

(7) D. Lalka, M. B. Meyer, B. R. Duce, and A. T. Elvin, *Clin. Pharmacol. Ther.*, **19**, 757 (1976).

(8) A. Berlin-Wahlen, J. C. Barkus, J. B. Keenaghan, M. Lebeaux, and P. A. Tenthorey, *Acta Pharm. Suec.*, **14**, 417 (1977).

(9) N. Lofgren, "Studies on Local Anesthetics—Xylocaine," Ivar Haeggstroms, Stockholm, Sweden, 1948, p. 25.

(10) J. G. Lombardino and C. F. Gerber, *J. Med. Chem.*, **7**, 97 (1964).

(11) D. Lalka and N. Back, *Biochim. Biophys. Acta*, **236**, 47 (1971).

(12) J. V. Kilmartin and L. Rossi-Bernardi, *Physiol. Rev.*, **53**, 836 (1973).

ACKNOWLEDGMENTS

Presented in part at the American Society for Pharmacology and Experimental Therapeutics [*Pharmacologist*, **18**, 114 (1976)].

The authors thank Ms. L. Trahan for manuscript preparation.

Secondary Products of Itanoxone

JEAN-PIERRE RIEU *, GILBERT MOUZIN *, HENRI COUSSE *x, and ANDRÉ BOUCHERLE ‡

Received February 26, 1979, from the **P. Fabre S.A. Research Center, 17 avenue Jean Moulin, 81106 Castres, France*, and the ‡*U.E.R. of Pharmaceutical and Biological Sciences, 38240 Meylan, France.* Accepted for publication August 7, 1979.

Abstract □ Itanoxone synthesis by Friedel–Crafts reaction between itaconic anhydride and 2-chlorobiphenyl was studied. Five isomers corresponding to possible impurities were prepared and studied to perfect a reliable and practical method to detect these impurities in itanoxone.

Keyphrases □ Itanoxone—synthesis, synthesis and detection of impurities □ Hypolipidemic agents—itanoxone, synthesis, synthesis and detection of impurities □ Hypouricemic agents—itanoxone, synthesis, synthesis and detection of impurities

The Friedel–Crafts reaction between itaconic anhydride and an aromatic derivative was reported (1–3). This reaction was adapted to many aromatic substrates and led to the synthesis of a chemical series with interesting pharmacological properties (4, 5). Pharmacological and toxicological studies yielded a new compound, 4-[4′-(2-chlorophenyl)phenyl]-4-oxo-2-methylenebutanoic acid (F 1379) (I), whose International General Designation is itanoxone. Compound I is a powerful hypolipidemic and hypouricemic agent (6–8).

The impurities that might be found in I were defined, isolated, or synthesized. With both chemical and physicochemical data of secondary products and samples, a detection method for these impurities in the end-product was investigated.

BACKGROUND

The Friedel–Crafts reaction between itaconic anhydride and 2-chlorobiphenyl gave I as the main product as reported previously (4, 5) (Scheme I).

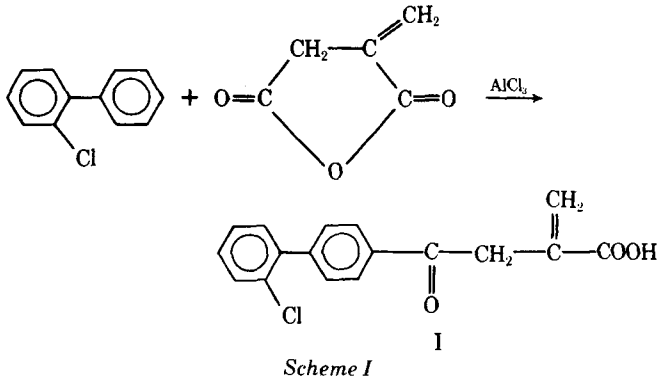

I

Scheme I

0022-3549/80/0100-0049$01.00/0

© 1980, American Pharmaceutical Association

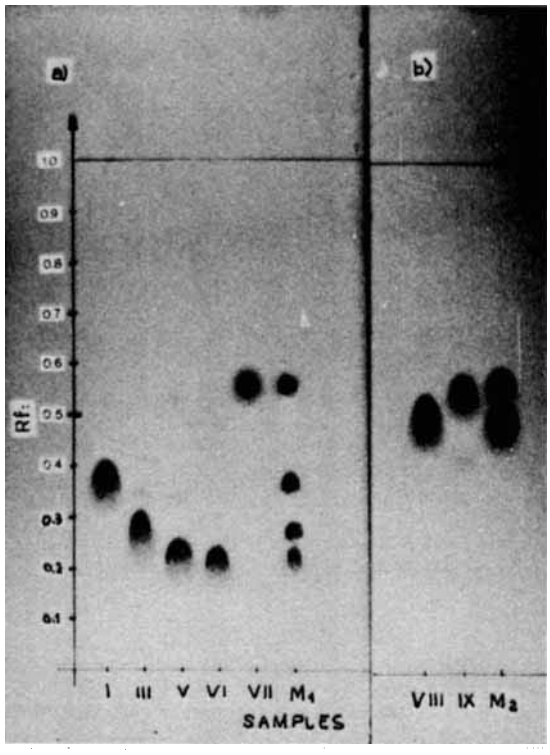

Figure 1—*Comparative thin-layer chromatograms of I, its isomers (III, V, VI, and VII), and M_1 (a mixture of I and its isomers) (a), and VIII and IX (hydrogenation products from III and I, respectively), and M_2 (a mixture of VIII and IX) (b).*

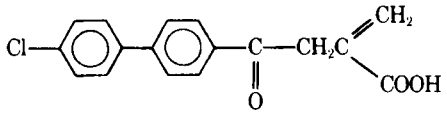

II

Impurities may be due to the raw material, unspecific reaction, or I degradation. The raw material, 2-chlorobiphenyl, may contain 4-chlorobiphenyl as an impurity. 2-Chlorobiphenyl, synthesized from 2-chloroaniline by a Gomberg–Bachmann–Hey reaction, must be analyzed for the 4-chlorobiphenyl impurity before itanoxone synthesis. After the Friedel–Crafts reaction with itaconic anhydride, 4-chlorobiphenyl gave another itanoxone isomer [4-[4′-(4-chlorophenyl)phenyl]-4-oxo-2-methylenebutanoic acid, II].

Secondary products are formed in the reaction since itaconic anhydride is asymmetric. Although the acylation is selective (1–3), it could give equally another derivative [4-[4′-(2-chlorophenyl)phenyl]-4-oxo-3-methylenebutanoic acid, III].

Furthermore, chlorobiphenyl acylation takes place preferentially in the *para*-position of the nonchlorinated ring, but the formation of IV is conceivable. This derivative has not been observed and was not prepared as a reference sample.

Degradation products also may be present as impurities. In I and III, the double bond can shift, as was found (1–3) with similar compounds. Shifting the double bond of I to an adjacent carbon gave a more highly conjugated isomer [4-[4′-(2-chlorophenyl)phenyl]-4-oxo-2-methyl-2-butenoic acid, V].

Compound V exists as two geometrical isomers, *Z* and *E*. Theoretically, the *Z* form is more stable in the cyclized form [5-[4′-(2-chlorophenyl)-phenyl]-5-hydroxy-3-methyl-2,5-dihydrofuran-2-one, VI] (1–3, 9, 10). Since VI is a lactone, V can be regarded as the *E*-isomer. Compound VI

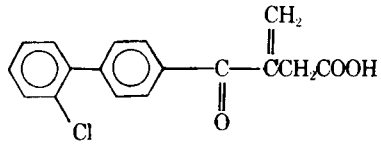

III

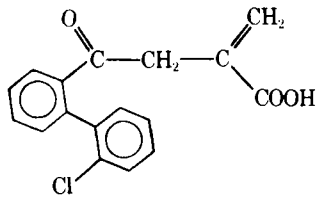

IV

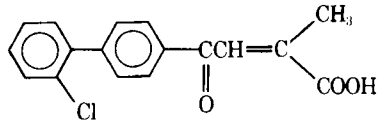

V

was prepared by sunlight isomerization of V (1–3, 10). Analogous reasoning applied to III led to the postulation of a derivative 5-[4′-(2-chlorophenyl)phenyl]-5-hydroxy-4-methyl-2,5-dihydrofuran-2-one (VII).

Compounds V and VII also may be obtained by Friedel–Crafts reaction of 2-chlorobiphenyl with citraconic anhydride, as reported for similar products (1–3, 10–12). This anhydride may be an impurity of itaconic anhydride, but not when the latter compound is crystallized. The isomerization of III or VII to the open *E* form is more difficult, as was shown (1, 11, 13) with similar compounds, and was not investigated. These derivatives are isomers with the formula $C_{17}H_{13}ClO_3$; their presence in I was not revealed by elemental analysis. These compounds, except IV, were synthesized.

EXPERIMENTAL

General Methods—NMR spectra were recorded on a 60-MHz apparatus[1] with tetramethylsilane as an internal reference; the chemical shifts were expressed in δ relative to tetramethylsilane. IR[2] and UV[3] spectra were obtained in a double-beam spectrometer. Melting points were taken on a hot stage[4] and were not corrected. TLC utilized precoated silica gel plates[5] with chloroform–methanol (85:15); after development to 12–15 cm, the plate was exposed to 254-nm UV radiation or iodine vapor for visualization (Figs. 1*a* and 1*b*).

Synthesis of I—A solution of 47.3 g (0.25 mole) of 2-chlorobiphenyl and 28 g (0.25 mole) of itaconic anhydride (rhombic bipyramidal prisms, mp 68–69°) in 120 ml of methylene chloride was preheated to 30° and placed in a 500-ml round-bottom flask. The flask was fitted with a mechanical stirrer, a thermometer, a dropping funnel, and a reflux condenser connected to a hydrochloric acid absorber. Freshly ground anhydrous aluminum chloride (74 g, 0.55 mole) was added in portions. After boiling

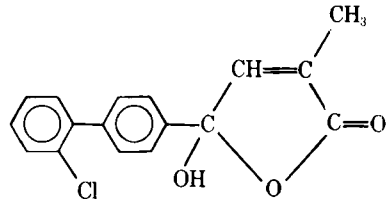

VI

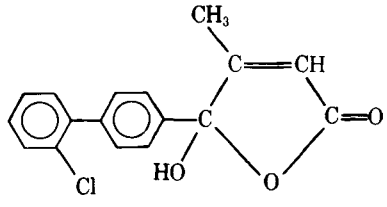

VII

[1] Model R-24B, Hitachi Perkin-Elmer, Hitachi Ltd., Tokyo, Japan.
[2] Model DK-2A, Beckman Instruments, GMBH, München 45, West Germany.
[3] Model 177, Perkin-Elmer Ltd., Beaconsfield, Buckinghamshire, England.
[4] Kofler stage, C. Reichert AG, Wein XVII, Austria.
[5] Silica gel 60 F 254 precoated plates, E. Merck, Darmstadt, West Germany.

under reflux for 3 hr, 350 ml of concentrated hydrochloric acid mixed with 200 g of crushed ice was added to the mixture.

The organic phase was separated and washed with water until the wash water was neutral. It then was poured into a mixture of 200 ml of acetone and 100 ml of 95% ethanol, which gave a first crop of crystals. These crystals were filtered off and rinsed with acetone (yield of 43.7 g). The mother liquor was evaporated to dryness, giving an oil (27 g) containing some crystals. This oil was taken up in 100 ml of 95% ethanol, and a second crop of crystals precipitated. These crystals were filtered off and washed with acetone (yield of 4.7 g). The solution (A) was retained.

The crystals were combined and purified by recrystallization from dioxane to give 46.5 g (62% yield) of I as small colorless needles, mp 212–214°; IR (potassium bromide): 1690 (COOH), 1675 (C=O), and 1610 (C=C aromatic) cm^{-1}; UV (95% ethanol): λ_{max} 267 (log ϵ 4.24) nm; NMR (dimethyl sulfoxide-d_6): δ 4.1 (s, 2H, $COCH_2$), 5.85 (d, 1H, J = 1.2 Hz, *trans*-HC=CCOOH), 6.3 (d, 1H, J = 1.2 Hz, *cis*-HC=CCOOH), 7.3–7.9 (m, 7H, COOH and aromatic protons), and 8.1 (d, 2H, J = 8 Hz, aromatic protons *ortho* to C=O) ppm; TLC: R_f 0.41.

Anal.—Calc. for $C_{17}H_{13}ClO_3$: C, 67.89; H, 4.35; Cl, 11.78. Found: C, 67.52; H, 4.30; Cl, 11.76.

Isolation of III—Solution A was evaporated to dryness under reduced pressure, and the residue was taken up in 250 ml of ether. The ethereal solution was washed with water and then dried over anhydrous sodium sulfate. On evaporation, it gave a yellow-orange oil (22 g) containing some crystals. This oil was extracted continuously for 8 hr with petroleum ether in a soxhlet apparatus. The resulting solution contained only unreacted 2-chlorobiphenyl and a small quantity of I.

The insoluble matter was purified by recrystallization from boiling isopropyl ether and gave 1.58 g (2.1% yield) of III as colorless crystals, mp 120°; IR (potassium bromide): 1705 (COOH), 1650 (C=O), and 1630 and 1605 (C=C) cm^{-1}; UV (95% ethanol): λ_{max} 269 (log ϵ 4.15) nm; NMR (chloroform-d and dimethyl sulfoxide-d_6): δ 3.5 (s, 2H, CH_2COOH), 5.75 (d, 1H, J = 0.6 Hz, *trans*-HC=CC=O), 6 (d, 1H, J = 0.6 Hz, *cis*-HC=CC=O), 7.2–7.7 (m, 6H, aromatic protons), 7.9 (d, 2H, J = 10 Hz, aromatic protons *ortho* to carbonyl), and 9.6 (s, 1H, COOH) ppm; TLC: R_f 0.32.

Anal.—Calc. for $C_{17}H_{13}ClO_3$: C, 67.89; H, 4.35; Cl, 11.78. Found: C, 68.02; H, 4.18; Cl, 11.74.

Determination of Structure of III—Compound III was hydrogenated to give a derivative [4-[4′-(2-chlorophenyl)phenyl]-4-oxo-3-methylbutanoic acid, VIII], which also could be obtained unequivocally by the action of citraconic anhydride on 2-chlorobiphenyl followed by reduction by a literature method (12).

Hydrogenation of III—A solution of 300.7 mg (10 mmoles) of III in 5 ml of ethanol was hydrogenated under normal pressure in the presence of 30 mg of 10% palladium-on-charcoal. After the catalyst was removed, the solvent was evaporated under reduced pressure, and the residue was recrystallized from boiling benzene–cyclohexane (2:1) to give 172 mg (58% yield) of colorless crystals, mp 139°; IR (potassium bromide): 1705 (COOH), 1680 (C=O), and 1605 (C=C aromatic) cm^{-1}; UV (95% ethanol): λ_{max} 266 (log ϵ 4.23) nm; NMR (dimethyl sulfoxide-d_6): δ 1.25 (d, 3H, J_{ad} = 7 Hz, $CHCH_{a3}$), 2.4 (q, 1H, J_{bd} = 6 Hz, J_{bc} = 16.5 Hz, CH_bCOOH), 2.9 (q, 1H, J_{cd} = 8 Hz, J_{cb} = 16.5 Hz, CH_cCOOH), 3.95 (m, 1H, CH_dCH_3), 7.2–7.7 (m, 6H, aromatic), 8 (d, 2H, J = 10 Hz, aromatic protons *ortho* to C=O), and 8.6 (s, 1H, COOH) ppm; TLC: R_f 0.46.

Anal.—Calc. for $C_{17}H_{15}ClO_3$: C, 67.44; H, 4.99; Cl, 11.71. Found: C, 67.64; H, 5.27; Cl, 11.61.

Preparation of VII—A suspension of 30 g (0.23 mole) of freshly ground anhydrous aluminum chloride in 80 ml of anhydrous carbon disulfide was treated dropwise with 11.2 g (0.1 mole) of citraconic anhydride. The solution was stirred for 30 min, and a solution of 18.8 g (0.1 mole) of 2-chlorobiphenyl in 30 ml of anhydrous carbon disulfide was added over 40 min. When the addition was complete, the mixture was refluxed for 2 hr.

The usual workup with hydrochloric acid and crushed ice gave 28 g of yellow-green crystals. When these crystals were recrystallized in boiling isopropyl ether, 15.5 g (52% yield) of VII was obtained as colorless crystals, mp 146°; IR (potassium bromide): 3280 (OH), 1740 (C=O lactone), and 1640 (C=C) cm^{-1}; UV (95% ethanol): λ_{max} 248 (log ϵ 4.16) nm: NMR (chloroform-d, dimethyl sulfoxide-d_6): δ 1.9 (s, 3H, CH_3), 5.7 (s, 1H, CH=CCH_3), and 7.8 (m, 9H, aromatic protons and OH) ppm; TLC: R_f 0.55.

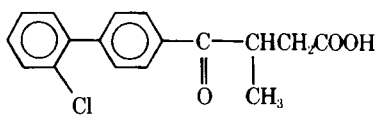

VIII

Anal.—Calc. for $C_{17}H_{13}ClO_3$: C, 67.89; H, 4.35; Cl, 11.78. Found: C, 67.41; H, 4.17; Cl, 11.81.

Hydrogenation of VII to VIII—An intimate mixture of 4.5 g (0.015 mole) of VII in 10 ml of acetic acid and 25 ml of water was refluxed in the presence of 3 g of zinc powder in a 100-ml round-bottom flask. After 1 hr, the mixture was filtered while still boiling. The insoluble matter was extracted several times with ethyl acetate, which also was used to extract the filtrate.

The combined organic extracts were washed with 50 ml of 5 N HCl and with water and then were dried over anhydrous sodium sulfate and evaporated. The residue was purified with boiling benzene–cyclohexane (2:1) and gave 2 g (45% yield) of VIII as colorless flakes, mp 139° (not depressed by mixing with the sample prepared by hydrogenation of III); IR (potassium bromide): 1705, 1680, and 1605 cm^{-1}; UV (95% ethanol): λ_{max} 266 (log ϵ 4.24) nm; NMR (dimethyl sulfoxide-d_6): δ 1.25, 2.4, 2.9, 3.95, 7.2–7.7, and 8 ppm; TLC: R_f 0.46.

Anal.—Calc. for $C_{17}H_{15}ClO_3$: C, 67.44; H, 4.99; Cl, 11.71. Found: C, 67.69; H, 5.09; Cl, 11.69.

Isomerization of I to V—Compound I was isomerized to V by the procedure of Lutz *et al.* (1) as adapted by Bailey and Dien (13) and Fateen *et al.* (3). Pure triethylamine (12.5 ml) was added to 5 g (16.6 mmoles) of I, suspended in 25 ml of water. The yellow solution that formed was stirred for 12 hr at room temperature. After a small quantity of insoluble matter was removed, the filtrate was diluted with 50 g of crushed ice and was acidified with 6 N HCl to pH 2–3. The yellow crystals were collected on a fritted filter, dried, and rinsed with distilled water until the wash water was neutral.

After drying, the crystals were recrystallized from 15 volumes of boiling isopropyl alcohol to give 3.5 g (70% yield) of V as yellow needles, mp 196°; IR (potassium bromide): 1690 (COOH), 1665 (C=O), 1630 and 1610 (C=C), and 975 (*trans*-CH_3C=C–H) cm^{-1}; UV (95% ethanol): λ_{max} 287 (log ϵ 4.25) nm; NMR (dimethyl sulfoxide-d_6): δ 2.15 (d, 3H, J = 1.4 Hz, CH_3) and 7.2–8.2 (m, 10H, other protons) ppm; TLC: R_f 0.28.

Anal.—Calc. for $C_{17}H_{13}ClO_3$: C, 67.89; H, 4.35; Cl, 11.78. Found: C, 68.06; H, 4.52; Cl, 11.59.

Isomerization of V to VI—Compound VI was obtained by sunlight isomerization of V according to the procedure of Lutz *et al.* (1) as adapted by Bowden and Henry (10). Compound V (15 g, 50 mmoles) was dissolved in methanol–dioxane, and the solution was exposed to sunlight for 12 hr. After the solvents were evaporated, the residue was purified by extraction with anhydrous ether. Petroleum ether was added, and 12 g (80% yield) of VI as colorless crystals precipitated, mp 130°; IR (potassium bromide): 3400 (OH), 1730 (C=O lactone), and 1610 (C=C) cm^{-1}; UV (95% ethanol): λ_{max} 249 (log ϵ 4.12) nm; NMR (dimethyl sulfoxide-d_6): δ 2.0 (d, 3H, J = 1 Hz, CH_3), 7 (d, 1H, J = 1 Hz, =C–H), and 7.15–7.8 (m, 9H, aromatic protons and COOH) ppm; TLC: Rf 0.26.

Anal.—Calc. for $C_{17}H_{13}ClO_3$: C, 67.89; H, 4.35; Cl, 11.78. Found: C, 67.64; H, 4.92; Cl, 11.62.

Synthesis of II—A solution of 20.6 g (0.1093 mole) of 4-chlorobiphenyl and 12.26 g (0.1093 mole) of itaconic anhydride in 70 ml of anhydrous methylene chloride was added with vigorous stirring to a suspension of 32.4 g (0.24 mole) of ground anhydrous aluminum chloride in 70 ml of anhydrous methylene chloride. After 2 hr at room temperature, the reaction mixture was refluxed for 3 hr and then left overnight at room temperature. The mixture was hydrolyzed in the usual manner. The organic phase was separated and rinsed several times by shaking with water. The solvent was removed under vacuum without heating.

The crystals obtained were rinsed with water until the wash water was neutral and were allowed to dry in the air. They finally were recrystallized from 11 volumes of boiling ethyl acetate to give 17 g (52% yield) of II as pale-beige powdery crystals, mp 192°; IR (potassium bromide): 1700 (COOH), 1675 (C=O), and 1630 and 1610 (C=C) cm^{-1}; UV (95% ethanol): λ_{max} 285 (log ϵ 4.47) nm; NMR (dimethyl sulfoxide-d_6): δ 4.05 (s, 2H, $COCH_2$), 5.75 (s, 1H, *trans*-HC=CCOOH), 6.3 (s, 1H, *cis*-HC=CCOOH), and 7.3–8.3 (m, 9H, other protons) ppm; TLC: R_f 0.38.

Anal.—Calc. for $C_{17}H_{13}ClO_3$: C, 67.89; H, 4.35; Cl, 11.78. Found: C, 67.12; H, 4.55; Cl, 11.49.

Hydrogenation of I to 4-[4′-(2-Chlorophenyl)phenyl]-4-oxo-2-methylbutanoic Acid (IX)—A semisolution of 54 g (0.179 mole) of I in 1080 ml of dioxane containing 36 ml of acetic acid was treated with 2.7 g of 10% palladium-on-charcoal in a 3-liter erlenmeyer flask connected to a hydrogen gas holder. After the apparatus was purged with nitrogen and hydrogen, the stirrer was started and hydrogenation began after induction for 40 min. The theoretical quantity of hydrogen was absorbed in 6 hr. The gas holder was disconnected, the catalyst was removed by

filtration through kieselguhr, and the filtrate was evaporated to dryness and gave beige crystals.

The solid was recrystallized from boiling alcohol, and 34.2 g (63% yield) of IX was produced as brilliant-beige needles on cooling, mp 172°. When IX was mixed with VIII, the melting point was depressed to 128–131°, and TLC gave a spot with two parts (Fig. 1*b*); IR (potassium bromide): 1700 (COOH), 1680 (C=O), and 1610 (aromatic C=C) cm^{-1}; UV (95% ethanol): λ_{max} 262.5 (log ϵ 4.21) nm; NMR (dimethyl sulfoxide-d_6): δ 1.25 (d, 3H, J = 7 Hz, $-CH_3$), 2.7–3.8 (m, 3H, $-COCH_2CHCOOH$), 7.2–7.8 (m, 7H, aromatic protons and COOH), and 8 (d, 2H, J = 8 Hz, aromatic protons *ortho* to the carbonyl) ppm; TLC: R_f 0.50.

Anal.—Calc. for $C_{17}H_{15}ClO_3$: C, 67.44; H, 4.99; Cl, 11.71. Found: C, 67.41; H, 5.10; Cl, 11.49.

DISCUSSION

Structure of III—The results of the experimental analysis confirmed the structure of III. The IR spectrum of III compared to that of I showed a shift of the acidic carboxyl band toward the shortwave region, which indicates that the carboxyl group was attached to an sp^3 carbon. Moreover, the shift of the ketonic carbonyl band toward the longwave region suggested that this function was adjacent to a double bond. Furthermore, the UV spectrum showed the presence of an absorption maximum at 269 nm (which excluded the existence of conjugation between the carbonyl and the carboxyl groups as in V).

In comparison with I, there also was a slight bathochromic effect (λ_{max} 269 *versus* 267 nm), which indicated that IV was not present since in that case there would have been a conjugation breakdown leading to a hypsochromic effect. This observation was in agreement with the slight bathochromic effect observed previously (14) in passing from α-methylpropiophenone or α-methylbutyrophenone to α-methylenepropiophenone. Finally, the NMR spectrum gave an identical picture for the block representing the aromatic protons of I and of III, which proved that the two isomers had the *para* structure. Shielding was also noticeable for the two signals of the ethylenic protons, but this shielding was especially remarkable for the methylenic protons since the chemical shift passed from δ 4.1 for I to δ 3.5 for III. Such a shift could be explained only by chain isomerism. Its intensity made it possible to note the presence of I in III and to calculate the percentage of it by integration ($\simeq$4% in the sample obtained).

These results were confirmed by the conversion into the saturated derivative. The saturated derivative was identical to an authentic sample prepared unequivocally by chemical reduction of the hydroxylactone (VII) formed by the reaction between citraconic anhydride and 2-chlorobiphenyl. The hydrogenated derivative (VIII) differs from its isomer (IX) obtained by hydrogenating I (different IR and NMR spectra). The melting point of a mixture of VIII and IX showed a distinct depression. Upon TLC, the mixture of VIII and IX gave a stain consisting of two parts (Fig. 1*b*). Therefore, the formation of this isomer showed that, contrary to the opinion of several investigators (1–3, 13), opening of the itaconic anhydride ring by an aryl group does not give a single product but instead leads to the formation of the two isomers in unequal proportions. NMR carried out on a crude reaction mixture after hydrolysis, washing with water, and solvent evaporation showed that the ratio by weight of I to III was ~80:20.

Structure of V—The method of formation of V showed that it is not easy to purify I by converting it into the water-soluble alkali metal salt followed by acidification after separating insoluble matter, unless the conditions are chosen carefully. The isomer structure was deduced from spectral analysis. The NMR spectrum agreed with a 4-aryl-4-oxo-2-methyl-2-butenoic acid. The presence of the doublet with δ 2.15, J = 1.4 Hz, was concordant with the values [δ 2.2, 2.14, and 2.18 (average)] reported (11, 12, 15) for similar aryl-substituted acids. With IR spectroscopy, two absorption bands were found at 1690 (COOH) and 1665 (C=O) cm^{-1}, which showed that the compound had an open structure. The stretching frequency observed at 975 cm^{-1} is characteristic of $=C-CH_3$ in the *trans*-$CH_3-C=C-H$ group (15, 16). As reported by various investigators (1, 3, 9–11), the *trans*-geometrical isomers of these acids are linked to the open form, the *cis*-isomer being stable only as the cyclized hydroxylactone.

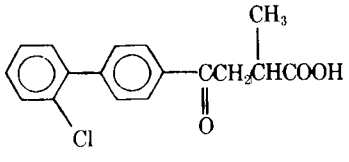

IX

Structure of VII—The IR spectrum of VII showed the absence of a ketonic carbonyl group and the very strong absorption of the lactone group at 1740 cm^{-1}. In addition, the presence of a hydroxyl group was indicated by an absorption band at 3280 cm^{-1}. The UV spectrum confirmed this result by the absence of conjugation between the aromatic ring and the carboxyl group through the intermediary of the carbonyl group excited by the double bond (λ_{max} 248 nm). Finally, the NMR spectrum agreed with the values of the signals given (10, 12) by analogous compounds.

The NMR spectrum was close to that of the isomeric hydroxylactone, VI. However, the signal relating to the ethylenic proton was more depressed with VI (7.0 *versus* 5.8), which confirmed the position assigned to the methyl group in these two compounds. The values of the chemical shifts observed for the ethylenic protons in VI and VII were in good agreement with those given by Bowden and Henry (10) in a review of ring–chain tautomerism for the derivatives:

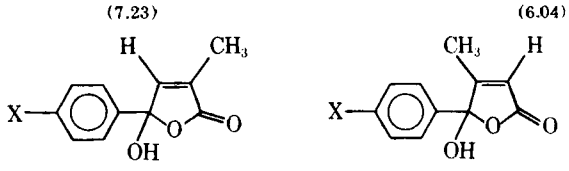

CONCLUSIONS

With the samples prepared as described and after comparative studies of R_f values, specific absorptions in the UV range, and specific NMR signals, a method was developed for detecting these impurities. The most suitable method for routine analysis is TLC on silica gel using methanol–chloroform (15:85) and developing to 15 cm. With these conditions, four isomers exhibited sufficient R_f differences to permit their detection in I (Fig. 1*a*). The respective R_f values for I, II, III, V, VI, and VII were 0.41, 0.38, 0.32, 0.28, 0.26, and 0.55. Nevertheless, considering the close R_f values for I and II, this method is not sufficiently accurate for the determination of II; in this case, GLC of 2-chlorobiphenyl provides a better control for the absence of II in I.

The most frequent impurity is V, which can be formed even when starting with pure I. Compound VI, formed with greater difficulty in the solid state, is present to a lesser extent in industrial samples. Compounds V and VI correspond to the evolution products of the I molecule, and their absence in the starting material does not exclude their detection in the finished pharmaceutical form. The other secondary products are manufacturing impurities, which must be tested for in the starting material. Their absence in the starting material is adequate to guarantee the quality of the pharmaceutical form since they cannot be formed spontaneously from I.

Systematic tests have shown that this method makes possible the detection of these main impurities in I concentrations as low as 0.2%. Levels as low as 1% of V can be detected in I by NMR using a routine 60-MHz apparatus. A standard range has been carried out in dimethyl sulfoxide-d_6 with I containing increasing quantities of V (0.5, 1, 2, 3, 5, and 7.5%); at 1%, the signal at δ 2.1 ppm clearly was distinct from the background noise. These UV or NMR physicochemical methods do not provide any advantage for detecting the impurities studied in comparison with TLC.

REFERENCES

(1) R. E. Lutz, P. S. Bailey, C. K. Dien, and J. W. Rinker, *J. Am. Chem. Soc.*, **75,** 5039 (1953).

(2) S. Dixon, H. Gregory, and L. F. Wiggins, *J. Chem. Soc.*, **1949,** 2139.

(3) A. K. Fateen, A. M. Sammour, and M. F. Ismail, *J. Chem. U.A.R.*, **10,** 331 (1967).

(4) H. Cousse, G. Mouzin, and J. P. Rieu, French pat. 2,265,409 (1974).

(5) H. Cousse, G. Mouzin, J. P. Rieu, and A. Delhon, French pat. 2,300,551 (1975).

(6) A. Delhon, J. P. Tarayre, H. Lauressergues, and S. Casadio, "International Conference on Atherosclerosis," Milan, Italy, Nov. 1975.

(7) J. Lubetzki and A. Mose, "International Conference on Atherosclerosis," Milan, Italy, Nov. 1975.

(8) A. Bizzi, M. T. Tacconi, E. Veneroni, and M. Cini, "7ème Congres

International de Pharmacologie," Paris, France, 1978.
(9) R. Escale and J. Verducci, *Bull. Soc. Chim. Fr.*, **1974**, 1203.
(10) K. Bowden and M. P. Henry, *J. Chem. Soc. Perkin Trans. II*, **1972**, 201.
(11) *Ibid.*, **1972**, 209.
(12) W. V. Curran and A. Ross, *J. Med. Chem.*, **17**, 273 (1974).
(13) P. S. Bailey and C. K. Dien, *J. Org. Chem.*, **21**, 624 (1956).
(14) A. F. Casy and J. L. Myers, *J. Chem. Soc.*, **1964**, 4639.
(15) G. Leclerc, C. G. Wermuth, and J. Schreiber, *Bull. Soc. Chim. Fr.*, **1967**, 1302.
(16) L. J. Belamy, "The Infrared Spectra of Complex Molecules," 2nd ed., Methuen, London, England, 1966, p. 52.

Chemical Constituents of Gentianaceae XXVIII: Flavonoids of *Enicostemma hyssopifolium* (Willd.) Verd.

S. GHOSAL ˣ **and D. K. JAISWAL**

Received January 16, 1978, from the *Pharmaceutical Chemistry Research Laboratory, Department of Pharmaceutics, Banaras Hindu University, Varanasi-5, India.* Accepted for publication June 20, 1979.

Abstract □ The whole plant of *Enicostemma hyssopifolium* (Willd.) Verd. (Gentianaceae) was collected at different growth stages and was shown to contain seven flavonoids: apigenin (I), genkwanin (II), isovitexin (III), swertisin (IV), saponarin (V), 5-*O*-glucosylswertisin (VI), and 5-*O*-glucosylisoswertisin (VII). Compounds VI and VII previously were unreported in nature. The yields of the flavonoids varied with the growth stage. The biochemical and chemotaxonomic significance of these results is appraised.

Keyphrases □ Flavonoids—isolation from *Enicostemma hyssopifolium*, identification □ Medicinal plants—isolation of flavonoids from *Enicostemma hyssopifolium*, identification □ Gentianaceae—isolation of flavonoids from *Enicostemma hyssopifolium*, identification □ *Enicostemma hyssopifolium*—isolation and identification of flavonoids

The genus *Enicostemma* (Gentianaceae) is monotypic; the only recorded species is *E. hyssopifolium* (Willd.) Verd. (synonymous with *E. littorale* Blume) (1). The plant is found throughout India up to 450 m (1500 ft). Extracts of the plant are used in Indian medicine to treat cardiac dropsy, rheumatism, and certain mental disorders. Significant antipsychotic (3), anti-inflammatory (4), and anthelmintic (5) activities were reported for its major alkaloid, gentianine; the corresponding heteroside, swertiamarin, was reported to produce central nervous system depressant (6) and cardiostimulant (7) activity.

The chemicals previously reported in this species were monoterpene alkaloids (8–12), heterosides (6, 7, 10, 13, 14), and a triterpene (14). This paper describes the isolation and characterization of the flavonoids of this species. The biochemical significance of the chemical constituent changes during vegetation is appraised in light of its separation as a monotypic genus.

EXPERIMENTAL[1]

All solutions were dried with anhydrous sodium sulfate. Silica gel[2] (60–120 mesh) was used for column chromatography. TLC was performed on silica gel[3] with chloroform–acetic acid (98:2, Solvent 1) and *n*-butanol–acetic acid–water (4:1:2, Solvent 2). Iodine vapor and ferric chloride solution were used for staining. Glucose was detected by partition paper chromatography[4] using sodium metaperiodate–benzidine reagent for staining (15).

Dried and milled whole plants of *E. hyssopifolium*[5] at the flowering stage (5.2 kg) were extracted continuously with light petroleum ether (bp 60–80°) in a soxhlet apparatus for 30 hr. The defatted plant material was extracted with ethanol for 30 hr. The petroleum ether extract contained alkanes and alkanols and was not processed further. The alcoholic extract was concentrated under reduced pressure and processed as shown in Scheme I.

The relative percent yields of the individual compounds at various stages of plant development are given in Table I. Determination of the mixed minor entities was accomplished by preparative layer chromatography of mixture extracts and absorptiometry of the layers after the components in these layers were identified by the usual methods.

Treatment of Fraction A—Fraction A was dissolved in 250 ml of hot ethyl acetate, the solution was concentrated, and a yellow solid (14.2 g) was separated. The solid showed two major spots on TLC at R_f 0.68 and 0.74 (Solvent 2). The two components were separated by fractional crystallization from methanol.

Swertisin (IV)—The sparingly methanol-soluble solid crystallized from methanol–dioxane as cream-colored crystals (7.65 g), mp 240–242°; $[\alpha]_D^{24}$ −9° (c 0.33, pyridine); UV: λ_{max} (ethanol) 272 (log ϵ 4.28) and 334 (4.38) nm; IR: ν_{max} 3360, 1668, and 1610 cm^{-1}; NMR (deuterodimethyl sulfoxide): δ 7.88 (2H, d, J = 9 Hz, H-2′,6′), 6.80 (2H, d, J = 9 Hz, H-3′,5′), 6.54 (1H, s, H-8), 6.50 (1H, s, H-3), 4.78 (1H, broad, glucosyl H-1), and 3.98 (3H, methoxyl). The hexaacetate, formed with acetic anhydride and pyridine under reflux, crystallized from alcohol as colorless needles, mp 150–151°; mass spectrum: *m/e* 698 (M$^+$, relative intensity 8%), 656 (22), 639 (12), 597 (20), 537 (12), 463 (80), 421 (98), 313 (100), 297 (60), and 139 (20).

Methylation with ethereal diazomethane gave swertisin-4′,5-di-*O*-methyl ether, mp 298–300°. Acetylation of the di-*O*-methyl ether with acetic anhydride and pyridine under reflux afforded swertisin-di-*O*-methyl ether tetraacetate, mp 128–129°; mass spectrum: *m/e* 642 (M$^+$, 5%), 583 (100), 582 (22), 523 (8), 341 (55), 325 (62), 294 (5), and 139 (5). The physical and spectral properties of the parent compound and its derivatives were indistinguishable from those of swertisin (16, 17).

Isovitexin (III)—After separation of swertisin, the methanol mother liquor was concentrated and diluted with acetone. It was kept at ordinary temperature overnight, and a yellow solid precipitated. Repeated crystallization of the solid from acetone–methanol gave isovitexin (18, 19) as yellow needles (6.4 g), mp 229–230°; $[\alpha]_D^{28}$ +15.4° (c 0.37, ethanol); UV: λ_{max} (ethanol) 272 (log ϵ 4.45) and 338 (4.42) nm; IR: ν_{max} 3300 (broad), 1662, 1628, 1600, and 1588 cm^{-1}; NMR (deuterodimethyl sulfoxide): δ 7.95 (2H, d, J = 9 Hz, H-2′,6′), 6.95 (2H, d, J = 9 Hz, H-3′,5′), 6.72 (1H, s, H-3), 6.54 (1H, s, H-8), and 4.70 (1H, broad, glucosyl H-1); mass spectrum: *m/e* 414 (M − 18, 20%), 396 (8.5), 378 (14), 295 (18), 283 (100), and 165 (20). The 4′,5,7-tri-*O*-methyl ether tetraacetate, prepared as de-

[1] Melting points were taken on a Kofler block in open capillaries and are uncorrected. UV spectra were determined on a Cary model 14 recording spectrophotometer. IR spectra were taken in Nujol using a Perkin-Elmer model 337 spectrophotometer, and only the major bands are quoted. ^{1}H-NMR spectra were recorded on an XL 100 instrument with tetramethylsilane as the internal standard. Mass spectra were determined with an MS-9 or MS-50 spectrometer at 70 ev.
[2] British Drug Houses, Poole, England.
[3] Silica gel G, E. Merck, Darmstadt, West Germany.
[4] Whatman No. 50.
[5] The plants were collected from the Banaras Hindu University Campus area 12 times during June and August of 1973–1976. Voucher specimens have been preserved at the Pharmaceutical Chemistry Research Laboratory, Department of Pharmaceutics, Banaras Hindu University.

0022-3549/80/0100-0053$01.00/0
© 1980, American Pharmaceutical Association

International de Pharmacologie," Paris, France, 1978.
(9) R. Escale and J. Verducci, *Bull. Soc. Chim. Fr.*, **1974**, 1203.
(10) K. Bowden and M. P. Henry, *J. Chem. Soc. Perkin Trans. II*, **1972**, 201.
(11) *Ibid.*, **1972**, 209.
(12) W. V. Curran and A. Ross, *J. Med. Chem.*, **17**, 273 (1974).
(13) P. S. Bailey and C. K. Dien, *J. Org. Chem.*, **21**, 624 (1956).
(14) A. F. Casy and J. L. Myers, *J. Chem. Soc.*, **1964**, 4639.
(15) G. Leclerc, C. G. Wermuth, and J. Schreiber, *Bull. Soc. Chim. Fr.*, **1967**, 1302.
(16) L. J. Belamy, "The Infrared Spectra of Complex Molecules," 2nd ed., Methuen, London, England, 1966, p. 52.

Chemical Constituents of Gentianaceae XXVIII: Flavonoids of *Enicostemma hyssopifolium* (Willd.) Verd.

S. GHOSAL ˣ **and D. K. JAISWAL**

Received January 16, 1978, from the *Pharmaceutical Chemistry Research Laboratory, Department of Pharmaceutics, Banaras Hindu University, Varanasi-5, India.* Accepted for publication June 20, 1979.

Abstract □ The whole plant of *Enicostemma hyssopifolium* (Willd.) Verd. (Gentianaceae) was collected at different growth stages and was shown to contain seven flavonoids: apigenin (I), genkwanin (II), isovitexin (III), swertisin (IV), saponarin (V), 5-*O*-glucosylswertisin (VI), and 5-*O*-glucosylisoswertisin (VII). Compounds VI and VII previously were unreported in nature. The yields of the flavonoids varied with the growth stage. The biochemical and chemotaxonomic significance of these results is appraised.

Keyphrases □ Flavonoids—isolation from *Enicostemma hyssopifolium*, identification □ Medicinal plants—isolation of flavonoids from *Enicostemma hyssopifolium*, identification □ Gentianaceae—isolation of flavonoids from *Enicostemma hyssopifolium*, identification □ *Enicostemma hyssopifolium*—isolation and identification of flavonoids

The genus *Enicostemma* (Gentianaceae) is monotypic; the only recorded species is *E. hyssopifolium* (Willd.) Verd. (synonymous with *E. littorale* Blume) (1). The plant is found throughout India up to 450 m (1500 ft). Extracts of the plant are used in Indian medicine to treat cardiac dropsy, rheumatism, and certain mental disorders. Significant antipsychotic (3), anti-inflammatory (4), and anthelmintic (5) activities were reported for its major alkaloid, gentianine; the corresponding heteroside, swertiamarin, was reported to produce central nervous system depressant (6) and cardiostimulant (7) activity.

The chemicals previously reported in this species were monoterpene alkaloids (8–12), heterosides (6, 7, 10, 13, 14), and a triterpene (14). This paper describes the isolation and characterization of the flavonoids of this species. The biochemical significance of the chemical constituent changes during vegetation is appraised in light of its separation as a monotypic genus.

EXPERIMENTAL[1]

All solutions were dried with anhydrous sodium sulfate. Silica gel[2] (60–120 mesh) was used for column chromatography. TLC was performed on silica gel[3] with chloroform–acetic acid (98:2, Solvent 1) and *n*-butanol–acetic acid–water (4:1:2, Solvent 2). Iodine vapor and ferric chloride solution were used for staining. Glucose was detected by partition paper chromatography[4] using sodium metaperiodate–benzidine reagent for staining (15).

Dried and milled whole plants of *E. hyssopifolium*[5] at the flowering stage (5.2 kg) were extracted continuously with light petroleum ether (bp 60–80°) in a soxhlet apparatus for 30 hr. The defatted plant material was extracted with ethanol for 30 hr. The petroleum ether extract contained alkanes and alkanols and was not processed further. The alcoholic extract was concentrated under reduced pressure and processed as shown in Scheme I.

The relative percent yields of the individual compounds at various stages of plant development are given in Table I. Determination of the mixed minor entities was accomplished by preparative layer chromatography of mixture extracts and absorptiometry of the layers after the components in these layers were identified by the usual methods.

Treatment of Fraction A—Fraction A was dissolved in 250 ml of hot ethyl acetate, the solution was concentrated, and a yellow solid (14.2 g) was separated. The solid showed two major spots on TLC at R_f 0.68 and 0.74 (Solvent 2). The two components were separated by fractional crystallization from methanol.

Swertisin (IV)—The sparingly methanol-soluble solid crystallized from methanol–dioxane as cream-colored crystals (7.65 g), mp 240–242°; $[\alpha]_D^{24}$ −9° (c 0.33, pyridine); UV: λ_{max} (ethanol) 272 (log ϵ 4.28) and 334 (4.38) nm; IR: ν_{max} 3360, 1668, and 1610 cm^{-1}; NMR (deuterodimethyl sulfoxide): δ 7.88 (2H, d, J = 9 Hz, H-2′,6′), 6.80 (2H, d, J = 9 Hz, H-3′,5′), 6.54 (1H, s, H-8), 6.50 (1H, s, H-3), 4.78 (1H, broad, glucosyl H-1), and 3.98 (3H, methoxyl). The hexaacetate, formed with acetic anhydride and pyridine under reflux, crystallized from alcohol as colorless needles, mp 150–151°; mass spectrum: *m/e* 698 (M$^+$, relative intensity 8%), 656 (22), 639 (12), 597 (20), 537 (12), 463 (80), 421 (98), 313 (100), 297 (60), and 139 (20).

Methylation with ethereal diazomethane gave swertisin-4′,5-di-*O*-methyl ether, mp 298–300°. Acetylation of the di-*O*-methyl ether with acetic anhydride and pyridine under reflux afforded swertisin-di-*O*-methyl ether tetraacetate, mp 128–129°; mass spectrum: *m/e* 642 (M$^+$, 5%), 583 (100), 582 (22), 523 (8), 341 (55), 325 (62), 294 (5), and 139 (5). The physical and spectral properties of the parent compound and its derivatives were indistinguishable from those of swertisin (16, 17).

Isovitexin (III)—After separation of swertisin, the methanol mother liquor was concentrated and diluted with acetone. It was kept at ordinary temperature overnight, and a yellow solid precipitated. Repeated crystallization of the solid from acetone–methanol gave isovitexin (18, 19) as yellow needles (6.4 g), mp 229–230°; $[\alpha]_D^{28}$ +15.4° (c 0.37, ethanol); UV: λ_{max} (ethanol) 272 (log ϵ 4.45) and 338 (4.42) nm; IR: ν_{max} 3300 (broad), 1662, 1628, 1600, and 1588 cm^{-1}; NMR (deuterodimethyl sulfoxide): δ 7.95 (2H, d, J = 9 Hz, H-2′,6′), 6.95 (2H, d, J = 9 Hz, H-3′,5′), 6.72 (1H, s, H-3), 6.54 (1H, s, H-8), and 4.70 (1H, broad, glucosyl H-1); mass spectrum: *m/e* 414 (M − 18, 20%), 396 (8.5), 378 (14), 295 (18), 283 (100), and 165 (20). The 4′,5,7-tri-*O*-methyl ether tetraacetate, prepared as de-

[1] Melting points were taken on a Kofler block in open capillaries and are uncorrected. UV spectra were determined on a Cary model 14 recording spectrophotometer. IR spectra were taken in Nujol using a Perkin-Elmer model 337 spectrophotometer, and only the major bands are quoted. ^{1}H-NMR spectra were recorded on an XL 100 instrument with tetramethylsilane as the internal standard. Mass spectra were determined with an MS-9 or MS-50 spectrometer at 70 ev.
[2] British Drug Houses, Poole, England.
[3] Silica gel G, E. Merck, Darmstadt, West Germany.
[4] Whatman No. 50.
[5] The plants were collected from the Banaras Hindu University Campus area 12 times during June and August of 1973–1976. Voucher specimens have been preserved at the Pharmaceutical Chemistry Research Laboratory, Department of Pharmaceutics, Banaras Hindu University.

0022-3549/80/0100-0053$01.00/0
© 1980, American Pharmaceutical Association

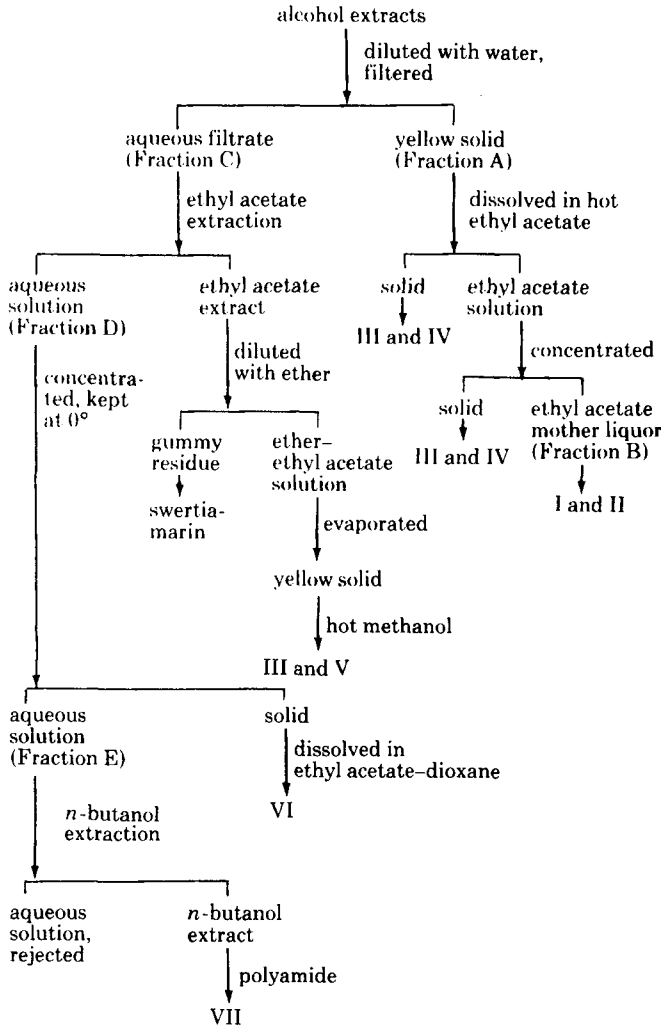

Scheme I—Isolation of flavonoids of E. hyssopifolium

scribed, was identified by melting-point, mixed melting-point, and co-TLC analyses as the di-*O*-methyltetraacetate derivative of IV.

Treatment of Fraction B—The ethyl acetate mother liquor was evaporated. The residue was dissolved in chloroform and chromatographed over silica gel (30 × 3 cm). Elution was carried out with benzene, benzene–chloroform (1:1), and chloroform (1 liter each), and 100-ml fractions were collected.

Genkwanin (II)—On evaporation, the middle benzene–chloroform eluates (fractions 14–17) afforded genkwanin (20) as yellow needles (0.37 g), mp 285–286°; R_f 0.48 (Solvent 1); UV: λ_{max} (ethanol) 268 (log ϵ 4.40) and 337 (4.47) nm; IR: ν_{max} 3250, 1660, 1600, 1592, and 1498 cm^{-1}; mass spectrum: *m/e* 284 (M^+, 100%), 256 (5), 255 (22), 254 (5), 167 (18), 166 (19), 138 (10), 128 (20), 118 (12), and 95 (11). The diacetate, prepared with acetic anhydride and pyridine under reflux, crystallized from ethanol as colorless needles, mp 195–198°. Correspondence of these properties with those reported previously (20–22) established the identity as II.

Apigenin (I)—The chloroform eluates were combined and evaporated. The residue crystallized from aqueous pyridine to give apigenin as yellow needles (0.46 g), mp 340–343° dec.; R_f 0.3 (Solvent 1); UV: λ_{max} (ethanol) 265 (log ϵ 4.44) and 336 (4.48) nm. 4′,5,7-Tri-*O*-methyl ether, prepared with dimethyl sulfate and potassium carbonate in anhydrous acetone under reflux for 40 hr, crystallized from ethanol as light-yellow needles, mp 153°; NMR (deuterochloroform): δ 7.91 (2H, d, J = 9 Hz, H-2′,6′), 6.94 (2H, d, J = 9 Hz, H-3′,5′), 6.70 (1H, s, H-3), 6.48 (1H, d, J = 3 Hz, H-8), 6.22 (1H, d, J = 3 Hz, H-6), and 4.0–3.98 (9H, methoxyl protons); mass spectrum: *m/e* 312 (M^+, 100%), 297 (22), 295 (10), 269 (22), and 254 (11). The melting point and spectral properties of the flavone and its permethyl ether were indistinguishable from those reported for apigenin (20, 21).

Treatment of Fraction C and Isolation of Saponarin (V)—The aqueous filtrate was extracted with ethyl acetate (5 × 1 liter), and the ethyl acetate extract was worked up in the usual fashion to give a brown concentrate (200 ml). It was diluted with 200 ml of ether, and swertiamarin (6) was precipitated as a brown gum. The ethyl acetate–ether mother liquor was evaporated to give a dull-yellow solid (0.28 g), which showed two major spots on TLC at R_f 0.42 and 0.7 (Solvent 2). Trituration of the residue with hot methanol gave 0.1 g of swertisin as the sparingly methanol-soluble solid.

Table I—Flavonoids of *E. hyssopifolium* during Growth [a] (Relative Percent Yield)

Flavone	2–3 Weeks Old	6–8 Weeks Old	Flowering Stage	Fruiting Stage
I	44	20	3	5
II	32	28	2	4
III	–	12	35	–
IV	–	7	42	–
V	–	14	+	8
VI	–	+	5	40
VII	–	–	+	24
Unidentified phenolic constituents	24	17	12	19
Yield, %	0.08	0.22	0.37	0.30

[a] n = 3; + denotes 1–2%; – denotes absence.

After separation of swertisin, the methanol mother liquor was evaporated to give a hygroscopic solid (0.11 g), mp 228–231°; R_f 0.4 (Solvent 2); $[\alpha]_D^{28}$ −8.5° (c 0.45, water) and −73.4° (c 0.55, pyridine); UV: λ_{max} (ethanol) 270 and 335 nm; NMR (deuterodimethyl sulfoxide): δ 7.95 (2H, d, J = 8 Hz, H-2′,6′), 6.98 (2H, d, J = 8 Hz, H-3′,5′), 6.92 (1H, s, H-8), 6.68 (1H, s, H-3), 4.95 (1H, broad, *O*-glucosyl H-1), and 4.8 (1H, d, J = 10 Hz, C-glucosyl H-1). Treatment with acetic anhydride and pyridine afforded a decaacetate, which crystallized from hexane–methylene chloride as a glassy solid, mp 142–144°. The physical and spectral properties of the compound and its acetate derivative were identical to those reported for saponarin (20, 23).

Treatment of Fraction D—The aqueous mother liquor was concentrated at 30° under reduced pressure to about 25 ml and kept at 0° for ~2 weeks, during which time a light-yellow solid precipitated. The solid was collected by filtration and dissolved in ethyl acetate–dioxane.

Swertisin-5-O-β-D-glucoside (VI)—On concentration and cooling, the ethyl acetate–dioxane solution gave an amorphous solid, which crystallized from methanol–dioxane as ivory-colored needles (0.93 g), mp 200–202°; R_f 0.32 (Solvent 2); $[\alpha]_D^{28}$ −77° (c 0.73, pyridine); UV: λ_{max} (ethanol) 271 (log ϵ 4.26) and 335 (4.30) nm; UV: λ_{max} (ethanol–0.2% sodium acetate) 262 sh, 268, and 388 nm; IR: ν_{max} 3300 (broad), 1668, 1662, 1630, 1612, 1295, 1255, 1020, and 838 cm^{-1}; NMR (deuterodimethyl sulfoxide): δ 7.98 (2H, d, J = 8.5 Hz, H-2′,6′), 6.95 (2H, d, J = 8.5 Hz, H-3′,5′), 6.82 (1H, s, H-8), 6.38 (1H, s, H-3), 5.0 (1H, broad, *O*-glucosyl H-1), 4.80 (1H, d, J = 10 Hz, C-glucosyl H-1), 3.94 (3H, methoxyl), and 3.35 (complex multiplet, 12 glucosyl protons plus water); ^{13}C-NMR (deuterodimethyl sulfoxide): δ 161.40 (C-2), 103.07 (C-3), 182.30 (C-4), 156.90 (C-5), 90.88 (C-6), 161.42 (C-7), 104.8 (C-8), 159.86 (C-9), 109.57 (C-10), 121.08 (C-1′), 128.46 (C-2′), 116.08 (C-3′), 164.05 (C-4′), 116.02 (C-5′), 128.46 (C-6′), 56.28 (methoxyl-C), and 56.0–100.5 (12 lines, C,*O*-glucosyl-C) (24).

Anal.—Calc. for $C_{28}H_{32}O_{15}\cdot H_2O$: C, 53.67; H, 5.43. Found: C, 52.99; H, 5.86.

Hydrolysis of VI with Emulsin—Compound VI, 52 mg, was dissolved in 20 ml of pH 5 aqueous buffer (0.5 *M* sodium acetate adjusted to pH 5 with acetic acid) to which 20 mg of powdered emulsin[6] was added. The mixture was kept at ambient temperature overnight. The reaction product was concentrated and subjected to paper chromatography[7] along with glucose, rhamnose, and glucuronic acid. Only glucose was detected as the sugar component in the hydrolyzed product. The aglucone was extracted with ethyl acetate, the solvent was removed, and the residue was crystallized from methanol–dioxane. Direct comparison of the aglucone by melting-point, mixed melting-point, and co-TLC analyses with swertisin established that they were identical.

Methylation of VI—Compound VI, 48 mg, was methylated by repeated addition of ethereal diazomethane daily for 7 days. After the usual workup, the methyl ether was obtained as a light-yellow solid.

[6] Sigma Corp.
[7] Whatman No. 1.

Isovitexin-4′,7-di-O-methyl Ether—The methyl ether of VI was dissolved in 20 ml of 10% aqueous acetic acid and kept at ambient temperature overnight. The solvent was removed under high vacuum, and a straw-colored residue was obtained. It was triturated with hot methanol. The methanol solution was concentrated and afforded 38 mg of a microcrystalline solid, mp 268–270°; R_f 0.42 (Solvent 2); UV: λ_{max} (ethanol) 268 (log ϵ 4.28) and 324 (4.36) nm; UV: λ_{max} (ethanol–aluminum chloride) 278, 300, and 345 nm (indicating the presence of a C_5-OH group); mass spectrum: *m/e* 460 (M^+, 3%), 445 (7), 442 (100), 431 (7), 430 (8), 422 (3), 417 (5), 311 (34), 296 (17), 281 (24), and 179 (7). The physical and spectral properties of the compound suggested its identity as isovitexin-4′,7-di-*O*-methyl ether.

Isovitexin-4′,5,7-tri-O-methyl Ether Tetraacetate—Further methylation of isovitexin-4′,7-di-*O*-methyl ether with excess ethereal diazomethane followed by acetylation with acetic anhydride and pyridine on a steam bath for 4 hr afforded isovitexin-tri-*O*-methyl ether tetraacetate, mp 127–129° (25); mass spectrum: *m/e* 642 (M^+, 3%), 583 (100), 541 (2), 523 (10), 481 (8), 463 (18), 421 (12), 408 (2), 341 (68), 339 (44), 31 (22), 294 (2), 179 (2), and 139 (25).

Permethylation of VI—The diglucoside, 24 mg, in 5 ml of *N,N*-dimethylformamide was treated with 1 ml of methyl iodide and 60 mg of sodium hydride under nitrogen. After 1 hr at ambient temperature, the reaction mixture was diluted with 50 ml of water and extracted with chloroform. The chloroform layer was worked up in the usual fashion, and the chloroform concentrate was subjected to preparative layer chromatography with Solvent 1 as the developer. The blue fluorescent zone at R_f 0.5 under a shortwave UV lamp was cut out and eluted with chloroform. Evaporation of the solvent from the chloroform solution gave a pale-yellow gum, which crystallized from benzene as yellow needles, mp 168–171°; mass spectrum (no M^+ was observed, only fragment ions were recorded): *m/e* 516 (relative intensity 12%), 501 (22), 485 (20), 469 (8), 341 (100), 311 (5), 101 (55), and 88 (47).

Treatment of Fraction E—Fraction E was extracted with *n*-butanol (4 × 250 ml). The residue from the butanol extract was dissolved in ethyl acetate and subjected to preparative layer chromatography on polyamide[8] plates (20 × 20 cm) with methanol–acetic acid–water (90:5:5) as the developer.

Isoswertisin-5-O-β-D-glucoside (VII)—The zone at R_f 0.4 was eluted with methanol, and the solvent was evaporated. The residue crystallized from methanol–dioxane as light-yellow microcrystals (0.1 g), mp 212–215°; R_f 0.37 (Solvent 2); $[\alpha]_D^{28}$ −91° (c 0.51, pyridine); UV: λ_{max} (ethanol) 270 (log ϵ 4.23) and 336 (4.26) nm; UV: λ_{max} (ethanol–0.2% sodium acetate) 262 sh, 268, and 390–395 nm; IR: ν_{max} 3300 (broad), 1665, 1610, 1502, 1362, 1295, 1258, 1212, 1196, 1035, and 842 cm^{-1}; NMR (deuterodimethyl sulfoxide): δ 7.92 (2H, d, J = 8.5 Hz, H-2′,6′), 6.95 (2H, d, J = 8.5 Hz, H-3′,5′), 6.34 (1H, s, H-6/H-3), 6.32 (1H, s, H-3/H-6), 5.0 (1H, broad, *O*-glucosyl H-1), 4.78 (1H, d, J = 10 Hz, C-glucosyl H-1), 3.92 (3H, methoxyl), and 3.50 (complex multiplet, 12 glucosyl protons plus water).

Anal.—Calc. for $C_{28}H_{32}O_{15}\cdot H_2O$: C, 53.67; H, 5.43. Found: C, 53.18; H, 5.82.

Hydrolysis of VII—Compound VII, 23 mg, was hydrolyzed with 10 mg of emulsin as described when glucose was detected as the only glucone moiety present. The aglucone, mp 295–298°, showed UV: λ_{max} (ethanol) 272 (log ϵ 4.17) and 335 (4.30) nm, identical to that reported for isoswertisin (17). It afforded a hexaacetate, mp 128–131°.

Methylation of VII—Compound VII, 22 mg, was methylated with excess ethereal diazomethane. After the usual workup, the methyl ether was obtained as an amorphous solid (21 mg).

Vitexin-4′,7-di-O-methyl Ether—The methyl ether of VII was hydrolyzed with acetic acid as described, and vitexin-4′,7-di-*O*-methyl ether was obtained as yellow microcrystals (9 mg), mp 260–262°; UV: λ_{max} (ethanol) 270 (log ϵ 4.27) and 324 (4.22) nm; UV: λ_{max} (ethanol–aluminum chloride) 277, 300, 345, and 383 nm.

Vitexin-4′,5,7-tri-O-methyl Ether Tetraacetate—Further methylation of vitexin-4′,7-di-*O*-methyl ether with ethereal diazomethane and subsequent acetylation afforded vitexin-4′,5,7-tri-*O*-methyl ether tetraacetate (26), mp 220–221°; mass spectrum: *m/e* 642 (M^+, 100%), 583 (8), 541 (12), 523 (18), 481 (5), 463 (4), 341 (35), 339 (11), 311 (28), 294 (6), 179 (5), and 139 (10). The mass fragmentation data of this compound are consistent with those reported for vitexin-4′,5,7-tri-*O*-methyl ether tetraacetate (16).

Permethylation of VII—Compound VII was permethylated as described for VI. The derivative crystallized from acetone–benzene as a light-brown solid, mp 122–125°; mass spectrum (no M^+ was observed, only fragment ions were recorded): *m/e* 516 (relative intensity 80%), 486 (5), 341 (100), 327 (22), 311 (8), 101 (70), and 88 (68). The mass spectral data were consistent with those reported (27) for the permethyl ether of vitexin-5-*O*-glucoside.

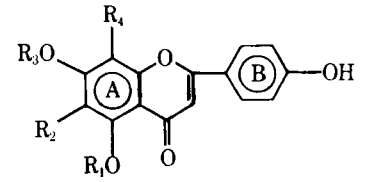

I: $R_1 = R_2 = R_3 = R_4 = H$
II: $R_1 = R_2 = R_4 = H$, $R_3 = CH_3$
III: $R_1 = R_3 = R_4 = H$, R_2 = glucosyl
IV: $R_1 = R_4 = H$, R_2 = glucosyl, $R_3 = CH_3$
V: $R_1 = R_4 = H$, $R_2 = R_3$ = glucosyl
VI: $R_1 = R_2$ = glucosyl, $R_3 = CH_3$, $R_4 = H$
VII: $R_1 = R_4$ = glucosyl, $R_3 = CH_3$, $R_2 = H$

RESULTS AND DISCUSSION

Seven flavonoids (22) were isolated from the whole plants of *E. hyssopifolium* at different vegetation periods by solvent extraction and column and preparative layer chromatography. These compounds, apigenin (I), gerkwanin (II), isovitexin (III), swertisin (IV), saponarin (V), swertisin-5-*O*-β-D-glucoside (VI), and isoswertisin-5-*O*-β-D-glucoside (VII), were characterized by chemical transformation and the UV, IR, NMR, and mass spectra of the compounds and their methyl ether and acetate derivatives. The structural elucidation of the two new compounds (VI and VII) that were not encountered before in nature or prepared synthetically is described.

Flavonoid VI—Compound VI ($C_{28}H_{32}O_{15}\cdot H_2O$), mp 200–202°, showed UV absorption maxima in neutral ethanol and in the presence of the usual shift reagents (21), characteristic of 4′,5,7-trioxygenated flavones with a free 4′-hydroxyl group (21). The 100-MHz PMR spectrum of the compound in deuterodimethyl sulfoxide exhibited signals due to 12 glucosyl protons, one aromatic methoxyl proton, two glucose anomeric protons, and six aromatic protons ascribable to C-3, C-8, and C-2′,3′,5′,6′-H (21). Its ^{13}C-NMR spectrum, interpreted on the basis of two recent reports of the ^{13}C-spectra of hydroxy–methoxy flavones (27, 28), also was consistent with this assignment.

On hydrolysis with emulsin, the compound gave IV and glucose. Methylation with ethereal diazomethane and subsequent acid hydrolysis afforded isovitexin-4′,7-di-*O*-methyl ether, which showed a mass spectrum consistent with this structure (16, 18). Likewise, the mass spectrum of the permethyl ether of the parent compound produced fragment ion peaks characteristic of 6-C,*O*-diglucosyl flavones (29). Based on these observations, the flavonoid was identified as 5-*O*-β-D-glucopyranosyl-6-C-β-D-glucopyranosyl genkwanin (VI).

Flavonoid VII—Compound VII ($C_{28}H_{32}O_{15}\cdot H_2O$), mp 212–215°, showed a close similarity in its UV absorption spectra in neutral ethanol and in the presence of the usual shift reagents (21) with those of VI. In the 100-MHz PMR spectrum, a significant difference from that of VI was discernible in the A-ring proton singlet, which appeared near the signal due to C_3-H. Therefore, the A-ring proton was assigned to C_6-H. The downfield shift was due to the glucosyloxy function at C-5. On hydrolysis with emulsin, it afforded isoswertisin and glucose. Methylation with ethereal diazomethane followed by acid hydrolysis under mild conditions yielded vitexin-4′,7-di-*O*-methyl ether. The permethyl ether of the parent compound produced fragment ion peaks in its mass spectrum that are characteristic of 8-C,*O*-diglucoside flavones (29). Based on these observations, the compound was identified as 5-*O*-β-D-glucopyranosyl-8-C-β-D-glucopyranosyl genkwanin (VII).

The glycoflavones (III–VII) were absent in the seedling stage (2–3 weeks) of the plant. At this stage, only the free flavones (I and II) were detected in the roots, stalks, and leaves of *E. hyssopifolium*. From the onset of maturity (6–8 weeks), biosynthesis of the C-glycoflavones (III and IV) started. At the flowering stage, the free flavones were largely replaced by these entities. At the fruiting stage, III and IV were represented by the C,*O*-diglycoflavones (V–VII). However, at this stage, I and II reappeared as minor entities.

Since previous results of biosynthetic experiments suggested that C-glycosylation of flavones takes place at the chalcone stage (30), it seemed plausible that elaboration of the free flavones (I and II) in *E.*

[8] Powder D, Riedel, Haen AG.

hyssopifolium was interrupted during the early growth of its stalk and leaves and substituted by the synthesis of the C-glycoflavones (III and IV). Toward the end of vegetation, synthesis of the free flavones revived, while the C-glycoflavones were further *O*-glycosylated to afford V–VII. This time lag in the *O*-glycosylation is surprising because *O*-glycosides are less toxic to plants than the free phenols (31); the reaction, therefore, was expected at an early stage of plant growth but was not observed in *E. hyssopifolium*. However, a similar ontogenic variation in the content of free xanthones and of xanthone-*O*-glycosides was reported recently in *Swertia angustifolia* (32).

Another noteworthy feature of *E. hyssopifolium*, whose certain chemical characters, *e.g.*, monoterpene alkaloids, heterosides, and flavonoids, are similar to those of *Gentiana* species (12), is the apparent complete absence of xanthones. Xanthones occur almost ubiquitously in *Gentiana* species (33, 34). From the chemotaxonomic point of view, this observation is significant since *E. hyssopifolium* was known previously as *Gentiana verticillata* Linn. but later was separated from the *Gentiana* genus on other taxonomic grounds (1). The chemical results reported in this paper support this separation of *E. hyssopifolium* as a monotypic species.

REFERENCES

(1) J. K. Maheswari, "Flora of Delhi," C.S.I.R., New Delhi, India, 1963, p. 223.

(2) R. N. Chopra, S. L. Nayar, and I. C. Chopra, "Glossary of Indian Medicinal Plants," C.S.I.R., New Delhi, India, 1956, p. 107.

(3) S. K. Bhattacharya, S. Ghosal, R. K. Chaudhuri, A. K. Singh, and P. V. Sharma, *J. Pharm. Sci.*, **63,** 1341 (1974).

(4) F. Sadritdinov, in "Farmakol Alkaloidov Serdechnykh Glikozidov," M. B. Sultanov, Ed., Fan: Tashkent, USSR, 1971, p. 146; through *Chem. Abstr.*, **78,** 79634 (1973).

(5) A. I. Taraeva, *Med. Parazitol. Parazit. Bolezni*, **27,** 432 (1958).

(6) S. K. Bhattacharya, P. K. S. P. Reddy, S. Ghosal, A. K. Singh, and P. V. Sharma, *J. Pharm. Sci.*, **65,** 1547 (1976).

(7) S. Ghosal, D. K. Jaiswal, A. K. Singh, and P. V. Sharma, "Abstracts of the Indo-German Symposium on Medicinal Plants with Cardiovascular Activity," Central Drug Research Institute, Lucknow, India, 1977, p. 1.

(8) T. R. Govindachari, K. Nagarajan, and S. Rajappa, *J. Chem. Soc. C*, **1957,** 2725.

(9) S. Ghosal, R. K. Chaudhuri, M. P. Tiwari, A. K. Singh, and F. W. Wehrli, *Tetrahedron Lett.*, **1974,** 403.

(10) S. Ghosal, A. K. Singh, P. V. Sharma, and R. K. Chaudhuri, *J. Pharm. Sci.*, **63,** 944 (1974).

(11) R. K. Chaudhuri, A. K. Singh, and S. Ghosal, *Chem. Ind. (London)*, **1975,** 127.

(12) A. K. Singh, Ph.D. thesis, Banaras Hindu University, Varanasi, India, 1976.

(13) W. C. Wildman, J. Le Men, and K. Wiesner, in "Cyclopentanoid Terpene Derivatives," W. I. Taylor and A. R. Battersby, Eds., Dekker, New York, N.Y., 1969, p. 198.

(14) J. Rai and K. A. Thaker, *Curr. Sci. (India)*, **35,** 148 (1966).

(15) S. Ghosal, P. V. Sharma, and R. K. Chaudhuri, *Phytochemistry*, **14,** 2671 (1975).

(16) M. Aritomi, T. Komori, and T. Kawasaki, *Justus Liebigs Ann. Chem.*, **734,** 91 (1970).

(17) M. Komatsu, T. Tomimori, and M. Ito, *Chem. Pharm. Bull.*, **15,** 263 (1967).

(18) A. Prox, *Tetrahedron Lett.*, **1969,** 943.

(19) R. M. Horowitz and B. Gentili, *Chem. Ind. (London)*, **1964,** 498.

(20) I. Heilbron, "Dictionary of Organic Compounds," Eyre & Spottiswoode, London, England, 1965.

(21) T. J. Mabry, K. R. Markham, and M. B. Thomas, "The Systematic Identification of Flavonoids," Springer-Verlag, New York, N.Y., 1970.

(22) J. B. Harborne, in "The Flavonoids," J. B. Harborne, T. J. Mabry, and H. Mabry, Eds., Chapman & Hall, London, England, 1975, chap. 19.

(23) M. K. Seikel, A. J. Bushnell, and R. Birzgalis, *Arch. Biochem. Biophys.*, **99,** 415 (1962).

(24) K. Bock and C. Pedersen, *Acta Chem. Scand.*, **29,** 258 (1975).

(25) M. Aritomi and T. Kawasaki, *Chem. Pharm. Bull.*, **16,** 1842 (1968).

(26) C. B. Rao and V. Venkataswarlu, *Curr. Sci. (India)*, **25,** 328 (1956).

(27) C. A. Kingsbury and J. H. Looker, *J. Org. Chem.*, **40,** 1120 (1975).

(28) B. Ternai and K. R. Markham, *Tetrahedron*, **32,** 565 (1976).

(29) M. L. Bouillant, J. Favre-Bonvin, and J. Chopin, *Phytochemistry*, **14,** 2267 (1975).

(30) R. E. Alston, in "Recent Advances in Phytochemistry," vol. I, T. J. Mabry, R. E. Alston, and V. C. Runeckles, Eds., Appleton-Century-Crofts, New York, N.Y., 1968, p. 305.

(31) L. P. Miller, in "Phytochemistry," vol. I, L. P. Miller, Ed., Van Nostrand, New York, N.Y., 1973, p. 297.

(32) S. Ghosal, P. V. Sharma, and D. K. Jaiswal, *J. Pharm. Sci.*, **67,** 55 (1978).

(33) I. Carpenter, H. D. Locksley, and F. Scheinmann, *Phytochemistry*, **8,** 2013 (1969).

(34) S. Ghosal, P. V. Sharma, and R. K. Chaudhuri, *ibid.*, **14,** 1393 (1975).

ACKNOWLEDGMENTS

Supported in part by a grant from the University Grants Commission, New Delhi, India.

For the previous paper in this series, see S. Ghosal, K. Biswas, and D. K. Jaiswal, *Phytochemistry*, in press.

The authors thank the Director of the Ciba-Geigy Research Center, Bombay, India; Dr. F. W. Wehrli, NMR Applications Laboratory, Varian AG, Zug, Switzerland; Dr. B. C. Das, CNRS, Gif-Sur-Yvette, France; and Dr. S. C. Pakrashi, Indian Institute of Experimental Medicine, Calcutta, India, for some of the spectral and optical rotation data.

New Compartment- and Model-Independent Method for Rapid Calculation of Drug Absorption Rates

WIN L. CHIOU

Received April 16, 1979, from the *Department of Pharmacy, College of Pharmacy, University of Illinois at the Medical Center, Chicago, IL 60612.* Accepted for publication August 22, 1979.

Abstract □ A simple and rapid method for the absorption rate calculation for drugs exhibiting linear pharmacokinetics is proposed. The method employs the novel instantaneous midpoint-input principle, which assumes that all drug absorbed during a given interval, regardless of the complexity of the absorption kinetics, is absorbed instantaneously at the midpoint of the interval. The drug amount absorbed is calculated by comparing the net plasma level resulting from the absorption during that interval with the plasma drug level obtained after intravenous dosing at the midpoint of the absorption interval. The method does not assume any compartments or models commonly used in pharmacokinetic studies. In examples with markedly different pharmacokinetic properties, the new method yielded accurate results almost identical to those obtained with the standard Wagner–Nelson and Loo–Riegelman methods. The method often is accurate to two to four significant figures in absorption rate calculations. For first-order absorption, the new method appears to be less subject to the influence of timing of the first blood sample. Theoretically, information on only a small portion of the intravenous plasma level–time profile is sufficient for the analysis. Data on plasma levels shortly after intravenous dosing and the terminal biological half-life are not always needed. Thus, the method might be particularly useful for drugs with long or uncertain biological half-lives. Theoretically, the method also can be applied to urine or saliva data. The method assumes the same drug disposition kinetics between the intravenous and absorption studies.

Keyphrases □ Drug absorption—compartment- and model-independent calculation for drugs with linear pharmacokinetics □ Pharmacokinetics, linear—compartment- and model-independent drug absorption calculation □ Absorption—compartment- and model-independent calculation for drugs with linear pharmacokinetics □ Instantaneous midpoint–input principle—drug absorption, linear pharmacokinetics

Calculation of the drug absorption rate from various dosage forms or administration routes is important in biopharmaceutical and pharmacokinetic studies. Many methods for calculating the absorption rate have been reported or reviewed (1–17). The original Wagner–Nelson (1) and Loo–Riegelman (2) methods have been the most widely and successfully used numerical methods in the past decade.

BACKGROUND

The original Wagner–Nelson method (1) is based on the linear one-compartment open model for drug disposition. Since the disposition kinetics of almost all drugs can be described more accurately by multicompartment models (2, 18), its use in many cases can be viewed only as an approximation. Precautions for using this method were discussed previously (2–4).

The Loo–Riegelman method (2) can be used for drugs exhibiting linear multicompartment properties. The method was derived based on multicompartment models in which drug elimination was assumed to take place exclusively from the central compartment (2). Although such an assumption probably is correct for most drugs, for some drugs various degrees of elimination probably also can take place in the tissue or peripheral compartments. However, it was shown subsequently that such an assumption is not necessary for the correct calculation of absorption rates (10, 15). In addition, the pharmacokinetic parameters of the drug in the body are assumed to remain the same during intravenous and absorption studies (2). For intrasubject variation in the terminal biological half-life during intravenous and oral studies, a new elimination rate constant from the central compartment must be used. This new rate constant is calculated based on the assumption that the central compartment volume and the intercompartmental first-order transfer rate constants remain the same (19).

Three approximations are made in the derivation of the final equations used in the original Loo–Riegelman method:

1. The linear trapezoidal rule method is used to estimate the area under the plasma level–time curve for the calculation of the drug amount eliminated from the body during a time interval. Such an approximation method also is employed in the Wagner–Nelson method. The accuracy of the linear trapezoidal rule method for calculating the area under the curve was discussed (15, 20, 21). An improper blood sampling schedule during absorption might result in significant errors in the estimate of the plasma area and, hence, the absorption rate calculation.
2. The plasma level is assumed to change linearly with time in the calculation of the drug distribution rate from the central compartment to the tissue or peripheral compartment. Again, various degrees of under- or overestimation probably occur if an improper blood sampling schedule is employed.
3. The two-term Taylor expansion series is used as a substitution for the exponential term in the equation. Such an approximation occasionally may result in serious errors. As a result, a three-term Taylor expansion series (4) or one without the Taylor series (16) was recommended.

Despite the assumptions and approximations for solving the absorption differential equation, the method has yielded excellent results (16).

This article reports a new, simple, compartment- and model-independent method for the rapid calculation of the absorption rate of drugs exhibiting linear pharmacokinetics. No assumptions regarding specific pharmacokinetic models or the drug elimination site from the body are necessary. Although the development of this method is empirical, it generally is highly accurate when properly used and might be satisfactory for many pharmacokinetic studies. Such use is analogous to the empirical use of the linear trapezoidal rule method for estimation of the area under the curve (20, 21).

THEORETICAL

It was shown (22, 23) that the plasma drug concentration after the constant intravenous infusion period for the one-compartment open model system can be approximated by assuming that the entire infused dose is injected instantaneously into the body as a bolus dose at the midpoint of the infusion period. Errors in such an approximation are negligible or insignificant when the infusion period to biological half-life ratios are low (22). For example, the error is ~0.1% when the ratio is 0.25.

In absorption studies, the plasma drug concentration of the first blood sample shortly after dosing, $C^{o}_{pt_1}$, also might be approximated satisfactorily by assuming that all drug absorbed up to the first sampling time, t_1, is absorbed instantaneously at the midpoint of the absorption period (*i.e.*, $0.5t_1$). The drug amount absorbed into the general circulation up to t_1 then can be calculated by comparing the $C^{o}_{pt_1}$ value with the theoretical plasma drug concentration, $C^{iv}_{p0.5t_1}$, at the midpoint of the absorption period (*i.e.*, $0.5t_1$) after an intravenous bolus dose. The drug amount absorbed between the first (t_1) and second (t_2) blood sampling periods can be estimated by the same principle after correction for the plasma level contribution, $C^{o}_{pp_1}$, at t_2 from the drug absorbed prior to t_1. Again, to calculate $C^{o}_{pp_1}$, all drug absorbed prior to t_1 is assumed to be absorbed instantaneously at $0.5t_1$. This can be done as follows: $C^{o}_{pp_1}$ = fraction of dose absorbed during the first absorption period × $C^{iv}_{p(t_2-0.5t_1)}$, where $C^{iv}_{p(t_2-0.5t_1)}$ is the theoretical plasma concentration at $(t_2 - 0.5t_1)$ when the same extravascular dose is given intravenously as a bolus. The same principle then can be used to calculate the drug amounts absorbed during other sampling intervals. The known or estimated absorption lag time should be corrected for the calculation of absorption periods.

0022-3549/80/0100-0057$01.00/0
© 1980, American Pharmaceutical Association

Table I—Comparisons of the Absorption Rates Calculated by the Loo–Riegelman Method and the New Method for Example 1

Hours	C_p[a]	C_p[b]	Cumulative Fraction Absorbed			
			Reported[c]	Calculated[d]	Theoretical[e]	Calculated[f]
0.5	3.0	3.36	0.165	0.1654	0.1853	0.1852
1.0	5.2	5.48	0.316	0.3167	0.3364	0.3357
1.5	6.5	6.77	0.437	0.4378	0.4594	0.4587
2.0	7.30	7.48	0.540	0.5401	0.5596	0.5584
2.5	7.60	7.83	0.618	0.6184	0.6412	0.6404
3.0	7.75	7.92	0.687	0.6865	0.7077	0.7077
3.5	7.70	7.85	0.742	0.7410	0.7619	0.7619
4.0	7.60	7.68	0.790	0.7882	0.8060	0.8060
5.0	7.10	7.19	0.854	0.8529	0.8713	0.8711
6.0	6.60	6.64	0.901	0.8990	0.9146	0.9143
7.0	6.00	6.10	0.926	0.9245	0.9433	0.9430
9.0	5.10	5.16	0.958	0.9575	0.9750	0.9747

[a] Based on data reported in Ref. 2. [b] Based on data generated by the first-order input equation using Eq. A8 in the *Appendix* where $K = 0.41\ hr^{-1}$. [c] Based on data reported in Refs. 2 and 4. [d] Based on the new method. [e] Based on $(1 - e^{-K_a t})$, where $K_a = 0.41\ hr^{-1}$. [f] Based on the newly generated C_p data shown in Column 3 of this table and the new method for absorption rate calculations.

The proposed method also can be described mathematically:

$$f_1 = \frac{C^o_{pt_1}}{C^{iv}_{p0.5t_1}} \qquad \text{(Eq. 1)}$$

where f_1 is the dose fraction absorbed up to t_1, expressed in terms of the fraction of the intravenous bolus dose. If the same dose is used in both intravenous and oral absorption studies, then the f_1 value will equal exactly the fraction of the oral dose absorbed into the general circulation up to t_1. The dose fraction absorbed during each subsequent period can be calculated by:

$$f_2 = \frac{C^o_{pt_2} - C^o_{pp_1}}{C^{iv}_{p0.5(t_2-t_1)}} \qquad \text{(Eq. 2)}$$

$$f_3 = \frac{C^o_{pt_3} - (C^o_{pp_1} + C^o_{pp_2})}{C^{iv}_{p0.5(t_3-t_2)}} \qquad \text{(Eq. 3)}$$

$$f_n = \frac{C^o_{pt_n} - \sum_{i=1}^{n-1} C^o_{pp_i}}{C^{iv}_{p0.5(t_n-t_{n-1})}} \qquad \text{(Eq. 4)}$$

The $C^o_{pp_i}$ value for the calculation of absorption in each period (Eq. 1, 2, or 4) is different, although the same symbol is used in these equations. For example, for the calculation of f_n in Eq. 4, the values are: $C^o_{pp_1} = f_1 C^{iv}_{p(t_n-0.5t_1)}$, $C^o_{pp_2} = f_2 C^{iv}_{p(t_n-0.5t_1-0.5t_2)}$, $C^o_{pp_3} = f_3 C^{iv}_{p(t_n-0.5t_2-0.5t_3)}$, and $C^o_{pp_{n-1}} = f_{n-1} C^{iv}_{p(t_n-0.5t_{n-2}-0.5t_{n-1})}$.

EXPERIMENTAL

Since this method was developed empirically, its validity must be examined using many examples with different disposition kinetic characteristics under various conditions such as first-order and zero-order absorptions.

Example 1—Loo and Riegelman (2) discussed a detailed theoretical example to illustrate the application of their method for a two-compartment open model system. Their absorption profile was reanalyzed using the proposed method. Close agreement between the two methods would support the applicability of the new method. Based on their microscopic rate constants (2) and other relevant data, the following biexponential plasma level equation may be obtained if the entire dose is injected instantaneously into the general circulation:

$$C_p = 12.37e^{-0.684t} + 7.857e^{-0.0725t} \qquad \text{(Eq. 5)}$$

where t is in hours.

Table II—Comparisons of Absorption Rates of Sulfisoxazole Calculated by the Proposed Method with the Theoretical Values following First-Order Absorption Kinetics

Hours	C_p[a], mg/liter	Cumulative Dose Fraction Absorbed	
		Calculated	Theoretical[b]
0.5	65.58	0.2925	0.2928
1.0	98.20	0.4994[c]	0.5000
1.5	113.29	0.6457	0.6464
2.0	118.95	0.7491[d]	0.7499
2.5	119.45	0.8222	0.8232

[a] Plasma levels after absorption study. [b] Based on $(1 - e^{-K_a t})$, where $K_a = 0.693\ hr^{-1}$. [c] With the assumption that the first blood sample was obtained at 1.0 hr, the calculated dose fraction absorbed would be 0.4977. [d] With the assumption that the first blood sample was obtained at 2 hr, the calculated dose fraction would be 0.7349.

The first-order absorption rate constant used in their simulation was $0.41\ hr^{-1}$. Some detailed absorption rate calculations based on this new method are illustrated in the *Appendix*, and the analysis results are summarized in Table I.

Example 2—The following mean biexponential equation was obtained after a bolus intravenous injection of 2000 mg of sulfisoxazole to seven normal subjects (24):

$$C_p = 108.43e^{-1.393t} + 152.13e^{-0.12t} \qquad \text{(Eq. 6)}$$

where C_p is in micrograms per liter and t is in hours.

Theoretical plasma drug concentrations at various times using a first-order absorption rate constant of $0.693\ hr^{-1}$ were generated in part with a programmable calculator. The dose used for absorption simulation also was 2000 mg. The plasma level data up to 2.5 hr after dosing are summarized in Table II.

The absorption simulation data generated throughout this discussion are based on a compartment- and model-independent approach. This approach is in contrast with the more commonly used compartmental approach. The general equation of the plasma level profile after a first-order input with an initial one-unit dose into a system where drug disposition kinetics following the intravenous bolus injection of the same unit of dose can be described by a polyexponential equation ($C_p = \Sigma_{i=1}^{n} A_i e^{-K_i t}$) is shown in the *Appendix*.

Example 3—The following mean biexponential equation was obtained after a bolus intravenous injection of 615 mg of ampicillin to nine subjects (25):

$$C_p = 120.4e^{-2.40t} + 12.12e^{-0.39t} \qquad \text{(Eq. 7)}$$

where C_p is in milligrams per liter and t is in hours.

The plasma level profile (Table III) during the early absorption phase was generated based on an initial dose of 615 mg and a first-order absorption rate constant of $2.0\ hr^{-1}$.

Example 4—The mean plasma level profile following the intravenous rapid injection of 10 mg of diazepam to four subjects (26) can be expressed by the following triexponential equation:

$$C_p = 0.23e^{-4.62t} + 0.15e^{-0.41t} + 0.062e^{-0.0225t} \qquad \text{(Eq. 8)}$$

where C_p is in milligrams per liter and t is in hours.

Based on the same intravenous dose absorbed with a first-order rate constant of $0.693\ hr^{-1}$, the plasma level data during the first 2.5 hr after dosing are summarized in Table IV.

Example 5—The drugs described in Examples 1–4 were infused at a unit intravenous bolus dose (the same intravenous dose used individually in each example) per hour to the same subjects. Theoretical plasma

Table III—Comparisons of Absorption Rates of Ampicillin Calculated by the New Method with Theoretical Values following First-Order Absorption Kinetics

Hours	C_p[a], mg/liter	Cumulative Dose Fraction Absorbed	
		Calculated	Theoretical[b]
0.25	39.27	0.3898	0.3935
0.50	46.99	0.6263	0.6321
1.0	35.02	0.8510	0.8647

[a] Plasma levels after absorption study. [b] Based on $(1 - e^{-K_a t})$, where $K_a = 2.0\ hr^{-1}$.

Table IV—Comparisons of Absorption Rate Analysis of Diazepam (Three-Compartment Model) Calculated by Two Methods with the Theoretical Values following First-Order Absorption Kinetics (K_a = 0.693 hr^{-1})

Hours	C_p[a], mg/liter	Fractional Absorption Rate during Each Study Period		Cumulative Dose Fraction Absorbed		
		Theoretical[b]	Calculated[c]	Theoretical[d]	Calculated[c]	Calculated[e]
0.5	0.082204	0.2928	0.3050	0.2928	0.3050	0.2767
			(4.17)		(4.17)[f]	(−5.55)[f]
1.0	0.1106	0.2072	0.2085	0.5000	0.5135	0.4874
			(0.63)		(2.7)	(−2.53)
1.5	0.1223	0.1464	0.1451	0.6464	0.6586	0.6339
			(−0.89)		(1.89)	(−1.95)
2.0	0.1253	0.1035	0.1018	0.7499	0.7604	0.7388
			(−1.64)		(1.4)	(−1.74)
2.5	0.1233	0.0733	0.07189	0.8232	0.8323	0.8132
			(−1.92)		(1.1)	(−1.22)
1.0	0.1106	0.5000	0.5361[g]	0.5000	0.5361[g]	0.4497[g]
			(7.22)		(7.22)	(−10.1)

[a] Plasma levels after absorption study. [b] Calculated from Column 5 of this table. [c] Based on the new method. [d] Based on $(1 - e^{-K_a t})$. [e] Based on Loo–Riegelman method. [f] Percent over- or underestimation of the absorption of the new method as compared to theoretical results. [g] Based on the first blood sample collected 1 hr after dosing.

level data at various times after the beginning of infusion were generated by the programmable calculator based on a compartment- and model-independent equation (see *Appendix*).

RESULTS AND DISCUSSION

The results of the absorption rate calculation using the standard Loo–Riegelman method (2, 4) and the proposed method for Example 1 are summarized in Table I. The values for cumulative dose fractions absorbed from 0.5 to 9.0 hr after dosing obtained from the two methods were essentially identical (up to three significant figures for some data). Since absorption was assumed to follow first-order kinetics with a rate constant, K_a, of 0.41 hr^{-1}, the cumulative dose fraction, F_t, absorbed at various times can be determined theoretically by:

$$F_t = 1 - e^{-K_a t} \qquad \text{(Eq. 9)}$$

These theoretical values are summarized in Table I; compared to them, the absorption rates calculated by the two methods were underestimated. Recalculation of theoretical plasma level data based on Eq. A2 in the *Appendix* revealed slight discrepancies between the reported values (2, 4) and the newly generated values (Table I). Using these new plasma level data and the proposed absorption rate calculation, the calculated cumulative dose fractions (Table I) absorbed at various times were essentially identical (identical values up to four significant figures for data at 3, 3.5, and 4 hr) to the theoretical values. These results were encouraging during early evaluation of the new method.

The total area under the plasma level–time curve from Eq. 5 calculated by the integration method was essentially identical to the total area from the absorption study reported (4) (126.46 *versus* 126.44), indicating the correctness of Eq. 5. In the absorption rate analyses, 97.5% of the dose theoretically was absorbed at 9 hr after dosing.

The results of the absorption study on sulfisoxazole (Example 2), which exhibited two-compartment properties, are summarized in Table II. The excellent accuracy of the new method also was demonstrated in this example. The first blood sample, obtained 1 or 2 hr after dosing, gave calculated fractions of the dose absorbed of 0.4977 and 0.7349, respectively. These values compared well with the corresponding theoretical values: 0.5000 and 0.7491.

The results for ampicillin (Example 3) are shown in Table III. This drug was selected due to its relatively large contribution of the distribution phase (21.5% of the total area, AUC_∞). A high degree of accuracy also was observed with the new method.

The results of the absorption rate analysis of diazepam in Example 4 are summarized in Table IV. Despite its three-compartment characteristics, errors of the absorption rate estimate for each sampling period and the cumulative absorption calculated by the new method were insignificant, except for the first 0.5-hr point where absorption was overestimated by 4.17%. The overestimation for the 0.5–1.0-hr period was only 0.63%, and the underestimations for the next three sampling periods were <2% (Table IV). The accuracy of the new method was improved considerably if the first blood sample was obtained at an earlier time. For example, the overestimation was reduced to only 1.48% when the 0.25-hr plasma level (0.05382 mg/liter) was used for calculation.

The Loo–Riegelman method without the Taylor expansion series also was employed to calculate the diazepam absorption rate discussed in Example 4. The results are summarized in Table IV. The Loo–Riegelman method underestimated absorption up to 0.5 hr by 5.55%, which was slightly greater (based on absolute percent) than the 4.17% underestimation based on the new method. In this example, the new method always overestimated the cumulative absorption values (up to 2.5 hr) while the Loo–Riegelman method always underestimated them. However, the absolute percentages of over- or underestimation by these two methods were practically the same (Table IV). The accuracy of both methods for calculating the diazepam absorption rates was demonstrated by the fact that, at 2.5 hr after dosing when 82.32% of the dose had been absorbed, the new method overestimated the absorption by 1.1% while the Loo–Riegelman method underestimated it by 1.22% (Table IV).

The new method also had essentially the same accuracy as the Wagner–Nelson method on theoretical compounds with one-compartment characteristics.

These results clearly demonstrate the accuracy and applicability of the new simple method for the calculation of absorption rates of compounds with markedly different pharmacokinetic properties under first-order absorption. In Examples 1 and 4, both the new method and

Table V—Comparisons of Results of Absorption Rate Calculations Based on the Loo–Riegelman Method and the New Method for Example 1 if Only One Plasma Level at Various Times after Absorption Study Is Used

Time for First Sample, hr	C_p	Fraction Absorbed		Theoretical Fraction Absorbed
		Based on Loo–Riegelman Method	Based on New Method	
1	5.484	0.3283	0.3351	0.3364
		(−2.37)[a]	(−0.357)[a]	
2	7.481	0.5172	0.5521	0.5596
		(−7.58)	(−1.34)	
3	7.921	0.6135	0.6900	0.7077
		(−13.3)	(−2.50)	
4	7.681	0.6529	0.7723	0.8060
		(−19.0)	(−4.18)	
5	7.191	0.6613	0.8179	0.8713
		(−24.1)	(−6.13)	
6	6.638	0.6534	0.8392	0.9146
		(−28.6)	(−8.24)	

[a] Percent deviation from the theoretical value.

Table VI—Results of the Zero-Order Absorption Rate Analysis of a Hypothetical Drug in Examples 1 and 5 Calculated by the New Method

Hours	C_p	Cumulative Theoretical Fraction of Unit Intravenous Dose Absorbed	Fraction of Unit Intravenous Dose Absorbed Calculated by New Method
0.25	4.786	0.2500	0.2500
0.50	9.095	0.5000	0.5003
0.75	14.85	0.7500	0.7506
1.00	16.54	1.0000	1.0004

Table VII—Results of the Zero-Order Absorption Rate Analysis of Sulfisoxazole and Ampicillin Calculated by the New Method and the Loo–Riegelman Method

Drug	Hours	C_p, mg/liter	Theoretical Cumulative Fraction of Unit Intravenous Dose Absorbed	Fraction of Unit Intravenous Dose Absorbed	
				Calculated by New Method	Calculated by Loo–Riegelman Method
Sulfisoxazole	0.5	112.9	0.5000	0.5036 (0.72)[a]	0.4976 (−0.49)[a]
	1.0	201.9	1.0000	1.0062 (0.62)	0.9970 (−0.303)
	1.5	277.0	1.5000	1.5077 (0.513)	1.4968 (−0.216)
	2.0	343.5	2.0000	2.0091 (0.455)	1.9971 (−0.146)
Ampicillin	0.25	25.52	0.2500	0.2533 (1.32)	0.2454 (−1.85)
	0.50	40.56	0.5000	0.5065 (1.30)	0.4932 (−1.36)
	0.75	49.76	0.7500	0.7597 (1.29)	0.7425 (−1.00)
	1.00	55.65	1.0000	1.0127 (1.27)	0.9925 (−0.75)

[a] Percent difference from the theoretical value.

the standard Loo–Riegelman method yielded essentially the same results, indicating the similar accuracy of both methods.

In absorption rate studies, the first blood sample occasionally is not collected soon after dosing. Evaluation of the effect of the time of the first blood sample on the accuracy of the new method was important. This effect was evaluated thoroughly using the data in Example 1. Results of comparisons using the first plasma level at 1, 2, 3, 4, 5, or 6 hr are summarized in Table V. This example shows that the new method is much less subject to the influence of the timing of the first sample. For example, with samples at 4, 5, and 6 hr, the new method gave underestimations in absorption of 4.18, 6.13, and 8.24%, respectively, while the Loo–Riegelman method gave underestimations of 19.0, 24.1, and 28.6%, respectively. For diazepam (Example 4), the new method resulted in a 7.22% overestimation, and the Loo–Riegelman method (without the Taylor expansion series) yielded a 10.1% underestimation if the first sample at 1 hr was used. The results for the new method are encouraging since the majority of drug absorption kinetics reported in the literature appear to follow the first-order process. Frequent blood sampling and the use of interpolated plasma level data between adjacent observed points were recommended for obtaining greater accuracy when applying the Loo–Riegelman method to oral data (15).

The accuracy of the new method under zero-order absorption was evaluated also. Extremely accurate (identical up to three or four significant figures in many cases) results were obtained for the hypothetical drug discussed in Example 1, ampicillin, and sulfisoxazole (Tables VI and VII). For sulfisoxazole and ampicillin, the results from the Loo–Riegelman method without the Taylor approximation were equally accurate (Table VII). For diazepam, which exhibited triexponential decay after intravenous dosing, the new method overestimated the absorption (Table VIII) in the first 2.5 hr of simulation. The overestimation was the greatest (6.5%) in the first 0.5 hr of study and decreased gradually (only 1.2% between 2.0 and 2.5 hr). The overestimation was reduced to only 2.2% when the first blood sample was taken at 0.25 hr after the beginning of the zero-order absorption. Considering the variability in the biological system and the accuracy of the dose administered and the plasma levels analyzed, these overestimations can be regarded as insignificant. However, the Loo–Riegelman method yielded more accurate results in this example (Table VIII). For example, it resulted in only a 3.43% underestimation when the first sample at 0.5 hr was used for calculation.

The oral absorption kinetics of sulfadimethoxine in a steer were reported previously (16). The steer, 190.68 kg, was given an initial oral dose of 12.5 g; blood samples were collected at 4, 8, 12, and 24 hr after dosing. Approximately 5 months later, the same animal, weighing 266.8 kg, received a rapid intravenous injection of 17.502 g. The plasma level profile after intravenous injection was described by a triexponential equation, which corresponded to a three-compartment open model (16). The absorption rates were calculated by the Loo–Riegelman method with and without the Taylor approximation.

Since the body weights of the steer during the oral and intravenous studies were different, an approximation assuming that the intercompartmental distribution rate constants remained constant during the two studies was made (16). In other words, intercompartmental clearances were assumed to increase with increasing body weight, as reflected by changes in the volume of distribution. In applying the proposed method for the absorption rate calculation to this example, only the coefficients of the triexponential plasma level decay equation were inversely corrected for the body weight change (*i.e.*, the volume of the central or initial compartment was proportional to the body weight). Thus, the C_p profile after a 1.0-g intravenous bolus dose at the time of the oral study can be expressed by:

$$C_p = 16.00e^{-9.11t} + 5.281e^{-0.55t} + 15.36e^{-0.0580t} \quad \text{(Eq. 10)}$$

when C_p is in milligrams per liter and t is in hours.

The results of the absorption rate analysis using the new method and the Loo–Riegelman method without the Taylor approximation were similar and encouraging (Table IX); the difference in the cumulative absorption at 24 hr was only 1.56%. The facts that the absorption rate appeared to follow approximately the first-order process (16) and that the first sample was collected only 4 hr after dosing may partially explain why the cumulative absorption at 4 hr calculated by the new method was 8.17% higher than that obtained with the Loo–Riegelman method (in view of the data in Table V). The validity of the new method in the flip-flop absorption condition also was confirmed.

The results of the extensive example analyses clearly demonstrate that the new method might be potentially useful for absorption rate calculations. Its simplicity is shown clearly in the *Appendix*. In contrast to the standard Loo–Riegelman method, the present method does not require the assumption of any pharmacokinetic compartmental model and the calculation of microscopic compartmental constants. Such calculations would be complicated in the classical three-, four-, or five-compartment mammillary model systems (27, 28). The volume of the central compartment (the initial volume of distribution) also is not needed.

Furthermore, the plasma level profile shortly after intravenous dosing theoretically does not need to be known in the new method. For example, the intravenous plasma data before 0.25, 0.75, and 0.125 hr were not necessary in the absorption rate calculations in Examples 1, 2, and 4, respectively. This feature of the new method may be important since drug disposition kinetics immediately or shortly after intravenous dosing often are much more complicated than commonly assumed or understood in conventional pharmacokinetic studies (29). In addition, the apparent value of the volume of the central compartment and the apparent number of compartments in the multicompartment analysis often may be subject to the influence of the frequency and timing of the blood sampling schedule in intravenous studies (30).

Moreover, the new method requires an accurate plasma level profile in the intravenous study for only a short period. For example, the intravenous data up to only 8.75 hr were required for the absorption rate calculation in Example 1. The terminal biological half-life of this hypothetical compound is 9.56 hr. For sulfisoxazole in Example 2, the intravenous data up to 2.25 hr were sufficient for the absorption rate calculation. The terminal half-life of the drug in this example is 5.78 hr. Therefore, if the individual or mean pharmacokinetic parameters (*i.e.*, the disposition function discussed in the *Appendix*) between the intra-

Table VIII—Comparisons of the Zero-Order Absorption Rate Analysis of Diazepam in Examples 4 and 5 Calculated by the Loo–Riegelman Method and the New Method

Hours	C_p, mg/liter	Cumulative Fraction of Unit Intravenous Dose Absorbed: Theoretical	Calculated by New Method	Calculated by Loo–Riegelman Method
0.5	0.1435	0.5000	0.5325 (6.50)[a]	0.4829 (−3.43)[a]
1.0	0.2337	1.0000	1.0472 (4.72)	0.9875 (−1.25)
1.5	0.3092	1.5000	1.5558 (3.72)	1.4897 (−0.686)
2.0	0.3758	2.0000	2.0629 (3.15)	1.9908 (−0.457)
2.5	0.4351	2.5000	2.5690 (2.76)	2.4912 (−0.352)
0.25[b]	0.08520	0.25000	0.2555 (2.2)	0.2459 (−1.64)

[a] Percent deviation from the theoretical value. [b] Data are based on the first blood sample collected at 0.25 hr.

venous and oral studies in the same subject or same panel of subjects may be assumed to be the same, the present method may be applied without knowledge of the terminal biological half-life of the drug as long as the intravenous data during a certain period can be obtained or generated accurately. This feature could be valuable for drugs with long biological half-lives (*e.g.*, greater than several days or weeks). As an approximation for the absorption rate calculation, the needed plasma level data can be obtained directly from a semilogarithmic intravenous data plot.

Despite these advantages, experimental protocols for studying complete plasma level profiles are recommended. For more accurate determination of absorption kinetics, a sufficient number of blood samples should be collected in absorption studies. The present method also might be used (perhaps as a good approximation) for drugs showing unusual plasma level profiles due to extensive enterohepatic circulation. Similarly, the method probably can be used with some salivary or urinary data obeying linear pharmacokinetic principles. Precautions in using saliva level data for pharmacokinetic studies were discussed previously (31–34).

The most unique assumption made in the proposed method is that all of the drug absorbed during a given interval, regardless of the complexity of the true absorption kinetics, is absorbed instantaneously at the midpoint of the interval. This assumption now has been shown to result in useful and practical applications for the determination of the apparent volume of distribution and total body clearance after a constant-rate intravenous drug infusion (22, 23) and for the absorption rate calculation. The method using such an assumption will be referred to as the instantaneous midpoint-input method.

The absolute accuracy of this new method for absorption rate calculations is a function of many factors such as the absorption rate, the drug disposition function, and the blood sampling schedule. This dependence is similar to the problems of the accuracy of the trapezoidal rule method for the estimation of the area under the curve (21) and the instantaneous midpoint-input method for the estimation of the volume of distribution and total body clearance (22, 23). Many digital computer programs also are available for the calculation of drug absorption rates (3, 4, 35).

APPENDIX

Sample Calculations Using New Method for Example 1—Absorption rate calculations based on the oral data reported in the literature (2, 4) in the first 1.5 hr after dosing are used for illustration. The oral data were taken from Table I. The intravenous data were generated from Eq. 5. They are 18.14, 14.85, and 12.437 at 0.25, 0.75, and 1.25 hr, respectively.

The dose fraction absorbed up to 0.5 hr, $f_{0.5\text{ hr}}$, is:

$$f_{0.5\text{ hr}} = \frac{C^o_{p0.5\text{ hr}}}{C^{iv}_{p0.25\text{ hr}}} = \frac{3.0}{18.14} = 0.1654 \qquad \text{(Eq. A1)}$$

The dose fraction absorbed between 0.5 and 1 hr, $f_{1\text{ hr}}$, is calculated from:

$$\text{contribution from 0 to 0.5 hr } (C^o_{pp0.5\text{ hr}}) = C^{iv}_{p0.75\text{ hr}} \times f_{0.5\text{ hr}} \qquad \text{(Eq. A2}a\text{)}$$

$$= 14.85 \times 0.1654 \qquad \text{(Eq. A2}b\text{)}$$

$$= 2.456 \qquad \text{(Eq. A2}c\text{)}$$

Table IX—Comparisons of Absorption Rate Calculations of Sulfisoxazole in a Steer by the Loo–Riegelman Method and the New Method

Hours	Cumulative Amount Absorbed, mg: Based on Loo–Riegelman Method[a]	Based on New Method
4	3294	3563 (8.17)[b]
8	5445	5679 (4.30)
12	6525	6710 (2.83)
24	7610	7729 (1.56)

[a] Calculated from Ref. 16. [b] Percent overestimation as compared to the value obtained from the Loo–Riegelman method.

and:

$$f_{1\text{ hr}} = \frac{C^o_{p1\text{ hr}} - C^o_{pp0.5\text{ hr}}}{C^{iv}_{p0.25\text{ hr}}} = \frac{5.20 - 2.456}{18.14} = 0.1513 \qquad \text{(Eq. A3)}$$

Therefore, the cumulative dose fraction absorbed up to 1 hr = 0.1654 + 0.1513 = 0.3167.

The dose fraction absorbed between 1.0 and 1.5 hr, $f_{1.5\text{ hr}}$, is calculated from:

$$C^o_{pp0.5\text{ hr}} = C^{iv}_{p1.25\text{ hr}} \times f_{0.5\text{ hr}} = 12.437 \times 0.1654 = 2.057 \qquad \text{(Eq. A4)}$$

$$C^o_{pp1\text{ hr}} = C^{iv}_{p0.75\text{ hr}} \times f_{1\text{ hr}} = 14.85 \times 0.1513 = 2.247 \qquad \text{(Eq. A5)}$$

and:

$$f_{1.5\text{ hr}} = \frac{C^o_{p1.5\text{ hr}} - C^o_{pp0.5\text{ hr}} - C^o_{pp1\text{ hr}}}{C^{iv}_{p0.25\text{ hr}}} \qquad \text{(Eq. A6}a\text{)}$$

$$= \frac{6.5 - 2.057 - 2.247}{18.14} = 0.1211 \qquad \text{(Eq. A6}b\text{)}$$

Therefore, the cumulative dose fraction absorbed up to 1.5 hr = 0.3167 + 0.1211 = 0.4378. For the calculation of absorption between 7 and 9 hr, $C^{iv}_{p1.0\text{ hr}}$ rather than $C^{iv}_{p0.25\text{ hr}}$ should be used.

General Equation for Plasma Level Profile after First-Order Input—If it is assumed that after an instantaneous intravenous injection of a unit drug dose, the plasma level–time profile, $C_{p_{inst}}$, can be described adequately by the following polyexponential equation (disposition function):

$$C_{p_{inst}} = \sum_{i=1}^{n} A_i e^{-K_i t} \qquad \text{(Eq. A7)}$$

the general equation to describe its plasma level profile, C_p, after the same unit drug dose with a first-order absorption rate constant, K_a, can be derived by using the input–output convolution method with the assistance of the Laplace transform technique (36). The general equation derived is:

$$C_p = K_a \sum_{i=1}^{n} \frac{A_i}{K_i - K_a} (e^{-K_a t} - e^{-K_i t}) \qquad \text{(Eq. A8)}$$

In absolute terms, Eq. A7 is incorrect because the plasma drug level at the sampling site immediately after dosing (*i.e.*, time = zero) is zero due to a definite lag time of the drug to be transported from the injection site to the sampling site and the complicated disposition kinetics shortly after dosing (29).

General Equation for Plasma Level Profile after Zero-Order Input—When the zero-order absorption rate is K_0 unit of dose per unit of time, the general equation to show the plasma level profile, C_p, during the zero-order absorption can be derived similarly as:

$$C_p = K_0 \left(\sum_{i=1}^{n} \frac{A_i}{K_i} - \sum_{i=1}^{n} \frac{A_i}{K_i} e^{-K_i t} \right) \qquad \text{(Eq. A9)}$$

REFERENCES

(1) J. G. Wagner and E. Nelson, *J. Pharm. Sci.*, **52**, 610 (1963).

(2) J. C. K. Loo and S. Riegelman, *ibid.*, **57**, 918 (1968).

(3) J. G. Wagner, "Fundamentals of Clinical Pharmacokinetics," Drug Intelligence Publications, Hamilton Press, Hamilton, Ill., 1976.

(4) M. Gibaldi and D. Perrier, "Pharmacokinetics," Dekker, New York, N.Y., 1975.

(5) R. E. Notari, "Biopharmaceutics and Pharmacokinetics, An Introduction," 2nd ed., Dekker, New York, N.Y., 1976.

(6) W. A. Ritschel, "Handbook of Basic Pharmacokinetics," Drug Intelligence Publications, Hamilton Press, Hamilton, Ill., 1977.

(7) L. Z. Benet and C.-W. N. Chiang, in "Abstracts of Papers Presented at the 13th National Meeting of the APhA Academy of Pharmaceutical Sciences, Chicago," vol. 2, Nov. 5–9, 1972, pp. 169–171.
(8) D. J. Cutler, *J. Pharmacokinet. Biopharm.*, **6**, 265 (1978).
(9) S. A. Kaplan, *J. Pharm. Sci.*, **59**, 309 (1970).
(10) T. Suzuki and Y. Saitoh, *Chem. Pharm. Bull.*, **21**, 1458 (1973).
(11) K. C. Kwan and A. E. Till, *J. Pharm. Sci.*, **62**, 1494 (1973).
(12) J. G. Wagner, *J. Pharmacokinet. Biopharm.*, **2**, 469 (1974).
(13) A. Breckenridge and M. Orme, *Clin. Pharmacol. Ther.*, **14**, 955 (1973).
(14) A. E. Till, L. Z. Benet, and K. C. Kwan, *J. Pharmacokinet. Biopharm.*, **2**, 525 (1974).
(15) J. G. Wagner, *ibid.*, **3**, 51 (1975).
(16) H. G. Boxenbaum and S. A. Kaplan, *ibid.*, **3**, 257 (1975).
(17) P. R. Byron and R. E. Notari, *J. Pharm. Sci.*, **65**, 1140 (1976).
(18) S. Riegelman, J. C. K. Loo, and M. Rowland, *ibid.*, **57**, 117 (1968).
(19) "Guidelines for Biopharmaceutical Studies," APhA Academy of Pharmaceutical Sciences, Washington, D.C., 1972.
(20) W. L. Chiou, M. A. F. Gadalla, and G. W. Peng, *J. Pharmacokinet. Biopharm.*, **6**, 135 (1978).
(21) W. L. Chiou, *ibid.*, **6**, 539 (1978).
(22) W. L. Chiou, G. W. Peng, and R. L. Nation, *J. Clin. Pharmacol.*, **18**, 266 (1978).
(23) W. L. Chiou, S. M. Huang, and Y. C. Huang, *Int. J. Clin. Pharmacol.*, in press.
(24) S. A. Kaplan, R. E. Weinfeld, C. W. Abruzzo, and M. Lewis, *J. Pharm. Sci.*, **61**, 773 (1972).
(25) G. P. Lewis and W. J. Jusko, *Clin. Pharmacol. Ther.*, **18**, 475 (1975).
(26) S. A. Kaplan, M. L. Jack, K. Alexander, and R. E. Weinfeld, *J. Pharm. Sci.*, **62**, 1789 (1973).
(27) A. Rescigno and G. Segre, "Drugs and Trace Kinetics," Blaisdell, New York, N.Y., 1966.
(28) J. G. Wagner, *J. Pharmacokinet. Biopharm.*, **4**, 443 (1976).
(29) W. L. Chiou, *ibid.*, **7**, 527 (1979).
(30) W. L. Chiou, presented at the APhA Academy of Pharmaceutical Sciences, Kansas City meeting, 1979.
(31) K. Chang and W. L. Chiou, *Res. Commun. Chem. Pathol. Pharmacol.*, **13**, 357 (1976).
(32) W. L. Chiou, K. Chang, and G. W. Peng, *J. Clin. Pharmacol.*, **16**, 158 (1976).
(33) J. C. Mucklow, M. R. Benoling, G. C. Kahn, and C. T. Dollery, *Clin. Pharmacol. Ther.*, **24**, 563 (1978).
(34) W. L. Chiou and F. S. Pu, *ibid.*, **25**, 777 (1979).
(35) C. M. Metzler, "NONLIN: A Computer Program for Parameter Estimation in Nonlinear Situations," Technical Report 7292/69/7292/005, Upjohn Co., Kalamazoo, Mich., Nov. 1969.
(36) J. C. K. Loo and S. Riegelman, *J. Pharm. Sci.*, **59**, 53 (1970).

ACKNOWLEDGMENTS

The author thanks Ms. Marie Zajac for manuscript preparation and Chung-Yuen Lui, Gilbert Lam, and Shiew-Mei Huang for assistance in performing some absorption rate calculations.

Oxygen Solubilization in Egg Lecithin Dispersed in Distilled Water and Physiological Electrolyte Fluids

R. SAUL LEVINSON *[x], SERAP BUYUKYAYLACI [‡], and LOYD V. ALLEN, Jr. [§]

Received April 10, 1979, from the **Arnold & Marie Schwartz College of Pharmacy and Health Sciences, Long Island University, Brooklyn, NY 11201*, the [‡]*School of Pharmacy and Pharmacal Sciences, Purdue University, West Lafayette, IN 47907*, and the [§]*College of Pharmacy, University of Oklahoma, Oklahoma City, OK 73190.* Accepted for publication July 31, 1979.

Abstract □ Gaseous oxygen solubilization in egg lecithin dispersed in distilled water, saline, and a multi-ion physiological electrolyte solution was determined and compared to controls deficient in egg lecithin. Significant oxygen solubilization occurred in the presence of egg lecithin. Oxygen solubilization was significantly greater in saline and in the multi-ion physiological electrolyte solution than in distilled water.

Keyphrases □ Solubilization—of oxygen in egg lecithin dispersed in distilled water and physiological electrolyte fluids □ Lecithin, egg—dispersions in distilled water and physiological electrolyte fluids, oxygen solubilization □ Pulmonary surfactant model systems—egg lecithin dispersions in distilled water and physiological electrolyte fluids, oxygen solubilization □ Model systems, pulmonary surfactant—egg lecithin dispersions in distilled water and physiological electrolyte fluids, oxygen solubilization □ Oxygen—solubilization in egg lecithin dispersions in distilled water and physiological electrolyte fluids

Several studies (1–5) demonstrated that respiratory disease syndrome[1] is a direct result of a pulmonary surfactant deficiency. Mammalian lung surfactant was shown to be primarily dipalmitoyl phosphatidylcholine (I) (6–8). Since I also is the major constituent of egg (*Gallus domesticus*) lecithin (9), egg lecithin dispersions serve as convenient and relatively inexpensive pulmonary surfactant model systems.

[1] Hyaline membrane disease.

Micellar oxygen solubilization in lung surfactant was proposed (10) as a mechanism for oxygen transposition at the alveolar membrane. Other studies (11–14) demonstrated the ability of lung surfactant to solubilize oxygen and other nonpolar gases.

The effect of the presence of electrolytes at physiological concentrations on oxygen solubilization in aqueous egg lecithin dispersions is reported here.

EXPERIMENTAL

Glass reaction vials were cleaned ultrasonically[2] in 2% aqueous detergent[3], rinsed three times with tap water, and rinsed three times with deionized, glass-distilled water[4]. The vials were air dried in a ventilated oven at 200°.

Egg lecithin[5] was weighed accurately to yield 50-ml samples of 0.25, 0.50, 0.75, and 1.00% (w/v) phospholipid in normal saline[6], physiological electrolyte solution[7], and deionized, glass-distilled water. A magnetic

[2] Cole Palmer Co., Chicago, Ill.
[3] Alconox, New York, N.Y.
[4] Deionized through an exchange resin deionizer (Continental Water Service, Oklahoma City, Okla.) and then glass distilled.
[5] Lot 12073, United States Biochemical Corp., Cleveland, Ohio.
[6] Travenol Laboratories, Deerfield, Ill.
[7] Normosol-R, Abbott Laboratories, North Chicago, Ill. Contains sodium, potassium, magnesium, chloride, and bicarbonate ions in isotonic aqueous solution.

0022-3549/80/0100-0062$01.00/0
© 1980, American Pharmaceutical Association

(7) L. Z. Benet and C.-W. N. Chiang, in "Abstracts of Papers Presented at the 13th National Meeting of the APhA Academy of Pharmaceutical Sciences, Chicago," vol. 2, Nov. 5–9, 1972, pp. 169–171.
(8) D. J. Cutler, *J. Pharmacokinet. Biopharm.*, **6**, 265 (1978).
(9) S. A. Kaplan, *J. Pharm. Sci.*, **59**, 309 (1970).
(10) T. Suzuki and Y. Saitoh, *Chem. Pharm. Bull.*, **21**, 1458 (1973).
(11) K. C. Kwan and A. E. Till, *J. Pharm. Sci.*, **62**, 1494 (1973).
(12) J. G. Wagner, *J. Pharmacokinet. Biopharm.*, **2**, 469 (1974).
(13) A. Breckenridge and M. Orme, *Clin. Pharmacol. Ther.*, **14**, 955 (1973).
(14) A. E. Till, L. Z. Benet, and K. C. Kwan, *J. Pharmacokinet. Biopharm.*, **2**, 525 (1974).
(15) J. G. Wagner, *ibid.*, **3**, 51 (1975).
(16) H. G. Boxenbaum and S. A. Kaplan, *ibid.*, **3**, 257 (1975).
(17) P. R. Byron and R. E. Notari, *J. Pharm. Sci.*, **65**, 1140 (1976).
(18) S. Riegelman, J. C. K. Loo, and M. Rowland, *ibid.*, **57**, 117 (1968).
(19) "Guidelines for Biopharmaceutical Studies," APhA Academy of Pharmaceutical Sciences, Washington, D.C., 1972.
(20) W. L. Chiou, M. A. F. Gadalla, and G. W. Peng, *J. Pharmacokinet. Biopharm.*, **6**, 135 (1978).
(21) W. L. Chiou, *ibid.*, **6**, 539 (1978).
(22) W. L. Chiou, G. W. Peng, and R. L. Nation, *J. Clin. Pharmacol.*, **18**, 266 (1978).
(23) W. L. Chiou, S. M. Huang, and Y. C. Huang, *Int. J. Clin. Pharmacol.*, in press.
(24) S. A. Kaplan, R. E. Weinfeld, C. W. Abruzzo, and M. Lewis, *J. Pharm. Sci.*, **61**, 773 (1972).
(25) G. P. Lewis and W. J. Jusko, *Clin. Pharmacol. Ther.*, **18**, 475 (1975).
(26) S. A. Kaplan, M. L. Jack, K. Alexander, and R. E. Weinfeld, *J. Pharm. Sci.*, **62**, 1789 (1973).
(27) A. Rescigno and G. Segre, "Drugs and Trace Kinetics," Blaisdell, New York, N.Y., 1966.
(28) J. G. Wagner, *J. Pharmacokinet. Biopharm.*, **4**, 443 (1976).
(29) W. L. Chiou, *ibid.*, **7**, 527 (1979).
(30) W. L. Chiou, presented at the APhA Academy of Pharmaceutical Sciences, Kansas City meeting, 1979.
(31) K. Chang and W. L. Chiou, *Res. Commun. Chem. Pathol. Pharmacol.*, **13**, 357 (1976).
(32) W. L. Chiou, K. Chang, and G. W. Peng, *J. Clin. Pharmacol.*, **16**, 158 (1976).
(33) J. C. Mucklow, M. R. Benoling, G. C. Kahn, and C. T. Dollery, *Clin. Pharmacol. Ther.*, **24**, 563 (1978).
(34) W. L. Chiou and F. S. Pu, *ibid.*, **25**, 777 (1979).
(35) C. M. Metzler, "NONLIN: A Computer Program for Parameter Estimation in Nonlinear Situations," Technical Report 7292/69/7292/005, Upjohn Co., Kalamazoo, Mich., Nov. 1969.
(36) J. C. K. Loo and S. Riegelman, *J. Pharm. Sci.*, **59**, 53 (1970).

ACKNOWLEDGMENTS

The author thanks Ms. Marie Zajac for manuscript preparation and Chung-Yuen Lui, Gilbert Lam, and Shiew-Mei Huang for assistance in performing some absorption rate calculations.

Oxygen Solubilization in Egg Lecithin Dispersed in Distilled Water and Physiological Electrolyte Fluids

R. SAUL LEVINSON *[x], SERAP BUYUKYAYLACI [‡], and LOYD V. ALLEN, Jr. [§]

Received April 10, 1979, from the **Arnold & Marie Schwartz College of Pharmacy and Health Sciences, Long Island University, Brooklyn, NY 11201*, the [‡]*School of Pharmacy and Pharmacal Sciences, Purdue University, West Lafayette, IN 47907*, and the [§]*College of Pharmacy, University of Oklahoma, Oklahoma City, OK 73190.* Accepted for publication July 31, 1979.

Abstract □ Gaseous oxygen solubilization in egg lecithin dispersed in distilled water, saline, and a multi-ion physiological electrolyte solution was determined and compared to controls deficient in egg lecithin. Significant oxygen solubilization occurred in the presence of egg lecithin. Oxygen solubilization was significantly greater in saline and in the multi-ion physiological electrolyte solution than in distilled water.

Keyphrases □ Solubilization—of oxygen in egg lecithin dispersed in distilled water and physiological electrolyte fluids □ Lecithin, egg—dispersions in distilled water and physiological electrolyte fluids, oxygen solubilization □ Pulmonary surfactant model systems—egg lecithin dispersions in distilled water and physiological electrolyte fluids, oxygen solubilization □ Model systems, pulmonary surfactant—egg lecithin dispersions in distilled water and physiological electrolyte fluids, oxygen solubilization □ Oxygen—solubilization in egg lecithin dispersions in distilled water and physiological electrolyte fluids

Several studies (1–5) demonstrated that respiratory disease syndrome[1] is a direct result of a pulmonary surfactant deficiency. Mammalian lung surfactant was shown to be primarily dipalmitoyl phosphatidylcholine (I) (6–8). Since I also is the major constituent of egg (*Gallus domesticus*) lecithin (9), egg lecithin dispersions serve as convenient and relatively inexpensive pulmonary surfactant model systems.

[1] Hyaline membrane disease.

Micellar oxygen solubilization in lung surfactant was proposed (10) as a mechanism for oxygen transposition at the alveolar membrane. Other studies (11–14) demonstrated the ability of lung surfactant to solubilize oxygen and other nonpolar gases.

The effect of the presence of electrolytes at physiological concentrations on oxygen solubilization in aqueous egg lecithin dispersions is reported here.

EXPERIMENTAL

Glass reaction vials were cleaned ultrasonically[2] in 2% aqueous detergent[3], rinsed three times with tap water, and rinsed three times with deionized, glass-distilled water[4]. The vials were air dried in a ventilated oven at 200°.

Egg lecithin[5] was weighed accurately to yield 50-ml samples of 0.25, 0.50, 0.75, and 1.00% (w/v) phospholipid in normal saline[6], physiological electrolyte solution[7], and deionized, glass-distilled water. A magnetic

[2] Cole Palmer Co., Chicago, Ill.
[3] Alconox, New York, N.Y.
[4] Deionized through an exchange resin deionizer (Continental Water Service, Oklahoma City, Okla.) and then glass distilled.
[5] Lot 12073, United States Biochemical Corp., Cleveland, Ohio.
[6] Travenol Laboratories, Deerfield, Ill.
[7] Normosol-R, Abbott Laboratories, North Chicago, Ill. Contains sodium, potassium, magnesium, chloride, and bicarbonate ions in isotonic aqueous solution.

0022-3549/80/0100-0062$01.00/0
© 1980, American Pharmaceutical Association

Table I—Three-Factor Analysis of Variance with Repeat Measures for Oxygen Solubilization in Egg Lecithin Dispersions Excluding Controls

Source of Variation	*df*	*SS*	*MS*	*F*[a]
Media	2	15.0288	7.5144	60.41
Concentration	3	4.5492	1.5164	12.19
Media × concentration	6	12.3654	2.0609	16.57
Subjects (G)	60	7.4632	0.1233	—
Time	4	1012.0422	253.0106	10,120.42
Time × media	8	48.9936	6.1242	244.97
Time × concentration	12	2.4318	0.2027	8.11
Time × media × concentration	24	3.4116	0.1422	5.69
Time × subjects (G)	240	5.9930	0.0250	—

[a] $p < 0.01$.

Table II—Three-Factor Analysis of Variance with Repeat Measures for Oxygen Solubilization in Egg Lecithin Dispersions Including Controls

Source of Variation	*df*	*SS*	*MS*	*F*[a]
Media	2	10.771	5.385	26.28
Concentration	4	351.825	87.956	429.26
Media × concentration	8	17.869	2.233	10.90
Subjects (G)	75	15.371	0.205	—
Time	4	827.529	206.882	9577.87
Time × media	8	40.475	5.059	234.21
Time × concentration	16	187.558	11.722	542.69
Time × media × concentration	32	12.129	0.379	17.55
Time × subjects (G)	300	6.484	0.022	—

[a] $p < 0.01$.

stirring bar was included in each sample vial before addition of the dispersion medium. Each vial was sealed with a rubber septum and an aluminum crimp seal and then was flushed with ultrapure (99.99%) humidified nitrogen[8]. Accurately measured volumes of the dispersion media were added after an equivalent volume of nitrogen gas was withdrawn from the vial. Each vial then was stirred gently on a magnetic stirring plate until homogeneous dispersion was effected.

Ten milliliters of nitrogen gas was withdrawn accurately from each vial, and an equivalent volume of ultrapure oxygen[9] was added with gas-tight gas transfer syringes[10]. While the dispersions were stirred gently on the magnetic stirring plate, 10-μl samples of the gaseous phase were withdrawn at 0, 24, 48, 96, and 120 hr.

Vials of normal saline, physiological electrolyte solution, and distilled water were prepared deficient in egg lecithin to serve as controls.

Each egg lecithin sample and its corresponding control sample were prepared and analyzed in triplicate, and each experiment was done in duplicate.

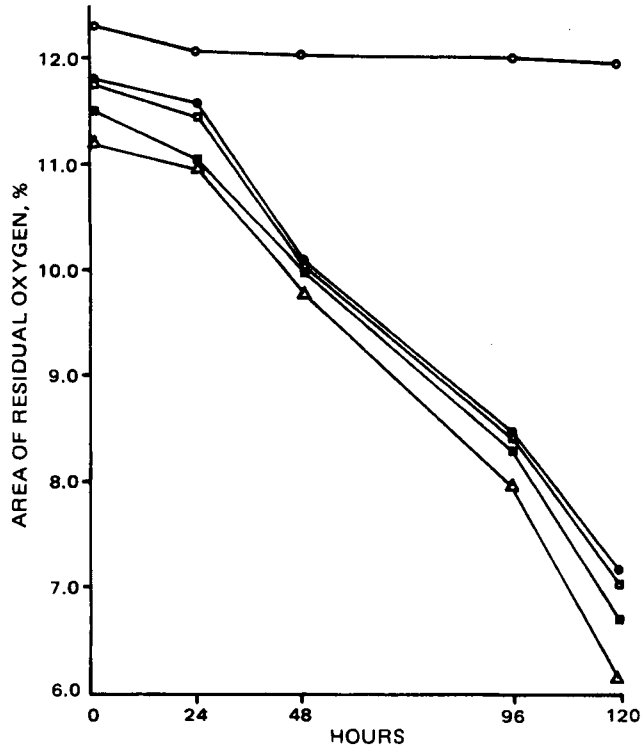

Figure 1—*Effect of egg lecithin concentration in normal saline on the extent of oxygen solubilization with time. Key: ○, normal saline (control); ●, 0.25% egg lecithin; □, 0.50% egg lecithin; ■, 0.75% egg lecithin; and △, 1.00% egg lecithin.*

[8] Union Carbide Corp., New York, N.Y.
[9] Ultrahigh purity, Union Carbide Corp., New York, N.Y.
[10] Models 1710 SN and 1020 LTN, Hamilton Syringe Co., Reno, Nev.

Analysis of the residual oxygen at the indicated times was accomplished by GLC[11]. The nitrogen–oxygen mixture was resolved on a molecular sieve[12] with thermal conductivity detection[13]. The peak area as the percent of detector response for oxygen was calculated and recorded with an electronic integrator[14].

Helium[8] was the carrier gas at 21 ml/min. The inlet, detector, and column temperatures were 100, 100, and 50°, respectively.

Since the sealed experimental and control vials were flushed with nitrogen to an open atmosphere and an equivalent volume of nitrogen gas was withdrawn when oxygen was added, the pressure in the closed system was equal to atmospheric pressure during sample preparation. Minor pressure effects due to the withdrawal of 10-μl gas samples at the indicated times were regarded as insignificant. Furthermore, any manipulative error introduced was offset in the statistical analysis because the control samples were treated the same as the experimental samples.

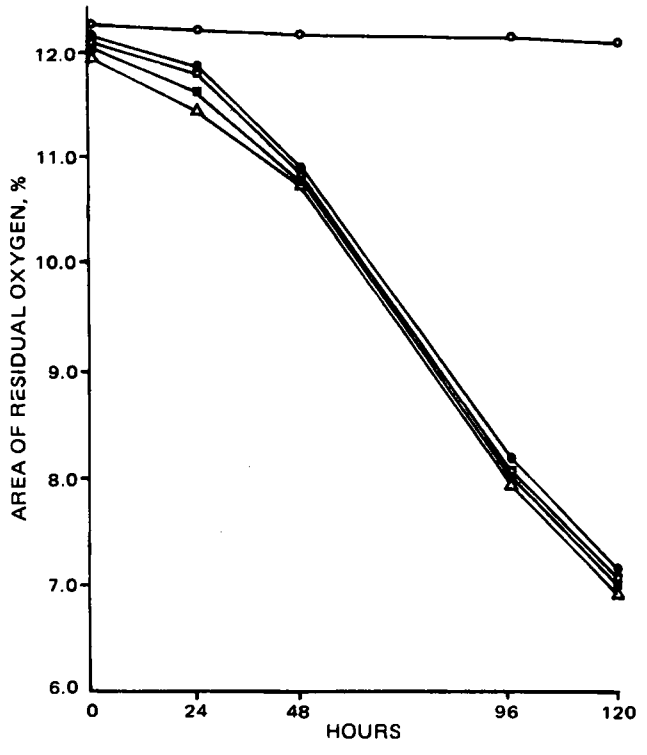

Figure 2—*Effect of egg lecithin concentration in a multi-ion physiological electrolyte fluid on the extent of oxygen solubilization with time. Key: ○, multi-ion physiological electrolyte solution (control); ●, 0.25% egg lecithin; □, 0.50% egg lecithin; ■, 0.75% egg lecithin; and △, 1.00% egg lecithin.*

[11] Model 2300 dual-column gas–liquid chromatograph, Bendix Corp., Ronceverte, W. Va.
[12] Molecular sieve 5-A, 80–100 mesh, and a 183-cm stainless steel column, Alltech Associates, Arlington Heights, Ill.
[13] Type 2300, four element, Bendix Corp., Ronceverte, W. Va.
[14] CDS IIIC, Varian Associates, Palo Alto, Calif.

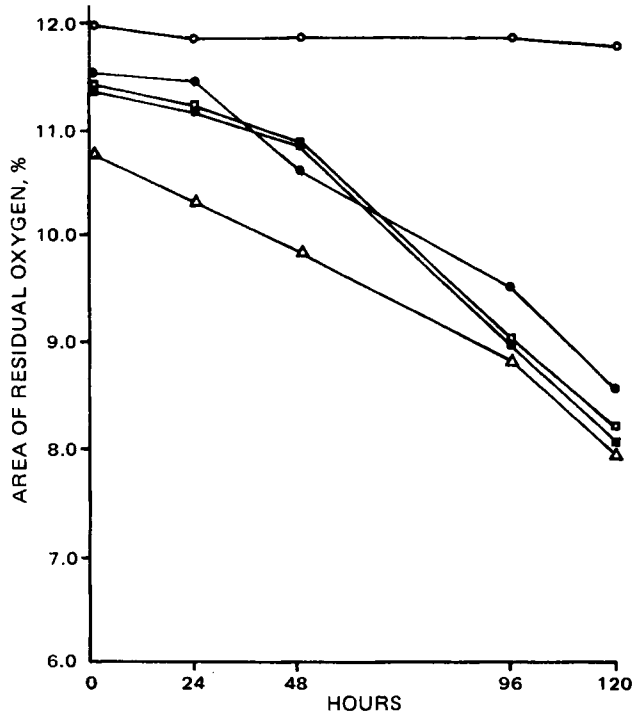

Figure 3—*Effect of egg lecithin concentration in distilled water on the extent of oxygen solubilization with time. Key:* ○, *deionized distilled water (control);* ●, *0.25% egg lecithin;* □, *0.50% egg lecithin;* ■, *0.75% egg lecithin; and* △, *1.00% egg lecithin.*

RESULTS AND DISCUSSION

Figures 1–3 indicate that, in comparison to the controls, considerable oxygen solubilization occurred in aqueous egg lecithin dispersions. Furthermore, differences in the amount of gaseous oxygen solubilized can be demonstrated for all three aqueous media used, with the multi-ion physiological electrolyte fluid and saline exhibiting the greatest solubilization. Statistical analysis of the data (Tables I and II) utilizing a three-factor analysis of variance indicated statistically valid differences in gaseous oxygen solubilization among the media employed, the egg lecithin concentration, and time.

Table II presents the statistical data including the control samples, while Table I excludes the controls. This contrast was done to identify the greatest variance ratio components. The incubation time had the greatest influence on oxygen solubilization, followed by the medium employed and then the egg lecithin concentration. This egg lecithin concentration effect, as determined statistically, is not surprising because solubilization requires only that micelles be present. Apparently, the egg lecithin concentration range used (0.25, 0.50, 0.75, and 1.00%) was above the critical micelle concentration for the surfactant in the media.

The presence of electrolytes can affect the size of surfactant micelles by forcing surfactant molecules into micellar units similar to the way in which electrolytes can be used to dehydrate or salt out sparingly soluble organic molecules from water.

The diffusional aspect of oxygen transposition was the rate limiter because the effect of time on oxygen transposition can be demonstrated statistically to be the predominant factor controlling oxygen solubilization.

This study indicated that, in the development of synthetic, natural, or semisynthetic lung surfactant for treatment of respiratory disease syndrome and other pulmonary surfactant diseases, the medium employed may overshadow the particular surfactant used. Further study with the egg lecithin pulmonary surfactant model system is warranted.

REFERENCES

(1) P. Gruenwald, *Am. J. Obstet. Gynecol.*, **53**, 996 (1947).

(2) R. E. Pattle, *Nature*, **175**, 1125 (1955).

(3) R. E. Pattle, A. E. Claireaux, P. A. Davies, and A. H. Cameron, *Lancet*, **2**, 469 (1962).

(4) M. E. Avery and J. Mead, *Am. J. Dis. Child.*, **97**, 517 (1959).

(5) J. A. Clements, R. F. Husted, R. Johnson, and I. Gribetz, *J. Appl. Physiol.*, **16**, 444 (1961).

(6) T. Fujiwara and F. H. Adams, *Tohoku J. Exp. Med.*, **84**, 46 (1964).

(7) E. S. Brown, *Am. J. Physiol.*, **207**, 402 (1964).

(8) S. Mulay, F. Khamsi, and S. Solomon, *Anal. Biochem.*, **77**, 350 (1977).

(9) L. Saunders, J. Perrin, and D. Gammack, *J. Pharm. Pharmacol.*, **14**, 567 (1962).

(10) B. Ecanow, B. H. Gold, R. Balagot, and R. S. Levinson, in "Micellization, Solubilization, and Microemulsions," vol. 2, K. L. Mittal, Ed., Plenum, New York, N.Y., 1977.

(11) B. Ecanow, R. Balagot, and V. Santelices, *Nature*, **215**, 1400 (1967).

(12) W. Stanaszek, B. Ecanow, and R. S. Levinson, *J. Pharm. Sci.*, **65**, 142 (1976).

(13) B. Ecanow, R. Balagot, and V. Bandelin, *Am. Rev. Resp. Dis.*, **99**, 106 (1969).

(14) W. Stanaszek and B. Ecanow, *J. Pharm. Sci.*, **61**, 860 (1972).

ACKNOWLEDGMENTS

Abstracted in part from a thesis submitted by S. Buyukyaylaci to the University of Oklahoma in partial fulfillment of the Master of Science degree requirements.

Kinetics and Mechanisms of Monolayer Interactions V: Surface Activities of Alkylamides, Alkylmonocarboxylic Acids, and Alkylketones and Their Interaction Energies with Phospholipid Monolayers

FEDERICO A. VILALLONGA ˣ **and EDWARD W. PHILLIPS**

Received May 2, 1979, from the *College of Pharmacy, University of Florida, Gainesville, FL 32610.* Accepted for publication July 24, 1979.

Abstract □ The adsorption free energies of the C_1–C_6 alkylamides, C_3–C_8 alkylketones, and C_1–C_{10} alkylmonocarboxylic acids at the air–water interface, estimated from plots of the surface pressure (≤5 dynes/cm) *versus* the bulk concentration, were linear functions of the total surface area per molecule (square angstroms per molecule), with a slope 46% higher for the alkylamides and 25% lower for the alkylketones than that for the monocarboxylic acids. The interaction energies of alkylamides with dipalmitoyl lecithin and dipalmitoyl phosphatidylethanolamine spread at the air–water interface, estimated from the surface pressure increase with increasing concentrations of the injected C_1–C_5 compounds, were linear functions of the total surface area per molecule. The diffusion free energies, ΔG_{dif}, of the alkylamides within a phospholipid bilayer, predicted from the permeability equation and their interaction energies with dipalmitoyl lecithin monolayers by assuming the additivity of their free energies of adsorption and dehydration at the solution–bilayer interface, agreed with the literature data.

Keyphrases □ Surface activity—alkylamides, alkylmonocarboxylic acids, and alkylketones, interaction energies with phospholipid monolayers □ Phospholipid monolayers—interaction energies with alkylamides, alkylmonocarboxylic acids, and alkylketones □ Interaction energies—alkylamides, alkylmonocarboxylic acids, and alkylketones with phopholipid monolayers

The adsorption free energies of alkanols at the air–aqueous interface estimated from plots of the surface pressure *versus* the bulk concentration were compared (1) with their interaction energies with dipalmitoyl lecithin (I) and dipalmitoyl phosphatidylethanolamine (II) monolayers, estimated from the variation of the equilibrium surface pressure with varying concentrations of subphase-injected alkanols based on a collision model and a constant entropy factor (2, 3).

The present work compares the adsorption free energies at the air–aqueous interface of alkylamides, their *N*-methyl derivatives, alkylmonocarboxylic acids, and alkylketones with those of the alkanols and with their interaction energies with I and II monolayers. Correlations between the surface activities and the molecular surface areas of the compounds are considered, and the implications with partition coefficients and permeabilities of these substances through biomembranes and liposomes are discussed.

EXPERIMENTAL

Reagents—Dipalmitoyl lecithin[1] and dipalmitoyl phosphatidylethanolamine[1] were homogeneous by TLC (4). Reagent grade formamide[2], acetamide[3], propionamide[4], butyramide[5], valeramide[2], hexanamide[2], *N*-methyl-[2] and *N,N*-dimethylformamide[2], *N*-methyl-[2] and *N,N*-dimethylacetamide[5], *N*-methyl-[2] and *N,N*-dimethylpropionamide[2], *N*-methyl-[6] and *N,N*-dimethylbutyramide[6], *N,N*-dimethylvaleramide[2], *N,N*-dimethylhexanamide[2], formic acid[4], propionic acid[3], butyric acid[5], valeric acid[5], hexanoic acid[5], octanoic acid[5], decanoic acid[5], propanone[5], 2-butanone[5], 2-pentanone[5], 2-hexanone[5], and 2-octanone[5] were used without further purification. The hexane[7] used to prepare the spreading solution and the distilled water used to prepare the aqueous solution and as a subphase for the phospholipid monolayers fulfilled the requirements described previously (2, 3).

Instruments—A 9-cm diameter polytef dish with two identical microburets[8] and a polytef-coated stirring bar (1.25 × 0.8 cm) was used as a trough in the closed system described previously (2, 3). Surface tension was measured with a Wilhelmy platinum plate (2.5 × 1.25 × 0.01 cm) attached to an electrobalance[9] whose output was fed into a recorder[10].

Surface Tensions of Aqueous Solutions—The surface tension of the aqueous solutions was measured as described previously (1). The reproducibility was within ±0.2 dyne/cm. All experiments were performed at 21 ± 1°. The surface pressure, π, obtained by the difference between the previously determined surface tension of the pure water and the surface tension of the aqueous solution, was fitted to an exponential function of the concentration, C (moles per liter), by digital computerized nonlinear regression (1). The Gibbs adsorption equation was used in the form described previously (1):

$$\Gamma_2 = \frac{d\pi}{d \ln C_2}\left(\frac{1}{kT}\right) \qquad \text{(Eq. 1)}$$

where Γ_2 is the solute surface concentration (molecules per square centimeter), π is the surface pressure (dynes per centimeter), C_2 is the solute concentration in the bulk solution (moles per liter), k is the Boltzmann constant (ergs per molecule per degree), and T is the absolute temperature (°K). The derivative ($d\pi/d \ln C_2$) of the exponential function that approximates the surface pressure dependence on concentration was computed with respect to the logarithm of the concentration. Substitution of these values into Eq. 1 permitted calculation of Γ_2 at any C_2.

Injection under Phospholipid Monolayers—Spreading of the phospholipid monolayers and injection of the test substance were performed as described previously (1–3). The initial phospholipid monolayer surface pressure was 5 ± 0.1 dynes/cm in all experiments. The criterion of equilibrium after the injection of the studied substance was the constancy (±0.1 dyne/cm) of the surface pressure increment, $\Delta\pi$, during 30 min.

RESULTS

Adsorption at Clean Air–Aqueous Interface—Typical plots of the surface pressure *versus* the logarithm of the concentration for some compounds are given in Figs. 1–4. Plots of surface pressure *versus* log concentration obtained with 0.1 *M* HCl solutions of the alkylmonocarboxylic acids coincided with those of their pure water solutions within reproducibility limits.

The standard free energy change, ΔG°_{ad} (ergs per molecule), associated with solute adsorption at the clean air–aqueous interface was estimated from (1, 5):

$$\Delta G^\circ_{ad} = -kT \ln \frac{\pi}{x_2^*} \qquad \text{(Eq. 2)}$$

where x_2^* is the solute activity. The ΔG°_{ad} values were calculated from the slope (π/x_2^*) of the plot of π (≤5 dynes/cm) *versus* the solute mole fraction

[1] Mann Research Laboratories, Orangeburg, N.Y.
[2] Pfalz and Bauer, Stanford, Conn.
[3] J. T. Baker Chemical Co., Rochester, N.Y.
[4] Eastman Kodak Co., Rochester, N.Y.
[5] Aldrich Chemical Co., Milwaukee, Wis.
[6] Prepared by K. V. Rao.
[7] Matheson, Coleman and Bell, East Rutherford, N.J.
[8] Manostat, New York, N.Y.
[9] Cahn Division, Ventron Instruments Corp., Paramount, Calif.
[10] Leeds and Northrup, North Wales, Pa.

0022-3549/80/0100-0065$01.00/0
© 1980, American Pharmaceutical Association

Table I—Total Molecular Surface Area, Adsorption Free Energies at the Air–Water Interface, ΔG°_{ad}, and Interaction Energies, ψ, with I and II Monolayers

Compound	TSA, Å²/molecule	Air–Water			I-Water,	II-Water,
		r	$\frac{\pi}{X_2}$	$-\Delta G^{\circ}_{ad} \times 10^{13}$, ergs/molecule	$\psi_I \times 10^{13}$, ergs/molecule	$\psi_{II} \times 10^{13}$, ergs/molecule
Formamide	64.2	0.9945	39.0	1.5	0.3	0.7
Acetamide	84.6	0.9916	1.8×10^2	2.1	0.6	1.3
Propionamide	103.1	0.9889	1.7×10^3	3.0	1.3	2.3
Butyramide	121.3	0.9833	7.7×10^3	3.6	2.2	2.9
Valeramide	139.4	0.9967	2.0×10^4	4.0	2.5	3.5
Hexanamide	157.5	0.9999	3.1×10^4	4.4	3.2	3.5
N,N-Dimethylformamide	105.9	0.9923	8.9×10^2	2.8	0.7	1.1
N,N-Dimethylacetamide	121.7	0.9892	1.4×10^3	2.9	1.0	1.3
N,N-Dimethylpropionamide	140.3	0.9875	3.3×10^3	3.3	—	—
N,N-Dimethylbutyramide	158.4	0.9797	1.0×10^4	3.8	1.8	1.8
N,N-Dimethylvaleramide	176.5	0.9952	3.4×10^4	4.3	2.0	2.1
N,N-Dimethylhexanamide	194.7	0.9975	1.2×10^5	4.7	2.3	3.2
Formic acid	59.1	0.9977	2.7×10^2	2.3	0.6	1.0
Acetic acid	73.7	0.9979	1.2×10^3	3.1	0.9	1.0
Propionic acid	98.1	0.9969	3.2×10^3	3.3	1.6	1.5
Butyric acid	116.2	0.9974	2.0×10^4	4.0	2.2	2.5
Valeric acid	134.3	0.9998	7.0×10^4	4.5	3.0	3.2
Hexanoic acid	152.5	0.9967	1.2×10^5	4.8	3.5	3.4
Octanoic acid	188.7	0.9983	1.2×10^6	5.7	4.4	4.8
Decanoic acid	261.3	0.9368	1.9×10^7	6.8	—	—
Propanone	82.0	0.9967	1.3×10^3	2.9	0.8	1.2
2-Butanone	109.2	0.9966	3.4×10^3	3.3	0.7	1.4
2-Pentanone	127.2	0.9961	5.2×10^3	3.5	0.9	1.6
2-Hexanone	145.4	0.9838	8.8×10^3	3.7	2.2	2.1
2-Octanone	181.6	0.9968	9.0×10^4	4.6	—	3.0
Methanol	61.9	0.9972	4.7×10^2	2.5	0.0	0.2
Ethanol	79.6	0.9983	1.3×10^3	2.9	0.7	0.9
Propanol	99.7	0.9983	4.0×10^3	3.4	1.2	1.5
Butanol	115.8	0.9994	1.1×10^4	3.8	1.7	1.9
Pentanol	134.0	0.9998	4.0×10^4	4.3	2.4	2.3
Hexanol	152.1	0.9922	1.1×10^5	4.7	3.6	4.2
Heptanol	170.3	0.9999	3.3×10^5	5.2	3.8	4.6
Octanol	188.4	0.9917	1.2×10^6	5.7	4.3	4.7

in the bulk solution, x_2, when $x_2 \rightarrow 0$ and $x_2^* \rightarrow x_2$ at low mole fractions. For all compounds, plots of the surface pressure ($\pi \leq 5$ dynes/cm) *versus* the solute mole fraction in the bulk solution were reasonably linear. The correlation coefficients (r), the slopes, and the estimated ΔG°_{ad} values obtained from such plots are given in Table I.

It was shown previously (1) that the simultaneous effect of the chain length and the position of the hydroxyl group on the alkanol surface activity is described best by the total molecular surface area, TSA (square angstroms per molecule), of the alkanol molecule. Molecular surface areas of the compounds were calculated by a modified version (6) of the original computer program MOLAREA (7). The molecule was considered as a collection of spherical groups and individual atoms. The methyl, methylene, and hydroxyl groups were approximated as single spheres, and standard geometry and interatomic bond lengths and angles (8, 9) were used in the construction of the molecules. These molecular surface areas are listed in Table I.

Plots of ΔG°_{ad} *versus* the total molecular surface area of alkylamides, their *N*-methyl derivatives, alkylmonocarboxylic acids, and alkylketones are compared in Fig. 5 with those for the alkanols. The experimental points yielded reasonably straight lines within the estimated experimental error (0.14 erg/molecule or 0.2 kcal/mole). The correlation coefficients and the slopes are listed in Table II.

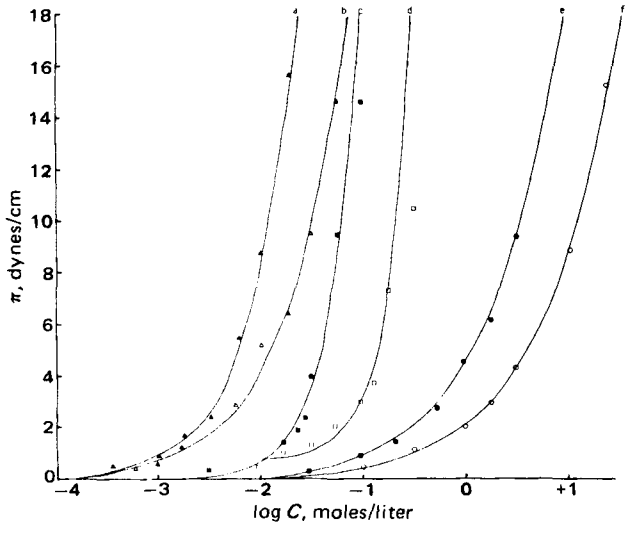

Figure 1—*Plots of the surface pressure, π, against the logarithm of the bulk concentration, C, for alkylamides from C_1 to C_6. Key: a, hexamide; b, valeramide; c, butyramide; d, propionamide; e, acetamide; and f, formamide. The lines through the experimental points were the best fit obtained with the computer (1).*

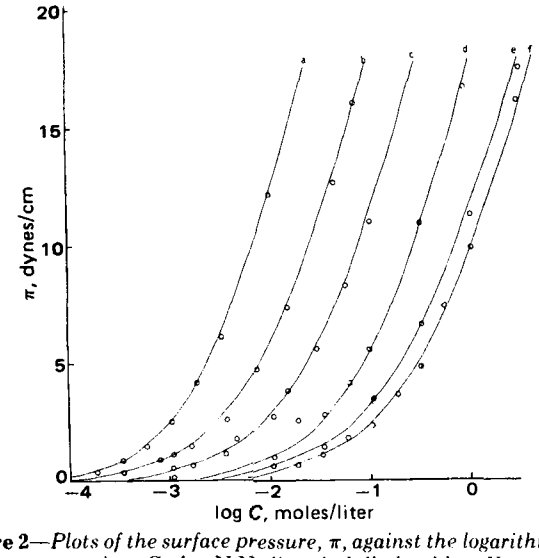

Figure 2—*Plots of the surface pressure, π, against the logarithm of the bulk concentration, C, for N,N-dimethylalkylamides. Key: a, N,N-dimethylhexanamide; b, N,N-dimethylvaleramide; c, N,N-dimethylbutyramide; d, N,N-dimethylpropionamide; e, N,N-dimethylacetamide; and f, N,N-dimethylformamide. The lines through the experimental points were the best fit obtained with the computer (1).*

Table II—Adsorption Free Energies per Methylene Group, ΔG_{CH_2}, at the Air–Water and Hydrocarbon–Water Interfaces, Interaction Energies per Methylene Group, ψ_{CH_2}, with I and II Monolayers, and Transfer Free Energies per Methylene Group, $\Delta G_{tr_{CH_2}}$, from Water to Oil

	Air–Water			Decane–[a] or Petroleum Ether[b]–Water			I–Water			II–Water			Oil–Water[c]		
Series	r	$\frac{\Delta G^\circ}{TSA}$, ergs/Å^2 × 10^{15}	$\Delta G^\circ_{CH_2}$, kcal/mole	r	$\frac{\Delta G_{ad}}{TSA}$, ergs/Å^2, × 10^{15}	$\psi G^\circ_{CH_2}$, kcal/mole	r	$\frac{\psi}{TSA}$, ergs/Å^2 × 10^{15}	ψ_{CH_2}, kcal/mole	r	$\frac{\psi}{TSA}$, ergs/Å^2 × 10^{15}	ψ_{CH_2}, kcal/mole	r	ΔG°_{tr}, ergs/Å^2 × 10^{15}	$\Delta G^\circ_{tr_{CH_2}}$, kcal/mole
Alkanols (C_1–C_5)[d]	0.9993	2.53	0.66	0.9954	3.26	0.85[b]	0.9942	3.21	0.84	0.9863	2.89	0.75	0.9983	3.0	0.79
Alkylketones (C_3–C_8)[d]	0.9638	1.65	0.43	—	—	—	—	—	—	—	—	—	0.9995	3.1	0.81
Alkylmonocarboxylic acids (C_1–C_{10})[d]	0.9750	2.20	0.57	—	—	—	0.9930	3.07	0.80	0.9817	3.35	0.87	0.9874	2.7	0.71
Alkylamides (C_1–C_6)[d]	0.9811	3.21	0.84	0.9997	3.22	0.84[a]	0.9803	3.25	0.85	0.9909	3.85	1.00	0.9831	3.2	0.83
N-Methylalkylamides (C_1–C_6)[d]	0.9811	2.26	0.59	—	—	—	—	—	—	—	—	—			
N,*N*-Dimethyl alkylamides (C_1–C_6)[d]	0.9811	2.27	0.59	—	—	—	0.9910	1.83	0.48	0.9979	1.4	0.37			

[a] From Ref. 31. [b] From Ref. 12. [c] From Ref. 33. [d] Number of carbon atoms in the hydrocarbon chain.

The slopes of the plots of the alkylmonocarboxylic acids and the *N*-methyl- and *N*-dimethylalkylamides were 13 and 10% smaller than those of the alkanols, respectively. The slopes of the plots of the alkylamides and alkylketones were 27% greater and 35% smaller than those of the alkanols, respectively.

Interaction with Phospholipid Monolayers—The interaction energies, ψ, were estimated from the slopes of the plots of the reciprocals of the equilibrium surface pressure, $\Delta\pi_{eq}$, after injection *versus* the reciprocals of the final concentration, n (molecules per cubic centimeter), of the subphase-injected substance (1–3). They are listed in Table I and are plotted in Figs. 6 and 7 *versus* the total surface area per molecule.

The plots for I monolayers were reasonably linear for alkylmonocarboxylic acids (C_1–C_8) and alkylamides (C_1–C_6) and their *N*-dimethyl derivatives. The interaction energies per methylene group, ψ_{CH_2}, estimated from the slopes of the plots of alkylmonocarboxylic acids and alkylamides (Table II), were similar to those of the alkanols (7), but the interaction energy of the *N*-dimethylalkylamides was 50% smaller.

For II monolayers, the interaction energies of formic acid, hexanamide, and *N*,*N*-dimethylhexanamide presented gross departures from linearity. The interaction energies per methylene group were higher for alkylamides and alkylmonocarboxylic acids and smaller for *N*-dimethylalkylamides than those of the alkanols.

The interaction energies of the first three compounds of the alkylketone series with I monolayers showed the same value within the estimated experimental error. In the interaction with II monolayers, the correlation coefficient was 0.93.

DISCUSSION

Adsorption at Clean Air–Aqueous Interface—From one compound of each of the studied homologous series to the next compound, there was a constant surface area increase of the hydrophobic moiety that progressively changed the hydrophilic–hydrophobic balance of the molecules. The slopes of the linear plots of the adsorption free energy *versus* the total

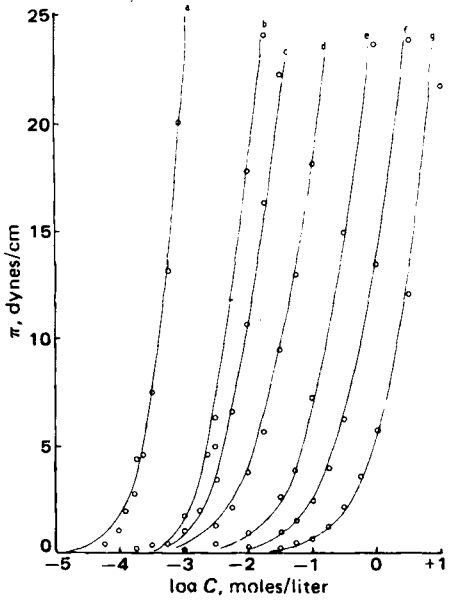

Figure 3—*Plots of the surface pressure, π, against the logarithm of the bulk concentrations, C, for alkylmonocarboxylic acids from C_1 to C_8. Key: a, octanoic; b, hexanoic; c, valeric; d, butyric; e, propanoic; f, acetic; and g, formic. The lines through the experimental points were the best fit obtained with the computer (1).*

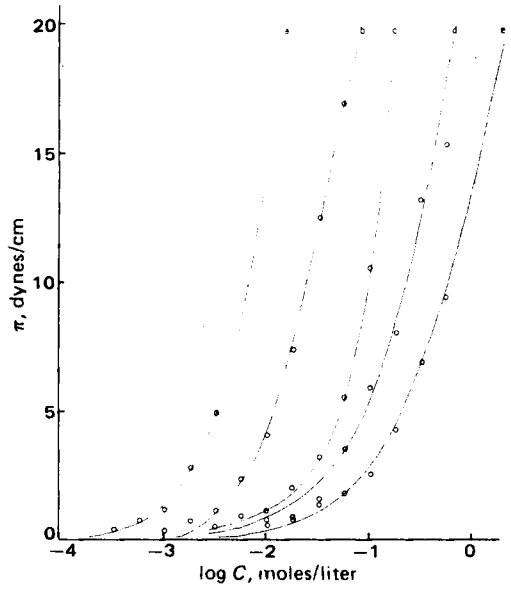

Figure 4—*Plots of the surface pressure, π, against the logarithm of the bulk concentration, C, for alkylketones from C_3 to C_8. Key: a, 2-octanone; b, 2-hexanone; c, 2-pentanone; d, 2-butanone, and e, propanone. The lines through the experimental points were the best fit obtained with the computer (1).*

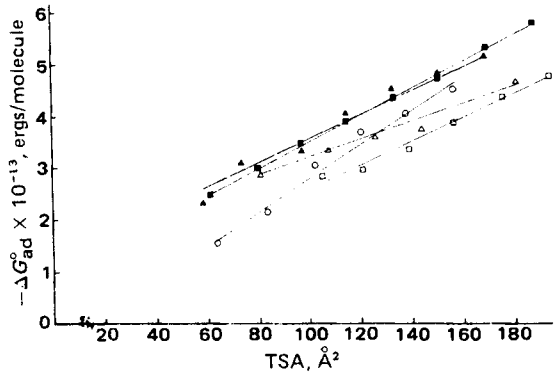

Figure 5—*Plots of the adsorption free energy of the air–aqueous solution interface, ΔG°_{ad} (ergs per molecule), against the total molecular surface area (square angstroms per molecule). Key: ▲, alkylmonocarboxylic acids; ■, alkanols; △, alkylketones; ○, alkylamides; and □, N,N-dimethylalkylamides.*

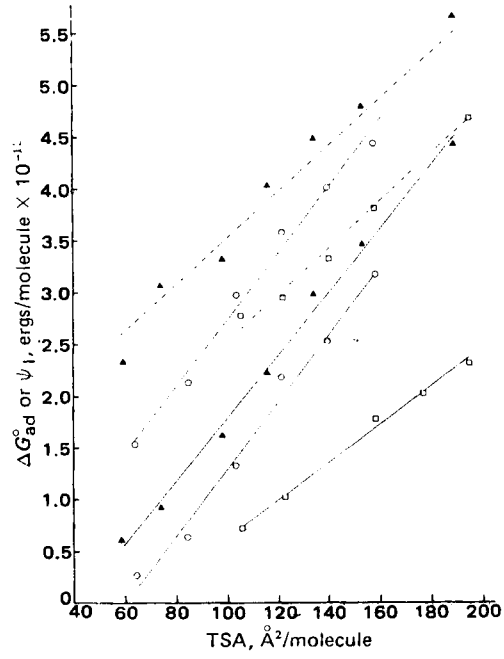

Figure 6—*Plots of the adsorption free energies at the air–aqueous solution interface (- - -) and of interaction energies with I monolayers (—) versus the total molecular surface area. Key: ▲, alkylmonocarboxylic acids; ○, alkylamides; and □, N,N-dimethylalkylamides.*

molecular surface area thus represent the contribution of each square angstrom increment of the hydrophobic surface area of the molecules to their total adsorption free energy.

The contribution to the molecular surface area due to an incremental methylene group in a straight chain extended conformation was estimated recently to be 18.1 Å² (6). The adsorption free energies per methylene group, ΔG_{CH_2}, of the studied homologous series calculated using this surface area contribution are listed in kilocalories per mole in Table II.

Since early findings obtained mainly with aliphatic alcohols, acids, and their esters (10, 11) were confirmed by several subsequent studies (1, 12–15), it generally has been accepted that the adsorption free energy increase produced by an incremental methylene group addition to a saturated straight hydrocarbon chain that adsorbs at the air–water interface is between 0.600 and 0.625 kcal/mole. The average value (0.603 ± 0.07 kcal/mole) obtained in the present study (Table II) for alkanols, alkylmonocarboxylic acids, and *N*-dimethylalkylamides reasonably agreed.

It is difficult to understand why the slope corresponding to the plot of the adsorption free energy *versus* the total molecular surface area for the alkylamides is 39% higher and that of the alkylketones is 29% lower than the average value (0.603 ± 0.07 kcal/mole) obtained for the rest of the homologous series.

The possibility existed that a different polar group attached to the same hydrocarbon chain might cause a different charge to be transferred along the methylene groups of the hydrocarbon chain, thus altering their interaction with the solvent molecules. Molecular orbital calculations performed on isolated molecules of 23 selected alkylamides, alkylmonocarboxylic acids, and alkanols failed to show evidence of a charge perturbation of the methylene groups beyond the first that could account for the observed effects of the amide group.

The fact that the adsorption free energy per methylene group of the *N*-methyl- and *N,N*-dimethylalkylamides is practically the same as that of the alkanols and alkylmonocarboxylic acids seems to indicate that the unsubstituted amino (NH_2) group is responsible for the higher adsorption free energy per methylene group in amides. Of the studied series, the amide group presents the higher hydrogen bonding capability. On the basis of *ab initio* self-consistent field method (SCF) computations of various polyhydrates, evidence was presented (16) for the structure of formamide in aqueous solutions consistent with a model of four water molecules in the primary hydration sphere, two of them hydrogen bonded to the amino group acting as a proton donor.

The standard adsorption free energy, ΔG°_{ad} (Eq. 2), is the free energy change associated with the transfer of one molecule from infinite dilution in bulk solution to infinite dilution at the interfacial region (5) and thus is a measure of the work of transfer. Kinetic data obtained for the time-dependent effect of cetrimonium ions injected beneath an air–aqueous interface on the water surface tension showed (17) excellent fit and consistency with a model that postulates an intermediate compartment (subinterface) between the plane of the interface and the bulk aqueous solution. This compartment is assumed to be a thin region with a thickness of 10–10^3 water molecule diameters (18) where the water molecules are oriented in a given array (19–21). Consequently, adsorption might be assumed to be energetically equivalent to the transfer of a solute molecule from a normal water environment in the bulk solution to the subinterface region where the water molecules are abnormally oriented.

Solute molecules such as those studied in the present work may interact with water molecules through hydrogen bonding of the polar hydrophilic group and through London dispersion forces generated mainly from its hydrophobic moiety. The negative standard adsorption free energies of formamide (−2.2 kcal/mole), formic acid (−3.3 kcal/mole), and methanol (−3.6 kcal/mole) indicate that the spontaneous tendency to perform the transfer from the bulk solution to the subinterface increases in the order: methanol > formic acid > formamide. Methanol and formamide present the minimum and maximum capabilities, respectively, to hydrogen bond with water; therefore, these results seem to indicate that, for these short-chain molecules, a correlation exists between their adsorption free energies at the air–aqueous interface and the hydrogen bonding capability of their hydrophilic moieties. The facts that aqueous urea solutions showed (22) a negative excess surface concentration (*i.e.*, $\Delta G^{\circ}_{ad} > 0$) and that thiourea in aqueous solution showed a negative adsorption free energy in preliminary experiments performed in this laboratory seem to corroborate this hypothesis.

The increase of the hydrocarbon chain length increases the surface area of the hydrophobic moiety only, enhancing its interaction through London dispersion forces with the water molecules. It seems reasonable that, at a given chain length, the adsorption free energy difference provoked by the different hydrophilic groups should be minimized due to the preponderant effect of the hydrophobic moiety. The adsorption free energies of hexanol, hexanoic acid, and hexamide are −6.8, −6.9, and −6.3 kcal/mole, respectively, in accord with this expectation; however, even for this chain length, hexanamide shows a significantly smaller value.

Experiments performed in this laboratory showed that, at constant temperature, the surface tension of heptanol–heptane mixtures adheres to the additivity rule represented by:

$$\gamma_{12} = \gamma_1 X_1 + \gamma_2 X_2 \qquad \text{(Eq. 3)}$$

where γ_{12} is the surface tension of the mixture and γ_1, γ_2, X_1, and X_2 are the surface tensions in the pure state (26.4 and 20.6 dynes/cm) and the mole fractions of heptanol and heptane in the mixture, respectively.

The surface tension of an aqueous solution containing 5.8×10^{-5} mole fraction of heptanol is 55 dynes/cm at 20°; *i.e.*, the surface tension of pure water (72.6 dynes/cm) is decreased 23% by the initial presence in the bulk solution of approximately six heptanol molecules/10^5 water molecules. A heptanol–heptane mixture containing this same heptanol mole fraction has the same surface tension as pure heptane within experimental error. In this last case, Eq. 1 predicts that the heptanol concentration at the interface is identical to that of the bulk solution. This fact suggests that

Table III—Diffusion Free Energies, ΔG_{dif}, of Alkylamides within a Phospholipid Bilayer

Compound	K, water–ether	$P^a \times 10^5$, cm/sec	$\Delta G_{dif}^{\ddagger a}$, kcal/mole	$\frac{\lambda^2}{l}\left(\frac{kT}{h}\right) \times 10^{-4}$, cm/sec	$-\psi_I$, kcal/mole	$\Delta G_{tr}^{\circ} - \Delta G_{ad}^{\circ}$ (o/w), kcal/mole	$\Delta G_{dif}^{calc\ b}$, kcal/mole
Formamide	0.0014	7.8 ± 0.5	6.15	1.61	0.43	5.61	6.10
Acetamide	0.0025	2.4 ± 0.4	7.55	2.11	0.86	5.61	7.46
Propionamide	0.013	6.1 ± 0.6	7.90	2.36	1.87	5.61	7.98
Valeramide	0.23	18.3 ± 1.1	8.00	2.98	3.60	5.61	9.18

[a] From Ref. 26. [b] Calculated from the equation: $\Delta G_{dif} = kT \ln [(\lambda^2/l)(kT/h)] + \psi_I - [\Delta G_{tr}^{\circ} - \Delta G_{ad}^{\circ}(o/w)] - kT \ln P$.

the different surface tension effects of the solvent produced by the presence of the same number of solute molecules in the two solutions may be related to some differential property between the water and heptane solvents.

The surface tension of a pure liquid is essentially a manifestation of the unbalanced molecular interactions on the surface molecules. The main intermolecular forces in liquid hydrocarbons are London dispersion forces. The hydrogen bond and London dispersion forces are the main intermolecular forces in water. The hydrogen bond component has been estimated to be responsible for two-thirds of the total surface energy of water (23).

The difference between the effect of heptanol on the surface tension of water and heptane could be related to the effect on the hydrogen bond component of the surface energy of water. The total molecular surface area of heptanol and the accepted water molecule radius (1.5 Å) lead to an estimated 25 water molecules packed closely around a heptanol molecule; *i.e.*, only 25 × 6 molecules out of 10^5 water molecules in this solution can be affected directly by the presence of heptanol molecules at that concentration.

If the assumption that the subinterface compartment with water molecules oriented in a given array (and, consequently, in a comparatively low entropic state) is valid, a plausible explanation of the magnitude of the observed effect on water could be that direct solute molecule interaction with a relatively small number of water molecules generates and propagates significant disruption of the water structure in the bulk solution. The entropic contribution thus created could be the driving force of the spontaneous heptanol molecule adsorption at the air–aqueous solution interface.

Interaction with Phospholipid Monolayers—Plots of the interaction energies, ψ, of alkylamides, *N*-dimethylalkylamides, and alkylmonocarboxylic acids with I monolayers *versus* the total molecular surface area are compared in Fig. 6 with those of their adsorption free energy at the clean air–water interface. The regression coefficients, the slopes, and the adsorption free energy per methylene group are listed in Table II.

The linearity of the plots of the compounds from C_1 to C_6 in the main hydrocarbon chain of the alkylamide and *N*-dimethylalkylamide series and from C_1 to C_8 in the alkylmonocarboxylic acids contrasts with the reported departure from linearity observed for the C_6 and C_8 compounds of the alkanol series in their interaction with I monolayers (1).

The interaction energies per methylene group of the alkylamides and alkylmonocarboxylic acids were practically identical to the adsorption free energies per methylene group at the hydrocarbon–water interface. This finding seems to indicate that I monolayers behave as ultrathin oil phases for these compounds, as was observed previously with alkanols (1). The observed 50% reduction of the interaction energy per methylene group of the hydrocarbon chain of the *N*-dimethylalkylamides compared with that of the adsorption free energies at the clean air–water interface. No literature data were found on the adsorption free energy of these compounds at the hydrocarbon–water interface.

The plots corresponding to II monolayers (Fig. 7) indicate a marked departure from linearity for hexanamide and *N*-dimethylhexamide and compare with that reported recently (7) for hexanol and octanol in their interaction with I and II monolayers. The interaction free energies per methylene group compare with those of the interaction with I monolayers. The small differences observed within the experimental error could be reasonably attributed to the different molecular surface density of I and II monolayers.

Correlations with Permeability—Three important variables govern nonelectrolyte permeation across biomembranes: (*a*) the partition coefficient of the membrane–bathing solution, (*b*) the rate constant for entrance into the membrane from the aqueous environment, and (*c*) the diffusion coefficient within the membrane (24). Solute permeation across the lipid regions of biomembranes can be separated into three successive events that contribute to the total permeation rate: (*a*) adsorption of the hydrated solute at the lipid–bathing solution interface, (*b*) dehydration, and (*c*) solute diffusion through the lipid region (25).

Kinetic analysis of membrane permeability (26, 27) based on the absolute rate theory treatment of diffusion (28) shows the permeation rate to be proportional to the product of the probability of occurrence of the three successive events (25):

$$P = \left(\frac{\lambda^2}{l}\right)\left(\frac{kT}{h}\right) \exp(-\Delta G_{ad}/RT) \exp(-\Delta G_{deh}/RT) \exp(-\Delta G_{dif}/RT) \quad \text{(Eq. 4)}$$

where P is the permeability (centimeters per second), λ is the average distance between equilibrium positions (angstroms), l is the membrane thickness (angstroms), h is the Planck constant (ergs × seconds), and ΔG_{ad}, ΔG_{deh}, and ΔG_{dif} are the contributions to the total activation energy of the adsorption, dehydration, and diffusion steps, respectively.

The ΔG_{ad} and ΔG_{deh} terms of Eq. 4 correspond to the first energetic barrier found by the solute molecule during its permeation, *i.e.*, the crossing of the bathing solution–lipid interface. Adsorption of the amides at the water–air or decane–water interface is spontaneous so that ΔG_{ad} is intrinsically negative. On the contrary, the nonspontaneity of dehydration indicates that ΔG_{deh} is intrinsically positive. Consequently, the total energetic cost of crossing the interfacial region is $-\Delta G_{ad} + \Delta G_{deh}$.

The free energy change, ΔG_{tr}, associated with the transfer of a solute from an aqueous solution to dimyristoyl lecithin liposomes was estimated by (29):

$$\Delta G_{tr}^{\circ} = -kT \ln P \quad \text{(Eq. 5)}$$

where P is the molal partition coefficient, which can be related to the thermodynamic partition coefficient through an expression containing

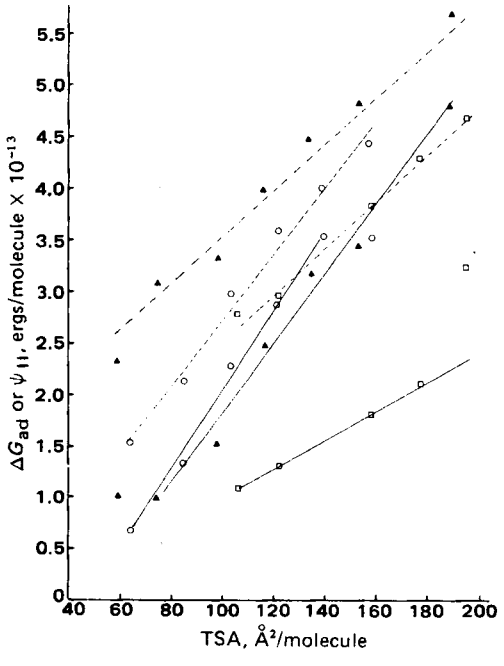

Figure 7—*Plots of the adsorption free energies at the air–aqueous solution interface (- - -) and the interaction energies with II monolayers (—)* versus *the total molecular surface area. Key:* ▲, *alkylmonocarboxylic acids;* ○, *alkylamides; and* □, N,N-*dimethylalkylamides.*

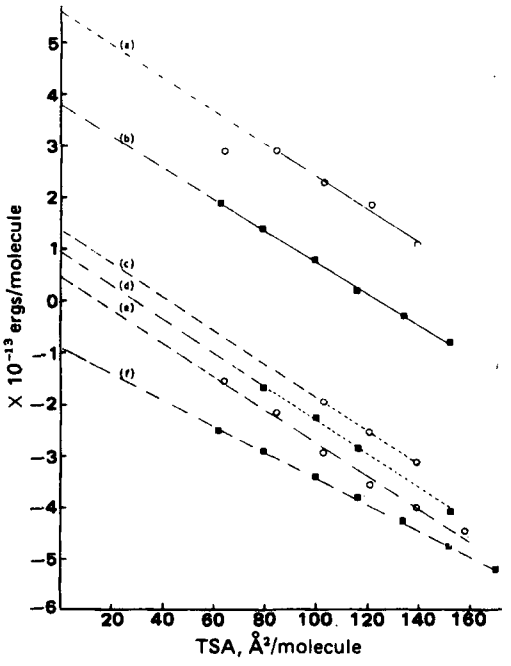

Figure 8—*Plots of the transfer free energies of the oil–water solution, ΔG°_{tr} (a, b); the adsorption free energies at the hydrocarbon–water interface, ΔG°_{ad} (o/w) (c, d); and the adsorption free energies at the air–water interface, ΔG°_{ad} (e, f), against the total molecular surface area. Key:* ○, *alkylamides; and* ■, *alkanols.*

the natural logarithm of the ratio of the molecular weights of the nonpolar and polar phases (29). However, for comparative purposes, the P values can be used to estimate a relative free energy change.

The plots of ΔG°_{tr} obtained from literature data (30) on partition coefficients of oil–aqueous solutions of alkylamides and alkanols *versus* the total surface area per molecule are compared in Fig. 8 with those of the adsorption free energy, $\Delta G^{o/w}_{ad}$, at the hydrocarbon–aqueous (obtained from Refs. 31 and 12, respectively) and at the air–aqueous interfaces. With the exception of formamide in the ΔG°_{tr} plot, the points determined reasonably straight lines. The slopes, intercepts, and correlation coefficient are given in Table II.

Parallelism of the plots of ΔG°_{tr} and ΔG°_{ad} at the hydrocarbon–water interface permitted estimation of the constant difference $(\Delta G^{\circ}_{tr} - \Delta G^{o/w}_{ad})_{TSA=0}$ for the alkylamides and the alkanols, 3.91×10^{-13} and 2.84×10^{-13} erg/molecule, respectively.

The partition of a surface-active solute between aqueous and nonaqueous phases can be separated into two successive events: the spontaneous adsorption of the hydrated solute at the interface ($\Delta G_{ad} < 0$) and its subsequent dehydration ($\Delta G_{deh} > 0$) that permits penetration into the nonaqueous phase (31). It can be reasonably assumed that the total free energy change of the partition, ΔG_{tr}, should reflect both events so that $\Delta G_{tr} = \Delta G^{o/w}_{ad} + \Delta G_{deh}$ and $\Delta G_{deh} = \Delta G_{tr} - \Delta G^{o/w}_{ad}$.

It is generally accepted (27, 32) that the amide group and the hydroxyl group form three and two hydrogen bonds with water, respectively. However, from *ab initio* SCF computations of various polyhydrates, evidence was presented recently (16) for the structure of formamide in aqueous solution consistent with a model of four water molecules in the primary hydration sphere, two of them hydrogen bonded to the amino group acting as a proton donor.

By assuming that the constant difference $(\Delta G^{\circ}_{tr} - \Delta G^{o/w}_{ad})_{TSA=0}$ is related to the free energy change that corresponds to dehydration, the contribution of each hydrogen bond to the total dehydration free energy can be estimated by dividing $(\Delta G_{tr} - \Delta G^{o/w}_{ad})_{TSA=0}$ by three for alkylamides and by two for alkanols. The values obtained, 1.31×10^{-13} and 1.42×10^{-13} erg/molecule, respectively, seem to indicate the validity of this assumption for the two series.

The equation used to estimate the interaction energies of subphase-injected solutes with phospholipid monolayers was derived originally (2) based on the statistical thermodynamic treatment of the Langmuir adsorption equation (33, 34). The Boltzmann–Maxwell exponential factor consequently contained an activation energy term about which, under the experimental conditions, no valid assumption could be made on the thermodynamic function (ΔE, ΔH, or ΔG) that it really represents. The ambiguous interaction energy term was coined, and the symbol ψ was used to represent it.

The order of magnitude of the experimentally measured interaction energies, ψ, of alkylamides and alkanols with phospholipid monolayers and their dependence on the total surface area per molecule strongly suggest that they could be related to the adsorption free energy of the solute at the phospholipid monolayer–aqueous solution interface. The validity of this suggested relationship and the former assumption of the dependence of ΔG_{deh} on $(\Delta G_{tr} - \Delta G^{o/w}_{ad})$ can be tested with Eq. 4.

The activation free energies for the diffusion, ΔG_{dif}, of formamide, acetamide, propionamide, and valeramide within egg lecithin bilayers estimated recently (26) from their measured permeability coefficients by assuming that the unknown bathing solution–lipid bilayer partition coefficients are proportional to the known water–ether partition coefficients are compared in Table III with those obtained by substituting ΔG_{ad} for the interaction energies with dipalmitoyl lecithin monolayers, ψ_I (Table I), and ΔG_{deh} for the corresponding values of $(\Delta G_{tr} - \Delta G^{o/w}_{ad})_{TSA=0}$ in Eq. 4. The coincidence of the calculated values of the activation free energy of the diffusion within the lipid bilayer for formamide, acetamide, and propionamide favors the validity of the former assumptions. The discrepancy between the calculated values of ΔG^{calc}_{dif} and $\Delta G^{\ddagger}_{dif}$ in the case of valeramide could be explained on the basis that as the solute size increases, the crossing of the interface becomes the rate-determining step; for valeramide, it constitutes 90% of the total resistance to permeation (24). The fact that in this case ΔG^{calc}_{dif} compares with ΔG°_{dif}, which contains the contribution corresponding to the partition coefficient $[\Delta G^{\circ}_{dif} = \Delta G^{\ddagger}_{dif} - \ln A/A'$ (24)], favors this explanation.

The results presented here seem to indicate that the interaction energy of alkylamides with dipalmitoyl lecithin monolayers spread at the air–water interface can be reasonably identified with the adsorption free energy at the aqueous solution–monolayer interface, which constitutes the first energetic step involved in alkylamide permeation across a phospholipid bilayer, and that the dehydration free energy constituting the second energetic step can be identified with the difference between the transfer free energy from an aqueous phase to an oil phase and the adsorption free energy at the water–hydrocarbon interface.

REFERENCES

(1) F. A. Vilallonga, E. R. Garrett, and J. S. Hunt, *J. Pharm. Sci.*, **66**, 1229 (1977).

(2) F. A. Vilallonga, E. R. Garrett, and M. Cereijido, *ibid.*, **61**, 1720 (1972).

(3) F. A. Vilallonga and E. R. Garrett, *ibid.*, **62**, 1605 (1973).

(4) G. M. Adams and T. L. Sallee, *J. Chromatogr.*, **49**, 552 (1970).

(5) J. H. Clint, J. M. Corkill, J. F. Goodman, and J. A. Tate, *J. Colloid Interface Sci.*, **28**, 522 (1968).

(6) S. C. Valvani, S. H. Yalkowsky, and G. L. Amidon, *J. Phys. Chem.*, **80**, 829 (1976).

(7) R. B. Hermann, *ibid.*, **76**, 2754 (1972).

(8) "Handbook of Chemistry and Physics," H. C. West, Ed., CRC Press, Cleveland, Ohio, 1970.

(9) L. Pauling, "The Nature of the Chemical Bond," Cornell University Press, Ithaca, N.Y., 1960, p. 260.

(10) J. Traube, *Ann.*, **265**, 27 (1891).

(11) I. Langmuir, *J. Am. Chem. Soc.*, **39**, 1883 (1917).

(12) D. A. Haydon and F. H. Taylor, *Phil. Trans. R. Soc.*, **A252**, 255 (1960).

(13) H. Kimizuka, L. G. Abood, F. Tahara, and K. Kaibara, *J. Colloid Interface Sci.*, **40**, 27 (1972).

(14) J. L. Llopis and P. Artalejo, *An. Fis. Quim. (Madrid)*, **58**, 367 (1962).

(15) M. Nakagaki and T. Handa, *Bull. Chem. Soc., Jpn.*, **48**, 630 (1975).

(16) A. Pullman, H. Berthod, C. Giessner-Pettre, J. F. Hinton, and D. Harpool, *J. Am. Chem. Soc.*, **100**, 3991 (1978).

(17) E. R. Garrett and F. A. Vilallonga, *J. Pharm. Sci.*, **64**, 1782 (1975).

(18) A. F. H. Ward and L. Tordai, *J. Chem. Phys.*, **14**, 453 (1946).

(19) W. Drost-Hansen, in "Chemistry of the Cell Interface," H. Darrow-Brown, Ed., Academic, New York, N.Y., 1971.

(20) M. S. Metzik, V. D. Perevertaev, V. A. Liopo, G. T. Timostchenko, and A. B. Kiseler, *J. Colloid Interface Sci.*, **43**, 662 (1973).

(21) R. E. Phares, *J. Pharm. Sci.*, **54**, 408 (1965).

(22) D. F. Sears, *J. Colloid Interface Sci.*, **29**, 288 (1969).

(23) F. M. Fowkes, *Ind. Eng. Chem.*, **56**, 40 (1964).

(24) M. Poznansky, S. Tong, P. C. White, J. M. Milgram, and A. K. Solomon, *J. Gen. Phys.*, **67**, 45 (1976).
(25) B. E. Cohen, *J. Membrane Biol.*, **20**, 205 (1975).
(26) H. Davson and J. F. Danielli, "The Permeability of Natural Membranes," Cambridge University Press, Cambridge, England, 1941.
(27) B. S. Zwolinski, H. Eyring, and C. E. Reese, *J. Phys. Colloid Chem.*, **53**, 1426 (1949).
(28) S. Glasstone, K. J. Laidler, and H. Eyring, "The Theory of Rate Processes," McGraw-Hill, New York, N.Y., 1941.
(29) Y. Katz and J. M. Diamond, *J. Membrane Biol.*, **17**, 101 (1974).
(30) A. Leo, C. Hansch, and D. Elinns, *Chem. Rev.*, **71**, 525 (1971).
(31) J. Wang, G. T. Tich, W. R. Galey, and A. K. Solomon, *Biochim. Biophys. Acta*, **255**, 691 (1972).
(32) W. D. Stein, "The Movement of Molecules Across Cell Membranes," Academic, New York, N.Y., 1967, p. 76.
(33) H. Hughes, "Physical Chemistry," Pergamon, London, England, 1961, pp. 46, 952, 956.
(34) T. L. Hill, "Introduction to Statistical Thermodynamics," Addison-Wesley, Reading, Mass., 1960, pp. 89, 127.

ACKNOWLEDGMENTS

The authors thank Professor J. R. Sabin for making the CNDO program of the Quantum Theory Project of the University of Florida available.

Protein Concentration Effects on Binding of ^{14}C-Codeine, ^{14}C-Morphine, and ^{3}H-Methadone to Human Serum Albumin

JOSEPH JUDIS

Received February 26, 1979, from the *College of Pharmacy, University of Toledo, Toledo, OH 43606.* Accepted for publication August 8, 1979.

Abstract □ The binding of ^{14}C-codeine, ^{14}C-morphine, and ^{3}H-methadone to human serum albumin was studied at a constant ligand concentration and varying albumin concentrations. Scatchard plots of the data were linear and had positive slopes. The curves for the three ligands had similar data values and slopes. With increasing albumin concentrations, β (fraction bound) values increased. The β change per albumin concentration change $[d(\beta)/d(\text{albumin})]$ dropped most markedly at lower albumin concentrations and changed less as the albumin concentrations approached those normally observed in human blood. Values of nK, the number of binding sites or systems on the protein times the association constant, calculated from β and the albumin concentrations decreased with an increase in albumin concentration increase. The curves were similar for codeine and morphine, while the methadone curve indicated less of a decrease in nK with an increasing albumin concentration. For data published previously on the binding of various ligands at different albumin concentrations, plots of β values or calculated nK values *versus* albumin concentration revealed that β generally increased and nK decreased with an increasing albumin concentration. Desipramine, propoxyphene, prednisone, and phenylbutazone were exceptions to these relationships.

Keyphrases □ Codeine—binding to human serum albumin, varying albumin concentration □ Morphine—binding to human serum albumin, varying albumin concentration □ Methadone—binding to human serum albumin, varying albumin concentration □ Binding, protein—codeine, morphine, and methadone to human serum albumin, varying albumin concentration

In most studies of drug binding to serum proteins, a single protein concentration was used and the ligand concentration was varied (1–3). Scatchard plots of the data gave either a straight line or curve and almost invariably had a negative slope. However, studies of cortisol binding to serum albumin were conducted in which the cortisol concentration was constant and the albumin concentration was varied (4). The resulting Scatchard plot was a straight line with a positive slope. The results could not be explained on the basis of microheterogeneity or by variations of the albumin activity coefficient. This observation was not investigated further.

Several subsequent studies involved the binding of various ligands to serum proteins using a constant ligand concentration and varying protein concentrations. Scatchard plots with a positive slope were observed with thiopental (5), phenytoin (6, 7), and L-tryptophan (6, 7). Bowmer and Lindup (8) recently commented on the several published studies involving data yielding Scatchard plots with positive slopes and the significance of obtaining binding data when the protein concentration is varied and the ligand concentration is constant.

Previous studies involving the binding of ^{14}C-codeine, ^{14}C-morphine, and ^{3}H-methadone to human serum albumin yielded Scatchard plots with positive slopes when the albumin concentration was constant and the ligand concentration was varied (9). No explanation for the positive slopes (rather than the usually observed negative slopes) could be offered. This report is an extension of the earlier studies and involves variation of the albumin concentration and constant ligand concentrations.

EXPERIMENTAL

Methods—All protein binding determinations were performed by the equilibrium dialysis method (9) using multiple-cell blocks. Each cell had 1 ml on each side of the cellulose membrane. Radioactivity was determined in a liquid scintillation system as described previously (9).

Materials—^{14}C-Codeine[1], ^{14}C-morphine[1], ^{3}H-methadone[2], and crystalline human serum albumin[3] were obtained commercially. All chemicals were reagent grade.

RESULTS AND DISCUSSION

The human serum albumin concentration was varied between 0.217×10^{-4} and 0.87×10^{-3} *M*. The ligand concentration was kept constant (^{14}C-morphine, 0.00356; ^{14}C-codeine, 0.00339; and ^{3}H-methadone, 0.00332 *M*). Scatchard plots of the data for the three ligands are shown in Fig. 1. The albumin concentrations for each ligand fell in the same sequence on the curve as found in studies (4, 5, 7) involving a constant ligand concentration and varying albumin concentrations. The slopes

[1] Amersham Corp.
[2] New England Nuclear Corp.
[3] ICN Life Sciences Group.

0022-3549/80/0100-0071$01.00/0
© 1980, American Pharmaceutical Association

(24) M. Poznansky, S. Tong, P. C. White, J. M. Milgram, and A. K. Solomon, *J. Gen. Phys.*, **67**, 45 (1976).
(25) B. E. Cohen, *J. Membrane Biol.*, **20**, 205 (1975).
(26) H. Davson and J. F. Danielli, "The Permeability of Natural Membranes," Cambridge University Press, Cambridge, England, 1941.
(27) B. S. Zwolinski, H. Eyring, and C. E. Reese, *J. Phys. Colloid Chem.*, **53**, 1426 (1949).
(28) S. Glasstone, K. J. Laidler, and H. Eyring, "The Theory of Rate Processes," McGraw-Hill, New York, N.Y., 1941.
(29) Y. Katz and J. M. Diamond, *J. Membrane Biol.*, **17**, 101 (1974).
(30) A. Leo, C. Hansch, and D. Elinns, *Chem. Rev.*, **71**, 525 (1971).
(31) J. Wang, G. T. Tich, W. R. Galey, and A. K. Solomon, *Biochim. Biophys. Acta*, **255**, 691 (1972).
(32) W. D. Stein, "The Movement of Molecules Across Cell Membranes," Academic, New York, N.Y., 1967, p. 76.
(33) H. Hughes, "Physical Chemistry," Pergamon, London, England, 1961, pp. 46, 952, 956.
(34) T. L. Hill, "Introduction to Statistical Thermodynamics," Addison-Wesley, Reading, Mass., 1960, pp. 89, 127.

ACKNOWLEDGMENTS

The authors thank Professor J. R. Sabin for making the CNDO program of the Quantum Theory Project of the University of Florida available.

Protein Concentration Effects on Binding of ^{14}C-Codeine, ^{14}C-Morphine, and ^{3}H-Methadone to Human Serum Albumin

JOSEPH JUDIS

Received February 26, 1979, from the *College of Pharmacy, University of Toledo, Toledo, OH 43606.* Accepted for publication August 8, 1979.

Abstract □ The binding of ^{14}C-codeine, ^{14}C-morphine, and ^{3}H-methadone to human serum albumin was studied at a constant ligand concentration and varying albumin concentrations. Scatchard plots of the data were linear and had positive slopes. The curves for the three ligands had similar data values and slopes. With increasing albumin concentrations, β (fraction bound) values increased. The β change per albumin concentration change $[d(\beta)/d(\text{albumin})]$ dropped most markedly at lower albumin concentrations and changed less as the albumin concentrations approached those normally observed in human blood. Values of nK, the number of binding sites or systems on the protein times the association constant, calculated from β and the albumin concentrations decreased with an increase in albumin concentration increase. The curves were similar for codeine and morphine, while the methadone curve indicated less of a decrease in nK with an increasing albumin concentration. For data published previously on the binding of various ligands at different albumin concentrations, plots of β values or calculated nK values *versus* albumin concentration revealed that β generally increased and nK decreased with an increasing albumin concentration. Desipramine, propoxyphene, prednisone, and phenylbutazone were exceptions to these relationships.

Keyphrases □ Codeine—binding to human serum albumin, varying albumin concentration □ Morphine—binding to human serum albumin, varying albumin concentration □ Methadone—binding to human serum albumin, varying albumin concentration □ Binding, protein—codeine, morphine, and methadone to human serum albumin, varying albumin concentration

In most studies of drug binding to serum proteins, a single protein concentration was used and the ligand concentration was varied (1–3). Scatchard plots of the data gave either a straight line or curve and almost invariably had a negative slope. However, studies of cortisol binding to serum albumin were conducted in which the cortisol concentration was constant and the albumin concentration was varied (4). The resulting Scatchard plot was a straight line with a positive slope. The results could not be explained on the basis of microheterogeneity or by variations of the albumin activity coefficient. This observation was not investigated further.

Several subsequent studies involved the binding of various ligands to serum proteins using a constant ligand concentration and varying protein concentrations. Scatchard plots with a positive slope were observed with thiopental (5), phenytoin (6, 7), and L-tryptophan (6, 7). Bowmer and Lindup (8) recently commented on the several published studies involving data yielding Scatchard plots with positive slopes and the significance of obtaining binding data when the protein concentration is varied and the ligand concentration is constant.

Previous studies involving the binding of ^{14}C-codeine, ^{14}C-morphine, and ^{3}H-methadone to human serum albumin yielded Scatchard plots with positive slopes when the albumin concentration was constant and the ligand concentration was varied (9). No explanation for the positive slopes (rather than the usually observed negative slopes) could be offered. This report is an extension of the earlier studies and involves variation of the albumin concentration and constant ligand concentrations.

EXPERIMENTAL

Methods—All protein binding determinations were performed by the equilibrium dialysis method (9) using multiple-cell blocks. Each cell had 1 ml on each side of the cellulose membrane. Radioactivity was determined in a liquid scintillation system as described previously (9).

Materials—^{14}C-Codeine[1], ^{14}C-morphine[1], ^{3}H-methadone[2], and crystalline human serum albumin[3] were obtained commercially. All chemicals were reagent grade.

RESULTS AND DISCUSSION

The human serum albumin concentration was varied between 0.217×10^{-4} and 0.87×10^{-3} *M*. The ligand concentration was kept constant (^{14}C-morphine, 0.00356; ^{14}C-codeine, 0.00339; and ^{3}H-methadone, 0.00332 *M*). Scatchard plots of the data for the three ligands are shown in Fig. 1. The albumin concentrations for each ligand fell in the same sequence on the curve as found in studies (4, 5, 7) involving a constant ligand concentration and varying albumin concentrations. The slopes

[1] Amersham Corp.
[2] New England Nuclear Corp.
[3] ICN Life Sciences Group.

0022-3549/80/0100-0071$01.00/0
© 1980, American Pharmaceutical Association

Table I—Relationship between β and Human Serum Albumin Concentration in the Binding of ^{14}C-Codeine, ^{14}C-Morphine, and ^{3}H-Methadone

Albumin Concentration, M	Ligand					
	^{14}C-Codeine		^{14}C-Morphine		^{3}H-Methadone	
	β	$d(\beta)/d$(albumin)	β	$d(\beta)/d$(albumin)	β	$d(\beta)/d$(albumin)
0.217×10^{-4}	—	—	—	—	0.0158	636.6
0.870×10^{-4}	0.0438	273.2	0.0512	329.7	—	—
0.145×10^{-3}	0.05	222.4	0.07	263.3	0.09	446.3
0.29×10^{-3}	0.074	168.2	0.095	194.1	0.145	391.9
0.58×10^{-3}	0.132	127.3	0.154	143.1	0.252	344.2
0.870×10^{-3}	0.16	108.1	0.184	119.8	0.305	319.0

Table II—Literature Data for Drug Binding at Varying Human Serum Albumin Concentrations

Reference	Ligand	Plot of Human Serum Albumin Concentrations, M, *versus*			
		β		nK	
		r[a]	Slope	r	Slope
10	Prednisone	0.8	+621	0.176	$+0.999 \times 10^{6}$
11	Methadone	0.945	+490	0.912	-0.904×10^{6}
12	Phenylbutazone	0.947	+53.8	0.986	$+0.104 \times 10^{9}$
13	Diphenylhydantoin	0.496	+148	0.383	-0.937×10^{7}
13	Desipramine	0.212	−22.2	0.826	-0.337×10^{8}
14	Morphine	0.373	+116	0.482	-0.549×10^{6}
14	Diphenylhydantoin	0.496	+197	0.158	-0.277×10^{8}
15	Furosemide	0.873	+88.2	0.91	-0.101×10^{9}
16	Propoxyphene	0.43	−244	0.712	-0.22×10^{8}

[a] The r value is the correlation coefficient for the best fit of the data points to a straight line. The slope given is that calculated for the best fit straight line.

for the curves for all three ligands were on the same order of magnitude.

When the extent of binding *versus* albumin concentration was examined, β (fraction of ligand bound) increased with albumin concentration (Fig. 2). The slopes of the curves were relatively close for codeine and morphine and slightly higher for methadone. Since it generally is recognized that drug binding to serum proteins may affect pharmacological activity because the active drug form is the free or unbound drug, serum albumin concentration changes could be important. Serum albumin concentrations vary among normal individuals to a limited extent and may be reduced in certain pathological circumstances.

To understand the relative effects of differences in the serum albumin concentration and the fraction of ligand bound, $d(\beta)/d$(albumin) was calculated for each albumin concentration and its corresponding β value. This parameter is the rate of change in β with respect to a change in albumin concentration. The value was calculated by fitting albumin concentrations and corresponding β values to a curve for which a statistically significant fit could be obtained by a computer. The first derivative of the curve then was taken at each albumin concentration.

The $d(\beta)/d$(albumin) values dropped rapidly as the albumin concentration increased from the low values and then dropped less as the higher albumin concentrations were reached (Table I). These values are represented in Fig. 3. At the higher albumin concentrations, β changed less per albumin concentration change. Since the higher albumin concentrations are those generally encountered, even in individuals with albumin concentrations considered somewhat below normal, β would not be reduced drastically, and only moderate modifications (if any) of the dose level would be indicated with slightly decreased albumin concentrations. The large β change per change in albumin concentration would exist at the much lower albumin concentrations, which generally are not encountered clinically.

Numerous studies were identified (8) in the literature in which binding was affected by albumin concentration changes. A protein concentration increase corresponding to an nK decrease was common to these studies[4]. The data obtained in this study were analyzed similarly, and nK was calculated using an equation (2) that permitted calculation of nK from β and the protein concentration. Figure 4 shows the curves obtained when the calculated nK values were plotted *versus* albumin concentration. For all three ligands, an albumin concentration increase was accompanied by an nK decrease.

Numerous investigators (10–16) have published data for drug binding

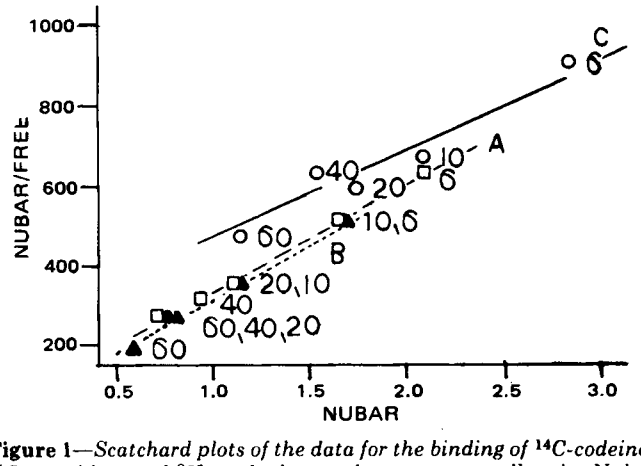

Figure 1—*Scatchard plots of the data for the binding of ^{14}C-codeine, ^{14}C-morphine, and ^{3}H-methadone to human serum albumin. Nubar refers to the moles of ligand bound per mole of albumin in the system. Numbers near the data points represent the milligrams of albumin per dialysis cell (1-ml cell). Key: A, □, ^{14}C-morphine; B, ▲, ^{14}C-codeine; and C, ○, ^{3}H-methadone.*

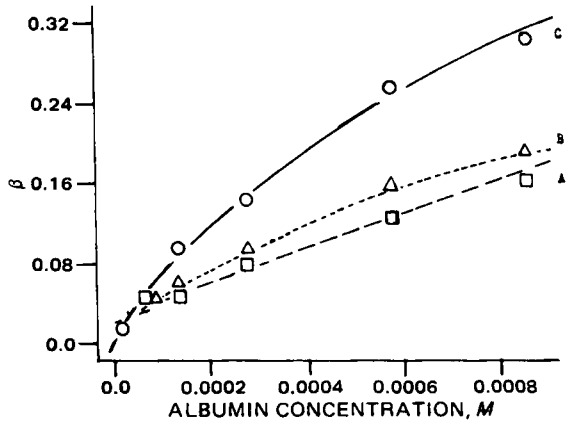

Figure 2—*Relationship between β and the human serum albumin concentration for the binding of ^{14}C-codeine, ^{14}C-morphine, and ^{3}H-methadone to human serum albumin. Key: A, □, ^{14}C-codeine; B, △, ^{14}C-morphine; and C, ○, ^{3}H-methadone.*

[4] The n refers to the number of binding sites or systems on the protein, and K refers to the association constant.

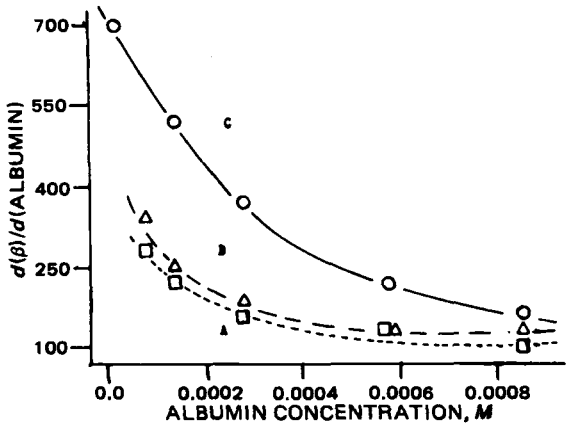

Figure 3—*Change in β per human serum albumin concentration change* [d(β)/d(*albumin*)] versus *albumin concentration for the binding of* ^{14}*C-codeine,* ^{14}*C-morphine, and* ^{3}*H-methadone to human serum albumin. Key: A,* □, ^{14}*C-codeine; B,* △, ^{14}*C-morphine; and C,* ○, ^{3}*H-methadone.*

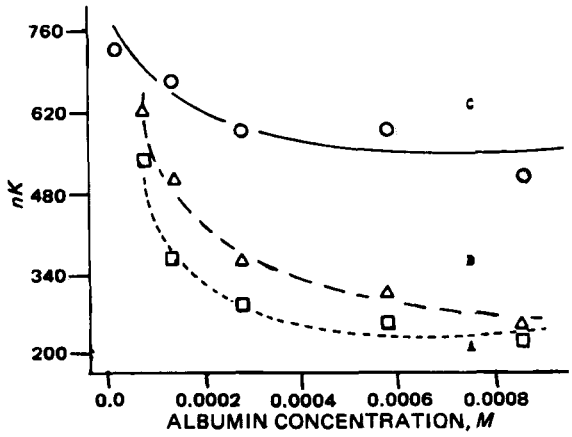

Figure 4—*Relationship between* nK *and human serum albumin concentration for the binding of* ^{14}*C-codeine,* ^{14}*C-morphine, and* ^{3}*H-methadone to human serum albumin. Key: A,* □, ^{14}*C-codeine; B,* △, ^{14}*C-morphine; and C,* ○, ^{3}*H-methadone.*

(β) at varying human serum albumin concentrations. The data in these reports were plotted as β *versus* albumin concentration (molar) and calculated *nK* values (calculated as described) *versus* albumin concentration.

The results are summarized in Table II. In many cases, the plots did not follow closely a straight line, as evidenced by statistically insignificant correlation coefficients (*i.e.*, <0.9); the slopes calculated thus represent a trend of the scattered points rather than a precise slope. In general, β increased with an albumin concentration increase except for desipramine and propoxyphene. The *nK* values decreased with an albumin concentration increase, as found by Bowmer and Lindup (8) in their study of literature for binding data. Table II reveals two other exceptions, prednisone and phenylbutazone. Thus, *nK* values apparently do decrease with an albumin concentration increase but with some exceptions. These exceptions merit further study for other possible unique albumin binding characteristics.

Bowmer and Lindup (8) suggested that positive-slope Scatchard curves might be explained by cooperativity if the positive-slope curves are obtained from data where the protein concentration was constant and the ligand concentration was varied, as well as from data for the same system where the ligand concentration was constant and the protein concentration was varied. This cooperativity seems to apply to the binding of codeine, morphine, and methadone to human serum albumin. Positive-slope Scatchard plots were obtained in a previous study (9) where the albumin concentration was constant and the ligand concentration was varied. In the present study in which the ligand concentration was constant and the albumin concentration was varied, Scatchard plots with positive slopes also were obtained.

More ligand–protein systems should be reinvestigated by keeping the ligand concentration constant and varying the protein concentration, not only for more complete characterization of these systems but also for the determination of the relative effects on the fraction bound with protein concentration changes, especially where blood proteins are involved. For drugs that are highly bound and very potent, the dosage may have to be adjusted for a reduction in serum protein concentration when the latter deviates significantly from normal.

REFERENCES

(1) A. Goldstein, *Pharmacol. Rev.*, **1**, 102 (1949).
(2) M. Meyer and D. Guttman, *J. Pharm. Sci.*, **57**, 1627 (1968).
(3) J. Vallner, *ibid.*, **66**, 447 (1977).
(4) W. Brunkhorst and E. Hess, *Arch. Biochem. Biophys.*, 111, 54 (1965).
(5) D. Shen and M. Gibaldi, *J. Pharm. Sci.*, **63**, 1698 (1974).
(6) W. Lindup, *Biochem. Soc. Trans.*, **3**, 635 (1975).
(7) C. Bowmer and W. Lindup, *Biochem. Pharmacol.*, **27**, 937 (1978).
(8) C. Bowmer and W. Lindup, *J. Pharm. Sci.*, **67**, 1193 (1978).
(9) J. Judis, *ibid.*, **66**, 802 (1977).
(10) G. Lewis and W. Jusko, *Lancet*, **2**, 778 (1971).
(11) G. Olsen, *Science*, **176**, 525 (1972).
(12) W. Wosilait, *Res. Commun. Chem. Pathol. Pharmacol.*, **9**, 681 (1974).
(13) M. Reidenberg, I. Odar-Cederlof, C. Bahr, O. Borga, and F. Sjoqvist, *N. Engl. J. Med.*, **285**, 264 (1971).
(14) G. Olsen, W. Bennett, and G. Porter, *Clin. Pharmacol. Ther.*, 17, 677 (1975).
(15) J. Prandota and A. Pruitt, *ibid.*, **17**, 159 (1975).
(16) K. Giacomini, T. Gibson, and G. Levy, *J. Clin. Pharmacol.*, 18, 106 (1978).

ACKNOWLEDGMENTS

The author thanks Mrs. Virginia Matusek for technical assistance.

Small Animal Model for Evaluating Neuroleptic Potency

JACK M. ROSENBERG *x and CESAR A. LAU-CAM

Received January 22, 1979, from the *Department of Pharmaceutical Sciences, St. John's University College of Pharmacy and Allied Health Professions, Jamaica, NY 11439.* Accepted for publication July 31, 1979. *Present address: Arnold and Marie Schwartz College of Pharmacy and Health Sciences, Brooklyn, NY 11201.

Abstract □ The prolactin response in the rat is proposed as a convenient and inexpensive test system for the assessment of the clinical potency of neuroleptic agents. Times of maximum elevation ($p < 0.01$) of serum prolactin levels were determined by a one-way analysis of variance and the Newman–Keuls test for a period of 180 min following intraperitoneal administration of chlorpromazine hydrochloride, fluphenazine hydrochloride, perphenazine, prochlorperazine edisylate, and trifluoperazine hydrochloride (phenothiazines); haloperidol (a butyrophenone); chlorprothixene (a thioxanthene); loxapine succinate (a dibenzoxazepine); and molindone hydrochloride (a dihydroindolene). Maximum serum prolactin elevations occurred as follows: chlorpromazine hydrochloride, 30–90 min; chlorprothixene and trifluoperazine hydrochloride, 30–150 min; fluphenazine hydrochloride, 90–150 min; haloperidol, 90 min; loxapine succinate, 30 min; molindone hydrochloride, 30 and 60 min; and perphenazine and prochlorperazine edisylate, 30–180 min. For drugs that exhibited statistically indistinguishable maximum serum prolactin elevations at more than one sampling time, one of these times was selected arbitrarily for construction of a log dose–prolactin response curve. Log dose–serum prolactin curves were constructed at a time of maximum serum prolactin elevation for each drug. Thirty minutes was utilized for loxapine succinate and molindone hydrochloride, and 90 min was used otherwise. These curves were nearly parallel, and each had an excellent linear fit. Based on these curves, the ratio of the weights of the neuroleptic and chlorpromazine hydrochloride required to produce the same prolactin-stimulating potency was determined for each drug. This ratio was compared to the clinically accepted ratio of the weights of the neuroleptic and chlorpromazine hydrochloride required to produce the same antipsychotic potency. This technique demonstrated a close correlation between the prolactin-stimulating potencies of neuroleptics in rats and accepted antipsychotic potency relationships in humans.

Keyphrases □ Neuroleptic agents—model for evaluation of potency, prolactin response in rats □ Phenothiazines—model for evaluation of potency, prolactin response in rats □ Models—evaluation of neuroleptic potency, prolactin response in rats □ Prolactin response, rats—model for evaluation of neuroleptic potency

Prolactin, an anterior pituitary hormone in animals, is structurally similar to growth hormone (1). The dominant hypothalamic regulation of prolactin secretion in mammals appears to be inhibitory and under the control of prolactin-inhibitory factor (2). Prolactin-inhibitory factor is liberated by the hypothalamus into the portal vessels as a result of afferent dopaminergic impulses (3). It is unclear whether dopamine is a constituent of prolactin-inhibitory factor or is the factor itself (4).

Evidence of a prolactin-releasing factor exists, but its activity in controlling prolactin secretion clearly is less important than prolactin-inhibitory factor (5). Thyrotropin-releasing hormone also stimulates the secretion of prolactin- and thyroid-stimulating hormone, but thyrotropin-releasing hormone presumably does not play an important role in physiological prolactin regulation (5).

BACKGROUND

Enhanced prolactin secretion was reported following neuroleptic administration to humans (6, 7) and is associated with galactorrhea and other endocrine disturbances which may accompany the use of such drugs (8). A fairly good correlation between the antipsychotic potency of various neuroleptics and their human prolactin-stimulating response was found (6, 9, 10). A notable exception is clozapine, which does not seem to be a potent or consistent prolactin stimulator in humans; however, it does stimulate prolactin in rats (11, 12). Despite this exception, the prolactin response to a test dose of a new neuroleptic in normal human volunteers was proposed as a useful means to screen its efficacy and potency prior to clinical studies in humans (6, 10).

In addition to the various neurochemical techniques using animals to assess antipsychotic activity and/or potency (13–16), Clemens *et al.* (17) reported that when chlorpromazine and thioridazine, two phenothiazines of comparable antipsychotic potency, were given to rats, serum prolactin levels were stimulated to a similar extent. This observation was based on serum samples obtained 2 hr after drug administration. Meltzer *et al.* (18) demonstrated that the rank orders of average daily doses of nine neuroleptic agents in rat serum samples obtained 30 min after drug administration correlated with their corresponding doses needed to double serum prolactin levels. These correlation studies as well as other studies (11, 12) did not consider the possibly significant variation in serum prolactin profiles with respect to time for individual antipsychotic drugs and the effects of this parameter on observed magnitudes of prolactin stimulation. Furthermore, it was suggested that pituitary dopamine receptors that influence prolactin secretion in rats may differ significantly from those relevant to the antipsychotic action of neuroleptics (12).

A study was designed in rats to determine the times of maximum elevation of serum prolactin for representative antipsychotic drugs following their intraperitoneal administration and to investigate thoroughly the correlation between prolactin-stimulating potency of neuroleptics in rats and their clinical potency.

EXPERIMENTAL

In Stage 1 of this study, experiments were conducted to determine the times of maximum serum prolactin elevation for representative neuroleptics following their intraperitoneal administration. In Stage 2, experiments were conducted to determine the potency of each neuroleptic in inducing prolactin release at a time of maximum serum prolactin elevation.

Drugs—The following nine pharmacological agents, representing all five classes of antipsychotics approved for clinical use in the United States, were investigated: chlorpromazine hydrochloride[1], fluphenazine hydrochloride[2], perphenazine[3], prochlorperazine edisylate[1], and trifluoperazine hydrochloride[1] (phenothiazines); haloperidol[4] (a butyrophenone); chlorprothixene[5] (a thioxanthene); loxapine succinate[6] (a dibenzoxazepine); and molindone hydrochloride[7] (a dihydroindolone).

Animals—Male Sprague–Dawley rats[8], 225–300 g, were housed for 21 days in a temperature-controlled environment (23 ± 3°) which was illuminated artificially (lights on daily from 7:00 am to 7:00 pm). The animals were given food[9] and water *ad libitum*.

Times of Statistically Significant Maximum Serum Prolactin Elevation—Rats were divided into 11 groups of 48. The following antipsychotics were administered in equipotent dose equivalents for humans (19): chlorpromazine hydrochloride (10 mg/kg), chlorprothixene (10 mg/kg), fluphenazine hydrochloride (0.2 mg/kg), haloperidol (0.2 mg/kg), loxapine succinate (1 mg/kg), molindone hydrochloride (1 mg/kg), perphenazine (1 mg/kg), prochlorperazine edisylate (1.5 mg/kg), and trifluoperazine hydrochloride (0.5 mg/kg).

Solutions of these drugs were prepared to contain the indicated mil-

[1] Smith Kline and French, Philadelphia, Pa.
[2] E. R. Squibb & Sons, Princeton, N.J.
[3] Schering Corp., Kenilworth, N.Y.
[4] McNeil Laboratories, Fort Washington, Pa.
[5] Roche Laboratories, Nutley, N.J.
[6] Lederle Laboratories, Pearl River, N.Y.
[7] Endo Inc., Garden City, N.Y.
[8] Taconic Farms, Germantown, N.Y.
[9] Purina Lab Chow, Ralston Purina Co., St. Louis, Mo.

0022-3549/80/0100-0074$01.00/0
© 1980, American Pharmaceutical Association

Table I—Prolactin-Stimulating and Therapeutic Potencies of Neuroleptics Relative to Chlorpromazine Hydrochloride

Neuroleptic	Prolactin-Stimulating Potency[a]	Antipsychotic Potency[b]
Chlorpromazine hydrochloride	1.0	1
Chlorprothixene	1.0	1–2.3
Prochlorperazine edisylate	5.7	6.2–7.7
Perphenazine	9.1	10–11.9
Molindone hydrochloride	9.3	5–19.6
Loxapine succinate	10.6	8–12
Trifluoperazine hydrochloride	33.3	20–35
Fluphenazine hydrochloride	62.5	50–90.9
Haloperidol	86.0	50–91

[a] Calculated from log dose–response regression curves (Figs. 4 and 5). [b] From Refs. 19, 24, and 26.

ligram-per-kilogram doses in 1 ml of physiological saline or, with haloperidol, chlorprothixene, and perphenazine, in 1 ml of 0.1 *M* tartaric acid to solubilize these agents. These solutions or equal volumes of vehicles were given intraperitoneally to experimental and control groups, each group consisting of eight subgroups of six animals each. Blood samples were collected by decapitation at 0, 30, 45, 60, 90, 120, 150, and 180 min after drug or vehicle administration.

Potency of Neuroleptics in Inducing Prolactin Secretion—Rats were divided into nine groups of 42. For each drug, six subgroups of seven rats were utilized. One animal in each subgroup served as a control. Every drug was administered in six serial dilutions. The concentrations in 1 ml of vehicle were: chlorpromazine hydrochloride and chlorprothixene, 25–0.781 mg/kg; fluphenazine hydrochloride, 1–0.031 mg/kg; haloperidol, 0.5–0.012 mg/kg; loxapine succinate and molindone hydrochloride, 1.25–0.078 mg/kg; perphenazine and prochlorperazine edisylate, 5–0.156 mg/kg; and trifluoperazine hydrochloride, 2–0.062 mg/kg.

Blood samples were obtained by decapitation at a statistically significant ($p < 0.01$) time of maximum serum prolactin elevation for each drug as determined by a one-way analysis of variance (20) and the Newman–Keuls test (21) from Stage 1 of this study.

Sample Collection and Assay—All decapitations were conducted between 2:00 and 4:00 pm. Blood was collected from the trunk portion and allowed to stand for 10 min at 4°; the serum was separated and frozen at −40° until hormone analysis could be performed. Serum samples were measured for prolactin using a radioimmunoassay kit[10]. The assays, using a double antibody radioimmunoassay, were performed according to the instructions.

The rat prolactin was iodinated by a modification of the Hunter–Greenwood method (22). Each serum sample was assayed in duplicate, and the average was taken as representative of the true prolactin concentration[11]. All test and control samples were determined concurrently for each drug. The intra- and interassay variations were 4.2 and 9.4%, respectively.

RESULTS

Time Course of Prolactin Response to Neuroleptics—Evaluation of the serum prolactin levels over 180 min following intraperitoneal injection of the various neuroleptic agents indicated that statistically significant ($p < 0.01$) maximum serum prolactin elevations occurred at the following times: chlorpromazine hydrochloride, 30–90 min; chlorprothixene and trifluoperazine hydrochloride, 30–150 min; fluphenazine hydrochloride, 90–150 min; haloperidol, 90 min; loxapine succinate, 30 min; molindone hydrochloride, 30 and 60 min; and perphenazine and prochlorperazine edisylate, 30–180 min (Figs. 1–3).

For drugs that exhibited statistically indistinguishable maximum serum prolactin elevations at more than one sampling time, one of these times was selected arbitrarily for each drug for subsequent experiments performed in Stage 2. Thirty minutes was utilized for loxapine succinate and molindone hydrochloride, and 90 min was used otherwise.

[10] National Institute of Arthritis, Metabolism, and Digestive Disease (NIAMDD) Rat Pituitary Hormone Distribution Program, National Pituitary Agency, Baltimore, Md.

[11] All results are expressed in terms of NIAMDD rat prolactin.

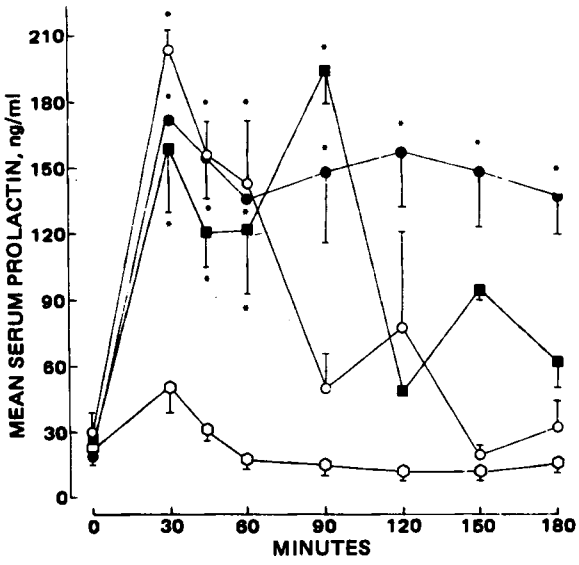

Figure 1—*Effect of intraperitoneally administered chlorpromazine hydrochloride (■), molindone hydrochloride (○), and prochlorperazine edisylate (●) on serum prolactin levels in male rats over 180 min. The control groups received normal saline (○). Each point is the mean for six animals. Vertical lines show the standard error of the means. Maximum serum prolactin elevations ($p < 0.01$) as determined by a one-way analysis of variance and the Newman–Keuls test are indicated by asterisks.*

Neuroleptic Dose–Prolactin Response Curves at Times of Maximum Serum Prolactin Elevation—Figures 4 and 5 show the log dose–prolactin response curves for the nine drugs studied as calculated by standard linear regression analyis (23). The slopes of the regression lines were: chlorpromazine hydrochloride, fluphenazine hydrochloride, haloperidol, and prochlorperazine edisylate, 1.9; chlorprothixene, loxapine succinate, and perphenazine, 1.8; and molindone hydrochloride and trifluoperazine, 1.6. The correlation coefficients for the log dose–prolactin curves were significant ($df = 4$) as follows: chlorpromazine, 0.91 ($p < 0.005$); chlorprothixene, 0.93 ($p < 0.005$); fluphenazine hydrochloride, 0.97 ($p < 0.005$); haloperidol, 0.95 ($p < 0.005$); loxapine succinate, 0.87 ($p < 0.01$); and prochlorperazine edisylate and trifluoperazine hydrochloride, 0.94 ($p < 0.005$).

Prolactin-Releasing Potency of Neuroleptics at Times of Maxi-

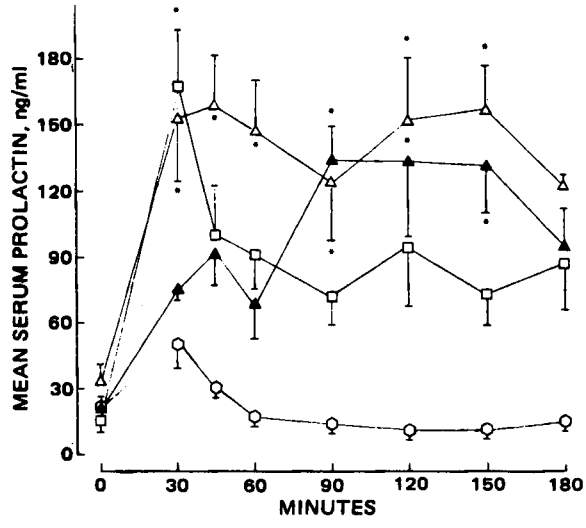

Figure 2—*Effect of intraperitoneally administered fluphenazine hydrochloride (▲), loxapine succinate (□), and trifluoperazine hydrochloride (△) on serum prolactin levels in male rats over 180 min. The control groups received normal saline (○). Each point is the mean for six animals. Vertical lines show the standard error of the means. Maximum serum prolactin elevations ($p < 0.01$) as determined by a one-way analysis of variance and the Newman–Keuls test are indicated by asterisks.*

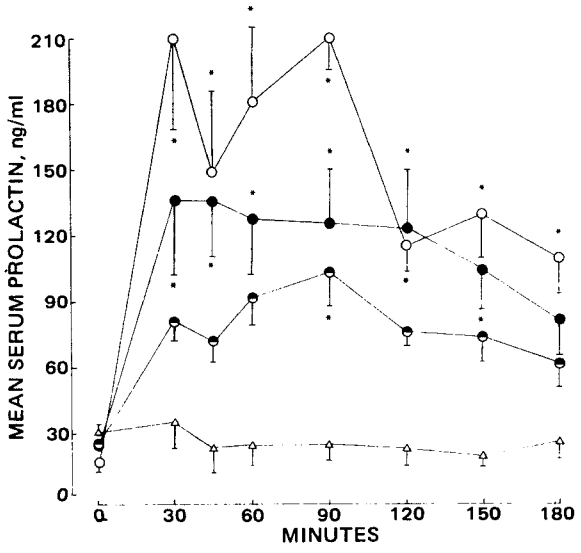

Figure 3—*Effect of intraperitoneally administered haloperidol (◓), chlorprothixene (●), and perphenazine (○) on serum prolactin levels in male rats over 180 min. The control group received 0.1* M *tartaric acid (△). Each point is the mean for six animals; vertical lines show the standard error of the means. Maximum serum prolactin elevations ($p < 0.01$) as determined by a one-way analysis of variance and the Newman–Keuls test are indicated by asterisks.*

mum Serum Prolactin Elevation—Doses (milligrams per kilogram) of neuroleptics calculated from log dose–response curves (Figs. 4 and 5) that were equipotent to 5.0 mg of chlorpromazine hydrochloride/kg in releasing prolactin are presented in Table I. In addition, the clinically defined therapeutic potencies of these drugs are compared on a weight to weight basis and related to their prolactin-stimulating potency. A commonly used chlorpromazine hydrochloride dose was selected as the reference because comparison of the activity of other antipsychotics to this neuroleptic is common (24–26).

DISCUSSION

Neuroleptic drugs belonging to three chemical groups, prochlorperazine, haloperidol, and thiothixene, produce parallel log dose–prolactin response curves in humans, presumably due to their antidopaminergic effects (10). When nine representative drugs belonging to five chemical classes of neuroleptics were administered to rats at experimentally determined times of maximum serum prolactin elevation [which do not vary

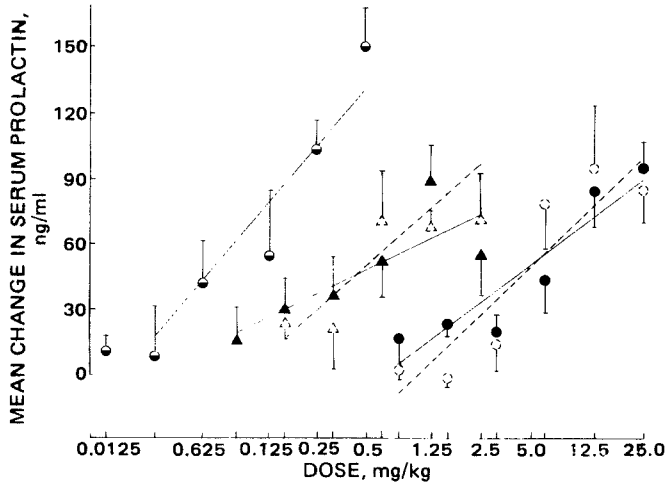

Figure 4—*Log dose–prolactin regression lines of chlorpromazine hydrochloride (○), chlorprothixene (●), haloperidol (◒), loxapine succinate (△), and molindone hydrochloride (▲). The y axis (mean change in serum prolactin) expresses the mean elevation of the prolactin concentration above the mean of the corresponding control group values. Each point represents the mean response of six experiments; vertical lines show the standard error of the means.*

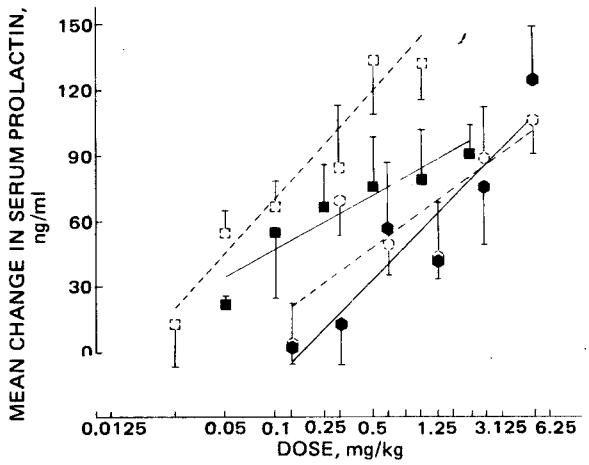

Figure 5—*Log dose–prolactin regression lines of fluphenazine hydrochloride (□), perphenazine (○), prochlorperazine edisylate (●), and trifluoperazine hydrochloride (■). The y axis (mean change in serum prolactin) expresses the mean elevation of the prolactin concentration above the mean of the corresponding control group values. Each point represents the mean response of six experiments; vertical lines show the standard error of the means.*

significantly for an individual neuroleptic in response to dose variations (6, 10)], nine nearly parallel log dose–prolactin response regression lines were calculated. The correlation coefficient for each drug was highly significant and indicated excellent linear fit. These results indicate that there also is a common mechanism for inducing prolactin release in rats, presumably due to their antidopaminergic effects.

To evaluate the prolactin-releasing potency of each drug at an experimentally determined time of maximum serum prolactin elevation, the log dose–prolactin response curves were utilized. Based on these curves, the calculated ratio of the neuroleptic to the chlorpromazine hydrochloride prolactin-stimulating potency was compared to its reported antipsychotic potency ratio. For seven of the nine drugs, the neuroleptic to chlorpromazine potency ratios in rats were consistent with the accepted neuroleptic to chlorpromazine potency relationships for humans. The prolactin potency ratios of perphenazine and prochlorperazine to chlorpromazine were only slightly below the accepted clinical potency relationships.

The data indicated a better relationship between the prolactin-releasing potency of neuroleptics in rats and the clinically accepted therapeutic potency in humans than was reported elsewhere in an animal system (18). For example, haloperidol was reported to be only 16.6 times more potent than chlorpromazine in inducing prolactin secretion using a fixed 30-min comparison of serum prolactin levels (18). For the experimentally derived 90-min maximum elevation of serum prolactin for haloperidol, which also was its peak prolactin response time observed in humans following intramuscular adminstration (10), a much better correlation was obtained between prolactin stimulation potency and the accepted clinical potency range (19, 24).

Due to the variability in the time–serum prolactin profiles of the individual neuroleptics following intraperitoneal administration, their potency and prolactin response ratios would have been altered if a fixed time comparison of all prolactin levels was made rather than a comparison at the time of each drug's maximum serum prolactin elevation. The different times for maximum elevation of serum prolactin observed for several neuroleptics in this study, as well as those cited by other investigators but involving humans (6), suggest a variation in the onset of action for different drugs due to their molecular characteristics. Future work should evaluate this possible relationship.

For the nine drugs studied, which represent all chemical classes of antischizophrenic agents approved for clinical use in the United States, there is evidence to suggest that clinically accepted neuroleptic potency relationships in humans closely correlate with prolactin-stimulating properties in male rats when measured at a time of maximum serum prolactin elevation. This technique may be a convenient alternative to the proposed use of normal volunteers (6, 10) as a screening test for establishing the potency of new neuroleptics.

REFERENCES

(1) A. G. Frantz and D. L. Kleinberg, *Science*, **170**, 745 (1970).

(2) M. T. Buckman and G. T. Peake, *J. Am. Med. Assoc.*, **236**, 871 (1976).
(3) I. A. Kamberi, R. S. Mical, and J. C. Porter, *Experientia*, **26**, 1150 (1970).
(4) E. Fluckiger, *Bull. Schweiz. Akad. Med. Wiss.*, **34**, 191 (1978).
(5) M. Szabo and L. A. Frohman, *Endocrinology*, **98**, 1451 (1976).
(6) E. J. Sachar, P. H. Gruen, N. Altman, F. S. Halpern, and A. G. Frantz, in "Hormones, Behavior, and Psychopathology," Raven, New York, N.Y., 1976, pp. 161–176.
(7) E. J. Sachar, P. H. Gruen, N. Altman, G. Langer, F. S. Halpern, and M. Liefer, in "Neuroregulators and Psychiatric Disorders," E. Usdin, D. Hamburg, and J. Barchas, Eds., Oxford University Press, New York, N.Y., 1977, pp. 242–249.
(8) R. Dickey and S. Stone, *Clin. Obstet. Gynecol.*, **18**, 95 (1975).
(9) H. Y. Meltzer and V. S. Fang, *Arch. Gen. Psychiat.*, **33**, 279 (1976).
(10) G. Langer, E. J. Sachar, F. S. Halpern, P. H. Gruen, and M. Solomon, *J. Clin. Endocrinol. Metab.*, **45**, 996 (1977).
(11) H. Y. Meltzer, S. Daniels, and V. S. Fang, *Life Sci.*, **17**, 339 (1976).
(12) H. Y. Meltzer, R. G. Fessler, and V. S. Fang, *Psychopharmacology*, **54**, 183 (1977).
(13) P. Seeman and T. Lee, *Science*, **188**, 1217 (1975).
(14) M. Goldstein, R. L. Bronaugh, T. Ohashi, and D. Eberstein, in "Neuroregulators and Psychiatric Disorders," E. Usdin, D. Hamburg, and J. Barchas, Eds., Oxford University Press, New York, N.Y., 1977, pp. 538–545.
(15) P. Seeman, M. Chou-Wong, J. Tadesco, and K. Wong, *Proc. Natl. Acad. Sci. USA*, **72**, 4376 (1975).
(16) S. H. Snyder, *Am. J. Psychiat.*, **133**, 197 (1976).
(17) J. A. Clemens, E. B. Smalstig, and B. D. Sawyer, *Psychopharmacologia*, **40**, 123 (1974).
(18) H. Y. Meltzer, D. J. Goode, and V. S. Fang, in "Psychopharmacology: A Generation of Progress," M. A. Lipton, A. DiMascio, and K. F. Killam, Eds., Raven, New York, N.Y., 1978, p. 509.
(19) American Medical Association Department of Drugs, "A.M.A. Drug Evaluations," Publishing Sciences Group, Littleton, Mass., 1977, pp. 444–448.
(20) B. J. Winer, "Statistical Principles in Experimental Design," 2nd ed., McGraw-Hill, New York, N.Y., 1961, p. 776.
(21) *Ibid.*, p. 191.
(22) W. M. Hunter and F. C. Greenwood, *Nature*, **194**, 495 (1962).
(23) B. J. Winer, "Statistical Principles in Experimental Design," 2nd ed., McGraw-Hill, New York, N.Y., 1961, p. 94.
(24) J. M. Davis, *Arch. Gen. Psychiat.*, **33**, 858 (1976).
(25) G. L. LaVigne and R. J. Baldessarini, *Am. J. Psychiat.*, **133**, 852 (1976).
(26) J. M. Davis, *Curr. Psychiatr. Ther.*, **17**, 209 (1977).

ACKNOWLEDGMENTS

Presented at the Natural Products and Medicinal Chemistry Section, APhA Academy of Pharmaceutical Sciences, Anaheim meeting, April 1979.

The authors thank the National Institute of Arthritis, Metabolism, and Digestive Disease Rat Pituitary Hormone Distribution Program and Dr. A. F. Parlow for their gift of radioimmunoassay materials. The authors also thank Dr. Howard McGuire, Long Island University, for assistance with the statistical analysis.

Further Considerations on Model-Independent Bioavailability Estimation

S. HWANG ˣ and K. C. KWAN

Received December 8, 1978, from *Merck Sharp & Dohme Research Laboratories, West Point, PA 19486.* Accepted for publication July 31, 1979.

Abstract □ Assumptions attendant to model-independent bioavailability estimation were reexamined. Particular attention was given to the situation where an intravenous reference is not available and nonrenal clearance is assumed to be constant between treatments. Under these circumstances, the previously proposed approximation was compared with other bioavailability estimators. On the basis of error analysis, a procedure was devised to yield optimal relative bioavailability estimates.

Keyphrases □ Bioavailability—model-independent estimation □ Drug availability—model-independent estimation □ Models—bioavailability estimation, equations

In a previous report (1), a model-independent method to assess bioavailability was suggested. The procedure calls for an initial determination of plasma clearance from an intravenous reference and assumptions concerning changes therein following the test dose(s). The proposed solutions are exact except when an intravenous reference is not available and nonrenal clearance is assumed to be unchanged between treatments. For this latter situation, an approximate solution was suggested initially with the support of a simulated example (1) and verified subsequently with experimental results (2).

This report provides a rigorous analysis of this approximation and the means to optimize its solutions. Its merits are examined relative to those of the dose-adjusted ratio of urinary recoveries of unchanged drug and of the area under the plasma concentration–time curve. It will be shown that where the nonrenal clearances are unchanged, the proposed approximation (1) is always superior to area ratios and often is better than urine ratios. Conditions under which relative bioavailability estimates should be optimal are discussed.

THEORETICAL

Bioavailability following a nonintravascular treatment, x, can be estimated by:

$$F^x = \frac{\dot{V}^x_{cl,p} AUC^x_\infty}{D^x} = \frac{\dot{V}^x_{cl,p} U^x_\infty}{D^x \dot{V}^x_{cl,r}} \qquad \text{(Eq. 1)}$$

where F is the fraction of the dose, D, absorbed; AUC_∞ is the total area under the plasma concentration–time curve; U_∞ is the total amount of unchanged drug excreted in the urine; and $\dot{V}_{cl,p}$ and $\dot{V}_{cl,r}$ are the plasma and plasma renal clearances, respectively. Except for $\dot{V}^x_{cl,p}$, the terms on the right side of Eq. 1 are known or can be calculated from plasma and/or urinary excretion data following treatment x.

On the other hand, plasma clearance must be determined by an independent experiment. Ideally, an intravenous tracer dose is administered concurrently with x such that the plasma clearance of the labeled drug becomes the estimate of $\dot{V}^x_{cl,p}$. An alternative solution was proposed (3, 4) whereby plasma clearance is estimated from separate treatments in which the renal drug clearance is perturbed in a controlled manner. The assumptions are that the perturbing influence on the kidney remains constant with time and that the same dose fraction is absorbed between

0022-3549/80/0100-0077$01.00/0
© 1980, American Pharmaceutical Association

(2) M. T. Buckman and G. T. Peake, *J. Am. Med. Assoc.*, **236**, 871 (1976).
(3) I. A. Kamberi, R. S. Mical, and J. C. Porter, *Experientia*, **26**, 1150 (1970).
(4) E. Fluckiger, *Bull. Schweiz. Akad. Med. Wiss.*, **34**, 191 (1978).
(5) M. Szabo and L. A. Frohman, *Endocrinology*, **98**, 1451 (1976).
(6) E. J. Sachar, P. H. Gruen, N. Altman, F. S. Halpern, and A. G. Frantz, in "Hormones, Behavior, and Psychopathology," Raven, New York, N.Y., 1976, pp. 161–176.
(7) E. J. Sachar, P. H. Gruen, N. Altman, G. Langer, F. S. Halpern, and M. Liefer, in "Neuroregulators and Psychiatric Disorders," E. Usdin, D. Hamburg, and J. Barchas, Eds., Oxford University Press, New York, N.Y., 1977, pp. 242–249.
(8) R. Dickey and S. Stone, *Clin. Obstet. Gynecol.*, **18**, 95 (1975).
(9) H. Y. Meltzer and V. S. Fang, *Arch. Gen. Psychiat.*, **33**, 279 (1976).
(10) G. Langer, E. J. Sachar, F. S. Halpern, P. H. Gruen, and M. Solomon, *J. Clin. Endocrinol. Metab.*, **45**, 996 (1977).
(11) H. Y. Meltzer, S. Daniels, and V. S. Fang, *Life Sci.*, **17**, 339 (1976).
(12) H. Y. Meltzer, R. G. Fessler, and V. S. Fang, *Psychopharmacology*, **54**, 183 (1977).
(13) P. Seeman and T. Lee, *Science*, **188**, 1217 (1975).
(14) M. Goldstein, R. L. Bronaugh, T. Ohashi, and D. Eberstein, in "Neuroregulators and Psychiatric Disorders," E. Usdin, D. Hamburg, and J. Barchas, Eds., Oxford University Press, New York, N.Y., 1977, pp. 538–545.
(15) P. Seeman, M. Chou-Wong, J. Tadesco, and K. Wong, *Proc. Natl. Acad. Sci. USA*, **72**, 4376 (1975).
(16) S. H. Snyder, *Am. J. Psychiat.*, **133**, 197 (1976).
(17) J. A. Clemens, E. B. Smalstig, and B. D. Sawyer, *Psychopharmacologia*, **40**, 123 (1974).
(18) H. Y. Meltzer, D. J. Goode, and V. S. Fang, in "Psychopharmacology: A Generation of Progress," M. A. Lipton, A. DiMascio, and K. F. Killam, Eds., Raven, New York, N.Y., 1978, p. 509.
(19) American Medical Association Department of Drugs, "A.M.A. Drug Evaluations," Publishing Sciences Group, Littleton, Mass., 1977, pp. 444–448.
(20) B. J. Winer, "Statistical Principles in Experimental Design," 2nd ed., McGraw-Hill, New York, N.Y., 1961, p. 776.
(21) *Ibid.*, p. 191.
(22) W. M. Hunter and F. C. Greenwood, *Nature*, **194**, 495 (1962).
(23) B. J. Winer, "Statistical Principles in Experimental Design," 2nd ed., McGraw-Hill, New York, N.Y., 1961, p. 94.
(24) J. M. Davis, *Arch. Gen. Psychiat.*, **33**, 858 (1976).
(25) G. L. LaVigne and R. J. Baldessarini, *Am. J. Psychiat.*, **133**, 852 (1976).
(26) J. M. Davis, *Curr. Psychiatr. Ther.*, **17**, 209 (1977).

ACKNOWLEDGMENTS

Presented at the Natural Products and Medicinal Chemistry Section, APhA Academy of Pharmaceutical Sciences, Anaheim meeting, April 1979.

The authors thank the National Institute of Arthritis, Metabolism, and Digestive Disease Rat Pituitary Hormone Distribution Program and Dr. A. F. Parlow for their gift of radioimmunoassay materials. The authors also thank Dr. Howard McGuire, Long Island University, for assistance with the statistical analysis.

Further Considerations on Model-Independent Bioavailability Estimation

S. HWANG ˣ and K. C. KWAN

Received December 8, 1978, from *Merck Sharp & Dohme Research Laboratories, West Point, PA 19486.* Accepted for publication July 31, 1979.

Abstract □ Assumptions attendant to model-independent bioavailability estimation were reexamined. Particular attention was given to the situation where an intravenous reference is not available and nonrenal clearance is assumed to be constant between treatments. Under these circumstances, the previously proposed approximation was compared with other bioavailability estimators. On the basis of error analysis, a procedure was devised to yield optimal relative bioavailability estimates.

Keyphrases □ Bioavailability—model-independent estimation □ Drug availability—model-independent estimation □ Models—bioavailability estimation, equations

In a previous report (1), a model-independent method to assess bioavailability was suggested. The procedure calls for an initial determination of plasma clearance from an intravenous reference and assumptions concerning changes therein following the test dose(s). The proposed solutions are exact except when an intravenous reference is not available and nonrenal clearance is assumed to be unchanged between treatments. For this latter situation, an approximate solution was suggested initially with the support of a simulated example (1) and verified subsequently with experimental results (2).

This report provides a rigorous analysis of this approximation and the means to optimize its solutions. Its merits are examined relative to those of the dose-adjusted ratio of urinary recoveries of unchanged drug and of the area under the plasma concentration–time curve. It will be shown that where the nonrenal clearances are unchanged, the proposed approximation (1) is always superior to area ratios and often is better than urine ratios. Conditions under which relative bioavailability estimates should be optimal are discussed.

THEORETICAL

Bioavailability following a nonintravascular treatment, x, can be estimated by:

$$F^x = \frac{\dot{V}^x_{cl,p} AUC^x_\infty}{D^x} = \frac{\dot{V}^x_{cl,p} U^x_\infty}{D^x \dot{V}^x_{cl,r}} \qquad \text{(Eq. 1)}$$

where F is the fraction of the dose, D, absorbed; AUC_∞ is the total area under the plasma concentration–time curve; U_∞ is the total amount of unchanged drug excreted in the urine; and $\dot{V}_{cl,p}$ and $\dot{V}_{cl,r}$ are the plasma and plasma renal clearances, respectively. Except for $\dot{V}^x_{cl,p}$, the terms on the right side of Eq. 1 are known or can be calculated from plasma and/or urinary excretion data following treatment x.

On the other hand, plasma clearance must be determined by an independent experiment. Ideally, an intravenous tracer dose is administered concurrently with x such that the plasma clearance of the labeled drug becomes the estimate of $\dot{V}^x_{cl,p}$. An alternative solution was proposed (3, 4) whereby plasma clearance is estimated from separate treatments in which the renal drug clearance is perturbed in a controlled manner. The assumptions are that the perturbing influence on the kidney remains constant with time and that the same dose fraction is absorbed between

0022-3549/80/0100-0077$01.00/0
© 1980, American Pharmaceutical Association

treatments. More typically, however, the intravenous reference is administered to the test subject separately so that some assumption must be made concerning the constancy of plasma clearance between treatments. For example, if plasma clearance remains unchanged, *i.e.*, $\dot{V}^x_{cl,p} = \dot{V}^{iv}_{cl,p}$, the bioavailability of x is given by the dose-adjusted ratio of the areas under the plasma concentration curve:

$$F^x = \frac{D^{iv}(AUC^x_\infty)}{D^x(AUC^{iv}_\infty)} \qquad \text{(Eq. 2)}$$

However, if plasma clearance changes in proportion to the observed renal clearance change[1], the dose-adjusted ratio of urinary recoveries is the more accurate estimator, *i.e.*:

$$F^x = \frac{D^{iv}U^x_\infty}{D^xU^{iv}_\infty} \qquad \text{(Eq. 3)}$$

Finally, if nonrenal clearance is constant between treatments:

$$F^x = \frac{AUC^x_\infty}{D^x}(\dot{V}^{iv}_{cl,p} - \dot{V}^{iv}_{cl,r} + \dot{V}^x_{cl,r}) \qquad \text{(Eq. 4}a\text{)}$$

$$F^x = \frac{U^x_\infty}{D^x\dot{V}^x_{cl,r}}(\dot{V}^{iv}_{cl,p} - \dot{V}^{iv}_{cl,r} + \dot{V}^x_{cl,r}) \qquad \text{(Eq. 4}b\text{)}$$

In the absence of an intravenous reference and when $\dot{V}_{cl,p}$ is assumed constant, the bioavailability of treatment x relative to another nonintravascular treatment, s, is given by:

$$\frac{F^x}{F^s} = \frac{D^sAUC^x_\infty}{D^xAUC^s_\infty} \qquad \text{(Eq. 5)}$$

and when the ratio of $\dot{V}_{cl,r}/\dot{V}_{cl,p}$ remains constant between treatments:

$$\frac{F^x}{F^s} = \frac{D^sU^x_\infty}{D^xU^s_\infty} \qquad \text{(Eq. 6)}$$

By analogy to Eqs. 4*a* and 4*b*, the corresponding expression for relative bioavailability when nonrenal clearance remains constant is:

$$\frac{F^x}{F^s} = \frac{U^x_\infty}{D^x\dot{V}^x_{cl,r}}\left[\frac{\dot{V}^s_{cl,p}}{F^s} - \frac{(\dot{V}^s_{cl,r} - \dot{V}^x_{cl,r})}{F^s}\right] \qquad \text{(Eq. 7)}$$

Equations 2–7 are exact insofar as their respective assumptions hold. While the application of Eqs. 2–6 is straightforward, Eq. 7 cannot be evaluated because of the presence of unknowns $\dot{V}^s_{cl,p}$ and F^s on the right side. As an approximation to Eq. 7, it was suggested by Kwan and Till (*K–T*) that (1):

$$\left(\frac{F^x}{F^s}\right)_{K-T} = \frac{1}{[\dot{V}^x_{cl,p}]_{ex}}([\dot{V}^s_{cl,p}]_{ex} - \dot{V}^s_{cl,r} + \dot{V}^x_{cl,r}) \qquad \text{(Eq. 8)}$$

where $[\dot{V}_{cl,p}]_{ex}$ is defined as an experimentally derivable clearance such that:

$$[\dot{V}^{niv}_{cl,p}]_{ex} = \frac{\dot{V}^{niv}_{cl,p}}{F^{niv}} = \frac{D^{niv}(\dot{V}^{niv}_{cl,r})}{U^{niv}_\infty} \qquad \text{(Eq. 9)}$$

and niv refers to a nonintravascular treatment such as x or s. The error incurred by the use of Eq. 8 instead of Eq. 7 therefore is:

$$|(F^x/F^s)_{K-T} - (F^x/F^s)_{Eq.\ 7}| = \frac{|\delta|}{[\dot{V}^x_{cl,p}]_{ex}}\left(\frac{1}{F^s} - 1\right) \qquad \text{(Eq. 10)}$$

where:

$$\delta = \dot{V}^s_{cl,r} - \dot{V}^x_{cl,r} \qquad \text{(Eq. 11)}$$

Since treatments x and s are nonintravascular, one should be able to estimate the bioavailability of s relative to that of x by the same approximate method:

$$\left(\frac{F^s}{F^x}\right)_{K-T} = \frac{1}{[\dot{V}^s_{cl,p}]_{ex}}([\dot{V}^x_{cl,p}] - \dot{V}^x_{cl,r} + \dot{V}^s_{cl,r}) \qquad \text{(Eq. 12)}$$

in which treatment x is designated as the reference for calculation purposes. Then, the bioavailability of x relative to s is simply the reciprocal of $(F^s/F^x)_{K-T}$:

$$\frac{1}{(F^s/F^x)_{K-T}} = \frac{[\dot{V}^s_{cl,p}]_{ex}}{[\dot{V}^x_{cl,p}] - \dot{V}^x_{cl,r} + \dot{V}^s_{cl,r}} \qquad \text{(Eq. 13)}$$

The error resulting from the use of Eq. 13 as an approximation to Eq. 7 is:

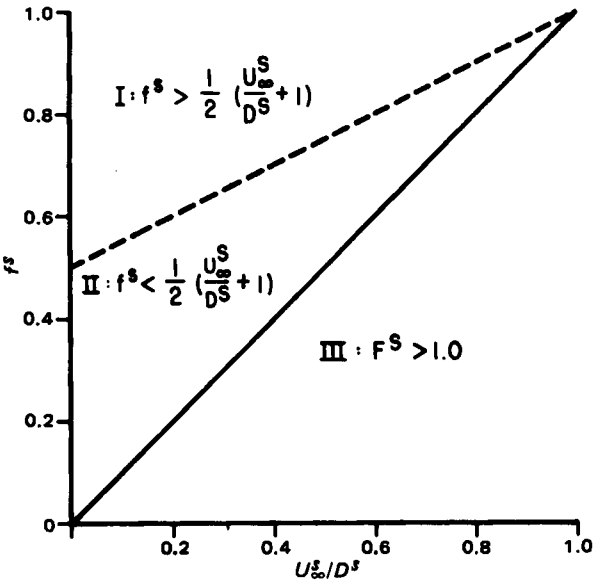

Figure 1—*Plot of* f^s versus U^s_∞/D^s. *On the dashed line,* $f^s = 0.5 + 0.5(U^s_\infty/D^s)$, *the errors associated with the uses of* $(U^x_\infty D^s/U^s_\infty D^x)$ *and* $(F^x/F^s)_{K-T}$ *are equal. In Region I,* $(U^x_\infty D^s)/(U^s D^x)$ *is preferred over* $(F^x/F^s)_{K-T}$, *and vice versa in Region II.*

$$\left|\frac{1}{(F^s/F^x)_{K-T}} - \left(\frac{F^x}{F^s}\right)_{Eq.\ 7}\right| = \frac{|\delta|}{[\dot{V}^x_{cl,p}]_{ex}}\frac{[\dot{V}^x_{cl,p}]_{ex} - \dot{V}^x_{cl,p}}{F^s([\dot{V}^x_{cl,p}]_{ex} + \delta)} \qquad \text{(Eq. 14)}$$

In addition to the trivial case where $\delta = 0$, it is evident from Eqs. 10 and 14 that the error term vanishes as F^s approaches 1.0 and as $[\dot{V}^x_{cl,p}]_{ex}$ approaches $\dot{V}^x_{cl,p}$, respectively. Equation 15 shows that estimates of bioavailability from Eq. 8 generally will differ from those from Eq. 13. The choice between the two can be made by considering the difference between their respective errors, Eqs. 14 and 10:

$$\left|\frac{1}{(F^s/F^x)_{K-T}} - \left(\frac{F^x}{F^s}\right)_{Eq.\ 7}\right| - \left|\left(\frac{F^x}{F^s}\right)_{K-T} - \left(\frac{F^x}{F^s}\right)_{Eq.\ 7}\right| = \frac{|\delta|}{[\dot{V}^x_{cl,p}]_{ex}([\dot{V}^x_{cl,p}]_{ex} + \delta)}|([\dot{V}^x_{cl,p}]_{ex} - \dot{V}^x_{cl,r}) - ([\dot{V}^s_{cl,p}]_{ex} - \dot{V}^s_{cl,r})| \qquad \text{(Eq. 15)}$$

All terms on the right side of Eq. 15 are experimentally derivable. Since the quotient preceding the braces, { }, always is positive, the sign of Eq. 15 is determined by the relative magnitude of $[\dot{V}_{cl,p}]_{ex} - \dot{V}_{cl,r}$ for the two treatments. If $[\dot{V}^x_{cl,p}]_{ex} - \dot{V}^x_{cl,r}$ is greater than $[\dot{V}^s_{cl,p}]_{ex} - \dot{V}^s_{cl,r}$, $(F^x/F^s)_{K-T}$ is closer to the true value and is preferred. If the converse holds, $1/(F^s/F^x)_{K-T}$ should be chosen. In the unlikely event that the two quantities within braces are identical, the same relative bioavailability estimate would result. The same criteria apply in studies involving three or more nonintravascular dosages. In other words, the treatment yielding the smallest value for $[\dot{V}_{cl,p}]_{ex} - \dot{V}_{cl,r}$ should be the reference for calculation.

According to Eq. 15, the first step in the estimation of relative bioavailability under the assumption of constant nonrenal clearance is to calculate $[\dot{V}_{cl,p}]_{ex} - \dot{V}_{cl,r}$ for all treatments in all subjects. For each subject, the treatment with the smallest $[\dot{V}_{cl,p}]_{ex} - \dot{V}_{cl,r}$ then is selected as the reference to which the bioavailability of all other treatments is compared. The resulting bioavailability ratios are rearranged or combined so that the desired reference, s, appears in the denominator.

In view of the approximate nature of Eqs. 8 and 13, their merits relative to other estimators should be examined. Conceivably, either the ratio of the dose fraction recovered in the urine or the ratio of the area under the plasma curve may be similarly adequate as an approximation even though nonrenal clearance is unchanged between treatments. Therefore, if nonrenal clearance truly is constant between treatments, the error associated with the use of the dose-adjusted area ratio (*i.e.*, Eq. 5) as a relative bioavailability estimate would be:

$$\left|\frac{AUC^x_\infty/D^x}{AUC^s_\infty/D^s} - \left(\frac{F^x}{F^s}\right)_{Eq.\ 7}\right| = \frac{|\delta|}{F^s[\dot{V}^x_{cl,p}]_{ex}} \qquad \text{(Eq. 16)}$$

Comparison of the uncommon terms on the right side of Eq. 10 with those of Eq. 16 shows that $(1/F^s) > (1/F^s) - 1$. Thus, under the prescribed

[1] This assumption is synonymous with saying that the fractional urinary recovery, $f = \dot{V}_{cl,r}/\dot{V}_{cl,p}$, remains constant between treatments.

Table I—Simulated Data for Relative Bioavailability Calculation

Oral Treatment	Dose, mg	Dose Fraction Absorbed, F^a	Dose Fraction Excreted in Urine, U_∞/D	Renal Clearance $\dot{V}_{cl,r}$, ml/min	$[\dot{V}_{cl,p}]_{ex} - \dot{V}_{cl,r}$
1	500	0.536	0.265	223.1	618.8
2	500	0.680	0.306	186.6	423.2

[a] As estimated in Table II of Ref. 1.

conditions, Eq. 8 estimates the true bioavailability better than does the ratio of dose-adjusted areas under the plasma curve. In light of the previous discussion on optimization, estimates by Eq. 13, when applicable, should be even better than those by Eq. 8.

Similarly, the absolute difference between the dose-adjusted ratio of urinary recoveries (*i.e.*, Eq. 6) and the true value is:

$$\left|\frac{U^x_\infty/D^x}{U^s_\infty/D^s} - \left(\frac{F^x}{F^s}\right)_{Eq.\ 7}\right| = \frac{|\delta|}{[\dot{V}^x_{cl,p}]_{ex}}\left(\frac{D^s}{U^s_\infty} - \frac{1}{F^s}\right) \quad \text{(Eq. 17)}$$

Comparison of the uncommon terms on the right side of Eqs. 10 and 17 shows that $(D^s/U^s_\infty) - (1/F^s)$ may be greater than, equal to, or less than $(1/F^s) - 1$. Thus, even when the nonrenal clearance is constant between treatments, the urinary excretion ratio approximates relative bioavailability better than does Eq. 8 in some situations. Intuitively, such situations prevail when renal excretion is the dominant drug elimination route. A quantitative assessment of situations in which one method is superior to the other is as follows.

The difference between Eqs. 10 and 17 can be expressed as:

$$\left|\left(\frac{F^x}{F^s}\right)_{K\text{-}T} - \left(\frac{F^x}{F^s}\right)_{Eq.\ 7}\right| - \left|\frac{U^x_\infty/D^x}{U^s_\infty/D^s} - \left(\frac{F^x}{F^s}\right)_{Eq.\ 7}\right| = \frac{|\delta|}{[\dot{V}^x_{cl,p}]_{ex}}\frac{D^s}{U^s_\infty}\left(2f^s - 1 - \frac{U^s_\infty}{D^s}\right) \quad \text{(Eq. 18)}$$

where f^s is the ratio of the renal clearance to plasma clearance. When the right side of Eq. 18 is positive, the urinary recovery ratio is better; when it is negative, $(F^x/F^s)_{K\text{-}T}$ is preferred. Whether Eq. 18 is greater or less than zero depends on the relative magnitude of f^s and U^s_∞/D^s. When Eq. 18 is zero:

$$f^s = \tfrac{1}{2}\left(1 + \frac{U^s_\infty}{D^s}\right) \quad \text{(Eq. 19)}$$

A plot of f^s *versus* U^s_∞/D^s is shown in Fig. 1, which is clearly divided into three regions. Equation 19 separates Region I, representing situations where $f^s > \frac{1}{2}[1 + (U^s_\infty/D^s)]$ when urinary excretion ratios should be used,

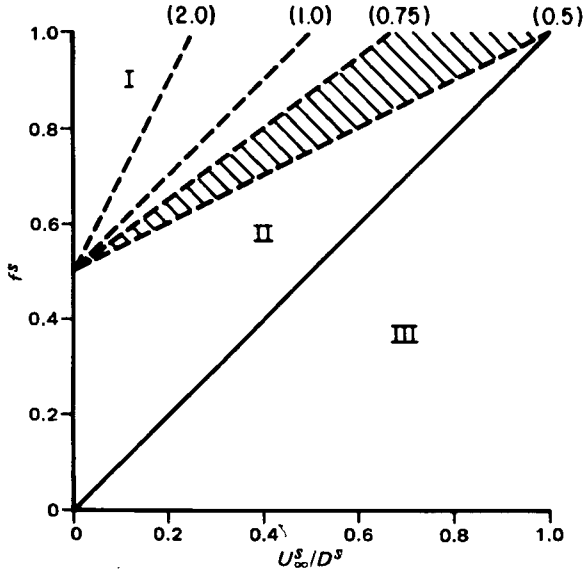

Figure 2—*Plot of* $f^s = 0.5 + \alpha(U^s_\infty D^s)$ *(Eq. 20). The* α *value for each line is specified in parentheses. The shaded area indicates the expansion of Region II by using* $1/(F^s/F^x)_{K\text{-}T}$ *instead of* $(F^x/F^s)_{K\text{-}T}$ *as* α *increases from 0.5 to 0.75.*

Table II—Sample Calculation of Relative Bioavailability of Oral Treatment 1 to Oral Treatment 2

True Value F^1/F^2	$\frac{AUC^1_\infty}{AUC^2_\infty}$[a]	$\frac{U^1_\infty}{U^2_\infty}$	$\left(\frac{F^1}{F^2}\right)_{K\text{-}T}$	$\frac{1}{(F^2/F^1)_{K\text{-}T}}$
0.788	0.724	0.866	0.768	0.757

[a] The *AUC* values were estimated by dividing total urinary recovery by renal clearance.

from Region II, where $f^s < \frac{1}{2}[1 + (U^s_\infty/D^s)]$ when $(F^x/F^s)_{K\text{-}T}$ should be favored. Region III, representing $f^s < (U^s_\infty/D^s)$ (or $\dot{F}^s > 1$), is not experimentally relevant.

In accord with the preceding discussion on the optimal choice of a reference in relative bioavailability calculations, there will be times when $1/(F^s/F^x)_{K\text{-}T}$ is a better estimator than $(F^x/F^s)_{K\text{-}T}$. Under these circumstances, the demarcation between Regions I and II must change so as to enlarge Region II. Therefore, the difference between Eqs. 14 and 17 is:

$$\left|\frac{1}{(F^s/F^x)_{K\text{-}T}} - \left(\frac{F^x}{F^s}\right)_{Eq.\ 7}\right| - \left|\frac{U^x_\infty/D^x}{U^s_\infty/D^s} - \left(\frac{F^x}{F^s}\right)_{Eq.\ 7}\right| = \frac{|\delta|}{[\dot{V}^x_{cl,p}]_{ex}}\frac{D^s}{U^s_\infty}\left\{2f^s - 1 - \frac{U^s_\infty}{D^s} - \frac{U^s_\infty}{D^s}\frac{([\dot{V}^s_{cl,p}]_{ex} - \dot{V}^s_{cl,r}) - ([\dot{V}^x_{cl,p}]_{ex} - \dot{V}^x_{cl,r})}{[\dot{V}^x_{cl,p}]_{ex} - \dot{V}^x_{cl,r} + \dot{V}^s_{cl,r}}\right\} \quad \text{(Eq. 20)}$$

Evidently, the critical value at which Eq. 20 becomes zero is when:

$$f^s = \frac{1}{2} + \left\{\frac{([\dot{V}^s_{cl,p}]_{ex} - \dot{V}^s_{cl,r}) - ([\dot{V}^x_{cl,p}]_{ex} - \dot{V}^x_{cl,r})}{[\dot{V}^x_{cl,p}]_{ex} - \dot{V}^x_{cl,r} + \dot{V}^s_{cl,r}} + \frac{1}{2}\right\}\frac{U^s_\infty}{D^s} \quad \text{(Eq. 21)}$$

Like Eq. 19, Eq. 21 is a straight line with an intercept of 0.5. Unlike Eq. 19, the slope of Eq. 21 varies with each specific pair of treatments x and s. However, since $1/(F^s/F^x)_{K\text{-}T}$ is used only when $[\dot{V}^s_{cl,p}]_{ex} - \dot{V}^s_{cl,r}$ is greater than $[\dot{V}^x_{cl,p}]_{ex} - \dot{V}^x_{cl,r}$, a positive contribution to the slope is assured. Thus, Eq. 20 represents a family of lines with slopes equal to or greater than 0.5 and a common intercept at $x = 0, y = 0.5$. Figure 2 illustrates the moving boundary between Regions I and II for a range of slopes. The shaded area in Fig. 2 represents the expansion of Region II at the expense of Region I if the slope increases from 0.5 to 0.75.

Application of Eqs. 19 and 21 requires some knowledge of the excretion characteristics of the drug. In the absence of an intravenous reference, f^s is an unknown, while all terms on the right side of Eqs. 19 and 21 are experimental observations. If it is known from previous studies that f generally is less than 0.5, Eq. 8 or 13 clearly is preferable to urinary excretion ratios. For given f values greater than 0.5, the superior estimator can be deduced from observed U_∞/D values with the aid of Eqs. 15, 19, and 21 and Fig. 2. That is to say, the choice between $(F^x/F^s)_{K\text{-}T}$ and $1/(F^s/F^x)_{K\text{-}T}$ depends on the criterion set by Eq. 15. Whether either of these terms is preferable to the urinary recovery ratio then depends on f for the drug and the actual observations, *e.g.*, U_∞ and $\dot{V}_{cl,r}$, for a given subject.

For comparisons involving $(F^x/F^s)_{K\text{-}T}$, Eq. 19 or the line having a slope equal to 0.5 in Fig. 2 applies. When $1/(F^s/F^x)_{K\text{-}T}$ is more appropriate, a slope first must be calculated in accordance with Eq. 21, and the proper line must be constructed in Fig. 2. For example, when $U^s_\infty/D^s = 0.4$ and the slope by Eq. 21 is 1.0, Fig. 2 shows that the urinary excretion ratio would be a better estimator of relative bioavailability than $(F^x/F^s)_{K\text{-}T}$ if f^s is >0.7 and superior to $1/(F^s/F^x)_{K\text{-}T}$ if f^s is >0.9.

EXAMPLE

To test the conclusions from the forgoing error analyses, it is necessary to use an example for which the correct answer is known. The simulated data from the previous report (1) are suitable for this purpose because all aspects of drug disposition except renal clearance were kept constant between treatments and the bioavailability of the two oral treatments was fixed *a priori* (and confirmed by comparison to the intravenous reference). Table I summarizes the information necessary to the present discussion.

Various bioavailability estimates of Treatment 2 relative to Treatment 1 are shown in Table II. The accuracy of each approximation can be ranked according to its proximity to the true value, which is the ratio of their absolute bioavailabilities. Since $[\dot{V}_{cl,p}]_{ex} - \dot{V}_{cl,r}$ is smaller after Treatment 2, $(F^1/F^2)_{K\text{-}T}$ should be closer to the true value than $1/(F^2/F^1)_{K\text{-}T}$. This is the case. Also, as predicted, the result by the *AUC*

ratio is worse than that by $(F^1/F^2)_{K\text{-}T}$. Finally, the urinary recovery ratio is the worst approximation of all, which is not unexpected since renal excretion is only a minor elimination route ($f < 0.50$).

DISCUSSION

An approximate solution for relative bioavailability estimation between nonintravascular doses was suggested previously (1). Since then, numerous inquiries have been received concerning the nature and source of its inexactitude, particularly under the assumption of constant nonrenal clearance between treatments. Simulation studies were not revealing; reasonably accurate estimates usually were obtained except when unrealistically large perturbations were considered. On the other hand, the present theoretical analysis appears to offer new insights.

Whereas the ratio of areas under the plasma curve and of urinary excretions are exact relative bioavailability determinants when their respective assumptions prevail, Eqs. 8 and 13 are only approximations when nonrenal clearance remains constant between treatments. In addition, Eqs. 8 and 13 give different answers for a given data set. However, criteria were established so that the more accurate of the two estimates always can be identified. The choice of reference for calculations should be made for each comparison within a study to ensure the best possible estimates.

Despite their approximate nature, Eqs. 8 and 13 always are preferable to area ratios and often are superior to urinary excretion ratios when nonrenal clearance is constant. The only exception is when the drug is eliminated predominantly by renal excretion. Predominance now has been defined as when $\dot{V}_{cl,r}/\dot{V}_{cl,p}$ is greater than either $\frac{1}{2}(1 + U^s_\infty/D^s)$ or:

$$\frac{1}{2} + \left\{\frac{1}{2} + \frac{([\dot{V}^s_{cl,p}]_{ex} - \dot{V}^s_{cl,r}) - ([\dot{V}^x_{cl,p}]_{ex} - \dot{V}^x_{cl,r})}{[\dot{V}^x_{cl,p}]_{ex} - \dot{V}^x_{cl,r} + \dot{V}^s_{cl,r}}\right\} \frac{U^s_\infty}{D^s}$$

depending on whether Eq. 8 or 13 is to be used, respectively. Thus, given some idea of the usual fraction excreted unchanged following an intravenous dose, a decision can be made whether the urinary excretion ratio, Eq. 8, or Eq. 13 should be chosen.

The constant nonrenal clearance assumption ordinarily is favored for another reason. Given that observed renal clearances differ between treatments, the likelihood that compensatory nonrenal clearance changes will occur to maintain a constant plasma clearance or a constant ratio of renal to plasma clearance seems remote. On the other hand, adjustments in plasma clearance based only on observed changes in renal clearance simply corroborate experimental evidence.

REFERENCES

(1) K. C. Kwan and A. E. Till, *J. Pharm. Sci.*, **62**, 1494 (1973).

(2) K. C. Kwan, G. O. Breault, E. R. Umbenhauer, F. G. McMahon, and D. E. Duggan, *J. Pharmacokinet. Biopharm.*, **4**, 255 (1976).

(3) D. Lalka and H. Feldman, *J. Pharm. Sci.*, **63**, 1812 (1974).

(4) D. Lalka, P. duSouich, A. J. McLean, and M. Gibaldi, *ibid.*, **67**, 591 (1978).

Mass Spectrometry of Chlorambucil, Its Degradation Products, and Its Metabolite in Biological Samples

S. Y. CHANG ˣ, B. J. LARCOM, D. S. ALBERTS, B. LARSEN, P. D. WALSON, and I. G. SIPES

Received December 22, 1978, from the *College of Medicine, University of Arizona, Tucson, AZ 85724.* Accepted for publication August 1, 1979.

Abstract □ A sensitive and specific method for the determination of chlorambucil and its metabolite in biological fluids is reported. The method is based on selected-ion monitoring detection following simple extraction of the parent compound, its metabolite, and an internal standard (chlorambucil-d_8) from plasma and urine samples. The precision (reproducibility) of the method was 94.3 ± 1.3% with 200 ng of chlorambucil added to 1 ml of plasma. Chlorambucil degradation or alkylation of plasma proteins was minimal with plasma incubated at 24° for 4 hr. However, chloroambucil recovery decreased to 56% after plasma incubation at 37° for 4 hr. Three chlorambucil degradation products in ethyl acetate solution were found, and their structures were studied by mass spectrometry.

Keyphrases □ Chlorambucil—analysis, mass spectrometry, degradation products and metabolite, human plasma and urine □ Antineoplastic agents—chlorambucil, degradation products and metabolite, mass spectrometry, human plasma and urine □ Mass spectrometry, selected-ion monitoring—chlorambucil, degradation products and metabolite, human plasma and urine

The anticancer drug chlorambucil (I) is useful in the treatment of chronic lymphocytic leukemia, ovarian carcinoma, nodular lymphocytic lymphoma, and myelocytic leukemia (1, 2). Various analytical methods were reported for the quantitation of I, including the colorimetric determination of 4-(*p*-nitrobenzyl)pyridine derivatives (3, 4) and UV spectrophotometric (5) and chlorine titrimetric (6) methods. None of these methods provides the sensitivity and accuracy needed to study I pharmacokinetics and metabolism in humans. The mass spectrometric determination of I in plasma was reported recently (7). This

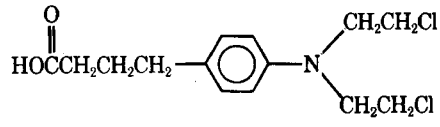

I

method requires several extraction steps, including a back-extraction of I from the aqueous solution at alkaline pH.

The quantitative method presented here is based on a one-step extraction followed by a determination of I and a metabolite in plasma and urine by mass spectrometry using a deuterated I internal standard. This method was used to study the *in vitro* I stability in plasma as well as to characterize the *in vitro* degradation products. The method was applied to the quantitation of I and a metabolite in human plasma and urine samples.

EXPERIMENTAL

Chlorambucil-d_8 Synthesis—The synthesis of chlorambucil-d_8 (labeled at *N*-chloroethyl) was adapted from a literature method (8). 4-(*p*-Nitrophenyl)butyric acid[1], 500 mg, was reacted with ethereal diazomethane[1]. The resulting methylnitrophenylbutyrate was dissolved in ethyl acetate–methanol (9:1 v/v) through which hydrogen gas was bubbled continuously for 8 hr in the presence of palladium[2] with the solvent

[1] Aldrich Chemical Co., Milwaukee, Wis.
[2] Ventron Corp., Danver, Mass.

0022-3549/80/0100-0080$01.00/0

© 1980, American Pharmaceutical Association

ratio is worse than that by $(F^1/F^2)_{K\text{-}T}$. Finally, the urinary recovery ratio is the worst approximation of all, which is not unexpected since renal excretion is only a minor elimination route ($f < 0.50$).

DISCUSSION

An approximate solution for relative bioavailability estimation between nonintravascular doses was suggested previously (1). Since then, numerous inquiries have been received concerning the nature and source of its inexactitude, particularly under the assumption of constant nonrenal clearance between treatments. Simulation studies were not revealing; reasonably accurate estimates usually were obtained except when unrealistically large perturbations were considered. On the other hand, the present theoretical analysis appears to offer new insights.

Whereas the ratio of areas under the plasma curve and of urinary excretions are exact relative bioavailability determinants when their respective assumptions prevail, Eqs. 8 and 13 are only approximations when nonrenal clearance remains constant between treatments. In addition, Eqs. 8 and 13 give different answers for a given data set. However, criteria were established so that the more accurate of the two estimates always can be identified. The choice of reference for calculations should be made for each comparison within a study to ensure the best possible estimates.

Despite their approximate nature, Eqs. 8 and 13 always are preferable to area ratios and often are superior to urinary excretion ratios when nonrenal clearance is constant. The only exception is when the drug is eliminated predominantly by renal excretion. Predominance now has been defined as when $\dot{V}_{cl,r}/\dot{V}_{cl,p}$ is greater than either $\frac{1}{2}(1 + U^s_\infty/D^s)$ or:

$$\frac{1}{2} + \left\{\frac{1}{2} + \frac{([\dot{V}^s_{cl,p}]_{ex} - \dot{V}^s_{cl,r}) - ([\dot{V}^x_{cl,p}]_{ex} - \dot{V}^x_{cl,r})}{[\dot{V}^x_{cl,p}]_{ex} - \dot{V}^x_{cl,r} + \dot{V}^s_{cl,r}}\right\} \frac{U^s_\infty}{D^s}$$

depending on whether Eq. 8 or 13 is to be used, respectively. Thus, given some idea of the usual fraction excreted unchanged following an intravenous dose, a decision can be made whether the urinary excretion ratio, Eq. 8, or Eq. 13 should be chosen.

The constant nonrenal clearance assumption ordinarily is favored for another reason. Given that observed renal clearances differ between treatments, the likelihood that compensatory nonrenal clearance changes will occur to maintain a constant plasma clearance or a constant ratio of renal to plasma clearance seems remote. On the other hand, adjustments in plasma clearance based only on observed changes in renal clearance simply corroborate experimental evidence.

REFERENCES

(1) K. C. Kwan and A. E. Till, *J. Pharm. Sci.*, **62**, 1494 (1973).

(2) K. C. Kwan, G. O. Breault, E. R. Umbenhauer, F. G. McMahon, and D. E. Duggan, *J. Pharmacokinet. Biopharm.*, **4**, 255 (1976).

(3) D. Lalka and H. Feldman, *J. Pharm. Sci.*, **63**, 1812 (1974).

(4) D. Lalka, P. duSouich, A. J. McLean, and M. Gibaldi, *ibid.*, **67**, 591 (1978).

Mass Spectrometry of Chlorambucil, Its Degradation Products, and Its Metabolite in Biological Samples

S. Y. CHANG ˣ, B. J. LARCOM, D. S. ALBERTS, B. LARSEN, P. D. WALSON, and I. G. SIPES

Received December 22, 1978, from the *College of Medicine, University of Arizona, Tucson, AZ 85724.* Accepted for publication August 1, 1979.

Abstract □ A sensitive and specific method for the determination of chlorambucil and its metabolite in biological fluids is reported. The method is based on selected-ion monitoring detection following simple extraction of the parent compound, its metabolite, and an internal standard (chlorambucil-d_8) from plasma and urine samples. The precision (reproducibility) of the method was 94.3 ± 1.3% with 200 ng of chlorambucil added to 1 ml of plasma. Chlorambucil degradation or alkylation of plasma proteins was minimal with plasma incubated at 24° for 4 hr. However, chloroambucil recovery decreased to 56% after plasma incubation at 37° for 4 hr. Three chlorambucil degradation products in ethyl acetate solution were found, and their structures were studied by mass spectrometry.

Keyphrases □ Chlorambucil—analysis, mass spectrometry, degradation products and metabolite, human plasma and urine □ Antineoplastic agents—chlorambucil, degradation products and metabolite, mass spectrometry, human plasma and urine □ Mass spectrometry, selected-ion monitoring—chlorambucil, degradation products and metabolite, human plasma and urine

The anticancer drug chlorambucil (I) is useful in the treatment of chronic lymphocytic leukemia, ovarian carcinoma, nodular lymphocytic lymphoma, and myelocytic leukemia (1, 2). Various analytical methods were reported for the quantitation of I, including the colorimetric determination of 4-(*p*-nitrobenzyl)pyridine derivatives (3, 4) and UV spectrophotometric (5) and chlorine titrimetric (6) methods. None of these methods provides the sensitivity and accuracy needed to study I pharmacokinetics and metabolism in humans. The mass spectrometric determination of I in plasma was reported recently (7). This

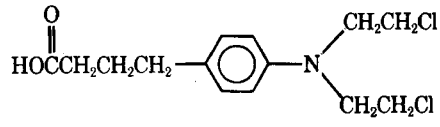

I

method requires several extraction steps, including a back-extraction of I from the aqueous solution at alkaline pH.

The quantitative method presented here is based on a one-step extraction followed by a determination of I and a metabolite in plasma and urine by mass spectrometry using a deuterated I internal standard. This method was used to study the *in vitro* I stability in plasma as well as to characterize the *in vitro* degradation products. The method was applied to the quantitation of I and a metabolite in human plasma and urine samples.

EXPERIMENTAL

Chlorambucil-d_8 Synthesis—The synthesis of chlorambucil-d_8 (labeled at *N*-chloroethyl) was adapted from a literature method (8). 4-(*p*-Nitrophenyl)butyric acid[1], 500 mg, was reacted with ethereal diazomethane[1]. The resulting methylnitrophenylbutyrate was dissolved in ethyl acetate–methanol (9:1 v/v) through which hydrogen gas was bubbled continuously for 8 hr in the presence of palladium[2] with the solvent

[1] Aldrich Chemical Co., Milwaukee, Wis.
[2] Ventron Corp., Danver, Mass.

0022-3549/80/0100-0080$01.00/0

© 1980, American Pharmaceutical Association

at constant volume. The ethyl acetate then was evaporated using nitrogen gas, yielding the reddish-brown aminophenylbutyric acid methyl ester, which was dissolved immediately in 20 ml of 50% acetic acid (CH_3COOD[3] in D_2O[3]). In a cold room (4°), 2 ml of ethylene oxide-d_4[3] (99% isotopic purity) was added.

The reaction mixture was allowed to stand at room temperature for 24 hr. The reaction was terminated by adding ~10 ml of water and sodium bicarbonate until no significant carbon dioxide evolved. The yellowish solution was extracted with 5 × 8 ml of ethyl acetate, and the ethyl acetate was dried with anhydrous sodium sulfate and then evaporated using nitrogen gas. All traces of water were removed by azeotroping with methylene chloride.

The gummy, dark-brown product was refluxed with 4 ml of freshly distilled phosphorus oxychloride for 45 min. Excess reagent was removed by partitioning several times with water–methylene chloride. The methylene chloride layer was evaporated using a nitrogen stream and refluxed with concentrated hydrochloric acid for 6 hr at 100°. The product was extracted with ethyl acetate–hexane (1:1) and partitioned with 0.01 *M* phosphate buffer (pH 9.0)–0.01 *M* NaCl. The aqueous phase was removed and washed twice with methylene chloride, and the pH was adjusted to 3 using 2 *N* HCl.

Chlorambucil-d_8 was extracted from the acidic aqueous solution with methylene chloride. The final product in methylene chloride was examined by high-performance liquid chromatography[4] and mass spectrometry[5]. The product had >95% chemical purity and >99% isotope purity as revealed by mass spectrometry for the molecular and base ions of deuterated and undeuterated chlorambucil. The yield was ~30%.

Chlorambucil-d_8 Standardization—Synthetic chlorambucil-d_8 was used as an internal standard without further purification. Its chlorambucil-d_8 concentration was determined against a known amount of I[6] by monitoring *m/e* 326 (M − CH_2Cl) and 328 for I and *m/e* 332 (M − CD_2Cl) and 334 for chlorambucil-d_8. Also, *m/e* 326 and 328 of I were monitored against *m/e* 383 and 385 of chlorambucil-d_8. Interferences due to other ions were not observed.

Extraction of I—Deuterated I (five to 10 times the maximum I amount expected) and 0.5 ml of 4% perchloric acid were added to 0.5 ml of plasma or urine. Ethyl acetate–hexane (1:1 v/v), 0.75 ml, was added to the precipitated sample, and I was extracted into the organic layer. The sample was centrifuged for 5 min at 3000 rpm[7], and the organic layer was transferred into a 1-ml microvial with a polytef-lined cap[8]. The solvent was evaporated with purified nitrogen gas at room temperature, and several drops of dry methylene chloride were added to the dried residue. Any water present in the dried residue was removed azeotropically with methylene chloride.

Derivatization of I—Dried samples were converted to their trimethylsilyl (TMS) derivatives for GLC–mass spectrometric analysis. *N,O* - Bis(trimethylsilyl)trifluoroacetamide[8]–acetonitrile–methylene chloride (20:10:1 v/v/v) solution, 100 μl, was added to the samples and allowed to react at 100° for 10 min. The trimethylsilyl derivatives were analyzed by GLC–mass spectrometry.

GLC–Mass Spectrometry—A mass spectrometer[5] was interfaced with a gas–liquid chromatograph[9]. All analyses were performed at 70 ev. The derivatized samples were injected directly onto a GLC column (0.5 m × 2 mm, 3% OV-17 on 100–120-mesh Gas Chrom Q) at 190°. After the solvent was vented for 45 sec at 190°, the column temperature was raised directly to 310°. A I trimethylsilyl derivative eluted at 230°.

Trimethylsilyl I was monitored at *m/e* 326 (M − CH_2Cl) and 328, and the internal standard (trimethylsilyl chlorambucil-d_8) was monitored at *m/e* 383 (M^+) and 385. Deuterated I was monitored at its molecular and chlorine isotope ions (*m/e* 383 and 385) instead of at its most intense fragment ions [*m/e* 332 (M − CD_2Cl) and 334] due to an interfering ion at *m/e* 332. Because *m/e* 383 was ~10 times less abundant than *m/e* 332, 10 times more of the internal standard relative to the expected I concentration was added to give an approximately equal height compared to that of *m/e* 326.

Animal and Human Studies—Rats were given 5.6 mg of I/kg by intravenous bolus injections over 1 min into a jugular venous catheter (9) Patients were given 0.6 mg of oral I[10]/kg. Animal and human plasma and urine samples were kept on ice during collection and stored at −70° until extracted for I.

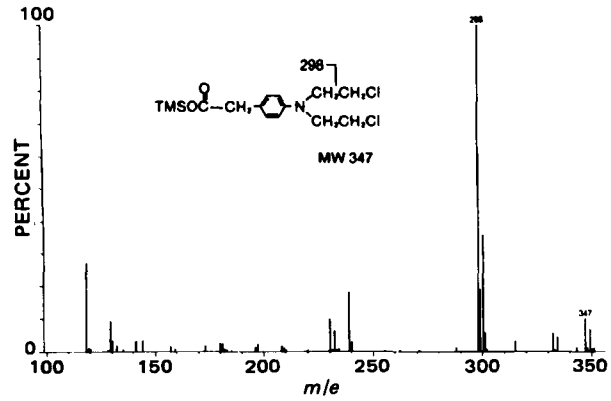

Figure 1—*Mass spectrum of metabolite, p-[4-N,N-bis(2-chloroethyl)]aminophenylacetic acid, isolated from human plasma and urine.*

Recovery Studies—Quantitative extraction was studied with ^{14}C-labeled I. ^{14}C-I[11] (505 ng, 3.5 × 10^4 cpm) was added to 1 ml of plasma, the solution was extracted three times, and the ^{14}C-recovery in the organic layer was examined in each extraction. The precision (reproducibility) of the recovery was studied by mass spectrometry. At least three samples of 5 and 1 μg and 200, 100, and 50 ng of I and appropriate amounts of the internal standard were added to 1-ml plasma samples. A single extraction was then carried out. The expected ratio of I to the internal standard was used to calculate recovery precision.

Stability of I—The I stability (10 μg/ml) in plasma at 37° was studied. At designated times, a sample was taken, the internal standard was added, and the extraction, derivatization, and analyses were performed. The disappearance rate constant, κ, of I was calculated according to $\kappa = 2.3 \log([C]_0/[C]_t)/t$, where $[C]_0$ and $[C]_t$ are the concentrations of I in the medium at times zero and t.

Drug stability in a nonaqueous medium also was studied. A solution of I in ethyl acetate was left at room temperature under ordinary laboratory conditions (with fluorescent light) for 2 weeks. The intensity of the brown color of the ethyl acetate solution increased with prolonged exposure to light. This brownish I solution was examined by GLC–mass spectrometry as the trimethylsilyl derivatives.

Calculations—The I concentrations in plasma and urine were calculated as follows:

$$\text{nanograms of I/aliquot} = \frac{\text{response of I sample}}{\text{response of internal standard sample}} \times \frac{1}{\text{relative equal weight response}} \times \text{nanograms of internal standard} \quad \text{(Eq. 1)}$$

where:

$$\text{relative equal weight response} = \frac{\text{response of I}}{\text{response of internal standard}} \quad \text{(Eq. 2)}$$

for standards of equal weight.

Identification and Determination of Phenylacetic Acid Mustard (p-[4-*N,N*-Bis(2-chloroethyl)]aminophenylacetic Acid)—Plasma and urine samples were extracted and derivatized as described for chlorambucil. Trimethylsilyl derivatives of samples were introduced directly into the GLC system, and the mass spectra of the resolved peaks were examined. Phenylacetic acid mustard was synthesized and highly purified.

The spectrum of the trimethylsilyl derivative of synthetic phenylacetic acid was compared directly to the GLC spectra of plasma and urine. The trimethylsilyl derivative of phenylacetic acid mustard eluted earlier than that of chlorambucil. For routine analysis of phenylacetic acid mustard in biological samples, *m/e* 298 (M − CH_2Cl) was monitored simultaneously with chlorambucil. The quantitation was performed as with

[3] Merck and Co., St. Louis, Mo.
[4] Waters Associates, St. Louis, Mo.
[5] Model 3300, Finnigan, Sunnyvale, Calif.
[6] Supplied by Burroughs-Wellcome Co., Research Triangle Park, N.C.
[7] GLC-2B, DuPont Instrument Co., Wilmington, Del.
[8] Regis Chemical Co., Morton Grove, Ill.
[9] Model 950 GC, Finnigan, Sunnyvale, Calif.
[10] Leukeran, supplied by Burroughs-Wellcome Co., Research Triangle Park, N.C.
[11] ^{14}C-Chlorambucil (labeled at the chloroethyl moiety) was supplied by Dr. R. Engles, Division of Cancer Treatment, National Cancer Institute, Bethesda, Md.

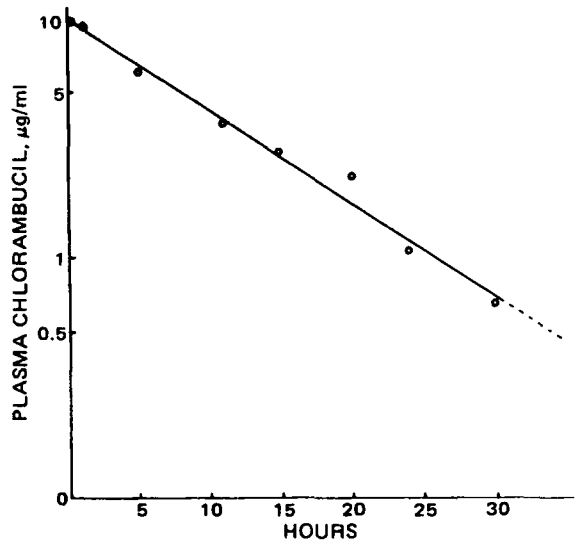

Figure 2—*Disappearance of I from plasma at 37°. Ten micrograms of I was added to 1.0 ml of plasma and incubated at 37°.*

chlorambucil. The initial calibration was carried out using the synthetic compound against chlorambucil-d_8.

Linearity—Linearity of the I determination was studied at 1 μg and 100, 50, 10, 5, 2, 1, and 0.5 ng. Each sample was derivatized independently along with the appropriate amount of internal standard and analyzed. The linearity was evaluated against $y = x$.

Since an excess of the internal standard was used, the dynamic range of the relative equal weight response also was examined. Both a 100-fold excess of the internal standard to I and a fivefold excess of I to the internal standard were studied. The concentration range used was 5 μg–0.5 ng for I and 10 μg–50 ng for the internal standard.

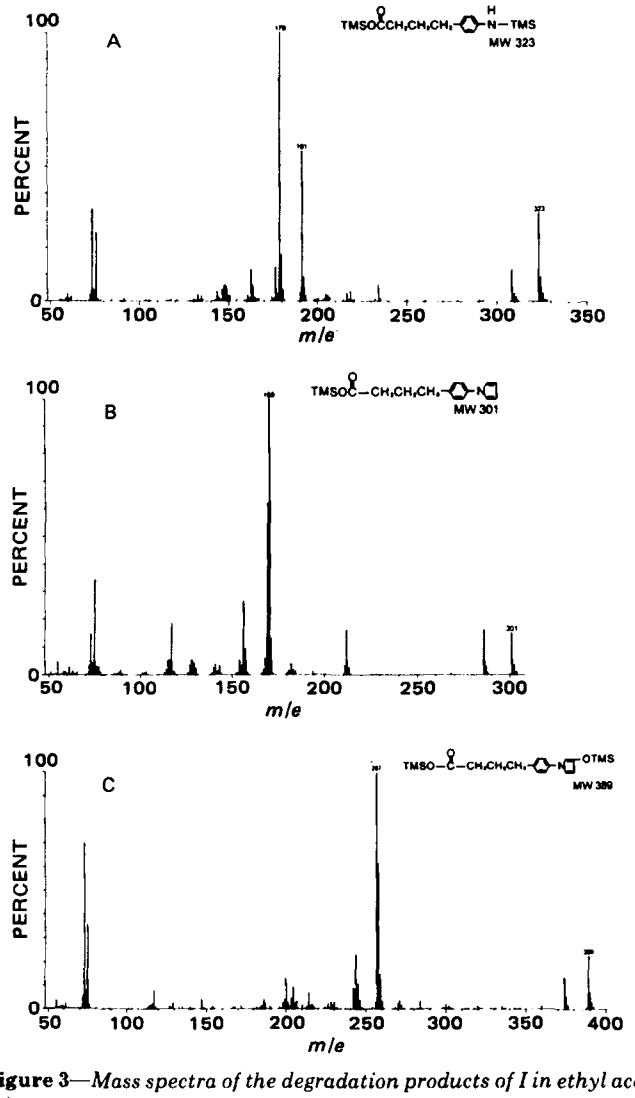

Figure 3—*Mass spectra of the degradation products of I in ethyl acetate.*

RESULTS

The spectrum of *p*-[4-*N*,*N*-bis(2-chloroethyl)]aminophenylacetic acid, a metabolite detected in human plasma and urine (Fig. 1), was identical to that of the synthesized compound.

Studies with ^{14}C-labeled I indicated that more than 70% of added I was recovered from plasma at 25°. Eighty-four percent of the I was recovered when the extraction was repeated three times. The extraction of I at concentrations of 5 and 1 μg and 200, 100, and 50 ng added to 1 ml of plasma showed percent recoveries and standard deviations of 100.4 ± 2.0, 90.5 ± 3.0, 94.3 ± 1.3, 88.2 ± 4.2, and 91.3 ± 12.8, respectively. At least three samples of each concentration were used for statistical calculations.

The linearity of the I determination between 1 μg and 500 pg showed a correlation coefficient, r, of 0.999. There was no statistical difference from $y = x$ ($p > 0.05$). The relative equal weight response calculated from either a 100-fold excess of the internal standard to I or a fivefold excess of I to the internal standard was consistent.

The disappearance of I incubated in plasma (10 μg/ml) is shown in Fig. 2. The disappearance rate constant of I was $\kappa = 0.09\ hr^{-1}$ for the plasma (Fig. 2). The correlation coefficient, r, for all data points to $C = C_0e^{-kt}$ was 0.993. Depending on the source of the plasma used, there was an ~10% variation in the disappearance rate constant.

In contrast to its degradation in an aqueous medium, I stored in a nonaqueous solution (ethyl acetate) at room temperature under fluorescent light resulted in three major products (Fig. 3). With deuterated *N*,*O*-bis(trimethylsilyl)trifluoroacetamide-d_8, the number of trimethylsilyl groups per molecule was two for Compound A (Fig. 3A), one for Compound B (Fig. 3B), and two for Compound C (Fig. 3C).

Stability data for I in plasma at 25 and 37° are presented in Table I. About 90% of the I was recovered from the plasma after 4 hr of incubation at 25° whereas only 56% of the I was recovered at 37° after that time.

Figure 4 shows a plasma I disappearance curve following an intravenous bolus injection of 5.6 mg/kg in a rat. The plasma disappearance of 0.55 mg of I/kg given orally and of *p*-[4-*N*,*N*-bis(2-chloroethyl)]aminophenylacetic acid in a patient with chronic lymphocytic leukemia is shown in Fig. 5. The selected-ion chromatograms of plasma I and the background are shown in Fig. 6.

DISCUSSION

The method presented is based on a one-step extraction from biological fluids, and the selected-ion monitoring method was used for the subsequent determination of I and a metabolite. The method can be used to study pharmacokinetics and metabolism in cancer patients. Compound I was monitored at *m/e* 326 and 328 with deuterated I at *m/e* 383 and 385. When 500 pg was derivatized and analyzed, there was sufficient sensitivity to detect quantities at the 100-pg level. However, to prevent I adsorption, the column had to be preconditioned with two to three repeated injections of I (~0.5 μg). The chlorine isotope ratio gave additional selectivity. The deuterated I synthesis can be carried out in most laboratories using basic organic chemistry techniques and starting materials readily available commercially.

A method for the determination of I in plasma was published recently (7) that depends on several extraction steps followed by mass spectrometric analysis. This method is not only lengthy, but it also requires back-extraction from the buffer at pH 9.0. The instability of the chloroethyl group at alkaline pH is well documented (6, 10, 11). At room temperature, there was ~13% hydrolysis of I in aqueous solution at pH 9.0 over 30 min (7). Alkaline exposure at higher temperatures could result in even greater hydrolysis. Although such hydrolysis is a spontaneous phenomenon observed in *in vitro* situations, the *in vivo* hydrolysis rate may be far greater. Quantitative determination of the formation of hydroxy products is necessary for an overall understanding of the pharmacokinetic behavior of I.

Table I shows the effect of the incubation time and temperature on the stability and recovery of plasma I. Compound I was stable in plasma at room temperature, but recovery decreased significantly at 37°. This low recovery probably resulted from both alkylation and hydrolysis. There

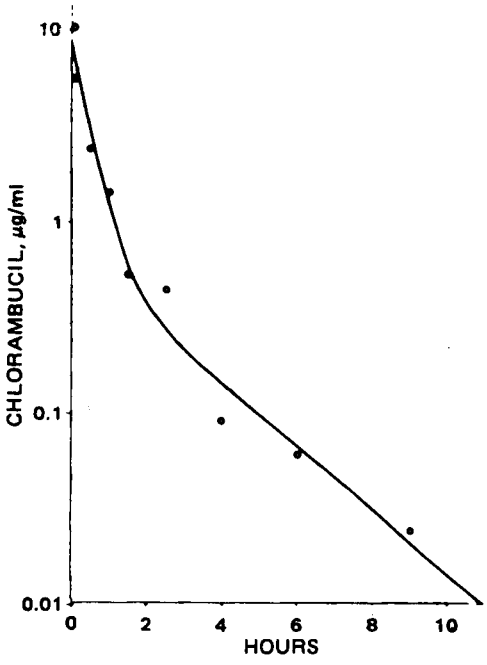

Figure 4—*Disappearance of I in rat plasma.*

may be a protective effect against hydrolysis by plasma proteins, as was shown previously for I and phenylalanine mustard (6, 12).

Three major compounds were observed in the nonaqueous system. The mass spectra with deuterated *N,O*-bis(trimethylsilyl)trifluoroacetamide

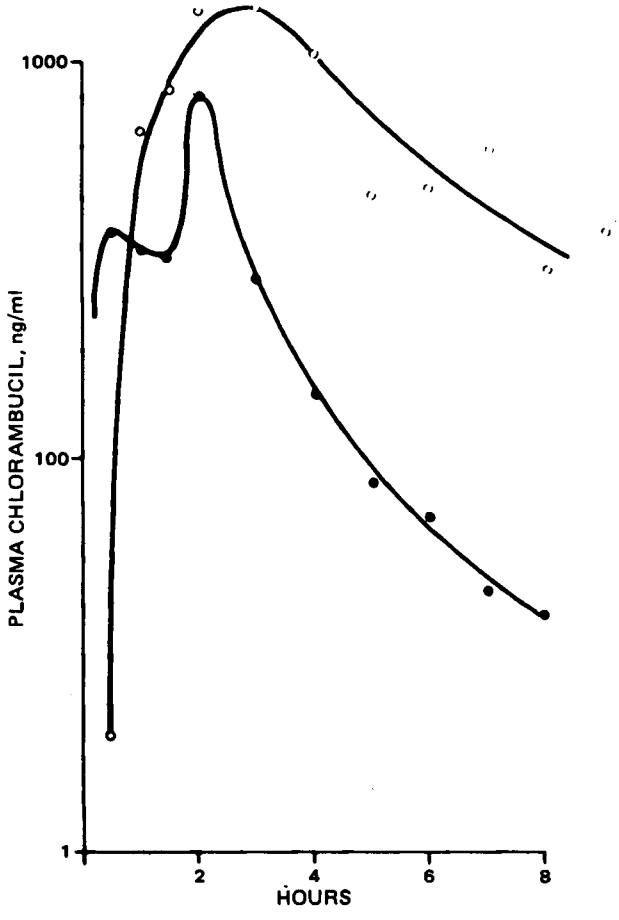

Figure 5—*Plasma I disappearance in a patient with chronic lymphocytic leukemia. The patient was given 0.55 mg/kg orally, and samples were drawn at designated times and analyzed for* p-*[4-*N,N-*bis(2-chloroethyl)]aminophenylacetic acid (○) and I (●).*

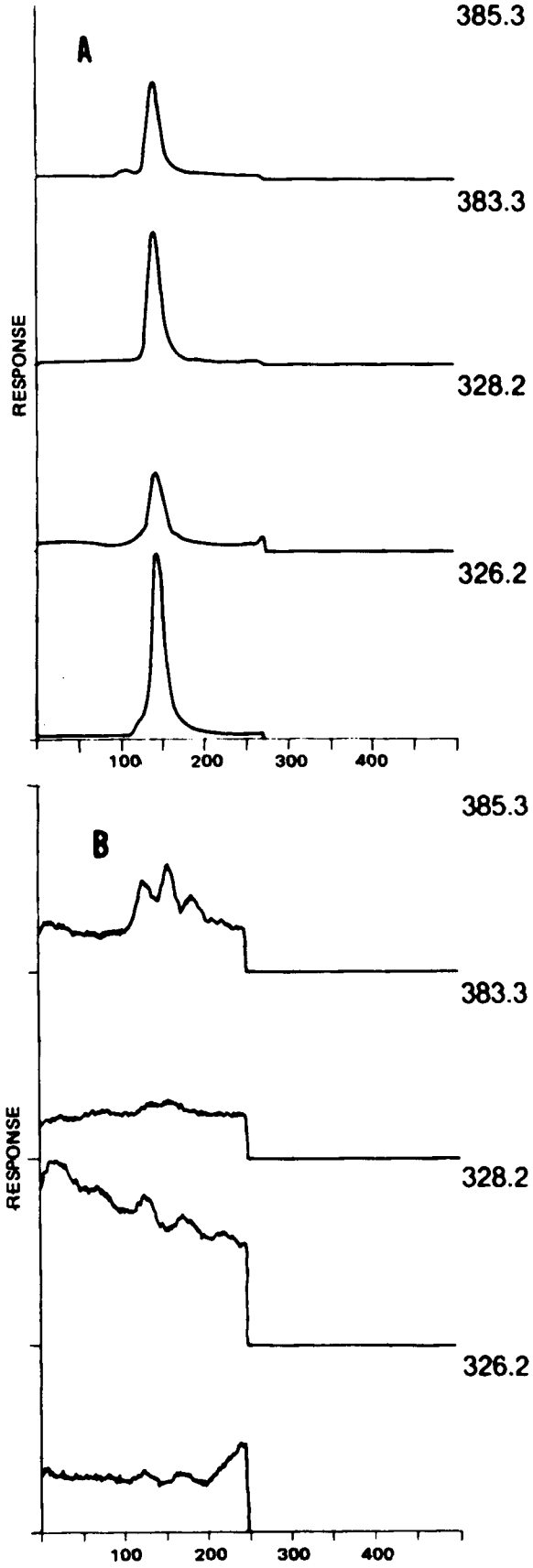

Figure 6—*Ion chromatograms of plasma I and plasma background. Compound I, 200 ng, and 2.0 μg of the internal standard were added to 1.0 ml of plasma. After extraction and derivatization, 0.1 ml of equivalent plasma was analyzed (Fig. 6A). In Fig. 6B, 1.0 ml of plasma was extracted and derivatized, and 0.5 ml of equivalent plasma was analyzed.*

Table I—Temperature and Time Effects on I Recovery from Plasma

Hours	Recovery[a] 25°	37°
0.0	90.5 ± 3.0	80.4 ± 3.0
0.5	82.5 ± 4.8	76.6 ± 3.7[b]
4.0	91.7 ± 2.6	55.6 ± 1.2[b]

[a] Percent recovery and percent relative standard deviation of quadruplicate analyses. [b] Percent relative standard deviation of a minimum of five samples.

of Compound A indicated that there were two replaceable hydrogens. The highest mass observed was 323 (odd mass), indicating that *m/e* 323 was either a fragment produced from a higher even mass or a molecular ion containing an odd number of nitrogens. Furthermore, there was no indication of chlorine in *m/e* 323. When compared to the chlorambucil molecule, it is most likely that *m/e* 323 was the molecular ion and the chlorambucil nitrogen was preserved. The carbon isotope ratio ($^{12}C/^{13}C$) indicated that 16 carbons was a reasonable assignment. Two major fragments, *m/e* 191 and 179, most likely were due to a highly stable styrene-like fragment and the *p*-aminobenzyl ion.

All three compounds showed the loss of 131 amu [$(CH_3)_3SiOCOCH_2$], indicating that the carboxyl group of I was intact. Based on these observations, Compound A (Fig. 3A) was suggested to be *p*-aminophenylbutyric acid. From similar observations, Compounds B and C (Figs. 3B and 3C) were suggested to be 4-pyrrolylphenylbutyric acid and 4-[3-(hydroxy)pyrrolyl]phenylbutyric acid. No *p*-aminobenzyl-like ion was observed in Compound B or C, probably due to the stabilization by the pyrrole group. The dark-brown color observed in the nonaqueous solution as well as in powdered preparations such as ^{14}C-I most likely was due to these pyrrole derivatives.

The α,β-unsaturated compounds 2-[4-*N*,*N*-bis(2-chloroethyl)]-aminophenyl-2-butenoic acid and 2-[4-bis(2-chloroethyl)]aminophenylacetic acid were found in rats given 8 mg of I/kg ip (13). Both compounds are products of the β-oxidation of I. The phenylacetic acid derivative in human urine and plasma was found (Figs. 1 and 5), and attempts to find the α,β-unsaturated compound were unsuccessful. More extensive studies of I metabolism are in progress.

REFERENCES

(1) R. B. Livingston and S. K. Carter, "Single Agents in Cancer Chemotherapy," Plenum, New York, N.Y., 1970, p. 81.

(2) A. C. Sartorelli and D. G. Johns, "Antineoplastic and Immunosuppressive Agents," vol. 1, Springer-Verlag, New York, N.Y., 1974, p. 7.

(3) H. G. Petering and G. J. van Giessen, *J. Pharm. Sci.*, **52**, 1159 (1963).

(4) R. Truhaut, E. Delacoux, G. Brule, and C. Bohuon, *Clin. Chim. Acta*, **8**, 235 (1963).

(5) J. M. Linford, *Biochem. Pharmacol.*, **11**, 693 (1962).

(6) *Ibid.*, **8**, 343 (1961).

(7) T. Jakhammer, A. Olsson, and L. Svensson, *Acta Pharm. Suec.*, **14**, 485 (1977).

(8) F. Bergel and J. A. Stock, *J. Chem. Soc.*, **76**, 2409 (1954).

(9) S. Nicolaidis, N. Rowland, M. Meile, P. Margaing-Jallat, and A. Perez, *Pharmacol. Biochem. Behav.*, **2**, 131 (1974).

(10) M. A. Chirigos and J. A. R. Mead, *Anal. Biochem.*, **7**, 259 (1964).

(11) R. Furner, L. Mellett, R. Brown, and G. Duncan, *Drug Metab. Disp.*, **4**, 577 (1976).

(12) S. Y. Chang, D. S. Alberts, D. Farquhar, L. R. Melnick, P. D. Walson, and S. E. Salmon, *J. Pharm. Sci.*, **67**, 682 (1978).

(13) A. McLean, D. Newell, and G. Baker, *Biochem. Pharmacol.*, **25**, 2331 (1976).

ACKNOWLEDGMENTS

Supported in part by Grant CA-17094 from the National Cancer Institute, by Grants T32-MO7533 and 5T32GMO7533-03 from the National Institutes of Health, and by a donation from Burroughs-Wellcome Co., Research Triangle Park, N.C.

Antiradiation Compounds XVII: Binding Ability of Radiation-Protective *N*-Heterocyclic Aminoethyl Disulfides and Thiosulfates to DNA

WILLIAM O. FOYE ˣ, MAHRUKH M. KARKARIA, and WILLIAM H. PARSONS

Received August 2, 1979, from the *Samuel M. Best Research Laboratory, Massachusetts College of Pharmacy, Boston, MA 02115.* Accepted for publication August 22, 1979.

Abstract □ Binding parameters for a series of *N*-heterocyclic aminoethyl disulfides and thiosulfates to DNA were determined at different ionic strengths and pH values. None of the thiosulfates showed any binding ability, but the disulfides revealed DNA binding abilities that were suppressed both by increased ionic strength and hydrogen-ion concentration. No correlation between DNA binding ability and radiation protective activity in mice was evident.

Keyphrases □ Antiradiation compounds—binding ability of radioprotective *N*-heterocyclic aminoethyl disulfides and thiosulfates to DNA □ Radioprotective compounds—*N*-heterocyclic aminoethyl disulfides and thiosulfates, DNA binding ability □ DNA—binding by radioprotective *N*-heterocyclic aminoethyl disulfides and thiosulfates □ *N*-Heterocyclic aminoethyl disulfides and thiosulfates—DNA binding ability, radiation protection evaluated

The ability of the radioprotective aminothiols cystamine and bis(2-guanidinoethyl) disulfide to bind reversibly to DNA, RNA, and other nucleoproteins has been demonstrated (1), but the significance of this ability in radiation protection of mammals is not clear. Evidence has accumulated that the aminothiol protecting agents cause a temporary inhibition of nucleoprotein synthesis and facilitate repair of radiation damage (2–5), but the necessity for complexation in this process has not been shown.

To demonstrate whether or not DNA binding is important to radiation protection or repair, a series of *N*-heterocyclic substituted aminoethyl disulfides and thiosulfates showing varying degrees of radiation protection to mice was observed for the ability to bind to DNA. A correlation with protecting ability could show DNA-binding ability to be essential to the protective or repair process.

Most studies of the mechanism of radiation protection in mammals utilized the *N*-unsubstituted aminothiols and simple *S*-derivatives, such as 2-mercaptoethylamine, its phosphorothioate, thiosulfate, or disulfide (cystamine), or 2-mercaptoethylguanidine. Since *N*-substituted de-

0022-3549/80/0100-0084$01.00/0

© 1980, American Pharmaceutical Association

Table I—Temperature and Time Effects on I Recovery from Plasma

Hours	Recovery[a] 25°	37°
0.0	90.5 ± 3.0	80.4 ± 3.0
0.5	82.5 ± 4.8	76.6 ± 3.7[b]
4.0	91.7 ± 2.6	55.6 ± 1.2[b]

[a] Percent recovery and percent relative standard deviation of quadruplicate analyses. [b] Percent relative standard deviation of a minimum of five samples.

of Compound A indicated that there were two replaceable hydrogens. The highest mass observed was 323 (odd mass), indicating that *m/e* 323 was either a fragment produced from a higher even mass or a molecular ion containing an odd number of nitrogens. Furthermore, there was no indication of chlorine in *m/e* 323. When compared to the chlorambucil molecule, it is most likely that *m/e* 323 was the molecular ion and the chlorambucil nitrogen was preserved. The carbon isotope ratio ($^{12}C/^{13}C$) indicated that 16 carbons was a reasonable assignment. Two major fragments, *m/e* 191 and 179, most likely were due to a highly stable styrene-like fragment and the *p*-aminobenzyl ion.

All three compounds showed the loss of 131 amu [$(CH_3)_3SiOCOCH_2$], indicating that the carboxyl group of I was intact. Based on these observations, Compound A (Fig. 3A) was suggested to be *p*-aminophenylbutyric acid. From similar observations, Compounds B and C (Figs. 3B and 3C) were suggested to be 4-pyrrolylphenylbutyric acid and 4-[3-(hydroxy)pyrrolyl]phenylbutyric acid. No *p*-aminobenzyl-like ion was observed in Compound B or C, probably due to the stabilization by the pyrrole group. The dark-brown color observed in the nonaqueous solution as well as in powdered preparations such as ^{14}C-I most likely was due to these pyrrole derivatives.

The α,β-unsaturated compounds 2-[4-*N*,*N*-bis(2-chloroethyl)]-aminophenyl-2-butenoic acid and 2-[4-bis(2-chloroethyl)]aminophenylacetic acid were found in rats given 8 mg of I/kg ip (13). Both compounds are products of the β-oxidation of I. The phenylacetic acid derivative in human urine and plasma was found (Figs. 1 and 5), and attempts to find the α,β-unsaturated compound were unsuccessful. More extensive studies of I metabolism are in progress.

REFERENCES

(1) R. B. Livingston and S. K. Carter, "Single Agents in Cancer Chemotherapy," Plenum, New York, N.Y., 1970, p. 81.

(2) A. C. Sartorelli and D. G. Johns, "Antineoplastic and Immunosuppressive Agents," vol. 1, Springer-Verlag, New York, N.Y., 1974, p. 7.

(3) H. G. Petering and G. J. van Giessen, *J. Pharm. Sci.*, **52**, 1159 (1963).

(4) R. Truhaut, E. Delacoux, G. Brule, and C. Bohuon, *Clin. Chim. Acta*, **8**, 235 (1963).

(5) J. M. Linford, *Biochem. Pharmacol.*, **11**, 693 (1962).

(6) *Ibid.*, **8**, 343 (1961).

(7) T. Jakhammer, A. Olsson, and L. Svensson, *Acta Pharm. Suec.*, **14**, 485 (1977).

(8) F. Bergel and J. A. Stock, *J. Chem. Soc.*, **76**, 2409 (1954).

(9) S. Nicolaidis, N. Rowland, M. Meile, P. Margaing-Jallat, and A. Perez, *Pharmacol. Biochem. Behav.*, **2**, 131 (1974).

(10) M. A. Chirigos and J. A. R. Mead, *Anal. Biochem.*, **7**, 259 (1964).

(11) R. Furner, L. Mellett, R. Brown, and G. Duncan, *Drug Metab. Disp.*, **4**, 577 (1976).

(12) S. Y. Chang, D. S. Alberts, D. Farquhar, L. R. Melnick, P. D. Walson, and S. E. Salmon, *J. Pharm. Sci.*, **67**, 682 (1978).

(13) A. McLean, D. Newell, and G. Baker, *Biochem. Pharmacol.*, **25**, 2331 (1976).

ACKNOWLEDGMENTS

Supported in part by Grant CA-17094 from the National Cancer Institute, by Grants T32-MO7533 and 5T32GMO7533-03 from the National Institutes of Health, and by a donation from Burroughs-Wellcome Co., Research Triangle Park, N.C.

Antiradiation Compounds XVII: Binding Ability of Radiation-Protective *N*-Heterocyclic Aminoethyl Disulfides and Thiosulfates to DNA

WILLIAM O. FOYE ˣ, MAHRUKH M. KARKARIA, and WILLIAM H. PARSONS

Received August 2, 1979, from the *Samuel M. Best Research Laboratory, Massachusetts College of Pharmacy, Boston, MA 02115.* Accepted for publication August 22, 1979.

Abstract □ Binding parameters for a series of *N*-heterocyclic aminoethyl disulfides and thiosulfates to DNA were determined at different ionic strengths and pH values. None of the thiosulfates showed any binding ability, but the disulfides revealed DNA binding abilities that were suppressed both by increased ionic strength and hydrogen-ion concentration. No correlation between DNA binding ability and radiation protective activity in mice was evident.

Keyphrases □ Antiradiation compounds—binding ability of radioprotective *N*-heterocyclic aminoethyl disulfides and thiosulfates to DNA □ Radioprotective compounds—*N*-heterocyclic aminoethyl disulfides and thiosulfates, DNA binding ability □ DNA—binding by radioprotective *N*-heterocyclic aminoethyl disulfides and thiosulfates □ *N*-Heterocyclic aminoethyl disulfides and thiosulfates—DNA binding ability, radiation protection evaluated

The ability of the radioprotective aminothiols cystamine and bis(2-guanidinoethyl) disulfide to bind reversibly to DNA, RNA, and other nucleoproteins has been demonstrated (1), but the significance of this ability in radiation protection of mammals is not clear. Evidence has accumulated that the aminothiol protecting agents cause a temporary inhibition of nucleoprotein synthesis and facilitate repair of radiation damage (2–5), but the necessity for complexation in this process has not been shown.

To demonstrate whether or not DNA binding is important to radiation protection or repair, a series of *N*-heterocyclic substituted aminoethyl disulfides and thiosulfates showing varying degrees of radiation protection to mice was observed for the ability to bind to DNA. A correlation with protecting ability could show DNA-binding ability to be essential to the protective or repair process.

Most studies of the mechanism of radiation protection in mammals utilized the *N*-unsubstituted aminothiols and simple *S*-derivatives, such as 2-mercaptoethylamine, its phosphorothioate, thiosulfate, or disulfide (cystamine), or 2-mercaptoethylguanidine. Since *N*-substituted de-

0022-3549/80/0100-0084$01.00/0

© 1980, American Pharmaceutical Association

Table I—Preparation of ^{35}S-Thiosulfates [a]

$R_2{}^+NHCH_2CH_2S{}^*SO_3{}^-$

$R_2{}^+NHC$-H_2CH_2X R_2N	X	Weight, g[a]	Yield, g	Melting Point	Literature Melting Point
NH_2	Br	0.1640	0.040	178–180°	189° (18)
O⟨⟩N	Cl	0.1488	0.055	180–182°	181–183° (9)
⟨⟩N	Cl	0.1472	0.150	179–181°	180–182° (9)
⟨⟩N	Cl	0.1360	0.077	159–161°	165–167° (9)

[a] All compounds were prepared using 1.1 ml of sodium ^{35}S-thiosulfate solution; these quantities represent equal moles (0.8 mmole).

rivatives of 2-mercaptoethylamine have shown greater protection in mammalian tests and provided compounds having activities ranging from good to nonprotective, such a series should be suitable for observing a possible correlation between DNA binding ability and radiation protective ability. Accordingly, a series of *N*-heterocyclic substituted 2-mercaptoethylamine derivatives (6) having the $HetNHCH_2CH_2SX$ structure (I) was utilized (Het = aromatic or alicyclic heterocycle and X = SO_3H, SCH_2CH_2NHHet). The possible mechanisms by which the aminothiols act as radiation-protective agents were reviewed (7).

EXPERIMENTAL[1]

Synthesis of Radiolabeled Thiosulfates and Disulfides—Synthesized compounds were identified[2] by comparison of IR spectra with those of authentic samples (6). Purity was checked by TLC on silica gel plates with detection of spots by exposure to iodine vapor. Both radiolabeled and nonradiolabeled compounds were prepared on a small scale.

Preparation of Sodium ^{35}S-Thiosulfate Solution—An ampul of sodium ^{35}S-thiosulfate[3] (22.5 mCi/mmole) was broken, and ~0.0074 g was weighed and spiked with cold sodium thiosulfate to give a weight of 0.5745 g (3.6 mmoles). The sodium thiosulfate was transferred to a 5-ml volumetric flask, and distilled water was added to the mark. Each milliliter of this solution contained 0.114 g (0.72 mmole) of sodium thiosulfate. The remaining sodium thiosulfate was stored *in vacuo* over phosphorus pentoxide.

The synthetic procedures for the organic thiosulfates were essentially those already described (6). Weights of starting materials, yields, and melting points are listed in Table I. The disulfides were prepared as follows.

2-Aminoethyl ^{35}S-Disulfide Dihydrochloride—A solution of iodine (0.2487 g, 0.98 mmole) in 5 ml of alcohol was added dropwise to a solution of ^{35}S-2-aminoethanethiosulfuric acid in 1 ml of water. The solution was refluxed for 90 min, and ethanol was removed by distillation. The aqueous residue was extracted with chloroform after the pH was adjusted to 9.0 with 10% NaOH.

The chloroform extract was dried over magnesium sulfate, and the chloroform was evaporated under reduced pressure (40°). The resulting oil was treated with hydrochloric acid in ethanol, and the hydrochloride was twice recrystallized from absolute ethanol, giving 0.042 g (20% yield), mp 219–221° dec. [lit. (8) mp 211°].

2-(N-Morpholinyl)ethyl ^{35}S-Disulfide Dihydrochloride—A solution of ^{35}S-2-(*N*-morpholinyl)ethanethiosulfuric acid (0.449 g, 1.96 mmoles) and potassium iodide (0.065 g, 0.392 mmole) in 1 ml of water was heated, and a solution of iodine (0.2487 g, 0.98 mmole) in 5 ml of alcohol was added dropwise. The solution was refluxed for 90 min, and the ethanol was removed under vacuum at 40° in a rotary evaporator. A little water was added, the solution was filtered, and the filtrate was extracted with ether after the pH was adjusted to 9.0 with 10% NaOH.

The ether layer was dried over magnesium sulfate and evaporated under reduced pressure to an oil, which was treated with hydrochloric acid in ethanol. The solution was evaporated to dryness, and the residue was twice recrystallized from absolute ethanol, giving 0.1056 g (30% yield) of white crystals, mp 225–226° dec. [lit. (9) mp 229–230°]; R_f 0.53 (methanol–water, 6:4).

2-(N-Piperidinyl)ethyl ^{35}S-Disulfide Dihydrochloride—The preceding procedure was followed with ^{35}S-2-(*N*-piperidinyl)ethanethiosulfuric acid (0.441 g, 1.96 mmoles), giving 0.11 g (31% yield) of white crystals, mp 267–269° dec. [lit. (9) mp 270–271°]; R_f 0.28 (*n*-butanol–water–acetic acid, 49.5:49.5:1).

Anal.—Calc. for $C_{14}H_{28}N_2S_2{\cdot}2HCl$: C, 46.52; H, 8.37; N, 7.75; S, 17.74. Found: C, 46.6; H, 8.5; N, 7.7; S, 17.4.

2-(N-Pyrrolidinyl)ethyl ^{35}S-Disulfide Dihydrochloride—The preceding procedure was used with ^{35}S-2-(*N*-pyrrolidinyl)ethanethiosulfuric acid (0.4135 g, 1.96 mmoles), giving 0.067 g (20% yield), mp 231–233° dec. [lit. (9) mp 227–228°]; R_f 0.25 (*n*-butanol–water–acetic acid, 49.5:49.5:1).

Preparation of Stock DNA Solutions—Stock solutions of DNA[4] were prepared in phosphate buffers of the following ionic strengths and pH:

Ionic Strength 0.14, pH 7.2—potassium phosphate (monobasic), 0.0158 *M*; sodium phosphate (dibasic), 0.0404 *M*; sodium diethylenediaminetetraacetate, 0.003 *M*; and carbon dioxide-free distilled water, *qs*, 1000 ml.

Ionic Strength 0.021, pH 7.2—phosphate buffer of ionic strength 0.14 and pH 7.2, 75 ml; and carbon dioxide-free distilled water, *qs*, 1000 ml.

Ionic Strength 0.02, pH 6.0—potassium phosphate (monobasic), 0.0132 *M*; sodium phosphate (dibasic), 0.0013 *M*; sodium diethylenediaminetetraacetate, 0.003 *M*; and carbon dioxide-free distilled water, *qs*, 1000 ml.

The DNA concentration was measured[5] at 259 nm using the molar absorptivity $E(P)$ = 6650 (10). Appropriate dilutions were made, and a Beer–Lambert plot was constructed using the regressed absorption values. Spectral scans of DNA in the different stock solutions were identical. The DNA concentration in micromoles of DNA phosphorus per milliliter was determined:

$$\text{concentration of DNA phosphorus } (\mu\text{moles/ml}) = \frac{1000}{6650} \times 12.5 \times \text{dilution factor} \times \text{absorbance} \quad \text{(Eq. 1)}$$

The concentration values ranged from 1.7 to 2.1 μmoles of DNA phosphorus/ml for the different stock solutions.

Preparation of Stock Solutions of Radiolabeled Thiosulfates and Disulfides—Stock solutions containing 3 μmoles/ml of radiolabeled thiosulfates and disulfides were prepared in the appropriate phosphate buffer and stored at 4°. For the equilibrium dialysis experiments, concentrations of 0.5, 1.0, 1.5, 2.0, and 2.5 μmoles/ml were prepared at the time of the experiments.

Equilibrium Dialysis—The equilibrium dialysis experiments were performed as described by Wagner and Arav (11), using 5-ml glass or acrylic dialysis cells (12). A cellular dialysis membrane (mol. wt. cutoff 12,000) was pretreated by five consecutive 30-min boilings in distilled water and storage at 4° in phosphate buffer for 3–4 hr. The filled dialysis cells were immersed in a thermostated shaker bath at 37 ± 0.5° and shaken until equilibrium was reached (generally 24 hr).

The concentrations of compound in each chamber were determined by radioactivity measurements, or by absorbance measurements in the case of the quinoxalinyl derivative. For radioactivity determinations, 2-ml aliquots from each chamber were transferred to liquid scintillation vials (20 ml). To each was added 15 ml of a liquid scintillation cocktail[6], and the solution was shaken vigorously and counted[7]. An average of five readings was taken, and experiments were carried out in triplicate.

Concentrations of free (C_F) and bound (C_B) species were calculated:

$$C_F = \frac{CT_F}{CT_T} \times \text{total concentration of radiolabeled compound} \quad \text{(Eq. 2)}$$

$$C_B = \frac{CT_T - CT_F}{CT_T} \times \text{total concentration of radiolabeled compound} \quad \text{(Eq. 3)}$$

[1] Elemental analyses were carried out by Dr. F. B. Strauss, Oxford, England. Melting points were determined on a Mel-Temp capillary melting-point block.
[2] Perkin-Elmer 457 S grating spectrometer.
[3] Amersham-Searle Corp.
[4] Type I, sodium salt, Sigma Chemical Co., St. Louis, Mo.
[5] Beckman DB spectrophotometer.
[6] Phase Combining System, Amersham-Searle Corp.
[7] Packard Tri-Carb liquid scintillation spectrometer.

Table II—Binding Parameters of Disulfides with DNA [a]

pH	Ionic Strength	Compound	K_a, mM^{-1}	$1/n$	n
7.2	0.14	2-Aminoethyl disulfide	0.51	3.57	0.28
		2-(*N*-Morpholinyl)ethyl disulfide	0.0	0.0	—
		2-(*N*-Piperidinyl)ethyl disulfide	0.40	3.70	0.27
		2-(*N*-Pyrrolidinyl)ethyl disulfide	0.49	5.05	0.20
7.2	0.021	2-Aminoethyl disulfide	10.84	2.48	0.41
		2-(*N*-Morpholinyl)ethyl disulfide	0.0	0.0	—
		2-(*N*-Piperidinyl)ethyl disulfide	5.22	1.81	0.55
6.0	0.020	2-Aminoethyl disulfide	6.93	1.65	0.61

[a] The values were determined from reciprocal (Klotz) plots.

The mathematical treatment of the dialysis experiment data to give association constants, if all binding sites of DNA exhibit the same affinity toward a small molecule, can be expressed as:

$$K_a = \frac{r}{C_F(n - r)} \quad \text{(Eq. 4)}$$

where K_a is the intrinsic association constant, r is the number of adsorbates bound per reference unit (DNA base pair), n is the number of available binding sites per reference unit (DNA base pair), and C_F is the equilibrium concentration of free unbound species.

Plots of both r/C_F *versus* r according to Scatchard (13):

$$r/C_F = nK_a - rK_a \quad \text{(Eq. 5)}$$

and $1/r$ *versus* $1/C_F$ according to Klotz (14):

$$1/r = 1/n + 1/K_a(n)(C_F) \quad \text{(Eq. 6)}$$

were used to determine K_a and n. The binding data were plotted according to both equations. Both gave linear plots, but the correlation coefficient for the Klotz equation was better (>0.91). Values of K_a and n are listed in Table II as determined by the Klotz equation.

DISCUSSION

Binding studies of the heterocyclic aminoethyl disulfides and thiosulfates were carried out by equilibrium dialysis (11), and the concentrations of free and bound species at equilibrium were determined by radioactivity measurements. Radiolabeled thiosulfates were synthesized using sodium ^{35}S-thiosulfate and the heterocyclic aminoethyl chlorides where the heterocycles were morpholine, piperidine, and pyrrolidine; 2-bromoethylamine was also converted to the thiosulfate. The thiosulfates were converted to the radiolabeled disulfides by oxidation with iodine (15) since the thiosulfate was labeled on the outer sulfur atom. Yields from both reactions were generally in the 30–40% range, but piperidinyl thiosulfate was obtained in an 83% yield.

2-(2-Quinoxalinyl)aminoethanethiosulfuric acid (6) also was studied but was not labeled with sulfur 35. It exhibited strong UV absorption at 249 and 359 nm, which did not interfere with the absorption peak of DNA (256 nm at pH 7.2) and could be used as such. The concentration of bound compound was found by breaking the complex with dimethyl sulfoxide (16).

The results of the equilibrium dialysis experiments for the *N*-heterocyclic aminoethyl thiosulfates indicate that no binding took place with DNA. In mice (Table III), the quinoxalinyl derivative and aminoethanethiosulfuric acid had high radiation protective activity (>50% survival at 30 days), the piperidinyl derivative had moderate radiation protective activity, and the morpholinyl and pyrrolidinyl derivatives were inactive. Apparently, DNA binding is not a requirement for protective activity by the aminoalkyl thiosulfates, at least of the intact molecule. The negatively charged thiosulfate probably is repelled by the phosphate groups of DNA and the positively charged amino groups probably remain associated with the thiosulfate groups. *In vivo*, it is possible that the thiosulfates are metabolized to the disulfides, a reaction that occurs readily under hydrolytic conditions (17).

The binding parameters for the heterocyclic aminoethyl disulfides are listed in Table II. Comparison of the radioprotective activities (Table III) with the DNA binding data indicates that the heterocyclic compound with good activity (morpholinyl) did not exhibit binding ability whereas

Table III—Intraperitoneal Radiation Protective Activities of Thiosulfates and Disulfides in Mice

Compound	Drug Dose, mg/kg	Radiation Dose, rads[a]	Survival at 30 Days, %
2-Aminoethanethiosulfuric acid[b]	150	800R[c]	73
2-(*N*-Morpholinyl)ethanethiosulfuric acid	100	849	0
2-(*N*-Piperidinyl)ethanethiosulfuric acid	60	849	20
2-(*N*-Pyrrolidinyl)ethanethiosulfuric acid	70	849	0
2-(*N*-Quinoxalinyl)ethanethiosulfuric acid	400	849	70
2-Aminoethyl disulfide[d]	146	650R[c]	60
2-(*N*-Morpholinyl)ethyl disulfide	20	849	50
2-(*N*-Piperidinyl)ethyl disulfide	30	849	10
2-(*N*-Pyrrolidinyl)ethyl disulfide	20	849	10

[a] Radiation dosage was from ^{137}Cs γ-irradiation given at a rate of 141.5 rads/min except where indicated otherwise. [b] Data from D. L. Klayman, M. M. Grenan, and D. P. Jacobus, *J. Med. Chem.*, **12**, 510 (1969). [c] Dose is expressed in roentgens of X-radiation. [d] Data from M. L. Beaumariage, *C. R. Soc. Biol.*, **151**, 1788 (1957), using rats.

the poor protective agents (piperidinyl and pyrrolidinyl) showed some binding at ionic strength 0.14 and good binding at ionic strength 0.021. However, 2-aminoethyl disulfide showed both good binding ability and radioprotective ability, although the binding ability was depressed at the higher ionic strength which would resemble physiological conditions more closely. Obviously, no correlation can be drawn between DNA binding ability and radiation protective ability for the disulfides.

Some useful information may be deduced from the binding parameters. Straight-line plots were obtained with both Scatchard and Klotz equation, but the Klotz equation, after linear regression analysis, gave the best correlation coefficient (>0.91). The linear binding isotherms for the disulfides indicate that only one type of binding site on the DNA molecule interacted with these compounds. Comparison of the association constants at two different ionic strengths, 0.14 and 0.021, shows that binding at the higher ionic strength was suppressed, probably through competition with other ions. Comparison of the n values also indicates that the number of available binding sites was reduced. In addition, the lower binding constants at pH 6.0, in comparison to those at pH 7.2, indicate competition with hydrogen ions. At the lower pH, the greater degree of protonation of the amino groups might be expected to lead to greater association with phosphate groups of DNA.

The inability of the morpholine derivative to bind to DNA might be assumed to result from the polar nature of the hetero oxygen atom. However, the fact that the piperidinyl derivative gave lower association constants than the unsubstituted 2-aminoethyl disulfide at both ionic strengths suggests that steric hindrance prevented the association of the charged nitrogen with DNA phosphate groups. Apparently, only ionic interactions occurred. Also, since the association constants were suppressed at the higher ionic strength, it is questionable that the disulfides, including cystamine, would bind to DNA appreciably under physiological conditions. From the effects of ionic strength and pH on the binding constants and the lack of correlation with radiation protective activity, it may be concluded that binding to DNA is not a requisite for radiation protection or nucleic acid repair.

REFERENCES

(1) E. Jellum, *Int. J. Radiat. Biol.*, **9**, 185 (1965).

(2) J. H. Stuy, *Radiat. Res.*, **14**, 56 (1961).

(3) F. Hernadi, Z. Nagy, P. Kovacs, and C. Kari, in "Radiation Protection and Sensitization," Proceedings of the Second International Symposium, 1969, H. Moroson and M. Quintiliani, Eds., Barnes & Noble, New York, N.Y., 1970, p. 167.

(4) E. F. Romantsev, N. N. Koshcheenko, and I. V. Fillipovich, *ibid.*, p. 421.

(5) R. Goutier and L. Baugnet-Mahieu, *ibid.*, p. 445.

(6) W. O. Foye, Y. H. Lowe, and J. J. Lanzillo, *J. Pharm. Sci.*, **65**, 1247 (1976).

(7) W. O. Foye, *Int. J. Sulfur Chem.*, **8**, 161 (1973).

(8) T. P. Johnston and A. Gallagher, *J. Org. Chem.*, **26**, 3780 (1961).
(9) W. O. Foye, J. J. Lanzillo, Y. H. Lowe, and J. M. Kauffman, *J. Pharm. Sci.*, **64**, 211 (1975).
(10) H. J. Lin and E. Chargaff, *Biochim. Biophys. Acta*, **123**, 66 (1966).
(11) K. G. Wagner and R. Arav, *Biochemistry*, **7**, 1771 (1968).
(12) F. Karush and S. S. Karush, "Methods in Immunology and Immunochemistry," vol. 3, Academic, New York, N.Y., 1967.
(13) G. Scatchard, *Ann. N.Y. Acad. Sci.*, **51**, 660 (1949).
(14) I. M. Klotz, *Cold Spring Harbor Symp. Quant. Biol.*, **14**, 97 (1949).
(15) H. Bretschneider, *Oesterr. Akad. Wiss. Math. Naturwiss. Kl., Sitzungsber., Abt. 2b*, **159**, 385 (1950).
(16) M. J. Waring, L. P. G. Wakelin, and J. S. Lee, *Biochim. Biophys. Acta*, **407**, 200 (1975).
(17) D. L. Klayman and R. J. Shine, *Q. Rep. Sulfur Chem.*, **3**, 231 (1968).
(18) H. Z. Lecher and E. M. Hardy, *J. Org. Chem.*, **20**, 475 (1955).

ACKNOWLEDGMENTS

Abstracted from a thesis submitted by M. M. Karkaria to the Massachusetts College of Pharmacy in partial fulfillment of the Master of Science degree requirements.

The authors express their appreciation to The Gillette Co. for financial assistance.

Biodistribution of ^{14}C-Lomustine in an Animal Tumor Model

FRANK P. CASTRONOVO, Jr.[x], MAJIC S. POTSAID, and SUSAN Y. KOPIWODA

Received May 14, 1979, from the *Department of Radiology, Massachusetts General Hospital, Boston, MA 02114.* Accepted for publication August 13, 1979.

Abstract □ A formulation of ^{14}C-lomustine in propylene glycol–ethanol (4:1) was administered intravenously to rats infiltrated with glioma tumors of the astrocytic series (RT6). The organ and tumor distribution of this agent was followed at 1, 4, 12, and 24 hr. Rapid blood disappearance (0–1 hr) of the label concomitant with an increase in all organs except the lung, muscle, and brain was observed. Only the blood, liver, and muscle contained >1% of the dose after 24 hr. The bladder, liver, small bowel, and kidneys concentrated the highest percentages throughout the study. The distribution of ^{14}C-lomustine in the tumor relative to the brain, muscle, and blood showed a maximum 4–12 hr after administration.

Keyphrases □ Lomustine, ^{14}C-labeled—biodistribution, rat tumor model □ Antineoplastic agents—^{14}C-lomustine, biodistribution, rat tumor model □ Biodistribution—^{14}C-lomustine, rat tumor model

Early detection of malignant tumors serves as a basis for improving cancer control. One experimental approach is to label minute quantities of antineoplastic drugs with appropriate radionuclides and to follow their biodistribution in a suitable animal tumor model. One example involved the *N*-nitrosoureas, a class of chemotherapeutic drugs for various malignant tumors (1). The structures of several *N*-substituted nitrosoureas are shown in Table I, where the chlorine- or fluorine-substituted haloethyl derivatives are the most active, with the methyl-substituted nitrosourea possessing the least chemotherapeutic activity (2).

The agent investigated in this study, lomustine [1-(2-chloroethyl)-3-cyclohexyl-1-nitrosourea[1], CCNU, I], is an asymmetrical *N*-substituted nitrosourea used for the palliative treatment of primary and metastatic brain tumors and for Hodgkin's disease (3). This investigation followed the radiopharmacodynamics of ^{14}C-I in tumor-bearing rats for 24 hr after intravenous injection.

EXPERIMENTAL

Materials and Methods—The *N*-nitrosoureas are lipophilic agents whose solubility characteristics require formulations with hydroalcoholic vehicles (4). Propylene glycol–ethanol (4:1) was the vehicle chosen for intravenous administration of ^{14}C-I[1] (5).

The ^{14}C-I [1-(2-chloroethyl-U-^{14}C)-3-cyclohexyl-1-nitrosourea] had a specific activity of 12.156 mCi/mmole (52.017 μCi/mg; 1.0195 mCi in 19.6 mg) and a radiochemical purity of 99.7%. The ^{14}C-I was labeled at the chloroethyl moiety (Table I). Prior to the animal studies, the ^{14}C-I was added to 10 ml of the propylene glycol–ethanol mixture.

Tissue Distribution—The rat tumor model (RT6) was a brain malignancy induced by repeated intravenous injections of *N*-nitrosomethylurea (6). The induced tumors were gliomas of the astrocytic series, the histology of which did not vary significantly with serial passage through tissue culture, subcutaneous implantation, or freezing (6). This model was used previously for the determination of the tumor affinity of various ^{99m}Tc-labeled compounds (7). Early detection of this type of tumor in patients with glioblastoma multiforme would be advantageous since the current survival estimate for this pathology 2 years after surgery is ~10% (8).

To determine the pharmacodynamics of ^{14}C-I, 0.2 ml was injected intravenously *via* the tail vein in adult male rats. Three rats were sacrificed at 1, 4, 12, and 24 hr postadministration. Each 0.2 ml of solution had 0.385 mg (1.65 μmoles) of ^{14}C-I (20 μCi of ^{14}C).

At the time of sacrifice, the blood (7% of the body weight), brain, liver, spleen, pancreas, lungs, small bowel, kidneys, heart, bladder, bone marrow, muscle, and tumor fluid, capsule, and necrotic center were isolated from each animal, and their radioactivity content was measured. The dose percentage per gram of tissue, the dose percentage per organ, and the mean ± standard deviation (n = 3) were calculated.

Activity Measurement—Approximately 100 mg of each tissue was placed in a glass scintillation vial containing 2 ml of tissue solubilizer (9).

Table I—Structures of Several *N*-Substituted Nitrosoureas

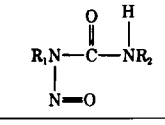

R_1	R_2	Name
Methyl	H	1-Methyl-1-nitrosourea
Fluoroethyl	Fluoroethyl	1,3-Bis(2-fluoroethyl)-1-nitrosourea
Chloroethyl	Chloroethyl	1,3-Bis(2-chloroethyl)-1-nitrosourea
Chloroethyl	Cyclohexyl	1-(2-Chloroethyl-U-^{14}C)-3-cyclohexyl-1-nitrosourea

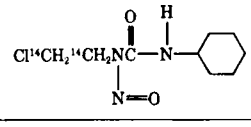

[1] Synthesized by the Monsanto Chemical Co. under contract with the National Institutes of Health and provided by Dr. R. Engle of the National Cancer Institute (sample NSC-79037,350-4H).

0022-3549/80/0100-0087$01.00/0
© 1980, American Pharmaceutical Association

(8) T. P. Johnston and A. Gallagher, *J. Org. Chem.*, **26**, 3780 (1961).
(9) W. O. Foye, J. J. Lanzillo, Y. H. Lowe, and J. M. Kauffman, *J. Pharm. Sci.*, **64**, 211 (1975).
(10) H. J. Lin and E. Chargaff, *Biochim. Biophys. Acta*, **123**, 66 (1966).
(11) K. G. Wagner and R. Arav, *Biochemistry*, **7**, 1771 (1968).
(12) F. Karush and S. S. Karush, "Methods in Immunology and Immunochemistry," vol. 3, Academic, New York, N.Y., 1967.
(13) G. Scatchard, *Ann. N.Y. Acad. Sci.*, **51**, 660 (1949).
(14) I. M. Klotz, *Cold Spring Harbor Symp. Quant. Biol.*, **14**, 97 (1949).
(15) H. Bretschneider, *Oesterr. Akad. Wiss. Math. Naturwiss. Kl., Sitzungsber., Abt. 2b*, **159**, 385 (1950).
(16) M. J. Waring, L. P. G. Wakelin, and J. S. Lee, *Biochim. Biophys. Acta*, **407**, 200 (1975).
(17) D. L. Klayman and R. J. Shine, *Q. Rep. Sulfur Chem.*, **3**, 231 (1968).
(18) H. Z. Lecher and E. M. Hardy, *J. Org. Chem.*, **20**, 475 (1955).

ACKNOWLEDGMENTS

Abstracted from a thesis submitted by M. M. Karkaria to the Massachusetts College of Pharmacy in partial fulfillment of the Master of Science degree requirements.

The authors express their appreciation to The Gillette Co. for financial assistance.

Biodistribution of ^{14}C-Lomustine in an Animal Tumor Model

FRANK P. CASTRONOVO, Jr.[x], MAJIC S. POTSAID, and SUSAN Y. KOPIWODA

Received May 14, 1979, from the *Department of Radiology, Massachusetts General Hospital, Boston, MA 02114.* Accepted for publication August 13, 1979.

Abstract □ A formulation of ^{14}C-lomustine in propylene glycol–ethanol (4:1) was administered intravenously to rats infiltrated with glioma tumors of the astrocytic series (RT6). The organ and tumor distribution of this agent was followed at 1, 4, 12, and 24 hr. Rapid blood disappearance (0–1 hr) of the label concomitant with an increase in all organs except the lung, muscle, and brain was observed. Only the blood, liver, and muscle contained >1% of the dose after 24 hr. The bladder, liver, small bowel, and kidneys concentrated the highest percentages throughout the study. The distribution of ^{14}C-lomustine in the tumor relative to the brain, muscle, and blood showed a maximum 4–12 hr after administration.

Keyphrases □ Lomustine, ^{14}C-labeled—biodistribution, rat tumor model □ Antineoplastic agents—^{14}C-lomustine, biodistribution, rat tumor model □ Biodistribution—^{14}C-lomustine, rat tumor model

Early detection of malignant tumors serves as a basis for improving cancer control. One experimental approach is to label minute quantities of antineoplastic drugs with appropriate radionuclides and to follow their biodistribution in a suitable animal tumor model. One example involved the *N*-nitrosoureas, a class of chemotherapeutic drugs for various malignant tumors (1). The structures of several *N*-substituted nitrosoureas are shown in Table I, where the chlorine- or fluorine-substituted haloethyl derivatives are the most active, with the methyl-substituted nitrosourea possessing the least chemotherapeutic activity (2).

The agent investigated in this study, lomustine [1-(2-chloroethyl)-3-cyclohexyl-1-nitrosourea[1], CCNU, I], is an asymmetrical *N*-substituted nitrosourea used for the palliative treatment of primary and metastatic brain tumors and for Hodgkin's disease (3). This investigation followed the radiopharmacodynamics of ^{14}C-I in tumor-bearing rats for 24 hr after intravenous injection.

EXPERIMENTAL

Materials and Methods—The *N*-nitrosoureas are lipophilic agents whose solubility characteristics require formulations with hydroalcoholic vehicles (4). Propylene glycol–ethanol (4:1) was the vehicle chosen for intravenous administration of ^{14}C-I[1] (5).

The ^{14}C-I [1-(2-chloroethyl-U-^{14}C)-3-cyclohexyl-1-nitrosourea] had a specific activity of 12.156 mCi/mmole (52.017 μCi/mg; 1.0195 mCi in 19.6 mg) and a radiochemical purity of 99.7%. The ^{14}C-I was labeled at the chloroethyl moiety (Table I). Prior to the animal studies, the ^{14}C-I was added to 10 ml of the propylene glycol–ethanol mixture.

Tissue Distribution—The rat tumor model (RT6) was a brain malignancy induced by repeated intravenous injections of *N*-nitrosomethylurea (6). The induced tumors were gliomas of the astrocytic series, the histology of which did not vary significantly with serial passage through tissue culture, subcutaneous implantation, or freezing (6). This model was used previously for the determination of the tumor affinity of various ^{99m}Tc-labeled compounds (7). Early detection of this type of tumor in patients with glioblastoma multiforme would be advantageous since the current survival estimate for this pathology 2 years after surgery is ~10% (8).

To determine the pharmacodynamics of ^{14}C-I, 0.2 ml was injected intravenously *via* the tail vein in adult male rats. Three rats were sacrificed at 1, 4, 12, and 24 hr postadministration. Each 0.2 ml of solution had 0.385 mg (1.65 μmoles) of ^{14}C-I (20 μCi of ^{14}C).

At the time of sacrifice, the blood (7% of the body weight), brain, liver, spleen, pancreas, lungs, small bowel, kidneys, heart, bladder, bone marrow, muscle, and tumor fluid, capsule, and necrotic center were isolated from each animal, and their radioactivity content was measured. The dose percentage per gram of tissue, the dose percentage per organ, and the mean ± standard deviation (n = 3) were calculated.

Activity Measurement—Approximately 100 mg of each tissue was placed in a glass scintillation vial containing 2 ml of tissue solubilizer (9).

Table I—Structures of Several *N*-Substituted Nitrosoureas

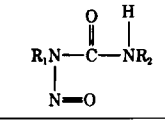

R_1	R_2	Name
Methyl	H	1-Methyl-1-nitrosourea
Fluoroethyl	Fluoroethyl	1,3-Bis(2-fluoroethyl)-1-nitrosourea
Chloroethyl	Chloroethyl	1,3-Bis(2-chloroethyl)-1-nitrosourea
Chloroethyl	Cyclohexyl	1-(2-Chloroethyl-U-^{14}C)-3-cyclohexyl-1-nitrosourea

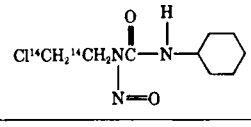

[1] Synthesized by the Monsanto Chemical Co. under contract with the National Institutes of Health and provided by Dr. R. Engle of the National Cancer Institute (sample NSC-79037,350-4H).

0022-3549/80/0100-0087$01.00/0
© 1980, American Pharmaceutical Association

Table II—Biodistribution of ^{14}C-I in Rat Tumors (RT6) (n = 3)

Organ	Dose Percent after 1 hr		Dose Percent after 4 hr		Dose Percent after 12 hr		Dose Percent after 24 hr	
	Mean	±*SD*	Mean	±*SD*	Mean	±*SD*	Mean	±*SD*
Blood	7.851	3.031	2.899	1.450	2.461	0.229	2.218	1.764
Brain	0.112	0.005	0.056	0.020	0.091	0.003	0.009	0.003
Liver	6.133	1.550	6.150	1.700	1.763	0.846	1.017	0.346
Spleen	0.320	0.003	0.422	0.143	0.129	0.073	0.040	0.022
Pancreas	0.289	0.207	0.208	0.124	0.282	0.138	0.075	0.057
Lungs	0.204	0.006	0.154	0.046	0.114	0.016	0.033	0.009
Small bowel	1.432	0.711	2.789	0.288	0.316	0.228	0.231	0.028
Kidney cortex	1.230	0.205	1.883	0.301	0.339	0.074	0.074	0.055
Kidney medulla	0.964	0.150	0.995	0.230	0.181	0.066	0.011	0.015
Heart	0.091	0.030	0.045	0.006	0.019	0.002	0.007	0.002
Bone marrow	0.198	0.088	0.051	0.089	0.099	0.012	0.023	0.016
Muscle	13.602	3.980	6.568	0.798	1.459	0.132	1.156	0.084
Bladder	0.072	0.041	0.165	0.016	0.030	0.020	0.051	0.017
Tumor fluid	0.726	0.851	5.460	0.548	1.678	0.232	0.523	0.015
Tumor capsule	0.718	0.419	3.560	0.621	1.463	1.073	0.482	0.443
Tumor necrotic	0.641	0.474	0.310	0.149	0.189	0.129	Background	Background

Each sample was minced with a scissors, and the capped vials were stored at room temperature until dissolution occurred. A toluene-based scintillation solution [4.2 mg of 2,5-diphenyloxazole/ml and 52.5 mg of 1,4-bis[2-(5-phenyloxazolyl)]benzene/ml], 15 ml, was added to each vial, and the radioactivity content was determined for each sample (10).

RESULTS

The initial biodistribution (1 hr) and subsequent translocation data for 24 hr for ^{14}C-I are shown in Tables II and III and are illustrated in Figs. 1–3. The data are displayed *versus* time as the mean dose percentage per organ (±*SD*) (Table II), the log of the mean dose percentage per gram (Figs. 1–3), and the dose percent per gram ratio of the tumor to the brain, muscle, and blood (Table III). Each point represents the mean for three determinations.

After intravenous administration, the whole body blood level of ^{14}C-I dropped rapidly from ~8% after 1 hr to <3% after 4 hr (Table II); therefore, the amount of tracer in the vascular compartment remained constant through the termination of the experiment at 24 hr. Concomitant with its clearance from the blood, the ^{14}C-I activity showed an increased concentration in all organs except for the brain, lungs, and muscle. Thereafter, the remaining organs exhibited a tracer concentration decrease. The muscle, liver, small bowel, and kidneys concentrated the highest dose percentage after 1 hr whereas the blood, liver, and muscle contained >1% of the dose after 24 hr (Table II).

The bladder and kidney cortex contained the greatest quantity of activity per gram (Fig. 1), emphasizing the rapid kidney excretion of ^{14}C-I. In fact, the bladder activity remained maximum up to 24 hr whereas the other organs decreased to a greater extent. Figure 2 illustrates the ^{14}C-I change per gram in the blood, muscle, and brain with time. The vascular compartment remained constant after 4 hr (protein binding), but the muscle and brain decreased rapidly up to 24 hr.

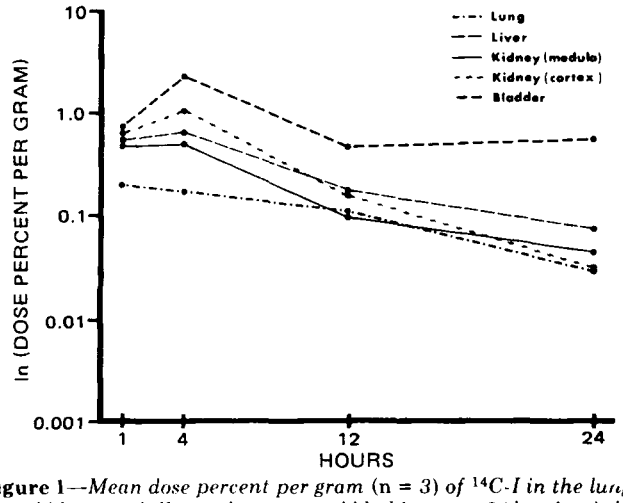

Figure 1—*Mean dose percent per gram* (n = 3) *of* ^{14}*C-I in the lungs, liver, kidney medullar and cortex, and bladder up to 24 hr after injection.*

For the tumor, a consistent ^{14}C-I uptake was observed at all times in the order: fluid > capsule > necrotic portion (Table II). The dose percentage per gram ratio of the tumor capsule to the brain rose rapidly to a maximum of 8.31 after 12 hr and decreased thereafter (Table III). Tumor to muscle and tumor to blood ratios were maximum after 4 hr and also decreased rapidly thereafter.

DISCUSSION

The localization and sizing of neoplasms were demonstrated with various tumor-specific radiopharmaceuticals (11). However, current radiodiagnostic agents are limited in their ability to be specific markers for tumors. Better definition not only could help in the identification of the histology but also could more precisely delineate and assist with effective treatment. Tumors may be defined better if radiopharmaceuticals are developed whose structures are based on chemotherapeutic agents.

The *N*-substituted nitrosoureas, a class of synthetic drugs currently studied for their anticancer properties (12), were selected for study. Their structural diversity (Table I) and limited chemical stability *in vivo* led investigators to hypothesize that their mechanism of action is alkylation (13–15). The 1-alkyl-1-nitrosoureas are believed to decompose under physiological conditions to yield alkyl diazohydroxides, which are progenitors of carbonium ions, and isocyanic acid or alkyl isocyanates, which undergo further reaction (13).

Compound I initially metabolizes to an alkyl diazohydroxide and an alkyl isocyanate. The former structure undergoes further decomposition to yield a vinyl carbonium ion, which eventually breaks down to acetaldehyde. The alkyl isocyanate reacts with water to form the corresponding carbamic acids, which decompose to yield cyclohexylamine. If the concentration of the latter compound is high, as is the case when therapeutic amounts are administered, a symmetrical urea is formed. Under the conditions of this investigation, nontherapeutic amounts of I were administered (0.385 mg of I/0.3-kg rat or 1.28 mg/kg), thus reducing the probability of a symmetrical urea. The production of alkylating agents during the *in vivo* decomposition of I results in the attack of nucleophilic

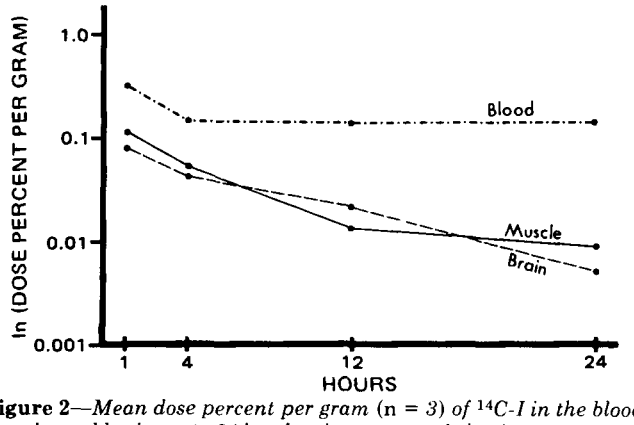

Figure 2—*Mean dose percent per gram* (n = 3) *of* ^{14}*C-I in the blood, muscle, and brain up to 24 hr after intravenous injection.*

Table III—Dose Percent Mean ^{14}C-I per Gram Ratios of Tumor to Various Organs (n = 3)

Hours	Tumor / Brain	Tumor / Muscle	Tumor / Blood
1	0.765	0.566	0.153
4	5.94	4.58	1.66
12	8.31	1.36	1.25
24	6.41	3.77	0.238

centers of biologically important molecules by these products. Reactions with amino, sulfhydryl, or hydroxyl groups yield alkylated materials, which alter the functional ability of biological materials. Such alkylation is thought to produce the mutagenic, teratogenic, carcinogenic, and cytotoxic activity of this class of chemotherapeutic agents (16).

Previous work with ^{14}C-chloroethyl-labeled I showed the label to be bound to nucleic acids and proteins both *in vitro* and *in vivo* (17). Specifically, the carbon-14 attached to nucleic acid bases and tRNA. Several investigators studied cyclohexyl derivatives of I in aninals, where extensive fixation of the label to the plasma proteins was found (18, 19). The tissue biodistribution of ^{14}C-cyclohexyl-I was studied in rabbits, where most of the label was found in the plasma, liver, kidneys, and lungs; after 12 hr, almost all of the carbon-14 label was eliminated *via* the kidneys and bile (5). The preparation and biodistribution of ^{13}N-bis(2-chloroethyl)nitrosourea, labeled primarily to the nitroso group, was reported recently (20). This positron-labeled agent was detected in a human neuroblastoma (mouse model) shortly after administration.

The results with ^{14}C-I correlate well with the literature relative to rapid blood disappearance and uptake in the liver and intestine (5, 18). The maximum tumor to organ ratios (Table III) suggest that γ-emitting radionuclides such as ^{99m}Tc ($t_{1/2p}$ = 6 hr) and ^{111}In ($t_{1/2p}$ = 2.6 days) labeled to I have potential as brain tumor scanning agents.

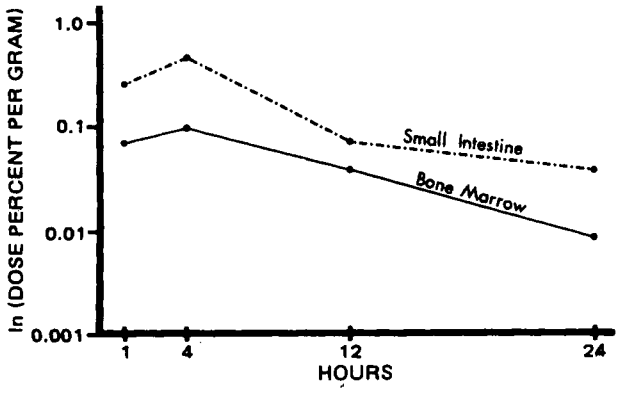

Figure 3—*Mean dose percent per gram* (n = 3) *of* ^{14}*C-I in the small intestine and bone marrow up to 24 hr after intravenous injection.*

REFERENCES

(1) W. C. J. Ross, in "Antineoplastic and Immunosuppressive Agents," part II, A. Sartorelli and D. O. Johns, Eds., Springer-Verlag, New York, N.Y., 1975.

(2) T. P. Johnson, G. S. McCaleb, P. S. Oplinger, W. R. Laster, and J. A. Montgomery, *J. Med. Chem.*, **14**, 600 (1971).

(3) CeeNu^{Tm} (Lomustine, CCNU) package insert, Bristol Laboratories, 1979.

(4) J. P. Davignon, K. W. Yang, H. B. Wood, and J. C. Craddock, *Cancer Chemother. Rep.*, **4**, 7 (1973).

(5) C. L. Litterst, E. G. Mimnaugh, A. C. Cowles, T. E. Gram, and A. M. Guarino, *J. Pharm. Sci.*, **63**, 1718 (1974).

(6) H. H. Schmidek, S. L. Neilson, A. L. Schiller, and J. Messer, *J. Neurol. Surg.*, **34**, 335 (1971).

(7) F. P. Castronovo, M. S. Potsaid, and P. L. Kornblith, *J. Nucl. Med.*, **17**, 566 (1976).

(8) National Program for the Conquest of Cancer, "Report of the National Panel of Consultants on the Conquest of Cancer, April 14, 1971," U.S. Government Printing Office, Washington, D.C., 1971.

(9) "Nuclear Medicine in Vitro," B. Rothfeld, Ed., Lippincott, Philadelphia, Pa., 1974.

(10) V. T. Oliverio, *Cancer Chemother. Rep.*, **4**, 13 (1973).

(11) A. G. H. Paterson and V. R. McCready, *Br. J. Med.*, **44**, 520 (1975).

(12) *Cancer Chemother.*, **20**, 81 (Sept. 22, 1978).

(13) J. A. Montgomery, R. James, G. S. McCaler, and T. P. Johnston, *J. Med. Chem.*, **10**, 668 (1967).

(14) G. P. Wheeler and S. Chumley, *ibid.*, **10**, 259 (1967).

(15) D. C. Chatterji, R. F. Freene, and J. E. Gallelli, *J. Pharm. Sci.*, **67**, 1527 (1978).

(16) P. N. Magee, *Ann. N.Y. Acad. Sci.*, **163**, 717 (1969).

(17) C. J. Cheng, S. Fujimura, D. Grunberger, and B. Weinstein, *Cancer Res.*, **32**, 22 (1972).

(18) J. T. Oliverio, W. M. Vietkze, M. K. Williams, and R. H. Adamsen, *ibid.*, **30**, 1330 (1970).

(19) T. A. Connors and J. R. Hare, *Br. J. Cancer*, **30**, 477 (1974).

(20) W. A. Piette, R. S. Tilbury, G. A. Digenis, M. S. Zedick, L. R. Nelson, G. R. Russ, and R. H. Mortara, *J. Nucl. Med.*, **17**, 558 (1966).

ACKNOWLEDGMENTS

Supported in part by U.S. Public Health Service Grant RR-05486-12.

New Calculation Method of Mean Total Body Clearance of Drugs and Its Application to Dosage Regimens

WIN L. CHIOU

Received May 17, 1979, from the *Clinical Pharmacokinetics Laboratory and Department of Pharmacy, College of Pharmacy, University of Illinois at the Medical Center, Chicago, IL 60612.* Accepted for publication July 3, 1979.

Abstract □ A new method for calculating the mean total body drug clearance is proposed for determining the mean dosing rate for patients. In this method, the mean clearance can be calculated from the individual clearance values by the harmonic mean method, or it can be determined by dividing the same absorbed dose by the arithmetic mean of the areas under the plasma level–time curve from time zero to infinity from all of the subjects or patients studied. In this method, the arithmetic mean method is assumed to have been used for calculation of literature mean plasma levels. Various methods for calculating mean clearances also are evaluated. These methods yield different mean clearance values from the same set of individual data, resulting in different dosage regimen recommendations.

Keyphrases □ Total body clearance—mean calculation, harmonic mean method, dosage rate □ Pharmacokinetics—mean total body clearance, calculation, harmonic mean method □ Dosage regimens—mean total body clearance, calculation, harmonic mean method

The total body clearance, Cl_p, of drugs is an important clinical pharmacokinetic parameter since, in linear pharmacokinetics, the intravenous dosing rate for maintaining the desired steady-state plasma level in an ith patient, C_{pi}^{ss}, is theoretically equal to the product of C_{pi}^{ss} and the total body drug clearance of the patient, Cl_{pi} (1). This principle also should be applied to the mean dosing rate for achieving a certain mean plasma level in multiple dosing after correction for the dose fraction absorbed.

BACKGROUND

Although it occasionally is feasible to individualize a patient's dosage regimen by studying or predicting the patient's Cl_p of the drug (1), the mean total body clearance obtained from group studies of normal subjects or patients often is used as a guide for initiating drug therapy (1–8). Therefore, proper calculation of the mean total body clearance might be important in pharmacokinetic studies.

There appear to be no serious questions in the literature regarding the validity of methods for calculating the individual Cl_p from plasma data obtained after intravenous administration. For example, the individual Cl_p can be calculated by any of the following three equations, which should yield the same result in linear pharmacokinetics (6, 7):

$$Cl_p = \frac{\text{intravenous dose}}{AUC} \qquad \text{(Eq. 1)}$$

$$Cl_p = V_{d,\text{area}}\beta \qquad \text{(Eq. 2)}$$

$$Cl_p = V_p K_{el} \qquad \text{(Eq. 3)}$$

where AUC is the area under the plasma level–time curve from time zero to infinity, $V_{d,\text{area}}$ is the apparent volume of distribution determined by the area method, β is the terminal exponential rate constant in the plasma level decay profile, V_p is the apparent volume of distribution of the central compartment, and K_{el} is the first-order elimination rate constant from the central compartment in a multicompartmental open model (7, 9). In a one-compartment open model system, Cl_p can be calculated by Eq. 1 or as the product of the apparent volume of distribution, V_d, and the apparent first-order elimination rate constant, K. Such methods will be referred to as the product-of-means method.

The arithmetic mean method is commonly used for calculating the mean Cl_p from a group of subjects (8, 10–19). In this method, all of the individual clearance values ($Cl_{p1}, Cl_{p2}, \ldots, Cl_{pn}$) are added and the sum is divided by the total number of subjects, n. In another commonly used method, apparently based on Eq. 3, the arithmetic mean V_p is multiplied by the arithmetic mean K_{el} (10). A recent study (10) on theophylline clinical pharmacokinetics reported that, depending on which of the two methods was used for calculation of the mean Cl_p, a 25–30% difference could occur. Therefore, depending on the method used, the recommended intravenous theophylline infusion rate can vary similarly (10). This inconsistency was considered to be unfortunate by the authors (10). Undoubtedly, different mean Cl_p values also will result for other drugs when these two methods are employed.

The purpose of this note is to propose a new method for calculation of the mean total body clearance that might be useful for the determination of mean dosage regimens in patients. In addition, several existing methods will be evaluated.

THEORETICAL

There are many ways to calculate the mean value of a data set. For example, the mean can be determined by the arithmetic mean, geometric mean, and harmonic mean methods (20). In pharmacokinetic studies, the arithmetic mean method has been used almost exclusively to calculate the means of the steady-state trough, peak, or averaged plasma drug levels after multiple or constant-rate dosing. This method also is used most often in calculation of the mean plasma levels of many endogenous substances such as creatinine and urea. Therefore, it is logical to propose that when a mean dosage regimen is recommended to obtain a targeted mean steady-state plasma level, $\overline{C_p^{ss}}$, for a group of patients, the arithmetic mean of the individual steady-state plasma levels achieved should be used to evaluate the recommended dosage regimen. Based on this assumption, it will be shown that the harmonic mean method should be used for calculating the mean total body clearance to achieve the desired arithmetically averaged steady-state blood, plasma, or serum level.

Since:

$$C_{pi}^{ss} = \frac{K_{0i}}{Cl_{pi}} \qquad \text{(Eq. 4)}$$

where K_{0i} is the zero-order dosing rate for the ith patient, therefore:

$$\overline{C_p^{ss}} = \frac{1}{n}\sum_{i=1}^{n} C_{pi}^{ss} \qquad \text{(Eq. 5)}$$

$$\overline{C_p^{ss}} = \frac{1}{n}\sum_{i=1}^{n} \frac{K_{0i}}{Cl_{pi}} \qquad \text{(Eq. 6)}$$

If $K_{01} = K_{02} = \ldots = K_{0n} = K_0$, then:

$$\overline{C_p^{ss}} = \frac{K_0}{n}\sum_{i=1}^{n} \frac{1}{Cl_{pi}} \qquad \text{(Eq. 7)}$$

$$\overline{C_p^{ss}} = \frac{K_0}{\overline{Cl_p}} \qquad \text{(Eq. 8)}$$

where:

$$\frac{1}{\overline{Cl_p}} = \frac{1}{\text{harmonic mean } Cl_p} = \frac{1}{n}\sum_{i=1}^{n} \frac{1}{Cl_{pi}} \qquad \text{(Eq. 9)}$$

Since for each individual the Cl_p also is related to the dose and to the AUC according to Eq. 1, Eq. 9 becomes:

$$\frac{1}{\overline{Cl_p}} = \frac{1}{n}\left(\frac{AUC_1}{\text{dose}_1} + \frac{AUC_2}{\text{dose}_2} + \ldots + \frac{AUC_n}{\text{dose}_n}\right) \qquad \text{(Eq. 10)}$$

0022-3549/80/0100-0090$01.00/0
© 1980, American Pharmaceutical Association

Table I—Relevant Pharmacokinetic Parameters[a] Based on Blood Theophylline Levels in Seven Asthmatic Subjects after Intravenous Study and the Resulting Steady-State Blood Levels after Different Infusion Rates Calculated from Different Mean Cl_p Values (Mean × 10 mg/liter) for Achieving the Targeted Mean Steady-State Blood Level of 10 mg/liter

Subject	β, hr^{-1}	K_{el}, hr^{-1}	V_p, liter/kg	Total Body Clearance, $K_{el}V_p$, liter/kg/hr	$V_d\beta$[b], liter/kg	C_p^{ssc}, mg/liter	C_p^{ssd}, mg/liter	C_p^{sse}, mg/liter	C_p^{ssf}, mg/liter
HW	0.130	0.149	0.464	0.0691	0.5315	9.20	9.78	12.50	9.82
VW	0.114	0.119	0.336	0.0400	0.3509	15.90	16.90	21.60	17.05
AG	0.171	0.359	0.225	0.0808	0.4725	7.88	8.38	10.71	8.45
AE	0.141	0.267	0.212	0.0566	0.4014	11.24	11.94	15.27	12.05
VM	0.241	0.750	0.119	0.0893	0.3705	7.12	7.57	9.68	7.64
JL	0.168	0.181	0.407	0.0737	0.4387	8.63	9.17	11.72	9.25
TS	0.166	0.361	0.176	0.0635	0.3825	10.02	10.65	13.61	10.74
Arithmetic mean	0.162	0.312	0.277	0.0676	0.4209	10.00	10.63	13.58	10.72

[a] Data from Ref. 18. [b] Determined by $(K_{el}V_p)/\beta$. [c] Based on the mean Cl_p calculated by the harmonic mean method (0.0636 liter/kg/hr). [d] Based on the mean Cl_p calculated by the arithmetic mean method (0.0676 liter/kg/hr). [e] Based on the mean Cl_p calculated by the $\overline{K}_{el}\overline{V}$ method (0.0864 liter/kg/hr). [f] Based on the mean Cl_p calculated by the $\overline{V}_{d,area}\overline{\beta}$ method (0.0682 liter/kg/hr).

When all of the doses used are the same or all of the obtained AUC values are corrected for the same dose when different doses are used, Eq. 10 can be simplified and rearranged to:

$$\overline{Cl}_p = \frac{\text{dose}}{(AUC_1 + AUC_2 + \ldots + AUC_n)/n} \qquad \text{(Eq. 11)}$$

$$\overline{Cl}_p = \frac{\text{dose}}{\text{arithmetic mean } AUC} \qquad \text{(Eq. 12)}$$

The method employing Eq. 12 for calculating the mean Cl_p will be referred to as the mean area method. This method and the harmonic mean (Eq. 9) method theoretically should yield the same mean Cl_p.

DISCUSSION

An example based on reported theophylline data (18) illustrates the consequence of employing different methods for the calculation of the mean total body clearance when the targeted mean blood level is set at 10 mg/liter. Relevant pharmacokinetic data in seven asthmatic subjects and analytical results are summarized in Table I. The mean Cl_p values determined by the harmonic mean, arithmetic mean, and two product-of-means ($\overline{K}_{el}\overline{V}_p$ and $\overline{V}_{d,area}\overline{\beta}$) methods are 0.0636, 0.0676, 0.0864, and 0.0682 liter/kg/hr, respectively. The largest difference among these methods is 35.8%.

Only the newly proposed harmonic method results in a correct arithmetic mean of 10 mg/liter of the steady-state blood level. The $\overline{K}_{el}\overline{V}_p$ method yields a mean blood level of 13.5 mg/liter. These results are based on the assumption that the dosing rate for all patients is equal to 10 mg/liter times the mean Cl_p. The difference in the mean Cl_p of propranolol in three subjects (14) estimated by the harmonic and arithmetic mean methods is 41.8%. In all of the methods studied, the harmonic mean method yields the lowest mean clearance values in the discussed and other simulated examples.

When employing the mean AUC method (Eqs. 11 and 12), the dose used for the entire test population should be the same. If not, the AUC for each individual should be corrected to the same dose in terms of the total dose or dose per unit of body weight or body surface area. The potential error of using the linear trapezoidal rule method for the estimation of the AUC was discussed recently (21). In estimating the individual total body drug clearance after oral dosing, the potential first-pass effect in the liver and lungs was ignored in many pharmacokinetic studies. Appropriate equations for such corrections are available (22–24).

It was pointed out recently (24) that the conventional concept for obtaining the initial plasma level at time zero after intravenous bolus dosing by the summation of the exponential coefficients (*i.e.*, $\Sigma_{i=1}^{n} A_i$ in $\Sigma_{i=1}^{n} A_i e^{-K_i t}$) and also for obtaining the AUC by $\Sigma_{i=1}^{n} (A_i)/(K_i)$ is not correct in terms of absolutes and could result in serious errors under certain circumstances. However, such conventional methods of pharmacokinetic analysis might be adequate as a reasonable approximation for most studies (24).

This discussion is based on the assumption that the arithmetic mean method is used for averaging the steady-state blood or plasma level data. Statistically speaking, if other methods such as the harmonic or geometric mean methods could be shown to be superior for averaging these blood or plasma data, a different conclusion regarding the best approach for estimating the mean Cl_p could be reached. Based on the rationale discussed under *Theoretical*, it also was concluded recently that the harmonic mean method is best for calculating the mean volumes of distribution for designing a rational dosage regimen (25). For general purposes, the conventional arithmetic mean method is acceptable for averaging the apparent volumes of distribution and the total body clearances of drugs. The harmonic mean method has been recommended for calculation of the mean biological half-life of drugs (12).

REFERENCES

(1) W. L. Chiou, M. A. F. Gadalla, and G. W. Peng, *J. Pharmacokinet. Biopharm.*, **6**, 135 (1978).

(2) W. L. Chiou, G. W. Peng, and R. L. Nation, *J. Clin. Pharmacol.*, **18**, 266 (1978).

(3) W. L. Chiou, S. M. Huang, and Y. C. Huang, *Int. J. Clin. Pharmacol. Biopharm.*, in press.

(4) W. L. Chiou, *J. Pharm. Sci.*, **67**, 1776 (1978).

(5) M. Gibaldi and G. Levy, *J. Am. Med. Assoc.*, **235**, 1987 (1976).

(6) J. G. Wagner, "Fundamentals of Clinical Pharmacokinetics," Drug Intelligence Publications, Hamilton, Ill., 1976.

(7) M. Gibaldi and D. Perrier, "Pharmacokinetics," Dekker, New York, N.Y., 1975.

(8) J. R. Powell, J. F. Thiercelin, S. Vozeh, L. Sansom, and S. Riegelman, *Am. Rev. Respir. Dis.*, **116**, 17 (1977).

(9) W. L. Chiou, *J. Pharm. Pharmacol.*, **24**, 342 (1972).

(10) F. A. Chrzanowski, P. J. Niebergall, R. L. Mayock, J. M. Taubin, and E. T. Sugita, *Clin. Pharmacol. Ther.*, **22**, 188 (1977).

(11) F. A. Chrzanowski and P. J. Niebergall, *ibid.*, **22**, 936 (1977).

(12) F. B. Eatman, W. A. Colburn, H. G. Boxenbaum, H. N. Posmanter, R. E. Weinfeld, R. Ronfeld, L. Weissman, J. D. Moore, M. Gibaldi, and S. A. Kaplan, *J. Pharmacokinet. Biopharm.*, **5**, 481 (1977).

(13) P. Gal, W. J. Jusko, A. M. Yurchak, and B. A. Franklin, *Clin. Pharmacol. Ther.*, **23**, 438 (1978).

(14) R. Gomeni, G. Bianchetti, R. Sega, and P. L. Morselli, *J. Pharmacokinet. Biopharm.*, **5**, 183 (1977).

(15) J. R. Koup, W. J. Jusko, C. M. Elwood, and R. K. Kohli, *Clin. Pharmacol. Ther.*, **18**, 9 (1975).

(16) P. M. Loughnan, D. S. Sitar, R. I. Ogilivie, A. Eisen, Z. Fox, and A. H. Heims, *J. Pediatr.*, **88**, 874 (1976).

(17) A. Mangione, T. E. Imhoff, R. V. Lee, L. Y. Hum, and W. J. Jusko, *Chest*, **73**, 616 (1978).

(18) P. A. Mitenko and R. I. Ogilivie, *Clin. Pharmacol. Ther.*, **14**, 509 (1973).

(19) K. M. Piafsky, D. S. Sitar, R. E. Rangno, and R. I. Ogilivie, *N. Engl. J. Med.*, **296**, 1495 (1977).

(20) E. B. Mode, "Elements of Statistics," 3rd ed., Prentice-Hall, Englewood Cliffs, N.J., 1961.

(21) W. L. Chiou, *J. Pharmacokinet. Biopharm.*, **6**, 539 (1978).

(22) *Ibid.*, **3**, 193 (1975).

(23) W. L. Chiou, *J. Pharm. Sci.*, **67**, 260 (1978).

(24) W. L. Chiou, *J. Pharmacokinet. Biopharm.*, in press.

(25) W. L. Chiou, *J. Pharm. Sci.*, **68**, 1067 (1979).

ACKNOWLEDGMENTS

The author thanks Ms. Marie Zajac for manuscript preparation.

Simultaneous GLC Determination of Clofibrate and Clofibric Acid in Human Plasma

MICHAEL S. WOLF and JAMES J. ZIMMERMAN ˣ

Received February 6, 1979, from the *Department of Pharmaceutics, School of Pharmacy, Temple University, Philadelphia, PA 19140.* Accepted for publication July 24, 1979.

Abstract □ A simultaneous assay for the detection of clofibrate and its metabolite, clofibric acid [2-(*p*-chlorophenoxy)-2-methylpropionic acid], is described. This GLC method is rapid and does not require a derivatization step. It is sensitive to 1-μg/ml levels of either compound in biological samples and can be used to characterize the *in vivo* conversion of clofibrate ester to the free acid.

Keyphrases □ Clofibrate—simultaneous GLC assay with clofibric acid, human plasma □ Clofibric acid—simultaneous GLC assay with clofibrate, human plasma □ Hypolipemic agents—clofibrate, simultaneous GLC assay with clofibric acid, human plasma

Clofibrate, an oral hypolipemic agent, is administered traditionally as the intact ester and assayed as the free acid, clofibric acid [2-(*p*-chlorophenoxy)-2-methylpropionic acid]. In the past decade, considerable attention has been devoted to the development of assays for these compounds (1–12). These methods have been used to generate pharmacokinetic data for clofibric acid.

Clofibric acid assays include spectrophotometric (1), radiometric (2), GLC (3–8), and high-pressure liquid chromatographic (9) techniques, all having approximately the same sensitivity. Clofibrate can be assayed easily by both spectrophotometric and GLC (1) methods, but clofibric acid determinations usually are tedious and time consuming, involving numerous extraction and evaporation steps. A major obstacle in the development of a GLC method for the simultaneous determination of clofibrate and clofibric acid has been the lack of a liquid phase sufficiently polar to yield reproducible clofibric acid peaks without derivatization. A flash derivatization would be ideal for the simultaneous determination, but the heat required would degrade the parent ester.

This paper describes a simultaneous assay method for clofibrate and clofibric acid that is rapid and does not require a derivatization step. It is sensitive to 1-μg/ml levels of either compound in biological samples and can be used to characterize the conversion of clofibrate to clofibric acid.

EXPERIMENTAL

Reagents—Fresh reagent grade ether was used without prior distillation. Purified granular ammonium sulfate was used in the salting-out procedure, and a 50% (w/v) NaF solution was used for plasma esterase deactivation. Commercially available benzocaine was recrystallized and used as the internal standard.

Clofibric acid was prepared by alkaline hydrolysis of clofibrate[1]. Clofibrate, 10 g, was combined with 80 ml of 30% KOH and 40 ml of alcohol USP, and the solution was refluxed for 4 hr as described previously (10). The hydrolysate was cooled to room temperature, extracted with 20 ml of ether to remove any remaining clofibrate, and acidified with 5% H_2SO_4 until litmus paper showed it to be strongly acidic. The acidified solution was extracted with ether (3 × 15 ml), and the extracts were combined and evaporated to dryness. The resulting crystalline residue was recrystallized with hot methanol, yielding ~70%, mp 118–118.5°. Qualitative confirmation was obtained by mass spectrometry[2] and NMR spectroscopy[3].

Sample Preparation—Human plasma, 1 ml, spiked with clofibrate and clofibric acid was added to a 10-ml test tube containing 20 μl of sodium fluoride solution and 550 mg of ammonium sulfate. The mixture was agitated for 30 sec with a vortex mixer[4] and then centrifuged for 10 min at 3500 rpm. The supernate (0.5 ml) was transferred to a fresh test tube, and 100 μg of benzocaine was added. The resulting solution was extracted with 1 ml of ether by agitating for 3 min. The sample tubes were sealed[5] and then centrifuged at 3500 rpm for 30 min to separate the phases. After centrifugation, the ether layer was withdrawn, and 1 μl was injected into the gas chromatograph.

GLC Conditions—The gas chromatograph[6] was equipped with a hydrogen flame-ionization detector. The glass column (1 m × 2 mm i.d.) was packed with 100–120-mesh Gas Chrom Q coated with 10% Silar 10 C[7]. Nitrogen was used as the carrier gas at a 24-ml/min flow rate. The oxygen and hydrogen flow rates were 240 and 40 ml/min, respectively; the injection port, oven, and detector temperatures were 200, 220, and 250°, respectively.

Hydrolysis—A 250-ml three-necked flask was placed in a heating mantle supported on a magnetic stirrer. Two necks were sealed, and a thermometer was placed in the third neck. The temperature control was calibrated and maintained at 37°. Clofibrate, 5 mg, was added within the reaction vessel to a pH 10.5 buffer system consisting of 0.1 *N* Na_2CO_3 and 30 ml of 0.1 *N* $NaHCO_3$. Samples were withdrawn and assayed by the simultaneous method.

RESULTS

Clofibric Acid Identification—The free acid of clofibrate, clofibric acid, when subjected to chemical-ionization mass spectrometry, provided a M + H ion at *m/e* 216. This mass is consistent with the formula of clofibric acid and is supported further by abundant ions at *m/e* 169 (equivalent to the loss of –COOH from the protonated compound) and at *m/e* 128 (corresponding to *p*-C_6H_4ClOH). The structure was confirmed further by other small peaks corresponding to the expected mass fragments.

Further confirmation was provided by an independent NMR spectrum. NMR demonstrated the presence of an aromatic ring (δ 6.75–7.3), –COOH (δ 10.1), and $-C(CH_3)_2-$ (δ 1.55), consistent with the clofibric acid structure. Chloroform was the solvent.

Assay—Under the described GLC conditions, clofibrate and clofibric acid eluted with retention times of 1.8 and 2.5 min, respectively (Fig. 1). Blank plasma samples did not produce any interfering peaks with retention times similar to either clofibrate or clofibric acid.

The standard curves of peak height ratio *versus* concentration in the 10–200-μg/ml range were linear for both compounds. The least-squares estimate for the line fitting a plot of the mean of the peak height ratios obtained on different days *versus* the clofibric acid concentration ($n = 7$, $r = 0.999$) was $y = (6.17 \times 10^{-3})x + 0.024$. For clofibrate ($n = 9$, $r = 0.999$), the regression line was $y = (3.04 \times 10^{-2})x - 0.012$. The standard errors of the estimate were 1.53×10^{-2} and 1.02×10^{-1}, respectively. There was a systematic reduction in all peak height ratios over 1 month, but the change was not statistically significant.

While the assay as outlined has a lower sensitivity limit of ~10 μg/ml for both compounds, the sensitivity can be increased 10-fold to ~1 μg/ml by evaporating the solvent after extraction and redissolving the residue in 100 μl of ether.

[1] Provided by Ayerst Laboratories, New York, N.Y.

[2] Hewlett-Packard model 5930 A.
[3] Varian model 60.
[4] Vortex-Genie, Scientific Industries, Springfield, Mass.
[5] Parafilm, American Can Co., Neenah, Wis.
[6] Hewlett-Packard model 5710 A.
[7] Applied Science Laboratories, State College, Pa.

0022-3549/80/0100-0092$01.00/0
© 1980, American Pharmaceutical Association

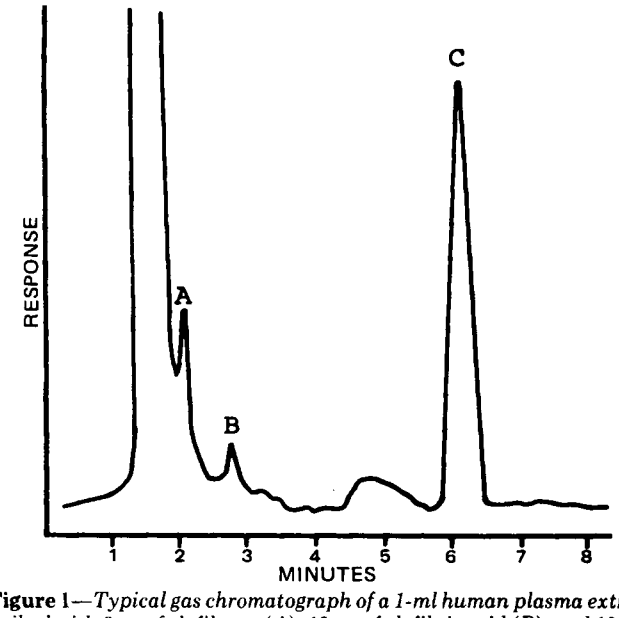

Figure 1—*Typical gas chromatograph of a 1-ml human plasma extract spiked with 6 μg of clofibrate (A), 10 μg of clofibric acid (B), and 100 μg of benzocaine (C).*

Recovery—To achieve maximum recovery of both the ester and the acid, a salting-out technique was utilized. The technique was based on a literature method (11) in which the efficacy of ammonium chloride as an agent for salting drugs out of plasma was examined. A later study (12) showed the effectiveness of ammonium sulfate for the same purpose. A standard mixture of 200 μg of clofibrate and 50 μg of benzocaine was used to study this technique for clofibrate recovery from aqueous solution and plasma. A peak height ratio of 12 was obtained from 1 ml of an aqueous solution of this mixture. For the plasma determination, varying amounts of ammonium sulfate were used to determine the amount needed to achieve the same peak height ratio. Amounts ranged from 300 (ratio of 9.45) to 900 (ratio of 6.65) mg/ml, with the maximum peak height ratio of 11.95 obtained using 550 mg of ammonium sulfate/ml of plasma.

Table I—Recovery of Clofibrate and Clofibric Acid after Alkaline Hydrolysis at 37° and pH 10.51 [a]

Minutes	Clofibrate, μmole/ml	Clofibric Acid, μmole/ml	Recovery, μmole/ml	Percent of Initial Concentration
10	0.190	0.019[b]	0.190	101
20	0.161	0.051	0.212	102
30	0.149	0.060	0.209	101
45	0.145	0.069	0.214	103
60	0.128	0.079	0.207	100
90	0.099	0.102	0.201	97
120	0.074	0.133	0.207	100

[a] Initial clofibrate concentration was 0.207 μmole/ml. Constant pH was maintained with a carbonate buffer. [b] This value was close to the assay sensitivity limit and could not be measured as accurately as other values.

Hydrolysis—The accuracy of the simultaneous assay was tested by following the disappearance of clofibrate and the appearance of clofibric acid during alkaline hydrolysis of the ester at pH 10.51 and 37°. There was excellent recovery at each period, indicating that the assay accurately measured the ester and the hydrolysis product simultaneously (Table I). Degradation of the ester followed pseudo-first-order kinetics over the 2-hr run, yielding a least-squares estimate for the degradation rate constant of 7.98×10^{-3} min^{-1}.

DISCUSSION

The described GLC method has several advantages over previously described assays. It is fast and specific. About 10 samples can be determined in 1 hr by one person. Its specificity is of particular interest because the disappearance of the parent ester and the appearance of the acid metabolite can be followed simultaneously, facilitating the determination of their respective pharmacokinetic parameters. The method does not require derivatization, which can introduce an additional variable.

The method sensitivity may be increased severalfold by evaporating the solvent and redissolving the residue in an appropriate amount of solvent. Column degradation by the free acid cannot be avoided. Under heavy use and with an overnight oven temperature of 200° or greater, column repacking may be necessary every 6–8 weeks.

REFERENCES

(1) H. Bruderlein, W. T. Robinson, M. Kraml, and D. Dvornik, *Clin. Biochem.*, **8**, 261 (1975).

(2) A. Sedaghat and E. H. Ahrens, Jr., *Eur. J. Clin. Invest.*, **5**, 177 (1975).

(3) R. Gugler and C. Janson, *J. Chromatogr.*, **117**, 175 (1976).

(4) W. G. Crouthamel and R. J. Cenedella, *Pharmacology*, **13**, 465 (1975).

(5) G. Mouin, J. J. Thebault, P. D.'Athis, J. P. Tillement, and J. L. Beaumont, *Eur. J. Clin. Pharmacol.*, **8**, 433 (1975).

(6) A. Karmen and H.Haut, *Biochem. Med.*, **12**, 154 (1975).

(7) T. C. Tuong and A. Tuong, *J. Chromatogr.*, **106**, 97 (1975).

(8) L. H. Olesen and K. Holch, *Arch. Pharm. Chem. Sci. Ed.*, **2**, 65 (1974).

(9) A. Sedaghat, H. Nakamura, and E. H. Ahrens, Jr., *J. Lipid Res.*, **15**, 352 (1974).

(10) D. L. Trout, E. H. Estes, and S. J. Friedberg, *ibid.*, **4**, 407 (1963).

(11) B. Davidow, N. L. Petri, and B. Quame, *Am. J. Clin. Pathol.*, **50**, 714 (1968).

(12) J. H. Speaker, *J. Chromatogr. Sci.*, **12**, 297 (1974).

ACKNOWLEDGMENTS

The authors acknowledge the aid of Dr. M. A. Abou-Gharbia and Dr. Mark Lichtenwalner in interpreting spectral data and Mr. Robert Norton for assistance in the chromatographic technique.

Cactus Alkaloids XLII: 3,4-Dimethoxy-β-phenethylamine and Heliamine from the Mexican Cereoid *Backebergia militaris*

RACHEL MATA and JERRY L. McLAUGHLIN ˣ

Received May 31, 1979, from the *Department of Medicinal Chemistry and Pharmacognosy, School of Pharmacy and Pharmacal Sciences, Purdue University, West Lafayette, IN 47907.* Accepted for publication July 16, 1979.

Abstract □ *Backebergia militaris* (Andot) Bravo ex Sánchez Mejorada yielded alkaloid crystals from a fractionated ethanol extract of only 20 g of plant material. The alkaloid was identified as heliamine (6,7-dimethoxy-1,2,3,4-tetrahydroisoquinoline) hydrochloride. A second alkaloid, 3,4-dimethoxy-β-phenethylamine hydrochloride, was crystallized after preparative TLC of the mother liquors. Both compounds were isolated previously from other cactus species.

Keyphrases □ Alkaloids, cactus—heliamine, 3,4-dimethoxy-β-phenethylamine, isolation, identification □ Heliamine—isolation from cacti, identification, 3,4-dimethoxy-β-phenethylamine □ 3,4-Dimethoxy-β-phenethylamine—isolation from cacti, identification, heliamine □ Cactus alkaloids—heliamine, 3,4-dimethoxy-β-phenethylamine, isolation, identification

In a chemotaxonomic analysis of several giant Mexican cereoid species of cacti, the new technique of mass-analyzed, ion kinetic energy spectrometry was used to detect and identify alkaloids in ethanol extracts of small (1-g) samples of dried cactus material (1). This survey included *Backebergia militaris* (Andot) Bravo ex Sánchez Mejorada, in which alkaloids at *m/e* 194 and 208 were detected; the major components at these peaks were identified on the basis of fragmentation patterns as heliamine (6,7-dimethoxy-1,2,3,4-tetrahydroisoquinoline) and *N*-methylheliamine (oxymethylcorypalline). Both alkaloids were identified previously in other cactus species (2–4). Alkaloid ions at *m/e* less than 194 were not examined.

DISCUSSION

In a previous TLC screening of this species as part of a continuing search for cactus alkaloids, two major compounds (a primary amine and a secondary amine) were detected in the screening extracts. Subsequently, an ethanol extract of only 20 g of plant material was subjected to anion exchange chromatography to resolve phenolic and nonphenolic alkaloids (5). Analytical TLC of the phenolic fraction was negative for any major alkaloids, but analytical TLC of the nonphenolic fraction detected two major and at least two minor alkaloid components. After acid–base partitioning of the nonphenolic fraction, one of the major alkaloids (I) crystallized directly as the hydrochloride. Preparative TLC of the mother liquor permitted resolution of the second major alkaloid from I and a third unidentified minor alkaloid; the second major alkaloid (II) then crystallized as the hydrochloride.

Analytical TLC of I with a series of reference cactus alkaloids suggested that it was heliamine (6,7-dimethoxy-1,2,3,4-tetrahydroisoquinoline); this identification was confirmed by melting-point comparisons, IR spectroscopy, and electron-impact mass spectrometry. TLC of II tentatively identified it as 3,4-dimethoxy-β-phenethylamine, and this identification was confirmed by its melting point and its IR and electron-impact mass spectra. Heliamine was reported initially as a natural product from the related cereoid cactus, *Pachycereus pecten-aboriginum* (Engelm.) Br. and R. (2); concurrently, it was crystallized from another Mexican cereoid, *Lemaireocereus weberi* (Coult.) Br. and R. (3). 3,4-Dimethoxy-β-phenethylamine was detected or isolated previously from several cactus species representing all three major cactus tribes (6–8).

Heliamine biogenesis would likely involve cyclization of a primary amine such as 3,4-dimethoxy-β-phenethylamine (or, perhaps, its 3-*O*-demethylated derivative) (9); consequently, the cooccurrence of heliamine and 3,4-dimethoxy-β-phenethylamine is not surprising. Heliamine reportedly has inhibitory activity against sarcoma 45 in rats (10), while 3,4-dimethoxy-β-phenethylamine has questionable involvement in certain mental processes (11).

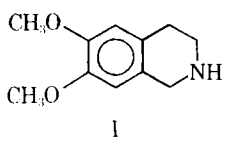

I

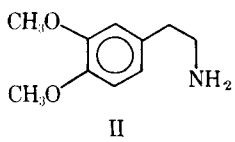

II

EXPERIMENTAL

Plant Material—Cuttings of fresh *B. militaris* (2.8 kg) conforming to published taxonomic descriptions (12) were obtained[1]. The fresh sections were sliced, frozen, freeze dried, and reduced to a powder through a 2-mm screen in a Wiley mill.

Alkaloid Extraction and Fractionation—Twenty grams of the powdered plant material was macerated with stirring in 1 liter of ethanol for 24 hr. After filtration to remove the marc, the ethanol extract was concentrated and subjected to anion-exchange chromatography on 20 g of resin[2] prepared in the hydroxide form (5). Upon analytical TLC using solvent systems and procedures as described previously (14), the phenolic fraction was devoid of any major alkaloids while the nonphenolic fraction contained two major and at least three minor compounds.

The residue from the nonphenolic extract was dissolved in 100 ml of 1 *N* HCl and partitioned with chloroform and ether (three times with 100 ml of each solvent). The aqueous solution pH was adjusted to 9.5 with sodium hydroxide, and the partitions were repeated. The combined chloroform–ether extracts from the basic solutions were dried over anhydrous sodium sulfate, concentrated, and acidified with 5% HCl in ethanol.

Isolation and Identification—*Heliamine (I)*—Upon further concentration of the acidic solution and addition of ether, a precipitate (300 mg) of alkaloid hydrochlorides formed. This precipitate was recrystallized (ethanol–ether) to produce 150 mg (0.75% yield) of the hydrochloride of I (mp 255°)[3]. Analytical TLC with Systems A, B, F, and G (14) identified I as heliamine; when the plate was sprayed with fluorescamine, the purple chromophore observed under UV light was diagnostic for the secondary amine function (15). IR[4] and electron-impact mass[5] spectra were essentially identical to those observed with previously isolated (mp 248°) and synthesized (mp 252°) heliamine hydrochloride (3).

3,4-Dimethoxy-β-phenethylamine (II)—The mother liquors from the crystallization of I were subjected to preparative TLC [eight plates, Solvent A (14)]. Three bands were scraped from the plates and eluted with ethanol: one was additional heliamine; a second was an unidentified compound which failed to crystallize; and the third, II, formed a crystalline hydrochloride (8 mg). Recrystallizations (ethanol–ether) raised the melting point to 149° (5 mg, 0.025% yield). Analytical TLC (14) identified II as 3,4-dimethoxy-β-phenethylamine; when the plate was sprayed with fluorescamine, the bright-yellow fluorescence observed under UV light was diagnostic for the primary amine function (15). IR and electron-impact mass spectra were indistinguishable from those of reference 3,4-dimethoxy-β-phenethylamine hydrochloride[6] (mp 150°).

[1] From Dr. Arthur C. Gibson, Department of Ecology and Evolutionary Biology, University of Arizona, Tucson, AZ 85721, who recently studied the phylogeny of the Mexican columnar cacti (13). The samples were collected June 25, 1978, 10 km west of Apatzingan on Highway 120, state of Michoacán, Mexico, from plants approximately 8 m in height. A voucher specimen is filed at the University of Arizona Herbarium: Gibson 3433 (ARIZ).

[2] Amberlite IRA 401S, Mallinckrodt Chemical Co.

[3] Mel-Temp apparatus, uncorrected.

[4] Beckman IR 33, potassium bromide pellets.

[5] DuPont 21-492B mass spectrometer (low resolution).

[6] Calbiochem.

0022-3549/80/0100-0094$01.00/0
© 1980, American Pharmaceutical Association

REFERENCES

(1) S. E. Unger, R. G. Cooks, R. Mata, and J. L. McLaughlin, *J. Am. Chem. Soc.*, in press.

(2) J. Strombom and J. G. Bruhn, *Acta Pharm. Suec.*, **15**, 127 (1978).

(3) R. Mata and J. L. McLaughlin, *Phytochemistry*, in press.

(4) J. E. Lindgren and J. G. Bruhn, *Lloydia*, **39**, 464 (1976).

(5) J. L. McLaughlin and A. G. Paul, *ibid.*, **29**, 315 (1966).

(6) R. Mata, M.S. thesis, Purdue University, West Lafayette, Ind., Dec. 1976, pp. 107–122.

(7) P. W. Doetsch, J. M. Cassady, and J. L. McLaughlin, *J. Chromatogr.*, in press.

(8) B. N. Meyer, Y. A. H. Mohamed, and J. L. McLaughlin, *Phytochemistry*, in press.

(9) A. G. Paul, *Lloydia*, **36**, 36 (1973).

(10) A. A. Chachoyan, B. T. Garibdzhanyan, and E. Z. Markaryan, *Biol. Zh. Arm.*, **25**, 102 (1972) (Russ.); through *Chem. Abstr.*, **78**, 52538m (1973).

(11) L. E. Hollister and A. J. Friedhoff, *Nature*, **210**, 1377 (1966).

(12) C. Backeberg, "Cactus Lexicon," English ed., Blandford, Poole, Dorset, England, 1977, p. 80.

(13) A. C. Gibson and K. E. Horak, *Ann. Mo. Bot. Gard.*, **65**, 999 (1978).

(14) R. L. Ranieri and J. L. McLaughlin, *J. Org. Chem.*, **41**, 319 (1976).

(15) R. L. Ranieri and J. L. McLaughlin, *J. Chromatogr.*, **111**, 234 (1975).

ACKNOWLEDGMENTS

Supported in part by BRSG RR-05586 from the National Institutes of Health and a grant from the Cactus and Succulent Society of America. R. Mata acknowledges fellowship support from the Departmento de Becas del Consejo de Desarrollo Cientifico y Humanistico de la Universidad Central de Venezuela.

Thanks are given to Dr. Arthur C. Gibson for suggesting this project and for supplying the plant material.

Determination of Two Fenamates in Plasma by High-Performance Liquid Chromatography

CHIEN K. LIN, CHING S. LEE ˣ, and JOHN H. PERRIN

Received March 6, 1979, from the *Department of Pharmacy, College of Pharmacy, University of Florida, Gainesville, FL 32610.* Accepted for publication July 2, 1979.

Abstract □ A high-performance liquid chromatographic determination of two fenamates in human plasma is described. Plasma samples, 1.0 ml, to which 4 μg of internal standard had been added, were extracted with carbon tetrachloride under acidic conditions. Portions of the organic layer were transferred and evaporated to dryness under nitrogen. Residues were dissolved in methanol, and an aliquot was injected into the liquid chromatograph. An intermediate polarity, bonded cyanopropylsilane column was used with a mobile phase of water–acetonitrile–acetic acid (60:30:10 v/v/v). The flow rate was 1 ml/min, and the effluent was monitored at 254 nm. Flufenamic acid and mefenamic acid had retention times of 10.4 and 9.2 min, respectively. In the 1–10-μg range, the mean flufenamic acid recovery from control plasma was 100.7 ± 3.4% (n = 18). A typical calibration curve had a regression equation of $y = 0.132x - 0.04$ with $\gamma^2 = 0.99$. Preliminary stability tests showed that flufenamic acid is stable for at least 2 weeks in plasma after freezing.

Keyphrases □ Flufenamic acid—analysis, high-performance liquid chromatography, plasma, rats, humans □ Mefenamic acid—analysis, high-performance liquid chromatography, plasma, rats, humans □ High-performance liquid chromatography—analysis, flufenamic acid, mefenamic acid, plasma, rats, humans

Flufenamic acid[1] (I) and mefenamic acid[1] (II) are potent nonsteroidal analgesic and anti-inflammatory agents used in the management of rheumatoid arthritis. Spectrophotometric (1, 2), colorimetric (3), and fluorometric (2, 4, 5) methods have been applied for fenamate analysis in aqueous solution and in biological samples such as plasma, urine, and milk. A fluorometric method for the determination of I in the nanogram range used a chamber paper analysis apparatus (6). A convenient TLC technique was reported for screening three fenamates and their metabolites (7).

Only one GLC method (8) utilizing electron-capture detection has been reported. Although it was described for II, it could be adapted to the analysis of I in blood and urine. However, details of the assay were not provided (8).

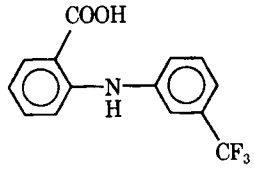

I

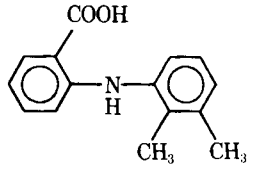

II

This article describes the high-performance liquid chromatographic (HPLC) determination of plasma fenamate levels. A single extraction step is followed by reversed-phase chromatography, eliminating the tedious and time-consuming procedures required by the previously reported methods (3, 7). Flufenamic acid and mefenamic acid can be internal standards for each other during either assay. The use of an internal standard improves both the precision and the accuracy of plasma level determination.

EXPERIMENTAL

Apparatus—Fenamate analyses were carried out on a liquid chromatograph[2] equipped with dual-delivery pumps[3], a single injector[4], and a single-chamber UV absorbance detector[5].

Reagents—Carbon tetrachloride[6], acetic acid[6], and sulfuric acid[7] were analytical reagent grade. Methanol[8] and acetonitrile[8] were distilled in glass. Solvents including distilled, deionized water were filtered routinely through 0.45-μm filters[9] prior to use in the liquid chromatograph.

[1] Provided by Parke-Davis and Co., Detroit, Mich.

[2] Model 204, Waters Associates, Milford, Mass.
[3] Model 6000A, Waters Associates, Milford, Mass.
[4] U6K, Waters Associates, Milford, Mass.
[5] Model 440, Waters Associates, Milford, Mass.
[6] Mallinckrodt, St. Louis, Mo.
[7] Eastman Kodak, Rochester, N.Y.
[8] Burdick & Jackson, Muskegon, Mich.
[9] Millipore Corp., Bedford, Mass.

0022-3549/80/0100-0095$01.00/0

© 1980, American Pharmaceutical Association

REFERENCES

(1) S. E. Unger, R. G. Cooks, R. Mata, and J. L. McLaughlin, *J. Am. Chem. Soc.*, in press.

(2) J. Strombom and J. G. Bruhn, *Acta Pharm. Suec.*, **15**, 127 (1978).

(3) R. Mata and J. L. McLaughlin, *Phytochemistry*, in press.

(4) J. E. Lindgren and J. G. Bruhn, *Lloydia*, **39**, 464 (1976).

(5) J. L. McLaughlin and A. G. Paul, *ibid.*, **29**, 315 (1966).

(6) R. Mata, M.S. thesis, Purdue University, West Lafayette, Ind., Dec. 1976, pp. 107–122.

(7) P. W. Doetsch, J. M. Cassady, and J. L. McLaughlin, *J. Chromatogr.*, in press.

(8) B. N. Meyer, Y. A. H. Mohamed, and J. L. McLaughlin, *Phytochemistry*, in press.

(9) A. G. Paul, *Lloydia*, **36**, 36 (1973).

(10) A. A. Chachoyan, B. T. Garibdzhanyan, and E. Z. Markaryan, *Biol. Zh. Arm.*, **25**, 102 (1972) (Russ.); through *Chem. Abstr.*, **78**, 52538m (1973).

(11) L. E. Hollister and A. J. Friedhoff, *Nature*, **210**, 1377 (1966).

(12) C. Backeberg, "Cactus Lexicon," English ed., Blandford, Poole, Dorset, England, 1977, p. 80.

(13) A. C. Gibson and K. E. Horak, *Ann. Mo. Bot. Gard.*, **65**, 999 (1978).

(14) R. L. Ranieri and J. L. McLaughlin, *J. Org. Chem.*, **41**, 319 (1976).

(15) R. L. Ranieri and J. L. McLaughlin, *J. Chromatogr.*, **111**, 234 (1975).

ACKNOWLEDGMENTS

Supported in part by BRSG RR-05586 from the National Institutes of Health and a grant from the Cactus and Succulent Society of America. R. Mata acknowledges fellowship support from the Departmento de Becas del Consejo de Desarrollo Cientifico y Humanistico de la Universidad Central de Venezuela.

Thanks are given to Dr. Arthur C. Gibson for suggesting this project and for supplying the plant material.

Determination of Two Fenamates in Plasma by High-Performance Liquid Chromatography

CHIEN K. LIN, CHING S. LEE ˣ, and JOHN H. PERRIN

Received March 6, 1979, from the *Department of Pharmacy, College of Pharmacy, University of Florida, Gainesville, FL 32610.* Accepted for publication July 2, 1979.

Abstract □ A high-performance liquid chromatographic determination of two fenamates in human plasma is described. Plasma samples, 1.0 ml, to which 4 μg of internal standard had been added, were extracted with carbon tetrachloride under acidic conditions. Portions of the organic layer were transferred and evaporated to dryness under nitrogen. Residues were dissolved in methanol, and an aliquot was injected into the liquid chromatograph. An intermediate polarity, bonded cyanopropylsilane column was used with a mobile phase of water–acetonitrile–acetic acid (60:30:10 v/v/v). The flow rate was 1 ml/min, and the effluent was monitored at 254 nm. Flufenamic acid and mefenamic acid had retention times of 10.4 and 9.2 min, respectively. In the 1–10-μg range, the mean flufenamic acid recovery from control plasma was 100.7 ± 3.4% (n = 18). A typical calibration curve had a regression equation of $y = 0.132x - 0.04$ with $\gamma^2 = 0.99$. Preliminary stability tests showed that flufenamic acid is stable for at least 2 weeks in plasma after freezing.

Keyphrases □ Flufenamic acid—analysis, high-performance liquid chromatography, plasma, rats, humans □ Mefenamic acid—analysis, high-performance liquid chromatography, plasma, rats, humans □ High-performance liquid chromatography—analysis, flufenamic acid, mefenamic acid, plasma, rats, humans

Flufenamic acid[1] (I) and mefenamic acid[1] (II) are potent nonsteroidal analgesic and anti-inflammatory agents used in the management of rheumatoid arthritis. Spectrophotometric (1, 2), colorimetric (3), and fluorometric (2, 4, 5) methods have been applied for fenamate analysis in aqueous solution and in biological samples such as plasma, urine, and milk. A fluorometric method for the determination of I in the nanogram range used a chamber paper analysis apparatus (6). A convenient TLC technique was reported for screening three fenamates and their metabolites (7).

Only one GLC method (8) utilizing electron-capture detection has been reported. Although it was described for II, it could be adapted to the analysis of I in blood and urine. However, details of the assay were not provided (8).

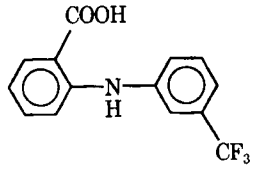

I

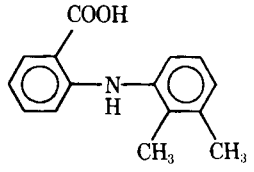

II

This article describes the high-performance liquid chromatographic (HPLC) determination of plasma fenamate levels. A single extraction step is followed by reversed-phase chromatography, eliminating the tedious and time-consuming procedures required by the previously reported methods (3, 7). Flufenamic acid and mefenamic acid can be internal standards for each other during either assay. The use of an internal standard improves both the precision and the accuracy of plasma level determination.

EXPERIMENTAL

Apparatus—Fenamate analyses were carried out on a liquid chromatograph[2] equipped with dual-delivery pumps[3], a single injector[4], and a single-chamber UV absorbance detector[5].

Reagents—Carbon tetrachloride[6], acetic acid[6], and sulfuric acid[7] were analytical reagent grade. Methanol[8] and acetonitrile[8] were distilled in glass. Solvents including distilled, deionized water were filtered routinely through 0.45-μm filters[9] prior to use in the liquid chromatograph.

[1] Provided by Parke-Davis and Co., Detroit, Mich.

[2] Model 204, Waters Associates, Milford, Mass.
[3] Model 6000A, Waters Associates, Milford, Mass.
[4] U6K, Waters Associates, Milford, Mass.
[5] Model 440, Waters Associates, Milford, Mass.
[6] Mallinckrodt, St. Louis, Mo.
[7] Eastman Kodak, Rochester, N.Y.
[8] Burdick & Jackson, Muskegon, Mich.
[9] Millipore Corp., Bedford, Mass.

0022-3549/80/0100-0095$01.00/0

© 1980, American Pharmaceutical Association

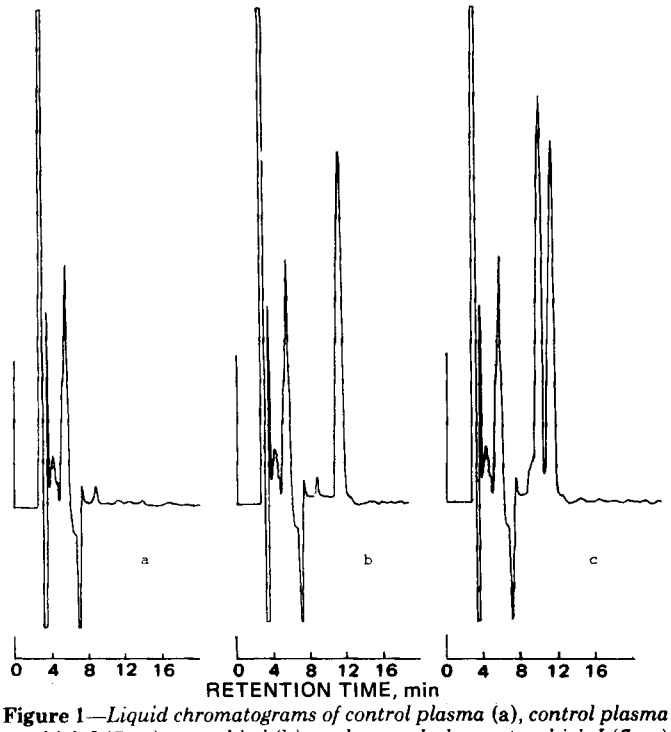

Figure 1—*Liquid chromatograms of control plasma* (a), *control plasma to which I* (7 μg) *was added* (b), *and control plasma to which I* (7 μg) *and II* (4 μg) *were added* (c).

Preparation of Standards—Ten milligrams of each fenamate was dissolved in methanol to yield a 100-μg/ml stock solution. Working standard solutions of I containing 1, 2, 3, 5, 7, and 10 μg/ml were prepared by diluting the stock solution with methanol–water (1:1 v/v). Six calibration samples were used in each run to establish the HPLC standard curve and to determine recovery reproducibility. Mefenamic acid solution, 4 μg/ml, served as the internal standard.

Measurement of Plasma I—Plasma samples, 1.0 ml, to which 4 μg of internal standard had been added, were mixed thoroughly by hand shaking and acidified with 0.9 *M* H_2SO_4. After the addition of 8 ml of carbon tetrachloride, the sample tubes were spun on a test tube rotator for 15 min and centrifuged. The aqueous phase was removed by aspiration. Portions of the carbon tetrachloride were transferred to another tube and evaporated to dryness under nitrogen. Residues were dissolved in 0.5 ml of methanol, and a 40-μl aliquot was injected into the liquid chromatograph.

The standard plasma curve was constructed by plotting the peak height ratios (I/II) *versus* the weight content of I. The peak height ratio of an unknown sample was used to determine the amount of I present. The standard samples were run concurrently with the unknown samples as described previously.

Chromatographic Conditions—A stainless steel column (30 cm × 4 mm i.d.) was packed with a stable reversed-phase stationary phase of porous silica beads (mean diameter 10 μm) coated with chemically bonded cyanopropylsilane monolayers[10]. The mobile phase was water–acetonitrile–acetic acid (60:30:10 v/v/v). The operating temperature was ambient, and the flow rate was 1 ml/min with an operating pressure of 1000 psi. The column effluent was monitored continuously at 254 nm with a full-scale deflection of 0.02 aufs. A short wash (acetonitrile for 15 min followed by chloroform for 10 min at 1 ml/min) at the end of each analytical day removed strongly retained solutes.

RESULTS AND DISCUSSION

Acceptable separation of the fenamates in this reversed-phase system was dependent on the amount of organic solvent in the mobile phase and on the effective pH of the aqueous component. A simple acetonitrile–water system (30:70 v/v) with an effective pH of 5.5 did not resolve the solutes. Since the fenamates are moderate acids (pKa 3.9 for I and 4.2 for II), their capacity factors were increased by lowering the effective pH of this solvent, and the water–acetonitrile–acetic acid system (60:30:10 v/v/v, effective pH 2.7) resolved the two solute peaks.

[10] μBondapak CN, Waters Associates, Milford, Mass.

Table I—Flufenamic Acid (I) Recovery from Human Plasma (n = 3)

I Added, μg	I Found, μg	Recovery[a], %
1	1.028 ± 0.031	102.8 ± 3.1
2	2.090 ± 0.430	104.5 ± 4.3
3	2.760 ± 0.079	92.0 ± 7.9
5	5.260 ± 0.051	105.0 ± 5.0
7	7.000 ± 0.000	100.0 ± 0.0
10	10.000 ± 0.000	100.0 ± 0.0
1–10[b]	—	100.7 ± 3.4

[a] Expressed as mean ± *SD*. [b] n = 18.

Table II—Peak Height Ratios for the Calibration Curve

I Added, μg	Peak Height Ratios	*SD*
1	0.099	0.003
2	0.230	0.010
3	0.355	0.026
5	0.605	0.025
7	0.857	0.015
10	1.297	0.021

Figure 1 presents liquid chromatograms of control human plasma, control plasma to which I was added, and control plasma to which both fenamates were added. As indicated in Fig. 1*a*, negligible interfering peaks were found in the control plasma specimens. Under the described chromatographic conditions, I and II had retention times of 10.4 and 9.2 min, respectively. Better resolution for the two fenamates can be obtained at a slower flow rate. However, no real benefits (*e.g.*, precision in the measurement of peak height ratios) were gained using prolonged retention times.

The results obtained following analyses of various amounts of I in control human plasma are summarized in Table I. In the 1–10-μg range, the mean I recovery from control plasma was 100.7 ± 3.4% (n = 18). Table II contains peak height ratios obtained from calibration curves prepared with human plasma. Each value represents the average of four samples at each concentration. A typical calibration curve prepared by extracting human plasma samples containing different concentrations of I and 4 μg of II had a regression equation of $y = 0.132x - 0.04$ with $\gamma^2 = 0.99$. The UV absorption was linear between 1 and 10 μg, where therapeutic concentrations can be interpolated conveniently. The lower detection sensitivity limit was 1 μg/ml of plasma.

When UV absorption spectra of I and II were obtained in methanolic solutions, the maximum absorption wavelength, λ_{max}, was 290 nm. Since the chromatograph was equipped with a single-wavelength detector at 254 nm, the optimal condition has not yet been achieved in this assay. Higher detecting sensitivity can be obtained by monitoring the absorption at 290 nm with a variable-wavelength UV detector.

Preliminary 2-week stability tests were performed by dissolving 1–10 μg of I in 1 ml of plasma, which was then frozen for 3, 7, or 15 days; I was stable in frozen plasma for at least 2 weeks (Table III).

Table III—Effect of Frozen Storage on the Flufenamic Acid Stability in Human Plasma

I Added, μg	Days			
	0	3	7	15
1	0.98	1.20	1.04	1.00
2	1.91	2.35	2.19	1.93
3	3.21	3.11	3.12	2.72
5	4.79	—	4.96	4.88
7	7.03	6.76	7.07	6.74
10	10.07	9.85	10.57	9.76

Table IV—Plasma Flufenamic Acid Levels in Two Rats at Various Times after Intravenous Sublingual Administration of 5 mg of I/kg in 0.2 *N* NaOH

Minutes	Plasma Levels, μg/ml	
	Rat 1	Rat 2
15	—	120
20	134	—
30	110	128
60	82.3	90.6

Experiments utilizing this procedure in animals are in progress. Plasma flufenamic acid levels in two rats at various times after intravenous sublingual administration of 5 mg of I/kg in 0.2 *N* NaOH are shown in Table IV. Due to the high plasma I concentrations at the dose administered, only 50 μl of the plasma sample was taken for analysis. The assays described here may be used to measure therapeutic levels of I in patients.

REFERENCES

(1) J. B. Carey, *J. Clin. Invest.*, **40**, 1028 (1961).

(2) A. R. Rosenberg and T. R. Bates, *Proc. Soc. Exp. Biol. Med.*, **145**, 93 (1974).

(3) G. Deveaux, P. Mesnard, and A. M. Brisson, *Ann. Pharm. Fr.*, **27**, 239 (1969).

(4) A. J. Glazko, *Ann. Phys. Med. Suppl.*, **9**, 24 (1967).

(5) H. D. Dell and R. Kamp, *Arch. Pharm.*, **303**, 785 (1970).

(6) W. S. Schmollack and U. Wenzel, *Pharmazie*, **29**, 583 (1974).

(7) B. Demetriou and B. G. Osborne, *J. Chromatogr.*, **90**, 405 (1974).

(8) S. A. Bland, J. W. Blake, and R. S. Ray, *J. Chromatogr. Sci.*, **14**, 201 (1976).

ACKNOWLEDGMENTS

Presented at the APhA Academy of Pharmaceutical Sciences, Anaheim meeting, April 1979.

Supported in part by the Division of Sponsored Research, University of Florida.

The authors thank Ms. Judy Fuller for manuscript preparation.

Antitumor Activity of Hydrazones and Adducts between Aromatic Aldehydes and *p*-(3,3-Dimethyl-1-triazeno)benzoic Acid Hydrazide

TULLIO GIRALDI *, PHYLLIS M. GODDARD ‡, CARLO NISI §x, and FABIO SIGON §

Received May 3, 1978, from the **Istituto di Farmacologia, Università di Trieste, I 34100, Trieste, Italy, the* ‡*Chester Beatty Research Institute, Institute of Cancer Research, Royal Cancer Hospital, London SW3 6JB, England,* and the §*Istituto di Chimica Farmaceutica, Università di Trieste, I 34100, Trieste, Italy.* Accepted for publication June 1, 1979.

Abstract □ Hydrazones and adducts between aromatic aldehydes and *p*-(3,3-dimethyl-1-triazeno)benzoic acid hydrazide were synthesized and tested for antitumor activity. Two adducts derived from 2,6-dinitro- and 4-cyanobenzaldehyde were active against TLX5 lymphoma in mice. The hydrazone of the latter aldehyde was significantly more active than the adducts.

Keyphrases □ *Antineoplastic agents, potential*—hydrazones and adducts between aromatic aldehydes and *p*-(3,3-dimethyl-1-triazeno)-benzoic acid hydrazide, structure–activity relationships □ *p*-(3,3-Dimethyl-1-triazeno)benzoic acid hydrazide—antineoplastic activity, hydrazones and adducts with aromatic aldehydes, structure–activity relationships

A series of 1-aryl-3,3-dimethyltriazene derivatives, characterized by the presence of a carbonyl group and a triazene function in the *para*-position on the aromatic nucleus, was previously synthesized and examined for antitumor activity against TLX5 lymphoma in mice (1). Among these compounds, the *o*-nitrophenylhydrazone of the *p*-(3,3-dimethyl-1-triazeno)benzoic acid hydrazide and the adduct between this hydrazide and *p*-nitrobenzaldehyde showed considerable activity. Therefore, a further group of adducts and related hydrazones carrying electron-withdrawing substituents was synthesized and tested for their antitumor activity. Their structures and activities are reported in Tables I and II.

EXPERIMENTAL[1]

Adducts I–IV—Adducts I, II, and IV were prepared by the addition of a solution of the aldehyde in hot ethanol to an equimolar solution of *p*-(3,3-dimethyl-1-triazeno)benzoic acid hydrazide (2) in the same solvent. After standing for a few minutes, the products precipitated and were washed with a few milliliters of cold ethanol. Methanol was used as a solvent for preparing adduct III, and this reaction mixture was heated gently for 15 min before allowing the precipitation.

The structures assigned to I–IV are in accordance with their elemental analyses and are supported by the following data:

1. When these substances were heated to 120°, they lost a molecule of water, yielding the corresponding hydrazone, except for III which decomposed.

2. TLC mobilities and UV spectra of these compounds were quite different from those of the relevant hydrazones, so they cannot be simply monohydrates of these substances. Furthermore, all of these compounds exhibited a strong characteristic band at 1040 cm^{-1} attributable to CO stretching, which disappeared after heating. In addition, the UV spectra of I–IV in ethanol corresponded to the sum of the spectra of the starting hydrazide and aldehydes. TLC on silica gel of these substances at very low concentrations showed that they are split, giving two spots corresponding to the starting reagents; the hydrazones, however, gave single spots. The very poor solubilities of these substances did not allow any NMR investigations of their structures.

Hydrazones V–VII—These hydrazones were prepared by heating the corresponding adducts for a few hours at 120°. The completion of the conversion was determined by TLC and by the disappearance of the strong characteristic band at ~1040 cm^{-1}; the yield was quantitative since no further recrystallization was required.

RESULTS AND DISCUSSION

Tests of the triazene derivatives against TLX5 lymphoma[2] in mice are reported in Table III. The activities observed for each compound were compared on the basis of the number of dose levels at which an ILS of ~50% was observed and by considering also the maximum ILS values obtained when >50%. The compounds carrying nitro groups as substit-

[1] Melting points were determined in open glass capillaries using a Büchi apparatus and are uncorrected. IR spectra were recorded on a Perkin-Elmer model 225 spectrophotometer, and UV spectra were determined on a Hitachi Perkin-Elmer model 124. Kieselgel HF 254 + 366 (Merck) and methanol–ethyl acetate–ligroin (3:2:1) were used for TLC.

[2] TLX5 lymphoma cells (10^5) were injected subcutaneously in the inguinal region of CBA/LAC female mice, 20–25 g, bred in the Chester Beatty Research Institute. The drugs were used as a solution freshly prepared by sonication in acetone–arachis oil (10:90 v/v); the treatment was performed by daily intraperitoneal administration from Day 3 to 7 after tumor inoculation. For each substance, 10 control mice and groups of five mice for each dose level were used. ILS is the percent increase of the mean survival time of each treated group to that of the relevant controls.

0022-3549/80/0100-0097$01.00/0

© 1980, American Pharmaceutical Association

Experiments utilizing this procedure in animals are in progress. Plasma flufenamic acid levels in two rats at various times after intravenous sublingual administration of 5 mg of I/kg in 0.2 *N* NaOH are shown in Table IV. Due to the high plasma I concentrations at the dose administered, only 50 μl of the plasma sample was taken for analysis. The assays described here may be used to measure therapeutic levels of I in patients.

REFERENCES

(1) J. B. Carey, *J. Clin. Invest.*, **40**, 1028 (1961).

(2) A. R. Rosenberg and T. R. Bates, *Proc. Soc. Exp. Biol. Med.*, **145**, 93 (1974).

(3) G. Deveaux, P. Mesnard, and A. M. Brisson, *Ann. Pharm. Fr.*, **27**, 239 (1969).

(4) A. J. Glazko, *Ann. Phys. Med. Suppl.*, **9**, 24 (1967).

(5) H. D. Dell and R. Kamp, *Arch. Pharm.*, **303**, 785 (1970).

(6) W. S. Schmollack and U. Wenzel, *Pharmazie*, **29**, 583 (1974).

(7) B. Demetriou and B. G. Osborne, *J. Chromatogr.*, **90**, 405 (1974).

(8) S. A. Bland, J. W. Blake, and R. S. Ray, *J. Chromatogr. Sci.*, **14**, 201 (1976).

ACKNOWLEDGMENTS

Presented at the APhA Academy of Pharmaceutical Sciences, Anaheim meeting, April 1979.

Supported in part by the Division of Sponsored Research, University of Florida.

The authors thank Ms. Judy Fuller for manuscript preparation.

Antitumor Activity of Hydrazones and Adducts between Aromatic Aldehydes and *p*-(3,3-Dimethyl-1-triazeno)benzoic Acid Hydrazide

TULLIO GIRALDI *, PHYLLIS M. GODDARD ‡, CARLO NISI §x, and FABIO SIGON §

Received May 3, 1978, from the **Istituto di Farmacologia, Università di Trieste, I 34100, Trieste, Italy, the* ‡*Chester Beatty Research Institute, Institute of Cancer Research, Royal Cancer Hospital, London SW3 6JB, England,* and the §*Istituto di Chimica Farmaceutica, Università di Trieste, I 34100, Trieste, Italy.* Accepted for publication June 1, 1979.

Abstract □ Hydrazones and adducts between aromatic aldehydes and *p*-(3,3-dimethyl-1-triazeno)benzoic acid hydrazide were synthesized and tested for antitumor activity. Two adducts derived from 2,6-dinitro- and 4-cyanobenzaldehyde were active against TLX5 lymphoma in mice. The hydrazone of the latter aldehyde was significantly more active than the adducts.

Keyphrases □ *Antineoplastic agents, potential*—hydrazones and adducts between aromatic aldehydes and *p*-(3,3-dimethyl-1-triazeno)-benzoic acid hydrazide, structure–activity relationships □ *p*-(3,3-Dimethyl-1-triazeno)benzoic acid hydrazide—antineoplastic activity, hydrazones and adducts with aromatic aldehydes, structure–activity relationships

A series of 1-aryl-3,3-dimethyltriazene derivatives, characterized by the presence of a carbonyl group and a triazene function in the *para*-position on the aromatic nucleus, was previously synthesized and examined for antitumor activity against TLX5 lymphoma in mice (1). Among these compounds, the *o*-nitrophenylhydrazone of the *p*-(3,3-dimethyl-1-triazeno)benzoic acid hydrazide and the adduct between this hydrazide and *p*-nitrobenzaldehyde showed considerable activity. Therefore, a further group of adducts and related hydrazones carrying electron-withdrawing substituents was synthesized and tested for their antitumor activity. Their structures and activities are reported in Tables I and II.

EXPERIMENTAL[1]

Adducts I–IV—Adducts I, II, and IV were prepared by the addition of a solution of the aldehyde in hot ethanol to an equimolar solution of *p*-(3,3-dimethyl-1-triazeno)benzoic acid hydrazide (2) in the same solvent. After standing for a few minutes, the products precipitated and were washed with a few milliliters of cold ethanol. Methanol was used as a solvent for preparing adduct III, and this reaction mixture was heated gently for 15 min before allowing the precipitation.

The structures assigned to I–IV are in accordance with their elemental analyses and are supported by the following data:

1. When these substances were heated to 120°, they lost a molecule of water, yielding the corresponding hydrazone, except for III which decomposed.

2. TLC mobilities and UV spectra of these compounds were quite different from those of the relevant hydrazones, so they cannot be simply monohydrates of these substances. Furthermore, all of these compounds exhibited a strong characteristic band at 1040 cm^{-1} attributable to CO stretching, which disappeared after heating. In addition, the UV spectra of I–IV in ethanol corresponded to the sum of the spectra of the starting hydrazide and aldehydes. TLC on silica gel of these substances at very low concentrations showed that they are split, giving two spots corresponding to the starting reagents; the hydrazones, however, gave single spots. The very poor solubilities of these substances did not allow any NMR investigations of their structures.

Hydrazones V–VII—These hydrazones were prepared by heating the corresponding adducts for a few hours at 120°. The completion of the conversion was determined by TLC and by the disappearance of the strong characteristic band at ~1040 cm^{-1}; the yield was quantitative since no further recrystallization was required.

RESULTS AND DISCUSSION

Tests of the triazene derivatives against TLX5 lymphoma[2] in mice are reported in Table III. The activities observed for each compound were compared on the basis of the number of dose levels at which an ILS of ~50% was observed and by considering also the maximum ILS values obtained when >50%. The compounds carrying nitro groups as substit-

[1] Melting points were determined in open glass capillaries using a Büchi apparatus and are uncorrected. IR spectra were recorded on a Perkin-Elmer model 225 spectrophotometer, and UV spectra were determined on a Hitachi Perkin-Elmer model 124. Kieselgel HF 254 + 366 (Merck) and methanol–ethyl acetate–ligroin (3:2:1) were used for TLC.

[2] TLX5 lymphoma cells (10^5) were injected subcutaneously in the inguinal region of CBA/LAC female mice, 20–25 g, bred in the Chester Beatty Research Institute. The drugs were used as a solution freshly prepared by sonication in acetone–arachis oil (10:90 v/v); the treatment was performed by daily intraperitoneal administration from Day 3 to 7 after tumor inoculation. For each substance, 10 control mice and groups of five mice for each dose level were used. ILS is the percent increase of the mean survival time of each treated group to that of the relevant controls.

0022-3549/80/0100-0097$01.00/0

© 1980, American Pharmaceutical Association

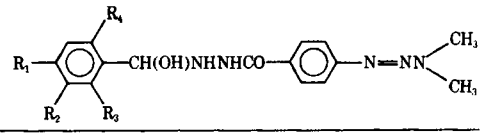

Table I—Physical Constants of the Adducts

Compound	R_1	R_2	R_3	R_4	Melting Point	Yield, %	Formula	Analysis, %	Calc.	Found
I	H	NO_2	H	H	210° dec.	31	$C_{16}H_{18}N_6O_4$	C	53.62	53.58
								H	5.06	5.08
								N	23.45	23.50
II	NO_2	H	NO_2	H	238° dec.	76	$C_{16}H_{17}N_7O_6$	C	47.64	47.55
								H	4.25	4.20
								N	24.31	24.38
III	H	H	NO_2	NO_2	116–118° dec.	59	$C_{16}H_{17}N_7O_6$	C	47.64	47.50
								H	4.25	4.12
								N	24.31	24.17
IV	CN	H	H	H	254–256° dec.	61	$C_{17}H_{18}N_6O_2$	C	60.34	60.40
								H	5.36	5.40
								N	24.84	24.90

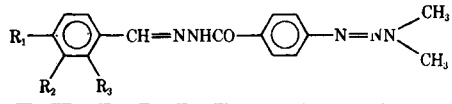

Table II—Physical Constants of the Hydrazones

Compound	R_1	R_2	R_3	Melting Point	Yield, %	Formula	Analysis, %	Calc.	Found
V	H	NO_2	H	210° dec.	100	$C_{16}H_{16}N_6O_3$	C	56.46	56.40
							H	4.74	4.80
							N	24.69	24.71
VI	NO_2	H	NO_2	243° dec.	100	$C_{16}H_{15}N_7O_5$	C	49.87	49.93
							H	3.92	3.95
							N	25.44	25.25
VII	CN	H	H	254–256° dec.	100	$C_{17}H_{16}N_6O$	C	63.74	63.80
							H	5.03	5.03
							N	26.23	26.21

Table III—Antitumor Activity of Compounds III, IV, and VII against TLX5 Lymphoma in Mice

Compound	Dose, mg/kg/day	Average Day of Death ± *SE*	ILS, %
III	—	10.1 ± 0.1	—
	12.5	14.0 ± 0.8	38.6
	25	16.6 ± 0.8	64.3
	50	16.2 ± 0.6	60.8
	100	16.0 ± 0.5	58.4
	200	4.0 ± 0.0	−60.4
IV	—	9.9 ± 0.2	—
	25	11.4 ± 0.2	15.1
	50	14.4 ± 0.5	45.4
	100	15.0 ± 0.3	51.5
	200	15.4 ± 0.7	55.5
	400	7.0 ± 0.9	−29.3
VII	—	10.2 ± 0.2	—
	12.5	11.0 ± 0.3	7.8
	25	16.2 ± 1.6	58.8
	50	19.8 ± 0.4	94.1
	100	20.2 ± 1.7	98.0
	200	17.6 ± 0.8	72.5
	400	17.4 ± 0.2	70.5

uents (I, II, V, and VI) were inactive over a dosage range that included maximum tolerated doses, with the exception of III which was effective at three dose levels. The adduct of *p*-cyanobenzaldehyde (IV) also was active at three dose levels, whereas the corresponding hydrazone (VII) was effective at the five highest dosages employed. An analysis of variance (3) indicated that the ILS values obtained for this compound at 50 and 100 mg/kg/day were significantly higher than those observed for the other compounds tested ($F = 17.2$, $p < 0.0002$).

These results, together with those already reported for a related series of compounds (1), indicate a marked antileukemic activity for derivatives characterized by single electron-withdrawing substituents in either the *ortho*- or *para*-position. High activity does not appear to be peculiar for hydrazones or adducts. In this series, the hydrazone derived from *p*-cyanobenzaldehyde (VII) was significantly more active than the corresponding adduct (IV). For the previously examined *p*-nitro-substituted derivatives, the hydrazone proved completely inactive and the adduct showed remarkable activity. The effects of these compounds on other experimental tumors is being examined.

REFERENCES

(1) T. Giraldi, C. Nisi, T. A. Connors, and P. M. Goddard, *J. Med. Chem.*, **20**, 850 (1977).

(2) Y. F. Shealy, C. A. O'Dell, and C. A. Krauth, *J. Pharm. Sci.*, **60**, 1426 (1971).

(3) G. W. Snedecor and W. G. Cochran, "Statistical Methods," 6th ed., Iowa State University Press, Ames, Iowa, 1967, pp. 258–298.

ACKNOWLEDGMENTS

Supported by Grants CT 77.01370.04 and CT 76.01049.03 from the Consiglio Nazionale delle Ricerche, Italy, and by Grant N-Ct 973/787/K to the Chester Beatty Research Institute from the Medical Research Council.

Electron-Capture GLC Determination of Bromhexine in Human Plasma

A. P. De LEENHEER ˣ **and L. M. R. VANDECASTEELE-THIENPONT**

Received March 26, 1979, from the *Laboratoria voor Medische Biochemie en voor Klinische Analyse, Faculteit van de Farmaceutische Wetenschappen, Rijksuniversiteit, Academisch Ziekenhuis, 135 De Pintelaan, 9000-Gent, Belgium.* Accepted for publication July 12, 1979.

Abstract □ A specific and sensitive GLC analysis of bromhexine in human plasma is described. After addition of the internal standard and an aqueous triethanolamine solution, bromhexine is extracted at alkaline pH into *n*-hexane, transferred to an acidic aqueous solution, and back-extracted into *n*-hexane after alkalinization. Both compounds are derivatized with trifluoroacetic anhydride and quantified by GLC using a ^{63}Ni-electron-capture detector. The method has a sensitivity of ~1.0 ng/ml of plasma. Linearity of plasma working curves was good. The extraction recovery from spiked plasma was 90.1 ± 5.68% (*SD*). The within-run and within-day precisions (*CV*) were 6.0% (4.3 ng/ml, $n = 8$) and 8.6% (11.0 ng/ml, $n = 13$), respectively. The procedure was applied successfully to measurement of the plasma concentration–time profile in a human volunteer after oral drug administration.

Keyphrases □ Bromhexine—electron-capture GLC analysis, human plasma □ GLC—bromhexine, electron-capture detection, human plasma □ Mucolytic agents—bromhexine, electron-capture GLC analysis, human plasma

Bromhexine hydrochloride[1] [*N*-cyclohexyl-*N*-methyl-2-(2-amino-3,5-dibromo)benzylammonium chloride] (I) is used as a mucolytic agent (1, 2). The low drug dosage (3) sufficient for pharmacological effectiveness and its extensive metabolism (4, 5) result in low levels in circulating blood (nanograms per milliliter) (6, 7). Thus, to follow the rapidly declining levels of the unchanged drug, highly sensitive and specific methodology is required.

Studies on the absorption, metabolism, and excretion of ^{14}C-labeled I were performed by liquid scintillation spectrometry after extraction of the plasma and urine samples and TLC separation of the drug and metabolites (6–8). Eichler and Kreuger (9) described an electron-capture GLC assay for the quantitation of I residues in the milk and tissues of treated animals. A previous paper[2] described a new GLC assay for the determination of standard I solutions at the nanogram level. The chromatographic properties and electron-capture sensitivity of the trifluoroacetyl derivatives of I and a synthesized, structurally analogous internal standard, *N*-cyclohexyl-*N*-*n*- propyl-2-(2-amino-3,5-dibromo)benzylammonium chloride (II) were investigated.

The present report describes a GLC assay with electron-capture detection for the determination of plasma bromhexine in the low nanogram range.

EXPERIMENTAL

Reagents and Materials—The hydrochloride of I[3] was used as received, and II was synthesized as described (10). Pesticide grade *n*-hexane[4] and methanol[5], fluorometric grade ethyl acetate[6], and trifluoroacetic anhydride[7], obtained in 1-ml sealed glass ampuls, were used as supplied.

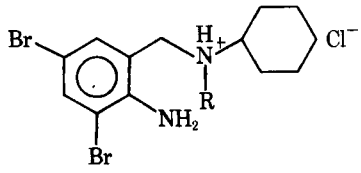

I: R = CH_3
II: R = $CH_2CH_2CH_3$

Aqueous 5 *N* NaOH[6], 2 *N* HCl[6], and 1 *N* triethanolamine[6] solutions were prepared with freshly double-distilled water.

Apparatus—GLC was conducted on a gas chromatograph[8] equipped with a 15-mCi ^{63}Ni-electron-capture detector[9] (pulsed, variable-frequency type). The stationary liquid phase, 4% SE-30[10], was coated on 100–120-mesh Gas Chrom Q[11] and packed into a 2.2-m × 2-mm i.d. spiral silanized glass column. The temperatures were: oven, 255°; injection port, 280°; and detector, 330°. Argon–methane (95:5) was the carrier and purge gas at a total flow rate of 28 ml/min.

Extraction—Plasma, 1.0 ml, was placed in a 20-ml polytef screw-capped test tube. The following were added by pipet: 80 μl of internal standard solution (1.2 ng of II/μl in methanol), methanol to a total volume of 200 μl/ml of plasma, 2 ml of 1.0 *N* aqueous triethanolamine, and 0.1 ml of 5.0 *N* NaOH. The solution was mixed well. *n*-Hexane, 15 ml, was added, and the tube contents were mixed on a rotary mixer[12] for 20 min. After centrifugation, the *n*-hexane was transferred to a tube containing 2 ml of 2.0 *N* HCl. The tube was shaken for 20 min, and the *n*-hexane was discarded after separation of the two layers. The extraction was repeated with 10 ml of *n*-hexane.

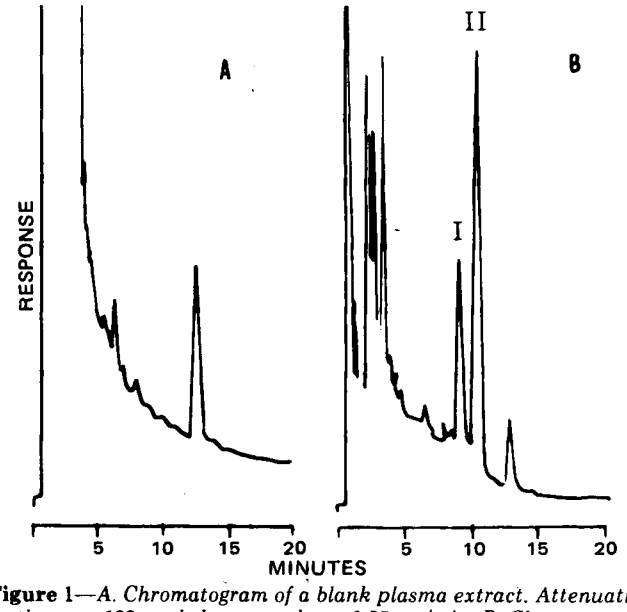

Figure 1—*A. Chromatogram of a blank plasma extract. Attenuation setting was 128, and chart speed was 0.25 cm/min. B. Chromatogram of a plasma extract 90 min after oral administration of 4 mg of bromhexine hydrochloride, representing a level of 3.9 ng of I/ml. Attenuation setting was 256.*

[1] Bisolvon.
[2] To be published.
[3] Supplied by Boehringer, Ingelheim, West Germany.
[4] Carlo Erba, Milan, Italy.
[5] Riedel-de Haën A.G., Seelze-Hannover, West Germany.
[6] E. Merck A.G., Darmstadt, West Germany.
[7] Pierce Eurochemie B.V., Rockford, Ill.
[8] Model 5830 A, Hewlett-Packard, Avondale, Pa.
[9] Model 18803 B, Hewlett-Packard, Avondale, Pa.
[10] R. S. L., St. Martens-Latem, Belgium.
[11] Supelco Inc., Bellefonte, Pa.
[12] Cenco Instrumenten B.V., Breda, The Netherlands.

0022-3549/80/0100-0099$01.00/0
© 1980, American Pharmaceutical Association

Table I—Recovery of I in Human Plasma by Electron-Capture GLC Analysis (n = 3)

I Added to 1.0 ml of Plasma, mg	Mean I Amount Recovered after Extraction, ng	Mean Recovery ± *SD*, %
6.6	6.5	98.5 ± 3.02
13.3	11.6	87.5 ± 8.90
26.6	23.4	88.0 ± 1.84
53.1	45.9	86.3 ± 4.75
Mean		90.1 ± 5.68

The acid solution was made basic with 1.5 ml of 5 *N* NaOH and was extracted twice with 5 ml of *n*-hexane during 20 min. After centrifugation, the organic layer was evaporated in a 3-ml glass-stoppered conical vial in a heating block[13] at 45° under a nitrogen stream. The residue was redissolved in ~100 μl of ethyl acetate. A slight excess of trifluoroacetic anhydride was added and mixed. After 5 min, excess trifluoroacetic anhydride was removed at 45° under nitrogen. The residue was dissolved in 100 μl of methanol, and ~2 μl was injected with a 10-μl syringe[14] onto the GLC column.

Linearity—Linearity was tested from 1.6 to 12.7 ng/ml and from 7.0 to 115.8 ng/ml. Solutions of I in methanol were added to plasma to give 1.6, 3.2, 6.4, and 12.7 ng/ml and 7.0, 11.6, 23.2, 46.3, 69.5, 92.7, and 115.8 ng/ml. An adjusted constant amount of II was added. The samples were extracted as described and analyzed by GLC. Peak height ratios of I to II were plotted *versus* the concentration ratio of I to II.

Recovery—Known I amounts were added to 1.0 ml of drug-free plasma to give drug concentrations as detailed in Table I. The internal standard was added after the extraction just before derivatization. Percentage recoveries were calculated from a standard curve of the same amounts of I and II derivatized without extraction.

RESULTS AND DISCUSSION

Figures 1A and 1B show representative chromatograms of drug-free plasma and an extract after a single 4-mg oral dose, respectively. Back-extraction from an organic solvent into an acidic aqueous solution was essential for sample cleanup prior to electron-capture GLC. Based on its retention on the 4% SE-30 stationary phase, the extraneous peak at a retention time of 12.6 min was supposed to represent dioctyl phthalate, used as a plasticizer. The component also was present after extraction

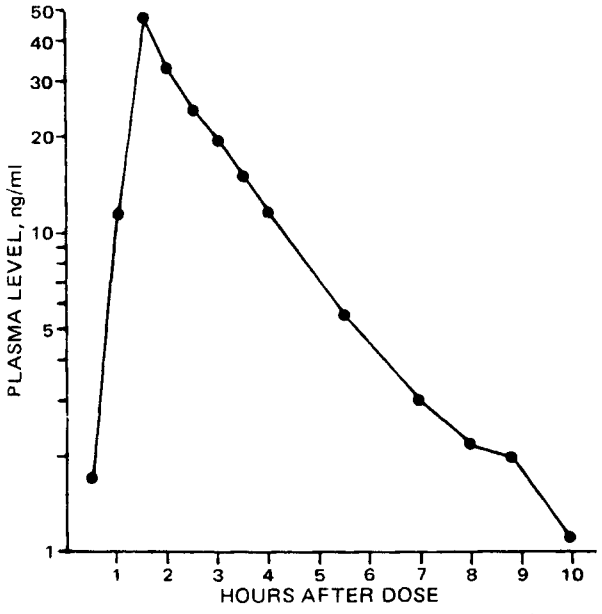

Figure 2—*Mean plasma bromhexine levels in a human volunteer following oral administration.*

[13] Dri-Bath, Thermolyne, Dubuque, Iowa.
[14] Hamilton 701, Bonaduz, Switzerland.

Table II—Assay Precision

Within-Day Precision, ng/ml		Day-to-Day Precision	
		Day	ng/ml
	4.3	1	10.2
	4.3	2	11.6
	4.4	3	10.3
	4.4	4	11.5
	4.1	5	11.9
	4.1	6	10.1
	4.2	7	11.2
	4.9	8	10.7
		9	11.0
Mean	4.3	10	10.1
SD	0.26	11	13.0
CV, %	6.0	12	12.0
		13	9.8
		Mean	11.0
		SD	0.95
		CV, %	8.6

of an aqueous solution. Therefore, it was not an endogenous compound. This peak can be eliminated by solvent distillation and storage in glass equipment.

Compound II was synthesized and chosen as the internal standard for GLC experiments[2] on the basis of its structural similarity to I. However, the extraction characteristics from plasma of I and II were different. In contrast, the extraction recovery from water was the same for I and II. Plasma extracts alkalinized only with sodium hydroxide without the triethanolamine solution afforded a relative recovery for II of only 32.1 ± 2.70% (*SD*); after the addition of the triethanolamine solution, the recovery increased to 81.3 ± 6.51% (*SD*). A plot of the response ratios of I to II *versus* the plasma concentration ratio of I to II in the 1.6–12.7- and 7.0–115.8-ng/ml ranges demonstrated a linear relationship (regression lines: $y = 2.5x + 0.04$, $r = 0.9997$, and $y = 2.3x + 0.01$, $r = 0.9996$, respectively).

A detection limit of ~1.0 ng of I/ml was obtained using 1.0 ml of plasma for the analysis.

The within-run precision of the overall procedure (*CV*) of 6.0% was obtained on analyzing eight samples of pooled plasma having a mean value of 4.3 ± 0.26 (*SD*) ng/ml. The day-to-day precision (*CV*) over 8 weeks was 8.6% at a mean concentration of 11.0 ± 0.95 (*SD*) ng/ml. For this study, plasma samples were stored at −20°. These data are presented in Table II. The I recovery studies in the 6.6–53.1-ng/ml range showed a mean of 90.1 ± 5.68% (*SD*) (Table I).

The utility of the technique developed for the determination of I was demonstrated in the establishment of plasma levels in a volunteer after oral administration of 24 mg of I as tablets. Two standard curves were constructed by adding quantities of I to plasma samples in the range of the expected levels, as mentioned under the linearity experiments. A typical time course for the I concentration is shown in Fig. 2. For an exact estimate of the pharmacokinetics of the drug after oral administration in humans, the levels below 3 ng/ml are of limited value since they are too close to the detection limit.

REFERENCES

(1) R. Engelhorn and S. Püschmann, *Arzneim.-Forsch.*, **13**, 474 (1963).

(2) E. M. Boyd and P. Sheppard, *Arch. Int. Pharmacodyn. Ther.*, **163**, 284 (1966).

(3) F. Arch, *Arzneim.-Forsch.*, **13**, 480 (1963).

(4) E. Schraven, F. W. Koss, J. Keck, and G. Beisenherz, *Eur. J. Pharmacol.*, **1**, 445 (1967).

(5) Z. Kopitar, R. Jauch, R. Hankwitz, and H. Pelzer, *ibid.*, **21**, 6 (1973).

(6) R. Jauch and R. Hankwitz, *Arzneim.-Forsch.*, **25**, 1954 (1975).

(7) H. D. Renovanz, *Wien. Med. Wochenschr., Suppl.*, **7**, 1 (1973).

(8) H. T. Nilsson, C. G. A. Persson, and K. Tegner, *Acta Pharm. Suec.*, **13**, 241 (1976).

(9) D. Eichler and H. Kreuzer, *Arzneim.-Forsch.*, **25**, 615 (1975).

(10) J. Keck, *Justus Liebigs Ann. Chem.*, **662**, 171 (1963).

ACKNOWLEDGMENTS

Supported by the I.W.O.N.L. through a bursary to one author.

Quantitative Determination of Titanium in a Commercial Sunscreen Formulation by Atomic Absorption Spectrometry

JAMES T. MASON, Jr.

Received May 7, 1979, from *Texas Pharmacal Company, San Antonio, TX 78296.* Accepted for publication June 29, 1979.

Abstract □ An atomic absorption spectrophotometric method was developed for the determination of titanium in a sunscreen formulation containing iron oxides and a complex organic base. Matrix matching between the samples and the standard was essential. A recovery study was conducted using a placebo base. Standard absorbance–concentration curves were linear in the 0–120-ppm range.

Keyphrases □ Titanium—analysis, atomic absorption spectrometry, sunscreens □ Atomic absorption spectrometry—analysis, titanium in sunscreens □ Sunscreens—titanium, analysis, atomic absorption spectrometry

Titanium dioxide is an effective sunscreen (1) for the prevention of sunburn and suntan. It reflects and scatters UV and visible light rays, providing a protective physical barrier against the damaging effects of the sun. The increasing use of sunscreens, along with the stringent and changing regulations on their use, makes a simple method for quantitating titanium dioxide desirable.

The commercial formulation[1] examined was a viscous, oil-in-water cream tinted with synthetic iron oxides. The analysis of titanium dioxide in the presence of iron oxides and a complex organic base requires either an intricate separation or a highly specific method to obtain significant results. Atomic absorption spectrometry promises a simple and specific analytical technique for pharmaceutical analyses. This technique offers an accurate and precise alternative to the titrimetric (2) and colorimetric (3) methods used to analyze titanium compounds. No atomic absorption spectrophotometric method was reported previously for the determination of titanium in pharmaceuticals.

EXPERIMENTAL

Equipment—The atomic absorption spectrophotometer[2] was equipped with a heavy solids, nitrous oxide burner head and a single-element titanium hollow cathode lamp[3]. The instrument settings were: wavelength, 364.3 nm; spectral band width, 0.3 nm; lamp current, 10 mamp; nitrous oxide flow, 10 SCFH; and acetylene flow, 9 SCFH.

Reagents—All reagents were ACS or USP grade. Purified water, USP grade, was used to make the solutions and to rinse the glassware.

Titanium Stock Solution—A standard stock solution containing 1000 ppm of titanium was prepared by heating vigorously 1.6681 g of titanium dioxide[4] with 40 g of ammonium sulfate and 200 ml of concentrated sulfuric acid until dissolution was complete. The solution was transferred to a 1000-ml volumetric flask and diluted to volume with purified water.

Iron Stock Solution—A stock solution containing 1000 ppm of iron was prepared by dissolving 0.50 g of iron wire in 20 ml of dilute nitric acid (1:1) and diluting to 500.0 ml with purified water.

Titanium Standards—The titanium stock solution was diluted to 80.0, 100.0, and 120.0 ppm. All standards were made to contain 0.8% (w/v) ammonium sulfate and 16 ppm of iron by the addition of appropriate quantities of ammonium sulfate and the iron stock solution.

[1] A-Fil Cream, Dark, Texas Pharmacal Co., San Antonio, Tex.
[2] Model 651, Instrumentation Laboratory.
[3] Intensitron, Perkin-Elmer.
[4] Pure Atlas White (99.6% pure), H. Kohnstamm and Co.

Table I—Absorbance Data for Standard Titanium Solutions

Solution	Titanium, ppm	Absorbance Trial 1	Trial 2	Trial 3
1	0	0.000	0.000	0.000
2	80	0.175	0.172	0.154
3	100	0.211	0.201	0.182
4	120	0.253	0.237	0.221
Correlation coefficient		0.9996	0.9980	0.9993

Table II—Titanium Dioxide Recovery from Placebo

Sample	Titanium Dioxide, mg Theoretical	Experimental	Recovery, %
1	47.5	48.0	101.0
2	39.6	39.5	99.7
3	49.0	47.9	97.8
4	34.7	35.6	102.6
5	43.3	42.2	97.5
6	37.3	37.3	100.0
Mean			99.8
RSD			1.9

Placebo—A placebo was prepared utilizing the ingredients and the manufacturing procedure prescribed for the commercial product but omitting the titanium dioxide.

Sample Preparation—Known titanium dioxide quantities, 35–50 mg, were weighed into separate 250-ml erlenmeyer flasks. Approximately 800 mg of placebo was added to each flask to approximate the commercial product at various strengths. After the addition of 7 ml of concentrated sulfuric acid and 2.0 g of ammonium sulfate, each flask was subjected to wet oxidation (4) to destroy the organic matter.

Each sample was digested on a hot plate in a fume hood until charring began. After the sample was decomposed initially by the acid, 30% hydrogen peroxide was added, dropwise, until all organic matter was destroyed and the solution was not more than slightly brown[5]. Fifty milliliters of water was added, and the solution was filtered through filter paper[6] into a 250-ml volumetric flask and brought to volume with purified water.

Procedure—The instrument was allowed to warm up for a minimum of 1 hr or until a stable absorbance reading was obtained using the 100-ppm standard. The nebulizer flow, lamp position, fuel flow, and burner head position were adjusted for maximum absorption. The absorbances of the sample and standard solutions were determined alternately, using the 10 read-average mode and 1-sec integration time, to verify conformance with the standard curve.

Each solution was aspirated at least three times, and the absorbance values were averaged. The two-variable linear regression of the absorbance–concentration curve through zero was determined for the standards using a statistical calculator[7]. The calibration curve was redetermined for each sample run.

RESULTS AND DISCUSSION

Table I contains the absorbance data obtained for three typical standard curves; the relationship of titanium to absorbance was linear in the 0–120-ppm range. This linearity permits the use of these data in determining the titanium in unknown samples, provided the instrument conditions remain unchanged.

Table II contains the titanium dioxide recovery data obtained from

[5] The solution was orange until all hydrogen peroxide was removed.
[6] Whatman No. 1.
[7] Monroe 1860.

0022-3549/80/0100-0101$01.00/0
© 1980, American Pharmaceutical Association

Table III—Iron Interference on 100 ppm of Titanium

Iron, ppm	Absorbance Increase, %
25	2
50	4
100	7
300	11
500	13
1000	13
3000	26

samples of placebo-prepared sunscreen product. In all samples, the placebo weight was the same.

Iron in the presence of sulfuric acid concentrations below 1 *N* was reported to depress titanium absorption (5). Iron at 2000 ppm in the presence of 2% HF enhanced titanium absorption, while iron at 200 ppm had no detectable effect (6). A third study indicated no interference on the absorbance of a 100-ppm titanium sample by 50 ppm of iron but a depression of absorbance by iron above 200 ppm (7). Attempts to determine the degree of interference caused by the presence of iron yielded the results in Table III. The iron amount present in the final dilutions varied from 11 to 22 ppm, depending on the shade[8] of the sunscreen. Iron, 16 ppm, was added to the standards to approximate the quantity in the samples to match the matrix and to minimize enhancement.

[8] Neutral and dark shades; iron levels were determined by the atomic absorption spectrophotometric method.

Examination of the effects on titanium absorption caused by a difference in the ammonium sulfate or sulfuric acid levels between the standards and the samples showed that a twofold increase in sulfuric acid produced a 2% enhancement of absorbance while a twofold increase in ammonium sulfate produced a 3% enhancement.

The fuel to oxidizer ratio was verified to be critical (5); when the flow rate of one gas varied slightly, the flame condition and the titanium absorption value changed significantly.

The described atomic absorption spectrophotometric method for the determination of titanium is simple, reliable, and accurate. The procedure, including standard preparation, can be performed in ~3 hr.

REFERENCES

(1) T. M. Macleod and W. Frain-Bell, *Br. J. Dermatol.*, **84**, 266 (1971).

(2) J. M. Thompson, *Anal. Chem.*, **24**, 1632 (1952).

(3) W. W. Scott, "Standard Methods of Chemical Analysis," vol. I, 5th ed., D. Van Nostrand, Princeton, N.J., 1939, p. 987.

(4) T. T. Gorouch, "The Destruction of Organic Matter," Pergamon, Elmsford, N.Y., 1970, pp. 19–27.

(5) J. A. Bowman and J. B. Willis, *Anal. Chem.*, **39**, 1210 (1967).

(6) M. D. Amos and J. B. Willis, *Spectrochim. Acta*, **22**, 1325 (1966).

(7) J. Y. Marks and G. G. Welcher, *Anal. Chem.*, **42**, 1033 (1970).

ACKNOWLEDGMENTS

The author thanks E. L. Anderson for valuable discussions.

Surface Activities of Barbital, Phenobarbital, and Pentobarbital and Their Interaction Energies with Phospholipid Monolayers

FEDERICO A. VILALLONGA ˣ and E. W. PHILLIPS

Received December 18, 1978, from the *College of Pharmacy, University of Florida, Gainesville, FL 32610.* Accepted for publication July 3, 1979.

Abstract □ The adsorption free energies of barbital, phenobarbital, and pentobarbital at the air–water interface were estimated from plots of the surface pressure ($\pi \leq 5$ dynes/cm) against the bulk concentration. Their energies of interaction with dipalmitoylphosphatidylethanolamine and dipalmitoyllecithin monolayers spread at the air–water interface were estimated from the surface pressure increase with increasing concentrations of the subphase-injected barbituric acid derivatives. Adsorption free energies and interaction energies were barbital < phenobarbital < pentobarbital, which correlate with their nerve blocking concentration.

Keyphrases □ Barbiturates—adsorption free energy, phospholipid monolayers, barbital, phenobarbital, pentobarbital □ Free energy—adsorption, barbital, phenobarbital, pentobarbital, phospholipid monolayers □ Phospholipid monolayers—adsorption free energy, barbital, phenobarbital, pentobarbital □ Surface activity—barbital, phenobarbital, pentobarbital, interaction with phospholipid monolayers

The interaction energies of procaine, lidocaine, and tetracaine with phospholipid monolayers were correlated recently with their anesthetic and nerve conduction blocking potencies (1).

The present work concerned the surface activities of barbital, phenobarbital, and pentobarbital at the air–water interface and their interaction energies with dipalmitoylphosphatidylethanolamine and dipalmitoyllecithin monolayers spread at the air–water interface.

EXPERIMENTAL

Reagents—Sodium salts of barbital[1], phenobarbital[1], and pentobarbital[1] were used without further purification. Dipalmitoyllecithin[2], dipalmitoylphosphatidylethanolamine[3], the hexane[4] used to prepare the phospholipid spreading solutions, and the water used to prepare the solutions fulfilled the requirements previously specified (2, 3). Analytical reagent grade sodium chloride[1] was roasted for 6 hr at 700° prior to preparation of the aqueous solutions to remove surface-active impurities.

Instruments and Methods—The instruments and methods for the measurement of the surface tension of aqueous solutions (γ) and of the surface pressure change ($\Delta\pi$) of the phospholipid monolayer after drug injection in the subphase already were described (2, 3). The experiments reported here were performed in 0.15 *M* NaCl at 20 ± 1°. In the injection experiments, the initial surface pressure of the phospholipid monolayer was 5 dynes/cm (±0.1 dyne/cm). Surface pressures (π) of the 0.15 *M* NaCl drug solutions were fitted to a function of the logarithm of the drug concentration, *C*, by digital-computerized, nonlinear regression (1, 4). Drug solution densities were determined using 10-ml specific gravity bottles.

RESULTS

Adsorption at Air–Aqueous Interface—Typical plots of the surface pressure (π) against the logarithm of the concentration (*C*, moles per liter)

[1] Mallinckrodt Chemical Works, St. Louis, Mo.
[2] Applied Science Laboratories, State College, Pa.
[3] Schwarz-Mann Research Laboratories, Orangeburg, N.Y.
[4] J. T. Baker Chemical Co., Phillipsburg, N.J.

0022-3549/80/0100-0102$01.00/0

© 1980, American Pharmaceutical Association

Table III—Iron Interference on 100 ppm of Titanium

Iron, ppm	Absorbance Increase, %
25	2
50	4
100	7
300	11
500	13
1000	13
3000	26

samples of placebo-prepared sunscreen product. In all samples, the placebo weight was the same.

Iron in the presence of sulfuric acid concentrations below 1 *N* was reported to depress titanium absorption (5). Iron at 2000 ppm in the presence of 2% HF enhanced titanium absorption, while iron at 200 ppm had no detectable effect (6). A third study indicated no interference on the absorbance of a 100-ppm titanium sample by 50 ppm of iron but a depression of absorbance by iron above 200 ppm (7). Attempts to determine the degree of interference caused by the presence of iron yielded the results in Table III. The iron amount present in the final dilutions varied from 11 to 22 ppm, depending on the shade[8] of the sunscreen. Iron, 16 ppm, was added to the standards to approximate the quantity in the samples to match the matrix and to minimize enhancement.

[8] Neutral and dark shades; iron levels were determined by the atomic absorption spectrophotometric method.

Examination of the effects on titanium absorption caused by a difference in the ammonium sulfate or sulfuric acid levels between the standards and the samples showed that a twofold increase in sulfuric acid produced a 2% enhancement of absorbance while a twofold increase in ammonium sulfate produced a 3% enhancement.

The fuel to oxidizer ratio was verified to be critical (5); when the flow rate of one gas varied slightly, the flame condition and the titanium absorption value changed significantly.

The described atomic absorption spectrophotometric method for the determination of titanium is simple, reliable, and accurate. The procedure, including standard preparation, can be performed in ~3 hr.

REFERENCES

(1) T. M. Macleod and W. Frain-Bell, *Br. J. Dermatol.*, **84**, 266 (1971).

(2) J. M. Thompson, *Anal. Chem.*, **24**, 1632 (1952).

(3) W. W. Scott, "Standard Methods of Chemical Analysis," vol. I, 5th ed., D. Van Nostrand, Princeton, N.J., 1939, p. 987.

(4) T. T. Gorouch, "The Destruction of Organic Matter," Pergamon, Elmsford, N.Y., 1970, pp. 19–27.

(5) J. A. Bowman and J. B. Willis, *Anal. Chem.*, **39**, 1210 (1967).

(6) M. D. Amos and J. B. Willis, *Spectrochim. Acta*, **22**, 1325 (1966).

(7) J. Y. Marks and G. G. Welcher, *Anal. Chem.*, **42**, 1033 (1970).

ACKNOWLEDGMENTS

The author thanks E. L. Anderson for valuable discussions.

Surface Activities of Barbital, Phenobarbital, and Pentobarbital and Their Interaction Energies with Phospholipid Monolayers

FEDERICO A. VILALLONGA ˣ and E. W. PHILLIPS

Received December 18, 1978, from the *College of Pharmacy, University of Florida, Gainesville, FL 32610.* Accepted for publication July 3, 1979.

Abstract □ The adsorption free energies of barbital, phenobarbital, and pentobarbital at the air–water interface were estimated from plots of the surface pressure ($\pi \leq 5$ dynes/cm) against the bulk concentration. Their energies of interaction with dipalmitoylphosphatidylethanolamine and dipalmitoyllecithin monolayers spread at the air–water interface were estimated from the surface pressure increase with increasing concentrations of the subphase-injected barbituric acid derivatives. Adsorption free energies and interaction energies were barbital < phenobarbital < pentobarbital, which correlate with their nerve blocking concentration.

Keyphrases □ Barbiturates—adsorption free energy, phospholipid monolayers, barbital, phenobarbital, pentobarbital □ Free energy—adsorption, barbital, phenobarbital, pentobarbital, phospholipid monolayers □ Phospholipid monolayers—adsorption free energy, barbital, phenobarbital, pentobarbital □ Surface activity—barbital, phenobarbital, pentobarbital, interaction with phospholipid monolayers

The interaction energies of procaine, lidocaine, and tetracaine with phospholipid monolayers were correlated recently with their anesthetic and nerve conduction blocking potencies (1).

The present work concerned the surface activities of barbital, phenobarbital, and pentobarbital at the air–water interface and their interaction energies with dipalmitoylphosphatidylethanolamine and dipalmitoyllecithin monolayers spread at the air–water interface.

EXPERIMENTAL

Reagents—Sodium salts of barbital[1], phenobarbital[1], and pentobarbital[1] were used without further purification. Dipalmitoyllecithin[2], dipalmitoylphosphatidylethanolamine[3], the hexane[4] used to prepare the phospholipid spreading solutions, and the water used to prepare the solutions fulfilled the requirements previously specified (2, 3). Analytical reagent grade sodium chloride[1] was roasted for 6 hr at 700° prior to preparation of the aqueous solutions to remove surface-active impurities.

Instruments and Methods—The instruments and methods for the measurement of the surface tension of aqueous solutions (γ) and of the surface pressure change ($\Delta\pi$) of the phospholipid monolayer after drug injection in the subphase already were described (2, 3). The experiments reported here were performed in 0.15 *M* NaCl at 20 ± 1°. In the injection experiments, the initial surface pressure of the phospholipid monolayer was 5 dynes/cm (±0.1 dyne/cm). Surface pressures (π) of the 0.15 *M* NaCl drug solutions were fitted to a function of the logarithm of the drug concentration, *C*, by digital-computerized, nonlinear regression (1, 4). Drug solution densities were determined using 10-ml specific gravity bottles.

RESULTS

Adsorption at Air–Aqueous Interface—Typical plots of the surface pressure (π) against the logarithm of the concentration (*C*, moles per liter)

[1] Mallinckrodt Chemical Works, St. Louis, Mo.
[2] Applied Science Laboratories, State College, Pa.
[3] Schwarz-Mann Research Laboratories, Orangeburg, N.Y.
[4] J. T. Baker Chemical Co., Phillipsburg, N.J.

0022-3549/80/0100-0102$01.00/0

© 1980, American Pharmaceutical Association

Table I—Adsorption Free Energies at the Air–Water Interface (ΔG_{ad}), Interaction Energies with Phospholipid Monolayers (Ψ), and Free Energies of Transfer (ΔG_{tr}) to Erythrocyte Membranes and to Octanol of Barbital, Phenobarbital, and Pentobarbital

Barbiturate	Air–0.15 *M* NaCl, ΔG_{ad}, kcal/mole	Dipalmitoyllecithin–0.15 *M* NaCl, Ψ, kcal/mole	Dipalmitoylphosphatidylethanolamine–0.15 *M* NaCl, Ψ, kcal/mole	Erythrocyte[a] Membrane–Buffer Solution, ΔG_{tr}, kcal/mole	Octanol[b]–Water, ΔG_{tr}, kcal/mole	Nerve Blocking[c] Concentration (Frog, Sciatic), mole/liter
Barbital	−4.0	−3.2	−4.0	+0.2	+0.2	28×10^{-3}
Phenobarbital	−4.6	−4.2	−5.2	−1.1	−0.2	5.7×10^{-3}
Pentobarbital	−6.4	−6.0	−5.7	−1.3	−0.4	1.7×10^{-3}

[a] Calculated from Ref. 10. [b] Calculated from Ref. 9. [c] From Ref. 10.

for barbital, phenobarbital, and pentobarbital in 0.15 *M* NaCl are given in Fig. 1.

The adsorption free energy at the air–aqueous solution interface can be estimated from (1, 4, 5):

$$\Delta G = -RT \ln \frac{\pi}{X_2^*} \qquad \text{(Eq. 1)}$$

where ΔG is the standard free energy change associated with solute adsorption at the air–water interface, π is the surface pressure, X_2^* is the solute activity, R is the universal gas constant, and T is the absolute temperature.

The ΔG value can be calculated from the slope (π/X_2^*) of a linear plot of the surface pressure (π) against the solute mole fraction (X_2) in the bulk solution when $X_2 \rightarrow 0$ and $X_2 \rightarrow X_2^*$ at low mole fractions. Plots of the surface pressure (π) against the mole fraction (X_2) for barbital, phenobarbital, and pentobarbital were linear in the region $\pi \leq 5$ dynes/cm (regression coefficients of 0.9988, 0.9918, and 0.9975, respectively). The estimated ΔG values from such plots are given in Table I and were barbital < phenobarbital < pentobarbital.

Interaction with Phospholipid Monolayers—The interaction of the subphase-injected drugs with dipalmitoylphosphatidylethanolamine and dipalmitoyllecithin was virtually completed in the first 15–25 min. The equilibrium criterion was the constancy (±0.1 dyne/cm) of the surface pressure increment ($\Delta\pi$) during 30 min. The interaction energies (Ψ) were estimated (1–4, 6) from the slopes of the linear plots of the reciprocals of the equilibrium surface pressures ($\Delta\pi_{eq}$) against the reciprocals of the final concentrations (n, molecules per cubic centimeter) of the subphase-injected drug. Such energies (Table I) were barbital < phenobarbital < pentobarbital for both monolayers.

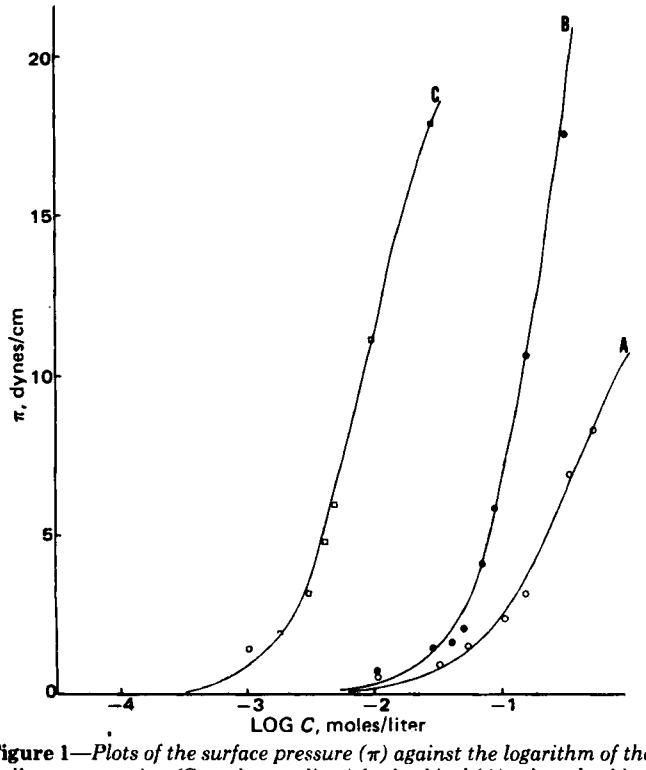

Figure 1—*Plots of the surface pressure (π) against the logarithm of the bulk concentration (C, moles per liter) for barbital (A), phenobarbital (B), and pentobarbital (C). The lines drawn through the experimental points were the best fit obtained from the computer.*

DISCUSSION

The amount of surfactant ions in an adsorbed monolayer at the air–water interface can be estimated directly from measurements of the surface tension variation with surfactant bulk concentration at a constant counterion concentration (1, 7):

$$\Gamma_2^m = \left(\frac{1}{RT}\right)\left(\frac{d\pi}{d \ln m_2}\right)_{m_3} \qquad \text{(Eq. 2)}$$

where Γ_2^m is the monolayer surface concentration of surfactant (moles per square centimeter), R is the universal gas constant (ergs per degree per mole), T is the absolute temperature (degrees Kelvin), π is the surface pressure (dynes per centimeter), and m_2 and m_3 are the molalities (moles per kilogram) of the surfactant ion and the counterion in the bulk solution.

The computed derivative ($d\pi/d \ln m_2$) of the exponential equation that characterized the surface pressure dependence on the concentration permitted (1–4, 6) calculation of the surfactant ion amount in the monolayer (Γ_2^m, moles per square centimeter) at any bulk concentration. Apparent molecular volume calculations performed using crystal density values (8) and space-filling molecular models indicate that the molecular dimensions of these barbituric acid derivatives can be accommodated into a thin interfacial region 8–12 Å thick. On the premises that the barbituric acid derivatives that form the adsorbed monolayer at the air–aqueous interface are immersed completely in the aqueous phase and that the average thickness is 10 Å, the volume, V_s, of the interfacial region that contains the amount of barbituric acid derivative, Γ_2^m (moles per square centimeter), can be estimated reasonably for comparison.

Concentration plots in such a thin interfacial region ($\Gamma'_2 = \Gamma_2^m/V_s$, in moles per liter) estimated from these volumes and from the surface concentration (Γ_2^m, mole per square centimeter) against the bulk concentration C (moles per liter) are given in Fig. 2 for barbital, phenobarbital, and pentobarbital and indicate that the adsorbed pentobarbital concentration at the thin interfacial region could be up to 500 times

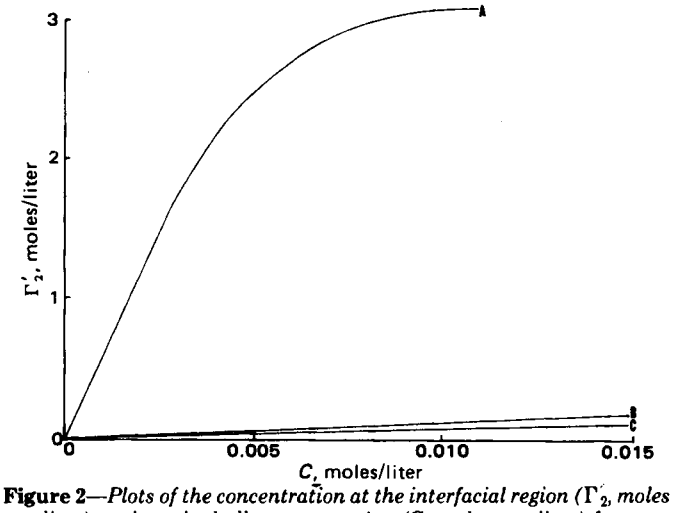

Figure 2—*Plots of the concentration at the interfacial region (Γ'_2, moles per liter) against the bulk concentration (C, moles per liter) for pentobarbital (A), phenobarbital (B), and barbital (C).*

greater than that of phenobarbital and barbital at the same conditions.

Partition coefficients have been measured between octanol–aqueous solution (9) and between erythrocyte membrane–buffer solution (10) for barbital, phenobarbital, and pentobarbital. With the assumptions that the numerical values of the interaction energies of barbital, phenobarbital, and pentobarbital are valid estimates (*i.e.*, the entropies are invariant) and that the same energies are operative for comparative purposes under the conditions in which partition coefficients were measured, the corresponding changes in free energies of transfer to the nonaqueous phase were calculated from literature data (9):

$$\Delta G_{tr} = RT \ln P \qquad \text{(Eq. 3)}$$

where P is the partition coefficient and ΔG_{tr} is the standard free energy associated with solute transfer from the aqueous to the nonaqueous phase. The order of such energies (ΔG_{tr}) (Table I) correlates with the interaction energies of barbital, phenobarbital, and pentobarbital with dipalmitoylphosphatidylethanolamine and with dipalmitoyllecithin monolayers and with their blocking concentrations.

These results show that the interaction energies of pentobarbital with the phospholipid monolayers are higher than those of barbital and phenobarbital and seem to indicate that its increased nerve blocking potency may be due to the comparatively greater interfacial concentration.

REFERENCES

(1) F. A. Vilallonga and E. W. Phillips, *J. Pharm. Sci.*, **68**, 314 (1979).

(2) F. A. Vilallonga, E. R. Garrett, and M. Cereijido, *ibid.*, **61**, 1720 (1972).

(3) F. A. Vilallonga and E. R. Garrett, *ibid.*, **62**, 1605 (1973).

(4) F. A. Vilallonga, E. R. Garrett, and J. S. Hunt, *ibid.*, **66**, 1226 (1977).

(5) J. H. Clint, J. M. Corkill, J. F. Goodman, and J. R. Tate, *J. Colloid Interface Sci.*, **28**, 522 (1968).

(6) F. A. Vilallonga and E. W. Phillips, *J. Pharm. Sci.*, **67**, 773 (1978).

(7) D. G. Hall, B. A. Pethica, and K. Shinoda, *Bull. Chem. Soc. Jpn.*, **48**, 324 (1975).

(8) "Handbook of Chemistry and Physics," 56th ed., C.R.C. Press, Cleveland, Ohio, 1976.

(9) A. Leo, C. Hansch, and D. Elkins, *Chem. Rev.*, **71**, 525 (Table XVII) (1971).

(10) P. Seeman, *Pharmacol. Rev.*, **24**, 583 (1972).

Rationalization of Drug Complexation in Aqueous Solution by Use of Hückel Frontier Molecular Orbitals

M. B. FAWZI, E. DAVISON, and M. S. TUTE ˣ

Received May 31, 1979, from *Pfizer Central Research, Sandwich, Kent, CT13 9NJ, England.* Accepted for publication July 25, 1979.

Abstract □ The complexation of certain drug molecules with niacinamide in aqueous solution was explained by the application of Hückel frontier molecular orbital calculations. A linear relationship was observed between the association constants derived from phase solubility studies and the interaction energy predicted by frontier molecular orbital calculations.

Keyphrases □ Niacinamide—complexation with drug molecules, aqueous solution, frontier molecular orbital calculations □ Complexation—of niacinamide with drug molecules, aqueous solution, frontier molecular orbital calculations □ Solubility—modification, niacinamide complexation with drug molecules, aqueous solution, frontier molecular orbital calculations

The solubility of drug substances often is modified by the use of additives. The discovery of the solubilizing (or solubility inhibiting) action of these additives frequently is made empirically; but in many cases, the system can be described by specific interactions between the drug and additive molecules. The use of phase solubility techniques to derive the association constants that quantitatively define the extent of interaction between the species involved was established (1). The nature of the specific interaction often is well understood.

Many potential interactions can be exploited to modify drug solubility. The present work concerns the use of Hückel frontier molecular orbital (FMO) calculations to confirm a π-donor–π-acceptor mechanism for the interaction of 6,7-dimethoxy-1-[4-(ethylcarbamoyloxy)piperidino]phthalazine (I), 2-[4-(2-furoyl)piperazin-1-yl]-4-amino-6,7-dimethoxyquinazoline (II), 4-(4-amino-6,7,8-trimethoxyquinazolin-2-yl)piperazine-1-carboxylic acid 2-methyl-2-hydroxypropyl ester (III), and 6,7-dime-

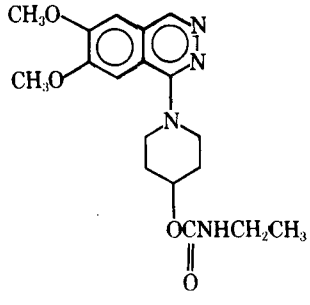

I

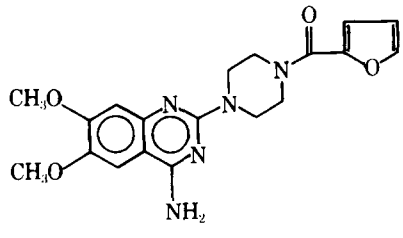

II

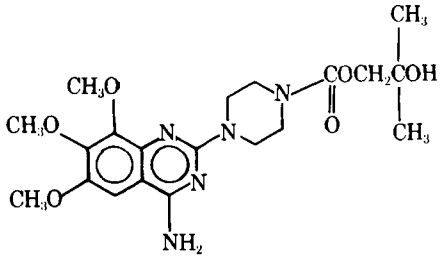

III

0022-3549/80/0100-0104$01.00/0

© *1980, American Pharmaceutical Association*

greater than that of phenobarbital and barbital at the same conditions.

Partition coefficients have been measured between octanol–aqueous solution (9) and between erythrocyte membrane–buffer solution (10) for barbital, phenobarbital, and pentobarbital. With the assumptions that the numerical values of the interaction energies of barbital, phenobarbital, and pentobarbital are valid estimates (*i.e.*, the entropies are invariant) and that the same energies are operative for comparative purposes under the conditions in which partition coefficients were measured, the corresponding changes in free energies of transfer to the nonaqueous phase were calculated from literature data (9):

$$\Delta G_{tr} = RT \ln P \qquad \text{(Eq. 3)}$$

where P is the partition coefficient and ΔG_{tr} is the standard free energy associated with solute transfer from the aqueous to the nonaqueous phase. The order of such energies (ΔG_{tr}) (Table I) correlates with the interaction energies of barbital, phenobarbital, and pentobarbital with dipalmitoylphosphatidylethanolamine and with dipalmitoyllecithin monolayers and with their blocking concentrations.

These results show that the interaction energies of pentobarbital with the phospholipid monolayers are higher than those of barbital and phenobarbital and seem to indicate that its increased nerve blocking potency may be due to the comparatively greater interfacial concentration.

REFERENCES

(1) F. A. Vilallonga and E. W. Phillips, *J. Pharm. Sci.*, **68**, 314 (1979).

(2) F. A. Vilallonga, E. R. Garrett, and M. Cereijido, *ibid.*, **61**, 1720 (1972).

(3) F. A. Vilallonga and E. R. Garrett, *ibid.*, **62**, 1605 (1973).

(4) F. A. Vilallonga, E. R. Garrett, and J. S. Hunt, *ibid.*, **66**, 1226 (1977).

(5) J. H. Clint, J. M. Corkill, J. F. Goodman, and J. R. Tate, *J. Colloid Interface Sci.*, **28**, 522 (1968).

(6) F. A. Vilallonga and E. W. Phillips, *J. Pharm. Sci.*, **67**, 773 (1978).

(7) D. G. Hall, B. A. Pethica, and K. Shinoda, *Bull. Chem. Soc. Jpn.*, **48**, 324 (1975).

(8) "Handbook of Chemistry and Physics," 56th ed., C.R.C. Press, Cleveland, Ohio, 1976.

(9) A. Leo, C. Hansch, and D. Elkins, *Chem. Rev.*, **71**, 525 (Table XVII) (1971).

(10) P. Seeman, *Pharmacol. Rev.*, **24**, 583 (1972).

Rationalization of Drug Complexation in Aqueous Solution by Use of Hückel Frontier Molecular Orbitals

M. B. FAWZI, E. DAVISON, and M. S. TUTE ˣ

Received May 31, 1979, from *Pfizer Central Research, Sandwich, Kent, CT13 9NJ, England.* Accepted for publication July 25, 1979.

Abstract □ The complexation of certain drug molecules with niacinamide in aqueous solution was explained by the application of Hückel frontier molecular orbital calculations. A linear relationship was observed between the association constants derived from phase solubility studies and the interaction energy predicted by frontier molecular orbital calculations.

Keyphrases □ Niacinamide—complexation with drug molecules, aqueous solution, frontier molecular orbital calculations □ Complexation—of niacinamide with drug molecules, aqueous solution, frontier molecular orbital calculations □ Solubility—modification, niacinamide complexation with drug molecules, aqueous solution, frontier molecular orbital calculations

The solubility of drug substances often is modified by the use of additives. The discovery of the solubilizing (or solubility inhibiting) action of these additives frequently is made empirically; but in many cases, the system can be described by specific interactions between the drug and additive molecules. The use of phase solubility techniques to derive the association constants that quantitatively define the extent of interaction between the species involved was established (1). The nature of the specific interaction often is well understood.

Many potential interactions can be exploited to modify drug solubility. The present work concerns the use of Hückel frontier molecular orbital (FMO) calculations to confirm a π-donor–π-acceptor mechanism for the interaction of 6,7-dimethoxy-1-[4-(ethylcarbamoyloxy)piperidino]phthalazine (I), 2-[4-(2-furoyl)piperazin-1-yl]-4-amino-6,7-dimethoxyquinazoline (II), 4-(4-amino-6,7,8-trimethoxyquinazolin-2-yl)piperazine-1-carboxylic acid 2-methyl-2-hydroxypropyl ester (III), and 6,7-dime-

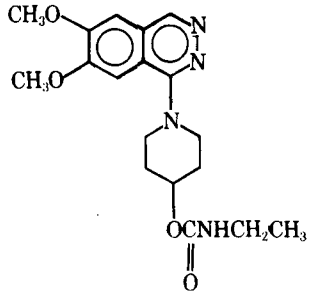

I

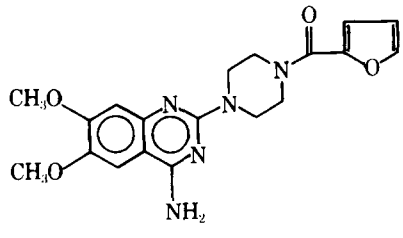

II

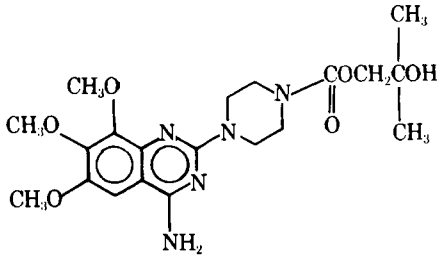

III

0022-3549/80/0100-0104$01.00/0

© *1980, American Pharmaceutical Association*

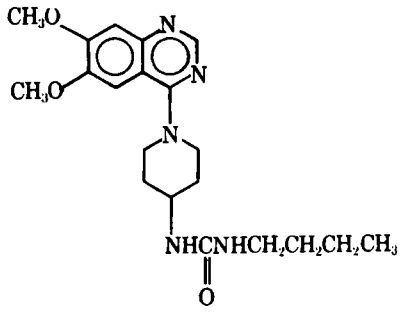

IV

thoxy-4-[4-(3-*n*-butylureido)piperidino]quinazoline (IV) with niacinamide in aqueous solution. The association constants derived from phase solubility experiments were linearly related to the interaction energy predicted by frontier molecular orbital calculations.

EXPERIMENTAL

The phase solubility technique described previously (1) was used to investigate the influence of niacinamide on the solubility of Compounds I–IV. Aqueous niacinamide solutions of known concentration were equilibrated with the test compound by stirring at 25° for 24 hr so that a small excess of compound remained undissolved. The total concentration of the test compound in the filtered solutions was measured by UV spectrophotometry after dilution in methanolic hydrochloric acid. Suitable blanks were prepared from the niacinamide solutions.

RESULTS AND DISCUSSION

Association Constants—The phase solubility diagram of I–IV in niacinamide solution showed increased test compound solubility as the niacinamide concentration increased. The slight pH change accompanying the increased concentrations of niacinamide and the test compound did not explain the increased compound solubility since previous experiments showed the solubility of I–IV to be independent of pH in this region. The phase solubility diagrams all showed positive deviations from linearity. This behavior has been interpreted in terms of first- and second-order interactions between the compound (S) and the solubilizing agent (L):

$$S + L \rightleftharpoons SL$$

Scheme I

$$K_{1:1} = \frac{[SL]}{[S][L]} \qquad \text{(Eq. 1)}$$

$$SL + L \rightleftharpoons SL_2$$

Scheme II

$$K_{1:2} = \frac{[SL_2]}{[SL][L]} \qquad \text{(Eq. 2)}$$

The equations for the association constants $K_{1:1}$ and $K_{1:2}$ involve the free solubilizing agent concentration, $[L]$, in solution. Since only the total concentration of solubilizing agent can be defined, an iterative procedure was developed to isolate values for $K_{1:1}$ and $K_{1:2}$ (2). The values obtained by a similar iterative procedure are shown in Table I.

Molecular Orbital Calculations—The expected π-donor nature of the methoxy-substituted heteroaromatic centers in I–IV led to the choice of the π-acceptor niacinamide as a potential solubilizing agent. The remarkable successes of the simple Hückel frontier molecular orbital approach in rationalizing not only the classical cycloaddition reaction (3) but also numerous other organic reactions (4) encouraged the exploration of a frontier molecular orbital correlation based on the perturbation approach.

Table I—Equilibrium Constants and Calculated Stabilization Energies for Niacinamide [a] Complexes

Compound	$K_{1:1}$	$K_{1:2}$	ΔE	log $K_{1:1}$	Calculated Log $K_{1:1}$
I	12.31	14.76	0.598	1.090	1.022
II	7.36	0.33	0.561	0.861	0.876
III	18.45	0.51	0.660	1.266	1.267
IV	9.88	2.26	0.607	0.995	1.058

[a] Niacinamide concentration was 0.0–2.0 M for II and 0.0–0.2 M otherwise.

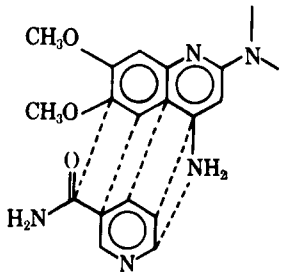

V

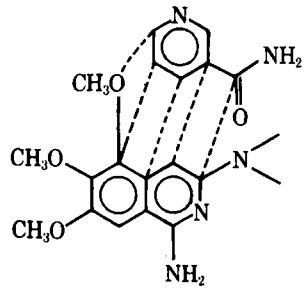

VI

In Eq. 3, ΔE is a partial measure of stabilization of the complex between a drug molecule S and the additive L (niacinamide in this case):

$$\Delta E = 2\gamma^2 \left[\frac{(\sum C_s^O C_l^U)^2}{E_s^O - E_l^U} + \frac{(\sum C_s^U C_l^O)^2}{E_l^O - E_s^U} \right] \qquad \text{(Eq. 3)}$$

The ΔE value is analogous to the stabilization energy of the transition state between two reactants (5). Positions s of S and l of L are juxtaposed, and γ is the resonance integral for the interacting molecular orbital lobes at each site. The C and E values are eigenvectors and eigenvalues appropriate to the occupied (O) and unoccupied (U) interacting frontier orbitals. Consideration of secondary orbital overlap was necessary to rationalize certain cycloaddition reactions (6). Similarly, the highest and the next-to-highest occupied orbitals as well as the lowest unoccupied orbitals are included in the summation.

Several assumptions are inherent in the use of Eq. 3:

1. Electrostatic force variations are small compared with frontier molecular orbital interactions (7) so coulombic interaction is neglected.
2. Only the delocalized π-electron systems are involved in complexation.
3. Because the complexing agent is constant, changes in solvation from one complex to another can be considered constant.

In using Eq. 3, the overlap and orientation principle (8) is invoked, and it is considered that the ring systems of the two partners occupy parallel planes for complexes in water (9).

The program used to obtain molecular orbital indexes was developed previously (10). The coulombic and resonance values were obtained from the literature (11). The maximum ΔE value corresponds to the most favorable overlap of orbitals; V shows the most favorable overlap for I, II, and IV; and VI shows the most favorable overlap for the trimethoxy Compound III. The ΔE values obtained from Eq. 3 for these overlaps are shown in Table I.

Equation 4 gives the regression line for the $K_{1:1}$ association constants and the ΔE values for these four complexes ($n = 4$, $r = 0.95$, $p < 0.05$):

$$\log K_{1:1} = 3.95\,\Delta E - 1.34 \qquad \text{(Eq. 4)}$$

This result is believed to justify the assumptions made and is sufficient to encourage further use of frontier molecular orbital theory in attempting to rationalize solution complexation.

The complexation of III shown in VI demonstrates that a simple change in substituent position can alter totally the complexation topology. The frontier molecular orbital theory applied to drug–receptor interactions could throw light on structure–activity relationships. Previously inexplicable "outliers" in regression analyses between biological activity and linear combinations of free energy-related parameters, as used in pioneering methods (12), now might be explained in terms of orbital symmetry if the receptor contains a conjugated π-electron system.

REFERENCES

(1) T. Higuchi and K. A. Connors, *Adv. Anal. Chem. Instr.*, **4**, 117 (1965).

(2) T. Higuchi and H. Kristiansen, *J. Pharm. Sci.*, **59**, 1601 (1970).

(3) K. L. Mok and M. J. Nye, *J. Chem. Soc. Perkin I*, **1975**, 1810.

(4) I. Fleming, "Frontier Orbitals and Organic Chemical Reactions," Wiley, New York, N.Y., 1976.

(5) R. Sustmann and H. Trill, *Angew. Chem. Int. Ed.*, **11**, 838 (1972).
(6) N. Dennis, B. Ibrahim, and A. R. Katritzky, *J. Chem. Commun.*, **1975**, 425.
(7) W. C. Herndon, *Chem. Rev.*, **72**, 257 (1972).
(8) R. Foster, "Organic Charge-Transfer Complexes," Academic, New York, N.Y., 1969.
(9) V. L. Antonovsky, A. S. Gukovskaja, G. V. Nekrasova, B. I. Sukhorukov, and I. I. Tchervin, *Biochim. Biophys. Acta*, **331**, 9 (1973).
(10) B. Novak and N. B. Furlong, *Tex. Rept. Biol. Med.*, **27**, 1041 (1969).
(11) B. Pullman and A. Pullman, *Rev. Mod. Phys.*, **32**, 428 (1960).
(12) C. Hansch, "Quantitative Approaches to Pharmacological Structure-Activity Relationships," International Encyclopaedia of Pharmacology and Therapeutics, section 5, vol. 1, Pergamon, Oxford, England, 1973, p. 75.

Fluorescence Assay of Nitrofurantoin with *o*-Aminothiophenol in Plasma and Urine

NOBUTOSHI WATARI, TOMOO FUNAKI, and NOBUYOSHI KANENIWA ˣ

Received February 1, 1979, from the *School of Pharmaceutical Sciences, Showa University, Hatanodai, Shinagawa-ku, Tokyo, 142, Japan.* Accepted for publication August 1, 1979.

Abstract □ A fluorescence method is presented for the determination of nitrofurantoin based on conversion of the drug to a fluorescent substance. The method requires 0.1–0.5 ml of plasma or diluted urine and is 10 times more sensitive than the commonly used colorimetric method.

Keyphrases □ Nitrofurantoin—fluorescence assay, plasma and urine □ Spectrophotofluorometry—analysis, nitrofurantoin, plasma and urine □ Antibacterials—nitrofurantoin, fluorescence assay, plasma and urine

Nitrofurantoin, 1-(5-nitro-2-furfurylideneamino)hydantoin (I), is used to treat urinary tract infections. The determination of drug levels in body fluids is important for pharmacokinetic and bioavailability studies. The content of I in plasma and urine commonly is determined by a colorimetric method based on the formation of a hyamine complex of I after its extraction into nitromethane (1, 2).

An electrochemical determination of I in urine that is faster and more accurate than the colorimetric method was reported (3). However, both methods require large sample volumes and are insufficiently sensitive for pharmacokinetic studies.

The reaction products obtained by heating some aromatic aldehydes with *o*-aminothiophenol (II) are fluorescent (4), and some drugs were assayed with II utilizing this reaction (5, 6). This paper discusses the application of this reaction to the fluorescence assay of I in plasma and urine.

EXPERIMENTAL

Reagents—Nitrofurantoin[1] (I) was obtained commercially. *o*-Aminothiophenol hydrochloride was prepared by recrystallization of crude crystals obtained from a mixture of 1 ml of hydrochloric acid/g of *o*-aminothiophenol[2] (II) in ethanol (4). The other reagents were reagent grade.

Procedure—Plasma, 0.1–0.5 ml, was deproteinized by mixing with 1 ml of ethanol. After centrifugation at 3000 rpm for 10 min, 0.5 ml of the supernate was transferred to a 15-ml test tube. Then 1 ml of 0.001% sodium nitrite, 2 ml of hydrochloric acid, 1 ml of 0.1% *o*-aminothiophenol hydrochloride, and 0.5 ml of distilled water were added. After mixing, the solution was heated at 70° in a water bath for 10 min. After cooling to room temperature, UV irradiation was carried out for 3 min; the relative fluoresence intensity was measured with excitation and emission at 375 and 422 nm, respectively.

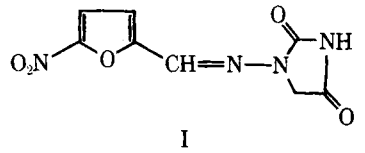

I

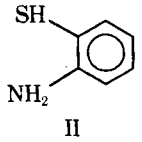

II

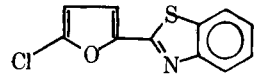

III

The content of I in urine was determined similarly. If the urine was diluted eightfold or more with distilled water, 1 ml of the diluted urine could be assayed directly without deproteinization.

The spectrophotofluorometer[3] was standardized with quinine sulfate[4] in 0.1 *N* H_2SO_4.

The concentration of I in a sample was determined by comparing its fluorescence intensity with that of a standard solution prepared by adding a known concentration of I dissolved in ethanol to plasma or urine free of I and processing it in the same way as the test sample.

RESULTS AND DISCUSSION

A fluorescent substance, 2-(5-chloro-2-furyl)benzothiazole (III), was formed by the reaction of the 2-furaldehyde obtained by hydrochloric acid hydrolysis of I with II (6). However, the conversion of I to III varied due to a steric effect of the side chain of I (7) and incomplete replacement of the nitro group of 2-(5-nitro-2-furyl)benzothiazole with chlorine to give III (6). The nitro group can be replaced with chlorine by UV irradiation (6). The hydrolysis of I is reversible and is promoted by sodium nitrite, acetylacetone, formaldehyde, *etc.*

The maximum relative intensity of fluorescence was obtained in the presence of 0.001% sodium nitrite and with UV irradiation after heating. Therefore, these conditions were adopted for the assay of I with II. Typical results are summarized in Table I.

A linear relationship was obtained between the relative fluorescence intensity and the I concentration up to 5 μg/ml. The means of the relative fluorescence intensity of plasma samples varied slightly within a given analysis, but the standard deviations were similar. For this reason, it is necessary to run a standard I solution with each plasma and urine analysis. Under these conditions, quantitative measurements are possible.

To check the fluorescence method, plasma and urine samples from

[1] Fukuju Seiyaku Co.
[2] Tokyo Kasei Kogyo Co., Tokyo, Japan.
[3] Hitachi MPF-2A.
[4] Wako Pure Chemical Industries, Osaka, Japan.

0022-3549/80/0100-0106$01.00/0
© 1980, American Pharmaceutical Association

(5) R. Sustmann and H. Trill, *Angew. Chem. Int. Ed.*, **11**, 838 (1972).
(6) N. Dennis, B. Ibrahim, and A. R. Katritzky, *J. Chem. Commun.*, **1975**, 425.
(7) W. C. Herndon, *Chem. Rev.*, **72**, 257 (1972).
(8) R. Foster, "Organic Charge-Transfer Complexes," Academic, New York, N.Y., 1969.
(9) V. L. Antonovsky, A. S. Gukovskaja, G. V. Nekrasova, B. I. Sukhorukov, and I. I. Tchervin, *Biochim. Biophys. Acta*, **331**, 9 (1973).
(10) B. Novak and N. B. Furlong, *Tex. Rept. Biol. Med.*, **27**, 1041 (1969).
(11) B. Pullman and A. Pullman, *Rev. Mod. Phys.*, **32**, 428 (1960).
(12) C. Hansch, "Quantitative Approaches to Pharmacological Structure-Activity Relationships," International Encyclopaedia of Pharmacology and Therapeutics, section 5, vol. 1, Pergamon, Oxford, England, 1973, p. 75.

Fluorescence Assay of Nitrofurantoin with *o*-Aminothiophenol in Plasma and Urine

NOBUTOSHI WATARI, TOMOO FUNAKI, and NOBUYOSHI KANENIWA ˣ

Received February 1, 1979, from the *School of Pharmaceutical Sciences, Showa University, Hatanodai, Shinagawa-ku, Tokyo, 142, Japan.* Accepted for publication August 1, 1979.

Abstract □ A fluorescence method is presented for the determination of nitrofurantoin based on conversion of the drug to a fluorescent substance. The method requires 0.1–0.5 ml of plasma or diluted urine and is 10 times more sensitive than the commonly used colorimetric method.

Keyphrases □ Nitrofurantoin—fluorescence assay, plasma and urine □ Spectrophotofluorometry—analysis, nitrofurantoin, plasma and urine □ Antibacterials—nitrofurantoin, fluorescence assay, plasma and urine

Nitrofurantoin, 1-(5-nitro-2-furfurylideneamino)hydantoin (I), is used to treat urinary tract infections. The determination of drug levels in body fluids is important for pharmacokinetic and bioavailability studies. The content of I in plasma and urine commonly is determined by a colorimetric method based on the formation of a hyamine complex of I after its extraction into nitromethane (1, 2).

An electrochemical determination of I in urine that is faster and more accurate than the colorimetric method was reported (3). However, both methods require large sample volumes and are insufficiently sensitive for pharmacokinetic studies.

The reaction products obtained by heating some aromatic aldehydes with *o*-aminothiophenol (II) are fluorescent (4), and some drugs were assayed with II utilizing this reaction (5, 6). This paper discusses the application of this reaction to the fluorescence assay of I in plasma and urine.

EXPERIMENTAL

Reagents—Nitrofurantoin[1] (I) was obtained commercially. *o*-Aminothiophenol hydrochloride was prepared by recrystallization of crude crystals obtained from a mixture of 1 ml of hydrochloric acid/g of *o*-aminothiophenol[2] (II) in ethanol (4). The other reagents were reagent grade.

Procedure—Plasma, 0.1–0.5 ml, was deproteinized by mixing with 1 ml of ethanol. After centrifugation at 3000 rpm for 10 min, 0.5 ml of the supernate was transferred to a 15-ml test tube. Then 1 ml of 0.001% sodium nitrite, 2 ml of hydrochloric acid, 1 ml of 0.1% *o*-aminothiophenol hydrochloride, and 0.5 ml of distilled water were added. After mixing, the solution was heated at 70° in a water bath for 10 min. After cooling to room temperature, UV irradiation was carried out for 3 min; the relative fluoresence intensity was measured with excitation and emission at 375 and 422 nm, respectively.

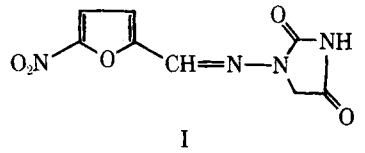

I

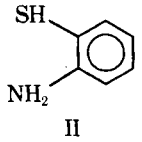

II

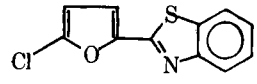

III

The content of I in urine was determined similarly. If the urine was diluted eightfold or more with distilled water, 1 ml of the diluted urine could be assayed directly without deproteinization.

The spectrophotofluorometer[3] was standardized with quinine sulfate[4] in 0.1 *N* H_2SO_4.

The concentration of I in a sample was determined by comparing its fluorescence intensity with that of a standard solution prepared by adding a known concentration of I dissolved in ethanol to plasma or urine free of I and processing it in the same way as the test sample.

RESULTS AND DISCUSSION

A fluorescent substance, 2-(5-chloro-2-furyl)benzothiazole (III), was formed by the reaction of the 2-furaldehyde obtained by hydrochloric acid hydrolysis of I with II (6). However, the conversion of I to III varied due to a steric effect of the side chain of I (7) and incomplete replacement of the nitro group of 2-(5-nitro-2-furyl)benzothiazole with chlorine to give III (6). The nitro group can be replaced with chlorine by UV irradiation (6). The hydrolysis of I is reversible and is promoted by sodium nitrite, acetylacetone, formaldehyde, *etc.*

The maximum relative intensity of fluorescence was obtained in the presence of 0.001% sodium nitrite and with UV irradiation after heating. Therefore, these conditions were adopted for the assay of I with II. Typical results are summarized in Table I.

A linear relationship was obtained between the relative fluorescence intensity and the I concentration up to 5 μg/ml. The means of the relative fluorescence intensity of plasma samples varied slightly within a given analysis, but the standard deviations were similar. For this reason, it is necessary to run a standard I solution with each plasma and urine analysis. Under these conditions, quantitative measurements are possible.

To check the fluorescence method, plasma and urine samples from

[1] Fukuju Seiyaku Co.
[2] Tokyo Kasei Kogyo Co., Tokyo, Japan.
[3] Hitachi MPF-2A.
[4] Wako Pure Chemical Industries, Osaka, Japan.

0022-3549/80/0100-0106$01.00/0
© 1980, American Pharmaceutical Association

Table I—Fluorescence Method for Nitrofurantoin Determination (Relative Fluorescence Intensity per Microgram [a])

Sample[b]	Trial[c]	Nitrofurantoin Reacted, μg							
		0.25	0.50	0.75	1.00	5.00	10.00	Mean[d]	SD
Water (1.0 ml)	1	124.8	100.7	99.9	100.3	100.1	62.7	106.4	10.7
	2	95.1	100.3	99.1	94.1	109.2	90.0	99.6	6.0
	3	113.3	93.6	93.9	92.9	88.6	72.5	96.5	9.7
Rabbit plasma (0.1 ml)	1	109.5	95.1	95.8	108.3	94.1	84.0	100.6	7.6
	2	109.5	119.5	107.8	119.3	115.9	107.5	114.4	5.5
	3	75.9	88.3	79.5	85.0	84.5	64.8	82.6	4.9
Rabbit plasma (0.5 ml)	1				87.3				
	2				99.0				
	3				102.5				

[a] Blank values were subtracted. [b] Blank values for water and 0.1 and 0.5 ml of rabbit plasma were 7.8, 10.6, and 27.6 relative fluorescence intensity units, respectively. [c] $n = 3$. [d] The mean and standard deviation were calculated between 0.25 and 5 μg since the 10-μg values seemed unreliable.

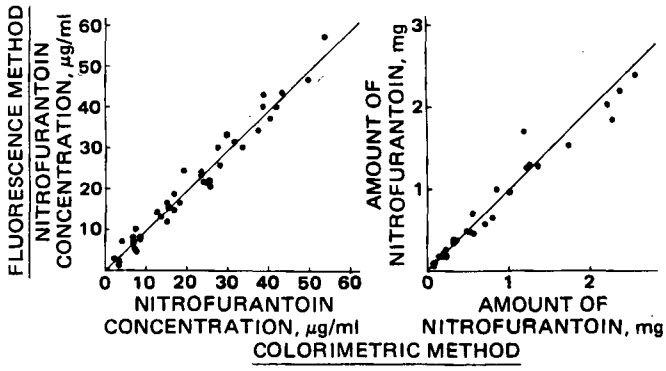

Figure 1—*Comparison of values obtained by the fluorescence and colorimetric methods for the determination of I in plasma (left) and urine (right).*

three rabbits dosed with I were assayed by the fluorescence and colorimetric methods. Figure 1 shows that good correlations were obtained for the values determined by the two methods in both plasma ($y = 0.980x + 0.125$, $r = 0.982$) and urine ($y = 0.980x - 0.026$, $r = 0.999$).

The fluorescence method for I is 10 times more sensitive than the colorimetric method, and it appears to be specific for I. It should be useful for the determination of microamounts of the drug for pharmacokinetic studies and other purposes.

REFERENCES

(1) J. D. Conklin and R. D. Hollifield, *Clin. Chem.*, 11, 925 (1965).
(2) *Ibid.*, 12, 690 (1966).
(3) W. D. Manson and B. Sandmann, *J. Pharm. Sci.*, 65, 599 (1976).
(4) T. Uno and H. Taniguchi, *Jpn. Anal.*, 21, 76 (1972).
(5) S. Nakano, H. Taniguchi, and T. Furuhashi, *Yakugaku Zasshi*, 92, 411 (1972).
(6) H. Taniguchi, K. Mikoshiba, K. Tsuge, and S. Nakano, *ibid.*, 94, 717 (1974).
(7) J. A. Buzard, D. M. Vrablic, and M. F. Paul, *Antibiot. Chemother.*, 6, 702 (1956).

ACKNOWLEDGMENTS

The authors thank Professor T. Miyasaka and Dr. H. Arai, Showa University, for valuable advice.

Phenylfurans IV: Spasmolytic 3-Diethylamino-2,2-(dimethyl)propyl Esters of 5-Substituted Phenyl-2-furancarboxylic Acids

HOMER A. BURCH *x, RONALD E. WHITE *, GEORGE C. WRIGHT *, and MARVIN M. GOLDENBERG ‡

Received February 15, 1979, from the **Chemical Research Division and the* ‡*Biological Research Division, Norwich-Eaton Pharmaceuticals, Division of Morton-Norwich Products, Inc., Norwich, NY 13815.* Accepted for publication August 1, 1979.

Abstract □ A series of 3-diethylamino-2,2-(dimethyl)propyl 5-substituted phenyl-2-furancarboxylates was prepared and found to be pharmacologically active *in vitro* as GI tract nonanticholinergic smooth muscle spasmolytic agents. One of the more active compounds in the series contained the 5-(4-nitrophenyl) group.

Keyphrases □ Phenylfurans—3-diethylamino -2,2- (dimethyl)propyl esters of 5-substituted phenyl-2-furancarboxylic acids, synthesis, potential use as spasmolytic agents □ Spasmolytic agents—3-diethylamino-2,2-(dimethyl)propyl esters of 5-substituted phenyl-2-furancarboxylic acids, synthesis and pharmacological properties

The syntheses and pharmacological properties of 1- and 3-amino- and 1-amino-5-hydroxy-2,4-imidazolidinedione derivatives of 5-phenyl-2-furancarboxaldehydes have been described (1–3). This paper discusses the synthesis and *in vitro* pharmacological evaluation of a series of esters (I) derived from 3-diethylamino-2,2-(dimethyl)propanol (III) and 5-phenyl-2-furancarboxylic acids (II) (4). These compounds have potential use as spasmolytic agents (5).

DISCUSSION

Synthesis—The key intermediates in the synthesis of the esters were the appropriately substituted 5-phenyl-2-furancarboxylic acids (II). The acids generally were obtained in modest yields through the coupling of a substituted phenyldiazonium salt with 2-furancarboxylic acid. Several acids were prepared by oxidation of the corresponding 5-phenyl-2-fur-

0022-3549/80/0100-0107$01.00/0
© 1980, American Pharmaceutical Association

Table I—Fluorescence Method for Nitrofurantoin Determination (Relative Fluorescence Intensity per Microgram [a])

Sample[b]	Trial[c]	Nitrofurantoin Reacted, μg							
		0.25	0.50	0.75	1.00	5.00	10.00	Mean[d]	SD
Water (1.0 ml)	1	124.8	100.7	99.9	100.3	100.1	62.7	106.4	10.7
	2	95.1	100.3	99.1	94.1	109.2	90.0	99.6	6.0
	3	113.3	93.6	93.9	92.9	88.6	72.5	96.5	9.7
Rabbit plasma (0.1 ml)	1	109.5	95.1	95.8	108.3	94.1	84.0	100.6	7.6
	2	109.5	119.5	107.8	119.3	115.9	107.5	114.4	5.5
	3	75.9	88.3	79.5	85.0	84.5	64.8	82.6	4.9
Rabbit plasma (0.5 ml)	1				87.3				
	2				99.0				
	3				102.5				

[a] Blank values were subtracted. [b] Blank values for water and 0.1 and 0.5 ml of rabbit plasma were 7.8, 10.6, and 27.6 relative fluorescence intensity units, respectively. [c] $n = 3$. [d] The mean and standard deviation were calculated between 0.25 and 5 μg since the 10-μg values seemed unreliable.

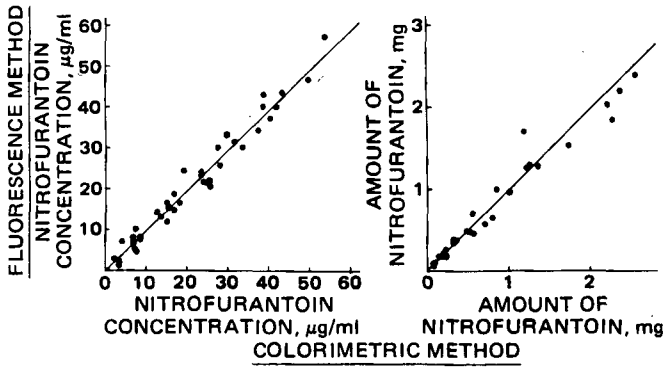

Figure 1—*Comparison of values obtained by the fluorescence and colorimetric methods for the determination of I in plasma (left) and urine (right).*

three rabbits dosed with I were assayed by the fluorescence and colorimetric methods. Figure 1 shows that good correlations were obtained for the values determined by the two methods in both plasma ($y = 0.980x + 0.125$, $r = 0.982$) and urine ($y = 0.980x - 0.026$, $r = 0.999$).

The fluorescence method for I is 10 times more sensitive than the colorimetric method, and it appears to be specific for I. It should be useful for the determination of microamounts of the drug for pharmacokinetic studies and other purposes.

REFERENCES

(1) J. D. Conklin and R. D. Hollifield, *Clin. Chem.*, 11, 925 (1965).
(2) *Ibid.*, 12, 690 (1966).
(3) W. D. Manson and B. Sandmann, *J. Pharm. Sci.*, 65, 599 (1976).
(4) T. Uno and H. Taniguchi, *Jpn. Anal.*, 21, 76 (1972).
(5) S. Nakano, H. Taniguchi, and T. Furuhashi, *Yakugaku Zasshi*, 92, 411 (1972).
(6) H. Taniguchi, K. Mikoshiba, K. Tsuge, and S. Nakano, *ibid.*, 94, 717 (1974).
(7) J. A. Buzard, D. M. Vrablic, and M. F. Paul, *Antibiot. Chemother.*, 6, 702 (1956).

ACKNOWLEDGMENTS

The authors thank Professor T. Miyasaka and Dr. H. Arai, Showa University, for valuable advice.

Phenylfurans IV: Spasmolytic 3-Diethylamino-2,2-(dimethyl)propyl Esters of 5-Substituted Phenyl-2-furancarboxylic Acids

HOMER A. BURCH *x, RONALD E. WHITE *, GEORGE C. WRIGHT *, and MARVIN M. GOLDENBERG ‡

Received February 15, 1979, from the **Chemical Research Division and the* ‡*Biological Research Division, Norwich-Eaton Pharmaceuticals, Division of Morton-Norwich Products, Inc., Norwich, NY 13815.* Accepted for publication August 1, 1979.

Abstract □ A series of 3-diethylamino-2,2-(dimethyl)propyl 5-substituted phenyl-2-furancarboxylates was prepared and found to be pharmacologically active *in vitro* as GI tract nonanticholinergic smooth muscle spasmolytic agents. One of the more active compounds in the series contained the 5-(4-nitrophenyl) group.

Keyphrases □ Phenylfurans—3-diethylamino -2,2- (dimethyl)propyl esters of 5-substituted phenyl-2-furancarboxylic acids, synthesis, potential use as spasmolytic agents □ Spasmolytic agents—3-diethylamino-2,2-(dimethyl)propyl esters of 5-substituted phenyl-2-furancarboxylic acids, synthesis and pharmacological properties

The syntheses and pharmacological properties of 1- and 3-amino- and 1-amino-5-hydroxy-2,4-imidazolidinedione derivatives of 5-phenyl-2-furancarboxaldehydes have been described (1–3). This paper discusses the synthesis and *in vitro* pharmacological evaluation of a series of esters (I) derived from 3-diethylamino-2,2-(dimethyl)propanol (III) and 5-phenyl-2-furancarboxylic acids (II) (4). These compounds have potential use as spasmolytic agents (5).

DISCUSSION

Synthesis—The key intermediates in the synthesis of the esters were the appropriately substituted 5-phenyl-2-furancarboxylic acids (II). The acids generally were obtained in modest yields through the coupling of a substituted phenyldiazonium salt with 2-furancarboxylic acid. Several acids were prepared by oxidation of the corresponding 5-phenyl-2-fur-

0022-3549/80/0100-0107$01.00/0
© 1980, American Pharmaceutical Association

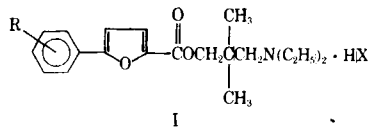

I

Table I—Evaluation of 5-Substituted Phenyl-2-furancarboxylic Esters

Compound	R	Melting Point	Yield, %	Crystallization Solvent[a]	Formula		Analysis, % Calc.	Analysis, % Found	Concentration, μg/ml	Inhibitory Action on Ileal Contractions *In Vitro*[b]	Acetylcholine-Induced Contractions, % of control[c]
Ia	4-F	134–138°	49	I	$C_{20}H_{26}FNO_3 \cdot HCl$	C	62.58	62.55	0.3	0.7	90
						H	7.09	7.02	1	0.09	93
						N	3.65	3.56			
Ib	4-Cl	139–143°	53	E	$C_{20}H_{26}ClNO_3 \cdot HCl$	C	60.00	60.03	1	1.4	119
						H	6.80	6.84	3	0.01	80
						N	3.50	3.45			
Ic	4-Br	154–157°	25.5	A	$C_{20}H_{26}BrNO_3 \cdot HCl$	C	54.01	54.16	1	1.7	93
						H	6.12	6.23	3	0.05	105
						N	3.15	3.02			
Id	2,3-Cl_2	168–175°	82	I	$C_{20}H_{25}Cl_2NO_3 \cdot HCl$	C	55.25	55.06	1	0.7	57
						H	6.03	5.94	10	0.01[d]	96
						N	3.22	3.13			
Ie	3,4-Cl_2	136–138°	41	I	$C_{20}H_{25}Cl_2NO_3 \cdot HCl$	C	55.25	55.42	1	2.1	103
						H	6.03	6.06	3	0.006	95
						N	3.22	3.14			
If	4-NO_2	179–182°	45	E	$C_{20}H_{26}N_2O_5 \cdot HCl$	C	58.46	58.51	1	0.1	100
						H	6.62	6.84	3	0.01	100
						N	6.82	6.96			
Ig	2-NO_2, 4-CH_3	146–148°	58	I	$C_{21}H_{28}N_2O_5 \cdot HCl$	C	59.36	59.38	1	1.1	107
						H	6.88	7.04	10	0.001	84
						N	6.59	6.49			
Ih	3-CF_3	119–123°	39	I	$C_{21}H_{26}F_3NO_3 \cdot HCl$	C	58.13	58.37	1	0.9	108
						H	6.27	6.33	3	0.1	92
						N	3.23	3.19			
Ii	4-CF_3	162–164°	65	EA	$C_{21}H_{26}F_3NO_3 \cdot HCl$	C	58.13	58.23	1	0.7	57
						H	6.27	6.50	10	0.01[d]	96
						N	3.23	3.15			
Ij	3,4-F_2	133–135°	47	EA–A	$C_{20}H_{25}F_2NO_3 \cdot HCl \cdot 1/2H_2O$[e]	C	58.74	58.60	1	0.3	117
						H	6.66	6.50	3	—[f]	101
						N	3.43	3.37			
Ik	3-CH_3O	138–140°	52	E	$C_{21}H_{29}NO_4 \cdot C_4H_4O_4$	C	63.14	63.17	1	0.5	93
						H	6.99	7.14	3	0.7	99
						N	2.95	3.01			
Il	4-CH_3O	133–136°	46	EA	$C_{21}H_{29}NO_4 \cdot HCl$	C	63.71	63.40	1	0.4	86
						H	7.64	7.65	3	0.008	102
						N	3.54	3.56			
Im	H	113–115°	75	BP	$C_{20}H_{27}NO_3 \cdot HCl$	C	65.65	65.45	1	0.7	108
						H	7.71	7.74	3	0.09	94
						N	3.83	3.85			

[a] E = ethanol, I = 2-propanol, A = acetone, BP = benzene–petroleum ether, and EA = ethyl acetate. [b] As determined by the ratio of two frequencies of electrical stimulation, one before and one after the drug, that caused equal muscle contraction (8). The estimation of inhibition is predicted on the lines representing contractions (at frequencies of electrical stimulation of 0.3, 1, 3, and 10 Hz) being parallel before and after drug administration. Two to 10 ileal strips were used to ascertain the activity of each compound. [c] Concentration of acetylcholine in the bath was 0.01 μg/ml. [d] The estimate of activity given in this case applied only to a frequency of 1 Hz and is different at other frequencies of stimulation because the lines are nonparallel. [e] Water by Karl Fischer method: calc., 2.20; found, 2.0%. [f] The frequency–response lines are nonparallel, and values do not apply.

ancarboxaldehydes (IV). Evidence for arylation of the furan ring at the 5-position was presented previously (6).

Subsequent ester formation occurred readily *via* the reaction of the acid chloride of II with III (Scheme I).

Pharmacology—This series of compounds was evaluated to discover

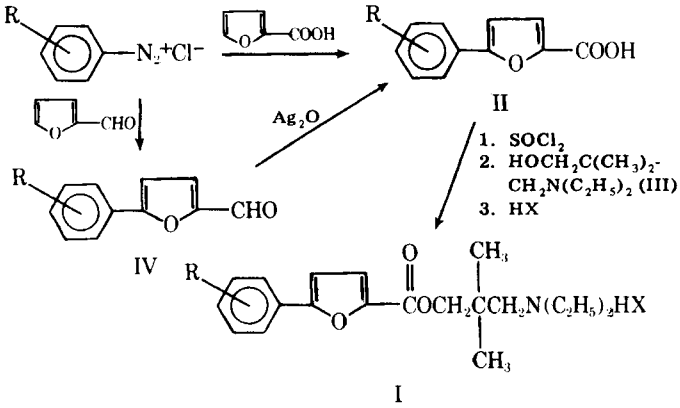

I

Scheme I

nonanticholinergic therapeutic agents capable of exerting a spasmolytic effect through inhibition of contraction of the small and large intestines induced by motor nerve electrical stimulation. The activity of each compound was determined initially by using the isolated rabbit ileum following transmural electrical- and acetylcholine-induced excitation of the smooth muscle (7).

A compound's efficacy was judged by whether it caused parallel displacement or depression of the contractile responses of the isolated rabbit ileum evoked by increasing electrical stimulation frequencies. An inactive compound did not shift the frequency–response line. If the contractile responses at any particular stimulation frequency were equal before and after drug administration, a numerical value of 1 was assigned to describe the lack of response change. An active inhibitory compound had a value of <1. A nonspecific depression of contractile responses following the various stimulation frequencies elicited a nonparallel shift of these responses.

The results of *in vitro* pharmacological testing are found in Table I. When tested at 1 μg/ml, six esters (Ia, If, and Ii–Il) displaced contractile responses of the isolated rabbit ileum. The estimation of inhibitory action for these compounds was ≤0.7. Increasing the concentration of each agent to 3 or 10 μg/ml shifted the frequency–response curves and caused profound inhibition by nearly all of the esters.

Another criterion for evaluating activity was the ability of the compound not to exhibit substantial antagonism of acetylcholine-induced

Table II—5-Substituted Phenyl-2-furancarboxylic Acids

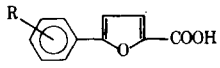

Compound	R	Melting Point	Synthetic Method[a]	Yield, %	Crystallization Solvent[b]	Formula	Analysis, %	Calc.	Found
II*a*	4-F	199–202°	A	13.9	A	$C_{11}H_7FO_3$	C	64.08	64.10
							H	3.42	3.48
II*b*	4-Cl	195–197°	A	34	A	$C_{11}H_7ClO_3$	C	59.35	59.36
							H	3.17	3.13
II*c*	4-Br	205–206°	A	31	B	$C_{11}H_7BrO_3$	C	49.47	49.54
							H	2.64	2.60
							Br	29.29	30.19
II*d*	2,3-Cl_2	259–261°	A	35.9	A	$C_{11}H_6Cl_2O_3$	C	51.39	51.36
							H	2.35	2.38
							Cl	27.58	27.37
II*e*	3,4-Cl_2	234–238°	A	44.4	A	$C_{11}H_6Cl_2O_3$	C	51.39	51.54
							H	2.35	2.41
II*f*	4-NO_2	255–257°	A	56	C	$C_{11}H_7NO_5$	C	56.66	56.86
							H	3.03	3.09
							N	5.67	5.91
II*g*	2-NO_2, 4-CH_3	197–200°	A	32.5	A	$C_{12}H_9NO_5$	C	58.30	58.04
							H	3.67	3.68
							N	5.67	5.59
II*h*	3-CF_3	208–210°	A	21.3	A	$C_{12}H_7F_3O_3$	C	56.26	56.24
							H	2.75	2.84
II*i*	4-CH_3	180–183°	B	20	D	$C_{12}H_{10}O_3$	C	56.26	55.92
							H	2.75	2.80
II*j*	3,4-F_2	212–214°	B	47	D	$C_{11}H_6F_2O_3$	C	58.94	58.55
							H	2.70	2.76
II*k*	3-CH_3O	163–166°	B	25	A	$C_{12}H_{10}O_4$	C	66.05	65.93
							H	4.62	4.67
II*l*	4-CH_3O	172–176°	B	32	D	$C_{12}H_{10}O_4$	C	66.05	66.38
							H	4.62	4.56
II*m*	H	151–152°	B	78	E	$C_{11}H_8O_3$	C	70.21	69.92
							H	4.29	4.27

[a] A = arylation of 2-furancarboxylic acid, and B = oxidation of 5-substituted phenyl-2-furancarboxaldehyde. [b] A = acetone, B = acetonitrile, C = acetic acid, D = benzene, and E = ether.

contractions. All esters failed to cause a dose-related inhibition of acetylcholine-induced contractions.

These findings demonstrate this class of compounds to be pharmacologically active as GI tract nonanticholinergic smooth muscle spasmolytic agents. The spectra of pharmacological effectiveness of I*f* were reported elsewhere (8).

EXPERIMENTAL[1]

5-Substituted Phenyl-2-furancarboxylic Acids (II)—*Method A*—To the diazonium salt of 2,3-dichloroaniline (289 g, 1.78 moles) in a mixture of 400 ml of water and 900 ml of concentrated hydrochloric acid at 0° were added a solution of 2-furancarboxylic acid (184 g, 1.6 moles) in 660 ml of acetone and a solution of cupric chloride (40 g) in 80 ml of water. Cooling was necessary to keep the temperature below 35°. After the exothermic reaction ceased, the mixture was stored at room temperature for 2 days; it was then poured into 6 liters of water, and the resulting mixture was stirred for 2 hr. The crude II*d* was collected by filtration, washed with water, and dried at 60°. Purification was achieved by recrystallization.

Compounds II*a*–II*h* were prepared similarly from the appropriately substituted anilines.

Method B—A solution of silver nitrate (120 g, 0.71 mole) in 243 ml of water was added with stirring to a solution of sodium hydroxide (56 g, 1.4 moles) in 243 ml of water. 5-Phenyl-2-furancarboxyaldehyde (6) (63 g, 0.37 mole) was added in portions to the resulting brown mixture. The reaction mixture was stirred for 0.5 hr at room temperature and filtered, and the residue was washed with 500 ml of hot water. The chilled filtrate was acidified to pH 2 with concentrated hydrochloric acid. The product was collected by filtration, washed with water, and recrystallized. Compound II*m* was described previously as an oil, bp 120–122°/30 mm (9).

Compounds II*i*–II*l* were prepared similarly from the appropriately substituted 5-phenyl-2-furancarboxaldehydes.

The IR spectra of II showed broad carbonyl absorption (COOH) at 5.85–6.0 μm. Other pertinent data are summarized in Table II.

Procedure for 5-Substituted Phenyl-2-furancarboxaldehydes (IV)—Thirty minutes after the formation of the diazonium salt from the appropriately substituted aniline (1.0 mole), the mixture was gravity filtered; the filtrate was added to a mixture of 2-furancarboxaldehyde (123 g, 1.28 moles) in 200 ml of water. A solution of cupric chloride (46 g) in 200 ml of water was added. The resulting mixture was heated with stirring at 56° for 4 hr and then stirred overnight at room temperature.

The product was extracted with 1 liter of chloroform in portions. After the extracts were dried over anhydrous magnesium sulfate and charcoal, the product was isolated by filtration and evaporation under reduced pressure. The crude aldehydes were obtained in 9–40% yields and were used for Method B without further purification.

5-(4-Trifluoromethyl)phenyl-, 3,4-difluorophenyl-, 4-methoxyphenyl- (10), and 3-methoxyphenyl-2-furancarboxaldehydes were prepared in this manner.

3-Diethylamino-2,2-(dimethyl)propyl-5-(4-nitrophenyl) -2- furancarboxylate Hydrochloride (I*f*)—Acid II*f* (55 g, 0.24 mole) was added with rapid stirring at room temperature to 84 ml of thionyl chloride. The resulting mixture was heated until dissolution occurred (~45 min), refluxed for an additional 0.5 hr, and cooled. Excess thionyl chloride was evaporated under reduced pressure. The residue was taken up in 1.3 liters of dry benzene, and III (11) (38.5 g, 0.24 mole) was added. The resulting solution was heated under reflux for 3 hr, cooled, diluted with 750 ml of petroleum ether, and allowed to stand overnight.

After removal of the benzene–petroleum ether by decantation, the residue was suspended in 2 liters of water containing 4 ml of concentrated hydrochloric acid. The mixture was stirred for 0.5 hr, and the pH was adjusted to ~8 by the cautious addition of 200 ml of saturated aqueous sodium carbonate solution. The mixture was extracted with 2.1 liters of benzene in portions, and the extracts were dried over anhydrous magnesium sulfate. The benzene extracts were treated with an ethereal hydrogen chloride solution to pH 3, diluted with 800 ml of petroleum ether, and allowed to stand for 1 hr. After filtration and recrystallization of the residue, I*f* was obtained as colorless needles.

The remaining I esters were prepared similarly from the appropriately substituted II acids. Ester I*k* was isolated as the fumarate salt rather than as the hydrochloride salt as follows. The benzene extracts, containing the free base of I*k*, were evaporated to dryness under reduced pressure. The residue was dissolved in 2-propanol and treated with a 2-propanol solution of fumaric acid. After cooling, the precipitated I*f* was isolated by filtration; IR: 6.8 (I*a*–I*d* and I*f*–I*m*) and 6.9 (I*e*) (ester carbonyl) μm; NMR (dimethyl sulfoxide-d_6): I*f*: δ 0.78 [s, 6, $C(CH_3)_2$], 0.89 (t, 6, J = 7

[1] All melting points were determined using a hot-stage apparatus and are uncorrected.

Hz, CH_2CH_3), 2.74 [m, 6, $N(CH_2)_3$], 3.9 (s, 2, OCH_2), 7.06, 7.18 (doublets, J = 3.5 Hz, 2, 3,4-furan CH), 7.61, 7.89 (doublets, J = 9.0 Hz, 4, phenyl CH), and 10.8 (b, 1, HCl)

Other I esters had similar NMR spectra except for expected variations due to various phenyl substitutents. Other pertinent data are summarized in Table I.

The I esters were evaluated initially *in vitro* on the rabbit ileum as described previously (7). Each drug was dissolved in distilled water for administration.

REFERENCES

(1) H. R. Snyder, Jr., C. S. Davis, R. K. Bickerton, and R. P. Halliday, *J. Med. Chem.*, **10**, 807 (1967).

(2) T. J. Schwan and K. O. Ellis, *J. Pharm. Sci.*, **64**, 1047 (1975).

(3) R. L. White and T. J. Schwan, *ibid.*, **65**, 135 (1976).

(4) G. C. Wright, H. A. Burch, and M. M. Goldenberg, U.S. pat. 3,856,825 (Dec. 1974).

(5) C. M. Suter, "Medicinal Chemistry," vol. I, Wiley, New York, N.Y., pp. 151–220.

(6) C. S. Davis and G. S. Lougheed, *J. Heterocycl. Chem.*, **4**, 153 (1967).

(7) M. M. Goldenberg, *Arzneim.-Forsch.*, **26**, 341 (1976).

(8) M. M. Goldenberg, *Arch. Int. Pharmacodyn. Ther.*, **222**, 27 (1976).

(9) H. Akashi and R. Oda, *J. Chem. Soc. Jpn., Ind. Sect.*, **55**, 271 (1952); through *Chem. Abstr.*, **48**, 3953f (1954).

(10) *Ibid.*, **53**, 202 (1950); through *Chem. Abstr.*, **46**, 9312i (1952).

(11) K. Hayes and G. Drake, *J. Org. Chem.*, **15**, 873 (1950).

ACKNOWLEDGMENTS

F. Abbott, R. Burns, J. Clark, J. Curtis, P. Curtis, R. Finch, D. George, G. Gustin, C. Jeffrey, G. Lougheed, N. Miles, W. Smith, B. Stevenson, M. Tefft, and A. Winterstein are acknowledged for their technical assistance in the preparation, analysis, and biological evaluation of the compounds.

Simultaneous Quantitation of Acetaminophen, Aspirin, Caffeine, Codeine Phosphate, Phenacetin, and Salicylamide by High-Pressure Liquid Chromatography

V. DAS GUPTA

Received May 7, 1979, from the *Department of Pharmaceutics, College of Pharmacy, University of Houston, Houston, TX 77004.* Accepted for publication July 31, 1979.

Abstract □ A method for the simultaneous quantitation of acetaminophen, aspirin, caffeine, codeine phosphate, phenacetin, and salicylamide was developed. The method is based on reversed-phase high-pressure liquid chromatography with a mobile phase buffered with phosphate (pH 2.3). The procedure not only separated these six active ingredients but also salicylic acid, the major decomposition product of aspirin. The method gave excellent results for three commercial products and a synthetic mixture containing four active ingredients. Lowering the pH increased the retention time of some weak acids and decreased that of some weak bases. Only these changes in the retention times made the separation possible.

Keyphrases □ High-pressure liquid chromatography—simultaneous quantitation of acetaminophen, aspirin, caffeine, codeine phosphate, phenacetin, and salicylamide □ Acetaminophen—simultaneous quantitation with aspirin, caffeine, codeine phosphate, phenacetin, and salicylamide, high-pressure liquid chromatography □ Aspirin—simultaneous quantitation with acetaminophen, caffeine, codeine phosphate, phenacetin, and salicylamide, high-pressure liquid chromatography □ Caffeine—simultaneous quantitation with acetaminophen, aspirin, codeine phosphate, phenacetin, and salicylamide, high-pressure liquid chromatography □ Codeine phosphate—simultaneous quantitation with acetaminophen, aspirin, caffeine, phenacetin, and salicylamide, high-pressure liquid chromatography □ Phenacetin—simultaneous quantitation with acetaminophen, aspirin, caffeine, codeine phosphate, and salicylamide, high-pressure liquid chromatography □ Salicylamide—simultaneous quantitation with acetaminophen, aspirin, caffeine, codeine phosphate, and phenacetin, high-pressure liquid chromatography

About 80 commercially available nonprescription drugs (1) contain one or more pain relievers such as acetaminophen, aspirin, phenacetin, and salicylamide. Many of them also contain caffeine and buffering agents such as aluminum hydroxide and magnesium hydroxide (1). At least two commercial products contain a combination of acetaminophen, aspirin, caffeine, and salicylamide (1). Other products contain a combination of acetaminophen or aspirin, caffeine, phenacetin, and salicylamide (1). Many prescription drugs contain codeine phosphate, usually combined with aspirin, caffeine, and phenacetin.

BACKGROUND

The simultaneous quantitation of these ingredients is difficult. The NF methods (2) for the quantitation of aspirin, caffeine, codeine phosphate, and phenacetin in combination are tedious and time consuming. The colorimetric (3) and fluorometric (4) methods for aspirin quantitation are based on its hydrolysis to salicylic acid. Since salicylic acid is the principal decomposition product of aspirin, these methods are not specific. The GLC method (5) for aspirin quantitation is more specific but requires derivatization, which takes ~1 hr and can be complicated by the hydrolysis of aspirin to salicylic acid.

Previous investigators (6) reported that aspirin-containing combinations were difficult to chromatograph using nonpolar solvents and normal-phase chromatography. They preferred (7) paired-ion chromatography using the tetrabutylammonium ion to separate aspirin from muscle relaxants. They did not apply this method to separate combinations of the various pain relievers mentioned.

An automated high-pressure liquid chromatographic (HPLC) method (8) for the quantitation of aspirin, caffeine, and phenacetin was reported. The investigators used a controlled pore glass support as the stationary column and 8% acetic acid in chloroform as the mobile phase. This method was not tried on other pain relievers or in the presence of codeine phosphate.

Another HPLC method (9) analyzed small aspirin quantities in plasma in the presence of large salicylic acid quantities. However, the salicylic acid quantity is very small and the aspirin quantity is high in the dosage forms.

One study (10) used macroporous poly(methyl methylacrylate) resin to assay aspirin. This method was tedious and complicated. Two columns and two solvents were used to analyze some pain reliever combinations.

The purposes of the present investigations were to: (*a*) develop a rapid

0022-3549/80/0100-0108$01.00/0

© 1980, American Pharmaceutical Association

Hz, CH_2CH_3), 2.74 [m, 6, $N(CH_2)_3$], 3.9 (s, 2, OCH_2), 7.06, 7.18 (doublets, J = 3.5 Hz, 2, 3,4-furan CH), 7.61, 7.89 (doublets, J = 9.0 Hz, 4, phenyl CH), and 10.8 (b, 1, HCl)

Other I esters had similar NMR spectra except for expected variations due to various phenyl substitutents. Other pertinent data are summarized in Table I.

The I esters were evaluated initially *in vitro* on the rabbit ileum as described previously (7). Each drug was dissolved in distilled water for administration.

REFERENCES

(1) H. R. Snyder, Jr., C. S. Davis, R. K. Bickerton, and R. P. Halliday, *J. Med. Chem.*, **10**, 807 (1967).

(2) T. J. Schwan and K. O. Ellis, *J. Pharm. Sci.*, **64**, 1047 (1975).

(3) R. L. White and T. J. Schwan, *ibid.*, **65**, 135 (1976).

(4) G. C. Wright, H. A. Burch, and M. M. Goldenberg, U.S. pat. 3,856,825 (Dec. 1974).

(5) C. M. Suter, "Medicinal Chemistry," vol. I, Wiley, New York, N.Y., pp. 151–220.

(6) C. S. Davis and G. S. Lougheed, *J. Heterocycl. Chem.*, **4**, 153 (1967).

(7) M. M. Goldenberg, *Arzneim.-Forsch.*, **26**, 341 (1976).

(8) M. M. Goldenberg, *Arch. Int. Pharmacodyn. Ther.*, **222**, 27 (1976).

(9) H. Akashi and R. Oda, *J. Chem. Soc. Jpn., Ind. Sect.*, **55**, 271 (1952); through *Chem. Abstr.*, **48**, 3953f (1954).

(10) *Ibid.*, **53**, 202 (1950); through *Chem. Abstr.*, **46**, 9312i (1952).

(11) K. Hayes and G. Drake, *J. Org. Chem.*, **15**, 873 (1950).

ACKNOWLEDGMENTS

F. Abbott, R. Burns, J. Clark, J. Curtis, P. Curtis, R. Finch, D. George, G. Gustin, C. Jeffrey, G. Lougheed, N. Miles, W. Smith, B. Stevenson, M. Tefft, and A. Winterstein are acknowledged for their technical assistance in the preparation, analysis, and biological evaluation of the compounds.

Simultaneous Quantitation of Acetaminophen, Aspirin, Caffeine, Codeine Phosphate, Phenacetin, and Salicylamide by High-Pressure Liquid Chromatography

V. DAS GUPTA

Received May 7, 1979, from the *Department of Pharmaceutics, College of Pharmacy, University of Houston, Houston, TX 77004.* Accepted for publication July 31, 1979.

Abstract □ A method for the simultaneous quantitation of acetaminophen, aspirin, caffeine, codeine phosphate, phenacetin, and salicylamide was developed. The method is based on reversed-phase high-pressure liquid chromatography with a mobile phase buffered with phosphate (pH 2.3). The procedure not only separated these six active ingredients but also salicylic acid, the major decomposition product of aspirin. The method gave excellent results for three commercial products and a synthetic mixture containing four active ingredients. Lowering the pH increased the retention time of some weak acids and decreased that of some weak bases. Only these changes in the retention times made the separation possible.

Keyphrases □ High-pressure liquid chromatography—simultaneous quantitation of acetaminophen, aspirin, caffeine, codeine phosphate, phenacetin, and salicylamide □ Acetaminophen—simultaneous quantitation with aspirin, caffeine, codeine phosphate, phenacetin, and salicylamide, high-pressure liquid chromatography □ Aspirin—simultaneous quantitation with acetaminophen, caffeine, codeine phosphate, phenacetin, and salicylamide, high-pressure liquid chromatography □ Caffeine—simultaneous quantitation with acetaminophen, aspirin, codeine phosphate, phenacetin, and salicylamide, high-pressure liquid chromatography □ Codeine phosphate—simultaneous quantitation with acetaminophen, aspirin, caffeine, phenacetin, and salicylamide, high-pressure liquid chromatography □ Phenacetin—simultaneous quantitation with acetaminophen, aspirin, caffeine, codeine phosphate, and salicylamide, high-pressure liquid chromatography □ Salicylamide—simultaneous quantitation with acetaminophen, aspirin, caffeine, codeine phosphate, and phenacetin, high-pressure liquid chromatography

About 80 commercially available nonprescription drugs (1) contain one or more pain relievers such as acetaminophen, aspirin, phenacetin, and salicylamide. Many of them also contain caffeine and buffering agents such as aluminum hydroxide and magnesium hydroxide (1). At least two commercial products contain a combination of acetaminophen, aspirin, caffeine, and salicylamide (1). Other products contain a combination of acetaminophen or aspirin, caffeine, phenacetin, and salicylamide (1). Many prescription drugs contain codeine phosphate, usually combined with aspirin, caffeine, and phenacetin.

BACKGROUND

The simultaneous quantitation of these ingredients is difficult. The NF methods (2) for the quantitation of aspirin, caffeine, codeine phosphate, and phenacetin in combination are tedious and time consuming. The colorimetric (3) and fluorometric (4) methods for aspirin quantitation are based on its hydrolysis to salicylic acid. Since salicylic acid is the principal decomposition product of aspirin, these methods are not specific. The GLC method (5) for aspirin quantitation is more specific but requires derivatization, which takes ~1 hr and can be complicated by the hydrolysis of aspirin to salicylic acid.

Previous investigators (6) reported that aspirin-containing combinations were difficult to chromatograph using nonpolar solvents and normal-phase chromatography. They preferred (7) paired-ion chromatography using the tetrabutylammonium ion to separate aspirin from muscle relaxants. They did not apply this method to separate combinations of the various pain relievers mentioned.

An automated high-pressure liquid chromatographic (HPLC) method (8) for the quantitation of aspirin, caffeine, and phenacetin was reported. The investigators used a controlled pore glass support as the stationary column and 8% acetic acid in chloroform as the mobile phase. This method was not tried on other pain relievers or in the presence of codeine phosphate.

Another HPLC method (9) analyzed small aspirin quantities in plasma in the presence of large salicylic acid quantities. However, the salicylic acid quantity is very small and the aspirin quantity is high in the dosage forms.

One study (10) used macroporous poly(methyl methylacrylate) resin to assay aspirin. This method was tedious and complicated. Two columns and two solvents were used to analyze some pain reliever combinations.

The purposes of the present investigations were to: (*a*) develop a rapid

0022-3549/80/0100-0108$01.00/0

© 1980, American Pharmaceutical Association

Table I—Assay Results [a] of Commercial Dosage Forms and Synthetic Mixture

Ingredient	Commercial Sample 1		Commercial Sample 2		Commercial Sample 3		Synthetic Mixture	
	Claim per Tablet, mg	Found, % claim	Claim per Tablet, mg	Found, % claim	Claim per Tablet, mg	Found, % claim	Added, g	Found, % claim
Acetaminophen (I)	97.2	98.6	—	—	325	99.0	1.00	99.4
Aspirin (II)	194.4	99.6	226.8	99.6	—	—	1.00	99.1
Salicylamide (III)	129.6	100.0	—	—	—	—	1.00	99.9
Caffeine (V)	64.8	99.1	32.4	100.9	—	—	0.30	100.7
Codeine phosphate (VI)	—	—	—	—	30	99.1[b]	—	—
Phenacetin (VII)	—	—	162.0	99.2[c]	—	—	0.30	100.5

[a] The relative percent standard deviations based on five repeated injections were: 1.8, 1.6, 1.5, 1.3, 1.2, and 1.5 for I, II, III, V, VI, and VII, respectively. [b] Assayed at 285 nm for better sensitivity. [c] Assayed at a sensitivity of 0.1 instead of further dilution and reinjection.

and simple HPLC method for the simultaneous quantitation of six active ingredients (acetaminophen, aspirin, caffeine, codeine phosphate, phenacetin, and salicylamide), and (*b*) develop a method free of interference from salicylic acid, the principal aspirin decomposition product.

EXPERIMENTAL

Reagents and Chemicals—All reagents and chemicals were ACS, USP, or NF quality and were used without further purification.

Apparatus—The high-pressure liquid chromatograph[1] was connected to a multiple-wavelength[2] detector, a recorder[3], and an integrator[4].

Column—The nonpolar column[5] (30 cm × 4 mm i.d.) consisted of a monomolecular layer of octadecyltrichlorosilane permanently bonded by silicone–carbon bonds.

Chromatographic Conditions—Solvent A consisted of 0.01 *M* KH_2PO_4 in water with 19% (v/v) methanol (±1%) whose pH[6] was adjusted to 2.3 with an 85% aqueous phosphoric acid solution (~1.1 ml/liter was required). Any methanol concentration between 18 and 20% could be used, but the retention times differed slightly. The exact concentrations used were reported with the sample chromatograms. Solvent B was the same as Solvent A, except that no phosphoric acid was added and the pH was ~4.85.

The temperature was ambient. The flow rate was 2.0 ml/min. The detector sensitivity was 0.04 (254 nm), except for acetaminophen peaks where it was 0.2. For the phenacetin analysis, the sensitivity was 0.1. For codeine analysis, 285 nm was preferred due to greater sensitivity. The chart speed was 30.5 cm/hr.

Solution Preparation—The stock solutions of acetaminophen (I), aspirin (II), salicylamide (III), and salicylic acid (IV) were prepared by dissolving 0.100 g in 5 ml of ethanol and bringing the solution to 100.0 ml with water. Aspirin solutions always were prepared immediately before use. Similar stock solutions of caffeine (V) and codeine phosphate (VI) were prepared without ethanol. The stock solution of phenacetin (VII) was prepared by dissolving 0.05 g of the drug in 5 ml of ethanol and bringing the solution to 100.0 ml with water. The lower concentration was used due to its poor water solubility. The standard solutions and mixture of solutions were prepared as needed by diluting the stock solutions with water.

Synthetic Mixture Preparation—A synthetic mixture was prepared by mixing 1.0 g each of I, II, and III and 0.3 g each of V and VII.

Preparation of Assay Solutions of Commercial Dosage Forms and Synthetic Mixture—For VI, an appropriate quantity of the powder representing 10.0 mg of VI was mixed with enough water to bring to 100.0 ml. The mixture was shaken for a few minutes and filtered. The first 15–20 ml of the filtrate was rejected, and a sample was collected for analysis.

For the other compounds, an appropriate quantity of the fine powder was stirred thoroughly with 5 ml of ethanol and brought to 100.0 ml with water. The mixture was filtered, the first 15–20 ml of the filtrate was rejected, and a sample was collected for further dilution. In general, 10.0 ml of the clear filtrate was diluted to 50.0 ml with water. For aspirin-containing products, the solution always was prepared fresh.

The appropriate quantity of the powder required was determined based on the concentrations of various active ingredients in multicomponent dosage forms. In general, the final dilution(s) for analysis contained the following active ingredient concentrations (micrograms per milliliter): I, 30–50; II, 100–250; III, 100–200; V, 15–30; and VII, 30–50. With these concentrations, sensitivity was 0.2 for I and 0.04 for all others. With one commercial dosage form containing I, V, and VII, instead of preparing another dilution for the analysis of VII, a higher concentration (~2.5 times more) was assayed at a sensitivity of 0.1. The standard mixtures used for comparison contained identical or similar concentrations of all active ingredients. The exact ingredient concentrations used for the sample chromatograms are reported in the figures.

Assay—A 20.0-μl aliquot of the assay solution was injected into the chromatograph using the described conditions (Solvent A). An identical volume of the appropriate standard solution or mixture was injected for comparison after the assay solution was eluted. The standard solution or mixture contained identical or similar active ingredient concentrations.

Calculations—Since preliminary investigations indicated that the peak heights (and the peak areas) were directly related to the concentrations tested (in micrograms: I, 0.5–1.2; II, 1.6–6.0; III, 1.6–5.0; V,

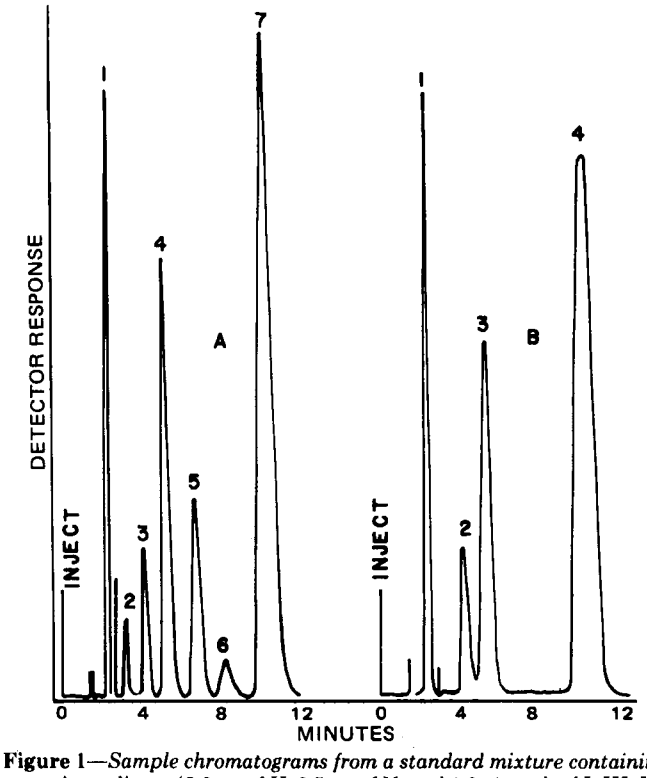

Figure 1—*Sample chromatograms from a standard mixture containing seven ingredients (2.0 μg of II, 0.5 μg of V, and 1.0 μg each of I, III, IV, VI, and VII). Chromatogram A was developed using Solvent A (20% methanol) and chromatogram B was developed using Solvent B. The sensitivity was 0.2 for peak 1 and 0.04 otherwise. The lines after peak 1 indicate the time when the sensitivity was changed. Peaks 1–7 in chromatogram A are from I, VI, III, V, II, IV, and VII, respectively. In chromatogram B, peak 1 is from I, II, and IV; peak 2 is from VI and III; peak 3 is from V; and peak 4 is from VII.*

[1] Waters ALC 202 equipped with a U6K universal injector, Waters Associates, Milford, Mass.
[2] Spectroflow monitor SF770, Schoeffel Instrument Corp., Westwood, N.J.
[3] Omniscribe 5213-12, Houston Instruments, Austin, Tex.
[4] Autolab minigrator, Spectra-Physics, Santa Clara, Calif.
[5] μBondapak C_{18}, catalog No. 27324, Waters Associates, Milford, Mass.
[6] Model 4500 digital pH meter, Beckman Instruments, Irvine, Calif.

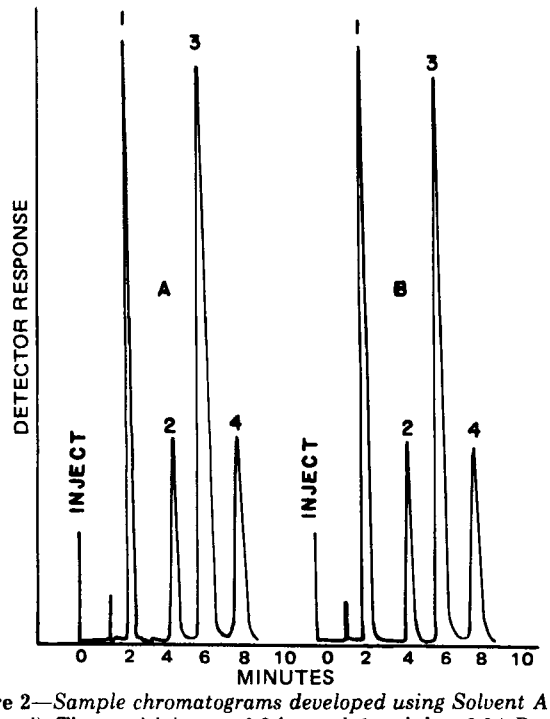

Figure 2—*Sample chromatograms developed using Solvent A (18% methanol). The sensitivity was 0.2 for peak 1 and then 0.04. Peaks 1–4 are from I (0.972 μg), III (1.296 μg), V (0.648 μg), and II (1.944 μg), respectively. Chromatogram A is from a standard mixture, and chromatogram B is from a commercial product.*

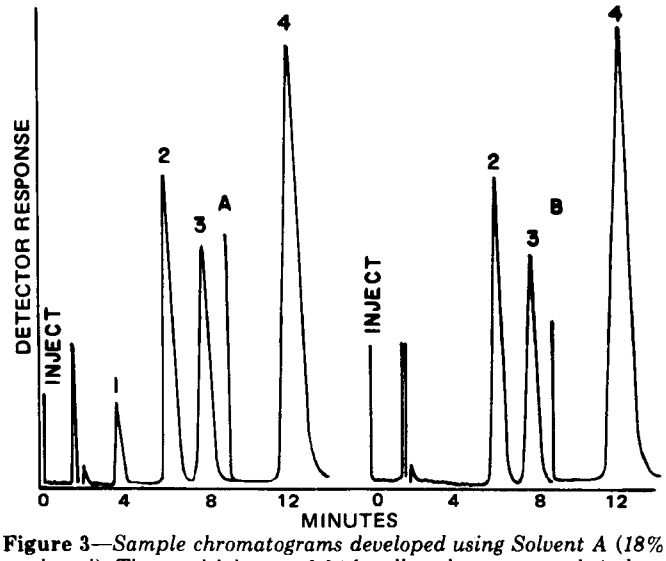

Figure 3—*Sample chromatograms developed using Solvent A (18% methanol). The sensitivity was 0.04 for all peaks except peak 4 where it was 0.1. The lines after peak 3 indicate the time when sensitivity was changed. Peaks 2–4 in both chromatograms are from V, II, and VII, respectively. Peak 1 in chromatogram A is from VI (1.0 μg). The quantities of II, V, and VII injected in chromatogram A (from a standard mixture) were 2.36, 0.32, and 1.56 μg, respectively. In chromatogram B (from a commercial product), the quantities were 2.268, 0.324, and 1.62 μg, respectively.*

0.2–0.7; VI, 1.5–4.0; and VIII, 0.5–1.2), the results were calculated using:

$$\frac{Ph_a}{Ph_s} \times 100 = \% \text{ label claim} \qquad \text{(Eq. 1)}$$

where Ph_a is the peak height of the assay solution and Ph_s is the peak height of the standard.

The ranges given are for a sensitivity of 0.2 for I and 0.04 for all other ingredients. In one commercial sample, VII was assayed using a sensitivity of 0.1. In this assay, peak heights *versus* concentrations were linear between 1.25 and 3.0 μg.

Two sample chromatograms (Fig. 1) were developed by injecting a 20-μl aliquot of a mixture containing 50 μg/ml each of I, III, IV, VI, and VII, 100 μg/ml of II, and 25 μg/ml of V. In the first chromatogram (Fig. 1A), Solvent A containing 20% (v/v) methanol was used; Solvent B (20% methanol) was used in the second chromatogram (Fig. 1B). The results are presented in Table I, and some sample chromatograms are shown in Figs. 2 and 3.

RESULTS AND DISCUSSION

Figure 1A clearly indicates that it is possible to separate seven active ingredients, I–VII, from each other using Solvent A, whose pH was adjusted to 2.3. The same ingredients could not be separated (Fig. 1B) using Solvent B (pH 4.85), which was similar to Solvent A but whose pH had not been adjusted with phosphoric acid. Figure 1B shows only four peaks since aspirin (II) and salicylic acid (IV) were eluted with acetaminophen (I) (peak 1) and codeine phosphate (VI) was eluted with salicylamide (III) (peak 2). The separation between peaks 2 and 3 also was not as good as in Fig. 1A.

By adjusting the solvent pH, the retention times of II and IV were increased and that of VI was decreased, which made the separation possible. Apparently, these changes result because, at a lower pH, both II and IV are predominantly in the undissociated forms while codeine is in the dissociated form. The undissociated forms were expected to be retained for longer times than dissociated forms on a nonpolar column.

With a solvent pH of 2.6–2.7, the retention times of II and IV increased, but these compounds did not separate from one another. It was important to separate these two compounds since IV is the major decomposition product of II. As the pH was decreased, separation became more effective. The pH is very important and functions similar to paired-ion chromatography, in which the retention times are increased.

The analytical results of three commercial dosage forms and a synthetic mixture (Table I and Figs. 2 and 3) indicate that the proposed method can be used for the simultaneous quantitation of active ingredients in various commercial products. Since none of the commercial dosage forms contain all seven ingredients, it is easy to select an internal standard if desired. The peak heights (also peak areas) *versus* concentrations were followed in wide ranges (see *Calculations*). These investigations were not intended to assay IV. Salicylic acid (IV), a major decomposition product of II, was investigated to determine its interference with the analysis of II. It is obvious (Fig. 1A) that it did not interfere. Investigators (11) reported recently that the USP method (12) for the quantitation of II in dosage forms is not stability indicating.

The standard and assay solutions can be prepared in ethanol if desired. Since peak heights vary with the solvent used, both the standard and assay solutions should be prepared in the same solvent. The peak heights were slightly smaller with ethanol as the solvent. Ethanol may be preferred for products containing II since it is less susceptible to hydrolysis in ethanol than in water. The solutions containing II must be prepared immediately before use. Since the optimum stability of II is at about pH 2.3 (13), the mobile phase should have a minimal adverse effect on hydrolysis. With ethanol as the solvent for the assay solution, I did not separate from the ethanol peak. Therefore, ethanol should not be used if I is to be assayed.

The possibilities of assaying very small quantities of IV (0.1% or more) in products containing II are now being studied since USP (12) requires such analysis.

REFERENCES

(1) "Handbook of Nonprescription Drugs," 5th ed., American Pharmaceutical Association, Washington, D.C., 1977, pp. 129–133.

(2) "The National Formulary," 13th ed., Mack Publishing Co., Easton, Pa., 1970, pp. 178, 179.

(3) J. R. Leonards, *Clin. Pharmacol. Ther.*, **4**, 476 (1976).

(4) P. A. Harris and S. Riegelman, *J. Pharm. Sci.*, **56**, 713 (1967).

(5) S. Ali, *Chromatographia*, **8**, 33 (1975).

(6) I. L. Honigberg, J. T. Stewart, and M. Smith, *J. Pharm. Sci.*, **67**, 675 (1978).

(7) J. T. Stewart, I. L. Honigberg, and J. W. Coldren, *ibid.*, **68**, 32 (1979).

(8) P. P. Ascione and J. P. Chrekrian, *ibid.*, **64**, 1029 (1975).

(9) G. W. Peng, M. A. F. Gadalla, V. Smith, A. Peng, and W. L. Chiou,

ibid., **67**, 710 (1978).
(10) R. G. Baum and F. F. Cantwell, *ibid.*, **67**, 1066 (1978).
(11) J. R. Luber, A. G. Visalli, and D. M. Patel, *ibid.*, **68**, 780 (1979).
(12) "The United States Pharmacopeia," 19th rev., Mack Publishing Co., Easton, Pa., 1975, pp. 38, 39.
(13) A. N. Martin, J. Swarbrick, and A. Cammarata, "Physical Pharmacy," 2nd ed., Lea & Febiger, Philadelphia, Pa., 1969, p. 388.

High-Pressure Liquid Chromatographic Determination of Salicylic Acid in Aspirin Powder and Pharmaceutical Dosage Forms

V. DAS GUPTA

Received May 10, 1979, from the *Department of Pharmaceutics, College of Pharmacy, University of Houston, Houston, TX 77004.*
Accepted for publication July 31, 1979.

Abstract □ A sensitive, simple, and rapid method for the quantitation of salicylic acid in aspirin powders and its dosage forms was developed. The method is based on reversed-phase high-pressure liquid chromatography using a mobile phase containing 20% methanol in aqueous phosphate buffer of pH 2.3. Other common ingredients present with aspirin such as acetaminophen, caffeine, codeine phosphate, phenacetin, and salicylamide do not interfere. Salicylic acid quantities as low as 0.1 μg can be assayed with a relative standard deviation of ±2.3%. Sensitivity can be increased by using lower sensitivity settings. The method was tried on numerous commercial products and an old aspirin powder. The results generally were excellent, except that all of the aspirin and salicylic acid could not be extracted from suppositories. The old aspirin powder failed the USP limit test for salicylic acid. The powder apparently absorbed moisture and contained salicylamide as an impurity.

Keyphrases □ High-pressure liquid chromatography—analysis, salicylic acid in aspirin powder and dosage forms □ Aspirin—powder and dosage forms, analysis of salicylic acid, high-pressure liquid chromatography □ Salicylic acid—analysis in aspirin powder and dosage forms, high-pressure liquid chromatography

Salicylic acid is the major decomposition product of aspirin. Because free salicylic acid can cause gastric upset, the USP (1) prescribes limit tests for salicylic acid in aspirin powder and in pharmaceutical dosage forms containing aspirin. The limits are 0.1% for aspirin powder, 0.3% for tablets without buffers, 3.0% for buffered aspirin dosage forms, and 1.0% for suppositories. However, the USP method for the quantitation of salicylic acid in aspirin dosage forms is tedious and time consuming. For aspirin powder, the test is qualitative.

A high-pressure liquid chromatographic (HPLC) method (2) was reported which analyzes small aspirin quantities in the presence of large salicylic acid quantities in plasma. However, in dosage forms and aspirin powder, the assay of small salicylic acid quantities in the presence of large aspirin quantities was a problem. A tedious and complicated method was used for the separation of salicylic acid from aspirin (3).

The simultaneous quantitation of acetaminophen, aspirin, caffeine, codeine phosphate, phenacetin, and salicylamide was reported (4). In this method, the salicylic acid did not interfere. Small salicylic acid quantities could not be determined due to a lack of sensitivity in the analytical method. The purpose of these investigations was to develop a simple and rapid HPLC method for the quantitation of small salicylic acid quantities in aspirin powder and its pharmaceutical dosage forms.

EXPERIMENTAL

Reagents and Chemicals—All reagents and chemicals were ACS, USP, or NF quality and were used without further purification.

Apparatus—The high-pressure liquid chromatograph[1] was connected to a multiple-wavelength[2] detector, a recorder[3], and an integrator[4].

Column—The nonpolar column[5] (30 cm × 4 mm i.d.) consisted of a monomolecular layer of octadecyltrichlorosilane permanently bonded by silicone–carbon bonds.

Chromatographic Conditions—The solvent consisted of 0.01 *M* KH_2PO_4 in water with 20% (v/v) methanol, and its pH[6] was adjusted to 2.3 with an 85% aqueous phosphoric acid solution (~1.1 ml/liter). The temperature was ambient. The flow rate was 2.0 ml/min. The detector sensitivity was 0.04 (300 nm), and the chart speed was 30.5 cm/hr.

Solution Preparation—A stock solution of salicylic acid was prepared by dissolving 0.100 g in enough ethanol to bring to 100.0 ml. This solution was diluted with ethanol for the preparation of the standard solution or other solutions.

A stock solution of a standard mixture was prepared by dissolving 48.6 mg of acetaminophen, 97.2 mg of aspirin, 32.4 mg of caffeine, 50.0 mg of phenacetin, 64.8 mg of salicylamide, and 25.0 mg of salicylic acid in 10 ml of ethanol and bringing the solution to 100.0 ml with water. A solution of the standard mixture was prepared by diluting 10.0 ml of the stock solution to 100.0 ml with water. Both the stock and standard mixture solutions were prepared immediately before use.

Preparation of Assay Solutions from Aspirin Powder—All solutions were prepared immediately before injection into the chromatograph. Aspirin powder, 250.0 mg, was dissolved in enough ethanol to bring to 25.0 ml. Another solution of identical strength was prepared from an old aspirin powder (~10 years), which appeared to have decomposed. These solutions were used for the free salicylic acid determination.

Two other aspirin solutions were prepared by diluting the first solution to 250 μg/ml. Solution 1 was prepared by diluting with water, and Solution 2 was prepared with ethanol. These solutions were allowed to stand for ~50 hr and were then analyzed for free salicylic acid. This analysis was done to compare the hydrolysis rate of aspirin in water *versus* ethanol.

Assay Solutions from Solid Dosage Forms—An appropriate quantity of the fine powder was mixed with enough ethanol to bring to 25.0 ml, and the mixture was shaken for 2–3 min and filtered. The first 5–8 ml of the filtrate was rejected, and samples were collected for analysis. The solutions were prepared immediately before analysis. The quantity of the powder weighed represented at least 80 mg (for all nonbuffered tablets) or 50 mg (for buffered tablets) of aspirin. These quantities were determined by considering USP (1) salicylic acid limits. Exact concentrations of the aspirin solutions are reported in Table I.

Suppository Assay Solutions—A suppository containing 600 mg of aspirin was transferred to a 150-ml beaker. The beaker was warmed by

[1] Waters ALC 202 equipped with a U6K universal injector, Waters Associates, Milford, Mass.
[2] Spectroflow monitor SF770, Schoeffel Instrument Corp., Westwood, N.J.
[3] Omniscribe 5213-12, Houston Instruments, Austin, Tex.
[4] Autolab minigrator, Spectra-Physics, Santa Clara, Calif.
[5] μBondapak C_{18}, catalog No. 27324, Waters Associates, Milford, Mass.
[6] Model 4500 digital pH meter, Beckman Instruments, Irvine, Calif.

0022-3549/80/0100-0113$01.00/0
© 1980, American Pharmaceutical Association

ibid., **67**, 710 (1978).
(10) R. G. Baum and F. F. Cantwell, *ibid.*, **67**, 1066 (1978).
(11) J. R. Luber, A. G. Visalli, and D. M. Patel, *ibid.*, **68**, 780 (1979).
(12) "The United States Pharmacopeia," 19th rev., Mack Publishing Co., Easton, Pa., 1975, pp. 38, 39.
(13) A. N. Martin, J. Swarbrick, and A. Cammarata, "Physical Pharmacy," 2nd ed., Lea & Febiger, Philadelphia, Pa., 1969, p. 388.

High-Pressure Liquid Chromatographic Determination of Salicylic Acid in Aspirin Powder and Pharmaceutical Dosage Forms

V. DAS GUPTA

Received May 10, 1979, from the *Department of Pharmaceutics, College of Pharmacy, University of Houston, Houston, TX 77004.*
Accepted for publication July 31, 1979.

Abstract □ A sensitive, simple, and rapid method for the quantitation of salicylic acid in aspirin powders and its dosage forms was developed. The method is based on reversed-phase high-pressure liquid chromatography using a mobile phase containing 20% methanol in aqueous phosphate buffer of pH 2.3. Other common ingredients present with aspirin such as acetaminophen, caffeine, codeine phosphate, phenacetin, and salicylamide do not interfere. Salicylic acid quantities as low as 0.1 μg can be assayed with a relative standard deviation of ±2.3%. Sensitivity can be increased by using lower sensitivity settings. The method was tried on numerous commercial products and an old aspirin powder. The results generally were excellent, except that all of the aspirin and salicylic acid could not be extracted from suppositories. The old aspirin powder failed the USP limit test for salicylic acid. The powder apparently absorbed moisture and contained salicylamide as an impurity.

Keyphrases □ High-pressure liquid chromatography—analysis, salicylic acid in aspirin powder and dosage forms □ Aspirin—powder and dosage forms, analysis of salicylic acid, high-pressure liquid chromatography □ Salicylic acid—analysis in aspirin powder and dosage forms, high-pressure liquid chromatography

Salicylic acid is the major decomposition product of aspirin. Because free salicylic acid can cause gastric upset, the USP (1) prescribes limit tests for salicylic acid in aspirin powder and in pharmaceutical dosage forms containing aspirin. The limits are 0.1% for aspirin powder, 0.3% for tablets without buffers, 3.0% for buffered aspirin dosage forms, and 1.0% for suppositories. However, the USP method for the quantitation of salicylic acid in aspirin dosage forms is tedious and time consuming. For aspirin powder, the test is qualitative.

A high-pressure liquid chromatographic (HPLC) method (2) was reported which analyzes small aspirin quantities in the presence of large salicylic acid quantities in plasma. However, in dosage forms and aspirin powder, the assay of small salicylic acid quantities in the presence of large aspirin quantities was a problem. A tedious and complicated method was used for the separation of salicylic acid from aspirin (3).

The simultaneous quantitation of acetaminophen, aspirin, caffeine, codeine phosphate, phenacetin, and salicylamide was reported (4). In this method, the salicylic acid did not interfere. Small salicylic acid quantities could not be determined due to a lack of sensitivity in the analytical method. The purpose of these investigations was to develop a simple and rapid HPLC method for the quantitation of small salicylic acid quantities in aspirin powder and its pharmaceutical dosage forms.

EXPERIMENTAL

Reagents and Chemicals—All reagents and chemicals were ACS, USP, or NF quality and were used without further purification.

Apparatus—The high-pressure liquid chromatograph[1] was connected to a multiple-wavelength[2] detector, a recorder[3], and an integrator[4].

Column—The nonpolar column[5] (30 cm × 4 mm i.d.) consisted of a monomolecular layer of octadecyltrichlorosilane permanently bonded by silicone–carbon bonds.

Chromatographic Conditions—The solvent consisted of 0.01 *M* KH_2PO_4 in water with 20% (v/v) methanol, and its pH[6] was adjusted to 2.3 with an 85% aqueous phosphoric acid solution (~1.1 ml/liter). The temperature was ambient. The flow rate was 2.0 ml/min. The detector sensitivity was 0.04 (300 nm), and the chart speed was 30.5 cm/hr.

Solution Preparation—A stock solution of salicylic acid was prepared by dissolving 0.100 g in enough ethanol to bring to 100.0 ml. This solution was diluted with ethanol for the preparation of the standard solution or other solutions.

A stock solution of a standard mixture was prepared by dissolving 48.6 mg of acetaminophen, 97.2 mg of aspirin, 32.4 mg of caffeine, 50.0 mg of phenacetin, 64.8 mg of salicylamide, and 25.0 mg of salicylic acid in 10 ml of ethanol and bringing the solution to 100.0 ml with water. A solution of the standard mixture was prepared by diluting 10.0 ml of the stock solution to 100.0 ml with water. Both the stock and standard mixture solutions were prepared immediately before use.

Preparation of Assay Solutions from Aspirin Powder—All solutions were prepared immediately before injection into the chromatograph. Aspirin powder, 250.0 mg, was dissolved in enough ethanol to bring to 25.0 ml. Another solution of identical strength was prepared from an old aspirin powder (~10 years), which appeared to have decomposed. These solutions were used for the free salicylic acid determination.

Two other aspirin solutions were prepared by diluting the first solution to 250 μg/ml. Solution 1 was prepared by diluting with water, and Solution 2 was prepared with ethanol. These solutions were allowed to stand for ~50 hr and were then analyzed for free salicylic acid. This analysis was done to compare the hydrolysis rate of aspirin in water *versus* ethanol.

Assay Solutions from Solid Dosage Forms—An appropriate quantity of the fine powder was mixed with enough ethanol to bring to 25.0 ml, and the mixture was shaken for 2–3 min and filtered. The first 5–8 ml of the filtrate was rejected, and samples were collected for analysis. The solutions were prepared immediately before analysis. The quantity of the powder weighed represented at least 80 mg (for all nonbuffered tablets) or 50 mg (for buffered tablets) of aspirin. These quantities were determined by considering USP (1) salicylic acid limits. Exact concentrations of the aspirin solutions are reported in Table I.

Suppository Assay Solutions—A suppository containing 600 mg of aspirin was transferred to a 150-ml beaker. The beaker was warmed by

[1] Waters ALC 202 equipped with a U6K universal injector, Waters Associates, Milford, Mass.
[2] Spectroflow monitor SF770, Schoeffel Instrument Corp., Westwood, N.J.
[3] Omniscribe 5213-12, Houston Instruments, Austin, Tex.
[4] Autolab minigrator, Spectra-Physics, Santa Clara, Calif.
[5] μBondapak C_{18}, catalog No. 27324, Waters Associates, Milford, Mass.
[6] Model 4500 digital pH meter, Beckman Instruments, Irvine, Calif.

0022-3549/80/0100-0113$01.00/0
© 1980, American Pharmaceutical Association

Table I—Assay Results of Aspirin Powders and Commercial Dosage Forms

Sample	Claim per Dosage Form, mg	Concentration of Aspirin in Assay Solution, mg/ml	Assay Results	
			Aspirin, % label claim	Salicylic Acid[a] Based on Percent Label Claim of Aspirin
Aspirin powder	—	10.0	—	0.07
Old aspirin powder	—	10.0	95.6[b]	0.61
Tablet 1	Aspirin, 325	10.0	99.8	0.06
Tablet 2	Aspirin, 325; magnesium-aluminum hydroxide, 300	2.6	100.4	0.41
Tablet 3	Aspirin, 600; magnesium hydroxide, 150; aluminum hydroxide dried gel, 150	2.4	99.6	0.54
Tablet 4	Aspirin, 227; phenacetin, 162; caffeine, 32	6.8	100.0	0.14
Tablet 5	Aspirin, 195; acetaminophen, 97; caffeine, 65; salicylamide, 130	7.8	100.1	0.13
Suppository	Aspirin, 600	1.0	31.4	0.64[c]
Aspirin solution (50 hr old)				
In ethanol	—	0.25	—	2.8
In water	—	0.25	—	6.6[d]

[a] Relative standard deviation based on five injections was ±2.3%. [b] This old aspirin powder apparently had absorbed moisture. It also failed the USP limit test for salicylic acid. [c] Calculated based on label claim of aspirin; percent found was divided by 0.314. Since the salicylic acid peak was small, the margin of error is ~3.8%. [d] To determine salicylic acid in a water solution, the standard salicylic acid solution also was made in water by diluting the stock solution. The peaks were slightly higher for the standard solution in water *versus* in ethanol.

immersion in a water bath (~50°) to melt the suppository, and the melt was mixed with enough ethanol to make 60.0 ml of mixture. The mixture was shaken for 4–5 min, and the decanted alcoholic solution was diluted (from 10.0 to 100.0 ml) with ethanol to prepare the assay solution.

Assay Method—A 20.0-μl aliquot of the assay solution was injected into the chromatograph using the described conditions. An identical volume of salicylic acid solution in ethanol (10.0 μg/ml) was injected for comparison after the assay solution eluted.

Two chromatograms (Fig. 1) were developed by injecting a 20.0-μl aliquot of the standard mixture. One chromatogram used a detector wavelength of 300 nm, and the other chromatogram used 254 nm.

Calculations—Since preliminary investigations indicated that peak heights were directly related to concentrations (0.10–0.6 μg) of salicylic acid, the results were calculated by:

$$\frac{Ph_a}{Ph_s} \times 10 = \text{micrograms of salicylic acid per milliliter of solution} \quad \text{(Eq. 1)}$$

where Ph_a is the peak height of the assay solution and Ph_s is the peak height of the standard solution. To ensure quantitative extraction of aspirin from the dosage forms, aspirin was assayed using the method reported previously (4) (Table I and Figs. 2–4).

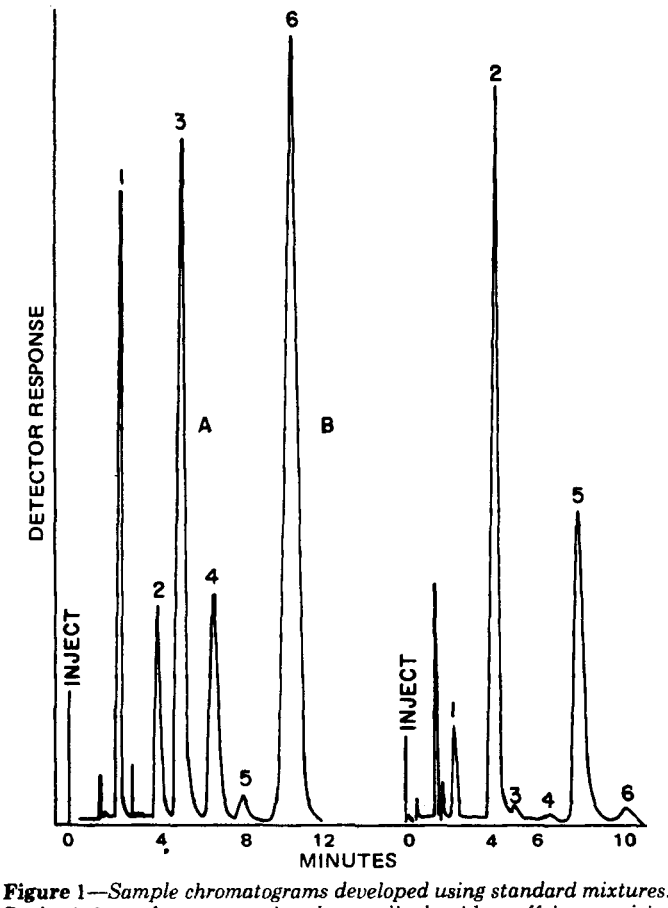

Figure 1—*Sample chromatograms developed using standard mixtures. Peaks 1–6 are from acetaminophen, salicylamide, caffeine, aspirin, salicylic acid, and phenacetin, respectively. Chromatogram A was developed at 254 nm, and B was developed at 300 nm.*

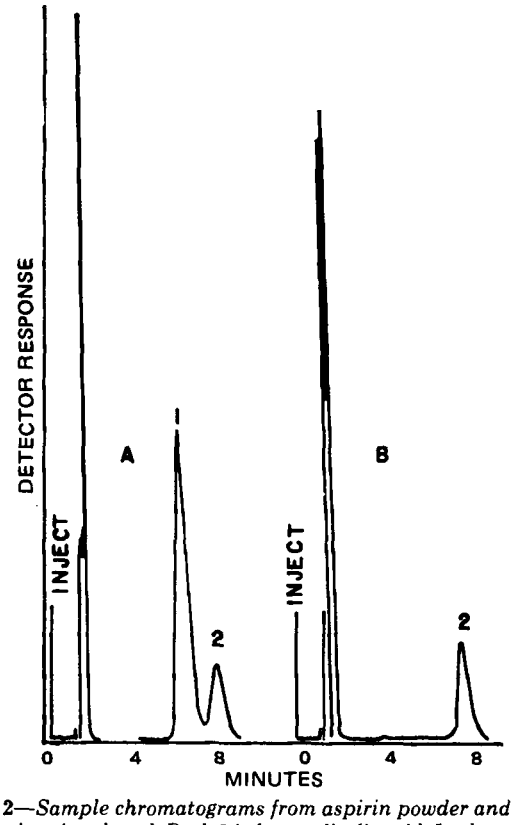

Figure 2—*Sample chromatograms from aspirin powder and salicylic acid solutions in ethanol. Peak 2 is from salicylic acid. In chromatogram A, peak 1 is from aspirin (0.2 mg). In B, 0.2 μg of salicylic acid was injected.*

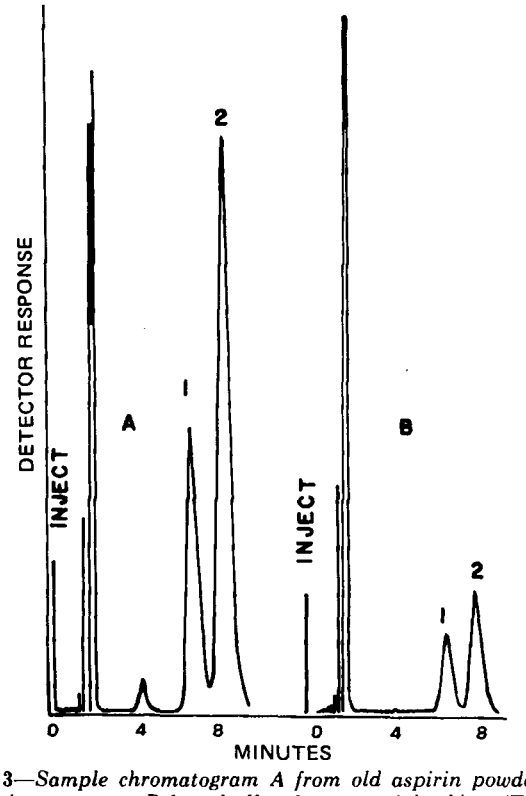

Figure 3—*Sample chromatogram A from old aspirin powder and sample chromatogram B from buffered commercial tablets (Tablet 3 in Table I). Peak 1 is from aspirin, and 2 is from salicylic acid. In A, there is an additional peak after ~4 min, which may be due to salicylamide impurity.*

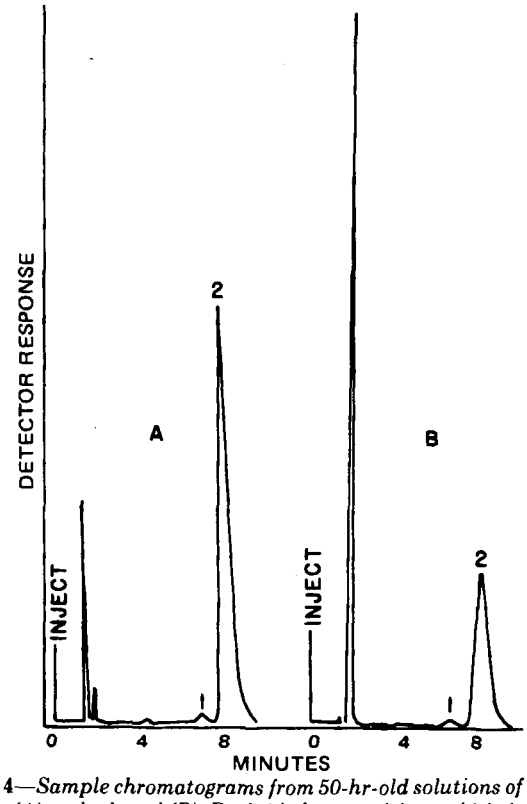

Figure 4—*Sample chromatograms from 50-hr-old solutions of aspirin in water (A) and ethanol (B). Peak 1 is from aspirin, and 2 is from salicylic acid.*

RESULTS AND DISCUSSION

It was reported (4) that it was not possible to assay salicylic acid using the solvent system developed for the simultaneous quantitation of acetaminophen, aspirin, caffeine, codeine phosphate, phenacetin, and salicylamide due to the lack of sensitivity at 254 nm (sensitivity 0.04). Otherwise, separation of salicylic acid from the six active ingredients was excellent (4). Preliminary investigations subsequently indicated that the spectral absorption of salicylic acid solution in the mobile phase was very high at 300 nm, the wavelength of maximum absorption. When considering weight per weight concentrations, the absorption of aspirin solution at 300 nm was almost negligible (Fig. 1B, peak 4). For comparison, chromatograms A and B (Fig. 1) were developed at 254 and 300 nm, respectively. In A, peak 1 was obtained at a sensitivity of 0.2; the sensitivity for peak 1 in B was 0.04. A sensitivity of 0.04 was used otherwise. Even with a sensitivity of 0.04, peak 1 (from acetaminophen) in chromatogram B was very small as compared with peak 1 in chromatogram A (Fig. 1).

The results (Table I) and the sample chromatograms indicate that very small quantities of salicylic acid can be assayed in aspirin powder and its dosage forms using a simple HPLC method. The mobile phase pH (2.3) was almost the optimum pH for aspirin stability (5). Therefore, the adverse effect from the mobile phase was minimal. Aspirin could not be extracted from the suppositories quantitatively with ethanol (Table I). Chloroform was not used for this extraction because it is not miscible with the mobile phase.

Salicylic acid determinations were made at a sensitivity of 0.04. The sensitivity of this method can be increased by changing the setting to 0.01; however, there was some noise problem at this low sensitivity. In the proposed assay, salicylic acid concentrations as low as 5 μg/ml can be determined with a relative standard deviation of ±2.3%. If the salicylic acid assay results are less than 5 μg/ml, the error could be higher. Therefore, the assay should be repeated either with a higher aspirin concentration or with a lower sensitivity.

The old aspirin powder did not pass the USP limit test (Table I) of 0.1% for salicylic acid. Moreover, the old aspirin powder assayed only 95.6%, which may have been due to the moisture absorption. Also, it showed an additional peak (Fig. 3A) after 4 min, which may have been due to salicylamide as an impurity since the retention time of the peak was identical to that of salicylamide (Fig. 1). Although no internal standard was used, one of the following (if not present in the dosage form) may be used as an internal standard: caffeine, 1–2 mg/ml; phenacetin, 1–2 mg/ml; and salicylamide, ~20 μg/ml.

REFERENCES

(1) "The United States Pharmacopeia," 19th rev., Mack Publishing Co., Easton, Pa., 1975, pp. 38, 39.

(2) G. W. Peng, M. A. F. Gadalla, V. Smith, A. Peng, and W. L. Chiou, *J. Pharm. Sci.*, **67**, 710 (1978).

(3) R. G. Baum and F. F. Cantwell, *ibid.*, **67**, 1066 (1978).

(4) V. D. Gupta, *ibid.*, **69**, 110 (1980).

(5) A. N. Martin, J. Swarbrick, and A. Cammarata, "Physical Pharmacy," 2nd ed., Lea & Febiger, Philadelphia, Pa., 1969, p. 388.

Dipole Moments and Conformational Structures of 2-Substituted Phenothiazines as Solutes

C. LEVAYER *, A.-M. GALY ‡, and J. BARBE ‡x

Received April 4, 1979, from the *Service de Chimie Minérale, U.E.R. de Pharmacie, Rue Gaston-Veil, B.P. 1024, 44035 Nantes Cedex, France, and the ‡Service de Chimie Minérale, U.E.R. de Pharmacie, Boulevard Jean-Moulin, 13385 Marseille Cedex 4, France. Accepted for publication August 7, 1979.

Abstract □ Experimental dipole moments measured in anhydrous benzene and dioxane are compared to the calculated values of some 2-substituted phenothiazine derivatives. The dipole moments and the solvent effects support the existence of a conformational mixture of these compounds as solutes.

Keyphrases □ Phenothiazines—2-substituted, dipole moments and conformational structures as solutes □ Dipole moments—of 2-substituted phenothiazines as solutes □ Conformations—of 2-substituted phenothiazines as solutes

A previous report (1) on *N*-methylphenothiazine and its 2-chloro derivative suggested a mixture of conformers of these compounds in solution. This finding is important for a possible conformational explanation of phenothiazine polybiovalency. The conformational structures of some other 2-substituted molecules, which are the chemical forerunners of the clinically used phenothiazine drugs, were determined by comparing the theoretical dipole moments of peculiar conformations to experimental values. The experiment dipole moments were measured with the compounds as solutes due to the physical state of the biophase.

EXPERIMENTAL

Materials—The following compounds[1] were studied: phenothiazine (I), 2-chlorophenothiazine (II), 2-cyanophenothiazine (III), 2-methoxyphenothiazine (IV), 2-thiomethylphenothiazine (V), 2-acetylphenothiazine (VI), and 2-propionylphenothiazine (VII).

Method—The dipole moments of the compounds as solutes in anhydrous benzene and in anhydrous dioxane were measured at different temperatures. The permittivity[2] and refractive index[3] of the solutions were extrapolated to infinite dilution according to Guggenheim (2) and Smith (3). The quantity $(\epsilon_{12} - n_{12}^2) - (\epsilon_1 - n_1^2)$ was plotted *versus* the molar concentration, C, of the solute. The slope of the curve at $C = 0$ then was used to calculate the dipole moment, μ, by:

$$\mu^2 = \frac{9kT}{4\pi N} \frac{3}{(\epsilon_1 + 2)(n_1^2 + 2)} \frac{(\epsilon_{12} - n_{12}^2) - (\epsilon_1 - n_1^2)}{C} \quad \text{(Eq. 1)}$$

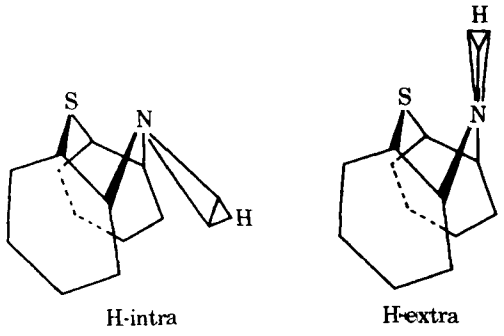

where k is the Boltzmann constant, N is Avogadro's number, T is the absolute temperature, and ϵ_i and n_i are the permittivities and refractive indexes, respectively, of the solutes (Index 1) and of the solutions (Index 12).

Table I—Experimental Dipole Moments of 2-Substituted Phenothiazines

Compounds[a]	Dipole Moment, Debye units 10°	25°	37°
I (B)	2.20 ± 0.02	2.14 ± 0.02	2.12 ± 0.03
I (D)	2.49 ± 0.02	2.50 ± 0.02	2.51 ± 0.03
II (B)	2.02 ± 0.03	1.93 ± 0.02	1.89 ± 0.08
II (D)	2.19 ± 0.02	2.15 ± 0.02	2.16 ± 0.01
III (B)	3.72 ± 0.07	3.60 ± 0.04	3.55 ± 0.08
III (D)	3.63 ± 0.05	3.67 ± 0.03	3.69 ± 0.04
IV (B)	2.57 ± 0.07	2.49 ± 0.02	2.44 ± 0.03
IV (D)	2.80 ± 0.03	2.84 ± 0.03	—
V (B)	2.19 ± 0.02	2.16 ± 0.03	2.11 ± 0.04
V (D)	2.55 ± 0.04	2.54 ± 0.02	—
VI (B)	2.46 ± 0.05	2.38 ± 0.03	2.40 ± 0.05
VI (D)	2.40 ± 0.01	2.42 ± 0.01	2.41 ± 0.02
VII (B)	—	2.30 ± 0.03	2.29 ± 0.05
VII (D)	2.35 ± 0.05	2.35 ± 0.02	2.34 ± 0.02

[a] The solvent was benzene (B) or dioxane (D).

Table II—Dipole Moments of Molecular Increments Used in Calculations

Compound	Dipole Moment, Debye units
Dimethylsulfide	1.49
Diphenylamine	1.11
Chlorobenzene	1.59
Anisole	1.25
Methylphenylsulfide	1.27
Benzonitrile	3.90
Acetophenone	2.89
Propiophenone	2.88

Table III—Experimental and Calculated Dipole Moments of Amines

Compound	Dipole Moment, Debye units Exp. (4, 5)	Calc.[a]
Trimethylamine	0.86	0.83 (U)
N-Methyldiphenylamine	1.56	1.54 (C)
		1.12 (U)
Diphenylamine	1.11	1.08 (C)
		1.29 (U)
Triphenylamine	0.51	1.12 (C)
		0.49 (U)
Aniline	1.53	1.50 (C)
		1.65 (U)
N-Methylaniline	1.68	1.62 (C)
		1.08 (U)
N,N-Dimethylaniline	1.61	1.65 (C)
		0.76 (U)

[a] Conjugated (C) and unconjugated (U) structures generally were considered.

[1] Compound I was crystallized from a commercial sample. Rhône-Poulenc Co., Paris, France, supplied samples of II-V. Clin-Midy Co., Paris, France, supplied samples of VI and VII.
[2] W.T.W. DM01 dipolmeter with a DFL 1 cell.
[3] O.P.L. Abbe type refractometer.

0022-3549/80/0100-0116$01.00/0
© 1980, American Pharmaceutical Association

Table IV—Calculated Dipole Moments of 2-Substituted Phenothiazines [a] for Selected α Values

α	I_i	I_e	II_i	II_e	III_i	III_e	IV_i	IV_e	V_i	V_e	VI or VII_i	VI or VII_e
180°	1.80	1.80	1.81	1.81	3.52	3.52	2.49	2.49	2.00	2.00	3.96	3.96
170°	2.12	1.45	1.97	1.65	3.48	3.56	2.77	0.94	2.14	1.68	4.07	2.02
160°	2.32	1.18	2.05	1.56	3.39	3.69	2.90	0.89	2.29	1.51	4.14	2.17
150°	2.51	0.87	2.12	1.46	3.31	3.64	3.04	0.93	2.41	1.35	4.22	2.40
140°	2.64	0.61	2.15	1.40	3.19	3.65	3.12	1.03	2.50	1.24	4.25	2.59
130°	2.73	0.39	2.15	1.25	3.09	3.67	3.14	1.23	2.54	1.18	4.21	2.84

[a] When necessary, H-intra structures (i) are distinguished from H-extra structures (e).

RESULTS AND DISCUSSION

The experimental dipole moments are given in Table I. The theoretical values were calculated using a vectorial incremental addition. The molecular increments and their dipole moments (4, 5) are listed in Table II.

Because folding along an NS axis is well known in phenothiazine derivatives (6–8), calculations were performed for different values of the angle, α, between each aromatic moiety of the heterocycle. Both H-intra (quasiequatorial) and H-extra (quasiaxial) limit conformations (9) were considered. Consequently, the following assumptions were used (10): $\mu_{CN\ conjugated}$ (*e.g.*, H-intra structure) = 1.7 *D*, and $\mu_{CN\ unconjugated}$ (*e.g.*, H-extra structure) = 0.8 *D*. Such values followed from a study of dipole moment geometrical structural relationships (Table III).

Theoretical dipole moments of the studied compounds are presented in Table IV.

The comparison between experimental and theoretical dipole moments agreed with a folded structure for these molecules. However, there were different α values with each. Compounds I–V sometimes had a quasiaxial structure and sometimes a quasiequatorial one, demonstrated by the dielectric behavior of the compounds in dioxane. Dioxane interacts with conformable solutes by hydrogen bonds (11). Such an interaction is included in the dipole moment value of the solute. Here, there were solute–solvent interactions only with an H-intra conformation because of the electronic hindrances of the H-extra conformer, as can be shown by a molecular framework. Dipole moments measured in benzene and dioxane must agree with one another only for an H-extra structure. The experimental values agreed. Unfortunately, the structures of VI and VII could not be elucidated by correlating experimental and calculated dipole moments except when the following classical relation was used:

$$\mu^2_{experimental} = \mu^2_{H\text{-intra structure}} x_1 + \mu^2_{H\text{-extra structure}} x_2 \qquad \text{(Eq. 2)}$$

Table V—Molar Fractions of the H-Intra Structure Calculated for Several α Values

α	I	II	III	IV	V	VI or VII
142°	0.65	0.67	0.21	0.60	0.67	0.46
146°	0.66	0.67	0.22	0.62	0.69	0.49
150°	0.69	0.68	0.23	0.64	0.71	0.52
154°	0.72	0.70	0.23	0.66	0.74	0.55
158°	0.77	0.73	0.19	0.69	0.78	0.58

where x_1 and x_2 are the molar fractions of the selected conformers. Thus, a conformational mixture was admitted. Results obtained by applying this conclusion to all of the compounds are listed in Table V.

These results were in agreement with those of the previous study of *N*-methylphenothiazine derivatives (1). Moreover, contradictory results about NH phenothiazine compounds from theoretical calculations (9), NMR studies (12, 13), and crystallographic data (14) could be explained if the prevalence of this or that conformer was considered for each molecule. Thus, a mixture of conformations is suggested for dibenzoparathiazine and its substituted derivatives in solution. This result supports the action pattern proposed (15, 16) for phenothiazine drugs.

REFERENCES

(1) C. Levayer, A.-M. Galy, and J. Barbe, *C.R.*, **287**, 569 (1978).

(2) E. A. Guggenheim, *Trans. Faraday Soc.*, **45**, 714 (1949).

(3) J. W. Smith, *ibid.*, **46**, 394 (1950).

(4) A. L. McClellan, "Tables of Experimental Dipole Moments," vol. 1, W. H. Freeman, San Francisco, Calif., 1963.

(5) A. L. McClellan, "Tables of Experimental Dipole Moments," vol. 2, Rahara Enter., El Cerrito, Calif., 1974.

(6) N. J. Leonard and L. E. Sutton, *J. Am. Chem. Soc.*, **70**, 1564 (1948).

(7) M. J. Aroney, G. M. Hoskins, and R. J. W. LeFèvre, *J. Chem. Soc. B*, **1968**, 1206.

(8) N. S. Angerman and S. S. Danyluk, *Org. Magn. Reson.*, **4**, 895 (1972).

(9) J. P. Malrieu and B. Pullman, *Theor. Chim. Acta*, **2**, 293 (1964).

(10) C. W. N. Cumper, *Tetrahedron*, **25**, 3131 (1969).

(11) O. Exner, "Dipole Moments in Organic Chemistry," G. Thieme, Stuttgart, West Germany, 1975.

(12) D. A. Simov, L. L. Kamenov, and S. I. Stoyanov, *C. R. Acad. Bulg. Sci.*, **24**, 1035 (1971).

(13) G. Fronza, R. Mondelli, G. Scapini, G. Ronsisvalle, and F. Vittorio, *J. Magn. Reson.*, **23**, 437 (1976).

(14) J. D. Bell, J. F. Blount, O. V. Briscol, and H. C. Freeman, *Chem. Commun.*, **1968**, 1656.

(15) J. Barbe, *Trav. Soc. Pharm. Montpellier*, **33**, 307 (1973).

(16) J. Barbe, in "Molecular Pharmacology 1978," F. Le Goffic, A. Rey, and C. Crescioni, Eds., Ed. Santé, Paris, France, 1979, p. 149.

GLC–Mass Spectral Determination of Mescaline in Plasma of Rabbits after Intravenous Injection

C. VAN PETEGHEM [x], A. HEYNDRICKX, and W. VAN ZELE

Received February 21, 1978, from the *Toxicology Laboratory, University of Ghent, 9000 Ghent, Belgium.* Accepted for publication August 7, 1979.

Abstract □ A GLC–mass spectral analysis with a deuterated internal standard was developed to measure plasma mescaline concentrations after intravenous administration to rabbits. The drug and the internal standard were extracted with benzene, derivatized with trifluoroacetic acid anhydride, and chromatographed on 2.5% QF-1 with mass fragmentographic detection. The detection limit is 5 ng/ml of plasma. The relative standard deviation was ~5%. The main advantage of this method is that it combines the specificity of the GLC retention time and mass spectral fragmentation pattern with the sensitivity of the mass fragmentographic detection.

Keyphrases □ Mescaline— GLC–mass spectral determination, rabbit plasma, intravenous injection □ Hallucinogenics—mescaline, GLC–mass spectral determination, rabbit plasma, intravenous injection □ GLC–mass spectrometry—analysis, mescaline in rabbit plasma

Mescaline (3,4,5-trimethoxyphenethylamine), an alkaloid isolated in 1896 from the peyote cactus *Lophophora Williamsii*, causes unusual psychic effects and visual hallucinations. In the United States, it is not considered a narcotic drug; but in most countries, it is on the list of illicit drugs. A review of its chemistry, biogenesis, and biological effects was published previously (1).

In clinical toxicological laboratories, identification and quantitation of mescaline are sometimes requested. Only a few methods relate to biological samples (2–4). Most references concern systematic mescaline identification by combined TLC (5–7), GLC and/or mass spectrometry (8–10), or high-pressure liquid chromatography (11). A radioimmunological method also was described (12).

Mescaline is excreted primarily in the urine in humans: subjects given 500 mg po excreted 87% of the dose in 24 hr. The unchanged compound accounted for 60%, and 3,4,5-trimethoxyphenylacetic acid accounted for ~30% (13).

This paper reports a specific and sensitive method for the quantitative determination of mescaline as trifluoroacetylmescaline (I) with trifluoroacetyl-$^2H_2$-mescaline (II) as the internal standard.

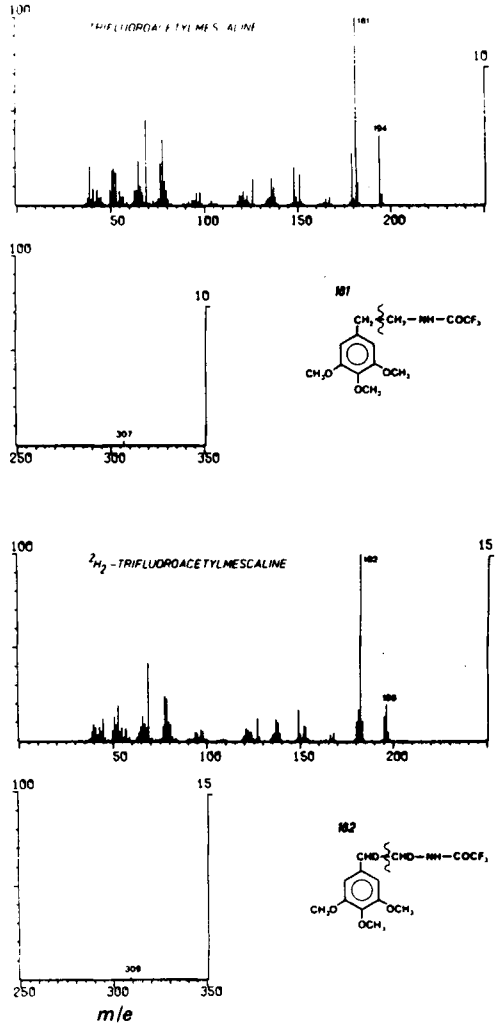

Figure 1—*The 70-ev electron-impact mass spectra of I (top) and II (bottom).*

EXPERIMENTAL

Materials—All chemicals were analytical reagent grade and used as received. Mescaline[1] was 99% pure. ^2H-Labeled mescaline was synthesized from 3,4,5-trimethoxybenzaldehyde by condensation with nitromethane and subsequent reduction with lithium aluminum deuteride. All labeled and nonlabeled standards were prepared in methanol at concentrations permitting use of 10–50-μl aliquots.

Table I—Influence of Overnight Storage Temperature (4 or −18°) on Plasma Mescaline Contents

Sample	Corrected Areas Ratio: Storage at 4°	Corrected Areas Ratio: Storage at −18°
1	0.416	0.417
2	0.443	0.455
3	0.441	0.458
4	0.464	0.471
5	0.457	0.487
6	0.444	0.460
$\bar{x}$	0.444	0.458
σ	0.017	0.023
CV	3.7%	5.1%

Subjects—Rabbits, 2 ± 0.1 kg, were given 1 ml of an aqueous solution of mescaline at a 10-mg/kg dose by rapid intravenous injection in the ear. Blood (1 ml) was drawn from the other ear and collected in heparinized tubes. The samples were centrifuged, and the plasma was stored at 4° until analysis on the next day.

Apparatus—Determinations were performed by GLC[2] with a mass spectrometer as a specific detector[3] coupled to a data system[4]. A silanized

[1] Koch and Light Laboratories.
[2] Varian model 1400.
[3] Finnigan model 3000.
[4] Finnigan model 6000 interactive data system.

0022-3549/80/0100-0118$01.00/0
© 1980, American Pharmaceutical Association

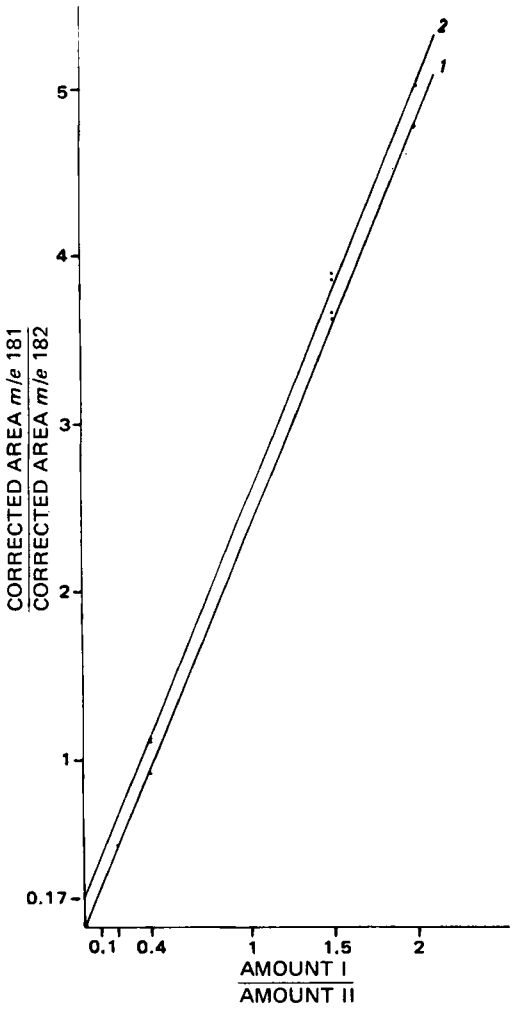

Figure 2—*Calibration graphs after correction for mutual contribution (1) and for the contribution of I to II (2) only.*

glass column, 1.5 m × 0.63 cm, was packed with 2.5% QF-1 on 100–120-mesh Varaport. Helium carrier gas flow was maintained at 30–35 ml/min. Injection port and oven temperatures were 210 and 195°, respectively. The mass spectrometer was operated at a pressure of 5×10^{-6} torr; the ionizing energy in the ion source was 70 ev.

Extraction—To 0.5 ml of plasma was added 20 μl of internal standard solution (200 ng of II). The pH was adjusted to 10 with 1 ml of ammonia–ammonium chloride buffer. The sample was then extracted with 4 ml of benzene. The extracts were dried over anhydrous sodium sulfate (~2 g) and evaporated to dryness under nitrogen.

The residue was dissolved in 0.2 ml of ethyl acetate and 0.2 ml of trifluoroacetic acid anhydride. The solution was allowed to react at 60° in a warm water bath for 30 min, after which the solvents were evaporated with a nitrogen stream. Then the residue was dissolved in 10–20 μl of methanol, and 1–2-μl aliquots were analyzed. The retention time for mescaline and the internal standard was 2.60 min.

Quantitation—Standard solutions in methanol, containing quantities equivalent to 20, 40, 80, 200, and 400 ng of mescaline/μl and 200 ng of internal standard/μl, were used to establish the calibration curve.

RESULTS AND DISCUSSION

The mass spectra of mescaline and of the internal standard are shown in Fig. 1. From the intensity ratio of the *m/e* 181 and 182 ions, the plasma concentrations could be calculated. The problem was that the *m/e* 181 ion in the mescaline spectrum had an isotopic peak at *m/e* 182, while the fragmentation pattern of the internal standard showed both *m/e* 181 and 182 peaks. Consequently, the standard calibration graph shows a curved line with an intercept different from zero, depending on the relative intensity of the *m/e* 181 ion to the *m/e* 182 ion in the mass spectrum of the internal standard. However, this problem could be overcome by correcting

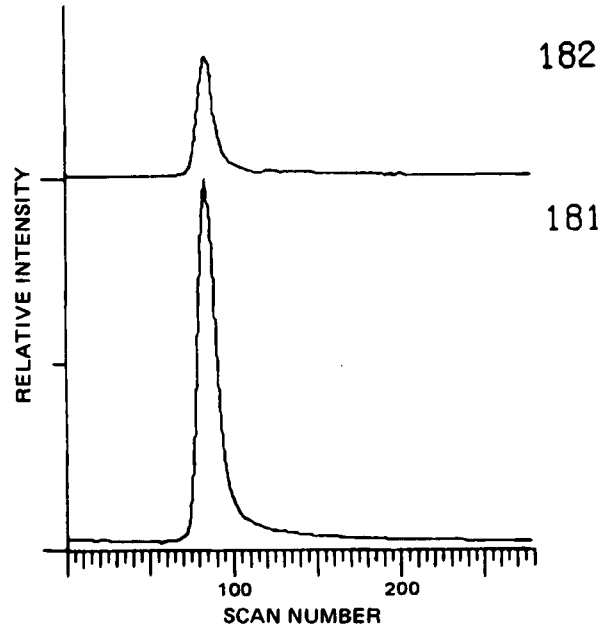

Figure 3—*Mass fragmentogram of a plasma extract (*m/e *181 = trace of I, and* m/e *182 = trace of II).*

for those mutual interferences using:

$$S_{181} = (f_x)(C_x) + (a)(f_s)(C_s) \quad \text{(Eq. 1)}$$

$$S_{182} = (f_s)(C_s) + (b)(f_x)(C_x) \quad \text{(Eq. 2)}$$

where:

C_x = amount of mescaline present in the extract
f_x = factor relating concentration to intensity of the *m/e* 181 ion in the mescaline spectrum
C_s = amount of internal standard in the extract
f_s = factor relating concentration to intensity of the *m/e* 182 ion in the internal standard spectrum
a = relative intensity of the *m/e* 181 ion to the *m/e* 182 ion in the mass spectrum of the internal standard
b = relative intensity of the *m/e* 182 ion to the *m/e* 181 ion in the mescaline mass spectrum
S_{181} = integrated area of the 181 channel
S_{182} = integrated area of the 182 channel

Equations 1 and 2 can be rewritten as:

$$\frac{S_{181} - (a)(S_{182})}{S_{182} - (b)(S_{181})} = (A)(C_x) \quad \text{(Eq. 3)}$$

where:

$$A = \left(\frac{f_x}{f_s}\right)\left(\frac{1}{C_s}\right) \quad \text{(Eq. 4)}$$

The ratio of the corrected areas is now directly proportional to the concentration of the unknown in the standard (Fig. 2). Curve 1 is calculated

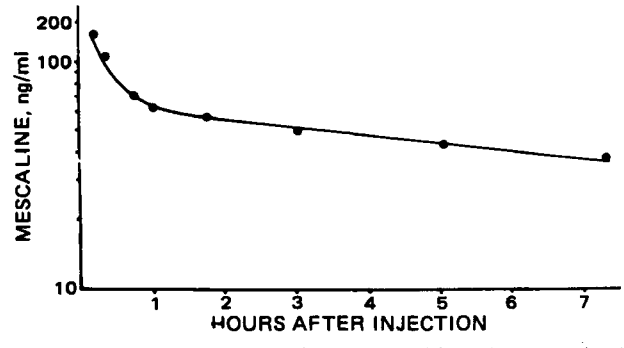

Figure 4—*Profile curve of mescaline in one subject after 10 mg/kg iv.*

by linear regression from the experimental data with $a = 0.165$ and $b = 0.105$. The latter values are obtained by injecting standard solutions of I and II and measuring the ratios of *m/e* 182 to 181 and of *m/e* 181 to 182, respectively. The equation is given by:

$$y = 0.05x + 0.0013 \qquad \text{(Eq. 5)}$$

where y is the corrected areas ratio and x is the mescaline concentration.

Curve 2 is calculated with $a = 0$ and $b = 0.105$ when no corrections are made for the constant contribution of the internal standard's *m/e* 181 ion to the compound to be measured. In this case, the intercept is 0.17, which is in reasonably good agreement with the expected value of 0.165.

An example of a mass fragmentogram of a plasma extract is shown in Fig. 3. No coeluting substances were found when blank plasma samples were analyzed. Therefore, the method, due to the combined specificity of both retention time and mass spectrometric fragmentation pattern, is suitable for pharmacokinetic studies.

The influence of the overnight storage temperature was examined by analyzing a 0.05-ppm spiked pool serum sample, part of which had been kept at 4° and another part at −18° overnight (Table I). The mean values ($n = 6$) of each set of assays were not significantly different (Student *t* test).

The precision of this analytical procedure, expressed as the coefficient of variation, is on the order of 5%. For the GLC–mass spectral quantitative assay, it was 1.7% (six repetitive injections of the same extract).

Although the apparent extraction efficiency with a labeled internal standard added before the extraction was 100%, the actual efficiency was checked; it was about 95% for spiked serum samples. To illustrate that the method is suitable for biological profile studies, the profile curve of one subject is shown in Fig. 4.

REFERENCES

(1) G. J. Kapadia and M. B. E. Fayez, *J. Pharm. Sci.*, **59,** 1699 (1970).

(2) I. Cohen and W. H. Vogel, *Experientia*, **26,** 1231 (1971).

(3) J. Cochin and J. W. Daly, *ibid.*, **18,** 294 (1962).

(4) M. P. Kullberg and C. W. Gorodetzky, *Clin. Chem.*, **20,** 177 (1974).

(5) R. J. Bussey and R. C. Backer, *ibid.*, **20,** 302 (1974).

(6) J. A. Vinson, J. E. Hooyman, and C. E. Ward, *J. Forensic Sci.*, **20,** 552 (1975).

(7) A. N. Masoud, *J. Pharm. Sci.*, **65,** 1585 (1976).

(8) A. C. Moffat, A. H. Stead, and K. W. Smalldon, *J. Chromatogr.*, **90,** 19 (1974).

(9) A. Wu, *Clin. Toxicol.*, **8,** 225 (1975).

(10) R. C. Gupta and G. D. Lundberg, *ibid.*, **11,** 437 (1977).

(11) M. L. Chan, C. Whetsell, and J. D. McChesney, *J. Chromatogr. Sci.*, **12,** 512 (1974).

(12) L. J. Riceberg, H. Van Vunakis, and L. Levine, *Anal. Biochem.*, **60,** 551 (1974).

(13) K. D. Charalampous, K. E. Walker, and J. Kinross-Wright, *Psychopharmacologia*, **9,** 48 (1966).

New Compounds: Reissert Compound Studies XXXII: Facile Synthesis of 3-Azapapaverine

DEBKUMAR BHATTACHARJEE and F. D. POPP ˣ

Received June 18, 1979, from the *Department of Chemistry, University of Missouri–Kansas City, Kansas City, MO 64110.* Accepted for publication July 31, 1979.

Abstract □ 6,7-Dimethoxyphthalazine was obtained in four steps from veratric acid and converted to its Reissert compound. Alkylation of this Reissert compound with 3,4-dimethoxybenzyl chloride followed by hydrolysis gave 3-azapapaverine.

Keyphrases □ Reissert compounds—synthesis of 3-azapapaverine from veratric acid □ 3-Azapapaverine—synthesis from veratric acid *via* a Reissert compound □ Phthalazines—synthesis of 3-azapapaverine from veratric acid *via* Reissert compound derivative of 6,7-dimethoxyphthalazine

The application of Reissert compounds (1, 2) to the synthesis of natural products and compounds of potential medicinal interest is well documented (2, 3) in the field of quinolines and, particularly, isoquinolines. Although phthalazine also yields a Reissert compound (4, 5), its use in the synthesis of potential medicinal agents has not been studied. This paper reports a convenient synthesis of 3-azapapaverine (I) using the Reissert compound (II) of 6,7-dimethoxyphthalazine (III) and demonstrates the potential utility of Reissert compounds derived from phthalazine.

DISCUSSION

A convenient synthesis of III from commercially available veratric acid (IV) was developed using modifications of several literature procedures. Chloromethylation of IV gave the lactone (V) (6), which yielded 4,5-dimethoxyphthalyl alcohol (VI) on reduction with lithium aluminum hydride (7). Oxidation of VI with activated manganese dioxide gave 4,5-dimethoxyphthalaldehyde (VII). Treatment of this dialdehyde (VII) with hydrazine hydrate gave III (8). The overall yield of III from IV was 36%.

Compound III was converted to its Reissert compound (II) by a phase transfer procedure (5) or by a trimethylsilyl cyanide procedure (9). Alkylation of II with 3,4-dimethoxybenzyl chloride in the presence of sodium hydride gave the alkylated Reissert compound VIII. Hydrolysis of VIII with potassium hydroxide gave I.

This procedure should be valuable in the synthesis of phthalazine analogs of isoquinolines of medicinal interest.

EXPERIMENTAL

***m*-Meconin (V)**—Formaldehyde (230 ml, 37% solution) was saturated with hydrogen chloride gas at 15–20°, and 32 g (0.176 mole) of IV[1] was added. The mixture was heated to 60–70° for 7 hr, during which hydrogen chloride gas was bubbled slowly through it. The mixture was cooled, kept overnight, and concentrated *in vacuo*. Water, 100 ml, was added, and the mixture was neutralized with 2:3 dilute ammonium hydroxide. A solid formed and was filtered, washed several times with water, and dried. Recrystallization from methanol gave 22.4 g (65.6%) of V, mp 154–155° [lit. (6) mp 154–156°]; IR (KBr): 3080, 3020 (m), 2940 (w), 1755–1740 (s), 1600 (s), 1500 (s), 1350 (s), and 1300 (s) cm^{-1}.

4,5-Dimethoxyphthalyl Alcohol (VI)—A warm solution of 14 g (0.072 mole) of V in 150 ml of anhydrous tetrahydrofuran was added continuously to a suspension of 7.5 g of lithium aluminum hydride in 80 ml of tetrahydrofuran, and the mixture was refluxed for 4 hr. The mixture was cooled in an ice bath, and the excess lithium aluminum hydride was

[1] Aldrich.

0022-3549/80/0100-0120$01.00/0

© 1980, American Pharmaceutical Association

by linear regression from the experimental data with $a = 0.165$ and $b = 0.105$. The latter values are obtained by injecting standard solutions of I and II and measuring the ratios of *m/e* 182 to 181 and of *m/e* 181 to 182, respectively. The equation is given by:

$$y = 0.05x + 0.0013 \qquad \text{(Eq. 5)}$$

where y is the corrected areas ratio and x is the mescaline concentration.

Curve 2 is calculated with $a = 0$ and $b = 0.105$ when no corrections are made for the constant contribution of the internal standard's *m/e* 181 ion to the compound to be measured. In this case, the intercept is 0.17, which is in reasonably good agreement with the expected value of 0.165.

An example of a mass fragmentogram of a plasma extract is shown in Fig. 3. No coeluting substances were found when blank plasma samples were analyzed. Therefore, the method, due to the combined specificity of both retention time and mass spectrometric fragmentation pattern, is suitable for pharmacokinetic studies.

The influence of the overnight storage temperature was examined by analyzing a 0.05-ppm spiked pool serum sample, part of which had been kept at 4° and another part at −18° overnight (Table I). The mean values ($n = 6$) of each set of assays were not significantly different (Student *t* test).

The precision of this analytical procedure, expressed as the coefficient of variation, is on the order of 5%. For the GLC–mass spectral quantitative assay, it was 1.7% (six repetitive injections of the same extract).

Although the apparent extraction efficiency with a labeled internal standard added before the extraction was 100%, the actual efficiency was checked; it was about 95% for spiked serum samples. To illustrate that the method is suitable for biological profile studies, the profile curve of one subject is shown in Fig. 4.

REFERENCES

(1) G. J. Kapadia and M. B. E. Fayez, *J. Pharm. Sci.*, **59,** 1699 (1970).

(2) I. Cohen and W. H. Vogel, *Experientia*, **26,** 1231 (1971).

(3) J. Cochin and J. W. Daly, *ibid.*, **18,** 294 (1962).

(4) M. P. Kullberg and C. W. Gorodetzky, *Clin. Chem.*, **20,** 177 (1974).

(5) R. J. Bussey and R. C. Backer, *ibid.*, **20,** 302 (1974).

(6) J. A. Vinson, J. E. Hooyman, and C. E. Ward, *J. Forensic Sci.*, **20,** 552 (1975).

(7) A. N. Masoud, *J. Pharm. Sci.*, **65,** 1585 (1976).

(8) A. C. Moffat, A. H. Stead, and K. W. Smalldon, *J. Chromatogr.*, **90,** 19 (1974).

(9) A. Wu, *Clin. Toxicol.*, **8,** 225 (1975).

(10) R. C. Gupta and G. D. Lundberg, *ibid.*, **11,** 437 (1977).

(11) M. L. Chan, C. Whetsell, and J. D. McChesney, *J. Chromatogr. Sci.*, **12,** 512 (1974).

(12) L. J. Riceberg, H. Van Vunakis, and L. Levine, *Anal. Biochem.*, **60,** 551 (1974).

(13) K. D. Charalampous, K. E. Walker, and J. Kinross-Wright, *Psychopharmacologia*, **9,** 48 (1966).

New Compounds: Reissert Compound Studies XXXII: Facile Synthesis of 3-Azapapaverine

DEBKUMAR BHATTACHARJEE and F. D. POPP ˣ

Received June 18, 1979, from the *Department of Chemistry, University of Missouri–Kansas City, Kansas City, MO 64110.* Accepted for publication July 31, 1979.

Abstract □ 6,7-Dimethoxyphthalazine was obtained in four steps from veratric acid and converted to its Reissert compound. Alkylation of this Reissert compound with 3,4-dimethoxybenzyl chloride followed by hydrolysis gave 3-azapapaverine.

Keyphrases □ Reissert compounds—synthesis of 3-azapapaverine from veratric acid □ 3-Azapapaverine—synthesis from veratric acid *via* a Reissert compound □ Phthalazines—synthesis of 3-azapapaverine from veratric acid *via* Reissert compound derivative of 6,7-dimethoxyphthalazine

The application of Reissert compounds (1, 2) to the synthesis of natural products and compounds of potential medicinal interest is well documented (2, 3) in the field of quinolines and, particularly, isoquinolines. Although phthalazine also yields a Reissert compound (4, 5), its use in the synthesis of potential medicinal agents has not been studied. This paper reports a convenient synthesis of 3-azapapaverine (I) using the Reissert compound (II) of 6,7-dimethoxyphthalazine (III) and demonstrates the potential utility of Reissert compounds derived from phthalazine.

DISCUSSION

A convenient synthesis of III from commercially available veratric acid (IV) was developed using modifications of several literature procedures. Chloromethylation of IV gave the lactone (V) (6), which yielded 4,5-dimethoxyphthalyl alcohol (VI) on reduction with lithium aluminum hydride (7). Oxidation of VI with activated manganese dioxide gave 4,5-dimethoxyphthalaldehyde (VII). Treatment of this dialdehyde (VII) with hydrazine hydrate gave III (8). The overall yield of III from IV was 36%.

Compound III was converted to its Reissert compound (II) by a phase transfer procedure (5) or by a trimethylsilyl cyanide procedure (9). Alkylation of II with 3,4-dimethoxybenzyl chloride in the presence of sodium hydride gave the alkylated Reissert compound VIII. Hydrolysis of VIII with potassium hydroxide gave I.

This procedure should be valuable in the synthesis of phthalazine analogs of isoquinolines of medicinal interest.

EXPERIMENTAL

***m*-Meconin (V)**—Formaldehyde (230 ml, 37% solution) was saturated with hydrogen chloride gas at 15–20°, and 32 g (0.176 mole) of IV[1] was added. The mixture was heated to 60–70° for 7 hr, during which hydrogen chloride gas was bubbled slowly through it. The mixture was cooled, kept overnight, and concentrated *in vacuo*. Water, 100 ml, was added, and the mixture was neutralized with 2:3 dilute ammonium hydroxide. A solid formed and was filtered, washed several times with water, and dried. Recrystallization from methanol gave 22.4 g (65.6%) of V, mp 154–155° [lit. (6) mp 154–156°]; IR (KBr): 3080, 3020 (m), 2940 (w), 1755–1740 (s), 1600 (s), 1500 (s), 1350 (s), and 1300 (s) cm^{-1}.

4,5-Dimethoxyphthalyl Alcohol (VI)—A warm solution of 14 g (0.072 mole) of V in 150 ml of anhydrous tetrahydrofuran was added continuously to a suspension of 7.5 g of lithium aluminum hydride in 80 ml of tetrahydrofuran, and the mixture was refluxed for 4 hr. The mixture was cooled in an ice bath, and the excess lithium aluminum hydride was

[1] Aldrich.

0022-3549/80/0100-0120$01.00/0

© 1980, American Pharmaceutical Association

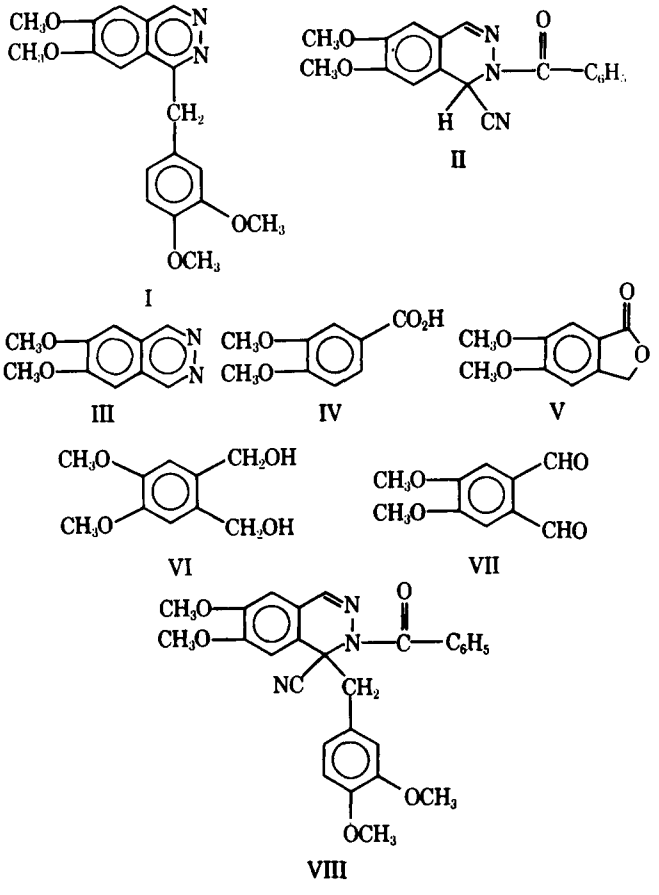

decomposed by the dropwise addition, with stirring, of 7.5 ml of water, 7.5 ml of 15% NaOH, and 22.5 ml of water. The precipitate was extracted with hot tetrahydrofuran, the combined tetrahydrofuran solutions were evaporated, and the residue was extracted with chloroform. Evaporation of the dried chloroform extract gave 13 g (91%) of VI, mp 110–111° (from benzene) [lit. (7) mp 111°].

4,5-Dimethoxyphthalaldehyde (VII)—To a vigorously stirred suspension of 20 g of activated manganese dioxide in 200 ml of chloroform was added 3 g of VI, and the mixture was stirred at room temperature for 3 days. The manganese dioxide was filtered and washed several times with chloroform, and the combined solvent was distilled to give 1.9 g (64.6%) of VII, mp 168–169° (from benzene) [lit. (7) mp 165°]; IR (KBr): 3100, 3000, 2930, 2870 (w), 1675 (vs), 1585 (s), 1510–1500 (s), 1460 (s), 1440 (s), and 1285 (s) cm^{-1}; NMR ($CDCl_3$): δ 10.7 (s, 2H), 7.36 (s, 2H), and 3.98 (s, 6H).

6,7-Dimethoxyphthalazine (III)—Compound VII (3.5 g, 0.018 mole) was warmed with 175 ml of absolute ethanol, and 1.1 g of 85% hydrazine hydrate was added dropwise with stirring. When VII had dissolved, the solution was refluxed for 5 hr and concentrated *in vacuo* to give 3.2 g (93.4%) of III, mp 198–200° (from chloroform–benzene) [lit. (8) mp 181–183°]; IR ($CHCl_3$): 3050 (m), 1605 (w), 1505 (m), 1470 (m), 1430 (s), 1335 (m), 1250 (s), 1225 (vs), and 1160 (s) cm^{-1}; NMR ($CDCl_3$): δ 9.27 (s, 2H), 7.1 (s, 2H), and 4.04 (s, 6H).

Anal.—Calc. for $C_{10}H_{10}N_2O_2$: C, 63.14; H, 5.30. Found: C, 63.41; H, 5.53.

1-Cyano-2-benzoyl-6,7-dimethoxy-1,2-dihydrophthalazine (II)—To a solution of 3.2 g (0.0168 mole) of III in 200 ml of dry methylene chloride were added a catalytic amount (50 mg) of anhydrous aluminum chloride and 5 g (0.0504 mole) of trimethylsilyl cyanide. After 10 min, 7.1 g (0.0504 mole) of benzoyl chloride was added, and the mixture was stirred at room temperature for 24 hr. The mixture was washed with water, 5% HCl, water, 5% NaOH, and water. The mixture was dried, and the solvent was removed. The residue was recrystallized from benzene–chloroform to give 5 g (92.6%) of II, mp 204–207°; IR (KBr): 3080 (w), 2975 (m), 2945 (w), 1640 (s), 1600 (s), 1570 (w), 1515 (s), 1450 (s), 1380 (s), 1315 (s), 1280 (s), 1250 (s), 1130 (s), 1010 (s), and 910 (s) cm^{-1}; NMR ($CDCl_3$): δ 7.78–7.20 (m, 6H), 6.86 (s, 1H), 6.82 (s, 1H), 6.55 (1H), 3.95 (s, 3H), and 3.92 (s, 3H).

Anal.—Calc. for $C_{18}H_{15}N_3O_3$: C, 67.28; H, 4.70; N, 13.08. Found: C, 67.28; H, 4.63; N, 13.02.

1-Cyano-1-(3,4-dimethoxybenzyl) -2- benzoyl-6,7-dimethoxy-1,2-dihydrophthalazine (VIII)—To a stirred solution of 3.21 g (0.01 mole) of II in 30 ml of dimethylformamide at −15° under a nitrogen atmosphere were added 1.87 g (0.01 mole) of 3,4-dimethoxybenzyl chloride and 0.48 g of 50% NaH in oil. The mixture was allowed to warm to room temperature and was stirred for an additional 2 hr. Then the solution was poured onto 300 g of ice. The product was filtered, washed with water, and dried to give 4.48 g (95%) of VIII, mp 198–201° (from chloroform–methanol); IR (KBr): 3070 (w), 3045 (w), 3010 (m), 2945 (w), 2850 (m), 1655 (s), 1600 (s), 1570 (m), 1510 (s), 1410 (s), 1330 (s), 1260 (s), 1240 (s), and 1120 (s) cm^{-1}; NMR ($CDCl_3$): δ 7.78–6.20 (m, 11H), 3.9 (s, 3H), 3.8 (s, 6H), 3.65 (s, 3H), and 3.56 (s, 2H).

Anal.—Calc. for $C_{27}H_{25}N_3O_5$: C, 68.78; H, 5.34; N, 8.91. Found: C, 68.85; H, 5.24; N, 8.88.

3-Azapapaverine (I)—A solution of 4.4 g of VIII and 47 g of potassium hydroxide in 140 ml of ethanol and 140 ml of water was refluxed for 3 hr. The mixture was concentrated *in vacuo* to less than half the volume, and 140 ml of water was added. The mixture was extracted with chloroform, and the dried chloroform extract was evaporated to give I (74% yield), mp 120° (from ethyl acetate–petroleum ether) [lit. (10) mp 120–121°].

Treatment of I in methanol with methyl iodide gave I methiodide, mp 203–208° (from ethanol); IR (KBr): 3010 (m), 2965 (m), 2920 (w), 2850 (m), 1595 (s), 1510 (vs), 1415 (s), 1300 (s), 1220 (s), 1150 (s), and 1030 (s) cm^{-1}; NMR (acetone-d_6): δ 10.35 (s, 1H), 7.98 (s, 1H), 7.9 (s, 1H), 7.05 (s, 1H), 6.83 (broad s, 2H), 4.73 (s, 2H), 4.68 (s, 3H), 4.11 (s, 3H), 4.08 (s, 3H), and 3.71 (s, 6H).

Anal.—Calc. for $C_{20}H_{23}IN_2O_4$: C, 49.80; H, 4.80; N, 5.80. Found: C, 49.77; H, 4.81; N, 5.89.

REFERENCES

(1) F. D. Popp, *Adv. Heterocycl. Chem.*, **9**, 1 (1968).

(2) *Ibid.*, **24**, 187 (1979).

(3) F. D. Popp, *Heterocycles*, **1**, 165 (1973).

(4) F. D. Popp, J. M. Wefer, and C. W. Klinowski, *J. Heterocycl. Chem.*, **5**, 879 (1968).

(5) D. Bhattacharjee and F. D. Popp, *Heterocycles*, **6**, 1905 (1977).

(6) T. Ikeda, S. Kanahara, and T. Ujiie, *Kanazawa Daigaku Yakugukubu, Kenkya Nempo*, **8**, 1 (1958).

(7) J. Blair, W. R. Logan, and G. T. Newbold, *J. Chem. Soc.*, **1956**, 2443.

(8) A. V. El'tsov and A. A. Ginesina, *Zh. Org. Khim.*, **3**, 191 (1967).

(9) S. Ruchirawat, N. Phadungkul, M. Chaunkamnerdkarn, and C. Thebtaranonth, *Heterocycles*, **6**, 43 (1977).

(10) T. Ikeda and S. Kanahara, *Kanazawa Daigaku Yakugukubu, Kenkya Nempo*, **10**, 15 (1960).

New Compounds: Derivatives of Fluorene XXXVII: 9-Substituted 3-Nitrofluorenes

HSI-LUNG PAN, CAROL-ANN COLE, and T. LLOYD FLETCHER ˣ

Received April 30, 1979, from the *Department of Oncological Organic Chemistry, The Fred Hutchinson Cancer Research Center, Seattle, WA 98104.* Accepted for publication July 10, 1979.

Abstract □ New 9-substituted 3-nitrofluorenes were prepared as potential intermediates in a study of modified electrophilicity and mutagenicity of the carcinogen 3-*N,O*-diacetylhydroxylaminofluorene. The reported derivatives, together with some already known 9-substituted 3-nitrofluorenes, were too unstable to survive the reducing conditions required to transform the nitro group to the corresponding hydroxylamine.

Keyphrases □ Fluorenes—synthesis of 3-nitro-9-substituted derivatives, potential enhancement of 3-*N,O*-diacetylhydroxylaminofluorene carcinogenicity □ 3-*N,O*-Diacetylhydroxylaminofluorene—synthesis of 9-substituted 3-nitrofluorene intermediates, effect on carcinogenicity □ Carcinogens—synthesis of 9-substituted 3-nitrofluorene intermediates for study of 3-*N,O*-diacetylhydroxylaminofluorene mutagenicity

Oncogenic arylamines and amides generally are believed to exert their baneful effects by undergoing enzymatic oxidation to an *N*-hydroxy derivative (a proximate carcinogen) and then by further reaction to form an ester such as the acetate or sulfate (1). Many of these esters are ultimate carcinogens, and they cleave heterolytically, with differing facility, at the nitrogen–oxygen bond. The electron-deficient nitrogen atom is left as an electrophilic center (acetamidonium ion). Such moieties are capable of an *in vivo* attack on various nucleophiles in tissue constituents such as DNA, RNA, and proteins. Some of these reactions appear to be crucial in carcinogenesis.

DISCUSSION

Much of the knowledge supporting the foregoing concepts was developed from studies on 2-fluorenamine and *N*-acetyl-2-fluorenamine, a strong hepatocarcinogen (1). A closely related isomer, *N*-acetyl-3-fluorenamine, is of interest because its *N*-acetoxy derivative, 3-*N,O*-diacetylhydroxylaminofluorene, is a much weaker carcinogen (mammary) and is not hepatocarcinogenic (2). It is possible that one major reason for this difference in biological activity between the 2-substituted and 3-substituted compounds is simply the lower tendency of the acetoxy group of the latter to act as a leaving group and the lower electrophilicity of the resulting acetamidonium ion.

Accordingly, 3-nitrofluorene (I) derivatives were designed with various 9-substituents to increase the leaving group facility of the acetoxy group and, after reduction and acetylation to the *N*-acetoxyamide, to produce a compound with enhanced mutagenicity and carcinogenicity. The presence of an electron donor group in the single-ring compound *O*-acetyl-*N*-benzoylphenylhydroxylamine was shown to enhance heterolytic acyloxy migration to a nucleophilic carbon (3). 2-Methoxy-3-*N,O*-diacetylhydroxylaminofluorene showed slightly enhanced mutagenicity over that of 3-*N,O*-diacetylhydroxylaminofluorene[1]. Since it was assumed that the effect sought was lessened by steric hindrance and since other methoxylated 3-nitrofluorenes were not readily available, the 9-position was investigated.

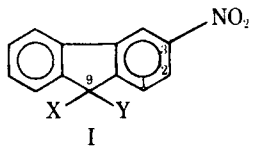

I

Ia: X = H, Y = Br
Ib: X = H, Y = OCH_3
Ic: X = H, Y = OC_2H_5
Id: X = H, Y = $P^+(C_6H_5)_3Br^-$
Ie: X = H, Y = $SC(NH_2)=N^+H_2Br^-$
If: XY = $=NNHSO_2C_6H_4CH_3$-*p*

Unfortunately, *Ia–If* were either too unstable for the reducing conditions required to transform the nitro group to the corresponding hydroxylamine (ammonium sulfide in ethanol–dimethylformamide) (4) or gave relatively intractable mixtures in the workup. Since these compounds may be of interest in other areas and since known 3,9-disubstituted fluorenes are comparatively few, this report is pertinent. Ways of stabilizing the 9-position are being studied and will be the subject of a future article.

Attempts to make 9-methoxy-3-nitrofluorene (*Ib*) from 3-nitrofluorene-9-ol (5) with methyl iodide, dimethylformamide, and silver oxide (6) or with trimethylsulfoxonium iodide and silver oxide (7) led to recovery of 3-nitrofluorenone as the only recognizable product.

Attempts to make an ylid from *Id* (8) failed, as did efforts to produce 9-mercapto-3-nitrofluorene from *Ie* (9). Attempts to prepare 9-fluoro- or 9-cyano-3-nitrofluorene did not yield the desired products. Previously known 9-chloro-3-nitrofluorene and 9-acetoxy-3-nitrofluorene were included in the nitro reduction attempts.

EXPERIMENTAL[2]

9-Bromo-3-nitrofluorene (Ia)—3-Nitrofluoren-9-ol (7.5 g, 0.033 mole), prepared by sodium borohydride reduction of 3-nitrofluoren-9-one (5), was mixed with 100% acetic acid (120 ml). Aqueous 48% HBr (16 ml) was added to the stirred mixture all at once. The mixture was heated with stirring to boiling, and the solvent was distilled off. The residue was allowed to cool to room temperature and then was dissolved in hot benzene. The benzene solution was treated with activated charcoal[3], filtered, and concentrated to a small volume. Addition of petroleum ether (bp 30–60°) caused the product to crystallize as white needles, 9.5 g (99%), mp 154.5–156°. Recrystallization from benzene–petroleum ether (bp 30–60°) gave 9.1 g, mp 157–158°.

Anal.—Calc. for $C_{13}H_8BrNO_2$: C, 53.82; H, 2.78; Br, 27.54; N, 4.83. Found: C, 53.81; H, 2.81; Br, 27.75; N, 4.86.

9-Methoxy-3-nitrofluorene (Ib)—9-Chloro-3-nitrofluorene (10) (1 g, 0.004 mole) was mixed with powdered silver nitrate (0.7 g, 0.004 mole) and absolute methanol (40 ml). The mixture was refluxed under dry nitrogen for 2 hr and cooled to room temperature. The suspension was filtered into a slurry of crushed ice and water. The crystallized product in the ice slurry then was collected, washed with water, and dried over concentrated sulfuric acid *in vacuo* to give 0.9 g. Chromatography on silica gel and recrystallization from methanol–water gave a pure product, 0.45 g (47%), mp 103.5–104.5°; IR (mineral oil): 1060 cm^{-1}.

Anal.—Calc. for $C_{14}H_{11}NO_3$: C, 69.70; H, 4.60; N, 5.81. Found: C, 69.87; H, 4.37; N, 5:62.

9-Ethoxy-3-nitrofluorene (Ic)—In a manner similar to that for *Ib*, equimolar amounts of 9-chloro-3-nitrofluorene and silver nitrate in refluxing absolute ethanol gave crude *Ic*. Chromatography and recrystallization from ethanol–water gave a 40% yield of pure product, mp 88–89°; IR (mineral oil): 1060 cm^{-1}.

Anal.—Calc. for $C_{15}H_{13}NO_3$: C, 70.58; H, 5.13; N, 5.49. Found: C, 70.52; H, 5.01; N, 5.42.

9-(3-Nitrofluorenyl)triphenylphosphonium Bromide (Id)—To a stirred solution of *Ia* (1.5 g, 0.005 mole) in benzene (50 ml) was added triphenylphosphine (1.3 g, 0.005 mole) in one portion. The mixture was

[1] H.-L. Pan, C.-A. Cole, and T. L. Fletcher, unpublished results.

[2] Melting points were determined on a Fisher-Johns apparatus and are corrected. IR spectra were obtained using a Beckman IR-33 spectrophotometer. Elemental analyses were performed by commercial analytical laboratories.

[3] Darco.

0022-3549/80/0100-0122$01.00/0
© 1980, American Pharmaceutical Association

stirred further in nitrogen for 1 hr and then refluxed for 0.5 hr and stirred to cool. After filtration from the reaction mixture, the gray solid (0.7 g, 25%) was washed twice with benzene and then with ether and dried *in vacuo*, mp 210–214° dec.

Anal.—Calc. for $C_{31}H_{23}BrNO_2P$: C, 67.40; H, 4.20; N, 2.54. Found: C, 67.27; H, 4.18; N, 2.64.

9-(3-Nitrofluorenyl)isothiuronium Bromide (Ie)—Compound Ia (2.9 g, 0.01 mole) and thiourea (0.76 g, 0.01 mole) were ground together thoroughly. To the mixture were added 1-butanol (8 ml) and aqueous 48% HBr (1 ml). The mixture was refluxed with occasional shaking for 0.5 hr and cooled. The crystalline product was collected, washed successively with small amounts of 1-butanol, carbon tetrachloride, chloroform, and ether, and air dried, giving 3.45 g (93%), mp 210–215° dec.

Anal.—Calc. for $C_{14}H_{12}BrN_3O_2S$: C, 45.91; H, 3.30; N, 11.47; S, 8.75. Found: C, 45.77; H, 3.22; N, 11.28; S, 8.76.

3-Nitrofluoren-9-*p*-toluenesulfonylhydrazone (If)—*p*-Toluenesulfonylhydrazine (11) (15.4 g, 0.083 mole) and 3-nitrofluoren-9-one (15 g, 0.067 mole) were suspended in absolute ethanol (150 ml). The suspension was heated with stirring under reflux for 1.5 hr and cooled. The brown crystalline product was collected, washed with 100 ml of boiling ethanol, and dried, giving 20.5 g (78%), mp 194–197° dec.

The product (0.5 g) was purified by repeated washing with boiling ethanol and recrystallization from chloroform–benzene to give lustrous orange crystals, 0.3 g, mp 205–206° dec.; IR (mineral oil): 3230, 1583, 1515, 1365, 1330, and 1150 cm^{-1}.

Anal.—Calc. for $C_{20}H_{15}N_3O_4S$: C, 61.06; H, 3.84; N, 10.68. Found: C, 60.94; H, 3.93; N, 10.24.

REFERENCES

(1) E. C. Miller and J. A. Miller, in "Chemical Carcinogens," C. E. Searle, Ed., ACS Monograph 173, American Chemical Society, Washington, D.C., 1976, chap. 16.

(2) Y. Yost, H. R. Gutmann, and R. E. Rydell, *Cancer Res.*, **35**, 447 (1975).

(3) T. Ohta, K. Skudo, and T. Okamoto, *Tetrahedron Lett.*, **1978**, 1983.

(4) J. D. Scribner and N. K. Naimy, *Cancer Res.*, **33**, 1159 (1973).

(5) H.-L. Pan, C.-A. Cole, and T. L. Fletcher, *Synthesis*, **1975**, 716.

(6) R. Kuhn, H. Trischmann, and I. Löw, *Angew. Chem.*, **67**, 32 (1955).

(7) R. Kuhn and H. Trischmann, *Ann.*, **611**, 117 (1958).

(8) T. L. Fletcher, M. J. Namkung, J. R. Dice, and S. K. Schaefer, *J. Med. Chem.*, **8**, 347 (1965).

(9) H.-L. Pan and T. L. Fletcher, *Chem. Ind.*, **1968**, 546.

(10) C. L. Arcus and M. M. Coombs, *J. Chem. Soc.*, **1954**, 3977.

(11) L. F. Fieser and M. Fieser, "Reagents for Organic Synthesis," vol. 2, Wiley, New York, N.Y., 1969, p. 417.

ACKNOWLEDGMENTS

Supported by Research Grant CA-19279 and Cancer Center Support Grant CA-15704 from the National Cancer Institute.

COMMUNICATIONS

Decarboxylation Kinetics of 5-(Tetradecyloxy)-2-furoic Acid

Keyphrases □ Decomposition—solid-state reactions, decarboxylation kinetics, hypolipidemic agent, 5-(tetradecyloxy)-2-furoic acid □ Kinetics—solid-state activation energy, decarboxylation, decomposition, 5-(tetradecyloxy)-2-furoic acid □ 2-Furoic acid, 5-tetradecyloxy—hypolipidemic agent, solid-state decomposition, kinetics

To the Editor:

Single-component solid reactions are of several types: *e.g.*, a solid can form a solid and a gas (type I) or a liquid and a gas (type II). A type I reaction is exemplified by oxygen formation from permanganates, whereas the formation of liquid aniline and gaseous carbon dioxide from decarboxylation of *p*-aminobenzoic acid denotes a type II reaction. This paper reports a type II reaction of a pharmaceutical solid, 5-(tetradecyloxy)-2-furoic acid[1], which is a novel hypolipidemic agent (1).

Decarboxylation kinetics in the solid state have been reported (2–7), and several reported reactions (3, 5, 6) were type II. This paper deals with carboxylic acid, RCOOH, where R = $C_{14}H_{29}O$–(C_4H_2O)– and where (C_4H_2O)– is a furan moiety. The compound decomposes *via* the reaction shown in Scheme I, where RH is liquid in the temperature range studied; hence, the reaction is type II.

$$RCOOH \rightarrow RH + CO_2$$

Scheme I

An apparatus such as the one described by Carstensen and Musa (Fig. 6 of Ref. 3) was constructed for the studies at each temperature. The assembly was completely tight since it was fused by glass blowing and sealed under vacuum (<0.1 μm Hg). The entire assembly was placed in a thermostated mineral oil bath or, for lower temperatures, in a water bath. The pressure evolution was followed as a function of time with a cathetometer[2]. All pertinent volumes were determined by water weight calibration. With knowledge of the volumes, the pressures were converted to moles of gas, thus yielding a decomposition *versus* time curve (Fig. 1). The gas evolution eventually accounted for 100% decomposition.

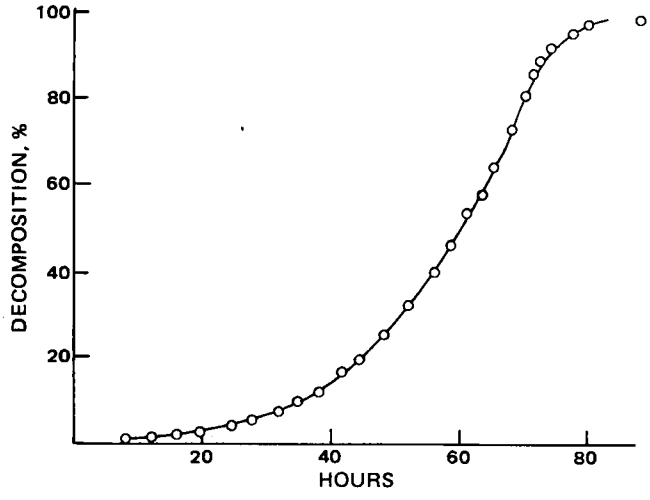

Figure 1—*Percent of parent compound decomposed as a function of time at 90°.*

[1] This agent is known as RMI 14514 and was supplied by R. A. Parker and M. A. Zoglio, Merrell National Laboratories, Cincinnati, OH 45215.

[2] Model M-911, Gaertner Scientific Corp., Chicago, IL 60614.

0022-3549/80/0100-0123$01.00/0

© 1980, American Pharmaceutical Association

stirred further in nitrogen for 1 hr and then refluxed for 0.5 hr and stirred to cool. After filtration from the reaction mixture, the gray solid (0.7 g, 25%) was washed twice with benzene and then with ether and dried *in vacuo*, mp 210–214° dec.

Anal.—Calc. for $C_{31}H_{23}BrNO_2P$: C, 67.40; H, 4.20; N, 2.54. Found: C, 67.27; H, 4.18; N, 2.64.

9-(3-Nitrofluorenyl)isothiuronium Bromide (Ie)—Compound Ia (2.9 g, 0.01 mole) and thiourea (0.76 g, 0.01 mole) were ground together thoroughly. To the mixture were added 1-butanol (8 ml) and aqueous 48% HBr (1 ml). The mixture was refluxed with occasional shaking for 0.5 hr and cooled. The crystalline product was collected, washed successively with small amounts of 1-butanol, carbon tetrachloride, chloroform, and ether, and air dried, giving 3.45 g (93%), mp 210–215° dec.

Anal.—Calc. for $C_{14}H_{12}BrN_3O_2S$: C, 45.91; H, 3.30; N, 11.47; S, 8.75. Found: C, 45.77; H, 3.22; N, 11.28; S, 8.76.

3-Nitrofluoren-9-*p*-toluenesulfonylhydrazone (If)—*p*-Toluenesulfonylhydrazine (11) (15.4 g, 0.083 mole) and 3-nitrofluoren-9-one (15 g, 0.067 mole) were suspended in absolute ethanol (150 ml). The suspension was heated with stirring under reflux for 1.5 hr and cooled. The brown crystalline product was collected, washed with 100 ml of boiling ethanol, and dried, giving 20.5 g (78%), mp 194–197° dec.

The product (0.5 g) was purified by repeated washing with boiling ethanol and recrystallization from chloroform–benzene to give lustrous orange crystals, 0.3 g, mp 205–206° dec.; IR (mineral oil): 3230, 1583, 1515, 1365, 1330, and 1150 cm^{-1}.

Anal.—Calc. for $C_{20}H_{15}N_3O_4S$: C, 61.06; H, 3.84; N, 10.68. Found: C, 60.94; H, 3.93; N, 10.24.

REFERENCES

(1) E. C. Miller and J. A. Miller, in "Chemical Carcinogens," C. E. Searle, Ed., ACS Monograph 173, American Chemical Society, Washington, D.C., 1976, chap. 16.

(2) Y. Yost, H. R. Gutmann, and R. E. Rydell, *Cancer Res.*, **35**, 447 (1975).

(3) T. Ohta, K. Skudo, and T. Okamoto, *Tetrahedron Lett.*, **1978**, 1983.

(4) J. D. Scribner and N. K. Naimy, *Cancer Res.*, **33**, 1159 (1973).

(5) H.-L. Pan, C.-A. Cole, and T. L. Fletcher, *Synthesis*, **1975**, 716.

(6) R. Kuhn, H. Trischmann, and I. Löw, *Angew. Chem.*, **67**, 32 (1955).

(7) R. Kuhn and H. Trischmann, *Ann.*, **611**, 117 (1958).

(8) T. L. Fletcher, M. J. Namkung, J. R. Dice, and S. K. Schaefer, *J. Med. Chem.*, **8**, 347 (1965).

(9) H.-L. Pan and T. L. Fletcher, *Chem. Ind.*, **1968**, 546.

(10) C. L. Arcus and M. M. Coombs, *J. Chem. Soc.*, **1954**, 3977.

(11) L. F. Fieser and M. Fieser, "Reagents for Organic Synthesis," vol. 2, Wiley, New York, N.Y., 1969, p. 417.

ACKNOWLEDGMENTS

Supported by Research Grant CA-19279 and Cancer Center Support Grant CA-15704 from the National Cancer Institute.

COMMUNICATIONS

Decarboxylation Kinetics of 5-(Tetradecyloxy)-2-furoic Acid

Keyphrases □ Decomposition—solid-state reactions, decarboxylation kinetics, hypolipidemic agent, 5-(tetradecyloxy)-2-furoic acid □ Kinetics—solid-state activation energy, decarboxylation, decomposition, 5-(tetradecyloxy)-2-furoic acid □ 2-Furoic acid, 5-tetradecyloxy—hypolipidemic agent, solid-state decomposition, kinetics

To the Editor:

Single-component solid reactions are of several types: *e.g.*, a solid can form a solid and a gas (type I) or a liquid and a gas (type II). A type I reaction is exemplified by oxygen formation from permanganates, whereas the formation of liquid aniline and gaseous carbon dioxide from decarboxylation of *p*-aminobenzoic acid denotes a type II reaction. This paper reports a type II reaction of a pharmaceutical solid, 5-(tetradecyloxy)-2-furoic acid[1], which is a novel hypolipidemic agent (1).

Decarboxylation kinetics in the solid state have been reported (2–7), and several reported reactions (3, 5, 6) were type II. This paper deals with carboxylic acid, RCOOH, where R = $C_{14}H_{29}O$–(C_4H_2O)– and where (C_4H_2O)– is a furan moiety. The compound decomposes *via* the reaction shown in Scheme I, where RH is liquid in the temperature range studied; hence, the reaction is type II.

$$RCOOH \rightarrow RH + CO_2$$

Scheme I

An apparatus such as the one described by Carstensen and Musa (Fig. 6 of Ref. 3) was constructed for the studies at each temperature. The assembly was completely tight since it was fused by glass blowing and sealed under vacuum (<0.1 μm Hg). The entire assembly was placed in a thermostated mineral oil bath or, for lower temperatures, in a water bath. The pressure evolution was followed as a function of time with a cathetometer[2]. All pertinent volumes were determined by water weight calibration. With knowledge of the volumes, the pressures were converted to moles of gas, thus yielding a decomposition *versus* time curve (Fig. 1). The gas evolution eventually accounted for 100% decomposition.

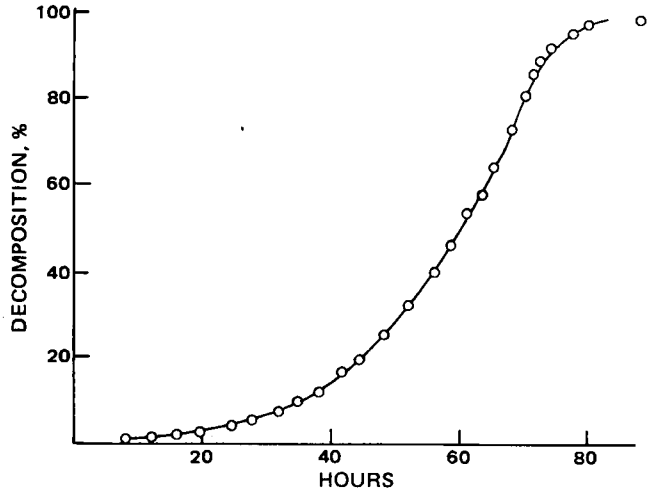

Figure 1—*Percent of parent compound decomposed as a function of time at 90°.*

[1] This agent is known as RMI 14514 and was supplied by R. A. Parker and M. A. Zoglio, Merrell National Laboratories, Cincinnati, OH 45215.

[2] Model M-911, Gaertner Scientific Corp., Chicago, IL 60614.

0022-3549/80/0100-0123$01.00/0

© 1980, American Pharmaceutical Association

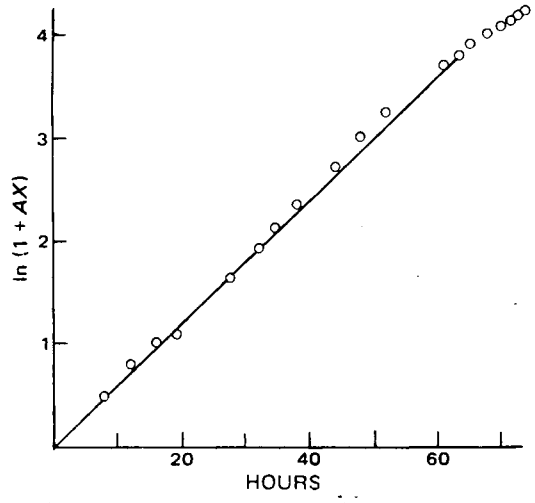

Figure 2—*Data from Fig. 1 treated according to Eq. 3* (A = 70).

The data treatment (3–6) of the curve is as follows. If the amount is n moles and if there are x moles decomposed at time t, then x is present as liquid. If the solubility of parent compound in the liquid is S moles of RCOOH/mole of RH, then the amount of solid present is $n - x - Sx$; the rate equation then is:

$$dx/dt = -k_s(n - X - Sx) - k_lSx \qquad \text{(Eq. 1)}$$

where k_s and k_l are solid and liquid first-order rate constants, respectively. If the mole fraction $X = x/n$ is used in place of moles decomposed, the equation becomes:

$$dX/dt = -k_s(1 - x - SX) - k_lSX \qquad \text{(Eq. 2)}$$

By integration:

$$\ln(1 + AX) = -\alpha t \qquad \text{(Eq. 3)}$$

where $A = \alpha/k_s$ and $\alpha = k_lS - k_sS - k_s$. The value of A is found by iteration, and linearization according to Eq. 3 is shown in Fig. 2. Once all solid has disappeared, the model no longer holds and simply reverts to solution kinetics as pointed out by Carstensen and Musa (3).

The values at four temperatures are shown in Table I. The least-squares fit for the Arrhenius plot (Fig. 3) is:

$$\ln k_s = (-38{,}650/R)(1/T) + 46.25 \qquad \text{(Eq. 4)}$$

with a correlation coefficient of −0.992. The activation

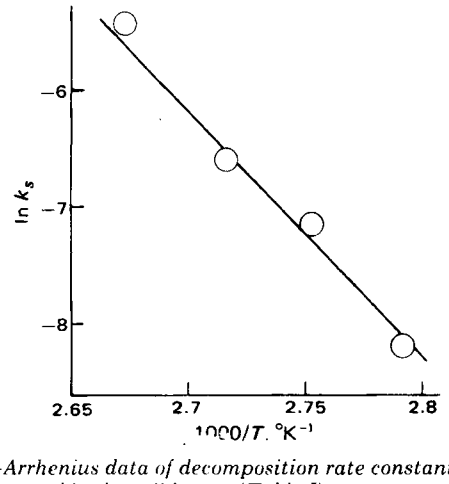

Figure 3—*Arrhenius data of decomposition rate constants,* k_s, *of the parent compound in the solid state (Table I).*

Table I—Parameter Values at Different Temperatures

Temperature	1000/T	A^a	α^b, hr^{-1}	$k_s{}^c$, hr^{-1}	ln k_s
85°	2.792	28	0.0070	0.00025	−8.094
90°	2.754	70	0.0594	0.00085	−7.070
95°	2.716	110	0.116	0.00151	−6.496
101°	2.673	175	0.571	0.00327	−5.723

[a] The A denotes the iteration constant in Eq. 3. [b] The α denotes the slope of the line according to Eq. 3. [c] The k_s is the solid-state decomposition constant.

energy for k_s is high compared to usual solution kinetics (although within range) but is lower than that for, for instance, the solid-state decomposition of substituted benzoic (3) or salicylic (6) acids. Solid-state activation energies are extremely high (3–7, 9–13). When they are wholly dictated by physical propagation (type I), the energy of activation supersedes the normal range for solution kinetics by a factor of two to three. Type II reactions usually have intermediate activation energies.

(1) R. A. Parker, T. Karyia, J. M. Grisar, and V. Petrow, *J. Med. Chem.*, **20**, 781 (1977).
(2) C. E. H. Bawn, in "Chemistry of the Solid State," W. E. Gardner, Ed., Butterworths Scientific Publication, London, England, 1955, p. 254.
(3) J. T. Carstensen and M. N. Musa, *J. Pharm. Sci.*, **61**, 112 (1972).
(4) J. T. Carstensen and P. Pothisiri, *ibid.*, **64**, 37 (1975).
(5) J. T. Carstensen, *ibid.*, **63**, 1 (1974).
(6) P. Pothisiri and J. T. Carstensen, *ibid.*, **64**, 1931 (1975).
(7) S. Kornblum and B. Sciarrone, *ibid.*, **53**, 935 (1964).
(8) R. R. A. Abou-Shaaban and A. P. Simonelli, *Thermochim. Acta*, **26**, 67 (1978).
(9) *Ibid.*, **26**, 89 (1978).
(10) *Ibid.* **26**, 111 (1978).
(11) R. R. A. Abou-Shaaban, J. A. Reffner, and A. P. Simonelli, *Thermochim. Acta*, **26**, 125 (1978).
(12) *Ibid.*, **26**, 137 (1978).

J. T. Carstensen [x]
Rohit C. Kothari
School of Pharmacy
University of Wisconsin
Madison, WI 53706

Received June 25, 1979.
Accepted for publication September 17, 1979.
The authors are indebted to Dr. R. A. Parker and Dr. M. A. Zoglio for valuable help and assistance.

Structure–Activity Analysis of Hydrazide Monoamine Oxidase Inhibitors Using Molecular Connectivity

Keyphrases □ Molecular connectivity analysis—hydrazide monoamine oxidase inhibitors, structure–activity relationships □ Structure–activity relationships—hydrazide monoamine oxidase inhibitors, molecular connectivity analysis □ Monoamine oxidase inhibitors—hydrazides, structure–activity relationships, molecular connectivity analysis

To the Editor:

Fulcrand *et al.* (1) recently analyzed a series of monoamine oxidase inhibitors and found good correlations between pI_{50} values and electronic and steric parameters for 24 compounds. The methods of Hansch *et al.* (2) and Free and Wilson (3), as employed by Fulcrand *et al.* (1), were equally successful in correlating physical properties with

0022-3549/80/0100-0124$01.00/0
© 1980, American Pharmaceutical Association

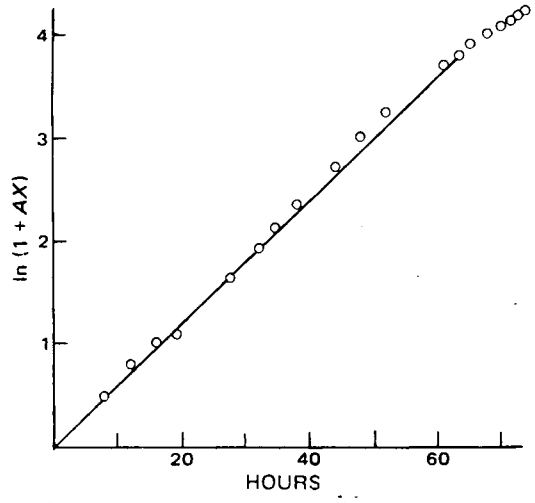

Figure 2—*Data from Fig. 1 treated according to Eq. 3* (A = 70).

The data treatment (3–6) of the curve is as follows. If the amount is n moles and if there are x moles decomposed at time t, then x is present as liquid. If the solubility of parent compound in the liquid is S moles of RCOOH/mole of RH, then the amount of solid present is $n - x - Sx$; the rate equation then is:

$$dx/dt = -k_s(n - X - Sx) - k_lSx \qquad \text{(Eq. 1)}$$

where k_s and k_l are solid and liquid first-order rate constants, respectively. If the mole fraction $X = x/n$ is used in place of moles decomposed, the equation becomes:

$$dX/dt = -k_s(1 - x - SX) - k_lSX \qquad \text{(Eq. 2)}$$

By integration:

$$\ln(1 + AX) = -\alpha t \qquad \text{(Eq. 3)}$$

where $A = \alpha/k_s$ and $\alpha = k_lS - k_sS - k_s$. The value of A is found by iteration, and linearization according to Eq. 3 is shown in Fig. 2. Once all solid has disappeared, the model no longer holds and simply reverts to solution kinetics as pointed out by Carstensen and Musa (3).

The values at four temperatures are shown in Table I. The least-squares fit for the Arrhenius plot (Fig. 3) is:

$$\ln k_s = (-38{,}650/R)(1/T) + 46.25 \qquad \text{(Eq. 4)}$$

with a correlation coefficient of −0.992. The activation

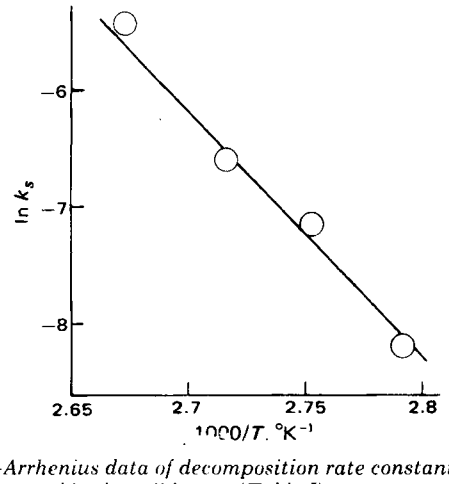

Figure 3—*Arrhenius data of decomposition rate constants,* k_s, *of the parent compound in the solid state (Table I).*

Table I—Parameter Values at Different Temperatures

Temperature	1000/T	A^a	α^b, hr^{-1}	$k_s{}^c$, hr^{-1}	ln k_s
85°	2.792	28	0.0070	0.00025	−8.094
90°	2.754	70	0.0594	0.00085	−7.070
95°	2.716	110	0.116	0.00151	−6.496
101°	2.673	175	0.571	0.00327	−5.723

[a] The A denotes the iteration constant in Eq. 3. [b] The α denotes the slope of the line according to Eq. 3. [c] The k_s is the solid-state decomposition constant.

energy for k_s is high compared to usual solution kinetics (although within range) but is lower than that for, for instance, the solid-state decomposition of substituted benzoic (3) or salicylic (6) acids. Solid-state activation energies are extremely high (3–7, 9–13). When they are wholly dictated by physical propagation (type I), the energy of activation supersedes the normal range for solution kinetics by a factor of two to three. Type II reactions usually have intermediate activation energies.

(1) R. A. Parker, T. Karyia, J. M. Grisar, and V. Petrow, *J. Med. Chem.*, **20**, 781 (1977).

(2) C. E. H. Bawn, in "Chemistry of the Solid State," W. E. Gardner, Ed., Butterworths Scientific Publication, London, England, 1955, p. 254.

(3) J. T. Carstensen and M. N. Musa, *J. Pharm. Sci.*, **61**, 112 (1972).

(4) J. T. Carstensen and P. Pothisiri, *ibid.*, **64**, 37 (1975).

(5) J. T. Carstensen, *ibid.*, **63**, 1 (1974).

(6) P. Pothisiri and J. T. Carstensen, *ibid.*, **64**, 1931 (1975).

(7) S. Kornblum and B. Sciarrone, *ibid.*, **53**, 935 (1964).

(8) R. R. A. Abou-Shaaban and A. P. Simonelli, *Thermochim. Acta*, **26**, 67 (1978).

(9) *Ibid.*, **26**, 89 (1978).

(10) *Ibid.* **26**, 111 (1978).

(11) R. R. A. Abou-Shaaban, J. A. Reffner, and A. P. Simonelli, *Thermochim. Acta*, **26**, 125 (1978).

(12) *Ibid.*, **26**, 137 (1978).

J. T. Carstensen [x]
Rohit C. Kothari
School of Pharmacy
University of Wisconsin
Madison, WI 53706

Received June 25, 1979.
Accepted for publication September 17, 1979.
The authors are indebted to Dr. R. A. Parker and Dr. M. A. Zoglio for valuable help and assistance.

Structure–Activity Analysis of Hydrazide Monoamine Oxidase Inhibitors Using Molecular Connectivity

Keyphrases □ Molecular connectivity analysis—hydrazide monoamine oxidase inhibitors, structure–activity relationships □ Structure–activity relationships—hydrazide monoamine oxidase inhibitors, molecular connectivity analysis □ Monoamine oxidase inhibitors—hydrazides, structure–activity relationships, molecular connectivity analysis

To the Editor:

Fulcrand *et al.* (1) recently analyzed a series of monoamine oxidase inhibitors and found good correlations between pI_{50} values and electronic and steric parameters for 24 compounds. The methods of Hansch *et al.* (2) and Free and Wilson (3), as employed by Fulcrand *et al.* (1), were equally successful in correlating physical properties with

0022-3549/80/0100-0124$01.00/0
© 1980, American Pharmaceutical Association

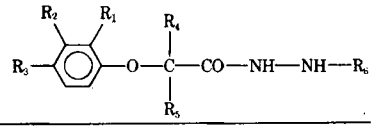

Table I—Hydrazide Monoamine Oxidase Inhibitors

Compound	R_1	R_2	R_3	R_4	R_5	R_6	E	pI_{50}
I	H	H	H	H	H	$CH(CH_3)_2$	−0.4310	5.42
II	Cl	H	H	H	H	$CH(CH_3)_2$	−0.4425	5.60
III	H	Cl	H	H	H	$CH(CH_3)_2$	−0.4368	5.40
IV	H	H	Cl	H	H	$CH(CH_3)_2$	−0.4433	5.96
V	CH_3	H	H	H	H	$CH(CH_3)_2$	−0.4390	5.54
VI	H	CH_3	H	H	H	$CH(CH_3)_2$	−0.4333	5.05
VII	H	H	CH_3	H	H	$CH(CH_3)_2$	−0.4355	5.40
VIII	OCH_3	H	H	H	H	$CH(CH_3)_2$	−0.4365	5.62
IX	H	OCH_3	H	H	H	$CH(CH_3)_2$	−0.4365	5.42
X	H	H	OCH_3	H	H	$CH(CH_3)_2$	−0.4353	5.52
XI	H	H	H	H	CH_3	$CH(CH_3)_2$	−0.4125	5.00
XII	Cl	H	H	H	CH_3	$CH(CH_3)_2$	−0.4148	5.16
XIII	H	Cl	H	H	CH_3	$CH(CH_3)_2$	−0.4118	4.96
XIV	H	H	Cl	H	CH_3	$CH(CH_3)_2$	−0.4155	5.00
XV	H	H	H	CH_3	CH_3	$CH(CH_3)_2$	−0.4025	4.34
XVI	H	H	Cl	CH_3	CH_3	$CH(CH_3)_2$	−0.4133	4.80
XVII	H	CH_3	H	H	CH_3	$CH(CH_3)_2$	−0.4115	4.90
XVIII	H	H	H	H	H	C_2H_5	−0.4232	5.82
XIX	H	H	Cl	H	H	C_2H_5	−0.4262	6.00
XX	H	H	H	H	H	$CH_2C_6H_5$	−0.4448	6.14
XXI	H	H	H	H	H	$CH(CH_3)C_6H_5$	−0.4340	5.70
XXII	H	H	CH_3	H	H	$CH(CH_3)C_6H_5$	−0.4340	6.05
XXIII	H	H	OCH_3	H	H	$CH(CH_3)C_6H_5$	−0.4368	6.00
XXIV	H	H	Cl	H	H	$CH_2C_6H_5$	−0.4560	6.96

the activity of the molecules whose structures are shown in Table I. Electronic effects, reflected in polarographic half-wave potentials, and steric effects were the most important parameters examined in the correlations. It was concluded that the monoamine oxidase inhibitory activity of the series was due to the hydrazide group, which could form an unstable diazene with the monoamine oxidase flavine coenzyme before rearrangement to bind on the enzyme.

An alternative approach to determining structure–activity relationships and to improving the understanding of the mechanism of action of a series of compounds evolved from the work of Kier and Hall (4, 5) and has been used extensively in structure–activity analyses (6–8). This approach, the molecular connectivity method, has its roots in the topology of the molecules, from which a set of indexes may be calculated. These indexes encode molecular structural information into the regression analysis. The indexes may be used alone or in conjunction with other physical parameters to discover correlations concerning biological or chemical activity within a series of molecules.

Molecular connectivity indexes were calculated for the monoamine oxidase inhibitors of Fulcrand *et al.* (1). Linear regression analysis by computer search for the three variables that gave the best correlation with activity as monoamine oxidase inhibitors yielded:

$$pI_{50} = -5.2 - 29E - 0.82\,{}^2\chi + 1.8\,{}^3\chi_p^v \qquad \text{(Eq. 1)}$$
$$n = 24 \quad r = 0.941 \quad s = 0.201 \quad F = 52$$

where E represents the half-wave potential; the other indexes calculated for the molecules were shown previously (4). This equation clearly indicates that electronic effects contribute to the monoamine oxidase inhibitor activity of the hydrazides, in agreement with Fulcrand *et al.* (1). The ${}^2\chi$ index gives weight to structural features of two-bond lengths in the molecules, whereas the ${}^3\chi_p^v$ index represents three-bond path lengths within the molecules and also emphasizes the importance of the heteroatoms in the substituents.

To gain further insight into structural influences on the interaction between the inhibitors and the active enzyme site, regression analyses were run on a subseries of molecules formed by the deletion of certain substituent groups. In particular, the nitrogen substituent (R_6) was kept constant with the isopropyl group to determine if this substituent was governing the inhibitory potency. This subset of 17 molecules correlates with pI_{50}:

$$pI_{50} = -4.1 + 0.59\,{}^0\chi^2 - 0.94\,{}^2\chi - 23E \qquad \text{(Eq. 2)}$$
$$n = 17 \quad r = 0.951 \quad s = 0.134 \quad F = 41$$

Again, E and ${}^2\chi$ emerge as significant parameters, but ${}^3\chi_p^v$ is replaced by ${}^0\chi^v$. However, this new valency chi index retains an indication of a contribution of heteroatoms in the substituents to activity. If the R_4 and R_5 substituents are limited to hydrogen while R_6 is kept as isopropyl, then only 10 molecules remain and the correlation is:

$$pI_{50} = -34 - 94E - 2.6\,{}^4\chi_{pc}^v \qquad \text{(Eq. 3)}$$
$$n = 10 \quad r = 0.923 \quad s = 0.100 \quad F = 20$$

Electronic effects again contribute to the relationship. The ${}^4\chi_{pc}^v$ index relates well to systems where ring substitutions have been made and indicates that monoamine oxidase inhibitor activity of the hydrazides is related to the ring in some fashion, perhaps indirectly through its effects on the neighboring ether linkage. A further argument can be made for this point if all substituents from R_1 through R_5 are restricted to hydrogen and R_6 is varied. Only four molecules remain in the set, but there is no hint of correlation with electronic or chi parameters to the monoamine oxidase inhibitor activity.

Although the R_6 substituents certainly must affect the hydrazide, these observations would clearly argue against the hydrazide moiety as the sole contributor to biological activity. Therefore, it may be concluded that monoamine oxidase inhibitor activity of these hydrazides depends

largely on the nature of the ring substitution as well as on the half-wave reduction potential of the ring, its substituents, or the ether oxygen.

(1) P. Fulcrand, G. Berge, A. Noel, P. Chevallet, J. Castel, and H. Orzalesi, *Eur. J. Med. Chem.*, **13**, 177 (1978).
(2) C. Hansch, R. M. Muir, T. Fujita, P. O. Maloney, F. Gerer, and M. Strejc, *J. Am. Chem. Soc.*, **85**, 2817 (1963).
(3) S. M. Free and J. R. Wilson, *J. Med. Chem.*, **7**, 395 (1964).
(4) L. B. Kier and L. H. Hall, "Molecular Connectivity in Chemistry and Drug Research," Academic, New York, N.Y, 1976.
(5) L. B. Kier and L. H. Hall, *J. Med. Chem.*, **20**, 1631 (1977).
(6) L. B. Kier and R. A. Glennon, *Life Sci.*, **22**, 1589 (1978).
(7) R. A. Glennon and L. B. Kier, *Eur. J. Med. Chem.*, **13**, 219 (1978).
(8) R. A. Glennon, L. B. Kier, and A. T. Shulgin, *J. Pharm. Sci.*, **68**, 906 (1979).

Alfred J. Richard ˣ
Lemont B. Kier
Department of Pharmaceutical Chemistry
Medical College of Virginia
Virginia Commonwealth University
Richmond, VA 23298

Received March 15, 1979.
Accepted for publication October 26, 1979.

Calculation of Cutaneous Metabolic Rate Constant from Diffusion Model

Keyphrases □ Rotating disk—analysis, cutaneous metabolism of vidarabine, guinea pig, *in vitro* study □ Skin—metabolism of vidarabine, rotating-disk method, guinea pig, *in vitro* study □ Antiviral agents—vidarabine, cutaneous metabolism, rotating-disk method, guinea pig, *in vitro* study □ Vidarabine—cutaneous metabolism, analysis by rotating-disk method, guinea pig, *in vitro* study

To the Editor:

A method for the determination of the cutaneous metabolic rate constant for vidarabine (I) from a rotating-disk diffusion model was reported recently by Leung and Ando (1). They calculated the enzyme rate constant from the observed flux using:

$$k_m = 1 \Big/ \left[\frac{C_A(h)}{-F_A} - \frac{h}{D_{aqA}}\right](m) \qquad \text{(Eq. 1)}$$

where k_m is the first-order enzyme rate constant, $C_A(h)$ is the initial substrate concentration, F_A is the flux of the substrate in the system, h is the aqueous diffusion layer thickness, D_{aqA} is the aqueous diffusion coefficient, and m is the membrane thickness. Equation 1 was derived from Eq. 25 of a previous publication by Ando *et al.* (2) by taking the limit of $\theta \to 0$ such that $\tanh \theta \to \theta$:

$$\frac{1}{\kappa} = C_1 \tanh \kappa m \qquad \text{(Eq. 2)}$$

where:

$$\kappa = \sqrt{k_m/D_A}$$

$$C_1 = D_A\left[\frac{C_A(h)}{-F_A} - \frac{h}{D_{aqA}}\right]$$

$$\theta = \kappa m$$

and D_A is the diffusion coefficient of the substrate for the cutaneous tissue.

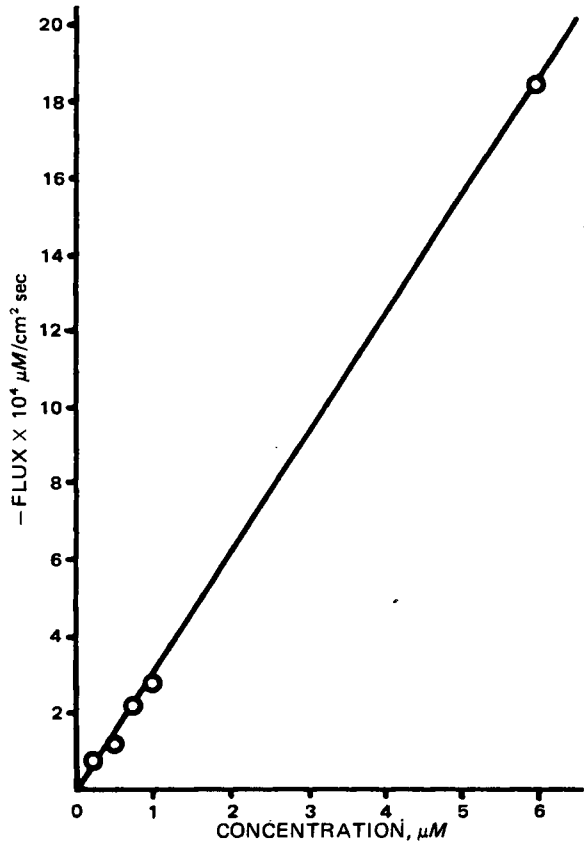

Figure 1—*Plot of flux* versus *substrate concentration. The slope of the linear regression line is 3.11 × 10⁻⁴ cm⁻² sec⁻¹ (r = 0.9997).*

The k_m of the deaminase enzyme in guinea pig epidermis was calculated to be 0.156 sec^{-1}, which contradicts the $\theta \to 0$ assumption by giving θ values of 0.25 and 24.9 for D_A values of 1.0×10^{-5} and 1.0×10^{-9} cm^2/sec, respectively. Obviously, the validity of Eq. 1 is questionable when D_A is smaller than 1.0×10^{-5} cm^2/sec. Strictly speaking, the $\theta \to 0$ assumption should never be valid because it leads to either $D_A \to \infty$, *i.e.*, no diffusional barrier exists, or $m \to 0$, *i.e.*, no membrane exists, since k_m is finite. In neither case will the simultaneous diffusion and metabolism theory

Table I—Fluxes [a] of I at Different Concentrations

Concentration, μM	Flux, %/cm^2 min	Mean Flux %/cm^2 min	Mean Flux $\mu M/cm^2$ sec
0.25	1.630 1.956 1.892	1.826	7.61×10^{-5}
0.50	1.888 0.797 1.164	1.283	1.07×10^{-4}
0.75	1.662 1.713 1.717	1.679	2.10×10^{-4}
1.0	1.691 1.921 1.230	1.616	2.69×10^{-4}
6.0	1.568 1.787 2.144	1.839	1.84×10^{-3}
600.0	0.388 0.399 0.346	0.378	3.78×10^{-2}

[a] Negative signs for all flux values, which indicate directions of the fluxes, are omitted in this table.

0022-3549/80/0100-0126$01.00/0
© 1980, American Pharmaceutical Association

largely on the nature of the ring substitution as well as on the half-wave reduction potential of the ring, its substituents, or the ether oxygen.

(1) P. Fulcrand, G. Berge, A. Noel, P. Chevallet, J. Castel, and H. Orzalesi, *Eur. J. Med. Chem.*, **13**, 177 (1978).
(2) C. Hansch, R. M. Muir, T. Fujita, P. O. Maloney, F. Gerer, and M. Strejc, *J. Am. Chem. Soc.*, **85**, 2817 (1963).
(3) S. M. Free and J. R. Wilson, *J. Med. Chem.*, **7**, 395 (1964).
(4) L. B. Kier and L. H. Hall, "Molecular Connectivity in Chemistry and Drug Research," Academic, New York, N.Y, 1976.
(5) L. B. Kier and L. H. Hall, *J. Med. Chem.*, **20**, 1631 (1977).
(6) L. B. Kier and R. A. Glennon, *Life Sci.*, **22**, 1589 (1978).
(7) R. A. Glennon and L. B. Kier, *Eur. J. Med. Chem.*, **13**, 219 (1978).
(8) R. A. Glennon, L. B. Kier, and A. T. Shulgin, *J. Pharm. Sci.*, **68**, 906 (1979).

Alfred J. Richard ˣ
Lemont B. Kier
Department of Pharmaceutical Chemistry
Medical College of Virginia
Virginia Commonwealth University
Richmond, VA 23298

Received March 15, 1979.
Accepted for publication October 26, 1979.

Calculation of Cutaneous Metabolic Rate Constant from Diffusion Model

Keyphrases □ Rotating disk—analysis, cutaneous metabolism of vidarabine, guinea pig, *in vitro* study □ Skin—metabolism of vidarabine, rotating-disk method, guinea pig, *in vitro* study □ Antiviral agents—vidarabine, cutaneous metabolism, rotating-disk method, guinea pig, *in vitro* study □ Vidarabine—cutaneous metabolism, analysis by rotating-disk method, guinea pig, *in vitro* study

To the Editor:

A method for the determination of the cutaneous metabolic rate constant for vidarabine (I) from a rotating-disk diffusion model was reported recently by Leung and Ando (1). They calculated the enzyme rate constant from the observed flux using:

$$k_m = 1 \Big/ \left[\frac{C_A(h)}{-F_A} - \frac{h}{D_{aqA}}\right](m) \qquad \text{(Eq. 1)}$$

where k_m is the first-order enzyme rate constant, $C_A(h)$ is the initial substrate concentration, F_A is the flux of the substrate in the system, h is the aqueous diffusion layer thickness, D_{aqA} is the aqueous diffusion coefficient, and m is the membrane thickness. Equation 1 was derived from Eq. 25 of a previous publication by Ando *et al.* (2) by taking the limit of $\theta \to 0$ such that $\tanh \theta \to \theta$:

$$\frac{1}{\kappa} = C_1 \tanh \kappa m \qquad \text{(Eq. 2)}$$

where:

$$\kappa = \sqrt{k_m/D_A}$$

$$C_1 = D_A\left[\frac{C_A(h)}{-F_A} - \frac{h}{D_{aqA}}\right]$$

$$\theta = \kappa m$$

and D_A is the diffusion coefficient of the substrate for the cutaneous tissue.

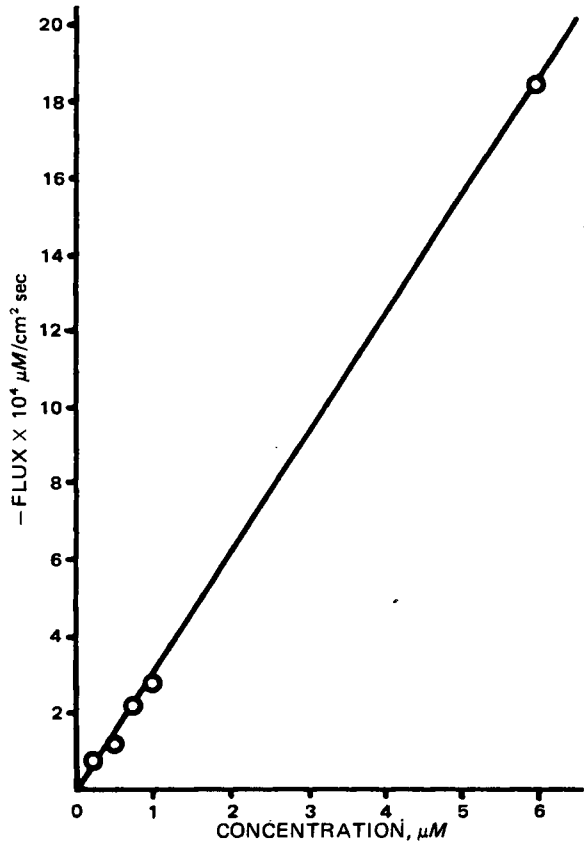

Figure 1—*Plot of flux* versus *substrate concentration. The slope of the linear regression line is 3.11 × 10⁻⁴ cm⁻² sec⁻¹ (r = 0.9997).*

The k_m of the deaminase enzyme in guinea pig epidermis was calculated to be 0.156 sec^{-1}, which contradicts the $\theta \to 0$ assumption by giving θ values of 0.25 and 24.9 for D_A values of 1.0×10^{-5} and 1.0×10^{-9} cm^2/sec, respectively. Obviously, the validity of Eq. 1 is questionable when D_A is smaller than 1.0×10^{-5} cm^2/sec. Strictly speaking, the $\theta \to 0$ assumption should never be valid because it leads to either $D_A \to \infty$, *i.e.*, no diffusional barrier exists, or $m \to 0$, *i.e.*, no membrane exists, since k_m is finite. In neither case will the simultaneous diffusion and metabolism theory

Table I—Fluxes [a] of I at Different Concentrations

Concentration, μM	Flux, %/cm^2 min	Mean Flux %/cm^2 min	Mean Flux $\mu M/cm^2$ sec
0.25	1.630 1.956 1.892	1.826	7.61×10^{-5}
0.50	1.888 0.797 1.164	1.283	1.07×10^{-4}
0.75	1.662 1.713 1.717	1.679	2.10×10^{-4}
1.0	1.691 1.921 1.230	1.616	2.69×10^{-4}
6.0	1.568 1.787 2.144	1.839	1.84×10^{-3}
600.0	0.388 0.399 0.346	0.378	3.78×10^{-2}

[a] Negative signs for all flux values, which indicate directions of the fluxes, are omitted in this table.

0022-3549/80/0100-0126$01.00/0
© 1980, American Pharmaceutical Association

apply. It would be a surprise if the calculation of k_m did not require a D_A value, as in the use of Eq. 1, since the model is based on the simultaneous diffusion and metabolism process.

The correct estimation of k_m can be drawn only from Eq. 2. From Eq. 2, one expects F_A to be a linear function of $C_A(h)$ for a given membrane. Figure 1 shows a plot of F_A *versus* $C_A(h)$. The data were taken from Table III of Leung and Ando's report (1) with a column added to list the mean fluxes in micromolar per square centimeter per second (Table I). With Eq. 2, the reciprocal of the slope of the line in Fig. 1 gives k_m values of 0.207, 1.148, 11.48, and 114.8 sec^{-1} for D_A values of 10^{-6}, 10^{-7}, 10^{-8}, and 10^{-9} cm^2/sec, respectively.

(1) L. C. Leung and H. Y. Ando, *J. Pharm. Sci.*, **68**, 571 (1979).
(2) H. Y. Ando, N. F. Ho, and W. I. Higuchi, *ibid.*, **66**, 1525 (1977).

Cheng-Der Yu
Institute of Pharmaceutical Science
Syntex Research
Palo Alto, CA 94304

Received June 11, 1979.
Accepted for publication September 19, 1979.

A Rebuttal and Some Insights into Cutaneous Metabolism and Diffusion

Keyphrases □ Rotating disk—analysis, cutaneous metabolism of vidarabine, guinea pig, *in vitro* study □ Skin—metabolism of vidarabine, rotating-disk method, guinea pig, *in vitro* study □ Antiviral agents—vidarabine, cutaneous metabolism, rotating-disk method, guinea pig, *in vitro* study □ Vidarabine—cutaneous metabolism, analysis by rotating-disk method, guinea pig, *in vitro* study

To the Editor:

Dr. Yu's communication (1) refers critically to the report of Leung and Ando (2); the basis for this criticism evidently stems from some of his recent research (3).

It appears from Dr. Yu's communication (1) that this research was based on a model derived by Ando *et al.* (4). One must assume that Dr. Yu used this model to measure k_m for the same enzyme and for the same drug as in the paper of Leung and Ando (2). The methodology is not stated; however, it is a good assumption that he used a diffusion cell similar to that used by Ando *et al.* (4) instead of the rotating disk in our system. It will be assumed that the D_A values for the epidermis that Dr. Yu cites for hairless mice skin were obtained after removal of the stratum corneum.

The basis of Dr. Yu's criticism is our interpretation of Eq. 25 of the model (4). His Eq. 2 is a rearrangement of this equation. In my comments, I shall show that Dr. Yu made two classical errors. First, he applied a model verbatim without due cognizance of the stated limitations of the model. Second, he made inappropriate comparisons.

The basic equation Dr. Yu disagrees with is Eq. 1 in his communication. We arrived at this equation by taking the limit of tanh $\theta \rightarrow 0$. The basic validity of this approximation is evident from the nature of the power series expansion for tanh θ (5):

$$\tanh\theta = \theta - \frac{\theta^3}{3} + \frac{2}{15}\theta^5 - \frac{17}{315}\theta^7 + \ldots + (-1)^{n-1}\frac{2^{2n}(2^{2n}-1)}{(2n)!}B_{2n-1}\theta^{2n-1} + \ldots \quad \text{(Eq. 1)}$$

where $|\theta| < \pi/2$ and B_{2n-1} are Bernoulli's numbers. The approximation of:

$$\tanh\theta \simeq \theta \quad \text{(Eq. 2)}$$

as $\theta \rightarrow 0$ is one of the most common forms of linearization. The basis for this approximation is that as θ becomes small, θ^3 decreases much more rapidly. For this reason, in the simple pendulum (6, 7):

$$F = mg\sin\theta \quad \text{(Eq. 3)}$$

can be replaced by:

$$F = -mg\theta \quad \text{(Eq. 4)}$$

for small θ since (5):

$$\sin\theta = \theta - \frac{\theta^3}{3!} + \frac{\theta^5}{5!} - \frac{\theta^7}{7!} + \ldots \quad \text{(Eq. 5)}$$

Using this approximation, $\theta \times \tanh\theta$ of Dr. Yu's Eq. 2 becomes:

$$\theta \times \tanh\theta = \theta^2 - \frac{\theta^4}{3} + \frac{2}{15}\theta^6 - \frac{17}{315}\theta^8 + \ldots \quad \text{(Eq. 6)}$$

In Table I, we show the percent error in using θ^2 instead of $\theta \times \tanh\theta$ computed from the first four terms of the series. Although θ^2 always overestimates $\theta \times \tanh\theta$, values of $\theta > 0.75$ are reasonable considering that the biological variability in determining the skin thickness in unmatched guinea pigs has a standard deviation of 18% for eight or more animals (8). Note also that $\theta = 0.11$ gives a 0.0% error.

The major thrust of Dr. Yu's criticism is that he believes that D_A must be measured to determine the linear metabolic rate constant, k_m. Current methodology, including Dr. Yu's, does not justify this degree of refinement. He is, as I have stated before, applying the model verbatim without due cognizance of the stated limitations of the model. In the model that I derived (4), the skin was envisioned as a two-ply laminate composed of the relatively impermeable stratum corneum and the viable epidermis. The distribution of enzymes in the epidermis was assumed to be homogeneous. A caveat was given: "The epidermis contains most of the catabolic enzymes that render the drug inactive by metabolism, but it is not clear how the distribution of catabolic enzymes might vary with epidermal depth. Presumably, one would expect a gradual increase in metabolic activity as the basal epithelial layer is approached from the stratum corneum."As we shall see, the distribution of the enzyme adenosine deaminase, the most likely catabolic enzyme responsible for the metabolism of 9-β-D-arabinofuranosylhypoxanthine (I), is not homogeneous; apparently, there is not even a gradual

Table I—Approximation of $\theta \times \tanh\theta$ by θ^2 and Percent Error

θ	θ^2	$\theta^4/3$	$2(\theta^6/15)$	$17(\theta^8/315)$	$\theta \times \tanh\theta$	Percent Error
0.90	0.8100	0.2903	0.0708	0.0232	0.5673	42.8
0.75	0.5625	0.1054	0.0237	0.0054	0.4754	18.3
0.71	0.5041	0.0847	0.0171	0.0035	0.4330	16.4
0.50	0.2500	0.0208	0.0020	0.0002	0.2310	8.2
0.25	0.0625	0.0013	0	0	0.0612	2.1
0.18	0.0324	0.0003	0	0	0.0327	0.9
0.11	0.0121	0	0	0	0.0121	0.0

0022-3549/80/0100-0127$01.00/0
© 1980, American Pharmaceutical Association

apply. It would be a surprise if the calculation of k_m did not require a D_A value, as in the use of Eq. 1, since the model is based on the simultaneous diffusion and metabolism process.

The correct estimation of k_m can be drawn only from Eq. 2. From Eq. 2, one expects F_A to be a linear function of $C_A(h)$ for a given membrane. Figure 1 shows a plot of F_A *versus* $C_A(h)$. The data were taken from Table III of Leung and Ando's report (1) with a column added to list the mean fluxes in micromolar per square centimeter per second (Table I). With Eq. 2, the reciprocal of the slope of the line in Fig. 1 gives k_m values of 0.207, 1.148, 11.48, and 114.8 sec^{-1} for D_A values of 10^{-6}, 10^{-7}, 10^{-8}, and 10^{-9} cm^2/sec, respectively.

(1) L. C. Leung and H. Y. Ando, *J. Pharm. Sci.*, **68**, 571 (1979).
(2) H. Y. Ando, N. F. Ho, and W. I. Higuchi, *ibid.*, **66**, 1525 (1977).

Cheng-Der Yu
Institute of Pharmaceutical Science
Syntex Research
Palo Alto, CA 94304

Received June 11, 1979.
Accepted for publication September 19, 1979.

A Rebuttal and Some Insights into Cutaneous Metabolism and Diffusion

Keyphrases □ Rotating disk—analysis, cutaneous metabolism of vidarabine, guinea pig, *in vitro* study □ Skin—metabolism of vidarabine, rotating-disk method, guinea pig, *in vitro* study □ Antiviral agents—vidarabine, cutaneous metabolism, rotating-disk method, guinea pig, *in vitro* study □ Vidarabine—cutaneous metabolism, analysis by rotating-disk method, guinea pig, *in vitro* study

To the Editor:

Dr. Yu's communication (1) refers critically to the report of Leung and Ando (2); the basis for this criticism evidently stems from some of his recent research (3).

It appears from Dr. Yu's communication (1) that this research was based on a model derived by Ando *et al.* (4). One must assume that Dr. Yu used this model to measure k_m for the same enzyme and for the same drug as in the paper of Leung and Ando (2). The methodology is not stated; however, it is a good assumption that he used a diffusion cell similar to that used by Ando *et al.* (4) instead of the rotating disk in our system. It will be assumed that the D_A values for the epidermis that Dr. Yu cites for hairless mice skin were obtained after removal of the stratum corneum.

The basis of Dr. Yu's criticism is our interpretation of Eq. 25 of the model (4). His Eq. 2 is a rearrangement of this equation. In my comments, I shall show that Dr. Yu made two classical errors. First, he applied a model verbatim without due cognizance of the stated limitations of the model. Second, he made inappropriate comparisons.

The basic equation Dr. Yu disagrees with is Eq. 1 in his communication. We arrived at this equation by taking the limit of tanh $\theta \rightarrow 0$. The basic validity of this approximation is evident from the nature of the power series expansion for tanh θ (5):

$$\tanh\theta = \theta - \frac{\theta^3}{3} + \frac{2}{15}\theta^5 - \frac{17}{315}\theta^7 + \ldots + (-1)^{n-1}\frac{2^{2n}(2^{2n}-1)}{(2n)!}B_{2n-1}\theta^{2n-1} + \ldots \quad \text{(Eq. 1)}$$

where $|\theta| < \pi/2$ and B_{2n-1} are Bernoulli's numbers. The approximation of:

$$\tanh\theta \simeq \theta \quad \text{(Eq. 2)}$$

as $\theta \rightarrow 0$ is one of the most common forms of linearization. The basis for this approximation is that as θ becomes small, θ^3 decreases much more rapidly. For this reason, in the simple pendulum (6, 7):

$$F = mg\sin\theta \quad \text{(Eq. 3)}$$

can be replaced by:

$$F = -mg\theta \quad \text{(Eq. 4)}$$

for small θ since (5):

$$\sin\theta = \theta - \frac{\theta^3}{3!} + \frac{\theta^5}{5!} - \frac{\theta^7}{7!} + \ldots \quad \text{(Eq. 5)}$$

Using this approximation, $\theta \times \tanh\theta$ of Dr. Yu's Eq. 2 becomes:

$$\theta \times \tanh\theta = \theta^2 - \frac{\theta^4}{3} + \frac{2}{15}\theta^6 - \frac{17}{315}\theta^8 + \ldots \quad \text{(Eq. 6)}$$

In Table I, we show the percent error in using θ^2 instead of $\theta \times \tanh\theta$ computed from the first four terms of the series. Although θ^2 always overestimates $\theta \times \tanh\theta$, values of $\theta > 0.75$ are reasonable considering that the biological variability in determining the skin thickness in unmatched guinea pigs has a standard deviation of 18% for eight or more animals (8). Note also that $\theta = 0.11$ gives a 0.0% error.

The major thrust of Dr. Yu's criticism is that he believes that D_A must be measured to determine the linear metabolic rate constant, k_m. Current methodology, including Dr. Yu's, does not justify this degree of refinement. He is, as I have stated before, applying the model verbatim without due cognizance of the stated limitations of the model. In the model that I derived (4), the skin was envisioned as a two-ply laminate composed of the relatively impermeable stratum corneum and the viable epidermis. The distribution of enzymes in the epidermis was assumed to be homogeneous. A caveat was given: "The epidermis contains most of the catabolic enzymes that render the drug inactive by metabolism, but it is not clear how the distribution of catabolic enzymes might vary with epidermal depth. Presumably, one would expect a gradual increase in metabolic activity as the basal epithelial layer is approached from the stratum corneum."As we shall see, the distribution of the enzyme adenosine deaminase, the most likely catabolic enzyme responsible for the metabolism of 9-β-D-arabinofuranosylhypoxanthine (I), is not homogeneous; apparently, there is not even a gradual

Table I—Approximation of $\theta \times \tanh\theta$ by θ^2 and Percent Error

θ	θ^2	$\theta^4/3$	$2(\theta^6/15)$	$17(\theta^8/315)$	$\theta \times \tanh\theta$	Percent Error
0.90	0.8100	0.2903	0.0708	0.0232	0.5673	42.8
0.75	0.5625	0.1054	0.0237	0.0054	0.4754	18.3
0.71	0.5041	0.0847	0.0171	0.0035	0.4330	16.4
0.50	0.2500	0.0208	0.0020	0.0002	0.2310	8.2
0.25	0.0625	0.0013	0	0	0.0612	2.1
0.18	0.0324	0.0003	0	0	0.0327	0.9
0.11	0.0121	0	0	0	0.0121	0.0

0022-3549/80/0100-0127$01.00/0
© 1980, American Pharmaceutical Association

distribution of the enzyme from the stratum corneum to the basal layer.

Adenosine deaminase is a salvage pathway enzyme in the skin (9) and converts the purine nucleoside adenosine to inosine. This intermediate may be degraded or possibly converted by other salvage pathway enzymes in the skin into guanosine (10). These salvage pathways permit reutilization of purines and may be necessary since the continuous cellular renewal occurring in the epidermis requires active synthesis and breakdown of nucleic acids. Indeed, the absence of effective salvage pathways for the reutilization of inosine forms the biochemical basis for some inherited disorders (11, 12). Similar salvage pathways exist for the synthesis of pyrimidines in the skin (13, 14).

With respect to Dr. Yu's comments, there is every reason to believe that there is not a homogeneous or even a gradual distribution of the enzyme adenosine deaminase in the skin; rather, there is every reason to believe that the enzyme resides exclusively in the basal layer of the epidermis. The basal layer of the epidermis can be separated from the upper differentiated spinous and granular layers (15). Studies with these cells have shown that only the basal cells have proliferative capabilities and that only the basal cells can be used to establish successful primary cultures. Irreversible changes in the spinous and granular cells of the upper epidermal layers probably are responsible for the absence of mitosis in these cells. A concomitant change with this loss of mitotic ability in the upper epidermal layer is the complete loss of salvage pathway pyrimidine enzymes (16). Only the basal cells have these enzymes. For this reason, only the basal cells probably contain the purine salvage enzyme, adenosine deaminase.

Studies have shown that the basal cells incorporate thymidine 205-fold faster than do the upper epidermal cells in the spinous and granular layers (16). This observation raises serious questions as to the utility of measuring the epidermal diffusion coefficient, D_A, for the entire epidermis, as Dr. Yu evidently has done. The fact that the diffusion coefficient for a drug would be much slower in the spinous and granular layers is reasonable from considerations of epidermal differentiation. Basal cells would be expected to be the most permeable because they are the only cells undergoing mitosis. Essential nutrients must permeate these cells from the dermal capillaries. For this reason, one would suppose that the diffusion coefficient of the basal cells would be on the order of the diffusion coefficient of the dermis. In this way, nutrient transport would be optimized. The diffusion coefficient of the differentiating spinous and granular layer cells of the upper epidermis should be *intermediate* between that of the basal cells and that of the very impermeable stratum corneum.

Further support for a faster diffusion coefficient for the basal cells is evident from a comparison of the unesterified cholesterol content (with respect to total lipid) of the epidermal cells (17): basal cells, 8.4 ± 0.3; granular cells, 18.0 ± 2.6; and stratum corneum, 23 ± 4.7. Since unesterified cholesterol is found primarily in the plasma membrane of these cells (18) and since levels of unesterified cholesterol and sphingomyelin render membranes more lipophilic, less permeable, and less easily degraded (19), one might justifiably conclude that the basal cells are much more permeable than the spinous and granular cells.

With these facts on hand, let us examine Dr. Yu's criticisms. Dr. Yu assumed D_A values of 1.0×10^{-5} and 1.0×10^{-9} cm^2/sec and, using the value for the membrane thickness that we used, 20.85×10^{-4} cm, and our value of k_m, he computed θ values of 0.25 and 24.9, respectively. He claims that this result contradicts our $\theta \to 0$ assumption. This is not true. Dr. Yu is making an inappropriate comparison. We viewed the epidermal layer as a whole and felt that it would be pedantic to try to define the model any further experimentally because of the inherent limitations of the model. The distribution of the enzyme, adenosine deaminase, is not homogeneous throughout the epidermal layer but rather resides exclusively in the basal cell layer.

Furthermore, a determination of D_A for the entire epidermis, exclusive of the stratum corneum, as Dr. Yu evidently has done experimentally, is equally pedantic and misleading. As we have shown, the diffusion coefficient of the basal cell layer where the enzyme almost exclusively resides is most likely on the order of the diffusion coefficient of the dermis and not the epidermis as a whole. Therefore, determination of D_A for the entire epidermis as Dr. Yu has done is in error, because D_A is defined as the diffusion coefficient in the region of a homogeneous enzyme distribution.

Dr. Yu also questions the validity of our approximation since the $\theta \to 0$ assumption, strictly speaking according to him, implies that either $D_A \to \infty$, *i.e.*, no diffusional barrier exists, or $M \to 0$, *i.e.*, no membrane exists. This conclusion is incorrect; as shown in Table I, the error in our approximation is less than 0.0% for a value of $\theta = 0.11$. It is not necessary for the θ value to equal 0 for this accuracy. Therefore, one would never reach Dr. Yu's conclusion. Moreover, the condition $\theta \to 0$ does not necessarily mean that either $D_A \to \infty$ or $M \to 0$. In real skin, all of these variables change because real skin is not homogeneous. If we chose to make a Yu-type computation of θ, a more appropriate calculation would be based on the evidence I have presented. The thickness of guinea pig epidermis has been determined from the upper border of the stratum granulosum to the lower border of the basal cell layer (8). This measurement included one basal cell layer, one or two spinous cell layers, and one to three granular cell layers or a range of three to six cell layers (20, 21). If we take the number of cell layers to be four and divide the number of cell layers into the thickness of the epidermis, 20.85 μm (*SE* 0.40, $n = 39$), we obtain an approximate thickness for the basal cell layer of 5.21 μm. Since we have argued that this layer is the only one containing the enzyme adenosine deaminase and that the diffusion coefficient in this layer would be very close to the dermis, we can calculate θ using Dr. Yu's value for D_A for the dermis of 1.34×10^{-6} cm^2/sec from:

$$\theta = M\sqrt{k_m/D_A} \qquad \text{(Eq. 7)}$$

This calculation yields a θ value of 0.178. From Table I, we see that a θ of 1.8 will only produce an error of 0.9%. We can even improve on this result. In the previous calculation, we used the reported k_m value of 0.156 cm^{-1}, which was based on a membrane thickness of 20.85 μm. If k_m is recomputed based on a membrane thickness of 5.21 μm, then

θ = 0.039. The approximation that we have made then gives an error of 0.05%.

(1) C.-D. Yu, *J. Pharm. Sci.*, **69**, 126 (1980).
(2) L. C. Leung and H. Y. Ando, *ibid.*, **68**, 571 (1979).
(3) C.-D. Yu, PhD thesis, University of Michigan, Ann Arbor, Mich., 1978.
(4) H. Y. Ando, N. F. H. Ho, and W. I. Higuchi, *J. Pharm. Sci.*, **66**, 1525 (1977).
(5) M. Abramowitz and I. A. Stegun, "Handbook of Mathematical Functions," Dover, New York, N.Y., 1965.
(6) R. Resnick and D. Halliday, "Physics, Part I," Wiley, New York, N.Y., 1961.
(7) A. Sommerfeld, "Mechanics, Volume 1," Academic, New York, N.Y., 1964.
(8) P. M. Gaylarde and I. Sarkany, *Trans. St. John's Hosp. Dermatol. Soc.*, **59**, 235 (1973).
(9) W. D. Block and D. V. Johnson, *J. Invest. Dermatol.*, **23**, 471 (1954).
(10) J. DeBersaques, *ibid.*, **48**, 169 (1967).
(11) F. M. Rosenbloom, W. N. Kelley, J. Miller, J. F. Henderson, and J. E. Seegmiller, *J. Am. Med. Assoc.*, **202**, 103 (1967).
(12) J. E. Seegmiller, F. M. Rosenbloom, and W. N. Kelley, *Science*, **155**, 1682 (1967).
(13) R. A. Lewis and M. Karasek, *J. Invest. Dermatol.*, **59**, 317 (1972).
(14) N. W. DeLapp and M. A. Karasek, *ibid.*, **66**, 306 (1976).
(15) F. L. Vaughan and I. A. Bernstein, *ibid.*, **56**, 454 (1971).
(16) J. T. Moore and M. A. Karasek, *ibid.*, **56**, 318 (1971).
(17) G. M. Gray and H. J. Yardley, *J. Lipid Res.*, **16**, 441 (1975).
(18) G. M. Gray, I. A. King, and H. J. Yardley, *J. Invest. Dermatol.*, **71**, 131 (1978).
(19) S. Patton, *J. Theoret. Biol.*, **29**, 489 (1970).
(20) I. Sarkany and P. M. Gaylarde, *Trans. St. John's Hosp. Dermatol. Soc.*, **59**, 241 (1973).
(21) I. Sarkany and R. B. Fountain, *Br. J. Dermatol.*, **79**, 174 (1967).

H. Y. Ando
Philadelphia College of Pharmacy and Science
Philadelphia, PA 19104

Received July 13, 1979.
Accepted for publication September 19, 1979.

Elimination of Tablet Air Entrapment Using USP 1 Rotating-Basket Dissolution Apparatus

Keyphrases □ Drug dissolution—USP 1 rotating-basket dissolution testing apparatus, modification to eliminate tablet air entrapment □ Rotating-basket apparatus—dissolution testing, modification to eliminate tablet air entrapment

To the Editor:

Dissolution testing using the USP 1 rotating-basket apparatus (1) is subject to variability due to an artifact of the method. For certain dosage forms, this artifact results in entrapment of the test specimen in an air bubble at the top of the basket assembly. This air bubble is entrapped if the 2-mm vent hole in the top of the basket assembly is blocked by the tablet as the assembly is lowered into the dissolution fluid or if the bubble is positioned elsewhere on the top of the assembly and does not migrate toward the vent.

Since the rim around the detachable part of the basket protrudes below the top of the assembly by about 3 mm, a dead space is available to prevent the bubble from migrating out of the basket at the edge (Fig. 1C). When a tablet is entrapped in this way, the apparent dissolution rate is very low and the dissolution run is invalid.

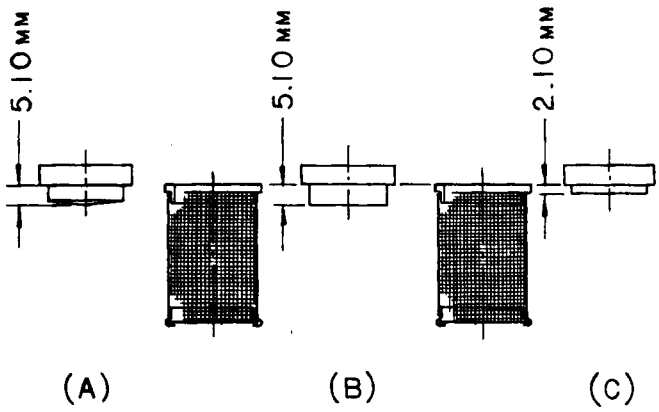

Figure 1—*Conical head design (A), extended head design (B), and conventional head design (C).*

It was noted in our laboratories that this air entrapment occurred occasionally during dissolution tests on the nondisintegrating USP dissolution calibrator salicylic acid 300-mg tablet. A basket top was fabricated to eliminate the dead space around the basket rim (Fig. 1B), and this simple modification essentially eliminated the problem. However, the problem recurred during testing of an experimental film-coated tablet. For the film-coated tablets, the problem was so severe that several runs were needed to obtain valid six-tablet results. Use of the modified design (Fig. 1B) did not totally eliminate the problem.

To circumvent air entrapment with the film-coated tablets, the top of the basket assembly was modified further by fabricating a slight conical shape such that the center protrudes about 1 mm below the edge. This shape imparts enough of a slope to permit an entrapped bubble to escape and to allow the tablet to return to the bottom of the basket (Fig. 1A). The improvement is dramatic. For example, in one series of six-tablet runs, seven of 18 USP salicylic acid calibrators were air entrapped with the conventional head while the conical head design completely eliminated the problem. For the experimental film-coated tablets, 10 of 18 tablets were air entrapped with the conventional head but only one of 18 was air entrapped with the conical head design.

The conical head modification of the basket top design (Fig. 1A) may be of sufficient utility to warrant general use. It is not inconsistent with the present apparatus description (1); however, it may be advantageous to define explicitly the dimensions in the USP to permit its use.

(1) "Fifth Supplement to USP XIX and NF XIV," United States Pharmacopeial Convention, Rockville, Md., 1979, pp. 221, 222.

A. C. Sarapu ˣ
L. Clark, Jr.
Control Laboratory Operations
The Upjohn Company
Kalamazoo, MI 49001

Received August 10, 1979.
Accepted for publication October 10, 1979.

© 1980, American Pharmaceutical Association

θ = 0.039. The approximation that we have made then gives an error of 0.05%.

(1) C.-D. Yu, *J. Pharm. Sci.*, **69**, 126 (1980).
(2) L. C. Leung and H. Y. Ando, *ibid.*, **68**, 571 (1979).
(3) C.-D. Yu, PhD thesis, University of Michigan, Ann Arbor, Mich., 1978.
(4) H. Y. Ando, N. F. H. Ho, and W. I. Higuchi, *J. Pharm. Sci.*, **66**, 1525 (1977).
(5) M. Abramowitz and I. A. Stegun, "Handbook of Mathematical Functions," Dover, New York, N.Y., 1965.
(6) R. Resnick and D. Halliday, "Physics, Part I," Wiley, New York, N.Y., 1961.
(7) A. Sommerfeld, "Mechanics, Volume 1," Academic, New York, N.Y., 1964.
(8) P. M. Gaylarde and I. Sarkany, *Trans. St. John's Hosp. Dermatol. Soc.*, **59**, 235 (1973).
(9) W. D. Block and D. V. Johnson, *J. Invest. Dermatol.*, **23**, 471 (1954).
(10) J. DeBersaques, *ibid.*, **48**, 169 (1967).
(11) F. M. Rosenbloom, W. N. Kelley, J. Miller, J. F. Henderson, and J. E. Seegmiller, *J. Am. Med. Assoc.*, **202**, 103 (1967).
(12) J. E. Seegmiller, F. M. Rosenbloom, and W. N. Kelley, *Science*, **155**, 1682 (1967).
(13) R. A. Lewis and M. Karasek, *J. Invest. Dermatol.*, **59**, 317 (1972).
(14) N. W. DeLapp and M. A. Karasek, *ibid.*, **66**, 306 (1976).
(15) F. L. Vaughan and I. A. Bernstein, *ibid.*, **56**, 454 (1971).
(16) J. T. Moore and M. A. Karasek, *ibid.*, **56**, 318 (1971).
(17) G. M. Gray and H. J. Yardley, *J. Lipid Res.*, **16**, 441 (1975).
(18) G. M. Gray, I. A. King, and H. J. Yardley, *J. Invest. Dermatol.*, **71**, 131 (1978).
(19) S. Patton, *J. Theoret. Biol.*, **29**, 489 (1970).
(20) I. Sarkany and P. M. Gaylarde, *Trans. St. John's Hosp. Dermatol. Soc.*, **59**, 241 (1973).
(21) I. Sarkany and R. B. Fountain, *Br. J. Dermatol.*, **79**, 174 (1967).

H. Y. Ando
Philadelphia College of Pharmacy and Science
Philadelphia, PA 19104

Received July 13, 1979.
Accepted for publication September 19, 1979.

Elimination of Tablet Air Entrapment Using USP 1 Rotating-Basket Dissolution Apparatus

Keyphrases □ Drug dissolution—USP 1 rotating-basket dissolution testing apparatus, modification to eliminate tablet air entrapment □ Rotating-basket apparatus—dissolution testing, modification to eliminate tablet air entrapment

To the Editor:

Dissolution testing using the USP 1 rotating-basket apparatus (1) is subject to variability due to an artifact of the method. For certain dosage forms, this artifact results in entrapment of the test specimen in an air bubble at the top of the basket assembly. This air bubble is entrapped if the 2-mm vent hole in the top of the basket assembly is blocked by the tablet as the assembly is lowered into the dissolution fluid or if the bubble is positioned elsewhere on the top of the assembly and does not migrate toward the vent.

Since the rim around the detachable part of the basket protrudes below the top of the assembly by about 3 mm, a dead space is available to prevent the bubble from migrating out of the basket at the edge (Fig. 1C). When a tablet is entrapped in this way, the apparent dissolution rate is very low and the dissolution run is invalid.

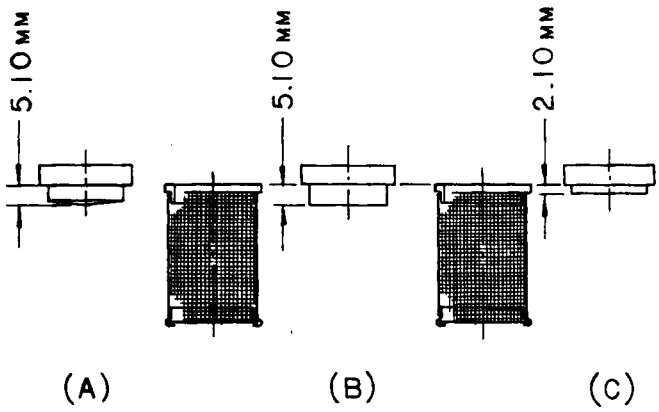

Figure 1—*Conical head design (A), extended head design (B), and conventional head design (C).*

It was noted in our laboratories that this air entrapment occurred occasionally during dissolution tests on the nondisintegrating USP dissolution calibrator salicylic acid 300-mg tablet. A basket top was fabricated to eliminate the dead space around the basket rim (Fig. 1B), and this simple modification essentially eliminated the problem. However, the problem recurred during testing of an experimental film-coated tablet. For the film-coated tablets, the problem was so severe that several runs were needed to obtain valid six-tablet results. Use of the modified design (Fig. 1B) did not totally eliminate the problem.

To circumvent air entrapment with the film-coated tablets, the top of the basket assembly was modified further by fabricating a slight conical shape such that the center protrudes about 1 mm below the edge. This shape imparts enough of a slope to permit an entrapped bubble to escape and to allow the tablet to return to the bottom of the basket (Fig. 1A). The improvement is dramatic. For example, in one series of six-tablet runs, seven of 18 USP salicylic acid calibrators were air entrapped with the conventional head while the conical head design completely eliminated the problem. For the experimental film-coated tablets, 10 of 18 tablets were air entrapped with the conventional head but only one of 18 was air entrapped with the conical head design.

The conical head modification of the basket top design (Fig. 1A) may be of sufficient utility to warrant general use. It is not inconsistent with the present apparatus description (1); however, it may be advantageous to define explicitly the dimensions in the USP to permit its use.

(1) "Fifth Supplement to USP XIX and NF XIV," United States Pharmacopeial Convention, Rockville, Md., 1979, pp. 221, 222.

A. C. Sarapu ˣ
L. Clark, Jr.
Control Laboratory Operations
The Upjohn Company
Kalamazoo, MI 49001

Received August 10, 1979.
Accepted for publication October 10, 1979.

© 1980, American Pharmaceutical Association

REVIEWS

Handbook of Aerosol Technology, 2nd Ed. By P. A. SANDERS. Van Nostrand Reinhold Co., 135 W. 50th St., New York, NY 10020. 1979. 526 pp. 15 × 25 cm. Price $27.50

This book is an updated version of "Principles of Aerosol Technology," which was published in 1970. It has become available at a time when the aerosol industry has completed the changeover from the predominant use of fluorocarbons as the propellant to other alternative propellant systems. The "Handbook of Aerosol Technology" is the first book that considers the development of aerosols in the light of the restrictions placed on the use of fluorocarbons as propellants.

The text is divided into three major sections: homogeneous systems and their properties; emulsions, foams, and suspensions; and miscellaneous. While Dr. Sanders is the major author, five chapters were written by several of his former associates from the Freon Products Division of Du Pont, and much of the new experimental data presented was developed at Du Pont.

Chapters 3 and 4 will be particularly valuable to the experienced aerosol chemist in that the use of the fluorocarbon and hydrocarbon propellants for aerosol products is discussed in light of the restricted use of fluorocarbon propellants. The chapters include all of the necessary physicochemical data of value to those formulating aerosol products. While the author includes much information about the fluorocarbon propellants, these propellants can be used only for inhalation-type aerosol products that are covered by a New Drug Application and for an extremely limited number of vaginal foams.

The chapters on containers and valves have been updated and supply the reader with the required knowledge of these components. The chapter on filling methods is adequate but should have included greater details about the filling of products utilizing hydrocarbon propellants. Since the hydrocarbon propellants are flammable, they must be handled differently from the fluorocarbons. A thorough discussion of vapor pressure, spray characteristics, solvency, viscosity, and density is presented. Much of the data in these chapters deal with fluorocarbons and are of limited value based on present regulations. However, data are given for other fluorocarbons such as fluorocarbon 22, which may be approved for use in the future.

The chapter on stability is especially well written and includes the various test methods used to determine the stability of aerosols. Since aerosols now utilize a hydrocarbon propellant, the chapter concerned with flammability is essential. Dr. Sanders also indicates the various regulations involved.

Section II deals with emulsions, foams, and suspensions. The basic aspect of emulsion technology is covered, and much research data of tremendous value to the formulating chemist are supplied. Both aqueous and nonaqueous foams and other systems are discussed, which should interest developers of pharmaceutical aerosol dosage foams. This section alone is worth more than the cost of the book. The material presented is of value to anyone interested in surface chemistry and emulsions, not only to those interested in aerosols.

Section III concerns fluorocarbons in the atmosphere and technical programs in the atmospheric sciences. These chapters are of limited value but present the concerns of various organizations as to the use of fluorocarbons as propellants. However, the final chapters dealing with the sampling and analysis of aerosol products and the toxicity of fluorocarbon propellants are related to the development of these products and are of interest.

This book is recommended for use by both the experienced and the newcomer and should be part of the required library of all laboratories.

Reviewed by John J. Sciarra
Arnold & Marie Schwartz College of Pharmacy and Health Sciences of Long Island University
Brooklyn, NY 11201

Alicyclic Chemistry, Vol. 6. (A Specialist Periodical Report). Edited by M. A. McKERVEY *et al.* The Chemical Society. 1978. 357 pp. 13 × 22 cm. Price $56.00. (Available from Special Issues Sales, American Chemical Society, 1155 16th St., N.W., Washington, DC 20036.)

This sixth volume of an annual series is devoted to a summary of the literature of 1976 describing the chemistry of alicyclic compounds. Each chapter is devoted to a different alicyclic system, beginning in Chapter 1 with three-membered rings and progressing through four-, five-, and six-membered ring systems in subsequent chapters. The last two chapters in the book deal with surveys of literature describing the chemistry of medium- and large-ring compounds and bridged carbocyclic compounds.

Each chapter contains summaries of the literature dealing with structural studies of the various alicyclic systems including both molecular orbital and spectroscopic investigations. The literature of 1976 describing conformational aspects of a variety of alicyclic systems also is summarized in the appropriate chapters. In addition, reports of novel syntheses and chemical reactions of the various alicyclic systems are provided.

Each chapter is well illustrated with structural and chemical formulas. The literature citations are provided conveniently on the same page as the text material. While this book does not have a subject index, a useful author index is included.

Volume 6 of "Alicyclic Chemistry" would be a useful addition to the personal library of chemists and spectroscopists interested in having a concise and thorough review of the literature (of 1976) in this area. Natural products chemists should find this publication useful in terms of an annual review of the chemistry of a variety of alicyclic compounds of natural origin. It is refreshing to note that the current volume of this series sells for the same price as Volume 5.

Reviewed by Thomas N. Riley
Department of Medicinal Chemistry
University of Mississippi
University, MS 38677

Forensic Toxicology: Controlled Substances and Dangerous Drugs. By W. T. LOWRY and J. C. GARRIOTT. Plenum Press, 227 W. 17th St., New York, NY 10011. 1979. xvii + 445 pp. 15 × 23 cm. Price $37.50.

A retrieval of archival data organized in alphabetical order is the purpose of this new hard-covered book. After eight introductory and explanatory chapters comprising 116 pages, the book covers information in monograph form. For each drug entity, which includes both American and foreign manufacturers, the structural formula is presented along with its synonyms, chemical name, trade name, pharmacological classification, biochemical consideration, toxicity data with blood levels, when available, and even some pharmacognosy data where applicable. In addition, each drug is boldly classified as: (*a*) noncontrolled, (*b*) dangerous, or (*c*) scheduled with the specific schedule.

The title is misleading in that one does not find classical forensic toxicology, but the authors did not intend it to be a forensic toxicology text. Apparently, the authors used the title for lack of a better description. It is a reference book intended for attorneys, toxicologists, or chemists who need legal, chemical, and toxicity information on various drugs.

For pharmacists who know the drug laws, the introductory chapters are of little value. The first seven chapters, covering some 100 pages, include definitions and explanations of pharmaceutical dosage forms (from aerosols to tinctures) and scheduled, legend, excluded, and excepted substances. Chapter 4 deals specifically with the regulation of controlled

REVIEWS

Handbook of Aerosol Technology, 2nd Ed. By P. A. SANDERS. Van Nostrand Reinhold Co., 135 W. 50th St., New York, NY 10020. 1979. 526 pp. 15 × 25 cm. Price $27.50

This book is an updated version of "Principles of Aerosol Technology," which was published in 1970. It has become available at a time when the aerosol industry has completed the changeover from the predominant use of fluorocarbons as the propellant to other alternative propellant systems. The "Handbook of Aerosol Technology" is the first book that considers the development of aerosols in the light of the restrictions placed on the use of fluorocarbons as propellants.

The text is divided into three major sections: homogeneous systems and their properties; emulsions, foams, and suspensions; and miscellaneous. While Dr. Sanders is the major author, five chapters were written by several of his former associates from the Freon Products Division of Du Pont, and much of the new experimental data presented was developed at Du Pont.

Chapters 3 and 4 will be particularly valuable to the experienced aerosol chemist in that the use of the fluorocarbon and hydrocarbon propellants for aerosol products is discussed in light of the restricted use of fluorocarbon propellants. The chapters include all of the necessary physicochemical data of value to those formulating aerosol products. While the author includes much information about the fluorocarbon propellants, these propellants can be used only for inhalation-type aerosol products that are covered by a New Drug Application and for an extremely limited number of vaginal foams.

The chapters on containers and valves have been updated and supply the reader with the required knowledge of these components. The chapter on filling methods is adequate but should have included greater details about the filling of products utilizing hydrocarbon propellants. Since the hydrocarbon propellants are flammable, they must be handled differently from the fluorocarbons. A thorough discussion of vapor pressure, spray characteristics, solvency, viscosity, and density is presented. Much of the data in these chapters deal with fluorocarbons and are of limited value based on present regulations. However, data are given for other fluorocarbons such as fluorocarbon 22, which may be approved for use in the future.

The chapter on stability is especially well written and includes the various test methods used to determine the stability of aerosols. Since aerosols now utilize a hydrocarbon propellant, the chapter concerned with flammability is essential. Dr. Sanders also indicates the various regulations involved.

Section II deals with emulsions, foams, and suspensions. The basic aspect of emulsion technology is covered, and much research data of tremendous value to the formulating chemist are supplied. Both aqueous and nonaqueous foams and other systems are discussed, which should interest developers of pharmaceutical aerosol dosage foams. This section alone is worth more than the cost of the book. The material presented is of value to anyone interested in surface chemistry and emulsions, not only to those interested in aerosols.

Section III concerns fluorocarbons in the atmosphere and technical programs in the atmospheric sciences. These chapters are of limited value but present the concerns of various organizations as to the use of fluorocarbons as propellants. However, the final chapters dealing with the sampling and analysis of aerosol products and the toxicity of fluorocarbon propellants are related to the development of these products and are of interest.

This book is recommended for use by both the experienced and the newcomer and should be part of the required library of all laboratories.

Reviewed by John J. Sciarra
Arnold & Marie Schwartz College of Pharmacy and Health Sciences of Long Island University
Brooklyn, NY 11201

Alicyclic Chemistry, Vol. 6. (A Specialist Periodical Report). Edited by M. A. McKERVEY *et al.* The Chemical Society. 1978. 357 pp. 13 × 22 cm. Price $56.00. (Available from Special Issues Sales, American Chemical Society, 1155 16th St., N.W., Washington, DC 20036.)

This sixth volume of an annual series is devoted to a summary of the literature of 1976 describing the chemistry of alicyclic compounds. Each chapter is devoted to a different alicyclic system, beginning in Chapter 1 with three-membered rings and progressing through four-, five-, and six-membered ring systems in subsequent chapters. The last two chapters in the book deal with surveys of literature describing the chemistry of medium- and large-ring compounds and bridged carbocyclic compounds.

Each chapter contains summaries of the literature dealing with structural studies of the various alicyclic systems including both molecular orbital and spectroscopic investigations. The literature of 1976 describing conformational aspects of a variety of alicyclic systems also is summarized in the appropriate chapters. In addition, reports of novel syntheses and chemical reactions of the various alicyclic systems are provided.

Each chapter is well illustrated with structural and chemical formulas. The literature citations are provided conveniently on the same page as the text material. While this book does not have a subject index, a useful author index is included.

Volume 6 of "Alicyclic Chemistry" would be a useful addition to the personal library of chemists and spectroscopists interested in having a concise and thorough review of the literature (of 1976) in this area. Natural products chemists should find this publication useful in terms of an annual review of the chemistry of a variety of alicyclic compounds of natural origin. It is refreshing to note that the current volume of this series sells for the same price as Volume 5.

Reviewed by Thomas N. Riley
Department of Medicinal Chemistry
University of Mississippi
University, MS 38677

Forensic Toxicology: Controlled Substances and Dangerous Drugs. By W. T. LOWRY and J. C. GARRIOTT. Plenum Press, 227 W. 17th St., New York, NY 10011. 1979. xvii + 445 pp. 15 × 23 cm. Price $37.50.

A retrieval of archival data organized in alphabetical order is the purpose of this new hard-covered book. After eight introductory and explanatory chapters comprising 116 pages, the book covers information in monograph form. For each drug entity, which includes both American and foreign manufacturers, the structural formula is presented along with its synonyms, chemical name, trade name, pharmacological classification, biochemical consideration, toxicity data with blood levels, when available, and even some pharmacognosy data where applicable. In addition, each drug is boldly classified as: (*a*) noncontrolled, (*b*) dangerous, or (*c*) scheduled with the specific schedule.

The title is misleading in that one does not find classical forensic toxicology, but the authors did not intend it to be a forensic toxicology text. Apparently, the authors used the title for lack of a better description. It is a reference book intended for attorneys, toxicologists, or chemists who need legal, chemical, and toxicity information on various drugs.

For pharmacists who know the drug laws, the introductory chapters are of little value. The first seven chapters, covering some 100 pages, include definitions and explanations of pharmaceutical dosage forms (from aerosols to tinctures) and scheduled, legend, excluded, and excepted substances. Chapter 4 deals specifically with the regulation of controlled

REVIEWS

Handbook of Aerosol Technology, 2nd Ed. By P. A. SANDERS. Van Nostrand Reinhold Co., 135 W. 50th St., New York, NY 10020. 1979. 526 pp. 15 × 25 cm. Price $27.50

This book is an updated version of "Principles of Aerosol Technology," which was published in 1970. It has become available at a time when the aerosol industry has completed the changeover from the predominant use of fluorocarbons as the propellant to other alternative propellant systems. The "Handbook of Aerosol Technology" is the first book that considers the development of aerosols in the light of the restrictions placed on the use of fluorocarbons as propellants.

The text is divided into three major sections: homogeneous systems and their properties; emulsions, foams, and suspensions; and miscellaneous. While Dr. Sanders is the major author, five chapters were written by several of his former associates from the Freon Products Division of Du Pont, and much of the new experimental data presented was developed at Du Pont.

Chapters 3 and 4 will be particularly valuable to the experienced aerosol chemist in that the use of the fluorocarbon and hydrocarbon propellants for aerosol products is discussed in light of the restricted use of fluorocarbon propellants. The chapters include all of the necessary physicochemical data of value to those formulating aerosol products. While the author includes much information about the fluorocarbon propellants, these propellants can be used only for inhalation-type aerosol products that are covered by a New Drug Application and for an extremely limited number of vaginal foams.

The chapters on containers and valves have been updated and supply the reader with the required knowledge of these components. The chapter on filling methods is adequate but should have included greater details about the filling of products utilizing hydrocarbon propellants. Since the hydrocarbon propellants are flammable, they must be handled differently from the fluorocarbons. A thorough discussion of vapor pressure, spray characteristics, solvency, viscosity, and density is presented. Much of the data in these chapters deal with fluorocarbons and are of limited value based on present regulations. However, data are given for other fluorocarbons such as fluorocarbon 22, which may be approved for use in the future.

The chapter on stability is especially well written and includes the various test methods used to determine the stability of aerosols. Since aerosols now utilize a hydrocarbon propellant, the chapter concerned with flammability is essential. Dr. Sanders also indicates the various regulations involved.

Section II deals with emulsions, foams, and suspensions. The basic aspect of emulsion technology is covered, and much research data of tremendous value to the formulating chemist are supplied. Both aqueous and nonaqueous foams and other systems are discussed, which should interest developers of pharmaceutical aerosol dosage foams. This section alone is worth more than the cost of the book. The material presented is of value to anyone interested in surface chemistry and emulsions, not only to those interested in aerosols.

Section III concerns fluorocarbons in the atmosphere and technical programs in the atmospheric sciences. These chapters are of limited value but present the concerns of various organizations as to the use of fluorocarbons as propellants. However, the final chapters dealing with the sampling and analysis of aerosol products and the toxicity of fluorocarbon propellants are related to the development of these products and are of interest.

This book is recommended for use by both the experienced and the newcomer and should be part of the required library of all laboratories.

Reviewed by John J. Sciarra
Arnold & Marie Schwartz College of Pharmacy and Health Sciences of Long Island University
Brooklyn, NY 11201

Alicyclic Chemistry, Vol. 6. (A Specialist Periodical Report). Edited by M. A. McKERVEY *et al.* The Chemical Society. 1978. 357 pp. 13 × 22 cm. Price $56.00. (Available from Special Issues Sales, American Chemical Society, 1155 16th St., N.W., Washington, DC 20036.)

This sixth volume of an annual series is devoted to a summary of the literature of 1976 describing the chemistry of alicyclic compounds. Each chapter is devoted to a different alicyclic system, beginning in Chapter 1 with three-membered rings and progressing through four-, five-, and six-membered ring systems in subsequent chapters. The last two chapters in the book deal with surveys of literature describing the chemistry of medium- and large-ring compounds and bridged carbocyclic compounds.

Each chapter contains summaries of the literature dealing with structural studies of the various alicyclic systems including both molecular orbital and spectroscopic investigations. The literature of 1976 describing conformational aspects of a variety of alicyclic systems also is summarized in the appropriate chapters. In addition, reports of novel syntheses and chemical reactions of the various alicyclic systems are provided.

Each chapter is well illustrated with structural and chemical formulas. The literature citations are provided conveniently on the same page as the text material. While this book does not have a subject index, a useful author index is included.

Volume 6 of "Alicyclic Chemistry" would be a useful addition to the personal library of chemists and spectroscopists interested in having a concise and thorough review of the literature (of 1976) in this area. Natural products chemists should find this publication useful in terms of an annual review of the chemistry of a variety of alicyclic compounds of natural origin. It is refreshing to note that the current volume of this series sells for the same price as Volume 5.

Reviewed by Thomas N. Riley
Department of Medicinal Chemistry
University of Mississippi
University, MS 38677

Forensic Toxicology: Controlled Substances and Dangerous Drugs. By W. T. LOWRY and J. C. GARRIOTT. Plenum Press, 227 W. 17th St., New York, NY 10011. 1979. xvii + 445 pp. 15 × 23 cm. Price $37.50.

A retrieval of archival data organized in alphabetical order is the purpose of this new hard-covered book. After eight introductory and explanatory chapters comprising 116 pages, the book covers information in monograph form. For each drug entity, which includes both American and foreign manufacturers, the structural formula is presented along with its synonyms, chemical name, trade name, pharmacological classification, biochemical consideration, toxicity data with blood levels, when available, and even some pharmacognosy data where applicable. In addition, each drug is boldly classified as: (*a*) noncontrolled, (*b*) dangerous, or (*c*) scheduled with the specific schedule.

The title is misleading in that one does not find classical forensic toxicology, but the authors did not intend it to be a forensic toxicology text. Apparently, the authors used the title for lack of a better description. It is a reference book intended for attorneys, toxicologists, or chemists who need legal, chemical, and toxicity information on various drugs.

For pharmacists who know the drug laws, the introductory chapters are of little value. The first seven chapters, covering some 100 pages, include definitions and explanations of pharmaceutical dosage forms (from aerosols to tinctures) and scheduled, legend, excluded, and excepted substances. Chapter 4 deals specifically with the regulation of controlled

substances and includes a copy of the Drug Enforcement Administration form for registration under the Controlled Substances Act of 1970. It also includes general information known to all practicing pharmacists concerning security requirements, order forms, *etc.*

Chapter 6 gives the requirements for exception of a preparation from all or part of the Act. This information is followed by 21 pages of alphabetically listed drug preparations indicating which are excepted. For some preparations, an indication is given that none is excepted. Chapter 5 (3 pages long) lists preparations that are excluded from any schedule and that can be sold over the counter, such as Vicks Inhaler which contains L-methamphetamine (L-desoxyephedrine). Some of these items are excluded from the Act only in a given preparation; L-methamphetamine is a Schedule II substance but is excluded only in a preparation like Vicks Inhaler.

Chapter 8 deals with the analytical techniques used for drug identification and serves only to familiarize the reader with the names of the techniques and with what might be accomplished by a chemist using the instrument or technique.

Chapter 9 is the bulk of the book and deviates from the subtitle because it includes controlled and noncontrolled substances. The implication from the title of Chapter 9 is that commonly abused substances are included. However, many listings do not constitute abused drugs; misused but not abused! For example, the noncontrolled substances acetaminophen, acetanilide, lactose, and salicylate are included. The information supplied is useful from a clinical or forensic view point.

During the 1st week that I had the book, I referred to it twice and both times I found the data and/or information I needed on a specific drug. The book is useful in my work; the same may not be true for the community or hospital pharmacist.

Reviewed by Charles L. Winek
Duquesne University
Pittsburgh, PA 15219

Encyclopaedia of Antibiotics, 2nd Ed. By JOHN S. GLASBY. Wiley, One Wiley Drive, Somerset, NJ 08873. 1979. 467 pp. 18 × 26 cm. Price $60.00.

The second edition has been expanded to include over 400 new antibiotics which have been discovered since publication of the first edition. As in the previous edition, formulas, structures, melting points, origin, methods of purification and preparation, and patent references are given for the antibiotics. Toxicity and activity are indicated for many of the antibiotics. This book would be a valuable reference source for scientists and students working with antibiotics.

Staff Review

The Family Prescription & Medication Guide. By ALBERT M. PAWLINA. Prentice-Hall, Englewood Cliffs, NJ 07632. 1979. 367 pp. 15 × 21 cm. Price $13.95 hard cover, $6.95 soft cover.

This nontechnical book is intended to guide the individual patient on appropriate drug use. The first section lists alphabetically about 250 commonly used drugs and summarizes their brand names, medical use, and possible side effects. An alphabetical arrangement of both generic and brand names, identifying the manufacturers and components of each product, follows. Common medical and pharmaceutical terms are defined in the third section. The Appendix tables list some common and serious food–drug and drug–drug interactions.

Staff Review

NOTICES

Applied Therapeutics for Clinical Pharmacists. 2nd Ed. Edited by MARY ANNE KODA-KIMBLE, LLOYD Y. YOUNG, and S. KATCHER. Applied Therapeutics Inc., P.O. Box 31-747, San Francisco, CA 94131. 1978. 944 pp. 20 × 26 cm. Price $31.50.

Molecular Structure by Diffraction Methods. Vol. 6. By L. E. SUTTON *et al.* The Chemical Society. 1979. 338 pp. 13 × 22 cm. Price $72.50. (Available from the American Chemical Society, 1155 16th St., N.W., Washington, DC 20036.)

Piroxicam. No. 1. International Congress and Symposium Series. Edited by W. M. O'BRIEN and E. H. WISEMAN. The Royal Society of Medicine. 1978. 111 pp. 16 × 24 cm. Price $10.25. (Available from Grune and Stratton, 111 5th Ave., New York, NY 10003.)

Pregnancy Metabolism, Diabetes and the Fetus. Ciba Foundation Symposium 63 (new series). Elsevier/North-Holland, 52 Vanderbilt Ave., New York, NY 10017. 1979. 326 pp. 16 × 24 cm. Price $39.50.

Principles of Organic Stereochemistry. Vol. 6. Studies in Organic Chemistry Series. By BERNARD TESTA. Dekker, 270 Madison Ave., New York, NY 10016. 1979. 248 pp. 15 × 23 cm. Price $14.50.

The Alkaloids. Chemistry and Physiology. Vol. XVII. Edited by R. H. F. MANSKE and R. G. A. RODRIGO. Academic, 111 5th Ave., New York, NY 10003. 1979. 611 pp. 15 × 23 cm. Price $55.00.

Progress in Pharmacology. Vol. 2, No. 2. Action of Cardiac Glycosides on the Excitation–Contraction Coupling in Heart Muscle. By HEINZ LULLMANN and THIES PETERS. *Drug Absorption from Abnormal Gastrointestinal Tract.* By M. J. MATTILA and V. M. K. VENHO. Gustav Fischer Verlag, Postfach 72 0143, D 7000 Stuttgart 70, West Germany. 1979. 86 pp. 16 × 24 cm. Price DM 41.50 (for the series).

Advances in Cancer Chemotherapy. Vol. 1. Edited by ANDRE ROSOWSKY. Dekker, 270 Madison Ave., New York, NY 10016. 1979. 297 pp. 15 × 23 cm. Price $29.75.

Disposition of Toxic Drugs and Chemicals in Man. Vol. 2. Peripherally-Acting Drugs and Common Toxic Chemicals. By RANDALL C. BASELT. Biomedical, P.O. Box 495, Davis, CA 95676. 1978. 281 pp. 15 × 23 cm. Price $22.50.

Carbohydrate Chemistry. Vol. 10. A Specialist Periodical Report. By J. S. BRIMACOMBE *et al.* The Chemical Society. 1978. 524 pp. 13 × 22 cm. Price $64.00. (Available from the American Chemical Society, 1155 16th St., N.W., Washington, DC 20036.)

Carbon-13 NMR Shift Assignments of Amines and Alkaloids. By MAURICE SHAMMA and DAVID M. HINDENLANG. Plenum, 227 W. 17th St., New York, NY 10011. 1979. 303 pp. 15 × 23 cm. Price $29.50.

Central Nervous System Pharmacology: A Self-Instruction Text, 2nd Ed. By DONALD E. McMILLAN. Little, Brown, 34 Beacon St., Boston, MA 02106. 1979. 166 pp. 21 × 26 cm. Price $12.50.

A Color Atlas Of The Rat. Dissection Guide. By RONALD J. OLDS and JOAN R. OLDS. Wiley, 605 Third Ave., New York, NY 10016. 1979. 112 pp. 13 × 19 cm.

Handbook on Drug Abuse. Edited by ROBERT I. DUPONT, AVRAM GOLDSTEIN, and JOHN O'DONNELL. National Institute on Drug Abuse, U.S. Department of Health, Education, and Welfare and Office of Drug Abuse Policy. 1979. 452 pp. 19 × 26 cm.

IARC Monographs on the Evaluation of the Carcinogenic Risk of Chemicals to Humans. Vol. 19. Some Monomers, Plastics and Synthetic Elastomers, and Acrolein. World Health Organization, 1211 Geneva 27, Switzerland. 1979. 513 pp. 17 × 24 cm. Price Sw. fr. 60.

Issues in Pharmaceutical Economics. Edited by ROBERT I. CHIEN. Lexington Books, D.C. Heath, Lexington, MA 02173. 1979. 246 pp. 16 × 23 cm. Price $17.95.

The Alkaloids. Vol. 8. By M. F. GRUNDON *et al.* The Chemical Society. 1978. 276 pp. 13 × 22 cm. Price $52.75. (Available from the American Chemical Society, 1155 16th St., N.W., Washington, DC 20036.)

Biosynthetic Products for Cancer Chemotherapy. Vol. 3. By GEORGE R. PETTIT and RICHARD H. ODE. Plenum, 227 W. 17th St., New York, NY 10011. 1979. 15 × 23 cm. 197 pp. Price $32.50.

Quantitative Structure Activity Relationships of Analgesics, Narcotic Antagonists, and Hallucinogens. National Institute on Drug Abuse. U.S. Government Printing Office, Washington, DC 20402 (Stock No. 017-024-00786-2). 487 pp. 14 × 23 cm.

substances and includes a copy of the Drug Enforcement Administration form for registration under the Controlled Substances Act of 1970. It also includes general information known to all practicing pharmacists concerning security requirements, order forms, *etc.*

Chapter 6 gives the requirements for exception of a preparation from all or part of the Act. This information is followed by 21 pages of alphabetically listed drug preparations indicating which are excepted. For some preparations, an indication is given that none is excepted. Chapter 5 (3 pages long) lists preparations that are excluded from any schedule and that can be sold over the counter, such as Vicks Inhaler which contains L-methamphetamine (L-desoxyephedrine). Some of these items are excluded from the Act only in a given preparation; L-methamphetamine is a Schedule II substance but is excluded only in a preparation like Vicks Inhaler.

Chapter 8 deals with the analytical techniques used for drug identification and serves only to familiarize the reader with the names of the techniques and with what might be accomplished by a chemist using the instrument or technique.

Chapter 9 is the bulk of the book and deviates from the subtitle because it includes controlled and noncontrolled substances. The implication from the title of Chapter 9 is that commonly abused substances are included. However, many listings do not constitute abused drugs; misused but not abused! For example, the noncontrolled substances acetaminophen, acetanilide, lactose, and salicylate are included. The information supplied is useful from a clinical or forensic view point.

During the 1st week that I had the book, I referred to it twice and both times I found the data and/or information I needed on a specific drug. The book is useful in my work; the same may not be true for the community or hospital pharmacist.

Reviewed by Charles L. Winek
Duquesne University
Pittsburgh, PA 15219

Encyclopaedia of Antibiotics, 2nd Ed. By JOHN S. GLASBY. Wiley, One Wiley Drive, Somerset, NJ 08873. 1979. 467 pp. 18 × 26 cm. Price $60.00.

The second edition has been expanded to include over 400 new antibiotics which have been discovered since publication of the first edition. As in the previous edition, formulas, structures, melting points, origin, methods of purification and preparation, and patent references are given for the antibiotics. Toxicity and activity are indicated for many of the antibiotics. This book would be a valuable reference source for scientists and students working with antibiotics.

Staff Review

The Family Prescription & Medication Guide. By ALBERT M. PAWLINA. Prentice-Hall, Englewood Cliffs, NJ 07632. 1979. 367 pp. 15 × 21 cm. Price $13.95 hard cover, $6.95 soft cover.

This nontechnical book is intended to guide the individual patient on appropriate drug use. The first section lists alphabetically about 250 commonly used drugs and summarizes their brand names, medical use, and possible side effects. An alphabetical arrangement of both generic and brand names, identifying the manufacturers and components of each product, follows. Common medical and pharmaceutical terms are defined in the third section. The Appendix tables list some common and serious food–drug and drug–drug interactions.

Staff Review

NOTICES

Applied Therapeutics for Clinical Pharmacists. 2nd Ed. Edited by MARY ANNE KODA-KIMBLE, LLOYD Y. YOUNG, and S. KATCHER. Applied Therapeutics Inc., P.O. Box 31-747, San Francisco, CA 94131. 1978. 944 pp. 20 × 26 cm. Price $31.50.

Molecular Structure by Diffraction Methods. Vol. 6. By L. E. SUTTON *et al.* The Chemical Society. 1979. 338 pp. 13 × 22 cm. Price $72.50. (Available from the American Chemical Society, 1155 16th St., N.W., Washington, DC 20036.)

Piroxicam. No. 1. International Congress and Symposium Series. Edited by W. M. O'BRIEN and E. H. WISEMAN. The Royal Society of Medicine. 1978. 111 pp. 16 × 24 cm. Price $10.25. (Available from Grune and Stratton, 111 5th Ave., New York, NY 10003.)

Pregnancy Metabolism, Diabetes and the Fetus. Ciba Foundation Symposium 63 (new series). Elsevier/North-Holland, 52 Vanderbilt Ave., New York, NY 10017. 1979. 326 pp. 16 × 24 cm. Price $39.50.

Principles of Organic Stereochemistry. Vol. 6. Studies in Organic Chemistry Series. By BERNARD TESTA. Dekker, 270 Madison Ave., New York, NY 10016. 1979. 248 pp. 15 × 23 cm. Price $14.50.

The Alkaloids. Chemistry and Physiology. Vol. XVII. Edited by R. H. F. MANSKE and R. G. A. RODRIGO. Academic, 111 5th Ave., New York, NY 10003. 1979. 611 pp. 15 × 23 cm. Price $55.00.

Progress in Pharmacology. Vol. 2, No. 2. Action of Cardiac Glycosides on the Excitation–Contraction Coupling in Heart Muscle. By HEINZ LULLMANN and THIES PETERS. *Drug Absorption from Abnormal Gastrointestinal Tract.* By M. J. MATTILA and V. M. K. VENHO. Gustav Fischer Verlag, Postfach 72 0143, D 7000 Stuttgart 70, West Germany. 1979. 86 pp. 16 × 24 cm. Price DM 41.50 (for the series).

Advances in Cancer Chemotherapy. Vol. 1. Edited by ANDRE ROSOWSKY. Dekker, 270 Madison Ave., New York, NY 10016. 1979. 297 pp. 15 × 23 cm. Price $29.75.

Disposition of Toxic Drugs and Chemicals in Man. Vol. 2. Peripherally-Acting Drugs and Common Toxic Chemicals. By RANDALL C. BASELT. Biomedical, P.O. Box 495, Davis, CA 95676. 1978. 281 pp. 15 × 23 cm. Price $22.50.

Carbohydrate Chemistry. Vol. 10. A Specialist Periodical Report. By J. S. BRIMACOMBE *et al.* The Chemical Society. 1978. 524 pp. 13 × 22 cm. Price $64.00. (Available from the American Chemical Society, 1155 16th St., N.W., Washington, DC 20036.)

Carbon-13 NMR Shift Assignments of Amines and Alkaloids. By MAURICE SHAMMA and DAVID M. HINDENLANG. Plenum, 227 W. 17th St., New York, NY 10011. 1979. 303 pp. 15 × 23 cm. Price $29.50.

Central Nervous System Pharmacology: A Self-Instruction Text, 2nd Ed. By DONALD E. McMILLAN. Little, Brown, 34 Beacon St., Boston, MA 02106. 1979. 166 pp. 21 × 26 cm. Price $12.50.

A Color Atlas Of The Rat. Dissection Guide. By RONALD J. OLDS and JOAN R. OLDS. Wiley, 605 Third Ave., New York, NY 10016. 1979. 112 pp. 13 × 19 cm.

Handbook on Drug Abuse. Edited by ROBERT I. DUPONT, AVRAM GOLDSTEIN, and JOHN O'DONNELL. National Institute on Drug Abuse, U.S. Department of Health, Education, and Welfare and Office of Drug Abuse Policy. 1979. 452 pp. 19 × 26 cm.

IARC Monographs on the Evaluation of the Carcinogenic Risk of Chemicals to Humans. Vol. 19. Some Monomers, Plastics and Synthetic Elastomers, and Acrolein. World Health Organization, 1211 Geneva 27, Switzerland. 1979. 513 pp. 17 × 24 cm. Price Sw. fr. 60.

Issues in Pharmaceutical Economics. Edited by ROBERT I. CHIEN. Lexington Books, D.C. Heath, Lexington, MA 02173. 1979. 246 pp. 16 × 23 cm. Price $17.95.

The Alkaloids. Vol. 8. By M. F. GRUNDON *et al.* The Chemical Society. 1978. 276 pp. 13 × 22 cm. Price $52.75. (Available from the American Chemical Society, 1155 16th St., N.W., Washington, DC 20036.)

Biosynthetic Products for Cancer Chemotherapy. Vol. 3. By GEORGE R. PETTIT and RICHARD H. ODE. Plenum, 227 W. 17th St., New York, NY 10011. 1979. 15 × 23 cm. 197 pp. Price $32.50.

Quantitative Structure Activity Relationships of Analgesics, Narcotic Antagonists, and Hallucinogens. National Institute on Drug Abuse. U.S. Government Printing Office, Washington, DC 20402 (Stock No. 017-024-00786-2). 487 pp. 14 × 23 cm.

substances and includes a copy of the Drug Enforcement Administration form for registration under the Controlled Substances Act of 1970. It also includes general information known to all practicing pharmacists concerning security requirements, order forms, *etc.*

Chapter 6 gives the requirements for exception of a preparation from all or part of the Act. This information is followed by 21 pages of alphabetically listed drug preparations indicating which are excepted. For some preparations, an indication is given that none is excepted. Chapter 5 (3 pages long) lists preparations that are excluded from any schedule and that can be sold over the counter, such as Vicks Inhaler which contains L-methamphetamine (L-desoxyephedrine). Some of these items are excluded from the Act only in a given preparation; L-methamphetamine is a Schedule II substance but is excluded only in a preparation like Vicks Inhaler.

Chapter 8 deals with the analytical techniques used for drug identification and serves only to familiarize the reader with the names of the techniques and with what might be accomplished by a chemist using the instrument or technique.

Chapter 9 is the bulk of the book and deviates from the subtitle because it includes controlled and noncontrolled substances. The implication from the title of Chapter 9 is that commonly abused substances are included. However, many listings do not constitute abused drugs; misused but not abused! For example, the noncontrolled substances acetaminophen, acetanilide, lactose, and salicylate are included. The information supplied is useful from a clinical or forensic view point.

During the 1st week that I had the book, I referred to it twice and both times I found the data and/or information I needed on a specific drug. The book is useful in my work; the same may not be true for the community or hospital pharmacist.

Reviewed by Charles L. Winek
Duquesne University
Pittsburgh, PA 15219

Encyclopaedia of Antibiotics, 2nd Ed. By JOHN S. GLASBY. Wiley, One Wiley Drive, Somerset, NJ 08873. 1979. 467 pp. 18 × 26 cm. Price $60.00.

The second edition has been expanded to include over 400 new antibiotics which have been discovered since publication of the first edition. As in the previous edition, formulas, structures, melting points, origin, methods of purification and preparation, and patent references are given for the antibiotics. Toxicity and activity are indicated for many of the antibiotics. This book would be a valuable reference source for scientists and students working with antibiotics.

Staff Review

The Family Prescription & Medication Guide. By ALBERT M. PAWLINA. Prentice-Hall, Englewood Cliffs, NJ 07632. 1979. 367 pp. 15 × 21 cm. Price $13.95 hard cover, $6.95 soft cover.

This nontechnical book is intended to guide the individual patient on appropriate drug use. The first section lists alphabetically about 250 commonly used drugs and summarizes their brand names, medical use, and possible side effects. An alphabetical arrangement of both generic and brand names, identifying the manufacturers and components of each product, follows. Common medical and pharmaceutical terms are defined in the third section. The Appendix tables list some common and serious food–drug and drug–drug interactions.

Staff Review

NOTICES

Applied Therapeutics for Clinical Pharmacists. 2nd Ed. Edited by MARY ANNE KODA-KIMBLE, LLOYD Y. YOUNG, and S. KATCHER. Applied Therapeutics Inc., P.O. Box 31-747, San Francisco, CA 94131. 1978. 944 pp. 20 × 26 cm. Price $31.50.

Molecular Structure by Diffraction Methods. Vol. 6. By L. E. SUTTON *et al.* The Chemical Society. 1979. 338 pp. 13 × 22 cm. Price $72.50. (Available from the American Chemical Society, 1155 16th St., N.W., Washington, DC 20036.)

Piroxicam. No. 1. International Congress and Symposium Series. Edited by W. M. O'BRIEN and E. H. WISEMAN. The Royal Society of Medicine. 1978. 111 pp. 16 × 24 cm. Price $10.25. (Available from Grune and Stratton, 111 5th Ave., New York, NY 10003.)

Pregnancy Metabolism, Diabetes and the Fetus. Ciba Foundation Symposium 63 (new series). Elsevier/North-Holland, 52 Vanderbilt Ave., New York, NY 10017. 1979. 326 pp. 16 × 24 cm. Price $39.50.

Principles of Organic Stereochemistry. Vol. 6. Studies in Organic Chemistry Series. By BERNARD TESTA. Dekker, 270 Madison Ave., New York, NY 10016. 1979. 248 pp. 15 × 23 cm. Price $14.50.

The Alkaloids. Chemistry and Physiology. Vol. XVII. Edited by R. H. F. MANSKE and R. G. A. RODRIGO. Academic, 111 5th Ave., New York, NY 10003. 1979. 611 pp. 15 × 23 cm. Price $55.00.

Progress in Pharmacology. Vol. 2, No. 2. Action of Cardiac Glycosides on the Excitation–Contraction Coupling in Heart Muscle. By HEINZ LULLMANN and THIES PETERS. *Drug Absorption from Abnormal Gastrointestinal Tract.* By M. J. MATTILA and V. M. K. VENHO. Gustav Fischer Verlag, Postfach 72 0143, D 7000 Stuttgart 70, West Germany. 1979. 86 pp. 16 × 24 cm. Price DM 41.50 (for the series).

Advances in Cancer Chemotherapy. Vol. 1. Edited by ANDRE ROSOWSKY. Dekker, 270 Madison Ave., New York, NY 10016. 1979. 297 pp. 15 × 23 cm. Price $29.75.

Disposition of Toxic Drugs and Chemicals in Man. Vol. 2. Peripherally-Acting Drugs and Common Toxic Chemicals. By RANDALL C. BASELT. Biomedical, P.O. Box 495, Davis, CA 95676. 1978. 281 pp. 15 × 23 cm. Price $22.50.

Carbohydrate Chemistry. Vol. 10. A Specialist Periodical Report. By J. S. BRIMACOMBE *et al.* The Chemical Society. 1978. 524 pp. 13 × 22 cm. Price $64.00. (Available from the American Chemical Society, 1155 16th St., N.W., Washington, DC 20036.)

Carbon-13 NMR Shift Assignments of Amines and Alkaloids. By MAURICE SHAMMA and DAVID M. HINDENLANG. Plenum, 227 W. 17th St., New York, NY 10011. 1979. 303 pp. 15 × 23 cm. Price $29.50.

Central Nervous System Pharmacology: A Self-Instruction Text, 2nd Ed. By DONALD E. McMILLAN. Little, Brown, 34 Beacon St., Boston, MA 02106. 1979. 166 pp. 21 × 26 cm. Price $12.50.

A Color Atlas Of The Rat. Dissection Guide. By RONALD J. OLDS and JOAN R. OLDS. Wiley, 605 Third Ave., New York, NY 10016. 1979. 112 pp. 13 × 19 cm.

Handbook on Drug Abuse. Edited by ROBERT I. DUPONT, AVRAM GOLDSTEIN, and JOHN O'DONNELL. National Institute on Drug Abuse, U.S. Department of Health, Education, and Welfare and Office of Drug Abuse Policy. 1979. 452 pp. 19 × 26 cm.

IARC Monographs on the Evaluation of the Carcinogenic Risk of Chemicals to Humans. Vol. 19. Some Monomers, Plastics and Synthetic Elastomers, and Acrolein. World Health Organization, 1211 Geneva 27, Switzerland. 1979. 513 pp. 17 × 24 cm. Price Sw. fr. 60.

Issues in Pharmaceutical Economics. Edited by ROBERT I. CHIEN. Lexington Books, D.C. Heath, Lexington, MA 02173. 1979. 246 pp. 16 × 23 cm. Price $17.95.

The Alkaloids. Vol. 8. By M. F. GRUNDON *et al.* The Chemical Society. 1978. 276 pp. 13 × 22 cm. Price $52.75. (Available from the American Chemical Society, 1155 16th St., N.W., Washington, DC 20036.)

Biosynthetic Products for Cancer Chemotherapy. Vol. 3. By GEORGE R. PETTIT and RICHARD H. ODE. Plenum, 227 W. 17th St., New York, NY 10011. 1979. 15 × 23 cm. 197 pp. Price $32.50.

Quantitative Structure Activity Relationships of Analgesics, Narcotic Antagonists, and Hallucinogens. National Institute on Drug Abuse. U.S. Government Printing Office, Washington, DC 20402 (Stock No. 017-024-00786-2). 487 pp. 14 × 23 cm.

substances and includes a copy of the Drug Enforcement Administration form for registration under the Controlled Substances Act of 1970. It also includes general information known to all practicing pharmacists concerning security requirements, order forms, *etc.*

Chapter 6 gives the requirements for exception of a preparation from all or part of the Act. This information is followed by 21 pages of alphabetically listed drug preparations indicating which are excepted. For some preparations, an indication is given that none is excepted. Chapter 5 (3 pages long) lists preparations that are excluded from any schedule and that can be sold over the counter, such as Vicks Inhaler which contains L-methamphetamine (L-desoxyephedrine). Some of these items are excluded from the Act only in a given preparation; L-methamphetamine is a Schedule II substance but is excluded only in a preparation like Vicks Inhaler.

Chapter 8 deals with the analytical techniques used for drug identification and serves only to familiarize the reader with the names of the techniques and with what might be accomplished by a chemist using the instrument or technique.

Chapter 9 is the bulk of the book and deviates from the subtitle because it includes controlled and noncontrolled substances. The implication from the title of Chapter 9 is that commonly abused substances are included. However, many listings do not constitute abused drugs; misused but not abused! For example, the noncontrolled substances acetaminophen, acetanilide, lactose, and salicylate are included. The information supplied is useful from a clinical or forensic view point.

During the 1st week that I had the book, I referred to it twice and both times I found the data and/or information I needed on a specific drug. The book is useful in my work; the same may not be true for the community or hospital pharmacist.

Reviewed by Charles L. Winek
Duquesne University
Pittsburgh, PA 15219

Encyclopaedia of Antibiotics, 2nd Ed. By JOHN S. GLASBY. Wiley, One Wiley Drive, Somerset, NJ 08873. 1979. 467 pp. 18 × 26 cm. Price $60.00.

The second edition has been expanded to include over 400 new antibiotics which have been discovered since publication of the first edition. As in the previous edition, formulas, structures, melting points, origin, methods of purification and preparation, and patent references are given for the antibiotics. Toxicity and activity are indicated for many of the antibiotics. This book would be a valuable reference source for scientists and students working with antibiotics.

Staff Review

The Family Prescription & Medication Guide. By ALBERT M. PAWLINA. Prentice-Hall, Englewood Cliffs, NJ 07632. 1979. 367 pp. 15 × 21 cm. Price $13.95 hard cover, $6.95 soft cover.

This nontechnical book is intended to guide the individual patient on appropriate drug use. The first section lists alphabetically about 250 commonly used drugs and summarizes their brand names, medical use, and possible side effects. An alphabetical arrangement of both generic and brand names, identifying the manufacturers and components of each product, follows. Common medical and pharmaceutical terms are defined in the third section. The Appendix tables list some common and serious food–drug and drug–drug interactions.

Staff Review

NOTICES

Applied Therapeutics for Clinical Pharmacists. 2nd Ed. Edited by MARY ANNE KODA-KIMBLE, LLOYD Y. YOUNG, and S. KATCHER. Applied Therapeutics Inc., P.O. Box 31-747, San Francisco, CA 94131. 1978. 944 pp. 20 × 26 cm. Price $31.50.

Molecular Structure by Diffraction Methods. Vol. 6. By L. E. SUTTON *et al.* The Chemical Society. 1979. 338 pp. 13 × 22 cm. Price $72.50. (Available from the American Chemical Society, 1155 16th St., N.W., Washington, DC 20036.)

Piroxicam. No. 1. International Congress and Symposium Series. Edited by W. M. O'BRIEN and E. H. WISEMAN. The Royal Society of Medicine. 1978. 111 pp. 16 × 24 cm. Price $10.25. (Available from Grune and Stratton, 111 5th Ave., New York, NY 10003.)

Pregnancy Metabolism, Diabetes and the Fetus. Ciba Foundation Symposium 63 (new series). Elsevier/North-Holland, 52 Vanderbilt Ave., New York, NY 10017. 1979. 326 pp. 16 × 24 cm. Price $39.50.

Principles of Organic Stereochemistry. Vol. 6. Studies in Organic Chemistry Series. By BERNARD TESTA. Dekker, 270 Madison Ave., New York, NY 10016. 1979. 248 pp. 15 × 23 cm. Price $14.50.

The Alkaloids. Chemistry and Physiology. Vol. XVII. Edited by R. H. F. MANSKE and R. G. A. RODRIGO. Academic, 111 5th Ave., New York, NY 10003. 1979. 611 pp. 15 × 23 cm. Price $55.00.

Progress in Pharmacology. Vol. 2, No. 2. Action of Cardiac Glycosides on the Excitation–Contraction Coupling in Heart Muscle. By HEINZ LULLMANN and THIES PETERS. *Drug Absorption from Abnormal Gastrointestinal Tract.* By M. J. MATTILA and V. M. K. VENHO. Gustav Fischer Verlag, Postfach 72 0143, D 7000 Stuttgart 70, West Germany. 1979. 86 pp. 16 × 24 cm. Price DM 41.50 (for the series).

Advances in Cancer Chemotherapy. Vol. 1. Edited by ANDRE ROSOWSKY. Dekker, 270 Madison Ave., New York, NY 10016. 1979. 297 pp. 15 × 23 cm. Price $29.75.

Disposition of Toxic Drugs and Chemicals in Man. Vol. 2. Peripherally-Acting Drugs and Common Toxic Chemicals. By RANDALL C. BASELT. Biomedical, P.O. Box 495, Davis, CA 95676. 1978. 281 pp. 15 × 23 cm. Price $22.50.

Carbohydrate Chemistry. Vol. 10. A Specialist Periodical Report. By J. S. BRIMACOMBE *et al.* The Chemical Society. 1978. 524 pp. 13 × 22 cm. Price $64.00. (Available from the American Chemical Society, 1155 16th St., N.W., Washington, DC 20036.)

Carbon-13 NMR Shift Assignments of Amines and Alkaloids. By MAURICE SHAMMA and DAVID M. HINDENLANG. Plenum, 227 W. 17th St., New York, NY 10011. 1979. 303 pp. 15 × 23 cm. Price $29.50.

Central Nervous System Pharmacology: A Self-Instruction Text, 2nd Ed. By DONALD E. McMILLAN. Little, Brown, 34 Beacon St., Boston, MA 02106. 1979. 166 pp. 21 × 26 cm. Price $12.50.

A Color Atlas Of The Rat. Dissection Guide. By RONALD J. OLDS and JOAN R. OLDS. Wiley, 605 Third Ave., New York, NY 10016. 1979. 112 pp. 13 × 19 cm.

Handbook on Drug Abuse. Edited by ROBERT I. DUPONT, AVRAM GOLDSTEIN, and JOHN O'DONNELL. National Institute on Drug Abuse, U.S. Department of Health, Education, and Welfare and Office of Drug Abuse Policy. 1979. 452 pp. 19 × 26 cm.

IARC Monographs on the Evaluation of the Carcinogenic Risk of Chemicals to Humans. Vol. 19. Some Monomers, Plastics and Synthetic Elastomers, and Acrolein. World Health Organization, 1211 Geneva 27, Switzerland. 1979. 513 pp. 17 × 24 cm. Price Sw. fr. 60.

Issues in Pharmaceutical Economics. Edited by ROBERT I. CHIEN. Lexington Books, D.C. Heath, Lexington, MA 02173. 1979. 246 pp. 16 × 23 cm. Price $17.95.

The Alkaloids. Vol. 8. By M. F. GRUNDON *et al.* The Chemical Society. 1978. 276 pp. 13 × 22 cm. Price $52.75. (Available from the American Chemical Society, 1155 16th St., N.W., Washington, DC 20036.)

Biosynthetic Products for Cancer Chemotherapy. Vol. 3. By GEORGE R. PETTIT and RICHARD H. ODE. Plenum, 227 W. 17th St., New York, NY 10011. 1979. 15 × 23 cm. 197 pp. Price $32.50.

Quantitative Structure Activity Relationships of Analgesics, Narcotic Antagonists, and Hallucinogens. National Institute on Drug Abuse. U.S. Government Printing Office, Washington, DC 20402 (Stock No. 017-024-00786-2). 487 pp. 14 × 23 cm.

Fundamentals of Oncology. By HENRY C. PITOT. Dekker, 270 Madison Ave., New York, NY 10016. 1978. 192 pp. 15 × 23 cm. Price $9.95.

Hagers Handbuch der Pharmazeutischen Praxis. 4th Ed., Vol. 6. Edited by P. H. LIST and L. HORHAMMER. Springer-Verlag, 175 5th Ave., New York, NY 10010. 1979. 720 pp. 16 × 24 cm. Price $101.80.

Reagents for Organic Synthesis. Vol. 7. By MARY FIESER and LOUIS F. FIESER. Wiley, 605 Third Ave., New York, NY 10016. 1979. 487 pp. 15 × 23 cm. Price $32.50.

75 Years of Chromatography—A Historical Dialogue. Edited by LESLIE S. ETTRE and ALBERT ZLATKIS. Elsevier/North-Holland, 52 Vanderbilt Ave., New York, NY 10017. 1979. 502 pp. 16 × 24 cm. Price $49.75.

Amino-acids, Peptides, and Proteins, Vol. 10. Senior Reporter, R. C. SHEPPARD. The Chemical Society. 1979. 537 pp. 13 × 23 cm. Price $68.00. (Available from the American Chemical Society, 1155 16th St., N.W., Washington, DC 20036.)

Medicine Before Columbus. By ABNER J. WEISMAN. Pre-Cortesian Publications, 162 E. 95th St., New York, NY 10028. 1979. 152 pp. 21 × 27 cm. Price $14.50.

Cigarette Smoking as a Dependence Process. NIDA Research Monograph 23. Edited by NORMAN A. KRASNEGOR. National Institute on Drug Abuse, 5600 Fishers Lane, Rockville, MD 20857. 1979. 194 pp. 15 × 23 cm.

Immobilized Enzymes Preparation and Engineering: Recent Advances. By J. C. JOHNSON. Noyes Data Corp., Mill Rd. at Grand Ave., Park Ridge, NJ 07656. 1979. 305 pp. 15 × 24 cm. Price $42.00.

International Drug Use. Research Issues 23. Edited by GREGORY A. AUSTIN, MARY A. MACARI, and DON J. LETTIERI. National Institute on Drug Abuse, 5600 Fishers Lane, Rockville, MD 20857. 1978. 199 pp. 20 × 27 cm.

Perspectives on the History of Psychoactive Substance Use. Research Issues 24. By GREGORY A. AUSTIN. National Institute on Drug Abuse, 5600 Fishers Lane, Rockville, MD 20857. 1978. 280 pp. 20 × 26 cm.

The Concept of a Blood–Brain Barrier. By MICHAEL BRADBURY. Wiley, 1 Wiley Dr., Somerset, NJ 08873. 1979. 465 pp. 15 × 24 cm. Price $56.00

NEW JOURNALS

Journal of Immunopharmacology. Edited by ALAN M. REYNARD, JOSEPH R. GERBASI, and MORRIS REICHLIN. Dekker, 270 Madison Ave., New York, NY 10016. 1979. 14 × 23 cm. Price $40.00 (4 issues per year).

Journal of Ethnopharmacology. An interdisciplinary journal devoted to bioscientific research on indigenous drugs. Edited by LAURENT RIVIER and JAN G. BRUHN. Elsevier/Sequoia S.A., Avenue de la Gare 50, P.O. Box 851, 1001 Lausanne #1, Switzerland. 1979. 16 × 24 cm. Price $83.25 (4 issues per year).

FEBRUARY 1980
VOLUME 69 NUMBER 2

JOURNAL OF PHARMACEUTICAL SCIENCES

MARY H. FERGUSON
Editor

SHELLY ELLIOTT
Production Editor

MARCIA GARTRELL
Copy Editor

NICOLETTE TRIANTAFELLU
Copy Editor

EDWARD G. FELDMANN
Contributing Editor

SAMUEL W. GOLDSTEIN
Contributing Editor

BELLE R. BECK
Editorial Secretary

DAVID BOHARDT
Director of Publications

L. LUAN CORRIGAN
Assistant Director of Publications

EDITORIAL ADVISORY BOARD

JOHN AUTIAN
HERBERT A. LIEBERMAN
NORMAN R. FARNSWORTH
DAVID E. MANN, JR.
WILLIAM O. FOYE
GERALD J. PAPARIELLO
WILLIAM J. JUSKO
EDWARD G. RIPPIE

The *Journal of Pharmaceutical Sciences* (ISSN 0022-3549) is published monthly by the American Pharmaceutical Association (APhA) at 2215 Constitution Ave., N.W., Washington, DC 20037. Second-class postage paid at Washington, D.C., and at additional mailing office.

All expressions of opinion and statements of supposed fact appearing in articles or editorials carried in this journal are published on the authority of the writer over whose name they appear and are not to be regarded as necessarily expressing the policies or views of APhA.

Offices—Editorial, Advertising, and Subscription: 2215 Constitution Ave., N.W., Washington, DC 20037. Printing: 20th & Northampton Streets, Easton, PA 18042.

Annual Subscriptions—United States and foreign, industrial and government institutions $60, educational institutions $60, individuals *for personal use only* $30; single copies $5. All foreign subscriptions add $5 for postage. Subscription rates are subject to change without notice. Members of APhA may elect to receive the *Journal of Pharmaceutical Sciences* as a part of their annual $80 (foreign $85) APhA membership dues.

Claims—Missing numbers will not be supplied if dues or subscriptions are in arrears for more than 60 days or if claims are received more than 60 days after the date of the issue, or if loss was due to failure to give notice of change of address. APhA cannot accept responsibility for foreign delivery when its records indicate shipment was made.

Change of Address—Members and subscribers should notify at once both the Post Office and APhA of any change of address.

Photocopying—The code at the foot of the first page of an article indicates that APhA has granted permission for copying of the article beyond the limits permitted by Sections 107 and 108 of the U.S. Copyright Law provided that the copier sends the per copy fee stated in the code to the Copyright Clearance Center, Inc., P.O. Box 8891, Boston, MA 02114. Copies may be made for personal or internal use only and not for general distribution.

Microfilm—Available from University Microfilms International, 300 N. Zeeb Road, Ann Arbor, MI 48106.

© Copyright 1980, American Pharmaceutical Association, 2215 Constitution Ave., N.W., Washington, DC 20037; all rights reserved.

CARCINOGENICITY TESTING—A NATIONAL CATASTROPHE

"What you have described to us is a national catastrophe!"

That strong language was used by a prominent clinical researcher who had just heard a presentation by a National Cancer Institute (NCI) staff scientist at a meeting of the National Council on Drugs (NCD). In an audio-visual presentation, the NCI scientist had provided a rather complete description of the NCI's Carcinogenicity Testing Program, and the apparent unanimous reaction of the NCD members present closely corresponded to that articulated by the clinical scientist quoted above.

In late spring 1979, the NCI released to the public press the test results on several well-known and long-used drugs which had been studied under that Institute's Carcinogenicity Testing Program. Included among those drugs was reserpine, and it was assigned a positive classification as a carcinogenic substance. Because of the current wide use of reserpine in medical treatment, classification of this drug as a carcinogenic agent caused considerable anxiety, apprehension, concern, and confusion among health care practitioners, as well as the general public including many patients under treatment with the drug.

Subsequent reports regarding the potential risks involving reserpine seemed only to confuse the matter further rather than to clarify it. Hence, the NCD invited the NCI to provide the group with a first-hand, detailed explanation of the entire testing program.

Beyond hearing that the project costs approximately 65 million dollars a year to conduct the screening program to detect possible carcinogenic effects of chemicals (including drugs), the NCD was also informed regarding the test protocol in use. The latter essentially involves the administration of maximally tolerated doses of the test chemical to two species of rodents for one generation.

Beyond the general view that such testing is virtually meaningless by itself, the NCD was shocked to learn, among other things, that the NCI has not:

(*a*) done any studies to correlate their animal results to humans;

(*b*) tested any known human carcinogens in animals to ascertain whether common relationships exist;

(*c*) attempted to establish whether there is any dose relationship for known carcinogens, much less what such a relationship might be;

(*d*) ascertained "background effects" for the test animals in their test environment—that is, the frequency of tumors in control animals due to heredity, feed, drinking water, or other factors; and

(*e*) conducted any replicate experiments whatsoever to confirm their initial findings—hence, even such questionable "positives" as reserpine have never been repeated.

During the ensuing discussion, the NCI official was subjected to sharp questioning regarding the basic scientific faults and omissions in the program. And incredibly, he clarified that he and his associates equally recognized those deficiencies, but they were constrained by legislative factors to follow their present course.

Incidentally, more than half of the substances tested in the NCI's bioassay program provided some evidence of carcinogenicity. Projections are that this is probably an accurate forecast of the eventual outcome of the total program. Imagine the devastating consequences on life as we know it if half the chemicals to which we are presently exposed are summarily banned from further use. The very thought is mind-boggling!

Yet such disproportionate findings of carcinogenicity potential should not be too surprising considering the massive doses used, the lifetime of exposure, and the other radical conditions comprising the "test protocol" employed.

But as explained by the NCI official, the agency is primarily restricted by the unrealistic provisions in the legislation Congress enacted. Given such a mandate, the Institute has little choice. Moreover, the enormous cost to conduct such tests on even a single chemical means that only a relatively few substances can be tested, thereby making simple retesting an "unaffordable luxury."

Clearly, Congressional review, restudy, reconsideration, and amendment of this law are in order to rectify what, in this writer's view, was accurately labeled "a national catastrophe."

Edward G. Feldmann

FEBRUARY 1980
VOLUME 69 NUMBER 2

JOURNAL OF PHARMACEUTICAL SCIENCES

MARY H. FERGUSON
Editor

SHELLY ELLIOTT
Production Editor

MARCIA GARTRELL
Copy Editor

NICOLETTE TRIANTAFELLU
Copy Editor

EDWARD G. FELDMANN
Contributing Editor

SAMUEL W. GOLDSTEIN
Contributing Editor

BELLE R. BECK
Editorial Secretary

DAVID BOHARDT
Director of Publications

L. LUAN CORRIGAN
Assistant Director of Publications

EDITORIAL ADVISORY BOARD

JOHN AUTIAN
HERBERT A. LIEBERMAN
NORMAN R. FARNSWORTH
DAVID E. MANN, JR.
WILLIAM O. FOYE
GERALD J. PAPARIELLO
WILLIAM J. JUSKO
EDWARD G. RIPPIE

The *Journal of Pharmaceutical Sciences* (ISSN 0022-3549) is published monthly by the American Pharmaceutical Association (APhA) at 2215 Constitution Ave., N.W., Washington, DC 20037. Second-class postage paid at Washington, D.C., and at additional mailing office.

All expressions of opinion and statements of supposed fact appearing in articles or editorials carried in this journal are published on the authority of the writer over whose name they appear and are not to be regarded as necessarily expressing the policies or views of APhA.

Offices—Editorial, Advertising, and Subscription: 2215 Constitution Ave., N.W., Washington, DC 20037. Printing: 20th & Northampton Streets, Easton, PA 18042.

Annual Subscriptions—United States and foreign, industrial and government institutions $60, educational institutions $60, individuals *for personal use only* $30; single copies $5. All foreign subscriptions add $5 for postage. Subscription rates are subject to change without notice. Members of APhA may elect to receive the *Journal of Pharmaceutical Sciences* as a part of their annual $80 (foreign $85) APhA membership dues.

Claims—Missing numbers will not be supplied if dues or subscriptions are in arrears for more than 60 days or if claims are received more than 60 days after the date of the issue, or if loss was due to failure to give notice of change of address. APhA cannot accept responsibility for foreign delivery when its records indicate shipment was made.

Change of Address—Members and subscribers should notify at once both the Post Office and APhA of any change of address.

Photocopying—The code at the foot of the first page of an article indicates that APhA has granted permission for copying of the article beyond the limits permitted by Sections 107 and 108 of the U.S. Copyright Law provided that the copier sends the per copy fee stated in the code to the Copyright Clearance Center, Inc., P.O. Box 8891, Boston, MA 02114. Copies may be made for personal or internal use only and not for general distribution.

Microfilm—Available from University Microfilms International, 300 N. Zeeb Road, Ann Arbor, MI 48106.

© Copyright 1980, American Pharmaceutical Association, 2215 Constitution Ave., N.W., Washington, DC 20037; all rights reserved.

CARCINOGENICITY TESTING—A NATIONAL CATASTROPHE

"What you have described to us is a national catastrophe!"

That strong language was used by a prominent clinical researcher who had just heard a presentation by a National Cancer Institute (NCI) staff scientist at a meeting of the National Council on Drugs (NCD). In an audio-visual presentation, the NCI scientist had provided a rather complete description of the NCI's Carcinogenicity Testing Program, and the apparent unanimous reaction of the NCD members present closely corresponded to that articulated by the clinical scientist quoted above.

In late spring 1979, the NCI released to the public press the test results on several well-known and long-used drugs which had been studied under that Institute's Carcinogenicity Testing Program. Included among those drugs was reserpine, and it was assigned a positive classification as a carcinogenic substance. Because of the current wide use of reserpine in medical treatment, classification of this drug as a carcinogenic agent caused considerable anxiety, apprehension, concern, and confusion among health care practitioners, as well as the general public including many patients under treatment with the drug.

Subsequent reports regarding the potential risks involving reserpine seemed only to confuse the matter further rather than to clarify it. Hence, the NCD invited the NCI to provide the group with a first-hand, detailed explanation of the entire testing program.

Beyond hearing that the project costs approximately 65 million dollars a year to conduct the screening program to detect possible carcinogenic effects of chemicals (including drugs), the NCD was also informed regarding the test protocol in use. The latter essentially involves the administration of maximally tolerated doses of the test chemical to two species of rodents for one generation.

Beyond the general view that such testing is virtually meaningless by itself, the NCD was shocked to learn, among other things, that the NCI has not:

(*a*) done any studies to correlate their animal results to humans;

(*b*) tested any known human carcinogens in animals to ascertain whether common relationships exist;

(*c*) attempted to establish whether there is any dose relationship for known carcinogens, much less what such a relationship might be;

(*d*) ascertained "background effects" for the test animals in their test environment—that is, the frequency of tumors in control animals due to heredity, feed, drinking water, or other factors; and

(*e*) conducted any replicate experiments whatsoever to confirm their initial findings—hence, even such questionable "positives" as reserpine have never been repeated.

During the ensuing discussion, the NCI official was subjected to sharp questioning regarding the basic scientific faults and omissions in the program. And incredibly, he clarified that he and his associates equally recognized those deficiencies, but they were constrained by legislative factors to follow their present course.

Incidentally, more than half of the substances tested in the NCI's bioassay program provided some evidence of carcinogenicity. Projections are that this is probably an accurate forecast of the eventual outcome of the total program. Imagine the devastating consequences on life as we know it if half the chemicals to which we are presently exposed are summarily banned from further use. The very thought is mind-boggling!

Yet such disproportionate findings of carcinogenicity potential should not be too surprising considering the massive doses used, the lifetime of exposure, and the other radical conditions comprising the "test protocol" employed.

But as explained by the NCI official, the agency is primarily restricted by the unrealistic provisions in the legislation Congress enacted. Given such a mandate, the Institute has little choice. Moreover, the enormous cost to conduct such tests on even a single chemical means that only a relatively few substances can be tested, thereby making simple retesting an "unaffordable luxury."

Clearly, Congressional review, restudy, reconsideration, and amendment of this law are in order to rectify what, in this writer's view, was accurately labeled "a national catastrophe."

Edward G. Feldmann

JOURNAL OF PHARMACEUTICAL SCIENCES

FEBRUARY 1980
VOLUME 68 NUMBER 10

RESEARCH ARTICLES

Effect of Self-Association of Phenol on Its Transport across Polyethylene Film

T. J. MIKKELSON ˣ, S. WATANABE *, J. H. RYTTING, and T. HIGUCHI

Received July 30, 1979, from the *Department of Pharmaceutical Chemistry, University of Kansas, Lawrence, KS 66044.* Accepted for publication September 10, 1979. *Present address: Eisai Co. Ltd., Tokyo, Japan.

Abstract □ Phenol diffusion across a high density polyethylene film from isooctane, in which phenol self-associates, demonstrated nonideal behavior. The steady-state flux of phenol across the film was not directly proportional to its concentration in the donor phase. At higher donor phase concentrations, negative steady-state flux deviations were observed. These negative deviations were due to phenol self-association in the donor phase and the resulting decreases in thermodynamic activity. By using a monomer–pentamer model for phenol self-association in isooctane, the steady-state flux was shown to be directly proportional to the phenol monomer concentration in the donor phase. Although steady-state flux concentration deviations were observed, the diffusion time lag was independent of the permeant concentration and reflected the intrinsic diffusivity of the film to phenol.

Keyphrases □ Phenol—effect of self-association on transport across polyethylene film □ Self-association—phenol, effect on transport across polyethylene film □ Mass transfer—phenol self-association, effect on membrane transport □ Diffusion—phenol self-association, effect on membrane transport □ Flux, steady state—effect of phenol self-association on transport across polyethylene film

Mass transfer processes in drug delivery include those that are involved in drug release from a dosage unit and those that are involved in drug transport across biological membranes. The rate and extent of these processes depend on the film or absorbing membrane, the physicochemical characteristics of the permeating drug, and the properties of the drug delivery unit. The dependency of these mass transfer processes on physicochemical drug properties and membrane characteristics has been extensively studied because it is an integral part of drug research and development. Determinants such as molecular size, crystalline form, solubility, pH and ionization, charge, complexation, and partitioning have been identified and continue to be characterized relative to their significance.

There is continuing interest in these laboratories in the effects of specific molecular interactions in solution. For example, many molecules with polar functional groups undergo pronounced self-association in nonpolar solvent systems, resulting in changes in thermodynamic activity (1–3).

The properties of alcohols in hydrocarbon solvents have been studied extensively. Self-association is a dominant factor in the lower than expected vapor pressures of alcohols (1–3). The anomalous solubility behavior of phenol in hydrocarbon solvents is a function of self-association (3). Furthermore, dissolution characteristics of an alcohol deviating from a modified Noyes–Whitney prediction (4) can be rationalized on the basis of self-association.

This report describes specifically the effects of phenol self-association in isooctane on phenol transport across a high density polyethylene film. The effect of self-association on transport was described previously only in general and descriptive terms (5–7). This report describes quantitatively the changes in transport properties resulting from the self-association of a permeating species in the donor phase of a diffusion assembly in terms of an exact molecular association model.

THEORETICAL

Steady-State Permeation—Fick's first law was formulated as:

$$J = -D\left(\frac{dC}{dx}\right) \qquad \text{(Eq. 1)}$$

where J is the flux of material across a unit area of film, D is the diffusion coefficient, and (dC/dx) is the concentration differential across the film. The negative sign implies that the material flow is from an element of higher concentration to an element of lower concentration. For an isotropic or homogeneous film of a given cross-sectional area and a constant thickness, Fick's law can be expressed as:

$$J = PA\,\Delta C \qquad \text{(Eq. 2)}$$

where J is the net flux of material or the appearance of permeant on the receptor side, P is the permeability coefficient, A is the cross-sectional area of the film or membrane, and ΔC is the concentration difference across the total film thickness.

0022-3549/80/0200-0133$01.00/0
© 1980 American Pharmaceutical Association

Under sink conditions, ΔC is replaced with the concentration of permeant in the donor phase, C_d, and the permeability coefficient or permeability, P, becomes:

$$P = \frac{D_m K}{h_m} \qquad \text{(Eq. 3)}$$

where D_m is the permeant diffusivity or diffusion coefficient in the membrane, K is the membrane–donor phase partition coefficient, and h_m is the membrane thickness. This development assumes a partition–diffusion mass transfer mechanism, in contrast to a pore permeation mechanism. A partition–diffusion mechanism has been demonstrated for polyethylene films and the transport of numerous solute materials of general and pharmaceutical interest (8–10).

From measurements of the permeant concentration appearing in the receptor phase as a function of time, the parameters descriptive of the transfer process can be obtained readily, in part from the steady-state permeation. By utilizing the expression:

$$J = \frac{dQ}{dt} = V\left(\frac{dC}{dt}\right) \qquad \text{(Eq. 4)}$$

(where Q is the amount of permeant reaching the receptor site, V is the volume of the receptor phase or compartment, and C is the permeant concentration reaching the receptor side), and combining it with the expression $\Delta C = C_d$ and with Eq. 2, the result is:

$$\frac{V}{A}\left(\frac{dC}{dt}\right) = PC_d \qquad \text{(Eq. 5)}$$

In a steady-state experiment, where C_d remains essentially unchanged (*i.e.*, where the amount of permeant transported or the concentration of permeant achieved in the receptor phase is small compared to C_d), a plot of C *versus* t following an initial time lag will be linear. From the slope, dC/dt, of the linear portion of the plot, the steady-state flux, SSF, is obtained by:

$$SSF = \frac{V}{A}\left(\frac{dC}{dt}\right) \qquad \text{(Eq. 6)}$$

which, in turn, results in:

$$SSF = PC_d \qquad \text{(Eq. 7)}$$

allowing for the determination of permeability by:

$$P = \frac{SSF}{C_d} \qquad \text{(Eq. 8)}$$

Equations 6 and 8 provide a means of computing the steady-state flux and permeability from observed data obtained in a steady-state experiment. Further system elucidation is achieved by defining and solving the permeability coefficient, P, which is a function of the diffusion coefficient of the permeant in the membrane, D_m, the thickness of the membrane, h_m, and the membrane–donor phase partition coefficient, K. The contribution of the partition coefficient to permeability results from use of the donor phase concentration as a reference to the actual concentration of the permeant in the membrane at the donor phase–membrane interface. The relationship is presented in Eq. 3. Of these three parameters (D_m, h_m, and K), only the h_m term, which is experimentally defined, is known. To obtain values of D_m and K, one of them must be independently determined; evaluation of the nonsteady-state data from the same experiments permits the calculation of D_m. Therefore, to elucidate the mass transfer process taking place, an analysis of nonsteady-state permeation is used.

Nonsteady-State Permeation—The necessary equation for determining the diffusivity, D_m, from the nonsteady-state permeation characteristics across an isotropic or homogeneous film was reported (11) and is:

$$t_L = \frac{h_m^2}{6D_m} \qquad \text{(Eq. 9)}$$

where t_L is the diffusion time lag. From Eq. 9, it can be seen that, for a homogeneous film, the time lag is a function only of the membrane thickness and the membrane diffusivity. The time lag is obtained by extrapolation of the linear steady-state data back to its time axis intercept. As a result, for a membrane of known thickness, the membrane diffusivity can be computed. With this information, the membrane–donor phase partition coefficient can be computed using Eq. 3.

Self-Association—The mass transfer characteristics of a self-associating permeant may demonstrate nonideal behavior when interpreted directly through Fick's laws. The nonideal behavior arises from a dependency on the effective concentration (thermodynamic activity or chemical potential) of the permeant, rather than the total concentration, and/or a dependency on the effective diffusion coefficient, which changes as a function of the size of the associated species and the extent of its formation. The contribution of self-association to a particular mass transfer process depends on the experimental conditions. Self-association can potentially occur in the phases contacting a membrane, such as the donor phase, and/or within the membrane itself, depending on donor phase and membrane characteristics.

For a nonassociating permeant diffusing through a homogeneous membrane in the steady state, Eq. 1 is directly applicable. For this simple system, the activity or concentration gradient across the film is linear.

For a system of a self-associating solute diffusing through a homogeneous membrane, Eq. 1 is not directly applicable. If it is assumed that this self-association is an equilibrium between a monomer and a single polymer species, there exists a gradient of each species, monomer and polymer, across the film, and the reaction between them will be at equilibrium within all elements within the film. As a result, the gradients of the two species across the film are nonlinear.

Approaches to quantitating the system can be empirical or modelistic. In the empirical approach, the total flux of permeant (monomer and polymer) can be described in terms of an observed or apparent diffusion coefficient, which is concentration dependent. Such an approach was suggested by Barrer (12); the equation for the diffusivity relates diffusivity to concentration:

$$D = BRT\frac{d\ln a}{d\ln c} \qquad \text{(Eq. 10)}$$

where R and T have their usual meaning, a is activity, and B is a coefficient reflecting the mobility of the permeant. Barrer (12) pointed out that both B and $(d\ln a/d\ln c)$ can depend on permeant concentration. Such an approach was taken by Longsworth (5), who interpreted the mass transfer of self-associating acids and alcohols in carbon tetrachloride in terms of an apparent diffusion coefficient, which decreases as a function of increasing total permeant concentration.

Under experimental conditions where permeant self-association occurs in the donor phase but only the monomeric species diffuses across the film, the observed nonideal characteristics of transport are explained in terms of effective concentration or chemical potential of permeant in the donor phase. This type of system is being reported here. The experimental results indicate that only the phenol monomer is transported across the polyethylene film and that the intrinsic membrane permeability remains unchanged. However, over the donor concentrations studied, phenol self-association in the isooctane donor phase, which decreases the effective donor phase concentration or activity of the permeant, appreciably influences mass transfer.

The literature affords significant data on the self-association of alcohols and its effect on vapor pressure (1, 2), spectral properties (13), solubility (3), and transport characteristics from an empirical standpoint (5). The effect of donor phase self-association on permeation characteristics across a membrane can be more systematically described by incorporation of a model describing the donor phase self-association rather than interpretation of experimental results in terms of a changing apparent or observed diffusion coefficient.

Phenol self-association in isooctane and cyclohexane has been studied in detail (3). These systems are adequately described in terms of a monomer–pentamer model. Given the information that a monomer–pentamer model is appropriate ($n = 5$) and given the equilibrium or association constant, $K_{1,5}$, monomer concentrations for a given total concentration can be calculated.

Permeation Model—The system of a solute that self-associates in a donor solvent but permeates a membrane only in its monomer form can be described by extending Eq. 7 to account for self-association. This system is diagrammed in Scheme I. A mathematical description of Scheme I is given in the following two equations:

$$SSF = PC_{\text{mon}} \qquad \text{(Eq. 11)}$$

$$SSF = \left(\frac{D_m K}{h_m}\right) C_{\text{mon}} \qquad \text{(Eq. 12)}$$

where P is the intrinsic membrane permeability and K is the intrinsic membrane–donor phase partition coefficient. These equations relate the steady-state flux to the monomer concentration of permeant in the donor phase. The expression $C_{\text{mon}} = (f_{\text{mon}})(C_T)$ allows Eq. 11 to be written as:

$$SSF = (P_{\text{obs}})(C_T) \qquad \text{(Eq. 13)}$$

where P_{obs} is the observed permeability and is related to the other pa-

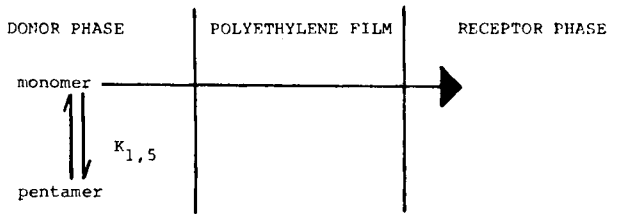

Scheme I

rameters by $P_{obs} = (D_m K/h_m)(f_{mon})$. This relationship indicates that the the observed permeability is equal to the product of the intrinsic permeability and the monomer fraction of permeant in the donor phase, $P_{obs} = Pf_{mon}$. This approach allows the system to be interpreted in terms of an observed permeability.

The system can also be interpreted in terms of an apparent or observed partition coefficient, K_{obs}. This approach results in:

$$SSF = \left(\frac{D_m}{h_m}\right)(K_{obs})(C_T) \qquad \text{(Eq. 14)}$$

where $K_{obs} = Kf_{mon}$.

This approach, beginning with Eq. 13, allows studies (permeant self-association in the donor phase, but membrane transport of only the monomer species) to be described in terms of an observed permeability or an observed partition coefficient when the reference concentration parameter is the total permeant concentration, C_T, in the donor phase. However, the most precise description is in terms of the intrinsic parameters, the intrinsic permeability, P, and the intrinsic partition coefficient, K, and by fully describing the donor phase self-association in terms of n and $K_{1,n}$.

The system can be resolved partially using only permeation data, without precise knowledge of the self-association equilibrium. The full mathematical expression for the system in terms of permeation is:

$$SSF = \left(\frac{D_m K}{h_m}\right)(f_{mon})(C_T) \qquad \text{(Eq. 15)}$$

From each experiment in a series of permeation experiments, SSF is determined as a function of C_T. Since the membrane thickness, h_m, is defined experimentally, the measured diffusion time lags permit calculation of D_m using Eq. 9; K and f_{mon} remain unsolved. However, K can be obtained by proper experimental design. Since f_{mon} goes to unity at low concentrations, experimental runs at low concentrations, where the self-association is negligible, allow determination of K; *i.e.*, $K_{obs} = K$ as f_{mon} goes to unity. As a result, experiments conducted at higher C_T can be interpreted in terms of f_{mon}, P, and K using the information obtained from the experiments conducted at low concentrations.

The approach of resolving the system only from interpretation of permeation data permits an estimation of f_{mon}, which is, however, a general description of the self-association. An accurate and complete understanding of the processes, both permeation and self-association, is best provided by a direct and independent equilibrium determination of C_{mon} as a function of C_T, such that n and $K_{1,n}$ are precisely known. For the phenol–isooctane mixtures used as the donor phases in this study, the values of n and $K_{1,n}$ were measured independently (3). This information permitted the processes to be more readily interpreted and modeled by providing independent verification of the experimental results.

EXPERIMENTAL

Materials—High density polyethylene films[1] were used. Phenol[2], analytical reagent grade, was used without further purification. The isooctane[3] had a labeled purity of 99+ mole %. It was stored over a molecular sieve and otherwise used as received. All other chemicals were analytical reagent grade.

Analytical Method—All phenol concentrations were determined by direct spectrophotometric[4] measurement at 269 nm ($\log \epsilon = 3.18$) in 0.1 M aqueous sulfuric acid.

Diffusion Cells—Pyrex glass diffusion cells were constructed. They consisted of identical cylindrical half-cells between which the polyethylene film was mounted. The half-cell chambers were slightly tapered and had a mean inside diameter of approximately 5.5 cm and an inside height or depth of approximately 6.0 cm, resulting in a half-cell volume of 145 ml. Each half-cell was constructed with a cylindrical portal extending off the cylinder side, allowing for filling of the compartments and withdrawing of samples. The open or contact end of the half-cells was of ground glass and grooved to accept an O-ring. The sequence of half-cell–O-ring–polyethylene membrane–O-ring–half-cell was firmly maintained using a metal clamp.

The assembled cell was immersed in a well-stirred constant-temperature bath, and the contents were well stirred by positioning magnetic stirrers directly below the half-cells beneath the water bath. Rapid mixing and homogeneity of the half-cell solutions were verified visually by use of a dye.

The cross-sectional area of the membrane over which the transport occurred was 29.7 cm^2, which resulted in an area to volume ratio of 0.20 cm^{-1}.

Diffusion Study—Prior to assembly, the polyethylene films were soaked to an equilibrium swelling in isooctane. The swelled film thickness was determined to be 0.078 ± 0.002 cm using a screw micrometer graduated to 0.001 cm.

Following assembly, the cell was immersed in a constant-temperature bath maintained at 25.0 ± 0.1°. The receptor compartment was filled with 145 ml of an aqueous solution of 0.1 M H_2SO_4. The donor compartment was filled with 145 ml of the test solutions of phenol in isooctane. The stir bars were immediately rotated at greater than 200 rpm, which commenced the experiment. This degree of stirring ensured membrane, and not diffusion layer, rate-limited transport.

At preselected intervals, 1.0-ml samples were withdrawn from the receptor compartment and immediately analyzed spectrophotometrically for phenol. The receptor compartment volume was maintained at 145 ml by addition of 1.0 ml of 0.1 M H_2SO_4 following sample removal. Aqueous sulfuric acid was used as the receptor phase to facilitate the analytical measurement for greater chemical stability and to suppress phenol ionization.

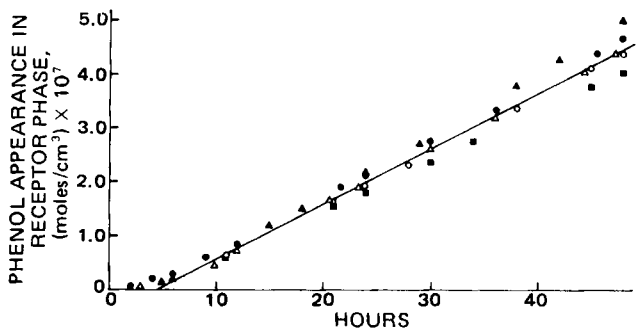

Figure 1—*Phenol concentration appearing in the receptor phase as a function of time. The donor phase phenol concentration was 2.00 × 10^{-4} mole/cm³. The different symbols represent five individual experiments. The drawn line is that obtained by linear regression analysis of the data points for times equal to or greater than 15 hr from all five individual experiments.*

RESULTS AND DISCUSSION

Permeation studies were conducted at 12 donor phase concentrations of phenol in isooctane over 0.05–2.00 × 10^{-4} mole/cm³. Figure 1, a plot of the phenol concentration in the receptor phase as a function of time, shows the data from five runs using a donor phase concentration of 2.0 × 10^{-4} mole/cm³. The linear steady-state portion and the time lag, which are typical of an experiment conducted under sink conditions with a constant donor phase concentration, are evident.

From the data obtained at each donor phase concentration, the steady-state flux was determined from the slope of the linear portion of the curve using Eq. 6 and linear regression data analysis. Since the experimental time lags were approximately 5 hr at each donor phase concentration, only data obtained at times greater than 15 hr were used in calculating the steady-state flux values. The line drawn in Fig. 1 is the regression line and corresponds to a steady-state flux of 1.36 × 10^{-11} mole/sec/cm². The 32 data points obtained at 15 hr or longer from the five experiments gave a correlation coefficient of 0.987. Extrapolation of the regression line to the time axis resulted in a time lag of 4.6 hr.

The steady-state flux and the extrapolated time lag, t_L, values calculated for the 12 donor phase concentrations are given in Table I. Figure

[1] Cadillac Plastic and Chemical Co., Kansas City, Kans.
[2] Mallinckrodt Chemical Works.
[3] Phillips Petroleum Co.
[4] Cary model 118 spectrophotometer, Varian Instrument Division.

Table I—Experimentally Observed Steady-State and Nonsteady-State Diffusion Parameters of Phenol across High Density Polyethylene Film for the Phenol Concentrations Studied

C_T[a], (moles/cm³) × 10⁴	q[b]	m[c]	SSF[d], (moles/sec/cm²) × 10¹¹	r[e]	t_L[f], hr
2.00	5	32	1.36	0.987	4.6
1.75	6	41	1.22	0.976	5.2
1.50	6	41	1.17	0.983	5.2
1.25	5	33	1.17	0.990	5.4
1.00	5	32	1.02	0.969	5.1
0.75	5	34	0.853	0.982	4.9
0.50	5	34	0.676	0.972	5.0
0.25	3	21	0.396	0.993	5.3
0.20	3	21	0.331	0.985	5.3
0.15	3	21	0.234	0.973	5.2
0.10	3	21	0.165	0.974	5.1
0.05	3	21	0.079	0.987	5.8
					$\bar{M}$ = 5.2
					σ = 0.3

[a] Total phenol concentration in the donor phase. [b] Number of experimental runs. [c] Number of individual data points used in the calculation of the steady-state flux. [d] Steady-state flux. [e] Correlation coefficient using m data points. [f] Time lag of diffusion.

Table II—Phenol Monomer Concentrations and Fractions, Observed Permeabilities, and Observed Partition Coefficients for the Phenol Concentrations Studied

C_T[a], (moles/cm³) × 10⁴	C_{mon}[b], (mole/cm³) × 10⁴	f_{mon}[c]	P_{obs}[d], (cm/sec) × 10⁸	K_{obs}[e]
2.0	0.82	0.41	6.8	0.09
1.75	0.79	0.45	6.9	0.10
1.50	0.75	0.50	7.8	0.11
1.25	0.71	0.57	9.3	0.14
1.00	0.65	0.65	10.2	0.14
0.75	0.57	0.76	11.4	0.16
0.50	0.44	0.88	13.5	0.19
0.25	0.25	1.00	15.9[f]	0.23[g]
0.20	0.20	1.00	16.5[f]	0.24[g]
0.15	0.15	1.00	15.6[f]	0.23[g]
0.10	0.10	1.00	16.5[f]	0.23[g]
0.05	0.05	1.00	15.9[f]	0.25[g]
			M = 16.1	M = 0.24
			σ = 0.4	σ = 0.01

[a] Total phenol concentration in the donor phase. [b] Concentration of phenol monomer in the donor phase. [c] Fraction of phenol monomer in the donor phase. [d] Experimentally observed permeability. [e] Experimentally observed membrane–donor phase partition coefficient. [f] The P_{obs} values used to calculate the mean value of 16.1 × 10⁻⁸ cm/sec. [g] The K_{obs} values used to calculate the mean value of 0.24.

2*a* shows the steady-state permeation data given in Table I, where the calculated steady-state flux values are plotted as a function of the total phenol concentration in the donor phase. This plot is linear at low donor phase concentrations up to ~0.25 × 10⁻⁴ mole/cm³. At donor phase concentrations greater than 0.25 × 10⁻⁴ mole/cm³, a negative deviation from linearity is observed, which increases in severity at larger values of C_T.

The time lags, t_L, at each donor phase concentration (Table I) are plotted in Fig. 2*b* as a function of C_T. The time lag is seen to be independent of the donor phase permeant concentration. An averaged value of the time lag computed from the experiments at the 12 donor phase concentrations is 5.2 ± 0.3 hr. By using this value and applying Eq. 9, the membrane diffusion coefficient for phenol was found to be 5.4 × 10⁻⁸ cm²/sec.

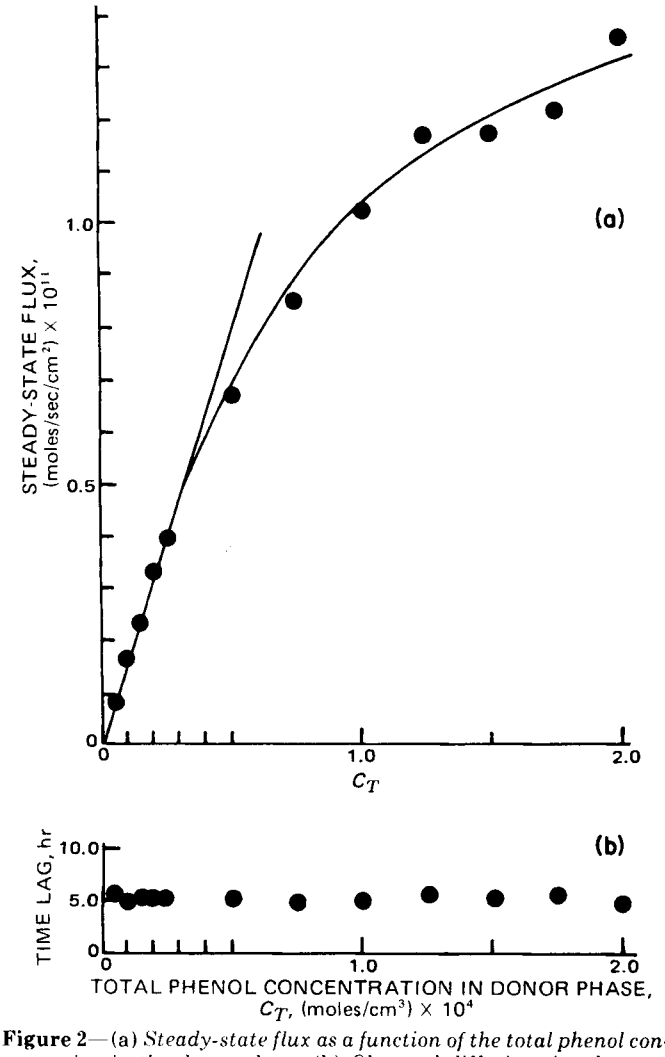

Figure 2—(a) *Steady-state flux as a function of the total phenol concentration in the donor phase.* (b) *Observed diffusion time lag as a function of the total phenol concentration in the donor phase.*

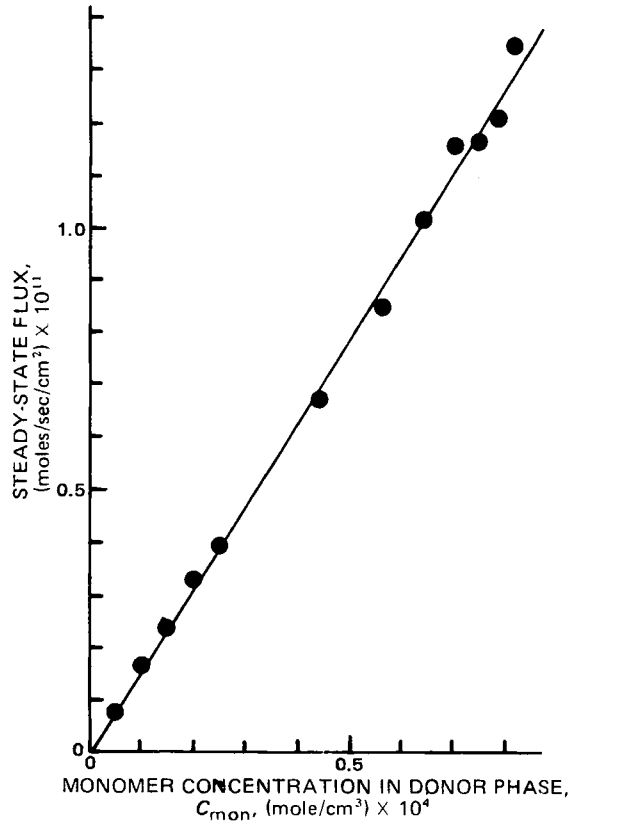

Figure 3—*Steady-state flux as a function of the donor phase phenol monomer concentration. The slope of the line, which was obtained by regression analysis, equals 15.9 × 10⁻⁸ cm/sec and represents the intrinsic permeability of the film to phenol contained in a donor phase of isooctane.*

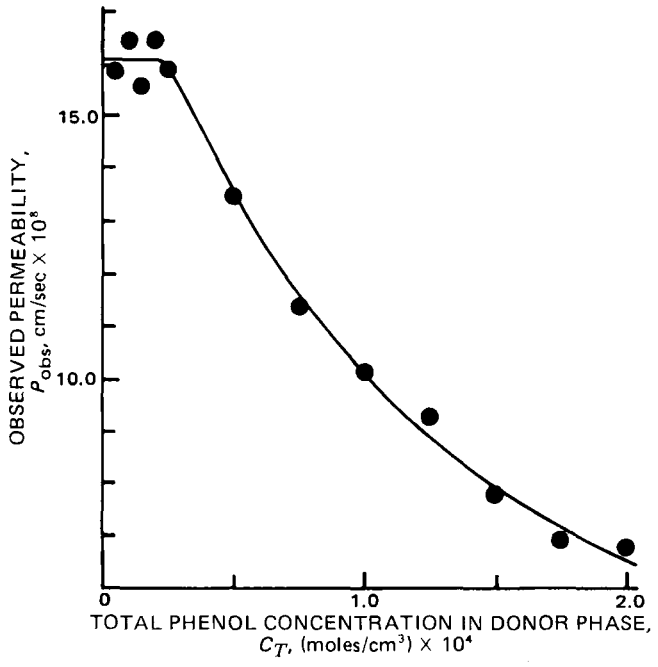

Figure 4—*Observed permeability coefficients as a function of the total phenol concentration in the donor phase.*

Ideally, these experiments would conform with Eq. 7, which predicts linearity in a plot of steady-state flux against donor phase concentration. The resulting slope would equal membrane permeability. Equation 7 is an expression of Fick's first law and includes the term C_d, the concentration difference across the film, which is typically taken to be the driving force for diffusion. However, as pointed out by Flynn *et al.* (14), the fundamental flux determinant is the chemical potential difference across the film. The nonlinearity actually observed was accounted for by relating the steady-state flux to the concentration gradient of the phenol monomer rather than to its total concentration.

With recently published data (3) on phenol self-association, the phenol monomer concentration in the isooctane donor solutions was calculated using an association constant, $K_{1,5}$, of 6.26×10^3 liters^4/mole^4. These concentrations and the fraction of phenol monomer, f_{mon}, are given in Table II. In the concentrations studied, the phenol exists totally as a monomer (negligible self-association) at or below 0.25×10^{-4} mole/cm^3.

A plot of the steady-state flux as a function of the donor phase concentration of the phenol monomer, C_{mon}, is presented in Fig. 3. The figure, a plot of Eq. 11 or 12, is linear. The slope of the line equals 15.9×10^{-8} cm/sec (correlation coefficient of 0.998) and represents the intrinsic permeability of the polyethylene film under the experimental conditions. This slope or intrinsic permeability value obtained from Fig. 3 should be identical to the initial slope value in Fig. 2, where the total phenol concentration is plotted as the abscissa, because at the phenol concentrations corresponding to the first five data points in Fig. 2, the phenol exists in effect totally as a monomer. This can be demonstrated by two different calculations. From the initial slope in Fig. 2, generated using the paired (C_T, SSF) data points for the five lowest phenol concentrations, a permeability of 16.0×10^{-8} cm/sec is obtained, in comparison to the value of 15.9×10^{-8} cm/sec obtained from the slope in Fig. 3. Alternatively, as can be seen in Table II, the individual P_{obs} values corresponding to the five lowest phenol concentrations yield an average value of 16.1×10^{-8} cm/sec.

Apparent or observed permeability values, P_{obs}, were calculated from the steady-state flux values at each donor phase concentration using Eq. 13 (Table II). These P_{obs} values are plotted in Fig. 4 as a function of C_T. This plot displays the significant decline in the apparent permeability at the higher donor phase concentrations where there is significant phenol self-association. The dependence of permeation on the monomer concentration is further substantiated by comparing the observed permeabilities to the monomer fractions. For the data in Table II, at a C_T of 2.00×10^{-4} mole/cm^3, the monomer fraction is 0.41. By comparison, the P_{obs} is 6.8×10^{-8} cm/sec, 0.43 times the value of 15.9×10^{-8} cm/sec obtained from the slope of Fig. 3. Similarly, at a C_T of 1.00×10^{-4} mole/cm^3, the monomer fraction is 0.65. In comparison, the P_{obs} is 10.2×10^{-8} cm/sec, 0.64 times the Fig. 3 slope value.

The data in Fig. 2*a* indicate that permeant self-association decreases the ability of the phenol to undergo transport across the polyethylene film. At total phenol concentrations greater than 0.25×10^{-4} mole/cm^3, there is not a proportionate increase in its steady-state flux across the polyethylene film. However, these steady-state flux data do not indicate whether the self-association effect is restricted only to the level of the donor phase or also occurs within the membrane.

An interpretation of the nonsteady-state data provides insight into the location of the self-association effect. As is evident in Fig. 2*b*, the experimentally determined time lags are independent of the donor phase phenol concentration, which indicates that the membrane diffusion coefficient is concentration independent. If permeant self-association occurred within the membrane, it would occur to an increasing extent as the donor phase permeant concentration increased. This increasing occurrence in the membrane of a polymer species at higher levels of C_T should increase the experimentally observed time lag. The time lag increase would result from a decrease in the effective diffusion coefficient, because of the inverse dependency of a diffusion coefficient on the effective molecular weight. However, since the diffusion coefficient is concentration independent, it can be concluded that (*a*) phenol self-association does not occur within the polyethylene film, or (*b*) if self-association is occurring within the membrane, its extent is negligible or the transport of the polymer species across the membrane is not sufficient to affect transport parameters, *i.e.*, it does not alter the diffusion coefficient.

The linearity seen in Fig. 3 suggests that the contribution of the self-association is restricted to the donor phase. Since there is an apparent direct dependency of the steady-state flux on the monomer concentration of phenol in the donor phase, it appears that only the monomer is partitioning into the membrane. This interpretation is further supported by the K_{obs} values found in Table II. The K_{obs} values, which are the experimentally observed polyethylene–isooctane partition coefficients, are closely approximated by calculating the product of the independently calculated f_{mon} values and the average intrinsic partition coefficient of 0.24, which is the observed value obtained from the experiments at the five lowest donor phase concentrations.

REFERENCES

(1) B. D. Anderson, J. H. Rytting, and T. Higuchi, *Int. J. Pharm.*, **1**, 15 (1978).

(2) J. H. Rytting, B. D. Anderson, and T. Higuchi, *J. Phys. Chem.*, **82**, 2240 (1978).

(3) B. D. Anderson, J. H. Rytting, and T. Higuchi, *J. Am. Chem. Soc.*, **101**, 5194 (1979).

(4) T. Higuchi, S. Dayal, and I. H. Pitman, *J. Pharm. Sci.*, **61**, 695 (1972).

(5) L. G. Longsworth, *J. Colloid Interface Sci.*, **22**, 3 (1966).

(6) I. Auerbach, W. R. Miller, W. C. Kuryla, and S. D. Gehman, *J. Polym. Sci.*, **28**, 129 (1958).

(7) J. T. Edward, *J. Chem. Educ.*, **47**, 261 (1970).

(8) M. Salame, *SPE Trans.*, **1961**, 153.

(9) D. G. Serota, M. C. Meyer, and J. Autian, *J. Pharm. Sci.*, **61**, 416 (1972).

(10) K. Nasim, M. C. Meyer, and J. Autian, *ibid.*, **61**, 1775 (1972).

(11) R. M. Barrer, *Trans. Faraday Soc.*, **35**, 628 (1939).

(12) R. M. Barrer, *Discuss. Faraday Soc.*, **21**, 138 (1956).

(13) A. N. Fletcher and C. A. Heller, *J. Phys. Chem.*, **71**, 3742 (1967).

(14) G. L. Flynn, S. H. Yalkowsky, and T. J. Roseman, *J. Pharm. Sci.*, **63**, 479 (1974).

ACKNOWLEDGMENTS

Supported by Grant GM22357 from the National Institutes of Health.

Simultaneous High-Performance Liquid Chromatographic Determination of Chlordiazepoxide and Amitriptyline Hydrochloride in Two-Component Tablet Formulations

D. BURKE and H. SOKOLOFF ˣ

Received December 5, 1978, from the *Quality Control Department, Hoffmann-La Roche Inc., Nutley, NJ 07110.* Accepted for publication August 21, 1979.

Abstract □ A rapid, precise, and accurate high-performance liquid chromatographic procedure is presented for the simultaneous determination of amitriptyline hydrochloride and chlordiazepoxide in two-component tablet formulations. The impurities and decomposition products of both components were separated, making the determination specific for amitriptyline hydrochloride and chlordiazepoxide. The method was used for the assay, content uniformity, and dissolution testing of dosage forms containing 5–30 mg of chlordiazepoxide and 12.5–75 mg of amitriptyline.

Keyphrases □ Chlordiazepoxide—simultaneous determination with amitriptyline hydrochloride, high-performance liquid chromatography □ Amitriptyline hydrochloride—simultaneous determination with chlordiazepoxide, high-performance liquid chromatography □ High-performance liquid chromatography—simultaneous determination of chlordiazepoxide and amitriptyline hydrochloride

Numerous high-performance liquid chromatographic (HPLC) methods for the determination of amitriptyline hydrochloride (V), chlordiazepoxide (III), and related compounds have been reported (1–4). However, none of the methods is applicable to the simultaneous determination of these compounds in two-component tablet formulations.

Conventional analyses, such as pharmacopeial procedures for the individual drugs (5), also are not suited for simultaneous determination. Traditional procedures, such as the spectrophotometric determination of the bromcresol green complex of amitriptyline hydrochloride and of the diazotization and coupling product of chlordiazepoxide, are tedious and time consuming, especially for content uniformity and dissolution testing.

This report presents an HPLC method for the quantitative determination of both substances in two-component tablet formulations. The analysis can be performed in a reasonable time and eliminates interference due to possible impurities: 10,11-dihydro-5-[3-(dimethylamino)propyl]-5*H*-dibenzo[*a*,*d*]cycloheptene-5-ol (IV) and 10,11-dihydro-5*H*-dibenzo[*a*,*d*]cycloheptene-5-one (VI) in amitriptyline hydrochloride and 7-chloro-1,3-dihydro-5-phenyl-2*H*-1,4-benzodiazepin-2-one-4-oxide (II) and 2-amino-5-chlorobenzophenone (VII) in chlordiazepoxide.

EXPERIMENTAL

Apparatus—The liquid chromatograph consisted of a pump[1] with a flow capacity of 16–160 ml/hr and a fixed-wavelength UV detector[2] (254 nm). Solutions were injected with a valve loop[3] with a capacity of 20 or 50 μl. A 30 × 0.39-cm i.d. column containing an octadecyl bonded-phase packing[4] was used.

Chromatographic Conditions—The mobile phase consisted of 0.01 *M* sodium lauryl sulfate in tetrahydrofuran–methanol–pH 2.5 Britton–Robinson buffer (120:30:150). A flow rate of ~1 ml/min was established.

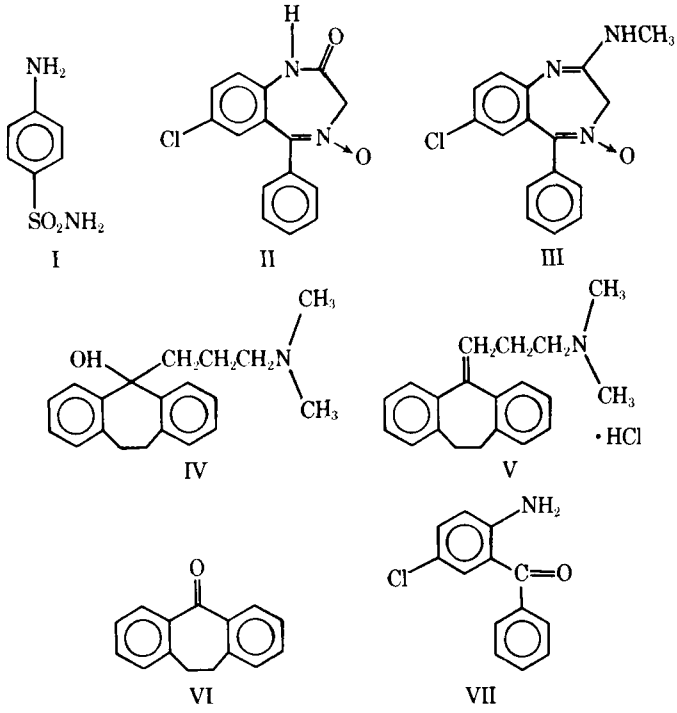

Reagents and Samples—The solvents were commercial analytical grade, and the water was double distilled. The Britton–Robinson buffer was prepared by adding 10.5 ml of 0.2 *N* NaOH to 100 ml of stock solution consisting of 0.04 *M* acetic acid, 0.04 *M* phosphoric acid, and 0.04 *M* boric acid to obtain pH 2.5 (6). The sample solvent was water–tetrahydrofuran–methanol (150:120:30). Sulfanilamide[5] (I) solution in the sample solvent at ~1 mg/ml was the internal standard. The standard solution contained ~0.3 mg of amitriptyline hydrochloride[6]/ml, 0.1 mg of chlordiazepoxide[7]/ml, and 0.1 mg of sulfanilamide/ml.

All standard and sample solutions were prepared and stored in low-actinic glassware.

Assay and Calculation—For the content uniformity test and tablet composite assay, one tablet or the equivalent tablet mass was triturated with the sample solvent and transferred quantitatively to a volumetric flask. The internal standard was added, and the flask contents were diluted to volume with the sample solvent to obtain ~0.3 mg of amitriptyline hydrochloride/ml, 0.1 mg of chlordiazepoxide/ml, and 0.1 mg of sulfanilamide/ml. An aliquot was filtered, and 20 μl was injected.

For analysis of the tablets after dissolution, a portion of the sample solution was withdrawn after an appropriate time and filtered, and an aliquot was transferred to a volumetric flask. The pH was adjusted to 2.5, and the aliquot was diluted to volume with the sample solvent to obtain 0.011 mg of amitriptyline hydrochloride/ml and 0.004 mg of chlordiazepoxide/ml. A solution of reference standards of the same amitriptyline hydrochloride and chlordiazepoxide concentrations was prepared similarly, and 50 μl of each solution was injected.

[1] Model 396/2396, Laboratory Data Control, Riviera Beach, Fla.
[2] Model 1285, Laboratory Data Control, Riviera Beach, Fla.
[3] Model 7010, Rheodyne, Inc., Berkeley, Calif.
[4] μBondapak C_{18}, Waters Associates, Milford, Mass.
[5] Eastman Organic Chemicals, Rochester, N.Y.
[6] USP reference standard.
[7] Chlordiazepoxide (99.3% pure), Hoffmann-La Roche Inc., Nutley, N.J.

0022-3549/80/0200-0138$01.00/0
© 1980, American Pharmaceutical Association

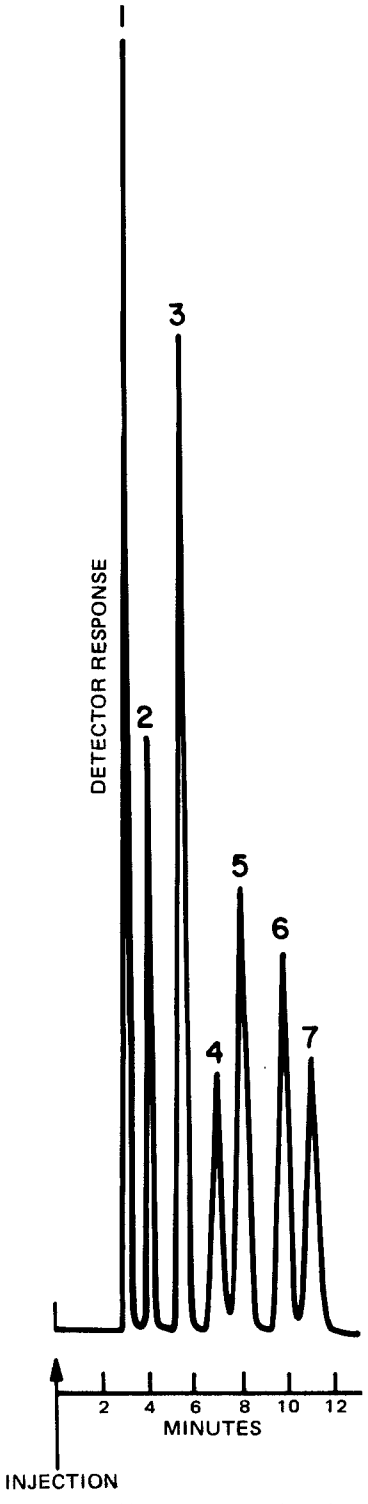

Figure 1—*Chromatogram of a mixture of I (1), II (2), III (3), IV (4), V (5), VI (6), and VII (7).*

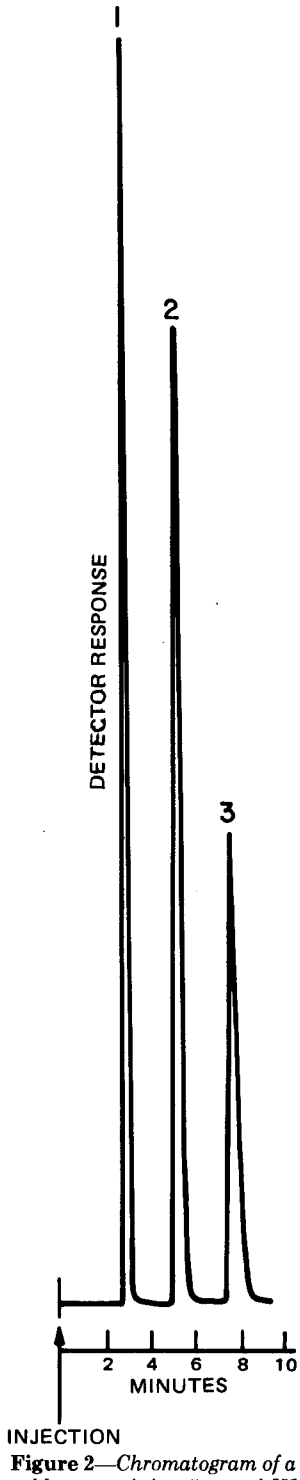

Figure 2—*Chromatogram of a tablet containing 5 mg of III (2) and 12.5 mg of V (3) with I (1) (internal standard) added.*

Quantitation was by the peak height ratio of the reference standards and sample to the internal standard for the content uniformity test and tablet composite assay and by comparison of the peak height of the sample to that of the external standard for dissolution calculations.

RESULTS AND DISCUSSION

This investigation was initiated for use in control laboratories where rapid and simple methods are required. Simple and rapid sample preparation was needed, particularly for content uniformity and dissolution tests. The aqueous sample solution in the latter test can be used as is or with minimal sample treatment for reversed-phase chromatography.

To determine the appropriate HPLC parameters, some preliminary TLC was performed using silica gel plates coated with silicone oil. A mobile phase containing tetrahydrofuran and pH 3 Britton–Robinson buffer was selective in the migration of the six compounds chromatographed. The use of a μBondapak C_{18} column with the buffered mobile phase failed to separate V, II, and IV from each other. Variation of the mobile phase composition was unsuccessful. Complete separation was achieved by the addition to a mobile phase of sodium lauryl sulfate and methanol and by adjustment of the pH to 2.5. The paired-ion species were eluted within 12 min.

Table I—Chromatographic Characteristics of Amitriptyline Hydrochloride, Chlordiazepoxide, Their Impurities, and the Internal Standard

Compound[a]	Retention Time, min	Number of Theoretical Plates, N^b	Capacity Factor, k^c	Selectivity, α
I	3.0	580	0.6	
				1.9
II	4.5	660	1.1	
				1.6
III	5.5	780	1.8	
				1.4
IV	7.5	730	2.6	
				1.2
V	8.0	960	3.1	
				1.3
VI	10.0	1440	4.1	
				1.2
VII	11.0	1870	4.8	

[a] The calculations were made from the chromatogram in Fig. 1. [b] The number of plates was calculated from $N = 16\ (t_r/t_w)^2$. [c] The column void volume was 2.0 ml.

Table II—Comparison of HPLC and Spectrophotometric Tablet Assays

	Amitriptyline Found, %		Chlordiazepoxide Found, %	
Sample	HPLC	Spectrophotometric	HPLC	Spectrophotometric
1	101.9	104.9	104.9	104.1
2	101.4	103.9	104.7	104.4
3	99.9	104.2	103.9	103.6
4	102.5	102.8	104.8	101.8
5	102.3	103.8	104.9	103.2
6	102.3	102.6	104.6	101.0
Average	101.7	103.7	104.6	103.0
RSD, %	0.96	0.84	0.36	1.3

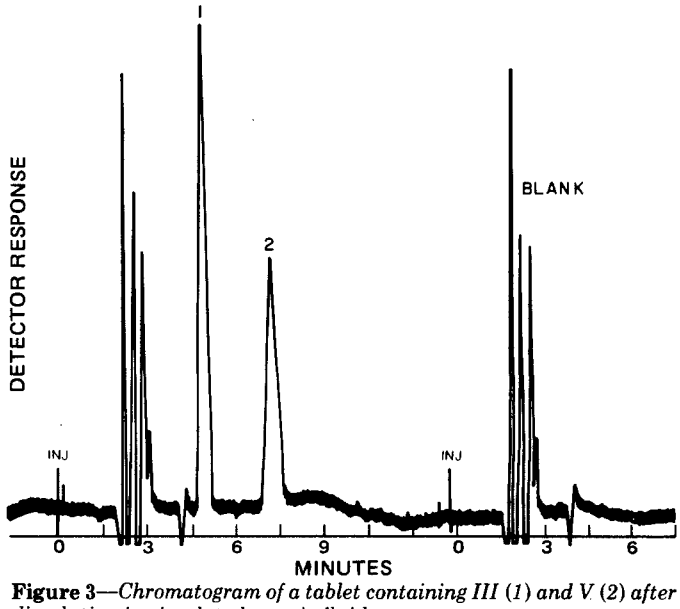

Figure 3—*Chromatogram of a tablet containing III (1) and V (2) after dissolution in simulated gastric fluid.*

Several tricyclic compounds and benzodiazepine derivatives were chromatographed in the selection of the internal standard necessary for the quantitation of amitriptyline hydrochloride and chlordiazepoxide, but a stable material with a suitable retention time was not found. Sulfanilamide eluted before amitriptyline hydrochloride and chlordiazepoxide and was well separated from their respective impurities, so it was chosen as the internal standard. Separation of the compounds including sulfanilamide is shown in Fig. 1, and the calculated chromatographic characteristics are listed in Table I.

Linearity—A plot of peak height *versus* the amount of the two components injected was linear between 0.3 and 11 μg of amitriptyline hydrochloride and 0.13 and 4 μg of chlordiazepoxide. The working concentration was ~5.7 μg of amitriptyline hydrochloride and 2 μg of chlordiazepoxide for the content uniformity test and assay. For dissolution measurements, the working concentration was 0.6 μg of amitriptyline hydrochloride and 0.2 μg of chlordiazepoxide.

Precision—Chromatographic system reproducibility was determined by injecting six 20-μl aliquots of a sample solution containing 0.1 mg of internal standard/ml, 0.3 mg of amitriptyline hydrochloride/ml, and 0.1 mg of chlordiazepoxide/ml as well as corresponding amounts of the reference standards. The relative standard deviation was ±0.16 and ±0.18% for amitriptyline hydrochloride and chlordiazepoxide, respectively. Six replicate samples of composite tablet mass also were assayed. The relative standard deviations were 0.96% for amitriptyline hydrochloride and 0.36% for chlordiazepoxide.

Recovery—A known amount of both active components was added to an assayed sample, and 97.7% of the amitriptyline hydrochloride and 100.2% of the chlordiazepoxide were recovered.

Figure 2 shows a typical chromatogram of the tablet assay. No interference due to a placebo was found. The completeness of the extraction of the tablet mass during sample preparation was checked; no active components remained in the tablet mass after filtering. Good agreement was obtained between the HPLC method and the spectrophotometric procedures, *i.e.*, measurements of the bromcresol green complex of amitriptyline hydrochloride and of the diazotization and coupling product of chlordiazepoxide (Table II).

For the dissolution test, external rather than internal standards were used since, at low concentrations, the sensitivity had to be increased and the blank interfered in the region of the internal standard. A typical chromatogram is shown in Fig. 3.

The described procedure subsequently was used for experimental tablet and capsule formulations containing only amitriptyline hydrochloride. The assay and content uniformity results correlated well with the data obtained using the pharmacopeial (5) procedures.

REFERENCES

(1) J. H. Knox and J. Jurand, *J. Chromatogr.*, **103**, 311 (1975).

(2) J. H. M. Van Den Berg, H. J. J. De Ruwe, and R. S. Deelder, *ibid.*, **138**, 431 (1977).

(3) C. G. Scott and P. Bommer, *J. Chromatogr. Sci.*, **8**, 446 (1970).

(4) J. R. Salmon and P. R. Wood, *Analyst*, **101**, 611 (1976).

(5) "The United States Pharmacopeia," 19th rev., Mack Publishing Co., Easton, Pa., 1975.

(6) M. Brezina and P. Zuman, "Polarography," Interscience, New York, N.Y., 1958, p. 731.

ACKNOWLEDGMENTS

The authors thank Mr. Paul Tracy for validating the method and performing the assay, content uniformity, and dissolution testing on numerous samples.

Validation of Washing Procedures for Maintaining a Microbiologically Clean Gel Filtration Column

L.-F. WEN ˣ, T. BOHANNON, A. CRABB, S. NG, and F. MAMARIL

Received March 26, 1979, from the *Quality Control Department, Hoffmann-La Roche Inc., Nutley, NJ 07110.* Accepted for publication September 10, 1979.

Abstract □ Chromatographic gel filtration matrixes used in various separation techniques are subject to microbial contamination. The need for a microbe-free column is critical when preparing materials that require a low or zero microbial count. This report proposes two alternative washing systems: 0.02 *N* HCl containing 0.81% NaCl, and 0.1 *M* tromethamine–hydrochloride buffer (pH 7.0) containing 0.81% NaCl and 0.02% thimerosal. These washing systems were validated using a 100 × 2.6-cm column packed with a modified dextran gel slurry previously inoculated with known counts of USP test organisms. After each wash, the column separation characteristics were verified further with appropriate test proteins.

Keyphrases □ Chromatography—gel filtration, washing procedures for columns contaminated with microorganisms □ Contamination—microorganisms in gel filtration columns, washing procedures for column disinfection

Chromatographic column packing materials such as gel filtration and ion-exchange matrixes used in separation and the buffer systems usually employed with such matrixes are subject to microbial contamination and proliferation. Excessive microbial growth obstructs the flow, affects the chromatographic properties of these columns, and contaminates material that is affected adversely by microorganisms.

Gel filtration matrixes can be sterilized in the wet or dry state by autoclaving (1, 2), but such techniques are not feasible for a working column. Gaseous sterilization with formaldehyde or ethylene oxide is ineffective and unsafe due to the limited sterilant penetration and the residual toxic effects (2, 3). Organic solvents such as chloroform and toluene are incompatible with the matrixes and some column components. Several antimicrobial agents are compatible with the column packing matrixes. Thimerosal is one of the most commonly used preservatives because of its highly biostatic effect (2, 4). Its routine use as an applicable and effective antimicrobial agent in chromatographic columns has to be evaluated.

The present investigation was undertaken to develop effective methods to minimize or eliminate microbial contamination in a gel filtration column and to validate the antimicrobial effectiveness and applicability of these methods.

EXPERIMENTAL

Microbial Inoculum Suspension Preparation—The bacterial cultures, *Staphylococcus aureus* (ATCC 6538), *Escherichia coli* (ATCC

0022-3549/80/0200-0140$01.00/0

© 1980, American Pharmaceutical Association

Several tricyclic compounds and benzodiazepine derivatives were chromatographed in the selection of the internal standard necessary for the quantitation of amitriptyline hydrochloride and chlordiazepoxide, but a stable material with a suitable retention time was not found. Sulfanilamide eluted before amitriptyline hydrochloride and chlordiazepoxide and was well separated from their respective impurities, so it was chosen as the internal standard. Separation of the compounds including sulfanilamide is shown in Fig. 1, and the calculated chromatographic characteristics are listed in Table I.

Linearity—A plot of peak height *versus* the amount of the two components injected was linear between 0.3 and 11 μg of amitriptyline hydrochloride and 0.13 and 4 μg of chlordiazepoxide. The working concentration was ~5.7 μg of amitriptyline hydrochloride and 2 μg of chlordiazepoxide for the content uniformity test and assay. For dissolution measurements, the working concentration was 0.6 μg of amitriptyline hydrochloride and 0.2 μg of chlordiazepoxide.

Precision—Chromatographic system reproducibility was determined by injecting six 20-μl aliquots of a sample solution containing 0.1 mg of internal standard/ml, 0.3 mg of amitriptyline hydrochloride/ml, and 0.1 mg of chlordiazepoxide/ml as well as corresponding amounts of the reference standards. The relative standard deviation was ±0.16 and ±0.18% for amitriptyline hydrochloride and chlordiazepoxide, respectively. Six replicate samples of composite tablet mass also were assayed. The relative standard deviations were 0.96% for amitriptyline hydrochloride and 0.36% for chlordiazepoxide.

Recovery—A known amount of both active components was added to an assayed sample, and 97.7% of the amitriptyline hydrochloride and 100.2% of the chlordiazepoxide were recovered.

Figure 2 shows a typical chromatogram of the tablet assay. No interference due to a placebo was found. The completeness of the extraction of the tablet mass during sample preparation was checked; no active components remained in the tablet mass after filtering. Good agreement was obtained between the HPLC method and the spectrophotometric procedures, *i.e.*, measurements of the bromcresol green complex of amitriptyline hydrochloride and of the diazotization and coupling product of chlordiazepoxide (Table II).

For the dissolution test, external rather than internal standards were used since, at low concentrations, the sensitivity had to be increased and the blank interfered in the region of the internal standard. A typical chromatogram is shown in Fig. 3.

The described procedure subsequently was used for experimental tablet and capsule formulations containing only amitriptyline hydrochloride. The assay and content uniformity results correlated well with the data obtained using the pharmacopeial (5) procedures.

REFERENCES

(1) J. H. Knox and J. Jurand, *J. Chromatogr.*, **103**, 311 (1975).

(2) J. H. M. Van Den Berg, H. J. J. De Ruwe, and R. S. Deelder, *ibid.*, **138**, 431 (1977).

(3) C. G. Scott and P. Bommer, *J. Chromatogr. Sci.*, **8**, 446 (1970).

(4) J. R. Salmon and P. R. Wood, *Analyst*, **101**, 611 (1976).

(5) "The United States Pharmacopeia," 19th rev., Mack Publishing Co., Easton, Pa., 1975.

(6) M. Brezina and P. Zuman, "Polarography," Interscience, New York, N.Y., 1958, p. 731.

ACKNOWLEDGMENTS

The authors thank Mr. Paul Tracy for validating the method and performing the assay, content uniformity, and dissolution testing on numerous samples.

Validation of Washing Procedures for Maintaining a Microbiologically Clean Gel Filtration Column

L.-F. WEN ˣ, T. BOHANNON, A. CRABB, S. NG, and F. MAMARIL

Received March 26, 1979, from the *Quality Control Department, Hoffmann-La Roche Inc., Nutley, NJ 07110.* Accepted for publication September 10, 1979.

Abstract □ Chromatographic gel filtration matrixes used in various separation techniques are subject to microbial contamination. The need for a microbe-free column is critical when preparing materials that require a low or zero microbial count. This report proposes two alternative washing systems: 0.02 *N* HCl containing 0.81% NaCl, and 0.1 *M* tromethamine–hydrochloride buffer (pH 7.0) containing 0.81% NaCl and 0.02% thimerosal. These washing systems were validated using a 100 × 2.6-cm column packed with a modified dextran gel slurry previously inoculated with known counts of USP test organisms. After each wash, the column separation characteristics were verified further with appropriate test proteins.

Keyphrases □ Chromatography—gel filtration, washing procedures for columns contaminated with microorganisms □ Contamination—microorganisms in gel filtration columns, washing procedures for column disinfection

Chromatographic column packing materials such as gel filtration and ion-exchange matrixes used in separation and the buffer systems usually employed with such matrixes are subject to microbial contamination and proliferation. Excessive microbial growth obstructs the flow, affects the chromatographic properties of these columns, and contaminates material that is affected adversely by microorganisms.

Gel filtration matrixes can be sterilized in the wet or dry state by autoclaving (1, 2), but such techniques are not feasible for a working column. Gaseous sterilization with formaldehyde or ethylene oxide is ineffective and unsafe due to the limited sterilant penetration and the residual toxic effects (2, 3). Organic solvents such as chloroform and toluene are incompatible with the matrixes and some column components. Several antimicrobial agents are compatible with the column packing matrixes. Thimerosal is one of the most commonly used preservatives because of its highly biostatic effect (2, 4). Its routine use as an applicable and effective antimicrobial agent in chromatographic columns has to be evaluated.

The present investigation was undertaken to develop effective methods to minimize or eliminate microbial contamination in a gel filtration column and to validate the antimicrobial effectiveness and applicability of these methods.

EXPERIMENTAL

Microbial Inoculum Suspension Preparation—The bacterial cultures, *Staphylococcus aureus* (ATCC 6538), *Escherichia coli* (ATCC

0022-3549/80/0200-0140$01.00/0

© 1980, American Pharmaceutical Association

8739), and *Pseudomonas aeruginosa* (ATCC 9027), were grown for 24 hr at 35° on soybean–casein digest agar[1] slants. The yeast culture, *Candida albicans* (ATCC 10231), was grown for 48 hr at 23° on Sabouraud dextrose agar[2] slants. On the slurry inoculation day, individual culture suspensions were prepared in 0.9% NaCl[3] contained in sterile colorimeter tubes (150 × 15 mm). Each culture was scraped aseptically with a loop from the agar slants and carefully emulsified in colorimeter tubes until the uniform turbidity, as determined at 420 nm[4], equaled an approximate viability count of 1–5 × 10^8 organisms/ml of suspension.

The bacterial culture, *Bacillus subtilis* (ATCC 9372), and the mold culture, *Aspergillus niger* (ATCC 16404), were prepared as spore suspensions in 0.9% NaCl solution, with the later suspension containing 0.05% polysorbate 80[5]. These spore suspensions had viability counts of ~1–5 × 10^8 organisms/ml.

Quantitative Determination of Microbial Viability—The individual inoculum suspensions and the initially inoculated samples of slurry and effluents were diluted serially in 10-fold increments to 10^{-9} in pH 7.2 phosphate buffer[6]. All other samples of effluents and slurry were similarly diluted to 10^{-5}. Then, in duplicate, 1.0 ml of each diluted sample was placed in sterile plastic petri dishes (150 × 25 mm) with a sterile glass serological pipet (1 in 1/100 ml). In addition, 1.0- and 0.1-ml quantities of each undiluted sample were placed aseptically in plastic petri dishes with glass serological pipets (1 in 1/100 ml and 1/10 in 1/100 ml, respectively).

For samples without thimerosal[7], Sabouraud dextrose agar was added to one set of plates to enumerate molds or yeasts, and soybean–casein digest agar was added to the other set of plates to enumerate bacteria. In the samples containing thimerosal, the appropriate media were supplemented with sodium thioglycolate[8] (500 mg/liter). After incubation of the soybean–casein digest agar plates for 3–5 days at 35° and the Sabouraud dextrose agar plates at room temperature for 7–11 days, colony-forming units were counted.

Qualitative Determination of Microbial Viability—To monitor the viability of *S. aureus*, *E. coli*, and *P. aeruginosa*, 0.1 ml of each sample was placed onto mannitol salt[9], MacConkey[10], and cetrimide[11] agar plates, which were incubated for ≥3 days at 35° and checked by Gram-stain or appearance for characteristic growth. In addition, the viability count plates were checked for colonies characteristic of each inoculated contaminant.

pH Determination—The pH of each sample was determined with a digital pH meter[12].

Mercury Determination—To monitor mercury as thimerosal in the effluents and slurries treated with the tromethamine–thimerosal wash solution, flameless atomic absorption spectroscopy was used.

Reagent blanks were prepared by pipetting water, 3 ml, into 300-ml bottles[13]. A working standard solution of 0.5 ppm of mercury was prepared by diluting a 1000-ppm mercury standard solution. Then 1.0, 2.0, and 3.0 ml of the working standard were pipetted into one of three 300-ml bottles[13].

Each sample from the tromethamine–thimerosal wash solution was acidified with an equal volume of concentrated nitric acid to kill any microorganisms. All samples were stored at 5° prior to the atomic absorption analyses. At that time, each sample was diluted with double-distilled water to obtain ~1 ppm of mercury, and 1-ml samples were pipetted into 300-ml bottles[13].

To each blank, standard, and sample solution were added 5 ml of 35% HNO_3, 5 ml of 50% (v/v) H_2SO_4, and 5 drops of 5.0% potassium permanganate to produce a purple color. After standing for 30 min, each preparation was diluted to volume (100 ml) with distilled water. Hydroxylamine hydrochloride (1.5%), 5 ml, was added to decolorize each solution, the solution was treated with 5 ml of 10.0% stannous chloride, and the flask was stoppered immediately with the aspirator tube of the instrument[14]. The enclosed atmosphere of each solution was circulated through the apparatus drying train using the electric pump. The maximum absorbance was recorded when the mercury vapor concentration reached an equilibrium value. Between runs of each solution, the vapor was circulated through the mercury scrubber to clean the system.

The average blank absorbance was subtracted from the standard and sample absorbances. The quantity of mercury in each diluted sample was read from a calibration curve prepared by plotting the mercury quantities in the standards in micrograms against the corrected standard absorbances. The mercury concentration in the original sample was calculated by:

$$\text{concentration (ppm) of mercury} = \frac{C \times D}{S} \qquad \text{(Eq. 1)}$$

where C is the amount of mercury (parts per million) in 1 ml of diluted sample, D is the dilution factor, and S is the amount of sample (milliliters).

Antimicrobial Activity Determination of Acid Wash Solution—Dry modified polymeric dextran gel[15] (~50 g) was added to ~1500 ml of sterile distilled water. After 3 days of equilibration at room temperature, the distilled water in the slurry was decanted and replaced with sterile 0.81% NaCl. Following an additional 2-day equilibration at room temperature, the supernate was decanted, leaving ~1000 ml of slurry. This slurry was inoculated with either 10 ml of each inoculum suspension (*S. aureus*, *E. coli*, *P. aeruginosa*, and *C. albicans*) or 10 ml of each spore suspension (*A. niger* and *B. subtilis*).

Over 24 hr, the inoculated slurry was packed by gravity into the column[16] to a height of ~95 cm. The column was maintained at 5° by circulating controlled-temperature water through the column jacket. The slurry and column effluent were sampled immediately and tested for microbial count and pH.

The packed column, continuously maintained at 5°, was washed with ~3–4 liters of the sterile, filtered, pH 1.8 acid wash solution at a flow rate of ~0.8 ml/min. Column effluent samples were collected in sterile screw-capped test tubes (150 × 20 mm) after 1 and 4 days to determine the microbial count and pH. The remaining effluent was pooled for determining the total acid wash elution volume.

After this acid wash treatment, the column was rinsed by washing with 1.5–2.5 liters of 0.1 *M* tromethamine–hydrochloride buffer (pH 7.0) containing 0.81% NaCl and 0.02% sodium azide (rinsing buffer) at the same flow rate.

After 1 and 2 days of rinsing, the column effluent samples were collected in sterile screw-capped test tubes for microbial counting and pH determination. The remaining effluent was pooled for determination of the total rinsing buffer elution volume. Five days after the rinse termination, a sample of the effluent was aseptically collected for microbial counting and pH determination. The slurry was removed immediately from the column and sampled aseptically from the top, middle, and bottom for the microbial count and pH determination.

Antimicrobial Activity Determination of Tromethamine–Thimerosal Wash Solution—The described washing and rinsing protocol and the time schedule were followed in using the tromethamine–thimerosal wash solution to clean the inoculated columns. In addition to the microbial count and pH determination, column effluents and slurry were assayed for mercury by flameless atomic absorption spectroscopy to monitor the thimerosal concentration.

Separation Properties of Columns Treated with Acid and Tromethamine–Thimerosal Wash Solution—Two milligrams each of cytochrome c[17], bovine serum albumin[18], and a dextran indicator[19] were added separately to 2-ml aliquots of the rinsing buffer. The test solution was prepared by combining 1.0 ml of each of these solutions. This test solution was fractionated on the same uninoculated column after each of the following procedures: (*a*) rinsed and equilibrated with ~2 liters of rinsing buffer over 24 hr (control run); (*b*) rinsed and equilibrated with

[1] Bacto-tryptic soy agar, Difco Laboratories, Detroit, Mich.
[2] Bacto-Sabouraud dextrose agar, Difco Laboratories, Detroit, Mich.
[3] Saline TS, USP XIX.
[4] Spectronic-20 colorimeter, Bausch & Lomb, Rochester, N.Y.
[5] Saline TS, USP XIX, as specified for preparation of mold spore suspensions.
[6] Butterfield's phosphate buffer.
[7] Ethylmercurithiosalicylic acid sodium salt, item 11228, Eastman Kodak Co., Rochester, N.Y.
[8] Difco Laboratories, Detroit, Mich.
[9] BBL Division, Becton, Dickinson & Co., Cockeysville, Md.
[10] Bacto-MacConkey agar, Difco Laboratories, Detroit, Mich.
[11] Pseudosel agar, BBL Division, Becton, Dickinson & Co., Cockeysville, Md.
[12] Corning digital 112 research pH meter, Corning Scientific Instruments, Medfield, Mass.
[13] Biological oxygen demand bottles.
[14] Model AA5, Techtron atomic absorption spectrophotometer, Varian, Palo Alto, Calif. The instrument conditions include a mercury tube and the following settings: wavelength, 253.65 nm; current, 3.5 mamp; and slit, 100 μm. The absorption cell was obtained from Perkin-Elmer Corp., Instrument Division, Norwalk, Conn. A mercury analysis kit, model 303-0830, with a drying train was also used.
[15] Sephadex G-100, Pharmacia Fine Chemicals, Piscataway, N.J.
[16] Column type K26/100 (100 × 2.6 cm i.d.), Pharmacia Fine Chemicals, Piscataway, N.J.
[17] Type VI, from horse heart, 95–100%, Item C-7752, Sigma Chemical Co., St. Louis, Mo.
[18] Crystallized and lyophilized, item A-4378, Sigma Chemical Co., St. Louis, Mo.
[19] Blue dextran 2000, Pharmacia Fine Chemicals, Piscataway, N.J.

Table I—Acid Wash Treatment of a Column Slurry Contaminated with Nonspore-Forming Bacteria and Yeast

Sampling Time, days	Column Eluting Solution Used between Sampling	Total Effluent Volume between Sampling, ml	Sample Analyses: Nature of Sample	pH	Microorganism Count per Milliliter: Total Bacteria	Yeast
0	Acid wash solution	0	Slurry	6.0	8.0×10^6	5.2×10^6
			Effluent	6.7	5.0×10^6	3.0×10^6
1	Acid wash solution	800	Effluent	1.8	0	1.8×10^4
4	Rinsing buffer	2325	Effluent	1.8	0	1.1×10^2
5	Rinsing buffer	640	Effluent	7.0	0	4.2×10^1
6	Rinsing buffer[a]	575	Effluent	7.0	0	2.2×10^1
11	Rinsing buffer[a]	0	Effluent	7.0	0	3.5×10^3
			Slurry from top	7.0	0	1.8×10^2
			Slurry from middle	7.0	0	6.0×10^2
			Slurry from bottom	7.0	0	2.2×10^4

[a] Standing in the slurry.

Table II—Acid Wash Treatment of a Column Slurry Contaminated with Bacterial and Mold Spores

Sampling Time, days	Column Eluting Solution Used between Sampling	Total Effluent Volume between Sampling, ml	Sample Analyses: Nature of Sample	pH	Microorganism Count per Milliliter: Bacteria Spores	Mold Spores
0	Acid wash solution	0	Slurry	6.4	2.2×10^6	3.0×10^6
			Effluent	6.3	1.9×10^6	1.6×10^4
1	Acid wash solution	1000	Effluent	1.9	2.1×10^2	3.0×10^0
4	Rinsing buffer	2150	Effluent	1.8	3.7×10^1	4.0×10^0
5	Rinsing buffer	1130	Effluent	7.0	2.3×10^2	8.0×10^1
6	Rinsing buffer[a]	930	Effluent	7.0	8.0×10^1	4.0×10^1
11	Rinsing buffer[a]	0	Effluent	7.1	1.6×10^4	8.5×10^2
			Slurry from top	7.1	3.8×10^5	8.0×10^5
			Slurry from middle	7.0	3.8×10^5	1.2×10^6
			Slurry from bottom	7.0	3.8×10^5	1.4×10^6

[a] Standing in the slurry.

~2 liters of rinsing buffer and treated with ~1 liter of the acid wash solution over 24 hr followed by rinsing and equilibration with ~2 liters of rinsing buffer over 48 hr (acid wash run); and (c) rinsed and reequilibrated with ~2 liters of rinsing buffer and treated with ~1 liter of the tromethamine–thimerosal wash solution over 24 hr followed by rinsing and equilibration with ~2 liters of rinsing buffer over 48 hr (tromethamine–thimerosal wash run). These solutions were allowed to flow through the slurry in the column by gravity at 0.8 ml/min.

After each of the three column treatments, the test solution was added to the column and was allowed to flow ~2.5 cm into the slurry before initiation of the rinsing buffer eluent, which flowed by gravity at a similar rate. Six-milliliter fractions were collected[20], and each fraction was monitored visually and/or spectrophotometrically[21] for components of the test solution.

The column void volume was estimated from the elution volume of the blue dextran, which was detected spectrophotometrically by its absorbance at 625 nm and visually by its blue color. The elution volume of cytochrome c was determined spectrophotometrically from its absorbance at 407 nm and visually by its red color. The elution volume of bovine serum albumin was determined by its absorbance at 280 nm. Then the relative elution volumes were calculated after each run by dividing the elution volume of each test protein, V_e, by the respective void volume, V_0, for each respective run. In addition, the Ouchterlony double-diffusion technique was used to confirm the separation of bovine serum albumin from cytochrome c.

Ouchterlony Double-Diffusion Technique—In the Ouchterlony technique, 50 μl from each of the three fractions of the bovine serum albumin peak was added to each of three outer wells of an Ouchterlony plate[22]. Fifty microliters from each of the two fractions of the cytochrome c peak was added to each of two additional outer wells on the same Ouchterlony plate. Fifty microliters of a control solution (2 mg of bovine serum albumin/ml) was added to the sixth outer well of the Ouchterlony plate. Fifty microliters of rabbit antibovine serum albumin[23] (2 mg/ml) was added to the center well of the plate, which was incubated for 24 hr in a moisture chamber at room temperature and subsequently examined for precipitin bands.

[20] LKB ultrorac fraction collector, instrument group 7000, LKB-Produktor AB, S-16125, Bromma 1, Sweden.

[21] Model 25 spectrophotometer, Beckman Instruments, Fullerton, Calif.

[22] IDF cell 1, Cordis Laboratories, Miami, Fla.

[23] Antibovine serum albumin (rabbit), code 65-111, Miles–Yeda Ltd.; distributed by Research Division, Miles Laboratories, Kankakee, Ill.

RESULTS

Validation of Antimicrobial Activity of Column Wash Solutions—The results indicate that both the acid wash and the tromethamine–thimerosal wash solutions are capable of eliminating microbial contamination from the gel filtration slurry packed into a column maintained at 5°. The acid wash was more effective than the tromethamine–thimerosal wash solution against both the nonspore-forming bacteria and the spores of *B. subtilis* (Tables I–IV). The acid wash solution was extremely active against the nonspore-forming bacteria since the combined bacterial count of *S. aureus* (Gram-positive cocci), *E. coli*, and *P. aeruginosa* (both Gram-negative bacilli) was reduced from 5.0×10^6 bacteria/ml of effluent to zero in 1 treatment day (Table I).

In comparison, the combined viability count for a mixture of the same three nonspore-forming bacteria was reduced from 3.8×10^6 to 1.6×10^3 organisms/ml of effluent sample following 4 days of treatment with the tromethamine–thimerosal wash (Table III). Visual (qualitative) examination of the viability count plates indicated that, after 4 days of treatment, *P. aeruginosa* was eliminated completely, that *E. coli* contamination was reduced significantly, and that most of the remaining nonspore-forming contamination was *S. aureus*.

The acid wash produced almost a 100,000-fold reduction in the number of *B. subtilis* spores per milliliter of effluent with 4 days of treatment (Table II). On the other hand, only a 1000-fold reduction in the number of *B. subtilis* spores per milliliter of effluent was produced with 4 days of treatment with the tromethamine–thimerosal wash solution (Table IV).

The tromethamine–thimerosal wash solution was more effective than the acid wash solution against yeast and the *A. niger* mold spores. *A. niger* spores, initially at concentrations of 1.5×10^6/ml of slurry and of 1.5×10^4/ml of effluent, were reduced to zero per milliliter of effluent with 1 day of treatment with the tromethamine–thimerosal wash solution (Table IV). This reduction was permanent since no mold spores were recovered from the treated slurry. Similarly, this same wash produced a 100,000-fold reduction in the *C. albicans* count per milliliter of effluent (Table III).

Table III—Tromethamine–Thimerosal Wash Treatment of a Column Slurry Contaminated with Nonspore-Forming Bacteria and Yeast

Sampling Time, days	Column Eluting Solution Used between Sampling	Total Effluent Volume between Sampling, ml	Sample Analyses				
			Nature of Sample	pH	Mercury Content, %	Microorganism Count per Milliliter	
						Total Bacteria	Yeast
0	Tromethamine–thimerosal wash solution	0	Slurry	6.6	—[a]	3.8×10^6	3.5×10^6
			Effluent	6.4	—[a]	3.8×10^6	2.4×10^6
1	Tromethamine–thimerosal wash solution	1000	Effluent	7.0	0.01	3.8×10^4	4.0×10^3
4	Rinsing buffer	2720	Effluent	7.1	0.01	1.6×10^3	3.5×10^1
5	Rinsing buffer	1000	Effluent	7.0	—[a]	7.6×10^2	1.0×10^1
6	Rinsing buffer[b]	1560	Effluent	7.0	—[a]	6.0×10^2	0
11	Rinsing buffer[b]	0	Effluent	7.0	—[a]	1.2×10^3	0
			Slurry from top	7.0	—[a]	1.6×10^3	0
			Slurry from middle	7.0	—[a]	3.2×10^3	0
			Slurry from bottom	7.0	—[a]	3.2×10^4	0

[a] Negligible mercury content. [b] Standing in the slurry.

Table IV—Tromethamine–Thimerosal Wash Treatment of a Column Slurry Contaminated with Bacterial and Mold Spores

Sampling Time, days	Column Eluting Solution Used between Sampling	Total Effluent Volume between Sampling, ml	Sample Analyses				
			Nature of Sample	pH	Mercury Content, %	Microorganism Count per Milliliter	
						Bacteria Spores	Mold Spores
0	Tromethamine–thimerosal wash solution	0	Slurry	6.4	—[a]	1.5×10^6	1.5×10^6
			Effluent	6.5	—[a]	2.0×10^6	1.5×10^4
1	Tromethamine–thimerosal wash solution	825	Effluent	7.0	0.01	5.5×10^3	0
4	Rinsing buffer	2250	Effluent	7.0	0.01	2.4×10^3	0
5	Rinsing buffer	1000	Effluent	7.0	—[a]	1.2×10^3	0
6	Rinsing buffer[b]	1150	Effluent	7.0	—[a]	8.0×10^2	0
11	Rinsing buffer[b]	0	Effluent	6.8	—[a]	9.0×10^4	0
			Slurry from top	6.8	—[a]	3.5×10^5	0
			Slurry from middle	6.8	—[a]	5.6×10^5	0

[a] Negligible mercury content. [b] Standing in the slurry.

Table V—Relative Elution Volumes of the Test Solution Components after Each Run

Test Solution Components	Relative Elution Volumes (V_e/V_0)[a]		
	Control Run	Acid Wash Run	Tromethamine–Thimerosal Wash Run
Bovine serum albumin[b]	1.04	1.05	1.00
Cytochrome c[b]	2.07	2.56	2.60

[a] The column void volume (V_0) was determined using blue dextran; V_e is the test protein elution volume. [b] Fractions were verified further by the Ouchterlony double-diffusion technique.

At the conclusion of this experiment, no viable *C. albicans* cells were recovered from the slurry (Table III).

The acid wash solution produced a less dramatic reduction in the number of yeast and mold spores. The yeast spore count per milliliter of effluent was reduced 10,000-fold with 4 days of treatment, although the count increased after the treatment ended (Table I). The mold spore count per milliliter of effluent was reduced almost 10,000-fold with 1 day of treatment, and as with the *C. albicans*, the number of colony-forming units of *A. niger* increased following termination of the 4-day flow of the acid wash solution (Table II).

Each wash solution was eliminated from the column within ~24 hr by continuous elution with the rinsing buffer, as shown by the pH or mercury determination (Tables I–IV). Only a trace of mercury was detected in the gel slurry after rinsing the column previously treated with the tromethamine–thimerosal wash (Tables III and IV).

Validation of Separation Properties of Treated Column—The test protein elution patterns (bovine serum albumin and cytochrome c) obtained from the control run, the acid wash run, and the tromethamine–thimerosal run showed no significant differences, indicating that the column separation properties were not affected by either washing procedure. The relative elution volumes of the test proteins after both the acid wash run and the tromethamine–thimerosal wash run were similar to the relative elution volumes obtained after the control run (Table V). In addition, the Ouchterlony double-diffusion technique verified that there was no cross-contamination of the cytochrome c fraction with bovine serum albumin.

DISCUSSION

Selection of Suitable Wash Solutions—Several disinfectant solutions other than the tromethamine–thimerosal and the acid wash solutions were considered, but they were not studied because of their undesirable characteristics. Formaldehyde (3–8%) and glutaraldehyde (2%) were reported to be sporocidal (4), but formaldehyde is corrosive and damaging to the plastic parts of the column equipment, and glutaraldehyde is expensive and unstable upon storage (4). Other substances, such as chloroform, butanol, and toluene, cause the gel particles of certain gel filtration matrixes to shrink (2), are effective only at high concentrations (2, 5), and are incompatible with the plastic parts of the column equipment (2).

Thimerosal, a well-known antimicrobial agent (4), commonly is used as a preservative in multiple-dose containers and in topical preparations (4, 6). Furthermore, it is compatible with gel filtration and cation-exchange matrixes (2, 5). Dilute hydrochloric acid was examined since its acidity is expected to be antimicrobial and since gel filtration matrixes can be exposed to 0.02 *N* HCl for at least 6 months without deleterious effects (2). The 0.02% sodium azide included in the rinsing buffer does not interact with proteins or carbohydrates or affect their chromatographic behavior (2). The inclusion of isotonic sodium chloride concentrations in the wash solutions and rinsing buffer keeps the ionic strengths constant to avoid gel volume shrinkage or swelling upon changes in the eluents.

Antimicrobial Activity Determination and Monitoring of Wash Solution Removal—The washing procedures were examined under working conditions in a typical gel filtration column maintained at 5°. To investigate their antimicrobial effectiveness, the gel slurry was inoculated with high counts of the five test microorganisms recommended by USP XIX for antimicrobial effectiveness testing (7). To ensure meaningful results with the tromethamine–thimerosal wash, the static effects of mercury (7, 8) were neutralized by the addition of sodium

thioglycolate to a final concentration of 500 mg/liter (7) to all culture media possibly containing thimerosal. To substantiate the microbial counts and pH or mercury concentrations of effluent samples taken at the end of each wash and rinse cycle, column slurry samples were also analyzed at the conclusion of each antimicrobial effectiveness test.

To monitor the acid wash removal, pH determination was the most appropriate method. Since thimerosal contains ~50% mercury by weight (9), the tromethamine–thimerosal wash removal was monitored by cold vapor, flameless atomic absorption spectroscopy (10).

Washing Solution Effects on Treated Column Separation Properties—The proteins cytochrome c and bovine serum albumin were selected because, based on their respective molecular weights of 12,400 and 67,000, they can be readily fractionated by the slurry used in this investigation (2). Each protein, as well as the blue dextran void volume indicator, was readily assayed spectrophotometrically. In addition, the Ouchterlony double-diffusion procedure, based on a literature method (11), confirmed the clear separation of bovine serum albumin and cytochrome c in the control column and in treated columns.

It is feasible to apply both wash solutions, 0.02 *N* HCl containing 0.81% NaCl and the 0.1 *M* tromethamine–hydrochloride buffer (pH 7.0) containing 0.81% NaCl and 0.02% thimerosal, for disinfecting a modified gel filtration slurry under typical working conditions. Both wash solutions demonstrate antimicrobial activity against high concentrations of various microorganisms in the gel slurry packed into a column maintained at 5°.

Since the acid wash is more effective against nonspore-forming bacteria, including the more resistant species *P. aeruginosa* (4), and since the tromethamine–thimerosal wash is more active against mold and yeast, both wash solutions can be used routinely on an alternating basis or as needed. The wash solutions cannot be used in combination, however, since thimerosal is unstable in acidic solutions (4). In addition, both wash solutions can be removed from the slurry within 24 hr with no more than 1 liter of the rinsing buffer. Both wash solutions do not adversely affect the matrix separation properties and should be compatible with similar column packing materials.

REFERENCES

(1) R. R. Ernst, in "Disinfection, Sterilization, and Preservation," 2nd ed., S. S. Block, Ed., Lea & Febiger, Philadelphia, Pa., 1977, p. 481.

(2) "Sephadex, Gel Filtration in Theory and Practice," Pharmacia Fine Chemicals AB, Uppsala 1, Sweden, 1976, pp. 9, 12, and 32.

(3) C. R. Phillips, in "Disinfection, Sterilization, and Preservation," 2nd ed., S. S. Block, Ed., Lea & Febiger, Philadelphia, Pa., 1977, p. 592.

(4) C. A. Lawrence and S. S. Block, "Disinfection, Sterilization, and Preservation," Lea & Febiger, Philadelphia, Pa., 1968, pp. 511, 517–530, 571, 645.

(5) "Sephadex Ion Exchangers, a Guide to Ion Exchange Chromatography," Pharmacia Fine Chemicals AB, Uppsala 1, Sweden, 1976, p. 35.

(6) "The National Formulary," 14th ed., Mack Publishing Co., Easton, Pa., 1975, p. 705.

(7) "The United States Pharmacopeia," 19th rev., Mack Publishing Co., Easton, Pa., 1975, pp. 587, 588, 592, 621.

(8) "Manual of Microbiological Methods," McGraw-Hill, New York, N.Y., 1957, p. 43.

(9) "The Merck Index," 8th ed., Merck & Co., Rahway, N.J., 1968, p. 1040.

(10) W. R. Hatch and W. L. Ott, *Anal. Chem.*, **40**, 2085 (1968).

(11) E. A. Kabat and M. M. Mayer, "Experimental Immunochemistry," 2nd ed., Charles C Thomas, Springfield, Ill., 1964, pp. 85–90.

ACKNOWLEDGMENTS

Presented in part at the APhA Academy of Pharmaceutical Sciences, Hollywood, Fla., meeting, November 1978.

The authors thank Dr. F. Bogdansky, Quality Control Department, Hoffmann-La Roche Inc., for reviewing this manuscript.

High-Performance Liquid Chromatographic Analysis of Trimethoprim and Sulfamethoxazole in Dosage Forms

R. O. SINGLETARY, Jr., and F. D. SANCILIO ˣ

Received April 29, 1979, from *Burroughs Wellcome Co., Greenville, NC 27834.* Accepted for publication August 30, 1979.

Abstract □ A rapid, sensitive, and automatable high-performance liquid chromatographic method is presented for the determination of sulfamethoxazole, trimethoprim, and a preservative in dosage forms in the presence of excipients and degradation products.

Keyphrases □ Trimethoprim—simultaneous analysis with sulfamethoxazole and methylparaben, high-performance liquid chromatography, oral suspension and solid dosage forms □ Sulfamethoxazole—simultaneous analysis with trimethoprim and methylparaben, high-performance liquid chromatography, oral suspension and solid dosage forms □ Antibacterial agents—trimethoprim and sulfamethoxazole, simultaneous high-performance liquid chromatographic analysis, oral suspension and solid dosage forms

The antibacterials sulfamethoxazole and trimethoprim are the active ingredients in several oral suspension and solid dosage forms. The official analyses of their dosage forms are spectrophotometric methods following extraction (1, 2). These methods are time consuming and relatively difficult. A high-performance liquid chromatographic (HPLC) method, presented for the analysis of various sulfonamides in combination with trimethoprim, does not separate the various degradation products and the active components and cannot be used as a stability-indicating assay (3).

This study was undertaken to establish a rapid, quantitative, and stability-indicating procedure for routine quality control testing of trimethoprim and sulfamethoxazole in dosage forms. Methylparaben, a commonly used preservative, also may be determined in the analysis of the oral suspension.

EXPERIMENTAL

Apparatus—A high-pressure liquid chromatograph[1] with a 254-nm detector and a stainless steel column (30 cm × 4 mm i.d.) was used. The column packing[2] was porous silica particles with an octadecylsilane-bonded coating. The system was operated at 2.0 ml/min with a column pressure of ~1800 psi for solid dosage forms and at 3.0 ml/min with a column pressure of ~2800 psi for oral suspensions.

[1] Model 6000A pump and 440 detector, Waters Associates, Milford, Mass.
[2] μBondapak C_{18}, Waters Associates, Milford, Mass.

0022-3549/80/0200-0144$01.00/0

© 1980, American Pharmaceutical Association

thioglycolate to a final concentration of 500 mg/liter (7) to all culture media possibly containing thimerosal. To substantiate the microbial counts and pH or mercury concentrations of effluent samples taken at the end of each wash and rinse cycle, column slurry samples were also analyzed at the conclusion of each antimicrobial effectiveness test.

To monitor the acid wash removal, pH determination was the most appropriate method. Since thimerosal contains ~50% mercury by weight (9), the tromethamine–thimerosal wash removal was monitored by cold vapor, flameless atomic absorption spectroscopy (10).

Washing Solution Effects on Treated Column Separation Properties—The proteins cytochrome c and bovine serum albumin were selected because, based on their respective molecular weights of 12,400 and 67,000, they can be readily fractionated by the slurry used in this investigation (2). Each protein, as well as the blue dextran void volume indicator, was readily assayed spectrophotometrically. In addition, the Ouchterlony double-diffusion procedure, based on a literature method (11), confirmed the clear separation of bovine serum albumin and cytochrome c in the control column and in treated columns.

It is feasible to apply both wash solutions, 0.02 *N* HCl containing 0.81% NaCl and the 0.1 *M* tromethamine–hydrochloride buffer (pH 7.0) containing 0.81% NaCl and 0.02% thimerosal, for disinfecting a modified gel filtration slurry under typical working conditions. Both wash solutions demonstrate antimicrobial activity against high concentrations of various microorganisms in the gel slurry packed into a column maintained at 5°.

Since the acid wash is more effective against nonspore-forming bacteria, including the more resistant species *P. aeruginosa* (4), and since the tromethamine–thimerosal wash is more active against mold and yeast, both wash solutions can be used routinely on an alternating basis or as needed. The wash solutions cannot be used in combination, however, since thimerosal is unstable in acidic solutions (4). In addition, both wash solutions can be removed from the slurry within 24 hr with no more than 1 liter of the rinsing buffer. Both wash solutions do not adversely affect the matrix separation properties and should be compatible with similar column packing materials.

REFERENCES

(1) R. R. Ernst, in "Disinfection, Sterilization, and Preservation," 2nd ed., S. S. Block, Ed., Lea & Febiger, Philadelphia, Pa., 1977, p. 481.

(2) "Sephadex, Gel Filtration in Theory and Practice," Pharmacia Fine Chemicals AB, Uppsala 1, Sweden, 1976, pp. 9, 12, and 32.

(3) C. R. Phillips, in "Disinfection, Sterilization, and Preservation," 2nd ed., S. S. Block, Ed., Lea & Febiger, Philadelphia, Pa., 1977, p. 592.

(4) C. A. Lawrence and S. S. Block, "Disinfection, Sterilization, and Preservation," Lea & Febiger, Philadelphia, Pa., 1968, pp. 511, 517–530, 571, 645.

(5) "Sephadex Ion Exchangers, a Guide to Ion Exchange Chromatography," Pharmacia Fine Chemicals AB, Uppsala 1, Sweden, 1976, p. 35.

(6) "The National Formulary," 14th ed., Mack Publishing Co., Easton, Pa., 1975, p. 705.

(7) "The United States Pharmacopeia," 19th rev., Mack Publishing Co., Easton, Pa., 1975, pp. 587, 588, 592, 621.

(8) "Manual of Microbiological Methods," McGraw-Hill, New York, N.Y., 1957, p. 43.

(9) "The Merck Index," 8th ed., Merck & Co., Rahway, N.J., 1968, p. 1040.

(10) W. R. Hatch and W. L. Ott, *Anal. Chem.*, **40**, 2085 (1968).

(11) E. A. Kabat and M. M. Mayer, "Experimental Immunochemistry," 2nd ed., Charles C Thomas, Springfield, Ill., 1964, pp. 85–90.

ACKNOWLEDGMENTS

Presented in part at the APhA Academy of Pharmaceutical Sciences, Hollywood, Fla., meeting, November 1978.

The authors thank Dr. F. Bogdansky, Quality Control Department, Hoffmann-La Roche Inc., for reviewing this manuscript.

High-Performance Liquid Chromatographic Analysis of Trimethoprim and Sulfamethoxazole in Dosage Forms

R. O. SINGLETARY, Jr., and F. D. SANCILIO ˣ

Received April 29, 1979, from *Burroughs Wellcome Co., Greenville, NC 27834.* Accepted for publication August 30, 1979.

Abstract □ A rapid, sensitive, and automatable high-performance liquid chromatographic method is presented for the determination of sulfamethoxazole, trimethoprim, and a preservative in dosage forms in the presence of excipients and degradation products.

Keyphrases □ Trimethoprim—simultaneous analysis with sulfamethoxazole and methylparaben, high-performance liquid chromatography, oral suspension and solid dosage forms □ Sulfamethoxazole—simultaneous analysis with trimethoprim and methylparaben, high-performance liquid chromatography, oral suspension and solid dosage forms □ Antibacterial agents—trimethoprim and sulfamethoxazole, simultaneous high-performance liquid chromatographic analysis, oral suspension and solid dosage forms

The antibacterials sulfamethoxazole and trimethoprim are the active ingredients in several oral suspension and solid dosage forms. The official analyses of their dosage forms are spectrophotometric methods following extraction (1, 2). These methods are time consuming and relatively difficult. A high-performance liquid chromatographic (HPLC) method, presented for the analysis of various sulfonamides in combination with trimethoprim, does not separate the various degradation products and the active components and cannot be used as a stability-indicating assay (3).

This study was undertaken to establish a rapid, quantitative, and stability-indicating procedure for routine quality control testing of trimethoprim and sulfamethoxazole in dosage forms. Methylparaben, a commonly used preservative, also may be determined in the analysis of the oral suspension.

EXPERIMENTAL

Apparatus—A high-pressure liquid chromatograph[1] with a 254-nm detector and a stainless steel column (30 cm × 4 mm i.d.) was used. The column packing[2] was porous silica particles with an octadecylsilane-bonded coating. The system was operated at 2.0 ml/min with a column pressure of ~1800 psi for solid dosage forms and at 3.0 ml/min with a column pressure of ~2800 psi for oral suspensions.

[1] Model 6000A pump and 440 detector, Waters Associates, Milford, Mass.
[2] μBondapak C_{18}, Waters Associates, Milford, Mass.

0022-3549/80/0200-0144$01.00/0

© 1980, American Pharmaceutical Association

Samples were injected by an autosampler[3] equipped with a 10-μl loop, and all analyses were performed at ambient temperature. A laboratory computer system[4] was used to gather data and to calculate the percentage of the theoretical component amounts.

Materials—Methanol[5], methylparaben[6], phenacetin[6], trimethoprim[6], sulfamethoxazole[6], acetonitrile[7], and acetic acid[8] were used as received. The oral suspensions and tablets were obtained from marketed batches[9].

Mobile Phase—The mobile phase was degassed acetonitrile–1% aqueous acetic acid (16:84) for tablets and degassed acetonitrile–1% aqueous acetic acid (10:90) for oral suspensions.

Internal Standard Solution—A 2-mg/ml solution of phenacetin in methanol was prepared as the internal standard.

Reference Standard Solution—Approximately 20 mg of trimethoprim and 100 mg of sulfamethoxazole were weighed accurately into a 100-ml volumetric flask. After 6.0 ml of the internal standard was added and the trimethoprim and sulfamethoxazole were dissolved in methanol[10], the flask was filled to volume with methanol.

Sample Preparation for Solid Dosage Forms—Twenty intact tablets from each sample were weighed accurately to obtain the average tablet weight and were ground to a fine powder. An amount of the powder equivalent to 100 mg of sulfamethoxazole was weighed accurately and placed in a 100-ml volumetric flask. Sufficient methanol to dissolve the active ingredients[10] and 6.0 ml of the internal standard solution were added, and the solution was diluted to volume with methanol. A portion of this solution was centrifuged or filtered before use.

Sample Preparations for Oral Suspension—Approximately 2.7 g of the oral suspension sample was weighed accurately and placed in a 100-ml volumetric flask. After 6.0 ml of the internal standard solution was added and the active ingredients were dissolved in methanol[10], the flask was diluted to volume with methanol. A portion of this solution was filtered or centrifuged before use. The specific gravity of the suspension was required for the calculations.

Chromatography—Each sample analysis consisted of two 10-μl injections of the sample solution bracketed by two 10-μl injections of a standard solution. Sample chromatograms for the oral suspension and tablet samples are shown in Figs. 1 and 2, respectively. The detector attenuation was 0.1 aufs.

The peak area or height ratios were used to quantitate the chromatograms. The ratios were calculated by:

$$SP \text{ or } ST = \frac{PA_1}{PA_2} \qquad \text{(Eq. 1)}$$

where SP is the sample ratio, ST is the standard ratio, PA_1 is the area or height of the sample or standard component peak, and PA_2 is the area or height of the internal standard peak. The percent of the theoretical amount of each component was calculated by:

$$\left(\frac{SP}{ST}\right)\left(\frac{W_1}{W_2}\right)\left(\frac{AS}{TA}\right) \times 100 = \% \text{ of theoretical amount} \qquad \text{(Eq. 2)}$$

where W_1 and W_2 are the standard and sample weights, respectively; AS is the average tablet weight or specific gravity; and TA is the theoretical amount per tablet or milliliter. Peak areas were used in the trimethoprim and sulfamethoxazole calculations, and peak heights were used in the methylparaben calculations.

RESULTS AND DISCUSSION

A nonpolar column was selected due to the polarity of the components to be determined. The high efficiency of the reversed-phase, small particle column resolved all of the formulation components and potential degradation products.

The presence of methylparaben as a preservative in the oral suspension required a different mobile phase from that used for the tablets. A slightly more polar mobile phase was used to resolve methylparaben from sulfamethoxazole in the oral suspension to quantitate both components accurately. The less polar mobile phase allowed faster analysis for the tablets.

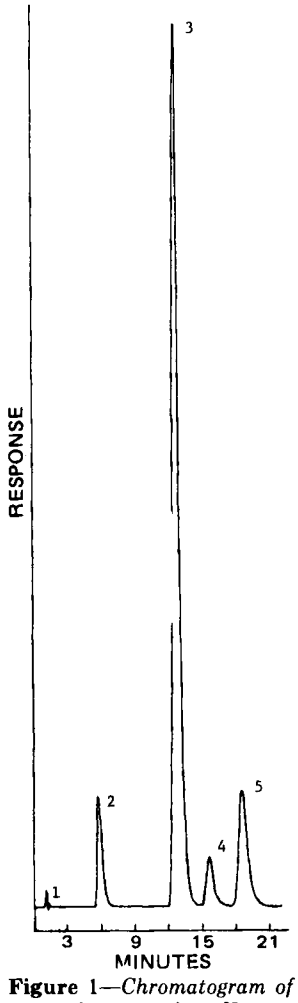

Figure 1—*Chromatogram of an oral suspension. Key: 1, solvent; 2, trimethoprim; 3, sulfamethoxazole; 4, methylparaben; and 5, phenacetin.*

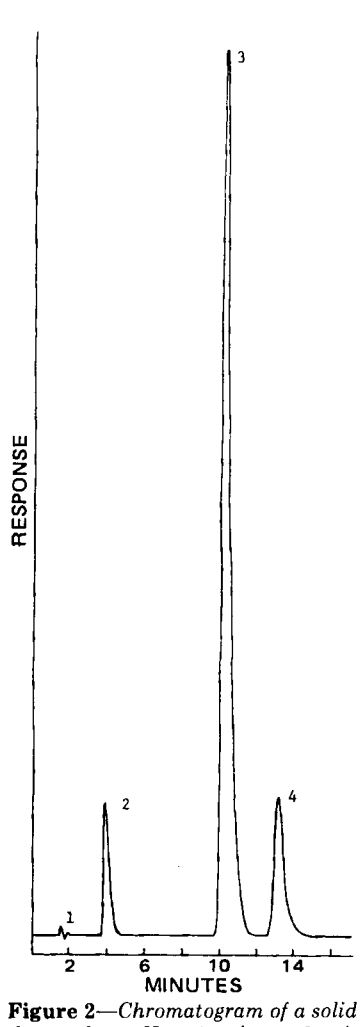

Figure 2—*Chromatogram of a solid dosage form. Key: 1, solvent; 2, trimethoprim; 3, sulfamethoxazole; and 4, phenacetin.*

An internal standard method was chosen to minimize errors resulting from both the apparatus and the injection technique. The peak exhibited by phenacetin, the internal standard, was resolved well from the peaks exhibited by trimethoprim, sulfamethoxazole, methylparaben, and the degradation products.

Linearity of the method for sulfamethoxazole and trimethoprim was determined by plotting the peak area response *versus* the concentration of each component. Peak height response was plotted *versus* concentration for the methylparaben linearity determination. Solutions containing various amounts of the component and a constant amount of the internal standard were chromatographed. The results proved that the method was linear in accordance with Beer's law.

Method reproducibility was determined by 13 consecutive injections of a standard solution equivalent to 100% of the theoretical amount of each component. The relative standard deviations were 0.16, 0.36, and 5.30%, using the peak area for sulfamethoxazole, trimethoprim, and methylparaben, respectively. The relative standard deviation for methylparaben was 0.97% using peak height measurements. Since this reproducibility is greater than that obtained using peak area, peak heights were used for the methylparaben calculations.

Each component was heat degraded in acid, base, and water. These solutions were chromatographed to show the retention times for the degradation products. Sulfamethoxazole exhibited no noticeable degradation, and trimethoprim exhibited two peaks identified as 2-amino-4-hydroxy-5-(3′,4′,5′-trimethoxybenzyl)pyrimidine and 4-amino-2-hydroxy-5-(3′,4′,5′-trimethoxybenzyl)pyrimidine. The retention times of the two degradation products using the mobile phase for solid dosage

[3] Model 725, Micromeritics, Norcross, Ga.
[4] HP3354, Hewlett-Packard, Avondale, Pa.
[5] Certified ACS, Fisher Scientific.
[6] Reference standards, Burroughs Wellcome Co., Greenville, N.C.
[7] HPLC grade, Fisher Scientific.
[8] ACS grade, Mallinckrodt.
[9] Septra suspension and Septra tablets, Burroughs Wellcome Co., Greenville, N.C.
[10] Samples or standards may have to be sonicated or shaken to effect dissolution.

Table I—Comparative Analyses Using HPLC and Extraction–Spectrophotometric Methods

Sample	Percent of Theoretical Amount[a]					
	Trimethoprim		Sulfamethoxazole		Methylparaben	
	Extraction	HPLC	Extraction	HPLC	Previous[b]	HPLC
1	96.6	99.8 ± 0.7	100.6	100.1 ± 0.0	—	—
2	98.7	100.0 ± 0.2	98.0	100.6 ± 0.1	—	—
3	99.8	99.7 ± 0.3	98.9	99.5 ± 0.7	—	—
4	99.4	98.8 ± 0.4	100.6	99.4 ± 0.0	—	—
5	97.5	95.1 ± 0.2	102.7	98.0 ± 0.2	—	—
6	101.8	100.4 ± 0.6	100.3	100.0 ± 0.8	—	—
7	101.0	99.5 ± 0.2	100.3	99.5 ± 0.3	—	—
8	102.1	97.7 ± 0.1	101.7	100.1 ± 0.3	—	—
Suspension 1	96.6	100.1 ± 1.5	99.8	102.2 ± 0.8	100.5	99.8 ± 0.4
Suspension 2	97.6	97.5 ± 0.3	101.5	100.0 ± 0.4	97.4	100.1 ± 0.0
Suspension 3	94.1	95.6 ± 0.8	101.5	99.4 ± 0.6	99.8	99.3 ± 0.8
Suspension 4	97.3	97.0 ± 1.1	99.3	99.9 ± 0.8	97.8	99.6 ± 0.0
Suspension 5	98.6	96.4 ± 1.1	97.6	100.4 ± 0.4	98.6	99.5 ± 0.6
Suspension 6	95.2	95.4 ± 1.3	98.9	98.7 ± 0.7	97.0	97.2 ± 0.6

[a] Each HPLC result is an average of two values. The percent of the theoretical amount is the amount of active ingredient found based on the amount claimed. [b] The previous assay was a different HPLC assay that used an acetonitrile–0.1% acetic acid (25:75) mobile phase and an ODS-2, 25-cm column at a flow rate of 2.0 ml/min.

Table II—Reproducibility of HPLC Method Results

Sample	Percent of Theoretical Amount[a]					
	Trimethoprim		Sulfamethoxazole		Methylparaben	
	Assay I	Assay II	Assay I	Assay II	Assay I	Assay II
1	99.8 ± 0.7	99.4 ± 0.4	100.1 ± 0.0	100.5 ± 1.1	—	—
2	95.1 ± 0.2	96.4 ± 0.3	98.0 ± 0.2	99.8 ± 0.4	—	—
3	100.4 ± 0.6	100.6 ± 0.6	100.0 ± 0.8	101.6 ± 0.4	—	—
Suspension 1	95.0 ± 0.1	95.3 ± 0.5	98.0 ± 0.1	98.7 ± 0.2	98.0 ± 0.3	99.2 ± 0.1
Suspension 2	94.2 ± 0.1	94.1 ± 0.4	99.3 ± 0.3	99.1 ± 0.6	99.3 ± 0.6	98.5 ± 0.5
Suspension 3	94.5 ± 0.2	94.5 ± 0.1	98.7 ± 0.0	98.3 ± 0.1	98.7 ± 0.2	97.7 ± 0.4

[a] Each assay result is an average of two analyses. Samples were weighed for each analysis. The percent of the theoretical amount is the amount of active ingredient found based on the amount claimed.

forms were ~4.9 and 3.1 min, respectively. The retention times using the mobile phase for the oral suspension were ~10.0 and 4.2 min, respectively. These degradation products were identified by chromatographing standard solutions containing the impurities, the degradation solutions containing the products of interest, and degradation solutions spiked with these products and noting the retention times of the peaks. Placebos were chromatographed and showed that the excipients did not interfere.

The values obtained using the HPLC method compared favorably with those obtained using the extraction–spectrophotometric determination (Table I). In most cases, the HPLC assay gave slightly higher values than the extraction method. This difference may have been caused by a loss of sample during the extraction. In some cases, absorbing impurities or degradation products may have caused the extraction–spectrophotometric method to give a higher result than the more specific HPLC method. The HPLC assay was performed on 2 days and showed that the precision of the instrumentation and the assay reproducibility results were good. A different sample was weighed each day the assay was performed (Table II).

The HPLC method is accurate and is shorter and easier than the extraction–spectrophotometric method. In addition, the HPLC method can be automated easily using automatic samplers and laboratory computers or integrators.

REFERENCES

(1) "British Pharmacopoeia, 1973," Her Majesty's Stationery Office, London, England, 1973, pp. 128, 129.

(2) "USP XX Comment Proof," vol. 2, no. 47, United States Pharmacopeial Convention, Rockville, Md., 1977, pp. 3360–3367.

(3) P. Helboe and M. Thomsen, *Arch. Pharm. Chem. Sci. Ed.*, **5**, 453 (1977).

Stability-Indicating Assay for Tolmetin Sodium in Solid Dosage Forms

CASIMIR A. JANICKI ˣ **and KATHERINE F. DALY** *

Received December 12, 1978, from the *Pharmacy Research Department, McNeil Laboratories, Fort Washington, PA 19034.* Accepted for publication August 22, 1979. *Present address: Instrument Products, E. I. du Pont de Nemours and Co., Wilmington, DE 19898.

Abstract □ A spectrophotometric assay for determining tolmetin sodium in pharmaceutical solid dosage forms is described. Tolmetin sodium is separated from common pharmaceutical excipients and probable degradation products. Recovery, precision, and accuracy data are provided. Two TLC methods are included which can be used to monitor qualitatively the stability of aged dosage forms.

Keyphrases □ Tolmetin sodium—stability-indicating assay, solid dosage forms □ Anti-inflammatory agents—tolmetin sodium, stability-indicating assay, solid dosage forms □ Stability—tolmetin sodium, spectrophotometric assay, solid dosage forms

Tolmetin[1] sodium [sodium 1-methyl-5-(4-methylbenzoyl)-1*H*-pyrrole-2-acetate dihydrate] was introduced commercially as an anti-inflammatory drug for the treatment of rheumatoid arthritis. Since it is a pyrrole derivative (1), it differs chemically from other anti-inflammatory agents. During the development of a suitable dosage form, a precise and accurate stability assay was needed. GLC and spectrophotometric assays were developed (2–4) to evaluate the absorption, distribution, and excretion of tolmetin sodium in human subjects. High-pressure liquid chromatographic methods were developed recently for assessing the purity of tolmetin sodium (5) and for determining tolmetin and its major metabolite in plasma (6).

A spectrophotometric assay is described that can determine tolmetin sodium in the presence of probable degradation products and common pharmaceutical tablet and capsule excipients. Precision and accuracy data also are provided. The method is quick and simple, requires only readily available equipment, and has the specificity needed for stability studies. Two TLC methods also are included which can be used to monitor qualitatively the stability of aged dosage forms.

EXPERIMENTAL

Reagents—All reagents met ACS specifications. Reference standard tolmetin sodium[2] was used as the standard. The TLC plates were 5 × 20-cm precoated silica gel GF[3]. Commercial tolmetin sodium tablets containing the equivalent of 200 mg of tolmetin were used[2].

Standard Preparation—Tolmetin sodium reference standard, 122.6 mg (equivalent to 100.0 mg of tolmetin), was placed in a 120-ml screw-capped bottle. Water, 25 ml, was added, and the mixture was swirled. Ethylene dichloride, 50 ml, and 5 ml of 6 *N* HCl were added by pipet. The standards were analyzed as described under *Procedure*.

Procedure—At least 20 tablets were weighed and finely powdered. A portion of the powder equivalent to 100 mg of tolmetin was weighed accurately and transferred to a 120-ml screw-capped bottle. Ethylene dichloride, 50 ml, and 25 ml of 1 *N* HCl were added by pipet, and the mixture was shaken mechanically[4] for 15 min.

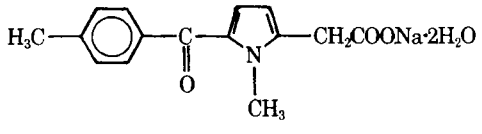

tolmetin sodium dihydrate

The solution was centrifuged to separate the phases and aspirated, and the aqueous layer was discarded. Five milliliters of the ethylene dichloride layer (2 mg/ml) was pipetted into a 100-ml volumetric flask, and the solution was diluted to volume with ethylene dichloride and mixed (0.1 mg/ml). Five milliliters of this solution was pipetted into a 120-ml screw-capped bottle containing exactly 50 ml of 0.1 *N* NaOH. The solution was shaken mechanically for 30 min and centrifuged. Then the sodium hydroxide layer was transferred to a clean container (0.01 mg/ml).

The UV absorption spectrum of the sample was recorded concomitantly with the reference standard in 1-cm cells, using 0.1 *N* NaOH saturated with ethylene dichloride as the blank. The percent tolmetin was calculated by:

$$\% \text{ tolmetin} = \frac{A_u}{A_s} \times \frac{C_s}{C_u} \times 100 \qquad \text{(Eq. 1)}$$

where A_u and A_s are the absorbances of the sample and standard, respectively, at the wavelength of maximum absorbance near 322 nm and C_s and C_u are the concentrations in milligrams per milliliter of the standard and sample, respectively.

Recovery—A stock solution of 24.6 mg of tolmetin sodium/ml of methanol was prepared. Two 5-ml samples were evaporated to dryness. One sample was assayed by the described procedure, and the second sample was diluted directly to the same final concentration with 0.1 *N* NaOH. Thirteen such experiments were run by five analysts.

Specificity—Twenty-five milligrams of I (*p*-toluic acid), III, IV, IX, and XI (Table I) were weighed directly into 120-ml screw-capped bottles and assayed as described.

Precision and Accuracy—An aqueous stock solution containing 1.23 mg of tolmetin sodium/ml was prepared, and 25-ml portions were assayed. The dilution was changed accordingly in the second assay step. Twelve assays were performed by six analysts.

In a second experiment, 40 tablets from a stability test program were ground to a fine powder and samples were assayed. Sixteen assays were performed by seven analysts.

Hydrolysis—Tolmetin sodium samples, 250 mg, were added to separate round-bottom flasks containing 50 ml of 1 *N* NaOH, water, or 1 *N* HCl. The samples were refluxed for 72, 72, or 24 hr, respectively.

Another sample of 615 mg of tolmetin sodium was dissolved in 500 ml of water and placed in a water-jacketed quartz immersion well and irradiated with a high-pressure mercury arc lamp for 24 hr. The resulting solutions and precipitants were assayed for intact tolmetin.

TLC—Tolmetin sodium and the 10 test compounds (Table I) were dissolved in methanol. The TLC chambers were 1.89-liter, wide-mouth Mason jars fitted with standard lids. The solvent systems were acetic acid–chloroform (5:95 v/v) (A) and *n*-butanol saturated with ammonia test solution (USP XIX) (B). For the *n*-butanol–ammonia solution, the plates were developed in preequilibrated paper-lined jars. Each plate was developed until the solvent front was ~2.5 cm from the top. The plates were air dried and viewed under short-wavelength UV light. The plates then were stained with iodine vapor. The plates also may be scanned with a densitometer[5].

RESULTS AND DISCUSSION

To determine the specificity of the assay for tolmetin sodium, I, III, IV, IX, and XI were assayed. The resulting UV spectra showed absorbance only from the sample derived from I. Since there was no interference

[1] Tolectin, McNeil Laboratories.
[2] McNeil Laboratories.
[3] Analtech Inc., Wilmington, Del.
[4] Wrist-action shaker, Burrell Corp., Pittsburgh, Pa.
[5] Schoeffel model SD3000 spectrodensitometer.

0022-3549/80/0200-0147$01.00/0
© 1980, American Pharmaceutical Association

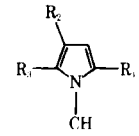

Table I—TLC R_f Values of the Test Compounds[a]

Compound	R_1	R_2	R_3	R_f Values Solvent A	R_f Values Solvent B
I (*p*-toluic acid)	—	—	—	0.69	0.78
II	$CH_2COOC_2H_5$	H	*p*-$CH_3C_6H_4CO$	0.66	0.79
III	CH_2COOCH_3	H	*p*-$CH_3C_6H_4CO$	0.66	0.80
IV	CH_2COOH	H	H	0.67	0.42
V	COOH	*p*-$CH_3C_6H_4CO$	CH_3	0.66	0.82
VI (tolmetin)	CH_2COOH	H	*p*-$CH_3C_6H_4CO$	0.54	0.50
VII	$CONH_2$	*p*-$CH_3C_6H_4CO$	CH_3	0.37	0.75
VIII	CH_2COOH	*p*-$CH_3C_6H_4CO$	H	0.29	0.44
IX	CH_2CONH_2	H	*p*-$CH_3C_6H_4CO$	0.18	0.92
X	CH_2CONH_2	*p*-$CH_3C_6H_4CO$	H	0.07	0.64
XI	CH_3	H	*p*-$CH_3C_6H_4CO$	0.68	0.79

[a] Detection limits under UV light ranged from 0.1 to 0.5 μg.

from *p*-toluic acid from 360 to 275 nm (Fig. 1), this compound does not interfere in the tolmetin sodium assay. The other compounds either did not extract into the sodium hydroxide layer or, in the case of IV, did not have any UV absorbance.

Compound I is *p*-toluic acid, and IV is the pyrrole acetic acid fragment of the tolmetin molecule. Both compounds are probable degradation products of tolmetin sodium. Compound III is the methyl ester of tolmetin, IX is the amide of tolmetin and a precursor in tolmetin synthesis, and XI is the decarboxylated tolmetin product. Compound III was used as a model compound in the event that esterification became a degradation route.

Since the five model compounds could be considered only as possible degradation or reaction products, attempts were made to degrade tolmetin sodium. Tolmetin sodium solutions were hydrolyzed as discussed under *Experimental*. The alkaline hydrolysis solution assayed 88% for intact tolmetin sodium, while the water hydrolysis solution assayed 94%. The solution from the attempted UV light degradation assayed 82%. TLC data showed many minor degradation products, but their identification was not attempted.

The acid solution was orange and contained a violet precipitate. The acid hydrolysis mixture assayed 64% for intact tolmetin sodium. The major TLC spots were at the origin and at R_f 0.5 and 0.7 using acetic acid–chloroform. With UV and IR, the sample at R_f 0.5 was identified as tolmetin, and the spot at R_f 0.7 was *p*-toluic acid. The spot at the origin was believed to be a highly polar molecule or a species of relatively high molecular weight containing many polar groups. *N*-Methylpyrroles are known to form polymers in acidic media, which are highly colored when polymerized under aerobic conditions (7).

To demonstrate the efficiency of the tolmetin sodium extraction, an aqueous stock solution of tolmetin sodium was prepared. Five analysts assayed 13 portions of it as directed for the tablets, and other portions were diluted simultaneously with 0.1 *N* NaOH. The data (Table II) indicated essentially complete drug extraction.

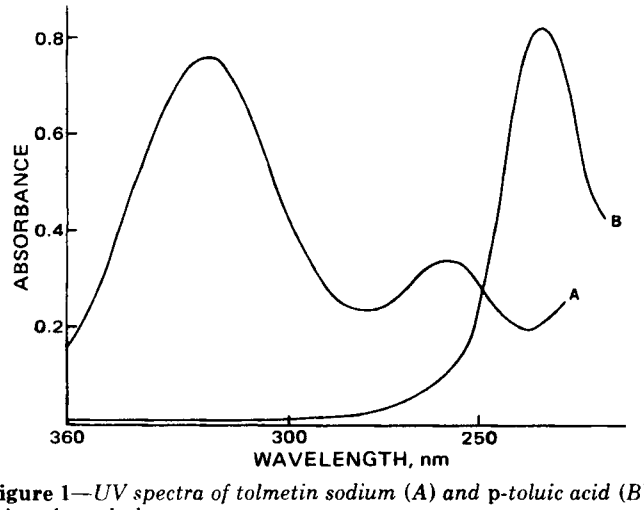

Figure 1—*UV spectra of tolmetin sodium (A) and p-toluic acid (B) taken through the assay.*

Another experiment was conducted to demonstrate the efficiency of the extraction for powdered tablet samples. Duplicate tablet powder samples were taken through the assay along with duplicate samples extracted with 25- and 75-ml samples of ethylene dichloride. The acid solution volume remained as described. The assay varied only in the dilution step with the last extraction step remaining as described. The mean of the six assays was 99.7% label with a standard deviation of 0.16.

To show that the initial extraction step in the assay did not affect tolmetin stability, reference standard tolmetin sodium was treated as described under *Experimental*, except that sufficient 12 *N* HCl was added to make the aqueous layer 3 *N* instead of 1 *N*. The solution was shaken, and samples were removed after 1 and 24 hr for TLC analysis. Using a densitometer, <0.2% degradation was determined after 1 hr and <0.8% was determined after 24 hr. Less than 0.1% degradation was detected by TLC using the method under *Procedure*.

Precision and accuracy were tested initially on an aqueous tolmetin

Table II—Recovery Data for Tolmetin Sodium

Analyst	Absorbance at Maximum near 322 nm Through Assay	Diluted Directly
1	0.756	0.765
	0.753	0.763
2	0.763	0.761
	0.756	0.761
3	0.757	0.759
	0.761	0.763
4	0.759	0.764
	0.775	0.764
	0.768	0.768
5	0.772	0.777
	0.772	0.783
	0.773	0.782
	0.766	0.778
Mean	0.764	0.769
SD	0.0075	0.0084

Table III—Precision and Accuracy Data

Analyst	Label Amount, % Solution	Tablets
1	100.8, 100.9	99.5, 99.6
2	100.1, 99.8	102.2, 101.9
3	100.7, 100.3	100.2, 99.2
4	100.1, 99.4	98.3, 98.8
5	99.9, 99.7	99.7, 99.9, 99.6
6	99.9, 100.4	100.1, 100.5
7		98.9, 99.4, 98.6
Mean	100.2	99.8
SD	0.47	1.07

sodium solution. The data had an accuracy of 100.2% with a standard deviation of 0.47% for the 12 assays (Table III). The experiment was conducted over 18 days. A precision study was conducted on a composite sample obtained by grinding 40 commercial tablets. The mean from the 16 assays was 99.8% over 2 months with a standard deviation of 1.07%. The data demonstrated that the method gives precise and accurate data.

Common tablet and capsule excipients such as starch, lactose, cellulose, and stearate lubricants were taken through the assay and did not interfere.

The assay was used to follow the stability of aged tablets and capsules containing up to an equivalent of 400 mg of tolmetin (490.1 mg of tolmetin sodium). Tablets were assayed for up to 5 years at room temperature and at various temperatures up to 80° for 3 months. The stability data demonstrated that the tablets and capsules were very stable. TLC was conducted on the aged samples using the two solvent mixtures. The data showed that tolmetin sodium remained intact in the dosage forms even after aging for 5 years at room temperature and accelerated aging at temperatures up to 80°. Less than 2% degradation was noted under the accelerated conditions.

Two solvent mixtures of different polarity were chosen for TLC to minimize the possibility of unresolved degradation products that could not be predicted. The compounds chosen to demonstrate the specificity of the TLC methods were, with one exception, previously postulated to be theoretical impurities in tolmetin sodium (5). The data (Table I) demonstrated that the solvent systems are suitable for separating tolmetin sodium from possible degradation products as well as theoretical impurities. Further confirmation was made on an aged tablet sample that was chromatographed and isolated from the TLC plate. The material was found to be identical to tolmetin sodium by UV, IR, and mass spectrometry.

The assay was used additionally to follow the stability of tolmetin sodium solutions buffered from pH 4.5 to 10.0 at 80°[6]. The data supported the reflux experiments, which showed that tolmetin sodium is relatively stable at neutral and alkaline pH values but unstable at acidic pH.

The data demonstrated that the method is capable of monitoring the stability of tolmetin sodium in solid dosage forms. The method is precise and accurate and utilizes common laboratory equipment. The hydrolysis experiments illustrated that tolmetin is stable under neutral and alkaline conditions but not under acidic conditions. The TLC methods can monitor qualitatively tolmetin sodium stability in aged dosage forms.

REFERENCES

(1) J. R. Carson, D. N. McKinstry, and S. Wong, *J. Med. Chem.*, **14**, 646 (1971).

(2) M. L. Selley, J. Thomas, and E. J. Triggs, *J. Chromatogr.*, **94**, 143 (1974).

(3) W. A. Cressman, B. Lopez, and D. Sumner, *J. Pharm. Sci.*, **64**, 1965 (1975).

(4) K. T. Ng, *J. Chromatogr.*, **166**, 527 (1979).

(5) R. K. Gilpin and C. A. Janicki, *ibid.*, **147**, 501 (1978).

(6) J. W. Ayres, E. Sakmar, M. R. Hallmark, and J. G. Wagner, *Res. Commun. Chem. Pathol. Pharmacol.*, **16**, 475 (1977).

(7) G. F. Smith, in "Advances in Heterocyclic Chemistry," vol. 2, A. R. Katritzky, Ed., Academic, New York, N.Y., 1963, pp. 287–309.

ACKNOWLEDGMENTS

The authors acknowledge the technical assistance of Mrs. R. Rocco, Dr. J. S. Ranweiler, Dr. C. Y. Ko, Mrs. C. M. Moral, Mr. L. T. Olszewski, and Dr. R. H. Erlich.

[6] W. A. Cressman, McNeil Laboratories, Fort Washington, PA 19034, personal communication.

Preparation and Biological Actions of *N*-2,2,2-Trifluoroethyl-2-(3,4-dihydroxyphenyl)ethylamine

JOHN P. O'DONNELL *x, A. J. AZZARO ‡, and P. R. URQUILLA ‡

Received April 9, 1979, from the **School of Pharmacy and the* ‡*Departments of Neurology and Pharmacology, School of Medicine, West Virginia University Medical Center, Morgantown, WV 26506.* Accepted for publication August 22, 1979.

Abstract □ *N*-2,2,2-Trifluoroethyl-2-(3,4-dihydroxyphenyl)ethylamine was synthesized and compared to *N*-ethyl-2-(3,4-dihydroxyphenyl)-ethylamine and dopamine for activity on adenylate cyclase in the rat striatum. Both dopamine and *N*-ethyl-2-(3,4-dihydroxyphenyl)ethylamine stimulated adenylate cyclase activity in a dose-dependent fashion. The *N*-trifluoroethyldopamine analog at 1×10^{-4} *M* induced a weak effect. The compounds were evaluated further by studying their relaxant effects in isolated rabbit renal and ear arteries. Both the *N*-ethyl- and *N*-trifluoroethyldopamine analogs produced a relaxant effect but demonstrated no selectivity for dopamine receptors.

Keyphrases □ Adenylate cyclase activity—dopamine, *N*- and *N,N*-substituted dopamine analogs, peripheral and central dopamine receptors, isolated striata and blood vessels □ Dopamine—antiparkinson drug, adenylate cyclase activity, dopamine analogs □ *N*-Ethyl-2-(3,4-dihydroxyphenyl)ethylamine—dopamine analog, adenylate cyclase activity □ *N*-2,2,2-Trifluoroethyl-2-(3,4-dihydroxyphenyl)ethylamine—dopamine analog, adenylate cyclase activity

The treatment of parkinsonism with levodopa has beneficial effects; however, in some patients with severely impaired dopaminergic neurons, the use of levodopa may be ineffective because the tissue cannot perform the necessary enzymatic decarboxylation to form dopamine (1, 2). An effort to generate new dopaminergic drugs for parkinsonism led to the synthesis of *N*- and *N,N*-substituted dopamine analogs (3–9). The binding of simple dopaminergic ligands to the receptor appears to be independent of substitution on the nitrogen (5). Unlike dopamine, the *N*- and *N,N*-substituted dopamine analogs cross the blood–brain barrier (3, 4). In addition, these agents are resistant to deamination by monoamine oxidase since they are secondary and tertiary amines. Moreover, these *N*- and *N,N*-substituted dopamine analogs act in the central nervous system as direct acting dopamine receptor agonists and, therefore, are independent of prejunctional dopaminergic mechanisms (4, 8).

To improve absorption and distribution of the *N*-alkyl-substituted dopamine analogs, *N*-2,2,2-trifluoroethyl-2-(3,4-dihydroxyphenyl)ethylamine (I) was prepared. The 2,2,2-trifluoroethyl group is well suited to replace the ethyl group because of similar steric properties and because the fluorine atom increases both lipid solubility and membrane penetration.

The agonistic properties of I, *N*-ethyl-2-(3,4-dihy-

0022-3549/80/0200-0149$01.00/0

© 1980, American Pharmaceutical Association

sodium solution. The data had an accuracy of 100.2% with a standard deviation of 0.47% for the 12 assays (Table III). The experiment was conducted over 18 days. A precision study was conducted on a composite sample obtained by grinding 40 commercial tablets. The mean from the 16 assays was 99.8% over 2 months with a standard deviation of 1.07%. The data demonstrated that the method gives precise and accurate data.

Common tablet and capsule excipients such as starch, lactose, cellulose, and stearate lubricants were taken through the assay and did not interfere.

The assay was used to follow the stability of aged tablets and capsules containing up to an equivalent of 400 mg of tolmetin (490.1 mg of tolmetin sodium). Tablets were assayed for up to 5 years at room temperature and at various temperatures up to 80° for 3 months. The stability data demonstrated that the tablets and capsules were very stable. TLC was conducted on the aged samples using the two solvent mixtures. The data showed that tolmetin sodium remained intact in the dosage forms even after aging for 5 years at room temperature and accelerated aging at temperatures up to 80°. Less than 2% degradation was noted under the accelerated conditions.

Two solvent mixtures of different polarity were chosen for TLC to minimize the possibility of unresolved degradation products that could not be predicted. The compounds chosen to demonstrate the specificity of the TLC methods were, with one exception, previously postulated to be theoretical impurities in tolmetin sodium (5). The data (Table I) demonstrated that the solvent systems are suitable for separating tolmetin sodium from possible degradation products as well as theoretical impurities. Further confirmation was made on an aged tablet sample that was chromatographed and isolated from the TLC plate. The material was found to be identical to tolmetin sodium by UV, IR, and mass spectrometry.

The assay was used additionally to follow the stability of tolmetin sodium solutions buffered from pH 4.5 to 10.0 at 80°[6]. The data supported the reflux experiments, which showed that tolmetin sodium is relatively stable at neutral and alkaline pH values but unstable at acidic pH.

The data demonstrated that the method is capable of monitoring the stability of tolmetin sodium in solid dosage forms. The method is precise and accurate and utilizes common laboratory equipment. The hydrolysis experiments illustrated that tolmetin is stable under neutral and alkaline conditions but not under acidic conditions. The TLC methods can monitor qualitatively tolmetin sodium stability in aged dosage forms.

REFERENCES

(1) J. R. Carson, D. N. McKinstry, and S. Wong, *J. Med. Chem.*, **14**, 646 (1971).

(2) M. L. Selley, J. Thomas, and E. J. Triggs, *J. Chromatogr.*, **94**, 143 (1974).

(3) W. A. Cressman, B. Lopez, and D. Sumner, *J. Pharm. Sci.*, **64**, 1965 (1975).

(4) K. T. Ng, *J. Chromatogr.*, **166**, 527 (1979).

(5) R. K. Gilpin and C. A. Janicki, *ibid.*, **147**, 501 (1978).

(6) J. W. Ayres, E. Sakmar, M. R. Hallmark, and J. G. Wagner, *Res. Commun. Chem. Pathol. Pharmacol.*, **16**, 475 (1977).

(7) G. F. Smith, in "Advances in Heterocyclic Chemistry," vol. 2, A. R. Katritzky, Ed., Academic, New York, N.Y., 1963, pp. 287–309.

ACKNOWLEDGMENTS

The authors acknowledge the technical assistance of Mrs. R. Rocco, Dr. J. S. Ranweiler, Dr. C. Y. Ko, Mrs. C. M. Moral, Mr. L. T. Olszewski, and Dr. R. H. Erlich.

[6] W. A. Cressman, McNeil Laboratories, Fort Washington, PA 19034, personal communication.

Preparation and Biological Actions of *N*-2,2,2-Trifluoroethyl-2-(3,4-dihydroxyphenyl)ethylamine

JOHN P. O'DONNELL *x, A. J. AZZARO ‡, and P. R. URQUILLA ‡

Received April 9, 1979, from the **School of Pharmacy and the* ‡*Departments of Neurology and Pharmacology, School of Medicine, West Virginia University Medical Center, Morgantown, WV 26506.* Accepted for publication August 22, 1979.

Abstract □ *N*-2,2,2-Trifluoroethyl-2-(3,4-dihydroxyphenyl)ethylamine was synthesized and compared to *N*-ethyl-2-(3,4-dihydroxyphenyl)-ethylamine and dopamine for activity on adenylate cyclase in the rat striatum. Both dopamine and *N*-ethyl-2-(3,4-dihydroxyphenyl)ethylamine stimulated adenylate cyclase activity in a dose-dependent fashion. The *N*-trifluoroethyldopamine analog at 1×10^{-4} *M* induced a weak effect. The compounds were evaluated further by studying their relaxant effects in isolated rabbit renal and ear arteries. Both the *N*-ethyl- and *N*-trifluoroethyldopamine analogs produced a relaxant effect but demonstrated no selectivity for dopamine receptors.

Keyphrases □ Adenylate cyclase activity—dopamine, *N*- and *N,N*-substituted dopamine analogs, peripheral and central dopamine receptors, isolated striata and blood vessels □ Dopamine—antiparkinson drug, adenylate cyclase activity, dopamine analogs □ *N*-Ethyl-2-(3,4-dihydroxyphenyl)ethylamine—dopamine analog, adenylate cyclase activity □ *N*-2,2,2-Trifluoroethyl-2-(3,4-dihydroxyphenyl)ethylamine—dopamine analog, adenylate cyclase activity

The treatment of parkinsonism with levodopa has beneficial effects; however, in some patients with severely impaired dopaminergic neurons, the use of levodopa may be ineffective because the tissue cannot perform the necessary enzymatic decarboxylation to form dopamine (1, 2). An effort to generate new dopaminergic drugs for parkinsonism led to the synthesis of *N*- and *N,N*-substituted dopamine analogs (3–9). The binding of simple dopaminergic ligands to the receptor appears to be independent of substitution on the nitrogen (5). Unlike dopamine, the *N*- and *N,N*-substituted dopamine analogs cross the blood–brain barrier (3, 4). In addition, these agents are resistant to deamination by monoamine oxidase since they are secondary and tertiary amines. Moreover, these *N*- and *N,N*-substituted dopamine analogs act in the central nervous system as direct acting dopamine receptor agonists and, therefore, are independent of prejunctional dopaminergic mechanisms (4, 8).

To improve absorption and distribution of the *N*-alkyl-substituted dopamine analogs, *N*-2,2,2-trifluoroethyl-2-(3,4-dihydroxyphenyl)ethylamine (I) was prepared. The 2,2,2-trifluoroethyl group is well suited to replace the ethyl group because of similar steric properties and because the fluorine atom increases both lipid solubility and membrane penetration.

The agonistic properties of I, *N*-ethyl-2-(3,4-dihy-

0022-3549/80/0200-0149$01.00/0

© 1980, American Pharmaceutical Association

droxyphenyl)ethylamine, and dopamine at central and peripheral dopamine receptors were analyzed pharmacologically. These studies measured the effects of each agent on the activity of dopamine-sensitive adenylate cyclase in rat neostriatum and evaluated their relaxant effects on isolated rabbit renal and ear arteries.

EXPERIMENTAL

Chemistry[1]—*N-Trifluoroacetyl -2- (3,4-dimethoxyphenyl)ethylamine (III)*—Trifluoroacetic anhydride (20 ml, 0.129 mole) was added very slowly, with stirring, to 20 g (0.115 mole) of 2-(3,4-dimethoxyphenyl)ethylamine. The resulting glassy solid was allowed to set overnight. Trituration of the solid mass with water gave a white suspension, which was filtered and washed with water. The crude amide was recrystallized from benzene–hexane to afford 27.4 g (86%), mp 84°; IR (neat): 1715 cm^{-1} (C=O); NMR ($CDCl_3$): δ 2.60–3.70 (m, 4H, CH_2), 3.84 (s, 6H, OCH_3), and 6.60–6.80 (m, 3H, 3 aromatic H).

Anal.—Calc. for $C_{12}H_{14}F_3NO_3$: C, 51.99; H, 5.08; N, 5.05. Found: C, 51.89; H, 5.11; N, 5.04.

N-(2,2,2-Trifluoroethyl) -2- (3,4-dimethoxyphenyl)ethylamine (IV)—To an ice-chilled mixture of tetrahydrofuran (100 ml) and 27.4 g of III (0.999 mole) was added slowly, with stirring, 233 ml (0.23 mole) of 1 *M* diborane in tetrahydrofuran[2] under nitrogen. The resulting mixture was stirred at 0° for 1 hr and then refluxed for 12 hr. The reaction mixture again was cooled to 0°, 50 ml of water was added, and the volatiles were removed from the reaction mixture. The residue was taken up in water and extracted three times with chloroform. The combined chloroform extracts were dried over magnesium sulfate and filtered, and the filtrate was treated with anhydrous hydrochloric acid. The volatiles were again removed, and the residue was recrystallized from ether to afford 27.8 g (90%) of crystals, mp 208°; NMR (free base) ($CDCl_3$): δ 2.50–3.45 (m, 6H, CH_2), 3.85 (s, 6H, OCH_3), and 6.68 (s, 3H, aromatic H).

Anal.—Calc. for $C_{12}H_{17}ClF_3NO_2$: C, 48.25; H, 5.39; N, 4.69. Found: C, 48.27; H, 5.48; N, 4.63.

N-(2,2,2-Trifluoroethyl)-2-(3,4-dihydroxyphenyl)ethylamine (I)—Compound IV (3.0 g, 0.01 mole) was dissolved in 48% HBr (20 ml). The system was flushed with nitrogen for 0.25 hr and then heated to 150° for 2 hr. Excess acid was removed under reduced pressure to give a residue. Two recrystallizations from isopropyl alcohol–ether afforded 2.12 g (70%) of product, mp 179–180°. The pKa of I was determined by titration (10); IR (KBr): 3250 cm^{-1} (broad, OH); NMR (D_2O): δ 2.60–4.20 (m, 6H, CH_2) and 6.62–6.80 (m, aromatic H).

Anal.—Calc. for $C_{10}H_{13}BrF_3NO_2$: C, 37.99; H, 4.11; N, 4.28. Found: C, 37.95; H, 4.22; N, 4.41.

Adenylate Cyclase Activity—Adult male Sprague–Dawley rats[3], 200–250 g, were decapitated, and their brains were removed rapidly and placed in ice-cold saline. Each corpus striatum was dissected in the cold, as described by Glowinski and Iverson (11), and placed in ice-cold pH 7.4 Krebs–Henseleit bicarbonate buffer. A cell-free striatal homogenate was prepared in 25 volumes (w/v) of 2 m*M* tris(hydroxymethyl)aminomethane maleate buffer (pH 7.4) containing 2 m*M* edetic acid (ethylenediaminetetraacetic acid) using a polytef–glass tissue homogenizer[4]. Aliquots (50 μl) of this cell-free homogenate were assayed for adenylate cyclase activity using the procedure of Kebabian *et al.* (12). 3-Isobutyl-1-methylxanthine[5] (1 m*M*) was used to inhibit phosphodiesterase activity. A 25-μl aliquot of each sample was assayed for cyclic AMP content by the method of Gilman (13) as modified by Tovey *et al.* (14).

A wide concentration range (*i.e.*, 10^{-7}–10^{-3} *M*) of dopamine and of each experimental agent was tested for striatal adenylate cyclase activity. Haloperidol[6] was dissolved in propylene glycol–3 *N* HCl. The haloperidol solution was adjusted to pH 7.4 and brought to 50 ml with normal saline. In experiments where haloperidol was employed, an equal volume of the vehicle used to dissolve haloperidol was added to samples without haloperidol.

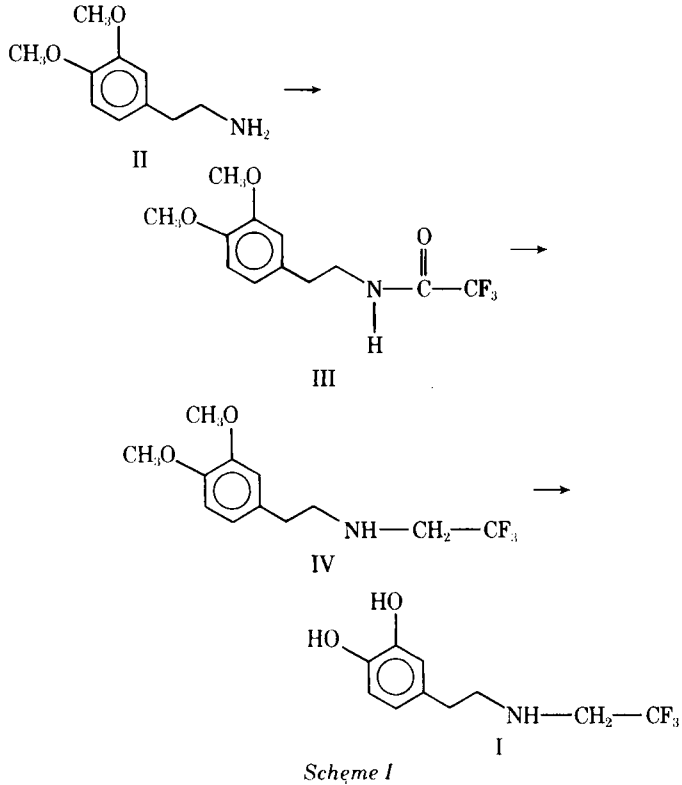

Scheme I

Statistical analysis to determine differences between sample means was performed using the Student *t* test or the Student *t* test for paired sample comparisons (15).

Isolated Rabbit Renal and Ear Arteries—Albino rabbits, 3–4 kg, were killed by air embolism, and the left renal artery and the central ear arteries were removed carefully. Two cylindrical segments (5 mm × 0.5 mm o.d.) were taken from each artery. The cylinders were set up for isometric recording of tension changes in the manner described for cerebral vessels (16, 17). The recording system included a polygraph[7] and force-displacement transducer[8]. A resting tension of 0.5 g was applied to the tissue and readjusted every 15 min during the initial 1-hr equilibration. The organ bath (pH 7.3–7.4) contained 10 ml of Krebs–Henseleit buffer continuously bubbled with 95% O_2–5% CO_2 and maintained at 37°. Edetic acid (30 m*M*) was added to minimize oxidation of dopamine and its analogs. Solutions of dopamine and its analogs were prepared in saline containing 0.01% (w/v) ascorbic acid.

To avoid possible concomitant activation of α- and β-adrenergic receptors by dopamine and the test compounds, the experiments were carried out in tissues pretreated with 29 m*M* phenoxybenzamine for 0.5 hr and in the presence of propranolol (3.4×10^{-7} *M*). Since phenoxybenzamine also has been reported (18) to inhibit neuronal uptake of catecholamines, its use in this study might have the additional advantage of preventing dopamine diversion from the receptor region toward the adrenergic nerve endings.

Active development of tension to 0.99 ± 0.089 g (mean ± *SEM*) was induced with 28–38 m*M* KCl. At the plateau level of the response to potassium chloride, dopamine and its analogs were added in increasing concentrations (*i.e.*, 10^{-7}–10^{-4} *M*) to the tissue segment, while the other segment served as a control to check for a decline of the plateau tension that might have occurred with time. Only one analog was tested in each segment. The plateau tension was stable, and no correction of the changes observed with dopamine was necessary. Dose–response curves for sodium nitrite also were determined in both arteries to assess vascular relaxation independently of the dopaminergic mechanism.

DISCUSSION

N-(2,2,2-Trifluoroethyl)-2-(3,4-dihydroxyphenyl)ethylamine (I) was prepared according to Scheme I. 2-(3,4-Dimethoxyphenyl)ethylamine (II) was reacted with trifluoroacetic anhydride to form the amide III, which was reduced with diborane to give the amide IV. The methyl ethers

[1] Melting points were determined in open glass capillaries using a Thomas-Hoover Uni-Melt apparatus and are uncorrected. IR absorption spectra were recorded on a Beckman model 18A spectrophotometer on liquid films or as potassium bromide pellets. NMR spectra were recorded on a Varian T-60 spectrometer with tetramethylsilane as the internal standard. Elemental analyses were performed by Galbraith Laboratories, Knoxville, Tenn.

[2] Aldrich Chemical Co., Milwaukee, Wis.

[3] ARS-Sprague-Dawley, Madison, Wis.

[4] Kontes, Vineland, N.J.

[5] Sigma Chemical Co., St. Louis, Mo.

[6] McNeil Laboratories, Fort Washington, Pa.

[7] Model 7, Grass, Quincy, Mass.

[8] Model FT03, Grass, Quincy, Mass.

Table I—Relaxant Effects of Dopamine, Dopamine Analogs, and Sodium Nitrite in Rabbit Renal and Ear Arteries

Compound	$ED_{40} \times 10^{-6} M$		Relaxation Ratio, Ear Artery/ Renal Artery	Number of Experiments
	Renal Artery	Ear Artery		
Dopamine hydrochloride	14.3 ± 8.4[a]	395.8 ± 7.8	27.6	5
6,7-Dihydroxy-2-aminotetrahydronaphthalene hydrobromide	10.4 ± 5.8	288.5 ± 4.8	27.7	6
Compound V	25.3 ± 6.2	44.3 ± 6.4	1.7	5
Compound I	76.3 ± 6.1	76.4 ± 5.8	1.0	5
Sodium nitrite	45.5 ± 2.1	89.1 ± 1.6	1.9	4

[a] Values are means ± *SEM*.

of IV were cleaved with hydrobromic acid. *N*-Ethyl-2-(3,4-dihydroxyphenyl)ethylamine (V) was prepared in an analogous procedure and also was evaluated for biological activity as a structural comparison to I.

One problem in characterizing dopaminergic activity in isolated blood vessels is the lack of a specific dopamine antagonist. Recent work (19) demonstrated that typical dopamine antagonists cannot be used to characterize peripheral dopamine activity in isolated vessels. In contrast, the induced vasodilator activity in dogs may be attenuated selectively by butyrophenone and phenothiazine neuroleptic agents (20). An alternative to the lack of vascular specificity and a specific dopamine antagonist is the use of two vascular preparations with different sensitivities to dopamine (19). The ED_{40} values and the ratios of rabbit ear arteries to renal arteries for dopamine and analogs are presented in Table I. The ED_{40} was selected because certain dopamine analogs at doses above the ED_{40} demonstrated contractile effects. A comparison of the relaxation ratio in the very responsive renal artery *versus* the less responsive ear artery for dopamine and the specific renal dopamine agonist, 6,7-dihydroxy-2-aminotetrahydronaphthalene (21), gave a similar ratio for dopamine receptor agonist activity. A nonspecific relaxant, sodium nitrite, has a similar potency on both vessels. Since the effect of I and V was comparable to that of sodium nitrite, these compounds demonstrated no specific activity.

The activity of dopamine-sensitive adenylate cyclase in rat neostriatum is a useful biochemical measure of the effectiveness of agents as agonists or antagonists at central dopamine receptors (3, 22–24). Agents that act as dopamine receptor agonists stimulate striatal adenylate cyclase activity (12). In addition, dopamine receptor antagonists attenuate the stimulating effect of dopamine or other dopamine receptor agonists on striatal adenylate cyclase activity.

Dopamine, I, and V were tested for their ability to enhance adenylate cyclase activity in rat corpus striatum (Table II). Dopamine and V stimulated the adenylate cyclase activity in a dose-dependent fashion. In this regard, both agents were similar in potency. Compound I induced only a weak stimulating effect on adenylate cyclase at $1 \times 10^{-4} M$.

To determine the specificity of dopamine and V on adenylate cyclase activity, both agents were tested in the presence of haloperidol, a dopamine receptor antagonist (12, 25, 26). Haloperidol ($10^{-4} M$) did not alter the control level of adenylate cyclase activity (Fig. 1). However, haloperidol completely attenuated the stimulating action of dopamine and *N*-ethyldopamine on striatal adenylate cyclase. Although not shown here, the weak stimulation of adenylate cyclase activity by I ($10^{-4} M$) was attenuated completely by haloperidol ($10^{-4} M$).

Table II—Adenylate Cyclase Activity in Striatal Homogenates [a]

Agent	Concentration, μM	Cyclic AMP[b], pmoles above control	Percent of Control
Dopamine	10	3.6 ± 2.4	105
	100	28.8 ± 3.9[c]	138
	1000	33.8 ± 6.3[c]	144
Compound V	10	13.0 ± 5.4[c]	117
	100	23.3 ± 4.5[c]	131
	1000	27.6 ± 4.3[c]	137
Compound I	10	7.4 ± 4.8	108
	100	11.7 ± 3.0[c]	113
	1000	−0.8 ± 3.4	99

[a] Cell-free homogenates of rat corpus striatum were assayed for adenylate cyclase activity by measuring the conversion of ATP (0.5 m*M*) to cyclic AMP. [b] Mean ± *SEM* of six to eight experiments. Controls for each agent were as follows: dopamine, 76.7 ± 5.2 pmoles/mg/2.5 min; V, 75.3 ± 8.1 pmoles/mg/2.5 min; and I, 89.7 ± 5.1 pmoles/mg/2.5 min. [c] $p < 0.05$ as compared to control.

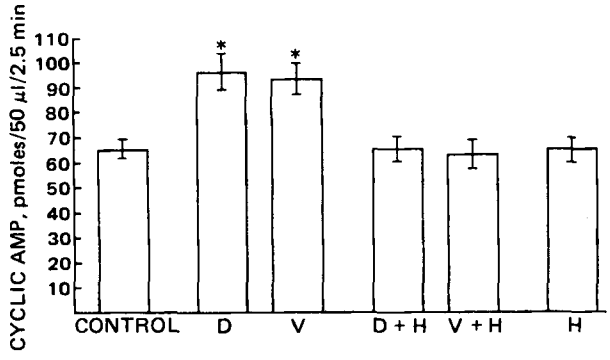

Figure 1—*Effect of haloperidol (H) (10^{-4} M) on the dopamine (D) and Compound V stimulation of adenylate cyclase in striatal homogenates. Cell-free homogenates of rat corpus striata were assayed for adenylate cyclase activity. Each value for cyclic AMP represents the mean* ± SEM *of five experiments. A concentration of 1×10^{-4} M dopamine or V was used to stimulate adenylate cyclase activity (* = $p < 0.05$ with respect to control).*

These results show that even if I would demonstrate improved absorption and distribution characteristics, it cannot stimulate adenylate cyclase. However, V stimulated adenylate cyclase but to a lesser degree than dopamine. These findings were unexpected due to the close structural similarity of I to V. An explanation for the lack of dopaminergic activity may be attempted by comparing the ionization ratios of the amine groups. The amine groups of dopamine (10) and V have pKa values of 9.74 and 10.61, respectively. Compound I has a pKa value of 5.10. Thus, altering the alkyl substitution by replacement of the protons with the electronegative fluorine atoms changes the ratio at physiological pH from the zwitterion to predominantly the uncharged species, in contrast to dopamine and V at physiological pH, at which the predominant species is the phenolic ammonium salt.

It was proposed recently (10) that the active species at dopamine receptors may be the neutral uncharged form of dopamine. The limited data of this study suggest that the activity of dopaminergic agonists may depend on the ability of the dopamine ligand to undergo readily an equilibrium transformation on the receptor between the zwitterion and the uncharged species.

REFERENCES

(1) A. N. Lieberman, A. L. Goodgold, and M. Goldstein, *Neurology*, **22**, 1205 (1972).

(2) O. Hornykiewicz, *Fed.Proc.*, **32**, 183 (1973).

(3) J. Ginos, G. C. Cotzias, E. Tolosa, L. C. Tang, and A. LoMonte, *J. Med. Chem.*, **18**, 1194 (1975).

(4) J. G. Cannon, F. L. Hsu, J. P. Long, J. R. Flynn, B. Costall, and R. J. Naylor, *ibid.*, **21**, 248 (1978).

(5) R. Miller, A. Horn, L. Iverson, and R. Pinder, *Nature*, **250**, 238 (1974).

(6) L. I. Goldberg, P. F. Sonneville, and J. L. McNay, *J. Pharmacol. Exp. Ther.*, **163**, 188 (1968).

(7) J. G. Cannon, J. P. O'Donnell, T. Lee, C. R. Hoppin, J. P. Long, M. I. Ilhan, B. Costall, and R. J. Naylor, *J. Med. Chem.*, **18**, 1212 (1975).

(8) J. Z. Ginos and F. C. Brown, *ibid.*, **21**, 155 (1978).

(9) J. Z. Ginos, G. C. Cotzias, and D. Doroski, *ibid.*, **21**, 160 (1978).
(10) J. L. Armstrong and R. B. Barlow, *Br. J. Pharmacol.*, **57**, 501 (1976).
(11) J. Glowinski and L. L. Iverson, *J. Neurochem.*, **13**, 655 (1966).
(12) J. W. Kebabian, G. L. Petzold, and P. Greengard, *Proc. Natl. Acad. Sci. USA*, **69**, 2145 (1972).
(13) A. Gilman, *ibid.*, **67**, 305 (1970).
(14) K. C. Tovey, K. G. Oldham, and J. A. Whelan, *Clin. Chim. Acta*, **56**, 221 (1974).
(15) R. R. Sokal and F. J. Rohlf, "Introduction to Biostatistics," W. H. Freeman, San Francisco, Calif., 1973.
(16) K. C. Nielsen and C. Owman, *Brain Res.*, **27**, 33 (1971).
(17) P. R. Urquilla, E. J. Marco, and S. Luch, *Blood Vessels*, **12**, 53 (1975).
(18) R. F. Furchgott, in "Handbuch der Experimentelles Pharmackologie," vol. 33, H. Blaschko and E. Muschall, Eds., Springer, Berlin, Germany, 1972, p. 283.
(19) L. I. Goldberg and N. Toda, *Circ. Res.* **36**, I-97 (1975).
(20) L. I. Goldberg and B. K. Yeh, *Eur. J. Pharmacol.*, **15**, 36 (1971).
(21) L. I. Goldberg, P. H. Volkman, and J. D. Kohli, *Ann. Rev. Pharmacol. Toxicol.*, **18**, 57 (1978).
(22) R. J. Miller and L. Iverson, *Naunyn-Schmiedebergs Arch. Pharmacol.*, **282**, 213 (1974).
(23) R. J. Miller, A. S. Horn, and L. Iverson, *Mol. Pharmacol.*, **10**, 759 (1974).
(24) R. J. Baldessarini, R. H. Walton, and R. J. Borgman, *Neuropharmacology*, **14**, 725 (1975).
(25) A. Carlsson and M. Lindqvist, *Acta Pharmacol. Toxicol.*, **20**, 140 (1963).
(26) N. E. Anden, H. Corrodi, K. Fuxe, and U. Ungerstedt, *Eur. J. Clin. Pharmacol.*, **15**, 193 (1971).

High-Performance Liquid Chromatographic Analysis of Codeine in Syrups Using Ion-Pair Formation

E. J. KUBIAK and J. W. MUNSON ˣ

Received July 25, 1979, from *Quality Control, The Upjohn Company, Kalamazoo, MI 49001.* Accepted for publication September 13, 1979.

Abstract □ The chromatographic behavior of morphine, codeine, and ethylmorphine was examined using reversed-phase high-performance liquid chromatography and ion-pair formation. Alkyl sulfonates and sulfates significantly increased the retention times for these compounds. The carbon chain length of the pairing ions was linearly related to the log of the capacity factors of these amine drugs. A mechanism for the increased retention based on ion-pair formation in the mobile phase is proposed. The use of dioctyl sodium sulfosuccinate as a pairing ion for codeine is described, and a method utilizing this pairing ion was developed for the quantitation of codeine in syrups. This method was applied successfully to various syrups containing codeine or codeine phosphate.

Keyphrases □ Codeine—analysis, high-performance liquid chromatography, ion-pair formation, effect of carbon chain length of pairing ions, syrups □ Ethylmorphine—analysis, high-performance liquid chromatography, ion-pair formation, effect of carbon chain length of pairing ions □ Morphine—analysis, high-performance liquid chromatography, ion-pair formation, effect of carbon chain length of pairing ions □ High-performance liquid chromatography, ion-pair formation—analysis of codeine, ethylmorphine, and morphine, effect of carbon chain length of pairing ion

The use of ion-pair formation to enhance retention time is becoming popular in reversed-phase high-performance liquid chromatography (HPLC). The counterions used to form ion-pairs generally are detergents such as alkyl sulfates and sulfonates or tetraalkylammonium salts. Anionic surfactants (sulfates and sulfonates) generally are used to form ion-pairs with cationic eluates, and cationic tetraalkylammonium salts are used with anionic eluates. By formation of the ion-pair, the apparent polarity of the eluate is decreased, leading to increased retention times in reversed-phase HPLC.

Since many drugs contain either acidic or basic functional groups, pH conditions can be chosen such that numerous drugs will form ion-pairs with these surfactants. The surfactant molecule often is referred to as the pairing ion, which gives rise to the term ion-pair HPLC. While ion-pair formation can be used in normal-phase HPLC, it is used more widely in reversed-phase HPLC. This technique also has been called soap chromatography (1, 2) because of the surfactants used.

BACKGROUND

The mechanism of retention enhancement has been attributed to two phenomena. The original concept closely follows classical ion-pair extraction techniques in which two oppositely charged molecules form an ion-pair in an aqueous solution and then partition as a complex into a nonpolar organic solvent. In the chromatographic analog of this concept, the analyte forms a complex with a pairing ion added to the mobile phase. The complex then partitions into the stationary phase (nonpolar), thus accounting for the increased analyte retention. An alternative mechanism suggests that the pairing ion first binds to the stationary phase to form an ion-exchanging surface due to the adsorbed charged pairing ions (3). Complex formation at the surface of the stationary phase thus is responsible for the increased analyte retention. Recently, application of solvophobic theory to a reversed-phase ion-pair chromatographic study led to the conclusion that the retention of the analyte involves ion-pair formation in the mobile phase and subsequent partitioning of the neutral complex to the stationary phase (4).

Codeine analysis by HPLC has been of interest. An early study (5) utilized columns of pellicular silica gel coated with polyethylene glycol 300 with an ethanol–heptane (1:10) mobile phase saturated with the stationary phase. In this system, codeine was well resolved from morphine, thebaine, and papaverine. However, quantitative codeine analysis at levels near 3 μg gave a relative error of ~9%. In a study of the liquid chromatographic behavior of alkaloids, the retention times of codeine and morphine on a microparticulate silica column were measured (6). Codeine eluted slightly before morphine with mobile phases of chloroform–methanol (three volume ratios) and ether–methanol (three volume ratios).

The quantification of morphine, codeine, and thebaine was accomplished by isocratic reversed-phase HPLC (7). With a microparticulate (10-μm) octadecylsilane column and a mobile phase of 0.1 *N* monobasic sodium phosphate in 25% acetonitrile–water, codeine in gum opium was measured with a relative standard deviation of 1.3%. Codeine also was separated from other opium alkaloids using a pellicular silica column and

0022-3549/80/0200-0152$01.00/0
© 1980, American Pharmaceutical Association

(9) J. Z. Ginos, G. C. Cotzias, and D. Doroski, *ibid.*, **21**, 160 (1978).
(10) J. L. Armstrong and R. B. Barlow, *Br. J. Pharmacol.*, **57**, 501 (1976).
(11) J. Glowinski and L. L. Iverson, *J. Neurochem.*, **13**, 655 (1966).
(12) J. W. Kebabian, G. L. Petzold, and P. Greengard, *Proc. Natl. Acad. Sci. USA*, **69**, 2145 (1972).
(13) A. Gilman, *ibid.*, **67**, 305 (1970).
(14) K. C. Tovey, K. G. Oldham, and J. A. Whelan, *Clin. Chim. Acta*, **56**, 221 (1974).
(15) R. R. Sokal and F. J. Rohlf, "Introduction to Biostatistics," W. H. Freeman, San Francisco, Calif., 1973.
(16) K. C. Nielsen and C. Owman, *Brain Res.*, **27**, 33 (1971).
(17) P. R. Urquilla, E. J. Marco, and S. Luch, *Blood Vessels*, **12**, 53 (1975).
(18) R. F. Furchgott, in "Handbuch der Experimentelles Pharmackologie," vol. 33, H. Blaschko and E. Muschall, Eds., Springer, Berlin, Germany, 1972, p. 283.
(19) L. I. Goldberg and N. Toda, *Circ. Res.* **36**, I-97 (1975).
(20) L. I. Goldberg and B. K. Yeh, *Eur. J. Pharmacol.*, **15**, 36 (1971).
(21) L. I. Goldberg, P. H. Volkman, and J. D. Kohli, *Ann. Rev. Pharmacol. Toxicol.*, **18**, 57 (1978).
(22) R. J. Miller and L. Iverson, *Naunyn-Schmiedebergs Arch. Pharmacol.*, **282**, 213 (1974).
(23) R. J. Miller, A. S. Horn, and L. Iverson, *Mol. Pharmacol.*, **10**, 759 (1974).
(24) R. J. Baldessarini, R. H. Walton, and R. J. Borgman, *Neuropharmacology*, **14**, 725 (1975).
(25) A. Carlsson and M. Lindqvist, *Acta Pharmacol. Toxicol.*, **20**, 140 (1963).
(26) N. E. Anden, H. Corrodi, K. Fuxe, and U. Ungerstedt, *Eur. J. Clin. Pharmacol.*, **15**, 193 (1971).

High-Performance Liquid Chromatographic Analysis of Codeine in Syrups Using Ion-Pair Formation

E. J. KUBIAK and J. W. MUNSON ˣ

Received July 25, 1979, from *Quality Control, The Upjohn Company, Kalamazoo, MI 49001.* Accepted for publication September 13, 1979.

Abstract □ The chromatographic behavior of morphine, codeine, and ethylmorphine was examined using reversed-phase high-performance liquid chromatography and ion-pair formation. Alkyl sulfonates and sulfates significantly increased the retention times for these compounds. The carbon chain length of the pairing ions was linearly related to the log of the capacity factors of these amine drugs. A mechanism for the increased retention based on ion-pair formation in the mobile phase is proposed. The use of dioctyl sodium sulfosuccinate as a pairing ion for codeine is described, and a method utilizing this pairing ion was developed for the quantitation of codeine in syrups. This method was applied successfully to various syrups containing codeine or codeine phosphate.

Keyphrases □ Codeine—analysis, high-performance liquid chromatography, ion-pair formation, effect of carbon chain length of pairing ions, syrups □ Ethylmorphine—analysis, high-performance liquid chromatography, ion-pair formation, effect of carbon chain length of pairing ions □ Morphine—analysis, high-performance liquid chromatography, ion-pair formation, effect of carbon chain length of pairing ions □ High-performance liquid chromatography, ion-pair formation—analysis of codeine, ethylmorphine, and morphine, effect of carbon chain length of pairing ion

The use of ion-pair formation to enhance retention time is becoming popular in reversed-phase high-performance liquid chromatography (HPLC). The counterions used to form ion-pairs generally are detergents such as alkyl sulfates and sulfonates or tetraalkylammonium salts. Anionic surfactants (sulfates and sulfonates) generally are used to form ion-pairs with cationic eluates, and cationic tetraalkylammonium salts are used with anionic eluates. By formation of the ion-pair, the apparent polarity of the eluate is decreased, leading to increased retention times in reversed-phase HPLC.

Since many drugs contain either acidic or basic functional groups, pH conditions can be chosen such that numerous drugs will form ion-pairs with these surfactants. The surfactant molecule often is referred to as the pairing ion, which gives rise to the term ion-pair HPLC. While ion-pair formation can be used in normal-phase HPLC, it is used more widely in reversed-phase HPLC. This technique also has been called soap chromatography (1, 2) because of the surfactants used.

BACKGROUND

The mechanism of retention enhancement has been attributed to two phenomena. The original concept closely follows classical ion-pair extraction techniques in which two oppositely charged molecules form an ion-pair in an aqueous solution and then partition as a complex into a nonpolar organic solvent. In the chromatographic analog of this concept, the analyte forms a complex with a pairing ion added to the mobile phase. The complex then partitions into the stationary phase (nonpolar), thus accounting for the increased analyte retention. An alternative mechanism suggests that the pairing ion first binds to the stationary phase to form an ion-exchanging surface due to the adsorbed charged pairing ions (3). Complex formation at the surface of the stationary phase thus is responsible for the increased analyte retention. Recently, application of solvophobic theory to a reversed-phase ion-pair chromatographic study led to the conclusion that the retention of the analyte involves ion-pair formation in the mobile phase and subsequent partitioning of the neutral complex to the stationary phase (4).

Codeine analysis by HPLC has been of interest. An early study (5) utilized columns of pellicular silica gel coated with polyethylene glycol 300 with an ethanol–heptane (1:10) mobile phase saturated with the stationary phase. In this system, codeine was well resolved from morphine, thebaine, and papaverine. However, quantitative codeine analysis at levels near 3 μg gave a relative error of ~9%. In a study of the liquid chromatographic behavior of alkaloids, the retention times of codeine and morphine on a microparticulate silica column were measured (6). Codeine eluted slightly before morphine with mobile phases of chloroform–methanol (three volume ratios) and ether–methanol (three volume ratios).

The quantification of morphine, codeine, and thebaine was accomplished by isocratic reversed-phase HPLC (7). With a microparticulate (10-μm) octadecylsilane column and a mobile phase of 0.1 *N* monobasic sodium phosphate in 25% acetonitrile–water, codeine in gum opium was measured with a relative standard deviation of 1.3%. Codeine also was separated from other opium alkaloids using a pellicular silica column and

0022-3549/80/0200-0152$01.00/0
© 1980, American Pharmaceutical Association

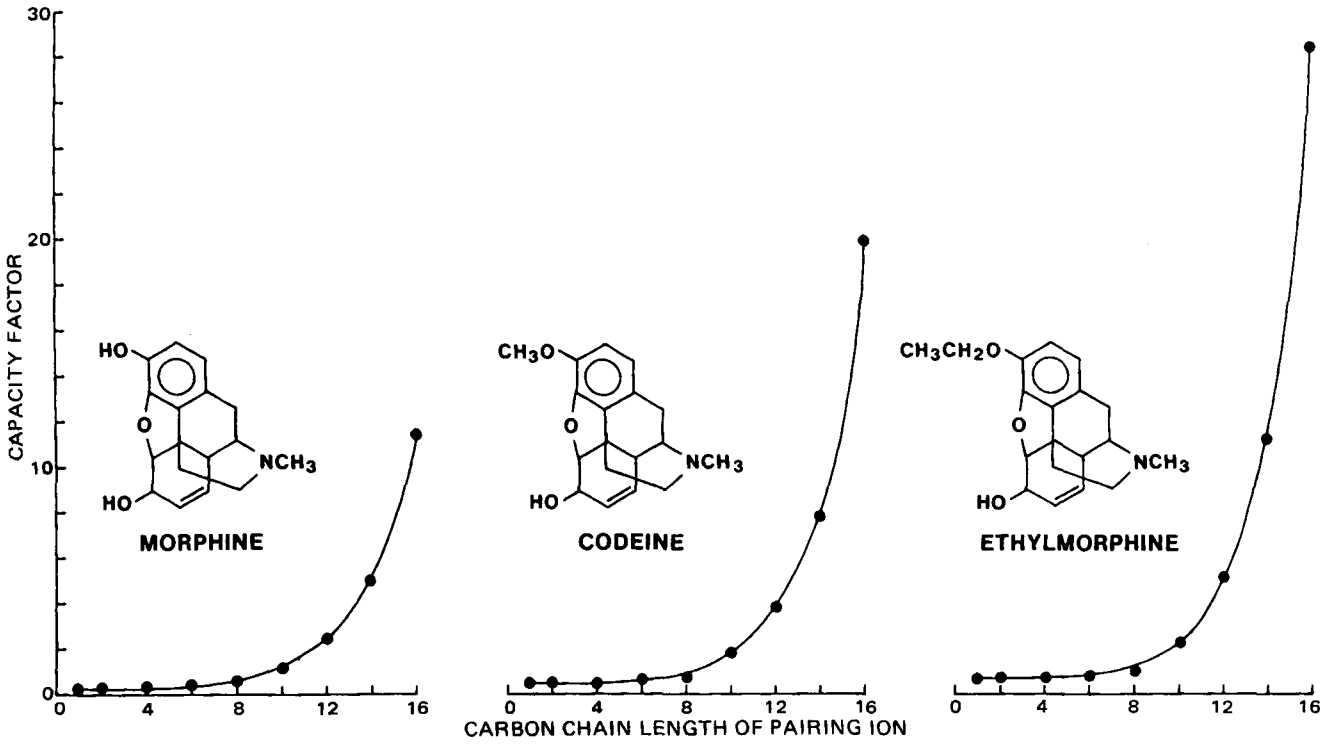

Figure 1—*Capacity factors of morphine, codeine, and ethylmorphine as a function of the carbon chain length of the alkylsulfonate and sulfate pairing ions using a microparticulate octadecylsilane column (10 μm).*

gradient elution with hexane and chloroform–methanol–diethylamine (400:300:1) (8). This methodology was applied to the analysis of morphine, cryptopine, thebaine, papaverine, codeine, and noscapine in opium (9).

The liquid chromatographic behavior of opium alkaloids using ion-pairing reagents in the mobile phase has been studied. With a microparticulate (10-μm) octadecylsilane column and a mobile phase of 0.005 *M* *n*-heptanesulfonic acid in methanol–water (40:60), several morphinan derivatives were separated (10). In this system, morphine eluted before codeine. Mixtures of morphine, codeine, thebaine, noscapine, and papaverine were separated with a similar chromatographic system (11). Codeine also was analyzed in liquid dosage forms with an octadecylsilane (10-μm) column and a water–methanol (87:13) mobile phase containing 0.05 *M* dibasic potassium phosphate (12). With this system, codeine was analyzed in the presence of guaifenesin, pheniramine maleate, phenylpropanolamine hydrochloride, and pyrilamine maleate.

This paper describes the effects of the carbon chain length of the pairing ion on the capacity factors for codeine, morphine, and ethylmorphine. Mechanisms are proposed to account for the retention of these compounds in reversed-phase ion-pair HPLC. The properties of dioctyl sodium sulfosuccinate as a pairing ion for codeine are described. An HPLC method for codeine syrups that requires minimum sample treatment is presented.

EXPERIMENTAL

Materials—Methanesulfonic acid[1], ethanesulfonic acid[1], sodium butanesulfonate[1], sodium hexanesulfonate[1], sodium hexanesulfate[1], sodium octanesulfonate[1], sodium decylsulfate[1], sodium dodecylsulfate[1], sodium tetradecylsulfonate[2], sodium tetradecylsulfate[1], sodium hexadecylsulfate[1], dioctyl sodium sulfosuccinate[3], codeine *N*-oxide[4], morphine hydrochloride[5], codeine phosphate[5], and ethylmorphine hydrochloride[5] were used as received.

Distilled-in-glass acetonitrile[6] and deionized water were used for all mobile phase preparations. The internal standard, diphenylamine, also was used as received. All other chemicals were reagent grade. Codeine syrups were obtained from a local drug wholesale distributor.

Apparatus—The modular high-performance liquid chromatograph consisted of a reciprocating piston pump equipped with a pulse dampener[7], an automated loop injector[8], a UV detector[9] (254 nm), and a recorder[10]. For quantitative measurements, data were collected and processed by a digital computer[11].

Mobile Phase—All mobile phases contained 0.005 *M* pairing ion and 0.01 *M* ammonium nitrate in acetonitrile–water (375:625). After mixing, the mobile phases were adjusted to pH 3.3 with acetic acid and filtered through a 5-μm filter. (Considerable foaming was observed with most mobile phases upon filtration.)

Columns—A microparticulate octadecylsilane column[12] (10 μm, 30 cm × 4 mm) and a microparticulate octasilane column[13] (10 μm, 25 cm × 4.6 mm) were obtained commercially. When not in use, these columns were flushed with acetonitrile–water (80:20) and stored in the same solvent. Flow rates of 2–3 ml/min gave adequate resolution with reasonable analysis time.

Quantitation of Codeine in Syrups—*Internal Standard Method*—Exactly 5.0 ml of the syrup was transferred quantitatively to a 125-ml erlenmeyer flask containing 40.0 ml of the internal standard solution (diphenylamine, 0.05 mg/ml in the mobile phase). After thorough mixing, 25-μl aliquots were chromatographed with a detector setting of 0.032 aufs. Concentrations were determined by comparison of the peak height ratios from sample preparations to those from a standard preparation (USP codeine phosphate reference standard).

External Standard Method—Exactly 5.0 ml of the syrup was added to 40.0 ml of the mobile phase and chromatographed in the same manner as the internal standard method. Concentrations were calculated by comparison of the peak heights of the codeine peaks.

RESULTS AND DISCUSSION

In preliminary studies, nitrate ions (as ammonium or sodium salts) significantly improved the peak shape and reduced tailing. This effect possibly was due to occupation of uncoated sites on the solid support

[1] Eastman Kodak Co., Rochester, NY 14650.
[2] Research Plus Laboratories, Denville, NJ 07834.
[3] Aldrich Chemical Co., Milwaukee, WI 53233.
[4] Courtesy of Dr. Arthur Jacobson, National Institute of Arthritis, Metabolism, and Digestive Disease.
[5] The Upjohn Co.
[6] Burdick & Jackson Laboratories, Muskegon, MI 49442.
[7] Model 110, Altex Corp., Berkeley, CA 94710.
[8] Upjohn LC Autosampler.
[9] UV III, Laboratory Data Control, Riviera Beach, Fla.
[10] Model XKR, Sargent Welch Co., Skokie, IL 60076.
[11] PDP 11, Digital Equipment Co., Maynard, MA 01754.
[12] μBondapak C_{18}, Waters Associates, Milford, MA 01757.
[13] RP-10A, Brownlee Laboratories, Santa Clara, CA 95050.

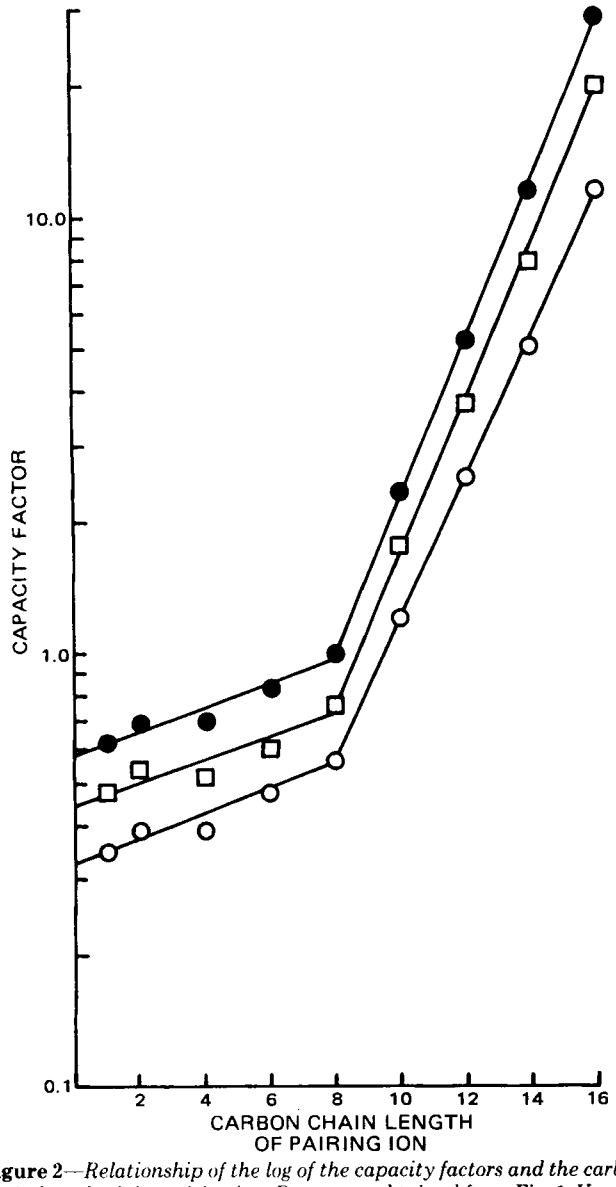

Figure 2—*Relationship of the log of the capacity factors and the carbon chain length of the pairing ion. Data were obtained from Fig. 1. Key:* ○, *morphine;* □, *codeine; and* ●, *ethylmorphine.*

material by the nitrate ions. Consequently, all mobile phase solutions contained 0.01 *M* ammonium nitrate. The mobile phase pH was adjusted to 3.3 to ensure that the amines would be protonated.

The effects of the carbon chain length of the pairing ion on the capacity factors of morphine, codeine, and ethylmorphine are shown in Fig. 1. Relatively minor effects were observed as the chain length was increased to eight carbons (octanesulfonate). Above this point, the capacity factors increased dramatically as the chain length was increased. The elution order for all systems was morphine, codeine, and ethylmorphine. This order is consistent with the polarity of the substitution on the aromatic ring (hydroxy, methoxy, and ethoxy, respectively). The shape of this curve suggests that the capacity factors are related logarithmically to the number of carbons in the pairing ions.

A plot of the log of the capacity factors of morphine, codeine, and ethylmorphine *versus* the carbon chain length of the pairing ion is shown in Fig. 2 (octadecylsilane column). A similar plot is shown in Fig. 3 for the octasilane column. The slopes of both plots are similar. The distinct break between the two linear portions of the curve suggests that two mechanisms may be operative in analyte retention.

Two distinct ion-pair mechanisms can be postulated to explain the behavior shown in Figs. 2 and 3. The first mechanism involves ion-pair formation in the mobile phase with subsequent partitioning into the stationary phase. This process is outlined in Scheme I, where D^+ is the protonated form of the amine drug, A^- is the anionic form of the pairing ion, and DA is the charge neutralized ion-pair:

$$D^+_M + A^-_M \rightleftharpoons DA_M$$

$$DA_M \rightleftharpoons DA_S$$

Scheme I

The subscripts *M* and *S* refer to the species in the mobile phase and the stationary phase, respectively.

The second mechanism, dynamic ion exchange, involves adsorption of the pairing ion onto the stationary phase surface followed by ion-pair formation at the interface (Scheme II):

$$A^-_M \rightleftharpoons A^-_S$$

$$A^-_S + D^+_M \rightleftharpoons DA_S$$

Scheme II

If the first mechanism is operative, one would expect the capacity factor to increase as the pairing-ion size increases. The increased chain length of the pairing ion should cause an increase in the hydrophobicity of the complex, thus favoring partitioning into the stationary phase. The portions of the curves in Figs. 2 and 3 that lie above a chain length of eight carbons show this behavior. This portion of the curve shows that each two additional methylene groups in the pairing ion increase the capacity by a factor of 2.2 (for the octadecylsilane column). This increase is in good agreement with the predicted value of 2.5 obtained from consideration of enhancement factors in a study of chromatographic retention of catecholamines paired with alkyl sulfates (4). In the same study, solvophobic theory was employed to deduce that ion-pair formation in the mobile phase was the primary mechanism for analyte retention.

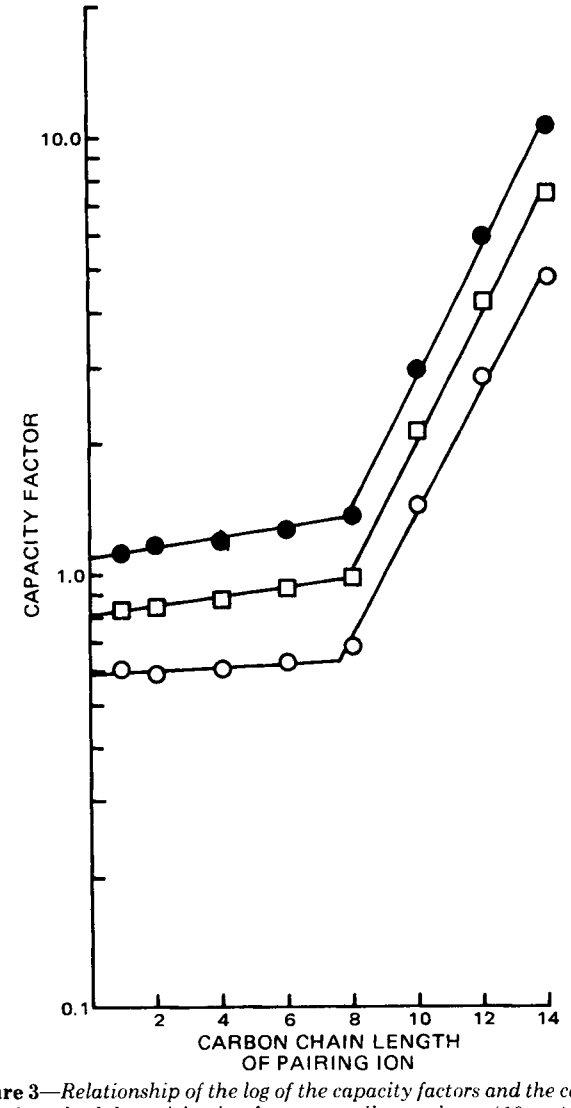

Figure 3—*Relationship of the log of the capacity factors and the carbon chain length of the pairing ion for an octasilane column (10 μm). Key:* ○, *morphine;* □, *codeine; and* ●, *ethylmorphine.*

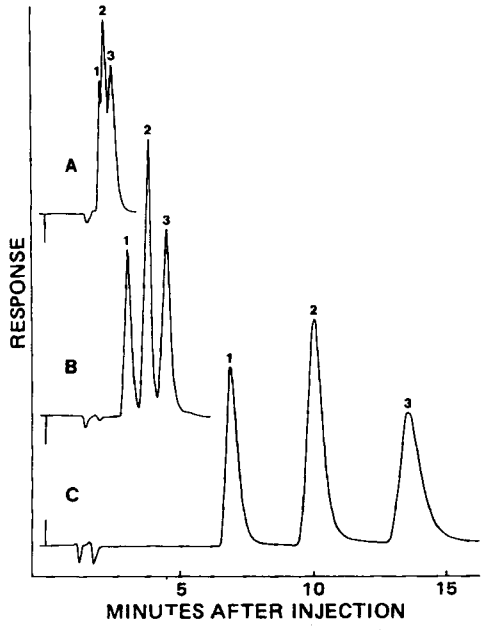

Figure 4—*Chromatograms of a mixture of morphine (1), codeine (2), and ethylmorphine (3) using various pairing ions. Key: A, sodium hexanesulfonate; B, sodium decylsulfate; and C, sodium tetradecylsulfate (octadecylsilane column).*

The retention mechanism when the ion-pairing reagent contains eight carbons or less is not straightforward. Since the shorter chain pairing ions were sulfonates and the longer chain pairing ions were sulfates, the possibility of sulfonates behaving differently from sulfates was considered. However, capacity factors measured with sodium hexanesulfonate and sodium hexanesulfate were the same (within experimental error); they also were the same for sodium tetradecylsulfonate and sodium tetradecylsulfate.

One is tempted to attribute this behavior to an ion-exchange mechanism, but the similarity of the curves in Figs. 2 and 3 weigh against it. If pairing-ion adsorption is significant, a difference in behavior when the chain length of the alkyl portion of the stationary phase is changed from eight to 18 would be expected. The plots presented in Figs. 2 and 3 are too similar to suggest that this mechanism is important. The behavior of the short chain pairing ions may be due to the ion-pair complex formed. Since there appears to be little increase in complex hydrophobicity with an increasing chain length up to eight, a mechanism is proposed to account for this behavior.

Examination of molecular models of codeine and octanesulfonate suggests that these molecules could form an ion-pair complex in which the hydrocarbon chain of the pairing ion aligns along the carbon backbone of the codeine molecule (ionic moieties of each molecule are juxtaposed), with essentially no portion of the carbon chain protruding beyond the codeine molecule. This type of complex formation would minimize the hydrophobic interactions of each molecule with the primarily aqueous solvent. For short carbon chains (eight or less), the ion-pair apparently is not appreciably less polar than the ion-pair formed from methanesulfonate and the protonated amine. In other words, the polarity is controlled primarily by the amine molecule. Consequently, little change in the capacity factor (Figs. 2 and 3) is observed with short pairing ions. On the other hand, pairing ions that contain more than eight carbon atoms would form ion-pairs in which the alkyl chain of the pairing ion would protrude beyond the codeine molecule. This protrusion results in greater complex hydrophobicity and hence greater retention. While these arguments can explain qualitatively the observed behavior, they do not rule out the possibility of dynamic ion exchange.

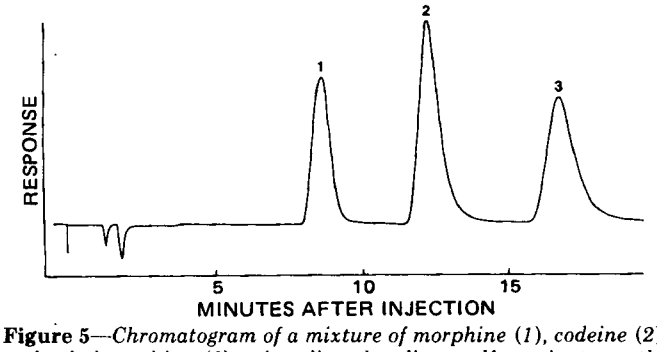

Figure 5—*Chromatogram of a mixture of morphine (1), codeine (2), and ethylmorphine (3) using dioctyl sodium sulfosuccinate as the pairing ion.*

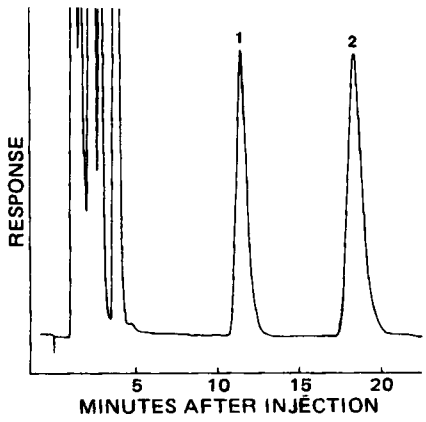

Figure 6—*Chromatogram of a codeine syrup using dioctyl sodium sulfosuccinate as the pairing ion. Peak 1 is codeine and peak 2 is diphenylamine, the internal standard (0.032 aufs).*

Data obtained in a study of the ion-pairing behavior of 4-methyl-1-tetradecylpyridinium chloride (I) lend support to the arguments presented here[14]. In this study, the capacity factor was measured as a function of the carbon chain length of the pairing ion (octadecylsilane column). Alkyl sulfates and sulfonates ranging from butanesulfonate to octadecylsulfate were used as pairing ions. No significant increase in capacity factor was observed until the alkyl chain length exceeded 12 carbons. These data are consistent with the concept of complex formation with association of the alkyl portions of both molecules of the ion-pair.

The effect of pairing ion chain length on compound resolution is shown in Fig. 4. Hexanesulfonate did not adequately resolve morphine, codeine, and ethylmorphine under these conditions, while decylsulfate and tetradecylsulfate gave resolutions adequate for peak height and peak area measurements, respectively. Furthermore, increasing the chain length increased the retention time to such an extent that nonionic species would have eluted well ahead of the amines. This latter aspect is important when direct injections of diluted syrups are contemplated.

In early studies, problems with pairing-ion solubilization were encountered with tetradecyl- and hexadecylsulfates. To circumvent this problem, dioctyl sodium sulfosuccinate (II) was investigated as a possible pairing ion for codeine. This molecule has the requisite solubility and a sufficiently long alkyl chain to produce adequate retention for codeine. Furthermore, this compound is readily available at low cost. The chromatogram for a morphine, codeine, and ethylmorphine mixture using II as the pairing ion is shown in Fig. 5. Under these conditions, II produced capacity factors similar to those produced by tetradecylsulfate. Also, II solubilization in the mobile phase was accomplished easily with stirring. Consequently, all assay development for codeine syrups was carried out using II as the pairing ion.

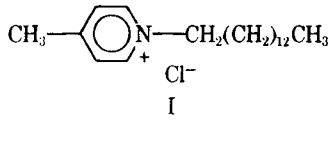

I

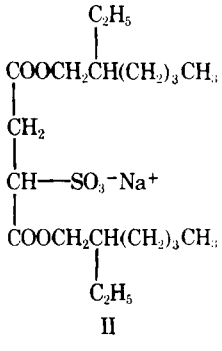

II

[14] Unpublished data.

Table I—Replicate Analyses [a] of Codeine Phosphate in a Single Syrup Lot

Day	Milligrams per 5 ml							
1	9.89,	9.96,	10.00,	10.00,	9.92,	9.97,	9.96,	9.89
2	10.12,	10.06,	10.08,	10.12,	10.07,	10.13		

[a] Internal standard method.

Table II—Analyses of Codeine Syrups (Milligrams per 5 ml)

Sample	Trial 1	Trial 2
A[a]	9.69[b]	9.66
B[c]	9.96[d]	9.99
C[e]	10.02	9.92
D[f]	10.21	10.05
E[g]	10.10	9.97

[a] Syrup contained 85 mg of terpin hydrate/5 ml and 10 mg of codeine/5 ml. [b] Expressed as free base. [c] Syrup contained (in 5 ml) 12.5 mg of phenylpropanolamine hydrochloride, 6.25 mg of pheniramine maleate, 6.25 mg of pyrilamine maleate, 100 mg of guaifenesin, and 10 mg of codeine phosphate. [d] Expressed as phosphate salt. [e] Syrup contained 100 mg of guaifenesin/5 ml and 10 mg of codeine phosphate/5 ml. [f] Syrup contained (in 5 ml) 5 mg of promethazine, 44 mg of potassium guaiacolsulfonate, and 10 mg of codeine phosphate. [g] Syrup contained (in 5 ml) 2 mg of brompheniramine maleate, 5 mg of phenylephrine hydrochloride, 5 mg of phenylpropanolamine hydrochloride, 100 mg of guaifenesin, and 10 mg of codeine phosphate.

Figure 6 shows a typical chromatogram of a 5.0-ml syrup sample (10.0 mg of codeine phosphate and 100 mg of guaifenesin/5 ml) diluted with 40.0 ml of the internal standard solution (diphenylamine, 0.05 mg/ml in the mobile phase). Excellent separation was obtained, with all syrup excipients (and guaifenesin) eluting at or near the solvent front. Codeine phosphate recovery from spiked placebo syrups averaged 100.5% with a relative standard deviation of 0.5% (n = 13) over 2.2–16.4 mg/5 ml (internal standard method). Replicate analyses of one lot of codeine syrup gave an average value of 9.95 mg/5 ml (theory is 10.0 mg/5 ml) with a relative standard deviation of 0.4% (n = 8). Analysis of the same lot on a different day gave an average of 10.10 mg/5 ml with a relative standard deviation of 0.3% (n = 6). The overall average of these data is 10.0 mg/5 ml with a relative standard deviation of 0.8% (n = 14) (Table I).

Five samples of syrups containing codeine or codeine phosphate were obtained through commercial sources and analyzed by the external standard method (Table II). Excellent agreement with the labeled codeine content was obtained. Even though some products contained other

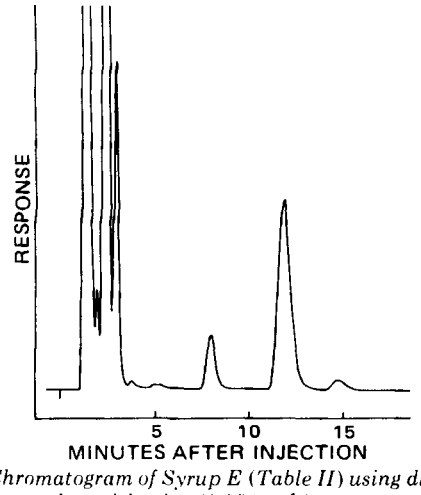

Figure 7—*Chromatogram of Syrup E (Table II) using dioctyl sodium sulfosuccinate as the pairing ion (0.064 aufs).*

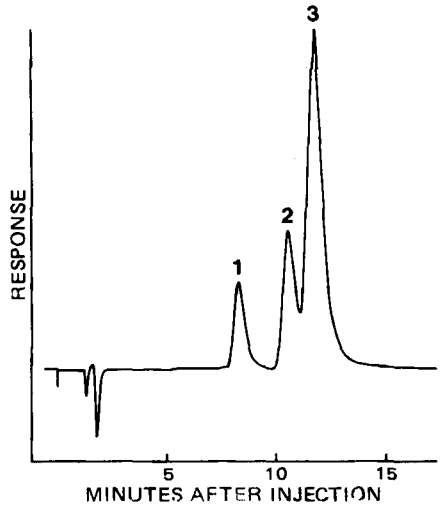

Figure 8—*Chromatogram of a mixture of morphine (1), codeine N-oxide (2), and codeine (3) using conditions used for the codeine assay.*

amine drugs, adequate resolution was obtained in all cases without modification of the mobile phase. The chromatographic tracing of the most complex mixture is shown in Fig. 7 (Product E).

The separation of codeine from its synthetic precursor, morphine, and a possible oxidation product, codeine N-oxide, is shown in Fig. 8. Even though the N-oxide was not completely resolved from codeine, it did not interfere when peak height measurements were used. No extraneous peaks were observed in any samples analyzed by this method, even though some samples were >1 year old.

The method described here is precise and accurate. Since the codeine elutes well after the solvent front, simple dilution of the syrups was the only sample preparation necessary. Total sample preparation and chromatographic analysis time is <20 min/sample. Dioctyl sodium sulfosuccinate has been shown to be a useful, inexpensive pairing ion for codeine analysis.

REFERENCES

(1) J. H. Knox and G. R. Laird, *J. Chromatogr.*, **122**, 17 (1976).

(2) J. H. Knox and J. Jurand, *ibid.*, **125**, 39 (1976).

(3) P. T. Kissinger, *Anal. Chem.*, **49**, 883 (1977).

(4) C. Horvath, W. Melander, I. Molnar, and P. Molnar, *ibid.*, **49**, 2295 (1977).

(5) C. Wu, S. Siggia, T. Robinson, and R. D. Waskiewicz, *Anal. Chim. Acta*, **63**, 393 (1973).

(6) R. Verpoorte and A. B. Svendsen, *J. Chromatogr.*, **100**, 227 (1974).

(7) C. U. Wu and J. J. Wittick, *Anal. Chem.*, **49**, 359 (1977).

(8) T. H. Beasley, D. W. Smith, H. W. Ziegler, and R. L. Charles, *J. Assoc. Offic. Anal. Chem.*, **57**, 585 (1974).

(9) H. W. Ziegler and T. H. Beasley, *ibid.*, **58**, 888 (1975).

(10) C. Olieman, L. Maat, K. Waliszewski, and H. C. Beyerman, *J. Chromatogr.*, **133**, 382 (1977).

(11) J. Lurie, *J. Assoc. Offic. Anal. Chem.*, **60**, 1035 (1977).

(12) V. D. Gupta and A. G. Ghanekar, *J. Pharm. Sci.*, **66**, 895 (1977).

ACKNOWLEDGMENTS

The authors thank Steve Mecker for assistance in obtaining morphine and ethylmorphine samples and Mark Fitch for preparation of placebo syrup formulations.

Tissue Distribution and Metabolism of Drugs VI: Effect of Second Drugs on Pancreatic Distribution and Insulin-Releasing Activity of Sulfonylureas in Perfused Rat Pancreas

KATSUHIKO OKUMURA *, MASATO ARAKAWA *§, and RYOHEI HORI ‡×

Received June 25, 1979, from the *Institute of Pharmaceutical Sciences, Hiroshima University School of Medicine, Hiroshima 734, Japan, and the ‡Department of Pharmacy, Kyoto University Hospital, Sakyo-ku, Kyoto, 606, Japan. Accepted for publication September 13, 1979. §Present address: General Research Center, Wakunaga Pharmaceutical Co. Ltd., Kotachi, Hiroshima, 729-64, Japan.

Abstract □ The distribution of sulfonylureas and their insulin-releasing potency as a pharmacological response were studied in isolated perfused rat pancreas. Sulfonylurea concentrations in the perfused pancreas in the presence or absence of a second drug were determined after perfusion for 15 min. Sulfonylureas could be distributed throughout the pancreas readily, and the tissue sulfonylurea concentration was reduced by the addition of sulfaphenazole, sulfadimethoxine, and salicylic acid. The insulin secretion rate stimulated by tolbutamide also was reduced by these three drugs; sulfanilamide, which could not displace the tolbutamide distribution, did not affect the tolbutamide-mediated secretion of insulin. These results document the importance of drug concentration in the tissue or receptor site with regard to insulin secretion and show that the sulfonylurea-mediated secretion of insulin can be modified easily by concomitant perfusion of a second drug that displaces sulfonylurea in the pancreas. These findings suggest that the drug interaction at the target organ or receptor site should be understood to provide adequate drug therapy.

Keyphrases □ Pancreas—distribution of sulfonylureas, displacement of sulfonylurea by second drug □ Distribution—sulfonylureas in the perfused pancreas, correlation with pharmacological response □ Sulfonylureas—distribution in pancreas, displacement by second drug □ Insulin secretion—stimulation by sulfonylurea, inhibition by presence of second drug

Hypoglycemic sulfonylureas are generally accepted to bind strongly to serum protein (1, 2). In 5% albumin solution, only 10% or less of tolbutamide was present in active unbound molecules at clinical levels (1, 2).

Even minute alteration of the protein binding capability changes the amount of the active unbound form of sulfonylureas. Clinically, ineffective therapy or toxic responses could result.

Displacement of such sulfonylurea–protein binding by other drugs has been demonstrated in plasma and in albumin solutions (3, 4). These phenomena may also occur in various organs or tissues (5, 6), but little is known about drug binding in tissues. The displacement at the receptor or binding site in the target organ may directly reflect therapeutic efficacy.

It has been generally accepted that the distribution dynamics of a drug are closely related to its efficacy or adverse reaction (6). However, technical difficulties in performing such investigations have limited available information. It is difficult to determine accurately the drug concentration in organs as compared to the blood, and it is almost impossible to measure the amount at isolated receptors. Moreover, it is particularly hard to obtain a simple and precise pharmacological marker.

In a previous paper (7), drug disposition dynamics in the exocrine pancreas were reported. Drugs are transported to the pancreas through the lipid barrier and excreted into the pancreatic juice through the rather tight lipoid and molecular sieve barriers.

In the present paper, the pancreatic distribution of sulfonylureas is correlated with insulin secretagogic capacity as the pharmacological marker using isolated perfused rat pancreas.

EXPERIMENTAL

Materials—Dextran (mol. wt. 60,000–90,000) was purchased in powder[1] or liquid[2] form (dextran 70 JP IX). Tolbutamide[3] and carbutamide[4] were the sulfonylureas studied. All other chemicals were obtained from commercially available sources and were analytical reagent grade.

Animals—Male Wistar rats, 200–300 g, were housed in a constant-temperature room with free access to water and food.

Procedure—The technique for pancreas isolation was practically the same as the reported pancreas–duodenum isolation method (8). The insertion of the cannulas was modified and directed upward just below the superior mesenteric artery. Furthermore, to simplify the procedure, the left renal, internal spermatic, and iliolumbar vessels were not occluded. The pancreas–duodenum was isolated from the rat and perfused on a constant-temperature table (37.4°).

The perfusion medium was Krebs–Henseleit bicarbonate solution supplemented with glucose (100 mg %). Colloidal osmotic pressure was maintained by the addition of dextran (4.5%) in accordance with the method of Toyota *et al.* (9). The perfusate was supplied by a peristaltic pump at the rate of 2 ml/min (net perfusion pressure was 30–60 mm Hg) and oxygenated with 95% O_2–5% CO_2 through a fiber-type oxygenator[5]. The perfusion time was 15 min for study of the pancreatic uptake of sulfonylureas. The perfusion experiment was carried out for 45 min to permit comparative study of insulin secretion stimulated by sulfonylureas with or without second drugs. The first 10 min was used as a stabilizing control period, and the next three 10-min periods and the last 5 min served as the experimental period to determine the effect of sulfonylurea and second drugs.

Four kinds of experiments were conducted in this comparative study. The first was a control experiment using basal Krebs–Henseleit bicarbonate solution, the second determined the direct effect of second drugs, the third was the tolbutamide control study, and the last was a combined experiment using tolbutamide and a second drug. Every 2.5 min, samples of effluent from the cannula in the portal vein were collected for insulin assay.

Analytical Methods—Tolbutamide and carbutamide were determined by the methods of Martin and Rowland (10) and of Bratton and Marshall (11), respectively, after Somozyi's deproteinization. Insulin secreted in each experimental period was assayed as immunoreactive insulin (IRI) by a single-antibody precipitation method using polyethylene glycol (12). Rat insulin was used as the reference standard. Aprotinin[6] was added to each borosilicated culture tube[7] (1.2 × 75 mm) in accordance with the method of Toyota *et al.* (13).

[1] Wako Chemicals Co., Osaka, Japan.
[2] Green Cross Co., Osaka, Japan.
[3] Provided by Dr. R. Konishi.
[4] Provided by Dr. H. Matsui.
[5] Bio-Fiber 5 minitube, Bio-Rad Laboratories, or microporous hollow fiber, Mitsubishi Rayon Co. & Hiromaito Manufacturing Co., Hiroshima, Japan.
[6] Trasylol (10,000 KIU/ml), Bayer Co. Ltd.
[7] Corning Co., Corning, N.Y.

0022-3549/80/0200-0157$01.00/0
© 1980, American Pharmaceutical Association

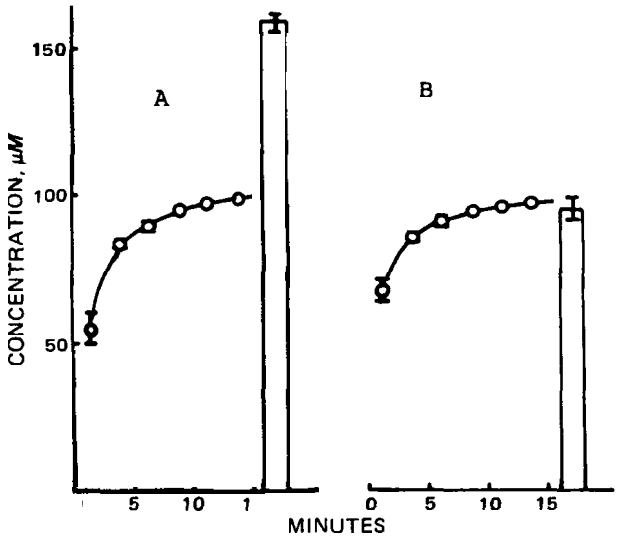

Figure 1—*Concentration profile of sulfonylureas in the portal effluent of the perfusate. Key: A, tolbutamide (100 μM) perfused; and B, carbutamide (100 μM) perfused. Open bars denote drug concentration in the pancreas.*

The effect of the second drug on the insulin secretion stimulated by tolbutamide was judged by the total amount of insulin secreted during the perfusion period of 15–45 min, because the insulin secretion stimulated by tolbutamide alone was almost stable during this period. The insulin secretion from 15 to 20 min and from 30 to 40 min was expressed as secretion in a combined experiment (microunits per minute), and the insulin secretion from 20 to 30 min and from 40 to 45 min was adopted as the control experiment in which only tolbutamide was perfused. The two values obtained from the two periods were compared. Statistical analysis was performed using the Student t test of paired samples.

RESULTS AND DISCUSSION

The concentration profile of tolbutamide and carbutamide in the effluent of the perfusate from the cannula in the portal vein when both drug solutions of 100 μM were perfused in the pancreas is shown in Fig. 1. After perfusion for 15 min, the sulfonylurea concentration in the whole pancreas was determined since equilibrium between the perfusate and the pancreas was nearly achieved within 15 min. The control data of pancreatic uptake of tolbutamide and carbutamide were 158 and 95 μM, respectively. These values were compared with the data based on concomitant use of second drugs.

Although serum albumin is used in almost every laboratory to maintain the colloidal osmotic pressure in the perfused pancreas, dextran was selected to differentiate between effects caused by competition for plasma protein binding sites as opposed to β-cell binding sites. The fact that dextran had no binding capacity with tolbutamide was confirmed by an ultrafiltration technique (14). Next, the effects of sulfaphenazole, sulfadimethoxine, sulfanilamide, and salicylic acid were examined to determine how they affect sulfonylurea distribution in the pancreas. Sulfaphenazole, sulfadimethoxine, and salicylic acid inhibited the pancreatic uptake of sulfonylureas by 30–40% (Table I), but sulfanilamide had little or no effect on the pancreatic uptake of tolbutamide.

These results correlated well with the displacement phenomenon of these drugs in the plasma or in an albumin solution (3). Christensen *et al.* (15) reported on the severe hypoglycemia provoked by the concomitant administration of tolbutamide and sulfaphenazole. Other investigators (16, 17) also reported that a similar phenomenon occurred with phenylbutazone or dicumarol. Hypoglycemia was attributable to a

Table I—Effect of the Second Drug on the Pancreatic Uptake of Sulfonylureas

Sulfonylurea	Second Drug	Pancreatic Uptake[a], μM	Uptake Ratio, %
Tolbutamide (100 μM)	None	158 ± 3[b] (6)[c]	100
	Sulfanilamide (2.5 mM)	150 ± 7 (3)	95
	Sulfaphenazole (2.5 mM)	109 ± 7 (5)	69[d]
	Salicylic acid (2.5 mM)	105 ± 6 (5)	67[d]
	Sulfadimethoxine (1 mM)	92 ± 9 (5)	58[d]
Carbutamide (100 μM)	None	95 ± 4 (8)	100
	Salicylic acid (2.5 mM)	70 ± 2 (9)	73[d]

[a] These values are of 15-min perfusion. [b] Values are mean ± *SEM*. [c] Values in parentheses are the number of experiments. [d] Significant differences were detected at $p < 0.001$.

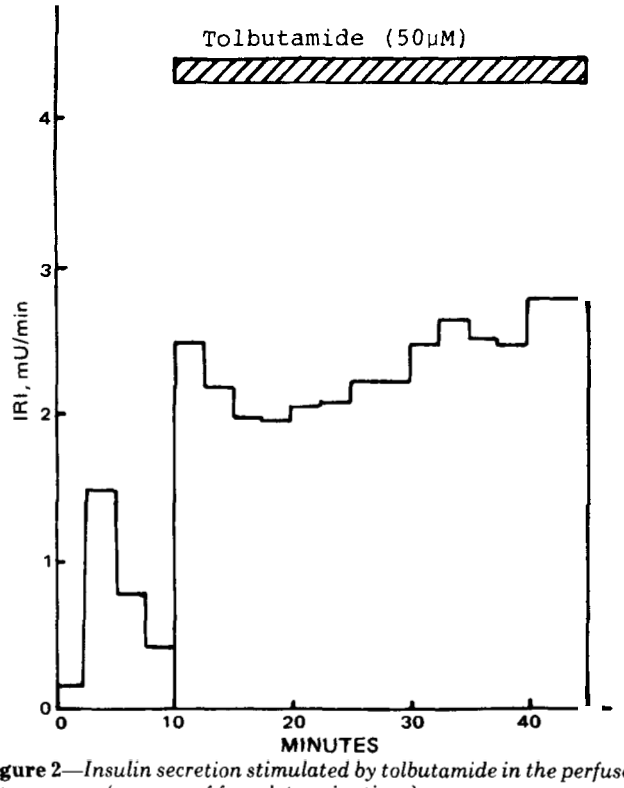

Figure 2—*Insulin secretion stimulated by tolbutamide in the perfused rat pancreas (average of four determinations).*

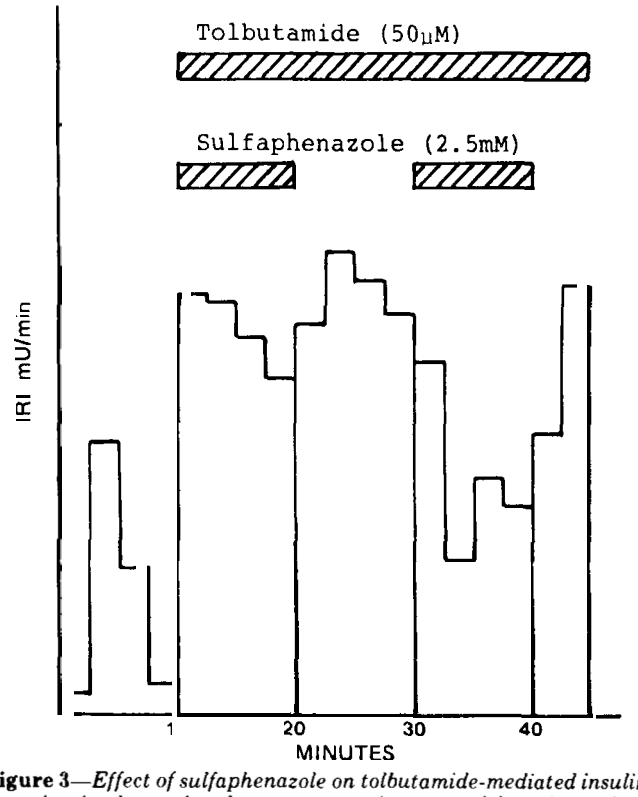

Figure 3—*Effect of sulfaphenazole on tolbutamide-mediated insulin secretion in the perfused rat pancreas (average of four determinations).*

Table II—Effect of the Second Drug on the Insulin Secretion in the Absence of Tolbutamide

Second Drug	Secreted Insulin, mU/min: Basal Medium[a]	Basal Medium plus Second Drug[b]	Statistics[c]
None	0.31	0.37	NS (3)[d]
Sulfanilamide (2.5 m*M*)	0.21	0.22	NS (3)
Sulfaphenazole (2.5 m*M*)	0.40	0.55	NS (4)
Salicylic acid (2.5 m*M*)	0.51	0.42	NS (5)
Sulfadimethoxine (1 m*M*)	0.23	0.36	NS (4)

[a] Insulin secretion during the 20–30- and 40–45-min periods. [b] Insulin secretion during the 15–20- and 30–40-min periods. [c] Paired *t* test. [d] Values in parentheses are the number of experiments.

Table III—Effect of the Second Drug on the Insulin Secretion Stimulated by Tolbutamide

Second Drug	Secreted Insulin, mU/min[a]: Tolbutamide Only[b]	Tolbutamide plus Second Drug[c]	Statistics[d]
None	2.35	2.34	NS (4)[e]
Sulfanilamide (2.5 m*M*)	1.81	1.99	NS (3)
Sulfaphenazole (2.5 m*M*)	2.68	1.89	$p < 0.01$ (4)
Salicylic acid (2.5 m*M*)	2.21	1.99	$p < 0.05$ (4)
Sulfadimethoxine (1 m*M*)	1.93	1.71	$p < 0.05$ (4)

[a] Concentration of tolbutamide was 50 μM. [b] Insulin secretion during the 20–30- and 40–50-min periods. [c] Insulin secretion during the 15–20- and 30–40-min periods. [d] Paired *t* test. [e] Values in parentheses are the number of experiments.

combination of causes, *i.e.*, inhibition of hepatic metabolism, increased protein-unbound sulfonylurea, and its displacement from tissue-binding sites in the liver (18). The displacement phenomenon in the blood is one main cause of hypoglycemia, but it is not totally responsible. The results of the present study showed that the pancreatic uptake of sulfonylureas decreased in accordance with their displacement phenomenon in plasma by the addition of second drugs with high hydrophobicity.

In considering the action site of sulfonylureas in the pancreas, the possibility that drug binding to the β-cell membrane may be related to secretagogic action (19–23) has received much attention. Drug displacement may occur at the receptor site as demonstrated in plasma or in the whole pancreas, and a converse pharmacological effect of what happened as a result of displacement in plasma may be seen. The possibility of displacement of tolbutamide at the receptor or binding site also was investigated in this study using the secreted insulin as a marker of the pharmacological effect. The basal pattern and tolbutamide-stimulated pattern are illustrated in Fig. 2.

Since it has been considered that sulfonylurea binding to the β-cell membranes is closely related to the secretagogic potency, it was expected that the drug interaction at the receptor level might be detected effectively by this experimental system. Sulfaphenazole, sulfadimethoxine, and salicylic acid, which inhibited the pancreatic uptake of tolbutamide, were investigated to determine their effect on the insulin secretion stimulated by tolbutamide. As shown in Fig. 3, the insulin secretory rate during the concomitant perfusion of tolbutamide and sulfaphenazole was significantly lower than that obtained during tolbutamide perfusion alone. When only sulfaphenazole was perfused, no significant effect was detected in the insulin secretory rate (Table II).

The effect of sulfadimethoxine and salicylic acid on insulin secretion stimulated by tolbutamide also was examined; smaller, but significant, inhibitory effects were observed. Insulin secretion rates when tolbutamide alone was perfused and when tolbutamide and a second drug were perfused are listed in Table III. These results are well explained by the hypothesis that expects competition at the binding or receptor site between tolbutamide and the second drug on the β-cell membrane.

Hellman *et al.* (22) reported on a similar phenomenon using 4-acetamide-4′-isothiocyanate-stilben-2,2′-disulfonic acid in incubated rat Langerhans islet. It depressed the islet uptake of glyburide (glibenclamide) and, when present solely with the islets, it activated the insulin secretion strongly. When it coexisted with glyburide, the two secretagogues acted less actively than the additive effect of glyburide and 4-acetamide-4′-isothiocyanate-stilben-2,2′-disulfonic acid. Hellman *et al.* (22) pointed out the possibility that 4-acetamide-4′-isothiocyanate-stilben-2,2′-disulfonic acid, a membrane probe, prevented the secretagogic recognition of glyburide by displacing this sulfonylurea from the β-cell membranes. Although their hypothesis may explain the present data, tolbutamide possibly could react directly with sulfaphenazole, sulfadimethoxine, or salicylic acid and form a less active complex compound. To exclude this possibility, the complex formation of these drugs was examined by the solubility method (24). The complex formation was no more than merely 1% of tolbutamide in the perfusate (stability constant = 5.3 M^{-1}). Thus, it could not explain the remarkably decreased insulin secretion.

On the other hand, the finding that tolbutamide-mediated secretion was inhibited by the addition of these three drugs could have been caused by their direct action if they had the capacity to inhibit insulin secretion. A perfusion study indicated that these drugs made a small, but insignificant, change in the insulin secretion (Table II). Consequently, direct inhibition of insulin secretion by these drugs apparently was not the reason for this phenomenon.

When sulfanilamide was perfused concomitantly with tolbutamide, the insulin secretion rate was slightly, but not significantly, stimulated (Table III). Since sulfanilamide was hardly able to displace the pancreatic uptake of tolbutamide, this result is consistent with the hypothesis that drug concentration at the tissue level might reflect the pharmacological response.

The importance of the drug protein binding in plasma has been stressed. It has been postulated widely that the unbound free fraction of a drug in plasma could serve as the marker of therapeutic efficacy. However, a correlation between the serum free fraction value and the tissue free fraction value is unlikely in the presence of some specific accumulation of drug in the tissue. From this point of view, drug–tissue binding or interaction in connection with pharmacological or toxicological response has received attention recently. The presented data show the important role of drug disposition dynamics in tissues, especially in target organs. Thus, drug disposition in target organs or receptor sites should always be considered when preparing a dosing regimen for optimal therapy.

REFERENCES

(1) M. J. Crooks and K. F. Brown, *J. Pharm. Pharmacol.*, **26**, 304 (1974).

(2) S. Goto, H. Yoshitomi, and M. Kishi, *Yakugaku Zasshi*, **97**, 1219 (1977).

(3) J. Judis, *J. Pharm. Sci.*, **61**, 89 (1972).

(4) J. J. Thiessen and M. Rowland, *ibid.*, **66**, 1063 (1977).

(5) C.-M. Lai and G. Levy, *ibid.*, **67**, 1492 (1978).

(6) G. Levy, C.-M. Lai, and A. Yacobi, *ibid.*, **67**, 299 (1978).

(7) R. Hori, M. Arakawa, and K. Okumura, *Chem. Pharm. Bull.*, **26**, 1135 (1978). M. Arakawa, K. Okumura, and R. Hori, *J. Pharm. Sci.*, **69**, 27 (1980).

(8) J. C. Penhos, C.-H. Wu, J. C. Basabe, N. Lopez, and F. W. Wolff, *Diabetes*, **18**, 733 (1969).

(9) T. Toyota, K. Abe, M. Kubo, H. Kikuchi, and K. Kimura, *Diabetes J.*, **3**, 99 (1975).

(10) S. B. Martin and M. Rowland, *J. Pharm. Pharmacol.*, **25**, 186 (1973).

(11) A. C. Bratton and E. K. Marshall, Jr., *J. Biol. Chem.*, **128**, 537 (1939).

(12) B. Desbuquios and G. D. Aurbach, *J. Clin. Endocrinol. Metab.*, **33**, 732 (1971).

(13) T. Toyota, S. Sato, M. Kubo, K. Abe, and Y. Goto, *ibid.*, **41**, 81 (1975).

(14) R. L. Diron, E. S. Owens, and D. P. Rall, *J. Pharm. Sci.*, **58**, 1106 (1969).

(15) L. K. Christensen, J. M. Hansen, and M. Kristensen, *Lancet*, **2**, 1298 (1963).

(16) J. B. Field, M. Ohta, C. Boyle, and A. Remers, *N. Engl. J. Med.*, **277**, 889 (1967).

(17) M. Kristensen and J. M. Hansen, *Diabetes*, **16**, 211 (1967).

(18) M. Rowland, S. B. Martin, J. Thiessen, and J. Karam, in "Drug Interactions," P. L. Mor Selli, S. Garattini, and S. N. Cohen, Eds., Raven, New York, N.Y., 1974, p. 199.

(19) J. Shelin, *Acta Diabetol. Lat.*, **10**, 1052 (1973).

(20) I.-B. Täljedal, *Horm. Res.*, **5**, 211 (1974).

(21) B. Hellman, A. Lernmark, J. Sehlin, and I.-B. Täljedal, *Biochem. J.*, **132**, 775 (1973).

(22) B. Hellman, A. Lernmark, J. Sehlin, and I.-B. Täljedal, *FEBS Lett.*, **34**, 347 (1973).

(23) V. Bowen and N. R. Lazarus, *Biochem. J.*, **142**, 385 (1974).

(24) K. A. Connors and J. A. Mollica, Jr., *J. Pharm. Sci.*, **55**, 772 (1966).

Serum Levels of Butorphanol by Radioimmunoassay

KENNETH A. PITTMAN ˣ, ROBERT D. SMYTH, and ROBERT F. MAYOL *

Received March 19, 1979, from *Bristol Laboratories, Syracuse, NY 13201.* Accepted for publication September 18, 1979. *Mead-Johnson Research Center, Evansville, IN 47721.

Abstract □ A radioimmunoassay was developed for the analysis of butorphanol in human serum. The procedure involves extraction of serum with hexane containing 2% isoamyl alcohol, followed by evaporative solvent removal and radioimmunoassay of the reconstituted residue. The antibody significantly cross-reacts with unidentified butorphanol metabolites but not with two known metabolites, hydroxybutorphanol and norbutorphanol. Extraction eliminated interference from the butorphanol metabolites normally present in serum. The antibody also cross-reacts with pentazocine and cyclazocine but not with morphine, hydromorphone, oxymorphine, codeine, methadone, and meperidine. Butorphanol tartrate was administered intravenously (2 mg) to normal male volunteers. Serum butorphanol levels declined biexponentially with an average terminal half-life of 2.7 hr. Enzymatic serum hydrolysis prior to extraction yielded additional butorphanol, indicating the presence of butorphanol conjugates. The specificity of the assay for butorphanol was confirmed by GLC–mass fragmentography.

Keyphrases □ Butorphanol—radioimmunoassay in human serum, pharmacokinetics in human serum □ Pharmacokinetics—butorphanol in human serum □ Radioimmunoassay—butorphanol in human serum □ Narcotic agonist–antagonist—serum butorphanol pharmacokinetics by radioimmunoassay

Butorphanol (I), a totally synthetic morphinan (1) with narcotic agonist–antagonist properties, has been shown to be a potent analgesic in animals (2) and humans (3–5). Studies with ^{3}H-butorphanol in normal human subjects demonstrated the presence of hydroxybutorphanol (II), norbutorphanol (III), and conjugates of I, II, and III as metabolites of I[1]. Additional unidentified metabolites were present. The plasma I levels indicated that conventional GLC or high-pressure liquid chromatographic procedures could not achieve the detection level necessary to define fully the serum concentration profile after parenteral administration. A specific radioimmunoassay procedure was needed to determine the pharmacokinetics and bioavailability of I.

Rabbit antibutorphanol antibody was prepared *via* I conjugation to bovine serum albumin, followed by injection of this antigen into rabbits to obtain the antiserum[2]. Radiolabeled antigen was prepared by a chloramine-T procedure for the introduction of iodine 125 into the aromatic ring of I, and this hapten was bound by the antiserum and displaced by comparable amounts of pure I. The conventional second antibody (goat antirabbit globulin) technique was utilized to separate free from bound antigen. No significant cross-reactivity with the butorphanol metabolites II or III was observed. Cross-reactivity from unknown metabolites, however, necessitated the development of a technique specific for I, so an extraction procedure prior to radioimmunoassay was included.

A combined GLC–mass fragmentography assay was developed to demonstrate that the final method was specific for I in the presence of its metabolites.

The purposes of these studies were to develop and validate a radioimmunoassay method for I and to demonstrate the utility of the method in the determination of serum levels of I after administration of therapeutic doses.

EXPERIMENTAL

Chemicals and Reagents—Na^{125}I (carrier free)[3], *N*-chloro-4-methylbenzenesulfonamide sodium salt[4] (chloramine-T), diethylamine[4], normal human serum[5], normal rabbit serum[5], goat antirabbit γ-globulin antiserum[6], 3,14-dihydroxy-*N*-cyclobutylmethylmorphinan hydrogen tartrate[7] (butorphanol tartrate, I-tartrate, lot 75F1355-2), 3,14-dihydroxy-*N*-(*trans*-3′-hydroxycyclobutylmethyl)morphinan hydrogen tartrate[7] (hydroxybutorphanol tartrate, II-tartrate, lot 1099-21), 3,14-dihydroxymorphinan[7] (norbutorphanol, III, lot 923-19), 3,14-dihydroxy-*N*-cyclopropylmethylmorphinan hydrogen tartrate[7] (internal standard, IV, lot 75F1878), *N,O*-bis(trimethylsilyl)trifluoroacetamide[8] (V), *N,O*-bis(perdeuterotrimethylsilyl)trifluoroacetamide[9] (VI), and rabbit antibutorphanol antiserum[2] were used as received.

All other chemicals and reagents were USP, NF, or ACS grade or better and were used without further purification.

Radioiodinated Butorphanol Hapten—To a 1-dram vial with a stirring bar were added, with stirring, 20 mCi of Na^{125}I (200 μl), 3.5 μl of a solution of 1.46 mg of I-tartrate (1 mg of base)/ml of distilled water, and 100 μl of 0.25 *M*, pH 7.6 phosphate buffer. Then 10 μl of a fresh solution of 3 mg of chloramine-T/ml was added, followed within 5–10 sec by 10 μl of a fresh solution of 7 mg of sodium metabisulfite/ml. Carbonate buffer (50 μl) and hexane (2 ml) were added, and stirring was continued for 10 min.

The aqueous phase was frozen on dry ice; the hexane phase was removed, washed once with 1 ml of distilled water, and aliquoted into individual vials after its activity was determined. The iodinated butorphanol was stored at −20°, and aliquots were reconstituted with radioimmunoassay buffer just prior to use. After 1–3 months, the stock preparation becomes unsatisfactory due to the accumulation of degradation products.

Solutions—The butorphanol standard solution was prepared to yield 145.8 pg of I-tartrate (100 pg of base)/ml; 1-ml amounts were transferred to 0.5-dram vials and stored at −20°. The radioimmunoassay buffer was 0.05 *M*, pH 7.6 phosphate buffer. It was prepared fresh for use. The carbonate buffer was a saturated solution of sodium bicarbonate and sodium carbonate. The extraction solvent was 2 parts (v/v) of isoamyl alcohol to 98 parts (v/v) of hexane. The protein solution consisted of 4 parts (v/v) of normal rabbit serum diluted with 96 parts (v/v) of radioimmunoassay buffer. It was prepared from frozen (−20°) serum aliquots and kept on ice[6].

Rabbit antibutorphanol antiserum was diluted in protein solution in the ratio of 1 μl to 5 ml, respectively. It was made fresh from frozen (−20°) antiserum aliquots and kept on ice. [Other lots of antibody than the one used may require a different dilution to obtain useful standard curves (7).] The goat antirabbit γ-globulin solution was prepared by diluting the antiserum in radioimmunoassay buffer to obtain about 13 units/ml, *e.g.*, 8 ml of antiserum plus 22 ml of buffer. It was made fresh from frozen (−20°) antiserum aliquots and kept on ice[8].

To prepare the radioiodinated butorphanol hapten solution, the ethanolic stock solution of ^{125}I-butorphanol was diluted to obtain (*a*) about 180,000 cpm/ml or (*b*) about 100,000 cpm, depending on whether

[1] R. C. Gaver, R. D. Smyth, M. Vasiljev, and D. R. Van Harken, Bristol Laboratories, Syracuse, N.Y., unpublished results.

[2] R. F. Mayol, Mead-Johnson Research Center, Evansville, Ind., unpublished results.

[3] Amersham Corp., Arlington Heights, Ill.

[4] Eastman Kodak Co., Rochester, N.Y.

[5] Glusulase, containing β-glucuronidase and arylsulfatase, Grand Island Biological Co., Grand Island, N.Y.

[6] Calbiochem, East Rutherford, N.J.

[7] Bristol Laboratories, Syracuse, N.Y.

[8] Pierce Chemical Co., Rockford, Ill.

[9] Regis Chemical Co., Morton Grove, Ill.

0022-3549/80/0200-0160$01.00/0
© 1980, American Pharmaceutical Association

Table I—Accuracy and Precision of Butorphanol Radioimmunoassay

Parameter	Added Butorphanol, pg					
	25	150	300	100	300	600
	"Low" Standard Curve (0–300 pg)			"High" Standard Curve (0–600 pg)		
Number of curves	8	8	8	12	13	13
Number of replicates per curve	3	3	3	3	3	3
Total number of samples	24	24	24	36	39	39
Mean predicted value	26	154	295	95	308	567
Intraassay variability, %[a]	14	10	15	11	8	12
Interassay variability, %[b]	10	6	10	8	6	9

[a] Mean coefficient of variation for triplicate samples. [b] Coefficient of variation for all samples (three times number of curves).

a high or low standard curve was prepared. It was made fresh and kept on ice. The counts per minute may need to be adjusted if a different γ-counter is used.

Radioimmunoassay—For a given analytical run, a constant volume of serum was taken from all samples, and the same volume of human serum was used for the standard curve, because of the variable effect of serum volume on nonspecific and control binding values. Volumes of human serum from 0.1 to 0.5 ml were suitable; 0.2 ml is used as an example.

Into sets of triplicate extraction tubes[10] were pipetted[11] 0.25, 0.50, 1.0, 1.5, 2.0, 2.5, and 3.0 μl of butorphanol standard solution. Three additional sets of tubes were reserved for background (BKG), nonspecific binding (NSB), and maximum binding (B_0). Human serum (0.2 ml) was pipetted[12] into all of the tubes, and duplicate 0.2-ml portions of the desired test samples were pipetted into additional tubes. Carbonate buffer (50 μl) and the extraction solvent (2 ml) were added; then the tubes were racked, and each rack was shaken gently by hand for 1 min. The racks were centrifuged[13] for 10 min at 3000 rpm at −5° and then placed in a shallow bath of dry ice–ethanol for about 3 min.

Each organic phase was decanted into a clean tube[14] and reduced to dryness, using a manifold[15] supplied with dry, filtered nitrogen gas. All subsequent solutions were added to the tubes with a diluter–pipeter[16] set to deliver 0.1 ml of reagent solution followed by 0.4 ml of radioimmunoassay buffer. The final volume in each tube was 1.5 ml. Solutions were kept in an ice bath when not in use. Radioiodinated hapten was added to all tubes except the background tubes, to which extra radioimmunoassay buffer was added. Antibutorphanol antiserum was added to all tubes except the nonspecific binding tubes, to which protein solution was added. Antirabbit serum antibody was added to all tubes.

The tubes were centrifuged at 3000 rpm for 3 min at −5° and stored at 5–7° for 16 hr (overnight). Free and bound haptens were separated by centrifugation at 3000 rpm for 30 min, and 1.0 ml of each supernate was transferred to fresh tubes. The ^{125}I-activity was determined in a γ-counter[17] with automatic correction for background. Calculations were carried out automatically in the system by a modified log–logit analysis (6). In this procedure, the bound radioactivity for each sample or standard (B) was estimated, and the ratio:

$$y = \frac{B - \text{NSB}}{B_0 - \text{NSB}} \qquad \text{(Eq. 1)}$$

was calculated and transformed to:

$$\text{logit } y = \ln\left(\frac{y}{1-y}\right) = \ln\left(\frac{B - \text{NSB}}{B_0 - B}\right) \qquad \text{(Eq. 2)}$$

The slope and intercept were obtained by linear regression for logit y *versus* ln p, where p equals the amount of standard in each tube. The amount of I in each sample tube was estimated by standard inverse prediction techniques.

Cross-Reactivity—Fifty micrograms each of II, III, morphine sulfate, hydromorphone, oxymorphone hydrochloride, codeine, pentazocine, cyclazocine, methadone hydrochloride, and meperidine hydrochloride were dissolved in 500 ml of 0.01 *N* HCl. Amounts of each of these solutions were added to control human serum to give concentrations of 0.2, 2, and 20 ng/ml, and the serum samples were carried through the radioimmunoassay as unknowns to determine the relative ability of the compounds to displace radioiodinated hapten from the antibutorphanol antibody.

Enzymatic Hydrolysis—To 1.0-ml samples of spiked or test human plasma were added 25 μl of enzyme solution[18], 5 μl of chloroform, and 4.0 ml of 0.1 *M*, pH 5.5 acetate buffer. The samples were incubated at 37° for 72 hr under a nitrogen atmosphere, and portions were carried through the radioimmunoassay.

GLC–Mass Fragmentography—To 3-ml samples of spiked or test human plasma was added 0.3 μg of IV. The samples were made basic and extracted with chloroform. The chloroform was extracted with 0.1 *N* H_2SO_4, which, in turn, was made basic and extracted with chloroform, which was reduced to dryness under a nitrogen stream. Compound V (25 μl) was added to each sample, and the samples were agitated and held at room temperature for 30 min to form the trimethylsilyl derivatives of I and IV. To each sample was added 2 μl of a solution containing 25 ng of I/ml of VI. This addition of the perdeuterotrimethylsilyl derivative of I provided a carrier for the picogram amounts of the trimethylsilyl derivative of I so that it was not lost in the chromatographic system.

The instrument used was a gas chromatograph[19] coupled to a quadrupole mass spectrometer[20] equipped with a chemical-ionization source. Conditions were: carrier–reactant gas, methane; injection port temperature, 250°; oven temperature, 235°; transfer line temperature, 250°; ion chamber pressure, 0.5–1 torr; and electron beam intensity, 100 ev. The methane flow rate was adjusted to maximize the mass 29 ion in the methane spectrum, resulting in a carrier gas flow rate between 10 and 20 ml/min. Four microliters from each sample was injected into a 91-cm × 2.5-mm i.d. column containing 3% OV-1 on Gas Chrom Q[21].

The column effluent was scanned continuously in the single-ion monitoring mode using a cycle time of 1 sec. Three mass numbers were monitored in each cycle, corresponding to the pseudomolecular ions (MH^+) of the trimethylsilyl derivative of IV (386.4 amu), the trimethylsilyl derivative of I (400.4 amu), and the perdeuterotrimethylsilyl derivative of I (409.4 amu). The derivatives of I eluted at 3.5 min, and the derivative of IV eluted at 2.0 min. A response ratio of the trimethylsilyl derivative of I to the trimethylsilyl derivative of IV was calculated, and the regression of the ratio on the I concentration in the plasma standards was used to calculate the I concentration in the test samples by inverse prediction.

Subjects—A signed informed consent was obtained from each normal, healthy, adult male subject. Complete physical examinations, hematology, blood chemistries, and urinalysis were performed on each subject on the day prior to the 1st study day. All parameters were within the normal range.

In Study 1, each subject in one group received 2 mg of butorphanol tartrate intramuscularly whereas each subject in the other group received 16 mg of butorphanol tartrate orally. Subjects were fasted overnight prior to drug administration in the morning. Blood samples were obtained at 0, 2, 4, and 8 hr.

In Study 2, subjects received 2 mg of butorphanol tartrate intravenously. Blood samples were obtained 0.5 hr prior to drug administration and at 5, 10, 15, 20, 30, and 45 min and at 1, 1.25, 2, 3, 4, 6, and 8 hr. Subjects abstained from solid food and liquid, except water, from midnight of the beginning of the test day. Subjects were instructed to walk around for at least 5 min after each blood collection. They received a light breakfast 4 hr after dose administration and were discharged after the

[10] Screw-capped glass tubes (13 × 100 mm) with Teflon-lined caps (catalog No. 99447), Corning Glass, Corning, N.Y.
[11] With a 2-μl syringe, Hamilton Co., Reno, Nev.
[12] MLA micropipets, Fisher Scientific Co., Pittsburgh, Pa.
[13] Model PR-6000 refrigerated centrifuge equipped with IEC No. 418 radioimmunoassay head, Damon/IEC Division, Needham Heights, Mass.
[14] Catalog No. 2053 12 × 75-mm polypropylene tubes, Falcon Plastic Co.
[15] Evap-O-Rac, Cole-Parmer Instrument Co., Chicago, Ill.
[16] Model 25004 equipped with a 200-μl sampling pump and a 1-ml dispensing pump, Micromedic Systems, Horsham, Pa.
[17] PACE-1 γ-counter with PAC-5 programmable automatic calculator, Picker Corp., Northford, Conn.
[18] Endo Laboratories, Garden City, N.J.
[19] Model 2500, Finnegan Corp., Sunnyvale, Calif.
[20] Model 3300, Finnegan Corp., Sunnyvale, Calif.
[21] Applied Science Laboratories, State College, Pa.

Table II—Butorphanol Concentrations as Determined by the Radioimmunoassay in Human Serum after Oral (16 mg) or Intramuscular (2 mg) Administration of Butorphanol Tartrate

Route of Administration	Subject	Butorphanol, ng/ml 0 hr	2 hr	4 hr	8 hr
Oral	1	0.14	0.80	0.82	0.36
	2	0.11	0.31	0.24	0.12
	3	0.12	2.68	2.99	1.51
	4	0	0.35	0.42	0.14
Intramuscular	5	0	1.46	0.96	0.21
	6	0	1.38	0.90	0.29
	7	0.10	1.13	0.63	0.10
	8	0	1.30	0.66	0.21

Table III—Butorphanol Concentrations as Determined by GLC–Mass Fragmentography in Human Serum after Oral (16 mg) or Intramuscular (2 mg) Administration of Butorphanol Tartrate

Route of Administration	Subject	Butorphanol, ng/ml 0 hr	2 hr	4 hr	8 hr
Oral	1	0	0.32	0.87	0.09
	2	0	0.07	0	0
	3	0	2.97	2.27	0.74
	4	0	0.08	0	0
Intramuscular	5	0.07	1.63	0.98	—
	6	0.56	1.69	1.22	0.44
	7	0	1.04	0.47	0.18
	8	0.03	1.27	0.74	0

last blood sample was obtained.

Blood samples were obtained in plain evacuated tubes, allowed to clot at room temperature for 30 min, and centrifuged at 5°. Serum samples were removed and immediately flash frozen, stored, and shipped frozen; they were maintained frozen at −20° until analyzed.

Pharmacokinetic Analysis—The serum concentration data for each subject in Study 2 were plotted on semilog paper with time as the abscissa. Judgments then were made as to the nature and trend of the time course of serum concentration; also at this time, certain data points were judged to be outliers if they deviated widely (by ~25%) from the general trend. With the outliers excluded, all of the data sets were run through the program CSTRIP (7) to obtain initial polyexponential parameter estimates. These estimates were then passed, along with their associated data sets, to the program GUESS (8) for parameter optimization by a nonlinear technique. The optimized polyexponential parameters then were used to calculate pharmacokinetic parameters.

RESULTS AND DISCUSSION

Preliminary experiments[22] showed that increasing amounts of human serum or of the residue of hexane extracts of human serum increasingly reduced the binding of radioiodinated hapten to the antibody. For a given serum volume, there was little variability in the reduction of this binding; for serum volumes of ≤0.5 ml, the effect was not of sufficient magnitude to interfere with the usefulness of the radioimmunoassay. Data on the accuracy and precision of the radioimmunoassay are presented in Table I. The data were obtained from the same standard curves used to estimate butorphanol concentrations in the discussed serum samples. As expected, the best precision was obtained for samples near the center of the range of the standard curve.

The potential interference of known[1] metabolites of butorphanol (II and III) and of various narcotics and agonist–antagonists (see *Experimental*) was tested at levels up to 20 ng/ml. Only pentazocine and cyclazocine cross-reacted; they gave apparent butorphanol values of 0.1–0.2 ng/ml at their highest level of 20 ng/ml. Therefore, misleading values for butorphanol may be observed in any subject who may have received large doses of pentazocine within 24 hr of assaying for butorphanol by the radioimmunoassay.

The plasma I concentrations as determined by the radioimmunoassay in human subjects after intramuscular and oral dosing (Table II) and those determined by GLC–mass fragmentography (Table III) were compared by least-squares analysis, assuming a linear relationship between the two analytical methods. The slope, y-intercept, and regression coefficient were calculated, and the null hypotheses that the slope was equal to unity and that the y-intercept was equal to zero were tested. The results (Table IV) indicate that the methods are equivalent and that the radioimmunoassay is specific for butorphanol in the presence of its metabolites.

Table IV—Correlation of Radioimmunoassay and GLC–Mass Fragmentography Methods for Determination of Serum Butorphanol [a]

Sample Source (n)	Slope ± 95% Confidence Interval	Intercept ± 95% Confidence Interval	Correlation Coefficient
Oral (16)	0.98 ± 0.18	0.24[b] ± 0.05	0.96
Intramuscular (15)	0.87 ± 0.19	0.01 ± 0.08	0.94
Oral plus intramuscular (31)	0.92 ± 0.14	0.13[b] ± 0.04	0.93

[a] Each value obtained by GLC–mass fragmentography was used as an independent variable (x values), and the corresponding value obtained by radioimmunoassay was used as the dependent variable (y value). [b] Significantly different than 0 ($p < 0.05$).

The slight, but significant, intercept in the radioimmunoassay results on subjects given I orally could indicate that the radioimmunoassay was measuring an immunoreactive moiety other than butorphanol, but one that was present in the serum in a constant amount. Or it could indicate that there was a slight positive bias in the radioimmunoassay for the analyses run on that day. Subsequent experience with many other subjects given oral butorphanol suggests that the latter explanation is

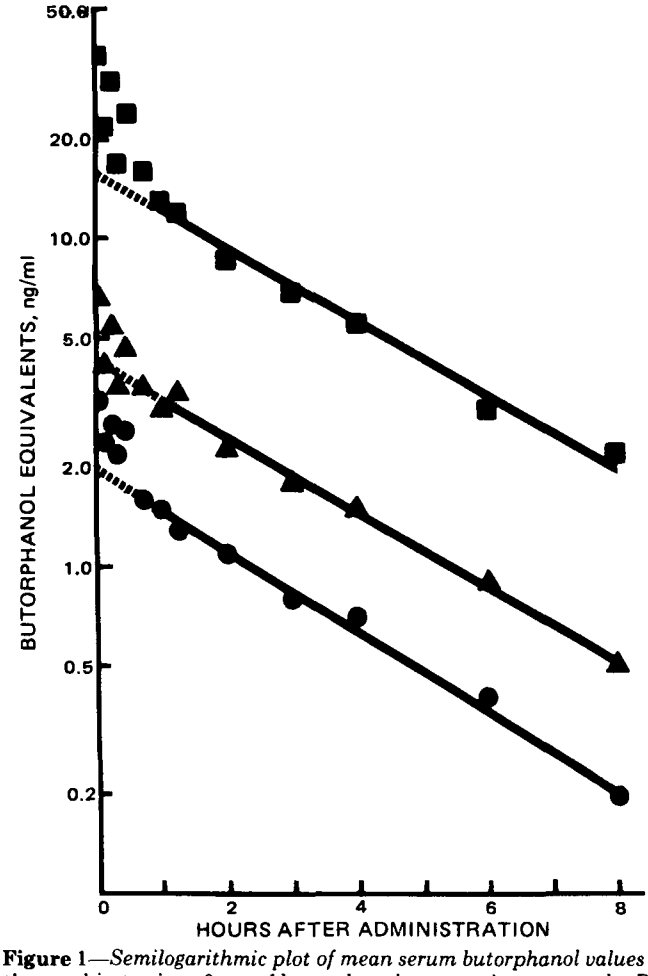

Figure 1—*Semilogarithmic plot of mean serum butorphanol values in three subjects given 2 mg of butorphanol tartrate intravenously. Butorphanol was determined by a complete radioimmunoassay (●) involving an extraction to separate butorphanol from its metabolites, by radioimmunoassay directly on serum (▲), and by radioimmunoassay after enzymatic hydrolysis to release butorphanol from conjugates (■), followed by extraction. Least-squares lines (solid and dashed) were calculated for log serum value* versus *time from 1 to 8 hr after dosing.*

[22] K. A. Pittman, unpublished data.

Table V—Serum Butorphanol in Subjects Given 2 mg of Butorphanol Tartrate Intravenously [a]

Hours after Administration	Butorphanol Equivalents, ng/ml								
	Subject 1			Subject 2			Subject 3		
	Complete RIA	Direct RIA	Hydrolysis RIA	Complete RIA	Direct RIA	Hydrolysis RIA	Complete RIA	Direct RIA	Hydrolysis RIA
0	0.1	0.3	1.2	0	0.4	1.2	0	0.3	1.3
0.08	2.4	4.9	31	3.6	9.6	40	3.6	5.2	38
0.17	1.6	2.6	13	3.0	5.5	29	2.5	4.3	24
0.25	2.7	4.9	29	2.5	5.9	30	2.9	5.5	30
0.33	1.7	2.5	13	3.0	4.6	20	2.0	3.5	19
0.50	1.5	3.1	18	3.2	5.8	24	3.2	4.9	29
0.75	1.2	1.9	10	1.9	5.4	22	1.6	3.3	16
1.0	1.1	2.3	9.7	1.7	3.3	16	1.7	3.3	12
1.25	1.0	1.9	7.9	1.6	4.2	8.4	1.4	4.0	21
2.0	0.9	1.5	6.0	1.2	3.1	10	1.1	2.3	9.7
3.0	0.6	1.2	4.8	0.9	2.1	7.3	1.0	2.1	8.5
4.0	0.4	0.9	3.2	0.7	1.7	5.4	1.0	2.0	7.9
6.0	0.2	0.4	1.9	0.5	1.3	3.6	0.4	1.0	3.5
8.0	0.1	0.3	1.8	0.2	0.8	2.4	0.2	0.5	2.3

[a] Determinations were made by a complete radioimmunoassay (RIA) involving an extraction to remove butorphanol from its metabolites, by radioimmunoassay directly on serum, and by radioimmunoassay after enzymatic hydrolysis of conjugates and extraction of butorphanol. See *Experimental* for details.

correct. Regression, using the log–logit transformation of Hatch *et al.* (6), often leads to an overestimate of very low concentrations, especially those below the lowest standard. Particular caution must be taken when estimating values between zero and the low standard with this procedure.

Serum samples for three subjects who received intravenous butorphanol were analyzed directly by the radioimmunoassay by omitting the extraction procedure. The values obtained (Table V) for serum butorphanol were 1.5–3 times higher (average 2.1 ± *SE*) than the values obtained (Table V) by including hexane extraction in the radioimmunoassay. The same samples also were analyzed by the radioimmunoassay after being subjected to enzymes (β-glucuronidase and arylsulfatase), which hydrolyze common conjugates of phenolic drugs. The values obtained (Table V) were 5–15 times higher (average 9.5 ± *SE* = 0.4) than those obtained without enzymatic hydrolysis.

Semilog plots of the mean serum butorphanol concentrations for those three subjects as determined by the complete radioimmunoassay, the radioimmunoassay without the extraction step, and the complete radioimmunoassay preceded by enzymatic hydrolysis are shown in Fig. 1. Lines of best fit were calculated for each set of data from 1 to 8 hr after dose administration. The slopes were not significantly different, suggesting that butorphanol elimination may be rate limiting in the clearance of it and its metabolites from the body.

When the data for each of the 18 subjects given butorphanol intravenously (Study 2) were plotted as log concentration *versus* time, log serum concentration in most subjects appeared to decline biexponentially, showing a rapid distributive phase (α-phase) and a slower postdistributive phase (β-phase). When the data for each subject were analyzed using CSTRIP, the decline in serum concentration was biexponential for 17 of the data sets and monoexponential for one in which the distributive phase was missed entirely. The equation used for biexponential decline was:

$$C_s = Ae^{-\alpha t} + Be^{-\beta t} \quad \text{(Eq. 3)}$$

where C_s is the serum concentration in nanograms per milliliter and A and B are the y-intercepts and α and β are the slopes of the fastest declining and the slowest declining exponentials, respectively; A and B are in nanograms per milliliter, and α and β are in reciprocal hours. Similarly, the equation used for the monoexponential decline observed for one subject was:

$$C_s = Be^{-\beta t} \quad \text{(Eq. 4)}$$

where B and β describe the same exponential (β-phase) as in Eq. 3.

The initial estimates for A, B, α, and β otained by CSTRIP were optimized to obtain a curve of best fit by GUESS. The average values and their standard errors for α, β, and the serum half-life (0.693/β) were 7.7 ± 2.5 hr^{-1}, 0.262 ± 0.009 hr^{-1}, and 2.70 ± 0.09 hr, respectively. As the standard errors indicate, the values for α were quite variable from subject to subject while those for β were consistent. Pharmacokinetic studies of narcotics and other narcotic agonists and antagonists have revealed polyexponential declines in plasma concentration following intravenous administration. Meperidine (9, 10), naloxone (11), and pentazocine (12, 13), for example, declined exponentially while fentanyl (14) and morphine (15, 16) declined triexponentially. Terminal plasma or serum half-lives for codeine (17), meperidine (9, 10), morphine (15, 16), and pentazocine (12, 13, 18) fell in the 2–4-hr range, as did butorphanol. In pharmacokinetic terms, the behavior of butorphanol after intravenous dosing appears to be typical of the narcotic and narcotic agonist–antagonist drugs.

REFERENCES

(1) I. Monkovic, T. T. Conway, H. Wong, Y. G. Perron, I. J. Pachter, and B. Belleau, *J. Am. Chem. Soc.*, **95**, 7910 (1973).

(2) A. W. Pircio, J. A. Gylys, R. L. Cavanaugh, J. P. Buyniski, and M. E. Bierwagen, *Arch. Int. Pharmacodyn. Ther.*, **220**, 231 (1976).

(3) A. B. Dobkin, S. Eamkaow, and F. S. Caruso, *Clin. Pharmacol. Ther.*, **18**, 547 (1975).

(4) M. S. Gilbert, R. M. Hanover, D. S. Moylan, and F. S. Caruso, *ibid.*, **20**, 359 (1976).

(5) M. Tavakoli, G. Corrsen, and F. S. Caruso, *Anesth. Analg.*, **55**, 394 (1976).

(6) K. F. Hatch, E. Coles, H. Busey, and S. C. Goldman, *Clin. Chem.*, **22**, 1383 (1976).

(7) A. J. Sedman and J. G. Wagner, *J. Pharm. Sci.*, **65**, 1006 (1976).

(8) E. Ackerman, L. C. Gatewood, J. W. Rosevear, and G. D. Molnar, in "Biomathematics, Volume 1, Concepts and Models of Biomathematics," F. Heinmets, Ed., Dekker, New York, N.Y., 1969, pp. 139–143.

(9) L. E. Mather and G. T. Tucker, *Clin. Pharmacol. Ther.*, **17**, 21 (1975).

(10) J. E. Stambaugh, J. W. Wainer, J. K. Sanstead, and D. M. Hemphill, *J. Clin. Pharmacol.*, **16**, 245 (1976).

(11) S. H. Ngai, B. A. Berkowitz, J. C. Yang, J. Hempstead, and S. Spector, *Anesthesiology*, **44**, 398 (1976).

(12) S. Agurell, L. O. Boreus, E. Gordon, J. E. Lindgren, M. Ehrnebo, and U. Lonroth, *J. Pharm. Pharmacol.*, **26**, 1 (1974).

(13) M. Ehrnebo, L. O. Boreus, and U. Lonroth, *Clin. Pharmacol. Ther.*, **22**, 888 (1977).

(14) R. Schleimer, E. Benjamini, J. Eisele, and G. Henderson, *ibid.*, **23**, 188 (1978).

(15) B. A. Berkowitz, S. H. Ngai, J. C. Yang, J. Hempstead, and S. Spector, *ibid.*, **17**, 629 (1975).

(16) B. E. Dahlstrom, L. K. Paalzow, G. Segre, and A. J. Agren, *J. Pharmacokinet. Biopharm.*, **6**, 41 (1978).

(17) J. W. A. Findlay, R. F. Butz, and R. M. Welch, *Clin. Pharmacol. Ther.*, **22**, 439 (1977).

(18) A. H. Beckett, P. Kourounakis, D. P. Vaughan, and M. Mitchard, *J. Pharm. Pharmacol.*, **22**, 169S (1970).

ACKNOWLEDGMENTS

The assistance of Mr. B. J. Floor and Ms. Ruth Van Buskirk in performing the radioimmunoassay is gratefully acknowledged.

Metabolites and Analogs of 2-Ethyl-2,3-dihydro-5-benzofuranacetic Acid (Furofenac): Chemical and Pharmacological Properties

CLAUDIO CASALINI *, GIUSEPPE MASCELLANI *x, GIANFRANCO TAMAGNONE *, GIULIA CESARANO *, and ANGELO GIUMANINI ‡

Received April 11, 1979, from the **Alfa Farmaceutici Research Laboratories, 40133 Bologna, Italy,* and the ‡*Centre for Gas Chromatography and Mass Spectrometry, University of Bologna, 40126 Bologna, Italy.* Accepted for publication September 19, 1979.

Abstract □ The *in vivo* metabolism of 2-ethyl-2,3-dihydro-5-benzofuranacetic acid (furofenac), a new drug, was studied in rats, dogs, and humans. The drug has antiplatelet-aggregation activity and anti-inflammatory activity combined with low ulcerogenic power. Hydroxylated derivatives and analogous compounds were prepared, and their syntheses and chemical characteristics are described. TLC, GLC, high-pressure liquid chromatography, and GLC–mass spectrometry were applied to urine extracts, and authentic synthetic specimens were used for comparison. The products identified in human and dog urine were mainly conjugation compounds of the drug, while the products in rat urine were hydroxylated derivatives. Some pharmacological characteristics of the metabolites are discussed.

Keyphrases □ 2-Ethyl-2,3-dihydro-5-benzofuranacetic acid—*in vivo* metabolism, rats, dogs, humans □ Drug metabolism—2-ethyl-2,3-dihydro-5-benzofuranacetic acid, *in vivo*, rats, dogs, humans □ Anti-inflammatory agents—2-ethyl-2,3-dihydro-5-benzofuranacetic acid, *in vivo* metabolism, rats, dogs, humans

2-Ethyl-2,3-dihydro-5-benzofuranacetic acid[1] (furofenac, I) was synthesized during a research project aimed at finding compounds with potential anti-inflammatory activity (1, 2). Pharmacotoxicological investigations showed that I has marked anti-inflammatory and antiplatelet-aggregation activity, low toxicity, and very slight ulcerogenicity. It interferes with the biosynthesis of prostaglandins (3), and some *in vivo* pharmacological tests showed that it has good inhibitory activity against thromboxane synthetase (4).

The synthesis of I was optimized (5, 6) in view of clinical trials, and pharmacokinetic studies were undertaken to define its metabolic fate and to search for metabolites of pharmacological interest. The purposes of the present study were to identify and synthesize some of the metabolites of I and to evaluate their anti-inflammatory activity.

EXPERIMENTAL[2]

2-(1-Acetoxyethyl)-2,3-dihydrobenzofuran-5-ylacetic Acid Methyl Ester (IV)—2-(1-Acetoxyethyl)-2,3-dihydrobenzofuran (3.3 g, 16 mmoles) (7) was added at 5° to a solution of zinc chloride (2.5 g, 18 mmoles) in acetic anhydride (5 ml) with stirring. The reaction mixture was poured into 0.5 *N* HCl after 4 hr at 5°, and the methylene chloride extract was dried over sodium sulfate and filtered over 70–230-mesh silica gel (5 g). The solvent was distilled off.

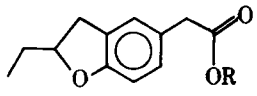

I: R = H
II: R = CH_3

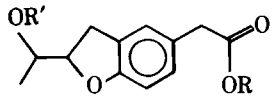

IV: R = CH_3, R′ = CH_3CO
V: R = R′ = H

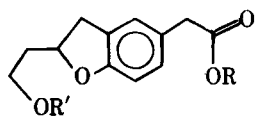

IX: R = CH_3, R′ = CH_3CO
X: R = R′ = H

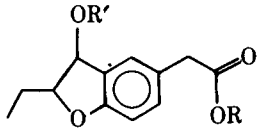

XV: R = R′ = H
XVII: R = CH_3, R′ = CH_3CO

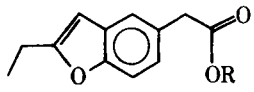

XVI: R = H
XVIII: R = CH_3

2-(1-Acetoxyethyl)-5-acetyl-2,3-dihydrobenzofuran (III), bp 155–158°/2 mm Hg, was obtained in a 58% yield. Compound III (1.6 g, 6.5 mmoles) was added at 5° to a solution of thallium trinitrate (3.1 g, 7 mmoles) in methanol (20 ml) and 70% perchloric acid (4 ml). After 3 hr at 5°, the mixture was kept at room temperature for 2 hr. The mixture then was filtered, diluted, and finally extracted with methylene chloride. The solvent was evaporated to give IV (79% yield).

2-(1-Hydroxyethyl)-2,3-dihydrobenzofuran-5-ylacetic Acid (V)—A mixture of IV (1.6 g, 7 mmoles) and sodium bicarbonate (1.6 g, 19 mmoles) in methanol–water was refluxed for 4 hr. It then was cooled to room temperature and extracted with ethyl acetate. The organic layer was washed (2 *N* HCl and water) and dried over sodium sulfate, and the solvent was evaporated.

Crystallization of the residue from hexane–methylene chloride gave pure V (78% yield), mp 85–87°; IR: 3400, 2960, 2900, 1690, 1490, 1410, 1255, 1210, and 1085 cm^{-1}; UV (CH_3OH): 232 (log ϵ 3.801) and 286 (3.468) nm; mass spectrum: *m/e* 131 (100%) and 222 (M^+, 13); ^1H-NMR: δ 6.60–7.10 (m, 3), 4.59 (m, 1), 3.85 (m, 1), 3.50 (s, 2), 3.14 (d, 2), and 1.22 (d, 3) ppm.

Anal.—Calc. for $C_{12}H_{14}O_4$: C, 64.85; H, 6.35. Found: C, 65.06; H, 6.31.

2-(2-Acetoxyethyl)-2,3-dihydrobenzofuran-5-ylacetic Acid Methyl Ester (IX)—A solution of 2,3-dihydrobenzofuran-2-ylacetic acid ethyl ester (6.9 g, 33.5 mmoles) (8) in ether was added to a slurry of lithium aluminum hydride (2.5 g, 66 mmoles) in ether (50 ml) over 30 min. The reaction mixture was refluxed for 10 hr and then chilled and quenched with 2 *N* HCl. 2-(2-Hydroxyethyl)-2,3-dihydrobenzofuran (VI), obtained from evaporation of the ether extract, was treated with acetic anhydride (10 ml) and pyridine (8 ml). The mixture was heated at 40° for 1 hr, and then ether and 0.5 *N* HCl were added. Usual workup gave 2-(2-acetoxyethyl)-2,3-dihydrobenzofuran (VII) (87% yield), bp 140–142°/2 mm Hg. The IR and UV spectra were as expected.

Compound VII (6 g, 29 mmoles) was added to a solution of anhydrous zinc chloride (4.8 g, 36 mmoles) in acetic anhydride (12 ml, 128 mmoles) with stirring over 30 min at 5°. After 2.5 hr at this temperature, the reaction mixture was extracted with ether. The workup gave 2-(2-acetoxyethyl)-5-acetyl-2,3-dihydrobenzofuran (VIII), bp 202–204°/2 mm Hg, mp 43–44°. The IR and UV spectra agreed with the expected structure.

[1] Furofenac has been patented by Schiapparelli, Turin, Italy.

[2] Melting points were determined in open capillary tubes and are uncorrected. IR spectra were obtained with a Perkin-Elmer 257 spectrophotometer in a potassium bromide disk. UV spectra were obtained with a Perkin-Elmer 550 spectrophotometer in methanol. ^1H-NMR spectra were obtained in deuteromethanol with a Jeol 60 HL spectrometer with tetramethylsilane as the internal standard. Mass spectra were obtained with an LKB 9000 gas–liquid chromatograph–mass spectrometer. GLC analyses were carried out on a Perkin-Elmer 3920 instrument equipped with a flame-ionization detector. HPLC analyses were performed on a Perkin-Elmer 601 instrument equipped with a UV/visible variable-wavelength detector. Elemental analyses were performed by Istituto di Chimica degli Intermedi, University of Bologna. All reagents and solvents were of analytical reagent grade and were used without further purification.

0022-3549/80/0200-0164$01.00/0
© 1980, American Pharmaceutical Association

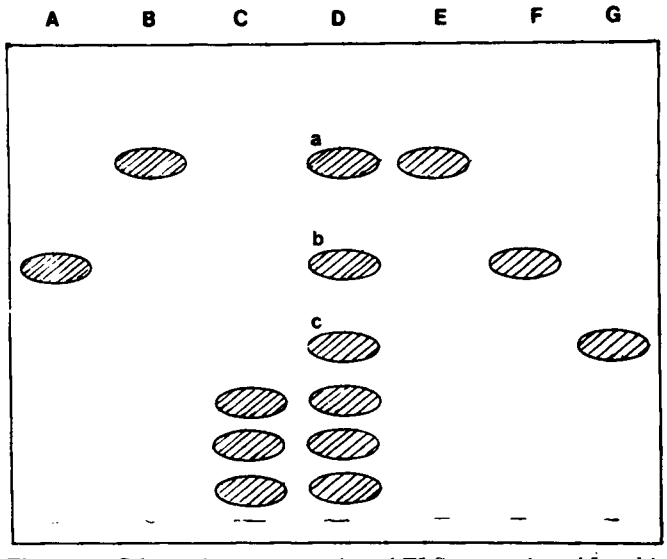

Figure 1—*Schematic representation of TLC separation of I and its metabolites. Key: A, XV; B, I; C, urine blank; D, chloroform extract A of rat urine samples; E, XVI; F, V; and G, X.*

Compound IX was obtained (85% yield) from VIII by treatment with thallium trinitrate as described for the preparation of IV.

2-(2-Hydroxyethyl)-2,3-dihydrobenzofuran-5-ylacetic Acid (X)—Crude IX was hydrolyzed with sodium hydroxide in ethanol–water to afford X (77% yield), mp 111–113° (dichloroethane); IR: 3400, 2920, 1690, 1495, 1410, 1255, 1210, and 1055 cm^{-1}; UV (CH_3OH): 232 (log ϵ 3.823) and 286 (3.475) nm; mass spectrum: *m/e* 222 (M^+, 100%); ^1H-NMR: δ 6.54–7.05 (m, 3), 4.93 (m, 1), 3.73 (t, 2), 3.48 (s, 2), 3.00 (m, 2), and 1.90 (m, 2) ppm.

Anal.—Calc. for $C_{12}H_{14}O_4$: C, 64.85; H, 6.35. Found: C, 64.58; H, 6.34.

2-Ethyl-3-hydroxy-2,3-dihydrobenzofuran-5-ylacetic Acid (XV)—Butyryl chloride (10.5 g, 0.1 mole) was added to a solution of *p*-hydroxyphenylacetic acid ethyl ester (18 g, 0.1 mole) and pyridine (7.9 g, 0.1 mole) in methylene chloride (50 ml) over 30 min. The mixture was refluxed for 2 hr and worked up to give *p*-butyryloxyphenylacetic acid ethyl ester (XI).

Compound XI (25 g, 0.1 mole) and aluminum chloride (32 g, 0.24 mole) were heated at 120–130°. The mixture was stirred with 2 *N* HCl, and the precipitate obtained was filtered. Crystallization from carbon tetrachloride yielded 3-butyryl-4-hydroxyphenylacetic acid (XII) (69% yield), mp 115–117°.

Bromine (8.3 g, 52 mmoles) was added to a solution of XII (11.1 g, 0.05 mole) in dichloroethane (60 ml) over 2.5 hr. After standing overnight, the solution was treated with hexane to afford 3-[(α-bromo)butyryl]-4-hydroxyphenylacetic acid (XIII) (88% yield), mp 135–137°.

Treatment of XIII (13 g, 43 mmoles) with a solution of sodium bicarbonate (13 g, 0.15 mole) in water (90 ml) gave 2-ethyl-3-oxo-2,3-dihydrobenzofuran-5-ylacetic acid (XIV) (78%), mp 118–120° (cyclohexane–ethyl acetate).

A solution of XIV (6.6 g, 33 mmoles) and sodium bicarbonate (2.8 g, 33 mmoles) in 30 ml of water was treated slowly with sodium borohydride (0.8 g, 21 mmoles). After 1.5 hr at room temperature, the reaction mixture was quenched with ethanol (8 ml) and chloroacetic acid (8.5 g, 90 mmoles) to give XV, mp 122–123° (80% yield); IR: 3200, 2940, 1680, 1625, 1485, 1415, 1300, 1270, 1240, 1210, 1145, 1060, 1025, 980, 925, 890, 815, 785, 755, and 710 cm^{-1}; UV: 232 (log ϵ 3.850) and 286 (3.426) nm; ^1H-NMR: δ 7.30–6.60 (m, 3), 4.20 (m, 1), 3.42 (s, 2), 1.70 (m, 2), and 1.00 (t, 3) ppm; mass spectrum: *m/e* 189 (100%) and 222 (M^+, 98).

Anal.—Calc. for $C_{12}H_{14}O_4$: C, 64.85; H, 6.35. Found: C, 65.25; H, 6.26.

After heating in 2 *N* HCl for 0.5 hr, XV was dehydrated to XVI.

2-Ethylbenzofuran-5-ylacetic Acid (XVI)—*N*-Bromosuccinimide (1.8 g, 10 mmoles) was added over 30 min to a carbon tetrachloride solution (30 ml) of I (2.05 g, 10 mmoles) and a catalytic amount of benzoyl peroxide. The mixture was refluxed for 1 hr, cooled, and filtered on a small silica gel column, from which XVI was eluted with methylene chloride–methanol (50:1, v/v). Pure XVI was obtained (60% yield) by crystallization from cyclohexane, mp 90–92°; IR: 2960, 2900, 1690, 1590, 1465, 1410, 1295, 1265, 1235, 1190, 1150, and 930 cm^{-1}; UV: 249 (log ϵ 4.129), 281 (3.514), and 288 (3.537) nm; mass spectrum: *m/e* 159 (100%) and 204 (M^+, 71); ^1H-NMR (*d*-chloroform): δ 10.86 (s, 1), 7.10–7.48 (m, 3), 6.38 (s, 1), 3.70 (s, 2), 2.81 (s, 2), and 1.30 (t, 3) ppm.

Anal.—Calc. for $C_{12}H_{12}O_3$: C, 70.57; H, 5.92. Found: C, 70.90; H, 5.99.

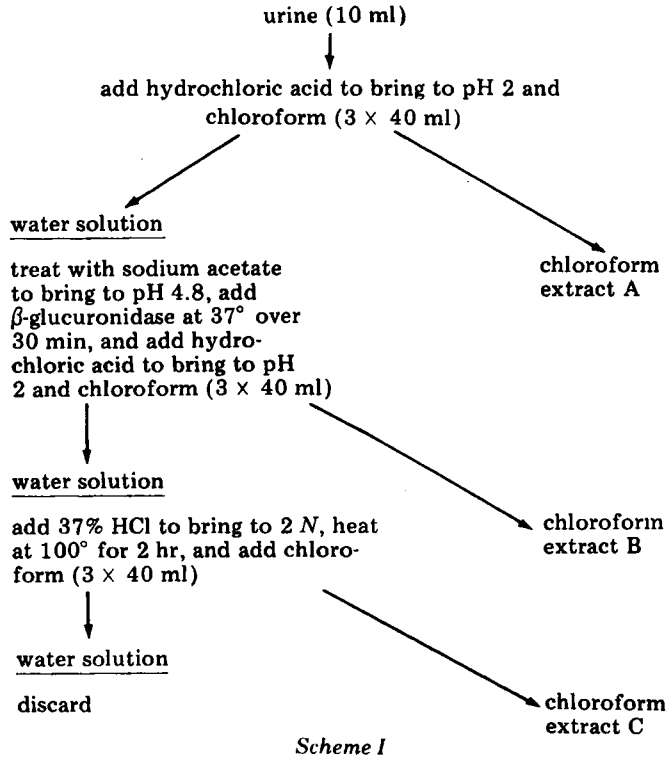

Scheme I

***In Vivo* Metabolism**—Adult male rats (Wistar), 250 g, and male beagle dogs, ~12 kg, were fed normally during drug administration. The cages were equipped with a urine–feces separator. No metabolic inducers were used. Tests also were performed on human volunteers in good health.

Compound I was administered orally in single doses to rats (500 mg/kg in arabic gum), dogs (100 mg/kg in a jelly capsule), and human volunteers (6.5 mg/kg in a hard jelly capsule). Individual 24-hr urine was collected after administration.

Urine Extraction—The drug and metabolites were extracted from collected urine according to Scheme I. Each chloroform extract was dried

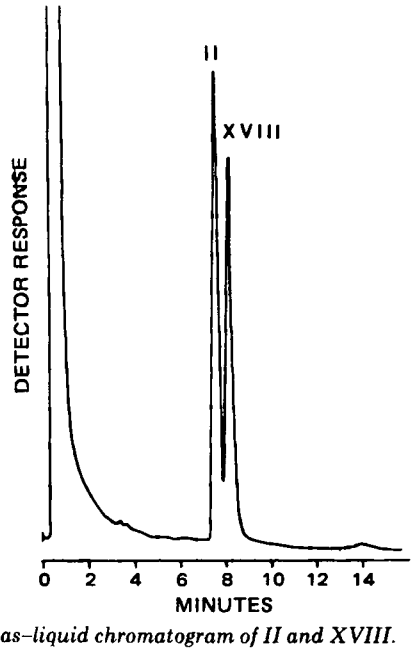

Figure 2—*Gas–liquid chromatogram of II and XVIII.*

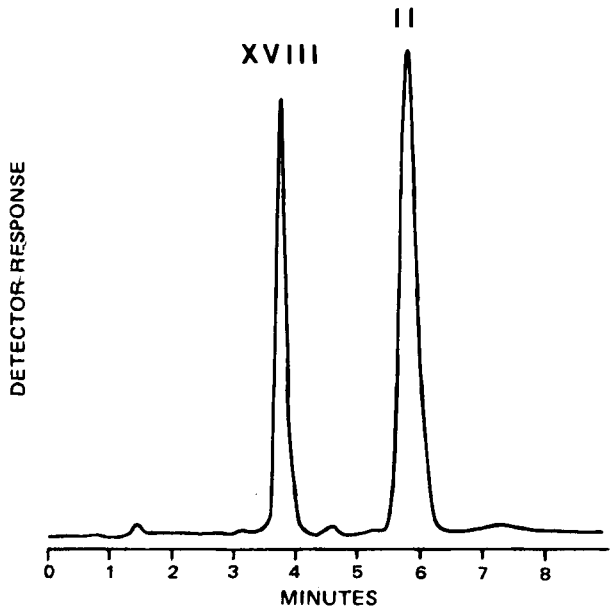

Figure 3—*High-pressure liquid chromatogram of II and XVIII.*

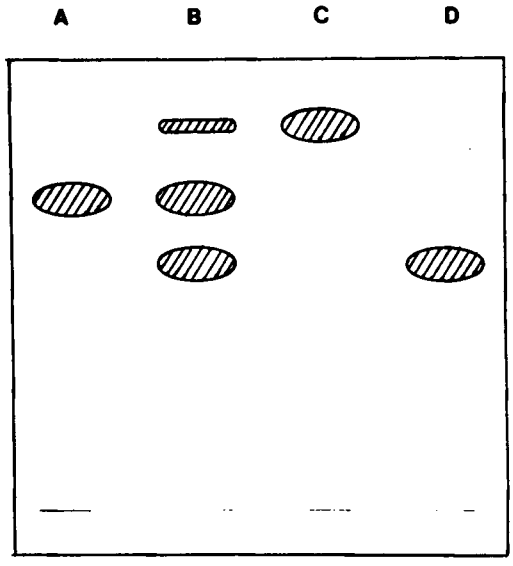

Figure 4—*Schematic representation of the TLC separation of IV, XVII, and XVIII. Key: A, XVII; B, urine band with* R_f *equal to that of V and XV eluted from the plate and treated with diazomethane and then acetic anhydride; C, XVIII; and D, IV.*

over sodium sulfate and concentrated to about 1 ml. The blanks were obtained according to the same procedure.

TLC—The chloroform extract (0.3 ml of the concentrated solution) was deposited on silica gel F-254 layers using benzene–dioxane–acetic acid (90:10:2, v/v/v) as the eluent and appropriate blanks and authentic samples for comparison.

TLC spots other than those common to the blank were scraped off and extracted with methanol. A UV spectrum was recorded for each solution, which was evaporated subsequently to dryness and then treated with an ether solution of diazomethane. The methyl esters were acetylated at 40° over 2 hr with pyridine and acetic anhydride, the excess of which was destroyed with methanol.

Derivatives IV, IX, XVII, and XVIII thus were obtained from V, X, XV[3], and XVI, respectively. These derivatives were analyzed for homogeneity by GLC, TLC, and high-pressure liquid chromatography (HPLC). Final identification was by mass spectrometry, with the appropriate inlet (direct or GLC), through comparison with the corresponding authentic sample.

Derivatives IV, XVII, and XVIII also were separated by TLC using a 0.75% solution of ethanol in chloroform as the eluent.

GLC—Compounds II and XVIII were separated using a steel column (2 m × 2.5 mm i.d.), packed with SP-1000 (3%) on Chromosorb HP (80–100 mesh) at 190°, with nitrogen as the carrier gas (30 ml/min). An E-301 (3%) on Chromosorb G (80–100 mesh) packing was used for IV and IX at 170°.

HPLC—Separations were performed with a steel column (25 × 0.26 cm) packed with Cyano-Sil-X-1 and set at 40° with a UV detector (285 nm). Chloroform–hexane (1:4, v/v, 1 ml/min) was the eluent.

Mass Spectrometry—Electron-impact mass spectra at 70 ev (source temperature 270–290°) were recorded *via* direct inlet at room temperature. When suitable, previous GLC separation was performed using helium as the carrier gas and a Ryhage separator at 300°. The spectral characteristics were reported previously (9).

Pharmacological and Toxicological Evaluations—The activity of the metabolites was tested in the carrageenan edema test (10). Mouse LD_{50} was determined according to the Spearman–Kärber procedure (11). All metabolites were less active than I and had similar toxicity.

RESULTS AND DISCUSSION

The preliminary data obtained by examination of the thin-layer chromatogram of the urine of rats treated with I suggested the likely formation of metabolites with the same dihydrobenzofuranic structure as I but with higher polarity. However, the neat benzofuranic UV spectrum of the spot corresponding to I was unexpected. The high reactivity toward acetic anhydride of the more polar metabolites and other chemical evidence, as well as known pharmacokinetic transformations [*e.g.*, benzylic hydroxylation (12) and ω and $\omega - 1$ side-chain hydroxylations (13)], indicated that the more polar metabolites were hydroxylated, nonphenolic compounds.

The puzzle of the benzofuranic spot was resolved upon observation of its variable intensity in different extraction conditions of the same urine pool. In particular, a nearly complete disappearance of the benzofuranic spot, accompanied by a slight increase in intensity of one of the polar spots, was observed under strictly defined extraction conditions. This observation suggested that it was a possible chemical artifact due to the decomposition of one of the actual metabolites to the benzofuranic analog of I. The following procedure was followed specifically for the identification of metabolites.

Chloroform extract A of rat urine was resolved into three TLC spots (a, b, and c in Fig. 1) which were not present in the chromatograms of the corresponding blanks. Spot a consisted of two components that could be separated and identified by GLC (Fig. 2) and HPLC (Fig. 3) of the corresponding methyl esters by comparison of their behavior with that of the analogous derivatives of authentic specimens of I and XVI. Spot b was resolved after the methylation–acetylation procedure into two spots (Fig. 4) with R_f values identical to those of independently prepared XVII and IV. Mass spectral analysis confirmed that spot b consisted of XV and

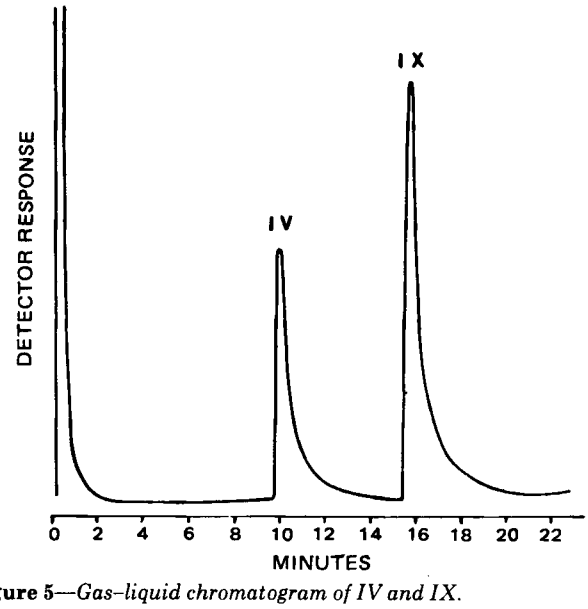

Figure 5—*Gas–liquid chromatogram of IV and IX.*

[3] On methylation and acylation, XV gave rise to XVII and to small amounts of XVIII.

Table I—Drug and Urinary Metabolites Separated from Different Animal Species [a]

Compound	Rats	Dogs	Humans
I	Trace	+	Trace
I glucuronide	−	+++	+++++
I labile acid derivative	−	+++++	++++
XV	+++	+	+
V	+++	+	−
X	++++	++	−

[a] The + indicates the relative abundance of the metabolites in the species.

V. Finally, spot c proved to be X on the basis of TLC and GLC data. The gas–liquid chromatogram of IV and IX is shown in Fig. 5.

In chloroform extracts B and C of rat urine, neither I nor compounds structurally related to I could be detected; a single spot with the same R_f as I was observed in the thin-layer chromatogram of the chloroform extracts B and C of both humans and dogs.

The mass spectra of the compounds extracted from the urine samples were identical to those of the derivatives of I, V, X, XV, and XVI. A comparative examination of the results obtained by the various techniques showed that rats metabolize I to the hydroxylated Compounds X, V, and XV.

Compound XVI is not a true metabolite, and its formation was due to a chemical artifact. In fact, it was only present in substantial amounts when the extraction was made in strongly acidic conditions, whereas the true Metabolite XV was detected in the extracts obtained in weakly acidic conditions. Compound XVI is formed from XV by dehydration.

In rat urine, traces of I also were present. In contrast to the findings for rats, the qualitative pattern of the metabolites of I in dogs was closer to that found in humans. Compound I was eliminated in a form conjugated with glucuronic acid, as shown by TLC of the extracts before and after treatment with β-glucuronidase.

Another conjugate, which gives I when treated with acid, was found in the urine of dogs and humans, but its identity was not elucidated. Amino acid conjugation is a possibility and was observed previously in the metabolism of other arylacetic anti-inflammatory drugs (14, 15). The results of the metabolism of I in different species are shown in Table I.

The initial stage of many biological oxidations is believed to be the abstraction of a hydrogen atom from the substrate. Lowering of the activation barrier for the homolytic cleavage of the CH bonds in I is expected only for the benzylic positions and the CH bond alpha to the ether oxygen. Interestingly, only the ring benzylic position was hydroxylated.

The toxicities of the metabolites were on the same order as the toxicity of the parent drug, and their activities in the carrageenan edema test were lower. Further detailed pharmacological and pharmacokinetic studies on I and its analogs are in progress in these laboratories.

REFERENCES

(1) G. F. Tamagnone and F. De Marchi, German Offen. 2,526,089 (1975); through *Chem. Abstr.*, **84**, P 135469 (1976).

(2) G. F. Tamagnone, M. V. Torrielli, and F. De Marchi, in "Simposio Internazionale sulla Ricerca Scientifica," GIRF-SISF, Eds., Ferro, Milan, Italy, 1975, p. 507.

(3) F. Berti, G. P. Velo, D. Bertoli, C. Casalini, G. Mascellani, E. Palazzini, and G. F. Tamagnone, "International Congress of Inflammation," Bologna, Italy, Oct.–Nov. 1978.

(4) A. K. Sim, M. E. Davies, and A. E. Scott, Inveresk Research International, Edinburgh, Scotland, unpublished results.

(5) G. F. Tamagnone, G. Mascellani, C. Casalini, and M. Fantuz, *Boll. Chim. Farm.*, **116**, 81 (1977).

(6) G. F. Tamagnone, Italian pat. appl. 3520 A/78 (1978).

(7) R. L. Shriner and J. Anderson, *J. Am. Chem. Soc.*, **61**, 2705 (1939).

(8) D. Misiti, F. De Marchi, and V. Rosnati, *Gazz. Chim. Ital.*, **93**, 52 (1963).

(9) C. Casalini, G. Cesarano, G. Mascellani, G. F. Tamagnone, and A. G. Giumanini, "Fifth International Symposium on Mass Spectrometry in Biochemistry and Medicine," Rimini, Italy, June 1978.

(10) C. A. Winter, E. A. Risley, and G. W. Nuss, *J. Pharmacol. Exp. Ther.*, **369**, 141 (1963).

(11) D. J. Finney, "Statistical Methods in Biological Assay," Griffin, London, England, 1964, p. 254.

(12) R. E. McMahon, H. R. Sullivan, C. J. Cymerman, and W. E. Pereira, Jr., *Arch. Biochem. Biophys.*, **132**, 575 (1969).

(13) E. C. Schreiber, *J. Pharm. Sci.*, **63**, 1177 (1974).

(14) A. Rubin, B. E. Rodda, P. Warrick, A. S. Ridolfo, and C. M. Gruber, *ibid.*, **61**, 739 (1972).

(15) G. F. Thompson and J. M. Collins, *ibid.*, **62**, 937 (1973).

GLC Determination of α- and β-Tribenosides in Human Plasma

ANTOINE SIOUFI ˣ and FRANÇOISE POMMIER

Received July 6, 1979, from the *Biopharmaceutical Research Center, Ciba-Geigy, B.P. 308, 92506 Rueil-Malmaison, France.* Accepted for publication August 30, 1979.

Abstract □ The determination of α-tribenoside at concentrations down to 10 ng/ml and β-tribenoside at concentrations down to 5 ng/ml in human plasma is described. After addition of an internal standard, α- and β-tribenosides are extracted at basic pH into benzene. Both compounds are derivatized with *N*-heptafluorobutyrylimidazole. The derivatives are determined by GLC using a ^{63}Ni-electron-capture detector.

Keyphrases □ Tribenoside—GLC determination of α- and β-anomers, human plasma □ Anti-inflammatory agents—tribenoside, GLC determination of α- and β-anomers, human plasma □ Antiphlebotic agents—tribenoside, GLC determination of α- and β-anomers, human plasma

Tribenoside[1] (ethyl 3,5,6-tri-*O*-benzyl-D-glucofuranoside) is an anti-inflammatory and antiphlebotic agent. It is a mixture of about 33% of the α-anomer and 67% of the β-anomer.

No analytical technique is available for the quantitative assay of the two anomers in plasma. Tribenoside metabolism was studied in rats and dogs after administration of the ^{14}C-labeled drug (1); the blood concentration of the β-anomer remained higher than that of the α-anomer for the first few hours, but the situation was reversed after 20 hr. Metabolism splits the three benzyl groups and the ethyl group, giving several metabolites from each anomer.

This paper describes the GLC determination in plasma of α-tribenoside down to 10 ng/ml and of β-tribenoside down to 5 ng/ml, using β-clobenoside as the internal standard.

[1] Glyvenol, Ciba-Geigy.

0022-3549/80/0200-0167$01.00/0

© 1980, American Pharmaceutical Association

Table I—Drug and Urinary Metabolites Separated from Different Animal Species [a]

Compound	Rats	Dogs	Humans
I	Trace	+	Trace
I glucuronide	−	+++	+++++
I labile acid derivative	−	+++++	++++
XV	+++	+	+
V	+++	+	−
X	++++	++	−

[a] The + indicates the relative abundance of the metabolites in the species.

V. Finally, spot c proved to be X on the basis of TLC and GLC data. The gas–liquid chromatogram of IV and IX is shown in Fig. 5.

In chloroform extracts B and C of rat urine, neither I nor compounds structurally related to I could be detected; a single spot with the same R_f as I was observed in the thin-layer chromatogram of the chloroform extracts B and C of both humans and dogs.

The mass spectra of the compounds extracted from the urine samples were identical to those of the derivatives of I, V, X, XV, and XVI. A comparative examination of the results obtained by the various techniques showed that rats metabolize I to the hydroxylated Compounds X, V, and XV.

Compound XVI is not a true metabolite, and its formation was due to a chemical artifact. In fact, it was only present in substantial amounts when the extraction was made in strongly acidic conditions, whereas the true Metabolite XV was detected in the extracts obtained in weakly acidic conditions. Compound XVI is formed from XV by dehydration.

In rat urine, traces of I also were present. In contrast to the findings for rats, the qualitative pattern of the metabolites of I in dogs was closer to that found in humans. Compound I was eliminated in a form conjugated with glucuronic acid, as shown by TLC of the extracts before and after treatment with β-glucuronidase.

Another conjugate, which gives I when treated with acid, was found in the urine of dogs and humans, but its identity was not elucidated. Amino acid conjugation is a possibility and was observed previously in the metabolism of other arylacetic anti-inflammatory drugs (14, 15). The results of the metabolism of I in different species are shown in Table I.

The initial stage of many biological oxidations is believed to be the abstraction of a hydrogen atom from the substrate. Lowering of the activation barrier for the homolytic cleavage of the CH bonds in I is expected only for the benzylic positions and the CH bond alpha to the ether oxygen. Interestingly, only the ring benzylic position was hydroxylated.

The toxicities of the metabolites were on the same order as the toxicity of the parent drug, and their activities in the carrageenan edema test were lower. Further detailed pharmacological and pharmacokinetic studies on I and its analogs are in progress in these laboratories.

REFERENCES

(1) G. F. Tamagnone and F. De Marchi, German Offen. 2,526,089 (1975); through *Chem. Abstr.*, **84**, P 135469 (1976).

(2) G. F. Tamagnone, M. V. Torrielli, and F. De Marchi, in "Simposio Internazionale sulla Ricerca Scientifica," GIRF-SISF, Eds., Ferro, Milan, Italy, 1975, p. 507.

(3) F. Berti, G. P. Velo, D. Bertoli, C. Casalini, G. Mascellani, E. Palazzini, and G. F. Tamagnone, "International Congress of Inflammation," Bologna, Italy, Oct.–Nov. 1978.

(4) A. K. Sim, M. E. Davies, and A. E. Scott, Inveresk Research International, Edinburgh, Scotland, unpublished results.

(5) G. F. Tamagnone, G. Mascellani, C. Casalini, and M. Fantuz, *Boll. Chim. Farm.*, **116**, 81 (1977).

(6) G. F. Tamagnone, Italian pat. appl. 3520 A/78 (1978).

(7) R. L. Shriner and J. Anderson, *J. Am. Chem. Soc.*, **61**, 2705 (1939).

(8) D. Misiti, F. De Marchi, and V. Rosnati, *Gazz. Chim. Ital.*, **93**, 52 (1963).

(9) C. Casalini, G. Cesarano, G. Mascellani, G. F. Tamagnone, and A. G. Giumanini, "Fifth International Symposium on Mass Spectrometry in Biochemistry and Medicine," Rimini, Italy, June 1978.

(10) C. A. Winter, E. A. Risley, and G. W. Nuss, *J. Pharmacol. Exp. Ther.*, **369**, 141 (1963).

(11) D. J. Finney, "Statistical Methods in Biological Assay," Griffin, London, England, 1964, p. 254.

(12) R. E. McMahon, H. R. Sullivan, C. J. Cymerman, and W. E. Pereira, Jr., *Arch. Biochem. Biophys.*, **132**, 575 (1969).

(13) E. C. Schreiber, *J. Pharm. Sci.*, **63**, 1177 (1974).

(14) A. Rubin, B. E. Rodda, P. Warrick, A. S. Ridolfo, and C. M. Gruber, *ibid.*, **61**, 739 (1972).

(15) G. F. Thompson and J. M. Collins, *ibid.*, **62**, 937 (1973).

GLC Determination of α- and β-Tribenosides in Human Plasma

ANTOINE SIOUFI ˣ and FRANÇOISE POMMIER

Received July 6, 1979, from the *Biopharmaceutical Research Center, Ciba-Geigy, B.P. 308, 92506 Rueil-Malmaison, France.* Accepted for publication August 30, 1979.

Abstract □ The determination of α-tribenoside at concentrations down to 10 ng/ml and β-tribenoside at concentrations down to 5 ng/ml in human plasma is described. After addition of an internal standard, α- and β-tribenosides are extracted at basic pH into benzene. Both compounds are derivatized with *N*-heptafluorobutyrylimidazole. The derivatives are determined by GLC using a ^{63}Ni-electron-capture detector.

Keyphrases □ Tribenoside—GLC determination of α- and β-anomers, human plasma □ Anti-inflammatory agents—tribenoside, GLC determination of α- and β-anomers, human plasma □ Antiphlebotic agents—tribenoside, GLC determination of α- and β-anomers, human plasma

Tribenoside[1] (ethyl 3,5,6-tri-*O*-benzyl-D-glucofuranoside) is an anti-inflammatory and antiphlebotic agent. It is a mixture of about 33% of the α-anomer and 67% of the β-anomer.

No analytical technique is available for the quantitative assay of the two anomers in plasma. Tribenoside metabolism was studied in rats and dogs after administration of the ^{14}C-labeled drug (1); the blood concentration of the β-anomer remained higher than that of the α-anomer for the first few hours, but the situation was reversed after 20 hr. Metabolism splits the three benzyl groups and the ethyl group, giving several metabolites from each anomer.

This paper describes the GLC determination in plasma of α-tribenoside down to 10 ng/ml and of β-tribenoside down to 5 ng/ml, using β-clobenoside as the internal standard.

[1] Glyvenol, Ciba-Geigy.

0022-3549/80/0200-0167$01.00/0

© 1980, American Pharmaceutical Association

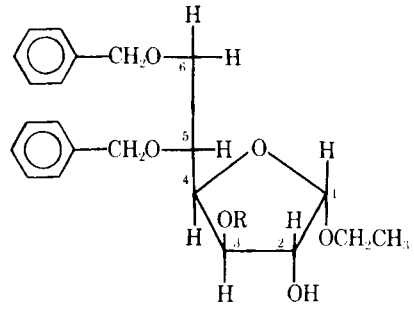

α-tribenoside: R = —CH_2—

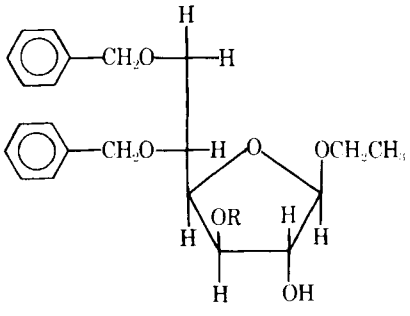

β-tribenoside: R = —CH_2—

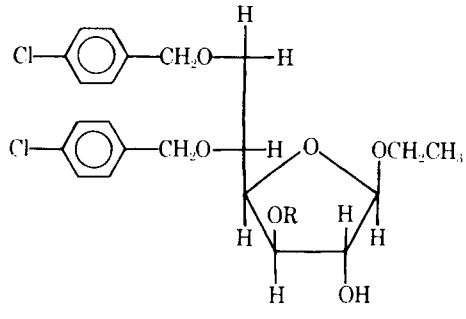

β-clobenoside: R = —C_7H_7

EXPERIMENTAL

Reagents—The benzene[2], sodium hydroxide[3], and heptane[3] were analytical grade. *N*-Heptafluorobutyrylimidazole[4] was stored at 4° in glass ampuls under nitrogen. The methanolic internal standard solution contained 500 ng of β-clobenoside[5]/ml.

Materials—The glassware was washed for 30 min in an ultrasonic bath, first with water and then with methanol.

The gas chromatograph[6] was equipped with a 15-mCi-^{63}Ni-electron-capture detector[7]. Peak areas were given by an electronic integrator[8]. The column was operated at 270°, the injector temperature was 300°, and the detector was set at 300° with argon–methane (90:10) at a 60-ml/min flow rate.

Glass columns (2 m × 3 mm i.d.) were washed with 1 *M* HCl, distilled water, acetone, and benzene and then were silanized with a 1% (v/v) solution of hexamethyldisilazane in benzene. The columns were washed again with benzene and dried at 100°.

The column packing[9] was 3% OV-17 on 100–120-mesh Gas Chrom Q. The filled columns were flushed with the carrier gas at a flow rate of 40 ml/min and heated to 300° at 1°/min. The column temperature was held overnight at 300° and at 270° throughout the next day. The temperature then was increased repeatedly from 150 to 250° for 24 hr. During these programmed cycles, the columns were conditioned further by the injection of 100 μl of a silylating agent[10] in portions between 150 and 220°. After this procedure, the columns were ready for use.

Extraction—The internal standard solution, 300 μl, was measured into a stoppered glass tube and dried under a nitrogen stream in a water bath at 37°. One milliliter of the sample, 2 ml of 0.1 *M* NaOH, and 4 ml of benzene were added. The tube was shaken mechanically[11] for 15 min and centrifuged at 5000 rpm for 10 min.

An aliquot of the benzene phase was transferred to another tube and dried under a nitrogen stream in a water bath at 37°.

Derivatization and Chromatography—To the dry residue were added 100 μl of heptane and 50 μl of *N*-heptafluorobutyrylimidazole. The solution was mixed thoroughly[12] for 30 sec and allowed to stand for 10 min at room temperature. Then 3 ml of water and 2 ml of heptane were added, and the tube was shaken thoroughly[12] for 30 sec and centrifuged for 3 min at 4000 rpm.

An aliquot of the heptane phase was transferred to another tube and dried under a nitrogen stream in a water bath at 37°; 500 μl of heptane was added, and the tube was shaken on a mixer[12].

[2] Mallinckrodt.
[3] Merck.
[4] Regis.
[5] Ciba-Geigy.
[6] Model 5710 A, Hewlett-Packard.
[7] Model 18713 A, Hewlett-Packard.
[8] Model 3380 A, Hewlett-Packard.
[9] Applied Science Laboratories.

Table I—Precision and Reproducibility of α-Tribenoside Assay (n = 6)

Concentration Added, ng/ml	Mean Concentration Found, ng/ml	95% Confidence Interval	Coefficient of Variation, *SD* %
10	10	8.5–11.5	12.2
25	25	23–27	5.9
50	49	47–51	4.2
75	77	74–80	3.2
100	100	94–106	4.8
150	150	145–154	2.9

Table II—Precision and Reproducibility of β-Tribenoside Assay (n = 6)

Concentration Added, ng/ml	Mean Concentration Found, ng/ml	95% Confidence Interval	Coefficient of Variation, *SD* %
5	4.8	4.4–5.3	8.9
10	9.8	8.2–11.4	13.2
25	26	25–27	3.2
50	50	49–51	2.3
75	75	74–76	1.2
100	100	97–102	2.3
150	150	148–152	1.1

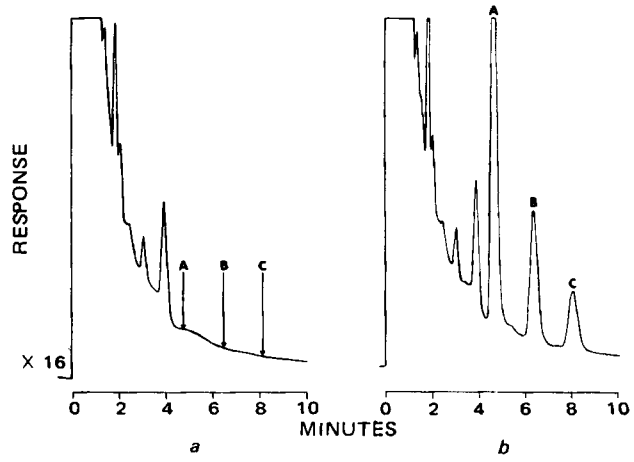

Figure 1—*Sample chromatograms of human plasma blank* (a) *and the same plasma spiked with 150 ng of internal standard/ml (A), 100 ng of β-tribenoside/ml (B), and 100 ng of α-tribenoside/ml (C)* (b).

[10] Silyl 8, Pierce.
[11] Infors.
[12] Vortex

Table III—α- and β-Tribenosides (Nanograms per Milliliter) in the Plasma of a Human Subject Given 800 mg of Tribenoside Orally for 7 Days

Anomer	Time after Administration								
	0 hr	1 hr	2 hr	3 hr	4 hr	6 hr	8 hr	Day 2	Day 8
α-Tribenoside	ND[a]	41	53	20	10	6	6	11	14
β-Tribenoside	ND	94	92	51	36	24	24	52	47

[a] ND = not detected.

A 2-μl portion of the heptane solution was injected into the gas chromatograph by the solvent flush technique.

The α- and β-tribenoside content was calculated from the ratio of the peak areas by reference to a calibration curve prepared from a series of dried methanolic α- and β-tribenoside solutions to which plasma was added to yield concentrations between 2 and 150 ng/ml.

Human Subject—A healthy male subject, who had not received any drug for 8 days prior to the experiment and did not take any other drug during the study, received two 400-mg tribenoside capsules before breakfast for 7 days.

Blood samples were collected on the 1st day before and 1, 2, 3, 4, 6, and 8 hr after drug administration. Blood was collected on Days 2 and 3, just before the morning drug administration.

RESULTS AND DISCUSSION

Reaction Time—The derivatization was applied to 10, 25, and 500 ng of α- and β-tribenosides, and the reaction time was varied from 1 to 30 min. Derivative formation was evaluated by peak areas; derivatization was immediate, and the yield of the α- and β-tribenosides was the same over 1–30 min. For convenience and safety, the suggested derivatization time is 10 min.

Sensitivity and Precision—Tables I and II show that when the concentrations of α- and β-tribenosides reached the lower limits, the coefficient of variation increased to ~10. These lower concentrations (10 and 5 ng/ml for α- and β-tribenosides, respectively) may be taken as the assay sensitivity limits; lower concentrations could be detected but could not be determined accurately.

Plasma Interferences—Figures 1*a* and 1*b* show the chromatograms of a blank human plasma extract and the same plasma spiked with 100 ng of α- and β-tribenosides and 150 ng of β-clobenoside, respectively. No interference of the normal plasma components was noted.

Specificity—The four main metabolites (all a mixture of the corresponding α- and β-anomers) were derivatized under the same conditions as tribenoside. These metabolites were ethyl 3,5-di-*O*-benzyl-D-glucofuranoside, ethyl 3,6-di-*O*-benzyl-D-glucofuranoside, ethyl 5,6-di-*O*-benzyl-D-glucofuranoside, and 3,5,6-tri-*O*-benzyl-D-glucofuranoside. Their derivatives were not recorded when chromatographed under the same conditions as tribenoside at concentrations of ≤1 mg/ml.

Application—The technique was used to study the elimination of α- and β-tribenosides after daily oral administration to humans. The plasma concentrations of α- and β-tribenosides are given in Table III. The determinations were done in duplicate.

REFERENCE

(1) H. Keberle and K. Schmid, in "Aspects Importants de l'Insuffisance Veineuse Chronique," Symposium de Porto Cervo (Italy), Ciba-Geigy, Basel, Switzerland, 1970, pp. 128–139.

ACKNOWLEDGMENTS

The authors thank Dr. K. Schmid, Pharmacological Chemistry Department, Ciba-Geigy, Basel, Switzerland, for helpful discussions and Dr. J. P. Schoeller, Medical Department, Ciba-Geigy, France, for conducting the clinical trial.

Effect of Polyols on Interaction of Paraben Preservatives with Polysorbate 80

JAMES BLANCHARD

Received April 3, 1979, from the *Department of Pharmaceutical Sciences, College of Pharmacy, University of Arizona, Tucson, AZ 85721.* Accepted for publication September 14, 1979.

Abstract □ A quantitative study of the interaction of the methyl, ethyl, propyl, and butyl esters of *p*-hydroxybenzoic acid with polysorbate 80 in the presence and absence of two polyols (propylene glycol and glycerol), which were potential competitors, was performed. The results indicate that neither competitor displaced significant amounts of the parabens from their binding sites on polysorbate 80. The previously observed synergistic antimicrobial effects of these polyols appear to be due to a mechanism other than the displacement of the parabens from their micellar binding sites.

Keyphrases □ Polyols—effect of propylene glycol and glycerol on interaction of parabens with polysorbate 80 □ Propylene glycol—effect on interaction of parabens with polysorbate 80 □ Glycerol—effect on interaction of parabens with polysorbate 80 □ Parabens—interaction with polysorbate 80, effect of propylene glycol and glycerol □ Preservatives—parabens, interaction with polysorbate 80, effect of propylene glycol and glycerol □ Polysorbate 80—interaction with paraben preservatives, effect of propylene glycol and glycerol

Several reports described the ability of nonionic surfactants (including polysorbates) to interfere with the activity of phenolic preservatives such as the parabens (1–4). This inactivation is believed to be due to the formation of a complex between the preservative molecules and the surfactant micelle, based on the assumption that the preservative antimicrobial activity is primarily due to the unbound form (3).

Previous work indicated that polyols such as propylene glycol or glycerol could function as preservatives or synergists to preservatives (5–7). Since these studies were designed to determine only whether preservative activity was enhanced by polyol addition, a systematic study was needed to evaluate the mechanism underlying the increased preservative activity associated with the polyols. Thus, a model system was developed to evaluate the ability

0022-3549/80/0200-0169$01.00/0
© 1980, American Pharmaceutical Association

Table III—α- and β-Tribenosides (Nanograms per Milliliter) in the Plasma of a Human Subject Given 800 mg of Tribenoside Orally for 7 Days

Anomer	Time after Administration								
	0 hr	1 hr	2 hr	3 hr	4 hr	6 hr	8 hr	Day 2	Day 8
α-Tribenoside	ND[a]	41	53	20	10	6	6	11	14
β-Tribenoside	ND	94	92	51	36	24	24	52	47

[a] ND = not detected.

A 2-μl portion of the heptane solution was injected into the gas chromatograph by the solvent flush technique.

The α- and β-tribenoside content was calculated from the ratio of the peak areas by reference to a calibration curve prepared from a series of dried methanolic α- and β-tribenoside solutions to which plasma was added to yield concentrations between 2 and 150 ng/ml.

Human Subject—A healthy male subject, who had not received any drug for 8 days prior to the experiment and did not take any other drug during the study, received two 400-mg tribenoside capsules before breakfast for 7 days.

Blood samples were collected on the 1st day before and 1, 2, 3, 4, 6, and 8 hr after drug administration. Blood was collected on Days 2 and 3, just before the morning drug administration.

RESULTS AND DISCUSSION

Reaction Time—The derivatization was applied to 10, 25, and 500 ng of α- and β-tribenosides, and the reaction time was varied from 1 to 30 min. Derivative formation was evaluated by peak areas; derivatization was immediate, and the yield of the α- and β-tribenosides was the same over 1–30 min. For convenience and safety, the suggested derivatization time is 10 min.

Sensitivity and Precision—Tables I and II show that when the concentrations of α- and β-tribenosides reached the lower limits, the coefficient of variation increased to ~10. These lower concentrations (10 and 5 ng/ml for α- and β-tribenosides, respectively) may be taken as the assay sensitivity limits; lower concentrations could be detected but could not be determined accurately.

Plasma Interferences—Figures 1*a* and 1*b* show the chromatograms of a blank human plasma extract and the same plasma spiked with 100 ng of α- and β-tribenosides and 150 ng of β-clobenoside, respectively. No interference of the normal plasma components was noted.

Specificity—The four main metabolites (all a mixture of the corresponding α- and β-anomers) were derivatized under the same conditions as tribenoside. These metabolites were ethyl 3,5-di-*O*-benzyl-D-glucofuranoside, ethyl 3,6-di-*O*-benzyl-D-glucofuranoside, ethyl 5,6-di-*O*-benzyl-D-glucofuranoside, and 3,5,6-tri-*O*-benzyl-D-glucofuranoside. Their derivatives were not recorded when chromatographed under the same conditions as tribenoside at concentrations of ≤1 mg/ml.

Application—The technique was used to study the elimination of α- and β-tribenosides after daily oral administration to humans. The plasma concentrations of α- and β-tribenosides are given in Table III. The determinations were done in duplicate.

REFERENCE

(1) H. Keberle and K. Schmid, in "Aspects Importants de l'Insuffisance Veineuse Chronique," Symposium de Porto Cervo (Italy), Ciba-Geigy, Basel, Switzerland, 1970, pp. 128–139.

ACKNOWLEDGMENTS

The authors thank Dr. K. Schmid, Pharmacological Chemistry Department, Ciba-Geigy, Basel, Switzerland, for helpful discussions and Dr. J. P. Schoeller, Medical Department, Ciba-Geigy, France, for conducting the clinical trial.

Effect of Polyols on Interaction of Paraben Preservatives with Polysorbate 80

JAMES BLANCHARD

Received April 3, 1979, from the *Department of Pharmaceutical Sciences, College of Pharmacy, University of Arizona, Tucson, AZ 85721.* Accepted for publication September 14, 1979.

Abstract □ A quantitative study of the interaction of the methyl, ethyl, propyl, and butyl esters of *p*-hydroxybenzoic acid with polysorbate 80 in the presence and absence of two polyols (propylene glycol and glycerol), which were potential competitors, was performed. The results indicate that neither competitor displaced significant amounts of the parabens from their binding sites on polysorbate 80. The previously observed synergistic antimicrobial effects of these polyols appear to be due to a mechanism other than the displacement of the parabens from their micellar binding sites.

Keyphrases □ Polyols—effect of propylene glycol and glycerol on interaction of parabens with polysorbate 80 □ Propylene glycol—effect on interaction of parabens with polysorbate 80 □ Glycerol—effect on interaction of parabens with polysorbate 80 □ Parabens—interaction with polysorbate 80, effect of propylene glycol and glycerol □ Preservatives—parabens, interaction with polysorbate 80, effect of propylene glycol and glycerol □ Polysorbate 80—interaction with paraben preservatives, effect of propylene glycol and glycerol

Several reports described the ability of nonionic surfactants (including polysorbates) to interfere with the activity of phenolic preservatives such as the parabens (1–4). This inactivation is believed to be due to the formation of a complex between the preservative molecules and the surfactant micelle, based on the assumption that the preservative antimicrobial activity is primarily due to the unbound form (3).

Previous work indicated that polyols such as propylene glycol or glycerol could function as preservatives or synergists to preservatives (5–7). Since these studies were designed to determine only whether preservative activity was enhanced by polyol addition, a systematic study was needed to evaluate the mechanism underlying the increased preservative activity associated with the polyols. Thus, a model system was developed to evaluate the ability

0022-3549/80/0200-0169$01.00/0
© 1980, American Pharmaceutical Association

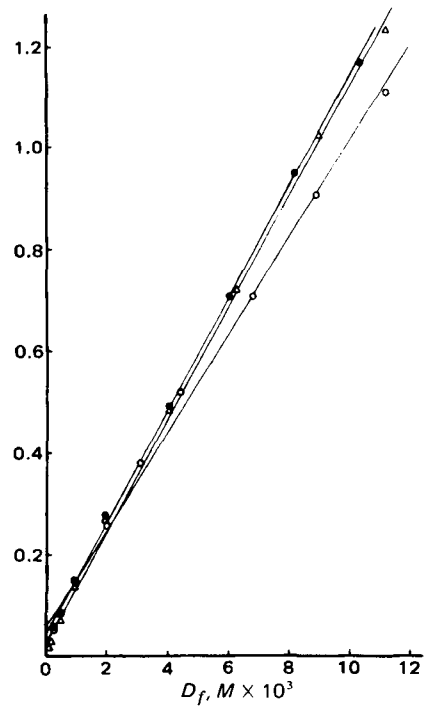

Figure 1—*Influence of polyol on methylparaben binding to polysorbate 80 at 23–25°. Key: ○, methylparaben alone; ●, methylparaben plus propylene glycol (10:1); and △, methylparaben plus glycerol (5:1). All data points represent the average of duplicate determinations.*

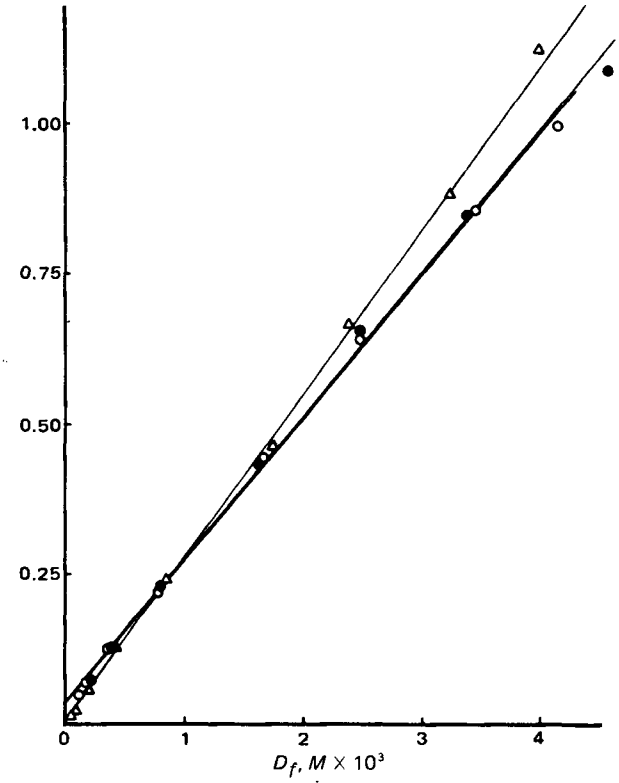

Figure 2—*Influence of polyol on ethylparaben binding to polysorbate 80 at 23–25° Key: ○, ethylparaben alone; ●, ethylparaben plus propylene glycol (10:1); and △, ethylparaben plus glycerol (5:1). All data points represent the average of duplicate determinations.*

of various polyols to inhibit the complexation of several paraben preservatives with polysorbate 80.

In initial efforts (8), sorbitol was the polyol chosen for study because of its compatibility with ingredients common to pharmaceutical formulations. Since sorbitol proved to be an ineffective competitive complexing agent, presumably because of its relatively high polarity, less polar polyols such as propylene glycol and glycerol were selected; these agents had previously been reported to act as synergists to preservatives (6, 7).

EXPERIMENTAL

Reagents—The following were used: methylparaben[1] (I), mp 130°; ethylparaben[2] (II), mp 117°; propylparaben[3] (III), mp 96–97°; butylparaben[4] (IV), mp 70°; polysorbate 80[5]; propylene glycol (reagent grade)[6]; and glycerol[7] (spectrophotometric grade).

The parabens were recrystallized from distilled water (9, 10) and dried in a desiccator for at least 48 hr prior to use. Polysorbate 80, propylene glycol, and glycerol were used without further purification. All solutions were prepared with double-distilled water from an all-glass apparatus.

Procedures—The dialysis procedures and equipment were similar to those described previously (8). Commercially available[8] acrylic plastic dialysis cells were employed. Nylon[9] membranes, previously washed for 1 hr in distilled water and heated to 80° to remove contaminants, were satisfactory. These membranes were previously shown to be impermeable to the polysorbate yet permeable to the parabens, thereby allowing equilibration of the latter (2, 11).

After the cells were assembled, 5 ml of distilled water was added to one cell compartment (the aqueous compartment) and 5 ml of a mixture of varying volume ratios of preservative in 10% (w/v) polysorbate 80 and polysorbate 80 (10% w/v) was added to the other cell compartment (the surfactant compartment). This procedure was employed to vary the amount of preservative present in the surfactant compartment while maintaining the polysorbate concentration constant at 10% (w/v). The cells were then placed on a shaker bath[10] and agitated at 120 oscillations/min for 20 hr at room temperature (23–25°) to achieve equilibrium.

Samples of preservative were removed from both sides of the membrane and assayed spectrophotometrically at 255 nm (2, 12) against blanks prepared identically, except for the omission of the parabens. This procedure was essential to compensate for any polysorbate absorption. Polysorbate 80 solutions stored for more than 4 weeks sometimes gave evidence of microbial growth. To avoid this problem, fresh polysorbate 80-containing solutions were prepared every 3 weeks.

In developing the spectrophotometric assay, it was noted that the absorption spectra of the parabens were pH dependent. As the pH was increased, the peak at 255 nm gradually decreased in intensity and a peak, centered at about 296 nm (13–15), increased in intensity. This second peak was likely due to the ionization of the weakly acidic phenolic proton of the parabens, which have pKa values of 8.4–8.5 (14). The simultaneous existence of the two paraben forms (*i.e.*, ionized and unionized) was undesirable in assaying the solutions accurately and in studying the binding of only the more active unionized form (16, 17), which reportedly binds more avidly to polysorbate 80 than the ionic form (18).

In addition, the parabens are reported to be relatively unstable at pH values above 6 (18, 19). Since the absorption spectra of the parabens should be pH independent at pH 6 or below (where they would be essentially 100% unionized), a study was performed to determine whether the paraben binding profile in a system buffered to pH 5.5 (0.1 *M* acetate) would differ significantly from that observed with an aqueous unbuffered system, as employed by Patel and Kostenbauder (2). The results of this comparison indicated that the use of unbuffered aqueous systems provides binding data that are equivalent to data obtained using a pH 5.5 system. Thus, in subsequent experiments, unbuffered aqueous systems were employed. Measurements at the start and completion of several

[1] Lot L49260, Ruger Chemical Co., Irvington, NJ 10533.
[2] Eastman Organic Chemicals, Rochester, NY 14650.
[3] Lot C708922, Ruger Chemical Co., Irvington, NJ 10533.
[4] Lot 750543, Calbiochem, La Jolla, CA 92037.
[5] Lot 1546, ICI Americas Inc., Atlas Chemicals Division, Wilmington, DE 19899.
[6] Mallinckrodt Chemical Works, St. Louis, MO 63160.
[7] Aldrich Chemical Co., Milwaukee, WI 53233.
[8] Model 289, Bel-Art Products, Pequannock, NJ 07440.
[9] Capran 77C, 0.6-mil, Allied Chemical Corp., Morristown, NJ 07960.
[10] Model 50, GCA/Precision Scientific, Chicago, IL 60647.

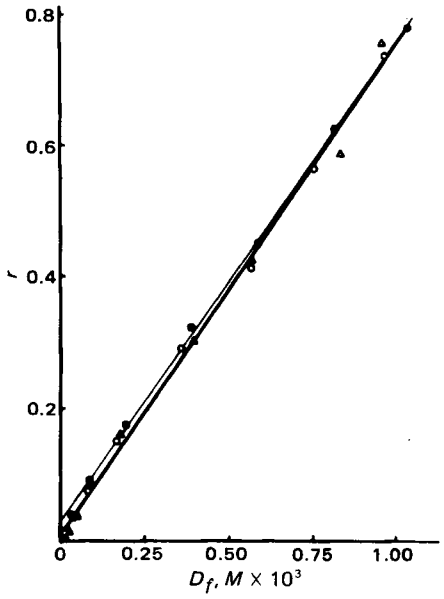

Figure 3—*Influence of polyol on propylparaben binding to polysorbate 80 at 23–25°. Key: ○, propylparaben alone; ●, propylparaben plus propylene glycol (10:1); and △, propylparaben plus glyercol (5:1). All data points represent the average of duplicate determinations.*

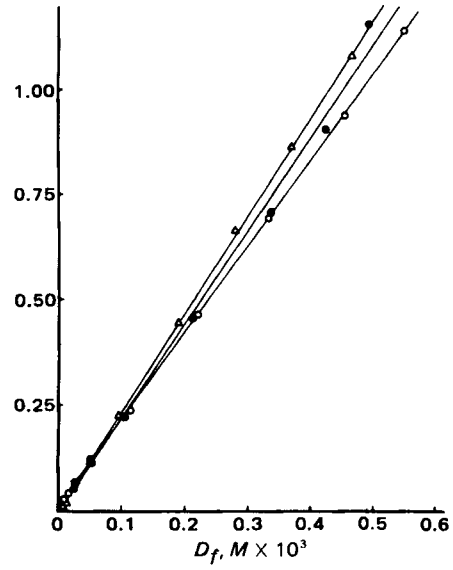

Figure 4—*Influence of polyol on butylparaben binding to polysorbate 80 at 23–25°. Key: ○, butylparaben alone; ●, butylparaben plus propylene glycol (10:1); and △, butylparaben plus glycerol (5:1). All data points represent the average of duplicate determinations.*

experimental runs indicated that the pH remained relatively constant (pH ≤ 6).

Propylene glycol and glycerol were added as possible competitors to the preservative in 10% (w/v) polysorbate 80 solution such that, in any aliquot portion, the molar ratio of polyol to paraben was constant at either 10:1 (propylene glycol) or 5:1 (glycerol). The assays were identical to those in the experiments involving no competitor since neither polyol interfered with the preservative assay at the dilutions necessary to assay for the parabens.

RESULTS AND DISCUSSION

The degree of interaction of each paraben with polysorbate 80 was determined by assaying spectrophotometrically the surfactant compartment of the dialysis cell to determine the total paraben concentration, D_t, and then assaying the aqueous compartment to determine the free (unbound) paraben concentration, D_f. The bound paraben concentration, D_b, was calculated as the difference between these two values.

To obtain information about the binding mechanism, the following mass action treatment was employed (20). It is applicable to binding phenomena in undersaturated systems such as those utilized here.

For a macromolecule with m classes of independent and equivalent binding sites, with each class i having n_i sites with an intrinsic association (binding) constant K_i, the following expression may be written:

$$r = \frac{[D_b]}{[M_t]} = \sum_{i=1}^{m} \frac{n_i K_i [D_f]}{1 + K_i [D_f]} \qquad \text{(Eq. 1)}$$

where r is the number of moles of paraben bound per mole of surfactant; $[D_b]$ and $[D_f]$ are the concentrations of bound and free (unbound) paraben, respectively; and $[M_t]$ is the concentration of macromolecule (surfactant). Theoretically, $[M_t]$ should be the micelle concentration, n the number of binding sites per micelle, and K the association constant for the reaction with the micelles since the binding interaction reportedly occurs between the preservative and the surfactant micelles rather than the monomer surfactant molecules (11, 21). From a practical standpoint, however, it is more convenient to express K, n, and M_t in terms of the surfactant concentration since the micellar molecular weight is not known precisely. Since the critical micelle concentration of polysorbate 80 is very low (21, 22), the monomer concentration may be neglected (11). In analyzing the data, the molecular weight of polysorbate 80 was assumed to be 1470[11].

A Scatchard (23) plot results when $r/[D_f]$ *versus* r is plotted. By rearranging Eq. 1, it can be observed that this type of plot should be linear with a slope of $-K$ and ordinate and abscissa intercepts of nK and n, respectively, when only one class of binding sites is present.

This simplest of binding models is referred to as the "two-parameter model" (24) since only n and K need to be determined to describe the binding adequately. However, as noted previously (9, 11, 25), Scatchard plots frequently exhibit curvature indicative of more than one class of binding sites. To describe these more complex binding processes, Eq. 1 may be rewritten as:

$$r = \sum_{i=1}^{m-1} \frac{n_i K_i [D_f]}{1 + K_i [D_f]} + n_m K_m [D_f] \qquad \text{(Eq. 2)}$$

when one association constant becomes very small. This can occur when the second class of binding sites is not saturable within the experimentally investigated range of ligand concentrations. In such instances, $[D_t] \ll 1/K_2$, where $[D_t]$ = the total drug (ligand) concentration employed. The second term on the right-hand side of Eq. 2 is, therefore, indicative of a class of binding sites that possesses an "infinite" (nonsaturable) binding capacity but "zero" affinity, thereby producing a horizontal asymptote on the Scatchard plot. This binding process can be described by a three-parameter model, which corresponds to a value of $m = 2$ in Eq. 2, and may be written as:

$$\frac{r}{[D_f]} = \frac{n_1 K_1}{1 + K_1 [D_f]} + C \qquad \text{(Eq. 3)}$$

where $C = n_2 K_2$. Often these two different classes of binding sites are designated as "specific" (subscript 1) and "nonspecific" (subscript 2) binding (26).

As illustrated by Winkler and Hubner (26), it is often necessary to use other plots in conjunction with the Scatchard plot to ascertain the binding models correctly. For example, if it is assumed that the smallest unbound ligand (preservative) concentration in the experiment is large relative to $1/K_1$, Eq. 3 can be rewritten as:

$$r = n_1 + C[D_f] \qquad \text{(Eq. 4)}$$

Equation 4 indicates that a plot of r *versus* $[D_f]$ should produce a straight line of slope C and an ordinate intercept of n_1.

To determine the applicability of Eq. 4 in describing the binding, the equation was fitted to the data plotted in Figs. 1–4. These plots illustrate the interaction between 10% (w/v) polysorbate 80 and I–IV, alone and in the presence of propylene glycol or glycerol. The best-fit binding parameters for the interaction of the various parabens with polysorbate 80 (Table I) were calculated by least-squares linear regression.

The linearity of these plots, as indicated by the high coefficients of determination for the linear regressions, is good evidence of the adherence of the binding data to Eq. 4. The values of C listed in Table I may be interpreted as being indicative of a weak, nonspecific (nonsaturable) type of binding analogous to a partitioning of the preservative between the micellar and aqueous phases (17, 21). In a Scatchard plot, they would

[11] Dr. Paul Becher, ICI Americas Inc., Wilmington, DE 19897, personal communication.

Table I—Binding Parameters for the Interaction of Parabens with Polysorbate 80 (at 23–25°) in the Presence and Absence of Polyols

Preservative	Competitor[a]	Coefficient of Determination (r^2)	n_1	C	Partition Coefficient[b]
Methylparaben	None	0.9944	0.0565 ± 0.0101[c]	95.5 ± 1.80	91.2
	Propylene glycol (10:1)	0.9991	0.0424 ± 0.0049	109.6 ± 0.90	
	Glycerol (5:1)	0.9973	0.0263 ± 0.0078	109.4 ± 1.43	
Ethylparaben	None	0.9984	0.0357 ± 0.0057	236.2 ± 2.56	295.1
	Propylene glycol (10:1)	0.9969	0.0367 ± 0.0081	236.2 ± 3.54	
	Glycerol (5:1)	0.9993	0.0006 ± 0.0037	277.4 ± 1.84	
Propylparaben	None	0.9979	0.0093 ± 0.0040	746.2 ± 8.56	1096.5
	Propylene glycol (10:1)	0.9975	0.0267 ± 0.0061	730.9 ± 10.66	
	Glycerol (5:1)	0.9933	0.0067 ± 0.0075	747.1 ± 15.33	
Butylparaben	None	0.9989	0.0106 ± 0.0048	2048.9 ± 17.13	3715.4
	Propylene glycol (10:1)	0.9940	0.0034 ± 0.0112	2221.1 ± 43.13	
	Glycerol (5:1)	0.9998	0.0033 ± 0.0020	2345.5 ± 8.60	

[a] Molar ratio of competitor to preservative is shown in parentheses (r^2, n_1, and C are derived from r *versus* D_f plots). [b] Octanol–water partition coefficient data from Ref. 27. [c] All parameter uncertainties are expressed as standard errors.

represent a constant value of $r/[D_f]$ (*i.e.*, a horizontal asymptote) at large r values. The partitioning phenomenon may be envisioned as a process whereby preservative molecules, in an attempt to lower their free energy, migrate from a thermodynamically less stable aqueous environment in the bulk phase to a more stable (less polar) micellar phase, with the degree of penetration and affinity being proportional to their lipophilicity.

The data also indicate that the values of C observed for the parabens are in excellent agreement with their reported (27) octanol–water partition coefficients (Fig. 5), which further substantiates that the binding process described by the term C is a type of partitioning phenomenon. The coefficient of determination for the regression of the calculated values of C on the partition coefficients was 0.9968. This excellent agreement between C and the lipophilicity of the preservative molecules also supports the notion that the binding sites are less polar than their surrounding aqueous environment.

The values of C obtained for each of the four parabens are also illustrated in Fig. 6 since the values of C plotted as the ordinate in Fig. 5 are equal to the slopes of the respective lines plotted in Fig. 6. This plot illustrates that the relative binding affinities of the four parabens for polysorbate 80 are in the order butyl > propyl > ethyl > methyl. This relative binding order was previously noted by other investigators (28–30).

In addition to the simple partitioning mechanism described, Higuchi and Lach (31) proposed that phenolic compounds that possess an acidic hydrogen could associate with electrophilic atoms such as oxygen, found in the polyether ethylene oxide chains of nonionic surfactants. They suggested that this type of interaction could be enhanced by the "squeezing together" of the hydrophobic portions of the interacting molecules by water molecules. This rationale provides a possible explanation for the progressive increase in binding to polysorbate 80 observed as the nonpolar character of the paraben was increased from the methyl to the butyl esters. The relative binding affinities based on the data of Fig. 6 (*i.e.*, the slopes of each plot) are in the order 1:2.5:7.8:21.5, from the methyl to the butyl esters, respectively.

Barr and Tice (4) and deNavarre (32) postulated that the inactivation of phenolics by nonionic surfactants was due to this type of complex formation. Other investigators, however, postulated that these interactions may be explained adequately in terms of solubilization within surfactant micelles (33). Some investigators (34, 35) suggested that, because inactivation occurs between preservatives and surfactants of extremely diverse chemical structure, solubilization is a more probable explanation than specific complex formation.

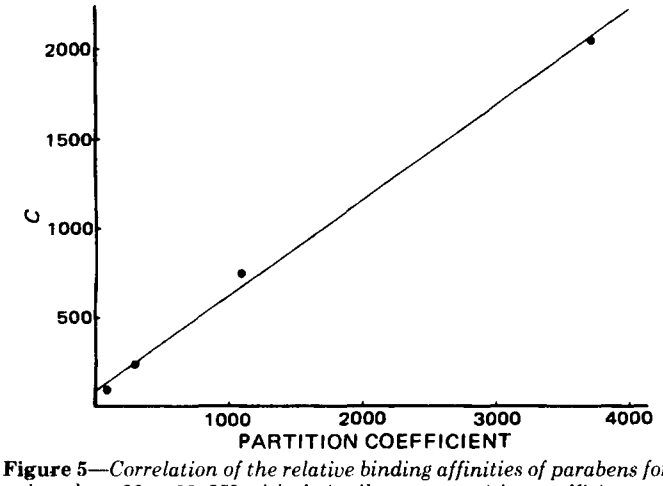

Figure 5—*Correlation of the relative binding affinities of parabens for polysorbate 80 at 23–25° with their oil–water partition coefficients.*

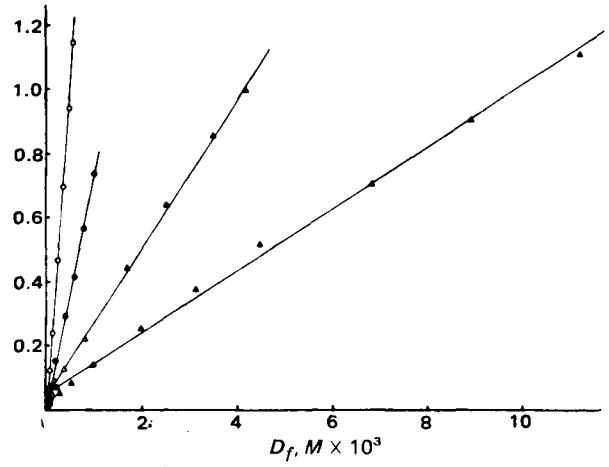

Figure 6—*Relative binding affinities of parabens to polysorbate 80 at 23–25°. Key: ▲, methylparaben; △, ethylparaben; ●, propylparaben; and ○, butylparaben. All data points represent the average of duplicate determinations.*

The literature indicates that a significant preservative–surfactant interaction requires micelles regardless of which mechanism is operative. In fact, micelles of nonionic surfactants probably provide an environment highly suited for both hydrogen bonding and micellar solubilization to operate simultaneously.

The r *versus* $[D_f]$ plots (Figs. 1–4) that illustrate the binding of the various paraben derivatives to polysorbate 80 also indicate that neither propylene glycol or glycerol displaced significant amounts of bound preservative from the polysorbate micelle. This result is shown by the virtual superimposability of these plots and the close agreement of the binding parameters (Table I) in the presence and absence of either polyol. These polyols probably are too polar to partition deeply enough into the polysorbate 80 micelle to displace the bound preservative. The previously reported synergistic antimicrobial effects of these polyols with the parabens apparently occur *via* a mechanism other than the simple displacement of the preservative molecules from their micellar binding sites. The antimicrobial activity enhancement associated with these agents possibly may be due to an osmotic effect or to their ability to hydrogen bond preferentially with available water, thereby preventing microorganism metabolism (5, 36–38) even though the polyol concentrations used (<6% w/v for propylene glycol and <5% w/v for glycerol) were considerably less than the levels (20–50%) described by Barr and Tice (37). An alternative possibility is that the polyol concentrations were too low to produce a measurable displacement of the bound paraben species.

REFERENCES

(1) M. A. Bolle and A. Mirimanoff, *J. Pharm. Pharmacol.*, **2**, 685 (1950).

(2) N. K. Patel and H. B. Kostenbauder, *J. Am. Pharm. Assoc., Sci. Ed.*, **47**, 289 (1958).

(3) F. D. Pisano and H. B. Kostenbauder, *ibid.*, **48**, 310 (1959).
(4) M. Barr and L. F. Tice, *ibid.*, **46**, 445 (1957).
(5) P. S. Prickett, H. L. Murray, and N. H. Mercer, *J. Pharm. Sci.*, **50**, 316 (1961).
(6) M. G. deNavarre, *Am. Perfum. Aromat.*, **73**, 23 (1959).
(7) J. Poprzan and M. G. deNavarre, *J. Soc. Cosmet. Chem.*, **12**, 280 (1961).
(8) J. Blanchard, W. T. Fink, and J. P. Duffy, *J. Pharm. Sci.*, **66**, 1470 (1977).
(9) K. F. Brown and M. J. Crooks, *Pharm. Acta Helv.*, **48**, 494 (1973).
(10) T. C. Corby and P. H. Elworthy, *J. Pharm. Pharmacol., Suppl.*, **23**, 39S (1971).
(11) S. J. A. Kazmi and A. G. Mitchell, *J. Pharm. Pharmacol.*, **23**, 482 (1971).
(12) T. C. Corby and P. H. Elworthy, *J. Pharm. Pharmacol., Suppl.*, **23**, 49S (1971).
(13) R. T. Coutts, N. Nagabhushan, and N. K. Patel, *Can. J. Pharm. Sci.*, **4**, 96 (1969).
(14) D. W. Fink, H. C. Fink, J. W. Tolan, and J. Blodinger, *J. Pharm. Sci.*, **67**, 837 (1978).
(15) T. Higuchi, K. P. Patel, E. R. Bonow, and J. Landsman, *J. Am. Pharm. Assoc., Sci. Ed.*, **41**, 293 (1952).
(16) T. R. Aalto, M. C. Firman, and N. E. Rigler, *ibid.*, **42**, 449 (1953).
(17) E. L. Barkley, *Am. Perfum. Aromat.*, **73**, 33 (1959).
(18) L. Lachman, *Bull. Parenteral Drug Assoc.*, **22**, 127 (1968).
(19) S. M. Blaug and D. E. Grant, *J. Soc. Cosmet. Chem.*, **25**, 495 (1974).
(20) E. R. Garrett, *J. Pharm. Pharmacol.*, **18**, 589 (1966).
(21) T. Shimamoto and Y. Ogawa, *Chem. Pharm. Bull.*, **23**, 3088 (1975).
(22) B. Farhadieh, *J. Pharm. Sci.*, **62**, 1685 (1973).
(23) G. F. Scatchard, *Ann. N.Y. Acad. Sci.*, **51**, 660 (1949).
(24) D. Rodbard and H. A. Feldman, in "Methods in Enzymology," vol. 36, "Hormone Action, Part A, Steroid Hormones," B. W. O'Malley and J. G. Hardman, Eds., Academic, New York, N.Y., 1975, pp. 3–16.
(25) M. J. Crooks and K. F. Brown, *J. Pharm. Pharmacol.*, **26**, 235 (1974).
(26) E. Winkler and G. Hubner, *Stud. Biophys.*, **66**, 211 (1977).
(27) A. Leo, C. Hansch, and D. Elkins, *Chem. Rev.*, **71**, 525 (1971).
(28) S. M. Blaug and S. S. Ahsan, *J. Pharm. Sci.*, **50**, 441 (1961).
(29) N. K. Patel and N. E. Foss, *ibid.*, **53**, 94 (1964).
(30) N. K. Patel, *Can. J. Pharm. Sci.*, **2**, 97 (1967).
(31) T. Higuchi and J. L. Lach, *J. Am. Pharm. Assoc., Sci. Ed.*, **43**, 465 (1954).
(32) M. G. deNavarre, *J. Soc. Cosmet. Chem.*, **8**, 68 (1957).
(33) W. P. Evans, *J. Pharm. Pharmacol.*, **16**, 323 (1964).
(34) W. P. Evans and S. F. Dunbar, in "Surface Activity and the Microbial Cell," Monograph 19, Society of Chemical Industries, London, England, 1965, pp. 169–190.
(35) D. L. Wedderburn, in "Advances in Pharmaceutical Sciences," vol. 1, H. S. Bean, A. H. Beckett, and J. E. Carless, Eds., Academic, New York, N.Y., 1964, pp. 195–245.
(36) M. Barr and L. F. Tice, *J. Am. Pharm. Assoc., Sci. Ed.*, **46**, 217 (1957).
(37) *Ibid.*, **46**, 219 (1957).
(38) *Ibid.*, **46**, 221 (1957).

ACKNOWLEDGMENTS

Presented in part at the APhA Academy of Pharmaceutical Sciences, Montreal meeting, May 1978.

Supported by the University of Arizona Foundation.

The author thanks Ms. Margaret Cork for technical assistance and Mr. William T. Fink for constructive comments.

trans-Cinnamic Acid–α-Cyclodextrin System as Studied by Solubility, Spectral, and Potentiometric Techniques

KENNETH A. CONNORS ˣ **and THOMAS W. ROSANSKE**

Received July 18, 1979, from the *School of Pharmacy, University of Wisconsin, Madison, WI 53706.* Accepted for publication September 19, 1979.

Abstract □ Complex formation in aqueous solutions of *trans*-cinnamic acid or *trans*-cinnamate ion (the substrate, S) and α-cyclodextrin (the ligand, L) can be described quantitatively as the 1:1 and 1:2 complexes, SL and SL_2. The solubility, spectral, and potentiometric data over a wide range of ligand concentrations yielded consistent estimates of the complex association constants. For cinnamic acid at 25°, $K_{11} = 2260\ M^{-1}$, $\Delta H^\circ_{11} = -9.3$ kcal/mole, and $\Delta S^\circ_{11} = -8$ e.u.; and $K_{12} = 60\ M^{-1}$, $\Delta H^\circ_{12} = -12$ kcal/mole, and $\Delta S^\circ_{12} = -26$ e.u. For cinnamate ion at 25°, $K_{11} = 110\ M^{-1}$, $\Delta H^\circ_{11} = -1.9$ kcal/mole, and $\Delta S^\circ_{11} = +11$ e.u.; and $K_{12} = 15\ M^{-1}$, $\Delta H^\circ_{12} = -9$ kcal/mole, and $\Delta S^\circ_{12} = -15$ e.u. (all entropy changes are unitary quantities). Thermodynamic cycles for the complexes, using solubility data, reveal that complex formation in the solid phase is thermodynamically spontaneous but that complex stability is greater in aqueous solution than in the solid phase.

Keyphrases □ Complexation—*trans*-cinnamic acid with α-cyclodextrin, thermodynamic analysis, stoichiometry, stability equilibria, determined by spectral, solubility, and pH measurements □ Thermodynamics—complexation analysis, determined by spectral, solubility, and pH measurements, *trans*-cinnamic acid–α-cyclodextrin complex □ *trans*-Cinnamic acid—analysis of complexation with α-cyclodextrin, thermodynamics □ α-Cyclodextrin—analysis of complexation with *trans*-cinnamic acid, thermodynamics □ Solubility measurements—complexation of *trans*-cinnamic acid with α-cyclodextrin □ UV spectrometry—complexation of *trans*-cinnamic acid–α-cyclodextrin □ pH measurements—complexation of *trans*-cinnamic acid–α-cyclodextrin

The chemical and physical properties of *trans*-cinnamic acid and its derivatives make these compounds highly useful substrates[1] in studies of molecular complex formation (1–7). Preliminary studies in this laboratory on the *trans*-cinnamic acid–α-cyclodextrin (cyclohexaamylose) system in aqueous solution showed that simple 1:1 stoichiometry in the complex does not adequately describe the equilibrium system. This observation seemed to be worth pursuing because cinnamic acid reportedly forms a 1:1 complex with α-cyclodextrin (8) and because this substrate does not seem to be an atypical one in such studies; hence,

[1] The substrate is the compound whose measured properties constitute the dependent variable; the ligand is the substance (α-cyclodextrin in this case) whose concentration is the independent variable.

0022-3549/80/0200-0173$01.00/0
© 1980, American Pharmaceutical Association

(3) F. D. Pisano and H. B. Kostenbauder, *ibid.*, **48**, 310 (1959).
(4) M. Barr and L. F. Tice, *ibid.*, **46**, 445 (1957).
(5) P. S. Prickett, H. L. Murray, and N. H. Mercer, *J. Pharm. Sci.*, **50**, 316 (1961).
(6) M. G. deNavarre, *Am. Perfum. Aromat.*, **73**, 23 (1959).
(7) J. Poprzan and M. G. deNavarre, *J. Soc. Cosmet. Chem.*, **12**, 280 (1961).
(8) J. Blanchard, W. T. Fink, and J. P. Duffy, *J. Pharm. Sci.*, **66**, 1470 (1977).
(9) K. F. Brown and M. J. Crooks, *Pharm. Acta Helv.*, **48**, 494 (1973).
(10) T. C. Corby and P. H. Elworthy, *J. Pharm. Pharmacol., Suppl.*, **23**, 39S (1971).
(11) S. J. A. Kazmi and A. G. Mitchell, *J. Pharm. Pharmacol.*, **23**, 482 (1971).
(12) T. C. Corby and P. H. Elworthy, *J. Pharm. Pharmacol., Suppl.*, **23**, 49S (1971).
(13) R. T. Coutts, N. Nagabhushan, and N. K. Patel, *Can. J. Pharm. Sci.*, **4**, 96 (1969).
(14) D. W. Fink, H. C. Fink, J. W. Tolan, and J. Blodinger, *J. Pharm. Sci.*, **67**, 837 (1978).
(15) T. Higuchi, K. P. Patel, E. R. Bonow, and J. Landsman, *J. Am. Pharm. Assoc., Sci. Ed.*, **41**, 293 (1952).
(16) T. R. Aalto, M. C. Firman, and N. E. Rigler, *ibid.*, **42**, 449 (1953).
(17) E. L. Barkley, *Am. Perfum. Aromat.*, **73**, 33 (1959).
(18) L. Lachman, *Bull. Parenteral Drug Assoc.*, **22**, 127 (1968).
(19) S. M. Blaug and D. E. Grant, *J. Soc. Cosmet. Chem.*, **25**, 495 (1974).
(20) E. R. Garrett, *J. Pharm. Pharmacol.*, **18**, 589 (1966).
(21) T. Shimamoto and Y. Ogawa, *Chem. Pharm. Bull.*, **23**, 3088 (1975).
(22) B. Farhadieh, *J. Pharm. Sci.*, **62**, 1685 (1973).
(23) G. F. Scatchard, *Ann. N.Y. Acad. Sci.*, **51**, 660 (1949).
(24) D. Rodbard and H. A. Feldman, in "Methods in Enzymology," vol. 36, "Hormone Action, Part A, Steroid Hormones," B. W. O'Malley and J. G. Hardman, Eds., Academic, New York, N.Y., 1975, pp. 3–16.
(25) M. J. Crooks and K. F. Brown, *J. Pharm. Pharmacol.*, **26**, 235 (1974).
(26) E. Winkler and G. Hubner, *Stud. Biophys.*, **66**, 211 (1977).
(27) A. Leo, C. Hansch, and D. Elkins, *Chem. Rev.*, **71**, 525 (1971).
(28) S. M. Blaug and S. S. Ahsan, *J. Pharm. Sci.*, **50**, 441 (1961).
(29) N. K. Patel and N. E. Foss, *ibid.*, **53**, 94 (1964).
(30) N. K. Patel, *Can. J. Pharm. Sci.*, **2**, 97 (1967).
(31) T. Higuchi and J. L. Lach, *J. Am. Pharm. Assoc., Sci. Ed.*, **43**, 465 (1954).
(32) M. G. deNavarre, *J. Soc. Cosmet. Chem.*, **8**, 68 (1957).
(33) W. P. Evans, *J. Pharm. Pharmacol.*, **16**, 323 (1964).
(34) W. P. Evans and S. F. Dunbar, in "Surface Activity and the Microbial Cell," Monograph 19, Society of Chemical Industries, London, England, 1965, pp. 169–190.
(35) D. L. Wedderburn, in "Advances in Pharmaceutical Sciences," vol. 1, H. S. Bean, A. H. Beckett, and J. E. Carless, Eds., Academic, New York, N.Y., 1964, pp. 195–245.
(36) M. Barr and L. F. Tice, *J. Am. Pharm. Assoc., Sci. Ed.*, **46**, 217 (1957).
(37) *Ibid.*, **46**, 219 (1957).
(38) *Ibid.*, **46**, 221 (1957).

ACKNOWLEDGMENTS

Presented in part at the APhA Academy of Pharmaceutical Sciences, Montreal meeting, May 1978.

Supported by the University of Arizona Foundation.

The author thanks Ms. Margaret Cork for technical assistance and Mr. William T. Fink for constructive comments.

trans-Cinnamic Acid–α-Cyclodextrin System as Studied by Solubility, Spectral, and Potentiometric Techniques

KENNETH A. CONNORS ˣ **and THOMAS W. ROSANSKE**

Received July 18, 1979, from the *School of Pharmacy, University of Wisconsin, Madison, WI 53706.* Accepted for publication September 19, 1979.

Abstract □ Complex formation in aqueous solutions of *trans*-cinnamic acid or *trans*-cinnamate ion (the substrate, S) and α-cyclodextrin (the ligand, L) can be described quantitatively as the 1:1 and 1:2 complexes, SL and SL_2. The solubility, spectral, and potentiometric data over a wide range of ligand concentrations yielded consistent estimates of the complex association constants. For cinnamic acid at 25°, $K_{11} = 2260\ M^{-1}$, $\Delta H^\circ_{11} = -9.3$ kcal/mole, and $\Delta S^\circ_{11} = -8$ e.u.; and $K_{12} = 60\ M^{-1}$, $\Delta H^\circ_{12} = -12$ kcal/mole, and $\Delta S^\circ_{12} = -26$ e.u. For cinnamate ion at 25°, $K_{11} = 110\ M^{-1}$, $\Delta H^\circ_{11} = -1.9$ kcal/mole, and $\Delta S^\circ_{11} = +11$ e.u.; and $K_{12} = 15\ M^{-1}$, $\Delta H^\circ_{12} = -9$ kcal/mole, and $\Delta S^\circ_{12} = -15$ e.u. (all entropy changes are unitary quantities). Thermodynamic cycles for the complexes, using solubility data, reveal that complex formation in the solid phase is thermodynamically spontaneous but that complex stability is greater in aqueous solution than in the solid phase.

Keyphrases □ Complexation—*trans*-cinnamic acid with α-cyclodextrin, thermodynamic analysis, stoichiometry, stability equilibria, determined by spectral, solubility, and pH measurements □ Thermodynamics—complexation analysis, determined by spectral, solubility, and pH measurements, *trans*-cinnamic acid–α-cyclodextrin complex □ *trans*-Cinnamic acid—analysis of complexation with α-cyclodextrin, thermodynamics □ α-Cyclodextrin—analysis of complexation with *trans*-cinnamic acid, thermodynamics □ Solubility measurements—complexation of *trans*-cinnamic acid with α-cyclodextrin □ UV spectrometry—complexation of *trans*-cinnamic acid–α-cyclodextrin □ pH measurements—complexation of *trans*-cinnamic acid–α-cyclodextrin

The chemical and physical properties of *trans*-cinnamic acid and its derivatives make these compounds highly useful substrates[1] in studies of molecular complex formation (1–7). Preliminary studies in this laboratory on the *trans*-cinnamic acid–α-cyclodextrin (cyclohexaamylose) system in aqueous solution showed that simple 1:1 stoichiometry in the complex does not adequately describe the equilibrium system. This observation seemed to be worth pursuing because cinnamic acid reportedly forms a 1:1 complex with α-cyclodextrin (8) and because this substrate does not seem to be an atypical one in such studies; hence,

[1] The substrate is the compound whose measured properties constitute the dependent variable; the ligand is the substance (α-cyclodextrin in this case) whose concentration is the independent variable.

0022-3549/80/0200-0173$01.00/0
© 1980, American Pharmaceutical Association

knowledge of its stoichiometric relationships may be of wider utility. Attempts to correlate and to explain complex stability or to explicate complex structures and the forces involved cannot be successful unless the stoichiometries and stabilities of the complexes are known.

Although 1:1 stoichiometric ratios commonly are found for cyclodextrin complexes, different ratios have been reported for some substrates. Among organic acids and acid anions, solid phase stoichiometries other than 1:1 have been found for cinnamic acid (acid–β-cyclodextrin, 2:1) (9), salicylic acid (acid–β-cyclodextrin, 3:1) (10), and some normal aliphatic acids (11). More recently, Laufer and coworkers (12–14) studied some acids and acid anions and found 1:2 (SL_2) complexes of 4-biphenylcarboxylate and *p*-methylcinnamate ions with α-cyclodextrin in aqueous solution.

The present approach to sorting out stoichiometric relationships in complex systems is to use more than one experimental technique capable of providing estimates of stability constants (15). Disagreement of apparent 1:1 stability constants evaluated by several methods is definitive evidence for the presence of at least one complex with a stoichiometry other than 1:1; quantitative agreement among several methods strengthens the argument for a model leading to such consistency. In this study, solubility (16), spectral (17), and potentiometric (18) methods were used.

EXPERIMENTAL

Materials—α-Cyclodextrin[2] was used directly. Drying to constant weight at 90° indicated 9.77% water, corresponding closely to the hexahydrate[3] ($[\alpha]_D^{25} = 150.4 \pm 2.1°$). *trans*-Cinnamic acid was recrystallized from water, mp 133.5–133.7° [lit. (19) mp 133–134°]. Tris(hydroxymethyl)aminomethane base and hydrochloride[4] were used directly. Other chemicals were reagent grade. Water was deionized and distilled from alkaline permanganate.

Apparatus—Spectrophotometric measurements were made on spectrophotometers[5] fitted with jacketed cell compartments for temperature control. The pH measurements were made with a combination electrode[6]. Solubility studies were carried out in a constant-temperature water bath equipped to rotate the sample vessels end-over-end at 32 rpm.

Solubility Method—Equal amounts (50 mg) of cinnamic acid were weighed into each of several 10-ml glass ampuls. To each ampul were added 0.50 ml of 0.10 *M* HCl and graded measured volumes of an aqueous stock solution of α-cyclodextrin. Water was added to make the total volume 5.0 ml. The ampuls were sealed and rotated end-over-end in a 25.0° water bath until solubility equilibrium was reached. (Twenty-four hours was adequate in the initial rising portion of the phase diagram, whereas 10 days was necessary in the plateau regions, as determined by numerous trials.)

The ampuls then were placed upright and motionless at 25° overnight to permit the precipitate to settle. A portion of the clear supernate was withdrawn with a 1-ml disposable syringe equipped with a 3.8-cm (1.5-in.) 20-gauge needle. A 2.0-ml sample of the supernate was titrated to the phenolphthalein end-point with standard sodium hydroxide; a correction was applied to account for the hydrochloric acid present in the sample solution.

The solid phases in the ampuls were collected by filtration and were dried; weighed samples were analyzed for cinnamic acid by titration. The cyclodextrin content was obtained by difference.

Spectral Method—Unionized cinnamic acid was studied by weighing increasing amounts of α-cyclodextrin into each of several 10-ml volumetric flasks; to each flask were added 1.0 ml of 0.1 *M* HCl, 5.0 ml of a stock solution of cinnamic acid, and water to bring to volume. Reference solutions were prepared for each sample solution, containing the same concentrations of cyclodextrin and hydrochloric acid but no cinnamic acid. Absorbance was measured at 279 nm in a 1.0-cm cell. For studies at temperatures other than 25°, concentrations at the experimental temperature were corrected from the concentrations at the temperature of preparation using the density of water.

Cinnamate anion was studied similarly, except that the pH was brought to 9 with tris(hydroxymethyl)aminomethane buffer, ensuring that essentially all of the substrate (pKa 4.35) was ionized whereas essentially none of the α-cyclodextrin (pKa 12) (20) was in anionic form. [Separate potentiometric measurements showed that this buffer does not significantly complex with α-cyclodextrin[7].] Measurements were made at 269 nm. The ionic strength in these and all studies was constant at 0.01 *M*. Control of pH with sodium hydroxide led to essentially the same results as with tris(hydroxymethyl)aminomethane buffers.

Potentiometric Method—A stock solution was prepared to contain equal concentrations of cinnamic acid and sodium cinnamate by exactly half-neutralizing a weighed sample of cinnamic acid with standard sodium hydroxide. The ionic strength was brought to 0.01 *M* with sodium chloride. Increasing amounts of α-cyclodextrin were weighed into each of several flasks, to which equal volumes of the cinnamic acid–cinnamate-ion stock solution were added. The pH of each solution, measured at 25°, was interpreted as pKa′, the apparent pKa of cinnamic acid in that solution.

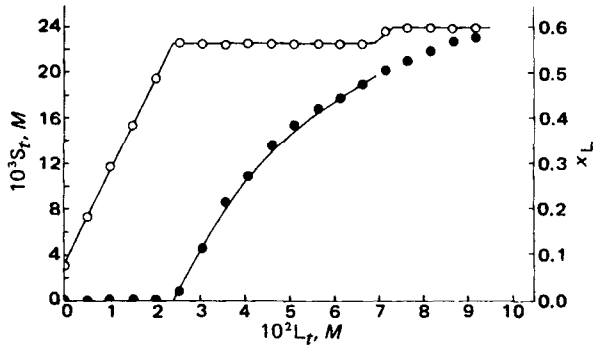

Figure 1—*Solubility of the* trans*-cinnamic acid–α-cyclodextrin system at 25°. Key:* ○ *(left vertical axis), total solution phase concentration of substrate; and* ● *(right vertical axis), mole fraction of cyclodextrin in the solid phase. The total added concentration of ligand (cyclodextrin) is given on the horizontal axis. The smooth lines were calculated as described in the text.*

RESULTS

Solubility Study—Figure 1 shows the experimental results of the solubility study. On the abscissa is specified L_t, the total molar concentration of ligand (α-cyclodextrin) in the system. The left-hand ordinate gives S_t, the total molar concentration of substrate found in the solution phase after equilibration. The right-hand ordinate gives the mole fraction of ligand in the solid phase.

The appearance of the solution phase diagram proves that at least two complexes of different stoichiometry are present, and the solid phase data indicate that a complex is present with an L/S ratio greater than unity. Therefore, these observations suggest that the simplest description of the system will invoke the complexes SL and SL_2. This conclusion may seem inconsistent with the linear nature of the initial rising portion of the solution data, but this will be shown not to be a problem.

To extract numerical estimates from Fig. 1, a quantitative description is required. The complex formation equilibria and stability constants are defined as:

$$S + L \rightleftharpoons SL$$

Scheme I

$$SL + L \rightleftharpoons SL_2$$

Scheme II

$$K_{11} = \frac{[SL]}{[S][L]} \qquad \text{(Eq. 1)}$$

[2] Lot 106C-0046-1, Sigma.
[3] Aldrich.
[4] Sigma.
[5] Cary model 14 or 16.
[6] Orion model 801 pH meter.
[7] A. B. Wong, unpublished results in these laboratories.

$$K_{12} = \frac{[SL_2]}{[SL][L]} \qquad \text{(Eq. 2)}$$

where K_{11} and K_{12} are concentration constants at the experimental ionic strength of 0.01 *M*. Assumptions include the constancy of activity coefficients, a negligible general medium effect, and negligible volume changes (this last assumption was the least well founded but was a relatively unimportant factor).

The following variables need to be defined: S_t is the total solution molar concentration of S, L_t is the total formal molar concentration of L, s_0 is the molar solubility of free S, s_{11} is the molar solubility of SL, and s_{12} is the molar solubility of SL_2. Throughout the initial rising portion of the solution phase diagram, solid substrate is present; hence, the concentration of S is held constant at the solubility limit. The mass balance on S gives:

$$S_t = [S] + [SL] + [SL_2] \qquad \text{(Eq. 3)}$$

which, with the given condition and Eqs. 1 and 2, becomes:

$$S_t = s_0 + K_{11}s_0[L] + K_{11}K_{12}s_0[L]^2 \qquad \text{(Eq. 4)}$$

where [L] is the free ligand concentration. The mass balance on L gives:

$$L_t = [L] + [SL] + 2[SL_2] \qquad \text{(Eq. 5)}$$

which becomes:

$$L_t = [L] + K_{11}s_0[L] + 2K_{11}K_{12}s_0[L]^2 \qquad \text{(Eq. 6)}$$

Eliminating [L] between Eqs. 4 and 6 yields:

$$S_t = s_0 + \frac{L_t}{2} + \frac{ab}{c} - \frac{b}{c}(a^2 + 8K_{11}K_{12}s_0L_t)^{1/2} \qquad \text{(Eq. 7)}$$

where:

$$a = 1 + K_{11}s_0$$

$$b = \frac{a}{2K_{11}s_0} - 1$$

$$c = 4K_{12}$$

Equation 7, which is valid only for finite values of K_{11} and K_{12}, is the equation of the rising portion of the solubility curve for the SL + SL_2 system before the solubility limit of either complex has been reached. The slope is given by dS_t/dL_t (Eq. 8):

$$\frac{dS_t}{dL_t} = \frac{1}{2}\left[1 - \frac{8bK_{11}K_{12}s_0}{c(a^2 + 8K_{11}K_{12}s_0L_t)^{1/2}}\right] \qquad \text{(Eq. 8)}$$

Since a and c must be positive, the curvature in the slope depends upon the sign of b. If $b = 0$, the slope is constant with the value 0.5; this implies that $K_{11} = 1/s_0$. If b is negative, the slope decreases as L_t increases; if b is positive, the slope increases as L_t increases. Whether these cases can be distinguished experimentally will be determined by the magnitudes of the parameters and the range of L_t over which the variable S_t can be observed. The value of the slope at $L_t = 0$ obtained from Eq. 9 is:

$$\left(\frac{dS_t}{dL_t}\right)_{L_t=0} = \frac{1}{2} - \frac{1}{2}\left[\frac{1 - K_{11}s_0}{1 + K_{11}s_0}\right] \qquad \text{(Eq. 9)}$$

The discontinuity giving rise to the segment that is invariant in S_t (the first plateau) needs to be considered. As L_t increases, S_t rises because of the formation of soluble SL and SL_2 complexes. Ultimately, the solubility limit of one of these complexes is reached (as long as the solid S phase is not exhausted first and the solubility limit of L is not reached). Suppose that the solubility of SL is reached before that of SL_2. Then [S] = s_0 and [SL] = s_{11}, and from Eq. 3 one gets:

$$S_t = s_0 + s_{11} + \frac{K_{12}(s_{11})^2}{K_{11}s_0} \qquad \text{(Eq. 10)}$$

That is, S_t becomes invariant as soon as one of the complexes reaches its solubility limit, with the complexation equilibria ensuring that the second complex concentration then also is fixed. This conclusion is general for any number of complexes and no matter which complex reaches its solubility first as long as solid S is present. Thus, the first plateau is accounted for. Of course, the interpretation of S_t in this region depends on which complex has reached its solubility limit. Because of the solid phase data, the argument leading to Eq. 10 appears to apply to Fig. 1.

As L_t continues to increase, the solid S eventually is depleted by its conversion into complexes and its precipitation as solid SL. At the point where solid S disappears, the constraint on S_t is lost (although the condition [SL] = s_{11} still applies). An equation for the dependence of S_t on L_t can be obtained (21); but since it plays no role in the quantitative interpretation of the present data, it can be overlooked. The S_t value rises until the solubility limit of the second complex (SL_2) is reached, when S_t again becomes invariant; its value, given by Eq. 11, is reached by an argument similar to that leading to Eq. 10:

$$S_t = \frac{K_{12}(s_{11})^2}{K_{11}s_{12}} + s_{11} + s_{12} \qquad \text{(Eq. 11)}$$

Thus, a "second plateau" is observed. (If L_t could be made sufficiently large, eventually all solid SL would disappear, and S_t would decrease to a final value approximately equal to s_{12}.)

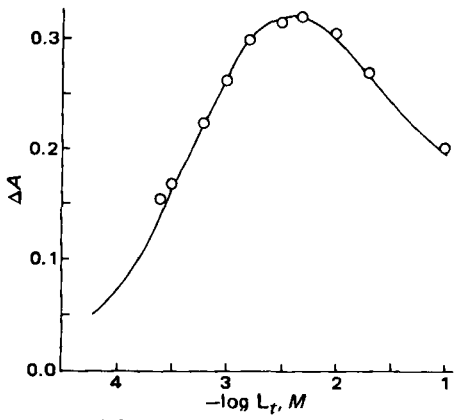

Figure 2—*Spectra of the* trans*-cinnamic acid–α-cyclodextrin system at 25°. The vertical axis gives the change in absorbance in a 1-cm path length of cinnamic acid at 279 nm produced by a total concentration L_t of ligand. The total substrate concentration, S_t, was 8.48 × 10^{-5} M. The ΔA values at the two points corresponding to the highest L_t were corrected for a general medium effect based on an equivalent weight/volume concentration of α-methylglucoside; at L_t = 0.1 M, this correction was 0.009 aufs. The smooth curve was calculated with Eqs. 15 and 16.*

The composition of the solid phase is now considered. From $L_t = 0$ up to the discontinuity marking the beginning of the first plateau, it is postulated that the complex species are soluble so that only solid substrate is present; thus, the mole fraction of cyclodextrin in the solid phase, x_L, should be zero, as is found experimentally (Fig. 1). Throughout the first plateau, the essential feature is that solid S is being replaced by solid SL; therefore, at the beginning of the plateau, $x_L = 0$; at the end of this plateau, $x_L = 0.5$, as is observed. At the beginning of the second plateau, the value of x_L should begin to rise as solid SL is replaced by solid SL_2, the eventual value of x_L being 0.667 (if L_t can be made large enough). Figure 1 shows that x_L does increase in this region, reaching a value of 0.58 at the highest ligand concentration studied.

Equations can be derived relating x_L to L_t in these regions (21), and the smooth line in the first plateau region was calculated with one of these equations, the experimental quantities, and system parameters estimated from the solution phase data. Some ambiguity is introduced by the varying solution phase and total system volumes in these calculations; hence, the qualitative interpretation previously given will suffice for present purposes.

The solubility data were not interpreted independently of the spectral and potentiometric data; rather, for unionized cinnamic acid, the solubility and spectral studies were analyzed to give K_{11} and K_{12} values that best fit both sets of results. These K_{11} and K_{12} values then were imposed as constraints on the potentiometric results. Therefore, uncertainties attached to these values represent limits outside of which the quantitative consistency among the independent sets of data is seriously degraded. These results are obtained at 25°: $K_{11} = 2260 \pm 50\ M^{-1}$, $K_{12} = 60 \pm 5\ M^{-1}$, $s_0 = 3.01 \pm 0.05 \times 10^{-3}\ M$ (the uncertainty is the standard deviation of 11 determinations for s_0), $s_{11} = 1.7 \pm 0.2 \times 10^{-2}\ M$, and $s_{12} = 5.5 \pm 0.5 \times 10^{-3}\ M$ or $1.4 \pm 0.6 \times 10^{-3}\ M$ (because of the ambiguity in a quadratic solution).

Spectral Study—The UV spectrum of cinnamic acid is altered in the presence of α-cyclodextrin. At low cyclodextrin concentrations, isosbestic points are observed at 231 and 296 nm, but these isosbestic points are lost at ligand concentrations greater than ~0.003 *M*. (At such low ligand concentrations, a general medium effect on the spectra cannot account for departure from the isosbestic behavior, as demonstrated by incorporation of α-methylglucoside.) This finding is evidence for at least two

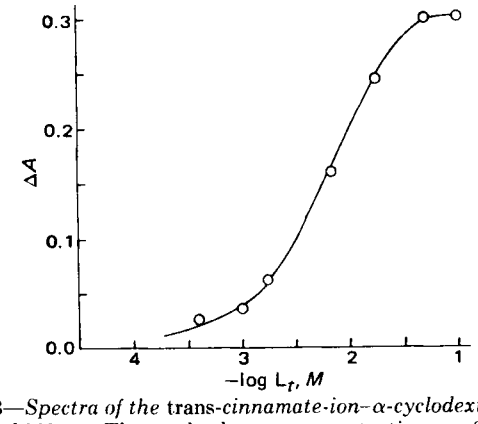

Figure 3—*Spectra of the* trans-*cinnamate-ion–α-cyclodextrin system at 25° and 269 nm. The total substrate concentration was 8.56 × 10^{-5} M. The smooth curve was calculated with Eqs. 15 and 16.*

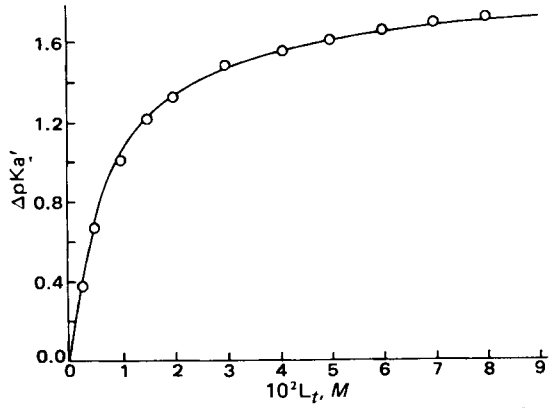

Figure 4—*Potentiometric study of the* trans-*cinnamic acid–α-cyclodextrin system at 25°. The smooth curve was calculated with Eqs. 26 and 34. The total substrate concentration, A_t, was 4.83 × 10^{-3} M.*

complexes. Figure 2 shows the change in absorbance at a fixed wavelength produced by α-cyclodextrin over a wide concentration range.

The analysis of this system assumes SL plus SL_2 complexes for consistency with the solubility results. This system has been treated before (15, 22) but primarily in terms of conventional double-reciprocal graphical analysis, which is not effective for extracting the stability constants. If adherence to Beer's law is assumed for all species, the absorbance for unit path length in a substrate solution containing nonabsorbing ligand is:

$$A = \epsilon_S[S] + \epsilon_{11}[SL] + \epsilon_{12}[SL_2] \qquad \text{(Eq. 12)}$$

In a solution without ligand, it is:

$$A_0 = \epsilon_S S_t \qquad \text{(Eq. 13)}$$

where ϵ_i is the molar absorptivity of species i. The total substrate concentration, S_t, is held constant. Defining $\Delta A = A_0 - A$, $\Delta\epsilon_{11} = \epsilon_S - \epsilon_{11}$, and $\Delta\epsilon_{12} = \epsilon_S - \epsilon_{12}$ and incorporating the relationship between S and free S:

$$S_t = [S](1 + K_{11}[L] + K_{11}K_{12}[L]^2) \qquad \text{(Eq. 14)}$$

relates ΔA to the free ligand concentration:

$$\Delta A = \frac{S_t K_{11}[L](\Delta\epsilon_{11} + \Delta\epsilon_{12}K_{12}[L])}{1 + K_{11}[L] + K_{11}K_{12}[L]^2} \qquad \text{(Eq. 15)}$$

From the mass balance on L:

$$L_t = [L] + \frac{S_t K_{11}[L](1 + 2K_{12}[L])}{1 + K_{11}[L] + K_{11}K_{12}[L]} \qquad \text{(Eq. 16)}$$

It is not practical to express ΔA as an explicit function of L_t, but a numerical curve-fitting procedure is straightforward. Estimates of K_{11}, K_{12}, $\Delta\epsilon_{11}$, and $\Delta\epsilon_{12}$ are obtained from preliminary trials or from supplementary data (*i.e.*, the solubility study). An arbitrary but realistic value of [L] is selected, and the corresponding quantities ΔA and L_t are calculated with Eqs. 15 and 16. These quantities are compared with the experimental values, and the parameters are adjusted until a satisfactory agreement is achieved. As noted earlier, K_{11} and K_{12} were not permitted to vary freely but were constrained by the condition that the final values must account for both the spectral and the solubility data. The smooth curve in Fig. 2 was calculated in this way; at 25°, the results are $K_{11} = 2260\ M^{-1}$, $K_{12} = 60\ M^{-1}$, $\Delta\epsilon_{11} = 4700$, and $\Delta\epsilon_{12} = 1900$. (At 279 nm, $\epsilon_S = 1.98 \times 10^4$.)

Figure 3 is the plot of ΔA *versus* log L_t for the cinnamate-ion–α-cyclodextrin system at 25°. This curve has a sigmoidal shape characteristic of simple 1:1 complexing, and a Benesi–Hildebrand plot of $1/\Delta A$ *versus* $1/L_t$ is linear; evidently, the system can be described in terms of a 1:1 complex. The potentiometric data, however, appear to require the presence of both the SL and SL_2 complexes in the cinnamate-ion system; hence, both complexes are considered to be present in the spectral study. The K_{11} and K_{12} values were required to give consistent fits to both the spectral and the potentiometric data. The smooth curve in Fig. 3 was drawn with Eqs. 15 and 16 and the values $K_{11} = 110 \pm 3\ M^{-1}$, $K_{12} = 15 \pm 2\ M^{-1}$, $\Delta\epsilon_{11} = 4300$, and $\Delta\epsilon_{12} = 3300$. (At 269 nm, $\epsilon_S = 2.04 \times 10^4$.)

Potentiometric Study—The potentiometric method for studying cyclodextrin complexes of weak acids was introduced in 1976 and applied to some 1:1 complexing systems (18). Let pKa represent the negative logarithm of the dissociation constant of the weak acid in the absence of ligand (pKa refers to the experimental conditions and is not the thermodynamic constant), and let pKa′ be the corresponding quantity in the presence of cyclodextrin. Define ΔpKa = pKa′ − pKa. Figure 4 shows the dependence of ΔpKa′ on L_t for the cinnamic acid–α-cyclodextrin system. This curve cannot be accounted for satisfactorily in terms of only 1:1 complexes between cyclodextrin and the unionized and ionized forms of the substrate. Therefore, the theory of this method for the SL + SL_2 case was developed.

Let HA, A^-, and L represent cinnamic acid, cinnamate ion, and cyclodextrin, respectively. Then the three acid–base equilibria are presented as:

$$HA \rightleftharpoons H^+ + A^-$$
Scheme III

$$HAL \rightleftharpoons H^+ + AL^-$$
Scheme IV

$$HAL_2 \rightleftharpoons H^+ + AL_2^-$$
Scheme V

with their acid–base dissociation constants given by:

$$K_a = \frac{[H^+][A^-]}{[HA]} \qquad \text{(Eq. 17)}$$

$$K_{a11} = \frac{[H^+][AL^-]}{[HAL]} \qquad \text{(Eq. 18)}$$

$$K_{a12} = \frac{[H^+][AL_2^-]}{[HAL_2]} \qquad \text{(Eq. 19)}$$

The four complexation equilibria are given by:

$$HA + L \rightleftharpoons HAL$$
Scheme VI

$$A^- + L \rightleftharpoons AL^-$$
Scheme VII

$$HAL + L \rightleftharpoons HAL_2$$
Scheme VIII

$$AL^- + L \rightleftharpoons AL_2^-$$
Scheme IX

with their corresponding stability constants:

$$K_{11a} = \frac{[HAL]}{[HA][L]} \qquad \text{(Eq. 20)}$$

$$K_{11b} = \frac{[AL^-]}{[A^-][L]} \qquad \text{(Eq. 21)}$$

$$K_{12a} = \frac{[HAL_2]}{[HAL][L]} \qquad \text{(Eq. 22)}$$

$$K_{12b} = \frac{[AL_2^-]}{[AL^-][L]} \qquad \text{(Eq. 23)}$$

The apparent acid dissociation constant, K_a', is defined by:

$$K_a' = \frac{[H^+][A^-]_{total}}{[HA]_{total}} = \frac{[H^+]([A^-] + [AL^-] + [AL_2^-])}{[HA] + [HAL] + [HAL_2]} \qquad \text{(Eq. 24)}$$

Table I—Thermodynamic Quantities for Cinnamic Acid–α-Cyclodextrin and Cinnamate-Ion–α-Cyclodextrin Complexes

T, °K	Complex[a]	K, M^{-1}	ΔH°, kcal/mole	ΔS°, e.u. Molar Basis	ΔS°, e.u. Mole Fraction Basis
		trans-Cinnamic Acid			
289	SL	3700 ± 100	−9.3 ± 0.6	−16 ± 2	−8
298	SL	2260 ± 50			
308	SL	1350 ± 80			
318	SL	850 ± 50			
289	SL_2	120 + 10	−12 ± 1	−34 ± 4	−26
298	SL_2	60 ± 5			
308	SL_2	30 ± 3			
318	SL_2	17 ± 2			
		trans-Cinnamate Ion			
298	SL	110 ± 3	−1.9 ± 0.6	+3 ± 2	+11
308	SL	100 ± 3			
318	SL	90 ± 3			
298	SL_2	15 ± 2	−9 ± 3	−23 ± 9	−15
308	SL_2	10 ± 1			
318	SL_2	6 ± 1			

[a] S = substrate (cinnamic acid or anion) and L = ligand (cyclodextrin).

Substitution leads to:

$$K_a' = K_a \frac{[1 + K_{11b}[L] + K_{11b}K_{12b}[L]^2]}{[1 + K_{11a}[L] + K_{11a}K_{12a}[L]^2]} \quad \text{(Eq. 25)}$$

or:

$$\Delta pKa' = \log \frac{[1 + K_{11a}[L] + K_{11a}K_{12a}[L]^2]}{[1 + K_{11b}[L] + K_{11b}K_{12b}[L]^2]} \quad \text{(Eq. 26)}$$

As in the spectral study, it is not feasible to find ΔpKa′ as an explicit function of L_t, but L_t can be related to [L] to give a practical method for evaluating the stability constants. The mass balances on ligand and substrate are written as:

$$L_t = [L] + [HAL] + [AL^-] + 2[HAL_2] + 2[AL_2^-] \quad \text{(Eq. 27)}$$

$$A_t = [HA] + [A^-] + [HAL] + [AL^-] + [HAL_2] + [AL_2^-] \quad \text{(Eq. 28)}$$

Substitution with the equilibrium expressions yields functions of L_t and A_t in terms of the variables [L], [HA], and [H^+]. Under the experimental conditions, [H^+] = K_a', so:

$$C = \frac{K_a}{[H^+]} = \frac{K_a}{K_a'} = \frac{1 + K_{11a}[L] + K_{11a}K_{12a}[L]^2}{1 + K_{11b}[L] + K_{11b}K_{12b}[L]^2} \quad \text{(Eq. 29)}$$

giving:

$$L_t = [L] + [HA](K_{11a}[L] + CK_{11b}[L] + 2K_{11a}K_{12a}[L]^2 + 2CK_{11b}K_{12b}[L]^2) \quad \text{(Eq. 30)}$$

and:

$$A_t = [HA](1 + C + K_{11a}[L] + CK_{11b}[L] + K_{11a}K_{12a}[L]^2 + CK_{11b}K_{12b}[L]^2) \quad \text{(Eq. 31)}$$

Define:

$$K_{11}' = K_{11a} + K_{11b}C \quad \text{(Eq. 32)}$$

and:

$$K_{12}' = K_{11a}K_{12a} + K_{11b}K_{12b}C \quad \text{(Eq. 33)}$$

Then Eq. 34 is obtained:

$$L_t = [L]\left[1 + \frac{K_{11}'A_t + 2K_{12}'A_t[L]}{1 + C + K_{11}'[L] + K_{12}'[L]^2}\right] \quad \text{(Eq. 34)}$$

The procedure is to assign a value to [L] and, with Eqs. 26 and 34 and estimates of the stability constants, to calculate ΔpKa′ and L_t for comparison with the experimental results.

Not all of the constants defined for the system are independent. From the definitions, one obtains:

$$K_{11a}K_{a11} = K_aK_{11b} \quad \text{(Eq. 35)}$$

and:

$$K_{12a}K_{a12} = K_{a11}K_{12b} \quad \text{(Eq. 36)}$$

The smooth curve in Fig. 4 was calculated with Eqs. 26 and 34. In this calculation, K_{11a} and K_{12a} were fixed at 2260 and 60 M^{-1}, respectively, as determined from the solubility and spectral studies; thus, only K_{11b} and K_{12b} were treated as adjustable parameters. Even these parameters, however, were not completely free since they had to account for both the potentiometric data and the spectral study on the cinnamate ion. The final values, as given previously, were K_{11b} = 110 M^{-1} and K_{12b} = 15 M^{-1}. It was necessary to incorporate a finite value for K_{12b} to achieve a satisfactory fit at the higher L_t range in Fig. 4.

Thermodynamic Quantities—Since the comparative studies demonstrated that these systems can be described in terms of SL and SL_2 complexes, any of the experimental techniques suffices to make subsequent estimates of the stability constants. The spectral technique was applied to the cinnamic acid–α-cyclodextrin and cinnamate-ion–α-cyclodextrin systems at several temperatures to obtain enthalpy and entropy changes for the complexation equilibria. The data were analyzed in terms of SL and SL_2 complexes (Table I). Entropy changes on a mole fraction basis (unitary entropy changes) (23) were obtained for Schemes I and II from:

$$\Delta S° \text{ (unitary)} = \Delta S° \text{ (molar)} + 8.0 \text{ e.u.} \quad \text{(Eq. 37)}$$

DISCUSSION

Complex Stoichiometry and Stability—Several kinds of evidence show that the cinnamic acid–α-cyclodextrin system cannot be described solely in terms of 1:1 complexes:

1. The isosbestic points seen at low ligand concentrations are lost at higher concentrations.
2. The shape of the plot of Δ*A versus* log L_t (Fig. 2) requires some process in addition to 1:1 complexation.
3. Apparent 1:1 stability constants, evaluated assuming only 1:1 stoichiometry and using data at low ligand concentration, are 1300 M^{-1} for the solubility method and 2900 M^{-1} for the spectral method, the disagreement being inconsistent with the assumption.
4. The increase of total dissolved substrate after the initial plateau portion of the solubility diagram cannot occur if only 1:1 complexation occurs.
5. The solid phase composition in the solubility study requires an L/S ratio greater than 1:1.
6. The potentiometric curve cannot be fitted with the assumption of 1:1 stoichiometry.

Few modern workers use the solubility method to study molecular complexes, and the technique has been criticized because it does not permit the estimation of stability constants unless the stoichiometry of the interaction is known. This criticism is correct, but the limitation applies equally to every other experimental technique. In the present investigation, the solubility method was the single most useful tool because it not only showed that more than one type of complex must be present, but it also indicated the probable stoichiometric ratios. But the strongest evidence for the interpretation of the cinnamic acid–α-cyclodextrin system in terms of SL and SL_2 complexes is the quantitative

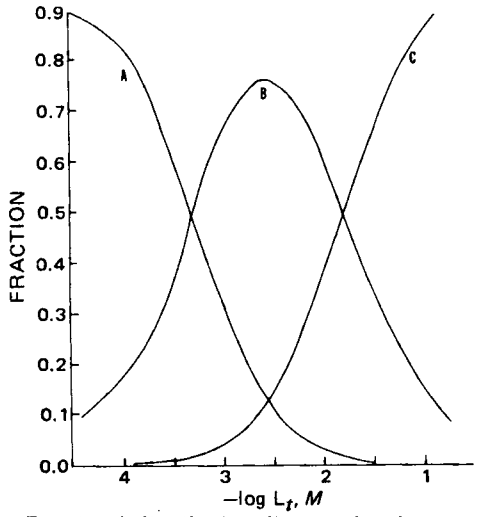

Figure 5—*Fractional distribution diagram for the* trans-*cinnamic acid–α-cyclodextrin system at 25°. The total cinnamic acid concentration was 8.5 × 10⁻⁵* M. *Curves A, B, and C are S, SL, and SL_2, respectively.*

agreement among the three experimental techniques when analyzed according to this model. Such comparative study by independent techniques is one desirable feature of investigations into complex stoichiometries and stabilities; another advantage is extension of the measurements over as wide a range of ligand concentrations as is feasible, preferably over essentially the full binding isotherm.

Should the small values of K_{12} relative to K_{11} (Table I) be thought to render the incursion of SL_2 formation negligible except at a high ligand concentration, it should be noted that the fractional distribution of species S, SL, and SL_2 depends on the product $K_{11}K_{12}$. These distributions (*e.g.*, for SL_2) can be calculated with Eqs. 16 and 38:

$$\text{fraction of } SL_2 = \frac{[SL_2]}{S_t} = \frac{K_{11}K_{12}[L]^2}{1 + K_{11}[L] + K_{11}K_{12}[L]^2} \quad \text{(Eq. 38)}$$

Figure 5 is a fractional distribution diagram for the cinnamic acid–α-cyclodextrin system at 25° with $S_t = 8.5 \times 10^{-5}$ *M*, corresponding to the conditions for the spectral study. At the relatively low total cyclodextrin concentration of 0.01 *M*, about 37% of the cinnamic acid is present as the ternary SL_2 complex. Diagrams of this type should be valuable in selecting experimental conditions for studying complex properties.

The evidence for a ternary SL_2 complex in the cinnamate-ion system is less compelling, consisting of the need to include the term containing K_{12b} in Eq. 26 to achieve a satisfactory fit to the potentiometric data.

Complex Properties and Structures—The symbolism of Schemes VI–IX is adopted here to discuss the several complexes with brevity and without ambiguity. Thus, HA represents cinnamic acid and A^- is cinnamate ion.

Several properties of the complexes (other than the standard thermodynamic quantities to be considered later) were measured in the present study and may be helpful in determining the complex structures. The complex molar absorptivities for HAL, HAL_2, AL^-, and AL_2^- were obtained but only at a single wavelength. The general spectral shifts in the presence of cyclodextrin are not dramatic and do not seem helpful at this point.

With Eqs. 35 and 36, one calculates $pKa_{11} = 5.66$ and $pKa_{12} = 6.27$, compared with pKa = 4.35 for uncomplexed cinnamic acid. Complexing between carboxylic acids and α-cyclodextrin leads to a decrease in the acid strength of the substrate; this is equivalent to saying that the unionized carboxylic acid complexes more strongly than does the carboxylate ion (18). Since the two statements are equivalent, a rationalization of one of them equally accounts for the other. Consider the acidity of HAL (*i.e.*, the acidity of complexed cinnamic acid) relative to that of cinnamic acid in water. Spectroscopic data (24) indicate that the α-cyclodextrin cavity is apolar. If the cinnamic acid group is included within the ligand cavity, it experiences an environment that is comparable (except for "end" effects and restricted molecular motion) to that provided by a solvent such as dioxane or a ketone. In such a medium, having an effective dielectric constant smaller than that of water, the extent of ionization of the carboxylic acid will be less than in water. Therefore, it is anticipated that $K_{a11} < K_a$ for neutral carboxylic acids, from which it follows that $K_{11a} > K_{11b}$, as is observed for these substrates[8]. The same argument applies to the ternary complex HAL_2, which also must be an inclusion complex[9].

The solubility of HAL was determined to be 1.7×10^{-2} *M*. If the substrate HA is included within the cavity, it is not surprising that HAL would have a solubility intermediate to that of the hydrophobic HA ($s_0 = 3.01 \times 10^{-3}$ *M*) and the hydrophilic L ($s_L = 0.125$ *M*). The solubility of HAL_2 is 5.5×10^{-3} *M* (or 1.4×10^{-3} *M*), considerably smaller than that of L or HAL and comparable with that of HA. If HA is included in a channel formed by an end-to-end association of two cyclodextrins, the solubility of HAL_2 will be determined in part by solvent interactions with a dimer-like species L_2; this species is twice as large as L or HAL and provides no additional sites for solvent interaction; hence, its solubility probably will be smaller.

The solubility of the cinnamate-ion–α-cyclodextrin complex was not determined; if it is an inclusion complex with the carboxylate group buried in the cavity, its solubility might be as low as that of HAL. On the other hand, if the carboxylate function is exposed, the complex may be as soluble as the substrate; sodium cinnamate had a solubility of 0.505 *M*. These limits will be used later.

The picture that results from these several kinds of evidence and lines of reasoning is of binary (1:1) inclusion complexes, probably with the side chain in the cavity. The ternary (1:2) complexes may have the substrate in a cavity formed by two ligand molecules associated end-to-end. Although α-cyclodextrin does not form a dimer (28), the SL_2 complex is formed in the presence of cinnamic acid or cinnamate ion. In a sense, cyclodextrin dimerization is promoted by the substrate molecule, the complex structure possibly being much like a dowel joint. Such SL_2 complexes are formed by cinnamic acid, cinnamate ion, *p*-methylcinnamate ion (13), and 4-biphenylcarboxylate ion (12) whereas benzoic acid, benzoate ion (14), and *p*-nitrophenolate ion (18, 27) apparently form only 1:1 complexes. The length of the substrate molecule is possibly a factor determining whether an SL_2 complex forms (11).

Thermodynamic Analysis—The values of free energy and entropy changes depend on the concentration units used in evaluating them, and these quantities can be corrected for the entropy of mixing if the concentrations are expressed on the mole fraction scale (29). The resulting values are called unitary quantities. Table I gives unitary entropy changes (in the last column) for the process studied here[10].

The favorable free energy changes are manifested for the HAL, HAL_2, and AL_2^- complexes as favorable $\Delta H°$ and unfavorable $\Delta S°$ values; for the AL^- complex, the entropy change is favorable and the enthalpy change is very small. Another observation is that, for each substrate, $\Delta H°$ is more favorable and $\Delta S°$ is less favorable for the 1:2 complexes than for the 1:1 complex. (The $\Delta H°$ and $\Delta S°$ for the 1:2 complexes refer to the stepwise process, $SL + L \rightleftharpoons SL_2$, not to the overall process, $S + 2L \rightleftharpoons SL_2$.)

The conventional interpretation of favorable enthalpy changes and of entropy decreases invokes the role of water structure or ordering in the complexation. The negative $\Delta S°$ may signify an increase in solvent ordering in the product state (complex) compared with the individual solvated species. Nonpolar solutes, upon association, show entropy increases, but moderately polar solutes lead to entropy decreases. Jencks (31) pointed out that a favorable $\Delta H°$ may result from solute–solute interactions or from increased solvent–solvent interactions, which are made possible by the greater solvent order. Cyclodextrins are rather special solutes because the cavity contains highly ordered solvent molecules, which must be displaced upon inclusion of a substrate. Van Etten *et al.* (24) suggested that these water molecules cannot form the normal complement of hydrogen bonds because of steric restrictions and that

[8] The same argument applied to phenols may seem to lead to the same prediction. However, phenols behave differently from carboxylic acids in nonaqueous media. For example, in pyridine, the acid strengths of phenols are enhanced relative to those of carboxylic acids, with the result that, for example, *p*-nitrophenol is a stronger acid than is benzoic acid in this solvent (25). Similar behavior is seen in acetone (26). Thus, it is likely that phenol acidity will be increased in the cyclodextrin cavity, with the consequence that $K_{11b} > K_{11a}$, as is seen (18, 27).

[9] The conclusion that HAL and HAL_2 are inclusion complexes follows from the abnormally large equilibrium constants for their formation. (The overall constant for $HA + 2L \rightleftharpoons HAL_2$ is equal to $K_{11}K_{12}$.) When two species interact noncovalently in solution in a simple stacking manner, the stability constant for the process is proportional to the area of contact between the molecules (6). For a molecule the size of cinnamic acid, the maximum value to be expected is on the order of $10^2\ M^{-1}$. Since K_{11} for cinnamic acid–α-cyclodextrin is much higher that this value, some extraordinary stabilizing phenomenon, presumably inclusion, must be occurring. The ternary complex HAL_2 is formed from L and the inclusion complex HAL, so it too is an inclusion complex.

[10] For other discussions of unitary quantities, see Refs. 23 and 30. The authors thank Professor P. Mukerjee, who first called their attention to unitary quantities.

Table II—Thermodynamic Analysis of the Cinnamic Acid–α-Cyclodextrin System

Process[a]	$\Delta G°$ (unitary)[b], cal/mole
1. $S(s) \rightleftharpoons S(aq)$	$+5820 \pm 10$
2. $L(s) \rightleftharpoons L(aq)$	$+3610 \pm 50$
3. $SL(aq) \rightleftharpoons SL(s)$	-4800 ± 70
4. $S(aq) + L(aq) \rightleftharpoons SL(aq)$	-6950 ± 15
5. $S(s) + L(s) \rightleftharpoons SL(s)$	-2320 ± 90
6. $SL(s) \rightleftharpoons SL(aq)$	$+4800 \pm 70$
7. $L(s) \rightleftharpoons L(aq)$	$+3610 \pm 50$
8. $SL_2(aq) \rightleftharpoons SL_2(s)$	-5460 ± 100 (-6280 ± 260)
9. $SL(aq) + L(aq) \rightleftharpoons SL_2(aq)$	-4810 ± 50
10. $SL(s) + L(s) \rightleftharpoons SL_2(s)$	-1860 ± 140 (-2680 ± 280)

[a] The *s* represents solid phase and aq represents solution. [b] Uncertainties represent standard deviation estimates calculated from experimental estimates of the uncertainties in the solubilities and stability constants.

Table III—Thermodynamic Analysis of the 1:1 Cinnamate-Ion–α-Cyclodextrin Complex

Process	$\Delta G°$ (unitary)[a], cal/mole
1. $M^+S^-(s) \rightleftharpoons M^+S^-(aq)$	$+2790 \pm 120$
2. $L(s) \rightleftharpoons L(aq)$	$+3610 \pm 50$
3. $M^+SL^-(aq) \rightleftharpoons M^+SL^-(s)$	[-2790 ± 120 to -4800 ± 70][b]
4. $M^+S^-(aq) + L(aq) \rightleftharpoons M^+SL^-(aq)$	-5160 ± 20
5. $M^+S^-(s) + L(s) \rightleftharpoons M^+SL^-(s)$	[-1550 ± 200 to -2430 ± 150]

[a] Uncertainties represent standard deviation estimates calculated from experimental estimates of the uncertainties in solubilities and stability constants. [b] Estimated limits.

their release to bulk solvent is manifested as a favorable enthalpy change for complex formation. Restriction of rotational motion of an included substrate molecule could lead to an entropy decrease.

Such rationalizations do not provide much predictive power. For the AL^- complex, an entropy increase is seen, and the enthalpy change is very small. If the carboxylate enters the cavity, the net result may be a considerable decrease in solvent order by release of water from the cavity and from the carboxylate group. Presumably, the counterion remains outside the cyclodextrin. Komiyama and Bender (32) interpreted similar $\Delta H°$ and $\Delta S°$ values in complexation of 1-adamantanecarboxylate with α-cyclodextrin as evidence for apolar binding of the nonpolar substrate to the top of the cavity. This interpretation does not seem applicable to the cinnamate-ion system.

The $\Delta H°$ and $\Delta S°$ values for HAL_2 and AL_2^- are similar, considering the uncertainties. In each case, the process may be much the same: a ligand cavity is evacuated, the ligand slides over the portion of substrate protruding in an SL complex, S readjusts its position within the L_2 aggregate, and solvent reordering occurs.

The solubility data provide an opportunity for a different kind of analysis. Table II gives unitary free energy changes for the processes described in this paper. Processes 1–4 are for the formation of complex HAL; these processes, when added, give the net Process 5. Process 5 is solvent independent (if solid L is understood to represent the hydrated ligand); it is expected that the same value would be obtained for its $\Delta G°$ if corresponding experimental values were available for Processes 1–4 in another solvent (such as a mixed aqueous–organic solvent). Thus, $\Delta G°$ for Process 5 can be compared with $\Delta G°$ for Process 4, indicating that the complex formation is more favorable in water than in the solid state. Tables II and III show a similar relationship for the HAL_2 and AL^- complexes. Formation of these complexes in the solid phase is thermodynamically favorable.

These processes can be represented as a cycle as for the complex SL (Scheme X):

$$\begin{array}{ccccc} S(aq) & + & L(aq) & \rightleftharpoons & SL(aq) \\ \Updownarrow & & \Updownarrow & & \Updownarrow \\ S(s) & + & L(s) & \rightleftharpoons & SL(s) \end{array}$$

Scheme X

Just as other solvents should lead to the same free energy change for the solid phase process, the solid phases in this cycle also could be replaced by liquid phases, and rather than using solubilities in the model, partition coefficients would be employed. This cycle suggests why, for a series of closely related compounds, limited correlations between complex stability constants and substrate solubility or partition coefficient may be observed.

This analysis suggests new lines of experimental work. It will be necessary to establish that the free energy change for the solid phase process is, in fact, independent of the solvent used. It will be interesting to partition this free energy change into enthalpy and entropy changes. Since a long-term goal is to predict complex stability constants in aqueous solution (*i.e.*, Process 4 in Table II), these thermodynamic cycles offer a promising route; after study of numerous systems, it may be easier to estimate the free energy change of Process 5 than of Process 4. The cycle then provides a path for the calculation of the free energy change of Process 4.

REFERENCES

(1) K. A. Connors and J. A. Mollica, *J. Am. Chem. Soc.*, **87**, 123 (1965).

(2) J. A. Mollica and K. A. Connors, *ibid.*, **89**, 308 (1967).

(3) P. A. Kramer and K. A. Connors, *ibid.*, **91**, 2600 (1969).

(4) K. A. Connors, M. H. Infeld, and B. J. Kline, *ibid.*, **91**, 3597, 5697 (1969).

(5) H. Stelmach and K. A. Connors, *ibid.*, **92**, 863 (1970).

(6) J. L. Cohen and K. A. Connors, *J. Pharm. Sci.*, **59**, 1271 (1970).

(7) K. A. Connors and S. Sun, *J. Am. Chem. Soc.*, **93**, 7239 (1971).

(8) K. Uekama, M. Otagiri, Y. Kanie, S. Tanaka, and K. Ideka, *Chem. Pharm. Bull.*, **23**, 1421 (1975).

(9) W. A. Pauli and J. L. Lach, *J. Pharm. Sci.*, **54**, 1745 (1965).

(10) J. Cohen and J. L. Lach, *ibid.*, **52**, 132 (1963).

(11) H. Schlenk and D. M. Sand, *J. Am. Chem. Soc.*, **83**, 2312 (1961).

(12) R. I. Gelb, L. M. Schwartz, C. T. Murray, and D. A. Laufer, *ibid.*, **100**, 3553 (1978).

(13) R. I. Gelb, L. M. Schwartz, and D. A. Laufer, *ibid.*, **100**, 5875 (1978).

(14) R. I. Gelb, L. M. Schwartz, R. F. Johnson, and D. A. Laufer, *ibid.*, **101**, 1869 (1979).

(15) K. A. Connors and J. A. Mollica, *J. Pharm. Sci.*, **55**, 772 (1966).

(16) T. Higuchi and K. A. Connors, *Adv. Anal. Chem. Instrum.*, **4**, 117 (1965).

(17) H. Benesi and J. H. Hildebrand, *J. Am. Chem. Soc.*, **70**, 2832 (1948).

(18) K. A. Connors and J. M. Lipari, *J. Pharm. Sci.*, **65**, 379 (1976).

(19) M. L. Bender, G. R. Schonbaum, and B. Zerner, *J. Am. Chem. Soc.*, **84**, 2540 (1962).

(20) M. L. Bender and M. Komiyama, "Cyclodextrin Chemistry," Springer-Verlag, Berlin, Germany, 1978.

(21) T. W. Rosanke, Ph.D. thesis, University of Wisconsin, Madison, Wis., 1979.

(22) G. D. Johnson and R. E. Bowen, *J. Am. Chem. Soc.*, **87**, 1655 (1965).

(23) K. A. Connors, "Reaction Mechanisms in Organic Analytical Chemistry," Wiley-Interscience, New York, N.Y., 1973, pp. 17–20.

(24) R. L. Van Etten, J. F. Sebastian, G. A. Clowes, and M. L. Bender, *J. Am. Chem. Soc.*, **89**, 3242 (1967).

(25) C. A. Streuli, *Anal. Chem.*, **32**, 407 (1960).

(26) J. S. Fritz and S. S. Yamamura, *ibid.*, **29**, 1079 (1957).

(27) F. Cramer, W. Saenger, and H.-C. Spatz, *J. Am. Chem. Soc.*, **89**, 14 (1967).

(28) R. I. Gelb, L. M. Schwartz, J. E. Markinac, and D. A. Laufer, *ibid.*, **101**, 1864 (1979).

(29) R. W. Gurney, "Ionic Processes in Solution," McGraw-Hill, New York, N.Y., 1953 (Dover Publications, New York, N.Y., reprint, 1962), chap. 6.

(30) C. Tanford, "The Hydrophobic Effect," Wiley-Interscience, New York, N.Y., 1973, chap. 2.

(31) W. P. Jencks, "Catalysis in Chemistry and Enzymology," McGraw-Hill, New York, N.Y., 1969, chap. 7.

(32) M. Komiyama and M. L. Bender, *J. Am. Chem. Soc.*, **100**, 2259 (1978).

ACKNOWLEDGMENTS

Supported in part by National Science Foundation Grant GP-36567 and in part by a grant from The Upjohn Co.

NMR Spectral Study of Proton Transfer in Amitriptyline Hydrochloride–Chlordiazepoxide Hydrochloride Combinations in Dipolar Aprotic Solvent

PRANAB K. BHATTACHARYYA

Received July 9, 1979, from the *Quality Control Department, Hoffmann-La Roche Inc., Nutley, NJ 07110.* Accepted for publication September 19, 1979.

Abstract □ The singlet resonance due to the two equivalent methyl groups of amitriptyline hydrochloride in dimethyl sulfoxide-d_6 solution changed into a doublet with the addition of chlordiazepoxide hydrochloride. A spin decoupling experiment revealed that the doublet originated because of the emergence of observable spin–spin coupling between the tertiary amine proton and the methyl groups. The phenomenon was interpreted to be due to the nature of proton transfer caused by the relative magnitudes of the basicities of the amines in these compounds, which were determined by the inductive and steric effects of the substituents, leading to the formation of hydrogen-bonded ion-pairs in the aprotic diluent. The enthalpy of the exchange process was 6.4 ± 0.5 kcal/mole.

Keyphrases □ NMR spectroscopy—proton transfer in amitriptyline hydrochloride–chlordiazepoxide hydrochloride mixtures, dipolar aprotic solvent □ Amitriptyline hydrochloride—effect of chlordiazepoxide hydrochloride on NMR spectra, proton transfer in a dipolar aprotic solvent □ Chlordiazepoxide hydrochloride—effect of amitriptyline hydrochloride on NMR spectra, proton transfer in a dipolar aprotic solvent

The relative magnitudes of the basicities of amines in solution essentially determine the outcome of the competition between the bases for available acidic protons. In an analytical study with a formulation containing amitriptyline hydrochloride and chlordiazepoxide free base, it was observed that mixtures of the hydrochloride salts of amitriptyline and chlordiazepoxide provide an interesting example of the proton exchange equilibrium caused by the relative orders of basicities of the amines in these compounds. However, since hydrogen bonding plays a vital role in acid–base behavior leading to the formation of many types of aggregates, which vary widely in stability, the protic solvents such as water and alcohols are not suitable for such an investigation because they are actively involved in hydrogen bonding and exchange reactions.

EXPERIMENTAL

The hydrochloride samples were prepared in NMR grade dimethyl sulfoxide-d_6 (99.8 atom % D), which was shaken with molecular sieves type 13 X. Spectra were obtained with an NMR spectrometer[1] equipped with accessories for performing double-resonance and temperature-dependence experiments.

RESULTS

The NMR spectra of chlordiazepoxide hydrochloride and amitriptyline hydrochloride in dimethyl sulfoxide-d_6 are presented in Figs. 1A and 1B. Table I contains the assignments of the NMR spectra of the hydrochloride salts and free bases of amitriptyline and chlordiazepoxide. The NMR spectrum (Fig. 1C) shows that the singlet resonance due to the two equivalent *N*-methyl groups of amitriptyline hydrochloride changes strikingly into a doublet when chlordiazepoxide hydrochloride is added to the amitriptyline hydrochloride solution. The doublet is observed when the mole ratio of chlordiazepoxide hydrochloride to amitriptyline hydrochloride is ≥0.1. The doublet (splitting ~4.5 Hz) collapses into a singlet (Fig. 2) when the tertiary amine proton resonance region (δ ~10.5–11.5 ppm) in amitriptyline hydrochloride is saturated by the double-resonance technique.

[1] Varian XL-100/Nicolet TT-100.

Table I—Assignments[a] of the PMR Spectra of Amitriptyline Hydrochloride and Free Base and of Chlordiazepoxide Hydrochloride and Free Base

Compound	Proton	δ, ppm (in Dimethyl Sulfoxide-d_6) HCl Salt	Free Base
Amitriptyline	$>CH_2 \times 4$	2.3–3.5 (m)	2.0–3.4 (m)
	$-CH_3 \times 2$	2.64 (s)	2.0 (s)
	$=CH-$	5.82 (t, 7.5 Hz)	5.8 (t, 7.5 Hz)
	Aromatic	6.9–7.4 (m)	$6.9–7.3_5$ (m)
	HCl	10.8–11.4 (b)	
Chlordiazepoxide	$-CH_3$	3.28 (s)	2.83 (d, 4.5 Hz)
	$>CH_2$	5.0 (s)	4.4 (s)
	Aromatic	$6.3–7.0_5$ (m)	6.3–7.7 (m)
	>NH	11.4 (b)	8.08 (q, 4.5 Hz)
	HCl	11.4 (b)	

[a] Multiplicities and, where applicable, coupling constants in Hertz are noted within parentheses; s = singlet, d = doublet, t = triplet, m = multiplet, and b = broad peak.

This experiment conclusively proves that the doublet in the NMR spectrum of amitriptyline hydrochloride is caused by the protons in the methyl groups becoming spin-coupled to the tertiary amine proton when chlordiazepoxide hydrochloride is added. This finding is confirmed by the experiments where the doublet collapses into a singlet when the amine proton is deuterated by the addition of deuterium oxide. The splitting does not arise from nonequivalent *N*-methyl groups or from stereoisomers protonated on opposite sides of the nitrogen atom.

The spin–spin coupling originates because of the emergence of the following predominant rate-determining step (Scheme I) in the acid–base equilibrium of amitriptyline hydrochloride in the presence of chlordiazepoxide hydrochloride in dimethyl sulfoxide-d_6 solvent:

$$N\text{:}\cdots HCl \rightarrow N^+H\cdots Cl^-$$

Scheme I

where the N:- - -H bond is electrostatic with no charge transfer and the N^+H bond is covalent with charge transfer.

With amitriptyline hydrochloride, the proton donor and acceptor are both strong enough so that the proton shifts toward the nitrogen nucleus under the condition where slightly more than one acid is attracted (probably by aggregation) per amine molecule. The product, symbolized by $N^+H\cdots Cl^-$, is called a hydrogen-bonded ion-pair (1). Thus, the transfer of acidity between the two compounds results in the neutral molecule changing into a positive ion where the intermolecular distance between the nitrogen and the proton is smaller than in the neutral molecule.

Since the doublet formation indicating that protonation has occurred on the nitrogen atom is a reflection of ion-pair formation, the criterion of splitting is a qualitative indication of the covalent character of the bond between the nitrogen atom and proton. Since the precise character of the sp^3 orbital occupied by the lone pair of electrons of the nitrogen atom depends on the groups linked to this atom, the energy of the N^+H bond produced and the thermodynamic stability of the positive ion depend on the nature of these groups.

The spin–spin coupling is an interaction that provides two magnetic environments for the *N*-methyl protons, depending on the spin state of the N^+H proton. Whether or not the *N*-methyl protons of amitriptyline appear as a doublet depends on the lifetime of the spin states of the N^+H protons. Development of the theory for intermediate rates of exchange was first published by Gutowsky *et al.* (2). Later extension of the theory

0022-3549/80/0200-0180$01.00/0
© 1980, American Pharmaceutical Association

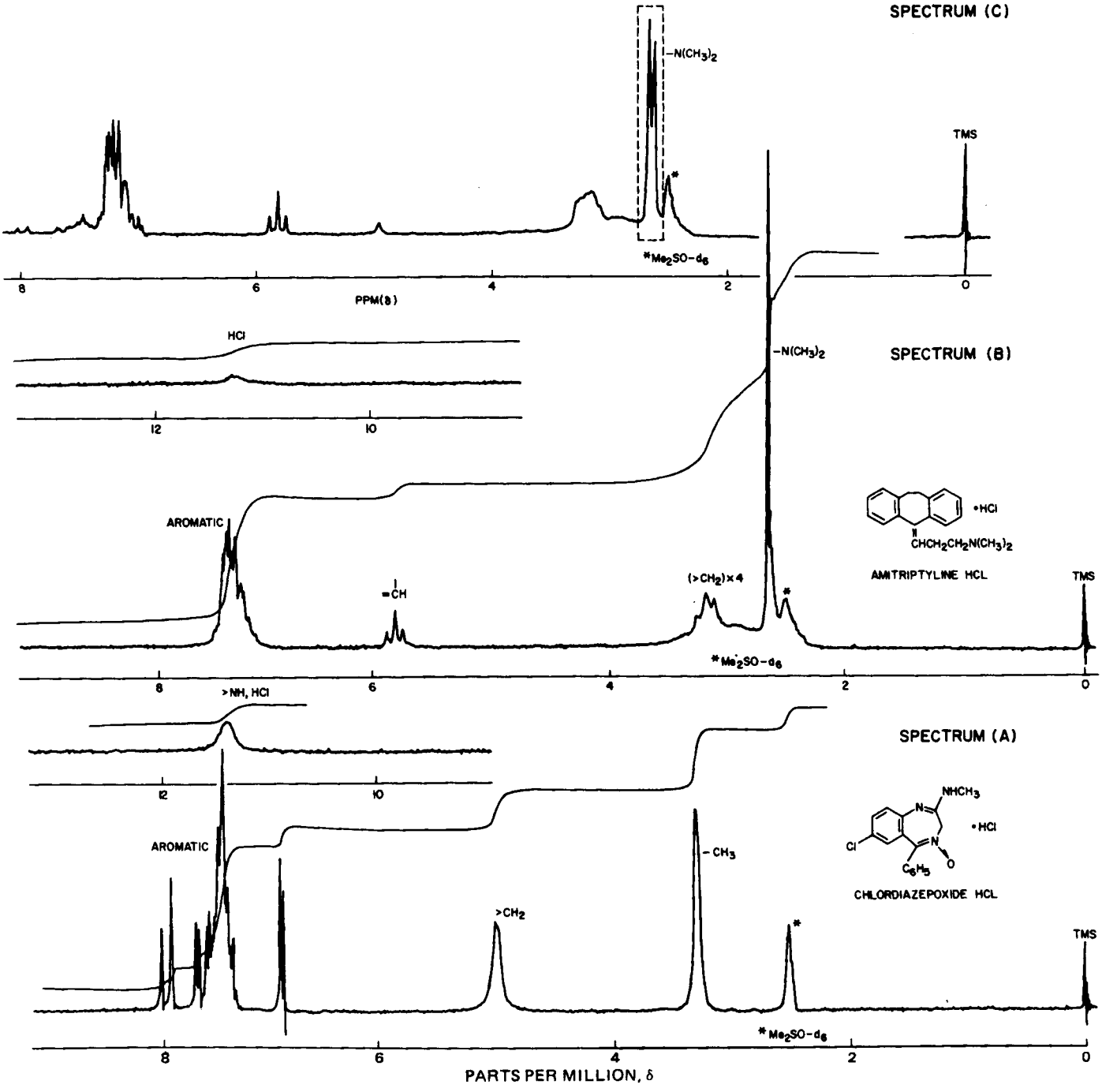

Figure 1—*PMR spectra (A) of chlordiazepoxide hydrochloride (50 mg) in 0.5 ml of dimethyl sulfoxide-d_6 solvent, (B) of amitriptyline hydrochloride (50 mg) in 0.5 ml of dimethyl sulfoxide-d_6 solvent, and (C) of the combination of amitriptyline hydrochloride (50 mg) and chlordiazepoxide hydrochloride (5 mg) in 0.5 ml of dimethyl sulfoxide-d_6 solvent. The doublet is marked with a dashed rectangle. (TMS = tetramethylsilane.)*

(3) was not very general in that it did not account for an asymmetric pair of lines. Rogers and Woodbrey (4) developed a general treatment in which a precise measure of lifetime, τ, is obtained from the line shape parameter, p. In the case of a doublet, the lifetime is given by the following expression:

$$2\pi\tau|J| = \pm[2p \pm 2(p^2 - p)^{1/2}]^{1/2} \quad \text{for } \sqrt{2}\pi\tau|J| > 1 \quad \text{(Eq. 1)}$$

where p is the ratio of the mean of the peak maxima to the minimum between them and J is the spin–spin coupling constant.

At the point of coalescence, the lifetime is given by:

$$2\pi\tau|J| = \sqrt{2} \quad \text{(Eq. 2)}$$

The proton exchange rates are obtained from the relation:

$$r = \frac{1}{\tau} \quad \text{(Eq. 3)}$$

The exchange process can be accelerated by raising the temperature (Fig. 3). Increasing the temperature increases r since a heat of activation, ΔH, is associated with it according to the Arrhenius equation:

$$r \propto \exp(-\Delta H/RT) \quad \text{(Eq. 4)}$$

where T is the absolute temperature and R is the gas constant.

The values of the lifetime and proton transfer rate of the positive ions at different temperatures, which are calculated from Eqs. 1–3, are listed in Table II. The doublet collapses into a singlet when the probe temperature is raised to 50° or higher (ambient probe temperature is 32°). The activation energy associated with the exchange process is obtained from the slope of the plot of:

$$\ln\frac{r(322)}{r(T)} = -\frac{\Delta H}{R}\left(\frac{1}{322} - \frac{1}{T}\right) \quad \text{(Eq. 5)}$$

The ΔH value is determined to be 6.4 ± 0.5 kcal/mole. In this example,

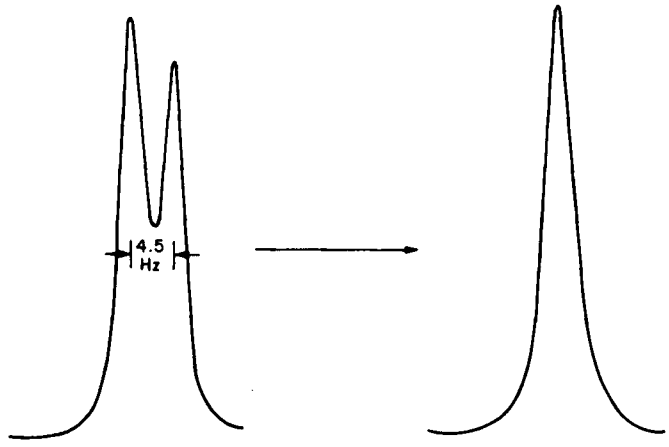

Figure 2—*Transformation of the doublet into a singlet when the tertiary amine proton resonance is decoupled.*

the spin–spin splitting averages to zero by the transfer process having a mean lifetime in the various states of <0.05 sec. Incidentally, the chemical shifts of the singlet and doublet due to the methyl groups of amitriptyline in the forms of associated complex and ion-pairs, respectively, are essentially the same (2.64 ppm), probably because (5) of the similar wave functions of the species rather than lack of sensitivity of the nuclei to changes in electron densities in the two forms of the compound.

It is also obvious from Figs. 1B and 1C that the *N*-methyl doublet splitting, which stands out as an observable effect caused by the intermolecular competition for acidic protons in this experiment, is not detectable in the following combinations since the amount of available exchangeable acidic protons is below the necessary threshold: amitriptyline hydrochloride and chlordiazepoxide base, amitriptyline base and chlordiazepoxide hydrochloride, and amitriptyline base and chlordiazepoxide base. This finding is confirmed by the doublet splitting in the competition-free model experiment where 5 μl of 0.01 *N* HCl is added to 20 mg of amitriptyline hydrochloride in dimethyl sulfoxide-d_6 solvent.

DISCUSSION

The overall acid–base behavior of compounds and, therefore, the observed competitive behavior of amines for acidic protons are determined by the relative proton donor–acceptor affinities and the role of intermolecular hydrogen bonding in dimethyl sulfoxide-d_6. The relative orders of basicities of amines, which can be considered as nucleophilic agents whose exact nature depends on the position of the unshared electron pair at the coordinatively active nitrogen atom, are determined (6) by the inductive and steric effects of the substituents attached to this atom. The introduction of electron donor groups with positive inductive effects into the tertiary amine molecule increases the basicity, and the introduction of electron acceptor groups with negative inductive effects lowers the basicity. Thus, in one direction, the increasing substitution of the nitrogen atom in going from the primary to tertiary amine results in an increase in base strength because of the electron-donating property of the alkyl group. In the other direction, the increasing steric hindrance due to the bulk of the alkyl groups decreases the apparent basicity. With amitriptyline, there is a fairly large amount of positive inductive effect on the tertiary nitrogen owing to the methylene and two methyl groups. The doublet splitting indicates that the steric hindrance is not large enough to neutralize this increase of basicity. In chlordiazepoxide, on the other hand, the positive inductive effect induced by the methyl group on the nitrogen atom of the secondary amine is reduced by the neighboring unsaturation in the ring. Thus, a significant difference in the electronic contributions to base strengths exists in the two compounds. The imines of chlordiazepoxide, which are expected to be comparatively weak in the relative order of basicity, will have a negligible influence on the competitive acid–base behavior in this study because the competition for the acidic protons obviously will be restricted mainly to the secondary amine proton of chlordiazepoxide and the tertiary amine proton of amitriptyline.

At this point, it is important to remember that the dipolar aprotic solvents such as dimethyl sulfoxide-d_6 are not truly inert but show proton donor–acceptor behavior, thus affecting quantitative relationships (7) observed in studying interactions between bases and acids. The aprotic solvents are thus admirably suited for ascertaining differentiating kinds of acid–base behavior, which are masked in amphiprotic and other active solvents. These solvents display significant and differing hydrogen bonding tendencies since the interactions of principal interest in such solvents are the much stronger interactions between dissolved species, including long-range Coulomb effects caused by the general electrostatic

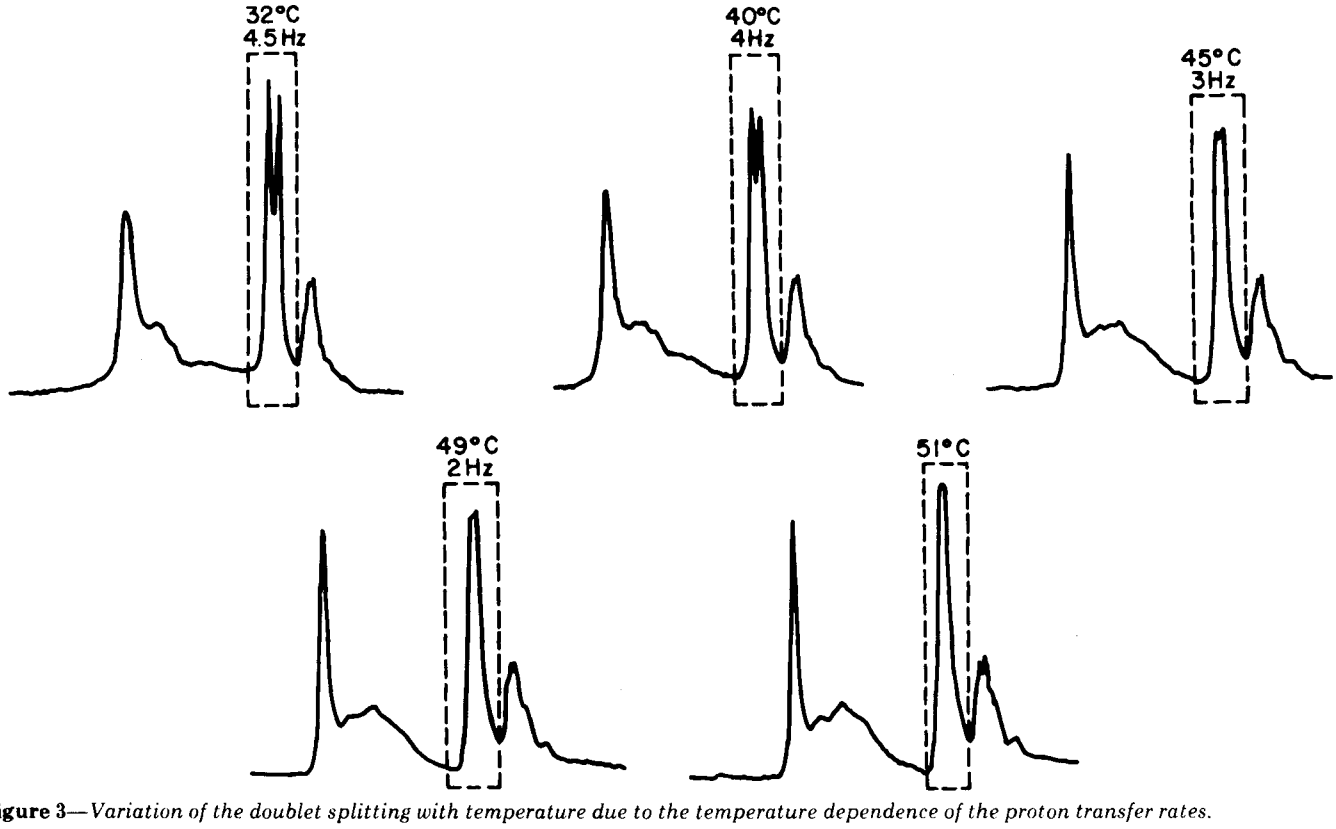

Figure 3—*Variation of the doublet splitting with temperature due to the temperature dependence of the proton transfer rates.*

Table II—Temperature Dependence of the Proton Exchange Rate (r) and Mean Lifetime (τ) of the Positive Ion

Temperature	$2\pi\tau\lvert J\rvert$[a]	τ, sec	r, sec^{-1}
32°	2.5	0.09	11
40°	2.0	0.07	14
45°	1.6	0.06	17
49°	1.4	0.05	20

[a] $|J|$ = 4.5 Hz.

solvation of the ammonium cation or the ion-pair by both the static and induced moments of the diluent molecules. Consequently, intermolecular hydrogen bonding assumes greater importance in aprotic solvents than in leveling solvents in the detection of competitive basic sites.

The relative degree of dissociation exhibited by amitriptyline hydrochloride and chlordiazepoxide hydrochloride in dimethyl sulfoxide-d_6 results from two opposing effects: the positive inductive effect, which tends to increase the stability of the salts, and the steric influence, which tends to decrease the stability. The observed base strengths are determined by the relative ease by which the respective amine hydrochlorides can form aggregates of ion-pairs by intermolecular hydrogen bonding (8). The tertiary amine hydrochlorides have one proton, which is presumably bonded to the chloride and unavailable for participation in aggregate formation. This condition delays aggregation until a higher concentration of acidic protons is reached by transfer of acidity caused by the migration of acidic protons from chlordiazepoxide molecules to amitriptyline molecules, particularly in a high dielectric constant solvent like dimethyl sulfoxide-d_6. When this happens, owing to the mobility of protons (9) within the hydrogen bonds, proton transfer can occur within the hydrogen bond representing the joining of the Brönsted acid–base pair N- - -HCl to yield the polar form N^+H- - -Cl^-.

At this time, the tertiary amine hydrochlorides are induced to form aggregates of ion-pairs (7) by intermolecular hydrogen bonding in response to the need to stabilize the ion-pairs of the salt. Therefore, the proton exchange equilibrium shifts toward the direction of reduced proton mobility of the tertiary amine proton of the amitriptyline salt, which results in the covalent N^+H bond being time resolved in the NMR spectrum. This phenomenon is reinforced by the fact that the tertiary amine forms stronger N^+H- - -Cl^- bonds than does the secondary amine due to the greater concentration of positive charge in the tertiary ammonium ion (10). The stronger the cation–anion hydrogen bonding, the less is the extent of the aggregation of the resulting ion-pairs by electrostatic solvation. While the number of molecules forming an aggregate is not determined in this example, it is disrupted when the temperature is raised. The existence of a doublet splitting requires that the N-methyl protons with fixed orientations of the magnetic moment vector remain coupled with the spin state of the N^+H group for a time greater than τ (Table II). The value of the heat of activation for the exchange process (~6.4 kcal/mole) probably leads to the suggestion of dimeric aggregates being the means of effecting exchange (11).

In conclusion, NMR spectroscopy is a useful tool for investigating proton exchange equilibrium between compounds possessing basic sites that compete for acidic protons, particularly in an aprotic solvent. An indication of the formation of ion-pairs and, hence, the covalent character of the nitrogen–proton bond are provided by the appropriate line splitting, which also gives an estimate of the mobility of protons existing in the exchange environment influenced by varied types of intermolecular hydrogen bonding and solute-solvent interactions.

REFERENCES

(1) H. Zimmermann, *Angew. Chem., Int. Ed. Engl.*, **3**, 157 (1964).

(2) H. S. Gutowsky, D. W. McCall, and C. P. Slichter, *J. Chem. Phys.*, **21**, 279 (1953).

(3) H. S. Gutowsky and C. H. Holm, *ibid.*, **25**, 1228 (1956).

(4) M. T. Rogers and J. C. Woodbrey, *J. Phys. Chem.*, **66**, 540 (1962).

(5) G. Fraenkel and J. P. Kim, *J. Am. Chem. Soc.*, **88**, 4203 (1966).

(6) "Chemistry of the Amino Group," S. Patai, Ed., Interscience, New York, N.Y., 1968.

(7) M. M. Davis, "Acid-Base Behavior in Aprotic Organic Solvents," Monograph 105, National Bureau of Standards, Washington, D.C., 1968.

(8) R. R. Grinstead and J. C. Davis, *J. Phys. Chem.* **72**, 1630 (1968).

(9) M. Eigen *et al.*, in "Kinetics of Proton Transfer Processes, Discussions of the Faraday Society," no. 39, The Faraday Society, London, England, 1965.

(10) B. Chinon and C. Sandorfy, *Can. J. Chem.*, **36**, 1181 (1958); C. Brisetti and C. Sandorfy, *ibid.*, **38**, 34 (1960).

(11) J. W. Emsley, J. Feeney, and L. H. Sutcliffe, "High Resolution Nuclear Magnetic Resonance Spectroscopy," vol. 1, Pergamon, New York, N.Y., 1965, pp. 530, 531.

ACKNOWLEDGMENTS

Presented in part at the APhA Academy of Pharmaceutical Sciences, Montreal meeting, 1978.

The author is grateful to Mr. Y. G. Bankawala for assistance, Dr. S. A. Moros for suggestions and comments, and Dr. A. Mlodozeniec and Dr. J. Sheridan for support.

Rapid Determination of Chlorpromazine Hydrochloride and Two Oxidation Products in Various Pharmaceutical Samples Using High-Performance Liquid Chromatography and Fluorescence Detection

DAVID M. TAKAHASHI

Received June 11, 1979, from the *Food and Drug Administration, 50 United Nations Plaza, San Francisco, CA 94102.* Accepted for publication September 20, 1979.

Abstract □ A rapid, simple, and accurate high-performance liquid chromatographic procedure using an amino-bonded microparticulate column is reported for the determination of chlorpromazine hydrochloride (I) and its two oxidation products, the sulfoxide (II) and the sulfone (III), in commercially available pharmaceutical dosage preparations. Simultaneous identification and quantitation of II and III in the presence of at least 100 times the amount of parent compound were achieved with selective fluorometric detection. Identification and quantitation of I were achieved by changing the fluorescence detection mode. A typical chromatographic run was completed within 15 min. The described procedure is simpler, more sensitive, and more accurate than the USP XIX methods, particularly for the analysis of II in injectables. Quantitation of II and III at levels as low as 0.1 μg, representing 0.1% contamination, was demonstrated.

Keyphrases □ Chlorpromazine hydrochloride—and oxidation products, high-performance liquid chromatography and fluorescence detection, dosage forms □ High-performance liquid chromatography—rapid determination of chlorpromazine hydrochloride and two oxidation products, dosage forms □ Phenothiazines—chlorpromazine hydrochloride and two oxidation products, rapid determination by high-performance liquid chromatography and fluorescence detection, dosage forms

Tricyclic antidepressants of the phenothiazine type are important psychopharmacological agents in modern psychotherapy and have continuously attracted interest since their discovery. One clinically useful member of this class is chlorpromazine hydrochloride (I). It readily undergoes sulfoxidation at the sulfur atom in position 5 to form the sulfoxide (II), which may be further oxidized to the sulfone (III).

BACKGROUND

The USP XIX monographs (1) specify limits for certain impurities and degradation products in various dosage formulations of chlorpromazine and its hydrochloride salt. For instance, a maximum of 0.5% for "other alkylated phenothiazines" is allowed. Although the widespread occurrence of both alkylated and nonalkylated compounds was recently demonstrated in various tablet formulations, many of the impurities found are also used as therapeutic agents and thus were not considered as a health hazard (2). However, the presence of these artifacts deserves attention during manufacturing quality control procedures (2) as an index to adherence with recognized Current Good Manufacturing Practices.

The USP XIX permits II in injectables up to a maximum of 5%, but the TLC identification test used is only semiquantitative at best. Furthermore, this test lacks the specificity desired since the comparison is made with the TLC spot of the USP chlorpromazine hydrochloride reference standard and not with that of the sulfoxide reference material. Similar TLC identification tests are also used for the other alkylated phenothiazines. One is never certain whether II, III, the other alkylated or nonalkylated phenothiazines, or other degradation products are being determined.

The quantitative determination of chlorpromazine and its hydrochloride salt in dosage preparations is based on the differential UV absorption of the drug using two absorption maxima (254 and 277 nm). Pure drug substances are assayed by perchloric acid titration.

In general, it is inherently more desirable to use simpler and more accurate techniques and to avoid complex and nonspecific analytical methods. Thus, there is a need for developing a suitable analytical method to identify and quantitate I and its degradation products rapidly (especially II).

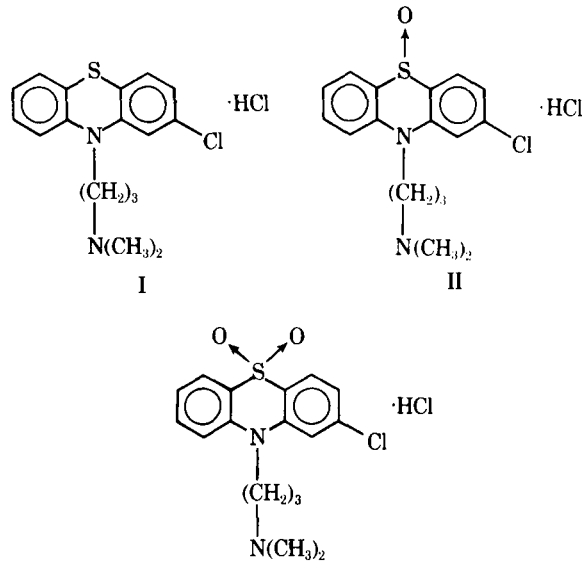

Many procedures have been reported for the determination of I and its metabolites. Previously reported fluorescence properties of phenothiazine drugs (3–6) indicate spectrofluorometry to be useful for qualitative and quantitative analyses of these compounds. The differences in the fluorescence spectra of I and its *S*-oxidation products may be particularly useful in the development of a rapid and simultaneous determination. However, it has been virtually impossible to differentiate between II and III by conventional spectrofluorometry when present in a mixture (6).

In recent years, high-performance liquid chromatography (HPLC) has been employed in the determination of I and its derivatives (7–11). In general, UV detection has been used. However, a method for the simultaneous determination of I–III has not been previously reported. This article describes the development of such a method, combining both the HPLC separation and fluorescence detection techniques for determining these three compounds in mixtures with other constituents normally present in commercial pharmaceutical preparations.

EXPERIMENTAL

Reagents and Chemicals—Compounds I[1], II[2], and III[2] were used as received. All other reagents were analytical reagent grade except *d*-araboascorbic acid[3]. All solvents were glass distilled[4].

Apparatus—The liquid chromatograph[5] was equipped with reciprocating dual-piston constant-flow rate pumps, a rotary valve injector[6],

[1] United States Pharmacopeial Convention, Rockville, Md.
[2] Smith Kline and French Laboratories, Philadelphia, Pa.
[3] Eastman Kodak Co., Rochester, N.Y.
[4] Burdick & Jackson Laboratories, Muskegon, Mich.
[5] Model 3500B, Spectra-Physics, Santa Clara, Calif.
[6] Six-port rotary valve (7000-psi capacity) with a 100-μl external loop, Valco Instrument Co., Houston, Tex.

0022-3549/80/0200-0184$01.00/0
© 1980, American Pharmaceutical Association

a filter fluorescence detector[7], a variable-wavelength UV detector[8], a computing integrator[9], and a recorder[10]. The HPLC columns were: (*a*) a 25-cm × 4.6-mm i.d. stainless steel column commercially packed with 10-μm amino-bonded microparticle packing[11] and (*b*) a 30-cm × 4-mm i.d. stainless steel column commercially packed with 10-μm amino-bonded microparticle packing[12]. Ambient temperature was used throughout these experiments.

Mobile Phase—The mobile phase consisted of acetonitrile–benzene–water (16:4:1), with the water containing 0.01% each of sodium metabisulfite and *d*-araboascorbic acid as antioxidants. The prepared mobile phase was filtered[13], degassed, and stored in the solvent reservoir of the instrument.

Standard Solutions—All standard materials were dissolved in and made to volume with acetonitrile. All solutions were protected from light.

Linearity Standards—Five standard solutions, ranging in concentration from 1.00 to 50.0 μg/ml, were individually prepared in acetonitrile for II or III. The I standard solutions (10.0–500 μg/ml) also were prepared in acetonitrile. Duplicate 100-μl aliquots of each solution were chromatographed.

Daily Calibration Standard Mixture—A mixture of the three standard materials in acetonitrile was made fresh each day and contained 10.0 μg/ml each of II and III and 1000 μg/ml of I.

Analysis of Pharmaceutical Dosage Preparations—For II or III determination, sample solutions were accurately prepared as indicated so that the final concentration of I, based on the declared potency, was 1 mg/ml. For I determination, sample solutions were accurately prepared so that the final concentration of I, based on the declared potency, was 100–250 μg/ml.

Injectables—A sample aliquot was diluted and made to volume with acetonitrile.

Tablets—Tablets were powdered, weighed, warmed over a steam bath in acetonitrile, and shaken vigorously for 1 min. The solution was allowed to cool and then was filtered and made to volume with acetonitrile.

Concentrates—An aliquot was diluted and made to volume with acetonitrile.

Syrup—An aliquot was mixed with acetonitrile, warmed over a steam bath, and shaken vigorously for 1 min. The solution was allowed to cool and then was filtered and concentrated under nitrogen to volume before injection.

Suppositories—A sample was warmed over a steam bath in acetonitrile until dissolution was complete. After cooling, the sample solution was filtered and made to volume with acetonitrile.

Detection—The HPLC eluates were monitored by the UV absorption at 345 nm and by fluorometry with excitation at 280 nm and emission at 385 nm for II and III or at 450 nm for I. All three compounds in approximately equal amounts can be simultaneously detected by fluorometry if the emission detection is set at 400 nm. Peak height was used for quantitation.

RESULTS AND DISCUSSION

HPLC Column—Polar bonded phases used in the normal mode frequently produce separations similar, but often more efficient, to those obtained on silica gel packings. One highly polar hydrogen bonded phase that is readily available commercially is a chemically bonded aminosilane. It is stable toward hydrolysis, can be used for normal or reversed-phase chromatography, and is less sensitive to water adsorption than is silica gel.

This material performed well in the normal phase HPLC separation of I and its two oxidation products, II and III (Fig. 1). Its unique selectivity and speed were amply demonstrated. Since these materials eluted rapidly, the expenditure of time and expensive organic solvents was greatly minimized.

HPLC Mobile Phase—Various isocratic and gradient mobile phase systems were tried before acetonitrile–benzene–water (16:4:1) was selected. Water-free mobile phases were undesirable since the elution of II was delayed considerably. They also resulted in a badly tailing peak. With the addition of water to the mobile phase, II rapidly eluted in a sharp and symmetrical peak. The amount of water added was carefully controlled as soon as it was optimized since varying the amount of water produced changes in the retention time of II. However, unlike silica gel, the amino-bonded packing was less sensitive to water adsorption, and lengthy equilibration was not required as the water content of the mobile phase was varied.

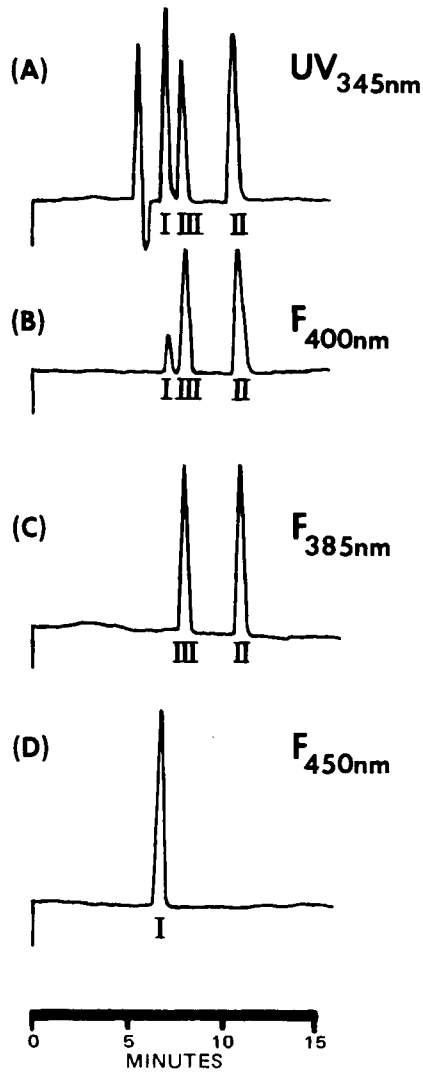

Figure 1—*Chromatograms of standard mixtures of chlorpromazine hydrochloride (I) and its two S-oxidation products, sulfoxide (II) and sulfone (III) (5 μg each). UV absorption was at 345 nm (A) and fluorescence emission was at 400 (B), 385 (C), or 450 (D) nm. The HPLC column was μBondapak NH_2, the pressure was 140 psi, and the flow rate was 1.0 ml/min.*

The inclusion of benzene in the mobile phase also was desirable to stabilize the retention time of II. Without benzene, II always eluted a little slower when injected in a mixture with I (a 100:1 ratio) and III. When the amount of benzene in the mobile phase was increased, the resolution of the three compounds greatly improved, although it took longer for a complete chromatographic run (*e.g.*, 12 *versus* 30 min). However, an increase in the amount of benzene limited the amount of water that could be mixed into the mobile phase. For instance, when benzene was increased from 20 to 50%, water had to be reduced to ~1% to keep the mobile phase homogeneous.

Selection of Fluorescence Detection Mode—Compound I displayed three UV maxima while II and III each had four UV maxima (12, 13). Since benzene was used as a component of the HPLC system, the absorbance below 280 nm of these phenothiazine derivatives was lost. However, this loss did not present problems since the compounds were monitored at wavelengths longer than 280 nm.

Simultaneous quantitation of I and its two oxidation products was possible with the aid of a UV detector only when all three compounds were present in approximately equal amounts and were completely free

[7] Fluorichrom with deuterium lamp source, Varian Associates, Palo Alto, Calif.
[8] Model 837 spectrophotometer, DuPont Instruments, Wilmington, Del.
[9] Model 3385A, Hewlett-Packard Co., Palo Alto, Calif.
[10] Model 285, Linear Instrument Corp., Irvine, Calif.
[11] Lichrosorb NH_2, Altex Scientific, Berkeley, Calif.
[12] μBondapak NH_2, Waters Associates, Milford, Mass.
[13] A 5.0-μm type LS filter, Millipore Corp., Bedford, Mass.

Table I—Analysis of Pharmaceutical Dosage Preparations [a]

Dosage Preparation	Declared Potency of Chlorpromazine Hydrochloride	Number of Samples Analyzed	Chlorpromazine Hydrochloride Content (Average), %	Chlorpromazine Sulfoxide Content, %
Tablet	10 mg/tablet	2	100	ND[b]
Suppository[c]	25 mg/suppository	4	99	ND
Syrup	10 mg/5 ml	4	95	ND
Injection, single dose (1 ml)	25 mg/ml	10	103	ND
Injection, multiple dose (10 ml)	25 mg/ml	2	102	ND
Concentrate (120 ml)	30 mg/ml	4	102	1.03, 0.69, 0.73, 0.90

[a] Chlorpromazine sulfone was not detected in any pharmaceutical dosage preparation tested. [b] ND = none detected. [c] Contained chlorpromazine.

from other UV-absorbing interferences. When I was present in a 100-fold excess, III was completely obscured by I. Furthermore, when such a large amount of I was chromatographed, other strong UV-absorbing impurities, although present in small amounts relative to the parent compound, became detectable and interfered with the determination of II.

Fluorescence detection is more selective and, therefore, better suited for this type of analysis. The differences in the fluorescence characteristics of I, II, and III were useful in developing this rapid HPLC procedure for their determination. To determine II and III, the fluorescence emission signal of I was completely eliminated by selectively choosing the emission signals of the oxidation products at 385 nm while I was similarly determined by switching to an emission wavelength of 450 nm. The impurities in I observed in its UV chromatogram were completely eliminated in its fluorescence chromatogram when the emission signal was set at 385 nm.

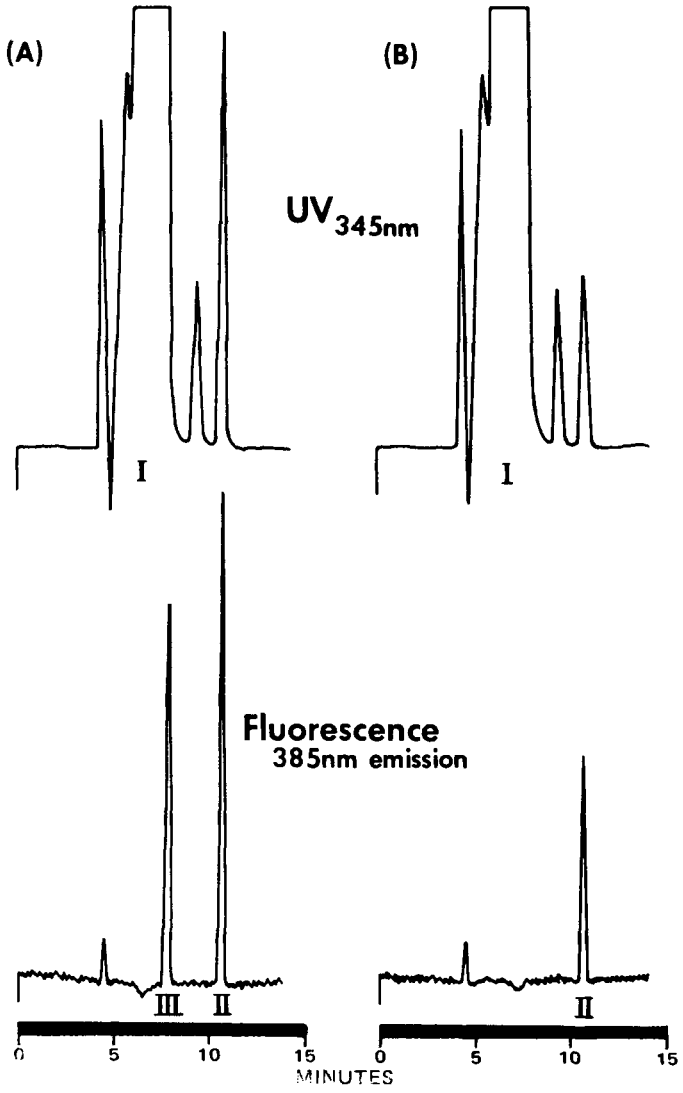

Figure 2—*Typical chromatograms of chlorpromazine hydrochloride (I) concentrate. Key: A, sample spiked with sulfoxide (II) and sulfone (III) at 1% (1 μg) level; and B, unspiked sample. The HPLC column was Lichrosorb NH_2, the pressure was 110 psi, and the flow rate was 1.0 ml/min.*

An alternative means of quickly and simultaneously identifying these three compounds was to determine selectively their fluorescence emission at 400 nm. At this wavelength, all three compounds could be detected if they were present in approximately equal amounts.

One problem encountered in the quantitative fluorescence determination of very low concentrations of phenothiazines is the interference from Raman scattering (3). This interference becomes particularly critical in the determination of II (6) or III. In the HPLC procedure described, a deuterium lamp source was used at 280 nm to lessen the Raman scatter influence. It also provided the stronger energy available at this wavelength.

The detection limit for UV and fluorescence modes remained about the same for I. For II and III, fluorescence was relatively more sensitive. However, unlike UV photometric detection, fluorescence detection is generally free from interferences caused by pump pulses and changes in the refractive index due to solvent peaks. Fluorescence detection also provides a convenient option of selectively eliminating all unwanted signals. All peaks obtained were well defined, sharp, and symmetrical and eluted within 15 min.

Linearity, Reproducibility, and Sensitivity—Fluorescence response curves of I–III were all linear in the ranges examined (1–50 μg for I and 0.1–5 μg for both II and III).

Good reproducibility of the described HPLC procedure using fluorescence detection was demonstrated when six 100-μl aliquots of a standard mixture containing 1.0 μg each of II and III in the presence of 100 μg of I were chromatographed. The relative standard deviations were 1.5 and 2.1% for II and III, respectively. This standard mixture was then diluted with acetonitrile so that each 100-μl injection represented 25 μg of I. The reproducibility of the method for I was determined by chromatographing six 100-μl diluted aliquots. The relative standard deviation was 1.2%.

The minimum detectable limit of I–III under the fluorescence conditions described was 0.05 μg for all three compounds. Under the sample conditions described, this limit represents, in most cases, a minimum detectable contamination level of 0.05% for II and III with respect to the parent compound.

Sample Analysis and Recovery—Various I formulations (Table I) were analyzed by this HPLC procedure using fluorescence detection. The UV detection mode was useless for III since it was completely obscured by the 100-fold amount of the parent drug. Furthermore, UV-absorbing impurities of the parent drug interfered with the determination of II. In addition, the UV detection mode was sensitive to changes in the refractive index of the solvent passing through it.

Table I indicates that, in almost all samples analyzed, neither II nor III was detected at the detection limit of 0.05%, even though the samples assayed were a few years old and were not representative of current formulations. (All samples were obtained during December 1975 and stored intact in the dark at room temperature. Samples were analyzed during November 1977.) The notable exceptions were the four samples of I concentrate that contained 0.7–1.0% of II. Figure 2 shows a typical chromatogram of I concentrate containing a low level of II.

All samples were also analyzed for I; the diluted aliquots of the sample solutions prepared for II and III assays were used. The same HPLC parameter was used throughout, except that the fluorometric detection was monitored at the 450-nm emission. All pharmacopeial samples were

within the USP XIX monograph limits. The I content of nonpharmacopeial concentrate was also satisfactory.

For a recovery study, five samples (tablet, concentrate, suppository, single-dose injectable, and multiple-dose injectable) were each spiked at 1% levels of II and III and analyzed. The mean recoveries ($n = 5$) were 98.3 and 97.5% with relative standard deviations of 1.8 and 2.4% for II and III, respectively. A syrup sample was spiked at 5% levels of II and III; 104 and 103% recoveries were obtained, respectively.

USP Reference Standard—Analysis of freshly obtained USP I reference standard (200 μg) by the UV absorption mode revealed 0.18% of "apparent" II. However, this peak was totally absent in the fluorescence chromatogram, proving that no II was present in the reference standard. The minimum detection level in this case was at 0.025%. When this standard solution was again analyzed 10 days later, its fluorescence chromatogram demonstrated the presence of II (0.03%). This change appeared to be due to the autoxidation of I. Although the solution was stored in the dark when not in use, dissolved oxygen was not purged and the solution was under a normal atmosphere at room temperature during its storage.

CONCLUSIONS

A novel approach of using an amino-bonded HPLC packing for the rapid and quantitative determination of I and two of its oxidation products was presented. Unlike the UV photometric determination, the selective fluorescence detection approach permitted a fast, qualitative, and quantitative determination of a mixture of trace components, II and III, in the presence of at least a 100-fold excess of parent drug. It also permitted a fast and selective determination of the major component, I. Interferences from other impurities were not encountered. A typical HPLC analysis was completed within 15 min. For all three compounds, the fluorescence response was linear in the ranges tested, and the minimum detectable amount was 0.05 μg.

The described HPLC procedure allows the injection of diluted raw samples directly into the HPLC system. The recoveries of II and III from commercial samples at 1% contamination levels were satisfactory. The described method is also simpler, more sensitive, and more accurate than the USP XIX methods for determining I or II.

REFERENCES

(1) "The United States Pharmacopeia," 19th rev., Mack Publishing Co., Easton, Pa., 1975.

(2) W. N. French, F. Matsui, D. L. Robertson, and S. J. Smith, *Can. J. Pharm. Sci.*, **10**, 27 (1975).

(3) S. Udenfriend, D. E. Duggan, B. M. Vasta, and B. B. Brodie, *J. Pharmacol. Exp. Ther.*, **120**, 26 (1957).

(4) T. J. Mellinger and C. E. Keeler, *Anal. Chem.*, **35**, 554 (1963).

(5) *Ibid.*, **36**, 1840 (1964).

(6) J. B. Ragland and V. J. Kinross-Wright, *Anal. Chem.*, **36**, 1356 (1964).

(7) D. H. Rogers, *J. Chromatogr. Sci.*, **12**, 742 (1974).

(8) M. Caude, J. P. Lefebre, and R. Rosset, *Chromatographia*, **8**, 217 (1975).

(9) M. Caude, L. X. Phan, B. Terlain, and J. P. Thomas, *J. Chromatogr. Sci.*, **13**, 390 (1975).

(10) P. J. Twitchett and A. C. Moffat, *J. Chromatogr.*, **111**, 149 (1975).

(11) C. Gonnet and J. L. Rocca, *ibid.*, **120**, 419 (1976).

(12) R. J. Warren, I. B. Eisdorfer, W. E. Thompson, and J. E. Zarembo, *J. Pharm. Sci.*, **55**, 144 (1966).

(13) A. De Leenheer, *J. Assoc. Offic. Anal. Chem.*, **56**, 105 (1973).

ACKNOWLEDGMENTS

The author thanks Smith Kline and French Laboratories, Philadelphia, Pa., for supplying 50 mg each of II and III. He also thanks Harvey K. Hundley, Research Coordinator, San Francisco District, Food and Drug Administration, and Neal Castagnoli, Professor of Chemistry, University of California, San Francisco, for helpful discussions during this work and for reviewing this paper.

Impurities in Drugs IV: Indomethacin

N. M. CURRAN, E. G. LOVERING, K. M. McERLANE *, and J. R. WATSON ˣ

Received July 27, 1979, from the *Pharmaceutical Chemistry Division, Drug Research Laboratories, Health Protection Branch, Tunney's Pasture, Ottawa, Ontario K1A 0L2, Canada.* Accepted for publication September 20, 1979. *Present address: Faculty of Pharmaceutical Sciences, University of British Columbia, Vancouver, British Columbia, Canada.

Abstract □ One lot of indomethacin raw material, five lots of capsule preparations, and three lots of suppository formulations were screened for impurities by TLC. Only the suppository products exhibited impurities above trace levels. The two main impurities were present at levels estimated at ~0.5 and 2%. After isolation from preparative TLC plates, they were identified by NMR, IR, and mass spectroscopy as the α-substituted monoglyceryl esters of 4-chlorobenzoic acid and indomethacin, respectively.

Keyphrases □ Indomethacin—impurities, detection by NMR, IR, and mass spectroscopy □ Anti-inflammatory agents—indomethacin, detection of impurities by NMR, IR, and mass spectroscopy

Indomethacin is an analgesic and anti-inflammatory agent used to treat rheumatoid arthritis and other joint diseases. The NF XIV (1) contains monograph specifications for the drug substance and capsules, and BP 1973 (2) includes monograph specifications for the drug substance, capsule, and suppository. However, the compendia do not contain tests and limits for impurities in indomethacin formulations, nor are there publications dealing with their occurrence in commercial preparations. Indomethacin may be synthesized by several routes (3–7). However, these methods are generally modifications of the original procedure described by Shen *et al.* (3).

This paper deals with impurities observed in a routine TLC screening program of indomethacin drug substances and formulations. The main impurities found in suppository preparations were isolated and identified and serve to underline a classical instance of drug–excipient interaction.

EXPERIMENTAL

Materials—All drug substances (one sample) and formulations (five capsule and three suppository samples) were obtained directly from the manufacturers. Indomethacin [1-(4-chlorobenzoyl)-5-methoxy-2-methylindole-3-acetic acid] (I) was the NF reference standard material. 4-Chlorobenzoic acid[1] (II), 4-chlorobenzoyl chloride[1], 5-methoxy-2-

[1] Aldrich Chemical Co., Milwaukee, Wis.

0022-3549/80/0200-0187$01.00/0

© 1980, American Pharmaceutical Association

within the USP XIX monograph limits. The I content of nonpharmacopeial concentrate was also satisfactory.

For a recovery study, five samples (tablet, concentrate, suppository, single-dose injectable, and multiple-dose injectable) were each spiked at 1% levels of II and III and analyzed. The mean recoveries ($n = 5$) were 98.3 and 97.5% with relative standard deviations of 1.8 and 2.4% for II and III, respectively. A syrup sample was spiked at 5% levels of II and III; 104 and 103% recoveries were obtained, respectively.

USP Reference Standard—Analysis of freshly obtained USP I reference standard (200 μg) by the UV absorption mode revealed 0.18% of "apparent" II. However, this peak was totally absent in the fluorescence chromatogram, proving that no II was present in the reference standard. The minimum detection level in this case was at 0.025%. When this standard solution was again analyzed 10 days later, its fluorescence chromatogram demonstrated the presence of II (0.03%). This change appeared to be due to the autoxidation of I. Although the solution was stored in the dark when not in use, dissolved oxygen was not purged and the solution was under a normal atmosphere at room temperature during its storage.

CONCLUSIONS

A novel approach of using an amino-bonded HPLC packing for the rapid and quantitative determination of I and two of its oxidation products was presented. Unlike the UV photometric determination, the selective fluorescence detection approach permitted a fast, qualitative, and quantitative determination of a mixture of trace components, II and III, in the presence of at least a 100-fold excess of parent drug. It also permitted a fast and selective determination of the major component, I. Interferences from other impurities were not encountered. A typical HPLC analysis was completed within 15 min. For all three compounds, the fluorescence response was linear in the ranges tested, and the minimum detectable amount was 0.05 μg.

The described HPLC procedure allows the injection of diluted raw samples directly into the HPLC system. The recoveries of II and III from commercial samples at 1% contamination levels were satisfactory. The described method is also simpler, more sensitive, and more accurate than the USP XIX methods for determining I or II.

REFERENCES

(1) "The United States Pharmacopeia," 19th rev., Mack Publishing Co., Easton, Pa., 1975.

(2) W. N. French, F. Matsui, D. L. Robertson, and S. J. Smith, *Can. J. Pharm. Sci.*, **10**, 27 (1975).

(3) S. Udenfriend, D. E. Duggan, B. M. Vasta, and B. B. Brodie, *J. Pharmacol. Exp. Ther.*, **120**, 26 (1957).

(4) T. J. Mellinger and C. E. Keeler, *Anal. Chem.*, **35**, 554 (1963).

(5) *Ibid.*, **36**, 1840 (1964).

(6) J. B. Ragland and V. J. Kinross-Wright, *Anal. Chem.*, **36**, 1356 (1964).

(7) D. H. Rogers, *J. Chromatogr. Sci.*, **12**, 742 (1974).

(8) M. Caude, J. P. Lefebre, and R. Rosset, *Chromatographia*, **8**, 217 (1975).

(9) M. Caude, L. X. Phan, B. Terlain, and J. P. Thomas, *J. Chromatogr. Sci.*, **13**, 390 (1975).

(10) P. J. Twitchett and A. C. Moffat, *J. Chromatogr.*, **111**, 149 (1975).

(11) C. Gonnet and J. L. Rocca, *ibid.*, **120**, 419 (1976).

(12) R. J. Warren, I. B. Eisdorfer, W. E. Thompson, and J. E. Zarembo, *J. Pharm. Sci.*, **55**, 144 (1966).

(13) A. De Leenheer, *J. Assoc. Offic. Anal. Chem.*, **56**, 105 (1973).

ACKNOWLEDGMENTS

The author thanks Smith Kline and French Laboratories, Philadelphia, Pa., for supplying 50 mg each of II and III. He also thanks Harvey K. Hundley, Research Coordinator, San Francisco District, Food and Drug Administration, and Neal Castagnoli, Professor of Chemistry, University of California, San Francisco, for helpful discussions during this work and for reviewing this paper.

Impurities in Drugs IV: Indomethacin

N. M. CURRAN, E. G. LOVERING, K. M. McERLANE *, and J. R. WATSON ˣ

Received July 27, 1979, from the *Pharmaceutical Chemistry Division, Drug Research Laboratories, Health Protection Branch, Tunney's Pasture, Ottawa, Ontario K1A 0L2, Canada.* Accepted for publication September 20, 1979. *Present address: Faculty of Pharmaceutical Sciences, University of British Columbia, Vancouver, British Columbia, Canada.

Abstract □ One lot of indomethacin raw material, five lots of capsule preparations, and three lots of suppository formulations were screened for impurities by TLC. Only the suppository products exhibited impurities above trace levels. The two main impurities were present at levels estimated at ~0.5 and 2%. After isolation from preparative TLC plates, they were identified by NMR, IR, and mass spectroscopy as the α-substituted monoglyceryl esters of 4-chlorobenzoic acid and indomethacin, respectively.

Keyphrases □ Indomethacin—impurities, detection by NMR, IR, and mass spectroscopy □ Anti-inflammatory agents—indomethacin, detection of impurities by NMR, IR, and mass spectroscopy

Indomethacin is an analgesic and anti-inflammatory agent used to treat rheumatoid arthritis and other joint diseases. The NF XIV (1) contains monograph specifications for the drug substance and capsules, and BP 1973 (2) includes monograph specifications for the drug substance, capsule, and suppository. However, the compendia do not contain tests and limits for impurities in indomethacin formulations, nor are there publications dealing with their occurrence in commercial preparations. Indomethacin may be synthesized by several routes (3–7). However, these methods are generally modifications of the original procedure described by Shen *et al.* (3).

This paper deals with impurities observed in a routine TLC screening program of indomethacin drug substances and formulations. The main impurities found in suppository preparations were isolated and identified and serve to underline a classical instance of drug–excipient interaction.

EXPERIMENTAL

Materials—All drug substances (one sample) and formulations (five capsule and three suppository samples) were obtained directly from the manufacturers. Indomethacin [1-(4-chlorobenzoyl)-5-methoxy-2-methylindole-3-acetic acid] (I) was the NF reference standard material. 4-Chlorobenzoic acid[1] (II), 4-chlorobenzoyl chloride[1], 5-methoxy-2-

[1] Aldrich Chemical Co., Milwaukee, Wis.

0022-3549/80/0200-0187$01.00/0

© 1980, American Pharmaceutical Association

Table I—TLC Characteristics of Indomethacin and Its Impurities

Compound	R_f[a]	R_f[b]	Detection Limit, μg
Indomethacin (I)	0.80	0.40	0.1
4-Chlorobenzoic acid (II)	0.90	0.50	0.2
5-Methoxy-2-methyl-3-indoleacetic acid (III)	0.75	0.38	0.1
Indomethacin-α-monoglyceride (IV)	0.24	0.33	0.1
4-Chlorobenzoic acid-α-monoglyceride (V)	0.35	0.28	0.2
VI	0.64	0.53	—
VII	0.70	0.55	—

[a] In ether–acetic acid (100:3). [b] In benzene–methanol–acetic acid (90:10:3).

methyl-3-indoleacetic acid, (III), glycerin[1] (ACS grade), pyridine[1] (ACS grade), ether[2] (USP grade), acetic acid[3] (ACS grade), benzene[4] (ACS grade), methanol[4] (ACS grade), anhydrous sodium sulfate[4] (ACS grade), and sodium hydrogen carbonate[4] (analytical reagent) were obtained commercially.

TLC plates were precoated with silica gel 60 F-25[4] (20 × 20 cm, 0.25 mm) or silica gel GF[5] (20 × 20 cm, 1.0 mm).

Standard Solutions—Ether solutions of the following were prepared: I, 20 mg/ml; II, 0.25 mg/ml; and III, 0.25 mg/ml.

TLC Systems—Two developing systems were used: A, ether–acetic acid (100:3); and B, benzene–methanol–acetic acid (90:10:3). Both solutions were placed in filter paper-lined chromatographic tanks and allowed to equilibrate for 1 hr prior to use. Spots were visualized with UV light at 254 nm.

Drug Substance, Capsule, and Suppository Extraction—About 100 mg of indomethacin drug substance, accurately weighed, was dissolved in 5 ml of ether. The solution was analyzed by TLC.

The contents of 10 capsules were emptied and weighed. An amount of powder equivalent to about 100 mg of indomethacin was accurately weighed into a screw-capped tube, 10 ml of ether–water (1:1) was added, and the mixture was shaken vigorously for 15 min and then centrifuged. A portion of the ether layer was used for TLC analysis.

Five suppositories, equivalent to 500 mg of drug, were stirred vigorously in a stoppered flask for 30 min in 50 ml of ether–water (1:1). The heterogeneous solution was transferred to a screw-capped tube and centrifuged. The ether layer was used for TLC analysis.

Screening for Impurities—The R_f values of the drug and each impurity were determined in both TLC systems, and the lower limits of detectability of I, II, III, IV (indomethacin-α-monoglyceride), and V (4-chlorobenzoic acid-α-monoglyceride) were established (Table I). Aliquots of 1, 10, and 25 μl (20, 200, and 500 μg of I) of the ether extracts of each formulation and drug substance were spotted (0.25-mm plate) beside 1-, 10-, and 25-μl (20-, 200-, and 500-μg) aliquots of the standard solution of I and 1-, 5-, 10-, and 20-μl (0.25-, 1.25-, 2.5-, and 5-μg) portions of each standard solution of II and III.

The concentrations of impurities in the formulations (Table II) were estimated by comparison of the spot diameters and intensities with the corresponding spots of the standard solutions.

Isolation of Impurities—Impurities IV and V (Tables I and II) were isolated from Suppository Formulation A using the following procedure. Ten suppositories were shaken vigorously for 30 min in 100 ml of ether–water (1:1) in a separator. The ether layer was transferred to an erlenmeyer flask and dried over anhydrous sodium sulfate for 15 min. The mixture was filtered, and 1 ml of the filtrate was applied to a silica gel GF (1.0-mm) plate using a commercial TLC sample streaker[6]. The streaking operation was repeated on several plates. Each plate was developed in System A until the solvent front reached the top of the plate.

After development and hot air drying of each plate, the bands corresponding to IV and V were scraped off the plate into separate flasks; the total scrapings of each of these impurities were stirred in 75 ml of ether for 2 hr. The mixtures were filtered, and the filtrates were dried over anhydrous sodium sulfate and filtered again. The plate extract solutions of impurities IV and V were brought to dryness under a stream of pure dry nitrogen, and the separate residues were dried *in vacuo* at 60° overnight. Pale-yellow oils were obtained. The purity of each compound as isolated was checked by TLC in both solvent systems.

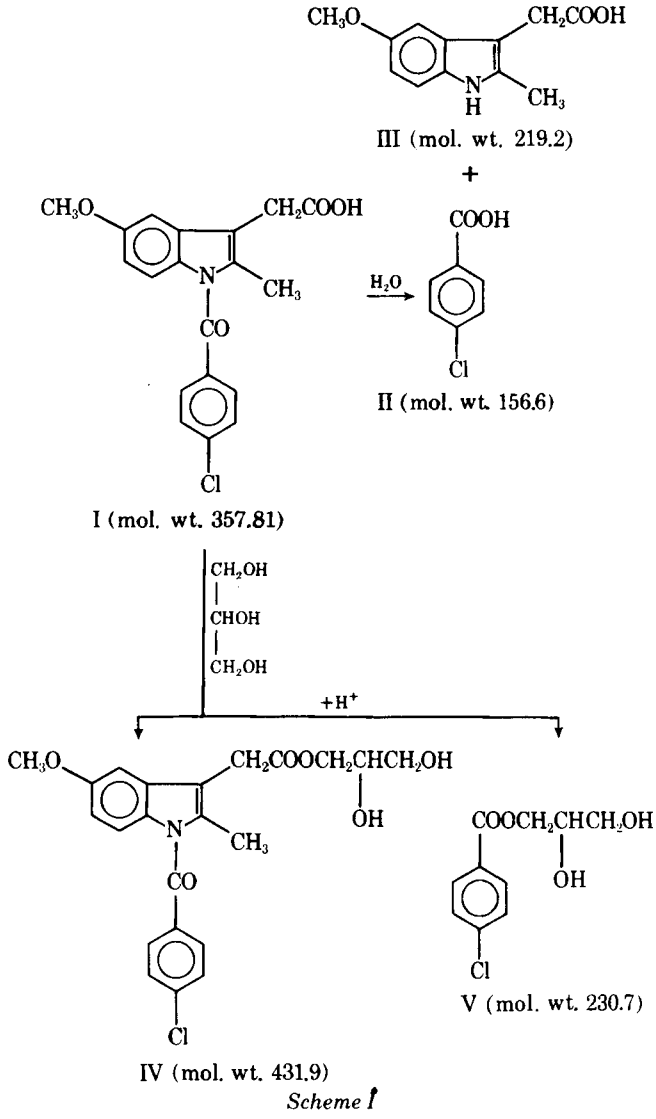

Scheme I

Synthesis of 4-Chlorobenzoic Acid-α-monoglyceride (V in Scheme I)—4-Chlorobenzoyl chloride (3.5 g, 0.02 mole) was slowly added dropwise with constant stirring to a solution of glycerin (4.0 g, 0.04 mole) in dry pyridine (10 ml) at 0°. Then the solution was allowed to warm to ambient temperature for 2 hr. The reaction mixture was diluted to 30 ml with water and extracted with three 25-ml portions of ether. The ether extracts were combined and shaken with four 15-ml portions of 5% aqueous sodium bicarbonate solution followed by two 10-ml portions of water. The ether layer was dried for 30 min over anhydrous sodium sulfate, the mixture was filtered, and the filtrate was evaporated to dryness under a stream of pure dry nitrogen. The oily residue was dried overnight *in vacuo* over phosphorus pentoxide at 50°. Recrystallization from benzene afforded white crystals (mp 88–89°).

The product was checked by TLC in both solvent systems against impurity V isolated from the plates and was subjected to NMR[7], IR[8], and mass spectral[9] analyses.

Characterization and Elucidation of IV and V Structures—*Indomethacin-α-monoglyceride (IV)*—IR (liquid film): 3200 (OH, br), 1725 (ester carbonyl), 1670 (amide carbonyl), and 1500 cm^{-1}; NMR[10] ($CDCl_3$): δ 7.69 [d, 2H, ArH (2′,6′), J = ~9 Hz], 7.47 [d, 2H, ArH (3′,5′), J = ~9 Hz], 6.97 [d, 1H, ArH (4), J = ~2.5 Hz], 6.90 [d, 1H, ArH (7), J = ~9 Hz], 6.67 [d, d, 1H, ArH (6), J = ~9 and 2.5 Hz], 4.22 (d, 2H, $COOCH_2$, J = ~5 Hz), 3.84 (s, 3H, OCH_3), 3.72 (s, 2H, CH_2COO), 3.62–3.53 (m, 3H, $OCHCH_2O$), 2.39 (s, 3H, CH_3), and 2.05 (s, 2H, OH, disappears on D_2O exchange) ppm;

[2] Mallinckrodt Canada Ltd., Toronto, Ontario, Canada.
[3] J. T. Baker Chemical Co., Phillipsburg, N.J.
[4] BDH Chemicals Ltd., Toronto, Ontario, Canada.
[5] Uniplates, Mandel Scientific Co. Ltd., Ville St-Pierre, Quebec, Canada.
[6] Applied Science Laboratories, State College, Pa.

[7] Brüker WP80 Fourier transform spectrometer.
[8] Perkin-Elmer model 621 grating IR spectrophotometer.
[9] Hewlett-Packard GLC–MS system 5985 with ionization potential of 70 ev.
[10] The aromatic protons on the indole ring are designated as 4, 6, and 7 while the aromatic protons on the 4-chlorobenzoyl ring are designated as *ortho* (2′ and 6′) and *meta* (3′ and 5′) to the carbonyl group.

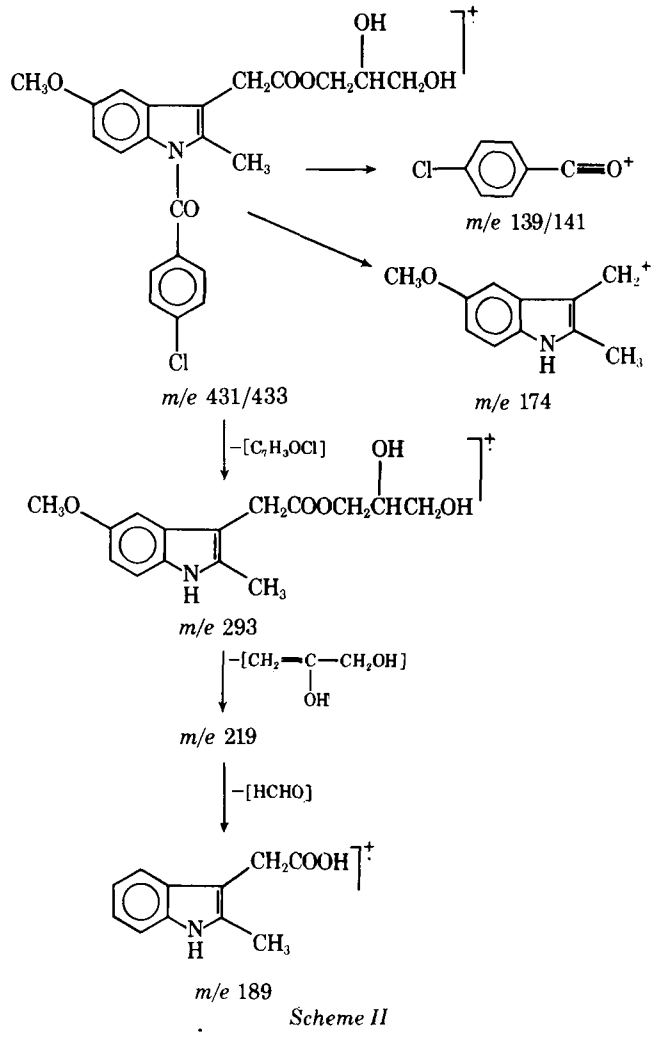

Scheme II

mass spectrum: electron-impact mode, *m/e* 431/433 (M^+, 100/36%), 293 (16), 219 (1.8), 189 (23), 174 (35), and 139/141 (82/33). The fragmentation pattern of this impurity is illustrated in Scheme II.

4-Chlorobenzoic Acid-α-monoglyceride (V) (TLC Isolate and Synthesized Product)—IR (liquid film): 3200 (OH, br) and 1725 (ester carbonyl) cm^{-1}; NMR[11] ($CDCl_3$): δ 8.01 [d, 2H, ArH (2, 6), J = ~9 Hz], 7.43 [d, 2H, ArH (3, 5), J = ~9 Hz], 4.44 (d, 2H, $COOCH_2$, J = ~5 Hz), 4.09–3.48 (m, 3H, $OCHCH_2O$), and 2.05 (s, 2H, OH, disappears on D_2O exchange) ppm; mass spectrum: chemical-ionization mode (CH_4), *m/e* 231/233 ($M^+ + 1$, 100/35%) and 213/215 ($M^+ + 1 - H_2O$, 93/31).

RESULTS AND DISCUSSION

The ethereal indomethacin solutions used were saturated and, as such, were prone to precipitation if not kept well capped. Alternatively, more dilute solutions could be prepared by increasing the amount of ether for dissolution or extraction by 50%. However, for application of the same amounts of drug to the TLC plates, the larger sample volumes required resulted in somewhat more diffuse spots and bands.

[11] The aromatic protons are designated as *ortho* (2 and 6) and *meta* (3 and 5) to the carbonyl group.

Table II—Impurity Levels in Indomethacin Drug Substance and Formulations

Form	Dosage Level, mg/unit	Impurities[a], % II	III	IV	V	VI	VII
Bulk drug	—	Tr[b]	Tr	ND[c]	ND	ND	ND
Capsule	40	Tr	Tr	ND	ND	ND	ND
Capsule	25	Tr	Tr	ND	ND	ND	ND
Capsule	25	Tr	Tr	ND	ND	ND	ND
Capsule	25	Tr	Tr	ND	ND	ND	ND
Capsule	50	Tr	Tr	ND	ND	ND	ND
Suppository	100	Tr	Tr	2	0.5	Tr	Tr
Suppository	100	Tr	Tr	2	0.5	Tr	Tr
Suppository	100	Tr	Tr	2	0.5	Tr	Tr

[a] Estimated by TLC and expressed as a percentage of the label claim of drug. [b] Trace (<0.05%). [c] None detected.

The data given in Table II indicate that only the suppository products exhibited impurities (IV and V) above trace levels. Compounds IV and V were estimated by TLC to be present at levels of ~2 and 0.5%, respectively. Both impurities are formed through chemical interaction of the drug with glycerin present in the suppository. Indomethacin produced these materials in significant amounts when heated with glycerin in the presence of trace mineral acid at 80° for 24 hr. Moreover, when reacted with glycerin under the same conditions, 4-chlorobenzoic acid gave appreciable amounts of V. Reaction of III with glycerin gave rise to an oily product (R_f 0.19, System A), which did not correspond to any of the observed impurities but which was consistent (NMR and IR) with an α-monoglyceride structure. In addition to IV and V and trace levels of II and III, two other impurities (VI and VII) were observed in the suppositories. Since only traces of these impurities appeared to be present, they were not investigated further.

The bulk drug sample and the capsule formulations gave traces of II and III, confirmed by comparison of R_f values in the two solvent systems with authentic specimens of these compounds. No other impurities were observed in the bulk drug and capsule preparations.

REFERENCES

(1) "The National Formulary," 14th ed., Mack Publishing Co., Easton, Pa., 1975, pp. 352–355.

(2) "British Pharmacopoeia 1973," Her Majesty's Stationery Office, London, England, 1973, pp. 239, 240, and Addendum 1977, p. 25.

(3) T. Y. Shen, T. B. Windholz, A. Rosegay, B. E. Witzel, A. N. Wilson, J. D. Willett, W. J. Holtz, R. L. Ellis, A. R. Matzuk, S. Lucas, C. H. Stammer, F. W. Holly, L. H. Sarett, E. A. Risley, G. W. Nuss, and C. A. Winter, *J. Am. Chem. Soc.*, **85**, 488 (1963).

(4) T. Y. Shen, U.S. pat. 3,161,654 (1964).

(5) T. Y. Shen, Belgian pat. 649,169 (1964); through *Chem. Abstr.*, **64**, 6622 (1966).

(6) H. Yamamoto, V. Nakamura, and T. Kobayashi, Japanese pat. 7,036,745 (1970); through *Chem. Abstr.*, **75**, 5692 (1971).

(7) D. Bertazzoni, B. Bortoletti, and T. Perlotto, *Boll. Chim. Farm.*, **109**, 60 (1970); through *Chem. Abstr.*, **73**, 14610t (1970).

ACKNOWLEDGMENTS

The authors thank Dr. M. A. Poirier and Dr. A. By for help in interpreting the spectral data and Mr. R. J. Wood for technical assistance.

Synthesis of Propranolol Mustard as a Possible Lung-Specific Antitumor Agent

L. V. FEYNS *, J. A. BEISLER *x, J. S. DRISCOLL *, and R. A. ADAMSON ‡

Received September 4, 1979, from the **Laboratory of Medicinal Chemistry and Biology and the* ‡*Laboratory of Chemical Pharmacology, Division of Cancer Treatment, National Cancer Institute, National Institutes of Health, Bethesda, MD 20205.* Accepted for publication September 28, 1979.

Abstract □ A nitrogen mustard analog of propranolol was synthesized as a potential lung-specific antitumor agent. Since *dl*-propranolol concentrates in lung tissue and β-blocking activity resides only with the *l*-enantiomer, the *d*-modification could serve as a lung-directed carrier for a cytotoxic group. Reaction of 1-(1-naphthyloxy)-3-[bis(2-hydroxyethyl)amino]-2-propanol with thionyl chloride resulted in replacement of all three hydroxyl groups with chlorine. The necessary chlorination selectivity was achieved with *p*-toluenesulfonyl chloride in dimethylformamide solution to provide propranolol mustard, 1-(1-naphthyloxy)-3-[bis(2-chloroethyl)amino]-2-propanol. Both the trichloro compound and propranolol mustard showed reproducible activity against P-388 leukemia. Neither compound was active against the B16 tumor or Lewis lung carcinoma.

Keyphrases □ Propranolol—nitrogen mustard analog, synthesis, potential lung-specific antitumor activity □ Antitumor agents, potential—lung specific, propranolol mustard, synthesis □ Alkylating agents—propranolol mustard, synthesis, potential lung-specific antitumor activity

Alkylating agents, especially the nitrogen mustards, continue to be an important class of drugs in the management of clinical cancer. Although early analogs involved the attachment of the mustard group to carriers seemingly randomly selected (1), cancer chemotherapists of the last decade have attempted to design new mustard derivatives based on exploitable differences between cell types and with the best attainable cytotoxic specificity toward neoplastic tissue (2).

A carrier moiety that has potential for selectively directing a mustard group to lung tissue was suggested recently (3) as having possible utility in the treatment of pulmonary carcinoma. It was reported (4) that high levels of *dl*-propranolol (I) concentrate in the lungs. Although the *l*-enantiomer produces a β-adrenergic blockade, the antipode is inactive as a β-blocker. Therefore, *d*-propranolol might serve effectively as a carrier for lung-directed alkylating agents that would be devoid of undesired effects on the peripheral autonomic nervous system. For example, replacement of the isopropylamino substituent of I with a bis(2-chloroethyl)amino group would result in mustard V shown in Scheme I.

As a continuation of the development of drugs for the treatment of lung cancer (5), the synthesis of a propranolol mustard (V) was initiated. Although the preliminary plan called for working with racemic synthetic intermediates leading to racemic V, the synthetic sequence (Scheme I) provided the option of resolution of optical isomers if biological test data of the racemic mixtures were encouraging.

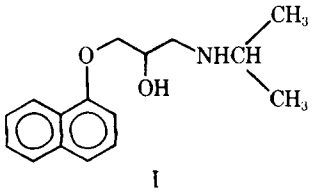

I

RESULTS AND DISCUSSION

Chemistry—Condensation of (1-naphthyloxy)methyloxirane (II) with diethanolamine (Scheme I) gave a triol (III), which was isolated in excellent yield as the hydrochloride salt. Conversion of III to V necessitated a regioselective chlorination of the two primary hydroxyl groups to generate the mustard functionality. Chlorination of III with thionyl chloride, using a procedure (6) that was utilized successfully in the preparation of a similar nitrogen mustard, nonspecifically gave the trichloro compound IV as the only isolated product.

The ^{13}C-NMR spectrum[1] of IV showed chemical shifts at 42.0 and 57.2 ppm due to the carbon atoms bearing the chlorine substituents and the carbon atoms bonded to the nitrogen atom of the mustard group, respectively. These assignments compare well with those reported (7) for the bis(2-chloroethyl)amino group of cyclophosphamide. The remaining aliphatic carbon atoms gave resonance signals at 69.2 (OCH_2), 58.6 (ClCH), and 57.5 (CH_2N) ppm. These assignments were verified by observing the chemical shift multiplicities in a spectrum obtained in the partially decoupled mode. The shifts recorded for the carbon atoms of the aromatic nucleus were in line with those reported (8) for I.

The necessary regiospecific chlorination of III was obtained using *p*-toluenesulfonyl chloride in dimethylformamide solution to provide the targeted compound, propranolol mustard (V). The poor water solubility of the hydrochloride salt of V allowed it to be separated easily in a 44% yield from other reaction products. Although used to advantage in the present work, the formation of alkyl chlorides first was reported (9) as a side reaction occurring with the tosylation of primary alcohols with *p*-toluenesulfonyl chloride in dimethylformamide solution.

The mass spectra of mustards IV and V showed molecular ions at *m/e* 359 and 341, respectively, and both gave their base peaks at *m/e* 154 due to the $[CH_2{=}N(CH_2CH_2Cl)_2]^+$ ion, which resulted from cleavage of the

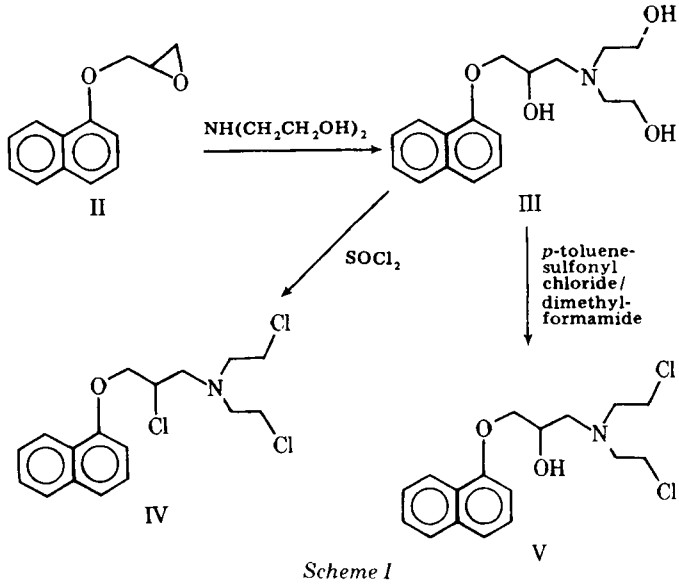

Scheme I

[1] Determined in deuterochloroform solution (0.3 *M*) by R. J. Highet, National Heart, Lung, and Blood Institute, National Institutes of Health, with a JEOL FX-60 spectrometer.

0022-3549/80/0200-0190$01.00/0
© 1980, American Pharmaceutical Association

Table I—Antitumor Evaluations

Compound	Dose[b], mg/kg/day	Percentage Increase of Lifespan[a] P-388 Leukemia Trial 1	P-388 Leukemia Trial 2	B16 Melanoma Trial 1	B16 Melanoma Trial 2	Lewis Lung Carcinoma (Subcutaneous) Trial 1	Lewis Lung Carcinoma (Subcutaneous) Trial 2	Lewis Lung Carcinoma (Intravenous) Trial 1	Lewis Lung Carcinoma (Intravenous) Trial 2
IV	40	33	39	2	30	−3	T[c]	13	−2
	20	34	41	22	24	6	−4	5	−2
	10	19	27	12	15	10	−8	−3	0
	5	27	20	2	11	1	−3	−2	−10
	2.5			3	13	−4	3	−3	
	1.25			9		3	−8	−8	−9
V	40	T	T	T	T	T	T	T	T
	20	−9	−9	T	T	T	T	T	T
	10	49	44	12	6	T	T	−8	12
	5	46	40	17	17	3	3	−4	−5
	2.5	40	31	19	15	1	0	−6	−2
	1.25	30	22	13	11	4	−6	5	−11

[a] The percentage increase (decrease) of the median lifespan of test animals beyond the median survival time of untreated control animals was used to evaluate antitumor activity. Activity is defined as a percentage increase of lifespan of ≥25%. [b] Drugs were suspended in 0.9% saline with hydroxypropylcellulose and administered daily for 9 days after tumor implantation. [c] The T indicates that deaths occurred due to drug-related toxicity.

carbon–carbon bond located α,β to the nitrogen atom. The ^{1}H-NMR spectra of IV and V were consistent with the structures assigned.

Antitumor Evaluation—Propranolol mustard (V) as well as the trichloro Compound IV was evaluated extensively *in vivo* for antitumor activity using three transplantable murine tumors: P-388 leukemia (PS), B16 melanoma (B16), and Lewis lung carcinoma (LL). The last tumor was employed in one system (10) where Lewis lung carcinoma tumor cells were given intravenously and in another system (11) where the Lewis lung carcinoma tumor inoculum was implanted subcutaneously. The P-388 and B16 test systems were used according to established protocols (12). In each of the four test systems, test compounds were administered intraperitoneally daily for 9 days beginning 24 hr after tumor implantation. Dose–response data for IV and V against each test system are recorded in Table I; duplicate determinations were carried out for each system.

Both IV and V prolonged the lifespan of mice bearing P-388 leukemia beyond that of untreated control animals. The percentage increase of lifespan achieved in leukemic mice by IV was between 34 and 41% at a dosage of 20 mg/kg/day. Propranolol mustard (V) gave a somewhat more potent antileukemic effect than IV since just 10 mg/kg/day was sufficient to produce a similar range increase (44–49%). That the bis(2-chloroethyl)amino group is necessary for activity was supported by the lack of activity observed with triol III against P-388 leukemia over a dose range of 400–12.5 mg/kg/day.

Neither IV nor V gave significant activity indications against B16 melanoma, a test system model for solid tumors (Table I). Table I also indicates that neither IV nor V was active in the lung tumor models. The Lewis lung tumor, both in the subcutaneous and intravenous implantation procedures, was completely unaffected by mustards IV and V.

The absence of activity shown by propranolol mustard in the Lewis lung system could be attributed to the net increase in the partition coefficient (log P) resulting from replacement of the $NHCH(CH_3)_2$ group in propranolol with the more lipophilic $N(CH_2CH_2Cl)_2$ group. However, the lack of activity also could be ascribed to an inappropriate utilization of propranolol as a carrier moiety. If the aliphatic portion of I is the essential element in the molecule to effect preferential concentration in lung tissue, then a rational design of a lung-specific antitumor agent would suggest attachment of the cytotoxic mustard group at a point distant from the side chain. Future work also might consider the use of a nitrosourea substituent as the cytotoxic functionality since members of the nitrosourea series have greater incidence of activity against the Lewis lung tumor than do the nitrogen mustards (13).

EXPERIMENTAL[2]

(1-Naphthyloxy)methyloxirane (II)—A literature method (14) was used to convert 110 g (0.76 mole) of 1-naphthol into II. It was obtained as a pale-yellow oil in a 21% yield after distillation, bp 141–144° (0.07 mm) [lit. (15) bp 140° (2 mm)]. The integrated NMR spectrum (60 Hz) was consistent with the assigned structure.

1-(1-Naphthyloxy)-3-[bis(2-hydroxyethyl)amino]-2-propanol (III)—A solution of 16.0 g (0.08 mole) of II and 10.1 g (0.096 mole) of diethanolamine in 200 ml of 1-propanol was refluxed for 2 hr. The reaction solution was concentrated under vacuum at 40°, and the residue was treated with excess methanolic hydrogen chloride. Four volumes of ether were added, and the mixture was allowed to stand overnight at 4°, giving 24.8 g (91% yield) of III as the crystalline hydrochloride salt, mp 140–142°. The melting point was raised to 142–142.5° after recrystallization from methanol–ether (1:2).

Anal.—Calc. for $C_{17}H_{23}NO_4$·HCl: C, 59.73; H, 7.08; Cl, 10.37; N, 4.10. Found: C, 59.71; H, 6.88; Cl, 10.13; N, 4.13.

The free base was extracted with chloroform from an aqueous solution of III·HCl, which was made basic with dilute sodium hydroxide solution. Evaporation of the dried extracts gave the liberated base (III) as a pale-yellow syrup. This syrup could not be induced to crystallize but was homogeneous by TLC; IR: 3360, 1627, 1596, 1579, 1458, 1397, 1262, 1100, 1066, and 1033 cm^{-1}; NMR (60 MHz): δ 2.68 (t, J = 5.5 Hz, 4H, NCH_2CH_2) and 3.52 (t, J = 5.5 Hz, 4H, CH_2OH).

The picrate of III was formed from ethanol and gave a melting point of 161–162° after recrystallization from ethanol [lit. (16) mp 161–163°].

1-(1-Naphthyloxy)-2-chloro-3-[bis(2-chloroethyl)amino]propane (IV)—To a solution of purified (17) thionyl chloride (16.3 g, 0.137 mole) in 60 ml of dry (sodium) benzene, which was stirred and cooled to 2°, was added dropwise a solution of II (10.45 g, 0.0342 mole) in 60 ml of dry benzene at a rate such that the solution temperature did not exceed 5°. After the addition was complete, the reaction solution was refluxed and stirred for 2.5 hr and then evaporated under reduced pressure at room temperature. Thionyl chloride traces were removed by codistillation with two 100-ml portions of dry benzene.

The residue was partitioned between 100 ml of benzene and 100 ml of 2 N aqueous NaOH solution. The layers were separated, and the aqueous layer was saturated with sodium chloride and extracted twice with benzene. The combined benzene solutions were washed twice with water, dried with anhydrous sodium sulfate, treated with activated charcoal, and evaporated to give 9.5 g of an oil. The oil was distilled in a short-path apparatus (150–170°, 0.2 mm) in 0.5–1.7-g portions to give a combined distillate of 7.0 g as a pale-yellow oil. The oil was extracted with hot petroleum ether.

Storage of the extract overnight at ~−15° gave 4.72 g (38%) of white crystals (IV), mp 45–46°; IR: 1583, 1510, 1460, 1404, 1267, 1240, and 1103 cm^{-1}; NMR (100 MHz): δ 2.96 (t, J = 6 Hz, 4H, NCH_2CH_2), 3.08–3.26 (m, 2H, $CHCH_2N$), 3.48 (t, J = 6 Hz, 4H, CH_2Cl), 4.23–4.56 (m, 3H, $ArOCH_2CH$), and 6.78–8.30 (m, 7H, aromatic); mass spectrum: m/e 359 (M^+, 4.4%), 323 (M − HCl, 1.2), 310 (M − CH_2Cl, 8.8), 216 (8.2), 202 (M − $CH_2OC_{10}H_7$, 8.2), 183 (13), 154 [$CH_2{=}N(CH_2CH_2Cl)_2$, 100], 144 (20), 127 (9.8), and 115 (32).

Anal.—Calc. for $C_{17}H_{20}Cl_3NO$: C, 56.61; H, 5.59; Cl, 29.49; N, 3.88. Found: C, 56.71; H, 5.62; Cl, 29.44; N, 4.02.

The picrate of IV was formed from chloroform and gave a melting point of 123–124° after recrystallization from ethanol.

[2] PMR spectra were determined with a Varian T-60 or HA100 spectrometer in deuterochloroform solution. Chemical shifts are reported in parts per million (δ) downfield from tetramethylsilane, which was used as an internal standard. IR spectra were recorded in chloroform solution with a Perkin-Elmer model 621 spectrophotometer. Mass spectra were obtained by direct probe insertion with a DuPont 21-492 spectrometer operated with a 75-ev ionizing voltage. Melting points were measured on a Thomas-Hoover capillary melting-point apparatus and are uncorrected. Elemental analyses were performed by the Section on Microanalytical Services and Instrumentation, National Institute of Arthritis, Metabolism, and Digestive Disease, National Institutes of Health.

Anal.—Calc. for $C_{17}H_{20}Cl_3NO \cdot C_6H_3N_3O_7$: C, 46.84; H, 3.93; Cl, 18.03; N, 9.50. Found: C, 46.87; H, 4.09; Cl, 17.83; N, 9.45.

1-(1-Naphthyloxy)-3-[bis(2-chloroethyl)amino] -2- propanol (V)—*p*-Toluenesulfonyl chloride (6.25 g, 0.0328 mole) was added to a solution of III (5.0 g, 0.0164 mole) in 50 ml of dry (molecular sieves) dimethylformamide. The reaction mixture was stirred and heated for 2 hr at 55–65°. The solvent was removed under reduced pressure at 40° with a rotary evaporator, and the residual syrup was partitioned between 250 ml of benzene and 100 ml of 1 *N* aqueous NaOH solution. The benzene layer was separated, washed with water, and dried over anhydrous sodium sulfate.

Under vigorous stirring, 250 ml of 2 *N* HCl was added dropwise over 30 min to the benzene solution. The stirring was continued for an additional hour after the addition was completed. The white crystals that formed were removed by filtration and washed with 2 *N* HCl, benzene, and ether to give 2.71 g (44% yield) of V as the hydrochloride salt, mp 149–153°. Analytically pure hydrochloride was obtained by chromatographing the free base and by converting the purified base back to the hydrochloride. Accordingly, the base was liberated by benzene extraction from 1 *N* NaOH.

After evaporation of the dried extracts, the residue was chromatographed over silica[3]. Elution of the column with chloroform gave V as a noncrystallizable oil, which was treated with ethanol saturated with hydrogen chloride. The resulting crystalline hydrochloride was recrystallized from the same solvent, mp 155.5–157°; IR (mineral oil mull): 3260 (br), 2580 (br), 1580, 1400, 1391, 1270, 1239, 1126, and 1100 cm^{-1}.

Anal.—Calc. for $C_{17}H_{21}Cl_2NO_2 \cdot HCl$: C, 53.91; H, 5.86; Cl (total), 28.08; Cl (ionic), 9.36; N, 3.70. Found: C, 53.80; H, 5.83; Cl (total), 27.98; Cl (ionic), 9.50; N, 3.70.

The free base appeared as one spot when analyzed by TLC (silica, chloroform); NMR (100 MHz): δ 2.78 (d, J = 7 Hz, 2H, $CHCH_2N$), 2.95 (t, J = 6 Hz, 4H, NCH_2CH_2), 3.55 (t, J = 6 Hz, 4H, CH_2Cl), 4.02–4.32 (m, 3H, $ArOCH_2CH$), and 6.76–8.26 (m, 7H, aromatic); mass spectrum: *m/e* 341 (M^+, 2.3%), 305 (M − HCl, 2.1), 292 (M − CH_2Cl, 1.7), 256 (M − CH_2Cl − HCl, 3.3), 198 (1.1), 186 (2.3), 183 (2.9), 154 [$CH_2{=}N(CH_2CH_2Cl)_2$, 100], 144 (13), and 115 (17).

[3] Bio-Sil A, Bio-Rad Laboratories, Richmond, CA 94804.

REFERENCES

(1) C. Heidelberger, *Cancer Res.*, **29**, 2435 (1969).

(2) W. C. J. Ross, in "Antineoplastic and Immunosuppressive Agents," part I, A. C. Sartorelli and D. G. Johns, Eds., Springer-Verlag, Berlin, Germany, 1975, p. 33.

(3) S. M. Sieber and R. A. Adamson, *Cancer Treat. Rep.*, **60**, 217 (1976).

(4) J. W. Black, W. A. M. Duncan, and R. G. Shanks, *Br. J. Pharmacol.*, **25**, 577 (1965).

(5) M. Takai, Y. Uehara, and J. A. Beisler, *J. Med. Chem.*, **22**, 1380 (1979).

(6) R. C. Elderfield, M. Israel, J. H. Ross, and J. A. Waters, *J. Org. Chem.*, **26**, 2827 (1961).

(7) R. F. Struck, M. C. Thorpe, W. C. Coburn, and W. R. Laster, *J. Am. Chem. Soc.*, **96**, 313 (1974).

(8) S. J. Pasaribu and G. C. Brophy, *Aust. J. Chem.*, **31**, 2629 (1978).

(9) R. A. Edington, *J. Chem. Soc.*, **1964**, 3499.

(10) A. A. Ovejera, R. K. Johnson, and A. Goldin, *Cancer Chemother. Rep., Part 2*, **5**, 111 (1975).

(11) R. I. Geran, N. H. Greenberg, M. M. Macdonald, A. M. Schumacher, and B. J. Abbott, *Cancer Chemother. Rep., Part 3*, **3**, 13 (1972).

(12) *Ibid.*, **3**, 9, 11 (1972).

(13) J. G. Mayo, *Cancer Chemother. Rep., Part 2*, **3**, 325 (1972).

(14) E. J. Rauckman, G. M. Rosen, and R. J. Lefkowitz, *J. Med. Chem.*, **19**, 1254 (1976).

(15) T. Kurihara, K. Osawa, and N. Iino, *Tohoku Yakka Daigaku Nenkyu Nempo*, **11**, 93 (1964); through *Chem. Abstr.*, **64**, 12664 (1966).

(16) A. F. Crowther and L. H. Smith, *J. Med. Chem.*, **11**, 1009 (1968).

(17) L. Fieser and M. Fieser, "Reagents for Organic Synthesis," vol. I, Wiley, New York, N.Y., 1967, p. 1158.

ACKNOWLEDGMENTS

The authors thank Ms. Pamela J. Kirchoff and Dr. Katsuhide Okada for their contributions to the initial stages of this work. They also thank Dr. James A. Kelley of this Laboratory for mass spectral measurements, Mr. George Congleton of Hazleton Laboratories, Vienna, Va., for the P-388 and B16 testing, and Dr. David P. Houchens of Battelle Memorial Institute, Columbus, Ohio, for the Lewis lung evaluations. The authors are grateful to Dr. Robert J. Highet, National Heart, Lung, and Blood Institute, National Institutes of Health, Bethesda, Md., for helpful discussions and for providing the ^{13}C-NMR spectra.

L. V. Feyns was a visiting Postdoctoral Fellow with the National Institutes of Health from 1976 to 1978.

Centrally Active *N*-Substituted Analogs of 3,4-Methylenedioxyphenylisopropylamine (3,4-Methylenedioxyamphetamine)

ULRICH BRAUN *, ALEXANDER T. SHULGIN ‡x, and GISELA BRAUN *

Received April 29, 1979, from the **Institute of Pharmacology, University of Bonn, 53 Bonn, West Germany*, and ‡*1483 Shulgin Road, Lafayette, CA 94549.* Accepted for publication September 20, 1979.

Abstract □ The known central nervous system activity of 3,4-methylenedioxyphenylisopropylamine and its *N*-methyl homolog prompted the synthesis of a series of analogs with substituents on the nitrogen atom. Most of these analogs (R = alkyl, alkenyl, hydroxy, alkoxy, and alkoxyalkyl) were prepared by the reductive alkylation of 3,4-methylenedioxyphenylacetone with the appropriate amine and sodium cyanoborohydride. Hindered isomers were synthesized indirectly. Measurements of their pharmacological activity in several animal assays and in human subjects indicated that the central activity decreased with the increasing bulk of the *N*-substituent.

Keyphrases □ Amines, phenylalkyl, substituted—*N*-substituted analogs of psychotomimetic agents □ Psychotomimetic agents—*N*-substituted analogs of known centrally active agents □ 3,4-Methylenedioxyphenylisopropylamine—synthesis of centrally active *N*-substituted analogs

The structural nucleus of amphetamine has served as the basis of numerous compounds of pharmacological interest. Amphetamine itself is a sympathomimetic stimulant at nominal dosages and leads to a psychotomimetic syndrome only at high dose levels (1). Nuclear alkyl substitution maintains the stimulant properties of the parent compound (2, 3), but the substitution of methoxyl groups leads to compounds that are primarily psychotomimetic

0022-3549/80/0200-0192$01.00/0

© 1980, American Pharmaceutical Association

Anal.—Calc. for $C_{17}H_{20}Cl_3NO \cdot C_6H_3N_3O_7$: C, 46.84; H, 3.93; Cl, 18.03; N, 9.50. Found: C, 46.87; H, 4.09; Cl, 17.83; N, 9.45.

1-(1-Naphthyloxy)-3-[bis(2-chloroethyl)amino] -2- propanol (V)—*p*-Toluenesulfonyl chloride (6.25 g, 0.0328 mole) was added to a solution of III (5.0 g, 0.0164 mole) in 50 ml of dry (molecular sieves) dimethylformamide. The reaction mixture was stirred and heated for 2 hr at 55–65°. The solvent was removed under reduced pressure at 40° with a rotary evaporator, and the residual syrup was partitioned between 250 ml of benzene and 100 ml of 1 *N* aqueous NaOH solution. The benzene layer was separated, washed with water, and dried over anhydrous sodium sulfate.

Under vigorous stirring, 250 ml of 2 *N* HCl was added dropwise over 30 min to the benzene solution. The stirring was continued for an additional hour after the addition was completed. The white crystals that formed were removed by filtration and washed with 2 *N* HCl, benzene, and ether to give 2.71 g (44% yield) of V as the hydrochloride salt, mp 149–153°. Analytically pure hydrochloride was obtained by chromatographing the free base and by converting the purified base back to the hydrochloride. Accordingly, the base was liberated by benzene extraction from 1 *N* NaOH.

After evaporation of the dried extracts, the residue was chromatographed over silica[3]. Elution of the column with chloroform gave V as a noncrystallizable oil, which was treated with ethanol saturated with hydrogen chloride. The resulting crystalline hydrochloride was recrystallized from the same solvent, mp 155.5–157°; IR (mineral oil mull): 3260 (br), 2580 (br), 1580, 1400, 1391, 1270, 1239, 1126, and 1100 cm^{-1}.

Anal.—Calc. for $C_{17}H_{21}Cl_2NO_2 \cdot HCl$: C, 53.91; H, 5.86; Cl (total), 28.08; Cl (ionic), 9.36; N, 3.70. Found: C, 53.80; H, 5.83; Cl (total), 27.98; Cl (ionic), 9.50; N, 3.70.

The free base appeared as one spot when analyzed by TLC (silica, chloroform); NMR (100 MHz): δ 2.78 (d, J = 7 Hz, 2H, $CHCH_2N$), 2.95 (t, J = 6 Hz, 4H, NCH_2CH_2), 3.55 (t, J = 6 Hz, 4H, CH_2Cl), 4.02–4.32 (m, 3H, $ArOCH_2CH$), and 6.76–8.26 (m, 7H, aromatic); mass spectrum: *m/e* 341 (M^+, 2.3%), 305 (M − HCl, 2.1), 292 (M − CH_2Cl, 1.7), 256 (M − CH_2Cl − HCl, 3.3), 198 (1.1), 186 (2.3), 183 (2.9), 154 [$CH_2{=}N(CH_2CH_2Cl)_2$, 100], 144 (13), and 115 (17).

[3] Bio-Sil A, Bio-Rad Laboratories, Richmond, CA 94804.

REFERENCES

(1) C. Heidelberger, *Cancer Res.*, **29**, 2435 (1969).

(2) W. C. J. Ross, in "Antineoplastic and Immunosuppressive Agents," part I, A. C. Sartorelli and D. G. Johns, Eds., Springer-Verlag, Berlin, Germany, 1975, p. 33.

(3) S. M. Sieber and R. A. Adamson, *Cancer Treat. Rep.*, **60**, 217 (1976).

(4) J. W. Black, W. A. M. Duncan, and R. G. Shanks, *Br. J. Pharmacol.*, **25**, 577 (1965).

(5) M. Takai, Y. Uehara, and J. A. Beisler, *J. Med. Chem.*, **22**, 1380 (1979).

(6) R. C. Elderfield, M. Israel, J. H. Ross, and J. A. Waters, *J. Org. Chem.*, **26**, 2827 (1961).

(7) R. F. Struck, M. C. Thorpe, W. C. Coburn, and W. R. Laster, *J. Am. Chem. Soc.*, **96**, 313 (1974).

(8) S. J. Pasaribu and G. C. Brophy, *Aust. J. Chem.*, **31**, 2629 (1978).

(9) R. A. Edington, *J. Chem. Soc.*, **1964**, 3499.

(10) A. A. Ovejera, R. K. Johnson, and A. Goldin, *Cancer Chemother. Rep., Part 2*, **5**, 111 (1975).

(11) R. I. Geran, N. H. Greenberg, M. M. Macdonald, A. M. Schumacher, and B. J. Abbott, *Cancer Chemother. Rep., Part 3*, **3**, 13 (1972).

(12) *Ibid.*, **3**, 9, 11 (1972).

(13) J. G. Mayo, *Cancer Chemother. Rep., Part 2*, **3**, 325 (1972).

(14) E. J. Rauckman, G. M. Rosen, and R. J. Lefkowitz, *J. Med. Chem.*, **19**, 1254 (1976).

(15) T. Kurihara, K. Osawa, and N. Iino, *Tohoku Yakka Daigaku Nenkyu Nempo*, **11**, 93 (1964); through *Chem. Abstr.*, **64**, 12664 (1966).

(16) A. F. Crowther and L. H. Smith, *J. Med. Chem.*, **11**, 1009 (1968).

(17) L. Fieser and M. Fieser, "Reagents for Organic Synthesis," vol. I, Wiley, New York, N.Y., 1967, p. 1158.

ACKNOWLEDGMENTS

The authors thank Ms. Pamela J. Kirchoff and Dr. Katsuhide Okada for their contributions to the initial stages of this work. They also thank Dr. James A. Kelley of this Laboratory for mass spectral measurements, Mr. George Congleton of Hazleton Laboratories, Vienna, Va., for the P-388 and B16 testing, and Dr. David P. Houchens of Battelle Memorial Institute, Columbus, Ohio, for the Lewis lung evaluations. The authors are grateful to Dr. Robert J. Highet, National Heart, Lung, and Blood Institute, National Institutes of Health, Bethesda, Md., for helpful discussions and for providing the ^{13}C-NMR spectra.

L. V. Feyns was a visiting Postdoctoral Fellow with the National Institutes of Health from 1976 to 1978.

Centrally Active *N*-Substituted Analogs of 3,4-Methylenedioxyphenylisopropylamine (3,4-Methylenedioxyamphetamine)

ULRICH BRAUN *, ALEXANDER T. SHULGIN ‡x, and GISELA BRAUN *

Received April 29, 1979, from the **Institute of Pharmacology, University of Bonn, 53 Bonn, West Germany*, and ‡*1483 Shulgin Road, Lafayette, CA 94549.* Accepted for publication September 20, 1979.

Abstract □ The known central nervous system activity of 3,4-methylenedioxyphenylisopropylamine and its *N*-methyl homolog prompted the synthesis of a series of analogs with substituents on the nitrogen atom. Most of these analogs (R = alkyl, alkenyl, hydroxy, alkoxy, and alkoxyalkyl) were prepared by the reductive alkylation of 3,4-methylenedioxyphenylacetone with the appropriate amine and sodium cyanoborohydride. Hindered isomers were synthesized indirectly. Measurements of their pharmacological activity in several animal assays and in human subjects indicated that the central activity decreased with the increasing bulk of the *N*-substituent.

Keyphrases □ Amines, phenylalkyl, substituted—*N*-substituted analogs of psychotomimetic agents □ Psychotomimetic agents—*N*-substituted analogs of known centrally active agents □ 3,4-Methylenedioxyphenylisopropylamine—synthesis of centrally active *N*-substituted analogs

The structural nucleus of amphetamine has served as the basis of numerous compounds of pharmacological interest. Amphetamine itself is a sympathomimetic stimulant at nominal dosages and leads to a psychotomimetic syndrome only at high dose levels (1). Nuclear alkyl substitution maintains the stimulant properties of the parent compound (2, 3), but the substitution of methoxyl groups leads to compounds that are primarily psychotomimetic

0022-3549/80/0200-0192$01.00/0

© 1980, American Pharmaceutical Association

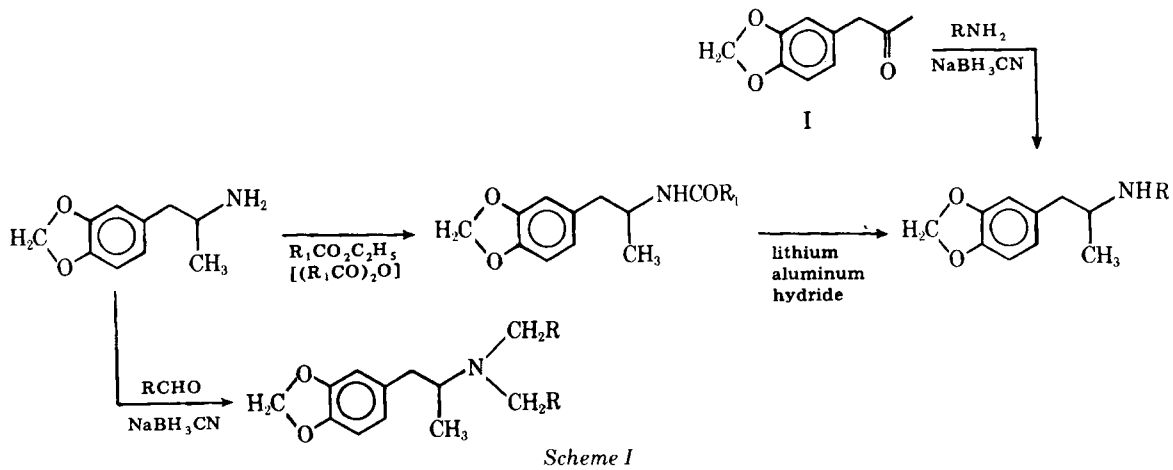

Scheme I

(4); this property is enhanced by the additional inclusion of alkyl (5), halo (6), or alkylmercapto (7) groups. A methylenedioxy group on the aromatic nucleus, either without (8, 9) or with (10) methoxyl groups, maintains this latter pharmacological property. Removal of the α-methyl group of these substituted amphetamine analogs inevitably decreases potency but leaves their qualitative nature intact (11).

Less is known about the effects of *N*-substitution. With amphetamine itself, *N*-methylation provides methamphetamine, which is similar to amphetamine in both potency and action (12), but only sparse information exists concerning the human pharmacology of higher homologs (13). One psychotomimetic (methylenedioxyphenylisopropylamine, IIa) is known to maintain its central action in humans with both *N*-methylation (7) and *N*-ethylation (14).

This report describes the preparation of some related *N*-substituted analogs of IIa and outlines their pharmacological properties with respect to motor activity and analgesia in animals and central activity in humans.

RESULTS AND DISCUSSION

Several bases were prepared by one or more of the three general procedures shown in Scheme I. Procedure I, employing the reductive amination of a ketone with amines in the presence of sodium cyanoborohydride (15), gave acceptable yields with piperonylacetone (I) and most primary amines as their hydrochloride salts in methanol. The products were isolated conventionally except for the long chain homologs which, as salts, were extremely water insoluble but soluble in methylene chloride. This procedure was unsatisfactory with hindered primary amines (*tert*-butylamine and 4-aminoheptane); with the secondary amines studied, it was effective only with dimethylamine.

The simpler homologs could be prepared by acylation of IIa itself, followed by reduction of the resulting amide with lithium aluminum hydride (Procedure II). The *N,N*-diethyl homolog IIv could not be formed from I and diethylamine, and it was prepared by the reductive alkylation of IIa with an excess of acetaldehyde and with sodium cyanoborohydride (Procedure III). Compound IIr formed readily from I and hydroxylamine, but attempts to distill the isolated product led to an erratic degree of decomposition by disproportionation, in part, to IIa. An alternative procedure leading to IIr was the reduction of the I oxime. The product amines and their physical properties are shown in Table I. Representative synthetic procedures are outlined under *Experimental*.

Several bases were evaluated as centrally active drugs in assays that measured analgesia or motor stimulation. Analgesia studies included hot-plate and light–warmth stimuli, as well as diminished response to injected acetic acid as determined by the loss of the stretch reflex response. Motor stimulation was determined in automated activity cages. Human psychotomimetic efficacy was determined for several of these materials by standard procedures (4).

In all animal assays, IIa was significantly more active as an analgesic than control saline. The results (Table II) were normalized with IIa as a standard, with increasing values indicating increased effectiveness. The motor stimulation observed in mice and the effective psychotomimetic levels found in humans are given in Table III. A full report of the pharmacological procedures and related experimental details was published separately (19).

The direct determination of central activity of these materials in animal studies is compromised by the use of dosages close to the LD_{50} values and may represent a more generalized somatic challenge than simple analgesia or stimulation. This problem was apparent for higher dosages of IIa and IIb but not for IIm and IIo where there was little stimulation despite high LD_{50} levels. Throughout these assays, it was apparent that the simplest homologs of IIa (IIb, IIc, and IIr) were somewhat similar in action and efficacy. The two simplest compounds (IIa and IIb) have been studied most frequently, and the reported facts are compared with the results of this study in Table IV. Generally, both the toxicity (and the risk) of a drug and its central activity decrease with homologation, maintaining a constant therapeutic index. The metabolic explanation that the activity of IIb in humans is due to its conversion to IIa is contradicted by the qualitative differences of their actions and by the fact that opposite optical isomers are responsible for their actions (22). Compound IIr, a potential metabolite of IIa, has been studied only as the racemate.

EXPERIMENTAL

Melting points were determined in open capillaries and are uncorrected. Boiling points were recorded from bulb-to-bulb distillation. Microanalyses of all new compounds are included in Table I. All new compounds had IR and NMR spectra consistent with the assigned structures[1].

N-Ethyl-3,4-methylenedioxyphenylisopropylamine (IIc)—*Procedure I*—To a solution of 31.0 g of ethylamine hydrochloride in 110 ml of methanol were added 6.6 g of piperonylacetone (I, 37 mmoles) and then 3 g of sodium cyanoborohydride. The mixture was stirred at ambient temperature, and 12 *N* HCl was added as required to maintain the pH at neutrality (determined by the use of external damp universal pH paper). The reaction was complete in 36 hr. Following addition to 1 liter of water containing 5 ml of 12 *N* HCl, the reaction mixture was extracted twice with 150 ml of methylene chloride (discarded), made basic with 25% NaOH, and reextracted with 3 × 150 ml of methylene chloride. The extracts were pooled, and the solvent was removed *in vacuo*.

Distillation of the residual oil (8.3 g) at 0.20 mm Hg yielded 6.0 g of product as a viscous colorless oil, bp 85–95°. This product was dissolved in 60 ml of isopropanol and acidified with 12 *N* HCl (titration end-point determined with external damp universal pH paper), and an equal volume of ether was added. There was a spontaneous crystallization of the product as a white solid. It was removed by filtration and washed first

[1] IR spectra were obtained on a Perkin-Elmer Infracord spectrophotometer, and NMR spectra were obtained on a Perkin-Elmer 60-mHz permanent magnet NMR spectrometer. Microanalyses were performed by Galbraith Laboratories, Knoxville, TN 37921.

Table I—*N*-Substituted 3,4-Methylenedioxyphenylisopropylamines

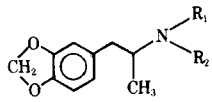

Compound	R_1	R_2	Procedure	Boiling Point of Base	Melting Point of Hydrochloride	Yield, %	Analysis of Nitrogen, % Calc.	Found
IIa[a]	—H	H	I[b]	80–90°/0.2 mm	187–188°	31[c]	—[d]	—
IIb[a]	$-CH_3$	H	I	100–110°/0.4 mm	152–153°	74	—[e]	—
			II	100–110°/0.4 mm	151–152°	46[f]	—	—
IIc	$-CH_2CH_3$	H	I	85–95°/0.2 mm	201–202°	68	5.75	5.74
			II	90–100°/0.2 mm	198–199°	37[g]	—	—
IId	$-(CH_2)_2CH_3$	H	I	90–100°/0.3 mm	194–195°	52	5.43	5.43
IIe	$-CH(CH_3)_2$	H	I	95–110°/0.3 mm	186–186.5°	25	5.43	5.40
IIf	$-(CH_2)_3CH_3$	H	I	90–100°/0.15 mm	200–200.5°	26	5.15	5.21
IIg	$-CH_2CH(CH_3)_2$	H	I	95–105°/0.15 mm	179–180°	64	5.15	5.13
IIh	$-CH_2\underline{CHCH_2}CH_2$	H	I	90–100°/0.1 mm	218–220°	15	5.19	5.20
IIi	$-(CH_2)_4CH_3$	H	I	110–120°/0.2 mm	164–166°	7	4.90	4.86
IIj	$-(CH_2)_5CH_3$	H	I	135–145°/0.3 mm	188–189°	38	4.67	4.59
IIk	$-(CH_2)_7CH_3$	H	I	130–135°/0.2 mm	206–208°	61	4.27	4.22
IIl	$-CH_2CN$	H	I	150–160°/0.3 mm	156–158°	21[h]	11.00	11.01
IIm	$-CH_2CH_2OH$	H	I	155–160°/0.15 mm	147–148°	35	5.39	5.48
IIn	$-CH_2CH_2OCH_3$	H	I	100–120°/0.2 mm	182.5–183°	72	5.12	5.10
IIo	$-CH_2CH{=}CH_2$	H	I	90–95°/0.2 mm	174–176°	39	5.48	5.37
IIp	$-CH_2C{\equiv}CH$	H	I	105–110°/0.2 mm	189–190°	39	5.52	5.57
IIq	$-CH_2C_6H_5$	H	I	135–145°/0.2 mm	170–171°	13	4.58	4.77
IIr	—OH	H	I	—[i]	149–150°	31	6.05	6.04
IIs	$-OCH_3$	H	I	90–95°/0.5 mm	143–146°	28	5.70	5.71
IIt	$-NHC(CH_3)_3$	H	I	95–105°/0.1 mm	220–222° dec.	3	9.77	10.67
								10.84
IIu	$-CH_3$	$-CH_3$	I	85–90°/0.5 mm	172–173°	27	5.75	5.70
IIv	$-CH_2CH_3$	$-CH_2CH_3$	III	85–88°/0.15 mm	177–178°	62	5.15	5.13

[a] Compound IIa has been referred to in the literature as MDA and EA-1299. Compound IIb has been referred to in the literature as MDM, MDMA, and EA-1475. The EA codes are from the Edgewood Arsenal, U.S. Army Chemical Warfare Service. [b] Ammonia was employed as the acetate salt. [c] The conventional preparation of IIa by the lithium aluminum hydride reduction of 1-(3,4-methylenedioxyphenyl)-2-nitropropene gave a yield of 87%. [d] Lit. (16) mp 186–187°. [e] Lit. (17) mp 148–149° and mp 147–148° (18). [f] Overall yield from IIa, with isolation and purification of the intermediate formamide. [g] Overall yield from IIa, with isolation and purification of the intermediate acetamide. [h] The major product was IIa from ammonia formed by the *in situ* decomposition of cyanomethylamine. [i] Unstable to distillation (see text). Free base from isopropanol, mp 94–95°. Nitrogen analysis was: calc., 7.08; found, 7.09.

with isopropanol–ether and finally with ether alone, giving 6.1 g of the air-dried product (68% yield), mp 201–202°.

Procedure II—A solution of 3.6 g of IIa as the free base (20 mmoles) in 20 ml of pyridine was treated with 2.4 ml of acetic anhydride and stirred at ambient temperature for 18 hr. The reaction mixture was added to 200 ml of water, stirred several hours, acidified with hydrochloric acid, and extracted with 2 × 80 ml of methylene chloride. The extracts were pooled, and the solvent was removed *in vacuo* to yield an off-white solid (mp 89–90°), which crystallized from 80 ml of ethyl acetate–hexane (1:1). The acetamide was obtained as white crystals (2.6 g, 58% yield, mp 92–93°).

A solution of 1.7 g of the acetamide (7.7 mmoles) in 8 ml of dry tetrahydrofuran was added to a solution of 1.6 g of lithium aluminum hydride in 150 ml of tetrahydrofuran and stirred at reflux temperature. After being held at reflux with stirring for 72 hr, the reaction mixture was cooled (external ice water), and treated sequentially with 1.6 ml of water in several milliliters of tetrahydrofuran, 1.6 ml of 15% NaOH, and finally with 4.8 ml of additional water. The white solids were removed by filtration and washed with tetrahydrofuran. The filtrate and washes were combined, and the solvent was removed *in vacuo*.

The residual oil was distilled (90–100° at 0.2 mm Hg), dissolved in 8 ml of isopropanol, acidified with 12 *N* HCl (external damp pH paper), and diluted with ether. Resulting white solids were filtered, washed with isopropanol–ether and then with ether, and air dried. The product weighed 1.0 g, mp 198–199° (mixed melting point with the product from Procedure I, 198–199°); the yield was 53% from the acetamide and 31% overall from IIa.

***N* - Cyanomethyl - 3,4 - methylenedioxyphenylisopropylamine (III)**—The crude reaction product (following Procedure I) obtained from I (2.67 g, 15 mmoles), cyanomethylamine sulfate (20 g, 130 mmoles) in 100 ml of methanol adjusted to neutral pH with 25% NaOH, and 1.3 g of sodium cyanoborohydride was a mixture of III and IIa. The latter was undoubtedly formed by the *in situ* decomposition of free cyanometh-

Table II—Central Analgesia [a]

Compound	Hot Plate[b]	Tail Flick[c]	Stretch Reflex[d]
IIa	1	1	1
IIb	1.09	1.25	5.33
IIc	1.04	0.66	0.71
IId	1.50	0.78	0.30
IIe	1.00	0.90	0.22
IIf	0.75	0.87	0.37
IIg	1.18	0.87	0.45
IIh	0.77	0.84	0.61
IIm	1.99	1.08	0.26
IIn	0.83	0.87	0.32
IIo	1.67	1.06	0.29
IIp	0.87	0.92	0.37
IIs	1.34	0.86	0.36
IIu	1.53	0.91	0.35

[a] Values obtained in mice, with oral administration, and normalized to IIa = 1. [b] With 20 mg/kg; IIa = 133% of saline control. [c] With 100 mg/kg; IIa = 119% of saline control. [d] With 20 mg/kg; IIa gave a 47% response of the saline control at 10 mg/kg, a 32% response at 20 mg/kg, and a 0% response (complete analgesia) at 100 mg/kg.

Table III—Central Stimulation

Compound	Motor Activity (Mice)[a]	Psychotomimetic Activity (Humans)[b]
IIa	640	60–120
IIb	1530	100–160
IIc	1780	140–200
IId	—	>160
IIe	910	>160
IIn	176	>160
IIo	153	>160
IIp	—	>160
IIq	—	>160
IIr	—	80–120
IIs	149	>160
IIu	40	>160
Saline	160	

[a] Averaged activity responses (events per hour) 1–4 hr following drug administration (20 mg/kg po). [b] Range of effective dosages, in milligrams, orally. Values given as greater than (>) represent the absence of significant activity at this maximum dosage.

Table IV—Comparison of Pharmacological Properties of IIa and IIb

Assay	Species	IIa	IIb	Reference[a]
Toxicity, LD_{50}, mg/kg	Mouse (intraperitoneal)	68	97	20
	Rat (intraperitoneal)	27	49	20
	Guinea pig (intraperitoneal)	60	98	20
	Dog (intravenous)	7	14	20
	Monkey (intravenous)	6	22	20
Central analgesia	Mouse, relative potency at stated dosages			
	hot plate (20 mg/kg)	1	1.09	—
	tail flick (100 mg/kg)	1	1.38	—
	stretch reflex (20 mg/kg)	1	5.34	—
Central stimulation	Mouse, relative potency at 20 mg/kg	1	2.4	—
	Dog, mg/kg	0.5–15	5–50	20
	Monkey, mg/kg	1–20	10–75	20
Human activity	Man			
	active dosage, mg	60–120	100–160	8, 9, 21
	active isomer	*R*[b]	*S*[b]	22
	qualitative feature	Moderately complex	Simple	7, 9, 23

[a] Published literature data have been commingled with results from this study for comparison. [b] *R* and *S* represents the absolute configurations of the pharmacologically active isomers, and are the levo- and dextrorotatory forms, respectively.

ylamine to ammonia. Upon distillation, the first fraction (1.3 g, bp 90–110° at 0.4 mm Hg) was substantially free of the cyanomethylene group (by NMR), but the second fraction (0.8 g, bp 150–160° at 0.3 mm Hg) had the proper NMR spectrum in deuterium oxide as the hydrochloride salt: δ 1.30 and 1.42 (2s, 3H, CH_3), 3.00 (m, 2H, aromatic CH_2), ~3.6 (m, 1H, CH), 4.38 (s, 2H, CH_2CN), 4.75 (s, NH and DOH), 6.05 (s, 2H, OCH_2O), and 6.95 (s, 3H, aromatic H). The analytical sample was recrystallized from boiling isopropanol (50 ml/g).

***N*-Hydroxy-3,4-methylenedioxyphenylisopropylamine (IIr)**—The crude reaction product (*via* Procedure I) obtained from I (7.2 g, 40 mmoles), hydroxylamine hydrochloride in methanol (29.6 g in 240 ml), and sodium cyanoborohydride (2 g) gave evidence, on attempted distillation, of the generation of water by pyrolytic disproportionation. At bath temperatures of <90°, the distillate was mainly IIt; but above 100°, there was extensive decomposition to IIa, which was the major product isolated (verified by IR spectral comparison of the hydrochloride salt with reference IIa·HCl). The free base could be obtained as a solid and was best purified by recrystallization as described below.

Compound IIr also could be prepared *via* the I oxime. A solution of 10 g of I (56 mmoles) and 10 g of hydroxylamine hydrochloride in 50 ml of pyridine and 50 ml of ethanol was held at reflux for 2 hr. Removal of the solvents *in vacuo* left an oil, which crystallized upon trituration under water. The crude oxime was removed by filtration and recrystallized from ethanol–water to yield 5.5 g (51% yield) of a white crystalline product, mp 84–87°. The oxime was dissolved in 50 ml of methanol and treated with 2.5 g of sodium cyanoborohydride. While being stirred at ambient temperature, 12 *N* HCl was added dropwise (about 10 drops every 12 hr) over 3 days. The methanol was removed *in vacuo*, and the residue was suspended in acidified water (5 ml of 12 *N* HCl in 500 ml). The reaction mixture was extracted with 3 × 100 ml of methylene chloride (unreacted oxime was discarded), made basic with sodium hydroxide, and reextracted with 3 × 100 ml of methylene chloride. The extracts were pooled, and the solvent was removed *in vacuo* to provide IIr (free base) as a white solid (1.4-g crude yield after vacuum drying at 0.2 mm Hg).

After recrystallization from isopropanol (6 ml/g), the product had a melting point of 92–94° (mixed melting point with the oxime, 56–62°). In the IR spectrum, both the NH and the OH stretch vibration absorptions were visible at 3040 (broad) and 3135 (sharp) cm^{-1} (in mineral oil). The free base was converted to the hydrochloride salt by dissolution in 20 ml of warm isopropanol, acidification with 12 *N* HCl (external damp pH paper), and the addition of 200 ml of ether. The clear solution slowly deposited white crystals of IIr·HCl, 0.8 g (12% yield from the oxime, overall yield of 6%), mp 149–150° (mixed melting point with IIa·HCl was 128–138°).

***N,N*-Diethyl-3,4-methylenedioxyphenylisopropylamine (IIv) (Procedure III)**—A stirred solution of 1.4 g of IIa·HCl (6.5 mmoles) in 30 ml of methanol was treated with 7.0 g of acetaldehyde and 1.5 g of sodium cyanoborohydride. Then 12 *N* HCl was added dropwise as needed to maintain the pH at neutrality (as determined by external damp universal pH paper). After 48 hr, the reaction mixture was added to 600 ml of water, acidified with hydrochloric acid (5 ml), and extracted with 2 × 100 ml of methylene chloride. The residual aqueous phase was made basic with 25% NaOH and reextracted with 3 × 100 ml of methylene chloride. The extracts were combined and the solvent was removed *in vacuo*. The residual pale-yellow oil (1.1 g of crude weight) was distilled (85–88° at 0.15 mm Hg) to yield 1.0 g of a colorless oil. This oil was dissolved in 8 ml of isopropanol, acidified with 12 *N* HCl, and diluted with 30 ml of ether. After the product had crystallized completely, it was removed by filtration and washed first with 75% ether (with isopropanol) and finally with ether. Air drying yielded 1.1 g of IIv·HCl as white crystals (62% of theory), mp 177–178°.

REFERENCES

(1) P. H. Connell, "Maudsley Monographs Number Five," Oxford University Press, London, England, 1958.

(2) D. F. Marsh and D. A. Herring, *J. Pharmacol. Exp. Ther.*, **100,** 298 (1950).

(3) S. C. Harris and R. C. Worley, *Proc. Soc. Exp. Biol. Med.*, **95,** 212 (1957).

(4) A. T. Shulgin, T. Sargent, and C. Naranjo, *Nature*, **221,** 537 (1969).

(5) A. T. Shulgin and D. C. Dyer, *J. Med. Chem.*, **18,** 1201 (1975).

(6) A. T. Shulgin, T. Sargent, and C. Naranjo, *Pharmacology*, **5,** 103 (1971).

(7) A. T. Shulgin and D. E. Nichols, in "The Psychopharmacology of Hallucinogens," R. C. Stillman and R. E. Willette, Eds., Pergamon, New York, N.Y., 1978, p. 74.

(8) G. A. Alles, in "Neuropharmacology, Transactions of the Fourth Conference," H. A. Abramson, Ed., Madison Printing Co., Madison, N.J., 1959, p. 181.

(9) C. Naranjo, A. T. Shulgin, and T. Sargent, *Med. Pharmacol. Exp.*, **17,** 359 (1967).

(10) A. T. Shulgin, *Experientia*, **20,** 366 (1964).

(11) U. Braun, G. Braun, P. Jacob, III, D. E. Nichols, and A. T. Shulgin, in "QuaSAR Research Monograph 22," G. Barnett, M. Trsic, and R. E. Willette, Eds., National Institute on Drug Abuse, Washington, D.C., 1978, p. 27.

(12) F. Hauschild, *Arch. Exp. Pathol. Pharmacol.*, **191,** 465 (1938).

(13) T. B. Vree, "Pharmacokinetics and Metabolism of Amphetamines," Brakkenstein Press, Nijmegen, Holland, 1973.

(14) A. T. Shulgin, in "Handbook of Psychopharmacology," vol. 11, L. L. Iversen, S. D. Iversen, and S. H. Snyder, Eds., Plenum, New York, N.Y., 1978, p. 243.

(15) R. F. Borch, M. D. Bernstein, and H. D. Durst, *J. Am. Chem. Soc.*, **93,** 2897 (1971).

(16) M. D. Fairchild, Ph.D. thesis, University of California, Los Angeles, Calif., 1963.

(17) S. Biniecki and E. Krajewski, *Acta Pol. Pharm.*, **17,** 421 (1960).

(18) K. Bailey, A. W. By, D. Legault, and D. Verner, *J. Assoc. Offic. Anal. Chem.*, **58,** 62 (1975).

(19) U. Braun, A. T. Shulgin, and G. Braun, *Arzneim.-Forsch.*, in press.

(20) H. F. Hardman, C. O. Haavic, and M. H. Seevers, *Toxicol. Appl. Pharmacol.*, **25,** 299 (1973).

(21) R. Yensen, F. B. DiLeo, J. C. Rhead, W. A. Richards, R. A. Soskin, B. Turek, and A. A. Kurland, *J. Nerv. Ment. Dis.*, **163,** 233 (1976).

(22) G. M. Anderson, III, G. Braun, U. Braun, D. E. Nichols, and A. T. Shulgin, in "QuaSAR Research Monograph 22," G. Barnett, M. Trsic, and R. E. Willette, Eds., National Institute on Drug Abuse, Washington, D.C., 1978, p. 8.

(23) C. Naranjo, "The Healing Journey," Pantheon Books, New York, N.Y., 1973, p. 26.

Topical Mosquito Repellents XIII: Cyclic Analogs of Lactic Acid

W. A. SKINNER [x], F. FUHRMANN, L. C. RUTLEDGE [*], M. A. MOUSSA [‡], and C. E. SCHRECK [§]

Received August 6, 1979, from the *Life Sciences Division, SRI International, Menlo Park, CA 94025.* Accepted for publication September 24, 1979. [*]Present address: Letterman Army Institute of Research, Presideo of San Francisco, CA 94129. [‡]Present address: Office of the Surgeon-General, Washington, DC 20310. [§]Present address: Insects Affecting Man and Animals Research Laboratory, Agricultural Research, Science and Education Administration, U.S. Department of Agriculture, Gainesville, FL 32604.

Abstract □ Numerous cyclic analogs of lactic acid were synthesized to ascertain whether they might act as agonists or antagonists of lactic acid, a known attractant for mosquitoes. These compounds were evaluated with an *in vitro* blood-feeding test system and an *in vivo* cloth test. Two of the compounds in the blood-feeding test system showed biphasic results, acting as attractants at low concentrations and as repellents at higher concentrations. Several compounds (III, V, VII, and X) repelled *Aedes aegypti* mosquitoes in the blood-feeding test system. However, in the *in vivo* cloth test system, only III repelled the mosquitoes significantly.

Keyphrases □ Lactic acid cyclic analogs—topical mosquito repellents, *in vivo* testing, humans □ Mosquitoes—topical repellents, lactic acid cyclic analogs, *in vivo* testing, humans □ Repellents, mosquito—topical use in humans, lactic acid cyclic analogs

Numerous cyclic analogs of lactic acid have been synthesized and evaluated as mosquito repellents using an *in vitro* blood-feeding test system (1). Some of these compounds also were evaluated by an *in vivo* cloth test[1].

In addition to L-lactic acid, several compounds related to lactic acid attract *Aedes aegypti* mosquitoes (2). Certain receptors on the antennae of the female *A. aegypti* mosquito respond to lactic acid, but *N,N*-diethyl-*m*-toluamide blocks this response (3). Thus, an antagonist to lactic acid may exhibit repellent activity and an agonist may attract the mosquitoes.

A survey of chemical classes with repellent behavior (4, 5) indicated that α-keto and α-hydroxy carbonyl compounds were among those showing increased frequency of repellent activity.

The structure–activity relationships of these compounds were investigated in structures that varied in the separation of the oxygen functions (hydroxyl or RO) from the carbonyl functions. The alkyl substituents were varied to give a boiling-point range since volatility is an important variable affecting the duration of topical repellency. Table I indicates the structures, boiling points or melting points, and repellency data for compounds used against *A. aegypti* (yellow fever) mosquitoes.

EXPERIMENTAL[2]

Chemistry—*Ethyl 2-Butyl-1-hydroxycyclopentanecarboxylate (6) (IV)*—2-*n*-Butyl-1-hydroxycyclopentanecarbonitrile (7) (5.0 g, 29.9 mmoles), anhydrous ethanol (1.38 g, 29.9 mmoles), *p*-toluenesulfonic acid monohydrate (5.69 g, 29.9 mmoles), and 5 ml of anhydrous benzene were stirred overnight at 90°. Water and benzene were added, the organic layer was washed with 20% Na_2CO_3 and water and then dried over sodium sulfate, and the solvent was evaporated. Distillation of the residue afforded IV (bp 71–72°/0.5 mm Hg) as a colorless liquid, 1.0 g (16% yield); IR (film): 3460, 2900, 2830, 1720, 1430, 1370, 1230, 1050, 880, and 760 cm^{-1}; NMR ($CDCl_3$): δ 4.27 (q, 2H), 3.1 (s, 1H), 1.6–2.2 (m, 7H), 1.27 (t, 3H), 1.05–1.4 (m, 6H), and 0.87 (t, 3H) ppm.

Anal.—Calc. for $C_{12}H_{22}O_3$: C, 67.25; H, 10.35. Found: C, 67.70; H, 10.60.

Methyl 2-Butyl-1-hydroxycyclohexanecarboxylate (V)—2-*n*-Butyl-1-hydroxycyclohexanecarbonitrile (7) (7.2 g, 39.7 mmoles) and 20 volume % H_2SO_4 (26 ml) in acetic acid (35 ml) were stirred at 110° for 27 hr. After cooling, the reaction mixture was poured into cold water and extracted with ether. The carboxylic acid was extracted with dilute sodium hydroxide, the aqueous alkaline solution was acidified with concentrated hydrochloric acid, and the solution was extracted with ether. The combined ether layers were dried over sodium sulfate–charcoal and were concentrated to yield 0.91 g of a yellow oil.

A solution of diazomethane in ether was added slowly at 0° to a stirred solution of 2-*n*-butyl-1-hydroxycyclohexanecarboxylic acid (0.91 g, 4.54 mmoles) in 10 ml of ether until nitrogen evolution ceased. The reaction mixture was stirred for 40 min at 0° and for 30 min at room temperature. After the addition of 1 ml of 3 *N* acetic acid, the solution was extracted with sodium bicarbonate and water, and the extract was dried over magnesium sulfate and concentrated. Distillation afforded V (bp 85–86°/0.5 mm Hg) as a colorless liquid, 0.90 g (93% yield); IR (film): 3480, 2920, 2850, 1730, 1460, 1390, 1240, 1160, 1100, and 1020 cm^{-1}; NMR ($CDCl_3$): δ 3.76 (s) and 3.64 (s, 3H), 3.36 (s, 1H), 2.2–2.5 (m, 3H), 1.0–1.9 (m, 12H), and 0.86 (t, 3H) ppm.

Anal.—Calc. for $C_{12}H_{22}O_3$: C, 67.26; H, 10.35. Found: C, 67.20; H, 10.22.

(1-Acetoxy-2-heptylcyclohexyl)carbonitrile—Five grams (0.022 mole) of (2-heptyl-1-hydroxycyclohexyl)carbonitrile was dissolved in 50 ml of acetic anhydride. After addition of 0.1 g of 4-dimethylaminopyridine as a catalyst, the mixture was allowed to stand at room temperature for 2 days. The excess acetic anhydride was removed *in vacuo*. The residue was taken up with saturated sodium bicarbonate and extracted three times with ether. After drying with anhydrous magnesium sulfate and

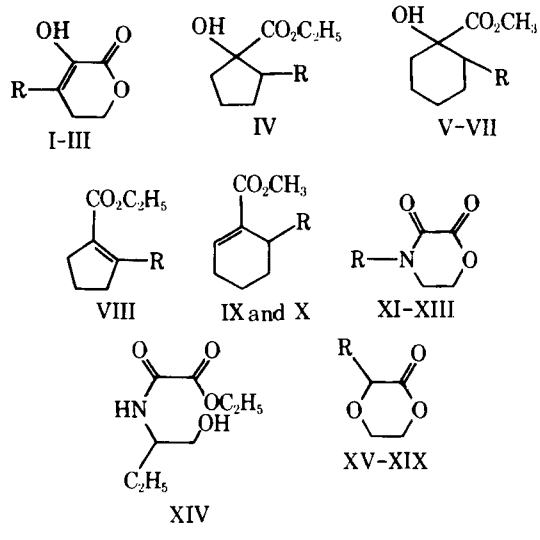

[1] The *in vivo* cloth test system was developed by the Agricultural Research Laboratories, U.S. Department of Agriculture, Gainesville, Fla.

[2] Melting points were determined on a capillary melting-point apparatus and are uncorrected. Boiling points were determined using a short-path distillation apparatus and are uncorrected. IR (Perkin-Elmer 735B) and NMR (Varian Associates T-60 or EM-390) spectra were taken of all compounds and were completely consistent with the assigned structures. Elemental analyses were performed by the Microanalytical Laboratory, Department of Chemistry, Stanford University, Stanford, Calif.

0022-3549/80/0200-0196$01.00/0
© 1980, American Pharmaceutical Association

Table I—Physical and Biological Properties of Cyclic Analogs of Lactic Acid

Compound	R	Boiling Poing or Melting Point	Reference	Repellent Activity (Membrane Feeder Test) ED_{50}	ED_{90}	r	Repellent Activity (Cloth Test), days	Minimum Effective Dose, mg/cm² 15 min	24 hr
I	CH_3	72–75°	8		No effect		—	—	—
II	CH_2CH_3	—	—[a]	0.10	0.64	−0.77	0	0.25	>1.0
III	$(CH_2)_4CH_3$	—	—[b]	0.035	0.094	−0.93	6	0.063	0.25
IV	$(CH_2)_3CH_3$	71–72°/0.5 mm Hg	—[c]		No effect		—	—	—
V	$(CH_2)_3CH_3$	85–86°/0.5 mm Hg	—[c]	0.0060	0.31	−0.87	>1	0.125	>1.0
VI	$(CH_2)_4CH_3$	92–93°/0.5 mm Hg	—[d]	0.096	0.27	−0.95	>1	0.5	>1.0
VII	$(CH_2)_6CH_3$	130°/0.5 mm Hg	—[c]	0.0073	0.064	−0.93	0	>1.0	—
VIII	$(CH_2)_3CH_3$	74–75°/0.5 mm Hg	—[c]		No effect		—	—	—
IX	$(CH_2)_4CH_3$	88°/0.5 mm Hg	—[e]		Bimodal effect		0	>1.0	—
X	$(CH_2)_6CH_3$	124°/0.5 mm Hg	—[c]	0.058	13	−0.33	0	>1.0	—
XI	CH_2CH_3	56–66°	—[f]		—		—	—	—
XII	$(CH_2)_3CH_3$	63–64°	—[c]		Bimodal effect		—	—	—
XIII	$(CH_2)_5CH_3$	62.5°	—[g]		—		—	—	—
XIV	—	—	—[c]		No effect		0	>1.0	—
XV	CH_2CH_3	52–55°/0.5 mm Hg	9	0.31	12	−0.80	—	—	—
XVI	$(CH_2)_3CH_3$	85–88°/0.5 mm Hg	9		No effect		0	0.25	>1.0
XVII	$(CH_2)_4CH_3$	90–92°/0.5 mm Hg, 48–49°	—[h]		—		—	—	—
XVIII	$(CH_2)_5CH_3$	100–102°/0.5 mm Hg, 47–49°	—[i]		—		—	—	—
XIX	$(CH_2)_6CH_3$	111–113°/0.5 mm Hg, 60–62°	—[j]		—		—	—	—
Diethyl toluamide		100°/0.5 mm Hg	—	0.031	0.10	−0.81	6	0.016	0.25

[a] Compound II was prepared as described previously for I (8). IR ($CDCl_3$): 3400, 2950, 2880, 1705, 1475, 1430, 1390, 1280, and 1190 cm^{-1}; NMR ($CDCl_3$): δ 5.6–6.1 (m, 1H), 4.4 (t, 2H), 2.05–2.65 (m, 4H), and 1.07 (t, 3H) ppm. *Anal.*—Calc. for $C_7H_{10}O_3$: C, 59.14; H, 7.09. Found: C, 57.42; H, 7.21 (hygroscopic because a part of the lactone always is hydrolyzed). [b] Compound III was prepared as described previously for I (8). IR ($CDCl_3$): 3450, 2940, 2860, 1710, 1480, 1430, 1390, 1295, 1200, and 1100 cm^{-1}; NMR ($CDCl_3$): δ 5.6–6.1 (m, 1H), 4.37 (t, 2H), 2.05–2.65 (m, 4H), 1.03–1.7 (m, 6H), and 0.9 (t, 3H) ppm. *Anal.*—Calc. for $C_{10}H_{16}O_3$: C, 65.19; H, 8.75. Found: C, 63.98; H, 8.53 (hygroscopic because a part of the lactone always is hydrolyzed). [c] See *Experimental*. [d] Compound VI was prepared as described under *Experimental* for V. IR ($CDCl_3$): 3500, 2920, 2850, 1720, 1460, 1390, 1245, 1160, 1095, and 1010 cm^{-1}; NMR ($CDCl_3$): δ 3.76 (s, 3H), 3.38 (s, 1H), 1.05–2.5 (m, 17H), and 0.86 (t, 3H) ppm. *Anal.*—Calc. for $C_{13}H_{24}O_3$: C, 68.38; H, 10.59. Found: C, 68.60; H, 10.74. [e] Compound IX was prepared as described under *Experimental* for X. IR (film): 2900, 2840, 1710, 1645, 1460, 1440, 1390, 1360, 1250, 1090, and 770 cm^{-1}; NMR ($CDCl_3$): δ 6.86 (t, 1H), 3.7 (s, 3H), 2.4–2.7 (m, 1H), 2.0–2.3 (m, 2H), 1.5–1.7 (m, 4H), 1.1–1.5 (m, 8H), and 0.87 (t, 3H) ppm. *Anal.*—Calc. for $C_{13}H_{22}O_2$: C, 74.24; H, 10.54. Found: C, 74.13; H, 10.47. [f] Compound XI was prepared as described under *Experimental* for XII. IR (film): 2960, 2930, 2870, 1760, 1680, 1490, 1450, 1375, 1325, 1200, 1080, 1030, 960, 890, and 820 cm^{-1}; NMR ($CDCl_3$): δ 4.58 (t, 2H), 3.2–3.9 (m, 4H), and 1.2 (t, 3H) ppm. [g] Compound XIII was prepared as described under *Experimental* for XII. IR (film): 2900, 2830, 1750, 1675, 1460, 1370, 1325, 1190, and 1075 cm^{-1}; NMR ($CDCl_3$): δ 4.53 (t, 2H), 3.70 (t, 2H), 3.50 (t, 2H), 1.1–1.8 (m, 8H), and 0.87 (t, 3H) ppm. *Anal.*—Calc. for $C_{10}H_{17}NO_3$: C, 60.28; H, 8.60; N, 7.03. Found: C, 60.00; H, 8.51; N, 6.93. [h] Compound XVII was prepared as described previously (9). IR (film): 2920, 2840, 1745, 1470, 1415, 1385, 1350, 1290, 1225, 1205, 1140, 1125, 1090, and 940 cm^{-1}; NMR ($CDCl_3$): δ 4.17–4.60 (m, 3H), 3.74–4.10 (m, 2H), 1.7–2.2 (m, 2H), 1.1–1.7 (m, 6H), and 0.9 (t, 3H) ppm. *Anal.*—Calc. for $C_9H_{16}O_3$: C, 62.77; H, 9.36. Found: C, 62.89; H, 9.32. [i] Compound XVIII was prepared as described previously (9). IR (film): 2900, 2820, 1720, 1465, 1410, 1380, 1340, 1300, 1280, 1210, 1180, 1120, 1070, 1005, 940, 880, and 740 cm^{-1}; NMR ($CDCl_3$): δ 4.2–4.6 (m, 3H), 3.7–4.1 (m, 2H), 1.7–2.2 (m, 2H), 1.1–1.7 (m, 8H), and 0.9 (t, 3H) ppm. *Anal.*—Calc. for $C_{10}H_{18}O_3$: C, 64.49; H, 9.74. Found: C, 64.40; H, 9.80. [j] Compound XIX was prepared as described previously (9). IR (mineral oil): 2900, 2820, 1740, 1460, 1420, 1380, 1310, 1230, 1150, 1080, 960, 905, 860, and 740 cm^{-1}; NMR ($CDCl_3$): δ 4.2–4.65 (m, 3H), 3.75–4.1 (m, 2H), 1.7–2.2 (m, 2H), 1.1–1.7 (m, 10H), and 0.9 (t, 3H) ppm. *Anal.*—Calc. for $C_{11}H_{20}O_3$: C, 65.97; H, 10.07. Found: C, 66.22; H, 9.94.

evaporating, 5.3 g of a yellow oil was obtained and was sufficiently pure for the following reaction.

(2-Heptyl-1-hydroxycyclohexyl)carbonitrile—A mixture of 15 g (0.076 mole) of 2-heptylcyclohexanone, 19 g (0.22 mole) of acetone cyanohydrin, and 0.3 g of triethylamine was allowed to stand at room temperature for 2 hr. After acidification with sulfuric acid in acetone, the excess acetone cyanohydrin was distilled *in vacuo* (60°/1.0 mm Hg). The residue was taken up in ether and washed with water. After drying over sodium sulfate and evaporating, 15 g of a reddish oil was obtained and was sufficiently pure for further reactions.

Methyl (2-Heptyl-1-hydroxycyclohexyl)carboxylate (VII)—Five grams (0.0187 mole) of (1-acetoxy-2-heptylcyclohexyl)carbonitrile was dissolved in a mixture of 19 ml of acetic acid, 1 ml of acetic anhydride, and 4 ml of sulfuric acid. After standing at room temperature for 4 hr, 3 ml of water was added. Three grams (0.0435 mole) of granular sodium nitrite was added slowly to the cooled and stirred mixture. The suspension was stirred under cooling for 30 min and at room temperature for 1 hr. The mixture was poured into ice water and extracted three times with ether.

The combined extracts were evaporated *in vacuo*, and the residue was taken up with 20 ml of methanol. After addition of 10 ml of 40% KOH, the mixture was refluxed for 1 hr, poured into water, and extracted three times with ether. The aqueous phase was acidified with 10% H_2SO_4 and extracted three times with dichloromethane. After drying with anhydrous magnesium sulfate, an ethereal solution of diazomethane was added slowly to the stirred and cooled acid solution. After decolorization with activated charcoal and evaporation, the crude product was distilled *in vacuo* to give 2.5 g of a colorless oil (130° air bath temperature/0.35 mm Hg). A second distillation gave 2.4 g (50% yield) of pure product, bp 118°/0.3 mm Hg.

Anal.—Calc. for $C_{15}H_{28}O_3$: C, 70.27; H, 11.01. Found: C, 69.42; H, 10.70.

Ethyl 2-Butyl-1-cyclopentene-1-carboxylate (VIII)—Compound IV (2.3 g, 10.73 mmoles) in 2.5 ml of pyridine was treated dropwise at 0° with 1.4 ml of thionyl chloride, heated for 1 hr at 140° (oil bath temperature), and poured after cooling into ice water. The ester was extracted with ether, and the extract was dried over sodium sulfate–charcoal and concentrated *in vacuo*. Distillation (bp 74–75°/0.5 mm Hg) afforded VIII as a colorless liquid, 1.8 g (86% yield); IR (film): 2940, 2850, 1700, 1640, 1470, 1380, 1270, 1210, 1105, and 1045 cm^{-1}; NMR ($CDCl_3$): δ 4.18 (q, 2H), 1.6–2.8 (m, 8H), 1.26 (t, 3H), 1.1–1.16 (m, 4H), and 0.9 (t, 3H) ppm.

Anal.—Calc. for $C_{12}H_{20}O_2$: C, 73.43; H, 10.27. Found: C, 73.03; H, 10.03.

Methyl 6-Heptyl-1-cyclohexene-1-carboxylate (X)—2-*n*-Heptyl-1-hydroxycyclohexanecarbonitrile (7) (2.0 g, 8.95 mmoles) in 2.2 ml of pyridine was treated dropwise at 0° with 1.2 ml of thionyl chloride, and the mixture was heated for 1 hr at 140° (oil bath temperature) and poured after cooling into ice water. The desired product was extracted with ether, and the extract was dried over sodium sulfate–charcoal and concentrated *in vacuo* to yield 1.6 g of a light-yellow oil.

A solution of 6-*n*-heptylcyclohex-1-enecarbonitrile (1.3 g, 6.33 mmoles) in 2.6 ml of 50 volume % H_2SO_4 and 6.5 ml of acetic acid was stirred at 110° for 18 hr. To this ice-cooled and well-stirred reaction mixture, a solution of sodium nitrite (0.52 g, 7.6 mmoles) in 2 ml of water was added slowly. After stirring for 20 min at room temperature and 1.5 hr at 80°, the reaction mixture was poured into water and extracted with ether. The ether solution was extracted several times with dilute sodium hydroxide, and the combined alkaline layers were acidified with concentrated hydrochloric acid and extracted with ether. The ether layers were dried over sodium sulfate–charcoal and concentrated to yield 0.93 g of a yellow oil.

Esterification of 6-*n*-heptylcyclohex-1-enecarboxylic acid (0.93 g, 4.14 mmoles) with diazomethane (as described for V) afforded X after distillation (bp 124°/0.5 mm Hg) as a light-yellow oil, 0.84 g (95% yield); IR (film): 2900, 2840, 1715, 1645, 1440, 1390, 1360, 1250, 1090, and 770 cm^{-1}; NMR ($CDCl_3$): δ 6.84 (t, 1H), 3.7 (s, 3H), 2.4–2.65 (m, 1H), 2.0–2.3 (m, 2H), 1.1–1.7 (m, 16H), and 0.87 (t, 3H) ppm.

Anal.—Calc. for $C_{13}H_{26}O_2$: C, 75.58; H, 10.99. Found: C, 75.34; H, 10.82.

4-Butyl-2,3-morpholinedione (XII)—A mixture of diethyl oxalate (6.24 g, 42.7 mmoles), 2-(butylamino)ethanol (5.0 g, 42.7 mmoles), and potassium hydroxide (0.1 g) was heated at 110° for 2 hr, and the ethanol

that formed was distilled off. To remove all of the ethanol, the reaction mixture was heated for another 2 hr at 100° under reduced pressure (40 mm). After cooling to room temperature, the partially crystallized residue was acidified by the addition of 0.2 ml of concentrated sulfuric acid and dissolved in methylene chloride. The solution was washed several times with water, dried over sodium sulfate, and concentrated *in vacuo*. Recrystallization from ether afforded XII as colorless flakes, 5.5 g (75% yield); IR (KBr): 2920, 2840, 1745, 1670, 1480, 1440, 1360, 1180, 1070, 1030, and 940 cm^{-1}; NMR ($CDCl_3$): δ 4.53 (t, 2H), 3.70 (t, 2H), 3.50 (t, 2H), 1.14–1.8 (m, 4H), and 0.93 (t, 3H) ppm.

Anal.—Calc. for $C_8H_{13}NO_3$: C, 56.13; H, 7.65. Found: C, 56.39; H, 7.77.

Ethyl [[1-(Hydroxymethyl)propyl]amino]oxoacetate (XIV)—2-Amino-1-butanol (5.0 g, 56.1 mmoles) in 70 ml of anhydrous ethanol was added over 2.5 hr to a stirred solution of diethyl oxalate (8.2 g, 56.1 mmoles) in 50 ml of anhydrous ethanol at 50°. After cooling, some crystalline by-product was filtered off, and the solution was concentrated *in vacuo*. The residue was purified by low-pressure liquid chromatography (8% ethanol in dichloromethane) to give XIV as a light-yellow oil, 5.2 g (49% yield); IR ($CDCl_3$): 3370, 2960, 2880, 1740, 1690, 1540, 1470, 1385, 1320, 1280, 1220, and 1040 cm^{-1}; NMR ($CDCl_3$): δ 7.7 (d, 1H), 4.4 (q, 2H), 3.5–4.2 (m, 4H), 1.35 (t, 3H), 1.2–1.8 (m, 2H), and 0.93 (t, 3H) ppm.

Anal.—Calc. for $C_8H_{15}NO_4$: C, 50.78; H, 7.99; N, 7.40. Found: C, 50.65; H, 8.01; N, 7.30.

***In Vivo* Testing Cloth Test**—The cloth test screens limited quantities of chemicals as mosquito repellents. The test compound (50 mg) was placed in a 2-dram vial to which 0.75 ml of acetone or other solvent was added. When the chemical was thoroughly dissolved, a 50-cm^2 (5 × 10-cm) piece of muslin bandage was rolled, placed in the vial, and mixed with the solution, and the vial was sealed until the chemicals were tested. The rate of cloth treatment was 1.0 mg/cm^2. After treatment, the cloths were kept refrigerated in the vials for at least 24 hr.

At the start of a test, vials were removed from the refrigerator and allowed to warm to room temperature. The cloth then was removed from the vial, stapled over a 4 × 9-cm opening cut into a 12.7 × 20.3-cm file card, and allowed to dry for 15 min before testing.

The subject testing the compounds covered his or her arm with a nylon stocking and wore a rubber glove over the hand and wrist to protect against bites. The card and attached cloth patch were then taped over the nylon-covered forearm so that only the treated cloth allowed access to the skin by the mosquitoes. The arm was then exposed to a stock cage of *A. aegypti* mosquitoes (~1500) for 1 min. More than three bites through the treated cloth in 1 min denoted failure of the chemical. If the chemical did not fail, it was stored at room temperature and retested in 24 hr and daily thereafter until it failed. Two standard repellents, diethyltoluamide and dimethyl phthalate, were tested concurrently.

When a sufficient quantity of the candidate material was available, the minimum effective dose (MED) was determined. The testing method was the same, but the treatment rate was reduced by one-half until more than three bites per minute were received at the lowest dose. The minimum effective doses were determined only on the fresh (air dried for 15 min) and 1-day-old treatments.

RESULTS AND DISCUSSION

Several of the synthesized compounds were solids; and although two compounds (I and XII) were evaluated in the membrane feeder test (1), the others (XI, XIII, and XVII–XIX) were not evaluated since solids with melting points greater than 40° do not repel significantly.

Two compounds (IX and XII) showed weak repellent activity at high concentrations and attracted the mosquitoes at lower concentrations in the membrane feeder test. These compounds are under study in these laboratories for their effects on the lactic acid receptor of *A. aegypti* mosquitoes.

There is not always good agreement between the *in vitro* membrane feeder test and the *in vivo* cloth test. However, the membrane feeder test is useful as a rapid screening method when many compounds are studied.

The most interesting compounds from this series were III and VII, which will be studied further on mice and Mexican hairless dogs prior to any human skin tests. From the cloth test results, III seems to be the most promising.

REFERENCES

(1) L. C. Rutledge, M. A. Moussa, and C. J. Belletti, *Mosquito News*, **36**, 283 (1976).

(2) D. A. Carlson, C. Smith, H. K. Gouck, and D. R. Godwin, *J. Entomol.*, **66**, 329 (1973).

(3) E. E. Davis and P. G. Sokolove, *J. Comp. Physiol.*, **105**, 43 (1976).

(4) U. S. Department of Agriculture, Agricultural Handbook No. 69, May 1954.

(5) U. S. Department of Agriculture, Agricultural Handbook No. 340, Aug. 1967.

(6) F. L. James and W. H. Bryan, *J. Org. Chem.*, **23**, 1225 (1958).

(7) I. N. Nazarov *et al.*, *Zh. Obsch. Khim.*, **25**, 1345 (1955); through *Chem. Abstr.*, **50**, 4950e.

(8) L. Laloi, N. Noel, and H. Gault, French pat. 1,329,011 (June 7, 1963).

(9) S. Piekarski, *Oleagineux*, **17**, 785 (1962).

ACKNOWLEDGMENTS

Supported by U.S. Army Medical Research and Development Command Contract DADA 17-70-C-0112.

Technical assistance from U. Rosentreter is gratefully acknowledged.

Tissue Distribution of Antitumor Drugs Associated with Polyalkylcyanoacrylate Nanoparticles

P. COUVREUR *x, B. KANTE *, V. LENAERTS *, V. SCAILTEUR *, M. ROLAND *, and P. SPEISER ‡

Received July 26, 1979, from the **Laboratoire de Pharmacie Galénique, Faculté de Médecine, Université Catholique de Louvain, 1200 Brussels, Belgium*, and the ‡*School of Pharmacy, Federal Institute of Technology, 8006 Zürich, Switzerland.* Accepted for publication September 24, 1979.

Abstract □ Polymethylcyanoacrylate nanoparticles, polyethylcyanoacrylate nanoparticles, and free ^{3}H-dactinomycin and ^{3}H-vinblastine were studied with emphasis on their distribution pattern in rat tissues after intravenous administration. The adsorption of cytostatic drugs to polyalkylcyanoacrylate nanoparticles can modify drug distribution in tissues. Particularly with vinblastine, modification of drug disposition is important. Data are given concerning the formation and stability of nanoparticle–drug complexes. Polyalkylcyanoacrylate nanoparticles seem to be an interesting drug carrier owing to their size, structure, degradability, and drug sorptive properties.

Keyphrases □ Polymethylcyanoacrylate nanoparticles—with adsorbed dactinomycin and vinblastine, distribution patterns in rats, compared to polyethylcyanoacrylate nanoparticles □ Polyethylcyanoacrylate nanoparticles—with adsorbed dactinomycin and vinblastine, distribution patterns in rats, compared to polymethylcyanoacrylate nanoparticles □ Dactinomycin—on polymethylcyanoacrylate and polyethylcyanoacrylate nanoparticles, distribution patterns in rats □ Vinblastine—on polymethylcyanoacrylate and polyethylcyanoacrylate nanoparticles, distribution patterns in rats □ Drug carriers—polymethylcyanoacrylate and polyethylcyanoacrylate nanoparticles, distribution patterns of adsorbed dactinomycin and vinblastine in rats

The problem of directing a cytostatic agent to specific sites is a current topic of research. Specific targeting of drug carriers may improve the anticancer activity and lower the general toxicity.

The use of endocytizable and lysosomotropic carriers such as liposomes (1–3) and DNA complexes (4, 5) appears promising, and new lysosomotropic carriers like albumin microspherules (6) and acrylic nanocapsules (7, 8) have been developed. Entrapment of fluorescein in such polyacrylamide nanocapsules significantly increases dye uptake by cultured fibroblasts and allows its accumulation into lysosomes, which are cell compartments in which fluorescein does not spontaneously accumulate (9, 10). However, the polymer used to prepare nanocapsules is unlikely to be digested by lysosomal enzyme, which might restrict its clinical use.

It has been demonstrated that polyalkylcyanoacrylate nanoparticles are potential lysosomotropic carriers because of their size, structure, and sorptive properties (11, 12). Such degradable nanoparticles are able to adsorb various molecules, including antimitotic drugs, reproducibly (11, 13, 14). The hydrolysis rate is dependent on the alkyl chain length of the cyanoacrylic monomer, which allows the drug release kinetics to be selected (13).

This study compared the tissue distribution of free dactinomycin and vinblastine with that of the adsorbed drugs on polymethylcyanoacrylate and polyethylcyanoacrylate nanoparticles after intravenous administration to rats.

EXPERIMENTAL

Preparation of ^{3}H-Dactinomycin and ^{3}H-Vinblastine Nanoparticles—Either ^{3}H-dactinomycin[1] (40 μl) or ^{3}H-vinblastine[1] (75 μl) was added to 1.5 ml of an aqueous solution containing 0.5% polysorbate[2] 20 in 0.01 *M* HCl. Then 17 μl of monomer[3] (methyl- or ethylcyanoacrylate) was dispersed under mechanical stirring.

After polymerization (30 min), the milky suspensions obtained were buffered to pH 7 using 0.05 ml of 1.0 *M* NaOH and 2.0 ml of phosphate buffer [containing 25% (v/v) of 0.2 *M* KH_2PO_4 and 15% (v/v) of 0.2 *M* NaOH]. The colloidal suspension obtained after filtration through a 0.8-μm filter[4] was diluted with an equal volume of the phosphate buffer.

The solutions of free ^{3}H-dactinomycin and ^{3}H-vinblastine were prepared as described for the nanoparticles but without monomer addition.

Determination of Drug Adsorbed on Nanoparticles—*Dactinomycin*—Dactinomycin (3.3 mg) and ^{3}H-dactinomycin (20 μl) were dissolved in 50 ml of acid containing polysorbate 20. Monomers were then added and polymerized as already described.

The nanospherule suspensions (10 ml) were centrifuged at 20,000 rpm. After separation and dissolution of the sediment in dimethylformamide, the ^{3}H-dactinomycin was measured in both the sediment and the supernate by scintillation counting as described.

Vinblastine—Vinblastine (17.5 mg) and ^{3}H-vinblastine (20 μl) were dissolved in 50 ml of acid containing polysorbate 20. The determination of the amount of vinblastine adsorbed on polymethyl- and polyethylcyanoacrylate nanoparticles was made in the same manner as for ^{3}H-dactinomycin.

Sample Preparation for Scintillation Counting—One milliliter of the supernatant and sediment solutions was pretreated with 0.5 *N* quaternary ammonium hydroxide in toluene[5] (0.75 ml). Isopropanol (0.75 ml) and 30% H_2O_2 (0.5 ml) were added to decolorize the samples. After 60 min, xylol–0.5 *M* HCl[6] (9:1) (15 ml) was added, and counting was performed in a liquid scintillation counter[7]. Quench correction was obtained using a channels ratio method. The results are expressed in percent of the drug adsorbed on the nanospherules.

Injection of ^{3}H-Dactinomycin and ^{3}H-Vinblastine in Free Form and Nanoparticle-Associated Forms—Three groups of 20 male Wistar rats (180–220 g), anesthetized with ether, were injected by puncture in femoral vena. Each group received one of the following forms of ^{3}H-dactinomycin in a single injection of 0.80 ml: free drug and polymethyl- and polyethylcyanoacrylate nanoparticles. At 0.5, 3, and 24 hr, six, eight, and six rats, respectively, were killed by decapitation in each of the three groups. Samples of blood and various tissues were removed for ^{3}H-analysis.

The differential tissue distribution of ^{3}H-vinblastine was determined in the same manner on two groups of 18 rats. Each group received free or adsorbed ^{3}H-vinblastine, and six rats were killed in each of the two groups at the same time intervals.

Preparation of Rat Tissues for ^{3}H-Analysis—Samples of fresh tissues including spleen, small intestine, muscle, kidneys, liver, and lungs were taken. For each organ except the spleen, three samples weighing 45–55 mg were each solubilized in 1 ml of 0.5 *N* quaternary ammonium hydroxide. For the spleen, 20-mg samples were used. After solubilization (about 4 hr), samples were decolorized using 0.2 ml of 30% H_2O_2, followed by warming at 40° for 30 min.

For the blood analysis, 200 μl was solubilized in 1.5 ml of quaternary

[1] M.B.L.E., Radiochemical Centre, Amersham, England.
[2] Tween 20, I.C.I., Atlas International Division, Everberg, Belgium.
[3] Loctite, Dublin, Ireland.
[4] Millipore, Buc, France.
[5] Soluene, Packard Instruments S.A., Brussels, Belgium.
[6] Instagel, Packard Instruments S.A., Brussels, Belgium.
[7] Computer Philips PW 4510, M.B.L.E., Brussels, Belgium.

0022-3549/80/0200-0199$01.00/0
© 1980, American Pharmaceutical Association

Table I—Efficiency of Drug Sorption on Nanoparticles

Drug	Concentration of Suspension, μg/ml	Sorption, % Polymethyl-cyanoacrylate	Sorption, % Polyethyl-cyanoacrylate
Dactinomycin	55	92.8	86.5
Vinblastine	350	35.8	80.0
Vinblastine	45	67.2	85.0

ammonium hydroxide in toluene–isopropanol (1:1) and decolorized with 0.5 ml of 30% H_2O_2.

After cooling at room temperature, 15 ml of the scintillation fluid was added to each sample, and counting was performed in the liquid scintillation analyzer.

For each form of ^{3}H-dactinomycin or ^{3}H-vinblastine used, the amount of radioactivity injected was calculated on the basis of analysis of triplicate samples of 0.2 ml measured with the same syringe used for injection. These samples were treated as described for the tissues.

Drug concentration in each tissue analyzed was expressed in microcuries × 10^{-3} per gram of tissue and per microcurie injected in the whole animal.

RESULTS AND DISCUSSION

Formation and Stability of Nanoparticle–Drug Complexes—Dactinomycin and vinblastine were adsorbed on the nanoparticles with high efficiency (Table I). Although the percentage of adsorbed drug declined with increasing amounts, substantial amounts of dactinomycin and vinblastine can be sorbed. The percentages of drug adsorbed to the nanoparticles were in all cases higher than those obtained with entrapment in liposomes (15, 16). Furthermore, the amounts of drug adsorbed on nanoparticles were reproducible.

For a 55-μg/ml suspension of dactinomycin, 92.8 and 86.5% of the drug were adsorbed on polymethyl- and polyethylcyanoacrylate nanoparticles, respectively, when the drug was incorporated before polymerization. In contrast, when a suspension of prepared nanoparticles was mixed with an aqueous solution of free dactinomycin, the percentage of the drug adsorbed on the particles decreased to 66.0 and 64.5% for polymethyl- and polyethylcyanoacrylate nanoparticle forms, respectively. These results are in agreement with the porous structure of particles observed after cryofracture by electron microscopy (11). Indeed, when the drug is added after the nanoparticles are formed, the inner surface of the carrier probably is no longer available for adsorption.

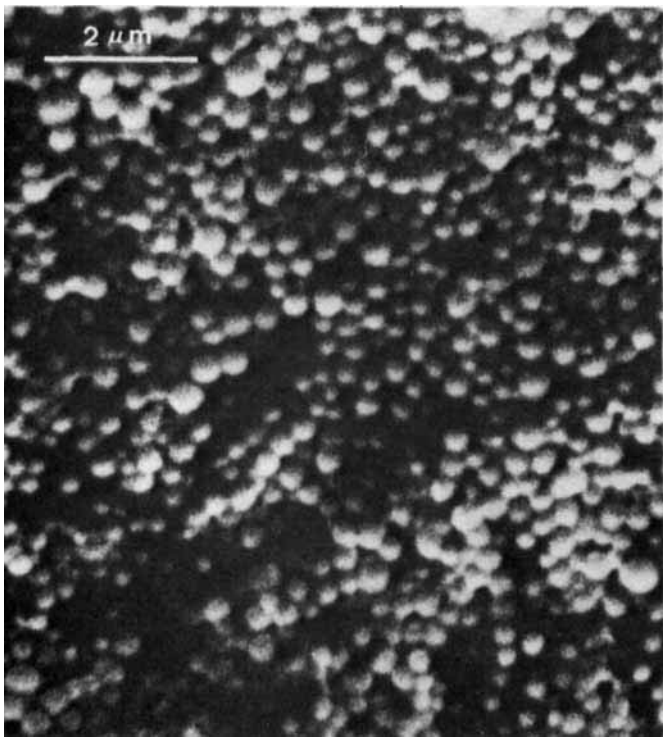

Figure 1—*Morphological appearance of dactinomycin associated to polymethylcyanoacrylate nanoparticles at the scanning electron microscope. Thickness of the gold layer was 100 nm.*

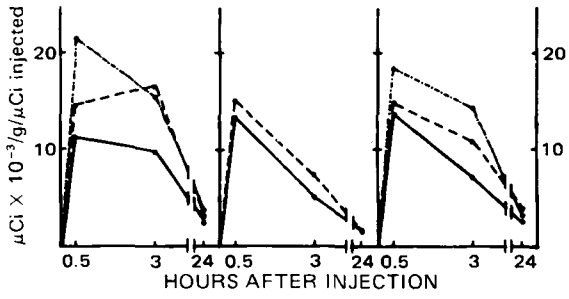

Figure 2—*Tissue concentrations [small intestine (left), liver (center), and lungs (right)] in rats at various times after administration of ^{3}H-dactinomycin. A single intravenous injection of polymethyl- (·–·) or polyethyl- (– –) cyanoacrylate nanoparticles or free (—) dactinomycin was given to each rat. Each point is the mean value from at least six animals.*

A scanning electron microscopic[8] study showed that drug adsorption at the surface of the particles induces no morphological modification of these nanoparticles. Figure 1 shows spherical dactinomycin–polymethylcyanoacrylate nanoparticles with a diameter of ~200–300 nm, considering the thickness of the gold layer (100 nm) used for sample preparation.

Dactinomycin Distribution in Rat Tissues—Table II shows the concentrations of ^{3}H-dactinomycin found in the blood, spleen, small intestine, muscle, kidney, liver, and lung samples after administration of either free dactinomycin or nanoparticle-adsorbed forms. Each value at various times after the injection represents a mean result obtained with six or eight animals and with three pretreatment levels from each tissue analyzed. A statistical analysis (Student t test) was carried out to determine, with a probability of 0.975, the significant differences in the tissue distributions induced by adsorption.

Significant increases of ^{3}H-dactinomycin uptake were obtained for the small intestine and lungs of polymethylcyanoacrylate nanoparticle-injected rats at 0.5 hr (Fig. 2). Three hours after the injection, the ^{3}H-dactinomycin content in both of these two tissues decreased, but the radioactivity levels remained higher than those found in the small in-

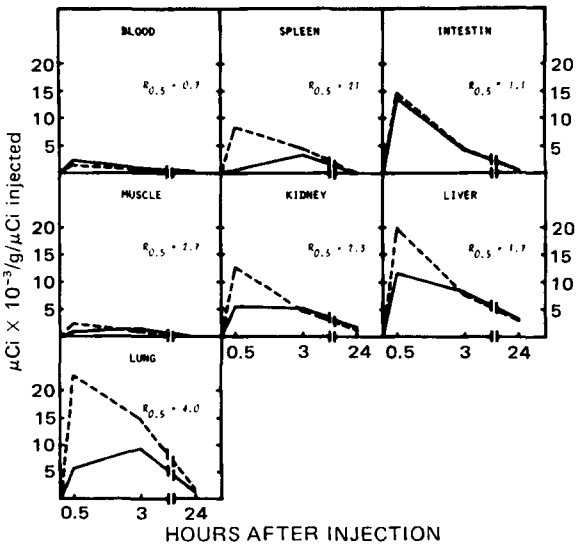

Figure 3—*Tissue concentrations (blood, spleen, intestine, muscle, kidneys, liver, and lungs) of free (—) and polyethylcyanoacrylate nanoparticle (– –) ^{3}H-vinblastine forms at various times after intravenous administration. Each point is the mean value from a minimum of six animals. The $R_{0.5}$ represents the relation between vinblastine adsorbed on polyethylcyanoacrylate nanoparticles and free vinblastine tissue concentration at 30 min after injection ($R_{0.5} = PEN_{0.5}/F_{0.5}$).*

[8] "Super Mini SM," International Scientific Instruments, Mountain View, Calif.

Table II—Tissue Distribution of Drug at 3 hr Postinjection

Organ	F^a	PMN[a]	PEN[a]	t_{stud} ($p = 0.975$) PMN	t_{stud} ($p = 0.975$) PEN	PNM or PEN / F PMN	PNM or PEN / F PEN
Blood	1.2	0.5	1.2	4.17	0.37	0.42	1.00
Spleen	15.0	15.3	17.5	0.16	1.51	1.02	1.17
Small intestine	9.8	15.3	16.8	2.70	3.76	1.56	1.71
Muscle	2.2	3.1	2.2	1.33	0.06	1.41	1.00
Kidneys	9.6	14.1	12.8	1.79	3.29	1.47	1.33
Liver	4.9	5.6	6.9	0.93	3.69	1.14	1.41
Lungs	6.8	14.3	10.5	3.85	3.80	2.10	1.54

[a] Units are microcuries × 10^{-3} per gram per microcurie injected. t_{stud} ($p = 0.975$) represents the results of the statistical analysis (Student test) for a probability of 0.975. Underlined numbers correspond to a significant difference between free (F), polymethyl- (PMN), and polyethyl- (PEN) cyanoacrylate nanoparticle forms for the chosen probability.

testine and lungs of rats injected with the free drug. No significant difference was found 24 hr after injection.

Similar observations were made for polyethylcyanoacrylate nanoparticles. Thus, the small intestine and lungs of the injected rats showed significantly higher contents of ^{3}H-dactinomycin at 3 hr in comparison with free drug. Furthermore, the ^{3}H-dactinomycin concentration in the liver was higher for the polyethylcyanoacrylate nanoparticle form; this observed difference was slight but significant (Table II).

In both the spleen and kidneys, the decrease of radioactivity remained similar for all three forms of ^{3}H-dactinomycin during the experiment. Except for the lungs and small intestine, the tissue distribution of ^{3}H-dactinomycin was poorly modified by adsorbing it on nanoparticles, in spite of generally higher drug levels in tissues of rats injected with nanoparticles. Previous studies on dactinomycin tissue distribution in mice showed that the small intestine retains high dactinomycin concentrations (17, 18). The present results are similar to these observations, but it was surprising to find still higher concentrations of radioactivity in the intestinal wall of rats injected with ^{3}H-dactinomycin adsorbed on nanoparticles. Likewise, the poor accumulation of the nanoparticle forms in the liver and the spleen is difficult to explain. The tissue distribution of dactinomycin nanoparticles was comparable to that observed when the drug was incorporated into the aqueous phase of multilamellar liposomes (18).

^{3}H-Vinblastine in Rat Tissues—Table III lists the ^{3}H-concentration after the injection of free drug or polyethylcyanoacrylate nanoparticle–^{3}H-vinblastine. Concentrations of ^{3}H-vinblastine found in tissues after administration of nanoparticles were generally higher than those obtained with the free form. This result was particularly remarkable at 0.5 hr after the injection and for tissues rich in reticuloendothelial macrophage cells such as the liver, spleen, and lungs (Fig. 3). Thus, 0.5 hr after injection, the spleen accumulated 21-fold more nanoparticles with adsorbed ^{3}H-vinblastine than free drug. Likewise, after the same time, the drug concentrations observed with nanoparticles were 1.7-fold higher in the liver, fourfold higher in the lungs, and 2.3-fold higher in the kidneys compared to levels with free vinblastine.

More surprising was the higher concentration of the nanoparticles compared to the free form in the muscle. Indeed, the muscle retained 2.7-fold more vinblastine when the drug was adsorbed on polyethylcyanoacrylate nanoparticles. At 30 min after injection, the tissue concentrations observed with nanoparticles were generally two- to 20-fold higher than with the free drug (Table III). Thus, the kinetics of tissue uptake of the nanoparticles were quite different compared to those of the free form (Fig. 3). Maximum levels were observed after 0.5 hr for the nanoparticle formulation and after 3 hr for the free form, except for the liver and blood. Differences in the tissue drug concentrations were more marked a short time after injection.

Table III—Tissue Accumulation of Drug at 0.5 hr Postinjection

Organ	F^a	PEN[a]	t_{stud} ($p = 0.975$)	PEN / F
Blood	2.2	1.5	1.54	0.7
Spleen	0.4	8.4	6.17	21.0
Small intestine	13.8	14.9	0.17	1.1
Muscle	0.8	2.2	4.69	2.7
Kidneys	5.5	12.8	8.34	2.3
Liver	11.6	20.0	3.84	1.7
Lungs	5.6	22.7	8.97	4.0

[a] Units are microcuries × 10^{-3} per gram per microcurie injected. t_{stud} ($p = 0.975$) represents the results of the statistical analysis (Student test). Underlined numbers correspond to a significant difference between free (F) and polyethylcyanoacrylate nanoparticle (PEN) forms for a probability of 0.975.

Earlier studies with liposomes (19, 20) showed preferential cellular capture by the liver and spleen. The present results show that the ^{3}H-vinblastine nanoparticles have a broader tissue distribution than liposomes and provide evidence that nanoparticles can be used to modify tissue distribution of vinblastine. The significant difference in the accumulation in the muscle between free and nanoparticle-adsorbed vinblastine cannot now be explained, but it is interesting to note that cultured fibroblasts, which have a moderate endocytic capacity, accumulate polyacrylamide nanoparticles (9).

These results agree qualitatively with previous reports in that the favored sites for free vinblastine include the spleen, intestine, lungs, and liver (19, 21).

CONCLUSIONS

The present study provides evidence that the adsorption of cytotoxic drugs to polyalkylcyanoacrylate nanoparticles can modify the drug distribution pattern in tissues. This effect was particularly marked for the vinblastine nanoparticles. Furthermore, the results obtained with dactinomycin and vinblastine show that the differential tissue distribution (between free and adsorbed forms) was not only related to the carrier but also depended on the active molecule. For example, both free vinblastine and dactinomycin had a marked affinity for the small intestine, which was enhanced with dactinomycin adsorbed on nanoparticles but unchanged with vinblastine nanoparticles. In contrast, the increase of the uptake of nanoparticle-adsorbed drugs by the liver and spleen was more marked, comparatively, for vinblastine than for dactinomycin.

Such results are in agreement with the observations reported for liposomes (22, 23). Indeed, 3 hr after injection of radiolabeled free drug or the liposome-encapsulated form, the tissue distribution was quite different for dactinomycin, cytosine arabinose, vinblastine, $^{86}Rb^+$, or ethylenediaminetetraacetate.

All modifications of distribution patterns of the examined drugs were observed at the earlier times after administration (0.5 or 3 hr). Thus, the effect of the carrier seems rapid, especially with vinblastine nanoparticles. Such observations are compatible with the rapidity of endocytosis, which may be carried out in minutes (24).

Moreover, these results show that there is a general increased uptake of cytostatic drugs when they are adsorbed on nanoparticles. But this increase is not uniform for all tissues. Differential and selective increases in tissue uptake of cytotoxic drugs will be of interest in cancer chemotherapy. Polyalkylcyanoacrylate nanoparticles could be useful in this area. The action of nanoparticles associated with cytostatic agents on tumor-bearing animals and the selective uptake by different cell types will be investigated.

REFERENCES

(1) G. Gregoriadis, *FEBS Lett.*, **36**, 292 (1973).

(2) G. Gregoriadis, E. J. Wills, C. P. Swain, and A. S. Tavill, *Lancet*, **1**, 1313 (1974).

(3) M. J. Kosloski, F. Rosen, R. J. Milholland, and D. Papahajopoulos, *Cancer Res.*, **38**, 2848 (1978).

(4) A. Trouet, D. Deprez-Decampeneere, and C. de Duve, *Nature*, **239**, 110 (1972).

(5) A. Trouet, D. Deprez-Decampeneere, M. De Smedt-Malengreaux, and G. Atassi, *Eur. J. Cancer*, **10**, 405 (1974).

(6) P. Kramer and T. Burnstein, *Life Sci.*, **19**, 515 (1976).

(7) P. Speiser, *Prog. Colloid Polym. Sci.*, **59**, 48 (1976).

(8) J. Marty, R. C. Oppenheim, and P. Speiser, *Pharm. Acta Helv.*, **53**, 17 (1978).
(9) P. Couvreur, P. Tulkens, M. Roland, A. Trouet, and P. Speiser, *FEBS Lett.*, **84**, 323 (1977).
(10) P. Couvreur, M. Roland, P. Speiser, A. Trouet, and P. Tulkens, *Acta Pharm. Technol., Suppl. 7*, **1979**, 185.
(11) P. Couvreur, B. Kante, M. Roland, P. Guiot, P. Baudhuin, and P. Speiser, *J. Pharm. Pharmacol.*, **31**, 331 (1979).
(12) P. Couvreur, B. Kante, and M. Roland, *Pharm. Acta Helv.*, **53**, 341 (1978).
(13) P. Couvreur, M. Roland, and P. Speiser, Belgian pat. 189.366 (1978).
(14) P. Couvreur, B. Kante, M. Roland, and P. Speiser, *J. Pharm. Sci.*, **68**, 1521 (1979).
(15) G. Gregoriadis, *FEBS Lett.*, **36**, 292 (1973).
(16) J. H. Fendler and A. Romero, *Life Sci.*, **20**, 1109 (1977).
(17) H. S. Schwartz, J. E. Sodergren, and R. Y. Ambaye, *Cancer Res.*, **28**, 192 (1968).
(18) Y. E. Rahman, W. E. Kisieleski, E. M. Buess, and E. A. Cerny, *Eur. J. Cancer*, **11**, 883 (1975).
(19) R. L. Juliano and D. Stamp, *Biochem. Pharmacol.*, **27**, 21 (1978).
(20) H. K. Kimelberg, T. F. Tracy, S. M. Biddlecome, and R. S. Bourke, *Cancer Res.*, **36**, 2949 (1976).
(21) R. J. Owellen and D. W. Donnigan, *J. Med. Chem.*, **15**, 894 (1972).
(22) H. K. Kimelberg, E. Mayhew, and D. Papahajopoulos, *Life Sci.*, **17**, 715 (1975).
(23) M. M. Jonah, E. A. Cerny, and Y. E. Rahman, *Biochim. Biophys. Acta*, **401**, 336 (1975).
(24) P. Tulkens, thesis, University of Louvain, Louvain-en-Woluwe, Belgium, 1979, p. 23.

ACKNOWLEDGMENTS

Supported in part by the Belgian "Fonds National de la Recherche Scientifique" and by the "Fonds de Developpement Scientifique" of the University of Louvain, Belgium. P. Couvreur is "Chargé de Recherches" to the Belgian "Fonds National de la Recherche Scientifique."

The authors thank Dr. Dunn, Loctite Co., Ireland, for a generous gift of the monomer samples and Dr. Kramp, Merck Sharp & Dohme, Brussels, Belgium, for a generous gift of dactinomycin.

Effect of Carnitine Analogs on Carnitine Acetyltransferase

MARVIN R. BOOTS *x, MARY LYNN WOLFE ‡, SHARON G. BOOTS *§, and JESSE L. BOBBITT ‡

Received June 1, 1979, from the **Department of Pharmaceutical Chemistry, Health Sciences Division, Medical College of Virginia, Virginia Commonwealth University, Richmond, VA 23298*, and the ‡*Biochemical Research Department, Lilly Research Laboratories, Division of Eli Lilly and Company, Indianapolis, IN 46240.* Accepted for publication September 20, 1979. §Present address: Department of Chemistry, Stanford University, Stanford, CA 94305.

Abstract □ Carnitine analogs with various substituents on the nitrogen were tested for their effect on carnitine acetyltransferase from rat sperm and pigeon breast. A radiometric assay was used to measure the formation of acetylcarnitine in the presence of other enzymes that competed for acetyl coenzyme A in the sperm preparation. The apparent enzyme inhibition caused by the analogs was explained by the analogs serving as alternative substrates with higher K_m and lower V_{max} values. The analogs had no effect on whole sperm.

Keyphrases □ Carnitine analogs—effect on carnitine acetyltransferase, spectrophotometric and radiometric measurements, kinetic parameters, *in vitro* □ Kinetics—analysis of carnitine analogs on carnitine acetyltransferase activity, spectrophotometric and radiometric measurements □ Spectrophotometry—analysis of carnitine analogs on carnitine acetyltransferase activity, kinetics

The primary importance of carnitine acetyltransferase (EC 2.3.1.7) in mitochondria is not known. Since the enzyme is found in high levels in cells that derive much of their energy requirements from lipid metabolism, it was thought that its major function was in lipid metabolism (1). For example, pigeon breast and heart muscle are common sources of the enzyme. The enzyme also is abundant in sperm (2), where the acetylation of carnitine may serve as an important regulator of both lipid and carbohydrate metabolism (3, 4).

Carnitine analogs that inhibit the enzyme may alter the path of energy metabolism (5). Rat and mouse sperm offer a convenient means of testing the biological activity of carnitine analogs. Carnitine appears to be important for sperm metabolism. Not only are carnitine acetyltransferase levels high in sperm, but carnitine is also in high concentration in epididymal fluid (6). The sperm can be isolated easily with little contamination by other cells, and they can be checked easily for viability by examining their motility under a microscope.

Unfortunately, the most commonly used spectrophotometric assay for carnitine acetyltransferase cannot be used with crude sperm enzyme; this assay measures the disappearance of the thiol ester bond of acetyl coenzyme A, and competing reactions using acetyl coenzyme A interfere with this measurement unless the enzyme is purified. However, crude enzyme can be assayed by measuring the transfer of labeled acetate to acetylcarnitine, which can be precipitated as the periodide (7). Since carnitine acetyltransferase probably is essential for sperm function, any inhibitor also should be detected with whole sperm by changes in the fertilization rate.

In this study, carnitine analogs were examined for their effect on the enzyme in both crude sperm preparations and crystalline pigeon breast enzyme. In addition, selected analogs were examined in various test systems to determine the cellular effects of the analogs.

EXPERIMENTAL

Carnitine Analogs—The *dl*-carnitine analogs (I–VII) were prepared as described previously (5).

Spectrophotometric Assay—The spectrophotometric assay of carnitine acetyltransferase activity measured the decrease in absorbance[1] of the thiol ester bond of acetyl coenzyme A at 232 nm (8). The reaction mixture in each cell contained 1.0 m*M* L-carnitine[2], 0.1 m*M* acetyl coenzyme A[2], and the carnitine analog of the desired concentration. The reaction was carried out at 25° in 100 m*M* tromethamine buffer, pH 8.0,

[1] Gilford spectrophotometer.
[2] Acetyl coenzyme A, PL Biochemicals.

0022-3549/80/0200-0202$01.00/0
© 1980, American Pharmaceutical Association

(8) J. Marty, R. C. Oppenheim, and P. Speiser, *Pharm. Acta Helv.*, **53**, 17 (1978).
(9) P. Couvreur, P. Tulkens, M. Roland, A. Trouet, and P. Speiser, *FEBS Lett.*, **84**, 323 (1977).
(10) P. Couvreur, M. Roland, P. Speiser, A. Trouet, and P. Tulkens, *Acta Pharm. Technol., Suppl. 7*, **1979**, 185.
(11) P. Couvreur, B. Kante, M. Roland, P. Guiot, P. Baudhuin, and P. Speiser, *J. Pharm. Pharmacol.*, **31**, 331 (1979).
(12) P. Couvreur, B. Kante, and M. Roland, *Pharm. Acta Helv.*, **53**, 341 (1978).
(13) P. Couvreur, M. Roland, and P. Speiser, Belgian pat. 189.366 (1978).
(14) P. Couvreur, B. Kante, M. Roland, and P. Speiser, *J. Pharm. Sci.*, **68**, 1521 (1979).
(15) G. Gregoriadis, *FEBS Lett.*, **36**, 292 (1973).
(16) J. H. Fendler and A. Romero, *Life Sci.*, **20**, 1109 (1977).
(17) H. S. Schwartz, J. E. Sodergren, and R. Y. Ambaye, *Cancer Res.*, **28**, 192 (1968).
(18) Y. E. Rahman, W. E. Kisieleski, E. M. Buess, and E. A. Cerny, *Eur. J. Cancer*, **11**, 883 (1975).
(19) R. L. Juliano and D. Stamp, *Biochem. Pharmacol.*, **27**, 21 (1978).
(20) H. K. Kimelberg, T. F. Tracy, S. M. Biddlecome, and R. S. Bourke, *Cancer Res.*, **36**, 2949 (1976).
(21) R. J. Owellen and D. W. Donnigan, *J. Med. Chem.*, **15**, 894 (1972).
(22) H. K. Kimelberg, E. Mayhew, and D. Papahajopoulos, *Life Sci.*, **17**, 715 (1975).
(23) M. M. Jonah, E. A. Cerny, and Y. E. Rahman, *Biochim. Biophys. Acta*, **401**, 336 (1975).
(24) P. Tulkens, thesis, University of Louvain, Louvain-en-Woluwe, Belgium, 1979, p. 23.

ACKNOWLEDGMENTS

Supported in part by the Belgian "Fonds National de la Recherche Scientifique" and by the "Fonds de Developpement Scientifique" of the University of Louvain, Belgium. P. Couvreur is "Chargé de Recherches" to the Belgian "Fonds National de la Recherche Scientifique."

The authors thank Dr. Dunn, Loctite Co., Ireland, for a generous gift of the monomer samples and Dr. Kramp, Merck Sharp & Dohme, Brussels, Belgium, for a generous gift of dactinomycin.

Effect of Carnitine Analogs on Carnitine Acetyltransferase

MARVIN R. BOOTS *x, MARY LYNN WOLFE ‡, SHARON G. BOOTS *§, and JESSE L. BOBBITT ‡

Received June 1, 1979, from the **Department of Pharmaceutical Chemistry, Health Sciences Division, Medical College of Virginia, Virginia Commonwealth University, Richmond, VA 23298*, and the ‡*Biochemical Research Department, Lilly Research Laboratories, Division of Eli Lilly and Company, Indianapolis, IN 46240.* Accepted for publication September 20, 1979. §Present address: Department of Chemistry, Stanford University, Stanford, CA 94305.

Abstract □ Carnitine analogs with various substituents on the nitrogen were tested for their effect on carnitine acetyltransferase from rat sperm and pigeon breast. A radiometric assay was used to measure the formation of acetylcarnitine in the presence of other enzymes that competed for acetyl coenzyme A in the sperm preparation. The apparent enzyme inhibition caused by the analogs was explained by the analogs serving as alternative substrates with higher K_m and lower V_{max} values. The analogs had no effect on whole sperm.

Keyphrases □ Carnitine analogs—effect on carnitine acetyltransferase, spectrophotometric and radiometric measurements, kinetic parameters, *in vitro* □ Kinetics—analysis of carnitine analogs on carnitine acetyltransferase activity, spectrophotometric and radiometric measurements □ Spectrophotometry—analysis of carnitine analogs on carnitine acetyltransferase activity, kinetics

The primary importance of carnitine acetyltransferase (EC 2.3.1.7) in mitochondria is not known. Since the enzyme is found in high levels in cells that derive much of their energy requirements from lipid metabolism, it was thought that its major function was in lipid metabolism (1). For example, pigeon breast and heart muscle are common sources of the enzyme. The enzyme also is abundant in sperm (2), where the acetylation of carnitine may serve as an important regulator of both lipid and carbohydrate metabolism (3, 4).

Carnitine analogs that inhibit the enzyme may alter the path of energy metabolism (5). Rat and mouse sperm offer a convenient means of testing the biological activity of carnitine analogs. Carnitine appears to be important for sperm metabolism. Not only are carnitine acetyltransferase levels high in sperm, but carnitine is also in high concentration in epididymal fluid (6). The sperm can be isolated easily with little contamination by other cells, and they can be checked easily for viability by examining their motility under a microscope.

Unfortunately, the most commonly used spectrophotometric assay for carnitine acetyltransferase cannot be used with crude sperm enzyme; this assay measures the disappearance of the thiol ester bond of acetyl coenzyme A, and competing reactions using acetyl coenzyme A interfere with this measurement unless the enzyme is purified. However, crude enzyme can be assayed by measuring the transfer of labeled acetate to acetylcarnitine, which can be precipitated as the periodide (7). Since carnitine acetyltransferase probably is essential for sperm function, any inhibitor also should be detected with whole sperm by changes in the fertilization rate.

In this study, carnitine analogs were examined for their effect on the enzyme in both crude sperm preparations and crystalline pigeon breast enzyme. In addition, selected analogs were examined in various test systems to determine the cellular effects of the analogs.

EXPERIMENTAL

Carnitine Analogs—The *dl*-carnitine analogs (I–VII) were prepared as described previously (5).

Spectrophotometric Assay—The spectrophotometric assay of carnitine acetyltransferase activity measured the decrease in absorbance[1] of the thiol ester bond of acetyl coenzyme A at 232 nm (8). The reaction mixture in each cell contained 1.0 m*M* L-carnitine[2], 0.1 m*M* acetyl coenzyme A[2], and the carnitine analog of the desired concentration. The reaction was carried out at 25° in 100 m*M* tromethamine buffer, pH 8.0,

[1] Gilford spectrophotometer.
[2] Acetyl coenzyme A, PL Biochemicals.

0022-3549/80/0200-0202$01.00/0
© 1980, American Pharmaceutical Association

Table I—Radiometric Precipitation Assay of Carnitine Acetyltransferase Inhibition

Compound	Inhibitors, mg/ml					
	1	2	4	1	2	4
	Inhibition of Sperm Enzyme, %			Inhibition of Pigeon Breast Enzyme, %		
I	15	24	50	12	25	45
II	25	38	45	30	45	50
III	28	38	42	30	45	45
IV	12	20	35	10	18	25
V	0	3	10	10	18	—
VI	5	12	38	10	20	30
VII	0	5	12	5	12	25

after addition of ~20 microunits (80 units/mg of protein) of pigeon breast enzyme[3].

Radiometric Assay—The assay using precipitation of labeled acetylcarnitine was a modification of the semimicro method described by McCaman *et al.* (7). The 0.25-ml reaction mixture contained 24 m*M* DL-carnitine (4.8 mg/ml), 0.5 m*M* ^{3}H-acetyl coenzyme A[4] tritium-labeled to ~1 mCi/mmole, the carnitine analog at various concentrations, and 0.1 *M* phosphate buffer, pH 7.5, with 0.5 m*M* ethylenediaminetetraacetate. The exact amount of sperm or pigeon breast enzyme was adjusted to stay within the linear portion of the standard curve.

After 30 min at 37°, the reaction was stopped, and the solution was deproteinized with 10 μl of cold 50% (w/v) trichloroacetic acid. After centrifugation, 0.20 ml of the supernate was transferred to another small centrifuge tube, and 0.30 ml of potassium iodide–iodine solution was added to precipitate the carnitine, labeled acetylcarnitine, and carnitine analogs as the periodides. The precipitate usually was allowed to stand overnight at 4° to ensure precipitation when the analogs were present. The precipitate was washed with 0.6 ml of cold 2 *N* H_2SO_4, dissolved in 10 ml of scintillator solution[5], and decolorized with 0.3 ml of an organic base[6].

Enzymes—Crystalline pigeon breast carnitine acetyltransferase was purchased[3]. The sperm enzyme was obtained from the mitochondria of rat or mouse epididymal sperm using a differential centrifugation procedure similar to that described previously (2). Fat-free epididymal tissue was homogenized in 0.25 *M* sucrose (5 ml/rat) and centrifuged for 10 min at 1000×*g*. The pellet was rehomogenized, and the combined supernate was centrifuged for 15 min at 10,000×*g* to sediment the mitochondria.

The mitochondria were homogenized twice at 20-min intervals with pH 8.0 phosphate buffer–ethylenediaminetetraacetate solution containing 0.1% deoxycholate (2), using 2 ml of buffer/rat. The homogenate was centrifuged at 10,000×*g* for 20 min. The enzyme was in the supernate, and the protein concentration was ~10 mg/ml. The preparation was stable in the frozen state.

Kinetic Measurements—Kinetic parameters for the carnitine analogs were determined spectrophotometrically using substrate concentrations less than or equal to 1 m*M*. Both K_m and V_{max} values were determined graphically from Lineweaver–Burk plots.

Whole Sperm Effects—Epididymal sperm from mice were expressed and washed twice in Tyrode's solution containing 0.1% glucose and 0.1% bovine serum albumin. The sperm were resuspended in the modified Tyrode's solution. To this suspension was added, in the desired concentration, the analog adjusted to neutral pH.

After 15 min at 37°, the sperm were washed again, and the enzyme was extracted for assay as already described. Comparison was made with control sperm without analog.

***In Vitro* Fertilization and Egg Culture**—Some analogs were tested in an assay designed to detect substances that interfered with sperm function, egg fertilization, or early embryo development. The system contained a measured number of mouse sperm and mouse eggs in an appropriate medium cultured under normal conditions (9). In the absence of test substances, the eggs were fertilized and developed to the morula stage at a known rate. Compounds that interfered with any part of the process, *i.e.*, from sperm viability to early egg metabolism, could be detected by an analysis of the cell types present at the end of the culture period. At 1 μg of the test substance/ml, ~14% of 1000 randomly selected organic compounds showed some activity. At 10 mg/ml, ~40% of the tested compounds interfered with some aspect of egg development.

[3] Sigma Chemical Co.
[4] New England Nuclear.
[5] The liquid scintillation fluid consisted of 2-ethoxyethanol–toluene (1:1) with 0.1 g of 1,4-bis[2-(5-phenyloxazolyl)]benzene and 5 g of 2,5-diphenyloxazole/liter.
[6] Soluene, Packard Instruments.

Table II—Kinetic Parameters for Carnitine Analogs as Substrates for Carnitine Acetyltransferase[a]

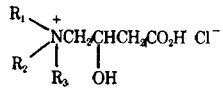

Compound	R_1	R_2	R_3	K_m, m*M*	V_{max}, nmoles/min/mg
Carnitine	CH_3	CH_3	CH_3	0.3	11
I	CH_3CH_2	CH_3	CH_3	0.4	8.6
II	CH_3CH_2	CH_3CH_2	CH_3	0.6	6.0
III	$CH_3(CH_2)_3$	CH_3	CH_3	0.6	6.2
IV	CH_3CH_2	CH_3CH_2	H	1.0	3.2
V	$CH_2CH_2OCH_2CH_2$		H	1.0	<1
VI	$CH_2CH_2CH_2CH_2CH_2$		H	1.0	<1
VII	$CH_2CH_2CH_2CH_2$		H	2.0	<1

[a] Data was obtained *via* the spectrophotometric assay using crystalline pigeon breast enzyme.

RESULTS

The radiometric assay for carnitine acetyltransferase, based on precipitation of acetylcarnitine, was linear with the amount of sperm enzyme until ~40% of the labeled acetyl coenzyme A was consumed. It also was linear with time until the same amount of acetyl coenzyme A was consumed. Acetyl coenzyme A was limiting under the assay conditions since excess carnitine was needed to get complete precipitation. The amount of enzyme used for assaying the inhibitory properties of the analogs was adjusted to give 25–30% conversion of acetyl coenzyme A (corresponding to approximately 3 milliunits of the commercial pigeon breast enzyme). Addition of the analogs to the reaction mixture appeared to inhibit the sperm enzyme (Table I). The same inhibition patterns were seen with purified pigeon breast enzyme using the precipitation assay (Table I): I–III were better inhibitors than V–VII.

When the analogs were tested as substrates for the enzyme in the absence of carnitine, they served as substrates to varying degrees. The precipitation of the acetyl analog as the periodide was more variable, however, and K_m and V_{max} values for each analog were determined spectrophotometrically using concentrations up to 1 m*M* (Table II).

Whole Sperm Enzyme Effects—Analogs IV and V were tested for their effect on carnitine acetyltransferase levels in whole sperm. Enzyme levels were unchanged in sperm incubated for 15 min with the analogs and then washed. Compound V was tested at 1 μ*M* and IV was tested at concentrations as high as 100 m*M* without effect on the enzyme extracted from treated sperm.

Effect on *In Vitro* Sperm and Egg Culture—Compounds III–V and VII were tested at 0.1, 1.0, and 10 μg/ml of media. The fertilization rate in the presence of the analogs was indistinguishable from controls.

DISCUSSION

The radiometric assay permitted the measurement of small amounts of sperm carnitine acetyltransferase without extensive purification. Enzyme levels in the epididymal sperm of one mouse could be measured, and numerous assays could be made without large numbers of animals.

Under the usual assay procedures, the analogs first appeared to be typical competitive inhibitors except that inhibition leveled off at high levels. When examined as substrates, the apparent inhibition occurred because they were poorer substrates than carnitine. The 4-mg/ml analog concentration was about twice the concentration of L-carnitine in the radiometric assay. Exact kinetics of the radiometric assay were obscured by the presence of D-carnitine (also an inhibitor) and the variables introduced by the precipitation of the acetyl analog periodides. The spectrophotometric system was used to measure K_m and V_{max} of the analogs with the purified pigeon breast enzyme. The similarity of the enzymes toward the analog effects in the radiometric assay suggested that the data obtained spectrophotometrically with the crystalline enzyme were applicable to the crude sperm enzyme.

The K_m value generally increased and the V_{max} value decreased with increasing bulk and rigidity of the nitrogen substituents. Analogs I–IV accepted the transfer of the acetyl group to the β-hydroxyl if the posi-

tively charged nitrogen atom of the analog fit the binding site on the enzyme. Attempts to isolate the labeled, acetylated analog from the reaction mixture were unsuccessful. The label trailed badly in all separation systems tried.

Although the analogs acted as enzyme inhibitors, they had no effect on the sperm. Whether the analogs were excluded from the cells or entered the cell and were ineffective in altering the enzyme activity cannot be discerned from the available data. These studies confirmed previous work that showed that the analogs had no biological activity (5).

REFERENCES

(1) I. B. Fritz, *Physiol. Rev.*, **41**, 52 (1961).

(2) N. R. Marquis and I. B. Fritz, *J. Biol. Chem.*, **240**, 2197 (1965).

(3) R. G. Vernon, V. L. W. Go, and I. B. Fritz, *Can. J. Biochem.*, **49**, 761 (1971).

(4) E. R. Casillas and B. J. Erickson, *Biol. Reprod.*, **12**, 275 (1975).

(5) S. G. Boots and M. R. Boots, *J. Pharm. Sci.*, **64**, 1949 (1975).

(6) E. R. Casillas, *Biochim. Biophys. Acta*, **280**, 545 (1972).

(7) R. E. McCaman, M. W. McCaman, and M. L. Stafford, *J. Biol. Chem.*, **241**, 930 (1966).

(8) J. F. A. Chase and P. K. Tubbs, *Biochem. J.*, **99**, 32 (1966).

(9) J. D. Biggers, W. K. Whitten, and D. G. Whittingham, in "Methods in Mammalian Embryology," J. C. Daniel, Jr., Ed., W. H. Freeman, San Francisco, Calif., 1971, pp. 86–116.

ACKNOWLEDGMENTS

The authors thank Mr. James F. Hutchins, Lilly Research Laboratories, for testing the analogs in the *in vitro* fertilization system.

Pharmacokinetics of Doxycycline Reabsorption

PETER VENG PEDERSEN [*x] **and RAYMOND MILLER** [‡]

Received August 20, 1979, from the [*]*Department of Pharmacy, School of Pharmacy, and the* [‡]*Division of Clinical Pharmacology, Department of Medicine, University of California, San Francisco, CA 94143.* Accepted for publication September 28, 1979.

Abstract □ Two cyclic linear compartment models are proposed to investigate the reabsorption mechanism of doxycycline. In one model, reabsorption is considered to be continuous; in the other model, it is discontinuous. The continuous model, when fitted, leads to one real and two complex conjugate eigenvalues, corresponding to a regression equation consisting of a regular exponential term and an exponentially damped trigonometric expression. In spite of the apparent oscillatory nature of this regression equation, the fitted curves show no secondary peaks or humps apparent in the data. Simulation studies indicate that it may not be possible to get response profiles showing secondary peaks or humps that are experimentally detectable with linear compartment systems with cyclic pathways and continuous transfer. The model with discontinuous cyclic transfer was more flexible in describing the discrepancies in the data and appeared to be preferable to the continuous cyclic transfer model judged by the Akaike information criterion.

Keyphrases □ Doxycycline—pharmacokinetics of reabsorption, two cyclic linear compartment models proposed □ Pharmacokinetics—doxycycline reabsorption, two cyclic linear compartment models proposed □ Models—pharmacokinetics of doxycycline reabsorption

There does not appear to be general agreement about the pharmacokinetic behavior of doxycycline in humans. Gibaldi (1) claimed that the persistence of serum doxycycline levels is due to a relatively slow absorption compounded by enterohepatic cycling, while other authors proposed that it is due to an intrinsically slow rate of elimination (2, 3). The pharmacokinetic parameters for doxycycline were calculated from the data of Fabre *et al.* (3), assuming a single-compartment model (1). The elimination rate was calculated using the data points from 35 to 72 hr after administration; these values were assumed to be true postabsorptive data (1). The mean half-life for doxycycline of 9.8 hr obtained in this way does not differ greatly from the half-life of other tetracyclines. An apparent absorption half-life of 5.3 hr was calculated by the method of residuals. It was suggested (1) that the persistence of appreciable serum concentrations of doxycycline relative to other tetracyclines is a function of absorption kinetics rather than elimination kinetics.

Using the same data, a subsequent investigator (2) calculated a substantially different absorption half-life of 50 min and a quite different elimination half-life of 22–24 hr and suggested that the persistent serum levels are primarily due to slow elimination. Schach von Witteman (2) pointed out that the low values found 72 hr after dosing are not very accurate and that the emphasis placed on this limited segment of the data is not justified. However, this investigator ignored the last two data points entirely in calculating the elimination rate constant. Inclusion of these two data points results in a considerably shorter half-life.

Although it is difficult to resolve properly the absorption and elimination kinetics from oral data alone, the data (3) show signs of secondary peaks, which support the hypothesis of reabsorption. This hypothesis is further supported by a high affinity to the bile reported for doxycycline and other tetracyclines (4). If reabsorption occurs, then the calculation of intrinsic absorption and elimination half-lives using classical pharmacokinetic approaches as discussed may not apply. It is not valid to assume a postabsorptive phase in a pharmacokinetic system with significant reabsorption.

Therefore, it is of interest to investigate the kinetic behavior of doxycycline using kinetic models that do consider the drug's reabsorption. It is also valuable to investigate whether the reabsorption occurs through a continuous process as suggested previously (4) or whether it is of a discontinuous nature, possibly related to biliary intestinal secretion that occurs primarily in the form of squirts of bile into the intestine (5). This work proposes two simple pharmacokinetic models to investigate these matters using the data of Fabre *et al.* (3).

THEORY

The two linear pharmacokinetic models proposed represent simple forms of drug reabsorption. Both models contain a cyclic disposition and do not belong to the categories of models (mammillary, catenary, and other noncyclic systems) proposed most frequently in pharmacokinetics.

Model 1—This linear model proposes first-order absorption, central

0022-3549/80/0200-0204$01.00/0

© 1980, American Pharmaceutical Association

tively charged nitrogen atom of the analog fit the binding site on the enzyme. Attempts to isolate the labeled, acetylated analog from the reaction mixture were unsuccessful. The label trailed badly in all separation systems tried.

Although the analogs acted as enzyme inhibitors, they had no effect on the sperm. Whether the analogs were excluded from the cells or entered the cell and were ineffective in altering the enzyme activity cannot be discerned from the available data. These studies confirmed previous work that showed that the analogs had no biological activity (5).

REFERENCES

(1) I. B. Fritz, *Physiol. Rev.*, **41**, 52 (1961).

(2) N. R. Marquis and I. B. Fritz, *J. Biol. Chem.*, **240**, 2197 (1965).

(3) R. G. Vernon, V. L. W. Go, and I. B. Fritz, *Can. J. Biochem.*, **49**, 761 (1971).

(4) E. R. Casillas and B. J. Erickson, *Biol. Reprod.*, **12**, 275 (1975).

(5) S. G. Boots and M. R. Boots, *J. Pharm. Sci.*, **64**, 1949 (1975).

(6) E. R. Casillas, *Biochim. Biophys. Acta*, **280**, 545 (1972).

(7) R. E. McCaman, M. W. McCaman, and M. L. Stafford, *J. Biol. Chem.*, **241**, 930 (1966).

(8) J. F. A. Chase and P. K. Tubbs, *Biochem. J.*, **99**, 32 (1966).

(9) J. D. Biggers, W. K. Whitten, and D. G. Whittingham, in "Methods in Mammalian Embryology," J. C. Daniel, Jr., Ed., W. H. Freeman, San Francisco, Calif., 1971, pp. 86–116.

ACKNOWLEDGMENTS

The authors thank Mr. James F. Hutchins, Lilly Research Laboratories, for testing the analogs in the *in vitro* fertilization system.

Pharmacokinetics of Doxycycline Reabsorption

PETER VENG PEDERSEN [*x] **and RAYMOND MILLER** [‡]

Received August 20, 1979, from the [*]*Department of Pharmacy, School of Pharmacy, and the* [‡]*Division of Clinical Pharmacology, Department of Medicine, University of California, San Francisco, CA 94143.* Accepted for publication September 28, 1979.

Abstract □ Two cyclic linear compartment models are proposed to investigate the reabsorption mechanism of doxycycline. In one model, reabsorption is considered to be continuous; in the other model, it is discontinuous. The continuous model, when fitted, leads to one real and two complex conjugate eigenvalues, corresponding to a regression equation consisting of a regular exponential term and an exponentially damped trigonometric expression. In spite of the apparent oscillatory nature of this regression equation, the fitted curves show no secondary peaks or humps apparent in the data. Simulation studies indicate that it may not be possible to get response profiles showing secondary peaks or humps that are experimentally detectable with linear compartment systems with cyclic pathways and continuous transfer. The model with discontinuous cyclic transfer was more flexible in describing the discrepancies in the data and appeared to be preferable to the continuous cyclic transfer model judged by the Akaike information criterion.

Keyphrases □ Doxycycline—pharmacokinetics of reabsorption, two cyclic linear compartment models proposed □ Pharmacokinetics—doxycycline reabsorption, two cyclic linear compartment models proposed □ Models—pharmacokinetics of doxycycline reabsorption

There does not appear to be general agreement about the pharmacokinetic behavior of doxycycline in humans. Gibaldi (1) claimed that the persistence of serum doxycycline levels is due to a relatively slow absorption compounded by enterohepatic cycling, while other authors proposed that it is due to an intrinsically slow rate of elimination (2, 3). The pharmacokinetic parameters for doxycycline were calculated from the data of Fabre *et al.* (3), assuming a single-compartment model (1). The elimination rate was calculated using the data points from 35 to 72 hr after administration; these values were assumed to be true postabsorptive data (1). The mean half-life for doxycycline of 9.8 hr obtained in this way does not differ greatly from the half-life of other tetracyclines. An apparent absorption half-life of 5.3 hr was calculated by the method of residuals. It was suggested (1) that the persistence of appreciable serum concentrations of doxycycline relative to other tetracyclines is a function of absorption kinetics rather than elimination kinetics.

Using the same data, a subsequent investigator (2) calculated a substantially different absorption half-life of 50 min and a quite different elimination half-life of 22–24 hr and suggested that the persistent serum levels are primarily due to slow elimination. Schach von Witteman (2) pointed out that the low values found 72 hr after dosing are not very accurate and that the emphasis placed on this limited segment of the data is not justified. However, this investigator ignored the last two data points entirely in calculating the elimination rate constant. Inclusion of these two data points results in a considerably shorter half-life.

Although it is difficult to resolve properly the absorption and elimination kinetics from oral data alone, the data (3) show signs of secondary peaks, which support the hypothesis of reabsorption. This hypothesis is further supported by a high affinity to the bile reported for doxycycline and other tetracyclines (4). If reabsorption occurs, then the calculation of intrinsic absorption and elimination half-lives using classical pharmacokinetic approaches as discussed may not apply. It is not valid to assume a postabsorptive phase in a pharmacokinetic system with significant reabsorption.

Therefore, it is of interest to investigate the kinetic behavior of doxycycline using kinetic models that do consider the drug's reabsorption. It is also valuable to investigate whether the reabsorption occurs through a continuous process as suggested previously (4) or whether it is of a discontinuous nature, possibly related to biliary intestinal secretion that occurs primarily in the form of squirts of bile into the intestine (5). This work proposes two simple pharmacokinetic models to investigate these matters using the data of Fabre *et al.* (3).

THEORY

The two linear pharmacokinetic models proposed represent simple forms of drug reabsorption. Both models contain a cyclic disposition and do not belong to the categories of models (mammillary, catenary, and other noncyclic systems) proposed most frequently in pharmacokinetics.

Model 1—This linear model proposes first-order absorption, central

0022-3549/80/0200-0204$01.00/0

© 1980, American Pharmaceutical Association

elimination, and drug distribution into an intermediate compartment. The intermediate compartment can be considered to be either the bile or a virtual compartment representing a secreted nonabsorbable compound or complex that releases the drug to the "absorption compartment" where it is subject to reabsorption.

The equation for this model is readily derived by the Veng Pedersen approach[1] (6). Equation 12 from Ref. 6 gives:

$$x_1 = L^{-1}\sum_{j=1}^{3}\frac{|\mathbf{S}|_{1j}}{|\mathbf{S}|}[x_j(0)+\bar{f}_j] = L^{-1}\frac{|\mathbf{S}|_{13}}{|\mathbf{S}|}D_F \qquad \text{(Eq. 1)}$$

Using Heaviside's expansion theorem and $c = x_1/V$, Eq. 1 becomes:

$$c = \frac{D_F}{V}\sum_{j=1}^{3}P(\lambda_j)\exp\lambda_j(t-T_L)_+ \qquad \text{(Eq. 2)}$$

where:

$$P(s) = |\mathbf{S}(s)|_{13}/|\mathbf{S}'(s)| \qquad \text{(Eq. 3)}$$

$$|\mathbf{S}(s)| = s^3 + a_2s^2 + a_1s + a_0 = (s-\lambda_1)(s-\lambda_2)(s-\lambda_3) \qquad \text{(Eq. 4)}$$

$$|\mathbf{S}'(s)| = 3s^2 + 2a_2s + a_1 \qquad \text{(Eq. 5)}$$

$$a_2 = E_1 + E_2 + E_3 \qquad \text{(Eq. 6)}$$

$$a_1 = E_1E_2 + E_1E_3 + E_2E_3 - (k_{21}k_{12} + k_{31}k_{13} + k_{23}k_{32}) \qquad \text{(Eq. 7)}$$

$$a_0 = E_1E_2E_3 - k_{23}k_{32}E_1 - k_{21}k_{12}E_3 - k_{31}k_{13}E_2 - k_{31}k_{12}k_{23} - k_{13}k_{32}k_{21} \qquad \text{(Eq. 8)}$$

$$|\mathbf{S}|_{13} = k_{31}(s+E_2) \qquad \text{(Eq. 9)}$$

If the system shows significant reabsorption, then two of the eigenvalues of the linear system will be complex conjugate while the third will be real; otherwise, all eigenvalues will be real. In any case, the real part of any eigenvalue is negative. In the complex case, Eq. 2 can also be written:

$$c = \frac{D_F}{V}\{2[Re(P(\lambda))\cos\lambda_{Im}(t-T_L)_+ - Im[P(\lambda)]\sin\lambda_{Im}(t-T_L)_+]\exp\lambda_{Re}(t-T_L)_+ + P(\lambda_1)\exp\lambda_1(t-T_L)_+\} \qquad \text{(Eq. 10)}$$

where λ_1 is the real eigenvalue and λ_{Im} and λ_{Re} are the imaginary and real parts, respectively, of a complex eigenvalue λ satisfying $|\mathbf{S}(\lambda)| = 0$.

Although explicit formulas exist for finding the complex and/or real roots of the characteristic polynomial $|\mathbf{S}(s)|$, it is not advisable to use them because of the possibility of severe numerical instability (10). Instead, the eigenvalues were determined to the proper degree of accuracy using Laguerre's method (11) and the interactive nonlinear regression program FUNFIT (12), which was used for all curve fittings. Equation 2 was programmed to accommodate both the real and complex cases. Therefore, the microparameters and the form of the response function are not constrained but lead to a convergence to either a real or complex case, depending on the data.

Model 2—This model is identical to Model 1, except that drug transfer between Compartments 2 and 3 is not a continuous first-order process but a bolus impulse. At some time, $t = T_b$, some fraction, F_b, of the drug cumulated in the bile is spontaneously released to the intestine by a bile squirt. The equation describing this process is readily derived by standard means (6):

$$c = \left(\frac{D_F}{V}\right)\frac{k_{31}}{k_{31}+\lambda}\{\exp\lambda(t-T_L)_+ - \exp[-k_{31}(t-T_L)_+] + A[\exp\lambda(t-T_b)_+ - \exp[-k_{31}(t-T_b)_+]]\} \qquad \text{(Eq. 11)}$$

where:

$$A = \frac{F_bk_{31}k_{12}}{k_{31}+\lambda}\left\{\frac{1}{\lambda}[\exp\lambda(T_b-T_s)-1] + \frac{1}{k_{31}}[\exp[-k_{31}(T_b-T_L)]-1]\right\} \qquad \text{(Eq. 12)}$$

and:

$$\lambda = E_1 = k_{12} + k_{10} \qquad \text{(Eq. 13)}$$

RESULTS AND DISCUSSION

In the real case with real eigenvalues, the response function for Model 1 consists of three regular exponential terms. However, in the complex case (Eq. 10), the function consists of two terms: an exponentially damped, oscillating trigonometric term superimposed on a regular exponential term. Thus, for a linear system behaving according to Model 1 and showing significant reabsorption, one may believe that the response function will show secondary peaks or humps judged from the functional form of Eq. 10. However, this does not appear to be the case. Although the curve fittings for all subjects using Eq. 2 lead to a convergence with complex eigenvalues (Eq. 10), no secondary peaks or humps were observed in the fitted curves (Fig. 1).

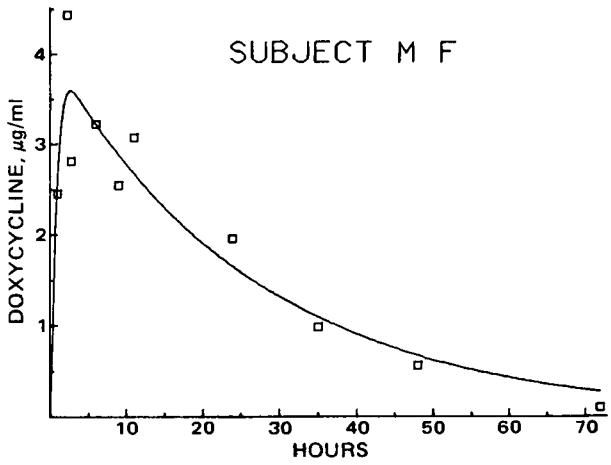

Figure 1—*Least-squares fit of Model 1 (Eq. 2) to plasma doxycycline level data. The fitting resulted in complex eigenvalues, with an estimated response function as given by Eq. 10.*

Extensive simulation studies were done on an interactive computer graphic system to investigate whether any perturbation of the microparameters of the model may result in secondary peaks or humps in the regression curve. Apparently, this effect does not occur even for systems with a substantial degree of reabsorption or for systems constructed numerically by maximizing the "degree of complexity" on the basis of the discriminant of the characteristic polynomial.

From a purely theoretical point of view, some support apparently exists for the claim that linear systems with cyclic pathways and continuous transfer do not give rise to secondary peaks and that humps may be difficult to detect, but there is no formal proof (13). This behavior is related to a relatively long period of the trigonometric expression and a relatively strong exponential damping term inherent in such systems.

When dealing with cyclic models with complex eigenvalues, as opposed to noncyclic systems, it is improper to fit the macroparametric form instead of the microparametric form of the response function. For example, if Eq. 10 is fitted in its macroparametric form, the curve may approximate an extra peak or a hump in the data. However, if the macroparameters are used to calculate the microparameters, then some of them may turn out to be complex or negative, in disagreement with the model proposed.

Table I shows that the reabsorption rate constant k_{23} is relatively large compared to the elimination rate constant k_{el} and k_{12} for all subjects, indicating substantial reabsorption. In spite of this significant reabsorption, the fitted curves do not appear distinguishable from ordinary absorption curves for noncyclic linear systems (Fig. 1). Reabsorption and cyclic transport processes in pharmacokinetics have usually been considered only when dealing with data containing secondary peaks or an extra hump. These results show that a "typical" drug level profile may be associated with a strong degree of reabsorption. Therefore, a greater number of drugs could be subject to reabsorption than currently known.

The average absorption half-life estimated using Model 1 is 0.5 hr (Table I), which is considerably shorter than the 5.3 hr determined by the method of residuals by Gibaldi (1) but comparable to the half-life of 50 min determined by Schach von Witteman (2). The average elimination half-life of 13 hr is larger than the 9–8 hr determined by Gibaldi (1) but considerably shorter than that determined by Schach von Witteman (2). These differences are mainly due to the different models used. Gibaldi (1) suggested that the slow decline of plasma doxycycline levels relative to other tetracyclines is due to relatively slow absorption compounded by enterohepatic cycling. However, the absorption and elimination half-lives were calculated assuming a one-compartment model without considering reabsorption (1, 2).

[1] The model contains a cyclic pathway. Thus, neither the Benet approach (7) nor the Vaughan *et al.* approach (8, 9) can be used for this reabsorption model.

Table I—Least-Squares Parameter Estimates for Model 1

Parameter	Subject						Mean	CV, %
	JN	CS	RV	MF	FF	GP		
k_a[a], hr^{-1}	3.27	1.82	1.52	1.03	0.678	2.79	1.85	54.4
$t_{1/2}$(abs), hr^{-1}	0.212	0.381	0.456	0.673	1.02	0.248	0.499	61.2
k_{el}[b], hr^{-1}	0.0446	0.0632	0.0473	0.0548	0.0770	0.0502	0.0562	21.6
$t_{1/2}$ el, hr	15.5	11.0	14.7	12.6	9.00	13.8	12.8	19.1
T_L, hr	2.15	0.719	0.108	0.131	1.13	0.122	0.727	111
k_{12}, hr^{-1}	0.546	0.590	0.355	0.245	0.217	0.392	0.391	39.1
k_{23}, hr^{-1}	1.13	2.09	1.31	1.19	0.643	1.76	1.354	37.5
D_F/V, g/ml	4.20	4.62	4.71	5.77	4.79	4.13	4.70	12.5
RSS[c]	0.393	0.322	1.22	1.83	0.298	0.242	0.718	91.5
AIC[d]	2.67	0.679	14.0	18.0	−0.091	−2.21		

[a] $k_a = k_{31}$. [b] $k_{el} = k_{12} + k_{10}$. [c] RSS = residual sum of squares. [d] Akaike's information criterion.

Table II—Least-Squares Parameter Estimates for Model 2

Parameter	Subject						Mean	CV, %
	JN	CS	RV	MF	FF	GP		
k_a[a], hr^{-1}	1.04	6.34	5.29	3.67	0.619	2.89	3.31	68.7
$t_{1/2}$(abs), hr	0.666	0.109	0.131	0.189	1.12	0.240	0.409	98.7
k_{el}[b], hr^{-1}	0.499	0.553	0.0407	0.050	0.067	0.044	0.0511	18.2
$t_{1/2}$ el, hr	13.9	12.5	17.0	13.9	10.3	15.8	13.9	16.9
T_L, hr	1.99	0.904	0.711	0.737	0.915	0.024	0.880	72.1
T_b, hr	23.8	16.4	9.27	10.8	24.7	5.91	15.2	51.7
F_b	0.570	0.488	0.436	0.952	0.368	0.338	0.525	42.8
k_{12}, hr^{-1}	0.0568	0.0624	0.0777	0.0412	0.0743	0.103	0.0692	30.5
D_F/V, g/ml	2.94	3.00	3.07	3.97	3.12	2.92	3.17	12.6
RSS[c]	0.0898	0.139	0.866	1.24	0.136	0.0875	0.426	117.3
AIC[d]	−10.1	−5.71	12.6	16.2	−6.0	−10.4		

[a] $k_a = k_{31}$. [b] $k_{el} = k_{12} + k_{10}$. [c] RSS = residual sum of squares. [d] Akaike's information criterion.

It appears that plasma level data showing secondary peaks or extra humps are not well approximated by linear compartment models with continuous first-order intercompartment drug transfer. However, such behavior may be related to discontinuous transfer processes. The doxycycline data appear to show secondary peaks that are not described by Model 1. Model 2 is identical to Model 1 except that drug transfer back into the intestine is a discontinuous bolus transfer *via* the bile. This model appears physiologically more meaningful than Model 1, considering the discontinuous nature of biliary secretion (5).

The average absorption half-life of 0.4 hr is somewhat smaller than that obtained using Model 1 (0.5 hr) while the average elimination half-life of 14 hr is greater than the 13 hr previously determined (Tables I and II). Although the average absorption and elimination half-lives are not very different from those determined using Model 1, Model 2 fits the data consistently better than Model 1 judged from the residual sum of squares and the Akaike information criterion values (Table II and Fig. 2).

Almost complete absorption takes place from the upper intestine following oral doxycycline administration (4). To account for the 70–80% doxycycline eventually recovered in the feces (14), intestinal secretion has been proposed as primarily responsible with biliary secretion playing a minor role (14, 15). It was proposed that after essentially complete absorption, the drug in the blood diffuses into the alkaline medium of the intestinal lumen where cationic chelation occurs, in which form doxycycline cannot be reabsorbed and is ultimately eliminated in the feces (16). Some investigations indicated that average concentrations of doxycycline are about five times greater than serum concentrations and that bile concentrations of the gallbladder are 10–15 times greater than serum concentrations (4). It was estimated that 10–15% of a 200-mg dose

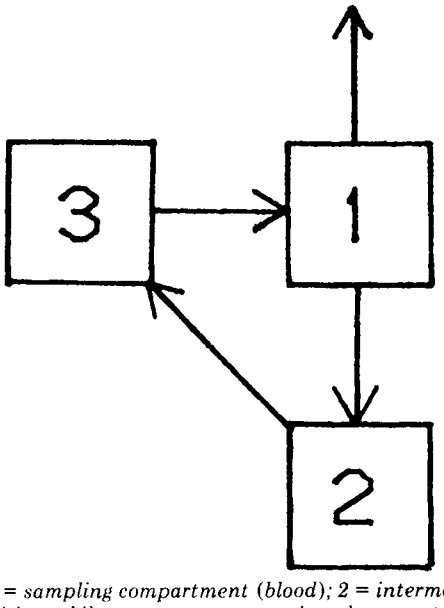

Model 1—1 = sampling compartment (blood); 2 = intermediate compartment, either a bile compartment or a virtual compartment representing a secreted nonabsorbable compound or complex from which an absorbable form of the drug is released; and 3 = compartment from which absorption takes place.

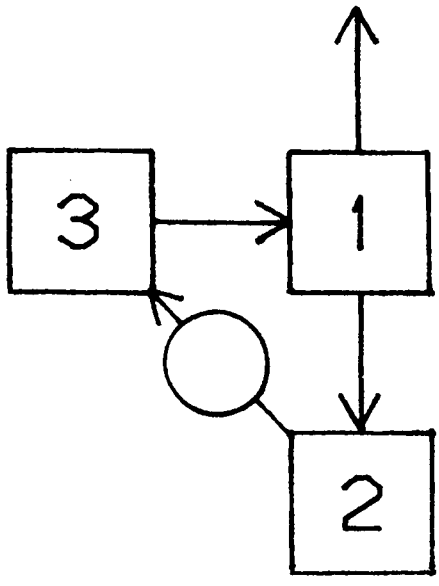

Model 2—1 = sampling compartment (blood); 2 = bile compartment from which bile containing drug is released spontaneously as a bolus squirt to the absorption compartment; and 3 = compartment from which absorption takes place.

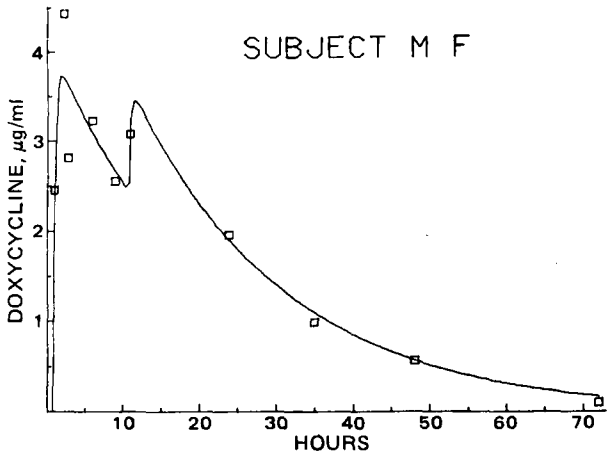

Figure 2—*Least-squares fit of Model 2 (Eq. 11) to plasma doxycycline level data.*

would be eliminated in the bile per day if an average of 500 ml of bile was secreted (4). If doxycycline's metabolism rate, urinary excretion rate, and excretion rate of chelate complex are first-order processes, or if the combined elimination rate by these processes is approximately first order (k_{10}), then Model 2 may be physiologically meaningful if the absorption rate is first order.

In humans, bile is retained in the gallbladder until it is spontaneously released, usually after a meal (5). The estimated times of bile release, T_b, in six subjects varied from 5 to 24 hr. Food and especially fats promote contraction of the gallbladder so that the timing and fat content of the meal play a role in the estimated time and magnitude of bile release.

It is difficult to speculate about the feasibility of these times and the degree of reabsorption because of the limited data and the inaccuracy of the assay methodology and because no specific information is available about the food intake of the subjects after drug administration. However, the data appear to show a consistent trend of reabsorption, and the Akaike information criterion (17, 18) seems to indicate, in comparing the two linear compartment models (Tables I and II), that the reabsorption mechanism is discontinuous rather than continuous.

NOTATIONS

c = drug concentration in sampleable compartment (blood plasma) at time t

D_F = amount of dose available in the compartment where absorption takes place

$E_i = \sum_{j=0}^{n} k_{ij}$, where $n = 3$

$\bar{f}_i$ = Laplace transform of input rate into the ith compartment

F_b = fraction of the amount of drug cumulated in the bile that is released by a squirt of bile at time $t = T_b$

$Im(z)$ = imaginary part of complex number z

k_{ij} = first-order rate constant for drug transfer from compartment i to compartment j

L^{-1} = inverse Laplace transform operator

λ = eigenvalue of linear pharmacokinetic system (real or complex)

$Re(z)$ = real part of complex number z

s = Laplace transform variable

$|\mathbf{S}|$ = $|\mathbf{S}(s)|$, determinant of $\mathbf{S}$ matrix defined in Ref. 6.

$|\mathbf{S}|_{ij}$ = $|\mathbf{S}(s)|_{ij}$ cofactor corresponding to the i,jth position of $\mathbf{S}$ matrix

T_b = time when bile containing drug is released to absorption compartment

T_L = absorption lag time

V = volume of distribution of sampleable compartment

x_i = amount in ith compartment at time t

$(y)_+$ = max(0,y), the "truncation function"

REFERENCES

(1) M. Gibaldi, *Chemotherapy*, **12**, 265 (1967).

(2) M. Schach von Witteman, *Chemotherapy, Suppl.*, **13**, 41 (1968).

(3) J. Fabre, J. S. Pitton, and J. P. Kuntz, *Chemotherapia*, **11**, 73 (1966).

(4) J. Fabre, E. Milek, P. Kaljopoulos, and G. Merier, *Schweiz. Med. Wochenschr.*, **101**, 593 (1971).

(5) E. A. Boyden, *Anat. Rec.*, **40**, 147 (1928).

(6) P. Veng Pedersen, *J. Pharm. Sci.*, **67**, 187 (1978).

(7) L. Z. Benet, *ibid.*, **61**, 536 (1972).

(8) D. P. Vaughan and A. Trainor, *J. Pharmacokinet. Biopharm.*, **3**, 203 (1975).

(9) D. P. Vaughan, D. J. H. Mallard, A. Trainor, and M. Mitchard, *Eur. J. Clin. Pharmacol.*, **8**, 141 (1975).

(10) G. Dahlquist and Å. Björck, "Numerical Methods," Prentice-Hall, New York, N.Y., 1974.

(11) B. T. Smith, "ZERPOL," Department of Computer Science, University of Toronto, Toronto, Canada, 1967.

(12) P. Veng Pedersen, *J. Pharmacokinet. Biopharm.*, **5**, 513 (1977).

(13) C. D. Thorn, *Bull. Math. Biophys.*, **34**, 277 (1972).

(14) M. Schach von Witteman and T. M. Twoney, *Chemotherapy*, **16**, 217 (1971).

(15) J. Fabre, J. P. Kuntz, C. Virieux, J. L. Laurend, and J. S. Pitton, *Chemotherapy, Suppl.*, **13**, 23 (1968).

(16) A. Whelton, M. Schach von Witteman, T. M. Twoney, W. G. Walker, and J. R. Bianchine, *Kidney Int.*, **5**, 365 (1974).

(17) H. Akaike, *IEEE Trans. Automat. Contr.*, **19**, 716 (1973).

(18) H. Akaike, *Math. Sci.*, **14** (1976).

ACKNOWLEDGMENTS

Supported in part by the South African Medical Research Council.

Insulin Permeability of Hydrophilic Polyacrylate Membranes

M. V. SEFTON ˣ **and E. NISHIMURA**

Received May 11, 1979, from the *Department of Chemical Engineering and Applied Chemistry, University of Toronto, Toronto, Ontario, M5S 1A4, Canada.* Accepted for publication August 22, 1979.

Abstract □ The diffusive permeability of insulin in polyhydroxyethyl methacrylate (37.1% water), polyhydroxyethyl acrylate (51.8% water), polymethacrylic acid (67.5% water), and cuprophane PT-150 membranes was determined and correlated with the weight fraction of water in the membrane. Insulin diffusivity in the membranes was determined to be 1.0×10^{-6} cm²/sec, which is in reasonable agreement with literature values for insulin diffusivity in water.

Keyphrases □ Polyacrylate membrane—effect on insulin diffusivity, extent of cross-linkage, hydration effect □ Insulin diffusivity—permeability through hydrophilic polyacrylate membranes □ Membrane permeability—hydrophilic polyacrylate membranes, effect on insulin diffusivity, extent of cross-linkage, hydration effect

Controlled-release insulin is desirable because of the recognized relationship between poor glycemia control associated with conventional insulin therapy and the degenerative sequelae of juvenile diabetes (1). Specifically, the development of a micropump for controlled-release delivery of insulin at variable rates (2) necessitated the investigation of the insulin permeability of a series of highly swollen polyacrylate membranes. In this device, basal delivery of insulin occurs through a polymeric membrane under a concentration and/or small pressure gradient while augmented delivery results when the membrane is repeatedly squeezed between the moving core of a solenoid and the membrane support. Augmentations as high as 50 times basal can be achieved to match insulin delivery to the postprandial insulin needs of a diabetic patient.

BACKGROUND

The diffusive permeability of solutes in hydrophilic membranes has been thoroughly studied (3–10). The effects of membrane hydration (3, 4), solute size (5–8), and cross-linker content (9, 10) were investigated. Various models were considered in analyzing the data. According to Yasuda *et al.* (3–5), the diffusive permeability, P, is related to the membrane diffusivity, D, by:

$$P = KD = \alpha HD \qquad \text{(Eq. 1)}$$

where H is the hydration or volume fraction of solvent in the membrane and K is the solute partition coefficient in the membrane. The parameter α reflects the proportionality between the partition coefficient and hydration and is unity for high hydration values (4). The solute diffusivity in the membrane generally is less than that in free solution because of the lower free volume (3) and the sieve effect (5) of the membrane. Yasuda *et al.* (5) found that the sieve effect was not evident for cellulose-based membranes with solutes up to the size of albumin (mol. wt. 66,000).

This study concerned the insulin permeability of highly swollen acrylate-based membranes and the membrane hydration effect on insulin permeability.

EXPERIMENTAL

Materials and Methods—Hydroxyethyl acrylate (I), hydroxyethyl methacrylate (II), and methacrylic acid (III) were polymerized *in situ* between two shim-separated glass plates over 24 hr. Triethylene glycol dimethacrylate was the cross-linking agent. Formulations are presented in Table I. The membranes were equilibrated in 0.9% saline prior to testing. A sample of cuprophane PT-150 was obtained from a Kolff twin-coil dialyzer[1].

The hydration, H, was assumed to be proportional to the weight fraction of water since the membrane densities were all 1.25 ± 0.05 g/cm³. The water fraction was determined by weighing the swollen membrane samples before and after drying *in vacuo*. The swollen membrane thickness was determined with a micrometer.

The membrane was supported by rubber gaskets between two Lucite chambers for permeability testing. It was tested in the horizontal position. The lower chamber, containing 65 ml of a radiolabeled insulin solution, was stirred by a magnetic stirrer. Initially, the upper chamber contained insulin-free saline and was agitated by an overhead stirrer, which was closely controlled because of frothing. The lower chamber was sealed to prevent bulk flow so that samples could be taken from this chamber only at the beginning and end of each run. The concentrations in this chamber were calculated by mass balance. The effective membrane area was 5.07 cm². The initial insulin solution was pH 7.4 phosphate-buffered saline containing 0.4 unit of insulin/ml[2] and 0.5 nCi of I-125 insulin/ml[3]. All experiments were conducted at $22 \pm 1°$.

Samples (1.3 ml) were removed at regular intervals from the upper chamber and were replaced by an equal volume of 0.9% saline. These samples, the two samples from the lower reservoir, and a background sample were each mixed with 10 ml of liquid scintillation cocktail[4] in

Table I—Formulations and Properties of Highly Swollen Polyacrylate Membranes

	Primary Monomer		
	Methacrylic Acid (III)	Hydroxyethyl Acrylate (I)	Hydroxyethyl Methacrylate (II)
Formulation (by volume)			
Monomer	10.0	10.0	10.0
Water	2.0	2.0	2.0
Triethylene glycol dimethacrylate	0.8	0.2	0.04
Ethylene glycol	3.0	3.0	3.0
Ammonium persulfate (40 g/100 ml of H_2O)	0.3	1.0	1.0
Sodium metabisulfite (15 g/100 ml of H_2O)	0.3	1.0	1.0
Reaction temperatures	20–25°	40–50°	20–25°
Properties			
Weight percent water[a,b]	67.5	51.8	37.1
Insulin permeability[c], $cm^2/sec \times 10^{-7}$	4.8	3.9	1.0
Compression modulus, $N/m^2 \times 10^5$	—	2.26	5.28
M_c, molecular weight between cross-links, g/mole	—	41,400	17,600

[a] Swollen in 0.9% saline. [b] Weight percent water for cuprophane PT-150 membrane was 44.7. [c] Insulin permeability through cuprophane PT-150 membrane was 1.4×10^{-7} cm²/sec.

[1] Ultra-Flow 145, Travenol Laboratories, Toronto, Ontario, Canada.
[2] Toronto Insulin.
[3] Amersham-Searle, Toronto, Ontario, Canada.
[4] ReadySolv GP, Beckman Instruments, Fullerton, Calif.

0022-3549/80/0200-0208$01.00/0
© 1980, American Pharmaceutical Association

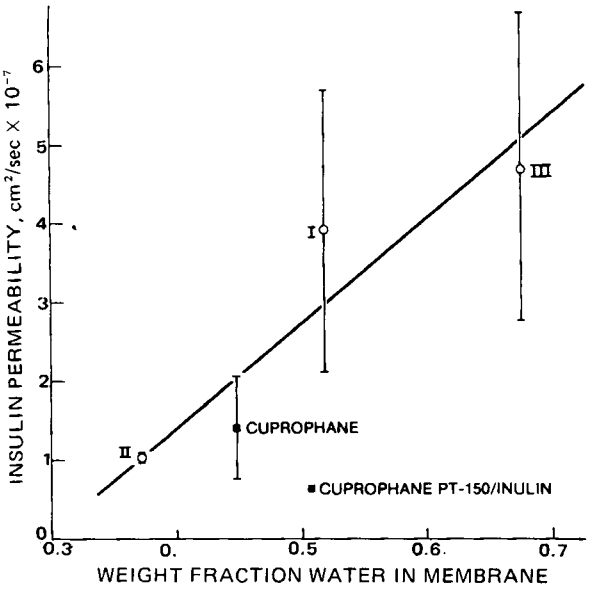

Figure 1—*Effect of weight fraction of water on insulin permeability of highly swollen polyacrylate membranes. Permeability of inulin in cuprophane PT-150(6) (■) is shown for comparison.*

polyethylene vials and counted using a liquid scintillation spectrometer.

Calculation of Membrane Permeability—Permeability was calculated using the following equations (6):

$$\ln \prod_{i=0}^{i=n} \left[\frac{(C_2 - C_1)_{i+1}}{(C_2' - C_1)_i}\right] = \frac{PA}{t_m}\left(\frac{1}{V_1} + \frac{1}{V_2}\right)\theta_n \quad \text{(Eq. 2)}$$

$$C_{2,i}' = (1 - V_r/V_2)C_{2,i} \quad \text{(Eq. 3)}$$

where:

$C_{1,i}$ = concentration of ith sample in lower (concentrated) reservoir, calculated by mass balance
$C_{2,i}$ = concentration of ith sample in upper (dilute) reservoir
$C_{2,i}'$ = concentration in upper reservoir corrected for dilution
V_1 = volume of lower reservoir
V_2 = volume of upper reservoir
V_r = sample volume (1.3 ml)
A = effective membrane area
t_m = membrane thickness
θ_n = time for sample n

The left side of Eq. 2 was plotted against time to determine the slope for calculating the membrane permeability, P. To compensate for mass balance errors, the lower reservoir concentration, C_1, was calculated forward from the initial concentration and backward from the final concentration. These two permeability values rarely differed by more than 10%; this variation was less than the intrasample variation. The averaged results are presented in Table I and were plotted against the weight fraction of water (Fig. 1). At least two experiments were performed for each membrane.

The compression moduli of 2-mm thick samples of I and II water-swollen hydrogels were determined at 10% strain on a tensile testing machine[5] having a crosshead speed of 0.1 cm/min. The hydrogels were prepared as given in Table I in 7-mm o.d. glass tubes at 10°. The molecular weight between cross-links, M_c, was determined (Table I) from these moduli and the hydrogel densities (11).

DISCUSSION

Despite the differences in membrane chemical structure, insulin permeability correlated well with the weight fraction of water in the membrane. Specific interactions between membrane chemical structure and solute were apparently negligible (within experimental error). With the assumption that α (Eq. 1) was unity, the membrane diffusivity of insulin was proportional to the slope of the line (Fig. 1) and was 1.0×10^{-6} cm²/sec. This value agrees with the literature values of 0.73×10^{-6} and 1.6×10^{-6} cm²/sec for insulin diffusivity in water at infinite dilution at 20° measured by ultracentrifugation techniques (12). The differences in the free volume and the molecular state within the membrane relative to that in free solution should account for this deviation.

The effect of cross-linking is as expected. At a higher M_c value (lower extent of cross-linking), the permeability is higher since the membrane swells more. Although the hydrogels absorbed more water than saline, the M_c values should not be different in saline. However, the differences in reaction conditions (temperature and geometry) may be significant despite the longer reaction times; for example, the number of free chain ends was ignored in this calculation. The dramatic increase in permeability at a low extent of cross-linking noted by others (9, 10) was not detected since the extent of cross-linking was greater in this work.

REFERENCES

(1) G. F. Cahill, D. D. Etzwiler, and N. Freinkel, *Diabetes*, **25**, 237 (1976).

(2) M. U. Waher, B.A.Sc. thesis, Department of Chemical Engineering and Applied Chemistry, University of Toronto, Toronto, Canada, 1977.

(3) H. Yasuda, C. E. Lamaze, and L. D. Ikenberry, *Makromol. Chem.*, **118**, 19 (1968).

(4) H. Yasuda, L. D. Ikenberry, and C. E. Lamaze, *ibid.*, **125**, 108 (1969).

(5) H. Yasuda, A. Peterlin, C. K. Colton, K. A. Smith, and E. W. Merrill, *ibid.*, **126**, 177 (1969).

(6) C. K. Colton, K. A. Smith, E. W. Merrill, and P. C. Farrell, *J. Biomed. Mater. Res.*, **5**, 459 (1971).

(7) B. D. Ratner and I. F. Miller, *ibid.*, **7**, 353 (1973).

(8) P. C. Farrell and A. L. Babb, *ibid.*, **7**, 272 (1973).

(9) S. J. Wisniewski, D. E. Gregonis, S. W. Kim, and J. D. Andrade, in "Hydrogels for Medical and Related Applications," J. D. Andrade, Ed., ACS Symposium Series, **31**, 80 (1976).

(10) K. H. Lee, J. G. Jee, M. S. Jhon, and T. Ree, *J. Bioeng.*, **2**, 269 (1978).

(11) E. F. Cluff, E. K. Gladding, and R. Pariser, *J. Polym. Sci.*, **45**, 341 (1960).

(12) M. H. Smith, in "Handbook of Biochemistry," 2nd ed., H. A. Sober, Ed., C.R.C., Cleveland, Ohio, 1970, pp. C3-C35.

ACKNOWLEDGMENTS

Supported by the National Research Council of Canada.

The authors thank Ms. E. Bobet for the establishment of the formulations and the measurements of compression modulus.

[5] Instron Corp, Canton, Mass.

Membrane Transport of Alkyl Homologs: Role of Fluid Flow in Aqueous Diffusion Region

ASHOK C. SHAH *x **and KENNETH G. NELSON** ‡§

Received April 4, 1979, from the *Pharmacy Research Unit, The Upjohn Company, Kalamazoo, MI 49001, and the ‡College of Pharmacy, University of Minnesota, Minneapolis, MN 55455. Accepted for publication August 24, 1979. §Present address: Pharmacy Research Unit, The Upjohn Company, Kalamazoo, MI 49001.

Abstract □ Passive drug transport across a membrane involves the resistances in series offered by the membrane and the liquid layer immediately adjacent to it. The liquid layers generally are referred to as unstirred aqueous diffusion layers, suggesting that solute transport across these layers occurs solely by molecular diffusion. In accord with convective diffusion theory, recent studies showed that the transport from either a dissolving surface or a membrane surface depends not only on molecular diffusion but also on fluid convection in the liquid adjacent to the membrane. Membrane permeation rates were determined for a series of alkyl *p*-aminobenzoates, and the results correlated with a model comprised of membrane diffusion and convective diffusion in the adjacent liquid region.

Keyphrases □ Drug transport—alkyl *p*-aminobenzoates, membrane permeation, fluid flow in aqueous diffusion region □ *p*-Aminobenzoates—membrane permeation, fluid flow in aqueous diffusion region □ Permeation—*p*-aminobenzoates, membrane transport, fluid flow in aqueous diffusion region

Passive drug transport across a membrane involves the resistance offered by the membrane itself as well as by the passage through the liquid immediately adjacent to the membrane. At steady state, the two processes occur simultaneously; because they are in series, limiting cases exist in which one process or the other may be rate limiting. Recent studies demonstrated that under conditions of aqueous boundary layer control, the permeation rate of butamben through a dimethicone membrane was described accurately by a mathematical model based on convective diffusion theory (1).

Models for steady-state transport across membranes generally have been based on the assumption of unstirred solvent layers adjacent to the membrane (2). Such layers are included as a resistance in series with the membrane. However, this concept of a static liquid layer adjacent to a solid and continuous with a moving liquid has been criticized (3) on the basis of empircal evidence as well as hydrodynamic theory.

The purposes of this work were to study the membrane permeation of a series of alkyl *p*-aminobenzoates and to evaluate the data in terms of a model comprised of membrane diffusion and convective diffusion in the adjacent liquid.

EXPERIMENTAL

The permeation studies for the methyl through pentyl *p*-aminobenzoates were carried out using a dimethicone membrane (thickness of 0.0254 cm) in a laminar flowcell (1, 4). On the donor side of the membrane, a well-stirred aqueous suspension of the permeant provided the source at a constant concentration. On the other side, water flowing under laminar conditions removed the solute from the vicinity of the membrane and also served as the means to monitor the permeation rate spectrophotometrically.

Table I gives the aqueous solubilities and partition coefficients for the compounds studied. The aqueous solubilities at 25° were determined previously (4). The partition coefficients were obtained by equilibrating dimethicone membranes with aqueous suspensions of the esters for 48 hr at 25°, extracting the ester from the membrane by successive equilibration with water, and analyzing the extract spectrophotometrically (λ_{max} 285 nm) to determine the ester concentration in the membrane. Partition coefficients were taken as the ratio of the concentration in the membrane to the aqueous solubility.

THEORETICAL

The diffusional resistance, R_m, of the circular membrane is given by:

$$R_m = \frac{h}{D_m K \pi r^2} \qquad \text{(Eq. 1)}$$

where h is the membrane thickness, D_m is the solute diffusivity in the membrane, K is the partition coefficient of the solute in the membrane relative to water, and r is the membrane radius. The analogous resistance term, R_w, for the convective diffusion transport through the liquid adjacent to the membrane may be expressed as:

$$R_w = \frac{1}{2.16 r^{5/3} D_w^{2/3} \alpha^{1/3}} \qquad \text{(Eq. 2)}$$

where D_w is the aqueous diffusivity of the solute and α is the rate of shear adjacent to the membrane which is directly proportional to the fluid flow rate (4). The steady-state permeation rate is given by the concentration difference across the membrane divided by the resistance, which is the sum of the individual layer resistances for a classical composite membrane (5). If it is assumed that the resistances as given in Eqs. 1 and 2 are additive, the steady-state permeation rate, J, may be written as:

$$J = \frac{2.16 \pi r^{11/3} D_w^{2/3} \alpha^{1/3} D_m K C}{\pi r^2 D_m K + 2.16 h r^{5/3} D_w^{2/3} \alpha^{1/3}} \qquad \text{(Eq. 3)}$$

where C is the constant solute concentration on the donor side of the membrane.

Two limiting cases of Eq. 3 are represented schematically in Fig. 1. In one case, diffusion across the membrane becomes rate controlling under conditions that favor minimizing Eq. 2 relative to Eq. 1, *e.g.*, a very large α or h, so that Eq. 3 becomes:

$$J = \frac{\pi r^2 D_m K C}{h} \qquad \text{(Eq. 4)}$$

Alternatively, if the resistance in the membrane (Eq. 1) is minimized with respect to that in the liquid (Eq. 2) by such factors as a small h or a large K, then:

$$J = 2.16 r^{5/3} D_w^{2/3} \alpha^{1/3} C \qquad \text{(Eq. 5)}$$

This limiting case was discussed previously (1) and is the same expression as for the dissolution from a solid solute surface in the cell. Equation 3 in effect is an interpolation formula; it combines the two limiting cases to describe permeation for conditions in which the two resistances are comparable in magnitude.

Figure 1 was drawn ignoring the partitioning effect ($K = 1$). In Case II, the profile in the liquid is dependent on the distance along the mem-

Table I—Aqueous Solubilities and Partition Coefficients of *p*-Aminobenzoate Esters at 25°

Ester	Aqueous Solubility, moles/liter	Partition Coefficient
Methyl	1.04×10^{-2}	0.26
Ethyl	6.19×10^{-3}	0.78
Propyl	2.78×10^{-3}	2.59
Butyl	9.39×10^{-4}	9.61
Pentyl	2.72×10^{-4}	38.11

0022-3549/80/0200-0210$01.00/0
© 1980, American Pharmaceutical Association

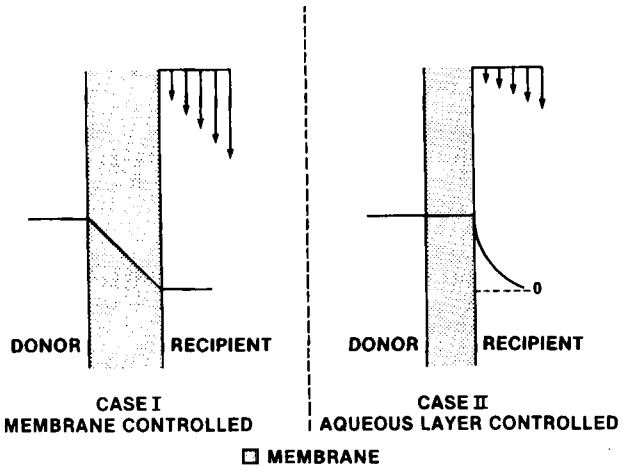

Figure 1—*Concentration profile for the two limiting cases of permeation according to Eq. 4 (Case I) and Eq. 5 (Case II). Arrows indicate the velocity of laminar liquid flow within the aqueous boundary layer.*

brane. Thus, the gradient would be steeper and the extent of penetration into the liquid would be less near the upstream edge of the membrane than at points along the membrane further downstream.

RESULTS AND DISCUSSION

The steady-state permeation rates of the methyl through pentyl *p*-aminobenzoates were determined as a function of the fluid flow rate under laminar conditions. These rates are shown in Fig. 2 as the data points. Because the parameters on the right side of Eq. 3 are known independently, the rates predicted by Eq. 3 also are included in Fig. 2 as the solid lines. The experimental results are in reasonably good agreement with

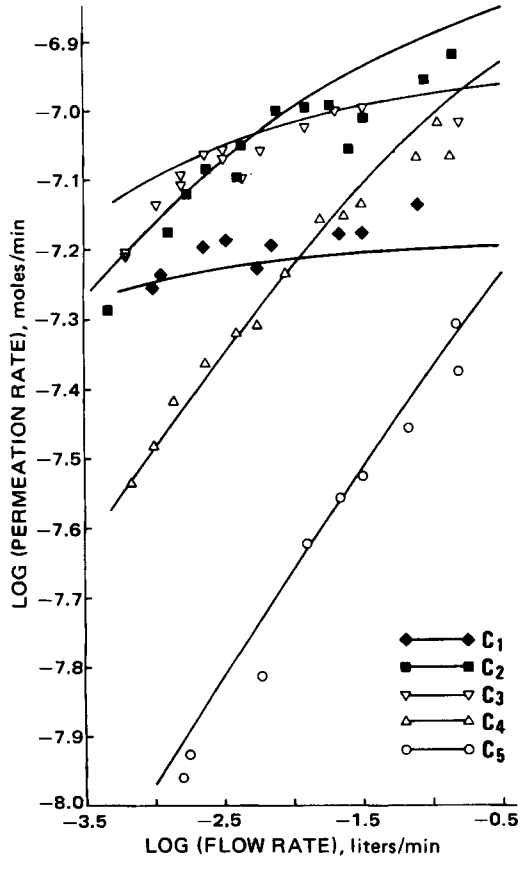

Figure 2—*Permeation rates of C_1–C_5 alkyl homologs of* p-*aminobenzoates determined as a function of the fluid flow rate. Curves represent relationships predicted by Eq. 3.*

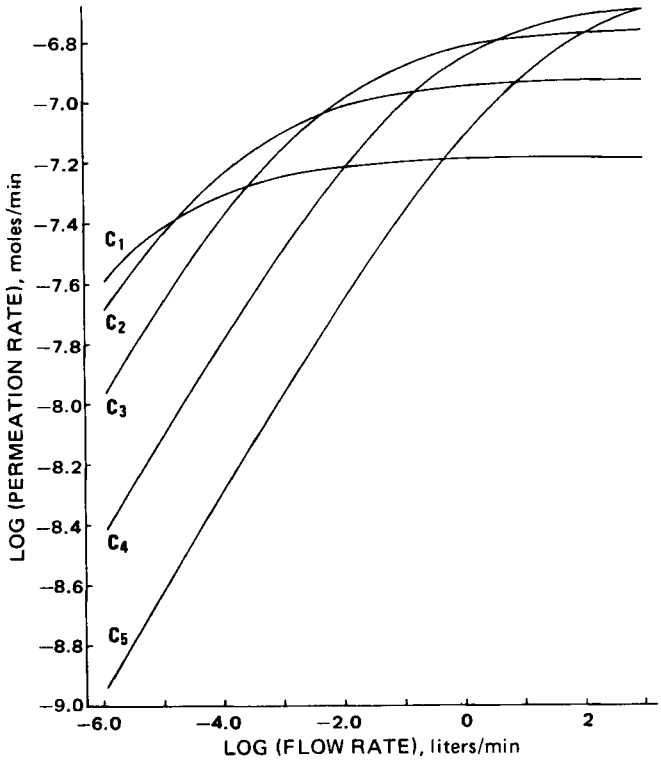

Figure 3—*Permeation rates of C_1–C_5 alkyl homologs of* p-*aminobenzoates estimated by Eq. 3 over a wide range of fluid flow rates.*

Eq. 3, especially for the butyl and pentyl esters. For the others, predicted trends exist in the rates of the various esters relative to each other.

To demonstrate the ramifications of Eq. 3, predicted rates are shown in Fig. 3 for a much wider range of fluid flow rates. At low flow rates, the lines became parallel with a slope of one-third because the solute transport rate was controlled by the simultaneous diffusion and convection in the liquid adjacent to the membrane, which is commonly termed the aqueous boundary layer control. This limiting case is given by Eq. 5. The

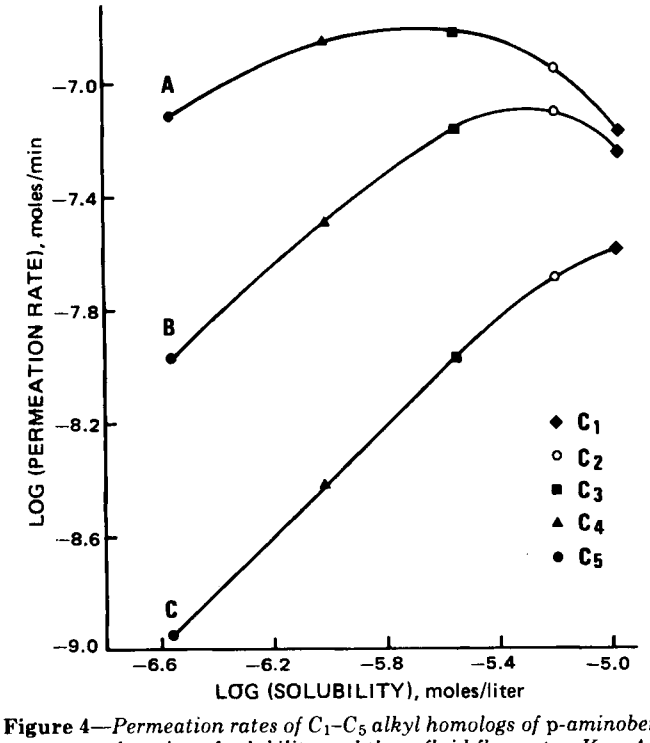

Figure 4—*Permeation rates of C_1–C_5 alkyl homologs of* p-*aminobenzoates as a function of solubility and three fluid flow rates. Key: A, 1 liter/min; B, 1×10^{-3} liter/min; and C, 1×10^{-6} liter/min.*

vertical spacing is governed by the solubilities of the various esters.

At high flow rates, the permeation rates leveled off and became independent of flow in accordance with Eq. 4, wherein the permeation rate becomes only a function of the transport across the membrane. Thus, K and C determined the relative positions of the plateaus in Fig. 3.

In the permeation simulations calculated with Eq. 3, values of D_m and D_w reported previously (2, 4) were assumed to be the same ($D_m = 2.72 \times 10^{-6}$ cm^2/sec and $D_w = 6 \times 10^{-6}$ cm^2/sec) for all members of the series because the change in molecular weight would change the diffusivity insignificantly (6) compared with the order-of-magnitude changes in the other parameters, *e.g.*, solubility and flow rate. Although the diffusivity was not evaluated as an independent parameter in the present work, it has been observed experimentally (7) that the resistance in the aqueous boundary layer film adjacent to a membrane is proportional to the diffusivity raised to the power −0.6. This observation is in reasonably good agreement with Eq. 2.

Equation 3 arises from an assumption that the resistances in the membrane and in the adjacent liquid are additive. This combination permits calculation of the permeation rate under conditions of membrane control or aqueous convective diffusion control or at intermediate points. It is apparent from the permeation data that the predictions were reasonably good. However, in the intermediate region, Eq. 3 should be considered as an interpolation formula rather than as an expression arising directly from basic theory because the instantaneous transport rate decreases somewhat with increasing distance along the membrane in the direction of flow. This decrease is a characteristic of convective diffusion theory. With intermediate cases, there would be a concentration gradient within the membrane in the direction of flow. This gradient is not accounted for in Eq. 3. However, such a gradient would be much smaller than the gradient normal to the membrane because of the relative distances involved and, therefore, may be ignored.

If the data in Fig. 3 are replotted as log permeation rate *versus* log solubility, the curves obtained at different flow rates appear as in Fig. 4. The maximum permeation rate is shifted to the left, *i.e.*, to permeants having a lower solubility, with an increase in flow rate. This is similar to the concepts of Flynn and Yalkowsky (2), who evaluated the effect of fluid flow agitation in terms of a change in the thickness of the stagnant or unstirred layer. The thickness of the unstirred layer is a model-dependent parameter; it cannot be measured independently of permeation experiments. In the present work, the effect of fluid flow is incorporated as the rate of shear adjacent to the membrane. Because hydrodynamic theory permits one to determine the shear rate from the fluid flow rate and the geometry of the cell, the effect of fluid flow on permeation and the position of maximum permeation can be calculated readily *a priori* for a given membrane thickness using Eq. 3.

REFERENCES

(1) K. G. Nelson and A. C. Shah, *J. Pharm. Sci.*, **66**, 137 (1977).

(2) G. L. Flynn and S. H. Yalkowsky, *ibid.*, **61**, 838 (1972).

(3) V. G. Levich, "Physicochemical Hydrodynamics," Prentice-Hall, Englewood Cliffs, N.J., 1962, pp. 43–45.

(4) A. C. Shah and K. G. Nelson, *J. Pharm. Sci.*, **64**, 1518 (1975).

(5) J. Crank, "The Mathematics of Diffusion," Clarendon, Oxford, England, 1956, p. 44.

(6) S. H. Yalkowsky and G. L. Flynn, *J. Pharm. Sci.*, **62**, 210 (1973).

(7) R. E. Beck and J. S. Schultz, *Biochim. Biophys. Acta*, **255**, 273 (1972).

Simultaneous High-Pressure Liquid Chromatographic Determination of Acetaminophen, Guaifenesin, and Dextromethorphan Hydrobromide in Cough Syrup

W. O. McSHARRY *x and I. V. E. SAVAGE ‡

Received April 12, 1979, from the **Quality Control Department, Hoffmann-La Roche Inc., Nutley, NJ 07110,* and ‡*Roche Products Pty. Ltd., Dee Why 2099, Australia.* Accepted for publication August 23, 1979.

Abstract □ Acetaminophen (I), guaifenesin (II), and dextromethorphan hydrobromide (III) were separated and quantitated simultaneously in cough syrup by high-pressure liquid chromatography. A chemically bonded octadecylsilane stationary phase was used with a mobile phase of 45% (v/v) aqueous methanol. The mobile phase pH was stabilized to 4.2 by adding formic acid–ammonium formate buffer (~0.4%). The internal standard was *o*-dinitrobenzene. Retention volumes were 4 ml for I, 6 ml for II, 11 ml for the internal standard, and 20 ml for III. Inactive syrup components did not interfere, permitting direct diluted sample injection. Results on active ingredients were essentially 100% of the claim, with standard deviations of ±1.5, 1.2, and 2.1% for I, II, and III, respectively.

Keyphrases □ High-pressure liquid chromatography—simultaneous determination of acetaminophen, guaifenesin, and dextromethorphan hydrobromide, analysis of cough syrup active ingredients □ Pharmaceutical preparations—simultaneous determination of cough syrup active ingredients by high-pressure liquid chromatography □ Acetaminophen—simultaneous determination with guaifenesin and dextromethorphan hydrobromide, high-pressure liquid chromatography □ Guaifenesin—simultaneous determination with acetaminophen and dextromethorphan hydrobromide, high-pressure liquid chromatography □ Dextromethorphan hydrobromide—simultaneous determination with acetaminophen and guaifenesin, high-pressure liquid chromatography

Characterization of numerous drugs (1–4) and analyses of specific dosage forms have been conducted through the use of high-pressure liquid chromatography (HPLC). Recent investigations of pharmaceutical preparations included acetaminophen (paracetamol)–chlorpheniramine maleate–dextromethorphan hydrobromide (5) and codeine phosphate–guaifenesin (glyceryl guaiacolate)–pheniramine maleate–phenylpropanolamine hydrochloride–pyrilamine maleate (6). A liquid chromatographic analysis of 29 drug compounds in acidic, neutral, and alkaline media included syrups containing phenylephrine hydrochloride, acetaminophen, guaifenesin, and dextromethorphan hydrobromide (4). However, it was not clear if the last three compounds could be analyzed using a single mobile phase.

Simultaneous determination of acetaminophan (I), guaifenesin (II), and dextromethorphan hydrobromide (III) in a liquid preparation has not been reported. Routine analysis of a cough syrup was required, and HPLC was the method of choice. A chemically bonded nonpolar-sta-

0022-3549/80/0200-0212$01.00/0

© 1980, American Pharmaceutical Association

vertical spacing is governed by the solubilities of the various esters.

At high flow rates, the permeation rates leveled off and became independent of flow in accordance with Eq. 4, wherein the permeation rate becomes only a function of the transport across the membrane. Thus, K and C determined the relative positions of the plateaus in Fig. 3.

In the permeation simulations calculated with Eq. 3, values of D_m and D_w reported previously (2, 4) were assumed to be the same ($D_m = 2.72 \times 10^{-6}$ cm^2/sec and $D_w = 6 \times 10^{-6}$ cm^2/sec) for all members of the series because the change in molecular weight would change the diffusivity insignificantly (6) compared with the order-of-magnitude changes in the other parameters, *e.g.*, solubility and flow rate. Although the diffusivity was not evaluated as an independent parameter in the present work, it has been observed experimentally (7) that the resistance in the aqueous boundary layer film adjacent to a membrane is proportional to the diffusivity raised to the power −0.6. This observation is in reasonably good agreement with Eq. 2.

Equation 3 arises from an assumption that the resistances in the membrane and in the adjacent liquid are additive. This combination permits calculation of the permeation rate under conditions of membrane control or aqueous convective diffusion control or at intermediate points. It is apparent from the permeation data that the predictions were reasonably good. However, in the intermediate region, Eq. 3 should be considered as an interpolation formula rather than as an expression arising directly from basic theory because the instantaneous transport rate decreases somewhat with increasing distance along the membrane in the direction of flow. This decrease is a characteristic of convective diffusion theory. With intermediate cases, there would be a concentration gradient within the membrane in the direction of flow. This gradient is not accounted for in Eq. 3. However, such a gradient would be much smaller than the gradient normal to the membrane because of the relative distances involved and, therefore, may be ignored.

If the data in Fig. 3 are replotted as log permeation rate *versus* log solubility, the curves obtained at different flow rates appear as in Fig. 4. The maximum permeation rate is shifted to the left, *i.e.*, to permeants having a lower solubility, with an increase in flow rate. This is similar to the concepts of Flynn and Yalkowsky (2), who evaluated the effect of fluid flow agitation in terms of a change in the thickness of the stagnant or unstirred layer. The thickness of the unstirred layer is a model-dependent parameter; it cannot be measured independently of permeation experiments. In the present work, the effect of fluid flow is incorporated as the rate of shear adjacent to the membrane. Because hydrodynamic theory permits one to determine the shear rate from the fluid flow rate and the geometry of the cell, the effect of fluid flow on permeation and the position of maximum permeation can be calculated readily *a priori* for a given membrane thickness using Eq. 3.

REFERENCES

(1) K. G. Nelson and A. C. Shah, *J. Pharm. Sci.*, **66**, 137 (1977).

(2) G. L. Flynn and S. H. Yalkowsky, *ibid.*, **61**, 838 (1972).

(3) V. G. Levich, "Physicochemical Hydrodynamics," Prentice-Hall, Englewood Cliffs, N.J., 1962, pp. 43–45.

(4) A. C. Shah and K. G. Nelson, *J. Pharm. Sci.*, **64**, 1518 (1975).

(5) J. Crank, "The Mathematics of Diffusion," Clarendon, Oxford, England, 1956, p. 44.

(6) S. H. Yalkowsky and G. L. Flynn, *J. Pharm. Sci.*, **62**, 210 (1973).

(7) R. E. Beck and J. S. Schultz, *Biochim. Biophys. Acta*, **255**, 273 (1972).

Simultaneous High-Pressure Liquid Chromatographic Determination of Acetaminophen, Guaifenesin, and Dextromethorphan Hydrobromide in Cough Syrup

W. O. McSHARRY *x and I. V. E. SAVAGE ‡

Received April 12, 1979, from the **Quality Control Department, Hoffmann-La Roche Inc., Nutley, NJ 07110,* and ‡*Roche Products Pty. Ltd., Dee Why 2099, Australia.* Accepted for publication August 23, 1979.

Abstract □ Acetaminophen (I), guaifenesin (II), and dextromethorphan hydrobromide (III) were separated and quantitated simultaneously in cough syrup by high-pressure liquid chromatography. A chemically bonded octadecylsilane stationary phase was used with a mobile phase of 45% (v/v) aqueous methanol. The mobile phase pH was stabilized to 4.2 by adding formic acid–ammonium formate buffer (~0.4%). The internal standard was *o*-dinitrobenzene. Retention volumes were 4 ml for I, 6 ml for II, 11 ml for the internal standard, and 20 ml for III. Inactive syrup components did not interfere, permitting direct diluted sample injection. Results on active ingredients were essentially 100% of the claim, with standard deviations of ±1.5, 1.2, and 2.1% for I, II, and III, respectively.

Keyphrases □ High-pressure liquid chromatography—simultaneous determination of acetaminophen, guaifenesin, and dextromethorphan hydrobromide, analysis of cough syrup active ingredients □ Pharmaceutical preparations—simultaneous determination of cough syrup active ingredients by high-pressure liquid chromatography □ Acetaminophen—simultaneous determination with guaifenesin and dextromethorphan hydrobromide, high-pressure liquid chromatography □ Guaifenesin—simultaneous determination with acetaminophen and dextromethorphan hydrobromide, high-pressure liquid chromatography □ Dextromethorphan hydrobromide—simultaneous determination with acetaminophen and guaifenesin, high-pressure liquid chromatography

Characterization of numerous drugs (1–4) and analyses of specific dosage forms have been conducted through the use of high-pressure liquid chromatography (HPLC). Recent investigations of pharmaceutical preparations included acetaminophen (paracetamol)–chlorpheniramine maleate–dextromethorphan hydrobromide (5) and codeine phosphate–guaifenesin (glyceryl guaiacolate)–pheniramine maleate–phenylpropanolamine hydrochloride–pyrilamine maleate (6). A liquid chromatographic analysis of 29 drug compounds in acidic, neutral, and alkaline media included syrups containing phenylephrine hydrochloride, acetaminophen, guaifenesin, and dextromethorphan hydrobromide (4). However, it was not clear if the last three compounds could be analyzed using a single mobile phase.

Simultaneous determination of acetaminophan (I), guaifenesin (II), and dextromethorphan hydrobromide (III) in a liquid preparation has not been reported. Routine analysis of a cough syrup was required, and HPLC was the method of choice. A chemically bonded nonpolar-sta-

0022-3549/80/0200-0212$01.00/0

© 1980, American Pharmaceutical Association

Table I—Typical Results and Precision

Sample	Acetaminophen (I)	Guaifenesin (II)	Dextromethorphan Hydrobromide (III)
1[a]	100.1	99.8	98.3
2[a]	102.1	101.2	101.3
3[a]	100.4	99.7	100.0
Response ratio only, %[b]	±1.3	±1.3	±1.7
Overall procedure, %[b]	±1.5	±1.2	±2.1

[a] Expressed as percent of claim. [b] Standard deviation of a single determination calculated from six replicates.

tionary phase was chosen because it is not adversely affected by the polar components of the syrup, making prior separation unnecessary. The aim was to develop a procedure in which all three components could be determined simultaneously in a single injection.

EXPERIMENTAL

Reagents—Acetaminophen (paracetamol) BP[1] (I), guaifenesin (glyceryl guaiacolate) BPC[1] (II), dextromethorphan hydrobromide[2] (III), and *o*-dinitrobenzene[3] (the internal standard) were used as supplied.

Mobile Phase Preparation—Thirty-four milliliters of 28–30% ammonia[4] was diluted with 30 ml of water. Then 30 ml of formic acid[4] (minimum 98%) was added slowly with stirring. When cool, the solution (pH ~ 3.9) was diluted to 100 ml with water (ammonium formate buffer).

Ammonium formate buffer (10 ml) was added to 450 ml of methanol[4] (ACS grade) and diluted with water to make 1 liter (pH ~ 4.2) at room temperature. The mobile phase was filtered with vacuum.

Standard Solutions—*Internal Standard Solution Preparation*—*o*-Dinitrobenzene, 50 mg, was dissolved in 125 ml of methanol and diluted to 250 ml.

Standard Solution Preparation—Separate standard stock solutions were prepared in 50% (v/v) methanol in water containing ~9.0 mg of I/ml, 3.7 mg of II/ml, or 0.4 mg of III/ml. A standard solution of all three components was prepared by pipetting 10.0 ml of I solution, 10.0 ml of II solution, 15.0 ml of III solution, and 5.0 ml of internal standard solution into a 50-ml volumetric flask and diluting to volume with 50% (v/v) methanol in water.

Sample Preparation—A 3-ml sample was transferred to a 50-ml volumetric flask and weighed. Then 5 ml of internal standard solution was added, and the mixture was diluted to volume with 50% (v/v) methanol in water.

Instrumentation—The liquid chromatograph consisted of a constant-flow pump[5], a low pressure injector[6], a 30-cm × 4-mm i.d. octadecylsilane column[7], and an absorbance detector[8] at 280 nm. The flow rate was 2.0 ml/min, and the injection volume was 15 μl. Peak heights were monitored with a strip-chart recorder[9] adjusted for maximum on-scale deflection for the internal standard and III. An electronic integrator[10] was used to monitor peak areas. Settings on the integrator were chosen to minimize noise.

Calculations—Results for I and II were calculated from the integrated area relative to the internal standard area. Results for III were calculated from the peak height relative to the height of the internal standard peak.

RESULTS AND DISCUSSION

The simultaneous analysis of all three components in this cough syrup was difficult for two reasons. First, the wide response range between I and III limited the amount of sample that could be injected without either overloading the detector or losing precision in the smaller component measurement. Second, the wide difference in polarity between I and III made it difficult to separate I and II from interfering impurities while eluting III in a reasonable time.

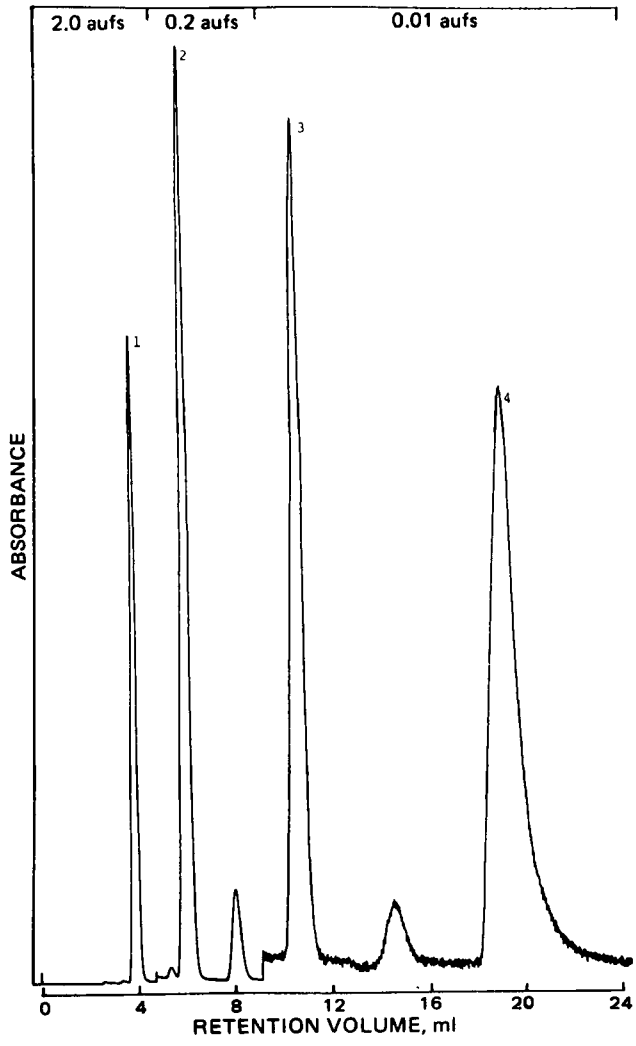

Figure 1—*High-pressure liquid chromatogram of a cough syrup preparation. Peaks 1, 2, and 4 are acetaminophen, guaifenesin, and dextromethorphan hydrobromide, respectively. Peak 3 is the internal standard (o-dinitrobenzene). Other peaks are unidentified components of the syrup. Absorbance units at full scale (aufs) are shown at the top.*

Heptanesulfonic acid and pentanesulfonic acid were tried as ion-pairing agents but retained III at methanol concentrations sufficiently low to separate I and II. Ammonium acetate buffer significantly reduced III retention without affecting I and II. Ammonium formate finally was chosen because it further reduced III retention, again without affecting I and II.

In all mobile phases tried, III tailed badly. Due to the tailing and low concentration of III, electronic integration was not reproducible (coefficient of variation ±5%). Therefore, peak height measurement was used. The possibility of interfering peaks was checked by injecting: a blank syrup preparation containing all ingredients except I, II, and III; a syrup preparation with no internal standard added; and the internal standard only, at a concentration 10 times that used in the analysis.

None of the inactive syrup components coeluted with the active ingredients or internal standard, nor did the internal standard contain any impurities that coeluted with the active ingredients (Fig. 1). Separation of I from its potential hydrolysis product, *p*-aminophenol, was confirmed by injecting a freshly prepared solution of *p*-aminophenol, which eluted separately from I. Detector response was linear within ±2% for all components between 80 and 110% of the claim.

Altogether nine samples were analyzed (Table I). Method precision was evaluated in two ways. The precision of the response ratio mea-

[1] Rhone-Poulenc Industries, Paris, France.
[2] F. Hoffmann-La Roche, Basel, Switzerland.
[3] British Drug Houses, Poole, England.
[4] Ajax Chemicals, Sydney, Australia.
[5] Model 6000 A, Waters Associates, Milford, Mass.
[6] Model U6K, Waters Associates, Milford, Mass.
[7] μBondapak C_{18}, Waters Associates, Milford, Mass.
[8] Model 440, Waters Associates, Milford, Mass.
[9] Series 5000, Fisher.
[10] Model CRS-204, Infotronics.

surement was determined by making six replicate injections of a single standard preparation. The overall precision was evaluated by making one injection for each of six separate sample preparations and calculating the result by comparison with the six replicate single injections. Most of the error resulted from the response ratio measurement (Table I), which can be reduced by replicate injections.

Instrument setup and preparation of the standard required ~2 hr. Individual analyses, including calculations, can be carried out at a rate of more than one sample per hour.

REFERENCES

(1) P. J. Twitchett and A. C. Moffat, *J. Chromatogr.*, **111**, 149 (1975).

(2) R. G. Achari and E. E. Theimer, *J. Chromatogr. Sci.*, **15**, 320 (1977).

(3) I. L., Honigberg, J. T. Stewart, and A. P. Smith, *J. Pharm. Sci.*, **63**, 766 (1974).

(4) H. Y. Mohammed and F. F. Cantwell, *Anal. Chem.*, **50**, 491 (1978).

(5) A. Menyharth, F. P. Mahn, and J. E. Heveran, *J. Pharm. Sci.*, **63**, 431 (1974).

(6) V. D. Gupta and A. G. Ghanekar, *ibid.*, **66**, 895 (1977).

ACKNOWLEDGMENTS

The authors thank Michael Meade of Roche Products Pty. Ltd. for the blank syrup preparation.

Work was performed at Roche Products Pty. Ltd., Dee Why, N.S.W. Australia.

Nonvariance of LD_{50} Values of Drugs in Gravid and Nongravid Mice

JAMES A. RUSSELL, MICHAEL P. MAHALIK, JOSEPH M. McDEVITT, and RONALD F. GAUTIERI ˣ

Received April 5, 1979, from the *Department of Pharmacology, School of Pharmacy, Temple University, Philadelphia, PA 19140.* Accepted for publication August 22, 1979.

Abstract □ This study showed that the LD_{50} values for morphine sulfate, cobalt chloride, and phenytoin sodium did not vary significantly on Day 9 of gestation in CF-1 mice when compared to values of nongravid animals.

Keyphrases □ LD_{50} testing—gravid and nongravid mice, morphine sulfate, cobalt chloride, phenytoin sodium, teratological study □ Teratological study—gravid and nongravid mice, morphine sulfate, cobalt chloride, phenytoin sodium, LD_{50} testing □ Morphine sulfate—LD_{50} testing, gravid and nongravid mice □ Phenytoin sodium—LD_{50} testing, gravid and nongravid mice □ Cobalt chloride—LD_{50} testing, gravid and nongravid mice

The LD_{50} value is the dose of a drug that proves lethal to 50% of a population. Despite the frequent use of this parameter to determine dosage schedules in teratological studies, it is often utilized with reservation due to its variance in gravid mice.

Therefore, to determine the LD_{50} variance in gravid and nongravid mice, it was decided to utilize drugs from different classes (morphine sulfate, cobalt chloride, and phenytoin sodium) and to subject the mice to a typical LD_{50} screen. Gravid mice were challenged on Day 9 of gestation, which corresponds to the midpoint in mouse pregnancy and also with the appearance of overt birth defects (1).

EXPERIMENTAL

Male and female CF-1 mice[1], ≥25 g, were utilized. Males were caged individually, and females were maintained in groups of 10 in large aggregate cages until exposure to the males. All mice were allowed water and food[2] *ad libitum*.

For morphine sulfate[3] and cobalt chloride[4] testing, 40 nongravid females were assigned to one of five groups of eight using a table of random numbers. Fifty-five animals, 11 per group, were used for phenytoin sodium testing[5] in the same manner. Dosage levels then were assigned to the groups (Tables I–III). Each mouse was weighed to the closest 0.1 g, caged individually, and administered the respective drug subcutaneously on the medial side of the right inguinal region.

Morphine sulfate (2%) and cobalt chloride (1 or 2%) were prepared daily in double-distilled water; phenytoin sodium (1%) was prepared in 70% propylene glycol in 0.9% NaCl. If the injected volume exceeded 1 ml, it was divided into two equal portions and was injected in separate inguinal regions. After injection, each mouse was observed for 24 hr, at which time the fatalities were observed (Tables I–III).

Breeding was accomplished as follows. Two females were placed

Table I—Observed Deaths [a] with Morphine Sulfate after 24 hr

Mice	Dosage, mg/kg				
	250	400	450	500	750
Nongravid	0/8	2/8	2/8	5/8	8/8
Gravid	0/8	1/8	2/8	5/8	7/8

[a] Deaths per number of mice tested.

Table II—Observed Deaths [a] with Cobalt Chloride after 24 hr

Mice	Dosage, mg/kg				
	100	125	150	200	300
Nongravid	0/8	2/8	4/8	6/8	8/8
Gravid	0/8	1/8	3/8	5/8	8/8

[a] Deaths per number of mice tested.

Table III—Observed Deaths [a] with Phenytoin Sodium after 24 hr

Mice	Dosage, mg/kg				
	200	250	300	325	400
Nongravid	0/11	3/11	7/11	10/11	11/11
Gravid	0/11	6/11	9/11	9/11	11/11

[a] Deaths per number of mice tested.

[1] Charles River Breeding Laboratories, Wilmington, Mass.
[2] Purina Laboratory Chow.
[3] USP, Merck & Co., Rahway, N.J.
[4] Lot 713262, Fisher Scientific, Fair Lawn, N.J.
[5] Lot PE338, Parke-Davis Co., Detroit, Mich.

0022-3549/80/0200-0214$01.00/0

© 1980, American Pharmaceutical Association

surement was determined by making six replicate injections of a single standard preparation. The overall precision was evaluated by making one injection for each of six separate sample preparations and calculating the result by comparison with the six replicate single injections. Most of the error resulted from the response ratio measurement (Table I), which can be reduced by replicate injections.

Instrument setup and preparation of the standard required ~2 hr. Individual analyses, including calculations, can be carried out at a rate of more than one sample per hour.

REFERENCES

(1) P. J. Twitchett and A. C. Moffat, *J. Chromatogr.*, **111**, 149 (1975).

(2) R. G. Achari and E. E. Theimer, *J. Chromatogr. Sci.*, **15**, 320 (1977).

(3) I. L., Honigberg, J. T. Stewart, and A. P. Smith, *J. Pharm. Sci.*, **63**, 766 (1974).

(4) H. Y. Mohammed and F. F. Cantwell, *Anal. Chem.*, **50**, 491 (1978).

(5) A. Menyharth, F. P. Mahn, and J. E. Heveran, *J. Pharm. Sci.*, **63**, 431 (1974).

(6) V. D. Gupta and A. G. Ghanekar, *ibid.*, **66**, 895 (1977).

ACKNOWLEDGMENTS

The authors thank Michael Meade of Roche Products Pty. Ltd. for the blank syrup preparation.

Work was performed at Roche Products Pty. Ltd., Dee Why, N.S.W. Australia.

Nonvariance of LD_{50} Values of Drugs in Gravid and Nongravid Mice

JAMES A. RUSSELL, MICHAEL P. MAHALIK, JOSEPH M. McDEVITT, and RONALD F. GAUTIERI ˣ

Received April 5, 1979, from the *Department of Pharmacology, School of Pharmacy, Temple University, Philadelphia, PA 19140.* Accepted for publication August 22, 1979.

Abstract □ This study showed that the LD_{50} values for morphine sulfate, cobalt chloride, and phenytoin sodium did not vary significantly on Day 9 of gestation in CF-1 mice when compared to values of nongravid animals.

Keyphrases □ LD_{50} testing—gravid and nongravid mice, morphine sulfate, cobalt chloride, phenytoin sodium, teratological study □ Teratological study—gravid and nongravid mice, morphine sulfate, cobalt chloride, phenytoin sodium, LD_{50} testing □ Morphine sulfate—LD_{50} testing, gravid and nongravid mice □ Phenytoin sodium—LD_{50} testing, gravid and nongravid mice □ Cobalt chloride—LD_{50} testing, gravid and nongravid mice

The LD_{50} value is the dose of a drug that proves lethal to 50% of a population. Despite the frequent use of this parameter to determine dosage schedules in teratological studies, it is often utilized with reservation due to its variance in gravid mice.

Therefore, to determine the LD_{50} variance in gravid and nongravid mice, it was decided to utilize drugs from different classes (morphine sulfate, cobalt chloride, and phenytoin sodium) and to subject the mice to a typical LD_{50} screen. Gravid mice were challenged on Day 9 of gestation, which corresponds to the midpoint in mouse pregnancy and also with the appearance of overt birth defects (1).

EXPERIMENTAL

Male and female CF-1 mice[1], ≥25 g, were utilized. Males were caged individually, and females were maintained in groups of 10 in large aggregate cages until exposure to the males. All mice were allowed water and food[2] *ad libitum*.

For morphine sulfate[3] and cobalt chloride[4] testing, 40 nongravid females were assigned to one of five groups of eight using a table of random numbers. Fifty-five animals, 11 per group, were used for phenytoin sodium testing[5] in the same manner. Dosage levels then were assigned to the groups (Tables I–III). Each mouse was weighed to the closest 0.1 g, caged individually, and administered the respective drug subcutaneously on the medial side of the right inguinal region.

Morphine sulfate (2%) and cobalt chloride (1 or 2%) were prepared daily in double-distilled water; phenytoin sodium (1%) was prepared in 70% propylene glycol in 0.9% NaCl. If the injected volume exceeded 1 ml, it was divided into two equal portions and was injected in separate inguinal regions. After injection, each mouse was observed for 24 hr, at which time the fatalities were observed (Tables I–III).

Breeding was accomplished as follows. Two females were placed

Table I—Observed Deaths [a] with Morphine Sulfate after 24 hr

Mice	Dosage, mg/kg				
	250	400	450	500	750
Nongravid	0/8	2/8	2/8	5/8	8/8
Gravid	0/8	1/8	2/8	5/8	7/8

[a] Deaths per number of mice tested.

Table II—Observed Deaths [a] with Cobalt Chloride after 24 hr

Mice	Dosage, mg/kg				
	100	125	150	200	300
Nongravid	0/8	2/8	4/8	6/8	8/8
Gravid	0/8	1/8	3/8	5/8	8/8

[a] Deaths per number of mice tested.

Table III—Observed Deaths [a] with Phenytoin Sodium after 24 hr

Mice	Dosage, mg/kg				
	200	250	300	325	400
Nongravid	0/11	3/11	7/11	10/11	11/11
Gravid	0/11	6/11	9/11	9/11	11/11

[a] Deaths per number of mice tested.

[1] Charles River Breeding Laboratories, Wilmington, Mass.
[2] Purina Laboratory Chow.
[3] USP, Merck & Co., Rahway, N.J.
[4] Lot 713262, Fisher Scientific, Fair Lawn, N.J.
[5] Lot PE338, Parke-Davis Co., Detroit, Mich.

0022-3549/80/0200-0214$01.00/0

© 1980, American Pharmaceutical Association

Table IV—Statistical Comparison [a] of Drugs Tested in Gravid and Nongravid CF-1 Mice

Test Group	LD_{50}, mg/kg	Slope	Slope Ratio	Slope Ratio Function	Potency Ratio	Potency Ratio Function
Morphine sulfate			1.11	1.20	1.08	1.22
Nongravid mice	480 (428–538)	1.17				
Gravid mice	520 (488–603)	1.30				
Cobalt chloride			1.04	1.60	1.11	1.26
Nongravid mice	157 (138–179)	1.33				
Gravid mice	174 (144–210)	1.28				
Phenytoin sodium			1.09	1.33	1.11	1.19
Nongravid mice	273 (250–298)	1.16				
Gravid mice	246 (214–283)	1.26				

[a] Values calculated by the method of Litchfield and Wilcoxon (2).

overnight in cages containing one male. On the next morning (Day 0), all females were observed for the presence of coagulated intravaginal semen, which was the criterion used for determining pregnancy. Then all those deemed pregnant were weighed and placed in individual cages. All of the nonpregnant mice were returned to the aggregate cages for later use.

On Day 9, gravid mice were randomly assigned to one of the appropriate dosage groups, and the respective solutions were administered subcutaneously; the same number of animals were used as for the nongravid groups. After 24 hr, fatalities were recorded. All gravid mice then were cervically dislocated and laparotomized to confirm pregnancy by the presence of fetal swellings.

RESULTS AND DISCUSSION

The teratogenic effects of morphine sulfate, cobalt chloride, and phenytoin sodium were reported previously (1, 3, 4). The determination of dosage schedules in these studies was made under the assumption that the LD_{50} of each drug did not vary between gravid and nongravid mice.

The data in Tables I–III were subjected to probit analysis according to the method of Litchfield and Wilcoxon (2). Because the slope ratios were less than the slope ratio functions, it can be concluded, with 95% confidence, that the dose–response curves did not deviate significantly from parallelism (Table IV). Furthermore, because the potency ratios were calculated to be less than the potency ratio functions, it can be concluded, with 95% confidence, that the LD_{50} of the respective drugs did not change significantly on Day 9 of gestation in CF-1 mice.

The range of the conclusions in this study is limited by the strain of mouse and the peculiarities of the drugs. However, because the drugs from three different classes did not vary in gravid and nongravid mice with respect to their LD_{50} curves, these results possibly can be extrapolated to other drugs. Hence, one LD_{50} curve obtained from nongravid mice may serve as a valid reference to determine the dose of an agent to be tested for teratogenicity.

REFERENCES

(1) H. S. Harpel, Jr., and R. F. Gautieri, *J. Pharm. Sci.*, **57**, 1590 (1968).

(2) J. T. Litchfield and F. Wilcoxon, *J. Pharmacol. Exp. Ther.*, **96**, 99 (1949).

(3) G. Kasirsky, W. T. Sherman, R. F. Gautieri, and D. E. Mann, Jr., *J. Pharm. Sci.*, **58**, 766 (1969).

(4) J. J. Mitala, D. E. Mann, Jr., and R. F. Gautieri, *ibid.*, **67**, 377 (1978).

Rapid Colorimetric Analysis of Chlorhexidine in Pharmaceutical Preparations

G. ANDERMANN ˣ, M. O. BUHLER, and M. ERHART

Received April 30, 1979, from the *Analytical Research and Development Department, P.O.S. Laboratories, 68240 Kaysersberg, France.* Accepted for publication August 21, 1979.

Abstract □ A colorimetric determination of chlorhexidine is described. The method is based on the formation of a yellow complex between the drug and bromcresol green. The absorption peak of this complex, extracted by chloroform, is at 410 nm, and linear response is obtained from 2.5 to 30 μg of chlorhexidine/ml. The accuracy and reproducibility of this rapid method make it useful for chlorhexidine determination in the manufacturing control of pharmaceutical mixtures.

Keyphrases □ Chlorhexidine—analysis, colorimetric determination in commercial dosage forms □ Antimicrobial agents—chlorhexidine, colorimetric determination in commercial dosage forms □ Colorimetry—analysis of chlorhexidine in commercial dosage forms

Chlorhexidine (I), an antimicrobial agent, is a common ingredient in antiseptic preparations. The presence of chlorhexidine as a preservative in other pharmaceutical dosage forms (eye drops) and cosmetics necessitated a rapid, economical, and sensitive determination.

BACKGROUND

The primary method available previously was a colorimetric procedure (1), but several components in pharmaceutical formulations interfere in the determination. Another colorimetric assay using *N*-(1-naphthyl)-ethylenediamine was reported for the determination of chlorhexidine in biological fluids (2), but it is time consuming and has background interference. A direct spectrophotometric assay of chlorhexidine using bromthymol blue was reported recently (3). Chlorhexidine is estimated based on differences in the absorbance before and after complexation with the acid dye. These techniques yield rather large errors.

Polarographic estimation (4) and an automated liquid chromatographic determination (5) also were reported recently. Chlorhexidine also has been determined successfully by GLC after hydrolysis to *p*-chloroaniline and suitable derivatization to *p*-chloroiodobenzene (6, 7), but this technique is time consuming and unsuitable for multiple analyses.

This paper describes a rapid colorimetric method that is based on the solvent extraction of a dye complex and is suitable for chlorhexidine analysis in pharmaceutical mixtures and cosmetics.

EXPERIMENTAL

Instrumentation—A double-beam spectrophotometer[1] and a shaker[2]

[1] Perkin-Elmer model 554.
[2] Lab-Line.

0022-3549/80/0200-0215$01.00/0

© 1980, American Pharmaceutical Association

Table IV—Statistical Comparison [a] of Drugs Tested in Gravid and Nongravid CF-1 Mice

Test Group	LD_{50}, mg/kg	Slope	Slope Ratio	Slope Ratio Function	Potency Ratio	Potency Ratio Function
Morphine sulfate			1.11	1.20	1.08	1.22
Nongravid mice	480 (428–538)	1.17				
Gravid mice	520 (488–603)	1.30				
Cobalt chloride			1.04	1.60	1.11	1.26
Nongravid mice	157 (138–179)	1.33				
Gravid mice	174 (144–210)	1.28				
Phenytoin sodium			1.09	1.33	1.11	1.19
Nongravid mice	273 (250–298)	1.16				
Gravid mice	246 (214–283)	1.26				

[a] Values calculated by the method of Litchfield and Wilcoxon (2).

overnight in cages containing one male. On the next morning (Day 0), all females were observed for the presence of coagulated intravaginal semen, which was the criterion used for determining pregnancy. Then all those deemed pregnant were weighed and placed in individual cages. All of the nonpregnant mice were returned to the aggregate cages for later use.

On Day 9, gravid mice were randomly assigned to one of the appropriate dosage groups, and the respective solutions were administered subcutaneously; the same number of animals were used as for the nongravid groups. After 24 hr, fatalities were recorded. All gravid mice then were cervically dislocated and laparotomized to confirm pregnancy by the presence of fetal swellings.

RESULTS AND DISCUSSION

The teratogenic effects of morphine sulfate, cobalt chloride, and phenytoin sodium were reported previously (1, 3, 4). The determination of dosage schedules in these studies was made under the assumption that the LD_{50} of each drug did not vary between gravid and nongravid mice.

The data in Tables I–III were subjected to probit analysis according to the method of Litchfield and Wilcoxon (2). Because the slope ratios were less than the slope ratio functions, it can be concluded, with 95% confidence, that the dose–response curves did not deviate significantly from parallelism (Table IV). Furthermore, because the potency ratios were calculated to be less than the potency ratio functions, it can be concluded, with 95% confidence, that the LD_{50} of the respective drugs did not change significantly on Day 9 of gestation in CF-1 mice.

The range of the conclusions in this study is limited by the strain of mouse and the peculiarities of the drugs. However, because the drugs from three different classes did not vary in gravid and nongravid mice with respect to their LD_{50} curves, these results possibly can be extrapolated to other drugs. Hence, one LD_{50} curve obtained from nongravid mice may serve as a valid reference to determine the dose of an agent to be tested for teratogenicity.

REFERENCES

(1) H. S. Harpel, Jr., and R. F. Gautieri, *J. Pharm. Sci.*, **57**, 1590 (1968).

(2) J. T. Litchfield and F. Wilcoxon, *J. Pharmacol. Exp. Ther.*, **96**, 99 (1949).

(3) G. Kasirsky, W. T. Sherman, R. F. Gautieri, and D. E. Mann, Jr., *J. Pharm. Sci.*, **58**, 766 (1969).

(4) J. J. Mitala, D. E. Mann, Jr., and R. F. Gautieri, *ibid.*, **67**, 377 (1978).

Rapid Colorimetric Analysis of Chlorhexidine in Pharmaceutical Preparations

G. ANDERMANN ˣ, M. O. BUHLER, and M. ERHART

Received April 30, 1979, from the *Analytical Research and Development Department, P.O.S. Laboratories, 68240 Kaysersberg, France.* Accepted for publication August 21, 1979.

Abstract □ A colorimetric determination of chlorhexidine is described. The method is based on the formation of a yellow complex between the drug and bromcresol green. The absorption peak of this complex, extracted by chloroform, is at 410 nm, and linear response is obtained from 2.5 to 30 μg of chlorhexidine/ml. The accuracy and reproducibility of this rapid method make it useful for chlorhexidine determination in the manufacturing control of pharmaceutical mixtures.

Keyphrases □ Chlorhexidine—analysis, colorimetric determination in commercial dosage forms □ Antimicrobial agents—chlorhexidine, colorimetric determination in commercial dosage forms □ Colorimetry—analysis of chlorhexidine in commercial dosage forms

Chlorhexidine (I), an antimicrobial agent, is a common ingredient in antiseptic preparations. The presence of chlorhexidine as a preservative in other pharmaceutical dosage forms (eye drops) and cosmetics necessitated a rapid, economical, and sensitive determination.

BACKGROUND

The primary method available previously was a colorimetric procedure (1), but several components in pharmaceutical formulations interfere in the determination. Another colorimetric assay using *N*-(1-naphthyl)-ethylenediamine was reported for the determination of chlorhexidine in biological fluids (2), but it is time consuming and has background interference. A direct spectrophotometric assay of chlorhexidine using bromthymol blue was reported recently (3). Chlorhexidine is estimated based on differences in the absorbance before and after complexation with the acid dye. These techniques yield rather large errors.

Polarographic estimation (4) and an automated liquid chromatographic determination (5) also were reported recently. Chlorhexidine also has been determined successfully by GLC after hydrolysis to *p*-chloroaniline and suitable derivatization to *p*-chloroiodobenzene (6, 7), but this technique is time consuming and unsuitable for multiple analyses.

This paper describes a rapid colorimetric method that is based on the solvent extraction of a dye complex and is suitable for chlorhexidine analysis in pharmaceutical mixtures and cosmetics.

EXPERIMENTAL

Instrumentation—A double-beam spectrophotometer[1] and a shaker[2]

[1] Perkin-Elmer model 554.
[2] Lab-Line.

0022-3549/80/0200-0215$01.00/0

© 1980, American Pharmaceutical Association

Table I—Chlorhexidine Digluconate Absorbance–Concentration Relationship

Concentration, μg/ml	Absorbance at 410 nm (Average ± *SD*, $n = 4$)	*RSD*, %
2.5	0.0380 ± 0.0005	1.3
5	0.0740 ± 0.0021	3.2
10	0.192 ± 0.001	0.7
15	0.1880 ± 0.0066	3.5
20	0.225 ± 0.012	5.5
25	0.285 ± 0.006	2.1
30	0.343 ± 0.002	0.6

Table II—Assay of Solutions of Known Chlorhexidine Digluconate Concentrations

Amount, mg	Concentration, μg/ml	Amount Found, mg ($\bar{X} \pm SD$, $n = 4$)	Amount Found, %
5	10	5.3 ± 0.2	106
10	10	10.4 ± 0.4	104
40	10	39.2 ± 2.1	98
50	10	50 ± 1.7	100

Table III—Assay of Commercially Available Chlorhexidine Digluconate Formulations

Formulation	Amount Claimed, mg/100 ml	Amount Found, mg/100 ml	Average Label Claim, %
Eye drops[a]	5	5.3	106
		5.2	104
		4.9	98
Viscous solutions[b]	5	5.3	106
		5.15	103
		5.24	105
Shampoos[c]	20	19.4	97

[a] Contains niacinamide, inosine monophosphate, and sodium glycerophosphate. [b] Contains thimerosal, hydroxyethylcellulose, sodium phosphate, and potassium phosphate. [c] Contains saponins, hydroxyethylcellulose, and bronidox.

Table IV—Within-Day Reproducibility of Color Extraction of Replicate 10-μg/ml Samples of Chlorhexidine Digluconate

Sample	Absorbance at 410 nm
1	0.128
2	0.129
3	0.128
4	0.121
5	0.123
6	0.123
7	0.124
8	0.126
9	0.128
10	0.132
11	0.127
12	0.127
Average	0.126
SD	0.003
RSD, %	2.37

were used. To prevent adsorption of the drug–dye complex onto the glass, screw-top plastic tubes were required (8).

Reagents—A pH 5.70 buffer was prepared by mixing 100 ml of 0.1 *M* citric acid with 140 ml of 0.2 *M* anhydrous Na_2HPO_4. The bromcresol green solution was prepared by dissolving 30 mg of bromcresol green[3] in 100 ml of the pH 5.70 buffer and filtering. The solution was stable for 1 week. A 1:100 dilution had an absorbance of 0.154 ± 0.003 at 617 nm.

Chlorhexidine digluconate[4], 5 mg, was dissolved in 100 ml of distilled water. This stock solution was diluted to give 2.5–30-μg/ml working standards, which were prepared fresh for each run.

Procedure for Chlorhexidine Standard Solutions—One milliliter of standard solution was transferred to a screw-top plastic tube, and 3 ml of the bromcresol green reagent and 2.5 ml of chloroform were added. The tubes were stoppered, shaken for 3 min, and centrifuged at 3000 rpm for 3 min. The aqueous supernate was discarded. The chloroform layer was transferred carefully with an automatic pipet[5] to a 1-cm light path cell, and the absorbance was measured against a blank (1 ml of distilled water instead of the chlorhexidine solution) at 410 nm.

[3] Pechiney Ugine-Kuhlmann.
[4] ICI Chemicals.

Table V—Between-Day Reproducibility of Samples Containing 10 μg of Chlorhexidine Digluconate/ml

Sample	Day 1	Day 2	Day 3
1	0.128	0.120	0.122
2	0.129	0.126	0.123
3	0.128	0.129	0.123
4	0.121	0.128	0.122
5	0.123	0.132	0.124
6	0.123	0.128	0.120
7	0.124	0.132	0.122
8	0.126	0.134	0.120
9	0.128	0.131	0.139
10	0.132	0.132	0.120
Average	0.126	0.127	0.123
SD	0.003	0.006	0.005
RSD, %	2.4	4.7	4.0

Procedure for Chlorhexidine Viscous Solutions, Shampoos, and Lotions—The chlorhexidine base was extracted from ~10–25 mg of chlorhexidine digluconate-containing samples by adding 50 μl of 10 *N* NaOH and shaking the solution for 15 min with 5 ml of chloroform. After centrifugation for 3 min at 3000 rpm, 2.5 ml of the chloroform layer was transferred to a screw-top plastic tube, 3 ml of bromcresol green reagent was added, and the procedure was followed as described for the standard solutions beginning with: "The tubes were stoppered . . . ."

RESULTS AND DISCUSSION

Color Stability—The yellow color was monitored with a recording spectrophotometer and was stable for 8 hr.

Linearity—The absorption peak of the bromcresol green–chlorhexidine complex was at ~410 nm. At this wavelength, the reaction followed Beer's law to an absorbance of 1.0, and linear response was obtained for 2.5–30 μg of chlorhexidine/ml (Table I).

The linear regression line was $A_{410} = (11.1C + 17.1)\ 10^{-3}$, where A_{410} is the absorbance at 410 nm and C is the concentration expressed in micrograms per milliliter. The calculated molar absorptivity, ϵ, was 11,302 ± 270. The correlation coefficient was 0.998.

Accuracy—The mean recoveries of known chlorhexidine amounts added to the formulations are shown in Table II. The precision was calculated by a literature method (9) as ~3.8% and was similar for viscous solutions and formulated products.

Table III shows the method to be fairly precise for chlorhexidine in eye drops, contact lens cleaning solutions, and shampoos, so the method can be used for manufacturing controls. No interference was observed with formulations of alcoholic solutions, eye drops, viscous solutions, and gels.

Detection Limits—The detection limit, as determined on 20 samples at the 95% confidence level, was 2.5 μg of chlorhexidine digluconate/ml.

Reproducibility—To show the within-batch variation, the chlorhexidine digluconate content of a 10-μg/ml standard solution was determined 12 times (Table IV). To show the between-batch variation, duplicate determinations were carried out on several days. The results were highly reproducible (Table V). Interanalyst variations of five chemists were determined at five levels by the proposed method, and rectilinear results were obtained (Table VI).

Method Limitations—Attempts to extend the method to chlorhexidine creams were unsuccessful due to coextraction of the formulation excipients that complex with bromcresol green. Emulsions also can be formed with the solvent and the chlorhexidine-containing creams.

This colorimetric determination of chlorhexidine salts offers improved precision, convenience, and speed over the previously reported methods. The high color stability offers an advantage over the colorimetric procedure of Holbrook (1). These considerations make the method suitable for the automated analysis of chlorhexidine salt formulations.

[5] Gilson.

Table VI—Results (Mean ± *SD*) of Intralaboratory Collaborative Study on Chlorhexidine Digluconate ($n = 4$)

Concentration, μg/ml	Chemist A	Chemist B	Chemist C	Chemist D	Chemist E
3.5	0.057 ± 0.001	0.050 ± 0.001	0.044 ± 0.002	0.045 ± 0.002	0.036 ± 0.002
8.5	0.118 ± 0.005	0.115 ± 0.002	0.107 ± 0.002	0.109 ± 0.001	0.096 ± 0.001
16	0.236 ± 0.003	0.216 ± 0.002	0.208 ± 0.004	0.220 ± 0.003	0.215 ± 0.003
23	0.313 ± 0.005	0.299 ± 0.017	0.300 ± 0.010	0.320 ± 0.002	0.306 ± 0.001
28	0.392 ± 0.008	0.367 ± 0.008	0.376 ± 0.013	0.420 ± 0.012	0.380 ± 0.005
Correlation coefficient	0.997	0.974	0.997	0.996	0.998

REFERENCES

(1) A. Holbrook, *J. Pharm. Pharmacol.*, **10,** 370 (1958).

(2) W. T. Robinson, L. Cosyns, and M. Kraml, *Clin. Biochem.*, **10,** 197 (1977).

(3) J. B. Lowry, *J. Pharm. Sci.*, **68,** 110 (1979).

(4) E. Jacobsen and B. Glyseth, *Talanta*, **22,** 1001 (1975).

(5) F. Bailey, P. N. Brittain, and B. F. Williamson, *J. Chromatogr.*, **109,** 305 (1975).

(6) K. Siefert, D. Casagrande, and H. Silberman, *ibid.*, **109,** 193 (1975).

(7) E. Cropper, R. Platt, and A. Puttnam, *J. Soc. Cosmet. Chem.*, **26,** 355 (1975).

(8) C. MacMartin, P. Simpson, and N. Thorpe, *J. Chromatogr.*, **43,** 72 (1969).

(9) R. B. Dean and W. B. Dixon, *Anal. Chem.*, **23,** 636 (1951).

Brain-to-Blood and Saliva-to-Blood Mepivacaine Ratios in Rats

KATHLEEN R. GANS, DEBRA J. WOOD, and G. VICTOR ROSSI ˣ

Received June 18, 1979, from the *Department of Biological Sciences, Philadelphia College of Pharmacy and Science, Philadelphia, PA 19104.* Accepted for publication August 24, 1979.

Abstract □ Mepivacaine hydrochloride, 25 and 50 mg/kg sc (with sacrifice at 15 min) produced higher ($p < 0.005$) drug levels in neonate (24–36-hr-old) rat brain and blood than in adult rat brain and blood; however, there was no significant difference in the brain-to-blood ratio of the drug between neonates and adults at either dose level. Intraarterial infusion of mepivacaine hydrochloride (20 μg/min) in adult rats resulted in measurable (GLC) mepivacaine base levels in pilocarpine-induced parotid salivary secretions collected throughout 30- and 45-min infusion periods. The saliva-to-blood ratios (±*SEM*) of mepivacaine base were 0.64 ± 0.13 after a 30-min infusion and 2.13 ± 0.48 after a 45-min infusion.

Keyphrases □ Mepivacaine—brain-to-blood and saliva-to-blood ratios, rats □ Anesthetics—mepivacaine, brain-to-blood and saliva-to-blood ratios, rats □ Models, animal—mepivacaine, brain-to-blood and saliva-to-blood ratios, rats

Several clinical studies demonstrated behavioral deficiencies and toxic manifestations in newborn infants whose mothers received local anesthesia during labor (1–8). Mepivacaine, widely used for such anesthesia, has been implicated in neonatal bradycardia, depression, apnea, convulsions, and death (1–4, 9, 10).

Because critical determinations of drug levels in the blood and tissues of healthy infants rarely are feasible, an animal model was employed to explore quantitative aspects of mepivacaine-related neural toxicity in neonates. Brain-to-blood ratios of mepivacaine base were determined for both neonate (24–36-hr-old) and adult rats after subcutaneous administration (25 and 50 mg/kg) of mepivacaine hydrochloride. Mepivacaine levels in adult rat whole blood and parotid saliva were compared to determine whether the salivary mepivacaine level could serve as an index of the blood drug concentration.

EXPERIMENTAL

Female Sprague–Dawley rats were supplied with food and water *ad libitum*. One group consisted of nonpregnant adult rats (250–300 g). Another group contained newborn rats (6–9 g) which remained with their mothers and nursed freely until drug or saline administration 24–36 hr postpartum.

Adult rats were prepared for saliva collection by anesthetization with urethan (1.2 mg/kg ip) followed by tracheotomy and cannulation of the parotid ducts according to a literature method (11). Tapered polyethylene tubing (PE 50) was inserted into each duct with the aid of a binocular dissecting microscope. Pilocarpine hydrochloride[1], 0.25 mg/ml, was infused at 0.2 ml/min into the right brachial artery to stimulate parotid salivary secretion. Mepivacaine hydrochloride[2], 1 mg/ml, was infused intraarterially (0.2 ml/min) concomitantly with the pilocarpine solution. Saliva was collected continuously throughout either a 30- or 45-min pilocarpine–mepivacaine infusion period, immediately after which 2–4 ml of blood was withdrawn *via* cardiac puncture into a heparinized vacutainer.

In another study, nonpregnant adult female rats were injected subcutaneously with 25 or 50 mg of mepivacaine hydrochloride/kg in 1.0 ml of saline; after 15 min, blood was collected *via* cardiac puncture into a heparinized vacutainer. The animals then were decapitated, and the brain was removed.

Two neonates were selected randomly from each of 15 litters and were injected subcutaneously with mepivacaine hydrochloride; one littermate received 25 mg/kg and the other received 50 mg/kg in 0.1 ml of saline. Animals were sacrificed 15 min after drug administration. Procedures for blood collection from neonates combined two techniques (12, 13). Brain tissue was removed after the spinal cord was severed at the neck.

Newborn and adult rat tissue and fluid samples also were collected from saline-injected animals, spiked with mepivacaine, and extracted for standard curves constructed each day for each tissue type. Mepiva-

[1] Aldrich Chemical Co., Milwaukee, Wis.

[2] Courtesy of Sterling-Winthrop Research Institute, Rensselaer, N.Y.

0022-3549/80/0200-0217$01.00/0

© 1980, American Pharmaceutical Association

Table VI—Results (Mean ± *SD*) of Intralaboratory Collaborative Study on Chlorhexidine Digluconate ($n = 4$)

Concentration, μg/ml	Chemist A	Chemist B	Chemist C	Chemist D	Chemist E
3.5	0.057 ± 0.001	0.050 ± 0.001	0.044 ± 0.002	0.045 ± 0.002	0.036 ± 0.002
8.5	0.118 ± 0.005	0.115 ± 0.002	0.107 ± 0.002	0.109 ± 0.001	0.096 ± 0.001
16	0.236 ± 0.003	0.216 ± 0.002	0.208 ± 0.004	0.220 ± 0.003	0.215 ± 0.003
23	0.313 ± 0.005	0.299 ± 0.017	0.300 ± 0.010	0.320 ± 0.002	0.306 ± 0.001
28	0.392 ± 0.008	0.367 ± 0.008	0.376 ± 0.013	0.420 ± 0.012	0.380 ± 0.005
Correlation coefficient	0.997	0.974	0.997	0.996	0.998

REFERENCES

(1) A. Holbrook, *J. Pharm. Pharmacol.*, **10,** 370 (1958).

(2) W. T. Robinson, L. Cosyns, and M. Kraml, *Clin. Biochem.*, **10,** 197 (1977).

(3) J. B. Lowry, *J. Pharm. Sci.*, **68,** 110 (1979).

(4) E. Jacobsen and B. Glyseth, *Talanta*, **22,** 1001 (1975).

(5) F. Bailey, P. N. Brittain, and B. F. Williamson, *J. Chromatogr.*, **109,** 305 (1975).

(6) K. Siefert, D. Casagrande, and H. Silberman, *ibid.*, **109,** 193 (1975).

(7) E. Cropper, R. Platt, and A. Puttnam, *J. Soc. Cosmet. Chem.*, **26,** 355 (1975).

(8) C. MacMartin, P. Simpson, and N. Thorpe, *J. Chromatogr.*, **43,** 72 (1969).

(9) R. B. Dean and W. B. Dixon, *Anal. Chem.*, **23,** 636 (1951).

Brain-to-Blood and Saliva-to-Blood Mepivacaine Ratios in Rats

KATHLEEN R. GANS, DEBRA J. WOOD, and G. VICTOR ROSSI ˣ

Received June 18, 1979, from the *Department of Biological Sciences, Philadelphia College of Pharmacy and Science, Philadelphia, PA 19104.* Accepted for publication August 24, 1979.

Abstract □ Mepivacaine hydrochloride, 25 and 50 mg/kg sc (with sacrifice at 15 min) produced higher ($p < 0.005$) drug levels in neonate (24–36-hr-old) rat brain and blood than in adult rat brain and blood; however, there was no significant difference in the brain-to-blood ratio of the drug between neonates and adults at either dose level. Intraarterial infusion of mepivacaine hydrochloride (20 μg/min) in adult rats resulted in measurable (GLC) mepivacaine base levels in pilocarpine-induced parotid salivary secretions collected throughout 30- and 45-min infusion periods. The saliva-to-blood ratios (±*SEM*) of mepivacaine base were 0.64 ± 0.13 after a 30-min infusion and 2.13 ± 0.48 after a 45-min infusion.

Keyphrases □ Mepivacaine—brain-to-blood and saliva-to-blood ratios, rats □ Anesthetics—mepivacaine, brain-to-blood and saliva-to-blood ratios, rats □ Models, animal—mepivacaine, brain-to-blood and saliva-to-blood ratios, rats

Several clinical studies demonstrated behavioral deficiencies and toxic manifestations in newborn infants whose mothers received local anesthesia during labor (1–8). Mepivacaine, widely used for such anesthesia, has been implicated in neonatal bradycardia, depression, apnea, convulsions, and death (1–4, 9, 10).

Because critical determinations of drug levels in the blood and tissues of healthy infants rarely are feasible, an animal model was employed to explore quantitative aspects of mepivacaine-related neural toxicity in neonates. Brain-to-blood ratios of mepivacaine base were determined for both neonate (24–36-hr-old) and adult rats after subcutaneous administration (25 and 50 mg/kg) of mepivacaine hydrochloride. Mepivacaine levels in adult rat whole blood and parotid saliva were compared to determine whether the salivary mepivacaine level could serve as an index of the blood drug concentration.

EXPERIMENTAL

Female Sprague–Dawley rats were supplied with food and water *ad libitum*. One group consisted of nonpregnant adult rats (250–300 g). Another group contained newborn rats (6–9 g) which remained with their mothers and nursed freely until drug or saline administration 24–36 hr postpartum.

Adult rats were prepared for saliva collection by anesthetization with urethan (1.2 mg/kg ip) followed by tracheotomy and cannulation of the parotid ducts according to a literature method (11). Tapered polyethylene tubing (PE 50) was inserted into each duct with the aid of a binocular dissecting microscope. Pilocarpine hydrochloride[1], 0.25 mg/ml, was infused at 0.2 ml/min into the right brachial artery to stimulate parotid salivary secretion. Mepivacaine hydrochloride[2], 1 mg/ml, was infused intraarterially (0.2 ml/min) concomitantly with the pilocarpine solution. Saliva was collected continuously throughout either a 30- or 45-min pilocarpine–mepivacaine infusion period, immediately after which 2–4 ml of blood was withdrawn *via* cardiac puncture into a heparinized vacutainer.

In another study, nonpregnant adult female rats were injected subcutaneously with 25 or 50 mg of mepivacaine hydrochloride/kg in 1.0 ml of saline; after 15 min, blood was collected *via* cardiac puncture into a heparinized vacutainer. The animals then were decapitated, and the brain was removed.

Two neonates were selected randomly from each of 15 litters and were injected subcutaneously with mepivacaine hydrochloride; one littermate received 25 mg/kg and the other received 50 mg/kg in 0.1 ml of saline. Animals were sacrificed 15 min after drug administration. Procedures for blood collection from neonates combined two techniques (12, 13). Brain tissue was removed after the spinal cord was severed at the neck.

Newborn and adult rat tissue and fluid samples also were collected from saline-injected animals, spiked with mepivacaine, and extracted for standard curves constructed each day for each tissue type. Mepiva-

[1] Aldrich Chemical Co., Milwaukee, Wis.

[2] Courtesy of Sterling-Winthrop Research Institute, Rensselaer, N.Y.

0022-3549/80/0200-0217$01.00/0

© 1980, American Pharmaceutical Association

Table I—Mepivacaine Base Concentration in Adult and Neonate Rat Whole Brain and Blood

Mepivacaine Hydrochloride[a] Dose, mg/kg sc	Brain Mepivacaine, μg/g ± SEM		Blood Mepivacaine, μg/g ± SEM		Mepivacaine Brain-to-Blood Ratio	
	Adult	Neonate	Adult	Neonate	Adult	Neonate
25	5.16 ± 0.54 $n = 18$[c]	15.50 ± 2.2[b] $n = 14$	2.61 ± 0.30	8.76 ± 1.5[b]	2.58 ± 0.39	2.01 ± 0.26
50	5.31 ± 0.52 $n = 17$	21.98 ± 2.2[b] $n = 15$	2.73 ± 0.38	11.26 ± 1.3[b]	3.84 ± 1.6	2.54 ± 0.44

[a] Animals sacrificed 15 min after mepivacaine hydrochloride administration. [b] $p < 0.005$. [c] n = number of animals.

Table II—Concentration of Mepivacaine Base in Adult Rat Parotid Saliva and Blood [a]

Infusion Time, min	n[b]	Saliva Mepivacaine, μg/g ± SEM	Blood Mepivacaine, μg/g ± SEM	Mepivacaine Saliva-to-Blood Ratio
30	17	4.79 ± 0.84	8.57 ± 1.07	0.64 ± 0.13
45	12	14.30 ± 4.64	8.10 ± 0.85	2.13 ± 0.48

[a] Mepivacaine hydrochloride was infused intraarterially at 200 μg/min. Pilocarpine hydrochloride (50 μg/min) was infused intraarterially concomitantly to stimulate parotid secretion. [b] Number of animals.

caine hydrochloride concentrations added to control samples ranged from 0.5 to 20 mg/g.

Immediately after collection, the blood, brain, and saliva samples were weighed and frozen (−15°). Because significant deterioration of mepivacaine in biological fluids stored for more than 72 hr was reported (14), extraction was performed within 3 days of tissue collection.

Published procedures were used for mepivacaine extraction from blood and saliva and for GLC analysis (14). Brain samples were homogenized with 1 ml of phosphate buffer (pH 7.4) in ground-glass tubes using a homogenizer[3]. An additional 2 ml of buffer was used to wash tissue from the homogenizing vessel into conical extraction tubes. After centrifugation at 2000 rpm for 10 min, ether was added to the supernate and the standard extraction protocol (14) was commenced.

Following evaporation of the final ether extract, the residue of each sample was reconstituted with 20 μl of chloroform. One microliter of the reconstituted sample was injected into a gas–liquid chromatograph[4] equipped with a hydrogen detector and preset to optimum conditions for detection of mepivacaine and procainamide (internal standard). The free (unbound) mepivacaine concentration (micrograms per gram of tissue) in each sample was determined *via* the method of internal standards with the use of standard curves constructed for each sample species. Relative ratios of brain-to-blood and parotid saliva-to-blood mepivacaine concentrations were calculated.

RESULTS AND DISCUSSION

Acute Mepivacaine Hydrochloride Toxicity—Dose studies (12.5–400 mg/kg) indicated that the approximate subcutaneous LD_{50} of mepivacaine hydrochloride in 24–36-hr-old neonate rats was 150 mg/kg. The subcutaneous LD_{50} of mepivacaine in rats weighing 65–75 g was reported to be 500 ± 53 mg/kg (15). None of the neonates that received 25 mg of mepivacaine hydrochloride/kg sc manifested gross toxic symptoms, but four of the 14 newborns injected with 50 mg/kg exhibited decreased spontaneous motor activity. Subcutaneous doses of 25 and 50 mg/kg produced no remarkable symptomatology in adult female rats. These subtoxic doses resulted in quantifiable mepivacaine levels in neonate and adult rat tissues.

Adult and Neonate Blood Mepivacaine Levels—Concentrations of mepivacaine base in adult and neonate rat whole brain and blood and calculated brain-to-blood ratios of mepivacaine appear in Table I. Following subcutaneous administration of 25- and 50-mg/kg mepivacaine hydrochloride doses, the mepivacaine levels were significantly higher in neonate rat brain and blood than in the corresponding adult female rat tissues. However, there was no significant difference between the brain-to-blood mepivacaine concentration ratios calculated for adults and for neonates at either of the two doses of local anesthetic agent.

Other investigators reported that a significantly greater fraction of bupivacaine, an anesthetic structurally related to mepivacaine, is bound to human maternal plasma proteins than is bound to fetal plasma proteins over a wide drug concentration range (16, 17). Although protein binding determinations were not performed, the slope of standard GLC curves (as determined by linear regression analysis) constructed with mepivacaine-spiked neonate rat brain and blood were consistently steeper than those obtained with adult rat tissue.

Acute neonatal intoxication without concomitant signs of local anesthetic intoxication in the mother was observed in humans born to mothers who received epidural or paracervical block anesthesia with mepivacaine hydrochloride during labor (1, 4, 7, 9, 18). The neurological deficiencies observed in the newborn might be related to incomplete development of the neonatal blood–brain barrier; however, this study revealed no significant differences in the brain-to-blood ratios of mepivacaine between neonate and adult rats. The study did demonstrate considerably higher levels of unbound mepivacaine in the brain tissue and blood of 24–36-hr-old rats than in these tissues of adult female rats 15 min after subcutaneous injection of equivalent body weight doses of the local anesthetic.

Mepivacaine in Adult Rat Blood and Saliva—The saliva-to-blood ratio of mepivacaine was explored to evaluate the sensitivity and reproducibility of this salivary assay as a noninvasive technique relevant to clinical monitoring of the blood level of a local anesthetic in the newborn. Intravenous infusion of mepivacaine hydrochloride (200 μg/min) in adult rats established blood and salivary drug levels well within the quantitation range by the GLC assay (14). The mepivacaine base concentrations in blood and pilocarpine-stimulated parotid saliva collected throughout 30- and 45-min intraarterial mepivacaine hydrochloride infusions and the saliva-to-blood mepivacaine ratio for each collection period are summarized in Table II.

Although the salivary drug concentration data were reasonably consistent within any collection period (*i.e.*, 30 or 45 min), the saliva-to-blood mepivacaine ratio differed considerably, depending on the infusion time and the total dose of local anesthetic. Thus, this study failed to demonstrate a consistent relationship between the mepivacaine level in these two body fluid compartments that would support saliva sampling and analysis as a means of estimating the blood drug level. The salivary secretion rate in the rat necessitated collection of a 20–30-min sample for drug extraction; a larger animal model, permitting simultaneous sampling of saliva and blood, would be advantageous to explore the relative compartmentalization of mepivacaine.

[3] Dorenmeyer.
[4] GOW-MAC model 750, Bound Brook, N.J.

REFERENCES

(1) W. E. Dodson, R. E. Hillman, and L. S. Hillman, *J. Pediatr.*, **86,** 624 (1975).

(2) H. R. Gordon, *N. Engl. J. Med.*, **279,** 910 (1968).

(3) I. Nyirjesy, B. L. Hawks, J. Herbert, J. Hopwood, Jr., and H. Falis, *Am. J. Obstet. Gynecol.*, **87,** 231 (1963).

(4) J. C. Sinclair, H. A. Fox, J. F. Lentz, G. L. Fuld, and J. Murphy, *N. Engl. J. Med.*, **273,** 1173 (1965).

(5) H. O. Morishima, S. S. Daniel, M. Finster, P. J. Poppers, and L. S. James, *Anesthesiology*, **27,** 147 (1966).

(6) K. Standley, A. B. Soule, S. A. Copans, and M. S. Duchowny, *Science*, **186,** 634 (1974).

(7) J. W. Scanlon, W. V. Brown, J. P. Weiss, and M. H. Alper, *Anesthesiology*, **40,** 121 (1974).

(8) B. T. Brazelton, *Am. J. Psychol.*, **126,** 95 (1970).

(9) J. B. Rosefsky, and M. E. Petersiel, *N. Engl. J. Med.*, **278,** 530 (1968).

(10) M. Finster, H. O. Morishima, R. N. Boyes, and B. G. Covino, *Anesthesiology*, **36,** 159 (1972).

(11) W. S. Chernick, E. Bobyock, and G. J. DiGregorio, *J. Dent. Res.*, **50,** 165 (1971).

(12) C. C. Korenbrot, D. C. Paup, and R. A. Gorski, *Endocrinology*, **97**, 709 (1975).
(13) C. J. Dunn and D. A. Willoughby, *J. Pathol.*, **116**, 167 (1975).
(14) J. H. Asling, S. M. Shnider, G. Wilkenson, and E. L. Way, *Anesthesiology*, **31**, 458 (1969).
(15) G. Aberg, *Acta Pharmacol. Toxicol.*, **31**, 273 (1972).
(16) L. E. Mather, G. J. Long, and J. Thomas, *J. Pharm. Pharmacol.*, **23**, 359 (1971).
(17) J. Thomas, G. Long, G. Moore, and D. Morgan, *Clin. Pharmacol. Ther.*, **19**, 426 (1976).
(18) L. J. Graziani, B. H. Korberly, and G. D'Amato, in "Topics in Pediatric Neurology," M. Blau, I. Rapin, and M. Kinsbourne, Eds., Spectrum, Jamaica, N.Y., 1977, pp. 11–41.

ACKNOWLEDGMENTS

The authors acknowledge the clinical observations of neurological deficiencies in the newborn by L. J. Graziani, Thomas Jefferson University School of Medicine, and Barbara H. Korberly, Philadelphia College of Pharmacy and Science, which prompted this investigation.

GLC Microdetermination of Indomethacin in Plasma

MICHAEL A. EVANS

Received May 18, 1979, from the *Department of Pharmacology, University of Illinois at the Medical Center, Chicago, IL 60680.* Accepted for publication August 27, 1979.

Abstract □ A GLC method utilizing an electron-capture detector is described for analysis of indomethacin in blood plasma. Indomethacin is extracted with ethyl acetate from plasma buffered to pH 5.0. The ethyl acetate is evaporated to dryness, and indomethacin is derivatized to a pentafluoropropionyl ester prior to chromatography. A GLC standard is used for peak height quantitation of indomethacin. The extraction efficiency from plasma is 92 ± 3%, and as little as 1 ng of indomethacin can be quantitatively determined.

Keyphrases □ Indomethacin—GLC analysis, human plasma □ GLC—analysis, indomethacin in human plasma □ Anti-inflammatory agents—indomethacin, GLC analysis in human plasma

Indomethacin[1] is an extensively used anti-inflammatory drug with potent inhibitory action on prostaglandin synthesis. Recent studies demonstrated that the drug is also successful in the management of patent ductus arteriosus in the premature infant (1). Since complications of indomethacin therapy in the premature infant are associated with high plasma levels, a rapid and sensitive assay was needed for monitoring therapeutic plasma drug levels utilizing small samples. Several investigators recently reported sensitive analytical procedures for indomethacin in biological fluid; however, these procedures require several extractions (2, 3), lack an internal standard (4), and require an initial plasma sample of 0.5 ml (5). Therefore, an electron-capture GLC method was developed for monitoring therapeutic indomethacin levels in limited plasma samples (0.1 ml) utilizing a GLC standard for quantitation.

EXPERIMENTAL

Apparatus—A gas chromatograph[2] equipped with a ^{63}Ni-electron-capture detector was maintained with a high purity nitrogen column gas flow of 70 ml/min. The column oven temperature was 295°; the injection port and detector temperatures were maintained at 310°.

Column—A glass column, 2 m × 2 mm, was packed with 10% SP 2250 on 100–120-mesh Supelcoport[3]. The column was rinsed before packing with methanol and acetone; it was then dried and conditioned for 2 hr with a 20% solution of dimethyldichlorosilane[4] in toluene. Following silylation, the column was rinsed with acetone and dried under nitrogen before packing.

Procedures—Plasma (0.1 ml) was transferred to 1.5-ml polypropylene disposable micro test tubes[5], buffered to pH 5.0 with 0.1 ml of 0.2 *M* acetate buffer, and extracted with 1.0 ml of ethyl acetate. The ethyl acetate (0.9 ml) was transferred by disposable pipet to a dry, clean 1.5-ml micro test tube and evaporated to dryness using a vacuum centrifuge[6]. The residue was mixed with 10 μl of a mixture of 2,2,3,3,3-pentafluoro-1-propanol in pentafluoropropionic anhydride[7] (1:4, v/v) and heated to 75° for 20 min. Following derivatization, the sample was evaporated to dryness using the vacuum centrifuge; the residue was redissolved in 10 μl of ethyl acetate containing 2.5 μg of *p*-bromobenzaldehyde isonicotinoylhydrazone/ml as the internal standard.

One-microliter samples were injected into the gas chromatograph for analysis. The internal standard was prepared according to Timbrell *et al.* (6) by mixing equimolar amounts of isoniazid and *p*-bromobenzaldehyde in methanol and refluxing for 1 hr at 60°. After cooling for 24 hr at −20°, the crystalline product was filtered, washed twice with warm methanol, and recrystallized. The final product, *p*-bromobenzaldehyde isonicotinoylhydrazone, was found to be better than 98% pure by GLC and TLC.

A standard calibration curve was prepared by adding 0.1 ml of plasma to known amounts of indomethacin to give final indomethacin concentrations ranging from 0.01 to 1 μg/ml. Thirty samples, five per concentration, were analyzed to prepare the standard curve. Each sample was injected in duplicate, and the determination of the entire standard curve was replicated at once. 2-^{14}C-Indomethacin[8] was used to estimate the extraction efficiency of indomethacin from plasma by measurement of the total radioactivity in the extract.

RESULTS AND DISCUSSION

The electron-capture GLC retention times for derivatized indomethacin and the internal standard were 5.2 and 6.8 min, respectively. Chromatograms from a control human plasma and a plasma sample containing 31 ng of indomethacin, both with the internal standard, are shown in Fig. 1. Since peaks for both agents were symmetrical, quantitation was made by comparison of peak heights. Detector response and the calibration curve were linear over 0.01–1.0-μg/ml range. Blanks were prepared from plasma of drug-free subjects, and no peaks were observed that would interfere with the measurement of indomethacin or the internal standard. Plasma samples containing 5 μg/ml of salicylate or furosemide also did not interfere with indomethacin quantitation.

Linear regression analysis of the individual data points (n = 60) from the standards plotted as the ratio of the peak height of derivatized in-

[1] Indocin, Merck & Co.
[2] Varian model 3700.
[3] Supelco, Inc., Bellefonte, Pa.
[4] Applied Science Laboratories, State College, Pa.
[5] Bio-Rad Laboratories, Richmond, Calif.
[6] Savant Instruments, Hicksville, N.Y.
[7] Regis Chemical, Morton Grove, Ill.
[8] New England Nuclear, Boston, Mass.

0022-3549/80/0200-0219$01.00/0
© 1980, American Pharmaceutical Association

(12) C. C. Korenbrot, D. C. Paup, and R. A. Gorski, *Endocrinology*, **97**, 709 (1975).
(13) C. J. Dunn and D. A. Willoughby, *J. Pathol.*, **116**, 167 (1975).
(14) J. H. Asling, S. M. Shnider, G. Wilkenson, and E. L. Way, *Anesthesiology*, **31**, 458 (1969).
(15) G. Aberg, *Acta Pharmacol. Toxicol.*, **31**, 273 (1972).
(16) L. E. Mather, G. J. Long, and J. Thomas, *J. Pharm. Pharmacol.*, **23**, 359 (1971).
(17) J. Thomas, G. Long, G. Moore, and D. Morgan, *Clin. Pharmacol. Ther.*, **19**, 426 (1976).
(18) L. J. Graziani, B. H. Korberly, and G. D'Amato, in "Topics in Pediatric Neurology," M. Blau, I. Rapin, and M. Kinsbourne, Eds., Spectrum, Jamaica, N.Y., 1977, pp. 11–41.

ACKNOWLEDGMENTS

The authors acknowledge the clinical observations of neurological deficiencies in the newborn by L. J. Graziani, Thomas Jefferson University School of Medicine, and Barbara H. Korberly, Philadelphia College of Pharmacy and Science, which prompted this investigation.

GLC Microdetermination of Indomethacin in Plasma

MICHAEL A. EVANS

Received May 18, 1979, from the *Department of Pharmacology, University of Illinois at the Medical Center, Chicago, IL 60680.* Accepted for publication August 27, 1979.

Abstract □ A GLC method utilizing an electron-capture detector is described for analysis of indomethacin in blood plasma. Indomethacin is extracted with ethyl acetate from plasma buffered to pH 5.0. The ethyl acetate is evaporated to dryness, and indomethacin is derivatized to a pentafluoropropionyl ester prior to chromatography. A GLC standard is used for peak height quantitation of indomethacin. The extraction efficiency from plasma is 92 ± 3%, and as little as 1 ng of indomethacin can be quantitatively determined.

Keyphrases □ Indomethacin—GLC analysis, human plasma □ GLC—analysis, indomethacin in human plasma □ Anti-inflammatory agents—indomethacin, GLC analysis in human plasma

Indomethacin[1] is an extensively used anti-inflammatory drug with potent inhibitory action on prostaglandin synthesis. Recent studies demonstrated that the drug is also successful in the management of patent ductus arteriosus in the premature infant (1). Since complications of indomethacin therapy in the premature infant are associated with high plasma levels, a rapid and sensitive assay was needed for monitoring therapeutic plasma drug levels utilizing small samples. Several investigators recently reported sensitive analytical procedures for indomethacin in biological fluid; however, these procedures require several extractions (2, 3), lack an internal standard (4), and require an initial plasma sample of 0.5 ml (5). Therefore, an electron-capture GLC method was developed for monitoring therapeutic indomethacin levels in limited plasma samples (0.1 ml) utilizing a GLC standard for quantitation.

EXPERIMENTAL

Apparatus—A gas chromatograph[2] equipped with a ^{63}Ni-electron-capture detector was maintained with a high purity nitrogen column gas flow of 70 ml/min. The column oven temperature was 295°; the injection port and detector temperatures were maintained at 310°.

Column—A glass column, 2 m × 2 mm, was packed with 10% SP 2250 on 100–120-mesh Supelcoport[3]. The column was rinsed before packing with methanol and acetone; it was then dried and conditioned for 2 hr with a 20% solution of dimethyldichlorosilane[4] in toluene. Following silylation, the column was rinsed with acetone and dried under nitrogen before packing.

Procedures—Plasma (0.1 ml) was transferred to 1.5-ml polypropylene disposable micro test tubes[5], buffered to pH 5.0 with 0.1 ml of 0.2 *M* acetate buffer, and extracted with 1.0 ml of ethyl acetate. The ethyl acetate (0.9 ml) was transferred by disposable pipet to a dry, clean 1.5-ml micro test tube and evaporated to dryness using a vacuum centrifuge[6]. The residue was mixed with 10 μl of a mixture of 2,2,3,3,3-pentafluoro-1-propanol in pentafluoropropionic anhydride[7] (1:4, v/v) and heated to 75° for 20 min. Following derivatization, the sample was evaporated to dryness using the vacuum centrifuge; the residue was redissolved in 10 μl of ethyl acetate containing 2.5 μg of *p*-bromobenzaldehyde isonicotinoylhydrazone/ml as the internal standard.

One-microliter samples were injected into the gas chromatograph for analysis. The internal standard was prepared according to Timbrell *et al.* (6) by mixing equimolar amounts of isoniazid and *p*-bromobenzaldehyde in methanol and refluxing for 1 hr at 60°. After cooling for 24 hr at −20°, the crystalline product was filtered, washed twice with warm methanol, and recrystallized. The final product, *p*-bromobenzaldehyde isonicotinoylhydrazone, was found to be better than 98% pure by GLC and TLC.

A standard calibration curve was prepared by adding 0.1 ml of plasma to known amounts of indomethacin to give final indomethacin concentrations ranging from 0.01 to 1 μg/ml. Thirty samples, five per concentration, were analyzed to prepare the standard curve. Each sample was injected in duplicate, and the determination of the entire standard curve was replicated at once. 2-^{14}C-Indomethacin[8] was used to estimate the extraction efficiency of indomethacin from plasma by measurement of the total radioactivity in the extract.

RESULTS AND DISCUSSION

The electron-capture GLC retention times for derivatized indomethacin and the internal standard were 5.2 and 6.8 min, respectively. Chromatograms from a control human plasma and a plasma sample containing 31 ng of indomethacin, both with the internal standard, are shown in Fig. 1. Since peaks for both agents were symmetrical, quantitation was made by comparison of peak heights. Detector response and the calibration curve were linear over 0.01–1.0-μg/ml range. Blanks were prepared from plasma of drug-free subjects, and no peaks were observed that would interfere with the measurement of indomethacin or the internal standard. Plasma samples containing 5 μg/ml of salicylate or furosemide also did not interfere with indomethacin quantitation.

Linear regression analysis of the individual data points (n = 60) from the standards plotted as the ratio of the peak height of derivatized in-

[1] Indocin, Merck & Co.
[2] Varian model 3700.
[3] Supelco, Inc., Bellefonte, Pa.
[4] Applied Science Laboratories, State College, Pa.
[5] Bio-Rad Laboratories, Richmond, Calif.
[6] Savant Instruments, Hicksville, N.Y.
[7] Regis Chemical, Morton Grove, Ill.
[8] New England Nuclear, Boston, Mass.

0022-3549/80/0200-0219$01.00/0
© 1980, American Pharmaceutical Association

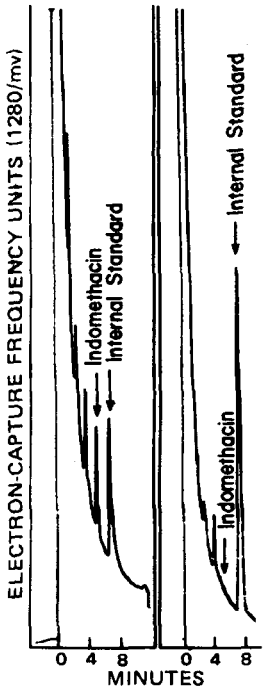

Figure 1—*Gas chromatograms of human plasma. Key: left: plasma (0.1 ml) containing 31 ng of indomethacin and internal standard; and right: control plasma with internal standard.*

domethacin divided by the peak height of the internal standard *versus* the plasma indomethacin concentration gave a computed slope of 42.8/ng of derivatized indomethacin and a coefficient of determination (r^2), a measure of accuracy, of 0.994. Extraction efficiency based on results from 10 samples using ^{14}C-indomethacin was estimated at 92 ± 3%.

Results of indomethacin analysis in a premature infant with patent ductus arteriosus following therapeutic intravenous administration of a 0.2-mg/kg dose of indomethacin sodium trihydrate are shown in Fig. 2. The pharmacokinetic parameters for the intravenous study were evaluated using a modified IGPHARM program (7). The calculated half-life was 15.5 hr, but further study is needed before any definitive statements can be made concerning the indomethacin half-life in the premature infant. Alvan *et al.* (8) demonstrated that the half-life of the β-phase of indomethacin in adults ranged from 2.6 to 11.2 hr. This rapid and sensitive method for indomethacin analysis has been useful in the

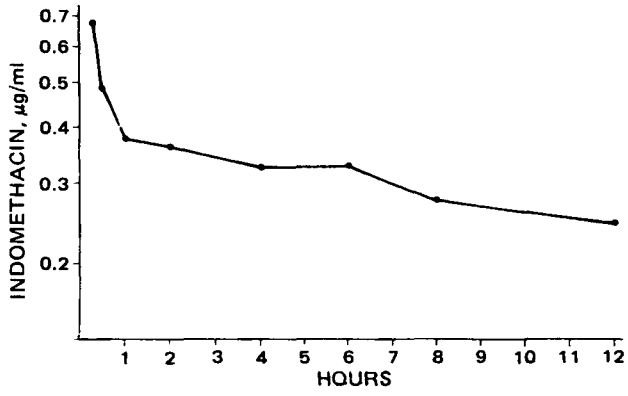

Figure 2—*Plasma concentration–time profile for indomethacin in a premature infant receiving intravenous indomethacin sodium trihydrate ($t_{1/2}$ = 15.5 hr, V_D = 0.37 liter/kg, and Cl_p = 15.3 ml/kg/hr). Sample size ranged from 0.05 to 0.15 ml of plasma.*

therapeutic monitoring of plasma drug levels when the sample volume is necessarily limited.

REFERENCES

(1) W. F. Friedman, M. J. Hirschklow, M. P. Printz, P. T. Pitlick, and S. E. Kirkpatrick, *N. Engl. J. Med.*, **295**, 526 (1976).

(2) B. Plazonnet and W. J. A. VandenHeuval, *J. Chromatogr.*, **142**, 587 (1977).

(3) R. G. Sibeon, J. D. Baty, N. Baber, K. Chan, and M. Orme, *ibid.*, **153**, 189 (1978).

(4) D. G. Ferry, D. M. Ferry, P. W. Moller, and E. G. McQueen, *ibid.*, **89**, 110 (1974).

(5) L. Helleberg, *ibid.*, **117**, 167 (1976).

(6) J. A. Timbrell, J. W. Wright, and C. M. Smith, *ibid.*, **138**, 165 (1977).

(7) G. Gomeni and Gomeni, *Comp. Biomed. Res.*, **11**, 1345 (1978).

(8) G. Alvan, M. Orme, L. Bertilson, R. Ekstrand, and L. Palmer, *Clin. Pharmacol. Ther.*, **18**, 364 (1975).

ACKNOWLEDGMENTS

Supported in part by U.S. Public Health Service Grant DA 01877 and University of Illinois Research Grant 7658.

Peristaltic Dissolution Apparatus: Prediction of Relative *In Vivo* Performance of Prednisone Tablets in Humans

D. L. SIMMONS ˣ, A. A. LEGORE, and P. PICOTTE

Received March 23, 1979, from the *R & D Laboratories, Frank W. Horner Limited, Montreal H3C 2W6, Canada.* Accepted for publication August 29, 1979.

Abstract □ By utilizing a previously established correlation concept, the relative *in vivo* performance in humans of seven unknown prednisone tablets was predicted accurately from peristaltic dissolution rate data. A general discussion is presented on the role of the peristaltic apparatus in selecting a suitable dosage form at the developmental stage.

Keyphrases □ Prednisone—tablets, prediction of relative *in vivo* performance in humans, peristaltic dissolution apparatus □ Dissolution apparatus, peristaltic—prednisone tablets, prediction of relative *in vivo* performance in humans □ *In vitro–in vivo* correlation—prednisone tablets, prediction of relative *in vivo* performance in humans, peristaltic dissolution apparatus

In 1975, a peristaltic dissolution rate apparatus was developed that was capable of predicting the *in vivo* performance of tolbutamide tablets in beagle dogs (1). This work was extended later to include meprobamate tablets (2) and tolbutamide tablets marketed in Canada (3). Despite the excellent *in vitro–in vivo* correlations obtained, a prime concern was the reliance on beagles as an *in vivo* model and the absence of human data in the correlations.

The performance of the apparatus on tablets that had been evaluated in a human bioavailability study was tested in this study. Seven prednisone tablets commercially available in the United States, each containing 5 mg of prednisone, were submitted in coded form by the Food and Drug Administration (FDA). Based on the peristaltic dissolution data, the relative *in vivo* performance of the tablets was predicted accurately.

0022-3549/80/0200-0220$01.00/0
© 1980, American Pharmaceutical Association

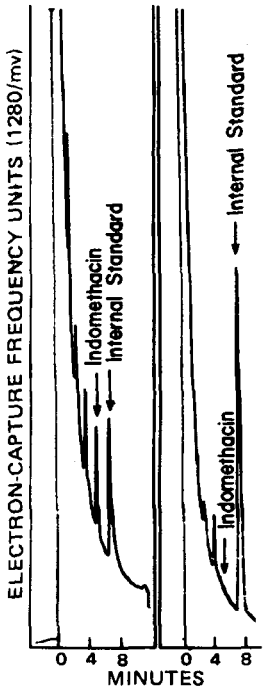

Figure 1—*Gas chromatograms of human plasma. Key: left: plasma (0.1 ml) containing 31 ng of indomethacin and internal standard; and right: control plasma with internal standard.*

domethacin divided by the peak height of the internal standard *versus* the plasma indomethacin concentration gave a computed slope of 42.8/ng of derivatized indomethacin and a coefficient of determination (r^2), a measure of accuracy, of 0.994. Extraction efficiency based on results from 10 samples using ^{14}C-indomethacin was estimated at 92 ± 3%.

Results of indomethacin analysis in a premature infant with patent ductus arteriosus following therapeutic intravenous administration of a 0.2-mg/kg dose of indomethacin sodium trihydrate are shown in Fig. 2. The pharmacokinetic parameters for the intravenous study were evaluated using a modified IGPHARM program (7). The calculated half-life was 15.5 hr, but further study is needed before any definitive statements can be made concerning the indomethacin half-life in the premature infant. Alvan *et al.* (8) demonstrated that the half-life of the β-phase of indomethacin in adults ranged from 2.6 to 11.2 hr. This rapid and sensitive method for indomethacin analysis has been useful in the

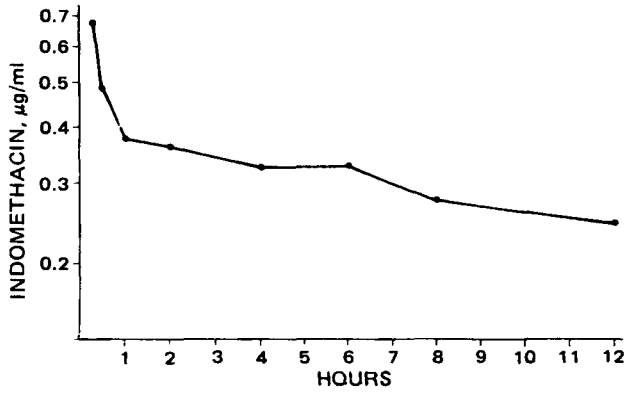

Figure 2—*Plasma concentration–time profile for indomethacin in a premature infant receiving intravenous indomethacin sodium trihydrate ($t_{1/2}$ = 15.5 hr, V_D = 0.37 liter/kg, and Cl_p = 15.3 ml/kg/hr). Sample size ranged from 0.05 to 0.15 ml of plasma.*

therapeutic monitoring of plasma drug levels when the sample volume is necessarily limited.

REFERENCES

(1) W. F. Friedman, M. J. Hirschklow, M. P. Printz, P. T. Pitlick, and S. E. Kirkpatrick, *N. Engl. J. Med.*, **295**, 526 (1976).

(2) B. Plazonnet and W. J. A. VandenHeuval, *J. Chromatogr.*, **142**, 587 (1977).

(3) R. G. Sibeon, J. D. Baty, N. Baber, K. Chan, and M. Orme, *ibid.*, **153**, 189 (1978).

(4) D. G. Ferry, D. M. Ferry, P. W. Moller, and E. G. McQueen, *ibid.*, **89**, 110 (1974).

(5) L. Helleberg, *ibid.*, **117**, 167 (1976).

(6) J. A. Timbrell, J. W. Wright, and C. M. Smith, *ibid.*, **138**, 165 (1977).

(7) G. Gomeni and Gomeni, *Comp. Biomed. Res.*, **11**, 1345 (1978).

(8) G. Alvan, M. Orme, L. Bertilson, R. Ekstrand, and L. Palmer, *Clin. Pharmacol. Ther.*, **18**, 364 (1975).

ACKNOWLEDGMENTS

Supported in part by U.S. Public Health Service Grant DA 01877 and University of Illinois Research Grant 7658.

Peristaltic Dissolution Apparatus: Prediction of Relative *In Vivo* Performance of Prednisone Tablets in Humans

D. L. SIMMONS ˣ, A. A. LEGORE, and P. PICOTTE

Received March 23, 1979, from the *R & D Laboratories, Frank W. Horner Limited, Montreal H3C 2W6, Canada.* Accepted for publication August 29, 1979.

Abstract □ By utilizing a previously established correlation concept, the relative *in vivo* performance in humans of seven unknown prednisone tablets was predicted accurately from peristaltic dissolution rate data. A general discussion is presented on the role of the peristaltic apparatus in selecting a suitable dosage form at the developmental stage.

Keyphrases □ Prednisone—tablets, prediction of relative *in vivo* performance in humans, peristaltic dissolution apparatus □ Dissolution apparatus, peristaltic—prednisone tablets, prediction of relative *in vivo* performance in humans □ *In vitro–in vivo* correlation—prednisone tablets, prediction of relative *in vivo* performance in humans, peristaltic dissolution apparatus

In 1975, a peristaltic dissolution rate apparatus was developed that was capable of predicting the *in vivo* performance of tolbutamide tablets in beagle dogs (1). This work was extended later to include meprobamate tablets (2) and tolbutamide tablets marketed in Canada (3). Despite the excellent *in vitro–in vivo* correlations obtained, a prime concern was the reliance on beagles as an *in vivo* model and the absence of human data in the correlations.

The performance of the apparatus on tablets that had been evaluated in a human bioavailability study was tested in this study. Seven prednisone tablets commercially available in the United States, each containing 5 mg of prednisone, were submitted in coded form by the Food and Drug Administration (FDA). Based on the peristaltic dissolution data, the relative *in vivo* performance of the tablets was predicted accurately.

0022-3549/80/0200-0220$01.00/0
© 1980, American Pharmaceutical Association

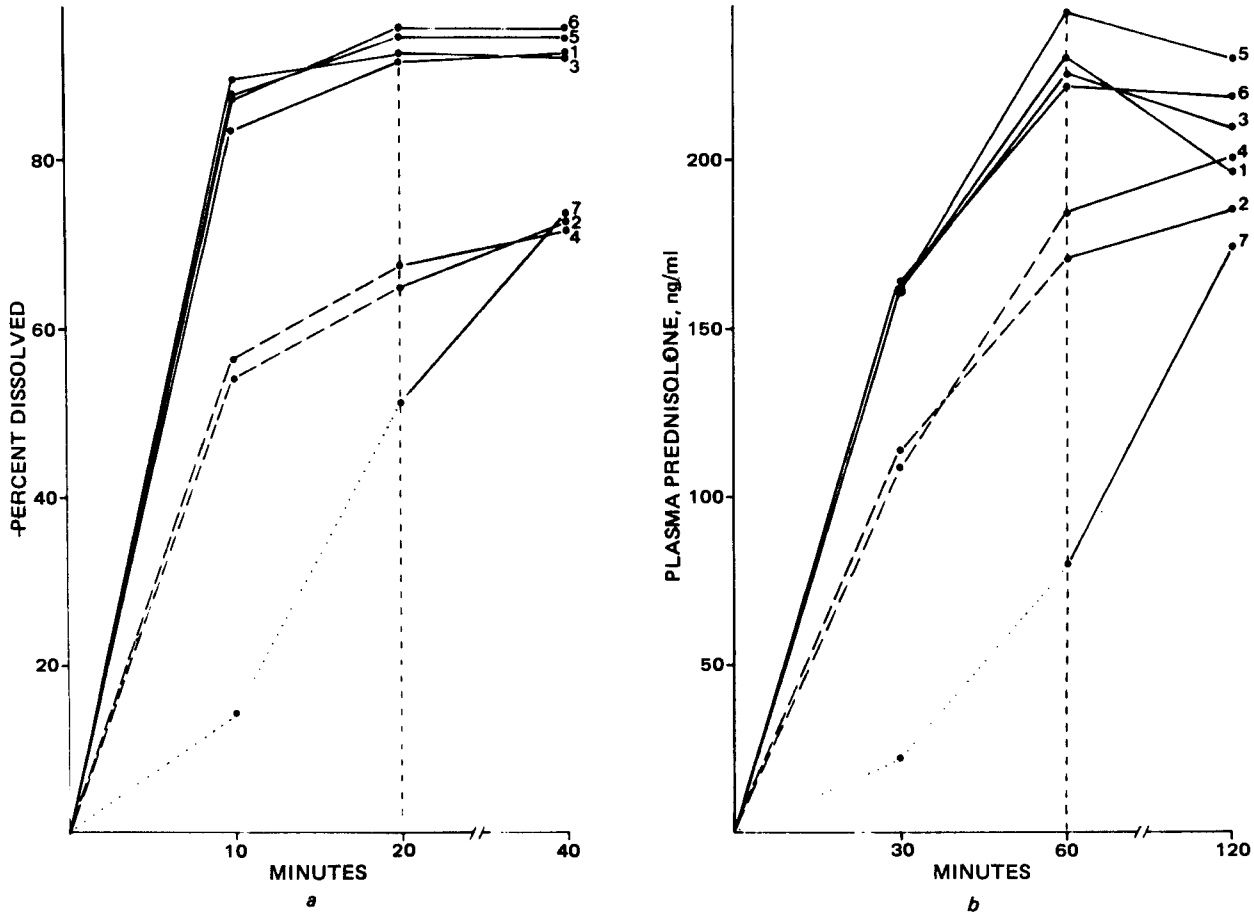

Figure 1—*Peristaltic dissolution plots of prednisone tablets* (a) *and prednisolone concentration–time plots of tablets* (b). *Key: See Table I. Dotted vertical lines at 20 and 60 min represent the maximum time intervals for* in vitro–in vivo *correlation. Relative performances of tablets from 0 to these times are categorized by solid, broken, and dotted lines.*

EXPERIMENTAL

Dissolution Rate Determinations—Dissolution rate profiles (Fig. 1*a*) for the prednisone tablets (5 mg) were obtained from the peristaltic dissolution rate assembly according to the conditions described previously (1). Aliquots (20 ml) of the dissolution medium, pH 7.6 tromethamine buffer, were removed at 10, 20, and 40 min and replenished with fresh buffer. Duplicate filtered aliquots (9 ml) were extracted separately with chloroform (3 × 5 ml), and the combined extracts from each sample were evaporated to dryness under nitrogen on a water bath.

The residues were dissolved in alcohol–chloroform (1:1, 0.5 ml) containing cholesteryl acetate[1] as an internal standard and were assayed for prednisone by GLC. The standard curve was obtained by spiking dissolution medium aliquots with known prednisone[2] quantities and performing the workup as described.

Chromatographic Conditions—The gas–liquid chromatograph[3] was equipped with a flame-ionization detector and a glass column (1.8 m × 6.2 mm o.d.) packed with 3% OV-17 on 80–100-mesh Gas Chrom Q. The column, detector, and injection port temperatures were 265, 295, and 278°, respectively. The carrier gas (nitrogen) flow rate was 48 ml/min. Air and hydrogen flow rates were adjusted for maximum sensitivity. The retention times for prednisone and cholesteryl acetate were 6.1 and 8.4 min, respectively.

RESULTS

In previous *in vitro–in vivo* correlation experiments (1–3) conducted with the peristaltic dissolution rate apparatus and blood drug level studies in beagles during the initial absorption phase, a direct relationship was established between *in vitro* data at t min and *in vivo* data at $3t$ min. By determining the dissolution rate profiles for the tablets during a 40-min period, their relative *in vivo* performance during a corresponding 120-min period was predicted accurately.

In this study, the average percent dissolved values also were obtained during the same *in vitro* period at 10, 20, and 40 min on the seven coded FDA prednisone tablets using the peristaltic dissolution assembly. These values are depicted graphically in Fig. 1*a*. Tablets 1, 3, 5, and 6 demonstrated comparable and excellent dissolution characteristics. Tablets 2 and 4 displayed mediocre dissolution profiles. Tablet 7 provided extremely poor initial performance and showed different intertablet disintegration characteristics, *e.g.*, two tablets in 23 min and one tablet in 32 min.

According to the correlation concept, these dissolution profiles were expected to reflect the relative *in vivo* performance of the tablets during a corresponding 120-min period. Tablets 1, 3, 5, and 6 were expected to exhibit identical drug absorption profiles. Conversely, Tablets 2, 4, and 7 were expected to display delayed drug absorption patterns, with a pronounced difference for Tablet 7.

This information was submitted to the FDA, which subsequently deciphered the code and confirmed that these prednisone tablets were from the same manufacturers and same lot numbers as those utilized in a comparative bioavailability study in human volunteers (4, 5). Figure 1*b* is a plot of the actual plasma prednisolone concentration *versus* time up to 120 min for 12 volunteers administered two 5-mg prednisone tablets. The data revealed that prednisone was absorbed and metabolized rapidly from Tablets 1, 3, 5, and 6 with a peak plasma prednisolone concentration of 222–244 ng/ml at 60 min. Tablets 2, 4, and 7 exhibited delayed drug absorption profiles. An examination of the two profiles in Figs. 1*a* and 1*b* demonstrates the ability of the peristaltic dissolution rate apparatus to simulate effectively the relative *in vivo* performance of the tablets.

Statistical treatment by regression analysis of the percent dissolved values for the tablets at 10 and 20 min *versus* plasma prednisolone concentrations at 30 and 60 min (Table I) revealed an extremely good fit with correlation coefficients of 0.995 and 0.923, respectively.

[1] Cholesteryl acetate, mp 113–116° (lot mp 115–116°) prepared by treating cholesterol with acetyl chloride and acetic acid.
[2] Courtesy of Merck-Frosst Laboratories, Montreal, Canada.
[3] Mikrotek MT 220, Tracor Inc., Austin, Tex.

Table I—Comparison of *In Vitro* and *In Vivo* Data [a]

Tablet	Percent Dissolved [b] 10 min	Percent Dissolved [b] 20 min	Plasma Prednisolone [c], ng/ml 30 min	Plasma Prednisolone [c], ng/ml 60 min
1	83.3	91.5	162	231
2	54.1	64.9	108	186
3	89.6	92.4	162	225
4	56.4	67.4	113	172
5	87.7	94.5	162	244
6	87.2	95.5	164	222
7	14.1	51.2	22	79.7

[a] Manufacturers and lot numbers of the tablets were: 1, Nysco Laboratories, 49571; 2, Barr Laboratories, 4126111; 3, McKesson Laboratories, 3K668; 4, Rexall Drug Co., E11499; 5, Lemmon Pharmacal, 1382; 6, The Upjohn Co., 786AEFI; and 7, Danbury Pharmacal Inc., 4539. The products were submitted by the FDA National Center for Drug Analysis, St. Louis, Mo. [b] Average of three runs. [c] From Ref. 4, Table IV, p. 163, and Table IX, p. 170.

DISCUSSION

The peristaltic dissolution apparatus has provided the authors with complete assurance that a new product launched on the market is bioequivalent to an originator's product or formulated to present optimum drug release characteristics. This assurance has been demonstrated by the excellent *in vitro–in vivo* correlations obtained in beagle dog studies, comparative bioavailability evaluations in humans, and results from clinical studies.

The utility of the peristaltic apparatus in drug product design can be exemplified in the following manner. If the drug substance (*e.g.*, prednisone) has limited water solubility, a drug suspension is screened for dissolution characteristics in dilute hydrochloric acid solutions (0.1–0.001 *N*), distilled water, and pH 7.6 tromethamine buffer. This procedure is followed in the event that the drug exhibits polymorphism or possesses amphoteric characteristics and because of pH variations observed in gastric fluids (6). If the drug is available commercially, a minimum of six lots of the originator's product is subjected to the same dissolution treatment. Any tablet or capsule formulation developed in the laboratories then must comply with the dissolution profiles exhibited by the originator's product. This routine is followed through to production scaleup, and the first six production batches of a new product are monitored carefully by the peristaltic apparatus. Any formulation change including an increase in batch size is investigated for possible changes in drug release characteristics before the product is released for sale.

Additional *in vitro–in vivo* correlations obtained with the peristaltic dissolution apparatus and initial drug absorption profiles in beagles are under investigation.

REFERENCES

(1) D. L. Simmons, A. A. Legore, P. Picotte, K. S. Lee, and N. N. Joshi, *J. Pharmacokinet. Biopharm.*, **3**, 39 (1975).

(2) D. L. Simmons, A. A. Legore, P. Picotte, K. S. Lee, and R. Jasmin, *Can. J. Pharm. Sci.*, **12**, 1 (1977).

(3) D. L. Simmons, A. A. Legore, P. Picotte, M. Chenier, and R. Jasmin, *ibid.*, **12**, 85 (1977).

(4) T. J. Sullivan, M. R. Hallmark, E. Sakmar, D. J. Weidler, R. H. Earhart, and J. G. Wagner, *J. Pharmacokinet. Biopharm.*, **4**, 157 (1976).

(5) T. J. Sullivan, E. Sakmar, and J. G. Wagner, *ibid.*, **4**, 173 (1976).

(6) S. Kuna, *Arch. Int. Pharmacodyn. Ther.*, **151**, 79 (1964).

ACKNOWLEDGMENTS

The authors acknowledge the collaboration of Dr. B. E. Cabana and Dr. V. K. Prasad, Food and Drug Administration, Washington, D.C., and Dr. John G. Wagner, University of Michigan, for permission to reproduce his data.

High-Performance Liquid Chromatographic Determination of Isoniazid and 1-Isonicotinyl-2-lactosylhydrazine in Isoniazid Tablet Formulations

A. G. BUTTERFIELD ˣ, E. G. LOVERING, and R. W. SEARS

Received August 6, 1979, from the *Drug Research Laboratories, Health Protection Branch, Tunney's Pasture, Ottawa, Ontario K1A 0L2, Canada.* Accepted for publication August 30, 1979.

Abstract □ A high-performance liquid chromatographic procedure is presented for the simultaneous determination of isoniazid and 1-isonicotinyl-2-lactosylhydrazine (I) in isoniazid tablet formulations. An aliquot of a diluted aqueous tablet extract is introduced onto a microparticulate cyanopropyl bonded-phase column using a valve-loop injector and chromatographed using a mobile phase of acetonitrile–0.01 *M*, pH 3.5 aqueous acetate buffer (5:95). Compound I can be determined at levels as low as 0.5% of the isoniazid label claim. The relative standard deviations are 0.4 and 0.7% for the simultaneous determination of isoniazid and I, respectively. Seven commercial tablet formulations contained 93.8–97.0% of the labeled isoniazid amounts and 0.3–5.8% of I, expressed as equivalent isoniazid relative to the labeled isoniazid level.

Keyphrases □ High-performance liquid chromatography—simultaneous determination of isoniazid and 1-isonicotinyl-2-lactosylhydrazine, isoniazid tablet formulation analysis □ Isoniazid—high-performance liquid chromatography, isoniazid tablet formulation analysis, simultaneous determination with 1-isonicotinyl-2-lactosylhydrazine □ 1-Isonicotinyl-2-lactosylhydrazine—high-performance liquid chromatography, isoniazid tablet analysis, simultaneous determination with isoniazid

1-Isonicotinyl-2-lactosylhydrazine (I) has been reported in isoniazid tablets formulated with lactose (1, 2). The formation of I from the interaction of isoniazid and lactose is marked at high humidity and/or elevated temperatures (3). TLC of various isoniazid tablet formulations available in Canada showed appreciable levels of I. The USP XIX (4) nitrite titration assay for isoniazid responds quantitatively to the isoniazid moiety of I (5); therefore, an alternative procedure was required to monitor isoniazid formulations for I. Several colorimetric procedures (2, 6) are specific for isoniazid in the presence of I but cannot directly measure I.

A chromatographic method would be applicable to the rapid, simultaneous determination of isoniazid and I. TLC was unsuitable because of the difficulty in obtaining quantitative data, and GLC was rejected because of chromatographic difficulties with I. High-performance liquid chromatography (HPLC) has been used for isoniazid analysis in single- (1) and dual- (7) component formulations but has not been applied to the analysis of I except (1) to show that such compounds do not interfere with the isoniazid peak. A forward-phase HPLC system was developed recently for the simultaneous analysis of isoniazid and α- and β-1-glucopyranosyl-2-isonicotinylhydrazine

0022-3549/80/0200-0222$01.00/0

© 1980, American Pharmaceutical Association

Table I—Comparison of *In Vitro* and *In Vivo* Data [a]

Tablet	Percent Dissolved [b] 10 min	Percent Dissolved [b] 20 min	Plasma Prednisolone [c], ng/ml 30 min	Plasma Prednisolone [c], ng/ml 60 min
1	83.3	91.5	162	231
2	54.1	64.9	108	186
3	89.6	92.4	162	225
4	56.4	67.4	113	172
5	87.7	94.5	162	244
6	87.2	95.5	164	222
7	14.1	51.2	22	79.7

[a] Manufacturers and lot numbers of the tablets were: 1, Nysco Laboratories, 49571; 2, Barr Laboratories, 4126111; 3, McKesson Laboratories, 3K668; 4, Rexall Drug Co., E11499; 5, Lemmon Pharmacal, 1382; 6, The Upjohn Co., 786AEFI; and 7, Danbury Pharmacal Inc., 4539. The products were submitted by the FDA National Center for Drug Analysis, St. Louis, Mo. [b] Average of three runs. [c] From Ref. 4, Table IV, p. 163, and Table IX, p. 170.

DISCUSSION

The peristaltic dissolution apparatus has provided the authors with complete assurance that a new product launched on the market is bioequivalent to an originator's product or formulated to present optimum drug release characteristics. This assurance has been demonstrated by the excellent *in vitro–in vivo* correlations obtained in beagle dog studies, comparative bioavailability evaluations in humans, and results from clinical studies.

The utility of the peristaltic apparatus in drug product design can be exemplified in the following manner. If the drug substance (*e.g.*, prednisone) has limited water solubility, a drug suspension is screened for dissolution characteristics in dilute hydrochloric acid solutions (0.1–0.001 *N*), distilled water, and pH 7.6 tromethamine buffer. This procedure is followed in the event that the drug exhibits polymorphism or possesses amphoteric characteristics and because of pH variations observed in gastric fluids (6). If the drug is available commercially, a minimum of six lots of the originator's product is subjected to the same dissolution treatment. Any tablet or capsule formulation developed in the laboratories then must comply with the dissolution profiles exhibited by the originator's product. This routine is followed through to production scaleup, and the first six production batches of a new product are monitored carefully by the peristaltic apparatus. Any formulation change including an increase in batch size is investigated for possible changes in drug release characteristics before the product is released for sale.

Additional *in vitro–in vivo* correlations obtained with the peristaltic dissolution apparatus and initial drug absorption profiles in beagles are under investigation.

REFERENCES

(1) D. L. Simmons, A. A. Legore, P. Picotte, K. S. Lee, and N. N. Joshi, *J. Pharmacokinet. Biopharm.*, **3**, 39 (1975).

(2) D. L. Simmons, A. A. Legore, P. Picotte, K. S. Lee, and R. Jasmin, *Can. J. Pharm. Sci.*, **12**, 1 (1977).

(3) D. L. Simmons, A. A. Legore, P. Picotte, M. Chenier, and R. Jasmin, *ibid.*, **12**, 85 (1977).

(4) T. J. Sullivan, M. R. Hallmark, E. Sakmar, D. J. Weidler, R. H. Earhart, and J. G. Wagner, *J. Pharmacokinet. Biopharm.*, **4**, 157 (1976).

(5) T. J. Sullivan, E. Sakmar, and J. G. Wagner, *ibid.*, **4**, 173 (1976).

(6) S. Kuna, *Arch. Int. Pharmacodyn. Ther.*, **151**, 79 (1964).

ACKNOWLEDGMENTS

The authors acknowledge the collaboration of Dr. B. E. Cabana and Dr. V. K. Prasad, Food and Drug Administration, Washington, D.C., and Dr. John G. Wagner, University of Michigan, for permission to reproduce his data.

High-Performance Liquid Chromatographic Determination of Isoniazid and 1-Isonicotinyl-2-lactosylhydrazine in Isoniazid Tablet Formulations

A. G. BUTTERFIELD ˣ, E. G. LOVERING, and R. W. SEARS

Received August 6, 1979, from the *Drug Research Laboratories, Health Protection Branch, Tunney's Pasture, Ottawa, Ontario K1A 0L2, Canada.* Accepted for publication August 30, 1979.

Abstract □ A high-performance liquid chromatographic procedure is presented for the simultaneous determination of isoniazid and 1-isonicotinyl-2-lactosylhydrazine (I) in isoniazid tablet formulations. An aliquot of a diluted aqueous tablet extract is introduced onto a microparticulate cyanopropyl bonded-phase column using a valve-loop injector and chromatographed using a mobile phase of acetonitrile–0.01 *M*, pH 3.5 aqueous acetate buffer (5:95). Compound I can be determined at levels as low as 0.5% of the isoniazid label claim. The relative standard deviations are 0.4 and 0.7% for the simultaneous determination of isoniazid and I, respectively. Seven commercial tablet formulations contained 93.8–97.0% of the labeled isoniazid amounts and 0.3–5.8% of I, expressed as equivalent isoniazid relative to the labeled isoniazid level.

Keyphrases □ High-performance liquid chromatography—simultaneous determination of isoniazid and 1-isonicotinyl-2-lactosylhydrazine, isoniazid tablet formulation analysis □ Isoniazid—high-performance liquid chromatography, isoniazid tablet formulation analysis, simultaneous determination with 1-isonicotinyl-2-lactosylhydrazine □ 1-Isonicotinyl-2-lactosylhydrazine—high-performance liquid chromatography, isoniazid tablet analysis, simultaneous determination with isoniazid

1-Isonicotinyl-2-lactosylhydrazine (I) has been reported in isoniazid tablets formulated with lactose (1, 2). The formation of I from the interaction of isoniazid and lactose is marked at high humidity and/or elevated temperatures (3). TLC of various isoniazid tablet formulations available in Canada showed appreciable levels of I. The USP XIX (4) nitrite titration assay for isoniazid responds quantitatively to the isoniazid moiety of I (5); therefore, an alternative procedure was required to monitor isoniazid formulations for I. Several colorimetric procedures (2, 6) are specific for isoniazid in the presence of I but cannot directly measure I.

A chromatographic method would be applicable to the rapid, simultaneous determination of isoniazid and I. TLC was unsuitable because of the difficulty in obtaining quantitative data, and GLC was rejected because of chromatographic difficulties with I. High-performance liquid chromatography (HPLC) has been used for isoniazid analysis in single- (1) and dual- (7) component formulations but has not been applied to the analysis of I except (1) to show that such compounds do not interfere with the isoniazid peak. A forward-phase HPLC system was developed recently for the simultaneous analysis of isoniazid and α- and β-1-glucopyranosyl-2-isonicotinylhydrazine

0022-3549/80/0200-0222$01.00/0

© 1980, American Pharmaceutical Association

in isoniazid sugar syrup formulations[1]. However, this system is not applicable to the determination of I in isoniazid tablet formulations because of the late elution of and low sensitivity for I.

This article describes the HPLC system developed for the quantitation of low levels of I and isoniazid in isoniazid tablet formulations.

EXPERIMENTAL

Reagents and Chemicals—Isoniazid[2] raw material was assayed before use by the USP (4) procedure (100.5%), and its purity was confirmed by HPLC. Compound I was synthesized from 0.2 mole of isoniazid and 0.2 mole of lactose[3] in 200 ml of water at room temperature (23 ± 1°). After 7 days, a white, crystalline product was precipitated by the addition of a small amount of methanol and cooling to 4°. The product was filtered, washed with acetone, and recrystallized from water–methanol until the HPLC[4] and TLC[5] tests for residual isoniazid and lactose, respectively, were negative. The product purity, mp 214–216° (uncorr.) [lit. (8) mp 202°], was determined by the isoniazid moiety titration using the USP XIX (4) nitrite titration procedure.

All other reagents and chemicals were commercial analytical reagent grade except for the distilled water, which was double distilled and filtered through a 0.2-μm filter[6] before use.

Chromatography—The liquid chromatograph consisted of a single-piston metering pump[7], a valve-loop injector[8] equipped with a 10-μl loop, a fixed-wavelength UV detector[9] [254 nm, 0.02 absorbance unit full scale (aufs)], a 10-mv strip-chart recorder[10] connected to the recorder output, and an electronic-computing integrator[11] connected to the detector absorbance terminals.

The mobile phase, aqueous 0.01 *M* acetate buffer (pH 3.5)–acetonitrile (95:5 v/v), was pumped through a 3.2 × 250-mm cyanopropyl bonded-phase column[12] at 1.5 ml/min (80 bar).

Calibration Curves—Aqueous stock solutions of isoniazid, 5.0 mg/ml, and of I, 0.125 mg/ml, were prepared. Standard solutions were prepared by pipetting 1, 2, 3, 5, or 10 ml of the isoniazid stock solution into each of five 50-ml volumetric flasks along with 1, 2, 5, 10, or 20 ml of the I stock solution. Each standard solution was diluted to volume with water, and duplicate 10-μl aliquots of each were chromatographed.

Calibration Standard Solutions—Compound I, ~5 mg, and isoniazid, 50 mg, were weighed accurately, transferred to a 100-ml volumetric flask, dissolved, and diluted to volume with distilled water (Solution A). A second calibration standard was prepared by diluting 5.0 ml of Solution A to 25.0 ml with water (Solution B). Duplicate 10-μl aliquots of each calibration standard were chromatographed periodically to check the slopes of the calibration curves.

Analysis of Pharmaceuticals—*Single-Tablet Assay*—A tablet was placed in a 20 × 150-mm screw-capped culture tube[13] and finely powdered with a glass rod. Sufficient distilled water was added to give a theoretical isoniazid concentration of 5.0 mg/ml, *e.g.*, 20.0 ml of water for a 100-mg tablet. The tightly capped tube was rotated[14] at 30 rpm for 15 min and then centrifuged[15] briefly at 1000 rpm. Five milliliters of the clear aqueous supernate was transferred to a 50-ml volumetric flask and diluted to volume with distilled water. Duplicate 10-μl aliquots of the resulting solution were chromatographed.

Tablet Composite Assay—A tablet composite was prepared by grinding 20 tablets in a mechanical mill[16]. A quantity of powdered tablet material equivalent to 50 mg of isoniazid was transferred to a 20 × 150-mm screw-capped culture tube, 10 ml of water was added, and the sample was centrifuged and chromatographed as described under *Single-Tablet Assay*.

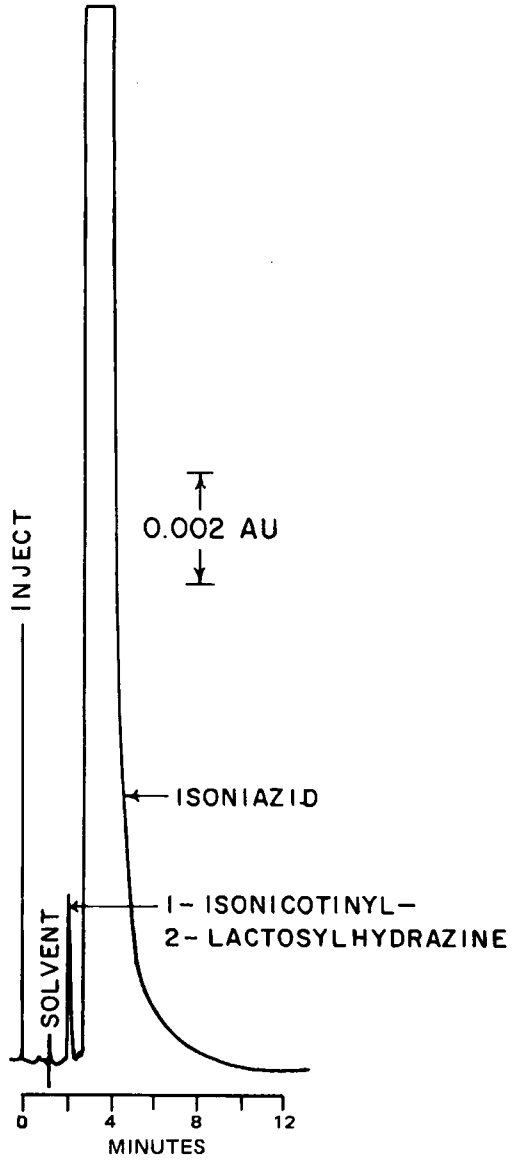

Figure 1—*High-performance liquid chromatogram of a typical isoniazid tablet extract.*

Quantitation—Quantitation was by comparison of the peak height for I and the peak area for isoniazid to the calibration standards and was based on absolute injection of 10-μl samples.

RESULTS AND DISCUSSION

Chromatographic System—Previous reports of HPLC systems for isoniazid analysis either did not describe the chromatographic behavior of I (7) or indicated a long retention time and, therefore, poor sensitivity (1). To achieve maximum sensitivity, reversed-phase HPLC was necessary to elute I ahead of isoniazid. Octadecyl bonded-phase columns[17] provided the desired elution order but gave retention times that decreased over a few days until both I and isoniazid eluted at the solvent front.

A cyanopropyl bonded-phase column[12] gave comparatively good results with the mobile phase described under *Experimental*. Satisfactory separations were obtained on three replicate cyanopropyl columns, each requiring somewhat different mobile phases. A simple water–acetonitrile

[1] To be published.
[2] Sigma Chemical Co., St. Louis, Mo.
[3] British Drug Houses, Toronto, Ontario, Canada.
[4] Conditions as described under *Experimental*.
[5] TLC conditions were silica gel GF 60 (Merck), 0.25 mm with a developing solvent of acetone–methanol–acetic acid (50:50:10). The R_f values were: lactose, 0.31; isoniazid, 0.42; and 1-isonicotinyl-2-lactosylhydrazine, 0.20. UV visualization was at 254 nm after spraying with *p*-methoxybenzaldehyde–ethanol–sulfuric acid (1:18:1) and heating at 100° to show the lactose spot.
[6] FGLP 04700, Millipore Ltd., Mississauga, Ontario, Canada.
[7] Model 110A, Altex Scientific, Berkeley, Calif.
[8] Model CV-6-UHPa-N60, Valco Instruments Co., Houston, Tex.
[9] Model 440, Waters Associates, Milford, Mass.
[10] Model 56, Perkin-Elmer Corp, Norwalk, Conn.
[11] System I, Spectra-Physics, Santa Clara, Calif.
[12] Spherisorb CN (5 μm), Altex Express Series, Altex Scientific, Berkeley, Calif.
[13] Canadian Laboratory Supplies, Montreal, Canada.
[14] Multipurpose rotator, Scientific Industries, Springfield, Mass.
[15] Model K, International Equipment Co., Needham Heights, Mass.
[16] Micro mill, Chemical Rubber Co., Cleveland, Ohio.
[17] RP18, E. Merck, West Germany (through British Drug Houses, Toronto, Canada).

Table I—Retention Times for Isoniazid and Various Related Compounds

Compound	Retention Time[a], sec
Isoniazid	258
1-Isonicotinyl-2-lactosylhydrazine (I)	133
Isonicotinic acid	75[b]
Isonicotinamide	184
1-Isonicotinyl-2-glucosylhydrazine (II)	128
1-Isonicotinyl-2-galactosylhydrazine (III)	130
4-Aminosalicylic acid	79
Pyridoxine hydrochloride	>900

[a] The column was a 3.2 × 250-mm Spherisorb CN (5 μm), the flow rate was 1.5 ml/min, and the mobile phase was 5% acetonitrile in aqueous 0.01 *M* sodium acetate buffer (pH 3.5). [b] Solvent front (t_0).

(95:5) mobile phase initially eluted isoniazid as a retained peak, but retention decreased to zero over a few days. Substitution of a dilute aqueous acetate buffer for water in the mobile phase stabilized the retention time at a value dependent on the buffer pH and concentration. Increased retention times were obtained as the pH or ionic strength was decreased. Since retention times also increased as the acetonitrile proportion in the mobile phase was reduced, the separation mode can be described as reverse phase.

After several weeks, the retention times for isoniazid and I decreased to an unacceptable degree. The column was regenerated by pumping 1% aqueous HCl at 1.5 ml/min for 1 hr. On returning to the original mobile phase conditions, this procedure initially led to much longer retention times followed by a slow return to the original separation.

Figure 1 shows a chromatogram obtained when a representative tablet formulation was analyzed. The compounds were eluted in less than 12 min, a major portion of this time being necessary for the elution of the long tail on the isoniazid peak.

Various isoniazid-related compounds were chromatographed (Table I), either because of their possible occurrence as impurities or because they are sometimes formulated with isoniazid in two-component tablets. 1-Isonicotinyl-2-glucosylhydrazine (II) and 1-isonicotinyl-2-galactosylhydrazine (III) may be present in tablet formulations through isoniazid interaction with lactose hydrolysis products, glucose and galactose. Since I–III are not resolved, the procedure is not specific for I in the presence of these impurities. However, since the three compounds exhibited the same molar detector response, due entirely to the isoniazid moiety, total isoniazid in the form of sugar hydrazones may be determined by quantifying the peak at the retention time of I.

Linearity and Standard Curves—The isoniazid standard curve (peak area *versus* amount injected) was linear with a negligible intercept ($y = mx$) over 1.0–10.1 μg/injection (0.1–1.10 mg/ml). Similarly, the I standard curve (peak height *versus* amount injected) was linear with a negligible intercept ($y = mx$) over 25–500 ng/injection (2.5–50 μg/ml). Therefore, the standard curves are applicable to tablets containing 20–200% of the isoniazid label claim level and 0.5–10% of I (or 0.15–3.0% of I expressed as equivalent isoniazid).

Response factors were determined by two or more injections of two calibration solutions at the start of each day or whenever the mobile phase was replenished. Agreement of the response factors within 3% at the two levels was considered adequate but was typically better than 2%. After checking the response at two levels to show linearity, a single calibration standard was chromatographed periodically to check for response changes. Due to gradual hydrolysis of I, calibration standards must be prepared daily.

Sample Preparation—The time required for constant extraction of isoniazid and I from the tablet mass was determined by tumbling crushed single tablets of a representative formulation, 100 mg, for 5, 10, 15, 20, and 30 min in 20 ml of water. Each sample was centrifuged briefly at 1000 rpm, and 1.0 ml was diluted to 10.0 ml with water. Duplicate 10-μl aliquots of each diluted sample were chromatographed. The peak heights for I and the peak areas for isoniazid were the same in all samples, indicating constant extraction of both compounds in less than 5 min. Based on response factor data and the label claim for the formulation used, extraction also appeared to be complete, and a geometric dilution procedure substantiated this finding. When tablet composite samples equivalent to one-half, one, and two tablets were analyzed (15-min tumbling time), the I and isoniazid concentrations were both in the ratio 1:2:4, showing that complete extraction took <15 min.

Table II—HPLC Analysis of Isoniazid Tablet Formulations[a]

Formulation	Label Claim, mg	Compound I[b,c], %	Isoniazid, % label claim[b]
A	50	0.39	93.9
B	300	ND[d]	95.9
C	100	0.35	96.8
D	100	0.31	94.4
E	100	5.81	93.8
F	100	0.29	96.3
G	100	0.96	97.0

[a] Tablet composite assay. [b] Mean of duplicate assays. [c] Based on the isoniazid moiety of I, *i.e.*, isoniazid equivalent. [d] None detected.

Quantitation—Samples, 10 μl, were introduced *via* a valve-loop injector using the loop-fill mode. This absolute injection technique gave precise, accurate results and eliminated the need for an internal standard. Initially, peak area was used for both compounds; but during the procedure testing, the separation of isoniazid and I on different columns was usable over a wider resolution range when peak height was used for quantitation of I. Ten injections of a representative formulation extract gave relative standard deviations of 0.7 and 0.4% for I and isoniazid, respectively.

Analysis of five replicate composite samples of a representative isoniazid tablet formulation containing 3.3% of I (0.96% expressed as equivalent isoniazid) and 97.0% of the isoniazid label claim level gave relative standard deviations of 1.8 and 0.9%, respectively.

Seven commercial formulations were analyzed in duplicate (Table II). In tablets formulated with lactose, the I levels varied between 0.3 and 5.8%, expressed as equivalent isoniazid, while isoniazid levels varied between 93.8 and 97.0% of the label claim.

REFERENCES

(1) L. C. Bailey and H. Abdou, *J. Pharm. Sci.*, **66**, 564 (1977).

(2) M. B. Devani, C. J. Shishoo, M. A. Patel, and D. D. Bhalara, *ibid.*, **67**, 661 (1978).

(3) W. H. Wu, T. F. Chu, and J. L. Lach, *ibid.*, **59**, 1234 (1970).

(4) "The United States Pharmacopeia," 19th rev., Mack Publishing Co., Easton, Pa., 1975, pp. 272, 273.

(5) M. I. Blake, D. Bode, and H. J. Rhodes, *J. Pharm. Sci.*, **63**, 1303 (1974).

(6) K. V. N. Rao, S. Kailasam, N. K. Menon, and S. Radhakrishna, *Indian J. Med. Res.*, **59**, 1343 (1971).

(7) J. T. Stewart, I. L. Honigberg, J. P. Brant, W. A. Murray, J. L. Webb, and J. B. Smith, *J. Pharm. Sci.*, **65**, 1536 (1976).

(8) R. Yamamoto and H. Tanaka, *Yukuzaigaku*, **17**, 219 (1957).

Comparative Analgesic, Behavioral, and Dependence Properties of Morphine and *O*-(4-Methoxylphenylcarbamoyl)-3-diethylaminopropiophenone Oxime Hydrochloride

NATHAN WATZMAN * **and JOSEPH P. BUCKLEY** ‡x

Received July 9, 1979, from the *Research Laboratories, Department of Pharmacology, School of Pharmacy, University of Pittsburgh, Pittsburgh, PA 15261.* Accepted for publication August 30, 1979. *Present address: Health Resources Administration, Department of Health, Education, and Welfare, Hyattsville, MD 20782. ‡Present address: College of Pharmacy, University of Houston, Houston, TX 77004.

Abstract □ The analgesic activity of *O*-(4-methoxylphenylcarbamoyl)-3-diethylaminopropiophenone oxime hydrochloride was investigated in Swiss–Webster mice using an electroshock technique in which the pain threshold was the minimum voltage producing tonic extension of the hindlimbs in response to an electroshock delivered to the feet. The analgesic potency of *O*-(4-methoxylphenylcarbamoyl)-3-diethylaminopropiophenone oxime hydrochloride was equal to, or greater than, that of morphine. Neither nalorphine nor withdrawal produced visible behavioral effects in rats treated with *O*-(4-methoxylphenylcarbamoyl)-3-diethylaminopropiophenone oxime hydrochloride for 21 days, suggesting that the physical dependency liability of the compound may be less than that of morphine.

Keyphrases □ Morphine sulfate—comparative effects with *O*-(4-methoxylphenylcarbamoyl)-3-diethylaminopropiophenone oxime hydrochloride in rodents, pain threshold, physical dependency, tolerance, analgesic, withdrawal syndrome □ *O*-(4-Methoxylphenylcarbamoyl)-3-diethylaminopropiophenone oxime hydrochloride—analgesic, behavioral, and dependence properties, compared to morphine sulfate □ Analgesics—morphine sulfate, *O*-(4-methoxylphenylcarbamoyl)-3-diethylaminopropiophenone oxime hydrochloride, comparative studies in rodents

The clinical use of morphine has been limited by its undesirable capacity to induce tolerance and physical and psychogenic dependence. The synthesis of meperidine[1] (1) gave impetus to the search for new chemical molecules possessing the same pharmacological properties as morphine without the undesirable characteristics. Compounds such as methadone[2], unlike morphine in chemical structure, have been reported to possess the same or greater analgesic effects as morphine (2); unfortunately, they also possess the undesirable ability to produce the same three adaptive processes.

The present study investigated the analgesic activity of *O* - (4-methoxylphenylcarbamoyl)-3-diethylaminopropiophenone oxime hydrochloride (I) in rodents.

EXPERIMENTAL

Pain sensitivity was determined in 48 male albino mice[3] utilizing a modified flinch jump method (3). The aluminum test chamber contained four (10.2 × 10.2 × 10.2-cm) compartments with a grid floor designed so that 2-sec shocks of increasing intensity were delivered to the feet every 8 sec; timers and a grid scrambler[4] with a 1.5-megaohm resistor were used. Beginning with 143 v (0.1 mamp), the current was increased progressively until the pain threshold was reached or a maximum of 385 v (0.25 mamp) was applied without the pain response. The threshold was designed as the minimum voltage that produced tonic extension of the hindlimbs and jumping in response to three successive shocks applied at each voltage level. Four of the eight groups (six animals each) received placebo (0.9% saline, 0.1 ml/10 g body weight) or one of three doses of morphine sulfate (2, 5, or 10 mg/kg sc) 30 min before testing; the four other groups received placebo treatment or one of three doses of I identical to morphine.

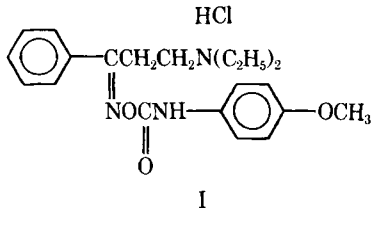

I

To observe the chronic effects of the two test compounds as well as to monitor the morphine tolerance behavior, male Sprague–Dawley rats were administered the test compounds for 3 weeks in doses regarded as sufficient to produce addiction. Both compounds were administered subcutaneously according to the following dose schedule: 5, 10, and 20 mg/kg twice daily during the 1st, 2nd, and 3rd weeks, respectively. When 20 mg of I/kg was administered on the 15th day (Day 1 of the 3rd week), convulsions and death occurred in three of six animals. A similar morphine sulfate dose did not produce any marked changes.

Based on preliminary trials, 18 male Sprague–Dawley rats were divided into three equal treatment groups. Each group received, subcutaneously, I, morphine sulfate, or normal saline twice daily for 21 consecutive days according to the following morphine dosage schedule utilized by Gunne (4). For I, the initial dose (2.5 mg/kg/injection) was doubled every 7th day so that the dose level for each of the 3 weeks was 2.5, 5.0, and 10

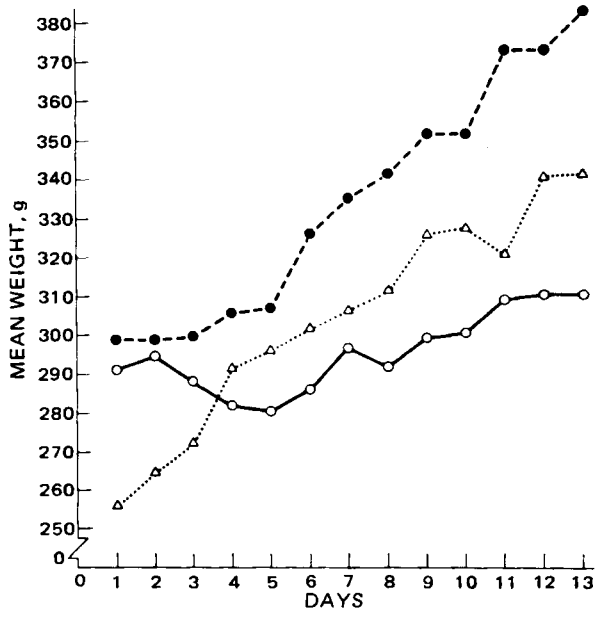

Figure 1—*Comparative effects of morphine sulfate and I on the weight gain of rats. Key:* ●, *saline;* △, *I; and* ○, *morphine sulfate.*

[1] Demerol, Winthrop Laboratories, New York, N.Y.
[2] Dolophine, Eli Lilly & Co., Indianapolis, Ind.
[3] Swiss–Webster, Hilltop Caviary, Scottdale, Pa.
[4] Lehigh Valley Electronics, Fogelsville, Pa.

0022-3549/80/0200-0225$01.00/0
© 1980, American Pharmaceutical Association

Table I—Comparative Effects of Subcutaneously Administered Morphine Sulfate and I on the Pain Threshold of Mice

Mouse	Volts Delivered							
	Group I, Saline	Group II, Morphine, 2 mg/kg	Group III, Morphine, 5 mg/kg	Group IV, Morphine, 10 mg/kg	Group V, Saline	Group VI, I, 2 mg/kg	Group VII, I, 5 mg/kg	Group VIII, I, 10 mg/kg
1	231	242	330	385[a]	220	231	308	385[a]
2	220	231	341	330	220	297	319	374
3	220	319	319	374	231	308	330	385
4	220	286	319	319	242	242	352	385[a]
5	187	297	319	165	187	220	374	374
6	242	297	275	385	187	275	253	385[a]
	1320	1672	1903	1958[a]	1287	1573	1936	2288[a]
$\bar{X}$	220	279	317	326[a]	214	262	323	381[a]

[a] Maximum voltage tested; threshold not achieved.

mg/kg/injection, respectively. For morphine sulfate, the initial dose (20 mg/kg/injection) was tripled every 7th day so that the dose level for each of the 3 weeks was 20, 60, and 180 mg/kg/injection, respectively.

One animal died from the initial morphine dose. On the 22nd day (Day 1 of drug withdrawal), half of the animals of each group (two of the morphine-treated animals) were administered a single 10-mg/kg sc dose of the narcotic antagonist nalorphine[5] to precipitate withdrawal symptoms. The other half of the groups (three animals each) received no drugs. All animals were observed for 1 week in their individual observation cages and home cages.

RESULTS

Table I shows the response threshold to electrical shock for each of the 48 mice and the average threshold for each drug dosage. The thresholds for the two saline control groups were similar, and the effects of the compounds did not differ statistically in thresholds produced at the two lowest doses (2 and 5 mg/kg). However, I produced a greater increase in pain threshold than did morphine at the highest dose level (10 mg/kg). Three of six animals receiving the highest dose of I did not reach the response criteria, whereas only one of six animals treated with the same dose of morphine failed to reach the criteria.

The early stages of chronic morphine administration initially produced hyperactivity and headbobbing, with the head carried close to the ground. After 10 min, the hyperactivity was replaced by a cataleptic-like state in which the animals remained in peculiar postures with a fixed stare. By the 16th day (Day 2 of 180-mg/kg dose), the animals were sedated but their bodies were stiff when handled, indicating an increase in muscular tone and stimulation of the spinal cord. Water and food intake decreased with time, and the animals became increasingly more difficult to handle. They were hyperactive only immediately after injection, jumping onto the back of the cage and over each other, and then they assumed trance-like postures similar to the description by Gunne (4). No behavioral effects were noted at any I dose level. Manifestations of central nervous system depression (ataxia, *etc.*) as well as autonomic effects were reported (5) in rhesus monkeys chronically administered I for 40 days.

Figure 1 shows the weight gains for each drug group. Compound I-treated animals and the saline controls had similar weight gains, and their fur appeared normal throughout the study. However, the weight gain of the morphine-treated animals was far below that of the other two groups, and their fur was off-white or brownish. On the last weighing day (19th day), the mean weights ± *SE* for the saline-, I-, and morphine-treated groups were 383 ± 11.9, 341 ± 11.1, and 310 ± 5,1 g, respectively. These data were statistically different ($p < 0.05$) by the Student t test. There were no visible physical effects among the saline control animals.

A single nalorphine injection to the morphine-treated rats on the 1st withdrawal day produced extreme sedation, ptosis, and increased defecation with diarrhea, reflecting the expected precipitation of the withdrawal syndrome (6). These symptoms, except the diarrhea, disappeared by Day 5 of withdrawal. Withdrawn morphine-treated animals (no nalorphine) also showed sedation, ptosis, and diarrhea and they returned to normal by Day 5 of withdrawal. Compound I- and saline-treated animals were not affected visibly by nalorphine, and I did not demonstrate withdrawal-like symptoms. Compound I partially suppressed morphine abstinence in morphine-dependent rhesus monkeys, reflecting some morphine antagonist properties of its own (7).

[5] Nalline, Merck Sharp & Dohme, West Point, Pa.

DISCUSSION

Data from the pain threshold study indicate that I has analgesic potency equal to or greater than morphine. Although the compounds did not differ in the pain thresholds produced at the two lowest doses, I induced a greater threshold increase at the highest dose (10 mg/kg). The differences in potency between the two compounds would have been greater had the trials continued beyond the maximum experimental voltage (385 v) and every animal reached criteria. Three of the six I-treated animals did not reach criteria compared to only one of the six in the morphine group.

The basic behavior elicited by chronic morphine administration to rats was an initial hyperactivity followed by a cataleptic-like immobile state with fixed stare. As the program progressed, the initial hyperactivity increased and the animals became more difficult to handle. The major effects of morphine withdrawal and nalorphine in morphine-treated rats were sedation, ptosis, and increased defecation with diarrhea. No such behavioral effects were produced by chronic I administration.

There were no qualitative differences between the morphine–nalorphine-treated animals and the morphine-withdrawn animals, except that diarrhea persisted longer in the former group. Thus, nalorphine apparently precipitated withdrawal-like symptoms. Neither nalorphine-administered I animals nor withdrawal from I produced any visible behavioral effects. The marked difference between the doses of I and morphine sulfate should not negate the results since, within experimental design limits, the animals did not develop a tolerance to the experimental compounds. Therefore, the data suggest that I does not produce the same autonomic and behavioral effects as morphine, nor do I-treated animals display the same syndrome of effects when withdrawn from the drug.

REFERENCES

(1) O. Eisleb and O. Schaumann, *Dtsch. Med. Wochenschr.*, **65**, 967 (1939).

(2) "The Pharmacological Basis of Therapeutics," 4th ed., L. S. Goodman and A. Gilman, Eds., Macmillan, New York, N.Y., 1970.

(3) W. O. Evans, *Psychopharmacologia*, **3**, 51 (1962).

(4) L. M. Gunne, *Acta Physiol. Scand., Suppl. 204*, **58**, 5 (1963).

(5) "Report to Committee on Problems of Drug Dependence," National Academy of Science–National Research Council, Washington, D.C., Addendum 1, 1970, p. 18.

(6) S. Kaymakcalan and L. A. Woods, *J. Pharmacol. Exp. Ther.*, **117**, 112 (1956).

(7) "Report to Committee on Problems of Drug Dependence," National Academy of Science–National Research Council, Washington, D.C., Addendum 2, 1969, p. 9.

Oral and Rectal Absorption of Chloral Hydrate and Its Betaine Complex

MICHAEL SIMPSON and EUGENE L. PARROTT ˣ

Received July 30, 1979, from the *Division of Pharmaceutics, College of Pharmacy, University of Iowa, Iowa City, IA 52242.* Accepted for publication September 21, 1979.

Abstract □ Chloral hydrate and its betaine complex were administered orally and rectally to nine healthy male subjects. The urinary excretion, which was a reflection of absorption, of a metabolite, trichloroacetic acid, was determined. No statistically significant difference was found between the oral absorption of chloral hydrate and its betaine complex and between the rectal absorption of chloral hydrate and its betaine complex. A statistical difference was found between the oral and rectal absorption of chloral hydrate and between the oral and rectal absorption of chloral betaine.

Keyphrases □ Chloral hydrate—oral and rectal absorption, compared to chloral betaine □ Chloral betaine—oral and rectal absorption, compared to chloral hydrate □ Absorption—oral and rectal, comparison of chloral hydrate and chloral betaine

The solubility, diffusivity, and lipid–water partition coefficient of drug complexes can differ significantly from these properties of the respective free drug. Therefore, some drug complexes may not penetrate biological membranes and thus have no biological activity (1). Conversely, if a complex is highly dissociated when diluted in biological fluids, complexation has little effect on absorption.

Several derivatives of chloral hydrate have been prepared and tried clinically to reduce or eliminate its bitter taste and gastric irritation (2, 3). Chloral betaine is a 1:1 complex of chloral hydrate and betaine (4). The purpose of this study was to determine if complexation influenced the absorption of an equivalent weight of chloral hydrate and chloral betaine by the oral and rectal routes. The availability of chloral hydrate and chloral betaine from rectal and oral administrations also was compared.

EXPERIMENTAL

Preparation—Chloral betaine was prepared by mixing 135.2 g of betaine monohydrate[1] with 200.2 g of chloral hydrate[2] and warming the mixture on a water bath at 60° (4). The pasty mixture was stirred continuously at 60° for 30 min. The solid residue was crystallized three times from a minimum of distilled water and was stored in a desiccator.

The crystals were compared to the NF reference standard[3] and to NF specifications (5). The melting point of the chloral betaine was determined[4] to be 121.5–123°. With sodium hydroxide TS, the chloral betaine produced chloroform, which was recognized by its odor (5). Measurement[5] of the IR spectra showed that the NF reference standard and the chloral betaine were similar. Differential thermal analysis[6] of the NF reference standard and the chloral betaine showed a single melting point at the same temperature.

The chloral betaine contained 7.97% of moisture by Karl Fischer titration; the NF specification is 5.9–7.5% (5). The excessive moisture was considered in the dose administered, so 881.5 mg of chloral betaine was equivalent to 500 mg of chloral hydrate in this study. The content of chloral hydrate in the chloral betaine assayed as 57.71%, within the NF specification of 56.0–59.5% (5). The amount of betaine was 41.54%, within the NF specification of 40–44% (5).

In the preparation of capsules, each compound was passed through a 60-mesh screen; then 500 mg of chloral hydrate and 881 mg of chloral betaine were placed in 00 and 000 hard gelatin capsules, respectively. Each capsule was stored in a coded, amber, screw-capped bottle.

The suppository base consisted of 24% beeswax[7] in cocoa butter[8] prepared by the fusion method. The base was stored in a cool room for 4 weeks prior to use. In the preparation of suppositories, each compound was passed through a 60-mesh screen; then equivalent weights of chloral hydrate and chloral betaine were manually incorporated in 2.5 g of the base. Each suppository was wrapped in aluminum foil with an inner lining of Parafilm and stored in a screw-capped bottle in a refrigerator until 10–15 min before insertion.

Protocol—All dosage forms were coded and were distributed by a crossover design with overnight fasting; 2 weeks elapsed between the administration of each dosage form. Three subjects did not continue the study after the first dose so the study was completed utilizing nine male subjects from 23 to 39 years of age and weighing 60–73 kg.

Upon arising, the bladder was voided, and a capsule was ingested with 300 ml of water. With rectal administration, the bladder was voided upon arising, the bowel was evacuated, a suppository was inserted high in the rectum, and 300 ml of water was ingested. At least 2 hr was allowed to elapse before food was eaten. Subjects were instructed not to ingest alcoholic beverages and coffee and not to operate machinery during the day.

Urine samples were collected at 2, 4, 6, 8, 10, 12, 16, and 24 hr after drug administration. Volumes were measured, and aliquots were retained in amber vials for analysis. No attempt was made to control the urinary pH. The urinary pH was determined at the time of each sample collection; for a given subject, the fluctuation of pH did not exceed 1.2 pH units.

Analytical Method—Since chloral hydrate has a very short half-life in the body and is not excreted as such, the urine was analyzed for trichloroacetic acid, one of the metabolites. The trichloroacetic acid excreted in the urine was determined by the method of Cabana and Gessner (6).

Statistics—The significance of the difference between the means was calculated using the Student t test, two tail ($p = 0.05$).

RESULTS AND DISCUSSION

Chloral hydrate is rapidly and completely absorbed after oral administration (7, 8), and relatively high concentrations of trichloroacetic acid are found in the blood coincident with the appearance of trichloroethanol after oral administration (9). After rectal administration, chloral hydrate is also converted to trichloroacetic acid and trichloroethanol (10). It appears that chloral hydrate is converted to its metabolites during the first pass through the liver (10), and chloral hydrate is not detectable in the blood at levels as low as 0.5 μg/ml 10 min after administration (10, 11). Chloral hydrate is biotransformed and is excreted as trichloroacetic acid, trichloroethanol, and trichloroethanol glucuronide. Trichloroacetic acid is also formed from trichloroethanol and is excreted in the urine (8, 10, 12).

Since the biotransformation of chloral hydrate is complex with a wide biological variation, a comparative study of chloral hydrate and chloral betaine administered by oral and rectal routes was based on the urinary excretion of trichloroacetic acid with the assumption that in a given subject this biotransformation would be essentially the same. In the crossover study, 500 mg of chloral hydrate or an equivalent weight of chloral betaine was administered in a hard gelatin capsule and in a cocoa butter suppository to nine male subjects. Plots of the milligrams excreted against time to each subject are not given; however, the individual plots

[1] Lot 26C-0292, Sigma Chemical Co.
[2] USP, lot AAZ50, City Chemical Co.
[3] Lot 69140.
[4] Thomas-Hoover melting-point apparatus, A. H. Thomas.
[5] Model 267 IR spectrophotometer, Perkin-Elmer.
[6] Model 900, DuPont Instruments.
[7] White wax USP, Fisher.
[8] USP, Ruger.

0022-3549/80/0200-0227$01.00/0
© 1980, American Pharmaceutical Association

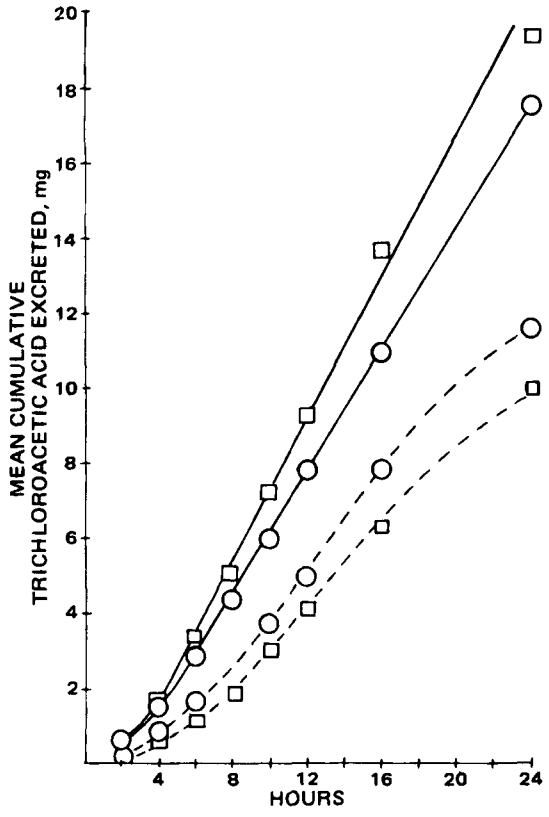

Figure 1—*Mean cumulative milligrams of trichloroacetic acid excreted by nine subjects in 24 hr after administration of 500 mg equivalent of chloral hydrate and chloral betaine in a capsule and in a suppository. Key: —, capsule; – –, suppository; ○, chloral hydrate; and □, chloral betaine.*

follow the general pattern shown in Fig. 1 for the mean cumulative amount of trichloroacetic acid for nine subjects as given in Table I.

It has been observed that complexes may alter absorption (1). Perhaps the most often observed complex formation is between various drugs and macromolecules such as gums, cellulose derivatives, and high molecular weight polyols. The nonabsorbable nature of this type of interaction (amphetamine with carboxymethylcellulose sodium; phenobarbital with polyethylene glycol 4000) provides ample explanation for the nonabsorbable character of the drug complex. With other types of complexes, the dilution of the drug complex in the biological fluids after administration may result in its complete dissociation so that the complexation has little or no effect on absorption. Soci and Parrott (13) noted that methylcellulose and carbomer complexed with nitrofurantoin *in vitro* but that this complexation did not interfere with GI absorption in humans. It was of interest to consider the influence of complexation by comparing the excretion of trichloroacetic acid after the administration of chloral hydrate and its betaine complex.

The significance of the difference between the means in Table I was calculated using the Student *t* test. There was no significant difference between the oral administration of an equivalent weight of chloral hydrate and chloral betaine. Likewise, there was no statistically significant difference between the rectal administration of an equivalent weight of chloral hydrate and chloral betaine (Fig. 1).

Table I—Mean Cumulative Milligrams (±*SD*) of Trichloroacetic Acid Excreted in 24 hr after Oral and Rectal Administration of 500 mg Equivalent of Chloral Hydrate and Chloral Betaine

	Oral		Rectal	
Hours	Chloral Hydrate	Chloral Betaine	Chloral Hydrate	Chloral Betaine
2	0.63 ± 0.52	0.69 ± 0.39	0.29 ± 0.20	0.18 ± 0.17
4	1.52 ± 0.87	1.65 ± 0.63	0.86 ± 0.51	0.51 ± 0.38
6	2.87 ± 0.97	4.44 ± 1.61	1.65 ± 0.81	1.07 ± 0.86
8	4.28 ± 1.74	5.06 ± 1.87	—	1.87 ± 1.45
10	6.01 ± 2.16	7.17 ± 2.55	3.76 ± 1.67	3.04 ± 2.34
12	7.41 ± 2.91	9.31 ± 3.48	4.92 ± 2.08	4.16 ± 3.20
16	11.49 ± 4.58	13.76 ± 4.92	7.84 ± 4.18	6.31 ± 4.53
24	17.17 ± 7.67	19.48 ± 7.15	11.62 ± 6.30	10.04 ± 7.17

Chloral hydrate may be administered rectally, especially in infants and children, to avoid bad taste and gastric irritation (14); however, it may be irritating to the rectal mucosa. The Student *t* test and the data in Table I indicated a significant difference between the oral and rectal administration of chloral hydrate. As shown in Fig. 1, more trichloroacetic acid was excreted after the oral administration of 500 mg of chloral hydrate than after rectal administration by means of a suppository.

There was also a significant difference between the oral and rectal administration of chloral betaine. As shown in Fig. 1, more trichloroacetic acid was excreted after oral administration than after rectal administration. Thus, although the chloral betaine complex is absorbed rectally, it appears that the rectal dose required is somewhat greater than the oral dose.

REFERENCES

(1) M. Gibaldi, in "The Theory and Practice of Industrial Pharmacy," 2nd ed., Lea & Febiger, Philadelphia, Pa., 1976, chap. 3, p. 106.

(2) W. B. Rice and J. C. McColl, *J. Am. Pharm. Assoc., Sci. Ed.*, **45**, 137 (1956).

(3) L. S. Shatin, L. J. Tsauaris, and R. P. Nenno, *Curr. Ther. Res.*, **4**, 12 (1962).

(4) British pat. 874,246 (June 26, 1959).

(5) "The National Formulary," 14th ed., Mack Publishing Co., Easton, Pa., 1975, p. 128.

(6) B. E. Cabana and P. K. Gessner, *Anal. Chem.*, **39**, 1449 (1967).

(7) "The Pharmacological Basis of Therapeutics," 5th ed., L. S. Goodman and A. Gilman, Eds., Macmillan, New York, N.Y., 1975, p. 126.

(8) E. K. Marshall, Jr., and A. H. Owens, *Bull. Johns Hopkins Hosp.*, **95**, 1 (1954).

(9) T. C. Butler, *J. Pharmacol. Exp. Ther.*, **92**, 49 (1948).

(10) D. D. Breimer, H. L. M. Cox, and J. M. VanRossum, *Pharm. Weekbl.*, **108**, 1101 (1973).

(11) D. D. Breimer, H. C. J. Ketelaars, and J. M. VanRossum, *J. Chromatogr.*, **88**, 55 (1974).

(12) E. R. Garrett and H. J. Lambert, *J. Pharm. Sci.*, **62**, 551 (1973).

(13) M. M. Soci and E. L. Parrott, *ibid.*, in press.

(14) "Martindale The Extra Pharmacopoeia," 27th ed., Pharmaceutical Press, London, England, 1977, p. 753.

ACKNOWLEDGMENTS

Abstracted in part from a dissertation submitted by M. Simpson to the University of Iowa in partial fulfillment of the Master of Science degree requirements.

^{13}C-NMR Spectroscopy of Three Tetracycline Antibiotics: Minocycline Hydrochloride, Meclocycline, and Rolitetracycline

EUGENE P. MAZZOLA *x, JUDITH A. MELIN §, and LOLA G. WAYLAND ‡

Received March 16, 1979, from the **Division of Chemistry and Physics, Bureau of Foods, Food and Drug Administration, Washington, DC 20204,* and the ‡*National Center for Antibiotics Analysis, Bureau of Drugs, Food and Drug Administration, Washington, DC 20204.* Accepted for publication September 13, 1979. §Undergraduate Federal Summer Intern, Radcliffe College, Cambridge, Mass.

Abstract □ ^{13}C-NMR data and spectral assignments are presented for tetracycline antibiotics minocycline hydrochloride, meclocycline, and rolitetracycline.

Keyphrases □ Tetracyclines—^{13}C-NMR spectra, chemical shifts assigned □ ^{13}C-NMR spectroscopy—tetracyclines, chemical shifts assigned □ Antibacterials—tetracyclines, ^{13}C-NMR spectra, chemical shifts assigned

PMR and, recently, ^{13}C-NMR spectroscopy have been widely applied to the characterization of tetracycline antibiotics (1–11). ^{13}C-NMR spectral analyses have been reported for tetracycline hydrochloride (I) and base (II) and the following related hydrochloride salts: chlortetracycline (III), methacycline (IV) (6-methyleneoxytetracycline), oxytetracycline, doxycycline (6-deoxyoxytetracycline), and demeclocycline (demethylchlortetracycline) (12).

This paper reports the ^{13}C-NMR data and spectral assignments for rolitetracycline (V) (*N*-pyrrolidinomethyltetracycline), minocycline hydrochloride (VI) (7-dimethylamino-6-demethyldeoxytetracycline hydrochloride), and meclocycline (VII) (7-chloro-6-methyleneoxytetracycline). These three tetracyclines gave rise to ^{13}C-NMR signals that could be tentatively assigned by virtue of their similarity to those of the six tetracycline antibiotics examined by Asleson and Frank (12). However, because several groups of resonance lines in the three tetracyclines were sufficiently closely spaced and different from those of the previously characterized tetracyclines, further study was necessary to clarify the assignments.

EXPERIMENTAL

NMR Spectra—^{13}C-NMR spectra, described by 4096 data points, were obtained at 20 MHz[1]. Pulse widths of 10 μsec were used, which correspond to tip angles of 45° with 10-mm sample tubes. Single-frequency off-resonance decoupled (SFORD) ^{13}C-NMR spectra were obtained with proton-decoupling frequencies about 600 Hz upfield from tetramethylsilane and at full decoupling power levels. Spin-lattice relaxation times, T_1, were determined for two particular ^{13}C-nuclei of VII using the inversion–recovery method (13, 14).

The delay time, T, between sequences was 15 sec; the intervals between the 180 and 90° pulses, τ, were 0.1, 0.2, 0.6, 0.8, 1.2, 1.4, 1.8, 2.2, 2.8, and 4.0 sec. Approximately 0.2 *M* solutions of these tetracyclines were prepared in dimethyl sulfoxide-d_6, and ~0.1 *M* solutions were prepared in deuterium oxide. The latter were used to locate carbon signals obscured by the dimethyl sulfoxide-d_6 solvent.

Compounds—Minocycline hydrochloride, meclocyline, and rolitetracycline official and proposed FDA working standards were obtained from the National Center for Antibiotics Analysis.

RESULTS AND DISCUSSION

The ^{13}C-NMR spectrum of V (Table I), as expected, closely resembled that of II, so assignment of most resonance lines was straightforward. One notable exception in terms of chemical shift value was the amide carbon which, at 168.3 ppm, was more shielded than that of II at 172.6 ppm. Such a change in shielding for amide carbons is, however, expected upon conversion of a primary to a secondary amide (15). Four triplet signals at 22.5, 23.6, 50.1, and 56.6 ppm in an SFORD spectrum corresponded to the pyrrolidine α- and β-carbons, C-5, and the pyrrolidino *N*-methylene carbon. The pyrrolidine carbons at 23.6 and 50.1 ppm were readily distinguished from C-5 (22.5 ppm) and the pyrrolidino *N*-methylene carbon (56.6 ppm) on the basis of their double intensities, due to symmetry, in the nuclear Overhauser effect-suppressed proton noise-decoupled spectrum used to count carbon atoms (16). Moreover, the signals at 50.1 and 56.6 ppm were in the range expected for methylene carbons bonded to nitrogen and were so assigned (16).

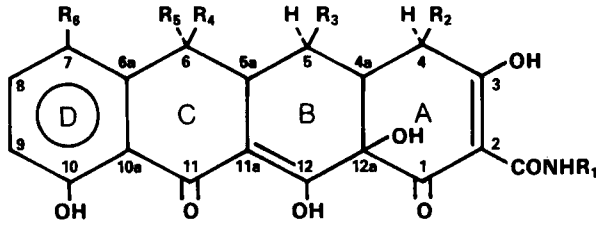

general tetracycline structure

	R_1	R_2	R_3	R_4	R_5	R_6
I	H	$N(CH_3)_2$·HCl	H	CH_3	OH	H
II	H	$N(CH_3)_2$	H	CH_3	OH	H
III	H	$N(CH_3)_2$·HCl	H	CH_3	OH	Cl
IV	H	$N(CH_3)_2$·HCl	OH	$=CH_2$		H
V	$CH_2NC_4H_8$	$N(CH_3)_2$	H	CH_3	OH	H
VI	H	$N(CH_3)_2$·HCl	H	H	H	$N(CH_3)_2$
VII	H	$N(CH_3)_2$	OH	$=CH_2$		Cl

The carbon spectrum of VI was somewhat different from the spectra of the other tetracyclines (12) partly because VI is the only member of this family possessing methylene carbons in both the B- and C-rings—*viz.*, C-5 and C-6, and a dimethylamino group attached to the D-ring. With respect to the D-ring, the signals at 136.6 and 157.4 ppm are characteristic of quaternary carbons bonded to nitrogen and oxygen, respectively (16), and were assigned to C-7 and C-10, respectively. The two methine carbons in the D-ring, C-8 and C-9, were easily identified in an SFORD spectrum as the doublets at 115.6 and 128.5 ppm. The former was assigned to C-9 by comparison with C-9 signals of the other tetracyclines (16). The latter (C-8) was shielded by the *o*-dimethylamino group relative to the other tetracyclines, as is C-6a, to which the signal at 142.2 ppm was assigned (16).

Assignment of the triplets due to C-5 and C-6 and of the close-lying doublets due to C-4a and C-5a in the SFORD spectrum was developed in the following manner. The triplet at 33.8 ppm was assigned to C-6 because this carbon is benzylic and is expected to be more deshielded than the other methylene carbon, C-5, which appears at 29.6 ppm (16). The doublet at 35.1 ppm was assigned to C-4a by comparison with C-4a signals of the other tetracyclines (12), leaving C-5a at 31.6 ppm. With I as a model, removal of the methyl and hydroxyl groups from C-6 to produce a structure like VI is expected to have a much greater effect on C-5a, which is shielded by about 10 ppm, than on C-4a, which is essentially unchanged. The quartet at 41.2 ppm was assigned to the carbons of the D-ring dimethylamino group, and that at 44.4 ppm was assigned to those of the A-ring dimethylammonium group. The carbons of the latter group are expected to be more deshielded because of the positively charged nitrogen atom.

[1] Varian CFT-20 spectrometer.

0022-3549/80/0200-0229$01.00/0
© 1980, American Pharmaceutical Association

Table I—^{13}C-NMR Data [a] and Spectral Assignments for Several Tetracyclines [b]

Position	I[c]	II[c]	III[c]	IV[c]	V[d]	VI	VII
1	193.0	192.4	192.0	192.1	191.8	193.0	190.3
2	95.5	98.3	95.6	94.8	101.2	95.6	98.8
3	187.3	192.4	187.3	187.3	189.6	187.5	187.1
4	67.9 d	69.4 d	68.1 d	65.1 d	72.5 d	68.0 d	64.9 d
4a	34.8 d	37 d	34.9 d	41 d	38.6 d	35.1 d	40.0 d
5	27.0 t	22.4 t	27.1 t	63.9 d	22.5 t	29.6 t	65.5 d
5a	41 d	40 d	42 d	44.0 d	41.6 d	31.6 d	45.4 d
6	67.8	68.1	70.4	140.6	68.0	33.8 t	136.9
6a	148.0	148.0	143.6	142.6	148.0	142.2	138.6
7	116.9 d	116.8 d	121.2	117.2 d	116.7 d	136.6	119.6
8	136.5 d	136.4 d	139.7 d	137.0 d	135.9 d	128.5 d	137.8 d
9	115.2 d	115.4 d	118.9 d	116.4 d	115.1 d	115.6 d	118.3 d
10	161.4	161.4	160.7	160.7	161.4	157.4	159.8
10a	114.4	114.4	117.0	114.4	114.5	116.0	116.6
11	193.5	192.9	193.4	193.5	192.0	193.7	191.3
11a	106.9	105.8	106.1	105.1	105.3	108.3	105.4
12	175.1	176.8	175.7	173.6	180.1	174.3	178.2
12a	73.1	74.3	73.2	73.5	74.8	73.9	75.4
$N(CH_3)_2$	41 q	42 q	41 q	41 q	42.3 q	44.4 q	41.7 q
CONHR	172.1	172.6	172.1	171.6	168.3	171.9	170.5
CH_3	22.5 q	22.9 q	25.0 q	113.7 t[e]	22.9 q	41.2 q[f]	117.7 t[e]

[a] In dimethyl sulfoxide-d_6; parts per million from tetramethylsilane. [b] See text for numerical designation of compounds. [c] From Ref. 12. [d] Also 23.6 (t), β-pyrrolidine carbons; 50.1 (t), α-pyrrolidine carbons; 56.6 (t), CH_2N-pyrrolidine group. [e] $=CH_2$. [f] $N(CH_3)_2$.

As anticipated, the carbon spectrum of VII was similar to spectra of III and IV. Like VI, the methine carbons, C-8 and C-9, were readily identified in an SFORD spectrum and assigned to the doublets at 137.8 and 118.3 ppm, respectively, by comparison with corresponding carbon signals of III. Further examination permitted differentiation of the doublet due to C-4 from that of C-5, these two signals being observed at 64.9 and 65.5 ppm, respectively. However, the components of the low-field doublet were relatively sharp while those of the high-field doublet exhibited considerable splitting due to long-range coupling, *i.e.*, two bonds or more. Since C-4 should be coupled to the six methyl protons of the 4-dimethylamino group and C-5 does not appear to have as extensive coupling possibilities, the signal at 64.9 ppm was assigned to C-4. Moreover, the doublets assigned to C-4 in I, III, IV, and VI all displayed similar long-range coupling compared with other doublet signals.

Examination of a fully coupled spectrum of meclocycline allowed the signal of C-7 to be distinguished from that of C-10a. Two singlet signals were observed at 116.6 and 119.6 ppm in the SFORD spectrum and were ascribed to the quaternary carbons C-7 and C-10a. In the fully coupled spectrum, however, the low-field signal appeared as a doublet of doublets, with coupling constants of 4 and 7 Hz, while the high-field signal was observed as a 7-Hz doublet. Since both carbons should exhibit *trans*-oriented three-bond couplings to H-9 and since C-7 should be coupled to H-8 as well, the four-line signal at 119.6 ppm was assigned to C-7 and the doublet at 116.6 ppm was assigned to C-10a. The remaining doublets at 40 and 45.4 ppm were assigned to C-4a and C-5a, respectively, by comparison with analogous carbon signals of the other tetracyclines (12). In these compounds, C-4a resonances were consistently ~5 ppm upfield from those attributed to C-5a carbons; in IV, these two carbons appeared at 41 and 44 ppm, respectively.

Several lines of reasoning led to the assignment of signals at 136.9 and 138.6 ppm to C-6 and C-6a, respectively. First, in the SFORD spectrum the low-field signal was considerably broader than the high-field one, which was only 1 Hz wider than the corresponding resonance line in the proton noise-decoupled spectrum. Inspection of VII revealed that C-6a should be *trans*-coupled to one exocyclic methylene proton and *cis*-coupled to the other and should exhibit a *trans*-oriented three-bond coupling to H-8. While C-6 ought, in principle, to be coupled to these same exocyclic methylene protons, the olefinic *cis* and *trans* three-bond couplings of C-6a should be larger and result in a wider signal for this carbon in the SFORD spectrum (17–19). Therefore, the low-field signal was tentatively assigned to C-6a.

Second, a selective heteronuclear decoupling experiment was carried out in which H-8, at 7.67 ppm, was irradiated while an otherwise fully coupled spectrum of VII was obtained. The signal at 138.6 ppm (tentatively assigned to C-6a) appeared to sharpen compared with the corresponding signal in a control, fully coupled spectrum, while that at 136.9 ppm apparently remained unchanged. Since C-6a is expected to show a larger coupling to H-8 than is C-6 (*trans*-oriented three-bond coupling *versus* allylic-type four-bond coupling) (17–19), the low-field signal was assigned to C-6a, consistent with the first results.

Third, spin-lattice relaxation times, T_1, were determined for the two signals. The resonance at 136.9 ppm had a T_1 value of 0.7 sec while that of the 138.6-ppm signal was 2.5 sec. Examination of a Dreiding model of VII demonstrated that C-6 is situated approximately 2 Å from both the two exocyclic methylene protons and H-5a while C-6a is located about 2.5 Å from the nearer exocyclic methylene proton and about 3 Å, or greater, from H-9, H-5a, and the further exocyclic methylene proton. Due to the substantial decrease in effectiveness of the dipole–dipole relaxation mechanism with increasing internuclear distance (13), C-6 would be expected to have a shorter T_1 value than C-6a. Therefore, the signal at 136.9 ppm was assigned to C-6, again consistent with the initial assignment.

REFERENCES

(1) M. Schach von Wittenau, F. A. Hochstein, and C. R. Stephens, *J. Org. Chem.*, **28**, 2454 (1963).

(2) C. R. Stephens, J. J. Beereboom, H. H. Rennhard, P. N. Gordon, K. Murai, R. K. Blackwood, and M. Schach von Wittenau, *J. Am. Chem. Soc.*, **85**, 2643 (1963).

(3) R. K. Blackwood, J. J. Beereboom, H. H. Rennhard, M. Schach von Wittenau, and C. R. Stephens, *ibid.*, **85**, 3943 (1963).

(4) M. Schach von Wittenau, *J. Org. Chem.*, **29**, 2746 (1964).

(5) M. Schach von Wittenau, R. K. Blackwood, L. H. Conover, R. H. Glauert, and R. B. Woodward, *J. Am. Chem. Soc.*, **87**, 134 (1965).

(6) F. Barbatschi, M. Dann, T. H. Martin, P. Miller, L. A. Mitscher, and N. Bohonos, *Experientia*, **21**, 162 (1965).

(7) M. Schach von Wittenau and R. K. Blackwood, *J. Org. Chem.*, **31**, 613 (1966).

(8) L. A. Mitscher, J. V. Juvarkar, W. Rosenbrook, Jr., W. W. Andres, J. Schenck, and R. S. Egan, *J. Am. Chem. Soc.*, **92**, 6070 (1970).

(9) G. L. Asleson, L. J. Stoel, E. C. Newman, and C. W. Frank, *J. Pharm. Sci.*, **63**, 1144 (1974).

(10) N. V. Sheberstova, M. E. Perel'son, and A. D. Kuzovkov, *Khim. Prir. Soedin.*, **10**, 67 (1974).

(11) J. Gulbis and G. W. Everett, Jr., *J. Am. Chem. Soc.*, **97**, 6248 (1975).

(12) G. L. Asleson and C. W. Frank, *ibid.*, **97**, 6246 (1975).

(13) F. W. Wehrli and T. Wirthlin, "Interpretation of Carbon-13 NMR Spectra," Heyden, New York, N.Y., 1976, chap. 4.

(14) K. Mullen and P. S. Pregosin, "Fourier Transform NMR Techniques: A Practical Approach," Academic, New York, N.Y., 1976, chap. 4.

(15) G. C. Levy and G. L. Nelson, "Carbon-13 Nuclear Magnetic Resonance for Organic Chemists," Wiley-Interscience, New York, N.Y., 1972, p. 123.

(16) F. W. Wehrli and T. Wirthlin, "Interpretation of Carbon-13 NMR Spectra," Heyden, New York, N.Y., 1976, chap. 2.

(17) A. S. Perlin, in "Isotopes in Organic Chemistry," vol. 3, E. Buncel and C. Lee, Eds., Elsevier, New York, N.Y., 1977, pp. 215–219.

(18) R. J. Abraham and P. Loftus, "Proton and Carbon-13 NMR Spectroscopy," Heyden, London, England, 1978, chap. 3.

(19) D. F. Ewing, *Annu. Rep. NMR Spectrosc.*, **6A**, 389 (1975).

Synthesis of 1-*O*-(2′-Acetoxy)benzoyl-α-D-2-deoxyglucopyranose, a Novel Aspirin Prodrug

J. E. TRUELOVE *, A. A. HUSSAIN ˣ, and H. B. KOSTENBAUDER

Received March 23, 1979, from the *College of Pharmacy, University of Kentucky, Lexington, KY 40506.* Accepted for publication September 12, 1979. *Present address: Wyeth Laboratories, Paoli, PA 19301.

Abstract □ The synthesis and characterization of 1-*O*-(2′-acetoxy)-benzoyl-α-D-2-deoxyglucopyranose, a novel aspirin prodrug, are described. 3,4,6-Tri-*O*-benzyl-α-D-2-deoxyglucopyranose was synthesized by methylating the anomeric hydroxyl group of 2-deoxyglucose, benzylating the 3-, 4-, and 6-hydroxy functional groups, and cleaving hydrolytically the anomeric methyl group. Reaction of the tribenzylated sugar with the acid chloride of aspirin and subsequent hydrogenolysis of the benzyl groups resulted in the prodrug, mp 128°. The compound was further characterized by elemental analysis and PMR and ^{13}C-NMR spectroscopy. *In vitro*, the compound cleaved to aspirin with a half-life of 7 min at 37°. Prodrug cleavage was independent of pH over the pH 3–9 range.

Keyphrases □ 1-*O*-(2′-Acetoxy)benzoyl -α-D- 2-deoxyglucopyranose —aspirin prodrug, synthesis □ Aspirin prodrugs—synthesis of 1-*O*-(2′-acetoxy)benzoyl-α-D-2-deoxyglucopyranose □ Prodrugs—aspirin, synthesis of 1-*O*-(2′-acetoxy)benzoyl-α-D-2-deoxyglucopyranose

Aspirin, probably the most widely used drug in the world, is a potent, effective, and low cost medicament. However, it produces occult GI blood loss in a large percentage of patients (1–6). Studies have also shown that gastric irritation is a local effect (6) of contact of the mucosa with the highly acidic aspirin particles or the saturated solution surrounding those particles. Although GI bleeding can be prevented by administration of aspirin in a highly buffered solution (7), the high sodium content of such buffered products makes their chronic use impractical (6).

Previous communications showed that the acylal derivative 1-ethoxy(ethyl-2-acetoxy)benzoate is an oily, insoluble compound which cleaves very rapidly, generating aspirin (8), and that the acylal 1-*O*-(2′-acetoxy)benzoyl-α-D-glucopyranose is a more soluble, crystalline compound which only slowly generates aspirin in solution (9).

The present report describes the synthesis of the prodrug 1-*O*-(2′-acetoxy)benzoyl-α-D-2-deoxyglucopyranose (V), a crystalline compound that cleaves to aspirin *in vitro* in a reaction that is independent of pH; it has a half-life of 7 min at 37° (10). The prodrug, a neutral compound, should generate a nonirritating aspirin solution upon contact with the gastric milieu.

EXPERIMENTAL

Materials—The following materials were reagent grade or equivalent: methanol, sodium carbonate, acetone, absolute ethanol, ethyl acetate, potassium hydroxide, dry dioxane, dry pyridine, ethyl ether, sodium sulfate, acetic acid, sulfuric acid, dichloromethane, sodium bicarbonate, palladium-on-carbon, petroleum ether, and chloroform. 2-Deoxyglucose[1] and *o*-acetylsalicyloyl chloride[2] were used as received. Benzyl chloride[2] was redistilled at 175 ± 0.5°.

Synthesis—The general procedure for the synthesis of the prodrug (V) was a modification of that of Glaudemans and Fletcher (11).

α-Methyl-2-deoxyglucopyranose (I)—A solution of the starting material, 2-deoxyglucose (15 g, 0.09 mole), in 2% methanolic hydrochloric acid (540 ml) was warmed to 40° and shaken for 1 hr. After cooling to 20°, the mixture was stirred with excess sodium carbonate (32 g) for 15 min. After filtration, the solvent was removed under reduced pressure to give an oil containing a small amount of white solid.

The oil was dissolved in acetone (750 ml) and, after filtration and solvent removal, crystallized from 5 ml of ethanol at −5°. The crystalline material (I) was recovered by filtration and washed with cold (−5°) ethyl acetate. The yield was 10 g (61%), mp 91–92°[3] [lit. (12) mp 91–92°]; NMR[4] (dimethyl sulfoxide-d_6): δ 4.1–4.8 (m, 3H, OH), 3.1–4.1 (m, 9H, 3-6-H's, 1-H, OCH_3), and 1.1–2.3 (m, 2H, 2-H's).

*α-Methyl-3,4,6-tri-*O*-benzyl-2-deoxy-D-glucopyranose (II)*—Nine grams (0.05 mole) of I was added to a suspension of finely powdered potassium hydroxide (44.8 g) in dry dioxane (110 ml), and the mixture was warmed to reflux. As soon as reflux was smooth, colorless benzyl chloride (62 ml) was added dropwise over 45 min. After an additional 40 min of refluxing, the dioxane was distilled off during 3 hr. After cooling, the residue was diluted to 350 ml with water and extracted with ether.

The ether portions were dried and, after filtration, evaporated at reduced pressure to give an oil. The oil was subjected to vacuum distillation (bath temperature of 200°, 0.4 mm Hg). The oily product (II) remained in the distillation vessel in ~100% yield; NMR ($CDCl_3$): δ 6.7–7.7 (m, 15H, ArH), 4.2–5.0 (m, 7H, ring-CH_2–, 1-H), 3.3–4.2 (m, 5H, 3-6-H's), 3.2 (s, 3H, OCH_3), and 1.4–2.5 (m, 2H, 2-H's).

*3,4,6-Tri-*O*-benzyl-α-D-2-deoxyglucopyranose (III)*—Compound II (22.3 g, 0.05 mole) was dissolved in hot (70°) acetic acid, slowly treated with hot (70°) 1 *M* H_2SO_4, and stirred at 70° for 1 hr. The reaction mixture was slowly added to cold water (3 liters, 10°), stirred for 2 hr, and kept at 10° for 24 hr. The product (III) was recovered by filtration and washed with methanol. The yield was 14 g (65%), mp 96–97°; NMR ($CDCl_3$): δ 6.7–7.7 (m, 15H, ArH), 5.1–5.4 (s, 1H, 1-H), 4.2–5.1 (m, 6, H ring-CH_2–), 3.2–4.2 (m, 6H, 3-6-H's, 1-OH), and 1.4–2.5 (m, 2H, 2-H's).

1-O-(2′-Acetoxy)benzoyl -3,4,6- tri-O-benzyl-α-D-2-deoxyglucopyranose (IV)—A solution of III (13.7 g, 0.032 mole) in dichloromethane (130 ml) was treated with a solution of *O*-acetylsalicyloyl chloride (6.93 g, 0.035 mole) and pyridine (2.8 ml) in dichloromethane (50 ml) and

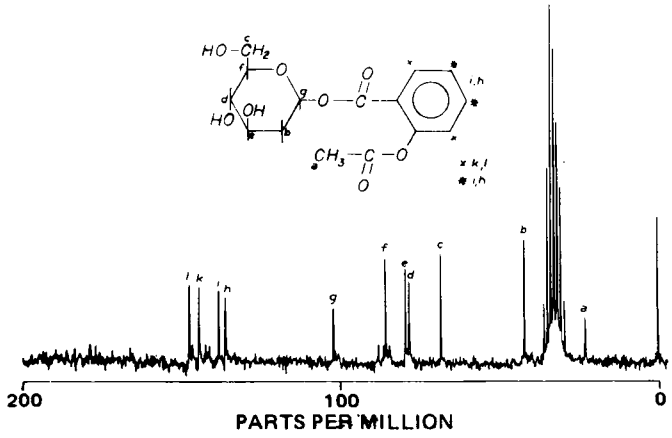

Figure 1—^{13}C-*NMR spectrum of 1-*O*-(2′-acetoxy)benzoyl-α-D-2-deoxyglucopyranose in acetone-*d_6.

[1] Sigma Chemical Co., St. Louis, Mo.
[2] Aldrich Chemical Co.

[3] All melting points were obtained using a Hoover Uni-melt capillary apparatus and are uncorrected.
[4] PMR spectra were obtained using a Varian EM-360 spectrophotometer with tetramethylsilane as the internal reference.

0022-3549/80/0200-0231$01.00/0
© 1980, American Pharmaceutical Association

stirred at 20° for 23 hr. Then 100 g of ice was added, and the mixture was left for an additional 1 hr. The dichloromethane layer was separated and washed with water, 3 *N* H_2SO_4, water, and a saturated solution of sodium bicarbonate. It then was dried and evaporated under reduced pressure to yield an oil.

The crude product separated as a waxy solid from a solution of the oil in methanol (200 ml). Recrystallization from ethanol gave IV (4.7 g, 25%); NMR ($CDCl_3$): δ 6.7–8.0 (m, 19H, ArH), 5.8 (d, 1H, 1-H), 4.4–4.9 (m, 6H, ring-CH_2–), 3.4–3.9 (m, 5H, 3-6-H's), and 1.0–2.5 (m, 5H, 2-H, –$OCOCH_3$). The ^{13}C-NMR[5] (deuterochloroform) was also consistent with the structure of IV.

1-O-(2′-Acetoxy)benzoyl-α-D-2-deoxyglucopyranose (V)—Compound IV (1 g, 0.002 mole) was dissolved in ethanol (150 ml), and 10% palladium-on-carbon (0.6 g) was added. Hydrogenolysis at 60 psig for 12 hr, filtration, and solvent evaporation at reduced pressure gave an oil. The oil was washed with petroleum ether (50 ml), and it crystallized spontaneously upon the addition of chloroform (15 ml). The yield was 0.52 g (95%), mp 128–129°; NMR (acetone-d_6): δ 7.0–8.2 (m, 4H, ArH), 5.8–5.9 (d, 1H, 1-H), 3.0–4.1 (m, 8H, 3-6-H's, OH's), 2.3 (s, 3H, –$OCOCH_3$), and 1.0–2.3 (m, 2H, 2-H's). The ^{13}C-NMR (acetone-d_6) was also consistent with the structure of V (Fig. 1).

Anal.[6]—Calc. for $C_{15}H_{18}O_8$: C, 55.20; H, 5.57. Found: C, 55.35; H, 5.59.

DISCUSSION

The method described here for Compound V provides a synthetic route for the preparation of acylal prodrugs of aspirin in which the acidic carboxyl function is masked by a sugar molecule. Compound V was characterized by elemental analysis and PMR and ^{13}C-NMR spectroscopy. The ^{13}C-NMR spectrum shown in Fig. 1 is consistent with the assigned structure (V).

Since the regeneration rate of the parent compound from V occurs *in vitro* with a half-life of 7 min at 37° (10) and since preliminary data (9) indicate that the glucose analog hydrolyzes much more slowly, application of the method to other sugars (or other parent drugs) may provide additional useful drug substances.

[5] The ^{13}C-NMR spectra were obtained using a Varian CFT-20 NMR spectrometer.

[6] Elemental analysis was performed by Micro-Analysis, Inc., Wilmington, Del.

REFERENCES

(1) L. Stubbé, *Br. Med. J.*, **2**, 1062 (1958).

(2) P. Holt, *J. Lab. Clin. Med.*, **56**, 717 (1960).

(3) R. Pierson, P. Holt, R. Watson, and R. Keating, *Am. J. Med.*, **31**, 259 (1961).

(4) P. Wood, E. Harvey-Smith, and A. Dixon, *Br. Med. J.*, **1**, 669 (1962).

(5) D. Croft and P. Wood, *ibid.*, **1**, 137 (1967).

(6) J. Leonards and G. Levy, *J. Pharm. Sci.*, **59**, 1511 (1970).

(7) J. Leonards, *Gastroenterology*, **44**, 617 (1963).

(8) A. Hussain, M. Yamasaki, and J. Truelove, *J. Pharm. Sci.*, **63**, 627 (1974).

(9) J. Truelove, Ph.D. thesis, University of Kentucky, Lexington, Ky., 1978.

(10) A. Hussain, J. Truelove, and H. Kostenbauder, *J. Pharm. Sci.*, **68**, 299 (1979).

(11) C. Glaudemans and H. Fletcher, in "Methods in Carbohydrate Chemistry," vol. VI, R. Whistler and J. BeMiller, Eds., Academic, New York, N.Y., 1972, p. 373.

(12) R. Deriaz, W. Overend, M. Stacey, and L. Wiggins, *J. Chem. Soc.*, **1949**, 2836.

New Compounds: Synthesis of 2-Chloromethylbenzo[*b*]furans

WAYNE K. ANDERSON ˣ, JEFFREY C. BOTTARO, and MICHAEL J. HALAT

Received June 20, 1979, from the *Department of Medicinal Chemistry, School of Pharmacy, State University of New York at Buffalo, Buffalo, NY 14260.* Accepted for publication August 8, 1979.

Abstract □ 2-Chloromethylbenzo[*b*]furans were prepared in high overall yield from the corresponding chloroethylphenyl ethers through chloroepoxide and α-chlorophenylacetone intermediates.

Keyphrases □ Benzo[*b*]furans—synthesis of 2-chloromethyl compounds □ 2-Chloromethylbenzo[*b*]furans—synthesis □ Heterocycles—synthesis of 2-chloromethylbenzo[*b*]furans

The benzo[*b*]furan ring system has provided a focus for the development of new agents in several classes, and new synthetic approaches to this heterocyclic system continue to be significant. The synthesis of 2-methylbenzo[*b*]furans from aryl 2-chloroprop-2-enyl ethers was described (1), but low yields were obtained when the starting phenol contained an *o*-chlorine substituent. This report describes an alternative procedure which circumvents this problem and gives a reactive chloromethyl group in the 2-position of the benzo[*b*]furan.

DISCUSSION

The starting phenol was added to a solution of sodium in absolute ethanol. 2,3-Dichloropropene was added, and the mixture was heated under reflux for 24 hr to give the aryl 2-chloroprop-2-enyl ethers (I) in almost quantitative yield. Rearrangement of I to II as described previously (1, 2) and acetylation of II gave III. This acetylation was necessary since the next step, epoxidation, yielded only decomposed material in the presence of the free phenol. Epoxidation of III gave chloroepoxides (IV), usually in crude yields greater than 90%, which were converted directly to the chloroketone (V).

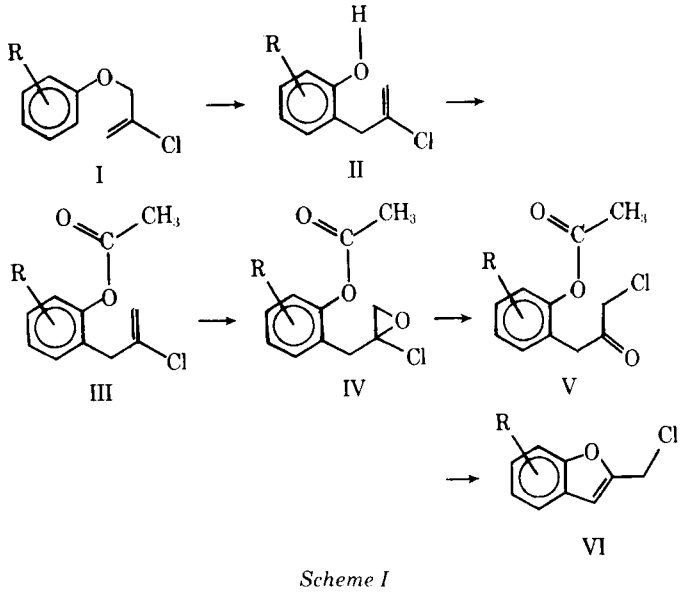

Scheme I

The rearrangement of IV occurred when the chloroepoxide was allowed

0022-3549/80/0200-0232$01.00/0

© 1980, American Pharmaceutical Association

stirred at 20° for 23 hr. Then 100 g of ice was added, and the mixture was left for an additional 1 hr. The dichloromethane layer was separated and washed with water, 3 *N* H_2SO_4, water, and a saturated solution of sodium bicarbonate. It then was dried and evaporated under reduced pressure to yield an oil.

The crude product separated as a waxy solid from a solution of the oil in methanol (200 ml). Recrystallization from ethanol gave IV (4.7 g, 25%); NMR ($CDCl_3$): δ 6.7–8.0 (m, 19H, ArH), 5.8 (d, 1H, 1-H), 4.4–4.9 (m, 6H, ring-CH_2–), 3.4–3.9 (m, 5H, 3-6-H's), and 1.0–2.5 (m, 5H, 2-H, –$OCOCH_3$). The ^{13}C-NMR[5] (deuterochloroform) was also consistent with the structure of IV.

1-O-(2′-Acetoxy)benzoyl-α-D-2-deoxyglucopyranose (V)—Compound IV (1 g, 0.002 mole) was dissolved in ethanol (150 ml), and 10% palladium-on-carbon (0.6 g) was added. Hydrogenolysis at 60 psig for 12 hr, filtration, and solvent evaporation at reduced pressure gave an oil. The oil was washed with petroleum ether (50 ml), and it crystallized spontaneously upon the addition of chloroform (15 ml). The yield was 0.52 g (95%), mp 128–129°; NMR (acetone-d_6): δ 7.0–8.2 (m, 4H, ArH), 5.8–5.9 (d, 1H, 1-H), 3.0–4.1 (m, 8H, 3-6-H's, OH's), 2.3 (s, 3H, –$OCOCH_3$), and 1.0–2.3 (m, 2H, 2-H's). The ^{13}C-NMR (acetone-d_6) was also consistent with the structure of V (Fig. 1).

Anal.[6]—Calc. for $C_{15}H_{18}O_8$: C, 55.20; H, 5.57. Found: C, 55.35; H, 5.59.

DISCUSSION

The method described here for Compound V provides a synthetic route for the preparation of acylal prodrugs of aspirin in which the acidic carboxyl function is masked by a sugar molecule. Compound V was characterized by elemental analysis and PMR and ^{13}C-NMR spectroscopy. The ^{13}C-NMR spectrum shown in Fig. 1 is consistent with the assigned structure (V).

Since the regeneration rate of the parent compound from V occurs *in vitro* with a half-life of 7 min at 37° (10) and since preliminary data (9) indicate that the glucose analog hydrolyzes much more slowly, application of the method to other sugars (or other parent drugs) may provide additional useful drug substances.

[5] The ^{13}C-NMR spectra were obtained using a Varian CFT-20 NMR spectrometer.

[6] Elemental analysis was performed by Micro-Analysis, Inc., Wilmington, Del.

REFERENCES

(1) L. Stubbé, *Br. Med. J.*, **2**, 1062 (1958).

(2) P. Holt, *J. Lab. Clin. Med.*, **56**, 717 (1960).

(3) R. Pierson, P. Holt, R. Watson, and R. Keating, *Am. J. Med.*, **31**, 259 (1961).

(4) P. Wood, E. Harvey-Smith, and A. Dixon, *Br. Med. J.*, **1**, 669 (1962).

(5) D. Croft and P. Wood, *ibid.*, **1**, 137 (1967).

(6) J. Leonards and G. Levy, *J. Pharm. Sci.*, **59**, 1511 (1970).

(7) J. Leonards, *Gastroenterology*, **44**, 617 (1963).

(8) A. Hussain, M. Yamasaki, and J. Truelove, *J. Pharm. Sci.*, **63**, 627 (1974).

(9) J. Truelove, Ph.D. thesis, University of Kentucky, Lexington, Ky., 1978.

(10) A. Hussain, J. Truelove, and H. Kostenbauder, *J. Pharm. Sci.*, **68**, 299 (1979).

(11) C. Glaudemans and H. Fletcher, in "Methods in Carbohydrate Chemistry," vol. VI, R. Whistler and J. BeMiller, Eds., Academic, New York, N.Y., 1972, p. 373.

(12) R. Deriaz, W. Overend, M. Stacey, and L. Wiggins, *J. Chem. Soc.*, **1949**, 2836.

New Compounds: Synthesis of 2-Chloromethylbenzo[*b*]furans

WAYNE K. ANDERSON ˣ, JEFFREY C. BOTTARO, and MICHAEL J. HALAT

Received June 20, 1979, from the *Department of Medicinal Chemistry, School of Pharmacy, State University of New York at Buffalo, Buffalo, NY 14260.* Accepted for publication August 8, 1979.

Abstract □ 2-Chloromethylbenzo[*b*]furans were prepared in high overall yield from the corresponding chloroethylphenyl ethers through chloroepoxide and α-chlorophenylacetone intermediates.

Keyphrases □ Benzo[*b*]furans—synthesis of 2-chloromethyl compounds □ 2-Chloromethylbenzo[*b*]furans—synthesis □ Heterocycles—synthesis of 2-chloromethylbenzo[*b*]furans

The benzo[*b*]furan ring system has provided a focus for the development of new agents in several classes, and new synthetic approaches to this heterocyclic system continue to be significant. The synthesis of 2-methylbenzo[*b*]furans from aryl 2-chloroprop-2-enyl ethers was described (1), but low yields were obtained when the starting phenol contained an *o*-chlorine substituent. This report describes an alternative procedure which circumvents this problem and gives a reactive chloromethyl group in the 2-position of the benzo[*b*]furan.

DISCUSSION

The starting phenol was added to a solution of sodium in absolute ethanol. 2,3-Dichloropropene was added, and the mixture was heated under reflux for 24 hr to give the aryl 2-chloroprop-2-enyl ethers (I) in almost quantitative yield. Rearrangement of I to II as described previously (1, 2) and acetylation of II gave III. This acetylation was necessary since the next step, epoxidation, yielded only decomposed material in the presence of the free phenol. Epoxidation of III gave chloroepoxides (IV), usually in crude yields greater than 90%, which were converted directly to the chloroketone (V).

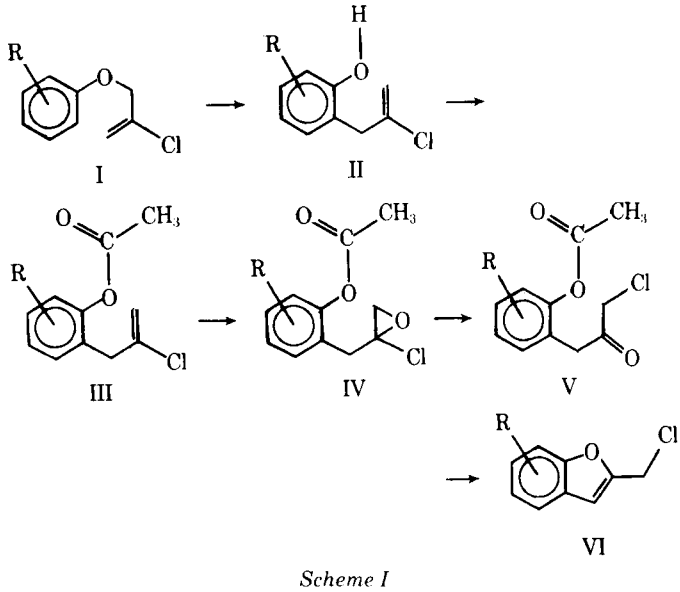

Scheme I

The rearrangement of IV occurred when the chloroepoxide was allowed

0022-3549/80/0200-0232$01.00/0

© 1980, American Pharmaceutical Association

Table I—Yields, Physical Properties, and Microanalytical Data [a]

Compound	R	Melting or Boiling Point (Recrystallization Solvent)	Yield, %	Molecular Formula	Analysis, %	Calc.	Found
IIIa	4-Cl	90°/0.20 torr	98	$C_{11}H_{10}Cl_2O_2$	C	53.90	53.82
					H	4.11	4.12
					Cl	28.93	28.81
IIIb	6-Cl	89°/0.25 torr	96	$C_{11}H_{10}Cl_2O_2$	C	53.90	53.97
					H	4.11	4.13
					Cl	28.93	28.83
IIIc	4-OCH_3	100°/0.90 torr	100	$C_{12}H_{13}ClO_3$	C	59.88	59.91
					H	5.44	5.49
					Cl	14.73	14.84
IIId	6-OCH_3	95°/1.00 torr	98	$C_{12}H_{13}ClO_3$	C	59.88	59.87
					H	5.44	5.47
					Cl	14.73	14.83
IIIe	6-CH_3	80°/0.15 torr	99	$C_{12}H_{13}ClO_2$	C	64.15	64.08
					H	5.83	5.88
					Cl	15.78	15.81
Va	4-Cl	98–100° (Carbon tetrachloride–hexane)	70[b]	$C_{11}H_{10}Cl_2O_3$	C	50.60	50.56
					H	3.86	3.87
					Cl	27.16	27.14
Vb	6-Cl	91–93° (Carbon tetrachloride–hexane)	75[b]	$C_{11}H_{10}Cl_2O_3$	C	50.60	50.66
					H	3.86	3.87
					Cl	27.16	27.09
Vc	4-OCH_3	104.5–105° (Methylene chloride–petroleum ether)	81[b]	$C_{12}H_{13}ClO_4$	C	56.15	56.16
					H	5.11	5.15
					Cl	13.81	13.74
Vd	6-OCH_3	85–86° (Carbon tetrachloride–petroleum ether)	60[b]	$C_{12}H_{13}ClO_4$	C	56.15	56.07
					H	5.11	5.13
					Cl	13.81	13.88
Ve	6-CH_3	94–95° (Carbon tetrachloride)	95[b]	$C_{12}H_{13}ClO_3$	C	59.88	59.65
					H	5.44	5.49
					Cl	14.73	14.64
VIa	5-Cl	54–55° (Hexane)	99	$C_9H_6Cl_2O$	C	53.77	53.74
					H	3.01	3.06
					Cl	35.27	35.16
VIb	7-Cl	84–86° (Methylene chloride–petroleum ether)	99	$C_9H_6Cl_2O$	C	53.77	53.70
					H	3.01	2.99
					Cl	35.27	37.18

[a] IR, UV, and NMR data are consistent with the reported structures and are similar to data reported under *Experimental*. [b] The yield of V is based on III (*i.e.*, on the two-step conversion).

to stand (neat) at room temperature for several days; this reaction was accelerated markedly by a trace of anhydrous hydrogen chloride. The phenylacetone derivatives (V) are potentially useful intermediates in the synthesis of substituted phenethylamines and phenpropylamines.

Treatment of Va or Vb with hot concentrated hydrochloric acid resulted in facile cyclization to VIa or VIb, respectively. Excessive decomposition accompanied attempted cyclization of Vc–Ve.

EXPERIMENTAL

Table I summarizes the yields, physical properties, and microanalyses for the compounds prepared[1]. Scheme I illustrates the steps in the synthesis.

2-(2′-Chloroprop-2-enyl)-4-chlorophenyl Acetate (IIIa)—A solution of IIa (6.09 g, 0.03 mole) and acetic anhydride (10 ml) in anhydrous pyridine (30 ml) was stirred magnetically and allowed to stand for 12 hr at room temperature. The pyridine and excess anhydride were removed *in vacuo*, and the residue was distilled to yield IIIa (7.21 g, 98%), bp 90°/0.20 torr; IR: 2899, 1757, 1634, 1475, 1427, 1404, 1366, 1190 (br), 1164, 1043, 1009, 943, 909, and 890 cm^{-1}; NMR: δ 2.25 (s, 3H), 3.59 (s, 2H), 5.29 (d, J = 13 Hz, 2H), and 7.08–7.60 (m, 3H); UV: λ_{max} 228 (Σ 3170) and 278 (55) nm.

2-(3′-Chloropropan-2′-one)-4-chlorophenyl Acetate (Va)—A stirred solution of IIIa (30 g, 0.115 mole) and *m*-chloroperbenzoic acid (85%, 36 g) in methylene chloride (300 ml) was allowed to stand at room temperature for 9 days. It was then concentrated to dryness *in vacuo*, and the residue was dissolved in ether (200 ml). The ethereal solution was washed successively with saturated aqueous sodium carbonate solution (200 ml), water (200 ml), and 10% aqueous hydrochloric acid (200 ml); the solution was dried over sodium sulfate and concentrated *in vacuo*.

The residual acid catalyzed the conversion of IVa to Va; the reaction was monitored by TLC (silica gel, methylene chloride); after several days, none of the chloroepoxide remained. The product was crystallized from carbon tetrachloride–hexane to yield 21 g (70%) of Va, mp 98–100°; IR: 2907, 1761, 1718, 1481, 1368, 1196, 1163, 1111, 1009, and 881 cm^{-1}; NMR: δ 2.27 (s, 3H), 3.78 (s, 2H), 4.07 (s, 2H), and 6.93–7.43 (m, 3H); UV: λ_{max} 226 (Σ 3260), 270 (550), and 278 (520) nm.

2-Chloromethyl-5-chlorobenzo[*b*]furan (VIa)—A vigorously stirred solution of Va (2.0 g, 7.66 mmoles) in concentrated hydrochloric acid (60 ml) was heated at 90° for 1 hr, and the cooled solution then was extracted with chloroform (3 × 60 ml). The chloroform solution was washed with water (100 ml), dried over sodium sulfate, and concentrated *in vacuo* to give 1.53 g (99%) of VIa, mp 53–55°. Crystallization from hexane at −78° gave VIa, mp 54–55°; IR: 2941, 1855, 1730, 1610, 1577, 1460, 1445, 1429, 1314, 1272, 1263, 1192, 1130, 1064, 961, 925, 889, 870, 833, 719, and 698 cm^{-1}; NMR: δ 4.52 (s, 2H), 6.51 (s, 1H), and 7.13–7.40 (m, 3H); UV: λ_{max} 215 (Σ 19,600), 256 (13,700), 288 (3460), and 298 (2990) nm.

[1] Melting points (uncorrected) were determined in an open capillary with a Thomas–Hoover Unimelt apparatus. IR spectra were determined for carbon tetrachloride solutions (unless otherwise specified) with a Perkin-Elmer 237 spectrophotometer. UV data were determined for 95% ethanol solutions with a Beckman DB-G spectrophotometer. NMR spectra were determined with a Varian T-60 spectrometer for carbon tetrachloride solutions (unless otherwise specified) containing ~1% tetramethylsilane as the internal standard. Microanalyses were performed by Atlantic Microlab, Atlanta, Ga.

REFERENCES

(1) W. K. Anderson, E. J. LaVoie, and J. C. Bottaro, *J. Chem. Soc., Perkin Trans. I*, **1976**, 1.

(2) H. Christensen, B. M. F. Lundt, F. G. Gronwald, and W. Andersen, U.S. pat. 3,860,619 (Jan. 14, 1975).

ACKNOWLEDGMENTS

Supported in part by Grant CA-11880, National Cancer Institute, National Institutes of Health.

Drug Interactions I: Folic Acid and Calcium Gluconate

Keyphrases □ Drug interactions—folic acid and calcium gluconate, low concentrations □ Folic acid—interaction with calcium gluconate, low concentrations □ Calcium gluconate—interaction with folic acid, low concentrations

To the Editor:

The interaction of folic acid and calcium salts is well documented (1–5). These references state that these compounds combine to yield a precipitate, but quantitative information on this interaction is lacking. Thus, it is of interest to determine the extent of this interaction at high dilutions and to investigate its reversibility with ethylenediaminetetraacetic acid (I), a known calcium-sensitive ligand. This study is important in view of the possible use of these agents in intravenous admixtures in pediatric patients in which a precipitate may not be obtained. This communication reports the results of a preliminary study that showed that calcium gluconate does inhibit significantly the reactivity of folic acid at low concentrations when a precipitate is not apparent.

The official assay (6) was modified by replacing the 2-min centrifuge period with a 10-min shaking period on a mechanical shaker[1]. The procedure yielded 4 μg of folic acid (mean = 0.1 μg, n = 16). The interaction procedure was conducted by diluting a volume of the same intravenous solution of folic acid[2] with 3.03% K_2HPO_4 to yield a solution containing 10 μg of folic acid/ml. This solution was treated with a volume of calcium gluconate solution[3], suitably diluted to yield the appropriate concentration of calcium ion (0.5, 1, or 10 μg/ml). This mixture was used as the assay preparation in the official assay after the volume was adjusted to 5 ml with distilled water. The quenching procedure was conducted as follows. After exactly 10 min, a quantity of I equimolar to the calcium concentration was added to the folic acid–calcium assay preparation, the volume was adjusted to 5 ml with distilled water, the preparation was mixed thoroughly, and the assay was followed as indicated previously.

Compound I in the same concentrations did not interfere with the folic acid determination when calcium gluconate was omitted (Fig. 1). As noted, the quantity of folic acid recovered by pretreatment with calcium gluconate diminished linearly (T = 26°, K = 0.228 min^{-1}). Furthermore, this folic acid–calcium interaction can be reversed quantitatively by the addition of I.

This study demonstrates that the folic acid–calcium interaction is significant at all concentrations, regardless of whether the interaction yields a precipitate. The stability constant of the folic acid–calcium interaction and the effect of pH on the reaction are being investigated further.

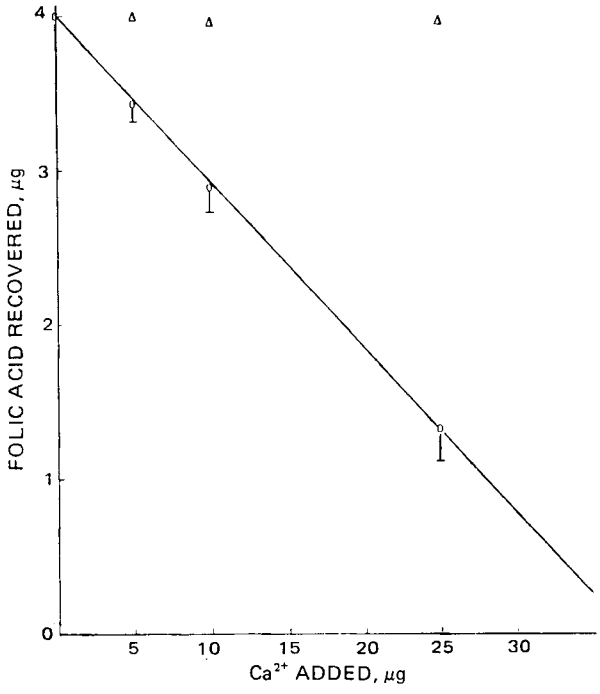

Figure 1—*Effect of calcium gluconate on the folic acid concentration (10 μg/ml). Folic acid concentrations (○) (mean + or − SD, n = 16) are shown as a function of the micrograms of Ca^{2+} added. Pretreatment with ethylenediaminetetraacetic acid (△) also is shown.*

(1) B. L. Gahart, "Intravenous Medications," 2nd ed., C. V. Mosby, St. Louis, Mo., 1977, p. 88.

(2) D. Michalski and M. S. Cohon, "Intravenous Incompatibilities," University of Wisconsin Hospitals, Madison, Wis., 1974, pp. 61, 62.

(3) L. A. Trissel, "Handbook on Injectable Drugs," American Society of Hospital Pharmacists, Washington, D.C., 1977, pp. 48–52, 155.

(4) "Martindale: the Extra Pharmacopeia," 26th ed., N. W. Blacow, Ed., Pharmaceutical Press, London, England, 1972, p. 1958.

(5) W. S. Kramer, A. Inglott, and R. Cluxton, *Drug. Intell. Clin. Pharm.*, **5**, 211 (1971).

(6) "The United States Pharmacopeia," 19th rev., Mack Publishing Co., Easton, Pa., 1975, p. 624.

K. R. Scott ˣ
Alexander F. Bell
Vasant G. Telang
Department of Biomedicinal Chemistry
College of Pharmacy and Pharmacal Sciences
Howard University
Washington, DC 20059

Received July 13, 1979.
Accepted for publication November 21, 1979.

[1] Model 6000, Eberbach.
[2] Folvite, Lederle.
[3] Calcium gluconate injection (10%), Parke-Davis.

0022-3549/80/0200-0234$01.00/0
© 1980, American Pharmaceutical Association

REVIEWS

Textbook of Biopharmaceutics and Clinical Pharmacokinetics. By S. NIAZI. Appleton-Century-Crofts, 292 Madison Ave., New York, NY 10017. 1979. 332 pp. 17 × 23 cm. Price $18.50.

The author claims that this book presents the principles needed to understand and control drug therapy with sufficient depth and breadth for the undergraduate pharmacy student.

The first chapter briefly describes the disciplines of biopharmaceutics, pharmacokinetics, and clinical pharmacokinetics and defines the scope of the book.

Chapters 2–4 concern the introduction of a drug into the body. In Chapter 2, definitions are presented and various formulation factors are described. Chemical form, ionization constant, polymorphism, solvation, complexation, particle size, and surface-active agents are mentioned. Each topic is described, and numerous examples are cited. The evaluation of dosage forms is the topic of Chapter 3. Different types of dosage forms and the various *in vitro* tests required of a dosage form are described. Bioavailability testing and evaluation also are covered. Chapter 4 describes various routes of drug administration with descriptions of numerous factors that can influence absorption.

The distribution of drugs is the subject of Chapter 5. Protein binding, tissue distribution, and volume of distribution are included. Drug excretion and metabolism are included in Chapter 6 as ways in which the body terminates drug action. Factors influencing renal, biliary, salivary, and mammary excretion are detailed and referenced. Metabolism pathways and Michaelis–Menten kinetics also are described.

Pharmacokinetic principles, with full development of numerous useful equations, are the subject of Chapter 7. One- and two-compartment plasma and urine data are treated. Administration as a bolus, infusion or absorption, single and multiple dose is included. The final sections briefly discuss nonlinear, physiologically based, and pharmacological models.

In Chapters 8 and 9, the effect of various factors on the value of pharmacokinetic parameters and the development of suitable dosage regimens for various drug classes based on the clinical status of the patient are described.

This book covers all of the topics of importance in an undergraduate biopharmaceutics and pharmacokinetics course. There are many referenced examples and tables of data given for each phenomenon discussed. Many questions are included at the end of most chapters. Although advanced material is at times given with only brief explanation, this text should serve admirably as a textbook accompanying a lecture course in biopharmaceutics and pharmacokinetics.

Reviewed by David Bourne
Division of Pharmaceutics
College of Pharmacy
University of Kentucky
Lexington, KY 40506

Sterile Dosage Forms: Their Preparation and Clinical Application. 2nd ed. By S. TURCO and R. E. KING. Lea & Febiger, Philadelphia, PA 19106. 1979. 456 pp. 15 × 24 cm. Price $18.50.

This book represents an updated version of the text introduced in 1974. The major changes include the addition of a chapter on Blood and Blood Substitutes and an Appendix entitled "Hazards Associated with Parenteral Therapy." Other major revisions include six pages added to the end of Chapter 7 (Biopharmaceutic Factors Influencing Drug Availability), pages 209–225 added to the end of Chapter 8 (Large Volume Sterile Solutions), and a complete rewriting of Chapter 13 (Radiopharmaceuticals). All of these new sections are worthwhile additions, especially the discussions of hospital-based intravenous teams, flow control devices for intravenous therapy, and the work of the National Coordinating Committee on Large Volume Parenterals (NCCLVP). Another significant improvement throughout the text is the use of *numbered* references. In the first edition, it was virtually impossible to match the discussion with the *unnumbered* reference listing at the end of each chapter.

Thus, the second edition of what was a reasonably good text to begin with is improved significantly. However, I feel that a number of considerations could improve the text even further. For example, some additional discussion of parenteral stability and the fundamental equations for calculating the shelflife of various admixtures could have been added to Chapter 11 (Parenteral Admixtures and Incompatibilities). Since the book appears to be directed toward the hospital pharmacist, I believe that it is well within their spectrum of duties to have to research a stability problem. Thus, the fundamental information necessary for performing simple stability studies would have been a worthwhile addition.

In the discussion of osmolality (pp. 262–263), it is stated that 0.9% sodium chloride injection has an osmotic pressure of 308 mOsm/liter since sodium chloride *ionizes* into two ions. In fact, it is only at infinite dilution that discrete "particles" exist since in more concentrated solutions the sodium and chloride ions are not completely *dissociated*. The net effect of this incomplete dissociation is that for electrolytes such as sodium chloride, the osmotic pressure will not normally be equal to the molarity of the salt multiplied by the number of ions formed. Instead, the molarity must be multiplied by an effective concentration or "*i* value" (van't Hoff term), which for 0.9% (w/v) NaCl is ~1.9, thereby producing an osmotic pressure of about 293 mOsm/liter for normal saline.

The discussion of particulate matter provided in Chapter 3 is adequate. It could be improved with a somewhat expanded description of the official standards presently in effect in the United States and other countries and some further mention of the present methodology. This is an area in which hospital pharmacists have made extensive contributions, and additional discussion is warranted.

The bimolecular leaflet model of the cell membrane proposed by Danielli and Davson (p. 148) seems to have fallen into disfavor among membrane biologists and has been largely replaced by the fluid mosaic model of Singer and Nicolson. Thus, a picture of the fluid mosaic model might have been more appropriate for Fig. 7–3.

Some references in the extensive listing on pages 431–441 use *et al.*, presumably because this section is appended since this procedure was not used in earlier sections of the book. I am opposed to the use of *et al.* in reference listings since it fails to give credit to deserving cocontributors.

Finally, some typographical errors noticed are as follows: in the index (p. ix), line 4, Flow Control in I.V. Therapy starts on p. 212, not 203; the caption to Fig. 1–2 in both the first and second editions refers to Johann Daniel "Taylor", which should be Johann Daniel "Major."

In spite of these limitations and suggestions for improvement, I still recommend this text as a major contribution in the area of parenterals. It should find use as a reference work for hospital and research pharmacists and will no doubt become a required text for course offerings in pharmacy and nursing colleges. It is attractively packaged and well illustrated through the use of numerous photographic plates, and the price is reasonable in relation to other texts of comparable size.

Reviewed by James Blanchard
Department of Pharmaceutical Sciences
College of Pharmacy
University of Arizona
Tucson, AZ 85721

REVIEWS

Textbook of Biopharmaceutics and Clinical Pharmacokinetics. By S. NIAZI. Appleton-Century-Crofts, 292 Madison Ave., New York, NY 10017. 1979. 332 pp. 17 × 23 cm. Price $18.50.

The author claims that this book presents the principles needed to understand and control drug therapy with sufficient depth and breadth for the undergraduate pharmacy student.

The first chapter briefly describes the disciplines of biopharmaceutics, pharmacokinetics, and clinical pharmacokinetics and defines the scope of the book.

Chapters 2–4 concern the introduction of a drug into the body. In Chapter 2, definitions are presented and various formulation factors are described. Chemical form, ionization constant, polymorphism, solvation, complexation, particle size, and surface-active agents are mentioned. Each topic is described, and numerous examples are cited. The evaluation of dosage forms is the topic of Chapter 3. Different types of dosage forms and the various *in vitro* tests required of a dosage form are described. Bioavailability testing and evaluation also are covered. Chapter 4 describes various routes of drug administration with descriptions of numerous factors that can influence absorption.

The distribution of drugs is the subject of Chapter 5. Protein binding, tissue distribution, and volume of distribution are included. Drug excretion and metabolism are included in Chapter 6 as ways in which the body terminates drug action. Factors influencing renal, biliary, salivary, and mammary excretion are detailed and referenced. Metabolism pathways and Michaelis–Menten kinetics also are described.

Pharmacokinetic principles, with full development of numerous useful equations, are the subject of Chapter 7. One- and two-compartment plasma and urine data are treated. Administration as a bolus, infusion or absorption, single and multiple dose is included. The final sections briefly discuss nonlinear, physiologically based, and pharmacological models.

In Chapters 8 and 9, the effect of various factors on the value of pharmacokinetic parameters and the development of suitable dosage regimens for various drug classes based on the clinical status of the patient are described.

This book covers all of the topics of importance in an undergraduate biopharmaceutics and pharmacokinetics course. There are many referenced examples and tables of data given for each phenomenon discussed. Many questions are included at the end of most chapters. Although advanced material is at times given with only brief explanation, this text should serve admirably as a textbook accompanying a lecture course in biopharmaceutics and pharmacokinetics.

Reviewed by David Bourne
Division of Pharmaceutics
College of Pharmacy
University of Kentucky
Lexington, KY 40506

Sterile Dosage Forms: Their Preparation and Clinical Application. 2nd ed. By S. TURCO and R. E. KING. Lea & Febiger, Philadelphia, PA 19106. 1979. 456 pp. 15 × 24 cm. Price $18.50.

This book represents an updated version of the text introduced in 1974. The major changes include the addition of a chapter on Blood and Blood Substitutes and an Appendix entitled "Hazards Associated with Parenteral Therapy." Other major revisions include six pages added to the end of Chapter 7 (Biopharmaceutic Factors Influencing Drug Availability), pages 209–225 added to the end of Chapter 8 (Large Volume Sterile Solutions), and a complete rewriting of Chapter 13 (Radiopharmaceuticals). All of these new sections are worthwhile additions, especially the discussions of hospital-based intravenous teams, flow control devices for intravenous therapy, and the work of the National Coordinating Committee on Large Volume Parenterals (NCCLVP). Another significant improvement throughout the text is the use of *numbered* references. In the first edition, it was virtually impossible to match the discussion with the *unnumbered* reference listing at the end of each chapter.

Thus, the second edition of what was a reasonably good text to begin with is improved significantly. However, I feel that a number of considerations could improve the text even further. For example, some additional discussion of parenteral stability and the fundamental equations for calculating the shelflife of various admixtures could have been added to Chapter 11 (Parenteral Admixtures and Incompatibilities). Since the book appears to be directed toward the hospital pharmacist, I believe that it is well within their spectrum of duties to have to research a stability problem. Thus, the fundamental information necessary for performing simple stability studies would have been a worthwhile addition.

In the discussion of osmolality (pp. 262–263), it is stated that 0.9% sodium chloride injection has an osmotic pressure of 308 mOsm/liter since sodium chloride *ionizes* into two ions. In fact, it is only at infinite dilution that discrete "particles" exist since in more concentrated solutions the sodium and chloride ions are not completely *dissociated*. The net effect of this incomplete dissociation is that for electrolytes such as sodium chloride, the osmotic pressure will not normally be equal to the molarity of the salt multiplied by the number of ions formed. Instead, the molarity must be multiplied by an effective concentration or "*i* value" (van't Hoff term), which for 0.9% (w/v) NaCl is ~1.9, thereby producing an osmotic pressure of about 293 mOsm/liter for normal saline.

The discussion of particulate matter provided in Chapter 3 is adequate. It could be improved with a somewhat expanded description of the official standards presently in effect in the United States and other countries and some further mention of the present methodology. This is an area in which hospital pharmacists have made extensive contributions, and additional discussion is warranted.

The bimolecular leaflet model of the cell membrane proposed by Danielli and Davson (p. 148) seems to have fallen into disfavor among membrane biologists and has been largely replaced by the fluid mosaic model of Singer and Nicolson. Thus, a picture of the fluid mosaic model might have been more appropriate for Fig. 7–3.

Some references in the extensive listing on pages 431–441 use *et al.*, presumably because this section is appended since this procedure was not used in earlier sections of the book. I am opposed to the use of *et al.* in reference listings since it fails to give credit to deserving cocontributors.

Finally, some typographical errors noticed are as follows: in the index (p. ix), line 4, Flow Control in I.V. Therapy starts on p. 212, not 203; the caption to Fig. 1–2 in both the first and second editions refers to Johann Daniel "Taylor", which should be Johann Daniel "Major."

In spite of these limitations and suggestions for improvement, I still recommend this text as a major contribution in the area of parenterals. It should find use as a reference work for hospital and research pharmacists and will no doubt become a required text for course offerings in pharmacy and nursing colleges. It is attractively packaged and well illustrated through the use of numerous photographic plates, and the price is reasonable in relation to other texts of comparable size.

Reviewed by James Blanchard
Department of Pharmaceutical Sciences
College of Pharmacy
University of Arizona
Tucson, AZ 85721

Pathophysiology and Pharmacotherapy of Asthma: An Overview

LAWRENCE W. CHAKRIN ˣ and ROBERT D. KRELL

Received May 4, 1979, from the *Department of Biological Research, Section on Respiratory and Allergic Diseases, Smith Kline and French Laboratories, Philadelphia, PA 19101.* Accepted for publication July 27, 1979.

Abstract □ The pathophysiology of allergic and "nonallergic" asthma is presented, and several classes of antiallergic agents are discussed.

Keyphrases □ Antiallergic drugs—cromolyn sodium, adrenergic bronchodilators, corticosteroids, anticholinergic agents □ Pathophysiology—asthma, immunologically induced release of primary and secondary mediators, membrane permeability changes, calcium-ion dependency, antiallergic drugs □ Asthma—review of current theories, clinical evaluation, symposium, antiallergic drugs

Asthma is a disease marked by recurrent, quickly developing, bronchial obstruction leading to paroxysmal dyspnea. The condition results from a spasm of hypersensitive bronchial smooth muscle, generally in the segmental and smaller bronchi. The spasm is often accompanied by a mucosal edema and respiratory mucus hypersecretion. The principal types of the disease are allergic or extrinsic asthma and "nonallergic" or intrinsic asthma, the latter of uncertain origin (1). The prevalence of asthma is slightly higher in children than in adults; ~5% of all children in the United States below the age of 15 suffer from the disease (2).

An early clinical impression of the disease was accurately given by Dr. Michael Ryan, writing in "Observations on the History and Cure of the Asthma" (for review, see Ref. 3), who observed in 1793 that few diseases can be considered more formidable. The prospect of instant suffocation is so alarming as to weaken and depress a mind endowed even with the utmost fortitude and resignation. Dr. Ryan concluded that any remedy capable of permanent relief must be looked upon as of the utmost importance to mankind.

PATHOPHYSIOLOGY

The symptomatology of immediate-type allergic diseases, including extrinsic asthma and allergic rhinitis, presumably results from the immunologically (antigen) induced release of various pharmacologically active substances from mast cells, and basophilic leukocytes previously sensitized with an antibody generally of the immunoglobulin E class (4), and possibly from other cells as well. The substances thus released and referred to as primary mediators of anaphylaxis, *i.e.*, those released as a direct consequence of antigen–antibody interaction, include histamine, slow-reacting substance, eosinophil chemotactic factor, and platelet-activating factor (5). There are probably other primary mediators as well as secondary mediators released indirectly, such as some of the prostaglandins and kinins involved in the modulation of allergic processes (5). The sequence of biochemical events associated with mediator release is not clearly understood and has been the subject of a substantial research effort, particularly during the past decade (5).

Considerable evidence now supports immunoglobulin E (4) as the immunoglobulin class essential to acute allergic reactions, although some data indicate that such reactions also can be mediated by subclasses of immunoglobulin G-type antibodies. Immunoglobulin E may be synthesized locally in the respiratory tract or by the systemic immune system. It is a heat-labile glycoprotein of 198,000 molecular weight, which, as do the other immunoglobulin classes, contains two heavy and two light polypeptide chains linked by sulfhydryl bonds in fundamentally a Y-shaped structure. Presumably, the most significant biological property of the molecule is its ability to bind to homologous mast cells and basophils, thus sensitizing these cells for subsequent allergic reactions (4, 6). The Fc region of immunoglobulin E is that portion of the stem of the immunoglobulin molecule responsible for the highly specific binding to the receptors (4, 6) on the membranes of the tissue-fixed mast cells and blood basophils.

The remaining branched portion of the molecule, the Fab portion, contains the antigen binding sites thought to be made up of parts of the heavy and light chains. While not completely understood, evidence suggests that bridging of two cell-bound immunoglobulin E molecules by antigen (4, 6) is the initial step in a cascade of reactions resulting in mediator release. Presumably, an allosteric change in the structure of the Fc portion of the antibody then leads to the development of activated sites (7) on the mast cell or basophil membrane. Resulting changes in the charge distribution of the membrane are thought to increase the membrane permeability and alter the intracellular ionic milieu, initiating further biochemical steps of which relatively little is known (7).

It has been suggested that an early event in the release is an activation of a membrane-bound chymotrypsin-like proesterase (5). Esterase activation presumably requires calcium ion and results in an enzyme that can be inhibited by isofluorphate (diisopropyl fluorophosphate). Later in the sequence, there appear to be an energy-requiring step that can be inhibited by 2-deoxyglucose, an intracellular calcium-ion-requiring step capable of being suppressed by edetic (ethylenediaminetetraacetic) acid, and a step regulated by the relative levels of cyclic adenosine monophosphate and/or cyclic guanosine monophosphate. Presumbly, the mechanism of action of many compounds clinically effective in asthma is at the cyclic nucleotide step(s) (5).

Moreover, the cellular secretion of histamine, at least, may involve microtubules and microfilaments (7), although the supporting data are generally indirect and involve inhibition of histamine release by the alkaloid colchicine, thought to be an inhibitor of microtubule function. Conversely, heavy water, which is considered to stabilize microtubules, enhances histamine release. Little is known about the process of limiting immunological histamine release, although a series of feedback controls governed by the cyclic nucleotides and histamine itself has been suggested. Somewhat more is known about some mediators of anaphylaxis, which are thought to contribute collectively to the clinical syndrome of the disease (5, 6).

Histamine is β-imidazolylethylamine, and it is synthesized principally by a specific *l*-histidine decarboxylase enzyme. Histamine involved in hypersensitivity reactions of the immediate type appears to be stored in discrete mast cell (or basophil) secretory granules as a complex with heparin and protein. This stored amine undergoes slow turnover by comparison to the extra mast cell histamine of the GI mucosa and the central nervous system.

While still the subject of controversy, it is believed that the immunological, calcium-dependent release of histamine involves two processes, perhaps including the exocytosis of the subcellular cytoplasmic granules and the disassociation of histamine from the granule matrix (7). The heparin–protein complex of mast cell granules has ion-exchange properties, and exposure of the granule matrix to an altered ionic environment results in an exchange of histamine for sodium ions, which have an affinity for the binding sites. Once released, histamine presumably contributes to portions of the clinical syndrome of immediate hypersensitivity reactions. Apart from tissue uptake, histamine then apparently undergoes metabolism by one of two pathways. One, through methylation of the ring structure by imidazole-*N*-methyltransferase, yields methylhistamine, which is then oxidized through monoamine oxidase to methylimida-

0022-3549/80/0200-0236$01.00/0
© 1980, American Pharmaceutical Association

zoleacetic acid. Alternatively, histamine can undergo an oxidative deamination by histaminase or diaminoxidase to imidazoleacetic acid. The products of this metabolism are excreted in the urine.

As with histamine, the mast cell has been implicated as a source of slow-reacting substance of anaphylaxis (5, 8), although other cell types also appear to serve that function. Two experimental systems that generate slow-reacting substance of anaphylaxis are the sensitized fragmented lung and peripheral blood leukocyte preparations. The material is measured by bioassay utilizing the guinea pig ileum, and it produces a sustained contraction in the presence of an H_1-antihistamine and an anticholinergic agent. While the chemical structure of slow-reacting substance of anaphylaxis has only just been disclosed, some information was available concerning its physicochemical and biological properties. Slow-reacting substance of anaphylaxis was thought to be an acidic lipid of ~400–600 molecular weight and presumably contained an esterified sulfate group. It was considered resistant to proteases and phospholipases but labile to arylsulfatases and oxidation (5, 8). Furthermore, it was thought that slow-reacting substance of anaphylaxis could be derived from arachidonic acid, perhaps through a lipoxygenase pathway, but it appeared to be more polar than, and could be separated from, conventional prostaglandins (8).

Recently (9), it was suggested that slow-reacting substance of anaphylaxis may be "identical" to leukotriene C, one of a group of compounds related to the prostaglandins identified by Samuelsson, Borgeat, and colleagues of the Karolinska Institute in Sweden. Leukotriene C contains the amino acid cysteine covalently linked to the 20-carbon fatty acid derivative of the prostaglandin precursor, arachidonic acid. While there have been occasional reports of a small amount of preformed slow-reacting substance of anaphylaxis in lung tissue, it is presumably formed *de novo* and released on immunological challenge.

Eosinophils occur in relatively large numbers in pulmonary tissues and mucosal secretions of asthmatics, although their role is not precisely understood (10). Investigations that demonstrated that neither relatively pure slow-reacting substance of anaphylaxis nor histamine was chemotactic for these cells provided the basis for discovery of eosinophil chemotactic factor of anaphylaxis, another preformed primary mediator. Eosinophil chemotactic factor has a molecular weight of ~500, and chromatographic and electrophoretic evaluation suggests that eosinophil chemotactic factor of anaphylaxis is a low molecular weight acidic peptide. Two tetrapeptides with amino acid sequence Val-Gly-Ser-Glu and Ala-Gly-Ser-Glu were recovered from extracts of human lung fragments and were shown to be chemotactic for eosinophils (5, 10). Whether these tetrapeptides are, in fact, eosinophil chemotactic factor remains to be determined conclusively.

Additionally, other pharmacologically potent materials have been shown to be released from previously sensitized lung tissues on immunological challenge. Prostaglandins of the E and F classes are presumably rapidly synthesized (5, 8) and released, and they affect bronchial smooth muscle in an opposing fashion: prostaglandin E_2 producing relaxation and prostaglandin $F_{2\alpha}$ producing contraction (8). Their pharmacological activities are probably mediated by intracellular messengers, the cyclic nucleotides, cyclic guanosine monophosphate, and cyclic adenosine monophosphate, and they themselves are considered as secondary mediators whose synthesis and release may be governed by histamine or slow-reacting substance of anaphylaxis.

In addition to the prostaglandins, other chemicals, yet poorly characterized, probably contribute to the symptomatology of allergic asthma. Platelet-activating factor is possibly a lipid material, released on an immunoglobulin E–antigen interaction on basophils or lung tissue (5). Platelet-activating factor induces aggregation of platelets and the subsequent release of serotonin, which can cause tracheobronchial smooth muscle contraction.

In addition to the direct spasmogenic effects of many mediators of anaphylaxis, parasympathetic reflexes mediated through the vagus nerve also may contribute to the bronchoconstriction in the human asthmatic. Furthermore, individuals with asthma disclose a substantial hyperresponsiveness of their airways to several pharmacological agents such as histamine, prostaglandins, and cholinergic agonists as well as to such nonspecific irritants as cold air and noxious gases. This hyperresponsiveness may enhance the pathophysiological effects of the mediators released on antigen exposure.

PHARMACOTHERAPY

Following an established diagnosis and evidence for the reversibility of airway obstruction, the process of selecting an appropriate course of pharmacotherapy may be initiated. Management of the acute bronchospasm has the first priority; when it is initially controlled, etiological factors can be determined. In status asthmaticus (1, 11), a severe continuous state of asthmatic dyspnea, hospital management is indicated. Treatment must provide rapid bronchodilation, perhaps best achieved in this instance with intravenous aminophylline.

For less severe clinical situations, new drugs have been introduced during the last decade (11–14). Still others have been reevaluated for their utility among various patient populations.

Cromolyn Sodium—In 1956, a Fisons Pharmaceutical Corporation research team (3) initiated a search for compounds having selective actions on smooth muscle. The team chose khellin, extracted from a Mediterranean plant, as the chemical prototype since its seeds had been used since ancient times as a smooth muscle relaxant. A series of chromone-2-carboxylic acids was developed, but the compounds were inactive as smooth muscle relaxants and as antagonists to chemical spasmogens. However, they did partially inhibit, but not reverse, antigen-induced bronchospasm in an asthmatic volunteer. The interest in chromones led to the bis-chromones (3); in January 1965, one of these bis-chromones, cromolyn sodium (disodium cromoglycate), was synthesized and tested. In January 1968, it was introduced into therapy in the United Kingdom.

Although the cellular events responsible for the release of the mediators of anaphylaxis is not clearly understood (5), inhibition of their release would seem to be effective therapy. Presumably, the effectiveness of cromolyn sodium (3) is based on its ability to inhibit the immunologically induced release of mediators from sensitized cells (15). The compound has no bronchodilator or anti-inflammatory activity, and it is not effective for the treatment of the acute asthmatic episode. Rather, it is a clinically effective, prophylactic antiallergic agent in a limited patient population consisting principally of children. The compound is poorly absorbed from the GI tract, so it is administered as a powder inhalation.

Although some inconvenience and a need for education are associated with its use, cromolyn sodium offers a rather substantial degree of safety, with only occasional cough or bronchospasm generally associated with its use. While enjoying broader use elsewhere, in the United States the compound is indicated as an adjunctive therapy in the management of patients with severe bronchial asthma (3). Cromolyn sodium is continued on a more chronic basis if it significantly reduces the severity of symptoms, allows for a reduction in or elimination of steroids, or allows for satisfactory management of individuals who have "intolerable" side effects to sympathomimetic drugs or the methylxanthines.

The clinical efficacy of cromolyn sodium as an antiasthmatic agent has prompted a significant worldwide research effort directed to the discovery of more potent, orally active antiallergic drugs (15).

In addition to cromolyn sodium, the pharmacological armamentarium for the management of asthma consists of several adrenergic bronchodilators (16) including epinephrine and isoproterenol and the new, β_2-selective adrenergic drugs, theophylline and its several preparations, both systemic and inhaled corticosteroids, and anticholinergic agents such as atropine and its derivatives (11–14, 16, 17). Concern as to potential side effects with some of these agents, as well as the relative inconvenience attendant to cromolyn sodium administration, suggests that an orally active prophylactic antiallergic agent with a rather broad therapeutic index would be of significant value.

Adrenergic Drugs—Adrenergic receptors have been pharmacologically classified into α, β-1, and β-2 types. Among various other activities, adrenergic agents can stimulate α-receptors and cause vasoconstriction, β-1 receptors and cause cardiac stimulation, and β-2 receptors and provide bronchodilation (13, 16).

The use of adrenergic drugs in asthma dates from the use of the herb *Ma Huang* in Chinese folk medicine. The active ingredient, ephedrine, was introduced into Occidental medicine in the 1920's. Ephedrine stimulates α- and β-adrenergic receptors and, apart from its direct actions, releases norepinephrine stores from peripheral sympathetic nerve endings. Tachyphylaxis can develop to its activity, and subsequent doses are less effective, presumably due to norepinephrine depletion.

Epinephrine and isoproterenol, the prototype β-adrenergic stimulant, have been used in the management of bronchospasm for many years. Their use is limited, however, by the occasional development of undesirable side effects of tremor and cardiac stimulation. Beyond their lack of selectivity for β-2 receptors, the compounds have a relatively short duration of action because of rapid tissue inactivation, in part due to catechol-*O*-methyltransferase.

In the mid-1960's, Lands and coworkers demonstrated that a substantial selectivity for β-adrenergic receptors could be realized by chemical modifications of the phenylethylamine moiety of catecholamines (16). More recent attempts to improve selectivity and metabolic

stability have involved altering the catechol structure (16). Thus, in the past few years, some relatively selective β-2 adrenergic agonists have been developed including salbutamol, carbuterol, terbutaline, metaproterenol, and isoetharine (11, 13). Many of these compounds provide prolonged bronchodilation after aerosol or oral administration while producing relatively few cardiovascular side effects at effective bronchodilator dose levels.

Methylxanthine Phosphodiesterase Inhibitors—Theophylline and its various salts (11–13) are presumably effective in asthma by preventing the intracellular conversion of cyclic adenosine monophosphate to 5′-adenosine monophosphate. By elevating cyclic adenosine monophosphate, theophylline is capable of inhibiting immunologically induced mediator release and of potentiating the effect of β-2 selective adrenergic agonists, which stimulate the production of increased concentrations of cyclic adenosine monophosphate. First introduced as a therapy for asthma in the 1930's, oral theophylline now is widely used because it provides effective bronchodilation with minimal side effects in many patients. Occasional side effects with oral administration and, perhaps more frequently, with rapid intravenous administration include insomnia, nervousness, and cardiac arrhythmias.

Corticosteroids—Generally, corticosteroids (11–13) of relatively short duration are highly effective for the clinical management of severe asthma. Such compounds as prednisone, hydrocortisone, and prednisolone provide excellent anti-inflammatory, antiallergic activity in asthma. When utilized in an alternate day therapy, they are less likely to cause adrenal suppression, osteoporosis, or other adverse effects.

Recently, a variety of inhaled steroids have been introduced, and beclomethasone or other compounds have been shown to be locally effective at relatively low doses that do not cause substantial systemic effects. Adrenal insufficiency has occurred in some individuals when transferred to these topical inhaled steroids from systemic dose forms. The mechanisms by which the corticosteroids are effective in allergic inflammation is unknown but may be related in part to adenyl cyclase and the relative levels of cyclic adenosine monophosphate and cyclic guanosine monophosphate.

Anticholinergic Agents—In recent years, there has been a substantial renewal of interest in anticholinergic agents for the clinical management of asthma. It has been suggested that an imbalance of the autonomic nervous system function contributes to the disease. The characteristic hyperirritability of the airway smooth muscle may be due to a parasympathetic nervous system predominance (11–13, 17). Stimulation of subepithelial receptors of tracheobronchial tissue by particulate, gaseous, or immunological irritants can induce vagal reflex-mediated bronchoconstriction. The resulting increase in airway resistance can be reduced by atropine administration. Moreover, cholinergic agonists enhance immunologically induced mediator release, and atropine can inhibit such release, thus suggesting activity at sites other than the muscle. Recent interest has been shown in the bronchodilation produced by ipratropium bromide, an atropine-like investigational drug.

In addition to these classes of compounds, other agents have been studied, including the E-series prostaglandins and α-adrenergic antagonists (8, 13). Prostaglandins E_1 and E_2 are apparently effective bronchodilators in some individuals, but respiratory tract irritation and cough have precluded their extensive study. α-Adrenergic antagonists such as phentolamine may be useful, although the extent of α-adrenergic tone to tracheobronchial smooth muscle is relatively minor. The potential for adverse effects with these antagonists has limited their study.

The selection of appropriate therapy was reviewed recently (11–13, 17). In summary, a substantial number of individuals respond with effective bronchodilation and little adverse reaction to an oral theophylline preparation. Oral, relatively β-2-selective adrenergic drugs provide good bronchodilation, but adverse effects including tremor may limit their use. Asthmatics who fail to achieve adequate relief with either of these classes of drugs may benefit from cromolyn sodium. Individuals with persistent, severe disease likely will require corticosteroids, and aerosols of these agents may preclude the need for larger doses of systemic steroids. Many of the therapies can be combined, and often lower doses of each agent in combination may be *as* effective (and perhaps offer fewer side effects) as single-drug therapy.

The past decade has seen substantial progress in the understanding of cellular processes that presumably account for the clinical syndrome of allergic asthma. As even greater understanding develops, we can expect more sophisticated drugs to supplement the existing agents.

REFERENCES

(1) H. Herxheimer, "A Guide to Bronchial Asthma," Academic, London, England, 1975.

(2) National Institute of Allergy and Infectious Diseases Task Force Report No. 79-387, Bethesda, Md., 1979, p. 7.

(3) "Intal—Cromolyn Sodium, A Monograph," Fisons Corp., Bedford, Mass., 1973.

(4) K. Ishizaka and T. Ishizaka, *Arch. Pathol. Lab. Med.*, **100**, 289 (1976).

(5) M. Kaliner and K. F. Austen, *Ann. Rev. Pharmacol.*, **15**, 177 (1975).

(6) R. Hamburger, *Am. Sci.*, **64**, 157 (1976).

(7) W. Kazimierczak and B. Diamant, *Prog. Allergy*, **24**, 295 (1978).

(8) C. W. Parker, *J. Allergy Clin. Immunol.*, **63**, 1 (1979).

(9) J. L. Fox, *Chem. Eng. News*, **57** (24), 19 (1979).

(10) E. Goetzl and K. F. Austen, *Proc. Natl. Acad. Sci. USA*, **72**, 4123 (1975).

(11) *The Medical Letter*, **20**, 69 (Aug. 11, 1978).

(12) M. Weinberger and L. Hendeles, *Am. J. Hosp. Pharm.*, **33**, 1071 (1976).

(13) E. Middleton, *Pediatr. Clin. North Am.*, **22**, 111 (1975).

(14) A. Oronsky and J. Wasley, "Annual Reports in Medicinal Chemistry," vol. 11, Academic, New York, N.Y., 1976, chap. 6, pp. 51–60.

(15) L. W. Chakrin and R. D. Krell, *J. Pharmacol. Exp. Ther.*, **207**, 756 (1978).

(16) J. R. Wardell, D. J. Colella, A. Shetzline, and P. Fowler, *ibid.*, **189**, 167 (1974).

(17) A. K. Pierce, "Hospital Formulary," part 2, Feb. 1979, pp. 154–167.

ACKNOWLEDGMENTS

Presented as part of the Symposium on New Approaches to the Treatment of Asthma, APhA Academy of Pharmaceutical Sciences, Anaheim meeting, April 1979.

Preclinical Evaluation of Antiallergic Agents

ROBERT D. KRELL and LAWRENCE W. CHAKRIN ˣ

Received May 4, 1979, from the *Department of Biological Research, Section on Respiratory and Allergic Diseases, Smith Kline and French Laboratories, Philadelphia, PA 19101.* Accepted for publication July 27, 1979.

Abstract □ This paper examines the advantages and disadvantages of many *in vivo* and *in vitro* experimental model systems employed in the preclinical testing of antiallergic drugs.

Keyphrases □ Antiallergic drugs—inhibition of mediator release, *in vivo* and *in vitro* models □ α-Adrenoceptor agonist—cyclic adenosine monophosphate levels, effects on mediator release, antiallergic drugs □ β-Adrenoceptor agonists—cyclic guanosine monophosphate levels, effects on mediator release, antiallergic drugs □ Asthma—review of current theories, clinical evaluation, symposium, antiallergic drugs □ Cromolyn sodium—prophylactic antiallergic drug

The primary purpose of this report is to provide insight into the drug discovery process by examining several commonly used animal models as well as to illustrate the type of data that may be obtained. It is not intended as a thorough review of all methods currently available for the detection of antiallergic activity of novel molecules. The merits and limitations of these various systems, at least as presently viewed, are addressed. Allergic asthma will serve as a focus for allergic disorders in general. It is hoped that agents efficacious in this disease will prove beneficial for other allergic conditions as well.

Most experimental animal models commonly are based on the "mediator concept" of allergic disorders discussed in the preceding paper (1). The rationale for this approach to pharmacotherapy lies almost totally with the known pharmacology of the prototype prophylactic antiallergic agent cromolyn sodium and its well-established clinical utility (2).

Before beginning a discussion as to the type of technology employed, it is pertinent to examine the question of why a search for antiallergic agents beyond cromolyn sodium should continue. Cromolyn sodium is not orally active and is, therefore, administered as a powdered aerosol by a clever but cumbersome technique. The drug is efficacious in only a portion of the asthmatic patients for reasons that are not presently understood (2). Consequently, a compound that is orally active or that can be administered by more conventional aerosol techniques and/or that can protect a broader group or preferably all asthmatics would be a significant advance in therapy.

IN VIVO MODELS

By far, the most widely used paradigm is the 48-hr rat passive cutaneous anaphylaxis test (3), which frequently serves as the primary laboratory experimental system (Fig. 1). Briefly, adult female rats are immunized on Day 0 with an appropriate dose of ovalbumin along with *Bordetella pertussis*, which serves as an adjuvant. Often, rats receive a subcutaneous injection of larva from the nematode *Nippostrongylus brasiliensis* several days after primary immunization to enhance the production of antiovalbumin reaginic antibody. The rats are killed and bled 10–14 days later, and serum containing the antibody is prepared.

Appropriate dilutions of the serum are subsequently injected into discrete areas of the dorsal surface of the skin of a recipient rat. Since certain subclasses of immunoglobulin G antibodies may also bind to cutaneous mast cells, a 48-hr period is interposed between sensitization and antigen challenge to allow these antibodies to dissipate. Immunoglobulin E-type antibodies directed against ovalbumin remain firmly fixed to the mast cells for much longer periods (4). Test compounds are administered to the animals immediately prior to challenge with ovalbumin, which is often mixed with Evans blue dye. The short time between administration of the test compound and antigen is essential to ensure optimal activity. Unaccountably, there is a well-established inverse relationship regarding the time interval between drug and antigen administration and efficacy (3).

Upon injection, the antigen interacts with the antibodies fixed to the mast cell surface, which leads to a series of intracellular biochemical events culminating in the release of the vasoactive amines, histamine and serotonin, from the cells. When the animal is killed 30 min later and the dorsal skin reflected, the pharmacological effect of these mediators is visualized as an area of dye infiltration (wheals), which can be quantitated. Antiallergic agents are expected to reduce mediator release, which is manifested as a reduction in wheal size as compared to controls. Those compounds that demonstrate efficacy often undergo secondary testing in the rodent. Wheal size reduction in rats may be brought about by interfering with the antigen-induced release of the mediators of anaphylaxis from mast cells or by antagonizing the ability of histamine and/or serotonin to increase vascular permeability. To discriminate between these types of activity, the ability of the test compound to block wheals produced by the direct intracutaneous injection of histamine and/or serotonin is evaluated. Compounds that antagonize the vascular response to histamine and/or serotonin are often discarded as having a potentially unsuitable mechanism of action. One shortcoming of this approach is the possibility that molecules that possess antiallergic as well as antagonist types of activity may be overlooked.

The principal advantages of the rat passive cutaneous anaphylaxis model are that it is simple, rapid, economical, and semiquantitative. Furthermore, the potential oral efficacy of compounds may be assessed at an early stage in the pharmacological testing sequence. Major disadvantages are that it provides only circumstantial evidence as to the mechanism of action of the compounds and that efficacy is established in cutaneous tissue rather than in the designated therapeutic site, pulmonary and tracheobronchial tissue.

Various *in vivo* models of "allergic asthma" have been developed in several species to gain information on the potential efficacy of compounds in preventing antigen-induced bronchospasm. Since these models are considerably more complex than the rat passive cutaneous anaphylaxis, compound evaluation in these paradigms generally occupies the terminal step in the pharmacological testing sequence. Models have been developed in small animals such as the rat and guinea pig, utilizing either active or passive sensitization, most frequently with ovalbumin or dinitrophenol–ovalbumin combinations (5–7). Antigen may be presented parenterally for precipitation of systemic anaphylaxis or by aerosol to induce pulmonary anaphylaxis. Pretreatment with an efficacious antiallergic agent would be expected to reduce the severity of the response to antigen. The major advantages of these models are that the principal mediators of pulmonary anaphylaxis have been determined in both species (5–7) and that the sensitized animals are easily and economically prepared in large numbers.

A major disadvantage of these models is that, until recently, they have not allowed for the use of sophisticated technology for measurement of pulmonary mechanics due to the small size of the animals (8). Determination of the effects of antigen or drug–antigen combinations usually involves an indirect assessment of lung compliance rather than a true determination of resistance to air flow in large and small airways.

In contrast, some large animal models of allergic asthma are amenable to measurement of large and small airway resistance (9–11). The principal models used are dogs and rhesus monkeys with a spontaneously occurring hypersensitivity to an antigen prepared from *Ascaris suum* roundworms. The basis of the hypersensitivity is believed to involve neonatal infestation by nematodes, which provokes immunoglobulin E-type antibodies directed against the worm. Although neither dogs nor monkeys are normally subject to infestation with *A. suum* roundworms, a cross-reactivity between common antigenic determinants of the host's natural parasite—*viz.*, *Toxocara canis* in the case of the dog, and *A. suum* is assumed

0022-3549/80/0200-0239$01.00/0
© 1980, American Pharmaceutical Association

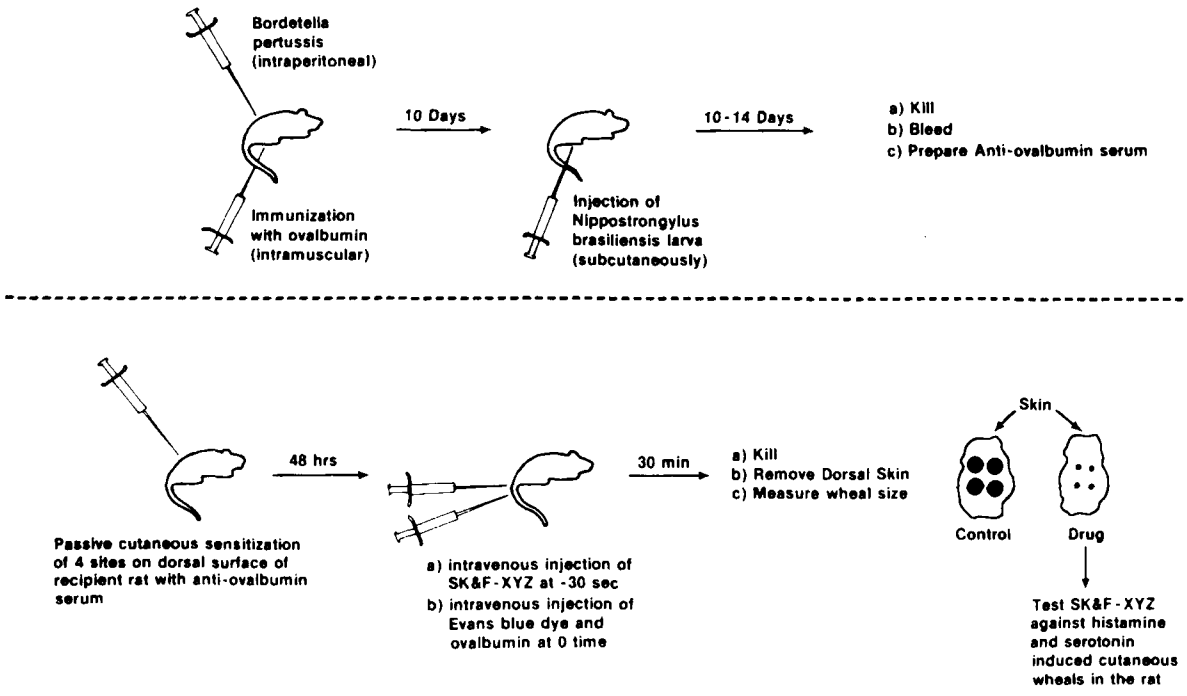

Figure 1—*Schematic of the rat passive cutaneous anaphylaxis model.*

to exist, allowing for the use of this more readily available nematode as an antigen source.

Dogs and rhesus monkeys with hypersensitivity to *Ascaris* antigen are separated from the nonhypersensitive population by a cutaneous testing procedure (Fig. 2). Briefly, the technique consists of injecting Evans blue dye intravenously followed by intracutaneous administration of appropriate dilutions of *Ascaris* antigen. Animals with the appropriate hypersensitivity level respond with wheals and dye infiltration at the antigen injection site. The reaction mechanism is thought to be similar to the rat cutaneous anaphylaxis test in that reaginic antibodies directed against the nematode are firmly fixed to cutaneous mast cells. Subsequent interaction with antigen causes cellular release of the vasoactive substances, leading to an increase in vascular permeability and leakage of dye from the vasculature.

In dogs reared in less than optimal environments, about 50% of adult animals demonstrate a cutaneous hypersensitivity whereas only about 5–10% of the wild adult rhesus monkey population display such hypersensitivity. Animals with appropriate cutaneous sensitivity are subse-

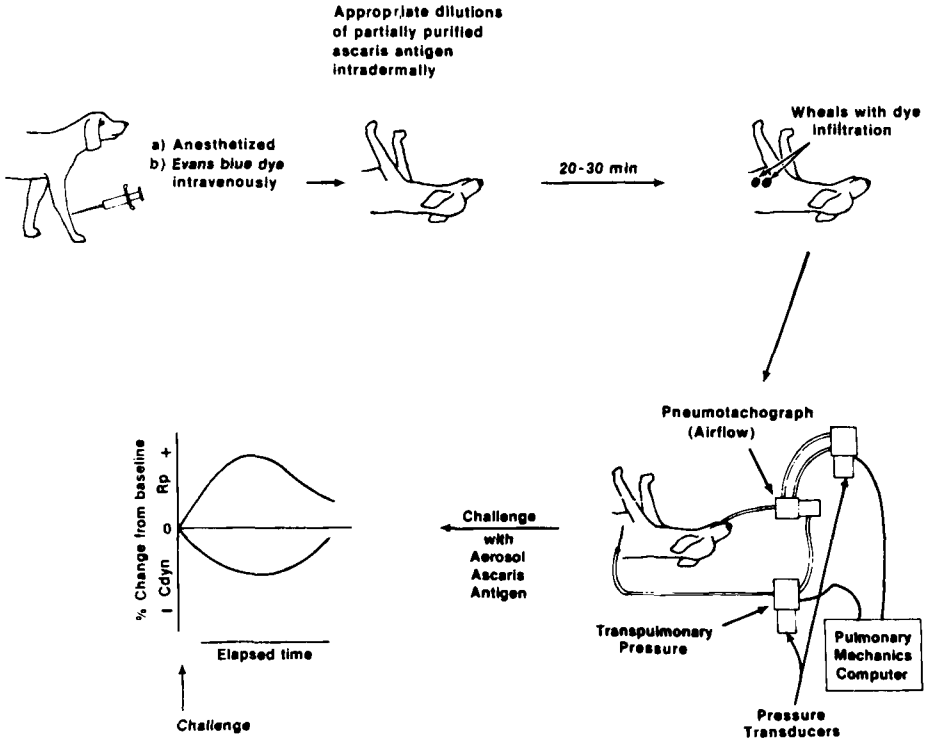

Figure 2—*Schematic of the procedures utilized in the* Ascaris *hypersensitive* in vivo *canine model of allergic asthma. The identical techniques are used for the* Ascaris *hypersensitive rhesus monkey model of allergic asthma.*

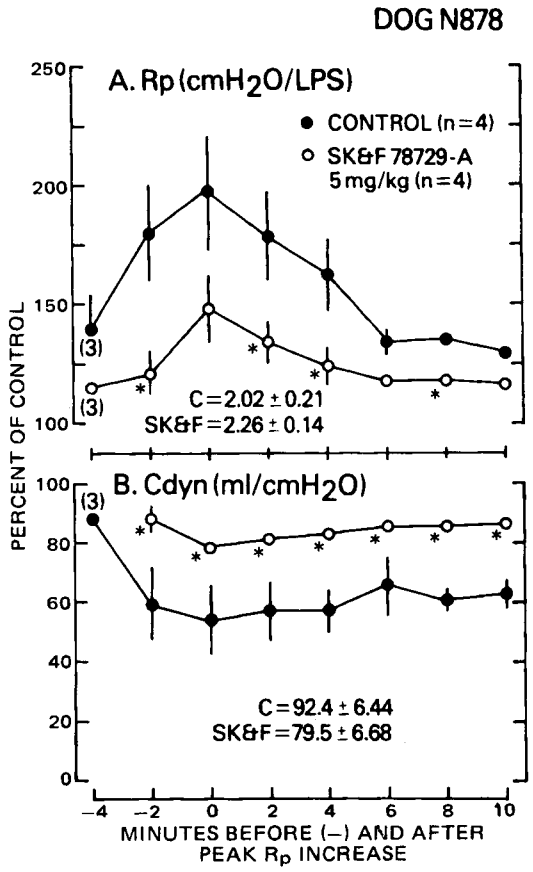

Figure 3—*Effect of I (SK&F 78729-A) on* Ascaris *antigen-induced pulmonary anaphylaxis in the* Ascaris *hypersensitive-canine model of allergic asthma. Compound I was administered (5 mg/kg iv) 30 min prior to seven inhalations of a 1:10 dilution of partially purified* Ascaris *antigen. Rp = pulmonary resistance, Cdyn = dynamic lung compliance, and* n *= number of observations. Numbers in parentheses associated with data points refer to the number of observations for that point only. Each data point signifies the mean* ± SEM. *Baseline values for Rp and Cdyn immediately prior to antigen challenge are illustrated within the graph. (Reprinted, with permission of the publisher, from* J. Pharm. Exp. Ther., *Williams & Wilkins, Baltimore Md.)*

quently challenged with aerosols of the partially purified antigen for determination of airway hypersensitivity. For reasons that are not clear, only a portion of those animals with a cutaneous hypersensitivity demonstrate bronchial responsiveness to the antigen. As with the small animal models, compounds with antiallergic activity are expected to inhibit anaphylaxis when administered prior to antigen provocation. An example of an appropriate pharmacological profile is provided in Figs. 3 and 4 where the antiallergic agent, 5-acetyl-4-hydroxy-3-[1-[(3-amino-4-hydroxyphenyl)amino]ethylidene]-2*H*-pyran-2,6(3*H*)-dione hydrochloride (I) (3), was evaluated against *Ascaris* antigen-induced alterations in pulmonary resistance and dynamic lung compliance in dogs and rhesus monkeys, respectively. Increases in pulmonary resistance and decreases in dynamic lung compliance represent narrowing of large and small airways, respectively. As is apparent, this compound significantly lessened the response in both species.

An alternative to these actively sensitized models is passive sensitization of the airways of nonhypersensitive dogs and monkeys with high titer reaginic serum obtained from hypersensitive donors (10). With monkeys, human serums directed against known allergens may be used because of immunological cross-reactivity between species. Although both systemic and aerosol sensitization may be employed, the latter is most efficient because it requires smaller quantities of serum. While usually successful in the dog, this technique is less applicable to monkeys for unknown reasons, which may relate to the presence or absence of pharmacological airway hyperresponsiveness in the recipient animals.

Rhesus monkeys bronchially hypersensitive to *Ascaris* antigen display an airway hyperresponsiveness to several pharmacological agents including histamine, prostaglandin $F_{2\alpha}$, and cholinergic agonists (12, 13). Dogs do not demonstrate such hyperresponsiveness (14). As noted in the preceding article (1), airway hyperresponsiveness to nonspecific irritants and pharmacological agents is one cardinal clinical feature of the asthmatic. This hyperresponsiveness apparently amplifies the pathophysiological effects of the mediators released on antigen exposure. The demonstration of this phenomenon in monkeys provides an experimental model that may be of utility in uncovering mechanisms underlying this aspect of the disease and perhaps eventually lead to therapeutic agents capable of alleviating the hyperresponsiveness. To date, however, comparatively few investigations have been undertaken with this aspect of the model.

Major disadvantages of large animal models include:

1. Animals with positive bronchial antigen hypersensitivity, particularly rhesus monkeys, are relatively scarce.
2. Antigen challenge can be no more frequent than every 2 weeks. Shorter intervals lead to highly erratic pathophysiological pulmonary responses. Thus, large numbers of animals are required to evaluate reasonable numbers of experimental compounds.
3. Pulmonary responses may be extremely variable, even in the same animal.
4. Large animal models are costly to develop and maintain routinely.
5. No clear insight has yet been gained regarding the biochemical pharmacology underlying the pulmonary pathophysiology. Therefore, unexpected results are difficult to understand.
6. Various pharmacological mechanisms other than inhibition of mediator release can account for a reduction in the response. For example, end-organ antagonism of prominent mediators and smooth muscle bronchodilator activity both reduce response severity.
7. Apparently, humans uniquely suffer from asthma. To our knowledge, no case of allergic asthma in a nonhuman species has been reported. Therefore, while there is presently no alternative, these laboratory models may ultimately prove irrelevant to the clinical syndrome.

For more information regarding these models, the reader is referred to several review articles (9–11, 15).

IN VITRO MODELS

In vitro models of allergic asthma generally occupy an intermediate step in the preclinical pharmacological testing sequence, most often interposed between passive cutaneous anaphylaxis and the more complex *in vivo* models. These systems allow for an assessment of the potential ability of novel molecules to interfere with the antigen-induced release process—the presumed mechanism of action of cromolyn sodium. The most commonly used *in vitro* systems include isolated mast cells (16), blood leukocytes (basophils) (17), and fragment lung tissue (18–21).

A commonly used technique for obtaining a relatively "pure" population of mast cells involves the rat peritoneal cavity. In brief, cells are removed from the peritoneal cavity of actively sensitized rats by a simple washing with a physiological salt solution, and the mast cell population is separated from other peritoneal cell types by centrifugation. Cells are then suspended in an appropriate physiological medium and challenged with antigen to induce histamine release. Preincubation with antiallergic agents is expected to reduce the amount of histamine released on challenge.

Similarly, blood leukocytes (basophils), which also contain histamine and IgE antibody Fc fragment binding sites, may be prepared from actively sensitized animals or allergic human donors, suspended in an artificial medium, and challenged with the appropriate antigen to release the mediators of anaphylaxis. One notable pharmacological peculiarity of human basophils is that immunologically induced mediator release is not susceptible to the inhibitory effect of cromolyn sodium (22). These types of systems are relatively simple and economical, and they provide an essentially homogeneous cell population with which to study antiallergic agents.

The next higher order of complexity in the testing sequence is the *in vitro* fragmented lung model prepared from various species including rats, guinea pigs, dogs, rhesus monkeys, and humans (18–21). Lungs obtained from normal or actively sensitized animals or humans are resected, chopped into small fragments, passively sensitized with high titer reaginic antibody (for those obtained from normal animals), placed in a physiological medium, and then challenged with the appropriate antigen. Many chemical substances can be released on immunological challenge from fragmented lung tissue, and some appear to be species specific. Without regard to species, a partial list of these "mediators" includes: histamine, slow-reacting substance of anaphylaxis, prostaglandins, eosinophil chemotactic factor of anaphylaxis, platelet-activating

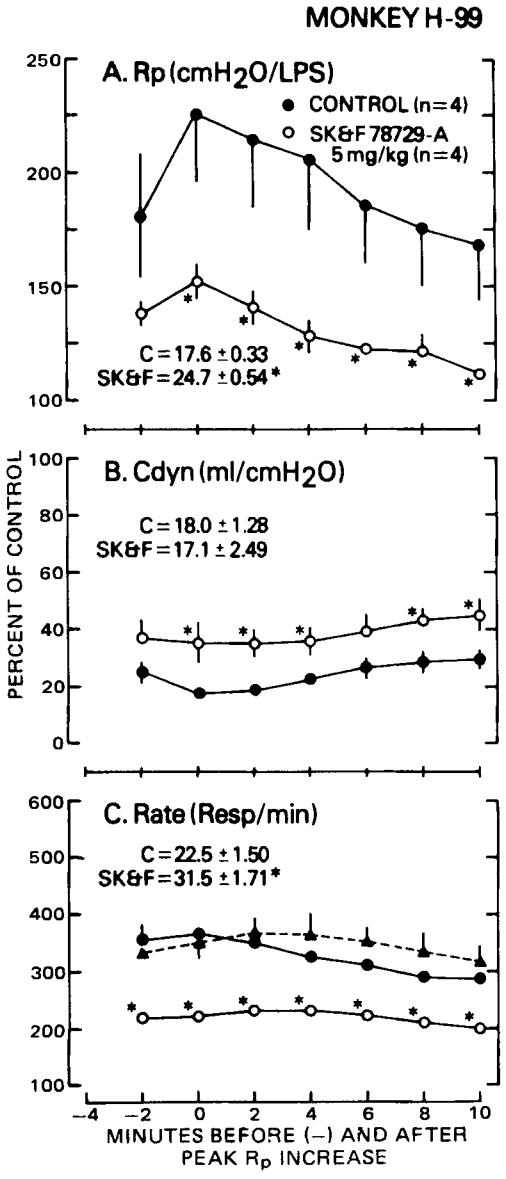

Figure 4—*Effect of I (SK&F 78729-A) on* Ascaris *antigen-induced pulmonary anaphylaxis in the* Ascaris *hypersensitive rhesus monkey model of allergic asthma. Compound I was administered (5 mg/kg iv) 5 min before 15 inhalations of a 1:3 dilution of partially purified* Ascaris *antigen. Rp = pulmonary resistance, and Cdyn = dynamic lung compliance. Baseline values for Rp, Cdyn, and rate immediately prior to antigen challenge are illustrated within the graph. The significant difference in the Rp baseline was not related to the administration of I. Each data point is the mean ± SEM of four separate experiments. (Reprinted, with permission of the publisher, from* J. Pharmacol. Exp. Ther., *Williams & Wilkins, Baltimore, Md.)*

factor, kinins, serotonin, rabbit aorta contracting substance releasing factor, and rabbit aorta contracting substance.

The sheer number of substances released, as well as the rather sophisticated technology required to assay each material, precludes the routine analysis of more than two or three substances. Consequently, many laboratories involved in the search for novel antiallergic agents often measure either histamine or slow-reacting substance of anaphylaxis or both. The selection of these two mediators is based on the observation that much of the body's histamine is sequestered within mast cells, the cells believed to play a major role in the pathophysiological process. Thus, inhibition of histamine release by antiallergic agents provides evidence that the molecule is altering the mast cell release process and, hopefully, that the inhibition will extend to all substances eminating from this cell. Unfortunately, recent experiments indicated that this assumption may not be valid.

The pharmacology of mediator release has been far more extensively studied in these models than in the large *in vivo* models of allergic asthma. It appears well established that agents capable of increasing intracellular levels of cyclic 3′,5′-adenosine monophosphate effectively inhibit histamine and slow-reacting substance of anaphylaxis release from most *in vitro* models (20). Such agents include β-adrenoceptor agonists such as isoproterenol and epinephrine, phosphodiesterase inhibitors including theophylline, and other agonists such as prostaglandins and, perhaps, histamine. Conversely, agents that increase intracellular levels of cyclic 3′,5′-guanosine monophosphate, including α-adrenoceptor and cholinergic stimulants, enhance the immunological release of the mediators (23).

Recently, it was demonstrated that slow-reacting substance of anaphylaxis release can be enhanced by several agents with little or no effect on histamine release, whereas amine release may be augmented or inhibited with no discernible effect on slow-reacting substance of anaphylaxis release (21, 24, 25). These observations suggest the lack of a common release process, at least as regards these two substances; the wider implication is that release of other mediators may also be pharmacologically distinct. Hence, inhibition of histamine and/or slow-reacting substance of anaphylaxis release by novel antiallergic agents cannot be extrapolated to other mediators without reservation. The obscurity of the important mediators of allergic asthma makes this observation unsettling to the preclinical pharmacologist because the inhibitory effects of antiallergic agents on histamine or slow-reacting substance of anaphylaxis release in laboratory models may not translate to an inhibition of the relevant mediators of allergic asthma in humans.

STATUS OF PROPHYLACTIC ANTIALLERGIC AGENTS

Several years of laboratory experimentation with these paradigms have led to the clinical introduction of almost 40 chemically novel antiallergic agents. Unfortunately, only one compound, ketotifen, has been added to the armamentarium and even it is currently limited to use in Switzerland (26). These discouraging clinical results have led to a reevaluation of these models, with attempts to determine which, if any, pharmacological commonalities of the 40 molecules may conceivably account for clinical failures. A number have been identified.

A rapid loss of efficacy as well as tachyphylaxis to the activity of these types of compounds is apparent following oral or parenteral administration in some *in vivo* models or on prolonged preincubation in some *in vitro* models. Although not orally active, cromolyn sodium demonstrates a similar pharmacological profile in these models, yet it remains clinically useful. On this basis, one may be tempted to speculate that such liability in laboratory models does not translate to the clinic and could not account for the clinical failures. However, a thorough determination as to whether this phenomenon occurs when compounds are administered by the aerosol route has not been conducted in laboratory models; thus, aerosol administration of cromolyn sodium may obviate tachyphylaxis and rapid loss of efficacy and prove a caveat for those unwilling to accept compounds not orally active.

Another area of concern is the recent demonstration, as already discussed, that some mediators can be selectively modulated (19, 21, 27). Since the important mediators of the allergic syndrome may be unknown, conceivably these compounds are not inhibiting release of the mediators most relevant to the pathophysiology. Alternatively, the major effects of these compounds may be on mediators of only secondary importance to the bronchospasm. Compounds with such activity may demonstrate marginal to no clinical activity.

Another interesting finding is that these types of molecules appear to be more potent inhibitors of histamine than slow-reacting substance of anaphylaxis release (3). In our experience, the concentration–response curve for these agents on histamine release often lies to the left and above that obtained for slow-reacting substance of anaphylaxis. If, as is often assumed, slow-reacting substance of anaphylaxis is an important mediator of human allergic asthma, a compound at least as potent for slow-reacting substance of anaphylaxis release as for histamine release may prove an interesting clinical candidate. Unfortunately, no new molecules appear to offer this profile.

And, finally, with relatively few exceptions, the newer compounds only partially inhibit the release of histamine and slow-reacting substance of anaphylaxis from most *in vitro* preparations. Frequently, "bell-shaped" concentration–response curves with maximal effects of between 40 and 60% inhibition are characteristic (3). However, cromolyn sodium shares this feature in many models but is clinically active. It is possible to compensate for this disparity by suggesting that cromolyn sodium may be completely efficacious in inhibiting other as yet unknown but important mediators of the human pathophysiology. Again, mechanisms

underlying this partial inhibition remain obscure; however, compounds offering 100% inhibition of both mediators or indeed all mediators would offer a potential clinical advantage.

In summary, as laboratory and clinical experience with both cromolyn sodium and novel antiallergic agents increases, a clearer understanding of the mechanism of action of this class of compounds undoubtedly will emerge. When this time approaches, many problems that concern us today will, hopefully, have fallen away and, perhaps, the design of and search for antiallergic drugs will be considerably less confusing and frustrating than they have been for the past decade.

REFERENCES

(1) L. W. Chakrin and R. D. Krell, *J. Pharm. Sci.*, **69**, 236 (1980).

(2) "Intal—Cromolyn Sodium, A Monograph," Fisons Corp., Bedford, Mass., 1973.

(3) L. W. Chakrin and R. D. Krell, *J. Pharmacol. Exp. Ther.*, **207**, 756 (1978).

(4) K. Ishizaka and T. Ishizaka, *Arch. Pathol. Lab. Med.*, **100**, 289 (1976).

(5) L. M. Stotland and N. N. Share, *Can. J. Physiol. Pharmacol.*, **52**, 1119 (1974).

(6) J. B. Farmer, I. M. Richards, P. Sheard, and A. M. Woods, *Br. J. Pharmacol.*, **55**, 57 (1975).

(7) P. Armitage, H. Herxheimer, and L. Rosa, *ibid.*, **7**, 625 (1952).

(8) L. Diamond and M. O'Donnell, *J. Appl. Physiol.*, **43**, 942 (1977).

(9) R. Patterson, *Prog. Allergy*, **13**, 332 (1969).

(10) R. Patterson and J. F. Kelly, *Arin. Rev. Med.*, **25**, 53 (1974).

(11) R. D. Krell, L. W. Chakrin, and J. R. Wardell, Jr., "Immunopharmacology," Spectrum, New York, N.Y., 1975, pp. 125–148.

(12) R. D. Krell, *Life Sci.*, **19**, 1777 (1976).

(13) R. Patterson, K. E. Harris, I. M. Suszko, and M. Roberts, *J. Lab. Clin. Invest.*, **57**, 586 (1976).

(14) R. D. Krell and L. W. Chakrin, *J. Allergy Clin. Immunol.*, **58**, 664 (1976).

(15) R. Patterson, *Yale J. Biol. Med.*, **40**, 495 (1968).

(16) T. J. Sullivan, K. L. Parker, W. Stenson, and C. W. Parker, *J. Immunol.*, **114**, 1473 (1975).

(17) L. M. Lichtenstein and E. Gillespie, *Nature*, **244**, 287 (1973).

(18) P. Sheard, P. G. Killingback, and A. M. J. N. Blair, *Nature*, **216**, 283 (1967).

(19) L. W. Chakrin, R. D. Krell, J. Mengel, D. Young, C. Zaher, and J. R. Wardell, Jr., *Agents Actions*, **4**, 297 (1974).

(20) R. P. Orange, W. G. Austen, and K. F. Austen, *J. Exp. Med.*, **134**, 136S (1971).

(21) R. D. Krell and L. W. Chakrin, *Int. Arch. Allergy Appl. Immunol.*, **56**, 39 (1978).

(22) E. S. K. Assem and J. L. Mongar, *ibid.*, **38**, 68 (1970).

(23) M. Kaliner, R. P. Orange, and F. K. Austen, *J. Exp. Med.*, **136**, 556 (1972).

(24) J. L. Walker, *Adv. Biosci.*, **9**, 235 (1973).

(25) R. P. Orange, *J. Immunol.*, **114**, 182 (1975).

(26) B. Wuethrich, P. Radielovic, and M. Debelic, *Int. J. Clin. Pharm.*, **16**, 424 (1978).

(27) R. D. Krell and L. W. Chakrin, *Eur. J. Pharm.*, **44**, 25 (1977).

ACKNOWLEDGMENTS

Presented as part of the Symposium on New Approaches to the Treatment of Asthma, APhA Academy of Pharmaceutical Sciences, Anaheim meeting, April 1979.

Antiasthmatic Drug Therapy and Calcium Ions: Review of Pathogenesis and Role of Calcium

ELLIOTT MIDDLETON, Jr.

Received May 18, 1979, from the *School of Medicine, State University of New York at Buffalo, Buffalo, NY 14203.* Accepted for publication July 27, 1979.

Abstract □ This paper presents the calcium-dependent pathophysiological features of allergic and nonallergic asthma. Various theories concerning the role of free calcium ions in the pathogenesis of asthma are discussed.

Keyphrases □ Antiallergic drugs—calcium antagonists, inhibition of calcium influx and intracellular calcium movements, inhibition of mediator release □ Calcium-ion dependency—asthma pathophysiology, cyclic adenosine and guanosine monophosphate levels, mediator release, smooth muscle contraction–excitation, mast cell and mucous cell secretion, vagus nerve activation □ Mediator release—antigen dependency, calcium dependency, antiallergic drugs □ Asthma—review of current theories, clinical evaluation, symposium, antiallergic drugs

The principal pathogenetic features of asthma are ultimately calcium-related phenomena: smooth muscle contraction, mast cell chemical mediator secretion, mucous gland secretion, and vagal cholinergic reflex activity. In these cell types, the availability of free calcium ions for excitation–contraction coupling, stimulus–secretion coupling, and nerve impulse conduction determines significantly the smooth muscle contractility, mast cell mediator secretion, mucous gland secretion, and vagus nerve activity. Increased free calcium-ion concentrations might account for heightened smooth muscle contractility and increased mucous gland secretion and perhaps also for an increased mast cell mediator secretion rate and vagal nerve activity.

If the critical pathogenetic pathways in asthma are ultimately related to free calcium-ion availability in smooth muscle, mast cells, mucous glands, and vagus nerve, it follows that effective asthma drug therapy must reduce calcium availability to the essential contractile, secretory, and vagus nerve functions. This concept places altered transmembrane and intracellular calcium movements at the level of final common pathway for the

0022-3549/80/0200-0243$01.00/0

© 1980, American Pharmaceutical Association

underlying this partial inhibition remain obscure; however, compounds offering 100% inhibition of both mediators or indeed all mediators would offer a potential clinical advantage.

In summary, as laboratory and clinical experience with both cromolyn sodium and novel antiallergic agents increases, a clearer understanding of the mechanism of action of this class of compounds undoubtedly will emerge. When this time approaches, many problems that concern us today will, hopefully, have fallen away and, perhaps, the design of and search for antiallergic drugs will be considerably less confusing and frustrating than they have been for the past decade.

REFERENCES

(1) L. W. Chakrin and R. D. Krell, *J. Pharm. Sci.*, **69**, 236 (1980).

(2) "Intal—Cromolyn Sodium, A Monograph," Fisons Corp., Bedford, Mass., 1973.

(3) L. W. Chakrin and R. D. Krell, *J. Pharmacol. Exp. Ther.*, **207**, 756 (1978).

(4) K. Ishizaka and T. Ishizaka, *Arch. Pathol. Lab. Med.*, **100**, 289 (1976).

(5) L. M. Stotland and N. N. Share, *Can. J. Physiol. Pharmacol.*, **52**, 1119 (1974).

(6) J. B. Farmer, I. M. Richards, P. Sheard, and A. M. Woods, *Br. J. Pharmacol.*, **55**, 57 (1975).

(7) P. Armitage, H. Herxheimer, and L. Rosa, *ibid.*, **7**, 625 (1952).

(8) L. Diamond and M. O'Donnell, *J. Appl. Physiol.*, **43**, 942 (1977).

(9) R. Patterson, *Prog. Allergy*, **13**, 332 (1969).

(10) R. Patterson and J. F. Kelly, *Arin. Rev. Med.*, **25**, 53 (1974).

(11) R. D. Krell, L. W. Chakrin, and J. R. Wardell, Jr., "Immunopharmacology," Spectrum, New York, N.Y., 1975, pp. 125–148.

(12) R. D. Krell, *Life Sci.*, **19**, 1777 (1976).

(13) R. Patterson, K. E. Harris, I. M. Suszko, and M. Roberts, *J. Lab. Clin. Invest.*, **57**, 586 (1976).

(14) R. D. Krell and L. W. Chakrin, *J. Allergy Clin. Immunol.*, **58**, 664 (1976).

(15) R. Patterson, *Yale J. Biol. Med.*, **40**, 495 (1968).

(16) T. J. Sullivan, K. L. Parker, W. Stenson, and C. W. Parker, *J. Immunol.*, **114**, 1473 (1975).

(17) L. M. Lichtenstein and E. Gillespie, *Nature*, **244**, 287 (1973).

(18) P. Sheard, P. G. Killingback, and A. M. J. N. Blair, *Nature*, **216**, 283 (1967).

(19) L. W. Chakrin, R. D. Krell, J. Mengel, D. Young, C. Zaher, and J. R. Wardell, Jr., *Agents Actions*, **4**, 297 (1974).

(20) R. P. Orange, W. G. Austen, and K. F. Austen, *J. Exp. Med.*, **134**, 136S (1971).

(21) R. D. Krell and L. W. Chakrin, *Int. Arch. Allergy Appl. Immunol.*, **56**, 39 (1978).

(22) E. S. K. Assem and J. L. Mongar, *ibid.*, **38**, 68 (1970).

(23) M. Kaliner, R. P. Orange, and F. K. Austen, *J. Exp. Med.*, **136**, 556 (1972).

(24) J. L. Walker, *Adv. Biosci.*, **9**, 235 (1973).

(25) R. P. Orange, *J. Immunol.*, **114**, 182 (1975).

(26) B. Wuethrich, P. Radielovic, and M. Debelic, *Int. J. Clin. Pharm.*, **16**, 424 (1978).

(27) R. D. Krell and L. W. Chakrin, *Eur. J. Pharm.*, **44**, 25 (1977).

ACKNOWLEDGMENTS

Presented as part of the Symposium on New Approaches to the Treatment of Asthma, APhA Academy of Pharmaceutical Sciences, Anaheim meeting, April 1979.

Antiasthmatic Drug Therapy and Calcium Ions: Review of Pathogenesis and Role of Calcium

ELLIOTT MIDDLETON, Jr.

Received May 18, 1979, from the *School of Medicine, State University of New York at Buffalo, Buffalo, NY 14203.* Accepted for publication July 27, 1979.

Abstract □ This paper presents the calcium-dependent pathophysiological features of allergic and nonallergic asthma. Various theories concerning the role of free calcium ions in the pathogenesis of asthma are discussed.

Keyphrases □ Antiallergic drugs—calcium antagonists, inhibition of calcium influx and intracellular calcium movements, inhibition of mediator release □ Calcium-ion dependency—asthma pathophysiology, cyclic adenosine and guanosine monophosphate levels, mediator release, smooth muscle contraction–excitation, mast cell and mucous cell secretion, vagus nerve activation □ Mediator release—antigen dependency, calcium dependency, antiallergic drugs □ Asthma—review of current theories, clinical evaluation, symposium, antiallergic drugs

The principal pathogenetic features of asthma are ultimately calcium-related phenomena: smooth muscle contraction, mast cell chemical mediator secretion, mucous gland secretion, and vagal cholinergic reflex activity. In these cell types, the availability of free calcium ions for excitation–contraction coupling, stimulus–secretion coupling, and nerve impulse conduction determines significantly the smooth muscle contractility, mast cell mediator secretion, mucous gland secretion, and vagus nerve activity. Increased free calcium-ion concentrations might account for heightened smooth muscle contractility and increased mucous gland secretion and perhaps also for an increased mast cell mediator secretion rate and vagal nerve activity.

If the critical pathogenetic pathways in asthma are ultimately related to free calcium-ion availability in smooth muscle, mast cells, mucous glands, and vagus nerve, it follows that effective asthma drug therapy must reduce calcium availability to the essential contractile, secretory, and vagus nerve functions. This concept places altered transmembrane and intracellular calcium movements at the level of final common pathway for the

0022-3549/80/0200-0243$01.00/0

© 1980, American Pharmaceutical Association

pathogenesis of asthma, regardless of the proximate stimulus (*e.g.*, allergy, infection, or exercise) and may be considered the *calcium hypothesis of asthma.*

DISCUSSION

Asthma is a clinically heterogeneous disorder. Examples of heterogeneity are noted in nonuniform heredity, variable airways reactivity and physiological abnormalities (large *versus* small airway involvement), immunologic features (allergic *versus* nonallergic asthma and the unique nonimmunologic form of aspirin-induced asthma), and variable therapeutic response with different drug classes. Furthermore, many asthma precipitants are recognized clinically including allergy, certain viral infections, exercise, cold air, respiratory irritants, aspirin (~10% of asthma patients), and emotional state, especially fear and anger. Does each of these aspects of clinical heterogeneity and variable precipitants represent different biochemical pathways? Perhaps in a proximate sense they do, yet the final expression of the pathological changes in asthma must finally be related to the translocation of calcium ions to activate the smooth muscle contractile system, the mast cell and mucous gland secretory systems, and nerve impulse initiation and conduction in vagal fibers.

It is reasonable to consider the interaction between an excitatory agent and specific tissue receptors (*e.g.*, antigen with mast cells or histamine or acetylcholine with smooth muscle) as the stimulus that activates some calcium membrane transport or membrane releasing system, or both. Following activation, the transport (or releasing) system promotes calcium-ion flow from intra- and/or extracellular storage sites into the cytoplasmic matrix. The result is an increase in free calcium ions near the contractile proteins in smooth muscle, the secretory apparatus in mast cells and mucous glands, and the nerve impulse initiation and conduction systems. The interaction of the calcium ions with the relevant specific sites then initiates a response.

When the excitatory agent is removed from the vicinity of the smooth muscle, mast cell, mucous gland, or nerve cell, calcium-ion flow into the cytoplasm is reduced and the cellular response is decreased. With smooth muscle, a gradual reduction in the calcium-ion level is accompanied by a gradual dissociation of calcium from the contractile elements and by a gradual decrease in the capacity of the contractile machinery to maintain increased tension. Removal of free cytoplasmic calcium is considered to be accomplished by a metabolically dependent calcium pump located in the plasma membrane and/or the membranes of intracellular organelles. The pump transports calcium from the cytoplasm to sequestration sites or to the external medium.

Based on these considerations, it is inferred that both the rate of inward flow or the release of calcium ions (from extra- or intracellular calcium stores) initiated by the excitatory agent and the simultaneous removal rate of free cytoplasmic calcium by the energy-linked calcium pump are important in determining the final cytosol calcium concentration. Since the calcium ions enter into a reversible interaction with specific contractile and secretory proteins, depending on cell type, their concentration in the cytoplasm determines the extent to which they elicit a response. It might be assumed, therefore, that the free calcium concentration in the cytoplasmic matrix and, therefore, the rate at which the calcium transport system delivers calcium to the cytoplasmic matrix would be important in the magnitude of the response.

The application of physiological techniques has uncovered energy-dependent calcium-concentrating systems in mitochondrial and microsomal preparations from smooth muscle. Therefore, it can be inferred that these structures possess a calcium-sequestering function, which, in the case of smooth muscle, induces relaxation. Conversely, these structures possibly may function as sites from which activator calcium can be mobilized for contraction. Comparable regulatory mechanisms may exist in mast cells and mucous glands.

The mechanisms by which excitatory agents mobilize calcium from different storage sites apparently vary from tissue to tissue. Vascular and nonvascular smooth muscle studies suggested that membrane depolarization is associated predominantly with the mobilization of extracellular or loosely bound calcium. It is difficult, however, to generalize about the manner in which an excitatory agent mobilizes calcium or about the calcium sources in smooth muscles, mast cells, mucous glands, or nerve tissues.

The manner in which the calcium transport system is coupled to the excitatory agent–receptor complex is not clear, and it is difficult to propose a model that accounts for graded increases in the activation of a calcium transport system that presumably occurs with incremental increases in the excitatory agent concentration (*e.g.*, antigen with mast cells or histamine or acetylcholine with smooth muscle).

Any exciting agent stimulating the relevant cell types in the lung in asthma (smooth muscle, mucous glands, mast cells, and nerve) may involve an induced shift of calcium ions from storage sites to the cytoplasmic matrix; this shift is carried out by a finite number of cellular transport sites which exist in cellular membranes. These calcium transport sites normally function at a low activity level unless activated by two independent cellular reactions. One of these reactions involves calcium transport site activation in an unknown fashion by the interaction of the excitatory agent with specific tissue receptors. The second involves reversible complex formation between calcium in storage depots and the activated calcium transport sites.

The entry rate of free calcium into the cytoplasmic matrix and, ultimately, the cellular response are dependent on the fraction of the total number of calcium transport sites participating in each type of reaction. Calcium transport site activation may be accomplished by a complex interaction between the excitatory agent and specific tissue receptors, which seem to be linked to the transport sites. The increase in calcium conductance that results from transport site activation is usually a graded response. It follows that calcium-ion transport by activated sites must be preceded by the formation of a reversible complex between the calcium transport sites and the calcium ions that are to be transported into the cytoplasmic matrix and, eventually, that are to interact with contractile, secretory, and nerve excitation systems.

Many recognized calcium-dependent processes are important in asthma pathogenesis: excitation–contraction coupling in smooth muscle, stimulus–secretion coupling in secretory cell types including mast cells and mucous glands, and microtubule function and calcium effects on certain enzyme systems such as adenyl cyclase, guanyl cyclase, and phosphodiesterase activator protein.

Currently utilized drugs presumably indirectly affect calcium movement and disposition by acting on the adenyl cyclase–cyclic adenosine monophosphate system (β-agonists) and, perhaps, through phosphodiesterase inhibition (theophylline); cromolyn sodium, however, may have some calcium-antagonistic properties, *i.e.*, inhibition of calcium uptake by activated mast cells. The relationship of the antiasthmatic effects of corticosteroids to calcium movement is obscure. The possibility of developing compounds with calcium-antagonistic properties selective for cells involved in asthma pathogenesis is attractive, and such compounds are being studied.

Calcium antagonists can be defined as compounds that affect the translocation of calcium ions across cell membranes and within cells; certain calcium antagonists appear to act by affecting transmembrane calcium translocations while others affect intracellular calcium movements. Their mechanism of action is complex and ill defined. Some calcium antagonists have been studied for their effects on myocardial and vascular smooth muscle responses to various agonists (and are in use therapeutically, *e.g.*, verapamil), a few have been studied for their effect on nonvascular smooth muscle, and several have been studied for their ability to block specific secretory processes (*e.g.*, catecholamine secretion from the adrenal medulla), but few investigations of calcium antagonists on mediator secretion from mast cells or basophils have been undertaken.

IMMUNOLOGICAL–CHEMICAL MEDIATOR THEORY: REGULATION OF CHEMICAL MEDIATOR RELEASE

Immunoglobulin E-sensitized mast cells and basophils can be triggered to release chemical mediators upon stimulation with a specific antigen, and the release process has an absolute requirement for calcium ions (*cf.*, 1–7). Indeed, calcium microinjection into mast cells provokes local granule extrusion (8). It was believed that the chemical mediators acted locally and directly on smooth muscle, blood vessels, and mucous glands and attracted eosinophils and other inflammatory cells to produce the characteristic pathological changes of asthma in the lung. Not all causes of asthma have an identifiable immunological basis, however, so it is safe to say that allergy is a sufficient, but not an exclusive, explanation for asthma.

The discovery of immunoglobulin E (*cf.*, 9) established the immunological basis of immediate-type hypersensitivity reactions and spurred research on the mechanisms by which chemical mediators are released from mast cells and basophils. It is now well recognized that immunoglobulin E antibody is firmly bound to special receptors in the cell membrane of mast cells and basophils and that interaction of the bound antibody with specific antigen initiates a series of intracellular biochemical reactions, which culminate in the noncytolytic secretion of

preformed mediators and the generation and release of several mediators that exist as precursors (1–7).

The essential role of immunoglobulin E receptors in mediator release from rat mast cells was demonstrated by Ishizaka and Ishizaka (10), who found that antibodies specifically directed against immunoglobulin E receptors caused histamine release and immediate skin reactions in normal rats. This important observation indicates that membrane perturbation, presumably involving the spatial relationships of the immunoglobulin E receptor and subtended functional units, is sufficient to initiate the biochemical sequence required for mediator release.

The list of mast cell- and basophil-derived mediators includes: (*a*) preformed mediators such as histamine, eosinophil chemotactic factor of anaphylaxis, eosinophil chemotactic factor oligopeptides, neutrophil chemotactic factor, heparin, chymase, lung kallikrein of anaphylaxis, superoxide radical, and superoxide dismutase; and (*b*) newly generated mediators such as slow-reacting substance of anaphylaxis, platelet-activating factor(s), lipid chemotactic factors, and prostaglandins. The source, nature, properties, and metabolism of these substances have been reviewed extensively (1–6, 11). Some or all of these substances may participate in the pathogenesis of the acute and chronic aspects of lung pathology and altered physiology in various types of asthma, acting through direct and reflex mechanisms. It is also pertinent that histamine and slow-reacting substance of anaphylaxis require calcium for stimulation of smooth muscle contraction.

Extensive studies (1–6) of immunoglobulin E-dependent immunological release of chemical mediators from mast cells and basophils have provided a partial picture of the biochemical events involved and, thus, the various loci for potential pharmacological intervention. Interaction of specific antigen with mast cell-bound immunoglobulin E antibody presumably results in membrane perturbation associated with extracellular calcium-ion transport into the cell. This initial step is accompanied by the activation of a proesterase, which is converted to an active chymotrypsin-like serine esterase, which subsequently engages in further autocatalytic activation. Possibly, calcium-ion influx is essential for initial activation and autocatalytic activation of the proesterase to the esterase. The active esterase decays quite rapidly.

A subsequent energy-dependent step can be inhibited by 2-deoxyglucose. Precisely what function in the mediator release sequence is subserved by the energy requirement is not certain, but it may be related to the function of a "contractile protein" since dense bands of microfilaments have been observed around mast cell granules, especially during degranulation. Microfilament function is probably involved in mediator release, and the function of microfilaments can be affected by cytochalasins A and B. Studies with these agents indicated that histamine release and slow-reacting substance of anaphylaxis generation and release can be dissociated. Although cytochalasins A and B enhance histamine release, they inhibit the concomitant formation of slow-reacting substance of anaphylaxis. An interesting study (12) indicated a significant difference in the cytochalasin sensitivity of histamine release in a comparison of asthmatic and normal basophils.

Several studies indicated an important function of microtubules in mediator release from mast cells and basophils. Colchicine, a compound that binds to the microtubular subunit protein, thereby preventing microtubule assembly and function, inhibits histamine release. Heavy water (D_2O), on the other hand, favors microtubule subunit aggregation and facilitates histamine release.

The metabolic regulation of chemical mediator release has been investigated intensively. One aspect of metabolic control of mediator release that is quite well worked out in several *in vitro* systems involves the effects of cyclic adenosine monophosphate, cyclic guanosine monophosphate, and agents that affect their intracellular concentration. Numerous studies (1–6) indicated that agents that increase cyclic adenosine monophosphate levels (*e.g.*, β-agonists, histamine, prostaglandin E, and cholera toxin) tend to decrease chemical mediator release, while agents that decrease cyclic adenosine monophosphate levels (*e.g.*, α-adrenergic agonists) tend to increase chemical mediator release. On the other hand, compounds that increase cyclic guanosine monophosphate levels (*e.g.*, cholinergic agents and, perhaps, α-adrenergic compounds) tend to increase chemical mediator release. Indeed, recent evidence appears to establish cyclic guanosine monophosphate as an important mediator of immunological mediator release in human lung (13).

The effect of each adrenergic or cholinergic agonist can be blocked by antagonists such as propranolol, phentolamine, and atropine, substantiating the β- and α-adrenergic and muscarinic cholinergic nature of the receptor systems involved. Thus, chemical mediator release can be modulated by products of the sympathetic and parasympathetic nervous system and other substances acting through specific receptor systems and affecting the intracellular levels of cyclic adenosine monophosphate and cyclic guanosine monophosphate. Calcium plays a critical role in control of intracellular cyclic nucleotide concentrations through its ability to inhibit adenyl cyclase (14), stimulate guanyl cyclase (15), and regulate the phosphodiesterase regulator protein (16).

NEUROGENIC THEORY

The neurogenic theory of asthma pathogenesis is grounded in the observation that stimulation of subepithelial airway receptors by released chemical mediators or other irritants results in a vagally mediated cholinergic bronchoconstrictor reflex, which can be markedly attenuated or abolished by atropine or experimental manipulations that attenuate vagal afferent and efferent impulse transmission. Atropine acts competitively to inhibit the calcium-dependent effects of released acetylcholine on smooth muscle and mucous glands. The asthma-worsening effect of viral respiratory infections that denude the epithelium is thought to be due to sensitization of these rapidly adapting subepithelial sensory receptors; in normal subjects with "colds," a transient (1–6 weeks) hyperirritability of the airways to inhaled histamine or citric acid aerosols has been demonstrated (17). Much evidence supports the neurogenic theory, and it has been reviewed extensively (18–21).

Mediators immunologically released from intraluminal airway mast cells or basophiloid cells (22) may stimulate vagal sensory endings and increase bronchial epithelial permeability to macromolecular antigens, allowing them to gain access to submucosal mast cells where further mediator release might occur. Although cholinergic agents increase immunological mediator release *in vitro*, there is no evidence that cholinergic stimulation *in vivo* does the same thing.

β-ADRENERGIC BLOCKADE THEORY

Another major theory concerned with asthma pathogenesis is that of β-adrenergic blockade proposed by Szentivanyi (23). Briefly, this theory states that there is diminished responsiveness of β-adrenergic receptors to stimulation by β-adrenergic agents. This theory implies that β-receptor-mediated relaxation of smooth muscle and β-receptor-mediated functions of other cells and organ systems might be reduced. It also implies a diminished accumulation of cyclic adenosine monophosphate following stimulation with β-agonists because of the linked relationship of β-receptors and adenyl cyclase to convert adenosine triphosphate to cyclic adenosine monophosphate. Adenyl cyclase is a membrane-bound, magnesium-dependent enzyme and is inhibited by calcium ions. Although not totally conclusive, considerable evidence supports this theory and the data have been reviewed extensively (23–27). An interesting recent supportive observation also was reported: salbutamol inhalation increased plasma and urinary cyclic adenosine monophosphate levels in both normal and asthmatic subjects, but the increase in asthmatics was significantly less (28).

A major objection to the β-adrenergic blockade theory arose when several investigators (29–32) noted that asthmatic patients or normal individuals given β-adrenergic drugs developed subsensitivity of leukocytes to stimulation by isoproterenol as determined by cyclic adenosine monophosphate accumulation. These studies indicated that the apparent state of "β-adrenergic blockade" was, in fact, drug induced. However, Busse (33) later studied asthmatic patients who had not received β-adrenergic drugs for 2 weeks and determined that the isoproterenol-induced inhibition of polymorphonuclear leukocyte lysosomal enzyme release was reduced as well as the isoproterenol-stimulated accumulation of cyclic adenosine monophosphate in these cells. These data are generally consistent with the β-adrenergic blockade theory. Bush *et al.* (34) also found a decreased isoproterenol polymorphonuclear leukocyte response in normal individuals during rhinovirus infection, indicating that the viral infection produces dysfunction of the β-receptor–adenyl cyclase system in nonpulmonary tissues. Thus, viral infections appear to have metabolic effects on cell function and direct airway effects. Precisely what aspect of enzymatic control of cyclic adenosine monophosphate synthesis (or degradation) is affected by the virus or the products of viral infection remains to be determined.

Recent experiments on asthmatic and nonasthmatic dogs (sensitive to *Ascaris suum*) compared trachael ring smooth muscle responsiveness to antigen, methacholine, and isoproterenol; isoproterenol induced consistently greater relaxation in nonasthmatic rings following standardized precontraction with methacholine (35). The finding of isoproterenol hyporesponsiveness in natively asthmatic dogs, under conditions excluding possible receptor densensitization due to prior exposure to β-agonists, is consistent with the β-adrenergic blockade theory but does

not exclude the importance of vagal mechanisms.

In summary, solid evidence apparently substantiates the possibility of β-adrenergic receptor–adenyl cyclase dysfunction in certain cells of asthmatic patients (and dogs). However, the studies do not shed any light on the locus of the biochemical–pharmacological defect. Since the β-receptor–adenyl cyclase system is considered to be composed of a recognition or discriminator (receptor) unit, a transducer unit, and a catalytic unit, dysfunction could occur at any (or all) of these levels.

It is now well recognized that guanosine triphosphate is an important regulator of adenyl cyclase in many hormone-stimulated systems (36). The data indicate that guanylyl nucleotide regulation of adenyl cyclase activity is not only ubiquitous but also independent of the receptor coupled to the enzyme. It is also known that the guanosine triphosphate concentration is under the control of a phosphatase (36–38). Thus, it is possible that cells of asthmatics may have abnormal function of this regulator site or possibly increased phosphatase activity, which would indirectly depress adenyl cyclase function. There are no data to support these ideas, but it is interesting to consider the therapeutic possibilities of agents that might act at the guanosine triphosphate regulator site to increase adenyl cyclase responsiveness to β-agonists or that might inhibit the phosphatase.

REDUCED FUNCTION OF NONADRENERGIC INHIBITORY SYSTEM THEORY

Another theory is reduced function of the nonadrenergic inhibitory system in the lungs of asthmatic patients (39). Human airways, from the midtrachea to the distal bronchi, have been studied *in vitro* for inhibitory nerves (40). Electrical field stimulation of the tissues demonstrated cholinergic excitatory nerves inhibitable by atropine. In the presence of atropine, field stimulation of the tissues relaxed smooth muscle, even when it was contracted by histamine. This relaxation was neither blocked nor modified by adrenergic antagonists. Nerve stimulation involvement in the field stimulation–induced relaxation was established when tetrodotoxin blocked the effect.

This airway relaxation system shares some characteristics of the nonadrenergic inhibitory system in the GI tract and of the comparable system reported in guinea pig tracheal smooth muscle. Moreover, no evidence of adrenergic inhibitory fibers in human bronchial muscle could be found by either pharmacological or histochemical techniques. The nonadrenergic inhibitory system may be the principal inhibitory system of human airway smooth muscle, and a defect in this system might be a possible explanation for the hyperreactivity of the airways noted in asthma patients.

The asthma theories reviewed are not mutually exclusive. Nevertheless, in each case, the final common denominator is considered to be the increased availability of free (activator) calcium ions for excitation–contraction coupling in smooth muscle, stimulus–secretion coupling in mast cells and mucous glands, and nerve impulse initiation and conduction in the vagus.

AIRWAY HYPERIRRITABILITY

Any asthma theory must explain the disease hallmark, namely, hyperirritability of the airways from various stimuli. Hyperirritability has been demonstrated in clinical investigations with various substances that are chemically unrelated but require calcium for their smooth muscle stimulating activity. These agents include acetylcholine, methacholine, histamine, slow-reacting substance of anaphylaxis, prostaglandin $F_{2\alpha}$, and bradykinin.

Airway hyperreactivity suggests that the airway smooth muscle is partially depolarized, *i.e.*, reactive to low doses of various chemically diverse substances or stimuli. The basic cause of the hyperreactivity (or postulated state of partial depolarization) is unknown but certainly suggests an increased permeability of smooth muscle cell membrane to calcium ions, which activate the contractile machinery. The single piece of evidence that possibly supports increased permeability (or partial depolarization) was provided by Simonsson *et al.* (41), who demonstrated that airway smooth muscle from a patient with chronic bronchitis responded *in vitro* to very low doses of carbachol and bradykinin as compared to normal bronchial smooth muscle. Whether such findings might obtain in asthma remains to be determined.

BIOLOGICAL PROPERTIES OF CALCIUM AND CALCIUM ANTAGONISTS

Calcium plays a critical and central role in many biological events at both the intra- and extracellular levels (42, 43). However, calcium distribution across the cell membrane is far from equilibrium; if the testing membrane potential (~−60 mv) were equal to the calcium equilibrium potential, then the intracellular calcium activity should be some 100-fold greater than the extracellular activity. This is clearly not so. Although accurate measurements of free ionized intracellular calcium concentrations have not been made in many systems, the consensus of evidence firmly indicates that the free intracellular calcium concentration is less than 10^{-7} *M* (44–46).

The very large driving force for calcium entry indicates that specific mechanisms must exist for intracellular calcium removal. Subsequent to entry, calcium may be removed through complexation with cytoplasmic constituents (including the internal membrane surface) or by sequestration into the intracellular structures, mitochondria (47, 48), and sarcoplasmic reticulum (49, 50) of smooth muscle, for example.

Although there can be no doubt as to the importance of calcium uptake by the active transport processes mediated by mitochondria and sarcoplasmic reticulum, the cell must, to maintain its total calcium reasonably constant, ultimately transport calcium to the external medium. Two major processes for intracellular calcium removal have been described. In one process, calcium extrusion is directly coupled to adenosine triphosphate hydrolysis; in the second process, calcium extrusion is coupled to an influx of sodium ions.

CALCIUM ENTRY PROCESS

Given the existence of the several mechanisms that operate to maintain a low intracellular free calcium concentration, there must also exist mechanisms that increase intracellular calcium concentrations and couple membrane excitation to intracellular calcium-modulated events. This calcium may be derived from intracellular stores or from extracellular sources. Although initial emphasis was placed by Hodgkin and Huxley (51) on Na^+ and K^+ as the current carrying species during squid axon excitation, there is now substantial evidence for this and many other tissues that calcium entry through "specific calcium channels" also contributes to the total membrane current (44, 46, 52, 53).

Of particular importance, pharmacological differentiation of the Na^+, K^+, and calcium channels is possible with selective antagonists. Tetrodotoxin and tetraethylammonium are well known for their actions on Na^+ and K^+ channels, respectively (54), and the inorganic ions Mg^{2+}, Mn^{2+}, Ni^{2+}, Co^{2+}, and La^{3+} and the organic agents verapamil, methoxyverapamil, and nifedipine have gained prominence as calcium channel antagonists (46, 55, 56). There is an obvious analogy between this differentiation of ion channels and the differentiation of pharmacological receptors through specific antagonist action.

There is not considerable evidence that the calcium entry process similar to that seen in the squid axon occurs in several excitable tissues and that a calcium channel is utilized distinct from that carrying the early sodium current. The basis for the differentiation of such a process rests on the following properties:

1. Membrane currents and potential changes in Na^+-free solution are basically identical to those seen in Na^+-containing media in the presence of tetrodotoxin or in preprations where the Na^+ channel has been inactivated by prior depolarization.
2. The calcium current is insensitive to tetrodotoxin and tetraethylammonium but is sensitive to antagonism by Mg^{2+}, Mn^{2+}, Co^{2+}, La^{3+}, verapamil, methoxyverapamil, and nifedipine.
3. Both Sr^{2+} and Ba^{2+} can substitute for calcium.
4. The threshold voltage- and time-dependent activation and inactivation parameters and gating currents are quite distinct from those determined for the early sodium current.

As judged by these criteria, calcium channels mediating calcium translocation have been described in various preparations, from protozoan to mammalian (57), although complete ionic, electrophysiological, and pharmacological characterization is not available in many instances.

CALCIUM CHANNEL ANTAGONISTS

The di- and trivalent cations Mn^{2+}, Ni^{2+}, Co^{2+}, and La^{3+} and the organic molecules verapamil, methoxyverapamil, and nifedipine are defined as calcium channel antagonists, and their actions serve as one important component of calcium channels. However, neither the sites nor the mechanisms of action of these antagonists have been defined precisely.

Certain data also suggest that the channels may possess gating mechanisms involving phosphatidylinositol breakdown as the initial event

required to open calcium channels following agonist–receptor interaction (58, 59). Phenoxybenzamine, an α-adrenergic blocker with antagonistic effects against several chemically unrelated agonists, was the only one of a number of compounds tested found to block phosphatidylinositol breakdown and to inhibit smooth muscle contraction (60). The nature and controlling mechanisms of calcium gates/channels is far from completely understood, but they are of central importance to the calcium hypothesis of asthma.

Various organic calcium antagonists have been developed which block entry of calcium ions from the outside to the inside of the cell and which can modify the effects of various calcium-dependent agonists (61). Some examples are verapamil, methoxyverapamil, nifedipine, benzyclane, prenylamine, and cinnarizine. These compounds have been studied mainly for their effect on myocardial cell function as well as on coronary and other vascular smooth muscles. Verapamil and methoxyverapamil have potent effects on excitation–contraction coupling in several vascular smooth muscle preparations and also in guinea pig ileal smooth muscle (57). Verapamil and methoxyverapamil are also quite potent inhibitors of stimulus–secretion coupling in several systems (57).

Other calcium antagonists such as the aminoindenes (62, 63) and mecinarone (66) appear not to block the calcium entry process but rather to affect the intracellular sites of calcium action. This was demonstrated in studies of cholinergically stimulated release of catecholamines from the adrenal medulla (62) and also with histamine- and carbachol-induced contraction of different smooth muscle preparations (63). Ketotifen, an effective antiasthmatic drug (64), inhibits calcium 45 uptake by rat mast cells (65) and also possesses antihistaminic activity (H_1). Compounds with such properties are of interest for both theoretical and practical considerations in drug design, *i.e.*, in the search for compounds that affect the essential intracellular calcium movements required for contractile and secretory phenomena. The effects of certain calcium antagonists on rat mast cell mediator release will be described later.

It is plausible that the calcium channel organization is basically similar to that suggested for the sodium channel by Hille (54). An important component of Hille's model is the channel cation coordination site, which constitutes a rate-limiting selectivity filter. The energetics of cation interaction at this site determine whether a cation is a permeant or nonpermeant species. In the case of the sodium channel, Na^+ binds the least well and is the most permeant. The geometry and ligand characteristics of this proposed site determine the selectivity between monovalent and divalent cations (67, 68) and, in the case of the calcium channel, divalent cations with ionic radii similar to those of calcium may be expected to interact with this site and to serve as substitutes for or antagonists of calcium permeation.

Little quantitative data exist for ion interactions at the calcium channel. However, for antagonism, it is clear that $M^{3+} > M^{2+}$ (69) and that among divalent cations the order of permeation is $Ba^{2+} > Sr^{2+} > Ca^{2+} \gg Mg^{2+}$; Ni^{2+} and Co^{2+} serve as antagonists, and Mn^{2+} acts as both an antagonist and permeant species (70). These findings suggest that the ionic radius and hydration energy may be important factors in determining cation interaction and permeation in the calcium channel. Many of these effects of di- and trivalent cations are likely related to a general adsorption to negatively charged membrane sites. Finally, the lanthanide series of cations are calcium channel antagonists, probably by virtue of their rather general ability to substitute for calcium at calcium-binding sites (71, 72).

The organic calcium antagonists verapamil, methoxyverapamil, and, to a lesser extent, nifedipine have achieved prominence recently and are classified, largely on the basis of electrophysiological evidence in cardiac preparations, as specific calcium channel antagonists (55, 56, 73–75). At 10^{-6}–10^{-8} M, these agents produce a selective antagonism of the slow calcium current with minimal effect on the fast sodium current and thus produce electromechanical decoupling of the heart in the activity sequence nifedipine > methoxyverapamil > verapamil (56, 74, 76–79). The effects of these agents are overcome by increased extracellular calcium.

Because of the high activity and apparent selectivity of action of these agents, their activity in other calcium-utilizing systems can be viewed as evidence that basically similar slow calcium channels are operative in secretory and mechanical processes (57). A complete characterization of the calcium current is not available for many of these processes. However, the similar activities of these antagonists in cardiac and smooth muscle and secretory systems certainly indicate a common basis of action. In a few preparations, widely different activities have been noted according to the stimulus employed; this finding is probably indicative of different modes of calcium translocation. Thus, in rabbit mesenteric artery, verapamil is ~1000 times more active against K^+ than against norepinephrine-induced contractions, suggesting that norepinephrine and K^+ employ principally intracellular and extracellular calcium sources, respectively (80). In contrast, K^+ and muscarinic receptor-induced contractions of guinea pig ileal longitudinal smooth muscle appear, as judged by antagonist activities, to employ identical calcium translocation mechanisms.

Where kinetic evidence is available, verapamil, methoxyverapamil, and nifedipine appear to act noncompetitively against agonists and competitively against calcium. An exceptional situation apparently exists in cardiac tissue where the effects of these agents can be overcome by increasing extracellular calcium and by catecholamines (55, 56, 74) so that a competitive relationship appears to exist also between β-agonists and the calcium antagonists (81, 82). A likely explanation is that the action of catecholamines at the cardiac β-receptor is to increase the available calcium channels, perhaps by a cyclic adenosine monophosphate-dependent mechanism (83). Nifedipine, which shows no apparent structural similarity to verapamil or methoxyverapamil, appears to behave similarly.

There is no question but that verapamil, methoxyverapamil, and nifedipine act as potent antagonists of the slow inward calcium current. There is also evidence that these agents may have important effects on other ionic processes. Verapamil and methoxyverapamil, at the fairly high concentrations used in the squid axon (2×10^{-4} M), do reduce the fast Na^+ current; in cardiac fibers, these agents also appear to have some effect on both the Na^+ and K^+ currents (84, 85). However, some part of their effects on K^+ currents probably is due to the dependence of the latter on calcium entry (86).

Whether nifedipine, which is generally assumed to be a calcium channel antagonist acting similarly to verapamil and methoxyverapamil but of higher activity, shares all of the actions of verapamil and methoxyverapamil is not fully established. However, nifedipine does exert a greater depressant effect on the guinea pig atria with increasing stimulus frequency, suggesting that it also modifies the kinetics of the calcium restitution processes (87). That compounds of such differing structure as verapamil and nifedipine exert similar effects on both the calcium permeation and restitution processes is perhaps suggestive that both processes are controlled through interaction at a common site.

EXCITATION–CONTRACTION COUPLING IN SMOOTH MUSCLE

The source of calcium utilized in smooth muscle excitation–contraction coupling remains ill-defined since, unlike fast skeletal muscle, the smaller less well-developed sarcoplasmic reticulum and slower and more sustained contractile responses of smooth muscle do not impose the dominant demands for an intracellular calcium mobilization–sequestration system that is seen in skeletal muscle. Hence, in smooth muscle, intracellular and extracellular sources of calcium may be utilized in excitation–contraction coupling; the relative usage depends on the tissue, the experimental conditions, and the stimulus (88–93).

Sarcoplasmic reticulum does exist in smooth muscle, and studies (94–96) showed that the amounts vary significantly, being greatest in rabbit main pulmonary artery and least in portal anterior mesenteric vein and taenia coli. A correlation exists between the sarcoplasmic reticulum volume and the ability to sustain contraction in the absence of extracellular calcium. Furthermore, the central and peripheral tubules of sarcoplasmic reticulum are continuous with each other, and the peripheral tubules enjoy a close relationship with the surface membrane in some tissues, suggesting that this arrangement may provide the structural basis for calcium release by the invasion of the action potential (94–98). Calcium-sequestering subcellular fractions have been isolated from several smooth muscles (89, 99–101). However, the quantitative contribution of sarcoplasmic reticulum calcium to excitation–contraction coupling is not established, and it is also clear that there is no obligatory association between electrical and mechanical events for some smooth muscles (94, 97, 102–105). Agonist and antagonist actions are identical or very similar to polarized and depolarized tissues, and excitation–contraction coupling can therefore be independent membrane potential changes.

Attempts to define intracellular or extracellular calcium pools as the source of calcium used in smooth muscle excitation–contraction coupling simply on the basis of dependence of responses on extracellular calcium is of questionable value. Thus, Keatinge (104) showed, for norepinephrine-induced contractions of sheep carotid artery, that a 30-min incubation in calcium-free media left sufficient extracellular calcium to sustain excitation–contraction coupling. Furthermore, in any experiments in which calcium is altered, significant "stabilizing" or "labilizing" actions

occur at the cell membrane level and may profoundly alter membrane excitability (105–108).

Finally, even where tissues do show extreme dependence on extracellular calcium, this does not imply equivalent utilization of extracellular calcium. Studies on guinea pig ileal longitudinal and rat vas deferens, both of which are extremely dependent on extracellular calcium, are illustrative of this fact (109, 110). Comparison of the action of calcium antagonists including La^{3+}, methoxyverapamil, nifedipine, 2-diethylaminoethyl-2,2-diphenyl valerate, and local anesthetics revealed significant differences in their activities in these two tissues. It was concluded: "that although qualitative similarities are apparent with respect to the dependence of agonist-induced activity in both the guinea pig ileum and rat vas deferens it is clear that calcium translocation processes in these two tissues, as examined by the use of a variety of calcium antagonists" are both tissue and agonist selective (110). The calcium ionophore A-23187 produces contractile responses in the guinea pig ileal but not in the rat vas deferens smooth muscle (111). Clearly, differences in calcium utilization are involved in these two smooth muscles which, however, show an equal apparent dependence on extracellular calcium.

It has been suggested that the lanthanide cations may provide a method for distinguishing between intracellular and extracellular calcium use (112–116) on the basis that the similar ionic radius of La^{3+} and calcium and the higher charge density of La^{3+} will enable it to replace calcium influx and efflux. If these assumptions are correct (53, 96, 117), then the use of La^{3+} may permit a qualitative diagnosis of intracellular *versus* extracellular calcium use. Moreover, because La^{3+} is presumed to displace the superficial, rapidly exchangeable calcium and prevent calcium flux, it can be used to "trap" intracellular calcium and, hence, to obtain a quantitative estimate of any change in intracellular calcium occurring during excitation–contraction coupling. Thus, in guinea pig ileal longitudinal muscle, phasic and tonic components of the acetylcholine- and K^+-induced responses are equally (and highly) sensitive to La^{3+}, suggesting that a similar or identical calcium source is involved (53). In rat uterus, acetylcholine responses are significantly more resistant than K^+ responses (115). In rabbit aorta, La^{3+} abolishes the slow phase of the norepinephrine response but leaves the fast phase unchanged (114, 115), suggesting that extracellular and intracellular calcium components are utilized, respectively.

The "lanthanum method" has also been used to determine quantitatively extracellular calcium uptake during excitation–contraction coupling. Thus, in rabbit aorta, Van Breemen *et al.* (114) showed that there were parallel changes in tension development and intracellular calcium content during K^+ or Li^+ stimulation but only after the complicating effects of extracellular calcium exchange had been eliminated by La^{3+} treatment.

Although progress is being made in the delineation of the relative use of intracellular and extracellular calcium in smooth muscle excitation–contraction coupling, the mechanisms by which drug–receptor interactions are linked to calcium mobilization are poorly understood. Several mechanisms must be considered:

1. Coupling of membrane potential changes to calcium release from sarcoplasmic reticulum. This may be regarded as some equivalent of skeletal muscle excitation–contraction coupling and may also include an influx of "trigger" calcium that initiates an intracellular calcium release.
2. Direct entry of calcium through action potentials that totally or partially use calcium as the current-carrying species.
3. Mobilization of calcium (intracellular or extracellular) by potential-independent changes, *i.e.*, the pharmacomechanical coupling of Somlyo and Somlyo (94, 97).
4. Influx of calcium through intracellular sodium–extracellular calcium exchange processes.

These processes are not mutually exclusive, and it is entirely possible that their combinations are used in a given smooth muscle. Additionally, it is obviously necessary to consider the roles of cyclic adenosine monophosphate and cyclic guanosine monophosphate because of their well-described relationships to receptor processes, notably to adrenergic (α and β) and cholinergic (muscarinic) processes (*cf.*, 118–121), and because of the mutual interrelationship of calcium and the cyclic nucleotides in many systems (122, 123). Increasing evidence suggests that the cyclic nucleotides may, through their activation of protein kinase, control membrane phosphorylation and that this may serve to control ion permeabilities (124, 125).

Finally, a comment must be made on the possible role of calcium as a component of membrane receptors such that agonist displacement of the calcium serves to labilize the membrane and initiate excitatory events and enhanced calcium binding serves to stabilize the membrane. Some implications of this proposal were considered previously (53, 108, 126).

As noted previously, calcium entry through specific calcium channels is one source of calcium for excitation–contraction coupling in smooth muscle. The guinea pig ileal longitudinal smooth muscle represents one such system (53, 126–128). This tissue is very sensitive to extracellular calcium for both K^+ and acetylcholine responses, and both responses are equally sensitive to La^{3+}, methoxyverapamil, and nifedipine.

Calcium 45 uptake has been measured by the "lanthanum procedure" and is equally sensitive to the calcium antagonists as the mechanical responses. A 1:1 relationship was found for calcium uptake and mechanical response and, in a series of muscarinic agonists and partial agonists, decreased calcium uptake was associated with partial agonists. The guinea pig ileal longitudinal smooth muscle is sensitive to stimulants including K^+, acetylcholine, and histamine, and the responses are all equally sensitive to the calcium antagonists methoxyverapamil and nifedipine. This finding suggests that several stimulants serve to activate a common pool of calcium channels.

Much of the reviewed material with respect to smooth muscle physiology and pharmacology may be relevant to calcium-ion involvement in chemical mediator releasing systems.

CALCIUM AND CHEMICAL MEDIATOR RELEASE

Lichtenstein's studies (129) with the basophil system indicated that the release reaction can be divided into two stages: first, an antigen-dependent, calcium-independent stage, and second, an antigen-independent, calcium-dependent stage. The agents affecting histamine release *via* increased accumulation of cyclic adenosine monophosphate appear to act only in the first stage whereas agents affecting microtubule function (colchicine and deuterium oxide) act in the calcium-dependent second stage.

Further investigation (130) of the mechanism of mediator release from chopped human lung revealed an additional edetic (ethylenediaminetetraacetic) acid-inhibitable, calcium-dependent step beyond the initial immunological stimulation of (presumed) increased permeability of the cell membrane to calcium and ingress of calcium ions. The experiments of Kaliner and Austen (130) also disclosed that isoproterenol increased cyclic adenosine monophosphate concentrations and prevented the observed calcium reversal of edetic acid inhibition of mediator release, suggesting that the second calcium-dependent step might relate to the action of a contractile protein susceptible to inhibition by phosphorylation by the cyclic adenosine monophosphate-dependent protein kinase system (130). In this connection, it is important to recall that calcium plays a critical role in the control of intracellular cyclic adenosine monophosphate and cyclic guanosine monophosphate concentrations through its ability to inhibit adenyl cyclase (14), stimulate guanyl cyclase (15), and control the phosphodiesterase regulator protein (16).

The most familiar pathophysiological stimulus to the mast cell is the antigen–antibody reaction, which leads to the release of histamine and other substances. In 1958, Mongar and Schild (7) observed that calcium was essential for this response. When it became apparent that calcium influx also mediated the effect of the physiological stimulus to adrenal chromaffin cell catecholamine release, Douglas (131) suggested that the role of calcium in immunological mast cell activation might be similar, namely, to act as a coupling agent between stimulus and response. Later, Douglas (132) cited the mast cell as an example of a class of secretory cells using calcium influx to activate exocytosis. Indeed, the microinjection of calcium ions into mast cells caused granule exocytosis (8).

The calcium inophore A-23187 also stimulates mediator release in rat mast cells (133) and human basophils (134). Comparisons of immunological and ionophore-induced mediator release from basophils have been made. Ionophore and antigen-stimulated histamine release in human basophils differ in several respects (134): the kinetics and total quantity of histamine released are different, depending on the concentrations of antigen or ionophore (with low antigen concentrations producing a slower rate and less total histamine release but low ionophore concentrations producing delayed onset but rapid and essentially complete histamine release); antigen-desensitized basophils release histamine with ionophore; cyclic adenosine monophosphate or agents that stimulate increased cyclic adenosine monophosphate concentrations do not reduce ionophore-induced histamine release as with antigen-induced release; the microtubule-active agents colchicine and deuterium oxide inhibit and augment ionophore-induced release, respectively, but quantitatively less so as compared to antigen-stimulated release; and the calcium antagonist lanthanum inhibits both processes, but the ionophore effect is slightly more sensitive. Thus, ionophore and antigen appear to share certain as-

pects of the codependent biochemical mechanisms involved in histamine release but clearly differ in some respects (134). The specific calcium channel(s) involved, their topography in relationship to the cell surface immunological event, and the mechanisms of opening and closing the calcium channels involved in immunological or ionophore-stimulated mediator release remain unknown.

The calcium antagonist lanthanum produces significant inhibition of histamine release not only in basophils but also in mast cells (135) following immunological challenge. Based on a series of experiments, Foreman and Mongar (*cf.*, 136) concluded that mast cell activation (by several different mechanisms) is accompanied by calcium uptake that is temporally and quantitatively related to histamine release, suggesting that the trigger to histamine release from mast cells is an increased mast cell membrane permeability to calcium and an influx of calcium ions to the intracellular compartment. In the stimulated cell, it is supposed that the equilibrium between "open" and "closed" calcium channels is shifted in favor of open, allowing increased influx of calcium, the magnitude of which determines the degree of histamine secretion. In their model, Foreman and Mongar (136) considered that cyclic adenosine monophosphate has an effect that closes calcium channels and reduces calcium influx.

The recent experiments of Payne (137) on histamine release in the rat mast cell system concerned the effects of quercitin, dantrolene sodium, and 8-(*N,N*-diethylamino)-octyl-3,4,5-trimethoxybenzoate, all calcium antagonists (137). Quercitin and a small number of other flavones of plant origin recently were shown to inhibit histamine release by immunological and nonimmunological stimuli (but no ionophore) (138). Flavones are chemically related to cromolyn sodium; it was suggested that they act similarly by interfering with the normal path of calcium entry into stimulated mast cells. Like quercitin, dantrolene sodium (130) and 8-(*N,N*-diethylamino)-octyl-3,4,5-trimethoxybenzoate (140) have been reported to interfere with calcium translocations. Dantrolene sodium is a peripherally acting smooth muscle relaxant thought to prevent intracellular mobilization of calcium. 8-(*N,N*-Diethylamino)-octyl-3,4,5-trimethoxybenzoate is an aliphatic reserpine analog, which has also been suggested to act as an intracellular calcium antagonist based on its inhibitory effects on smooth muscle contraction (140).

Payne's results (137) indicated that histamine release by compound 48/80 from peritoneal and pleural rat mast cells was inhibited in a concentration-dependent manner by quercitin, which also inhibited dextran-induced histamine release. Dantrolene sodium inhibited histamine release by either compound 48/80 or dextran whereas it produced only weak inhibition of histamine release induced by the calcium ionophore A-23187. On the other hand, histamine release by dextran and ionophore A-23187 was strongly inhibited by 8-(*N,N*-diethylamino)-octyl-3,4,5-trimethoxybenzoate. The results were interpreted to suggest that quercitin, dantrolene sodium, and 8-(*N,N*-diethylamino)-octyl-3,4,5-trimethoxybenzoate may act at different sites to inhibit calcium translocations required for histamine release. Also, Barrett-Bee (141) found that the calcium antagonist cinnarizine inhibited antigen-induced histamine release (50%) in the rat mast cell system.

SUMMARY

Asthma may be considered to be a calcium-dependent disease by virtue of the dependency of excitation–contraction coupling in smooth muscle, stimulus–secretion coupling in mast cells and mucous glands, and vagal nerve activity on the availability of increased cytoplasmic calcium-ion concentrations. The nature and regulation of the calcium channels or pathways involved in various cell types are unknown. Whether the increased responsiveness of the relevant cells in asthma is characterized by increased ease of calcium influx, release from intracellular storage sites, or decreased calcium sequestration mechanisms in the plasma membrane or intracellular organelles is a subject for future research.

Effective antiasthmatic therapy must act finally to reduce availability of cytoplasmic calcium to excitation–contraction, stimulus–secretion, and nerve activation systems. Many effective drugs presumably act in this fashion, but the mechanisms are poorly understood.

It is possible that new calcium antagonists could be synthesized that would inhibit calcium influx or intracellular calcium movements in airway smooth muscle, mast cells, mucous glands, and vagus nerve and that might prove of value in asthma treatment.

REFERENCES

(1) K. F. Austen and R. P. Orange, *Am. Rev. Resp. Dis.*, **112,** 423 (1975).

(2) K. F. Austen, in "Immunological Diseases," 3rd ed., M. Santer, Ed., Little, Brown, Boston, Mass., 1978, p. 183.

(3) T. J. Sullivan and C. W. Parker, *Am. J. Pathol.*, **85,** 437 (1976).

(4) M. Kaliner and K. F. Austen, *Biochem. Pharmacol.*, **23,** 763 (1974).

(5) R. G. Coffey and E. Middleton, Jr., in "Comprehensive Immunology, Part III: Immunopharmacology," J. W. Hadden, R. G. Coffey, and F. Spreafico, Eds., Plenum, New York, N.Y., 1977, p. 203.

(6) M. Plaut and L. M. Lichtenstein, in "Allergy: Principles and Practice," E. Middleton, Jr., C. E. Reed, and E. F. Ellis, Eds., Mosby, St. Louis, Mo., 1978, p. 115.

(7) J. L. Mongar and H. O. Schild, *J. Physiol.*, **140,** 272 (1958).

(8) T. Kanno, D. E. Cochrane, and W. W. Douglas, *Can. J. Physiol. Pharmacol.*, **51,** 1001 (1973).

(9) K. Ishizaka and T. Ishizaka, in "Allergy: Principles and Practice," E. Middleton, Jr., C. E. Reed, and E. F. Ellis, Eds., Mosby, St. Louis, Mo., 1978, p. 52.

(10) T. Ishizaka and K. Ishizaka, *J. Immunol.*, **120,** 800 (1978).

(11) R. A. Lewis and K. F. Austen, *Fed. Proc. Fed. Am. Soc. Exp. Biol.*, **36,** 2676 (1977).

(12) H. R. Colten and K. H. Gabbay, *J. Clin. Invest.*, **51,** 1972 (1972).

(13) M. Kaliner, *J. Allergy Clin. Immunol.*, **60,** 204 (1977).

(14) G. A. Robison, R. W. Butcher, and E. W. Suterland, "Cyclic AMP," Academic, New York, N.Y., 1971, p. 81.

(15) G. Schultz, in "Asthma: Physiology, Immunopharmacology and Treatment," K. F. Austen and L. M. Lichtenstein, Eds., Academic, New York, N.Y., 1978, p. 77.

(16) C. O. Brostorm, Y. Huang, B. M. Breckenridge, and D. J. Wolff, *Proc. Natl. Acad. Sci. USA*, **72,** 64 (1975).

(17) D. W. Empey, W. A. Laitinen, L. Jacobs, W. M. Gold, and J. A. Nadel, *Am. Rev. Resp. Dis.*, **113,** 131 (1976).

(18) J. A. Nadel, in "Asthma: Physiology, Immunopharmacology and Treatment," K. F. Austen and L. M. Lichtenstein, Eds., Academic, New York, N.Y., 1973, p. 29.

(19) J. A. Nadel, *Am. Rev. Resp. Dis.*, **115,** 117 (1977).

(20) W. M. Gold, *Postgrad. Med. J., Suppl. 7,* **51,** 53 (1975).

(21) W. M. Gold, in "Allergy: Principles and Practice," E. Middleton, Jr., C. E. Reed, and E. F. Ellis, Eds., Mosby, St. Louis, Mo., 1978, p. 499.

(22) R. Patterson, J. C. McKenna, I. M. Suszko, N. H. Solliday, J. J. Pruzansky, M. Roberts, and T. J. Kehoe, *J. Clin. Invest.*, **59,** 217 (1977).

(23) A. Szentivanyi, *J. Allergy,* **42,** 203 (1968).

(24) C. E. Reed and R. G. Townley, in "Allergy: Principles and Practice," E. Middleton, Jr., C. E. Reed, and E. F. Ellis, Eds., Mosby, St. Louis, Mo., 1978, p. 659.

(25) C. W. Parker, in "Asthma: Physiology, Immunopharmacology and Treatment," K. F. Austen and L. M. Lichtenstein, Eds., Academic, New York, N.Y., 1973, p. 185.

(26) E. Middleton, Jr., *Adv. Intern. Med.*, **18,** 177 (1972).

(27) R. G. Coffey and E. Middleton, Jr., in "Comprehensive Immunology, Part III: Immunopharmacology," J. W. Hadden, R. G. Coffey, and F. Spreafico, Eds., Plenum, New York, N.Y., 1977, p. 203.

(28) K. Raij, K. Alanko, A. Muittari, and M. Harkonen, *Scand. J. Resp. Dis.*, **57,** 223 (1976).

(29) M. E. Connolly and J. K. Greenacre, *J. Clin. Invest.*, **58,** 1307 (1976).

(30) H. S. Nelson, J. W. Black, L. B. Branch, B. Pfuetze, H. Spauling, R. Summers, and D. Wood, *J. Allery Clin. Immunol.*, **55,** 299 (1975).

(31) H. G. Morris, S. A. Rusnak, J. C. Selner, and J. Barnes, *Chest, June Suppl.*, **73,** 973 (1978).

(32) A. Kalisker, H. E. Nelson, and E. Middleton, Jr., *J. Allergy Clin. Immunol.*, **60,** 259 (1977).

(33) W. W. Busse, *Am. Rev. Resp. Dis.*, **115,** 783 (1977).

(34) R. K. Bush, W. W. Busse, D. K. Flaherty, D. Warshauer, E. C. Dick, and C. E. Reed, *J. Allergy Clin. Immunol.*, **61,** 80 (1978).

(35) G. A. Rinard, A. R. Rubinfeld, L. L. Brunton, and S. E. Mayer, *Proc. Natl. Acad. Sci. USA*, **76,** 1472 (1979).

(36) M. Rodbell, M. C. Lin, Y. Salmon, C. Londos, J. P. Harwood, B. R. Martin, M. Rendell, and M. Berman, *Acta Endocrinol., Suppl. 191,* **77,** 11 (1974).

(37) T. Pfeuffer and E. J. M. Helmreich, *J. Biol. Chem.*, **250,** 867 (1975).

(38) D. Cassel and Z. Selinger, *Biochim. Biophys. Acta,* **452,** 538 (1976).

(39) J. Richardson and T. Bouchard, *J. Allergy Clin. Immunol*, **56**, 473 (1975).
(40) J. Richard and J. Beland, *J. Appl. Physiol.*, **41**, 764 (1976).
(41) B. G. Simonsson, R. Andersson, N. P. Bergh, B. E. Skoogh, and N. Svedmyr, in "Bronchitis III," N. G. M. Orie and R. Van Der Lende, Eds., Charles C Thomas, Springfield, Ill., 1970, p. 334.
(42) C. J. Duncan, "Symposium of the Society for Experimental Biology, XXX," Cambridge University Press, Cambridge, England, 1976.
(43) R. H. Kretsinger, *Chem. Rev.*, **18**, 29 (1976).
(44) P. F. Baker, *Progr. Biophys. Mol. Biol.*, **24**, 177 (1972).
(45) M. P. Blaustein, *Rev. Physiol. Biochem. Pharmacol.*, **70**, 33 (1974).
(46) H. Rueter, *Progr. Biophys. Mol. Biol.*, **26**, 1 (1973).
(47) A. L. Lehninger, *Suppl. III, Circ. Res.*, **1974**, 83.
(48) E. Carafoli and M. Crampton, "Symposium of the Society for Experimental Biology, XXX," Cambridge University Press, Cambridge, England, 1976.
(49) D. H. MacLennan and P. C. Holland, *Ann. Rev. Biophys. Bioeng.*, **4**, 377 (1975).
(50) E. Carafoli, F. Clementi, W. Drabikowski, and A. Margreth, "Calcium Transport in Contraction and Secretion," North-Holland Amsterdam, The Netherlands, 1975.
(51) A. L. Hodgkin and A. F. Huxley, *J. Physiol. (London)*, **117**, 500 (1952).
(52) S. Hagiwara, in "Dynamic Properties of Lipid Membranes and Bilayers," vol. 3, G. Eisenman, Ed., Dekker, New York, N.Y., 1975.
(53) D. J. Triggle and C. R. Triggle, "Chemical Pharmacology of the Synapse," Academic, New York, N.Y., 1976, chap. IV.
(54) B. Hille, *Progr. Biophys. Mol. Biol.*, **21**, 1 (1970).
(55) A. Fleckenstein, in "Calcium and the Heart," P. Harris and L. H. Opie, Eds., Academic, New York, N.Y., 1971, p. 135.
(56) A. Fleckenstein, *Arzneim.-Forsch.*, **22**, 2019 (1972).
(57) L. Rosenberger and D. J. Triggle, in "Calcium in Drug Action," G. B. Weiss, Ed., Plenum, New York, N.Y., 1978, p. 3.
(58) S. S. Jafferji and R. H. Michell, *Biochem. J.*, **154**, 653 (1976).
(59) *Ibid.*, **160**, 397 (1976).
(60) *Ibid.*, **160**, 163 (1976).
(61) A. Fleckenstein, *Annu. Rev. Pharmacol, Toxicol.*, **17**, 149 (1977).
(62) M. F. Piascik, R. G. Rahwan, and D. T. Witiak, *J. Pharmacol. Exp. Ther.*, **205**, 155 (1978).
(63) R. G. Rahwan, M. M. Faust, and D. T. Witiak, *ibid.*, **201**, 126 (1977).
(64) J. P. Girard and M. Cuevas, *Allergol..Immunopathol., Suppl. V*, **1977**, 13.
(65) U. Martin and D. Roemer, *ibid.*, **1977**, 5.
(66) B. Pourrias and F. Friedrich, *Eur. J. Pharmacol.*, **49**, 203 (1978).
(67) J. M. Diamond and E. M. Wright, *Annu. Rev. Physiol.*, **31**, 581 (1969).
(68) R. J. P. Williams, *Q. Rev. Chem. Soc.*, **24**, 331 (1970).
(69) P. F. Baker and H. G. Glitsch, *Phil. Trans. R. Soc. London Ser. B.*, **270**, 389 (1975).
(70) R. Ochi, *J. Physiol. (London)*, **263**, 139 (1976).
(71) E. Nieboer, *Struc. Bonding*, **22**, 1 (1975).
(72) R. B. Mikkelsen, in "Biological Membranes," D. Chapman and D. F. H. Wallach, Eds., Academic, New York, N.Y., 1976, p. 153.
(73) A. Fleckenstein, *Adv. Cardiol.*, **12**, 183 (1974).
(74) A. Fleckenstein, in "New Therapy of Ischemic Heart Disease," W. Lochner, Ed., Springer, Berlin, Germany, 1976, p. 56.
(75) A. Fleckenstein, H. Tritthart, H. J. Doring, and K. Y. Byon, *Arzneim.-Forsch.*, **22**, 22 (1972).
(76) M. Kohlardt, B. Bauer, H. Krause, and A. Fleckenstein, *Pfluegers Arch.*, **335**, 309 (1972).
(77) *Ibid.*, **338**, 115 (1973).
(78) M. Kohlardt, A. Herdey, and M. Kubler, *ibid.*, **344**, 149 (1973).
(79) H. Tritthart, R. Volkman, R. Weiss, and A. Fleckenstein, *Naunyn-Schmeidebergs Arch. Pharmacol.*, **280**, 239 (1973).
(80) H. J. Schuman, B. D. Gorlitz, and J. Wager, *ibid.*, **289**, 409 (1975).
(81) B. D. Gorlitz, J. Wagner, and H. Schuman, *ibid.*, **283**, 311 (1975).
(82) M. Endoh, J. Wagner, and H. J. Schuman, *ibid.*, **287**, 61 (1975).
(83) H. Reuter and H. Scholz, *J. Physiol. (London)*, **264**, 17 (1977).
(84) P. F. Cranefield, R. S. Aronson, and A. L. Wit, *Circ. Res.*, **34**, 204 (1974).
(85) R. S. Kass and R. W. Tsien, *J. Gen. Physiol.*, **66**, 169 (1975).
(86) J. B. Bassingthwaighte, C. H. Fry, and J. A. S. McGuigan, *J. Physiol. (London)*, **262**, 15 (1976).
(87) K. Baumann, *Naunyn-Schmiedebergs Arch. Pharmacol.*, **294**, 161 (1976).
(88) E. E. Daniel, in "Muscle," Pual, Danile, and Monckton, Eds., Oxford University Press, New York, N.Y., 1965.
(89) L. Hurwitz and A. Suria, *Annu. Rev. Pharmacol.*, **11**, 303 (1971).
(90) D. J. Triggle, "Neurotransmitter-Receptor Interactions," Academic, New York, N.Y., 1971.
(91) D. J. Triggle, *Prog. Surf. Mem. Sci.*, **5**, 267 (1972).
(92) T. Tomita, *Prog. Biophys. Mol. Biol.*, **30**, 185 (1975).
(93) E. E. Daniel and R. A. Janis, *Pharmacol. Ther. B.*, **1**, 695 (1975).
(94) A. V. Somlyo and A. P. Somlyo, *Science*, **174**, 1955 (1971).
(95) C. E. Devine, A. V. Somlyo, and A. P. Somlyo, *J. Cell Biol.*, **52**, 690 (1972).
(96) C. E. Devine, A. V. Somlyo, and A. P. Somlyo, *Phil. Trans. Roy. Soc. London B*, **265**, 17 (1973).
(97) A. V. Somlyo and A. P. Somlyo, *J. Pharmacol. Exp. Ther.*, **159**, 129 (1968).
(98) A. P. Somlyo and A. V. Somlyo, in "Methods in Pharmacology," vol. 3, E. E. Daniel and D. M. Paton, Eds., Plenum, New York, N.Y., 1975, pp. 3–45.
(99) D. F. Fitzpatrick, E. J. Landon, G. Debbes, and L. Hurwitz, *Science*, **176**, 305 (1972).
(100) M. L. Hess and G. D. Ford, *J. Mol. Cell Cardiol.*, **6**, 275 (1974).
(101) R. C. Webb and R. C. Bhalla, *ibid.*, **8**, 145 (1976).
(102) K. A. P. Edman and H. O. Schild, *J. Physiol.*, **169**, 404 (1963).
(103) J. Axelsson, in "Smooth Muscle," E. Bulbring, A. F. Brading, A. W. Jones, and T. Tomita, Eds., Williams & Wilkens, Baltimore, Md., 1970.
(104) W. R. Keatinge, *J. Physiol.*, **224**, 21 (1972).
(105) D. J. Triggle and C. R. Triggle, "Chemical Pharmacology of the Synpase," Academic, New York, N.Y., 1976.
(106) B. Frenkenhaeuser and A. L. Hodgkin, *J. Physiol. (London)*, **137**, 218 (1957).
(107) A. M. Shanes, *Pharmacol. Rev.*, **10**, 59 (1958).
(108) D. J. Triggle, *Annu. Rev. Pharmacol.*, **12**, 185 (1972).
(109) C. R. Triggle and D. J. Triggle, *J. Physiol.*, **254**, 39 (1976).
(110) C. R. Triggle, V. C. Swamy, and D. J. Triggle, *Can. J. Physiol. Pharmacol.*, in press.
(111) V. C. Swamy, M. Ticku, C. R. Triggle, and D. J. Triggle, *ibid.*, **53**, 1108 (1975).
(112) M. Takata, W. F. Pickard, J. Y. Lettvin, and J. W. Moore, *J. Gen. Physiol.*, **50**, 461 (1966).
(113) C. Van Breemen, *Arch. Int. Physiol. Biochim.*, **77**, 710 (1969).
(114) C. Van Breemen, B. R. Farinas, P. Gerba, and E. McNaughton, *Circ. Res.*, **30**, 44 (1972).
(115) C. Van Breemen, B. R. Farinas, R. Casteels, P. Gerba, R. Wuytack, and R. Deth, *Phil. Trans. Roy. Soc. B*, **265**, 57 (1973).
(116) G. B. Weiss, *Annu. Rev. Pharmacol.*, **14**, 343 (1974).
(117) B. J. Hodgson, A. M. Kidwai, and E. E. Daniel, *Can. J. Physiol. Pharmacol.*, **50**, 730 (1972).
(118) R. G. G. Andersson, *Acta Physiol. Scand. Suppl.*, **1972**, 382.
(119) H. P. Bar, *Adv. Cyclic Nucleotides Res.*, **4**, 174 (1974).
(120) T. P. Lee, J. F. Kuo, and P. Greengard, *Proc. Natl. Acad. Sci. USA*, **69**, 3817 (1972).
(121) G. Schultz and J. G. Hardman, *Adv. Cyclic Nucleotide Res.*, **5**, 339 (1975).
(122) H. Rasmussen, *Science*, **170**, 404 (1971).
(123) M. J. Berridge, *Adv. Cyclic Nucleotide Res.*, **6**, 1 (1975).
(124) P. Greengard, *ibid.*, **5**, 582 (1975).
(125) P. Greengard, *Nature*, **260**, 101 (1976).
(126) K. J. Chang and D. J. Triggle, in "Membranes in Metabolic Regulation," M. Mehlmann, Ed., Academic, New York, N.Y., 1973.
(127) M. Ticku and D. J. Triggle, *Gen. Pharmacol.*, **7**, 133 (1976).
(128) L. Rosenberg, M. Ticku, and D. J. Triggle, *Can. J. Physiol. Pharmacol.*, **57**, 333 (1979).
(129) L. M. Lichtenstein, *J. Immunol.*, **107**, 1122 (1971).
(130) M. Kaliner and K. F. Austen, *J. Exp. Med.*, **138**, 1077 (1973).

(131) W. W. Douglas, in "Calcium Transport in Contraction and Secretion," E. Carafoli, F. Clementi, W. Drabikowski, and A. Margreth, Eds., American Elsevier, New York, N.Y., 1975, p. 167.
(132) W. W. Douglas, *Br. J. Pharmacol.*, **34**, 451 (1968).
(133) J. C. Foreman, J. L. Mongar, and B. D. Gomperts, *Nature*, **245**, 249 (1973).
(134) L. M. Lichtenstein, *J. Immunol.*, **114**, 1692 (1975).
(135) J. C. Foreman and J. L. Mongar, *Br. J. Pharmacol.*, **48**, 527 (1973).
(136) J. C. Foreman and J. L. Mongar, in "Calcium Transport in Contraction and Secretion," E. Carafoli, F. Clementi, W. Drabikowski, and A. Margreth, Eds., American Elsevier, New York, N.Y., 1975, p. 175.
(137) A. Payne, Ph.D. thesis, London University, London, England, 1978, chap. 8.
(138) C. M. S. Fewtrell and B. D. Gomperts, *Biochim. Biophys. Acta*, **469**, 52 (1977).
(139) K. G. Morgan and S. H. Bryant, *J. Pharmacol. Exp. Ther.*, **201**, 138 (1977).
(140) M. H. Malagodi and C. Y. Chiou, *Eur. J. Pharmacol.*, **27**, 25 (1974).
(141) K. J. Barrett-Bee, *Biochem. Soc. Trans.*, **5**, 965 (1977).

ACKNOWLEDGMENTS

Presented as part of the Symposium on New Approaches to the Treatment of Asthma at the APhA Academy of Pharmaceutical Sciences, Anaheim meeting, April 1979.

The author gratefully acknowledges many informative and stimulating conversations with Dr. David Triggle regarding the role of calcium in smooth muscle functions.

Clinical Evaluation of Antiallergic Agents

RICHARD R. ROSENTHAL

Received May 4, 1979, from the *School of Medicine, Johns Hopkins University, and the Good Samaritan Hospital, Baltimore, MD 21239.* Accepted for publication September 10, 1979.

Abstract □ Testing methods used to detect antiallergic activity are described for several pharmacological classes of drugs. The pharmacodynamics of each drug determine the type of testing required to detect antiallergic or antiasthmatic activity.

Keyphrases □ Pharmacokinetics—clinical testing in mildly asthmatic human volunteers, dose–response curve of antiallergic drugs □ Antiallergic drugs—pharmacokinetics, various clinical testing procedures in humans, inhibition of mediator release, cyclic adenosine monophosphate levels, potential asthma inhibitors □ β-Adrenoceptor agonists—antiallergic drug testing, bronchiolar smooth muscle, cyclic adenosine monophosphate levels, effects on mediator release □ Asthma—review of current theories, clinical evaluation, symposium, antiallergic drugs

Hypersensitivity involves an allergic reaction that is an immunological event characterized by the release of a chemical mediator, histamine or slow-reacting substance of anaphylaxis, in response to exposure to a foreign antigen. Foreign (environmental) antigens are usually complex protein mixtures such as cat dander or ragweed pollen. Initial antigen exposure results in the elaboration of antibody of the immunoglobulin E class, which, as circulating specific immunoglobulin E antibody, is in equilibrium with cell-fixed immunoglobulin E on circulating basophils or tissue mast cells. When a subsequent environmental antigenic insult occurs, the antigen combines with the cell-fixed immunoglobulin E antibody, whereupon histamine and other chemical mediators are released to act directly on target tissue. Accordingly, the characteristic allergic reactions seen in asthma, rhinitis, urticaria, and even systemic anaphylaxis reflect the anatomic sites where histamine and other chemical mediators are released as well as their respective tissue responses.

DISCUSSION

Histamine release induced by antigen can be modified by drugs that act on various stages within the release mechanism. For example, the β-agonists, isoproterenol, ephedrine, metaproterenol, and terbutaline, activate adenyl cyclase to increase intracellular levels of cyclic adenosine monophosphate, an enhancement that prevents histamine release. Because phosphodiesterase catalyzes the conversion of cyclic adenosine monophosphate to 5′-adenosine monophosphate, inhibition of this enzyme by drugs such as the xanthines (theophylline) arrests the breakdown of cyclic adenosine monophosphate, thereby preventing histamine release.

Cromolyn sodium is the prototype of a new class of compounds that act presumably by preventing mediator release, although the exact mechanism of action is unknown. The anti-inflammatory steroids appear to stabilize the mast cell membrane and also enhance β-receptor sensitivity. The prostaglandins not only influence intracellular cyclic adenosine monophosphate but also may prevent mediator release, whereas prostaglandin synthetase inhibitors may regulate allergic hypersensitivity reactions in either direction. At the cellular level, α-agonists (phenylephrine) and cholinergic agonists (acetylcholine) may increase intracellular cyclic guanosine monophosphate by stimulating guanyl cyclase and enhancing histamine release. On the basis of experimental evidence, α-blockers and cholinergic antagonists may have some usefulness as antiallergic agents.

The classical antihistamines, exemplified by diphenhydramine, compete with histamine at H_1-receptor sites to allay allergic reactions. This group has a new member with different pharmacological attributes, the H_2-receptor antagonist cimetidine, which blocks gastric acid secretion. Although this kind of blockade has not previously been associated with allergy treatment, preliminary studies suggest that H_1- and H_2-blockers in combination may be effective against urticaria (1–3). Drugs that alter the immune response also may be considered antiallergic. Ragweed extract or denatured antigens can raise the protective immunoglobulin G antibody titers and reduce the severity of an allergic reaction.

A number of clinical testing procedures can be used to evaluate new antiallergic medications. The inhalation challenge method elicits an asthmatic attack under laboratory conditions, enabling a test drug to be evaluated (4). In this technique, mildly asthmatic volunteers with near normal pulmonary function inhale graded doses of antagonists such as antigen, methacholine, or histamine, using a specialized inhalation dosing apparatus, the inhalation dosimeter. Spirometry and specific airway conductance are monitored, and the dose–response curves to the inhaled antagonists indicate patient sensitivity.

The provocation dose, defined as the amount of antagonist causing a 20% fall in forced expiratory volume in 1 sec, is interpolated from the dose–response curve and used as a reproducible index of patient sensitivity to the inhalant.

A change in the dose–response curve or a shift of the provocation dose toward a higher antigen requirement indicates an alteration of antigen sensitivity. By this procedure, antiasthma agents can be evaluated for

0022-3549/80/0200-0251$01.00/0
© 1980, American Pharmaceutical Association

(131) W. W. Douglas, in "Calcium Transport in Contraction and Secretion," E. Carafoli, F. Clementi, W. Drabikowski, and A. Margreth, Eds., American Elsevier, New York, N.Y., 1975, p. 167.
(132) W. W. Douglas, *Br. J. Pharmacol.*, **34**, 451 (1968).
(133) J. C. Foreman, J. L. Mongar, and B. D. Gomperts, *Nature*, **245**, 249 (1973).
(134) L. M. Lichtenstein, *J. Immunol.*, **114**, 1692 (1975).
(135) J. C. Foreman and J. L. Mongar, *Br. J. Pharmacol.*, **48**, 527 (1973).
(136) J. C. Foreman and J. L. Mongar, in "Calcium Transport in Contraction and Secretion," E. Carafoli, F. Clementi, W. Drabikowski, and A. Margreth, Eds., American Elsevier, New York, N.Y., 1975, p. 175.
(137) A. Payne, Ph.D. thesis, London University, London, England, 1978, chap. 8.
(138) C. M. S. Fewtrell and B. D. Gomperts, *Biochim. Biophys. Acta*, **469**, 52 (1977).
(139) K. G. Morgan and S. H. Bryant, *J. Pharmacol. Exp. Ther.*, **201**, 138 (1977).
(140) M. H. Malagodi and C. Y. Chiou, *Eur. J. Pharmacol.*, **27**, 25 (1974).
(141) K. J. Barrett-Bee, *Biochem. Soc. Trans.*, **5**, 965 (1977).

ACKNOWLEDGMENTS

Presented as part of the Symposium on New Approaches to the Treatment of Asthma at the APhA Academy of Pharmaceutical Sciences, Anaheim meeting, April 1979.

The author gratefully acknowledges many informative and stimulating conversations with Dr. David Triggle regarding the role of calcium in smooth muscle functions.

Clinical Evaluation of Antiallergic Agents

RICHARD R. ROSENTHAL

Received May 4, 1979, from the *School of Medicine, Johns Hopkins University, and the Good Samaritan Hospital, Baltimore, MD 21239.* Accepted for publication September 10, 1979.

Abstract □ Testing methods used to detect antiallergic activity are described for several pharmacological classes of drugs. The pharmacodynamics of each drug determine the type of testing required to detect antiallergic or antiasthmatic activity.

Keyphrases □ Pharmacokinetics—clinical testing in mildly asthmatic human volunteers, dose–response curve of antiallergic drugs □ Antiallergic drugs—pharmacokinetics, various clinical testing procedures in humans, inhibition of mediator release, cyclic adenosine monophosphate levels, potential asthma inhibitors □ β-Adrenoceptor agonists—antiallergic drug testing, bronchiolar smooth muscle, cyclic adenosine monophosphate levels, effects on mediator release □ Asthma—review of current theories, clinical evaluation, symposium, antiallergic drugs

Hypersensitivity involves an allergic reaction that is an immunological event characterized by the release of a chemical mediator, histamine or slow-reacting substance of anaphylaxis, in response to exposure to a foreign antigen. Foreign (environmental) antigens are usually complex protein mixtures such as cat dander or ragweed pollen. Initial antigen exposure results in the elaboration of antibody of the immunoglobulin E class, which, as circulating specific immunoglobulin E antibody, is in equilibrium with cell-fixed immunoglobulin E on circulating basophils or tissue mast cells. When a subsequent environmental antigenic insult occurs, the antigen combines with the cell-fixed immunoglobulin E antibody, whereupon histamine and other chemical mediators are released to act directly on target tissue. Accordingly, the characteristic allergic reactions seen in asthma, rhinitis, urticaria, and even systemic anaphylaxis reflect the anatomic sites where histamine and other chemical mediators are released as well as their respective tissue responses.

DISCUSSION

Histamine release induced by antigen can be modified by drugs that act on various stages within the release mechanism. For example, the β-agonists, isoproterenol, ephedrine, metaproterenol, and terbutaline, activate adenyl cyclase to increase intracellular levels of cyclic adenosine monophosphate, an enhancement that prevents histamine release. Because phosphodiesterase catalyzes the conversion of cyclic adenosine monophosphate to 5′-adenosine monophosphate, inhibition of this enzyme by drugs such as the xanthines (theophylline) arrests the breakdown of cyclic adenosine monophosphate, thereby preventing histamine release.

Cromolyn sodium is the prototype of a new class of compounds that act presumably by preventing mediator release, although the exact mechanism of action is unknown. The anti-inflammatory steroids appear to stabilize the mast cell membrane and also enhance β-receptor sensitivity. The prostaglandins not only influence intracellular cyclic adenosine monophosphate but also may prevent mediator release, whereas prostaglandin synthetase inhibitors may regulate allergic hypersensitivity reactions in either direction. At the cellular level, α-agonists (phenylephrine) and cholinergic agonists (acetylcholine) may increase intracellular cyclic guanosine monophosphate by stimulating guanyl cyclase and enhancing histamine release. On the basis of experimental evidence, α-blockers and cholinergic antagonists may have some usefulness as antiallergic agents.

The classical antihistamines, exemplified by diphenhydramine, compete with histamine at H_1-receptor sites to allay allergic reactions. This group has a new member with different pharmacological attributes, the H_2-receptor antagonist cimetidine, which blocks gastric acid secretion. Although this kind of blockade has not previously been associated with allergy treatment, preliminary studies suggest that H_1- and H_2-blockers in combination may be effective against urticaria (1–3). Drugs that alter the immune response also may be considered antiallergic. Ragweed extract or denatured antigens can raise the protective immunoglobulin G antibody titers and reduce the severity of an allergic reaction.

A number of clinical testing procedures can be used to evaluate new antiallergic medications. The inhalation challenge method elicits an asthmatic attack under laboratory conditions, enabling a test drug to be evaluated (4). In this technique, mildly asthmatic volunteers with near normal pulmonary function inhale graded doses of antagonists such as antigen, methacholine, or histamine, using a specialized inhalation dosing apparatus, the inhalation dosimeter. Spirometry and specific airway conductance are monitored, and the dose–response curves to the inhaled antagonists indicate patient sensitivity.

The provocation dose, defined as the amount of antagonist causing a 20% fall in forced expiratory volume in 1 sec, is interpolated from the dose–response curve and used as a reproducible index of patient sensitivity to the inhalant.

A change in the dose–response curve or a shift of the provocation dose toward a higher antigen requirement indicates an alteration of antigen sensitivity. By this procedure, antiasthma agents can be evaluated for

0022-3549/80/0200-0251$01.00/0
© 1980, American Pharmaceutical Association

relative efficacy and compared pharmacokinetically. Also, the premedication interval can be lengthened to provide information relative to the duration of the blocking activity after the administration of the protective dose of the test drug.

Isoproterenol kinetics have been studied with this procedure. When premedication with isoproterenol was accomplished 1 hr before antigen provocation, the sympathomimetic agent was effective as a bronchodilator but did not act long enough to inhibit the response to inhaled antigen 1 hr later. When isoproterenol was given every 0.5 hr in conjunction with inhaled antigen, the dose–response curve shifted significantly in the direction of increased antigen requirement. However, when isoproterenol was admixed with the antigen and given simultaneously, complete inhibition of the antigen response occurred. These observations correlate well with *in vitro* studies, which revealed that a peak accumulation of cyclic adenosine monophosphate occurred within 5 min of exposure to isoproterenol, as did a concomitant inhibition of antigen-induced histamine release (5).

Similar studies with selective adrenergic agonists have shed light on the pharmacology involved in the bronchomotor response. Phenylephrine, primarily an α-agonist, elicits bronchodilator responses and inhibits inhaled antigen effects in the manner of isoproterenol, a β-agonist, although less effectively. This observation refutes the popular belief that α-adrenergic receptors of bronchiolar smooth muscle cause bronchospasm when activated. On the contrary, the evidence suggests that there are few, if any, α-receptors in bronchiolar smooth muscle and that any activity caused by α-agonistic drugs is due to the unopposed weak β-specificity (6).

Bronchial provocation techniques have been used extensively to study the physiology of asthma and the pharmacology of antiallergic drugs. β-Agonists, xanthines, anticholinergics, prostaglandins, and the cromolyn-type inhibitors have all been evaluated by these methods. The most effective agents in preventing bronchospasm by inhalation are the β-adrenergic agonists. Isoproterenol is the most effective drug in this respect when given simultaneously with the antigen. Metaproterenol and terbutaline, the latter not yet approved for inhalation, have a longer duration (7).

Anticholinergic drugs, including atropine, are not yet available for inhalation in the United States, although they have been evaluated in bronchoprovocation studies. Atropine causes considerable baseline elevation and is a bronchodilator that diminishes the resting bronchial vagal tone (8). Irritant-induced bronchospasm caused by inhalation of dust or cold air is mediated by the vagus nerve, a cholinergic pathway, whose responses are effectively blocked by inhaled atropine (9). Antihistamines (H_1-blockers) are ineffective when inhaled before antigen challenge, suggesting that mediators other than histamine may be involved in allergic bronchospasm. The synthetic prostaglandins, while not yet in the clinical testing stage, represent another class of potential asthma inhibitors.

The exercise challenge is more physiological or "natural" than the inhalation challenge. Exercise protocols require the performance of pulmonary function tests after a suitable patient jogs on a treadmill for 6–8 min. Following this exercise, susceptible patients usually have a significant fall in their pulmonary function. A test drug can be introduced before the exercise challenge, and its inhibitory capabilities can be studied. This procedure seems best suited for evaluation of the cromolyn-type agents. Atropine, while raising the baseline, does not usually prevent the relative drop in pulmonary function that occurs after exercise (10, 11). Some protection is afforded by this anticholinergic, however, because of the elevated baseline pulmonary functions. The β-adrenergic agonists, isoproterenol and terbutaline, are quite effective through mechanisms of baseline elevation as well as prevention of the exercise response (7). On the other hand, inhaled antihistamines are ineffective against exercise challenge, although they possess varying degrees of anticholinergic activity (8).

The most widely employed experimental method of drug evaluation is the maintenance of a symptom diary often supplemented with routine pulmonary function tests. Diaries that measure chronic symptoms of wheezing, shortness of breath, chest tightness, and cough and that assign a score for intensity and duration are quite useful, especially when medication use and pulmonary function are integrated into the diary. Such diaries are also effective for monitoring the effects of immunotherapy (allergy shots) for the treatment of seasonal hay fever (12).

In summary, drugs representative of many pharmacological categories are useful in the treatment of asthma and other allergic illnesses. An understanding of their pharmacodynamics is critical to the design of appropriate clinical trials as well as to proper prescribing. When underlying mechanisms are not understood or are unclear, empiricism may be necessary for drug evaluation. As the mechanisms underlying the asthmatic state become better known, the potential for optimal therapy will emerge.

REFERENCES

(1) P. Phanuphak, A. Shocket, and P. F. Kohler, *Clin. Allergy*, **8**, 429 (1978).

(2) H. B. Kaiser, S. C. Weishers, and R. J. Morris, "Proceedings of the American Academy of Allergy," 35th Annual Meeting, Mar. 1979.

(3) R. P. Harvey and A. L. Shocket, *ibid.*

(4) H. Chai, R. S. Farr, L. A. Froehlich, D. A. Mathison, J. A. McLean, R. R. Rosenthal, A. L. Sheffer, II, S. L. Spector, and R. G. Townley, *J. Allergy Clin. Immunol.*, **56**, 323 (1975).

(5) R. R. Rosenthal, *Chest*, **73S**, 977S (1978).

(6) R. R. Rosenthal, D. W. Kordansky, G. I. Rosenberg, and P. S. Norman, *J. Allergy Clin. Immunol.*, **57**, 223 (1976).

(7) R. R. Rosenthal, J. Campbell, and P. S. Norman, *Am. Rev. Resp. Dis.*, **119**, 79 (1979).

(8) R. R. Rosenthal, P. S. Norman, E. R. Bleecker, H. Menkes, B. Laube, and D. Hood," Proceedings of the American Academy of Allergy," 35th Annual Meeting, Mar. 1979.

(9) J. G. Widdicombe, D. C. Kent, and J. A. Nadel, *J. Appl. Physiol.*, **17**, 613 (1962).

(10) S. Godfrey and P. Konig, *Thorax*, **31**, 137 (1976).

(11) R. M. Sly, E. M. Heimlich, R. J. Busser, and L. Strick, *J. Allergy*, **40**, 93 (1967).

(12) P. S. Norman, W. L. Winkenwerder, and L. M. Lichtenstein, *ibid.*, **42**, 93 (1968).

ACKNOWLEDGMENTS

Presented as part of the Symposium on New Approaches to the Treatment of Asthma at the APhA Academy of Pharmaceutical Sciences, Anaheim meeting, April 1979.

MARCH 1980
VOLUME 69 NUMBER 3

JOURNAL OF PHARMACEUTICAL SCIENCES

MARY H. FERGUSON
Editor

SHELLY ELLIOTT
Production Editor

MARCIA GARTRELL
Copy Editor

NICOLETTE TRIANTAFELLU
Copy Editor

EDWARD G. FELDMANN
Contributing Editor

SAMUEL W. GOLDSTEIN
Contributing Editor

BELLE R. BECK
Editorial Secretary

DAVID BOHARDT
Director of Publications

L. LUAN CORRIGAN
Assistant Director of Publications

EDITORIAL ADVISORY BOARD

JOHN AUTIAN
HERBERT A. LIEBERMAN
NORMAN R. FARNSWORTH
DAVID E. MANN, JR.
WILLIAM O. FOYE
GERALD J. PAPARIELLO
WILLIAM J. JUSKO
EDWARD G. RIPPIE

The *Journal of Pharmaceutical Sciences* (ISSN 0022-3549) is published monthly by the American Pharmaceutical Association (APhA) at 2215 Constitution Ave., N.W., Washington, DC 20037. Second-class postage paid at Washington, D.C., and at additional mailing office.

All expressions of opinion and statements of supposed fact appearing in articles or editorials carried in this journal are published on the authority of the writer over whose name they appear and are not to be regarded as necessarily expressing the policies or views of APhA.

Offices—Editorial, Advertising, and Subscription: 2215 Constitution Ave., N.W., Washington, DC 20037. Printing: 20th & Northampton Streets, Easton, PA 18042.

Annual Subscriptions—United States and foreign, industrial and government institutions $60, educational institutions $60, individuals *for personal use only* $30; single copies $5. All foreign subscriptions add $5 for postage. Subscription rates are subject to change without notice. Members of APhA may elect to receive the *Journal of Pharmaceutical Sciences* as a part of their annual $80 (foreign $85) APhA membership dues.

Claims—Missing numbers will not be supplied if dues or subscriptions are in arrears for more than 60 days or if claims are received more than 60 days after the date of the issue, or if loss was due to failure to give notice of change of address. APhA cannot accept responsibility for foreign delivery when its records indicate shipment was made.

Change of Address—Members and subscribers should notify at once both the Post Office and APhA of any change of address.

Photocopying—The code at the foot of the first page of an article indicates that APhA has granted permission for copying of the article beyond the limits permitted by Sections 107 and 108 of the U.S. Copyright Law provided that the copier sends the per copy fee stated in the code to the Copyright Clearance Center, Inc., P.O. Box 8891, Boston, MA 02114. Copies may be made for personal or internal use only and not for general distribution.

Microfilm—Available from University Microfilms International, 300 N. Zeeb Road, Ann Arbor, MI 48106.

© Copyright 1980, American Pharmaceutical Association, 2215 Constitution Ave., N.W., Washington, DC 20037; all rights reserved.

EVERY FIVE YEARS

A current series on public affairs television is titled "Every Four Years." The series examines various aspects of the presidency of the United States, and specifically the changing style of those who have sought and reached the office as well as the evolving impact those changes have had on the office itself. The title, of course, refers to the presidential term, and the timing of the series is most appropriate with national elections coming up again this fall.

But even sooner, in fact this April, a process will repeat itself, which used to occur every ten years since 1820, but more recently has been taking place at five-year intervals.

We refer to the United States Pharmacopeial Convention, the members of which will be gathering in Washington, D.C., from April 17 through April 19, immediately preceding the APhA Annual Meeting.

As provided for in the USPC Bylaws, a call goes out "*every five years*" to all the recognized organizations in medicine, pharmacy, and several related areas for each of them to appoint delegates who will then convene at the USPC's quinquennial meeting. These delegates are responsible for (*a*) electing a Board of Trustees to oversee the operation, (*b*) selecting a Committee of Revision to undertake the assigned tasks of developing and updating the standards to go into the next edition of the compendia, and (*c*) adopting a series of resolutions to serve as the expression of the will of the assembled convention concerning what particular subjects should be addressed, or what particular tasks should be undertaken, during the upcoming five-year period until the next convention. The delegates also deal with certain other matters such as extending recognition to additional organizations and proposed amendments to the USPC Bylaws.

But the task of broadly laying out the master plan which will point the direction for the coming revision period is a function that should not be taken casually. All too often, organizations fail to recognize ominous signs which suggest the need for corrective action.

In the case of the USPC, we see certain strong indications that the federal government is moving in the direction of impinging on traditional compendia turf. Although there have been a number of such intrusions over the years—such as the antibiotic certification amendments and the authority to establish nonproprietary drug names—the movement was given substantial impetus with the Office of Technology Assessment's Drug Bioequivalence Study Panel report in mid-1974. That report called for the replacement of the USP and NF with a new standards-setting organization.

Changes that occurred in 1975 served to buy some additional time for the official compendia to undertake and complete the job of developing standards and specifications that would pass the scrutiny of discerning critics including the OTA panel. There is, however, some question as to how well the USPC has responded to date in fully satisfying that challenge.

Whatever might be said along that line, the fact remains that significant compendia-related activity has been recently stirring within Food and Drug Administration circles. Indeed, these activities have caused some compendia-watchers to be concerned that the FDA could be laying the groundwork for an Afghanistan-style take-over. Whether or not the FDA may have such designs, we truly don't know.

However, at least two speeches by FDA officials, during recent months, point in the direction of a future turf-battle.

First, the staff director of FDA's new Compendial Monograph Evaluation and Development Program, speaking at the APhA Academy of Pharmaceutical Sciences' November meeting in Kansas City, told the audience that the agency expects his program to produce a "new generation of compendial standards which are highly reflective of both the market and the state-of-the-art." Begun only in late 1978, this program has two professed objectives: (*a*) to evaluate existing selected compendial monographs and to develop or improve analytical testing methods to assure that they will be suitable for regulatory purposes, and (*b*) to develop monographs where none currently exist in order to establish adequate public standards.

Second, the executive director of FDA's regional operations, appearing as a panelist during the Food and Drug Law Institute's annual conference in Washington last December, informed the audience of programs initiated by his department within the past year. One such program he mentioned is a critical review of USP/NF monographs with a view toward developing new and improved test and assay procedures at the various FDA regional laboratories.

Clearly, therefore, in FDA's eyes there is significant room for improvement in the compendial monographs. And how far FDA plans to pursue these projects of "improvement" remains to be seen.

But if the agency were ever to mount a take-over effort, this would clearly be the wisest strategy to follow in initiating such tactics. Consequently, the delegates who soon will be assembling for the USP Convention should be conscious of this possibility and lay out the best possible defense to meet that threat—namely, a program that will produce a new edition of the compendia that is so improved in the standards and specifications area as to approach a level of perfection that it will defy FDA challenges to "improve" it.

In conclusion, we feel it would be tragic if this country ever were to lose the present system whereby drug standards are established within the private sector under legal sanction and recognition. The 1980 USP Convention will have the prime challenge of producing a workable, no-frills blueprint to see that such a loss is not allowed to occur through oversight or neglect.

—EGF

JOURNAL OF PHARMACEUTICAL SCIENCES

MARCH 1980
VOLUME 69 NUMBER 3

RESEARCH ARTICLES

Fluorescence Properties of Pseudomorphine and Congeners: Structure–Activity Relationships

W. D. DARWIN and E. J. CONE ˣ

Received July 23, 1979, from the *National Institute on Drug Abuse, Division of Research, Addiction Research Center, Lexington, KY 40583.*
Accepted for publication October 1, 1979.

Abstract □ The fluorescence properties of morphine congeners oxidized with potassium ferro-ferricyanide are described. Fluorescence did not occur in congeners with the following structural features: an alkyl or acyl group at the 3-*O*-position, a C-6 carbonyl group, or absence of the furan oxygen. Masking the carbonyl group by ethylene ketal formation effectively restored fluorescence. Morphine congeners that fluoresced were most sensitive to structural changes at C-6, C-7, and C-8. Details of effects of structural changes on emission maxima, intensity, and Stokes' shift are reported.

Keyphrases □ Morphine congeners—ferro-ferricyanide oxidation, fluorescence characteristics □ Pseudomorphine—structural variations, fluorescence □ Fluorometry—structural effects, intensity, Stokes' shift, structural analysis □ Structure–activity relationships—pseudomorphine and congeners

Morphine (I, Table I) can be oxidized to the bimolecular base pseudomorphine (II) by reaction with potassium ferricyanide in aqueous solution (1). The structure of this derivative was shown to be 2,2′-bimorphine on the basis of spectral and chemical studies (2). Because of the extended conjugated system, the fluorescence properties of II are greatly enhanced over that of I.

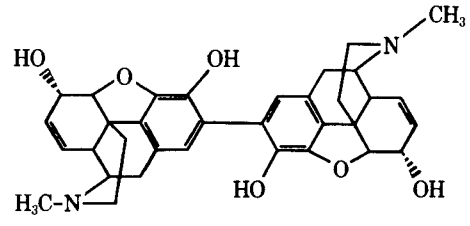

II

Several fluorometric assays of I in biological material are based on the conversion of I to a pseudomorphine derivative (3–6). The occurrence of fluorescence from oxidized solutions containing morphine congeners also has been observed (1) and used for structural verification of metabolites of naltrexone (XVII) (7) and naloxone (XXII) (8). However, a detailed understanding of the structural requirements for fluorescence of pseudomorphine congeners is not available for prediction of fluorescence of new compounds, and there is some ambiguity in the literature concerning the requirements for fluorescence of morphine congeners (1, 8). Consequently, a study was made of the fluorescence properties of a series of morphine analogs to determine their basic structural requirements for fluorescence under oxidizing conditions. An explanation is also proposed for the unusual quenching properties of XVII and XXII.

EXPERIMENTAL

Apparatus—A spectrofluorometer[1] equipped with an *x–y* recorder[2] was used for determining excitation and emission spectra and for measuring fluorescent intensities. Spectra were not corrected for variations in lamp intensity or photomultiplier sensitivity but were calibrated with quinine sulfate at 350 and 450 nm before each measurement.

Chemicals[3]—All chemicals were reagent grade quality.

TLC—Glass fiber sheets[4] were developed with ethyl acetate–methanol–aqueous ammonia (70:10:5 v/v/v). The developing chamber was allowed to equilibrate 10 min prior to elution. After the sheets were developed and dried, they were inspected for fluorescence under 250- and 360-nm UV light. The plates were then sprayed with potassium iodoplatinate solution for visualization of morphine and pseudomorphine-like components.

Preparation of Standard Solutions—Quinine sulfate solutions (1 mg/liter) were prepared in 0.1 *N* H_2SO_4. Solutions of morphine (10 μg/ml) and congeners were prepared in distilled water. The oxidant solution was a mixture of potassium ferricyanide (28.85 mg) and potassium ferrocyanide (2.45 mg) in 50 ml of distilled water (1). The latter solution was prepared fresh daily, and an aliquot was diluted 10-fold before use.

Oxidation and Measurement of Fluorescence—Equal volumes of drug solution (5 ml, 10 μg/ml) and phosphate buffer (5 ml, 0.1 *M* K_2HPO_4, pH 8.5) were mixed and treated with the freshly prepared oxidant solution (0.5 ml). The mixture was allowed to remain at room temperature for 10 min. During the waiting period, the instrument was

[1] Model MK-1, Farrand Optical Co., New York, N.Y.
[2] Model F-100, Varian Associates, Palo Alto, Calif.
[3] Fisher Scientific Co., Fair Lawn, N.J.
[4] Gelman I.T.L.C., type S.G., Gelman Instrument Co., Ann Arbor, Mich.

0022-3549/80/0300-0253$01.00/0
© 1980, American Pharmaceutical Association

Table I—Structures and Fluorescence Properties of Morphine Congeners Oxidized with Potassium Ferro-ferricyanide

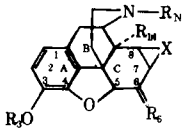

Compound	Structure					Fluorescence Characteristics[b]			
	R_3	R_6	R_{14}	R_N	X[a]	λ_{ex}	λ_{em}	I^{-1}	Stokes' Shift
I Morphine	H		H	CH_3	—	324	434	18.9	7823
III α-Isomorphine	H		H	CH_3	—	324	429	22.4	7554
IV Codeine	CH_3		H	CH_3	—	n.o.	n.o.		
V Normorphine	H		H	H	—	324	436	12.7	7928
VI Norcodeine	CH_3		H	H	—	n.o.	n.o.		
VII 6-Monoacetylmorphine	H		H	CH_3	—	323	433	22.0	7865
VIII Diacetylmorphine	CH_3CO		H	CH_3	—	n.o.[c]	n.o.[c]		
IX Nalorphine	H		H	$CH_2CH{=}CH_2$	—	323	437	127.1	8076
X Dihydromorphine	H		H	CH_3	H_2	321	427	22.5	7733
XI Dihydro-α-isomorphine	H		H	CH_3	H_2	322	422	28.6	7359
XII Hydromorphone	H	O	H	CH_3	H_2	n.o.	n.o.		
XIII Hydrocodone	CH_3	O	H	CH_3	H_2	n.o.	n.o.		
XIV Dihydrodesoxy-morphine-D	H		H	CH_3	H_2	322	422	17.0	7359
XV 6α-Naltrexol	H		OH	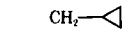	H_2	323	432	23.5	7812
XVI 6β-Naltrexol	H		OH	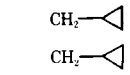	H_2	322	422	112.2	7359
XVII Naltrexone	H	O	OH	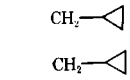	H_2	n.o.	n.o.		
XVIII *N*-Methylcyclo-propylnoroxymorphone cyclic ethylene ketal	H		OH		H_2	322	423	77.9	7415
XIX *N*-Methylcyclo-propylnoroxycodone	CH_3	O	OH	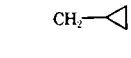	H_2	n.o.	n.o.		
XX 6α-Naloxol	H		OH	$CH_2CH{=}CH_2$	H_2	323	433	18.4	7865
XXI 6β-Naloxol	H		OH	$CH_2CH{=}CH_2$	H_2	322	423	30.3	7415
XXII Naloxone	H	O	OH	$CH_2CH{=}CH_2$	H_2	n.o.	n.o.		
XXIII 6α-Oxymorphol	H		OH	CH_3	H_2	323	431	38.9	7758
XXIV 6β-Oxymorphol	H		OH	CH_3	H_2	322	422	101.9	7359
XXV Oxymorphone	H	O	OH	CH_3	H_2	n.o.	n.o.		
XXVI Oxycodone	CH_3	O	OH	CH_3	H_2	n.o.	n.o.		

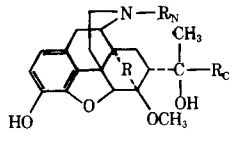

Compound	Structure			Fluorescence Characteristics[b]			
	R_N	R_C	R	λ_{ex}	λ_{em}	I^{-1}	Stokes' Shift
XXVII Etorphine	CH_3	$CH_2CH_2CH_3$	CH=CH	328	442	86.6	7863
XXVIII 6,14-*endo*-Etheno-7-(2-hydroxy-2-heptyl)-tetrahydrooripavine	CH_3	$(CH_2)_4CH_3$	CH=CH	327	441	500.1	7905
XXIX Diprenorphine		CH_3	CH_2CH_2	326	441	32.4	7999
XXX Buprenorphine		$C(CH_3)_3$	CH_2CH_2	326	439	298.3	7896

[a] The designations — and H_2 represent unsaturation and saturation of the 7,8-bond, respectively. [b] The constants λ_{ex} and λ_{em} are reported in nanometers, and Stokes' shift constant is reported in centimeters^{-1}. Intensity (I^{-1}) is equivalent to the concentration of the compound, in micrograms per milliliter, that will give the same fluorescence intensity as 1 μg/ml of quinine sulfate. The fluorescence of all compounds was measured at pH 8.5 at a concentration of 5 μg/ml, with the exception of XXVII–XXX which were measured at pH 7.0 due to insolubility at higher pH. n.o. indicates that fluorescence was not observed. [c] A small amount of fluorescence was observed due to contamination of VIII by hydrolysis to VII.

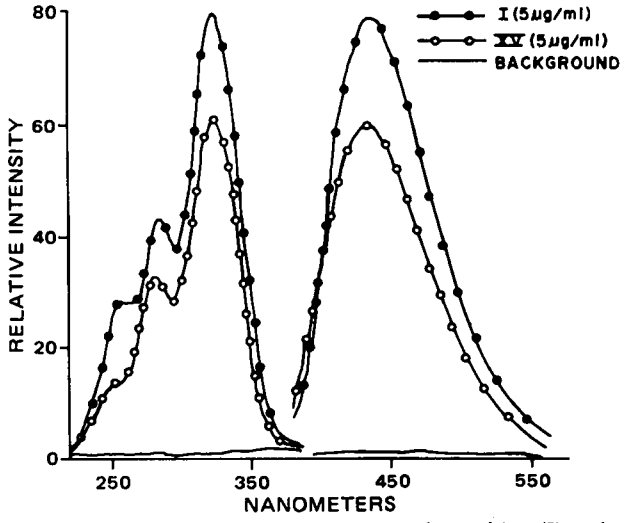

Figure 1—*Excitation and emission spectra of morphine (I) and 6α-naltrexol (XV) oxidized with potassium ferro-ferricyanide at pH 8.5. Both concentrations were 5 μg/ml; λ_{ex} = 324 nm and λ_{em} = 434 for I, and λ_{ex} = 323 nm and λ_{em} = 432 for XV.*

calibrated with quinine sulfate solution for wavelength and intensity corrections.

The excitation maximum, λ_{ex}, of the drug solution was located, and relative intensity was recorded. Background corrections were made using drug solutions treated similarly but without added oxidant. Contributions from background were generally <5%. All drugs were analyzed in triplicate, and the mean of the analyses is reported.

RESULTS AND DISCUSSION

Morphine congeners were oxidized with potassium ferro-ferricyanide solution to form pseudomorphine-like products similar to those formed from reaction of I. Fluorescence properties of these products were measured with a spectrofluorometer calibrated with quinine sulfate solution. The procedure used for the oxidation step was adapted from that of Kupferberg *et al.* (1) for the oxidation of I. Optimum conditions for production of fluorescence (pH and reaction time) were established prior to fluorescence measurement.

Typical excitation and emission spectra of the oxidation products of XV and I are shown in Fig. 1. The spectral similarities of XV to I are apparent. Three absorption bands were observed for all morphine congeners that exhibited fluorescence. Emission spectra characteristically showed a single maximum. The fluorescence properties of the oxidized morphine congeners are presented in Table I. The most intense absorption bands, λ_{ex} and λ_{em}, are reported. In addition, a measure of the reciprocal of the fluorescent intensity, I^{-1} (equivalent to the concentration of the compound in micrograms per milliliter that will give the same fluorescent intensity as 1 μg/ml of quinine sulfate), Stokes' shift constant (9, 10), and a structure are included. The Stokes' shift constant, a measure of the energy dissipated during the lifetime of the excited state before return to the ground state, also reflects energy differences in shifts of equal magnitude at different wavelengths.

Table II—Compounds that Did Not Fluoresce under Oxidizing Conditions and Associated Mechanisms Preventing Fluorescence

Compound	Apparent Structural Feature Involved in Prevention of Fluorescence
Codeine, α-isocodeine, norcodeine, 6α-hydrocodol, 6β-hydrocodol, 6α-oxycodol, 6β-oxycodol, hydrocodone[a], oxycodone[a], *N*-methylcyclopropylnoroxycodone[a], dextromethorphan[a], ethylmorphine, diacetylmorphine, 14-hydroxycodeine	Prevention of dimerization at C-2 by alkylation or acylation of the C-3 phenol group
Levallorphan, pentazocine, cyclazocine	Lack of a furan oxygen
Hydromorphone, naltrexone, naloxone, oxymorphone	Intramolecular quenching by C-6 keto group

[a] These compounds have additional structural features that would prevent fluorescence under these conditions.

Compounds that did not fluoresce under the mild oxidizing conditions of the potassium ferro-ferricyanide solution are listed in Table II. It is apparent that at least three structural features are important in the prevention of fluorescence of morphine congeners under these conditions. The dimerization process can be blocked by introduction of an alkyl or acetyl group at the 3-*O*-position. TLC analyses of the oxidized products of I, X, XII, XIII, XV, XVII, and 6β-hydrocodol for polar, pseudomorphine-like adducts provided evidence for their occurrence for I, X, XII, XV, and XVII. Thus, it is likely that the C-2 position of these compounds is activated by the presence of the C-3 phenolic group through tautomerization to a quinone-like structure, which may then undergo a coupling reaction. Blockade of this process with an alkyl or acyl group would prevent dimerization.

A second structural feature important in the prevention of fluorescence involves quenching by a carbonyl group located at C-6. Both XII and XVII reacted under the standard oxidizing conditions to produce a more polar product, as evidenced by iodoplatinate-positive spots on TLC. Although dimerization apparently occurred for XII and XVII, neither compound fluoresced. In contrast, fluorescence was observed for the 6α- and 6β-carbinol homologs of XII and XVII and for the ethylene ketal XVIII. Protection of the carbonyl group as a ketal, thus providing a fluorescent derivative, is a similar effect to that observed by Crowell and Varsel (11), who reported that the fluorescence quenching effect of aromatic aldehydes could be overcome by acetal formation.

The quenching effects of the carbonyl group result from the nonbonded electrons undergoing $n \rightarrow \pi^*$ transitions at lower energy levels and with lower molar absorptivity than the $\pi \rightarrow \pi^*$ transitions. In addition, the greater degree of *s* character in the sp^2 hybridized nonbinding orbital of the carbonyl oxygen than in the π orbitals of the biphenyl system results in a higher degree of spin-orbit coupling. Intersystem crossing is increased, thereby decreasing fluorescence and increasing the possibility of phosphorescence at lower temperatures. The conversion of XVII to XVIII results in less *s* character for the carbon–oxygen bond at C-6 (sp^3 orbitals) and eliminates the π bond, thereby restoring fluorescence.

The possibility that fluorescence quenching by the carbonyl group was occurring *via* an intermolecular process rather than by intramolecular quenching was ruled out by mixing the fluorescent species and measuring the resultant fluorescence. Three solutions were prepared: A, XVII (20 μg/ml); B, XV (20 μg/ml); and C, XVII (10 μg/ml) and XV (10 μg/ml). The compounds were oxidized and an additional solution, D, was prepared from equal parts of the oxidized Solutions A and B. This procedure gave the same concentration of drug in Solutions C and D.

The fluorescence of each solution was measured (Fig. 2). The fluorescent intensity of Solution D was approximately one-half of that observed for Solution B, as would be expected if intermolecular quenching

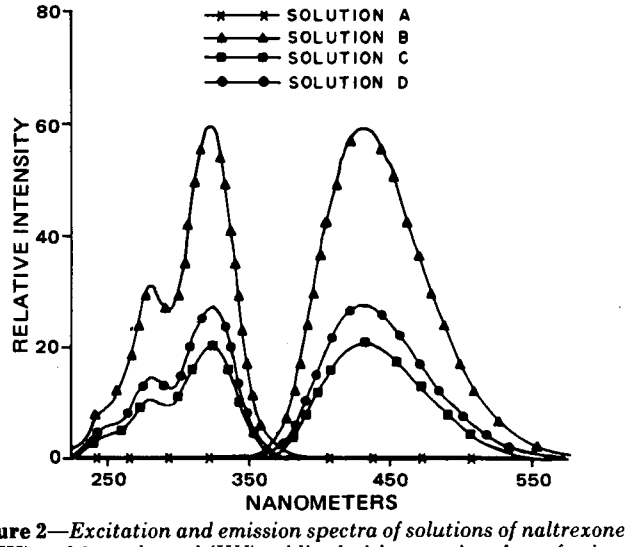

Figure 2—*Excitation and emission spectra of solutions of naltrexone (XVII) and 6α-naltrexol (XV) oxidized with potassium ferro-ferricyanide at pH 8.5. The contents of the solutions were: A, XVII (20 μg/ml); B, XV (20 μg/ml); and C, XVII (10 μg/ml) and XV (10 μg/ml). Solutions A–C were oxidized, and Solution D was prepared from equal parts of the oxidized Solutions A and B.*

Table III—Effects of Structural Changes on Fluorescence Characteristics

Comparison	Structural Change[a]	Effect[b]		
		$\Delta\lambda_{em}$, nm	Intensity Ratio	Δ Stokes' Shift, cm^{-1}
I → V	(N)CH_3 → H	+2	0.67	+105
I → IX	(N)CH_3 → $CH_2CH{=}CH_2$	+3	6.72	+253
XXIII → XX	(N)CH_3 → $CH_2CH{=}CH_2$	+2	0.47	+107
XXIV → XXI	(N)CH_3 → $CH_2CH{=}CH_2$	+1	0.30	+56
XXIII → XV	(N)CH_3 →	+1	0.60	+54
XXIV → XVI	(N)CH_3 →	0	1.10	0
V → IX	(N)H → $CH_2CH{=}CH_2$	+1	10.01	+148
XX → XV	(N)$CH_2CH{=}CH_2$ →	−1	1.28	−53
XXI → XVI	(N)$CH_2CH{=}CH_2$ →	−1	3.70	−56
I → X	HC(7)=C(8)H → CH_2CH_2	−7	1.19	−90
III → XI	HC(7)=C(8)H → CH_2CH_2	−7	1.28	−195
I → VII	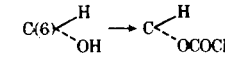	−1	1.16	+42
I → III	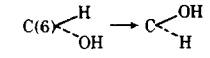	−5	1.18	−269
X → XI	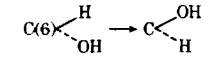	−5	1.27	−374
XV → XVI	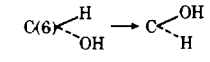	−10	4.77	−453
XX → XXI	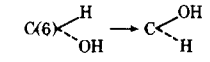	−10	1.65	−450
XXIII → XXIV	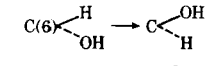	−9	2.62	−399
XV → XVIII	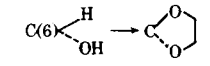	−9	3.31	−397
XVI → XVIII	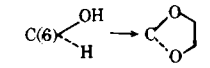	+1	0.69	+56
XIV → X	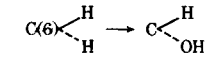	+5	1.32	+374
XIV → XI	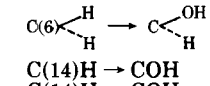	0	1.68	0
X → XXIII	C(14)H → COH	+4	1.73	+25
XI → XXIV	C(14)H → COH	0	3.56	0
XXIX → XXX	$CH_3(R_c)$ → $C(CH_3)_3$	−2	9.21	−103
XXVII → XXVIII	$CH_3CH_2CH_2(R_c)$ → $CH_3(CH_2)_4$	−1	5.77	+42

[a] The molecular site at which a structural comparison is made is indicated in parentheses. [b] $\Delta\lambda_{em}$ and ΔStokes' shift are expressed as differences in the fluorescence constants of the second compound minus those of the first compound. The intensity ratio is I^{-1} of the second compound divided by that of the first compound. When the intensity ratio is less than unity, the fluorescence intensity of the second compound is increased by the molecular change.

were not occurring. The fluorescence of Solution C was somewhat greater (75% of the intensity of Solution D) than would be accounted for by the dimers of XV formed in this mixture. This finding indicates that the mixed dimer forms (XV–XVII adduct) exhibit some fluorescence, although less intense than that of XV.

The third structural feature that was important in the production of fluorescence by pseudomorphine-like compounds was the furan oxygen bridge. Compounds lacking this group (*e.g.*, levallorphan, pentazocine, and cyclazocine) exhibited no fluorescence under oxidizing conditions. Delocalization of the nonbonding electrons of the furan oxygen into the biphenyl ring system, thereby extending the conjugated system, possibly accounts for the importance of this group.

Table IV—Effects of Substituents on the Fluorescence of Morphine Congeners Oxidized with Potassium Ferro-ferricyanide

Structural[a] Group	Substituent Change	Effect on λ_{em}	Effect on Intensity	Effect on Stokes' Shift
C(3)-OH	C—O-alkyl	Fluorescence not observed	—	—
	C=O	Fluorescence not observed	—	—
Furan oxygen bridge	Elimination	Fluorescence not observed	—	—
		Decrease	Decrease	Decrease
HC(7)=C(8)H	CH_2CH_2	Decrease	Decrease	Decrease
C(14)H	C—OH	None to small increase	Decrease	None to small increase
(N)H	NCH_3	Decrease	Decrease	Decrease
(N)CH_3	$CH_2CH{=}CH_2$ or 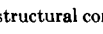	None to small increase	Increase or decrease	None to large increase

[a] The molecular site at which a structural comparison is made is indicated in parenthesis.

Overall, the structural requirements for the production of fluorescence from pseudomorphine-like congeners include the following structural features: an unsubstituted C-3 phenolic group, a furan oxygen bridge, and lack of a C-6 carbonyl group. Thus, the observation by Weinstein *et al.* (8) that a C-6 hydroxyl group is necessary for formation of a fluorescent derivative of XVII under these conditions appears to be incomplete.

Certain structural changes modified λ_{em}, intensity, and the Stokes' shift constant (Table III). Substitution of a larger group for the methyl group at the *N*-substituent position generally produced a shift to longer λ_{em} with a concurrent increase in the Stokes' shift constant. The effect of this change on intensity, however, was varied and could increase or decrease. Saturation of the 7,8-double bond caused a sizable shift to shorter λ_{em}, as well as a decrease in intensity and the Stokes' shift constant.

Changes in the carbinol configuration at C-6 from the α to the β orientation consistently decreased λ_{em}. This change also produced a decrease in intensity and a large decrease in the Stokes' shift constant. Inspection of Dreiding molecular models indicates that the alcoholic group in the β orientation is *anti* to the biphenyl ring system and, thus, would exhibit an electron-withdrawing effect, which would result in a shift to shorter wavelengths and higher energy. However, substitution of an alcoholic group at C-14 for hydrogen caused little change in the fluorescence pattern, probably due to its isolation from the biphenyl system.

Substitution of bulkier groups at R_C in the oripavine series of compounds, XXVII–XXX, caused a decrease in λ_{em} as well as large decreases in intensity.

General trends for effects of substituent changes on the fluorescent properties of the series of morphine agonists and antagonists tested are shown in Table IV. The most pronounced effects resulted from (*a*) structural changes at C-3, where fluorescence was abolished by prevention of dimerization; (*b*) loss of the furan oxygen; and (*c*) structural changes in ring C, where fluorescence could be quenched by the presence of a carbonyl group at C-6. Diminution of intensity was produced by structural changes at C-6, C-7, and C-8.

The structural effects on λ_{em} were so pronounced by epimerization at C-6 that it could provide a means of distinguishing isomers in newly synthesized compounds and metabolites of this series with unknown configurations. Furthermore, the methods used for measurement of fluorescence are readily adaptable for quantitative measurements of drug in biological samples. Thus, a general understanding of the requirements for fluorescence of morphine analogs with the ferricyanide reagent may assist in the development of sensitive and specific assays for these compounds.

REFERENCES

(1) H. J. Kupferberg, A. Burkhalter, and E. L. Way, *J. Chromatogr.*, **16**, 558 (1964).

(2) K. W. Bentley and S. F. Dyke, *J. Chem. Soc.*, **1959**, 2574.

(3) H. J. Kupferberg, A. Burkhalter, and E. L. Way, *J. Pharmacol. Exp. Ther.*, **145**, 247 (1964).

(4) A. E. Takemorei, *Biochem. Pharmacol.*, **17**, 1627 (1968).

(5) S. J. Mulé and P. L. Hushin, *Anal. Chem.*, **43**, 708 (1971).

(6) I. Jane and J. F. Taylor, *J. Chromatogr.*, **109**, 37 (1975).

(7) E. J. Cone, *Tetrahedron Lett.*, **1973**, 2607.

(8) S. H. Weinstein, M. Pfeffer, J. M. Schor, L. Indindoli, and M. Mintz, *J. Pharm. Sci.*, **60**, 1567 (1971).

(9) S. Udenfriend, "Fluorescence Assay in Biology and Medicine," vol. II, Academic, New York, N.Y., 1969, p. 7.

(10) H. G. Leeman, K. Stich, and M. Thomas, in "Progress in Drug Research," vol. 6, E. Jucker, Ed., Birkhauser Verlag, Basel, Switzerland, 1963, pp. 160–185.

(11) E. P. Crowell and C. J. Varsel, *Anal. Chem.*, **35**, 189 (1963).

ACKNOWLEDGMENTS

The authors are grateful to Ms. L. J. M. Sturdivant for aid in preparation of this manuscript.

High-Performance Liquid Chromatographic Determination of Pilocarpine in Aqueous Humor: Derivatization by Quaternization of Methylimidazole Tertiary Amine Group

A. K. MITRA, C. L. BAUSTIAN, and T. J. MIKKELSON ˣ

Received July 23, 1979, from the *Department of Pharmaceutical Chemistry, University of Kansas, Lawrence, KS 66044.* Accepted for publication October 1, 1979.

Abstract □ A derivatization procedure and a high-performance liquid chromatographic (HPLC) method of analysis for pilocarpine are described. The method is based on the quaternization of the 3′-tertiary amino group of the methylimidazole ring of pilocarpine with *p*-nitrobenzyl bromide. The HPLC system employs an RP-ODS column with a methanol–water mobile phase containing octanesulfonate as an ion-pairing agent. The sensitivity of the method permits the analysis of pilocarpine in biological fluids such as aqueous humor. The method is selective for pilocarpine in the presence of isopilocarpine. Its applicability to the analysis of aromatic heterocyclic and alkyl tertiary amines is demonstrated.

Keyphrases □ Pilocarpine—high-performance liquid chromatographic determination in aqueous humor, quaternization of the methylimidazole tertiary amine group □ High-performance liquid chromatography—determination of pilocarpine in aqueous humor, quaternization of the methylimidazole tertiary amine group □ Ocular agents—pilocarpine, high-performance liquid chromatographic determination in aqueous humor □ Tertiary amines—derivatization, quaternization, high-performance liquid chromatographic determination

Pilocarpine (I), a parasympathomimetic amine, is used widely as a topical ocular agent for the reduction of the elevated intraocular pressure associated with glaucoma. The UV absorption characteristics of pilocarpine are such that its direct spectrophotometric analysis is an alternative only when high sensitivity is not a requirement.

BACKGROUND

Various analytical methods are available for the determination of pilocarpine, but they are limited relative to sensitivity, specificity, selectivity, and/or reliability. The official colorimetric method (1) utilizes hydroxylamine to cleave the lactone ring. However, the official method is neither selective nor specific.

A kinetic method of analysis was reported (2). In the method, which is based on the imidazole- or substituted imidazole-catalyzed hydrolysis of 2,4-dinitrophenyl acetate, the extent of catalysis is dependent on the pilocarpine concentration. Microgram quantities of pilocarpine are measurable.

0022-3549/80/0300-0257$01.00/0

© 1980, American Pharmaceutical Association

Overall, the structural requirements for the production of fluorescence from pseudomorphine-like congeners include the following structural features: an unsubstituted C-3 phenolic group, a furan oxygen bridge, and lack of a C-6 carbonyl group. Thus, the observation by Weinstein *et al.* (8) that a C-6 hydroxyl group is necessary for formation of a fluorescent derivative of XVII under these conditions appears to be incomplete.

Certain structural changes modified λ_{em}, intensity, and the Stokes' shift constant (Table III). Substitution of a larger group for the methyl group at the *N*-substituent position generally produced a shift to longer λ_{em} with a concurrent increase in the Stokes' shift constant. The effect of this change on intensity, however, was varied and could increase or decrease. Saturation of the 7,8-double bond caused a sizable shift to shorter λ_{em}, as well as a decrease in intensity and the Stokes' shift constant.

Changes in the carbinol configuration at C-6 from the α to the β orientation consistently decreased λ_{em}. This change also produced a decrease in intensity and a large decrease in the Stokes' shift constant. Inspection of Dreiding molecular models indicates that the alcoholic group in the β orientation is *anti* to the biphenyl ring system and, thus, would exhibit an electron-withdrawing effect, which would result in a shift to shorter wavelengths and higher energy. However, substitution of an alcoholic group at C-14 for hydrogen caused little change in the fluorescence pattern, probably due to its isolation from the biphenyl system.

Substitution of bulkier groups at R_C in the oripavine series of compounds, XXVII–XXX, caused a decrease in λ_{em} as well as large decreases in intensity.

General trends for effects of substituent changes on the fluorescent properties of the series of morphine agonists and antagonists tested are shown in Table IV. The most pronounced effects resulted from (*a*) structural changes at C-3, where fluorescence was abolished by prevention of dimerization; (*b*) loss of the furan oxygen; and (*c*) structural changes in ring C, where fluorescence could be quenched by the presence of a carbonyl group at C-6. Diminution of intensity was produced by structural changes at C-6, C-7, and C-8.

The structural effects on λ_{em} were so pronounced by epimerization at C-6 that it could provide a means of distinguishing isomers in newly synthesized compounds and metabolites of this series with unknown configurations. Furthermore, the methods used for measurement of fluorescence are readily adaptable for quantitative measurements of drug in biological samples. Thus, a general understanding of the requirements for fluorescence of morphine analogs with the ferricyanide reagent may assist in the development of sensitive and specific assays for these compounds.

REFERENCES

(1) H. J. Kupferberg, A. Burkhalter, and E. L. Way, *J. Chromatogr.*, **16**, 558 (1964).

(2) K. W. Bentley and S. F. Dyke, *J. Chem. Soc.*, **1959**, 2574.

(3) H. J. Kupferberg, A. Burkhalter, and E. L. Way, *J. Pharmacol. Exp. Ther.*, **145**, 247 (1964).

(4) A. E. Takemorei, *Biochem. Pharmacol.*, **17**, 1627 (1968).

(5) S. J. Mulé and P. L. Hushin, *Anal. Chem.*, **43**, 708 (1971).

(6) I. Jane and J. F. Taylor, *J. Chromatogr.*, **109**, 37 (1975).

(7) E. J. Cone, *Tetrahedron Lett.*, **1973**, 2607.

(8) S. H. Weinstein, M. Pfeffer, J. M. Schor, L. Indindoli, and M. Mintz, *J. Pharm. Sci.*, **60**, 1567 (1971).

(9) S. Udenfriend, "Fluorescence Assay in Biology and Medicine," vol. II, Academic, New York, N.Y., 1969, p. 7.

(10) H. G. Leeman, K. Stich, and M. Thomas, in "Progress in Drug Research," vol. 6, E. Jucker, Ed., Birkhauser Verlag, Basel, Switzerland, 1963, pp. 160–185.

(11) E. P. Crowell and C. J. Varsel, *Anal. Chem.*, **35**, 189 (1963).

ACKNOWLEDGMENTS

The authors are grateful to Ms. L. J. M. Sturdivant for aid in preparation of this manuscript.

High-Performance Liquid Chromatographic Determination of Pilocarpine in Aqueous Humor: Derivatization by Quaternization of Methylimidazole Tertiary Amine Group

A. K. MITRA, C. L. BAUSTIAN, and T. J. MIKKELSON ˣ

Received July 23, 1979, from the *Department of Pharmaceutical Chemistry, University of Kansas, Lawrence, KS 66044.* Accepted for publication October 1, 1979.

Abstract □ A derivatization procedure and a high-performance liquid chromatographic (HPLC) method of analysis for pilocarpine are described. The method is based on the quaternization of the 3′-tertiary amino group of the methylimidazole ring of pilocarpine with *p*-nitrobenzyl bromide. The HPLC system employs an RP-ODS column with a methanol–water mobile phase containing octanesulfonate as an ion-pairing agent. The sensitivity of the method permits the analysis of pilocarpine in biological fluids such as aqueous humor. The method is selective for pilocarpine in the presence of isopilocarpine. Its applicability to the analysis of aromatic heterocyclic and alkyl tertiary amines is demonstrated.

Keyphrases □ Pilocarpine—high-performance liquid chromatographic determination in aqueous humor, quaternization of the methylimidazole tertiary amine group □ High-performance liquid chromatography—determination of pilocarpine in aqueous humor, quaternization of the methylimidazole tertiary amine group □ Ocular agents—pilocarpine, high-performance liquid chromatographic determination in aqueous humor □ Tertiary amines—derivatization, quaternization, high-performance liquid chromatographic determination

Pilocarpine (I), a parasympathomimetic amine, is used widely as a topical ocular agent for the reduction of the elevated intraocular pressure associated with glaucoma. The UV absorption characteristics of pilocarpine are such that its direct spectrophotometric analysis is an alternative only when high sensitivity is not a requirement.

BACKGROUND

Various analytical methods are available for the determination of pilocarpine, but they are limited relative to sensitivity, specificity, selectivity, and/or reliability. The official colorimetric method (1) utilizes hydroxylamine to cleave the lactone ring. However, the official method is neither selective nor specific.

A kinetic method of analysis was reported (2). In the method, which is based on the imidazole- or substituted imidazole-catalyzed hydrolysis of 2,4-dinitrophenyl acetate, the extent of catalysis is dependent on the pilocarpine concentration. Microgram quantities of pilocarpine are measurable.

0022-3549/80/0300-0257$01.00/0

© 1980, American Pharmaceutical Association

GLC methods for pilocarpine have been reported. The most recent utilizes the heptafluorobutyric anhydride acylation of the methylimidazole ring of pilocarpine (3). The method is selective and sensitive and is readily capable of measuring pilocarpine at levels found in biological fluids such as aqueous humor. However, it requires extensive sample handling and workup.

High-performance liquid chromotographic (HPLC) methods for pilocarpine (4) and other imidazole bases (5) have been reported. These methods are based on the direct spectrophotometric measurement of pilocarpine (4) and other imidazole bases (5) at 217 and 208 nm, respectively. Although the approach of direct UV detection of pilocarpine (4) is selective and reliable and is suitable for the analysis of levels contained in pilocarpine dosage forms, it lacks adequate sensitivity for pilocarpine at levels found in aqueous humor following topical administration.

This report describes a derivatization and HPLC procedure for the analysis of pilocarpine in aqueous humor. The method is based on the quaternization of the 3′-tertiary amino group of the methylimidazole ring of pilocarpine with the chromophore *p*-nitrobenzyl bromide. The utilization of a reversed-phase chromatographic system with an ion-pairing agent is described. The method is reliable, because little sample handling is required; the method is selective since pilocarpine and isopilocarpine are separated and determined; and the method is sensitive in that it is applicable to the determination of pilocarpine levels encountered experimentally in aqueous humor. The applicability of the quaternization procedure to the analysis of other tertiary amines, such as aliphatic and aromatic heterocyclic amines, is also described.

EXPERIMENTAL

Materials—Pilocarpine nitrate[1] and isopilocarpine nitrate[2] were used as received. *p*-Nitrobenzyl bromide[2] was recrystallized from water–acetonitrile. The ion-pairing agent, 1-octanesulfonic acid sodium salt[3], was used as received, as was acetonitrile[4]. Methylene chloride[5] (certified ACS grade) was distilled from phosphorus pentoxide prior to use. HPLC grade methanol[5] also was used. All other reagents and chemicals used were analytical reagent grade or high purity.

Equipment—The HPLC system was comprised of a solvent delivery system[6], a septumless injector[7], a UV absorbance detector[8], and a 10-mv strip-chart recorder[9]. Absorbance was measured at 254 nm. Sensitivity settings to 0.005 aufs were used. The column was a 30-cm RP-ODS column with an inside diameter of 3.9 mm and a 10-μm (spherical) particle size[10].

NMR spectra of pilocarpine and the derivative were obtained on a spectrometer[11] in the pulse mode. Spectra were obtained using solutions in deuterium oxide and acetone-d_6, with tetramethylsilane as the internal reference at concentrations of 10–20%.

Chromatographic Conditions—All chromatography was conducted at ambient temperature. The mobile phase consisted of an 80% (v/v) methanol in water mixture containing 1×10^{-3} *M* sodium octanesulfonate. The mobile phase was filtered and degassed prior to use. The flow rate was 1.6 ml/min, which generated a column pressure of 1000–1500 psig.

Glassware—The centrifuge tubes and ampuls used in the derivatization procedure were silanized by soaking for several hours in a solution of 5% dimethyldichlorosilane[1] in toluene and rinsing with toluene, methanol, and methylene chloride (3).

Derivatization—Volumes of 100 μl of either standard aqueous solutions of pilocarpine nitrate or aqueous humor samples were added to 500 μl of 0.3 *M* potassium bicarbonate solutions (pH 8.4) in silanized centrifuge tubes. The resulting solutions were each immediately extracted (vortexed for 1 min and centrifuged at 2000 rpm for 5 min at ambient temperature) with two 1.0-ml volumes of methylene chloride. Aliquots of the two extracts from each sample were combined in silanized glass ampuls and evaporated to dryness under nitrogen at 40°. To the dried samples, a 200-μl volume of a solution of *p*-nitrobenzyl bromide in acetonitrile (0.25 mg/ml) was added.

The ampuls were sealed at ambient pressure under a nitrogen atmosphere, using an oxygen torch flame, and reacted for 24 hr at 40°. Then they were cooled to ambient temperature and opened. The chromatography was conducted by direct injection of an aliquot of the reaction mixture or an internal standard solution was added, the mixture was vortexed, and an aliquot was injected. The internal standard solution was a 10-μl volume of phenylephrine hydrochloride in methanol at 2.0 mg/ml.

Milligram Quantities of Derivative—Pilocarpine nitrate, 50 mg, was dissolved in 25 ml of 0.3 *M* aqueous potassium bicarbonate and extracted with 25 ml of methylene chloride. The organic layer was separated, and the methylene chloride was removed under vacuum. The product obtained was a hydrated pilocarpine base as a clear or very slightly yellow, highly viscous fluid. The pilocarpine base, 50 mg, was combined with 500 mg of *p*-nitrobenzyl bromide in 10 ml of acetonitrile. The resulting solution was reacted at 40° for 24 hr, the reaction mixture was placed in a glass mortar, and the quaternary ammonium reaction product was precipitated by ether addition.

The precipitate was repeatedly washed and purified by trituration in the presence of ether. Then it was dried and stored under vacuum. After thorough drying, the solid was used for UV, mass spectral, and NMR analyses. In addition, the product was used to confirm the chromatographic peak used for quantitation of pilocarpine in the analytical procedure.

Standard Curves—Volumes of 100 μl of aqueous solutions of pilocarpine nitrate ranging in concentration from 0.3 to 10.0 μg/ml were used to develop standard curves. The previously described procedure for derivatization was followed. Standard curves were constructed on a basis of the measured peak heights of the analyte (II), which were compared to both an internal and an external standard. The internal standard, phenylephrine hydrochloride, was used in construction of the standard curve, which was applied to the analysis of samples obtained in *in vitro* transport studies across isolated, mounted corneal membranes.

In vivo pilocarpine absorption studies, where the test solutions were aqueous humor samples obtained as a function of time following topical dosing, and studies using spiked aqueous humor samples resulted in a contaminant that interfered with the internal standard. Therefore, all aqueous humor samples were measured against an external standard of II, which was pure analyte obtained in the milligram quantity preparation procedure described previously. When used, the internal standard was added to the reaction mixture after the derivatization reaction was completed and just prior to injection. This approach was suitable in view of the extraction efficiencies obtained.

Aqueous Humor Samples—New Zealand albino rabbits were sacrificed by marginal ear vein administration of pentobarbital sodium solution. The corneal surface was rinsed with normal saline solution and patted dry with tissue paper. Aqueous humor samples were obtained from the anterior chamber by paracentesis by entering at the limbus with a 1-ml tuberculin syringe fitted with a 27-gauge needle.

RESULTS AND DISCUSSION

Analyte Characteristics—The derivatizing reaction, which is the reaction of pilocarpine (I) with the chromophore *p*-nitrobenzyl bromide to form the quaternary ammonium analyte (II) *p*-nitrobenzyl pilocarpine bromide, is shown in Scheme I. The derivative II displayed a UV absorbance maximum at 263 nm with a molar absorptivity of 1.20×10^4. At 254 nm, this analyte displayed a molar absorptivity of 1.07×10^4.

Under the described chromatographic conditions, the capacity factor, k', for II was 4.87. In comparison, the capacity factor for derivatized isopilocarpine was 5.40. The resulting selectivity was evidenced by a separation factor, α, of 1.11; the degree of separation was evidenced by a resolution, R, of 0.80.

Kinetic experiments were conducted to optimize the reaction conditions in terms of the temperature required and the excess *p*-nitrobenzyl bromide required to achieve complete or near complete production of II in a reasonable time. Reactions forming quaternary salts from tertiary amines and alkyl halides, the Menschutkin reaction (6), are not fast (6–9). They are biomolecular and clearly second order (7). A significant sensitivity to the size and disposition of the nitrogen-substituted alkyl groups has been demonstrated; for example, quinuclidine, which has an exposed nitrogen, is 200-fold more reactive than triethylamine toward methyl chloride (7). Alkyl halide substitutions also significantly alter the quaternization rate. Approximately a 500-fold reduction in the conversion rate was detected through an alkyl series where the following reactivities were found: methyl > ethyl > higher normal alkyls > isopropyl (6, 8). The derivatizing agent, *p*-nitrobenzyl bromide, was chosen because of its UV

[1] Sigma Chemical Co.
[2] Aldrich Chemical Co.
[3] Eastman Kodak Co.
[4] Baker Analyzed HPLC reagent, J. T. Baker Chemical Co.
[5] Fisher Scientific Co.
[6] Model 6000A, Waters Associates.
[7] Model U6K, Waters Associates.
[8] Model 440, Waters Associates.
[9] Omniscribe model B-5117-1, Houston Instruments.
[10] μBondapak C_{18}, Waters Associates.
[11] Model R-24B, Hitachi/Perkin-Elmer Corp.

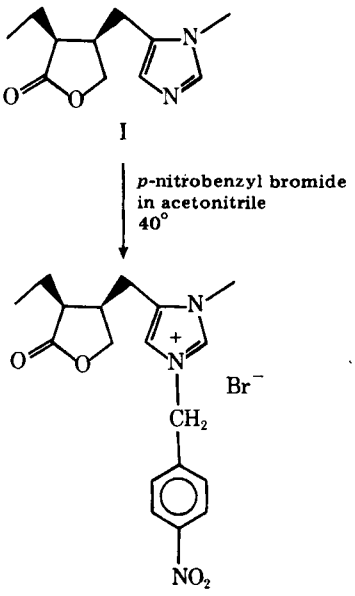

I II

Scheme I

absorption characteristics. However, it was not expected to react rapidly with pilocarpine because of its molecular size, even though the 3′-tertiary nitrogen of the methylimidazole group of pilocarpine is an exposed nitrogen.

Preliminary kinetic studies were conducted at several temperatures, and 40° was chosen for the analytical derivatization. Molar ratios of *p*-nitrobenzyl bromide to I of 40, 125, 420, and 600 were studied. Pseudo-first-order kinetic behavior was observed in each instance, and a decreasing reaction time (10) was observed as a function of increasing molar ratios.

The conditions selected, as described in the procedure for derivatization, corresponded to a molar ratio of *p*-nitrobenzyl bromide to pilocarpine of approximately 600 for a pilocarpine sample solution containing 1.0 μg/ml. These particular conditions were selected because the reaction proceeded with a half-life of ~3 hr without any detectable side reactions. As a result, the reaction was essentially complete in the 24-hr reaction time. In addition, the selected level of *p*-nitrobenzyl bromide did not affect resolution of the analyte or the internal standard.

Comparisons of the NMR spectrum of pilocarpine and the analyte are presented in Table I (the proton numbering system is given in Structure III). The protons of pilocarpine were all accounted for in the derivative. The protons of the ethyl-substituted lactone ring and the methylene bridge were essentially unchanged. However, the protons of the methylimidazole ring demonstrated significant downfield shifts. The *N*-methyl protons, which appeared as a singlet, underwent a downfield shift in the analyte of 0.26 ppm due to the flow of electrons toward the quaternary nitrogen. The 2′- and 4′-protons underwent extensive deshielding. The 2′-proton was found downfield at 11.1 ppm in the analyte compared to 8.6 ppm in pilocarpine. The 4′-proton was at 7.3 ppm in pilocarpine and at 8.1 ppm in the analyte. However, the 4′-proton did not appear as a singlet in the analyte but overlapped as a multiplet with the aromatic protons.

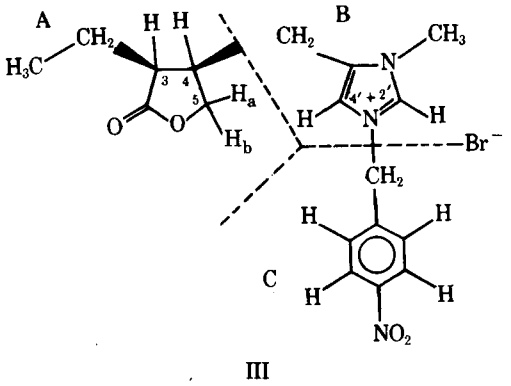

III

Table I—Chemical Shifts in Parts per Million Using Tetramethylsilane Standard for Pilocarpine in Deuterium Oxide and Analyte in Acetone-d_6 [a]

		Pilocarpine[b]	Analyte[b]
Lactone ring with bridge	CH_3–CH_2	1.02 (t)	1.03 (t)
	CH_3–CH_2	1.71 (m)	1.64 (m)
	$-CH_2$-bridge plus 3H,4H	2.81 (m)	3.15 (m)
	$5H_a$	4.17 (dd)	4.31 (dd)
	$5H_b$	4.19 (dd)	4.32 (dd)
Methylimidazole group	N–CH_3	3.77 (s)	4.04 (s)
	2′H	8.60 (s)	11.1 (s)
	4′H	7.30 (s)	8.1 (m)[c]
Chromophore	$-CH_2-$	—	5.96 (s)
	Aromatic	—	8.10 (m)[c]

[a] See Structure III for numbering. [b] s = singlet, dd = double doublet, t = triplet, and m = multiplet. [c] The 4′-proton in the analyte occurs as a multiplet with the aromatic protons.

The integration of the analyte spectrum clearly demonstrated the formation of a one-to-one reaction product. The multiplet at 8.1 ppm was indicative of five protons, the four aromatic protons of the chromophore plus the 4′-proton of the imidazole ring. The singlet at 5.96 ppm, which is the methylene group of the *p*-nitrobenzyl moiety, was indicative of two protons. In comparison, the *N*-methyl group, the lactone–imidazole methylene bridge, the methylene group of the lactone ethyl group at the 3-position, and the methyl group of the lactone ethyl group at the 3-position clearly were indicative of three, two, two, and three protons, respectively.

The mass spectrum of the analyte III did not display a molecular ion peak. The lability of the bond between the quaternary nitrogen of the methylimidazole ring and the methylene of the *p*-nitrobenzyl group was demonstrated by the abundance of *m/e* 208 and 136 fragments, corresponding to a fragment of A + B (pilocarpine), and a fragment of C in III. Further fragmentation was apparent as a function of the abundance of *m/e* 113 (A in III), 84 (A − $-C_2H_5$), 95 (B in III), and 80 (B − $-CH_3$) fragments.

The product sample used to obtain NMR and mass spectral data was isolated and purified from a reaction run at 40° for 24 hr, which indicated that the reaction conditions used to generate the analyte did not result in unexpected side reactions. *p*-Nitrobenzyl bromide and pilocarpine are stable under the conditions of the reaction in that all protons are accounted for and other structural integrity is observed. The reaction follows the expected bimolecular behavior, resulting in the quaternary derivative.

Standard Curve and Detection Limits—Following the procedure for derivatization, plots of calculated peak height ratios, where the analyzed solutions were sample aqueous solutions of pilocarpine nitrate in the concentration range of 0.3–10.0 μg/ml and the internal standard was phenylephrine hydrochloride, were constructed. These plots were linear and reproducible with typical results of $n = 10$, slope = 0.144, intercept = 0.018, and correlation coefficient = 0.995.

Figure 1*a* is the chromatographic result of the derivatization of a standard sample of an aqueous solution containing 6.0 μg/ml of pilocarpine nitrate, approximately equivalent to an injection of 100 ng of pilocarpine. The excess *p*-nitrobenzyl bromide did not interfere with the internal standard or the analyte peaks. Figure 1*b* is the chromatographic result obtained from spiked aqueous humor containing 1.8 μg/ml of pilocarpine nitrate. The internal standard was not added to aqueous humor or spiked aqueous humor samples because of overlapping and interfering substances. For aqueous humor samples, an external standard was employed. Standard curves of peak height plotted against concentration, which were constructed from standard pilocarpine nitrate solutions, from spiked aqueous humor samples, and directly from solutions of known concentrations of analyte, were linear.

The initial step in the derivatization procedure is the double extraction with methylene chloride of the aqueous solutions or samples to which bicarbonate has been added. The efficiency of this extraction was evaluated in two ways. First, several standard pilocarpine solutions were carried through the derivatizing procedure, including the extraction step. The chromatographic results or peak heights obtained were compared to the peak heights obtained from solutions prepared directly with known concentrations of analyte. The chromatographic results were within ±2%, which confirms the extraction efficiency.

Second, aqueous humor samples were spiked with several known concentrations of tritiated pilocarpine and split into two sets. One set

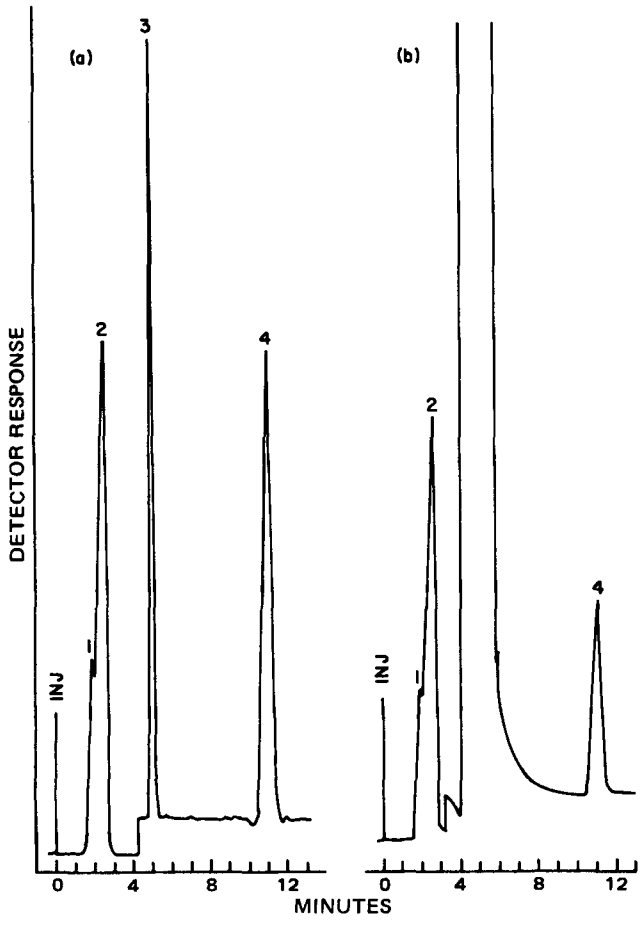

Figure 1—(a) *Chromatogram resulting from a standard pilocarpine nitrate solution. The peaks are: 1, solvent front; 2, excess* p*-nitrobenzyl bromide; 3, internal standard; and 4, analyte.* (b) *Chromatogram resulting from a spiked aqueous humor sample. No internal standard was added because of the broad overlapping contaminant peak.*

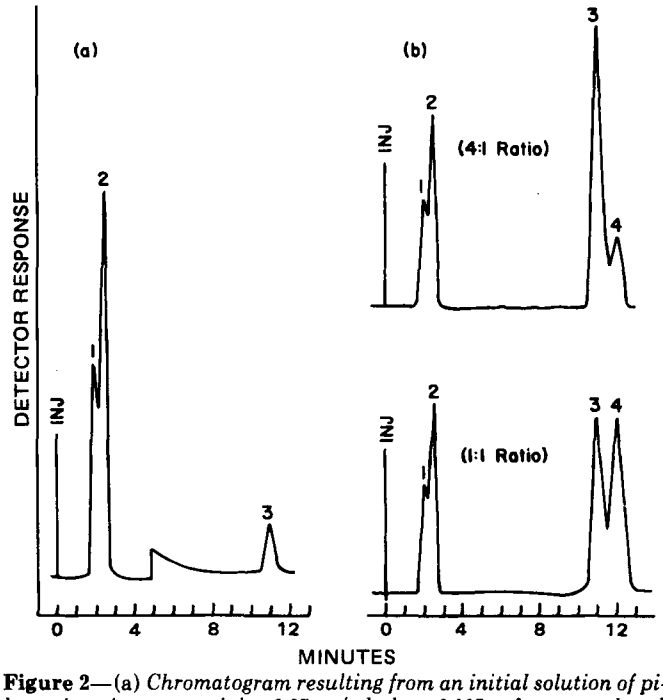

Figure 2—(a) *Chromatogram resulting from an initial solution of pilocarpine nitrate containing 0.05 μg/ml where 0.005 aufs was employed. This amount represents the equivalent of a 3.8-ng injection of pilocarpine. Peak height response linearity was observed at this level.* (b) *Chromatogram resulting from samples containing pilocarpine and isopilocarpine at ratios of 4:1 and 1:1. The peaks in both* a *and* b *are: 1, solvent front; 2, excess* p*-nitrobenzyl bromide; 3, analyte or derivatized pilocarpine (II); and 4, derivatized isopilocarpine.*

was assayed by the derivatization procedure, including the extraction step, and the other set was counted for radioactivity (11). The two sets of analytical results were within ±5%. In the procedure, the solutions containing pilocarpine to which a bicarbonate solution has been added are twice extracted with methylene chloride. The two extractions achieved a total transfer in excess of 98% of the pilocarpine, which is consistent with a previously reported extraction procedure for pilocarpine (2).

The results of the experiments conducted to determine the extraction efficiency support the use of the internal reference standard that is added just prior to injection and not added to the system prior to extraction. Also supported is the use of an external reference standard prepared directly from purified analyte rather than the use of standard solutions of pilocarpine nitrate which are carried through the complete derivatization procedure.

Of the pilocarpine nitrate solutions used to construct standard curves as outlined in the procedure for derivatization, the lowest concentration used was 0.3 μg/ml. To enhance sensitivity, experiments were conducted with 100-μl volumes of the *p*-nitrobenzyl bromide solutions in acetonitrile at 0.5 mg/ml (rather than 200 μl at 0.25 mg/ml). Decreasing the derivatizing reaction volume permitted the volume of the injected aliquot to approach the total volume of the reaction mixture.

Figure 2*a* gives the result of an experiment approximating the practical sensitivity limits of the procedure. The result was obtained from a pilocarpine nitrate solution at 0.05 μg/ml. The injection contained the equivalent of 3.8 ng of pilocarpine. Detection at this level was quantitative. The absolute limits of detection were not determined but are less than the 3.8 ng (or 0.05 μg/ml of pilocarpine nitrate) used previously.

Selectivity—To assess method selectivity, solutions were prepared that contained different ratios (4:1, 1:1, and 1:4) of pilocarine (I) to isopilocarpine (IV). These solutions were run through the described procedure and compared to samples of pure I and IV. A sample result is shown in Fig. 2*b*. The peak height ratios obtained (peak height of I to peak height of IV) were in excellent agreement with the concentration ratios of the initial solutions.

The results suggest that: (*a*) conversion of pilocarpine to isopilocarpine does not occur as a result of the procedure, (*b*) the method is quantitative for isopilocarpine and is applicable to the determination of the amount of isopilocarpine present in pilocarpine as a contaminant, and (*c*) the absorptivity of the pilocarpine and isopilocarpine derivatives is the same at 254 nm. In experiments conducted at the higher pilocarpine nitrate concentrations, *e.g.*, 10 μg/ml, the presence of contaminating isopilocarpine nitrate in the commercial pilocarpine nitrate was observed.

Other Nucleophiles—The primary intent of this study was to develop a method for the low level analysis of pilocarpine in aqueous humor. The method described is based on the reaction between the alkyl halide *p*-nitrobenzyl bromide and the 3′-tertiary amino group of the methylimidazole ring of pilocarpine, which results in the formation of the quaternary ammonium analyte II. Methods are readily available in the literature for the derivatization of primary and secondary amines for purposes of analysis (10, 12, 13), but this is not the case for tertiary amines.

The applicability of this derivatization procedure was investigated for other tertiary amines. Milligram samples of triethylamine, 4-methoxypyridine, and 1-methylimidazole were derivatized and chromatographed. The capacity factors, k', obtained for the resulting quaternary amine derivatives were 5.93, 6.47, and 6.73, respectively. The results indicate that the quaternization reaction using an alkyl halide, such as *p*-nitrobenzyl bromide, can be readily applied to the HPLC analysis of aromatic, heterocyclic, and alkyl tertiary amines in general. There is also flexibility relative to the choice of alkyl halide. An alternative for enhanced UV detection would be the selection of a chromophore with greater molar absorptivity. Another alternative would be the selection of an alkyl halide fluorophore, which would afford the advantage of greater sensitivity of fluorescence.

REFERENCES

(1) "The United States Pharmacopeia," 19th rev., Mack Publishing Co., Easton, Pa., 1975, pp. 385, 386.

(2) A. Repta and T. Higuchi, *J. Pharm. Sci.*, **60**, 1465 (1971).

(3) W. F. Bayne, L.-C. Chu, and F. T. Tau, *ibid.*, **65**, 1724 (1976).

(4) T. Urbanyi, A. Piedmont, E. Willis, and G. Manning, *ibid.*, **65**, 257 (1976).

(5) E. Gaetani and C. F. Laureri, *Farmaco, Ed. Prac.*, **33**, 26 (1978).
(6) N. Menschutkin, *Z. Phys. Chem.*, **5**, 589 (1890).
(7) C. G. Swain and N. D. Hershey, *J. Am. Chem. Soc.*, **94**, 1901 (1972).
(8) C. K. Ingold, "Structure and Mechanism in Organic Chemistry," 2nd ed., Cornell University Press, New York, N.Y., 1969, p. 435.
(9) R. B. Wagner and H. D. Zook, "Synthetic Organic Chemistry," Wiley, New York, N.Y., 1953, p. 665.
(10) W. Morozowich and M. Cho, in "GLC and HPLC Determination of Therapeutic Agents, Part 1," K. Tsuji and W. Morozowich, Eds., Dekker, New York, N.Y., 1978, pp. 222–224.
(11) T. Patton, *J. Pharm. Sci.*, **66**, 1058 (1977).
(12) T. H. Jupille, *Am. Lab.*, **1976**, 85.
(13) J. F. Lawrence and R. W. Frei, "Chemical Derivatization in Liquid Chromatography," Elsevier, New York, N.Y., 1976.

ACKNOWLEDGMENTS

Supported in part by National Eye Institute Grant EY02328, by National Institute of General Medical Sciences Grant GM22357, and by Biomedical Research Support Grant SO7-RR-5606.

Dosage Form Design for Improvement of Bioavailability of Levodopa II: Bioavailability of Marketed Levodopa Preparations in Dogs and Parkinsonian Patients

KUNIHIRO SASAHARA ˣ, TAKASHI NITANAI, TAEKO HABARA, TADASHI MORIOKA, and EIICHI NAKAJIMA

Received March 16, 1979, from the *Product Development Laboratories, Sankyo Company, Ltd., 1-2-58, Hiromachi, Shinagawa, Tokyo, Japan.* Accepted for publication September 14, 1979.

Abstract □ To estimate the absolute bioavailability of oral levodopa, plasma concentrations and urinary excretion of levodopa and its metabolites were determined in beagle dogs and in parkinsonian patients after intravenous and oral drug administration. The absolute bioavailability of orally administered levodopa was estimated to be about 35% in both dogs and patients; however, the total amount absorbed of intact drug and levodopa metabolites was estimated to be 80–90% of the administered dose. Due to the similarities of the pharmacokinetic characteristics of levodopa found in beagle dogs and in humans, beagle dogs can serve as a model to study bioavailability, absorption, and metabolic mechanisms.

Keyphrases □ Levodopa—bioavailability, dosage form design, dogs and humans □ Bioavailability—levodopa, dosage form design, dogs and humans □ Antiparkinsonian agents—levodopa, bioavailability, dosage form design, dogs and humans

Much higher oral doses than intravenous doses of levodopa are required to achieve a therapeutic effect in parkinsonian patients, and the resultant plasma levels after oral levodopa are markedly lower than those in patients receiving the drug intravenously.

Rivera-Calimlim *et al.* (1, 2) reported that when levodopa was administered orally to parkinsonian patients, a considerable portion apparently was metabolized *via* reactions in the stomach and intestines before it was absorbed. Other investigators (3–6) reported that 50–70% of the oral doses appeared to be metabolized in the intestinal mucosa of parkinsonian patients.

This paper reports part of a continuing study of levodopa to delineate mechanisms involved in the absorption profile in humans and to develop new dosage form designs to improve the bioavailability of levodopa. The absolute bioavailability of levodopa from marketed conventional preparations was determined by measuring the plasma levels and urinary excretion of levodopa and its metabolites after intravenous and oral administration of single doses to beagle dogs and to parkinsonian patients.

EXPERIMENTAL

Single Intravenous Doses in Dogs—After six healthy male beagle dogs, 10.3–12.5 kg, had been fasted for ~16 hr, levodopa[1] at a 50-mg dose was injected over 30 sec into the brachial vein. Blood samples were withdrawn with a heparinized syringe from the contralateral brachial vein. Samples were obtained 0, 2, 5, 15, and 45 min and 1, 1.5, 2, 3, 4, and 6 hr after dosing. Sodium metabisulfite solution (5% in a saline solution, 0.1 ml/5 ml of blood) and disodium ethylenediaminetetraacetate (2% in a saline solution, 0.1 ml/5 ml of blood) were added to the freshly drawn heparinized blood, and the plasma was separated immediately by centrifugation at 4°. All procedures were conducted in an ice bath.

Urine was collected before dosing and for 48 hr in bottles containing 5 ml of 6 *N* HCl and 3 ml of 0.2 *M* disodium ethylenediaminetetraacetate. The pH of the collected urine was adjusted to 2.0, and the urine was stored at −20° until assayed.

Single Oral Doses in Dogs—The same six beagle dogs used in the single intravenous dose studies were forcefully administered 250 mg of levodopa in capsule form[2] orally with 10 ml of warm water. The dogs' mouths were closed by hand to prevent emesis. Blood samples were withdrawn with a heparinized syringe 0, 0.5, 1, 2, 3, 4, and 6 hr after oral administration.

The blood samples were treated using the same procedures as in the intravenous study. The urine also was collected before dosing and for 48 hr after oral administration following the same procedure used for intravenous administration.

Single Intravenous Doses in Patients—Five parkinsonian patients (three men and two women) were studied. Their mean age was 63 years (range 51–71). Three days prior to the experiment, all levodopa preparations and other drugs that had been administered for the treatment of Parkinson's disease were withdrawn. Levodopa[1], 50 mg, diluted with 200 ml of physiological saline, was infused for 20 min at a constant rate into the brachial vein of these patients. Blood samples were withdrawn with a heparinized syringe at 0, 10, and 20 min during infusion and at 15 and 30 min and 1, 2, and 3 hr after infusion. The blood and urine samples were collected and processed in the same way as were those taken from the dogs.

Single Oral Doses in Patients—Six parkinsonian patients (three men and three women) were studied. Their mean age was 68 years (range 58–74). Three days before drug administration, all levodopa preparations and other drugs that had been administered for the treatment of Par-

[1] Dopaston Injection, Sankyo Co. Ltd., Tokyo, Japan.

0022-3549/80/0300-0261$01.00/0
© 1980, American Pharmaceutical Association

(5) E. Gaetani and C. F. Laureri, *Farmaco, Ed. Prac.*, **33**, 26 (1978).
(6) N. Menschutkin, *Z. Phys. Chem.*, **5**, 589 (1890).
(7) C. G. Swain and N. D. Hershey, *J. Am. Chem. Soc.*, **94**, 1901 (1972).
(8) C. K. Ingold, "Structure and Mechanism in Organic Chemistry," 2nd ed., Cornell University Press, New York, N.Y., 1969, p. 435.
(9) R. B. Wagner and H. D. Zook, "Synthetic Organic Chemistry," Wiley, New York, N.Y., 1953, p. 665.
(10) W. Morozowich and M. Cho, in "GLC and HPLC Determination of Therapeutic Agents, Part 1," K. Tsuji and W. Morozowich, Eds., Dekker, New York, N.Y., 1978, pp. 222–224.
(11) T. Patton, *J. Pharm. Sci.*, **66**, 1058 (1977).
(12) T. H. Jupille, *Am. Lab.*, **1976**, 85.
(13) J. F. Lawrence and R. W. Frei, "Chemical Derivatization in Liquid Chromatography," Elsevier, New York, N.Y., 1976.

ACKNOWLEDGMENTS

Supported in part by National Eye Institute Grant EY02328, by National Institute of General Medical Sciences Grant GM22357, and by Biomedical Research Support Grant SO7-RR-5606.

Dosage Form Design for Improvement of Bioavailability of Levodopa II: Bioavailability of Marketed Levodopa Preparations in Dogs and Parkinsonian Patients

KUNIHIRO SASAHARA ˣ, TAKASHI NITANAI, TAEKO HABARA, TADASHI MORIOKA, and EIICHI NAKAJIMA

Received March 16, 1979, from the *Product Development Laboratories, Sankyo Company, Ltd., 1-2-58, Hiromachi, Shinagawa, Tokyo, Japan.* Accepted for publication September 14, 1979.

Abstract □ To estimate the absolute bioavailability of oral levodopa, plasma concentrations and urinary excretion of levodopa and its metabolites were determined in beagle dogs and in parkinsonian patients after intravenous and oral drug administration. The absolute bioavailability of orally administered levodopa was estimated to be about 35% in both dogs and patients; however, the total amount absorbed of intact drug and levodopa metabolites was estimated to be 80–90% of the administered dose. Due to the similarities of the pharmacokinetic characteristics of levodopa found in beagle dogs and in humans, beagle dogs can serve as a model to study bioavailability, absorption, and metabolic mechanisms.

Keyphrases □ Levodopa—bioavailability, dosage form design, dogs and humans □ Bioavailability—levodopa, dosage form design, dogs and humans □ Antiparkinsonian agents—levodopa, bioavailability, dosage form design, dogs and humans

Much higher oral doses than intravenous doses of levodopa are required to achieve a therapeutic effect in parkinsonian patients, and the resultant plasma levels after oral levodopa are markedly lower than those in patients receiving the drug intravenously.

Rivera-Calimlim *et al.* (1, 2) reported that when levodopa was administered orally to parkinsonian patients, a considerable portion apparently was metabolized *via* reactions in the stomach and intestines before it was absorbed. Other investigators (3–6) reported that 50–70% of the oral doses appeared to be metabolized in the intestinal mucosa of parkinsonian patients.

This paper reports part of a continuing study of levodopa to delineate mechanisms involved in the absorption profile in humans and to develop new dosage form designs to improve the bioavailability of levodopa. The absolute bioavailability of levodopa from marketed conventional preparations was determined by measuring the plasma levels and urinary excretion of levodopa and its metabolites after intravenous and oral administration of single doses to beagle dogs and to parkinsonian patients.

EXPERIMENTAL

Single Intravenous Doses in Dogs—After six healthy male beagle dogs, 10.3–12.5 kg, had been fasted for ~16 hr, levodopa[1] at a 50-mg dose was injected over 30 sec into the brachial vein. Blood samples were withdrawn with a heparinized syringe from the contralateral brachial vein. Samples were obtained 0, 2, 5, 15, and 45 min and 1, 1.5, 2, 3, 4, and 6 hr after dosing. Sodium metabisulfite solution (5% in a saline solution, 0.1 ml/5 ml of blood) and disodium ethylenediaminetetraacetate (2% in a saline solution, 0.1 ml/5 ml of blood) were added to the freshly drawn heparinized blood, and the plasma was separated immediately by centrifugation at 4°. All procedures were conducted in an ice bath.

Urine was collected before dosing and for 48 hr in bottles containing 5 ml of 6 *N* HCl and 3 ml of 0.2 *M* disodium ethylenediaminetetraacetate. The pH of the collected urine was adjusted to 2.0, and the urine was stored at −20° until assayed.

Single Oral Doses in Dogs—The same six beagle dogs used in the single intravenous dose studies were forcefully administered 250 mg of levodopa in capsule form[2] orally with 10 ml of warm water. The dogs' mouths were closed by hand to prevent emesis. Blood samples were withdrawn with a heparinized syringe 0, 0.5, 1, 2, 3, 4, and 6 hr after oral administration.

The blood samples were treated using the same procedures as in the intravenous study. The urine also was collected before dosing and for 48 hr after oral administration following the same procedure used for intravenous administration.

Single Intravenous Doses in Patients—Five parkinsonian patients (three men and two women) were studied. Their mean age was 63 years (range 51–71). Three days prior to the experiment, all levodopa preparations and other drugs that had been administered for the treatment of Parkinson's disease were withdrawn. Levodopa[1], 50 mg, diluted with 200 ml of physiological saline, was infused for 20 min at a constant rate into the brachial vein of these patients. Blood samples were withdrawn with a heparinized syringe at 0, 10, and 20 min during infusion and at 15 and 30 min and 1, 2, and 3 hr after infusion. The blood and urine samples were collected and processed in the same way as were those taken from the dogs.

Single Oral Doses in Patients—Six parkinsonian patients (three men and three women) were studied. Their mean age was 68 years (range 58–74). Three days before drug administration, all levodopa preparations and other drugs that had been administered for the treatment of Par-

[1] Dopaston Injection, Sankyo Co. Ltd., Tokyo, Japan.

0022-3549/80/0300-0261$01.00/0
© 1980, American Pharmaceutical Association

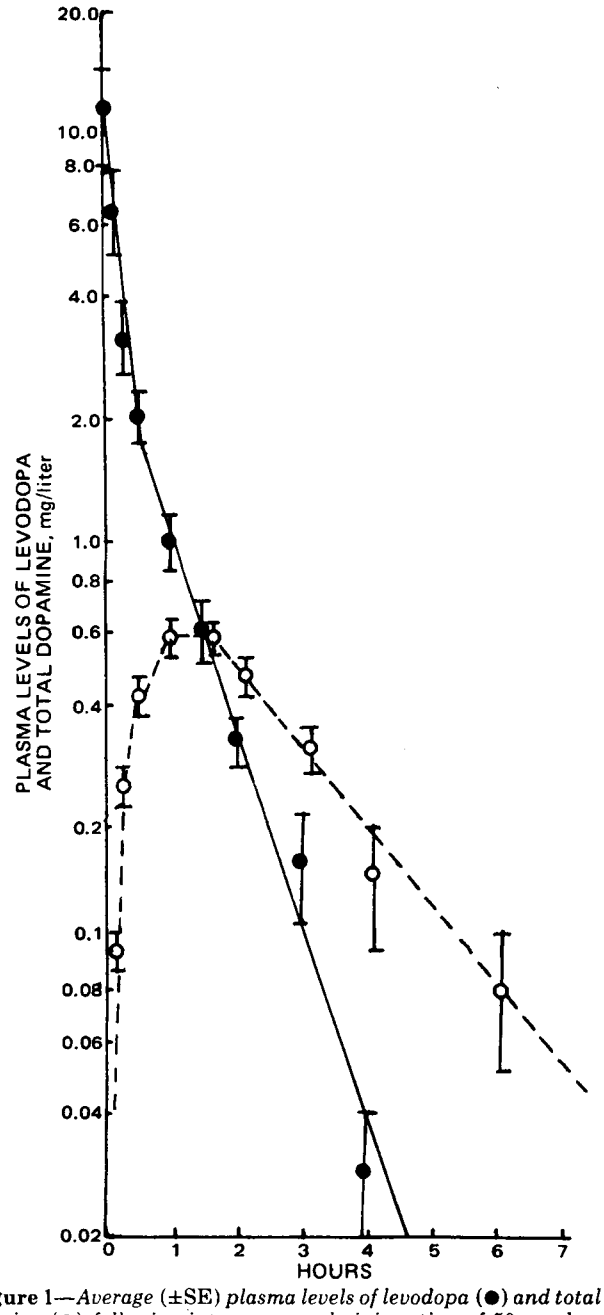

Figure 1—*Average* (±SE) *plasma levels of levodopa* (●) *and total dopamine* (○) *following intravenous administration of 50-mg doses of levodopa to six dogs.*

kinson's disease were withdrawn. A 1-g dose of levodopa in capsule form[2] was administered to the subjects with 1 cup of water at about 9:00 am.

On the day of the study, the subjects ate breakfast at about 7:00 am, lunch at about 12:00, and dinner at about 5:30 pm. Blood samples were withdrawn with a heparinized syringe before the drug was administered and at 0.5, 1, 2, 3, 4, and 6 hr after oral administration. The blood and urine samples were collected and processed using the same procedures as those used for the dogs.

Assay of Levodopa and Its Metabolites in Plasma and Urine—Levodopa and its metabolites in plasma and urine were assayed according to the methods reported previously (7).

Pharmacokinetics—The plasma levodopa concentration curves following intravenous administration to dogs were analyzed using the program of Hanano *et al.* (8). The plasma levodopa concentration curves following oral administration to dogs, infusion administration to patients, and oral administration to patients were analyzed using the BMDP-3R nonlinear regression program (9).

[2] Dopaston Capsules, Sankyo Co. Ltd., Tokyo, Japan.

Table I—Average Pharmacokinetic Parameters of Levodopa [a]

Parameter	Dogs[b], 50 mg iv	Patients[c], 50 mg iv
α, hr^{-1}	13.3 ± 3.4	11.7 ± 1.05
β, hr^{-1}	1.14 ± 0.11	1.12 ± 0.13
$0.693/\beta$, hr	0.58 ± 0.06	0.65 ± 0.069
k_{12}, hr^{-1}	6.5 ± 0.59	5.1 ± 0.52
k_{21}, hr^{-1}	3.3 ± 0.34	3.1 ± 0.29
k_{10}, hr^{-1}	4.5 ± 0.42	3.7 ± 0.35
V_1, liter/kg	0.29 ± 0.027	0.36 ± 0.037
AUC of levodopa, mg/kg/liter/hr	0.34 ± 0.025	0.0124 ± 0.0012
AUC of total dopamine, mg/kg/liter/hr	0.17 ± 0.014	0.0099 ± 0.00094
Clearance of levodopa, liters/kg/hr	1.21 ± 0.11	1.38 ± 0.19

[a] Average ± *SE*. [b] $n = 6$. [c] $n = 5$.

RESULTS

Absolute Bioavailability of Marketed Levodopa Preparations in Dogs—*Single Intravenous Doses*—The average plasma levels of levodopa and total dopamine[3] following intravenous administration of levodopa at a 50-mg dose to six dogs are presented in Fig. 1. Since the plasma levodopa concentration–time curve appeared to follow biexponential disposition characteristics, the data were fitted to the two-compartment open model using linear kinetics. Table I shows the results of the computer analysis. Visual inspection of the observed points around the fitted curve indicated satisfactory randomness of scatter. The average area under the plasma concentration–time curve (*AUC*) of levodopa corrected for body weight and the average plasma clearance of levodopa corrected for body weight also are shown in Table I to facilitate comparison between these parameters in dogs and in patients.

The average plasma levels of total dopamine formed by the metabolism of levodopa increased with time, reached a maximum value at ~1 hr after intravenous administration, and then decreased more slowly as compared to the elimination of levodopa in the plasma. The average *AUC* of total dopamine corrected for body weight is shown in Table I.

The intravenously administered levodopa was excreted in urine over 48 hr as total levodopa[4], total dopamine, total 3,4-dihydroxyphenylacetic acid[5], and total homovanillic acid[6], which represented 3.1 ± 0.43, 10.6 ± 0.92, 12.3 ± 1.24, and 37.3 ± 3.51% of the dose, respectively. Consequently, 63.3 ± 4.52% of the dose in terms of total urinary excretion[7] was eliminated within 48 hr after intravenous administration. The remainder of the drug probably was excreted in the feces or was undetermined metabolites.

Single Oral Doses—The average plasma levels of levodopa and total dopamine after oral administration of levodopa to six dogs are shown in Fig. 2. The maximum plasma level of 4.32 ± 0.42 mg/liter occurred 1 hr after oral administration. The levels then decreased rapidly to ~0.2 mg/liter 6 hr after oral administration, corresponding to 5% of the maximum plasma levels.

The average plasma levels of total dopamine changed more slowly than did those of levodopa. The elimination of total dopamine from the plasma also was slower compared to that of levodopa, and the plasma level of total dopamine 6 hr after oral administration was 0.42 ± 0.03 mg/liter, corresponding to about 25% of the maximum levels. The average *AUC* values of levodopa and total dopamine were 0.60 ± 0.053 and 0.56 ± 0.046 mg/liter/hr, respectively.

The orally administered levodopa was excreted in urine over 48 hr as total levodopa, total dopamine, total 3,4-dihydroxyphenylacetic acid, and total homovanillic acid, which represented 0.73 ± 0.93, 11.7 ± 1.21, 13.6 ± 0.91, and 25.6 ± 2.62% of the dose, respectively. Consequently, 51.6 ± 3.02% of the dose was excreted within 48 hr after oral administration.

Comparison of the absolute bioavailability of marketed levodopa capsules after oral administration with intravenous injection was accomplished using the plasma levodopa levels to estimate the intact amounts of levodopa absorbed into the circulation system, with the as-

[3] Total dopamine = conjugated dopamine + unconjugated dopamine.

[4] Total levodopa = unconjugated levodopa + conjugated levodopa.

[5] Total 3,4-dihydroxyphenylacetic acid = unconjugated 3,4-dihydroxyphenylacetic acid + conjugated 3,4-dihydroxyphenylacetic acid.

[6] Total homovanillic acid = unconjugated homovanillic acid + conjugated homovanillic acid.

[7] Total urinary excretion = total levodopa + total dopamine + total 3,4-dihydroxyphenylacetic acid + total homovanillic acid.

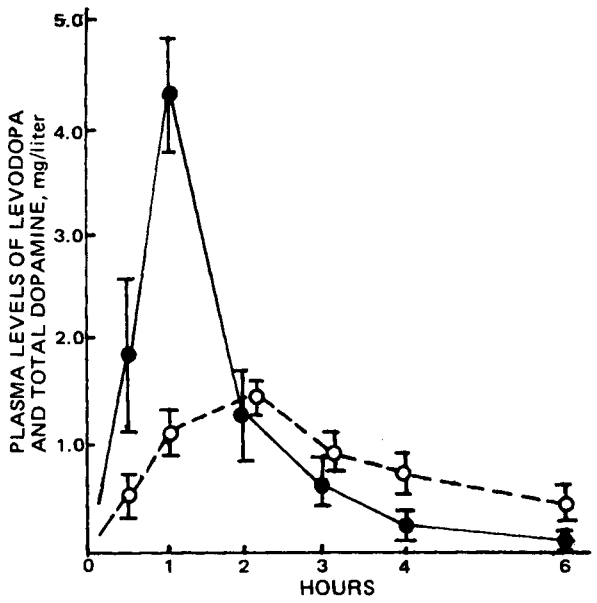

Figure 2—*Average* (±SE) *plasma levels of levodopa* (●) *and total dopamine* (○) *following oral administration of 250-mg doses of levodopa to six dogs.*

sumption that levodopa disposition in the body followed linear kinetics. On the other hand, the total amount absorbed from the GI tract, including levodopa and its metabolites, was calculated by the ratio of the total urinary excretion after oral administration to that after intravenous administration. The absolute bioavailability in the dogs and the total amount absorbed are shown in Table I. These results indicate that the difference between these values is due to presystemic metabolism and/or degradation of the drug.

Absolute Bioavailability of Marketed Levodopa Capsules in Parkinsonian Patients—*Single Intravenous Doses*—The average plasma levels of levodopa and total dopamine for 20 min following intravenous infusion of a 50-mg dose of levodopa to five parkinsonian patients are presented in Fig. 3. The plasma levodopa levels increased during the intravenous infusion and reached a maximum value of 0.89 ± 0.09 mg/liter at the conclusion of the infusion, *i.e.*, 20 min after the beginning of the intravenous infusion. The subsequent plasma levodopa levels decreased rapidly, and levodopa was almost undetectable in the plasma after 200 min. These plasma levodopa concentration–time curves were analyzed by appropriate procedures and linear kinetics presuming a two-compartment open model (Table I). The terminal half-life of levodopa in patients was 39 ± 4.1 min (mean ± *SE*). The *AUC* of levodopa corrected for body weight was 0.0124 ± 0.0012 mg/kg/liter/hr (Table II).

The plasma level of total dopamine increased with time and reached a maximum value of 0.18 ± 0.016 mg/liter 50 min after the intravenous infusion began. The levels then decreased more slowly compared to the elimination of levodopa in the plasma and were approximately 33% of the maximum plasma levels 200 min after the intravenous infusion began. Plasma levodopa and total dopamine were not detectable before dosing. The *AUC* of total dopamine was 0.0099 ± 0.00094 mg/kg/liter/hr.

The infused levodopa was excreted in urine over 8 hr as total levodopa, total dopamine, total 3,4-dihydroxyphenylacetic acid, and total homovanillic acid, which represented 2.5 ± 0.21, 11.2 ± 1.02, 11.8 ± 0.94, and 29.6 ± 2.43% of the dose, respectively. Consequently, 55.1 ± 4.24% of the dose was excreted within 48 hr after infusion.

Single Oral Administration—The average plasma levels of levodopa and total dopamine after oral administration of a 1-g dose of levodopa in capsule form to six patients are shown in Fig. 4. The maximum plasma levels occurred 1 hr after oral administration. The levels then decreased rapidly to <0.2 mg/liter at 6 hr after oral administration. The *AUC* of levodopa was 0.0826 ± 0.0105 mg/kg/liter/hr.

The average plasma levels of total dopamine reached a maximum after 2 hr and then decreased more slowly than did those of levodopa, with the concentration of 0.45 ± 0.05 mg/liter at 6 hr corresponding to about 33% of the maximum levels. The *AUC* of total dopamine was 0.104 ± 0.0102 mg/kg/liter/hr.

Orally administered levodopa was excreted in urine over 24 hr as total levodopa, total dopamine, total 3,4-dihydroxyphenylacetic acid, and total homovanillic acid, which represented 0.58 ± 0.065, 13.5 ± 1.25, 15.1 ± 1.62, and 18.2 ± 1.95% of the dose, respectively. Consequently, 48.4 ± 4.13% of the dose was excreted within 48 hr after oral administration.

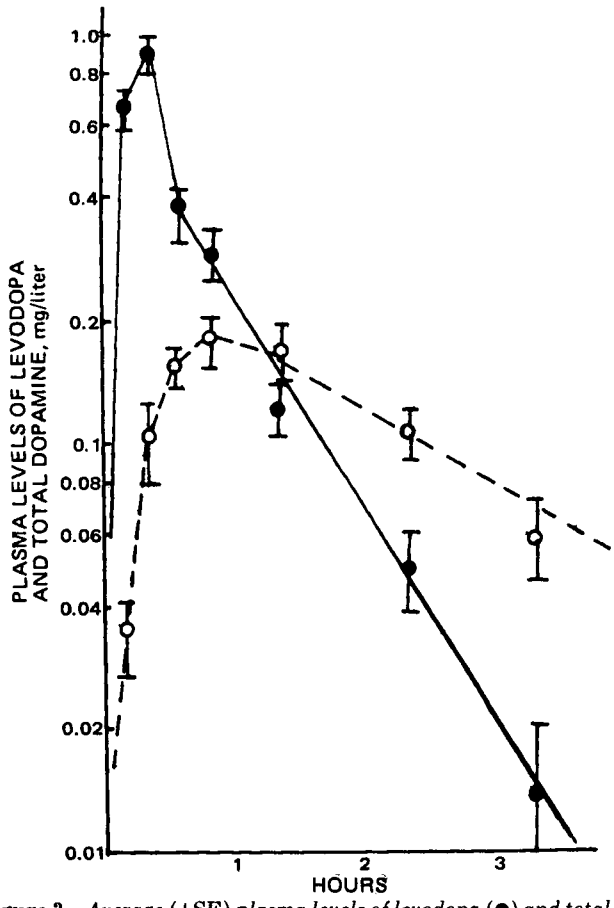

Figure 3—*Average* (±SE) *plasma levels of levodopa* (●) *and total dopamine* (○) *following infusion of 50-mg doses of levodopa to five parkinsonian patients.*

The absolute bioavailability and total percent of oral capsules that were absorbed by patients were calculated on the assumption that levodopa in the body obeys linear kinetics and that the two different population groups were comparable in this study. They are shown in Table II and were in good agreement with the values for the dogs.

DISCUSSION

The plasma concentration–time curves and the estimated pharmacokinetic parameters obtained in these studies compare well with the data obtained by Coutinho *et al.* (10) and Colter *et al.* (11) following intravenous administration of radiolabeled levodopa to dogs. However, Coutinho *et al.* (10) reported that ~75% of the intravenously administered dose, in terms of total radioactivity, was recovered in the urine within 72 hr. In contrast, ~65% of the intravenously administered dose, as the sum of total levodopa, total dopamine, total 3,4-dihydroxyphenylacetic acid, and total homovanillic acid, was excreted in the urine within 48 hr in the present studies. Both results seem to be consistent considering that the data of Coutinho *et al.* (10) involved total radioactivity measurements.

Table II—Absolute Bioavailability and Total Amount Absorbed, Including Metabolites, after Oral Administration of Levodopa to Dogs and Patients

Subject	Dose, mg	Absolute Bioavailability, %[a]	Total Amount Absorbed, %[a]
Dogs	250	36.3 ± 2.9[b]	81.0 ± 4.7
Patients	1000	33.3 ± 4.23	87.8 ± 7.4

[a] Based on the presumed linear kinetics using the dose-corrected *AUC* from the intravenous dose. [b] Average ± *SE*.

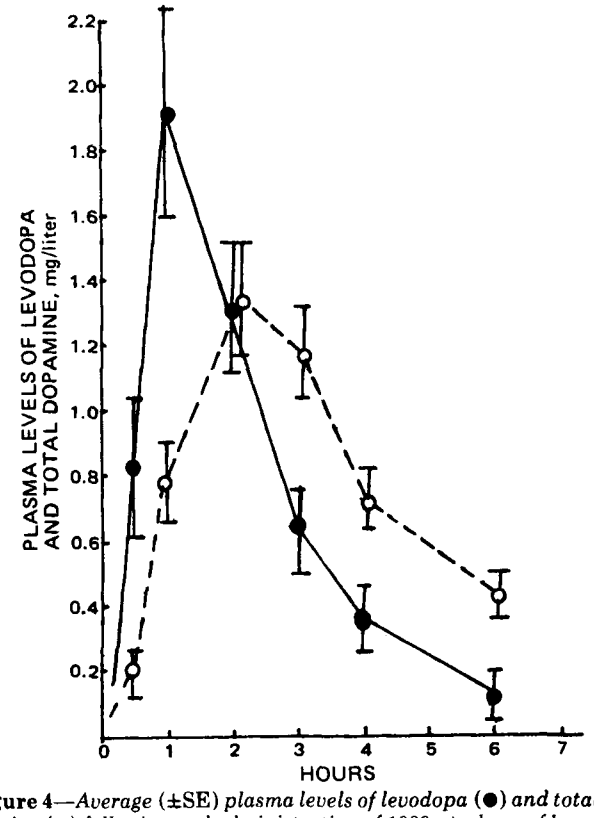

Figure 4—*Average* (±SE) *plasma levels of levodopa* (●) *and total dopamine* (○) *following oral administration of 1000-mg doses of levodopa to six parkinsonian patients.*

The profile of plasma levodopa levels and the pattern of urinary excretion obtained in this experiment following oral administration of levodopa, respectively, agree with the results and the observations reported previously (10–12). In the urine, 44–57% of the oral dose was excreted, including metabolites, but only small amounts of intact levodopa were excreted.

The absolute bioavailability and the extent of total oral absorption including levodopa and its metabolites following oral administration of levodopa to dogs were ~35 and 80%, respectively. These results showed that the bioavailability of levodopa was low but that the extent of total absorption of levodopa was good. It can be inferred that this difference is due to the degradation and/or metabolism of levodopa in the GI tract and liver during absorption. In fact, levodopa decarboxylase, believed to be responsible for metabolizing levodopa, is widely distributed in the liver (13–15), kidney (16), and GI tract (5, 6, 17). The activity of this enzyme is relatively high in the GI tract. Therefore, the proposal of gut and gut wall metabolism of levodopa by this enzyme probably is justified.

One way of evaluating the first-pass effect is to compare the ratio of the *AUC* of the metabolite, total dopamine, to that of the parent drug. These relationships may be represented as follows:

$$AUC_{\text{levodopa}} = FD/Cl_{\text{levodopa}} \qquad \text{(Eq. 1)}$$

$$AUC_{\text{total dopamine}} = fFD/Cl_{\text{total dopamine}} \qquad \text{(Eq. 2)}$$

where Cl_{levodopa} and $Cl_{\text{total dopamine}}$ represent the elimination clearance of the respective compounds, *FD* represents the levodopa dose absorbed, and *f* represents the fraction of the levodopa dose absorbed that is converted to total dopamine. The ratio of Eq. 2 to Eq. 1 gives:

$$\frac{AUC_{\text{total dopamine}}}{AUC_{\text{levodopa}}} = \frac{fCl_{\text{levodopa}}}{Cl_{\text{total dopamine}}} \qquad \text{(Eq. 3)}$$

Thus, the new ratio shown in Eq. 3 cancels out the *FD* term relating to the absorbed dose. The right side of Eq. 3 includes three parameters. The elimination clearance of dopamine, $Cl_{\text{total dopamine}}$, in the denominator should be unaffected by the administration route. Since Eq. 3 eliminates the effect of the absorbed dose, the observed elimination clearance for the parent drug, Cl_{levodopa}, should be unchanged as long as the system obeys linear kinetics.

Finally, Eq. 3 includes a term, *f*, in the numerator that represents the fraction of the parent drug converted to the metabolite, total dopamine. This term should increase after oral administration relative to an intravenous dose. Therefore, comparison of the *AUC* ratios obtained after oral and intravenous studies should reflect the increase in the metabolite formed *via* presystemic metabolism of the drug during oral absorption. The ratio in dogs was 0.56 ± 0.06 after intravenous injection *versus* 0.93 ± 0.10 after oral absorption. Therefore, the first-pass metabolism most likely results in more extensive metabolism of levodopa.

On the other hand, parkinsonian patients administered an intravenous dose of levodopa showed levodopa disposition kinetics similar to those observed in the dogs (Table I). As mentioned before, about 55% of the intravenous dose was recovered from the urine within 8 hr. Imai *et al.* (18) reported that following oral administration of levodopa to parkinsonian patients, >90% of the drug excreted within 24 hr was recovered from the urine within the first 8 hr. Therefore, even though these data are from urine collected within the first 8 hr after dose administration, it seems appropriate to assume that the results would be similar to the 24-hr data. In addition, Bronaugh *et al.* (19) determined the urinary excretion of total levodopa, total dopamine, total 3,4-dihydroxyphenylacetic acid, and total homovanillic acid separately after intravenous administration of radioactive levodopa to patients. They reported about 50% urinary excretion of these metabolites, which is in good agreement with our value. The plasma levodopa levels and the urinary excretion pattern following oral administration of levodopa in the parkinsonian patients in the present study were similar to previous (18, 20, 21) results.

The absolute bioavailability and the extent of total absorption calculated from results of intravenous infusion in parkinsonian patients were ~33 and 88%, respectively (Table II). These results show that bioavailability of levodopa was low in patients but that the extent of total absorption of levodopa was good, as in dogs. Also, the ratio of the *AUC* of total dopamine to the *AUC* of levodopa was 0.81 ± 0.06 after an intravenous dose in patients, while it was 1.26 ± 0.13 after oral administration. These values are consistent with the concept of first-pass metabolism, yielding a more extensive metabolism of levodopa during oral administration in patients as well as in dogs.

Furthermore, the results of these bioavailability studies using both dogs and patients indicate that beagle dogs and patients showed similar pharmacokinetic parameters following intravenous administration of levodopa (Table I) and similar bioavailability of oral levodopa (Table II). Therefore, this study supports the use of beagle dogs as model animals for pharmacokinetic and biopharmaceutical investigations to study the mechanism involved in the low bioavailability of marketed levodopa preparations. A subsequent paper of this series will discuss the possibility of nonlinear kinetics of levodopa in dogs and humans.

REFERENCES

(1) L. Rivera-Calimlim, C. A. Dujorvne, J. P. Morgan, L. Lasagna, and J. R. Bianchine, *Eur. J. Clin. Invest.*, **1**, 313 (1971).

(2) L. Rivera-Calimlim, C. Dujorvne, J. Morgan, L. Lasagna, and J. Bianchine, *Pharmacologist*, **12**, 269 (1970).

(3) J. Bergmark, A. Carlsson, A.-K. Granerus, R. Jagenburg, T. Magnusson, and A. Svanborg, *Naunyn-Schmiedebergs Arch. Pharmakol.*, **272**, 437 (1972).

(4) A.-K. Granerus, R. Jagenburg, and A. Svanborg, *ibid.*, **280**, 429 (1973).

(5) A.-K. Granerus, R. Jagenburg, S. Rödjer, and A. Svanborg, *Acta Med Scand.*, **196**, 459 (1974).

(6) I. Anderson, A.-K. Granerus, R. Jagenburg, and A. Svanborg, *ibid.*, **198**, 415 (1975).

(7) K. Sasahara, T. Nitanai, T. Habara, A. Ninomiya, T. Morioka, and E. Nakajima, *Ann. Rep. Sankyo Res. Lab.*, **30**, 65 (1978).

(8) M. Hanano, S. Awazu, K. Bun, T. Fuwa, R. Iga, and K. Nogami, presented at the 2nd Symposium of Metabolism, Effect and Toxicity of Drugs, Kyoto, Japan, Nov. 1972.

(9) W. J. Dixon and M. B. Brown, "BMDP Biomedical Computer Programs," University of California Press, Berkeley, Calif., 1977.

(10) C. B. Coutinho, H. E. Spiegel, S. A. Kaplan, M. Yu, R. P. Christian, J. J. Carbone, J. Symington, J. A. Cheripko, M. Lewis, A. Tonchen, and T. Crews, *J. Pharm. Sci.*, **60**, 1014 (1971).

(11) S. Cotler, A. Holazo, H. G. Boxenbaum, and S. A. Kaplan, *ibid.*, **65**, 822 (1976).

(12) W. B. Abrams, C. B. Coutinho, A. S. Leon, and H. E. Spiegel, *J. Am. Med. Assoc.*, **218**, 1912 (1971).

(13) T. L. Sourkes, *Pharmacol. Rev.*, **18**, 53 (1966).

(14) L. Calimlim, J. Morgan, C. A. Dujorvne, J. R. Bianchine, and L. Lasagna, *Biochem. Pharmacol.*, **20**, 3051 (1971).

(15) L. Landsberg and L. H. Taubin, *ibid.*, **22**, 2789 (1973).

(16) J. G. Christenson, W. Dairman, and S. Udenfriend, *Arch. Biochem. Biophys.*, **141**, 356 (1970).
(17) G. M. Tyce and C. A. Owen, *Biochem. Pharmacol.*, **21**, 2977 (1972).
(18) K. Imai, M. Sugiura, H. Kubo, Z. Tamura, K. Ohya, N. Tsunakawa, and K. Hirayama, *Chem. Pharm. Bull.*, **20**, 759 (1972).
(19) R. L. Bronaugh, R. J. McMurtry, M. M. Hoehn, and C. O. Rutledge, *Biochem. Pharmacol.*, **24**, 1317 (1975).
(20) S. Bergmann, G. Curzon, J. Friedel, R. B. Godwin-Austen, C. D. Marsden, and J. D. Parkes, *Br. J. Clin. Pharmacol.*, **1**, 417 (1974).
(21) J. G. L. Morris, R. L. Parsons, J. R. Trounce, and M. J. Groves, *ibid.*, **3**, 983 (1976).

ACKNOWLEDGMENTS

Presented in part at the Pharmaceutics Section, 97th Meeting of the Pharmaceutical Society of Japan, Tokyo, Japan, April 1977.

The authors are grateful to Dr. A. Noguchi for help in designing the protocol and supervising drug administration and blood and urine sampling in patients and to Mr. S. Yamane for technical assistance in the bioavailability studies in patients. The authors also thank Dr. T. Higuchi for valuable discussions; Dr. H. Negoro, Dr. S. Akagi, and Dr. T. Miki for the promotion of the research project; Dr. S. Riegelman for constructive comments on the manuscript; and Ms. Ellen Buoncristiani for typing the manuscript.

Polymers for Sustained Macromolecule Release: Procedures to Fabricate Reproducible Delivery Systems and Control Release Kinetics

WILLIAM D. RHINE, DEAN S. T. HSIEH, and ROBERT LANGER ˣ

Received May 31, 1979, from the *Department of Nutrition and Food Science, Massachusetts Institute of Technology, Cambridge, MA 02139,* and the *Department of Surgery, Childrens' Hospital Medical Center, Boston, MA 02115.* Accepted for publication October 8, 1979.

Abstract □ Matrixes composed of ethylene–vinyl acetate copolymer are useful vehicles for the sustained release of macromolecules such as proteins. A new procedure for fabricating these polymeric delivery systems involved mixing the dry, powdered macromolecule with a polymer solution and casting the mixture at −80°. The resulting matrix was dried in two 48-hr stages, first at −20° and then at 20°. These polymer systems had uniform drug distribution, and their release kinetics were reproducible. Fabrication parameters such as drug particle size, drug loading, and matrix coating all significantly affected release kinetics.

Keyphrases □ Kinetics, drug release—effects of particle size, drug loading, and matrix coating on polymer–drug mixtures □ Polymers—use in sustained-release film formation, preparation methods of polymer–drug matrix, low temperature effects on polymeric matrix □ Controlled-delivery system—preparation methods, polymer–drug matrix, drug release kinetics

A previous study described the first biocompatible polymeric delivery systems capable of continuously delivering macromolecules (mol. wt. > 1000) such as proteins for prolonged periods (1). In that study, a polymer–macromolecule matrix was formed by mixing powdered macromolecules in a polymer solution. This mixture was poured into small, conical, glass molds, and the solvent was evaporated. The resulting pellets, when exposed to an aqueous medium, released macromolecules in biochemically active form for >100 days (2). Although sustained release was achieved, the reproducibility of the release kinetics was poor. Difficulties in obtaining reproducible release rates were compounded when larger volume polymeric delivery systems were fabricated.

Significant drug settling and redistribution occurred during casting and drying due to the insolubility of the incorporated macromolecules in the polymer solvent. At room temperature, the drug migrated vertically, and visible lateral motion was caused by currents (possibly thermal) in the mixture. The low temperature casting procedures described were developed to minimize this drug movement during matrix formation. The reproducibility of release kinetics of matrixes prepared using these low temperature methods was improved markedly.

The reproducible kinetics permitted the study of the effects of certain fabrication factors, including drug particle size, drug loading, and matrix coating, on macromolecule release. The significant effects of these factors on release kinetics suggest possible means of utilizing and modifying macromolecular release systems according to research or clinical needs.

EXPERIMENTAL

Matrix Preparation—Ethylene–vinyl acetate copolymer[1] (40% vinyl acetate by weight) was dissolved in methylene chloride[2] to give a 10% solution (w/v). Protein or another macromolecular powder was sieved[3] to give particles of <75, 75–250, or 250–425 μm. A weighed amount of powder from a single size range was added to 15 ml of the polymer solution in a glass vial[4], and the mixture was vortexed[5] for at least 10 sec to yield a uniform suspension. This mixture was poured quickly into the center of a leveled glass mold (7 × 7 × 0.5 cm), which had been cooled previously on dry ice for 5 min. During precooling, the mold was covered with a glass plate to prevent excess frost formation.

After the mixture was poured, the mold remained on the dry ice for 10 min, and the mixture froze. (The mold was covered again for the last 7 min of this stage.) The frozen slab was easily pried loose with a cold spatula, transferred onto a wire screen[6], and kept at −20° for 2 days. The slab then was dried for 2 more days at room temperature in a desiccator[7] under a mild, houseline vacuum (600 mtorr). Drying caused the slabs to shrink to ~5 × 5 cm. The central 3 × 3-cm square was excised with a scalpel[8] and a straight edge and divided further into nine 1 × 1-cm squares.

Kinetics—Each square was weighed, its thickness was measured with

[1] Elvax 40, DuPont Chemical Co., Wilmington, Del. This polymer also may be obtained from Dr. Langer at the Massachusetts Institute of Technology.
[2] Fisher Scientific Co., Fair Lawn, N.J.
[3] American Standard sieves, Nos. 40, 60, and 200, Dual Manufacturing Co., Chicago, Ill.
[4] Wheaton Scientific Co., Millville, N.J.
[5] Scientific Industries, Bohemia, N.Y.; set at speed 10.
[6] Common steel mesh, 0.5-mm spacing.
[7] Bel Art, Pequannock, N.J.
[8] No. 10 blade, Bard-Parker, Rutherford, N.J.

0022-3549/80/0300-0265$01.00/0
© 1980, American Pharmaceutical Association

(16) J. G. Christenson, W. Dairman, and S. Udenfriend, *Arch. Biochem. Biophys.*, **141**, 356 (1970).
(17) G. M. Tyce and C. A. Owen, *Biochem. Pharmacol.*, **21**, 2977 (1972).
(18) K. Imai, M. Sugiura, H. Kubo, Z. Tamura, K. Ohya, N. Tsunakawa, and K. Hirayama, *Chem. Pharm. Bull.*, **20**, 759 (1972).
(19) R. L. Bronaugh, R. J. McMurtry, M. M. Hoehn, and C. O. Rutledge, *Biochem. Pharmacol.*, **24**, 1317 (1975).
(20) S. Bergmann, G. Curzon, J. Friedel, R. B. Godwin-Austen, C. D. Marsden, and J. D. Parkes, *Br. J. Clin. Pharmacol.*, **1**, 417 (1974).
(21) J. G. L. Morris, R. L. Parsons, J. R. Trounce, and M. J. Groves, *ibid.*, **3**, 983 (1976).

ACKNOWLEDGMENTS

Presented in part at the Pharmaceutics Section, 97th Meeting of the Pharmaceutical Society of Japan, Tokyo, Japan, April 1977.

The authors are grateful to Dr. A. Noguchi for help in designing the protocol and supervising drug administration and blood and urine sampling in patients and to Mr. S. Yamane for technical assistance in the bioavailability studies in patients. The authors also thank Dr. T. Higuchi for valuable discussions; Dr. H. Negoro, Dr. S. Akagi, and Dr. T. Miki for the promotion of the research project; Dr. S. Riegelman for constructive comments on the manuscript; and Ms. Ellen Buoncristiani for typing the manuscript.

Polymers for Sustained Macromolecule Release: Procedures to Fabricate Reproducible Delivery Systems and Control Release Kinetics

WILLIAM D. RHINE, DEAN S. T. HSIEH, and ROBERT LANGER ˣ

Received May 31, 1979, from the *Department of Nutrition and Food Science, Massachusetts Institute of Technology, Cambridge, MA 02139,* and the *Department of Surgery, Childrens' Hospital Medical Center, Boston, MA 02115.* Accepted for publication October 8, 1979.

Abstract □ Matrixes composed of ethylene–vinyl acetate copolymer are useful vehicles for the sustained release of macromolecules such as proteins. A new procedure for fabricating these polymeric delivery systems involved mixing the dry, powdered macromolecule with a polymer solution and casting the mixture at −80°. The resulting matrix was dried in two 48-hr stages, first at −20° and then at 20°. These polymer systems had uniform drug distribution, and their release kinetics were reproducible. Fabrication parameters such as drug particle size, drug loading, and matrix coating all significantly affected release kinetics.

Keyphrases □ Kinetics, drug release—effects of particle size, drug loading, and matrix coating on polymer–drug mixtures □ Polymers—use in sustained-release film formation, preparation methods of polymer–drug matrix, low temperature effects on polymeric matrix □ Controlled-delivery system—preparation methods, polymer–drug matrix, drug release kinetics

A previous study described the first biocompatible polymeric delivery systems capable of continuously delivering macromolecules (mol. wt. > 1000) such as proteins for prolonged periods (1). In that study, a polymer–macromolecule matrix was formed by mixing powdered macromolecules in a polymer solution. This mixture was poured into small, conical, glass molds, and the solvent was evaporated. The resulting pellets, when exposed to an aqueous medium, released macromolecules in biochemically active form for >100 days (2). Although sustained release was achieved, the reproducibility of the release kinetics was poor. Difficulties in obtaining reproducible release rates were compounded when larger volume polymeric delivery systems were fabricated.

Significant drug settling and redistribution occurred during casting and drying due to the insolubility of the incorporated macromolecules in the polymer solvent. At room temperature, the drug migrated vertically, and visible lateral motion was caused by currents (possibly thermal) in the mixture. The low temperature casting procedures described were developed to minimize this drug movement during matrix formation. The reproducibility of release kinetics of matrixes prepared using these low temperature methods was improved markedly.

The reproducible kinetics permitted the study of the effects of certain fabrication factors, including drug particle size, drug loading, and matrix coating, on macromolecule release. The significant effects of these factors on release kinetics suggest possible means of utilizing and modifying macromolecular release systems according to research or clinical needs.

EXPERIMENTAL

Matrix Preparation—Ethylene–vinyl acetate copolymer[1] (40% vinyl acetate by weight) was dissolved in methylene chloride[2] to give a 10% solution (w/v). Protein or another macromolecular powder was sieved[3] to give particles of <75, 75–250, or 250–425 μm. A weighed amount of powder from a single size range was added to 15 ml of the polymer solution in a glass vial[4], and the mixture was vortexed[5] for at least 10 sec to yield a uniform suspension. This mixture was poured quickly into the center of a leveled glass mold (7 × 7 × 0.5 cm), which had been cooled previously on dry ice for 5 min. During precooling, the mold was covered with a glass plate to prevent excess frost formation.

After the mixture was poured, the mold remained on the dry ice for 10 min, and the mixture froze. (The mold was covered again for the last 7 min of this stage.) The frozen slab was easily pried loose with a cold spatula, transferred onto a wire screen[6], and kept at −20° for 2 days. The slab then was dried for 2 more days at room temperature in a desiccator[7] under a mild, houseline vacuum (600 mtorr). Drying caused the slabs to shrink to ~5 × 5 cm. The central 3 × 3-cm square was excised with a scalpel[8] and a straight edge and divided further into nine 1 × 1-cm squares.

Kinetics—Each square was weighed, its thickness was measured with

[1] Elvax 40, DuPont Chemical Co., Wilmington, Del. This polymer also may be obtained from Dr. Langer at the Massachusetts Institute of Technology.
[2] Fisher Scientific Co., Fair Lawn, N.J.
[3] American Standard sieves, Nos. 40, 60, and 200, Dual Manufacturing Co., Chicago, Ill.
[4] Wheaton Scientific Co., Millville, N.J.
[5] Scientific Industries, Bohemia, N.Y.; set at speed 10.
[6] Common steel mesh, 0.5-mm spacing.
[7] Bel Art, Pequannock, N.J.
[8] No. 10 blade, Bard-Parker, Rutherford, N.J.

0022-3549/80/0300-0265$01.00/0
© 1980, American Pharmaceutical Association

a micrometer[9], and it was placed in a vial containing 10 ml of saline (0.154 *M* NaCl[10]). Vials were put on a shaker[11] at 20°. At each time point, the squares were transferred with forceps into fresh, saline-containing vials. During these transfers, excess solution on the matrix surface was removed by gentle blotting on a tissue. The concentrations of macromolecules in the vials were determined spectrophotometrically[12].

Release of Macromolecules—Kinetic studies were conducted on the release of three proteins[13]: bovine serum albumin (mol. wt. 68,000), β-lactoglobulin (mol. wt. 18,000), and lysozyme (mol. wt. 14,400). A standard particle size (75–250 μm) and loading (25% of matrix weight as protein) were used in the measurement of release kinetics. Protein concentrations were determined by absorbance at 220 or 280 nm.

Particle Size and Loading—A series of experiments was conducted to compare the release of albumin of three particle sizes (<75, 75–250, and 250–425 μm) at four drug loadings (10, 25, 37.5, and 50% protein by weight). With the smallest particle size, a 67% loading was possible and was tested for release kinetics. (With particle sizes greater than 75 μm, the polymer solution–protein powder mixture would not pour.)

For each particle size and loading, at least two slabs were cast and assayed for release characteristics. Release from each square was monitored for 4–8 weeks. *Table I lists the* weights and thicknesses of matrix squares containing albumin of various particle sizes and loadings.

Isotropic Studies—Experiments were conducted to examine matrix isotropy by comparing release from the top and bottom faces of polymer matrixes containing albumin. Conditions ranged from 25% loading and particle sizes of <75 μm to 50% loading and particle sizes of 250–425 μm. For each matrix square, all surfaces except for one face were covered by dripping molten paraffin wax[14] onto the square. The remaining face was protected by adhesive tape. The excess wax was trimmed off, and the adhesive tape was removed.

Release measurements were conducted with care taken to ensure that the unwaxed face always was exposed to the release medium. Release rates were compared between the top and bottom faces of matrixes for each combination of particle size and loading. Control squares containing albumin were covered completely with wax; these squares showed no effect on the spectrophotometric assay.

Coating—The effect of coating matrixes with an additional polymer layer was examined. Polymeric matrixes, 50% insulin[13] by weight, were prepared by the described procedures, except that the insulin powder was not sieved. (Commercial insulin powder, with a particle size of <50 μm, is more uniform than most protein powder preparations.) After the insulin–polymer matrixes were dried and weighed, the squares were coated by dropping each into a vial containing 15 ml of polymer solution, either 5 or 20% (w/v) ethylene–vinyl acetate in methylene chloride. After 1 min in solution, the square was grasped on its edges with forceps, removed from solution, and held to dry at room temperature for 2 min. The matrix was dried for an additional 24 hr at room temperature under mild vacuum.

Both coated and uncoated samples were measured for release kinetics for over 20 days. Because insulin can bind to glass, release was measured in silicone[15]-coated vials containing saline at 20°. Insulin concentrations were determined by adjusting the pH to 3.0 (50 μl of 1 *N* HCl[10] added/10 ml of saline) and measuring absorbance at 220 nm.

RESULTS

Uniformity and Reproducibility—The improvement in the uniformity of drug distribution using low temperature fabrication methods is shown in Fig. 1. Figure 1*a* is a photograph of a matrix containing albumin (particle size of 75–250 μm, 25% protein by weight), which was cast and dried at low temperature; under these conditions, the drug was distributed uniformly throughout the matrix. Figure 1*b* shows a matrix similarly prepared, except that casting and drying were conducted at room temperature. In this case, drug distribution was irregular, with some areas nearly void of protein (clear zones).

The low temperature fabrication procedure produced polymer matrixes that were essentially isotropic with respect to release. Experiments in which release rates from the top and bottom faces of the polymer matrix were studied separately showed that release rates never differed by more than 25%, which suggests that the low temperatures during the matrix casting and drying prevented significant vertical drug migration.

Figure 2 depicts the reproducibility of release kinetics from matrixes prepared at a low temperature. Three slabs were prepared with albumin, and all 27 1 × 1-cm squares were measured for release for >24 days. The mean daily release rates and their standard deviations are shown in Fig.

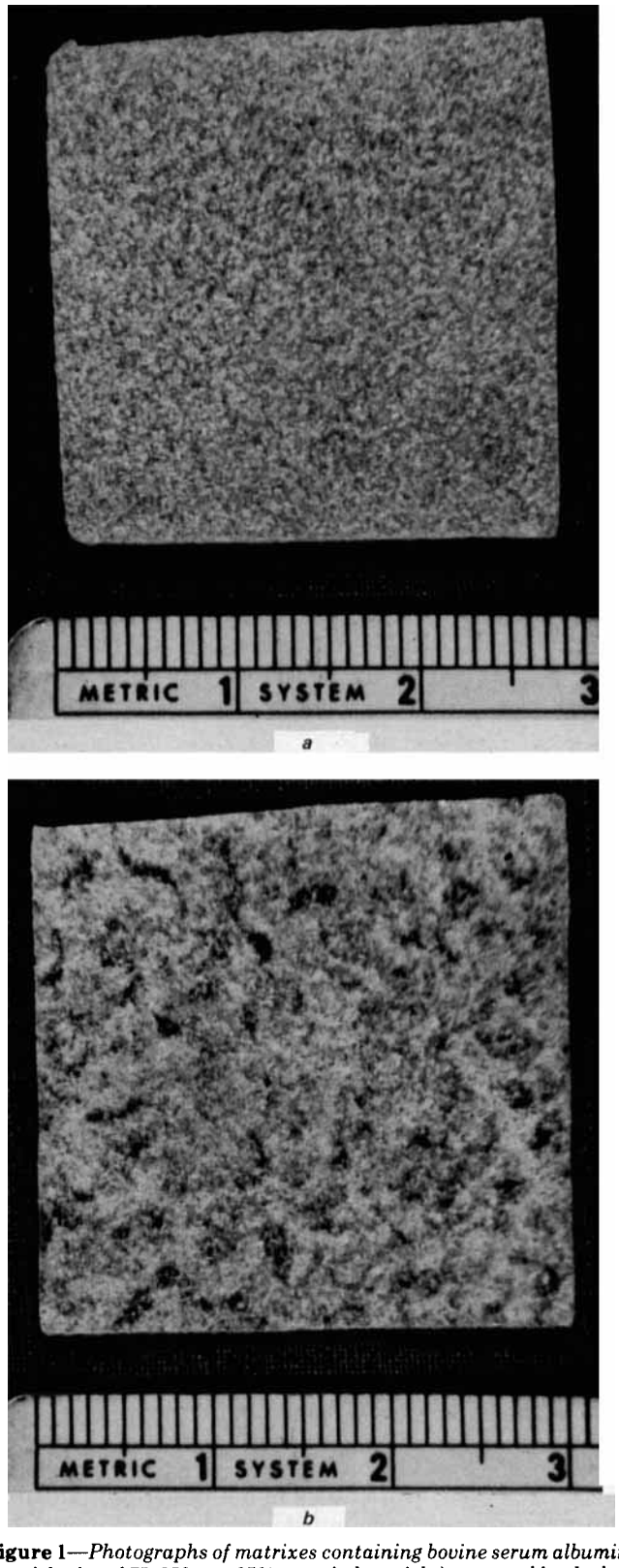

Figure 1—*Photographs of matrixes containing bovine serum albumin (particle size of 75–250 μm, 25% protein by weight) prepared by the low temperature procedure (Fig. 1a) and at room temperature (Fig. 1b). The scale is in centimeters.*

[9] Starret Co., Athol, Mass.
[10] USP grade, Mallinckrodt, St. Louis, Mo.
[11] Clinical rotating apparatus, Arthur H. Thomas, Philadelphia, Pa.; set at speed 3.
[12] Gilford Instrument Laboratories, Oberlin, Ohio.
[13] Sigma Chemical Co., St. Louis, Mo.
[14] Gulf Oil Corp., Houston, Tex.
[15] Siliclad, Clay-Adams, Parsippany, N.J.

Table I—Weights and Thicknesses[a] of 1 × 1-cm Matrixes Prepared with Albumin at Various Particle Sizes and Loadings

Loading, % by weight	Particles of <75 μm		Particles of 75–250 μm		Particles of 250–425 μm	
	Weight ± *SD*[b], mg	Thickness ± Range, mm	Weight ± *SD*[b], mg	Thickness ± Range, mm	Weight ± *SD*[b], mg	Thickness ± Range, mm
10	67.3 ± 3.6	0.75 ± 0.01	64.5 ± 3.6	0.75 ± 0.01	56.3 ± 2.3	0.81 ± 0.01
25	76.1 ± 3.5	0.80 ± 0.02	70.3 ± 4.3	0.83 ± 0.01	62.3 ± 2.3	1.00 ± 0.02
37.5	87.3 ± 3.4	0.94 ± 0.02	74.9 ± 3.0	1.13 ± 0.02	68.9 ± 4.3	1.23 ± 0.03
50	98.7 ± 4.4	1.13 ± 0.03	83.1 ± 5.2	1.47 ± 0.04	74.9 ± 5.3	1.43 ± 0.04
67	103.6 ± 6.3	1.74 ± 0.04	—[c]	—[c]	—[c]	—[c]

[a] All weights and thicknesses were measured before exposure to saline. Hydration increased the volume by ~5%. [b] $n \geq 8$. [c] This particular combination of particle size and loading was not prepared.

2. Standard deviations of release rates were within 15% of the respective means, except during the early release period (in which the standard deviations were still within 25%). Standard deviations of release rates from matrixes prepared at room temperature were only within 75%. In addition, more than 90% of the total variance of release for matrixes fabricated at a low temperature was due to variability within a single slab.

Other studies using different proteins, particle sizes, and loadings yielded release reproducibilities consistent with the described observation with one exception: at high loadings (≥50%), the center square had a significantly slower release rate than the other eight squares from the same slab. This observation may be because the center is the site of pouring and, therefore, is the last area to be fully cooled.

Figure 3 shows the release of different proteins of the same particle size and loading. In this graph, cumulative percent protein release is plotted *versus* time$^{1/2}$. The standard deviation of cumulative release was within 10% of the mean in all cases.

Particle Size and Loading—Figures 4 and 5 show the effects of drug particle size and loading on release kinetics. The profiles of cumulative release *versus* time$^{1/2}$ first are grouped by common loadings ranging from 10 to 50% (Figs. 4*a*–4*d*). These release profiles then are plotted by similar particle size (Figs. 5*a*–5*c*). In every case, the standard deviation of cumulative release was within 10% of the mean, and there appeared to be a release period roughly linear with respect to time$^{1/2}$. At higher loadings, this period was almost immediate (Fig. 4*d*). At lower loadings, there was an initial, nonlinear burst of release lasting about 48 hr, followed by a linear period (Figs. 4*a* and 4*b*).

Particle size significantly affected the drug release rates. In almost all cases, an increase in particle size increased the release kinetics. The only exception was at the highest loading; in this case, the difference between release rates of polymer matrixes containing protein in the two larger particle-size ranges was minimal. The effect of particle size was most significant at the intermediate loadings (25 and 37.5%). Here, the slopes of the regions linear with respect to time$^{1/2}$ varied as much as sixfold due to a change in particle size.

Increases in drug loading uniformly increased drug release rates (Fig. 5). Not only did total drug release increase, but the cumulative percent of matrix drug released over time increased. As much as a 50-fold increase in the percent released slopes was caused by increasing drug loading from 10 to 50% by weight (Fig. 5*a*).

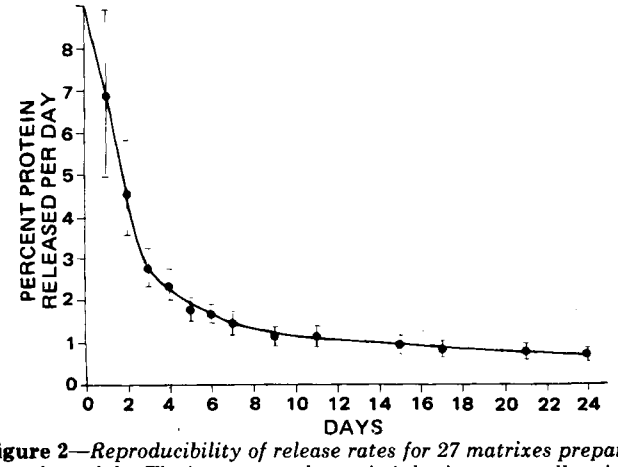

Figure 2—*Reproducibility of release rates for 27 matrixes prepared from three slabs. The incorporated protein is bovine serum albumin at a particle size of 75–250 μm and 25% loading.*

Coating—Coating the matrix also significantly affected drug release rates (Fig. 6). Release in coated matrixes again appeared to follow time$^{1/2}$ kinetics. Release kinetics decreased with increases in coating solution concentrations. A sevenfold difference in release rates was observed between uncoated samples and samples coated with 20% polymer solution. Standard deviations of cumulative release values were within 15% of the means.

DISCUSSION

These results show the effectiveness of low temperature fabrication procedures for the incorporation of macromolecules into polymeric matrixes. Procedures used for the incorporation of low molecular weight drugs (3–7) are inadequate for macromolecules. Compression molding and levigation (3, 4) would subject the relatively less stable proteins or macromolecules to denaturation. Therefore, macromolecules were added to a solution of polymer dissolved in a volatile solvent (methylene chloride). This mixture, when cast and dried, produced matrixes capable of sustained macromolecular release.

Sustained-release films for low molecular weight drugs have been cast from polymer solutions in which the drug also was dissolved (5–7). However, macromolecules such as proteins were insoluble in the polymer solution used and rapidly migrated when cast at room temperature. Low temperature casting and drying reduced protein migration and resulted in matrixes with uniform drug distribution and reproducible release kinetics. Similar low temperature techniques may prove useful in other systems that require uniform distribution of an insoluble compound in a polymer solution.

The reproducibility of release kinetics for matrixes prepared by low temperature methods was demonstrated for different proteins and for a range of particle sizes and loadings. However, it may be more difficult to incorporate some macromolecules uniformly if the drug particle density is much greater than that used in the present study since high density may cause the particles to settle significantly even at low temperatures. This settling may be alleviated by more rapid cooling during casting.

The polymer solution mixed with macromolecules quickly gelled when cast on dry ice at −80°. After 2 days at −20°, enough solvent had evaporated to allow further drying at room temperature (2 days under mild

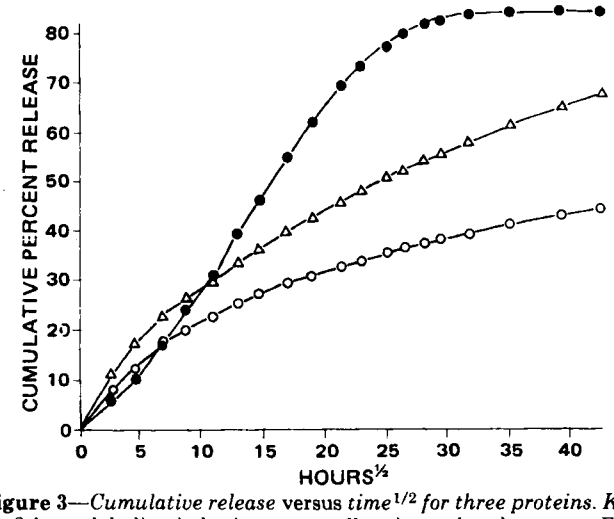

Figure 3—*Cumulative release* versus *time$^{1/2}$ for three proteins. Key: ●, β-lactoglobulin; Δ, bovine serum albumin; and ○, lysozyme. Each point represents the mean of at least eight samples. Standard deviations were <10% of the respective mean values.*

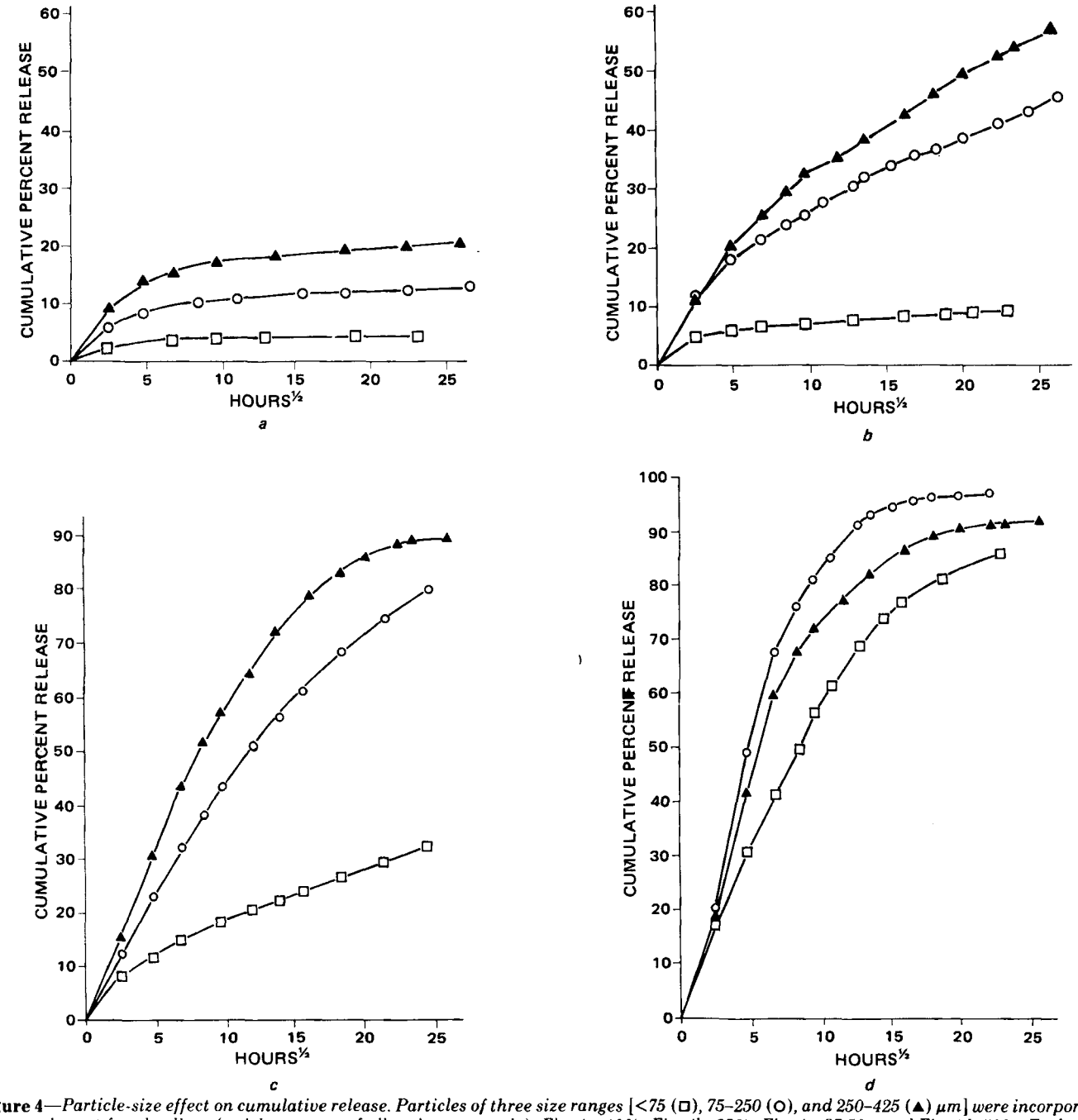

Figure 4—*Particle-size effect on cumulative release. Particles of three size ranges [<75 (□), 75–250 (○), and 250–425 (▲) μm] were incorporated into matrixes at four loadings (weight percent of albumin per matrix): Fig. 4a, 10%; Fig. 4b, 25%; Fig. 4c, 37.5%; and Fig. 4d, 50%. Each point represents the mean of eight samples. Standard deviations were <10% of the respective mean values.*

vacuum). In a separate experiment, more extensive drying (up to 60 days under vacuum) did not affect release kinetics.

There appeared to be three release phases: (*a*) a burst or initial period of rapid release; (*b*) a period when release was approximately linear with respect to time$^{1/2}$; and (*c*) a final period when release tapered off. The burst effect presumably was due to protein dissolution on the surface and cut edges of the matrix. The intermediate release phase that displayed time$^{1/2}$ kinetics resembled earlier release models of low molecular weight drugs from granular matrixes (8). Because macromolecules are too large to diffuse through a pure polymer film (1), it is possible that sustained release occurs *via* diffusion through channels in the matrix. The incorporation of the macromolecules during casting may introduce such channels through which the dissolved drug can diffuse. In this case, observed differences in release rates for different proteins would be attributable to differences in protein properties (solubility and diffusivity) and matrix characteristics (porosity and tortuosity). For example, the very slow release from the uncoated insulin–polymer matrixes (Fig. 6) may result from the small size of the incorporated insulin powder and the low insulin solubility in the release media.

Drug particle size and loading markedly affected release kinetics of the macromolecular polymeric delivery systems (Figs. 4 and 5). Similar observations have been made for low molecular weight drug release (9, 10), although the effects were not as significant. Release rate increases caused by increases in particle size may result from the formation of larger channels or pores in the polymer matrix. Similarly, increased loadings may provide simpler pathways (lower tortuosity) and greater porosity for diffusion, both of which would facilitate the movement of water into, and proteins out of, the matrix.

A coating also can be used to control macromolecular release kinetics. Its effects may be due to the reduced amount of macromolecule on the matrix surface as well as the decreased surface access of pores for channeled diffusion. It is assumed that the coating procedure does not cause a pure intact polymer film to form around the matrix since that would prevent any macromolecular diffusion into the surrounding media (1).

Systems for the sustained release of macromolecules have potential biological and pharmacological value. For example, these systems provided the basis for bioassays of growth factors derived from tumors (2), cartilage (11), the vitreous body (12), and macrophages (13). They also

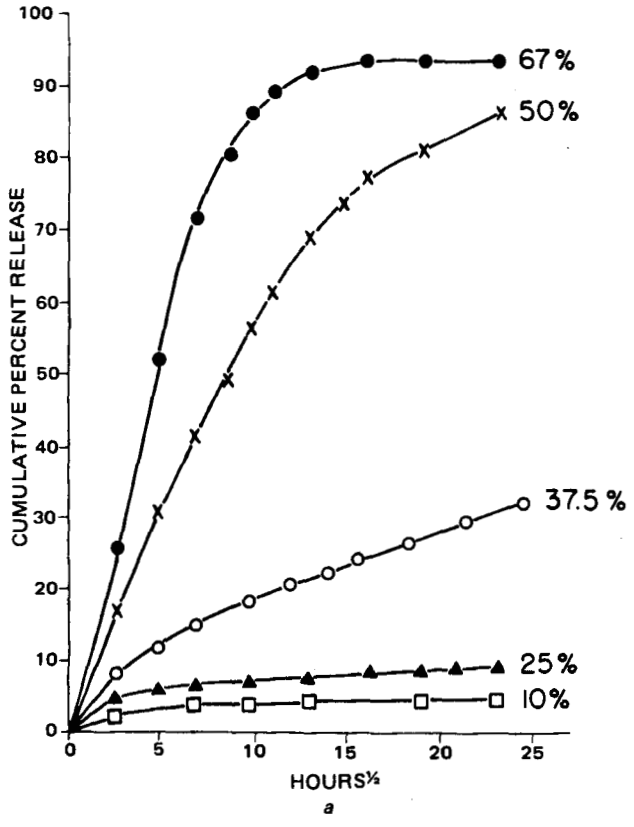

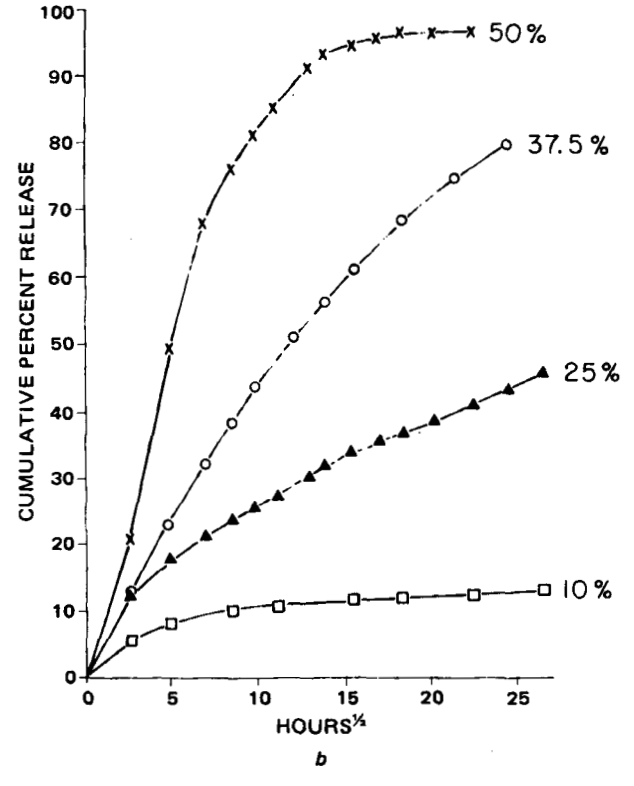

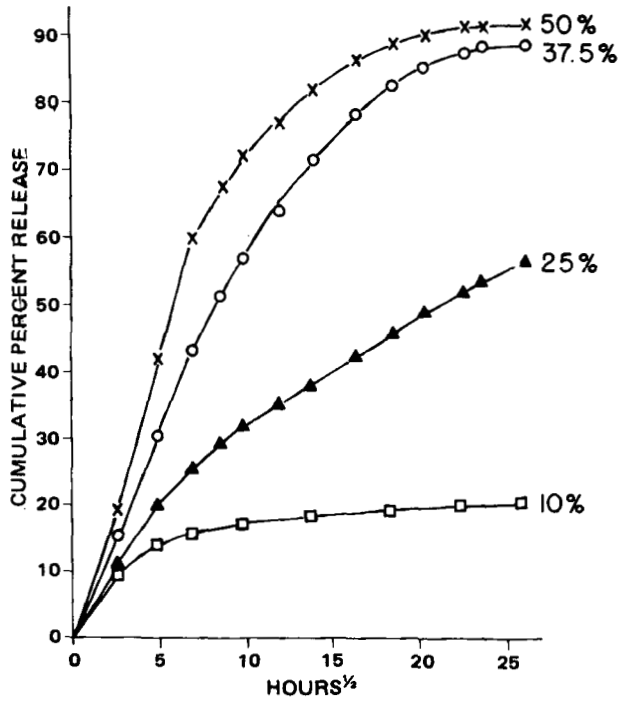

Figure 5—*Loading effect on cumulative release. Matrixes with loadings [10 (□), 25 (▲), 37.5 (○), 50 (×), and 67% (●) of albumin by weight] were made using albumin of three particle-size ranges: Fig. 5a, <75 μm; Fig. 5b, 75–250 μm; and Fig. 5c, 250–425 μm. Each point represents the mean of at least eight samples. Standard deviations were <10% of the respective mean values.*

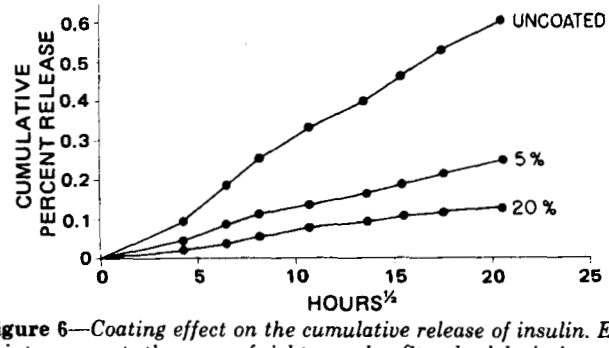

Figure 6—*Coating effect on the cumulative release of insulin. Each point represents the mean of eight samples. Standard deviations were <15% of the respective mean values.*

were used in studies of vascular proliferation (14), vascular regression (15), and chemotaxis (16). Clinically, these systems may prove valuable as single-step methods for immunization (17) or for the continuous delivery of insulin (18) and other high molecular weight drugs.

These low temperature fabrication procedures for macromolecular release systems are easy to perform and require standard, inexpensive laboratory apparatus. A wide spectrum of release rates can be achieved by altering drug particle size and loading and by coating the matrix; thus, these systems can be modified for various applications. Further work is being directed toward the development of physical and mathematical models to describe and predict macromolecular release.

REFERENCES

(1) R. Langer and J. Folkman, *Nature*, **263**, 797 (1976).

(2) R. Langer and J. Folkman, in "Polymeric Delivery Systems," Midland Macromolecular Monograph, vol. 5, R. J. Kostelnik, Ed., Gordon and Breach, New York, N.Y., 1978, pp. 175–196.

(3) S. J. Desai, A. P. Simonelli, and W. I. Higuchi, *J. Pharm. Sci.*, **54**, 1459 (1965).

(4) T. J. Roseman, *ibid.*, **61**, 46 (1972).

(5) S. Borodkin and F. E. Tucker, *ibid.*, **64**, 1289 (1975).

(6) Y. Samuelov, M. Donbrow, and M. Friedman, *ibid.*, **68**, 325 (1979).

(7) N. B. Shah and B. B. Sheth, *ibid.*, **61**, 412 (1972).

(8) T. Higuchi, *ibid.*, **52**, 1145 (1963).

(9) J. Lazarus, M. Pagliery, and L. Lachman, *ibid.*, **53**, 798 (1964).

(10) H. Lapidus and N. G. Lordi, *ibid.*, **55**, 840 (1966).

(11) R. Langer, H. Brem, K. Falterman, M. Klein, and J. Folkman, *Science*, **193**, 70 (1976).

(12) S. Brem, I. Preis, R. Langer, H. Brem, J. Folkman, and A. Patz, *Am. J. Ophthalmol.*, **84**, 323 (1977).
(13) P. Polverini, R. Cotran, M. Gimbrone, and E. Unanue, *Nature*, **269**, 804 (1977).
(14) H. Conn, M. Berman, K. Kenyon, R. Langer, and J. Gage, *Invest. Ophthalmol.*, in press.
(15) D. Ausprunk, K. Falterman, and J. Folkman, *J. Lab. Invest.*, **38**, 284 (1978).
(16) K. Bergman, M. Fefferman, and R. Langer, in "11th International Congress of Biochemistry," 1979, p. 576.
(17) I. Preis and R. Langer, *J. Immunol. Methods*, **28**, 193 (1979).
(18) A. Augustin and R. Langer, in "Proceedings of the Symposium on Ocular and Systemic Disorders," R. Fair, Ed., American Optometric Association, St. Louis, Mo., 1979, pp. 35–38.

ACKNOWLEDGMENTS

Supported by gifts from Monsanto Corp. and Alza Corp.
The authors thank Judah Folkman, Arthur Sanford, Andrew Braunstein, and Germaine Grant.

Solvent Effects on IR Spectra of Flurazepam

SAMUEL S. M. NG ˣ and PRANAB K. BHATTACHARYYA

Received April 6, 1979, from the *Quality Control Department, Hoffmann-La Roche Inc., Nutley, NJ 07110.* Accepted for publication October 5, 1979.

Abstract □ Differences among the IR spectra of flurazepam samples obtained by recrystallizing flurazepam dihydrochloride from different solvents were studied and found to be caused by different mixtures of flurazepam mono- and dihydrochlorides and the free base; these spectral differences are not caused by polymorphism or decomposition of flurazepam.

Keyphrases □ Flurazepam—IR spectral analysis, effects of various extraction solvents, transformation from dihydrochloride to monohydrochloride and free base, comparison of spectra of extracted, untreated, and solution samples □ Spectroscopy, IR—flurazepam analysis, effect of various extraction solvents □ Sedatives—flurazepam, IR spectroscopy

To identify the active ingredient in flurazepam dihydrochloride capsules, flurazepam dihydrochloride was extracted from the capsules and its IR spectrum was matched with a reference spectrum. The IR spectrum of the extracted substance in potassium bromide was significantly different from the spectrum of untreated flurazepam dihydrochloride in potassium bromide, as well as from that published previously (1). Different spectra also were obtained in potassium bromide when different extraction solvents were used. The observed differences in the IR spectra were investigated to determine their origin.

EXPERIMENTAL

The spectra were recorded by a grating IR spectrophotometer[1]. The samples were measured as potassium bromide disks, as solutions in cells with sodium chloride windows, and as a capillary film between two sodium chloride disks.

The samples were prepared using the following extraction methods.

1. The contents of three 15-mg flurazepam dihydrochloride capsules[2] were extracted with 10 ml of methanol or acetone and filtered. The filtrate was evaporated to dryness under a nitrogen stream, and the residue was collected.
2. Flurazepam dihydrochloride (0.5 g) was dissolved in 3 ml of methanol and evaporated to dryness under nitrogen.
3. Flurazepam dihydrochloride (0.5 g) was dissolved in 100 ml of chloroform with stirring, and the clear solution was evaporated to dryness under nitrogen.
4. Flurazepam dihydrochloride (0.5 g) was dissolved in 2 ml of distilled water and evaporated to dryness under nitrogen. The residue was dried in a vacuum oven at ~50°, if necessary.
5. The contents of two to three flurazepam dihydrochloride capsules (or 100 mg of flurazepam dihydrochloride) were mixed well with 10 ml of distilled water. The mixture was neutralized with 1.0 *N* NaOH, and the milky solution was extracted with 10 ml of chloroform. The chloroform layer (flurazepam free base) was passed through anhydrous sodium sulfate and evaporated to dryness under nitrogen.

[1] Model 283, Perkin-Elmer.
[2] Dalmane, Hoffmann-La Roche.

RESULTS AND DISCUSSION

The IR spectra of materials (in potassium bromide) extracted from three 15-mg flurazepam dihydrochloride capsules with methanol and acetone are presented in Fig. 1 (curves A and B, respectively). Figure 1 also includes the spectra of untreated flurazepam dihydrochloride, flurazepam monohydrochloride, and flurazepam free base as potassium bromide pellets (curves C, D, and E, respectively). The spectra of the materials extracted with methanol and acetone disagree with each other as well as with the spectra of untreated flurazepam dihydrochloride. At this point, the suggestion of polymorphism arose. The IR spectra (as potassium bromide pellets) of the substances recrystallized by dissolving flurazepam dihydrochloride in methanol, chloroform, and water were obtained (curves A, B, and C, respectively, Fig. 2). Again, these spectra are not identical to one another or to the spectrum of untreated flurazepam dihydrochloride. To investigate whether polymorphism was causing these differences, solution spectra of the same substances were obtained (Fig. 3). Figure 3 also contains the solution spectrum of untreated flurazepam dihydrochloride. Since significant differences were found in the solution spectra as well, these differences could not be attributed to polymorphism.

The differences among curves C–E in Fig. 1 are most pronounced between 1800 and 2500 cm^{-1} and at 1635 cm^{-1}. The 1800–2500-cm^{-1} region contains the absorption bands due to the R_3N^+H and $R_2C{=}N^+H$ ions. Saturated tertiary amine salts (R_3N^+H) exhibit a strong and broad ammonium band (2) centered between 2300 and 2500 cm^{-1}, particularly when a large asymmetric tertiary ammonium ion combines with a relatively small negative ion such as chloride. This band has been observed in many tertiary amine salts of hydrochloric acid and hydrobromic acid.

Unsaturated amine salts ($C{=}N^+H$) exhibit a characteristic immonium band between 1800 and 2000 cm^{-1} in addition to the ammonium band between 2300 and 2500 cm^{-1}, which overlaps with the ammonium band caused by the R_3N^+H ion. The IR spectrum of flurazepam dihydrochloride is characterized by the immonium band between 1800 and 2000 cm^{-1} as well as the ammonium band between 2300 and 2500 cm^{-1} (curve C, Fig. 1). The IR spectrum of flurazepam monohydrochloride is characterized only by the ammonium band between 2300 and 2500 cm^{-1} and the absence of the immonium band between 1800 and 2000 cm^{-1} (curve D, Fig. 1). In flurazepam monohydrochloride, where the hydrochloride

0022-3549/80/0300-0270$01.00/0
© 1980, American Pharmaceutical Association

(12) S. Brem, I. Preis, R. Langer, H. Brem, J. Folkman, and A. Patz, *Am. J. Ophthalmol.*, **84**, 323 (1977).
(13) P. Polverini, R. Cotran, M. Gimbrone, and E. Unanue, *Nature*, **269**, 804 (1977).
(14) H. Conn, M. Berman, K. Kenyon, R. Langer, and J. Gage, *Invest. Ophthalmol.*, in press.
(15) D. Ausprunk, K. Falterman, and J. Folkman, *J. Lab. Invest.*, **38**, 284 (1978).
(16) K. Bergman, M. Fefferman, and R. Langer, in "11th International Congress of Biochemistry," 1979, p. 576.
(17) I. Preis and R. Langer, *J. Immunol. Methods*, **28**, 193 (1979).
(18) A. Augustin and R. Langer, in "Proceedings of the Symposium on Ocular and Systemic Disorders," R. Fair, Ed., American Optometric Association, St. Louis, Mo., 1979, pp. 35–38.

ACKNOWLEDGMENTS

Supported by gifts from Monsanto Corp. and Alza Corp.
The authors thank Judah Folkman, Arthur Sanford, Andrew Braunstein, and Germaine Grant.

Solvent Effects on IR Spectra of Flurazepam

SAMUEL S. M. NG ˣ and PRANAB K. BHATTACHARYYA

Received April 6, 1979, from the *Quality Control Department, Hoffmann-La Roche Inc., Nutley, NJ 07110.* Accepted for publication October 5, 1979.

Abstract □ Differences among the IR spectra of flurazepam samples obtained by recrystallizing flurazepam dihydrochloride from different solvents were studied and found to be caused by different mixtures of flurazepam mono- and dihydrochlorides and the free base; these spectral differences are not caused by polymorphism or decomposition of flurazepam.

Keyphrases □ Flurazepam—IR spectral analysis, effects of various extraction solvents, transformation from dihydrochloride to monohydrochloride and free base, comparison of spectra of extracted, untreated, and solution samples □ Spectroscopy, IR—flurazepam analysis, effect of various extraction solvents □ Sedatives—flurazepam, IR spectroscopy

To identify the active ingredient in flurazepam dihydrochloride capsules, flurazepam dihydrochloride was extracted from the capsules and its IR spectrum was matched with a reference spectrum. The IR spectrum of the extracted substance in potassium bromide was significantly different from the spectrum of untreated flurazepam dihydrochloride in potassium bromide, as well as from that published previously (1). Different spectra also were obtained in potassium bromide when different extraction solvents were used. The observed differences in the IR spectra were investigated to determine their origin.

EXPERIMENTAL

The spectra were recorded by a grating IR spectrophotometer[1]. The samples were measured as potassium bromide disks, as solutions in cells with sodium chloride windows, and as a capillary film between two sodium chloride disks.

The samples were prepared using the following extraction methods.

1. The contents of three 15-mg flurazepam dihydrochloride capsules[2] were extracted with 10 ml of methanol or acetone and filtered. The filtrate was evaporated to dryness under a nitrogen stream, and the residue was collected.
2. Flurazepam dihydrochloride (0.5 g) was dissolved in 3 ml of methanol and evaporated to dryness under nitrogen.
3. Flurazepam dihydrochloride (0.5 g) was dissolved in 100 ml of chloroform with stirring, and the clear solution was evaporated to dryness under nitrogen.
4. Flurazepam dihydrochloride (0.5 g) was dissolved in 2 ml of distilled water and evaporated to dryness under nitrogen. The residue was dried in a vacuum oven at ~50°, if necessary.
5. The contents of two to three flurazepam dihydrochloride capsules (or 100 mg of flurazepam dihydrochloride) were mixed well with 10 ml of distilled water. The mixture was neutralized with 1.0 *N* NaOH, and the milky solution was extracted with 10 ml of chloroform. The chloroform layer (flurazepam free base) was passed through anhydrous sodium sulfate and evaporated to dryness under nitrogen.

[1] Model 283, Perkin-Elmer.
[2] Dalmane, Hoffmann-La Roche.

RESULTS AND DISCUSSION

The IR spectra of materials (in potassium bromide) extracted from three 15-mg flurazepam dihydrochloride capsules with methanol and acetone are presented in Fig. 1 (curves A and B, respectively). Figure 1 also includes the spectra of untreated flurazepam dihydrochloride, flurazepam monohydrochloride, and flurazepam free base as potassium bromide pellets (curves C, D, and E, respectively). The spectra of the materials extracted with methanol and acetone disagree with each other as well as with the spectra of untreated flurazepam dihydrochloride. At this point, the suggestion of polymorphism arose. The IR spectra (as potassium bromide pellets) of the substances recrystallized by dissolving flurazepam dihydrochloride in methanol, chloroform, and water were obtained (curves A, B, and C, respectively, Fig. 2). Again, these spectra are not identical to one another or to the spectrum of untreated flurazepam dihydrochloride. To investigate whether polymorphism was causing these differences, solution spectra of the same substances were obtained (Fig. 3). Figure 3 also contains the solution spectrum of untreated flurazepam dihydrochloride. Since significant differences were found in the solution spectra as well, these differences could not be attributed to polymorphism.

The differences among curves C–E in Fig. 1 are most pronounced between 1800 and 2500 cm^{-1} and at 1635 cm^{-1}. The 1800–2500-cm^{-1} region contains the absorption bands due to the R_3N^+H and $R_2C{=}N^+H$ ions. Saturated tertiary amine salts (R_3N^+H) exhibit a strong and broad ammonium band (2) centered between 2300 and 2500 cm^{-1}, particularly when a large asymmetric tertiary ammonium ion combines with a relatively small negative ion such as chloride. This band has been observed in many tertiary amine salts of hydrochloric acid and hydrobromic acid.

Unsaturated amine salts ($C{=}N^+H$) exhibit a characteristic immonium band between 1800 and 2000 cm^{-1} in addition to the ammonium band between 2300 and 2500 cm^{-1}, which overlaps with the ammonium band caused by the R_3N^+H ion. The IR spectrum of flurazepam dihydrochloride is characterized by the immonium band between 1800 and 2000 cm^{-1} as well as the ammonium band between 2300 and 2500 cm^{-1} (curve C, Fig. 1). The IR spectrum of flurazepam monohydrochloride is characterized only by the ammonium band between 2300 and 2500 cm^{-1} and the absence of the immonium band between 1800 and 2000 cm^{-1} (curve D, Fig. 1). In flurazepam monohydrochloride, where the hydrochloride

0022-3549/80/0300-0270$01.00/0
© 1980, American Pharmaceutical Association

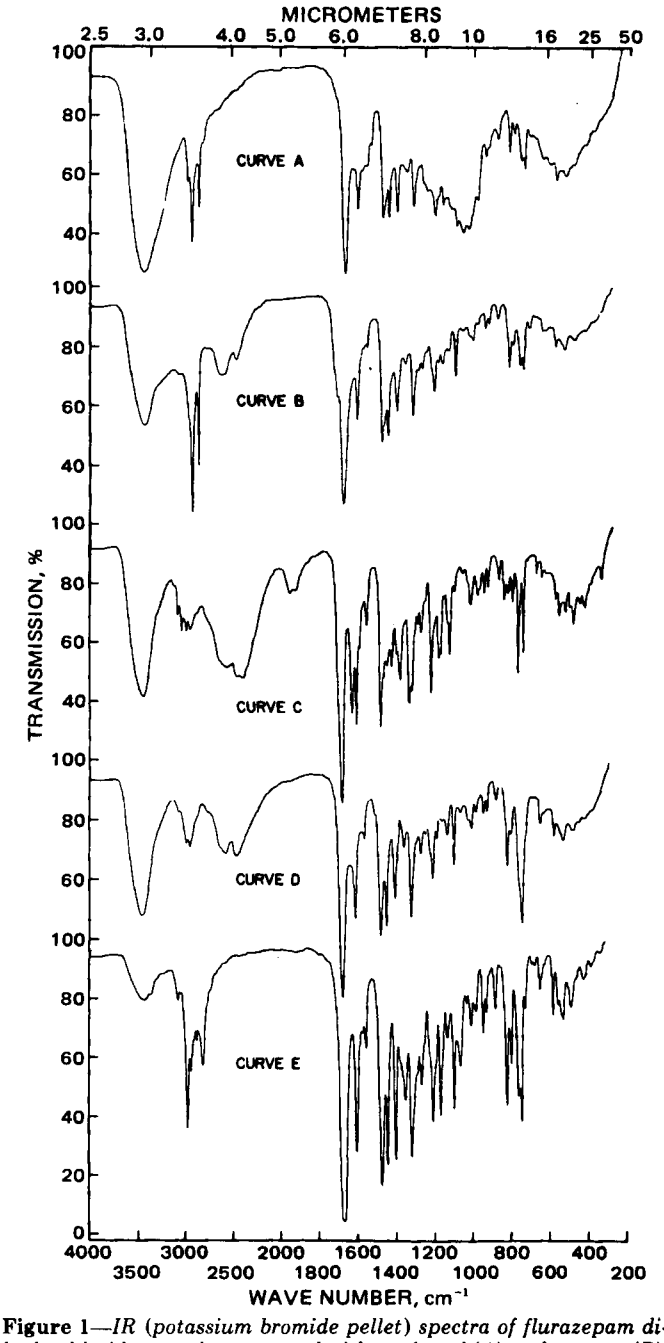

Figure 1—*IR (potassium bromide pellet) spectra of flurazepam dihydrochloride capsules extracted with methanol (A) and acetone (B). Curve C is the spectrum of untreated flurazepam dihydrochloride, curve D is that of flurazepam monohydrochloride, and curve E is that of flurazepam free base.*

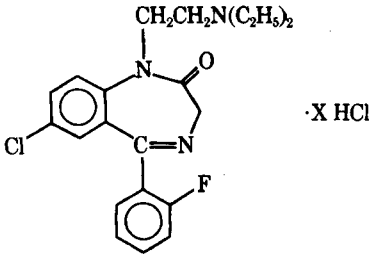

X = 2 (dihydrochloride)
X = 1 (monohydrochloride)
X = 0 (free base)

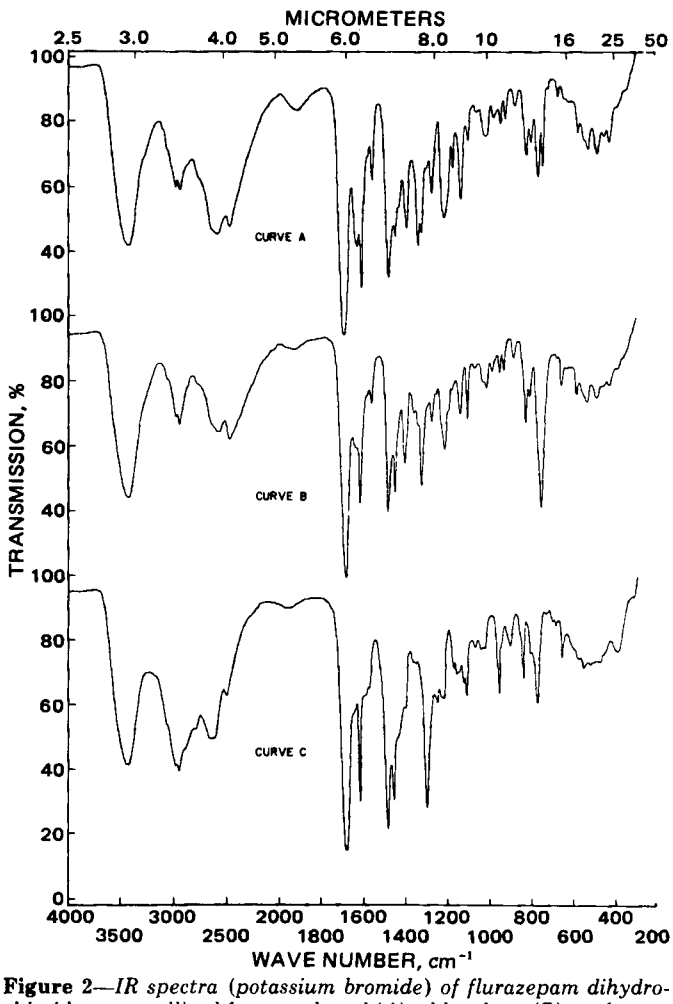

Figure 2—*IR spectra (potassium bromide) of flurazepam dihydrochloride recrystallized from methanol (A), chloroform (B), and water (C).*

concentration is less than that in flurazepam dihydrochloride, the acidic protons in flurazepam monohydrochloride participate in the formation of saturated tertiary ammonium ions (R_3N^+H) only because of the higher basicity of the tertiary amine (R_3N) than the imine (C=N—). The free base is recognized by the absence of such bands in the 1800–2500-cm^{-1} region (curve E, Fig. 1). The next most distinguishing feature of flurazepam dihydrochloride is the sharp band at 1635 cm^{-1} assigned to the $C{=}N^+$ stretching vibration; this band is absent in the spectra of the monohydrochloride and the free base. Furthermore, the carbonyl stretching band shifts from ~1680 cm^{-1} in the monohydrochloride and in the free base, to ~1700 cm^{-1} in the dihydrochloride.

Interpretation of Spectra from Capsules—The spectrum of flurazepam dihydrochloride capsules extracted with methanol lacks the ammonium and immonium absorption bands from 1800 to 2500 cm^{-1} (curve A, Fig. 1); this material is mostly flurazepam free base contaminated by other ingredients extracted from the capsule. The spectrum of flurazepam dihydrochloride capsules extracted with acetone displays only the ammonium band between 2300 and 2500 cm^{-1} (curve B, Fig. 1). Since the intensity of this band is weaker than that observed with the monohydrochloride, this material is a mixture of flurazepam monohydrochloride and flurazepam free base.

The intensities of the observed bands between 1800 and 2500 cm^{-1} and at 1635 cm^{-1} in Fig. 2 show that each spectrum is a linear superposition of the spectra of flurazepam dihydrochloride and flurazepam monohydrochloride, each having a different ratio of dihydrochloride to monohydrochloride. The material recrystallized by dissolving flurazepam dihydrochloride in methanol seemed to be approximately an equal mixture of mono- and dihydrochlorides (curve A, Fig. 2). The substances obtained from chloroform and water contain much more mono- than dihydrochlorides, as evidenced by the reduced intensities of the $C{=}N^+$ band at 1635 cm^{-1} and the immonium band at 1800–2000 cm^{-1} (curves B and C, Fig. 2).

Interpretation of Spectra from Solutions—These spectra (curves

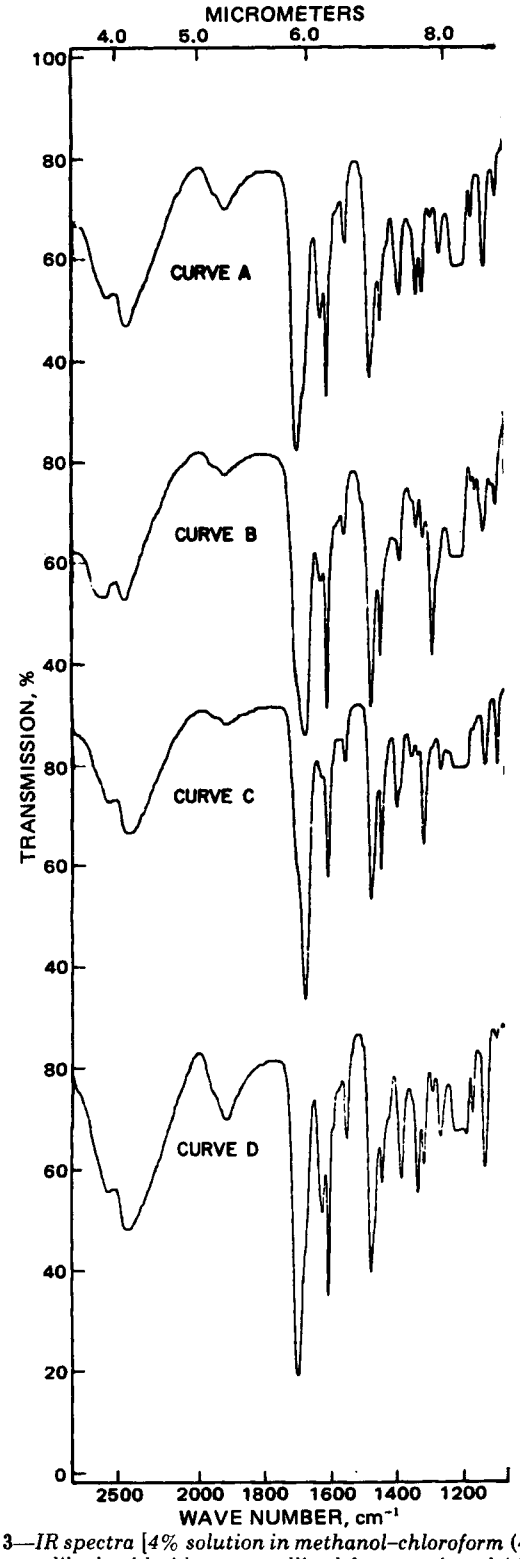

Figure 3—*IR spectra [4% solution in methanol–chloroform (4:96)] of flurazepam dihydrochloride recrystallized from methanol (A), chloroform (B), and water (C). Curve D is the solution spectrum of untreated flurazepam dihydrochloride.*

A–C, Fig. 3) display varying intensities of the ammonium, immonium, and C=N$^+$ bands, which can be attributed to different equilibrium mixtures of the mono- and dihydrochlorides in the materials recrystallized from methanol, chloroform, and water. The material recrystallized from water contained the lowest amount of dihydrochloride. The solution spectra were sharp enough to show the presence of two carbonyl stretching resonances due to the mono- and dihydrochlorides. The shift of the carbonyl band from 1700 to 1680 cm^{-1} provides further evidence of the transformation from the di- to the monohydrochloride.

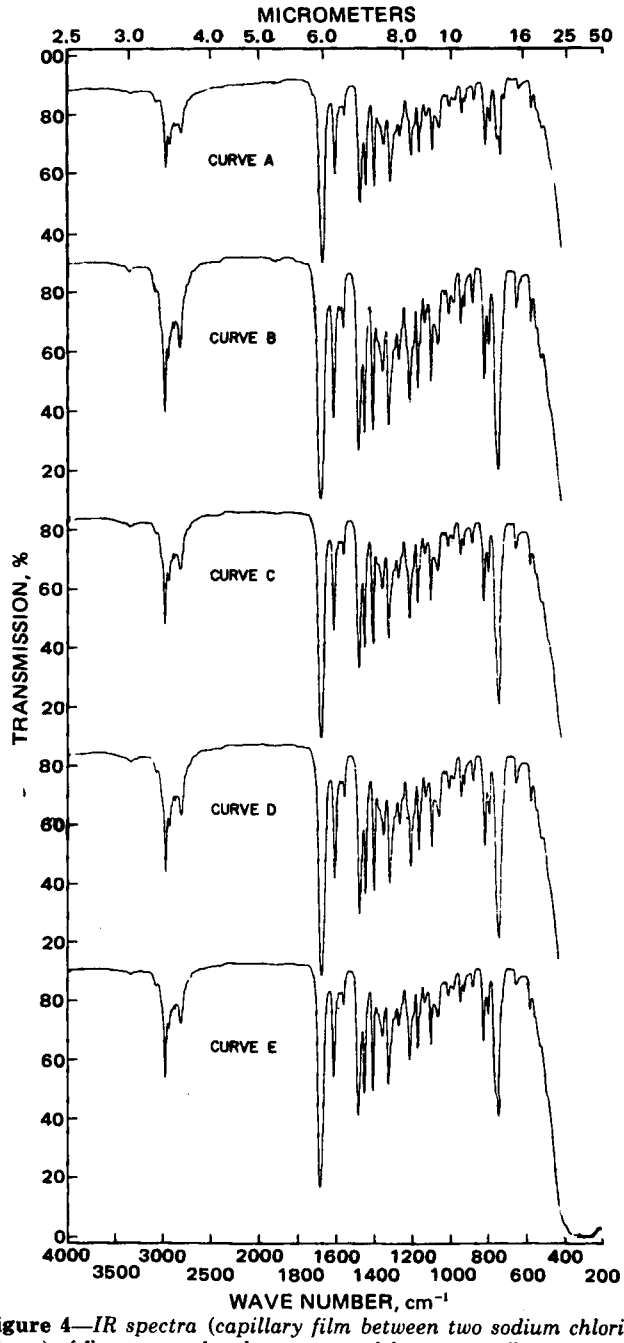

Figure 4—*IR spectra (capillary film between two sodium chloride plates) of flurazepam free base prepared from 15-mg flurazepam dihydrochloride capsules (A) and of flurazepam dihydrochloride recrystallized from methanol (B), chloroform (C), and water (D). Curve E is the spectrum of the free base prepared from untreated flurazepam dihydrochloride.*

In the spectrum (curve A) of the substance recrystallized from methanol, a small shoulder is observable at 1680 cm^{-1} on the right side of the carbonyl band at 1700 cm^{-1}. In the spectra (curves B and C) of the samples recrystallized from chloroform and water, the shoulder becomes the main carbonyl band at 1680 cm^{-1}, while the intensity of the band at 1700 cm^{-1} decreases such that it becomes a shoulder at 1680 cm^{-1} on the left side of the main band. The compatibility of the spectra (Fig. 4) of the flurazepam free base prepared from untreated flurazepam dihydrochloride, flurazepam dihydrochloride capsules, and flurazepam dihydrochloride recrystallized from methanol, chloroform, and water ruled out decomposition of flurazepam in the various studies.

CONCLUSIONS

The immonium and ammonium bands between 1800 and 2500 cm^{-1} and the C=N$^+$ stretching band at 1635 cm^{-1}, as well as the carbonyl band

position (1700 cm^{-1} for dihydrochloride and 1680 cm^{-1} for monohydrochloride and for free base), were the distinguishing diagnostic features used in this investigation to establish that the different IR spectra of flurazepam dihydrochloride recrystallized from different solvents result from different equilibrium mixtures of flurazepam mono- and dihydrochlorides and/or free base in these solvents. The solvent effect on the transformation of flurazepam di- to monohydrochloride was methanol < chloroform < water. The solution spectra also ruled out polymorphism, and the spectra in Fig. 4 show no compound decomposition.

In view of these findings, the IR identity test for the active ingredient in bulk flurazepam dihydrochloride or flurazepam dihydrochloride capsules should be based on extraction of flurazepam free base using the procedure described in the *Experimental* section and then on comparison of its IR spectrum with a spectrum of the free base similarly extracted from a standard flurazepam dihydrochloride sample, which can serve as a reference spectrum for future work.

REFERENCES

(1) "The Sadtler Standard Spectra, Spectrum R59," vol. 1, Sadtler Research Laboratories, Philadelphia, Pa., 1974.

(2) R. J. Warren, W. E. Thompson, and J. E. Zarembo, *J. Pharm. Sci.*, **54**, 1554 (1965).

ACKNOWLEDGMENTS

The authors are grateful to Dr. S. A. Moros, Dr. A. Mlodozeniec, and Dr. J. Sheridan for comments and support.

Determination of Nofedone in Human Serum by Electron-Capture GLC

D. HEUSSE *x, P. POPULAIRE *, A. RENARD *, P. PASQUIER ‡, and J. GREGOIRE ‡

Received February 23, 1979, from the **Institut de Biopharmacie, Rhône-Poulenc, 13 quai Jules Guesde, 94400 Vitry-sur-Seine, France*, and the ‡*Direction des Recherches Thérapeutiques, Rhône-Poulenc, 16 rue Clisson, 75013 Paris, France.* Accepted for publication October 5, 1979.

Abstract □ An electron-capture GLC method to measure nofedone in human serum was developed. A homolog of nofedone was added to the serum as an internal standard before the sample was alkalinized with pH 9.5 phosphate buffer and extracted with ethylene dichloride containing 0.5% isopentyl alcohol. This organic phase was extracted with 0.2 *N* HCl, the acidic aqueous phase was neutralized immediately, and the extraction with ethylene dichloride was repeated. The ethylene dichloride phase was evaporated to dryness, and the residue was reacted with heptafluorobutyric anhydride. The derivatives were chromatographed at 290° on a 1% Dexsil 300 column. Data on apparent recovery, accuracy, and specificity are given. The detection limit was 5 ng/ml of serum. Serum levels over time in one patient after intravenous administration of 1 mg/kg and after oral administration of 50, 100, and 150 mg of nofedone are presented.

Keyphrases □ Nofedone—analysis, electron-capture GLC, human serum □ GLC, electron capture—nofedone, human serum □ Antiarrhythmic agents—nofedone, analysis, electron-capture GLC, human serum

Nofedone[1] (I) fumarate, 3-[2-hydroxy-3-(isopropylamino)propoxy]-2-phenyl-1-isoindolinone B form, shows marked experimental and clinical antiarrhythmic activity after intravenous and oral administration (1). Compound I is under clinical study. To investigate its pharmacokinetics and to establish the optimal dose range, a procedure was developed for the determination of the drug in human serum. The described method involves GLC of a heptafluorobutyrate derivative with ^{63}Ni-electron-capture detection. A similar method was used for the determination of a β-adrenoreceptor antagonist with the same aminohydroxylated chain (2).

EXPERIMENTAL

Reagents—All solvents and reagents (0.2 *N* HCl[2], 1 *N* NaOH[3], and pH 9.5 phosphate buffer prepared from a 0.5 *M* aqueous solution of dibasic sodium phosphate[4]) were analytical grade. Ethylene dichloride[5], UV spectrophotometric grade, was freshly distilled before use. The heptafluorobutyric anhydride[6] was the derivatizing agent for the electron-capture analysis. It was kept at 4° in sealed vials to prevent the ingress of water from the atmosphere. Nofedone and the internal standard, 3-[2-hydroxy-3-(isopropylamino)propoxy]-2-(3-trifluoromethylphenyl)-1-isoindolinone[7] (II), were used as the free bases.

Apparatus and Operating Conditions—The gas chromatograph[8] was equipped with a ^{63}Ni-electron-capture detector[9] and a glass column (2 m long × 6.25 mm i.d.) packed with 1% Dexsil 300 on a 100–120-mesh support[10]. The column temperature was 290°, the injection port temperature was 300°, the detector temperature was 300°, the carrier gas (nitrogen) flow rate was 20 ml/min, and the scavenger gas (nitrogen) flow rate was 80 ml/min.

The column was conditioned for 24 hr by temperature programming from 250 to 350° at 1°/min and was regulated at 350° for 10 min. It was treated before analysis by several injections of the derivatized extract of serum blank with or without I and the internal standard to ensure maximal performance. Under the conditions described, the retention times of the derivatives of I and II were 2 and 1.5 min, respectively.

Glassware—All glassware was cleaned well and tested with an aqueous solution of I·HCl and II of known content.

Procedure—Compound II was used as a 100-μg/ml solution in ethyl acetate[11] and kept from bright light. This solution was diluted (1:100) with ethyl acetate and immediately inserted in a centrifuge tube. Samples of the internal standard, 50, 200, and 500 ng, were commonly used for such analyses. The quantity of the internal standard was selected to give a peak height greater than or equal to that of I. The solvent was evaporated under a nitrogen stream, and 0.25, 0.50, or 1 ml of serum was added. After vibrating for 30 sec, 2 ml of pH 9.5 phosphate buffer was added.

This aqueous solution was extracted with 6 ml of ethylene dichloride containing 0.5% isopentyl alcohol[12], mechanically shaken for 20 min, and centrifuged. The lower organic phase was removed by pipet and washed by shaking for 5 min with 2 ml of distilled water. The organic phase then was extracted with 2 ml of 0.2 *N* HCl and mechanically shaken for 20 min. The acidic aqueous phase was neutralized immediately with 0.5 ml of 1

[1] 30,356 RP.
[2] Catalog No. 20 252, Prolabo, 75011 Paris, France.
[3] Catalog No. 31 627, Prolabo, 75011 Paris, France.
[4] Catalog No. 28 028, Prolabo, 75011 Paris, France.
[5] Catalog No. 23 341, Prolabo, 75011 Paris, France.
[6] Puriss p.a., Fluka A.G., Buchs S.G., Switzerland.
[7] 28,731 RP.
[8] Model 419, Packard Instrument Co., Downers Grove, Ill.
[9] Model 714, Packard Instrument Co., Downers Grove, Ill.
[10] Supelcoport, Supelco, Bellefonte, Pa.
[11] Catalog No. 23 882, Prolabo, 75011 Paris, France.
[12] Catalog No. 20 799, Prolabo, 75011 Paris, France.

0022-3549/80/0300-0273$01.00/0
© 1980, American Pharmaceutical Association

position (1700 cm^{-1} for dihydrochloride and 1680 cm^{-1} for monohydrochloride and for free base), were the distinguishing diagnostic features used in this investigation to establish that the different IR spectra of flurazepam dihydrochloride recrystallized from different solvents result from different equilibrium mixtures of flurazepam mono- and dihydrochlorides and/or free base in these solvents. The solvent effect on the transformation of flurazepam di- to monohydrochloride was methanol < chloroform < water. The solution spectra also ruled out polymorphism, and the spectra in Fig. 4 show no compound decomposition.

In view of these findings, the IR identity test for the active ingredient in bulk flurazepam dihydrochloride or flurazepam dihydrochloride capsules should be based on extraction of flurazepam free base using the procedure described in the *Experimental* section and then on comparison of its IR spectrum with a spectrum of the free base similarly extracted from a standard flurazepam dihydrochloride sample, which can serve as a reference spectrum for future work.

REFERENCES

(1) "The Sadtler Standard Spectra, Spectrum R59," vol. 1, Sadtler Research Laboratories, Philadelphia, Pa., 1974.

(2) R. J. Warren, W. E. Thompson, and J. E. Zarembo, *J. Pharm. Sci.*, **54**, 1554 (1965).

ACKNOWLEDGMENTS

The authors are grateful to Dr. S. A. Moros, Dr. A. Mlodozeniec, and Dr. J. Sheridan for comments and support.

Determination of Nofedone in Human Serum by Electron-Capture GLC

D. HEUSSE *x, P. POPULAIRE *, A. RENARD *, P. PASQUIER ‡, and J. GREGOIRE ‡

Received February 23, 1979, from the **Institut de Biopharmacie, Rhône-Poulenc, 13 quai Jules Guesde, 94400 Vitry-sur-Seine, France*, and the ‡*Direction des Recherches Thérapeutiques, Rhône-Poulenc, 16 rue Clisson, 75013 Paris, France.* Accepted for publication October 5, 1979.

Abstract □ An electron-capture GLC method to measure nofedone in human serum was developed. A homolog of nofedone was added to the serum as an internal standard before the sample was alkalinized with pH 9.5 phosphate buffer and extracted with ethylene dichloride containing 0.5% isopentyl alcohol. This organic phase was extracted with 0.2 *N* HCl, the acidic aqueous phase was neutralized immediately, and the extraction with ethylene dichloride was repeated. The ethylene dichloride phase was evaporated to dryness, and the residue was reacted with heptafluorobutyric anhydride. The derivatives were chromatographed at 290° on a 1% Dexsil 300 column. Data on apparent recovery, accuracy, and specificity are given. The detection limit was 5 ng/ml of serum. Serum levels over time in one patient after intravenous administration of 1 mg/kg and after oral administration of 50, 100, and 150 mg of nofedone are presented.

Keyphrases □ Nofedone—analysis, electron-capture GLC, human serum □ GLC, electron capture—nofedone, human serum □ Antiarrhythmic agents—nofedone, analysis, electron-capture GLC, human serum

Nofedone[1] (I) fumarate, 3-[2-hydroxy-3-(isopropylamino)propoxy]-2-phenyl-1-isoindolinone B form, shows marked experimental and clinical antiarrhythmic activity after intravenous and oral administration (1). Compound I is under clinical study. To investigate its pharmacokinetics and to establish the optimal dose range, a procedure was developed for the determination of the drug in human serum. The described method involves GLC of a heptafluorobutyrate derivative with ^{63}Ni-electron-capture detection. A similar method was used for the determination of a β-adrenoreceptor antagonist with the same aminohydroxylated chain (2).

EXPERIMENTAL

Reagents—All solvents and reagents (0.2 *N* HCl[2], 1 *N* NaOH[3], and pH 9.5 phosphate buffer prepared from a 0.5 *M* aqueous solution of dibasic sodium phosphate[4]) were analytical grade. Ethylene dichloride[5], UV spectrophotometric grade, was freshly distilled before use. The heptafluorobutyric anhydride[6] was the derivatizing agent for the electron-capture analysis. It was kept at 4° in sealed vials to prevent the ingress of water from the atmosphere. Nofedone and the internal standard, 3-[2-hydroxy-3-(isopropylamino)propoxy]-2-(3-trifluoromethylphenyl)-1-isoindolinone[7] (II), were used as the free bases.

Apparatus and Operating Conditions—The gas chromatograph[8] was equipped with a ^{63}Ni-electron-capture detector[9] and a glass column (2 m long × 6.25 mm i.d.) packed with 1% Dexsil 300 on a 100–120-mesh support[10]. The column temperature was 290°, the injection port temperature was 300°, the detector temperature was 300°, the carrier gas (nitrogen) flow rate was 20 ml/min, and the scavenger gas (nitrogen) flow rate was 80 ml/min.

The column was conditioned for 24 hr by temperature programming from 250 to 350° at 1°/min and was regulated at 350° for 10 min. It was treated before analysis by several injections of the derivatized extract of serum blank with or without I and the internal standard to ensure maximal performance. Under the conditions described, the retention times of the derivatives of I and II were 2 and 1.5 min, respectively.

Glassware—All glassware was cleaned well and tested with an aqueous solution of I·HCl and II of known content.

Procedure—Compound II was used as a 100-μg/ml solution in ethyl acetate[11] and kept from bright light. This solution was diluted (1:100) with ethyl acetate and immediately inserted in a centrifuge tube. Samples of the internal standard, 50, 200, and 500 ng, were commonly used for such analyses. The quantity of the internal standard was selected to give a peak height greater than or equal to that of I. The solvent was evaporated under a nitrogen stream, and 0.25, 0.50, or 1 ml of serum was added. After vibrating for 30 sec, 2 ml of pH 9.5 phosphate buffer was added.

This aqueous solution was extracted with 6 ml of ethylene dichloride containing 0.5% isopentyl alcohol[12], mechanically shaken for 20 min, and centrifuged. The lower organic phase was removed by pipet and washed by shaking for 5 min with 2 ml of distilled water. The organic phase then was extracted with 2 ml of 0.2 *N* HCl and mechanically shaken for 20 min. The acidic aqueous phase was neutralized immediately with 0.5 ml of 1

[1] 30,356 RP.
[2] Catalog No. 20 252, Prolabo, 75011 Paris, France.
[3] Catalog No. 31 627, Prolabo, 75011 Paris, France.
[4] Catalog No. 28 028, Prolabo, 75011 Paris, France.
[5] Catalog No. 23 341, Prolabo, 75011 Paris, France.
[6] Puriss p.a., Fluka A.G., Buchs S.G., Switzerland.
[7] 28,731 RP.
[8] Model 419, Packard Instrument Co., Downers Grove, Ill.
[9] Model 714, Packard Instrument Co., Downers Grove, Ill.
[10] Supelcoport, Supelco, Bellefonte, Pa.
[11] Catalog No. 23 882, Prolabo, 75011 Paris, France.
[12] Catalog No. 20 799, Prolabo, 75011 Paris, France.

0022-3549/80/0300-0273$01.00/0
© 1980, American Pharmaceutical Association

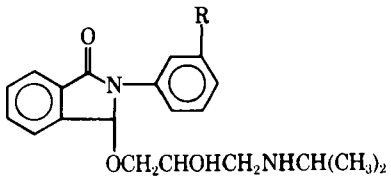

I: R = H

II: R = CF_3

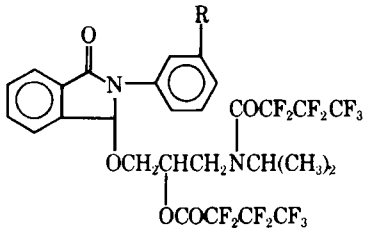

III

N NaOH, and 1 ml of pH 9.5 buffer was added. The extraction with ethylene dichloride was repeated.

The organic phase was transferred to a small tube fitted with a glass stopper and evaporated to dryness under a nitrogen stream in a 50° water bath. The residue was dissolved in a mixture of 0.1 ml of ethyl acetate and 0.4 ml of toluene[13]. After shaking for 30 sec, 50 μl of heptafluorobutyric anhydride was added, and the solution was allowed to stand for 5 min at room temperature. The excess reagent was eliminated by adding 1 ml of a 5% aqueous solution of sodium bicarbonate[14]. After gas release, 0.1 ml of isopentyl alcohol was added. The lower aqueous phase was removed by pipet and discarded. The organic phase was washed by shaking with 0.5 ml of a 2% solution of isopentyl alcohol in distilled water. The mixture

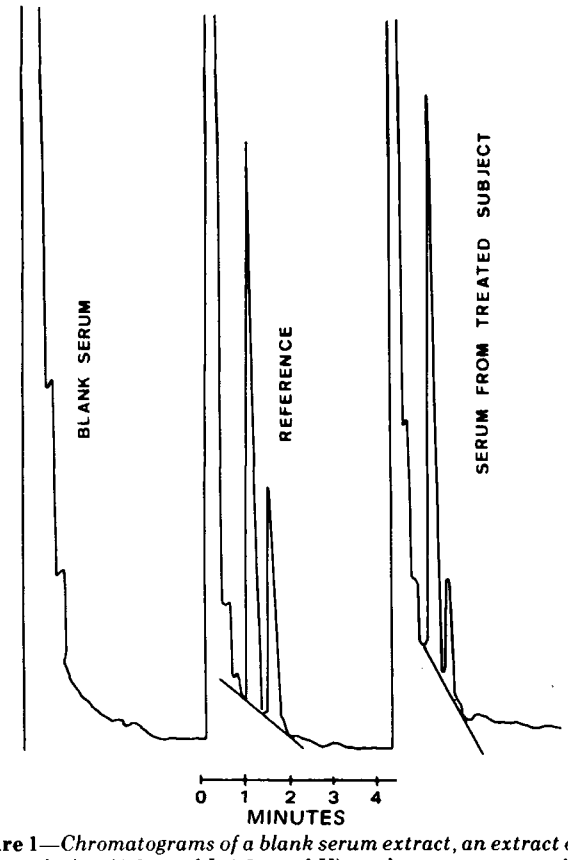

Figure 1—*Chromatograms of a blank serum extract, an extract of reference solution (1.6 ng of I–1.6 ng of II), and a serum extract from a treated subject.*

[13] Catalog No. 28 676, Prolabo, 75011 Paris, France.
[14] Catalog No. 27 778, Prolabo, 75011 Paris, France.

Table I—Apparent Recovery of Nofedone Added to Control Serum

Nofedone Added, ng/ml	Nofedone Found, ng/ml	Apparent Recovery[a], % (Mean ± *RSD*)
20	18.6	93 ± 16.4
50	49.7	99 ± 17.3
100	104	104 ± 10.7
250	270	108 ± 11.5
500	504	101 ± 3.2
1000	978	98 ± 5.0
2000	2070	103 ± 12.1
4000	4270	107 ± 9.72

[a] Average of seven determinations.

was allowed to stand, and 2 or 3 μl of the upper organic phase was injected into the gas chromatograph.

The ratio of the peak heights, H/H_1 (H is the derivative of I and H_1 is the derivative of II), was calculated and compared to a calibration curve. This calibration was obtained by performing derivations on a mixture of 0.025, 0.050, 0.1, or 0.2 ml of a 100-μg/ml stock solution of I in ethyl acetate with 0.1 ml of a 100-μg/ml stock solution of II in ethyl acetate. These reference samples were derivatized and diluted with a mixture of toluene–ethyl acetate–isopentyl alcohol (40:10:10) and were recorded in the best sensitivity range (1:25 dilution for an attenuation of $4 \times 2.5 \times 10^{-10}$). The highest reference sample was not linearly related to the lowest sample when the column was performing properly, but the samples were always derivatized to permit estimation of serum samples added with a too low an amount of internal standard.

To increase reliability, the calibration curve was checked for each series of samples. Each analysis on serum samples and each injection into the chromatograph were repeated at least twice. The injected volume was kept constant during a series of injections.

RESULTS AND DISCUSSION

The use of II as an internal standard was satisfactory because its physicochemical properties are closely related to those of I. The presence of the CF_3 radical in the molecule ensured a higher response for electron-capture detection (Fig. 1).

Several derivatization techniques were tested to form derivatives of I, and the method selected for use in this study was the most rapid. After neutralizing the excess heptafluorobutyric anhydride with sodium bicarbonate, no interfering peaks due to endogenous substances were noted in the upper organic phase. The bis-derivative of I (III) from the serum

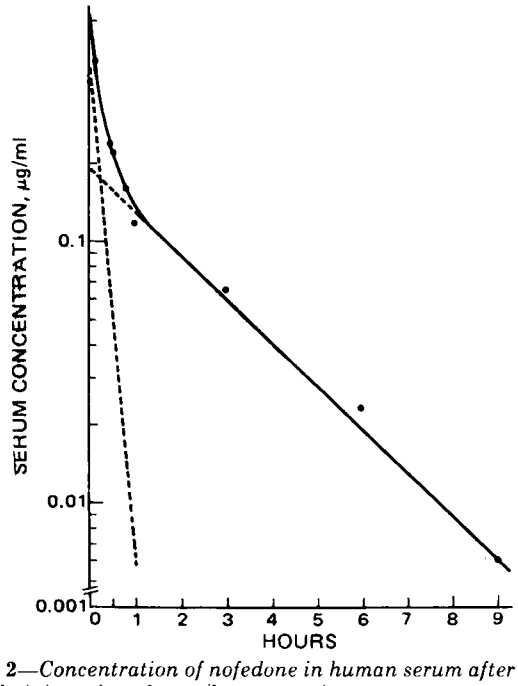

Figure 2—*Concentration of nofedone in human serum after intravenous administration of 1 mg/kg over 2 min.*

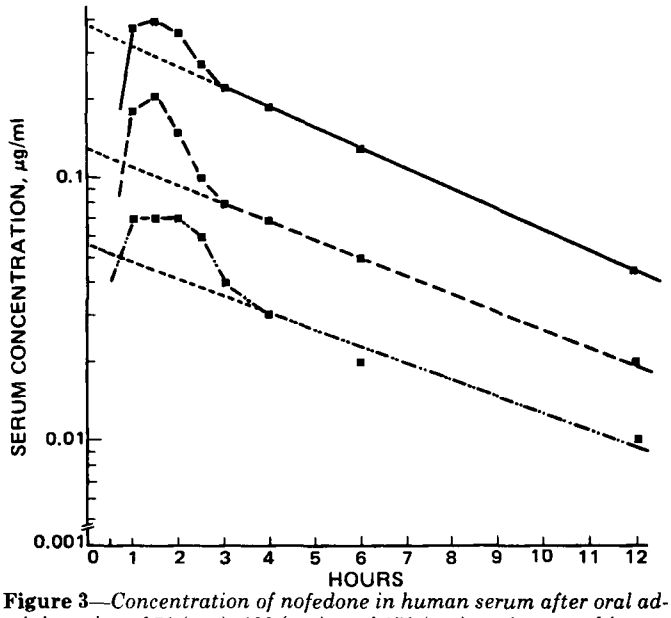

Figure 3—*Concentration of nofedone in human serum after oral administration of 50 (-·-·-), 100 (- - -), and 150 (——) mg in one subject.*

extract had the same chromatographic behavior as the authentic compound. The minimum detectable quantity was 100 pg, and the linearity of the ^{63}Ni-electron-capture detection response was observed from 0.5 to 2 ng in the organic phase injected (attenuation $4 \times 2.5 \times 10^{-10}$).

The theoretical sensitivity initially was 10 ng/ml, but it improved during use. The sensitivity limit for the quantitative determination of I in serum by electron-capture detection was 5 ng/ml of serum after a 2-ml sample extraction. We observed, as did Leitch *et al.* (3), that the sensitivity increased with the number of plasma extracts injected. At the beginning of the GLC analysis, plasma extracts were injected to obtain the plateau of best sensitivity. This plateau was maintained by alternating injections of serum extracts and reference samples. The apparent recovery of I compared with that of the internal standard and the accuracy of the results obtained are shown in Table I. The determinations were repeated seven times for each quantity. The last column in Table I shows the validity of the method. A plot of added drug *versus* found drug had a slope of unity. According to the data provided, a single determination is expected to be within about 12% of the true value, and multiple determinations should vary by ±12% (reproducibility).

The chromatographic analysis of the serum blanks showed that no compound extracted under the conditions described interfered with I or the internal standard (II) (Fig. 1). TLC of derivatized extracts from serum taken from patients treated with nofedone showed that there was no interfering substance with a close R_f value. In the urine of treated patients that contained metabolites, the concentrations of nofedone in the form of bis-derivatives were the same as those measured after elution of a silica plate and GLC analysis.

The sensitivity of this technique allowed determination of serum levels in humans for ~9 hr after an intravenous bolus injection (1 mg/kg in 2 min) and for 12 hr after a single oral dose (50–150 mg in a capsule or tablet). Figures 2 and 3 show the concentrations of nofedone in human serum after an intravenous bolus injection of 1 mg/kg and after an oral dose of 50, 100, and 150 mg in a capsule in another subject. Pharmacokinetic data can be derived from these distribution values. The selectivity of this method allows determination of the compound in saliva, urine, and feces.

Isopentyl alcohol was used because it prevents the molecule from adhering to the glass walls during extraction, derivatization, and GLC analysis. It also prevents tailing peaks and thus increases sensitivity. For serum concentrations below 50 ng/ml, optimal stability of the chromatograph is required to minimize background noise. For higher concentrations, the method provided good reproducibility and allowed calculation of pharmacokinetic parameters up to 9 hr following an intravenous bolus injection (1 mg/kg) and up to 12 and 24 hr after oral doses of 50, 100, and 150 mg.

REFERENCES

(1) J. Y. Detaille, C. G. Caillard, S. Mondot, J. C. Louis, and L. Julou, *C. R. Ser. D*, **288**, 555 (1979).

(2) E. Di Salle, K. M. Baker, S. R. Bareggi, W. D. Watkins, C. A. Chidsey, A. Frigerio, and P. L. Morselli, *J. Chromatogr.*, **84**, 347 (1973).

(3) W. E. Leitch, L. P. Stuart, and E. Forchielli, *Anal Biochem.*, **56**, 380 (1973).

ACKNOWLEDGMENTS

The authors thank Mr. C. Cotrel, Centre Nicolas Grillet, Rhône-Poulenc, Vitry, France, and Mr. C. Saturnin and Mrs. M. Besenval, Institut de Biopharmacie, Rhône-Poulenc, Vitry, France, for technical assistance; and Mrs. M. Eiglier, Rhône-Poulenc Santé, Paris, France, for English translation.

Fluorometric Determination of Thiazole-Containing Compounds

J.-S. K. SHIM, J. W. TOLAN *, and D. W. FINK ˣ

Received August 9, 1979, from the *Merck Sharp & Dohme Research Laboratories, Rahway, NJ 07065.* Accepted for publication October 11, 1979. *Present address: Ethicon, Somerville, NJ 08876.

Abstract □ Fluorescence spectroscopy was applied to the development of sensitive analytical methods for the determination of thiazole and several congeners that contain substituted thiazole rings. Treatment to yield thionine, previously used spectrophotometrically to measure thiazole and fluorometrically only for sulfur determinations in inorganic systems, is further characterized and illustrated with the determination of the antibiotic thiopeptin. This method is selective for submicrogram quantities of thiazole rings in the presence of fused-ring derivatives and reduced analogs. It has a precision of ±2% *RSD* (n = 11) at the 15-ng/ml thiazole concentration level with a signal-to-noise ratio of 3:1. For thiopeptin, this method has an accuracy of 5% mean relative error (n = 8) over the 5–20-ppm range in medicated feed.

Keyphrases □ Thiazole—thiazole-containing compounds, fluorometry □ Fluorometry—analysis, thiazole-containing compounds □ Spectroscopy, fluorescence—thiazole-containing compounds

The thiazole ring is a common structural element found in many compounds exhibiting biological and therapeutic activity and in several molecules used in agricultural products as well as in pharmaceutical formulations (1, 2). Because of these properties, sensitive analytical methods for thiazole-containing compounds are of interest for application in low concentration level formulations, bioavailability studies, and environmental samples.

0022-3549/80/0300-0275$01.00/0
© 1980, American Pharmaceutical Association

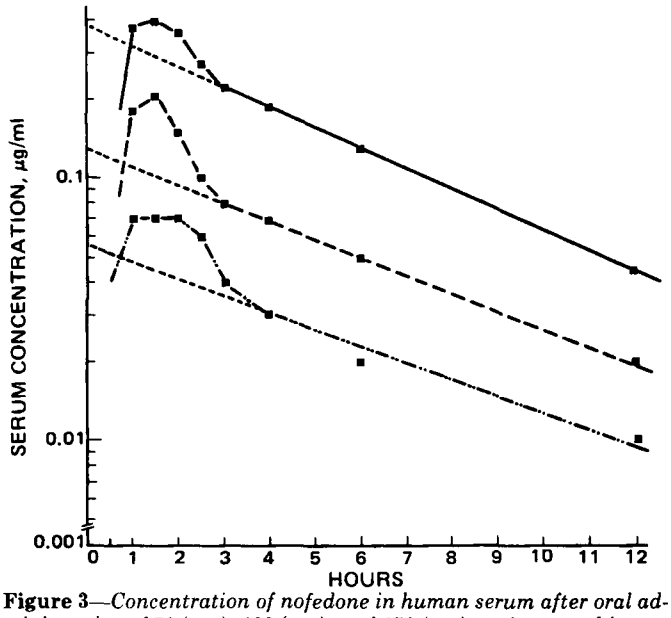

Figure 3—*Concentration of nofedone in human serum after oral administration of 50 (-·-·-), 100 (- - -), and 150 (——) mg in one subject.*

extract had the same chromatographic behavior as the authentic compound. The minimum detectable quantity was 100 pg, and the linearity of the ^{63}Ni-electron-capture detection response was observed from 0.5 to 2 ng in the organic phase injected (attenuation $4 \times 2.5 \times 10^{-10}$).

The theoretical sensitivity initially was 10 ng/ml, but it improved during use. The sensitivity limit for the quantitative determination of I in serum by electron-capture detection was 5 ng/ml of serum after a 2-ml sample extraction. We observed, as did Leitch *et al.* (3), that the sensitivity increased with the number of plasma extracts injected. At the beginning of the GLC analysis, plasma extracts were injected to obtain the plateau of best sensitivity. This plateau was maintained by alternating injections of serum extracts and reference samples. The apparent recovery of I compared with that of the internal standard and the accuracy of the results obtained are shown in Table I. The determinations were repeated seven times for each quantity. The last column in Table I shows the validity of the method. A plot of added drug *versus* found drug had a slope of unity. According to the data provided, a single determination is expected to be within about 12% of the true value, and multiple determinations should vary by ±12% (reproducibility).

The chromatographic analysis of the serum blanks showed that no compound extracted under the conditions described interfered with I or the internal standard (II) (Fig. 1). TLC of derivatized extracts from serum taken from patients treated with nofedone showed that there was no interfering substance with a close R_f value. In the urine of treated patients that contained metabolites, the concentrations of nofedone in the form of bis-derivatives were the same as those measured after elution of a silica plate and GLC analysis.

The sensitivity of this technique allowed determination of serum levels in humans for ~9 hr after an intravenous bolus injection (1 mg/kg in 2 min) and for 12 hr after a single oral dose (50–150 mg in a capsule or tablet). Figures 2 and 3 show the concentrations of nofedone in human serum after an intravenous bolus injection of 1 mg/kg and after an oral dose of 50, 100, and 150 mg in a capsule in another subject. Pharmacokinetic data can be derived from these distribution values. The selectivity of this method allows determination of the compound in saliva, urine, and feces.

Isopentyl alcohol was used because it prevents the molecule from adhering to the glass walls during extraction, derivatization, and GLC analysis. It also prevents tailing peaks and thus increases sensitivity. For serum concentrations below 50 ng/ml, optimal stability of the chromatograph is required to minimize background noise. For higher concentrations, the method provided good reproducibility and allowed calculation of pharmacokinetic parameters up to 9 hr following an intravenous bolus injection (1 mg/kg) and up to 12 and 24 hr after oral doses of 50, 100, and 150 mg.

REFERENCES

(1) J. Y. Detaille, C. G. Caillard, S. Mondot, J. C. Louis, and L. Julou, *C. R. Ser. D*, **288**, 555 (1979).

(2) E. Di Salle, K. M. Baker, S. R. Bareggi, W. D. Watkins, C. A. Chidsey, A. Frigerio, and P. L. Morselli, *J. Chromatogr.*, **84**, 347 (1973).

(3) W. E. Leitch, L. P. Stuart, and E. Forchielli, *Anal Biochem.*, **56**, 380 (1973).

ACKNOWLEDGMENTS

The authors thank Mr. C. Cotrel, Centre Nicolas Grillet, Rhône-Poulenc, Vitry, France, and Mr. C. Saturnin and Mrs. M. Besenval, Institut de Biopharmacie, Rhône-Poulenc, Vitry, France, for technical assistance; and Mrs. M. Eiglier, Rhône-Poulenc Santé, Paris, France, for English translation.

Fluorometric Determination of Thiazole-Containing Compounds

J.-S. K. SHIM, J. W. TOLAN *, and D. W. FINK ˣ

Received August 9, 1979, from the *Merck Sharp & Dohme Research Laboratories, Rahway, NJ 07065.* Accepted for publication October 11, 1979. *Present address: Ethicon, Somerville, NJ 08876.

Abstract □ Fluorescence spectroscopy was applied to the development of sensitive analytical methods for the determination of thiazole and several congeners that contain substituted thiazole rings. Treatment to yield thionine, previously used spectrophotometrically to measure thiazole and fluorometrically only for sulfur determinations in inorganic systems, is further characterized and illustrated with the determination of the antibiotic thiopeptin. This method is selective for submicrogram quantities of thiazole rings in the presence of fused-ring derivatives and reduced analogs. It has a precision of ±2% *RSD* (n = 11) at the 15-ng/ml thiazole concentration level with a signal-to-noise ratio of 3:1. For thiopeptin, this method has an accuracy of 5% mean relative error (n = 8) over the 5–20-ppm range in medicated feed.

Keyphrases □ Thiazole—thiazole-containing compounds, fluorometry □ Fluorometry—analysis, thiazole-containing compounds □ Spectroscopy, fluorescence—thiazole-containing compounds

The thiazole ring is a common structural element found in many compounds exhibiting biological and therapeutic activity and in several molecules used in agricultural products as well as in pharmaceutical formulations (1, 2). Because of these properties, sensitive analytical methods for thiazole-containing compounds are of interest for application in low concentration level formulations, bioavailability studies, and environmental samples.

0022-3549/80/0300-0275$01.00/0
© 1980, American Pharmaceutical Association

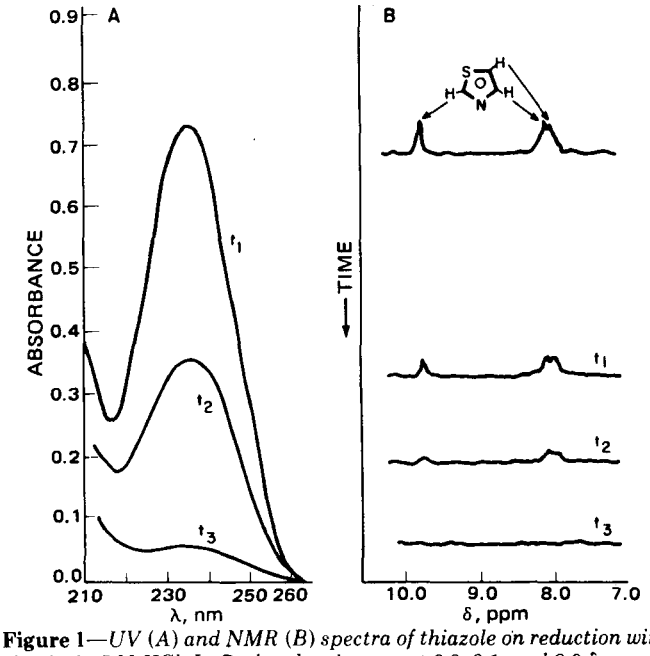

Figure 1—*UV (A) and NMR (B) spectra of thiazole on reduction with zinc in 0.15 N HCl. In B, the absorbances at 9.8, 8.1, and 8.0 δ are assigned to H(2), H(4), and H(5), respectively (20). This reaction was run with deuterium chloride in deuterium oxide.*

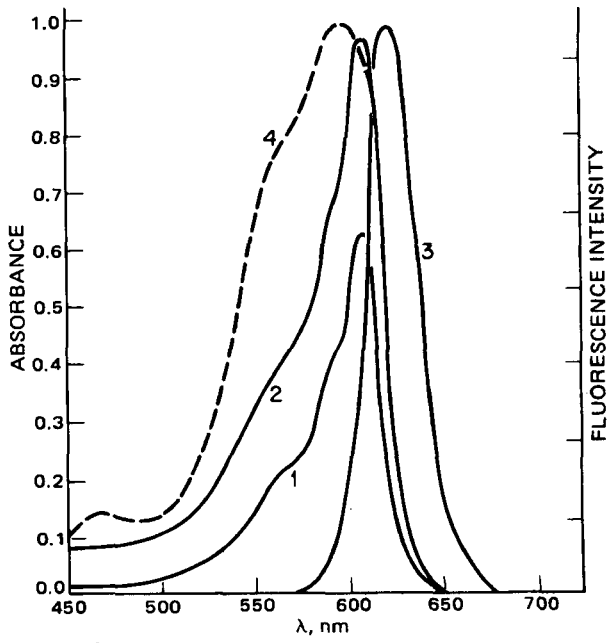

Figure 2—*Spectral properties of the thionine fluorophore in n-butyl alcohol. Key: 1, absorption spectrum of thionine, 10^{-5} M; 2, absorption spectrum obtained from treatment of thiazole according to the text (a solution containing 6 × 10^{-5} M thiazole was treated; the absorbance of this thionine reaction product represents a chemical yield of 26%); 3, uncorrected emission spectrum, λ_{excite} = 595 nm; and 4, uncorrected excitation spectrum, λ_{emit} = 620 nm.*

The condensation reactions of sulfides with *p*-phenylenediamine or its *N,N*-dimethyl derivative to yield thionine or methylene blue, respectively, have been known for many years. Most previous analytical applications of this reaction sequence primarily have been for spectrophotometric determinations of hydrogen sulfide (3, 4) and other sulfides (5, 6) and for sulfur in inorganic systems such as sulfate after reduction to sulfide (7). A prior inorganic application by luminescence measurement involved the determination of traces of sulfate and sulfite in semiconductors (8, 9).

This inorganic reaction sequence has had only one previous analytical application to the thiazole ring. In work in these laboratories, thiabendazole [2-(4-thiazolyl)-1*H*-benzimidazole] was determined spectrophotometrically by the generation of sulfide *via* pretreatment with zinc in acidic solution (10). The present report describes the extension of this technique to the development of a sensitive general analytical method for the determination of thiazole, substituted thiazoles, and other thiazole-containing compounds. The reaction is characterized further through the examination of model compounds, and its sensitivity is enhanced with the first application of fluorometric measurement instead of absorptiometric analysis for the organic system. Included is the determination of thiopeptin (an antibiotic that contains four thiazole rings) at the low parts-per-million concentration level.

EXPERIMENTAL

Apparatus—A spectrofluorometer[1] equipped with a xenon lamp and a 1P21 photomultiplier tube was used for all fluorescence measurements. The excitation and emission slit widths at the cell were both 1.0 mm, and a 0.2-mm slit was used at the entrance beam to the photomultiplier tube. The sample container was a fused quartz fluorescence cell, 10.5 mm i.d. square × 46 mm high.

All emission intensities were read on the microphotometer[1] and standardized relative to the fluorescence intensity (450 nm) of 1.0-ppm quinine sulfate in 0.1 *N* H_2SO_4 (350-nm excitation). Excitation and emission spectra were recorded on an *x–y* recorder[2] and are uncorrected for frequency dependence of source excitation intensity, photomultiplier output, or monochromators. Absorption spectra were recorded on a spectrophotometer[3].

Reagents and Solutions—Ferric ammonium sulfate[4], *n*-butyl alcohol[4], sodium sulfate[4], pyridine[4], *p*-phenylenediamine[5], zinc dust[6], thiazole[7], thiophene[8], thionine[5], thiabendazole[9], cambendazole[9], and the remaining substituted thiazoles[7] were used as received. Other chemicals were reagent grade.

Procedure—The fluorophore was developed according to the procedure described previously (10). To a 15-ml sample of thiopeptin in 0.15 *N* HCl were added 5.0 ml of 0.5-mg/ml aqueous *p*-phenylenediamine and 150 ± 5 mg of zinc dust, and the sample was mixed. After 7 min, 5.0 ml of ~0.65 *M* aqueous ferric ammonium sulfate was added, and the solution was mixed and allowed to remain at room temperature for 15 min.

The reaction vessel was placed in a water bath at 90 ± 3° for 20 min and then cooled in an ice bath for 5 min. An additional 2.0 ml of ferric ammonium sulfate solution was added, and the mixture was mixed again. After 30 min, ~5 g of sodium sulfate (anhydrous) and 5.0 ml of *n*-butyl alcohol were added, the phases were equilibrated for 2 min, and the fluorescence intensity of the *n*-butyl alcohol phase was measured at 620 nm under 475-nm excitation.

RESULTS AND DISCUSSION

In the present reaction sequence, thiazole was treated with zinc in acidic solution to yield an intermediate that might have been the result of two consecutive reactions, *i.e.*, zinc reduction of the ring followed by hydrolysis to sulfide. This unidentified product added 2 moles of *p*-phenylenediamine; in a ring-closing reaction with ferric ion as the oxidizing agent, the central ring was closed to yield thionine according to standard techniques. A boiling water bath was used for heating the reaction mixture. (When *N,N*-dimethyl-*p*-phenylenediamine was used, the product for colorimetric measurement was methylene blue.)

[1] Aminco-Bowman SPF, American Instrument Co.

[2] Aminco J4-8976, American Instrument Co.
[3] Cary model 15, Varian Associates.
[4] J. T. Baker.
[5] Eastman.
[6] Matheson, Coleman and Bell.
[7] Aldrich.
[8] Pfaltz & Bauer.
[9] Merck Sharp & Dohme.

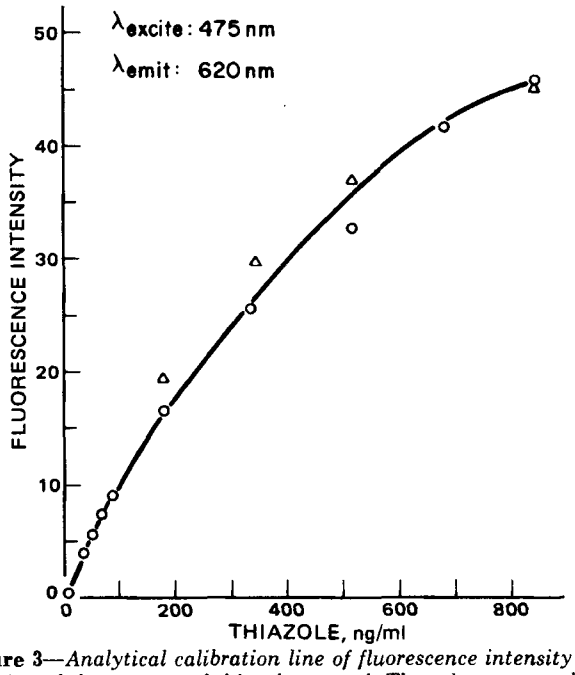

Figure 3—*Analytical calibration line of fluorescence intensity as a function of the amount of thiazole reacted. The solvent was n-butyl alcohol; λ_{excite} = 475 nm, λ_{emit} = 620 nm. Key: O, direct measurement; and Δ, dilutions of a more concentrated reaction product solution. For reaction conditions, see text.*

The identity of the thiazole reaction product was confirmed by chromatographic comparison with authentic thionine in three systems. The R_f values of the reaction product, neutral thionine, and the conjugate acid thionine hydrochloride on silica gel TLC plates[10] were 0.93, 0.91, and 0.17, respectively, with a mobile phase of *p*-dioxane–water (5:1); on silica gel RP-2 with a mobile phase of acetic acid–methanol (100:1), thionine appeared at R_f 0.70, and the reaction product obtained from thiazole appeared at R_f 0.72. This product also eluted with the same retention time as thionine from a silica gel high-pressure liquid chromatographic (HPLC) column[11] with acetic acid–methanol (0.1:200) as the mobile phase.

The first step of this reaction was monitored without the organic coupling reagent and the ferric oxidizing agent by treating thiazole with zinc in acidic solution (Fig. 1). As the reaction proceeded, the single-band, λ_{max} 236-nm electronic absorption spectrum of thiazole decreased in intensity, with no band shifts or new absorption transitions appearing. Eventually, the solution became transparent at λ greater than 210 nm, demonstrating a loss of aromatic π-character. Simultaneously, the intensity of the NMR[12] signals assigned to the three protons of thiazole also diminished and were ultimately lost, with no new NMR signals apparent.

Although proton exchange could have contributed to these lessening NMR signals with time, these results nevertheless were in accord with the UV absorbance spectral changes, confirming that this extremely stable heteroaromatic molecule was broken down by this treatment to furnish the sulfur for the succeeding condensation. This reaction was run with deuterium chloride in deuterium oxide[13]. The ratio of reducing agent to thiazole substrate can be regulated to govern the reaction rate; when microgram quantities of thiazole were treated with milligram quantities of zinc, the reaction proceeded too rapidly to record the UV and/or NMR spectra.

The absorption spectrum of the thionine reaction product is included in Fig. 2. The Beer's law deviation (metachromatic effect) exhibited by this fluorophore has been attributed to self-association to form dimers (or higher polymers) in a stacking, sandwich equilibrium (11–13) that can occur at concentrations as low as 10^{-7} *M* (12). The observed 600-nm λ_{max} in Fig. 2 has been assigned to the monomer, with the dimer evident as the shoulder at 560 nm (12–14).

[10] Whatman LK5DF.
[11] Spectra-Physics model 740B pump, 740C controller, 714 pressure monitor, and SP 8400 UV detector (254 nm) with Spherisorb silica 5-μm column.
[12] Perkin-Elmer R24B.
[13] Merck Sharp & Dohme Canada Ltd.

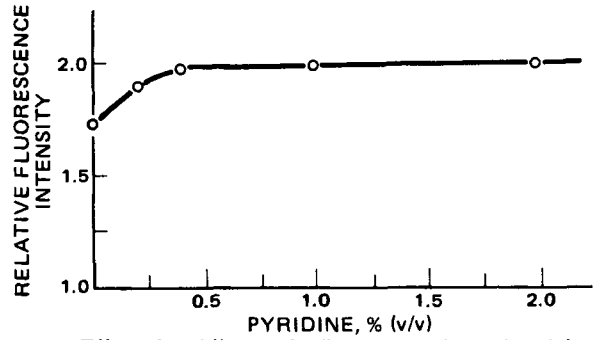

Figure 4—*Effect of pyridine on the fluorescence intensity of the thionine reaction product. The solvent was n-butyl alcohol; λ_{excite} = 475 nm, λ_{emit} = 620 nm. The product was obtained from a solution containing ~0.5μg of thiazole/ml. For reaction conditions, see text.*

The fluorescence spectrum of thionine in *n*-butyl alcohol (Fig. 2) has an emission maximum (uncorrected) at 620 nm, similar to the fluorescence in aqueous and in methanolic solution (13, 15). At least three features of these spectral properties attenuate the analytical signal:

1. The very small Stokes shift and overlap of the absorption and emission spectra cause self-absorption of emitted radiation.
2. Because of the high absorptivity of thionine in butyl alcohol ($\epsilon \sim 6.3 \times 10^4$ liters/mole-cm at 605 nm), the sample is excited at 475 nm so that absorbance at the excitation wavelength is low (Fig. 2) to reduce excitation energy loss near the entrance surface of the cell.
3. Dimerization causes a Beer's law deviation.

Figure 3 presents the fluorescence intensity calibration line as a function of the amount of thiazole treated. This line exhibits the usual attenuation at high concentrations predicted from these spectroscopic properties, although it does furnish a convenient linear range for dilute solutions. Included in Fig. 3 are fluorescence measurements of solutions obtained from dilutions of a more concentrated solution of the reaction product, as in the similar characterization of the Beer's law calibration line by Gustafsson (7). In accordance with the absorbance results, the fluorescence intensity from these solutions near the calibration line confirms that the attenuation results from optical and equilibrium effects and is not the result of decreased reaction yield with larger amounts of thiazole.

Because thionine is not fluorescent in its associated state (12, 13), this dimerization, which also would attenuate the analytical signal, should be avoided over the range of analytical calibration concentrations. To investigate the aggregation of thionine, pyridine was added to the solution to perturb the dimerization equilibrium; similar studies with methylene blue demonstrated that pyridine eliminates the self-association (16). Because of the structural similarity of pyridine to these thiazines, this nitrogen heterocycle can associate with the thionine molecules and thus dissociate the sandwich dimers.

Figure 4 illustrates the small effect pyridine exerts on this system. The increase in fluorescence intensity is only ~15%, suggesting that there is no significant dimerization in this solvent. (Most reports of dimerization have been for aqueous, not alcoholic, solutions.) Moreover, these data also demonstrate that the analytical signal cannot be significantly enhanced by this technique.

Structural Effects—Table I lists a series of model compounds that were examined by this fluorometric procedure using the same reaction conditions. The first column lists single-ring substrates with the fluorescence intensity obtained from thiazole. Thiazole *per se* is not fluorescent (17). Saturation of the aromatic ring inhibits the reaction, as demonstrated by the negative response from thiazolidine. In this aromatic system, the nitrogen heteroatom is necessary for the reaction to proceed; thiophene does not yield the sulfide under these conditions.

The second column of Table I demonstrates that fusing thiazole with a benzene nucleus also inhibits the reaction; neither benzothiazole nor its indicated derivative produced any fluorescence at 620 nm. Each monosubstituted and disubstituted thiazole in Table I gave approximately equimolar (±25%) fluorescence intensity with the parent compound. These compounds are each substituted only in the 2- and/or 4-positions.

Analytical Application—The last disubstituted entry in Table I provides an example of a thiazole-containing compound that was determined by the present method. Thiopeptin is an antibiotic administered to swine and chickens at 10–20 g of drug/ton of feed. The structure of this fermentation product recently was elucidated (18). Thiopeptin has seven

Table I—Relative Fluorescence Intensity from Some Model Compounds[a]

Single Rings	Fused Rings	Monosubstituted	Disubstituted
1.0	0.0	1.03	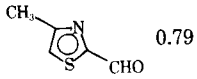 0.79
0.0	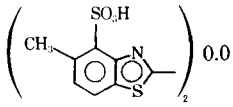 0.0	0.89	Thiopeptin 0.76/thiazole
0.0		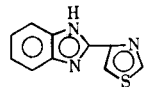 0.84	
		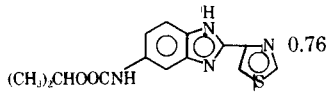 0.76	

[a] Reaction conditions optimized for thiopeptin; see text.

ring systems, including a partially reduced quinoxaline moiety, one piperidine ring, and five five-membered nitrogen–sulfur heterocyclic rings, one of which is a thiazoline nucleus. The remaining four heterocyclic rings are thiazole rings, each bound to the carbon–nitrogen–oxygen skeleton at the 2- and 4-positions.

Because the present reaction sequence is not stoichiometric, it must be optimized (7). Figure 5 presents the effects of four factors on the yield of thionine from thiopeptin, monitored by the absorbance of the fluorophore. Optimal levels for each factor were selected from these data: 2.5 mg of *p*-phenylenediamine was used to minimize the signal from the reagent blank, the amount of zinc and the reaction time were selected at points on the plateaus of each function, and the reaction medium was selected at the peak response for the effect of pH (*i.e.*, 0.15 *M* HCl). The residuals of the linear least-squares calibration line of $A_{605\ nm}$ obtained

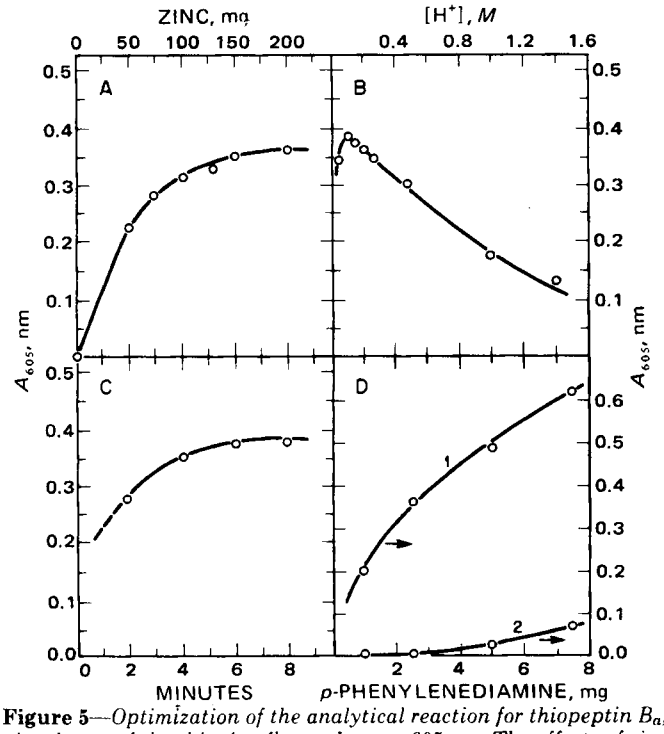

Figure 5—*Optimization of the analytical reaction for thiopeptin B_a; absorbance of the thionine fluorophore at 605 nm. The effects of zinc (A), [H+] (B), time (C), and reagent (D) are shown. Each sample contained ~30 μg of thiopeptin B_a in 15 ml of hydrochloric acid. Zinc, 150 mg, was used in B, C, and D; the reaction mixture was heated 15 min in A, B, and D; 2.5 mg of* p*-phenylenediamine was used in A, B, and C; 0.1 N HCl was used in A; and 0.15 N HCl was used in C and D. In D, line 1 presents the data from thiopeptin and line 2 is the reagent blank response. Each point in this figure is the mean of two, three, or four replicate measurements.*

Table II—Representative Analytical Results for the Determination of Thiopeptin B_a in Feed

Thiopeptin Added, ppm	Fluorescence Intensity	Thiopeptin Found ppm	Thiopeptin Found Relative %
5.0	4.35	5.0	100
	4.30	4.8	96
10.0	5.50	10	100
	4.95	7.6	76
15.0	7.10	17.0	113
	6.45	14.1	94
20.0	7.70	19.6	98
	7.10	17.0	85
Mean			95
Reagent blank	3.20	—	—
Unmedicated feed	3.45	1	—
	3.70	2	—
Analytical standard	5.90	—	—
	5.70	—	—
	5.70	—	—
	5.70[a]	—	—
	5.30[a]	—	—

[a] Processed through the separation scheme.

from seven samples covering the range of 2–15 μg of thiopeptin B_a[14] treated by this procedure averaged 2.9% relative to the line, demonstrating the precision possible with this method.

In the animal feed sample analyzed, thiopeptin was only a trace ingredient in a poorly defined complex matrix. An efficient isolation scheme was required to separate the drug from any other thiazole rings. Furthermore, in addition to thiazole-containing extraneous materials, protein that contains sulfur can also be a significant interference. For instance, these same reactions were used previously for cysteine determinations (19). In the present study, the drug was extracted from the feed into ethyl acetate in the presence of a pH 7 aqueous buffer; the aqueous phase was discarded, and the ethyl acetate extract was charged to the top of a magnesia–silica gel[15] adsorption column. After interfering substances were removed using successive elutions of increasing polarity with petroleum ether, ether, and acetone, the drug was eluted with 5% acetic acid in methanol. The sample was evaporated to dryness under nitrogen and taken up in the 0.15 *N* HCl reaction medium for the fluorogenic reaction, and the thionine fluorophore was partitioned into *n*-butyl alcohol for measurement.

Table II presents some representative analytical results obtained with this procedure. The range of fluorescence intensities from the five analytical reference standards illustrates the precision of replicate measurements. Furthermore, the comparison between the reaction of a pure thiopeptin solution with the same pure solution processed through the analytical isolation demonstrates that there is no loss of thiazole through

[14] Thiopeptin consists of several components, each containing four thiazole rings (18).

[15] Florisil, 100–200 mesh, Floridan Co.

this treatment. The unmedicated feed samples produced fluorescence representing 1–2 ppm of thiopeptin, furnishing sufficient selectivity to determine this drug at the 5-ppm level with an intensity 33% greater than the reagent blank. The mean of the eight analyses covering the 5–20-ppm range in the feed was 95% of the known thiopeptin concentration that was added to the feed. These results demonstrate the use of this treatment for the determination of one thiazole-containing analyte and suggest that this method also should be applicable to other analogous thiazole-containing compounds of pharmaceutical and biological interest.

REFERENCES

(1) J. P. Aune, H. J.-M. Dou, and J. Crousier, in "Thiazole and Its Derivatives. Part I," J. V. Metzger, Ed., "The Chemistry of Heterocyclic Compounds," vol. 34, A. Weissberger and E. C. Taylor, Eds., Wiley–Interscience, New York, N.Y., 1979, p. 399.

(2) G. Fenech, A. Chimirri, and R. Ficarra, *J. Pharm. Sci.*, **67**, 1432 (1978).

(3) L. H. Almy, *J. Am. Chem. Soc.*, **47**, 1381 (1925).

(4) S. E. Sheppard and J. H. Hudson, *Ind. Eng. Chem., Anal. Ed.*, **2**, 73 (1930).

(5) L. M. Siegel, *Anal. Biochem.*, **11**, 126 (1965).

(6) A. M. Krichevskaya and A. A. Fedorov, *J. Anal. Chem. USSR*, **32**, 903 (1977).

(7) L. Gustafsson, *Talanta*, **4**, 227, 236 (1960).

(8) C. A. Parker, "Photoluminescence of Solutions," Elsevier, Amsterdam, The Netherlands, 1968, p. 482.

(9) C. A. Parker and W. T. Rees, in "Trace Analysis of Semi-conductor Materials," J. P. Cali, Ed., Pergamon, Oxford, England, 1964, p. 243.

(10) C. R. Szalkowski and J. Kanora, *J. Assoc. Off. Anal. Chem.*, **48**, 288 (1965).

(11) T. G. Dewey, P. S. Wilson, and D. H. Turner, *J. Am. Chem. Soc.*, **100**, 4550 (1978).

(12) E. Rabinowitch and L. F. Epstein, *ibid.*, **63**, 69 (1941).

(13) G. Haugen and R. Hardwick, *J. Phys. Chem.*, **69**, 2988 (1965).

(14) R. E. Ballard and C. H. Park, *J. Chem. Soc. A*, **1970**, 1340.

(15) I. C. Ferreira and A. Harriman, *J. Chem. Soc. Faraday Trans. I*, **73**, 1085 (1977).

(16) W. J. Kirsten and V. J. Patel, *Microchem. J.*, **17**, 277 (1972).

(17) J. V. Metzger, E.-J. Vincent, J. Chouteau, and G. Mille, in "Thiazole and Its Derivatives. Part I," J. V. Metzger, Ed., "The Chemistry of Heterocyclic Compounds," vol. 34, A. Weissberger and E. C. Taylor, Eds., Wiley–Interscience, New York, N.Y., 1979, p. 51.

(18) O. D. Hensens and G. Albers-Schönberg, *Tetrahedron Lett.*, **1978**, 3649.

(19) B. Vassel, *J. Biol. Chem.*, **140**, 323 (1941).

(20) J. V. Metzger, E.-J. Vincent, J. Chouteau, and G. Mille, in "Thiazole and its Derivatives. Part I," J. V. Metzger, Ed., "The Chemistry of Heterocyclic Compounds," vol. 34, A. Weissberger and E. C. Taylor, Eds., Wiley–Interscience, New York, N.Y., 1979, pp. 66–72.

ACKNOWLEDGMENTS

Presented in part at the 13th Middle Atlantic Regional Meeting, American Chemical Society, West Long Branch, N.J., March 1979.

Decreased Activity of Proteins Adsorbed onto Glass Surfaces with Porous Glass as a Reference

TAKAHARU MIZUTANI

Received April 9, 1979, from the *Faculty of Pharmaceutical Sciences, Nagoya City University, Mizuho-ku, Nagoya 467, Japan.* Accepted for publication October 15, 1979.

Abstract □ The biological activity of proteins bound to controlled-pore glass surfaces was studied as a model of denaturation of biologicals upon storage in glass containers. After adsorption onto the glass for 1 week, the activities of alkaline phosphatase, catalase, and horse-radish peroxidase recovered from the glass column were 88, 63, and 97%, respectively. However, the phosphatase activity recovered after adsorption for 3 months was 14% of the total activity loaded onto the column, and the activities recovered of peroxidase and catalase were 48 and 2%, respectively. Insulin had almost full activity after adsorption for 3 months, but calcitonin activity was absent. The scission of peptide bonds of proteins eluted after adsorption for 3 months was not observed, but dissociation to the subunits was found. The proteins were active in the state adsorbed onto glass surfaces.

Keyphrases □ Adsorption—proteins, glass surfaces, activity decrease □ Proteins—adsorption onto glass surfaces, activity decrease □ Activity—proteins, decrease after adsorption onto glass surfaces

The reaction of biological materials on glass is well known (1–4). By use of controlled-pore glass (5) with a large surface area (97 m^2/g), it was shown that 5 μmoles of basic drugs and materials was adsorbed onto 97 m^2 of glass surface and that adsorption of proteins onto the surfaces was caused by amine–silanol bonding and a cooperative aggregative factor between silica and proteins (6–10). Proteins also were adsorbed in detergent solutions such as urea and guanidine hydrochloride (11). From the value of the maximum amount of protein adsorbed (233 mg/97 m^2), the amount of protein adsorbed onto the surfaces of a glass container (50 cm^2, 20 ml) and a glass injector was estimated to be >12 μg. The 12-μg/20 ml concentration must be a marginal point not affected by adsorption, and the biologicals used at lower concentrations would be affected by adsorption to glass surfaces (10).

Some biologicals composed of proteins are stored or maintained in pharmaceutical glass containers in a water medium (12). However, denaturation of proteins by their adsorptive aggregation on surfaces of glass containers upon storage for long periods is not clear. The purpose of this investigation was to show changes in the biological activity and the structure of proteins adsorbed onto glass surfaces upon storage as a model of denaturation of protein biologicals in glass containers. Enzymes and hormones were studied, and controlled-pore glass was used as a reference standard.

EXPERIMENTAL

Materials and Column Operation—The controlled-pore glass[1] was 96% silica and had a surface area of 97 m^2/g and a particle size of 100 μm. After being washed with water, 0.1% sodium dodecylsulfate, water, chromic acid mixture, and water, the glass was packed in columns (0.6

[1] CPG-10, Electro-Nucleonics, Fairfield, N.J.

0022-3549/80/0300-0279$01.00/0

© 1980, American Pharmaceutical Association

this treatment. The unmedicated feed samples produced fluorescence representing 1–2 ppm of thiopeptin, furnishing sufficient selectivity to determine this drug at the 5-ppm level with an intensity 33% greater than the reagent blank. The mean of the eight analyses covering the 5–20-ppm range in the feed was 95% of the known thiopeptin concentration that was added to the feed. These results demonstrate the use of this treatment for the determination of one thiazole-containing analyte and suggest that this method also should be applicable to other analogous thiazole-containing compounds of pharmaceutical and biological interest.

REFERENCES

(1) J. P. Aune, H. J.-M. Dou, and J. Crousier, in "Thiazole and Its Derivatives. Part I," J. V. Metzger, Ed., "The Chemistry of Heterocyclic Compounds," vol. 34, A. Weissberger and E. C. Taylor, Eds., Wiley–Interscience, New York, N.Y., 1979, p. 399.

(2) G. Fenech, A. Chimirri, and R. Ficarra, *J. Pharm. Sci.*, **67**, 1432 (1978).

(3) L. H. Almy, *J. Am. Chem. Soc.*, **47**, 1381 (1925).

(4) S. E. Sheppard and J. H. Hudson, *Ind. Eng. Chem., Anal. Ed.*, **2**, 73 (1930).

(5) L. M. Siegel, *Anal. Biochem.*, **11**, 126 (1965).

(6) A. M. Krichevskaya and A. A. Fedorov, *J. Anal. Chem. USSR*, **32**, 903 (1977).

(7) L. Gustafsson, *Talanta*, **4**, 227, 236 (1960).

(8) C. A. Parker, "Photoluminescence of Solutions," Elsevier, Amsterdam, The Netherlands, 1968, p. 482.

(9) C. A. Parker and W. T. Rees, in "Trace Analysis of Semi-conductor Materials," J. P. Cali, Ed., Pergamon, Oxford, England, 1964, p. 243.

(10) C. R. Szalkowski and J. Kanora, *J. Assoc. Off. Anal. Chem.*, **48**, 288 (1965).

(11) T. G. Dewey, P. S. Wilson, and D. H. Turner, *J. Am. Chem. Soc.*, **100**, 4550 (1978).

(12) E. Rabinowitch and L. F. Epstein, *ibid.*, **63**, 69 (1941).

(13) G. Haugen and R. Hardwick, *J. Phys. Chem.*, **69**, 2988 (1965).

(14) R. E. Ballard and C. H. Park, *J. Chem. Soc. A*, **1970**, 1340.

(15) I. C. Ferreira and A. Harriman, *J. Chem. Soc. Faraday Trans. I*, **73**, 1085 (1977).

(16) W. J. Kirsten and V. J. Patel, *Microchem. J.*, **17**, 277 (1972).

(17) J. V. Metzger, E.-J. Vincent, J. Chouteau, and G. Mille, in "Thiazole and Its Derivatives. Part I," J. V. Metzger, Ed., "The Chemistry of Heterocyclic Compounds," vol. 34, A. Weissberger and E. C. Taylor, Eds., Wiley–Interscience, New York, N.Y., 1979, p. 51.

(18) O. D. Hensens and G. Albers-Schönberg, *Tetrahedron Lett.*, **1978**, 3649.

(19) B. Vassel, *J. Biol. Chem.*, **140**, 323 (1941).

(20) J. V. Metzger, E.-J. Vincent, J. Chouteau, and G. Mille, in "Thiazole and its Derivatives. Part I," J. V. Metzger, Ed., "The Chemistry of Heterocyclic Compounds," vol. 34, A. Weissberger and E. C. Taylor, Eds., Wiley–Interscience, New York, N.Y., 1979, pp. 66–72.

ACKNOWLEDGMENTS

Presented in part at the 13th Middle Atlantic Regional Meeting, American Chemical Society, West Long Branch, N.J., March 1979.

Decreased Activity of Proteins Adsorbed onto Glass Surfaces with Porous Glass as a Reference

TAKAHARU MIZUTANI

Received April 9, 1979, from the *Faculty of Pharmaceutical Sciences, Nagoya City University, Mizuho-ku, Nagoya 467, Japan.* Accepted for publication October 15, 1979.

Abstract □ The biological activity of proteins bound to controlled-pore glass surfaces was studied as a model of denaturation of biologicals upon storage in glass containers. After adsorption onto the glass for 1 week, the activities of alkaline phosphatase, catalase, and horse-radish peroxidase recovered from the glass column were 88, 63, and 97%, respectively. However, the phosphatase activity recovered after adsorption for 3 months was 14% of the total activity loaded onto the column, and the activities recovered of peroxidase and catalase were 48 and 2%, respectively. Insulin had almost full activity after adsorption for 3 months, but calcitonin activity was absent. The scission of peptide bonds of proteins eluted after adsorption for 3 months was not observed, but dissociation to the subunits was found. The proteins were active in the state adsorbed onto glass surfaces.

Keyphrases □ Adsorption—proteins, glass surfaces, activity decrease □ Proteins—adsorption onto glass surfaces, activity decrease □ Activity—proteins, decrease after adsorption onto glass surfaces

The reaction of biological materials on glass is well known (1–4). By use of controlled-pore glass (5) with a large surface area (97 m^2/g), it was shown that 5 μmoles of basic drugs and materials was adsorbed onto 97 m^2 of glass surface and that adsorption of proteins onto the surfaces was caused by amine–silanol bonding and a cooperative aggregative factor between silica and proteins (6–10). Proteins also were adsorbed in detergent solutions such as urea and guanidine hydrochloride (11). From the value of the maximum amount of protein adsorbed (233 mg/97 m^2), the amount of protein adsorbed onto the surfaces of a glass container (50 cm^2, 20 ml) and a glass injector was estimated to be >12 μg. The 12-μg/20 ml concentration must be a marginal point not affected by adsorption, and the biologicals used at lower concentrations would be affected by adsorption to glass surfaces (10).

Some biologicals composed of proteins are stored or maintained in pharmaceutical glass containers in a water medium (12). However, denaturation of proteins by their adsorptive aggregation on surfaces of glass containers upon storage for long periods is not clear. The purpose of this investigation was to show changes in the biological activity and the structure of proteins adsorbed onto glass surfaces upon storage as a model of denaturation of protein biologicals in glass containers. Enzymes and hormones were studied, and controlled-pore glass was used as a reference standard.

EXPERIMENTAL

Materials and Column Operation—The controlled-pore glass[1] was 96% silica and had a surface area of 97 m^2/g and a particle size of 100 μm. After being washed with water, 0.1% sodium dodecylsulfate, water, chromic acid mixture, and water, the glass was packed in columns (0.6

[1] CPG-10, Electro-Nucleonics, Fairfield, N.J.

0022-3549/80/0300-0279$01.00/0

© 1980, American Pharmaceutical Association

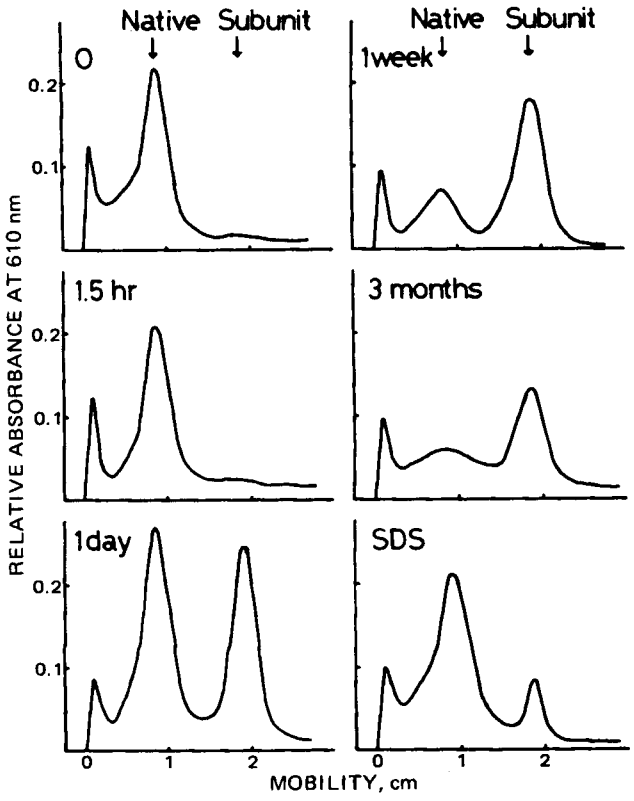

Figure 1—*Densitometric tracing of stained gel patterns of alkaline phosphatase on 10% polyacrylamide gel in the presence of 0.1% sodium dodecylsulfate. The times on the shoulder of each figure are those of adsorption. SDS is the sample incubated in 4* M *urea–0.1% sodium dodecylsulfate solution for 15 hr.*

× 10 cm, 1.3 g), which were used to preserve the proteins in the state in which they were bound to glass. After the column was equilibrated with buffer, the protein solution was applied on the column.

For experiments involving the retention of the activity of proteins bound to porous glass, the protein-bound columns were stored for 1 day, 1 week, 1 month, or 3 months in a cold room at 4°. After storage, the columns were eluted at a flow rate of 0.5 ml/cm^2/min, and 1-ml fractions were collected. Three columns were used for the measurement of each point, and the mean ● *SE* of the three measurements was calculated.

The enzymes and hormones used were alkaline phosphatase from *Escherichia coli*[2], horse-radish peroxidase[3], catalase[3], malate dehydrogenase[3], insulin[4], and porcine calcitonin[5]. For storage for 1 and 3 months, sodium azide was added at 0.1% to the enzyme solution as a preservative.

Activity Measurement—The activity of alkaline phosphatase was measured by the increase of the optical density at 405 nm in an assay mixture containing 0.95 *M* tromethamine [tris(hydroxymethyl)aminomethane] hydrochloride (pH 8.0), 4.8 m*M* *p*-nitrophenyl phosphate, and enzyme. Alkaline phosphatase was used after dialysis of ammonium sulfate contained in the commercial enzyme solution, and the specific activity was 10 units/mg. The activity of malate dehydrogenase was measured by the decrease of the optical density at 340 nm in the mixture of 94 m*M* phosphate buffer (pH 7.5), 0.5 m*M* oxaloacetate, 0.2 m*M* β-nicotinamide adenine dinucleotide in the reduced form, and enzyme. Commercial malate dehydrogenase was used without further purification.

The activity of peroxidase was determined according to a literature method (13) involving measurement of the time required to increase the optical density by 0.05 at 470 nm when 10 μl of 10 m*M* hydrogen peroxide was added to 3 ml of 13 m*M* guaiacol–enzyme. The activity of catalase was determined by direct measurements of the decreased light absorption at 230 nm caused by the decomposition of hydrogen peroxide by catalase.

The insulin activity was determined by measurement of the decreased glucose in rabbit serum. The glucose concentration in the serum derived from a group of six male rabbits was analyzed by a literature method using a mixture of 960 ml of 8% *o*-toluidine in acetic acid and 40 ml of 4% boric acid in water (14). Blood was drawn from the aural vein of six rabbits before and 1 hr after the injection of insulin. The rate of the fall of serum glucose after the injection compared with that before the injection was calculated, and the mean rate was taken as the glucose lowering rate.

The hypocalcemic activity of calcitonin was determined using six male rabbits (15). The sample was injected into the rabbit aural vein, and blood was drawn from another aural vein before and 1 hr after the injection. The calcium concentration in the serum was determined by atomic absorption[6] at 422.7 nm (16). The rate of fall of serum calcium after the injection compared with that before the injection was calculated. Bioassay data are expressed as the mean ± *SE*.

Other Methods—The molecular weights of the proteins were determined by sodium dodecylsulfate–polyacrylamide gel electrophoresis (17). The acrylamide gel concentration was 10% for alkaline phosphatase, peroxidase, and catalase and 20% for insulin and calcitonin. Densitometric tracing of the stained bands on the gel was carried out using an autodensitometer[7], and the ratio of proteins on the gel was calculated from the patterns.

RESULTS AND DISCUSSION

Activity of Proteins Eluted from Porous Glass Columns—Alkaline phosphatase was adsorbed onto a glass column in 0.2 *M* sodium chloride–0.01 *M* phosphate buffer (pH 7.0) and eluted with 0.2 *M* glycine at pH 9.0. After 1 mg of the phosphatase was adsorbed onto the column which can adsorb about 100 mg of protein, the column was washed with five column volumes of buffer, followed by glycine buffer (pH 9.0) for enzyme elution. After adsorption for 1.5 hr, the activity of phosphatase was completely recovered, and the specific activity was identical with that of the untreated enzyme.

The sodium dodecylsulfate–polyacrylamide gel pattern of the eluted enzyme was similar to that of the native enzyme (Fig. 1). After adsorption for 1 day in the sodium chloride–phosphate buffer, 95% of the activity of phosphatase applied on the column was eluted with the glycine solution, but 45% of the enzyme was separated into subunits with a molecular weight of 40,000 (Fig. 1). This separation did not originate from the treatment used in sodium dodecylsulfate electrophoresis, because the native phosphatase did not show the subunit pattern after incubation and treatment for 1 day in the sodium dodecylsulfate solution (Fig. 1).

In the case of adsorption for 1 week, 88% of the activity was recovered, and 61% of the total protein eluted from the column dissociated into subunits (Fig. 1). The phosphatase activity recovered after adsorption for 1 month was 62%. After phosphatase was adsorbed onto the porous glass column for 3 months, elution with glycine yielded the enzyme activity as only 14%; the yield of protein by elution with glycine was 24%. Subunits comprised 70% of the total protein eluted from the column with glycine buffer (Fig. 1).

The relationship between the activity and the binding time on glass surfaces is summarized in Table I. The half-life of the activity of phosphatase adsorbed onto glass surfaces was ~30 days. Phosphatase was eluted easily with glycine after adsorption for 1 week, and the activity was almost completely recovered. The enzyme was adsorbed strongly after standing for 3 months and was not completely eluted with glycine but was eluted with the 0.1% sodium dodecylsulfate solution, which has the strongest eluting force of proteins from the porous glass column among several buffers. The band showing a smaller molecular weight than the subunit was not found on the gel patterns (Fig. 1). Therefore, scission of the peptide bond did not occur on glass surfaces for the long preservation period. The decreased activity recovered from the glass column was believed to depend on a conformational change of proteins or desolubilization by aggregation of proteins on glass surfaces.

After adsorption of catalase for 1 week, 63% of the catalase activity was eluted from the column with the glycine solution, and residual protein was eluted with the 0.1% sodium dodecylsulfate solution. The sodium dodecylsulfate gel pattern of catalase after the 1-week adsorption showed that the subunit with a molecular weight of 6 × 10^4 was 80% of the total protein, even though the native enzyme preparation was comprised of 73% subunits by the gel pattern. The specific activity of catalase adsorbed for 1 week decreased to 75%.

After adsorption for 3 months, the catalase activity recovered from the

[2] P-L Biochemical Inc., Milwaukee, Wis.
[3] Boehringer Mannheim GmbH, Mannheim, West Germany.
[4] Fluka AG, Buchs, Switzerland.
[5] Armour Pharmaceutical Co., Chicago, Ill.
[6] AA 610 spectrophotometer, Shimadzu, Kyoto, Japan.
[7] FD-A IV, Fujiriken, Tokyo, Japan.

Table I—Protein Activity in Eluates after Adsorption onto Porous Glass Columns

Protein	Total Activity Recovered after Adsorption[a], % (Specific Activity, %)		
	1 Week	1 Month	3 Months
Horse-radish peroxidase	97 ± 1.5 (100)	77 ± 2.1 (98)	48 ± 3.1 (90)
Alkaline phosphatase	88 ± 1.1 (98)	62 ± 1.7 (92)	14 ± 1.0 (58)
Catalase	63 ± 3.2 (75)	26 ± 3.0 (73)	2 ± 0.9 (6)
Insulin	—	—	89 ± 2.3 (86)

[a] The values are given as the means of three experiments (±*SE*).

column with glycine buffer (pH 9.0) was only 2% of the total protein applied on the column. Residual catalase adsorbed onto porous glass surfaces was not eluted with the 0.1% sodium dodecylsulfate solution, and the colored band of catalase or heme was found on the top of the column. Catalase was adsorbed onto glass surfaces more strongly than was alkaline phosphatase.

Horse-radish peroxidase was not adsorbed onto the glass column in 0.2 *M* sodium chloride–0.01 *M* phosphate buffer (pH 7.0) but was adsorbed in a distilled water medium. Therefore, peroxidase was eluted with the sodium chloride–phosphate buffer from the column on which the enzyme was loaded in a water medium. After adsorption for 1 week, the recovery of the peroxidase activity was 97% of the initial activity. The recovery of the activity after adsorption for 3 months was 48%, and the residual protein adsorbed onto glass surfaces was eluted with the 0.1% sodium dodecylsulfate solution. The mobility of the eluted peroxidase on a gel did not change from that of the native protein.

The eluting order of proteins by adsorption chromatography was peroxidase, phosphatase, and catalase (7), and the adsorption of peroxidase was weak. The recoveries of the activity after adsorption for 3 months were 48% for peroxidase, 14% for phosphatase, and 2% for catalase (Table I). The stronger the proteins adsorbed onto glass surfaces, the lower was the activity recovery. The retention of the activity of proteins did not relate to the molecular weight and isoelectric point but instead to the inherent properties of proteins such as solubility and aggregative force. Since γ-globulin in serum was adsorbed strongly onto glass and the elution of the γ-globulin fraction from a porous glass column by adsorption chromatography was difficult, as reported previously (7), adsorption of antiserum samples onto the surface of glass containers must be considered. The inactivation of biologicals composed of proteins upon storage must be caused partially by adsorption onto the surface of glass containers.

Insulin (0.5 mg, 10 units) was dissolved in 0.5 ml of 0.01 *N* hydrochloric acid–1.5% glycerin isotonic solution and applied on the porous glass column. Insulin was adsorbed well onto porous glass in this condition (10). After adsorption for 3 months, adsorbed insulin was eluted with 0.2 *M* glycine (pH 9.0), and the pH of the eluate was adjusted with hydrochloric acid to pH 2. For injection, the protein concentration of insulin in the solution was estimated from the absorbance at 280 nm. The solution containing insulin was diluted to a concentration of 0.05 mg/ml with a 1.5% glycerin isotonic solution (pH 2.6), and 0.5 ml was injected subcutaneously into each rabbit. The molecular weight of insulin in the eluate from the column was studied by sodium dodecylsulfate gel electrophoresis using 20% gel, but the mobility on the gel was identical to that of native protein, and the scission to the A-chain and B-chain was not found. In a dose of 0.025 mg/rabbit, native insulin lowered the rabbit serum glucose concentration to 41.7 ± 10.3%, and insulin in the column eluate after adsorption for 3 months lowered the concentration to 36.3 ± 4.1%. The value of 36.3% was less than that of native insulin, but no significant difference between the two values was found. Insulin was not inactivated by adsorption for 3 months.

The calcium lowering rate of native porcine calcitonin was 12.7 ± 0.7% 1 hr after the injection of 4 MRC units/kg of rabbit. Calcitonin (100 MRC units) was dissolved in 1 ml of water and loaded onto a porous glass column, and the column was stored for 3 months at 4°. The column was eluted with 0.2 *M* glycine (pH 9.0), and the eluate of five column volumes was collected. The eluate was used for the hypocalcemic activity assay. The dose of 4 MRC units/kg of rabbit to be injected was calculated on the assumption that the eluate contained the total amount of calcitonin (100 MRC units) applied on the column. However, the hypocalcemic rate at 1 hr after the injection, 2.6 ± 1.4%, was insignificant, even though the band of calcitonin was found on the sodium dodecylsulfate–polyacrylamide gel of the eluate. After elution with glycine, the column was eluted with the 0.1% sodium dodecylsulfate solution, but the gel pattern of the eluate did not contain the band of calcitonin. Finally, active calcitonin was not recovered from the porous glass column after adsorption for 3 months.

These adsorption experiments for long periods showed that enzymes and hormones had a specific strength of activity on glass surfaces. Moreover, drugs might be inactivated on surfaces of glass containers upon storage. In this experiment, 96% silica glass was used, but proteins show different properties on other glass, such as soda-lime glass, from those on 96% silica glass. The stability of enzymes in the buffer at 4° was examined as a control experiment, and the enzymes stored for 3 months in the solution containing 0.1% sodium azide were fully active and the dissociation to the subunit was not found because the commercial enzymes used were stable and pure. Twenty-milliliter glass containers are able to adsorb about 10 μg of proteins. Therefore, for many biologicals composed of proteins at high concentration, the protein drugs in the containers might be inactivated more slowly than the time showed in these experiments.

Activity of Proteins in State Adsorbed onto Glass—After enzymes were adsorbed onto a glass column, the substrate solution was loaded onto the column at a constant flow rate, and the absorbance of the product in the eluate was measured. Malate dehydrogenase (23 μg) in 0.1 *M* phosphate buffer (pH 7.4) was adsorbed onto the column, and the substrate solution containing nicotinamide adenine dinucleotide in the reduced form and oxaloacetic acid was applied on the column at a flow rate of 1.2 ml/min/cm^2. The decreased absorbance in the eluate at 340 nm was 0.41, and thus confirmed that malate dehydrogenase on glass surfaces was active. The reaction rate of the enzyme immobilized on glass was about 1/600 compared with that in the free solution from the flow rate data, the thickness of the band adsorbing the enzyme, and the enzyme concentration in the band.

Alkaline phosphatase (3.4 μg) was adsorbed onto the column, and the column was washed with five column volumes of the 0.2 *M* sodium chloride–0.01 *M* phosphate buffer (pH 7.0). The substrate solution containing 5 m*M* *p*-nitrophenyl phosphate was applied on the column at a flow rate of 1.2 ml/min/cm^2, and the absorbance of the eluate at 405 nm was measured. The apparent reaction rate of the enzyme on glass surfaces was about one-fifth of that in the free solution. The absorbance of the solution was measured at 405 nm at 0 and 1 hr, but it had not changed. Therefore, the enzyme was not eluted and was not contained in the eluate. The change of the absorbance was caused by digestion with the enzyme bound to porous glass surfaces.

Peroxidase (2 mg) dissolved in a water medium was adsorbed onto the glass column, and the substrate solution containing guaiacol and hydrogen peroxide was loaded on the column. The eluate developed a brown color, confirming the reaction with peroxidase on the column. The activity of catalase bound to the porous glass column was ascertained by the evolution of gas (oxygen) with elution of the hydrogen peroxide solution. Bovine serum albumin (1 μmole) bound to glass surfaces adsorbed 0.42 μmole of aspirin and 0.59 μmole of sulfamethoxazole in 0.15 *M* sodium chloride–0.01 *M* phosphate (pH 6.0) by frontal analyses. After adsorption of albumin for 1 week, the amounts of aspirin and sulfamethoxazole bound to albumin (1 μmole) were 0.35 and 0.16 μmole, respectively. The reason for the lower values than those obtained using albumin coupled on agarose (18) must be that the site on albumin which adsorbs drugs was used for adsorption to glass silanol.

REFERENCES

(1) J. Schoenmakers, R. Matze, C. Haanen, and F. Zilliken, *Biochim. Biophys. Acta*, **101**, 166 (1965).

(2) P. Lehtinen, J. Pikkarainen, and E. Kulonen, *ibid.*, **439**, 393 (1976).

(3) H. Wigzell and B. Anderson, *J. Exp. Med.*, **129**, 23 (1969).

(4) J. Pouyssegur, M. Willingham, and I. Pastan, *Proc. Natl. Acad. Sci. USA*, **74**, 243 (1977).

(5) W. Haller, *Nature*, **206**, 693 (1965).

(6) T. Mizutani and A. Mizutani, *J. Chromatogr.*, **120**, 206 (1976).

(7) *Ibid.*, **168**, 143 (1979).

(8) T. Mizutani and A. Mizutani, *Anal. Biochem.*, **83**, 216 (1977).

(9) T. Mizutani and A. Mizutani, *J. Non-Cryst. Solids*, **30**, 23 (1978).

(10) T. Mizutani and A. Mizutani, *J. Pharm. Sci.*, **67**, 1102 (1978).

(11) T. Mizutani and A. Mizutani, *J. Non-Cryst. Solids*, **27**, 437 (1978).

(12) "The United States Pharmacopeia," 19th rev., Mack Publishing Co., Easton, Pa., 1975, pp. 642–647.

(13) B. Chance and A. C. Maehly, in "Methods in Enzymology," vol. II, S. P. Colowick and N. O. Kaplan, Eds., Academic, New York, N.Y.,

1955, p. 764.
(14) K. Sasaki, *Rinshoyakuri*, **12**, 434 (1964).
(15) P. Maier, R. Neher, W. Rittel, and M. Staehelin, in "Calcitonin," William Heineman Medical Books, London, England, 1969, p. 381.
(16) A. Mizutani, T. Mizutani, and P.-F. Kuo, *Chem. Pharm. Bull.*, **24**, 2733 (1976).
(17) A. K. Dunker and R. R. Rueckert, *J. Biol. Chem.*, **244**, 5074 (1969).
(18) N. I. Nakano, T. Oshio, Y. Fujimoto, and T. Amiya, *J. Pharm. Sci.*, **67**, 1005 (1978).

Synthesis and Anti-Inflammatory Evaluation of 3-Methylthio-1,2,4-triazines, 3-Alkoxy-1,2,4-triazines, and 3-Aryloxy-1,2,4-triazines

WILLIAM P. HEILMAN ˣ, R. D. HEILMAN, JAMES A. SCOZZIE, R. J. WAYNER, JAMES M. GULLO, and ZAVEN S. ARIYAN *

Received April 5, 1979, from the *T. R. Evans Research Center, Diamond Shamrock Corporation, Painesville, OH 44077.* Accepted for publication October 5, 1979. *Present address: Fairmont Chemical Co., Newark, NJ 07105.

Abstract □ To develop nonacidic, nonsteroidal anti-inflammatory agents without GI complications, a series of asymmetric triazines was synthesized and evaluated for anti-inflammatory efficacy in the carrageenan-induced pedal edema assay. Toxicity was estimated by determination of approximate LD_{50} values in mice. Twenty-five compounds possessed activity comparable to the standard, indomethacin. Thirteen of the 25 compounds were selected for dose–response evaluation in the carrageenan assay based on their relative toxicity and anti-inflammatory activity. Neurotoxicity of the 13 triazines was estimated by determination of NTD_{50} values in mice. Five of the 13 compounds tested in the dose–response assay were active in terms of anti-inflammatory efficacy (ED_{50} values) and lack of overt neurotoxicity (NTD_{50} values) when compared to indomethacin. To determine the effect of these five developmental triazines on chronic inflammation, they were evaluated in the adjuvant-induced polyarthritis assay. One was comparable to indomethacin in reducing adjuvant-induced inflammation in this assay.

Keyphrases □ Triazines, asymmetric—synthesis, evaluation of anti-inflammatory activity □ Anti-inflammatory agents—asymmetric triazines, synthesis, evaluation of activity □ Polyarthritis, adjuvant induced—assay, asymmetric triazines

In recent years, the literature on nonsteroidal anti-inflammatory agents has increased dramatically. From 1966 to 1976, 807 new compounds from 262 research laboratories were identified as new nonsteroidal anti-inflammatory agents. However, clinical reports were available on only 65 drugs; and of those that have been marketed, only a few have been commercially successful. GI irritation continues to be the principal complication with most developmental, clinical, and commercial nonsteroidal anti-inflammatory drugs.

The occurrence of GI effects in humans has been demonstrated by numerous investigators with administration of various salicylates (1–4), phenylbutazone (5, 6), indomethacin (7), tolmetin (8), naproxen (9), and ibuprofen (10). The ongoing search for novel classes of nonsteroidal anti-inflammatory agents in part reflects the continued inability to separate anti-inflammatory efficacy from GI toxicity. Although considerable controversy concerns the etiology of this toxicity, it generally is agreed that gastric irritation is associated, directly or indirectly, with the acidic nature of these drugs and their metabolites (11, 12).

DISCUSSION

To eliminate GI complications while maintaining anti-inflammatory activity, a series of 81 asymmetric triazines was synthesized and evaluated for potential anti-inflammatory efficacy. The carrageenan-induced pedal edema assay was utilized to detect primary level activity; acute toxicity was estimated by determination of LD_{50} values in mice. A dose–response carrageenan assay and neurotoxicity evaluation were used to determine the ED_{50} and NTD_{50} values of those compounds active at the primary level. Neurotoxicity was estimated by determination of NTD_{50} values in mice. Compounds that were comparable to indomethacin in the secondary stage of evaluation were tested in the adjuvant-induced polyarthritis assay to determine their effect on a chronic inflammatory condition.

Synthesis—3-Methoxy-5-substituted-1,2,4-triazines (III*a*–III*v*) and 3-alkoxy-5-substituted-phenyl-1,2,4-triazines (IV*a*–IV*l*) were synthesized. Melting points and recrystallization solvents are shown in Tables I–III. The 3-methylthio-1,2,4-triazines (II*a*–II*v*) served as common intermediates in the synthesis of all 3-alkoxy- and 3-aryloxy-1,2,4-triazines (III*a*–III*v*, IV*a*–IV*l*, X*a*–X*h*, and XI*a*–XI*i*). The 3-methylthio intermediates were synthesized according to the method of Paudler and Chen (13) with modifications by Heilman *et al.* (14).

Treatment of II with sodium methoxide in refluxing methanol resulted in nucleophilic displacement of the methylthio function to afford the corresponding 3-methoxy-5-substituted-1,2,4-triazines (III*a*–III*v*). Reaction of II with a variety of sodium alkoxides refluxing in dioxane afforded the corresponding 3-alkoxy-5-phenyl-1,2,4-triazines (IV*a*–IV*l*).

5,6-Disubstituted-3-alkoxy-1,2,4-triazines (VII*a*–VII*h* and VIII*a*–VIII*i*) were synthesized. Melting points and recrystallization solvents are shown in Tables IV and V. Cyclization of symmetrical 1,2-diones (V*a*–V*h*) under basic conditions with methylthiosemicarbazide hydrogen iodide afforded the 3-methylthio-5,6-disubstituted-1,2,4-triazines (VI*a*–VI*h*). Nucleophilic displacement of the methylthio group with the appropriate sodium alkoxide produced the desired 3-alkoxy-5,6-disubstituted-1,2,4-triazines (VII*a*–VII*h* and VIII*a*–VIII*i*).

Biology—The effect of the asymmetric triazines on the inflammatory response was evaluated at the primary level in the carrageenan-induced pedal edema assay (15). Carrageenan injected into the plantar tissue of the hindpaw of Sprague–Dawley rats produces an edematous condition, which simulates in part the inflammatory process found in human arthritis (16–18). Nonsteroidal anti-inflammatory drugs such as indomethacin, phenylbutazone, and aspirin inhibit the formation of this edema (19, 20).

Compounds were administered orally, using 0.25% methylcellulose as the vehicle. Five rats were used per dose, with the reported percent reduction in inflammation represented by the average of the reduction produced in the five animals. Compounds were administered at levels expected to be subtoxic by consideration of their approximate, measured LD_{50} values. The LD_{50} values in mice were determined in a standard,

0022-3549/80/0300-0282$01.00/0
© 1980, American Pharmaceutical Association

1955, p. 764.
(14) K. Sasaki, *Rinshoyakuri*, **12**, 434 (1964).
(15) P. Maier, R. Neher, W. Rittel, and M. Staehelin, in "Calcitonin," William Heineman Medical Books, London, England, 1969, p. 381.
(16) A. Mizutani, T. Mizutani, and P.-F. Kuo, *Chem. Pharm. Bull.*, **24**, 2733 (1976).
(17) A. K. Dunker and R. R. Rueckert, *J. Biol. Chem.*, **244**, 5074 (1969).
(18) N. I. Nakano, T. Oshio, Y. Fujimoto, and T. Amiya, *J. Pharm. Sci.*, **67**, 1005 (1978).

Synthesis and Anti-Inflammatory Evaluation of 3-Methylthio-1,2,4-triazines, 3-Alkoxy-1,2,4-triazines, and 3-Aryloxy-1,2,4-triazines

WILLIAM P. HEILMAN ˣ, R. D. HEILMAN, JAMES A. SCOZZIE, R. J. WAYNER, JAMES M. GULLO, and ZAVEN S. ARIYAN *

Received April 5, 1979, from the *T. R. Evans Research Center, Diamond Shamrock Corporation, Painesville, OH 44077.* Accepted for publication October 5, 1979. *Present address: Fairmont Chemical Co., Newark, NJ 07105.

Abstract □ To develop nonacidic, nonsteroidal anti-inflammatory agents without GI complications, a series of asymmetric triazines was synthesized and evaluated for anti-inflammatory efficacy in the carrageenan-induced pedal edema assay. Toxicity was estimated by determination of approximate LD_{50} values in mice. Twenty-five compounds possessed activity comparable to the standard, indomethacin. Thirteen of the 25 compounds were selected for dose–response evaluation in the carrageenan assay based on their relative toxicity and anti-inflammatory activity. Neurotoxicity of the 13 triazines was estimated by determination of NTD_{50} values in mice. Five of the 13 compounds tested in the dose–response assay were active in terms of anti-inflammatory efficacy (ED_{50} values) and lack of overt neurotoxicity (NTD_{50} values) when compared to indomethacin. To determine the effect of these five developmental triazines on chronic inflammation, they were evaluated in the adjuvant-induced polyarthritis assay. One was comparable to indomethacin in reducing adjuvant-induced inflammation in this assay.

Keyphrases □ Triazines, asymmetric—synthesis, evaluation of anti-inflammatory activity □ Anti-inflammatory agents—asymmetric triazines, synthesis, evaluation of activity □ Polyarthritis, adjuvant induced—assay, asymmetric triazines

In recent years, the literature on nonsteroidal anti-inflammatory agents has increased dramatically. From 1966 to 1976, 807 new compounds from 262 research laboratories were identified as new nonsteroidal anti-inflammatory agents. However, clinical reports were available on only 65 drugs; and of those that have been marketed, only a few have been commercially successful. GI irritation continues to be the principal complication with most developmental, clinical, and commercial nonsteroidal anti-inflammatory drugs.

The occurrence of GI effects in humans has been demonstrated by numerous investigators with administration of various salicylates (1–4), phenylbutazone (5, 6), indomethacin (7), tolmetin (8), naproxen (9), and ibuprofen (10). The ongoing search for novel classes of nonsteroidal anti-inflammatory agents in part reflects the continued inability to separate anti-inflammatory efficacy from GI toxicity. Although considerable controversy concerns the etiology of this toxicity, it generally is agreed that gastric irritation is associated, directly or indirectly, with the acidic nature of these drugs and their metabolites (11, 12).

DISCUSSION

To eliminate GI complications while maintaining anti-inflammatory activity, a series of 81 asymmetric triazines was synthesized and evaluated for potential anti-inflammatory efficacy. The carrageenan-induced pedal edema assay was utilized to detect primary level activity; acute toxicity was estimated by determination of LD_{50} values in mice. A dose–response carrageenan assay and neurotoxicity evaluation were used to determine the ED_{50} and NTD_{50} values of those compounds active at the primary level. Neurotoxicity was estimated by determination of NTD_{50} values in mice. Compounds that were comparable to indomethacin in the secondary stage of evaluation were tested in the adjuvant-induced polyarthritis assay to determine their effect on a chronic inflammatory condition.

Synthesis—3-Methoxy-5-substituted-1,2,4-triazines (III*a*–III*v*) and 3-alkoxy-5-substituted-phenyl-1,2,4-triazines (IV*a*–IV*l*) were synthesized. Melting points and recrystallization solvents are shown in Tables I–III. The 3-methylthio-1,2,4-triazines (II*a*–II*v*) served as common intermediates in the synthesis of all 3-alkoxy- and 3-aryloxy-1,2,4-triazines (III*a*–III*v*, IV*a*–IV*l*, X*a*–X*h*, and XI*a*–XI*i*). The 3-methylthio intermediates were synthesized according to the method of Paudler and Chen (13) with modifications by Heilman *et al.* (14).

Treatment of II with sodium methoxide in refluxing methanol resulted in nucleophilic displacement of the methylthio function to afford the corresponding 3-methoxy-5-substituted-1,2,4-triazines (III*a*–III*v*). Reaction of II with a variety of sodium alkoxides refluxing in dioxane afforded the corresponding 3-alkoxy-5-phenyl-1,2,4-triazines (IV*a*–IV*l*).

5,6-Disubstituted-3-alkoxy-1,2,4-triazines (VII*a*–VII*h* and VIII*a*–VIII*i*) were synthesized. Melting points and recrystallization solvents are shown in Tables IV and V. Cyclization of symmetrical 1,2-diones (V*a*–V*h*) under basic conditions with methylthiosemicarbazide hydrogen iodide afforded the 3-methylthio-5,6-disubstituted-1,2,4-triazines (VI*a*–VI*h*). Nucleophilic displacement of the methylthio group with the appropriate sodium alkoxide produced the desired 3-alkoxy-5,6-disubstituted-1,2,4-triazines (VII*a*–VII*h* and VIII*a*–VIII*i*).

Biology—The effect of the asymmetric triazines on the inflammatory response was evaluated at the primary level in the carrageenan-induced pedal edema assay (15). Carrageenan injected into the plantar tissue of the hindpaw of Sprague–Dawley rats produces an edematous condition, which simulates in part the inflammatory process found in human arthritis (16–18). Nonsteroidal anti-inflammatory drugs such as indomethacin, phenylbutazone, and aspirin inhibit the formation of this edema (19, 20).

Compounds were administered orally, using 0.25% methylcellulose as the vehicle. Five rats were used per dose, with the reported percent reduction in inflammation represented by the average of the reduction produced in the five animals. Compounds were administered at levels expected to be subtoxic by consideration of their approximate, measured LD_{50} values. The LD_{50} values in mice were determined in a standard,

0022-3549/80/0300-0282$01.00/0
© 1980, American Pharmaceutical Association

Table I—Melting Points or Boiling Points, Recrystallization Solvents, and Elemental Analyses of 3-Methylthio-5-substituted-1,2,4-triazines (II*a*–II*v*)

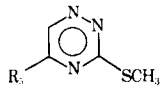

Compound	R_5	Melting Point or Boiling Point	Recrystallization Solvent	Elemental Analysis, % Calculated C, H, N	Elemental Analysis, % Found C, H, N
II*a*	Phenyl	99–100°[a]	Hexane	—	—
II*b*	3-Chlorophenyl	79–81°[b]	Hexane	—	—
II*c*	3-Trifluoromethylphenyl	123–125°[b]	Hexane	—	—
II*d*	4-Methylphenyl	160–161°[b]	Methanol	—	—
II*e*	4-Chlorophenyl	165–166°[b]	Methanol	—	—
II*f*	3,4-Dimethoxyphenyl	150–152°	Isopropanol	54.73, 4.98, 15.96	54.56, 5.02, 15.90
II*g*	4-Bromophenyl	153–154°	Heptane	42.55, 2.84, 14.89	42.55, 2.88, 15.03
II*h*	4-Methoxyphenyl	106–107°	Heptane	56.65, 4.72, 18.03	56.32, 4.74, 17.80
II*i*	2,4-Difluorophenyl	79–80°	Hexane	50.21, 2.93, 17.57	50.16, 2.96, 17.87
II*j*	2,4-Dichlorophenyl	106–107°	Heptane	44.12, 2.57, 15.44	44.16, 2.56, 15.50
II*k*	2,5-Dimethoxyphenyl	113–114°	Heptane	54.75, 4.94, 16.97	54.94, 5.02, 16.67
II*l*	4-Ethylphenyl	71–72°	Hexane	62.34, 5.63, 18.18	62.11, 5.66, 18.43
II*m*	4-Morpholinophenyl	127–128°	Heptane	58.33, 5.55, 19.44	57.93, 5.69, 19.77
II*n*	*tert*-Butyl	91–93°/ 0.1 mm Hg	—	52.46, 7.10, 22.95	52.30, 7.21, 22.90
II*o*	Cyclopropyl	44–46°	Hexane	50.27, 5.42, 25.13	50.11, 5.41, 25.07
II*p*	1-Adamantyl	140–141°	Ethyl acetate	64.37, 7.28, 16.09	64.22, 7.42, 16.32
II*q*	2-Furyl	88–90°	Hexane	49.74, 3.63, 21.76	50.01, 3.64, 21.82
II*r*	2-Thienyl	105–106°	Hexane	45.93, 3.35, 20.10	46.04, 3.40, 20.20
II*s*	2-Benzofuryl	134–135°	Heptane	59.26, 3.70, 17.39	59.63, 3.77, 17.87
II*t*	9-Anthracyl	181–183°	Acetone	71.26, 4.32, 13.85	70.79, 4.32, 14.01
II*u*	1-Naphthyl	99–100°	Hexane	66.40, 4.35, 16.60	66.33, 4.40, 16.89
II*v*	2-Naphthyl	117–118°	Heptane	66.40, 4.35, 16.60	66.30, 4.26, 16.64

[a] Identical to melting point given in Ref. 13. [b] Identical to melting point given in Ref. 14.

Table II—Melting Points or Boiling Points, Recrystallization Solvents, and Elemental Analyses of 3-Methoxy-5-substituted-1,2,4-triazines (III*a*–III*v*)

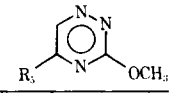

Compound	R_5	Melting Point or Boiling Point	Recrystallization Solvent	Elemental Analysis, % Calculated C, H, N	Elemental Analysis, % Found C, H, N
III*a*	Phenyl	75–76°[a]	Heptane	—	—
III*b*	3-Chlorophenyl	93–94°	Hexane	54.18, 3.61, 18.96	54.25, 3.64, 18.90
III*c*	3-Trifluoromethylphenyl	95–97°	Hexane	51.76, 3.14, 16.47	51.80, 3.10, 16.52
III*d*	4-Methylphenyl	139–140°	Benzene	65.67, 5.47, 20.90	65.52, 5.51, 21.01
III*e*	4-Chlorophenyl	131–132°	Benzene	54.18, 3.61, 18.96	54.22, 3.66, 19.04
III*f*	3,4-Dimethoxyphenyl	167–169°	Methanol	58.29, 4.30, 17.00	57.82, 5.38, 16.96
III*g*	4-Bromophenyl	108–109°	Ethyl acetate–hexane	46.11, 3.01, 15.79	46.83, 3.31, 15.98
III*h*	4-Methoxyphenyl	106–107°	Dioxane	60.82, 5.07, 19.35	60.77, 5.16, 19.35
III*i*	2,4-Difluorophenyl	91–93°	Heptane	53.81, 3.94, 18.83	53.41, 4.18, 18.78
III*j*	2,4-Dichlorophenyl	114–115°	Ethyl acetate–hexane	46.87, 2.73, 16.41	46.64, 2.68, 16.49
III*k*	2,5-Dimethoxyphenyl	108–109°	Heptane	58.30, 5.26, 17.00	58.43, 5.33, 16.99
III*l*	4-Ethylphenyl	50–51°	Hexane	66.97, 6.05, 19.53	66.60, 6.07, 19.49
III*m*	4-Morpholinophenyl	122–123°	Ethyl acetate–hexane	61.76, 5.88, 20.59	61.42, 5.91, 20.77
III*n*	*tert*-Butyl	45–46°	Hexane	57.48, 7.78, 25.15	57.52, 7.81, 25.20
III*o*	Cyclopropyl	119–120°/ 1.8 mm Hg	—	55.62, 6.00, 27.80	55.03, 6.04, 27.28
III*p*	1-Adamantyl	101–102°	Heptane	68.57, 7.75, 17.14	68.38, 7.88, 17.14
III*q*	2-Furyl	96–97°	Hexane	54.24, 3.95, 23.73	54.36, 3.99, 24.00
III*r*	2-Thienyl	129–130°	Hexane	49.74, 3.63, 21.76	50.05, 3.75, 21.80
III*s*	2-Benzofuryl	139–140°	Ethyl acetate	63.43, 3.97, 18.50	63.31, 3.99, 18.59
III*t*	9-Anthracyl	195–196°	Methanol	75.16, 4.53, 14.63	74.72, 4.53, 14.58
III*u*	1-Naphthyl	76–77°	Hexane	70.89, 4.64, 17.72	70.40, 4.51, 17.76
III*v*	2-Naphthyl	130–131°	Heptane	70.89, 4.64, 17.72	70.46, 4.69, 17.85

[a] Identical to melting point given in Ref 13.

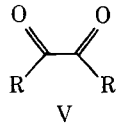

V

V*a*: R = phenyl
V*b*: R = 4-chlorophenyl
V*c*: R = 4-methylphenyl
V*d*: R = 3,4-dichlorophenyl
V*e*: R = 3,4-dimethoxyphenyl
V*f*: R = 2-furyl
V*g*: R = 2-pyridyl
V*h*: R = methyl

multidimensional observational assay and calculated according to the method of Litchfield and Wilcoxon (21). The anti-inflammatory and LD_{50} results are shown in Table VI.

Based on the anti-inflammatory performance of each compound relative to the indomethacin standard, 25 of the 81 compounds evaluated gave a reduction in edema equal to or greater than the standard. However, test compounds were administered at 200 mg/kg (unless overt toxicity necessitated a lower dose), while indomethacin was administered at 2.5 mg/kg. Of the 25 active triazines, 13 were selected for secondary evaluation based on their relative toxicity and anti-inflammatory activity. Those compounds selected had LD_{50} values greater than 300 mg/kg and produced a percent reduction in inflammation equal to or greater than the standard, which was run simultaneously.

Within the 3-methylthio-5-substituted-1,2,4-triazine series, seven of the 22 compounds screened were active; two were selected for secondary testing (II*c* and II*f*). Among the 3-methoxy-5-substituted-1,2,4-triazines, eight of the 22 compounds evaluated were active; five were selected for further testing (III*a*, III*b*, III*f*, III*n*, and III*o*). In the 3-alkoxy-5-substituted phenyl series, five of the 12 compounds tested were active; four were selected for secondary evaluation (IV*a*, IV*b*, IV*e*, and IV*i*). Within the 3-methylthio- and 3-methoxy-5,6-disubstituted-1,2,4-triazine series, only two of the 16 compounds evaluated were active; one was selected for secondary testing (VII*g*). In the 3-alkoxy-5,6-disubstituted-1,2,4-triazine

Table III—Melting Points or Boiling Points, Recrystallization Solvents, and Elemental Analyses of 3-Alkoxy-5-substituted-phenyl-1,2,4-triazines (IV*a*–IV*l*)

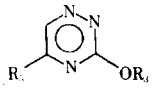

Compound	R_3	R_5	Melting Point or Boiling Point	Recrystallization Solvent	Elemental Analysis, % Calculated C, H, N	Found C, H, N
IV*a*	Ethyl	Phenyl	48–49°	Hexane	64.67, 5.47, 20.89	64.37, 5.40, 20.59
IV*b*	*n*-Propyl	Phenyl	44–45°	Hexane	64.98, 6.05, 19.03	64.62, 6.01, 18.71
IV*c*	*n*-Pentyl	Phenyl	36–38°	Hexane	69.11, 7.05, 17.27	68.92, 7.02, 17.06
IV*d*	Benzyl	Phenyl	78–80°	Heptane	72.99, 4.98, 15.96	73.26, 4.99, 16.26
IV*e*	Allyl	Phenyl	155°/0.3 mm Hg		67.59, 5.29, 19.71	67.78, 5.34, 19.66
IV*f*	4-Methoxyphenyl	Phenyl	149–151°	Ethyl acetate–heptane	68.81, 4.69, 15.05	68.89, 4.75, 14.66
IV*g*	Cyclohexyl	Phenyl	69–71°	Heptane	70.56, 6.71, 16.46	70.31, 6.62, 16.80
IV*h*	*n*-Decyl	Phenyl	46–47°	Hexane	72.80, 8.69, 13.41	73.00, 8.83, 13.12
IV*i*	Ethyl	3-Chlorophenyl	79–81°	Heptane	56.06, 4.28, 17.83	56.16, 4.28, 18.02
IV*j*	Isopropyl	3-Chlorophenyl	73–74°	Heptane	57.72, 4.85, 16.83	57.86, 4.86, 17.18
IV*k*	Phenyl	3-Chlorophenyl	125–127°	Heptane	63.50, 3.55, 14.81	63.43, 3.46, 14.95
IV*l*	Benzyl	3-Chlorophenyl	81–83°	Heptane	64.54, 4.06, 14.11	64.66, 4.16, 14.10

Table IV—Melting Points or Boiling Points, Recrystallization Solvents, and Elemental Analyses of 3-Methylthio- and 3-Methoxy-5,6-disubstituted-1,2,4-triazines (VI*a*–VI*h* and VII*a*–VII*h*)

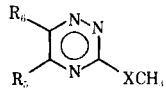

Compound	X	R_5, R_6	Melting Point or Boiling Point	Recrystallization Solvent	Elemental Analysis, % Calculated C, H, N	Found C, H, N
VI*a*	S	Phenyl	119–120°[a]	Ethyl acetate	—	—
VI*b*	S	4-Chlorophenyl	142–143°	Ethyl acetate	55.17, 3.16, 12.07	54.99, 3.16, 12.11
VI*c*	S	4-Methylphenyl	166–167°	Chloroform	70.36, 5.54, 13.68	70.27, 5.56, 13.52
VI*d*	S	3,4-Dichlorophenyl	127–128°	Hexane–chloroform	46.04, 2.16, 10.17	45.90, 2.12, 10.14
VI*e*	S	3,4-Dimethoxyphenyl	130–131°	Chloroform	60.15, 5.26, 10.53	60.01, 5.42, 10.68
VI*f*	S	2-Furyl	91–92°	Hexane	55.60, 3.47, 16.34	55.48, 3.46, 16.30
VI*g*	S	2-Pyridyl	122–123°	Hexane	59.79, 3.91, 24.91	59.57, 3.90, 25.35
VI*h*	S	Methyl	100–102°/ 0.1 mm Hg	—	46.45, 5.81, 27.10	46.48, 5.95, 26.94
VII*a*	O	Phenyl	78–79°	Hexane	73.00, 4.94, 15.97	72.63, 4.98, 16.39
VII*b*	O	4-Chlorophenyl	146–147°	Methanol	57.83, 3.31, 12.65	57.95, 3.32, 12.77
VII*c*	O	4-Methylphenyl	128–129°	Hexane	74.22, 5.84, 14.43	74.12, 5.73, 14.30
VII*d*	O	3,4-Dichlorophenyl	138–139°	Hexane	48.89, 2.24, 10.47	48.60, 2.24, 10.40
VII*e*	O	3,4-Dimethoxyphenyl	83–84°	Heptane	61.66, 5.48, 10.97	61.64, 5.40, 10.90
VII*f*	O	2-Furyl	105–107°	Hexane	59.26, 3.70, 17.28	59.24, 3.81, 17.35
VII*g*	O	2-Pyridyl	132–133°	Hexane	63.40, 4.15, 26.41	63.47, 4.18, 26.37
VII*h*	O	Methyl	55–57°/ 0.05 mm Hg	—	51.80, 6.47, 30.22	52.05, 6.46, 30.25

[a] Identical to melting point given in M. Gianturco, *Gazz. Chim. Ital.*, **82**, 595 (1952).

Table V—Melting Points or Boiling Points, Recrystallization Solvents, and Elemental Analyses of 3-Alkoxy-5,6-disubstituted-1,2,4-triazines (VIII*a*–VIII*i*)

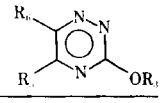

Compound	R_3	R_5, R_6	Melting Point or Boiling Point	Recrystallization Solvent	Elemental Analysis, % Calculated C, H, N	Found C, H, N
VIII*a*	Ethyl	Phenyl	73–74°	Hexane	73.63, 5.45, 15.15	73.67, 5.40, 15.11
VIII*b*	Isopropyl	Phenyl	96–97°	Heptane	74.20, 5.88, 14.42	73.97, 5.84, 14.39
VIII*c*	Phenyl	Phenyl	123–125°	Ethanol	77.52, 4.65, 12.92	76.97, 4.57, 12.77
VIII*d*	4-Chlorophenyl	Phenyl	162–164°	Heptane	70.10, 3.92, 11.68	70.00, 3.97, 11.61
VIII*e*	4-Methylphenyl	Phenyl	154–156°	Heptane	77.85, 5.05, 12.38	77.78, 5.00, 11.89
VIII*f*	3,4-Dichlorophenyl	Phenyl	133–135°	Hexane–benzene	63.97, 3.32, 10.66	63.98, 3.30, 10.65
VIII*g*	Ethyl	Methyl	74–75°/ 0.07 mm Hg	—	54.90, 7.19, 27.45	55.10, 7.24, 27.40
VIII*h*	Isopropyl	Methyl	75–78°/ 0.05 mm Hg	—	57.48, 7.78, 25.15	57.62, 7.84, 24.90
VIII*i*	Allyl	Methyl	84–86°/ 0.08 mm Hg	—	58.18, 6.66, 25.45	57.94, 6.72, 25.00

series, two of the nine compounds tested were active; one was selected for subsequent evaluation (VIII*i*).

The secondary evaluation consisted of a dose–response carrageenan assay and the determination of the NTD_{50} value in mice, based on the method of Swinyard *et al.* (22). The compounds were administered in the carrageenan assay at multiple doses (*e.g.*, 100, 30, 10, and 3 mg/kg) to obtain a three-point dose–response curve under identical conditions as used in the primary evaluation. If a dose–response relationship was observed, the ED_{50} value was determined according to the method of Litchfield and Wilcoxon (21). The NTD_{50} values were determined to provide additional information concerning the toxicity of the compounds relative to indomethacin.

The results of the secondary testing are shown in Table VII. Based on 50 determinations, indomethacin had a mean ED_{50} value of 2.5 mg/kg and an NTD_{50} value of 112 mg/kg. To compete successfully with this standard, compounds were expected to be less toxic and yet maintain similar levels of efficacy. Therefore, an NTD_{50} value of >300 mg/kg and an ED_{50} value of <30 mg/kg were established as limits for further testing. Five of the 13 compounds subjected to secondary testing fell within these arbitrary bounds (II*f*, III*o*, IV*b*, IV*e*, and VIII*i*).

To determine the effect of these five developmental compounds on a chronic inflammatory condition, each candidate was evaluated in the adjuvant-induced polyarthritis assay (23). An injection of heat-killed *Mycobacterium tuberculosis*, suspended in mineral oil, produced a highly

Table VI—Activity in the Carrageenan-Induced Anti-Inflammatory Assay and LD_{50} Values in Mice of 3-Methylthio- and 3-Alkoxy-1,2,4-triazines

Compound	Reduction, %	Carrageenan Dose, mg/kg	Standard[a] Reduction, %	LD_{50}, mg/kg
II*a*	27	175	35	237
II*b*	17	200	35	300
II*c*	57	200	35	300
II*d*	16	200	33	300
II*e*	22	200	33	300
II*f*	39	200	31	300
II*g*	20	200	20	300
II*h*	18	200	30	300
II*i*	10	150	31	178
II*j*	0	200	20	300
II*k*	37	200	40	300
II*l*	33	200	40	300
II*m*	19	200	31	300
II*n*	57	150	35	178
II*o*	86	200	33	316
II*p*	17	200	20	300
II*q*	39	200	37	316
II*r*	51	200	37	316
II*s*	2	200	20	300
II*t*	0	200	32	300
II*u*	8	200	24	300
II*v*	0	200	26	300
III*a*	86	200	40	300
III*b*	72	200	28	300
III*c*	77	100	35	133
III*d*	0	200	28	300
III*e*	23	200	28	300
III*f*	52	200	35	300
III*g*	33	200	38	300
III*h*	17	200	24	300
III*i*	36	150	37	178
III*j*	16	200	20	300
III*k*	49	200	43	300
III*l*	15	200	26	300
III*m*	14	200	22	300
III*n*	64	200	25	300
III*o*	57	200	33	300
III*p*	30	150	32	178
III*q*	70	175	25	237
III*r*	50	175	29	237
III*s*	12	200	28	300
III*t*	0	200	28	300
III*u*	22	200	28	300
III*v*	7	200	24	300
IV*a*	96	200	42	300
IV*b*	51	200	39	300
IV*c*	29	200	32	300
IV*d*	0	150	32	178
IV*e*	67	200	44	300
IV*f*	15	200	32	300
IV*g*	7	200	24	300
IV*h*	5	200	31	300
IV*i*	71	200	31	300
IV*j*	43	200	43	300
IV*k*	23	200	31	300
IV*l*	18	200	31	300
V*Ia*	0	200	37	300
V*Ib*	7	200	37	300
V*Ic*	0	200	28	300
V*Id*	0	200	28	300
V*Ie*	0	200	37	300
V*If*	2	200	28	300
V*Ig*	19	200	28	300
V*Ih*	54	70	37	100
VII*a*	17	200	31	316
VII*b*	0	200	31	300
VII*c*	12	200	28	300
VII*d*	0	200	28	300
VII*e*	0	200	31	300
VII*f*	5	200	28	316
VII*g*	46	200	42	300
VII*h*	4	40	37	178
VIII*a*	12	200	27	300
VIII*b*	0	200	27	300
VIII*c*	7	200	27	300
VIII*d*	0	200	42	300
VIII*e*	18	200	27	300
VIII*f*	0	200	32	300
VIII*g*	22	200	27	300
VIII*h*	37	200	37	300
VIII*i*	63	200	37	300

[a] Mean percent reduction in inflammation produced by the standard, indomethacin, at a dose of 2.5 mg/kg. An indomethacin standard was run simultaneously with each set of test compounds.

developed arthritic condition after 20 days when injected into the left hindfoot pad of male Wistar–Lewis rats. The developed arthritis was characterized by swelling of all four paws and secondary involvement of the tail and ears (24). The test compounds were administered by gastric intubation in a methylcellulose vehicle on Days 20 and 22. Both left and right hindpaw volumes were recorded daily on Days 20–24. The decrease in mean paw volume per group per day then was calculated as the percent change from Day 20. Efficacy was determined by a percent decrease in the paw volume of test compounds *versus* that of the standard, indomethacin. The test compounds were administered at a dose of 30 mg/kg, and the standard was given at a dose of 1 mg/kg.

The results of this assay are shown in Table VII. Only II*f* was active in the adjuvant-induced polyarthritis assay. This compound appeared to have a rapid onset of action compared to the standard. However, after several days, the activity level began to fall. Additional evaluation is needed to establish whether II*f* possesses a therapeutic advantage over current standards.

Physicochemical Parameters—Since compounds in each series (Tables I–V) differed from others in that series by only one substituent, hydrophobic substituent constants (π values) (25, 26), electronic substituent constants (σ values) (27), and steric substituent constants (E_s values) (28) were utilized to estimate the relative effect of these physicochemical parameters on anti-inflammatory activity. After detailed investigation, it was concluded that within each series, no apparent structure–activity correlation existed between any of these physicochemical parameters and anti-inflammatory activity. Nevertheless, several general trends deserve comment.

First, at the primary screening level, the 5-substituted triazine classes (II*a*–II*v*, III*a*–III*v*, and IV*a*–IV*l*) were inherently more active than the corresponding 5,6-disubstituted triazines (VI*a*–VI*h*, VII*a*–VII*h*, and VIII*a*–VIII*i*). Over 37% of the compounds in the 5-substituted classes were considered active, while only 16% of the compounds in the 5,6-disubstituted classes were active.

Second, the difluorinated triazines (II*i* and III*i*) were among the most toxic derivatives evaluated in this series. Perhaps the toxicity among these fluorinated derivatives is the result of increased susceptibility to nucleophilic attack by the amino and mercapto functions present in DNA

Table VII—ED_{50} Values in Carrageenan-Induced Anti-Inflammatory Assay, NTD_{50} Values in Mice, and Adjuvant-Induced Polyarthritis Activity of Selected 3-Methylthio- and 3-Alkoxy-1,2,4-triazines

Compound	Carrageenan-Induced Anti-Inflammatory Assay		Adjuvant-Induced Polyarthritis Assay[a], % reduction			
	ED_{50}, mg/kg	NTD_{50}, mg/kg	Day 21	Day 22	Day 23	Day 24
II*c*	30	170	NT[b]	NT	NT	NT
II*f*	10	1000	24	19	14	8
III*a*	10	170	NT	NT	NT	NT
III*b*	30	76	NT	NT	NT	NT
III*f*	100	1000	NT	NT	NT	NT
III*n*	100	100	NT	NT	NT	NT
III*o*	30	1000	5	6	0	NT
IV*a*	10	87	NT	NT	NT	NT
IV*b*	30	300	6	0	0	NT
IV*e*	30	300	0	0	0	NT
IV*i*	30	250	NT	NT	NT	NT
VII*g*	30	250	NT	NT	NT	NT
VIII*i*	30	300	4	0	0	NT
Indomethacin	2.5	112	12	19	18	21

[a] All test compounds were administered at 30 mg/kg, while indomethacin was given at 1 mg/kg. [b] Not tested.

and protein structure (29). It may be that the relatively labile fluorine atoms undergo displacement by these functional groups, resulting in interchelation and overt toxic effects.

EXPERIMENTAL[1]

3-Methoxy-5-substituted-1,2,4-triazines (IIIa–IIIv)—In a 1-liter round-bottom flask equipped with condenser and magnetic stirrer was placed the appropriate 3-methylthio-5-substituted-1,2,4-triazine (IIa–IIv) (13,14) dissolved in methanol (500 ml). To this stirred solution was added a molar excess of sodium methoxide, and the mixture was refluxed for 10 hr. (The methanethiol fumes were trapped by a sodium hydroxide scrubber system.) Upon cooling, the mixture was concentrated and treated with hexane–heptane to afford a crystalline product.

Recrystallization from the appropriate solvents (Table II) resulted in the corresponding 3-methoxy-1,2,4-triazine (IIIa–IIIv). The 3-methoxytriazines were characterized by carbon, hydrogen, and nitrogen analyses (Table II) and NMR spectroscopy. This class of triazines was characterized by the following chemical shifts relative to tetramethylsilane in deuterochloroform: δ 4.0–4.2 (s, 3, OCH_3), 7.0–8.2 (m, C-5 aromatic substituent protons), and 9.6–9.8 (s, 1, C-6 triazine proton).

3-Alkoxy-5-substituted-phenyl-1,2,4-triazines (IVa–IVl)—The 3-alkoxy-5-substituted-phenyl-1,2,4-triazines were synthesized in a similar manner as the 3-methoxy-1,2,4-triazines (IIIa–IIIv), except that a molar excess of the desired sodium alkoxide was reacted with the 3-methylthio-1,2,4-triazine (IIa or IIb) and the mixture was refluxed with dioxane. Crude products were recrystallized from the appropriate solvents (Table III) to yield the corresponding 3-alkoxy-1,2,4-triazine (IVa–IVl). The 3-alkoxytriazines were characterized by carbon, hydrogen, and nitrogen analyses (Table III) and NMR spectroscopy; chemical shifts were similar to the 3-methoxytriazines (IIIa–IIIv), but the methoxy shift was replaced by ethyl, *n*-propyl, *n*-pentyl, and higher homologs (Table III).

3-Methylthio-5,6-disubstituted-1,2,4-triazines (VIa–VIh)—In a 1-liter round-bottom flask equipped with a heating mantle, condenser, and magnetic stirrer was placed the appropriate symmetrical 1,2-dione (Va–Vh) dissolved in 80% ethanol (500 ml). To this stirred solution was added an equal molar solution of methylthiosemicarbazide hydrogen iodide and sodium bicarbonate in 80% ethanol. The mixture was refluxed for 10 hr, cooled to ambient temperature, and diluted with water to afford a solid.

The solid material was collected and recrystallized from the appropriate solvents (Table IV) to yield the desired 3-methylthio-5,6-disubstituted-1,2,4-triazine (VIa–VIh). The 3-methylthiotriazines were characterized by carbon, hydrogen, and nitrogen analyses (Table IV) and NMR spectroscopy. This class of triazines was characterized by the following chemical shifts relative to tetramethylsilane in deuterated dimethyl sulfoxide: δ 2.7–2.9 (s, 3, SCH_3) and 7.0–8.2 (m, C-5 and C-6 aromatic substituents).

3-Methoxy-5,6-disubstituted-1,2,4-triazines (VIIa–VIIh)—The 3-methoxy-5,6-disubstituted-1,2,4-triazines (VIIa–VIIh) were synthesized in the same fashion as the corresponding 3-methoxy-5-substituted triazines (IIIa–IIIv). Recrystallization of the solid product from the appropriate solvents (Table IV) afforded the desired 3-methoxy-5,6-disubstituted-1,2,4-triazines (VIIa–VIIh). The carbon, hydrogen, and nitrogen analyses are shown in Table IV; the NMR spectra were identical to those of the 3-methylthio precursor except that the δ 2.7–2.9 (s, 3, SCH_3) signal was replaced by a δ 4.0–4.2 (s, 3, OCH_3) signal further downfield.

3-Alkoxy-5,6-disubstituted-1,2,4-triazines (VIIIa–VIIIi)—The 3-alkoxy-5,6-disubstituted-1,2,4-triazine analogs (VIIIa–VIIIi) were synthesized by the same procedure as the 3-alkoxy-5-substituted-1,2,4-triazines (IVa–IVl). Recrystallization solvents are listed in Table V. The 3-alkoxytriazines (VIIIa–VIIIi) were characterized by carbon, hydrogen, and nitrogen analyses (Table V) and NMR spectroscopy. The 5,6-diphenyl derivatives (VIIIa–VIIIf) produced chemical shifts similar to those of their common precursor VIa, except that the methylthio singlet (δ 2.7–2.9) was replaced by a variety of alkoxy and aryloxy multiplets. The 5,6-dimethyl derivatives (VIIIg–VIIIi) were characterized by the two methyl singlets with δ 2.6–2.5 (s, 3, C-6 methyl) and 2.3–2.5 (s, 3, C-5 methyl) and a variety of multiplets resulting from substituents at C-3.

Carrageenan-Induced Pedal Edema Assay (15)—Male Sprague–Dawley rats, 100–140 g, were used in the pedal edema assay. Five rats were used in each treatment group, the known standard control group, and the vehicle control edema groups. The first and seventh groups were vehicle controls. Therefore, recalibration of the volume differential meter could be done after every 30 animals. All rats were fasted for 2 hr prior to the test, and water was available *ad libitum*.

The experimental drugs and the standard control were given orally and were dissolved or suspended in 0.25% methylcellulose. The volume given was 0.005 cm^3/g of body weight. The edema control groups were administered the vehicle. One hour after the administration of the test compounds, 0.05 cm^3 of a 1% sterile carrageenan solution was injected into the left hindfoot pad of each rat using a 1-cm^3 Cornwall syringe pipet. Three hours after this injection, the paw volumes of the injected paws were measured by means of mercury displacement on a volume differential meter. The apparatus used was a modification of that described by Adamkiewicz *et al.* (30).

The amount of edema was calculated, and the percent reduction of edema from control values was determined. The mean volume ($\pm SD$) of edema based on 50 determinations was 1.24 $\pm$0.226 cm^3. Compounds that reduced edema to a level less than that of indomethacin (dosed at 2.5 mg/kg) were considered active. The ED_{50} values for indomethacin and active test compounds were estimated according to the method of Litchfield and Wilcoxon (21).

Neurotoxicity Determination, NTD_{50} Values (22)—The mean neurotoxic dose was the dose administered orally or intraperitoneally to mice that caused minimal recognizable neurotoxicity in 50% of the animals tested as determined by the following five end-points.

1. Positional sense test: If the hindleg of a normal mouse is lowered gently over the end of a table, it will be lifted quickly back to a normal position. Neurological deficit was indicated by the inability to correct the abnormal position rapidly.
2. Righting test: If a mouse is placed on its back, it will right itself quickly and assume a normal posture. Neurological deficit was indicated by the inability to correct for the abnormal body posture rapidly.
3. Gait and stance test: Neurological deficit was indicated by a circular or zigzag gait, ataxia, abnormal spread of the legs, abnormal body posture, tremor, hyperactivity, lack of exploratory behavior, somnolence, stupor, catalepsy, *etc.*
4. Muscle tone test: Normal animals have a certain amount of skeletal muscle tone that is apparent to the observer on handling. Neurological deficit was indicated by a loss of skeletal muscle tone characterized by hypotonia or flaccidity.
5. Equilibrium test: If a normal mouse is placed on a narrow edge, such as the rim of a cage, it can maintain its equilibrium and walk along the rim. Neurological deficit was indicated by the inability to do so.

Abnormal neurological status disclosed by any of these five tests was taken as the end-point for the NTD_{50} determination. However, if other side effects (*e.g.*, hematuria and hypernea) consistently appeared at doses lower than those causing neurological deficit, they were taken as the end-point.

Adjuvant-Induced Polyarthritis Assay (23, 24)—Five male Wistar–Lewis rats, ~110 g each, were used in each group. On Day 1, 0.1 cm^3 of 3.5-mg/cm^3 suspension of heat-killed *M. tuberculosis* in mineral oil was injected into the left hindfoot pad of each rat. The animals then were kept in cages, with two or three rats per cage for 20 days; food and water were available *ad libitum*. On Day 20, all animals with developed arthritis, *i.e.*, swelling of all four paws and secondary involvement of the tail and ears, were used in the study.

The test compounds and the standard control were dissolved or suspended in methylcellulose and were given orally at doses of 30 and 1 mg/kg, respectively. The volume given was 0.005 cm^3/g of body weight. The control group was administered the vehicle alone. The animals were administered compounds by gavage on Days 20 and 22. The left hindpaw volumes were recorded daily on Days 20–24. The decrease or increase in mean paw volume per group per day was then calculated as the percent change from Day 20. Efficacy was determined by a percent decrease in paw volume of the test compounds compared to indomethocin.

[1] Elemental analyses were performed by the Analytical Group, Diamond Shamrock Corp., Painesville, Ohio. IR spectra were determined on a Perkin-Elmer model 137 spectrophotometer with sodium chloride optics. NMR spectra were recorded on a Varian A56/60D and a Bruker WH-90 spectrometer. Melting points were determined on a Thomas–Hoover capillary melting apparatus and are uncorrected.

REFERENCES

(1) "International Symposium on Salicylates" (London, 1962), A. J. Dixon, Ed., Churchill, London, England, 1963.

(2) "The Salicylates: A Critical Bibliographic Review," M. J. H. Smith and P. K. Smith, Eds., Wiley, New York, N.Y., 1966.

(3) A. R. Cooke, *Am. J. Dig. Dis.*, **18**, 225 (1973).
(4) H. E. Paulus and M. W. Whitehouse, *Annu. Rev. Pharmacol.*, **13**, 107 (1973).
(5) E. F. Mauer, *N. Engl. J. Med.*, **253**, 404 (1955).
(6) *Am. J. Med.*, **30**, 268 (1961).
(7) P. L. Boardman and E. D. Hart, *Br. Med. J.*, **4**, 264 (1967).
(8) S. S. Berkowitz, *Curr. Ther. Res.*, **16**, 442 (1974).
(9) A. Lussier, K. L. MacCannell, S. J. Alexander, C. V. Multz, G. Boost, and E. J. Segre, *Clin. Pharmacol. Ther.*, **13**, 146 (1972).
(10) S. S. Adams, R. G. Bough, E. E. Cliffe, B. Lessel, and R. F. N. Mills, *Toxicol. Appl. Pharmacol.*, **15**, 310 (1969).
(11) E. Arrigoni-Martelli, "Inflammation and Anti-inflammatories," Wiley, New York, N.Y., 1977, p. 208.
(12) K. D. Rainsford, K. Brane, and M. W. Whitehouse, "Aspirin and Related Drugs: Their Actions and Uses," Birkhauser Verlag, Basel, Switzerland, 1977, p. 67.
(13) W. W. Paudler and T. K. Chen, *J. Heterocycl. Chem.*, **7**, 767 (1970).
(14) W. P. Heilman, R. D. Heilman, J. A. Scozzie, R. J. Wayner, and J. M. Gullo, *J. Med. Chem.*, **22**, 671 (1979).
(15) C. A. Winter, E. A. Risley, and G. W. Nuss, *Proc. Soc. Exp. Biol. Med.*, **111**, 544 (1962).
(16) M. DiRosa and D. A. Willoughby, *J. Pharm. Pharmacol.*, **23**, 297 (1971).
(17) M. DiRosa, J. P. Giroud, and D. A. Willoughby, *J. Pathol.*, **104**, 15 (1971).
(18) R. Vinegar, J. F. Truax, and J. L. Selph, *Fed. Proc., Fed. Am. Soc. Exp. Biol.*, **35**, 2447 (1976).
(19) C. A. Winter, *Prog. Drug Res.*, **10**, 139 (1966).
(20) C. J. E. Niemegeers, F. J. Verbruggen, and P. A. J. Janssen, *J. Pharm. Pharmacol.*, **16**, 810 (1964).
(21) J. T. Litchfield and F. Wilcoxon, *J. Pharmacol. Exp. Ther.*, **96**, 99 (1949).
(22) E. A. Swinyard, W. C. Brown, and L. S. Goodman, *ibid.*, **106**, 319 (1952).
(23) M. L. Graeme, E. Fabry, and E. B. Sigg, *ibid.*, **153**, 373 (1966).
(24) R. D. Sofia, H. B. Vassar, and S. D. Nalepa, *Eur. J. Pharmacol.*, **24**, 108 (1973).
(25) C. Hansch, J. E. Quinlan, and G. L. Lawrence, *J. Org. Chem.*, **33**, 347 (1968).
(26) C. Hansch, E. J. Lien, and F. Helmer, *Arch. Biochem. Biophys.*, **128**, 319 (1968).
(27) L. P. Hammett, "Physical Organic Chemistry," McGraw-Hill, New York, N.Y., 1940, chap. 7.
(28) C. K. Hancock and C. P. Falls, *J. Am. Chem. Soc.*, **83**, 4214 (1961).
(29) N. J. Turner and R. D. Battershell, *Contrib. Boyce Thompson Inst.*, **24**, 139 (1969).
(30) V. W. Adamkiewicz, W. B. Rice, and J. D. McCall, *Can. J. Biochem. Physiol.*, **33**, 332 (1955).

Nonisothermal Kinetics with Programmed Temperature Steps

B. EDEL ˣ and M. O. BALTZER

Received April 30, 1979, from *Analytical Research and Development, Pharmaceutical Department, Sandoz Ltd., CH-4002 Basel, Switzerland.* Accepted for publication October 15, 1979.

Abstract □ Data required for predicting the stability of an active principle in solution can be obtained by two kinetic methods. With the isothermal method, the degradation rate constants are determined at different temperatures, which are kept constant throughout the experiment. With the nonisothermal method, the temperature is increased with time. This paper describes a nonisothermal kinetic method in which the temperature is increased in consecutive equal steps. The results are compared with those obtained by the conventional isothermal method. The values for the activation energy are approximately the same by both methods. Although the technique of nonisothermal kinetics demands sophisticated equipment and high experimental accuracy, it provides a continuous picture over a wide temperature range.

Keyphrases □ Stability—prediction, nonisothermal kinetic method, programmed temperature steps, comparison with isothermal kinetic method □ Drug degradation kinetics—nonisothermal method, programmed temperature steps, comparison with isothermal kinetic method □ Kinetics, degradation—nonisothermal method, programmed temperature steps, comparison with isothermal kinetic method

Degradation kinetics usually are studied under isothermal conditions by determining the reaction rate constant at different temperatures. These temperatures generally are fairly high and are kept constant throughout the experiment; in nonisothermal kinetic studies, the temperature changes continuously with time. Several such methods have been described, with the essential difference between them being the equation for the time–temperature relationship (1–3).

Calculations using a continuous temperature increase were carried out previously *via* a multistep model (3). Study of an experimental model with a stepwise temperature profile then was desired. This paper describes the application of nonisothermal kinetics in which the temperature is raised discontinuously in consecutive equal steps, whose number and duration are predetermined. The results are compared with those obtained in conventional isothermal kinetic studies.

EXPERIMENTAL

The investigation was carried out using an active principle, a substituted benzazepine, as a 0.2% solution in pH 5 buffer–ethanol (60:40). This pH was chosen to give appreciable degradation in a relatively short time[1].

The solution of the active principle was introduced into ampuls, which then were sealed and immersed in a thermostatically controlled bath[2] of glycerol–water. At predetermined times coinciding with the end of a temperature stage, ampuls were removed to determine the remaining amount of active ingredient. This determination was done by high-performance liquid chromatography (HPLC) or by spectrophotometry after separation by TLC followed by elution.

TLC—Plates precoated with silica gel and an indicator[3] were used as the stationary phase. The mobile phase was chloroform—ethanol–concentrated ammonia (90:10:0.8). The plates were developed to 12 cm. UV detection was performed at 254 nm with the use of Dragendorff's reagent and peroxide for visualization of degradation after elution.

The R_f values were 0.5 for the active principle and 0.4, 0.7, and 0.9 for the degradation products. After development, the spot corresponding to the unchanged active principle was eluted[4] with 2.50 ml of solvent

[1] M. O. Baltzer, unpublished results.
[2] Model FP thermostat, Haake.
[3] G 1500/LS 254, Schleicher and Schuell.
[4] Eluchrom apparatus, Camag.

0022-3549/80/0300-0287$01.00/0
© 1980, American Pharmaceutical Association

(3) A. R. Cooke, *Am. J. Dig. Dis.*, **18**, 225 (1973).
(4) H. E. Paulus and M. W. Whitehouse, *Annu. Rev. Pharmacol.*, **13**, 107 (1973).
(5) E. F. Mauer, *N. Engl. J. Med.*, **253**, 404 (1955).
(6) *Am. J. Med.*, **30**, 268 (1961).
(7) P. L. Boardman and E. D. Hart, *Br. Med. J.*, **4**, 264 (1967).
(8) S. S. Berkowitz, *Curr. Ther. Res.*, **16**, 442 (1974).
(9) A. Lussier, K. L. MacCannell, S. J. Alexander, C. V. Multz, G. Boost, and E. J. Segre, *Clin. Pharmacol. Ther.*, **13**, 146 (1972).
(10) S. S. Adams, R. G. Bough, E. E. Cliffe, B. Lessel, and R. F. N. Mills, *Toxicol. Appl. Pharmacol.*, **15**, 310 (1969).
(11) E. Arrigoni-Martelli, "Inflammation and Anti-inflammatories," Wiley, New York, N.Y., 1977, p. 208.
(12) K. D. Rainsford, K. Brane, and M. W. Whitehouse, "Aspirin and Related Drugs: Their Actions and Uses," Birkhauser Verlag, Basel, Switzerland, 1977, p. 67.
(13) W. W. Paudler and T. K. Chen, *J. Heterocycl. Chem.*, **7**, 767 (1970).
(14) W. P. Heilman, R. D. Heilman, J. A. Scozzie, R. J. Wayner, and J. M. Gullo, *J. Med. Chem.*, **22**, 671 (1979).
(15) C. A. Winter, E. A. Risley, and G. W. Nuss, *Proc. Soc. Exp. Biol. Med.*, **111**, 544 (1962).
(16) M. DiRosa and D. A. Willoughby, *J. Pharm. Pharmacol.*, **23**, 297 (1971).
(17) M. DiRosa, J. P. Giroud, and D. A. Willoughby, *J. Pathol.*, **104**, 15 (1971).
(18) R. Vinegar, J. F. Truax, and J. L. Selph, *Fed. Proc., Fed. Am. Soc. Exp. Biol.*, **35**, 2447 (1976).
(19) C. A. Winter, *Prog. Drug Res.*, **10**, 139 (1966).
(20) C. J. E. Niemegeers, F. J. Verbruggen, and P. A. J. Janssen, *J. Pharm. Pharmacol.*, **16**, 810 (1964).
(21) J. T. Litchfield and F. Wilcoxon, *J. Pharmacol. Exp. Ther.*, **96**, 99 (1949).
(22) E. A. Swinyard, W. C. Brown, and L. S. Goodman, *ibid.*, **106**, 319 (1952).
(23) M. L. Graeme, E. Fabry, and E. B. Sigg, *ibid.*, **153**, 373 (1966).
(24) R. D. Sofia, H. B. Vassar, and S. D. Nalepa, *Eur. J. Pharmacol.*, **24**, 108 (1973).
(25) C. Hansch, J. E. Quinlan, and G. L. Lawrence, *J. Org. Chem.*, **33**, 347 (1968).
(26) C. Hansch, E. J. Lien, and F. Helmer, *Arch. Biochem. Biophys.*, **128**, 319 (1968).
(27) L. P. Hammett, "Physical Organic Chemistry," McGraw-Hill, New York, N.Y., 1940, chap. 7.
(28) C. K. Hancock and C. P. Falls, *J. Am. Chem. Soc.*, **83**, 4214 (1961).
(29) N. J. Turner and R. D. Battershell, *Contrib. Boyce Thompson Inst.*, **24**, 139 (1969).
(30) V. W. Adamkiewicz, W. B. Rice, and J. D. McCall, *Can. J. Biochem. Physiol.*, **33**, 332 (1955).

Nonisothermal Kinetics with Programmed Temperature Steps

B. EDEL ˣ and M. O. BALTZER

Received April 30, 1979, from *Analytical Research and Development, Pharmaceutical Department, Sandoz Ltd., CH-4002 Basel, Switzerland.* Accepted for publication October 15, 1979.

Abstract □ Data required for predicting the stability of an active principle in solution can be obtained by two kinetic methods. With the isothermal method, the degradation rate constants are determined at different temperatures, which are kept constant throughout the experiment. With the nonisothermal method, the temperature is increased with time. This paper describes a nonisothermal kinetic method in which the temperature is increased in consecutive equal steps. The results are compared with those obtained by the conventional isothermal method. The values for the activation energy are approximately the same by both methods. Although the technique of nonisothermal kinetics demands sophisticated equipment and high experimental accuracy, it provides a continuous picture over a wide temperature range.

Keyphrases □ Stability—prediction, nonisothermal kinetic method, programmed temperature steps, comparison with isothermal kinetic method □ Drug degradation kinetics—nonisothermal method, programmed temperature steps, comparison with isothermal kinetic method □ Kinetics, degradation—nonisothermal method, programmed temperature steps, comparison with isothermal kinetic method

Degradation kinetics usually are studied under isothermal conditions by determining the reaction rate constant at different temperatures. These temperatures generally are fairly high and are kept constant throughout the experiment; in nonisothermal kinetic studies, the temperature changes continuously with time. Several such methods have been described, with the essential difference between them being the equation for the time–temperature relationship (1–3).

Calculations using a continuous temperature increase were carried out previously *via* a multistep model (3). Study of an experimental model with a stepwise temperature profile then was desired. This paper describes the application of nonisothermal kinetics in which the temperature is raised discontinuously in consecutive equal steps, whose number and duration are predetermined. The results are compared with those obtained in conventional isothermal kinetic studies.

EXPERIMENTAL

The investigation was carried out using an active principle, a substituted benzazepine, as a 0.2% solution in pH 5 buffer–ethanol (60:40). This pH was chosen to give appreciable degradation in a relatively short time[1].

The solution of the active principle was introduced into ampuls, which then were sealed and immersed in a thermostatically controlled bath[2] of glycerol–water. At predetermined times coinciding with the end of a temperature stage, ampuls were removed to determine the remaining amount of active ingredient. This determination was done by high-performance liquid chromatography (HPLC) or by spectrophotometry after separation by TLC followed by elution.

TLC—Plates precoated with silica gel and an indicator[3] were used as the stationary phase. The mobile phase was chloroform—ethanol–concentrated ammonia (90:10:0.8). The plates were developed to 12 cm. UV detection was performed at 254 nm with the use of Dragendorff's reagent and peroxide for visualization of degradation after elution.

The R_f values were 0.5 for the active principle and 0.4, 0.7, and 0.9 for the degradation products. After development, the spot corresponding to the unchanged active principle was eluted[4] with 2.50 ml of solvent

[1] M. O. Baltzer, unpublished results.
[2] Model FP thermostat, Haake.
[3] G 1500/LS 254, Schleicher and Schuell.
[4] Eluchrom apparatus, Camag.

0022-3549/80/0300-0287$01.00/0
© 1980, American Pharmaceutical Association

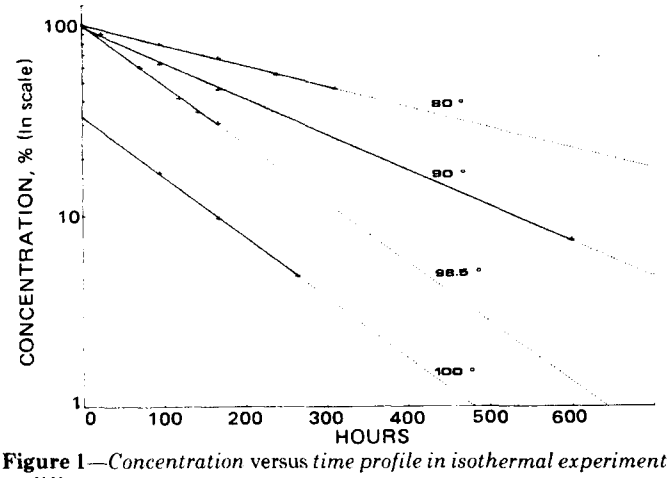

Figure 1—*Concentration* versus *time profile in isothermal experiment at different temperatures.*

(methanol–10% concentrated ammonia). A UV absorption spectrum of this solution was recorded between 200 and 320 nm with a spectrophotometer[5] linked to a recorder[6]. The value was measured at the extinction maximum of 230 nm. The recovery was 97%.

The values are the means of five samples from one ampul. A calibration curve was prepared under the same conditions. The equation was $y = 0.0726x + 0.0111$ ($r = 0.9995$) for concentrations between 1 and 9.5 μg/ml.

HPLC[7]—The stationary phase was Lichrosorb Si 100, 5 μm in a column of 10 cm length and 0.46 i.d. The mobile phase was 95% ethanol–methanol–saturated ammonium carbonate solution (900:100:0.4). A pump[8] maintained the flow rate at 1.5 ml/min with a pressure of ~175 × 10^5 Pa. The chart speed of the recorder[9] was 1 cm/min. The UV detector[10] wavelength was set at 230 nm. The sample loop of the injector[11] had an injection volume of 20 μl. The peak area was obtained by an integration system[12] connected to the detector.

The values are the means of three injections obtained after diluting the sample to give a concentration of unchanged active principle approximating that of the calibration curve. The equation was $y = 0.0258x + 0.0174$ ($r = 0.9999$) for injections from 0.2 to 6 μg.

The kinetic test at 100° carried out using TLC also was performed using HPLC and gave concentrations of 33.7, 19.6, 10.68, and 5.2% at 0, 96, 168, and 264 hr, respectively. These values are close to those shown in Fig. 1. This fact indicates the equivalence of the two methods.

Nonisothermal Temperature Programming—A programmer[13] was used to control the rise of temperature in the bath. This system enables the bath temperature to be altered automatically stepwise from a preset starting temperature over a range of 115° at 10 rates. The kinetic experiments were carried out between 40 and 97.6° in consecutive equal steps, which in this case were temperature changes, ΔT, of 0.3° every 3 hr (Fig. 2). The temperature was increased by 0.3° quickly at the beginning of each step and was kept constant for the remainder of the step time.

RESULTS

Nonisothermal Kinetics—Zoglio *et al.* (3) used a linear progression for temperature. The degradation curve, $f(C)$, is described by a series of straight lines (where the time interval during which the temperature remains constant is reduced) whose individual slopes (or rate constants), k_i, represent the instantaneous degradation rate at a given moment (or temperature). The shorter this time interval, the greater is the chance of the curve being linear in this interval. (For first-order reactions, the curve is log concentration as a function of time.)

This method is based on the hypothesis that the arithmetic mean of these rate constants is equal to the ratio of total degradation, $f(b) - f(a)$,

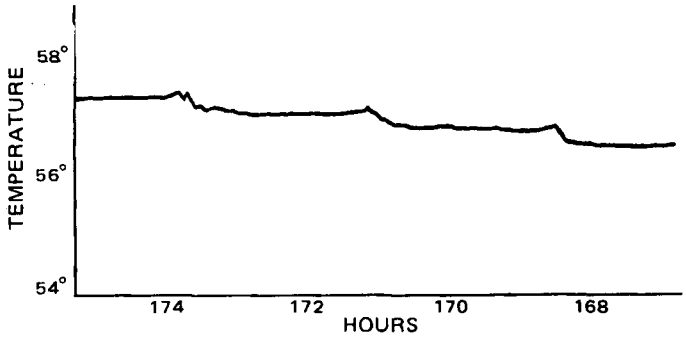

Figure 2—*Section of the experimental temperature profile.*

for the duration of the experiment, $b - a$:

$$\frac{f(b) - f(a)}{b - a} = \frac{k_1 + k_2 + \ldots + k_i + \ldots + k_n}{n} \qquad \text{(Eq. 1)}$$

The size of n is fixed to minimize the error.

The temperature programming in the present experiment represents a special case of this theory. The hypothesis according to which each interval can be described by a straight line becomes a reality. Each temperature stage can be regarded as a miniature isothermal kinetic model. For each step, the degradation is represented by a straight line whose slope corresponds to the rate constant at that temperature. The error due to the time required to raise the temperature between each stage can be regarded as negligible. The equation for the degradation is:

$$\ln C - \ln C_0 = \frac{t}{n}(k_1 + k_2 + \ldots + k_i + \ldots + k_n) \qquad \text{(Eq. 2)}$$

To solve this equation for any rate constant, the constant must be expressed in terms of all of the other constants in the equation. For constant k_i:

$$k_i = Ae^{-E(RT_i)^{-1}} \qquad \text{(Eq. 3)}$$

For constant $k_i + 1$:

$$k_{i+1} = Ae^{-E(RT_{i+1})^{-1}} \qquad \text{(Eq. 4)}$$

By dividing Eq. 4 by Eq. 3, the following expression is obtained:

$$k_{i+1} = k_i e^{E/R[(T_{i+1}-T_i)(T_iT_{i+1})^{-1}]} \qquad \text{(Eq. 5)}$$

Because the increment $T_{i+1} - T_i$ is constant and equal to ΔT, the solution for k_{i+2} with respect to k_i becomes:

$$k_{i+2} = k_i e^{E/R[\Delta T(T_{i+1}T_i)^{-1}]}\, e^{E/R[\Delta T(T_{i+2}T_{i+1})^{-1}]} \qquad \text{(Eq. 6)}$$

In the same way, each constant can be expressed with respect to k_i. The corresponding expressions can be substituted for the values of k_1 to k_n in Eq. 2.

If $k_1 = k_i$, then:

$$\ln C - \ln C_0 = k_1 \frac{t}{n}(1 + e^{E/R[\Delta T(T_1T_2)^{-1}]} + e^{E/R[\Delta T(T_1T_2)^{-1} + \Delta T(T_2T_3)^{-1}]} + \ldots + e^{E/R[\Delta T(T_1T_2)^{-1} + \ldots + \Delta T(T_{n-1}T_n)^{-1}]}) \qquad \text{(Eq. 7)}$$

or:

$$\ln C - \ln C_0 = k_1 \frac{t}{n}\left(1 + \sum_{m=1}^{n-1} \exp\left[E/R\ \Delta T \sum_{i=1}^{m} (T_iT_{i+1})^{-1}\right]\right) \qquad \text{(Eq. 8)}$$

Once the values of $\ln C - \ln C_0$ and t/n are determined experimentally, k_1 can be calculated for any activation energy.

Equations similar to Eq. 8 can be derived and solved for the constants k_2 to k_n in the same way. These constants then are used to plot the theoretical curves [$\ln C = f(t)$] for different activation energies using a scale that corresponds to the order of the degradation reaction (which must be determined).

Since extremely lengthy calculations are needed to solve these equations, a program was elaborated that enables the problem to be solved on a computer[12]. (Automatic calculation takes ~6 hr.) For a first-order reaction and for a particular activation energy, this program calculates (with the aid of Eq. 8) the k' value corresponding to the first temperature stage. With this value, it then is possible to determine the theoretical concentration at the end of this stage, which also is the concentration at the beginning of the next stage. By substituting the values of the con-

[5] Model SP 1800, Pye Unicam.
[6] Model AR 25, Pye Unicam.
[7] J. Meier and C. Morin, Sandoz Ltd., Basel, Switzerland, personal communication.
[8] Model 110, Altex.
[9] Model 312, W + W.
[10] Model LC 55, Perkin-Elmer.
[11] Model 7120, Rheodyne.
[12] System 3354, Hewlett-Packard.
[13] Model PG 12, Haake.

Table I—Values Obtained by Nonisothermal Conditions [a]

Hours	Percent of Unchanged Substance	ln C
0	100	4.60517
72	97.47	4.57954
144	94.95	4.55335
192	93.95	4.54276
240	91.60	4.51743
312	85.59	4.44957
360	73.06	4.29128
408	71.70	4.27249
480	58.37	4.06680
528	48.36	3.87867
576	35.61	3.57263

[a] Number of stages, n, = 576/3 = 192.

centration and initial temperature in the first stage with those in the second stage and by substituting n with the number of stages remaining, an analogous computation gives the k value corresponding to the second stage and so on to the last one.

The concentrations calculated theoretically are compared with the concentrations obtained experimentally. The value taken for the activation energy then is altered until the calculated concentrations approach the experimental data. Progressively smaller adjustments evaluate the activation energy at best fit to the nearest 100 J. When the sum of the squares of the difference between the experimental values and the theoretical values at the same moment is a minimum, the corresponding activation energy is regarded as the activation energy of the reaction. The constant of the Arrhenius equation is determined at the same time.

Quantitative analysis of the ampul produced the results shown in Table I over 576 hr. Automatic computation of the activation energy after scanning between 40,000 and 70,000 J yielded E = 62.2 kJ/mole. Although this value is purely arbitrary since the n value used corresponds to an actual number of temperature stages during which it remained constant, the same calculation also was performed with n twice the size, and there was no appreciable modification in the activation energy.

The theoretical degradation curves for each activation energy (Fig. 3) were plotted with the concentration values for each ΔT interval given by the computer. The points corresponding to experimental values also were plotted on the graph. One point is marked to show the considerable effect that an error of ±1% can have on the concentration at a given moment.

Isothermal Kinetics—Degradation kinetics were performed isothermally at 80, 90, 98.5, and 100° (Fig. 1). The reaction order was checked in each case as a function of time; the graph of C, ln C, and C^{-1} *versus* t is a straight line for zero-, first-, and second-order reactions, respectively, where C is the concentration of unaltered active ingredient.

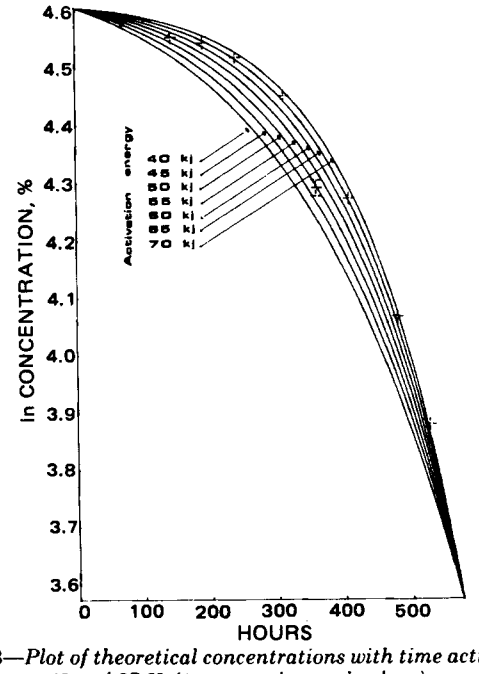

Figure 3—*Plot of theoretical concentrations with time activation energy between 40 and 97.6° (+ = experimental values).*

Table II—Correlation and k Values at Different Temperatures

Parameter	80°	90°	98.5°	100°
Correlation	0.9992	0.9994	0.9989	0.9997
$k \times 10^5$, hr^{-1}	248	431	716	728

When the linear regression was calculated on a programmable computer[14], the best correlation coefficient was obtained for a first-order reaction at the four temperatures. Therefore, the equation for calculating the degradation rate constant is:

$$C = C_0 e^{-kt} \qquad \text{(Eq. 9a)}$$

or:

$$\ln C = \ln C_0 - kt \qquad \text{(Eq. 9b)}$$

where k is the slope of the regression line (Table II).

With the Arrhenius equation, $k = Ae^{-E/RT}$, the graph of ln k as a function of T^{-1} is a straight line with a slope of $-E/R$ (Fig. 4). Calculation of the regression line of ln k as a function of T^{-1} at 80, 90, 98.5, and 100° gave a correlation coefficient of 0.9999. The equation for the straight line was ln k = 14.6 − 7290 T^{-1} in which ln A = 14.6 and E/R = 7290 °K. The activation energy was E = 60.6 kJ/mole.

DISCUSSION AND CONCLUSION

The value for activation energy obtained by the nonisothermal method was similar to that obtained by the isothermal method (62.2 and 60.6 kJ/mole). Therefore, the two methods may be regarded as equivalent with respect to their results. However, they generally are suitable only when the activation energy and the reaction order remain constant throughout the experiment, *i.e.*, the Arrhenius relationship is valid in the particular case.

Given these conditions, the major limitation of the nonisothermal procedure seems to be the experimental accuracy. This limitation is demonstrated by the fact that if the experimental points are measured inaccurately, the experimental and the theoretical degradation curves intersect in too broad a range of activation energies and this effect soon leads to a considerable scattering of the results. To control the experimental accuracy, it is essential to complement the computation by plotting the theoretical curves corresponding to each activation energy to compare them with the experimental curve. It also is necessary to have a prior idea of the degradation rate to select a suitable temperature program; this planning avoids alteration during the experiment.

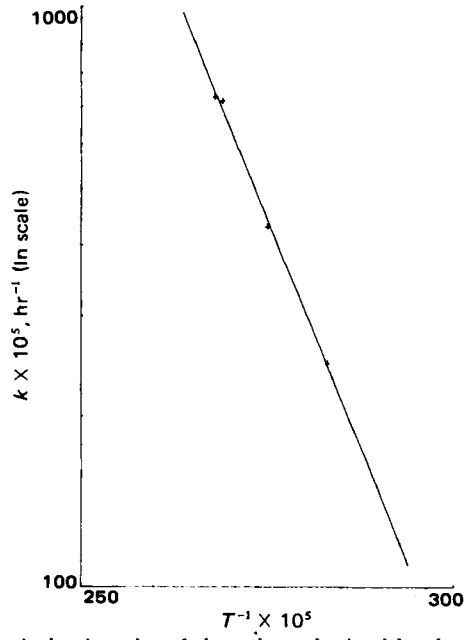

Figure 4—*Arrhenius plot of the values obtained by the isothermal experiment.*

[14] Model 9810 A, Hewlett-Packard.

One advantage of the method is that it examines a wider temperature range than does the isothermal kinetic method. Provided that the tests are sufficiently accurate, it is possible to detect any activation energy change.

Since three temperatures stages and three durations for each stage generally are considered as a minimum for isothermal kinetic studies, the nonisothermal method does not appear to offer any decisive advantage. The definitive need for more sophisticated equipment (temperature programmer, computer, and plotter) is a disadvantage. On the other hand, the nonisothermal method may lead to more precise results with less experimental effort, *e.g.*, data points. Furthermore, it requires only a fraction of the time an isothermal experiment does. Selection of a method depends on the equipment and the time available.

REFERENCES

(1) A. R. Rogers, *J. Pharm. Pharmacol.*, **15**, 101T (1975).

(2) S. P. Eriksen and H. Stelmach, *J. Pharm. Sci.*, **54**, 1029 (1965).

(3) M. A. Zoglio, J. J. Windheuser, R. Vatti, H. V. Maulding, S. S. Kornblum, A. Jacobs, and H. Hamot, *ibid.*, **57**, 2080 (1968).

Time and Temperature Dependence of Disintegration and Correlation between Dissolution and Disintegration Rate Constants

J. T. CARSTENSEN ˣ, ROHIT KOTHARI, V. K. PRASAD *, and JANE SHERIDAN ‡

Received June 25, 1979, from the *School of Pharmacy, University of Wisconsin, Madison, WI 53706.* Accepted for publication October 17, 1979.

*Biopharmaceutics Laboratory, Food and Drug Administration, Washington, D.C. ‡Hoffmann-La Roche Inc., Nutley, NJ 07110.

Abstract □ Commercial prednisone tablets were subjected to dissolution tests by USP basket and paddle methods. It was found experimentally that disintegration adheres to an exponential decay law: $\ln(W/W_0) = -d(t - t_i)$, where W is the nondisintegrated weight, d is a disintegration constant, t is time, and t_i is a lag time. Dissolution has been reported to adhere to a similar law, where the dissolution constant, K, follows a pseudo-Arrhenius relationship with changing temperature. Within a certain temperature range, this relationship also exists for the disintegration rate constant, d. A correlation exists in these tablets between K and d. The shaft length in the dissolution apparatus plays a part in the disintegration (and hence dissolution) rate and, therefore, is an important apparatus parameter affecting reproducibility.

Keyphrases □ Disintegration—commercial prednisone tablets, time and temperature dependence, correlation between dissolution and disintegration rate constants □ Prednisone—commercial tablets, time and temperature dependence of disintegration, correlation between dissolution and disintegration rate constants □ Dissolution—commercial prednisone tablets, time and temperature dependence of disintegration, correlation between dissolution and disintegration rate constants

Several recent articles correlated two- or three-component dissolution model parameters with those of disintegration in the same apparatus. These studies were aimed at elucidation of the type of dissolution curve obtained in dissolution experiments both for control and for research purposes. The curves usually are *s*-shaped. Wagner (1) and Wood (2) first recognized the importance of this type of curve, and a probit and a Weibul function were suggested later as a descriptive means (1–4).

Several investigators demonstrated that disintegration and dissolution in an apparatus can be correlated and that these factors lead to *s*-shaped curves (5–11). Carstensen *et al.* (7, 8) suggested that the best general trial function is one in which the weight of undisintegrated tablet is monitored as a function of time. The dimensions of the tablets remaining (such as thickness) as a function of time can be useful in certain cases; but since many tablets swell on contact with water, the functions become complicated. Furthermore, the thickness of a swelling, disintegrating tablet is difficult not only to monitor but also to define.

The simplest model of weight *versus* time that appears compatible with experimental data (8) is a simple exponential decay function. Double exponentials may apply in more complicated systems. This model has been recognized in compendial work, and disintegrating dissolution calibrators have been suggested. This article presents data showing the disintegration–dissolution behavior of a conventional prednisone tablet.

Excellent research and review articles regarding the mechanism of disintegration have been published (12–14), and the effect of temperature on dissolution has been elucidated (15). This article reports the dependence of tablet disintegration on temperature and also the effect of the length of the stirring shaft on dissolution.

EXPERIMENTAL

Commercial prednisone tablets were assayed and found to contain starch, lactose, metallic stearate, and prednisone. Two 20-mg tablets were placed in the basket of a USP basket dissolution apparatus in a thermostated bath. The apparatus was operated at 150 rpm. This agitation speed was chosen because problems with liquid homogeneity exist at lower rotational speeds (9). Samples were taken routinely at appropriate time intervals and, after filtration[1], were assayed using the spectrophotometric absorbance at 242 nm. The amount of prednisone then was determined by comparison with a standard curve of prednisone obtained with a USP reference standard. The experiment was repeated using a different shaft length (Fig. 1), *i.e.*, assembling the shaft onto the motor such that the length of free shaft was different from that first used. The two shaft "lengths" used are denoted as positions I and II (Fig. 1).

A set of experiments was performed (in both positions) to establish the disintegration rate of the tablets in the apparatus. These experiments were done as follows (6, 7). An experiment was carried out for t_i min and then was stopped. The basket was lifted out, and the tablets were removed and dried to constant weight, W, at 100°. This weight was compared with the weight, W_0, of a similarly dried tablet prior to the dissolution test. The experiment then was repeated for other t_i values.

The experiments were repeated using a USP paddle apparatus at 150 rpm. Experiments were carried out at 10, 20, and 30° for the paddle apparatus and at 0, 5, 10, 15, 20, 30, and 37° for the basket apparatus.

[1] Millipore filter.

0022-3549/80/0300-0290$01.00/0

© 1980, American Pharmaceutical Association

One advantage of the method is that it examines a wider temperature range than does the isothermal kinetic method. Provided that the tests are sufficiently accurate, it is possible to detect any activation energy change.

Since three temperatures stages and three durations for each stage generally are considered as a minimum for isothermal kinetic studies, the nonisothermal method does not appear to offer any decisive advantage. The definitive need for more sophisticated equipment (temperature programmer, computer, and plotter) is a disadvantage. On the other hand, the nonisothermal method may lead to more precise results with less experimental effort, *e.g.*, data points. Furthermore, it requires only a fraction of the time an isothermal experiment does. Selection of a method depends on the equipment and the time available.

REFERENCES

(1) A. R. Rogers, *J. Pharm. Pharmacol.*, **15**, 101T (1975).

(2) S. P. Eriksen and H. Stelmach, *J. Pharm. Sci.*, **54**, 1029 (1965).

(3) M. A. Zoglio, J. J. Windheuser, R. Vatti, H. V. Maulding, S. S. Kornblum, A. Jacobs, and H. Hamot, *ibid.*, **57**, 2080 (1968).

Time and Temperature Dependence of Disintegration and Correlation between Dissolution and Disintegration Rate Constants

J. T. CARSTENSEN ˣ, ROHIT KOTHARI, V. K. PRASAD *, and JANE SHERIDAN ‡

Received June 25, 1979, from the *School of Pharmacy, University of Wisconsin, Madison, WI 53706.* Accepted for publication October 17, 1979.

*Biopharmaceutics Laboratory, Food and Drug Administration, Washington, D.C. ‡Hoffmann-La Roche Inc., Nutley, NJ 07110.

Abstract □ Commercial prednisone tablets were subjected to dissolution tests by USP basket and paddle methods. It was found experimentally that disintegration adheres to an exponential decay law: $\ln(W/W_0) = -d(t - t_i)$, where W is the nondisintegrated weight, d is a disintegration constant, t is time, and t_i is a lag time. Dissolution has been reported to adhere to a similar law, where the dissolution constant, K, follows a pseudo-Arrhenius relationship with changing temperature. Within a certain temperature range, this relationship also exists for the disintegration rate constant, d. A correlation exists in these tablets between K and d. The shaft length in the dissolution apparatus plays a part in the disintegration (and hence dissolution) rate and, therefore, is an important apparatus parameter affecting reproducibility.

Keyphrases □ Disintegration—commercial prednisone tablets, time and temperature dependence, correlation between dissolution and disintegration rate constants □ Prednisone—commercial tablets, time and temperature dependence of disintegration, correlation between dissolution and disintegration rate constants □ Dissolution—commercial prednisone tablets, time and temperature dependence of disintegration, correlation between dissolution and disintegration rate constants

Several recent articles correlated two- or three-component dissolution model parameters with those of disintegration in the same apparatus. These studies were aimed at elucidation of the type of dissolution curve obtained in dissolution experiments both for control and for research purposes. The curves usually are *s*-shaped. Wagner (1) and Wood (2) first recognized the importance of this type of curve, and a probit and a Weibul function were suggested later as a descriptive means (1–4).

Several investigators demonstrated that disintegration and dissolution in an apparatus can be correlated and that these factors lead to *s*-shaped curves (5–11). Carstensen *et al.* (7, 8) suggested that the best general trial function is one in which the weight of undisintegrated tablet is monitored as a function of time. The dimensions of the tablets remaining (such as thickness) as a function of time can be useful in certain cases; but since many tablets swell on contact with water, the functions become complicated. Furthermore, the thickness of a swelling, disintegrating tablet is difficult not only to monitor but also to define.

The simplest model of weight *versus* time that appears compatible with experimental data (8) is a simple exponential decay function. Double exponentials may apply in more complicated systems. This model has been recognized in compendial work, and disintegrating dissolution calibrators have been suggested. This article presents data showing the disintegration–dissolution behavior of a conventional prednisone tablet.

Excellent research and review articles regarding the mechanism of disintegration have been published (12–14), and the effect of temperature on dissolution has been elucidated (15). This article reports the dependence of tablet disintegration on temperature and also the effect of the length of the stirring shaft on dissolution.

EXPERIMENTAL

Commercial prednisone tablets were assayed and found to contain starch, lactose, metallic stearate, and prednisone. Two 20-mg tablets were placed in the basket of a USP basket dissolution apparatus in a thermostated bath. The apparatus was operated at 150 rpm. This agitation speed was chosen because problems with liquid homogeneity exist at lower rotational speeds (9). Samples were taken routinely at appropriate time intervals and, after filtration[1], were assayed using the spectrophotometric absorbance at 242 nm. The amount of prednisone then was determined by comparison with a standard curve of prednisone obtained with a USP reference standard. The experiment was repeated using a different shaft length (Fig. 1), *i.e.*, assembling the shaft onto the motor such that the length of free shaft was different from that first used. The two shaft "lengths" used are denoted as positions I and II (Fig. 1).

A set of experiments was performed (in both positions) to establish the disintegration rate of the tablets in the apparatus. These experiments were done as follows (6, 7). An experiment was carried out for t_i min and then was stopped. The basket was lifted out, and the tablets were removed and dried to constant weight, W, at 100°. This weight was compared with the weight, W_0, of a similarly dried tablet prior to the dissolution test. The experiment then was repeated for other t_i values.

The experiments were repeated using a USP paddle apparatus at 150 rpm. Experiments were carried out at 10, 20, and 30° for the paddle apparatus and at 0, 5, 10, 15, 20, 30, and 37° for the basket apparatus.

[1] Millipore filter.

0022-3549/80/0300-0290$01.00/0

© 1980, American Pharmaceutical Association

Table I—Dissolution Constants and Disintegration Constants at Various Temperatures and Positions

Temperature	Position[a]	$10^5 K$, sec^{-1}	r^2	$10^3 d$, sec^{-1}	r^2
		Basket, 150 rpm			
0	I	8.3	0.99	2.7	0.98
0	II	8.3	0.99	2.8	0.99
5°	I	8.3	0.99	2.9	0.99
5°	II	8.7	0.996	3.5	0.998
10°	I	24.7	0.97	3.6	0.992
10°	II	28.1	0.98	4.1	0.98
15°	I	38.0	0.96	4.4	0.998
15°	II	38.3	0.96	4.9	0.99
20°	I	111	0.99	5.7	0.97
20°	II	125	0.97	6.7	0.95
30°	I	206	0.993	8.2	0.94
30°	II	248	0.996	8.7	0.90
37°	I	240	0.99	13.2	0.91
37°	II	284	0.992	14.6	0.96
		Paddle, 150 rpm			
10°	I	44.5	0.97	3.9	0.996
10°	II	58.9	0.97	4.0	0.99
20°	I	145	0.92	5.6	0.996
20°	II	164	0.96	7.0	0.97
30°	I	219	0.999	9.6	0.98
30°	II	228	0.97	9.7	0.96

[a] Positions I and II are 22 and 32 cm, respectively, and equal the shaft length.

RESULTS AND DISCUSSION

All dissolution and disintegration data show s-shaped curves as exemplified in Fig. 2. The data were recast in semilogarithmic form, and, as shown in Fig. 3 and Table I, follow the equations:

$$\ln(W/W_0) = -d(t - t_i) \quad \text{(Eq. 1)}$$

$$\ln(m/m_0) = -K(t - t_i') \quad \text{(Eq. 2)}$$

where m is the amount of undissolved drug, d is a disintegration rate constant ($time^{-1}$), K is a dissolution rate constant ($time^{-1}$), t_i and t_i' are lag times, and the subscript zero denotes zero time.

To present all of the data points graphically, they were converted to reduced parameters in the following fashion. The least-squares parameters d and t_i (and K and t_i') were calculated as shown in Table I. For disintegration, the experimental value of $\ln(W/W_0)$ at time $t^\dagger$ was used as the ordinate (y-axis) in Fig. 4. The corresponding abscissa value, x, then was obtained by inserting the $t^\dagger$ value and the least-squares values of d and t_i into $x = -d(t - t_i)$. A similar procedure was used for dissolution (Fig. 5).

This graphic method allows visualization of how all data points fit the two equations. Essentially straight lines of unit slope and zero intercept are obtained in Figs. 4 and 5. The graphical presentation is not statistical. Usual least-squares methods are not possible by the reduced presentation because both x and y have errors of comparable magnitude, and most methods addressing this situation fail when (as in the described treatment) the error on the y-axis is not independent of the error on the x-axis.

Statistical evidence is confined to comparison of the s_{yx}^2 values of the data treated according to Eq. 1 as compared to other functions, where s_{yx}^2 is the total sum of squares divided by the degrees of freedom ($n - 2$),

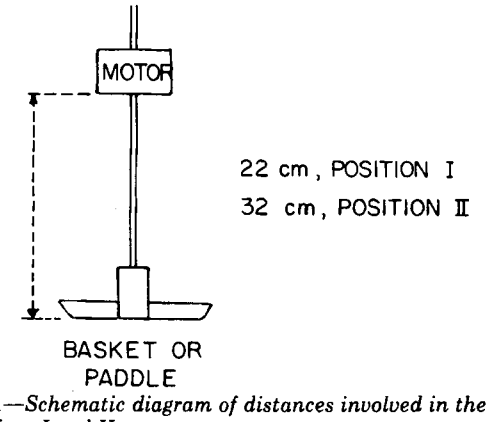

Figure 1—*Schematic diagram of distances involved in the assembly for positions I and II.*

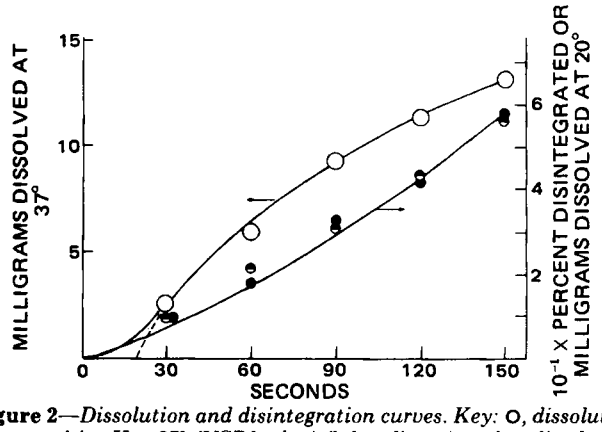

Figure 2—*Dissolution and disintegration curves. Key: ○, dissolution curve, position II at 37° (USP basket) (left ordinate); and ●, dissolution, and ◒, disintegration, at 20° (USP basket, position I) (right ordinate).*

where n is the number of experimental points. The data from the dissolution in USP basket position I at 15° are used as an example. Table II compares the data treated by Eq. 1 with the data treated by the function:

$$y = [1 - (W/W_0)] = (t/t_d)^n \quad \text{(Eq. 3a)}$$

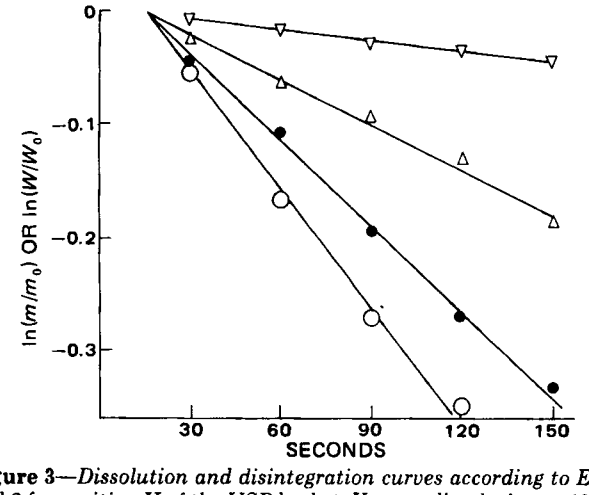

Figure 3—*Dissolution and disintegration curves according to Eqs. 1 and 2 for position II of the USP basket. Key: ▽, dissolution at 10°; △, dissolution at 20°; ●, dissolution at 30°; and ○, disintegration at 5°.*

Table II—Statistical Comparison for USP Basket (15°, Position I) Treated by Eq. 1 and by Eq. 3 as an Example

t, sec	ln t	100 y (Percent Dis-integrated)	$z_1 = \ln y$	$\bar{z}_1$	$\bar{y}_1$ × 100	Δ_1^2	$z_2 = \ln(1-y)$	$\bar{z}_2$	$\bar{y}_2$ × 100	Δ_2^2
30	3.4	7.9	−2.538	−2.500	8.2	0.09	−0.082	−0.076	7.3	0.36
60	4.09	18.2	−1.704	−1.746	17.5	1.69	−0.201	−0.207	18.7	0.25
90	4.50	28.9	−1.241	−1.298	27.3	2.56	−0.341	−0.339	27.7	1.44
120	4.79	36.8	−1.000	−0.982	37.5	0.49	−0.459	−0.470	37.5	1.69
150	5.01	45.7	−0.783	−0.742	47.6	1.21	−0.611	−0.602	45.2	0.25
						$\Sigma\Delta^2 = 6.04$				$\Sigma\Delta^2 = 3.99$
						$s_{yx}^2 = 2.01$				$s_{yx}^2 = 1.33$
				Slope		1.091				−0.0044
				Intercept		−6.209				0.056
				Correlation coefficient		−0.998				−0.999

which is the equation derived by Kitamori and Iga (11). In logarithmic form, this equation is:

$$z_1 = \ln[1 - (W/W_0)] = n \ln(t) - n \ln(t_d) \qquad \text{(Eq. 3}b\text{)}$$

where n is an equation parameter and t_d is the disintegration time. The least-squares fit for the data is $z_1 = 1.091 \ln t - 6.209$ ($r^2 = 0.996$), where r^2 is the square of the correlation coefficient.

The s_{yx}^2 values are obtained for Eq. 3a first by finding the line values, $\bar{z}_1$, corresponding to Eq. 3b for each t value and then by converting them to $\bar{y}_1$ values (percent disintegrated). These values are shown in Table II. A similar calculation is shown for the data plotted according to Eq. 1 [$z_2 = \ln(W/W_0)$ and $y_2 = 1 - (W/W_0)$]. The sums of squares were equally good whether obtained by Eq. 1 or by Eq. 2. The sums of squares obtained by Eq. 1 were always lower than those calculated from Eq. 3a but only by small amounts, and none of the s_{yx}^2 ratios exceeded the critical F values with (3,3) degrees of freedom.

The derivation of Eq. 3a (10) is based on an assumption (16) that the thickness of a tablet will decrease steadily as it disintegrates. This assumption usually is not the case since swelling initially will cause an increase in thickness. Even if the basis for the derivation of Eq. 3a may not be general, Eq. 3a as shown provides a good trial function. However, Eq. 1 will be used in the remainder of this article.

Correlation between Disintegration and Dissolution—The data in Table I concerning the values of K and d are plotted in Fig. 6. It is graphically evident that there is a correlation and that this correlation is not linear. Many curvilinear functions may fit this curve, one of which ($r = 0.97$) is $\ln[(300 - 10^5 k)] = -0.214 \times 10^3 d + 6.4$. This function is consistent with the theoretical models proposed elsewhere (5–8, 10). At high d values, K should become independent of d (7), and this result probably is the explanation for the curving off at high d values.

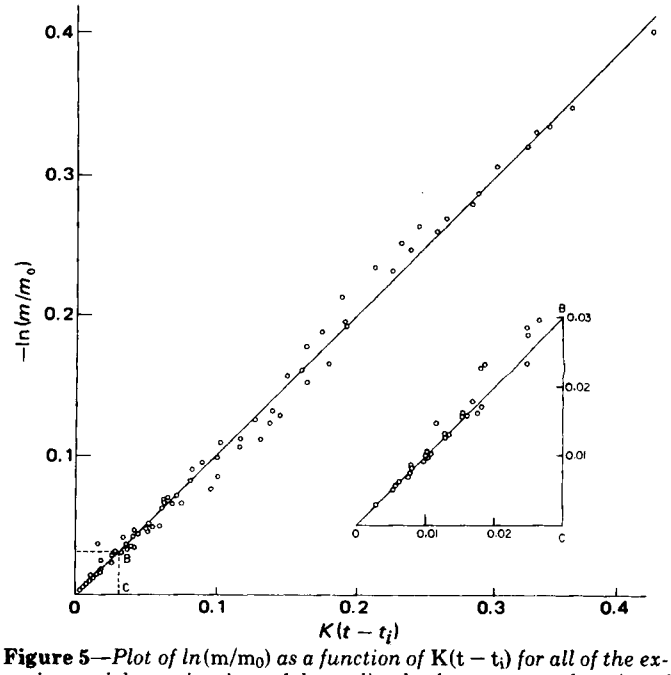

Figure 5—*Plot of* $\ln(m/m_0)$ *as a function of* $K(t - t_i)$ *for all of the experimental determinations of the undissolved amount as a function of time.*

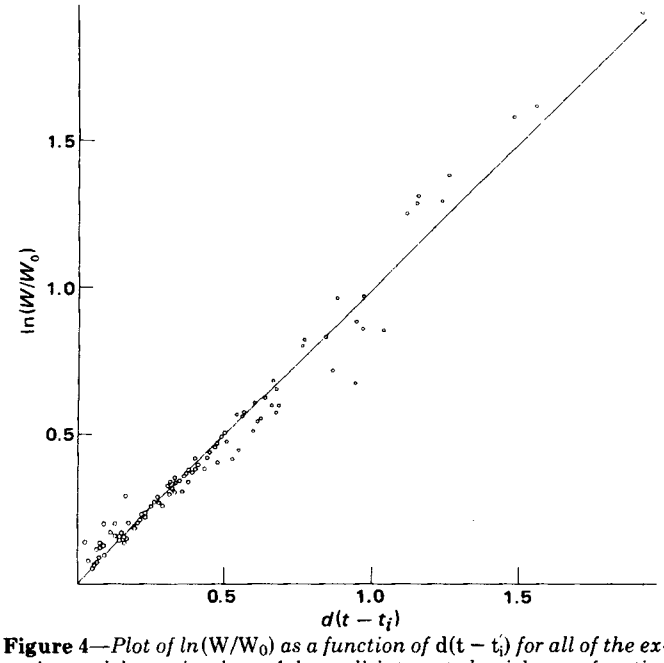

Figure 4—*Plot of* $\ln(W/W_0)$ *as a function of* $d(t - t_i)$ *for all of the experimental determinations of the undisintegrated weight as a function of* t.

Effect of Shaft Length—Table I shows that position II gave significantly ($p > 0.995$) higher results than did position I as far as both disintegration and dissolution are concerned. Since disintegration affects dissolution [$K = f(d)$], it is speculated that the change in disintegration is caused by the longer shaft length and that this effect is the cause for the observed differences.

Effect of Temperature—The logarithm of the disintegration constants, d, is plotted *versus* the reciprocal temperature in Fig. 7. The

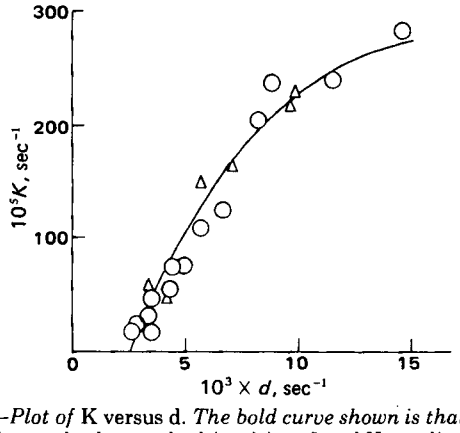

Figure 6—*Plot of* K versus d. *The bold curve shown is that expressed in Eq. 3. Key:* ○, *basket method (positions I and II not distinguished); and* △, *paddle method (positions I and II not distinguished).*

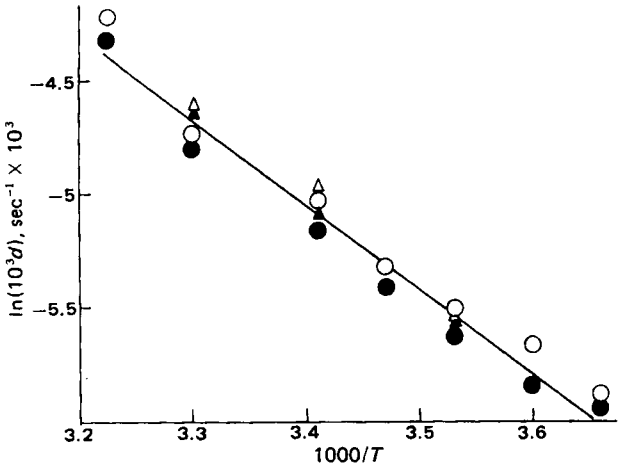

Figure 7—*Temperature dependence of the disintegration constant, d (seconds^{-1}). Key: O, USP basket method; and Δ, USP paddle method. Solid circles are position I, and open circles are position II.*

least-squares equation for the line is:

$$\ln d = -(7000/R)(1/T) - 0.0152 \quad \text{(Eq. 4)}$$

According to previous investigators (12–14), the disintegration of a tablet proceeds *via* two principal mechanisms: (*a*) penetration of liquid into the tablet pores, and (*b*) expansion of the disintegrant exposed in the pore walls. A large pore size facilitates penetration; but if it is too large, the expansion of the disintegrant will not cause sufficient strain to rupture the tablet (12, 17). Therefore, either mechanism or both simultaneously may be the rate-controlling step.

If the rate-controlling process is solely the penetration of pores of a radius *r*, then, as shown previously (12, 18, 19), the length of liquid penetration, *L*, into the capillaries is time dependent according to:

$$L^2 = (r\gamma \cos\theta)/(2\eta)t = q^2t \quad \text{(Eq. 5)}$$

where:

$$q = [r\gamma \cos\theta/(2\eta)]^{1/2} \quad \text{(Eq. 6)}$$

and where γ is the interfacial tension between the liquid and the solid, η is the viscosity, and θ is the contact angle.

If the amount penetrated disintegrates in a certain length of time, t^*, after the time of wetting and if the radius of the tablet is L_0 cm initially, then the weight remaining after t sec would be given by (20, 21):

$$W/W_0 = (L_0 - L)^3/L_0^3 \quad \text{(Eq. 7)}$$

Inserting Eq. 7 into Eq. 5 gives (21):

$$[1 - (W/W_0)^{1/3}]^2 = (q/L_0)^2(t - t^*) \quad \text{(Eq. 8)}$$

Data treated similarly are shown in Table III, and it is apparent that the equation does not hold. However, the model is simple, and more complicated relations could be visualized. But if *d*, the disintegration constant, is related more closely to the volume rate of penetration, then *d* would be expected to be linearly related to q^3, *i.e.*:

$$\ln d = 1.5 \ln(\gamma) + 1.5 \ln(\cos\theta) - 1.5 \ln(\eta) + Q \quad \text{(Eq. 9)}$$

where *Q* is a temperature-independent term.

Table III—Data from Table II Treated by Eq. 8

t, sec	100 (W/W_0), Experimental, %	$[1 - (W/W_0)^{1/3}]^2$	$\widetilde{100(W/W_0)}$, Predicted, %	Δ^2, %^{2}
30	92.1	0.00073	—[a]	—[a]
60	81.8	0.0042	78.7	9.6
90	71.1	0.0116	68.4	7.3
120	63.2	0.0201	61.5	2.9
150	54.3	0.0339	56.2	3.6
				$\Sigma\Delta^2 = 23.4$

[a] Least-squares parameters predicts a negative number for $[1 - (W/W_0)^{1/3}]^2$ at $t = 30$ sec. The least-squares fit was $[1 - (W/W_0)^{1/3}]^2 = 0.000274t - 0.01059$ with $r^2 = 0.95$ and $s^2_{yx} = 23.4/2 = 11.7\%^2$.

The dependence of θ on T is slight (22, 23) as shown. Stepanov *et al.* (24) gave θ values of water on sapphire of:

$$\theta = 8.8 + 8.2 \times 10^{-15}T^6 \quad \text{(Eq. 10)}$$

i.e., $\theta = 11.5$ [or $\ln(\cos\theta) = -0.0206$] at $T = 273°$ ($1/T = 0.00366$) and $\theta = 15.1$ [or $\ln(\cos\theta) = -0.0351$] at $T = 303°$ ($1/T = 0.00333$). On metals, θ decreased with temperature to the same extent (25). Linear Eq. 10 when expressed as $\ln(\cos\theta)$ as a function of $1/T$ is approximately as follows.

For sapphire:

$$\ln(\cos\theta) = 44(1/T) - 0.18 \quad \text{(Eq. 11}a\text{)}$$

For metals:

$$\ln(\cos\theta) = -44(1/T) + 0.13 \quad \text{(Eq. 11}b\text{)}$$

Hence, the activation energy, *E*, is negligible (-88 cal/mole $< E <$ 88 cal/mole). Equations 11*a* and 11*b* are approximations (but acceptable ones) of the experimental Eq. 10. No data exist for the θ values on the tablet matrix used, but it is expected to have a temperature dependence between that of an ionic and that of a covalently bonded surface.

The surface tension, γ, is dependent on temperature by the Ramsay–Shields rule (26):

$$\gamma(M/\rho)^{2/3} = k'(T_c - T - 6) \quad \text{(Eq. 12)}$$

where *M* is the molecular weight, ρ is the density, T_c is the critical temperature of the liquid, and k' is a constant (which equals about 2.1 for liquids that follow Trouton's rule). Since the critical temperature of water is high, γ is virtually temperature independent.

The dependence of viscosity on temperature is given by (25, 26):

$$\ln\eta = (4000/R)(1/T) + \ln\eta_0 \quad \text{(Eq. 13)}$$

This quantity is the only temperature-dependent term in Eq. 9, and it contributes substantially. Equation 9, when Eq. 13 is inserted, becomes:

$$\ln d = (6000/R)(1/T) + Q' \quad \text{(Eq. 14)}$$

where Q' is a nearly temperature-independent term. The slope predicted in Eq. 14 (3000) is on the same order as that found in Eq. 4. Therefore, the data in this case are not contradictory to the disintegration process as being penetration controlled.

REFERENCES

(1) J. Wagner, *J. Pharm. Sci.*, **58**, 1253 (1969).

(2) J. Wood, in "Abstracts of Papers Presented at the 113th Annual Meeting of the Academy of Pharmaceutical Sciences," American Pharmaceutical Association, Washington, D.C., 1974, p. 189.

(3) F. Langenbucher, *J. Pharm. Pharmacol.*, **24**, 979 (1972).

(4) I. Lippmann, in "Dissolution Technology," L. Leeson and J. T. Carstensen, Eds., Academy of Pharmaceutical Sciences, Washington, D.C., 1974, p. 193.

(5) K. G. Nelson and L. Y. Wang, *J. Pharm. Sci.*, **66**, 1758 (1977).

(6) *Ibid.*, **67**, 87 (1978).

(7) J. T. Carstensen, J. L. Wright, K. W. Blessel, and J. Sheridan, *J. Pharm. Sci.*, **67**, 48 (1978).

(8) *Ibid.*, **67**, 982 (1978).

(9) J. T. Carstensen, T. Y.-F. Lai, and V. K. Prasad, *J. Pharm. Sci.*, **67**, 1303 (1978).

(10) N. Kitamori and T. Shimamoto, *Chem. Pharm. Bull.*, **24**, 1789 (1976).

(11) N. Kitamori and K. Iga, *J. Pharm. Sci.*, **67**, 1436 (1978).

(12) P. Couvreur, Ph.D. thesis, Université Catholique de Louvain, Brussels, Belgium, 1975, p. 87.

(13) J. T. Ingram and W. Lowenthal, *J. Pharm. Sci.*, **55**, 614 (1966).

(14) *Ibid.*, **57**, 393 (1968).

(15) J. T. Carstensen and M. Patel, *J. Pharm. Sci.*, **64**, 1770 (1975).

(16) J. P. Cleave, *J. Pharm. Pharmacol.*, **17**, 698 (1965).

(17) H. Berry and C. W. Ridout, *ibid.*, **2**, 619 (1950).

(18) E. H. Washburn, *Phys. Rev.*, **17**, 273 (1921).

(19) H. Nogami, T. Nagai, and H. Uchida, *Chem. Pharm. Bull.*, **14**, 152 (1966).

(20) E. Nelson, D. Eppich, and J. T. Carstensen, *J. Pharm. Sci.*, **63**, 755 (1974).

(21) J. T. Carstensen, *ibid.*, **63**, 1 (1974).

(22) A. W. Adamson, "Physical Chemistry of Surfaces," 3rd ed., Wiley, New York, N.Y., 1976, p. 345.
(23) A. W. Neumann, *Z. Phys. Chem., Neue Folge*, **41**, 339 (1964).
(24) V. G. Stepanov, L. D. Volyak, and Y. V. Tarakov, *Zh. Fiz. Khim.*, **46**, 2397 (1972); through *Chem. Abstr.*, **77**, 169160c (1973).
(25) *Ibid.*, **49**, 2931 (1975); through *Chem. Abstr.*, **84**, 80161a (1976).
(26) W. J. Moore, "Physical Chemistry," 3rd ed., Prentice-Hall, Englewood Cliffs, N.J., 1963, p. 734.

ACKNOWLEDGMENTS

Supported by grants from Hoffmann-La Roche, Nutley, NJ 07110, and by Contract 223-76-3020 from the Food and Drug Administration.

Antitumor Agents XLI: Effects of Eupaformosanin on Nucleic Acid, Protein, and Anaerobic and Aerobic Glycolytic Metabolism of Ehrlich Ascites Cells

I. H. HALL ˣ, K. H. LEE, W. L. WILLIAMS, Jr., T. KIMURA, and T. HIRAYAMA

Received August 8, 1979, from the *Division of Medicinal Chemistry, School of Pharmacy, University of North Carolina, Chapel Hill, NC 27514.* Accepted for publication October 16, 1979.

Abstract □ The major effect of eupaformosanin as an antineoplastic agent on Ehrlich ascites cell metabolism was to inhibit deoxyribonucleic acid synthesis, specifically at deoxyribonucleic acid polymerase and thymidylate synthetase enzymatic sites. Both pyrimidine and purine systems of Ehrlich ascites were marginally inhibited. Ribonucleic acid synthesis and messenger and ribosomal polymerase activities also were suppressed. Cyclic adenosine monophosphate levels were increased significantly, which correlated with the drastic reduction of histone phosphorylation. Eupaformosanin also suppressed a number of glycolytic and Krebs cycle enzymes as well as oxidative phosphorylation *in vitro*. All of the inhibited enzymes are known thiol-bearing enzymes that can undergo a Michael-type addition with the α-methylene-γ-lactone moiety of eupaformosanin, as shown with other sesquiterpene lactones.

Keyphrases □ Antitumor agents—eupaformosanin, effect on nucleic acid, protein, and anaerobic and aerobic glycolytic metabolism, Ehrlich ascites cells □ Eupaformosanin—antitumor activity, effect on nucleic acid, protein, and anaerobic and aerobic glycolytic metabolism, Ehrlich ascites cells □ Deoxyribonucleic acid synthesis, inhibitors—eupaformosanin, effect on nucleic acid, protein, and anaerobic and aerobic glycolytic metabolism, Ehrlich ascites cells

A new germacranolide, eupaformosanin (I), has been isolated from the whole plant of *Eupatorium formosanum*, and its stereochemistry and physical characteristics were reported previously (1). As an antineoplastic agent, eupaformosanin is a potent inhibitor of Walker 256 carcinosarcoma cell proliferation at 2.5 mg/kg/day (T/C = 471) and of P-388 lymphocytic leukemia cell proliferation at 25 mg/kg/day (T/C = 147) (2). The effects of eupaformosanin on nucleic acid, chromatin protein, purine, pyrimidine, and protein metabolism, anaerobic and aerobic glycolysis, and oxidative phosphorylation of Ehrlich ascites tumor cells are reported here.

EXPERIMENTAL

Male CF_1 mice, ~30 g, were implanted intraperitoneally on Day 0 with 10^6 Ehrlich ascites tumor cells from donor mice housed in these laboratories. Eupaformosanin suspended by homogenization in 0.05% polysorbate 80–water was administered intraperitoneally at 25 mg/kg/day for 8 days to determine the inhibition of tumor growth (3). For the metabolic studies, mice were treated on Days 7–9 with a subacute dose of 0.25 mg ip. Animals were sacrificed on Day 10, and the ascites fluid was collected from the peritoneal cavity. *In vitro* metabolic studies were determined on untreated, harvested, Day 10 Ehrlich ascites cells. The number of tumor cells per milliliter and the 0.4% trypan blue uptake were determined with a hemocytometer (4).

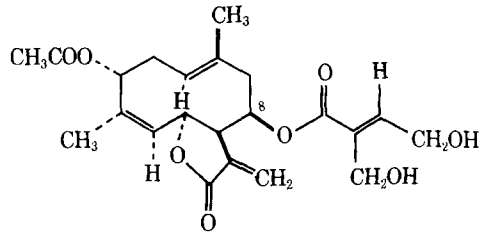

I

Incorporation of thymidine into deoxyribonucleic acid was determined by the method of Chae *et al.* (5). One hour prior to the animal sacrifice, 10 μCi of [^{14}C-*methyl*]-thymidine[1] (53.2 mCi/mmole) was injected intraperitoneally. The deoxyribonucleic acid was isolated, and the carbon-14 content was determined in two parts of toluene, one part of octoxynol, 0.4% 2,5-diphenyloxazole, and 0.01% 1,4-bis[2-(5-oxazolyl)]-benzene scintillation fluid and corrected for quenching. The deoxyribonucleic acid concentration was determined by UV spectrophotometry at 260 nm with calf thymus deoxyribonucleic acid as a standard.

Uridine incorporation into ribonucleic acid was determined in an analogous manner utilizing 10 μCi of 5-^{3}H-uridine (20.0 Ci/mmole). Ribonucleic acid was extracted by the method of Wilson *et al.* (6). Leucine incorporation into protein was determined by the method of Sartorelli (7) using 8 μCi of 1-^{14}C-leucine (54.4 mCi/mmole). The effect of eupaformosanin on 1-^{14}C-acetic acid (57.8 mCi/mmole) incorporation into cholesterol of Ehrlich ascites cells also was measured (8, 9).

Nuclear deoxyribonucleic acid polymerase activity was determined on isolated nuclei (10). The incubation medium was that of Sawada *et al.* (11), except that [^{3}H-*methyl*]-deoxyribothymidine-5′-triphosphate (53.1 mCi/mmole) was used and the insoluble nucleic acids were collected on glass fiber paper (GF/F) by vacuum suction. Deoxythymidine and deoxythymidylate monophosphate and diphosphate kinase activities were determined by the method of Maley and Ochoa (12), which is based on the disappearance of 0.1 μmole of reduced nicotinamide adenine dinucleotide at 340 nm.

Thymidine synthetase activity was assayed by the method of Kampf *et al.* (13) utilizing a postmitochondrial supernate (9000×*g* for 10 min) and 5 μCi of 5-^{3}H-deoxyuridine monophosphate (11 Ci/mmole). Mes-

[1] New England Nuclear was the source of all radioisotopes used in this study. Biochemical reagents were purchased from Sigma Chemical Co. and Calbiochem Co.

0022-3549/80/0300-0294$01.00/0
© 1980, American Pharmaceutical Association

(22) A. W. Adamson, "Physical Chemistry of Surfaces," 3rd ed., Wiley, New York, N.Y., 1976, p. 345.
(23) A. W. Neumann, *Z. Phys. Chem., Neue Folge*, **41**, 339 (1964).
(24) V. G. Stepanov, L. D. Volyak, and Y. V. Tarakov, *Zh. Fiz. Khim.*, **46**, 2397 (1972); through *Chem. Abstr.*, **77**, 169160c (1973).
(25) *Ibid.*, **49**, 2931 (1975); through *Chem. Abstr.*, **84**, 80161a (1976).
(26) W. J. Moore, "Physical Chemistry," 3rd ed., Prentice-Hall, Englewood Cliffs, N.J., 1963, p. 734.

ACKNOWLEDGMENTS

Supported by grants from Hoffmann-La Roche, Nutley, NJ 07110, and by Contract 223-76-3020 from the Food and Drug Administration.

Antitumor Agents XLI: Effects of Eupaformosanin on Nucleic Acid, Protein, and Anaerobic and Aerobic Glycolytic Metabolism of Ehrlich Ascites Cells

I. H. HALL ˣ, K. H. LEE, W. L. WILLIAMS, Jr., T. KIMURA, and T. HIRAYAMA

Received August 8, 1979, from the *Division of Medicinal Chemistry, School of Pharmacy, University of North Carolina, Chapel Hill, NC 27514.* Accepted for publication October 16, 1979.

Abstract □ The major effect of eupaformosanin as an antineoplastic agent on Ehrlich ascites cell metabolism was to inhibit deoxyribonucleic acid synthesis, specifically at deoxyribonucleic acid polymerase and thymidylate synthetase enzymatic sites. Both pyrimidine and purine systems of Ehrlich ascites were marginally inhibited. Ribonucleic acid synthesis and messenger and ribosomal polymerase activities also were suppressed. Cyclic adenosine monophosphate levels were increased significantly, which correlated with the drastic reduction of histone phosphorylation. Eupaformosanin also suppressed a number of glycolytic and Krebs cycle enzymes as well as oxidative phosphorylation *in vitro*. All of the inhibited enzymes are known thiol-bearing enzymes that can undergo a Michael-type addition with the α-methylene-γ-lactone moiety of eupaformosanin, as shown with other sesquiterpene lactones.

Keyphrases □ Antitumor agents—eupaformosanin, effect on nucleic acid, protein, and anaerobic and aerobic glycolytic metabolism, Ehrlich ascites cells □ Eupaformosanin—antitumor activity, effect on nucleic acid, protein, and anaerobic and aerobic glycolytic metabolism, Ehrlich ascites cells □ Deoxyribonucleic acid synthesis, inhibitors—eupaformosanin, effect on nucleic acid, protein, and anaerobic and aerobic glycolytic metabolism, Ehrlich ascites cells

A new germacranolide, eupaformosanin (I), has been isolated from the whole plant of *Eupatorium formosanum*, and its stereochemistry and physical characteristics were reported previously (1). As an antineoplastic agent, eupaformosanin is a potent inhibitor of Walker 256 carcinosarcoma cell proliferation at 2.5 mg/kg/day (T/C = 471) and of P-388 lymphocytic leukemia cell proliferation at 25 mg/kg/day (T/C = 147) (2). The effects of eupaformosanin on nucleic acid, chromatin protein, purine, pyrimidine, and protein metabolism, anaerobic and aerobic glycolysis, and oxidative phosphorylation of Ehrlich ascites tumor cells are reported here.

EXPERIMENTAL

Male CF_1 mice, ~30 g, were implanted intraperitoneally on Day 0 with 10^6 Ehrlich ascites tumor cells from donor mice housed in these laboratories. Eupaformosanin suspended by homogenization in 0.05% polysorbate 80–water was administered intraperitoneally at 25 mg/kg/day for 8 days to determine the inhibition of tumor growth (3). For the metabolic studies, mice were treated on Days 7–9 with a subacute dose of 0.25 mg ip. Animals were sacrificed on Day 10, and the ascites fluid was collected from the peritoneal cavity. *In vitro* metabolic studies were determined on untreated, harvested, Day 10 Ehrlich ascites cells. The number of tumor cells per milliliter and the 0.4% trypan blue uptake were determined with a hemocytometer (4).

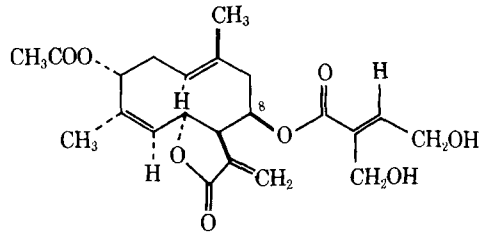

I

Incorporation of thymidine into deoxyribonucleic acid was determined by the method of Chae *et al.* (5). One hour prior to the animal sacrifice, 10 μCi of [^{14}C-*methyl*]-thymidine[1] (53.2 mCi/mmole) was injected intraperitoneally. The deoxyribonucleic acid was isolated, and the carbon-14 content was determined in two parts of toluene, one part of octoxynol, 0.4% 2,5-diphenyloxazole, and 0.01% 1,4-bis[2-(5-oxazolyl)]-benzene scintillation fluid and corrected for quenching. The deoxyribonucleic acid concentration was determined by UV spectrophotometry at 260 nm with calf thymus deoxyribonucleic acid as a standard.

Uridine incorporation into ribonucleic acid was determined in an analogous manner utilizing 10 μCi of 5-^{3}H-uridine (20.0 Ci/mmole). Ribonucleic acid was extracted by the method of Wilson *et al.* (6). Leucine incorporation into protein was determined by the method of Sartorelli (7) using 8 μCi of 1-^{14}C-leucine (54.4 mCi/mmole). The effect of eupaformosanin on 1-^{14}C-acetic acid (57.8 mCi/mmole) incorporation into cholesterol of Ehrlich ascites cells also was measured (8, 9).

Nuclear deoxyribonucleic acid polymerase activity was determined on isolated nuclei (10). The incubation medium was that of Sawada *et al.* (11), except that [^{3}H-*methyl*]-deoxyribothymidine-5′-triphosphate (53.1 mCi/mmole) was used and the insoluble nucleic acids were collected on glass fiber paper (GF/F) by vacuum suction. Deoxythymidine and deoxythymidylate monophosphate and diphosphate kinase activities were determined by the method of Maley and Ochoa (12), which is based on the disappearance of 0.1 μmole of reduced nicotinamide adenine dinucleotide at 340 nm.

Thymidine synthetase activity was assayed by the method of Kampf *et al.* (13) utilizing a postmitochondrial supernate (9000×*g* for 10 min) and 5 μCi of 5-^{3}H-deoxyuridine monophosphate (11 Ci/mmole). Mes-

[1] New England Nuclear was the source of all radioisotopes used in this study. Biochemical reagents were purchased from Sigma Chemical Co. and Calbiochem Co.

0022-3549/80/0300-0294$01.00/0
© 1980, American Pharmaceutical Association

senger, ribosomal, and hormone-sensitive ribonucleic acid polymerase activity were determined by the methods of Anderson *et al.* (14) and Hall *et al.* (15). Variation of ammonium sulfate concentrations was used to measure the respective type of ribonucleic acid polymerase. Insoluble ribonucleic acid was collected on nitrocellulose fiber paper by vacuum suction.

Phosphorylation of histones was determined by injecting intraperitoneally 10 μCi of γ-^{32}P-adenosine triphosphate (30.0 Ci/mmole) 1 hr prior to sacrifice. The nuclei were isolated (10), and the histone chromatin protein was extracted by the method of Raineri *et al.* (16). Nonhistone chromatin phosphorylation by nuclear protein kinase (17) was assayed utilizing 2 nmoles of γ-^{32}P-adenosine triphosphate (30.0 Ci/mmole). Chromatin protein was collected on nitrocellulose filter membranes. The effect of eupaformosanin on hydrolytic enzymes also was determined. Deoxyribonuclease activity was measured at pH 5.0 by a modification of the de Duve method (18). Ribonuclease activity and acid cathepsin activity were determined at pH 5.0 by the method of Cho-Chung and Gullino (19).

^{14}C-Formate incorporation into purine was measured by the method of Spassova *et al.* (20) using 0.5 μCi of ^{14}C-formic acid (4.95 mCi/mmole). Separation of purines was carried out on silica gel TLC plates eluted with *n*-butanol–acetic acid–water (4:1:5). The plates were scraped, and the radioactive content was determined. Phosphoribosyl–pyrophosphate amino transferase activity was determined by the method of Wyngaarden and Ashton (21), which is based on the reduction of 0.6 μmole of nicotinamide adenine dinucleotide at 340 nm. Carbamyl phosphate synthetase acitivity was determined with ornithine and ornithine transcarbamylase present by the method of Kalman *et al.* (22).

The colorimetric determination of citrulline was performed according to the method of Archibald (23). Aspartate carbamyl transferase activity was assessed by the method of Kalman *et al.* (22) in the presence of aspartate transcarbamylase. The colorimetric determination of carbamyl aspartate was carried out according to the method of Koritz and Cohen (24). Dihydrofolate reductase activity was determined by the procedure of Ho *et al.* (25), which is based on the disappearance of 0.1 μmole of reduced nicotinamide adenine dinucleotide phosphate at 340 nm. *S*-Adenosyl methionine transferase activity was determined by the method of Borchardt *et al.* (26) utilizing 0.05 μCi of [^{14}C-*methyl*]-*S*-adenosyl-L-methionine (53 mCi/mmole). Ribonucleotide reductase activity was determined by the method of Moore and Hurlbert (27) using 5-^{3}H-cytidine-5-diphosphate (26.1 Ci/mmole).

Cyclic-3′,5′-adenosine monophosphate levels were determined by the method of Gilman (28) using a ^{3}H(G)-adenosine-3′,5′-cyclic phosphate (39.8 Ci/mmole) radioimmunoassay.

UV binding studies (4) were conducted *in vitro* with eupaformosanin (85 μg/ml) with deoxyribonucleic acid or deoxyguanosine monophosphate (38 μg/ml) in 0.1 *M* phosphate buffer, pH 7.2, over a range of 200–340 nm for 24 hr at 22°.

The following *in vitro* glycolytic and Krebs cycle enzymatic activities were determined both for controls and in the presence of 1 μmole of eupaformosanin: hexokinase (29), phosphofructokinase (30), lactic dehydrogenase (31), glucose-6-phosphate dehydrogenase (32), glyceraldehyde-3-phosphate dehydrogenase (33), glucose-6-phosphatase (34), fructose-1,6-diphosphatase (35), malic dehydrogenase (36), succinic dehydrogenase (37), and adenosine phosphatase (38). *In vitro* effects of eupaformosanin on Ehrlich ascites tumor cell oxidative phosphorylation were measured in the presence and absence of adenosine diphosphate utilizing succinate, a flavin adenine dinucleotide-linked dehydrogenase, and α-ketoglutarate, a nicotinamide adenine dinucleotide-linked dehydrogenase (39). The inorganic phosphate was determined by the method of Chen *et al.* (40). The protein content for all assays was determined by the method of Lowry *et al.* (41).

Probable (*p*) significant differences were determined by the Student *t* test. Data are expressed in Tables I and II as percent of the control with standard deviations; *n* equals the number of animals per group.

RESULTS

Daily administration of eupaformosanin resulted in 97% inhibition of Ehrlich ascites tumor growth. The normal number of Ehrlich ascites cells per milliliter on Day 10 was 223 × 10^{6}. Eupaformosanin treatment at a subacute dose of 0.25 mg (12.5 mg/kg) on Days 7–9 reduced the cell count by 82%. Drug treatment resulted in no significant difference in the percentage of nonviable cells or in the size or general morphology of the cell as observed by light microscopy.

For the control animals, the thymidine incorporation into deoxyribonucleic acid was 241,675 dpm/mg of deoxyribonucleic acid. Drug treatment inhibited deoxyribonucleic acid synthesis by 76% (Table I). Uridine incorporation into ribonucleic acid for Day 10 Ehrlich ascites cells was 92,489 dpm/mg of ribonucleic acid. Eupaformosanin treatment reduced ribonucleic acid synthesis by an average of 23%. Leucine incorporation into protein for the control was 2484 dpm/mg of protein, which was not affected by drug treatment. Acetic acid incorporation into cholesterol for membrane synthesis for the control was 273,271 dpm/mg of protein. Drug treatment reduced cholesterol synthesis by 59%.

Table I—*In Vivo* Effects of Eupaformosanin on Nucleic Acid and Protein Metabolism of Ehrlich Ascites Tumor Cells (n = 6)

Parameter	Percent Control: Control (0.05% Polysorbate 80), $\bar{x} \pm SD$	Percent Control: Treated on Days 7–9 with 0.25 mg of Eupaformosanin, $\bar{x} \pm SD$
^{14}C-Thymidine incorporation into deoxyribonucleic acid	100 ± 22	24 ± 8[a]
^{3}H-Uridine incorporation into ribonucleic acid	100 ± 15	77 ± 17[b]
^{14}C-Leucine incorporation into protein	100 ± 19	102 ± 24
^{14}C-Acetic acid incorporation into cholesterol	100 ± 23	41 ± 13[a]
Number of tumor cells per milliliter of fluid	100 ± 14	18 ± 3[a]
Thymidine kinase	100 ± 2	102 ± 5
Thymidylate monophosphate kinase	100 ± 3	88 ± 4[a]
Thymidylate diphosphate kinase	100 ± 9	103 ± 7
Deoxyribonucleic acid polymerase	100 ± 8	58 ± 10[a]
Messenger ribonucleic acid polymerase	100 ± 15	69 ± 6[c]
Ribosomal ribonucleic acid polymerase	100 ± 10	73 ± 10[c]
Hormone-sensitive ribonucleic acid polymerase	100 ± 6	283 ± 7[a]
Thymidylate synthetase	100 ± 7	69 ± 4[a]
^{14}C-Formate incorporation into purines	100 ± 9	66 ± 8[a]
Phosphoribosyl–pyrophosphate amino transferase	100 ± 3	87 ± 2[a]
Carbamyl phosphate synthetase	100 ± 10	73 ± 9[c]
Aspartate carbamyl transferase	100 ± 11	77 ± 13[b]
Dihydrofolate reductase	100 ± 13	106 ± 7
S-Adenosyl-L-methionine transferase	100 ± 4	91 ± 3[c]
Ribonucleotide reductase	100 ± 5	89 ± 3[c]
Phosphorylation of histone proteins	100 ± 14	40 ± 6[a]
Phosphorylation of nonhistone proteins	100 ± 10	90 ± 9
Cyclic-3′,5′-adenosine monophosphate levels	100 ± 11	252 ± 49[a]
Deoxyribonuclease	100 ± 7	73 ± 7[a]
Ribonuclease activity	100 ± 9	97 ± 8
Cathepsin activity	100 ± 9	95 ± 10

[a] p = 0.001. [b] p = 0.025. [c] p = 0.005.

In vitro studies of the binding of eupaformosanin with deoxyribonucleic acid and deoxyguanosine monophosphate demonstrated that eupaformosanin possessed a maximum absorption peak at 230 nm. Combination with nucleic acids increased the absorption at 230 nm, indicating nonspecific binding. Untreated Day 10 Ehrlich ascites cells demonstrated a change in absorbance for thymidine kinase activity of 1.328 optical density units/hr/mg of protein. Thymidylate monophosphate kinase activity was 1.361 optical density units/hr/mg of protein, and thymidylate diphosphate kinase activity was 2.100 optical density units/hr/mg of protein. Eupaformosanin treatment had little effect on the kinase activities, with only a 12% reduction of thymidylate monophosphate kinase activity. Nuclear deoxyribonucleic acid polymerase activity, *i.e.*, alpha, beta, and gamma, for the control was 45,734 dpm/mg of nucleoprotein, which was reduced 42% by drug treatment.

^{14}C-Formate incorporation into purines for Day 10 Ehrlich ascites cells was 17,088 dpm/mg of protein, which was reduced 34% by drug therapy. Phosphoribosyl–pyrophosphate amino transferase activity for the control resulted in an absorption increase at 340 nm of 0.376 optical density unit/min/mg of protein based on 0.75 μmole of nicotinamide adenine dinucleotide, which was significantly reduced 13% by eupaformosanin. Dihydrofolate reductase activity for the control was 0.514 optical density unit/hr/mg of protein, which was unaffected by eupaformosanin treatment. *S*-Adenosyl-L-methionine transferase activity for the Day 10 Ehrlich ascites cells was 3268 dpm/mg of protein, which was suppressed 9% by drug treatment. Carbamyl phosphate synthetase activity for the control was 0.128 mg of carbamyl phosphate formed/hr/mg of protein,

Table II—*In Vitro* Effects of Eupaformosanin on Anaerobic and Aerobic Metabolism of Ehrlich Ascites Cells ($n = 6$)

Parameter	Percent Control: Control (0.05% Polysorbate 80), $\bar{x} \pm SD$	Percent Control: Treated on Days 7–9 with Eupaformosanin, $\bar{x} \pm SD$
Hexokinase activity	100 ± 4	85 ± 4[a]
Phosphofructokinase activity	100 ± 5	25 ± 9[a]
Lactic dehydrogenase activity	100 ± 9	43 ± 4[a]
Glucose-6-phosphate dehydrogenase activity	100 ± 16	3 ± 2[a]
Glyceraldehyde-3-phosphate dehydrogenase activity	100 ± 19	35 ± 4[a]
Glucose-6-phosphatase activity	100 ± 5	72 ± 12[a]
Fructose-1,6-diphosphatase activity	100 ± 9	59 ± 3[a]
Malic dehydrogenase activity	100 ± 4	26 ± 10[a]
Succinic dehydrogenase activity	100 ± 7	11 ± 6[a]
Adenosine triphosphatase activity	100 ± 16	96 ± 8
Oxidative phosphorylation processes		
Succinate: State 4	100 ± 3	69 ± 12[a]
Succinate: State 3	100 ± 4	69 ± 9[a]
α-Ketoglutarate: State 4	100 ± 5	52 ± 14[a]
α-Ketoglutarate: State 3	100 ± 11	53 ± 8[a]

[a] $p = 0.001$. [b] $p = 0.005$. [c] $p = 0.025$.

which was inhibited 27% by eupaformosanin treatment. Aspartate carbamyl transferase activity for the Day 10 Ehrlich ascites cells was 6.245 mg of carbamyl aspartate formed/hr/mg of protein, which was suppressed 23% by eupaformosanin.

Thymidylate synthetase activity for the control was 103,328 dpm/mg of protein, which was reduced 31% by drug treatment. Ribonucleotide reductase activity for the control was 155,065 dpm/mg of protein, which eupaformosanin reduced by 11%. Messenger ribonucleic acid polymerase activity for the control was 6434 dpm/mg of protein, ribosomal ribonucleic acid polymerase activity was 7340 dpm/mg of protein, and hormone-sensitive polymerase activity was 8254 dpm/mg of protein. Eupaformosanin reduced messenger activity by 31% and ribosomal activity by 27% and elevated hormone-sensitive polymerase activity by 183%. The cyclic adenosine monophosphate level for the control was 3.65 pmoles/10^6 cells, whereas the level rose by 152% after drug treatment. Histone phosphorylation of chromatin protein was at a rate of 2954 dpm/mg of chromatin protein, which was reduced 60% by eupaformosanin treatment. Nonhistone phosphorylation of chromatin protein was at a rate of 9803 dpm/mg of chromatin protein, which was inhibited 10% by drug treatment.

The catabolic rate of nucleic acids and proteins also was determined to eliminate the possibility that the drug accelerated hydrolytic enzymatic activity and thus indirectly lowered the incorporation of precursors into nucleic acids and proteins. Deoxyribonuclease activity for Day 10 Ehrlich ascites cells was 247 μg of deoxyribonucleic acid hydrolyzed/hr/mg of protein, which was inhibited 27% by eupaformosanin treatment. Ribonuclease activity for the control tumor cells was 43 μg of ribonucleic acid hydrolyzed/hr/mg of protein, which was unaffected by eupaformosanin. Cathepsin activity for the control was 869 μg of protein hydrolyzed/hr/mg of protein, which was unchanged by drug therapy.

Hexokinase activity for the control Ehrlich ascites tumor cells was calculated as a change in absorbance equal to 0.195 optical density unit/min/mg of protein based on 500 μmoles of nicotinamide adenine dinucleotide phosphate, which was suppressed 15% by 1 μmole of eupaformosanin *in vitro* (Table II). Phosphofructokinase activity for the control was a change of 0.176 optical density unit/min/mg of protein based on 1.125 μmoles of reduced nicotinamide adenine dinucleotide, which was reduced 75% by eupaformosanin presence. Lactic dehydrogenase activity resulted in an optical density unit change of 0.623/min/mg of protein based on 0.12 μmole of reduced nicotinamide adenine dinucleotide, which eupaformosanin reduced by 57%. Glyceraldehyde dehydrogenase activity for the control was 2.623 optical density units/min/mg of protein based on 20.3 μmoles of nicotinamide adenine dinucleotide, which was suppressed 65% by the drug.

Glucose-6-phosphate dehydrogenase activity for the control was 0.284 optical density unit/min/mg of protein based on the presence of 0.0056 μmole of nicotinamide adenine dinucleotide phosphate. Eupaformosanin inhibited this dehydrogenase activity by 97%. Glucose-6-phosphatase activity for the control was 20.15 μg of phosphorus released/hr/mg of protein, which was suppressed 28% by the drug treatment. Fructose-1,6-diphosphatase activity for the control was 24.87 μg of phosphorus released/hr/mg of protein, which was reduced 41% by eupaformosanin. Malic dehydrogenase activity for Day 10 Ehrlich ascites cells was 0.80 optical density unit/min/mg of protein, which was reduced 74% by the drug. Succinic dehydrogenase activity for the control was 0.069 optical density unit/min/mg of protein based on 15 μmoles of potassium ferricyanide, which eupaformosanin suppressed by 89%. Adenosine triphosphatase activity measured as inorganic phosphate released for the control was 17.02 μg of phosphorus hydrolyzed/hr/mg of protein. The presence of eupaformosanin resulted in no change in enzymatic activity.

The basal respiration (state 4) of Day 10 Ehrlich ascites tumor cells with succinate as the substrate was 5.273 μl of oxygen consumed/hr/mg of protein. In the presence of adenosine diphosphate (state 3), stimulated respiration on coupled oxidative phosphorylation was 8.725 μl of oxygen consumed/hr/mg of protein. Eupaformosanin inhibited state 4 and state 3 respiration by 31%. Use of α-ketoglutarate as a substrate resulted in a state 4 respiration of 3.569 μl of oxygen consumed/hr/mg of protein and in a state 3 respiration of 5.156 μl of oxygen consumed/hr/mg of protein. Eupaformosanin inhibited state 4 respiration by 48% and state 3 respiration by 47%.

DISCUSSION

Eupaformosanin administration significantly lowered deoxyribonucleic acid and cholesterol synthesis, whereas ribonucleic acid synthesis was only moderately inhibited in Day 10 Ehrlich ascites cells. One possible explanation of the reduction of radiolabeled precursor into these macromolecules is that drug treatment accelerated catabolism of macromolecules. However, treatment with eupaformosanin did not accelerate hydrolytic enzymatic activity responsible for the catabolism of these macromolecules; rather, the drug moderately reduced deoxyribonuclease activity and had no effect on ribonucleic and cathepsin activities at pH 5.0.

The major site of eupaformosanin inhibition of deoxyribonucleic acid synthesis was on the deoxyribonucleic acid polymerase nuclei enzymes, whereas thymidylate synthetase activity appeared to be reduced moderately. Purine synthesis also was inhibited, but the major site did not appear to be at the regulatory enzyme of the cycle, *i.e.*, phosphoribosylpyrophosphate amino transferase, which was only slightly inhibited. Pyrimidine synthesis was moderately inhibited at the carbamyl phosphate synthetase and aspartate carbamyl transfer steps. *S*-Adenosyl-L-methionine transferase and ribonucleotide reductase activity also were slightly inhibited.

It was demonstrated previously that compounds containing the O=CC=CH_2 system can undergo a rapid Michael-type addition with biological nucleophiles, *e.g.*, sulfhydryl groups (4). Both α- and γ-deoxyribonucleic acid polymerase of the nucleus (42), thymidylate synthetase (43), aspartate carbamyl transferase (44), and ribonucleotide reductase (44) possess exposed sulfhydryl groups which can be alkylated. Contained in the structure of eupaformosanin is the O=CC=CH_2 system both as an α-methylene-γ-lactone and within the C-8 ester side chain. The α-methylene-γ-lactone moiety undergoes a rapid Michael-type addition with L-cysteine and reduced glutathione (4, 45). A similar phenomenon occurs with the sesquiterpene lactones helenalin and tenulin (4, 45) and the germacranolide eupahyssopin (46).

Cellular proliferation is regulated by phosphorylation of chromatin histones, *e.g.*, the F-1 fraction by protein kinase (47). This effect occurs predominantly during G_1 and early S of the cell cycle, when cyclic adenosine monophosphate levels are decreasing and enzymes are synthesized for nucleic acid replication. Eupaformosanin treatment significantly inhibited phosphorylation of histone chromatin protein and increased the intracellular level of cyclic adenosine monophosphate levels in Day 10 Ehrlich ascites cells. The latter effect is associated with reversal of tumor morphology (48), reduced cellular proliferation, and enhanced cellular differentiation (49, 50).

The UV spectral studies suggest that eupaformosanin interacts with deoxyribonucleic acid. The fact that messenger ribonucleotide polymerase activity also was suppressed by drug treatment may indicate that the transcription processes utilizing deoxyribonucleic acid as a template were impaired. The inhibition of purine and pyrimidine nucleotide synthesis is not the reason why messenger and ribosomal ribonucleic acid polymerase activities are inhibited since triphosphate ribonucleotides were added to the medium. Hormone-sensitive ribonucleotide polymerase may be elevated due to the elevated level of cyclic adenosine monophosphate, a modulator of this polymerase (15).

Compounds containing the α-methylene-γ-lactone moiety inhibit

enzymes of the Embden–Meyerhof and Krebs cycles (35, 51–53). Eupaformosanin inhibited phosphofructokinase and lactic acid dehydrogenase significantly and hexokinase marginally *in vitro*. These enzymes contain sulfhydryl groups (35, 51–53) that can be alkylated by the O=CC=CH_2 moiety. Enzymes involved in reversed glycolysis, *e.g.*, glucose-6-phosphatase and fructose-1,6-diphosphatase, were inhibited significantly by eupaformosanin, as was observed previously with other germacranolides (46) and pseudoguaianolides (35). The regulatory enzyme of the hexose monophosphate shunt, glucose-6-phosphate dehydrogenase, was reduced drastically by eupaformosanin. Succinic and malic dehydrogenase activities were suppressed significantly *in vitro*. Dehydrogenases of the Krebs cycle contain sulfhydryl groups in the enzymes and iron inorganic sulfide flavin proteins as integral components of the dehydrogenase enzymes (54). Theoretically, this group also can be alkylated.

Eupaformosanin suppressed basal respiration and coupled oxidative phosphorylation or mitochondrial adenosine triphosphate synthesis *in vitro*, and this suppression was not due to an accelerated adenosine triphosphatase activity brought about by the presence of the drug. The drug inhibited respiration with α-ketoglutarate, a nicotinamide adenine dinucleotide-linked dehydrogenase that contains an iron–sulfur center (55) more than with succinate, which is a flavin adenine dinucleotide-linked enzyme. Numerous antitumor agents inhibit respiration and oxidative phosphorylation of Ehrlich ascites cells (56) including other sesquiterpene lactones (2).

REFERENCES

(1) K. H. Lee, T. Kimura, M. Haruna, A. T. McPhail, K. D. Onan, and H. C. Huang, *Phytochemistry*, **16**, 1068 (1977).

(2) I. H. Hall, K. H. Lee, C. O. Starnes, S. A. ElGebaly, T. Ibuka, Y. S. Wu, T. Kimura, and M. Haruna, *J. Pharm. Sci.*, **67**, 1235 (1978).

(3) C. Piantadosi, C. S. Kim, and J. L. Irvin, *ibid.*, **58**, 821 (1969).

(4) I. H. Hall, K. H. Lee, E. C. Mar, and C. O. Starnes, *J. Med. Chem.*, **20**, 333 (1977).

(5) C. B. Chae, J. L. Irvin, and C. Piantadosi, *Proc. Am. Assoc. Cancer Res.*, **9**, 44 (1968).

(6) R. G. Wilson, R. H. Bodner, and G. E. MacHorter, *Biochim. Biophys. Acta*, **378**, (1975).

(7) A. C. Sartorelli, *Biochem. Biophys. Res. Commun.*, **27**, 26 (1967).

(8) G. T. Haven, J. R. Krzemien, and T. T. Nquyea, *Res. Commun. Chem. Pathol. Pharmacol.*, **6**, 253 (1973).

(9) F. Wada, K. Hirata, and Y. Sakamoto, *J. Biol. Chem.*, **65**, 171 (1969).

(10) W. C. Hymer and E. L. Kuff, *J. Histochem. Cytochem.*, **12**, 359 (1964).

(11) H. Sawada, K. Tatsumi, M. Sasada, S. Shirakawa, T. Nakumuna, and G. Wakisaka, *Cancer Res.*, **34**, 3341 (1974).

(12) F. Maley and S. Ochoa, *J. Biol. Chem.*, **233**, 1538 (1958).

(13) A. Kampf, R. L. Barfknecht, P. J. Schoffer, S. Osaki, and M. P. Mertes, *J. Med. Chem.*, **19**, 903 (1976).

(14) K. M. Anderson, I. S. Mendelson, and G. Guzik, *Biochim. Biophys. Acta*, **383**, 56 (1975).

(15) I. H. Hall, G. L. Carlson, G. S. Abernethy, and C. Piantadosi, *J. Med. Chem.*, **17**, 1253 (1974).

(16) A. Raineri, R. C. Simsiman, and R. K. Boutwell, *Cancer Res.*, **33**, 134 (1973).

(17) Y. M. Kish and L. J. Kleinsmith, *Methods Enzymol.*, **40**, 201 (1975).

(18) I. H. Hall, K. S. Ishaq, and C. Piantadosi, *J. Pharm. Sci.*, **63**, 625 (1974).

(19) Y. S. Cho-Chung and P. M. Gullino, *J. Biol. Chem.*, **248**, 4743 (1973).

(20) M. K. Spassova, G. C. Russev, and E. V. Golovinsky, *Biochem. Pharmacol.*, **25**, 923 (1976).

(21) J. B. Wyngaarden and D. M. Ashton, *J. Biol. Chem.*, **234**, 1492 (1959).

(22) S. M. Kalman, P. H. Duffield, and T. Brzozouski, *Am. Biol. Chem.*, **24**, 1871 (1966).

(23) R. M. Archibald, *J. Biol. Chem.*, **156**, 121 (1944).

(24) S. B. Koritz and P. P. Cohen, *ibid.*, **209**, 145 (1954).

(25) M. K. Ho, T. Hakalo, and S. F. Zakrzwski, *Cancer Res.*, **32**, 1023 (1972).

(26) R. T. Borchardt, J. A. Huber, and Y. S. Wu, *J. Med. Chem.*, **19**, 1094 (1976).

(27) E. G. Moore and R. B. Hurlbert, *J. Biol. Chem.*, **241**, 4802 (1966).

(28) A. C. Gilman, *Proc. Natl. Acad. Sci., USA*, **67**, 305 (1970).

(29) D. G. Walker and J. J. Parry, *Methods Enzymol.*, **9**, 381 (1966).

(30) T. E. Mansour, *ibid.*, **9**, 430 (1966).

(31) M. K. Schwartz and O. Bodansky, *ibid.*, **9**, 294 (1966).

(32) P. Cohen and M. A. Rosemeyer, *Eur. J. Biochem.*, **8**, 1 (1969).

(33) W. S. Allison, *Methods Enzymol.*, **9**, 210 (1967).

(34) M. A. Swanson, *J. Biol. Chem.*, **184**, 647 (1950).

(35) I. H. Hall, K. H. Lee, and S. A. ElGebaly, *J. Pharm. Sci.*, **67**, 552 (1978).

(36) S. Ochoa, A. H. Mehler, and A. Kornberg, *J. Biol. Chem.*, **174**, 979 (1948).

(37) D. V. DerVartanian and C. Veerger, *Biochim. Biophys. Acta*, **92**, 233 (1964).

(38) E. M. Suolinna, R. N. Buchsbaum, and E. Racker, *Cancer Res.*, **35**, 1865 (1975).

(39) I. H. Hall, K. H. Lee, C. O. Starnes, S. A. ElGebaly, T. Ibuka, Y. S. Wu, T. Kimura, and M. Haruna, *J. Pharm. Sci.*, **67**, 1235 (1978).

(40) P. S. Chen, T. Y. Toribara, and H. Warner, *Anal. Chem.*, **28**, 1756 (1956).

(41) O. H. Lowry, N. J. Rosebrough, A. L. Farr, and R. J. Randall, *J. Biol. Chem.*, **193**, 265 (1951).

(42) L. A. Loeb, in "The Enzymes," 3rd ed., P. D. Boyer, Ed., Academic, New York, N.Y., 1974, p. 1973.

(43) M. Friedkin, *Adv. Enzymol.*, **38**, 235 (1973).

(44) A. White, P. Handler, E. L. Smith, R. L. Hill, and I. R. Lehman, "Principles of Biochemistry," McGraw-Hill, New York, N.Y., 1978, pp. 225, 386–389, 769.

(45) K. H. Lee, I. H. Hall, E. C. Mar, C. O. Starnes, S. A. ElGebaly, T. G. Waddell, R. I. Hadgnaft, C. G. Ruffner, and I. Weidner, *Science*, **196**, 533 (1977).

(46) I. H. Hall, K. H. Lee, and S. A. ElGebaly, *J. Pharm. Sci.*, **67**, 1232 (1978).

(47) C. S. Rubin and O. M. Roseu, *Ann. Rev. Biochem.*, **44**, 81 (1975).

(48) V. Stefanovich, *Res. Commun. Chem. Pathol. Pharmacol.*, **7**, 573 (1974).

(49) T. Posternak, *Annu. Rev. Pharmacol.*, **14**, 23 (1974).

(50) Y. S. Cho-Chung and P. M. Gullino, *Science*, **183**, 87 (1974).

(51) S. M. Kupchan, D. C. Fessler, M. A. Eakin, and T. J. Giacobbe, *Science*, **168**, 376 (1970).

(52) R. L. Hanson, H. A. Lardy, and S. M. Kupchan, *ibid.*, **168**, 378 (1970).

(53) C. H. Smith, J. Larner, A. M. Thomas, and S. M. Kupchan, *Biochim. Biophys. Acta*, **276**, 94 (1972).

(54) L. Stryer, "Biochemistry," Freeman, San Francisco, Calif., 1975, p. 32.

(55) E. Racker, *Am. Sci.*, **60**, 56 (1972).

(56) M. Gosalvez, R. Garcia-Canero, M. Blanco, and C. Gurmcharri-Lloyd, *Can. Chemother. Rep.*, **60**, 1 (1976).

ACKNOWLEDGMENTS

Supported by University of North Carolina Research Council Grant VF 785 awarded to I. H. Hall; American Cancer Society Grants CH-19A, CH-19B, and CH-19C; and National Institutes of Health Grant CA-17625 awarded to K. H. Lee.

Model-Independent Method of Analyzing Input in Linear Pharmacokinetic Systems Having Polyexponential Impulse Response I: Theoretical Analysis

PETER VENG PEDERSEN

Received September 22, 1978, from the *Department of Pharmacy, School of Pharmacy, University of California, San Francisco, CA 94143.* Accepted for publication October 11, 1979.

Abstract □ A rigorous treatment of linear compartmental systems is presented, which allows the input rate of drugs into the systemic circulation to be evaluated without assuming a specific kinetic model. The method allows the input to be evaluated in the presence or absence of any combination of intravenous bolus input and infusion input. Only data for the blood drug concentration are required; there are no requirements for specific sampling times. Applications of the equations are given in several examples. The input rate is evaluated with data obtained from a disposition experiment involving an intravenous bolus or zero-order infusion input and an experiment involving the input to be evaluated. The two experiments can be merged so that the input can be evaluated without a washout period between the two drug administrations. The equations also enable model-independent calculations of the optimal drug input control that produces any desirable drug concentration profile. The approach is a useful deconvolution method for any linear pharmacokinetic system where the impulse response can be approximated by a polyexponential expression.

Keyphrases □ Pharmacokinetic models, linear—model-independent method of input analysis, derivation of equations for linear compartmental systems, blood drug levels, polyexponential impulse response □ Blood drug levels—model-independent method of input analysis, linear pharmacokinetic model □ Models, pharmacokinetic—derivation of equations for linear compartmental systems, model-independent method of input analysis

The study of drug input plays such a fundamental role in biopharmaceutics that it has been suggested that biopharmaceutics be defined as the science of drug input (1). Numerous methods of evaluating the pharmacokinetics of drug input have been suggested (2–14), and they can be divided into model-dependent and model-independent methods.

The model-dependent methods assume a specific model for drug input (*e.g.*, first-order or zero-order input) and a specific model for drug disposition (*e.g.*, one- or multiple-compartment models). The blood profile of the drug is analyzed according to the model equation and the specific input parameter(s) that are determined graphically or by a regression technique (15). These methods often do not give a reliable estimate of the input kinetics because they are defined too specifically with respect to drug disposition and because the input is considered to be a simple process that can be described in simple mathematical terms (*e.g.*, zero- and first-order input).

With the many variables affecting the input, particularly in oral administration, it seems unlikely that the input can be approximated well in such simple terms. Nevertheless, it is not uncommon to have good agreement between such model equations and drug level data, as judged by goodness-of-fit when the equations are fitted to the data. However, the good fit may be explained by an inherent flexibility of the equations used. The equations are derived based on a model for the input and a model for the drug disposition. If the input model is wrong, the flexibility of the equation used may compensate for this error in that the disposition parameters in the iterative curve-fitting procedure take values that do not reflect the disposition but provide a good fit. Therefore, it is not uncommon when using model-dependent methods to obtain parameter values of unrealistic magnitude, even when the curve fitting is satisfactory.

Certain methods partly eliminate this problem by combining information about the drug's disposition, obtained from separate intravenous bolus or infusion data, with data resulting from the input to be evaluated. Among these methods are the deconvolution methods (9–14), which have the additional advantage of not assuming a model for the input.

This paper presents a novel method of input analysis; it is applicable to systems with central input and to certain systems with noncentral input. The method is model independent in that it does not assume any specific disposition model. The method enables an unknown input to be evaluated quantitatively in the presence or absence of any combination of intravenous bolus and infusion input. The method requires only blood drug level data with no special requirements for sampling times.

BACKGROUND

Drug input in a subject is studied most accurately by following the blood concentration–time profile. The aim of this theoretical analysis is to derive a suitable method for analyzing blood profiles to quantitate an unknown input.

The total input in the sampleable compartment is the sum of two kinds of input: the primary and the secondary. The primary input is the input into the sampleable compartment of those drug molecules that arrive there for the first time. The secondary input is the input into the sampleable compartment of those drug molecules that previously have been present there. The primary input, the object of this analysis, is of interest for bioavailability studies and for the evaluation of drug delivery systems. The secondary input encompasses ordinary back-transfer from reversible distributions between the sampleable compartment and other compartments, as well as previously presented cyclic processes (recycling) (16).

The present method uses two fundamental properties of linear response systems: the superposition property and the convolution integral property. These properties can be verified only for a known input, *i.e.*, an input made directly into the sampleable compartment. However, the primary input to be evaluated is not a direct input, so it is necessary to assume or verify that the primary input is noninteracting. It must not change the basic linear response property of the system that is evaluated from a direct input but is used to calculate an indirect input.

This requirement is basic for any model-independent and most model-dependent approaches. Its importance cannot be emphasized enough since several factors in the first-pass transfer of a drug may cause a significant interaction. Little attention has been given to this issue. The justification of linear pharmacokinetic principles in drug absorption studies often has been limited to verification of the superposition property. However, it is equally important to test for interaction, *e.g.*, by comparing the concentration profiles of a labeled drug introduced directly into the sampleable compartment in the absence and in the presence of absorption of the unlabeled drug.

0022-3549/80/0300-0298$01.00/0
© 1980, American Pharmaceutical Association

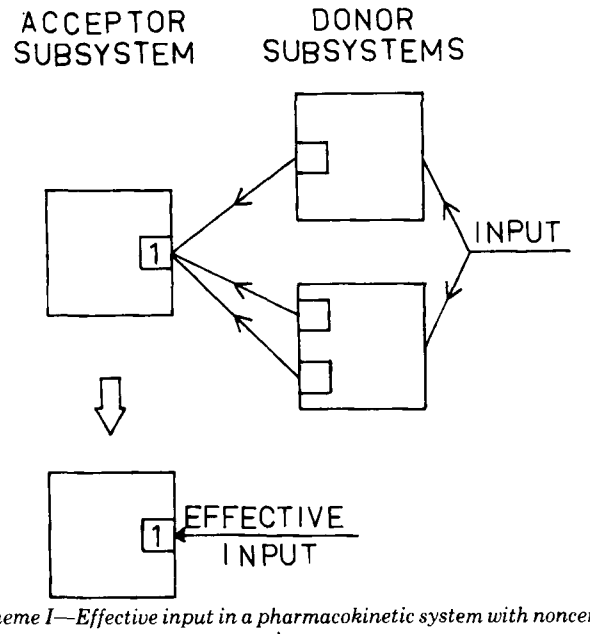

Scheme I—Effective input in a pharmacokinetic system with noncentral input

In the context of the classical linear compartmental systems discussed previously (16), a noninteracting input is either a direct input or an input reaching the sampleable compartment from one or more irreversibly connected donor subsystems (Scheme I).

The following theoretical analysis shows how a noninteracting primary input (subsequently to be referred to as the input) can be rigorously evaluated (blood = sampleable compartment) when blood level data from a known input such as an intravenous bolus or zero-order infusion input are available. The input may be of any linear or nonlinear kinetic form. Although the analysis forms a link to classical linear compartmental pharmacokinetics (16), it is not limited to such systems. The analysis applies to any linear response system where the unit impulse response is appropriately approximated by a polyexponential function with real and/or complex (conjugate) time coefficients.

In the context of compartmental principles (16), the method allows the kinetic processes in irreversibly connected donor subsystems to be of any nonlinear form. In the context of general linear system theory, the method allows individual kinetic processes to be of nonlinear form as long as the total effect of all of the processes results in an approximately linear input–response relationship.

THEORY

In a general treatment of linear compartmental pharmacokinetics, the following matrix–vector equation was presented (16):

$$\mathbf{x} = L^{-1}(\mathbf{Dv}) \qquad \text{(Eq. 1)}$$

where x_i, the ith component of the vector $\mathbf{x}$, is the amount in the ith compartment at time t; and v_i, the ith component of the input vector $\mathbf{v}$, is the sum of the initial amount in the ith compartment and the Laplace transform of the external input rate (*i.e.*, not coming from other compartments) into the ith compartment.

The disposition is defined uniquely by the disposition matrix, **D**. The operator L^{-1} denotes the inverse Laplace transform operator. In the case of central input only, the amount in the central compartment is given by:

$$x_1 = L^{-1}(d_{11}v_1) \qquad \text{(Eq. 2)}$$

where d_{11} is the 1,1 element of the disposition matrix. When a generalized function approach is used in the mathematical analysis, continuous and discontinuous input can be superimposed so that the central input, $v_1(t)$, is written as:

$$v_1(t) = f(t) + f_{bol}(t) + f_{inf}(t) \qquad \text{(Eq. 3)}$$

where $f(t)$ is the unknown input rate to be determined and $f_{bol}(t)$ and $f_{inf}(t)$ are the known bolus input rate and the infusion input rate, respectively. It is most accurate to determine $f(t)$ in the absence of other input. However, this may not always be possible. The following treatment enables $f(t)$ to be determined in the presence or absence of bolus and infusion input.

The bolus input component of Eq. 3 is described in terms of the unit impulse function or Dirac delta function, $\delta(t)$, by:

$$f_{bol}(t) = \sum_{i=1}^{R} q_i\delta(t - \tau_i) \qquad R = 1,2,..,N \qquad \text{(Eq. 4)}$$

where q_i is the quantity of the ith intravenous bolus, τ_i is the time for the ith bolus injection, R is the highest integer for which $\tau_R < t$ is satisfied, and N is the number of bolus inputs. If $\tau_R < t$ cannot be satisfied for any R, then R is defined as zero. Therefore, the right side of Eq. 4 becomes zero by definition. The Laplace transform (bars denote transformed functions) of Eq. 3 is:

$$\bar{v}_1(s) = \bar{f}(s) + \sum_{i=1}^{N} q_i e^{-\tau_i s} + \bar{f}_{inf}(s) \qquad \text{(Eq. 5)}$$

so that Eq. 2 can be written as:

$$c(t) = V^{-1}L^{-1}\left[d_{11}\bar{f}(s) + d_{11}\sum_{i=1}^{N} q_i e^{-\tau_i s} + d_{11}\bar{f}_{inf}(s)\right] \qquad \text{(Eq. 6)}$$

where the conversion from the amount, x_1, to the concentration, $c(t)$, has been done by the central volume term, V. The concentration profile following a single initial intravenous bolus input is:

$$c^*(t) = V^{-1}L^{-1}(d_{11}q^*) \qquad \text{(Eq. 7)}$$

where * distinguishes between the separate intravenous bolus experiment and the input experiment in further derivations. The transforms of Eqs. 6 and 7 are, respectively:

$$\bar{c}(s) = V^{-1}\left[d_{11}\bar{f}(s) + d_{11}\sum_{i=1}^{N} q_i e^{-\tau_i s} + d_{11}\bar{f}_{inf}(s)\right] \qquad \text{(Eq. 8)}$$

$$\bar{c}^*(s) = V^{-1}d_{11}q^* \qquad \text{(Eq. 9)}$$

When $d_{11} = V\bar{c}^*(s)/q^*$ from Eq. 9 is substituted into Eq. 8, Eq. 8 becomes:

$$\bar{c}(s) = \frac{1}{q^*}\left[\bar{c}^*(s)\bar{f}(s) + \bar{c}^*(s)\sum_{i=1}^{N} q_i e^{-\tau_i s} + \bar{c}^*(s)\bar{f}_{inf}(s)\right] \qquad \text{(Eq. 10)}$$

Therefore, the transform of the input rate can be written as:

$$\bar{f}(s) = \frac{\bar{g}(s)}{\bar{c}^*(s)} \qquad \text{(Eq. 11)}$$

where:

$$\bar{g}(s) = q^*\bar{c}(s) - \bar{c}^*(s)\sum_{i=1}^{N} q_i e^{-\tau_i s} - \bar{c}^*(s)\bar{f}_{inf}(s) \qquad \text{(Eq. 12)}$$

To facilitate a suitable solution of Eq. 11, it can be written as:

$$\bar{f}(s) = s\{[s\bar{g}(s)]\bar{h}(s)\} \qquad \text{(Eq. 13)}$$

where:

$$\bar{h}(s) = s^{-2}\bar{c}^*(s)^{-1} \qquad \text{(Eq. 14)}$$

Since $vg(0) = 0$, it follows that:

$$L^{-1}[s\bar{g}(s)] = g'(t) \qquad \text{(Eq. 15)}$$

It will be shown later that $c^*(t)$ has a functional form such that $L^{-1}[s^{-2}\bar{c}^*(s)^{-1}]$ exists. Thus, according to the convolution theorem, Eq. 13 can be transformed to:

$$f(t) = \frac{d}{dt}\int_0^t g'(u)h(t - u)du \qquad \text{(Eq. 16)}$$

According to the Leibnitz rule, Eq. 16 can be written as:

$$f(t) = \int_0^t g'(u)h'(t - u)du + g'(t)h(0) \qquad \text{(Eq. 17)}$$

Integrating by parts and noting that $g(0) = 0$, Eq. 17 becomes:

$$f(t) = h'(0)g(t) + h(0)g'(t) + \int_0^t g(u)h''(t - u)du \qquad \text{(Eq. 18)}$$

Equation 18 forms the basis for further deviations, leading to a final, more specific expression for the input, $f(t)$. The following sections deal with

the problem of deriving specific expressions for $h(0)$, $h'(0)$, $g(0)$, $g'(t)$, and $h''(t)$ in Eq. 18.

If the system has distinct eigenvalues, then the impulse response is given by:

$$c^*(t) = \sum_{i=1}^{n} a_i e^{\lambda_i t} \qquad \text{(Eq. 19)}$$

so that:

$$\bar{c}^*(s) = \sum_{i=1}^{n} \frac{a_i}{s - \lambda_i} \qquad \text{(Eq. 20)}$$

The relationship between the macroparameters in Eq. 19, the coefficient matrix, and the fundamental matrix of the compartmental system is given in the *Appendix*.

According to Eq. 20, Eq. 14 can be written as:

$$\bar{h}(s) = s^{-2}\left[\sum_{i=1}^{n} \frac{a_i}{s - \lambda_i}\right]^{-1} \qquad \text{(Eq. 21)}$$

so that, according to the initial value theorem and L'Hôspital's rule, $h(0)$ in Eq. 18 is:

$$h(0) = \lim_{s \to \infty} s\bar{h}(s) = \left[\sum_{i=1}^{n} a_i\right]^{-1} \qquad \text{(Eq. 22)}$$

Similarly, it can be shown that:

$$h'(0) = \lim_{s \to \infty} s\bar{h'}(s) = \lim_{s \to \infty} [s^2 h(s) - sh(0)] = -\frac{\sum_{i=1}^{n} a_i \lambda_i}{\left[\sum_{i=1}^{n} a_i\right]^2} \qquad \text{(Eq. 23)}$$

The $h(t)$ function can be written, according to Eq. 21, as:

$$h(t) = L^{-1} \frac{\prod_{i=1}^{n} (s - \lambda_i)}{s^2 \sum_{i=1}^{n} a_i \prod_{\substack{j=1 \\ \neq i}}^{n} (s - \lambda_j)} \qquad \text{(Eq. 24)}$$

where the numerator and denominator are polynomials of nth and $(n + 1)$th degree, respectively. Therefore, according to Heaviside's expansion theorem, Eq. 24 can be written as:

$$h(t) = A_1 t + A_2 + \sum_{i=1}^{n-1} E_i e^{\beta_i t} \qquad \text{(Eq. 25)}$$

where A_1 and A_2 are functions of $\{a_i, \lambda_i\}_1^n$ only and the $\{\beta_i\}_1^{n-1}$ are the roots of the $(n - 1)$th degree polynomial:

$$Q(s) = \sum_{i=1}^{n} a_i \prod_{\substack{j=1 \\ \neq i}}^{n} (s - \lambda_j) \qquad \text{(Eq. 26)}$$

The $\{E_i\}_1^{n-1}$ terms in Eq. 25 are given by:

$$E_\nu = \left.\frac{\prod_{i=1}^{n} (s - \lambda_i)}{\frac{d}{ds}\left[s^2 \sum_{i=1}^{n} a_i \prod_{\substack{j=1 \\ \neq i}}^{n} (s - \lambda_j)\right]}\right|_{s = \beta_\nu} \qquad \text{(Eq. 27)}$$

which leads to:

$$E_\nu = \frac{\prod_{i=1}^{n} (\beta_\nu - \lambda_i)}{2\beta_\nu \sum_{i=1}^{n} a_i \prod_{\substack{j=1 \\ \neq i}}^{n} (\beta_\nu - \lambda_j) + \beta_\nu^2 \sum_{i=1}^{n} a_i \sum_{\substack{j=1 \\ \neq i}}^{n} \prod_{\substack{m=1 \\ \neq i \text{and} j}}^{n} (\beta_\nu - \lambda_m)} \qquad \text{(Eq. 28)}$$

The first term in the denominator of Eq. 28 is equal to zero, according to the property of β_ν since $Q(\beta_\nu) = 0$ (Eq. 26). Therefore, after further simplification, Eq. 28 can be written as:

$$E_\nu = \left[\beta_\nu^2 \sum_{i=1}^{n} \frac{a_i}{\beta_\nu - \lambda_i} \sum_{\substack{j=1 \\ \neq i}}^{n} \frac{1}{\beta_\nu - \lambda_j}\right]^{-1} \qquad \text{(Eq. 29)}$$

For further simplification in later derivations, it is convenient to introduce $b_\nu = \beta_\nu^2 E_\nu$ so that:

$$b_\nu = \left[\sum_{i=1}^{n} \frac{a_i}{\beta_\nu - \lambda_i} \sum_{\substack{j=1 \\ \neq i}}^{n} \frac{1}{\beta_\nu - \lambda_j}\right]^{-1} \qquad \text{(Eq. 30)}$$

According to Eq. 25, h'' in Eq. 18 is given by:

$$h''(t - u) = \sum_{i=1}^{n-1} \beta_i^2 E_i e^{\beta_i t} e^{-\beta_i u} = \sum_{i=1}^{n-1} b_i e^{\beta_i t} e^{-\beta_i u} \qquad \text{(Eq. 31)}$$

By substituting $h''(t - u)$, $h'(0)$, and $h(0)$, as given by Eqs. 31, 23, and 21, respectively, into Eq. 18, this equation becomes:

$$f(t) = -\frac{\sum_{i=1}^{n} a_i \lambda_i}{\left[\sum_{i=1}^{n} a_i\right]^2} g(t) + \frac{g'(t)}{\sum_{i=1}^{n} a_i} + \sum_{i=1}^{n-1} b_i e^{\beta_i t} \int_0^t g(u) e^{-\beta_i u}\, du \qquad \text{(Eq. 32)}$$

This equation can also be written:

$$f(t) = -\frac{\sum_{i=1}^{n} a_i \lambda_i}{\left[\sum_{i=1}^{n} a_i\right]^2} g(t) + \frac{g'(t)}{\sum_{i=1}^{n} a_i} + z(t)^* g(t) \qquad \text{(Eq. 33)}$$

where:

$$z(t) = \sum_{i=1}^{n-1} b_i e^{\beta_i t} \qquad \text{(Eq. 34)}$$

and $z(t)^*g(t)$ is the convolution of $z(t)$ and $g(t)$.

The $g(t)$ function remains to be derived and substituted into Eq. 32 to yield the final expression for the input rate, $f(t)$. The $g(t)$ function is obtained as the inverse transform of Eq. 12. It is useful to partition $g(t)$ into a basic component, a bolus component, and an infusion component, according to their origin in Eq. 12, so that it can be written as:

$$g(t) = g_0(t) - g_{bol}(t) - g_{inf}(t) \qquad \text{(Eq. 35)}$$

where:

$$g_0(t) = q^* c(t) \qquad \text{(Eq. 36)}$$

$$g_{bol}(t) = L^{-1}\left[\bar{c}^*(s) \sum_{i=1}^{N} q_i e^{-\tau_i s}\right] \qquad \text{(Eq. 37)}$$

$$g_{inf}(t) = L^{-1}[\bar{c}^*(s)\bar{f}_{inf}(s)] \qquad \text{(Eq. 38)}$$

When each of the three components of $g(t)$ is substituted for $g(t)$ in Eq. 32, this substitution leads to three corresponding components of $f(t)$:

$$f(t) = U_0(t) - U_{bol}(t) - U_{inf}(t) \qquad \text{(Eq. 39)}$$

where $U_0(t)$ is the basic function, and $U_{bol}(t)$ and $U_{inf}(t)$ are the bolus corrector function and the infusion corrector function, respectively, because these functions are subtracted from the basic function if the unknown input rate, $f(t)$, is evaluated in the presence of bolus or infusion input.

The basic function, $U_0(t)$, is obtained by substituting q*c(t) for $g(t)$ in Eq. 32, which yields:

$$U_0(t) = q^*\left[-\frac{\sum_{i=1}^{n} a_i \lambda_i}{\left[\sum_{i=1}^{n} a_i\right]^2} c(t) + \frac{c'(t)}{\sum_{i=1}^{n} a_i} + \sum_{i=1}^{n-1} b_i e^{\beta_i t} \int_0^t c(u) e^{-\beta_i u}\, du\right] \qquad \text{(Eq. 40)}$$

According to Eq. 20, Eq. 37 can be written as:

$$g_{bol}(t) = \sum_{m=1}^{R} q_m \sum_{j=1}^{n} a_j e^{\lambda_j (t - \tau_m)} \qquad \text{(Eq. 41)}$$

which, when substituted for $g(t)$ in Eq. 32, yields:

$$\begin{aligned} U_{bol}(t) = &-\frac{\sum_{i=1}^{n} a_i \lambda_i}{\left[\sum_{i=1}^{n} a_i\right]^2} \sum_{m=1}^{R} q_m \sum_{j=1}^{n} a_j e^{\lambda_j (t - \tau_m)} \\ &+ \frac{\sum_{m=1}^{R} q_m \sum_{j=1}^{n} a_j \lambda_j e^{\lambda_j (t - \tau_m)}}{\sum_{i=1}^{n} a_i} \\ &+ \sum_{m=1}^{R} q_m \sum_{i=1}^{n-1} b_i \sum_{j=1}^{n} \frac{a_j}{\lambda_j - \beta_i} e^{\lambda_j (t - \tau_m)} \\ &- \sum_{m=1}^{R} q_m \sum_{i=1}^{n-1} b_i e^{\beta_i (t - \tau_m)} \sum_{j=1}^{n} \frac{a_j}{\lambda_j - \beta_i} \end{aligned} \qquad \text{(Eq. 42)}$$

The last two terms of Eq. 42 are obtained from:

$$\sum_{i=1}^{n-1} b_i e^{\beta_i t} \int_0^t \left[\sum_{m=1}^{R} q_m \sum_{j=1}^{n} a_j e^{\lambda_j(u-\tau_m)}\right] e^{-\beta_i u}\, du$$

$$= \sum_{m=1}^{R} q_m \sum_{i=1}^{n-1} b_i \sum_{j=1}^{n} \frac{a_j}{\lambda_j - \beta_i} e^{\lambda_j(t-\tau_m)}$$

$$- \sum_{m=1}^{R} q_m \sum_{i=1}^{n-1} b_i e^{\beta_i(t-\tau_m)} \sum_{j=1}^{n} \frac{a_j}{\lambda_j - \beta_i} \quad \text{(Eq. 43)}$$

It can be shown that the sum of the first three terms of Eq. 42 is zero[1]:

$$-\frac{\sum_{i=1}^{n} a_i\lambda_i}{\left[\sum_{i=1}^{n} a_i\right]^2} \sum_{m=1}^{R} q_m \sum_{j=1}^{n} a_j e^{\lambda_j(t-\tau_m)} + \frac{\sum_{m=1}^{R} q_m \sum_{j=1}^{n} a_j\lambda_j e^{\lambda_j(t-\tau_m)}}{\sum_{i=1}^{n} a_i}$$

$$+ \sum_{m=1}^{R} q_m \sum_{i=1}^{n-1} b_i \sum_{j=1}^{n} \frac{a_j}{\lambda_j - \beta_i} e^{\lambda_j(t-\tau_m)} = 0 \quad \text{(Eq. 44)}$$

The fact that the last term of Eq. 42 also equals zero is seen from the innermost summation term, which can be written as:

$$\sum_{j=1}^{n} \frac{a_j}{\lambda_j - \beta_i} = -\frac{\sum_{j=1}^{n} a_j \prod_{\substack{m=1 \\ \neq j}}^{n} (\beta_i - \lambda_m)}{\prod_{j=1}^{n} (\beta_i - \lambda_j)} \quad \text{(Eq. 45)}$$

It is apparent from Eq. 26 and the property of β_i that this term is zero because:

$$\sum_{j=1}^{n} a_j \prod_{\substack{m=1 \\ \neq j}}^{n} (\beta_i - \lambda_m) = Q(\beta_i) = 0 \quad \text{(Eq. 46)}$$

Therefore, the right side of Eq. 42 is zero; *i.e.*, the bolus correction function is zero:

$$U_{bol}(t) = 0 \quad \text{(Eq. 47)}$$

Therefore, the input, $f(t)$ (Eq. 39), can be evaluated in the presence of the bolus input without any correction.

Equation 38 can be written according to Eq. 9 as:

$$g_{inf}(t) = q^* \frac{L^{-1}[d_{11}\bar{f}_{inf}(s)]}{V} \quad \text{(Eq. 48)}$$

According to Eq. 2, the term $L^{-1}[d_{11}\bar{f}_{inf}(s)]/V$ is the blood level, $c_{inf}(t)$, resulting from the infusion input, $f_{inf}(t)$, so Eq. 48 can be written as:

$$g_{inf}(t) = q^* c_{inf}(t) \quad \text{(Eq. 49)}$$

The infusion correction function, $U_{inf}(t)$, is obtained by substituting $g_{inf}(t)$ for $g(t)$ in Eq. 32, which gives:

$$U_{inf}(t) = q^* \times \left[-\frac{\sum_{i=1}^{n} a_i\lambda_i}{\left[\sum_{i=1}^{n} a_i\right]^2} c_{inf}(t) + \frac{c'_{inf}(t)}{\sum_{i=1}^{n} a_i} + \sum_{i=1}^{n-1} b_i e^{\beta_i t} \int_0^t c_{inf}(u) e^{-\beta_i u}\, du\right] \quad \text{(Eq. 50)}$$

If the infusion input, $f_{inf}(t)$, is considered an unknown input to be evaluated in the absence of other inputs, then by substituting $c_{inf}(t)$ for $c(t)$ in Eq. 40, $f_{inf}(t)$ is given by:

$$f(t) = f_{inf}(t) = U_0(t) = q^* \left[-\frac{\sum_{i=1}^{n} a_i\lambda_i}{\left[\sum_{i=1}^{n} a_i\right]^2} c_{inf}(t) + \frac{c'_{inf}(t)}{\sum_{i=1}^{n} a_i} + \sum_{i=1}^{n-1} b_i e^{\beta_i t} \int_0^t c_{inf}(u) e^{-\beta_i u}\, du\right] \quad \text{(Eq. 51)}$$

[1] The derivations that show that Eq. 44 holds for $n \geq 1$ are extensive. They are omitted because they are not crucial for understanding the theoretical approach.

By comparing Eqs. 50 and 51, it follows that:

$$U_{inf}(t) = f_{inf}(t) \quad \text{(Eq. 52)}$$

Thus, the infusion correction function is the rate of infusion input. Analogous to Eqs. 48 and 49, it is seen that $g_{bol}(t) = q^* c_{bol}(t)$, where $c_{bol}(t)$ is the drug level resulting from bolus input only. From Eq. 47, it follows that when $c_{bol}(t)$ is substituted for $c(t)$ in Eq. 40, the basic function becomes zero.

To unify these findings in a simple way, it is useful to define the input-generating function, ψ:

$$\psi[c(t)] = q^* \left[-\frac{\sum_{i=1}^{n} a_i\lambda_i}{\left[\sum_{i=1}^{n} a_i\right]^2} c(t) + \frac{c'(t)}{\sum_{i=1}^{n} a_i} + \sum_{i=1}^{n-1} b_i e^{\beta_i t} \int_0^t c(u) e^{-\beta_i u}\, du\right] \quad \text{(Eq. 53)}$$

This function generates the input from the drug level profile, $c(t)$. It is evident from above that the input-generating function has the following remarkable properties:

$$\psi[c_{bol}(t)] = 0 \qquad t \neq \tau_i \quad \text{(Eq. 54)}$$

$$\psi[c_{inf}(t)] = f_{inf}(t) \quad \text{(Eq. 55)}$$

$$\psi[c(t)] = f(t) + f_{inf}(t) \qquad t \neq \tau_i \quad \text{(Eq. 56)}$$

Equation 54 states that there is no drug input between the bolus input in an experiment only involving bolus input. Equation 56 states that the input-generating function generates the sum of all nonbolus input. Independent of any bolus input, the drug input rate therefore is given by the input-generating function corrected for the rate of superimposed intravenous infusion input that may or may not be present:

$$f(t) = \psi[c(t)] - f_{inf}(t) \qquad t \neq \tau_i \quad \text{(Eq. 57)}$$

which is rewritten as:

$$f(t) = q^* \left[-\frac{\sum_{i=1}^{n} a_i\lambda_i}{\left[\sum_{i=1}^{n} a_i\right]^2} c(t) + \frac{c'(t)}{\sum_{i=1}^{n} a_i} + \sum_{i=1}^{n-1} b_i e^{\beta_i t} \int_0^t c(u) e^{-\beta_i u}\, du\right] - f_{inf}(t) \qquad t \neq \tau_i \quad \text{(Eq. 58)}$$

RESULTS AND DISCUSSION

If the eigenvalues of the A matrix are distinct, then the impulse response function always is given by Eq. 19. Systems with cyclic structures may give rise to complex conjugate eigenvalues. However, the method still can be applied. An eigenvalue is either zero, due to a subsystem being closed, or is functionally related to the dynamic processes. The input analysis deals with the transport and transition dynamics of drug molecules in a fairly random state. Consequently, nonzero eigenvalues show a stochastic behavior; therefore, the statistical probability of two nonzero eigenvalues being equal is zero.

It is evident that the rank of the coefficient matrix for a closed system is full rank minus one and that a lower rank than that contradicts the randomness condition. Therefore, in an applied (*i.e.*, not theoretical) closed system, there is one and only one zero eigenvalue. Open applied systems are of full rank with no zero eigenvalues (17). The eigenvalues for any applied linear compartmental system are distinct and give rise to a unit impulse response as given by Eq. 19. Therefore, the method of analysis is applicable to any applied linear compartmental system. However, the method is not applicable to every theoretical linear compartmental system because of the possibility of nondistinct eigenvalues, which would result in an equation different from Eq. 19.

The method also could have been derived from the linear system theory for linear systems, where the impulse response can be approximated by a polyexponential expression. As such, it represents a new deconvolution approach. The present derivation method is valuable because it forms a link between classical pharmacokinetics and the linear system approach,

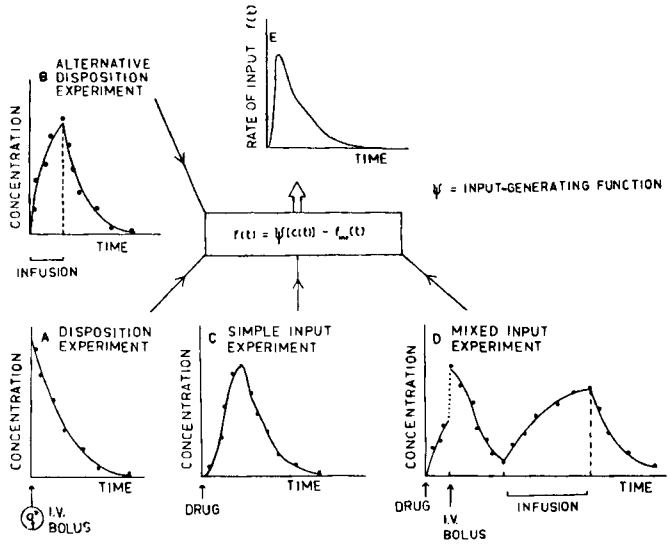

Figure 1—*Summary of model-independent approach of evaluating the drug input rate. The drug is given intravenously either as an initial bolus, q* (A), or alternatively as a zero-order infusion (B) to a subject as a nonprecipitating solution. Equation 19 or Eqs. 75 and 76 are fitted to the respective drug concentration data to give the parameters* $\{a_i, \lambda_i\}_1^n$ *and q* (A and B). The rate of drug input into the blood from a drug delivery system can be evaluated in the same subject in the absence of other input (C) or in the presence of any combination of intravenous bolus and infusion input (D). An appropriate arbitrary function,* c(t) *(e.g., a least-squares spline function), is fitted to the data from the input experiment (C and D). The rate of input is calculated from the parameters* $\{a_i, \lambda_i\}_1^n$, q*, *and the drug level profile,* c(t), *according to the input-generating function and corrected for any superimposed infusion input (E).*

thereby enabling classical pharmacokinetics to be analyzed in a new context.

The input rate can be determined quantitatively in the absence or presence of any combination of intravenous bolus input and infusion input.

The procedure for the evaluation of an input rate is mathematically defined by Eqs. 19, 26, 30, and 58. These equations are used as follows. Equation 19 is fitted to the drug level data from a single intravenous bolus input, q^*, to give $\{a_i, \lambda_i\}_1^n$ (Fig. 1A). If $n > 1$, these parameters are inserted into Eq. 26 to give the auxiliary parameters, $\{\beta_i\}_1^{n-1}$, which when subsequently inserted into Eq. 30 give another set of auxiliary parameters, $\{b_i\}_1^{n-1}$. An arbitrary function is fitted to the drug level data from the input to be evaluated (Fig. 1C). The arbitrary function is denoted briefly as $c(t)$ in the derivations. Since both b and β are functions of $\{a_i, \lambda_i\}_1^n$, only q^*, $\{a_i, \lambda_i\}_1^n$, and $c(t)$ are required to calculate $f(t)$ from Eq. 58. The input-generating function, ψ, is uniquely defined from the disposition experiment by the parameters q^* and $\{a_i, \lambda_i\}_1^n$.

Which arbitrary function, $c(t)$, is chosen to estimate the true drug level profile depends on the accuracy of the data and their general shape as well as any assumptions made about the variation and smoothness of the input process. The method by which a chosen function is fitted to the data should relate to assumptions made about the statistical properties of the errors in the data. For a fairly smooth input process, the best general choice of a function seems to be a weighted or unweighted least-squares spline function. Such a function is particularly suitable because of its smoothness, great flexibility, and optimal properties in estimating the rate of change [the $c'(t)$ term in Eq. 58] and the fact that it readily describes the disturbance(s) caused by bolus input (Fig. 1D). Due to the linear nature of the parameters defining the spline function, it also has desirable computational and statistical properties (18, 19).

If the drug level data are sampled frequently and are not too erratic, then a fitting of an ordinary polynomial may be quite appropriate. To avoid bias in the estimation of the drug level and to avoid an erratic behavior of the first derivative, it has been suggested that the degree of polynomial fitted by least squares should not exceed two times the square root of the number of data points (20). Use of exponential expressions for $c(t)$ can be troublesome because of the problem of getting initial parameter estimates and because of the computational problems associated with nonlinear curve fitting (21). If the drug levels range over several orders of magnitude, it is recommended that a logarithmic transformation or other suitable transformation be applied to the data before the curve fitting (22).

Although Eq. 58 involves an integral, no computational problems should be caused in the evaluation of $f(t)$ since the functions likely to be used for $c(t)$, such as spline functions, ordinary polynomials, and exponential expressions, lead to simple algebraic expressions without an integral that can be evaluated readily and exactly. Although the equations used to calculate $f(t)$ may seem complex, their use is straightforward.

Example 1, $n = 1$—This example represents a drug that behaves in a subject, following a single intravenous bolus, q^*, according to a one-compartment model so the intravenous bolus blood level data are described by:

$$c^*(t) = ae^{\lambda t} \qquad \text{(Eq. 59)}$$

The equation necessary for calculating the input rate of the drug administered to the same subject is simplified in this case with $n = 1$, since the summation term involving a summation to $i = n - 1$ is zero by definition. Thus, in the absence of intravenous infusion input, the input rate is given by:

$$f(t) = \frac{q^*}{a}[c'(t) - \lambda c(t)] \qquad \text{(Eq. 60)}$$

It is of interest to compare this equation with the Wagner–Nelson model-independent method of evaluating the absorption rate in a one-compartment system. The Wagner–Nelson equation is (15):

$$A_t = V\left[c(t) + K\int_0^t c(t)dt\right] \qquad \text{(Eq. 61)}$$

so that:

$$dA_t/dt = V[c'(t) + Kc(t)] \qquad \text{(Eq. 62)}$$

where A_t is the amount absorbed between time zero and time t and K is the first-order elimination rate constant. Since $dA_t/dt = f(t)$, $K = -\lambda$ and $V = q^*/a$, Eq. 62 can be written the same as Eq. 60. Therefore, for $n = 1$, the input-generating function reduces to an expression that is essentially identical to the Wagner–Nelson equation.

Example 2, $n = 2$—In this case, the intravenous bolus data are described by:

$$c^*(t) = a_1e^{\lambda_1 t} + a_2e^{\lambda_2 t} \qquad a_i > 0, \lambda_i < 0 \qquad \text{(Eq. 63)}$$

Equation 26 is used to obtain the auxiliary parameter, β_1:

$$Q(s) = a_1(s - \lambda_2) + a_2(s - \lambda_1) = (a_1 + a_2)s - (a_1\lambda_2 + a_2\lambda_1) \qquad \text{(Eq. 64)}$$

so that:

$$\beta_1 = \frac{a_1\lambda_2 + a_2\lambda_1}{a_1 + a_2} \qquad \text{(Eq. 65)}$$

The other auxiliary parameter, b_1, is obtained from β_1 using Eq. 30:

$$b_1 = \left[\frac{a_1}{(\beta_1 - \lambda_1)}\frac{1}{(\beta_1 - \lambda_2)} + \frac{a_2}{(\beta_1 - \lambda_2)}\frac{1}{(\beta_1 - \lambda_1)}\right]^{-1} = -\frac{a_1a_2(\lambda_1 - \lambda_2)^2}{(a_1 + a_2)^3} \qquad \text{(Eq. 66)}$$

The input-generating function then becomes:

$$\psi[c(t)] = q^*\left\{-\frac{a_1\lambda_1 + a_2\lambda_2}{(a_1 + a_2)^2}c(t) + \frac{c'(t)}{a_1 + a_2} - \frac{a_1a_2(\lambda_1 - \lambda_2)^2}{(a_1 + a_2)^3}\exp\left[\frac{a_1\lambda_2 + a_2\lambda_1}{a_1 + a_2}t\right] \times \int_0^t c(u)\exp\left[-\frac{a_1\lambda_2 + a_2\lambda_1}{a_1 + a_2}u\right]du\right\} \qquad \text{(Eq. 67)}$$

Example 3, $n = 3$— The intravenous bolus data are described by:

$$c^*(t) = a_1e^{\lambda_1 t} + a_2e^{\lambda_2 t} + a_3e^{\lambda_3 t} \qquad a_i > 0, \lambda_i < 0 \qquad \text{(Eq. 68)}$$

The $n - 1 = 2$ auxiliary parameters, β_1 and β_2, are obtained as the two roots of Eq. 26:

$$Q(s) = a_1(s - \lambda_2)(s - \lambda_3) + a_2(s - \lambda_1)(s - \lambda_3) + a_3(s - \lambda_1)(s - \lambda_2) \qquad \text{(Eq. 69)}$$

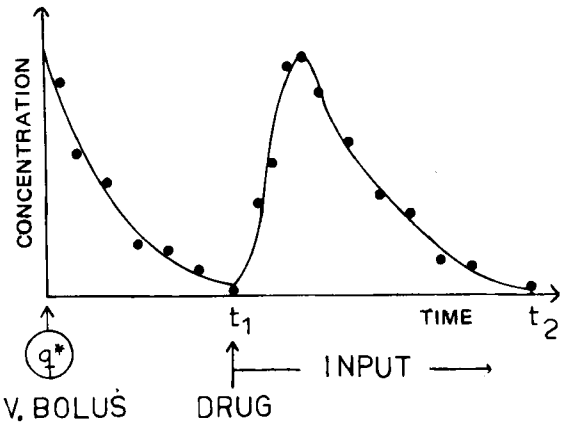

Figure 2—*Summary of input analysis based on a merged bolus and input approach. An initial intravenous bolus solution of the drug is given, and the drug level is followed for a sufficiently long time, t_1, to get proper estimates of $\{a_i, \lambda_i\}_1^n$ by fitting Eq. 19 to the drug level data for $0 < t \leq t_1$. Then, the drug delivery system is administered (t_1) and the drug level is followed for the appropriate length of time (t_2). The input rate is calculated from the input-generating function. The arbitrary function, c(t), fitted to the data must consist of Eq. 19 for the time period $0 < t \leq t_1$ and some other appropriate function (e.g., a least-squares spline function) for $t_1 < t \leq t_2$. This approach of input analysis is powerful because it does not require a washout period between the disposition and the input experiments and because errors arising from changes in the subject's drug disposition with time are reduced to a minimum by bringing the two drug administrations close together.*

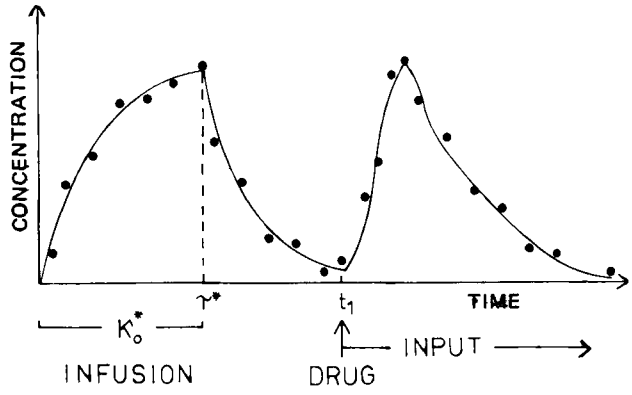

Figure 3—*Summary of input analysis based on a merged infusion and input approach. A zero-order (κ_0^*) infusion is given from $t = 0$ to $t = \tau^*$, and the drug level is allowed to drop to a proper level before the drug delivery system is administered at t_1. Equations 75 and 76 are fitted simultaneously to the data for $0 < t \leq \tau^*$ and $\tau^* < t \leq t_1$, respectively, to give the parameters $\{a_i, \lambda_i\}_1^n$ and q^*. The rate of drug input ($t > t_1$) is calculated from the input-generating function. The arbitrary function, c(t), must consist of Eq. 75 (with the estimated parameters) for $0 < t \leq \tau^*$, of Eq. 76 for $\tau^* < t \leq t_1$, and of some suitable function (e.g., a least-squares spline function) for $t > t_1$.*

so that:

$$Q(s) = [a_1 + a_2 + a_3]s^2 - [a_1(\lambda_2 + \lambda_3) + a_2(\lambda_1 + \lambda_3) + a_3(\lambda_1 + \lambda_2)]s + [a_1\lambda_2\lambda_3 + a_2\lambda_1\lambda_3 + a_3\lambda_1\lambda_2] \quad \text{(Eq. 70)}$$

The two other auxiliary parameters, b_1 and b_2, are obtained from Eq. 30:

$$b_1 = \left[\frac{a_1}{\beta_1 - \lambda_1}\left(\frac{1}{\beta_1 - \lambda_2} + \frac{1}{\beta_1 - \lambda_3}\right) + \frac{a_2}{\beta_1 - \lambda_2}\left(\frac{1}{\beta_1 - \lambda_1} + \frac{1}{\beta_1 - \lambda_3}\right) + \frac{a_3}{\beta_1 - \lambda_3}\left(\frac{1}{\beta_1 - \lambda_1} + \frac{1}{\beta_1 - \lambda_2}\right)\right]^{-1} \quad \text{(Eq. 71)}$$

so that:

$$b_1 = \frac{(\beta_1 - \lambda_1)(\beta_1 - \lambda_2)(\beta_1 - \lambda_3)}{(\beta_1 - \beta_2)(a_1 + a_2 + a_3)} \quad \text{(Eq. 72)}$$

and similarly:

$$b_2 = \frac{(\beta_2 - \lambda_1)(\beta_2 - \lambda_2)(\beta_2 - \lambda_3)}{(\beta_2 - \beta_1)(a_1 + a_2 + a_3)} \quad \text{(Eq. 73)}$$

The input-generating function is:

$$\psi[c(t)] = q^*\left[-\frac{a_1\lambda_1 + a_2\lambda_2 + a_3\lambda_3}{(a_1 + a_2 + a_3)^2}c(t) + \frac{c'(t)}{a_1 + a_2 + a_3} + b_1e^{\beta_1 t}\int_0^t c(u)e^{-\beta_1 u}\,du + b_2e^{\beta_2 t}\int_0^t c(u)e^{-\beta_2 u}\,du\right] \quad \text{(Eq. 74)}$$

where b_1, b_2, β_1, and β_2 are described in terms of $\{a_i, \lambda_i\}_1^2$.

Merged Bolus and Input Approach—The fact that the input-generating function automatically corrects for the disturbance in the drug level profile bolus input makes it particularly suitable for performing an input analysis in a single experiment. For example, it may be of interest to study the input rate from an oral administration. This study can be done by giving an initial intravenous bolus solution of the drug (Fig. 2) and following the drug profile for a sufficiently long time, t_1, to get proper estimates of $\{a_i, \lambda_i\}_1^n$ by fitting Eq. 19. Thereafter, the oral dosage form of the drug is administered and the drug level is followed for the appropriate length of time, t_2.

The input rate ($t > t_1$) is calculated from the input-generating function. The arbitrary function, $c(t)$, representing the data must consist of Eq. 19 for $0 < t \leq t_1$ and of some other appropriate function (*e.g.*, a least-squares spline function) for $t_1 < t \leq t_2$. This input analysis approach is powerful because it does not require a washout period between the disposition and the input experiments and because errors arising from changes in the subject's drug disposition with time are reduced to a minimum by bringing the two drug administrations close together.

Alternative Approach to Intravenous Bolus Input—It is assumed that the intravenous bolus administered to estimate $\{a_i, \lambda_i\}_1^n$ is given in a solution that does not precipitate on dilution with the blood so that it is available immediately to the systemic circulation. Some drugs may be so slightly soluble or so toxic that it is not feasible to administer an intravenous bolus dose to estimate $\{a_i, \lambda_i\}_1^n$. However, this study can be done by an alternative approach. It can be proven that if an intravenous bolus, q^*, produces a concentration profile in a linear pharmacokinetic system as described by Eq. 19, then the profile resulting from a zero-order (κ_0^*) infusion from $t = 0$ to $t = \tau^*$ in the same system is given by:

$$c_0^*(t) = \frac{\kappa_0^*}{q^*}\sum_{i=1}^{n}\frac{a_i}{\lambda_i}[e^{\lambda_i t} - 1] \qquad t \leq \tau^* \quad \text{(Eq. 75)}$$

and:

$$c_0^*(t) = \frac{\kappa_0^*}{q^*}\sum_{i=1}^{n}\frac{a_i e^{\lambda_i t}}{\lambda_i}[1 - e^{-\lambda_i \tau^*}] \qquad t > \tau^* \quad \text{(Eq. 76)}$$

Thus, q^* and $\{a_i, \lambda_i\}_1^n$ required for the calculation of the input rate are obtained by fitting Eqs. 75 and 76 to the infusion data.

Merged Infusion and Input Approach—The infusion disposition experiment can be merged with the input experiment by stopping the infusion after the proper length of time (τ^*, Fig. 3) and then letting the drug level drop to a proper level before the drug delivery system is administered (t_1, Fig. 3). The arbitrary function, $c(t)$, fitted to the data must consist of Eq. 75 (using the estimated parameters) for $0 < t \leq \tau^*$ and Eq. 76 for $\tau^* < t \leq t_1$ and an appropriate arbitrary function for the drug input interval $t > t_1$ (Fig. 3). The rate of drug input, $t > t_1$, is calculated from the input-generating function (without infusion correction). The rate of drug input, $t < t_1$, calculated according to Eq. 58 [with $f_{inf}(t) = \kappa_0^*$ for $0 < t < \tau^*$] is zero if the process has been correctly defined mathematically. This can be used to check the computations when the method is implemented on a computer.

Drug Input Control—Although the presented analysis is directed at a model-independent evaluation of drug input, it is equally applicable to control of drug input. Any desirable drug profile may be produced by a controlled intravenous input according to the equations presented. The application of the theory to model-independent optimized drug input is under investigation.

Although the equations used to calculate the input rate may appear complex, they are presented in a general form that readily allows them to be programmed and implemented on a computer. A general-purpose drug input analysis program can be developed from the equations presented. Ultimately, the investigator will need only to supply the blood level data and information about the experimental design, and the program will automatically compute and plot the drug input rate profile.

The practical application of the drug input analysis presented appears versatile and powerful. It provides some important tools for the evalua-

tion and design of drug delivery systems. In particular, it enables the rate and extent of drug bioavailability to be evaluated in a more intrinsic and accurate way than previous methods for linear systems with a polyexponential impulse response.

APPENDIX

The system of n linear differential equations describing the kinetics after an initial bolus input into a linear pharmacokinetic system is (16):

$$\mathbf{x}' = \mathbf{A}\mathbf{x} \qquad \text{(Eq. A1)}$$

where the square matrix **A** contains the first-order intercompartmental rate constants and the elimination rate constants (16). If the eigenvalues of **A** are distinct, then the solution of Eq. A1 is:

$$\mathbf{x} = \mathbf{P} \exp(t\mathbf{\Lambda})\mathbf{P}^{-1}\mathbf{x}(0) \qquad \text{(Eq. A2)}$$

where $\mathbf{\Lambda}$ is a diagonal matrix of the eigenvalues $\{\lambda_i\}_1^n$ of **A** and the columns of **P** are the corresponding eigenvectors.

From Eq. A2, the following equation is obtained:

$$x_i = \sum_{j=1}^{n} \Omega_{ij} e^{\lambda_j t} \qquad \text{(Eq. A3)}$$

where:

$$\Omega_{ij} = \mathbf{P}_{ij}[\mathbf{P}_{ij}^{-1}\mathbf{x}(0)]_j \qquad \text{(Eq. A4)}$$

An initial bolus input in the central compartment is described by $\mathbf{x}(0)^T = (q^*, 0, 0, \ldots, 0)$, which according to Eqs. A3 and A4 leads to:

$$c^*(t) = \sum_{j=1}^{n} \Omega_{1j} e^{\lambda_j t}/V \qquad \text{(Eq. A5)}$$

Thus, a_i in Eq. 19 is given by:

$$a_i = \Omega_{1i}/V = q^* \mathbf{P}_{1i}\mathbf{P}_{1i}^{-1}/V \qquad \text{(Eq. A6)}$$

Note that:

$$L^{-1}\mathbf{D} = \mathbf{\Phi}(t) = \mathbf{P} \exp(t\mathbf{\Lambda})\mathbf{P}^{-1} \qquad \text{(Eq. A7)}$$

where $\mathbf{\Phi}(t)$, introduced previously (16), is the fundamental matrix of the pharmacokinetic system.

NOTATIONS[2]

a_i = defined by Eq. 19
A_1, A_2 = defined by Eq. 25
A_t = amount absorbed between $t = 0$ and time t
A = coefficient matrix, Eq. A1
b_i = auxiliary parameter defined in terms of $\{a_i, \lambda_i\}_1^n$ by Eq. 30 (see β_i)
β_i = auxiliary parameter defined in terms of $\{a_i, \lambda_i\}_1^n$ by Eq. 26
$c(t)$ = arbitrary function(s) describing the drug concentration
$c^*(t)$ = function (Eq. 19) describing the drug concentration data following an initial intravenous bolus input, q^*
$c_0^*(t)$ = drug concentration resulting from a zero-order infusion starting at $t = 0$
$c_{bol}(t)$ = drug concentration resulting from one or more intravenous bolus input
$c_{inf}(t)$ = drug concentration resulting from continuous or discontinuous intravenous infusion input
d_{ij} = i-, jth element of disposition matrix **D**
D = disposition matrix
$\delta(t)$ = Dirac delta function
e = 2.71828 . . .
E_ν = expression defined by Eq. 27
$f(t)$ = rate of input to be evaluated (amount per unit of time)
$f_{bol}(t)$ = bolus input component
$f_{inf}(t)$ = rate of intravenous infusion input
$g(t)$ = function whose Laplace tranform is defined by Eq. 12
$g_{bol}(t)$ = bolus component of $g(t)$
$g_{inf}(t)$ = infusion component of $g(t)$
$g_0(t)$ = component of $g(t)$ corresponding to $f(t)$
$h(t)$ = function whose Laplace transform is defined by Eq. 16
i = index variable
j = index variable
K = first-order elimination constant in a one-compartment model
κ_0^* = zero-order infusion rate from $t = 0$ to $t = \tau^*$ used in the disposition experiment and in the merged infusion and input approach
λ_i = defined by Eq. 19, ith eigenvalue of matrix **A**
L, L^{-1} = Laplace and inverse Laplace transform operator
$\mathbf{\Lambda}$ = diagonal matrix defined by Eq. A3
m = index variable
n = defined by Eq. 19
N = number of bolus input
ν = index variable
p_{ij} = i-, jth element of the eigenvector matrix
$\mathbf{p}_i$ = ith column vector of the eigenvector matrix
P = eigenvector matrix defined by Eq. A2
π = product operator
q^* = bolus amount injected intravenously initially in the disposition experiment resulting in a drug level described by Eq. 19
q_i = ith bolus injected intravenously
$Q(s)$ = auxiliary function defining β_i (Eq. 26)
R = highest integer for which $\tau_R < t$ is satisfied or defined as zero if inequality cannot be satisfied
s = complex domain variable
t = time
t_1, t_2 = defined in Fig. 2
τ_i = time when the ith intravenous bolus is given
τ^* = time for zero-order infusion stop (Fig. 3)
$U_0(t)$ = basic function
$U_{bol}(t)$ = bolus corrector function
$U_{inf}(t)$ = infusion corrector function
v = input vector
v_1 = first element of input vector
V = constant with dimension of volume
x = vector containing the amounts in the n compartments at time t
x_1 = first element of vector **x**
y = vector defined by Eq. A6
$z(t)$ = auxiliary function defined in terms of $\{a_i, \lambda_i\}_1^n$ by Eq. 34 (see b_i and β_i)
$\Phi(t)$ = fundamental matrix of pharmacokinetic system
$\Psi[c(t)]$ = input-generating function

[2] Bars denote Laplace transforms, bold-faced capital letters denote matrixes, and bold-faced noncapital letters denote vectors.

REFERENCES

(1) L. Z. Benet, in "Drug Design," vol. IV, E. J. Ariens, Ed., Academic, New York, N.Y., 1973, chap. 1.
(2) J. G. Wagner and E. Nelson, *J. Pharm. Sci.*, **52**, 610 (1963).
(3) J. G. Wagner, *J. Pharmacokinet. Biopharm.*, **2**, 469 (1974).
(4) J. C. K. Loo and S. Riegelman, *J. Pharm. Sci.*, **57**, 918 (1968).
(5) J. G. Wagner, *J. Pharmacokinet. Biopharm.*, **3**, 51 (1975).
(6) D. Perrier and M. Gibaldi, *J. Pharm. Sci.*, **62**, 225 (1973).
(7) L. J. Leeson and H. Weintraub, *ibid.*, **62**, 1936 (1973).
(8) J. C. K. Loo and S. Riegelman, presented at the APhA Academy of Pharmaceutical Sciences, San Francisco meeting, Mar. 1971.
(9) A. Rescigno and G. Segre, "Drug and Tracer Kinetics," Blaisdell, Waltham, Mass., 1966, p. 102.
(10) L. Z. Benet and C. W. N. Chiang, presented at the APhA Academy of Pharmaceutical Sciences, Chicago meeting, Nov. 5–9, 1977.
(11) D. P. Vaughan and M. Dennis, *J. Pharm. Sci.*, **67**, 663 (1978).
(12) V. F. Smolen, *J. Pharmacokinet. Biopharm.*, **4**, 337 (1976).
(13) D. J. Cutler, *ibid.*, **6**, 227 (1978).
(14) *Ibid.*, **6**, 243 (1978).
(15) J. G. Wagner, "Fundamentals of Clinical Pharmacokinetics," Drug Intelligence Publications, Hamilton, Ill., 1975, chap. 4.
(16) P. Veng Pedersen, *J. Pharm. Sci.*, **67**, 187 (1978).
(17) J. Z. Hearon, *Ann. N.Y. Acad. Sci.*, **108**, 37 (1963).

(18) C. L. Lawson and R. J. Hanson, "Solving Least Squares Problems," Prentice-Hall, Englewood Cliffs, N.J., 1974.
(19) J. H. Ahlberg, E. N. Nilson, and J. L. Walsh, "The Theory of Splines and Their Applications," Academic, New York, N.Y., 1967.
(20) G. Dahlquist and Å. Björk, "Numerical Methods," Prentice-Hall, Englewood Cliffs, N.J., 1974, p. 128.
(21) P. Veng Pedersen, *J. Pharmacokinet. Biopharm.*, **5**, 513 (1977).
(22) S. Wold, *Chem. Scr.*, **1**, 97 (1971).

ACKNOWLEDGMENTS

Presented in part at the APhA Academy of Pharmaceutical Sciences, Hollywood, Fla., meeting, November 1978.

Model-Independent Method of Analyzing Input in Linear Pharmacokinetic Systems Having Polyexponential Impulse Response II: Numerical Evaluation

PETER VENG PEDERSEN

Received September 22, 1978, from the *Department of Pharmacy, School of Pharmacy, University of California, San Francisco, CA 94143.* Accepted for publication October 11, 1979.

Abstract □ The investigated method is based on an exact mathematical solution to the deconvolution problem of linear pharmacokinetic systems with a polyexponential impulse response. The accuracy of the method is determined only by how well the curves fitted to the intravenous and absorption data represent the true drug level. Consequently, the method enables objective evaluation of the input. It permits the user to assess whether discrepancies in a calculated input are due to an improper data representation, as judged from the fitted curves, to the inherent nature of the data, or to a violation of the pharmacokinetic assumptions. The method is compared to another method using simulated data containing various degrees of random noise. The accuracy of the two methods was not significantly different and was of the same magnitude as the noise level of the data. The theoretical properties of the two methods and their expected performance in various pharmacokinetic situations are discussed. The method is applied to pentobarbital data from oral and intravenous administrations.

Keyphrases □ Pharmacokinetics—linear systems, polyexponential impulse response, analysis of input, model-independent method □ Model-independent analysis—linear pharmacokinetic systems, polyexponential impulse response, analysis of input □ Drug input—linear pharmacokinetic systems, polyexponential impulse response, analysis by model-independent method

A previous article (1) presented the theoretical derivation and analysis of a novel input analysis method. The method allows a drug input to be evaluated in the presence or absence of any combination of intravenous bolus input and infusion input. Three approaches were discussed: evaluation of the input rate based on a separate intravenous bolus experiment and an input (absorption) experiment, evaluation based on a merged intravenous bolus and input experiment, and evaluation based on a merged infusion and input experiment.

The present work is confined to the first approach and is based on an exact mathematical solution to the deconvolution problem of linear pharmacokinetic systems with a polyexponential impulse response. Several methods for deconvolution have been presented (2–5). The Wagner–Nelson method usually is limited to one-compartment systems (6), and the methods investigated by Benet and Chiang (2) were shown to be very sensitive to errors in the data. The numerical deconvolution method presented by Gamel *et al.* (3) did not provide satisfactory results, possibly due to numerical ill conditioning. Cutler (5) improved Gamel's approach by using orthogonal polynomials to avoid the problem of ill conditioning. The improved method seems to be the most accurate method for numerical deconvolution. It appears to be superior to the many model-dependent methods (6–10) because it is based on fewer assumptions and, therefore, is more likely to result in a meaningful evaluation of the drug input.

This work compares the new method with Cutler's approach using Cutler's simulated test data that contain various degrees of random noise (4, 5).

THEORY

Let the concentration of drug in the blood, $c^*(t)$, following an initial intravenous bolus dose, q^*, be described by a multiexponential relationship (1):

$$c^*(t) = \sum_{i=1}^{n} a_i e^{\lambda_i t} \qquad \text{(Eq. 1)}$$

Let $c(t)$ denote the drug level resulting from an unknown input of a drug that, in the same subject with the same linear relationship between input and response, results in the blood level $c^*(t)$ (Eq. 1) when an intravenous bolus dose, q^*, is given. It has been shown (1) that the rate of input of the drug then is given by:

$$f(t) = q^* \left[-\frac{\sum_{i=1}^{n} a_i \lambda_i}{\left[\sum_{i=1}^{n} a_i\right]^2} c(t) + \frac{c'(t)}{\sum_{i=1}^{n} a_i} + \sum_{i=1}^{n-1} b_i e^{\beta_i t} \int_0^t c(u) e^{-\beta_i u}\, du \right] \qquad \text{(Eq. 2)}$$

where β_i, $i = 1, 2, \ldots, n-1$ are the roots of the $(n-1)$th-degree polynomial:

$$Q(x) = \sum_{i=1}^{n} a_i \prod_{\substack{j=1 \\ \neq i}}^{n} (x - \lambda_j) \qquad \text{(Eq. 3)}$$

and b_ν, $\nu = 1, 2, \ldots, n-1$ are obtained from:

$$b_\nu = \left[\sum_{i=1}^{n} \frac{a_i}{\beta_\nu - \lambda_i} \sum_{\substack{j=1 \\ \neq i}}^{n} \frac{1}{\beta_\nu - \lambda_j} \right]^{-1} \qquad \text{(Eq. 4)}$$

Integration of $f(t)$ from time zero to time t yields the cumulative amount of input:

$$A(t) = q^* \left[-\left\{ \frac{\sum_{i=1}^{n} a_i \lambda_i}{\left(\sum_{i=1}^{n} a_i\right)^2} + \sum_{i=1}^{n-1} \frac{b_i}{\beta_i} \right\} \int_0^t c(t)\, dt + \frac{c(t)}{\sum_{i=1}^{n} a_i} + \sum_{i=1}^{n-1} \frac{b_i}{\beta_i} e^{\beta_i t} \int_0^t c(u) e^{-\beta_i u}\, du \right] \qquad \text{(Eq. 5)}$$

0022-3549/80/0300-0305$01.00/0
© 1980, American Pharmaceutical Association

(18) C. L. Lawson and R. J. Hanson, "Solving Least Squares Problems," Prentice-Hall, Englewood Cliffs, N.J., 1974.
(19) J. H. Ahlberg, E. N. Nilson, and J. L. Walsh, "The Theory of Splines and Their Applications," Academic, New York, N.Y., 1967.
(20) G. Dahlquist and Å. Björk, "Numerical Methods," Prentice-Hall, Englewood Cliffs, N.J., 1974, p. 128.
(21) P. Veng Pedersen, *J. Pharmacokinet. Biopharm.*, **5**, 513 (1977).
(22) S. Wold, *Chem. Scr.*, **1**, 97 (1971).

ACKNOWLEDGMENTS

Presented in part at the APhA Academy of Pharmaceutical Sciences, Hollywood, Fla., meeting, November 1978.

Model-Independent Method of Analyzing Input in Linear Pharmacokinetic Systems Having Polyexponential Impulse Response II: Numerical Evaluation

PETER VENG PEDERSEN

Received September 22, 1978, from the *Department of Pharmacy, School of Pharmacy, University of California, San Francisco, CA 94143.* Accepted for publication October 11, 1979.

Abstract □ The investigated method is based on an exact mathematical solution to the deconvolution problem of linear pharmacokinetic systems with a polyexponential impulse response. The accuracy of the method is determined only by how well the curves fitted to the intravenous and absorption data represent the true drug level. Consequently, the method enables objective evaluation of the input. It permits the user to assess whether discrepancies in a calculated input are due to an improper data representation, as judged from the fitted curves, to the inherent nature of the data, or to a violation of the pharmacokinetic assumptions. The method is compared to another method using simulated data containing various degrees of random noise. The accuracy of the two methods was not significantly different and was of the same magnitude as the noise level of the data. The theoretical properties of the two methods and their expected performance in various pharmacokinetic situations are discussed. The method is applied to pentobarbital data from oral and intravenous administrations.

Keyphrases □ Pharmacokinetics—linear systems, polyexponential impulse response, analysis of input, model-independent method □ Model-independent analysis—linear pharmacokinetic systems, polyexponential impulse response, analysis of input □ Drug input—linear pharmacokinetic systems, polyexponential impulse response, analysis by model-independent method

A previous article (1) presented the theoretical derivation and analysis of a novel input analysis method. The method allows a drug input to be evaluated in the presence or absence of any combination of intravenous bolus input and infusion input. Three approaches were discussed: evaluation of the input rate based on a separate intravenous bolus experiment and an input (absorption) experiment, evaluation based on a merged intravenous bolus and input experiment, and evaluation based on a merged infusion and input experiment.

The present work is confined to the first approach and is based on an exact mathematical solution to the deconvolution problem of linear pharmacokinetic systems with a polyexponential impulse response. Several methods for deconvolution have been presented (2–5). The Wagner–Nelson method usually is limited to one-compartment systems (6), and the methods investigated by Benet and Chiang (2) were shown to be very sensitive to errors in the data. The numerical deconvolution method presented by Gamel *et al.* (3) did not provide satisfactory results, possibly due to numerical ill conditioning. Cutler (5) improved Gamel's approach by using orthogonal polynomials to avoid the problem of ill conditioning. The improved method seems to be the most accurate method for numerical deconvolution. It appears to be superior to the many model-dependent methods (6–10) because it is based on fewer assumptions and, therefore, is more likely to result in a meaningful evaluation of the drug input.

This work compares the new method with Cutler's approach using Cutler's simulated test data that contain various degrees of random noise (4, 5).

THEORY

Let the concentration of drug in the blood, $c^*(t)$, following an initial intravenous bolus dose, q^*, be described by a multiexponential relationship (1):

$$c^*(t) = \sum_{i=1}^{n} a_i e^{\lambda_i t} \qquad \text{(Eq. 1)}$$

Let $c(t)$ denote the drug level resulting from an unknown input of a drug that, in the same subject with the same linear relationship between input and response, results in the blood level $c^*(t)$ (Eq. 1) when an intravenous bolus dose, q^*, is given. It has been shown (1) that the rate of input of the drug then is given by:

$$f(t) = q^* \left[-\frac{\sum_{i=1}^{n} a_i \lambda_i}{\left[\sum_{i=1}^{n} a_i\right]^2} c(t) + \frac{c'(t)}{\sum_{i=1}^{n} a_i} + \sum_{i=1}^{n-1} b_i e^{\beta_i t} \int_0^t c(u) e^{-\beta_i u}\, du \right] \qquad \text{(Eq. 2)}$$

where β_i, $i = 1, 2, \ldots, n-1$ are the roots of the $(n-1)$th-degree polynomial:

$$Q(x) = \sum_{i=1}^{n} a_i \prod_{\substack{j=1 \\ \neq i}}^{n} (x - \lambda_j) \qquad \text{(Eq. 3)}$$

and b_ν, $\nu = 1, 2, \ldots, n-1$ are obtained from:

$$b_\nu = \left[\sum_{i=1}^{n} \frac{a_i}{\beta_\nu - \lambda_i} \sum_{\substack{j=1 \\ \neq i}}^{n} \frac{1}{\beta_\nu - \lambda_j} \right]^{-1} \qquad \text{(Eq. 4)}$$

Integration of $f(t)$ from time zero to time t yields the cumulative amount of input:

$$A(t) = q^* \left[-\left\{ \frac{\sum_{i=1}^{n} a_i \lambda_i}{\left(\sum_{i=1}^{n} a_i\right)^2} + \sum_{i=1}^{n-1} \frac{b_i}{\beta_i} \right\} \int_0^t c(t)\, dt + \frac{c(t)}{\sum_{i=1}^{n} a_i} + \sum_{i=1}^{n-1} \frac{b_i}{\beta_i} e^{\beta_i t} \int_0^t c(u) e^{-\beta_i u}\, du \right] \qquad \text{(Eq. 5)}$$

0022-3549/80/0300-0305$01.00/0
© 1980, American Pharmaceutical Association

It may be more convenient to describe the amount as a percentage of the dose, q, given, *i.e.*:

$$\mathrm{PCT}(t) = 100\frac{q^*}{q}\left[-\left\{\frac{\sum_{i=1}^{n} a_i\lambda_i}{\left(\sum_{i=1}^{n} a_i\right)^2} + \sum_{i=1}^{n-1}\frac{b_i}{\beta_i}\right\}\int_0^t c(t)dt + \frac{c(t)}{\sum_{i=1}^{n} a_i} + \sum_{i=1}^{n-1}\frac{b_i}{\beta_i}e^{\beta_i t}\int_0^t c(u)e^{-\beta_i u}\,du\right] \quad \text{(Eq. 6)}$$

Consider as an example the case where the drug level after an intravenous bolus dose, q^*, is described by a two-exponential expression:

$$c^*(t) = a_1e^{\lambda_1 t} + a_2e^{\lambda_2 t} \quad \text{(Eq. 7)}$$

The auxiliary parameters β_1 and b_1, according to Eqs. 3 and 4, are given by:

$$\beta_1 = \frac{a_1\lambda_2 + a_2\lambda_1}{a_1 + a_2} \quad \text{(Eq. 8)}$$

and:

$$b_1 = -\frac{a_1a_2(\lambda_1 - \lambda_2)^2}{(a_1 + a_2)^3} \quad \text{(Eq. 9)}$$

so that the rate of input becomes:

$$f(t) = q^*\left[-\frac{a_1\lambda_1 + a_2\lambda_2}{(a_1 + a_2)^2}c(t) + \frac{c'(t)}{a_1 + a_2} - \frac{a_1a_2(\lambda_1 - \lambda_2)^2}{(a_1 + a_2)^3} \times \exp\left(\frac{a_1\lambda_2 + a_2\lambda_1}{a_1 + a_2}t\right)\int_0^t c(u)\exp\left(-\frac{a_1\lambda_2 + a_2\lambda_1}{a_1 + a_2}u\right)du\right] \quad \text{(Eq. 10)}$$

and the cumulative amount of input expressed as a percentage of the dose, q, becomes:

$$\mathrm{PCT}(t) = 100\frac{q^*}{q}\left[-\left\{\frac{a_1\lambda_2 + a_2\lambda_1}{(a_1 + a_2)^2} - \frac{a_1a_2(\lambda_1 - \lambda_2)^2}{(a_1\lambda_2 + a_2\lambda_1)(a_1 + a_2)^2}\right\} \times \int_0^t c(t)dt + \frac{c(t)}{a_1 + a_2} - \frac{a_1a_2(\lambda_1 - \lambda_2)^2}{(a_1\lambda_2 + a_2\lambda_1)(a_1 + a_2)^2}\exp\left(\frac{a_1\lambda_2 + a_2\lambda_1}{a_1 + a_2}t\right) \times \int_0^t c(u)\exp\left(-\frac{a_1\lambda_2 + a_2\lambda_1}{a_1 + a_2}u\right)du\right] \quad \text{(Eq. 11)}$$

which simplifies to:

$$\mathrm{PCT}(t) = 100\frac{q^*}{q}\left[-\frac{\lambda_1\lambda_2}{a_1\lambda_2 + a_2\lambda_1}\int_0^t c(t)dt + \frac{c(t)}{a_1 + a_2} - \frac{a_1a_2(\lambda_1 - \lambda_2)^2}{(a_1\lambda_2 + a_2\lambda_1)(a_1 + a_2)^2}\exp\left(\frac{a_1\lambda_2 + a_2\lambda_1}{a_1 + a_2}t\right) \times \int_0^t c(u)\exp\left(-\frac{a_1\lambda_2 + a_2\lambda_1}{a_1 + a_2}u\right)du\right] \quad \text{(Eq. 12)}$$

The procedure for evaluating the input is as follows. The two-exponential expression (Eq. 7) is fitted by nonlinear regression to the intravenous bolus data to estimate a_1, a_2, λ_1, and λ_2. A suitable empirical function[1], $s(t)$, is fitted to the absorption data to estimate the true drug level, $c(t)$. The rate and extent of absorption then are estimated according to Eqs. 10 and 12 using the estimates obtained for a_1, a_2, λ_1, λ_2, and $c(t)$.

The function $s(t)$ chosen to estimate $c(t)$ is an adaptive least-squares cubic spline function (12)[2]. This function is fitted to the data by minimizing the following expression:

$$E = \sum_{i=1}^{m}[w_i|c_i - s(t_i)|]^2 + \sum_{i=2}^{N-1}[\theta_i d_i]^2 \quad \text{(Eq. 13)}$$

where w_i are weights and (c_i, t_i), $i = 1, 2, \ldots, m$ are the absorption data. This expression consists of the usual least-squares term (the first term) and a smoothing term that is determined automatically using statistical tests on errors (16). The function $s(t)$ is a cubic spline with knots $\xi_1, \xi_2, \xi_3, \ldots, \xi_N$ and d_i represents the discontinuity in $s'''(t)$ at ξ_i, *i.e.*:

$$d_i = s'''(\xi_i + 0) - s'''(\xi_i - 0) \quad \text{(Eq. 14)}$$

The θ_i values are weight factors used for smoothing $s(t)$. In the fitting procedure, the number of knots, N, their position, and the smoothing weight factors, θ_i, are optimized automatically so that the fitted spline function attempts to follow trends in the data but ignores random errors (16). The rate of input (Eq. 2) and the extent of input (Eq. 5 or 6) can be evaluated accurately without numerical integration errors[3] when a cubic spline function, $s(t)$, is used to estimate $c(t)$.

This evaluation leads to the following expressions:

$$f(t) = q^*\left[-\frac{\sum_{i=1}^{n} a_i\lambda_i}{\left(\sum_{i=1}^{n} a_i\right)^2}s(t) + \frac{s'(t)}{\sum_{i=1}^{n} a_i} + \sum_{i=1}^{n-1} b_i\left\{-\sum_{k=0}^{3}\frac{s^{(k)}(t)}{\beta_i^{k+1}} + e^{\beta_i t}\sum_{k=0}^{3}\frac{s^{(k)}(0)}{\beta_i^{k+1}} + \beta_i^{-4}\sum_{k=2}^{j} e^{\beta_i(t-\xi_k)}d_k\right\}\right] \quad \text{(Eq. 15)}$$

where j is the highest integer for which $t \le \xi_j$ is satisfied, *i.e.*:

$$j = \overset{\sup}{i}\,(t \le \xi_i) \quad \text{(Eq. 16)}$$

and:

$$\mathrm{PCT}(t) = 100\frac{q^*}{q}\left[-\left(\frac{\sum_{i=1}^{n} a_i\lambda_i}{\left[\sum_{i=1}^{n} a_i\right]^2} + \sum_{i=1}^{n-1}\frac{b_i}{\beta_i}\right)\int_0^t s(t)dt + \frac{s(t)}{\sum_{i=1}^{n} a_i} + \sum_{i=1}^{n-1}\frac{b_i}{\beta_i}\left\{-\sum_{k=0}^{3}\frac{s^{(k)}(t)}{\beta_i^{k+1}} + e^{\beta_i t}\sum_{k=0}^{3}\frac{s^{(k)}(0)}{\beta_i^{k+1}} + \beta_i^{-4}\sum_{k=2}^{j} e^{\beta_i(t-\xi_k)}d_k\right\}\right] \quad \text{(Eq. 17)}$$

EXPERIMENTAL

The simulated data used to test the new method consist of four sets of data presented by Cutler (4) and denoted as Data Sets 1–4. Each set consists of a set of 11 simulated unit impulse response data with random noise added and a set of 11 simulated input response data also containing noise from the same linear system. The method of analysis is model independent. Therefore, the models used to simulate data from a linear system to test the method can be chosen arbitrarily.

The models employed by Cutler to generate the test data (Table I) were chosen because of their resemblance to models commonly employed in drug release and drug absorption analyses. They can be considered, in the classical linear pharmacokinetic sense, as a two-compartment model with first-order input (Data Sets 1 and 2) and as a two-compartment model with dissolution rate-limited release from an intramuscular injection, where the drug release follows the well-known cube-root relationship (17) (Data Sets 3 and 4). The results shown for Cutler's method (Tables II–V) were chosen as the best results reported (5).

Data Treatment—Polyexponential expressions of increasing degree n (Eq. 1) were fitted to the unit impulse response data with equal weights using the nonlinear regression program FUNFIT (18). A two-exponential expression fit the data adequately (Table VI). The cubic spline function, $s(t)$, was fitted to the input response data using the subroutine VCO3A from the Harwell subroutine library (12). A subroutine was written that calls VCO3A and calculates, according to Eqs. 15 and 17, the rate and extent of input at the observation times and, optionally, at any number of equally spaced time points from time zero to the last observation time for graphical representation of the input[4]. The pentobarbital data used were those reported by Smith *et al.* (11).

[1] The term empirical function is used here to denote a function that describes empirical data in a low information situation where no specific mathematical model is assumed.

[2] References 13–15 give an introduction to the theory and applications of spline functions in data analysis.

[3] This is the case because analytical expressions exist for $s'(t)$, $s''(t)$, and $s'''(t)$ and because $\int_0^t s(t)dt$ (Eq. 17) leads to a polynomial expression that can be evaluated exactly.

[4] Plotted using a Tektronix 4662 penplotter using a FORTRAN IV graphical software package written by the author.

Table I—Origin of the Simulated Data in Data Sets 1–4 [a]

Data Set	Rate of Input	Amount of Input, $f(t)$	Random Noise Level[b], %	Unit Impulse Response Data	Input Response Data
1	$f(0)e^{-kt}$	$\frac{f(0)}{k}(1-e^{-kt})$	1	$a_1e^{\lambda_1 t}+a_2e^{\lambda_2 t}+\epsilon$	$c^*(t)*f(t)+\epsilon$
2	$f(0)e^{-kt}$	$\frac{f(0)}{k}(1-e^{-kt})$	10	$a_1e^{\lambda_1 t}+a_2e^{\lambda_2 t}+\epsilon$	$c^*(t)*f(t)+\epsilon$
3	$\frac{3D}{t_d}\left(1-\frac{t}{t_d}\right)_+^2$	$D\left[1-\left(1-\frac{t}{t_d}\right)_+^3\right]$	1	$a_1e^{\lambda_1 t}+a_2e^{\lambda_2 t}+\epsilon$	$c^*(t)*f(t)+\epsilon$
4	$\frac{3D}{t_d}\left(1-\frac{t}{t_d}\right)_+^2$	$D\left[1-\left(1-\frac{t}{t_d}\right)_+^3\right]$	10	$a_1e^{\lambda_1 t}+a_2e^{\lambda_2 t}+\epsilon$	$c^*(t)*f(t)+\epsilon$

[a] The following notations are used: $(1-x)_+ = \max(0, 1-x)$; and $c^*(t)*f(t)$ is the convolution of $c^*(t)$ and $f(t)$, where $c^*(t) = a_1\exp(\lambda_1 t) + a_2\exp(\lambda_2 t)$. The parameters used in the simulations are: $a_1 = a_2 = 1$, $\lambda_1 = -5$, $\lambda_2 = -1$, $k = 2$, $D = 0.6$, $t_d = 1.15$, and $f(0) = 1.2$. [b] See Ref. 4 for details.

Table II—Input Rates Calculated from Data Set 1 Using the New Method and the Cutler Method

Time	Exact Rate	New Method	Percent Difference[a]	Cutler Method	Percent Difference[a]
0.1	0.9825	0.9666	−1.32	0.967	−1.29
0.2	0.8044	0.8366	2.68	0.810	0.467
0.3	0.6586	0.6884	2.48	0.674	1.28
0.4	0.5392	0.5500	0.901	0.556	1.40
0.6	0.3614	0.3658	0.364	0.370	0.717
0.8	0.2423	0.2339	−0.701	0.240	−0.192
1.0	0.1624	0.1555	−0.577	0.156	−0.533
1.2	0.1089	0.1160	0.598	0.105	−0.325
1.4	0.0730	0.0790	0.506	0.076	0.250
1.6	0.0489	0.0404	−0.712	0.057	0.675
2.0	0.0220	0.0230	0.083	0.003	−1.583
Mean[b]			0.99		0.79
SD[b]			0.84		0.50

[a] Calculated as 100 × (calculated rate − exact rate)/1.2, where 1.2 is the initial exact input rate. [b] The mean and the standard deviation of the absolute values of the percent difference.

Table III—Input Rates Calculated from Data Set 2 Using the New Method and the Cutler Method

Time	Exact Rate	New Method	Percent Difference[a]	Cutler Method	Percent Difference[a]
0.1	0.9825	0.8784	−8.67	0.904	−6.54
0.2	0.8044	0.8087	0.36	0.813	0.72
0.3	0.6586	0.7242	5.47	0.724	5.45
0.4	0.5392	0.6358	8.05	0.639	8.32
0.6	0.3614	0.4771	9.64	0.479	9.80
0.8	0.2423	0.3308	7.37	0.338	7.98
1.0	0.1624	0.2199	4.79	0.219	4.72
1.2	0.1089	0.1409	2.67	0.125	1.34
1.4	0.0730	0.0708	−0.18	0.058	−1.25
1.6	0.0489	0.0129	−3.00	0.020	−2.41
2.0	0.0220	0.0091	−1.08	0.027	0.42
Mean[b]			4.65		4.41
SD[b]			3.46		3.45

[a] Calculated as 100 × (calculated rate − exact rate)/1.2, where 1.2 is the initial exact input rate. [b] The mean and the standard deviation of the absolute values of the percent difference.

The data treatment of the pentobarbital data (Table VII) was identical to the treatment of the simulated data with the exception of the additional determination of the absorption lag time. The lag time was determined by linear extrapolation using the line that agreed with the fitted spline function and its slope at the first observation time. The appropriate time transformation then was performed before the rate and extent of input were calculated. Although the intravenously administered pentobarbital was given by a 5-min infusion, it was considered computationally as a bolus input because of the short infusion time relative to the absorption time and the rate of drug elimination.

RESULTS AND DISCUSSION

The analysis method does not require the input of a particular linear or nonlinear form, nor does it assume a specific linear pharmacokinetic model. The method only assumes a time-invariant linearity between input and response and that the impulse response (intravenous bolus input) can be approximated adequately by a polyexponential expression.

The equations for the rate (Eq. 2) and the extent (Eqs. 5 and 6) of input are mathematically exact expressions. The accuracy with which the input is evaluated is determined solely by the accuracy with which $c^*(t)$ (as described by a_i, λ_i, $i = 1, 2, \ldots, n$) and $c(t)$ are estimated. Therefore, the accuracy of the estimation depends on the qualities of two curve fittings. The functional form of $c^*(t)$ has been established as Eq. 1 (1). The method estimates $c^*(t)$ by least-squares regression which, according to the central limit theorem and the Gauss–Markov theorem, can be considered to be statistically the best estimation when no prior information is available about the statistical properties of the errors. Appropriate weighting can be applied if the variances of the errors can be estimated (18).

The estimation of $c(t)$ is the most difficult step. Its functional form is unknown in any model-independent approach. The main problem is to find an empirical function that can be fitted so that it follows the trend and the intrinsic values of the data but ignores the errors. A proper choice of function must be based on assumptions about the properties of the errors and the real behavior of $c(t)$. The function chosen must be able, when fitted, to reflect and demonstrate these properties properly. The present method generally assumes random errors. Although it is difficult to make assumptions about the real behavior of $c(t)$, it seems important

Table IV—Input Rates Calculated from Data Set 3 Using the New Method and the Cutler Method

Time	Exact Rate	New Method	Percent Difference[a]	Cutler Method	Percent Difference[a]
0.1	1.3048	1.2780	−1.71	1.256	−3.11
0.2	1.0681	1.1080	2.55	1.060	−0.51
0.3	0.8551	0.8959	2.61	0.893	2.42
0.4	0.6657	0.6839	1.16	0.715	3.15
0.6	0.3580	0.3609	0.19	0.356	−0.13
0.8	0.1450	0.1312	−0.88	0.115	−1.92
1.0	0.0266	0.0202	−0.41	0.026	−0.04
1.2	0	0.0011	0.07	0.004	0.26
1.4	0	0.0010	0.06	−0.010	−0.64
1.6	0	0.0008	0.05	0.048	3.07
2.0	0	0.0007	0.04	−0.526	33.61
Mean[b]			0.88		4.44
SD[b]			1.00		9.76

[a] Calculated as 100 × (calculated rate − exact rate)/(1.8/1.15), where 1.8/1.15 is the exact initial input rate. [b] The mean and the standard deviation of the absolute values of the percent difference.

Table V—Input Rates Calculated from Data Set 4 Using the New Method and the Cutler Method

Time	Exact Rate	New Method	Percent Difference[a]	Cutler Method	Percent Difference[a]
0.1	1.3048	1.1761	−8.22	1.235	−4.46
0.2	1.0681	1.0614	−0.43	1.058	−0.65
0.3	0.8551	0.9224	4.30	0.895	2.55
0.4	0.6657	0.7740	6.92	0.744	5.00
0.6	0.3580	0.4934	8.65	0.481	7.86
0.8	0.1450	0.2480	6.58	0.270	7.99
1.0	0.0266	0.0859	3.79	0.109	5.26
1.2	0	0.0057	0.36	0.000	0.00
1.4	0	0.0008	0.05	−0.059	−3.77
1.6	0	0.0000	0.00	−0.066	−4.22
2.0	0	0.0000	0.00	0.074	4.73
Mean[b]			3.57		4.23
SD[b]			3.55		2.51

[a] Calculated as 100 × (calculated rate − exact rate)/(1.8/1.15), where 1.8/1.15 is the exact initial input rate. [b] The mean and the standard deviation of the absolute values of the percent difference.

to consider the concept of smoothness. It seems unrealistic to assume $c(t)$ to be as smooth as the functions fitted in model-dependent approaches, considering the natural oscillations in the many body functions affecting absorption. It is more realistic to consider $c(t)$ to have a certain degree of fluctuation.

The adaptive least-squares cubic spline function was chosen to estimate $c(t)$ because it has the following properties. It is flexible enough to follow whatever shape $c(t)$ may have (15). Due to the smoothing term (the second term of Eq. 13), it is not so floppy that it fits to the errors in the data, *i.e.*, by going through all of the data points. The fit of the spline function in one region bears little relationship to its behavior in another region (15). Polynomials and other continuous mathematical functions that are not defined in a piecemeal fashion have just the opposite property. Namely, their behavior in any region determines their behavior everywhere. This unique and important property of the spline function enables it to describe the local behavior of $c(t)$ with no interference from nonlocal data points. The spline function has a smoothness that seems realistic in relation to the response it attempts to describe. It is well recognized in numerical analysis that spline functions are excellent tools for differentiation and integration. Therefore, a spline function representation should provide good estimates for the rate and the extent of drug input, considering the algebraic form of Eqs. 2, 5, and 6. Spline functions, when fitted to data by the least-squares method, conserve the first two moments of the data (19). This statistical property makes spline functions suitable for the analysis of observations with random errors because estimates of the mean, variance, and confidence interval of the true response can be obtained.

The theoretical basis for the described properties of spline functions

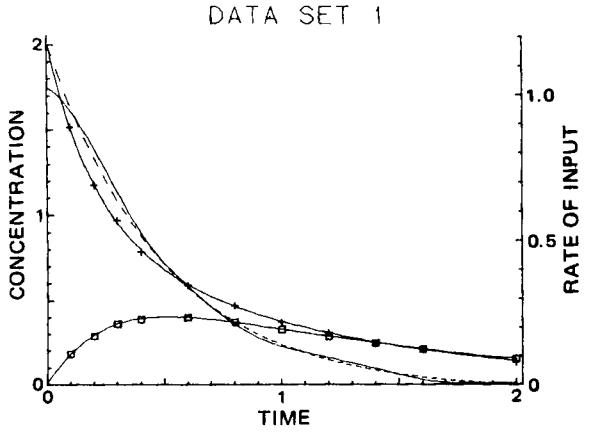

Figure 1—*Test of the new method on simulated data containing 1% random error. Equation 1* (n = 2) *is fitted to the impulse response data* (+). *An adaptive least-squares cubic spline function,* s(t), *is fitted to the input response data* (□). *The slightly sigmoid-shaped curve is the rate of input calculated from* a_i, λ_i, i = *1, 2 and* s(t) *according to Eq. 15. The broken curve is the exact rate of input.*

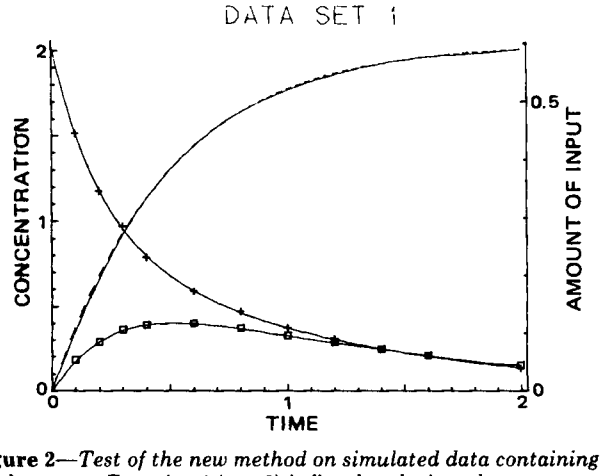

Figure 2—*Test of the new method on simulated data containing 1% random error. Equation 1* (n = 2) *is fitted to the impulse response data* (+). *An adaptive least-squares cubic spline function,* s(t), *is fitted to the input response data* (□). *The continuously increasing curve is the amount of input calculated from* a_i, λ_i, i = *1, 2 and* s(t) *according to Eq. 17.*

Table VI—Least-Squares Unit Impulse Response Parameters Used in the Calculation of the Input [a]

Data Set	a_1	a_2	λ_1	λ_2	Sum of Squares	Correlation Coefficient, r	Figure
1	1.0427	0.97617	−5.0526	−0.97567	4.54×10^{-4}	0.9998	1 and 2
2	1.3377	0.52381	−3.1851	−0.61065	3.14×10^{-2}	0.9919	3 and 4
3	1.0308	1.0487	−5.9131	−1.0262	2.18×10^{-4}	0.9999	5 and 6
4	1.3377	0.52381	−3.1851	−0.61065	3.14×10^{-2}	0.9919	7 and 8

[a] Determined with the FUNFIT program (18).

Table VII—Least-Squares Parameters Obtained from Plasma Pentobarbital Data from Intravenous Administration and Used in the Calculation of the Input [a]

Subject	a_1, μg/ml	a_2, μg/ml	λ_1, hr^{-1}	λ_2, hr^{-1}	Sum of Squares, $(\mu g/ml)^2$	Correlation Coefficient, r	Figure
R.M.	0.8014	0.5515	−1.7518	-2.391×10^{-2}	7.442×10^{-2}	0.9777	9
B.G.	0.8654	0.3396	−2.203	-9.940×10^{-3}	1.704×10^{-2}	0.9918	9
R.B.	0.6493	0.4222	−1.375	-1.984×10^{-2}	3.34×10^{-2}	0.9850	9

[a] Determined with the FUNFIT program (18).

and their relationship to their application in empirical data analysis have been discussed extensively (13–15, 19).

Numerical Results—The two linear systems from which the simulated data were generated will be denoted as Systems 1 and 2, corresponding to Data Sets 1 and 2 and 3 and 4, respectively.

Both the rate and the extent of input were evaluated from the four data sets, giving a total of eight determinations (Figs. 1–8 and Tables II–V).

System 1, Data Set 1 (Noise Level 1%)—There was no significant difference in the results obtained by the new method and Cutler's method (t test, $p = 0.95$). The pattern of the errors was similar for the two methods. The average percent relative error was on the same order of magnitude as the percent error added to the data. The methods appeared to be least accurate in the initial stage of the input (Table II and Figs. 1 and 2).

System 1, Data Set 2 (Noise Level 10%)—Raising the error level from 1 to 10% did not differentiate between the two methods. The pattern of the errors again was similar, and the average percent error was of the same order of magnitude as the noise added to the data (Table III and Figs. 3 and 4).

System 2, Data Set 3 (Noise Level 1%)—Although the Cutler method appeared to perform better in the initial stage of the input, it did not estimate the input as accurately as did the new method at later sampling times. The difference was particularly great at the last sampling point. The new method seemed to give an overall better estimate of the input (Table IV and Figs. 5 and 6).

System 2, Data Set 4 (Noise Level 10%)—The two methods did not seem to be significantly different in their overall accuracy when the error level was raised from 1 to 10%. However, the new method appeared to determine the input rate more accurately at the later sampling times. The average percent error for the two methods was on the same order of magnitude as the noise level and came close to the averages obtained for System 1 where the same degree of noise was added to the data (Table V and Figs. 7 and 8).

It is not possible to differentiate between the two methods on the basis of the test data. They both performed well considering that the average relative error in all estimations was of the same magnitude as the noise added to the simulated data. However, both methods appeared to underestimate the initial release rate consistently. Cutler's test problems could not discriminate between the two methods because the test data simulate rather ideal, somewhat synthetic cases. In practice, it is uncommon to have so many points sampled in the absorption phase, and the sampling is rarely taken so evenly and at the same times after intravenous and oral administrations. Also, it is uncommon not to have a lag time in the absorption phase.

An excessive number of simulation tests is required to establish experimentally, using a variety of linear systems and sampling schemes, the relative performance of the two methods. However, the following theoretical considerations should give an assessment of the methods and how they may perform in various situations.

Both methods use empirical functions. The Cutler method uses polynomials of various degrees to represent the input function and the unit impulse response. The new method uses an adaptive least-squares cubic spline function to represent the input response and a polyexponential expression (Eq. 1) to represent the impulse response. It is important to recognize the properties of polynomials relative to the properties of a

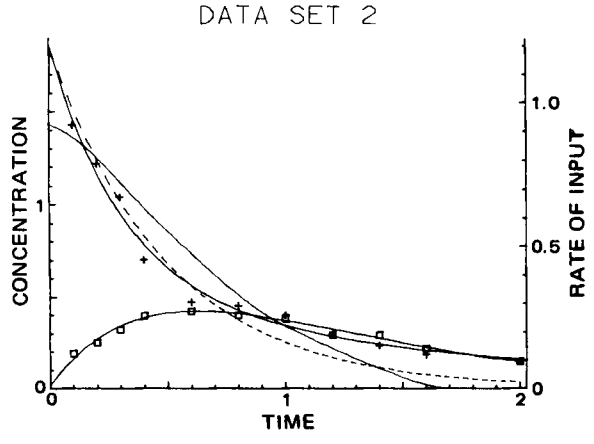

Figure 3—*Test of the new method on simulated data containing 10% random error. Equation 1 (n = 2) is fitted to the impulse response data (+). An adaptive least-squares cubic spline function, s(t), is fitted to the input response data (□). The slightly sigmoid-shaped curve is the rate of input calculated from a_i, λ_i, i = 1, 2 and s(t) according to Eq. 15. The broken curve is the exact rate of input.*

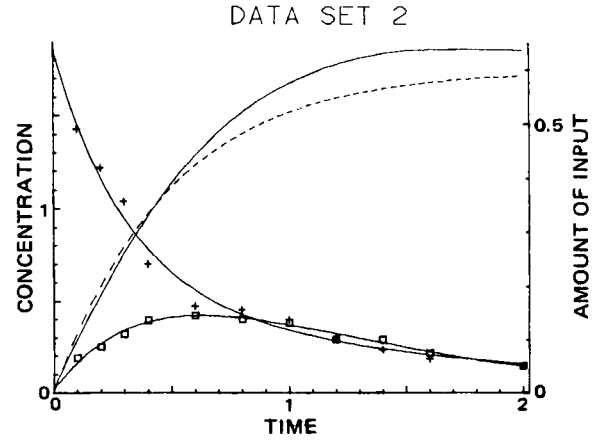

Figure 4—*Test of the new method on simulated data containing 10% random error. Equation 1 (n = 2) is fitted to the impulse response data (+). An adaptive least-squares cubic spline function, s(t), is fitted to the input response data (□). The continuously increasing curve is the amount of input calculated from a_i, λ_i, i = 1, 2 and s(t) according to Eq. 17.*

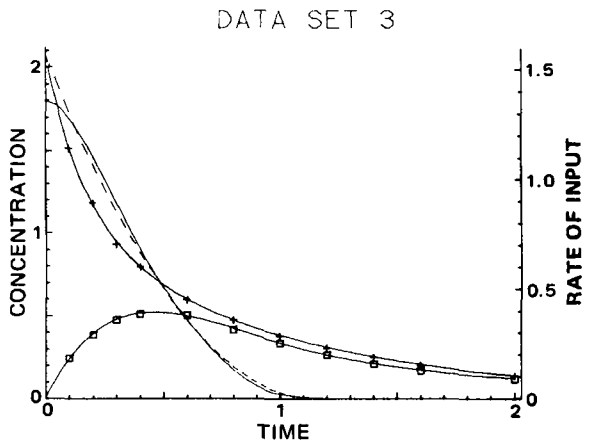

Figure 5—*Test of the new method on simulated data containing 1% random error. Equation 1* (n = 2) *is fitted to the impulse response data* (+). *An adaptive least-squares cubic spline function,* s(t), *is fitted to the input response data* (□). *The slightly sigmoid-shaped curve is the rate of input calculated from* a_i, λ_i, i = *1, 2 and* s(t) *according to Eq. 15. The broken curve is the exact rate of input.*

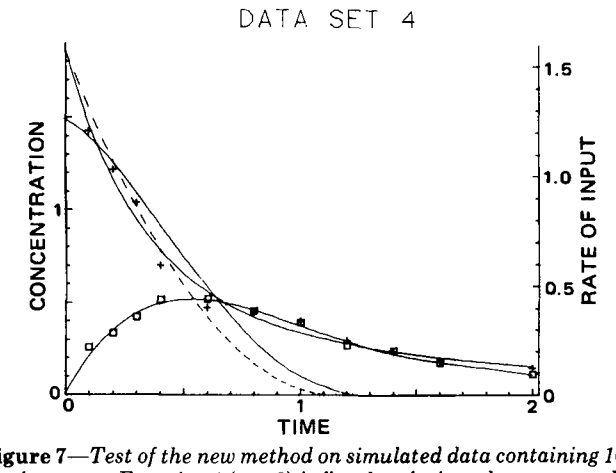

Figure 7—*Test of the new method on simulated data containing 10% random error. Equation 1* (n = 2) *is fitted to the impulse response data* (+). *An adaptive least-squares cubic spline function,* s(t), *is fitted to the input response data* (□). *The slightly sigmoid-shaped curve is the rate of input calculated from* a_i, λ_i, i = *1, 2 and* s(t) *according to Eq. 15. The broken curve is the exact rate of input.*

least-squares cubic spline function and a polyexponential expression since the differences may explain and predict how the two methods perform under various conditions. Least-squares polynomials usually give a good data representation when the data points are fairly equally spaced and do not change too rapidly or contain excessive errors as in the described simulation study. They then interpolate well but perform poorly when used for extrapolation beyond the end-points. The extrapolation error frequently increases rapidly with the distance from the end-point. Cutler used a polynomial to represent the impulse response (the intravenous bolus response). The polynomial is extrapolated from the first sampling time to time zero to calculate the convolution integral (p. 249, Ref. 5) that plays an essential role in his method. The chance of introducing a substantial error in this way becomes particularly significant if early intravenous data are lacking.

It sometimes is desirable to evaluate the absorption of a drug that has been sampled longer than its intravenous bolus response. Inaccurate results may be expected using Cutler's method in such cases because it requires a polynomial extrapolation beyond the last intravenous bolus data point to calculate the convolution integral. It is well known that polynomials may interpolate badly and show large oscillations between some data points if the data are not spaced fairly equally or contain one or more large gaps, due to missing data for example. The Cutler method is expected to be deficient when applied to such data. It is well known in empirical data fittings that cubic spline functions are superior to polynomials with respect to interpolation and extrapolation (20). It also is evident that the polyexponential expression, Eq. 1, is superior to a polynomial for interpolation and especially for extrapolation of the intravenous bolus response, considering the well-documented and successful use of Eq. 1 in pharmacokinetics. Therefore, the new method is expected to be more accurate with respect to the interpolations and the extrapolations that greatly influence the accuracy of the two methods.

Cutler's method should perform at its best when the sampling times from intravenous and nonintravenous administrations coincide as in the test examples. This result occurs because the polynomial representation of the input function is best defined under this condition, due to the local emphasis inherent in the sum of squares expression being minimized. The accuracy of the new method does not depend on whether the sampling times coincide because of the different approach used. Most absorption data in pharmacokinetics contain a lag time. Cutler did not discuss how his method should be applied to take this factor into account.

It seems apparent from the discussion that the test data used tend to give an optimistically biased evaluation of the performance of Cutler's method. A differentiation of the two methods may result if more realistic simulation studies are performed.

The user of Cutler's method is faced with several different estimations of the input corresponding to the various degrees of the polynomial used in the approximations of the input rate. The problem of picking the "best" results is complicated by possible multiple minima of the residual mean square function (5). If a polynomial of too high a degree is used, it will fit to the errors in the data and produce unreliable results. In favor-

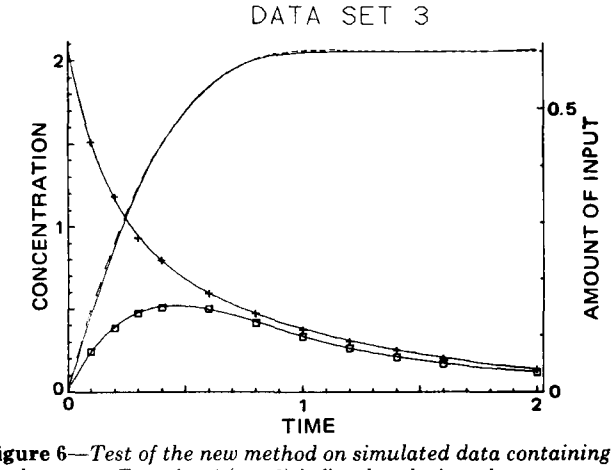

Figure 6—*Test of the new method on simulated data containing 1% random error. Equation 1* (n = 2) *is fitted to the impulse response data* (+). *An adaptive least-squares cubic spline function,* s(t), *is fitted to the input response data* (□). *The continuously increasing curve is the amount of input calculated from* a_i, λ_i, i = *1, 2 and* s(t) *according to Eq. 17.*

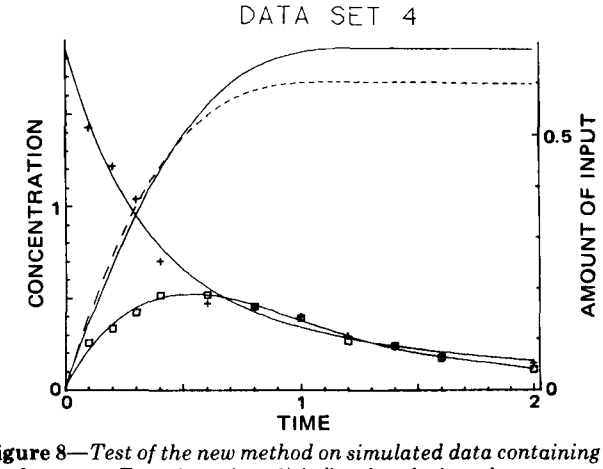

Figure 8—*Test of the new method on simulated data containing 10% random error. Equation 1* (n = 2) *is fitted to the impulse response data* (+). *An adaptive least-squares cubic spline function,* s(t), *is fitted to the input response data* (□). *The continuously increasing curve is the amount of input calculated from* a_i, λ_i, i = *1, 2 and* s(t) *according to Eq. 17.*

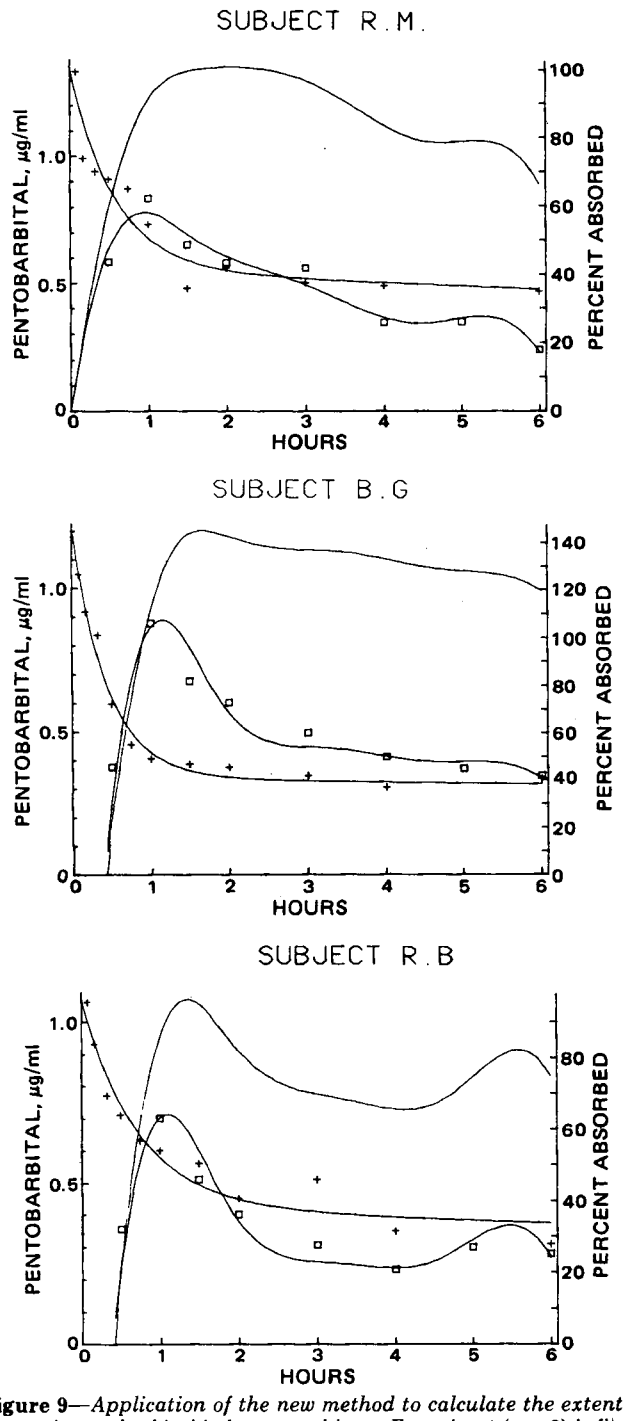

Figure 9—*Application of the new method to calculate the extent of input of pentobarbital in human subjects. Equation 1* (n = 2) *is fitted to the plasma drug level data* (+) *from intravenous administration. An adaptive least-squares cubic spline function,* s(t), *is fitted to the oral absorption data* (□). *The drug input (upper curves) is calculated from* a_i, λ_i, i = *1, 2 and* s(t) *according to Eq. 17.*

able cases, a suitable, well-defined minimum may exist, but the problem is expected to be particularly difficult in more realistic situations. The additional problem of choosing the proper polynomial to represent the impulse response was not discussed by Cutler. The number of multiple solutions is multiplied for each possible polynomial, thereby making a choice even more difficult.

The new method seems more appealing from the user's point of view because it gives clear, unambiguous results. It has the advantage that, contrary to Cutler's approximation method, it is based on an exact mathematical solution to the deconvolution problem of linear compartmental pharmacokinetics. The method also provides, as a by-product of the least-squares spline fitting to the absorption data, estimates of the important model-independent quantities, *i.e.*, time to the peak, maximum response, and area under the curve (truncated).

Pentobarbital Input—The pentobarbital data are difficult to treat because the absorption phase is defined by only three or four data points and because the absorption lag time is not well defined due to the lack of early sampling points (Fig. 9). Although the lag times for the absorption by Subjects R.B. and B.G. (0.36 and 0.46 hr, respectively) came close, it was not possible to detect a significant lag time for the absorption by Subject R.M. due to the low information density of the data in the absorption phase. It is satisfactory that the extent of absorption for R.M. and R.B. both came close to the label claim (100 and 96%, respectively) judged from the maximum of the percent absorbed curves (Fig. 9). However, the excessive value for Subject B.G. (144%) and the significant decline of the percent absorbed curves for all subjects indicate a pronounced violation of the assumption of time-invariant linearity between input and response.

The observed discrepancy was not caused by the method of analysis or the numerical treatment. The rate of decline of the absorption data after the absorption phase was significantly larger than the rate for the intravenous data, indicating apparently faster elimination after the oral administration. Under the given assumptions, this effect will computationally result in a negative input, *i.e.*, a decline in the percent absorbed curve after the absorption phase as shown due to an elimination rate that is faster than that expected judging from the intravenous data.

Several explanations may be investigated to explain this discrepancy between the oral and intravenous data. One possibility is that the linearity between input and response is only of a relatively short duration so that it changes significantly between administrations but not within the duration of a single administration. The merged intravenous bolus and input approach or the merged infusion and input approach (1) can be applied in such cases. These methods do not require a washout period between the intravenous and nonintravenous administrations. Therefore, the two administrations can be brought close together to minimize errors arising from a time-dependent input–response linearity. This ability should result in a more reliable drug input evaluation than is possible with other model-independent methods because these methods are based on a complete washout of drug between the administrations.

The new method appears to be a potentially powerful tool for the evaluation of drug input and bioavailability. It is based on an exact mathematical solution to the deconvolution problem of linear compartmental pharmacokinetics. The accuracy of the method is determined by how well the fitted curves represent the true response. The superimposed graphical representation of the estimated impulse and input responses and the calculated input, provided by the method (Fig. 9), consequently is of significant conceptual value. It enables the user to evaluate visually whether discrepancies or peculiarities in a calculated input are due to an improper data representation, judged from the fitted curves, or to the inherent nature of the impulse and input response data. The method is not used as a "black box" but enables the user to be critical about the results obtained and the assumptions made about the pharmacokinetics. Hopefully, this work will lead to a less assumptive and more objective approach in bioavailability testing.

REFERENCES

(1) P. Veng Pedersen, *J. Pharm. Sci.*, **69**, 298 (1980).

(2) L. Z. Benet and C. W. N. Chiang, paper presented at the APhA Academy of Pharmaceutical Sciences, Chicago meeting, Nov. 1977.

(3) J. Gamel, W. F. Rousseau, C. R. Katholi, and E. Messel. *Circ. Res.*, **32**, 516 (1973).

(4) D. J. Cutler, *J. Pharmacokinet. Biopharm.*, **6**, 227 (1978).

(5) *Ibid.*, **6**, 243 (1978).

(6) J. G. Wagner and E. Nelson, *J. Pharm. Sci.*, **52**, 610 (1963).

(7) J. C. K. Loo and S. Reigelman, *ibid.*, **57**, 918 (1968).

(8) C. Pidgeon and W. H. Pitlick, *Res. Commun. Chem. Pathol. Pharmacol.*, **18**, 467 (1977).

(9) J. G. Wagner, "Biopharmaceutics and Relevant Pharmacokinetics," Drug Intelligence Publications, Hamilton, Ill., 1971, chap. 37.

(10) M. Gibaldi, "Biopharmaceutics and Clinical Pharmacokinetics," Lea & Febiger, Philadelphia, Pa., 1977, chap. 4.

(11) R. B. Smith, L. W. Dittert, W. O. Griffen, Jr., and J. T. Doluisio, *J. Pharmacokinet. Biopharm.*, **1**, 5 (1973).

(12) M. J. Hopper, Theoretical Physics Division, Atomic Energy Research Establishment, Harwell Scientific Software Library, Harwell, Berkshire, England.

(13) S. Wold, *Technometrics*, **16**, 1 (1974).

(14) S. Wold, *Chem. Scr.*, **1**, 97 (1971).

(15) J. Ahlberg, E. N. Nilson, and J. L. Walsh, "The Theory of Splines and Their Applications," Academic, New York, N.Y., 1967.
(16) M. J. D. Powell, "Curve Fitting by Cubic Splines," Report T.P. 307, Theoretical Physics Division, Atomic Energy Research Establishment, Harwell, Berkshire, England, 1967.
(17) A. W. Hixson and J. H. Crowell, *Ind. Eng. Chem.*, **23**, 923 (1931).
(18) P. Veng Pedersen, *J. Pharmacokinet. Biopharm.*, **5**, 513 (1977).
(19) E. T. Whittaker and G. Robinson, "The Calculus of Observations," Blackie and Son Ltd., London, England, 1926.
(20) J. R. Rice, "The Approximation of Functions," vol. II, Addison-Wesley, Reading, Mass., 1969.

ACKNOWLEDGMENTS

Presented in part at the APhA Academy of Pharmaceutical Sciences, Hollywood, Fla., meeting, November 1978.

Novel Deconvolution Method for Linear Pharmacokinetic Systems with Polyexponential Impulse Response

PETER VENG PEDERSEN

Received November 15, 1978, from the *Department of Pharmacy, School of Pharmacy, University of California, San Francisco, CA 94143.* Accepted for publication March 28, 1979.

Abstract □ A novel least-squares deconvolution method for estimating the rate and the extent of drug input into the systemic circulation is presented. The method is based on a polyexponential approximation of the impulse response and a polynomial approximation of the input rate. The method, which is readily implemented on a computer using any multiple linear regression program with a zero-intercept option, is compared to two other deconvolution methods using simulated data with various degrees of random noise added. It appears to have several significant advantages. The method is applied to plasma pentobarbital level data from oral and intravenous administration. The assumptions and limitations of deconvolution methods for analyzing drug input into the blood are discussed.

Keyphrases □ Pharmacokinetics—deconvolution method, linear pharmacokinetics, polyexponential impulse response, drug input into blood □ Blood—drug input, deconvolution method for pharmacokinetic estimation □ Deconvolutions—pharmacokinetic estimation of drug input into blood □ Drug bioavailability—blood, deconvolution method for pharmacokinetic estimation

Drug input analysis is of utmost importance in biopharmaceutics because of its fundamental role in drug design, evaluation, and administration. Accurate quantitation of a drug's input–response relationship in a subject or patient population is, therefore, important. The relevant response is usually the drug concentration in the blood, in a certain tissue, or in an organ, but it may be a pharmacological or toxicological response.

The response environment is the destination for the input to be quantitated. There are two kinds of response environments: sampleable, *i.e.*, environments that can be quantitatively sampled for the drug, and nonsampleable. The blood, a tissue, or an organ are sampleable environments. Drug receptors and other biochemical structures responsible for a drug's pharmacological–toxicological response are usually nonsampleable environments. A drug's input can be experimentally verified only for sampleable environments. The evaluation of a drug's input into a nonsampleable environment would be based on some hypothesis about the quantitative relationship between the drug concentration in the nonsampleable response environment and the sampleable response. Therefore, it is not possible to quantitate drug input from pharmacological measurements if the input is defined with respect to a nonsampleable response environment, *e.g.*, drug receptors or "the biophase" (1).

For only a few drugs is it possible to establish experimentally a quantitative functional relationship between the drug concentration in a sampleable environment (*e.g.*, the blood) and the pharmacological response. In such cases, the pharmacological response may be used to evaluate the input into the sampleable environment. The possibility of noninvasive, nonanalytical techniques to quantitate drug input from pharmacological response measurements is exciting (1). However, the sources of errors are enormous and generally result in very inaccurate results. The blood is usually not the "site of action" for a drug and, therefore, may not represent the ultimate destination for the drug input. However, the transfer of a drug to the site of action from the blood is often direct, or the barriers involved are often insignificant compared to the physical, chemical, and biological barriers the drug encounters to get into the blood. Thus, it is adequate in most cases to evaluate the drug input with the blood as the response environment, as in the present approach.

The treatment presented is limited to linear pharmacokinetic systems, *i.e.*, systems where the input–response relationship follows the linear superposition principle. The classical linear compartmental systems (2, 3) belong to the family of linear systems. The method presented can be characterized in the classical (linear compartmental) pharmacokinetic sense as model independent. The various published approaches for evaluating drug input were discussed previously (4, 5).

THEORY

The drug level in the blood, $c^*(t)$, after an intravenous bolus dose, q^*, can often be well described by a polyexponential expression:

$$c^*(t) = \sum_{i=1}^{n} a_i e^{\lambda_i t} \qquad \text{(Eq. 1)}$$

If the blood drug level behaves linearly with respect to input into the blood, then the unit impulse response is $c^*(t)/q^*$, and the response to an arbitrary input rate, $f(t)$, is given by the general expression:

$$c(t) = \frac{1}{q^*} \int_0^t f(t-u)c^*(u)du \qquad \text{(Eq. 2)}$$

0022-3549/80/0300-0312$01.00/0
© 1980, American Pharmaceutical Association

(15) J. Ahlberg, E. N. Nilson, and J. L. Walsh, "The Theory of Splines and Their Applications," Academic, New York, N.Y., 1967.
(16) M. J. D. Powell, "Curve Fitting by Cubic Splines," Report T.P. 307, Theoretical Physics Division, Atomic Energy Research Establishment, Harwell, Berkshire, England, 1967.
(17) A. W. Hixson and J. H. Crowell, *Ind. Eng. Chem.*, **23**, 923 (1931).
(18) P. Veng Pedersen, *J. Pharmacokinet. Biopharm.*, **5**, 513 (1977).
(19) E. T. Whittaker and G. Robinson, "The Calculus of Observations," Blackie and Son Ltd., London, England, 1926.
(20) J. R. Rice, "The Approximation of Functions," vol. II, Addison-Wesley, Reading, Mass., 1969.

ACKNOWLEDGMENTS

Presented in part at the APhA Academy of Pharmaceutical Sciences, Hollywood, Fla., meeting, November 1978.

Novel Deconvolution Method for Linear Pharmacokinetic Systems with Polyexponential Impulse Response

PETER VENG PEDERSEN

Received November 15, 1978, from the *Department of Pharmacy, School of Pharmacy, University of California, San Francisco, CA 94143.* Accepted for publication March 28, 1979.

Abstract □ A novel least-squares deconvolution method for estimating the rate and the extent of drug input into the systemic circulation is presented. The method is based on a polyexponential approximation of the impulse response and a polynomial approximation of the input rate. The method, which is readily implemented on a computer using any multiple linear regression program with a zero-intercept option, is compared to two other deconvolution methods using simulated data with various degrees of random noise added. It appears to have several significant advantages. The method is applied to plasma pentobarbital level data from oral and intravenous administration. The assumptions and limitations of deconvolution methods for analyzing drug input into the blood are discussed.

Keyphrases □ Pharmacokinetics—deconvolution method, linear pharmacokinetics, polyexponential impulse response, drug input into blood □ Blood—drug input, deconvolution method for pharmacokinetic estimation □ Deconvolutions—pharmacokinetic estimation of drug input into blood □ Drug bioavailability—blood, deconvolution method for pharmacokinetic estimation

Drug input analysis is of utmost importance in biopharmaceutics because of its fundamental role in drug design, evaluation, and administration. Accurate quantitation of a drug's input–response relationship in a subject or patient population is, therefore, important. The relevant response is usually the drug concentration in the blood, in a certain tissue, or in an organ, but it may be a pharmacological or toxicological response.

The response environment is the destination for the input to be quantitated. There are two kinds of response environments: sampleable, *i.e.*, environments that can be quantitatively sampled for the drug, and nonsampleable. The blood, a tissue, or an organ are sampleable environments. Drug receptors and other biochemical structures responsible for a drug's pharmacological–toxicological response are usually nonsampleable environments. A drug's input can be experimentally verified only for sampleable environments. The evaluation of a drug's input into a nonsampleable environment would be based on some hypothesis about the quantitative relationship between the drug concentration in the nonsampleable response environment and the sampleable response. Therefore, it is not possible to quantitate drug input from pharmacological measurements if the input is defined with respect to a nonsampleable response environment, *e.g.*, drug receptors or "the biophase" (1).

For only a few drugs is it possible to establish experimentally a quantitative functional relationship between the drug concentration in a sampleable environment (*e.g.*, the blood) and the pharmacological response. In such cases, the pharmacological response may be used to evaluate the input into the sampleable environment. The possibility of noninvasive, nonanalytical techniques to quantitate drug input from pharmacological response measurements is exciting (1). However, the sources of errors are enormous and generally result in very inaccurate results. The blood is usually not the "site of action" for a drug and, therefore, may not represent the ultimate destination for the drug input. However, the transfer of a drug to the site of action from the blood is often direct, or the barriers involved are often insignificant compared to the physical, chemical, and biological barriers the drug encounters to get into the blood. Thus, it is adequate in most cases to evaluate the drug input with the blood as the response environment, as in the present approach.

The treatment presented is limited to linear pharmacokinetic systems, *i.e.*, systems where the input–response relationship follows the linear superposition principle. The classical linear compartmental systems (2, 3) belong to the family of linear systems. The method presented can be characterized in the classical (linear compartmental) pharmacokinetic sense as model independent. The various published approaches for evaluating drug input were discussed previously (4, 5).

THEORY

The drug level in the blood, $c^*(t)$, after an intravenous bolus dose, q^*, can often be well described by a polyexponential expression:

$$c^*(t) = \sum_{i=1}^{n} a_i e^{\lambda_i t} \qquad \text{(Eq. 1)}$$

If the blood drug level behaves linearly with respect to input into the blood, then the unit impulse response is $c^*(t)/q^*$, and the response to an arbitrary input rate, $f(t)$, is given by the general expression:

$$c(t) = \frac{1}{q^*} \int_0^t f(t-u)c^*(u)du \qquad \text{(Eq. 2)}$$

0022-3549/80/0300-0312$01.00/0
© 1980, American Pharmaceutical Association

A suitable method is to be derived whereby $f(t)$ can be estimated from samples of the bolus response, $c^*(t)$, and the input (absorption) response, $c(t)$.

Considering the many factors influencing the absorption process, it may be appropriate to approximate $f(t)$ with a model-independent empirical equation such as a polynomial:

$$f(t) = \sum_{i=0}^{N} x_i t^i \qquad \text{(Eq. 3)}$$

The problem is then to determine the polynomial coefficients $x_0, x_1, \ldots, x_N$. The following derivations (Eqs. 4–15) lead to an equation, Eq. 16, that is linear with respect to the coefficients. This equation can be used to calculate the coefficients by standard multiple linear regression techniques.

Inserting Eqs. 1 and 3 into Eq. 2 leads to:

$$c(t) = \frac{1}{q^*} \int_0^t \sum_{i=0}^{N} x_i (t-u)^i \sum_{j=1}^{n} a_j e^{\lambda_j t}\, du \qquad \text{(Eq. 4)}$$

The binomial expansion for $(t-u)^i$ leads to:

$$c(t) = \frac{1}{q^*} \int_0^t \sum_{i=0}^{N} x_i \sum_{j=0}^{i} \binom{i}{j} t^j (-1)^{i-j} u^{i-j} \sum_{k=1}^{n} a_k e^{\lambda_k u}\, du \qquad \text{(Eq. 5)}$$

so that:

$$c(t) = \frac{1}{q^*} \sum_{i=0}^{N} x_i \sum_{j=0}^{i} \binom{i}{j} t^j (-1)^{i-j} \sum_{k=1}^{n} a_k \int_0^t u^{i-j} e^{\lambda_k u}\, du \qquad \text{(Eq. 6)}$$

The following useful integral formula can be derived readily:

$$\int_0^t x^n e^{ax}\, dx = \frac{e^{at}}{a} \sum_{i=0}^{n} (-1)^i \frac{n!}{a^i (n-i)!} t^{n-i} - (-1)^n \frac{n!}{a^{n+1}} \qquad n \geq 0 \qquad \text{(Eq. 7)}$$

By applying this formula to the integral in Eq. 6, this equation becomes:

$$q^* c(t) = \sum_{i=0}^{N} x_i \sum_{j=0}^{i} \binom{i}{j} t^j (-1)^{i-j} \sum_{k=1}^{n} \frac{a_k}{\lambda_k} e^{\lambda_k t} \sum_{m=0}^{i-j} (-1)^m \times \frac{(i-j)!}{\lambda_k^m (i-j-m)!} t^{i-j-m} - \left[\sum_{i=0}^{N} x_i \sum_{j=0}^{i} \binom{i}{j} t^j (-1)^{i-j} \sum_{k=1}^{n} a_k (-1)^{i-j} \frac{(i-j)!}{\lambda_k^{i-j+1}} \right] \qquad \text{(Eq. 8)}$$

The second term in Eq. 8, indicated by a bracket, simplifies to:

$$\text{second term} = -\sum_{i=0}^{N} x_i i! \sum_{j=0}^{i} \frac{t^j}{j!} \sum_{k=1}^{n} \frac{a_k}{\lambda_k^{i-j+1}} \qquad \text{(Eq. 9)}$$

Multiplying through with t^j and rearranging terms in the first term of Eq. 8 lead to:

$$\text{first term} = \sum_{i=0}^{N} x_i i! \sum_{j=0}^{i} \frac{(-1)^{i-j}}{j!} \sum_{k=1}^{n} \frac{a_k}{\lambda_k} e^{\lambda_k t} \sum_{m=0}^{i-j} \frac{(-1)^{i-j-m}}{\lambda_k^m (i-j-m)!} t^{i-m} \qquad \text{(Eq. 10)}$$

By changing the order of the summation and rearranging terms, this expression becomes:

$$\text{first term} = \sum_{i=0}^{N} x_i i! \sum_{k=1}^{n} \frac{a_k}{\lambda_k} e^{\lambda_k t} \sum_{j=0}^{i} \sum_{m=0}^{i-j} \frac{(-1)^{i-j+m}}{\lambda_k^m j! (i-j-m)!} t^{i-m} \qquad \text{(Eq. 11)}$$

The coefficient to t^{i-m} resulting from the two innermost summations in Eq. 11 is:

$$\frac{1}{\lambda_k^m} \sum_{j=0}^{i-m} \frac{(-1)^{i-m-j}}{j!(i-m-j)!} = 0 \qquad m < i \qquad \text{(Eq. 12)}$$

Thus, only the term $1/\lambda_k^i (m = i)$ is left from the two innermost summations, which results in a substantial simplification of Eq. 11:

$$\text{first term} = \sum_{i=0}^{N} x_i i! \sum_{k=1}^{n} \frac{a_k}{\lambda_k^{i+1}} e^{\lambda_k t} \qquad \text{(Eq. 13)}$$

Equation 8, according to Eqs. 9 and 13, simplifies considerably to:

$$c(t) = \frac{1}{q^*} \sum_{i=0}^{N} x_i i! \left[\sum_{k=1}^{n} \frac{a_k}{\lambda_k^{i+1}} e^{\lambda_k t} - \sum_{j=0}^{i} \frac{t^j}{j!} \sum_{k=1}^{n} \frac{a_k}{\lambda_k^{i-j+1}} \right] \qquad \text{(Eq. 14)}$$

which also can be rearranged to give:

$$c(t) = \sum_{i=0}^{N} x_i \frac{1}{q^*} i! \sum_{j=1}^{n} \frac{a_j}{\lambda_j^{i+1}} \left[e^{\lambda_j t} - \sum_{k=0}^{i} \frac{(\lambda_j t)^k}{k!} \right] \qquad \text{(Eq. 15)}$$

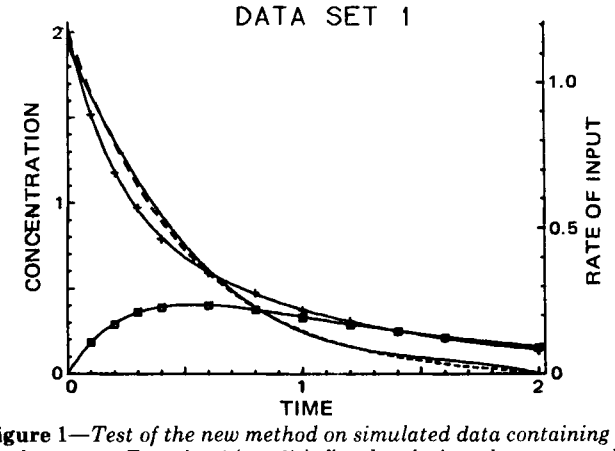

Figure 1—*Test of the new method on simulated data containing 1% random errors. Equation 1* (n = 2) *is fitted to the impulse response data* (+). *The curve representing the input response data* (□) *is calculated from Eq. 16 using the parameters* $x_0, x_1, \ldots, x_N$ *estimated by multiple linear regression and the parameters estimated from Eq. 1. The input curve is the input rate calculated according to Eq. 3. The broken curve is the exact input rate.*

For further simplification and to illustrate the linearity of $c(t)$ with respect to the polynomial coefficients $x_0, x_1, \ldots, x_N$, Eq. 15 can be written:

$$c(t) = \sum_{i=0}^{N} x_i \theta_i(t) \qquad \text{(Eq. 16)}$$

where:

$$\theta_i(t) = \frac{1}{q^*} i! \sum_{j=1}^{n} \frac{a_j}{\lambda_j^{i+1}} \left[e^{\lambda_j t} - \sum_{k=0}^{i} \frac{(\lambda_j t)^k}{k!} \right] \qquad \text{(Eq. 17)}$$

The expression inside the brackets in Eq. 17 is recognized as the difference between $e^{\lambda_j t}$ and a truncated Maclaurin series expansion of $e^{\lambda_j t}$. This difference becomes smaller when $\lambda_j t \to 0$ and when i increases, which may result in subtraction cancellation and loss of significant figures in the calculations. However, this result can be avoided by using alternative formulas for $\theta_i(t)$. When $|\lambda_j t|$ is small (<0.1), $\theta_i(t)$ is calculated most accurately from the tail of the Maclaurin series:

$$\theta_i(t) \doteq \frac{1}{q^*} i! \sum_{j=1}^{n} \frac{a_j}{\lambda_j^{i+1}} \sum_{k=i+1}^{K} \frac{(\lambda_j t)^k}{k!} \qquad \text{(Eq. 18)}$$

If the computer used represents floating-point numbers to m significant decimal digits, then K in Eq. 18 should be equal to $i + m + 1$ to get the best accuracy ($|\lambda_j t| < 0.1$). (The first neglected term in the summation of the series gives a strict error estimate because the series is alternating.) In the extreme cases where i (N) is large and $|\lambda_j t|$ is not small, $\theta_i(t)$ can be accurately evaluated using the integral representation of the tail of the Maclaurin series, which is:

$$\theta_i(t) = \frac{1}{q^*} \sum_{j=1}^{n} \frac{a_j}{(-\lambda_j)^{i+1}} \int_{\lambda_j t}^{0} e^u (u - \lambda_j t)^i\, du \qquad \text{(Eq. 19)}$$

where the integral is evaluated numerically. However, in most cases, it would not be necessary to use Eq. 19 because Eq. 17 is sufficiently accurate, particularly if the calculations are done in double precision. Furthermore, the number of sampling points in the absorption phase is frequently small. To avoid "fitting to the errors in the data," it is not advisable to use a polynomial of high degree in the approximation of the input rate $f(t)$ so N will not be large.

EXPERIMENTAL

The method presented was tested using the same simulated and real pharmacokinetic data used previously (5) so that it could be compared to two other deconvolution methods tested on the same data (5, 6). A function subprogram was written in FORTRAN IV which evaluated the theta function $\theta_i(t)$[1]. The subprogram algorithm automatically chooses among Eqs. 17–19 so that the best accuracy is obtained. The integral in Eq. 19 was evaluated using a product-type two-point Gauss–Legendre–

[1] A listing of the subprogram is available from the author.

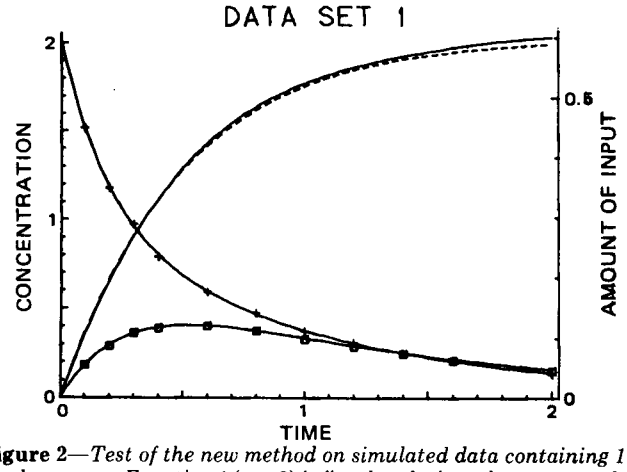

Figure 2—*Test of the new method on simulated data containing 1% random errors. Equation 1* (n = 2) *is fitted to the impulse response data* (+). *The curve representing the input response data* (□) *is calculated from Eq. 16 using the parameters* $x_0, x_1, \ldots, x_N$ *estimated by multiple linear regression and the parameters estimated from Eq. 1. The increasing curve is the amount of input calculated from the integrated form of Eq. 3. The broken curve is the exact cumulative amount of input.*

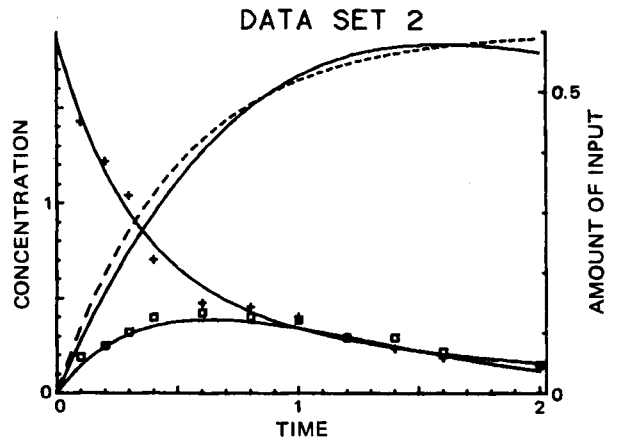

Figure 4—*Test of the new method on simulated data containing 10% random errors. Equation 1* (n = 2) *is fitted to the impulse response data* (+). *The curve representing the input response data* (□) *is calculated from Eq. 16 using the parameters* $x_0, x_1, \ldots, x_N$ *estimated by multiple linear regression and the parameters estimated from Eq. 1. The increasing curve is the amount of input calculated from the integrated form of Eq. 3. The broken curve is the exact cumulative amount of input.*

Simpson algorithm compounded 50 times (7), which gave excellent accuracy.

The subprogram was used to generate, from the M observations c_i, t_i, $i = 1, 2, \ldots, M$, an $M \times (M + 1)$ data matrix $\{d_{ij}\}$ for input to the multiple linear regression program that calculated $x_0, x_1, \ldots, x_N$ (Eq. 3). The first data matrix column contains the M observations of the dependent variable, *i.e.*, the observed drug concentrations $d_{i1} = c_i$, $i = 1, 2, \ldots, M$. The other data matrix columns contain the independent variables $d_{ij} = \theta_{j-2}(t_i)$, $i = 1, \ldots, M$, $j = 2, \ldots, M + 1$. The highest degree possible for the polynomial that approximates $f(t)$ is $N = M - 1$, which corresponds to a collocation approximation (zero residual sum of squares). Most of the many multiple linear regression programs available for statistical computations can be used to calculate the parameters $x_0, x_1, \ldots, x_N$ of the input function from this data matrix. The only requirement is that the regression program must have a zero-intercept option that is to be used in this regression situation (Eq. 16)[2].

The program P9R, "All Possible Subset Regression," from the BMDP-77 biomedical computer program package (9) was used with the zero-option and TOL = 10^{-5}. The program was used to automatically find, among $x_0, x_1, \ldots, x_{M-1}$, the best subset based on Mallow's criterion (10). The parameters of the polyexponential expression, Eq. 1, fitted to the intravenous bolus data were reported previously (5) and were determined using the FUNFIT nonlinear regression program (11). The drawings (Figs. 1–9) were done by a penplotter driven by a computer[3] using a software package written by the author. The lag times used in the calculation of the pentobarbital input were those reported earlier (5).

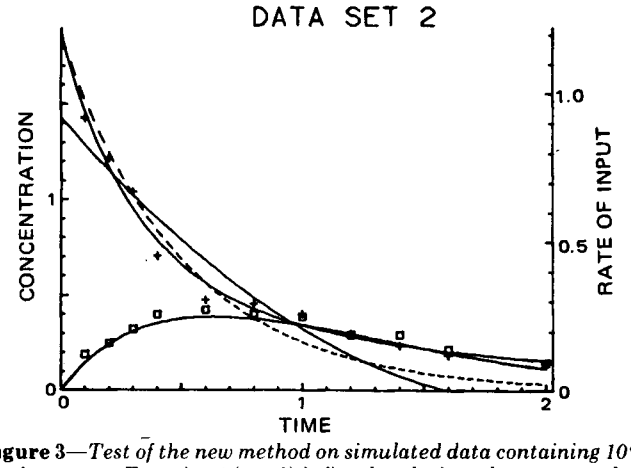

Figure 3—*Test of the new method on simulated data containing 10% random errors. Equation 1* (n = 2) *is fitted to the impulse response data* (+). *The curve representing the input response data* (□) *is calculated from Eq. 16 using the parameters* $x_0, x_1, \ldots, x_N$ *estimated by multiple linear regression and the parameters estimated from Eq. 1. The input curve is the input rate calculated according to Eq. 3. The broken curve is the exact input rate.*

RESULTS AND DISCUSSION

The proposed method is a least-squares deconvolution method, as is the method presented by Cutler (6). Both methods are based on a polynomial approximation of the input rate. However, the present method offers four significant advantages over Cutler's method:

1. The impulse response (bolus input response) is approximated by a polyexponential expression and not by a polynomial. A polyexponential expression does not tend to "fit to the errors" in the data as a polynomial

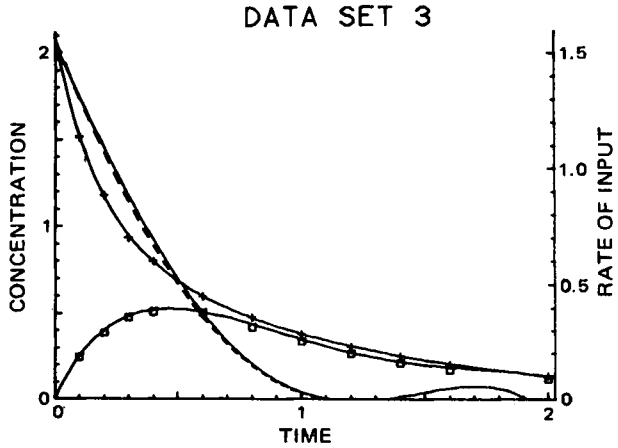

Figure 5—*Test of the new method on simulated data containing 1% random errors. Equation 1* (n = 2) *is fitted to the impulse response data* (+). *The curve representing the input response data* (□) *is calculated from Eq. 16 using the parameters* $x_0, x_1, \ldots, x_N$ *estimated by multiple linear regression and the parameters estimated from Eq. 1. The input curve is the input rate calculated according to Eq. 3. The broken curve is the exact input rate.*

[2] The two most widely used statistical software packages SPSS (8) and BMDP (9) contain several multiple linear regression programs. However, only the BMDP programs have the zero-intercept option. These programs allow the data to be weighted.

[3] IBM 370.

Table I—Rate and Extent of Input Calculated from Data Set 1

Time	Exact Rate	Rate	Percent Difference[a]	Exact Amount	Amount	Percent Difference[b]
0.1	0.9825	0.9712	−0.94	0.1088	0.1058	−0.49
0.2	0.8044	0.8146	0.86	0.1978	0.1950	−0.48
0.3	0.6586	0.6780	1.62	0.2707	0.2694	−0.21
0.4	0.5392	0.5598	1.72	0.3304	0.3312	0.13
0.6	0.3614	0.3732	0.98	0.4193	0.4234	0.69
0.8	0.2423	0.2434	0.10	0.4789	0.4842	0.90
1.0	0.1624	0.1590	−0.29	0.5188	0.5238	0.84
1.2	0.1089	0.1084	−0.04	0.5456	0.5501	0.75
1.4	0.0730	0.0803	0.61	0.5635	0.5687	0.86
1.6	0.0489	0.0631	1.18	0.5755	0.5829	1.23
2.0	0.0220	0.0160	−0.50	0.5890	0.6003	1.89
Mean[c]			0.80			0.77
SD[c]			0.56			0.49

[a] Calculated as 100 × (calculated rate − exact rate)/1.2, where 1.2 is the initial exact input rate. [b] Calculated as 100 × (calculated amount − exact amount)/0.6, where 0.6 is the exact total amount of input ($t = \infty$). [c] The mean and standard deviation of the absolute values of the percent difference.

Table II—Rate and Extent of Input Calculated from Data Set 2

Time	Exact Rate	Rate	Percent Difference[a]	Exact Amount	Amount	Percent Difference[b]
0.1	0.9825	0.8303	−12.68	0.1088	0.0876	−3.53
0.2	0.8044	0.7426	−5.15	0.1978	0.1662	−5.27
0.3	0.6586	0.6595	0.08	0.2707	0.2363	−5.74
0.4	0.5392	0.5810	3.48	0.3304	0.2983	−5.36
0.6	0.3614	0.4378	6.36	0.4193	0.3998	−3.24
0.8	0.2423	0.3129	5.89	0.4789	0.4746	−0.71
1.0	0.1624	0.2065	3.67	0.5188	0.5262	1.24
1.2	0.1089	0.1184	0.79	0.5456	0.5584	2.14
1.4	0.0730	0.0486	−2.03	0.5635	0.5748	1.88
1.6	0.0489	−0.0027	−4.30	0.5755	0.5791	0.59
2.0	0.0220	−0.0503	−6.02	0.5890	0.5660	−3.83
Mean[c]			4.59			3.05
SD[c]			3.41			1.88

[a] Calculated as 100 × (calculated rate − exact rate)/1.2, where 1.2 is the initial exact input rate. [b] Calculated as 100 × (calculated amount − exact amount)/0.6, where 0.6 is the exact total amount of input ($t = \infty$). [c] The mean and standard deviation of the absolute values of the percent difference.

does. It is smoother and does not oscillate between data points as a polynomial often does. It is also superior to a polynomial with respect to the extrapolation to time zero, which plays an important role in the accuracy of any deconvolution method. Polyexponential expressions have been used successfully and extensively in pharmacokinetics to describe intravenous bolus data, and many application programs are available for this curve-fitting procedure (8, 11, 12).

2. The rate and extent of input are given in a simple, explicit mathematical form by the new method. Cutler (6) expressed the input rate as a sum of polynomial functions which, through a linear transformation, gives a set of orthogonal functions. Although a back-transformation and summation of terms may provide a single polynomial expression, this approach substantially increases the complexity of the method.

3. The present method requires very little programming on a computer. Only a short program is needed that, according to Eq. 17 or 18 (or Eq. 19 in rare cases), generates the data matrix for input to a standard multiple linear regression program. This programming can be done even using an ordinary programmable pocket calculator. The input function is calculated directly by the linear regression program in terms of the polynomial coefficients. Implementation of Cutler's method requires the

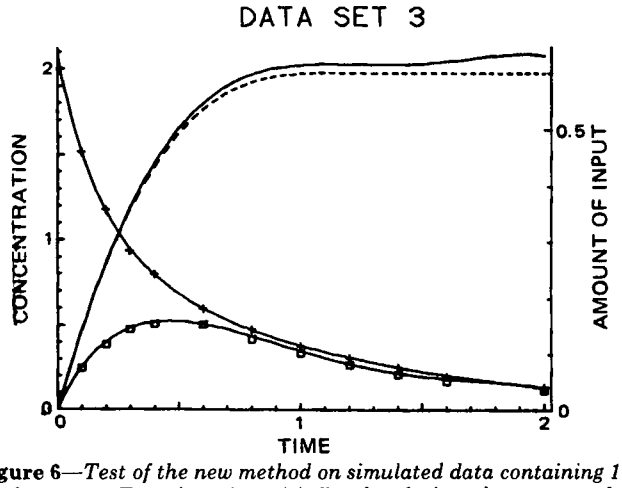

Figure 6—*Test of the new method on simulated data containing 1% random errors. Equation 1 (n = 2) is fitted to the impulse response data (+). The curve representing the input response data (□) is calculated from Eq. 16 using the parameters $x_0, x_1, \ldots, x_N$ estimated by multiple linear regression and the parameters estimated from Eq. 1. The increasing curve is the amount of input calculated from the integrated form of Eq. 3. The broken curve is the exact cumulative amount of input.*

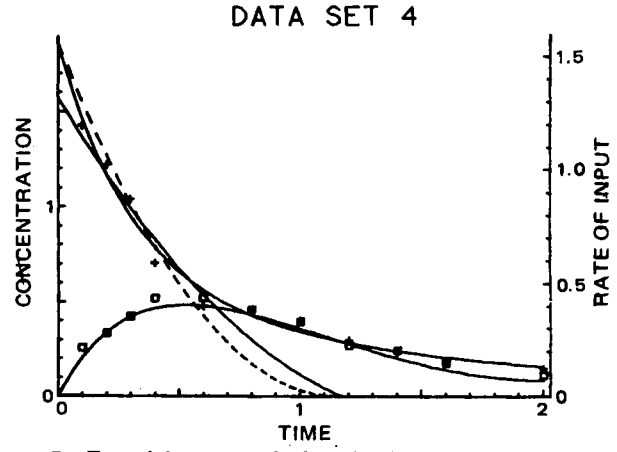

Figure 7—*Test of the new method on simulated data containing 10% random errors. Equation 1 (n = 2) is fitted to the impulse response data (+). The curve representing the input response data (□) is calculated from Eq. 16 using the parameters $x_0, x_1, \ldots, x_N$ estimated by multiple linear regression and the parameters estimated from Eq. 1. The input curve is the input rate calculated according to Eq. 3. The broken curve is the exact input rate.*

Table III—Rate and Extent of Input Calculated from Data Set 3

Time	Exact Rate	Rate	Percent Difference[a]	Exact Amount	Amount	Percent Difference[b]
0.1	1.3048	1.3133	0.54	0.1433	0.1427	−0.10
0.2	1.0681	1.0924	1.55	0.2618	0.2629	0.18
0.3	0.8551	0.8844	1.87	0.3577	0.3616	0.65
0.4	0.6657	0.6936	1.78	0.4336	0.4404	1.13
0.6	0.3580	0.3758	1.14	0.5344	0.5458	1.90
0.8	0.1450	0.1543	0.59	0.5831	0.5972	2.35
1.0	0.0266	0.0305	0.25	0.5987	0.6141	2.57
1.2	0	−0.0082	−0.52	0.6000	0.6151	2.52
1.4	0	0.0112	0.72	0.6000	0.6147	2.45
1.6	0	0.0478	3.05	0.6000	0.6207	3.45
2.0	0	−0.0625	−3.99	0.6000	0.6321	5.35
Mean[c]			1.45			2.06
SD[c]			1.18			1.54

[a] Calculated as 100 × (calculated rate − exact rate)/(1.8/1.15), where 1.8/1.15 is the exact initial input rate. [b] Calculated as 100 × (calculated amount − exact amount)/0.6, where 0.6 is the exact total amount of input ($t = \infty$). [c] The mean and standard deviation of the absolute values of the percent difference.

Table IV—Rate and Extent of Input Calculated from Data Set 4

Time	Exact Rate	Rate	Percent Difference[a]	Exact Amount	Amount	Percent Difference[b]
0.1	1.3048	1.1487	−9.97	0.1433	0.1235	−3.30
0.2	1.0681	0.9863	−5.23	0.2618	0.2301	−5.28
0.3	0.8551	0.8353	−1.27	0.3577	0.3211	−6.10
0.4	0.6657	0.6956	1.91	0.4336	0.3976	−6.00
0.6	0.3580	0.4504	5.90	0.5344	0.5114	−3.83
0.8	0.1450	0.2507	6.75	0.5831	0.5808	−0.38
1.0	0.0266	0.0964	4.46	0.5987	0.6147	2.67
1.2	0	−0.0125	−0.80	0.6000	0.6223	3.72
1.4	0	−0.0759	−4.85	0.6000	0.6127	2.12
1.6	0	−0.0938	−5.99	0.6000	0.5950	−0.83
2.0	0	0.0067	0.43	0.6000	0.5715	−4.75
Mean[c]			4.32			3.54
SD			2.95			1.93

[a] Calculated as 100 × (calculated rate − exact rate)/(1.8/1.15), where 1.8/1.15 is the exact initial input rate. [b] Calculated as 100 × (calculated amount − exact amount)/0.6, where 0.6 is the exact total amount of input ($t = \infty$). [c] The mean and standard deviation of the absolute values of the percent difference.

development of a fairly extensive and specialized program. Moreover, the user would not have many of the valuable statistical options that are supplied by the standard multiple linear regression programs (9).

4. The present method is computationally efficient and fast. With Cutler's method, a convolution integral (Ref. 6, p. 249) is evaluated numerically several times during the computations. The integration may introduce significant errors and may add significant cost to the computations if the results are to be presented graphically.

Simulation Results—The present results and comparisons are related to a similar investigation recently published (5). Comparing Tables I–IV with Tables II–V in Ref. 5 shows that the present method and Cutler's method do not differ significantly in the accuracy of estimating the input for Data Sets 1, 2, and 4 (Tables I, II, and IV). However, the present method appears to be significantly more accurate for Data Set 3 (Table III). Both methods perform well, considering that the average relative error in all estimations is of the same magnitude as the noise added to the simulated data.

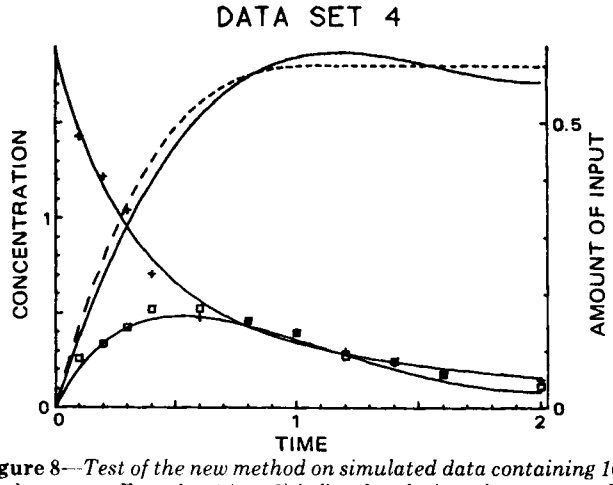

Figure 8—*Test of the new method on simulated data containing 10% random errors. Equation 1* (n = 2) *is fitted to the impulse response data* (+). *The curve representing the input response data* (□) *is calculated from Eq. 16 using the parameters* $x_0, x_1, \ldots, x_N$ *estimated by multiple linear regression and the parameters estimated from Eq. 1. The increasing curve is the amount of input calculated from the integrated form of Eq. 3. The broken curve is the exact cumulative amount of input.*

Each method tends consistently to underestimate the initial input rate. This trend is probably related to the use of a polynomial in the input approximation. It may be explained theoretically ["Runge's phenomenon" (13)]. A special sampling procedure may eliminate or reduce this trend and give an overall better estimation. This procedure, based on the min–max principle using a Tschebyscheff sampling (13), is as follows. Let it be known from preliminary investigations that the absorption of the drug is completed (*e.g.*, 95%) in approximately T hr after the lag time and that the lag time is approximately t_{lag} hr. If the experimental protocol allows m samples to be drawn, then these samples should be taken at the following times:

$$t_i = t_{lag} + \frac{T}{2}\left[1 + \cos\frac{(2i-1)\pi}{2m}\right] \qquad i = 1, 2, \ldots, m \quad \text{(Eq. 20)}$$

A few additional samples are required after $T + t_{lag}$ hr to check for a change in the disposition kinetics between the intravenous and the absorption experiments. However, these points should not be included in the actual calculation of the input because they may interact unfavorably with the curve fitting in the absorption region.

Calculation of Pentobarbital Input—It is of interest to compare the present method with the other deconvolution method presented by the author (Ref. 5, Fig. 9). The pentobarbital data are rather difficult to treat, because the absorption phase is defined by only three or four data points and the data contain rather large errors. However, it is surprising how similarly the two methods perform in the absorption region. The total percent absorbed, measured by the maximum of the percent absorbed curve, does not differ much between the methods. The times for the absorption are also rather close.

However, the present method does not perform as well with respect

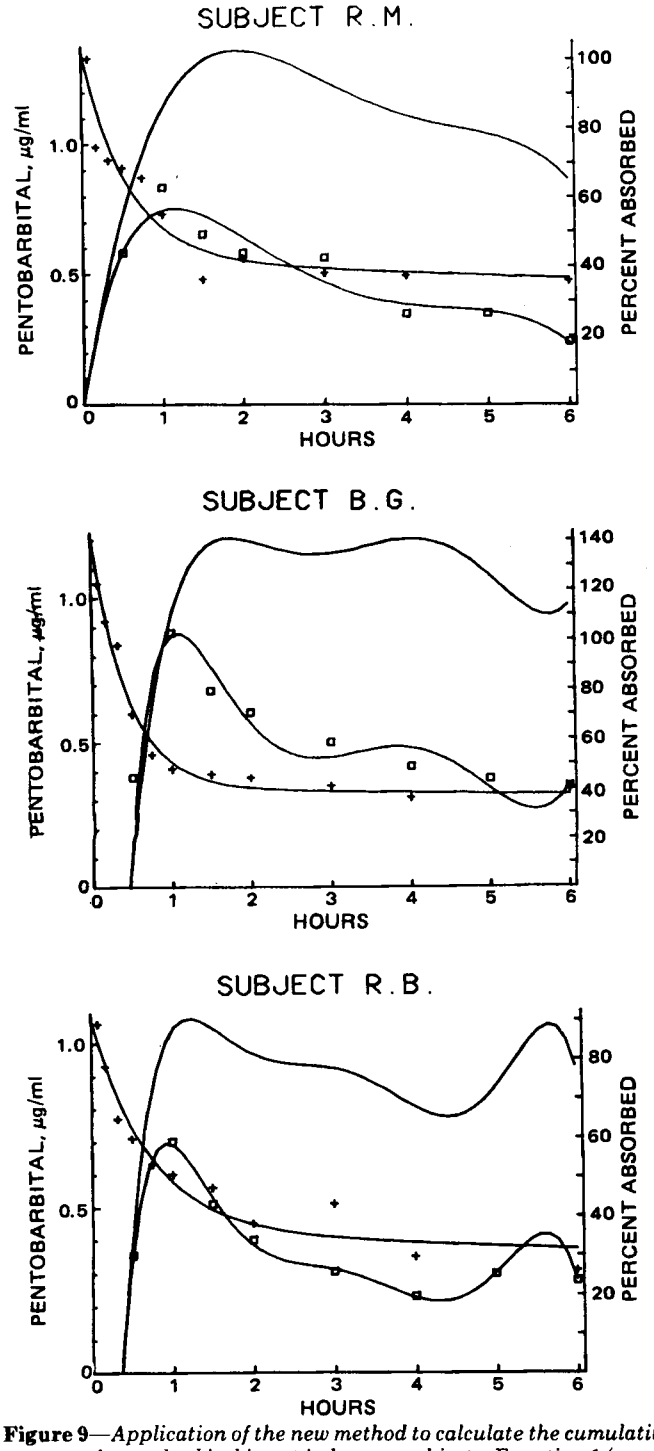

Figure 9—*Application of the new method to calculate the cumulative amount of pentobarbital input in human subjects. Equation 1* (n = 2) *is fitted to the plasma drug level data* (+) *from intravenous administration. The curve representing oral absorption data* (□) *is calculated from Eq. 16 using the parameters* $x_0, x_1, \ldots, x_N$ *estimated by multiple linear regression and the parameters estimated from Eq. 1. The input is calculated according to the integrated form of Eq. 3.*

to the curve fitting after the absorption phase. It demonstrates some of the undesirable effects originating from the polynomial approximation of the input rate; the absorption curve for Subject R.B. passes too close to all of the points, probably resulting in a poor filtering of the errors in the data. The curve for Subject B.G. shows excessive oscillations. However, the curve for Subject R.M. seems satisfactory overall. The same discrepancies between the intravenous and the absorption data reported previously (5) are also observed using the present method.

It is important to note that the calculation of the rate and extent of drug input at a given time, $t = t_0$, depends only on the fitted curves up to that time, t_0, according to the fundamental convolution integral equation (Eq. 2). Thus, the accuracy of the calculated input depends only on the goodness of the fit in the absorption phase. The goodness of the fit in the postabsorptive phase has no influence on the calculations. A fitting in this region is not required, but it provides a means of detecting discrepancies between the intravenous and absorption data (5). The fits in the absorption phase (Fig. 9) appear satisfactory considering the sparseness of the data in this region.

Table V—Calculated Polynomials that Describe the Rate of Input [a]

Data Set	Rate of Input
1	$f(t) = 1.149 - 1.891t + 1.139t^2 - 0.2385t^3$
2	$f(t) = 0.9225 - 0.9457t + 0.2297t^2$
3	$f(t) = 1.542 - 2.311t + 0.1076t^2 + 1.059t^3 - 0.3680t^4$
4	$f(t) = 1.322 - 1.794t + 0.5682t^2$

[a] $0.1 \leq t \leq 2.0$.

Assumptions and Limitations of Deconvolution Methods of Analysis of Drug Input into Blood—The deconvolution methods are based on the assumption of a time-invariant linearity between input and response in the sampleable response environment (the blood). A necessary condition for an environment to be linear is that the principle of superposition applies; *i.e.*, the sum or superposition of any two inputs, $f_1(t) + f_2(t)$, results in a response that is the superposition, $c_1(t) + c_2(t)$, of the individual responses (14). Corollaries to the superposition principle are:

1. No input affects the response of other inputs.
2. There is no interaction among the responses caused by different inputs.
3. The total response of several inputs into the environment can be determined by determining separately the response of the environment to each individual input and then superimposing the responses to get the total response.

These principles are well known from linear system theory (14). However, the real problem in applying these principles to pharmacokinetics apparently has not been discussed, namely, the effect of the input path on the response. The deconvolution methods can be used only if the response to a well-defined input is determined. The input is only well defined if it is direct intravenous (bolus and/or infusion). Consequently, the information about the system's input–response relationship is based only on a direct intravenous input. However, the inputs that are of interest are not direct intravenous. Therefore, the validity of the deconvolution approach is directly related to Corollary 1.

The crucial question is: Does the drug in its indirect path to the sampleable response environment affect the change in the concentration of the drug already in the environment so that the concentration change is different from that predicted had the input been direct? This question is identical to the question posed previously in dealing with the evaluation of input into linear compartmental systems (4): Is the input interacting?

Deconvolution methods can only be used to evaluate a noninteracting, primary input (4). Therefore, to verify the validity of the deconvolution approach, the system must be tested not only with respect to superposition but also with respect to interaction. A superposition test requires a minimum of two different direct intravenous bolus or intravenous infusion inputs. A test for interaction requires two experiments, one involving only a direct intravenous input and the other involving the indirect and direct inputs combined, where the drug in either the indirect or the direct input must be labeled in order to evaluate a possible interaction between the two inputs.

In spite of the crucial role that these aspects play in drug input evaluation, there does not seem to have been any work done in this fundamental area.

Table VI—Rate of Input of Pentobarbital

Subject	Rate[a], mg/hr	Lag Time, hr
B.G.	$f(t) = 159 - 266T + 150T^2 - 34.7T^3 + 2.77T^4$	0.46
R.M.	$f(t) = 69.9 - 64.7T + 17.8T^2 - 1.54T^3$	0.0
R.B.	$f(t) = 149 - 365T + 313T^2 - 122T^3 + 22.1T^4 - 1.49T^5$	0.36

[a] T = time − lag time.

The method presented, when applied with care, should be a valuable tool in drug absorption investigations. It seems to have some distinct advantages over the method proposed by Cutler (6). The simulation data generated by Cutler do not differentiate between the two approaches. However, these data represent rather ideal, somewhat unrealistic cases. More realistic tests might result in a definite distinction of the methods. The relative accuracy of the two approaches in practice is closely related to the issue of whether the impulse response data (*i.e.*, the intravenous bolus data) are best approximated by a polynomial or a polyexponential expression. It seems quite evident that the latter is the case, so the present method should be generally more accurate. Although this method seems promising, it appears from previous theoretical considerations (4) that the other deconvolution method presented by the author (5) is superior. However, the new method has the advantage that the rate and the amount (cumulative) of input are summarized in a simple polynomial form (Tables V and VI).

REFERENCES

(1) V. F. Smolen, *J. Pharmacokinet. Biopharm.*, **4**, 337 (1976).

(2) P. Veng Pedersen, *J. Pharm. Sci.*, **67**, 187 (1978).

(3) J. G. Wagner, "Fundamentals of Clinical Pharmacokinetics," Drug Intelligence Publications, Hamilton, Ill., 1975.

(4) P. Veng Pedersen, *J. Pharm. Sci.*, **69**, 298 (1980).

(5) *Ibid.*, **69**, 305 (1980).

(6) D. J. Cutler, *J. Pharmacokinet. Biopharm.*, **6**, 243 (1978).

(7) W. R. Boland and C. S. Duris, *BIT*, **11**, 139 (1971).

(8) N. H. Nie, C. H. Hull, J. G. Jenkins, K. Steinbrenner, and D. H. Bent, "SPSS, Statistical Package for the Social Sciences," McGraw-Hill, New York, N.Y., 1975.

(9) W. J. Dixon and M. B. Brown, "BMDP Biomedical Computer Programs," University of California Press, Berkeley, Calif., 1977.

(10) C. Daniel and F. S. Wood, "Fitting Equations to Data," Wiley, New York, N.Y., 1971, p. 86.

(11) P. Veng Pedersen, *J. Pharmacokinet. Biopharm.*, **5**, 513 (1977).

(12) C. M. Metzler, "A Users Manual for NONLIN," Tech. Rept. 7293/7292/005, Upjohn Co., Kalamazoo, Mich., 1969.

(13) G. Dahlquist and Å. Björk, "Numerical Methods," Prentice-Hall, Englewood Cliffs, N.J., 1974.

(14) B. M. Brown, "The Mathematical Theory of Linear Systems," Chapman and Hall, London, England, 1965.

Novel Approach to Bioavailability Testing: Statistical Method for Comparing Drug Input Calculated by a Least-Squares Deconvolution Technique

PETER VENG PEDERSEN

Received January 29, 1979, from the *Department of Pharmacy, School of Pharmacy, University of California, San Francisco, CA 94143.* Accepted for publication July 18, 1979.

Abstract □ A novel approach to bioavailability testing is presented. The approach is model independent because it does not assume a specific pharmacokinetic model and does not use absorption, distribution, or elimination rate constants or a volume term. The method, which requires intravenous administration, is compared to classical bioavailability evaluation methods. Evaluation of drug input is based on the same assumptions required for using the area under the curve. No extrapolation beyond the last data point is required. Two statistics are derived that enable a comparison of the rate and the cumulative amount of input of two inputs for various times. A differential confidence profile is calculated that allows a more detailed and intrinsic bioavailability comparison than previous methods. The approach is demonstrated on simulated data containing random noise and shows satisfactory performance.

Keyphrases □ Bioavailability—testing, drug input, least-squares deconvolution technique □ Deconvolution—least-squares technique, bioavailability testing, drug input □ Drug availability—testing, least-squares deconvolution technique

The quality of a drug product as a drug delivery system is determined by the rate and extent of delivery of the active form to the biological environment responsible for the pharmacological effect. In most cases, this environment is neither known nor may be sampled for the drug. However, a close relationship usually exists between the drug concentration in a sampled environment (*e.g.*, blood) and its pharmacological response. Therefore, this environment may be a useful indicator of the drug input into the response environment.

Drug delivery usually is characterized in bioavailability terms with the blood as the sampleable environment. Bioavailability commonly is defined by the rate and the extent of drug input into the systemic circulation (1). Bioavailability comparisons usually are based on three parameters from a single-dose blood level curve: (*a*) the area under the curve, AUC (extrapolated); (*b*) the time of the peak concentration, t_{max}; and (*c*) the peak concentration, C_{max} (2).

These parameters are associated conceptually with the extent (AUC) and the rate (t_{max} and C_{max}) of input. This association is related to linear pharmacokinetic assumptions. For example, AUC is a proper measure of the total input only if the response (concentration) is linear with respect to the input (3, 4). If the system is not linear, a larger AUC does not guarantee greater input. Comparisons of the drug input on the basis of AUC may be inaccurate for several reasons:

1. The tail area must be estimated by extrapolation. Consequently, this area can be determined only by a model-dependent approach that assumes a certain functional form for the tail or the total curve.

2. The tail area frequently is estimated from the last observations (*e.g.*, log-linear extrapolation), based on the assumption that these points predict the behavior in the tail. The tail area usually is determined poorly in this way due to low information density of the terminal set of points. This problem is complicated further by constraints in time and the number of samples when dealing with human subjects. The experimenter must decide whether more samples should be taken in the terminal phase, where little or no input takes place, to predict the tail area better or whether these samples would be more valuable in the input phase where the real information about the input is present and where C_{max} and t_{max} are to be estimated.

3. The problem is complicated by the fact that the tail

0022-3549/80/0300-0318$01.00/0

© 1980, American Pharmaceutical Association

The method presented, when applied with care, should be a valuable tool in drug absorption investigations. It seems to have some distinct advantages over the method proposed by Cutler (6). The simulation data generated by Cutler do not differentiate between the two approaches. However, these data represent rather ideal, somewhat unrealistic cases. More realistic tests might result in a definite distinction of the methods. The relative accuracy of the two approaches in practice is closely related to the issue of whether the impulse response data (*i.e.*, the intravenous bolus data) are best approximated by a polynomial or a polyexponential expression. It seems quite evident that the latter is the case, so the present method should be generally more accurate. Although this method seems promising, it appears from previous theoretical considerations (4) that the other deconvolution method presented by the author (5) is superior. However, the new method has the advantage that the rate and the amount (cumulative) of input are summarized in a simple polynomial form (Tables V and VI).

REFERENCES

(1) V. F. Smolen, *J. Pharmacokinet. Biopharm.*, **4**, 337 (1976).

(2) P. Veng Pedersen, *J. Pharm. Sci.*, **67**, 187 (1978).

(3) J. G. Wagner, "Fundamentals of Clinical Pharmacokinetics," Drug Intelligence Publications, Hamilton, Ill., 1975.

(4) P. Veng Pedersen, *J. Pharm. Sci.*, **69**, 298 (1980).

(5) *Ibid.*, **69**, 305 (1980).

(6) D. J. Cutler, *J. Pharmacokinet. Biopharm.*, **6**, 243 (1978).

(7) W. R. Boland and C. S. Duris, *BIT*, **11**, 139 (1971).

(8) N. H. Nie, C. H. Hull, J. G. Jenkins, K. Steinbrenner, and D. H. Bent, "SPSS, Statistical Package for the Social Sciences," McGraw-Hill, New York, N.Y., 1975.

(9) W. J. Dixon and M. B. Brown, "BMDP Biomedical Computer Programs," University of California Press, Berkeley, Calif., 1977.

(10) C. Daniel and F. S. Wood, "Fitting Equations to Data," Wiley, New York, N.Y., 1971, p. 86.

(11) P. Veng Pedersen, *J. Pharmacokinet. Biopharm.*, **5**, 513 (1977).

(12) C. M. Metzler, "A Users Manual for NONLIN," Tech. Rept. 7293/7292/005, Upjohn Co., Kalamazoo, Mich., 1969.

(13) G. Dahlquist and Å. Björk, "Numerical Methods," Prentice-Hall, Englewood Cliffs, N.J., 1974.

(14) B. M. Brown, "The Mathematical Theory of Linear Systems," Chapman and Hall, London, England, 1965.

Novel Approach to Bioavailability Testing: Statistical Method for Comparing Drug Input Calculated by a Least-Squares Deconvolution Technique

PETER VENG PEDERSEN

Received January 29, 1979, from the *Department of Pharmacy, School of Pharmacy, University of California, San Francisco, CA 94143.* Accepted for publication July 18, 1979.

Abstract □ A novel approach to bioavailability testing is presented. The approach is model independent because it does not assume a specific pharmacokinetic model and does not use absorption, distribution, or elimination rate constants or a volume term. The method, which requires intravenous administration, is compared to classical bioavailability evaluation methods. Evaluation of drug input is based on the same assumptions required for using the area under the curve. No extrapolation beyond the last data point is required. Two statistics are derived that enable a comparison of the rate and the cumulative amount of input of two inputs for various times. A differential confidence profile is calculated that allows a more detailed and intrinsic bioavailability comparison than previous methods. The approach is demonstrated on simulated data containing random noise and shows satisfactory performance.

Keyphrases □ Bioavailability—testing, drug input, least-squares deconvolution technique □ Deconvolution—least-squares technique, bioavailability testing, drug input □ Drug availability—testing, least-squares deconvolution technique

The quality of a drug product as a drug delivery system is determined by the rate and extent of delivery of the active form to the biological environment responsible for the pharmacological effect. In most cases, this environment is neither known nor may be sampled for the drug. However, a close relationship usually exists between the drug concentration in a sampled environment (*e.g.*, blood) and its pharmacological response. Therefore, this environment may be a useful indicator of the drug input into the response environment.

Drug delivery usually is characterized in bioavailability terms with the blood as the sampleable environment. Bioavailability commonly is defined by the rate and the extent of drug input into the systemic circulation (1). Bioavailability comparisons usually are based on three parameters from a single-dose blood level curve: (*a*) the area under the curve, AUC (extrapolated); (*b*) the time of the peak concentration, t_{max}; and (*c*) the peak concentration, C_{max} (2).

These parameters are associated conceptually with the extent (AUC) and the rate (t_{max} and C_{max}) of input. This association is related to linear pharmacokinetic assumptions. For example, AUC is a proper measure of the total input only if the response (concentration) is linear with respect to the input (3, 4). If the system is not linear, a larger AUC does not guarantee greater input. Comparisons of the drug input on the basis of AUC may be inaccurate for several reasons:

1. The tail area must be estimated by extrapolation. Consequently, this area can be determined only by a model-dependent approach that assumes a certain functional form for the tail or the total curve.

2. The tail area frequently is estimated from the last observations (*e.g.*, log-linear extrapolation), based on the assumption that these points predict the behavior in the tail. The tail area usually is determined poorly in this way due to low information density of the terminal set of points. This problem is complicated further by constraints in time and the number of samples when dealing with human subjects. The experimenter must decide whether more samples should be taken in the terminal phase, where little or no input takes place, to predict the tail area better or whether these samples would be more valuable in the input phase where the real information about the input is present and where C_{max} and t_{max} are to be estimated.

3. The problem is complicated by the fact that the tail

0022-3549/80/0300-0318$01.00/0

© 1980, American Pharmaceutical Association

area is determined by an asymptotic-type infinite extrapolation that is more complex than an intercept-type extrapolation.

A new approach to bioavailability testing is presented that enables a more detailed comparison of the rate and the extent of drug input than conventional methods. The method does not use *AUC* and does not require extrapolation beyond the last data point. The approach is model independent in the classical linear pharmacokinetic sense because it does not assume a specific pharmacokinetic model and does not use absorption, distribution, or elimination rate constants or a volume term. This method of evaluating drug input is based on the same assumptions as those required for using *AUC* as a proper measure of the drug input. These assumptions are: (*a*) the input evaluated is a noninteracting primary input, and (*b*) there is a time-invariant linearity between the response (concentration) measured in the sampled environment (the blood) and the input (4). These assumptions can be tested experimentally as discussed previously (4). Their violation invalidates the classical linear approaches to bioavailability testing (5) under the current bioavailability definition (1, 6).

THEORY

It was shown (4) that if the input rate into a linear response environment is given in polynomial form by[1]:

$$f(t) = \sum_{i=1}^{N} \beta_i t^{i-1} \qquad \text{(Eq. 1)}$$

and the unit impulse response (the characteristic response) of the environment is given by:

$$c_u(t) = \sum_{i=1}^{n} a_i e^{\lambda_i t} \qquad \text{(Eq. 2)}$$

then the response to $f(t)$ is:

$$c(t) = \sum_{i=1}^{N} \beta_i \phi_i(t) \qquad \text{(Eq. 3)}$$

which is linear with respect to the unknown parameters $\beta_1, \beta_2, \ldots, \beta_N$, and:

$$\phi_i(t) = (i-1)! \sum_{j=1}^{n} \frac{a_j}{\lambda_j^i} \left[e^{\lambda_j t} - \sum_{k=0}^{i-1} \frac{(\lambda_j t)^k}{k!} \right] \qquad \text{(Eq. 4)}$$

Without loss of generality, two brands or drug delivery systems may be compared by assuming the blood to be the response environment, the response to be the drug concentration, $c(t)$, and $c_m(t_{mi})$ to be the response measured at the time t_{mi}, $i = 1, 2, \ldots, M_m$, for the mth drug product ($m = 1, 2$). To facilitate the statistical analysis, the measured responses can be written in the form:

$$y_{mi} = \sum_{j=1}^{N_m} \beta_{mj} x_{mij} + \epsilon_{mi} \qquad \begin{matrix} i = 1, 2, \ldots, M_m \\ m = 1, 2 \end{matrix} \qquad \text{(Eq. 5)}$$

where:

$$x_{mij} = \phi_{mj}(t_{mi}) \qquad \begin{matrix} i = 1, 2, \ldots, M_m \\ j = 1, 2, \ldots, N_m \\ m = 1, 2 \end{matrix} \qquad \text{(Eq. 6)}$$

and:

$$y_{mi} = c(t_{mi}) \qquad \begin{matrix} i = 1, 2, \ldots, M_m \\ m = 1, 2 \end{matrix} \qquad \text{(Eq. 7)}$$

Equations 1 and 4 may be written similarly:

$$f_m(t) = \sum_{i=1}^{N_m} \beta_{mi} t^{i-1} \qquad m = 1, 2 \qquad \text{(Eq. 8)}$$

$$\phi_{mi}(t) = (i-1)! \sum_{j=1}^{n_m} \frac{a_{mj}}{\lambda_{mj}^i} \left[e^{\lambda_{mj} t} - \sum_{k=0}^{i-1} \frac{(\lambda_{mj} t)^k}{k!} \right] \qquad m = 1, 2 \qquad \text{(Eq. 9)}$$

It is of interest in bioavailability studies to test the significance of differences in the rate and/or extent of drug input between drug products. This is equivalent to testing the null hypothesis:

$$H_0: \quad \mu_1|t_0 = \mu_2|t_0 \qquad \text{(Eq. 10)}$$

against:

$$H_1: \quad \mu_1|t_0 \neq \mu_2|t_0 \qquad \text{(Eq. 11)}$$

where:

$$\mu_m|t_0 = f_m(t_0) = \sum_{i=1}^{N_m} \beta_{mi} t_0^{i-1} \qquad m = 1, 2 \qquad \text{(Eq. 12)}$$

for various values of $t = t_0$.

In matrix–vector notation, Eq. 5 is:

$$\mathbf{y}_m = \mathbf{X}_m \boldsymbol{\beta}_m + \boldsymbol{\epsilon}_m \qquad m = 1, 2 \qquad \text{(Eq. 13)}$$

The statistics to be derived for testing H_0 will be based on a normality assumption about the errors; *i.e.*, $\boldsymbol{\epsilon}_m$ is a random vector distributed $N(\mathbf{0}, \sigma_m^2 \mathbf{I})$, where $\mathbf{I}$ is the identity matrix and σ_m^2 is unknown. The unknown $N_m \times 1$ parameter vector, $\boldsymbol{\beta}_m$, is estimated by a multiple linear regression technique (4). It is assumed that the observed data are sufficient to ensure that the rank of the $M_m \times N_m$ matrix, $\mathbf{X}_m$, is $N_m \leq M_m$.

For this statistical model the least-squares estimates, denoted by $\hat{}$, are given by:

$$\hat{\boldsymbol{\beta}}_m = \mathbf{V}_m \mathbf{X}_m' \mathbf{y}_m \qquad m = 1, 2 \qquad \text{(Eq. 14)}$$

and:

$$\hat{\sigma}_m = \mathbf{e}_m' \mathbf{e}_m / (M_m - N_m) \qquad m = 1, 2 \qquad \text{(Eq. 15)}$$

where:

$$\mathbf{V}_m = (\mathbf{X}_m' \mathbf{X}_m)^{-1} \qquad m = 1, 2 \qquad \text{(Eq. 16)}$$

and:

$$\mathbf{e}_m = \mathbf{y}_m - \mathbf{X}_m \hat{\boldsymbol{\beta}}_m \qquad m = 1, 2 \qquad \text{(Eq. 17)}$$

are best linear unbiased estimates (BLUE) of $\boldsymbol{\beta}_m$ and σ_m^2. They are sufficient, efficient, complete, and consistent estimators. Furthermore, $\hat{\boldsymbol{\beta}}_m$ and $\hat{\sigma}_m$ are stochastically independent and $\hat{\boldsymbol{\beta}}_m$ is distributed $N(\boldsymbol{\beta}_m, \sigma_m^2 \mathbf{V}_m)$. Consequently, the least-squares estimate of the input rate at $t = t_0$ is the best linear unbiased estimate and is distributed:

$$\hat{f}_m(t_0) = \boldsymbol{\tau}_m' \hat{\boldsymbol{\beta}}_m \sim N(\mu_m|t_0, \sigma_m^2 \boldsymbol{\tau}_m' \mathbf{V}_m \boldsymbol{\tau}_m) \qquad m = 1, 2 \qquad \text{(Eq. 18)}$$

where:

$$\boldsymbol{\tau}_m' = (1, t_0, t_0^2, \ldots, t_0^{N_m - 1}) \qquad m = 1, 2 \qquad \text{(Eq. 19)}$$

Since $[\hat{f}_1(t_0) - \mu_1|t_0]$ and $[\hat{f}_2(t_0) - \mu_2|t_0]$ are stochastically independent, the random variable Q_1 given by:

$$Q_1 = \frac{[\hat{f}_1(t_0) - \hat{f}_2(t_0)] - (\mu_1|t_0 - \mu_2|t_0)}{[\sigma_1^2 \boldsymbol{\tau}_1' \mathbf{V}_1 \boldsymbol{\tau}_1 + \sigma_2^2 \boldsymbol{\tau}_2' \mathbf{V}_2 \boldsymbol{\tau}_2]^{1/2}} \qquad \text{(Eq. 20)}$$

is standard and normally distributed. Furthermore, $(M_m - N_m)\hat{\sigma}_m^2 / \sigma_m^2$ is χ^2-distributed with $(M_m - N_m)$ degrees of freedom. Thus, the random variable Q_2 given by:

$$Q_2 = (M_1 - N_1)\hat{\sigma}_1^2 / \sigma_1^2 + (M_2 - N_2)\hat{\sigma}_2^2 / \sigma_2^2 = \frac{\mathbf{e}_1' \mathbf{e}_1}{\sigma_1^2} + \frac{\mathbf{e}_2' \mathbf{e}_2}{\sigma_2^2} \qquad \text{(Eq. 21)}$$

is χ^2-distributed with $(M_1 - N_1) + (M_2 - N_2)$ degrees of freedom because $(M_1 - N_1)\hat{\sigma}_1^2 / \sigma_1^2$ and $(M_2 - N_2)\hat{\sigma}_2^2 / \sigma_2^2$ are stochastically independent. It can be shown that the standard normal random variable Q_1 and the χ^2-distributed random variable Q_2 are stochastically independent. Consequently, by definition, the random variable $T = Q_1 / [Q_2 / (M_1 - N_1 + M_2 - N_2)]^{1/2}$ is t-distributed with $(M_1 - N_1 + M_2 - N_2)$ degrees of freedom. If the two population variances are equal, $\sigma_1^2 = \sigma_2^2$, then T becomes independent of σ^2, so that the H_0-hypothesis can be tested by a t-test:

$$T = \frac{\hat{f}_1(t_0) - \hat{f}_2(t_0)}{\left[\dfrac{\mathbf{e}_1' \mathbf{e}_1 + \mathbf{e}_2' \mathbf{e}_2}{M_1 - N_1 + M_2 - N_2} (\boldsymbol{\tau}_1' \mathbf{V}_1 \boldsymbol{\tau}_1 + \boldsymbol{\tau}_2' \mathbf{V}_2 \boldsymbol{\tau}_2) \right]^{1/2}} \qquad \text{(Eq. 22)}$$

[1] Note that the notational expressions for the input rate (Eq. 1), the impulse response (Eq. 2), and the input response (Eq. 3) were changed from previous notations (4) to facilitate the present statistical analysis.

Table I—Origin of the Simulated Data Used

Data Set	Unit Impulse Response $a_1e^{\lambda_1 t} + a_2e^{\lambda_2 t}$				Input Rate $f(t) = kKe^{-kt}$	
	a_1	a_2	λ_1	λ_2	K	k
1	1	1	−4	−1	Unit impulse	
2	1.727	7.523	−16.30	−2.134	Unit impulse	
3	1	1	−4	−3	Unit impulse	
4	1	1	−4	−1	3.0	1.5
5	1.727	7.523	−16.30	−2.134	1.0	1.0
6	1	1	−4	−3	3.0	1.5

with a critical region (H_0 rejection region) $|T| > t\ (\alpha/2, M_1 - N_1 + M_2 - N_2)$ for a type 1 error probability α.

The equality of the population variances can be tested according to an F-test:

$$F = \frac{\mathbf{e}_1'\mathbf{e}_1}{\mathbf{e}_2'\mathbf{e}_2} \qquad \text{(Eq. 23)}$$

with a critical region $F > F\ (\alpha, M_1 - N_1, M_2 - N_2)$, since $\mathbf{e}_1'\mathbf{e}_1/\sigma^2$ and $\mathbf{e}_2'\mathbf{e}_2/\sigma^2$ are stochastically independent, χ^2-distributed, random variables with the respective degrees of freedom.

If the F-test shows that the variances are not equal, then the t-test (Eq. 22) should not be used. For such cases, the H_0-hypothesis can be tested using the following statistic (see *Appendix*):

$$w = \frac{\hat{f}_1(t_0) - \hat{f}_2(t_0)}{\left[\dfrac{\mathbf{e}_1'\mathbf{e}_1\tau_1'\mathbf{V}_1\tau_1}{M_1 - N_1} + \dfrac{\mathbf{e}_2'\mathbf{e}_2\tau_2'\mathbf{V}_2\tau_2}{M_2 - N_2}\right]^{1/2}} \qquad \text{(Eq. 24)}$$

The w-statistic is approximated by a t-distribution with degrees of freedom, DF, given by[2]:

$$DF = \left[\frac{u^2}{M_1 - N_1} + \frac{1 - u^2}{M_2 - N_2}\right]^{-1} \qquad \text{(Eq. 25)}$$

where:

$$u = \frac{\mathbf{e}_1'\mathbf{e}_1\tau_1'\mathbf{V}_1\tau_1/(M_1 - N_1)}{\mathbf{e}_1'\mathbf{e}_1\tau_1'\mathbf{V}_1\tau_1/(M_1 - N_1) + \mathbf{e}_2'\mathbf{e}_2\tau_2'\mathbf{V}_2\tau_2/(M_2 - N_2)} \qquad \text{(Eq. 26)}$$

The critical region (H_0 rejection region) is $|w| > t(\alpha/2, DF)$. A $100(1 - \alpha)$-percent confidence interval for the drug input rate at time $t = t_0$ is:

$$\hat{f}_m(t_0) - t\left(\frac{\alpha}{2}, M_m - N_m\right)\left[\frac{\mathbf{e}_m'\mathbf{e}_m\tau_m'\mathbf{V}_m\tau_m}{M_m - N_m}\right]^{1/2} \le \mu_m|t_0 \le \hat{f}_m(t_0) + t\left(\frac{\alpha}{2}, M_m - N_m\right)\left[\frac{\mathbf{e}_m'\mathbf{e}_m\tau_m'\mathbf{V}_m\tau_m}{M_m - N_m}\right]^{1/2} \qquad m = 1, 2 \quad \text{(Eq. 27)}$$

This treatment dealt with a statistical analysis of the *rate* of drug input.

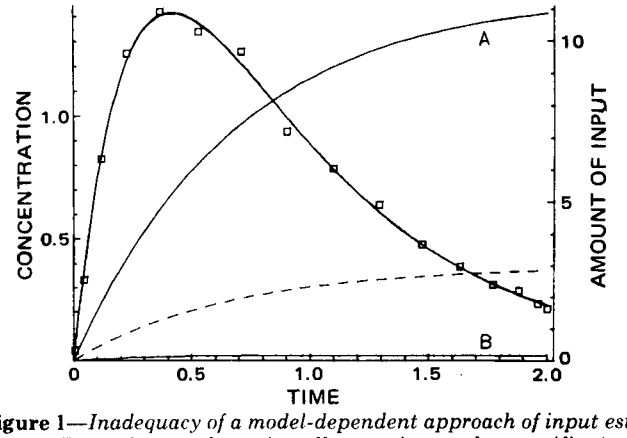

Figure 1—*Inadequacy of a model-dependent approach of input estimation. Examples are of two virtually superimposed curves (fits 1 and 2 in Table IV) fitted to Data Set 6. Curves A and B are the inputs calculated from the two fitted curves. The broken curve is the true input.*

[2] The degrees of freedom thereby is a real number, requiring interpolation in the t-table. However, most computer routines for the t-distribution permit noninteger degrees of freedom.

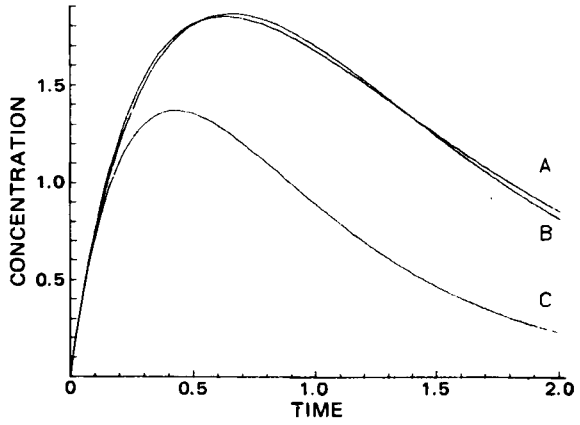

Figure 2—*Response curves A, B, and C from which the simulated Data Sets 4, 5, and 6, respectively, are derived by adding 5% random, normally distributed error. Curves A and B have widely different inputs; curves A and C have the same input (Table I).*

However, the *extent* of drug input given by:

$$A_m(t) = \int_0^t f_m(t)\,dt = \sum_{i=1}^{N_m} \frac{\beta_{mi}}{i!}\,t^i \qquad m = 1, 2 \qquad \text{(Eq. 28)}$$

can be treated similarly by replacing $f_m(t)$ with $A_m(t)$ in the respective equations and redefining τ_m' (Eq. 19) as:

$$\tau_m' = \left(t_0, \frac{t_0^2}{2}, \frac{t_0^3}{3}, \ldots, \frac{t_0^{Nm}}{N_m}\right) \qquad m = 1, 2 \qquad \text{(Eq. 29)}$$

The analysis was based on the ordinary least-squares Gauss–Markov statistical model. It is extended readily by standard means (7) to the generalized linear regression model involving correlated and/or heteroscedatic errors. The Gauss–Markov statistical model assumes no error in the independent variables, which is not true in the present case. However, the independent variables are stochastically independent random variables that do not depend on the β parameters, so the above estimation, testing, and prediction still apply. Only two aspects of the analysis are affected: (*a*) the probability in the t- and F-tests is not exact but only approximate, and (*b*) the power of the tests is different. The effect of these modifications becomes smaller the more accurately the unit impulse response is determined.

EXPERIMENTAL

The rate and the cumulative amount of input were determined by the least-squares deconvolution method presented previously (4). The data used for the demonstration of the proposed approach were generated from an arbitrarily chosen linear model with a two-exponential unit impulse response and a first-order input (Table I). Random, normally dis-

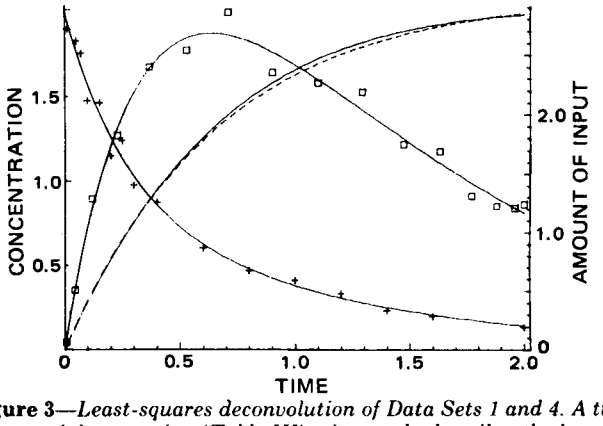

Figure 3—*Least-squares deconvolution of Data Sets 1 and 4. A two-exponential expression (Table III) adequately describes the impulse response data (+). The input function Eq. 1 is estimated subsequently by fitting Eq. 3 to the response data (□) by multiple linear regression. The continuously increasing curve is the calculated input amount (Table V). The broken curve is the exact input.*

Table II—Data Used in Simulations [a]

Unit Impulse Response				First-Order Input Response			
	Concentration				Concentration		
Time	Data Set 1	Data Set 2	Data Set 3	Time	Data Set 4	Data Set 5	Data Set 6
0.01	1.89	8.42	1.79	0.00482	0.0402	0.0467	0.0407
0.05	1.82	8.21	1.79	0.0431	0.352	0.343	0.331
0.07	1.75	6.99	1.52	0.118	0.895	0.891	0.826
0.10	1.47	6.76	1.43	0.227	1.27	1.25	1.25
0.15	1.46	5.59	1.06	0.366	1.67	1.54	1.42
0.20	1.15	4.97	1.04	0.529	1.77	1.88	1.34
0.25	1.24	4.49	0.812	0.710	1.99	1.96	1.26
0.30	0.977	4.40	0.714	0.902	1.64	1.74	0.938
0.40	0.873	3.54	0.519	1.10	1.58	1.57	0.787
0.60	0.603	1.95	0.270	1.29	1.53	1.42	0.640
0.80	0.468	1.32	0.130	1.47	1.22	1.39	0.479
1.00	0.413	0.926	0.0753	1.63	1.18	1.11	0.389
1.20	0.333	0.562	0.0389	1.77	0.916	1.03	0.313
1.40	0.233	0.385	0.0157	1.88	0.855	0.999	0.290
1.60	0.200	0.230	0.00997	1.96	0.845	0.841	0.237
2.00	0.137	0.112	0.00303	2.00	0.868	0.847	0.214

[a] The data were generated from the equations in Table I, and random normally distributed noise was added.

tributed noise was added to the exact concentration data at the 5% level, *i.e.*, with an expected coefficient of variation of 5%, using a pseudo-random normal generator based on the polar method (8) (Table II). To demonstrate the method, the unit impulse response parameters for Data Set 2 (Table I) were calculated by a nonlinear optimization technique so that Data Sets 4 and 5 (having different input) would not differ significantly. The parameters for Data Set 6 were chosen for the same reason so that Data Sets 4 and 6 would differ significantly but would have the same input (Tables I and II). The 16 sampling times for Data Sets 4–6 were chosen according to a Tschebyscheff sampling (Eq. 20 in Ref. 4) to avoid the "Runge effect" occurring in some linear regressions with fairly equally spaced sampling points.

The data matrix for the linear regression was generated from the simulated data as discussed previously (4). The matrix was executed stepwise with the BMDP-77 linear regression program P9R with a zero-intercept option and the option METHOD = NONE resulting in double-precision computations (9). The regression subsets were chosen on the basis of Mallow's criterion (10).

None of the BMDP linear regression programs provides output of the unscaled variance–covariance matrix required in the statistical computations. Therefore, a program was written to assemble the cross-product matrix and invert it using a Cholesky decomposition. A subroutine was written in FORTRAN IV to calculate and compare the rate and the cumulative amount of input of two inputs. The routine tests for heteroscedatic errors (Eq. 23) and chooses the appropriate type of statistic (Eq. 22 or 24) to calculate the significance of the input difference for various times. The α-values for the t-statistic were calculated according to the algorithm presented by Hill (11). The α-values for the F-statistic were calculated according to algorithms 26.6.15 and 26.2.17 reported in the literature (12). The parameters in Tables III and IV were obtained by nonlinear regression using the interactive program FUNFIT (13). All drawings were done by a penplotter[3] driven by a computer[4] using a software package written by the author.

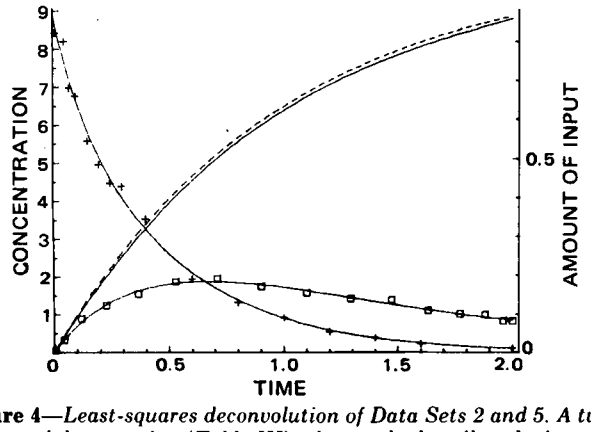

Figure 4—*Least-squares deconvolution of Data Sets 2 and 5. A two-exponential expression (Table III) adequately describes the impulse response data (+). The input function Eq. 1 is estimated subsequently by fitting Eq. 3 to the response data (□) by multiple linear regression. The continuously increasing curve is the calculated input amount (Table V). The broken curve is the exact input.*

RESULTS AND DISCUSSION

Simulated Model—Data Sets 1–3 (Tables I and II) can be considered to simulate, in the classical linear compartmental sense, intravenous bolus data normalized with respect to the dose for three subjects showing two-compartmental pharmacokinetic behavior with respect to a given drug. Data Sets 4–6 (Tables I and II) can be considered similarly as simulated first-order absorption blood concentration data adjusted for a possible lag time for the three subjects.

Comparison of Model-Dependent and Model-Independent Approaches—It is often impossible to administer a drug intravenously. It is of interest to see how accurately the drug input can be determined by a model-dependent approach from absorption blood level data alone, without knowledge of the system's response to intravenous administration of the drug. Data Sets 4–6 are generated from the convolution of $a_1 \exp(\lambda_1 t) + a_2 \exp(\lambda_2 t)$ and $kK \exp(-kt)$. The three data sets are based on:

$$c(t) = kK\left[\frac{a_1}{\lambda_1 + k}(e^{\lambda_1 t} - e^{-kt}) + \frac{a_2}{\lambda_2 + k}(e^{\lambda_2 t} - e^{-kt})\right] \qquad \lambda_1, \lambda_2 < 0 \quad \text{(Eq. 30)}$$

where K corresponds to FD (F = fraction of dose D available) and k corresponds to k_a (the first-order absorption rate constant) in classical linear compartmental modeling. This equation was fitted several times to Data Set 6 using the FUNFIT program (13) with the initial parameter estimates randomly chosen in a feasible parameter space. It is evident (Table IV and Fig. 1) that the parameters for the rate, k, and the extent, K, of input describe the input inadequately, even though the correct model is fitted to the data, the fits are excellent (Table IV and Fig. 1), and the data are as accurate as can be expected in a pharmacokinetic experiment. The input is determined poorly primarily because the parameters a_1, a_2, λ_1, and λ_2 from the unit impulse response $a_1 \exp(\lambda_1 t) + a_2 \exp(\lambda_2 t)$ (the characteristic response) are free to take nearly any values in the

Table III—Least-Squares Unit Impulse Response Parameters Used in Deconvolutions

Data Set	a_1	a_2	λ_1	λ_2
1	1.1055	0.88427	−3.7725	−0.91283
2	1.3170	7.5800	−9.0096	−2.1257
3	0.94748	0.99355	−3.3894	−3.2941

[3] Tektronix 4662.
[4] IBM 370.

Table IV—Estimates of the Input $f(t) = kKe^{-kt}$ obtained in a Model-Dependent Approach by Fitting Eq. 30 to Data Set 6

Fit	K	k	a_1	a_2	λ_1	λ_2	$RSS \times 10^{2a}$
1	0.170	3.31	10.8	6.10	−2.08	−1.13	1.0659
2	11.5	1.46	0.491	0.0797	−3.70	−3.64	1.0758
3	1.85	1.46	3.05	0.500	−3.69	−3.70	1.0758
4	0.233	3.65	9.39	1.85	−1.55	−1.18	1.0733
5	3.17	1.46	1.08	0.992	−3.70	−3.68	1.0758
6[b]	1.04	3.69	0	2.50	0	−1.46	1.0758
True values	3.0	1.5	1	1	−4	−3	

[a] Residual sum of squares. [b] The parameters a_1 and λ_1 were fixed as zero in the fitting procedure corresponding to a one-compartment model.

curve-fitting procedure at the expense of k and K. Furthermore, the nonlinear parameters are not unique due to the presence of multiple minima of the residual sum of the squares function (13). (The six fits in Table IV represent different local minima.)

The input could have been determined more accurately if the unit impulse response parameters had been determined first from an intravenous administration and then used as constants in the fitting of Eq. 30. However, this approach has the disadvantage of being model dependent since it assumes a first-order input $f(t) = kK \exp(-kt)$. Since many variables affect the input *via* the GI route (gastric emptying, GI motility, pH, blood flow, *etc.*), it may seem unreasonable that the input is described in such a smooth, functional form. The present least-squares deconvolution approach is more general. The input is approximated by a polynomial. As such, it is more flexible and can adapt to whatever fluctuations or functional form the input may have. Furthermore, the input is determined by linear rather than nonlinear regression, so it is easier to apply computationally (*e.g.*, no initial parameter estimates are required). The problem with multiple minima is eliminated, and the approach is more suitable for a statistical analysis of the input.

The present method requires the unit impulse response parameters to be determined by nonlinear regression. However, the nonuniqueness of these parameters and their actual values as such have no influence on the accuracy of the input determination. The input is not calculated from the parameters individually but collectively in the way that together they represent the unit impulse response. In estimating these parameters from data from an intravenous bolus or intravenous infusion administration, two or more sets of widely different parameters may be obtained that give nearly superimposed curves as in Fig. 1 (Table IV). However, contrary to a model-dependent approach, the individual parameter values are irrelevant. The important consideration is how well the curve fits the data. There are several methods for automatically handling this curve-fitting problem (14, 15).

Deficiencies in Using C_{max}, t_{max}, and AUC in Bioavailability Testing—Data Sets 4, 5, and 6 are generated from Fig. 2 curves A, B, and C, respectively, by adding 5% normally distributed noise to the exact concentration data (Table II). Curves A and B are very close, but the rate and the extent of input resulting in these curves differ substantially (Table I; A: $k = 1.5$, $K = 3.0$; B: $k = 1.0$, $K = 1.0$). Curves A and C differ widely, but they result from the same input (Table I; $k = 1.5$, $K = 3.0$). A comparison of the extent and the rate of input for Data Sets 4 and 5 (A and B, Fig. 2) on the basis of AUC, t_{max}, and C_{max} will not show a significant difference in their input. Furthermore, a comparison of Data Sets 4 and 6 (A and C, Fig. 2) by AUC, t_{max}, and C_{max} is likely to show a significant difference in both the rate and the extent of input when, in fact, there is no difference.

Because AUC, t_{max}, and C_{max} depend both on the input and the response properties of the system, they can be misleading measures of bioavailability if the comparison is not done within subjects, *i.e.*, for a constant unit impulse response. The deconvolution approach does not have this disadvantage. The response properties of the system are deconvoluted from the measured response to give a pure measure of the rate and the extent of input.

Deconvolution Approach—Deconvolution of Data Sets 4, 5, and 6 (corresponding to A, B, and C in Fig. 2) is done (Figs. 3, 4, and 5, respectively) using the responses measured for the three systems from a bolus input (Data Sets 1, 2, and 3, respectively)[5]. There is excellent agreement between the exact input and that calculated by deconvolution (Figs. 3–5). The regression function, Eq. 3, fits Data Sets 4–6 well. A Durbin–Watson analysis (16) and a runs test (17) show no systematic deviations among the residuals. The Tschebyscheff sampling strategy for Data Sets 4–6 appears to give a more stable behavior for the fitted curve (Eq. 3) and the calculated input for an increase in N (Eqs. 1 and 3) than the sampling scheme used previously (4).

Statistical Comparison of Input—The input rate calculated from Data Sets 1 and 4 and 3 and 6 (A and B, respectively, Fig. 6) does not appear to differ significantly throughout the input period $t = 0$–2. The differential confidence profile (curve C, Fig. 6) is largest in the initial input phase but shows no significant [$100(1 - \alpha) < 95$] difference in the input rate. The same is the case in comparing the cumulative input amount (Fig. 7). The input rates calculated from Data Sets 2 and 5 and 3 and 6 (A and B, respectively, Fig. 8) differ significantly in most of the input period. The respective cumulative input amounts differ significantly during the entire input period (Fig. 9). The input calculated from Data Sets 1 and 4 and 2 and 5 shows the same general behavior as the input calculated from Data Sets 2 and 5 and 3 and 6 (Figs. 10 and 11).

The method proposed performs satisfactorily. The inputs are well determined[6], and the method properly differentiates between the input

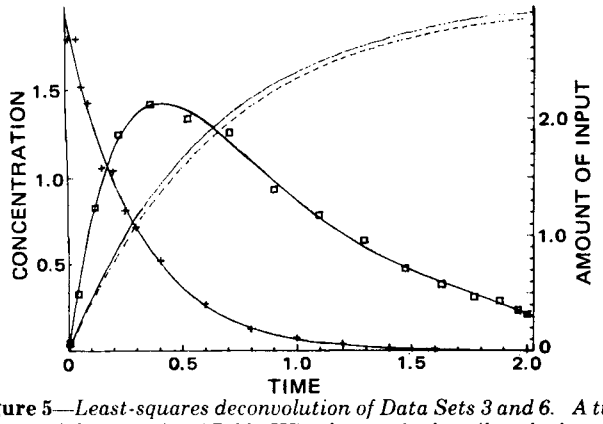

Figure 5—*Least-squares deconvolution of Data Sets 3 and 6. A two-exponential expression (Table III) adequately describes the impulse response data (+). The input function Eq. 1 is estimated subsequently by fitting Eq. 3 to the response data (□) by multiple linear regression. The continuously increasing curve is the calculated input amount (Table V). The broken curve is the exact input.*

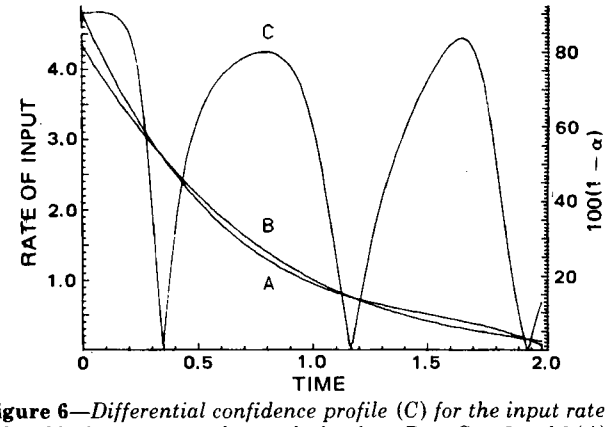

Figure 6—*Differential confidence profile (C) for the input rate calculated by least-squares deconvolution from Data Sets 3 and 6 (A) and 1 and 4 (B).*

[5] An infusion input also could have been used to obtain the unit impulse response parameters.

[6] The input might not have been approximated so well if the analysis had been performed using data extending substantially beyond the absorption phase. However, a beginning oscillatory behavior around zero of $f(t)$ in the postabsorption phase would result, indicating that the fitting is extended too far.

Table V—Input Rate Estimated by the Least-Squares Deconvolution Method, $0 \leq t \leq 2$

Data Sets	
1 and 4	$f(t) = 4.35 - 5.37t + 2.43t^2 - 0.403t^3$
2 and 5	$f(t) = 0.937 - 0.754t + 0.184t^2$
3 and 6	$f(t) = 4.81 - 7.32t + 4.45t^2 - 0.988t^3$

for the similar Data Sets 4 and 5. It also shows no significant difference between the widely different Data Sets 4 and 6 having the same input. However, the statistics appear rather sensitive (Figs. 6 and 7), as expected, since they are based on normality assumptions. Therefore, it would be appropriate to choose a more conservative hypothesis testing such as:

$$H_1: \quad \mu_1|t_0 \leq \mu_2^*|t_0 \qquad \text{(Eq. 31)}$$

against:

$$H_0: \quad \mu_1|t_0 > \mu_2^*|t_0 \qquad \text{(Eq. 32)}$$

$$\mu_2^*|t_0 = \frac{100 + D}{100}\mu_2|t_0 \qquad \text{(Eq. 33)}$$

where D, the differential index, is chosen appropriately. For example, with the differential index equal to 25, the hypothesis that the rate or cumulative amount of input differs by more than 25% could then be tested at various times by a simple extension of the present method. This approach seems to be more rational considering the large intersubject variations observed in the pharmacological response for many drugs. The application of the method to analyze real pharmacokinetic data is in progress.

APPENDIX

Several statistics have been proposed to test the equality of means for normal populations with unequal variances (18–21). Monte Carlo simulation studies comparing several of these statistics (21) indicate that the statistic proposed by Welch (19) is the most robust and appropriate for small samples.

This statistic can be stated for a two population problem in the following simplified form:

Theorem I: Let x_{ij} be the jth observation from the ith population, where $j = 1, \ldots, n_i$ and $i = 1, 2$. If x_{ij} are stochastically independent normal variates with expected values of μ_i and the variance σ_i^2, then the probability distribution of the statistic:

$$w = \frac{\bar{x}_1 - \bar{x}_2}{\left(\frac{s_1^2}{n_1} + \frac{s_2^2}{n_2}\right)^{1/2}} \qquad \text{(Eq. A1)}$$

is approximated by a t-distribution with degrees of freedom given by:

$$DF = \left[\frac{u^2}{n_1 - 1} + \frac{1 - u^2}{n_2 - 1}\right]^{-1} \qquad \text{(Eq. A2)}$$

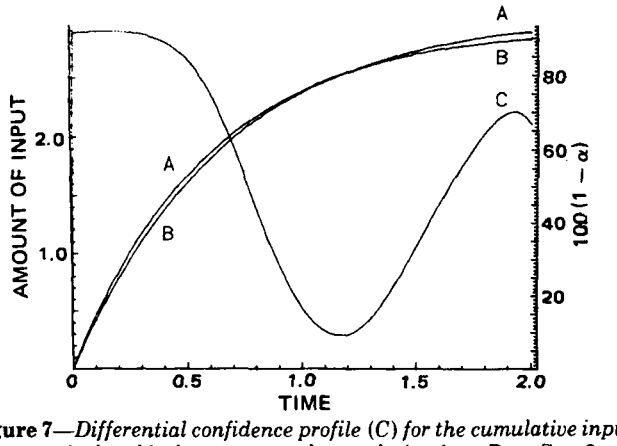

Figure 7—*Differential confidence profile (C) for the cumulative input amount calculated by least-squares deconvolution from Data Sets 3 and 6 (A) and 1 and 4 (B).*

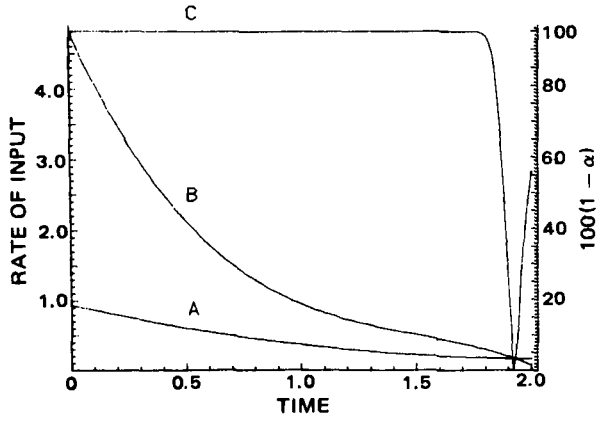

Figure 8—*Differential confidence profile (C) for the input rate calculated by least-squares deconvolution from Data Sets 2 and 5 (A) and 3 and 6 (B).*

where:

$$u = \frac{s_1^2/n_1}{s_1^2/n_1 + s_2^2/n_2} \qquad \text{(Eq. A3)}$$

$$s_i^2 = \sum_{j=1}^{n_i} (\bar{x}_i - x_{ij})^2/(n_i - 1) \qquad i = 1, 2 \qquad \text{(Eq. A4)}$$

and:

$$\bar{x}_i = \sum_{j=1}^{n_i} x_{ij}/n_i \qquad i = 1, 2 \qquad \text{(Eq. A5)}$$

This theorem deals with a differently formulated statistical problem than that of interest. However, the following extension of the theorem can be applied to test H_0 (Eq. 10) in the case of unequal population variances:

Corollary I: Let z_1 and z_2 be stochastically independent random variables distributed $N(\mu_1, \sigma_1^2)$ and $N(\mu_2, \sigma_2^2)$, respectively. Further, let s_{z1}^2 and s_{z2}^2 be stochastically independent random variables with moment-generating functions:

$$G_1(t) = \left(1 - 2\frac{\sigma_1^2}{\nu_1}t\right)^{-\nu_1/2} \qquad \nu_1 > 0 \qquad \text{(Eq. A6)}$$

$$G_2(t) = \left(1 - 2\frac{\sigma_2^2}{\nu_2}t\right)^{-\nu_2/2} \qquad \nu_2 > 0 \qquad \text{(Eq. A7)}$$

Then the probability distribution of the statistic:

$$w = \frac{z_1 - z_2}{(s_{z1}^2 + s_{z2}^2)^{1/2}} \qquad \text{(Eq. A8)}$$

is approximated by a t-distribution with degrees of freedom given by:

$$DF = \left[\frac{u^2}{\nu_1} + \frac{1 - u^2}{\nu_2}\right]^{-1} \qquad \text{(Eq. A9)}$$

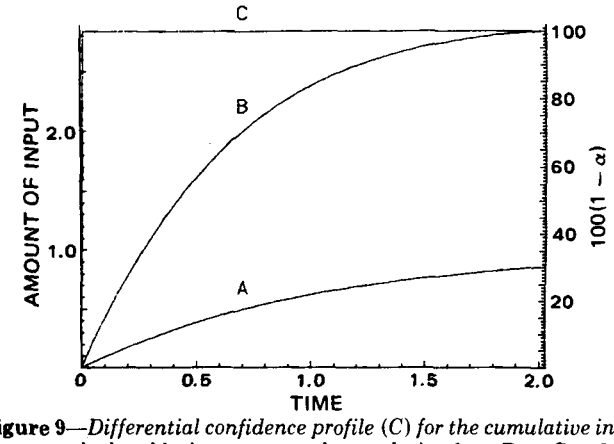

Figure 9—*Differential confidence profile (C) for the cumulative input amount calculated by least-squares deconvolution from Data Sets 2 and 5 (A) and 3 and 6 (B).*

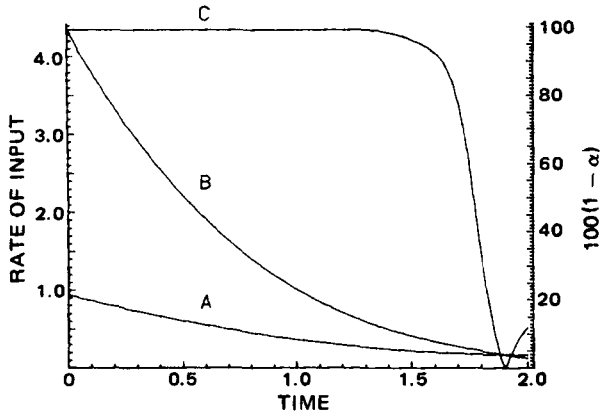

Figure 10—*Differential confidence profile (C) for the input rate calculated by least-squares deconvolution from Data Sets 2 and 5 (A) and 1 and 4 (B).*

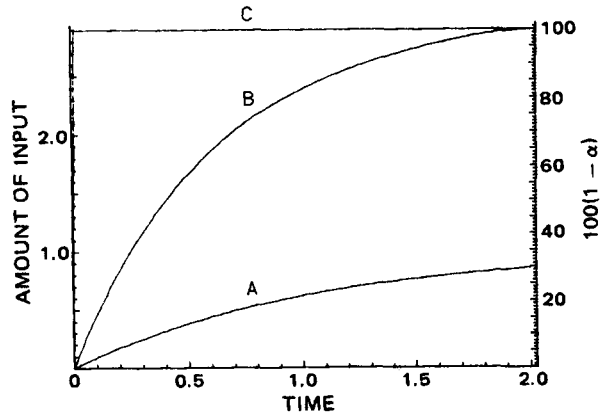

Figure 11—*Differential confidence profile (C) for the cumulative input amount calculated by least-squares deconvolution from Data Sets 2 and 5 (A) and 1 and 4 (B).*

where:

$$u = \frac{s_{z1}^2}{s_{z1}^2 + s_{z2}^2} \qquad \text{(Eq. A10)}$$

Proof: The random variables $z_i = \bar{x}_i$, $i = 1, 2$ (Eq. A5), are distributed $N(\mu_i, \sigma_i^2/n_i)$. The random variables $s_{zi}^2 = s_i^2/n_i$ have the moment-generating functions:

$$G_i(t) = \left(1 - 2\frac{\sigma_i^2/n_i}{n_i - 1}t\right)^{-(n_i-1)/2} \qquad i = 1, 2 \qquad \text{(Eq. A11)}$$

because $(n_i - 1)s_i^2/\sigma_i^2$ is χ^2-distributed with $n_i - 1$ degrees of freedom[7]. Equation A11 uniquely defines the probability distribution of s_{zi}^2. Letting $\nu_i = n_i - 1$ and replacing σ_i^2/n_i by σ_i^2 lead to the corollary.

The applicability of the corollary to test H_0 (Eq. 10) is seen as follows. With:

$$z_m = \hat{f}_m(t_0) \sim N(\mu_m | t_0, \sigma_m^2 \tau_m' \mathbf{V}_m \tau_m) \qquad m = 1, 2 \qquad \text{(Eq. A12)}$$

the moment-generating function of:

$$s_{zm}^2 = \hat{\sigma}_m^2 \tau_m' \mathbf{V}_m \tau_m = \frac{\mathbf{e}_m' \mathbf{e}_m}{M_m - N_m} \tau_m' \mathbf{V}_m \tau_m \qquad m = 1, 2 \qquad \text{(Eq. A13)}$$

is:

$$G_m(t) = \left(1 - 2\frac{\sigma_m^2 \tau_m' \mathbf{V}_m \tau_m}{M_m - N_m}t\right)^{-(M_m - N_m)/2} \qquad m = 1, 2 \qquad \text{(Eq. A14)}$$

because $(M_m - N_m)\hat{\sigma}_m^2/\sigma_m^2$ is χ^2-distributed with $M_m - N_m$ degrees of freedom. Comparison of Eqs. A12 and A14 in relation to Corollary I leads to Eqs. 24–26.

[7] The moment-generating function of a χ^2-distributed variable with n degrees of freedom is $(1 - 2t)^{-n/2}$.

REFERENCES

(1) "Guidelines for Biopharmaceutical Studies in Man," APhA Academy of Pharmaceutical Sciences, Washington, D.C., Feb. 1972.

(2) D. J. Chondos and A. R. DiSanto, "Basis of Bioavailability," The Upjohn Co., Kalamazoo, Mich., 1974.

(3) F. H. Dost, "Grundlagen der Pharmakokinetic," 2nd ed., Thieme, Stuttgart, West Germany, 1968, p. 155.

(4) P. Veng Pedersen, *J. Pharm. Sci.*, **69**, 312 (1980).

(5) J. G. Wagner, "Biopharmaceutics and Relevant Pharmacokinetics," Drug Intelligence Publications, Hamilton, Ill., 1971.

(6) *J. Pharmacokinet. Biopharm.*, **1**, 3 (1973).

(7) A. S. Goldberger, *JASA*, **57**, 369 (1962).

(8) D. E. Knuth, "The Art of Computer Programming," vol. 2, Addison-Wesley, Reading, Mass., 1969, p. 105.

(9) W. J. Dixon and M. B. Brown, "BMDP Biomedical Computer Programs," University of California Press, Berkeley, Calif., 1977.

(10) C. Daniel and F. S. Wood, "Fitting Equations to Data," Wiley, New York, N.Y., 1971, p. 86.

(11) G. W. Hill, *CACM*, **13**, 10 (1970).

(12) M. Abramowitz and I. A. Stegun, "Handbook of Mathematical Functions," Dover, New York, N.Y., 1970, pp. 932, 947.

(13) P. Veng Pedersen, *J. Pharmacokinet. Biopharm.*, **5**, 513 (1977).

(14) D. W. Kammler, *J. Approximation Theory*, **16**, 384 (1976).

(15) D. W. Kammler and R. J. McGlinn, *J. Computational Appl. Math.*, **4**, 167 (1978).

(16) J. Durbin and G. S. Watson, *Biometrica*, **37**, 409 (1950).

(17) F. S. Sweed and C. Eisenhart, *Ann. Math. Stat.*, **14**, 66 (1943).

(18) B. L. Welch, *Biometrics Bull.*, **1**, 80 (1951).

(19) B. L. Welch, *Biometrica*, **38**, 330 (1951).

(20) G. S. James, *ibid.*, **38**, 19 (1951).

(21) M. B. Brown and A. B. Forsythe, *Technometrics*, **16**, 129 (1974).

Kinetic Ratio as a Parameter for Product Stability Calculations

MARVIN SCHER

Received May 17, 1979, from *Miles Laboratories, Elkhart, IN 46515.* Accepted for publication October 12, 1979.

Abstract □ A new parameter, the kinetic ratio, is suggested for estimating product potency during storage under ambient warehouse temperatures. Actual warehouse temperature data were integrated using Arrhenius kinetics, and the resulting potency errors, due both to the integration method and to temperature averaging, were evaluated. Kinetic ratios and virtual temperatures then were compared to show seasonal and Arrhenius constant effects. Equations interrelating the kinetic ratio and virtual temperature are given. Finally, sample calculations using typical vitamin A data were analyzed to demonstrate the calculational and interpretation characteristics of the kinetic ratio compared to the virtual temperature.

Keyphrases □ Stability—product potency, calculation, kinetic ratio parameter □ Drug potency—product stability, calculation, kinetic ratio parameter □ Expiration dating—product stability, calculation, kinetic ratio parameter □ Arrhenius equation—calculation of product stability, kinetic ratio parameter

The useful concept of a single measurement, virtual temperature, to reflect the pattern of changing temperatures in a warehouse was introduced in 1971 (1). Since then, virtual temperature has been used widely in stability calculations. Although the physical meaning of virtual temperature is easily understood, it tends to be misleading and difficult to use because it causes a change two exponentiations away from the focus of interest.

Because temperature is a misleading criterion for kinetic change and is difficult to use in calculations, and because reference potencies commonly were calculated based on a reference temperature anyway, a new parameter, the kinetic ratio, was defined. Compared to virtual temperature, the kinetic ratio appears to relate more directly to potency, to separate temperature effects more effectively, to reflect important changes more sensitively, and to yield calculated results more conveniently.

EXPERIMENTAL

Data obtained at a Dallas warehouse were selected for analysis because this location offered extreme temperature variation. Temperature readings were used weekly from a circular chart recorder at 6-hr intervals for 364 days (September 1, 1975 through August 31, 1976). The data were collected as part of an ongoing stability evaluation program by a quality assurance unit.

In addition to the temperature data, typical constants for vitamin A in multivitamin tablets at a reference temperature of 24° were obtained from the same source and used in sample calculations. These constants were: Arrhenius "activation" constant (b_1), 13185.0 °K; Arrhenius factor (b_0), 2.0361×10^{16} weeks^{-1}; reference rate constant (T_{ref}), 297.16 °K; reference rate constant (k_{ref}), 0.0010943 week^{-1}; initial potency (P_0), 7300 units; reference potency at 52 weeks (P_{52}), 6896 units; reference potency at 78 weeks (P_{78}), 6703 units; reference potency at 156 weeks (P_{156}), 6154 units; and reference shelflife (τ_{sl}), 442 weeks.

RESULTS

Definitions and Relationships—Virtual temperature is the fixed temperature that produces the same kinetic constant as that which results from evaluating temperature that changes with time[1]. The kinetic ratio is a ratio of a rate constant that results from evaluating temperature that changes with time to the rate constant at a fixed reference temperature.

Quantitative relationships are given in Table I, and the nomenclature is appended. Both virtual temperature and the kinetic ratio are independent of reaction order for the simple models used in most cases. In this paper, temperature response is assumed to follow Arrhenius's law (Eq. 1). Mathematical definitions of the virtual temperature and kinetic ratio (Eqs. 2*a* and 2*b*, respectively) allow for temperature variation with time. At a given location, the observed temperature values can be integrated numerically to yield values of the two parameters. The remaining relationships in Table I are the result of combining and relating kinetic-order effects with the Arrhenius equation. Because reference temperature constants are a common form of reporting stability data, these constants normally would be readily available for the indicated calculations.

The resulting equations for α may be verified by direct derivation using definitions and kinetic relationships. For example, if a ratio of the first-order kinetic equations, $\ln(P_\tau/P_0) = -k\tau$ and $\ln(P_\tau/P_0)_{ref} = -k_{ref}\tau$, is formed and the definition of the kinetic ratio, $\alpha = k/k_{ref}$, is substituted therein, Eq. 3*b* results after antilogs are taken.

Temperature Data—Many questions might be asked about the process of transforming temperature data into a potency change. How frequently must temperature be measured? What errors are introduced by averaging temperatures to daily, weekly, and monthly values? What methods might be used to convert temperature–time data into potency effects? These questions are not fully answered here, but an efficient approach to the problem is suggested and the relative importance of several factors is weighed.

Potency changes were evaluated for two sets of Arrhenius constants, one set typical of vitamin A in a multivitamin tablet and another set arbitrarily formulated to approach the upper temperature–instability limit likely to be encountered in products stored at ambient temperatures. The conventional Arrhenius equation and first-order kinetics were combined as in Eq. 3*a*, except that actual temperatures were used in place of virtual temperature. The result was integrated numerically over time. With temperature readings at 6-hr intervals, three numerical integration methods were compared: Simpson's rule, the trapezoidal rule, and a fifth-order quadrature method[2]. Although errors resulting from all methods were small (Table II), the fifth-order quadrature method was used for subsequent comparisons because it reduced integration errors to insignificantly small values.

The effect of temperature averaging on the observed error in potency also was considered. Results for averaged temperature values for each day, week, and month showed very small errors for moderately stable materials, but these values would be subject to noticeable errors at the limit of practical stability. This effect has a direct bearing on the use of virtual temperature, the kinetic ratio, or any other temperature-averaging method. Either correction factors or averages over smaller time intervals probably would be required to reflect accurately the potency of very heat-sensitive materials stored at ambient temperatures.

Daily averaged temperatures and fifth-order quadrature were used with Eq. 2*a* from Table I to evaluate virtual temperatures. Kinetic ratios were determined similarly from Eq. 2*b* with a reference temperature of 24°. Results are presented in Table III.

DISCUSSION

Virtual Temperature and Kinetic Ratio—Close examination of Eq. 3*b* reveals that, for first-order kinetics, the kinetic ratio has an interpretation similar to the elasticity in economics. For every small percent change in the reference potency, the actual percent potency changes by a factor of approximately α times. Thus, with reference to Table III, a compound with an activation constant of 15,000 will drop approximately 13.24% for a 10% annual loss observed at the reference temperature. Actual calculation from Eq. 3*b* yields 13.02%. Although this simple interpretation of α becomes subject to larger errors with larger potency

[1] This statement is a general application of Haynes' definition, which related virtual temperature to a monthly average temperature (1).

[2] Scientific Subroutine Package, IBM.

0022-3549/80/0300-0325$01.00/0
© 1980, American Pharmaceutical Association

Table I—Relationships of Virtual Temperature and Kinetic Ratio Parameters [Arrhenius's Law: $k = b_0 e^{-b_1/T}$ (Eq. 1)]

Definition	Virtual Temperature		Kinetic Ratio	
	$T_v = \dfrac{-b_1}{\ln\left(\frac{1}{\tau}\int_0^\tau e^{-b_1/T}\,d\theta\right)}$	(Eq. 2a)	$\alpha = \dfrac{\frac{1}{\tau}\int_0^\tau e^{-b_1/T}\,d\theta}{e^{-b_1/T_{ref}}}$	(Eq. 2b)
	where $T = g(\theta)$ is an unspecified function of time			
First-order potency	$P_\tau = P_0 e^{-(b_0 e^{-b_1/T_v})\tau}$	(Eq. 3a)	$P_\tau = P_0\left(\frac{P_\tau}{P_0}\right)^\alpha_{ref}$	(Eq. 3b)
First-order shelflife	$\tau_{sl} = \dfrac{\ln(P_0/P_\tau)_{sl}}{b_0 e^{-b_1/T_v}}$	(Eq. 4a)	$\tau_{sl} = \dfrac{\ln(P_0/P_\tau)_{sl}}{\alpha k_{ref}}$	(Eq. 4b)
Zero-order potency	$(P_0 - P_\tau) = (b_0 e^{-b_1/T_v})\tau$	(Eq. 5a)	$(P_0 - P_\tau) = \alpha(P_0 - P_\tau)_{ref}$	(Eq. 5b)
Zero-order shelflife	$\tau_{sl} = \dfrac{(P_0 - P_\tau)_{sl}}{b_0 e^{-b_1/T_v}}$	(Eq. 6a)	$\tau_{sl} = \dfrac{(P_0 - P_\tau)_{sl}}{\alpha k_{ref}}$	(Eq. 6b)
For equal cumulative time periods	$(-b_1/T_v)_\tau = \ln\frac{1}{\tau}\sum_{i=1}^{\tau}(e^{-b_1/T_{vi}})$	(Eq. 7a)	$\alpha_\tau = \frac{1}{\tau}\sum_{i=1}^{\tau}\alpha_i$	(Eq. 7b)
Conversion, T_v/α	$T_v = \dfrac{b_1}{b_1/T_{ref} - \ln\alpha}$	(Eq. 8a)	$\ln\alpha = b_1\left(\frac{1}{T_{ref}} - \frac{1}{T_v}\right)$	(Eq. 8b)
Conversion, reference T	$k_v = \alpha k_{ref}$	(Eq. 9a)	$\alpha_{T_2} = \alpha_{T_1} e^{-b_1(1/T_1 - 1/T_2)}$	(Eq. 9b)

Table II—Annual Percent Error in Potency Calculations Relative to the Best Estimate Based on a Dallas Warehouse

Constants		Percent Potency Remaining, $100\,(P_\tau/P_0)_y$	Percent Error in Fraction Potency Remaining[a] by Time Interval/Method[b]					
			6 hr			Daily	Weekly	Monthly
b_0	b_1		DQSF	SIMP	TRAP	DQSF	DQSF	DQSF
2.0361×10^{16}	13,185	93.1	0	<0.01	−0.02	0.06	0.18	0.50
8.46×10^{33}	25,000	74.3	0	0.09	−0.30	1.5	5.5	12.6

[a] Percent error = $100\,[(P_\tau/P_0)_y - (P_\tau^{\sim}/P_0)_y]/(P_\tau/P_0)_y$. [b] DQSF is a fifth-order quadrature subroutine from IBM's Scientific Subroutine Package, and SIMP and TRAP are mnemonics for Simpson's rule and the trapezoidal rule, respectively.

Table III—Yearly and Quarterly Arrhenius Kinetic Parameters for a Dallas Warehouse [T_{ref} = 297.16 (24°)]

	Kinetic Ratios					Virtual Temperatures				
b_1	α_y	α_1	α_2	α_3	α_4	T_{vy}	T_{v1}	T_{v2}	T_{v3}	T_{v4}
5,000	1.009	0.708	0.998	1.404	0.927	297.32	291.17	297.13	303.27	295.83
10,000	1.112	0.507	1.027	1.999	0.915	298.15	291.28	297.39	303.41	296.37
15,000	1.324	0.367	1.088	2.886	0.955	298.82	291.38	297.66	303.53	296.89
20,000	1.679	0.270	1.187	4.214	1.046	299.47	291.48	297.92	303.64	297.36
25,000	2.236	0.200	1.331	6.221	1.190	300.03	291.58	298.17	303.76	297.77

changes, it is a quick and easy estimator and has a readily understood relationship to potency.

Seasonal effects are relatively easy to discern in the kinetic ratio (Table III). A compound with an activation constant of 15,000 and a warehouse potency loss of 13% for the year will have experienced a cycle of changes relative to the constant-temperature reference. In the cold winter months of the first quarter, the α value of 0.367 suggests a change of slightly more than one-third of the change of the reference potency. During the spring and fall, the reference and warehouse potencies change by about the same amount. However, in the summer, the warehouse potency loss was just under three times the reference loss.

For zero-order kinetics, the kinetic ratio is directly proportional to the drop in potency (Eq. 5b). Thus, if the reference potency for the example drops 500 units in a year, that same compound would drop $1.324 \times 500 = 662$ units in the Dallas warehouse.

Comparison of Virtual Temperature and Kinetic Ratio—No obvious deductions regarding potency changes can be made from the virtual temperatures in Table III. Interpolation may be used to obtain intermediate values for both parameters. Linear interpolation in Table III produced a maximum positive error of ~0.01. Because of the additional exponentiation, virtual temperature calculations require greater care. The constancy of virtual temperature has been emphasized as offering a special advantage (1). This constancy is an artifact of double exponentiation and demonstrates the insensitivity of virtual temperature to changes that can significantly affect potency. For example, according to Eq. 3a, a relatively small change in T_v will, after being exponentiated twice, magnify into a substantial potency change.

The interrelationship between the kinetic ratio and virtual temperature is given by Eqs. 8a and 8b, which quantify the relative sensitivity of α observed in Table III. Specifically, the entire range of virtual temperatures here changes by only 4%, while the corresponding range of the kinetic ratio changes by 3100%. It is evident that numerous significant digits must be carried for virtual temperature and that the leading constant digits tend to screen information.

Computation of virtual temperature and the kinetic ratio is similar, except that a reference temperature must be declared for the latter (Eq. 2b). This requirement is the only price paid for later ease of use, and reference temperature calculations appear to be widely used throughout the pharmaceutical industry. Because both parameters are dependent on ambient temperatures, which, in turn, are a function of the specific

Table IV—Comparison of Calculations for Potency at a Dallas Warehouse

Calculation	Virtual Temperature	Kinetic Ratio	Number of Arithmetic Operations: Virtual Temperature	Number of Arithmetic Operations: Kinetic Ratio	Vitamin A Results
Potency after 3 years	Eqs. 1 and 3*a*	Eq. 3*b*	6	3	5914 units
Potency after 18 months (six quarters) using seasonal values	Eqs. 7*a*, 1, and 3*a*	Eqs. 7*b* and 3*b*	17	8	664 units
Potency after 18 months (six quarters) using annual values	Eqs. 1 and 3*a*	Eq. 3*b*	6	3	6570 units
Shelflife	Eq. 4*a*	Eq. 4*b*	6	4	358 weeks

warehouse location and construction, each company would have to determine its individual parameters. The inclusion of a reference temperature in these calculations is a small matter. In addition, conversion from one reference temperature to another, should this be necessary, is straightforward (Eq. 9*b*).

Sample Calculations—Constants and reference data were combined with the data from Table III for sample calculations. Twice as many arithmetic operations usually are required for calculations involving virtual temperature (Table IV). The use of reference potencies eliminates the need to calculate rate constants. The kinetic ratio reference potency and initial potency are all that are required for direct calculations. Once the reference values are calculated, they remain constant and may be used to calculate potencies at each warehouse with the appropriate α value. Virtual temperature calculations invariably require exponentiation to obtain a rate constant needed for subsequent calculations. As also can be seen from Table IV, the seasonal effect over six quarters is not significant for vitamin A in multivitamin tablets (1.5%). Shelflife calculations using the kinetic ratio are particularly easy because they only involve dividing a constant by a different α for each warehouse.

CONCLUSIONS

Although it is only a simple extension of a generalized virtual temperature definition, the kinetic ratio offers clear practical advantages. The parameter has a direct, easily understood physical relationship to potency, and commonly performed calculations are simplified greatly.

NOMENCLATURE

α = kinetic ratio (dimensionless)
b_0 = Arrhenius factor, defined by Eq. 1 (weeks^{-1})
b_1 = Arrhenius activation factor, E/R, defined by Eq. 1 (°K)
θ = time (weeks)
g = general unspecified function
k = Arrhenius kinetic constant (weeks^{-1})
P = potency or concentration variable (units)
τ = specific time (weeks)
T = temperature (°K)

Subscripts:

0 = initial value of a variable
1, 2, 3, 4 = either a specific value denoted by the number or values that relate to enumerated quarters of the year
ref = reference value of a variable or quantity enclosed in brackets
sl = value of variables corresponding to the shelflife
v = virtual value
y = cumulative annual value

REFERENCES

(1) J. D. Haynes, *J. Pharm. Sci.*, **60**, 927 (1971).

Synthesis and Skeletal Muscle Relaxant Activity of Quaternary Ammonium Salts of Dantrolene and Clodanolene

K. O. ELLIS ˣ, R. L. WHITE, Jr., G. C. WRIGHT, and F. L. WESSELS

Received July 16, 1979, from the *Scientific Affairs Department, Norwich-Eaton Pharmaceuticals, Division of Morton-Norwich Products, Inc., Norwich, NY 13815.* Accepted for publication October 16, 1979.

Abstract □ A series of quaternary ammonium salts of dantrolene and clodanolene was prepared and evaluated for skeletal muscle relaxant activity. The quaternary ammonium salts exhibit greater aqueous solubility and, therefore, facilitate intravenous administration. One member of this series, although less effective orally, exhibited greater aqueous solubility than the sodium salt. When administered intravenously, it was a more potent antagonist of skeletal muscle contraction and yielded comparable therapeutic and muscle relaxant efficacy indexes.

Keyphrases □ Dantrolene—quaternary ammonium salts, synthesis, skeletal muscle relaxant activity □ Clodanolene—quaternary ammonium salts, synthesis, skeletal muscle relaxant activity □ Relaxants, skeletal muscle—dantrolene and clodanolene, quaternary ammonium salts, synthesis, activity

Several hydantoins have skeletal muscle relaxant activity (1). One member of this series, dantrolene[1], was shown subsequently to cause skeletal muscle relaxation by a unique mechanism involving direct action on the skeletal muscle (2, 3). Dantrolene sodium has been hypothesized to act by preventing the release of calcium ion (Ca^{2+}) from the sarcoplasmic reticulum (4, 5).

Dantrolene sodium recently was shown to have potential

[1] Dantrium, Morton-Norwich Products.

0022-3549/80/0300-0327$01.00/0
© 1980, American Pharmaceutical Association

Table IV—Comparison of Calculations for Potency at a Dallas Warehouse

Calculation	Virtual Temperature	Kinetic Ratio	Number of Arithmetic Operations: Virtual Temperature	Number of Arithmetic Operations: Kinetic Ratio	Vitamin A Results
Potency after 3 years	Eqs. 1 and 3*a*	Eq. 3*b*	6	3	5914 units
Potency after 18 months (six quarters) using seasonal values	Eqs. 7*a*, 1, and 3*a*	Eqs. 7*b* and 3*b*	17	8	664 units
Potency after 18 months (six quarters) using annual values	Eqs. 1 and 3*a*	Eq. 3*b*	6	3	6570 units
Shelflife	Eq. 4*a*	Eq. 4*b*	6	4	358 weeks

warehouse location and construction, each company would have to determine its individual parameters. The inclusion of a reference temperature in these calculations is a small matter. In addition, conversion from one reference temperature to another, should this be necessary, is straightforward (Eq. 9*b*).

Sample Calculations—Constants and reference data were combined with the data from Table III for sample calculations. Twice as many arithmetic operations usually are required for calculations involving virtual temperature (Table IV). The use of reference potencies eliminates the need to calculate rate constants. The kinetic ratio reference potency and initial potency are all that are required for direct calculations. Once the reference values are calculated, they remain constant and may be used to calculate potencies at each warehouse with the appropriate α value. Virtual temperature calculations invariably require exponentiation to obtain a rate constant needed for subsequent calculations. As also can be seen from Table IV, the seasonal effect over six quarters is not significant for vitamin A in multivitamin tablets (1.5%). Shelflife calculations using the kinetic ratio are particularly easy because they only involve dividing a constant by a different α for each warehouse.

CONCLUSIONS

Although it is only a simple extension of a generalized virtual temperature definition, the kinetic ratio offers clear practical advantages. The parameter has a direct, easily understood physical relationship to potency, and commonly performed calculations are simplified greatly.

NOMENCLATURE

α = kinetic ratio (dimensionless)
b_0 = Arrhenius factor, defined by Eq. 1 (weeks^{-1})
b_1 = Arrhenius activation factor, E/R, defined by Eq. 1 (°K)
θ = time (weeks)
g = general unspecified function
k = Arrhenius kinetic constant (weeks^{-1})
P = potency or concentration variable (units)
τ = specific time (weeks)
T = temperature (°K)

Subscripts:

0 = initial value of a variable
1, 2, 3, 4 = either a specific value denoted by the number or values that relate to enumerated quarters of the year
ref = reference value of a variable or quantity enclosed in brackets
sl = value of variables corresponding to the shelflife
v = virtual value
y = cumulative annual value

REFERENCES

(1) J. D. Haynes, *J. Pharm. Sci.*, **60**, 927 (1971).

Synthesis and Skeletal Muscle Relaxant Activity of Quaternary Ammonium Salts of Dantrolene and Clodanolene

K. O. ELLIS ˣ, R. L. WHITE, Jr., G. C. WRIGHT, and F. L. WESSELS

Received July 16, 1979, from the *Scientific Affairs Department, Norwich-Eaton Pharmaceuticals, Division of Morton-Norwich Products, Inc., Norwich, NY 13815.* Accepted for publication October 16, 1979.

Abstract □ A series of quaternary ammonium salts of dantrolene and clodanolene was prepared and evaluated for skeletal muscle relaxant activity. The quaternary ammonium salts exhibit greater aqueous solubility and, therefore, facilitate intravenous administration. One member of this series, although less effective orally, exhibited greater aqueous solubility than the sodium salt. When administered intravenously, it was a more potent antagonist of skeletal muscle contraction and yielded comparable therapeutic and muscle relaxant efficacy indexes.

Keyphrases □ Dantrolene—quaternary ammonium salts, synthesis, skeletal muscle relaxant activity □ Clodanolene—quaternary ammonium salts, synthesis, skeletal muscle relaxant activity □ Relaxants, skeletal muscle—dantrolene and clodanolene, quaternary ammonium salts, synthesis, activity

Several hydantoins have skeletal muscle relaxant activity (1). One member of this series, dantrolene[1], was shown subsequently to cause skeletal muscle relaxation by a unique mechanism involving direct action on the skeletal muscle (2, 3). Dantrolene sodium has been hypothesized to act by preventing the release of calcium ion (Ca^{2+}) from the sarcoplasmic reticulum (4, 5).

Dantrolene sodium recently was shown to have potential

[1] Dantrium, Morton-Norwich Products.

0022-3549/80/0300-0327$01.00/0
© 1980, American Pharmaceutical Association

Table I—Synthesized Imidazolidinedione Compounds and Their Corresponding Cations

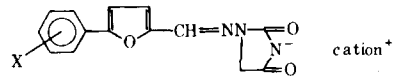

Compound	X	Cation	Water Solubility, mg/liter
I	4-NO_2	Benzyltrimethylammonium	>10
II	4-NO_2	Tetramethylammonium	—[a]
III	4-NO_2	*N*-Methylpyridinium	—[a]
IV	4-NO_2	Tetrabutylammonium	—[a]
V	3,4-Cl	2-(2,3-Dihydroxy-1-propylamino)-quinolizinium	550
VI	3,4-Cl	Safranine O	40
VII	4-NO_2	Quinolizinium	930
VIII	3,4-Cl	Quinolizinium	2000
IX	4-NO_2	2-Carbamoyl-1-methylpyridinium	90
X	4-NO_2	2,3-Dimethyl-1-phenyl-4-trimethyl-ammonium-3-pyrazolin-5-one	—[a]
XI	4-NO_2	Diethyldimethylammonium	9400
XII	4-NO_2	1,3-Dimethylimidazolium	—[a]
XIII	3,4-Cl	2,3-Dimethyl-1-phenyl-4-trimethyl-ammonium-3-pyrazolin-5-one	1200
XIV	4-NO_2	Choline	8000
XV	4-NO_2	2-(1-Hydroxy-2-methyl)propyltri-methylammonium	140
Dantrolene sodium			15
Clodanolene sodium			20

[a] The water solubility is greater than 1%.

utility for the treatment of malignant hyperthermia (6–8). The fulminating nature of this condition requires rapid institution of therapeutic measures including intravenous muscle relaxants. Because dantrolene sodium is relatively insoluble in aqueous solutions, other soluble salts have been synthesized for evaluation (Table I). This paper reports the preparation of a series of quaternary ammonium salts (9) of dantrolene and clodanolene and their pharmacological evaluation for skeletal muscle relaxant activity.

Salts of dantrolene and clodanolene, other than the sodium salts, were desired for comparative pharmacological evaluation. Since the hydantoin moiety of the two parent compounds is weakly acidic, a strong base was sought for salt formation. The broad class of quaternary ammonium hydroxides fills the requirement of a strong base and also provides versatility in selection of an organic cation. In practice, the acid–base reaction of dantrolene or clodanolene with quaternary ammonium hydroxides proceeded rapidly, and the salt products were stable to recrystallization from various solvents (Scheme I). The quaternary ammonium hydroxides were prepared from the appropriate quaternary ammonium halides by ion-exchange chromatography and then were used directly. Success of

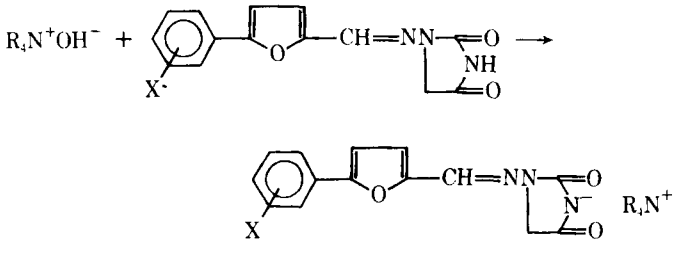

dantrolene: X = *p*-NO_2
clodanolene: X = 3,4-Cl

Scheme I

the acid–base reaction was easily discernible upon isolation of the product. The carbonyl bands of the hydantoins at 5.65 and 5.8 μm in the IR spectrum shifted to 5.9 and 6.2 μm.

EXPERIMENTAL

Chemistry[2]—*Quaternary Halides*—The following salts were prepared by literature methods: diethyldimethylammonium iodide (10), 1,3-dimethylimidazolium iodide (11), *N*-methylpyridinium iodide (12), 1,1-dimethyl-2-hydroxyethyltrimethylammonium iodide (13), 2-carbamyl-1-methylpyridinium iodide (14), aminopyridine methiodide (15), quinolizinium bromide (16), and 2-(2,3-dihydroxypropylamino)quinolizinium bromide (17). Tetramethylammonium hydroxide, benzyltrimethylammonium hydroxide, tetramethylammonium chloride, tetrabutylammonium iodide, benzyltrimethylammonium chloride, and Safranine O were purchased[3]. Choline chloride was obtained commercially[4].

The following four methods were used for preparation of quaternary salts of dantrolene and clodanolene, with dantrolene salts given as examples (Table II).

Dantrolene [1-[[5-(p-Nitrophenyl)furfurylidene]amino]hydantoin] Quinolizinium Salt Hemihydrate (VII) (Method A)—Resin[5] (65 ml) was activated by elution with 10% NaOH, and the column was washed with water to bring to pH 7–8. Quinolizinium bromide (4.7 g, 0.021 mole) (7) was passed through the basic anion-exchange resin with water (75 ml) at ~1 drop/sec until the eluent (pH 10–11) returned to pH 8–9.

Dantrolene (5.1 g, 0.016 mole) was added slowly to the quaternary hydroxide solution at room temperature to bring to pH 8–9. The resultant yellow solid was collected and washed with cold water (3 × 5 ml) and 2-propanol (2 × 5 ml) and then was allowed to dry to give 5.1 g (70% yield), mp 184–196° dec.; IR (mineral oil): 5.9 and 6.2–6.3 μm.

Dantrolene Diethyldimethylammonium Salt (XI) (Method B)—A resin[5] column (115 ml) was prepared as in Method A. Methanol (400 ml) was eluted slowly through the column followed by a solution of diethyldimethylammonium iodide in methanol (50 ml). The column was eluted to neutrality with methanol. The methanolic solution was added to dantrolene (15.7 g, 0.050 mole) in methanol (100 ml), and the mixture was stirred for 1.0 hr.

The mixture was filtered, and the filtrate was concentrated under reduced pressure to a red solid. Recrystallization from 2-propanol (150 ml) with activated charcoal[6] yielded 16.5 g (72% yield) of product, mp 198–200°. A sample again was recrystallized from 2-propanol to analytical purity, mp 201–202°; IR (mineral oil): 5.9 and 6.2–6.3 μm.

Dantrolene Tetramethylammonium Salt (II) (Method C)—To a stirred mixture of dantrolene (21 g, 0.066 mole) in 1.0 liter of methanol was added tetramethylammonium hydroxide (50 ml of 20% solution in methanol, 0.10 mole). The mixture was stirred for 1.0 hr and then heated while methanol (400 ml) was added to complete dissolution. Filtration and cooling allowed isolation of 15 g (59% yield) of a red product. Recrystallization from methanol gave analytical material, mp 218–220°; NMR: δ 3.23 (s, 12H, methyl CH), 3.80 (s, 2H, hydantoin CH), 6.87 (d, 1H, furan CH, J = 3.5 Hz), 7.46 (d, 1H, furan CH, J = 3.5 Hz), 7.58 (s, 1H, azomethine CH), 8.00 (d, 2H, phenyl CH, J = 8 Hz), and 8.32 (d, 2H, phenyl CH, J = 8 Hz); IR (mineral oil): 5.9 and 6.2 (broad) μm.

Dantrolene Benzyltrimethylammonium Salt (I) (Method D)—To a refluxing stirred solution of dantrolene (16 g, 0.050 mole) in methanol (1.0 liter) was added rapidly benzyltrimethylammonium hydroxide (25 ml of 40% solution in methanol, 0.060 mole). The solution was filtered and concentrated under reduced pressure to ~250 ml. Ether (750 ml) was added to the cooled solution, and the resulting red solid was collected and rinsed with ether (100 ml) to give 22 g (95% yield) of product, mp 150–160° dec.; IR (mineral oil): 5.9 and 6.25 μm.

Pharmacology—Initially selected quaternary ammonium salts were evaluated intravenously in rats by gross observation for skeletal muscle relaxant activity (cholinergic and/or toxic signs). Direct effects on skeletal

[2] Melting points were determined on a Mel-Temp apparatus and are uncorrected. A Varian Associates A-60A instrument was used for NMR spectra. All spectra were run in dimethyl sulfoxide-d_6 with tetramethylsilane as the internal standard. A Perkin-Elmer model 137B recording spectrophotometer was used for IR spectra. Solubilities were determined by agitation of a sample in water at room temperature, filtration of the saturated aqueous solution, and UV comparison with a standard sample (Table I).

[3] Aldrich Chemical Co.

[4] Merck Laboratory Chemicals.

[5] Amberlite IRA-410.

[6] Darco.

Table II—Analysis of Synthesized Imidazolidinedione Compounds

Compound	Recrystallization Solvent[a]	Synthetic Method	Yield, %	Melting Point	Empirical Formula	Analysis, %	Calc.	Found
I	E	D	95	150–160° dec.	$C_{24}H_{25}N_5O_5$	C	62.19	61.79
						H	5.44	5.80
						N	15.11	14.96
II	F	C	59	218–220°	$C_{18}H_{21}N_5O_5$	C	55.81	55.82
						H	5.46	5.45
						N	18.08	18.14
III	F	B	83	173–175°	$C_{20}H_{17}N_5O_5 \cdot 0.75\ H_2O$	C	57.07	56.98
						H	4.43	4.75
						N	16.64	16.64
IV	G	B	58	187–189°	$C_{30}H_{45}N_5O_5$	C	64.84	65.04
						H	8.16	8.14
						N	12.60	12.43
V	H	A	33	132–135°	$C_{26}H_{23}Cl_2N_5O_5 \cdot 0.5\ H_2O$	C	55.23	54.92
						H	4.28	4.52
						N	12.39	12.16
VI	H	A	38	194–197°	$C_{34}H_{27}Cl_2N_2O_3 \cdot 1.5\ H_2O$	C	60.09	60.00
						H	4.45	4.64
						N	14.43	14.23
VII	E	A	70	184–196° dec.	$C_{23}H_{17}N_5O_5 \cdot 0.5\ H_2O$	C	61.06	60.86
						H	4.01	3.79
						N	15.48	15.80
VIII	F[b]	A	62	160–162° dec.	$C_{23}H_{16}Cl_2N_4O_3 \cdot 0.167\ C_3H_8O$	C	59.12	58.94
						H	3.67	3.65
						N	11.74	11.66
IX	J	B	59	203–204°	$C_{21}H_{18}N_6O_6$	C	55.60	55.85
						H	4.03	4.02
						N	18.66	18.81
X	K	B	74	150–152°	$C_{28}H_{29}N_7O_6$	C	60.10	59.91
						H	5.22	5.47
						N	17.52	17.47
XI	L	B	72	198–200°	$C_{20}H_{25}N_5O_5$	C	57.82	57.64
						H	6.07	6.15
						N	16.86	17.02
XII	F	B	53	172–175°	$C_{19}H_{18}N_6O_5$	C	55.60	55.36
						H	4.42	4.42
						N	20.48	20.43
XIII	F	B	62	190–215° dec.	$C_{28}H_{28}Cl_2N_6O_4$	C	57.64	57.51
						H	4.84	5.01
						N	14.41	14.33
XIV	F	B	48	196–198° dec.	$C_{19}H_{23}N_5O_6$	C	54.67	54.31
						H	5.55	5.54
						N	16.78	16.78
XV	J	B	54	179–181°	$C_{21}H_{27}N_5O_6$	C	56.72	56.21
						H	6.11	6.10
						N	15.72	15.64

[a] The recrystallization solvents were methanol (F), acetone (G), ethanol (H), nitromethane (J), acetonitrile (K), and 2-propanol (L), or no recrystallization solvent was used (E). [b] Sample was rinsed with 2-propanol after recrystallization, and the NMR spectrum indicated the presence of 0.167 mole of 2-propanol.

Table III—Acute Lethality of Quaternary Salts Used to Prepare Dantrolene and Clodanolene Salts

Quaternary Salt	Gastrocnemius Muscle Twitch Response, maximum % change at 25 mg/kg	Acute Oral Lethality in Mice
Benzyltrimethylammonium chloride	+10.1 ± 1.5	100% at 1600 mg/kg
Tetramethylammonium chloride	+8 ± 0.9	100% at 125 mg/kg
N-Methylpyridinium iodide	+3 ± 3.0	30% at 1600 mg/kg
Tetrabutylammonium iodide	+14.2 ± 6.5	60% at 1600 mg/kg
2-(2,3-Dihydroxy-1-propylamino)quinolizinium bromide	−5.6 ± 5.6	10% at 1600 mg/kg
Safranine O	+5 ± 1.7	10% at 1600 mg/kg
Quinolizinium bromide	+18.7 ± 6.3	100% at 1600 mg/kg
2-Carbamoyl-1-methylpyridinium iodide	+7 ± 1.4	>1600 mg/kg
2,3-Dimethyl-1-phenyl-4-trimethylammonium-3-pyrazolin-5-one iodide	−1 ± 2.1	>1600 mg/kg
Diethyldimethylammonium iodide	+7 ± 4.5	LD_{50} = 712 mg/kg (584–853)
1,3-Dimethylimidazolium iodide	+3 ± 0.1	10% at 1600 mg/kg
Choline chloride	+7.5 ± 0.5	>1600 mg/kg
2-(1-Hydroxy-2-methyl)propyltrimethylammonium iodide	+20 ± 2.7	>1600 mg/kg

muscle also were evaluated in the gastrocnemius muscle preparation by the method to be described later. Only compounds (Table III) devoid of skeletal muscle relaxant activity were used for the preparation of the imidazolidinedione compounds.

Gross Observation—Groups of unfasted male mice (TAC:SWfBr), 20–27 g, were used. The drugs were administered orally as 2% concentrations suspended in 0.5% methylcellulose 4000 cps. Gross observations for pharmacological effects were made for 2 hr, utilizing a rating of drug effect signs similar to that described by Irwin (18). Muscle relaxation was rated on a scale from 0 to 4 with 0 = no effect, 1 = slight, 2 = moderate, 3 = marked, and 4 = extreme.

Pithed Rat Gastrocnemius Muscle Preparation—A literature method was used for direct stimulation of the gastrocnemius muscle in rats (TAC:SD/NfBr) (19). The test drugs were administered intravenously at logarithmically spaced doses in tetrahydrofurfuryl alcohol, and ED_{50} values for inhibition of skeletal muscle contractions were estimated by the method of Litchfield and Wilcoxon (20).

Rotarod Testing in Mice—A method similar to that described by Dunham and Miya (21) was used to test the effect of drugs on motor coordination. Male mice (TAC:SWfBr) were trained to walk a revolving rod (20 rpm) for over 1 min. The test drugs were administered orally at logarithmically spaced doses in methylcellulose[7] to the previously trained mice, and performance trials were conducted 30 min following drug administration. The inability of an animal to stay on the rotarod for more than 30 sec was considered a positive drug effect. The ED_{50} values (the drug dose that caused 50% of the animals to fall off the revolving rod within the 30 sec) were calculated using the method of Litchfield and Wilcoxon (20).

[7] Methocel, Dow.

Table IV—Oral Testing for Skeletal Muscle Relaxant Properties of Quaternary Ammonium Salts of Dantrolene and Clodanolene

Compound	Minimum Dose (mg/kg) for Maximum Activity[a]	ED_{50}, Straub Tail[b]	ED_{50}, Rotarod[c]	LD_{50}, mg/kg	Muscle Relaxant Efficacy Index, ED_{50} (Rotarod)/ ED_{50} (Straub Tail)	Therapeutic Index, LD_{50}/ED_{50} (Straub Tail)
I	800/0	—[d]	—	—	—	—
II	800/0	—[d]	—	—	—	—
III	800/4	70 (35–140)	13 (5–36)	>2300	0.2	>33
IV	800/0	—[d]	—	—	—	—
V	800/3	>180	—[e]	—	—	—
VI	400/3	70 (46–106)	120 (56–252)	>2300	1.7	>33
VII	800/3	>180	—[e]	—	—	—
VIII	200/4	>180	—[e]	—	—	—
IX	200/3	>180	—[e]	—	—	—
X	400/2	90 (63–128)	45 (25–81)	>2300	0.5	>26
XI	400/3	>300	—[e]	—	—	—
XII	200/2	62 (43–89)	60 (20–183)	>2300	1.0	>37
XIII	400/3	75 (52–108)	54 (27–108)	>2300	0.7	>31
XIV	400/2	>180	—[e]	—	—	—
XV	400/2	86 (54–138)	34 (13–88)	>2300	0.4	>27
Dantrolene sodium[f]	400/4	20 (12–34)	25 (16–36)	1110	1.3	54
Clodanolene sodium[f]	400/4	50 (30–82)	39 (26–54)	1335	0.8	21

[a] See *Experimental* for key to rating of drug-induced skeletal muscle relaxation. [b] Dose of test drug (milligrams per kilogram) causing 50% reduction in the morphine-induced Straub tail. [c] Dose of test drug (milligrams per kilogram) causing 50% of the animals to fall from the revolving rod prior to 1 min. [d] Inactive in gross observation; no further oral testing. [e] Inactive in Straub tail; no further oral testing. [f] Expressed as parent compounds on a milligram per kilogram basis.

Table V—Intravenous Testing for Skeletal Muscle Relaxant Properties of Quaternary Ammonium Salts of Dantrolene and Clodanolene

Compound	Gastrocnemius Muscle Twitch Tension[a], mean maximum % change ± *SE*	ED_{50}[b] mg/kg (95% confidence limits)	ED_{50}[b] μM/kg	Gross Effects[c]	LD_{50} in Rats, mg/kg	Therapeutic Index, LD_{50}/ED_{50} (Gastrocnemius Muscle Twitch Tension)	ED_{50} (Straub Tail)[d], mg/kg	LD_{50} in Mice, mg/kg	Therapeutic Index, LD_{50}/ED_{50} (Straub Tail)
I	−72 ± 3.6	3.0 (1.2–4.2)	5.3	Cholinergic	—[e]	—	—	—	—
II	−70 ± 3.7	6.0 (3.8–9.9)	21	Cholinergic	—[e]	—	—	—	—
III	−81 ± 1.8	3.0	8.5	Skeletal muscle relaxation	110 (71–172)	36.7	43 (33–57)	122 (73–205)	2.8
IV	−77 ± 1.4	4.1 (3.2–5.1)	7.4	Cholinergic	—[e]	—	—	—	—
V	−75 ± 3.2	5.0 (3.8–6.8)	9.0	Cholinergic	—[e]	—	—	—	—
VI	−72 ± 6.0	6.0 (3.7–8.6)	8.2	Skeletal muscle relaxation	—[f]	—	—	—	—
VII	−78 ± 3.4	4.0 (2.4–4.9)	7.7	—[f]	—[f]	—	—	—	—
VIII	−76 ± 2.5	7.0 (2.6–9.7)	10.7	Cholinergic	—[e]	—	—	—	—
IX[g]	—	—	—	—[f]	—[f]	—	—	—	—
X	−74 ± 0.1	4.0 (2.7–4.1)	5.9	Skeletal muscle relaxation	115 (85–155)	28.8	24 (19–31)	115 (68–196)	4.8
XI	−77 ± 1.8	3.0 (2.0–4.5)	7.5	Cholinergic	—[e]	—	—	—	—
XII	−71 ± 2.2	3.0 (0.7–4.0)	5.1	Skeletal muscle relaxation	145 (105–200)	48.3	21 (13–33)	>180–<200	>8–<8.9
XIII	−72 ± 3.0	6.0 (4.2–7.9)	9.8	Skeletal muscle relaxation	88 (69–113)	14.7	16 (10–26)	115 (91–146)	7.2
XIV	−76 ± 3.1	8.0 (4.5–11.0)	19.6	Skeletal muscle relaxation	45 (30–68)	5.6	18 (13–24)	66 (48–75)	3.7
XV	−74 ± 3.9	4.0 (2.8–5.8)	9.2	Skeletal muscle relaxation	102 (78–133)	25.5	22 (17–28)	111 (93–133)	5.0
Dantrolene sodium	−80 ± 1.0	2.6 (2.1–3.4)	7.7	Skeletal muscle relaxation	—[f]	—	—	—	—
Clodanolene sodium	−78 ± 3.7	3.7 (3.2–4.1)	10.2	Skeletal muscle relaxation	—[f]	—	—	—	—

[a] $n = 4$ for each compound: drugs were administered in tetrahydrofurfuryl alcohol at a maximum cumulative dose of 36.6 mg/kg. [b] Drug dose causing 50% inhibition of gastrocnemius muscle twitch tension. [c] Gross effects in rats following a 30-mg/kg dose in tetrahydrofurfuryl alcohol. [d] Drug dose causing 50% inhibition of morphine-induced Straub tail in mice. [e] Not tested further because of undesirable side effects. [f] Not tested further because of solubility. [g] Insoluble in tetrahydrofurfuryl alcohol or dimethyl sulfoxide.

Straub Tail in Mice—The method used was similar to that reported by Ellis and Carpenter (22). The drugs were administered either orally in 0.5% methylcellulose or intravenously in distilled water 20 min after the subcutaneous morphine injection to male mice (TAC:SWfBr). The drugs administered orally were evaluated 30 min after drug dosing, while the compounds administered intravenously were evaluated 5 min after drug administration. The drugs were judged effective if they caused the elevated Straub tail to lie flat on the table. The compounds were administered in logarithmically spaced doses, and ED_{50} values were obtained by the Litchfield and Wilcoxon method (20).

LD_{50} in Mice—The test compounds were administered orally or intravenously to groups of unfasted male mice (TAC:SWfBr). The drugs administered orally were suspended in saline to prevent the gel formation that occurred occasionally in methylcellulose at the higher concentrations. Drugs administered intravenously were dissolved in distilled water. The animals were held in cages for 72 hr, and deaths were recorded. The LD_{50} values were calculated using the Litchfield and Wilcoxon method (20).

Intravenous Injections in Rats—Adult male rats (TAC:SD/NfBr) were used to determine the intravenous muscle relaxant potential of each drug in unanesthetized animals. The drugs were injected intravenously at a dose of 30 mg/kg (0.25 ml) in 100% tetrahydrofurfuryl alcohol into the tail vein. This dose was more than three times the effective muscle relaxant dose and was selected to uncover undesirable cholinergic and/or toxic effects of the drug. The drugs were evaluated by gross observation for skeletal muscle relaxation, gross changes, and acute toxicity.

Intravenous LD_{50} in Rats—Groups of five male rats (TAC:SD/NfBr) were administered the drug intravenously in distilled water for acute toxicity. The animals were held in their cages for 72 hr, and all deaths were recorded. The LD_{50} values were calculated using the method of Litchfield and Wilcoxon (20).

RESULTS AND DISCUSSION

To increase the aqueous solubility of dantrolene and clodanolene, quaternary ammonium salts of these compounds were synthesized. Initially, representative quaternary ammonium halide salts were evaluated for skeletal muscle relaxant activity (cholinergic and toxic signs such as loss of the righting reflex and death), and only compounds devoid of these pharmacological activities were used to form salts (Table III).

Fifteen compounds were synthesized and evaluated, including four salts of clodanolene and 11 salts of dantrolene (Table I). The aqueous solubilities for these compounds as well as those for dantrolene sodium and clodanolene sodium are listed in Table I. The compounds were evaluated initially by gross observation in mice, and 12 of the 15 compounds were effective oral muscle relaxants (Table IV). Dantrolene sodium has been shown to relax the tail in the Straub tail mouse (22). The 12 active compounds then were tested orally in the Straub tail mouse, and six compounds were effective (Table IV). These six compounds then were evaluated for motor incoordination (rotating rod), and the activities of these compounds were compared to the parent structures (Table IV). From these data, VI and XII yielded muscle relaxant efficacy indexes equal to those of dantrolene and slightly superior to those of clodanolene.

The objective in the synthesis and pharmacological evaluation of these compounds was to increase aqueous solubility. This objective was achieved since the solubilities for the respective compounds represent increases in solubilities of 10–50 times over those of the parent sodium salts. This increased solubility facilitates the dosage flexibility, specifically for intravenous administration of a skeletal muscle contraction antagonist required for conditions such as malignant hyperthermia (6–8).

The compounds were tested intravenously for inhibition of the gastrocnemius muscle twitch response and for gross effects including cholinergic symptoms and skeletal muscle relaxation. Fourteen of the 15 compounds tested were equally effective in inhibiting the gastrocnemius muscle twitch tension (IX was insoluble in the standard solvents, tetrahydrofurfuryl alcohol and dimethyl sulfoxide) (Table V). Six compounds caused cholinergic effects and were not tested further.

The six compounds without cholinergic properties that exhibited sufficient aqueous solubility were evaluated further. The LD_{50} intravenous values in rats were calculated, and therapeutic indexes were calculated using the ED_{50} for gastrocnemius muscle twitch tension inhibition (Table V). All six compounds were effective intravenously in abolishing the Straub tail phenomenon (Table V). The LD_{50} intravenous values in mice were estimated for these active compounds, and the resulting therapeutic indexes were calculated (Table V).

REFERENCES

(1) H. R. Snyder, Jr., C. S. Davis, R. K. Bickerton, and R. P. Halliday, *J. Med. Chem.*, **10**, 807 (1967).

(2) L. J. Honkomp, R. P. Halliday, and F. L. Wessels, *Pharmacologist*, **12**, 301 (1970).

(3) K. O. Ellis and J. F. Carpenter, *Fed. Proc.*, **30**, 670 (1971).

(4) K. O. Ellis and J. F. Carpenter, *Naunyn-Schmiedebergs Arch. Pharmacol.*, **275**, 83 (1972).

(5) K. O. Ellis and S. H. Bryant, *ibid.*, **274**, 107 (1972).

(6) G. G. Harrison, *Br. J. Anaesth.*, **47**, 62 (1975).

(7) I. L. Anderson and E. W. Jones, *Anesthesiology*, **44**, 44 (1976).

(8) G. A. Gronert, J. H. Milde, and R. A. Theye, *ibid.*, **44**, 488 (1976).

(9) R. L. White, Jr., and G. C. Wright, U.S. pat. 4,137,402 (Jan. 30, 1979).

(10) H. Rapoport, E. Campion, and J. E. Gordon, *J. Am. Chem. Soc.*, **77**, 2389 (1955).

(11) C. G. Overberger, J. C. Salamone, and S. Yaroslavsky, *J. Org. Chem.*, **30**, 3580 (1965).

(12) E. M. Kosower and J. A. Skorcz, *J. Am. Chem. Soc.*, **82**, 2195 (1960).

(13) I. F. Halverstadt, W. R. Hardie, and A. R. Williams, *ibid.*, **81**, 3618 (1959).

(14) H. Hjedo, *Acta Chem. Scand.*, **17**, 2351 (1963).

(15) W. A. Madjar, French pat. 1,330,112 (June 21, 1963); through *Chem. Abstr.*, **60**, 529g (1964).

(16) E. E. Glover and G. Jones, *J. Chem. Soc.*, **1958**, 3021.

(17) R. J. Alaimo and M. M. Goldenberg, *J. Pharm. Sci.*, **63**, 1939 (1974).

(18) S. Irwin, *Psychopharmacologia*, **13**, 222 (1968).

(19) K. O. Ellis and F. L. Wessels, *Arzneim.-Forsch.*, **28**, 1100 (1978).

(20) J. T. Litchfield, Jr., and F. Wilcoxon, *J. Pharmacol. Exp. Ther.*, **96**, 99 (1949).

(21) N. W. Dunham and T. S. Miya, *J. Am. Pharm. Assoc., Sci. Ed.*, **46**, 208 (1957).

(22) K. O. Ellis and J. F. Carpenter, *Neuropharmacology*, **13**, 311 (1974).

ACKNOWLEDGMENTS

The authors thank Mr. R. Storrin and Mr. R. Finch for synthesis of chemicals and Ms. R. Turrell for assistance in the pharmacological studies. They also are grateful to the Physical and Analytical Chemistry Section for determining the elemental analyses.

Effects of *N*-Demethylated Carbachol on Iris and Ciliary Muscles

JEROME TRZECIAKOWSKI *§ **and GEORGE C. Y. CHIOU** ‡x

Received November 27, 1978, from the *Department of Pharmacology & Therapeutics, College of Medicine, University of Florida, Gainesville, FL 32610, and the ‡Department of Medical Pharmacology, College of Medicine, Texas A&M University, College Station, TX 77843. Accepted for publication October 18, 1979. §Present address: Department of Pharmacology, College of Medicine, Cornell University, New York, NY 10021.

Abstract □ The tertiary nitrogen derivative of carbachol, *N*-demethylated carbachol, was synthesized to produce a drug that could be used as an alternative to pilocarpine in the treatment of open-angle glaucoma. Unlike pilocarpine, *N*-demethylated carbachol appeared to be stable in alkaline solutions. Since pilocarpine has to be dissolved in an acidic medium (pH 5.5) to prevent its destruction, <10% of its molecules are in an unionized form. On the other hand, *N*-demethylated carbachol is very stable at pH values higher than 7.4 and thus has more molecules (>10%) in an unionized, penetrable form than does pilocarpine in high pH media. *N*-Demethylated carbachol acted as a full agonist on isolated dog iris and ciliary muscle preparations, whereas pilocarpine produced only 49 and 38% of the maximum tissue responses, respectively. These findings suggest that *N*-demethylated carbachol may be able to affect the outflow facility to a greater extent than is achievable with pilocarpine at high doses.

Keyphrases □ Carbachol, *N*-demethylated derivative—effect on iris and ciliary muscles, treatment of open-angle glaucoma □ *N*-Demethylated carbachol—effect on iris and ciliary muscles, treatment of open-angle glaucoma □ Antiglaucoma agents—*N*-demethylated carbachol, effect on iris and ciliary muscles, treatment of open-angle glaucoma □ Ophthalmic preparations—*N*-demethylated carbachol, effect on iris and ciliary muscles, treatment of open-angle glaucoma

Pilocarpine is one of the oldest antiglaucoma agents used in ophthalmology (1). It exerts its action primarily through the increase of aqueous humor outflow (2). However, it induces some side effects such as miosis, exocrine gland secretions, and local irritations, which prevent it from being used continuously in some patients (3).

N-Demethylated carbachol recently was reported to possess a potency similar to that of pilocarpine in its ability to lower the intraocular pressure of glaucomatous dogs but to cause only minor miotic effects and to be devoid of other untoward actions produced by pilocarpine (4). Therefore, the effects of these two antiglaucoma drugs in the isolated ocular tissues, iris, and ciliary muscles were compared. The pKa value of *N*-demethylated carbachol was determined, and the ionization curves were constructed for comparison with its penetrability.

EXPERIMENTAL

Chemistry—*N*-Demethylated carbachol hydrochloride was synthesized in this laboratory by a modification (4) of the method of Hazard *et al.* (5). Dimethylaminoethanol was refluxed with an excess of ethyl carbamate in toluene for 2 hr to remove water by using a trap receiver. Aluminum methoxide was added to catalyze the reaction, and the reaction mixture was refluxed for an additional 12 hr. The reaction by-product, ethanol, was removed by distillation along with toluene at a rate of 2–5 ml/min for 10 hr. Fresh toluene was added periodically to replenish the lost volume. Aluminum methoxide then was filtered off while the reaction mixture was still hot.

The product, *N*-demethylated carbachol base, was distilled with fractional distillation under vacuum to avoid overheating. (The distillation temperature should not exceed 130° to avoid polymerization and reduction in the yield.) The base product then was converted into the hydrochloride salt with dry hydrogen chloride gas in ether. The final product was recrystallized with absolute ethanol. *N*-Demethylated carbachol was tritiated commercially[1] with a specific activity of 31 mCi/mmole. The ^{3}H-*N*-demethylated carbachol was stored as a dried powder and was dissolved in an aqueous medium immediately before use to avoid tritium exchange. Pilocarpine nitrate and carbachol chloride were purchased from commercial sources.

The stability of aqueous solutions of *N*-demethylated carbachol was studied with NMR spectroscopy. Free *N*-demethylated carbachol base and its salt were dissolved in heavy water for NMR analysis.

The acid dissociation constants, pKa, of *N*-demethylated carbachol and pilocarpine were determined with a potentiometric titration method. The standardized carbonate-free potassium hydroxide solution (0.1 *M*) was obtained commercially[2] for titration. The drug quantities employed were selected to achieve concentrations of 1×10^{-5} *M* at the point of half-neutralization. Values of pKa and their scatter were calculated as described in the literature (6).

Penetrability—^{3}H-*N*-Demethylated carbachol solution (25 μl of 0.128 *M* and 31 mCi/mmole at pH 7.4) was instilled into the eyes of conscious rabbits, and the eyelids were held closed for 1 min. Rabbits were killed at 10, 20, 60, and 180 min after instillation. The eyes were rinsed with saline to remove surface radioactivity, and the tissues were obtained in the order of aqueous humor, cornea, iris, and ciliary body. All tissues were weighed, digested with a solubilizer[3], and counted in a scintillation medium[4] with a scintillation counter[5]. The tissue uptake of ^{3}H-*N*-demethylated carbachol was expressed in picomoles per milligram of tissue. The amount of *N*-demethylated carbachol taken up by ocular tissues at the approximate peak time was tabulated.

Isolated Iris and Ciliary Muscle Preparation—Mongrel dogs, 13–17 kg, were sacrificed with an intravenous injection of pentobarbital sodium. The eyes were removed and placed on a moist gauze, and the iris was dissected according to a literature method (7). After removal of the iris, an incision was made in the sclera to expose the interior of the glove. The lens and adhering vitreous humor were removed, and a shallow incision was made in the uvea anterior to the ora serrata. A strip of ciliary muscle, 4–5 mm wide and approximately 25 mm long, was carefully lifted free of the sclera. Sections of iris and ciliary muscles were suspended in 6-ml organ baths containing a Ringer solution (119.8 m*M* NaCl, 4.02 m*M* KCl, 1.98 m*M* $CaCl_2$, 1.27 m*M* $MgSO_4$, 26.2 m*M* $NaHCO_3$, 1.0 m*M* KH_2PO_4, and 11.1 m*M* glucose at pH 7.4) oxygenated with 95% O_2–5% CO_2 at 32°.

A microdisplacement force transducer[6] was used to detect the muscle contraction, and the contraction was recorded on a polygraph[7]. The initial tension placed on the iris was 100 mg and that on the ciliary muscle was 300 mg. Effects of *N*-demethylated carbachol were compared with those of pilocarpine and carbachol. The maximum contraction induced by carbachol was designated as the 100% response, and other responses induced were calculated as a percent of that maximum response.

RESULTS

The NMR spectrum of *N*-demethylated carbachol dissolved in heavy water produced the expected chemical shifts and splitting patterns. The spectrum consisted of a singlet at δ 4.72 (NH_2), two triplets at δ 4.27 and 2.65 (CH_2CH_2), and another singlet at δ 2.27 [$N(CH_3)_2$] relative to Tiers' salt, $(CH_3)_3Si(CH_2)_3SO_3Na$. The NMR spectra of the salt and free base of *N*-demethylated carbachol obtained at regular intervals after the compounds were dissolved in heavy water remained unchanged at room temperature for at least 3 months.

[1] ICN Pharmaceuticals.
[2] Baker Chemical Co.
[3] NCS solubilizer, Amersham/Searle Corp.
[4] Biofluor scintillation medium, New England Nuclear Co.
[5] Model LS100, Beckman Instruments.
[6] Myograph A, Narco BioSystems.
[7] Physiograph, Narco BioSystems.

0022-3549/80/0300-0332$01.00/0
© 1980, American Pharmaceutical Association

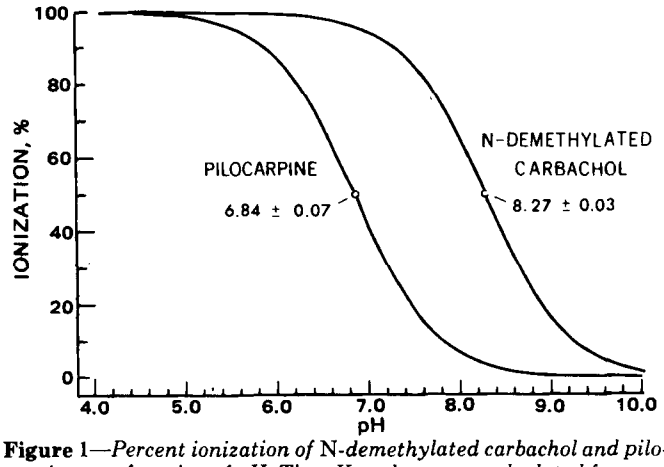

Figure 1—*Percent ionization of* N-*demethylated carbachol and pilocarpine as a function of pH. The pKa values were calculated from experimentally determined values at 25°* (n = 9).

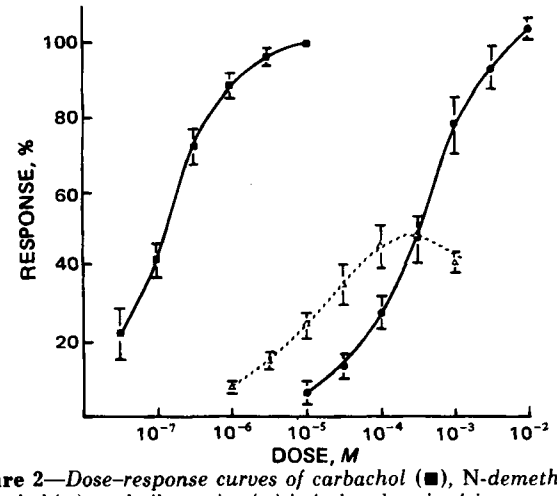

Figure 2—*Dose–response curves of carbachol* (■), N-*demethylated carbachol* (●), *and pilocarpine* (△) *in isolated canine iris preparations. Each point is the mean of four values, and the bars indicate standard errors.*

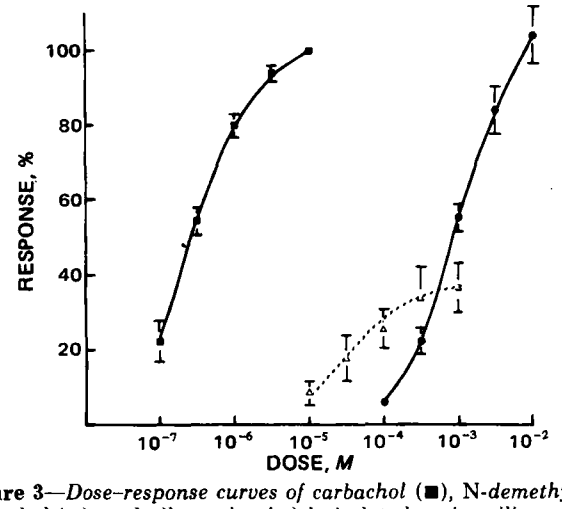

Figure 3—*Dose–response curves of carbachol* (■), N-*demethylated carbachol* (●), *and pilocarpine* (△) *in isolated canine ciliary muscle preparations. Each point is the mean of four values, and the bars indicate standard errors.*

The pKa values of *N*-demethylated carbachol and pilocarpine and the ionization curves constructed from these values are shown in Fig. 1. An additional pKa value for pilocarpine should be at 12.57 (8), but it was not observed in this laboratory. Titrations of *N*-demethylated carbachol revealed that this compound has a single pKa value of 8.27.

The penetrability of *N*-demethylated carbachol into the eyes is presented in Table I. The peak time for *N*-demethylated carbachol to reach intraocular tissues was ~20 min, and the penetrability was about the same as that of pilocarpine (9).

N-Demethylated carbachol contracted the isolated dog iris at doses of 1×10^{-5}–1×10^{-2} *M* (Fig. 2). The dose–response curve paralleled that of carbachol. Pilocarpine was more potent at lower doses (1×10^{-6}–1×10^{-4} *M*) than *N*-demethylated carbachol, but the maximum effect attainable with this drug was only 49% of that produced by carbachol or *N*-demethylated carbachol. Pilocarpine doses greater than 3×10^{-4} *M* decreased muscle tension.

The overall shape of the dose–response curves of *N*-demethylated carbachol, carbachol, and pilocarpine obtained with ciliary muscle was similar to that obtained with the iris preparation, except that the ciliary muscle appeared to be less sensitive to these agents (Fig. 3). The maximum response produced by pilocarpine was only 38% of that produced by *N*-demethylated carbachol or carbachol.

DISCUSSION

The usefulness of a drug as eye drops in the treatment of glaucoma depends primarily on its penetrability across the cornea. Although pilocarpine is a much less potent muscarinic agent than carbachol, it is more widely used than carbachol as an antiglaucoma agent because it can penetrate the cornea better than carbachol.

At the physiological pH of 7.4, 78% of pilocarpine is in the unionized, penetrable form (Fig. 1). However, pilocarpine is not stable at this pH because it undergoes base-catalyzed epimerization or is cleaved at the lactone ring (10, 11). For this reason, the pH of most ophthalmic preparations of pilocarpine is adjusted to 4.5–5.5 (12). At these pH values, >95% of the drug is ionized.

The ester linkage in *N*-demethylated carbachol is the same as that in carbachol, which is known to be quite stable in aqueous solution. This structure was confirmed in this laboratory with NMR studies. Thus, an ophthalmic solution of *N*-demethylated carbachol at pH 7.4 can be made.

Table I—Penetration of *N*-Demethylated Carbachol into Ocular Tissues

Tissue	Peak Time, min	Quantity at Peak, pmoles/mg	Tissue Weight, mg	Total Amount in Tissue, nmoles	Percent Absorbed[a]
Cornea	10	129[b]	64[c]	8.26	0.26
Iris	20	20	35	0.70	0.02
Ciliary muscle	20	15	27	0.41	0.01
Aqueous humor	20	21	287	6.03	0.20

[a] The calculation was based on the total amount of *N*-demethylated carbachol instilled (3.19 μmoles). [b] $n = 6$. [c] $n = 19$.

At pH 7.4, <90% of *N*-demethylated carbachol is ionized. Thus, in clinical situations (*N*-demethylated carbachol at pH 7.4, pilocarpine at pH 5.5 or less), *N*-demethylated carbachol could be more effective than pilocarpine because it has greater penetration. Moreover, a drug solution with a pH range of 6.6–8.7 may be instilled into the eye without producing unpleasant sensations (13). Therefore, it should be possible to increase the effectiveness of *N*-demethylated carbachol even further by administering it in solutions having pH values greater than 7.4 but less than 8.7. At pH 8.7, 70% of *N*-demethylated carbachol is unionized and penetrable.

In actual experimentation with ^{3}H-*N*-demethylated carbachol, the drug was absorbed to reach a concentration in the aqueous humor of 2.1×10^{-5} *M* 20 min after topical administration at pH 7.4.

Experiments with isolated iris and ciliary muscles demonstrated that *N*-demethylated carbachol has a greater intrinsic activity or efficacy than pilocarpine. However, pilocarpine possesses higher sensitivity to these muscles at lower doses (1×10^{-6}–1×10^{-4} *M* in the iris preparation and 1×10^{-5}–2×10^{-4} *M* in ciliary muscle). The combination of these two factors could explain the fact that, in *in vivo* studies, *N*-demethylated carbachol is as potent as pilocarpine in lowering the intraocular pressure but causes less miosis in the glaucomatous beagle eye.

REFERENCES

(1) A. Weber, *Albrecht Von Graefes Arch. Klin. Ophthalmol.*, **23**, 1 (1877).

(2) M. Flocks and H. C. Zweng, *Am. J. Ophthalmol.*, **44**, 380 (1957).
(3) C. S. O'Brein and K. C. Swan, *Trans. Am. Ophthalmol. Soc.*, **39**, 175 (1941).
(4) J. Trzeciakowski and C. Y. Chiou, *J. Pharm. Sci.*, **67**, 531 (1978).
(5) R. Hazard, J. Cheymol, P. Chabrier, A. Sekera, and R. Eche-Fialaire, *Bull Soc. Chim. Fr.*, **1961**, 2087.
(6) A. Albert and E. P. Serjeant, "Ionization Constants of Acids and Bases," Wiley, New York, N.Y., 1962.
(7) W. H. Morrison, *Am. J. Ophthalmol.*, **37**, 744 (1954).
(8) "The Merck Index," 9th ed., M. Windholz, Ed., Merck & Co., Rahway, N.J., 1976, p. 966.
(9) S. S. Chrai and J. R. Robinson, *Am. J. Ophthalmol.*, **77**, 735 (1974).
(10) P. H. Chung, T. F. Chin, and J. L. Lach, *J. Pharm. Sci.*, **59**, 1300 (1970).
(11) M. A. Nunes and E. Brochmann-Hanssen, *ibid.*, **63**, 716 (1974).
(12) A. Longwell, S. Birss, N. Keller, and D. Moore, *ibid.*, **65**, 1654 (1976).
(13) F. N. Martin and J. L. Mims, *Arch. Ophthalmol.*, **44**, 561 (1950).

ACKNOWLEDGMENTS

J. Trzeciakowski was supported in part by a predoctoral traineeship from the National Institutes of Health (GM-00760). The authors thank the National Eye Institute of the National Institutes of Health (Ey-01624) for research support.

The authors also thank Ms. Marilyn K. Martin for technical assistance.

Effect of Low and High Relative Humidity on Metered-Dose Bronchodilator Solution and Powder Aerosols

F. CHARLES HILLER ˣ, MALAY K. MAZUMDER, J. DOUGLAS WILSON, and ROGER C. BONE

Received August 9, 1979, from the *University of Arkansas for Medical Sciences, Little Rock, AR 72201.* Accepted for publication October 19, 1979.

Abstract □ Physical properties of two metered-dose bronchodilator aerosols packaged as solutions and two aerosols packaged as finely ground powders were measured at low and high relative humidity. The aerodynamic size distribution and particle concentration were measured in real time using the single-particle aerodynamic relaxation time analyzer, which can measure the aerodynamic diameter of single suspended particles in the respirable size range. The count median aerodynamic diameter, the mass median aerodynamic diameter, the total particles per dose, and the total aerodynamic mass per dose were calculated. Significant increases were noted in the count median aerodynamic diameter for three aerosols and in the mass median aerodynamic diameter for two aerosols. The number of particles in the measured size range increased 3.6- and 4.1-fold for the droplet aerosols and 1.4-fold for the powder preparations. The aerodynamic mass per dose in the measured size range increased 5.7- and 11.4-fold for the droplet aerosols and 3.1- and 1.6-fold for the powder aerosols. These data indicate that all aerosols tested increased in size at high humidity and that aerosols dispensed as droplets may be more unstable than those dispensed as powders.

Keyphrases □ Bronchodilators—metered-dose solution and powder aerosols, effect of low and high humidity □ Aerosols—bronchodilators, metered-dose solution and powder preparations, effect of low and high humidity □ Asthma products—metered-dose solution and powder aerosols, effect of low and high humidity □ Metered-dose aerosols—bronchodilators, solution and powder preparations, effect of low and high humidity

Metered-dose bronchodilator aerosols are used widely to treat obstructive lung disease. The efficacy of these medications is determined by their quantity and site of pulmonary deposition. Factors that affect pulmonary retention and distribution are the inhalation technique, airway patency, and particle size.

BACKGROUND

The particle-size distributions of aerosols produced by some of these devices have been reported (1–3), but the effect of hygroscopicity on particle size was not included. Any particle may grow by water condensation or shrink by water evaporation, depending on the humidity and physical characteristics of the particle. Such changes may affect the mass and site of aerosol deposition in the respiratory tract. Although particle growth during exposure to high humidity such as that occurring in the respiratory tract has been predicted for therapeutic aerosols (4) and the effect of humidity on the size of propylene glycol aerosols has been described (5), there is no information documenting or quantitating the effect of high humidity on bronchodilator aerosols.

Measurement of aerosol particle size is most relevant for prediction of deposition when the size is expressed as the aerodynamic diameter, defined as the diameter of a unit density spherical particle having the same terminal settling velocity as the particle in question. Methods currently used to measure the aerodynamic size distribution of aerosols require particle impaction and subsequent analysis of the quantity deposited (4, 6). The instability of water-containing particles has been described (7), and size changes may occur in <1 sec (8). This instability precludes extrapolation of the particle-size measurement following precipitation of unstable particles to the particle size in the suspended state. Measurement in the suspended state is necessary to assess accurately the effect of humidity on the size of unstable particles.

The purpose of this study was to determine the effect of high humidity, similar to that encountered in the respiratory tract, on the particle-size distribution of four commonly used metered-dose aerosol devices. Humidity in the trachea and more distal airways generally is regarded to be in the 99.0–99.8% range (9). The mass median aerodynamic diameter and count median aerodynamic diameter (the sizes below which are 50% of the particles by mass and number, respectively), the geometric standard deviation (84.1% size divided by 50% size), the mass per dose, and the number of particles per dose were measured. A new device, the single-particle aerodynamic relaxation time analyzer (hereafter called the analyzer) that measures the aerodynamic diameter of single particles in real time, was used for these studies.

EXPERIMENTAL

The following medications were studied: isoproterenol hydrochloride[1] and isoetharine mesylate[2], both packaged as solutions, and metaproterenol sulfate[3] and isoproterenol sulfate[4], both packaged as finely ground powders. In each case, the commercially available preparation was used. Each medication was injected into an environmental chamber for subsequent sampling by the analyzer.

The analyzer (Fig. 1) and the theoretical basis for its operation were described previously (3, 10, 11). The sensing volume, in which the signal

[1] Isuprel Mistometer, Winthrop Laboratories, New York, N.Y.
[2] Bronkometer, Breon Laboratories, New York, N.Y.
[3] Metaprel, Dorsey Laboratories, Lincoln, Neb.
[4] Medihaler-Iso, Riker Laboratories, Northridge, Calif.

0022-3549/80/0300-0334$01.00/0
© 1980, American Pharmaceutical Association

(2) M. Flocks and H. C. Zweng, *Am. J. Ophthalmol.*, **44**, 380 (1957).
(3) C. S. O'Brein and K. C. Swan, *Trans. Am. Ophthalmol. Soc.*, **39**, 175 (1941).
(4) J. Trzeciakowski and C. Y. Chiou, *J. Pharm. Sci.*, **67**, 531 (1978).
(5) R. Hazard, J. Cheymol, P. Chabrier, A. Sekera, and R. Eche-Fialaire, *Bull Soc. Chim. Fr.*, **1961**, 2087.
(6) A. Albert and E. P. Serjeant, "Ionization Constants of Acids and Bases," Wiley, New York, N.Y., 1962.
(7) W. H. Morrison, *Am. J. Ophthalmol.*, **37**, 744 (1954).
(8) "The Merck Index," 9th ed., M. Windholz, Ed., Merck & Co., Rahway, N.J., 1976, p. 966.
(9) S. S. Chrai and J. R. Robinson, *Am. J. Ophthalmol.*, **77**, 735 (1974).
(10) P. H. Chung, T. F. Chin, and J. L. Lach, *J. Pharm. Sci.*, **59**, 1300 (1970).
(11) M. A. Nunes and E. Brochmann-Hanssen, *ibid.*, **63**, 716 (1974).
(12) A. Longwell, S. Birss, N. Keller, and D. Moore, *ibid.*, **65**, 1654 (1976).
(13) F. N. Martin and J. L. Mims, *Arch. Ophthalmol.*, **44**, 561 (1950).

ACKNOWLEDGMENTS

J. Trzeciakowski was supported in part by a predoctoral traineeship from the National Institutes of Health (GM-00760). The authors thank the National Eye Institute of the National Institutes of Health (Ey-01624) for research support.

The authors also thank Ms. Marilyn K. Martin for technical assistance.

Effect of Low and High Relative Humidity on Metered-Dose Bronchodilator Solution and Powder Aerosols

F. CHARLES HILLER ˣ, MALAY K. MAZUMDER, J. DOUGLAS WILSON, and ROGER C. BONE

Received August 9, 1979, from the *University of Arkansas for Medical Sciences, Little Rock, AR 72201.* Accepted for publication October 19, 1979.

Abstract □ Physical properties of two metered-dose bronchodilator aerosols packaged as solutions and two aerosols packaged as finely ground powders were measured at low and high relative humidity. The aerodynamic size distribution and particle concentration were measured in real time using the single-particle aerodynamic relaxation time analyzer, which can measure the aerodynamic diameter of single suspended particles in the respirable size range. The count median aerodynamic diameter, the mass median aerodynamic diameter, the total particles per dose, and the total aerodynamic mass per dose were calculated. Significant increases were noted in the count median aerodynamic diameter for three aerosols and in the mass median aerodynamic diameter for two aerosols. The number of particles in the measured size range increased 3.6- and 4.1-fold for the droplet aerosols and 1.4-fold for the powder preparations. The aerodynamic mass per dose in the measured size range increased 5.7- and 11.4-fold for the droplet aerosols and 3.1- and 1.6-fold for the powder aerosols. These data indicate that all aerosols tested increased in size at high humidity and that aerosols dispensed as droplets may be more unstable than those dispensed as powders.

Keyphrases □ Bronchodilators—metered-dose solution and powder aerosols, effect of low and high humidity □ Aerosols—bronchodilators, metered-dose solution and powder preparations, effect of low and high humidity □ Asthma products—metered-dose solution and powder aerosols, effect of low and high humidity □ Metered-dose aerosols—bronchodilators, solution and powder preparations, effect of low and high humidity

Metered-dose bronchodilator aerosols are used widely to treat obstructive lung disease. The efficacy of these medications is determined by their quantity and site of pulmonary deposition. Factors that affect pulmonary retention and distribution are the inhalation technique, airway patency, and particle size.

BACKGROUND

The particle-size distributions of aerosols produced by some of these devices have been reported (1–3), but the effect of hygroscopicity on particle size was not included. Any particle may grow by water condensation or shrink by water evaporation, depending on the humidity and physical characteristics of the particle. Such changes may affect the mass and site of aerosol deposition in the respiratory tract. Although particle growth during exposure to high humidity such as that occurring in the respiratory tract has been predicted for therapeutic aerosols (4) and the effect of humidity on the size of propylene glycol aerosols has been described (5), there is no information documenting or quantitating the effect of high humidity on bronchodilator aerosols.

Measurement of aerosol particle size is most relevant for prediction of deposition when the size is expressed as the aerodynamic diameter, defined as the diameter of a unit density spherical particle having the same terminal settling velocity as the particle in question. Methods currently used to measure the aerodynamic size distribution of aerosols require particle impaction and subsequent analysis of the quantity deposited (4, 6). The instability of water-containing particles has been described (7), and size changes may occur in <1 sec (8). This instability precludes extrapolation of the particle-size measurement following precipitation of unstable particles to the particle size in the suspended state. Measurement in the suspended state is necessary to assess accurately the effect of humidity on the size of unstable particles.

The purpose of this study was to determine the effect of high humidity, similar to that encountered in the respiratory tract, on the particle-size distribution of four commonly used metered-dose aerosol devices. Humidity in the trachea and more distal airways generally is regarded to be in the 99.0–99.8% range (9). The mass median aerodynamic diameter and count median aerodynamic diameter (the sizes below which are 50% of the particles by mass and number, respectively), the geometric standard deviation (84.1% size divided by 50% size), the mass per dose, and the number of particles per dose were measured. A new device, the single-particle aerodynamic relaxation time analyzer (hereafter called the analyzer) that measures the aerodynamic diameter of single particles in real time, was used for these studies.

EXPERIMENTAL

The following medications were studied: isoproterenol hydrochloride[1] and isoetharine mesylate[2], both packaged as solutions, and metaproterenol sulfate[3] and isoproterenol sulfate[4], both packaged as finely ground powders. In each case, the commercially available preparation was used. Each medication was injected into an environmental chamber for subsequent sampling by the analyzer.

The analyzer (Fig. 1) and the theoretical basis for its operation were described previously (3, 10, 11). The sensing volume, in which the signal

[1] Isuprel Mistometer, Winthrop Laboratories, New York, N.Y.
[2] Bronkometer, Breon Laboratories, New York, N.Y.
[3] Metaprel, Dorsey Laboratories, Lincoln, Neb.
[4] Medihaler-Iso, Riker Laboratories, Northridge, Calif.

0022-3549/80/0300-0334$01.00/0
© 1980, American Pharmaceutical Association

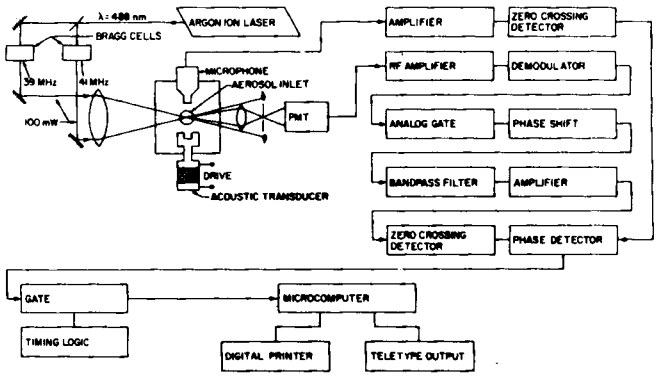

Figure 1—*Schematic outline of the SPART analyzer. The analyzer and ancillary signal processing equipment are shown.*

for particle-size measurement is generated, is formed by the intersection of two laser beams of slightly different frequencies (Fig. 2). Each particle entering the sensing volume is subjected to acoustic oscillation at 24.25 kHz. Particle oscillation lags behind acoustic field oscillation; this delay, the phase lag, is directly related to the aerodynamic diameter.

Particle oscillation is measured by a laser Doppler velocimeter using the Doppler principle (7). The Doppler frequency shift in the light scattered by a particle oscillating in this sensing volume is detected by a photomultiplier, which generates a frequency-modulated (FM) signal. The FM signal, which transmits particle velocity information, is demodulated and compared using data processing circuitry to the acoustic signal generated by a microphone to determine the phase lag. A microprocessor determines the aerodynamic diameter from the phase lag and stores the data for analysis (Fig. 1). The stored data are processed by a minicomputer to determine the count median aerodynamic diameter, mass median aerodynamic diameter, and geometric standard deviation (σg) and to plot the following distributions: (*a*) derivative of the number with respect to the aerodynamic diameter, (*b*) derivative of the aerodynamic mass with respect to the aerodynamic diameter, (*c*) the cumulative number, and (*d*) the cumulative aerodynamic mass. The aerodynamic mass is calculated from the aerodynamic diameter by:

$$\text{aerodynamic mass} = \tfrac{2}{3}\,\pi \text{ aerodynamic diameter}^3 \times \text{density} \quad \text{(Eq. 1)}$$

The density is assumed to be unity. The actual density of these multicomponent particles is difficult to determine. The actual mass differs from the aerodynamic mass as the difference between the actual and assumed density increases. There also is some error introduced for particles with an aerodynamic diameter of <1 μm since those particles behave somewhat differently than larger particles. For these studies, the error should be small since most of the mass is in particles with an aerodynamic diameter of <1 μm. The geometric standard deviation (Table I) was calculated by a computer from the cumulative aerodynamic mass distributions and was only slightly different from the geometric standard deviation calculated from cumulative number distributions.

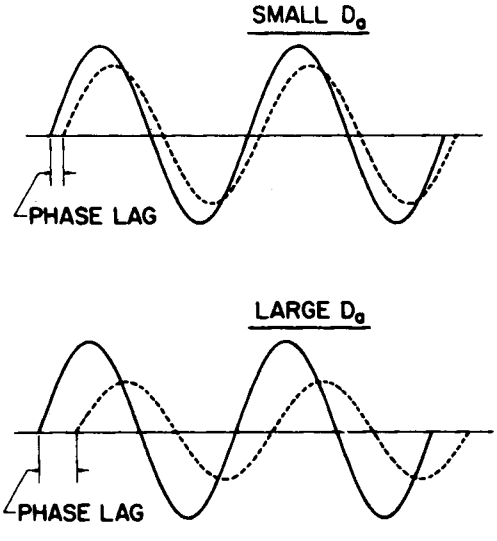

Figure 2—*The solid lines represent the wave form of the oscillatory motion of air caused by acoustic excitation. The broken lines represent particle motion, which lags behind air motion. The relative phase lag depends on the aerodynamic diameter of the particulate.* D_a = *aerodynamic diameter. (Reprinted from Ref. 3 with permission of the publisher.)*

Table I—Physical Properties of Aerosol Produced by Four Metered-Dose Bronchodilator Devices Measured at Low and High Humidity

Drug	Parameter	CMAD[a], μm		MMAD[b], μm		σg[c]	
Isoetharine mesylate	RH[d]	21	95	21	95	21	95
	x[e]	0.74	0.93	3.59	3.79	2.0	1.9
	SD[f]	0.02	0.08	0.73	0.63	0.07	0.06
	p[g]	<0.001		NS[h]		—	
Isoproterenol hydrochloride	RH	20	96	20	96	20	96
	x	0.70	0.92	3.21	4.03	2.1	1.9
	SD	0.03	0.12	0.50	0.38	0.1	0.1
	p	<0.001		<0.01		—	
Metaproterenol sulfate	RH	16	98	16	98	16	98
	x	0.68	0.80	4.05	5.22	2.0	2.0
	SD	0.01	0.04	0.32	0.54	0.1	0.2
	p	<0.001		<0.001		—	
Isoproterenol sulfate	RH	17	96	17	96	17	96
	x	0.70	0.71	2.88	3.26	2.0	2.0
	SD	0.02	0.08	0.24	0.43	0.1	0.1
	p	NS		NS		—	

[a] Average count median aerodynamic diameter (n = 7). [b] Average mass median aerodynamic diameter (n = 7). [c] Average geometric standard deviation (n = 7). [d] Average relative humidity for each group of studies. [e] Average of seven studies for measured characteristics. [f] Standard deviation. [g] Statistical significance of difference between measured characteristic at high and low humidity on basis of t test. [h] Not significant.

The aerosol is drawn from the environmental chamber to the analyzer at a rate of 55 cm^3/min. Only a portion of this sample passes through the sensing volume. The sensing volume is 1.3×10^{-6} cm^3, and the quantity of aerosol passing through it is 1.3×10^{-2} cm^3/sec. The analyzer coincidence loss is <2% at a counting rate of 40 particles/sec or less. In the present study, the count rate was maintained below this level by maintaining aerosol concentrations in the environmental chamber at <3000 particles/cm^3.

The environmental chamber was a 200-liter insulated plastic box. The temperature was maintained at 37 ± 0.5° by applying thermostatically controlled heat strips to the chamber walls and was monitored using a digital thermometer. The chamber was humidified for high humidity studies by bubbling chamber air through a heated water bath and was monitored with a hygrometer[5]. Ambient humidity studies were at 16–21% relative humidity (RH), and high humidity studies were at 95–98% RH. The analyzer was operated at 37°, and the relative humidity of the efflux from the analyzer was monitored[6] to ensure that no significant loss of humidity occurred during transport of the aerosol to the sensing volume.

Prior to each study, the environmental chamber was checked to ensure that it was free of residual aerosol. The aerosol and thermal mixing was provided using a fan inside the chamber. The decay rate for this chamber has been measured as a function of the aerodynamic diameter and is sufficiently low for the particle sizes involved in this study so as to be insignificant for the sampling time used. During testing, the environmental chamber was placed above the analyzer. The aerosol was sampled vertically with laminar flow in the sampling tubes to minimize particle loss from impaction in the sampling tubing.

For each of the four metered-dose devices, seven trials were performed. When appropriate environmental conditions were attained, the drug was injected into the chamber. The count rate was assessed, and the injection was repeated until the chamber concentration reached 3000 particles/cm^3. Injection was completed in <1 min. Following loading of the chamber with the aerosol, 30 sec was allowed for mixing; the analyzer sampling then was begun and continued for 5 min.

RESULTS

Seven trials were performed for each study, with 5000–9000 individual particles sized in each trial. The data reported are the average of these

[5] Model HTAB-176, Abbeon Corp., Santa Barbara, Calif.
[6] Model HM-111, Weathermeasure Corp., Sacramento, Calif.

Table II—Number of Particles and Total Mass Aerosolized in 0.10–10.0-μm Range per Dose by Metered-Dose Devices

Drug	Parameter	Particles per Dose ($\times 10^6$)		Dose, μg		Active Ingredient per Dose, μg[a]
Isoetharine mesylate	RH[b]	21	95	21	95	410
	x[c]	123	447	334	1907	
	SD[d]	38	771	164	566	
	p[e]	<0.001		<0.001		
Isoproterenol hydrochloride	RH	20	96	20	96	125
	x	49	202	89	1016	
	SD	2.5	68	18	297	
	p	<0.001		<0.001		
Metaproterenol sulfate	RH	16	98	16	98	650
	x	288	364	660	2215	
	SD	24	52	54	839	
	p	<0.01		<0.001		
Isoproterenol sulfate	RH	17	96	17	96	75
	x	140	200	225	509	
	SD	6	39	23	135	
	p	<0.01		<0.001		

[a] Active ingredient dispensed per dose according to the manufacturer's package insert. [b] Average relative humidity (n = 7). [c] Average of seven studies. [d] Standard deviation from seven studies. [e] Statistical significance of difference between measured characteristic at high and low humidity on basis of unpaired t test.

trials. The average results for the count median aerodynamic diameter, mass median aerodynamic diameter, and geometric standard deviation for each preparation at low and high humidity are shown in Table I. Also shown is the statistical significance of the comparison between the values at low and high humidity. The information indicates that there was a significant increase at high humidity in the count median aerodynamic diameter for isoetharine mesylate, isoproterenol hydrochloride, and metaproterenol sulfate but not for isoproterenol sulfate. Significant increases in the mass median aerodynamic diameter were noted for isoproterenol hydrochloride and metaproterenol sulfate. The geometric standard deviation for all of the aerosols was similar, did not change much with high humidity, and indicated a heterodisperse aerosol.

Table II describes the total number of particles and the total mass per dose of the aerosol measured in the 0.30–6.0-μm range. At high humidity, the total particles and total mass per dose of all aerosols increased significantly. The increase in total particles was 3.6- and 4.1-fold for isoetharine mesylate and isoproterenol hydrochloride, respectively, an increase considerably greater than the 1.4-fold change noted for both powdered preparations. The increases in total mass of 5.7- and 11.4-fold for isoetharine mesylate and isoproterenol hydrochloride were greater than the 3.4- and 1.6-fold increases in mass noted with the metaproterenol sulfate and isoproterenol sulfate powders.

Representative aerodynamic size distribution curves are shown in Figs. 3 and 4. In Fig. 3, the number distribution of the droplet isoproterenol hydrochloride aerosol measured at low humidity is compared to the number distribution measured at high humidity. The area under each curve represents the total number of particles measured at each humidity.

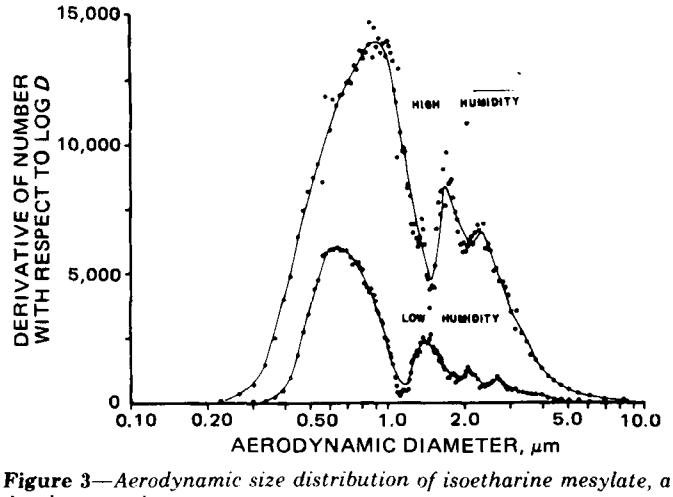

Figure 3—*Aerodynamic size distribution of isoetharine mesylate, a droplet aerosol.*

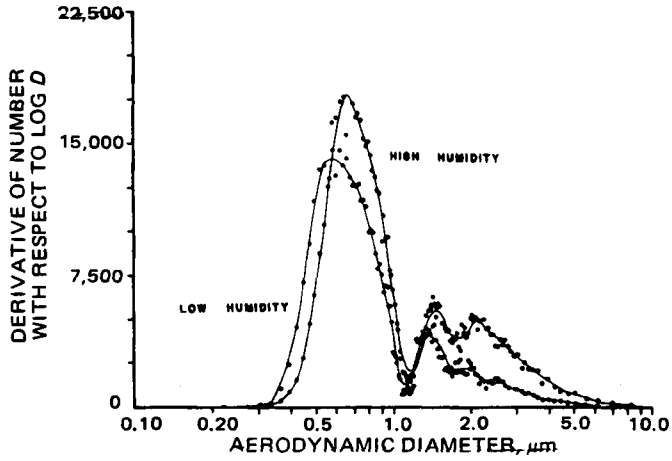

Figure 4—*Aerodynamic size distribution of isoproterenol sulfate, a powdered aerosol.*

The aerodynamic size distribution curves for the powdered isoproterenol sulfate aerosol are shown in Fig. 4, which is arranged similarly to Fig. 3. These figures illustrate the considerably smaller difference in the area under the curve between studies done at low and high relative humidity for the powdered aerosol compared to the droplet aerosol, a difference also shown in the particles per dose column of Table II.

DISCUSSION

The physical properties of all aerosols tested were different at low humidity compared to high humidity. In general, physical properties reflecting particle size increased at high humidity, and these increases were greater for droplet aerosols than for powder aerosols.

The number of particles per dose increased significantly for all four aerosols tested. The increase in particles per dose was especially marked for droplet aerosols. The number of particles per dose increased from 1.23×10^8 to 4.47×10^8 for isoetharine mesylate and from 4.0×10^7 to 2.02×10^8 for isoproterenol hydrochloride. One possible explanation for the increase in the particle number per dose is that many small particles exist at low humidity below the resolution limit (0.3 μm) of the analyzer and that these particles grow into the measurable size range at high humidity.

The mass per dose also increased significantly at high humidity for all four aerosols. The increase was greatest for droplet aerosols, changing from 334 to 1016 μg for isoproterenol hydrochloride at low and high humidity, respectively. The count median aerodynamic diameter increased significantly for three aerosols, while the mass median aerodynamic diameter increased for two aerosols.

The increase in the total mass and the number of particles per dose observed in these studies was considerable, especially for droplet aerosols, and may seem inconsistent with the modest increases in the count median aerodynamic diameter and mass median aerodynamic diameter. There are several possible explanations. At low humidity, the aerosol may contain many particles smaller than the lowest size the analyzer can measure. When the humidity increases, these particles grow and become measurable. Thus, in the measurable size range, there is an apparent increase in the number of particles in the smaller size range. This increase in the number of small particles would offset the increase in the count median aerodynamic diameter and the mass median aerodynamic diameter that would be expected had the aerosol not contained at low humidity many particles below the measurable size range. The size attained by a particle subjected to a given set of conditions is called the equilibrium diameter. The equilibrium diameter is determined by the relative humidity, hygroscopicity of the particle, and size of the dry particle. The severalfold increase in the total aerosol mass per dose without a significant change in the mass median aerodynamic diameter may be due in part to the fact that small hygroscopic particles have larger surface-to-mass ratios than do larger particles and undergo a higher relative growth when exposed to high humidity.

Another phenomenon pertains to the fact that the measured aerodynamic diameter depends in part on the particle density, ρ. If ρ of the dry particle is greater than 1 g/cm^3, then water absorbed by the particle increases the volume but reduces ρ, and, consequently, the aerodynamic diameter does not increase in proportion to the geometric diameter.

Therefore, the total particulate volume may increase out of proportion to the observed change in the mass median aerodynamic diameter. In considering these data and the hypothesized explanations, it is important to recognize that the relative contribution to particle growth at high humidity in a complex system of multicomponent particles, air, water vapor, and other vapors such as fluorocarbons and ethanol is not clear.

The increase in the number density and the mass of aerosol particles at high humidity must not be interpreted as an increase in the content of active ingredients. Although the growth is caused by the water uptake, any accompanying change in the mass distribution of the active ingredient may significantly change the amount and site of deposition of the active ingredient inside the lung. Additional information is needed to determine the content of the active ingredient at various size intervals, especially at high humidity.

The total mass of dry aerosol in the 0.30–6.0-μm range shown in Table II is similar for three of the four aerosols to the mass of the active ingredient claimed by the manufacturer to be dispensed from each device per valve activation. All aerosols contain stabilizing and dispensing agents that may contribute to the total mass. The portion of the active ingredient in the aerosol mass is not known. The active ingredient of droplet aerosols is dissolved in alcohol, which may contribute to the aerosol mass, although it probably evaporates fairly rapidly. The fluorocarbon propellants also contribute to the particle size as these aerosols leave the metered-dose device, but most are highly volatile and evaporate almost immediately upon aerosolization. In addition, all of these devices contain a dispersing agent present in variable quantities. The mass of isoproterenol sulfate measured in this study was greater than the mass of active ingredient reported to be dispensed per dose by the manufacturer. This difference probably was due to the relatively high ratio of dispersing agent to active ingredient for isoproterenol sulfate (~2.5:1) compared to metaproterenol sulfate (~1:1)[7].

The increase in particle size found in this study probably was not greatly influenced by particle aggregation since the aerosol concentration after injection into the environmental chamber was relatively dilute. Aggregation, which is related to the square of the concentration, may contribute along with water condensation to particle growth in the respiratory tract where the concentration should be much higher than in the chamber used for these studies.

Although the content of active ingredient per particle at high humidity is not known, the increase in total aerosol mass, which is considerable for the droplet aerosols, implies that the content of active ingredient shifts to particles of a larger size. A size shift similar to that observed in these high humidity studies may occur when these aerosols are inhaled into the human respiratory tract. Failure to consider particle-size changes may result in inaccurate prediction of respiratory tract deposition, especially for apparently highly unstable droplet aerosols.

[7] I. Porush, Director, Quality Assurance, Riker Laboratories, personal communication.

REFERENCES

(1) I. Porush, C. G. Thiel, and J. G. Young, *J. Am. Pharm. Assoc., Sci. Ed.*, **49**, 70 (1960).

(2) T. T. Mercer, R. F. Goddard, and R. L. Flores, *Ann. Allergy*, **23**, 314 (1965).

(3) C. Hiller, M. Mazumder, D. Wilson, and R. Bone, *Am. Rev. Resp. Dis.*, **118**, 311 (1978).

(4) P. E. Morrow, *ibid.*, **110**, 88 (1974).

(5) S. S. Davis and M. D. Budd, *Int. J. Pharm.*, **1**, 303 (1978).

(6) T. T. Mercer, *Arch. Intern. Med.*, **131**, 39 (1973).

(7) W. R. Lane, in "Proceedings of the 5th International Cystic Fibrosis Conference," D. Lawson, Ed., Cambridge University, Cambridge, England, 1969, pp 103–111.

(8) S. El Golli, G. Arnaud, J. Bricardi, and C. Treiner, *J. Aerosol Sci.*, **8**, 39 (1977).

(9) J. Porstendorfer, *ibid.*, **2**, 73 (1971).

(10) M. K. Mazumder and K. J. Kirsh, *Rev. Sci. Instrum.*, **48**, 622 (1977).

(11) M. K. Mazumder, *Appl. Phys. Lett.*, **16**, 462 (1970).

ACKNOWLEDGMENTS

Supported by National Institutes of Health Grant HL20024.

The authors thank Melinda Smith and Cindy Burris for assistance in manuscript preparation, Dr. D. L. Lattin for advice during manuscript preparation, and Dr. M. K. Testerman for support and encouragement.

Substituent Constants of Azulene

M. R. LICHTENWALNER * and T. J. SPEAKER ˣ

Received September 4, 1979, from the *School of Pharmacy, Temple University, Philadelphia, PA 19140.* Accepted for publication October 24, 1979. *Present address: Center for Laboratory Medicine, Trevose, PA 19047.

Abstract □ The ionization constants in water for six 3-substituted azuloic acids were determined spectrophotometrically. Conversion of these physical constants to their pKa values allowed a set of Hammett-type σ values for the substituents on these acids to be calculated. Determination of partition coefficients for nine 1-substituted azulenes allowed Hansch-type π values to be determined, using azulene as the model compound.

Keyphrases □ Azulenes, various—substituent constants, ionization and partition coefficients, spectral characteristics □ Substituent constants—various azulenes □ Ionization constants—various azuloic acids □ Partition constants—various azulenes

The σ constant of Hammett (1) and the π constant of Hansch *et al.* (2) are useful in estimating the relative effects of substituents on the reactivity (σ) and partitioning (π) characteristics (3) of aromatic compounds. There are extensive collections of correlations of biological activity with these substituent values within one or another series of benzenoid compounds (4–6). Thus, they can guide the selection of substituents with which to modify the bioactivity and other properties of benzenoid compounds (7).

BACKGROUND

Replacement of the benzenoid nucleus with nonbenzenoid aromatic systems has been used to prepare local anesthetic esters, amides, and carboxamides (8–10) and oxidative enzyme inhibitors (11). Few experimentally determined σ or π values are available for nonbenzenoid aromatic systems. Except for the work of McDonald *et al.* (12), only scattered reports of pKa and σ values and even fewer reports of partition coefficients and π values for nonbenzenoid aromatic compounds are available. These studies include the ionization constants of azuloic acids as determined in 50% aqueous ethanol (12, 13), the ionization constants of variously substituted ferrocenecarboxylic acids (14), and the octanol–water partition coefficient of azulene (15). This small set of values is restricted further in utility because, as Bright and Briscoe (16) reported, apparent

0022-3549/80/0300-0337$01.00/0

© 1980, American Pharmaceutical Association

Therefore, the total particulate volume may increase out of proportion to the observed change in the mass median aerodynamic diameter. In considering these data and the hypothesized explanations, it is important to recognize that the relative contribution to particle growth at high humidity in a complex system of multicomponent particles, air, water vapor, and other vapors such as fluorocarbons and ethanol is not clear.

The increase in the number density and the mass of aerosol particles at high humidity must not be interpreted as an increase in the content of active ingredients. Although the growth is caused by the water uptake, any accompanying change in the mass distribution of the active ingredient may significantly change the amount and site of deposition of the active ingredient inside the lung. Additional information is needed to determine the content of the active ingredient at various size intervals, especially at high humidity.

The total mass of dry aerosol in the 0.30–6.0-μm range shown in Table II is similar for three of the four aerosols to the mass of the active ingredient claimed by the manufacturer to be dispensed from each device per valve activation. All aerosols contain stabilizing and dispensing agents that may contribute to the total mass. The portion of the active ingredient in the aerosol mass is not known. The active ingredient of droplet aerosols is dissolved in alcohol, which may contribute to the aerosol mass, although it probably evaporates fairly rapidly. The fluorocarbon propellants also contribute to the particle size as these aerosols leave the metered-dose device, but most are highly volatile and evaporate almost immediately upon aerosolization. In addition, all of these devices contain a dispersing agent present in variable quantities. The mass of isoproterenol sulfate measured in this study was greater than the mass of active ingredient reported to be dispensed per dose by the manufacturer. This difference probably was due to the relatively high ratio of dispersing agent to active ingredient for isoproterenol sulfate (~2.5:1) compared to metaproterenol sulfate (~1:1)[7].

The increase in particle size found in this study probably was not greatly influenced by particle aggregation since the aerosol concentration after injection into the environmental chamber was relatively dilute. Aggregation, which is related to the square of the concentration, may contribute along with water condensation to particle growth in the respiratory tract where the concentration should be much higher than in the chamber used for these studies.

Although the content of active ingredient per particle at high humidity is not known, the increase in total aerosol mass, which is considerable for the droplet aerosols, implies that the content of active ingredient shifts to particles of a larger size. A size shift similar to that observed in these high humidity studies may occur when these aerosols are inhaled into the human respiratory tract. Failure to consider particle-size changes may result in inaccurate prediction of respiratory tract deposition, especially for apparently highly unstable droplet aerosols.

[7] I. Porush, Director, Quality Assurance, Riker Laboratories, personal communication.

REFERENCES

(1) I. Porush, C. G. Thiel, and J. G. Young, *J. Am. Pharm. Assoc., Sci. Ed.*, **49**, 70 (1960).

(2) T. T. Mercer, R. F. Goddard, and R. L. Flores, *Ann. Allergy*, **23**, 314 (1965).

(3) C. Hiller, M. Mazumder, D. Wilson, and R. Bone, *Am. Rev. Resp. Dis.*, **118**, 311 (1978).

(4) P. E. Morrow, *ibid.*, **110**, 88 (1974).

(5) S. S. Davis and M. D. Budd, *Int. J. Pharm.*, **1**, 303 (1978).

(6) T. T. Mercer, *Arch. Intern. Med.*, **131**, 39 (1973).

(7) W. R. Lane, in "Proceedings of the 5th International Cystic Fibrosis Conference," D. Lawson, Ed., Cambridge University, Cambridge, England, 1969, pp 103–111.

(8) S. El Golli, G. Arnaud, J. Bricardi, and C. Treiner, *J. Aerosol Sci.*, **8**, 39 (1977).

(9) J. Porstendorfer, *ibid.*, **2**, 73 (1971).

(10) M. K. Mazumder and K. J. Kirsh, *Rev. Sci. Instrum.*, **48**, 622 (1977).

(11) M. K. Mazumder, *Appl. Phys. Lett.*, **16**, 462 (1970).

ACKNOWLEDGMENTS

Supported by National Institutes of Health Grant HL20024.

The authors thank Melinda Smith and Cindy Burris for assistance in manuscript preparation, Dr. D. L. Lattin for advice during manuscript preparation, and Dr. M. K. Testerman for support and encouragement.

Substituent Constants of Azulene

M. R. LICHTENWALNER * and T. J. SPEAKER ˣ

Received September 4, 1979, from the *School of Pharmacy, Temple University, Philadelphia, PA 19140.* Accepted for publication October 24, 1979. *Present address: Center for Laboratory Medicine, Trevose, PA 19047.

Abstract □ The ionization constants in water for six 3-substituted azuloic acids were determined spectrophotometrically. Conversion of these physical constants to their pKa values allowed a set of Hammett-type σ values for the substituents on these acids to be calculated. Determination of partition coefficients for nine 1-substituted azulenes allowed Hansch-type π values to be determined, using azulene as the model compound.

Keyphrases □ Azulenes, various—substituent constants, ionization and partition coefficients, spectral characteristics □ Substituent constants—various azulenes □ Ionization constants—various azuloic acids □ Partition constants—various azulenes

The σ constant of Hammett (1) and the π constant of Hansch *et al.* (2) are useful in estimating the relative effects of substituents on the reactivity (σ) and partitioning (π) characteristics (3) of aromatic compounds. There are extensive collections of correlations of biological activity with these substituent values within one or another series of benzenoid compounds (4–6). Thus, they can guide the selection of substituents with which to modify the bioactivity and other properties of benzenoid compounds (7).

BACKGROUND

Replacement of the benzenoid nucleus with nonbenzenoid aromatic systems has been used to prepare local anesthetic esters, amides, and carboxamides (8–10) and oxidative enzyme inhibitors (11). Few experimentally determined σ or π values are available for nonbenzenoid aromatic systems. Except for the work of McDonald *et al.* (12), only scattered reports of pKa and σ values and even fewer reports of partition coefficients and π values for nonbenzenoid aromatic compounds are available. These studies include the ionization constants of azuloic acids as determined in 50% aqueous ethanol (12, 13), the ionization constants of variously substituted ferrocenecarboxylic acids (14), and the octanol–water partition coefficient of azulene (15). This small set of values is restricted further in utility because, as Bright and Briscoe (16) reported, apparent

0022-3549/80/0300-0337$01.00/0

© 1980, American Pharmaceutical Association

Table I—K_a and pKa Values of 3-Substituted Azuloic Acids and σ Constants of Azuloic and Benzoic Acids

Substituent	$K_a \times 10^6$	pKa	σ Azuloic Acid	σ_m (25)	σ_p (25)	σ_I (26)
H	7.80	5.11 ± 0.03	0	0	—	0
Cl	11.35	4.95 ± 0.05	0.16	0.37	0.23	0.47
Br	13.61	4.87 ± 0.05	0.24	0.39	0.23	0.47
$COCH_3$	17.22	4.76 ± 0.07	0.34	0.31	0.52	0.28
CHO	31.05	4.51 ± 0.04	0.60	0.36	0.22	0.31
NO_2	47.86	4.32 ± 0.06	0.79	0.71	0.78	0.63

Table II—Partition Coefficients of 1-Substituted Azulenes and π Constants for Azulene and Benzene

Substituent	K_p	log K_p	π Azulene	π Benzene
H	1671	3.22	0	0
$COOCH_2CH_3$	6730	3.83	+0.61	+0.51
COOH	754	2.88	−0.34	−0.32
$COCH_3$	743	2.87	−0.35	−0.35
CHO	434	2.64	−0.58	−0.65
NO_2	393	2.59	−0.63	−0.28
$NHCOCH_3$	301	2.48	−0.74	−0.97

pKa values and apparent σ constants calculated from them change substantially as the ethanol concentration in hydroalcoholic solutions changes. They showed that an apparent σ value could change sign as the alcohol concentration of the solution changed.

The present work involved the determination of σ and π values for azulene substituents for use in selecting candidate substances in drug design and the elucidation of drug action.

Although an acidic functional group is not essential (17), Hammett σ values are determined conveniently when the model substance is an acid. The ionization constants of some 3-substituted azuloic acids (Table I) and the partition coefficients of some 1-substituted azulenes (Table II) were measured spectrophotometrically. The corresponding σ and π constants for the azulene series were calculated from the experimental values.

EXPERIMENTAL

Materials—Azulene[1], reagents[1,2], and solvents[3] were purchased commercially. The following compounds were prepared by previously described methods: azuloic acid (18), 3-acetylazuloic acid (19), 3-bromoazuloic acid (19), 3-chloroazuloic acid (19), 3-formylazuloic acid (20), 3-nitroazuloic acid (9), acetamidoazulene (21), acetylazulene (21), azulenecarboxaldehyde (22), nitroazulene (21), and ethyl azuloate (18).

Ionization Constants—The method employed for the determination of ionization constants was adapted from that of Albert and Serjeant (23). The acid of interest was dissolved in 0.01 *N* HCl, 0.01 *N* NaOH, or a graded series of buffers having pH values that bracketed the anticipated pKa. The pH values of the resulting solutions were recorded to a thousandth of a pH unit[4], and the desired spectral characteristics were measured using a recording spectrophotometer[5]. All measurements were made between 20 and 25° to eliminate making temperature corrections (24).

All solutions except buffers were prepared fresh daily. Buffer solutions were prepared as needed from 0.1 *M* stock solutions of acetic acid, hydrochloric acid, sodium acetate, and sodium hydroxide. All water for the preparation of solutions was purified by ion exchange and reverse osmosis and then distilled in glass.

Saturated solutions of the azuloic acids in water containing 1% ethanol (to assist wetting) (23) were prepared as stock solutions from which exact 1:5 dilutions were made with 0.01 *N* HCl, acetate buffer, or NaOH. Volumes of 1% ethanol in water were similarly diluted to provide blanks. Spectra were recorded between 700 and 220 nm using cells with 10-cm light paths.

The absorption spectra of the most basic and most acidic solutions were recorded as superimposed traces on the same section of calibrated chart paper. With the aid of dividers, the optimal wavelength was found; the checklist of priorities regarding selection of this wavelength as described by Albert and Serjeant (23) was observed. All subsequent measurements were made at this wavelength.

In all instances, the pH value of each solution was measured just prior to measuring the absorbance. Sufficient time was allowed for electrode equilibration so that not more than a 0.001-pH unit drift occurred in 1 min.

Since the pKa values were assumed and found to lie between 4 and 5, acetate buffer was used; it has useful buffering properties between pH 4.1 and 5.3. The ionic strength of the buffer in the final measured solution was 8×10^{-3}. The molarity of the acids varied but was never greater than 1.5×10^{-4} mole/liter. A trial determination at pH 4.5 was made to obtain a first measure of the pKa of each acid. Once this value was obtained, a series of buffers with pH values bracketing it was used to provide a set of seven values for each compound. The averages of the K_a and pKa values determined for each compound are given in Table I together with the calculated σ values.

Partition Coefficients—The method for partition coefficients used was derived from that of Hansch and coworkers (25). Monosubstituted azulenes were partitioned between *n*-octanol and water. For the determination of the partition coefficient of azuloic acid only, the water was adjusted with acetic acid to a final acid concentration of 0.01 *N*; the resulting pH was about 3.4. This acid concentration was low enough that it did not interfere with the analysis but was sufficiently high to ensure that azuloic acid was <2% ionized.

Because the specific method employed is critical to the accuracy of the values determined, the procedure is described in detail. The octanol was purified by sequentially washing with nominally 2 *N* NaOH, 4 *N* H_2SO_4, 2 *N* Na_2CO_3, and water followed by distillation under reduced pressure. The water used for partitioning studies was purified by ion exchange, reverse osmosis, and distillation in glass and then was vigorously shaken with purified octanol to ensure saturation. The resulting milky suspension was passed through two 0.22-μm filters[6] saturated with octanol to assist in breaking the emulsion. The phases were separated and stored in ground-glass stoppered bottles.

A few milligrams of each purified 1-substituted azulene was dissolved separately in about 25 ml of water-saturated octanol. These solutions were used as stock solutions. Beer's law plots were established for each compound; correlations between absorbance values and concentration typically had values of r^2 greater than 0.999. A 5.00-ml aliquot of the stock solution and two dilutions of it were pipetted into volumetric flasks containing 1000.0 ml of octanol-saturated water. The mixtures were hand inverted 400 times and allowed to separate, and as much of each octanol layer as possible was withdrawn with the aid of a Pasteur pipet. The octanol layers were clarified by centrifugation at 1000×*g* for 30 min. The absorbances of the octanol solutions were measured immediately at three different absorbance maxima of the azulenoid, and the azulenoid concentration was calculated. Results are reported as the average of these nine values in Table II, expressed as partition coefficients, together with the corresponding values of π.

RESULTS AND DISCUSSION

The ionization constants of six azuloic acids were determined spectrophotometricallly using the method of Albert and Serjeant (23), and the corresponding pKa and Hammett σ values were calculated. These values are presented in Table I together with the corresponding benzenoid σ values. Azuloic acid, with a pKa of 5.11, is a weaker acid than naphthoic acid (pKa 4.17) (27), which is an isomer, or than benzoic acid (pKa 4.18) (27). This finding is consistent with the relatively high charge density of the parent hydrocarbon, azulene, as calculated by the Hückle LCAO–MO (linear combination of atomic orbitals–molecular orbitals) approach (28).

The observation that azuloic acid is about 10-fold weaker as an acid than either naphthoic or benzoic acid was confirmed indirectly by Leermakers and Bowman (13) who determined the apparent pKa of azuloic acid in 50% ethanol to be 6.67. A similar determination of the apparent pKa of benzoic acid gave 5.78.

Comparison of the σ values of the benzene and azulene series shows them to be substantially different. It is possible that inductive and resonance components may correlate with these values; however, the limited number of compounds in this study precludes such a test. The reversal

[1] Aldrich Chemical Co., Milwaukee, Wis.
[2] Matheson, Coleman and Bell, Norwood, Ohio.
[3] Fisher Scientific Co., Pittsburgh, Pa.
[4] Model 801 pH/mv meter, Orion Research, Cambridge, Mass.
[5] Model 15, Cary Instruments Division, Varian Associates, Monrovia, Calif.
[6] Millipore.

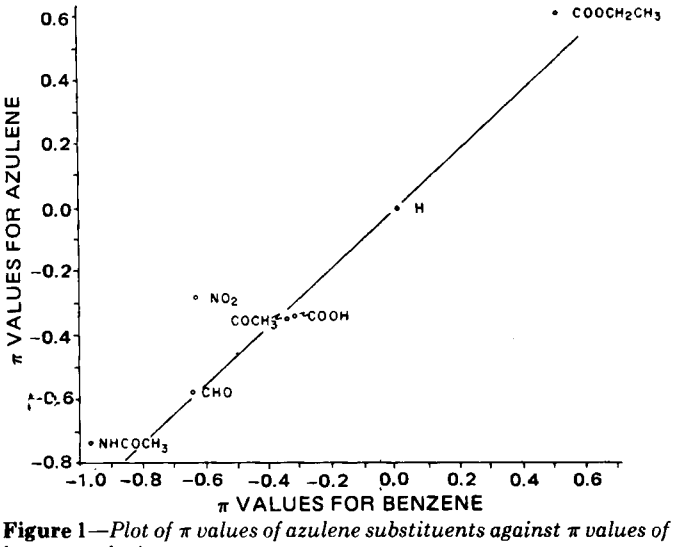

Figure 1—*Plot of π values of azulene substituents against π values of benzene substituents.*

of rank for the acetyl and formyl groups compared to σ_p is deserving of comment since the acetyl and formyl groups usually are considered similar in electronic behavior. They are, however, sterically different, and the difference in σ values may be attributed to a steric interaction between the methyl portion of the acetyl group and the *peri*-proton. Such steric interaction can reduce the coplanarity of the acetyl group with the ring bearing it, thereby decreasing the conjugation between the ring and the carbonyl function. Such a reduction of conjugation would reduce the electron-withdrawing ability of the carbonyl group. This interpretation is consistent with the observation that the UV absorbance maximum of acetylazulene shows a hypsochromic shift of about 7 nm with respect to that of formylazulene.

Another disparity between azulenoid and benzenoid σ values is seen with the bromo and chloro substituents. The benzenoid σ values for these substituents are nearly identical, but the azulenoid values differ distinctly. While this effect may be attributable to differing degrees of steric interaction with the *peri*-proton on the adjacent ring, it is explained more satisfactorily by the greater conjugative effect of the chloro over the bromo substituent.

The octanol–water partition coefficients of seven azulenoid compounds were determined spectrophotometrically, and the corresponding π values (2) were calculated. These values, together with the corresponding benzenoid π values, are presented in Table II.

Comparison of the azulenoid and benzenoid π values in Table II and Fig. 1 shows that a fair correlation exists between the two values (r^2 = 0.841). The correlation improves markedly (r^2 = 0.966) if the values for the nitro substituent are omitted from the regression equation:

$$\pi_{Az} = 0.925\ \pi_{Bz} + 0.041 \qquad \text{(Eq. 1)}$$

where the subscripts Az and Bz indicate azulenoid and benzenoid values, respectively. It is reasoned that the strongly electron-withdrawing character of the nitro group further accentuates the charge separation that exists in azulene itself (μ = 1*D*), thus increasing both its dipole moment and its water solubility.

In summary, while the π constants for azulene may be predicted reasonably and accurately from benzene π values except when the substituents are highly polar, the values of the azulene σ constants may not be inferred reliably from σ values of their benzenoid counterparts.

REFERENCES

(1) L. Hammett, "Phsyical Organic Chemistry," McGraw-Hill, New York, N.Y., 1940, p. 186.

(2) C. Hansch, R. Meir, T. Fujita, P. Maloney, F. Geiger, and M. Streich, *J. Am. Chem. Soc.*, **85**, 2818 (1963).

(3) R. Collander, *Acta Chem. Scand.*, **5**, 744 (1951).

(4) C. Hansch and T. Fujita, *J. Am. Chem. Soc.*, **86**, 1617 (1964).

(5) S. Free, Jr., and J. Wilson, *J. Med. Chem.*, **7**, 395 (1964).

(6) A. Cammarata and K. S. Rogers, in "Advances in Linear Free Energy Relationships," N. B. Chapman and J. Shorta, Eds., Plenum, New York, N.Y., 1972, p. 401.

(7) J. G. Topliss, *J. Med. Chem.*, **15**, 1006 (1972).

(8) T. J. Speaker and G. Redman, *J. Pharm. Sci.*, **55**, 479 (1966).

(9) P. H. Doukas and T. J. Speaker, *ibid.*, **60**, 184 (1971).

(10) P. H. Doukas, T. J. Speaker, and R. Thompson, *ibid.*, **64**, 158 (1975).

(11) T. B. Vree, P. T. Henderson, M. M. Van Rossum, and P. H. Doukas, *Xenobiotica*, **3**, 23 (1973).

(12) R. N. McDonald, R. R. Reitz, and J. M. Richmond, *J. Org. Chem.*, **41**, 1822 (1976).

(13) P. Leermakers and W. Bowman, *ibid.*, **29**, 3708 (1964).

(14) S. Gubin, K. Grandberg, E. Perevalova, and A. Nesmeyanov, *Dokl. Akad. Nauk SSSR*, **159**, 1075 (1964); through *Chem. Abstr.*, **62**, 7619b (1965).

(15) A. Leo, C. Hansch, and D. Elkins; through *Chem. Rev.*, **71**, 590 (1971).

(16) W. Bright and H. Briscoe, *J. Phys. Chem.*, **37**, 787 (1933).

(17) R. W. Taft, *ibid.*, **64**, 1805 (1960).

(18) W. Triebs, H. Neupert, and J. Heibsch, *Chem. Ber.*, **92**, 1216 (1959); through *Chem. Abstr.*, **53**, 17081c.

(19) A. G. Anderson, Jr., J. Nelson, and J. Tazuma, *J. Am. Chem. Soc.*, **75**, 4980 (1953).

(20) J. Billow, Ph.D. thesis, Temple University, Philadelphia, Pa., 1972, pp. 97, 98.

(21) A. G. Anderson, Jr., R. Scotini, E. Cowles, and C. Fritz, *J. Org. Chem.*, **22**, 1193 (1957).

(22) K. Hafner and C. Bernhard, *Ann.*, **625**, 108 (1959).

(23) A. Albert and E. Serjeant, "The Determination of Ionization Constants," Chapman and Hall, London, England, 1971, pp. 44–59.

(24) R. Pariser, *J. Chem. Phys.*, **25**, 1112 (1956).

(25) C. Hansch, in "Strategy of Drug Design," W. Purcell, G. Bass, and J. Clayton, Eds., Wiley–Interscience, New York, N.Y., 1973, pp. 126–142.

(26) O. Exner, in "Advances in Linear Free Energy Relationships," N. B. Chapman and J. Shorter, Eds., Plenum, New York, N.Y., 1972, p. 37.

(27) "Handbook of Chemistry and Physics," 34th ed., C. D. Hodgman, Ed., Chemical Rubber Publishing Co., Cleveland, Ohio, 1952, p. 1564.

(28) S. Fukushi and Y. Obata, *J. Ag. Chem. Soc. Jpn.*, **27**, 353 (1953).

ACKNOWLEDGMENTS

Abstracted in part from a dissertation submitted by M. R. Lichtenwalner to the Graduate School, Temple University, in partial fulfillment of the Master of Science degree requirements.

The authors thank Dr. Arthur Cammarata, Dr. Peter H. Doukas, and Dr. R. John Stedman, Temple University, for helpful suggestions and comments.

Antimicrobial Activity of *N*-Substituted *N*-(Triphenylstannyl)cyanamides and Triethylammonium (Organocyanoamino)chlorotriphenylstannates

EUGENE J. KUPCHIK *x, MICHAEL A. PISANO ‡, ANN M. CARROLL ‡, JOHN R. LUMPP ‡, and JOSEPH A. FEICCABRINO *

Received July 18, 1979, from the *Department of Chemistry and the ‡Department of Biological Sciences, St. John's University, New York, NY 11439. Accepted for publication September 21, 1979.

Abstract □ *N*-Substituted *N*-(triphenylstannyl)cyanamides were studied and found to be better antifungal agents than the previously tested *N*-substituted *N'*-cyano-*S*-(triphenylstannyl)isothioureas and *N*-substituted *N'*-cyano-*O*-(triphenylstannyl)isoureas. They were similar in activity to the previously tested ethyl *N*-aryl-*S*-(triphenylstannyl)-isothiocarbamates. The antifungal activity of triethylammonium (organocyanoamino)chlorotriphenylstannates, which are the triethylammonium chloride complexes of *N*-substituted *N*-(triphenylstannyl)-cyanamides, was similar to or better than that of the *N*-substituted *N*-(triphenylstannyl)cyanamides. Triethylammonium (acetylcyanoamino)chlorotriphenylstannate and triethylammonium dichlorotriphenylstannate were highly inhibitory toward Gram-positive bacteria.

Keyphrases □ *N*-(Triphenylstannyl)cyanamides, *N*-substituted—evaluated for antifungal activity □ Triethylammonium (organocyanoamino)chlorotriphenylstannates—evaluated for antifungal and antibacterial activity □ Antifungal activity—*N*-substituted *N*-(triphenylstannyl)cyanamides and triethylammonium (organocyanoamino)-chlorotriphenylstannates evaluated □ Antibacterial activity—triethylammonium (acetylcyanoamino)chlorotriphenylstannate and triethylammonium dichlorotriphenylstannate evaluated □ Organotin compounds—*N*-substituted *N*-(triphenylstannyl)cyanamides and triethylammonium (organocyanoamino)triphenylstannates evaluated for antibacterial activity, triethylammonium (acetylcyanoamino)triphenylstannate and triethylammonium dichlorostannate evaluated for antibacterial activity □ Structure–activity relationships—cyanamides evaluated for antifungal activity, chlorotriphenylstannates evaluated for antifungal and antibacterial activity

Many biocidal applications have been found or suggested for organotin compounds (1). The biological effects of organotin compounds were stressed in a recent symposium (2). Their use in agriculture as fungicides and pesticides is of special interest because they degrade to nontoxic inorganic compounds and, therefore, appear to pose little threat to the environment (3–7). Recently, ethyl *N*-aryl-*S*-(triphenylstannyl)isothiocarbamates (Series I) (8), which contain a tin–sulfur bond, were found to be generally better antifungal agents than another class of compounds having a tin–sulfur bond, namely, *N*-substituted *N'*-cyano-(triphenylstannyl)isothioureas (Series II) (9). The former compounds were also generally better antifungal agents than some previously studied compounds having a tin–oxygen bond, namely, *N*-substituted *N'*-cyano-*O*-(triphenylstannyl)isoureas (Series III) (10).

The purpose of the present study was to evaluate the antimicrobial activity of some recently reported compounds (11, 12) having a tin–nitrogen bond, namely, *N*-substituted *N*-(triphenylstannyl)cyanamides (Series IV) and triethylammonium (organocyanoamino)chlorotriphenylstannates (Series V). The latter compounds are anionic organotin complexes. The anionic organotin complex, triethylammonium dichlorotriphenylstannate (VI) (12), which is structurally simpler than V, also was evaluated.

RESULTS AND DISCUSSION

The data in Table I show that each of the Series IV compounds behaved essentially identically toward *Cladosporium carpophilum* (ATCC 12117), *Fusarium monoliforme* (ATCC 10052), *Myrothecium verrucaria* (ATCC 9095), *Penicillium notatum* (ATCC 9179), *Rhizopus stolonifer* (ATCC 10404), *Saccharomyces cerevisiae* (ATCC 9896), and *Trichoderma viride* (ATCC 8678). In the case of *C. carpophilum*, *F. monoliforme*, *M. verrucaria*, *P. notatum*, and *R. stolonifer*, each compound partially inhibited fungal growth at all three concentrations, with the exception of IV*a*, IV*c*, IV*e*, IV*f*, and IV*i*. Compounds IV*a*, IV*c*, and IV*f* were inactive toward *C. carpophilum* at 1 μg/ml, IV*i* was inactive toward both *P. notatum* and *R. stolonifer* at 1 μg/ml, and IV*e* was inactive toward *S. cerevisiae* at 10 μg/ml.

Each Series IV compound partially inhibited *Aspergillus niger* (ATCC 12845) at both 1 and 10 μg/ml. Each compound also completely inhibited growth at 100 μg/ml, with the exception of IV*e*–IV*g* and IV*i*, which only partially inhibited growth. The Series IV compounds exhibited partial inhibition of growth of *Chaetomium globosum* (ATCC 6205) at all concentrations, with the exception of IV*a*, IV*e*, and IV*i*, which completely inhibited growth at 100 μg/ml. The Series IV compounds showed the greatest activity toward *Trichophyton mentagrophytes* (ATCC 9129), with seven compounds completely inhibiting growth at 100 μg/ml.

In general, the Series IV compounds were much better antifungal agents than the previously tested Series II compounds and, with the exception of *T. mentagrophytes* toward which the antifungal activity was the same, were better fungal inhibitors than the Series III compounds. The Series IV compounds were more effective against *A. niger* but less effective against *C. globosum*, *T. mentagrophytes*, and *C. carpophilum* than the Series I compounds; the Series IV and Series I compounds exhibited essentially identical activity toward the other six fungi.

The antifungal activity of the Series V compounds (Table II), which are the triethylammonium chloride complexes of the Series IV compounds, was similar to or better than that of the Series IV compounds. The Series V compounds were more active than the Series IV compounds toward *C. globosum*, *P. notatum*, *S. cerevisiae*, and *T. viride*. For ex-

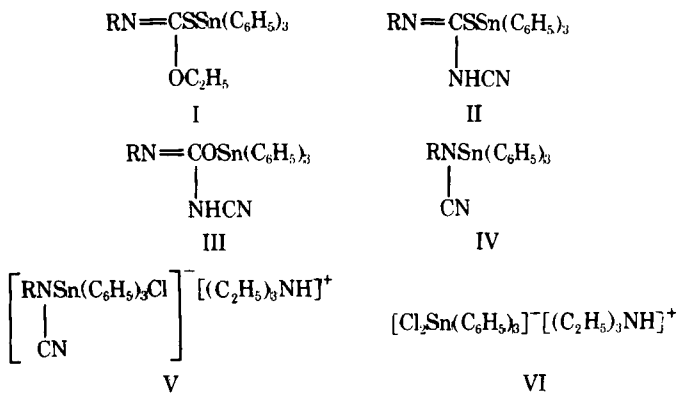

0022-3549/80/0300-0340$01.00/0
© 1980, American Pharmaceutical Association

Table I—Antifungal Activity of *N*-Substituted *N*-(Triphenylstannyl)cyanamides

Compound	R	*A. niger*			*C. globosum*			*C. carpophilum*			*F. moniliforme*			*M. verrucaria*			*P. notatum*			*R. stolonifer*			*S. cerevisiae*			*T. viride*			*T. mentagrophytes*		
		1[a]	10	100	1	10	100	1	10	100	1	10	100	1	10	100	1	10	100	1	10	100	1	10	100	1	10	100	1	10	100
IV*a*	$CH_3C(=O)$	+	+	2+	+	+	2+	—	+	+	+	+	+	+	+	+	+	+	+	+	+	+	—	+	+	—	+	+	+	+	2+
IV*b*	$C_2H_5C(=O)$	+	+	2+	+	+	+	+	+	+	+	+	+	+	+	+	+	+	+	+	+	+	—	+	+	—	+	+	+	+	2+
IV*c*	$C_6H_5C(=O)$	+	+	2+	+	+	+	—	+	+	+	+	+	+	+	+	+	+	+	+	+	+	—	+	+	—	+	+	+	+	2+
IV*d*	$C_6H_5CH_2C(=O)$	+	+	2+	+	+	+	+	+	+	+	+	+	+	+	+	+	+	+	+	+	+	—	+	+	—	+	+	+	+	2+
IV*e*	$p\text{-}O_2NC_6H_4C(=O)$	+	+	+	+	+	2+	+	+	+	+	+	+	+	+	+	+	+	+	+	+	+	—	—	+	—	+	+	+	+	2+
IV*f*	$CF_3C(=O)$	+	+	+	+	+	+	—	+	+	+	+	+	+	+	+	+	+	+	+	+	+	—	+	+	—	+	+	+	2+	2+
IV*g*	$CH_3OC(=O)$	+	+	+	+	+	+	+	+	+	+	+	+	+	+	+	+	+	+	+	+	+	—	+	+	—	+	+	+	+	+
IV*h*	$C_2H_5OC(=O)$	+	+	2+	+	+	+	+	+	+	+	+	+	+	+	+	+	+	+	+	+	+	—	+	+	—	+	+	+	+	+
IV*i*	$C_6H_5SO_2$	+	+	+	+	+	2+	+	+	+	+	+	+	+	+	+	—	+	+	—	+	+	—	+	+	—	+	+	+	+	2+

[a] Indicates concentrations of compounds employed in micrograms per milliliter; – indicates no inhibition of growth, + indicates partial inhibition, and 2+ indicates complete inhibition.

Table II—Antifungal Activity of Triethylammonium (Organocyanoamino)chlorotriphenylstannates and Triethylammonium Dichlorotriphenylstannate

Compound	R	*A. niger*			*C. globosum*			*C. carpophilum*			*E. moniliforme*			*M. verrucaria*			*P. notatum*			*R. stolonifer*			*S. cerevisiae*			*T. viride*			*T. mentagrophytes*		
		1[a]	10	100	1	10	100	1	10	100	1	10	100	1	10	100	1	10	100	1	10	100	1	10	100	1	10	100	1	10	100
V*a*	$CH_3C(=O)$	+	+	+	+	+	+	+	+	+	+	+	+	+	+	+	+	+	+	+	+	+	+	+	+	+	+	+	+	+	2+
V*b*	$C_2H_5C(=O)$	+	+	2+	+	+	2+	+	+	+	+	+	+	+	+	+	+	+	+	+	+	+	—	+	+	+	+	+	+	+	2+
V*c*	$C_6H_5C(=O)$	+	+	+	+	+	2+	+	+	+	—	+	+	+	+	+	+	+	+	+	+	+	+	+	+	+	+	+	+	+	+
V*d*	$CH_3OC(=O)$	+	+	2+	+	+	2+	+	+	+	+	+	+	+	+	+	+	+	2+	+	+	+	—	+	+	+	+	+	+	+	+
V*e*	$C_2H_5OC(=O)$	+	+	2+	+	+	+	+	+	+	+	+	+	+	+	+	+	+	2+	+	+	+	+	+	+	+	+	+	+	+	2+
V*f*	$C_6H_5CH_2OC(=O)$	+	+	+	+	2+	2+	+	+	+	+	+	+	+	+	+	+	+	+	+	+	+	—	+	2+	+	+	+	+	+	2+
V*g*	$C_6H_5SO_2$	+	+	2+	+	+	2+	+	+	+	+	+	2+	+	+	+	+	+	+	+	+	+	+	+	2+	+	+	+	+	2+	2+
VI	—	+	+	+	+	+	2+	+	+	+	+	+	+	+	+	+	+	+	+	+	+	+	—	+	+	+	+	+	+	+	+

[a] Indicates concentrations of compounds employed in micrograms per milliliter; – indicates no inhibition of growth, + indicates partial inhibition, and 2+ indicates complete inhibition.

Table III—Antibacterial Activity of Triethylammonium (Acetylcyanoamino)chlorotriphenylstannate and Triethylammonium Dichlorotriphenylstannate

Compound	*B. subtilis*[a]			*E. coli*			*S. aureus*		
	1[b]	10	100	1	10	100	1	10	100
Va	2+	2+	2+	—	—	+	2+	2+	2+
VI	2+	2+	2+	—	—	+	+	2+	2+

[a] Bacteria were obtained from the culture collection of the Department of Biological Sciences, St. John's University. [b] Indicates concentration of compounds employed in micrograms per milliliter; — indicates no inhibition of growth, + indicates partial inhibition of growth, and 2+ indicates complete inhibition of growth.

ample, only three of the Series IV compounds completely inhibited *C. globosum* at 100 μg/ml, whereas five of the Series V compounds exhibited this activity. Furthermore, none of the Series IV compounds inhibited *P. notatum* at 100 μg/ml, whereas two of the Series V compounds exhibited this activity. Furthermore, none of the Series IV compounds showed activity against *S. cerevisiae* and *T. viride* at 1 μg/ml, whereas four of the Series V compounds were partially active against *S. cerevisiae* and all of the Series V compounds were partially active against *T. viride* at this concentration. In addition, two of the Series V compounds completely inhibited *S. cerevisiae* at 100 μg/ml. The simple anionic complex, VI, exhibited equal or less activity than the Series V compounds.

The data in Table III show that Va and VI behaved in an almost identical manner toward specific test bacteria. Both compounds completely inhibited *Bacillus subtilus* at the lowest level (1 μg/ml) of organotin compound. Both compounds were equal to the previously tested *N*-phenyl-*N'*-cyano-*S*-(triphenylstannyl)isothioureas (II, R = C_6H_5) in this regard (9). On the other hand, the previously tested Series I compounds (8) were completely inactive at this concentration, while the previously tested *N*-phenyl-*N'*-cyano-*O*-(triphenylstannyl)isourea (III, R = C_6H_5) (10) only partially inhibited growth at this concentration. Compound Va behaved identically to the Series I compounds and to II (R = C_6H_5) in that it completely inhibited the growth of *Staphylococcus aureus* at 1 μg/ml. Compound III (R = C_6H_5) was inactive at this concentration (10). Compounds Va and VI were no more active than some previously studied compounds toward *Escherichia coli* (8–10).

EXPERIMENTAL

The Series IV compounds were individually dissolved in tetrahydrofuran. The Series V compounds and VI were individually dissolved in acetone. The preparation of sterile solutions of the compounds, the fungi employed, the antimicrobial testing procedures, and the determination of growth inhibition were reported previously (10).

Compounds Va and VI also were investigated for antibacterial activity according to the procedure reported earlier (10).

REFERENCES

(1) J. S. Thayer, *J. Organomet. Chem.*, **76**, 265 (1974).

(2) "Organotin Compounds: New Chemistry and Applications," J. J. Zuckerman, Ed., American Chemical Society, Washington, D.C., 1976.

(3) K.-D. Freitag and R. Bock, *Pestic. Sci.*, **5**, 731 (1974).

(4) R. D. Barnes, A. T. Bull, and R. C. Poller, *ibid.*, **4**, 305 (1973).

(5) M. E. Getzendaner and H. B. Corbin, *J. Agric. Food Chem.*, **20**, 881 (1972).

(6) R. Bock and K.-D. Freitag, *Naturwissenschaften*, **59**, 165 (1972).

(7) A. J. Chapman and J. W. Price, *Int. Pestic. Control*, 1, 11 (1972).

(8) E. J. Kupchik, M. A. Pisano, H. E. Hanke, and W.-C. R. Tseng, *J. Pharm. Sci.*, **67**, 576 (1978).

(9) E. J. Kupchik, M. A. Pisano, A. V. Raghunath, R. A. Cardona, N. Formaini, and C. Alleguez, *ibid.*, **64**, 1259 (1975).

(10) E. J. Kupchik, M. A. Pisano, D. K. Parikh, and M. A. D'Amico, *ibid.*, **63**, 261 (1974).

(11) E. J. Kupchik and J. A. Feiccabrino, *J. Organomet. Chem.*, **93**, 325 (1975).

(12) J. A. Feiccabrino and E. J. Kupchik, *ibid.*, **73**, 319 (1974).

Determination of Isophenindamine in Phenindamine Tartrate Using an Argentated High-Performance Liquid Chromatographic Mobile Phase

RONALD J. TSCHERNE ˣ and HERMINIA UMAGAT

Received May 7, 1979, from the *Quality Control Department, Hoffmann-La Roche Inc., Nutley, NJ 07110.* Accepted for publication September 13, 1979.

Abstract □ A high-performance liquid chromatographic procedure was developed for the determination of isophenindamine in phenindamine tartrate bulk powder. The method employs a reversed-phase column and a mobile phase containing methanol, 0.001 *M* HNO_3, and silver nitrate.

Keyphrases □ Isophenindamine—analysis, high-performance liquid chromatography, argentated mobile phase, phenindamine tartrate bulk powder □ High-performance liquid chromatography—isophenindamine, analysis in phenindamine tartrate bulk powder □ Phenindamine tartrate—analysis of isophenindamine in bulk powder, high-performance liquid chromatography, argentated mobile phase □ Antihistaminics—phenindamine tartrate, analysis of bulk powder for isophenindamine, high-performance liquid chromatography, argentated mobile phase

The role of histamine in anaphylactic shock and allergic conditions stimulated research for specific histamine antagonists. A series of antihistaminics including phenindamine (I) was synthesized (1). Distinct differences were observed between I and isophenindamine (II) when administered intravenously.

Because of the possible formation of II during the manufacture of phenindamine tartrate, a method for the determination of II was desired. A UV spectrophotometric procedure based on the fact that the wavelength of maximum absorbance for each compound is slightly different

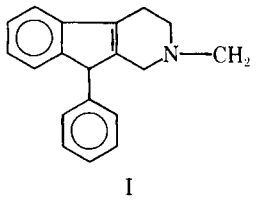

I

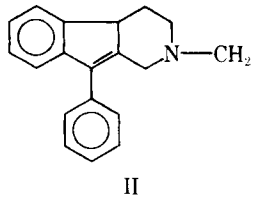

II

0022-3549/80/0300-0342$01.00/0

© 1980, American Pharmaceutical Association

Table III—Antibacterial Activity of Triethylammonium (Acetylcyanoamino)chlorotriphenylstannate and Triethylammonium Dichlorotriphenylstannate

Compound	*B. subtilis*[a]			*E. coli*			*S. aureus*		
	1[b]	10	100	1	10	100	1	10	100
Va	2+	2+	2+	—	—	+	2+	2+	2+
VI	2+	2+	2+	—	—	+	+	2+	2+

[a] Bacteria were obtained from the culture collection of the Department of Biological Sciences, St. John's University. [b] Indicates concentration of compounds employed in micrograms per milliliter; — indicates no inhibition of growth, + indicates partial inhibition of growth, and 2+ indicates complete inhibition of growth.

ample, only three of the Series IV compounds completely inhibited *C. globosum* at 100 μg/ml, whereas five of the Series V compounds exhibited this activity. Furthermore, none of the Series IV compounds inhibited *P. notatum* at 100 μg/ml, whereas two of the Series V compounds exhibited this activity. Furthermore, none of the Series IV compounds showed activity against *S. cerevisiae* and *T. viride* at 1 μg/ml, whereas four of the Series V compounds were partially active against *S. cerevisiae* and all of the Series V compounds were partially active against *T. viride* at this concentration. In addition, two of the Series V compounds completely inhibited *S. cerevisiae* at 100 μg/ml. The simple anionic complex, VI, exhibited equal or less activity than the Series V compounds.

The data in Table III show that Va and VI behaved in an almost identical manner toward specific test bacteria. Both compounds completely inhibited *Bacillus subtilus* at the lowest level (1 μg/ml) of organotin compound. Both compounds were equal to the previously tested *N*-phenyl-*N'*-cyano-*S*-(triphenylstannyl)isothioureas (II, R = C_6H_5) in this regard (9). On the other hand, the previously tested Series I compounds (8) were completely inactive at this concentration, while the previously tested *N*-phenyl-*N'*-cyano-*O*-(triphenylstannyl)isourea (III, R = C_6H_5) (10) only partially inhibited growth at this concentration. Compound Va behaved identically to the Series I compounds and to II (R = C_6H_5) in that it completely inhibited the growth of *Staphylococcus aureus* at 1 μg/ml. Compound III (R = C_6H_5) was inactive at this concentration (10). Compounds Va and VI were no more active than some previously studied compounds toward *Escherichia coli* (8–10).

EXPERIMENTAL

The Series IV compounds were individually dissolved in tetrahydrofuran. The Series V compounds and VI were individually dissolved in acetone. The preparation of sterile solutions of the compounds, the fungi employed, the antimicrobial testing procedures, and the determination of growth inhibition were reported previously (10).

Compounds Va and VI also were investigated for antibacterial activity according to the procedure reported earlier (10).

REFERENCES

(1) J. S. Thayer, *J. Organomet. Chem.*, **76**, 265 (1974).

(2) "Organotin Compounds: New Chemistry and Applications," J. J. Zuckerman, Ed., American Chemical Society, Washington, D.C., 1976.

(3) K.-D. Freitag and R. Bock, *Pestic. Sci.*, **5**, 731 (1974).

(4) R. D. Barnes, A. T. Bull, and R. C. Poller, *ibid.*, **4**, 305 (1973).

(5) M. E. Getzendaner and H. B. Corbin, *J. Agric. Food Chem.*, **20**, 881 (1972).

(6) R. Bock and K.-D. Freitag, *Naturwissenschaften*, **59**, 165 (1972).

(7) A. J. Chapman and J. W. Price, *Int. Pestic. Control*, 1, 11 (1972).

(8) E. J. Kupchik, M. A. Pisano, H. E. Hanke, and W.-C. R. Tseng, *J. Pharm. Sci.*, **67**, 576 (1978).

(9) E. J. Kupchik, M. A. Pisano, A. V. Raghunath, R. A. Cardona, N. Formaini, and C. Alleguez, *ibid.*, **64**, 1259 (1975).

(10) E. J. Kupchik, M. A. Pisano, D. K. Parikh, and M. A. D'Amico, *ibid.*, **63**, 261 (1974).

(11) E. J. Kupchik and J. A. Feiccabrino, *J. Organomet. Chem.*, **93**, 325 (1975).

(12) J. A. Feiccabrino and E. J. Kupchik, *ibid.*, **73**, 319 (1974).

Determination of Isophenindamine in Phenindamine Tartrate Using an Argentated High-Performance Liquid Chromatographic Mobile Phase

RONALD J. TSCHERNE ˣ and HERMINIA UMAGAT

Received May 7, 1979, from the *Quality Control Department, Hoffmann-La Roche Inc., Nutley, NJ 07110.* Accepted for publication September 13, 1979.

Abstract □ A high-performance liquid chromatographic procedure was developed for the determination of isophenindamine in phenindamine tartrate bulk powder. The method employs a reversed-phase column and a mobile phase containing methanol, 0.001 *M* HNO_3, and silver nitrate.

Keyphrases □ Isophenindamine—analysis, high-performance liquid chromatography, argentated mobile phase, phenindamine tartrate bulk powder □ High-performance liquid chromatography—isophenindamine, analysis in phenindamine tartrate bulk powder □ Phenindamine tartrate—analysis of isophenindamine in bulk powder, high-performance liquid chromatography, argentated mobile phase □ Antihistaminics—phenindamine tartrate, analysis of bulk powder for isophenindamine, high-performance liquid chromatography, argentated mobile phase

The role of histamine in anaphylactic shock and allergic conditions stimulated research for specific histamine antagonists. A series of antihistaminics including phenindamine (I) was synthesized (1). Distinct differences were observed between I and isophenindamine (II) when administered intravenously.

Because of the possible formation of II during the manufacture of phenindamine tartrate, a method for the determination of II was desired. A UV spectrophotometric procedure based on the fact that the wavelength of maximum absorbance for each compound is slightly different

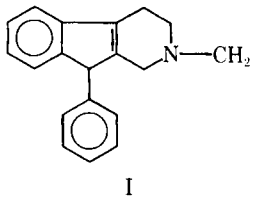

I

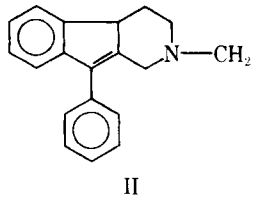

II

0022-3549/80/0300-0342$01.00/0

© 1980, American Pharmaceutical Association

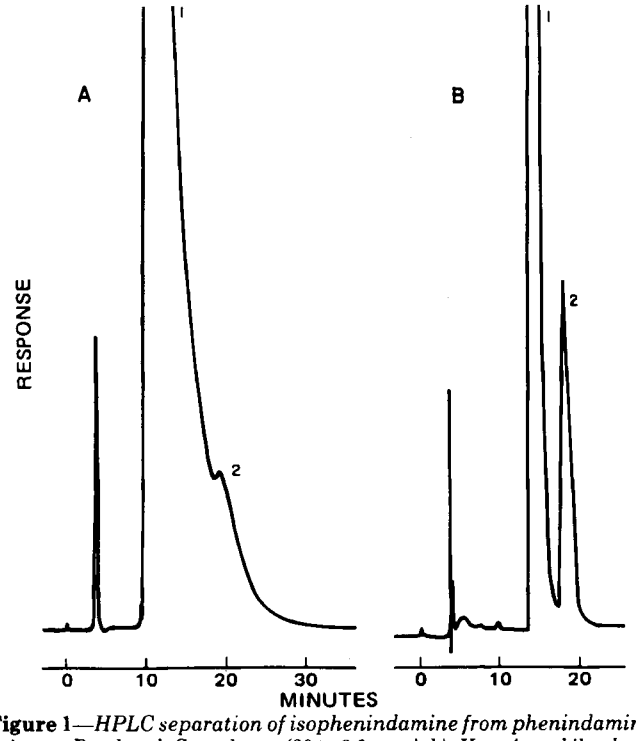

Figure 1—*HPLC separation of isophenindamine from phenindamine using a μBondapak C_{18} column (30 × 3.9 mm i.d.). Key: A, mobile phase of 0.001 M HNO_3–methanol (1:1) and a flow rate of 0.8 ml/min; B, mobile phase of 0.001 M HNO_3–methanol (1:1) containing 2% $AgNO_3$ (w/v) and a flow rate of 0.8 ml/min; 1, phenindamine; and 2, isophenindamine.*

(2) would allow quantitation using simultaneous equation treatment. NMR spectroscopy might be used for II detection, but quantitative results have not been reported[1].

A high-performance liquid chromatographic (HPLC) procedure that enables separation and quantitation of II in the presence of phenindamine tartrate bulk powder is described.

EXPERIMENTAL

Reagents and Chemicals—Glass-distilled water, methanol, nitric acid, and silver nitrate[2] were used for preparation of the mobile phase. The mobile phase was filtered[3] prior to use. Samples and standards were prepared using low-actinic glassware. Isophenindamine nitrate[4] was used for standard preparations.

Instrumentation and Apparatus—A constant-volume pump[5] was used in conjunction with a septum-type injector[6] and a variable-wavelength detector[7]. The separation was accomplished using a permanently bonded octadecylsilane partition column[8]. A high-pressure syringe[9] was used for injection of all samples and standards.

Mobile Phase—The mobile phase was prepared by dissolving 20 g of silver nitrate in 500 ml of 0.001 *M* HNO_3 and diluting with 500 ml of methanol. It was prepared fresh daily using low-actinic glassware and filtered through a 0.45-μm filter prior to use.

Standard Preparation—To prepare the standard solution, 13 mg of isophenindamine nitrate reference standard was weighed accurately into a 25-ml low-actinic volumetric flask, and 12.5 ml of 0.001 *M* HNO_3 was added. The flask was shaken until dissolution was nearly or totally complete (~5 min). Then 12.5 ml of methanol was added, and the flask was shaken again until dissolution occurred. A small degree of sonication usually was necessary to solubilize the reference material.

Sample Preparation—To prepare the sample solution, ~100 mg of phenindamine tartrate powder was weighed accurately into a low-actinic 10-ml volumetric flask. The sample was dispersed in 5 ml of 0.001 *M* HNO_3 by gentle shaking of the flask. Then 5 ml of methanol was added, and the solution was shaken until complete dissolution was observed.

Procedure—Five microliters each of the standard and sample solutions were injected alternately into the chromatograph. The peak heights of the isophenindamine standard and the peak that corresponded to it in retention time in the sample chromatogram were measured. The percent isophenindamine (as tartrate) was calculated by:

$$\%\ \text{isophenindamine (as tartrate)} = \left(\frac{W_{ISTD}}{P_{ISTD}}\right)\left(\frac{P_{ISAM}}{W_{SAM}}\right)\left(\frac{MW_{ITAR}}{MW_{INO3}}\right)\left(\frac{1000}{25}\right) \quad \text{(Eq. 1)}$$

where W_{ISTD} is the weight of isophenindamine nitrate standard in milligrams; W_{SAM} is the weight of the sample in milligrams; P_{ISTD} and P_{ISAM} are the heights, in millimeters, of isophenindamine in the standard and sample runs, respectively; and MW_{ITAR} and MW_{INO3} are the molecular weights of isophenindamine tartrate (411.44) and isophenindamine nitrate (324.37), respectively. The factor 1000/25 is a combination of the dilution factor (10/25) and the conversion to percent (×100).

Table I—Comparison of Results Obtained Using UV and Chromatographic Methods

Lot	Percent Isophenindamine	
	HPLC Determination	UV Determination
A	5.6	3.5
B	5.1	3.1
C	5.3	3.9
D	6.3	3.4
E	7.6	4.2

RESULTS AND DISCUSSION

The chromatographic separation of isophenindamine in the presence of phenindamine tartrate was obtained using a μBondapak C_{18} column and an argentated mobile phase. A 2% $AgNO_3$ (w/v) concentration in the mobile phase was necessary for complete compound separation. Lower silver nitrate concentrations reduced the resolution between I and II, while increased silver nitrate concentrations yielded little additional separation. Typical chromatograms using argentated and nonargentated mobile phases are shown in Fig. 1. Ion-pairing systems employing octanesulfonic acid and lauryl sulfate as pairing reagents were tried but did not produce resolution equivalent to the system containing 2% $AgNO_3$.

Several phenindamine tartrate samples were tested for their isophenindamine content using this method, and the results were compared with those obtained using a UV spectrophotometric procedure based on UV absorbance differences (Table I). Since poor correlation of results was found between the two methods, a standard addition study was done using the HPLC procedure. A straight line through the origin (within experimental error) was obtained for a plot of peak height response *versus* amount of isophenindamine added. This experiment showed conclusively that: (*a*) response *versus* concentration was linear between 0 and 10% isophenindamine in the samples and (*b*) discrepancy in results between the two methods must be linked to the inaccuracy of the UV procedure. Intuitively, these conclusions seem logical because the UV procedure suffers inherently from overlapping absorption bands in the measurement region. The relative standard deviation for 10 injections of the same solution into the chromatograph was 2.2%.

When using both the UV and the chromatographic procedures for quantitation studies, isophenindamine nitrate was the reference standard because no isophenindamine tartrate was available. Sample results were corrected for molecular weight differences between the tartrate and the nitrate salts.

Samples of phenindamine free base also were assayed for their isophenindamine content when the sample preparation was modified slightly. Free base samples had to be dissolved in methanol instead of 0.001 *M* HNO_3–methanol (1:1). This alteration did not affect method reliability.

A rechromatographed portion of an eluted phenindamine peak showed that no detectable amount of the iso-compound formed during the analysis. Also, a stability study on prepared solutions indicated that a

[1] J. H. Johnson and C. Condon, Hoffmann-La Roche Inc., unpublished data.
[2] Analyzed reagent, J. T. Baker Chemical Co.
[3] Millipore Corp.
[4] Hoffmann-La Roche Inc.
[5] Model 396, Laboratory Data Control.
[6] DuPont Instruments.
[7] Model 835, DuPont Instruments.
[8] μBondapak C_{18}, Waters Associates, Milford, Mass.
[9] HP-305, Hamilton Co.

small degree of transformation of isophenindamine to phenindamine occurred after standing in the mobile phase for ~1 day.

To take advantage of the properties of silver nitrate, it was necessary to ensure that all materials in contact with the mobile phase were made of 316 stainless steel or other noncorrodible material. The detector balance had to be electronically offset to monitor the effluent at 254 nm because of the relatively high absorbance of the mobile phase. By observing these relatively simple directions and precautions, the system was safe and reliable, producing no column deterioration over ~3 months of use.

REFERENCES

(1) G. Lehmann, *J. Pharmacol. Ther.*, **92**, 249 (1948).

(2) J. Plati and W. Wenner, *J. Org. Chem.*, **20**, 1412 (1955).

ACKNOWLEDGMENTS

The authors thank Dr. J. Plati for the isophenindamine nitrate reference standard, Mr. N. Beratti for spectroscopic data, and Ms. G. Capitano for technical assistance.

Effect of Exercise on Renal Clearance of Atenolol

WILLIAM D. MASON *x, GREGORY KOCHAK *, NATHANIEL WINER *, and IRVING COHEN ‡

Received April 30, 1979, from the **Pharmacokinetics Laboratory, Schools of Pharmacy and Medicine, University of Missouri-Kansas City, Kansas City, MO 64108,* and the ‡*Clinical Research Department, ICI Americas, Inc., Wilmington, DE 19897.* Accepted for publication October 1, 1979.

Abstract □ The effect of exercise on plasma atenolol was evaluated using a two-phase complete crossover study in 12 healthy volunteers. In one phase, the volunteers were subjected to physical exertion on a treadmill; in the other phase, they remained in a sitting or standing position. Following a single 100-mg atenolol dose, frequent blood samples and a complete urine collection were obtained over 24 hr. Plasma and urine atenolol levels were assayed by high-pressure liquid chromatography. Plasma atenolol was significantly ($p < 0.05$) higher during the exercise phase of the study, and this result was associated with approximately an 8% decrease in the renal clearance of the drug, probably due to decreased renal blood flow during exercise.

Keyphrases □ Atenolol—effect of exercise on renal clearance □ Pharmacokinetics—atenolol, effect of exercise on renal clearance □ Renal clearance—atenolol, effect of exercise □ β-Adrenergic blocking agents—atenolol, effect of exercise on renal clearance

Recently published reports described the pharmacokinetics (1) and pharmacodynamics (2) of atenolol, 2-[*p*-[2-hydroxy-3-(isopropylamino)propoxy]phenyl]acetamide, a new cardioselective (3–5) β-adrenergic blocking agent. More than 90% of the bioavailable dose of atenolol is excreted unchanged in the urine within 48 hr of dosing (6). To study the relationship of pharmacokinetics to pharmacodynamics, a two-phase complete crossover design was employed, with the phases differing only in the amount of exercise required of the subjects. A difference in the kinetics of atenolol between the two phases (exercise *versus* nonexercise) is reported.

EXPERIMENTAL

The 12 healthy male volunteers were 20–28 years old and weighed 63.6–85.5 kg (140–188 lb). Each subject was judged healthy based on the absence of any abnormality in his history, physical examination, ECG, hemogram, blood chemistries, and urinalysis.

The study design was a two-phase complete crossover, with the treatments being identical except for the exercise performed by each subject. Following a 10-hr fast, each subject received 100 mg of atenolol as an oral solution in 240 ml of water. The fast continued until after the 4th-hr blood sample was drawn; a standard meal was served at the 5th hr. Following the meal, water was allowed *ad libitum*. Blood samples were collected at 0, 0.5, 1.0, 2.0, 3.0, 4.0, 6.0, 8.0, 10.0, 12.0, 14.0, and 24.0 hr. Urine was collected prior to dosing, from 0.0 to 12.0 hr, and from 12.0 to 24.0 hr.

Plasma and urine atenolol levels were determined by a high-pressure liquid chromatographic (HPLC) method described previously (7) and modified as follows. The mobile phase consisted of a 4.00 m*M* solution of 1-heptanesulfonic acid sodium salt, 1.0% acetic acid, and 60.0% methanol in distilled water. The mobile phase was pumped at 1.5 ml/min and 20° through a stainless steel column packed with a high efficiency bonded-phase packing[1]. Aliquots of 150 μl of the reextraction solution were injected directly on-column through the injector. The atenolol peak was well separated from the procainamide internal standard peak and from artifacts. The retention times of atenolol and procainamide were 5.8 and 12.3 min, respectively.

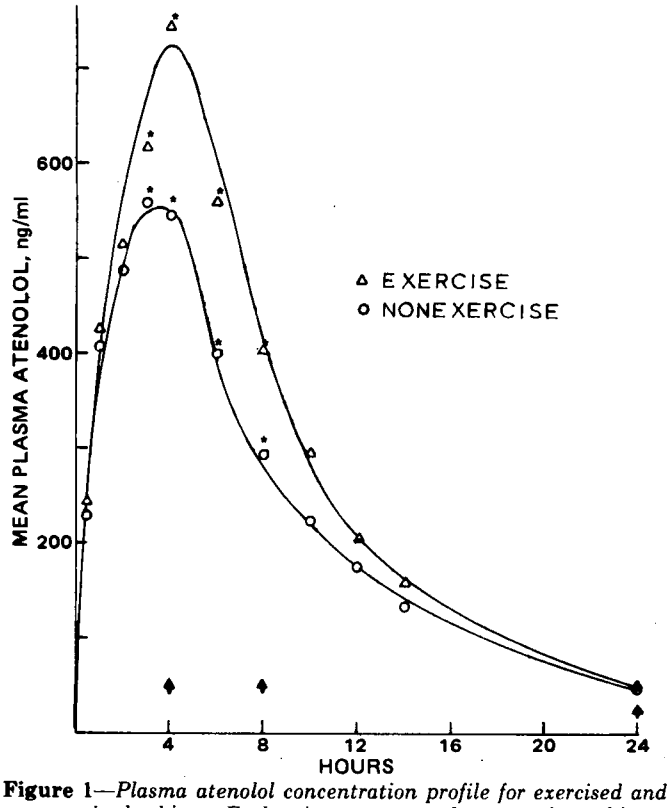

Figure 1—*Plasma atenolol concentration profile for exercised and nonexercised subjects. Each point represents the mean of 12 subjects. Starred (*) points represent significant differences ($p < 0.05$) between exercised and nonexercised subjects. Arrows indicate times of exercise.*

[1] Spherisorb 5-μm ODS, Laboratory Data Control, Riviera Beach, Fla.

0022-3549/80/0300-0344$01.00/0

© 1980, American Pharmaceutical Association

small degree of transformation of isophenindamine to phenindamine occurred after standing in the mobile phase for ~1 day.

To take advantage of the properties of silver nitrate, it was necessary to ensure that all materials in contact with the mobile phase were made of 316 stainless steel or other noncorrodible material. The detector balance had to be electronically offset to monitor the effluent at 254 nm because of the relatively high absorbance of the mobile phase. By observing these relatively simple directions and precautions, the system was safe and reliable, producing no column deterioration over ~3 months of use.

REFERENCES

(1) G. Lehmann, *J. Pharmacol. Ther.*, **92**, 249 (1948).

(2) J. Plati and W. Wenner, *J. Org. Chem.*, **20**, 1412 (1955).

ACKNOWLEDGMENTS

The authors thank Dr. J. Plati for the isophenindamine nitrate reference standard, Mr. N. Beratti for spectroscopic data, and Ms. G. Capitano for technical assistance.

Effect of Exercise on Renal Clearance of Atenolol

WILLIAM D. MASON *x, GREGORY KOCHAK *, NATHANIEL WINER *, and IRVING COHEN ‡

Received April 30, 1979, from the **Pharmacokinetics Laboratory, Schools of Pharmacy and Medicine, University of Missouri-Kansas City, Kansas City, MO 64108,* and the ‡*Clinical Research Department, ICI Americas, Inc., Wilmington, DE 19897.* Accepted for publication October 1, 1979.

Abstract □ The effect of exercise on plasma atenolol was evaluated using a two-phase complete crossover study in 12 healthy volunteers. In one phase, the volunteers were subjected to physical exertion on a treadmill; in the other phase, they remained in a sitting or standing position. Following a single 100-mg atenolol dose, frequent blood samples and a complete urine collection were obtained over 24 hr. Plasma and urine atenolol levels were assayed by high-pressure liquid chromatography. Plasma atenolol was significantly ($p < 0.05$) higher during the exercise phase of the study, and this result was associated with approximately an 8% decrease in the renal clearance of the drug, probably due to decreased renal blood flow during exercise.

Keyphrases □ Atenolol—effect of exercise on renal clearance □ Pharmacokinetics—atenolol, effect of exercise on renal clearance □ Renal clearance—atenolol, effect of exercise □ β-Adrenergic blocking agents—atenolol, effect of exercise on renal clearance

Recently published reports described the pharmacokinetics (1) and pharmacodynamics (2) of atenolol, 2-[*p*-[2-hydroxy-3-(isopropylamino)propoxy]phenyl]acetamide, a new cardioselective (3–5) β-adrenergic blocking agent. More than 90% of the bioavailable dose of atenolol is excreted unchanged in the urine within 48 hr of dosing (6). To study the relationship of pharmacokinetics to pharmacodynamics, a two-phase complete crossover design was employed, with the phases differing only in the amount of exercise required of the subjects. A difference in the kinetics of atenolol between the two phases (exercise *versus* nonexercise) is reported.

EXPERIMENTAL

The 12 healthy male volunteers were 20–28 years old and weighed 63.6–85.5 kg (140–188 lb). Each subject was judged healthy based on the absence of any abnormality in his history, physical examination, ECG, hemogram, blood chemistries, and urinalysis.

The study design was a two-phase complete crossover, with the treatments being identical except for the exercise performed by each subject. Following a 10-hr fast, each subject received 100 mg of atenolol as an oral solution in 240 ml of water. The fast continued until after the 4th-hr blood sample was drawn; a standard meal was served at the 5th hr. Following the meal, water was allowed *ad libitum*. Blood samples were collected at 0, 0.5, 1.0, 2.0, 3.0, 4.0, 6.0, 8.0, 10.0, 12.0, 14.0, and 24.0 hr. Urine was collected prior to dosing, from 0.0 to 12.0 hr, and from 12.0 to 24.0 hr.

Plasma and urine atenolol levels were determined by a high-pressure liquid chromatographic (HPLC) method described previously (7) and modified as follows. The mobile phase consisted of a 4.00 m*M* solution of 1-heptanesulfonic acid sodium salt, 1.0% acetic acid, and 60.0% methanol in distilled water. The mobile phase was pumped at 1.5 ml/min and 20° through a stainless steel column packed with a high efficiency bonded-phase packing[1]. Aliquots of 150 μl of the reextraction solution were injected directly on-column through the injector. The atenolol peak was well separated from the procainamide internal standard peak and from artifacts. The retention times of atenolol and procainamide were 5.8 and 12.3 min, respectively.

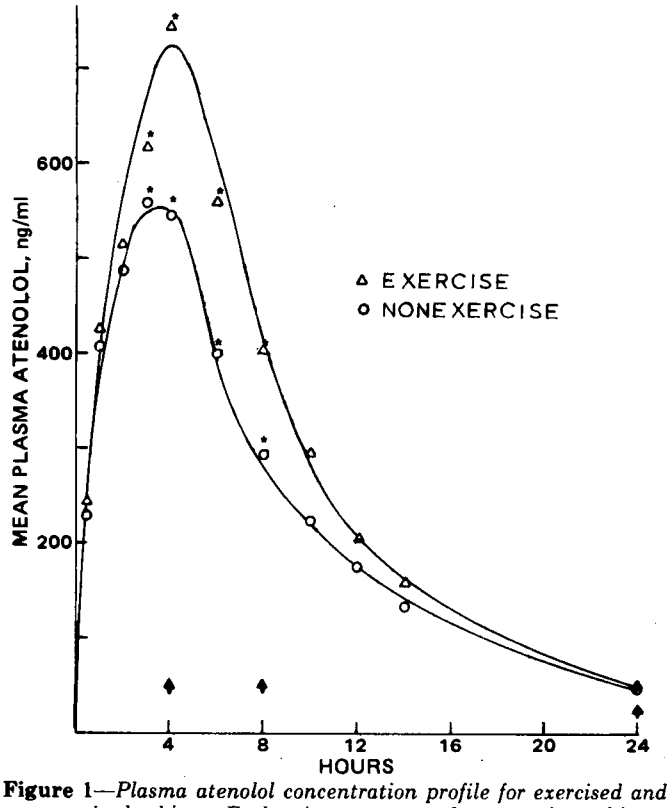

Figure 1—*Plasma atenolol concentration profile for exercised and nonexercised subjects. Each point represents the mean of 12 subjects. Starred (*) points represent significant differences ($p < 0.05$) between exercised and nonexercised subjects. Arrows indicate times of exercise.*

[1] Spherisorb 5-μm ODS, Laboratory Data Control, Riviera Beach, Fla.

0022-3549/80/0300-0344$01.00/0

© 1980, American Pharmaceutical Association

Table I—Bruce Protocol

Stage	Speed, mph	Grade, %	Duration, min	Total Time Elapsed, min
1	1.7	10	3	3
2	2.5	12	3	6
3	3.4	14	3	9
4	4.2	16	3	12

Table II—Plasma Atenolol Concentrations for Nonexercise Treatment *versus* Exercise Treatment

Hours	Nonexercise, ng/ml Mean	Nonexercise, ng/ml *SD*	Exercise, ng/ml Mean	Exercise, ng/ml *SD*	Statistics[a]
0.0	0.0	0.0	0.0	0.0	
0.5	229	94.1	244	200	NS
1.0	408	105	428	171	NS
2.0	488	161	515	205	NS
3.0	560	228	618	204	NS
4.0	547	188	746	222	S
6.0	400	168	561	157	S
8.0	296	89.5	403	105	S
10.0	226	72.7	297	79.0	S
12.0	177	56.3	207	53.4	NS
14.0	135	43.9	161	41.9	NS
24.0	49.1	13.3	51.6	21.2	NS
$AUC^{0\rightarrow 24}$[b], μg hr/ml	5.53	1.79	6.85	1.74	S
X_u^{24}[c], mg	49.4	15.7	56.1	12.3	NS
X_u^{12}[d], mg	39.4	13.4	42.0	13.3	NS
Cl_R[e], ml/min	150	18.6	139	14.3	S

[a] S denotes significant difference at 0.05 significance level by analysis of variance; NS denotes no significant difference. [b] Area under the plasma concentration–time profile from 0 to 24 hr. [c] Amount of drug collected in the urine in 24 hr. [d] Amount of drug collected in the urine in 12 hr. [e] Renal clearance = $X_u^{0\rightarrow 24}/AUC^{0\rightarrow 24}$ hr.

During the nonexercise phase, the subjects remained in a sitting or standing position while confined to a small room. Subjects were confined for the entire 24-hr period of each phase of the study. The exercise phase consisted of the four stages of the Bruce protocol (8) (Table I) prior to dosing and at 4, 8, and 24 hr following each dose.

The mean heart rate for the 12 subjects prior to atenolol administration was 174 beats/min at Stage 4 of exercise. Volunteers in the exercise group were subjected to further physical exertion by the need to walk from their location up one flight of stairs to the treadmill, a distance of 114.3 m (375 ft). The subjects then rested until a resting pulse was attained, and treadmill exercise was then performed.

RESULTS AND DISCUSSION

Table II and Fig. 1 present the mean plasma and urine atenolol with the individual and mean areas under the plasma–time profiles and the calculated renal clearances for each treatment with the corresponding statistics. Analysis of variance showed differences at the 4-, 6-, 8-, and 10-hr times in plasma atenolol ($p < 0.05$) such that plasma atenolol was higher during exercise. The $AUC^{0\rightarrow 24}$ and Cl_R also showed significant ($p < 0.05$) differences. All other times and $X_u^{0\rightarrow 24}$ did not show significant differences. Since the total amount of atenolol excreted in 24 hr did not differ between exercised and nonexercised subjects and the area under the curve ($AUC^{0\rightarrow 24}$) was significantly increased during exercise ($p < 0.05$), the computed renal clearance decreased during exercise.

With the commencement of exercise at 4 hr, a change in plasma atenolol was attained. This result is consistent with the fact that the change in $AUC^{0\rightarrow 24}$ and Cl_R with exercise is due to the exercising condition and not some other factor. Urinary recovery of atenolol verified previous recoveries (1), consistent with published results showing orally administered atenolol to be 0.58 ± 0.16 bioavailable.

The decrease in renal clearance of atenolol of ~8% can possibly be explained by changes in renal plasma flow. Decreases of up to 35% normal renal plasma flow were noted in a similar treadmill test as the Bruce treadmill protocol (9–11). During exercise, neurogenic and hormonal influences shunt blood away from the kidney to other areas (*i.e.*, heart, brain, and skeletal muscle). Since atenolol is essentially totally eliminated *via* the kidney, a decrease in renal clearance, Cl_R, would be expected during exercise.

A review (12) of the interrelationships among renal hemodynamics, drug kinetics, and drug action described the potential effects of reduced renal blood flow on the clearance and distribution of drugs but did not directly address the potential effects of exercise. Little is known of the effects of exercise on drug kinetics. An 8% increase in plasma atenolol during exercise would probably not be therapeutically significant, but it does demonstrate the importance of controlling exercise levels during pharmacokinetic and bioavailability studies.

REFERENCES

(1) W. D. Mason, N. Winer, G. Kochak, and I. Cohen, *Clin. Pharmacol. Ther.*, **25**, 408 (1979).

(2) N. Winer, W. D. Mason, C. H. Carter, T. L. Willoughby, G. Kochak, I. Cohen, and R. Bell, *ibid.*, **26**, 315 (1979).

(3) A. M. Barret, J. Carter, J. D. Fitzgerald, R. Hull, and D. DeCount, *Br. J. Clin. Pharmacol.*, **2**, 527 (1975).

(4) J. D. Harry, M. F. Knapp, and R. J. Linder, *Br. J. Pharmacol.*, **48**, 340 (1973).

(5) R. Hainsworth, F. Karim, and J. B. Stocker, *ibid.*, **48**, 342 (1973).

(6) J. C. Brown, S. G. Carruthers, G. D. Johnston, J. G. Kelly, J. McAnish, D. G. McDevitt, and R. G. Shanks, *ibid.*, **20**, 524 (1976).

(7) O. H. Weddle, E. N. Amick, and W. D. Mason, *J. Pharm. Sci.*, **67**, 1033 (1978).

(8) R. A. Bruce, J. R. Blackmon, J. W. Jones, and G. Strait, *Pediatrics, Suppl.*, **32**, 742 (1963).

(9) C. B. Chapman, A. Henschel, J. Minckler, A. Forsgren, and A. Keys, *J. Clin. Invest.*, **27**, 639 (1948).

(10) G. Grimby, *J. Appl. Physiol.*, **20**, 1294 (1965).

(11) C. B. Chapman, A. Henschel, and A. Forsgren, *Proc. Soc. Exp. Biol. Med.*, **69**, 170 (1948).

(12) K. L. Duchin and R. W. Schrier, *Clin. Pharmacokinet.*, **3**, 58 (1978).

Colorimetric Determination of Procaine Hydrochloride in Pharmaceutical Preparations

R. B. SALAMA *x and A. I. H. OMER ‡

Received June 16, 1978, from the **Department of Pharmaceutical Chemistry, University of Khartoum, Khartoum, Sudan,* and the ‡*Chemical Laboratories, Ministry of Health, Khartoum, Sudan.* Accepted for publication October 1, 1979.

Abstract □ A new rapid, specific, and convenient colorimetric method for the determination of procaine hydrochloride in pharmaceutical preparations is described. This method is based on measurement of the intensity of the orange-red color developed when procaine hydrochloride is allowed to react with 1,2-naphthoquinone-4-sulfonic acid sodium salt in aqueous solution. Beer's law is followed over 6.0–20.0 μg/ml. The method was applied to the determination of procaine hydrochloride in procaine hydrochloride, procaine hydrochloride injection with or without epinephrine, penicillin G procaine, penicillin G procaine injection, and fortified procaine penicillin injection (BP). The results were comparable to those obtained by official procedures. Because of its simplicity, sensitivity, and accuracy, this method is particularly suited for routine analysis of official preparations of procaine hydrochloride.

Keyphrases □ Procaine hydrochloride—colorimetric assay using 1,2-naphthoquinone-4-sulfonic acid sodium salt □ Colorimetry—analysis, procaine hydrochloride reaction with 1,2-naphthoquinone-4-sulfonic acid sodium salt

The USP (1) and BP (2) methods for the determination of procaine hydrochloride depend on diazotization and titration of the compound with standard sodium nitrite solution. For procaine hydrochloride injection, the USP assay requires prior isolation of the procaine by solvent extraction and then determination of the procaine spectrophotometrically (3). The BP (4) method for the determination of procaine hydrochloride in procaine hydrochloride injection depends on solvent extraction of the procaine from alkaline solution followed by acid–base titration. Both methods are lengthy and involve solvent extractions.

The BP (5) methods for the determination of procaine in penicillin G procaine, penicillin G procaine injection, and fortified procaine penicillin injection are all similar, depending on solvent extraction followed by acid–base titration. The method is lengthy and lacks sensitivity.

A colorimetric method for the determination of procaine hydrochloride was developed recently (6) based on the interaction of procaine hydrochloride with *p*-dimethylaminocinnamaldehyde in the presence of trichloroacetic acid in absolute methanol. This method requires a nonaqueous acidic medium.

A simple, time-saving, and sensitive method for the determination of procaine in pharmaceutical preparations is needed. The proposed method depends on the reaction between procaine hydrochloride and 1,2-naphthoquinone-4-sulfonic acid sodium salt in aqueous solution. 1,2-Naphthoquinone-4-sulfonic acid sodium salt was reported previously (7) to be a detecting agent for aromatic amines on TLC plates.

EXPERIMENTAL

Instruments—A visible UV spectrophotometer[1] was used.

Materials and Reagents—The following were used: procaine hydrochloride[2]; a 0.1% solution of 1,2-naphthoquinone-4-sulfonic acid sodium salt in water[3]; a 2% procaine hydrochloride injection; a 2% procaine hydrochloride injection containing 0.002% epinephrine; a procaine and epinephrine injection[4] containing 2.0% procaine hydrochloride, 0.002% epinephrine, 0.2% sodium chloride, 0.3% potassium sulfate, and 0.002% phenylmercuric nitrate; penicillin G procaine[5]; a penicillin G procaine injection containing 300 mg of penicillin G procaine; fortified penicillin and penicillin G (sodium salt), 60 mg; and fortified penicillin G injection BP[6].

Calibration Curve Preparation—Several aliquots of exactly 2.0–10.0 ml of procaine hydrochloride solution (100 μg/ml) were pipetted into 50-ml volumetric flasks. Then 20 ml of water and 2.0 ml of 1,2-naphthoquinone-4-sulfonic acid sodium salt were added. Each flask was mixed well, let stand for 60 min, and diluted to volume with water. The absorbance was measured at 482 nm in a 1-cm cell against a blank prepared under the same conditions but without procaine hydrochloride.

Table I—Effect of Time on Absorbance of Procaine Hydrochloride [a]–1,2-Naphthoquinone-4-sulfonic Acid Sodium Salt Color Complex

Minutes	Absorbance at 482 nm
10	0.202
20	0.222
30	0.240
40	0.250
50	0.260
60	0.260
120	0.262
180	0.260

[a] Concentration of 16 μg of procaine hydrochloride/ml.

Table II—Effect of pH on Absorbance of Procaine Hydrochloride–1,2-Naphthoquinone-4-sulfonic Acid Sodium Salt Color Complex [a]

pH	Absorbance at 482 nm
4	0.198
5	0.200
6	0.198
7	0.200
8	0.201
9	0.200
10	0.105

[a] Concentration of 12 μg of procaine hydrochloride/ml.

Table III—Reproducibility of Color Development of Replicate Samples of Procaine Hydrochloride Containing 6, 12, or 18 μg/ml (n = 10)

Concentration, μg/ml	Mean Absorbance at 482 nm	*CV*, %
6	0.0986	1.190
12	0.2001	0.684
18	0.2995	0.452

[1] DU-2, Beckman Instruments, Fullerton, Calif.

[2] BDH Laboratory, Poole, England.
[3] Fluka AG, Buchs SG, Switzerland.
[4] Planocaine, May and Baker Ltd., Dagenham, England.
[5] WHO, Geneva, Switzerland.
[6] Scurocilline, Specia, Paris, France.

0022-3549/80/0300-0346$01.00/0
© 1980, American Pharmaceutical Association

Table IV—Comparative Analysis of Preparations Containing Procaine Hydrochloride

Preparation	Labeled Amount, mg/ml	Amount Found, mg/ml[a] USP Method	BP Method	Proposed Method
Procaine hydrochloride, 2.0%	20.0	19.90 (CV = 0.34%)	19.93 (CV = 0.45%)	20.00 (CV = 0.25%)
Procaine hydrochloride, 2%, + 0.002% epinephrine	20.0	20.10 (CV = 0.66%)	19.91 (CV = 1.07%)	19.95 (CV = 0.66%)
Procaine hydrochloride, 2%, + 0.002% epinephrine + 0.2% sodium chloride + 0.3% potassium sulfate + 0.002% phenylmercuric nitrate	20.0	20.20 (CV = 0.74%)	19.81 (CV = 1.06%)	20.10 (CV = 0.20%)
Procaine hydrochloride, 2%, + 0.002% epinephrine + 5% sodium chloride + 0.1% chlorocresol	20.0	20.10 (CV = 1.79%)	19.70 (CV = 0.62%)	20.10 (CV = 0.50%)
Penicillin G procaine injection, 300,000 IU	139		130.00 (CV = 1.38%)	135.00 (CV = 0.74%)

[a] Mean of three results.

Table V—Recovery of Procaine Hydrochloride

Preparation	Procaine Hydrochloride, mg	Found, mg	Added, mg	Found after Addition, mg	Recovery, %
Injection (without epinephrine)	20	20.05	10.0	30.1	100.5
Injection (with epinephrine)	20	19.95	20.0	39.9	99.75
Solution	50	50.15	50.0	100.4	100.5

Procaine Hydrochloride—One hundred milligrams, accurately weighed, of procaine hydrochloride was dissolved in water to produce 100 ml. Then 0.8 ml of this solution was pipetted into a 50-ml volumetric flask, and the procedure described for the calibration curve was followed. The amount of procaine hydrochloride was calculated from the calibration curve.

Procaine Hydrochloride Injection with or without Epinephrine—Five milliliters of a 2% procaine hydrochloride injection was pipetted into a 100-ml volumetric flask and diluted to volume with water. Then 0.8 ml of this solution was pipetted into a 50-ml volumetric flask, and the procedure described for the calibration curve was followed. The amount of procaine hydrochloride was calculated from the calibration curve.

Penicillin G Procaine—Three hundred milligrams[7] of penicillin G procaine was dissolved in water to produce 100 ml. Then 0.5 ml of this solution was pipetted into a 50-ml volumetric flask, and the procedure described for the calibration curve was followed. The amount of procaine hydrochloride was calculated from the calibration curve.

Penicillin G Procaine Injection—An accurately measured volume of a well-shaken suspension, equivalent to 300 mg of penicillin G procaine, was diluted to 100 ml with water. Then 0.5 ml of this solution was pipetted into a 50-ml volumetric flask, and the procedure described for the calibration curve was followed. The amount of procaine hydrochloride was calculated from the calibration curve.

Fortified Procaine Penicillin Injection (BP)—The contents of the vial (containing 300 mg of penicillin procaine and 60 mg of penicillin G) were dissolved in water to produce 100 ml. Then 0.5 ml of this solution was pipetted into a 50-ml volumetric flask, and the procedure described for the calibration curve was followed. The amount of procaine hydrochloride was calculated from the calibration curve.

Interferences—The effect of epinephrine, sodium chloride, potassium sulfate, phenylmercuric nitrate, chlorocresol, and sodium metabisulfite on the determination of procaine hydrochloride was determined by preparing solutions containing these substances plus a known amount of procaine hydrochloride and performing the analysis according to the procedure for procaine hydrochloride. The effect of penicillin G on the determination of procaine in penicillin G procaine preparation was studied similarly.

RESULTS AND DISCUSSION

A characteristic orange-red color with an absorbance maximum at 482 nm developed when procaine hydrochloride was reacted with 1,2-naphthoquinone-4-sulfonic acid sodium salt in aqueous medium. When the observed absorbances were plotted against concentrations, a linear calibration curve with a slope of 0.01636 was obtained over the concentration range of 6.0–20.0 μg/ml, indicating obedience to Beer's law. This linearity was also confirmed when the correlation coefficient, r, was calculated from the values of absorbances and concentrations and was 0.9991.

The color reached maximum intensity after 60 min and remained stable for at least an additional 2 hr (Table I).

The effect of pH on the color intensity was studied. It was stable between pH 4 and 9 but dropped suddenly at pH 10 (Table II). Therefore, buffers were not used to adjust the pH since the method could be used at any pH between 4 and 9.

The concentration optimum of the color reagent was determined by adding various volumes of 0.1% 1,2-naphthoquinone-4-sulfonic acid sodium salt reagent to a series of 50-ml volumetric flasks, each containing 800 μg of procaine hydrochloride, diluting to volume with water, and measuring the absorbance of each solution at 482 nm against a blank[8]. Maximum color intensity was obtained with 1.5 ml of the reagent. Increasing the volume to 4.0 ml did not increase the absorbance. Therefore, it was decided to use 2.0 ml as the optimum concentration.

The precision study was performed at three different concentrations, 6, 12, and 18 μg/ml, by running 10 replicates of each. The coefficients of variation were 1.190, 0.684, and 0.452%, respectively (Table III).

The proposed method was compared to the official methods for prepared and commercially available procaine hydrochloride pharmaceutical preparations. There was a close relationship between the results obtained by the official procedures and those obtained by the suggested method (Table IV).

Samples of procaine hydrochloride preparation were analyzed before and after the addition of known quantities of procaine hydrochloride solution (Table V). The recovery data obtained proved that the suggested method is accurate. Temperature change had an insignificant effect on chromophore formation.

The presence of epinephrine, penicillin G, sodium chloride, potassium sulfate, phenylmercuric nitrate, chlorocresol, and sodium metabisulfite in the concentrations used produced no effect on the development, intensity, or stability of the color and, therefore, had no effect on the colorimetric assay.

REFERENCES

(1) "The United States Pharmacopeia," 19th rev., Mack Publishing Co., Easton, Pa., 1975, p. 408.

[7] Equivalent to 139.0 mg of procaine hydrochloride.

[8] Each blank contained the same amount of 1,2-naphthoquinone-4-sulfonic acid sodium salt reagent as in the solution studied.

(2) "British Pharmacopoeia 1973," Her Majesty's Stationery Office, London, England, 1973, p. 385.
(3) "The United States Pharmacopeia," 19th rev., Mack Publishing Co., Easton, Pa., 1975, p. 409.
(4) "British Pharmacopoeia 1973," Her Majesty's Stationery Office, London, England, 1973, p. 386.
(5) *Ibid.*, p. 387.
(6) H. S. I. Tan and D. Shelton, *J. Pharm. Sci.*, **63**, 916 (1974).
(7) R. B. Smyth and G. G. McKeown, *J. Chromatogr.*, **16**, 454 (1964).

Quantitation of Acetazolamide in Plasma by High-Performance Liquid Chromatography

R. D. HOSSIE ˣ, N. MOUSSEAU, S. SVED, and R. BRIEN

Received August 20, 1979, from the *Drug Research Laboratories, Health Protection Branch, Health and Welfare Canada, Tunney's Pasture, Ottawa, Ontario K1A 0L2, Canada.* Accepted for publication October 5, 1979.

Abstract □ A method for estimating acetazolamide concentrations in human plasma is described. Buffered plasma (pH 4.8) containing chlorothiazide as an internal standard is extracted twice with ethyl acetate. The extract is evaporated, redissolved, and chromatographed on silica gel with hexane–chloroform–methanol–acetic acid (65:25:10:0.25) as the mobile phase. The extraction efficiencies were >90%, the coefficients of variation at 1 and 30 μg/ml of plasma were 3.5 and 2.0%, respectively, and the calibration curves were linear and had an intercept of essentially zero. The suitability of the method for pharmacokinetic studies was verified in a normal volunteer dosed with 250-mg (solution) and 500-mg (sustained-release tablet) acetazolamide formulations.

Keyphrases □ Acetazolamide—analysis, high-performance liquid chromatography, plasma □ High-performance liquid chromatography—analysis, acetazolamide, plasma □ Carbonic anhydrase inhibitors—acetazolamide, high-performance liquid chromatography, plasma

Acetazolamide, a carbonic anhydrase inhibitor, is used to decrease the ocular aqueous humor secretion in certain types of glaucoma. Methods for the quantitation of this drug in biological fluids include measurement of the carbonic anhydrase inhibition (1, 2), colorimetry (3, 4), electron-capture GLC (5), and high-performance liquid chromatography (HPLC) (6). However, the GLC and HPLC procedures are time consuming (2), the colorimetric method is only partially successful (4, 6), and the modified enzymatic assay (2) lacks sufficient precision.

The present study was undertaken to develop an assay without the described deficiencies that could be used to quantitate acetazolamide in human or animal plasma following administration of single doses of 250 mg of a regular acetazolamide formulation or 500 mg of a sustained-release formulation.

EXPERIMENTAL

Materials—Hexane, chloroform, and methanol were HPLC grade[1,2]. Acetazolamide and chlorothiazide were USP reference standards. Sodium acetate, ethyl acetate, sodium bicarbonate, sodium hydroxide, and acetic acid were reagent grade.

One oral acetazolamide solution, used in the plasma profile experiments, was prepared by dissolving 250 mg of the USP standard in 20 ml of ethanol and diluting to 200 ml with fresh aqueous sodium bicarbonate (0.1 *M*). The final pH was 8. Another oral solution, used in determining the absence of interference, was prepared by dissolving a commercial parenteral preparation[3] in water.

Subjects—After an overnight fast, a healthy, 40-year-old male subject (90 kg) was administered 200 ml of the solution (250 mg) and separately one commercial 500-mg sustained-release formulation[3] with 150–250 ml of water at a 1-week interval.

Blood samples (10 ml) were collected in heparinized evacuated containers[4] at the various times (Figs. 1 and 2). The samples were centrifuged at 1000×*g*, and the separated plasma was stored at −18° until analysis.

Method—To tubes containing 1 ml of plasma were added 0.5 ml of internal standard (20 μg of chlorothiazide/ml of water), 2 ml of sodium acetate buffer (0.05 *M*, pH 4.8), and 10 ml of ethyl acetate. After mixing[5] for 10 min and centrifuging for 10 min at 1000×*g*, the organic layer was removed, and the extraction steps were repeated. The combined organic layers were evaporated at 60° to dryness using a nitrogen stream. After the residue was dissolved in 10 μl of 0.45 *N* NaOH by mixing[6], 1 ml of ethyl acetate was added, and the contents were mixed again. Aliquots (200 μl) of this solution were chromatographed.

The HPLC system consisted of a pump, an injector, and a detector[7] set at 280 nm. The silica gel column[8] (5 μm, 3.2 × 250 mm) was packed using a balanced density slurry method. The mobile phase was hexane–chloroform–methanol–acetic acid (65:25:10:0.25) at a flow rate of 3 ml/min (2900 psi). Quantitation was achieved by measuring the peak height ratio of the drug to the internal standard.

Calibration Curve—The linearity of the calibration curve was determined by adding 0.5, 2, 4, 8, and 12 μg of acetazolamide/ml to blank plasma samples. Two aliquots of each concentration were assayed as described. The coefficients of variation were determined using replicate samples of plasma standards containing 1 and 30 μg of acetazolamide/ml.

Determination of Extraction Efficiency—The extraction efficiency for the drug was estimated from the change in the peak height ratio when the drug was added to the plasma while the internal standard was added to the final extract compared to the peak height ratio when both were added to the final extract. The extraction efficiency for the internal standard was estimated from the change in the peak height ratio when the internal standard was added to the plasma while the drug was added to the final extract compared to the peak height ratio when both were added to the final extract.

Absence of Interferences—To verify the absence of metabolites and naturally occurring plasma constituents interfering with the internal standard or drug, plasma samples obtained from another volunteer 2 and 2.5 hr after ingestion of 500 mg of acetazolamide solution were pooled and extracted without the internal standard and chromatographed.

The effluents containing acetazolamide were combined and evaporated. One aliquot was rechromatographed on the same column using hexane–chloroform–methanol–acetic acid (70:25:5:0.25) as the mobile phase at a flow rate of 3 ml/min. Another aliquot was injected onto a bonded amino-silica gel column[9] (10 μm, 4.0 × 300 mm) using a mobile

[1] Burdick & Jackson Laboratories, Muskegon, Mich.
[2] Fisher Scientific, Ottawa, Canada.
[3] Diamox, Lederle, Canadian Cyanamide Ltd., Montreal, Canada.
[4] Vacutainers, Becton Dickinson, purchased through Canlab, Ottawa, Canada.
[5] Roto-rack, Fisher Scientific.
[6] Vortex, Fisher Scientific.
[7] Models 6000A, U6K, and 440, Waters Associates, Mississauga, Ontario, Canada.
[8] Li-Chrosorb Si-60, 5 μm, Brinkmann Instruments, Rexdale, Ontario, Canada.
[9] μBondapak-NH_2, Waters Associates.

0022-3549/80/0300-0348$01.00/0
© 1980, American Pharmaceutical Association

(2) "British Pharmacopoeia 1973," Her Majesty's Stationery Office, London, England, 1973, p. 385.
(3) "The United States Pharmacopeia," 19th rev., Mack Publishing Co., Easton, Pa., 1975, p. 409.
(4) "British Pharmacopoeia 1973," Her Majesty's Stationery Office, London, England, 1973, p. 386.
(5) *Ibid.*, p. 387.
(6) H. S. I. Tan and D. Shelton, *J. Pharm. Sci.*, **63**, 916 (1974).
(7) R. B. Smyth and G. G. McKeown, *J. Chromatogr.*, **16**, 454 (1964).

Quantitation of Acetazolamide in Plasma by High-Performance Liquid Chromatography

R. D. HOSSIE ˣ, N. MOUSSEAU, S. SVED, and R. BRIEN

Received August 20, 1979, from the *Drug Research Laboratories, Health Protection Branch, Health and Welfare Canada, Tunney's Pasture, Ottawa, Ontario K1A 0L2, Canada.* Accepted for publication October 5, 1979.

Abstract □ A method for estimating acetazolamide concentrations in human plasma is described. Buffered plasma (pH 4.8) containing chlorothiazide as an internal standard is extracted twice with ethyl acetate. The extract is evaporated, redissolved, and chromatographed on silica gel with hexane–chloroform–methanol–acetic acid (65:25:10:0.25) as the mobile phase. The extraction efficiencies were >90%, the coefficients of variation at 1 and 30 μg/ml of plasma were 3.5 and 2.0%, respectively, and the calibration curves were linear and had an intercept of essentially zero. The suitability of the method for pharmacokinetic studies was verified in a normal volunteer dosed with 250-mg (solution) and 500-mg (sustained-release tablet) acetazolamide formulations.

Keyphrases □ Acetazolamide—analysis, high-performance liquid chromatography, plasma □ High-performance liquid chromatography—analysis, acetazolamide, plasma □ Carbonic anhydrase inhibitors—acetazolamide, high-performance liquid chromatography, plasma

Acetazolamide, a carbonic anhydrase inhibitor, is used to decrease the ocular aqueous humor secretion in certain types of glaucoma. Methods for the quantitation of this drug in biological fluids include measurement of the carbonic anhydrase inhibition (1, 2), colorimetry (3, 4), electron-capture GLC (5), and high-performance liquid chromatography (HPLC) (6). However, the GLC and HPLC procedures are time consuming (2), the colorimetric method is only partially successful (4, 6), and the modified enzymatic assay (2) lacks sufficient precision.

The present study was undertaken to develop an assay without the described deficiencies that could be used to quantitate acetazolamide in human or animal plasma following administration of single doses of 250 mg of a regular acetazolamide formulation or 500 mg of a sustained-release formulation.

EXPERIMENTAL

Materials—Hexane, chloroform, and methanol were HPLC grade[1,2]. Acetazolamide and chlorothiazide were USP reference standards. Sodium acetate, ethyl acetate, sodium bicarbonate, sodium hydroxide, and acetic acid were reagent grade.

One oral acetazolamide solution, used in the plasma profile experiments, was prepared by dissolving 250 mg of the USP standard in 20 ml of ethanol and diluting to 200 ml with fresh aqueous sodium bicarbonate (0.1 *M*). The final pH was 8. Another oral solution, used in determining the absence of interference, was prepared by dissolving a commercial parenteral preparation[3] in water.

Subjects—After an overnight fast, a healthy, 40-year-old male subject (90 kg) was administered 200 ml of the solution (250 mg) and separately one commercial 500-mg sustained-release formulation[3] with 150–250 ml of water at a 1-week interval.

Blood samples (10 ml) were collected in heparinized evacuated containers[4] at the various times (Figs. 1 and 2). The samples were centrifuged at 1000×*g*, and the separated plasma was stored at −18° until analysis.

Method—To tubes containing 1 ml of plasma were added 0.5 ml of internal standard (20 μg of chlorothiazide/ml of water), 2 ml of sodium acetate buffer (0.05 *M*, pH 4.8), and 10 ml of ethyl acetate. After mixing[5] for 10 min and centrifuging for 10 min at 1000×*g*, the organic layer was removed, and the extraction steps were repeated. The combined organic layers were evaporated at 60° to dryness using a nitrogen stream. After the residue was dissolved in 10 μl of 0.45 *N* NaOH by mixing[6], 1 ml of ethyl acetate was added, and the contents were mixed again. Aliquots (200 μl) of this solution were chromatographed.

The HPLC system consisted of a pump, an injector, and a detector[7] set at 280 nm. The silica gel column[8] (5 μm, 3.2 × 250 mm) was packed using a balanced density slurry method. The mobile phase was hexane–chloroform–methanol–acetic acid (65:25:10:0.25) at a flow rate of 3 ml/min (2900 psi). Quantitation was achieved by measuring the peak height ratio of the drug to the internal standard.

Calibration Curve—The linearity of the calibration curve was determined by adding 0.5, 2, 4, 8, and 12 μg of acetazolamide/ml to blank plasma samples. Two aliquots of each concentration were assayed as described. The coefficients of variation were determined using replicate samples of plasma standards containing 1 and 30 μg of acetazolamide/ml.

Determination of Extraction Efficiency—The extraction efficiency for the drug was estimated from the change in the peak height ratio when the drug was added to the plasma while the internal standard was added to the final extract compared to the peak height ratio when both were added to the final extract. The extraction efficiency for the internal standard was estimated from the change in the peak height ratio when the internal standard was added to the plasma while the drug was added to the final extract compared to the peak height ratio when both were added to the final extract.

Absence of Interferences—To verify the absence of metabolites and naturally occurring plasma constituents interfering with the internal standard or drug, plasma samples obtained from another volunteer 2 and 2.5 hr after ingestion of 500 mg of acetazolamide solution were pooled and extracted without the internal standard and chromatographed.

The effluents containing acetazolamide were combined and evaporated. One aliquot was rechromatographed on the same column using hexane–chloroform–methanol–acetic acid (70:25:5:0.25) as the mobile phase at a flow rate of 3 ml/min. Another aliquot was injected onto a bonded amino-silica gel column[9] (10 μm, 4.0 × 300 mm) using a mobile

[1] Burdick & Jackson Laboratories, Muskegon, Mich.
[2] Fisher Scientific, Ottawa, Canada.
[3] Diamox, Lederle, Canadian Cyanamide Ltd., Montreal, Canada.
[4] Vacutainers, Becton Dickinson, purchased through Canlab, Ottawa, Canada.
[5] Roto-rack, Fisher Scientific.
[6] Vortex, Fisher Scientific.
[7] Models 6000A, U6K, and 440, Waters Associates, Mississauga, Ontario, Canada.
[8] Li-Chrosorb Si-60, 5 μm, Brinkmann Instruments, Rexdale, Ontario, Canada.
[9] μBondapak-NH_2, Waters Associates.

0022-3549/80/0300-0348$01.00/0
© 1980, American Pharmaceutical Association

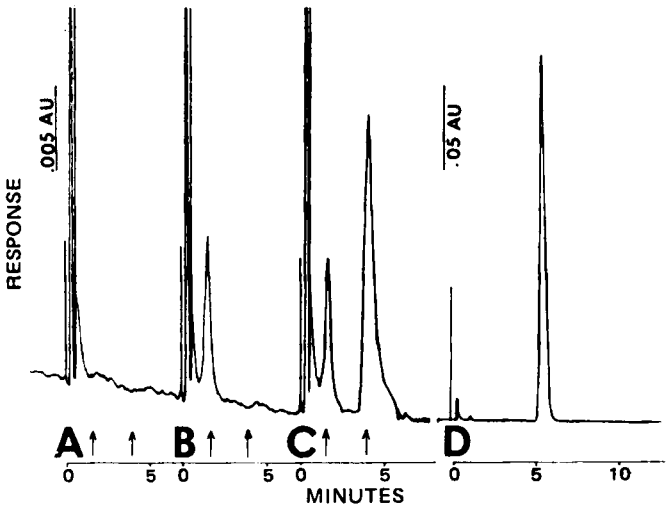

Figure 1—*Chromatograms of plasma extracts. Key: A, blank plasma; B and C, plasma of a human volunteer 4.5 hr after administration of 250 mg of an oral acetazolamide solution without (B) and with (C) the internal standard (estimated concentration, 6.03 μg/ml); and D, rechromatography of pooled acetazolamide peaks. Samples A, B, and C were chromatographed on a silica gel column with a mobile phase of hexane–chloroform–methanol–acetic acid (65:25:10:0.25). Sample D was chromatographed on a bonded amino-silica gel column with a mobile phase of 20% methanol in 0.01* M *ammonium formate. The expected locations of the drug and the internal standard are marked by arrows.*

phase of 20% methanol in 0.01 *M* aqueous ammonium formate at a flow rate of 2 ml/min.

RESULTS AND DISCUSSION

Preliminary experiments demonstrated the need for acetic acid in the mobile phase. In its absence, the peak height ratio of the drug to the internal standard diminished on successive injections of plasma extract, which may have been due to an accumulation of interfering substances. However, inclusion of acetic acid maintained the constancy of the peak height ratio in new columns, and old columns were restored to their original conditions by thorough flushing with the acidic mobile phase. Bayne *et al.* (6) had a similar problem with their acetazolamide assay. They attempted to overcome the problem by injecting alcohol between injections of the plasma extract. Unfortunately, in the present investigation this alcohol injection increased the analysis time and was not always successful.

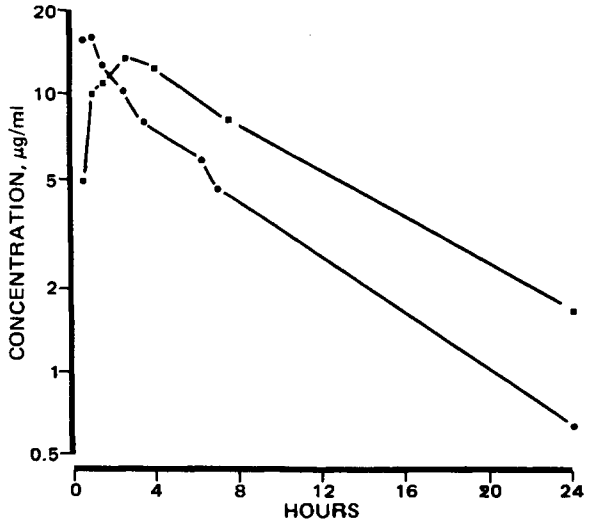

Figure 2—*Plasma concentration profiles of acetazolamide in a volunteer following the oral administration of 250 mg in solution (●) and a 500-mg sustained-release tablet (■).*

Table I—Typical Acetazolamide Calibration Curve

Drug Added, μg/ml	Peak Height Ratio[a]	Ratio[b]
0.5	0.062	0.125
2.0	0.264	0.132
4.0	0.521	0.130
8.0	1.043	0.130
12.0	1.595	0.133

[a] Ratio of the drug to the internal standard. [b] Ratio of the peak height ratio to the drug concentration.

The final method was evaluated in terms of extraction efficiency, interferences, linearity, and precision. The extraction efficiency of acetazolamide from plasma to ethyl acetate was 94% while that for chlorothiazide was 91%. Neither naturally occurring plasma constituents nor metabolites interfered with the peak height determination of either the drug or the internal standard. With blank plasma, when the internal standard was eliminated from the assay, no peaks absorbing at 280 nm and having the same retention times as acetazolamide or chlorothiazide were observed (Fig. 1A). Plasma extracts from a volunteer 4.5 hr after ingestion of 250 mg of drug (Fig. 1B) showed no peak with a retention time similar to that of the internal standard. Furthermore, the pooled effluents corresponding to the acetazolamide peak from the plasma of a volunteer 2–2.5 hr after a 500-mg drug dose showed a single peak when rechromatographed using a different column and mobile phase (Fig. 1D).

A typical calibration curve is shown in Table I. The excellent linearity of the method is illustrated by the constant values of the ratio of the peak height ratio to the drug concentration. The regression of the peak height ratio against drug concentrations gave a slope (±95% confidence interval) of 0.13 (±0.003) ml/μg and a peak height ratio intercept of nearly zero (−0.006 ± 0.02). In another series of experiments, the coefficients of variation determined at 1 and 30 μg/ml (n = 5 and 6, respectively) were 3.5 and 2.0%, respectively.

The suitability of the method for studying acetazolamide pharmacokinetics following single-dose administration was ascertained by administering separately 250 mg of the drug in solution and 500 mg in a sustained-release formulation to a normal human volunteer (Fig. 2). The solution showed rapid absorption with apparently biphasic elimination. A peak concentration of 16 μg/ml was produced at 1 hr compared to the lower peak concentration (13 μg/ml) produced at 2.5 hr with the larger dose, sustained-release product. These figures are in good agreement with values published previously (7).

This assay is relatively quick and precise and is not subject to interference either from metabolites or from naturally occurring plasma constituents.

REFERENCES

(1) T. H. Maren, *J. Pharmacol. Exp. Ther.*, **130**, 26 (1960).

(2) G. J. Yakatan, C. A. Martin, and R. V. Smith, *Anal. Chim. Acta*, **84**, 173 (1976).

(3) W. Harke, C. Schirren, and R. Wehrmann, *Klin. Wochenschr.*, **37**, 1040 (1959).

(4) T. H. Maren, V. I. Ash, and E. M. Bailey, Jr., *Bull. Johns Hopkins Med. J.*, **95**, 244 (1954).

(5) S. M. Wallace, V. P. Shah, and S. Riegelman, *J. Pharm. Sci.*, **66**, 527 (1977).

(6) W. F. Bayne, G. Rogers, and N. Crisologo, *ibid.*, **64**, 402 (1975).

(7) R. D. Schoenwald, M. E. Garabedian, and G. J. Yakatan, *Drug Dev. Ind. Pharm.*, **4**, 599 (1978).

Effect of Hyperthermically Elevated Serum Prolactin on Epididymal Cyclic AMP (Adenosine 3′,5′-Cyclic Monophosphate) Levels in Rats

J. M. ROSENBERG ×, I. S. KAMPA *, V. REID, J. M. HUNDERTMARK *, D. W. FRASCELLA ‡, and C. A. LAU-CAM §

Received June 21, 1979, from the *Arnold and Marie Schwartz College of Pharmacy and Health Sciences, Brooklyn, NY 11201.* Accepted for publication October 5, 1979. *Department of Pathology, Valley Hospital, Ridgewood, NJ 07451. ‡Hoechst-Roussel Pharmaceuticals, Somerville, NJ 08876. §Department of Pharmaceutical Sciences, St. John's University College of Pharmacy and Allied Health Professions, Jamaica, NY 11439.

Abstract □ To investigate whether increased blood prolactin concentration affects epididymal cyclic AMP (adenosine 3′,5′-cyclic monophosphate) levels during hyperthermic stress, a study was conducted on 40 Sprague–Dawley male rats divided into four equal groups. Two groups were injected intraperitoneally with bromocriptine, a potent inhibitor of prolactin release. Under identical experimental conditions, one group was subjected to hyperthermic stress, and the other group was maintained at room temperature. Two additional groups were injected with a control vehicle; one group was subjected to hyperthermic stress, and the other group was kept at normal body temperature. Blood samples were analyzed for serum prolactin, and epididymal fat pads were assayed for cyclic AMP. Serum prolactin levels increased significantly ($p < 0.01$) in hyperthermic rats, but this effect was suppressed completely by bromocriptine. Cyclic AMP levels were increased ($p < 0.01$) during elevated body temperature in all animals examined, with no significant difference ($p > 0.05$) occurring between the nonbromocriptine-treated and bromocriptine–prolactin-suppressed groups. This investigation suggested that elevation of epididymal fat cyclic AMP during hyperthermia is not the result of increased prolactin levels.

Keyphrases □ Cyclic AMP—epididymal levels, effect of hyperthermically elevated serum prolactin, rats □ Hyperthermia—elevation of serum prolactin, effect on epididymal cyclic AMP levels, rats □ Prolactin, serum—hyperthermic elevation, effect on epididymal cyclic AMP levels, rats

Hyperthermic stress induces changes in lipid metabolism, including a rise in epididymal fat pad cyclic AMP (adenosine 3′,5′-cyclic monophosphate) (1–3). It has been shown that insulin exerts an inhibiting effect on the rise of epididymal fat pad cyclic AMP during hyperthermia (1). However, the rise in cyclic AMP may result from a concomitant decrease in blood insulin (1), an increase in extrapituitary lipolytic hormones such as glucagon (1), and/or an increase in pituitary lipolytic hormones such as prolactin (4–6). The present study was designed to elucidate the role of prolactin on the elevation of epididymal cyclic AMP during hyperthermic stress.

EXPERIMENTAL

Animals—Forty male Sprague–Dawley adult rats[1], 225–300 g, were divided into four equal groups. They were housed for 21 days prior to the study in a temperature-controlled (23 ± 3°), artificially illuminated (lights on from 7:00 am to 7:00 pm daily) room. During this period, the rats were given food[2] and water *ad libitum*. Prior to all experiments, the animals were fasted for 12 hr.

Effect of Hyperthermia on Epididymal Fat Pad Cyclic AMP and Serum Prolactin—The first 10 animals (hyperthermic bromocriptine group) were injected intraperitoneally with 1 mg of bromocriptine[3], a known potent inhibitor of prolactin (7), in 0.5 ml of 5% ethanol. A second group of animals (hyperthermic control group) was injected intraperitoneally with 5% ethanol vehicle. Thirty minutes after injection, both groups were placed in an environmental chamber[4]. The relative humidity was maintained between 40 and 45% within the chamber, and the ambient temperature was controlled to allow the rectal temperature[5] to increase ~1°/30 min until a value of 42 ± 0.1° was reached. This rectal temperature was maintained for approximately 30 min, at which time blood samples were obtained by decapitation. A small portion of epididymal fat was removed immediately from each animal and frozen in liquid nitrogen.

The third group of animals (normothermic bromocriptine group) was treated as described for the first group, and the remaining 10 animals (normothermic control group) were treated identically to the second group. For the latter two groups, the temperature in the environmental chamber was maintained at 23 ± 3° for the 3 hr that the animals were contained in it. Blood and epididymal fat samples then were obtained.

Sample Collection and Assay—All decapitations were conducted between 3:30 and 5:00 pm. Blood was collected from the trunk portion and allowed to stand for 10 min at 4°, and the serum was separated and frozen at −40° until hormone analysis could be performed. Serum prolactin levels were measured using a double antibody radioimmunoassay kit[6] according to the instructions supplied. The rat prolactin was iodinated by a modification of the Hunter–Greenwood method (8). Each serum sample was assayed in duplicate, and the average was taken as representative of the true prolactin concentration. All results are expressed in terms of nanograms per milliliter of NIAMDD rat prolactin.

Cyclic AMP was extracted from the epididymal fat pads by a method described by Steiner *et al.* (9), and the concentrations were determined by radioimmunoassay[7] using a modification of a method reported by the same investigators (10). Each sample was assayed in duplicate, and the average was taken as representative of the concentration. Cyclic AMP results are expressed in picomoles per gram of wet epididymal fat tissue.

Statistical comparisons were determined by the Student t test (11).

RESULTS

Figure 1 shows the results of hyperthermic stress on serum prolactin levels following treatment with bromocriptine or control vehicle. Prolactin levels were elevated significantly ($p < 0.01$) in the hyperthermic control group compared to the normothermic control group [124.3 ± 20.6 (*SE*) *versus* 44.8 ± 7.7 (*SE*) ng/ml, respectively; $t = 3.4$, $df = 18$]. Prolactin levels were depressed significantly ($p < 0.01$) in the hyperthermic bromocriptine group compared to the hyperthermic control group [11.2 ± 1.2 (*SE*) *versus* 124.3 ± 20.6 (*SE*) ng/ml, respectively; $t = 39.0$, $df = 18$] and in the normothermic bromocriptine group compared to the normothermic control group [44.8 ± 7.7 (*SE*) *versus* 13.4 ± 1.2 (*SE*) ng/ml, respectively; $t = 3.5$, $df = 18$], with no significant difference ($p > 0.05$) between the bromocriptine–prolactin-suppressed groups [11.2 ± 1.2 (*SE*) *versus* 13.4 ■ 1.2 (*SE*) ng/ml, respectively; $t = 1.2$, $df = 18$].

Figure 2 indicates that epididymal cyclic AMP levels were elevated significantly ($p < 0.01$) in the hyperthermic control group compared to

[1] Taconic Farms, Germantown, N.Y.
[2] Purina Lab Chow, Ralston Purina Co., St. Louis, Mo.
[3] Sandoz Laboratories, East Hanover, N.J.
[4] Refrigerator incubator model 305500, Hotpack Corp., Philadelphia, Pa.
[5] Rectal thermister probe, Yellow Springs Instrument Co., Springfield, Ohio.
[6] Supplied by the National Institutes of Arthritis, Metabolism, and Digestive Diseases (NIAMDD) Rat Pituitary Hormone Distribution Program, National Pituitary Agency, Baltimore, Md.
[7] Cyclic AMP radioimmunoassay kit ^{125}I, Becton Dickinson, Orangeburg, N.Y.

0022-3549/80/0300-0350$01.00/0
© 1980, American Pharmaceutical Association

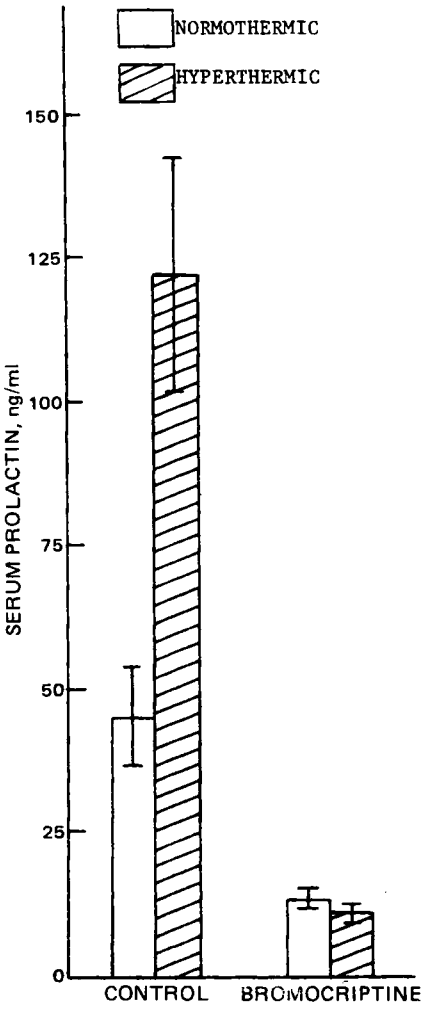

Figure 1—*Serum prolactin levels in rats treated with bromocriptine or vehicle during normal and elevated rectal temperatures. Each vertical bar represents the mean of 10 observations. The vertical brackets indicate standard errors of the mean. Prolactin levels in the hyperthermic control rats were significantly ($p < 0.01$) elevated compared to normothermic controls. Bromocriptine treatment significantly depressed serum prolactin levels in both hyperthermic and normothermic animals.*

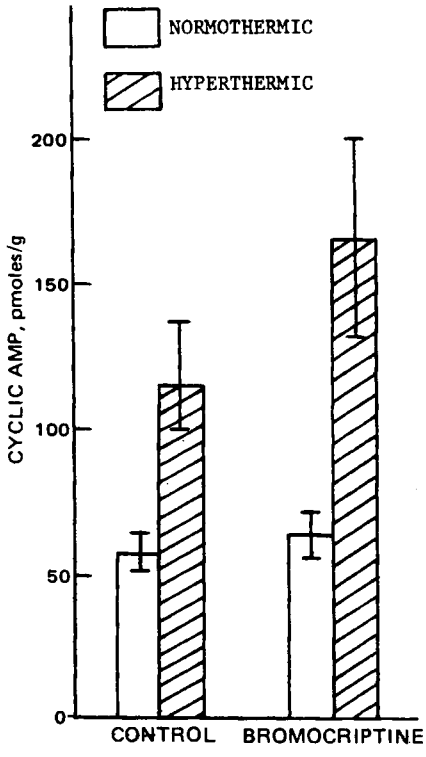

Figure 2—*Cyclic AMP concentrations in rats treated with bromocriptine or control vehicle during normal and elevated rectal temperatures. Each vertical bar represents the mean of 10 observations. The vertical brackets indicate standard errors of the mean. Hyperthermia significantly ($p < 0.01$) elevated cyclic AMP in both bromocriptine- and control vehicle-treated animals with no significant difference ($p > 0.05$) in the concentration of both groups.*

the normothermic control group [115.2 ± 20.9 (*SE*) *versus* 56.1 ± 6.7 (*SE*) pmoles/g, respectively; $t = 3.8$, $df = 18$] and in the hyperthermic bromocriptine group compared to the normothermic bromocriptine animals [165.7 ± 33.8 (*SE*) *versus* 63.4 ± 8.3 (*SE*) pmoles/g, respectively; $t = 3.9$, $df = 18$]. The cyclic AMP concentrations of the normothermic control and the normothermic bromocriptine groups were not significantly different ($p > 0.05$) [56.1 ± 6.7 (*SE*) *versus* 63.4 ± 8.3 (*SE*) pmoles/g, respectively; $t = 2.0$, $df = 18$], and there also was no significant difference ($p > 0.05$) in concentration between the hyperthermic control and the hyperthermic bromocriptine groups [115.2 ± 20.9 (*SE*) *versus* 165.7 ± 33.8 (*SE*) pmoles/g, respectively; $t = 1.2$, $df = 18$].

DISCUSSION

Serum prolactin levels are largely controlled by a hypothalamic prolactin-inhibiting factor related to dopamine which, indeed, may be dopamine (12). Pharmacological agents that reduce serum prolactin levels include dopamine agonists such as bromocriptine (7). Although bromocriptine also may transiently increase the prolactin clearance from plasma by stimulating its uptake into peripheral receptor sites, its exact inhibitory mechanism is not fully known (13).

In the present study, serum prolactin levels significantly increased in hyperthermic rats. Bromocriptine-treated animals exhibited suppressed serum prolactin levels, and no elevation of prolactin levels occurred during hyperthermia (Fig. 1). Previous studies (14, 15) showed that increased temperature raises blood prolactin. However, these changes were not attributed simply to stress since lowered temperature significantly decreased serum prolactin and elevated temperature produced the opposite effect (14, 15). Although it was reported previously that prolactin increases lipolysis in adipose tissue from mature rats, as indicated by an increased free fatty acid and glycerol release (16, 17), this effect has not been observed in young rats (16).

Prolactin also is known to increase cyclic AMP in some tissues but not in others (16). Since no significant change in the levels of cyclic AMP occurred among the bromocriptine-treated hyperthermic animals in contrast to nonbromocriptine-treated rats (Fig. 2), it appears that epididymal fat cyclic AMP elevations during hyperthermia occur independently of increases in serum prolactin levels. The role of extrapituitary lipolytic hormones such as glucagon is now being investigated to determine if they play a part in the epididymal fat cyclic AMP increase observed during elevated body temperature.

REFERENCES

(1) I. S. Kampa and D. W. Frascella, *Horm. Metab. Res.*, **9**, 282 (1977).

(2) I. S. Kampa and D. W. Frascella, *Bull. N.J. Acad. Sci.*, **23**, 74 (1978).

(3) S. Bergstrom, R. Eliasson, U. S. von Euler, and J. Sjovall, *Acta Physiol. Scand.*, **45**, 133 (1959).

(4) R. W. Butcher and E. W. Sutherland, *Ann. N.Y. Acad. Sci.*, **139**, 848 (1967).

(5) R. W. Turkington, *N. Engl. J. Med.*, **285**, 1455 (1971).

(6) D. F. Horrobin, "Prolactin Physiology and Clinical Significance," MTP Medical and Technical Publishing Co., Lancaster, England, 1973, p. 19.

(7) W. H. Utman, G. Begg, A. I. Vinik, M. Paul, and L. Shuman, *Br. J. Obstet. Gynaecol.*, **82**, 755 (1975).

(8) W. M. Hunter and F. C. Greenwood, *Nature*, **194**, 495 (1962).

(9) A. L. Steiner, C. W. Parker, and D. M. Kipnis, "Advances in Biochemical Psychopharmacology," vol. 3, Raven, New York, N.Y., 1970.

(10) A. L. Steiner, D. M. Kipnis, R. Utiger, and C. Parker, *Proc. Natl. Acad. Sci. USA*, **64**, 367 (1969).

(11) B. J. Winer, "Statistical Principles in Experimental Design," 2nd ed., McGraw-Hill, New York, N.Y., 1971, p. 471.

(12) C. H. Mortimer and G. M. Besser, in "Recent Advances in Medicine," 17th ed., D. N. Baron, N. Compston, and A. M. Dawson, Eds., Churchill Livingstone, London, England, 1977, p. 441.

(13) E. E. Muller, A. E. Panerai, D. Cocchi, and P. Mantegazza, *Life Sci.*, **21**, 1545 (1977).

(14) G. P. Mueller, H. T. Chen, J. A. Dibbet, H. J. Chen, and J. Meites, *Proc. Soc. Exp. Biol. Med.*, **147**, 698 (1974).

(15) R. P. Wettemann and A. L. Tucker, *ibid.*, **146**, 908 (1974).

(16) D. F. Horrobin, "Prolactin Physiology and Clinical Significance," MTP Medical and Technical Publishing Co., Lancaster, England, 1973, p. 15.

(17) J. Elsair and R. Denine, *Rev. Eur. Etud. Clin. Biol.*, **15**, 899 (1970).

ACKNOWLEDGMENTS

Presented at the APhA Academy of Pharmaceutical Sciences, Kansas City meeting, November 1979.

The authors thank the National Institutes of Arthritis, Metabolism, and Digestive Diseases, Rat Pituitary Hormone Distribution Program, and Dr. A. F. Parlow for their gift of radioimmunoassay materials for the prolactin assay. They also thank Sandoz Laboratories for the gift of bromocriptine.

In Vitro Adsorption Studies of Cimetidine

F. GANJIAN, A. J. CUTIE, and T. JOCHSBERGER ˣ

Received August 8, 1979, from the *Arnold & Marie Schwartz College of Pharmacy and Health Sciences, Brooklyn, NY 11201.* Accepted for publication October 5, 1979.

Abstract □ The adsorption of cimetidine on selected pharmaceuticals including kaolin, activated charcoal, talc, and nonsystemic antacids was determined at pH 5.0 and 25°. The Langmuir and Freundlich adsorption isotherms showed that cimetidine adsorption was significant with activated charcoal, kaolin, talc, and magnesium trisilicate and was virtually nonexistent with magnesium hydroxide and aluminum hydroxide. Equations expressing the Freundlich and Langmuir adsorption isotherms were evaluated for each adsorbent. The approximate amounts of cimetidine adsorbed per gram of adsorbent were 25.6, 0.402, 0.291, and 0.343 mg for charcoal, kaolin, talc, and magnesium trisilicate, respectively. These *in vitro* studies indicate that some cimetidine may be lost when it is administered concomitantly with pharmaceutical adsorbents.

Keyphrases □ Cimetidine—adsorption onto various pharmaceutical adsorbents, *in vitro* □ Adsorption—cimetidine, various pharmaceutical adsorbents, *in vitro* □ Interactions—adsorption of cimetidine onto various pharmaceutical adsorbents

Numerous pharmaceuticals contain substances that are capable of adsorbing various drugs and other compounds (1–8). These substances include clays such as kaolin and talc and silicates found in some antacid–antiflatulent preparations. The purpose of this study was to determine if any adsorption interaction occurred with some commonly employed pharmaceutical ingredients including kaolin, talc, magnesium trisilicate, aluminum hydroxide, magnesium hydroxide, activated charcoal, and the H_2-receptor antagonist cimetidine used for the treatment of duodenal ulcers and gastric hypersecretion. Since antacids are recommended commonly for concurrent therapy with cimetidine, it was of interest to determine if any *in vitro* interaction was evident. To evaluate the efficiency of the adsorption, activated charcoal was employed as a standard.

EXPERIMENTAL

Reagents—Activated charcoal[1], kaolin[1], talc[2], aluminum hydroxide[1], magnesium hydroxide[1], and magnesium trisilicate[3] were reagent grade. Cimetidine[4] was compendial grade and was used without further purification. Methanol was certified ACS spectroanalyzed grade[1].

Procedure—All potential adsorbents (aluminum hydroxide, charcoal, kaolin, magnesium hydroxide, magnesium trisilicate, and talc) employed were washed repeatedly with distilled water followed by spectroanalytical grade methanol until the wash solution exhibited no absorbance at 226 nm (the wavelength of maximum cimetidine absorption). The adsorbents were passed through a 20-mesh sieve[1] while still moist and permitted to dry in an oven at approximately 45°. The dried materials then were passed through a 100-mesh sieve to ensure that the particle sizes of all of the adsorbents were 100 mesh or smaller. One gram of adsorbent was used in all cases, except for charcoal where only 50 mg was utilized.

Adsorbate mixtures were prepared by diluting aqueous cimetidine solutions (~12 mg/liter) with appropriate amounts of distilled water. The final pH of the solutions was 5.0[1]. The solutions then were agitated vigorously[5] for 10 min at 25° and allowed to stand for 20 min. Twenty-five-milliliter aliquots of the supernate were drawn from each solution, centrifuged[6] for 20 min, and assayed spectrophotometrically[7] at 226 nm. The reference solutions were prepared in an identical manner as the sample, with the cimetidine solution replaced by distilled water.

RESULTS AND DISCUSSION

The results of the *in vitro* adsorption of cimetidine onto various substances are given in Tables I–III and Figs. 1 and 2. The data are presented as both Freundlich constants (Eq. 1) and Langmuir constants (Eq. 2) as well as in terms of the adsorption rate:

$$\frac{x}{m} = kC^n \qquad \text{(Eq. 1)}$$

$$\frac{x}{m} = \frac{\alpha C}{1 + \beta C} \qquad \text{(Eq. 2)}$$

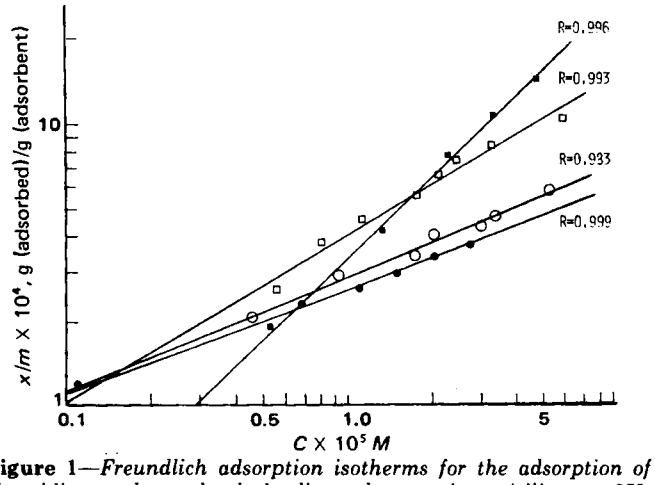

Figure 1—*Freundlich adsorption isotherms for the adsorption of cimetidine on charcoal, talc, kaolin, and magnesium trisilicate at 25°. Key:* ■, *magnesium trisilicate;* □, *kaolin;* ○, *talc; and* ●, *charcoal (values* × 10^2*).*

[1] Fisher Scientific Co., Fair Lawn, N.J.
[2] Matheson, Coleman and Bell, Norwood, Ohio.
[3] Mallinckrodt, St. Louis, Mo.
[4] Smith Kline and French Laboratories, Philadelphia, Pa.
[5] Shaker bath 6250, Eberbach Corp., Ann Arbor, Mich.
[6] Dynac centrifuge, Clay-Adams Co., New York, N.Y.
[7] Spectronic 200, Bausch & Lomb.

0022-3549/80/0300-0352$01.00/0
© 1980, American Pharmaceutical Association

(17) J. Elsair and R. Denine, *Rev. Eur. Etud. Clin. Biol.*, **15**, 899 (1970).

ACKNOWLEDGMENTS

Presented at the APhA Academy of Pharmaceutical Sciences, Kansas City meeting, November 1979.

The authors thank the National Institutes of Arthritis, Metabolism, and Digestive Diseases, Rat Pituitary Hormone Distribution Program, and Dr. A. F. Parlow for their gift of radioimmunoassay materials for the prolactin assay. They also thank Sandoz Laboratories for the gift of bromocriptine.

In Vitro Adsorption Studies of Cimetidine

F. GANJIAN, A. J. CUTIE, and T. JOCHSBERGER ˣ

Received August 8, 1979, from the *Arnold & Marie Schwartz College of Pharmacy and Health Sciences, Brooklyn, NY 11201.* Accepted for publication October 5, 1979.

Abstract □ The adsorption of cimetidine on selected pharmaceuticals including kaolin, activated charcoal, talc, and nonsystemic antacids was determined at pH 5.0 and 25°. The Langmuir and Freundlich adsorption isotherms showed that cimetidine adsorption was significant with activated charcoal, kaolin, talc, and magnesium trisilicate and was virtually nonexistent with magnesium hydroxide and aluminum hydroxide. Equations expressing the Freundlich and Langmuir adsorption isotherms were evaluated for each adsorbent. The approximate amounts of cimetidine adsorbed per gram of adsorbent were 25.6, 0.402, 0.291, and 0.343 mg for charcoal, kaolin, talc, and magnesium trisilicate, respectively. These *in vitro* studies indicate that some cimetidine may be lost when it is administered concomitantly with pharmaceutical adsorbents.

Keyphrases □ Cimetidine—adsorption onto various pharmaceutical adsorbents, *in vitro* □ Adsorption—cimetidine, various pharmaceutical adsorbents, *in vitro* □ Interactions—adsorption of cimetidine onto various pharmaceutical adsorbents

Numerous pharmaceuticals contain substances that are capable of adsorbing various drugs and other compounds (1–8). These substances include clays such as kaolin and talc and silicates found in some antacid–antiflatulent preparations. The purpose of this study was to determine if any adsorption interaction occurred with some commonly employed pharmaceutical ingredients including kaolin, talc, magnesium trisilicate, aluminum hydroxide, magnesium hydroxide, activated charcoal, and the H_2-receptor antagonist cimetidine used for the treatment of duodenal ulcers and gastric hypersecretion. Since antacids are recommended commonly for concurrent therapy with cimetidine, it was of interest to determine if any *in vitro* interaction was evident. To evaluate the efficiency of the adsorption, activated charcoal was employed as a standard.

EXPERIMENTAL

Reagents—Activated charcoal[1], kaolin[1], talc[2], aluminum hydroxide[1], magnesium hydroxide[1], and magnesium trisilicate[3] were reagent grade. Cimetidine[4] was compendial grade and was used without further purification. Methanol was certified ACS spectroanalyzed grade[1].

Procedure—All potential adsorbents (aluminum hydroxide, charcoal, kaolin, magnesium hydroxide, magnesium trisilicate, and talc) employed were washed repeatedly with distilled water followed by spectroanalytical grade methanol until the wash solution exhibited no absorbance at 226 nm (the wavelength of maximum cimetidine absorption). The adsorbents were passed through a 20-mesh sieve[1] while still moist and permitted to dry in an oven at approximately 45°. The dried materials then were passed through a 100-mesh sieve to ensure that the particle sizes of all of the adsorbents were 100 mesh or smaller. One gram of adsorbent was used in all cases, except for charcoal where only 50 mg was utilized.

Adsorbate mixtures were prepared by diluting aqueous cimetidine solutions (~12 mg/liter) with appropriate amounts of distilled water. The final pH of the solutions was 5.0[1]. The solutions then were agitated vigorously[5] for 10 min at 25° and allowed to stand for 20 min. Twenty-five-milliliter aliquots of the supernate were drawn from each solution, centrifuged[6] for 20 min, and assayed spectrophotometrically[7] at 226 nm. The reference solutions were prepared in an identical manner as the sample, with the cimetidine solution replaced by distilled water.

RESULTS AND DISCUSSION

The results of the *in vitro* adsorption of cimetidine onto various substances are given in Tables I–III and Figs. 1 and 2. The data are presented as both Freundlich constants (Eq. 1) and Langmuir constants (Eq. 2) as well as in terms of the adsorption rate:

$$\frac{x}{m} = kC^n \qquad \text{(Eq. 1)}$$

$$\frac{x}{m} = \frac{\alpha C}{1 + \beta C} \qquad \text{(Eq. 2)}$$

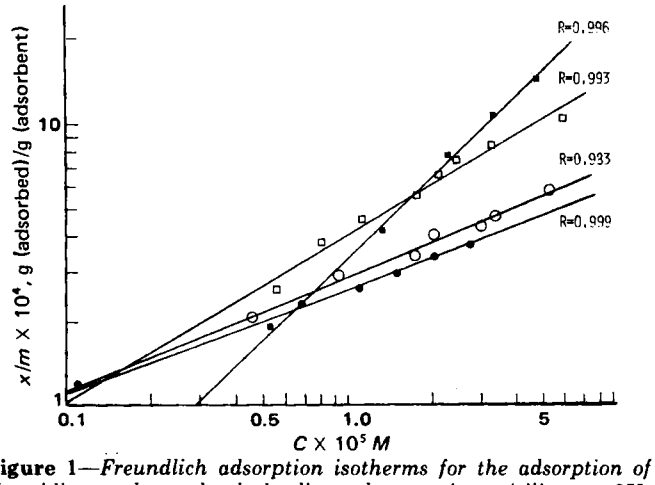

Figure 1—*Freundlich adsorption isotherms for the adsorption of cimetidine on charcoal, talc, kaolin, and magnesium trisilicate at 25°. Key:* ■, *magnesium trisilicate;* □, *kaolin;* ○, *talc; and* ●, *charcoal (values* × 10^2*).*

[1] Fisher Scientific Co., Fair Lawn, N.J.
[2] Matheson, Coleman and Bell, Norwood, Ohio.
[3] Mallinckrodt, St. Louis, Mo.
[4] Smith Kline and French Laboratories, Philadelphia, Pa.
[5] Shaker bath 6250, Eberbach Corp., Ann Arbor, Mich.
[6] Dynac centrifuge, Clay-Adams Co., New York, N.Y.
[7] Spectronic 200, Bausch & Lomb.

0022-3549/80/0300-0352$01.00/0
© 1980, American Pharmaceutical Association

Table I—Freundlich Constants for Adsorption of Cimetidine onto Various Adsorbents

Adsorbent	$k \times 10^4$, g (adsorbed)/g (adsorbent)	n
Kaolin	4.02	0.621
Magnesium trisilicate	3.43	0.943
Talc	2.91	0.384
Charcoal	256	0.347

Table II—Langmuir Constants for Adsorption of Cimetidine onto Various Adsorbents

Adsorbent	$\alpha \times 10^{-1}$, g (adsorbed)/mg (adsorbent)	$\beta \times 10^{-4}\ M^{-1}$
Kaolin	5.68	3.72
Talc	4.63	6.57
Magnesium trisilicate	3.83	0.475
Charcoal	877	21.6

where x/m is the grams of drug adsorbed per gram of adsorbent, C is the equilibrium concentration of the unbound drug, and k, n, α, and β are constants.

The data indicate that activated charcoal is about two orders of magnitude more efficient in the adsorption of cimetidine than are kaolin, talc, and magnesium trisilicate. Magnesium hydroxide and aluminum hydroxide did not adsorb cimetidine to any significant extent. This lack of adsorption is reflected in the adsorption rate as well as in the Freundlich constant k and the Langmuir constants α and β. These latter constants

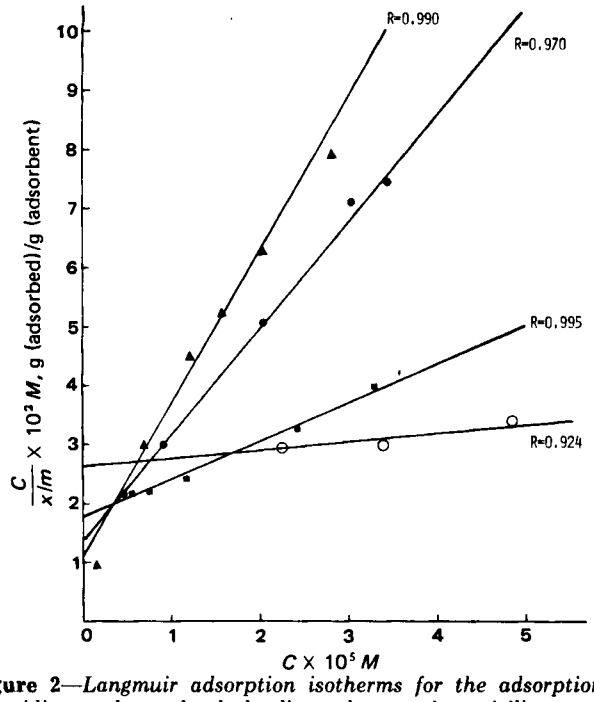

Figure 2—*Langmuir adsorption isotherms for the adsorption of cimetidine on charcoal, talc, kaolin, and magnesium trisilicate at 25°. Key: ▲, charcoal (values × 10⁴); ●, talc; ■, kaolin; and ○, magnesium trisilicate.*

Table III—Adsorption Rate of Cimetidine [a] with Different Adsorbents

Adsorbent	$(x/m)^b \times 10^4$, g (adsorbed)/ g (adsorbent)	Adsorption Rate $\times 10^3$, g (adsorbed)/ g(adsorbent) hr
Charcoal	118	35.4
Kaolin	4.69	1.41
Magnesium trisilicate	4.23	1.27
Talc	3.33	1.00
Magnesium hydroxide	0.00	0.00
Aluminum hydroxide	0.00	0.00

[a] The initial concentration was $3.20 \times 10^{-5}\ M$. [b] At equilibrium.

are directly related to the adsorption rate and inversely to the desorption rate. Therefore, the larger their values, the more efficient is the adsorbent. The Freundlich constant k represents the drug amount adsorbed per unit weight of adsorbent at a unit drug concentration (Eq. 1).

The Freundlich constant n is always less than unity (9) and represents the drug amount adsorbed for a given concentration change. Larger n values reflect a greater fraction of adsorbed drug to unbound drug. This value, in turn, reflects the ratio of the rate of adsorption to desorption and the relative strength of the bond between the drug and the binding site. The n value is largest for magnesium trisilicate, which appears to indicate that while the number of sites available on this adsorbent are somewhat less than for charcoal, as reflected in a lower per gram adsorption, the interaction of the magnesium trisilicate with cimetidine is stronger. This interaction could be the result of an electrostatic interaction between anionic silicate and the positive charge on the cimetidine molecules. The pKa of cimetidine (10) is 6.8; at pH 5.0, the drug exists almost entirely in the cationic form. Khalil (11) showed that adsorption of materials on magnesium trisilicate diminishes its uptake of hydrochloric acid, which could be significant in the use of antacids utilizing magnesium trisilicate concomitantly with cimetidine.

The results of aluminum hydroxide and magnesium hydroxide, although negative, are interesting. Bodemar *et al.* (12) showed that blood cimetidine levels are reduced in the presence of both compounds. The present work indicates that the source of this reduction is not due to the cimetidine adsorption.

The *in vitro* results with kaolin and talc indicate possible interference with cimetidine therapy by these substances. However, the clinical significance of this interaction has not been demonstrated.

REFERENCES

(1) E. M. Sellers, V. Khouw, and L. Dolman, *J. Pharm. Sci.*, **66**, 1640 (1977).

(2) T. Tsuchiya and G. Levy, *ibid.*, **61**, 586 (1972).

(3) C. A. Bainbridge, E. L. Kelly, and W. D. Walkling, *ibid.*, **66**, 481 (1977).

(4) G. Levy and P. R. Gwilt, *Pharmacologist*, **16**, 208 (1974).

(5) T. Tsuchiya and G. Levy, *J. Pharm. Sci.*, **61**, 624 (1972).

(6) L. S. Porubcan, G. S. Born, J. L. White, and S. L. Hem, *ibid.*, **67**, 1081 (1978).

(7) L. S. Porubcan, C. S. Serna, J. L. White, and S. L. Hem, *ibid.*, **68**, 358 (1979).

(8) A. A. Hincal and B. B. Sheth, *ibid.*, **68**, 472 (1979).

(9) P. C. Heimenz, "Principles of Colloid and Surface Chemistry," Dekker, New York, N.Y., 1977, p. 293.

(10) D. W. Newton and R. B. Kluza, *Drug Intell. Clin. Pharm.*, **12**, 546 (1978).

(11) S. A. H. Khalil, *J. Pharm. Sci.*, **66**, 289 (1977).

(12) G. Bodemar, B. Norlander, and A. Walan, *Lancet*, **1**, 444 (1979).

Serum Protein Binding Alterations of Selected Cephalosporin Antibiotics by Fatty Acids and Their Derivatives

D. H. PITKIN ˣ, P. ACTOR, and J. A. WEISBACH

Received June 11, 1979, from *Smith Kline Corp., Philadelphia, PA 19101.* Accepted for publication October 15, 1979.

Abstract □ Saturated fatty acids containing 10–14 carbon atoms were more potent inhibitors of serum protein binding than those containing shorter or longer carbon chains. Introduction of unsaturation into chains containing 16 or 18 carbons increased their inhibitory potency. Triglycerides and fatty acid esters, chlorides, thiols, and amides had no inhibitory activity. When inhibition was observed, it was concentration dependent and occurred when the molar ratio of fatty acid to protein equaled or exceeded three. The change in percent serum protein binding in the presence of an effective inhibitor was the greatest with cephalosporins that were most highly bound in the absence of an inhibitor.

Keyphrases □ Antibiotics—cephalosporins, serum protein binding, alteration by fatty acids and their derivatives □ Cephalosporins—serum protein binding, alteration by fatty acids and their derivatives □ Protein binding—cephalosporin antibiotics, alteration by fatty acids and their derivatives, serum

Serum protein binding can be diminished in several disease states, after administration of certain hormones, anticoagulants, and sulfa drugs, or by alteration of the levels of normally occurring metabolites such as bilirubin or fatty acids (1–6). Even small changes in serum protein binding can produce clinically significant physiological effects, particularly with drugs that are highly bound. These changes may affect not only the amount of free drug in the plasma but also its tissue concentration, tissue distribution, and elimination pharmacokinetics (1, 5, 7–9).

Kunin (4) showed that the content of free penicillin analogs in humans may be increased by coadministration of sulfamethoxypyridazine or sulfaethidole (sulfaethylthiadiazole), two *in vitro* inhibitors of serum protein binding. Spector (8) stressed the need to determine if the ability of albumin to transport a second compound can be influenced by free fatty acid concentrations in plasma. In this paper, data are presented on the relationship between the structure and serum protein binding inhibition of seven saturated and four unsaturated fatty acids in addition to the effects of chemical substituents on the carboxy terminus.

EXPERIMENTAL

Cephalothin and cefazolin were obtained from commercial sources. Cefonicid sodium [(6*R*,7*R*)-7-[(*R*)-mandelamido]-8-oxo-3-[[[1-(sulfomethyl)-1*H*-tetrazol-5-yl]thio]methyl]-5-thia -1- azabicyclo[4.2.0]oct-2-ene-2-carboxylic acid disodium salt], a new, long-acting parenteral cephalosporin (10), was synthesized[1]. Fatty acids were obtained commercially at a stated purity of >98%, while analogs were obtained at a stated purity of >95%. Fatty acids and their analogs were dissolved at high concentrations in ethanol or ethanol–chloroform, depending on solubility.

Human serum was obtained from a local commercial supplier of blood products. Serum pH was adjusted to 7.2–7.4 with carbon dioxide before use. Small volumes of fatty acid or other stock solutions or the diluent used in their preparation were added in varying concentrations to the serum, which was then held at 4° for 16–18 hr before use. This storage permitted the additive to interact with the serum proteins (9, 11). The additives to the serum were present at molar ratios of fatty acid to serum protein of 0:1, 1:1, 3:1, 5:1, 7.5:1, or 10:1, whereas the fatty acid analogs were tested at ratios of 0:1, 3:1, and 10:1 (5, 12, 13).

Samples were assayed using a disk agar diffusion test employing *Bacillus subtilis* (ATCC 6633) grown in penicillin assay seed agar as the indicator. Corrections were made for intergroup variation in the indicator response by assaying an internal standard. Serum protein binding determinations were made using the standard response line offset technique. In this technique, the response of the indicator to five concentrations of the selected antibiotic in 1% pH 7.4 phosphate buffer was compared to the response produced when the antibiotic was diluted in serum. The concentration of antibiotic in serum, S, producing a specified response was compared to the concentration of antibiotic in buffer, B, producing the identical response. The value $(1 - B)/S \times 100$ was computed and reported as the percent serum protein binding (11, 14).

RESULTS

The three antibiotics used, cephalothin, cefazolin, and cefonicid, were chosen in control experiments on the basis of their serum protein binding as being representatives of moderately, highly, and very highly bound cephalosporins.

The effects of adding C_6–C_{18}-saturated fatty acids at various fatty acid to protein molar ratios on the serum protein binding of the three cephalosporins are shown in Figs. 1–3. The data show the difference in percent serum protein binding with and without an inhibitor in the serum as a function of inhibitor chain length. The amount of inhibition was dependent on fatty acid concentrations and occurred at ratios of 3:1 or greater. The various fatty acids differed in their ability to inhibit serum protein binding. With cephalothin, maximal inhibition occurred at C_{10} (Fig. 1); it occurred at C_{10}–C_{12} (Fig. 2) for cefazolin and at C_{12} for cefonicid (Fig. 3).

Results obtained using the standard curve offset technique were confirmed using ultrafiltration techniques and radiolabeled cefonicid with intermediate or high concentrations of a C_{10}-fatty acid as a serum additive. These results indicate that data obtained using the standard curve offset technique are not attributable to artifacts introduced by the assay system. Fatty acids exerted their greatest effect on cephalosporins that were most highly bound in the absence of an inhibitor. The carbon chain length requirements for inhibition of cefazolin appear to be slightly less

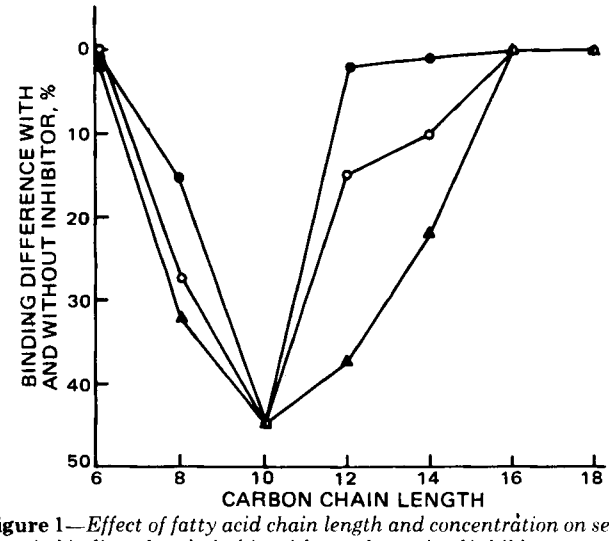

Figure 1—*Effect of fatty acid chain length and concentration on serum protein binding of cephalothin with a molar ratio of inhibitor to protein of 3:1 (●), 5:1 (○), and 10:1 (△).*

[1] Smith Kline & French Laboratories.

0022-3549/80/0300-0354$01.00/0
© 1980, American Pharmaceutical Association

Table I—Effect of Fatty Acid Unsaturation on Serum Protein Binding of Three Cephalosporins at a Fatty Acid to Protein Ratio of 10:1[a]

Fatty Acid	Cephalothin	Cefazolin	Cefonicid
Palmitic (16[b])	0	34	23
Palmitoleic (16:1)	38	50	83
Stearic (18)	0	9	7
Oleic (18:1)	25	42	61
Linoleic (18:2)	14	54	68
Linolenic (18:3)	41	47	69

[a] Data are shown as a change in the percent bound from the control. [b] Number of carbons to unsaturated bonds.

stringent than those for inhibition of cephalothin or cefonicid. In all cases, adding a potential inhibitor at inhibitor to serum protein ratios of 1:1 failed to affect the serum protein binding significantly.

The effect of structural modification of saturated fatty acids on their ability to act as serum protein binding inhibitors was examined. Fatty acids having carbon chain lengths of 16 (poorly effective) or 18 (ineffective) were used as examples. Introduction of monounsaturation or multiple unsaturation into these compounds profoundly changed their potency as serum protein binding inhibitors (Table I).

The next structural modification examined was substitution at the carboxy terminus. Fatty acids with a 12 carbon chain (lauric acid) and a monounsaturated 18 carbon chain (oleic acid) were studied. The results of substituting the carboxy group with sodium, alcohol, amide, chloride, methyl ester, or thiol groups or of using the triglyceride on the serum protein binding of the three cephalosporins are shown in Table II. These tests were carried out with a 10:1 inhibitor to protein ratio. Only the acid and its sodium salt were effective serum protein inhibitors.

DISCUSSION

These results show that saturated fatty acids having 10–14 carbon atom chains markedly inhibited serum protein binding of all tested cephalosporins whereas fatty acids with shorter or longer carbon chains were less effective. Introduction of unsaturation or substitution at the carboxy terminus also altered their potency. This effect suggests that the interaction is structure dependent and possibly is due to the degree of lipophilicity of the inhibitor. This idea is supported by the findings that introduction of unsaturation into 16–18 carbon atom chains markedly increase their inhibitory ability while substitution at the carboxy terminus with any of several negatively charged groups or esterification in the presence or absence of glycerol eliminated the serum protein binding inhibitory effect.

These findings are in agreement with earlier work (8) which indicated that the bond between fatty acids and human serum albumin was due

Table II—Effect of Chemical Substitution at the Carboxy Terminus on the Serum Protein Binding Inhibitory Potency of C_{12} or Monounsaturated C_{18} Fatty Acids

Inhibitor	Cephalothin	Cefazolin	Cefonicid
Lauric acid[a]	37	47	64
Sodium salt	33	44	64
Alcohol	0	4	4
Chloride	0	0	0
Methyl ester	0	4	0
Thiol	0	0	0
Triglyceride	5	0	0
Oleic acid[b]	33	41	61
Sodium salt	33	48	77
Alcohol	0	2	1
Chloride	0	7	2
Amide[c]	0	0	0
Methyl ester	0	1	0
Triglyceride	3	0	1

[a] Twelve carbon chain. [b] Eighteen carbon chain, with one unsaturated bond. [c] Tested at a ratio of 5:1 because of inhibition of the assay organism at a ratio of 10:1.

predominantly to lipophilic rather than electrostatic or hydrogen bond interactions. Fatty acid esters or triglycerides were not inhibitory (8). The findings of Vallner (12) and Rudman *et al.* (5) were verified in that maximal inhibitory effects were observed when the fatty acid to protein ratio was three or greater. Previous findings that highly bound drugs show a more pronounced response than drugs with lower binding also were confirmed (1).

In related studies, probenecid and novobiocin, both organic acids that are highly serum protein bound, also were effective *in vitro* inhibitors of serum protein binding using the three cephalosporins. These findings suggest that variation in the fatty acid content of human serum or coadministration of other highly serum protein bound compounds have the potential to affect dramatically the serum protein binding of commonly used antibiotics.

Changes in serum protein binding can be important clinically with regard to potential toxicity of highly bound drugs having a narrow therapeutic ratio. In addition, alterations in serum protein binding may affect

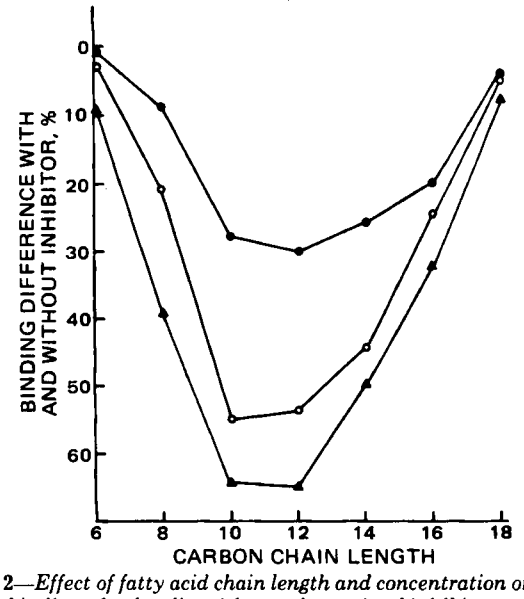

Figure 2—*Effect of fatty acid chain length and concentration on serum protein binding of cefazolin with a molar ratio of inhibitor to protein of 3:1 (●), 5:1 (○), and 10:1 (△).*

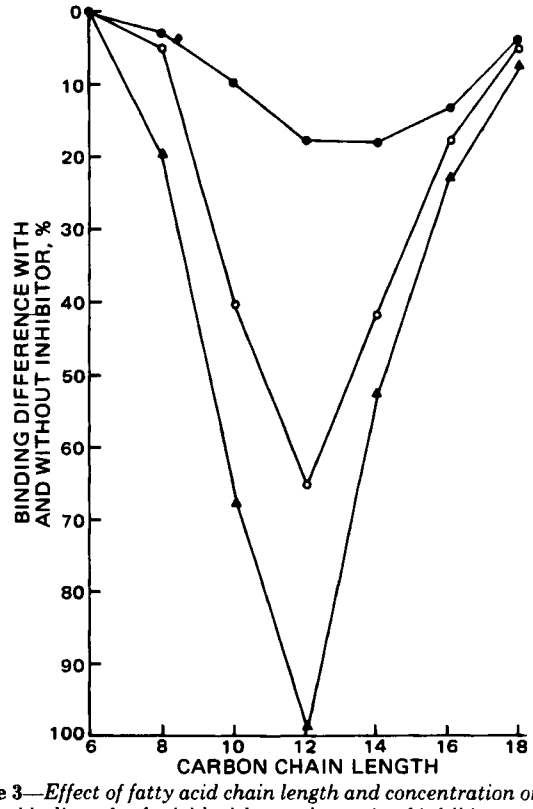

Figure 3—*Effect of fatty acid chain length and concentration on serum protein binding of cefonicid with a molar ratio of inhibitor to protein of 3:1 (●), 5:1 (○), and 10:1 (△).*

the bioassay of samples containing multiple drugs or abnormal levels of normally occurring metabolic products.

REFERENCES

(1) W. A. Craig and P. G. Welling, *Clin. Pharmacokinet.*, **2**, 252 (1977).

(2) D. S. Greene and A. Tice, "Abstracts," vol. 7, no. 2, APhA Academy of Pharmaceutical Sciences, Washington, D.C., 1977, p. 133 (abstract 75).

(3) C. S. Hollander, R. L. Scott, J. A. Burgess, D. Rabinowitz, T. J. Merimee, and J. H. Oppenheimer, *J. Clin. Endocrinol. Metab.*, **27**, 1219 (1967).

(4) C. M. Kunin, *J. Lab. Clin. Med.*, **65**, 406 (1965).

(5) D. Rudman, T. J. Bixler, III, and A. E. DelRio, *J. Pharmacol. Exp. Ther.*, **176**, 261 (1971).

(6) W. Shaw, I. L. Hubert, and F. W. Spierto, *Clin. Chem.*, **225**, 673 (1976).

(7) G. N. Rolinson, "Recent Advances in Medical Microbiology," A. P. Waterson, Ed., Little, Brown, Boston, Mass., 1966, pp. 254–283.

(8) A. A. Spector, *J. Lipid Res.*, **16**, 165 (1975).

(9) G. Wilding, R. C. Feldhoff, and E. S. Vesell, *Biochem. Pharmacol.*, **26**, 1143 (1977).

(10) P. Actor, J. V. Uri, I. Zajac, J. R. Guarini, L. Phillips, D. H. Pitkin, D. A. Berges, G. L. Dunn, J. R. E. Hoover, and J. A. Weisbach, *Antimicrob. Agents Chemother.*, **13**, 784 (1978).

(11) R. W. Joss and W. H. Hall, *J. Pharmacol. Exp. Ther.*, **166**, 133 (1969).

(12) J. J. Vallner, *J. Pharm. Sci.*, **66**, 447 (1977).

(13) J. D. Ashbrook, A. A. Spector, E. C. Santos, and J. E. Fletcher, *J. Biol. Chem.*, **250**, 2333 (1975).

(14) A. H. Anton, *J. Pharmacol. Exp. Ther.*, **134**, 291 (1961).

Absorption of Sodium γ-Hydroxybutyrate and Its Prodrug γ-Butyrolactone: Relationship between *In Vitro* Transport and *In Vivo* Absorption

C. ARENA and HO-LEUNG FUNG ˣ

Received August 20, 1979, from the *Department of Pharmaceutics, School of Pharmacy, State University of New York at Buffalo, Amherst, NY 14260.* Accepted for publication October 11, 1979.

Abstract □ A qualitative relationship between *in vitro* transport and *in vivo* absorption of sodium γ-hydroxybutyrate and γ-butyrolactone was demonstrated. As with other short-chain acids, sodium γ-hydroxybutyrate showed capacity-limited transport *in vitro*, consistent with the previous observation that this drug exhibited slower *in vivo* absorption with increasing dose. The prodrug lactone, on the other hand, showed a higher intestinal flux than the acid in the everted gut, and *in vivo* absorption also was more rapid. Capacity-limited transport and absorption of the lactone appeared less evident. Thus, the increased oral hypnotic activity of the lactone over that of the acid most likely is a result of its more favorable intestinal transport characteristics.

Keyphrases □ Sodium γ-hydroxybutyrate—relationship between *in vitro* transport and *in vivo* absorption □ γ-Butyrolactone—prodrug for sodium γ-hydroxybutyrate, relationship between *in vitro* transport and *in vivo* absorption □ Hypnotic agents—sodium γ-hydroxybutyrate and γ-butyrolactone, relationship between *in vitro* transport and *in vivo* absorption

γ-Hydroxybutyrate (I), a metabolite of γ-aminobutyric acid, is found endogenously in the human brain (1). When introduced intravenously, I is a useful anesthetic (2) and is beneficial in Parkinson's disease (3). However, oral administration of this compound results in decreased and variable pharmacological activity (4–6). Recently, oral doses of I totaling 50 mg/kg were shown to be useful in the treatment of narcolepsy and cataplexy in patients, but the duration of sleep induction after each oral dose lasted only for ~2 hr (7).

BACKGROUND

In previous animal studies in these laboratories (8–10), orally administered I was shown to be subject to first-pass metabolism at low doses (≤200 mg/kg) in rats. At higher doses (400–1600 mg/kg), systemic availability approached 100%, presumably due to saturation of first-pass metabolism, but the relative absorption rate appeared to decrease with increasing dose. Thus, although the extent of drug absorption was almost complete, peak plasma I concentrations were relatively insensitive to increases in the oral dose and, in most animals, threshold hypnotic concentrations in plasma were not reached in spite of high oral doses.

The lactone analog of I, γ-butyrolactone (II), is hydrolyzed rapidly and exclusively *in vivo* to I (11, 12) and, therefore, can be classified as a prodrug. Compound II is rapidly and completely absorbed *in vivo* after oral administration over a wide dose range. In contrast to I, the peak drug concentration after oral dosing of II was proportional to the dose, and II was equally effective as a hypnotic whether given orally or intravenously (9).

The reason for the apparent difference in *in vivo* absorption characteristics between I and II has not been delineated. In this paper, *in vitro* experiments that compared the transport properties of these two compounds across the everted rat gut are described.

EXPERIMENTAL

Reagents—Compound I, obtained as the sodium salt[1], and II[1] were used without purification. The buffer and assay reagents[1–3] were all reagent or analytical grade.

Everted Rat Gut Preparation—Male Sprague–Dawley rats, 260–310 g, were sacrificed by decapitation. An intestinal segment, ~12 cm long, was taken from a region 20 cm from the pylorus sphincter; it was everted and mounted according to the technique originally devised by Wilson and Wiseman (13) and modified by Crane and Wilson (14).

Flux Experiment—The everted gut was placed inside a test tube with the mucosal side exposed to 90 ml of a 0.05 *M* physiological tromethamine buffer (pH 7.4) containing the appropriate drug concentration. All flux studies were carried out at 37°. At 5-min intervals up to 25 min, the serosal solution (~1 ml) was removed for the assay and replaced with an equal volume of fresh buffer. Three or four replicate flux experiments were conducted at each initial mucosal concentration.

Spectrophotometric Analysis—The Hestrin (15) assay for short-chain *O*-acyl derivatives as adopted for I and II by Guidotti and Ballotti (16) was employed. Conversion of I to II was effected by reaction with two parts of concentrated sulfuric acid[2] and subsequent neutralization with 10 parts of 6 *N* NaOH[2].

[1] Eastman Kodak Co., Rochester, NY 14650.
[2] Fisher Scientific Co., Fair Lawn, NJ 07410.
[3] J. T. Baker Chemical Co., Phillipsburg, NJ 08865.

0022-3549/80/0300-0356$01.00/0
© 1980, American Pharmaceutical Association

the bioassay of samples containing multiple drugs or abnormal levels of normally occurring metabolic products.

REFERENCES

(1) W. A. Craig and P. G. Welling, *Clin. Pharmacokinet.*, **2**, 252 (1977).

(2) D. S. Greene and A. Tice, "Abstracts," vol. 7, no. 2, APhA Academy of Pharmaceutical Sciences, Washington, D.C., 1977, p. 133 (abstract 75).

(3) C. S. Hollander, R. L. Scott, J. A. Burgess, D. Rabinowitz, T. J. Merimee, and J. H. Oppenheimer, *J. Clin. Endocrinol. Metab.*, **27**, 1219 (1967).

(4) C. M. Kunin, *J. Lab. Clin. Med.*, **65**, 406 (1965).

(5) D. Rudman, T. J. Bixler, III, and A. E. DelRio, *J. Pharmacol. Exp. Ther.*, **176**, 261 (1971).

(6) W. Shaw, I. L. Hubert, and F. W. Spierto, *Clin. Chem.*, **225**, 673 (1976).

(7) G. N. Rolinson, "Recent Advances in Medical Microbiology," A. P. Waterson, Ed., Little, Brown, Boston, Mass., 1966, pp. 254–283.

(8) A. A. Spector, *J. Lipid Res.*, **16**, 165 (1975).

(9) G. Wilding, R. C. Feldhoff, and E. S. Vesell, *Biochem. Pharmacol.*, **26**, 1143 (1977).

(10) P. Actor, J. V. Uri, I. Zajac, J. R. Guarini, L. Phillips, D. H. Pitkin, D. A. Berges, G. L. Dunn, J. R. E. Hoover, and J. A. Weisbach, *Antimicrob. Agents Chemother.*, **13**, 784 (1978).

(11) R. W. Joss and W. H. Hall, *J. Pharmacol. Exp. Ther.*, **166**, 133 (1969).

(12) J. J. Vallner, *J. Pharm. Sci.*, **66**, 447 (1977).

(13) J. D. Ashbrook, A. A. Spector, E. C. Santos, and J. E. Fletcher, *J. Biol. Chem.*, **250**, 2333 (1975).

(14) A. H. Anton, *J. Pharmacol. Exp. Ther.*, **134**, 291 (1961).

Absorption of Sodium γ-Hydroxybutyrate and Its Prodrug γ-Butyrolactone: Relationship between *In Vitro* Transport and *In Vivo* Absorption

C. ARENA and HO-LEUNG FUNG ˣ

Received August 20, 1979, from the *Department of Pharmaceutics, School of Pharmacy, State University of New York at Buffalo, Amherst, NY 14260.* Accepted for publication October 11, 1979.

Abstract □ A qualitative relationship between *in vitro* transport and *in vivo* absorption of sodium γ-hydroxybutyrate and γ-butyrolactone was demonstrated. As with other short-chain acids, sodium γ-hydroxybutyrate showed capacity-limited transport *in vitro*, consistent with the previous observation that this drug exhibited slower *in vivo* absorption with increasing dose. The prodrug lactone, on the other hand, showed a higher intestinal flux than the acid in the everted gut, and *in vivo* absorption also was more rapid. Capacity-limited transport and absorption of the lactone appeared less evident. Thus, the increased oral hypnotic activity of the lactone over that of the acid most likely is a result of its more favorable intestinal transport characteristics.

Keyphrases □ Sodium γ-hydroxybutyrate—relationship between *in vitro* transport and *in vivo* absorption □ γ-Butyrolactone—prodrug for sodium γ-hydroxybutyrate, relationship between *in vitro* transport and *in vivo* absorption □ Hypnotic agents—sodium γ-hydroxybutyrate and γ-butyrolactone, relationship between *in vitro* transport and *in vivo* absorption

γ-Hydroxybutyrate (I), a metabolite of γ-aminobutyric acid, is found endogenously in the human brain (1). When introduced intravenously, I is a useful anesthetic (2) and is beneficial in Parkinson's disease (3). However, oral administration of this compound results in decreased and variable pharmacological activity (4–6). Recently, oral doses of I totaling 50 mg/kg were shown to be useful in the treatment of narcolepsy and cataplexy in patients, but the duration of sleep induction after each oral dose lasted only for ~2 hr (7).

BACKGROUND

In previous animal studies in these laboratories (8–10), orally administered I was shown to be subject to first-pass metabolism at low doses (≤200 mg/kg) in rats. At higher doses (400–1600 mg/kg), systemic availability approached 100%, presumably due to saturation of first-pass metabolism, but the relative absorption rate appeared to decrease with increasing dose. Thus, although the extent of drug absorption was almost complete, peak plasma I concentrations were relatively insensitive to increases in the oral dose and, in most animals, threshold hypnotic concentrations in plasma were not reached in spite of high oral doses.

The lactone analog of I, γ-butyrolactone (II), is hydrolyzed rapidly and exclusively *in vivo* to I (11, 12) and, therefore, can be classified as a prodrug. Compound II is rapidly and completely absorbed *in vivo* after oral administration over a wide dose range. In contrast to I, the peak drug concentration after oral dosing of II was proportional to the dose, and II was equally effective as a hypnotic whether given orally or intravenously (9).

The reason for the apparent difference in *in vivo* absorption characteristics between I and II has not been delineated. In this paper, *in vitro* experiments that compared the transport properties of these two compounds across the everted rat gut are described.

EXPERIMENTAL

Reagents—Compound I, obtained as the sodium salt[1], and II[1] were used without purification. The buffer and assay reagents[1–3] were all reagent or analytical grade.

Everted Rat Gut Preparation—Male Sprague–Dawley rats, 260–310 g, were sacrificed by decapitation. An intestinal segment, ~12 cm long, was taken from a region 20 cm from the pylorus sphincter; it was everted and mounted according to the technique originally devised by Wilson and Wiseman (13) and modified by Crane and Wilson (14).

Flux Experiment—The everted gut was placed inside a test tube with the mucosal side exposed to 90 ml of a 0.05 *M* physiological tromethamine buffer (pH 7.4) containing the appropriate drug concentration. All flux studies were carried out at 37°. At 5-min intervals up to 25 min, the serosal solution (~1 ml) was removed for the assay and replaced with an equal volume of fresh buffer. Three or four replicate flux experiments were conducted at each initial mucosal concentration.

Spectrophotometric Analysis—The Hestrin (15) assay for short-chain *O*-acyl derivatives as adopted for I and II by Guidotti and Ballotti (16) was employed. Conversion of I to II was effected by reaction with two parts of concentrated sulfuric acid[2] and subsequent neutralization with 10 parts of 6 *N* NaOH[2].

[1] Eastman Kodak Co., Rochester, NY 14650.
[2] Fisher Scientific Co., Fair Lawn, NJ 07410.
[3] J. T. Baker Chemical Co., Phillipsburg, NJ 08865.

0022-3549/80/0300-0356$01.00/0
© 1980, American Pharmaceutical Association

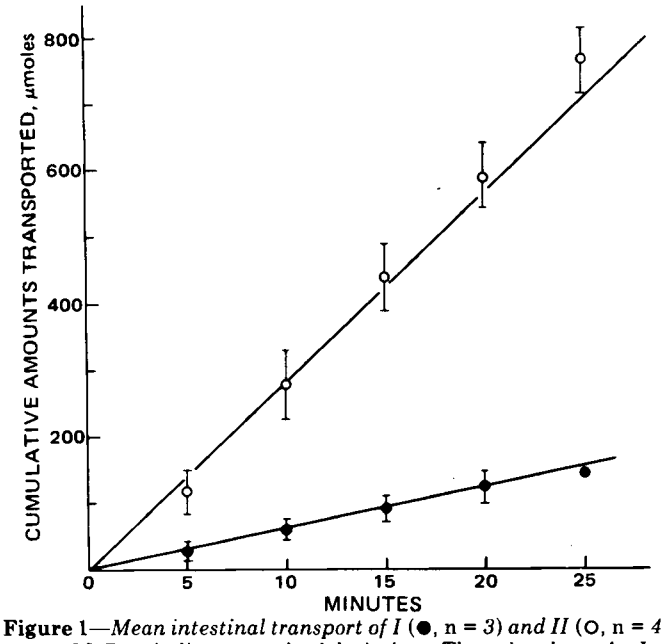

Figure 1—*Mean intestinal transport of I (●, n = 3) and II (○, n = 4) at 0.40* M. *Bars indicate standard deviations. The point shown for I at 25 min represents the mean value of two measurements.*

RESULTS AND DISCUSSION

Transport of I and II through the everted rat gut was examined at various initial mucosal drug concentrations. Intestinal flux was determined for each animal preparation by linear regression of a plot of cumulative amount transported to the serosal side *versus* time. Representative plots showing intestinal transport of I and II at 0.40 *M* are given in Fig. 1. At low mucosal concentrations, linearity of flux was maintained throughout the experiment. However, at high I concentrations, positive deviations (increased flux) occurred at the later time points, suggesting possible tissue damage with prolonged drug exposure. In these instances, initial rates of transport restricted to the linear portion of the curve (usually 0–20 min) were used to calculate flux. In all experiments, the total amounts transported to the serosal side were small (<0.4% for I and <2.5% for II) compared to the total drug available from the mucosal pool. Thus, the initial mucosal concentration remained essentially unchanged throughout each experiment.

Figure 2 shows the relationships between intestinal flux of I and II and their respective mucosal concentrations. Over the concentration range studied, intestinal transport of II was considerably more rapid than that of I. At equimolar mucosal concentrations, the differences in flux between I and II were statistically significant at $p < 0.001$ using the Student t test. Compound II fluxes were ~5, 7, and 10 times higher than I fluxes at 0.40, 0.79, and 1.19 *M*, respectively. In addition, I transport leveled off at concentrations above 0.40 *M*. If nonspecific effects on intestinal permeability could be ruled out, this flux behavior suggested the presence of a capacity-limited transport system for I in the rat intestine. In comparison, concentration-dependent transport of II was less evident.

In these experiments, the ionic strength in the mucosal solution was not constant over the concentration range studied. Although the mucosal solution was prepared with buffer, high I concentrations also could affect the pH slightly because I, as its sodium salt, is mildly basic. The leveling in I flux could, in principle, have been partially contributed to by nonspecific ionic strength and/or pH effects created by increasing mucosal concentrations of the ionic drug. The possibility of this artifact was ruled out by the following experiment.

Flux studies were carried out at 0.08 *M* I under two sets of conditions. In one case, no pH or salt adjustments were made (Condition A: pH 7.4, $\mu = 0.23$ *M*); in the other case, sodium chloride and sodium hydroxide were added so that the pH and ionic conditions were equivalent to those present when flux was studied at 1.19 *M* I (Condition B: pH 8.1, $\mu = 1.34$ *M*). If ionic strength and pH affected flux significantly, then the observed fluxes under Conditions A and B would be different, with the flux of B similar to that observed at 1.19 *M* I. In fact, the flux of I was identical whether or not additional salt or alkalinizing agents were added.

In duplicate determinations, the fluxes obtained under Condition A were 2.2 and 2.3 μ*M*/min; those under Condition B both were 2.4 μ*M*/min. Thus, minor differences in pH and ionic strength contributed by changes

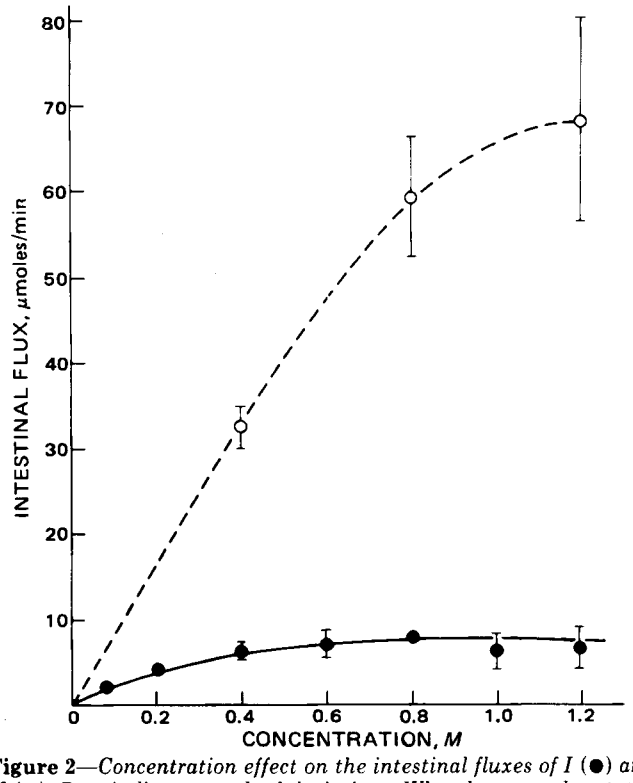

Figure 2—*Concentration effect on the intestinal fluxes of I (●) and II (○). Bars indicate standard deviations. When bars are absent, the standard deviations were too small to be shown.*

in the mucosal I concentration did not affect flux significantly. Since II is nonionic, ionic strength and pH effects produced by increasing II concentrations were presumed to be negligible. Bender *et al.* (17) found the second-order alkaline hydrolytic constant of II to be ~0.2 liter/mole-sec at 25°. At pH 7.4, the hydrolysis half-life would be about 1000 days. Thus, conversion of II to I in the buffered mucosal solution was insignificant during the experiment.

The *in vitro* transport characteristics of I and II are consistent with their *in vivo* absorption properties reported previously (8–10). Compound I, which showed capacity-limited transport *in vitro*, also exhibited relatively slower *in vivo* absorption rates with increasing oral dose (10). Other short-chain acids, such as acetic and butyric acids, also have been shown to be transported *via* an active system (18, 19). Therefore, a capacity-limited absorption mechanism might be a reason for the decreased and variable activity of I when given in high oral doses to humans (4–7). The prodrug lactone II, on the other hand, showed a much higher intestinal flux than I in the everted gut and was almost instantaneously absorbed when orally administered (9). Capacity-limited transport of II, if existent, appeared to occur at much higher drug concentrations.

The present study demonstrated a qualitative relationship between *in vitro* transport and *in vivo* absorption of the two compounds studied. Thus, the increased oral activity of the lactone over that of its open-chain hydroxy acid is most likely a result of its more favorable intestinal transport characteristics. The usefulness of II has not been investigated in humans.

REFERENCES

(1) S. P. Bessman and W. N. Fishbein, *Nature (London)*, **200**, 1207 (1963).

(2) A. S. Hunter, W. J. Long, and C. G. Ryrie, *Br. J. Anaesth.*, **43**, 620 (1971).

(3) A. Bonicinelli, G. Pranoi, A. Greggia, and L. Casalgrandi, *Riv. Farmacol. Ter.*, **11**, 29 (1971).

(4) E. H. Jenney, H. B. Murphee, L. Goldstein, and C. C. Pfeiffer, *Pharmacologist*, **4**, 166 (1962).

(5) D. R. Metcalf, R. N. Emde, and J. T. Stripe, *Electroencephalogr. Clin. Neurophysiol.*, **20**, 506 (1966).

(6) H. Laborit, *Int. J. Neuropharmacol.*, **3**, 433 (1964).

(7) R. Broughton and M. Mamelak, *Can. J. Neurol. Sci.*, **6**, 1 (1979).

(8) J. T. Lettieri and H.-L. Fung, *Res. Commun. Chem. Path.*

Pharmacol., **13**, 425 (1976).
(9) *Ibid.*, **22**, 107 (1978).
(10) J. T. Lettieri and H.-L. Fung, *J. Pharmacol. Exp. Ther.*, **208**, 7 (1979).
(11) R. H. Roth and N. J. Giarman, *Biochem. Pharmacol.*, **15**, 1333 (1966).
(12) J. T. Lettieri and H.-L. Fung, *Biochem. Med.*, **20**, 70 (1978).
(13) T. H. Wilson and G. Wiseman, *J. Physiol.*, **123**, 116 (1954).
(14) R. K. Crane and T. H. Wilson, *J. Appl. Physiol.*, **12**, 145 (1958).
(15) S. Hestrin, *J. Biol. Chem.*, **180**, 249 (1949).
(16) A. Guidotti and P. L. Ballotti, *Biochem. Pharmacol.*, **19**, 883 (1970).
(17) M. L. Bender, H. Matsui, R. J. Thomas, and S. W. Tobey, *J. Am. Chem. Soc.*, **83**, 4193 (1961).
(18) D. H. Smyth and C. B. Taylor, *J. Physiol. (London)*, **141**, 73 (1958).
(19) R. J. C. Barry and D. H. Smyth, *ibid.*, **152**, 48 (1960).

ACKNOWLEDGMENTS

Supported in part by Grant 20852 from the National Institutes of Health.

Temporal Variations in Trough Serum Theophylline Concentrations at Steady State

L. J. LESKO *x, D. BROUSSEAU ‡, A. T. CANADA *, and G. EASTWOOD *

Received June 21, 1979, from the **Drug Concentration Laboratory, University of Massachusetts Medical Center, Worcester, MA 01605*, and ‡*Fisons Corporation, Bedford, MA 01730.* Accepted for publication October 11, 1979.

Abstract □ Temporal variations in serum theophylline concentrations were observed in 14 healthy volunteers receiving multiple doses of theophylline. After repeated oral doses (6.9–18.2 mg/kg/day) of theophylline as either a nonalcoholic aminophylline solution or a controlled-release capsule, trough theophylline levels at steady state were significantly higher ($p < 0.05$) in the morning than in the afternoon or evening. With the solution, the mean ($\pm SE$) trough serum level at 7 am was 11.1 ± 0.9 μg/ml, and at 1 pm it was 9.6 ± 0.8 μg/ml. With the capsule, the mean ($\pm SE$) trough serum level at 8 am was 13.8 ± 0.9 μg/ml, and at 8 pm it was 10.7 ± 0.9 μg/ml. Temporal variations in serum theophylline concentrations have not been reported previously and may be important in therapeutic monitoring.

Keyphrases □ Theophylline—trough serum concentrations at steady state, temporal variations □ Bronchodilators—theophylline, trough serum concentrations at steady state, temporal variations □ Pharmacokinetics—theophylline, trough serum concentrations at steady state, temporal variations

Temporal variation in the absorption and disposition of drugs is an area of pharmacokinetics about which relatively little is known. In the few studies performed, the findings have not been consistent. For example, Shirley and Vesell (1) reported that temporal variations in the disposition of acetaminophen and phenacetin occur. However, Vesell *et al.* (2) observed no temporal variations in the pharmacokinetics of antipyrine (2), and Nakano and Hollister (3) reported no time-related changes in the disposition of nortriptyline. The causes of temporal variations in drug pharmacokinetics may be varied. Circadian rhythm apparently influences the distribution of potassium between body compartments (4), while changes in body posture alter the absorption of cephradine (5) and erythromycin (6) from the GI tract.

One mechanism suggested to account for the temporal variations in the disposition of phenacetin and acetaminophen was the occurrence of diurnal changes in the amount and activity of hepatic microsomal oxidases (1). Theophylline is a drug whose disposition also is determined by microsomal oxidases, so it seemed possible that temporal variations in theophylline disposition may occur. Since this aspect of theophylline kinetics had not been reported previously, one objective of this study was to determine if temporal variations exist.

EXPERIMENTAL

Subjects—The seven male and seven female volunteers were 21–40 years old, and their average weight was 67.5 kg. All volunteers were nonsmokers and were in good physical health with no history of alcoholism or cardiovascular disease.

Drug Administration and Blood Sampling—The volunteers randomly received either a nonalcoholic aminophylline solution or a controlled-release theophylline capsule. The oral theophylline dose was individualized for each volunteer, based on single-dose kinetics, to produce peak serum theophylline concentrations no larger than 18 μg/ml after repeated dosing. The daily doses ranged from 6.9 to 18.2 mg/kg. The solution was administered at 7 am, 1 pm, 7 pm, and 1 am, and the capsule was given at 8 am and 8 pm. Dosing was continued for 6 days prior to each study day. The study days were separated by 1 week during which the volunteers took the alternate formulation.

On each study day, 1 ml of serum was obtained immediately before the morning dose of each dosage form and 6 or 12 hr after administration of the solution or capsule, respectively.

Theophylline Assay—Serum theophylline determinations were made by high-pressure liquid chromatography using a method described previously (7).

Data Analysis—A paired t test was used to analyze within-subject differences between the am and pm trough theophylline concentrations observed for each dosage form.

RESULTS AND DISCUSSION

The am and pm trough serum theophylline concentrations determined for each dosage form are listed in Table I. The percentage changes in trough level are noted for each volunteer. The mean ($\pm SE$) serum theophylline concentration at 7 am for the solution was 11.1 ± 0.9 μg/ml, while at 1 pm the serum theophylline concentration was 9.6 ± 0.8 μg/ml, representing a change of 13%. For the capsule, the mean ($\pm SE$) serum theophylline concentration at 8 am was 13.8 ± 0.9 μg/ml, and at 8 pm it was 10.7 ± 0.9 μg/ml, reflecting a decrease of 24%. The differences between the am and pm serum theophylline concentrations were significant ($p < 0.05$) for each dosage form.

Based on these results, there appear to be temporal variations in theophylline pharmacokinetics. Higher trough levels at 7 or 8 am compared to those at 1 or 8 pm may be related to a shorter plasma half-life at the latter times. Indeed, Shirley and Vesell (1) reported that plasma half-lives of phenacetin and acetaminophen were ~15% shorter at 2 pm than at 6 am. Another possible cause of higher am trough levels may be

0022-3549/80/0300-0358$01.00/0
© 1980, American Pharmaceutical Association

Pharmacol., **13**, 425 (1976).
(9) *Ibid.*, **22**, 107 (1978).
(10) J. T. Lettieri and H.-L. Fung, *J. Pharmacol. Exp. Ther.*, **208**, 7 (1979).
(11) R. H. Roth and N. J. Giarman, *Biochem. Pharmacol.*, **15**, 1333 (1966).
(12) J. T. Lettieri and H.-L. Fung, *Biochem. Med.*, **20**, 70 (1978).
(13) T. H. Wilson and G. Wiseman, *J. Physiol.*, **123**, 116 (1954).
(14) R. K. Crane and T. H. Wilson, *J. Appl. Physiol.*, **12**, 145 (1958).
(15) S. Hestrin, *J. Biol. Chem.*, **180**, 249 (1949).
(16) A. Guidotti and P. L. Ballotti, *Biochem. Pharmacol.*, **19**, 883 (1970).
(17) M. L. Bender, H. Matsui, R. J. Thomas, and S. W. Tobey, *J. Am. Chem. Soc.*, **83**, 4193 (1961).
(18) D. H. Smyth and C. B. Taylor, *J. Physiol. (London)*, **141**, 73 (1958).
(19) R. J. C. Barry and D. H. Smyth, *ibid.*, **152**, 48 (1960).

ACKNOWLEDGMENTS

Supported in part by Grant 20852 from the National Institutes of Health.

Temporal Variations in Trough Serum Theophylline Concentrations at Steady State

L. J. LESKO *x, D. BROUSSEAU ‡, A. T. CANADA *, and G. EASTWOOD *

Received June 21, 1979, from the **Drug Concentration Laboratory, University of Massachusetts Medical Center, Worcester, MA 01605*, and ‡*Fisons Corporation, Bedford, MA 01730.* Accepted for publication October 11, 1979.

Abstract □ Temporal variations in serum theophylline concentrations were observed in 14 healthy volunteers receiving multiple doses of theophylline. After repeated oral doses (6.9–18.2 mg/kg/day) of theophylline as either a nonalcoholic aminophylline solution or a controlled-release capsule, trough theophylline levels at steady state were significantly higher ($p < 0.05$) in the morning than in the afternoon or evening. With the solution, the mean ($\pm SE$) trough serum level at 7 am was 11.1 ± 0.9 μg/ml, and at 1 pm it was 9.6 ± 0.8 μg/ml. With the capsule, the mean ($\pm SE$) trough serum level at 8 am was 13.8 ± 0.9 μg/ml, and at 8 pm it was 10.7 ± 0.9 μg/ml. Temporal variations in serum theophylline concentrations have not been reported previously and may be important in therapeutic monitoring.

Keyphrases □ Theophylline—trough serum concentrations at steady state, temporal variations □ Bronchodilators—theophylline, trough serum concentrations at steady state, temporal variations □ Pharmacokinetics—theophylline, trough serum concentrations at steady state, temporal variations

Temporal variation in the absorption and disposition of drugs is an area of pharmacokinetics about which relatively little is known. In the few studies performed, the findings have not been consistent. For example, Shirley and Vesell (1) reported that temporal variations in the disposition of acetaminophen and phenacetin occur. However, Vesell *et al.* (2) observed no temporal variations in the pharmacokinetics of antipyrine (2), and Nakano and Hollister (3) reported no time-related changes in the disposition of nortriptyline. The causes of temporal variations in drug pharmacokinetics may be varied. Circadian rhythm apparently influences the distribution of potassium between body compartments (4), while changes in body posture alter the absorption of cephradine (5) and erythromycin (6) from the GI tract.

One mechanism suggested to account for the temporal variations in the disposition of phenacetin and acetaminophen was the occurrence of diurnal changes in the amount and activity of hepatic microsomal oxidases (1). Theophylline is a drug whose disposition also is determined by microsomal oxidases, so it seemed possible that temporal variations in theophylline disposition may occur. Since this aspect of theophylline kinetics had not been reported previously, one objective of this study was to determine if temporal variations exist.

EXPERIMENTAL

Subjects—The seven male and seven female volunteers were 21–40 years old, and their average weight was 67.5 kg. All volunteers were nonsmokers and were in good physical health with no history of alcoholism or cardiovascular disease.

Drug Administration and Blood Sampling—The volunteers randomly received either a nonalcoholic aminophylline solution or a controlled-release theophylline capsule. The oral theophylline dose was individualized for each volunteer, based on single-dose kinetics, to produce peak serum theophylline concentrations no larger than 18 μg/ml after repeated dosing. The daily doses ranged from 6.9 to 18.2 mg/kg. The solution was administered at 7 am, 1 pm, 7 pm, and 1 am, and the capsule was given at 8 am and 8 pm. Dosing was continued for 6 days prior to each study day. The study days were separated by 1 week during which the volunteers took the alternate formulation.

On each study day, 1 ml of serum was obtained immediately before the morning dose of each dosage form and 6 or 12 hr after administration of the solution or capsule, respectively.

Theophylline Assay—Serum theophylline determinations were made by high-pressure liquid chromatography using a method described previously (7).

Data Analysis—A paired t test was used to analyze within-subject differences between the am and pm trough theophylline concentrations observed for each dosage form.

RESULTS AND DISCUSSION

The am and pm trough serum theophylline concentrations determined for each dosage form are listed in Table I. The percentage changes in trough level are noted for each volunteer. The mean ($\pm SE$) serum theophylline concentration at 7 am for the solution was 11.1 ± 0.9 μg/ml, while at 1 pm the serum theophylline concentration was 9.6 ± 0.8 μg/ml, representing a change of 13%. For the capsule, the mean ($\pm SE$) serum theophylline concentration at 8 am was 13.8 ± 0.9 μg/ml, and at 8 pm it was 10.7 ± 0.9 μg/ml, reflecting a decrease of 24%. The differences between the am and pm serum theophylline concentrations were significant ($p < 0.05$) for each dosage form.

Based on these results, there appear to be temporal variations in theophylline pharmacokinetics. Higher trough levels at 7 or 8 am compared to those at 1 or 8 pm may be related to a shorter plasma half-life at the latter times. Indeed, Shirley and Vesell (1) reported that plasma half-lives of phenacetin and acetaminophen were ~15% shorter at 2 pm than at 6 am. Another possible cause of higher am trough levels may be

0022-3549/80/0300-0358$01.00/0
© 1980, American Pharmaceutical Association

Table I—Trough Serum Theophylline Levels (Micrograms per Milliliter) in 14 Subjects after Administration of Either a Nonalcoholic Aminophylline Solution or a Controlled-Release Theophylline Capsule

Subject	Daily Dose, mg/kg	Solution			Capsule		
		7 am	1 pm	% Chg[a]	8 am	8 pm	% Chg[a]
A	8.1	6.6	5.0	24.2	6.1	4.1	32.8
B	18.2	14.1	12.7	9.9	16.3	13.8	15.3
C	18.0	7.4	6.0	18.9	15.0	9.1	39.3
D	6.9	7.0	6.6	5.7	12.0	7.3	43.0
E	11.1	14.0	13.0	7.1	17.1	13.1	23.3
F	16.2	15.0	12.0	20.0	15.7	12.7	19.1
G	14.5	14.2	12.4	12.7	16.5	13.2	20.0
H	12.0	14.4	11.5	13.2	14.4	13.4	6.9
I	8.0	8.0	6.5	18.8	11.7	6.3	46.2
J	11.5	14.6	13.6	6.8	13.3	10.8	18.8
K	14.3	11.3	9.7	14.2	13.8	10.4	24.6
L	9.4	7.7	6.1	20.8	8.1	6.2	23.5
M	9.2	11.6	11.6	0.0	13.9	13.2	6.0
N	16.1	8.9	8.3	6.7	18.5	15.7	15.1
Mean		11.1	9.6	12.8	13.8	10.7	23.8
±*SEM*		0.9	0.8	1.9	0.9	0.9	3.4

[a] Percent decrease in trough level from the am to pm period.

slower absorption of the nighttime dose. Nakano and Hollister (3) reported that nortriptyline was absorbed slower after an evening oral dose than after a morning dose. In this study of theophylline, the volunteers were primarily in the supine position after the 1-am and 8-pm doses, which may have slowed absorption. The supine position has been shown to account for slowed absorption of cephradine (5) and erythromycin (6).

Since serum level determinations are widely used to monitor theophylline therapy, temporal variations in theophylline kinetics may be important in the clinical setting. The results emphasize the importance of timing in therapeutic drug monitoring. Serum theophylline concentrations vary with time during a dosage interval at steady state and, based on this study, from one dosage interval to the next. In monitoring theophylline therapy from 1 day to another, it is important to obtain a trough serum theophylline concentration at the same time on each day.

REFERENCES

(1) C. A. Shirley and E. S. Vesell, *Clin. Pharmacol. Ther.*, **18**, 413 (1975).

(2) E. S. Vesell, C. A. Shirley, and G. T. Passananti, *ibid.*, **22**, 843 (1977).

(3) S. Nakano and L. E. Hollister, *ibid.*, **23**, 199 (1978).

(4) M. C. Moore-Ede, M. M. Meguid, G. F. Fitzpatrick, C. M. Boyden, and M. R. Bell, *ibid.*, **23**, 218 (1978).

(5) A. J. Rommel, R. A. Vukovich, J. R. Knill, and A. A. Sugerman, *ibid.*, **23**, 127 (1978).

(6) R. L. Parsons, M. Paccock, and A. Hussack, *Infection*, **5**, 23 (1978).

(7) J. J. Orcutt, P. O. Kozak, S. A. Gillman, and L. H. Cummins, *Clin. Chem.*, **23**, 599 (1977).

ACKNOWLEDGMENTS

Supported by a grant from Fisons Corp., Bedford, Mass.

The technical assistance of J. Palmeri and D. Walker is gratefully acknowledged.

Chemical Constituents of *Curatella americana* (Dilleniaceae)

M. M. EL-AZIZI *, A. M. ATEYA *, G. H. SVOBODA ‡, P. L. SCHIFF, Jr. *, D. J. SLATKIN *, and J. E. KNAPP *x

Received July 16, 1979, from the **Department of Pharmacognosy, School of Pharmacy, University of Pittsburgh, Pittsburgh, PA 15261*, and the ‡*Lilly Research Laboratories, Eli Lilly and Company, Indianapolis, IN 46206.* Accepted for publication October 15, 1979.

Abstract □ A phytochemical investigation of an ethanolic extract of the leaves of *Curatella americana* Linn. (Dilleniaceae) resulted in the isolation and identification of the flavonol glycoside avicularin and gallic acid.

Keyphrases □ *Curatella americana*—chemical constituents, isolation and identification □ Medicinal plants—*Curatella americana*, chemical constituents, isolation and identification □ Avicularin—isolation from *Curatella americana*, identification □ Gallic acid—isolation from *Curatella americana*, identification

Curatella americana Linn. (Dilleniaceae) (1) is a shrub indigenous to Australasia and the tropical Americas (2). The plant has been used in Mexico medicinally for unidentified conditions (3). This use, along with reports of the medicinal and/or toxic potential among other members of the Dilleniaceae (3), and the scarcity of in-depth phytochemical studies on the plant prompted this study.

DISCUSSION

The plant material was extracted by percolation with ethanol to exhaustion. The ethanolic extract was fractionated by successive solvent partitioning and precipitation to yield a fraction that was separated further by chromatography over a polyamide column. Elution of this column with methanol–water afforded avicularin (II) and gallic acid (V).

Compound II was identified by consideration of its physical properties as well as those of derivatives and hydrolysis products. Hydrolysis of II afforded quercetin (I) and L-arabinose. Methylation of II with diazomethane followed by acid hydrolysis afforded 5,7,3′,4′-*O*-methylquercetin (III) and L-arabinose. The identity of III was deduced largely from its mass spectrum, which readily differentiates it from the other tetra-*O*-methylquercetins (4). Peracetylation showed that II was a monoarabinoside.

The NMR spectrum of the peracetate (IV) clearly indicated the presence of phenolic and aliphatic acetate groups in a 4:3 ratio. The mass spectrum of IV showed a weak, but discernible, molecular ion at *m/e* 728, confirming the presence of a single arabinose residue.

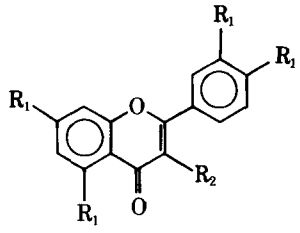

I: $R_1 = R_2 = OH$
II: $R_1 = OH$, R_2 = L-arabinose
III: $R_1 = OCH_3$, $R_2 = OH$
IV: $R_1 = CH_3COO$, $R_2 = CH_3COO$—L-arabinose

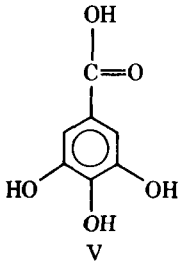

V

The identity of gallic acid (V) was established by comparison of its physical properties with those of an authentic sample.

The presence of a quercetin glycoside in *C. americana* was not unexpected since quercetin (I) was detected chromatographically in *Curatella* species previously (5). Avicularin (II), although not widely distributed in nature, was reported previously in *Polygonum aviculare* var. *buxifolium* (Polygonaceae), *Psidium guaijava* (Myrtaceae), and *Vaccinium myrtillus* (Ericaceae) (6–8). Compound II possesses antibiotic properties (6), which may account for some of the reputed medicinal activity of *C. americana*.

EXPERIMENTAL[1]

Plant Material—The leaves of *C. Americana* (Dilleniaceae) were used[2].

Extraction—The air-dried ground plant material (1.56 kg) was extracted by percolation with ethanol (20 liters). The extract was evaporated *in vacuo* at 40° to yield a syrupy extract (508 g).

Fractionation—The extract was partitioned between chloroform (2 liters) and water (2 liters). The aqueous layer was partitioned further with ethyl acetate (2 liters), and the solvents were removed from each layer to afford Fractions A (chloroform) (175 g), B (water) (268 g), and C (ethyl acetate) (59 g). Fraction C was dissolved in 100 ml of methanol, and 200 ml of chloroform was added. The resulting suspension was filtered to remove the insoluble matter (8.0 g), and the filtrate was evaporated to a residue. This residue was dissolved in 100 ml of ethyl acetate, and 1 liter of petroleum ether was added to the solution. The resulting precipitate (Fraction D) (9.22 g) was recovered by filtration, and the filtrate was set aside.

Chromatography—The precipitated Fraction D was dissolved in methanol (100 ml) and was adsorbed onto 20 g of polyamide[3] by evaporation of the solvent. The dry powder was packed on top of a column (5 × 23 cm, 100 g) of polyamide packed in water. The column was rinsed with 6 liters of water, and elution was carried out first with methanol–water and then with methanol. One-liter fractions were collected.

Isolation of II—Elution of the column with methanol–water (1:1) afforded a fraction (2.86 g) from which II (307 mg) was obtained by crystallization from methanol. The compound had a melting point of 224° [lit. (6) mp 217° (dilute ethanol) and 222° (dehydrated)]; $[\alpha]_D^{30}$ −60° (c 0.2, water); UV (CH_3OH): λ_{max} 215 (log ϵ 4.36), 258 (4.31), 296 (sh) (3.88), and 357 (4.27) nm; IR (KBr): ν_{max} 3420–3200 (br), 1650, 1600, 1500, 1450, 1120, 1050, and 1015 cm^{-1}; NMR (dimethyl sulfoxide): δ 5.35 (1H, d, J = 5 Hz), 6.20 (1H, d, J = 2 Hz), 6.40 (1H, d, J = 2 Hz), 6.85 (1H, d, J = 8 Hz), 7.52 (1H, s), and 7.60 (1H, d, J = 8 Hz).

The mass spectrum did not show a molecular ion. However, characteristic of flavonol glycosides (4), the spectrum was that of the aglycone, showing peaks at *m/e* 302 (100%), 286 (10), 237 (7), 153 (6), 151 (3), 137 (9), and 109 (5). Since no physical data on II other than the melting point have been reported and since a reference sample was unavailable, comparison of physical constants was not possible.

[1] Melting points were taken on a Thomas-Hoover Uni-Melt capillary apparatus and are corrected. IR spectra were determined on a Perkin-Elmer model 257 spectrometer in potassium bromide pellets. UV spectra were obtained on a Perkin-Elmer model 202 spectrometer. Optical rotations were measured on a Perkin-Elmer 241 automatic polarimeter. Mass spectra were taken with an LKB-9000 mass spectrometer. NMR spectra were obtained on a Perkin-Elmer R-24 spectrometer in the solvents specified with tetramethylsilane as the internal standard. Chemical shifts are reported as δ units (parts per million). GLC analysis was performed on a Perkin-Elmer model 3920B instrument operated isothermally at 150°. The column (2 × 0.0004 m, glass) was packed with 3% OV-17 on 80–100-mesh Supelcoport. Nitrogen was the carrier gas at a flow rate of 30 ml/min.

[2] Collected in Brazil and identified by Dr. Basset McGuire of the New York Botanical Gardens. A voucher specimen is on deposit at Eli Lilly and Co., Indianapolis, IN 46206.

[3] Polypenco Nylon 66, Molding Plastics Division, Polymer Corp., Pittsburgh, Pa.

0022-3549/80/0300-0360$01.00/0
© 1980, American Pharmaceutical Association

Hydrolysis of II—Compound II (80 mg) was dissolved in 20 ml of 6% aqueous HCl, and the solution was refluxed for 45 min. The solution was cooled and filtered to separate the precipitated I from the soluble sugar. The filtrate was extracted with chloroform (4 × 50 ml), the extract was dried (sodium sulfate) and evaporated to a residue, and the residue was added to the precipitated I to afford a total of 35 mg. The I obtained (mp 300°) was identical in all respects (UV, IR, NMR, and mass spectra, melting point, and mixed melting point) to an authentic sample[4].

The aqueous filtrate was evaporated to dryness to yield a residue (31 mg) of crude L-arabinose; $[\alpha]_D^{29}$ +34.1° (c 1.1, water). TLC of the material (silica gel G, *n*-butanol–acetic acid–ether–water 9:6:3:1) indicated that it was homogeneous. A comparison of the R_f value (0.42) and color reaction with anisaldehyde spray reagent (9) given by the material with known sugars indicated that it was arabinose. This conclusion was confirmed by converting the sugar to its trimethylsilyl derivative (10) and subjecting it, along with the trimethylsilyl derivatives of other known sugars, to GLC analysis. The trimethylsilyl derivative of the isolated sugar showed an identical retention time (7.5 min) to that of the trimethylsilyl derivative of L-arabinose when analyzed individually or as a mixture and was clearly different from the trimethylsilyl derivatives of other sugars.

5,7,3′,4′-*O*-Methylquercetin (III)—Compound II (50 mg) was treated for 48 hr with 30 ml of ethereal diazomethane solution prepared from 21.5 g of *N*-methyl-*N*-nitrosó-*p*-toluenesulfonamide[5]. The solution then was evaporated to give a residue (56 mg), the residue was suspended in 10 ml of 7% aqueous H_2SO_4, and the suspension was refluxed for 1 hr. The reaction mixture was cooled and extracted with ether (4 × 20 ml), and the ether extract was evaporated to yield 5,7,3′,4′-*O*-methylquercetin (III) (20 mg).

The compound had a melting point of 186–188° [lit. (8) mp 195–196°]; IR (KBr): ν_{max} 3290, 3000, 2925, 2820, 1635 (sh), 1615, 1570, 1515, 1490, 1090, and 1025 cm^{-1}; mass spectrum: *m/e* 358 (M^+) (85%), 312 (100), 181 (17), 197 (75), 165 (65), 150 (43), 149 (34), 142 (30), 137 (30), 135 (42), 122 (30), 119 (32), 107 (28), 92 (33), 79 (52), and 77 (48); NMR ($CDCl_3$): δ 3.90 (1H, s), 3.95 (9H, s), 6.26 (1H, d, J = 2 Hz), 6.43 (1H, d, J = 2 Hz), 6.90 (1H, d, J = 9 Hz), 7.70 (1H, d, J = 9 Hz), and 7.73 (1H, bs); UV: λ_{max} (methanol) 224 (log ε 4.54), 257 (4.43), 300 (6.65), and 3.61 (4.30) nm; λ_{max} (aluminum chloride–methanol) 227 (log ε 4.52), 265 (4.49), and 422 (4.40) nm; and λ_{max} (aluminum chloride–hydrochloric acid–methanol) 220 log ε 4.50), 262 (4.38), 360 (4.05), and 420 (4.03) nm. The UV spectrum was indicative of a 3-hydroxy flavonoid (11).

Avicularin Heptaacetate (IV)—Compound II (15 mg) was treated at room temperature with acetic anhydride and pyridine (5 ml each) for 16 hr. Water, 2 ml, was added to the reaction mixture, and the mixture was evaporated to a residue. This residue was dissolved in 1 ml of acetone, and 5 ml of hexane was added. The precipitated heptaacetate (IV) (16 mg) was recovered by filtration.

The compound had a melting point of 175° [lit. (4) mp 187°]; $[\alpha]_D^{28}$ −95.1° (c 1.20, chloroform) [lit. (4) $[\alpha]_D$ −136° (c 1.22, chloroform)]; IR (KBr): ν_{max} 2920, 1725, 1630, 1615, 1500, 1420, 1370, 1215, and 1070 cm^{-1}; mass spectrum: *m/e* 728 (M^+) (0.2%), 686 (1.0), 644 (0.3), 470 (2.0), 428 (30), 386 (53), 344 (67), 328 (10), 302 (100), 286 (30), 273 (17), 259 (77), 233 (27), 199 (13), 157 (43), 153 (10), 137 (27), 134 (7), and 109 (7). The NMR spectrum ($CDCl_3$) showed singlets at δ 2.10 (12H) and 2.30 (9H), attributable to aromatic and aliphatic acetate groups, respectively.

Isolation of Gallic Acid (V)—Elution of the polyamide column with methanol–water (3:1) afforded a fraction (332 mg) containing V. Treatment of this fraction with methanol–chloroform afforded crystals of V (12 mg) with a melting point of 230–235° whose physical properties (IR, UV, NMR, and mass spectra) were identical to those of an authentic sample[5].

[4] K & K Laboratories, Plainview, N.Y.

[5] Diazald, Aldrich Chemical Co., Milwaukee, Wis.

REFERENCES

(1) B. D. Jackson, "Index Kewensis," vol. I, University Press, Oxford, England, 1895, p. 671.

(2) G. H. M. Lawrence, "Taxonomy of Vascular Plants," Macmillan, New York, N.Y., 1951, p. 598.

(3) S. von Reis Altschul, "Drugs and Foods from Little-Known Plants," Harvard University, Cambridge, Mass., 1973, p. 191.

(4) J. B. Harborne, T. J. Mabry, and H. Mabry, "The Flavonoids," Academic, London, England, 1975, p. 79.

(5) K. Kubitzki, *Ber. Dsch. Bot. Ges.*, **81**, 238 (1968); through *Chem. Abstr.*, **70**, 84922h (1969).

(6) H. El Khadem and Y. S. Mohammed, *J. Chem. Soc. (London)*, **1958**, 3320.

(7) T. Ohta, *Hoppe-Seylers Z. Physiol. Chem.*, **263**, 221 (1940).

(8) C. H. Ice and S. H. Wender, *J. Am. Chem. Soc.*, **75**, 50 (1953).

(9) K. Randerath, "Thin Layer Chromatography," Academic, New York, N.Y., 1968, p. 235.

(10) C. C. Sweeley, R. Bently, M. Makita, and W. W. Wells, *J. Am. Chem. Soc.*, **85**, 2497 (1963).

(11) J. B. Harborne, T. J. Mabry, and H. Mabry, "The Flavonoids," Academic, London, England, 1975, p. 46.

ACKNOWLEDGMENTS

The mass spectrometer facility was supported by Research Grant 5S01RR05455-10 from the National Institutes of Health.

The authors are grateful to Mr. John Naworal, Graduate School of Public Health, University of Pittsburgh, for determining the mass spectra.

Improved GLC Determination of Ethambutol

Keyphrases □ Ethambutol—GLC analysis in biological fluids □ GLC—analysis, ethambutol in biological fluids □ Tuberculostatic antibacterials—ethambutol, GLC analysis in biological fluids

To the Editor:

Several GLC procedures have been reported for the determination of ethambutol in biological fluids (1–4). Only the methods (3, 4) using electron-capture detection are sensitive enough to measure ethambutol concentrations in patient samples of plasma and dialysate. We modified the previously published method (3, 4) to provide a more sensitive and precise procedure that is particularly useful for the determination of low ethambutol levels in biological samples.

Appropriate plasma aliquots (10–100 μl) were mixed with 50 μl of the internal standard [(+)-2,2′-(ethylenediimino)di-1-propanol] solution (10 μg/ml) and deionized water to give a final volume of 0.5 ml. The mixtures were extracted with 5 ml of chloroform for 10 min under alkaline conditions. Portions of the chloroform extract were transferred to another tube and evaporated to dryness under nitrogen. Residues were dissolved in 0.5 ml of spectroquality ethyl acetate.

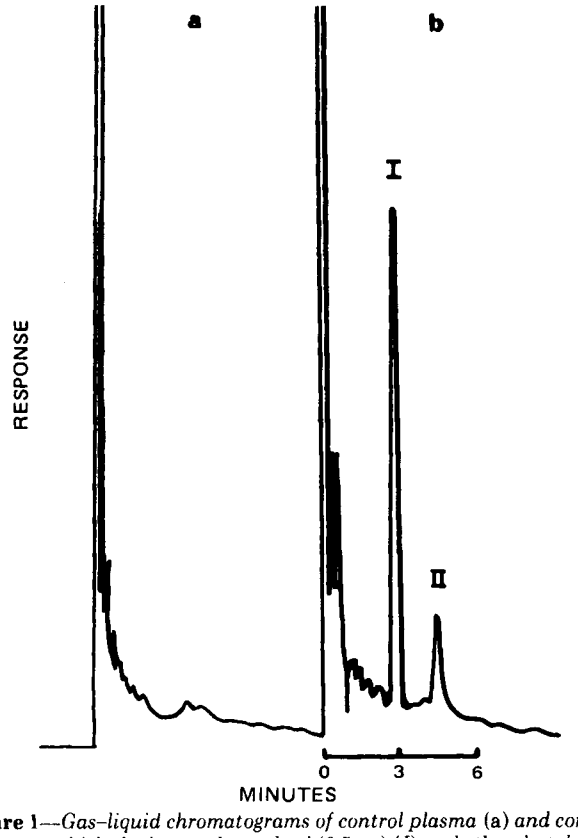

Figure 1—*Gas–liquid chromatograms of control plasma* (a) *and control plasma to which the internal standard (0.5 μg) (I) and ethambutol (0.01 μg) (II) were added* (b).

Table I—Recovery of Ethambutol from Plasma using Electron-Capture Detection (n = 5)

Ethambutol Added, ng	Ethambutol Found, ng	Recovery[a], %
10	9.37 ± 0.84	93.7 ± 8.4
20	18.79 ± 1.13	93.4 ± 5.7
30	30.15 ± 2.72	103.5 ± 9.1
50	51.19 ± 1.13	102.4 ± 2.3
70	68.49 ± 5.02	97.8 ± 7.2
100	98.70 ± 4.92	98.7 ± 4.9
10–100[b]	—	98.3 ± 4.2

[a] Expressed as mean ± *SD*. [b] n = 30.

Derivatization was initiated by adding 20 μl of trifluoroacetic anhydride and was complete in 1 hr at 50°. The contents of the tube were dried with a nitrogen stream to remove excess trifluoroacetic anhydride. Residues of the trifluoroacyl derivatives were reconstituted in 0.5 ml of anhydrous ethyl acetate, and 1–2 μl was injected into the gas–liquid chromatograph equipped with a ^{63}Ni-electron-capture detector. GLC conditions were the same as those described previously (3, 4).

Figure 1 presents gas–liquid chromatograms of control and blank plasma to which 0.01 μg of ethambutol and 0.5 μg of the internal standard were added. Retention times of 3 and 5 min were observed for the internal standard and the drug, respectively. No interfering peaks were found in the control plasma specimens (Fig. 1*a*). Table I summarizes the results obtained following electron-capture analysis of various amounts of ethambutol (10–100 ng) added to plasma. The mean recovery of ethambutol from control plasma in the 10–100-ng range was 98.3 ± 4.2% (n = 30).

The modified procedure offers the following advantages:

1. No catalyst is needed for derivatization. In the old procedure, pyridine is required.
2. The excess trifluoroacetic anhydride can be eliminated by direct evaporation. In the old procedure, the excess derivatizing agent was decomposed by the addition of 0.01 *M* HCl. The acid hydrolysis may adversely affect the yield of the trifluoroacyl derivative.
3. The detection sensitivity of the modified method, 10 ng/ml of plasma, is a significant improvement over that of the previous procedure, 100 ng/ml of plasma. Therefore, only a very small biological sample volume is required for ethambutol detection.

The minimum detectable quantity for ethambutol using this procedure is 10 ng. The optimal therapeutic plasma level in humans was reported as 3–5 μg/ml for ethambutol (5). In this concentration range, only 1–2 μl of plasma would be adequate for an accurate determination of the ethambutol content. This procedure would be helpful in pharmacokinetic studies where low ethambutol concentrations are encountered (6). It should be particularly useful for the microdetermination of ethambutol in bio-

0022-3549/80/0300-0362$01.00/0
© 1980, American Pharmaceutical Association

logical fluids such as saliva, cerebrospinal fluid, and dialysate.

(1) A. Calo, C. Cardini, and V. Quercia, *J. Chromatogr.*, **37**, 194 (1968).
(2) B. M. Richard, J. E. Manno, and B. R. Manno, *ibid.*, **89**, 80 (1974).
(3) C. S. Lee and L. Z. Benet, *ibid.*, **128**, 188 (1976).
(4) C. S. Lee and L. Z. Benet, *J. Pharm. Sci.*, **67**, 470 (1978).
(5) R. Kanther, *Antibiot. Chemother.*, **16**, 203 (1970).
(6) C. S. Lee, T. G. Gambertoglis, D. C. Brater, and L. Z. Benet, *Clin. Pharmacol. Ther.*, **22**, 615 (1977).

Charles S. Lee ˣ
Laurene H. Wang
College of Pharmacy
University of Florida
Gainesville, FL 32610

Received September 21, 1979.
Accepted for publication November 29, 1979.

Pharmacokinetic Studies of Propoxyphene IV: Effect of Renal Failure on Systemic Clearance in Rats

Keyphrases □ Propoxyphene—pharmacokinetics, effect of renal failure on systemic clearance, rats □ Pharmacokinetics—propoxyphene, effect of renal failure on systemic clearance, rats □ Analgesics—propoxyphene, pharmacokinetics, effect of renal failure on systemic clearance, rats

To the Editor:

There is considerable concern about the safety of the widely used analgesic agent propoxyphene (dextropropoxyphene) (1). Under certain circumstances, death from propoxyphene may occur following ingestion of quantities only slightly larger than the upper limit of the recommended therapeutic dosage (1).

Propoxyphene is subject to pronounced presystemic ("first-pass") biotransformation; only a small fraction of the absorbed dose enters the general circulation in unmetabolized form (2–4). This effect may be due to both hepatic and prehepatic biotransformation of the drug during absorption (5). Plasma concentrations of propoxyphene in patients without functioning kidneys are considerably higher than in normal subjects after oral administration of the drug (6). Indirect evidence suggests that this result is due to decreased presystemic biotransformation in the patients (6). However, since propoxyphene could not be administered by intravenous injection, a decreased systemic clearance or apparent volume of distribution of the drug in anephric patients could not be excluded definitively. For this reason, the systemic clearance and apparent volume of distribution of propoxyphene after intravenous injection have now been determined in normal rats and in rats with renal failure.

Male Sprague–Dawley rats, 260–350 g, received a single 5-mg/kg iv dose of either uranyl nitrate (7) or an equal volume of saline solution. Five days later, when serum urea nitrogen concentrations had increased to 150 ± 37 mg/100 ml (mean ± *SD*) in the uranyl nitrate-treated animals (as compared to 15 ± 8 mg/100 ml in normal rats), all animals received a single dose of tritium-labeled propoxyphene, 8.3 ± 1.9 μg/kg (mean ± *SD*), through an indwelling cannula in the jugular vein (8).

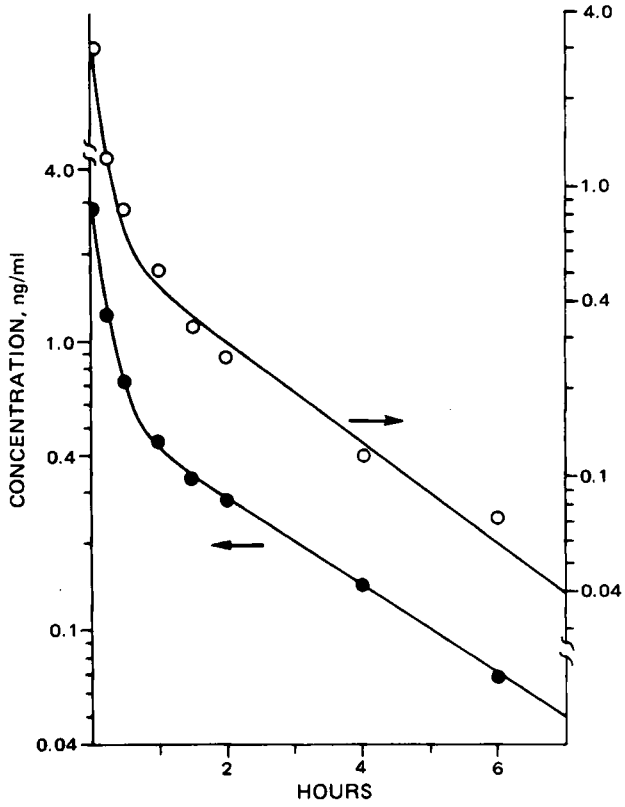

Figure 1—*Serum concentrations of propoxyphene as a function of time after intravenous injection of ^{3}H-propoxyphene at ~8 μg/kg. Key: ●, normal rat; and ○, rat with experimental renal failure. The curves were fitted to the data by nonlinear least-squares regression analysis. (The two vertical axes are displaced relative to one another.)*

Blood samples (0.25–1 ml) were obtained serially for 6–8 hr after injection. Serum was separated, adjusted to pH 9.8, and extracted with butyl chloride; the unmetabolized drug was isolated by TLC (9) and quantified by scintillation spectrometry. An aliquot of the injected solution was assayed similarly. The concentration–time curve was fitted to a biexponential equation by a digital computer (10), with the concentrations weighted as their reciprocals (Fig. 1). The systemic clearance was calculated from the injected dose and the area under the concentration–time curve. The apparent volume of distribution was calculated by dividing the systemic clearance by β.

Compared to surgical methods, injection of uranyl nitrate produces a more reproducible (as determined by serum creatinine and urea nitrogen concentrations) renal failure model. The animals appear to be in better health than after surgery. There was no evidence of hepatocellular damage after a single injection of uranyl nitrate in that glutamic–pyruvic transaminase concentrations in serum were normal[1]. Concomitant injection of tritium-labeled and unlabeled propoxyphene and assay of serum samples by scintillation spectrometry (after TLC) and by GLC

[1] K. M. Giacomini, S. M. Roberts, and G. Levy, unpublished data.

0022-3549/80/0300-0363$01.00/0
© 1980, American Pharmaceutical Association

logical fluids such as saliva, cerebrospinal fluid, and dialysate.

(1) A. Calo, C. Cardini, and V. Quercia, *J. Chromatogr.*, **37**, 194 (1968).
(2) B. M. Richard, J. E. Manno, and B. R. Manno, *ibid.*, **89**, 80 (1974).
(3) C. S. Lee and L. Z. Benet, *ibid.*, **128**, 188 (1976).
(4) C. S. Lee and L. Z. Benet, *J. Pharm. Sci.*, **67**, 470 (1978).
(5) R. Kanther, *Antibiot. Chemother.*, **16**, 203 (1970).
(6) C. S. Lee, T. G. Gambertoglis, D. C. Brater, and L. Z. Benet, *Clin. Pharmacol. Ther.*, **22**, 615 (1977).

Charles S. Lee ˣ
Laurene H. Wang
College of Pharmacy
University of Florida
Gainesville, FL 32610

Received September 21, 1979.
Accepted for publication November 29, 1979.

Pharmacokinetic Studies of Propoxyphene IV: Effect of Renal Failure on Systemic Clearance in Rats

Keyphrases □ Propoxyphene—pharmacokinetics, effect of renal failure on systemic clearance, rats □ Pharmacokinetics—propoxyphene, effect of renal failure on systemic clearance, rats □ Analgesics—propoxyphene, pharmacokinetics, effect of renal failure on systemic clearance, rats

To the Editor:

There is considerable concern about the safety of the widely used analgesic agent propoxyphene (dextropropoxyphene) (1). Under certain circumstances, death from propoxyphene may occur following ingestion of quantities only slightly larger than the upper limit of the recommended therapeutic dosage (1).

Propoxyphene is subject to pronounced presystemic ("first-pass") biotransformation; only a small fraction of the absorbed dose enters the general circulation in unmetabolized form (2–4). This effect may be due to both hepatic and prehepatic biotransformation of the drug during absorption (5). Plasma concentrations of propoxyphene in patients without functioning kidneys are considerably higher than in normal subjects after oral administration of the drug (6). Indirect evidence suggests that this result is due to decreased presystemic biotransformation in the patients (6). However, since propoxyphene could not be administered by intravenous injection, a decreased systemic clearance or apparent volume of distribution of the drug in anephric patients could not be excluded definitively. For this reason, the systemic clearance and apparent volume of distribution of propoxyphene after intravenous injection have now been determined in normal rats and in rats with renal failure.

Male Sprague–Dawley rats, 260–350 g, received a single 5-mg/kg iv dose of either uranyl nitrate (7) or an equal volume of saline solution. Five days later, when serum urea nitrogen concentrations had increased to 150 ± 37 mg/100 ml (mean ± *SD*) in the uranyl nitrate-treated animals (as compared to 15 ± 8 mg/100 ml in normal rats), all animals received a single dose of tritium-labeled propoxyphene, 8.3 ± 1.9 μg/kg (mean ± *SD*), through an indwelling cannula in the jugular vein (8).

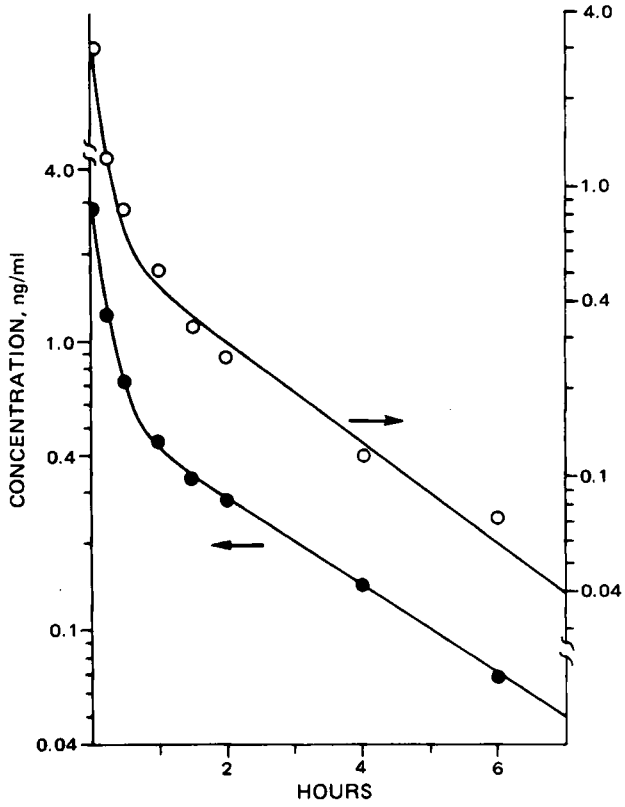

Figure 1—*Serum concentrations of propoxyphene as a function of time after intravenous injection of ^{3}H-propoxyphene at ~8 μg/kg. Key: ●, normal rat; and ○, rat with experimental renal failure. The curves were fitted to the data by nonlinear least-squares regression analysis. (The two vertical axes are displaced relative to one another.)*

Blood samples (0.25–1 ml) were obtained serially for 6–8 hr after injection. Serum was separated, adjusted to pH 9.8, and extracted with butyl chloride; the unmetabolized drug was isolated by TLC (9) and quantified by scintillation spectrometry. An aliquot of the injected solution was assayed similarly. The concentration–time curve was fitted to a biexponential equation by a digital computer (10), with the concentrations weighted as their reciprocals (Fig. 1). The systemic clearance was calculated from the injected dose and the area under the concentration–time curve. The apparent volume of distribution was calculated by dividing the systemic clearance by β.

Compared to surgical methods, injection of uranyl nitrate produces a more reproducible (as determined by serum creatinine and urea nitrogen concentrations) renal failure model. The animals appear to be in better health than after surgery. There was no evidence of hepatocellular damage after a single injection of uranyl nitrate in that glutamic–pyruvic transaminase concentrations in serum were normal[1]. Concomitant injection of tritium-labeled and unlabeled propoxyphene and assay of serum samples by scintillation spectrometry (after TLC) and by GLC

[1] K. M. Giacomini, S. M. Roberts, and G. Levy, unpublished data.

0022-3549/80/0300-0363$01.00/0
© 1980, American Pharmaceutical Association

Table I—Effect of Renal Failure on Pharmacokinetics of Propoxyphene in Rats

Pharmacokinetic Constant	Normal Rats	Renal Failure Rats
Systemic clearance, ml/min/kg	61.4 ± 11.7[a] (47.8–75.1)	59.1 ± 13.2 (38.5–78.0)
Apparent volume of distribution, liters/kg	10.4 ± 3.2 (6.24–13.4)	8.3 ± 2.1 (6.22–11.9)

[a] Mean ± SD, $n = 6$; the range is given in parentheses.

yielded essentially identical results, showing that the tritium exchange was negligible.

The propoxyphene clearance and apparent volume of distribution values for normal rats and rats with experimental renal failure are listed in Table I. Clearance was high and comparable in magnitude to the hepatic plasma flow rate (11). The apparent volume of distribution was very large and comparable to that reported for humans (4). There were no significant differences in the kinetic constants between rats with normal and impaired renal function.

Rats, like humans, eliminate propoxyphene almost exclusively by biotransformation (12). Systemic clearance of propoxyphene in humans is somewhat higher than the hepatic plasma flow rate (4); the two values are similar in the rat. Therefore, the systemic clearance of propoxyphene is primarily a function of the hepatic blood flow rate and should be relatively insensitive to changes in the activity of hepatic drug metabolizing enzyme systems. Hepatic blood flow is not reduced, and the blood plasma flow rate may actually increase in renal failure (13). The results of this study are consistent with these considerations in that the systemic clearance of propoxyphene was not affected by experimental renal dysfunction. This finding and the apparent lack of effect of renal dysfunction on the volume of distribution of propoxyphene support the conclusion that higher plasma propoxyphene concentrations in anephric patients following oral administration are probably due to decreased presystemic biotransformation of the drug (6).

(1) *Fed. Reg.*, **44**, 11837 (1979).

(2) R. L. Wolen, C. M. Gruber, Jr., G. F. Kiplinger, and N. E. Scholz, *Toxicol. Appl. Pharmacol.*, **19**, 480 (1971).

(3) D. Perrier and M. Gibaldi, *J. Clin. Pharmacol.*, **12**, 449 (1972).

(4) L. F. Gram, J. Schou, W. L. Way, J. Heltberg, and N. O. Bodin, *Clin. Pharmacol. Ther.*, **26**, 473 (1979).

(5) K. M. Giacomini, S. M. Nakeeb, and G. Levy, *J. Pharm. Sci.*, in press.

(6) T. P. Gibson, K. M. Giacomini, W. A. Briggs, W. Whitman, and G. Levy, *Clin. Pharmacol. Ther.*, **21**, 103 (1977).

(7) W. Flamenbaum, M. L. Huddleston, J. S. McNeil, and R. J. Hamburger, *Kidney Int.*, **6**, 408 (1974).

(8) J. R. Weeks and J. D. Davis, *J. Appl. Physiol.*, **19**, 540 (1964).

(9) P. J. Murphy, R. C. Nickander, G. M. Bellamy, and W. L. Kurtz, *J. Pharmacol. Exp. Ther.*, **199**, 415 (1976).

(10) C. M. Metzler, "NONLIN, A Computer Program for Parameter Estimation in Nonlinear Situations," The Upjohn Co., Kalamazoo, Mich., 1969.

(11) E. E. Ohnhaus and J. T. Locher, *Eur. J. Pharmacol.*, **31**, 161 (1975).

(12) R. E. McMahon, A. S. Ridolfo, H. W. Culp, R. L. Wolen, and F. J. Marshall, *Toxicol. Appl. Pharmacol.*, **19**, 427 (1971).

(13) P. Corvol, X. Bertagna, and J. Bedrossian, *Acta Endocrinol.*, **75**, 756 (1974).

Stephen M. Roberts
Gerhard Levy [x]

Department of Pharmaceutics
State University of New York at Buffalo
Amherst, NY 14260

Received September 24, 1979.

Accepted for publication December 6, 1979.

Supported in part by Grant GM 20852 and by postdoctoral fellowship GM 06774-02 to S. M. Roberts from the National Institute of General Medical Sciences, National Institutes of Health.

Reaction of *cis*-Platinum with Sodium Bisulfite

Keyphrases □ *cis*-Platinum—reaction with sodium bisulfite □ Sodium bisulfite—reaction with *cis*-platinum □ Antitumor agents, potential—*cis*-platinum(II) diaminedichloride, reaction of *cis*-platinum with sodium bisulfite

To the Editor:

cis-Platinum(II) diaminedichloride is a promising antitumor agent for the treatment of testicular cancer. Although the exact mechanism of its action is not fully understood, it is known that the agent reacts with DNA (1) and inhibits DNA synthesis (2). Recent studies showed that the antitumor agent reacts with DNA bases to form complexes of different composition (3).

In our study of the reaction of *cis*-platinum with pharmaceutical additives, we observed a rather unusual reaction between the antitumor agent and sodium bisulfite. When sodium bisulfite solutions (0.005–0.2 *M*) were mixed directly in the spectrophotometric cell with freshly prepared *cis*-platinum solution (10^{-4} *M*) in pH 4.2, 0.5 *M* acetate buffer, the absorbance at 280 nm increased. At this wavelength and concentration, *cis*-platinum has no absorbance; sodium bisulfite was present in both the sample and the blank.

The increase in the absorbance at 280 nm exhibited a lag time, followed by a rapid change, and finally leveled off (Fig. 1). However, the rate of change in absorbance varied

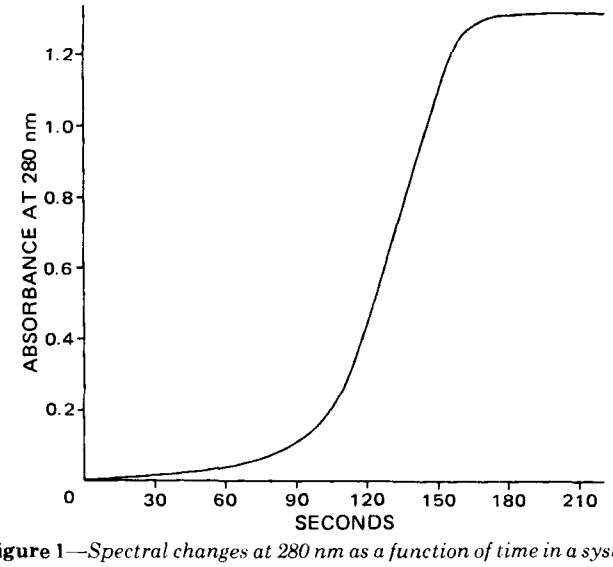

Figure 1—*Spectral changes at 280 nm as a function of time in a system containing 2 × 10^{-4} M cis-platinum and 0.01 M sodium bisulfite at pH 4.2 and 25°.*

0022-3549/80/0300-0364$01.00/0

© 1980, American Pharmaceutical Association

Table I—Effect of Renal Failure on Pharmacokinetics of Propoxyphene in Rats

Pharmacokinetic Constant	Normal Rats	Renal Failure Rats
Systemic clearance, ml/min/kg	61.4 ± 11.7[a] (47.8–75.1)	59.1 ± 13.2 (38.5–78.0)
Apparent volume of distribution, liters/kg	10.4 ± 3.2 (6.24–13.4)	8.3 ± 2.1 (6.22–11.9)

[a] Mean ± SD, $n = 6$; the range is given in parentheses.

yielded essentially identical results, showing that the tritium exchange was negligible.

The propoxyphene clearance and apparent volume of distribution values for normal rats and rats with experimental renal failure are listed in Table I. Clearance was high and comparable in magnitude to the hepatic plasma flow rate (11). The apparent volume of distribution was very large and comparable to that reported for humans (4). There were no significant differences in the kinetic constants between rats with normal and impaired renal function.

Rats, like humans, eliminate propoxyphene almost exclusively by biotransformation (12). Systemic clearance of propoxyphene in humans is somewhat higher than the hepatic plasma flow rate (4); the two values are similar in the rat. Therefore, the systemic clearance of propoxyphene is primarily a function of the hepatic blood flow rate and should be relatively insensitive to changes in the activity of hepatic drug metabolizing enzyme systems. Hepatic blood flow is not reduced, and the blood plasma flow rate may actually increase in renal failure (13). The results of this study are consistent with these considerations in that the systemic clearance of propoxyphene was not affected by experimental renal dysfunction. This finding and the apparent lack of effect of renal dysfunction on the volume of distribution of propoxyphene support the conclusion that higher plasma propoxyphene concentrations in anephric patients following oral administration are probably due to decreased presystemic biotransformation of the drug (6).

(1) *Fed. Reg.*, **44**, 11837 (1979).

(2) R. L. Wolen, C. M. Gruber, Jr., G. F. Kiplinger, and N. E. Scholz, *Toxicol. Appl. Pharmacol.*, **19**, 480 (1971).

(3) D. Perrier and M. Gibaldi, *J. Clin. Pharmacol.*, **12**, 449 (1972).

(4) L. F. Gram, J. Schou, W. L. Way, J. Heltberg, and N. O. Bodin, *Clin. Pharmacol. Ther.*, **26**, 473 (1979).

(5) K. M. Giacomini, S. M. Nakeeb, and G. Levy, *J. Pharm. Sci.*, in press.

(6) T. P. Gibson, K. M. Giacomini, W. A. Briggs, W. Whitman, and G. Levy, *Clin. Pharmacol. Ther.*, **21**, 103 (1977).

(7) W. Flamenbaum, M. L. Huddleston, J. S. McNeil, and R. J. Hamburger, *Kidney Int.*, **6**, 408 (1974).

(8) J. R. Weeks and J. D. Davis, *J. Appl. Physiol.*, **19**, 540 (1964).

(9) P. J. Murphy, R. C. Nickander, G. M. Bellamy, and W. L. Kurtz, *J. Pharmacol. Exp. Ther.*, **199**, 415 (1976).

(10) C. M. Metzler, "NONLIN, A Computer Program for Parameter Estimation in Nonlinear Situations," The Upjohn Co., Kalamazoo, Mich., 1969.

(11) E. E. Ohnhaus and J. T. Locher, *Eur. J. Pharmacol.*, **31**, 161 (1975).

(12) R. E. McMahon, A. S. Ridolfo, H. W. Culp, R. L. Wolen, and F. J. Marshall, *Toxicol. Appl. Pharmacol.*, **19**, 427 (1971).

(13) P. Corvol, X. Bertagna, and J. Bedrossian, *Acta Endocrinol.*, **75**, 756 (1974).

Stephen M. Roberts
Gerhard Levy [x]

Department of Pharmaceutics
State University of New York at Buffalo
Amherst, NY 14260

Received September 24, 1979.

Accepted for publication December 6, 1979.

Supported in part by Grant GM 20852 and by postdoctoral fellowship GM 06774-02 to S. M. Roberts from the National Institute of General Medical Sciences, National Institutes of Health.

Reaction of *cis*-Platinum with Sodium Bisulfite

Keyphrases □ *cis*-Platinum—reaction with sodium bisulfite □ Sodium bisulfite—reaction with *cis*-platinum □ Antitumor agents, potential—*cis*-platinum(II) diaminedichloride, reaction of *cis*-platinum with sodium bisulfite

To the Editor:

cis-Platinum(II) diaminedichloride is a promising antitumor agent for the treatment of testicular cancer. Although the exact mechanism of its action is not fully understood, it is known that the agent reacts with DNA (1) and inhibits DNA synthesis (2). Recent studies showed that the antitumor agent reacts with DNA bases to form complexes of different composition (3).

In our study of the reaction of *cis*-platinum with pharmaceutical additives, we observed a rather unusual reaction between the antitumor agent and sodium bisulfite. When sodium bisulfite solutions (0.005–0.2 *M*) were mixed directly in the spectrophotometric cell with freshly prepared *cis*-platinum solution (10^{-4} *M*) in pH 4.2, 0.5 *M* acetate buffer, the absorbance at 280 nm increased. At this wavelength and concentration, *cis*-platinum has no absorbance; sodium bisulfite was present in both the sample and the blank.

The increase in the absorbance at 280 nm exhibited a lag time, followed by a rapid change, and finally leveled off (Fig. 1). However, the rate of change in absorbance varied

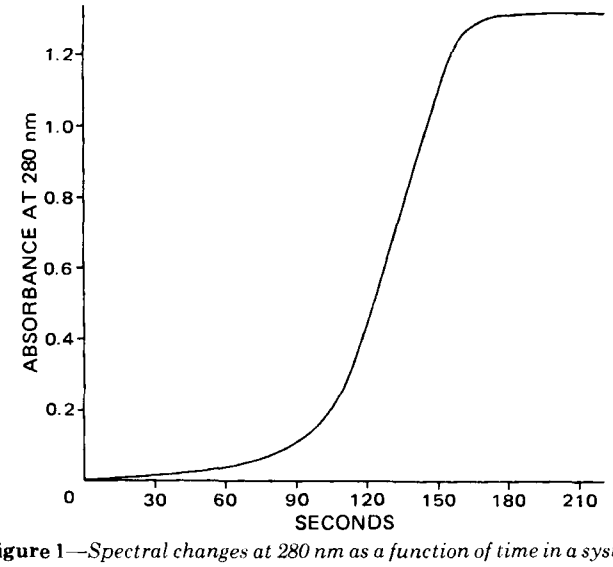

Figure 1—*Spectral changes at 280 nm as a function of time in a system containing 2 × 10^{-4} M cis-platinum and 0.01 M sodium bisulfite at pH 4.2 and 25°.*

0022-3549/80/0300-0364$01.00/0

© 1980, American Pharmaceutical Association

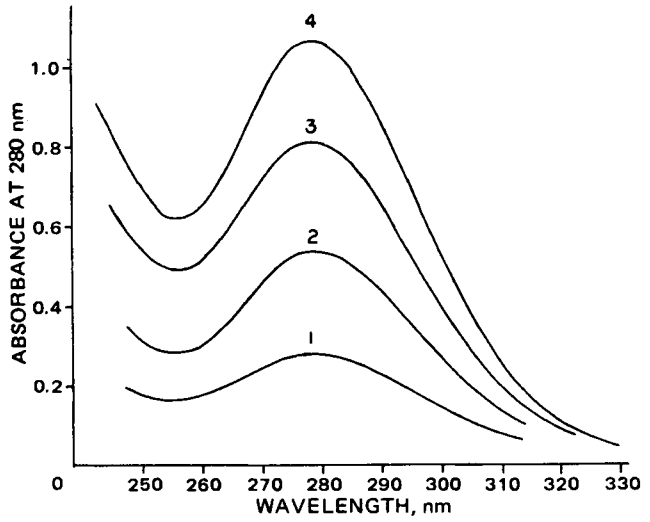

Figure 2—*UV spectra of solutions containing 1 × 10^{-2} M sodium bisulfite and varying amounts of* cis-*platinum. Key: 1, 4 μg/ml; 2, 8 μg/ml; 3, 12 μg/ml; and 4, 16 μg/ml.*

in nonlinear fashion as a function of the bisulfite concentration. Furthermore, in the presence of nitrogen or concentrations of ethanol or methanol as low as 1 × 10^{-3} *M*, no reaction was observed indicating autoxidation.

When 0.5 ml of 1 *M* sodium bisulfite (pH 4.2) was added to different concentrations of *cis*-platinum (0.1–0.5 ml of 1 mg of *cis*-platinum/ml) in water and the reaction mixture was left for 5 min at room temperature and diluted with pH 4.2 acetate buffer to 25 ml, the maximum absorbance at 280 nm varied linearly with the *cis*-platinum concentration (Fig. 2).

The absorbance at 280 nm remained constant for several hours. Although the exact mechanism of this interesting reaction is not known at this time, such a chemical reaction possibly may occur *in vivo* between the antitumor agent and the enzymes containing a sulfhydryl group found in the body.

Furthermore, in view of the enhancement of the UV absorbance of *cis*-platinum in the presence of bisulfite, this reaction can be used for the analysis of the drug in dosage forms. This observation also is important from the pharmaceutical standpoint when the drug is added to intravenous fluids containing antioxidants such as sodium bisulfite. It may be possible that the antioxidant will inactivate the drug in the intravenous fluids prior to administration.

(1) J. J. Roberts, in "Platinum Coordination Complexes in Cancer Chemotherapy," T. A. Connors and Roberts, Eds., Springer, Berlin, Germany, 1974, pp. 79–97.

(2) H. C. Harder and B. Rosenberg, *Inst. J. Cancer*, **6**, 207 (1970).

(3) V. Kleinwachter and R. Zaludova, *Chem. Biol. Interact.*, **16**, 207 (1977).

Anwar A. Hussain ˣ
Mawaffak Haddadin *
K. Iga
College of Pharmacy
University of Kentucky
Lexington, KY 40506

Received October 29, 1979.
Accepted for publication December 20, 1979.
* Present address: University of Jordan, Amman, Jordan.

Percutaneous Absorption of Nitroglycerin

Keyphrases □ Nitroglycerin—percutaneous absorption, rhesus monkeys □ Absorption, percutaneous—nitroglycerin, rhesus monkeys □ Vasodilators—nitroglycerin, percutaneous absorption, rhesus monkeys

To the Editor:

We wish to report the percutaneous absorption of nitroglycerin in the rhesus monkey, an animal model that has been shown to be similar to humans (1, 2).

Sublingual nitroglycerin therapy has been the principal treatment for the symptomatic relief of angina pectoris. Sublingual nitrates are very effective, but their symptomatic improvements are not long lasting. Recently, nitroglycerin administered topically as an ointment was shown to be clinically effective for angina (3), and the slower absorption rate after topical administration results in a longer duration of action than after sublingual administration. Oral administration of nitroglycerin is not effective.

Our objective was to study some parameters of the percutaneous absorption of nitroglycerin. We wanted first to determine if there is an optimal site for absorption because the anatomical site of application affects skin absorption (4, 5). We then wanted to ascertain if the size of the application area affects the absorption of nitroglycerin.

The study was done *in vivo* with the rhesus monkey (*Macaca mulata*). Nitroglycerin (40 mg, 5 μCi) labeled with carbon 14 was applied to a 2-cm^2 area of skin. The areas tested were the chest, arm (upper inside), inner thigh, and postauricular region. After the application, each area was occluded with aluminum foil and adhesive tape for 24 hr. Then the occlusion was removed, and the site was washed with soap and water.

In addition, absorption of an identical dose was determined on the chest using a surface area of 50 cm^2. For this larger surface area, it was necessary to dissolve the dose in 250 μl of absolute ethanol. This solution was applied, and the ethanol was gently evaporated. Alcohol does not significantly alter nitroglycerin absorption (6). Percutaneous absorption was determined by the urinary excretion of carbon 14.

Absorption was quantified on the basis of the percent of radioactivity excreted in urine for 5 days following application of a known amount of the labeled compound to the skin. Daily urinary excretion values were corrected for excretion of radioactivity by other routes and retention of radioactivity in the body by administration of an intravenous dose of [^{14}C]nitroglycerin (1). Urinary radioactivity represents only the apparent nitroglycerin absorption. The potential for skin metabolism of nitroglycerin during absorption is unknown.

After intravenous administration of [^{14}C]nitroglycerin, 59.0 ± 1.9 (*SEM*) % of the dose was excreted in the urine in 5 days. Percent absorptions were 13.4 ± 1.2 (chest), 12.9 ± 1.2 (arm), 8.9 ± 1.4 (postauricular), and 14.8 ± 2.2 (thigh). None of the absorption values for doses applied to the 2-cm^2 areas was statistically different from each other. The majority of the unabsorbed dose in each case was recovered in the wash. Absorption of an identical dose

0022-3549/80/0300-0365$01.00/0
© 1980, American Pharmaceutical Association

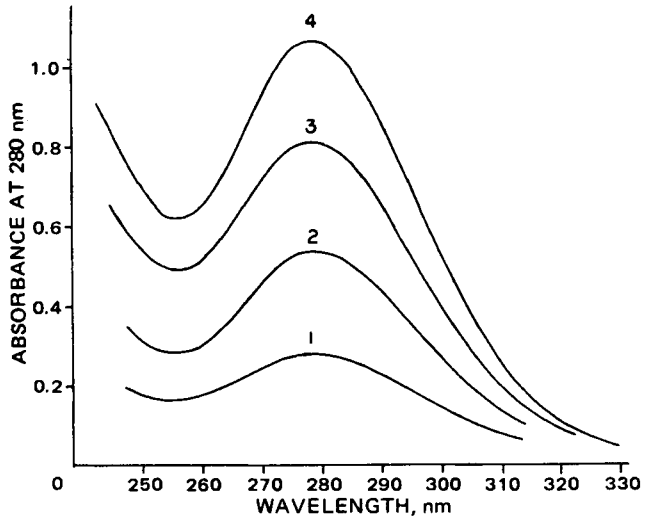

Figure 2—*UV spectra of solutions containing 1 × 10^{-2} M sodium bisulfite and varying amounts of* cis-*platinum. Key: 1, 4 μg/ml; 2, 8 μg/ml; 3, 12 μg/ml; and 4, 16 μg/ml.*

in nonlinear fashion as a function of the bisulfite concentration. Furthermore, in the presence of nitrogen or concentrations of ethanol or methanol as low as 1 × 10^{-3} *M*, no reaction was observed indicating autoxidation.

When 0.5 ml of 1 *M* sodium bisulfite (pH 4.2) was added to different concentrations of *cis*-platinum (0.1–0.5 ml of 1 mg of *cis*-platinum/ml) in water and the reaction mixture was left for 5 min at room temperature and diluted with pH 4.2 acetate buffer to 25 ml, the maximum absorbance at 280 nm varied linearly with the *cis*-platinum concentration (Fig. 2).

The absorbance at 280 nm remained constant for several hours. Although the exact mechanism of this interesting reaction is not known at this time, such a chemical reaction possibly may occur *in vivo* between the antitumor agent and the enzymes containing a sulfhydryl group found in the body.

Furthermore, in view of the enhancement of the UV absorbance of *cis*-platinum in the presence of bisulfite, this reaction can be used for the analysis of the drug in dosage forms. This observation also is important from the pharmaceutical standpoint when the drug is added to intravenous fluids containing antioxidants such as sodium bisulfite. It may be possible that the antioxidant will inactivate the drug in the intravenous fluids prior to administration.

(1) J. J. Roberts, in "Platinum Coordination Complexes in Cancer Chemotherapy," T. A. Connors and Roberts, Eds., Springer, Berlin, Germany, 1974, pp. 79–97.

(2) H. C. Harder and B. Rosenberg, *Inst. J. Cancer*, **6**, 207 (1970).

(3) V. Kleinwachter and R. Zaludova, *Chem. Biol. Interact.*, **16**, 207 (1977).

Anwar A. Hussain ˣ
Mawaffak Haddadin *
K. Iga
College of Pharmacy
University of Kentucky
Lexington, KY 40506

Received October 29, 1979.
Accepted for publication December 20, 1979.
* Present address: University of Jordan, Amman, Jordan.

Percutaneous Absorption of Nitroglycerin

Keyphrases □ Nitroglycerin—percutaneous absorption, rhesus monkeys □ Absorption, percutaneous—nitroglycerin, rhesus monkeys □ Vasodilators—nitroglycerin, percutaneous absorption, rhesus monkeys

To the Editor:

We wish to report the percutaneous absorption of nitroglycerin in the rhesus monkey, an animal model that has been shown to be similar to humans (1, 2).

Sublingual nitroglycerin therapy has been the principal treatment for the symptomatic relief of angina pectoris. Sublingual nitrates are very effective, but their symptomatic improvements are not long lasting. Recently, nitroglycerin administered topically as an ointment was shown to be clinically effective for angina (3), and the slower absorption rate after topical administration results in a longer duration of action than after sublingual administration. Oral administration of nitroglycerin is not effective.

Our objective was to study some parameters of the percutaneous absorption of nitroglycerin. We wanted first to determine if there is an optimal site for absorption because the anatomical site of application affects skin absorption (4, 5). We then wanted to ascertain if the size of the application area affects the absorption of nitroglycerin.

The study was done *in vivo* with the rhesus monkey (*Macaca mulata*). Nitroglycerin (40 mg, 5 μCi) labeled with carbon 14 was applied to a 2-cm^2 area of skin. The areas tested were the chest, arm (upper inside), inner thigh, and postauricular region. After the application, each area was occluded with aluminum foil and adhesive tape for 24 hr. Then the occlusion was removed, and the site was washed with soap and water.

In addition, absorption of an identical dose was determined on the chest using a surface area of 50 cm^2. For this larger surface area, it was necessary to dissolve the dose in 250 μl of absolute ethanol. This solution was applied, and the ethanol was gently evaporated. Alcohol does not significantly alter nitroglycerin absorption (6). Percutaneous absorption was determined by the urinary excretion of carbon 14.

Absorption was quantified on the basis of the percent of radioactivity excreted in urine for 5 days following application of a known amount of the labeled compound to the skin. Daily urinary excretion values were corrected for excretion of radioactivity by other routes and retention of radioactivity in the body by administration of an intravenous dose of [^{14}C]nitroglycerin (1). Urinary radioactivity represents only the apparent nitroglycerin absorption. The potential for skin metabolism of nitroglycerin during absorption is unknown.

After intravenous administration of [^{14}C]nitroglycerin, 59.0 ± 1.9 (*SEM*) % of the dose was excreted in the urine in 5 days. Percent absorptions were 13.4 ± 1.2 (chest), 12.9 ± 1.2 (arm), 8.9 ± 1.4 (postauricular), and 14.8 ± 2.2 (thigh). None of the absorption values for doses applied to the 2-cm^2 areas was statistically different from each other. The majority of the unabsorbed dose in each case was recovered in the wash. Absorption of an identical dose

0022-3549/80/0300-0365$01.00/0
© 1980, American Pharmaceutical Association

on the chest from a surface area of 50 cm^2 was significantly ($p < 0.002$) greater (36.4 ± 4.3%) than the absorption from the smaller surface area. Therefore, differences in these anatomical sites did not affect absorption, but increasing the size of the skin surface area did increase absorption.

The anatomical site of application has been shown to affect the percutaneous absorption of compounds in humans (4, 5) and the rhesus monkey (7). Site dependence for absorption of nitroglycerin has been reported in the rat (8) and humans (9). In the human study, the topical dose and the surface area were not controlled, but both of these parameters affect absorption (2).

Two points should be stressed. First, the topical dose and the surface area must be controlled in percutaneous absorption studies. Second, future studies may show that nitroglycerin absorption can vary with some anatomical sites. However, there also will be anatomical sites where absorption is similar. Therefore, a patient may have the convenience of choosing a preferred site.

(1) R. C. Wester and H. I. Maibach, *Toxicol. Appl. Pharmacol.*, **32**, 394 (1975).
(2) R. C. Wester and H. I. Maibach, *J. Invest. Dermatol.*, **67**, 518 (1976).
(3) D. L. Karsh, R. E. Umbach, L. S. Cohen, and R. A. Langou, *Am. Heart J.*, **96**, 587 (1978).
(4) H. I. Maibach, R. J. Feldmann, T. H. Milby, and W. F. Serat, *Arch. Environ. Health*, **23**, 208 (1971).
(5) R. J. Feldmann and H. I. Maibach, *J. Invest. Dermatol.*, **48**, 181 (1967).
(6) S. T. Horhota and H. Fung, *J. Pharm. Sci.*, **68**, 608 (1979).
(7) R. C. Wester, P. K. Noonan, and H. I. Maibach, *J. Soc. Cosmet. Chem.*, **30**, 297 (1979).
(8) S. T. Horhota and H. Fung, *J. Pharm. Sci.*, **67**, 1345 (1978).
(9) M. S. Hansen, *Am. J. Cardiol.*, **42**, 1061 (1978).

Patrick K. Noonan
Ronald C. Wester ˣ
Department of Drug Metabolism
G. D. Searle and Co.
Skokie, IL 60076

Received September 14, 1979.
Accepted for publication December 21, 1979.

BOOKS

REVIEWS

GLC and HPLC Determination of Therapeutic Agents, Parts I–III. (Chromatographic Science Series, Vol. 9).

Part I edited by K. TSUJI and W. MOROZOWICH.

Parts II and III edited by K. TSUJI.

Dekker, 270 Madison Ave., New York, NY 10016.

Part I: 1978, 415 pp., 18 × 26 cm, Price $37.50.

Part II: 1978, 432 pp., 18 × 26 cm, Price $45.00.

Part III: 1979, 528 pp., 18 × 26 cm, Price $45.00.

Part I has chapters entitled: Theory and Instrumentation, Column Selection in GLC, Column Selection in HPLC, Derivatization Techniques in Gas–Liquid Chromatography, Derivatization Techniques in HPLC, The Mass Spectrometer as a Detector for Gas–Liquid Chromatography, Isolation of Samples Prior to Chromatography, Preparative HPLC: Small Scale and Trace Collection, Preparative HPLC: Milligram Quantities, Quality Control in GLC, Automation and Quality Control in HPLC, Computer Interfacing, and Data Processing. Much new material as well as an exhaustive critical review of the literature is included. The writing has an immediacy and authority which are most welcome, indicating that the authors are directly involved with the techniques they describe. The volume is recommended to all in the field who wish to update their knowledge of the theory and practice of GLC and HPLC. It is particularly recommended to graduate students and would make an excellent course text except for one problem: an index is available only in Part III. Use of the index is made more annoying since the three parts are successively paginated so that the index does not immediately indicate the volume to open.

Part II is devoted to therapeutic drug monitoring with GLC and HPLC. It contains chapters 14–24, which give scientific methods and detailed directions for individual drugs. In addition to the literature review, there are author-preferred-and-tested methods for each drug. The drug classes covered are: narcotic analgesics, narcotic antagonists and related drugs, central nervous system (CNS) depressants, cocaine and phenylethylamines, hallucinogens, cannabis preparations, barbiturates, anticonvulsants, salicylates, aniline derivatives, pyrazolones, synthetic opiate-like drugs of low potency and low addictive potential, analgesic combinations, nonbarbiturate hypnotics, glutethimide, methaqualone, anorexigenics, antipsychotics, antianxiety agents, antidepressives, stimulants, antihypertensives, pulmonary and vasoactive drugs, antimicrobials, antimycotics, antiparasitics, adrenocorticosteroids, androgens, estrogens, and antifertility steroids. In addition, there are chapters on preservatives and on the determination of residues in gaseous sterilants.

The editor has been extremely careless in Part II, allowing the same material about the same drug to appear in two different chapters. For example, Fig. 9 of Chapter 14, showing GLC analysis of opium alkaloids, is reproduced as Fig. 15 of Chapter 16. The duplicated information involves the narcotic analgesics, barbiturates, amphetamine, papaverine, and, perhaps, others.

Part III continues with the drugs used in metabolic diseases, those that affect endocrine functions and nutritional agents. Drug classes included are: nonsteroidal anti-inflammatories, prostaglandins, cardiac glycosides, antiarrhythmics, vasodilators, oral anticoagulants (there are no methods for heparin in this collection), antidiabetics, diuretics, lipid- and cholesterol-lowering agents, thyroid agents, X-ray contrast agents, nucleosides and nucleotides, alkaloids, antihistamines and antitussives, water-soluble vitamins, fat-soluble vitamins, amino acids and peptides, sugar and sugar alcohols, and saccharin. The last chapter deals with serum lipid and fatty acid analysis.

The methods reported in Parts II and III include sample preparation (including separation from clinical samples or drug formulations and derivatization) as well as the determinations. Most chapters contain a summary table of the drugs included in it, choosing between GLC and HPLC as the method of choice and giving the chromatographic conditions.

It is an amusing coincidence that while this review was being prepared, the August issue of "Chromatography Newsletter" was received, which was devoted entirely (15 pages) to drug analysis, thus showing again that reviews, no matter how well done, can only supplement and not substitute for current periodicals.

These three volumes are an indispensible reference to all scientists who use or intend to use GLC and HPLC, particularly drug analysts, forensic scientists, clinical chemists, and biochemists. Good use of the collection will be made by "anyone concerned with the potency, purity, stability,

on the chest from a surface area of 50 cm^2 was significantly ($p < 0.002$) greater (36.4 ± 4.3%) than the absorption from the smaller surface area. Therefore, differences in these anatomical sites did not affect absorption, but increasing the size of the skin surface area did increase absorption.

The anatomical site of application has been shown to affect the percutaneous absorption of compounds in humans (4, 5) and the rhesus monkey (7). Site dependence for absorption of nitroglycerin has been reported in the rat (8) and humans (9). In the human study, the topical dose and the surface area were not controlled, but both of these parameters affect absorption (2).

Two points should be stressed. First, the topical dose and the surface area must be controlled in percutaneous absorption studies. Second, future studies may show that nitroglycerin absorption can vary with some anatomical sites. However, there also will be anatomical sites where absorption is similar. Therefore, a patient may have the convenience of choosing a preferred site.

(1) R. C. Wester and H. I. Maibach, *Toxicol. Appl. Pharmacol.*, **32**, 394 (1975).
(2) R. C. Wester and H. I. Maibach, *J. Invest. Dermatol.*, **67**, 518 (1976).
(3) D. L. Karsh, R. E. Umbach, L. S. Cohen, and R. A. Langou, *Am. Heart J.*, **96**, 587 (1978).
(4) H. I. Maibach, R. J. Feldmann, T. H. Milby, and W. F. Serat, *Arch. Environ. Health*, **23**, 208 (1971).
(5) R. J. Feldmann and H. I. Maibach, *J. Invest. Dermatol.*, **48**, 181 (1967).
(6) S. T. Horhota and H. Fung, *J. Pharm. Sci.*, **68**, 608 (1979).
(7) R. C. Wester, P. K. Noonan, and H. I. Maibach, *J. Soc. Cosmet. Chem.*, **30**, 297 (1979).
(8) S. T. Horhota and H. Fung, *J. Pharm. Sci.*, **67**, 1345 (1978).
(9) M. S. Hansen, *Am. J. Cardiol.*, **42**, 1061 (1978).

Patrick K. Noonan
Ronald C. Wester ˣ
Department of Drug Metabolism
G. D. Searle and Co.
Skokie, IL 60076

Received September 14, 1979.
Accepted for publication December 21, 1979.

BOOKS

REVIEWS

GLC and HPLC Determination of Therapeutic Agents, Parts I–III. (Chromatographic Science Series, Vol. 9).

Part I edited by K. TSUJI and W. MOROZOWICH.

Parts II and III edited by K. TSUJI.

Dekker, 270 Madison Ave., New York, NY 10016.

Part I: 1978, 415 pp., 18 × 26 cm, Price $37.50.

Part II: 1978, 432 pp., 18 × 26 cm, Price $45.00.

Part III: 1979, 528 pp., 18 × 26 cm, Price $45.00.

Part I has chapters entitled: Theory and Instrumentation, Column Selection in GLC, Column Selection in HPLC, Derivatization Techniques in Gas–Liquid Chromatography, Derivatization Techniques in HPLC, The Mass Spectrometer as a Detector for Gas–Liquid Chromatography, Isolation of Samples Prior to Chromatography, Preparative HPLC: Small Scale and Trace Collection, Preparative HPLC: Milligram Quantities, Quality Control in GLC, Automation and Quality Control in HPLC, Computer Interfacing, and Data Processing. Much new material as well as an exhaustive critical review of the literature is included. The writing has an immediacy and authority which are most welcome, indicating that the authors are directly involved with the techniques they describe. The volume is recommended to all in the field who wish to update their knowledge of the theory and practice of GLC and HPLC. It is particularly recommended to graduate students and would make an excellent course text except for one problem: an index is available only in Part III. Use of the index is made more annoying since the three parts are successively paginated so that the index does not immediately indicate the volume to open.

Part II is devoted to therapeutic drug monitoring with GLC and HPLC. It contains chapters 14–24, which give scientific methods and detailed directions for individual drugs. In addition to the literature review, there are author-preferred-and-tested methods for each drug. The drug classes covered are: narcotic analgesics, narcotic antagonists and related drugs, central nervous system (CNS) depressants, cocaine and phenylethylamines, hallucinogens, cannabis preparations, barbiturates, anticonvulsants, salicylates, aniline derivatives, pyrazolones, synthetic opiate-like drugs of low potency and low addictive potential, analgesic combinations, nonbarbiturate hypnotics, glutethimide, methaqualone, anorexigenics, antipsychotics, antianxiety agents, antidepressives, stimulants, antihypertensives, pulmonary and vasoactive drugs, antimicrobials, antimycotics, antiparasitics, adrenocorticosteroids, androgens, estrogens, and antifertility steroids. In addition, there are chapters on preservatives and on the determination of residues in gaseous sterilants.

The editor has been extremely careless in Part II, allowing the same material about the same drug to appear in two different chapters. For example, Fig. 9 of Chapter 14, showing GLC analysis of opium alkaloids, is reproduced as Fig. 15 of Chapter 16. The duplicated information involves the narcotic analgesics, barbiturates, amphetamine, papaverine, and, perhaps, others.

Part III continues with the drugs used in metabolic diseases, those that affect endocrine functions and nutritional agents. Drug classes included are: nonsteroidal anti-inflammatories, prostaglandins, cardiac glycosides, antiarrhythmics, vasodilators, oral anticoagulants (there are no methods for heparin in this collection), antidiabetics, diuretics, lipid- and cholesterol-lowering agents, thyroid agents, X-ray contrast agents, nucleosides and nucleotides, alkaloids, antihistamines and antitussives, water-soluble vitamins, fat-soluble vitamins, amino acids and peptides, sugar and sugar alcohols, and saccharin. The last chapter deals with serum lipid and fatty acid analysis.

The methods reported in Parts II and III include sample preparation (including separation from clinical samples or drug formulations and derivatization) as well as the determinations. Most chapters contain a summary table of the drugs included in it, choosing between GLC and HPLC as the method of choice and giving the chromatographic conditions.

It is an amusing coincidence that while this review was being prepared, the August issue of "Chromatography Newsletter" was received, which was devoted entirely (15 pages) to drug analysis, thus showing again that reviews, no matter how well done, can only supplement and not substitute for current periodicals.

These three volumes are an indispensible reference to all scientists who use or intend to use GLC and HPLC, particularly drug analysts, forensic scientists, clinical chemists, and biochemists. Good use of the collection will be made by "anyone concerned with the potency, purity, stability,

pharmacokinetics and mechanisms of actions of drugs. . . ."

The type is clear and readable. The books have glossy paper covered boards, are easy to open, and lie flat, as are typical of Marcel Dekker volumes.

Despite the nuisances and repetitiveness noted, the set is highly recommended.

Reviewed by Murray M. Tuckerman
School of Pharmacy
Temple University
Philadelphia, PA 19140

The Chemistry of Antitumor Antibiotics, Vol. 1. By WILLIAM A. REMERS. Wiley–Interscience, One Wiley Drive, Somerset, NJ 08873. 1979. 289 pp. 15 × 22.5 cm.

A lack of fundamental knowledge concerning many aspects of the biological sciences still restricts most oncologists to dealing with the treatment rather than the causes of cancer. Nevertheless, encouraging results have been attained with many drugs in the treatment of certain neoplastic diseases such as acute lymphocytic leukemia, Burkitt's lymphoma, choriocarcinoma, Hodgkin's disease, squamous cell cancer, and Wilm's tumor, Many of these remissions were achieved by the use of antitumor antibiotics.

Antibiotics are unique in their extreme diversity of chemical structures and in the fact that the "rational approach" followed so enthusiastically in the design of other classes of antineoplastic agents has played only a minor role in the discovery of their striking effects. As a result, information gained by assessing the antitumor activity of these antibiotics may be more objective than studies of more conventional drug classes. There can be little doubt that the information will contribute significantly to the future design of better antineoplastic agents and will provide a guide to the proper selection of agents for use in combination chemotherapy.

Since the discovery in 1952 that actinomycin D (dactinomycin) shows activity against experimental tumors, antibiotics have gained firm ground as a unique class of agents for the management of cancer. As a result, numerous studies on this subject mushroomed, and publications were scattered in every possible chemical, biological, pharmacological, and medical journal. Although some reviews and chapters were published occasionally on certain antitumor antibiotics, this book is the first of its type in which pertinent information in this area has been assembled in a comprehensive yet precise and clear manner. Dr. Remers' effort should be appreciated by investigators working in this field. His achievement is particularly admired by those who have tried to compile similar information, even on a smaller scale.

Volume 1 of this book is divided into five chapters: the actinomycins, the anthracyclines, the aureolic acid group, the bleomycins and phleomycins, and the mitomycins and porfiromycins. At least one member of each of these categories has recognition in cancer chemotherapy [*e.g.*, actinomycin D, adriamycin (doxorubicin), mithramycin, bleomycin B_2, and mitomycin C, respectively]. Each chapter has a concise, general introduction and is divided further into specific discussions including the discovery, isolation, and characterization, structural elucidation, possible mode of action, chemical synthesis and biosynthesis, and structure–activity relationships. Three of these five chapters also include the chemical transformations among related antibiotics.

Since many antibiotics discussed in this book tend to form chelates or complexes with certain metal ions, the author has emphasized repeatedly a significant point which, if not noticed, would cause confusion and misinterpretation by other investigators. This point is that physical properties such as optical rotation often are influenced by traces of metals and other impurities that are difficult to separate or remove from the pure compound. This case is especially true with antibiotics of the aureolic acid group in which samples with the same chemical structure were assigned as different antibiotics based on the observed discrepancy in specific rotation values.

This reviewer agrees with the author's comment that in a field where anticancer activity is the primary goal of synthesis and structural modification, it is surprising that not enough data have been published on the inhibition of experimental tumors. Judging from the many elegant total or partial syntheses recorded in this book, I cannot help but wonder whether the lengthy ones under the name of an alternate synthesis or a novel approach are of value to other investigators. Indeed, the aim of a chemical synthesis is to identify the structural assignment, to devise a practical method for more plentiful procurement of a specific antibiotic, or to facilitate analog synthesis. With the current limited funding in research, perhaps now is the best time for every dedicated investigator to reassess the true value and implication of his or her own work.

The order of tetracyclic rings in the anthracycline antibiotics (Chapter 2) given in this book was from the aromatic ring (ring A) toward the alicyclic ring (ring D) in which the glycoside is attached. However, on p. 88 and p. 102, ring A was designated as the alicyclic ring. In the literature, the conflicting order of rings A → D or D ← A has been assigned and has aroused unnecessary confusion. Since the original Italian investigators [Arcamone *et al.*, *Gazz. Chim. Ital.*, **100**, 949 (1970)] designated the alicyclic ring on the aglycone portion as ring A, perhaps such assignment should be honored rather than the general order of assignment in this book. The author also may wish to change the cell line of He La to HeLa in forthcoming books.

This reviewer also would like to add one piece of interesting information concerning the phleomycin antibiotics. Although it is known that the low therapeutic indexes of phleomycins hamper their use as antibacterial or antitumor agents, the addition of certain thioethers of purine or related heterocyclic compounds as potentiators ("amplifiers") permits the use of phleomycins at much lower levels, thereby raising their therapeutic indexes to potentially useful levels [Grigg *et al.*, *J. Bacteriol.*, **107**, 599 (1971); and Brown *et al.*, *Austr. J. Chem.*, **31**, 397 (1978) and the references cited therein].

All in all, this is a well-written and valuable book. Readers can follow easily the historical development of important antibiotics and recognize the work that has been accomplished as well as areas that still need to be studied. This book should be of interest to chemists, biochemists, toxicologists, pharmacologists, and clinicians who are interested in research.

Reviewed by C. C. Cheng
Mid-America Cancer Center
University of Kansas Medical Center
Kansas City, KS 66103

The Alkaloids: The Fundamental Chemistry—A Biogenetic Approach. (Studies in Organic Chemistry Series, Vol. 7). By D. R. DALTON. 270 Madison Ave., New York, NY 10016. 1979. x + 789 pp. 18 × 26 cm. Price $49.50 (A special price of $29.50 is available in the United States and Canada on orders of five or more copies).

The alkaloids represent the largest and most diverse group of plant-derived natural products, with well over 10,000 known members of the class involving 300 different ring systems. In view of their importance, including their significance in pharmacy and medicine, it is surprising that few textbooks on alkaloids have appeared in recent years. Thus, apart from reviews in "The Alkaloids" series, the Chemical Society Specialist Periodical Reports of the same name, and specialized reviews such as the one by Shamma and Moniot on isoquinoline alkaloids, no comprehensive general treatment of the alkaloids has appeared since that edited by Pelletier almost a decade ago. The publication of the book that is the subject of this review is thus a timely event and one that will be welcomed by all researchers involved in the alkaloid field.

The book is an outgrowth of a course taught by the author at Temple University, and this is the origin of its greatest strength and its greatest weakness. The strength of the book is that it provides for the first time, in one place, a unified account of the biosynthesis and chemistry of the alkaloids. It is organized along biosynthetic lines rather than along the traditional lines of previous works. Thus, instead of chapters on subjects such as the ipecac (ipecacuanha) alkaloids or the cinchona alkaloids, there are chapters on alkaloids derived from ornithine, lysine, nicotinic acid, tyrosine, and tryptophan and on alkaloids derived by introduction of nitrogen into a terpenoid skeleton. Although the traditional classification, largely by plant of origin, does group alkaloids of similar type, our present understanding of alkaloid biosynthesis makes the approach adopted in this book logical and desirable. Furthermore, the discussion of the biosynthesis and the chemistry of each alkaloid is integrated within each chapter rather than having the biosynthesis discussed in a separate chapter. This feature allows the reader to appreciate the synthetic approaches to the alkaloids more readily, particularly those that are modeled on an actual or presumed biosynthetic pathway.

The major weakness of the book as a standard reference on the alka-

pharmacokinetics and mechanisms of actions of drugs. . . ."

The type is clear and readable. The books have glossy paper covered boards, are easy to open, and lie flat, as are typical of Marcel Dekker volumes.

Despite the nuisances and repetitiveness noted, the set is highly recommended.

Reviewed by Murray M. Tuckerman
School of Pharmacy
Temple University
Philadelphia, PA 19140

The Chemistry of Antitumor Antibiotics, Vol. 1. By WILLIAM A. REMERS. Wiley–Interscience, One Wiley Drive, Somerset, NJ 08873. 1979. 289 pp. 15 × 22.5 cm.

A lack of fundamental knowledge concerning many aspects of the biological sciences still restricts most oncologists to dealing with the treatment rather than the causes of cancer. Nevertheless, encouraging results have been attained with many drugs in the treatment of certain neoplastic diseases such as acute lymphocytic leukemia, Burkitt's lymphoma, choriocarcinoma, Hodgkin's disease, squamous cell cancer, and Wilm's tumor, Many of these remissions were achieved by the use of antitumor antibiotics.

Antibiotics are unique in their extreme diversity of chemical structures and in the fact that the "rational approach" followed so enthusiastically in the design of other classes of antineoplastic agents has played only a minor role in the discovery of their striking effects. As a result, information gained by assessing the antitumor activity of these antibiotics may be more objective than studies of more conventional drug classes. There can be little doubt that the information will contribute significantly to the future design of better antineoplastic agents and will provide a guide to the proper selection of agents for use in combination chemotherapy.

Since the discovery in 1952 that actinomycin D (dactinomycin) shows activity against experimental tumors, antibiotics have gained firm ground as a unique class of agents for the management of cancer. As a result, numerous studies on this subject mushroomed, and publications were scattered in every possible chemical, biological, pharmacological, and medical journal. Although some reviews and chapters were published occasionally on certain antitumor antibiotics, this book is the first of its type in which pertinent information in this area has been assembled in a comprehensive yet precise and clear manner. Dr. Remers' effort should be appreciated by investigators working in this field. His achievement is particularly admired by those who have tried to compile similar information, even on a smaller scale.

Volume 1 of this book is divided into five chapters: the actinomycins, the anthracyclines, the aureolic acid group, the bleomycins and phleomycins, and the mitomycins and porfiromycins. At least one member of each of these categories has recognition in cancer chemotherapy [*e.g.*, actinomycin D, adriamycin (doxorubicin), mithramycin, bleomycin B_2, and mitomycin C, respectively]. Each chapter has a concise, general introduction and is divided further into specific discussions including the discovery, isolation, and characterization, structural elucidation, possible mode of action, chemical synthesis and biosynthesis, and structure–activity relationships. Three of these five chapters also include the chemical transformations among related antibiotics.

Since many antibiotics discussed in this book tend to form chelates or complexes with certain metal ions, the author has emphasized repeatedly a significant point which, if not noticed, would cause confusion and misinterpretation by other investigators. This point is that physical properties such as optical rotation often are influenced by traces of metals and other impurities that are difficult to separate or remove from the pure compound. This case is especially true with antibiotics of the aureolic acid group in which samples with the same chemical structure were assigned as different antibiotics based on the observed discrepancy in specific rotation values.

This reviewer agrees with the author's comment that in a field where anticancer activity is the primary goal of synthesis and structural modification, it is surprising that not enough data have been published on the inhibition of experimental tumors. Judging from the many elegant total or partial syntheses recorded in this book, I cannot help but wonder whether the lengthy ones under the name of an alternate synthesis or a novel approach are of value to other investigators. Indeed, the aim of a chemical synthesis is to identify the structural assignment, to devise a practical method for more plentiful procurement of a specific antibiotic, or to facilitate analog synthesis. With the current limited funding in research, perhaps now is the best time for every dedicated investigator to reassess the true value and implication of his or her own work.

The order of tetracyclic rings in the anthracycline antibiotics (Chapter 2) given in this book was from the aromatic ring (ring A) toward the alicyclic ring (ring D) in which the glycoside is attached. However, on p. 88 and p. 102, ring A was designated as the alicyclic ring. In the literature, the conflicting order of rings A → D or D ← A has been assigned and has aroused unnecessary confusion. Since the original Italian investigators [Arcamone *et al.*, *Gazz. Chim. Ital.*, **100**, 949 (1970)] designated the alicyclic ring on the aglycone portion as ring A, perhaps such assignment should be honored rather than the general order of assignment in this book. The author also may wish to change the cell line of He La to HeLa in forthcoming books.

This reviewer also would like to add one piece of interesting information concerning the phleomycin antibiotics. Although it is known that the low therapeutic indexes of phleomycins hamper their use as antibacterial or antitumor agents, the addition of certain thioethers of purine or related heterocyclic compounds as potentiators ("amplifiers") permits the use of phleomycins at much lower levels, thereby raising their therapeutic indexes to potentially useful levels [Grigg *et al.*, *J. Bacteriol.*, **107**, 599 (1971); and Brown *et al.*, *Austr. J. Chem.*, **31**, 397 (1978) and the references cited therein].

All in all, this is a well-written and valuable book. Readers can follow easily the historical development of important antibiotics and recognize the work that has been accomplished as well as areas that still need to be studied. This book should be of interest to chemists, biochemists, toxicologists, pharmacologists, and clinicians who are interested in research.

Reviewed by C. C. Cheng
Mid-America Cancer Center
University of Kansas Medical Center
Kansas City, KS 66103

The Alkaloids: The Fundamental Chemistry—A Biogenetic Approach. (Studies in Organic Chemistry Series, Vol. 7). By D. R. DALTON. 270 Madison Ave., New York, NY 10016. 1979. x + 789 pp. 18 × 26 cm. Price $49.50 (A special price of $29.50 is available in the United States and Canada on orders of five or more copies).

The alkaloids represent the largest and most diverse group of plant-derived natural products, with well over 10,000 known members of the class involving 300 different ring systems. In view of their importance, including their significance in pharmacy and medicine, it is surprising that few textbooks on alkaloids have appeared in recent years. Thus, apart from reviews in "The Alkaloids" series, the Chemical Society Specialist Periodical Reports of the same name, and specialized reviews such as the one by Shamma and Moniot on isoquinoline alkaloids, no comprehensive general treatment of the alkaloids has appeared since that edited by Pelletier almost a decade ago. The publication of the book that is the subject of this review is thus a timely event and one that will be welcomed by all researchers involved in the alkaloid field.

The book is an outgrowth of a course taught by the author at Temple University, and this is the origin of its greatest strength and its greatest weakness. The strength of the book is that it provides for the first time, in one place, a unified account of the biosynthesis and chemistry of the alkaloids. It is organized along biosynthetic lines rather than along the traditional lines of previous works. Thus, instead of chapters on subjects such as the ipecac (ipecacuanha) alkaloids or the cinchona alkaloids, there are chapters on alkaloids derived from ornithine, lysine, nicotinic acid, tyrosine, and tryptophan and on alkaloids derived by introduction of nitrogen into a terpenoid skeleton. Although the traditional classification, largely by plant of origin, does group alkaloids of similar type, our present understanding of alkaloid biosynthesis makes the approach adopted in this book logical and desirable. Furthermore, the discussion of the biosynthesis and the chemistry of each alkaloid is integrated within each chapter rather than having the biosynthesis discussed in a separate chapter. This feature allows the reader to appreciate the synthetic approaches to the alkaloids more readily, particularly those that are modeled on an actual or presumed biosynthetic pathway.

The major weakness of the book as a standard reference on the alka-

pharmacokinetics and mechanisms of actions of drugs. . . ."

The type is clear and readable. The books have glossy paper covered boards, are easy to open, and lie flat, as are typical of Marcel Dekker volumes.

Despite the nuisances and repetitiveness noted, the set is highly recommended.

Reviewed by Murray M. Tuckerman
School of Pharmacy
Temple University
Philadelphia, PA 19140

The Chemistry of Antitumor Antibiotics, Vol. 1. By WILLIAM A. REMERS. Wiley–Interscience, One Wiley Drive, Somerset, NJ 08873. 1979. 289 pp. 15 × 22.5 cm.

A lack of fundamental knowledge concerning many aspects of the biological sciences still restricts most oncologists to dealing with the treatment rather than the causes of cancer. Nevertheless, encouraging results have been attained with many drugs in the treatment of certain neoplastic diseases such as acute lymphocytic leukemia, Burkitt's lymphoma, choriocarcinoma, Hodgkin's disease, squamous cell cancer, and Wilm's tumor, Many of these remissions were achieved by the use of antitumor antibiotics.

Antibiotics are unique in their extreme diversity of chemical structures and in the fact that the "rational approach" followed so enthusiastically in the design of other classes of antineoplastic agents has played only a minor role in the discovery of their striking effects. As a result, information gained by assessing the antitumor activity of these antibiotics may be more objective than studies of more conventional drug classes. There can be little doubt that the information will contribute significantly to the future design of better antineoplastic agents and will provide a guide to the proper selection of agents for use in combination chemotherapy.

Since the discovery in 1952 that actinomycin D (dactinomycin) shows activity against experimental tumors, antibiotics have gained firm ground as a unique class of agents for the management of cancer. As a result, numerous studies on this subject mushroomed, and publications were scattered in every possible chemical, biological, pharmacological, and medical journal. Although some reviews and chapters were published occasionally on certain antitumor antibiotics, this book is the first of its type in which pertinent information in this area has been assembled in a comprehensive yet precise and clear manner. Dr. Remers' effort should be appreciated by investigators working in this field. His achievement is particularly admired by those who have tried to compile similar information, even on a smaller scale.

Volume 1 of this book is divided into five chapters: the actinomycins, the anthracyclines, the aureolic acid group, the bleomycins and phleomycins, and the mitomycins and porfiromycins. At least one member of each of these categories has recognition in cancer chemotherapy [*e.g.*, actinomycin D, adriamycin (doxorubicin), mithramycin, bleomycin B_2, and mitomycin C, respectively]. Each chapter has a concise, general introduction and is divided further into specific discussions including the discovery, isolation, and characterization, structural elucidation, possible mode of action, chemical synthesis and biosynthesis, and structure–activity relationships. Three of these five chapters also include the chemical transformations among related antibiotics.

Since many antibiotics discussed in this book tend to form chelates or complexes with certain metal ions, the author has emphasized repeatedly a significant point which, if not noticed, would cause confusion and misinterpretation by other investigators. This point is that physical properties such as optical rotation often are influenced by traces of metals and other impurities that are difficult to separate or remove from the pure compound. This case is especially true with antibiotics of the aureolic acid group in which samples with the same chemical structure were assigned as different antibiotics based on the observed discrepancy in specific rotation values.

This reviewer agrees with the author's comment that in a field where anticancer activity is the primary goal of synthesis and structural modification, it is surprising that not enough data have been published on the inhibition of experimental tumors. Judging from the many elegant total or partial syntheses recorded in this book, I cannot help but wonder whether the lengthy ones under the name of an alternate synthesis or a novel approach are of value to other investigators. Indeed, the aim of a chemical synthesis is to identify the structural assignment, to devise a practical method for more plentiful procurement of a specific antibiotic, or to facilitate analog synthesis. With the current limited funding in research, perhaps now is the best time for every dedicated investigator to reassess the true value and implication of his or her own work.

The order of tetracyclic rings in the anthracycline antibiotics (Chapter 2) given in this book was from the aromatic ring (ring A) toward the alicyclic ring (ring D) in which the glycoside is attached. However, on p. 88 and p. 102, ring A was designated as the alicyclic ring. In the literature, the conflicting order of rings A → D or D ← A has been assigned and has aroused unnecessary confusion. Since the original Italian investigators [Arcamone *et al.*, *Gazz. Chim. Ital.*, **100**, 949 (1970)] designated the alicyclic ring on the aglycone portion as ring A, perhaps such assignment should be honored rather than the general order of assignment in this book. The author also may wish to change the cell line of He La to HeLa in forthcoming books.

This reviewer also would like to add one piece of interesting information concerning the phleomycin antibiotics. Although it is known that the low therapeutic indexes of phleomycins hamper their use as antibacterial or antitumor agents, the addition of certain thioethers of purine or related heterocyclic compounds as potentiators ("amplifiers") permits the use of phleomycins at much lower levels, thereby raising their therapeutic indexes to potentially useful levels [Grigg *et al.*, *J. Bacteriol.*, **107**, 599 (1971); and Brown *et al.*, *Austr. J. Chem.*, **31**, 397 (1978) and the references cited therein].

All in all, this is a well-written and valuable book. Readers can follow easily the historical development of important antibiotics and recognize the work that has been accomplished as well as areas that still need to be studied. This book should be of interest to chemists, biochemists, toxicologists, pharmacologists, and clinicians who are interested in research.

Reviewed by C. C. Cheng
Mid-America Cancer Center
University of Kansas Medical Center
Kansas City, KS 66103

The Alkaloids: The Fundamental Chemistry—A Biogenetic Approach. (Studies in Organic Chemistry Series, Vol. 7). By D. R. DALTON. 270 Madison Ave., New York, NY 10016. 1979. x + 789 pp. 18 × 26 cm. Price $49.50 (A special price of $29.50 is available in the United States and Canada on orders of five or more copies).

The alkaloids represent the largest and most diverse group of plant-derived natural products, with well over 10,000 known members of the class involving 300 different ring systems. In view of their importance, including their significance in pharmacy and medicine, it is surprising that few textbooks on alkaloids have appeared in recent years. Thus, apart from reviews in "The Alkaloids" series, the Chemical Society Specialist Periodical Reports of the same name, and specialized reviews such as the one by Shamma and Moniot on isoquinoline alkaloids, no comprehensive general treatment of the alkaloids has appeared since that edited by Pelletier almost a decade ago. The publication of the book that is the subject of this review is thus a timely event and one that will be welcomed by all researchers involved in the alkaloid field.

The book is an outgrowth of a course taught by the author at Temple University, and this is the origin of its greatest strength and its greatest weakness. The strength of the book is that it provides for the first time, in one place, a unified account of the biosynthesis and chemistry of the alkaloids. It is organized along biosynthetic lines rather than along the traditional lines of previous works. Thus, instead of chapters on subjects such as the ipecac (ipecacuanha) alkaloids or the cinchona alkaloids, there are chapters on alkaloids derived from ornithine, lysine, nicotinic acid, tyrosine, and tryptophan and on alkaloids derived by introduction of nitrogen into a terpenoid skeleton. Although the traditional classification, largely by plant of origin, does group alkaloids of similar type, our present understanding of alkaloid biosynthesis makes the approach adopted in this book logical and desirable. Furthermore, the discussion of the biosynthesis and the chemistry of each alkaloid is integrated within each chapter rather than having the biosynthesis discussed in a separate chapter. This feature allows the reader to appreciate the synthetic approaches to the alkaloids more readily, particularly those that are modeled on an actual or presumed biosynthetic pathway.

The major weakness of the book as a standard reference on the alka-

loids is that is is not thoroughly referenced. It only has 480 references, fewer than 20 of which are from 1975 or later. In contrast, the earlier and somewhat shorter work by Pelletier, which dealt largely with alkaloid chemistry, boasted 1750 references. In the present work, the lack of references is made up to some extent by references to review articles at the end of each chapter, but these reviews are, of course, of even earlier vintage than the book itself. The book thus is not a good source for the latest information in alkaloid research, particularly in such rapidly developing fields as indole alkaloid biosynthesis. In addition, it also is not comprehensive; several classes of alkaloids are not discussed at all.

The book sets out to be a textbook, however, and it is within this framework that it should be judged. As the author modestly states in the epilogue, "The major objective . . . is to provide the beginning student with an appreciation of order in structure type and biogenetic reasoning. Hopefully, some chemistry was also learned." Any person who takes the time to work through this book is certain to achieve these objectives and much more. The discussion of both biosynthesis and chemistry is lucid and concise, and the structural diagrams are excellent in quality and abundant in quantity. The only minor improvements that could be suggested would be for the initial diagrams to carry the numbering system for that structural type and for more diagrams to be oriented so that the reader does not have to turn the book around to see them.

In conclusion, the author has written an excellent textbook on the alkaloids, and it can be recommended as the book of choice for any scientist wishing to become acquainted with this fascinating area of natural products. Persons needing detailed and up-to-date information in a specific area will have to supplement this book with material from review articles and the recent literature.

Reviewed by David G. I. Kingston
Department of Chemistry
Virginia Polytechnic Institute
and State University
Blacksburg, VA 24061

The Pharmaceutical Codex, 11th Ed. The Pharmaceutical Press, One Lambeth High St., London SE1 7JN, England. 1979. 1101 pp. 17 × 25 cm. Price £27.

The 11th edition of "The British Pharmaceutical Codex," now called "The Pharmaceutical Codex," contains over 1400 entries in a single alphabetical sequence. Over 900 monographs on synthetic drug substances and natural products used in medicine are included. A typical drug substance monograph features the full chemical name, structural and molecular formulas, molecular weights, synonyms and trade names, physical characteristics such as solubility and specific rotation, stability and storage information, identification tests, metabolism, actions and uses, and preparations. Entries for drug classes also are included.

Diseases and minor ailments are discussed with respect to the cause and nature of the disorder, its major signs and symptoms, and its treatment with reference to the use of drugs. Entries on analytical techniques such as IR and UV spectrophotometry are included.

The first appendix describes the analytical reagents mentioned in the text. The second appendix gives reduced facsimile reproductions of IR spectra for more than 300 drug substances to aid in their identification. A comprehensive index with over 10,000 entries concludes the book.

This book is a useful reference for those concerned with the manufacture, formulation, distribution, dispensing, and quality control of drugs and medicines for human or veterinary use.

Staff Review

NOTICES

Surface of Normal and Malignant Cells. Edited by RICHARD O. HYNES. Wiley, One Wiley Drive, Somerset, NJ 08873. 1979. 471 pp. 15 × 23 cm. Price $65.00.

Cell Substrates: Their Use in the Production of Vaccines and Other Biologicals. Edited by JOHN C. PETRICCIANI, HOPE E. HOPPS, and PAUL J. CHAPPLE. Plenum, 227 W. 17th St., New York, NY 10011. 1979. 220 pp. 16 × 25 cm. Price $29.50.

Reviews of Physiology, Biochemistry and Pharmacology, Vol. 86. Contributors, P. THORÉN, R. J. HOGG, J. P. KOKKO, and P. SCHEID. Springer-Verlag New York Inc., 44 Hartz Way, Secaucus, NJ 07094. 1979. 206 pp. 16 × 24 cm. Price $48.40.

Standard Operating Procedures in Toxicology. Edited by G. E. PAGET and R. THOMSON. University Park Press, 233 E. Redwood St., Baltimore, MD 21202. 1979. 650 pp. 21 × 30 cm. Price $39.50.

Common Medicines: An Introduction for Consumers. By DAVID J. GEORGE. W. H. Freeman, 660 Market St., San Francisco, CA 94104. 1979. 197 pp. 21 × 28 cm. Price $6.00.

Bailey's Industrial Oil and Fat Products, 4th Ed., Vol. 1. Edited by DANIEL SWERN. Wiley, One Wiley Drive, Somerset, NJ 08873. 1979. 841 pp. 15 × 23 cm. Price $45.95.

Circulating Catecholamines and Blood Pressure. Edited by W. H. BIRKENHAGER and H. E. FALKE. University Park Press, 233 E. Redwood St., Baltimore, MD 21202. 1979. 71 pp. 14 × 23 cm. Price $12.50.

Human Toxicology. Edited by AUBIN HEYNDRICKX. European Press, Ghent, Belgium. 1978. 221 pp. 17 × 24 cm.

The Interpretation of Quantal Responses in Biology. By P. S. HEWLETT and R. L. PLACKETT. University Park Press, 233 E. Redwood St., Baltimore, MD 21202. 1979. 82 pp. 14 × 23 cm. Price $11.95.

The Alkaloids, Vol. 9. A Specialist Periodical Report. Senior Reporter, M. F. GRUNDON. The Chemical Society. 1979. 273 pp. 14 × 22 cm. Price $70.00. (Available from the American Chemical Society, 1155 16th St., N.W., Washington, DC 20036.)

Inorganic Biochemistry, Vol. 1. A Specialist Periodical Report. Senior Reporter, H. A. O. HILL. The Chemical Society. 1979. 441 pp. 14 × 22 cm. Price $61.50. (Available from the American Chemical Society, 1155 16th St., N.W., Washington, DC 20036.)

Plant Metabolism. By GERHARD RICHTER. University Park Press, 233 E. Redwood St., Baltimore, MD 21202. 1978. 475 pp. 12 × 19 cm. Price $22.75.

Workshop on Ursodeoxycholic Acid. Edited by R. H. DOWLING, A. F. HOFMANN, and L. BARBARA. University Park Press, 233 E. Redwood St., Baltimore, MD 21202. 1979. 88 pp. 15 × 24 cm. Price $9.95.

Nucleosides As Biological Probes. By ROBERT J. SUHADOLNIK. Wiley, One Wiley Drive, Somerset, NJ 08873. 1979. 346 pp. 14 × 23 cm. Price $37.50.

Modern Organic Elemental Analysis. By T. S. MA and ROBERT C. RITTNER. Dekker, 270 Madison Ave., New York, NY 10016. 1979. 518 pp. 15 × 23 cm. Price $45.00.

Arachidonic Acid Metabolism in Inflammation and Thrombosis. Edited by K. BRUNE and M. BAGGIOLINI. Birkhäuser Boston Inc., 380 Green St., P.O. Box 2007, Cambridge, MA 02139. 1979. 301 pp. 17 × 24 cm. Price $38.00.

Against Ourselves: Disorders from Improvements under the Organic Limitedness of Man. By D. G. GARAN. Philosophical Library, 15 E. 40th St., New York, NY 10016. 1979. 310 pp. 14 × 22 cm. Price $9.75.

loids is that is is not thoroughly referenced. It only has 480 references, fewer than 20 of which are from 1975 or later. In contrast, the earlier and somewhat shorter work by Pelletier, which dealt largely with alkaloid chemistry, boasted 1750 references. In the present work, the lack of references is made up to some extent by references to review articles at the end of each chapter, but these reviews are, of course, of even earlier vintage than the book itself. The book thus is not a good source for the latest information in alkaloid research, particularly in such rapidly developing fields as indole alkaloid biosynthesis. In addition, it also is not comprehensive; several classes of alkaloids are not discussed at all.

The book sets out to be a textbook, however, and it is within this framework that it should be judged. As the author modestly states in the epilogue, "The major objective . . . is to provide the beginning student with an appreciation of order in structure type and biogenetic reasoning. Hopefully, some chemistry was also learned." Any person who takes the time to work through this book is certain to achieve these objectives and much more. The discussion of both biosynthesis and chemistry is lucid and concise, and the structural diagrams are excellent in quality and abundant in quantity. The only minor improvements that could be suggested would be for the initial diagrams to carry the numbering system for that structural type and for more diagrams to be oriented so that the reader does not have to turn the book around to see them.

In conclusion, the author has written an excellent textbook on the alkaloids, and it can be recommended as the book of choice for any scientist wishing to become acquainted with this fascinating area of natural products. Persons needing detailed and up-to-date information in a specific area will have to supplement this book with material from review articles and the recent literature.

Reviewed by David G. I. Kingston
Department of Chemistry
Virginia Polytechnic Institute
and State University
Blacksburg, VA 24061

The Pharmaceutical Codex, 11th Ed. The Pharmaceutical Press, One Lambeth High St., London SE1 7JN, England. 1979. 1101 pp. 17 × 25 cm. Price £27.

The 11th edition of "The British Pharmaceutical Codex," now called "The Pharmaceutical Codex," contains over 1400 entries in a single alphabetical sequence. Over 900 monographs on synthetic drug substances and natural products used in medicine are included. A typical drug substance monograph features the full chemical name, structural and molecular formulas, molecular weights, synonyms and trade names, physical characteristics such as solubility and specific rotation, stability and storage information, identification tests, metabolism, actions and uses, and preparations. Entries for drug classes also are included.

Diseases and minor ailments are discussed with respect to the cause and nature of the disorder, its major signs and symptoms, and its treatment with reference to the use of drugs. Entries on analytical techniques such as IR and UV spectrophotometry are included.

The first appendix describes the analytical reagents mentioned in the text. The second appendix gives reduced facsimile reproductions of IR spectra for more than 300 drug substances to aid in their identification. A comprehensive index with over 10,000 entries concludes the book.

This book is a useful reference for those concerned with the manufacture, formulation, distribution, dispensing, and quality control of drugs and medicines for human or veterinary use.

Staff Review

NOTICES

Surface of Normal and Malignant Cells. Edited by RICHARD O. HYNES. Wiley, One Wiley Drive, Somerset, NJ 08873. 1979. 471 pp. 15 × 23 cm. Price $65.00.

Cell Substrates: Their Use in the Production of Vaccines and Other Biologicals. Edited by JOHN C. PETRICCIANI, HOPE E. HOPPS, and PAUL J. CHAPPLE. Plenum, 227 W. 17th St., New York, NY 10011. 1979. 220 pp. 16 × 25 cm. Price $29.50.

Reviews of Physiology, Biochemistry and Pharmacology, Vol. 86. Contributors, P. THORÉN, R. J. HOGG, J. P. KOKKO, and P. SCHEID. Springer-Verlag New York Inc., 44 Hartz Way, Secaucus, NJ 07094. 1979. 206 pp. 16 × 24 cm. Price $48.40.

Standard Operating Procedures in Toxicology. Edited by G. E. PAGET and R. THOMSON. University Park Press, 233 E. Redwood St., Baltimore, MD 21202. 1979. 650 pp. 21 × 30 cm. Price $39.50.

Common Medicines: An Introduction for Consumers. By DAVID J. GEORGE. W. H. Freeman, 660 Market St., San Francisco, CA 94104. 1979. 197 pp. 21 × 28 cm. Price $6.00.

Bailey's Industrial Oil and Fat Products, 4th Ed., Vol. 1. Edited by DANIEL SWERN. Wiley, One Wiley Drive, Somerset, NJ 08873. 1979. 841 pp. 15 × 23 cm. Price $45.95.

Circulating Catecholamines and Blood Pressure. Edited by W. H. BIRKENHAGER and H. E. FALKE. University Park Press, 233 E. Redwood St., Baltimore, MD 21202. 1979. 71 pp. 14 × 23 cm. Price $12.50.

Human Toxicology. Edited by AUBIN HEYNDRICKX. European Press, Ghent, Belgium. 1978. 221 pp. 17 × 24 cm.

The Interpretation of Quantal Responses in Biology. By P. S. HEWLETT and R. L. PLACKETT. University Park Press, 233 E. Redwood St., Baltimore, MD 21202. 1979. 82 pp. 14 × 23 cm. Price $11.95.

The Alkaloids, Vol. 9. A Specialist Periodical Report. Senior Reporter, M. F. GRUNDON. The Chemical Society. 1979. 273 pp. 14 × 22 cm. Price $70.00. (Available from the American Chemical Society, 1155 16th St., N.W., Washington, DC 20036.)

Inorganic Biochemistry, Vol. 1. A Specialist Periodical Report. Senior Reporter, H. A. O. HILL. The Chemical Society. 1979. 441 pp. 14 × 22 cm. Price $61.50. (Available from the American Chemical Society, 1155 16th St., N.W., Washington, DC 20036.)

Plant Metabolism. By GERHARD RICHTER. University Park Press, 233 E. Redwood St., Baltimore, MD 21202. 1978. 475 pp. 12 × 19 cm. Price $22.75.

Workshop on Ursodeoxycholic Acid. Edited by R. H. DOWLING, A. F. HOFMANN, and L. BARBARA. University Park Press, 233 E. Redwood St., Baltimore, MD 21202. 1979. 88 pp. 15 × 24 cm. Price $9.95.

Nucleosides As Biological Probes. By ROBERT J. SUHADOLNIK. Wiley, One Wiley Drive, Somerset, NJ 08873. 1979. 346 pp. 14 × 23 cm. Price $37.50.

Modern Organic Elemental Analysis. By T. S. MA and ROBERT C. RITTNER. Dekker, 270 Madison Ave., New York, NY 10016. 1979. 518 pp. 15 × 23 cm. Price $45.00.

Arachidonic Acid Metabolism in Inflammation and Thrombosis. Edited by K. BRUNE and M. BAGGIOLINI. Birkhäuser Boston Inc., 380 Green St., P.O. Box 2007, Cambridge, MA 02139. 1979. 301 pp. 17 × 24 cm. Price $38.00.

Against Ourselves: Disorders from Improvements under the Organic Limitedness of Man. By D. G. GARAN. Philosophical Library, 15 E. 40th St., New York, NY 10016. 1979. 310 pp. 14 × 22 cm. Price $9.75.

loids is that is is not thoroughly referenced. It only has 480 references, fewer than 20 of which are from 1975 or later. In contrast, the earlier and somewhat shorter work by Pelletier, which dealt largely with alkaloid chemistry, boasted 1750 references. In the present work, the lack of references is made up to some extent by references to review articles at the end of each chapter, but these reviews are, of course, of even earlier vintage than the book itself. The book thus is not a good source for the latest information in alkaloid research, particularly in such rapidly developing fields as indole alkaloid biosynthesis. In addition, it also is not comprehensive; several classes of alkaloids are not discussed at all.

The book sets out to be a textbook, however, and it is within this framework that it should be judged. As the author modestly states in the epilogue, "The major objective . . . is to provide the beginning student with an appreciation of order in structure type and biogenetic reasoning. Hopefully, some chemistry was also learned." Any person who takes the time to work through this book is certain to achieve these objectives and much more. The discussion of both biosynthesis and chemistry is lucid and concise, and the structural diagrams are excellent in quality and abundant in quantity. The only minor improvements that could be suggested would be for the initial diagrams to carry the numbering system for that structural type and for more diagrams to be oriented so that the reader does not have to turn the book around to see them.

In conclusion, the author has written an excellent textbook on the alkaloids, and it can be recommended as the book of choice for any scientist wishing to become acquainted with this fascinating area of natural products. Persons needing detailed and up-to-date information in a specific area will have to supplement this book with material from review articles and the recent literature.

Reviewed by David G. I. Kingston
Department of Chemistry
Virginia Polytechnic Institute
and State University
Blacksburg, VA 24061

The Pharmaceutical Codex, 11th Ed. The Pharmaceutical Press, One Lambeth High St., London SE1 7JN, England. 1979. 1101 pp. 17 × 25 cm. Price £27.

The 11th edition of "The British Pharmaceutical Codex," now called "The Pharmaceutical Codex," contains over 1400 entries in a single alphabetical sequence. Over 900 monographs on synthetic drug substances and natural products used in medicine are included. A typical drug substance monograph features the full chemical name, structural and molecular formulas, molecular weights, synonyms and trade names, physical characteristics such as solubility and specific rotation, stability and storage information, identification tests, metabolism, actions and uses, and preparations. Entries for drug classes also are included.

Diseases and minor ailments are discussed with respect to the cause and nature of the disorder, its major signs and symptoms, and its treatment with reference to the use of drugs. Entries on analytical techniques such as IR and UV spectrophotometry are included.

The first appendix describes the analytical reagents mentioned in the text. The second appendix gives reduced facsimile reproductions of IR spectra for more than 300 drug substances to aid in their identification. A comprehensive index with over 10,000 entries concludes the book.

This book is a useful reference for those concerned with the manufacture, formulation, distribution, dispensing, and quality control of drugs and medicines for human or veterinary use.

Staff Review

NOTICES

Surface of Normal and Malignant Cells. Edited by RICHARD O. HYNES. Wiley, One Wiley Drive, Somerset, NJ 08873. 1979. 471 pp. 15 × 23 cm. Price $65.00.

Cell Substrates: Their Use in the Production of Vaccines and Other Biologicals. Edited by JOHN C. PETRICCIANI, HOPE E. HOPPS, and PAUL J. CHAPPLE. Plenum, 227 W. 17th St., New York, NY 10011. 1979. 220 pp. 16 × 25 cm. Price $29.50.

Reviews of Physiology, Biochemistry and Pharmacology, Vol. 86. Contributors, P. THORÉN, R. J. HOGG, J. P. KOKKO, and P. SCHEID. Springer-Verlag New York Inc., 44 Hartz Way, Secaucus, NJ 07094. 1979. 206 pp. 16 × 24 cm. Price $48.40.

Standard Operating Procedures in Toxicology. Edited by G. E. PAGET and R. THOMSON. University Park Press, 233 E. Redwood St., Baltimore, MD 21202. 1979. 650 pp. 21 × 30 cm. Price $39.50.

Common Medicines: An Introduction for Consumers. By DAVID J. GEORGE. W. H. Freeman, 660 Market St., San Francisco, CA 94104. 1979. 197 pp. 21 × 28 cm. Price $6.00.

Bailey's Industrial Oil and Fat Products, 4th Ed., Vol. 1. Edited by DANIEL SWERN. Wiley, One Wiley Drive, Somerset, NJ 08873. 1979. 841 pp. 15 × 23 cm. Price $45.95.

Circulating Catecholamines and Blood Pressure. Edited by W. H. BIRKENHAGER and H. E. FALKE. University Park Press, 233 E. Redwood St., Baltimore, MD 21202. 1979. 71 pp. 14 × 23 cm. Price $12.50.

Human Toxicology. Edited by AUBIN HEYNDRICKX. European Press, Ghent, Belgium. 1978. 221 pp. 17 × 24 cm.

The Interpretation of Quantal Responses in Biology. By P. S. HEWLETT and R. L. PLACKETT. University Park Press, 233 E. Redwood St., Baltimore, MD 21202. 1979. 82 pp. 14 × 23 cm. Price $11.95.

The Alkaloids, Vol. 9. A Specialist Periodical Report. Senior Reporter, M. F. GRUNDON. The Chemical Society. 1979. 273 pp. 14 × 22 cm. Price $70.00. (Available from the American Chemical Society, 1155 16th St., N.W., Washington, DC 20036.)

Inorganic Biochemistry, Vol. 1. A Specialist Periodical Report. Senior Reporter, H. A. O. HILL. The Chemical Society. 1979. 441 pp. 14 × 22 cm. Price $61.50. (Available from the American Chemical Society, 1155 16th St., N.W., Washington, DC 20036.)

Plant Metabolism. By GERHARD RICHTER. University Park Press, 233 E. Redwood St., Baltimore, MD 21202. 1978. 475 pp. 12 × 19 cm. Price $22.75.

Workshop on Ursodeoxycholic Acid. Edited by R. H. DOWLING, A. F. HOFMANN, and L. BARBARA. University Park Press, 233 E. Redwood St., Baltimore, MD 21202. 1979. 88 pp. 15 × 24 cm. Price $9.95.

Nucleosides As Biological Probes. By ROBERT J. SUHADOLNIK. Wiley, One Wiley Drive, Somerset, NJ 08873. 1979. 346 pp. 14 × 23 cm. Price $37.50.

Modern Organic Elemental Analysis. By T. S. MA and ROBERT C. RITTNER. Dekker, 270 Madison Ave., New York, NY 10016. 1979. 518 pp. 15 × 23 cm. Price $45.00.

Arachidonic Acid Metabolism in Inflammation and Thrombosis. Edited by K. BRUNE and M. BAGGIOLINI. Birkhäuser Boston Inc., 380 Green St., P.O. Box 2007, Cambridge, MA 02139. 1979. 301 pp. 17 × 24 cm. Price $38.00.

Against Ourselves: Disorders from Improvements under the Organic Limitedness of Man. By D. G. GARAN. Philosophical Library, 15 E. 40th St., New York, NY 10016. 1979. 310 pp. 14 × 22 cm. Price $9.75.

APRIL 1980
VOLUME 69 NUMBER 4

JOURNAL OF PHARMACEUTICAL SCIENCES

MARY H. FERGUSON
Editor

SHELLY ELLIOTT
Production Editor

MARCIA GARTRELL
Copy Editor

NICOLETTE TRIANTAFELLU
Copy Editor

EDWARD G. FELDMANN
Contributing Editor

SAMUEL W. GOLDSTEIN
Contributing Editor

BELLE R. BECK
Editorial Secretary

DAVID BOHARDT
Director of Publications

L. LUAN CORRIGAN
Assistant Director of Publications

EDITORIAL ADVISORY BOARD

JOHN AUTIAN
HERBERT A. LIEBERMAN
NORMAN R. FARNSWORTH
DAVID E. MANN, JR.
WILLIAM O. FOYE
GERALD J. PAPARIELLO
WILLIAM J. JUSKO
EDWARD G. RIPPIE

The *Journal of Pharmaceutical Sciences* (ISSN 0022-3549) is published monthly by the American Pharmaceutical Association (APhA) at 2215 Constitution Ave., N.W., Washington, DC 20037. Second-class postage paid at Washington, D.C., and at additional mailing office.

All expressions of opinion and statements of supposed fact appearing in articles or editorials carried in this journal are published on the authority of the writer over whose name they appear and are not to be regarded as necessarily expressing the policies or views of APhA.

Offices—Editorial, Advertising, and Subscription: 2215 Constitution Ave., N.W., Washington, DC 20037. Printing: 20th & Northampton Streets, Easton, PA 18042.

Annual Subscriptions—United States and foreign, industrial and government institutions $60, educational institutions $60, individuals *for personal use only* $30; single copies $5. All foreign subscriptions add $5 for postage. Subscription rates are subject to change without notice. Members of APhA may elect to receive the *Journal of Pharmaceutical Sciences* as a part of their annual $80 (foreign $85) APhA membership dues.

Claims—Missing numbers will not be supplied if dues or subscriptions are in arrears for more than 60 days or if claims are received more than 60 days after the date of the issue, or if loss was due to failure to give notice of change of address. APhA cannot accept responsibility for foreign delivery when its records indicate shipment was made.

Change of Address—Members and subscribers should notify at once both the Post Office and APhA of any change of address.

Photocopying—The code at the foot of the first page of an article indicates that APhA has granted permission for copying of the article beyond the limits permitted by Sections 107 and 108 of the U.S. Copyright Law provided that the copier sends the per copy fee stated in the code to the Copyright Clearance Center, Inc., P.O. Box 8891, Boston, MA 02114. Copies may be made for personal or internal use only and not for general distribution.

Microfilm—Available from University Microfilms International, 300 N. Zeeb Road, Ann Arbor, MI 48106.

© Copyright 1980, American Pharmaceutical Association, 2215 Constitution Ave., N.W., Washington, DC 20037; all rights reserved.

IDENTIFYING "THE BAD CHARACTERS"

The so-called "Lannett decision" threw into question the authority of the Food and Drug Administration to require its approval of a duplicative drug product before that product is placed in distribution on the open market. At this writing, the effect of the court decision is still in question for various reasons including FDA appeals and differing decisions by courts in other judicial districts.

In the meantime, however, certain manufacturers have proceeded to market products without submitting them for FDA review and approval. The FDA has been seizing many of these products—particularly in those judicial districts where decisions have not been handed down that are adverse to its claim that federal law gives it the authority to require premarketing drug approval.

Nevertheless, at least a few unapproved products have gotten into general distribution. Moreover, according to the FDA, several of these products have been poorly formulated in a manner to make them less than satisfactory for their intended clinical uses, and the problem presented by these defective products has been widely publicized.

In an effort to avoid creating therapeutic problems for patients, pharmacists have been strongly advised to avoid purchasing and dispensing any products lacking FDA's approval. Indeed, pharmacists have been warned that they expose themselves to potential legal liability and to possible malpractice suits by using such products—particularly if patient injury were to result.

This well-intended advice has been offered from a variety of sources. In addition to a veritable bombarding of mailings from certain major pharmaceutical companies, pharmacists have gotten such cautions from state boards of pharmacy, from editors in the pharmaceutical press, from various professional associations, from attorney-pharmacists at conferences and symposia, and so on.

Indeed, a report in the drug press even quoted FDA Commissioner Jere E. Goyan as telling his Bureau of Drugs staff in mid-February that the situation concerning "unapproved generics"—the problem that some manufacturers may be marketing drugs illegally—is one that calls for an information campaign directed at the pharmacist. According to the Commissioner, "We have to go very heavily to pharmacy and say, 'Look, you're taking a terrible risk.' "

We do not quarrel in the least with the Commissioner's assessment that dispensing unapproved drugs constitutes a very serious risk to both the pharmacist and the patient. But what we do wonder is whether the Commissioner, and all the other well-meaning dispensors of "Dutch-uncle advice" noted above, recognize or appreciate the pharmacist's real problem.

We are personally convinced that virtually all pharmacists would shun such unapproved drug products *if*—and that's a very big "if"—they could immediately identify which products are approved or which are not. Fully 99% of the nation's pharmacists have the integrity and intelligence to avoid dealing with products of such questionable quality; and most of the other 1% are at least wise enough to do so, even if they are not motivated out of professional integrity.

Imagine for a moment the confusion that would reign if the millions and millions of automobiles in this country were all being driven around without license plates. The vehicles themselves still might be properly registered with the respective state vehicle departments, but there would be no outward evidence of such registration, or verification of registration, or means of identification, or the like, displayed on each automobile for all to see. To say that this would be a chaotic situation is a gross understatement.

And yet, when it comes to marketed drug products, we have no reliable system—short of telephoning the FDA offices in Washington concerning each individual drug product—for identifying those that have been so approved. Hence, there is no ready means of being able to distinguish them from products that may be on the market without having gone through the FDA's new drug application (NDA) or abbreviated new drug application (ANDA) approval process.

In mid-December, APhA President William S. Apple and this writer met with FDA officials and made a strong pitch for the agency to permit (or to require) drug manufacturers to carry the NDA or ANDA approval number in the labeling of those drug products that do, in fact, have such approval. In the past, and continuing at least to the time of this writing, FDA has prohibited the inclusion of such information as part of the product labeling on grounds that it constituted a form of inappropriate advertising; that is, the FDA was concerned that the approval number would be interpreted by consumers as an FDA endorsement of the product or that the product had a "seal of approval" from the federal government.

However justified this prohibition may have been in the past, present circumstances have drastically changed. In our opinion, if pharmacists are going to be able to exercise due care in product selection and dispensing, and if the health and welfare of patients are to be duly guarded, then it is essential that the FDA rescind its restriction and permit approved products to be appropriately identified for the benefit of all pertinent parties. —EGF

JOURNAL OF PHARMACEUTICAL SCIENCES

APRIL 1980
VOLUME 69 NUMBER 4

RESEARCH ARTICLES

Determination of Extent of Hydration of Water-Miscible Organic Liquids in Aqueous Solution from Viscosity Data

HANS SCHOTT

Received March 12, 1979, from the *School of Pharmacy, Temple University, Philadelphia, PA 19140.* Accepted for publication September 20, 1979.

Abstract □ Three viscometric methods for estimating the extent of association in binary liquid mixtures were employed to determine the maximum hydration of acetone, dimethyl sulfoxide, dioxane, 1-propanol, and 2-pyrrolidinone in aqueous solution. Two of the methods are based on the increase in viscosity or the decrease in fluidity of binary aqueous solutions caused by association between water and the second component, *i.e.*, by hydration of the second component. The composition of maximum hydration is that at which the deviation of experimental viscosities or fluidities from additive viscosities or fluidities reaches a maximum. Additive values are calculated by interpolation between the viscosities or fluidities of water and the second liquid component. Additivity would be observed in ideal solutions, *i.e.*, in the absence of hydration. The first method of interpolation uses the Kendall equation, $\phi_{12calc} = \phi_1^{x_1}\phi_2^{x_2}$, to calculate the fluidities, ϕ, of the mixtures (subscript 12) from the fluidities and mole fractions, x, of water (subscript 1) and the second liquid (subscript 2). The Kendall equation has a theoretical basis and is applicable where the viscosities, η, of water and the second liquid are of the same order of magnitude, differing by less than a factor of five. The maximum number of bound water molecules per molecule of the second component was 3 for acetone and dimethyl sulfoxide, 4 for dioxane, and 5.7 for propanol. The second method of interpolation is based on the empirical Kendall–Monroe equation, $\eta_{12\,calc}^{1/3} = x_1\eta_1^{1/3} + x_2\eta_2^{1/3}$, which is applicable to mixtures where the viscosities of the two pure components differ by a factor of 10 or more. The resultant hydration ratio of one water molecule per molecule of pyrrolidinone is confirmed by the separation of the solid monohydrate at lower temperatures. A novel and universal method determines the maximum hydration as the composition at which the activation energy for viscous flow of the mixtures, indicative of the size of the flow units, goes through a maximum. This method requires viscosity data of higher accuracy and at more than one temperature. Its hydration results agreed with those of the other two methods where the latter were applicable. The change in the activation energy of water with temperature was used to obtain a relative measure of the degree of self-association in liquid water as a function of temperature.

Keyphrases □ Hydration—water-miscible organic liquids in aqueous solution, determination using three viscometric methods □ Binary liquid mixtures—extent of hydration, three viscometric methods □ Viscosity—determination of extent of hydration of water-miscible organic liquids in aqueous solution □ Organic solvents—extent of hydration in aqueous solution, viscosity data

The extent of hydration of water-miscible organic liquids is of interest because it affords estimates of the number of water molecules associated with the organic functional groups present in the molecules of these liquids as well as in other compounds containing the same functional groups, including drugs, polymers, and constituents of biological membranes and cells.

For example, a knowledge of the maximum number of water molecules associated with an ether group, obtained from studies of binary liquid systems comprising water and model ethers (1), was essential to understanding the hydration of micelles of nonionic polyoxyethylated surfactants, making it possible to distinguish between water molecules bound to ether groups by hydrogen bonding and those mechanically trapped in the coiled and interpenetrating chains of the polyoxyethylene moieties of the surfactants (2). Information concerning the maximum hydration of hydroxyl groups (3) may lead to a better understanding of the transport properties of aqueous solutions of natural or synthetic polyhydroxylated polymers and of the water vapor permeability of their films (4).

Finally, the composition of maximum hydration of solvents such as dimethyl sulfoxide (5) is important in connection with their use as vehicles for drugs and as reaction media.

THEORETICAL

Association in a binary liquid system usually can be detected by the deviation of the experimental values of an intensive property of the solutions from the additive values of the property. Additive values are calculated by linear interpolation between the two values of that property belonging to the two pure components as a function of composition. Additive values are observed experimentally in the absence of association between molecules of the two liquids in their binary mixtures. Association leads to deviations from additivity. Such deviations frequently reach maximum values at a stoichiometric composition corresponding to the complex formed between the two components or at the composition of maximum hydration when water is one of the two liquid components.

Among the properties tested as suitable indicators are density and partial molar volume, refractive index and molar refraction, dielectric

0022-3549/80/0400-0369$01.00/0
© 1980, American Pharmaceutical Association

constant, magnetic susceptibility, IR and UV absorption spectra, and heat of mixing (6). Fluidity, ϕ, or its reciprocal, viscosity, η, is a reliable and sensitive property for detecting association between strongly (7) and weakly (1, 3, 5, 8, 9) interacting components.

Kendall and Kendall–Monroe Equations—The first equation used to calculate the fluidities of binary aqueous mixtures by interpolation between the fluidity of water and that of the second liquid component was the Kendall equation (10):

$$\log \phi_{12\ \text{calc}} = x_1 \log \phi_1 + x_2 \log \phi_2 \qquad \text{(Eq. 1)}$$

where x represents mole fraction and subscripts 1, 2, and 12 refer to water, the second liquid component, and their mixtures, respectively. This equation is obeyed by ideal or nearly ideal solutions (11).

Association between the two components causes the observed fluidity of their mixtures to be smaller than that calculated by Eq. 1. The composition corresponding to the greatest deviation of the experimental fluidity from that calculated by Eq. 1 is the composition at which the association between the two liquids is most extensive. Deviations in fluidity are defined as:

$$\Delta\phi = \phi_{12\ \text{calc}} - \phi_{12\ \text{exp}} \qquad \text{(Eq. 2)}$$

while percent relative deviations in fluidity are calculated as:

$$\text{relative deviation } \phi = 100\Delta\phi/\phi_{12\ \text{exp}} \qquad \text{(Eq. 3)}$$

The Kendall equation is easily derived from Eyring's theory of the viscosity of liquids (12) for the case where the molar volumes and, hence, the viscosities of the two pure liquid components are of comparable orders of magnitude. Molar volume refers to the volume of 1 mole of the kinetic or flow unit. If the liquid is self-associated, *e.g.*, a dimer, the molar volume to be used is twice the ratio of the monomeric molecular weight to density. Molar volume is then related to the size of the holes or vacant sites which, according to the relaxation theory of transport phenomena, exist in liquids and determine their transport properties (13).

The Kendall equation is applicable to pairs of miscible liquids whose viscosities do not differ by too much, *e.g.*, by less than a factor of 5. In that case, the fluidities of the mixtures calculated by means of Eq. 1 are correct in the absence of association between the two components. Therefore, where association does occur, the composition of maximum interaction is that corresponding to the maximum difference, $\Delta\phi$, between calculated and observed fluidities.

When the fluidities of the two liquid components differ appreciably, Kendall and Monroe (14) proposed the following empirical equation to calculate the viscosities of binary mixtures by interpolation between the viscosities of the pure components:

$$\eta_{12\ \text{calc}}^{1/3} = x_1\eta_1^{1/3} + x_2\eta_2^{1/3} \qquad \text{(Eq. 4)}$$

Equation 4 correctly predicts the viscosity of binary mixtures of nonassociated liquids when there is an appreciable difference between the viscosities and, hence, the molar volumes of the two liquids (7, 14). Deviations of the observed viscosities of aqueous solutions from the viscosities calculated by means of Eq. 4 can be used to determine the composition corresponding to maximum hydration only if the second liquid is considerably more viscous than water, having a viscosity at room temperature of at least 10 or 15 cps. Deviations in viscosity are defined as:

$$\Delta\eta = \eta_{12\ \text{exp}} - \eta_{12\ \text{calc}} \qquad \text{(Eq. 5)}$$

while percent relative deviations in viscosity are calculated as:

$$\text{relative deviation } \eta = 100\ \Delta\eta/\eta_{12\ \text{exp}} \qquad \text{(Eq. 6)}$$

Neither Eq. 1 nor 4 is universally applicable. They are mutually exclusive; furthermore, Eq. 4 lacks a theoretical basis. Therefore, there is a need for a general method of determining the composition of most extensive hydration of binary systems. Such a method, while still based on rheology because of the large relative deviations observed, does not employ deviations from viscosities calculated by interpolation.

Activation Energy for Viscous Flow as a Measure of Association—The activation energy for viscous flow, ΔE, is defined by the Arrhenius–Gusman–Andrade equation (11):

$$\eta = A \exp(\Delta E/RT) \qquad \text{(Eq. 7)}$$

or:

$$\frac{d \log \eta}{d(1/T)} = \frac{\Delta E}{2.3026R} \qquad \text{(Eq. 8)}$$

where T is the absolute temperature; R is the gas constant, 1.98717 cal/mole/degree; A is another constant; and ΔE is expressed in calories per mole.

Mixtures of simple liquids generally exhibit Newtonian flow behavior, so that η and, hence, ΔE are independent of shear stress. Plots of log η *versus* $1/T$ are sometimes very slightly convex toward the reciprocal temperature axis, especially over temperature ranges broader than ~30°. The ΔE values used in the present study were calculated from viscosity data taken within temperature ranges of ≤20°. The Arrhenius equation was obeyed over these narrow ranges, and ΔE was calculated by the method of least squares.

When viscosity data at only two temperatures, T_1 and T_2, were considered, ΔE was calculated from the integrated form of Eq. 8:

$$\Delta E = \frac{(2.3026)(1.98717)}{\left(\frac{1}{T_2} - \frac{1}{T_1}\right)} \log \frac{(\eta_{12\ \text{exp}})_{T_2}}{(\eta_{12\ \text{exp}})_{T_1}} \qquad \text{(Eq. 9)}$$

The energy of activation for viscous flow of a single liquid is related to its latent heat of vaporization. Liquids are mobile because of the presence of holes or vacant sites. According to Eyring's theory for viscous flow, the flow of liquids in shear consists of molecules squeezing past their neighbors to occupy such vacant sites. The activation energy for viscous flow is used mostly to form new holes (11–13). The size of the holes and, hence, the magnitude of the activation energy must increase as the flow unit increases. For binary aqueous mixtures, more extensive hydration of the second liquid increases the size of the flow unit and should increase the activation energy. Accordingly, the activation energy should go through a maximum at the composition at which the association is most extensive, *i.e.*, at which the greatest number of water molecules are associated with each molecule of the second liquid. The composition corresponding to the highest activation energy is the composition of maximum hydration.

EXPERIMENTAL

Materials—Purification methods and properties of dimethyl sulfoxide (5), 1,4-dioxane (1, 15), and 1-propanol (3) were described previously; 2-pyrrolidinone[1] (also called 2-pyrrolidone or γ-butyrolactam) was purified by fractional distillation and repeated crystallization by freezing until the freezing point could not be increased further. The final value of 25.64° is in good agreement with the published values of 25.57° (16) and 25.67° (17). Because solid pyrrolidinone monohydrate separates at room temperature over a wide range of compositions (16), measurements for the water–pyrrolidinone system were made at temperatures above its melting point of 30.4°.

Acetone[2] was dried with anhydrous sodium sulfate and distilled twice from a 4-Å molecular sieve. Its normal boiling point, refractive index, and density at 25° (Table I) are in good agreement with published values (18, 19).

Water was double distilled. Water–solvent mixtures were prepared in batches of ~100 g by weighing the two liquids to the nearest milligram. Selected properties of the six purified liquids are listed in Table I.

Methods—The temperatures during the measurements were maintained constant within ±0.01°. Viscosities were measured with Cannon–Fenske glass capillary viscometers for which the flow times exceeded 250 sec. The kinetic energy correction was thus too small to be considered. Duplicate measurements, made on fresh portions of the solutions, agreed within 0.2 sec. Densities were determined with a Sprengel–Ostwald pycnometer of 25-ml capacity. Duplicate measurements were identical within ±0.00003 g/ml or better.

RESULTS

Evaluation of Three Methods—The three viscometric methods for determining the composition at which binary mixtures of miscible liquids are most extensively associated were applied to aqueous solutions of acetone, dimethyl sulfoxide, dioxane, propanol, and pyrrolidinone. The data are plotted in Figs. 1–9 and summarized in Table II.

The activation energies for viscous flow for the various aqueous solvent systems were computed as follows. For acetone, new viscosity data at 20 and 25° were obtained because the ΔE values calculated from Ref. 19 as a function of x_2 were too irregular. While ΔE went through a maximum at $x_2 = 0.24$, $\Delta\phi$ went through maxima at $x_2 = 0.26$ for 20° and at $x_2 =$

[1] Practical grade, Eastman Organic Chemicals.
[2] ACS reagent, spectro grade, Eastman Organic Chemicals.

Table I—Some Properties of Purified Materials

Solvent	Normal Boiling Point	Viscosity, cps, at 20.00°	Viscosity, cps, at 25.00°	Density at 25°, g/ml	Refractive Index at 25°[a]
Water	100.0°	1.0020	0.8903	0.9971	1.3325
Acetone	56.15°	0.3175	0.3028	0.7845	1.3563
Dimethyl sulfoxide	18.53°[b]	2.207	2.000	1.0957	1.4768
1,4-Dioxane	101.4° 11.81°[b]	1.310	1.196	1.0280	1.4198
1-Propanol	97.2°	2.193	1.938	0.7997	1.3833
2-Pyrrolidinone	25.64°[c]	9.109[d]	7.693[e]	1.0996[d] 1.0958[e]	—

[a] Sodium D line. [b] Melting point. [c] Freezing point. [d] At 35.00°. [e] At 40.00°.

0.25 for 25° (Figs. 1 and 3). These three values of x_2 are identical within the precision of the methods.

The ΔE values for water–dimethyl sulfoxide mixtures (Fig. 3) are based on viscosity data of Ref. 20 at 25 , 35, and 45°; of Ref. 21 at 25 and 45°; and on new data at 20° combined with published data at 25° (5). The three sets of data agree well with one another. The ΔE values for water–dioxane mixtures (Fig. 6) are based on data of Ref. 22 at 20, 25, and 30° plus new data at 20° combined with published data at 25° (1, 23).

The viscosity data of Refs. 3 and 24 for water–propanol mixtures are in good agreement. The ΔE values are based on data of both references at 25 and 30°. The melting points of solid pyrrolidinone and its monohydrate, 25.6 and 30.4°, respectively (16, 17), require higher working temperatures. Published viscosity data at 31, 35, 40, 45, and 50° (17) were supplemented by new data at 37 and 45°, especially for determining ΔE (Fig. 8).

The disparity between the viscosities of the second liquid and water is relatively small for acetone (1:3 ratio; seventh column of Table II), dimethyl sulfoxide and propanol (2:1 ratio), and dioxane (approximately equal). Therefore, the Kendall equation (Eq. 1) should provide the correct fluidity or viscosity in the absence of association. Consequently, the composition of maximum deviation, $\Delta\phi$, defined by Eq. 2 should be the composition corresponding to the highest hydration.

The applicability of the method based on the Kendall equation is corroborated by the excellent agreement between the composition of maximum hydration, x_2, obtained from $\Delta\phi$ and ΔE for the first four liquids in Table II (compare the x_2 values in the second and sixth columns). The x_2 values calculated by the Kendall–Monroe equation (Eq. 4) and $\Delta\eta$ (Eq. 5), shown in the fourth column, disagree with the x_2 values determined by the other two methods.

The following additional point confirms the use of $\Delta\phi$ rather than $\Delta\eta$ for the first four systems. The maximum deviation in $\Delta\phi$ and ΔE for water–dioxane mixtures occurred at $x_2 = 0.20$ and 0.19, corresponding to a maximum hydration ratio of four water molecules per dioxane molecule or two water molecules per ether group. This hydration ratio of two is to be expected because each ether oxygen has two lone or unshared electron pairs. The same ratio also was found experimentally for linear polyfunctional ethers (1, 8). The x_2 value corresponding to a maximum in $\Delta\eta$, 0.23, would result in a hydration ratio of 3.35 or only 1.67 water molecules per ether group.

The viscosity of pyrrolidinone is 12–13 times higher than that of water at comparable temperatures, indicating that the Kendall–Monroe equation and $\Delta\eta$ rather than the Kendall equation and $\Delta\phi$ should provide the composition corresponding to maximum hydration. Both ΔE and $\Delta\eta$ result in $x_2 = 0.51$ for maximum hydration, compared to $x_2 = 0.15$ from $\Delta\phi$. The following is direct evidence for the correctness of the unit hydration ratio in liquid water–pyrrolidinone mixtures and of the methods for determining this ratio. The solid monohydrate has a congruent melting point at 30.4°. The maximum in the water–pyrrolidinone phase diagram corresponding to this compound is relatively sharp rather than flat (16). These facts indicate that the monohydrate is stable in the liquid state above the melting point as well as in the solid state below it and that dissociation in the melt at temperatures close to the melting point is not extensive (25). Hence, the monohydrate largely persists over the 31–45° range in which the viscosity measurements were conducted.

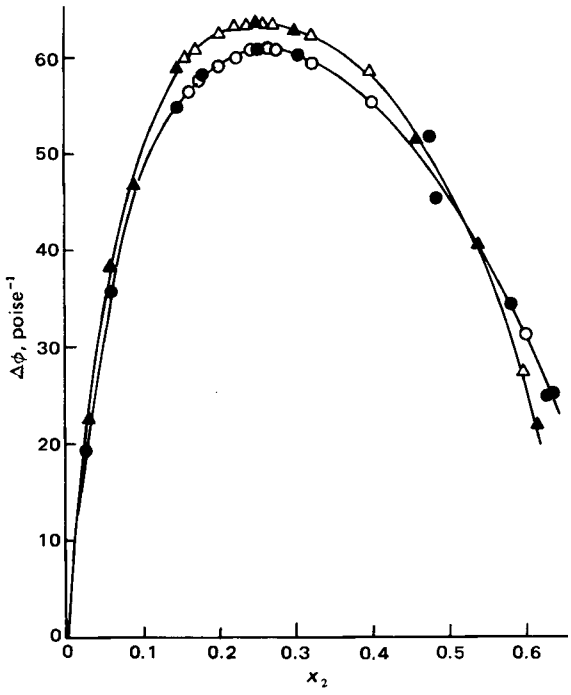

Figure 1—*Difference between calculated and experimental fluidities of water–acetone mixtures as a function of the mole fraction,* x_2, *of acetone. Key:* ●, *Ref. 19 at 20°;* ○, *present work at 20°;* ▲, *Ref. 19 at 25°; and* △, *present work at 25°.*

Precision of Three Methods—The points of most plots of $\Delta\phi$ and $\Delta\eta$ *versus* x_2 fell right on the curves because the usual experimental errors have only moderate effects on $\Delta\phi$ and $\Delta\eta$. Compositions of maximum deviation can be located with a precision of 0.005. Extensive sets of viscosity data by different investigators agreed within 0.01 of the x_2 value corresponding to maximum hydration.

The viscosities of water and the other five pure solvents were determined by five or more measurements each and were practically identical with the literature values reported for the carefully purified liquids at comparable temperatures. If the viscosities of the pure components are assumed to be free of experimental error, the standard deviation of $\Delta\eta$ is the same as that of $\eta_{12\ exp}$ according to Eq. 5. Since fluidity is the reciprocal of viscosity, the standard deviation of $\phi_{12\ exp}$ and $\Delta\phi$ is equal to the standard deviation of $\eta_{12\ exp}$ divided by the square of that viscosity (26).

Table II—Maximum Hydration of Organic Solvents According to the Three Viscometric Methods

Second Component	Compositions of Maximum Δ as Mole Fraction x_2 and Relative Deviations According to: $\Delta\phi$[a]	Relative Deviation ϕ[b], %	$\Delta\eta$[c]	Relative Deviation η[d], %	ΔE[e]	Ratio (η_2/η_{H_2O}) at 25°	Hydration Ratio[f] (Molecules Water / Molecule Second Component)
Acetone	0.25	78	0.17	—	0.24	0.34	3.0
Dimethyl sulfoxide	0.23	208	0.32	—	0.26	2.25	3.2
Dioxane	0.20	107	0.23	—	0.19	1.34	4.1
Propanol	0.15	142	0.24	—	0.15	2.18	5.7
Pyrrolidinone	0.15	—	0.51	49	0.51	12.7[g]	1.0

[a] Calculated with Eq. 2 at 25° except for pyrrolidinone. [b] Calculated with Eq. 3. [c] Calculated with Eq. 5 at 25° except for pyrrolidinone. [d] Calculated with Eq. 6. [e] Calculated with Eq. 8 or 9. [f] Based on weighted average of x_2 from $\Delta\phi$ (first four systems) or $\Delta\eta$ (last system) and ΔE. [g] At 35°.

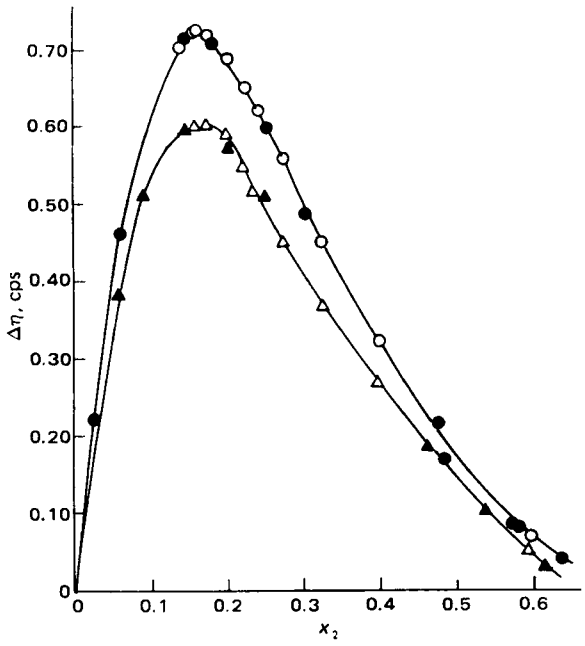

Figure 2—*Difference between experimental and calculated viscosities of water–acetone mixtures as a function of the mole fraction,* x_2, *of acetone. Key:* ●, *Ref. 19 at 20°;* ○, *present work at 20°;* ▲, *Ref. 19 at 25°; and* △, *present work at 25°.*

Experimental errors in the viscosity and temperature measurements greatly affect the activation energy values. Points of ΔE *versus* x_2 plots were more widely scattered about the curves than those of the other two methods, and some published sets of η *versus* x_2 values at different temperatures could not be used due to lack of precision in the viscosity measurements.

The experimental errors in maintaining and measuring temperatures were small compared to those incurred in measuring viscosities. Since ΔE and T are exponential terms in Eq. 7 or, alternatively, since viscosity appears as a logarithmic term in Eqs. 8 and 9, the experimental errors in η affect ΔE less than would comparable errors in T (26). However, two

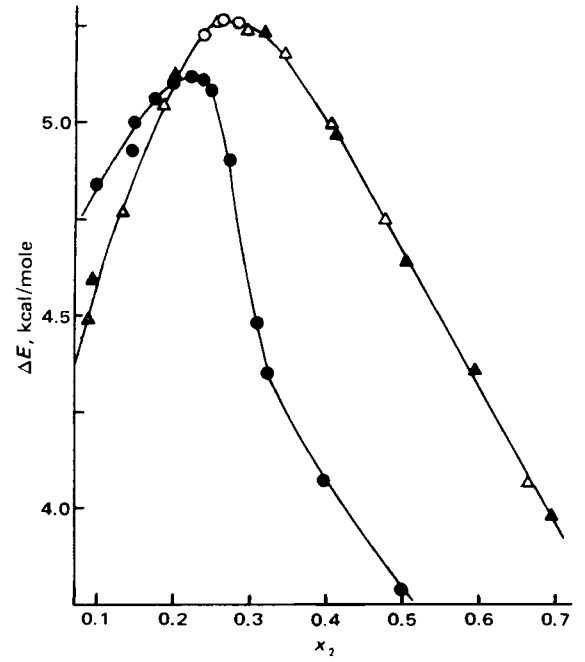

Figure 3—*Activation energies for viscous flow of water–acetone and water–dimethyl sulfoxide mixtures as a function of the mole fraction,* x_2, *of the organic liquids. Key:* ▲, *dimethyl sulfoxide, Ref. 20;* △, *dimethyl sulfoxide, Ref. 21;* ○, *dimethyl sulfoxide, present work; and* ●, *acetone, present work.*

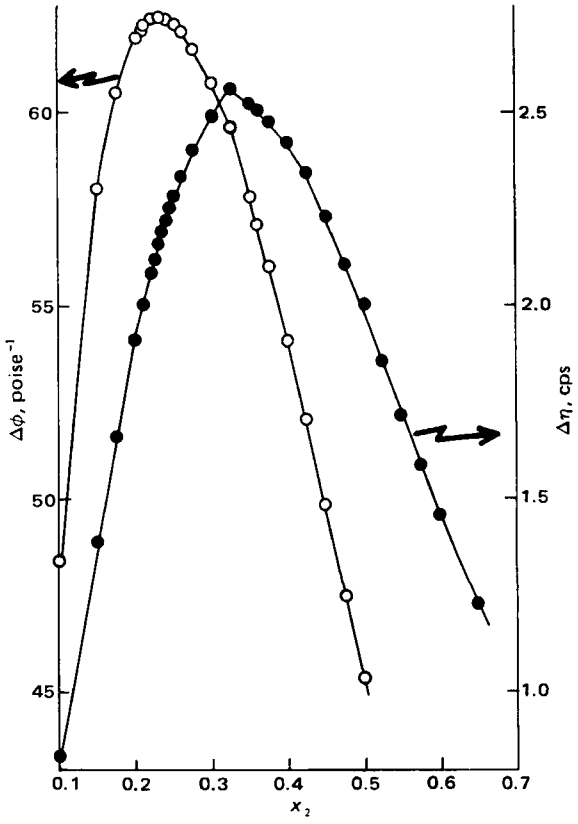

Figure 4—*Differences between calculated and experimental fluidities and viscosities of water–dimethyl sulfoxide mixtures as a function of the mole fraction,* x_2, *of dimethyl sulfoxide at 25°. Key:* ○, $\Delta\phi$; *and* ●, $\Delta\eta$.

or more pairs of η, T measurements are required to determine each value of the dependent variable ΔE to eliminate the unknown preexponential factor A, which varies with composition. This requirement raises the standard deviation of ΔE substantially, increasing it above the standard deviations of $\Delta\phi$ and $\Delta\eta$.

Use of the activation energy for viscous flow to determine the composition of maximum association between two liquids thus requires a larger number of more accurate viscosity measurements than does use of the maximum deviation in fluidity or viscosity. The present values for x_2 of maximum hydration obtained from maxima in activation energies are only good to ±0.015. The greatest uncertainty is in the water–dimethyl sulfoxide and water–pyrrolidinone systems, where the curves have flat peaks.

STRUCTURAL CONSIDERATIONS

Possible structures for the most extensively hydrated species prevalent in the water–solvent systems are discussed here. The 3:1 hydration ratio found in the acetone and dimethyl sulfoxide systems is probably represented (5) by Structure I, where two water molecules are hydrogen bonded to the carbonyl or sulfoxide oxygen while a third water molecule is associated with the organic molecule by attraction between the negative end of its dipole and the positive end of the carbonyl or sulfoxide dipole.

IR studies (27) showed that carbonyl groups can bind two water molecules through their two lone electron pairs. Hydrogen bonding increases

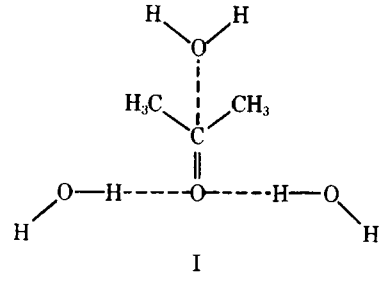

I

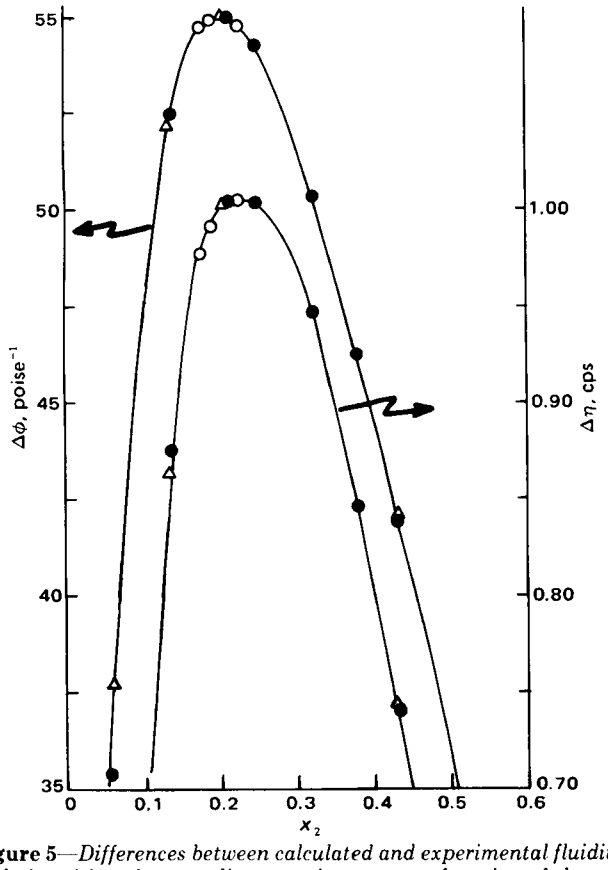

Figure 5—*Differences between calculated and experimental fluidities and viscosities of water–dioxane mixtures as a function of the mole fraction,* x_2, *of dioxane at 25°. Key:* ○, *Ref. 1;* ●, *Ref. 22; and* △, *Ref. 23.*

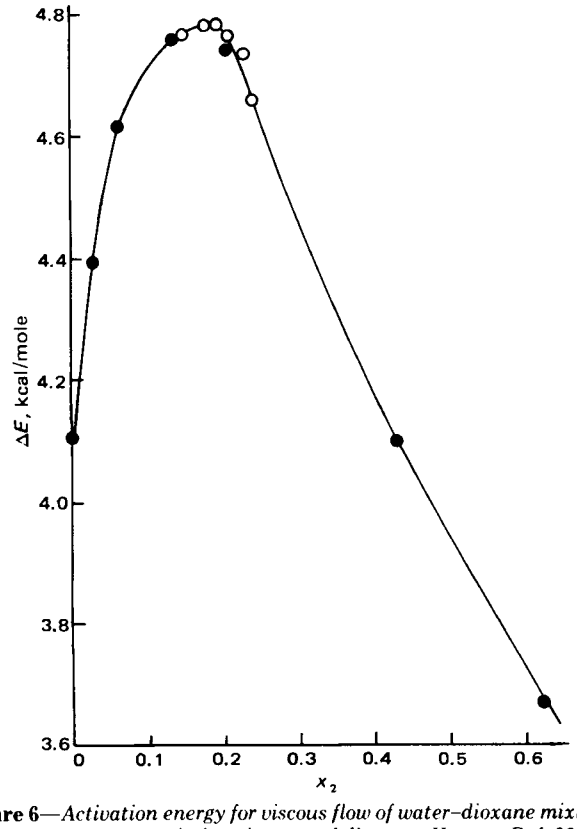

Figure 6—*Activation energy for viscous flow of water–dioxane mixtures as a function of the mole fraction,* x_2, *of dioxane. Key:* ●, *Ref. 22; and* ○, *present work.*

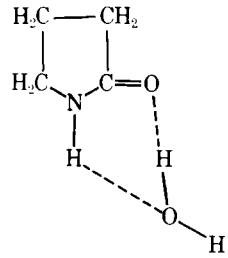

II

the dipole moment of the carbonyl group, enhancing its binding of a third water molecule by dipole–dipole attraction.

The three aprotic solvents acetone, dimethyl sulfoxide, and dioxane can only act as proton acceptors in hydrogen bonding with water. The simple and integer hydration ratios of 3:1 for the carbonyl and sulfoxide groups and 2:1 for the ether group may be due to this fact. The high and fractional hydration ratio of propanol probably results because this solvent acts as a proton donor as well as acceptor, forming hydrogen-bonded clusters consisting, on the average, of 5.67 water molecules for each propanol molecule. Hydrophobic interaction (28) probably plays a role in forming such clusters—*viz.*, the structure of the water molecules surrounding the normal propyl chain is enhanced or tightened. Accordingly, such clusters may consist of water molecules hydrogen bonded to the hydroxyl group of propanol and other water molecules bunched around its hydrocarbon chain and hydrogen bonded to each other.

The following two experimental observations are consistent with the existence of such clusters and with the enhancement of the water structure around the propyl chain (3). In the homologous series of lower alcohols, the hydration ratio at 25° decreases with the hydrocarbon chain length of the alcohol, from 5.7 for 1-propanol to 4.0 for ethanol and 1.4 for methanol. For propanol, the hydration ratio or cluster size decreases with increasing temperature, being 5.7, 5.3, 4.9, and 4.6 at 25, 30, 40, and 50°, respectively. The hydration ratio of ethanol decreases merely from 4.0 to 3.7 while that of methanol remains practically constant, increasing from 1.4 to 1.5 between 25 and 50° (3). The effect of alkyl chain length on the hydration of monofunctional alcohols and aprotic solvents is under investigation.

The monohydrate of pyrrolidinone is probably represented chiefly by Structure II, where the hydrogen-bonded water molecule participates in a six-membered ring.

COMPARISON WITH OTHER METHODS

Other Viscometric Methods—Viscosity maxima for binary liquid mixtures have frequently been reported. For instance, the compilation of Raridon and Kraus (29) covered 39 aqueous mixtures of organic sol-

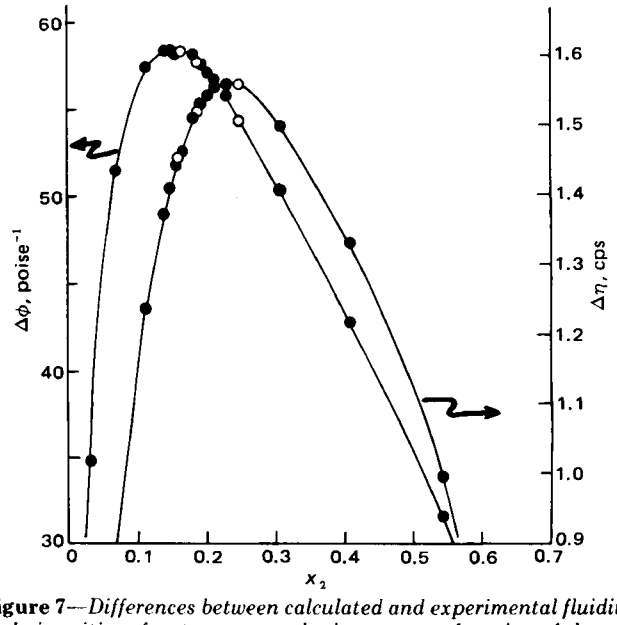

Figure 7—*Differences between calculated and experimental fluidities and viscosities of water–propanol mixtures as a function of the mole fraction,* x_2, *of propanol at 25°. Key:* ○, *Ref. 3; and* ●, *Ref. 24.*

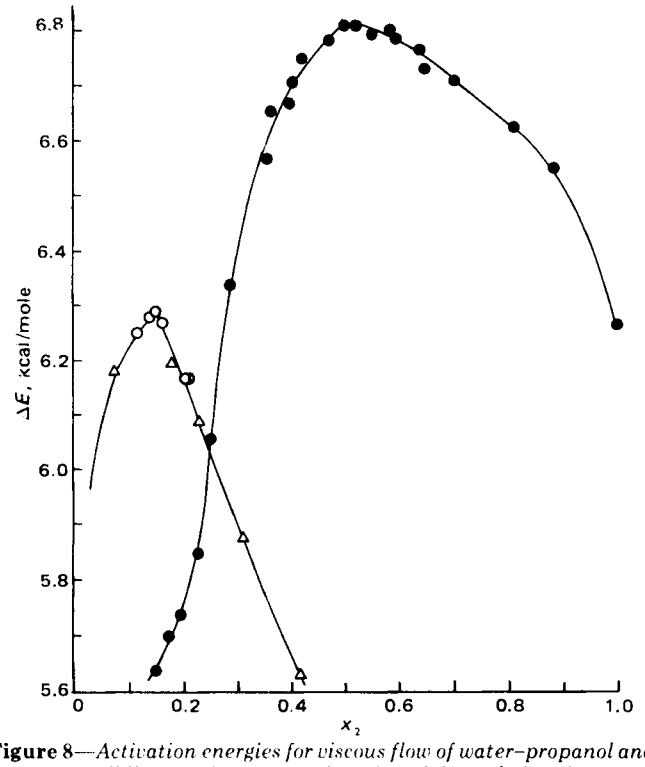

Figure 8—*Activation energies for viscous flow of water–propanol and water–pyrrolidinone mixtures as a function of the mole fraction,* x_2, *of the organic liquids. Key:* ○, *propanol, Ref. 3;* △, *propanol, Ref. 24; and* ●, *pyrrolidinone, present work.*

vents at 25°. Viscosities were measured at only five compositions for each binary system, making the determination of the composition of maximum viscosity by interpolation uncertain. Their estimated x_2 values corresponding to maximum viscosity were 0.14 for acetone, 0.35 for dimethyl sulfoxide, 0.24 for dioxane, and 0.29 for propanol (29).

Viscosity maxima in binary solvent mixtures are of practical importance, *e.g.*, when using such mixtures as reaction media, but do not necessarily coincide with the maximum association between the two solvents. As was pointed out in several publications as early as 1913 and 1917, the most extensive association between two liquids, as well as the possible formation of stoichiometric complexes of the highest solvation number between them, occurs at the composition at which the *deviation* of the experimental viscosity function goes through a maximum rather than at the composition of the viscosity maximum (1, 7, 10, 14, 22). Furthermore, the choice of the correct viscosity function for calculating additive viscosities is important. This requirement was demonstrated in the present work by the discrepancies between the compositions of maximum deviation from experimental viscosities or fluidities calculated with the Kendall (Eq. 1) and Kendall–Monroe (Eq. 4) equations.

Despite these considerations, the maximum in the viscosity of water–dimethyl sulfoxide mixtures at approximately $x_2 = 0.35$ (20, 21, 30–32) has been attributed to a 2:1 association complex (20, 21, 30, 31).

The following are additional arguments against equating the composition of maximum viscosity with the composition of maximum association. With water–acetone mixtures, maximum viscosity at room temperature was reached at $x_2 = 0.14$ (19, 29). This composition would correspond to a hydration ratio of 6, which is improbable, because six water molecules cannot be in close contact with a single carbonyl group. In the water–pyrrolidinone system, the highest viscosity is that of pure pyrrolidinone; *i.e.*, there is no viscosity maximum at an intermediate composition. However, there is a pronounced association maximum at the composition of the monohydrate, signaled by a maximum in the deviation of the experimental viscosity from that calculated by Eq. 4 at $x_2 = 0.50$, which amounts to one-half of the experimental viscosity.

Fort and Moore (32) introduced a correction term into the Kendall equation (Eq. 1), changing it to:

$$\log \eta_{12\,\mathrm{exp}} = x_1 \log \eta_1 + x_2 \log \eta_2 + x_1 x_2 d \qquad \text{(Eq. 10)}$$

Comparison of Eq. 10 with Eq. 1 results in:

$$d = \frac{\log (\phi_{12\,\mathrm{calc}}/\phi_{12\,\mathrm{exp}})}{x_1 x_2} \qquad \text{(Eq. 11)}$$

They claimed that the empirical parameter d provides a useful measure of the interaction between pairs of liquids, reaching a maximum at the composition of strongest interaction (32). One shortcoming of their work is that only four mixtures were determined for each of the 14 binary systems, making the location of the composition corresponding to the maximum value of d for each system vague.

A more serious shortcoming is that the 14 pairs of liquids studied all had viscosities of the same order of magnitude. If the present data for the water–pyrrolidinone system are used to calculate d by Eq. 11, the maximum value of d is reached at a mole fraction of pyrrolidinone close to unity, corresponding to a hydration ratio close to zero. Thus, Fort and Moore's treatment has the same shortcoming as the Kendall equation, which it resembles. It fails for binary systems where one of the two components has an appreciably higher viscosity than the other. The only universal viscometric method for determining the composition of maximum association, applicable to pairs of liquids of widely differing as well as of comparable viscosities, is the one based on the activation energies of viscous flow described previously.

Other Transport Properties—Differential diffusion coefficients in the water–acetone system at 25° (33, 34), as well as at 35, 45, and 55° (33), went through minima at a mole fraction of acetone of about 0.25, confirming the maximum hydration ratio of 3:1 obtained by the viscometric methods. Relative deviation, in percent, is defined by equations analogous to Eqs. 5 and 6, with viscosity replaced by the differential diffusion coefficient. The relative deviations of the latter at the composition of maximum deviation were in the −200 to −300% range.

For the systems of deuterated water–dimethyl sulfoxide and water–deuterated dimethyl sulfoxide at 26°, self-diffusion measurements were made in x_2 increments of 0.1. Minima in the self-diffusion coefficients of water and of dimethyl sulfoxide were observed at a mole fraction of dimethyl sulfoxide of ~0.3. This composition could correspond either to the present 3:1 or to the lower 2:1 hydration ratio. The measurements were made by NMR, using a pulsed magnetic field-gradient spin-echo technique (35).

Compound Formation—The most direct corroboration for the maximum hydration ratio is the existence, on the binary phase diagram, of a solid hydrate with a congruent melting point stable at lower temperatures. In agreement with the present hydration ratios of 3:1 for dimethyl sulfoxide and 1:1 for pyrrolidinone, a solid trihydrate was isolated for the former (36) and a monohydrate was isolated for the latter (16). The other solvents form no stable solid hydrates (37).

Thermodynamic Parameters—When water is mixed with aprotic solvents, hydrogen bonds between water molecules are broken while hydrogen bonds between water and solvent molecules are formed. Hydrogen bonds of protonated solvents like propanol are broken as well. The enthalpy of mixing depends in part on the difference between the numbers and energies of these two or three kinds of hydrogen bonds. The breaking up of clusters of water molecules when adding solvent or of clusters of solvent molecules when adding water increases the entropy of mixing while the association between water and solvent molecules decreases it. The net entropy change of mixing depends in part on the difference between the numbers and sizes of these two or three types of clusters. Enthalpy and entropy of mixing thus depend on the difference between two opposite processes, and their variation with composition does not provide a good indication of the composition of maximum association between water and the solvent.

Dimethyl sulfoxide and acetone can bind only two water molecules by hydrogen bonding (Ref. 27 and below). The third water molecule is held by Keesom forces, which are considerably weaker than hydrogen bonds and are probably not detected in calorimetric measurements. This difference in bond energies is another reason why thermodynamic functions are not reliable parameters for determining the maximum hydration of solvents. Excess functions are used in the discussion here since they represent the magnitude of deviation from ideality.

The maximum hydration ratio of dioxane is 4:1, with two water molecules hydrogen bonded to each ether group (1, 8, and present results, Table II). The excess enthalpy of mixing goes through a minimum at a mole fraction of dioxane of 0.14 or 0.15 (37–39), which would correspond to a hydration ratio of 6.1 or 5.7:1, while the excess entropy of mixing goes through a minimum at $x_2 = 0.27$ (37). Excess enthalpy and entropy of mixing are thus at variance with one another and with previous and present results.

Mixing of water and dimethyl sulfoxide is noticeably exothermic. The excess enthalpy of mixing at 25° goes through a minimum at mole frac-

Table III—Maximum Deviations of Density and Dielectric Constant for Five Water–Solvent Systems

	Maximum Deviations According to									
	Density					Dielectric Constant				
Solvent	Temperature	x_2	Hydration Ratio[a]	Relative Deviation[b], %	Reference	Temperature	x_2	Hydration Ratio[a]	Relative Deviation[b], %	Reference
Acetone	20°	0.45	1.2	−4.3	18, 19, p[c]	25°	0.39	1.6	−49	58
Dimethyl sulfoxide	25°	0.30	2.3	+5.6	5	25°	0.25	3.0	+4.1	5, 59
Dioxane	25°	0.24	3.2	+3.0	15	25°	0.32	2.1	−182	60, 61
Propanol	25°	0.37	1.7	−6.1	3, 24	20°	0.36	1.8	−72	58
Pyrrolidinone	35°	0.33	2.0	+4.8	17, p	35°	0.50	1.0	−17	17
	40°	0.31	2.2	+4.6	17, p	40°	0.50	1.0	−17	17

[a] Ratio water molecules to molecule solvent. [b] Calculated with equations analogous to Eqs. 5 and 6. [c] Present work.

tions of dimethyl sulfoxide of 0.34 (40, 41) or 0.36 (42), which would translate into hydration ratios of 1.9 or 1.8:1. The excess enthalpy of mixing in the water–acetone system at 20° goes through a minimum at a mole fraction of acetone of 0.18 (43). This composition would correspond to a hydration ratio of 4.6:1.

Heat capacities of liquid mixtures are perhaps more pertinent than enthalpies since they depend in part on the size of the clusters of associated molecules. The excess molal heat capacity at 25° goes through a maximum at a mole fraction of acetone of 0.24, corresponding to the present hydration ratio of 3:1. It is much smaller and nearly independent of composition in the water–dimethyl sulfoxide system (44). The cohesive energy density of binary mixtures depends in part on the extent of association since it represents the energy of vaporization per molar volume. The excess cohesive energy density at 25° goes through a maximum at a mole fraction of dimethyl sulfoxide of 0.25 (45), corresponding to the present hydration ratio of 3:1.

Spectroscopic Methods—The main difficulty in using absorption spectroscopy to determine the maximum hydration of organic solvents in binary mixtures with water is that spectroscopic methods are restricted almost exclusively to the strongest intermolecular bonds—*viz.*, hydrogen bonds. Dipole–dipole interactions between molecules have, in most cases, only minor effects on their IR, UV, Raman, and NMR spectra and usually go undetected. Additional reasons why spectroscopic methods are not well suited for determining maximum hydration are the frequent use of a third, "inert" solvent and the difficulty of proper band assignment.

The maximum hydration ratio of pyrrolidinone was identified correctly as unity from the IR spectra (46) because the attraction between water and pyrrolidinone is based mainly on hydrogen bonds. In the water–acetone system, a maximum of two water molecules can be bound to the carbonyl group by hydrogen bonds (27), which is to be expected in view of the fact that the carbonyl oxygen has two unshared electron pairs. IR (47–49), UV (49), and NMR (50) measurements have identified mainly water–acetone "complexes" of 1:1 and 1:2 molar ratios, in part because this was the range of compositions in which most spectra were investigated. Both 2:1 and 3:1 or 4:1 complexes were reported also, although it is difficult to reconcile the binding of more than two water molecules by hydrogen bonds to one carbonyl oxygen having two lone electron pairs. Water molecules bound to acetone by dipole–dipole forces (Structure I) could not have been detected by the spectroscopic techniques used in Refs. 47–50.

In the water–dimethyl sulfoxide system, IR (41, 51), UV (41), Raman (52, 53), and NMR (54) spectra have identified 2:1, 1:1, and 1:2 complexes. The third water molecule, bound to dimethyl sulfoxide by dipole–dipole forces (5, 36), cannot be disclosed by these spectroscopic techniques.

NMR relaxation techniques are better suited to determine maximum hydration because they depend largely on the size and symmetry of water–solvent clusters. The reorientation of these clusters or complexes is the most important motion in the relaxation process. In particular, excess nuclear spin-lattice relaxation times, T_1, reach a minimum and excess relaxation rates, $1/T_1$, reach a maximum at the composition corresponding to the maximum intermolecular association (55, 56). Use of mixtures of deuterated acetone with water and heavy water with acetone resulted in a maximum relaxation rate at 25° at a mole fraction of acetone of ~0.20 (55). Since the authors only studied compositions of $x_2 = 0.10$, 0.20, and 0.40 in the pertinent range, the maximum could equally well be located at $x_2 = 0.25$ but not as high as 0.33. Accordingly, the maximum hydration ratio of acetone lies between 4 and 2.7:1, a result compatible with the present 3.0:1 value. The use of excess functions might have shifted the x_2 value corresponding to maximum hydration.

The water–dimethyl sulfoxide system was investigated over narrower composition intervals. The absolute value of the excess relaxation time went through a maximum at a mole fraction of dimethyl sulfoxide of 0.25, leading the author to describe "compound formation" resulting in a 3:1 molecular complex (56). While this result does not preclude the existence of a 2:1 complex in mixtures of lower water content, the most highly hydrated complex has a 3:1 hydration ratio, in agreement with the present results. Other studies of proton spin-lattice plus spin-spin relaxation times over a range of temperatures found maxima in relaxation rates at a mole fraction of dimethyl sulfoxide of about 0.35 (57), but these authors used $1/T_1$. The use of excess relaxation rates would shift the maxima toward somewhat lower dimethyl sulfoxide mole fractions or higher hydration ratios.

Density—Compositions of maximum deviations and relative deviations of calculated from experimental densities for the five binary systems are summarized in Table III. Positive relative deviations indicate that experimental densities were higher than calculated densities, *i.e.*, that volume contractions occurred during mixing. In aqueous mixtures of acetone and propanol, experimental densities were actually smaller than those calculated. The absolute values of the relative deviations are small, ranging from 3 to 6%.

If the compositions of maximum density deviation corresponded to maximum hydration ratios, these would be quite different from the ratios obtained by viscometry. However, excess densities do not necessarily reach maxima at the composition of most extensive association for the following reason. When two highly structured liquids like water, propanol, or pyrrolidinone are mixed, the structures of both liquids are broken up and new structures or association complexes are formed. Even acetone and dioxane, which have little structure of their own in the pure state,

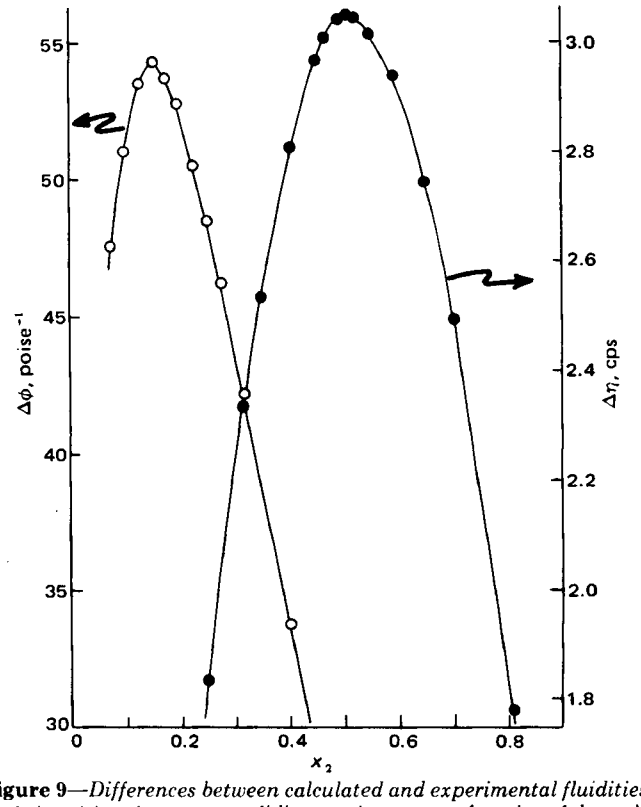

Figure 9—*Differences between calculated and experimental fluidities and viscosities of water–pyrrolidinone mixtures as a function of the mole fraction,* x_2, *of pyrrolidinone at 37°. Key:* ○, $\Delta\phi$; *and* ●, $\Delta\eta$.

are effective in breaking up the structure of water in aqueous mixtures. Calculated densities depend on the density and, hence, on the short-range order and structure in pure water and in the second pure liquid. These properties of one pure liquid are unrelated to corresponding properties of the second pure liquid and of the clusters formed by association between the two. A highly structured liquid like propanol and a liquid with little association like acetone both caused monotonic decreases in density when mixed with water while aqueous mixtures of the nonpolar dioxane had a density maximum at an intermediate composition. Therefore, excess density does not constitute a suitable property for determining the composition of maximum association, contrary to what had been assumed by the author (15).

Dielectric Constants—Deviations of experimental dielectric constants from those interpolated according to equations analogous to Eqs. 5 and 6 were calculated from literature data for the five aqueous systems. Compositions corresponding to the maximum deviations, hydration ratios corresponding to these compositions, and relative deviations are listed in Table III. Hydration ratios agree with those obtained from the viscometric methods in the cases of dimethyl sulfoxide and pyrrolidinone. However, in the former system, the experimental dielectric constants were higher than those calculated for the corresponding compositions, resulting in positive relative deviations; in the latter system and in the other three, the calculated dielectric constants were higher than the corresponding experimental values.

Pure propanol and, presumably, liquid pyrrolidinone as well have high values for the Kirkwood correlation factor (62). Those of the aprotic solvents acetone and dimethyl sulfoxide are low, namely, close to unity, while dioxane has a zero dipole moment (62). When added to water in low concentrations, propanol, acetone, and dioxane decrease the dielectric constant of water. In the water–acetone and water–dioxane systems, the correlation factors (62) and the experimental dielectric constants (58, 60, 61) decrease monotonically with increasing mole fraction of the organic component over the entire range of compositions. The addition of water to propanol and of propanol to water break their respective structures, and the correlation factor of the mixtures reaches a minimum around $x_2 = 0.5$ (62). Surprisingly, the experimental dielectric constants of water–propanol (58) and water–pyrrolidinone (17) mixtures decrease monotonically with increasing x_2 over the entire range of compositions.

The case of dimethyl sulfoxide is even more puzzling since its aqueous mixtures constitute the only one of the five systems studied in which experimental dielectric constants are larger than the corresponding calculated values. The cause for the high dielectric constant of pure dimethyl sulfoxide (46.4 at 25° from Ref. 59) is poorly understood (63). Therefore, it seems useless to speculate on why the deviations of the dielectric constants are positive in the water–dimethyl sulfoxide system and negative in the other four systems. The agreement between the compositions corresponding to a maximum positive deviation in the dimethyl sulfoxide mixtures and a maximum negative deviation in the pyrrolidinone mixtures and the compositions of maximum hydration obtained by the viscometric methods may be fortuitous. Until the theory for dielectric constants of aqueous solutions of nonelectrolytes is better understood (62), it seems preferable not to use the excess dielectric constants of such mixtures for determining the composition of maximum hydration.

Miscellaneous Methods—Ultrasonic velocity in water–dimethyl sulfoxide mixtures reaches a maximum at a mole fraction of dimethyl sulfoxide of 0.27 at 20° (64). The excess velocity, *i.e.*, the deviation of the experimental velocity from the velocity calculated by equations analogous to Eqs. 5 and 6, reaches a maximum at $x_2 = 0.25$. The maximum relative deviation, which occurs at that composition, amounts to 16%.

The adiabatic compressibility at 20°, calculated as the reciprocal of the product of density and the square of the sound velocity, goes through a minimum at $x_2 = 0.27$ (64). The excess adiabatic compressibility goes through a minimum at a slightly lower x_2 value. The relative deviation reaches a maximum value of −42% at that composition. The excess compressibility of a mixture is expected to reach a minimum and the excess sound velocity is expected to reach a maximum at the composition at which the intermolecular association is most extensive. Therefore, these data confirm the present hydration ratio of 3:1.

The solubility of hydrogen at 25° and a constant partial pressure of 1 atm in water–dimethyl sulfoxide mixtures goes through a minimum at a mole fraction of dimethyl sulfoxide of about 0.28 (65). Since solubilities were measured in mole fraction increments of 0.2, the minimum could be located equally well at $x_2 = 0.25$ or 0.33, corresponding to hydration ratios of 3:1 or 2:1. The hydrogen molecule, as a small and nonpolar probe, should cause only minimal disturbance of the association clusters between water and dimethyl sulfoxide molecules, so the minimum solubility should occur at the composition of maximum association. Symons (65) interprets his measurements in terms of an equilibrium between a 3:1 and a 2:1 water–dimethyl sulfoxide complex. His maximum hydration of 3:1 is in agreement with the present findings.

The reason why excess molar refraction is not suitable for determining the composition of maximum hydration is given in Ref. 5.

CONCLUSION

The composition at which water and the second liquid component are most extensively associated is marked by a minimum or maximum in an excess property of the binary mixture that expresses the difference between the experimental and the calculated values of this property rather than by a minimum or maximum in the experimental value of the property. Excess enthalpy and entropy of mixing as well as absorption spectroscopy methods only detect intermolecular association by hydrogen bonding but not by dipole–dipole attraction. When the two components interact mainly by hydrogen bonding, as in the water–pyrrolidinone system, maximum hydration ratios obtained from excess thermodynamic functions or by absorption spectroscopy agree with those obtained by viscometric methods. When additional water molecules are bound by dipole forces, spectroscopic methods result in erroneously low maximum hydration ratios comprising only hydrogen-bonded water molecules. This is the case with the water–dimethyl sulfoxide and water–acetone systems, where absorption spectra and thermodynamic excess functions identified the 2:1 hydrogen-bonded complex as possessing the highest hydration ratio, whereas transport and relaxation methods revealed the existence of the 3:1 complex.

Relaxation methods that depend on the size of the clusters or complexes give maximum hydration ratios in good agreement with viscometric methods. Since all transport properties depend on cluster size, they result in identical maximum hydration ratios when properly interpreted. These hydration ratios are relevant to chemical and biological processes affected by the solvation of functional groups.

The most direct validation of the hydration ratios determined by viscometric methods is that they agreed with the composition of solid hydrates stable at lower temperatures in the two instances where such solid hydrates exist. For instance, the fact that a solid dimethyl sulfoxide trihydrate was found demonstrates that dimethyl sulfoxide possesses the bonding capacity and geometric requirements to bind three water molecules. Any method producing a hydration ratio of <3:1 as the *maximum* ratio is in error.

The use of the activation energy for viscous flow of binary mixtures to determine the composition of maximum association requires a greater number and more accurate viscosity measurements than the use of isothermal viscosities or fluidities. By comparison with the other suitable methods already discussed, viscometric techniques require less elaborate equipment that is easier to operate, have comparable or better reproducibility, and result in relative deviations that are as large or larger.

APPENDIX: VARIATION IN SELF-ASSOCIATION OF LIQUID WATER WITH TEMPERATURE DETERMINED FROM TEMPERATURE DEPENDENCE OF ACTIVATION ENERGY FOR VISCOUS FLOW

In this section, the variation of the activation energy for viscous flow of water with temperature is used to provide a relative estimate of the degree of self-association in the pure liquid as a function of temperature. The activation energy of water, unlike that of most liquids, depends markedly on temperature because of an exceptionally extensive self-association (66–68).

The activation energies for viscous flow at constant volume of nonassociated liquids are small and independent of temperature. The experimental activation energies, ΔE, measured at constant pressure and defined by Eqs. 7–9 vary with temperature to the same limited extent as do the specific volumes and, hence, the free space or volume of the holes in these liquids (11, 13, 69). For associated liquids, the size of the holes and, therefore, the viscosities and activation energies for viscous flow are larger than for nonassociated liquids of comparable molecular size because the flow units are larger.

The degree of association decreases with increasing temperature. Since the activation energy for viscous flow is primarily expended in creating the holes or vacant sites required for flow, it too should decrease with increasing temperature. The activation energy is proportional to the size of a hole which, in turn, is proportional to the size of a flow unit and the degree of association. Therefore, any decrease of the latter with increasing

Table IV—Activation Energy for Viscous Flow, Slope of the ΔE *versus* Temperature Curve, and Median Cluster Size for Liquid Water

Temperature	ΔE, kcal/mole	$\frac{d(\Delta E)}{dT}$, kcal/mole/°K	j^a
0°	5.5		11.2[b]
10°	4.58	0.043	8.8[b]
20°	4.20	0.034	7.8[b]
30°	3.89	0.026	7.0[b]
40°	3.66	0.020	6.5[b]
50°	3.47	0.015	6.1[b]
60°	3.34	0.014	5.6[b]
70°	3.22	0.010	5.3[c]
80°	3.12	0.008	5.1[c]
90°	3.06	0.004	4.9[c]
100°	2.9		4.5[c]

[a] Median cluster size [b] From Ref. 68. [c] Calculated by Eq. 12.

temperature should be reflected in a comparable decrease in the activation energy. The variation of the activation energy with temperature can, therefore, be used as a measure of the variation in the degree of association of the liquid with temperature.

Three sets of data for the viscosity of water at 1 atm from 0 to 100° in increments of 5° are reported in the literature (66, 70). The activation energies for viscous flow derived from the three sets are in good agreement up to 70°. Table IV lists the best values of ΔE as a function of temperature and the values of the slope of the ΔE *versus* temperature curve, $\Delta(\Delta E)/\Delta T$, in kcal/mole/°K. As shown, ΔE decreases fast with increasing temperature near the melting point where the association of water molecules is extensive and, consequently, the reduction in association per degree temperature increase is appreciable. This reduction and the slope of the ΔE *versus* temperature curve level off as the temperature approaches the normal boiling point. Considering the association in liquid water in the range between its freezing point and normal boiling point, over half of the association disappears between 0 and 20° because over half of the drop in ΔE occurs over that temperature range.

The extensive dissociation of clusters of associated water molecules over a relatively narrow temperature interval above the melting point of ice is confirmed qualitatively by several techniques. Most of the investigations dealing with self-association in water are based on spectroscopic methods and provide estimates mainly for the fraction of unbonded and hydrogen-bonded protons. The various results differ considerably (51).

In a statistical thermodynamic treatment, water was assumed to consist of clusters in equilibrium having a continuous size distribution. The median cluster size, j, was calculated from partition functions and found to decrease with increasing temperature (68). These values of j, estimated between 0 and 60°, are included in Table IV. The following linear relation between ΔE and j is obtained from the tabulated data, with a correlation coefficient of 0.9995:

$$j = -2.884 + 2.555\,\Delta E \qquad \text{(Eq. A1)}$$

The close correlation between cluster size and activation energy for viscous flow corroborates the use of the latter in estimating the relative size of the flow unit and its variation with temperature for pure, extensively associated liquids like water.

REFERENCES

(1) H. Schott, *J. Chem. Eng. Data*, **11**, 417 (1966).

(2) H. Schott, *J. Colloid Interface Sci.*, **24**, 193 (1967).

(3) H. Schott, *J. Chem. Eng. Data*, **14**, 237 (1969).

(4) D. W. van Krevelen, "Properties of Polymers and Their Correlation with Chemical Structure," 2nd ed., Elsevier, Amsterdam, The Netherlands, 1976, chap. 18.

(5) H. Schott, *J. Pharm. Sci.*, **58**, 946 (1969).

(6) B. Castagna, R. Favier, R. Giavarini, M. Guerin, J. Roveillo, and M. Gomel, *Ann. Chim.*, **7**, 5 (1972).

(7) E. Hatschek, "The Viscosity of Liquids," Van Nostrand, New York, N.Y., 1928, chap. 9.

(8) W. J. Wallace, C. S. Shepard, and C. Underwood, *J. Chem. Eng. Data*, **13**, 11 (1968).

(9) R. P. Singh and S. S. Singh, *J. Indian Chem. Soc.*, **51**, 790 (1974).

(10) J. Kendall, *Medd. K. Vetenskapsakad. Nobelinst.*, **2** (25), 1 (1913).

(11) S. Glasstone, "Textbook of Physical Chemistry," 2nd ed., Van Nostrand, New York, N.Y., 1951, chap. 7.

(12) S. Glasstone, K. J. Laidler, and H. Eyring, "The Theory of Rate Processes," McGraw-Hill, New York, N.Y., 1941, chap. 9.

(13) T. Ree and H. Eyring, in "Rheology—Theory and Applications," vol. II, F. R. Eirich, Ed., Academic, New York, N.Y., 1958, chap. 3.

(14) J. Kendall and K. P. Monroe, *J. Am. Chem. Soc.*, **39**, 1787 (1917).

(15) H. Schott, *J. Chem. Eng. Data*, **6**, 19 (1961).

(16) L. J. Lohr, *J. Phys. Chem.*, **62**, 1150 (1958).

(17) R. L. Blumenshine and P. G. Sears, *J. Chem. Eng. Data*, **11**, 141 (1966).

(18) S. S. Kurtz, Jr., A. E. Wikingsson, D. L. Camin, and A. R. Thompson, *ibid.*, **10**, 330 (1965).

(19) K. S. Howard and R. A. McAllister, *AIChE J.*, **4**, 362 (1958).

(20) J. J. Lindberg and R. Lauren, *Finska Kemistsam. Medd.*, **71**, 37 (1962).

(21) J. M. G. Cowie and P. M. Toporowski, *Can. J. Chem.*, **39**, 2240 (1961).

(22) J. A. Geddes, *J. Am. Chem. Soc.*, **55**, 4832 (1933).

(23) J. E. Lind and R. M. Fuoss, *J. Phys. Chem.*, **65**, 999 (1961).

(24) S. Z. Mikhail and W. R. Kimel, *J. Chem. Eng. Data*, **8**, 323 (1963).

(25) S. Glasstone, "Textbook of Physical Chemistry," 2nd ed., Van Nostrand, New York, N.Y., 1951, chap. 10.

(26) T. B. Crumpler and J. H. Yoe, "Chemical Computations and Errors," Wiley, New York, N.Y., 1949, pp. 175–180.

(27) P. Combelas, C. Garrigou-Lagrange, and J. Lascombe, *Ann. Chim.*, **5**, 315 (1970).

(28) F. Franks, in "Water, a Comprehensive Treatise," vol. 4, F. Franks, Ed., Plenum, New York, N.Y., 1975, chap. 1.

(29) R. J. Raridon and K. A. Kraus, U.S. Department of the Interior Research and Development Progress Report No. 302, Washington, D.C., 1968, p. 52.

(30) R. G. LeBel and D. A. I. Goring, *J. Chem. Eng. Data*, **7**, 100 (1962).

(31) S. A. Schichman and R. L. Amey, *J. Phys. Chem.*, **75**, 98 (1971).

(32) R. J. Fort and W. R. Moore, *Trans. Faraday Soc.*, **62**, 1112 (1966).

(33) M. T. Tyn and W. F. Calus, *J. Chem. Eng. Data*, **20**, 310 (1975).

(34) D. K. Anderson, J. R. Hall, and A. L. Babb, *J. Phys. Chem.*, **62**, 404 (1958).

(35) K. J. Packer and D. J. Tomlinson, *Trans. Faraday Soc.*, **67**, 1302 (1971).

(36) D. H. Rasmussen and A. P. MacKenzie, *Nature*, **220**, 1315 (1968).

(37) J. R. Goates and R. J. Sullivan, *J. Phys. Chem.*, **62**, 188 (1958).

(38) G. N. Malcolm and J. S. Rowlinson, *Trans. Faraday Soc.*, **53**, 921 (1957).

(39) K. W. Morcom and R. W. Smith, *ibid.*, **66**, 1073 (1970).

(40) R. Philipe and C. Jambon, *J. Chim. Phys.*, **71**, 1041 (1974).

(41) M. F. Fox and K. P. Wittingham, *J. Chem. Soc., Faraday Trans., I*, **71**, 1407 (1975).

(42) J. Kenttamaa and J. J. Lindberg, *Suom. Kemistil., B*, **33**, 32, 98 (1960).

(43) V. P. Belousov and E. P. Sokolova, *Vestn., Lening. Univ.*, **21** (16); *Ser. Fiz. Khim.*, **3**, 90 (1966).

(44) R. Arnaud, L. Avedikian, and J.-P. Morel, *J. Chim. Phys.*, **69**, 45 (1972).

(45) D. D. Macdonald, *Can. J. Chem.*, **54**, 3559 (1976).

(46) Y. V. Moiseev, I. G. Orlov, and M. I. Vinnik, *Zh. Strukt. Khim.*, **6**, 387 (1965); through *Chem. Abstr.*, **63**, 10866 (1965).

(47) S. C. Mohr, W. D. Wilk, and G. M. Barrow, *J. Am. Chem. Soc.*, **87**, 3048 (1965).

(48) A. Burneau and J. Corset, *J. Phys. Chem.*, **76**, 449 (1972).

(49) M. Fox, *Trans. Faraday Soc.*, **68**, 1294 (1972).

(50) F. Takahashi and N. C. Li, *J. Am. Chem. Soc.*, **88**, 1117 (1966).

(51) O. D. Bonner and Y. S. Choi, *J. Phys. Chem.*, **78**, 1723, 1727 (1974).

(52) J. R. Scherer, M. K. Go, and S. Kint, *ibid.*, **77**, 2108 (1973).

(53) H. Kelm, J. Klosowski, and E. Steger, *J. Mol. Struct.*, **28**, 1 (1975).

(54) S. F. Ting, S. M. Wang, and N. C. Li, *Can. J. Chem.*, **45**, 425 (1967).
(55) L. W. Reeves and C. P. Yue, *ibid.*, **48**, 3307 (1970).
(56) J. A. Glasel, *J. Am. Chem. Soc.*, **92**, 372 (1970).
(57) K. J. Packer and D. J. Tomlinson, *Trans. Faraday Soc.*, **67**, 1302 (1971).
(58) G. Akerlof, *J. Am. Chem. Soc.*, **54**, 4125 (1932).
(59) J. J. Lindberg and J. Kenttamaa, *Suom. Kemistil., B*, **33**, 104 (1960).
(60) F. E. Critchfield, J. A. Gibson, and J. L. Hale, *J. Am. Chem. Soc.*, **75**, 1991 (1953).
(61) A. N. Paruta and S. A. Irani, *J. Pharm. Sci.*, **54**, 1334 (1965).
(62) J. B. Hasted, "Aqueous Dielectrics," Chapman & Hall, London, England, 1973, chap. 7.
(63) D. Martin, A. Weise, and H.-J. Niclas, *Angew. Chem.*, **79**, 340 (1967).
(64) D. E. Bowen, M. A. Priesand, and M. P. Eastman, *J. Phys. Chem.*, **78**, 2611 (1974).
(65) E. A. Symons, *Can. J. Chem.*, **49**, 3940 (1971).
(66) D. Eisenberg and W. Kauzmann, "The Structure and Properties of Water," Oxford University Press, New York, N.Y., 1969, chap. 4.
(67) H. S. Frank, *Science*, **169**, 635 (1970).
(68) A. T. Hagler, H. A. Scheraga, and G. Nemethy, *J. Phys. Chem.*, **76**, 3229 (1972).
(69) R. E. Powell, W. E. Roseveare, and H. Eyring, *Ind. Eng. Chem.*, **33**, 430 (1941).
(70) L. Korson, W. Drost-Hansen, and F. J. Millero, *J. Phys. Chem.*, **73**, 34 (1969).

Spectra of Radical Cations of Phenothiazine Derivatives in Solution and Solid State

A. ORTIZ, A. PARDO, and J. I. FERNÁNDEZ-ALONSO ˣ

Received July 21, 1978, from the *Departamento de Química Física y Química Cuántica, Centro Coordinado CSIC-UAM, Facultad de Ciencias C-XIV, Cantoblanco, Madrid 34, Spain.* Accepted for publication October 1, 1979.

Abstract □ The UV and visible spectra of radical cations of several phenothiazine derivatives were studied using different solvents. The establishment of a relationship between these bands and the R_2 and R_{10} substituents was attempted. The influence of the disolvents on the bands also was studied. The characteristic charge transfer band was observed in the solid state using diffuse reflectance spectroscopy. The R_2 substituent did not appear to influence the band, while the R_{10} substituent influenced the band considerably, probably due to steric effects.

Keyphrases □ Phenothiazine—derivatives, spectra in solution and solid state, effect of R_2 and R_{10} substituents □ Psychotropic drugs—phenothiazine derivatives, spectra in solution and solid state, effect of R_2 and R_{10} substituents □ Spectroscopy—UV and visible spectra of phenothiazine derivatives, solution and solid state

Psychotropic drugs are fundamental in the treatment of mental disorders. Increased knowledge of the physicochemical properties of these products would help in understanding their interaction with live organisms.

One important property of these drugs is that they are oxidized easily (1). The idea that phenothiazines could act in humans in an oxidized form (2) was supported by the fact that several oxidized compounds are observed in the degradation products (3). This paper describes a study of the oxidized form of these phenothiazine derivatives in solution and in the solid state.

An attempt was made to relate the derivatives according to their R_2 and R_{10} substituents, semiconductor properties, dissociation constants (4), and ability to form complexes (5). The phenothiazine derivative cation radicals were prepared in a solid state, and their diffuse reflectance spectra were studied. The UV and visible spectra of these radicals in solution also were studied.

EXPERIMENTAL

Materials—Phenothiazine derivatives with R_2 and R_{10} substituents were used (Table I). The products were pharmacologically pure and were used as supplied commercially. Perchloric acid (70%) and potassium dichromate were the oxidizing agents. The solvents were distilled water, acetonitrile, and sulfuric acid (2 and 9 *N*).

A UV–visible spectrophotometer was used to obtain the solution spectra; for the diffuse reflectance spectra, the corresponding attachment was used.

Method—A literature method (6) was used to obtain the cation radicals in the solid state. The proposed formula for these products is (6):

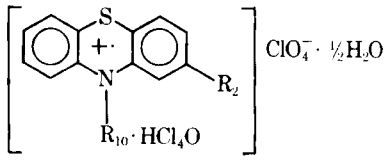

The melting points of the products ranged from 175 to 223°. The radicals rapidly dissolved in all of the solvents used. An intense color appeared, corresponding to the oxidized form. The radicals remained indefinitely stable only with 9 *N* H_2SO_4 due to its high acidity.

The formation of charge transfer complexes in the solid state was studied by diffuse reflectance spectroscopy. Tablet preparation was the same as that used for the IR method except that naphthalene (7) was the solvent.

RESULTS

Solutions were prepared from polycrystalline powder of the cation radicals in 9 *N* H_2SO_4. Table II gives the wavelengths corresponding to the absorption peaks of the radicals in 9 *N* H_2SO_4, both in the visible and the UV range (Fig. 1). The reference used to study the effect of the substituents was promazine.

UV Spectra—The UV spectra of derivatives with a constant R_2 substituent and various R_{10} substituents were studied. Derivatives with R_2 = H and various R_{10} substituents (I–V) showed no change from the reference spectrum. This observation showed that the R_{10} substituent does not influence the UV electron transitions. In derivatives with R_2 = Cl and various R_{10} substituents, the R_2 substituent caused a bathochromic shift of 4 nm throughout the spectrum (Table II). The second peak in the spectra of derivatives with R_2 = CF_3 and various R_{10} substituents disappeared.

Derivatives with a constant R_{10} substituent and various R_2 substituents were considered. The effect of the R_2 substituent was observed in the promazine (I and VI–VIII) and perazine (V and X–XIII) families (Table II). The chlorine derivatives featured a 4-nm bathochromic shift in all bands. The other substituents caused more pronounced shifts throughout the spectrum, together with the disappearance of the second peak [derivatives with R_2 = OCH_3 or $SO_2N(CH_3)_2$].

0022-3549/80/0400-0378$01.00/0
© 1980, American Pharmaceutical Association

(54) S. F. Ting, S. M. Wang, and N. C. Li, *Can. J. Chem.*, **45**, 425 (1967).
(55) L. W. Reeves and C. P. Yue, *ibid.*, **48**, 3307 (1970).
(56) J. A. Glasel, *J. Am. Chem. Soc.*, **92**, 372 (1970).
(57) K. J. Packer and D. J. Tomlinson, *Trans. Faraday Soc.*, **67**, 1302 (1971).
(58) G. Akerlof, *J. Am. Chem. Soc.*, **54**, 4125 (1932).
(59) J. J. Lindberg and J. Kenttamaa, *Suom. Kemistil., B*, **33**, 104 (1960).
(60) F. E. Critchfield, J. A. Gibson, and J. L. Hale, *J. Am. Chem. Soc.*, **75**, 1991 (1953).
(61) A. N. Paruta and S. A. Irani, *J. Pharm. Sci.*, **54**, 1334 (1965).
(62) J. B. Hasted, "Aqueous Dielectrics," Chapman & Hall, London, England, 1973, chap. 7.
(63) D. Martin, A. Weise, and H.-J. Niclas, *Angew. Chem.*, **79**, 340 (1967).
(64) D. E. Bowen, M. A. Priesand, and M. P. Eastman, *J. Phys. Chem.*, **78**, 2611 (1974).
(65) E. A. Symons, *Can. J. Chem.*, **49**, 3940 (1971).
(66) D. Eisenberg and W. Kauzmann, "The Structure and Properties of Water," Oxford University Press, New York, N.Y., 1969, chap. 4.
(67) H. S. Frank, *Science*, **169**, 635 (1970).
(68) A. T. Hagler, H. A. Scheraga, and G. Nemethy, *J. Phys. Chem.*, **76**, 3229 (1972).
(69) R. E. Powell, W. E. Roseveare, and H. Eyring, *Ind. Eng. Chem.*, **33**, 430 (1941).
(70) L. Korson, W. Drost-Hansen, and F. J. Millero, *J. Phys. Chem.*, **73**, 34 (1969).

Spectra of Radical Cations of Phenothiazine Derivatives in Solution and Solid State

A. ORTIZ, A. PARDO, and J. I. FERNÁNDEZ-ALONSO ˣ

Received July 21, 1978, from the *Departamento de Química Física y Química Cuántica, Centro Coordinado CSIC-UAM, Facultad de Ciencias C-XIV, Cantoblanco, Madrid 34, Spain.* Accepted for publication October 1, 1979.

Abstract □ The UV and visible spectra of radical cations of several phenothiazine derivatives were studied using different solvents. The establishment of a relationship between these bands and the R_2 and R_{10} substituents was attempted. The influence of the disolvents on the bands also was studied. The characteristic charge transfer band was observed in the solid state using diffuse reflectance spectroscopy. The R_2 substituent did not appear to influence the band, while the R_{10} substituent influenced the band considerably, probably due to steric effects.

Keyphrases □ Phenothiazine—derivatives, spectra in solution and solid state, effect of R_2 and R_{10} substituents □ Psychotropic drugs—phenothiazine derivatives, spectra in solution and solid state, effect of R_2 and R_{10} substituents □ Spectroscopy—UV and visible spectra of phenothiazine derivatives, solution and solid state

Psychotropic drugs are fundamental in the treatment of mental disorders. Increased knowledge of the physicochemical properties of these products would help in understanding their interaction with live organisms.

One important property of these drugs is that they are oxidized easily (1). The idea that phenothiazines could act in humans in an oxidized form (2) was supported by the fact that several oxidized compounds are observed in the degradation products (3). This paper describes a study of the oxidized form of these phenothiazine derivatives in solution and in the solid state.

An attempt was made to relate the derivatives according to their R_2 and R_{10} substituents, semiconductor properties, dissociation constants (4), and ability to form complexes (5). The phenothiazine derivative cation radicals were prepared in a solid state, and their diffuse reflectance spectra were studied. The UV and visible spectra of these radicals in solution also were studied.

EXPERIMENTAL

Materials—Phenothiazine derivatives with R_2 and R_{10} substituents were used (Table I). The products were pharmacologically pure and were used as supplied commercially. Perchloric acid (70%) and potassium dichromate were the oxidizing agents. The solvents were distilled water, acetonitrile, and sulfuric acid (2 and 9 *N*).

A UV–visible spectrophotometer was used to obtain the solution spectra; for the diffuse reflectance spectra, the corresponding attachment was used.

Method—A literature method (6) was used to obtain the cation radicals in the solid state. The proposed formula for these products is (6):

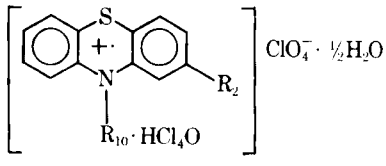

The melting points of the products ranged from 175 to 223°. The radicals rapidly dissolved in all of the solvents used. An intense color appeared, corresponding to the oxidized form. The radicals remained indefinitely stable only with 9 *N* H_2SO_4 due to its high acidity.

The formation of charge transfer complexes in the solid state was studied by diffuse reflectance spectroscopy. Tablet preparation was the same as that used for the IR method except that naphthalene (7) was the solvent.

RESULTS

Solutions were prepared from polycrystalline powder of the cation radicals in 9 *N* H_2SO_4. Table II gives the wavelengths corresponding to the absorption peaks of the radicals in 9 *N* H_2SO_4, both in the visible and the UV range (Fig. 1). The reference used to study the effect of the substituents was promazine.

UV Spectra—The UV spectra of derivatives with a constant R_2 substituent and various R_{10} substituents were studied. Derivatives with R_2 = H and various R_{10} substituents (I–V) showed no change from the reference spectrum. This observation showed that the R_{10} substituent does not influence the UV electron transitions. In derivatives with R_2 = Cl and various R_{10} substituents, the R_2 substituent caused a bathochromic shift of 4 nm throughout the spectrum (Table II). The second peak in the spectra of derivatives with R_2 = CF_3 and various R_{10} substituents disappeared.

Derivatives with a constant R_{10} substituent and various R_2 substituents were considered. The effect of the R_2 substituent was observed in the promazine (I and VI–VIII) and perazine (V and X–XIII) families (Table II). The chlorine derivatives featured a 4-nm bathochromic shift in all bands. The other substituents caused more pronounced shifts throughout the spectrum, together with the disappearance of the second peak [derivatives with R_2 = OCH_3 or $SO_2N(CH_3)_2$].

0022-3549/80/0400-0378$01.00/0
© 1980, American Pharmaceutical Association

Table I—Products and Their Characteristics

	Product	R_2	R_{10}	Salt	Clinical Use
I	Promazine[a]	H	$(CH_2)_3N(CH_3)_2$	HCl	Tranquilizer
II	Trimeprazine[b]	H	$CH_2CHCH_2N(CH_3)_2$ | CH_3	Tartrate	Antipruritic
III	Ethopropazine[b]	H	$CH_2CHN(CH_2CH_3)_2$ | CH_3	HCl	Antiparkinsonian, anticholinergic
IV	Diethazine[b]	H	$(CH_2)_2N(CH_2CH_3)_2$	HCl	Antiparkinsonian, anticholinergic
V	Perazine[c]	H	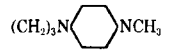	HCl	Tranquilizer
VI	Chlorpromazine[b]	Cl	$(CH_2)_3N(CH_3)_2$	HCl	Tranquilizer
VII	Triflupromazine[d]	CF_3	$(CH_2)_3N(CH_3)_2$	HCl	Tranquilizer
VIII	Methoxypromazine[b]	OCH_3	$(CH_2)_3N(CH_3)_2$	Maleate	Tranquilizer
IX	Methotrimeprazine[b]	OCH_3	$CH_2CHCH_2N(CH_3)_2$ | CH_3	Maleate	Analgesic
X	Prochlorperazine[e]	Cl	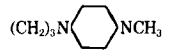	HCl	Tranquilizer
XI	Trifluoperazine[d]	CF_3	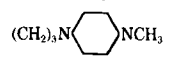	2 HCl	Tranquilizer
XII	Thiethylperazine[f]	SCH_2CH_3	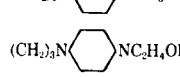	Dimaleate	Antiemetic
XIII	Thioproperazine[b]	$SO_2N(CH_3)_2$	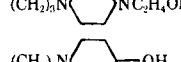	Maleate	Tranquilizer
XIV	Perphenazine[g]	Cl	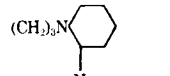	HCl	Tranquilizer
XV	Fluphenazine[a]	CF_3	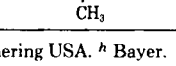	2 HCl	Tranquilizer
XVI	Properiziazine	CN	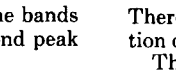	Base	—
XVII	Thioridazine[h]	SCH_3	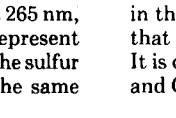	HCl	Tranquilizer

[a] Rhodia. [b] Specia. [c] Promonta. [d] Squibb. [e] Upjohn. [f] Sandoz. [g] Schering USA. [h] Bayer.

In derivatives where $R_2 = CF_3$, no shift was produced in the bands compared to the same derivatives with $R_2 = H$, but the second peak disappeared.

For derivatives where $R_2 = SCH_3$ or SC_2H_5, an intense bathochromic shift was present in the first peak, the second peak remained at 265 nm, and a transition peak appeared (245–228 nm) that seemed to represent a vibratory structure. This transition could have been caused by the sulfur atom in the substituent [the same bands also appeared at the same wavelengths in the spectra of identical neutral products (8)].

Visible Spectra—The influence of the R_2 substituent on the first band was studied.

For the molecular series of I and VI–VIII, the results in Table II indicate that the substituents caused bathochromic shifts except for $R_2 = CF_3$, where a hypsochromic effect existed in the first band. The same shift occurred with the perazine-derived molecules (V and X–XIII).

The effect of the R_{10} substituent in the first band of the visible zone was observed in I–V. The values in Table II for these compounds show that not only the reduction in the number of carbons between the two nitrogens of the alkyl chain and of the nucleus, but also the introduction of substituents in the chain, produced small bathochromic shifts.

For the second and third bands, where a vibratory structure appeared to exist, the R_{10} substituent produced bathochromic effects. Contrary to the case with the first band, the R_2 substituent did not exert such a pronounced effect as the R_{10} substituent (5).

Analysis of Spectra with Different Solvents—A comparison of spectra using different solvents showed that the characteristic bands did not undergo any change. As a result, it was deduced that a difference in the polarity of the solvent did not produce a shift in the bands assigned to these compounds. It follows that the transition cannot be of the $n-\pi$ type where any influence of the solvent polarity would be pronounced. Therefore, these bands correspond to $\pi-\pi^*$ transitions (with the exception of the SR type, which was not studied).

The bathochromic shifts could have been produced by an instability in the fundamental state caused by the substituent and possible stability in the excited state. Where bands remained unaltered, it was assumed that the substituents did not interact with the π-structure of the ring. It is difficult to explain the effect of certain substituents, such as OCH_3 and CF_3, which caused the disappearance of some bands. The influence

Table II—UV and Visible Spectra of the Radical Cations of Some Phenothiazines Derivatives in Solution

Product	UV λ_{max}, nm	Visible λ_{max}, nm
I	272, 264, 212	518, 775–865
II	272, 265, 212	520, 780–875
III	271, 264, 210	520, 792–890
IV	272, 265, 212	523, 785–882
V	272, 265, 212	517, 774–860
VI	276, 268, 212	534, 775–865
VII	272, 214	505, 770–858
VIII	282, 228	573, 760s–820
IX	282, 224	575, 770s–825
X	276, 268, 217	535, 775–865
XI	272, 212	505, 775–860
XII	296, 268, 246, 224, 210	405, 465s–493, 650, 830s, 910
XIII	276, 216	525, 778–865
XIV	276, 268, 215	537, 775–867
XV	272, 212	505, 775–860
XVI	278, 230, 208	530, 775–860
XVII	295, 265, 244, 232, 210	363, 400s–470, 495, 650, 830, 900

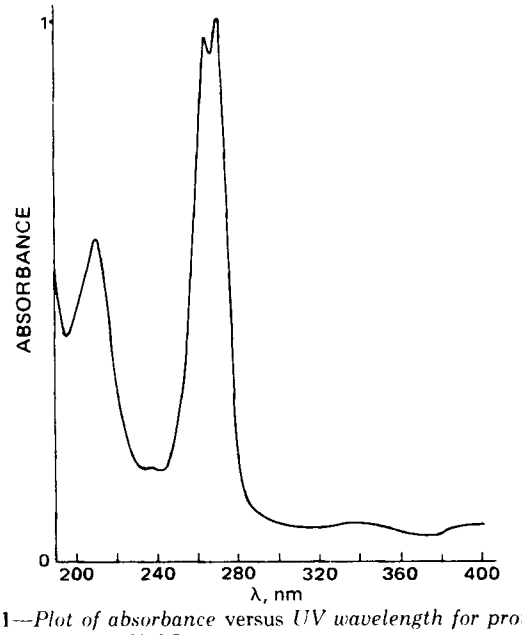

Figure 1—*Plot of absorbance* versus *UV wavelength for promazine radical cation in 9* N H_2SO_4.

of the R_{10} substituent appears on the electronic transition of the lowest energy transitions (with vibrational structure) in the visible range. This fact was attributed to the effect of the R_{10} interaction on the vibrational states.

Solid-State Spectra of Cation Radicals—The diffuse reflection spectra contained one band at 500 nm and another very wide band of equal intensity at 600–1200 nm. There were no other transitions in the field until 2000 nm.

A comparison was made with the visible spectrum of a cation radical in solution (curve e, Fig. 2). The location of the first band corresponded with the spectrum of the same radical in solution (515 nm), although it was slightly displaced toward the blue zone. These transitions of the monomer were affected by the field of the other cations and caused a shift in the π–π^* bands. The second band, wide and equal in intensity to the first band, was attributed to a charge transfer transition and appeared to superimpose on the electronic transition of the monomer in solution that appeared at 750–870 nm. This band exhibited the typical characteristics of a charge transfer; it was wide and without defined maxima.

To study the influence of the R_{10} substituent, I, II, IV, and V were considered (Fig. 2). If the maximum of this band is considered to be ~1000 nm, the promazine and perazine maxima were shifted toward the blue zone while the maxima of trimeprazine and diethazine were shifted toward the red zone.

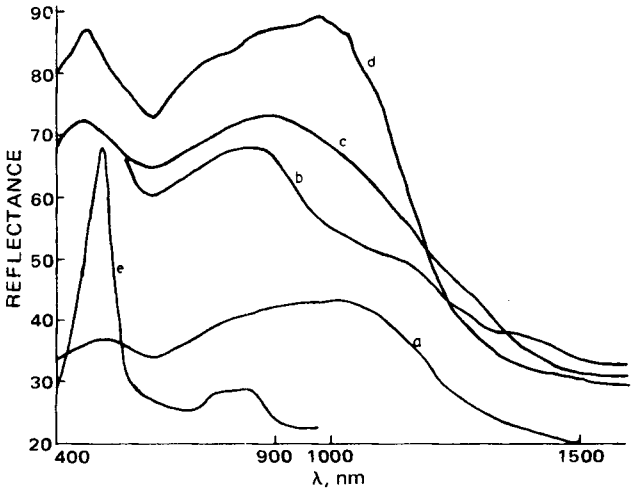

Figure 2—*Solid-state reflectance spectra of radical cations* (*reflectance* versus λ). *Key: a, diethazine; b, promazine; c, perazine; and d, trimeprazine. The visible spectrum of the perazine radical cation in sulfuric acid also is shown (e).*

Study of the influence of the R_2 substituent in the perazine family showed that the absorption peak varied slightly from 900 nm. Therefore, the R_{10} lateral chain appears to exert a greater effect than the R_2 substituents in the solid state. The influence of the R_{10} chain could be due to steric effects. This steric effect is augmented by an increase in the chain length and the different configurations that may result. This chain could insert itself between two radicals in the same column and the separation between them would increase, thus diminishing the possibility of a charge transfer and shifting the maximum toward the blue zone. Magnetic susceptibility studies could be conducted to verify this supposition. Promazine and perazine compounds should exhibit greater paramagnetism than the trimeprazine and diethazine compounds[1].

The transition was attributed to a charge transfer in the solid state and is thought to be caused through those ion radicals that are sufficiently close to overlap their half-complete π-orbitals.

Phenothiazine and its derivatives in neutral form are puckered by the heteroatoms (9).

In phenothazine oxidation, the positive charge is distributed throughout the nucleus, and the phenothiazine ion subsequently has to adopt a plane spatial structure for stability. On the other hand, it was concluded from electron–proton resonance studies (10, 11) that the positive charge is centered on the hetero ring. A definitive solution could be achieved by an X-ray diffraction study of these ions in the solid state. These ions could be in the form of infinitely long columns (12); this type of structure has been proposed for several ion salts (13).

The columns are believed to be formed by equidistant ion radicals (14). The separation of these ion radicals within the same column also could be studied by X-ray analysis. The columnar structure and the interplanar distance between the ions comprising the column can lead to charge transfer complexes. Here, the bond can be described as being formed by the overlap of half-complete π-orbitals of a donor molecule, *D*, and an acceptor, *A*. In this case, *A* and *D* are equal, and it follows that each molecule participates in the formation of overlapping orbitals. With two identical radicals, greatest interaction would take place when the two ions are superimposed.

The existence of distinct substituents capable of producing a large steric effect when interposed between two radicals of the same column appeared to have a marked influence on the packing distance of the cation derivatives in this study.

The apparent opposition that exists between the formation of solid structures with the participation of charge transfer bonding forces and the existence of unpaired electrons of these ion radicals, which in turn exhibit semiconductor properties associated with the unpaired electrons (15), should be considered. Likewise, the decrease in paramagnetic properties as a result of charge transfer interactions should be noted.

REFERENCES

(1) J. P. Billon, *Bull. Soc. Chim. Fr.*, **1960**, 1884. *Ibid.*, **1961**, 1923.

(2) A. Sentz-Gyorgi, "Introduction to Submolecular Biology," Academic, New York, N.Y., 1960.

(3) I. Forrest and M. Berger, *Biochim. Biophys. Acta*, **29**, 442 (1958).

(4) A. Pardo, S. Vivas, F. España, and J. I. Fernández-Alonso, *Afinidad*, **29**, 640 (1972).

(5) A. Pardo, F. Tomás, and J. I. Fernández-Alonso, *An. Quím.*, **73**, 20 (1977).

(6) F. H. Merkle and C. A. Discher, *J. Pharm. Sci.*, **53**, 965 (1964).

(7) Y. Iida, *Bull. Chem. Soc. Jpn.*, **45**, 624 (1972).

(8) J. González and J. I. Fernández-Alonso, *An. Fis. Quím.*, **66B**, 919 (1970).

(9) B. Pullman and A. Pullman, *Biochim. Biophys. Acta*, **35**, 525 (1969).

(10) D. W. Schieser and L. D. Tuck, *J. Phys. Chem.*, **51**, 7 (1962). M. Kamiya and A. Akahori, *Chem. Pharm. Bull.*, **18**, 11 (1970).

(11) G. Lagercrantz, *Acta Chem. Scand.*, **15**, 1545 (1961).

(12) Y. Iida, *Bull. Chem. Soc. Jpn.*, **45**, 624 (1972). *Ibid.*, **45**, 105 (1972).

(13) *Ibid.*, **43**, 772 (1969).

(14) R. G. Kepler, *J. Chem. Phys.*, **39**, 3528 (1963). Y. Matsunaga, *Bull. Chem. Soc. Jpn.*, **41**, 2615 (1968).

(15) A. Ortiz, A. Pardo, J. Llabrés, and J. I. Fernández-Alonso, *Mol. Pharmacol.*, in press.

[1] To be published.

Antifungal Properties of n-Alkanols, α,ω-n-Alkanediols, and ω-Chloro-α-alkanols

HERMAN GERSHON [x] **and LARRY SHANKS**

Received March 6, 1979, from the *Boyce Thompson Institute, Cornell University, Ithaca, NY 14853.* Accepted for publication October 22, 1979.

Abstract □ Fourteen n-alkanols (C_1–C_{12}, C_{14}, and C_{16}), 13 α,ω-n-alkanediols (C_2–C_{12}, C_{14}, and C_{16}), and 13 ω-chloro-α-alkanols (C_2–C_{12}, C_{14}, and C_{16}) were tested against *Aspergillus niger*, *Trichoderma viride*, and *Myrothecium verrucaria* in Sabouraud dextrose agar at pH 4.0 and 5.6. Toxicity to *Candida albicans*, *Trichophyton mentagrophytes*, and *Mucor mucedo* was determined in the same medium at pH 5.6 and 7.0 in the absence and presence of 10% beef serum. The fungitoxicity of these alcohols was influenced by chain length and insignificantly by the pH of the medium and the presence of beef serum. The C_{10}-member of each series was most active; the order of activity of the three groups was chloroalkanols > alkanols > alkanediols. Compared to the fatty acids, the order of fungitoxicity on a weight basis was 2-alkynoic acids > 2-alkenoic acids > ω-chloroalkanols > alkanoic acids > 2-bromoalkanoic acids > 2-fluoroalkanoic acids > n-alkoxyacetic acids > n-alkanols > α,ω-n-alkanediols.

Keyphrases □ Antifungal activity—n-alkanols, α,ω-n-alkanediols, and ω-chloro-α-alkanols, *in vitro*, effect of chain length, pH, and adsorbents □ Structure–activity relationships—n-alkanols, α,ω-n-alkanediols, and ω-chloro-α-alkanols, antifungal activity, *in vitro*, effect of chain length □ n-Alkanols—antifungal activity, *in vitro*, effect of chain length, pH, and adsorbents □ α,ω-n-Alkanediols—antifungal activity, *in vitro*, effect of chain length, pH, and adsorbents □ ω-Chloro-α-alkanols—antifungal activity, *in vitro*, effect of chain length, pH, and adsorbents

In the examination in these laboratories of the effect of structural modification on the antifungal activity of fatty acids, systematic studies were made on the fungitoxicity of alkanoic acids (1), 2-alkenoic acids (2), 2-alkynoic acids (3), 2-fluoroalkanoic acids (1), 2-bromoalkanoic acids (2), α,ω-alkanedicarboxylic acids (4), and alkoxyacetic acids (5). Two major factors that influence the fungitoxicity of fatty acids are the partition coefficient and the absence or presence of adsorbents such as albumin in the growth medium. Among the factors that determine the partition coefficient are chain length, pKa, and pH of the medium (3).

BACKGROUND

It was established that the intact carboxyl group was not essential for fungitoxicity. The alkyl carboxamides were less toxic than the carboxylic acids at pH 4.0 but were equally toxic at pH 5.6. The pH of the medium had little effect on the activity of the amides, but beef serum had a deactivating effect on both the acids and amides. Chain length was a determining factor for the toxicity of the amides as well as the acids (6).

Esters were reported to be markedly less fungitoxic than the acids (7). This finding was confirmed for the methyl esters of the alkanoic and 2-fluoroalkanoic acids (8) and 2-alkynoic acids (3). An exception to these observations was that *Trichophyton mentagrophytes* was inhibited equally by the esters and free acids. The pH of the medium and the absence or presence of beef serum in the medium did not greatly affect the toxicity of the esters to the fungus.

The antifungal activity of nonionizing compounds is affected only slightly by the pH of the medium. The serum effect on fatty acids, amides, and esters can be rationalized on the basis of hydrogen bonding. Compounds containing carboxyl and carboxamide functions are bound more strongly by beef serum because they possess both donor hydrogen atoms and acceptor oxygen atoms, whereas the esters possess only acceptor oxygen atoms (9).

The purpose of the present study was to examine the fungitoxic action of the n-alkanols, α,ω-n-alkanediols, and ω-chloro-α-alkanols. These nonionizing compounds would not be expected to undergo strong hydrogen bonding with adsorbents.

It was reported previously that the wood-destroying fungus, Madison 517 on an agar malt extract medium, was inhibited by n-alkanols. n-Decanol was the most inhibitory of the series (10). The same effect was observed for *Penicillium glaucum* in an inorganic medium containing sucrose or lactose as the carbon source (11). This observation was confirmed in agar media, but n-dodecanol was the most effective alcohol for the protection of wood (12). No systematic studies of the α,ω-n-alkanediols or ω-chloro-α-alkanols have been reported.

The present work concerns the *in vitro* testing of 14 n-alkanols (C_1–C_{12}, C_{14}, and C_{16}), 13 α,ω-n-alkanediols (C_2–C_{12}, C_{14}, and C_{16}), and 13 ω-chloro-α-alkanols (C_2–C_{12}, C_{14}, and C_{16}) against *Aspergillus niger*, *Trichoderma viride*, and *Myrothecium verrucaria* in Sabouraud dextrose agar at pH 4.0 and 5.6. *Candida albicans*, *T. mentagrophytes*, and *Mucor mucedo* also were tested in the same medium at pH 5.6 and 7.0 in the absence or presence of 10% beef serum. Also included in these tests were 11-bromo-1-undecanol for comparison of analogous chloro and bromo compounds and 1,6-dichlorohexane and 1,9-dichlorononane for comparisons with the corresponding chloroalkanols.

EXPERIMENTAL

Some compounds were obtained from commercial sources[1]. The ω-chloroalkanols [C_5 and C_7–C_{10} (13), C_{11} (14), and C_{12}, C_{14}, and C_{16} (15)] were prepared by published methods.

The test fungi included *A. niger* (ATCC 1004), *T. viride* (ATCC 8678), *M. verrucaria* (ATCC 9095C), *C. albicans* (ATCC 10231), *T. mentagrophytes* (ATCC 9129), and *M. mucedo* (ATCC 7941).

The compounds were tested against *A. niger*, *T. viride*, and *M. verrucari* in Sabouraud dextrose agar[2] at pH 4.0 and 5.6 according to published methods (1). Graded levels of test compound dissolved in dimethyl sulfoxide (I) were incorporated into the growth medium, which then was inoculated with the respective fungus. The inoculum consisted of 1 drop of spore suspension delivered from a 5-ml Mohr pipet containing 6×10^6 spores/ml in 0.85% NaCl solution. Incubation took place at 28° for 5 days.

For *T. mentagrophytes*, *C. albicans*, and *M. mucedo*, the methods described previously were used (16). Graded levels of test compounds dissolved in I were added to Sabouraud dextrose agar at pH 5.6 and 7.0 alone and supplemented with 10% beef serum[3]. The inocula of *T. mentagrophytes* and *M. mucedo* consisted of 1 drop of spore suspension containing 6×10^6 spores/ml, and the inoculum of *C. albicans* was 1 drop of a suspension obtained from a 20-hr culture in Sabouraud dextrose broth[2] incubated at 37°. The test plates with *T. mentagrophytes* were incubated at 28° for 5 days, and those with *C. albicans* and *M. mucedo* were incubated at 37° for 20 hr.

The results reported are the number of levels of compounds causing 100% inhibition of the test organisms. The compounds were tested at 10^4, 10^3, and 10^2 μg/ml. All tests were carried out in I-plate petri dishes[4].

The results were weighted by calculating the antifungal spectrum index, defined as the sum of the number of levels of complete inhibition multiplied by the number of organisms inhibited within the defined system (17, 18).

[1] The C_1-, C_3–C_{12}-, C_{14}-, C_{16}-, and C_{18}-alkanols, the C_2–C_{12}- and C_{16}-α,ω-alkanediols, and 3-chloro-1-propanol, 6-chloro-1-hexanol, 11-bromo-1-undecanol, 1,6-dichlorohexane, and 1,9-dichlorononane were obtained from Aldrich Chemical Co., Milwaukee, Wis. The C_2-alkanol was obtained from U.S. Industrial Chemicals Co., New York, N.Y. The C_{14}-α,ω-alkanediol was obtained from Eastman Kodak Co., Rochester, N.Y. 2-Chloro-1-ethanol and 4-chloro-1-butanol were obtained from Matheson, Coleman and Bell, Norwood, Ohio.

[2] Difco, Detroit, Mich.

[3] Miles Laboratories, Kankakee, Ill.

[4] Falcon, Oxnard, Calif.

0022-3549/80/0400-0381$01.00/0
© 1980, American Pharmaceutical Association

Table I—Antifungal Activity [a] of *n*-Alkanols, α,ω-*n*-Alkanediols, and ω-Chloro-α-alkanols at pH 4.0 and 5.6 against *A. niger*, *T. viride*, and *M. verrucaria* in Sabouraud Dextrose Agar

	Inhibition Levels at pH 4.0				Inhibition Levels at pH 5.6			
n [b]	*A. niger*	*T. viride*	*M. verrucaria*	Antifungal Spectrum Index [c]	*A. niger*	*T. viride*	*M. verrucaria*	Antifungal Spectrum Index
				$CH_3(CH_2)_nOH$				
0	0	0	0	0	0	0	0	0
1	0	0	1	1	0	0	1	1
2	0	0	1	1	0	0	1	1
3	0	1	1	4	0	1	1	4
4	1	1	1	9	1	1	1	9
5	1	1	1	9	1	1	1	9
6	1	1	1	9	1	1	1	9
7	1	1	1	9	1	1	1	9
8	1	3	1	15	1	3	1	15
9	2	3	3	24	2	3	2	21
10	2	2	2	18	2	2	2	18
11	0	2	3	10	0	2	3	10
13	0	0	0	0	0	0	0	0
15	0	0	0	0	0	0	0	0
				$HO(CH_2)_nOH$				
2	0	0	0	0	0	0	0	0
3	0	0	0	0	0	0	0	0
4	0	0	0	0	0	0	0	0
5	0	0	0	0	0	0	0	0
6	0	0	0	0	0	0	0	0
7	0	1	1	4	0	1	1	4
8	1	1	1	9	1	1	1	9
9	1	1	2	12	1	1	2	12
10	1	2	2	15	1	2	2	15
11	1	1	1	9	1	1	1	9
12	0	0	0	0	0	0	0	0
14	0	0	0	0	0	0	0	0
16	0	0	0	0	0	0	0	0
				$Cl(CH_2)_nOH$				
2	0	0	1	1	0	0	1	1
3	1	1	1	9	1	1	1	9
4	1	1	1	9	1	1	1	9
5	1	1	1	9	1	1	1	9
6	1	1	2	12	1	1	2	12
7	2	2	2	18	2	2	2	18
8	2	2	2	18	2	2	2	18
9	3	3	3	27	3	3	3	27
10	3	3	3	27	3	3	3	27
11	1	3	3	21	1	3	3	21
12	0	2	3	10	0	2	3	10
14	0	1	2	6	0	1	2	6
16	0	0	0	0	0	0	0	0
				Miscellaneous				
$Br(CH_2)_{11}OH$	0	1	0	1	0	1	1	4
$Cl(CH_2)_6Cl$	0	0	1	1	0	0	1	1
$Cl(CH_2)_9Cl$	0	0	1	1	0	0	0	0

[a] Compounds were incorporated in the test medium at 10^4, 10^3, and 10^2 μg/ml. Key to inhibition levels: 3 = inhibition at all levels of the compound, 2 = inhibition at the two highest levels, 1 = inhibition at the highest level only, and 0 = compound inactive at the highest level tested. [b] Number of methylene groups in the chain. [c] Sum of the number of levels of inhibition multiplied by the number of organisms inhibited.

RESULTS

The results of the tests of the *n*-alkanols, α,ω-*n*-alkanediols, and ω-chloro-α-alkanols against *A. niger*, *T. viride*, and *M. verrucaria* are given in Table I; the results of the tests against *C. albicans*, *T. mentagrophytes*, and *M. mucedo* are given in Table II.

A comparison of the fungitoxicity of the alkanols based on the combined antifungal spectrum indexes at pH 4.0 and 5.6 (Table I) reveals that the homologs of chain length C_5–C_{12} were most active against *A. niger*, *T. viride*, and *M. verrucaria*. The order of activity of the compounds tested was $C_{10} > C_{11} > C_9 > C_{12} > C_8 = C_7 = C_6 = C_5 > C_4 > C_3 = C_2$. Similarly, for the alkanediols, the most active members of the series were the C_7–C_{11}-compounds; the order of activity was $C_{10} > C_9 > C_{11} = C_8 > C_7$. For the ω-chloro-α-alkanols, the most fungitoxic compounds were between C_8 and C_{14}; the order of activity was $C_{10} = C_9 > C_{11} > C_8 = C_7 > C_6 > C_{12} > C_5 = C_4 = C_3 > C_{14} > C_2$. Varying the pH between 4.0 and 5.6 did not affect the fungitoxicity of the three classes of compounds significantly.

The most fungitoxic alkanols against *C. albicans*, *T. mentagrophytes*, and *M. mucedo* were the C_5–C_{12}-compounds; the overall order of toxicity was $C_{11} = C_{10} > C_{12} > C_9 = C_8 > C_7 > C_6 = C_5 > C_4 > C_{14} = C_3$. For the alkanediols, the C_7–C_{12}-compounds were the most toxic; the order of toxicity was $C_{10} > C_{11} > C_9 = C_8 = C_7 > C_{12}$. The chloroalkanols were most fungitoxic at chain lengths between C_2 and C_{11} in the order $C_{10} = C_9 > C_{11} = C_8 = C_7 > C_6 = C_5 = C_2 > C_4 = C_3 > C_{12}$. Raising the pH from 5.6 to 7.0 and adding beef serum to the growth medium caused no significant deactivation of the antifungal activity of the three classes of compounds.

11-Bromo-1-undecanol was less fungitoxic than the analogous alkanol, chloroalkanol, and alkanediol. 1,6-Dichlorohexane and 1,9-dichlorononane were markedly less toxic than the analogous alkanols, chloroalkanols, and alkanediols, with the 6-carbon compound being more active than the 9-carbon compound.

DISCUSSION

It is apparent (Tables I and II) that the chain length influences antifungal activity in each homologous series of compounds. A chain length of 10 carbon atoms seems to be optimal for maximal fungitoxicity. This result was observed previously for the alkanols (10–12). The relationship between the chain length and the partition coefficient with respect to the antifungal activity of fatty acids was discussed previously (3). This constant was employed in the application of regression analysis to fungitoxicity (19).

Table II—Antifungal Activity of *n*-Alkanols, α,ω-*n*-Alkanediols, and ω-Chloro-α-alkanols at pH 5.6 and 7.0 against *C. albicans*, *T. mentagrophytes*, and *M. mucedo* in Sabouraud Dextrose Agar in the Absence and Presence of Beef Serum [a]

	Inhibition Levels [b]												
	C. albicans				*T. mentagrophytes*				*M. mucedo*				
	pH 5.6		pH 7.0		pH 5.6		pH 7.0		pH 5.6		pH 7.0		Antifungal
n [c]	Without Serum	With Serum	Without Serum	With Serum	Without Serum	With Serum	Without Serum	With Serum	Without Serum	With Serum	Without Serum	With Serum	Spectrum Index [d]
						$CH_3(CH_2)_nOH$							
0	0	0	0	0	0	0	0	0	0	0	0	0	0
1	0	0	0	0	0	0	0	0	0	0	0	0	0
2	0	0	0	0	0	0	0	0	1	1	1	1	4
3	1	1	1	1	0	0	0	0	1	1	1	1	16
4	1	1	1	1	1	1	1	1	1	1	1	1	36
5	1	1	1	1	1	1	1	1	1	1	1	1	36
6	1	1	1	1	2	2	2	2	1	1	1	1	48
7	2	2	2	2	2	2	2	2	1	1	1	1	60
8	2	2	2	2	2	2	2	2	1	1	1	1	60
9	2	2	2	2	2	2	2	2	2	2	2	2	72
10	2	2	2	2	3	3	3	3	1	1	1	1	72
11	2	2	2	2	3	2	3	2	1	1	1	1	66
13	0	0	0	0	1	1	1	1	0	0	0	0	4
15	0	0	0	0	0	0	0	0	0	0	0	0	0
17	0	0	0	0	0	0	0	0	0	0	0	0	0
						$HO(CH_2)_nOH$							
2	0	0	0	0	0	0	0	0	0	0	0	0	0
3	0	0	0	0	0	0	0	0	0	0	0	0	0
4	0	0	0	0	0	0	0	0	0	0	0	0	0
5	0	0	0	0	0	0	0	0	0	0	0	0	0
6	0	0	0	0	1	1	1	1	0	0	0	0	4
7	1	1	1	1	1	1	1	1	1	1	1	1	36
8	1	1	1	1	1	1	1	1	1	1	1	1	36
9	1	1	1	1	1	1	1	1	1	1	1	1	36
10	2	2	1	1	1	1	1	1	2	2	2	2	54
11	1	1	1	1	2	2	2	2	1	1	1	1	48
12	0	0	0	0	3	3	3	3	0	0	0	0	12
14	0	0	0	0	1	1	1	1	0	0	0	0	4
16	0	0	0	0	0	0	0	0	0	0	0	0	0
						$Cl(CH_2)_nOH$							
2	1	1	1	1	2	2	2	2	1	1	1	1	48
3	1	1	1	1	1	1	1	1	1	1	1	1	36
4	1	1	1	1	1	1	1	1	1	1	1	1	36
5	1	1	1	1	2	2	2	2	1	1	1	1	48
6	1	1	1	1	2	2	2	2	1	1	1	1	48
7	2	2	2	2	2	2	2	2	2	2	2	2	72
8	2	2	2	2	2	2	2	2	2	2	2	2	72
9	2	2	2	2	3	3	3	3	2	2	2	2	84
10	2	2	2	2	3	3	3	3	2	2	2	2	84
11	2	2	2	2	3	3	3	3	1	1	1	1	72
12	1	1	1	1	0	0	0	0	0	0	0	0	4
14	0	0	0	0	0	0	0	0	0	0	0	0	0
16	0	0	0	0	0	0	0	0	0	0	0	0	0
						Miscellaneous							
$Br(CH_2)_{11}OH$	1	1	1	1	3	3	3	3	1	1	1	1	60
$Cl(CH_2)_6Cl$	0	0	0	0	1	1	1	1	1	1	1	1	16
$Cl(CH_2)_9Cl$	0	0	0	0	2	2	1	1	0	0	0	0	6

[a] *C. albicans* and *M. mucedo* were incubated at 37° for 30 hr, and *T. mentagrophytes* was incubated at 28° for 5 days. [b] Compounds were incorporated in the test medium at 10^4, 10^3, and 10^2 μg/ml. Key to inhibition levels: 3 = inhibition at all levels of the compound, 2 = inhibition at the two highest levels, 1 = inhibition at the highest level only, and 0 = compound inactive at the highest level tested. [c] Number of methylene groups in the chain. [d] Sum of the number of levels of inhibition multiplied by the number of organisms inhibited.

The order of fungitoxicity of the three classes of compounds was chloroalkanols > alkanols > alkanediols. This finding suggests that, in addition to possessing a certain degree of amphiphilicity, each compound also should have a lipophilic and a hydrophilic end. These concepts are consistent with the results obtained with the fatty acids and derivatives (1–6, 8).

Although these data do not indicate a mechanism of action for the alkanols and related compounds, it is clear that alkylation plays no part in the fungitoxic reaction. The bromoalkanol, which is a better alkylating agent than the corresponding chloro compound, is a poorer antifungal agent.

The antifungal activity of alkanols can be modified by altering the ω-end of the molecule. Conceivably, an ω-substituted alkanol could be prepared with superior antifungal activity. Such a compound also would have the advantage of its activity not being affected significantly by a pH change or the presence of serum.

Since an attempt is being made at generalizing the antifungal activity of the substituted straight-chain alkanes, it is not unreasonable to compare the activity of the alkanols with the carboxylic acids. Totaling the antifungal spectrum indexes of the seven most active members of each series of compounds at pH 4.0 and 5.6 for *A. niger*, *T. viride*, and *M. verrucaria* gives the order of fungitoxicity for six types of fatty acids and three types of alcohols, on a weight basis, as 2-alkynoic acids (336) > 2-alkenoic acids (288) > ω-chloroalkanols (266) > alkanoic acids (264) > 2-bromoalkanoic acids (253) > 2-fluoroalkanoic acids (228) > *n*-alkoxyacetic acids (220) > alkanols (205) > α,ω-alkanediols (98) (3, 5).

REFERENCES

(1) H. Gershon and R. Parmegiani, *J. Med. Chem.*, **10**, 186 (1967).

(2) H. Gershon, M. W. McNeil, R. Parmegiani, P. K. Godfrey, and J. M. Bariko, *Antimicrob. Agents Chemother.*, **4**, 435 (1973).

(3) H. Gershon and L. Shanks, *Can. J. Microbiol.*, **24**, 593 (1978).

(4) *Ibid.*, **22**, 1198 (1976).

(5) H. Gershon, L. Shanks, and A. DeAngelis, *J. Pharm. Sci.*, **68**, 82 (1979).

(6) H. Gershon, R. L. Rodin, R. Parmegiani, and P. K. Godfrey, *J. Med. Chem.*, **13**, 1237 (1970).

(7) G. Weitzel and E. Schraufstätter, *Hoppe-Seylers Z. Physiol.*

Chem., **285**, 172 (1950).
(8) H. Gershon, R. L. Rodin, R. Parmegiani, and P. K. Godfrey, *Contrib. Boyce Thompson Inst.*, **24**, 245 (1970).
(9) J. Donahue, in "Structural Chemistry and Molecular Biology," A. Rich and N. Davidson, Eds., W. H. Freeman, San Francisco, Calif., 1968, pp. 443–465.
(10) R. H. Baechler, *Proc. Am. Wood Preserv. Assoc.*, **1939**, 364.
(11) H. Engelhard, O. Müller, and K. Bertl, *Zentralbl. Bakteriol. Parasitenkd., Abt. I*, **153**, 326 (1949).
(12) R. W. Finholt, M. Weeks, and C. Hathaway, *Ind. Eng. Chem.*, **44**, 101 (1952).
(13) F. L. M. Pattison, W. C. Howell, A. J. McNamara, J. C. Schneider, and J. W. Walker, *J. Org. Chem.*, **21**, 739 (1956).
(14) S. Voerman and A. K. Minks, *Environ. Entomol.*, **2**, 751 (1973).
(15) G. M. Bennett and H. Gudgeon, *J. Chem. Soc.*, **1938**, 1679.
(16) H. Gershon and L. Shanks, *Can. J. Microbiol.*, **21**, 1317 (1975).
(17) H. Gershon and R. Parmegiani, *Appl. Microbiol.*, **10**, 348 (1962).
(18) H. Gershon, R. Parmegiani, and W. J. Nickerson, *ibid.*, **10**, 556 (1962).
(19) C. Hansch and E. J. Lien, *J. Med. Chem.*, **14**, 653 (1971).

New Instrumentation for Determining Flexure Breaking Strength of Capsule-Shaped Tablets

GERALD GOLD ˣ, RONALD N. DUVALL, and BLAZE T. PALERMO

Received June 14, 1978, from the *Applied Pharmaceutics Laboratory, Miles Laboratories, Inc., Elkhart, IN 46514.* Accepted for publication October 22, 1979.

Abstract □ New instrumentation to measure the flexure breaking strength of capsule-shaped tablets was developed. It consisted of a mechanical linkage to apply the breaking load at a uniform rate and a strain-gauge instrumented cantilever beam to convert the load to a proportional millivolt response on a recorder. A recorder tracing was obtained of increasing load with time, with a break in the tracing denoting the tablet's flexure breaking strength. Measurements were made for different tablet hardnesses, and a plot of tablet hardness *versus* flexure breaking strength yielded a profile of the mechanical strength of the tablet. The instrumentation was shown to have application for determining the effects of tablet thicknesses, tablet ingredients, tablet sizes, cup depths, and bisect dimensions on tablet strength.

Keyphrases □ Flexure breaking strength—determination for capsule-shaped tablets, new instrumentation □ Tablet breakage—capsule-shaped tablets, determination of flexure breaking strength, new instrumentation □ Hardness, tablets—flexure breaking strength, determination for capsule-shaped tablets, new instrumentation

Although tablet breakage is a problem often encountered in the manufacture, packaging, and distribution of capsule-shaped tablets, little information is available on the subject. Several factors that need to be studied for their effects on breakage are the ingredients, size, shape, and dimensions of the tablets. To evaluate these factors, the flexure breaking strength of the tablet must be determined. At present, there is no generally accepted mechanical method to measure the flexure breaking strength of tablets with sufficient accuracy and precision.

BACKGROUND

A widely used but subjective flexure test employed in practice is to break the tablet between the thumb and fingers and to evaluate both the force necessary to break the tablet and the sharpness of the snap. An instrument constructed to simulate the manual method was described (1) in which a pneumatic tablet hardness tester was modified by the addition of two auxiliary pieces, one attached to the plunger and the other to the anvil. Increasing pressure is applied through the plunger on the center of the tablet face until it breaks to measure the fracture resistance. These investigators found that the fracture resistance was directly proportional to tablet thickness and pointed out the importance of this finding for reducing tablet breakage. They also indicated that additional research was necessary to design an instrument that would be more versatile and accurate.

In another study, a flexure tester was constructed by attaching a knife edge and two fulcrums to the platens of a motorized tablet hardness tester (2). The flexure tester was found to be a rapid, reproducible instrument for determining the tablet tensile strength of very strong tablets but could not be used for very weak tablets.

Two related procedures have been developed to measure resistance to bending. In one procedure, mercury is added to provide the weight to break the tablet (3). In the other procedure, a special tablet form is used that is unrelated to the manufactured product (4). Both procedures, however, are impractical for use in industry.

The objective of this study was to develop new instrumentation that can be calibrated readily for increased accuracy, measure a wide range of tablet strengths, and be of practical use in a product development laboratory. This paper describes the instrument developed and indicates

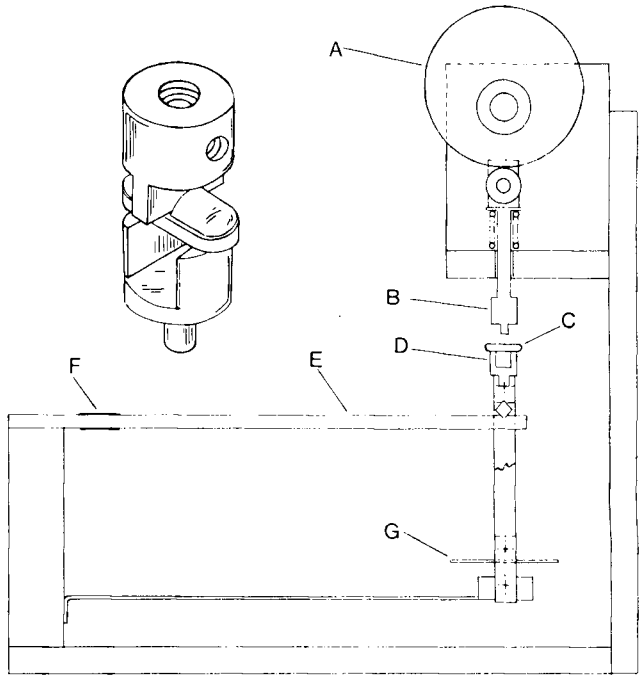

Figure 1—*Instrumentation for measuring flexure breaking strength. Key: A, motor-driven cam; B, plunger; C, capsule-shaped tablet; D, anvil; E, cantilever beam; F, strain gauges; and G, weight platform for calibration.*

0022-3549/80/0400-0384$01.00/0
© 1980, American Pharmaceutical Association

Chem., **285**, 172 (1950).
(8) H. Gershon, R. L. Rodin, R. Parmegiani, and P. K. Godfrey, *Contrib. Boyce Thompson Inst.*, **24**, 245 (1970).
(9) J. Donahue, in "Structural Chemistry and Molecular Biology," A. Rich and N. Davidson, Eds., W. H. Freeman, San Francisco, Calif., 1968, pp. 443–465.
(10) R. H. Baechler, *Proc. Am. Wood Preserv. Assoc.*, **1939**, 364.
(11) H. Engelhard, O. Müller, and K. Bertl, *Zentralbl. Bakteriol. Parasitenkd., Abt. I*, **153**, 326 (1949).
(12) R. W. Finholt, M. Weeks, and C. Hathaway, *Ind. Eng. Chem.*, **44**, 101 (1952).
(13) F. L. M. Pattison, W. C. Howell, A. J. McNamara, J. C. Schneider, and J. W. Walker, *J. Org. Chem.*, **21**, 739 (1956).
(14) S. Voerman and A. K. Minks, *Environ. Entomol.*, **2**, 751 (1973).
(15) G. M. Bennett and H. Gudgeon, *J. Chem. Soc.*, **1938**, 1679.
(16) H. Gershon and L. Shanks, *Can. J. Microbiol.*, **21**, 1317 (1975).
(17) H. Gershon and R. Parmegiani, *Appl. Microbiol.*, **10**, 348 (1962).
(18) H. Gershon, R. Parmegiani, and W. J. Nickerson, *ibid.*, **10**, 556 (1962).
(19) C. Hansch and E. J. Lien, *J. Med. Chem.*, **14**, 653 (1971).

New Instrumentation for Determining Flexure Breaking Strength of Capsule-Shaped Tablets

GERALD GOLD ˣ, RONALD N. DUVALL, and BLAZE T. PALERMO

Received June 14, 1978, from the *Applied Pharmaceutics Laboratory, Miles Laboratories, Inc., Elkhart, IN 46514.* Accepted for publication October 22, 1979.

Abstract □ New instrumentation to measure the flexure breaking strength of capsule-shaped tablets was developed. It consisted of a mechanical linkage to apply the breaking load at a uniform rate and a strain-gauge instrumented cantilever beam to convert the load to a proportional millivolt response on a recorder. A recorder tracing was obtained of increasing load with time, with a break in the tracing denoting the tablet's flexure breaking strength. Measurements were made for different tablet hardnesses, and a plot of tablet hardness *versus* flexure breaking strength yielded a profile of the mechanical strength of the tablet. The instrumentation was shown to have application for determining the effects of tablet thicknesses, tablet ingredients, tablet sizes, cup depths, and bisect dimensions on tablet strength.

Keyphrases □ Flexure breaking strength—determination for capsule-shaped tablets, new instrumentation □ Tablet breakage—capsule-shaped tablets, determination of flexure breaking strength, new instrumentation □ Hardness, tablets—flexure breaking strength, determination for capsule-shaped tablets, new instrumentation

Although tablet breakage is a problem often encountered in the manufacture, packaging, and distribution of capsule-shaped tablets, little information is available on the subject. Several factors that need to be studied for their effects on breakage are the ingredients, size, shape, and dimensions of the tablets. To evaluate these factors, the flexure breaking strength of the tablet must be determined. At present, there is no generally accepted mechanical method to measure the flexure breaking strength of tablets with sufficient accuracy and precision.

BACKGROUND

A widely used but subjective flexure test employed in practice is to break the tablet between the thumb and fingers and to evaluate both the force necessary to break the tablet and the sharpness of the snap. An instrument constructed to simulate the manual method was described (1) in which a pneumatic tablet hardness tester was modified by the addition of two auxiliary pieces, one attached to the plunger and the other to the anvil. Increasing pressure is applied through the plunger on the center of the tablet face until it breaks to measure the fracture resistance. These investigators found that the fracture resistance was directly proportional to tablet thickness and pointed out the importance of this finding for reducing tablet breakage. They also indicated that additional research was necessary to design an instrument that would be more versatile and accurate.

In another study, a flexure tester was constructed by attaching a knife edge and two fulcrums to the platens of a motorized tablet hardness tester (2). The flexure tester was found to be a rapid, reproducible instrument for determining the tablet tensile strength of very strong tablets but could not be used for very weak tablets.

Two related procedures have been developed to measure resistance to bending. In one procedure, mercury is added to provide the weight to break the tablet (3). In the other procedure, a special tablet form is used that is unrelated to the manufactured product (4). Both procedures, however, are impractical for use in industry.

The objective of this study was to develop new instrumentation that can be calibrated readily for increased accuracy, measure a wide range of tablet strengths, and be of practical use in a product development laboratory. This paper describes the instrument developed and indicates

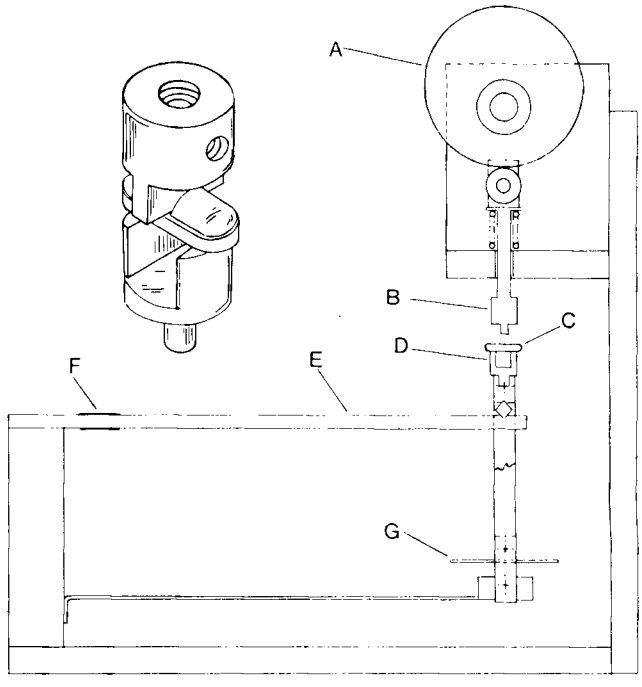

Figure 1—*Instrumentation for measuring flexure breaking strength. Key: A, motor-driven cam; B, plunger; C, capsule-shaped tablet; D, anvil; E, cantilever beam; F, strain gauges; and G, weight platform for calibration.*

0022-3549/80/0400-0384$01.00/0
© 1980, American Pharmaceutical Association

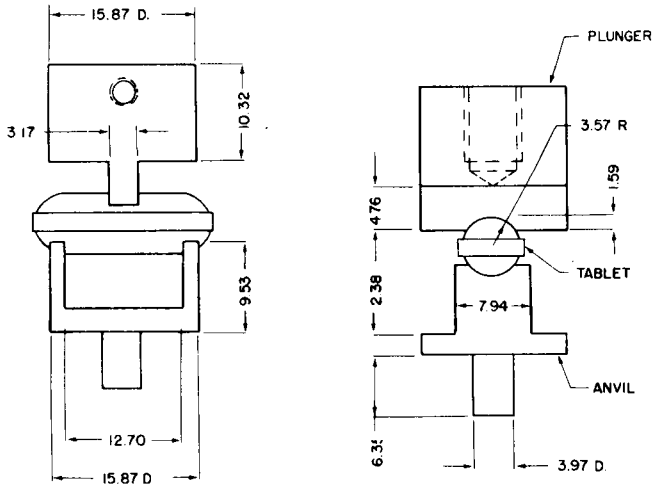

Figure 2—*Dimensions of the plunger and anvil in millimeters.*

how the measurements may be used in product development to evaluate factors affecting tablet breakage.

EXPERIMENTAL

The flexure tester (Fig. 1) was constructed by modifying the plunger tip and anvil of instrumentation described previously for measuring granule strength (5). Dimensions of the modified plunger tip and anvil are given in Fig. 2.

The flexure tester consists of a mechanical linkage for applying the load at a uniform rate and a strain-gauge instrumented cantilever beam and recorder for measuring the magnitude of the applied load. To measure flexure breaking strength, a single capsule-shaped tablet (C) is placed on the anvil (D), and the cam (A) is rotated at a uniform rate. Rotation of the cam at one revolution per 45 sec is controlled by a link chain, gear motor[1], and speed control switch[2].

The plunger (B) presses down across the middle of the tablet and bends the instrumented cantilever beam (E), thereby deforming the strain gauges (F). This deformation results in a millivolt response across the strain-gauge bridge circuit, which is measured on a recorder[3] with a 0–2-mv range for 25.4-cm full scale and a chart speed of 0.33 cm/sec. A tracing is obtained of increasing load with time, and a measurement of the tablet breaking strength is obtained at tablet breakage. The cam makes one complete revolution for each measurement.

The calibration procedure is built into the instrumentation and is performed each time the instrument is operated. A linear relationship exists between the weight on the calibration platform and the millivolt response on the recorder. The instrument is calibrated by adding weights to the calibration platform and adjusting the gain and zero controls to obtain the desired full-scale deflection on the recorder. Full-scale deflection can be varied from 200 g to 10 kg.

A typical recorder tracing of a flexure breaking strength measurement is shown in Fig. 3. The load is applied at a uniform rate by the speed control switch, which regulates the descent rate of the plunger. A break in the tracing of the increasing load with time indicates the tablet flexure breaking strength. In this tracing, the flexure breaking strength is 3 kg.

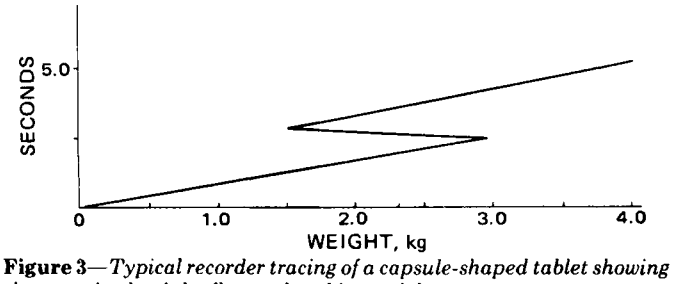

Figure 3—*Typical recorder tracing of a capsule-shaped tablet showing the magnitude of the flexure breaking weight.*

[1] Model 4K 868, Dayton Electric Manufacturing Co., Chicago, Ill.
[2] Model 4X 599, Dayton Electric Manufacturing Co., Chicago, Ill.
[3] Brown Electronik, Honeywell, Philadelphia, Pa.

Table I—Typical Flexure Breaking Strength and Tablet Hardness Values (±*SD*)

Tablet Thickness[a], mm	Tablet Weight, mg	Flexure Breaking Strength ± *SD*, kg[b]	Tablet Hardness ± *SD*, kg[c]
6.299	588	1.25 ± 0.05	4.97 ± 0.08
6.325	620	1.97 ± 0.15	7.80 ± 0.21
6.325	650	2.79 ± 0.14	11.01 ± 0.66
6.350	680	3.99 ± 0.30	15.34 ± 0.78

[a] All tablets were 7.035 mm wide and 17.900 mm long. [b] Mean of six measurements. [c] Mean of 10 measurements.

After the breaking point, the backswing develops because the load is relieved abruptly and the cantilever beam rapidly rises until it contacts the plunger. Six replicate measurements were made, and the mean is reported.

Tablet hardness[4] measurements were made by the diametral compression of capsule-shaped tablets through their major axes. Ten replicate measurements were made, and the mean is reported. Typical tablet hardness and flexure breaking strength measurements and their relative standard deviations are listed in Table I. The tablet mechanical strength profile was obtained by a least-squares line plot of tablet hardness *versus* flexure breaking strength.

Materials used in this study were USP, NF, or pharmaceutical grade. Lactose tablets contained 89.5% direct-compression lactose, 10% cornstarch, and 0.5% magnesium stearate. Capsule-shaped tablets, 7.035 × 17.900 mm, were prepared with one punch of a rotary tablet press[5] at a rate of 24 tablets/min using one station to minimize tooling variations. Tablets of other sizes were prepared on a modified single-punch tablet press[6].

RESULTS AND DISCUSSION

The effects of four different tablet thicknesses on the mechanical strength profile of lactose capsule-shaped tablets are shown in Fig. 4. From this profile, it is apparent that, at the same tablet hardness, an increase in tablet thickness resulted in an increase in flexure breaking strength. At 10-kg tablet hardness, for example, tablets prepared at a thickness of 5.08 mm (line A) had a flexure breaking strength of 2.2 kg, whereas tablets prepared at a thickness of 7.62 mm (line D) had a breaking strength of 3.4 kg.

The effects of various tablet formulations on the mechanical strength profile of tablets prepared at a constant thickness were studied. Measurements on 10 formulations are shown in Fig. 5. The formulations were prepared by either direct compression or wet granulation, and an attempt was made to vary the type and concentrations of fillers, binders, disintegrants, and lubricants. The formulation and ingredients did not significantly alter the mechanical strength of the tablet. The data indicate

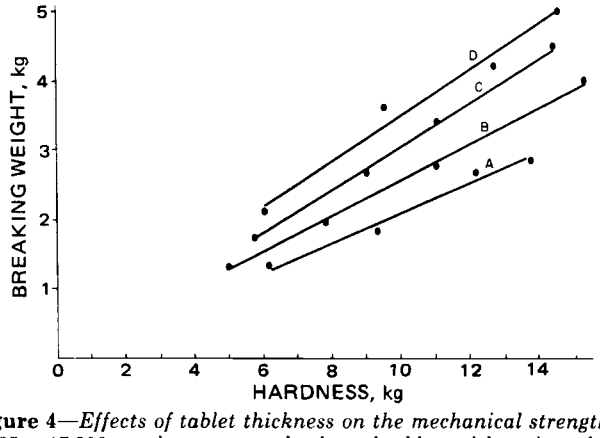

Figure 4—*Effects of tablet thickness on the mechanical strength of 7.035 × 17.900-mm lactose capsule-shaped tablets with various thicknesses. Key: A, 5.088 mm thick; B, 5.715 mm thick; C, 6.350 mm thick; and D, 7.620 mm thick.*

[4] Heberlein model 2E/106, series 7203, Key Industries, Farmingdale, N.Y.
[5] Colton 216, Cherry-Burrell Corp., Park Ridge, Ill.
[6] Colton T-12, Cherry-Burrell Corp., Park Ridge, Ill.

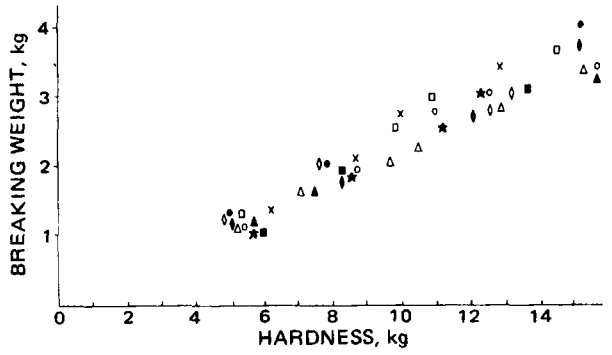

Figure 5—*Effects of 10 formulations on the mechanical strength of a 7.035 × 17.900 × 6.350-mm capsule-shaped tablet. Key: ●, direct-compression lactose (89.5%), cornstarch (10%), and magnesium stearate (0.5%); ×, unmilled dibasic calcium phosphate dihydrate (89.5%), cornstarch (10%), and magnesium stearate (0.5%); □, unmilled dibasic calcium phosphate dihydrate (44.75%), direct-compression lactose (44.75%), cornstarch (10%), and magnesium stearate (0.5%); ◇, direct-compression lactose (44.75%), microcrystalline cellulose (44.75%), cornstarch (10%), and magnesium stearate (0.5%); ○, unmilled dibasic calcium phosphate dihydrate (44.75%), microcrystalline cellulose (44.75%), cornstarch (10%), and magnesium stearate (0.5%); ★, unmilled dibasic calcium phosphate dihydrate (77%), microcrystalline cellulose (20%), and stearic acid (3%); ■, dibasic calcium phosphate granules prepared by wet granulation (89.5%), cornstarch (10%), and magnesium stearate (0.5%); ▲, calcium sulfate granules prepared by wet granulation (95%), sodium carboxymethyl starch (4%), and hydrogenated vegetable oil (1%); ♦, calcium sulfate granules prepared by wet granulation (89.5%), cornstarch (10%), and magnesium stearate (0.5%); and △, calcium sulfate granules prepared by wet granulation (64.5%), α-cellulose (25%), cornstarch (10%), and magnesium stearate (0.5%).*

that, for this specific tablet configuration, there is a linear relationship between the tablet crushing strength as determined by the tablet hardness measurement and the flexure breaking strength.

The mechanical strength of different size lactose tablets is shown in Fig. 6. At the lower tablet hardness values, the differences in breaking strengths between the different size tablets were small; at the higher tablet hardness values, the differences were significantly greater. The oval tablet (line D) had greater breaking strength than the capsule-shaped tablet. Since each breakage problem represents a unique set of conditions,

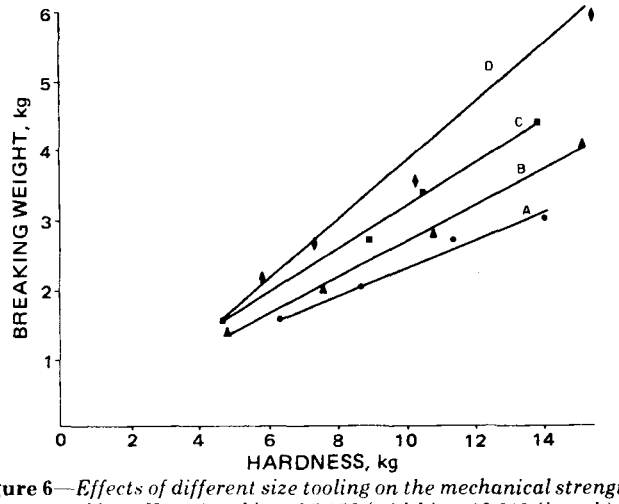

Figure 6—*Effects of different size tooling on the mechanical strength of lactose tablets. Key: A, tablet of 5.156 (width) × 16.612 (length) × 5.105 (thickness) mm; B, tablet of 7.035 (width) × 17.900 (length) × 6.350 (thickness) mm; C, tablet of 7.112 (width) × 22.987 (length) × 7.239 (thickness) mm; and D, oval-shaped tablet of 7.976 (width) × 19.177 (length) × 6.655 (thickness) mm.*

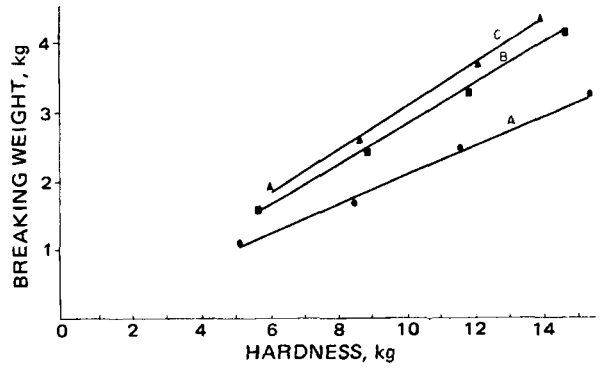

Figure 7—*Effects of tablet concavity on the mechanical strength of a 7.035-mm wide × 17.900-mm long × 6.350-mm thick lactose capsule-shaped tablet. Key: A, 1.143 mm deep; B, 1.8034 mm deep; and C, 2.235 mm deep.*

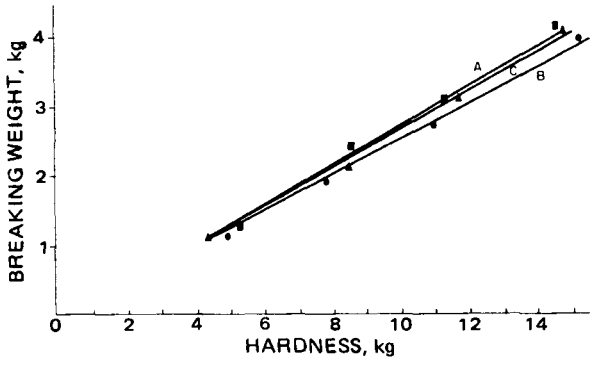

Figure 8—*Effects of the bisect bar dimensions on the mechanical strength of a 7.035-mm wide × 17.900-mm long × 6.350-mm thick lactose capsule-shaped tablet. Key: A, no bisect bar; B, 0.762-mm wide and 0.381-mm deep bisect bar; and C, 1.524-mm wide and 0.381-mm deep bisect bar.*

the size and configuration of the tablet must be evaluated in terms of the specific problem. Where the cross-sectional area of the tablet may be the critical parameter in coating tablets, the length may be the critical parameter in a bottle-filling operation.

The effect of the concavity of the tablet on the mechanical strength of lactose tablets was evaluated (Fig. 7). Tablets were prepared with shallow (1.143 mm), medium (1.803 mm), and deep (2.235 mm) cups in which the overall dimensions of the tablet were maintained at 7.035 × 17.900 × 6.350 mm. Tablets made with the shallow cup had significantly less breaking strength at the same tablet hardness than did either the medium or deep cup tablets. At 12-kg tablet hardness, the shallow cup had a breaking strength of only 2.4 kg compared to the standard cup value of 3.3 kg and the deep cup value of 3.6 kg.

The effect of the bisect on the mechanical strength of lactose tablets also was evaluated (Fig. 8). Using the same size tooling, tablets were prepared with no bisect, a 0.762-mm wide and 0.381-mm deep bisect, and a 1.524-mm wide and 0.381-mm deep bisect. Surprisingly, the bisect did not significantly alter the mechanical strength of these tablets.

REFERENCES

(1) C. J. Endicott, W. Lowenthal, and H. M. Gross, *J. Pharm. Sci.*, **50**, 343 (1961).

(2) S. T. David and L. L. Augsburger, *ibid.*, **63**, 933 (1974).

(3) H. Spengler and A. Kaelin, *Pharm. Acta Helv.*, **20**, 219, 239 (1945).

(4) K. Munzel and W. Kagi, *ibid.*, **32**, 305 (1957).

(5) G. Gold, R. N. Duvall, B. T. Palermo, and R. L. Hurtle, *J. Pharm. Sci.*, **60**, 922 (1971).

Vehicle Effects in Percutaneous Absorption: *In Vitro* Study of Influence of Solvent Power and Microscopic Viscosity of Vehicle on Benzocaine Release from Suspension Hydrogels

G. DI COLO ˣ, V. CARELLI, B. GIANNACCINI, M. F. SERAFINI, and F. BOTTARI

Received April 11, 1979, from the *Pharmaceutical Technology Laboratory, Institute of Pharmaceutical Chemistry, University of Pisa, 56100 Pisa, Italy.* Accepted for publication October 23, 1979.

Abstract □ The release through silicone rubber membranes of benzocaine suspended in carbomer hydrogels containing different concentrations of low molecular weight polyols (ethylene glycol, propylene glycol, glycerol, and sorbitol) was studied to establish general principles and procedures for control of the effects on percutaneous absorption caused by changes in drug solubility and/or diffusivity in the vehicle. The effect of the additives on the release is expressed in terms of the relative released amount, *i.e.*, the ratio, Q/Q_W, of the amount of drug released from each additive-containing gel to the amount released at the same time from the additive-free gel. The experimental Q/Q_W values are correlated with values calculated by a simple equation involving known or readily measurable parameters such as the drug concentration in the gel, the drug solubility in the pure liquid phase, and the viscosity of this phase. Derivation of such a relationship from a known equation describing the vehicle-controlled release of suspended drugs was possible because an inverse proportionality was observed between drug diffusivity in the gels and the viscosity of the respective solvents. This relationship is interpreted with respect to current theories on drug diffusion in diluted gels.

Keyphrases □ Absorption, percutaneous—benzocaine, release from suspension hydrogels, influence of solvent power and microscopic viscosity of vehicle, *in vitro* □ Benzocaine—percutaneous absorption, release from suspension hydrogels, influence of solvent power and microscopic viscosity of vehicle, *in vitro* □ Hydrogels, suspension—percutaneous absorption of benzocaine, influence of solvent power and microscopic viscosity of vehicle, *in vitro* □ Vehicles—suspension hydrogels, percutaneous absorption of benzocaine, influence of solvent power and microscopic viscosity of vehicle, *in vitro* □ Percutaneous absorption—benzocaine, release from suspension hydrogels, influence of solvent power and microscopic viscosity of vehicle, *in vitro*

Low molecular weight polyols are used extensively as humidity conditioners in dermatological hydrogels. Propylene glycol, glycerol, and sorbitol usually are introduced in these dosage forms to prevent undesirable solid films from forming on the skin following water evaporation. In addition to vehicle stability, drug bioavailability can be affected profoundly by these additives through their effect on physicochemical factors controlling passive absorption, such as the solubility and diffusivity of the drug in the vehicle and the resistance of the skin barrier to drug penetration.

The effect of varying the solubility of the penetrant in the vehicle on transepidermal penetration was investigated thoroughly (1–3). Other investigators (4) found that drug diffusion in the vehicle may provide a rate-limiting step in absorption if the drug is suspended in the vehicle. On the other hand, *in vivo* studies have not fully clarified, except in certain cases, the effect of excipients on skin resistance to drug penetration.

From the results of *in vivo* studies on propylene glycol, the most studied of these polyols (5), a precise conclusion cannot be drawn as to whether this substance exerts its effect on drug penetration by influencing the physicochemical properties of the vehicle or those of the skin or both. This uncertainty is due to the fact that, in most of these studies, the physicochemical parameters relative to the vehicle and the drug, namely, the solubility and apparent diffusivity of the drug in the vehicle, were not controlled suitably to allow assessment of the effects of the excipient on the skin barrier. These parameters must be considered for an appropriate evaluation of the release properties of topical vehicles.

This paper discusses an *in vitro* study of drug release from hydrogels containing low molecular weight polyols. The purpose of this study was to establish general principles and procedures for control of the effects on percutaneous absorption caused by the additive-induced changes in drug solubility and diffusivity in these vehicles. Although convenient methods for determining the solubility and the diffusion coefficient of drugs in semisolid media have been developed (6–9), investigation of possible correlations of these parameters with the more readily measurable drug solubility in the liquid phase of gels and the viscosity of this phase, respectively, was desired.

Propylene glycol, ethylene glycol, glycerol, and sorbitol were the additives studied because they are used widely in commercial preparations. Benzocaine (ethyl *p*-aminobenzoate) was selected as a model of a neutral, topical drug with low water solubility.

THEORETICAL

The effect on drug release to the skin by variations of the solubility and/or diffusivity of the drug in the vehicle depends on whether the rate-controlling step of release occurs in the skin (Case A), in the vehicle (Case B), or in both the skin and the vehicle (Case C).

In Case A, such variations are expected to exert no effect on the release rate since this rate depends on skin parameters, which are presumed constant, and on the thermodynamic activity of the drug in the vehicle, which is independent of the vehicle properties, above saturation (10). For two vehicles characterized by different values of drug solubility and/or diffusivity, $Q_2/Q_1 = 1$, where the ratio Q_2/Q_1 of the amount of drug released per unit area at any given time from Vehicle 2 to that released at the same time from Vehicle 1 is defined as the relative released amount from Vehicle 2 with respect to Vehicle 1.

Higuchi (11) derived the following equation for Case B:

$$Q = \sqrt{(2A - S)SDt} \qquad \text{(Eq. 1)}$$

where D, A, and S are the apparent diffusivity, the total concentration, and the solubility of the drug in the vehicle, respectively. Equation 1 is valid for vehicles in which the apparent diffusion coefficient is constant, the suspended drug is finely dispersed, the dissolution of the drug is much faster than its diffusion through the vehicle, and the total drug concentration is at least threefold greater than the solubility. With Eq. 1, the following expression for the relative released amount can be derived:

0022-3549/80/0400-0387$01.00/0
© 1980, American Pharmaceutical Association

$$Q_2/Q_1 = \sqrt{\frac{(2A - S_2)S_2D_2}{(2A - S_1)S_1D_1}} \quad \text{(Eq. 2)}$$

where the drug concentration is assumed to be the same in the two vehicles.

In Case C, Q_2/Q_1 is expected to vary from 1 to the value expressed by Eq. 2, depending on the resistance the drug encounters in its diffusion through the respective vehicles relative to that in the skin[1].

Equation 2 should be suitable for evaluating the maximum effect on the *in vivo* release of a drug to the skin attributable to variations of drug solubility and/or diffusivity in the vehicle. Greater or opposite effects should be ascribed to modifications of the barrier properties of skin due to skin–vehicle interactions.

The convenience of Eq. 2 for controlling the solubility and diffusivity effects obviously is connected with the ease of determination of these parameters. For gels, Eq. 2 can be modified to contain such readily measurable parameters as drug solubility in the solvent of the gel and the viscosity of this solvent. If the gel substance does not interact significantly with the drug, the solubility and diffusion coefficient of the drug in the gel should be practically the same as in the pure liquid. The diffusivity in homogeneous liquids, D_l, can be expressed through the viscosity of the liquid, η, and can be expected to range from:

$$D_l = \frac{kT}{4\pi\eta}\left(\frac{4\pi}{3v}\right)^{1/3} \quad \text{(Eq. 3)}$$

for solutes whose molar volume, v, is equal to the molar volume of the solvent, to:

$$D_l = \frac{kT}{6\pi\eta}\left(\frac{4\pi}{3v}\right)^{1/3} \quad \text{(Eq. 4)}$$

when the molar volume of the solute is significantly greater than that of the solvent[2] (12).

Substitution in Eq. 2 of the appropriate expressions of D_l (*i.e.*, Eq. 3 or 4) in place of the respective D and of the drug solubility in the solvent of the gel, Sl, in place of the respective S leads to:

$$Q_2/Q_1 = \sqrt{\frac{(2A - Sl_2)Sl_2\eta_1}{(2A - Sl_1)Sl_1\eta_2}} \quad \text{(Eq. 5)}$$

for Solvents 1 and 2, having either similar or different molecular volumes approximately equal to or smaller than that of the drug in the former case and considerably smaller than that of the drug in the latter, or to:

$$Q_2/Q_1 = \sqrt{\frac{2(2A - Sl_2)Sl_2\eta_1}{3(2A - Sl_1)Sl_1\eta_2}} \quad \text{(Eq. 6)}$$

where the molecular volume of Solvent 1 is significantly greater than that of Solvent 2 and approaches the value of the diffusing particle.

As stated, Eqs. 5 and 6 are applicable to gels where the interactions of the drug with the chains of the gel polymer are either absent or unimportant. Actually, these equations also are valid where such interactions are strictly mechanical if the volume fraction of the gel substance is the same in Gels 1 and 2, and is not so high that the diameter of the gel pores approaches the diffusing particle diameter. In these conditions, the diffusion coefficient in the gel is proportional to that in the solvent, D_l (12):

$$D = \frac{D_l}{1 + 2/3\phi} \quad \text{(Eq. 7)}$$

If ϕ, the volume fraction of the gel substance, is the same in Gels 1 and 2, then Eq. 2 for these gels again may be transformed into Eq. 5 or 6. On the other hand, the complications arising when the drug or some components of the liquid phase undergo complexation by the gel polymer rule out the application of simple Eq. 5 or 6 to such systems.

EXPERIMENTAL

Materials—Ethylene glycol[3], propylene glycol[3], glycerol[3], sorbitol[4], and carboxypolymethylene[5] (carboxyvinyl polymer) were used as received. The neutral sodium salt of carboxypolymethylene was prepared as described in the literature (13). Benzocaine[3] was crystallized to a constant melting point of 91.5° and micronized[6]. The average diameter of the particles (microscopic analysis) was 2.0 μm (geometric). Simethicone[7] (dimethyl polysiloxane, silicone rubber) sheeting in a labeled thickness of ~127 μm was used as the membrane.

Vehicles, Apparatus, and Procedures—Hydrophilic gels containing 1% (w/v) carboxypolymethylene sodium salt were obtained from water (Gel W) and from the following aqueous polyols: 25% (w/w) ethylene glycol (Gel EG 25), 36% (w/w) ethylene glycol (Gel EG 36), 17.5% (w/w) propylene glycol (Gel PG 17.5), 30% (w/w) propylene glycol (Gel PG 30), 50% (w/w) glycerol (Gel G 50), 66% (w/w) glycerol (Gel G 66), and 54.5% (w/w) sorbitol (Gel S 54.5).

Solution gels, each containing benzocaine concentrations corresponding to 20 and 40% of the solubility in the respective solvents, and suspension gels, each containing 11 mg of micronized benzocaine/ml, were prepared following literature procedures (7, 8). The apparatus and procedures used for the release experiments with the solution (9) and suspension (7) gels were reported previously.

The apparent impermeability of the membrane to the polyols was demonstrated by the use of a previously described permeation cell and an apparatus (14) where the nongelled polyol–water mixtures without the drug were the internal solutions and water was the external phase. The periodic acid test (15) performed on this phase after 8-hr runs gave a negative result in all cases. Each release experiment was performed at least three times, and the averaged data were used for the individual plots.

Solubility Determinations—Benzocaine solubility in the solvent systems of the gels was determined by equilibrating excess benzocaine with the solvent at 30°. Samples then were withdrawn and rapidly filtered through a 0.22-μm pore filter[8]. The clear solutions were diluted with distilled water and spectrophotometrically[9] analyzed at 286 nm.

Diffusivity Determinations—The diffusion coefficient of benzocaine in the gels at 30° was calculated from the release data obtained from the solution gels according to a reported numerical method of analysis (9). The computations were executed with a computer[10].

Table I—Solubility, Diffusivity, and Viscosity Data at 30°

Gel	Drug Solubility in Solvent, Sl, mg/ml	Drug Diffusivity in Gel, D, $cm^2/sec \times 10^6$	Solvent Viscosity, η, cps	$D\eta$, cm^2/sec cps $\times 10^6$
W[a]	1.31	8.6	0.8	6.88
EG 25	2.37	4.5	1.60	7.2
EG 36	3.35	4.1	2.08	8.53
PG 17.5	2.44	4.7	1.58	7.33
PG 30	4.07	3.7	2.16	7.99
G 50	2.50	1.7	4.60	7.8
G 66[a]	3.77	0.79	11.8	9.32
S 54.5[a]	1.05	—	12.3	—

[a] The solubility and diffusivity data for this gel were obtained from previous reports (7–9).

RESULTS AND DISCUSSION

Solubility of Drug, Microscopic Viscosity of Gels, and Drug Diffusivity in Gels—The values of the solubility, Sl, of benzocaine in the solvents of the gels studied are listed in Table I, together with the viscosity[11] of the solvents, η, and the diffusion coefficient, D, of drug in the gels. These values were determined by a recently developed method based on numerical analysis of release data (9). Accordingly, two drug concentrations, corresponding to 20 and 40% solubility in the solvent, were run for each gel; the respective values of diffusivity obtained from the computations were compared to ascertain the independence of concentration. This independence existed for all gels investigated since the diffusivity values determined at the two drug concentrations were within experimental error. Table I reports the average values. The diffusion coefficient of benzocaine in the gel containing sorbitol was not determined since previous work showed concentration dependence of this parameter (9).

[1] This analysis assumes the same release mechanism for the two vehicles being compared. The case of different mechanisms is not considered since it generally would require large variations of solubility and diffusivity.

[2] Strictly speaking, a correction for nonsphericity of the diffusant should be introduced in the expression of D for large particles. However, this correction has been ignored since it amounts to <10% for all but the most elongated structures (12).

[3] Carlo Erba S.p.A., Milan, Italy.

[4] Istituto Chemioterapico Italiano, Milan, Italy.

[5] Carbopol 934, B. F. Goodrich Chemical Co., Cleveland, Ohio.

[6] Jet mill model JMRS-80, Fryma Maschinen AG, Rheinfelden, Switzerland.

[7] Silastic, Medical Products Division, Dow Corning Corp., Midland, Mich.

[8] GSWP 01300, Millipore Filter Corp., Bedford, Mass.

[9] Beckman DU spectrophotometer.

[10] IBM 370/168.

[11] Rheomat-30 viscosimeter, Contraves, Zurich, Switzerland.

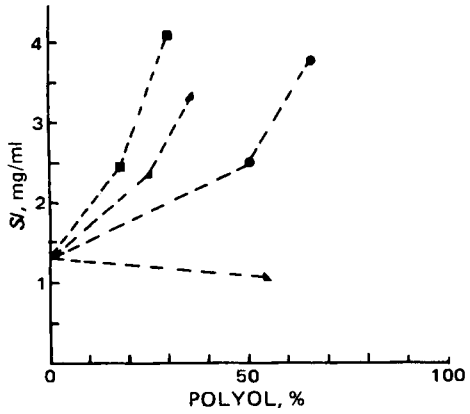

Figure 1—*Solubility of benzocaine in polyol–water mixtures at 30°. Key: ■, propylene glycol; ◢, ethylene glycol; ●, glycerol; and ◣, sorbitol.*

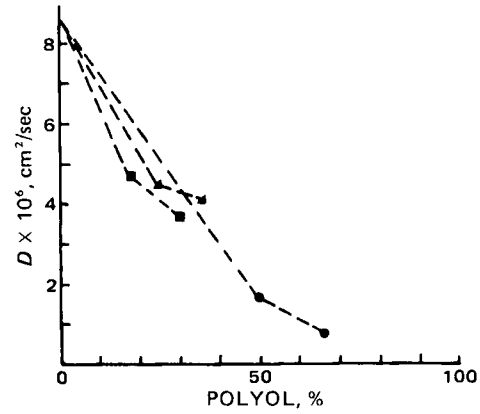

Figure 3—*Diffusivity of benzocaine in the polyol-containing hydrogels. Key: ■, propylene glycol; ◢, ethylene glycol; and ●, glycerol.*

The concentration independence of diffusivity in Gels W, G 50, G 66, EG 25, EG 36, PG 17.5, and PG 30 points to the absence of self-aggregation of the benzocaine molecules over the concentration ranges investigated (12). Complexation of the drug by the gel substance also can be excluded, because previous work indicated that the addition of carboxypolymethylene sodium salt to solutions of benzocaine in water or in water–glycerol did not alter the thermodynamic activity of the drug (8). Then the values reported in Table I for the solubility in the solvents also may be referred to as the drug solubility in the corresponding gels.

The dependence of the parameters in Table I on solvent composition can be visualized best in Figs. 1–3. Table I and Fig. 1 show that the solubility of benzocaine in the solvent mixtures increased with increasing content of propylene glycol, ethylene glycol, or glycerol, but the opposite effect was produced by sorbitol. For a given composition of the water–additive mixture, ascent in the polyol series from ethylene glycol to sorbitol resulted in a progressive solubility decrease. Such a decrease was more evident for higher additive concentrations. The greater solvent power of propylene glycol with respect to ethylene glycol probably was due to the moderately lower polarity of the propylene glycol molecule.

A substantial inverse proportionality between the diffusion coefficient in the gels and the viscosity of the respective solvents can be noticed on comparing the data in Figs. 2 and 3. This relationship is confirmed in Table I by the $D\eta$ products approximating a constant and in Fig. 4 by the linear trend of the D *versus* $1/\eta$ plot with a least-squares intercept approximating zero. Such a relationship agrees with the theory. Once complexation is excluded, only mechanical interactions between the diffusing species and the gel substance can be anticipated. Then, at the low concentrations of the gel polymer used in the present work, a proportionality between the diffusion coefficient of the drug in the gel and that in the solvent should exist and should be expressed by Eq. 7. Compliance of the latter coefficient with (or, in fact, an approximation to) Eq. 3 or 4 should account for the relationship between D and η emerging from the present data. Equation 4 seems more appropriate since the molecular volume either of water or of the polyols is in all cases smaller than that of the diffusing particle.

According to the foregoing considerations, the viscosity of the solvent mixtures should represent the effective microscopic viscosity of the respective gels; in turn, the composition of the liquid phase of gels should be substantially the same as that of the corresponding nongelled solvents. The assumption of an inverse proportionality between D and η, although substantially reasonable, is in fact an approximation. The nonzero intercept of the D *versus* $1/\eta$ plot in Fig. 4 hardly is attributable only to experimental errors. This observation may be better explained by admitting that in the presence of increasing additive concentrations, the diffusion coefficient in the liquid phase of gels deviates toward higher values than those expressed by Eq. 4. Furthermore, the volume fraction of solvent immobilized by the polymer might decrease, thus causing a decrease of the mechanical interactions of the diffusing particle with the gel network and, consequently, an increase of the diffusion coefficient in the gel with respect to that in the solvent (Eq. 7).

Influence of Solubility and Microscopic Viscosity on Release—Silicone rubber membranes similar to those used in this investigation were employed previously (4) for simulating skin. Their permeability to the drug is not supposed to be influenced by the polyols since none of them was found in the receiving phase. The degree of fineness of the suspended benzocaine, the concentration of the drug, and the concentration of the gel polymer all were kept constant so that the differences in release could not be attributed to these variables.

The plots in Fig. 5 show that either the solubility of the drug or the microscopic viscosity of the gels markedly affected release. Substantially

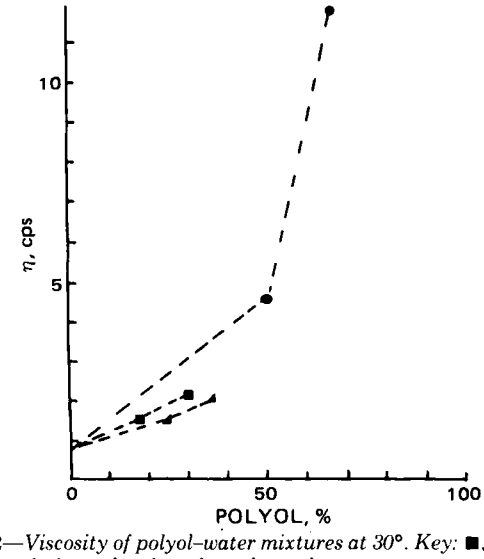

Figure 2—*Viscosity of polyol–water mixtures at 30°. Key: ■, propylene glycol; ◢, ethylene glycol; and ●, glycerol.*

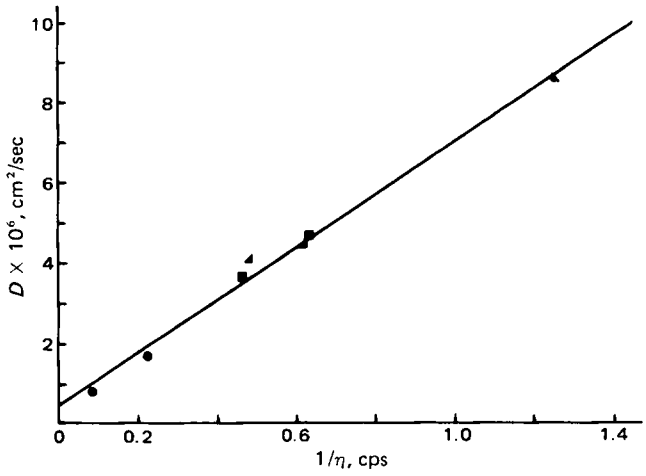

Figure 4—*Plot of benzocaine diffusivity in the hydrogels* versus *the inverse viscosity of the respective solvents. Key: ■, propylene glycol-containing gels; ◢, ethylene glycol-containing gels; ●, glycerol-containing gels; and ◣, additive-free Gel W. The linear regression parameters are slope = 6.65 and intercept = 0.44.*

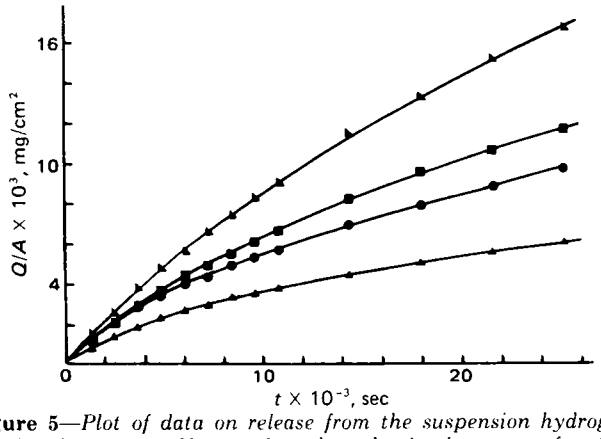

Figure 5—*Plot of data on release from the suspension hydrogels showing the amount of benzocaine released per unit area as a function of time. The total drug concentration was 11 mg/ml. Key: ◣, Gel W; ▲, Gel S 54.5; ●, Gel G 66; and ■, Gel G 50. The plots for Gels EG 25, EG 36, PG 17.5, and PG 30 are nearly superimposable on that for Gel W.*

distinct release patterns were shown by gels differing only in a single parameter (compare the data in Table I and Fig. 5 for Gels G 66 and S 54.5 and for Gels PG 17.5 and G 50). The data also indicate that the drug solubility and the gel microviscosity exerted their effects in opposite directions, with the former related directly and the latter related inversely to release. This effect can explain the substantially identical release pattern shown by gels differing in both parameters such as Gels W, EG 25 (or PG 17.5), and PG 30 (or EG 36) since any increase in the drug solubility was paralleled by an increase in the microscopic viscosity.

In light of the considerations stated under *Theoretical*, the results point to possible utilization of Eq. 5 for controlling the effect on release of varying the described parameters. Such an effect may be represented through the relative released amount, *i.e.*, the ratio, Q/Q_W, of the amount of drug released from each additive-containing gel to the amount released at the same time from the additive-free Gel W. The plots in Fig. 6 were intended to verify the time dependence of Q/Q_W for each gel; a comparison of the values of Q/Q_W determined at the end of the release experiments ($t = 25.2 \times 10^3$ sec) with those calculated by Eq. 5 is given in Table II.

The relative released amount was time dependent for gels (G 50, G 66, and S 54.5) that showed a marked deviation from the Q/Q_W value of unity determined at $t = 25.2 \times 10^3$ sec. Such a deviation was essentially less than that calculated by Eq. 5. On the other hand, a fair correspondence existed at all times between the experimental and the calculated Q/Q_W values when the latter value approximated one (see the data for PG 17.5, PG 30, EG 25, and EG 36). These results are in compliance with the theoretical considerations for Case C, and they appear to substantiate a vehicle–membrane-controlled release for the present gels. The increasing deviation of Q/Q_W from unity with time toward the value ex-

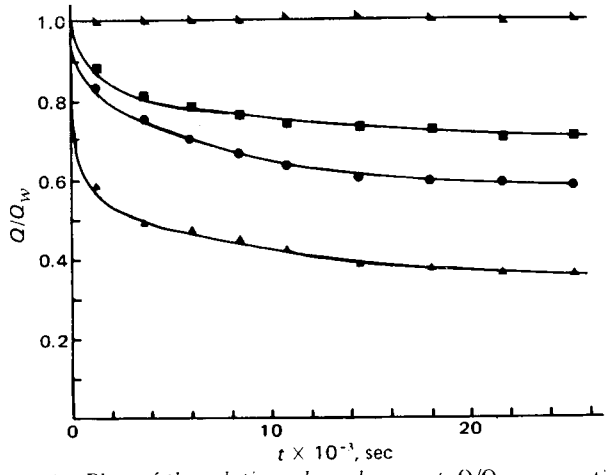

Figure 6—*Plots of the relative released amount, Q/Q_W, versus time. Key: ▲, Gel S 54.5; ●, Gel G 66; ■, Gel G 50; and ◣, Gel PG 17.5. The plots for Gels PG 30, EG 25, and EG 36 are nearly superimposable on that for Gel PG 17.5.*

Table II—Comparison of Experimental Relative Released Amount, Q/Q_W, with Values Calculated by Eq. 5

Gel	Experimental ($t = 25.2 \times 10^3$ sec)	Calculated
EG 25	1.04	0.93
EG 36	1.07	0.94
PG 17.5	1.01	0.94
PG 30	1.06	0.99
G 50	0.69	0.56
G 66	0.58	0.41
S 54.5	0.36	0.22

pressed by Eq. 5 is in agreement with the statement in previous reports (7, 16) that the vehicle–membrane-controlled release model evolves with time toward the vehicle-controlled model. Also, the present experimental evidence supports the view that Eq. 5 expresses the maximum effect on release produced by variations of the drug solubility and/or the gel microviscosity.

In Fig. 7, the experimental values of the relative released amount determined at $t = 1.2 \times 10^3$ sec, $t = 3.6 \times 10^3$ sec, and $t = 25.2 \times 10^3$ sec for all gels are plotted *versus* the values calculated by Eq. 5. The alignment of points clearly indicates that a definite relationship existed between the experimental vehicle–membrane-controlled Q/Q_W and the calculated vehicle-controlled values. This result points to the usefulness of such plots as calibration curves of the effects of the solubility and the diffusivity of the drug in the applied phase on quasi-steady-state[12] drug penetration through a membrane. Curves of this type, if obtained from *in vivo* experiments, should be indicative of the absence of vehicle-induced changes in skin permeability to drug; in this event, they could enable the prediction of the relative released amount once the parameters in Eq. 5 are determined. The more general Eq. 2 should be used to construct similar calibration curves when dealing with vehicles not meeting the requirements of Eq. 5.

CONCLUSIONS

In summary, Eq. 5 is proposed as a tool for controlling the effects of polyol additives, usually introduced in dermatological hydrogels, on important physicochemical factors influencing drug release such as the solubility and diffusivity of the drug in the vehicle. This equation has been shown to predict the maximum effect on benzocaine penetration through silicone rubber membranes associated with changes in the described parameters. A precise correlation exists between the experimental values of the relative released amount and the values calculated by Eq. 5. This finding points to the potential usefulness of this equation for constructing calibration curves of the effects of drug solubility and diffusivity in the vehicle on quasi-steady-state drug penetration through skin.

Although a silicone rubber membrane is far from being perfectly rep-

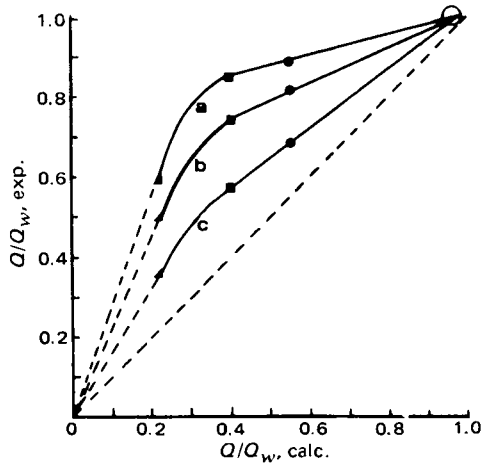

Figure 7—*Plots of the experimental relative released amount, Q/Q_W, versus the values calculated by Eq. 5. Key: a, $t = 1.2 \times 10^3$ sec; b, $t = 3.6 \times 10^3$ sec; c, $t = 25.2 \times 10^3$ sec; ○, Gels EG 25, EG 36, PG 17.5, and PG 30; ■, Gel G 66; ▲, Gel S 54.5; and ●, Gel G 50.*

[12] According to the results of a previous work (7), linear concentration gradients of the drug in the membrane should exist after the early times of the release experiments.

resentative of skin with regard to drug penetration, it nevertheless provides the requirements for the present comparative study where the following assumptions were made:

1. Skin transport is passive.
2. The skin parameters relevant to drug penetration are not influenced by the vehicle.
3. The vehicle composition does not change significantly during release.

Derivation of Eq. 5 from Higuchi's Eq. 1 (11) was possible because an inverse proportionality was observed between the diffusivity of drug in gels and the viscosity of the respective solvents. Such a relationship is justifiable considering the current theories on diffusion in diluted gels, as long as the viscosity of each solvent is accepted as the microscopic viscosity of the corresponding gel and self-aggregation or complexation of the drug is excluded. All of the gels studied in the present work (except, perhaps, the gel containing sorbitol) met the requirement of Eq. 5 that the molecular volume of the components of the liquid phase be substantially smaller than that of the diffusing drug. The cases of molecular volume of solvent approaching or exceeding that of the drug might deserve investigation for the applicability of Eq. 5 or 6.

It is hoped that the present study will help to rationalize the compounding of pharmaceutical gels and, furthermore, that the suggested principles and procedures for controlling the vehicle parameters will be useful in *in vivo* studies intended to assess the effects of excipients on skin permeability to drugs.

REFERENCES

(1) B. J. Poulsen, E. Young, V. Coquilla, and M. Katz, *J. Pharm. Sci.*, *57*, 928 (1968).

(2) J. Ostrenga, C. Steinmetz, and B. Poulsen, *ibid.*, **60**, 1175 (1971).

(3) J. Ostrenga, C. Steinmetz, B. Poulsen, and S. Yett, *ibid.*, **60**, 1180 (1971).

(4) S. S. Davis and M. S. Khanderia, "The Influence of the Rheological Properties of the Vehicle on the Release of Drugs from Semisolid Ointments," Proceedings of the 1st International Conference of Pharmaceutical Technology, vol. III, Paris, France, 1977, pp. 30–47.

(5) B. Idson, *J. Pharm. Sci.*, **64**, 901 (1975).

(6) J. Polderman, G. M. Basart-Westgeest, and J. A. R. Siemons, *Pharm. Weekbl.*, **109**, 325 (1974).

(7) F. Bottari, G. Di Colo, E. Nannipieri, M. F. Saettone, and M. F. Serafini, *J. Pharm. Sci.*, **66**, 926 (1977).

(8) F. Bottari, V. Carelli, G. Di Colo, M. R. Firinu, and E. Nannipieri, *Farmaco, Ed. Prat.*, **33**, 3 (1978).

(9) F. Bottari, V. Carelli, G. Di Colo, M. F. Saettone, and M. F. Serafini, *Int. J. Pharm.*, **2**, 63 (1979).

(10) T. Higuchi, *J. Soc. Cosmet. Chem.*, **11**, 85 (1960).

(11) T. Higuchi, *J. Pharm. Sci.*, **50**, 874 (1961).

(12) G. L. Flynn, S. H. Yalkowsky, and T. J. Roseman, *ibid.*, **63**, 479 (1974).

(13) A. G. Perotti, *Farmaco, Ed. Prat.*, **25**, 651 (1970).

(14) F. Bottari, G. Di Colo, E. Nannipieri, M. F. Saettone, and M. F. Serafini, *J. Pharm. Sci.*, **64**, 946 (1975).

(15) R. L. Shriner and R. C. Fuson, "The Systematic Identification of Organic Compounds," 3rd ed., Wiley, New York, N.Y., 1948, pp. 115, 116.

(16) T. J. Roseman and W. I. Higuchi, *J. Pharm. Sci.*, **59**, 353 (1970).

ACKNOWLEDGMENTS

Supported in part by a grant from Consiglio Nazionale delle Ricerche.

Effect of Particle Size on Ophthalmic Bioavailability of Dexamethasone Suspensions in Rabbits

R. D. SCHOENWALD ˣ and P. STEWART *

Received June 25, 1979, from the *Pharmaceutics Division, College of Pharmacy, University of Iowa, Iowa City, IA 52242.* Accepted for publication October 24, 1979. *Present address: Department of Pharmacy, University of Queensland, St. Lucia 4067, Queensland, Australia.

Abstract □ Three suspensions of 0.1% [^{3}H]dexamethasone were prepared with mean particle sizes of 5.75, 11.5, and 22.0 μm. The suspensions were dosed topically to the right eyes of rabbits. Their bioavailability was compared by measuring aqueous humor and corneal levels over 5 hr. A statistically significant rank-order correlation was observed between increasing drug levels and decreasing particle size.

Keyphrases □ Dexamethasone—ophthalmic suspensions, bioavailability, effect of particle size, rabbits □ Bioavailability—dexamethasone, ophthalmic suspensions, effect of particle size, rabbits □ Ophthalmic preparations—dexamethasone suspensions, bioavailability, effect of particle size, rabbits

In the development of an aqueous suspension for topical use in the eye, the size of the suspended particles often is governed by their irritation potential. Although the particle size is an important consideration in irritation and comfort, the ophthalmic bioavailability of the drug can be influenced by particle size according to one or two possible *in vivo* mechanisms. If the particle induces tearing, rapid drainage of the instilled dose could reduce bioavailability (1, 2). In addition, the dissolution rate of particles residing in the conjunctival sac just after dose instillation should influence ophthalmic bioavailability.

Few published articles have indicated the importance of particle size in ophthalmic bioavailability. Sieg and Robinson (2) studied the bioavailability of a 0.1% ophthalmic fluorometholone suspension and demonstrated that the particles were retained within the conjunctival sac longer than the corresponding saturated solution and contributed significantly to the quantity of drug penetrating the cornea. By comparing the area under the aqueous humor–time curve for the 0.1% suspension and the saturated solution, ~78% of the area was determined to come from the retained particles. Therefore, the dissolution rate for poorly soluble drugs may influence the rate and extent of penetration into eye fluids.

The present study was conducted in rabbits to determine the importance of particle size in the ophthalmic bioavailability of a 0.1% dexamethasone suspension. Dexamethasone was chosen because of its clinical significance and because of the availability of tritiated dexa-

0022-3549/80/0400-0391$01.00/0

© 1980, American Pharmaceutical Association

resentative of skin with regard to drug penetration, it nevertheless provides the requirements for the present comparative study where the following assumptions were made:

1. Skin transport is passive.
2. The skin parameters relevant to drug penetration are not influenced by the vehicle.
3. The vehicle composition does not change significantly during release.

Derivation of Eq. 5 from Higuchi's Eq. 1 (11) was possible because an inverse proportionality was observed between the diffusivity of drug in gels and the viscosity of the respective solvents. Such a relationship is justifiable considering the current theories on diffusion in diluted gels, as long as the viscosity of each solvent is accepted as the microscopic viscosity of the corresponding gel and self-aggregation or complexation of the drug is excluded. All of the gels studied in the present work (except, perhaps, the gel containing sorbitol) met the requirement of Eq. 5 that the molecular volume of the components of the liquid phase be substantially smaller than that of the diffusing drug. The cases of molecular volume of solvent approaching or exceeding that of the drug might deserve investigation for the applicability of Eq. 5 or 6.

It is hoped that the present study will help to rationalize the compounding of pharmaceutical gels and, furthermore, that the suggested principles and procedures for controlling the vehicle parameters will be useful in *in vivo* studies intended to assess the effects of excipients on skin permeability to drugs.

REFERENCES

(1) B. J. Poulsen, E. Young, V. Coquilla, and M. Katz, *J. Pharm. Sci.*, *57*, 928 (1968).

(2) J. Ostrenga, C. Steinmetz, and B. Poulsen, *ibid.*, **60**, 1175 (1971).

(3) J. Ostrenga, C. Steinmetz, B. Poulsen, and S. Yett, *ibid.*, **60**, 1180 (1971).

(4) S. S. Davis and M. S. Khanderia, "The Influence of the Rheological Properties of the Vehicle on the Release of Drugs from Semisolid Ointments," Proceedings of the 1st International Conference of Pharmaceutical Technology, vol. III, Paris, France, 1977, pp. 30–47.

(5) B. Idson, *J. Pharm. Sci.*, **64**, 901 (1975).

(6) J. Polderman, G. M. Basart-Westgeest, and J. A. R. Siemons, *Pharm. Weekbl.*, **109**, 325 (1974).

(7) F. Bottari, G. Di Colo, E. Nannipieri, M. F. Saettone, and M. F. Serafini, *J. Pharm. Sci.*, **66**, 926 (1977).

(8) F. Bottari, V. Carelli, G. Di Colo, M. R. Firinu, and E. Nannipieri, *Farmaco, Ed. Prat.*, **33**, 3 (1978).

(9) F. Bottari, V. Carelli, G. Di Colo, M. F. Saettone, and M. F. Serafini, *Int. J. Pharm.*, **2**, 63 (1979).

(10) T. Higuchi, *J. Soc. Cosmet. Chem.*, **11**, 85 (1960).

(11) T. Higuchi, *J. Pharm. Sci.*, **50**, 874 (1961).

(12) G. L. Flynn, S. H. Yalkowsky, and T. J. Roseman, *ibid.*, **63**, 479 (1974).

(13) A. G. Perotti, *Farmaco, Ed. Prat.*, **25**, 651 (1970).

(14) F. Bottari, G. Di Colo, E. Nannipieri, M. F. Saettone, and M. F. Serafini, *J. Pharm. Sci.*, **64**, 946 (1975).

(15) R. L. Shriner and R. C. Fuson, "The Systematic Identification of Organic Compounds," 3rd ed., Wiley, New York, N.Y., 1948, pp. 115, 116.

(16) T. J. Roseman and W. I. Higuchi, *J. Pharm. Sci.*, **59**, 353 (1970).

ACKNOWLEDGMENTS

Supported in part by a grant from Consiglio Nazionale delle Ricerche.

Effect of Particle Size on Ophthalmic Bioavailability of Dexamethasone Suspensions in Rabbits

R. D. SCHOENWALD ˣ and P. STEWART *

Received June 25, 1979, from the *Pharmaceutics Division, College of Pharmacy, University of Iowa, Iowa City, IA 52242.* Accepted for publication October 24, 1979. *Present address: Department of Pharmacy, University of Queensland, St. Lucia 4067, Queensland, Australia.

Abstract □ Three suspensions of 0.1% [^{3}H]dexamethasone were prepared with mean particle sizes of 5.75, 11.5, and 22.0 μm. The suspensions were dosed topically to the right eyes of rabbits. Their bioavailability was compared by measuring aqueous humor and corneal levels over 5 hr. A statistically significant rank-order correlation was observed between increasing drug levels and decreasing particle size.

Keyphrases □ Dexamethasone—ophthalmic suspensions, bioavailability, effect of particle size, rabbits □ Bioavailability—dexamethasone, ophthalmic suspensions, effect of particle size, rabbits □ Ophthalmic preparations—dexamethasone suspensions, bioavailability, effect of particle size, rabbits

In the development of an aqueous suspension for topical use in the eye, the size of the suspended particles often is governed by their irritation potential. Although the particle size is an important consideration in irritation and comfort, the ophthalmic bioavailability of the drug can be influenced by particle size according to one or two possible *in vivo* mechanisms. If the particle induces tearing, rapid drainage of the instilled dose could reduce bioavailability (1, 2). In addition, the dissolution rate of particles residing in the conjunctival sac just after dose instillation should influence ophthalmic bioavailability.

Few published articles have indicated the importance of particle size in ophthalmic bioavailability. Sieg and Robinson (2) studied the bioavailability of a 0.1% ophthalmic fluorometholone suspension and demonstrated that the particles were retained within the conjunctival sac longer than the corresponding saturated solution and contributed significantly to the quantity of drug penetrating the cornea. By comparing the area under the aqueous humor–time curve for the 0.1% suspension and the saturated solution, ~78% of the area was determined to come from the retained particles. Therefore, the dissolution rate for poorly soluble drugs may influence the rate and extent of penetration into eye fluids.

The present study was conducted in rabbits to determine the importance of particle size in the ophthalmic bioavailability of a 0.1% dexamethasone suspension. Dexamethasone was chosen because of its clinical significance and because of the availability of tritiated dexa-

0022-3549/80/0400-0391$01.00/0

© 1980, American Pharmaceutical Association

methasone, which permits determination of low drug levels in aqueous humor.

EXPERIMENTAL

Materials—Two millicuries of tritiated dexamethasone dissolved in benzene–ethanol (9:1) was obtained commercially[1]. Nontritiated dexamethasone[2] was used as received. Other chemicals were reagent grade.

Preparation of Particle-Size Dexamethasone Fractions—Tritiated dexamethasone in benzene–ethanol (9:1) was evaporated to dryness using a nitrogen stream and was redissolved in 0.5 ml of absolute alcohol. An alcoholic solution containing 120 mg of nontritiated dexamethasone in 5.6 ml was heated to 65° and was added to 0.4 ml of the tritiated alcoholic dexamethasone solution. This supersaturated solution was transferred to a test tube, submerged in an ice bath at 0°, and sonified[3] for 10 min until crystallization occurred.

Crystals were harvested 2, 9, and 24 hr following sonification by removing 2 ml of the resulting suspension at each time increment and filtering through a 0.45-μm membrane[4]. The three fractions of dexamethasone crystals were air dried and removed carefully from the membrane. The dried microfine powder was assumed to contain tracer homogeneously throughout its crystalline structure.

Suspension Preparation—Five milliliters of 0.1% dexamethasone suspension was prepared separately from the three microfine powder fractions using a vehicle consisting of 0.9% NaCl, 0.05% polysorbate 80, and water for injection. Each suspension was sonified for 30 sec to achieve uniform dispersion of the particles and was stored in several small vials at 4° for <4 weeks.

Particle-Size Measurement—Several suspensions were formulated with narrow and nearly nonoverlapping particle-size distributions using an adapted sonification technique (3–5). The suspensions were formulated as simply as possible. Viscosity-inducing agents were omitted because their effect on particle-size growth is not known. Particle-size distributions of each suspension were performed with a research microscope[5]. The eye-piece micrometer had been calibrated previously using a stage micrometer.

At least 300 particles were measured for each determination of the particle-size distribution. Microscopic examinations confirmed that the particles were well dispersed with no evidence of agglomeration. At the end of the study, the suspensions were examined again for the mean particle size and distribution; no differences were noted as a function of storage conditions.

Procedure—New Zealand White rabbits without observable eye defects, 1.5–3.0 kg[6] and 2–3 months old, were used. Four to six rabbits were studied at each time interval for each preparation. The animals were randomized with respect to the formulation each received. A single 50-μl dose[7] was administered to the right eye. The lower lid was pulled away from the globe, and the drop was allowed to fall onto the cornea, with the excess falling into the conjunctival sac. The eyelid was returned carefully to its normal position.

The rabbits were sacrificed by rapid injection of 20 cm of air into the marginal ear vein at intervals of 0, 0.33, 0.67, 1, 1.67, 2.5, and 5 hr. Aqueous humor samples of about 0.15 ml were removed from the anterior chamber with a 27-gauge needle attached to a 1-ml tuberculin syringe and were added quantitatively to a counting vial[8] in volumes of 0.125–0.175 ml. Ten milliliters of scintillation fluid[9] was added to each vial.

Immediately following removal of the aqueous humor samples, 8-mm corneal buttons were removed with the use of a trephine[10], blotted once on each side, weighed, and immediately place in a counting vial containing 1.0 ml of tissue solubilizer[11]. The mixture was allowed to stand overnight to permit dissolution of the cornea. Ten milliliters of scintillation fluid[12] then was added to each vial. The vials were allowed to adapt to the dark overnight before counting. A minimum of 10,000 counts was obtained (2% counting error) for each sample. The internal standardization method (6) was used to determine counting efficiencies and, therefore, permitted the quantity of steroid[13] present in each sample to be calculated.

Table I—Particle Statistics for Dexamethasone Suspensions

Suspension	d_{lm}[a], μm	d_{vn}[b], μm	d_{vs}[c], μm	Number of Particles per Dose[d]	*CV* for Randomized System[e], %
A	2.19	3.50	6.75	1,114,200	0.095
B	8.80	9.90	11.50	49,200	0.450
C	18.93	20.4	22.0	5,630	1.3

[a] Length number diameter or arithmetic mean, $\Sigma nd/\Sigma n$. [b] Volume number diameter, $(\Sigma nd^3/\Sigma n)^{1/3}$. [c] Volume surface diameter, $\Sigma nd^3/\Sigma nd^2$. [d] Calculated from the particle number, $6/\pi d_{vn}^3 p$. [e] Calculated from $\sigma = \sqrt{N}$ (from Ref. 7).

RESULTS AND DISCUSSION

The specific activities of Suspensions A, B, and C were 10.3, 11.4, and 11.2 μCi/mg, respectively. The radiochemical purity of each tracer before and after preparation of each suspension as well as at the end of the study was approximately 98%[14]. A particle-size analysis was performed on each suspension prior to use (Fig. 1).

The particle statistics and diameters of each 0.1% dexamethasone suspension are shown in Table I. The mean volume surface diameter, d_{vs}, which emphasizes surface characteristics (7), was used to express the mean particle size. Measurements of 5.75, 11.5, and 22.0 μm were obtained for Suspensions A, B, and C, respectively. The d_{vs} parameter was considered appropriate since the GI absorption rate of poorly soluble, weakly acidic, and, particularly, neutral drugs has been shown to be dissolution rate limited (8–10). After sonification, crystallization continued. The

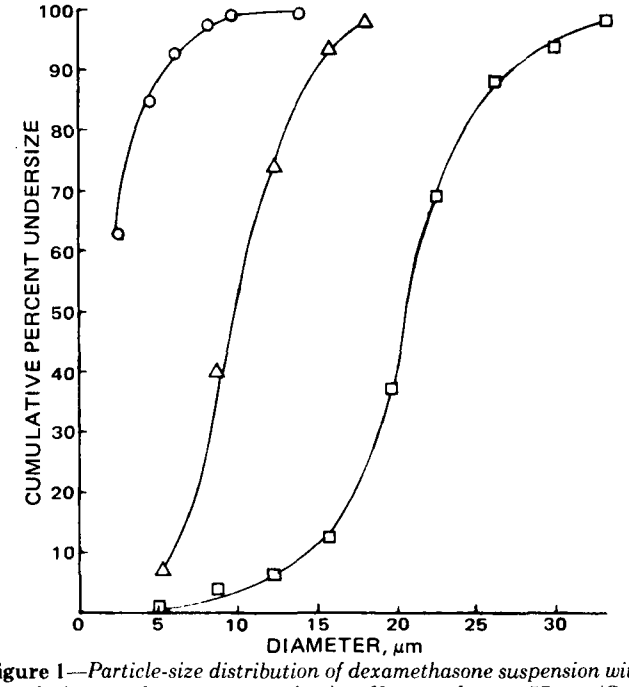

Figure 1—*Particle-size distribution of dexamethasone suspension with cumulative number percent undersize. Key:* ○, d_{vs} = *5.57 μm (Suspension A);* △, d_{vs} = *11.5 μm (Suspension B); and* □, d_{vs} = *22.0 μm (Suspension C).*

[1] Lot 1022-145, [6,7-^{3}H]dexamethasone, New England Nuclear, Boston, Mass.

[2] Lot 18C-01302, Sigma Chemical Co., St. Louis, Mo.

[3] Model W140 sonifier cell disruptor (Heat Systems-Ultrasonics, Plainview, N.Y.) equipped with a QBSP6 probe (Branson Sonic Power Co., Danbury, Conn.)

[4] Millipore.

[5] Bausch & Lomb Optical Co., Rochester, N.Y.

[6] Three rabbits weighed 3 kg, and the remainder weighed between 1.5 and 2.2 kg; data from the larger rabbits fell within the range of data from the smaller rabbits.

[7] Eppendorf pipet, Brinkmann Instruments, Westbury, NY 11590.

[8] Low-potassium glass vials with polyseal cone-lined screw caps, Packard Instrument Co., Downers Grove, IL 60515.

[9] Insta-gel, Packard Instrument Co., Downers Grove, IL 60515.

[10] Martinez disposable corneal trephine, 8 mm, Storz Surgical Instruments, St. Louis, MO 63122.

[11] Soluene 350, Packard Instrument Co., Downers Grove, IL 60515.

[12] Dimilume-30, Packard Instrument Co., Downers Grove, IL 60515.

[13] Quantification of total quantities of tracer does not permit differentiation between metabolites and intact drug. Therefore, *steroid,* as used here, should be considered apparent.

[14] Fifty microliters of each suspension was dissolved in an equal quantity of methanol and chromatographed with chloroform–methanol (9:1). The radiochemical purity was determined using a model 7230 radiochromatographic scanner, Packard Instrument Co., Downers Grove, IL 60515.

Table II—Dexamethasone Concentration in Aqueous Humor and Cornea following Topical Application of 0.1% Suspensions of Varying Mean Particle Size

		Micrograms per Milliliter of Aqueous Humor				Micrograms per Gram of Cornea			
t, hr	Number of Eyes	Suspension A[a]	Suspension B[b]	Suspension C[c]	p	Suspension A[a]	Suspension B[b]	Suspension C[c]	p
0.33	5	0.079 (0.016)[d]	0.061 (0.043)	0.024 (0.006)	<0.01[e]	5.8 (2.56)	4.11 (0.79)	2.50 (1.68)	<0.05
0.67	6	0.215 (0.151)	0.093 (0.013)	0.0696 (0.011)	<0.01[e]	5.01 (2.84)	3.46 (1.18)	2.05 (0.62)	<0.025[e]
1.0	6	0.249 (0.069)	0.103 (0.037)	0.064 (0.023)	<0.01	4.56 (1.14)	2.24 (0.84)	0.412 (0.81)	<0.01
1.67	5	0.193 (0.112)	0.139 (0.083)	0.082 (0.03)	NS	2.81 (2.47)	2.39 (1.22)	1.40 (0.93)	NS
2.5	5	0.106 (0.054)	0.098 (0.020)	0.037 (0.018)	<0.01[e]	1.44 (0.75)	1.44 (0.31)	0.519 (0.25)	<0.025
5.0	4	0.035 (0.091)	0.021 (0.009)	0.009 (0.003)	NS[e]	0.576 (0.36)	0.371 (0.19)	0.221 (0.09)	NS

[a] Mean particle size = 5.75 μm. [b] Mean particle size = 11.5 μm. [c] Mean particle size = 22.0 μm. [d] Number in parentheses represent 1 *SD*. [e] Determined by one-way analysis of variance for heterogeneous variances; all other data sets were determined by the standard one-way analysis of variance for homogeneous variances. NS = not significant or $p > 0.05$.

particle size increased after 2 hr. Relatively narrow distributions were achieved, but some overlap occurred. Removal of crystals from the filter after drying and subsequent handling produced some particle comminution that contributed to this overlap.

The averaged aqueous humor levels of dexamethasone obtained after dosing with the 0.1% preparations are shown in Fig. 2. A rank-order correlation is observed between increasing drug levels and decreasing particle size.

Because of the small sample size used at certain time intervals, a heterogeneous variance resulted. The assumption of homogeneous variances, which is required by a standard one-way analysis of variance, was tested with the use of Bartlett's test of homogeneity of variances (11). Of the 12 time points, five produced χ^2 distributions of $p < 0.05$, indicating heterogeneous variances for these data sets. The remaining seven data sets could be treated with the standard one-way analysis of variance (Table II).

When an equal number of cases (or eyes) is used in each treatment population, the effect of heterogeneous variances is less important in producing erroneous F distributions (12, 13). Nevertheless, an analysis of variance for heterogeneous variances was applied to the appropriate data sets (12, 13). This method differs from the standard method in that the means are weighted according to the reciprocal of the sample variance, and a corrected error mean square term takes the weighting into account (12). An analysis of variance indicated a statistically significant difference for the aqueous humor levels of dexamethasone at each sampling time except the 1.67- and 5-hr intervals. Table II lists the probability values calculated for the data.

Although dissolution rates were not determined for each formulation, the results agree with the expected findings. Suspension A, with its smaller particle size, would be expected to have a more rapid dissolution rate and, providing absorption is dissolution rate controlled, would show a higher C_{max} and an earlier time to peak than Suspension B or C. In comparing Suspensions B and C, Suspension B, which had a smaller particle size, showed a higher C_{max} but had an identical apparent time to peak. More frequent sampling may have permitted a separation of time to peak for Suspensions B and C. The area under the aqueous humor–time curves through the five sampling periods diminished for Suspensions A–C. This effect would occur if the residence time of particles in the conjunctival sac for each suspension was relatively short in comparison to their respective dissolution rates.

Figure 3 shows similar results obtained for corneal levels of drug with time. A statistical difference also was determined between Suspensions A–C for corneal drug levels for most sampling times (Table II). An apparent time to peak was observed at 0.33 hr; however, earlier sampling periods might have indicated an earlier time to peak. The area under each curve shows reduced absorption as the particle size increased.

Suspensions A and B, but not C, showed a parallel decline from 2.5 to 5 hr for the aqueous humor levels. For the corneal data, Suspensions A and C, but not B, showed a parallel decline. The reason for this observation may be related to each suspension; however, more data points in this region are needed to draw a firm conclusion.

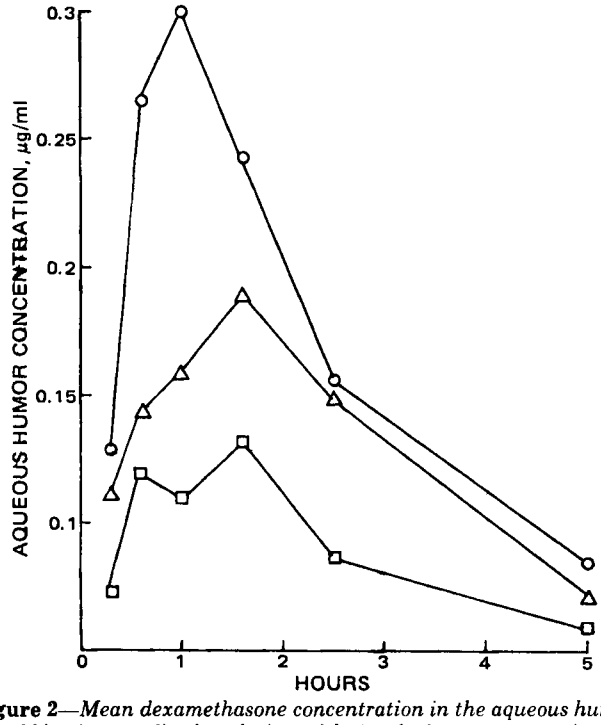

Figure 2—*Mean dexamethasone concentration in the aqueous humor of rabbits* (n = 4–6) *after dosing with 50 μl of 0.1% suspensions of varying particle size. Key:* ○, d_{vs} = *5.75 μm (Suspension A);* △, d_{vs} = *11.5 μm (Suspension B); and* □, d_{vs} = *22.0 μm (Suspension C).*

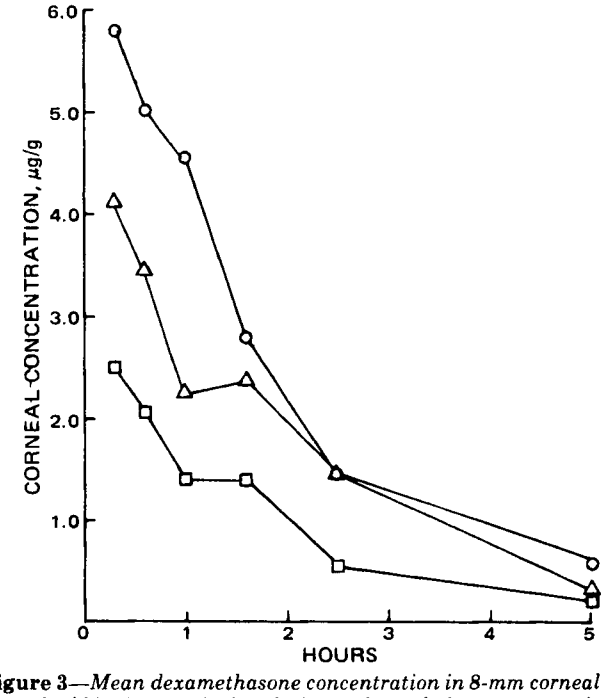

Figure 3—*Mean dexamethasone concentration in 8-mm corneal buttons of rabbits* (n = 4–6) *after dosing with 50 μl of 0.1% suspensions of varying particle size. Key:* ○, d_{vs} = *5.75 μm (Suspension A);* △, d_{vs} = *11.5 μm (Suspension B); and* □, d_{vs} = *22.0 μm (Suspension C).*

According to the data presented, Figs. 2 and 3 suggest that as the particles increase in size, the *in vivo* dissolution rate decreases such that the particles are removed from the conjunctival sac before dissolution is completed. Therefore, both the rate and the extent of penetration into aqueous humor are decreased.

It is possible that as particle size increases, a potential for discomfort is created. As a consequence, tearing could be induced and a progressively decreasing residence time might occur. No clear distinction has been made regarding an upper limit in particle size that would be considered comfortable and, therefore, would not induce tearing. Sieg and Robinson (2) stated that the particle size should be <10 μm to minimize particle irritation in the eye. However, shape and concentration are additional factors that make it difficult to select a specific particle size above which irritation or discomfort might result. From observing the animals during the study, there was no reason to believe that dexamethasone induced tearing at a concentration of 0.1% and an average size of 5.75–22 μm. Nevertheless, the present data do not rule out this possibility.

A potential source of variability between ophthalmic suspensions with different particle sizes could be differences in the amount of the administered dose. Table I lists the volume number diameter, d_{vn}, from which the number of particles per dose can be calculated. In low-strength suspensions such as 0.1% dexamethasone, as the drug particle size increases the number of particles per dose falls rapidly (*i.e.*, inversely with the cube of d_{vn}), potentially increasing the standard deviation of the drug concentration in a randomized dose. The last column in Table I illustrates this point.

Although a limited number of animals was used in the study, the results suggest that ophthalmic dexamethasone suspensions can be optimized for bioavailability by using suspensions with particles as small as possible. This approach would promote a rapid dissolution rate and reduce the chance of tearing and, therefore, would minimize rapid drainage as well as the variability in the quantity of dose administered.

REFERENCES

(1) J. W. Sieg and J. R. Robinson, *J. Pharm. Sci.*, **66**, 1222 (1977).

(2) *Ibid.*, **64**, 931 (1975).

(3) D. M. Skauen, *J. Pharm. Sci.*, **56**, 1373 (1967).

(4) J. R. Principe and D. M. Skauen, *ibid.*, **51**, 389 (1962).

(5) R. M. Cohen and D. M. Skauen, *ibid.*, **53**, 1040 (1964).

(6) C. H. Wang and D. C. Willis, "Radiotracer Methodology in Biological Science," Prentice Hall, Englewood Cliffs, N.J., 1965, pp. 134, 135.

(7) I. C. Edmundson, *Adv. Pharm. Sci.*, **2**, 95 (1967).

(8) J. Fincher, *J. Pharm. Sci.*, **57**, 1825 (1968).

(9) M. Gibaldi, "Biopharmaceutics and Clinical Pharmacokinetics," 2nd ed., Lea & Febiger, Philadelphia, Pa., 1977, pp. 35, 36.

(10) S. Niazi, "Textbook of Biopharmaceutics and Clinical Pharmacokinetics," Appleton-Century-Crofts, New York, N.Y., 1979, p. 29.

(11) G. W. Snedecor and W. G. Cochran, "Statistical Methods," 6th ed., Iowa State University Press, Ames, Iowa, 1967, pp. 296–298.

(12) *Ibid.*, p. 324.

(13) R. R. Sokal and F. J. Rohlf, "Biometry," W. H. Freeman, San Francisco, Calif., 1969, pp. 369–376.

Pharmacokinetics and Bioavailability of Cimetidine in Humans

PETER VENG PEDERSEN [*x] **and RAYMOND MILLER** [‡§]

Received August 28, 1979, from the [*]*Department of Pharmacy, School of Pharmacy, and the* [‡]*Division of Clinical Pharmacology, Department of Medicine, University of California, San Francisco, CA 94143.* Accepted for publication October 18, 1979. [§]Present address: Department of Pharmacology, University of Potchefstroom, Potchefstroom 2520, South Africa.

Abstract □ Cimetidine given orally without food after an overnight fast produces a blood concentration curve with a pronounced second peak that does not appear after parenteral administration or when the drug is taken with food. The following interpretation of this kinetic phenomenon is proposed: 1. The drug cumulates in a tissue or organ that is well perfused in the first-pass transfer. 2. The hepatic parenchymal tissue and the bile phase are the most likely storage areas. 3. The high capacity of the cumulation may be due to the formation of conjugates or other modifications of the drug with a pronounced affinity for the hepatic–biliary system. 4. The rate of cumulation is much higher in the first-pass transfer than from the systemic circulation, possibly due to the difference in the drug concentrations and the conjugation rate. 5. The cumulation appears to occur by a competitive process. 6. Absorbed elements of food seem to compete in this process. 7. The second peak apparently is the result of a rapid release of drug and bioreversible drug compounds from the hepatic–biliary system with subsequent reabsorption. 8. This release may occur spontaneously but appears to be triggered by food intake. A pharmacokinetic model constructed according to this interpretation showed good agreement with data from oral, intravenous, and intramuscular administration. The special problems associated with the evaluation of bioavailability in the presence of reabsorption are discussed.

Keyphrases □ Cimetidine—pharmacokinetics, bioavailability, humans □ Pharmacokinetics—cimetidine, humans □ Bioavailability—cimetidine, humans

Blood levels of cimetidine in humans after oral dosing (1–8) and intravenous administration (2, 5, 6) have been analyzed with respect to the pharmacological response (2), influence of a meal on absorption (3), biliary distribution and secretion (4), and bioavailability (1, 5, 6). The drug shows unusual pharmacokinetic behavior in producing a significant secondary peak in the drug concentration profile after oral dosing on a fasting stomach but not after intravenous administration (5–7). No attempts have been made to describe the pharmacokinetics of the phenomenon.

A conventional two-exponential model has been applied (6), but such a model does not account for the secondary peaks. Bodemar *et al.* (8) stated that: "A second absorption peak could be explained by enterohepatic circulation of cimetidine, although a preliminary report by Spence *et al.* (4) seems almost to exclude this possibility." Considering the possibility of delayed absorption of some of the cimetidine or a varying absorption rate at different segments of the GI tract (6), the same authors (1) stated that: "Calculations from the present results indicate that the consideration from a hypothetical delayed absorption is as much as 50% of total *AUC* in some patients. Delayed absorption of this magnitude, however, is unlikely and this second peak following oral administration of cimetidine remains to be explained."

This study was intended to evaluate the pharmacokinetics of cimetidine and to explain its kinetic discrepancy using the data of Walkenstein *et al.* (5). It is proposed that the phenomenon can be described best in terms of discontinuous reabsorption. The special problems associated with the evaluation of bioavailability in the presence of reabsorption are discussed.

0022-3549/80/0400-0394$01.00/0

© 1980, American Pharmaceutical Association

According to the data presented, Figs. 2 and 3 suggest that as the particles increase in size, the *in vivo* dissolution rate decreases such that the particles are removed from the conjunctival sac before dissolution is completed. Therefore, both the rate and the extent of penetration into aqueous humor are decreased.

It is possible that as particle size increases, a potential for discomfort is created. As a consequence, tearing could be induced and a progressively decreasing residence time might occur. No clear distinction has been made regarding an upper limit in particle size that would be considered comfortable and, therefore, would not induce tearing. Sieg and Robinson (2) stated that the particle size should be <10 μm to minimize particle irritation in the eye. However, shape and concentration are additional factors that make it difficult to select a specific particle size above which irritation or discomfort might result. From observing the animals during the study, there was no reason to believe that dexamethasone induced tearing at a concentration of 0.1% and an average size of 5.75–22 μm. Nevertheless, the present data do not rule out this possibility.

A potential source of variability between ophthalmic suspensions with different particle sizes could be differences in the amount of the administered dose. Table I lists the volume number diameter, d_{vn}, from which the number of particles per dose can be calculated. In low-strength suspensions such as 0.1% dexamethasone, as the drug particle size increases the number of particles per dose falls rapidly (*i.e.*, inversely with the cube of d_{vn}), potentially increasing the standard deviation of the drug concentration in a randomized dose. The last column in Table I illustrates this point.

Although a limited number of animals was used in the study, the results suggest that ophthalmic dexamethasone suspensions can be optimized for bioavailability by using suspensions with particles as small as possible. This approach would promote a rapid dissolution rate and reduce the chance of tearing and, therefore, would minimize rapid drainage as well as the variability in the quantity of dose administered.

REFERENCES

(1) J. W. Sieg and J. R. Robinson, *J. Pharm. Sci.*, **66**, 1222 (1977).

(2) *Ibid.*, **64**, 931 (1975).

(3) D. M. Skauen, *J. Pharm. Sci.*, **56**, 1373 (1967).

(4) J. R. Principe and D. M. Skauen, *ibid.*, **51**, 389 (1962).

(5) R. M. Cohen and D. M. Skauen, *ibid.*, **53**, 1040 (1964).

(6) C. H. Wang and D. C. Willis, "Radiotracer Methodology in Biological Science," Prentice Hall, Englewood Cliffs, N.J., 1965, pp. 134, 135.

(7) I. C. Edmundson, *Adv. Pharm. Sci.*, **2**, 95 (1967).

(8) J. Fincher, *J. Pharm. Sci.*, **57**, 1825 (1968).

(9) M. Gibaldi, "Biopharmaceutics and Clinical Pharmacokinetics," 2nd ed., Lea & Febiger, Philadelphia, Pa., 1977, pp. 35, 36.

(10) S. Niazi, "Textbook of Biopharmaceutics and Clinical Pharmacokinetics," Appleton-Century-Crofts, New York, N.Y., 1979, p. 29.

(11) G. W. Snedecor and W. G. Cochran, "Statistical Methods," 6th ed., Iowa State University Press, Ames, Iowa, 1967, pp. 296–298.

(12) *Ibid.*, p. 324.

(13) R. R. Sokal and F. J. Rohlf, "Biometry," W. H. Freeman, San Francisco, Calif., 1969, pp. 369–376.

Pharmacokinetics and Bioavailability of Cimetidine in Humans

PETER VENG PEDERSEN [*x] **and RAYMOND MILLER** [‡§]

Received August 28, 1979, from the [*]*Department of Pharmacy, School of Pharmacy, and the* [‡]*Division of Clinical Pharmacology, Department of Medicine, University of California, San Francisco, CA 94143.* Accepted for publication October 18, 1979. [§]Present address: Department of Pharmacology, University of Potchefstroom, Potchefstroom 2520, South Africa.

Abstract □ Cimetidine given orally without food after an overnight fast produces a blood concentration curve with a pronounced second peak that does not appear after parenteral administration or when the drug is taken with food. The following interpretation of this kinetic phenomenon is proposed: 1. The drug cumulates in a tissue or organ that is well perfused in the first-pass transfer. 2. The hepatic parenchymal tissue and the bile phase are the most likely storage areas. 3. The high capacity of the cumulation may be due to the formation of conjugates or other modifications of the drug with a pronounced affinity for the hepatic–biliary system. 4. The rate of cumulation is much higher in the first-pass transfer than from the systemic circulation, possibly due to the difference in the drug concentrations and the conjugation rate. 5. The cumulation appears to occur by a competitive process. 6. Absorbed elements of food seem to compete in this process. 7. The second peak apparently is the result of a rapid release of drug and bioreversible drug compounds from the hepatic–biliary system with subsequent reabsorption. 8. This release may occur spontaneously but appears to be triggered by food intake. A pharmacokinetic model constructed according to this interpretation showed good agreement with data from oral, intravenous, and intramuscular administration. The special problems associated with the evaluation of bioavailability in the presence of reabsorption are discussed.

Keyphrases □ Cimetidine—pharmacokinetics, bioavailability, humans □ Pharmacokinetics—cimetidine, humans □ Bioavailability—cimetidine, humans

Blood levels of cimetidine in humans after oral dosing (1–8) and intravenous administration (2, 5, 6) have been analyzed with respect to the pharmacological response (2), influence of a meal on absorption (3), biliary distribution and secretion (4), and bioavailability (1, 5, 6). The drug shows unusual pharmacokinetic behavior in producing a significant secondary peak in the drug concentration profile after oral dosing on a fasting stomach but not after intravenous administration (5–7). No attempts have been made to describe the pharmacokinetics of the phenomenon.

A conventional two-exponential model has been applied (6), but such a model does not account for the secondary peaks. Bodemar *et al.* (8) stated that: "A second absorption peak could be explained by enterohepatic circulation of cimetidine, although a preliminary report by Spence *et al.* (4) seems almost to exclude this possibility." Considering the possibility of delayed absorption of some of the cimetidine or a varying absorption rate at different segments of the GI tract (6), the same authors (1) stated that: "Calculations from the present results indicate that the consideration from a hypothetical delayed absorption is as much as 50% of total *AUC* in some patients. Delayed absorption of this magnitude, however, is unlikely and this second peak following oral administration of cimetidine remains to be explained."

This study was intended to evaluate the pharmacokinetics of cimetidine and to explain its kinetic discrepancy using the data of Walkenstein *et al.* (5). It is proposed that the phenomenon can be described best in terms of discontinuous reabsorption. The special problems associated with the evaluation of bioavailability in the presence of reabsorption are discussed.

0022-3549/80/0400-0394$01.00/0

© 1980, American Pharmaceutical Association

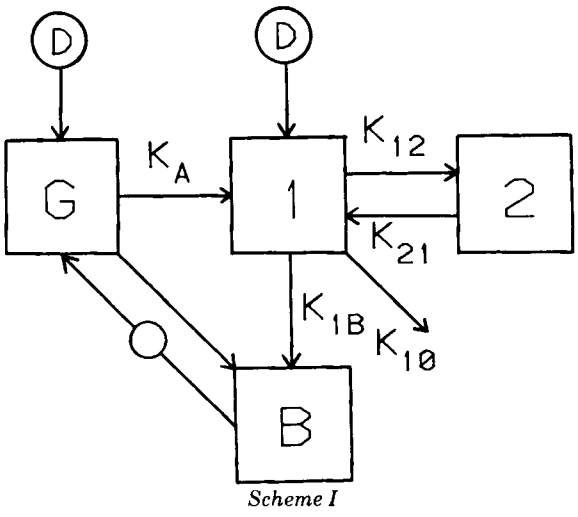

Scheme I

THEORY

The proposed pharmacokinetic model (Scheme I) was developed considering the reported kinetic behavior of cimetidine and encompasses the kinetics after oral, intravenous, and intramuscular administration.

Oral Administration—The drug is presented into the absorption compartment, G (the gut), where a fraction, F_{G1}, of the dose, D, is absorbed by a first-order process into the central, sampleable compartment, 1. The remaining fraction, $1 - F_{G1}$, of the drug goes into a compartment, B, in the first-pass transfer process. No assumptions are made about the type of transfer process from G to B because the kinetic behavior of the system does not depend on the rate of input into B but only on the amount of drug in B at a particular time, T_B. At this time, a fraction, F_B, of the drug cumulated in B is released momentarily into the absorption compartment.

The first-pass elimination reported for cimetidine (5, 6) is incorporated into $1 - F_{G1}$ for simplification. The drug is eliminated from the central compartment and transferred into compartment B and a peripheral compartment, 2, by first-order processes.

Intravenous and Intramuscular Administration—It has been shown that there are no significant differences in the blood level profiles between intravenous and intramuscular administration (5). The absorption from an intramuscular injection appears so rapidly that kinetically it can be considered as an intravenous administration. Therefore, the same model was applied for the two administrations. It is the same model as discussed, except that the input is a bolus input into the central compartment.

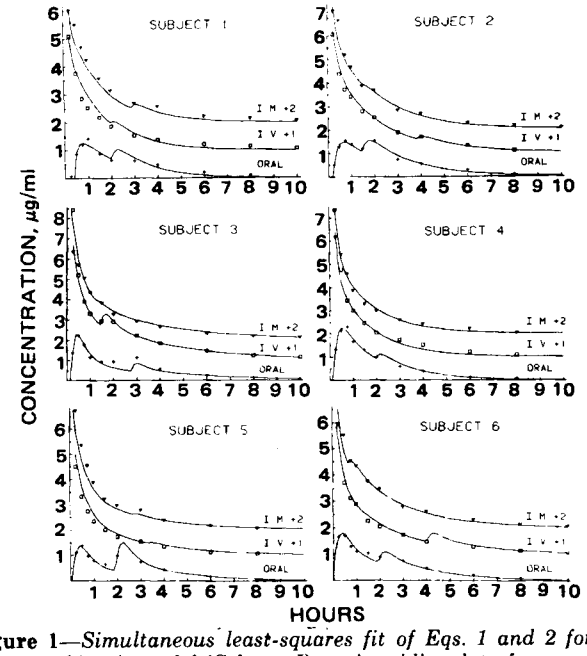

Figure 1—*Simultaneous least-squares fit of Eqs. 1 and 2 for the pharmacokinetic model (Scheme I) to cimetidine data from oral, intravenous, and intramuscular administration. The curves and data are staggered vertically one unit for clarity.*

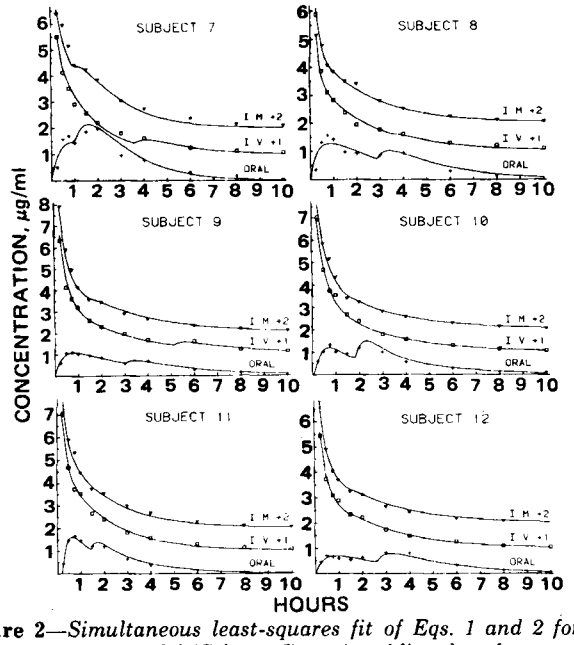

Figure 2—*Simultaneous least-squares fit of Eqs. 1 and 2 for the pharmacokinetic model (Scheme I) to cimetidine data from oral, intravenous, and intramuscular administration. The curves and data are staggered vertically one unit for clarity.*

The differences in the response profiles with respect to the presence or the absence of the secondary peak from an oral or parenteral administration is accounted for by the relative magnitude of the transfer rate of the drug from G to B and from 1 to B. A significant G to B transfer gives rise to a pronounced secondary peak. However, a slow 1 to B transfer, competing with elimination and distribution, results in only a small drug cumulation in B and an insignificant secondary peak, which may be difficult to detect in the blood level data (Figs. 1 and 2).

The choice of a discontinuous cyclic transfer process in the model is justified from physiological considerations (9, 10). Theoretical as well as simulation studies also indicate that secondary peaks cannot be obtained from linear compartmental systems with continuous cyclic transfer processes (11, 12).

Regression Equations—The following response equations are readily derived by standard means (13). After intravenous and intramuscular administration:

$$c = \frac{D}{V}[a_1e^{-\lambda_1 t} + a_2e^{-\lambda_2 t}] + \frac{K_A F_B D_B}{V}[a_3e^{-K_A(t-T_B)+} - a_4e^{-\lambda_1(t-T_B)+} - a_5e^{-\lambda_2(t-T_B)+}] \quad \text{(Eq. 1)}$$

and after oral administration:

$$c = \frac{K_A}{V}[F_{G1}D(a_3e^{-K_A(t-T_L)+} - a_4e^{-\lambda_1(t-T_L)+} - a_5e^{-\lambda_2(t-T_L)+}) + F_B D_B(a_3e^{-K_A(t-T_B)+} - a_4e^{-\lambda_1(t-T_B)+} - a_5e^{-\lambda_2(t-T_B)+})] \quad \text{(Eq. 2)}$$

where:

$$a_1 = (K_{21} - \lambda_1)/(\lambda_2 - \lambda_1) \quad \text{(Eq. 3)}$$

$$a_2 = (K_{21} - \lambda_2)/(\lambda_1 - \lambda_2) \quad \text{(Eq. 4)}$$

$$a_3 = (K_{21} - K_A)/(\lambda_1 - K_A)(\lambda_2 - K_A) \quad \text{(Eq. 5)}$$

$$a_4 = (K_{21} - \lambda_1)/(\lambda_1 - K_A)(\lambda_2 - \lambda_1) \quad \text{(Eq. 6)}$$

$$a_5 = (K_{21} - \lambda_2)/(\lambda_2 - K_A)(\lambda_1 - \lambda_2) \quad \text{(Eq. 7)}$$

and where after intravenous and intramuscular administration:

$$D_B = K_{1B}D\left[\frac{a_1}{\lambda_1}(1 - e^{-\lambda_1 T_B}) + \frac{a_2}{\lambda_2}(1 - e^{-\lambda_2 T_B})\right] \quad \text{(Eq. 8)}$$

while after oral administration:

$$D_B = X_B + (1 - F_{G1})D \quad \text{(Eq. 9)}$$

Table I—Least-Squares Parameter Estimates

Parameter	Subject 1	2	3	4	5	6	7	8	9	10	11	12	Mean (*CV*, %)
T_L	0.41	0.19	0.18	0.15	0.10	0.04	0.00	0.03	0.00	0.13	0.21	0.02	0.12 (99)
T_B (iv), hr	2.00	3.81	1.47	3.42	3.34	4.01	3.58	3.52	5.13	0.93	0.80	1.41	2.78 (50)
T_B (im), hr	2.88	1.51	1.25	1.25	2.70	0.65	0.96	0.75	1.50	1.51	0.45	1.50	1.41 (53)
T_B (po), hr	2.04	1.46	2.76	1.96	1.93	1.94	1.00	2.90	3.00	1.82	1.44	2.60	2.07 (30)
K_A, hr^{-1}	2.24	2.80	7.75	2.59	6.22	3.68	1.21	1.22	1.04	1.91	2.81	0.95	2.87 (74)
K_{12}, hr^{-1}	7.12	1.42	0.92	2.27	0.69	2.02	1.50	2.32	1.41	0.90	1.86	1.70	2.01 (84)
K_{21}, hr^{-1}	3.20	2.24	0.84	2.09	0.96	1.77	3.15	1.91	1.15	0.91	1.95	1.40	1.80 (45)
K_{1B}, hr^{-1}	0.95	0.19	0.44	0.0003	0.06	0.65	0.67	0.16	0.81	0.08	0.11	0.32	0.37 (88)
K_{el}, hr^{-1}	2.75	0.92	0.82	1.56	0.95	1.17	1.03	1.08	1.01	0.95	1.13	1.18	1.21 (43)
F_{G1}	0.37	0.39	0.41	0.57	0.37	0.48	0.62	0.62	0.44	0.36	0.39	0.36	0.45 (22)
F_B (iv)	0.21	0.27	0.50	0.21	0.42	0.21	0.20	0.27	0.13	0.64	0.19	0.34	0.30 (51)
F_B (im)	0.20	0.28	0.10	0.20	0.40	0.61	0.80	0.30	0.12	0.43	0.19	0.32	0.33 (63)
F_B (po)	0.20	0.28	0.10	0.20	0.50	0.20	0.80	0.50	0.12	0.44	0.20	0.32	0.32 (63)
V, liters	15.7	35.2	35.0	25.3	51.2	33.9	40.0	36.2	31.0	34.7	28.5	34.6	33.5 (25)

where:

$$X_B = K_{1B}K_AF_{G1}D\left[\frac{a_3}{K_A}(1 - e^{-K_A(T_B-T_L)}) - \frac{a_4}{\lambda_1}(1 - e^{-\lambda_1(T_B-T_L)}) - \frac{a_5}{\lambda_2}(1 - e^{-\lambda_2(T_B-T_L)})\right] \quad \text{(Eq. 10)}$$

The truncation function used in Eqs. 1 and 2 is defined by:

$$(x)_+ = \max(0,x) \quad \text{(Eq. 11)}$$

Data Treatment[1]—With the interactive program FUNFIT (14), Eqs. 1 and 2 were fitted simultaneously by nonlinear least-squares regression to the oral, intravenous, and intramuscular data for each of the 12 subjects (5). All estimated microparameters are common for the functions describing the intravenous, intramuscular, and oral data except for the time, T_B, and the fraction, F_B, of drug release from B (Table I).

RESULTS AND DISCUSSION

To elucidate the unusual kinetic behavior of cimetidine, it is appropriate to summarize the most pertinent findings in the literature:

F1. Cimetidine taken orally without food after an overnight fast produces a pronounced secondary peak in most subjects (1, 5).

F2. The secondary peak does not seem to be present when the drug is taken orally with food (1).

F3. Intravenous and intramuscular administrations of cimetidine do not result in secondary peaks as occur after oral administration (1, 5).

F4. With food, the initial rise in plasma cimetidine concentration appears more slowly than if the drug is taken without food on a fasting stomach (1, 3).

F5. Mean blood levels after equal doses of cimetidine given orally or parenterally do not differ significantly after 4 hr (5, 6).

F6. The drug appears to be completely and rapidly absorbed in the therapeutic dosing range after oral administration (1, 5).

F7. The extent of absorption apparently does not differ when the drug is administered on a fasting stomach with or without food (1).

F8. The bioavailability of the drug after oral administration is ~70% of the intravenous bioavailability. The reduction appears to be due to a first-pass effect rather than a drug release rate-limited absorption (1, 5).

F9. The *AUC* appears to be proportional to the oral dose in the therapeutic dosing range (1, 6).

F10. Cimetidine is eliminated mainly *via* the kidneys (2). An average of 0.75 of the drug is recovered unchanged in the urine after parenteral administration, while only 0.5 of it is recovered after oral administration (5).

F11. A small amount of material derived from cimetidine is excreted in the feces after intravenous administration of radiolabeled drug (6).

F12. The fecal radioactivity accounts for an average of 10% of orally administered labeled cimetidine regardless of the dose (400 or 800 mg) (6).

F13. An average of 70% of the radioactivity administered is recovered in the urine of healthy human subjects after an oral dose of 200 mg of labeled cimetidine.

F14. The concentration of cimetidine is approximately five times higher in the bile than in the blood of patients undergoing exploratory surgery of the common bile duct (4).

F15. The conjugation reaction is of considerable significance for the biliary excretion of a drug since it produces a substrate with particularly suitable properties for the hepatic system (15–17).

F16. Several isolated studies on the fate of orally administered conjugates indicate that they are reabsorbed largely after hydrolysis in the gut and that this step is important in relation to the enterohepatic cycle (15, 17, 18).

F17. Substances showing a bile–blood concentration ratio substantially larger than one appear to be transferred into the bile across the parenchymal cell wall by an active transport process (4, 15).

F18. Substances actively transferred by the liver cells compete for transport across the hepatic membrane into the bile (15, 19–22).

F19. Many compounds secreted in the bile have a marked affinity for localizing in hepatic parenchymal tissue (22–24).

F20. The gallbladder releases most of its bile content into the duodenum shortly after the intake of a meal, particularly when the meal is eaten on a fasting stomach (9, 10).

F21. The release of bile into the duodenum stimulates the flow of pancreatic juice (25).

F22. Spontaneous contractions of the gallbladder occur in the fasting stage (9).

F23. The volume difference between a full and contracted gallbladder is ~30–50 cm^3 (9).

F24. It takes the gallbladder 1.5–2 hr to fill after a full contraction (9).

F25. Cimetidine results in marked inhibition of both gastric acid and pepsin secretion (2).

Kinetic Interpretation—In studying the cimetidine data from intravenous, intramuscular, and oral administrations (1, 5) together with the described findings, the following interpretation of this drug's unusual kinetic behavior was reached:

1. The secondary peak appears to be due to a rapid release from a drug depot. The depot is located in a tissue or organ that is well perfused by the drug in the first-pass transfer. The bile and the hepatic parenchymal tissues are the most likely primary storage areas (F11, F14, F15, F19, and F20) (26).

2. The time for the release appears to coincide with the intake of food in most cases. The 2-hr interval between oral drug intake and breakfast agrees well with the start of the second peak (Figs. 1 and 2). The mean value of T_B is 2.1 hr (Table I) (F20 and F22).

3. Drug transfer into the depot occurs mainly in the first-pass process (F1 and F3).

4. This transfer is significantly inhibited, possibly by the way of competitive active membrane transport, when the drug is taken with food (F2, F17, and F18). The excretion of bile in response to food also may play a role if the smaller amount of bile in the hepatic system reduces the uptake rate or capacity of the system.

5. The transfer rate of drug into the depot from the systemic circulation is slow compared to the first-pass transfer (F1 and F3). This effect possibly is due to a pronounced drug concentration difference at the depot site for the two administration routes. The drug concentration is large in the first-pass perfusion of the depot organ before the drug reaches the general systemic circulation. However, when the drug is introduced parenterally in the systemic circulation, a substantial dilution takes place before it reaches the depot organ. The higher metabolic activity at the first-pass route also may contribute to a larger uptake of drug by the

[1] The figures were drawn by a Tektronix 4662 penplotter controlled by an IBM 370/145 computer.

Table II—Pharmacokinetic Parameters

Parameter	Subject 1	2	3	4	5	6	7	8	9	10	11	12	Mean (*CV*, %)
$t_{1/2}$, hr	0.98	1.37	2.28	1.13	1.67	1.51	1.08	1.64	1.92	1.92	1.40	1.70	1.55 (25)
AUC (iv), μg/ml/hr	7.35	9.73	11.85	7.60	6.32	8.35	8.13	7.89	10.49	9.31	9.38	7.74	8.68 (18)
AUC (im), μg/ml/hr	7.39	9.59	10.69	7.60	6.31	7.91	9.18	7.77	10.14	9.27	9.36	7.73	8.58 (15)
AUC (po), μ/ml/hr	3.57	5.32	5.06	5.01	4.29	4.67	7.30	6.41	5.13	5.86	4.84	4.27	5.14 (20)
D (iv)/ *AUC* (iv), liters/hr	40.8	30.8	25.3	39.5	47.5	35.9	36.9	38.0	28.6	32.2	32.0	38.7	35.5 (17)
D (im)/ *AUC* (im), liters/hr	40.6	31.3	28.1	39.5	47.6	37.9	32.7	38.6	29.6	32.5	32.0	38.8	35.8 (16)
D_T[a]/ *AUC* (po), liters/hr	43.1	32.4	28.8	39.5	48.5	39.6	41.3	39.3	31.2	33.0	32.2	40.8	37.5 (16)
$V \cdot K_{el}$, liters/hr	43.1	32.4	28.8	39.5	48.5	39.6	41.3	39.3	31.2	33.0	32.2	40.8	37.5 (16)
AUC (po)/ *AUC* (iv)	0.49	0.55	0.43	0.66	0.68	0.56	0.90	0.83	0.49	0.63	0.52	0.55	0.61 (23)
AUC (po)/ *AUC* (im)	0.48	0.56	0.47	0.66	0.68	0.59	0.80	0.81	0.51	0.63	0.52	0.55	0.64 (24)
D_T[a]/ *D* (po)	0.51	0.57	0.49	0.66	0.69	0.62	1.00	0.84	0.53	0.65	0.52	0.58	0.64 (24)

[a] $D_T = FD$ (po) + $F_B D_b$ (po).

depot (F8, F15, and F16).

6. Cimetidine possibly is stored in the depot both in the parent form and as conjugates or complexes. The large capacity of the hepatic system for storage and biliary excretion of conjugates may explain the magnitude of the secondary peak (F15 and F16).

Capacity of Hepatic System for Recycling—The theory of enterohepatic recycling to explain the second peak phenomenon has been criticized mainly because of the magnitude of the peak relative to the concentration of cimetidine found in the bile (4) and the estimated amount of bile secreted by the hepatic system into the intestine (9). However, it is difficult to evaluate the mechanism and capacity of the hepatic system for drug recycling. Data obtained with chronic biliary fistulas or with draining T-tubes after cholecystectomy may have to be interpreted with caution because of the inevitable loss of bile salts (27). In addition, liver disease in humans is a collection of functional and structural disabilities including inflammatory, neoplastic, and degenerative disorders in which the parenchyma, the biliary tree, and the vascular supply may be substantially affected (28, 29). Therefore, the disease state of the patient would play a significant role in the biliary excretion of the drug.

The studies of biliary secretion of cimetidine involved patients undergoing exploratory surgery of the common bile duct (4). Presumably, the patients did not have a normal hepatic–biliary function. The surgery seems to have had a pronounced effect on the pharmacokinetics since the peak venous concentration of cimetidine often differed by more than 100% in the same individual during the study. In contrast, the nonoperative studies involving healthy subjects showed a remarkably small intraindividual variation in the blood drug levels (1, 5). The concentration of cimetidine in the bile found in the operative study (4) apparently was based on an assay that considers only free, untransformed drugs (3). Conjugates or other modifications that may be present in high concentrations (F15) and may be responsible for a significant recycling (F16) apparently were not included.

Pharmacokinetic Model—The pharmacokinetic model proposed (Scheme I) is a highly simplified functional model constructed according to the given interpretation. The *B* compartment represents the depot of the drug that is partly released, F_B, at some time, T_B, soon after or during a meal or spontaneously before a meal (F22). The model appears to agree well with the data (Figs. 1 and 2) and shows that the transfer of the drug into *B* in the first pass (*G* to *B*) is primarily responsible for the cumulation of the drug in *B* while the systemic transfer (1 to *B*) only plays a minor role (Figs. 1 and 2 and Table I).

The least-squares estimate of T_B after oral administration is 2.1 hr, which is not significantly different from the time (2 hr) for the intake of food after oral drug administration (F20). Although it is difficult to detect a secondary peak or hump in the data from the parenteral administrations, nonlinear regression analysis indicates a small degree of recycling in some cases (Figs. 1 and 2). However, due to the sparseness and limited accuracy of the data, it is difficult to determine T_B and the magnitude of the recycling effect after parenteral administration. This situation is reflected in the coefficients of variation of the T_B values; they are approximately the same for intravenous and intramuscular administrations but significantly larger than those for oral administration (Table I).

Bioavailability—An interesting aspect of the recycling phenomenon is its influence on the *AUC* values and the interpretation of bioavailability calculations based on comparisons of such values. The ratio between *AUC* values in such cases cannot be used as a relative measure of the extent of drug absorption since the *AUC* is dependent on the extent of recycling. Therefore, the *AUC* does not properly reflect the extent of primary absorption. Thus, the evaluation of the extent of first-pass effect and the evaluation of bioequivalency of oral drug delivery systems are complicated using the model-independent *AUC* approach, so other techniques may be worth considering. However, the *AUC* still is a useful parameter since, physiologically and pharmacologically, it is a more meaningful parameter than a parameter that measures the extent of primary absorption.

By using the intravenous and intramuscular administrations as reference dosage forms and the integrated form of the regression equations to calculate the *AUC* values, the bioavailability of the oral dosage was 0.61 in both cases (Table II). This value corresponds well to the reported values of 0.62 and 0.59 obtained by log-linear trapezoidal integration (5).

It is evident that in the presence of recycling it is not possible to calculate *F*, the fraction of the dose given that reaches the systemic circulation, by a model-independent approach. With the present model, *F* can be calculated according to:

$$F = (F_{G1}D + F_B D_B)/D \qquad \text{(Eq. 12)}$$

The mean value of 0.64 obtained in this way (Table II) agrees with the quantities of drug and drug metabolites found in the urine and the feces (F10, F12, and F13).

The oral data showing the pronounced secondary peak were from an oral administration taken on a fasting stomach without food. Two hours was allowed to pass before food intake. Other investigations indicated that the second peak will not be present when cimetidine is taken orally with food (1). It has been recommended that cimetidine be taken with food to obtain the best therapeutic effect. Thus, the second peak seems to be an artifact from the experimental design and may not be of much significance in the practical therapeutic setting. This result raises the question of how appropriate it is to fast a subject before and during a pharmacokinetic study. It may not be appropriate if the objective is to estimate the normal pharmacokinetic behavior of a population or to provide practical guidelines for dosage regimens.

However, the particular experimental design does reveal an interesting pharmacokinetic phenomenon that may be of significance in organ and

tissue specific drug delivery, chemotherapy, and treatment of inflammatory and infectious diseases of the liver and biliary system.

NOTATIONS

$AUC = \int_0^\infty c\,dt$
B = drug depot compartment
c = blood cimetidine concentration
D = dose
$D_B = X_B + (1 - F_{G1})D$
$D_T = F_{G1}D + F_BD_B$, the apparent amount of the dose absorbed
$F = (F_{G1}D + F_BD_B)/D$, the apparent fraction of the dose absorbed
F_B = fraction of drug cumulated in B that is released to G at time $t = T_B$
F_{G1} = fraction of D absorbed by first-order absorption into the central compartment
$1 - F_{G1}$ = fraction of D transferred from G to B
G = compartment from which absorption takes place
K_{xx} = first-order transfer rate constants
$-\lambda_1, -\lambda_2$ = eigenvalues of the linear system
t = time
T_L = lag time
T_B = time when a part (F_BD_B) of the drug cumulated in B is released to G
V = volume of distribution
X_B = amount of drug transferred from compartment 1 to compartment B at time $t = T_B$

REFERENCES

(1) G. Bodemar, B. Norlander, L. Fransson, and A. Walan, *Br. J. Clin. Pharmacol.*, 7, 22 (1979).

(2) W. L. Burland, W. A. M. Duncan, T. Hesselbo, J. G. Mills, and P. C. Sharpe, *ibid.*, 2, 481 (1975).

(3) R. W. Spence, D. R. Creak, and L. R. Celestin, *Digestion*, **14**, 127 (1976).

(4) R. W. Spence, L. R. Celestin, R. De La Guardia, C. A. McMullen, and D. A. McCormick, "Proceedings of the Second International Symposium on Histamine H_2-Receptor Antagonists," Excerpta Medica, Amsterdam, The Netherlands, 1977, p. 81.

(5) S. S. Walkenstein, J. W. Dubb, W. C. Randolph, W. J. Westlake, R. M. Stote, and A. P. Intoccia, *Gastroenterology*, **74**, 360 (1978).

(6) R. Griffiths, R. M. Lee, and D. C. Taylor, "Proceedings of the Second International Symposium on Histamine H_2-receptor Antagonists, Excerpta Medica, Amsterdam, The Netherlands, 1977, p. 38.

(7) R. H. Henn, J. I. Isenberg, V. Maxwell, and R. A. L. Sturdevant, *N. Engl. J. Med.*, **293**, 371 (1975).

(8) G. Bodemar, B. Norlander, and A. Walan, "Proceedings of the Second International Symposium on Histamine H_2-receptor Antagonists," Excerpta Medica, Amsterdam, The Netherlands, 1977, p. 224.

(9) E. A. Boyden, *Anat. Rec.*, **40**, 147 (1928).

(10) *Ibid.*, **33**, 201.

(11) P. Veng Pedersen and R. Miller, *J. Pharm. Sci.*, **69**, 204 (1980).

(12) C. D. Thorn, *Bull. Math. Biophys.*, **34**, 277 (1972).

(13) P. Veng Pedersen, *J. Pharm. Sci.*, **67**, 187 (1978).

(14) P. Veng Pedersen, *J. Pharmacokinet. Biopharm.*, **5**, 513 (1977).

(15) R. L. Smith, *Prog. Drug. Res.*, **9**, 299 (1966).

(16) A. A. Sandberg and W. R. Slaunwhite, *J. Clin. Invest.*, **35**, 1331 (1956).

(17) K. E. Anderson, B. Bergdahl, and G. Wettrell, *Eur. J. Clin. Pharmacol.*, **11**, 273 (1977).

(18) A. J. Quick, *J. Biol. Chem.*, **97**, 403 (1932).

(19) W. B. Bradley and A. C. Ivy, *Proc. Soc. Exp. Biol. Med.*, **45**, 145 (1940).

(20) A. Cantarow and C. W. Wirts, *Am. J. Dig. Dis.*, **10**, 261 (1943).

(21) C. W. Wirts, A. Cantarow, W. J. Sanpe, and B. Delserone, *Am. J. Physiol.*, **165**, 680 (1951).

(22) V. Hanzon, *Acta Physiol. Scand., Suppl. 101*, **28**, 1 (1952).

(23) R. W. Brauer and R. L. Pessotti, *Am. J. Physiol.*, **162**, 565 (1950).

(24) R. Bine, M. Friedman, S. O. Byers, and C. Bland, *Circulation*, **4**, 105 (1951).

(25) J. Mellanky, *Lancet*, **2**, 215 (1926).

(26) S. A. M. Cross, "Proceedings, 18th Meeting of the European Society of Toxicology, Edinburgh," Excerpta Medica, Amsterdam, The Netherlands, 1977, p. 105.

(27) T. Hargreaves, "The Liver and Bile Metabolism," Appleton-Century-Crofts, New York, N.Y., 1968, p. 39.

(28) R. K. Roberts, P. V. Desmond, and S. Schenker, *Drugs*, **17**, 198 (1979).

(29) *Ibid.*, **17**, 198 (1979).

ACKNOWLEDGMENTS

Supported in part by the South African Medical Research Council.

Human Pharmacokinetics of a New Broad-Spectrum Parenteral Cephalosporin Antibiotic, Ceforanide

MORRIS PFEFFER ˣ, ROBERT C. GAVER, and DONALD R. VAN HARKEN

Received July 14, 1977, from the *Department of Drug Metabolism and Pharmacokinetics, Bristol Laboratories, Syracuse, NY 13201.* Accepted for publication October 26, 1979.

Abstract □ The pharmacokinetics of the *l*-lysine salt of ceforanide were studied after intravenous administration of 1132 and 2264 mg as 30-min constant-rate infusions and after intramuscular administration of 556 and 1132 mg. The peak intravenous plasma concentrations were 136 and 222 μg/ml at termination of infusion, and 12-hr trough concentrations were 5.9 and 9.0 μg/ml, respectively. The peak intramuscular plasma concentrations were 38 and 74 μg/ml at 1.0–1.3 hr after dosing, and 12-hr trough concentrations were 3.9 and 6.7 μg/ml, respectively. When 19 successive intravenous and intramuscular doses at these levels were administered at 12-hr intervals, there was no tendency toward drug accumulation. The major drug elimination route was urinary excretion; 85% of the dose was excreted unchanged in the urine within 12 hr, and no metabolites with antibiotic activity were observed in urine. The mean terminal plasma half-life was 2.98 hr, the mean plasma protein binding was 80.6%, the steady-state volume of distribution was 12 liters, the plasma clearance was 45.9 ml/min/1.73 m^2, and the renal clearance was 34.9 ml/min/1.73 m^2. The pharmacokinetic properties and antibacterial activity spectrum indicate that this antibiotic should be effective in treating human bacterial infections when administered at 12-hr intervals. It is presently under clinical investigation.

Keyphrases □ Ceforanide—pharmacokinetics, humans □ Antibiotics, cephalosporins—ceforanide, pharmacokinetics, humans □ Pharmacokinetics, humans—ceforanide

The *in vitro* antimicrobial activity and *in vivo* properties in rodents of ceforanide, 7-[*o*-(aminomethyl)phenylacetamido]-3-[[[1-(carboxymethyl)-1*H*-tetrazol-5-yl]thio]methyl]-3-cephem-4-carboxylic acid, a new parenterally

0022-3549/80/0400-0398$01.00/0

© 1980, American Pharmaceutical Association

tissue specific drug delivery, chemotherapy, and treatment of inflammatory and infectious diseases of the liver and biliary system.

NOTATIONS

$AUC = \int_0^\infty c\,dt$
B = drug depot compartment
c = blood cimetidine concentration
D = dose
$D_B = X_B + (1 - F_{G1})D$
$D_T = F_{G1}D + F_BD_B$, the apparent amount of the dose absorbed
$F = (F_{G1}D + F_BD_B)/D$, the apparent fraction of the dose absorbed
F_B = fraction of drug cumulated in B that is released to G at time $t = T_B$
F_{G1} = fraction of D absorbed by first-order absorption into the central compartment
$1 - F_{G1}$ = fraction of D transferred from G to B
G = compartment from which absorption takes place
K_{xx} = first-order transfer rate constants
$-\lambda_1, -\lambda_2$ = eigenvalues of the linear system
t = time
T_L = lag time
T_B = time when a part (F_BD_B) of the drug cumulated in B is released to G
V = volume of distribution
X_B = amount of drug transferred from compartment 1 to compartment B at time $t = T_B$

REFERENCES

(1) G. Bodemar, B. Norlander, L. Fransson, and A. Walan, *Br. J. Clin. Pharmacol.*, 7, 22 (1979).

(2) W. L. Burland, W. A. M. Duncan, T. Hesselbo, J. G. Mills, and P. C. Sharpe, *ibid.*, 2, 481 (1975).

(3) R. W. Spence, D. R. Creak, and L. R. Celestin, *Digestion*, **14**, 127 (1976).

(4) R. W. Spence, L. R. Celestin, R. De La Guardia, C. A. McMullen, and D. A. McCormick, "Proceedings of the Second International Symposium on Histamine H_2-Receptor Antagonists," Excerpta Medica, Amsterdam, The Netherlands, 1977, p. 81.

(5) S. S. Walkenstein, J. W. Dubb, W. C. Randolph, W. J. Westlake, R. M. Stote, and A. P. Intoccia, *Gastroenterology*, **74**, 360 (1978).

(6) R. Griffiths, R. M. Lee, and D. C. Taylor, "Proceedings of the Second International Symposium on Histamine H_2-receptor Antagonists, Excerpta Medica, Amsterdam, The Netherlands, 1977, p. 38.

(7) R. H. Henn, J. I. Isenberg, V. Maxwell, and R. A. L. Sturdevant, *N. Engl. J. Med.*, **293**, 371 (1975).

(8) G. Bodemar, B. Norlander, and A. Walan, "Proceedings of the Second International Symposium on Histamine H_2-receptor Antagonists," Excerpta Medica, Amsterdam, The Netherlands, 1977, p. 224.

(9) E. A. Boyden, *Anat. Rec.*, **40**, 147 (1928).

(10) *Ibid.*, **33**, 201.

(11) P. Veng Pedersen and R. Miller, *J. Pharm. Sci.*, **69**, 204 (1980).

(12) C. D. Thorn, *Bull. Math. Biophys.*, **34**, 277 (1972).

(13) P. Veng Pedersen, *J. Pharm. Sci.*, **67**, 187 (1978).

(14) P. Veng Pedersen, *J. Pharmacokinet. Biopharm.*, **5**, 513 (1977).

(15) R. L. Smith, *Prog. Drug. Res.*, **9**, 299 (1966).

(16) A. A. Sandberg and W. R. Slaunwhite, *J. Clin. Invest.*, **35**, 1331 (1956).

(17) K. E. Anderson, B. Bergdahl, and G. Wettrell, *Eur. J. Clin. Pharmacol.*, **11**, 273 (1977).

(18) A. J. Quick, *J. Biol. Chem.*, **97**, 403 (1932).

(19) W. B. Bradley and A. C. Ivy, *Proc. Soc. Exp. Biol. Med.*, **45**, 145 (1940).

(20) A. Cantarow and C. W. Wirts, *Am. J. Dig. Dis.*, **10**, 261 (1943).

(21) C. W. Wirts, A. Cantarow, W. J. Sanpe, and B. Delserone, *Am. J. Physiol.*, **165**, 680 (1951).

(22) V. Hanzon, *Acta Physiol. Scand., Suppl. 101*, **28**, 1 (1952).

(23) R. W. Brauer and R. L. Pessotti, *Am. J. Physiol.*, **162**, 565 (1950).

(24) R. Bine, M. Friedman, S. O. Byers, and C. Bland, *Circulation*, **4**, 105 (1951).

(25) J. Mellanky, *Lancet*, **2**, 215 (1926).

(26) S. A. M. Cross, "Proceedings, 18th Meeting of the European Society of Toxicology, Edinburgh," Excerpta Medica, Amsterdam, The Netherlands, 1977, p. 105.

(27) T. Hargreaves, "The Liver and Bile Metabolism," Appleton-Century-Crofts, New York, N.Y., 1968, p. 39.

(28) R. K. Roberts, P. V. Desmond, and S. Schenker, *Drugs*, **17**, 198 (1979).

(29) *Ibid.*, **17**, 198 (1979).

ACKNOWLEDGMENTS

Supported in part by the South African Medical Research Council.

Human Pharmacokinetics of a New Broad-Spectrum Parenteral Cephalosporin Antibiotic, Ceforanide

MORRIS PFEFFER ˣ, ROBERT C. GAVER, and DONALD R. VAN HARKEN

Received July 14, 1977, from the *Department of Drug Metabolism and Pharmacokinetics, Bristol Laboratories, Syracuse, NY 13201.* Accepted for publication October 26, 1979.

Abstract □ The pharmacokinetics of the *l*-lysine salt of ceforanide were studied after intravenous administration of 1132 and 2264 mg as 30-min constant-rate infusions and after intramuscular administration of 556 and 1132 mg. The peak intravenous plasma concentrations were 136 and 222 μg/ml at termination of infusion, and 12-hr trough concentrations were 5.9 and 9.0 μg/ml, respectively. The peak intramuscular plasma concentrations were 38 and 74 μg/ml at 1.0–1.3 hr after dosing, and 12-hr trough concentrations were 3.9 and 6.7 μg/ml, respectively. When 19 successive intravenous and intramuscular doses at these levels were administered at 12-hr intervals, there was no tendency toward drug accumulation. The major drug elimination route was urinary excretion; 85% of the dose was excreted unchanged in the urine within 12 hr, and no metabolites with antibiotic activity were observed in urine. The mean terminal plasma half-life was 2.98 hr, the mean plasma protein binding was 80.6%, the steady-state volume of distribution was 12 liters, the plasma clearance was 45.9 ml/min/1.73 m^2, and the renal clearance was 34.9 ml/min/1.73 m^2. The pharmacokinetic properties and antibacterial activity spectrum indicate that this antibiotic should be effective in treating human bacterial infections when administered at 12-hr intervals. It is presently under clinical investigation.

Keyphrases □ Ceforanide—pharmacokinetics, humans □ Antibiotics, cephalosporins—ceforanide, pharmacokinetics, humans □ Pharmacokinetics, humans—ceforanide

The *in vitro* antimicrobial activity and *in vivo* properties in rodents of ceforanide, 7-[*o*-(aminomethyl)phenylacetamido]-3-[[[1-(carboxymethyl)-1*H*-tetrazol-5-yl]thio]methyl]-3-cephem-4-carboxylic acid, a new parenterally

0022-3549/80/0400-0398$01.00/0

© 1980, American Pharmaceutical Association

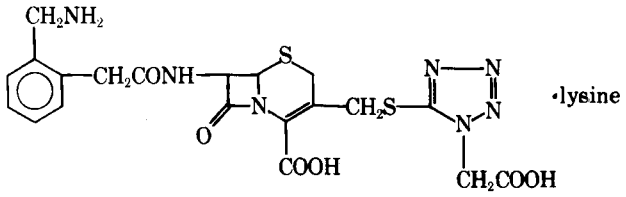

I

administered cephalosporin antibiotic, have been described in detail and compared with those of cephalothin, cephaloridine, and cefazolin (1). With few exceptions, ceforanide was more active than these reference antibiotics against major Gram-negative pathogens, and it inhibited their growth at plasma and urinary concentrations readily achievable in humans.

This report describes the pharmacokinetics of the lysine salt (I) of this cephalosporin antibiotic in normal subjects following single and multiple intravenous and intramuscular doses.

EXPERIMENTAL

Drug Doses and Administration Routes—All doses are expressed in terms of free acid equivalents of ceforanide. The drug was prepared immediately before administration as sterile solutions in vials containing 283 mg of drug. For intramuscular injection, the vial contents were reconstituted with sterile water USP to yield concentrations of 283 mg/ml. The intramuscular injections were administered in the outer quadrant of the gluteal muscle as 2 ml of solution for the 566-mg dose and as 4 ml of solution for the 1132-mg dose. For intravenous administration, the antibiotic was reconstituted in sterile physiological saline solution USP to give a final concentration of 1132 or 2264 mg in 50 ml of solution. Fifty milliliters of either solution was administered into an antecubital vein by 30-min constant-rate infusion using a compact infusion pump[1].

Volunteers and Study Design—The drug was administered to 24 normal adult males, 22–40 years old, with an average weight ($\pm SE$) of 72.5 ± 1.3 kg and an average body surface area ($\pm SE$) of 1.90 ± 0.02 m^2.

Six randomly selected subjects were given 556 and 1132 mg im and 1132 and 2264 mg iv twice daily at 12-hr intervals for a total of 19 successive doses over 10 dosing days (a second dose was not administered on the last dosing day). The morning dose was given before breakfast.

Sample Collection—Plasma and urine specimens were collected after the first, ninth, and 19th doses. Plasma samples were collected from the intravenous subjects immediately before dosing (zero time), at 15 and 30 min during the infusion (the 30-min sample was collected at the end of the infusion and also constituted the zero-time postinfusion sample), and then at 0.25, 0.50, 1.0, 2.0, 4.0, 6.0. 8.0, and 11.5 hr after infusion termination. Plasma samples were collected from the intramuscular subjects immediately before dosing (zero time) and at 0.25, 0.50, 0.75, 1.0, 1.5, 2.5, 4.0, 6.0, 9.0, and 12 hr after dosing.

Complete urine samples were collected from all subjects over the 0–2-, 2–4-, 4–6-, 6–9-, and 9–12-hr intervals after the start of dosing. After the 19th dose, a 12–24-hr urine sample also was collected.

Heparinized blood samples, 10 ml, were collected by venipuncture[2]. The contents of the tubes were mixed gently and then immediately placed in a chipped ice bath where they were kept until plasma was separated by centrifugation at 4°. At least 3 ml of plasma was withdrawn and placed in polypropylene tubes with caps.

The urine samples were refrigerated at 4° while being collected. The subjects were instructed to empty their bladders at the end of each collection interval. The total volume and pH of each urine sample were measured and recorded. Immediately thereafter, 10-ml aliquots of each urine sample were transferred to polypropylene bottles.

The plasma and urine samples were flash frozen by immersion in an ethanol–dry ice bath and stored at or below −20° until they were thawed for assay.

Antibiotic Assay—Plasma and urine concentrations of ceforanide were determined by standard cup-plate bioassay techniques (2) using *Klebsiella pneumoniae* (Bristol A9977)[3] as the bioassay organism. Other microorganisms cannot be expected to yield equivalent, valid results for the bioassay of ceforanide. All bioassay results are expressed in terms of free acid equivalent concentrations.

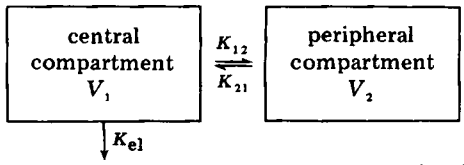

Scheme I—Open, first-order, two-compartment model of drug distribution

The lower sensitivity limit of the assay was equivalent to a plasma concentration of 2.0 μg/ml. The linear concentration ranges for the cup-plate assay were 0.5–5.0 μg/ml for plasma and 1–10 μg/ml for urine. The mean coefficient of variation [(standard deviation of zone diameter/mean zone diameter) × 100] of replicate cup-plate assays of the standards was 3.10%.

Determination of Plasma Protein Binding—Ceforanide was added to fresh, pooled, heparinized 90% human plasma at concentrations of 27, 53, 99, and 200 μg/ml, and the samples were incubated at 37° for 15 min with gentle shaking. Replicate solutions were prepared in aqueous pH 7.40 buffer containing 0.05 *M* NaCl and 0.10 *M* *N*-tris(hydroxymethyl)-methyl-2-aminoethanesulfonic acid[4] and were treated similarly. These samples were subjected to centrifugal ultrafiltration[5].

The drug concentrations in the filtrates were determined by the same cup-plate assay technique used for plasma and urine analyses. The concentration in the plasma filtrate as a percentage of the total concentration in the unfiltered plasma sample was subtracted from 100% to determine the percentage bound to plasma protein. Ceforanide did not bind to the ultrafiltration membrane.

Bioautographic Analysis for Urinary Metabolites with Antibiotic Activity—Urine samples were diluted with 0.1 *M* potassium phosphate buffer (pH 7.0) and spotted on 1.2 × 57-cm strips of filter paper[6]. The strips were developed overnight in the descending mode using *n*-butanol–acetic acid–water (60:15:25). Then they were air dried, overlaid on seed agar inoculated with *Bacillus subtilis* (A9506A), and incubated overnight at 28°. Inhibition zones were visualized by spraying with 1.2% triphenyltetrazolium chloride in 1.25% dextrose solution. The R_f value of ceforanide was 0.3.

Pharmacokinetic Analysis—Mean plasma concentrations during and after intravenous infusion of the first doses were fitted to an open, first-order, two-compartment model of drug distribution (Scheme I) (3). The fitting was performed according to Marquardt's algorithm (4) using a digital computer program. The best-fit parameters found by this procedure were corrected by the Loo–Riegelman procedure (5) to obtain the equivalent parameters that could be found on instantaneous bolus intravenous administration of the same drug doses. This procedure yielded an equation of the form $C = A \exp(-\alpha t) + B \exp(-\beta t)$, where C is the plasma concentration, t is time, A and B are coefficients, and α and β are exponents. The A, B, α, and β parameters and the urinary excretion data were processed further, allowing the various pharmacokinetic parameters to be calculated by standard procedures (6).

The individual subject's observed peak plasma concentrations, C_{max}, and the time to peak plasma concentrations, t_{max}, by both dosing routes and at all dose levels were tabulated, and the mean values and standard errors were calculated. The individual area under the plasma concentration–time curves from $t = 0$ to $t = \infty$ (AUC) were calculated for the first dose by the trapezoidal rule:

$$AUC = \sum_{i=1}^{n-1} (C_{i+1} + C_i)(t_{i+1} - t_i)/2 + C_n/\beta \qquad \text{(Eq. 1)}$$

where $C_1 = 0$ at $t_1 = 0$. The β term is the slope of a plot of the natural logarithms of the 3–12-hr plasma concentrations *versus* time as determined by linear regression analysis. The AUC values for the ninth and 19th doses were calculated between 0 and 12 hr. The observed terminal plasma half-life, $t_{1/2}$, was calculated from β by:

$$t_{1/2} = 0.693/\beta \qquad \text{(Eq. 2)}$$

for all subjects. The individual AUC and $t_{1/2}$ values also were tabulated, and their means and standard errors were calculated.

[1] Model 975, Harvard Apparatus Co., Millis, Mass.
[2] Vacutainer tubes, Becton-Dickinson, Rutherford, N.J.
[3] This microorganism is a mutant strain of *K. pneumoniae* (A9977) specifically selected by the Department of Microbiological Research, Bristol Laboratories.
[4] Calbiochem, Los Angeles, Calif.
[5] DF50A Centriflo membrane cones, Amicon, Lexington, Mass.
[6] Whatman No. 1.

Table I—Ceforanide Binding to Human Plasma Proteins

Plasma Concentration, μg/ml	Percent Bound[a]
27	83.0 (0.0)
53	82.8 (0.2)
99	80.7 (0.0)
200	76.0 (1.1)

[a] Mean (±*SE*) of triplicate determinations.

The absorption profile following intramuscular administration was determined from the mean plasma concentration data using the Loo–Riegelman method (7).

The absolute percentage bioavailability following intramuscular administration was determined by linear regression analysis of a plot of *AUC versus* dose for the intravenous and intramuscular data and by:

$$100F = (U_{im}/U_{iv}) \times 100 \qquad \text{(Eq. 3)}$$

where $100F$ is the absolute percentage bioavailability and U is the fraction of the dose excreted in the urine in 12 hr.

Statistical Analysis—The various observed and calculated pharmacokinetic parameters by each dosing route and at each dose level were compared between dosing groups by the *t* test for group comparisons. The statistical tests (both the *t* test and linear regression analyses) were analyzed for significance at $p = 0.05$. All references to significant or nonsignificant results refer to the tests for statistical significance.

When comparisons were performed between study days within a given dosing group, a *t* test for paired comparisons was used, except in one case. Since there were data for only four subjects for the first 1132-mg iv infusion dose but there were data for all six subjects for the ninth and 19th doses, these data sets also were compared by a *t* test for group comparisons so that two subjects did not have to be omitted at the ninth and 19th doses. These *t* tests for group comparisons yielded the same results as the *t* tests for paired comparisons.

The results of the absolute bioavailability analyses of urinary excretion data were subjected to a *t* test of the null hypothesis that the true mean bioavailability was 100%. These tests also were analyzed for significance at $p = 0.05$.

RESULTS

Plasma Protein Binding—These results are summarized in Table I. The binding over the 27–200-μg/ml range was essentially constant at 80.6%. Investigations of the binding of other cephalosporin antibiotics, using the same technique and the same pooled plasma sample as for ceforanide, indicated 89.7% protein binding for cefazolin between 25 and 205 μg/ml, 50.0% for cefoxitin between 11 and 88 μg/ml, 44.7% for cefuroxime between 9 and 75 μg/ml, and 82.7% for cefamandole (either as the sodium salt or as cefamandole nafate) between 8 and 88 μg/ml.

Bioautographic Analysis—No evidence was found for the presence of any ceforanide metabolite(s) with antibiotic activity in urine.

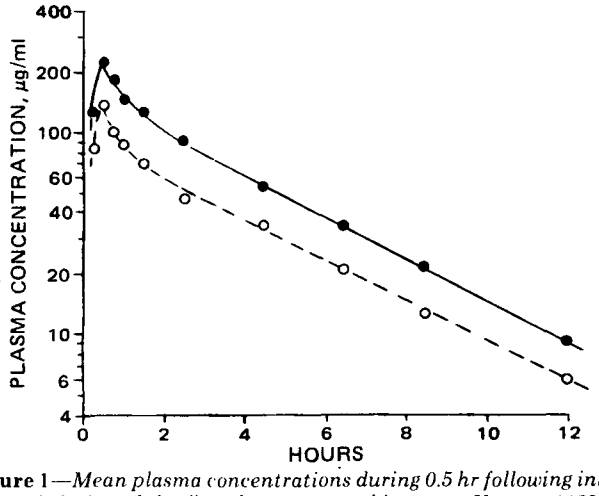

Figure 1—*Mean plasma concentrations during 0.5 hr following intravenous infusion of the first dose to normal humans. Key:* ○, *1132-mg dose; and* ●, *2264-mg dose.*

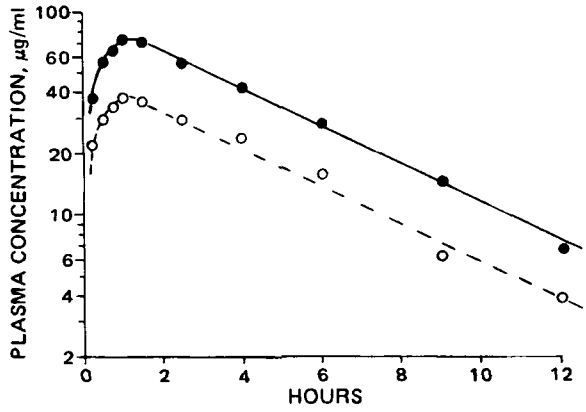

Figure 2—*Mean plasma concentrations following intramuscular administration of the first dose to normal humans. Key:* ○, *566-mg dose; and* ●, *1132-mg dose.*

Plasma and Urine Levels—Figures 1 and 2 are semilogarithmic plots of the mean concentration *versus* time data for the first intravenous and intramuscular doses. There were data from six subjects for each dosage route and dosage level on all dosing days, except for the first 1132-mg iv dose where there were only four subjects. At that time, one infusion pump developed a minor mechanical problem. Therefore, the starting time and exact dose administered to two of the subjects were unknown, although it was estimated that they received ~85% of the dose. Neither plasma nor urine samples were collected from these two subjects on the 1st day. The mechanical problem was resolved immediately, and there were no other difficulties with dosing throughout the study.

The various observed mean plasma parameters after intravenous and intramuscular administration are listed in Table II. The mean peak concentrations did not change significantly over the 19 drug doses by either route or at any given dose level, indicating that there was no tendency toward accumulation of ceforanide when administered every 12 hr, even though there was an appreciably detectable trough plasma concentration immediately before the next dose was given. The mean time of peak concentrations after intramuscular dosing did not change significantly over the duration of the study, indicating that the absorption profile of ceforanide did not change on repeated administration.

The terminal plasma half-lives (2.7–3.2 hr) remained essentially constant throughout the study by both routes and dose levels. Figure 3 is a rectilinear plot of the mean area under the plasma concentration–time curve *versus* dose for the intravenous and intramuscular data from the first, ninth, and 19th doses. Linear regression analysis indicated that the areas by the two dosage routes were on the same statistically significant straight line and that the *y* intercept was not significantly different from zero ($p = 0.05$). Therefore, the absolute bioavailability was 100% following intramuscular administration. The reciprocal of the slope of this line was the plasma clearance, Cl_p, of the drug, 50.2 ml/min/1.73 m^2.

The mean urinary recoveries are listed in Table III. The compound was excreted through the kidneys at high concentrations. On the average, 85% of the administered dose was recovered in the urine within 12 hr of the start of injection. There were no statistically significant differences in total excretion after intramuscular or intravenous administration, which

Table II—Mean Observed Plasma Parameters for Ceforanide[a]

Route	Dose, mg	Dose Number	Peak Concentration, μg/ml	Peak Time, hr	Plasma Half-Life, hr
Intravenous	1132	1	136 (14)	0.5	3.06 (0.16)
		9	128 (4)	0.5	2.83 (0.15)
		19	125 (2)	0.5	2.65 (0.11)
	2264	1	222 (10)	0.5	2.88 (0.09)
		9	240 (4)	0.5	2.80 (0.28)
		19	240 (4)	0.5	2.70 (0.08)
Intramuscular	566	1	38.0 (1.9)	1.04 (0.10)	3.25 (0.23)
		9	40.7 (2.7)	1.12 (0.12)	2.84 (0.31)
		19	39.8 (1.8)	1.08 (0.14)	3.04 (0.40)
	1132	1	74.3 (2.8)	1.33 (0.10)	3.24 (0.26)
		9	76.0 (1.8)	1.00 (0.11)	3.11 (0.34)
		19	75.7 (2.0)	0.92 (0.05)	2.78 (0.14)

[a] Standard errors in parentheses.

Table III—Mean Urinary Recovery of Ceforanide [a]

Route	Dose, mg	Dose Number	Percent Recovery during Collection Intervals after Start of Injection						
			0–2 hr	2–4 hr	4–6 hr	6–9 hr	9–12 hr	12–24 hr	Cumulative
Intravenous	1132	1	34.5 (2.5)	24.5 (0.8)	13.9 (1.1)	11.3 (0.5)	5.9 (0.6)	—[b]	91.2 (3.6)
		9	34.3 (7.3)	18.1 (3.3)	11.7 (1.1)	9.2 (1.0)	4.9 (0.7)	—	78.3 (9.3)
		19	30.2 (2.0)	34.8 (4.0)	12.7 (2.3)	8.6 (1.1)	4.8 (0.6)	3.5 (0.7)	83.9 (4.6)
	2264	1	33.3 (3.8)	26.8 (4.0)	11.1 (2.5)	9.4 (1.3)	4.5 (0.6)	—	85.1 (5.4)
		9	29.7 (4.9)	23.7 (2.7)	14.9 (1.6)	9.1 (1.1)	4.9 (0.6)	—	83.7 (17.8)
		19	32.6 (2.7)	32.7 (4.4)	15.8 (1.0)	9.1 (0.6)	4.3 (0.5)	4.0 (0.6)	98.6 (3.0)
Intramuscular	566	1	19.6 (1.5)	26.1 (0.7)	16.7 (0.8)	11.7 (1.0)	5.7 (0.2)	—	79.8 (1.7)
		9	23.7 (3.7)	30.1 (2.2)	14.4 (1.3)	15.0 (3.4)	6.4 (4.2)	—	89.5 (2.8)
		19	23.8 (6.6)	25.3 (1.7)	13.0 (2.4)	13.0 (0.5)	5.4 (1.0)	4.7 (1.9)	90.5 (1.2)
	1132	1	18.1 (2.5)	26.1 (0.6)	15.5 (2.3)	11.2 (1.2)	7.1 (0.9)	—	78.1 (3.3)
		9	23.2 (1.3)	28.2 (0.8)	14.9 (1.8)	11.4 (1.2)	6.1 (0.5)	—	83.9 (2.5)
		19	23.8 (2.6)	28.8 (1.9)	18.1 (1.3)	10.5 (1.4)	6.0 (1.1)	5.0 (0.6)	92.3 (2.2)

[a] Standard errors in parentheses. [b] Sample not collected.

also is indicative of 100% bioavailability of ceforanide on intramuscular administration.

The data in Table III were converted to urinary excretion rates during each urine collection interval and plotted *versus* the plasma concentrations at the midpoints of the collection intervals (Fig. 4). The data yielded a statistically significant straight line by linear regression analysis. The y intercept was not significantly different from zero. Therefore, urinary excretion of ceforanide may be treated as a reaction following apparent first-order kinetics. The slope of the plot was equivalent to the renal clearance, Cl_r, of ceforanide, 34.9 ml/min/1.73 m^2.

The mean plasma concentrations for the first intravenous doses of ceforanide were analyzed using the open, two-compartment model of drug distribution (Scheme I). The central compartment, with a volume of distribution of V_1, is comprised of well-perfused tissues and includes the blood plasma. The peripheral compartment, with a volume of distribution of V_2, is comprised of more poorly perfused tissues. Both K_{12} and K_{21} are first-order rate constants for drug transfer between the central and peripheral compartments; K_{el} is the first-order rate constant for drug elimination, which occurs only from the central compartment. The total volume of the drug distribution in the body is V_{dss} (the volume of distribution at steady state). If it is assumed that drug clearances from the central to the peripheral compartments and from the peripheral to the central compartments are equal (*i.e.*, $V_1K_{12} = V_2K_{21}$), then $V_2 = K_{12}V_1/K_{21}$ and V_{dss} can be calculated as $V_{dss} = V_1 + V_2$. According to this model, the plasma clearance can be calculated as $Cl_p = V_1K_{el}$.

The best-fit values for the pharmacokinetic parameters are listed in Table IV. The results for the 1132- and 2264-mg iv doses were essentially identical; the differences between doses were attributed to normal intersubject differences between two panels of subjects. The half-lives (3.08 and 2.89 hr) were almost identical to those found by direct linear regression analysis of the data of individual subjects (3.06 and 2.88 hr, Table II). The overall Cl_p found by direct pharmacokinetic analysis of the mean intravenous infusion data, 45.9 ml/min/1.73 m^2, was close to the Cl_p of 50.2 ml/min/1.73 m^2 found by plotting the area under the curve *versus* dose for all subjects for both the intravenous and intramuscular data.

The most important, but not exclusive, factor controlling the terminal half-life of ceforanide was the elimination rate constant, K_{el}. The rate constant for drug transfer from the peripheral to the central compartment, K_{21}, was about three times larger than K_{el} and, therefore, cannot be process limiting.

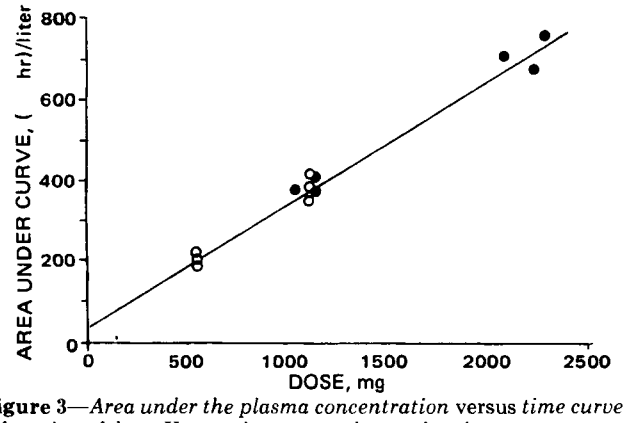

Figure 3—*Area under the plasma concentration* versus *time curve as a function of dose. Key:* ○, *intramuscular; and* ●, *intravenous.*

The mean values listed for the pharmacokinetic parameters in Table IV were used to determine the intrinsic intramuscular absorption profile according to the Loo–Riegelman procedure (7). The results are presented in Fig. 5 as a semilogarithmic plot of the percentage of dose unabsorbed *versus* time. The values for the 566- and 1132-mg doses essentially were superimposable and formed a straight line. Intramuscular absorption of the drug can be considered to be a passive process proceeding by apparent first-order kinetics. The first-order intramuscular absorption rate constant, K_a, was 1.19 hr^{-1}, yielding an absorption half-time of 35 min. Intramuscular absorption of ceforanide had no dose-dependent features.

DISCUSSION

Ceforanide has linear, dose-independent pharmacokinetic properties in humans. These properties are compared to those of several other parenteral cephalosporin antibiotics in Table V. Its plasma half-life, 2.9 hr, is the longest of any of these antibiotics; cefazolin, at 1.8 hr, has the next longest plasma half-life. Concomitant with its extended half-life, ceforanide has the lowest rates of plasma and renal clearance. These factors result in the prolonged *in vivo* duration of ceforanide. Peak plasma levels of ceforanide following intramuscular administration would be higher than those reported for equivalent doses of cephalothin, cephaloridine, cefoxitin, cefuroxime, and cefamandole and should be similar to peak plasma concentrations following the intramuscular administration of cefazolin. Volumes of distribution are in the range of the values of the two-compartment model reported for cephalothin and cefoxitin and are 1.4- to 1.8-fold higher than these volumes of distribution for cefazolin. These relatively high volumes of distribution, coupled with high peak plasma concentrations and prolonged duration, suggest favorable distribution of the drug to tissue sites. Ceforanide was excreted in the urine in 12 hr, suggesting little or no contribution of biliary excretion or metabolism to drug elimination.

The linear, dose-independent kinetics of ceforanide permit prediction of plasma concentrations that would result from different dosage regimens. For instance, the predicted mean peak plasma concentrations after intramuscular injection of 500 and 1000 mg should be about 34 and 66 μg/ml, respectively. The peak plasma concentration and time to peak on intravenous administration can be controlled by controlling the size and

Table IV—Pharmacokinetic Parameters for Ceforanide from Mean Plasma Concentration Data for First Intravenous Doses

Parameter	Dose, mg		Mean (*SE*)
	1132	2264	
A, μg/ml	75.5	11	—
α, hr^{-1}	1.89	1.80	1.84 (0.06)
B, μg/ml	81.7	151	—
β, hr^{-1}	0.225	0.240	0.232 (0.011)
K_{12}, hr^{-1}	0.638	0.523	0.580 (0.04)
K_{21}, hr^{-1}	0.387	0.377	0.382 (0.007)
$t_{1/2}$, hr	3.08	2.89	2.98 (0.13)
V_1, liters	7.20	8.64	7.92 (1.02)
V_{dss}, liters	11.4	12.6	12.0 (0.8)
Cl_p, ml/min/1.73 m^2	42.3	49.5	45.9 (5.1)

Table V—Comparison of Pharmacokinetic Parameters for Various Parenteral Cephalosporin Antibiotics [a]

Parameter	Ceforanide	Cephalothin	Cephaloridine	Cefazolin	Cefoxitin	Cefuroxime	Cefamandole
Cl_p, ml/min/1.73 m^2	45.9	472	167	62	331	150	241
Cl_r, ml/min/1.73 m^2	34.9	274	125	64	298–331	139	—
Renal excretion, % of dose	85	52	75	100	90–100	95	100
$t_{1/2}$, hr	2.98	0.56	0.6–1.5	1.80	0.666	1.17	0.90
Percent protein bound	81	65	8–31	90	50	45	83
Peak levels, μg/ml							
500 mg im	34	6–8	30	11–70	11	26	15
1000 mg im	66	15–20	40	38–75	22	40	36
V_1, liters	7.92	7.76	—	4.44	6.88	—	—
V_{dss}, liters	12.0	14.3	—	8.48	13.3	—	—

[a] Protein binding values for ceforanide, cefazolin, cefoxitin, cefuroxime, and cefamandole were obtained in this laboratory. All other cefuroxime values are from Ref. 8. All other cefamandole values are from Refs. 9 and 10. All other values for cephalothin, cephaloridine, cefazolin, and cefoxitin are from Ref. 11.

Table VI—Estimated Mean Duration of Plasma Ceforanide Concentrations

Mode of Administration	Dose, mg	Duration (hr) at Plasma Concentrations Greater Than or Equal to 6.25 μg/ml	8.0 μg/ml	12.5 μg/ml
Intramuscular	500	9.6	8.2	6.2
	1000	12.8	11.6	9.4
Intravenous bolus	1000	10.4	9.3	7.4
	2000	13.3	12.3	10.4
Constant rate intravenous infusion for 30 min	1000	10.5	9.5	7.6
	2000	13.5	12.5	10.5
Constant rate intravenous infusion for 60 min	1000	10.8	9.7	7.8
	2000	13.8	12.7	10.8

mode of the intravenous injection. The predicted mean peak plasma concentrations resulting from a 0.5-hr constant-rate infusion would occur at 0.5 hr and would be 103 μg/ml for a 1000-mg dose and 205 μg/ml for a 2000-mg dose. If the doses remain the same and are infused over 1 hr, the peak concentrations at 1 hr should be 88 μg/ml for 1000 mg and 176 μg/ml for 2000 mg. If these doses are given by true bolus intravenous injection, the immediate peak plasma concentrations should be 126 μg/ml at 1000 mg and 252 μg/ml at 2000 mg.

The varying modes of administration also would affect the periods over which observed plasma concentrations would exceed the given minimum

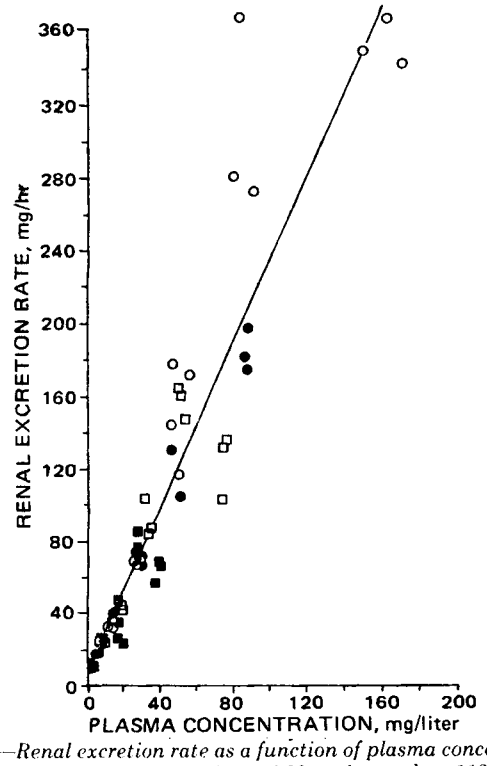

Figure 4—*Renal excretion rate as a function of plasma concentration. Key:* ●, *1132 mg iv;* ○, *2264 mg iv;* ■, *566 mg im; and* □, *1132 mg im.*

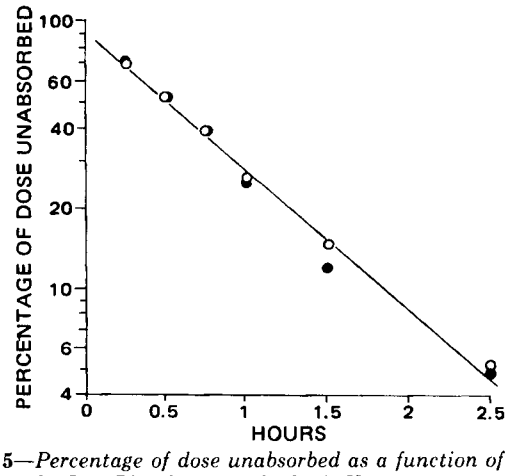

Figure 5—*Percentage of dose unabsorbed as a function of time according to the Loo–Riegelman method (7). Key:* ○, *566-mg dose; and* ●, *1132-mg dose.*

plasma concentrations. Table VI lists the estimated periods that plasma concentrations would exceed 6.25, 8.0, and 12.5 μg/ml (standard concentrations in a geometrically diluted minimum inhibitory concentration series) using these modes of parenteral administration. If ceforanide is dosed at 12-hr intervals, a 500-mg im dose would exceed 6.25 μg/ml for about 80% of that period and would exceed 12.5 μg/ml for about 52% of that period. If the intramuscular dose is increased to 1000 mg, the plasma concentration would exceed 6.25 μg/ml for the entire 12-hr period and would exceed 12.5 μg/ml for about 78% of that period. From the point of view of maintaining a proper peak-to-trough plasma concentration relationship, a 500-mg im dose every 12 hr is reasonable. The kinetic relationships pertaining to constant-rate intravenous infusion of ceforanide are such that increasing the infusion time for a given dose from 0.5 to 1 hr would lower the peak concentration without appreciably lengthening the duration of plasma concentrations above the given minimum levels.

Ceforanide demonstrated no tendency to accumulate. It yielded high and prolonged plasma concentrations and has useful distribution properties. These favorable properties, together with its good antibacterial activity, suggest that it could be effective in treating bacterial infections in humans when administered at 12-hr intervals. This regimen is undergoing clinical trials.

REFERENCES

(1) F. Leitner, M. Misiek, T. A. Pursiano, R. E. Buck, D. R. Chisholm, R. DeRegis, and Y. H. Tsai, *Antimicrob. Agents Chemother.*, **10**, 426 (1976).

(2) D. C. Grove and W. A. Randall, "Assay Methods of Antibiotics. A Laboratory Manual," Medical Encyclopedia, Inc., New York, N.Y., 1955.

(3) A. Rescigno and G. Segre, "Drug and Tracer Kinetics," Blaisdell, Waltham, Mass., 1966, p. 85.

(4) D. W. Marquardt, *J. Soc. Ind. Appl. Math.*, **11**, 431 (1963).

(5) J. C. K. Loo and S. Riegelman, *J. Pharm. Sci.*, **59**, 53 (1970).

(6) M. Gibaldi and D. Perrier, "Pharmacokinetics," Dekker, New York, N.Y., 1975, p. 48.

(7) J. C. K. Loo and S. Riegelman, *J. Pharm. Sci.*, **57**, 918 (1968).

(8) R. D. Foord, *Antimicrob. Agents Chemother.*, **9**, 741 (1976).

(9) M. Barza, S. Melethil, S. Berger, and E. C. Ernst, *ibid.*, **10**, 421 (1976).
(10) B. R. Myers, B. Ribner, S. Yancovitz, and S. Z. Hirschman, *ibid.*, **9**, 140 (1976).
(11) C. H. Nightingale, D. S. Green, and R. Quintiliani, *J. Pharm. Sci.*, **64**, 1899 (1975).

ACKNOWLEDGMENTS

The authors thank Dr. John C. Godfrey, clinical monitor of the study. They are grateful to Katherine Casson for direction of the cup-plate bioassays and to Violet Z. Rossomano for direction of the bioautographic urine analysis.

Influence of Viscosity on Absorption from Nitrofurantoin Suspensions

M. MIRTA SOCI * and EUGENE L. PARROTT ˣ

Received July 23, 1979, from the *Division of Pharmaceutics, College of Pharmacy, University of Iowa, Iowa City, IA 52242.* Accepted for publication October 31, 1979. *Present address: Caracas, Venezuela.

Abstract □ Nitrofurantoin, 200 mg, was administered orally to 11 subjects in an aqueous reference dispersion and in five suspensions having the same rheogram. Algin, carbomer, guar gum, methylcellulose, and colloidal magnesium aluminum silicate were the five suspending agents employed. Complexation was demonstrated by dialysis between nitrofurantoin and methylcellulose and between nitrofurantoin and carbomer; however, physiological availability was not altered by the interaction. The viscosity increase slowed absorption and urinary excretion, thus delaying the time of the maximum excretion rate without a decrease in bioavailability. A clinically acceptable urinary nitrofurantoin concentration was maintained for at least 2 hr longer by a viscosity increase.

Keyphrases □ Nitrofurantoin—suspensions, effect of viscosity on absorption □ Suspensions—nitrofurantoin, effect of viscosity on absorption □ Bioavailability—nitrofurantoin suspensions, effect of viscosity on absorption □ Antibacterial agents—nitrofurantoin suspensions, effect of viscosity on absorption

Based on the few literature reports, it is difficult to generalize the effect of viscosity on the absorption and availability of medicinal compounds from oral liquids. Malone *et al.* (1) noted that increasing viscosity by increasing the concentration of sucrose in aqueous solutions of phenobarbital sodium progressively lengthened the induction time of narcosis in rats. Davison *et al.* (2) found that methylcellulose delayed the absorption from orally administered sodium salicylate solutions as demonstrated by the reduction of brain and plasma salicylate levels.

Levy and Jusko (3) concluded that the decrease in absorption by the ligated rat stomach of alcohol and salicylic acid from solutions containing methylcellulose was due to the slower movement of the drug molecule to the absorbing membrane. Harper and Wordan (4) reported that the LD_{50} values of isoniazid (isonicotinic acid hydrazide) in rats were 3300, 2650, and 2000 mg/kg in acacia solution, gelatin solution, and water, respectively, and they concluded that the apparent toxicity was influenced by the vehicle. Hewitt and Levy (5) reported that, contrary to expectation, the oral administration of thiamine and riboflavin in highly viscous methylcellulose solutions did not affect the rate and extent of absorption. Ashley and Levy (6) showed that the absorption of phenolsulfonphthalein was decreased during the 1st hr by the addition of algin (sodium alginate) to the solution but that the total amount absorbed was unchanged.

BACKGROUND

Suspending agents are added to suspensions to increase the viscosity so that the sedimentation rate is slowed and the measurement of a proper dose is simplified. Because a suspending agent improves the physical properties of a suspension, it may concomitantly affect the absorption of the medicinal compound by the increased viscosity or by complexation. It has been shown that the dissolution rate of a solid is inversely proportional to the viscosity of the dissolution medium (7).

Since the dissolution rate often is the limiting factor in availability of a relatively insoluble medicinal compound in an orally administered suspension, viscosity would be expected to affect absorption. Seager (8) found that methylcellulose affected the excretion after the oral administration of a nitrofurantoin suspension so that less nitrofurantoin was excreted and the time of maximum excretion was delayed by 1 hr.

This study was conducted to determine, by a urinary recovery technique, the effect of suspending agents (algin, carbomer, guar gum, methylcellulose, and colloidal magnesium aluminum silicate) on the absorption of nitrofurantoin. Because the main concern was to determine if the viscosity affected GI absorption, all formulations containing a suspending agent had the same viscosity.

EXPERIMENTAL

Suspension Preparation—Nitrofurantoin[1] was classified by a sonic sifter[2], and the 70–140-mesh fraction (157 μm) was used. Nitrofurantoin, 200 mg, was dispersed in 20 g of vehicle. Each vehicle was prepared by making dispersions of various concentrations of the suspending agent, and their viscosities were measured by a rotational viscometer[3]. Guided by these results, more appropriate concentrations then were prepared, and their viscosities were measured. For each suspending agent, a concentration was found experimentally that provided a rheogram similar to that of a 2% aqueous solution of methylcellulose, 4000 cps.

Dialysis—Dialysis was carried out at 37° in cellophane tubing[4] tied into a sac with distilled water as the dialysis medium. The nitrofurantoin dispersion, 50 ml, was placed in the cellophane sac, which was soaked previously for 24 hr to achieve hydration; then the open end was tied. The sac was immersed in 100 ml of distilled water, sealed in the container, and attached to a submersion rotator[5].

At 3, 6, 12, 24, and 36 hr, one dialysis sac of a series was removed, fluid volume inside and outside of the sac was measured, and the nitrofurantoin concentration in the fluid inside and outside of the sac was determined from spectrophotometric measurements at 367 nm. Equilibrium was always attained in <36 hr.

Protocol—All suspensions were coded and distributed according to the Latin square law (9) so that two of the initial 12 volunteers received

[1] Lot 43C-1550, Sigma.
[2] Allen-Bradley.
[3] Brookfield LVT.
[4] Fisher 8-667E dialyzer tubing, 2.74 cm i.d.
[5] Model SR-25V, Scientific Industries.

0022-3549/80/0400-0403$01.00/0
© 1980, American Pharmaceutical Association

(9) M. Barza, S. Melethil, S. Berger, and E. C. Ernst, *ibid.*, **10**, 421 (1976).
(10) B. R. Myers, B. Ribner, S. Yancovitz, and S. Z. Hirschman, *ibid.*, **9**, 140 (1976).
(11) C. H. Nightingale, D. S. Green, and R. Quintiliani, *J. Pharm. Sci.*, **64**, 1899 (1975).

ACKNOWLEDGMENTS

The authors thank Dr. John C. Godfrey, clinical monitor of the study. They are grateful to Katherine Casson for direction of the cup-plate bioassays and to Violet Z. Rossomano for direction of the bioautographic urine analysis.

Influence of Viscosity on Absorption from Nitrofurantoin Suspensions

M. MIRTA SOCI * and EUGENE L. PARROTT ˣ

Received July 23, 1979, from the *Division of Pharmaceutics, College of Pharmacy, University of Iowa, Iowa City, IA 52242.* Accepted for publication October 31, 1979. *Present address: Caracas, Venezuela.

Abstract □ Nitrofurantoin, 200 mg, was administered orally to 11 subjects in an aqueous reference dispersion and in five suspensions having the same rheogram. Algin, carbomer, guar gum, methylcellulose, and colloidal magnesium aluminum silicate were the five suspending agents employed. Complexation was demonstrated by dialysis between nitrofurantoin and methylcellulose and between nitrofurantoin and carbomer; however, physiological availability was not altered by the interaction. The viscosity increase slowed absorption and urinary excretion, thus delaying the time of the maximum excretion rate without a decrease in bioavailability. A clinically acceptable urinary nitrofurantoin concentration was maintained for at least 2 hr longer by a viscosity increase.

Keyphrases □ Nitrofurantoin—suspensions, effect of viscosity on absorption □ Suspensions—nitrofurantoin, effect of viscosity on absorption □ Bioavailability—nitrofurantoin suspensions, effect of viscosity on absorption □ Antibacterial agents—nitrofurantoin suspensions, effect of viscosity on absorption

Based on the few literature reports, it is difficult to generalize the effect of viscosity on the absorption and availability of medicinal compounds from oral liquids. Malone *et al.* (1) noted that increasing viscosity by increasing the concentration of sucrose in aqueous solutions of phenobarbital sodium progressively lengthened the induction time of narcosis in rats. Davison *et al.* (2) found that methylcellulose delayed the absorption from orally administered sodium salicylate solutions as demonstrated by the reduction of brain and plasma salicylate levels.

Levy and Jusko (3) concluded that the decrease in absorption by the ligated rat stomach of alcohol and salicylic acid from solutions containing methylcellulose was due to the slower movement of the drug molecule to the absorbing membrane. Harper and Wordan (4) reported that the LD_{50} values of isoniazid (isonicotinic acid hydrazide) in rats were 3300, 2650, and 2000 mg/kg in acacia solution, gelatin solution, and water, respectively, and they concluded that the apparent toxicity was influenced by the vehicle. Hewitt and Levy (5) reported that, contrary to expectation, the oral administration of thiamine and riboflavin in highly viscous methylcellulose solutions did not affect the rate and extent of absorption. Ashley and Levy (6) showed that the absorption of phenolsulfonphthalein was decreased during the 1st hr by the addition of algin (sodium alginate) to the solution but that the total amount absorbed was unchanged.

BACKGROUND

Suspending agents are added to suspensions to increase the viscosity so that the sedimentation rate is slowed and the measurement of a proper dose is simplified. Because a suspending agent improves the physical properties of a suspension, it may concomitantly affect the absorption of the medicinal compound by the increased viscosity or by complexation. It has been shown that the dissolution rate of a solid is inversely proportional to the viscosity of the dissolution medium (7).

Since the dissolution rate often is the limiting factor in availability of a relatively insoluble medicinal compound in an orally administered suspension, viscosity would be expected to affect absorption. Seager (8) found that methylcellulose affected the excretion after the oral administration of a nitrofurantoin suspension so that less nitrofurantoin was excreted and the time of maximum excretion was delayed by 1 hr.

This study was conducted to determine, by a urinary recovery technique, the effect of suspending agents (algin, carbomer, guar gum, methylcellulose, and colloidal magnesium aluminum silicate) on the absorption of nitrofurantoin. Because the main concern was to determine if the viscosity affected GI absorption, all formulations containing a suspending agent had the same viscosity.

EXPERIMENTAL

Suspension Preparation—Nitrofurantoin[1] was classified by a sonic sifter[2], and the 70–140-mesh fraction (157 μm) was used. Nitrofurantoin, 200 mg, was dispersed in 20 g of vehicle. Each vehicle was prepared by making dispersions of various concentrations of the suspending agent, and their viscosities were measured by a rotational viscometer[3]. Guided by these results, more appropriate concentrations then were prepared, and their viscosities were measured. For each suspending agent, a concentration was found experimentally that provided a rheogram similar to that of a 2% aqueous solution of methylcellulose, 4000 cps.

Dialysis—Dialysis was carried out at 37° in cellophane tubing[4] tied into a sac with distilled water as the dialysis medium. The nitrofurantoin dispersion, 50 ml, was placed in the cellophane sac, which was soaked previously for 24 hr to achieve hydration; then the open end was tied. The sac was immersed in 100 ml of distilled water, sealed in the container, and attached to a submersion rotator[5].

At 3, 6, 12, 24, and 36 hr, one dialysis sac of a series was removed, fluid volume inside and outside of the sac was measured, and the nitrofurantoin concentration in the fluid inside and outside of the sac was determined from spectrophotometric measurements at 367 nm. Equilibrium was always attained in <36 hr.

Protocol—All suspensions were coded and distributed according to the Latin square law (9) so that two of the initial 12 volunteers received

[1] Lot 43C-1550, Sigma.
[2] Allen-Bradley.
[3] Brookfield LVT.
[4] Fisher 8-667E dialyzer tubing, 2.74 cm i.d.
[5] Model SR-25V, Scientific Industries.

0022-3549/80/0400-0403$01.00/0
© 1980, American Pharmaceutical Association

Table I—Mean Excretion Rate (±*SD*) and Mean Cumulative Milligrams (±*SD*) of Nitrofurantoin Excreted for 11 Subjects after Oral Administration of an Aqueous Reference Dispersion and Aqueous Suspensions Containing Various Suspending Agents

Hours	Reference Dispersion		Methylcellulose Suspension		Colloidal Magnesium Aluminum Silicate Suspension	
	Rate, mg/hr	Cumulative Excretion, mg	Rate, mg/hr	Cumulative Excretion, mg	Rate, mg/hr	Cumulative Excretion, mg
1	8.44 ± 9.82	8.44 ± 9.82	0.12 ± 6.75	6.12 ± 6.75	3.25 ± 3.49	3.25 ± 3.49
2	11.17 ± 4.08	19.61 ± 12.64	13.03 ± 8.00	19.15 ± 12.22	8.23 ± 6.49	11.48 ± 9.77
3	15.32 ± 5.76	34.93 ± 14.23	13.06 ± 6.60	32.21 ± 14.67	9.17 ± 3.36	20.65 ± 11.68
4	9.13 ± 6.34	44.06 ± 14.57	7.55 ± 5.00	39.76 ± 13.09	9.24 ± 5.16	29.89 ± 10.86
5	6.05 ± 4.34	50.11 ± 14.54	5.75 ± 5.88	45.51 ± 11.64	10.75 ± 7.73	40.64 ± 8.47
6	3.38 ± 3.03	53.49 ± 13.88	3.21 ± 5.39	48.73 ± 12.90	6.77 ± 6.58	47.41 ± 10.04
7	0.73 ± 0.67	54.22 ± 13.00	1.59 ± 2.09	50.32 ± 13.57	3.97 ± 5.30	51.38 ± 12.13
8	0.34 ± 0.21	54.56 ± 13.00	0.44 ± 0.38	50.76 ± 10.31	1.90 ± 3.97	53.28 ± 13.25
9	0.14 ± 0.12	54.70 ± 13.32	0.64 ± 1.27	51.40 ± 10.85	0.49 ± 0.42	53.77 ± 14.55
10	0.09 ± 0.11	54.79 ± 13.66	0.22 ± 0.23	51.62 ± 11.62	0.21 ± 0.16	53.98 ± 10.45
11	0.08 ± 0.08	54.87 ± 8.41	0.30 ± 0.40	51.92 ± 7.76	0.11 ± 0.06	54.09 ± 12.84
12	0.05 ± 0.03	54.92 ± 0.06	0.37 ± 0.48	52.29 ± 0.07	0.12 ± 0.02	54.21 ± 4.04
	Algin Suspension		Carbomer Suspension		Guar Gum Suspension	
Hours	Rate, mg/hr	Cumulative Excretion, mg	Rate, mg/hr	Cumulative Excretion, mg	Rate, mg/hr	Cumulative Excretion, mg
1	5.74 ± 4.72	5.74 ± 4.72	3.19 ± 3.38	3.19 ± 3.38	6.37 ± 6.64	6.37 ± 6.64
2	11.18 ± 8.34	16.92 ± 15.19	10.38 ± 7.38	13.57 ± 10.31	13.10 ± 8.79	19.47 ± 14.76
3	14.01 ± 6.34	30.93 ± 16.14	16.14 ± 8.29	29.71 ± 17.95	15.35 ± 7.94	34.82 ± 17.22
4	14.00 ± 8.30	44.93 ± 17.27	13.68 ± 5.19	43.39 ± 19.41	15.33 ± 9.79	50.15 ± 22.34
5	9.30 ± 5.66	54.23 ± 19.97	13.15 ± 6.11	56.54 ± 17.41	8.12 ± 6.27	58.27 ± 23.66
6	5.26 ± 4.31	59.49 ± 13.07	5.45 ± 6.14	16.99 ± 20.00	4.72 ± 5.76	62.99 ± 23.68
7	2.96 ± 4.08	62.45 ± 10.80	2.12 ± 2.85	64.11 ± 22.39	2.22 ± 4.52	65.21 ± 23.60
8	2.54 ± 5.91	64.99 ± 9.71	0.70 ± 1.09	64.81 ± 23.47	1.61 ± 3.08	66.82 ± 28.04
9	3.85 ± 7.36	68.84 ± 14.57	0.33 ± 0.49	69.14 ± 21.68	0.59 ± 0.98	67.41 ± 20.46
10	1.50 ± 3.00	70.34 ± 17.31	0.15 ± 0.18	65.29 ± 22.90	0.16 ± 0.10	67.57 ± 28.81
11	1.10 ± 1.87	71.44 ± 19.00	0.15 ± 0.08	65.44 ± 26.78	0.08 ± 0.09	67.65 ± 31.09
12	0.47 ± 0.49	71.91 ± 22.35	0.14 ± 0.06	65.58 ± 26.00	0	67.65 ± 31.05

Table II—Mean Time (±*SD*) of the Maximum Excretion Rate and Mean Percent (±*SD*) of the Oral Dose Excreted in 12 hr for 11 Subjects

Preparation	Maximum Rate, hr	Percent Oral Dose Excreted
Aqueous reference	2.6 ± 0.8	27.5 ± 6.9
Methylcellulose	2.9 ± 1.4	26.1 ± 6.5
Colloidal magnesium aluminum silicate	4.0 ± 1.7	27.1 ± 6.5
Algin	4.0 ± 1.6	35.9 ± 8.0
Carbomer	4.0 ± 1.3	32.9 ± 11.7
Guar gum	3.8 ± 0.7	33.8 ± 12.0

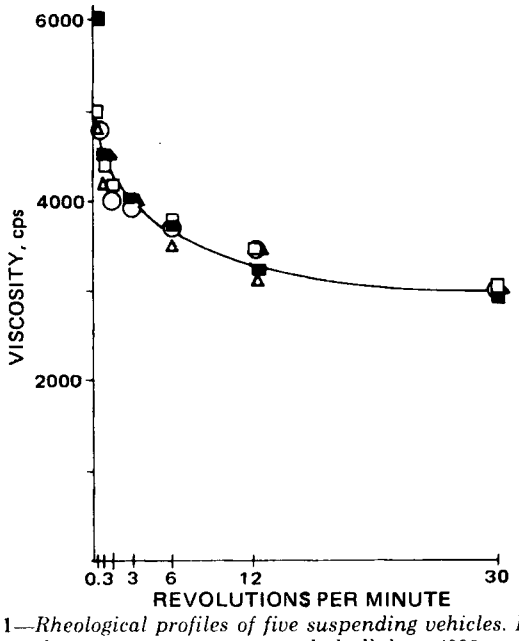

Figure 1—*Rheological profiles of five suspending vehicles. Key:* □, *algin;* △, *carbomer;* ■, *guar gum;* ○, *methylcellulose, 4000 cps; and* ▲, *colloidal magnesium aluminum silicate.*

the same suspension. Two weeks elapsed between each urinary study. One subject did not complete the study; the study was completed with two healthy female and nine healthy male subjects, 24–35 years old and 40–70 kg.

Each subject drank 300 ml of water upon arising. After 30 min, the bladder was voided, and the suspension was swallowed. The participants were instructed to allow adequate time for the suspension to drain from the container. Two 5-ml portions of water were used to rinse any residue from the container, and each portion was swallowed. No food or fluids were ingested for 6 hr.

Urine samples were collected at 1-hr intervals for 12 hr. Volumes were measured, and aliquots were retained in amber vials for analysis. The urinary pH was determined at the time of each sample collection, and the values ranged from 5.3 to 7.0. For a given subject, the pH fluctuation did not exceed 1 pH unit. No attempt was made to control the urinary pH.

Analytical Method—The urine analysis was carried out in duplicate by the method of Conklin and Hollifield (10) on the collection day. To protect the nitrofurantoin from light, amber glassware was used.

Statistics—The significance of the difference between suspensions containing different suspending agents and the reference dispersion was calculated using the Student two-tailed t test ($p = 0.05$).

RESULTS AND DISCUSSION

To compare the effect of several suspending agents on the absorption and urinary excretion of nitrofurantoin from an oral suspension, the viscosity should be the same for all suspensions. A 2% aqueous solution of methylcellulose, 4000 cps, was selected because it had a moderately high viscosity. This selection accented the factor of viscosity, but the suspension was pourable from the container. Figure 1 shows that the rheological characteristics of a 1.6% algin[6] solution, a 0.3% carbomer[7] solution, a 1.0% guar gum[8] solution, a 2.0% methylcellulose[9] solution, and a 5.0% colloidal magnesium aluminum silicate[10] dispersion are similar.

Shah and Sheth (11) demonstrated *in vitro* that the dialysis rate of nitrofurantoin was reduced by the presence of methylcellulose. They thought that this effect was due to the drug complexation in solution with

[6] Kelgin M.V., Kelco Co.
[7] Carbopol 934, B. F. Goodrich Chemical Co.
[8] Supercol GF, Henkel Co., General Mills Chemicals.
[9] Methocel 90 HG Premium, 4000 cps, Dow Chemical Co.
[10] Veegum, R. T. Vanderbilt Co.

Table III—Mean Nitrofurantoin Concentration in the Urine of 11 Subjects after Oral Administration of 200 mg of Nitrofurantoin

	Urinary Concentration					
Hours	Reference Dispersion	Algin Suspension	Carbomer Suspension	Guar Gum Suspension	Methylcellulose Suspension	Colloidal Magnesium Aluminum Silicate Suspension
1	1:12,000	1:25,000	1:50,000	1:20,000	1:25,000	1:50,000
2	1:8400	1:7700	1:9000	1:5500	1:10,000	1:10,000
3	1:4400	1:5000	1:5000	1:5000	1:10,000	1:10,000
4	1:5600	1:5000	1:5000	1:5000	1:10,000	1:10,000
5	1:8300	1:5000	1:5000	1:6600	1:10,000	1:10,000
6	1:15,000	1:11,100	1:8300	1:11,100	1:20,000	1:11,100
7	1:126,000	1:15,100	1:33,300	1:33,300	1:33,300	1:14,200
8	1:200,000	1:17,200	1:100,000	1:50,000	1:125,000	1:33,300
9	1:357,000	1:14,200	1:140,800	1:200,000	1:90,000	1:142,800
10		1:52,600				
11		1:52,600				
12		1:125,000				

the polymer. A nitrofurantoin–suspending agent interaction (complexation) possibly could affect absorption and urinary excretion. Nitrofurantoin and each suspending agent were dialyzed until equilibrium was attained. Aqueous dispersions of nitrofurantoin with carbomer and with methylcellulose gave ratios of the concentration in the internal compartment to that in the external compartment of 1.22 and 1.26, respectively, thus indicating interaction between nitrofurantoin and carbomer and between nitrofurantoin and methylcellulose such that less nitrofurantoin diffused through the membrane. Such an interaction could interfere with absorption and subsequent urinary excretion. No interaction occurred with algin, guar gum, and colloidal magnesium aluminum silicate.

In a blind study, 11 subjects ingested 200 mg of nitrofurantoin in various suspensions of the same viscosity and in an aqueous dispersion at 2-week intervals. No nitrofurantoin was detected in the urine of any subject after 12 hr. The half-life was determined by plotting the logarithm of the amount excreted after administration of the aqueous dispersion against time (12). The average half-life was 1.03 ± 0.45 hr. This result agrees with the literature values that range from 0.3 to 1.0 hr (13).

The excretion rate and the cumulative milligrams excreted were determined and plotted for each subject. From these data, the percent of the orally administered dose excreted in the urine and the time of the maximum excretion rate were determined for each subject. Data for each individual are not given to conserve space. The mean ($\pm SD$) excretion rate and the cumulative amount ($\pm SD$) excreted for 11 subjects are given in Table I for the aqueous reference dispersion and for the five suspensions. Figure 2 shows the mean cumulative amount of nitrofurantoin excreted as a function of time for each suspension.

The mean percent ($\pm SD$) of the oral dose excreted is given in Table II. The significance of the difference between the aqueous reference dispersion and the means in Table II was calculated using the Student t test. The percent of the oral dose recovered in the urine was not diminished significantly by any suspending agent, even though *in vitro* interaction had been demonstrated between nitrofurantoin and methylcellulose and between nitrofurantoin and carbomer. This result indicates that under physiological conditions, complexation, as demonstrated by dialysis, does not interfere with GI absorption. Because complexation did not alter physiological availability, any changes in urinary excretion may be attributed to the effect of viscosity.

The excretion rates were plotted against time for each subject. The times of the maximum excretion rate for each of the 11 subjects were averaged to give the mean time ($\pm SD$) of the maximum excretion rate given in Table II. The significance of the difference between the mean time of the maximum excretion rate of the aqueous reference dispersion and the suspensions with various suspending agents (Table II) was determined using the Student t test. The differences between the time of the maximum excretion rate of the aqueous reference dispersion and the test suspensions were significant.

Nitrofurantoin suspended with methylcellulose reportedly (8) delays the maximum absorption time by 1 hr relative to an aqueous reference dispersion. In this study, the time at which the average maximum excretion rate occurred for the preparation containing methylcellulose was only 0.3 hr longer than that of the aqueous reference dispersion, with the time of the maximum excretion rate varying from 1 to 6 hr for the 11 subjects. The reason for this wide variation without a significant difference between the aqueous reference dispersion and the suspension containing methylcellulose is unknown.

As shown in Table II, the mean time of the maximum excretion rate was increased by 1.4 hr for the experimental viscosity induced by algin, carbomer, guar gum, and colloidal magnesium aluminum silicate in comparison to an aqueous dispersion. Thus, the increased viscosity of these oral suspensions delayed absorption and excretion but did not diminish total absorption. Since increasing viscosity slows diffusion, mobility, and the dissolution rate, one would anticipate slower absorption and excretion.

Because nitrofurantoin is rapidly excreted in the urine, slower absorption could maintain a clinically recommended concentration of 1:100,000-1:200,000 (14) in the urine for a longer time. The mean nitrofurantoin concentration in the urine of 11 subjects after the oral administration of 200 mg of nitrofurantoin is given in Table III. With 1:100,000 as the nitrofurantoin concentration needed for the clinically acceptable bacteriostatic effect, the reference dispersion is acceptable for 6 hr. The suspensions containing carbomer, guar gum, and colloidal magnesium aluminum silicate are acceptable for 8 hr. The suspensions containing methylcellulose and algin are acceptable for 7 and 11 hr, respectively.

An increase in viscosity of the investigated suspensions delayed absorption; consequently, urinary excretion was delayed without a decrease in availability. As a result, the concentration in the urine was maintained

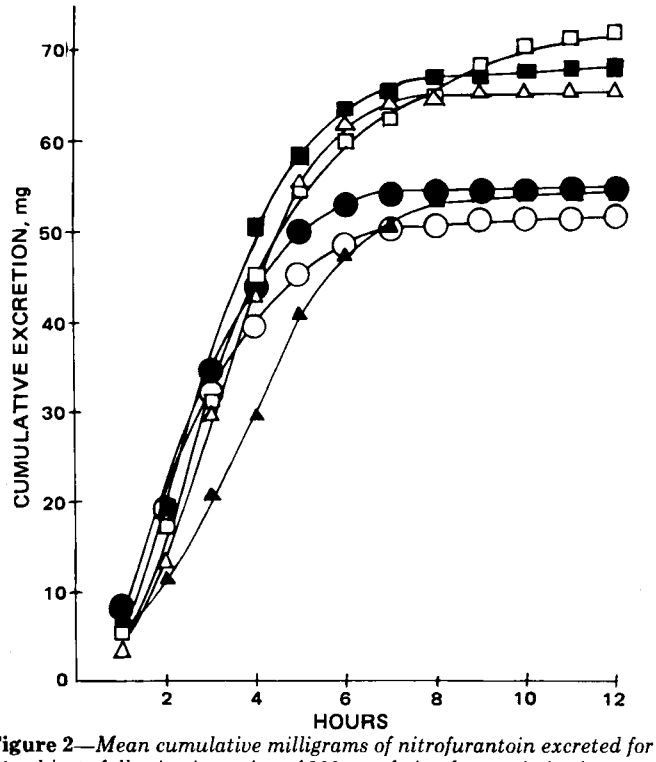

Figure 2—*Mean cumulative milligrams of nitrofurantoin excreted for 11 subjects following ingestion of 200 mg of nitrofurantoin in six preparations. Key: ●, aqueous reference dispersion; □, algin; △, carbomer; ■, guar gum; ○, methylcellulose, 4000 cps; and ▲, colloidal magnesium aluminum silicate.*

at a clinically useful concentration for a longer time. In the studied suspensions, the viscosity maintained an acceptable concentration in the urine for at least 2 hr longer than that obtained from an aqueous dispersion.

REFERENCES

(1) M. H. Malone, R. D. Gibson, and T. S. Miya, *J. Am. Pharm. Assoc., Sci. Ed.*, **49**, 529 (1960).

(2) C. Davison, J. L. Guy, M. Levitt, and P. R. Smith, *J. Pharmacol. Exp. Ther.*, **134**, 176 (1961).

(3) G. Levy and W. J. Jusko, *J. Pharm. Sci.*, **54**, 219 (1965).

(4) K. H. Harper and A. N. Wordan, *Toxicol. Appl. Pharmacol.*, **8**, 325 (1966).

(5) R. R. Hewitt and G. Levy, *ibid.*, **60**, 784 (1971).

(6) J. J. Ashley and G. Levy, *ibid.*, **62**, 688 (1973).

(7) R. J. Braun and E. L. Parrott, *ibid.*, **61**, 175 (1972).

(8) H. Seager, *J. Pharm. Pharmacol.*, **20**, 968 (1968).

(9) R. Larsen, "Statistics for the Health Sciences," Merrell Publishing, Columbus, Ohio, 1975, p. 350.

(10) J. D. Conklin and R. D. Hollifield, *Clin. Chem.*, **11**, 925 (1965).

(11) N. B. Shah and B. B. Sheth, *J. Pharm. Sci.*, **65**, 1618 (1976).

(12) J. R. Robinson, "Sustained and Controlled Release Drug Delivery Systems," Dekker, New York, N.Y., 1978, p. 641.

(13) "Remington's Pharmaceutical Sciences," 15th ed., Mack Publishing Co., Easton, Pa., 1975, chap. 63, p. 1153.

(14) "Physicians' Desk Reference," 32nd ed., Medical Economics Co., Oradell, N.J., 1978, p. 841.

ACKNOWLEDGMENTS

Abstracted in part from a dissertation submitted by M. M. Soci to the University of Iowa in partial fulfillment of the Master of Science degree requirements.

Surface Properties of Membrane Systems: Interaction of Electrolyte and Lipid with Ca^{2+} Ionophores

GIUSEPPE COLACICCO *x and MUKUL K. BASU

Received May 22, 1978, from the *Albert Einstein College of Medicine, Bronx, NY 10461.* Accepted for publication October 29, 1979. *Present address: Bioelectrochemistry Laboratory, Columbia University, New York, NY 10032.

Abstract □ When spread from organic solvents onto electrolyte solutions, the Ca^{2+} ionophores A23187 (I) and X537A (II) formed films with relatively high surface pressures and surface potentials. Ionophore I had collapse pressures between 16 and 19 dynes/cm and nearly equal surface activity on distilled water and on 1000 mEq of either sodium chloride or calcium chloride. Film pressure did not reveal appreciable ion selectivity. However, the surface potential of I on calcium chloride solution was higher than that on sodium chloride, and the potential difference, $\Delta(\Delta V)$, of 40 mv was independent of the electrolyte concentration. In contrast, the ion selectivity of II was dependent on the electrolyte concentrations since the $\Delta(\Delta V)$ value between calcium chloride and sodium chloride was maximal (130 mv) on 1000 mEq and negligible on 500- and 2000-mEq salt solutions. The isotherms of phospholipid–ionophore films were markedly different from those of the individual components, although they revealed ionophore characteristics at low film pressures and phospholipid behavior at high film pressures. The magnitude of the surface potential indicated that dipalmitoyl phosphatidylcholine enhanced, whereas mitochondrial lipid and cardiolipin reduced, the preference of the two ionophores for Ca^{2+} over Na^+. Since the ion selectivity was manifested most at both high electrolyte and high lecithin concentrations, the ionophore probably prefers the low dielectric constant of neutral lipid membranes to complex with the selected cation.

Keyphrases □ Membrane systems—surface properties, interaction of electrolytes and lipids with Ca^{2+} ionophores □ Surface pressure—films of Ca^{2+} ionophores on electrolyte solutions, effect of membrane lipids □ Surface potential—films of Ca^{2+} ionophores on electrolyte solutions, effect of membrane lipids □ Ionophores, Ca^{2+}—surface properties of films on electrolyte solutions, effect of membrane lipids

The ubiquitous occurrence and importance of Ca^{2+} in biological processes (enzymatic as well as mechanical) prompt interest in the modes of its availability, translocation, and action. The transport of ions in and out of cells may be aided by certain organic molecules, referred to as ionophores (1). These molecules are expected to influence metabolic (2) and physical (3) properties of cells in culture as well as *in vivo*.

Questions have been raised as to whether and how Ca^{2+} may stimulate or inhibit specific membrane and intracellular enzymes (4) and the contractile activity of systems within both the plasma membrane and the cytoplasm. Although extensive work has been published on the physicochemical properties of numerous ionophores and their interactions with natural and artificial membranes (1), little is known about the surface behavior of the Ca^{2+} ionophores A23187 (mol. wt. 523, I) and X537A (mol. wt. 590, II); this information is important since at least some of the action of the ionophore develops at membranes, whose structure and function are controlled by surface phenomena.

As in the case of valinomycin (5, 6), surface activity and surface potential should reflect certain structural char-

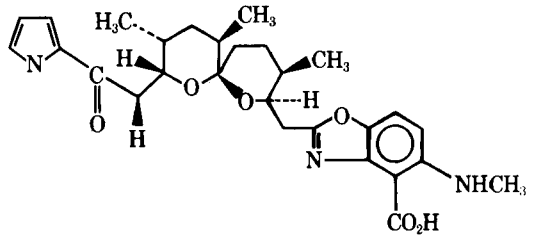

I

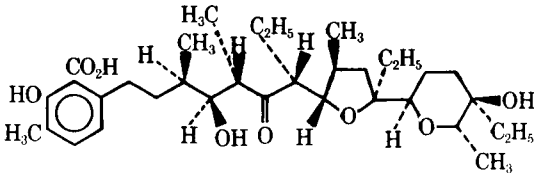

II

0022-3549/80/0400-0406$01.00/0

© 1980, American Pharmaceutical Association

at a clinically useful concentration for a longer time. In the studied suspensions, the viscosity maintained an acceptable concentration in the urine for at least 2 hr longer than that obtained from an aqueous dispersion.

REFERENCES

(1) M. H. Malone, R. D. Gibson, and T. S. Miya, *J. Am. Pharm. Assoc., Sci. Ed.*, **49**, 529 (1960).

(2) C. Davison, J. L. Guy, M. Levitt, and P. R. Smith, *J. Pharmacol. Exp. Ther.*, **134**, 176 (1961).

(3) G. Levy and W. J. Jusko, *J. Pharm. Sci.*, **54**, 219 (1965).

(4) K. H. Harper and A. N. Wordan, *Toxicol. Appl. Pharmacol.*, **8**, 325 (1966).

(5) R. R. Hewitt and G. Levy, *ibid.*, **60**, 784 (1971).

(6) J. J. Ashley and G. Levy, *ibid.*, **62**, 688 (1973).

(7) R. J. Braun and E. L. Parrott, *ibid.*, **61**, 175 (1972).

(8) H. Seager, *J. Pharm. Pharmacol.*, **20**, 968 (1968).

(9) R. Larsen, "Statistics for the Health Sciences," Merrell Publishing, Columbus, Ohio, 1975, p. 350.

(10) J. D. Conklin and R. D. Hollifield, *Clin. Chem.*, **11**, 925 (1965).

(11) N. B. Shah and B. B. Sheth, *J. Pharm. Sci.*, **65**, 1618 (1976).

(12) J. R. Robinson, "Sustained and Controlled Release Drug Delivery Systems," Dekker, New York, N.Y., 1978, p. 641.

(13) "Remington's Pharmaceutical Sciences," 15th ed., Mack Publishing Co., Easton, Pa., 1975, chap. 63, p. 1153.

(14) "Physicians' Desk Reference," 32nd ed., Medical Economics Co., Oradell, N.J., 1978, p. 841.

ACKNOWLEDGMENTS

Abstracted in part from a dissertation submitted by M. M. Soci to the University of Iowa in partial fulfillment of the Master of Science degree requirements.

Surface Properties of Membrane Systems: Interaction of Electrolyte and Lipid with Ca^{2+} Ionophores

GIUSEPPE COLACICCO *x and MUKUL K. BASU

Received May 22, 1978, from the *Albert Einstein College of Medicine, Bronx, NY 10461.* Accepted for publication October 29, 1979. *Present address: Bioelectrochemistry Laboratory, Columbia University, New York, NY 10032.

Abstract □ When spread from organic solvents onto electrolyte solutions, the Ca^{2+} ionophores A23187 (I) and X537A (II) formed films with relatively high surface pressures and surface potentials. Ionophore I had collapse pressures between 16 and 19 dynes/cm and nearly equal surface activity on distilled water and on 1000 mEq of either sodium chloride or calcium chloride. Film pressure did not reveal appreciable ion selectivity. However, the surface potential of I on calcium chloride solution was higher than that on sodium chloride, and the potential difference, $\Delta(\Delta V)$, of 40 mv was independent of the electrolyte concentration. In contrast, the ion selectivity of II was dependent on the electrolyte concentrations since the $\Delta(\Delta V)$ value between calcium chloride and sodium chloride was maximal (130 mv) on 1000 mEq and negligible on 500- and 2000-mEq salt solutions. The isotherms of phospholipid–ionophore films were markedly different from those of the individual components, although they revealed ionophore characteristics at low film pressures and phospholipid behavior at high film pressures. The magnitude of the surface potential indicated that dipalmitoyl phosphatidylcholine enhanced, whereas mitochondrial lipid and cardiolipin reduced, the preference of the two ionophores for Ca^{2+} over Na^+. Since the ion selectivity was manifested most at both high electrolyte and high lecithin concentrations, the ionophore probably prefers the low dielectric constant of neutral lipid membranes to complex with the selected cation.

Keyphrases □ Membrane systems—surface properties, interaction of electrolytes and lipids with Ca^{2+} ionophores □ Surface pressure—films of Ca^{2+} ionophores on electrolyte solutions, effect of membrane lipids □ Surface potential—films of Ca^{2+} ionophores on electrolyte solutions, effect of membrane lipids □ Ionophores, Ca^{2+}—surface properties of films on electrolyte solutions, effect of membrane lipids

The ubiquitous occurrence and importance of Ca^{2+} in biological processes (enzymatic as well as mechanical) prompt interest in the modes of its availability, translocation, and action. The transport of ions in and out of cells may be aided by certain organic molecules, referred to as ionophores (1). These molecules are expected to influence metabolic (2) and physical (3) properties of cells in culture as well as *in vivo*.

Questions have been raised as to whether and how Ca^{2+} may stimulate or inhibit specific membrane and intracellular enzymes (4) and the contractile activity of systems within both the plasma membrane and the cytoplasm. Although extensive work has been published on the physicochemical properties of numerous ionophores and their interactions with natural and artificial membranes (1), little is known about the surface behavior of the Ca^{2+} ionophores A23187 (mol. wt. 523, I) and X537A (mol. wt. 590, II); this information is important since at least some of the action of the ionophore develops at membranes, whose structure and function are controlled by surface phenomena.

As in the case of valinomycin (5, 6), surface activity and surface potential should reflect certain structural char-

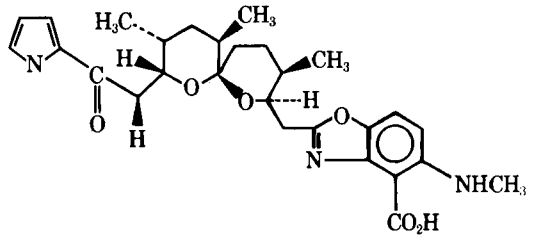

I

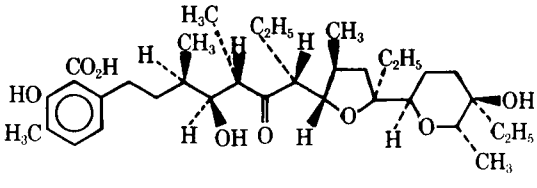

II

0022-3549/80/0400-0406$01.00/0

© 1980, American Pharmaceutical Association

acteristics of the ionophore molecule and could be related to two phenomena: (*a*) the ability of the ionophore to complex with the various ions, and (*b*) the modifications brought about in the architecture of the membrane when the ionophore picks up or delivers the ion or when the ionophore finally lodges in or crosses the membrane.

This paper describes the surface pressure and surface potential characteristics of films of ionophores I and II on various concentrations of sodium chloride and calcium chloride solutions. To evaluate the influence of membrane lipids on these parameters, films of mixtures of the ionophore with dipalmitoyl phosphatidylcholine, total mitochondrial lipids, and cardiolipin also were studied.

EXPERIMENTAL

The sodium salts of ionophores I and II were used[1]. Routine TLC (2) showed that the dipalmitoyl phosphatidylcholine and beef heart cardiolipin[2] were homogeneous, and they were not purified further. Rat liver mitochondria[3] were prepared according to published methods (7); the total lipid was extracted by shaking the aqueous mitochondrial suspension once with four volumes of chloroform–methanol (2:1) and then with four volumes of chloroform.

TLC was performed with precoated silica gel G plates[4], chloroform–methanol–water–concentrated ammonium hydroxide (70:30:2:4) as the solvent, and the appropriate lipid standards. The lipid pattern was typical of mitochondria, with phosphatidylcholine > phosphatidylethanolamine > cardiolipin > sphingomyelin. For all practical purposes, this lipid composition of mitochondria is independent of either the organ or the animal species (8).

The lipids for the film preparation were dissolved to give 1 mg/ml in chloroform–methanol (85:15), and the solutions were stored at −20° for no longer than 2 weeks. During the experiments, the lipid solutions were kept in ice. The organic solvents were of the highest spectroscopic grade. Water was distilled twice (9). The electrolyte solutions, prepared with freshly distilled water and reagent grade salts, were foamed to remove surface-active contaminants (10) and were stored for no longer than 3 days at room temperature.

The techniques for the determinations of surface pressure and surface potential were described previously (10), except that a circular constant area trough was used (11) instead of a rectangular trough. Measured volumes of the lipid or ionophore solution in organic solvent were applied onto a 20-cm^2 area, and the values of surface pressure and surface potentials were related to the quantity of the material applied per square centimeter or to the apparent molecular area of the ionophore and other lipid.

RESULTS AND DISCUSSION

The surface pressure and surface potential values are averages from three experiments, with deviations of ±0.2 dyne/cm and ±5 mv, respectively. The π and ΔV effects of the ionophores revealed characteristics that should be related to their molecular structures.

Theoretical Considerations—Since the two monocarboxylic acid ionophores, I and II, are complex molecules, the effects of the electrolyte on surface pressure and surface potential may not be predicted at once. Such a prediction, however, will contain information or suggestions about several possible phenomena: (*a*) interaction of the electrolyte cation with the ionized carboxylic group of the ionophore; (*b*) discrimination between Na^+ and Ca^{2+} in terms of surface pressure and/or surface potential; (*c*) conformational changes, which are known to occur during such interactions in bulk (1); (*d*) rigidity or flexibility of the ionophore molecule; (*e*) electrolyte penetration into the interface (12); and (*f*) changes in the interfacial structures of the water of hydration (13) and in the distribution of dipoles (13, 14).

Each of these effects is expected to contribute to both surface pressure and surface potential but, unfortunately, cannot be evaluated individually in the present state of the art. Nevertheless, determinations of surface pressure and surface potential of the Ca^{2+} ionophores can be used to establish empirical correlations between structure and function, correlations that are fundamental to future biological studies.

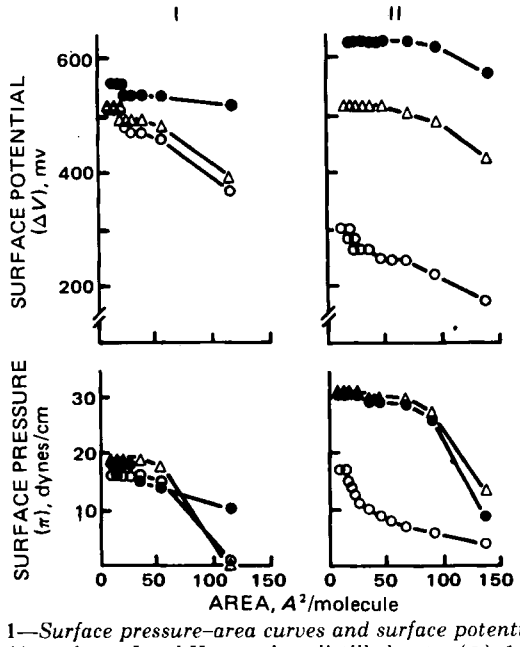

Figure 1—*Surface pressure–area curves and surface potential–area curves of ionophores I and II spread on distilled water* (○), *1 M NaCl* (△), *and 0.5 M* $CaCl_2$ (●) *at 25°.*

Effects of Electrolyte on Ionophore Surface Pressure–Area (π–*A*) and Surface Potential–Area (ΔV–*A*) Curves—Figures 1 and 2 describe experiments in which films of ionophores I and II were spread on distilled water and on aqueous solutions containing three concentrations of either sodium chloride or calcium chloride (150, 1000, and 2000 mEq). The film pressure, in dynes per centimeter, and the surface potential, in millivolts, are related to the apparent molecular area of each ionophore on water and on aqueous solutions of 1000 mEq of sodium chloride or calcium chloride in Fig. 1 and to the electrolyte concentration at the molecular area of 50 Å^2 for each ionophore in Fig. 2. The two ionophores were surface active with II more than I; according to their surface potentials, they discriminated differently between Na^+ and Ca^{2+}.

π–A *Curves*—Films of II were more expanded but had higher collapse pressures than those of I on the aqueous electrolytes; this difference could be ascribed to the greater flexibility of II, which requires constraints to build up pressure as compared to the more rigid I molecule, whose iso-

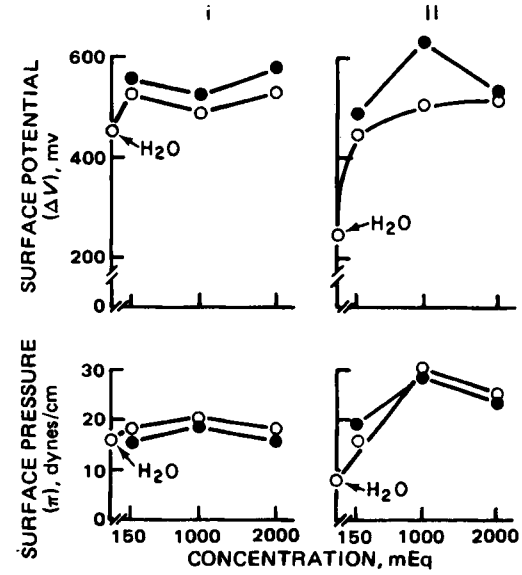

Figure 2—*Influence of electrolyte concentration on the surface pressure and surface potential of ionophores I and II at the molecular area of 50 Å^2 at 25°. Key:* ○, *sodium chloride; and* ●, *calcium chloride.*

[1] These salts were supplied by Dr. Robert J. Hosley of Eli Lilly, Indianapolis, Ind., and Dr. W. Scott of Hoffmann–La Roche, Nutley, N.J., respectively.

[2] Applied Science Laboratories, State College, Pa.

[3] Gift of Dr. R. Rezek, Departments of Neurology and Biochemistry, Albert Einstein College of Medicine, New York, NY 10461.

[4] Analtech, Newark, N.J.

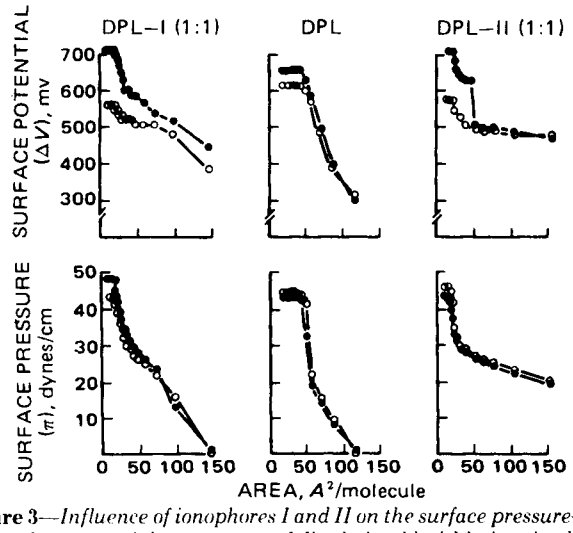

Figure 3—*Influence of ionophores I and II on the surface pressure–area and surface potential–area curves of dipalmitoyl lecithin in mixed films spread on 1.0 M NaCl (○) and 0.5 M $CaCl_2$ (●) at 25°. The apparent molecular areas are averages of the areas of lecithin and the ionophore.*

therm on distilled water did not differ much from that on the subphase containing various electrolyte concentrations. The slow rise of pressure with compression indicates that II must encounter difficulty in making a film on distilled water (Fig. 1); II was much more surface active than I on electrolyte solutions. The collapse pressures on 1000 mEq of sodium chloride or calcium chloride were 30 dynes/cm for II and 18 dynes/cm for I.

The virtual identity of the isotherms of II on solutions of 1000 mEq of sodium chloride or calcium chloride means that, at this electrolyte concentration, the ionophore cannot distinguish between Na^+ and Ca^{2+} on the basis of surface tension or surface pressure. Ionophore II did distinguish between the cations at lower concentration, where its isotherm on 150 mEq of calcium chloride (Fig. 2) was markedly more expanded (higher) than that on sodium chloride. At present, no explanation is available for this effect, which is the opposite of the film contraction expected from the interaction of Ca^{2+} with negatively charged lipids (15). The complexity of the ionophore molecule may be responsible for numerous deviations from the surface behavior of a straight-chain lipid.

The two ionophores were similar in that, on both electrolytes at all concentrations studied, they reached the different collapse or saturation pressures at an apparent molecular area of 50 Å², below which the π and ΔV values were quite stable. For reasons given earlier (6), interpretation of the apparent molecular area must be postponed until an exact determination is made of the effective number of ionophore molecules per square centimeter and their orientation in the film, parameters that are not accessible at present.

ΔV–A Curves—Unlike surface pressure, the surface potential revealed marked ion selectivities for both ionophores.

On distilled water, the surface potential of I was 200 mv higher than that of II. At all areas, I distinguished sodium chloride from water by 20 mv in favor of sodium chloride and sodium chloride from calcium chloride by 40 mv in favor of calcium chloride. Unlike I, II showed a marked dependence of π and ΔV on the electrolyte concentration (Fig. 2) and distinguished markedly well between Na^+ and Ca^{2+} at one electrolyte concentration (1000 mEq), although by a much greater difference (130 mv) as compared to 40 mv for I.

The π–A curves of II on 1000 mEq of sodium chloride and calcium chloride were nearly superimposable. The ΔV–A curve of II on sodium chloride was 300 mv higher than that on water; on calcium chloride, it was 130 mv higher than that on sodium chloride (Fig. 1). In contrast, the selectivity of I for Ca^{2+} was about the same (40 mv) at all electrolyte concentrations (Fig. 2).

These differences in surface behavior between the two ionophores are consistent with a rigid structure for I and a flexible structure for II. At present, it is not possible to relate these observations to the conformational changes that the ionophores undergo in bulk (1), primarily because of a lack of spectroscopic methods capable of viewing the interface directly *in situ*.

Lipid Influence on Ion Selectivity and Surface Behavior of the Ionophore—The foregoing data show that ionophores I and II are surface active and distinguish between Na^+ and Ca^{2+} in the absence of membrane lipids. Since the transport of Ca^{2+} by the ionophore across the membrane could imply some interaction of the ionophore with the membrane structures that negotiate Ca^{2+} with the ionophore, information about the membrane behavior of the ionophore may be attained by a study of the interaction of the electrolyte with films of ionophore and phospholipid mixtures.

Three mixtures were studied: dipalmitoyl phosphatidylcholine–ionophore, mitochondrial lipid–ionophore, and cardiolipin–ionophore. The lipid mixtures in chloroform–methanol (85:15) were spread on the aqueous subphase containing 1000 mEq of sodium chloride or calcium chloride. This electrolyte concentration was chosen for convenience, since the surface potential effects were largest; they were small at either lower or higher salt concentrations.

Dipalmitoyl Phosphatidylcholine—Figure 3 shows the π–A and ΔV–A curves of dipalmitoyl lecithin (DPL) and equal weight mixtures of it with I and II on 1000 mEq of sodium chloride or calcium chloride.

With this salt concentration, the dipalmitoyl lecithin films were slightly more expanded, and the ΔV values were appreciably higher than on more dilute solutions [*e.g.*, 100 mEq (12)]; dipalmitoyl lecithin did not significantly discriminate between Na^+ and Ca^{2+}. However, both ionophores influenced appreciably the π–A and ΔV–A curves of the phospholipid in the dipalmitoyl lecithin–ionophore film, in which dipalmitoyl lecithin seemed to enhance markedly the ion selectivity of the ionophore (Ca^{2+} over Na^+), especially in terms of surface potential.

The π–A and ΔV–A curves of the mixtures were quite different from those of individual components. The pressure–area curves of the mixed films had an ionophore character (expanded) at low pressure. At the average molecular area of 150 Å², the pressure was near zero for the dipalmitoyl lecithin–I system and near 20 dynes/cm for dipalmitoyl lecithin–II. This observation strengthens the suggestion that I is rigid whereas II is flexible and thus is more compressible than I.

Although the disappearance of the ionophore character from the mixed ionophore–lecithin film in terms of film pressure could suggest that, at high pressure, the ionophore may be squeezed out of the mixed film, which then resumes the lecithin character, this mechanism may not be valid because the surface potential increase at high pressure is that of a unique lecithin–ionophore mixture, far above the ΔV of lecithin alone. The mode of the ionophore–lecithin interaction thus remains to be investigated.

Whereas the dipalmitoyl lecithin–ionophore mixtures did not distinguish between Na^+ and Ca^{2+} by the surface pressure, they did distinguish between the cations markedly well by the surface potential, especially at high pressure where the $\Delta(\Delta V)$ difference between calcium chloride and sodium chloride reached ~150 mv for both ionophores as opposed to 40 mv for I and 130 mv for II in the absence of dipalmitoyl lecithin. The fact that the selectivity between Na^+ and Ca^{2+} was manifested at high film pressure and high electrolyte concentration is reminiscent of the Na^+–K^+ discrimination of valinomycin films, which required 700–1000 mEq of electrolyte and film pressures above 20 dynes/cm to show a dramatic effect of K^+ on the surface potential (5, 6, 16). Indeed, the presence of lipid brings about a low dielectric constant (favorable to ionic inter-

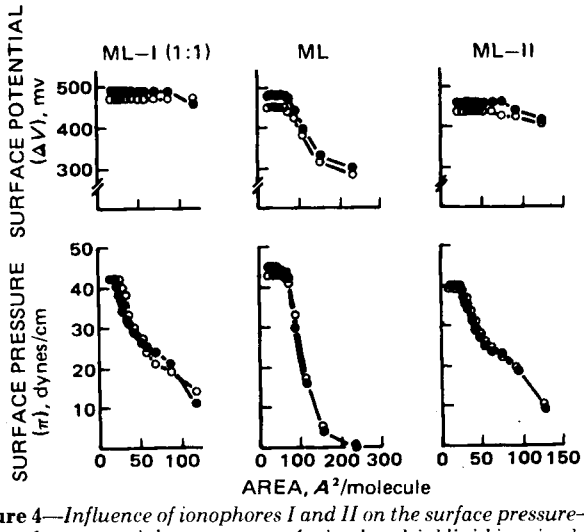

Figure 4—*Influence of ionophores I and II on the surface pressure–area and surface potential–area curves of mitochondrial lipid in mixed films spread on 1.0 M NaCl (○) and 0.5 M $CaCl_2$ (●) at 25°. The apparent molecular areas are calculated averages of the areas of ionophore and mitochondrial lipid.*

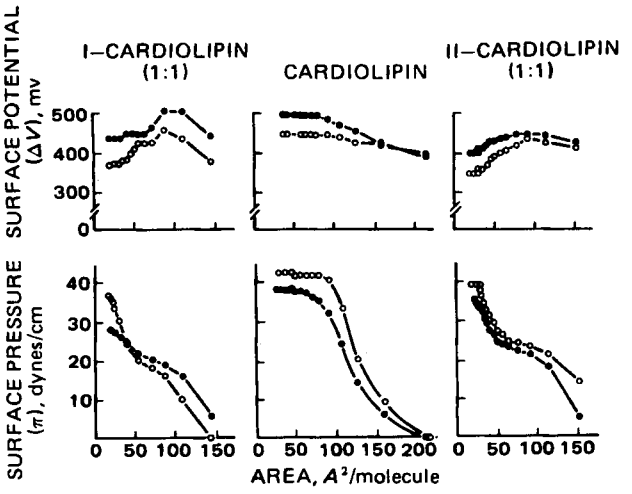

Figure 5—*Influence of ionophores I and II on the surface pressure–area and surface potential–area curves of cardiolipin on 1.0 M NaCl (○) and 0.5 M $CaCl_2$ (●) at 25°. The apparent molecular areas are averages of the areas of cardiolipin and the ionophore.*

actions) and high surface potentials (6, 13). The fact that this effect was not seen at higher electrolyte concentrations is interesting, has no explanation as yet, and clearly reflects a specificity that calls for optimal conditions of dose response in the interaction of Ca^{2+} with the ionophore.

Mitochondrial Lipid—The film was made by spreading the total lipid extract of rat liver mitochondria as a model of a membrane containing negatively charged groups, namely, the two phosphate groups of cardiolipin (diphosphatidylglycerol). Unlike dipalmitoyl lecithin, the mitochondrial lipid (ML) conferred little ion-discriminating ability to either ionophore (Fig. 4).

Although a high collapse pressure of the mitochondrial lipid was revealed in the isotherm of mixed films of the ionophore with this lipid, the surface potential of the mixture reflected an ionophore character in the sense that its ΔV–A curve was lifted to a constant saturation value that extended over the entire area range. However, the ΔV effect of the electrolyte in the two mixtures was not different from that of the mitochondrial lipid alone.

Cardiolipin—Since the major ionic component of mitochondrial lipid is cardiolipin, the behavior of the cardiolipin–ionophore mixed film was evaluated to see if the behavior of the mitochondrial lipid could be ascribed to cardiolipin. The results (Fig. 5) confirm that possibility.

More evident than with the total mitochondrial lipid was the contraction in the molecular area of cardiolipin in the presence of Ca^{2+} as compared to Na^+ (Fig. 5), a discrimination that is known for acidic phospholipids (15, 17) but was not so apparent and was modified partially with the mixed ionophore–cardiolipin films (Fig. 5). As with the mitochondrial lipid and with cardiolipin alone, the surface potential of the cardiolipin–ionophore mixed film showed a modest separation in ΔV between Na^+ and Ca^{2+}, with the value for Ca^{2+} higher as expected.

An unusual feature of the ionophore–cardiolipin mixed film was the maximum in surface potential, between pressures of 20 and 22 dynes/cm, above which, although the pressure continued to rise until saturation, the surface potential decreased appreciably on sodium chloride and on calcium chloride solutions. This unusual behavior is reminiscent of the ΔV–A curve of gangliosides (18). Since the film pressure continued to rise, one can argue that the film was not collapsing and that the fall in surface potential could be accounted for by reorganization of molecules and/or dipoles so as to produce a film with a higher dielectric constant, an excess of ∓-oriented ionic dipoles (including water), or both (6, 13, 19–21).

CONCLUSIONS

In the surface chemistry literature, there has been a misleading tendency to speculate or even make conclusions about the orientation of molecular groups and dipoles from surface potential data. That approach has been challenged; but for a variety of reasons that are given elsewhere (6, 12, 13, 19–22), quantitative models must be postponed until the molecular correlates of surface potentials are understood. Such models may be derived only after information is obtained about the detailed molecular topography of the films at the air–water interface; such experiments involving radiolabels and direct spectroscopy of the interface cannot be done in the present state of the art (12). Meanwhile, empirical comparisons and correlations are valuable.

The comparisons between Na^+ and Ca^{2+} were based on equivalent concentrations instead of uncomparable ionic strength (0.225 for calcium chloride and 0.150 for sodium chloride). This choice was made to avoid blurring of the data by electrostatic effects due to ion binding competition in such different equivalent concentrations. For similar reasons, in working with ionophore–phospholipid mixtures, the empirical π–A relationships were preferred to graphs of mean molecular area *versus* mole fraction.

Unlike prostaglandins (23) [carboxylic acids that produced films with very small surface pressures (0–9 dynes/cm) and surface potentials (−10 to +250 mv)], I and II were quite surface active and had fairly large surface potentials. Both the surface pressure and especially the surface potential values were influenced by certain electrolyte concentrations. As observed with acidic phospholipids (15, 17) and fatty acids (24) at pH 5.7, the ΔV values on calcium chloride were higher than those on sodium chloride, indicating preferential involvement or binding of Ca^{2+}. However, at certain low and high electrolyte concentrations, the two ionophores, especially II, could not distinguish between Na^+ and Ca^{2+}. Discrimination between Na^+ and Ca^{2+} in terms of surface potential was enhanced markedly when the ionophore was mixed with dipalmitoyl lecithin; it was diminished when the ionophore was mixed with acidic lipids, either mitochondrial lipids or cardiolipin, despite the fact that such lipids interacted with Ca^{2+} with a marked surface potential effect.

The monolayer experiments suggest that, in the presence of Ca^{2+}, both ionophores prefer the hydrophobic medium of membranes and are admitted more easily into membranes containing high doses of neutral or hydrophobic phospholipid. These concepts of surface science could be exploited in the interpretation of the behavior of ionophores in experiments that are aimed at differentiating between cell types on the basis of the ionophore's selectivity for Ca^{2+} and for the membrane lipid.

REFERENCES

(1) B. C. Pressman, *Ann. Rev. Biochem.*, **45**, 501 (1976).

(2) G. Colacicco, M. K. Basu, A. K. Ray, M. Wittner, and R. M. Rosenbaum, *Prostaglandins*, **14**, 283 (1977).

(3) G. Colacicco, C. F. Gillman, and A. K. Ray, "Abstract from 52nd National Colloid Surface Science Symposium (American Chemical Society)," Knoxville, Tenn., June 1978.

(4) W. C. Picket, R. L. Jesse, and P. Cohen, *Biochim. Biophys. Acta*, **486**, 209 (1977).

(5) G. Kemp and C. Wenner, *ibid.*, **282**, 1 (1972).

(6) G. Colacicco and E. E. Gordon, *J. Colloid Interface Sci.*, **63**, 76 (1978).

(7) D. Holtman and C. L. Moore, *Biol. Neonate*, **22**, 230 (1973).

(8) S. Fleischer and G. Rouser, *J. Am. Oil Chem. Soc.*, **42**, 588 (1965).

(9) G. Colacicco, M. K. Basu, and E. M. Scarpelli, *Resp. Physiol.*, **27**, 169 (1976).

(10) G. Colacicco and M. M. Rapport, *J. Lipid Res.*, **6**, 258 (1966).

(11) G. Colacicco, *J. Colloid Interface Sci.*, **29**, 345 (1969).

(12) G. Colacicco and M. K. Basu, *Biochim. Biophys. Acta*, **509**, 230 (1978).

(13) G. Colacicco, in "Biological Horizons in Surface Science," L. M. Prince and D. F. Sears, Eds., Academic, New York, N.Y., 1973, p. 247.

(14) G. Caines, Jr., "Insoluble Monolayers at Liquid–Gas Interfaces," Interscience, New York, N.Y., 1966.

(15) A. D. Bangham and D. Papahadjopoulos, *Biochim. Biophys. Acta*, **126**, 181 (1966).

(16) G. Colacicco, E. E. Gordon, and G. Berchenko, *Biophys. J.*, **8**, 22a (1968).

(17) D. O. Shah and J. H. Schulman, *J. Lipid Res.*, **6**, 341 (1965).

(18) G. Colacicco, J. M. Burnell, and M. K. Basu, *J. Pharm. Sci.*, **68**, 1246 (1979).

(19) G. Colacicco, *Biochim. Biophys. Acta*, **266**, 313 (1972).

(20) G. Colacicco, *Ann. N.Y. Acad. Sci.*, **195**, 224 (1972).

(21) G. Colacicco, *Biophys. J.*, **21**, 48a (1978).

(22) G. Colacicco, M. K. Basu, and F. A. Tansey, *Adv. Chem. Ser.*, in press.

(23) G. Colacicco and M. K. Basu, *Prostaglandins*, **16**, 189 (1978).

(24) E. D. Goddard, *Adv. Chem. Ser.*, **144**, 67 (1975).

ACKNOWLEDGMENTS

Supported by National Institutes of Health Grant and Contract N01-HR5-2952 from the Heart, Lung, and Blood Institute.

Digoxin Degradation in Acidic Dissolution Medium

TAKASHI SONOBE ˣ, SHUNJI HASUMI, TAKASHI YOSHINO, YOICHI KOBAYASHI, HIROITSU KAWATA, and TSUNEJI NAGAI *

Received January 8, 1979, from the *Institute of Research and Development, Yamanouchi Pharmaceutical Co., Ltd., 1-1-8 Azusawa, Itabashi-ku, Tokyo 174, Japan.* Accepted for publication October 31, 1979. *Present address: Hoshi Institute of Pharmaceutical Sciences, Hoshi College of Pharmacy, 2-4-41 Ebara, Shinagawa-ku, Tokyo 142, Japan.

Abstract □ The release of digoxin and its simultaneous conversion to digoxigenin bisdigitoxoside, digoxigenin monodigitoxoside, and digoxigenin in a USP dissolution test medium were followed by high-pressure liquid chromatography. Two products, Tablets A and B, were manufactured by solvent deposition and simple blending methods, respectively. Tablet A released digoxin faster than Tablet B in distilled water and in artificial intestinal juice, and no decomposition was observed. In the USP dissolution test medium, the rate of hydrolysis to digoxigenin bisdigitoxoside was almost equal to that of hydrolysis to digoxigenin monodigitoxoside, and a comparatively large formation rate of digoxigenin was observed. Concentrations of digoxin and its decomposition products were described by differential equations that included dissolution rates of digoxin (rapidly dissolving digoxin and digoxin crystals) and an apparent hydrolysis rate. In the earlier stage of dissolution, hydrolysis was rate determining; in the later stage, dissolution became the rate-determining step for overall digoxin degradation. To suppress digoxin hydrolysis in the USP dissolution test medium, a developmental formulation study was performed. The incorporation of magnesium oxide and magnesium hydroxide–aluminum hydroxide in the tablet formulations inhibited digoxin hydrolysis by 15.3 and 14.5%, respectively, after dissolution for 30 min without serious delay of drug release.

Keyphrases □ Digoxin—dissolution and degradation in acidic solution, high-pressure liquid chromatography, kinetic study □ Dissolution—digoxin tablets, biphasic dissolution □ Stability—digoxin in acidic solution, high-pressure liquid chromatography, kinetic study, incorporation of antacid □ Antacids—suppression of digoxin degradation

The bioavailability of digoxin preparations was reported to vary significantly among brands and batches (1–5). Many studies revealed the correlation between the dissolution rate and the bioavailability of digoxin, but little attempt was made to separate digoxin from its degraded glycosides (6–8). Digoxin reportedly was hydrolyzed in acidic media (9), and the therapeutic efficacy may have decreased as a result (10). Although the absorption kinetics of digoxin, digoxigenin bisdigitoxoside, and digoxigenin monodigitoxoside were in the same range, the blood concentrations of the latter two substances were five to six times lower than that of digoxin (11). The cardioactivity of digoxigenin was one-tenth of that of digoxin, but the other compounds possessed approximately the same activity (12).

It was of interest to study the dissolution and simultaneous hydrolysis of digoxin *in vitro* since they may be potential causes of the variation of bioavailability and clinical efficacy in different digoxin formulations. To investigate digoxin hydrolysis, a quantitative assay that distinguishes between digoxin and its decomposition products is required. All of the current assays (13–15) fail to determine digoxin and its decomposition products individually without additional separations, except for a high-performance liquid chromatographic method (16).

The purposes of the present investigation were to use high-pressure liquid chromatography (HPLC) to study the hydrolysis of digoxin released from tablets during dissolution and to establish a pharmaceutical method of preventing digoxin hydrolysis in an acidic medium.

EXPERIMENTAL

Materials—Digoxin, digoxigenin bisdigitoxoside, digoxigenin monodigitoxoside, and digoxigenin were used as received[1]. The following materials were USP grade: lactose, cornstarch, magnesium hydroxide–aluminum hydroxide, and magnesium oxide. Synthetic aluminum silicate was JP grade. The other reagents were reagent grade unless otherwise stated.

To prepare Tablet A, a 5% chloroform–ethanol solution (2:1 v/v) of digoxin was deposited on lactose–cornstarch (7:3 w/w) diluent and granulated with 10% cornstarch paste to make ~0.2% digoxin granules. The granules were compressed to tablets of 7 mm in diameter and 120 mg in weight by a single-punch tableting machine[2] (17).

To prepare Tablet B, digoxin crystals were blended with lactose–cornstarch (7:3 w/w) diluent to give a 10% digoxin powder. The powder was diluted repeatedly in the same manner to give a final digoxin content of ~0.2%. The resultant digoxin–diluent mixture was granulated and compressed to give tablets of the same size as Tablet A following the described procedure (17).

Tablets A and B each contained 0.25 mg of digoxin. A digoxin powder mixture also was prepared containing antacids to study the effect of antacids in suppressing digoxin hydrolysis in acidic media. This mixture was prepared by dissolving 0.25 g of digoxin crystals in 50 ml of ethanol–chloroform (1:2 v/v) solution and incorporating the resulting solution in 20 g of magnesium hydroxide–aluminum hydroxide, synthetic aluminum silicate, or magnesium oxide. After mixing, the solvents were evaporated by heating on a thermostated water bath at 40° for 4 hr. The powder mixture was blended with lactose–cornstarch (7:3 w/w) diluent and granulated with 10% cornstarch paste, and the mixture was dried and passed through a 32-mesh screen. The digoxin content of 120 mg of the powders was 0.25 mg.

Analyses of Digoxin and Glycosides—Spectrofluorometry was performed to determine the total amount of digoxin and glycosides. For the separate determination of digoxin and glycosides, an HPLC method was developed.

Spectrofluorometry—The digoxin concentration in solution was determined with a spectrofluorometer[3] following the assay described for the dissolution testing of digoxin tablets in USP XIX (13).

HPLC—The separation conditions developed by Castle (16) were modified for the present experiments. A high-pressure liquid chromatograph[4] was used. The eluent was monitored spectrophotometrically at 220 nm. The separation utilized a column[5] (4 mm × 15 cm) operating at 1.5 ml/min with 25% acetonitrile solution as the mobile phase.

The retention volumes for digoxin, digoxigenin bisdigitoxoside, digoxigenin monodigitoxoside, and digoxigenin were 12.1, 7.2, 4.5, and 3.8 ml, respectively. The practical detection limit for digoxin was 50 ng. The resolution between the closest peaks of digoxigenin and digoxigenin monodigitoxoside was maintained at >1.3.

For the quantitation of digoxin and glycosides, aqueous standard solutions were prepared by dissolving accurately weighed quantities of digoxin, digoxigenin bisdigitoxoside, digoxigenin monodigitoxoside, and digoxigenin and treating these solutions in the same manner as the sample solution. The amounts of the components were determined by comparing the peak heights with those of the standard solutions.

Dissolution Study—The dissolution tests for Tablets A and B were performed using a rotating-basket apparatus[6] described in USP XIX. Six tablets were used to determine the dissolution rate at 37° in 250 ml of distilled water, USP dissolution test medium (0.6% HCl), and artificial

[1] Boehringer, Mannheim GMBH, West Germany.
[2] Kimura KM-2, Okada Seiko Co., Tokyo, Japan.
[3] Hitachi MPF-4, Hitachi Ltd., Tokyo, Japan.
[4] The chromatographic system consisted of a 6000 A pump and a U6K universal injector (Waters Associates, Milford, Mass.) coupled with a SF-770 detector (Schoeffel Instrument Corp., Westwood, N.J.).
[5] LiChrosorb RP-18 (5 μm), Merck, Darmstadt, West Germany.
[6] Toyama Sangyo Co., Osaka, Japan.

0022-3549/80/0400-0410$01.00/0
© 1980, American Pharmaceutical Association

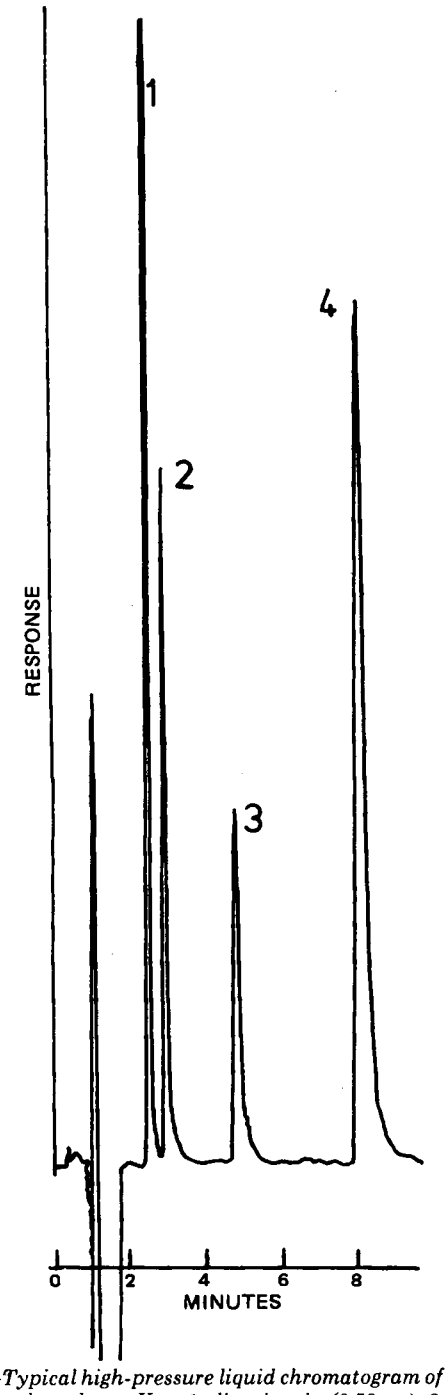

Figure 1—*Typical high-pressure liquid chromatogram of digoxin and its hydrolyzed products. Key: 1, digoxigenin (0.50 μg); 2, digoxigenin monodigitoxoside (0.50 μg); 3, digoxigenin bisdigitoxoside (0.50 μg); and 4, digoxin (2.5 μg).*

intestinal juice[7] at a basket rotation speed of 100 rpm. At the specified time, 5 ml of the test medium was withdrawn and filtered immediately through a membrane filter[8] (pore size of 0.22 μm).

With the USP dissolution test medium, 1.5 ml of Sørensen borate buffer (0.2 *M*, pH 10.0) was added to prevent further digoxin hydrolysis. Five milliliters of the dissolution medium was added at each sampling time to maintain a constant volume. Sample solutions were analyzed by spectrofluorometry and HPLC after appropriate dilution with distilled water.

[7] JP IX second disintegration test fluid: dissolve 35.8 g of dibasic sodium phosphate in 6 ml of 10% HCl and distilled water to make 1000 ml. The solution pH is ~7.5.

[8] Millipore, Japan Millipore Ltd., Tokyo, Japan.

RESULTS AND DISCUSSION

Dissolution—The individual determination of digoxin, digoxigenin bisdigitoxoside, digoxigenin monodigitoxoside, and digoxigenin was accomplished satisfactorily by HPLC as shown in Fig. 1. The total amount of digoxin detected by the conventional spectrofluorometric method was consistent with the HPLC results.

Digoxin instability in gastric juice was confirmed by analysis of digoxin and its degraded materials and was suggested as a possible cause of decreased oral efficacy (10). Degradation steps or pathways of digoxin in acidic media have been considered (18). The glycoside bond in the monoglycoside was suggested as being more resistant to acid hydrolysis than the bisglycoside and digoxin (9). Digoxin decomposition is closely related to reduced cardiac action. The rate constant of digoxigenin appearance might be clinically significant because of the lowered pharmacological action.

Figure 2 shows the dissolution of digoxin from Tablets A and B in distilled water and in artificial intestinal juice. Tablet A released digoxin faster than did Tablet B; their $t_{1/2}$ values were 1 and >60 min, respectively, which suggested that Tablet B would not meet the USP XIX requirement. This difference in the dissolution rates resulted mainly from the production procedure, because the same lot of digoxin crystals was incorporated in both digoxin tablets. For Tablet A, digoxin was deposited on diluents after complete dissolution in ethanol–chloroform, which might have resulted in easier dissolution of digoxin crystals. This deposit might be the amorphous layer, the existence of which was demonstrated by ball milling the digoxin crystals (19). No digoxin decomposition was observed in distilled water and in artificial intestinal juice; earlier work showed that digoxin mainly undergoes degradation at acidic pH (9, 10).

The amount of digoxin that dissolved from Tablet A in the USP XIX dissolution medium increased remarkably in a short time. Digoxin release reached a peak in ~6 min, and this release was followed by a gradual decrease that was related to the increase of decomposed digoxin. The digoxigenin bisdigitoxoside concentration reached a plateau in 10 min, while the digoxigenin monodigitoxoside concentration increased linearly with the time. These findings suggest that the degradation rate of digoxin to digoxigenin bisdigitoxoside is almost equal to the degradation rate of digoxin to digoxigenin monodigitoxoside and that a comparatively high formation rate of digoxigenin exists. In a previous study (20) with a conventional solvent extraction method, 75% of the dissolved digoxin was degraded 60 min after the initiation of the dissolution test in the USP XIX dissolution test medium; that finding supports results obtained in this study.

After the disintegration of digoxin tablets, the digoxin dissolution is assumed to consist of two stages; the dissolution of digoxin into the medium from crystals and the simultaneous hydrolysis of digoxin by acid. It also is assumed that a freely soluble amorphous layer exists in crystals (21) and that the hydrolysis of digoxin at the surface of the digoxin solid is negligibly small compared to that in solution.

With these assumptions, the following differential equations are obtained for the description of the dissolution and degradation:

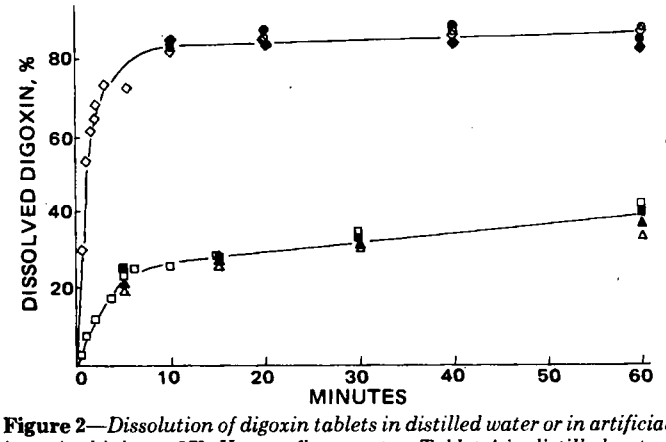

Figure 2—*Dissolution of digoxin tablets in distilled water or in artificial intestinal juice at 37°. Key: ♦, fluorometry, Tablet A in distilled water; ◇, HPLC, Tablet A in distilled water; ■, fluorometry, Tablet B in distilled water; □, HPLC, Tablet B in distilled water; ●, fluorometry, Tablet A in artificial intestinal juice; ○, HPLC, Tablet A in artificial intestinal juice; ▲, fluorometry, Tablet B in artificial intestinal juice; and △, HPLC, Tablet B in artificial intestinal juice.*

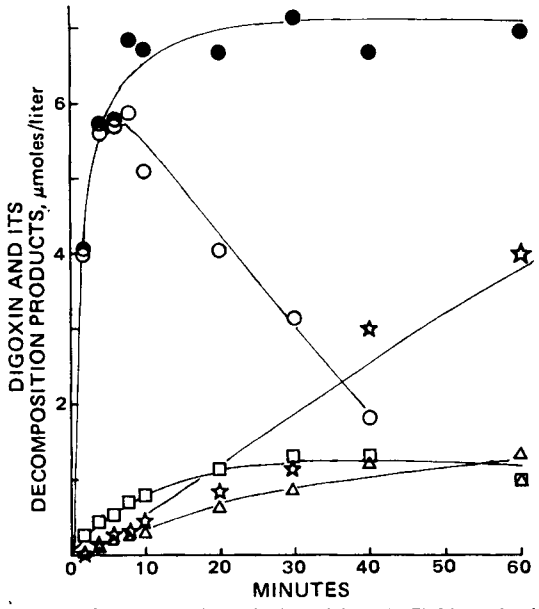

Figure 3—*Dissolution and degradation of digoxin Tablet A in the USP XIX dissolution test medium at 37°. Key: ●, total amount dissolved; ○, digoxin; ☆, digoxigenin; △, digoxigenin monodigitoxoside; and □, digoxigenin bisdigitoxoside.*

$$dA/dt = -K_{diss}A \quad \text{(Eq. 1)}$$

$$dB/dt = K_{diss}A - K_{degr}B \quad \text{(Eq. 2)}$$

$$dC/dt = K_{degr}B \quad \text{(Eq. 3)}$$

$$A + B + C = A_0 \quad \text{(Eq. 4)}$$

where $A = A_I + A_{II}$, $B = B_I + B_{II}$, $C = C_I + C_{II}$, and $A_0 = A_{0I} + A_{0II}$, in which A, B, C, and A_0 are the amounts of solid digoxin, digoxin in solution, digoxin degradation products (total amount of digoxigenin monodigitoxoside, digoxigenin bisdigitoxoside, and digoxigenin), and initial digoxin, respectively. The subscripts I and II denote the amorphous digoxin and digoxin crystals, respectively.

When $t = 0$, $A = A_0$ and $B = C = 0$. When t = infinity, $A = B = 0$ and $C = A_0$. Under these conditions, Eqs. 1–4 were integrated to give the following solutions:

$$A = A_0 \exp(-K_{diss}t) \quad \text{(Eq. 5)}$$

$$B = A_0\left(\frac{K_{diss}}{K_{degr} - K_{diss}}\right)[\exp(-K_{diss}t) - \exp(-K_{degr}t)] \quad \text{(Eq. 6)}$$

$$C = A_0\left[1 - \frac{K_{degr}\exp(-K_{diss}t) - K_{diss}\exp(-K_{degr}t)}{K_{degr} - K_{diss}}\right] \quad \text{(Eq. 7)}$$

For both solids I and II, the same solutions are given. Therefore, the residual digoxin dissolved in the solution could be described by the following equation:

$$B = A_{0I}\left(\frac{K_{dissI}}{K_{degr} - K_{dissI}}\right)[\exp(-K_{dissI}t) - \exp(-K_{degr}t)] + A_{0II}\left(\frac{K_{dissII}}{K_{degr} - K_{dissII}}\right)[\exp(-K_{dissII}t) - \exp(-K_{degr}t)] \quad \text{(Eq. 8)}$$

For Tablets A and B, the dissolution data were fitted to Eq. 8 by the least-squares method[9]. Figures 3 and 4 show the data points for the release of digoxin from Tablets A and B in the USP XIX dissolution test medium. Table I summarizes the rate constants calculated by the iterative least-squares method. The K_{degr} value is in good agreement with that determined in a hydrolysis study of digoxin in solution (20).

Tablet A should have essentially the same dissolution rate constants, K_{dissI} and K_{dissII}, as those of Tablet B. However, in this study, these kinetic constants were expressed as apparent constants which included

[9] Calculations were made by a digital computer, IBM S/370 model 158, with the NONLIN FORTRAN program developed by C. M. Metzler, G. L. Elfring, and A. J. McEwen, The Upjohn Co., Kalamazoo, Mich.

Table I—Values of K_{diss} and K_{degr} of Digoxin Obtained from Dissolution Tests of Tablet A and Tablet B

Parameter	Tablet A	Tablet B
K_{dissI}, min^{-1}	1.23	0.269
K_{dissII}, min^{-1}	0.00995	0.00429
K_{degr}, min^{-1}	0.0367 (0.0216)[a]	

[a] From Ref. 20.

effective surface area. Therefore, the differences of the diffusion rates indicate the existence of a more soluble layer and smaller digoxin crystals in Tablet A. The degradation rate constant was smaller than K_{dissI} but was larger than K_{dissII} in both Tablets A and B. This result indicates that degradation was rate determining in the earlier dissolution stage while dissolution became the rate-determining step in the later stage.

Suppression of Digoxin Hydrolysis—Digoxin is adsorbed by some antacids in aqueous solution (22). Moreover, when a large amount of an antacid is incorporated into a drug, the bioavailability of the drug may be reduced considerably (23). However, when specific antacids that have a large adsorption capability and dissolve comparatively quickly in acidic solution are selected, the stability of digoxin preparations can be enhanced without serious delay of drug release.

In this study, digoxin powders containing magnesium hydroxide–aluminum hydroxide, synthetic aluminum silicate, or magnesium oxide were placed in the dissolution apparatus in two positions, outside and inside the basket, to study the influence of granule dispersion on hydrolysis. The release of digoxin and hydrolyzed glycosides from digoxin powders in the USP XIX dissolution test medium was observed at different basket rotation speeds (Table II).

When the sample was placed inside the basket at a rotation speed of 50 rpm, magnesium oxide and magnesium hydroxide–aluminum hydroxide prevented the degradation of digoxin in the dissolution medium most, although the latter compound suppressed the release of digoxin. Aluminum silicate released digoxin more easily than did the other antacids but showed little antidegradation effect. When powders were placed outside the basket at a rotation speed of 100 rpm, synthetic aluminum silicate showed an inhibitory effect that probably was due to a reduced digoxin release rate because it released only 44.2% of the total amount of digoxin; magnesium hydroxide–aluminum hydroxide released 98.3% of the digoxin in 30 min. When samples were placed inside the basket at a rotation speed of 100 rpm, magnesium oxide and magnesium hydroxide–aluminum hydroxide released 100% of the digoxin in 30 min and still exerted a degradation inhibitory effect.

The dissolution rate was influenced considerably by the stirring conditions and the sample position in the dissolution apparatus. However, all samples showed reduced decomposition compared to that of the ref-

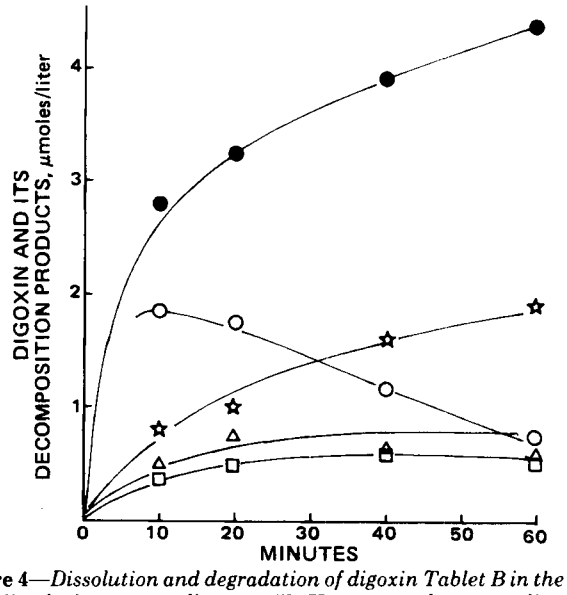

Figure 4—*Dissolution and degradation of digoxin Tablet B in the USP XIX dissolution test medium at 37°. Key: ●, total amount dissolved; ○, digoxin; ☆, digoxigenin; △, digoxigenin monodigitoxoside; and □, digoxigenin bisdigitoxoside.*

Table II—Effect of Antacids on Digoxin Hydrolysis in the USP XIX Dissolution Test Medium

Basket Rotation Speed, Sample Location	Antacid[a]	Total Amount Dissolved, %			Residual Digoxin in Solution, %		
		10 min	20 min	30 min	10 min	20 min	30 min
100 rpm, outside the basket	A	59.5	87.8	98.3	84.3	76.1	63.4
	B	30.0	39.8	44.2	78.3	65.7	53.6
	Reference	96.4	99.3	100	77.3	59.2	45.7
50 rpm, inside the basket	A	29.3	42.8	59.4	84.5	66.1	56.7
	B	37.1	55.4	73.7	70.4	59.2	48.4
	C	30.5	46.3	66.3	77.5	60.5	57.5
	Reference	56.4	60.4	69.4	76.4	55.2	42.2
100 rpm, inside the basket	A	94.8	99.7	100	75.4	53.7	39.3
	C	94.4	89.5	100	75.0	55.8	45.4
	Reference	94.7	94.0	100	72.5	47.4	30.5

[a] A = magnesium hydroxide–aluminum hydroxide, B = synthetic aluminum silicate, and C = magnesium oxide.

erence sample, which contained no antacid. Throughout the dissolution test, the dissolution medium pH was constant (1.3–1.4), and no significant influence of antiacidic agents on the medium pH was observed. This finding suggests that suppressed degradation of digoxin in the acidic medium by the incorporation of specific antacids is due to the antiacidic effect of those substances at the local dissolution site but is not due to an overall change in pH of the dissolution medium.

REFERENCES

(1) J. Lindenbaum, M. H. Mellow, M. O. Blackstone, and V. P. Butler, *N. Engl. J. Med.*, **285**, 1344 (1971).

(2) V. Manninen, J. Melin, and G. Hartel, *Lancet*, **2**, 934 (1971).

(3) T. R. D. Shaw, M. R. Howard, and J. Harmer, *ibid.*, **2**, 303 (1972).

(4) C. Ampolsuk, J. V. Mauro, A. A. Nyuis, N. Shah, and C. I. Jarowski, *J. Pharm. Sci.*, **63**, 117 (1974).

(5) P. R. Klink, R. I. Poust, J. L. Colaizzi, and R. H. McDonald, Jr., *ibid.*, **63**, 1231 (1974).

(6) B. F. Johnson and S. Lader, *Br. J. Clin. Pharmacol.*, **1**, 329 (1974).

(7) P. Ylitalo, G. Wilen, and S. Lundall, *J. Pharm. Sci.*, **64**, 1264 (1975).

(8) B. F. Johnson, H. Greer, J. McCredie, C. Bye, and A. Fowle, *Lancet*, **1**, 1473 (1973).

(9) J. Khulmann, U. Abshagen, and N. Rietbrock, *Naunyn-Schmiedebergs Arch. Pharmacol.*, **276**, 149 (1973).

(10) M. H. Gault, J. D. Charles, D. L. Sugden, and D. C. Kepkay, *J. Pharm. Pharmacol.*, **29**, 27 (1977).

(11) U. Abshagen, K. v. Bergmann, and N. Rietbrock, *Naunyn-Schmiedebergs Arch. Pharmacol.*, **275**, 1 (1972).

(12) G. Kroneberg, *Arch. Exp. Pathol. Pharmakol.*, **237**, 222 (1959).

(13) "The United States Pharmacopeia," 19th rev., Mack Publishing Co., Easton, Pa., 1975, p. 149.

(14) D. Wells, B. Katzung, and F. H. Meyers, *J. Pharm. Pharmacol.*, **13**, 389 (1961).

(15) T. W. Smith, V. P. Butler, Jr., and E. Harber, *N. Engl. J. Med.*, **281**, 1212 (1969).

(16) M. C. Castle, *J. Chromatogr.*, **115**, 437 (1975).

(17) T. Sonobe, S. Hasumi, T. Yoshino, Y. Kabayashi, and H. Kawata, *Yakuzaigaku*, **37**, 215 (1977).

(18) L. A. Sternson and R. D. Shaffer, *J. Pharm. Sci.*, **67**, 327 (1978).

(19) A. T. Florence and E. G. Salole, *J. Pharm. Pharmacol.*, **28**, 637 (1976).

(20) S. A. H. Khalil, *J. Pharm. Pharmacol., Suppl.*, **28**, 6 P (1976).

(21) A. T. Florence, E. G. Salole, and J. B. Stenlake, *J. Pharm. Pharmacol.*, **26**, 481 (1974).

(22) S. A. H. Khalil, *ibid.*, **26**, 961 (1974).

(23) D. D. Brown and R. P. Juhl, *N. Engl. J. Med.*, **295**, 1034 (1976).

ACKNOWLEDGMENTS

Presented at the 97th Japanese Pharmaceutical Conference, Tokyo, Japan, April 1977.

Adsorption of Lecithin by Cholesterol

ANNIE HOELGAARD *x and SVEN FRØKJAER ‡

Received September 17, 1979, from the **Department of Pharmaceutics, Royal Danish School of Pharmacy, 2 Universitetsparken, DK-2100 Copenhagen, Denmark*, and the ‡*NOVO Research Institute, Novo Allé, DK-2880 Bagsvaerd, Denmark.* Accepted for publication November 2, 1979.

Abstract □ Egg lecithin was adsorbed significantly by cholesterol monohydrate crystals. Adsorption data obtained at initial concentrations of <1.1 m*M* lecithin fitted the Langmuir equation. The calculated adsorption capacity suggested formation of a lecithin bilayer or a mixed bilayer of lecithin and cholesterol. The amount of lecithin adsorbed was highly dependent on the cholate concentration in the incubation medium. Minimal adsorption was observed at ~5 m*M* cholate. The presence of quaternary ammonium salts and dioctyl sodium sulfosuccinate caused desorption. The finding of an adsorptive layer supported the existence of an interfacial barrier that controls cholesterol dissolution.

Keyphrases □ Adsorption—formation of adsorptive lecithin layer on cholesterol, effect of detergents □ Lecithin—adsorption by cholesterol, effect of total bile acid concentration, lecithin concentration and type of bile acid □ Cholesterol—effect of lecithin adsorption on cholesterol dissolution, interfacial barrier formation

The main constituent of most gallstones is cholesterol monohydrate, which is insoluble in water. The bile containing bile acids and phospholipid can dissolve some cholesterol in mixed micelles. Recent investigations (1–4) established that the *in vitro* dissolution of both human cholesterol gallstones and cholesterol monohydrate crystals in bile salt–lecithin media and human bile is controlled largely by an interfacial barrier.[1] The cholesterol mono-

0022-3549/80/0400-0413$01.00/0

© 1980, American Pharmaceutical Association

Table II—Effect of Antacids on Digoxin Hydrolysis in the USP XIX Dissolution Test Medium

Basket Rotation Speed, Sample Location	Antacid[a]	Total Amount Dissolved, %			Residual Digoxin in Solution, %		
		10 min	20 min	30 min	10 min	20 min	30 min
100 rpm, outside the basket	A	59.5	87.8	98.3	84.3	76.1	63.4
	B	30.0	39.8	44.2	78.3	65.7	53.6
	Reference	96.4	99.3	100	77.3	59.2	45.7
50 rpm, inside the basket	A	29.3	42.8	59.4	84.5	66.1	56.7
	B	37.1	55.4	73.7	70.4	59.2	48.4
	C	30.5	46.3	66.3	77.5	60.5	57.5
	Reference	56.4	60.4	69.4	76.4	55.2	42.2
100 rpm, inside the basket	A	94.8	99.7	100	75.4	53.7	39.3
	C	94.4	89.5	100	75.0	55.8	45.4
	Reference	94.7	94.0	100	72.5	47.4	30.5

[a] A = magnesium hydroxide–aluminum hydroxide, B = synthetic aluminum silicate, and C = magnesium oxide.

erence sample, which contained no antacid. Throughout the dissolution test, the dissolution medium pH was constant (1.3–1.4), and no significant influence of antiacidic agents on the medium pH was observed. This finding suggests that suppressed degradation of digoxin in the acidic medium by the incorporation of specific antacids is due to the antiacidic effect of those substances at the local dissolution site but is not due to an overall change in pH of the dissolution medium.

REFERENCES

(1) J. Lindenbaum, M. H. Mellow, M. O. Blackstone, and V. P. Butler, *N. Engl. J. Med.*, **285**, 1344 (1971).

(2) V. Manninen, J. Melin, and G. Hartel, *Lancet*, **2**, 934 (1971).

(3) T. R. D. Shaw, M. R. Howard, and J. Harmer, *ibid.*, **2**, 303 (1972).

(4) C. Ampolsuk, J. V. Mauro, A. A. Nyuis, N. Shah, and C. I. Jarowski, *J. Pharm. Sci.*, **63**, 117 (1974).

(5) P. R. Klink, R. I. Poust, J. L. Colaizzi, and R. H. McDonald, Jr., *ibid.*, **63**, 1231 (1974).

(6) B. F. Johnson and S. Lader, *Br. J. Clin. Pharmacol.*, **1**, 329 (1974).

(7) P. Ylitalo, G. Wilen, and S. Lundall, *J. Pharm. Sci.*, **64**, 1264 (1975).

(8) B. F. Johnson, H. Greer, J. McCredie, C. Bye, and A. Fowle, *Lancet*, **1**, 1473 (1973).

(9) J. Khulmann, U. Abshagen, and N. Rietbrock, *Naunyn-Schmiedebergs Arch. Pharmacol.*, **276**, 149 (1973).

(10) M. H. Gault, J. D. Charles, D. L. Sugden, and D. C. Kepkay, *J. Pharm. Pharmacol.*, **29**, 27 (1977).

(11) U. Abshagen, K. v. Bergmann, and N. Rietbrock, *Naunyn-Schmiedebergs Arch. Pharmacol.*, **275**, 1 (1972).

(12) G. Kroneberg, *Arch. Exp. Pathol. Pharmakol.*, **237**, 222 (1959).

(13) "The United States Pharmacopeia," 19th rev., Mack Publishing Co., Easton, Pa., 1975, p. 149.

(14) D. Wells, B. Katzung, and F. H. Meyers, *J. Pharm. Pharmacol.*, **13**, 389 (1961).

(15) T. W. Smith, V. P. Butler, Jr., and E. Harber, *N. Engl. J. Med.*, **281**, 1212 (1969).

(16) M. C. Castle, *J. Chromatogr.*, **115**, 437 (1975).

(17) T. Sonobe, S. Hasumi, T. Yoshino, Y. Kabayashi, and H. Kawata, *Yakuzaigaku*, **37**, 215 (1977).

(18) L. A. Sternson and R. D. Shaffer, *J. Pharm. Sci.*, **67**, 327 (1978).

(19) A. T. Florence and E. G. Salole, *J. Pharm. Pharmacol.*, **28**, 637 (1976).

(20) S. A. H. Khalil, *J. Pharm. Pharmacol., Suppl.*, **28**, 6 P (1976).

(21) A. T. Florence, E. G. Salole, and J. B. Stenlake, *J. Pharm. Pharmacol.*, **26**, 481 (1974).

(22) S. A. H. Khalil, *ibid.*, **26**, 961 (1974).

(23) D. D. Brown and R. P. Juhl, *N. Engl. J. Med.*, **295**, 1034 (1976).

ACKNOWLEDGMENTS

Presented at the 97th Japanese Pharmaceutical Conference, Tokyo, Japan, April 1977.

Adsorption of Lecithin by Cholesterol

ANNIE HOELGAARD *x and SVEN FRØKJAER ‡

Received September 17, 1979, from the **Department of Pharmaceutics, Royal Danish School of Pharmacy, 2 Universitetsparken, DK-2100 Copenhagen, Denmark*, and the ‡*NOVO Research Institute, Novo Allé, DK-2880 Bagsvaerd, Denmark.* Accepted for publication November 2, 1979.

Abstract □ Egg lecithin was adsorbed significantly by cholesterol monohydrate crystals. Adsorption data obtained at initial concentrations of <1.1 m*M* lecithin fitted the Langmuir equation. The calculated adsorption capacity suggested formation of a lecithin bilayer or a mixed bilayer of lecithin and cholesterol. The amount of lecithin adsorbed was highly dependent on the cholate concentration in the incubation medium. Minimal adsorption was observed at ~5 m*M* cholate. The presence of quaternary ammonium salts and dioctyl sodium sulfosuccinate caused desorption. The finding of an adsorptive layer supported the existence of an interfacial barrier that controls cholesterol dissolution.

Keyphrases □ Adsorption—formation of adsorptive lecithin layer on cholesterol, effect of detergents □ Lecithin—adsorption by cholesterol, effect of total bile acid concentration, lecithin concentration and type of bile acid □ Cholesterol—effect of lecithin adsorption on cholesterol dissolution, interfacial barrier formation

The main constituent of most gallstones is cholesterol monohydrate, which is insoluble in water. The bile containing bile acids and phospholipid can dissolve some cholesterol in mixed micelles. Recent investigations (1–4) established that the *in vitro* dissolution of both human cholesterol gallstones and cholesterol monohydrate crystals in bile salt–lecithin media and human bile is controlled largely by an interfacial barrier.[1] The cholesterol mono-

0022-3549/80/0400-0413$01.00/0

© 1980, American Pharmaceutical Association

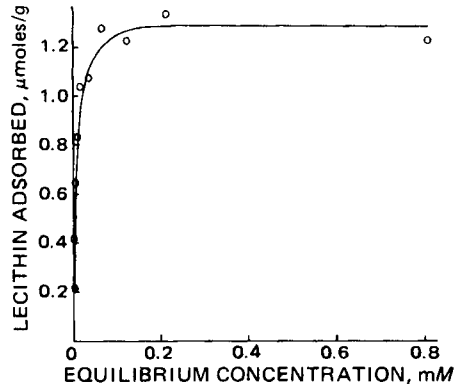

Figure 1—*Lecithin adsorption by cholesterol monohydrate in pH 7.4 tromethamine buffer with a constant cholate–lecithin molar ratio of 3.8.*

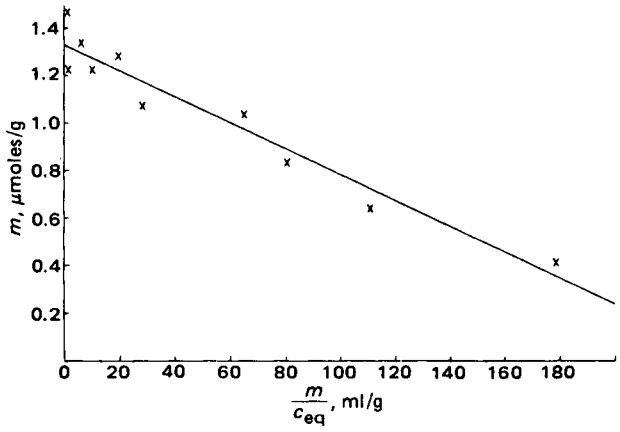

Figure 2—*Langmuir plot of lecithin adsorption in pH 7.4 tromethamine buffer with a constant cholate–lecithin molar ratio of 3.8.*

hydrate dissolution rate in artificial bile is ~20 times as slow as that predicted for diffusion-controlled dissolution.

The possibility arises that lecithin adsorbs onto the cholesterol surface and forms a condensed layer that restrains dissolution of cholesterol and thus acts as the interfacial barrier. The present study examined the *in vitro* adsorption of lecithin onto cholesterol and the effect of cholate concentration on binding.

EXPERIMENTAL

Materials—Commercial cholesterol[1] was ground in a mortar and stored in the dark in a desiccator saturated with water vapor. Differential scanning calorimetry[2] confirmed the hydrate nature of the crystals. The surface area of the cholesterol monohydrate powder was determined by an air permeability method (5).

Radioactive lecithin was prepared by mixing 10 mg of egg lecithin[3] in chloroform–methanol with 2 μCi of L-α-distearoyl[1-^{14}C]phosphatidylcholine[4] in benzene–ethanol. Before use, TLC confirmed the purity of the egg lecithin to be >99%, and the radiochemical purity of distearoylphosphatidylcholine was >95%.

The mixture was dried in an argon atmosphere and dissolved in 5 ml of pH 7.4, 0.1 *M* tromethamine buffer[5] containing 0.05 *M* NaCl and 4.6 m*M* sodium cholate[5]. The lecithin concentration was determined by measuring the phosphorus content by a method described previously (6).

Benzalkonium chloride Ph.Nord.63, lysolecithin[5], and dioctyl sodium sulfosuccinate[6] were used as received. Octadecyltrimethylammonium chloride[7] was dried *in vacuo*.

Adsorption Measurements—Cholesterol monohydrate, 0.50 g, was introduced into 2 ml of incubation medium in centrifuge tubes. The incubation medium was pH 7.4, 0.1 *M* tromethamine buffer containing 0.05 *M* NaCl with varying amounts of radioactive lecithin and sodium cholate. The tubes were filled with argon before closing. The powder was dispersed in the incubation medium by sonication in a bath-type instrument for 10 min.

After incubation in a circulating shaker at room temperature for 4 hr, the tubes were centrifugated. The supernate, 100 μl, was added to 5 ml of scintillation fluid[8], and the radioactivity was counted[9]. The amount of lecithin that was adsorbed was the difference between the initial and the equilibrium concentrations of the incubation medium. The effect of different substances on the adsorption of lecithin was measured by adding the substances at equilibrium, incubating for 4 hr, and remeasuring the radioactivity in the supernate.

[1] Merck, Darmstadt, West Germany.
[2] Perkin-Elmer DSC-1B.
[3] Lipid Products Ltd. (England).
[4] Applied Science Laboratories.
[5] Sigma Chemical Co.
[6] Aerosol OT, Cyanamid.
[7] Arquad 18/50, Akzo Chemie (United Kingdom).
[8] Pico-Fluor 15, Packard.
[9] Beckman LS-250.

RESULTS AND DISCUSSION

Adsorption at Constant Cholate–Lecithin Ratio—The adsorption of lecithin by cholesterol monohydrate from a medium with a cholate–lecithin molar ratio of 3.8 is shown in Figs. 1 and 2. The molar ratio of 3.8 is within the size range of physiological bile (4).

Figure 1 shows a plot of the amount of lecithin adsorbed per gram of cholesterol *versus* the equilibrium lecithin concentration. Since the isotherm becomes linear at low concentrations and shows a limiting value, the binding can be described by the Langmuir adsorption equation:

$$m = b\frac{Kc_{eq}}{1 + Kc_{eq}} \qquad \text{(Eq. 1)}$$

where m is the amount adsorbed, c_{eq} is the equilibrium concentration, and b and K are constants. By transformation of Eq. 1, the following expression is derived:

$$m = b - \frac{1}{K}\left(\frac{m}{c_{eq}}\right) \qquad \text{(Eq. 2)}$$

from which the constants can be determined. At sufficiently high concentrations, m approached the limiting value, b. Thus, b is a measure of the adsorbent capacity, and K is the adsorption intensity.

In Fig. 2, the results were plotted according to Eq. 2; the best straight line through the experimental data was calculated by the least-squares method. The values of b and K were determined from the intercept and the reciprocal of the regression line slope. The b value was 1.34 μmoles/g, and K was 1.8×10^5 liters/mole.

The effective area occupied by a lecithin molecule in a pure lecithin monolayer is 96 Å^2; but in mixtures with cholesterol (38 Å^2/molecule), the area occupied by a lecithin molecule is reduced, depending on the amount of cholesterol built into the layer (7). For example, when there are two or three lecithin molecules for one molecule of cholesterol, 1 m^2 is occupied by 1.67 or 1.76 μmoles of lecithin, respectively. A monolayer formed entirely of lecithin is occupied by 1.72 μmoles of lecithin/m^2.

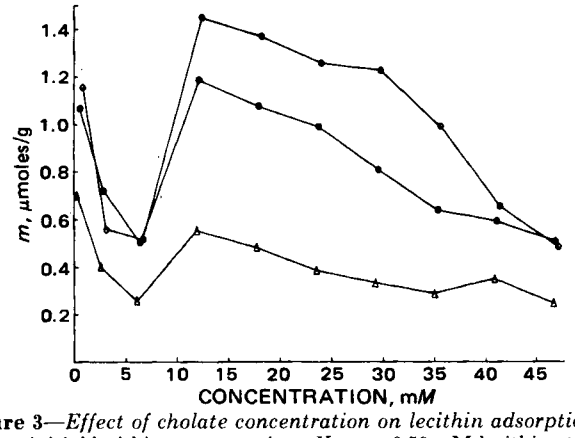

Figure 3—*Effect of cholate concentration on lecithin adsorption at various initial lecithin concentrations. Key:* ○, *0.50 mM lecithin;* ●, *0.38 mM lecithin; and* △, *0.18 mM lecithin.*

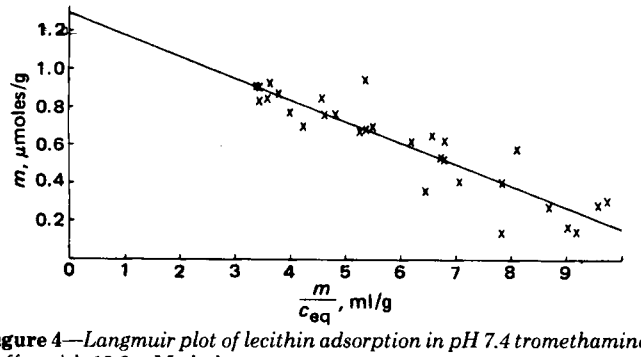

Figure 4—*Langmuir plot of lecithin adsorption in pH 7.4 tromethamine buffer with 12.2 mM cholate.*

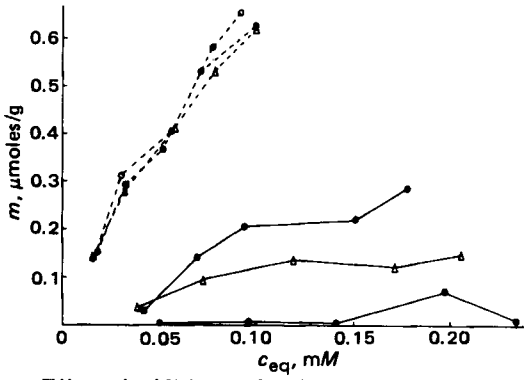

Figure 5—*Effect of additive on lecithin adsorption in pH 7.4 tromethamine buffer with 12.2 mM cholate. Key: - - -, no additive; ○, 1% octadecyltrimethylammonium chloride; △, 1% benzalkonium chloride; and ●, 1% dioctyl sodium sulfosuccinate.*

The surface area of the cholesterol powder was determined to be 0.4 m^2/g, which gives the experimental adsorptive capacity of 3.3 μmoles of lecithin/m^2 of cholesterol. Thus, the results are consistent with formation of a lecithin bilayer or a mixed bilayer.

A hydrophobic layer composed of lecithin or lecithin and cholesterol possibly could form the interfacial barrier for cholesterol dissolution in bile. A study conducted with liposomes showed that lecithin mixed with cholesterol forms condensed layers with reduced permeability (8).

Effect of Bile Salt Concentration—To investigate the effect of the bile salt concentration on adsorption, incubation was performed with cholate concentrations in the 0.05–50 m*M* range and at different initial lecithin concentrations. The results in Fig. 3 show that no simple correlation exists between cholate concentration and lecithin adsorption. The profiles showing a minimum at about 5 m*M* cholate, and decreased adsorption at concentrations greater than ~12 m*M* suggest that different mechanisms are involved.

A possible explanation of the minimum can be derived from the work of Shankland (9), who found that stable mixed micelles are formed only when the solution contains enough cholate to give the critical micelle concentration, which was 5 m*M* sodium cholate. This finding means that adsorption is highly dependent on how cholate molecules are associated in the solution. Since the detergent action of bile salts influences the structural integrity of liposomes (10), a similar effect on the adsorptive layer is expected at the higher cholate concentrations.

Adsorption experiments were carried out with a constant cholate concentration of 12.2 m*M*. The results are plotted in Fig. 4, and the constants of Eq. 2 were determined to be $b = 1.29$ μmoles/g and $K = 8.8 \times 10^3$ liters/mole. The result shows a low adsorption intensity but the same adsorption capacity as in the experiment with a constant cholate–lecithin molar ratio.

Desorption—Different substances were added to the incubation media to examine their effect on the adsorptive layer. Figure 5 shows the adsorption of lecithin from a 12.2 m*M* cholate solution measured before and after the addition of 1% octadecyltrimethylammonium chloride, benzalkonium chloride, or dioctyl sodium sulfosuccinate. These detergents caused desorption, especially dioctyl sodium sulfosuccinate, which prevented the formation of an adsorptive layer. Lysolecithin at 1% had no effect on adsorption.

If the adsorptive layer of lecithin is the interfacial barrier of dissolution, substances that cause desorption of lecithin may act as dissolution accelerators. Kwan *et al.* (11) found that amines and quaternary ammonium compounds were effective cholesterol dissolution accelerators.

The interfacial barrier is believed to be clinically important in gallstone dissolution (3). The observation of an adsorptive lecithin layer may contribute to the understanding of dissolution kinetics. The type of bile acid, the total bile acid concentration, and the lecithin concentration influence dissolution (12). These parameters also affect the formation of an adsorptive layer like the factors that increase the dissolution rate decrease adsorption. Preliminary experiments show that substitution of cholate with chenodeoxycholate leads to less lecithin adsorption onto cholesterol. The significance of the adsorptive layer in cholesterol dissolution as well as of the adsorption behavior under physiological conditions with various conjugated bile acids is not known.

By elucidating the type and structure of the rate-limiting barrier and the factors influencing it for dissolution, it may be possible to search for substances that reduce or destroy the barrier and thereby accelerate dissolution.

REFERENCES

(1) W. I. Higuchi, S. Prakongpan, and F. Young, *J. Pharm. Sci.*, **62**, 945 (1973).

(2) S. Prakongpan, W. I. Higuchi, K. H. Kwan, and A. M. Molokhia, *ibid.*, **65**, 685 (1976).

(3) K. H. Kwan, W. I. Higuchi, A. M. Molokhia, and A. F. Hofmann, *ibid.*, **66**, 1094 (1977).

(4) A. M. Molokhia, A. F. Hofmann, W. I. Higuchi, M. Tuchinda, K. Feld, S. Prakongpan, and R. G. Danzinger, *ibid.*, **66**, 1101 (1977).

(5) N. Möller, *Dan. Tidsskr. Farm.*, **46**, 47 (1972).

(6) C. W. F. McClare, *Anal. Biochem.*, **39**, 527 (1971).

(7) D. G. Dervichian, *Prog. Biophys. Mol. Biol.*, **14**, 263 (1964).

(8) R. A. Demel, S. C. Kinsky, C. B. Kinsky, and L. L. M. van Deenen, *Biochim. Biophys. Acta*, **150**, 655 (1968).

(9) W. Shankland, *Chem. Phys. Lipids*, **4**, 109 (1970).

(10) M. H. Richards and C. R. Gardner, *Biochim. Biophys. Acta*, **543**, 508 (1978).

(11) K. H. Kwan, W. I. Higuchi, A. M. Molokhia, and A. F. Hofmann, *J. Pharm. Sci.*, **66**, 1105 (1977).

(12) K. H. Kwan, W. I. Higuchi, and A. F. Hofmann, *ibid.*, **67**, 1711 (1978).

Molecular Structure Influencing Either a Sweet or Bitter Taste among Aldoximes

LEMONT B. KIER

Received July 5, 1979, from the *Department of Pharmaceutical Chemistry, Medical College of Virginia, Virginia Commonwealth University, Richmond, VA 23298.* Accepted for publication November 1, 1979.

Abstract □ A series of cyclohexylaldoximes was examined for their sweet or bitter taste using discriminant analysis. The structures of the molecules were described using molecular connectivity. A two-variable linear discriminant function and critical value were computed that correctly assigned 17 of the 20 molecules to their observed sweet or bitter taste categories. The same discriminant function can predict correctly the taste categories of seven of eight additional molecules.

Keyphrases □ Aldoximes—influence of molecular structure on sweet or bitter taste, discriminant analysis, molecular connectivity, taste category prediction □ Molecular connectivity indexes—aldoximes, influences of molecular structure on sweet or bitter taste □ Sweeteners, noncaloric—analysis of aldoximes for potential use as sweeteners, molecular connectivity indexes, discriminant analysis

A safe, stable, noncaloric sweetener continues to be an active research objective. The ban on cyclamate and the suspicion concerning the safe use of saccharin necessitate research for sweet-tasting molecules.

BACKGROUND

The prevailing hypothesis about the chemical structure governing sweet taste was proposed by Shallenberger and Acree (1) and extended by Kier (2). In essence, the hypothesis describes three structural features necessary, but not sufficient, for sweet taste. The first and second features are the presence of a potential hydrogen bond donor, designated AH, and the presence of a hydrogen bond acceptor, B (1). The optimum separation between A and B is about 3 Å. The third feature is a nonpolar region, X, capable of dispersion interaction at a receptor (2). It is a region of atoms located ~3.5 Å from A and ~5.5 Å from B.

One problem in the search for noncaloric sweeteners is the common occurrence of a bitter taste among a series of molecules under investigation. The bitter taste also can coexist with a sweet taste in the same molecule. A classic example is the perception of a bitter aftertaste with saccharin.

Some insight into structural influence on this taste dichotomy was revealed by Solms (3), who recorded that five D-amino acids are sweet while their L-forms are bitter. This finding implicates a stereochemical factor in the sweet and bitter response. Receptors for bitter and sweet taste have been shown to be activated by similar structural features so that closely related molecules impart either or both sensations (4).

The design of noncaloric sweeteners could be improved significantly if the structural characteristics influencing bitter and sweet taste could be discriminated. This knowledge would permit the design of molecules with an unambiguous taste.

A recent report (5) on a series of oximes presented an opportunity for such a discriminative structural analysis. In that study, 51 molecules were analyzed for taste potency and relative sweet–bitter contribution. The results from this oxime study (5) were used in these laboratories to analyze the structures by molecular connectivity, and a discrimination analysis was performed to find the best structural representation discriminating between these two tastes.

EXPERIMENTAL

Selection of Sweet- and Bitter-Tasting Molecules—Two taste characteristics that were defined previously (5) were considered in the present study to differentiate between sweet and bitter molecules. The first characteristic, taste potency compared to a 0.25 *M* sucrose solution, is a measure of taste intensity, regardless of whether the molecule is sweet or bitter. The other characteristic is the percentage of the taste identified as sweet and that identified as bitter.

For the present study, 10 molecules were selected from each taste category based on the largest percentage of sweet (or bitter) taste and the most potent taste response. All 20 molecules selected were aldoximes (Tables I and II).

Structural Analyses and Discrimination Analysis—The structural descriptions of the molecules in Tables I and II were made using molecular connectivity (6). Numerous studies on the structure–activity relationships of drug molecules have employed molecular connectivity to quantitate molecular structure effectively (6–9).

Discriminant analysis is an approach to differentiate between two or more classes of molecules. The procedure is a search for a linear combination of structural variables that describes a line, plane, or general surface that separates the molecule classes in the optimum manner. The value of y is related to the linear discriminant function by:

$$y = c_1x_1 + c_2x_2 + \ldots + c_nx_n \qquad \text{(Eq. 1)}$$

The function separates the categories with as little overlap as possible, thus providing discrimination between the categories. The coefficients, c_i, are determined so that the distance between the categories is maximized whereas the distance between members of the same category is minimized.

The analysis also produces the critical value, y^*, so that molecules with $y > y^*$ are assigned to one category and those with $y < y^*$ are assigned to the other category. The ratio of the between-category variance to the within-category variance is proportional to other statistical quantities such as D^2 (the Mahalanobis generalized distance), T^2 (defined by Hotelling), and the more standard F value (10).

The quality of the discriminant function may be assessed in three ways: comparison of the F value to tabulated values, determination of the

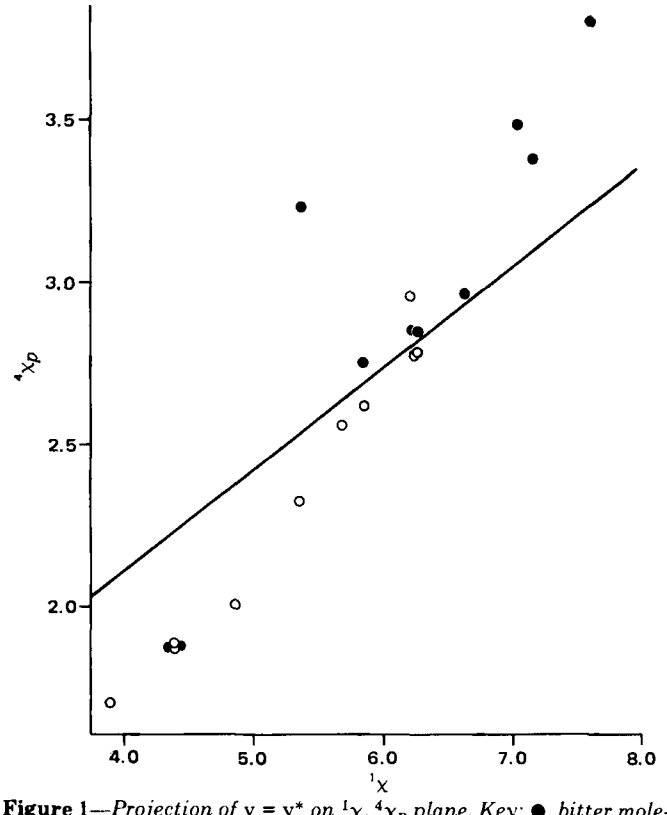

Figure 1—*Projection of* $y = y^*$ *on* $^1\chi$, $^4\chi_p$ *plane. Key:* ●, *bitter molecules; and* ○, *sweet molecules.*

0022-3549/80/0400-0416$01.00/0
© 1980, American Pharmaceutical Association

Table I—Discriminant Analysis of Sweet-Tasting Aldoximes R—CH=N—OH

Compound	R	Taste Potency Relative to Sucrose	Percent of Taste, Sweet/Bitter	$^1\chi$	$^4\chi_p$	$y - y^*$
I	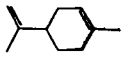	370	60/25	5.736	2.552	0.32
II	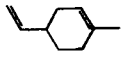	1150	50/10	5.364	2.337	0.70
III	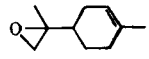	50	65/10	6.244	2.965	−0.67
IV		55	48/7	3.932	1.707	1.41
V		55	40/16	4.432	1.884	1.33
VI	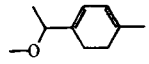	135	65/7	6.274	2.788	0.05
VII		200	70/3	4.432	1.884	1.33
VIII	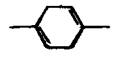	500	78/3	4.826	2.026	1.25
IX	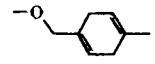	225	90/2	5.864	2.625	0.18
X	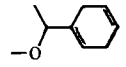	300	92/1	6.274	2.788	0.05

Table II—Discriminant Analysis of Bitter-Tasting Aldoximes R—CH=N—OH

Compound	R	Taste Potency Relative to Sucrose	Percent of Taste, Sweet/Bitter	$^1\chi$	$^4\chi_p$	$y - y^*$
I	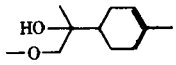	4	6/70	7.098	3.489	−1.67
II	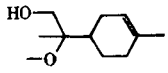	11	4/93	7.158	3.384	−1.19
III	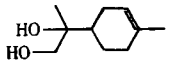	30	5/73	6.598	2.930	−0.11
IV		1.5	0/50	4.432	1.884	1.33
V		2	2/65	4.432	1.884	1.33
VI	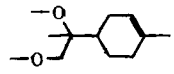	50	0/70	7.658	3.797	−2.19
VII	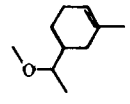	28	2/52	6.274	2.853	−0.20
VIII	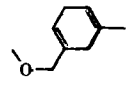	140	0/75	5.864	2.743	−0.27
IX	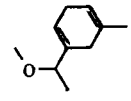	92	0/67	6.274	2.853	−0.20
X		320	0/50	5.398	3.240	−2.77

percentage of molecules correctly classified, and prediction of the classification of molecules not included in the original study.

RESULTS

The best linear discriminant function, using two molecular connectivity index variables, is:

$$y = 1.21^1\chi - 3.88^4\chi_p \quad \text{(Eq. 2)}$$

and the critical value is:

$$y^* = -3.27 \quad \text{(Eq. 3)}$$

When each y value is solved for the sweet (Table I) and bitter (Table II) molecules, values of $y > -3.27$ are assigned to the sweet category while

Table III—Taste Prediction from Discriminant Analysis R—CH=N—OH

Compound	R	Taste Potency Relative to Sucrose	Percent of Taste, Sweet/Bitter	$^1\chi$	$^4\chi_p$	$y - y^*$
I		90	50/15	4.432	1.884	1.32
II	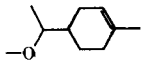	80	50/20	6.274	2.788	0.05
III	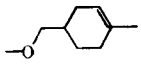	52	53/22	5.864	2.625	0.18
IV	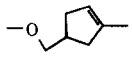	24	39/9	5.364	2.519	0.00
V		40	55/5	3.308	0.697	4.568
VI	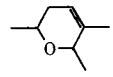	10	0/36	5.236	2.528	−0.20
VII	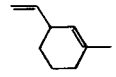	175	14/34	5.364	2.444	0.28
VIII	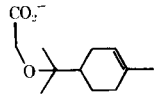	10	0/38	7.958	3.593	−1.04
IX	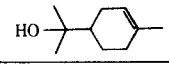	8	4/18	6.037	2.725	−0.01

values of $y < -3.27$ are assigned to the bitter category. Therefore, when $y - y^*$ is negative, the molecule is classified as bitter. The discriminant function is projected onto the $^1\chi$, $^4\chi_p$ plane for $y = y^*$ (Fig. 1) to illustrate the assignments to the two taste categories.

The discriminant function correctly assigns nine of the 10 sweet-tasting molecules (Table I) and eight of the 10 bitter-tasting molecules (Table II). The average percentage of correct assignment is 85%. The statistical significance can be stated as the T^2 value, which in this case is 5.9.

DISCUSSION

The linear discriminant function is an equation featuring two molecular connectivity indexes, $^1\chi$ and $^4\chi_p$. These indexes, weighted by the coefficients in the equation, describe two structural characteristics that influence whether a molecule is sweet or bitter.

The indexes convey structural information that is familiar to the medicinal chemist. The $^1\chi$ index describes the size of the molecule in terms of the number of bonds. Within the equation, the $^1\chi$ index indicates that the more bonds there are, the larger the y value will be. When $^1\chi$ is large enough, $y > y^*$ and the molecule is classified as sweet. The influence of size as expressed by $^1\chi$ is countered by the information conveyed by $^4\chi_p$. This index, as a negative term in the linear discriminant function, leads to lower y values when $^4\chi_p$ increases. The value of $^4\chi_p$ is influenced by the size of the molecule as well as by the substituents.

The indexes in the linear discriminant function indicate that the value of y is greater than that of y^* when the number of first-row atoms in the substituent of cyclohexylaldoxime is four or less. Thus, a *tert*-butyl group (*i.e.*, Compound IX, Table III) has a $y - y^*$ of virtually zero. Substituents with more than four first-row atoms, particularly if they are branched, give a y value less than y^* (Table II). The structural conclusions are that larger, more branched substituents on cyclohexylaldoximes increase the tendency for the molecule to be bitter. In contrast, smaller substituents, with four or fewer first-row atoms, influence sweet taste (Table I).

Another observation that can be made about the influence of structure on taste, based on the linear discriminant function, is that the two chi indexes are not of the valence class. This finding means that unsaturation or heteroatoms in the 20 molecules are not critical to the structures that influence the sweet or bitter taste. This conclusion is correct to the extent that 85% of the molecules are assigned correctly.

For the three incorrectly assigned molecules (III in Table I and IV and V in Table II), a molecular connectivity index of the valence type may be necessary for the correct assignment. However, the addition of a third molecular connectivity index in the discrimination analysis failed to improve the number of correctly assigned molecules in Tables I and II. The three incorrectly assigned molecules in Tables I and II have the lowest taste potencies among their respective taste classes. This observation suggests that high taste potency is important in the categorization of molecules as bitter or sweet tasting.

A test of the linear discriminant function and the molecular connectivity indexes that describe structures is the ability of the function and the associated critical value, y^*, to predict the taste categories of molecules not in the original study. For this test, nine additional molecules were selected from the study of Acton and Stone (5), based on their taste potencies and sweet–bitter taste ratios that favored one or the other category (Table III).

Calculation of the $^1\chi$ and $^4\chi_p$ indexes for each molecule and computation of $y - y^*$ for the linear discriminant function formed the basis of the taste category predictions shown in Table III. The first five molecules are reported to be sweet. The predictions for I–III and V are correct. The prediction for IV is ambiguous since $y = y^*$.

Compounds VI–IX are classified as bitter tasting. The solution of $y - y^*$ predicts VI, VIII, and IX to be bitter. Compound VII is predicted incorrectly.

Thus, seven of the predictions were correct, one was incorrect, and one was ambiguous. Without IV, the correct prediction for seven of eight compounds gave an accuracy of 87%, the same quality of classification as obtained with the assignments in Tables I and II combined.

The results of the study are encouraging in that molecular connectivity indexes appear to encode sufficient information about the structure influencing the taste category of cyclohexylaldoximes so that the discriminant analysis can assign correctly 17 of 20 molecules to the sweet or bitter taste category. Furthermore, the analysis based on these indexes can predict the taste category of additional molecules with the same accuracy. The study shows one approach to the possible separation of bitter taste from candidate molecules of interest as noncaloric sweeteners.

REFERENCES

(1) R. S. Shallenberger and T. E. Acree, *Nature*, **216**, 480 (1967).

(2) L. B. Kier, *J. Pharm. Sci.*, **61**, 1394 (1972).

(3) J. Solms, *J. Agr. Food Chem.*, **17**, 686 (1969).

(4) P. A. Temussi, F. Lelj, and T. Tancredi, *J. Med. Chem.*, **21**, 1154 (1978).

(5) E. M. Acton and H. Stone, *Science*, **193**, 584 (1976).

(6) L. B. Kier and L. H. Hall, "Molecular Connectivity in Chemistry and Drug Research," Academic, New York, N.Y., 1976.

(7) T. DiPaolo, L. B. Kier, and L. H. Hall, *Mol. Pharmacol.*, **13**, 31 (1977).

(8) L. B. Kier and L. H. Hall, *J. Med. Chem.*, **20**, 1631 (1977).
(9) L. B. Kier and L. H. Hall, *J. Pharm. Sci.*, **67**, 1408 (1978).
(10) B. W. Bolch and C. J. Huang, "Multivariate Statistical Methods for Business and Economics," Prentice-Hall, Englewood Cliffs, N.J., 1974.

ACKNOWLEDGMENTS

The author thanks Lowell H. Hall for the use of the program that computed the linear discriminant function. The author also acknowledges the helpful assistance of the Data Acquisition Laboratory at the Medical College of Virginia, Virginia Commonwealth University.

Biological Disposition of Sodium Dichloroacetate in Animals and Humans after Intravenous Administration

GEORGE LUKAS *x, KUNJBALA H. VYAS *, SHIRLEY D. BRINDLE *, ANNE R. Le SHER ‡, and WILLIAM E. WAGNER, Jr. ‡

Received April 27, 1979, from the *Research Department, Pharmaceuticals Division, Ciba-Geigy Corporation, *Ardsley, NY 10502, and ‡Summit, NJ 07901.* Accepted for publication October 5, 1979.

Abstract □ Sodium dichloroacetate, a potential antidote for lactic acidosis, was administered intravenously to rats, dogs, and four humans. In three rats, maximum plasma sodium dichloroacetate concentrations were 120–164 μg/ml after a 100-mg/kg dose and declined with half-lives of 2.1–4.4 hr. In two dogs, maximal concentrations of 447 and 508 μg/ml were attained after a 100-mg/kg dose. The subsequent decline was relatively slow with approximate half-lives of 17.1 and 24.6 hr. An intravenous infusion of 10 mg/kg was administered over 20 min to two human subjects. Two other subjects received 20 mg/kg. After the infusion, maximum plasma concentrations of 19.9 and 24.7 μg/ml were seen with the lower dose and 57.3 and 74.9 μg/ml were achieved with the higher dose. Thereafter, concentrations declined rapidly with half-lives of 20–36 min. The observed large interspecies differences in half-lives could be explained in terms of differences in the apparent volume of distribution and/or clearance.

Keyphrases □ Pharmacokinetics—sodium dichloroacetate, plasma concentration level-time curve, rats, dogs, humans □ Sodium dichloroacetate—pharmacokinetics, plasma concentration levels, rats, dogs, humans □ Clearance, intrinsic—plasma sodium dichloroacetate concentration, pharmacokinetics, rats, dogs, humans

Sodium dichloroacetate (I) has been reported to reduce normal or elevated blood lactate and pyruvate levels in animals by activating the pyruvate dehydrogenase enzyme complex (1–3). Oral administration of I to patients having nonketotic diabetes mellitus also led to an appreciable lowering of plasma lactate concentrations (4). The compound has been of possible interest as an intravenous antidote in patients suffering from lactic acidosis. This study was undertaken to provide information on the biological disposition of I in animals and humans since no data are available.

EXPERIMENTAL

Materials—Labeled[1] and unlabeled[2] sodium dichloroacetate were used. The material labeled in both carbon atom positions had a specific activity of 23.4 μCi/mg. Radiochemical purity, determined by TLC on silica gel plates in ethanol–chloroform–concentrated ammonium hydroxide–water (53:30:15:1.5), was >98%.

Animal Experiments—Each of three male Sprague–Dawley rats, 160–170 g, was given an intravenous injection of ^{14}C-I, diluted 1:20 with nonlabeled I, in a tail vein. The compound (100 mg/kg) was administered as a 10% aqueous solution. At specified times, animals were subjected to light ether anesthesia, and a 0.2–0.3-ml blood sample was collected in a heparinized centrifuge tube through a glass capillary by puncture of the suborbital sinus. Animals then were permitted to recover until the next sampling time.

Each of two male beagles, 9.0 and 10.5 kg, was given 100 mg of I/kg as a 20% aqueous solution intravenously in the cephalic vein. Animals were placed in individual metabolism cages. At specified times, blood was collected from a jugular vein without anesthesia.

Human Study—Four normal subjects, having given informed consent, participated after an overnight fast. Subjects 1 and 2, ages 42 and 38 years, respectively, each weighed ~70 kg. Subjects 3 and 4, ages 52 and 26 years, respectively, weighed 80 and 83 kg. In each case, the history, physical examination, ECG, and all laboratory tests were within normal limits.

Following the collection of the control urine sample and the drawing of a control blood specimen from Subjects 1 and 2, a 10-mg/kg dose of I dissolved in 100 ml of saline was infused over 20 min. Blood specimens were obtained from the contralateral antecubital vein at the time the infusion was completed. Specimens were drawn subsequently at 1 (40 min after termination of the infusion), 2, 3, 4, 6, 8, 10, 12, 24, 32, and 48 hr. All urine was collected for 96 hr with collection periods ending at 1, 2, 4, 8, 12, 24, 48, 72, and 96 hr.

Several weeks later, the procedure was repeated on Subjects 3 and 4, the sole change being that each received 20 mg/kg. All subjects were given a standard breakfast after the 4th hr. They remained under clinical observation for 8 hr.

Blood specimens were centrifuged as soon as they were collected. Plasma was separated and stored frozen until analysis. The urinary volume was measured and recorded. Aliquots of 20 ml from each urine sample were labeled and frozen for analysis.

Analysis of Unchanged I—Plasma and urine I concentrations were analyzed by a reported GLC method (5) as modified (6). Briefly, the method involved addition of trichloroacetic acid as an internal standard and 14% boron trifluoride in methanol as the derivatizing reagent. The resulting methyl esters of I and the internal standard were extracted with benzene and analyzed on a Chromosorb 101 column using an electron-capture detector.

Preliminary analyses of plasma samples obtained from human subjects indicated that many specimens contained very low I concentrations. Therefore, method sensitivity was improved from 300 ng/ml as reported previously (6) to 40–50 ng/ml by three minor modifications: (*a*) the volume of solvent used in the extraction was reduced from 2 to 0.5 ml; (*b*) between the extraction and centrifugation steps, the entire contents of the vial were transferred to a 5-ml centrifuge tube to facilitate aliquot removal; and (*c*) the volume of extract analyzed was changed from 2 to 3 μl. The linearity of standard curves obtained during analysis demonstrated that these changes had no effect on the accuracy and precision of the results.

Analysis of Total Radioactivity—A 10-μl aliquot of plasma or urine was dissolved in 15 ml of scintillation cocktail and counted[3]. External standardization was used to correct for quenching. The cocktail had the following composition: naphthalene, 400 g; 2,5-diphenyloxazole, 20 g; 2,2′-*p*-phenylenebis(4-methyl-5-phenyloxazole), 1.2 g; dioxane, 2920 ml; toluene, 540 ml; and methanol, 140 ml.

[1] New England Nuclear Corp., Boston, Mass.
[2] Synthesized in these laboratories.
[3] Intertechnique model SL-40 liquid scintillation spectrometer.

0022-3549/80/0400-0419$01.00/0
© 1980, American Pharmaceutical Association

(8) L. B. Kier and L. H. Hall, *J. Med. Chem.*, **20**, 1631 (1977).
(9) L. B. Kier and L. H. Hall, *J. Pharm. Sci.*, **67**, 1408 (1978).
(10) B. W. Bolch and C. J. Huang, "Multivariate Statistical Methods for Business and Economics," Prentice-Hall, Englewood Cliffs, N.J., 1974.

ACKNOWLEDGMENTS

The author thanks Lowell H. Hall for the use of the program that computed the linear discriminant function. The author also acknowledges the helpful assistance of the Data Acquisition Laboratory at the Medical College of Virginia, Virginia Commonwealth University.

Biological Disposition of Sodium Dichloroacetate in Animals and Humans after Intravenous Administration

GEORGE LUKAS *x, KUNJBALA H. VYAS *, SHIRLEY D. BRINDLE *, ANNE R. Le SHER ‡, and WILLIAM E. WAGNER, Jr. ‡

Received April 27, 1979, from the *Research Department, Pharmaceuticals Division, Ciba-Geigy Corporation, *Ardsley, NY 10502, and ‡Summit, NJ 07901.* Accepted for publication October 5, 1979.

Abstract □ Sodium dichloroacetate, a potential antidote for lactic acidosis, was administered intravenously to rats, dogs, and four humans. In three rats, maximum plasma sodium dichloroacetate concentrations were 120–164 μg/ml after a 100-mg/kg dose and declined with half-lives of 2.1–4.4 hr. In two dogs, maximal concentrations of 447 and 508 μg/ml were attained after a 100-mg/kg dose. The subsequent decline was relatively slow with approximate half-lives of 17.1 and 24.6 hr. An intravenous infusion of 10 mg/kg was administered over 20 min to two human subjects. Two other subjects received 20 mg/kg. After the infusion, maximum plasma concentrations of 19.9 and 24.7 μg/ml were seen with the lower dose and 57.3 and 74.9 μg/ml were achieved with the higher dose. Thereafter, concentrations declined rapidly with half-lives of 20–36 min. The observed large interspecies differences in half-lives could be explained in terms of differences in the apparent volume of distribution and/or clearance.

Keyphrases □ Pharmacokinetics—sodium dichloroacetate, plasma concentration level-time curve, rats, dogs, humans □ Sodium dichloroacetate—pharmacokinetics, plasma concentration levels, rats, dogs, humans □ Clearance, intrinsic—plasma sodium dichloroacetate concentration, pharmacokinetics, rats, dogs, humans

Sodium dichloroacetate (I) has been reported to reduce normal or elevated blood lactate and pyruvate levels in animals by activating the pyruvate dehydrogenase enzyme complex (1–3). Oral administration of I to patients having nonketotic diabetes mellitus also led to an appreciable lowering of plasma lactate concentrations (4). The compound has been of possible interest as an intravenous antidote in patients suffering from lactic acidosis. This study was undertaken to provide information on the biological disposition of I in animals and humans since no data are available.

EXPERIMENTAL

Materials—Labeled[1] and unlabeled[2] sodium dichloroacetate were used. The material labeled in both carbon atom positions had a specific activity of 23.4 μCi/mg. Radiochemical purity, determined by TLC on silica gel plates in ethanol–chloroform–concentrated ammonium hydroxide–water (53:30:15:1.5), was >98%.

Animal Experiments—Each of three male Sprague–Dawley rats, 160–170 g, was given an intravenous injection of ^{14}C-I, diluted 1:20 with nonlabeled I, in a tail vein. The compound (100 mg/kg) was administered as a 10% aqueous solution. At specified times, animals were subjected to light ether anesthesia, and a 0.2–0.3-ml blood sample was collected in a heparinized centrifuge tube through a glass capillary by puncture of the suborbital sinus. Animals then were permitted to recover until the next sampling time.

Each of two male beagles, 9.0 and 10.5 kg, was given 100 mg of I/kg as a 20% aqueous solution intravenously in the cephalic vein. Animals were placed in individual metabolism cages. At specified times, blood was collected from a jugular vein without anesthesia.

Human Study—Four normal subjects, having given informed consent, participated after an overnight fast. Subjects 1 and 2, ages 42 and 38 years, respectively, each weighed ~70 kg. Subjects 3 and 4, ages 52 and 26 years, respectively, weighed 80 and 83 kg. In each case, the history, physical examination, ECG, and all laboratory tests were within normal limits.

Following the collection of the control urine sample and the drawing of a control blood specimen from Subjects 1 and 2, a 10-mg/kg dose of I dissolved in 100 ml of saline was infused over 20 min. Blood specimens were obtained from the contralateral antecubital vein at the time the infusion was completed. Specimens were drawn subsequently at 1 (40 min after termination of the infusion), 2, 3, 4, 6, 8, 10, 12, 24, 32, and 48 hr. All urine was collected for 96 hr with collection periods ending at 1, 2, 4, 8, 12, 24, 48, 72, and 96 hr.

Several weeks later, the procedure was repeated on Subjects 3 and 4, the sole change being that each received 20 mg/kg. All subjects were given a standard breakfast after the 4th hr. They remained under clinical observation for 8 hr.

Blood specimens were centrifuged as soon as they were collected. Plasma was separated and stored frozen until analysis. The urinary volume was measured and recorded. Aliquots of 20 ml from each urine sample were labeled and frozen for analysis.

Analysis of Unchanged I—Plasma and urine I concentrations were analyzed by a reported GLC method (5) as modified (6). Briefly, the method involved addition of trichloroacetic acid as an internal standard and 14% boron trifluoride in methanol as the derivatizing reagent. The resulting methyl esters of I and the internal standard were extracted with benzene and analyzed on a Chromosorb 101 column using an electron-capture detector.

Preliminary analyses of plasma samples obtained from human subjects indicated that many specimens contained very low I concentrations. Therefore, method sensitivity was improved from 300 ng/ml as reported previously (6) to 40–50 ng/ml by three minor modifications: (*a*) the volume of solvent used in the extraction was reduced from 2 to 0.5 ml; (*b*) between the extraction and centrifugation steps, the entire contents of the vial were transferred to a 5-ml centrifuge tube to facilitate aliquot removal; and (*c*) the volume of extract analyzed was changed from 2 to 3 μl. The linearity of standard curves obtained during analysis demonstrated that these changes had no effect on the accuracy and precision of the results.

Analysis of Total Radioactivity—A 10-μl aliquot of plasma or urine was dissolved in 15 ml of scintillation cocktail and counted[3]. External standardization was used to correct for quenching. The cocktail had the following composition: naphthalene, 400 g; 2,5-diphenyloxazole, 20 g; 2,2′-*p*-phenylenebis(4-methyl-5-phenyloxazole), 1.2 g; dioxane, 2920 ml; toluene, 540 ml; and methanol, 140 ml.

[1] New England Nuclear Corp., Boston, Mass.
[2] Synthesized in these laboratories.
[3] Intertechnique model SL-40 liquid scintillation spectrometer.

0022-3549/80/0400-0419$01.00/0
© 1980, American Pharmaceutical Association

Table I—Daily Standard Curves (Peak Height Ratios) Generated during Analyses in Human Plasma

Day	Sodium Dichloroacetate				
	0.05 μg/ml	0.2 μg/ml	1 μg/ml	5 μg/ml	10 μg/ml
1	0.267	0.967	3.807	16.45	20.17
	0.282	1.027	3.809	16.81	22.07
2	0.376	1.178	3.684	15.57	22.42
	0.197	—	—	17.30	23.82
3	0.261	0.976	3.613	17.90	21.71
	0.303	1.023	3.473	17.17	22.08
4	0.226	1.187	3.636	18.58	25.30
	0.277	1.184	4.135	20.58	22.95
5	0.265	0.937	2.833	12.21	17.12
	0.255	—	3.622	13.96	20.36
Mean	0.271	1.060	3.623	16.65	21.80
CV[a]	17.45	10.00	9.66	14.10	10.24

[a] Overall coefficient of variation is 12.66%.

Table II—Plasma Sodium Dichloroacetate Levels (Micrograms per Milliliter) in Rats after a 100-mg/kg iv Dose [a]

Time	Rat A		Rat B		Rat C	
	^{14}C	GLC	^{14}C	GLC	^{14}C	GLC
10 min	195.0	150.0	126.5	85.7	209.0	163.5
20 min	178.0	122.0	165.9	120.0	191.8	149.0
30 min	171.8	117.5	160.8	100.5	181.0	131.8
1 hr	161.8	83.7	157.4	74.3	175.3	118.8
2 hr	153.6	50.0	153.9	47.5	171.4	87.5
3 hr	134.7	33.3	125.9	33.3	146.0	67.2
4 hr	116.9	22.0	120.2	19	142.7	52.5
6 hr	115.3	20.3	115.5	12	127.8	43.2
24 hr	28.5	NS[b]	51.2	ND[c]	48.8	3.8
28 hr	46.8	ND	44.6	ND	45.3	1
48 hr	26.7	ND	25.3	ND	23.7	0
52 hr	31.0	ND	26.1	ND	27.1	0.05
72 hr	17.4	ND	NS	NS	16.7	0
96 hr	16.6	ND	NS	NS	16.5	1

[a] Results are given in terms of both total radioactivity and GLC analysis. [b] NS = no sample. [c] ND = not detectable.

Distribution of I between Plasma and Erythrocytes—To 2 ml of heparinized fresh human blood obtained from three healthy volunteers was added 0.2 ml of an aqueous solution of ^{14}C-I to provide concentrations of 0.5, 5, and 50 μg/ml. The mixtures were incubated for 1 hr at 37° in a shaking water bath and cooled. Triplicate 0.1-ml aliquots were combusted in a sample oxidizer[4]. The resulting $^{14}CO_2$ was trapped and counted for the estimation of radioactivity in whole blood. The remaining blood samples were centrifuged, and radioactivity in triplicate 0.1-ml plasma aliquots was analyzed similarly by combustion and counting. In a separate experiment, the stability of I in whole blood for 1 hr at 37° was ascertained.

Stability of I in Frozen Plasma—To 1-ml aliquots of human plasma obtained from healthy volunteers was added 1 μg of I in 50 μl of water. The aliquots were sealed, stored at −20°, and analyzed in triplicate after periods ranging from 1 week to 6 months.

Pharmacokinetic Calculations—Pharmacokinetic parameters were calculated using standard procedures and assuming a one-compartment open model with constant-rate intravenous infusion (7). Half-lives were obtained with the least-squares method after logarithmic transformation of concentrations. Plasma clearance (8) was calculated as the ratio of the dose and the area under the concentration–time curve. The apparent volume of distribution was obtained as the ratio of clearance and the elimination rate constant, the latter value having been derived from the corresponding half-life estimate.

The importance of using blood clearance rather than plasma clearance in the calculation of intrinsic clearance was demonstrated previously (8, 9). Blood clearance was obtained from plasma clearance using a constant correction factor of 0.688. The value was obtained assuming a mean hematocrit of 0.45 and a mean distribution ratio of 4:1 between plasma and the cellular fraction of blood for I (see *Results*):

$$F = \frac{B(1 - H)}{P} \qquad \text{(Eq. 1)}$$

[4] Packard model 306.

where F is the correction factor, H is the hematocrit, and B and P represent concentrations in equal-volume aliquots of whole blood and plasma, respectively.

Intrinsic clearance was obtained from the blood clearance as described (9) by:

$$Cl_{in} = \frac{QCl_{bl}}{Q - Cl_{bl}} \qquad \text{(Eq. 2)}$$

where Cl_{in} and Cl_{bl} refer to the intrinsic and blood clearance, respectively, and Q indicates the hepatic blood flow rate. An approximate mean value of 1500 ml/min was used for the calculations in conformity with literature reports (9).

RESULTS

Reproducibility of GLC Method—Standard curves generated daily in conjunction with the analyses of human plasma samples are summarized in Table I. Each of the five curves represents five concentrations of I, usually in duplicate determinations, ranging from 0.05 to 10 μg/ml. Daily variations in the individual standard curves were acceptable, with the relative standard deviations ranging from 9.66 to 17.45% and giving an overall value of 12.66% over 5 days.

Animal Studies—Plasma levels in three rats after 100 mg/kg iv are summarized in Table II. Maximal concentrations of unchanged I ranged between 120 and 164 μg/ml. Subsequent declines of plasma concentrations occurred with half-lives of 2.1–4.4 hr. Total radioactive materials attained maximal concentrations of 166–209 μg/ml (expressed as unchanged I). Thus, at the peak concentration, unchanged I in plasma represented the bulk of total radioactivity. However, the subsequent decline of the total radioactivity concentrations was considerably less rapid, and apparent half-lives of 21–36 hr could be estimated, indicating extensive metabolism and slow elimination of metabolites.

Plasma levels of unchanged I in two dogs after 100 mg/kg iv are summarized in Table III. Maximum concentrations of 447 and 508 μg/ml were measured in the first plasma samples at 5 min. The subsequent decline was slow. Sampling in one animal was continued for 48 hr. In the other animal, sampling had to be discontinued after 24 hr because of collapsing veins and the formation of hematomas. Nevertheless, approximate half-lives of 17.1 and 24.6 hr could be estimated in the two animals.

Human Studies—No subjective or objective changes or signs of clinical activity were noted in any subject upon intravenous infusion of I.

Plasma concentrations of unchanged I are summarized in Table IV.

Table III—Plasma Sodium Dichloroacetate Levels (Micrograms per Milliliter) in Dogs following a 100-mg/kg iv Dose

Time	Dog 1	Dog 2
5 min	447	508
15 min	418	502
30 min	412	439
45 min	412	410
1 hr	390	418
1.5 hr	298	206
2 hr	300	384
3 hr	290	314
4 hr	266	341
5 hr	290	—
6 hr	278	—
24 hr	155	192
28 hr	163	—
48 hr	50	—

Table IV—Plasma Sodium Dichloroacetate Concentrations (Micrograms per Milliliter) in Humans after an Intravenous Infusion

Hours[a]	10-mg/kg Dose		20-mg/kg Dose	
	Subject 1	Subject 2	Subject 3	Subject 4
0.33[b]	24.7	19.9	57.3	74.9
1	3.27	4.44	29.3	46.8
2	0.304	0.585	5.96	11.2
3	0.086	0.117	0.623	4.68
4	<0.04	<0.04	0.140	0.608
6	<0.04	<0.04	<0.04	0.175
8	<0.04	--[c]	<0.04	<0.04

[a] All samples collected at 10, 12, 24, 32, and 48 hr after dosing contained <0.04 μg of I/ml. [b] End point of 20-min infusion. [c] Sample lost during analysis.

Table V—Pharmacokinetic Parameters of Sodium Dichloroacetate in Humans

Parameter[a]	Subject 1	2	3	4
Dose, mg	700	700	1600	1650
Weight, kg	69.5	69.1	80.0	83.3
$t_{1/2}$, min	19.6	21.6	24.3	36.6
$AUC_{0-\infty}$, (hr μg)/ml	15.46	14.35	59.85	93.61
V_d, liters	21.4	25.3	15.6	15.5
Cl_{plasma}, ml/min	755	813	446	294
Cl_{bl}, ml/min	1100	1180	648	427
Cl_{in}, ml/min	4125	5530	1140	600

[a] AUC = area under the plasma level-time curve, V_d = apparent volume of distribution, and Cl = clearance.

Table VI—Average Values (and Ranges) of Pharmacokinetic Parameters of Sodium Dichloroacetate in Humans, Rats, and Dogs [a]

Parameter	Humans 10 mg/kg	Humans 20 mg/kg	Rats, 100 mg/kg	Dogs, 100 mg/kg
$t_{1/2}$, hr	0.34 (0.33–0.36)	0.51 (0.41–0.61)	2.97 (2.1–4.4)	20.8 (17.1–24.6)
V_d, ml/kg	337 (308–366)	190 (186–195)	932 (701–1080)	256 (249–262)
Cl_{plasma}, ml/(min kg)	11.31 (10.86–11.76)	4.55 (3.53–5.58)	4.22 (1.84–5.94)	0.146 (0.123–0.168)
Cl_{in}, ml/(min kg)	69.7 (59.3–80.0)	10.7 (7.2–14.2)	6.9 (2.8–9.9)	0.21 (0.18–0.24)

[a] Values of 20, 67, and 40 ml/(min kg) were used in humans (9), rats (12), and dogs (13), respectively, for hepatic blood flow.

The highest concentrations were obtained immediately after the end of the infusion. Subjects 1 and 2, receiving 10 mg/kg, had maximum values of 19.9 and 24.7 μg/ml, respectively. Maximum concentrations of 57.3 and 74.9 μg/ml were seen in Subjects 3 and 4 after 20 mg/kg.

Concentrations of I declined rapidly following monoexponential kinetics. The values decreased to <0.04 μg/ml, the sensitivity of the method, at 4 hr after the lower dose and at 6 or 8 hr after the higher dose.

Urinary excretion of unchanged I became negligible after the first 8 hr; in all subjects, cumulative excretion amounted to considerably less than 1% of the dose.

The pharmacokinetic parameters are summarized in Table V. Half-lives in the four subjects ranged from 20 to 36 min. Values for the apparent volume of distribution were 15.5–25.3 liters. Plasma clearance ranged from 294 to 813 ml/min, and the corresponding values for blood clearance were 427–1180 ml/min. Hematocrit in the four subjects had a mean value of 0.45 (range of 0.43–0.49).

The following values were obtained for intrinsic clearance: Subjects 1 and 2, 4125 and 5530 ml/min; and Subjects 3 and 4, 1140 and 600 ml/min. Expressed on the basis of unit body weight, these values were 59.3, 80.0, 14.2, and 7.2 ml/(min kg), respectively.

The stability of I stored in frozen human plasma for 6 months was demonstrated in separate experiments.

In an *in vitro* study using fresh blood from three subjects, an average of 80% (range of 72–94%) of I present in whole blood was in the plasma. The distribution between plasma and the cellular fraction was independent of the concentration in the 0.5–50-μg/ml range.

DISCUSSION

After an intravenous infusion, I in human plasma declined monoexponentially over a 200–500-fold concentration range, corresponding to a range of 7–9 half-lives. These findings permitted a relatively simple pharmacokinetic analysis. Examination of the individual pharmacokinetic parameters (Table V) suggests some dose dependence because the apparent volume of distribution and the plasma clearance decreased with a doubling of the dose. Although this observation is necessarily limited by the size of the study, it suggests capacity-limited elimination.

Intrinsic clearance refers to the maximum capacity of an organ to remove the drug irreversibly by all pathways when blood flow to the organ is not rate limiting (10). The metabolism of I has not been explored in detail, but Demaugre *et al.* (11) demonstrated its hepatic biotransformation to oxalate. The present results show that the intrinsic clearance of I was considerably greater than, and the elimination presumably limited by, blood flow in subjects receiving 10 mg/kg. In subjects receiving 20 mg/kg, intrinsic clearance was considerably lower, lending support to the hypothesis of capacity-limited metabolism. Corresponding intrinsic values expressed on the basis of unit body weight indicated even more clearly the dose-dependent pharmacokinetics of I. A doubling of the dose led to an approximately sevenfold decrease in intrinsic clearance, yet the systemic (plasma or blood) clearance values decreased only by a factor of two or three. Thus, when the elimination rate is limited by hepatic blood flow, systemic clearance appears to reflect only partially any large changes occurring in intrinsic clearance.

Pharmacokinetic parameters also were estimated for rats and dogs. Average values and ranges of the animal and human data are summarized in Table VI for comparison. The large difference in the half-lives of I between humans and dogs may reflect the difference in clearance. In contrast, the observed difference in half-lives between humans and rats is consistent with the relatively high value of the apparent volume of distribution in the latter species.

In the present study, the I elimination rate in humans was dose dependent and limited by hepatic blood flow. The role of blood flow appeared to diminish with increasing dose. Elimination of high doses was not flow limited in rats and, particularly, in dogs since hepatic blood flow substantially exceeded intrinsic clearance[5]. The large differences seen show the difficulty in predicting the biological disposition and toxicity of therapeutic doses of a drug in humans from animals given large doses.

REFERENCES

(1) S. Whitehouse, R. H. Cooper, and P. J. Randle, *Biochem. J.*, **141**, 761 (1974).

(2) P. A. H. Holloway and K. G. M. M. Alberti, *Diabetologia*, **11**, 350 (1975).

(3) A. L. Loubatieres, G. Ribes, and G. Valette, *Br. J. Pharmacol.*, **58**, 429p (1976).

(4) P. W. Stacpoole, G. W. Moore, and D. M. Kornhauser, *N. Engl. J. Med.*, **298**, 526 (1978).

(5) L. T. Sennello, *Biochem. Med.*, **8**, 345 (1973).

(6) G. Lukas, K. H. Vyas, and S. D. Brindle, *Anal. Lett.*, **B11**, 953 (1978).

(7) J. G. Wagner, "Biopharmaceutics and Relevant Pharmacokinetics," Drug Intelligence Publications, Hamilton, Ill., 1971, p. 293.

(8) A. S. Nies, D. G. Shand, and G. R. Wilkinson, *Clin. Pharmacokinet.*, **1**, 135 (1976).

(9) G. R. Wilkinson and D. G. Shand, *Clin. Pharmacol. Ther.*, **18**, 377 (1975).

(10) M. Rowland, L. Z. Benet, and G. G. Graham, *J. Pharmacokinet. Biopharm.*, **1**, 123 (1973).

(11) F. Demaugre, C. Cepanec, and J. P. Leroux, *Biochem. Biophys. Res. Commun.*, **85**, 1180 (1978).

(12) D. G. McDevitt, A. S. Nies, and G. R. Wilkinson, *Biochem. Pharmacol.*, **26**, 1247 (1977).

(13) A. Fischer, in "The Liver, Morphology, Biochemistry, Physiology," vol. I, C. Rouiller, Ed., Academic, New York, N.Y., 1969, p. 336.

[5] The relative contributions of dose dependence and species difference were not determined. These factors could be assessed by additional studies wherein each subject or animal would receive both larger and smaller doses of I.

Analysis of Benzimidazoles in Body Fluids by High-Performance Liquid Chromatography

J. A. BOGAN ˣ **and S. MARRINER**

Received August 6, 1979, from the *Department of Veterinary Pharmacology, University of Glasgow, Bearsden Road, Bearsden, Glasgow, Scotland.* Accepted for publication November 2, 1979.

Abstract □ A simple assay for benzimidazole in plasma and GI fluids using high-performance liquid chromatography was developed. The benzimidazoles were extracted using ether and were chromatographed with methanol–ammonium carbonate mixtures as the eluting solvents. Benzimidazole was detectable in 4 ml of plasma or GI fluid to a limit of 20 ng/ml.

Keyphrases □ Benzimidazoles—analysis, high-performance liquid chromatography, GI fluids, plasma □ High-performance liquid chromatography—analysis, benzimidazoles, GI fluids, plasma □ Anthelmintics—benzimidazoles, high-performance liquid chromatographic analysis, GI fluids, plasma

The benzimidazole anthelmintics are characterized by low mammalian toxicity and a broad spectrum of activity against GI nematodes. Some members of the group also are active against lungworms, tapeworms, and liver flukes in humans, cattle, sheep, and other animals. This paper describes a simple assay for this important group of anthelmintics using high-performance liquid chromatography (HPLC).

BACKGROUND

The anthelmintic activity of the benzimidazole anthelmintics appears to be the result of the length of time over which the parasite is exposed to the drug rather than the peak concentration to which the parasite is exposed. Thus, administration of the drug in divided doses usually increases anthelmintic activity (1). The drugs exert their activity on the parasites by inhibiting glucose uptake (2) and/or by inhibiting the enzyme fumarate reductase (3). Differences between members of the group appear to be more a result of differing pharmacokinetics of the drugs in the host animal than of different inherent anthelmintic activity. However, there is a lack of data on the pharmacokinetics of these drugs, probably because of analytical problems.

Most published data on benzimidazole pharmacokinetics are from experiments using radiolabeled drug without distinguishing between the parent drug and the metabolites. A method was published for the analysis of fenbendazole using fluorescence spectrophotometry, but this method also fails to distinguish the parent drug from the metabolites (4). A radioimmunoassay for oxfendazole (5) was reported recently, but this complex method requires the raising of an antiserum, and some cross-reactivity with metabolites occurs.

This paper describes a sensitive HPLC method for the analysis of oxfendazole, fenbendazole, and albendazole, the most potent members of the group, in body fluids. The method can be adapted for the other five members of the group that are marketed in the United Kingdom.

EXPERIMENTAL

Materials—Analar reagents were used, and the HPLC solvents were distilled.

Extraction—The method is applicable to plasma, rumen fluid, abomasal fluid, and duodenal fluid.

To 4 ml of plasma or GI fluid in a 50-ml stoppered tube were added 4 ml of phosphate buffer (pH 7.4) and 20 ml of ether. The tube was shaken for 10 min on a rotary mixer. Then 16 ml of the ether layer was removed to a clean test tube, and 20 ml of ether was added to the first tube, which was shaken again for 10 min. Twenty milliliters of ether was removed and combined with the initial 16 ml of ether.

The ether was evaporated slowly on a dry bath at 60° under nitrogen to a volume of about 6 ml and then was transferred to a conical 10-ml glass tube. The 50-ml tube was washed with several milliliters of ether, and the washings were added to the conical tube. The ether then was evaporated to dryness, the walls of the conical tube were rinsed with ether, and the solution was evaporated again to dryness. The residue in the tube was redissolved in 50 μl of methanol with the aid of an ultrasonic bath. If higher concentrations were expected, larger volumes of methanol were used. Five microliters of this solution was used for HPLC analysis.

HPLC—The HPLC system consisted of a solvent delivery pump[1] and a variable-wavelength UV detector[2] with a 100 × 8-mm column[3] packed

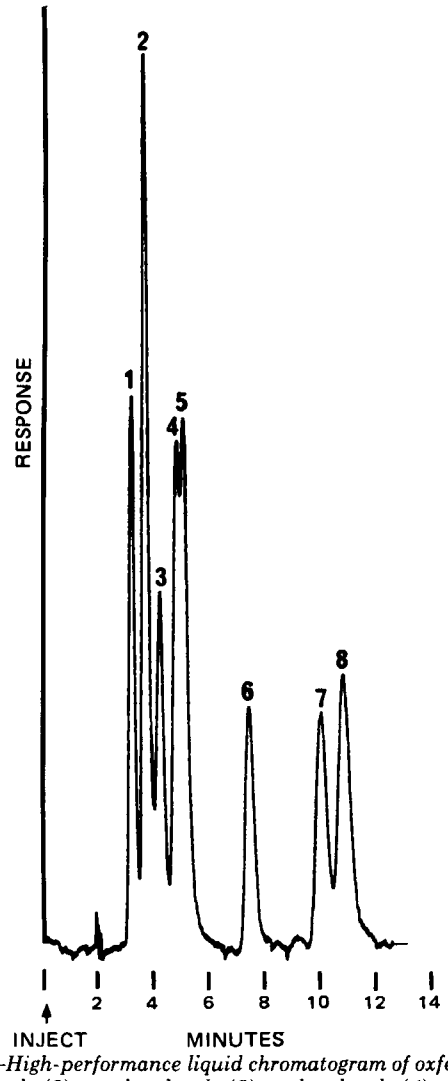

Figure 1—*High-performance liquid chromatogram of oxfendazole (1), thiabendazole (2), cambendazole (3), mebendazole (4), oxibendazole (5), albendazole (6), fenbendazole (7), and parbendazole (8) in methanol–ammonium carbonate (0.05 M) (65:35). Five microliters of a solution containing 10 μg/ml of each benzimidazole in methanol was used for injection.*

[1] Model 110, Altex, Berkeley, Calif.
[2] Model CE 2012, Cecil Instruments, Cambridge, England.
[3] Shandon Southern Products Ltd., Runcorn, Cheshire, England.

0022-3549/80/0400-0422$01.00/0
© 1980, American Pharmaceutical Association

Table I—Recoveries of Benzimidazoles added to Plasma, Rumen Fluid, and Abomasal Fluid

Compound	Recovery, %		
	Plasma	Rumen Fluid	Abomasal Fluid
Fenbendazole	83–100 (n = 10)	82–105 (n = 9)	83–112 (n = 8)
Oxfendazole	70–97 (n = 10)	70–97 (n = 6)	72–92 (n = 12)
Albendazole	73–103 (n = 9)	72–90 (n = 4)	87–93 (n = 4)

Table II—Estimation of Oxfendazole in Abomasal Fluid

Oxfendazole Added, μg	Oxfendazole Measured, μg	Mean ± SE	SEM, %	Ratio of Assayed to Added
1.5	1.03	1.08 ± 0.03	2.8	0.72
	1.08			
	1.13			
7.5	5.90	6.07 ± 0.09	1.5	0.81
	6.20			
	6.10			
15	12.10	11.57 ± 0.27	2.3	0.77
	11.20			
	11.40			
30	24.50	24.93 ± 0.59	2.4	0.83
	24.20			
	26.10			

with ODS-Hypersil 10[4]. The solvent flow rate was 1.5 ml/min, and the detector wavelength was 292 nm.

The drug concentration in the samples was calculated with the aid of calibration curves prepared by adding known drug amounts (0.05–10 μg/ml) to blank plasma or GI fluids. The standard samples were run through the procedure, and the peak heights of drug in the sample were compared with the calibration curve prepared from the standard samples.

RESULTS AND DISCUSSION

The new broad-spectrum benzimidazoles have limited solubility in both water and organic solvents. While this feature enhances their action by slowing drug dissolution after oral dosage, it also produces difficulties in analysis because the concentrations found in plasma and in the GI contents are low and are present for long periods. The method described here is sensitive and practical for the evaluation of the pharmacokinetics of the benzimidazoles.

The retention times of the benzimidazoles varied considerably, and Fig. 1 shows a chromatogram of the eight benzimidazoles using a solvent mixture of methanol—ammonium carbonate (0.05 M) (65:35). For the analysis of individual benzimidazoles with longer retention times, retention times can be shortened by increasing the proportion of methanol in the solvent mixture. For example, parbendazole has a retention time of 3.6 min in 85:15 methanol–ammonium carbonate.

Recoveries were determined by measuring standard concentrations (0.2–5.0 μg/ml) of some benzimidazoles added to plasma, rumen fluid, and abomasal fluid (Table I). The method is sufficiently sensitive to measure plasma and GI fluid concentrations down to 0.02 μg/ml with 4 ml of sample or 0.01 μg/ml with 8 ml of sample.

The accuracy and precision of the method for oxfendazole were determined by adding known amounts of oxfendazole to 4 ml of abomasal fluid. Samples of each known concentration then were assayed in triplicate (Table II). It was determined that the recovery losses were due to the extraction procedure rather than to benzimidazole degradation.

Fenbendazole, oxfendazole, and albendazole, which are the most potent compounds of the benzimidazole series and have the broadest spectrum of activity, were administered at 10 mg/kg to three sheep with permanent ruminal and abomasal fistulae. Samples of plasma, ruminal fluid, and abomasal fluid were withdrawn at intervals for measurement of the benzimidazole concentration[5].

[4] Whatman Co., Clifton, N.J.

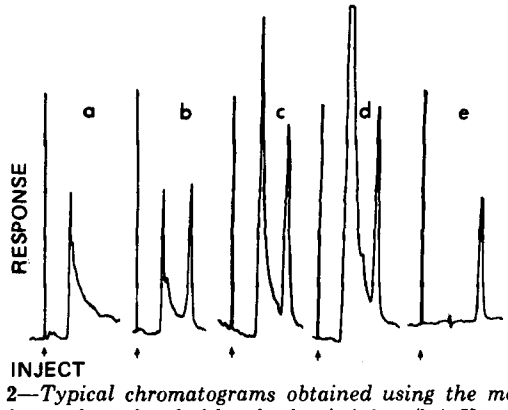

Figure 2—*Typical chromatograms obtained using the method on samples from a sheep dosed with oxfendazole (10 mg/kg). Key: a, plasma before oxfendazole administration; b, plasma at 12 hr after administration; c, abomasal fluid at 12 hr; d, ruminal fluid at 12 hr; and e, oxfendazole standard (10 μg/ml).*

Under the conditions described, no interfering substances were encountered in any fluid. The peaks encountered were symmetrical and, except at the lowest concentrations, were well defined. Typical chromatograms for oxfendazole are shown in Fig. 2.

The mean peak concentrations encountered in the three sheep for oxfendazole were 0.8, 0.4, and 4.6 μg/ml in plasma, ruminal fluid, and abomasal fluid, respectively. Oxfendazole was detectable for up to 11 days after administration. For fenbendazole, the mean peak concentrations were 0.13, 3.4, and 2.6 μg/ml, respectively, and it was detectable in all sheep 120 hr after administration. Fenbendazole was metabolized to oxfendazole (its equivalent sulfoxide metabolite), and the kinetics of the oxfendazole formed were similar to those of the administered oxfendazole.

Albendazole was not detectable in any plasma samples, although it could be detected in ruminal and abomasal fluids at maximum concentrations of 0.3 and 4.9 μg/ml, respectively. Albendazole was detectable in ruminal and abomasal fluids for at least 72 hr after administration. Metabolites (sulfoxide and sulfone) were found in high concentration in the plasma and abomasum after albendazole administration and were present for more than 48 hr. These metabolites did not interfere with the assay of the parent drug, but they also could be assayed by this method.

[5] A full description of the pharmacokinetics of these drugs in sheep will be the subject of a separate investigation.

REFERENCES

(1) R. K. Prichard, D. R. Hennessy, and J. W. Steel, *Vet. Parasitol.*, **4**, 309 (1978).

(2) H. Van den Bossche, "Comparative Biochemistry of Parasites," Academic, New York, N.Y., 1972, pp. 139–157.

(3) R. K. Prichard, *Int. J. Parasitol.*, **3**, 409 (1973).

(4) D. Duwel, P. Hajdu, and D. Damm, *Berl. Muench. Tieraerztl.*, **88**, 131 (1975).

(5) C. Nerenberg, R. A. Runkel, and S. B. Matin, *J. Pharm. Sci.*, **67**, 1553 (1978).

ACKNOWLEDGMENTS

Supported by the Agricultural Research Council.

S. Marriner is a Wellcome Veterinary Research Scholar.

The gifts of fenbendazole and oxfendazole from Hoechst and Syntex and the albendazole and metabolites from Smith Kline are acknowledged gratefully.

The authors also thank Mrs. A. Galbraith for excellent technical assistance.

Prostaglandin Prodrugs VI: Structure–Thermodynamic Activity and Structure–Aqueous Solubility Relationships

BRADLEY D. ANDERSON ˣ **and ROBERT A. CONRADI**

Received May 7, 1979, from *Pharmacy Research, The Upjohn Company, Kalamazoo, MI 49001.* Accepted for publication November 6, 1979.

Abstract □ Solubilities in isooctane and water were determined for several C_1-phenolic esters of prostaglandin $F_{2\alpha}$ and prostaglandin E_2 and acetates having the same phenol moiety. Linear free energy relationships for solubility among the series were observed with slopes of ~1. These results suggest that the contributions of the phenyl substituent to the free energies of these processes are similar in the three series, even though the structure of the acyl moiety is varied. In addition, aqueous solubility was separated into two thermodynamic components, reflecting transfer from the solid phase to an inert solvent and transfer from the inert solvent to water, to evaluate the relative effects of various substituents on the escaping tendency of the drug from the solid phase and on solution interactions. It was found that polar, hydrogen-bonding functional groups in many cases do not bring about increased water solubility because of a corresponding increase in intermolecular interaction in the solid phase.

Keyphrases □ Prostaglandins—prodrugs, structure–thermodynamic activity and structure–aqueous solubility relationships □ Prodrugs—prostaglandins, structure–thermodynamic activity and structure–aqueous solubility relationships □ Solubility—prostaglandin prodrugs, solubility in isooctane and water

The physicochemical properties of a drug affect every aspect of drug design, from initial purification to optimization of drug concentration in the receptor region. Consequently, relationships between molecular structure and physical properties are extremely useful to the pharmaceutical or medicinal chemist. Predictive relationships are particularly important in prodrug design since the primary goal often is the improvement of pharmaceutical or pharmacodynamic properties of already active compounds through modifications of physical properties.

A variety of prostaglandin prodrugs have been synthesized in an attempt to improve the pharmaceutical or biological properties of the parent compounds (1–5). Among the problems encountered with prostaglandins are solid-state instability and their frequent existence as liquids, which pose difficulties in handling and formulation. In the E_2 series, some crystalline high-melting C_1-phenolic esters with improved solid-state stability were reported (1). A rough correlation was observed between the melting points of the esters and the parent phenols, suggesting that strong intermolecular interactions existing in the crystalline phenols may be retained upon ester formation. Similar melting-point correlations were observed for C_1-phenolic esters in the prostaglandin $F_{2\alpha}$ series[1].

This report describes an attempt to gain a more quantitative understanding of the effect of various prodrug moieties on aqueous solubility and on the thermodynamic activity of drugs in the pure crystalline solid as reflected by alkane solubility. Alkane and aqueous solubilities have been determined for several phenolic C_1-esters of prostaglandins of the E_2 and $F_{2\alpha}$ series and for acetates having the same phenolic moieties. Linear free energy relationships between series with slopes of ~1 have been observed in the alkane and aqueous solubilities, suggesting that the effect of a given substituent on the free energies of these processes is similar in all three series. Such relationships may be useful in the prediction of solubilities of other prostaglandin derivatives.

[1] W. Morozowich, The Upjohn Co., Kalamazoo, Mich., personal communication.

EXPERIMENTAL

The compounds examined in this study and their melting points are listed in Table I[2]. The syntheses of the prostaglandin E_2 esters were reported previously (1). The C_1-phenolic esters of prostaglandin $F_{2\alpha}$ and the corresponding acetates were prepared by a similar procedure[3].

Solubilities were determined by various methods, depending on the particular difficulties encountered with each compound. For pure, relatively soluble compounds, 10–50-mg samples were shaken in vials containing 10–25 ml of solvent at 25° for at least 24 hr. These solutions were filtered or centrifuged to remove undissolved solid; after the appropriate dilutions or concentrations, they were analyzed for dissolved drug.

Solution concentrations were determined spectrophotometrically[4] only if solubilities were quite high. Thus, the isooctane and water solubilities of acetates having solubilities greater than 2×10^{-5} *M* were determined by UV analysis, as were the isooctane solubilities of the biphenyl, naphthyl, and *p*-acetylphenyl esters of prostaglandin E_2. In the spectrophotometric analyses, solubilities were determined as a function of the amount of solid added to the vials. A constant apparent solubility suggested that impurities did not contribute significantly to the UV absorbance reading.

All other analyses were performed by high-pressure liquid chromatography[5] (HPLC) using a reversed-phase column[6] and acetonitrile–water solvent systems. Sample detection was at 254 nm.

In many cases, especially for compounds having low aqueous solubility but much higher solubility in isooctane, the method proposed by Higuchi *et al.* (6) was utilized. Solid samples, 10–50 mg, were shaken in vials at 25° in both isooctane and water for not less than 24 hr. When possible, the saturation solubility in both phases was determined as described previously. Because of the low water solubility in isooctane and vice versa (7), it was assumed that solubilities in water-saturated isooctane or in isooctane-saturated water were equal within experimental error to the solubilities in the pure solvents.

Water solubilities of extremely insoluble compounds or compounds that appeared to adsorb readily to glassware, filters, *etc.*, were determined by recycling the solvent through a cartridge containing a filter[7] and a 1–20-mg sample. The change in UV absorbance was monitored at 254 nm[8]. The solvent was pumped[9] through the filtration system at ~10–15 ml/min.

This system offered several advantages over conventional methods:

1. By monitoring absorbance with time, one can ascertain whether equilibrium is established within the system.
2. Withdrawal of filtered samples can be done easily and rapidly with a minimum temperature change.
3. Possible adsorption onto extraneous glassware or onto the filter no longer is a problem since all components become saturated with solute.

Equilibrium solubilities generally were approached within 1 day for

[2] Compounds used in this study were provided by W. Morozowich and S. L. Douglas, The Upjohn Co., Kalamazoo, Mich.

[3] W. Morozowich and S. L. Douglas, The Upjohn Co., Kalamazoo, Mich., personal communication.

[4] Zeiss DMR-21.

[5] DuPont model 840 liquid chromatograph.

[6] Lichrosorb RP-8, 10 μ, Merck, Darmstadt, West Germany.

[7] Swinnex-13 filter unit with 0.45-μm pore size filters (type HA), Millipore Corp., Bedford, MA 01730.

[8] Altex detector 153-00.

[9] FMI RP-58 solvent pump.

0022-3549/80/0400-0424$01.00/0
© 1980, American Pharmaceutical Association

Table I—Melting Points of Investigated Compounds

Phenolic Moiety	Acyl Moiety: Prostaglandin $F_{2\alpha}$	Acyl Moiety: Prostaglandin E_2	Acyl Moiety: Acetic Acid
Phenyl	59–60.6°	Liquid	Liquid
p-Biphenyl	114.3–116.8°	91.8–92.8°	87.0–88.0°
β-Naphthyl	98.8–100°	79.3–80.3°	68.9–69.9°
p-Nitrophenyl	—	—	81–82°
p-Acetylphenyl	85.3–86.5°	76.8–77.8°	52.1–53.7°
p-Benzamidophenyl	139.8–143.8°	132.8–135.0°	172–173°
p-Acetamidophenyl	114–115.8°	102.3–103.3°	154–156°
p-Carbamoylphenyl	129.5–130.8°	106.3–108.3°	175–184.1°
p-(*p*-Acetamidobenzamido)phenyl	165.6–168.2°	173.2–176.2°	256–260°
p-Ureidophenyl	133.8–135°	105.3–108.3°	189.6–191.2°
N-Acetyl-L-tyrosinamide	109.8–113.8°	137.3–140.8°	222–225.7°
N-Benzoyl-L-tyrosinamide	142.5–144.3°	160.8–164.8°	221.7–228°
α-Semicarbazono-*p*-tolyl	110.8–113.3°	125.3–126.5°	194–198°
2-Oxo-5-indolinyl	109.8–112.0°	—	146–147°
p-(3-Phenylureido)phenyl	145.0–147.3°	—	198–199°

the major component, although impurities often leached out of the solid phase more slowly. Because impurities often contributed more to the UV absorbance than did the compound of interest, HPLC analysis of the saturated solution was necessary. All solubilities are reported in moles per liter.

RESULTS AND DISCUSSION

Molecular Structure–Aqueous Solubility Relationships—Aqueous solubilities of prostaglandin E_2 and $F_{2\alpha}$ derivatives and their corresponding acetates are listed in Table II. Plots of log solubility of the prostaglandin $F_{2\alpha}$ esters and the prostaglandin E_2 esters *versus* log solubility of the acetates are shown in Figs. 1 and 2. These quantities were obtained experimentally. Slopes of ~1 (Fig. 1: slope = 0.98, r = 0.9467; Fig. 2: slope = 1.03, r = 0.9468) are observed.

Since log solubility is proportional to the solution free energy, the plots in Figs. 1 and 2 are indicative of approximate linear free energy relationships for solubility; the effect of a substituent on the solution free energy in one series is linearly related to its effect in another series. Slopes of 1, as observed in the series of compounds examined, suggest that not only is there a proportionality in free energy but that the substituent effects on solubility are nearly the same for both prostaglandin series and the acetates. This effect was not known to be observed previously for polar crystalline materials. These observations should not be extrapolated to other series since the constancy in substituent group contributions probably depends on similar crystal lattice arrangements of molecules in all compounds examined.

The aqueous solubilities in Table II are listed from highest to lowest. There appears to be no correlation between the apparent polarity of the phenol moiety and aqueous solubility. This lack of correlation illustrates the inadequacy of simple maxims such as "like dissolves like" for predicting relative solubilities of solids in water. A more quantitative understanding of the relationship between molecular structure and aqueous solubility can be gained by separating aqueous solubility into two thermodynamic components.

Separation of Aqueous Solubility into Two Thermodynamic Components—As shown in Scheme I, the solution free energy of a drug in water can be expressed as a sum of the energies from the escape of the drug from the crystal into an inert solvent and the transfer of the drug from an inert solvent to water.

Table II—Water Solubilities of C_1-Phenolic Esters of Prostaglandin $F_{2\alpha}$ and Prostaglandin E_2 and Acetates Having the Same Phenol Moiety

Phenol Moiety	Water Solubility, *M*		
	Acetate	Prostaglandin E_2	Prostaglandin $F_{2\alpha}$
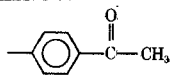	3.0×10^{-2}	1.6×10^{-5}	5.0×10^{-5}
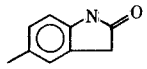	2.9×10^{-2}	—	6.0×10^{-5}
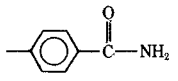	2.3×10^{-2}	4.4×10^{-5}	8.3×10^{-5}
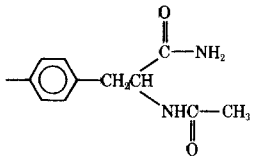	1.3×10^{-2}	1.7×10^{-4}	1.4×10^{-4}
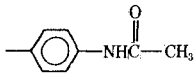	1.1×10^{-2}	5.4×10^{-5}	9.5×10^{-5}
	Liquid	Liquid	9.1×10^{-5}
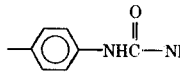	3.2×10^{-3}	2.8×10^{-5}	6.9×10^{-5}
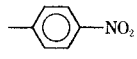	2.9×10^{-3}	1.1×10^{-5}	2.1×10^{-5}
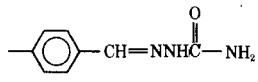	1.4×10^{-3}	2.5×10^{-6}	1.6×10^{-5}
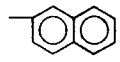	3.6×10^{-4}	3.9×10^{-7}	5.7×10^{-7}
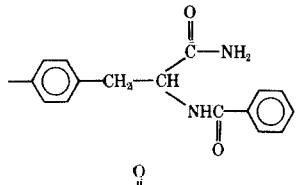	1.3×10^{-4}	4.7×10^{-7}	1.8×10^{-6}
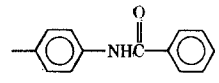	7.2×10^{-5}	2.3×10^{-7}	3.0×10^{-7}
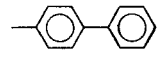	3.9×10^{-5}	6.6×10^{-8}	9.6×10^{-8}
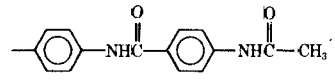	3.9×10^{-5}	~9.8×10^{-8}	2.8×10^{-7}
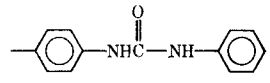	3.6×10^{-5}	—	—

Component 1: Drug Escape from Crystal into Inert Solvent—The excaping tendency of a compound from its solid phase obviously is dependent on the strength of the intermolecular forces in the crystal. *A priori* attempts to predict the magnitude of these forces from molecular structural considerations still are largely undeveloped. Ideally, partial

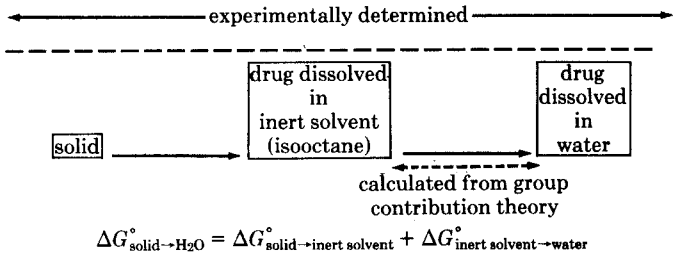

Scheme I—Separation of aqueous solubility into two thermodynamic components

vapor pressures of the drug above the solid phase give relative escaping tendencies directly (8), but these quantities are not easily measured for most compounds. Consequently, it has been suggested (9, 10) that solubility in a relatively inert solvent such as an aliphatic hydrocarbon should be employed to compare escaping tendencies of drugs from the solid phase.

By choosing the infinitely dilute solution of the solute in an alkane solvent as the reference state and setting the thermodynamic activity of a hypothetical 1 *M* solution equal to 1, the thermodynamic activity of a drug in the solid phase may be defined as its alkane solubility (providing that the solubility is low). Differences in the free energies thus obtained reflect differences in such interactions as hydrogen bonding and Debye forces and the entropic content between the two states (10). Whereas specific interactions may be quite significant in the solid phase, solution interactions between the drug substance and alkane solvent are expected to be nonspecific and not highly sensitive to minor changes in molecular structure.

Alkane Solubilities—The alkane solubilities of acetates reported here were determined by direct measurement as described under *Experi-*

Table III—Isooctane Solubilities of C_1-Phenolic Esters of Prostaglandin $F_{2\alpha}$ and Prostaglandin E_2 and Acetates Having the Same Phenol Moiety

Phenol Moiety	Isooctane Solubility, *M*		
	Acetate	Prostaglandin $F_{2\alpha}$	Prostaglandin E_2
	—	5.4×10^{-5}	—
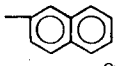	9.6×10^{-2}	3.3×10^{-6}	1.9×10^{-5}
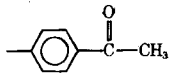	6.2×10^{-2}	1.7×10^{-6}	1×10^{-5}
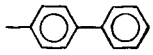	4.4×10^{-2}	2.8×10^{-6a}	2.7×10^{-5}
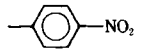	1.6×10^{-2}	4.1×10^{-6}	6.7×10^{-6}
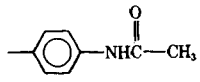	1.8×10^{-5}	3.9×10^{-9a}	1.4×10^{-8a}
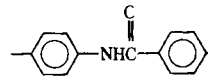	1.7×10^{-5}	1.8×10^{-9a}	8.7×10^{-9a}
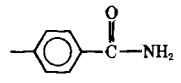	5.8×10^{-6}	5.4×10^{-10a}	1.8×10^{-9a}
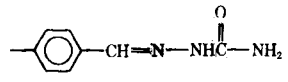	1.9×10^{-7}	5.5×10^{-11a}	5.5×10^{-11a}
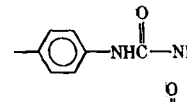	1.8×10^{-8}	1.1×10^{-11a}	2.8×10^{-11a}
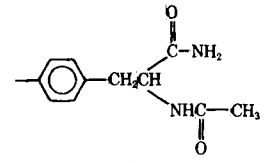	1.7×10^{-8}	6.2×10^{-12a}	1.0×10^{-11a}
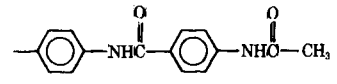	$\sim 1.3 \times 10^{-9}$	2.4×10^{-13a}	5.5×10^{-13a}

[a] Estimated from water solubility data (Table II) and alkane–water partition coefficients (Table V).

mental. Prostaglandin alkane solubilities were in many cases too low to measure experimentally. These values were estimated from their water solubilities and alkane–water partition coefficients estimated from group contribution theory (the method employed for calculating alkane–water partition coefficients of highly insoluble prostaglandin esters will be described).

Table III gives the alkane solubilities of the C_1-esters of prostaglandins E_2 and $F_{2\alpha}$ and the corresponding acetates. Plots of log alkane solubility in the prostaglandin series *versus* log alkane solubilities of the corresponding esters in the acetate series are shown in Figs. 3 and 4. The plots

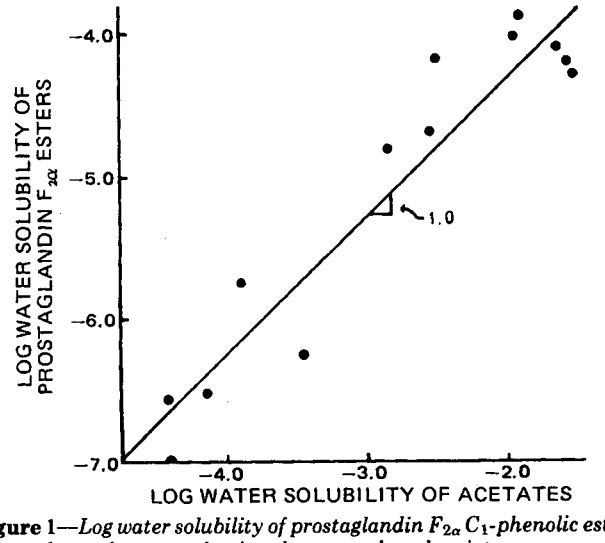

Figure 1—*Log water solubility of prostaglandin $F_{2\alpha}$ C_1-phenolic esters* versus *those of acetates having the same phenol moiety.*

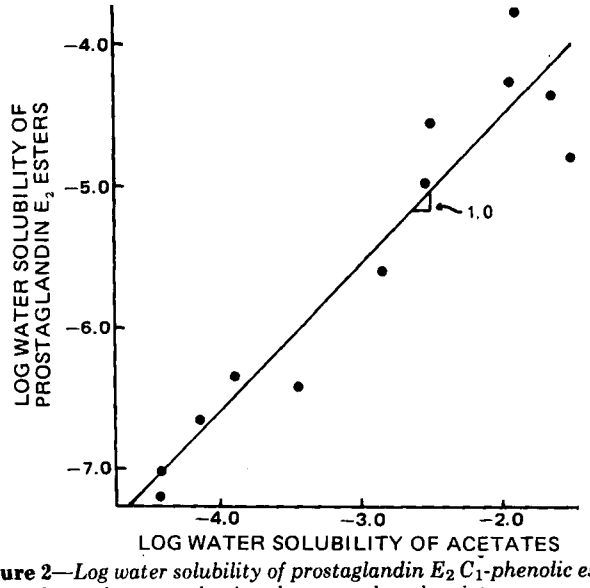

Figure 2—*Log water solubility of prostaglandin E_2 C_1-phenolic esters* versus *those of acetates having the same phenol moiety.*

Table IV—Log Isooctane–Water Partition Coefficient and Group Contribution to the Free Energy of Transfer of Phenyl Substituents in Various Acetates

X	Log Partition Coefficient of $CH_3CO-C_6H_4-X$	π_{alk}[a]	$\Delta(\Delta G^{\circ}_{H_2O\rightarrow alkane})_X$, kcal/mole
	3.05	1.92	−2.62
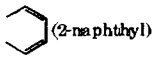 (2-naphthyl)	2.43	1.30	−1.77
—H	1.13	0.0	0.0
$-NO_2$	0.73	−0.39	0.53
	0.30	−0.83	1.13
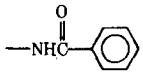	−0.64	−1.77	2.41
	−2.80	−3.92	5.3
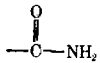	−2.60	−4.72	6.4
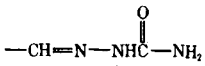	−3.87	−5.0	6.8
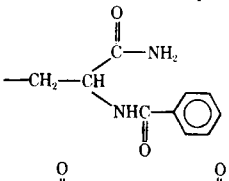	−3.78	−5.0	6.8
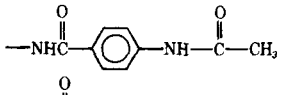	−4.5	−5.6	7.6
	−5.3	−6.4	8.7

[a] π_{alk} = log partition coefficient of $RCO-C_6H_4-X$ minus log partition coefficient of $RC-O-C_6H_4-H$ in isooctane–water systems.

are linear with slopes of ~1 (Fig. 3: slope = 0.89, r = 0.994; Fig. 4: slope = 0.96, r = 0.9967). The linear free energy correlations observed in the alkane solubilities are a direct consequence of the observed correlations in the aqueous solubilities since group contribution theory was employed in estimating the alkane–water partition coefficients used in calculating many of the alkane solubilities. Nevertheless, the exercise is useful because it enables one to separate structural effects on thermodynamic activity in the solid phase from structural effects on interactions in solution.

Some interesting observations can be made from Table III on the effect

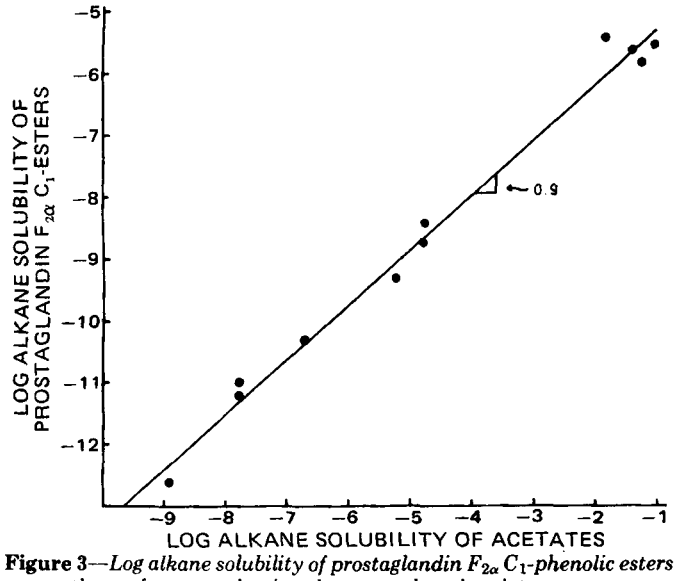

Figure 3—*Log alkane solubility of prostaglandin $F_{2\alpha}$ C_1-phenolic esters* versus *those of acetates having the same phenol moiety.*

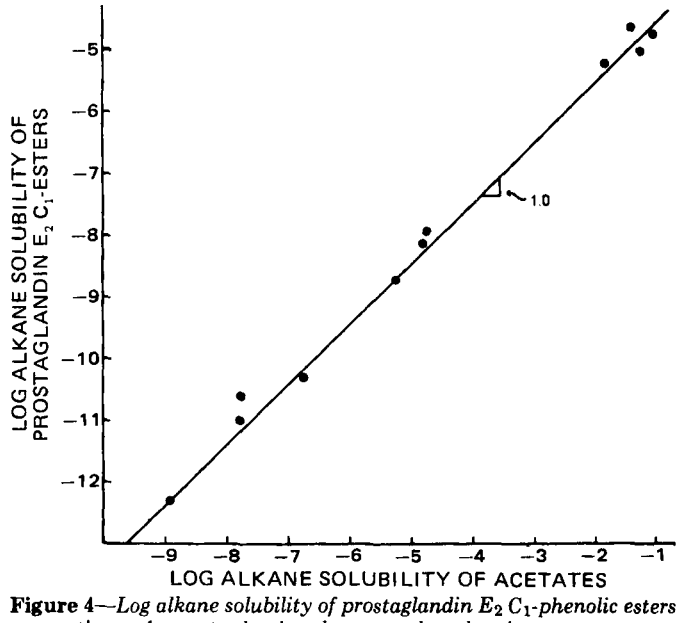

Figure 4—*Log alkane solubility of prostaglandin E_2 C_1-phenolic esters* versus *those of acetates having the same phenol moiety.*

Table V—Calculated [a] Log Isooctane–Water Partition Coefficients of Prostaglandin $F_{2\alpha}$ and Prostaglandin E_2 *para*-Substituted Phenyl Esters [b]

Phenol Moiety	Log Partition Coefficient: Prostaglandin $F_{2\alpha}$	Log Partition Coefficient: Prostaglandin E_2
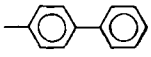	1.46	2.26 (2.61)
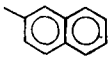	0.84 (0.77)	1.64 (1.69)
	(−0.46)	(0.34)
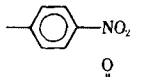	−0.85 (−0.71)	−0.05 (−0.20)
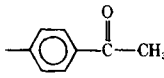	−1.28 (−1.47)	−0.48 (−0.22)
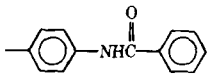	−2.2	−1.42
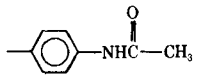	−4.4	−3.6
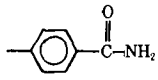	−5.2	−4.4
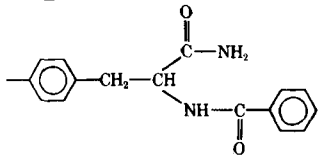	−5.4	−4.6
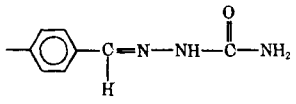	−5.4	−4.6
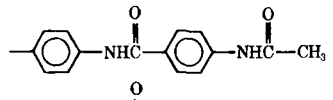	−6.1	−5.3
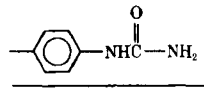	−6.8	−6.0

[a] Calculated values were obtained from:

log partition coefficient$_{\text{prostaglandin}}$ 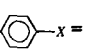 =

log partition coefficient$_{\text{prostaglandin}}$ 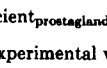 + $(\pi_{alk})_X$

where $(\pi_{alk})_X$ values are listed in Table IV. [b] Experimental values are given in parentheses.

of molecular structure, particularly the incorporation of hydrogen-bonding substituents into the molecule, on the escaping tendency of drug from the solid phase. For example, a difference of over 3000-fold in the alkane solubility of *p*-acetylphenyl acetate compared to *p*-acetamidophenyl acetate shows the dramatic influence of a single hydrogen-bonding moiety on crystalline energy. This factor represents a difference of ~4.8 kcal in free energy, a difference that can be rationalized in terms of hydrogen-bonding differences in the crystals. Replacement of a terminal methyl group with a phenyl group (*p*-acetamidophenyl acetate *versus* *p*-benzamidophenyl acetate) has a small influence on alkane solubility, while addition of another acetamido substituent again lowers the solubility by the equivalent of 5.6 kcal in free energy.

Clustering of points is evident in Figs. 3 and 4. Points at high alkane solubilities represent compounds containing no hydrogen-bonding phenyl substituents, while addition of a single hydrogen-bonding group results in a second cluster of points 3–4 log units lower in solubility.

Component 2: Transfer of Drug from Inert Solvent to Water—Prediction of organic solvent–water partition coefficients from molecular structures is complicated by the present lack of understanding of solute–solvent interactions at the molecular level. Consequently, a semiempirical approach often is employed based on the group contribution concept (11).

Briefly, it is assumed that the free energy of the partitioning process

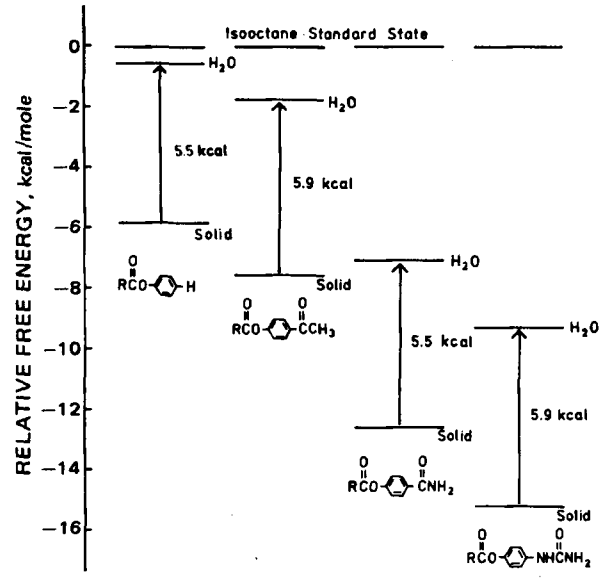

Figure 5—*Relative free energy diagram illustrating the effect of polar substituents on the thermodynamic activity of drug in the solid, on the free energy of transfer from alkane to water, and on aqueous solubility in which RCOO represents prostaglandin $F_{2\alpha}$.*

can be divided into independent contributions from the constituent groups in a molecule.

Alkane–Water Partitioning Behavior—Logs of the partition coefficients at 25° for acetates containing various substituted phenyl moieties are listed in Table IV. In most cases, these values were determined from solubility ratios, which are assumed to be reliable estimates of partition coefficients because isooctane and water are almost completely immiscible and because the solubilities usually were sufficiently low so that solute–solute interactions in solution were considered negligible.

Phenyl acetate was chosen as a reference compound for determining group contributions of various substituents to the free energy of transfer from water to isooctane. The standard free energy of transfer of a drug containing a substituent, X, from water to isooctane can be expressed as:

$$\Delta G^{\circ RX}_{H_2O\rightarrow alk} = -RT \ln PC_{RX} \qquad \text{(Eq. 1)}$$

where:

$$PC_{RX} = \frac{C_{alk}}{C_{H_2O}} \qquad \text{(Eq. 2)}$$

in which C is expressed in moles per liter.

The change in transfer free energy brought about by substitution is:

$$\Delta(\Delta G^{\circ}_{H_2O\rightarrow alk})_X = \Delta G^{\circ RX} - \Delta G^{\circ RH} = -RT \ln \frac{PC_{RX}}{PC_{RH}} \qquad \text{(Eq. 3)}$$

Values of $\Delta(\Delta G^{\circ}_{H_2O\rightarrow alk})_X$ for various substituents on the phenyl ring, derived from the acetate partition coefficients, also are listed in Table IV along with π_{alk} values that represent the quantity log PC_{RX}/PC_{RH}.

Partition coefficient data for the prostaglandin esters were generated from solubility ratios when possible or were estimated from group contributions. This calculation was done by adding the π_{alk} value for a phenyl substituent obtained from acetate partitioning data (Table IV) to the measured log of the partition coefficient of the unsubstituted phenyl ester of either prostaglandin E_2 or $F_{2\alpha}$ to obtain the log of the partition coefficient for the substituted phenyl prostaglandin ester. Calculated values of log partition coefficient for the substituted phenyl esters of prostaglandins $F_{2\alpha}$ and E_2 are shown in Table V (experimental values in parentheses).

Influence of Polar, Hydrogen-Bonding Substituents on Aqueous Solubility—Because of the large effect of polar groups on the partitioning behavior of a molecule, it occasionally is suggested that the introduction of polar groups into a molecule should increase aqueous solubility. The underlying assumption is that log solubility is inversely related to log partition coefficient, as has been shown for liquid solutes. However, the effect of polar groups capable of hydrogen bonding on the crystal lattice energies also must be considered for solids.

A diagram of relative free energy levels of solute in the solid phase, in

the aqueous solution standard state, and in the isooctane standard state (Fig. 5) illustrates the effect of polar groups in a series of prostaglandin $F_{2\alpha}$ esters. An alkane solution of drug at infinite dilution was chosen as the reference state according to the convention proposed previously (9, 10). Thus, the free energies of various derivatives in isooctane arbitrarily were set equal to zero so that relative energies in the solid phase and in water could be compared. Polar substituents dramatically lowered the energy level of a drug in the solid phase and in water relative to an alkane solution; but the free energy difference between solid and aqueous solution, which is reflected by aqueous solubility, remained similar upon addition of increasingly polar substituents.

The conclusion is that polar, hydrogen-bonding substituents may not result in increased aqueous solubility. Even though lipophilicity as measured by partition coefficients may be decreased drastically, the effect of polar groups on the thermodynamic activity of a drug in the solid may tend to offset the change in lipophilicity (Fig. 5). Both thermodynamic components of aqueous solubility must be considered in predicting aqueous solubility.

REFERENCES

(1) W. Morozowich, T. O. Oesterling, W. L. Miller, C. F. Lawson, J. R. Weeks, R. G. Stehle, and S. L. Douglas, *J. Pharm. Sci.*, **68**, 833 (1979).

(2) W. Morozowich, T. O. Oesterling, W. L. Miller, and S. L. Douglas, *ibid.*, **68**, 836 (1979).

(3) W. Morozowich, T. O. Oesterling, W. L. Miller, C. F. Lawson, J. C. Cornette, J. R. Weeks, and S. L. Douglas, *ibid.*, **68**, 949 (1979).

(4) M. J. Cho and W. Morozowich, *ibid.*, **68**, 1069 (1979).

(5) M. J. Cho, G. L. Bundy, and J. J. Biermacher, *J. Med. Chem.*, **20**, 15 (1977).

(6) T. Higuchi, F.-M. L. Shih, T. Kimura, and J. H. Rytting, *J. Pharm. Sci.*, **68**, 1267 (1979).

(7) S. S. Davis, *Sep. Sci.*, **10**, 1 (1975).

(8) G. N. Lewis and M. Randall, "Thermodynamics," 2nd ed., McGraw-Hill, New York, N.Y., 1961, pp. 145–156.

(9) J. H. Rytting, S. S. David, and T. Higuchi, *J. Pharm. Sci.*, **61**, 816 (1972).

(10) T. Higuchi, in "Design of Biopharmaceutical Properties through Prodrugs and Analogs," E. B. Roche, Ed., American Pharmaceutical Association, Washington, D.C., 1977, pp. 409–421.

(11) S. S. Davis, T. Higuchi, and J. H. Rytting, in "Advances in Pharmaceutical Sciences," vol. 4, Academic, London, England, 1974, pp. 73–261.

ACKNOWLEDGMENTS

The authors thank W. Morozowich and S. L. Douglas for providing the compounds used in this study and for enlightening discussions.

Preliminary Examination of Rabbit Conjunctival Mucins

VINCENT HON-LEUNG LEE * and JOSEPH R. ROBINSON ˣ

Received September 19, 1979, from the *School of Pharmacy, University of Wisconsin, Madison, WI 53706.* Accepted for publication November 16, 1979. *Present address: School of Pharmacy, University of Southern California, Los Angeles, CA 90033.

Abstract □ Conjunctival mucins from albino rabbits were fractionated using gel filtration and anion-exchange chromatography. Charge homogeneity of the various conjunctival mucin fractions was confirmed by polyacrylamide gel electrophoresis. The molecular weight characteristics of the isolated fractions varied with the analytical scheme employed. Two schemes yielded mucins with molecular weights of 10^4, 10^5, and 10^6. However, when anion-exchange chromatography was the first step in the fractionation scheme, the dominant mucin had a molecular weight of 1.7×10^5. In contrast, when gel filtration chromatography was the first step, the dominant mucin had a molecular weight of 5.7×10^4. It was postulated that during migration through the anion-exchange matrix, the low molecular weight conjunctival mucin underwent trimer formation. Comparison with the mucin fractions isolated from tear mucoid threads revealed that the scheme beginning with anion-exchange chromatography preserved the fractionation pattern seen in tear mucoid threads. This result implies that conjunctival mucins undergo an association prior to or after their entry into the tear film. The molecular event of interest in this process is self-association of the species with a molecular weight of 5.7×10^4, resulting in a trimer with a molecular weight of 1.7×10^5. This trimer appears to resist deaggregation on exposure to a medium of lesser ionic strength. Several explanations are offered for its formation as well as for its stability. The implication of multiple conjunctival (tear) mucins for tear film stability also is discussed.

Keyphrases □ Mucins—isolation from rabbit conjunctiva, fractionation by gel filtration and anion-exchange chromatography, determination of molecular weight, role in tear film stability □ Conjunctival mucins—isolation from rabbits, fractionation by gel filtration and anion-exchange chromatography, determination of molecular weight, role in tear film stability □ Ocular mucins—isolation from rabbit conjunctiva, fractionation by gel filtration and anion-exchange chromatography, determination of molecular weight, role in tear film stability

The strategic role assumed by conjunctival mucin in tear film stability has been recognized, but not understood, for many years. Alteration in either its chemical nature or quantity (probably both) has been implicated in keratoconjunctivitis sicca as well as other dry-eye syndromes (1–5), all of which are characterized by poor wetting of the corneal epithelium. It has been proposed that this fascinating substance derives its role from both the surface activity it is expected to exhibit at the air–tear and tear–corneal epithelium interfaces and the molecular events following its absorption at these two interfaces.

Principally because conjunctival mucins have never been isolated or identified, statements about their surface activity are based on experiments using bovine submaxillary mucin (6–9). In contrast, three tear mucins have been isolated (10), but the interrelationship between tear and conjunctival mucins is unknown. The tear mucins were shown to possess an amino acid and carbohydrate composition not shared by typical epithelial mucins (10, 11). Since the function it serves depends on its structure, considerable caution must be exercised in extrapolating the findings on surface activity of bovine submaxillary mucin to conjunctival and tear mucins. Successful isolation of conjunctival mucins, in reasonable quantity and purity, is important in understanding the mechanisms by which they confer stability to the tear film. This study is a first attempt in this direction; specifically, it concerns identifying conjunctival mucins present in a crude conjunctival extract.

The three tear mucins isolated by Iwata and Kabasawa (10) from tear mucoid threads on the conjunctival surface of albino rabbits possessed molecular weights of 4×10^5,

0022-3549/80/0400-0430$01.00/0

© 1980, American Pharmaceutical Association

the aqueous solution standard state, and in the isooctane standard state (Fig. 5) illustrates the effect of polar groups in a series of prostaglandin $F_{2\alpha}$ esters. An alkane solution of drug at infinite dilution was chosen as the reference state according to the convention proposed previously (9, 10). Thus, the free energies of various derivatives in isooctane arbitrarily were set equal to zero so that relative energies in the solid phase and in water could be compared. Polar substituents dramatically lowered the energy level of a drug in the solid phase and in water relative to an alkane solution; but the free energy difference between solid and aqueous solution, which is reflected by aqueous solubility, remained similar upon addition of increasingly polar substituents.

The conclusion is that polar, hydrogen-bonding substituents may not result in increased aqueous solubility. Even though lipophilicity as measured by partition coefficients may be decreased drastically, the effect of polar groups on the thermodynamic activity of a drug in the solid may tend to offset the change in lipophilicity (Fig. 5). Both thermodynamic components of aqueous solubility must be considered in predicting aqueous solubility.

REFERENCES

(1) W. Morozowich, T. O. Oesterling, W. L. Miller, C. F. Lawson, J. R. Weeks, R. G. Stehle, and S. L. Douglas, *J. Pharm. Sci.*, **68**, 833 (1979).

(2) W. Morozowich, T. O. Oesterling, W. L. Miller, and S. L. Douglas, *ibid.*, **68**, 836 (1979).

(3) W. Morozowich, T. O. Oesterling, W. L. Miller, C. F. Lawson, J. C. Cornette, J. R. Weeks, and S. L. Douglas, *ibid.*, **68**, 949 (1979).

(4) M. J. Cho and W. Morozowich, *ibid.*, **68**, 1069 (1979).

(5) M. J. Cho, G. L. Bundy, and J. J. Biermacher, *J. Med. Chem.*, **20**, 15 (1977).

(6) T. Higuchi, F.-M. L. Shih, T. Kimura, and J. H. Rytting, *J. Pharm. Sci.*, **68**, 1267 (1979).

(7) S. S. Davis, *Sep. Sci.*, **10**, 1 (1975).

(8) G. N. Lewis and M. Randall, "Thermodynamics," 2nd ed., McGraw-Hill, New York, N.Y., 1961, pp. 145–156.

(9) J. H. Rytting, S. S. David, and T. Higuchi, *J. Pharm. Sci.*, **61**, 816 (1972).

(10) T. Higuchi, in "Design of Biopharmaceutical Properties through Prodrugs and Analogs," E. B. Roche, Ed., American Pharmaceutical Association, Washington, D.C., 1977, pp. 409–421.

(11) S. S. Davis, T. Higuchi, and J. H. Rytting, in "Advances in Pharmaceutical Sciences," vol. 4, Academic, London, England, 1974, pp. 73–261.

ACKNOWLEDGMENTS

The authors thank W. Morozowich and S. L. Douglas for providing the compounds used in this study and for enlightening discussions.

Preliminary Examination of Rabbit Conjunctival Mucins

VINCENT HON-LEUNG LEE * and JOSEPH R. ROBINSON ˣ

Received September 19, 1979, from the *School of Pharmacy, University of Wisconsin, Madison, WI 53706.* Accepted for publication November 16, 1979. *Present address: School of Pharmacy, University of Southern California, Los Angeles, CA 90033.

Abstract □ Conjunctival mucins from albino rabbits were fractionated using gel filtration and anion-exchange chromatography. Charge homogeneity of the various conjunctival mucin fractions was confirmed by polyacrylamide gel electrophoresis. The molecular weight characteristics of the isolated fractions varied with the analytical scheme employed. Two schemes yielded mucins with molecular weights of 10^4, 10^5, and 10^6. However, when anion-exchange chromatography was the first step in the fractionation scheme, the dominant mucin had a molecular weight of 1.7×10^5. In contrast, when gel filtration chromatography was the first step, the dominant mucin had a molecular weight of 5.7×10^4. It was postulated that during migration through the anion-exchange matrix, the low molecular weight conjunctival mucin underwent trimer formation. Comparison with the mucin fractions isolated from tear mucoid threads revealed that the scheme beginning with anion-exchange chromatography preserved the fractionation pattern seen in tear mucoid threads. This result implies that conjunctival mucins undergo an association prior to or after their entry into the tear film. The molecular event of interest in this process is self-association of the species with a molecular weight of 5.7×10^4, resulting in a trimer with a molecular weight of 1.7×10^5. This trimer appears to resist deaggregation on exposure to a medium of lesser ionic strength. Several explanations are offered for its formation as well as for its stability. The implication of multiple conjunctival (tear) mucins for tear film stability also is discussed.

Keyphrases □ Mucins—isolation from rabbit conjunctiva, fractionation by gel filtration and anion-exchange chromatography, determination of molecular weight, role in tear film stability □ Conjunctival mucins—isolation from rabbits, fractionation by gel filtration and anion-exchange chromatography, determination of molecular weight, role in tear film stability □ Ocular mucins—isolation from rabbit conjunctiva, fractionation by gel filtration and anion-exchange chromatography, determination of molecular weight, role in tear film stability

The strategic role assumed by conjunctival mucin in tear film stability has been recognized, but not understood, for many years. Alteration in either its chemical nature or quantity (probably both) has been implicated in keratoconjunctivitis sicca as well as other dry-eye syndromes (1–5), all of which are characterized by poor wetting of the corneal epithelium. It has been proposed that this fascinating substance derives its role from both the surface activity it is expected to exhibit at the air–tear and tear–corneal epithelium interfaces and the molecular events following its absorption at these two interfaces.

Principally because conjunctival mucins have never been isolated or identified, statements about their surface activity are based on experiments using bovine submaxillary mucin (6–9). In contrast, three tear mucins have been isolated (10), but the interrelationship between tear and conjunctival mucins is unknown. The tear mucins were shown to possess an amino acid and carbohydrate composition not shared by typical epithelial mucins (10, 11). Since the function it serves depends on its structure, considerable caution must be exercised in extrapolating the findings on surface activity of bovine submaxillary mucin to conjunctival and tear mucins. Successful isolation of conjunctival mucins, in reasonable quantity and purity, is important in understanding the mechanisms by which they confer stability to the tear film. This study is a first attempt in this direction; specifically, it concerns identifying conjunctival mucins present in a crude conjunctival extract.

The three tear mucins isolated by Iwata and Kabasawa (10) from tear mucoid threads on the conjunctival surface of albino rabbits possessed molecular weights of 4×10^5,

0022-3549/80/0400-0430$01.00/0

© 1980, American Pharmaceutical Association

5×10^4, and 1.4×10^4. Conspicuously absent was the mucin with a molecular weight of 10^6, a species commonly seen in epithelial mucins. However, this result probably is an artifact since the gel filtration medium employed, Sephadex G-150, does not fractionate proteins with molecular weights exceeding 4×10^5. Nevertheless, the isolation of multiple tear mucin fractions is intriguing because multiple fractions rarely have been isolated for simple proteins such as insulin and growth hormone. Moreover, since mucins in the precorneal area of the eye are derived from both the conjunctival (12) and lacrimal (13) glands and their composition varies with the source, it was of interest to see if the three tear mucin fractions were primarily of conjunctival origin. The results of the present study indicate that this is the case.

The three objectives of this study were: (*a*) to examine the type of mucins derived from the conjunctiva, as well as the interrelationship among them; (*b*) to learn how these mucins are related to those identified in the tear film; and (*c*) to gain further insight into tear film stability. The interrelationship between tear and conjunctival mucins will be reported later. The present paper concerns the interrelationship among conjunctival mucins and their probable roles in tear film stability.

EXPERIMENTAL

Materials—Male albino rabbits[1], 1.8–2.4 kg, were used.

The following chemicals and reagents were used as received: synthetic *N*-acetylneuraminic acid[2], 3,5-diaminobenzoic acid dihydrochloride[2], chromatographic gel[3], polyacrylamide gel[4], polyacrylamide gel basic buffer[5] (pH 8.9), protein assay kit[6], anion-exchange chromatographic gel[7], tracking dye solution[8] (acidic), trichloroacetic acid[9], Blue Dextran 2000[10], Sephadex G-25[10] (fine), rabbit albumin[11], γ-globulin[11], bovine submaxillary mucin[12] (type I), Coomassie brilliant blue G-250[12], and fumarase[13].

Analytical Methods—*Protein Assay*—In addition to its absorbance at 280 nm, A_{280}, the protein content of the column eluate was monitored using the protein assay kit. This assay is based on the differential color change of the dye in response to various protein concentrations (14). It was performed following the procedure outlined by the manufacturer (15).

Fluorometric Assay for Sialic Acid—A fluorometric assay (16) that can detect as little as 0.2 ng of sialic acid was adopted; the more widely used thiobarbituric acid assay (17) was found to underestimate sialic acid levels as a result of sialic acid degradation following its liberation from mucins (11).

The procedure was conducted as follows. To 10 μl of a sample containing sialic acid in a 1-ml ampul[14] was added 500 μl of 0.005 *M* 3,5-diaminobenzoic acid dihydrochloride in 0.125 *N* HCl. The ampul was sealed and placed in an oven at 100° for 16 hr. After cooling to room temperature, the contents of the ampul were transferred to a 5-ml volumetric flask and brought to volume with 0.05 *N* HCl. The fluorescence intensity was measured in a fluorescence spectrophotometer[15] with the excitation wavelength set at 425.8 nm and the emission wavelength at 507.5 nm. A standard curve was established daily using freshly prepared *N*-acetylneuraminic acid solutions.

Collection of Rabbit Conjunctivas—Rabbits were sacrificed with a rapid intravenous injection of pentobarbital sodium into a marginal ear vein. The corneal and conjunctival surfaces were washed thoroughly with 0.9% NaCl solution and blotted dry with tissue. A single incision was made at the upper nasal palpebral conjunctiva and was continued clockwise along the lid margin and terminated at the bulbar conjunctiva around the limbus. Each conjunctiva was rinsed carefully in saline, frozen, and stored frozen at −20° for a period not to exceed 3 months. Approximately 98 g of conjunctivas was collected from 150 rabbits.

Extraction of Conjunctival Mucins—The entire extraction was conducted in a cold room maintained at 4°. Approximately 90 g of conjunctivas was suspended in 450 ml of 0.01 *M* ammonium acetate buffer at pH 7.2 and homogenized in a blender for 10 min. The mixture was stirred constantly for 24 hr in the presence of toluene.

The homogenate was filtered through four layers of adsorbent cheesecloth, prerinsed in the buffer, and centrifuged at 15,000 rpm for 30 min at 4° in a centrifuge[16]. The supernate was filtered first through filter paper[17] and then through a 0.65-μm filter[18], both of which were placed in a buchner funnel connected to a water aspirator. The filtrate was lyophilized in a freeze-drying apparatus[19] at 65 μm Hg and −55° for 48 hr. The residue, denoted as conjunctival crude extract, was a yellowish powder and was stored in a desiccator placed in a freezer at −20°. Lyophilization was assumed to cause no changes in the mucin; this assumption was shown to be the case with bovine submaxillary mucin (18).

The conjunctival crude extract represented about 2.5% of the initial conjunctival weight.

Anion-Exchange Chromatography of Conjunctival Crude Extract—Approximately 70 mg of conjunctival crude extract was dissolved in 2.5 ml of 0.01 *M* ammonium acetate buffer at pH 7.2. Two milliliters of the resulting solution was layered onto an anion-exchange column (1.5 × 20 cm) that had been preequilibrated for 16 hr at 4° with the buffer. After the entire sample entered the gel, the column was washed with two bed volumes (100 ml) of the buffer at a constant flow rate of 58.5 ml/hr controlled by a peristaltic pump. The column then was eluted at the same flow rate with a linear gradient consisting of 200 ml each of 0.1 and 1 *M* NaCl, both dissolved in 0.01 *M* ammonium acetate at pH 7.2. Fractions of 1.5 ml were collected. The content of every third tube was measured for its absorbance at 280 nm and for sialic acid, protein, and sodium chloride concentrations.

Finally, the contents of several tubes were pooled, followed by desalting on a column (5 × 60 cm) of Sephadex G-25 (fine). The column was eluted with double-distilled water at a constant flow rate of 150 ml/hr. Fractions of 18.5 ml were collected. The proteins emerged with the void volume (~30% of total bed volume), while the salt emerged with ~80% of the total bed volume. Fractions containing protein were lyophilized at −55° and 65 μm Hg for 48 hr.

The lyophilizate was reconstituted with 0.01 *M* ammonium acetate buffer at pH 7.2. The behavior of the proteins contained therein was studied next on a chromatographic gel filtration column.

Gel Filtration of Conjunctival Crude Extract—Sample preparation and layering onto a column (1.5 × 60 cm) of chromatographic gel were essentially the same as described for anion-exchange chromatography. The column was eluted at a constant flow rate of 8.8 ml/hr with the buffer. Fractions of 1.5 ml were collected. The contents of appropriate tubes were examined at 280 nm for their protein and sialic acid content. Based on the results of these assays, certain tubes were selected for polyacrylamide gel electrophoresis. The contents of several tubes were pooled and lyophilized, and selected fractions were chromatographed further on an anion-exchange column (1.5 × 30 cm).

Molecular Weight Estimation—The molecular weight of various mucin fractions was estimated by calibrating a gel filtration column in the manner described previously (19–23). This procedure has been employed to estimate the molecular weight of tear mucins (10); consequently, a meaningful molecular weight comparison can be made between conjunctival and tear mucins.

A gel chromatography column (1.5 × 60 cm) was calibrated using the following proteins (or protein mixture): bovine submaxillary mucin (2.26 mg/ml) and rabbit γ-globulin (8.76 mg/ml), rabbit serum albumin (5.0 mg/ml), fumarase (5.0 mg/ml), and Blue Dextran 2000 (2.62 mg/ml). All solutions were prepared in 0.01 *M* ammonium acetate buffer at pH 7.2. To the Blue Dextran 2000 solution was added also 0.1 *M* NaCl. Two milliliters of sample was layered onto the column, which then was eluted

[1] Klubertanz, Edgerton, Wis.
[2] Aldrich Chemical Co., Milwaukee, Wis.
[3] Bio-Gel A 5m, Bio-Rad Laboratories, Richmond, Calif.
[4] Bio-Phore 4, 7.5, 12%, Bio-Rad Laboratories, Richmond, Calif.
[5] Bio-Phore, Bio-Rad Laboratories, Richmond, Calif.
[6] Bio-Rad Protein Assay Kit II, Bio-Rad Laboratories, Richmond, Calif.
[7] DEAE Bio-Gel A, Bio-Rad Laboratories, Richmond, Calif.
[8] Bio-Rad Laboratories, Richmond, Calif.
[9] Mallinckrodt, St. Louis, Mo.
[10] Pharmacia Fine Chemicals AB, Uppsala, Sweden.
[11] Schwarz/Mann, Orangeburg, N.Y.
[12] Sigma Chemical Co., St. Louis, Mo.
[13] United States Biochemical Corp., Cleveland, Ohio.
[14] Wheaton Scientific, Millville, N.J.
[15] Model MPF-4, Perkin-Elmer, Norwalk, Conn.
[16] Sorvall RC-5B refrigerated superspeed centrifuge using an SS-34 rotor, DuPont Instruments, Newtown, Conn.
[17] Whatman No. 2.
[18] Millipore.
[19] New Brunswick Scientific Co., New Brunswick, N.J.

1. Anion-Exchange Chromatography

conjunctival crude extract
anion-exchange chromatography
wash | gradient

peak	A	B	C	D E	F (0.032 *M* NaCl)	G (0.008 *M* NaCl)
fraction	W1	W2	W3	G1	G2	G3
AUC ratio[a]	1	18	—[b]	—[b]	1.1	1
sialic acid, μg[c]	0.03	0.22	0.24	0.04	0.13	0.04
percent	1	9.4	1.2	0.8	4.7	0.2[d]
polyacrylamide gel electrophoresis (bands)	—[b]	—[b]	—[b]	—[b]	5 (Fig. 1)	7

2. Gel Filtration Chromatography

	W2 gel chromatography			G2 gel chromatography			G3 gel chromatography		
peak	A	B	C	A	B	C	A	B	C
molecular weight	2.4×10^4	5.5×10^3	465 120	3×10^6	1.7×10^5	4.9×10^3	2.5×10^6	1.7×10^5	480
AUC ratio[a]	1	1	—[b]	1	16	—[b]	1	14	—[b]
sialic acid, μg[c]	—[b]	—[b]	—[b]	0.12	0.35	0.12, 0.05	0.05	0.07	0.04, 0.02
percent	—[b]	—[b]	—[b]	4.4	4.6	5.8, 1.6	1.2	0.3	0.3
polyacrylamide gel electrophoresis (bands)	—[b]	—[b]	—[b]	0	3	—[b]	1	1	—[b]

Scheme I—Fractionation of Conjunctival Crude Extract by Procedure A. [[a] Area under the curve (referred to A_{280} *versus* the tube number profile). [b] Not performed or determined. [c] Sialic acid in 10 μl of solution. [d] Insufficient data to give an accurate estimate.]

with 0.01 *M* ammonium acetate buffer at pH 7.2 at a flow rate of 8.8 ml/hr. Fractions of 1.5 ml were collected, and the absorbance of every third tube was measured at 280 nm.

The position of the peak maximum in the elution diagram, *i.e.*, absorbance *versus* tube number, was taken as the elution volume, V_e. The correlation between molecular weight and elution behavior was analyzed by plotting K_{av} *versus* log molecular weight. The regression equation for the plot is:

$$K_{av} = 1.497 - 0.228 \log \text{molecular weight} \qquad \text{(Eq. 1)}$$

($r = -0.995$, $r^2 = 0.989$), where K_{av} is the partition coefficient of the solute between the liquid phase and the gel phase.

Polyacrylamide Gel Electrophoresis—Polyacrylamide gel electrophoresis was performed at 4° using precast 4, 7.5, and 12% polyacrylamide gels and basic buffer at pH 8.9. The sample solution was mixed with tracking dye solution in a ratio of ~3:1. Thirty microliters of the resulting mixture was layered onto a gel using a microbiopet[6].

At the end of electrophoresis, each gel was carried through three steps leading to the visualization of protein bands:

1. The proteins were fixed onto the gel by immersing the gel for 90 min in a mixture of 12.5% trichloroacetic acid and 25% isopropanol.
2. The precipitated proteins were stained by immersing the gel for 6 hr in a Coomassie brilliant blue G-250 solution (the staining solution was 0.05% dye, 10% isopropanol, and 10% acetic acid).
3. The excess stain on the gel was removed in a diffusion destainer[20] filled with a mixture of 7% acetic acid and 25% ethanol.

The procedure outlined by Wardi and Michos (24) for staining glycoproteins on polyacrylamide gels was unsatisfactory for conjunctival mucins, probably due to the low sialic acid content of the glycoproteins. No further attempt was made to improve visualization of these glycoproteins on the gels.

RESULTS

Fractionation Procedure A—Scheme I summarizes the results obtained by chromatographing the crude conjunctival extract. The results were displayed as the ratio of area under each elution peak in a chromatogram (*AUC*) relative to an appropriately chosen reference peak; as the sialic acid content, in both amount and percent, corresponding to each peak; and, where appropriate, as the molecular weight corresponding to each peak as well as the number of protein bands yielded by each peak upon performing polyacrylamide gel electrophoresis.

Thus, anion-exchange chromatography on the crude extract yielded seven fractions, in close agreement with the seven bands observed in electrophoresis of the extract on a 12% polyacrylamide gel (Gel C in Fig. 1). The chromatogram displayed in Fig. 2 indicates that three peaks (A–C) emerged with the wash and that four peaks (D–G) emerged with the gradient. The major peaks were F and G, hereafter referred to as

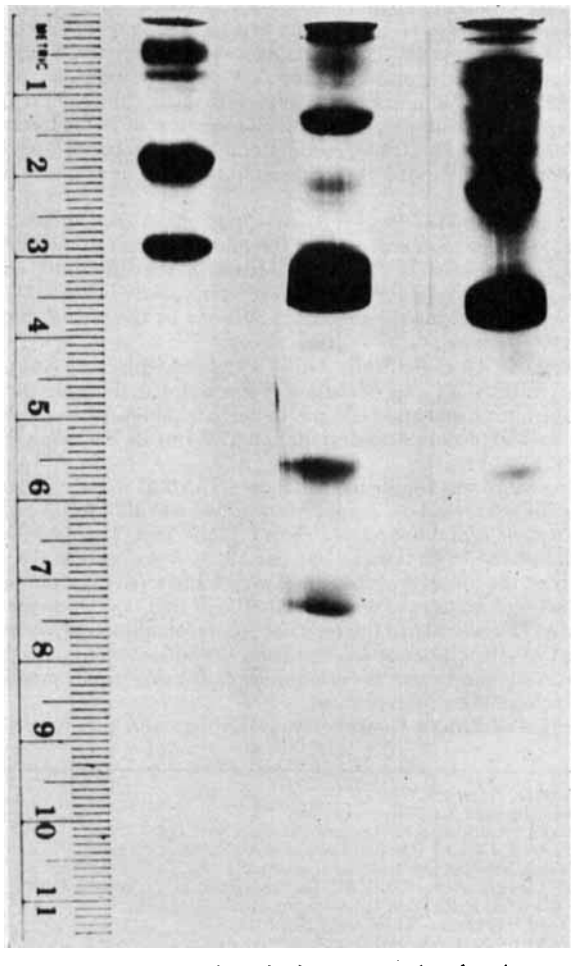

Figure 1—*Polyacrylamide gel electrophoresis of anion-exchange chromatography gradient Fractions 2 (G2) and 3 (G3) using 12% polyacrylamide gels. Key: Gel A, anion-exchange gel G2; Gel B, anion-exchange gel G3; and Gel C, conjunctival crude extract.*

[20] Model 172A, Bio-Rad Laboratories, Richmond, Calif.

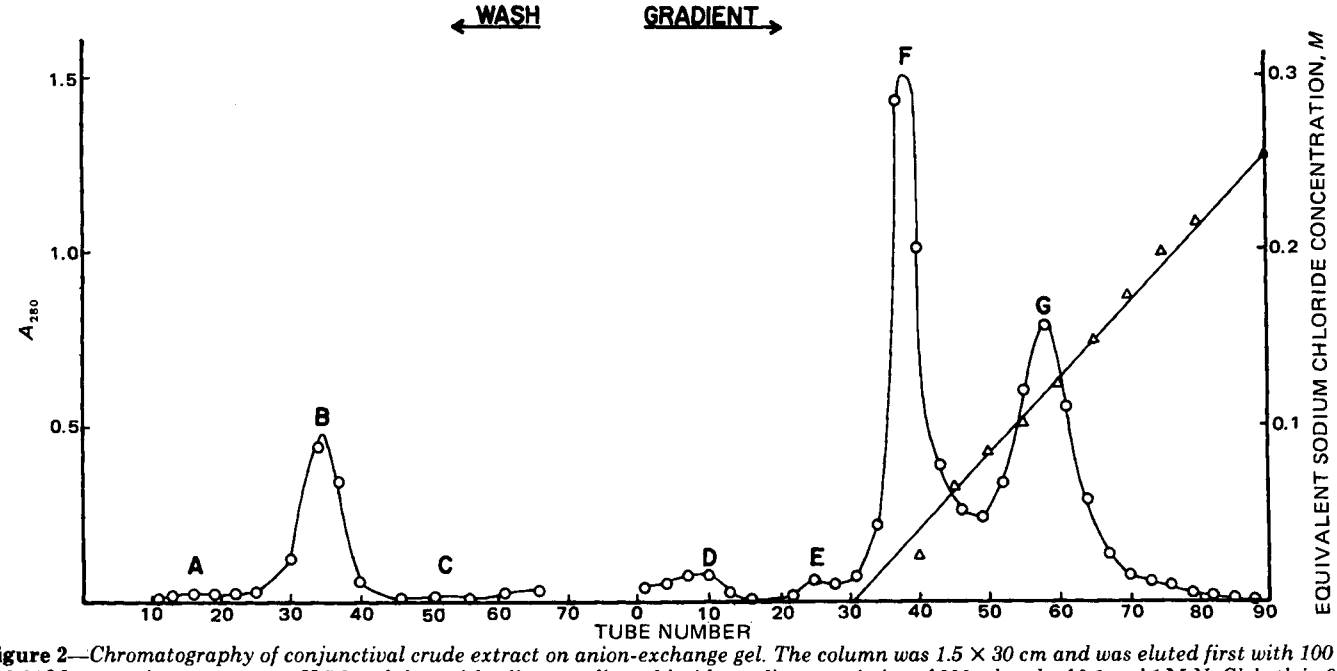

Figure 2—*Chromatography of conjunctival crude extract on anion-exchange gel. The column was 1.5 × 30 cm and was eluted first with 100 ml of 0.01* M *ammonium acetate at pH 7.2 and then with a linear sodium chloride gradient consisting of 200 ml each of 0.1 and 1* M *NaCl, both in 0.01* M *ammonium acetate at pH 7.2. The flow rate was 58.50 ml/hr. Fraction volumes were 1.5 ml.*

Fractions G2 and G3, respectively (Scheme I). Fraction G2 was eluted at 0.032 *M* NaCl, while Fraction G3 was eluted at 0.118 *M* NaCl. In contrast, under essentially the same chromatographic conditions, bovine submaxillary mucin eluted as a single peak at 0.146 *M* NaCl (Fig. 3).

The electrophoretic patterns due to Fractions G2 and G3 (Gels A and B) shown in Fig. 1 revealed that nearly all of the bands seen in the conjunctival crude extract (Gel C) represented these two fractions. At least three bands (0, 2, and 3 cm from the origin) due to Fractions G2 and G3 overlapped, reflecting, in part, the slight overlap between Fractions G2 and G3 as they were eluted from the anion-exchange column. Nevertheless, both fractions contained characteristic mucins. They were the two bands at 0.5 and 0.8 cm on Gel A, corresponding to Fraction G2, and the four bands at 1.3, 4, 5.5, and 7.4 cm on Gel B, corresponding to Fraction G3. The last three bands due to Fraction G3 were of higher charge density than the two bands due to Fraction G2. Together with the abundance of the band at 3 cm, this finding was consistent with the elution of Fraction G3 at a higher sodium chloride concentration. The major protein also was different for Fractions G2 and G3. In Fraction G2, the major protein migrated 1.8 cm into the gel; in Fraction G3, it migrated 3 cm into the gel.

The similarity in composition between Fractions G2 and G3 is apparent not only in their electrophoretic patterns (Fig. 4) but also in their chromatograms (Figs. 5 and 6). Moreover, according to Scheme I, both Fractions G2 and G3 contained mucins with molecular weights on the order of 10^5 and 10^6. The major fraction contained the lower molecular weight species; the area of the peak, B, containing it was approximately 15 times that of the peak containing the 10^6 species.

Two conclusions can be drawn from these observations. First, the elution of these two species, with a 10-fold difference in molecular weight, must be inversely related to their charge density since they eluted at the same sodium chloride concentration. Second, each species of a given molecular weight existed in two charge densities since it was eluted at sodium chloride concentrations differing by a factor of approximately four, *i.e.*, 0.032 and 0.118 *M*. These results indicate that four mucins, in suitable combinations of molecular weight and charge density, were present in Fractions G2 and G3.

In summary, Procedure A yielded mucins with molecular weights on the order of 10^4 (Fraction G2) and 10^5 and 10^6 (both from Fractions G2 and G3). Unlike other epithelial mucins, the major mucin was not the one with a molecular weight of 10^6. Rather, it was the one with a molecular weight of 10^5. This pattern is remarkedly consistent with that seen in tear mucins. The 10^5 and 10^6 species are heterogeneous with respect to charge.

Fractionation Procedure B—Scheme II summarizes the results obtained by chromatographing the conjunctival crude extract according to Procedure B.

As shown in Scheme II and Fig. 7, chromatography of the conjunctival crude extract on chromatographic gel yielded five peaks. Peak E did not contain proteins, as indicated by the protein assay. The molecular weight of the species contained in peak D was too low to be a protein. Therefore, proteins were detected only in peaks A, B, and C; this conclusion was confirmed by polyacrylamide gel electrophoresis (Fig. 8). Since all of the proteins reacted positively to the sialic acid assay, they were glycoproteins.

As with Procedure A, Procedure B did not yield the mucin with a molecular weight of ~10^6 as the major mucin. Unlike Procedure A, Procedure B yielded a major mucin with a molecular weight of ~10^4, not ~10^5. Clearly, the pattern seen in tear mucins was not preserved. The implication of this finding was elaborated upon previously. Briefly, trimer formation probably occurred as the mucin with a molecular weight of ~10^4 migrated through the anion-exchange matrix and a similar matrix may exist on the conjunctival surface.

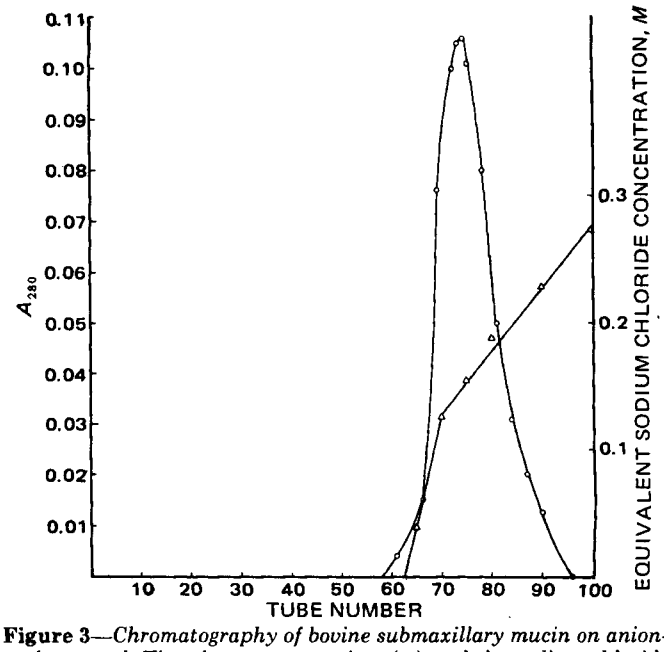

Figure 3—*Chromatography of bovine submaxillary mucin on anion-exchange gel. The plots represent* A_{280} (○) *and the sodium chloride concentration* (△). *The column was 1.5 × 30 cm and was eluted at 4° with a linear sodium chloride gradient at a flow rate of 58.5 ml/hr. Fraction volumes were 1.46 ml.*

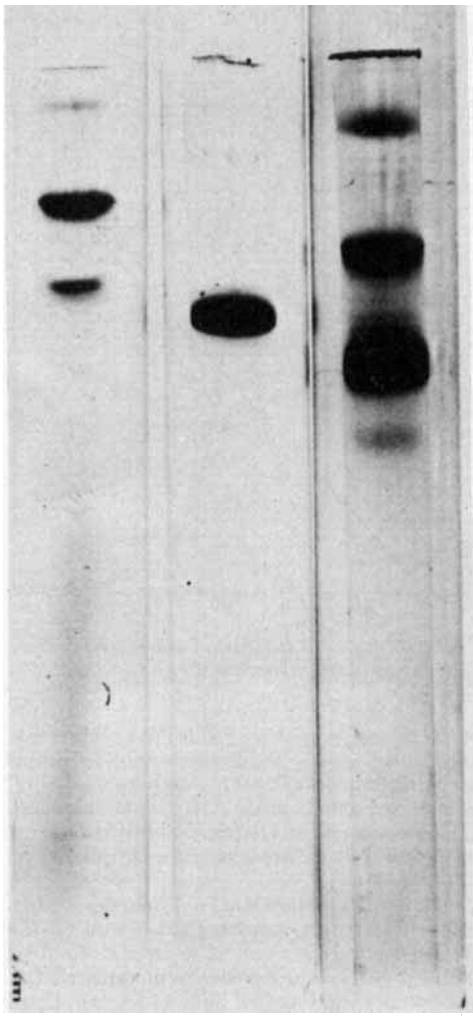

Figure 4—*Comparison of electrophoretic patterns of anion-exchange gel-chromatographic gel Fraction G2, peak B (Gel A); anion-exchange gel-chromatographic gel Fraction G3, peak B (Gel B); and chromatographic gel peak C (Gel C) on 12% polyacrylamide gels.*

The fact that the species with molecular weights of $\sim 10^4$ and $\sim 10^5$ were heterogeneous with respect to charge is evident in the electrophoretic patterns (Fig. 8) and the anion-exchange chromatograms (Figs. 9 and 10). The absence of multiple bands in the gel (A) layered with the 10^6 species should be expected from its inability to enter the gel. In contrast, anion-exchange chromatography resolved this species into three fractions, which eluted at 0.1, 0.105, and 0.135 *M* NaCl (Fig. 9). Similarly, four fractions were resolved for the mucins with a molecular weight of $\sim 10^4$. They eluted at 0, 0.02, 0.1, and 0.154 *M* NaCl (Fig. 10).

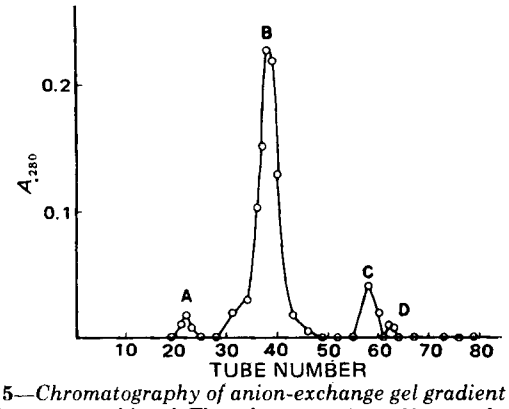

Figure 5—*Chromatography of anion-exchange gel gradient Fraction G2 on chromatographic gel. The column was 1.5 × 60 cm and was eluted with a flow rate of 8.8 ml/hr. Fraction volumes were 1.5 ml.*

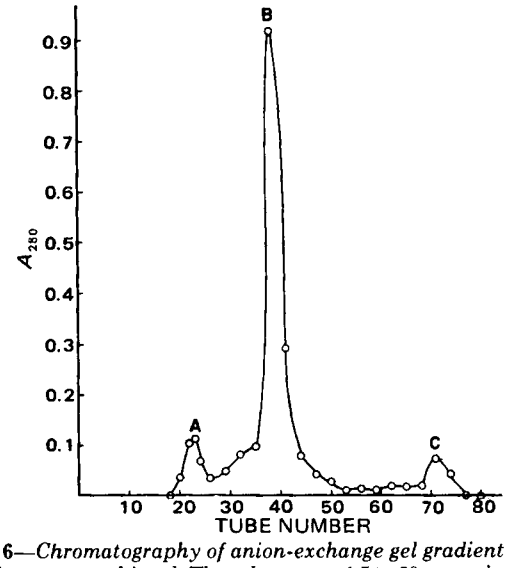

Figure 6—*Chromatography of anion-exchange gel gradient Fraction G3 on chromatographic gel. The column was 1.5 × 60 cm and was eluted with a flow rate of 8.8 ml/hr. Fraction volumes were 1.5 ml.*

DISCUSSION

This investigation showed that multiple conjunctival mucins exist, each differing in molecular weight and charge density. This finding is in accord with the isolation of multiple tear mucins in the precorneal area by Iwata and Kabasawa (10). There is evidence that the high molecular weight conjunctival mucins are aggregates of some monomer unit, and studies are underway to elucidate the mechanisms governing self-association and the factors contributing to stability of the resulting aggregates.

The remainder of this report will be devoted to an evaluation of the mucin extraction procedure, the conjunctival mucin fractionation schemes, postulated mechanisms of conjunctival mucin trimer formation, and the physiological significance of multiple conjunctival mucins in tear film stability.

Extraction of Mucin from Rabbit Conjunctivas—A caution exercised in this research was to isolate mucins from conjunctivas free from those in the precorneal area. To this end, each conjunctiva was rinsed with copious quantities of physiological saline following surgical removal from the eye. This rinsing should rid the surface of most of the adherent mucin and tear proteins since mucin was reported to be removed readily during increased tear secretion (25) and upon touching the conjunctival surface with a filter[18] (26, 27).

Another caution exercised in this research was to minimize denatur-

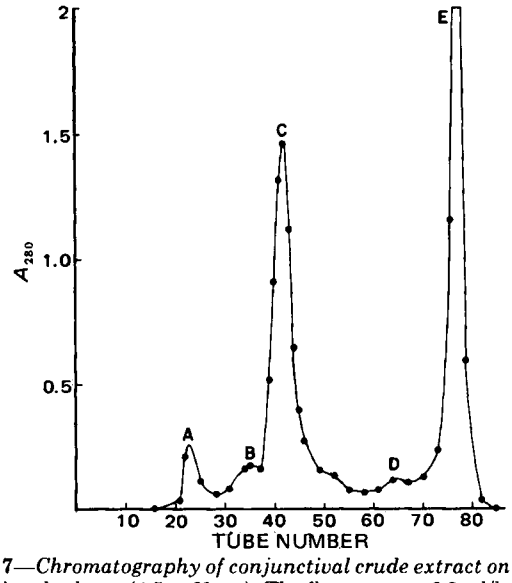

Figure 7—*Chromatography of conjunctival crude extract on chromatographic gel column (1.5 × 60 cm). The flow rate was 8.8 ml/hr, and the fraction volumes were 1.5 ml.*

1. Gel Filtration Chromatography

conjunctival crude extract

gel chromatography

	A	B	C	D	E
molecular weight	1.9×10^6	2.3×10^5	5.7×10^4	1.2×10^3	140
AUC ratio[a]	1	1	11	1	—[b]
sialic acid, %	16.4	2.4	2.4	10	5.6
polyacrylamide gel electrophoresis[c] (bands)	1	4	3	2	0

2. Anion-Exchange Chromatography

	Fraction A			Fraction C		
	anion-exchange gel			anion-exchange gel		
	wash	gradient		wash	gradient	
M NaCl	0.1	0.105	0.135	0	0.02	0.10	0.154
AUC ratio	1.2	1	1.3	0.8	1	2.9	14.5

Scheme II—Fractionation of Conjunctival Crude Extract by Procedure B. [[a] Ratio of area under the curve (referred to A_{280} *versus* tube number profile). [b] Not determined. [c] 12% gel.]

ation of conjunctival mucins during isolation. Gross fractionation of proteins from nonproteinaceous material by ammonium sulfate and ethanol precipitation is a step used in the fractionation schemes for many proteins (28). Such a treatment, while considered to be mild for most proteins, caused degradation of bovine and porcine submaxillary mucins (29–31). Because of this concern, the conjunctival crude extract was fractionated using chromatography as the first step.

In addition, since the slow process of denaturation would be delayed almost indefinitely if the temperature is low enough (32), all operations from tissue homogenization to chromatographic elution were conducted at 4° in a cold room. Similarly, to optimize stability of the glycoproteins on storage, the conjunctiva was frozen immediately following its removal at the temperature of a dry ice–acetone mixture. Thus, the ongoing glycoprotein synthesis is arrested and, depending on their quantities, such proteins may appear as mucin fractions when the crude extract is chromatographed. Similarly, unless they are membrane bound, the enzymes responsible for the biosynthesis (and, perhaps, degradation) of glycoproteins may be isolated. Neither possibility was vigorously investigated in this work.

An assumption made in this study was that little or none of the glycoproteins found in membranes (33) was isolated. Isolation of membrane glycoproteins often requires treatment of the cells with enzymes such as trypsin (34, 35) or chemicals such as lithium diiodosalicylate, phenol, aqueous pyridine, and sodium dodecylsulfate (36, 37). Since none of these agents was employed in the present study, the assumption seemed reasonable.

Influence of Fractionation Procedure on Conjunctival Mucin Trimer Formation—Two major findings emerged from fractionation of conjunctival mucins by Procedures A and B. First, both procedures yielded multiple mucin fractions. This finding agrees with the observation that mucins, unlike simple proteins, are polydisperse and microheterogeneous (38) and tend to yield several fractions during chromatographic separation. In general, the number of mucin fractions for a given mucin ranges from two to five; they differ primarily in their threonine, serine, sialic acid, and carbohydrate content as well as on their molecular weights (11). Conjunctival mucins with molecular weights on the order of 10^4, 10^5, and 10^6 were isolated in this work.

Second, the molecular weight of the dominant fraction was affected by the isolation procedure. When anion-exchange chromatography was the first step in fractionation, the dominant mucin possessed a molecular weight of 1.7×10^5. In contrast, when gel filtration was the first step, the dominant mucin possessed a lower molecular weight (5.7×10^4). The two fractions behaved similarly in polyacrylamide gel electrophoresis (Fig. 4). According to these electrophoretic patterns, the proteins concerned had the same charge density, suggesting that the mucin with a molecular weight of 5.7×10^4 underwent trimer formation when placed in an electrostatic field, which also was present at the positively charged surface of the anion-exchange gel. The trimer thus formed resisted deaggregation when it was exposed subsequently to the lesser charged media, Sephadex G-25 and the chromatographic gel. This finding indicates that simple electrostatic interaction was not the major stabilizing factor; short-range interactions such as hydrophobic bonding may play a more important role.

Conjunctival Mucin Trimer: Postulated Mechanisms of Its Formation and Stability—Self-association has been observed in over 300 proteins (39, 40) and is particularly prevalent in proteins with high molecular weights. According to Reithel (39), proteins with molecular weights exceeding 6.6×10^4 should be considered as aggregates. Consequently, it is reasonable to consider the conjunctival mucin with a molecular weight of 1.7×10^5 as an aggregate of a monomer with a molecular weight of 5.7×10^4, a value that is at the upper monomer molecular weight limit. The same probably is true of the conjunctival mucin with a molecular weight of 1.9×10^6. In proteins, dimers and tetramers are common; multimers with an odd number of monomers are rare. On this basis, the conjunctival mucin trimer may be an oddity.

Several glycoproteins exist in an associated form. They include canine tracheal mucin (41), several submaxillary mucins (41, 42), erythrocyte membrane glycoprotein (43, 44), and sucrase (invertase)–isomaltase, a membrane-bound glycoprotein complex located on the brush border of the small intestine (45–48). The majority of these glycoproteins resist deaggregation by urea, guanidine hydrochloride, and sodium dodecylsulfate, agents known to disrupt hydrogen and hydrophobic bonds. As indicated previously, the conjunctival mucin trimer appears to be stable to deaggregation in a medium of low ionic strength.

Figure 8—*Polyacrylamide gel electrophoresis on fractions obtained by chromatographing conjunctival crude extract on a chromatographic gel column (1.5 × 60 cm) using 12% polyacrylamide gels. Key: Gel A, peak A; Gel B, peak B; Gel C, peak C; Gel D, peak D; Gel E, peak E; and Gel F, conjunctival crude extract.*

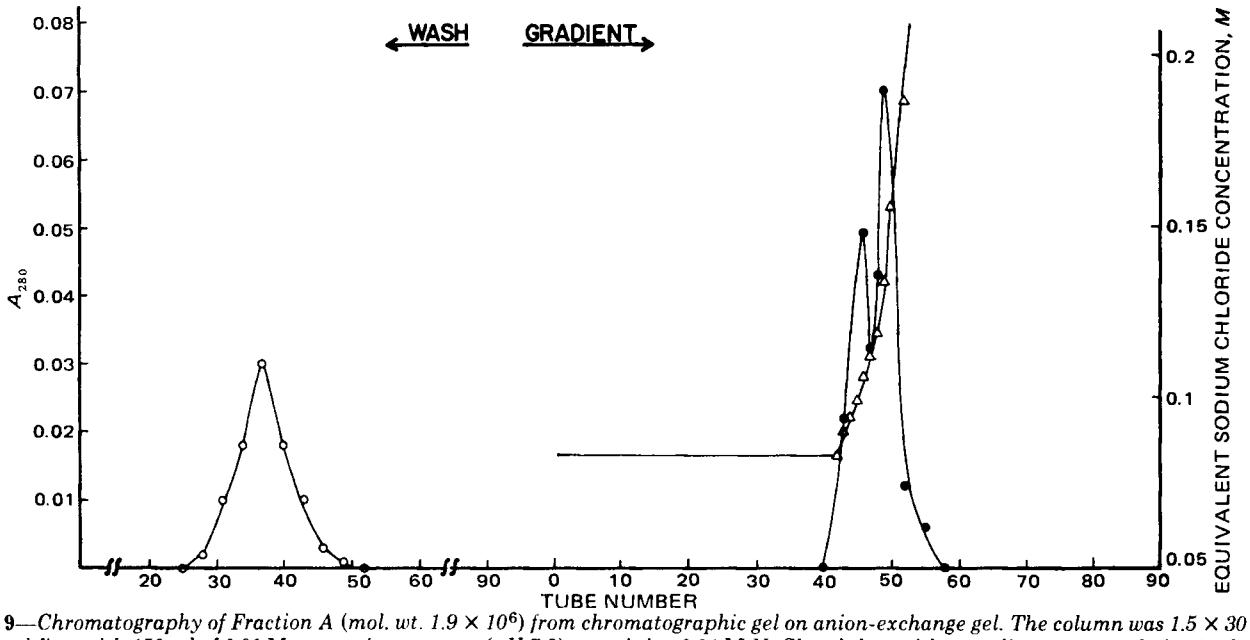

Figure 9—*Chromatography of Fraction A (mol. wt. 1.9 × 10^6) from chromatographic gel on anion-exchange gel. The column was 1.5 × 30 cm. It was eluted first with 150 ml of 0.01 M ammonium acetate (pH 7.2) containing 0.01 M NaCl and then with a gradient composed of 200 ml each of 0.1 and 1 M NaCl in the buffer. The flow rate was 62.4 ml/hr, and the fraction volumes were 1.6 ml.*

The mechanisms governing conjunctival mucin self-association, trimer formation in particular, have not been studied. However, two mechanisms can be postulated: the bulk mechanism and the surface mechanism. In the bulk mechanism, a monomer–trimer equilibrium already exists in the bulk. An ion-exchange gel promotes aggregation by preferentially adsorbing the trimers, thus effectively shifting the equilibrium in favor of the trimer.

At least three possibilities can be explored for the surface mechanism. A pH effect cannot be a possibility because the microenvironmental pH is higher than the bulk pH due to repulsion of hydrogen ions from the positively charged gel surface. The higher pH favors ionization of sialic, glutamic, and aspartic acids, and the attendant electrostatic repulsion among the molecules concerned hinders aggregation.

On the other hand, the ion-exchange gel may promote aggregation by providing the proper matrix to immobilize a glycoprotein molecule through electrostatic interaction between negative charges on the glycoprotein molecule and positive charges in the matrix.This interaction conceivably can initiate unfolding of the glycoprotein, thereby exposing its hydrophobic moieties and allowing hydrophobic interaction with another glycoprotein molecule to occur (Scheme III). Alternatively, as a glycoprotein binds to the ion-exchange gel, the Ca^{2+} ions known (49–51) to be associated with its sialic acid are displaced and become available for bridging the unbound sialic acids of two glycoprotein molecules (Scheme IV).

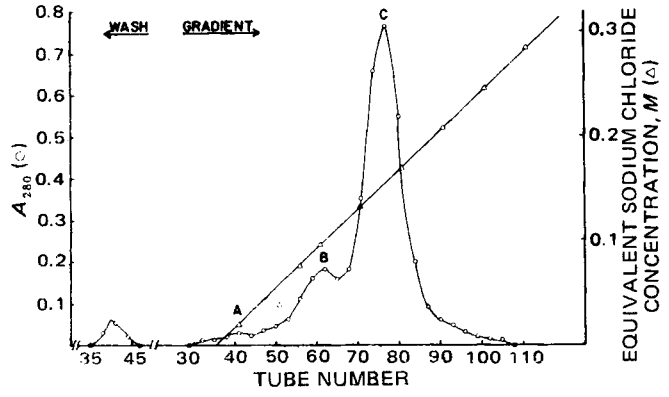

Figure 10—*Chromatography of Fraction C (mol. wt. 5.7 × 10^4) from chromatographic gel on anion-exchange gel. The column was 1.5 × 30 cm and was eluted with a 0.01 M ammonium acetate wash (100 ml) followed by a gradient composed of 200 ml each of 0.1 and 1 M NaCl in 0.01 M ammonium acetate buffer at pH 7.2. Fractions of 1.4 ml were collected. The flow rate was 56.0 ml/hr.*

The third possibility centers on elution of bound glycoprotein from the ion-exchange gel. As the ionic strength of the eluting buffer increases, the thickness of the electrical double layer about a glycoprotein molecule decreases. This effect allows two or more glycoprotein molecules to approach each other, thus favoring aggregation (Scheme V). However, in light of the stability of the aggregate in a medium whose ionic strength is 10 times less, this mechanism appears unlikely.

Like the mechanisms governing its formation, the apparent stability of the resulting aggregate has not been studied. Hill *et al.* (52) studied the aggregation of ovine submaxillary mucins and its desialylated (asialomucin) and deglycosylated (apomucin) variants. They found that the

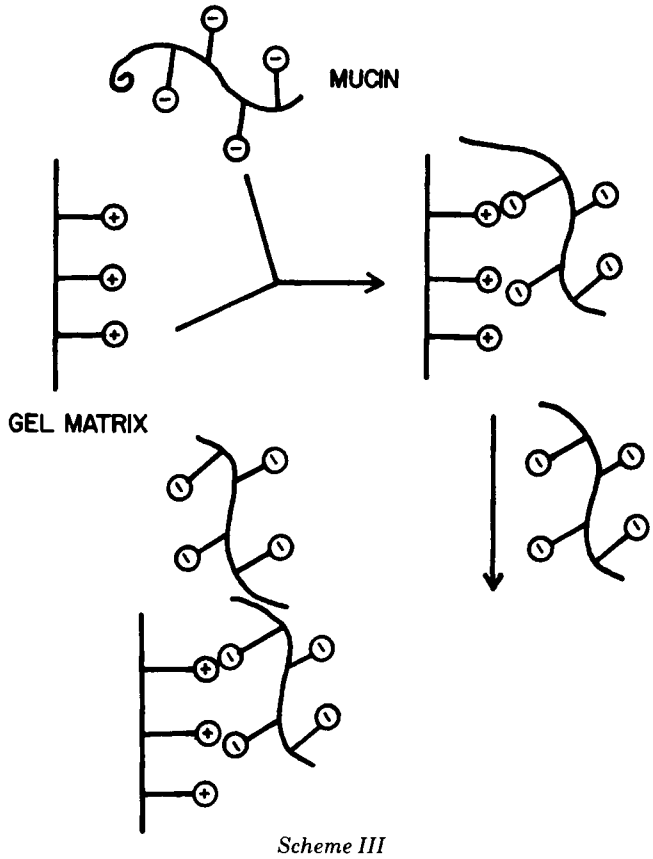

Scheme III

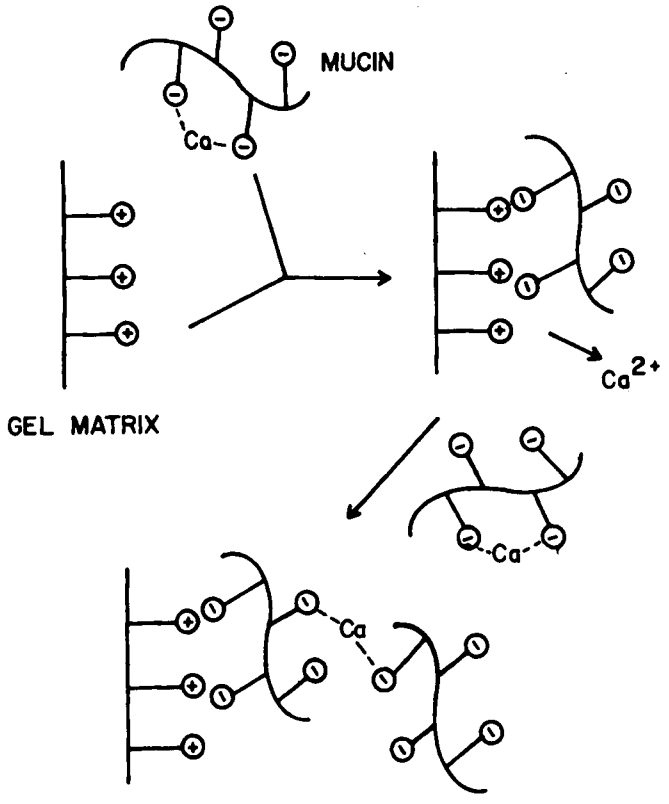

Scheme IV

apomucin did not aggregate whereas the asialomucin and parent mucin did, indicating that the carbohydrate portion of the molecule, with many hydrogen bonding sites, was necessary for aggregation.

Physiological Significance of Multiple Conjunctival Mucins in Tear Film Stability—A mucin layer adhering to the corneal surface has been considered an integral tear film component (53) since the tear film structure was proposed by Wolff (54) in 1946. The corneal epithelium is an intrinsically hydrophobic, low-energy surface, and a mucin layer at its surface generally is accepted as necessary to achieve complete wetting by tears. In fact, Mishima (55), as early as 1965, demonstrated that wiping the corneal surface rendered it unwettable by tears. This finding was confirmed subsequently by the *in vitro* experiments of Lemp *et al.* (8). Since then, the surface activity that mucin is expected to exhibit at the tear–corneal epithelium interface and, to a lesser extent, at the tear–lipid interface has captured the attention of researchers. To date, the mystery surrounding the driving force for tear film stability remains far from solved.

The principal reasons underlying this dilemma are the lack of information about the chemical nature of conjunctival mucins and the precise mechanisms by which they exercise their roles. Understanding the mechanisms by which each conjunctival mucin exercises its roles requires knowledge of factors contributing to thin film stability (or rupture).

Several factors contribute to rupture of thin liquid films (56). They include dissolution of the film liquid into the adjoining bulk phase, *e.g.*, evaporation, drainage of interlamellar liquid, gravitational convection, and marginal regeneration at the film borders. Although these factors originally were proposed for films that are at most 0.1 μm thick, they should also hold for a tear film that is 10 times thicker. Of course, some factors such as evaporation and drainage may predispose the tear film to rupture more readily than others.

Thus, conjunctival mucin can stabilize the tear film in several ways. For instance, it may interact with the meibomian lipids, resulting in a mixed film that is surface rheologically stable. This film, when coupled with another surface rheologically stable layer at the corneal epithelial surface, can resist drainage. Drainage also can be reduced by increased bulk viscosity due to mucin. On the other hand, the evaporation tendency of the tear may be diminished due to the mixed mucin–lipid film and the diffusional barrier secondary to hydration of mucin in the bulk. Additionally, the shape and net charge of the mucin molecule can affect tear film stability through their influence on the surface activity, hydration, and surface and bulk viscosity of the mucin. It is clear that the surface activity of the mucin is just one of the many elements contributing to tear film stability.

It is useful to speculate about the functions performed by each conjunctival mucin. There are at least three conjunctival mucins with molecular weights of 1.9×10^6, 1.7×10^5, and 5.7×10^4. It is reasonable to expect each conjunctival mucin to possess a characteristic shape, degree of hydration, solubility, and surface activity, although each mucin has not been studied with regard to each property. Thus, the mucin with a molecular weight of 5.7×10^4, being a monomer and like other epithelial mucins, may have clearly delineated hydrophobic and hydrophilic regions and, therefore, may be well suited to adsorb at the superficial meibomian lipid layer as well as at the corneal epithelial surface.

The trimer, with its hydrophobic regions being buried by the prominent oligosaccharide mantle, may be the most soluble mucin despite its molecular weight. This characteristic helps to retain water of hydration, thus establishing a diffusional barrier to tear evaporation and eventually stabilizing the tear film. The trimer may be the least surface-active mucin and may interact minimally with either the air–tear or tear–cornea interface.

As the molecular weight exceeds 1.7×10^5, aqueous solubility diminishes, meaning that the mucin with a molecular weight of 1.9×10^6 prefers the interface to the bulk. Due to its molecular inflexibility compared to the mucin monomer, it is unlikely to be the species forming the monolayer at the corneal surface. However, it may exercise an important role in multilayer formation because less of it is necessary to achieve extensive surface coverage. Multilayer formation by the high molecular weight mucin at the corneal surface is roughly equivalent to viscoelastic film formation at the surface. This result not only allows lubrication of the surface but also hinders drainage of the liquid film.

This discussion implies that tear film stability hinges on an intricate balance among various conjunctival mucins. Therefore, a strategy to control dry-eye syndromes must involve selection of a polymer that behaves similarly to conjunctival mucins, *i.e.*, one that has the ability to self-associate to yield various fractions in the proper proportion and with the proper degree of hydration and affinity for interfaces. Selection of

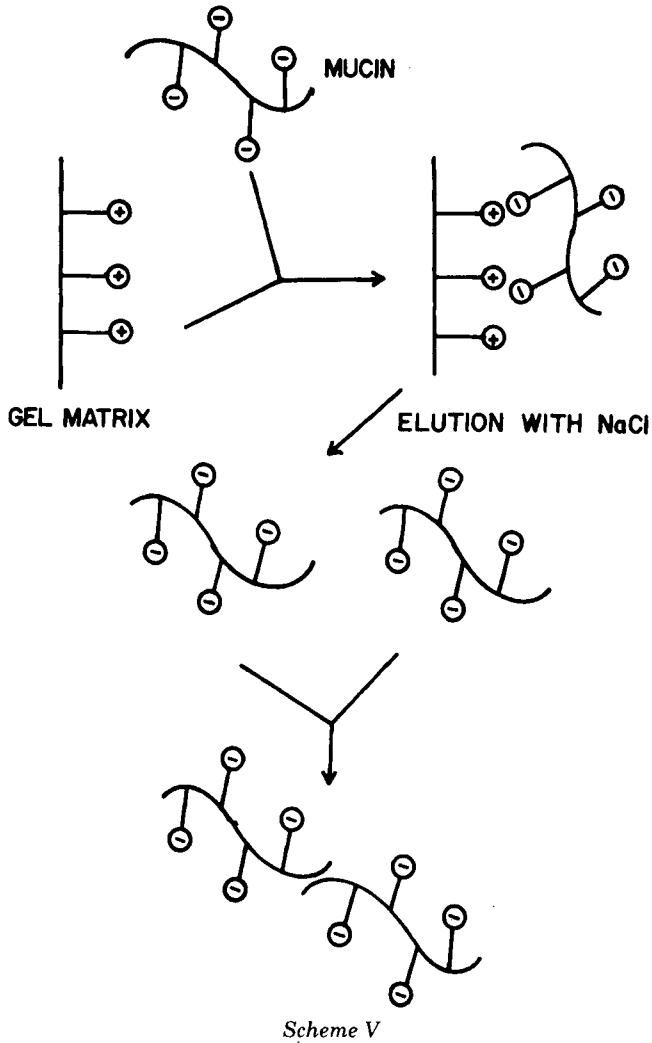

Scheme V

the proper polymer alone may not be sufficient; it may be necessary to fabricate it into a unit possessing anion-exchange properties.

SUMMARY

Several mucins have been isolated from the albino rabbit conjunctiva. The preponderance of each mucin depends on whether gel filtration or anion-exchange chromatography is the first step in fractionation. As reported previously, the conjunctival mucins bear a closer resemblance to the tear mucins in their molecular weights when anion-exchange chromatography is the first step. The discrepancy centers on the anion-exchange fraction with a molecular weight of 1.7×10^5 and the gel filtration fraction with a molecular weight of 5.7×10^4. It is postulated that self-association (trimer formation) induced by the microenvironment of the ion-exchange gel occurs. It is postulated also that the same sequence of events exists during transit of conjunctival mucin from the goblet cell to the precorneal area of the eye. The resulting scenario is one in which the mucin with a molecular weight of 1.7×10^5 is a major tear mucin component.

The physiological advantage of having multiple rather than single fractions in the precorneal area has yet to be elucidated. Nevertheless, it seems reasonable to expect each mucin to perform a specific role in tear film stability. An evaluation of each conjunctival mucin with regard to its amino acid and carbohydrate composition, hydration, shape, and structure is desirable. Factors conferring stability to the mucin possessing a molecular weight of 1.7×10^5, a trimer of the one with a molecular weight of 5.7×10^4, should be identified. Studies are underway in these laboratories to investigate trimer formation and stability.

REFERENCES

(1) R. A. Ralph, *Invest. Ophthalmol.*, **14**, 299 (1975).
(2) R. R. Pfister and M. E. Renner, *Invest. Ophthalmol. Vis. Sci.*, **17**, 874 (1978).
(3) J. M. Carroll and T. Kuwabara, *Arch. Ophthalmol.*, **80**, 683 (1968).
(4) A. Kreiker, *Graefes Arch. Ophthalmol.*, **124**, 191 (1930).
(5) L. M. R. Abdel-Khalek, J. Williamson, and W. R. Lee, *Br. J. Ophthalmol.*, **62**, 800 (1978).
(6) F. J. Holly, J. T. Patten, and C. H. Dohlman, *Exp. Eye Res.*, **24**, 479 (1977).
(7) F. J. Holly, *J. Colloid Interface Sci.*, **49**, 221 (1974).
(8) M. A. Lemp, F. J. Holly, S. Iwata, and C. H. Dohlman, *Arch. Ophthalmol.*, **83**, 89 (1970).
(9) M. A. Lemp and E. S. Szymanski, *ibid.*, **93**, 134 (1975).
(10) S. Iwata and I. Kabasawa, *Exp. Eye Res.*, **12**, 360 (1971).
(11) V. H.-L. Lee, Ph:D. thesis, University of Wisconsin, Madison, Wis., 1979.
(12) S. V. Kessing, *Acta Ophthalmol. Suppl.*, **95**, 133 (1968).
(13) I. Falbe-Hansen, O. A. Jensen, and J. K. Degn, *Acta Ophthalmol.*, **47**, 620 (1969).
(14) M. M. Bradford, *Anal. Biochem.*, **72**, 248 (1976).
(15) Bio-Rad Protein Assay Bulletin 1069, Bio-Rad Laboratories, Richmond, Calif., 1979.
(16) H. H. Hess and E. Rolde, *J. Biol. Chem.*, **239**, 3215 (1964).
(17) L. Warren, *ibid.*, **234**, 1971 (1959).
(18) K. Nisizawa and W. Pigman, *Arch. Oral Biol.*, **1**, 161 (1959).
(19) P. Andrews, *Nature*, **196**, 36 (1962).
(20) P. Andrews, *Biochem. J.*, **91**, 222 (1964).
(21) P. Andrews, *ibid.*, **96**, 595 (1965).
(22) W. K. Downey and P. Andrews, *ibid.*, **94**, 642 (1965).
(23) P. Andrews, *Methods Biochem. Anal.*, **18**, 1 (1970).
(24) A. H. Wardi and G. A. Michos, *Anal. Biochem.*, **49**, 607 (1972).
(25) S. V. Kessing, *Acta Ophthalmol.*, **44**, 439 (1966).
(26) P. R. Egbert, S. Lauber, and D. M. Maurice, *Am. J. Ophthalmol.*, **84**, 798 (1977).
(27) A. D. Adams, *Arch Ophthalmol.*, **97**, 730 (1979).
(28) R. H. Haschemeyer and A. E. V. Haschemeyer, "Proteins. A Guide to Study by Physical and Chemical Methods," Wiley, New York, N.Y., 1973, p. 32.
(29) S. Tsuiki, Y. Hashimoto, and W. Pigman, *J. Biol. Chem.*, **236**, 2172 (1961).
(30) C. C. Curtain and J. Pye, *Aust. J. Exp. Biol. Med. Sci.*, **33**, 315 (1955).
(31) R. L. Katzman and E. H. Eylar, *Arch. Biochem. Biophys.*, **117**, 623 (1966).
(32) P. Douzou and C. Balny, *Adv. Protein Chem.*, **32**, 77 (1978).
(33) R. Harrison and G. G. Lunt, "Biological Membranes—Their Structure and Function," Wiley, New York, N.Y., 1975, pp. 124, 125.
(34) M. C. Glick, Y. Kimhi, and U. Z. Littauer, *Proc. Natl. Acad. Sci., USA*, **70**, 1682 (1973).
(35) M. C. Glick, Z. Rabinowitz, and L. Sachs, *Biochemistry*, **12**, 4864 (1973).
(36) V. K. Jansons and M. M. Burger, *Biochim. Biophys. Acta*, **291**, 127 (1973).
(37) L. Liljas, P. Lundahl, and S. Hjerten, *ibid.*, **426**, 526 (1976).
(38) R. A. Gibbons, in "Glycoproteins—Their Composition, Structure and Function," part A, A. Gottschalk, Ed., Elsevier, Amsterdam, The Netherlands, 1972.
(39) F. J. Reithal, *Adv. Protein Chem.*, **18**, 123 (1963).
(40) I. M. Klotz, D. W. Darnall, and N. R. Langerman, in "The Proteins," vol. 1, 3rd ed., H. Neurath and R. L. Hill, Eds., Academic, New York, N.Y., 1975.
(41) K. G. Holden, N. C. F. Yim, L. J. Griggs, and J. A. Weisbach, *Biochemistry*, **10**, 3110 (1971).
(42) F. A. Bettelheim and T. C. Laurent, *Carbohydr. Res.*, **2**, 81 (1966).
(43) A. Morawiecki, *Biochim. Biophys. Acta*, **83**, 339 (1964).
(44) A. Bezkorovainy, G. F. Springer, and K. Hotta, *ibid.*, **115**, 501 (1966).
(45) A. Cogoli, A. Eberle, H. Sigrist, C. Joss, E. Robinson, H. Mosimann, and G. Semenza, *Eur. J. Biochem.*, **33**, 40 (1973).
(46) H. Mosimann, G. Semenza, and H. Sund, *ibid.*, **36**, 489 (1973).
(47) H. Sigrist, P. Ronner, and G. Semenza, *Biochim. Biophys. Acta*, **406**, 433 (1975).
(48) J. Brunner, H. Hauser, H. Braun, K. J. Wilson, H. Wacker, B. O'Neill, and G. Semenza, *J. Biol. Chem.*, **254**, 1821 (1979).
(49) J.-P. Behr and J.-M. Lehn, *FEBS Lett.*, **31**, 297 (1973).
(50) G. A. Langer, J. S. Frank, L. M. Nudd, and K. Seraydarian, *Science*, **193**, 1013 (1976).
(51) L. W. Jaques, E. B. Brown, J. M. Barrett, W. S. Brey, Jr., and W. Weltner, Jr., *J. Biol. Chem.*, **252**, 4533 (1977).
(52) H. D. Hill, J. A. Reynolds, and R. L. Hill, *ibid.*, **252**, 3791 (1977).
(53) F. J. Holly and M. A. Lemp, *Contact Lens. Soc. Am. J.*, **5**, 1 (1971).
(54) E. Wolff, *Trans. Ophthalmol. Soc., U.K.*, **66**, 291 (1946).
(55) S. Mishima, *Arch. Ophthalmol.*, **73**, 233 (1965).
(56) J. S. Clunie, J. F. Goodman, and B. T. Ingram, *Surf. Colloid Sci.*, **3**, 167 (1971).

ACKNOWLEDGMENTS

Supported by a grant from Allergan Pharmaceuticals, Irvine, Calif.

Measurement of Film-Coating Adhesiveness

RAYMOND M. FUNG * **and EUGENE L. PARROTT** ˣ

Received June 11, 1979, from the *Division of Pharmaceutics, College of Pharmacy, University of Iowa, Iowa City, IA 52242.* Accepted for publication November 9, 1979. *Present address: Hong Kong.

Abstract □ A modified balance was used to measure the adhesive force between the film coating and the tablet surface of 10 commercial film-coated tablets. The adhesiveness or force required to remove the film coating from a unit area of tablet surface ranged from 1.06 to 4.67 × 10^4 Nm^{-2}. Measurement of at least eight film coatings from the sides of four tablets was calculated to be required to obtain a result with 95% confidence. The method also was useful in studying the influence of solvents and humidity on bonding of the film coating to the tablet.

Keyphrases □ Adhesiveness—commercial film-coated tablets, measurement of force between film coating and tablet surface, effect of solvents and humidity on bonding of film to tablet surface □ Tablets—commercial film-coated preparations, measurement of adhesion of film coating to tablet surface, effect of solvents and humidity on bonding of film to tablet surface □ Film-coated tablets—measurement of adhesion of film coating to tablet surface, effect of solvents and humidity on bonding of film to tablet surface

Although film coating has been used in pharmacy for over 25 years, limited research has been conducted on the measurement of the adhesive force between the film coat and the tablet surface. The first method suggested for studying the adhesion of a film coating to a film-coated tablet was a peel test in which a section of the film coating was peeled from the tablet by a tensile tester (1, 2). To overcome the deficiencies of the peel test, an instrument was designed for removing the film normal to the interface between the film coating and the tablet surface (3, 4). Examination of the tablet and the film after removal showed that a rupture occurred at the boundary between the film surface and the tablet surface (5).

In the last 15 years, there has been an emphasis on quality assurance, increased testing, and stringent specifications for pharmaceuticals. Although coated tablets are evaluated in terms of exposure to moisture and chipping of the coating during handling, no test is used to express quantitatively the adhesiveness of a coating to a tablet. A method for measuring the adhesiveness would be useful in developmental work to evaluate tablet excipients (6), solvents (1), polymeric coating materials, humidity effects, formulations, and processes; it also would be useful in quality control to ensure uniformity of application.

This report demonstrates the feasibility of measuring the force required to remove a film coating from a film-coated tablet and explores the range of adhesiveness that has been acceptable on marketed film-coated tablets. The usefulness of the adhesive force measurement in determining solvent and humidity effects on adhesiveness also is demonstrated.

EXPERIMENTAL

Instrumentation—An analytical balance[1] was modified by replacing the left pan and pan support with a metal ring attached by a nylon cord. The coated tablet was attached to the metal ring by a hook with a 35-mm shaft, which was soldered at a right angle to an 18-mm circular stainless steel plate. A backing cut from a rubber stopper was carved on one side to fit any curvature of the tablet and was attached by double-sided adhesive tape[2] to the circular plate. Preliminary work showed that a backing was required to ensure even compressive force over the entire surface of the tablet when the adhesive tape was applied to the coated tablet. Another piece of double-sided adhesive tape was applied to the second surface of the backing.

The coated tablet was positioned carefully and pressed firmly onto the adhesive tape attaching it to the assembly (Fig. 1). The assembly holding the coated tablet was hooked onto the metal ring and nylon cord attached to the left arm, and the balance was balanced by counterweights. The tablet then was clamped on its edge into a fixed position during the measurement using two sets of screws attached to a heavy metal base. The weight applied to the right pan was increased until the film coating separated from the tablet.

In preparation for measurement, the coating on the edge of the tablet was removed with a razor blade to ensure that the force was used to remove only the film coating from the upper tablet surface and to eliminate any coating effect at the tablet edge.

The dimensions of each tablet and the film-coating thickness were measured by a micrometer[3]. For round, flat tablets, the surface area is πr^2. When the same relationship is used to estimate the surface area of tablets prepared with standard concave punches, an error of ~5% is introduced (4).

Humidity—Relative humidities (RH) of 0, 20, 45, 70, and 90% were obtained using various concentrations of sulfuric acid and water (7). Tablets of each commercial product were placed in aluminum cups and were kept at each of the five humidities for 2 weeks at room temperature. The adhesive force was measured immediately after removal from the humidity chamber.

Preparation of Film-Coated Tablets—Tablets with a hardness of 8 ± 1 kg were prepared in batches of 20,000 using a standard concave 11.11-mm punch and die set in a single-punch tablet machine[4]. Each tablet contained 10 mg of FD&C Red No. 3, 380 mg of dicalcium phosphate[5], 20 mg of cornstarch, 85 mg of microcrystalline cellulose[6], and 5 mg of magnesium stearate.

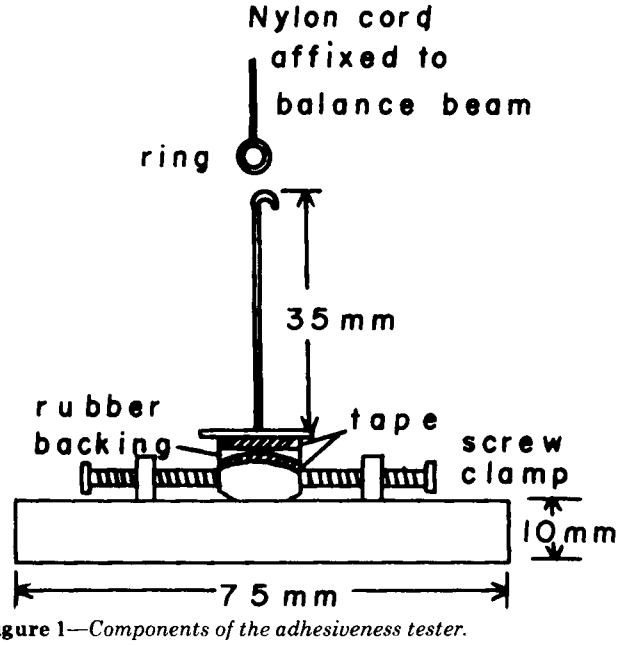

Figure 1—*Components of the adhesiveness tester.*

[1] Model 220, Voland & Sons, New Rochelle, N.Y.

[2] Tuck carpet bond.
[3] Screw gauge, Ames Co., Waltham, Mass.
[4] Stokes A-3.
[5] Encompress, Edward Mendell Co., Carmel, N.Y.
[6] Avicel PH 101, FMC Corp., Philadelphia, Pa.

0022-3549/80/0400-0439$01.00/0
© 1980, American Pharmaceutical Association

Table I—Average Adhesive Force (±*SD*), Adhesiveness, and Thickness

Product	Adhesive Force: Front[a] Surface, g	Adhesive Force: Back[a] Surface, g	Adhesive Force: Average[b], g	Adhesive Force: Average[b], N	Area, cm^2	Adhesiveness $\times 10^{-4}$, Nm^{-2}	Thickness[c], mm
A[d]	236 ± 21.3	235 ± 23.8	235 ± 18.2	2.31	1.31	1.76	0.108
B[e]	493 ± 52.7	492 ± 44.9	493 ± 44.0	4.83	1.30	3.72	0.085
C[f]	365 ± 56.0	356 ± 56.4	360 ± 44.6	3.53	1.31	2.69	0.100
D[g]	358 ± 60.0	357 ± 71.0	357 ± 49.6	3.51	1.28	2.74	0.100
E[h]	103 ± 16.4	112 ± 16.2	107 ± 16.5	1.05	0.99	1.06	0.062
F[i]	284 ± 24.6	292 ± 24.4	288 ± 22.3	2.82	1.41	2.00	0.108
G[j]	316 ± 29.5	296 ± 33.3	306 ± 27.7	3.00	1.51	1.99	0.245
H[k]	391 ± 36.0	386 ± 40.7	390 ± 28.6	3.81	1.89	2.02	0.138
I[l]	296 ± 31.3	275 ± 28.0	285 ± 29.0	2.80	0.60	4.67	0.097
J[m] (colored)	390 ± 32.1	—	—	3.82[a]	1.55	2.46	0.059
J[m] (white)	—	294 ± 45.5	—	2.88[a]	1.55	1.86	0.059

[a] Average of 10 measurements. [b] Average of measurements of 10 front and 10 back surfaces. [c] Average of four measurements. [d] Erythromycin stearate (250 mg), Lederle lot 437-113. [e] Bristamycin (250 mg), Bristol lot L3118. [f] SK-Erythromycin (250 mg), Smith Kline & French lot 142367. [g] Robimycin (250 mg), A. H. Robins lot 72-23-11. [h] Triaminic, Dorsey lot A53493. [i] Unipen (500 mg), Wyeth lot 1740664. [j] Stresstabs 600, Lederle lot 247-137. [k] Ethril (250 mg), Squibb lot 2G305. [l] Betaphen-VK (250 mg), Bristol lot B4544. [m] Cama Inlay, Dorsey lot M43438.

Approximately 2000 tablets were coated in a 20-cm coating pan that was rotating at 25 rpm. With the organic solvent systems, six applications of 25, 20, 15, 12, 8, and 5 ml of coating solution were applied, with drying between each application. The aqueous solution was applied in eight applications of 4 ml each. The coating solution contained 4.9% (w/v) hydroxypropylcellulose[7], 1.0% (w/v) propylene glycol 4000, and the solvent system to 100 ml. The solvent systems were methylene chloride–methanol (9:1), 95% ethanol, acetone–water (9:1), chloroform, and distilled water.

RESULTS AND DISCUSSION

Ten commercial film-coated tablets of various shapes and sizes were selected (Table I). With the modified balance, the intact film coating was pulled from these tablets without tearing or rending. Close examination showed that only traces of the substrate were pulled from the tablet surface with the film coating and that a rupture occurred at the interface between the film coating and the tablet as reported previously (5). The integrity of a removed film coating was not affected by the lettering indentations on the surfaces of Products D–G and J.

Adhesive force is the force required to pull a film coating from the tablet surface. Adhesiveness may be defined as the force required to remove the film coating from a unit area of the tablet surface.

The adhesive force was measured on both sides of 10 tablets of each product. For all tablets except Product J, there was no significant difference in the adhesive force measured on either tablet surface (Table I). Thus, there was no disturbance of the film coating on the opposite surface of the tablet when the adhesion of one side was measured (3).

Product J was a double-layered tablet with a white side and a colored side. Because the substrate was different on the two sides, the adhesive force would not necessarily be the same on each surface.

Since there was no difference in adhesive force on either side of the film-coated tablet, the adhesiveness was calculated using the average adhesive force of 20 film coatings. For the 10 products studied, adhesiveness ranged from 1.06 to 4.67 × 10^4 Nm^{-2}.

There presently is no standard for the adhesiveness of film coating. Because the adhesiveness of a coating reflects the bonding between the film coating and the substrate and the physical stability of the film-coated tablet, its evaluation is important in film-coating development and in product evaluation. Although the data were collected from commercial film-coated products of different formulations that probably were coated by more than a single process, they provide a range of values that describes the variation in coating adhesiveness of products that already were marketed and were regarded as acceptable from the viewpoint of processing, resistance to the environment, and handling.

In any test, the number of determinations must be decided to provide a statistically valid sample. To calculate the sample size, n, a tolerance interval containing a certain proportion, p, of the population must be developed. When both the population mean and the standard deviation are known, $\mu \pm k\sigma$ may be used as a tolerance level, where μ is the population mean, σ is the population standard deviation, and k is a constant.

When both the population mean and the standard deviation are unknown, the tolerance limits, which will include on the average a proportion, p, of the normal universe, are:

$$\bar{x} \pm t_{1-\alpha,n-1}\sqrt{\frac{n+1}{n}}S \qquad \text{(Eq. 1)}$$

where $\bar{x}$ is the mean of a sample of n observations, S is the sample standard deviation, and $t_{1-\alpha,n-1}$ is a Student t value for $n-1$ degrees of freedom that is exceeded in absolute value by the probability, α.

By equating the tolerance intervals, the minimum number of observations, n, needed to provide a significant result is obtained with:

$$K_{s,p} = t_{1-\alpha,n-1}\sqrt{\frac{n+1}{n}} \leq \frac{k\sigma}{S_{max}} \qquad \text{(Eq. 2)}$$

To determine the number of film-coated tablets needed, the adhesive force values of both sides of the tablet were averaged and the standard deviations were calculated (Table I). The estimated population mean of 313.6 ± 107.2 g was taken as the mean of the nine product means (Product J was excluded). A tolerance level of 313.6 ± 214.4 g was selected at which k equals 2.

The standard deviation, S_{max}, of Product D that had the highest value among the film-coated tablets was used. Thus:

$$K_{s,p} = t_{1-\alpha,n-1}\sqrt{\frac{n+1}{n}} \leq \frac{2 \times 107.2}{49.6} = 4.323 \qquad \text{(Eq. 3)}$$

The value of $K_{s,p}$, which relates sample size, n, and tolerance intervals, is obtained from the statistical table (8). For a 95% confidence limit, the minimum n that gives a $K_{s,p}$ value of ≤4.323 is 4. Thus, at least four film-coated tablets are required; the adhesive force is measured on their eight film coatings to give a statistically significant result with 95% confidence.

Influence of Humidity—The influence of humidity on the film-coating adhesiveness is shown in Table II. With Products E and F, there

Table II—Adhesiveness of Film-Coated Tablets at Various Relative Humidities

Product	Adhesiveness × 10^{-4}, Nm^{-2}: 0%	20%	45%	70%	90%
A	1.36	2.08	1.90	1.30	1.96
C	1.54	2.38	2.28	—[a]	—[a]
E	0.77	0.84	0.75	1.22	—[a]
F	1.38	1.52	1.71	1.66	2.30

[a] Spongy and deformed.

Table III—Adhesiveness of Hydroxypropylcellulose Coatings Applied from Various Solvent Systems

Solvent System	Adhesive Force[a]: g	Adhesive Force[a]: N	Area, cm^2	Adhesiveness × 10^{-4}, Nm^{-2}
Methylene chloride–methanol (9:1)	295.0	2.89	0.97	2.98
Ethanol, 95%	237.0	2.32	0.97	2.39
Acetone–water (9:1)	199.5	1.96	0.97	2.02
Chloroform	142.5	1.40	0.97	1.44
Water	70.5	0.69	0.97	0.71

[a] Average obtained from 10 film-coated tablets.

[7] Klucel, Hercules, Wilmington, Del.

was a linear relationship with a slight increase in adhesiveness as the relative humidity was increased.

With Products A and C, the maximum value of adhesiveness occurred at ~30% RH. With Product A, a minimum value of adhesiveness was reached at 70% RH, and then the adhesiveness increased with a further increase in humidity. With Product C at >50% RH, the tablet and the coating became spongy and deformed so that measurements could not be made.

Since the coating material, solvent, coating process, and substrate were unknown, speculation on these differences serves no useful purpose; however, the results confirm the applicability of this method to the detection of changes occurring in a film-coated product.

Influence of Solvent—The solvent from which a film coating is applied may affect the adhesion of the film to the substrate (2). When hydroxypropylcellulose was applied from the five solvent systems shown in Table III, there was a twofold difference ($1.44–2.98 \times 10^4$ Nm^{-2}) in adhesiveness among the organic solvents. When hydroxypropylcellulose was applied from aqueous solution, the adhesiveness (0.71×10^4 Nm^{-2}) was one-fourth to one-half as great as that from the organic solvents.

Applications—The method may be used to evaluate the stability of a film-coated tablet to moisture and its physical stability during shipment. The method also may be used in product development to express quantitatively the bonding between the film coating and the tablet surface and to compare the effect of various solvents on the bonding.

REFERENCES

(1) J. A. Wood and S. W. Harder, *Can. J. Pharm. Sci.*, **5**, 18 (1970).

(2) P. D. Nadkarni, D. O. Kildsig, P. A. Kramer, and G. S. Banker, *J. Pharm. Sci.*, **64**, 1554 (1975).

(3) D. G. Fisher and R. C. Rowe, *J. Pharm. Pharmacol.*, **28**, 886 (1976).

(4) R. C. Rowe, *ibid.*, **29**, 58 (1977).

(5) *Ibid.*, **30**, 343 (1978).

(6) *Ibid.*, **29**, 723 (1977).

(7) A. Wexler and W. G. Brombacker, *Natl. Bur. Stand. (U.S.) Circ.*, **1951**, 512.

(8) F. Proschan, *Am. Stat. Assoc. J.*, **48**, 550 (1953).

ACKNOWLEDGMENTS

Abstracted in part from a dissertation submitted by R. M. Fung to the University of Iowa in partial fulfillment of the Master of Science degree requirements.

Role of α- and β-Adrenergic Activation in Ventricular Fibrillation Death of Corticoid-Pretreated Rats

MARK GREEN ˣ, GIANCARLO GUIDERI, and DAVID LEHR

Received March 5, 1979, from the *Department of Pharmacology, New York Medical College, Valhalla, NY 10595.* Accepted for publication November 8, 1979.

Abstract □ Death in ventricular fibrillation was induced consistently in desoxycorticosterone acetate-pretreated rats by the β-adrenergic agonist isoproterenol but not by norepinephrine or epinephrine, both of which possess α- as well as β-adrenergic activity. Aminophylline, which enhances β-adrenergic activity, and phenoxybenzamine, an α-receptor blocking agent, were used to study the roles of α- and β-adrenergic stimulation in the production of ventricular fibrillation. With the addition of aminophylline, both norepinephrine and epinephrine produced death in ventricular fibrillation, and the existing cardiotoxicity of isoproterenol was potentiated. Similarly, in the presence of phenoxybenzamine, doses of norepinephrine and epinephrine that had been well tolerated became lethal. Interventions that favor β-adrenergic preponderance, either by enhancing β-effects or by blocking protective α-adrenergic activation, apparently increase the arrhythmogenic propensity of norepinephrine and epinephrine in steroid-pretreated rats. The similarity of some forms of stress to the experimental protocol of chronic steroid treatment followed by acute catecholamine exposure is discussed.

Keyphrases □ Ventricular fibrillation—role of α- and β-adrenergic activity, desoxycorticosterone acetate-pretreated rats □ Arrhythmias—catecholamine induced, effect of steroid pretreatment □ Aminophylline—effect on catecholamine-induced arrhythmias, steroid-pretreated rats □ Phenoxybenzamine—effect on catecholamine-induced arrhythmias, steroid-pretreated rats

Earlier studies in this laboratory showed that, following pretreatment of the albino rat with the steroid desoxycorticosterone acetate and saline as the drinking fluid, the administration of isoproterenol elicited severe cardiac arrhythmias at dose levels that otherwise are well tolerated (1, 2). The enhanced cardiotoxicity was reflected in a shift of the isoproterenol LD_{50} from 680 mg/kg (3) in untreated rats to 14.5 μg/kg in desoxycorticosterone acetate–saline-pretreated rats (4), a nearly 47,000-fold potentiation. The deaths produced by this drug–drug interaction usually occurred within 60 min and consistently were due to ventricular fibrillation, while the mortality observed in untreated rats developed over 24 hr and usually was attributable to acute heart failure, lung edema, and shock. Recent studies showed that prednisone, administered either subcutaneously or orally, also can sensitize the myocardium to the arrhythmogenic effect of isoproterenol (4). It has been suggested that this type of drug interaction may expose patients such as asthmatics, taking steroids and isoproterenol simultaneously, to potentially life-threatening cardiac arrhythmias (5).

The mechanism underlying this phenomenon is not well understood. Alterations in the myocardial electrolyte content may be a factor in the increased myocardial vulnerability to isoproterenol. Electrolyte changes such as those seen with this treatment (6) have been well documented as increasing the propensity of the heart to arrhythmias and ventricular fibrillation (7).

The ability of steroids to affect protein synthesis also might be important in the sensitization process. In preliminary studies, agents that inhibit protein synthesis blocked the steroid-induced myocardial sensitization to isoproterenol (8).

The present investigation was undertaken to determine: (*a*) whether norepinephrine and epinephrine, which are both α- and β-adrenergic agonists, exhibit enhanced arrhythmogenic activity following steroid pretreatment comparable to that observed with isoproterenol; and (*b*) whether aminophylline, an agent administered frequently

0022-3549/80/0400-0441$01.00/0

© 1980, American Pharmaceutical Association

was a linear relationship with a slight increase in adhesiveness as the relative humidity was increased.

With Products A and C, the maximum value of adhesiveness occurred at ~30% RH. With Product A, a minimum value of adhesiveness was reached at 70% RH, and then the adhesiveness increased with a further increase in humidity. With Product C at >50% RH, the tablet and the coating became spongy and deformed so that measurements could not be made.

Since the coating material, solvent, coating process, and substrate were unknown, speculation on these differences serves no useful purpose; however, the results confirm the applicability of this method to the detection of changes occurring in a film-coated product.

Influence of Solvent—The solvent from which a film coating is applied may affect the adhesion of the film to the substrate (2). When hydroxypropylcellulose was applied from the five solvent systems shown in Table III, there was a twofold difference ($1.44–2.98 \times 10^4$ Nm^{-2}) in adhesiveness among the organic solvents. When hydroxypropylcellulose was applied from aqueous solution, the adhesiveness (0.71×10^4 Nm^{-2}) was one-fourth to one-half as great as that from the organic solvents.

Applications—The method may be used to evaluate the stability of a film-coated tablet to moisture and its physical stability during shipment. The method also may be used in product development to express quantitatively the bonding between the film coating and the tablet surface and to compare the effect of various solvents on the bonding.

REFERENCES

(1) J. A. Wood and S. W. Harder, *Can. J. Pharm. Sci.*, **5**, 18 (1970).

(2) P. D. Nadkarni, D. O. Kildsig, P. A. Kramer, and G. S. Banker, *J. Pharm. Sci.*, **64**, 1554 (1975).

(3) D. G. Fisher and R. C. Rowe, *J. Pharm. Pharmacol.*, **28**, 886 (1976).

(4) R. C. Rowe, *ibid.*, **29**, 58 (1977).

(5) *Ibid.*, **30**, 343 (1978).

(6) *Ibid.*, **29**, 723 (1977).

(7) A. Wexler and W. G. Brombacker, *Natl. Bur. Stand. (U.S.) Circ.*, **1951**, 512.

(8) F. Proschan, *Am. Stat. Assoc. J.*, **48**, 550 (1953).

ACKNOWLEDGMENTS

Abstracted in part from a dissertation submitted by R. M. Fung to the University of Iowa in partial fulfillment of the Master of Science degree requirements.

Role of α- and β-Adrenergic Activation in Ventricular Fibrillation Death of Corticoid-Pretreated Rats

MARK GREEN ˣ, GIANCARLO GUIDERI, and DAVID LEHR

Received March 5, 1979, from the *Department of Pharmacology, New York Medical College, Valhalla, NY 10595.* Accepted for publication November 8, 1979.

Abstract □ Death in ventricular fibrillation was induced consistently in desoxycorticosterone acetate-pretreated rats by the β-adrenergic agonist isoproterenol but not by norepinephrine or epinephrine, both of which possess α- as well as β-adrenergic activity. Aminophylline, which enhances β-adrenergic activity, and phenoxybenzamine, an α-receptor blocking agent, were used to study the roles of α- and β-adrenergic stimulation in the production of ventricular fibrillation. With the addition of aminophylline, both norepinephrine and epinephrine produced death in ventricular fibrillation, and the existing cardiotoxicity of isoproterenol was potentiated. Similarly, in the presence of phenoxybenzamine, doses of norepinephrine and epinephrine that had been well tolerated became lethal. Interventions that favor β-adrenergic preponderance, either by enhancing β-effects or by blocking protective α-adrenergic activation, apparently increase the arrhythmogenic propensity of norepinephrine and epinephrine in steroid-pretreated rats. The similarity of some forms of stress to the experimental protocol of chronic steroid treatment followed by acute catecholamine exposure is discussed.

Keyphrases □ Ventricular fibrillation—role of α- and β-adrenergic activity, desoxycorticosterone acetate-pretreated rats □ Arrhythmias—catecholamine induced, effect of steroid pretreatment □ Aminophylline—effect on catecholamine-induced arrhythmias, steroid-pretreated rats □ Phenoxybenzamine—effect on catecholamine-induced arrhythmias, steroid-pretreated rats

Earlier studies in this laboratory showed that, following pretreatment of the albino rat with the steroid desoxycorticosterone acetate and saline as the drinking fluid, the administration of isoproterenol elicited severe cardiac arrhythmias at dose levels that otherwise are well tolerated (1, 2). The enhanced cardiotoxicity was reflected in a shift of the isoproterenol LD_{50} from 680 mg/kg (3) in untreated rats to 14.5 μg/kg in desoxycorticosterone acetate–saline-pretreated rats (4), a nearly 47,000-fold potentiation. The deaths produced by this drug–drug interaction usually occurred within 60 min and consistently were due to ventricular fibrillation, while the mortality observed in untreated rats developed over 24 hr and usually was attributable to acute heart failure, lung edema, and shock. Recent studies showed that prednisone, administered either subcutaneously or orally, also can sensitize the myocardium to the arrhythmogenic effect of isoproterenol (4). It has been suggested that this type of drug interaction may expose patients such as asthmatics, taking steroids and isoproterenol simultaneously, to potentially life-threatening cardiac arrhythmias (5).

The mechanism underlying this phenomenon is not well understood. Alterations in the myocardial electrolyte content may be a factor in the increased myocardial vulnerability to isoproterenol. Electrolyte changes such as those seen with this treatment (6) have been well documented as increasing the propensity of the heart to arrhythmias and ventricular fibrillation (7).

The ability of steroids to affect protein synthesis also might be important in the sensitization process. In preliminary studies, agents that inhibit protein synthesis blocked the steroid-induced myocardial sensitization to isoproterenol (8).

The present investigation was undertaken to determine: (*a*) whether norepinephrine and epinephrine, which are both α- and β-adrenergic agonists, exhibit enhanced arrhythmogenic activity following steroid pretreatment comparable to that observed with isoproterenol; and (*b*) whether aminophylline, an agent administered frequently

0022-3549/80/0400-0441$01.00/0

© 1980, American Pharmaceutical Association

Table I—Effect of Norepinephrine and Epinephrine on the Desoxycorticosterone Acetate–Saline-Pretreated Rat

Dose, μg/kg	l-Norepinephrine Bitartrate		l-Epinephrine Bitartrate	
	n	Mortality, %	n	Mortality, %
25	—	—	7	0
50	7	0	5	0
75	—	—	7	0
202	—	—	5	0
300	22	0	—	—
680	—	—	5	0
1360	—	—	5	0

to asthmatics alone or with steroids and catecholamines, affects the existing interaction between corticoids and adrenergic agonists.

EXPERIMENTAL

Male albino rats, 250–300 g, were pretreated with desoxycorticosterone acetate (I) and saline as the drinking fluid. Pellets of the steroid were implanted subcutaneously and provided a constant source of I over the entire 21-day pretreatment period. The methodology for the manufacture and implantation of these pellets was described previously (4). Except where noted, all animals received steroid pretreatment.

All drug solutions were prepared in normal saline immediately prior to injection, except for phenoxybenzamine, which was suspended in a 10% acacia solution. All drugs were administered subcutaneously. Aminophylline, 75 mg/kg, was administered to rats 10 min prior to the catecholamines; chlorisondamine, 10 mg/kg, and phenoxybenzamine, 4 mg/kg, were given 30 min before the catecholamines.

Animals were observed for 90 min following catecholamine administration, and mortality rates were noted. ECG's were monitored from selected animals in each group to observe arrhythmias and to verify that mortality was due to ventricular fibrillation. The ECG was obtained by taping gold-plated disk electrodes to each limb of the rat, which otherwise was unrestrained.

The data obtained are reported as mortality rates. This selection was made because mortality rates reflect both the relative toxicities of the various agents and their relative arrhythmogenic activity since early death was attributable consistently to ventricular fibrillation.

A χ-square analysis was used to determine significant differences between treatment groups. Linear regression was used to determine the best-fit lines through data points on the graphs and to calculate LD_{50} values.

RESULTS

Effect of Norepinephrine and Epinephrine—Several doses of norepinephrine and epinephrine were administered to I–saline-pretreated rats (Table I). Within the dose ranges used, there was no mortality. The ECG's recorded from some rats did not show any of the tachyarrhythmias usually seen with isoproterenol in I–saline-pretreated rats. The largest dose of epinephrine did elicit bradyarrhythmias, which often are seen with the substantial elevations of blood pressure produced by this dose of epinephrine. However, these bradyarrhythmias are unlike the arrhythmias produced by isoproterenol.

Table II—Toxicity of Aminophylline in the Desoxycorticosterone Acetate–Saline-Pretreated Rat

Treatment Group	n	Number of Deaths	Mortality, %
I Aminophylline (75 mg/kg)	9	7	77
II Aminophylline + handling	9	6	67
III Aminophylline + saline injection	17	14	82
IV Aminophylline + saline injection + chlorisondamine	15	1	7[a]
V No steroid; aminophylline + saline injection	10	0	0[a]

[a] $p < 0.001$ compared to Group III.

Table III—Effect of Aminophylline on Catecholamine Cardiotoxicity

	Dose, μg/kg	Aminophylline, I–Saline, and Chlorisondamine		LD_{50}, μg/kg	I–Saline and Chlorisondamine Mortality,	
		n	Mortality, %		n	%
l-Norepinephrine bitartrate	30	13	8			
	100	10	50	110		
	200	16	62			
	300	20	90		15	0[a]
l-Epinephrine bitartrate	10	11	18			
	30	10	60	28.2		
	100	8	87		10	0[a]
l-Isoproterenol bitartrate	2	10	20			
	3	9	44	3.63		
	10	10	90			

[a] $p < 0.001$ compared to the group with aminophylline.

Cardiotoxicity of Aminophylline—The administration of aminophylline, 75 mg/kg, to I–saline-pretreated rats resulted in a 77% incidence of mortality (Table II). Animals in Group II were handled 10 min after aminophylline administration and showed a 67% incidence of mortality. Group III animals were given an injection of normal saline (0.1 ml/100 g) 10 min after aminophylline administration, resulting in a mortality rate of 82%.

Although a direct effect of aminophylline on the heart could not be ruled out, past experience showed that β-adrenergic stimulation was necessary to produce these deaths in ventricular fibrillation. To determine whether reflex release of endogenous catecholamines in response to the stress of handling, the injections, or simply the laboratory environment was the cause of these deaths, the ganglionic blocking agent chlorisondamine, 10 mg/kg, was used. Animals in Group IV received this agent 30 min prior to aminophylline admininstration (Table II). Ganglionic blockage was expected to prevent reflex release of catecholamines and to help determine whether the observed toxic effect was attributable to a direct action of aminophylline on the heart.

Following chlorisondamine administration, the combination of aminophylline followed by a saline injection produced only a 7% mortality rate, a highly significant decrease from the 82% seen without chlorisondamine. This result was compatible with the assumption that stress-induced reflex release of catecholamines, and not a direct effect of aminophylline, was responsible for the observed high death rate.

The importance of steroid pretreatment to this response is illustrated by the data for Group V (Table II). These animals were given aminophylline, 75 mg/kg, followed by a saline injection, but they did not receive I–saline pretreatment. Their mortality rate was significantly different ($p < 0.001$) from that of Group III, which had received steroid pretreatment in addition to the aminophylline and saline injections.

Toxicity of Catecholamines following Aminophylline—In this study and all following studies, chlorisondamine was used routinely together with aminophylline to block endogenous catecholamine release in order to evaluate the effect of aminophylline on administered catecholamines.

Table III shows the effect of aminophylline on norepinephrine and epinephrine toxicity. Unlike the initial study in which administration of the two agonists produced no fatality, dose-dependent increases in the mortality rate were observed with both catecholamines. Data for isoproterenol have been included to show its relative potency. The calculated LD_{50} values show that isoproterenol was nearly seven times more potent than epinephrine, which, in turn, was about four times more active than norepinephrine. The role of aminophylline in eliciting this cardiotoxicity is seen when comparing the effect of equal catecholamine doses in its presence and absence. Table III shows that in the presence of aminophylline, chlorisondamine, and I–saline, norepinephrine, 300 μg/kg, and epinephrine, 100 μg/kg, produced mortality rates of 90 and 87%, respectively. Without aminophylline, neither drug produced any mortality at equal dose levels.

Unlike norepinephrine and epinephrine, isoproterenol produced ventricular fibrillation deaths without aminophylline, but its effect with aminophylline was enhanced greatly (Fig. 1). The isoproterenol used in this study was the racemic hydrochloride salt, not the l-isomer of the

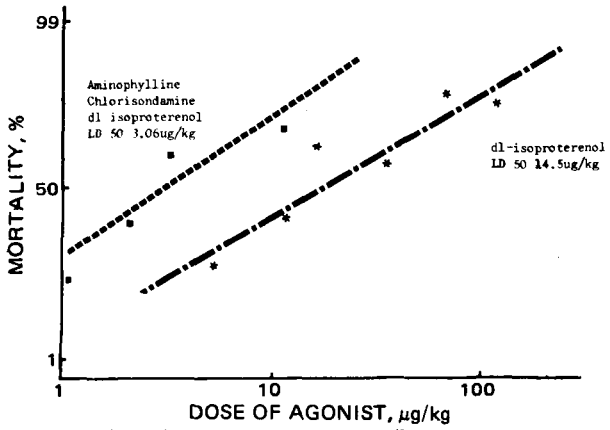

Figure 1—*Effect of aminophylline (75 mg/kg) on isoproterenol cardiotoxicity in desoxycorticosterone acetate-saline-pretreated rats after ganglionic blockage with chlorisondamine (10 mg/kg).*

bitartrate used in all other studies. The curve on the right represents isoproterenol toxicity following I–saline pretreatment alone. The addition of aminophylline (and chlorisondamine to prevent release of endogenous catecholamines) produced a marked shift to the left, decreasing the LD_{50} value from 14.5 to 3.06 μg/kg, a nearly fivefold potentiation (95% confidence limits of the potentiation were 2.48–9.4 times).

Effect of α-Blockage on Catecholamine Toxicity—While isoproterenol alone could produce ventricular fibrillation deaths in I–saline-pretreated rats, norepinephrine and epinephrine did so only in the presence of aminophylline. Phenoxybenzamine, an α-adrenergic blocking agent, was used to determine whether the potent α-agonist properties of norepinephrine and epinephrine were protecting the animals from fibrillation deaths (Fig. 2). Norepinephrine, 300 μg/kg, produced no deaths in I–saline-pretreated rats; but with the addition of the α-blocker, a 40% mortality rate was produced. Similarly, 100 μg of epinephrine/kg was nontoxic in steroid-pretreated rats; but in combination with phenoxybenzamine, it produced a 70% mortality rate.

Phenoxybenzamine itself did not show any acute toxicity in I–saline-pretreated rats. Ten animals injected with the drug followed by a saline injection did not exhibit any signs of the lethal interaction. Blockage of the α-adrenergic component of norepinephrine and epinephrine apparently allows the unopposed β-adrenergic activity to produce fibrillation deaths in these animals in a manner similar to that of the pure β-agonist isoproterenol.

Effect of Norepinephrine on Isoproterenol Cardiotoxicity—The interaction between α- and β-adrenergic stimulation was examined from a different perspective. In this study, a dose of *l*-isoproterenol, which produced a 75% mortality rate, was administered 10 min after 300 μg of norepinephrine/kg. As shown in Fig. 2, this dose of norepinephrine produced fibrillation deaths only if its α-adrenergic activity was blocked. Since the α-agonist component of norepinephrine prevented this catecholamine from inducing fibrillation deaths, it was expected that it also might attenuate the response of the pure β-agonist isoproterenol. This

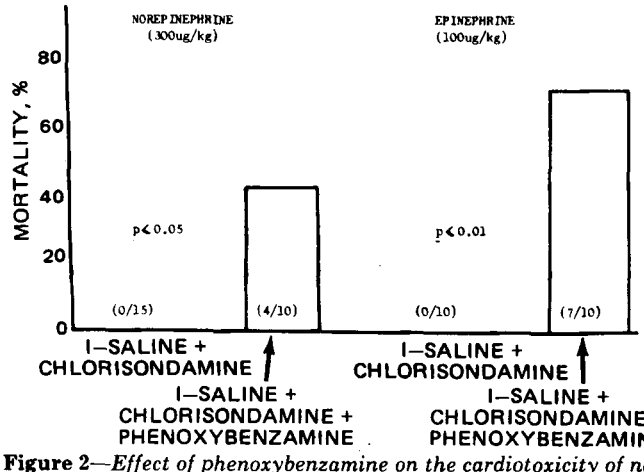

Figure 2—*Effect of phenoxybenzamine on the cardiotoxicity of norepinephrine and epinephrine in desoxycorticosterone acetate–saline-pretreated rats.*

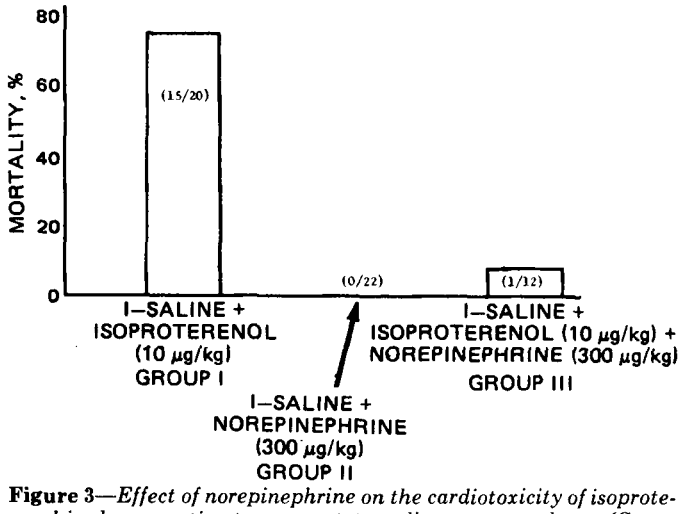

Figure 3—*Effect of norepinephrine on the cardiotoxicity of isoproterenol in desoxycorticosterone acetate–saline-pretreated rats (Group I* versus *Group III,* $p < 0.01$).

effect did, in fact, occur (Fig. 3). The addition of norepinephrine reduced the mortality rate attributable to isoproterenol alone from 75 to 8%.

DISCUSSION

Injections of norepinephrine and epinephrine can produce lethal cardiac arrhythmias in steroid-pretreated rats when combined with either aminophylline or the α-blocking agent phenoxybenzamine. The cardiotoxicity of isoproterenol, already established following steroid pretreatment alone, is enhanced greatly by aminophylline. Comparison of the LD_{50} value of isoproterenol in untreated rats to that of I–saline-pretreated rats also given aminophylline shows a decrease from 680 mg/kg to 3.06 μg/kg, a >200,000-fold increase in toxicity. The effect of aminophylline is so great that even the amounts of norepinephrine and epinephrine released endogenously as a stress response become lethal in its presence.

The ability of both phenoxybenzamine and aminophylline to increase the cardiotoxicity of adrenergic agonists may relate to the importance of β-adrenergic stimulation in this phenomenon. Norepinephrine and epinephrine contain potent α-adrenergic agonist activity in addition to their β-properties. Phenoxybenzamine and aminophylline each can upset, in a different way, the relative balance between α- and β-tone in favor of β-activity. The protective effect of α-stimulation may be due to its ability to raise the fibrillation threshold (9, 10). This effect would decrease the vulnerability of the heart to fibrillation induced by β-stimulation, reducing both the morbidity and mortality of the drug interaction.

Phenoxybenzamine may upset the α–β-balance by removing the α-component by receptor blockage. Aminophylline may produce its effect through its synergistic activity with β-adrenergic stimulation. This result might be accomplished through the adenylate cyclase system. β-Activity has been closely related to this system (11), and aminophylline, a potent phosphodiesterase inhibitor (12, 13), would prevent the degradation of formed adenosine-3′,5′-monophosphate (cyclic AMP) and enhance the activity of agents, such as β-agonists, whose actions depend on the elaboration of cyclic AMP. By either blocking α-receptors or enhancing β-stimulation, the net effect is to promote a β-preponderance, resulting in ventricular fibrillation.

The demonstrated beneficial effect of norepinephrine on isoproterenol cardiotoxicity is consistent with this theory. In this situation, potent α-adrenergic stimulation was added to an environment that was unbalanced favorably for β-adrenergic activity. By reestablishing a balance between α- and β-activity, the appearance of lethal arrhythmias was suppressed. The β-adrenergic component of norepinephrine may have played a small role in the diminution of the effect of isoproterenol. It is a weaker β-agonist than isoproterenol and, therefore, can act as a partial antagonist at certain dosage combinations with isoproterenol. However, this effect alone could not produce the observed decrease in mortality, from 75 to 8%. Hence, the potent α-activity of norepinephrine must have played the major role in decreasing the cardiotoxic response to isoproterenol.

The finding that endogenously released catecholamines can trigger ventricular fibrillation in steroid-pretreated rats fits well with current theories concerning the pathology of stress. Balazs *et al.* (14) found that

both cold and isolation stress increased the heart's sensitivity to isoproterenol and speculated that steroid hormones released by stress may have sensitized the myocardium to the β-agonist. Raab (15) also suggested that stress-induced discharge of adrenal corticoids may enhance the cardiotoxicity of endogenously released catecholamines. In discussing unexpected sudden death during sleep, he implicated a combination of 17-hydroxycorticosteroids, which reach peak levels during sleep, and dream-induced catecholamine discharges as being contributory to a fatal cardiotoxic interaction (16). The prolonged administration of steroids followed by exposure to catecholamines, as seen in the present study, may mimic the hormonal milieu produced by chronic stress, resulting in the similarity of toxic sequelae.

The applicability of these experimental findings to the clinical setting has to be determined. However, the data point out the potential danger of chronic steroid treatment. In such instances, there might be increased risk not only from administered catecholamines but also from agents that potentiate the effects of endogenous catecholamines, such as aminophylline and possibly monoamine oxidase inhibitors, and from agents that produce catecholamine discharge, such as tyramine, an ingredient of many foods.

REFERENCES

(1) G. Guideri, W. Goldman, and D. Lehr, *Fed. Proc. Fed. Am. Soc. Exp. Biol.*, **30**, 686 (1971).

(2) G. Guideri, M. Barletta, and D. Lehr, *Cardiovasc. Res.*, **8**, 775 (1974).

(3) G. Rona, C. I. Chappel, T. Balazs, and R. Gaudry, *Arch. Pathol.*, **67**, 443 (1959).

(4) G. Guideri, M. Green, and D. Lehr, *Res. Commun. Chem. Pathol. Pharmacol.*, **21**, 197 (1978).

(5) D. Lehr, *N. Engl. J. Med.*, **287**, 987 (1972).

(6) G. Guideri, M. Barletta, R. Chau, M. Green, and D. Lehr, in "Recent Advances in Studies on Cardiac Structure and Metabolism, Vol. 10, The Metabolism of Contraction," P. E. Roy and G. Rona, Eds., University Park Press, Baltimore, Md., 1975, pp. 671–679.

(7) B. F. Hoffman and P. F. Cranefield, "Electrophysiology of the Heart," McGraw-Hill, New York, N.Y., 1960.

(8) G. Guideri, C. Healy, and D. Lehr, *Fed. Proc. Fed. Am. Soc. Exp. Biol.*, **37**, 817 (1978).

(9) J. G. Papp and L. Szekeres, *Eur. J. Pharmacol.*, **3**, 4 (1968).

(10) A. J. Pappano, *J. Pharmacol. Exp. Ther.*, **177**, 85 (1971).

(11) E. W. Sutherland and T. W. Rall, *Pharmacol. Rev.*, **12**, 265 (1960).

(12) E. W. Sutherland and T. W. Rall, *J. Biol. Chem.*, **232**, 1077 (1958).

(13) R. W. Butcher, Jr., and E. W. Sutherland, *Pharmacologist*, **1**, 63 (1959).

(14) T. Balazs, J. B. Murphy, and H. C. Grice, *J. Pharm. Pharmacol.*, **14**, 750 (1962).

(15) W. Raab, *Am. Heart J.*, **72**, 538 (1966).

(16) W. Raab, in "Recent Advances in Studies on Cardiac Structure and Metabolism, Vol. 1, Myocardiology," E. Bajusz and G. Rona, Eds., University Park Press, Baltimore, Md., 1970, p. 707.

ACKNOWLEDGMENTS

Supported in part by National Institutes of Health Grant 1 R01 HL20052-01A2.

Application of High-Pressure Liquid Chromatography and Thermal Energy Analyzer to Analysis of Trinitroglycerin and Its Metabolites in Blood

RONALD J. SPANGGORD ˣ and RODNEY G. KECK

Received August 29, 1979, from the *Life Sciences Division, SRI International, Menlo Park, CA 94025.* Accepted for publication November 20, 1979.

Abstract □ A highly selective and sensitive analytical procedure for the determination of trinitroglycerin and four metabolites in whole blood was developed. Trinitroglycerin and its metabolites were extracted from whole blood with ethyl acetate and analyzed by high-pressure liquid chromatography using the thermal energy analyzer detector. Linearity of response was observed over the 1–1000-ng range. The applicability of this method to the analysis of whole blood from dogs orally dosed with trinitroglycerin is described.

Keyphrases □ Trinitroglycerin—high-pressure liquid chromatographic analysis of parent drug and metabolites in whole blood □ High-pressure liquid chromatography—analysis of trinitroglycerin and metabolites in whole blood □ Thermal energy analyzer—analysis of trinitroglycerin and metabolites in whole blood

The analysis of trinitroglycerin in blood has been performed primarily by electron-capture GLC (1–3). Although this method possesses high sensitivity and some selectivity for trinitroglycerin, it requires extensive cleanup procedures and solvent purification. Furthermore, it does not adequately account for the primary metabolites of trinitroglycerin, the isomeric mono- and dinitroglyceryl esters. A recent report (4) described the detection of ethylene glycol dinitrate esters in water by use of the thermal energy analyzer. It was thought that the analyzer detection system also may be applicable to the analysis of trinitroglycerin in complex matrixes such as whole blood.

This report describes the development of a high-pressure liquid chromatographic (HPLC) method to determine trinitroglycerin as well as the primary isomeric dinitro- and mononitroglyceryl metabolites in whole blood. The application of this methodology to the blood of dogs orally dosed with trinitroglycerin is described.

EXPERIMENTAL

Reagents—Acetone[1] and ethyl acetate[1] were glass distilled. Trinitroglycerin[2] was used as a powder (10% trinitroglycerin in lactose). *N*-Nitrosodipropylamine[3] was supplied as a standard solution in isooctane. All other chemicals and solvents were standard reagent grade and were used without further purification. Authentic samples of 1,3- and 1,2-dinitroglycerols and 1- and 2-mononitroglycerols were obtained[4].

Apparatus—The chromatographic system consisted of a liquid

[1] Burdick & Jackson Laboratory, Muskegon, MI 49442.
[2] ICI United States, Wilmington, DE 19897.
[3] ITT Research Institute, Chicago, IL 60616.
[4] Midwest Research Institute, Kansas City, MO 64110.

0022-3549/80/0400-0444$01.00/0

© 1980, American Pharmaceutical Association

both cold and isolation stress increased the heart's sensitivity to isoproterenol and speculated that steroid hormones released by stress may have sensitized the myocardium to the β-agonist. Raab (15) also suggested that stress-induced discharge of adrenal corticoids may enhance the cardiotoxicity of endogenously released catecholamines. In discussing unexpected sudden death during sleep, he implicated a combination of 17-hydroxycorticosteroids, which reach peak levels during sleep, and dream-induced catecholamine discharges as being contributory to a fatal cardiotoxic interaction (16). The prolonged administration of steroids followed by exposure to catecholamines, as seen in the present study, may mimic the hormonal milieu produced by chronic stress, resulting in the similarity of toxic sequelae.

The applicability of these experimental findings to the clinical setting has to be determined. However, the data point out the potential danger of chronic steroid treatment. In such instances, there might be increased risk not only from administered catecholamines but also from agents that potentiate the effects of endogenous catecholamines, such as aminophylline and possibly monoamine oxidase inhibitors, and from agents that produce catecholamine discharge, such as tyramine, an ingredient of many foods.

REFERENCES

(1) G. Guideri, W. Goldman, and D. Lehr, *Fed. Proc. Fed. Am. Soc. Exp. Biol.*, **30**, 686 (1971).

(2) G. Guideri, M. Barletta, and D. Lehr, *Cardiovasc. Res.*, **8**, 775 (1974).

(3) G. Rona, C. I. Chappel, T. Balazs, and R. Gaudry, *Arch. Pathol.*, **67**, 443 (1959).

(4) G. Guideri, M. Green, and D. Lehr, *Res. Commun. Chem. Pathol. Pharmacol.*, **21**, 197 (1978).

(5) D. Lehr, *N. Engl. J. Med.*, **287**, 987 (1972).

(6) G. Guideri, M. Barletta, R. Chau, M. Green, and D. Lehr, in "Recent Advances in Studies on Cardiac Structure and Metabolism, Vol. 10, The Metabolism of Contraction," P. E. Roy and G. Rona, Eds., University Park Press, Baltimore, Md., 1975, pp. 671–679.

(7) B. F. Hoffman and P. F. Cranefield, "Electrophysiology of the Heart," McGraw-Hill, New York, N.Y., 1960.

(8) G. Guideri, C. Healy, and D. Lehr, *Fed. Proc. Fed. Am. Soc. Exp. Biol.*, **37**, 817 (1978).

(9) J. G. Papp and L. Szekeres, *Eur. J. Pharmacol.*, **3**, 4 (1968).

(10) A. J. Pappano, *J. Pharmacol. Exp. Ther.*, **177**, 85 (1971).

(11) E. W. Sutherland and T. W. Rall, *Pharmacol. Rev.*, **12**, 265 (1960).

(12) E. W. Sutherland and T. W. Rall, *J. Biol. Chem.*, **232**, 1077 (1958).

(13) R. W. Butcher, Jr., and E. W. Sutherland, *Pharmacologist*, **1**, 63 (1959).

(14) T. Balazs, J. B. Murphy, and H. C. Grice, *J. Pharm. Pharmacol.*, **14**, 750 (1962).

(15) W. Raab, *Am. Heart J.*, **72**, 538 (1966).

(16) W. Raab, in "Recent Advances in Studies on Cardiac Structure and Metabolism, Vol. 1, Myocardiology," E. Bajusz and G. Rona, Eds., University Park Press, Baltimore, Md., 1970, p. 707.

ACKNOWLEDGMENTS

Supported in part by National Institutes of Health Grant 1 R01 HL20052-01A2.

Application of High-Pressure Liquid Chromatography and Thermal Energy Analyzer to Analysis of Trinitroglycerin and Its Metabolites in Blood

RONALD J. SPANGGORD ˣ and RODNEY G. KECK

Received August 29, 1979, from the *Life Sciences Division, SRI International, Menlo Park, CA 94025.* Accepted for publication November 20, 1979.

Abstract □ A highly selective and sensitive analytical procedure for the determination of trinitroglycerin and four metabolites in whole blood was developed. Trinitroglycerin and its metabolites were extracted from whole blood with ethyl acetate and analyzed by high-pressure liquid chromatography using the thermal energy analyzer detector. Linearity of response was observed over the 1–1000-ng range. The applicability of this method to the analysis of whole blood from dogs orally dosed with trinitroglycerin is described.

Keyphrases □ Trinitroglycerin—high-pressure liquid chromatographic analysis of parent drug and metabolites in whole blood □ High-pressure liquid chromatography—analysis of trinitroglycerin and metabolites in whole blood □ Thermal energy analyzer—analysis of trinitroglycerin and metabolites in whole blood

The analysis of trinitroglycerin in blood has been performed primarily by electron-capture GLC (1–3). Although this method possesses high sensitivity and some selectivity for trinitroglycerin, it requires extensive cleanup procedures and solvent purification. Furthermore, it does not adequately account for the primary metabolites of trinitroglycerin, the isomeric mono- and dinitroglyceryl esters. A recent report (4) described the detection of ethylene glycol dinitrate esters in water by use of the thermal energy analyzer. It was thought that the analyzer detection system also may be applicable to the analysis of trinitroglycerin in complex matrixes such as whole blood.

This report describes the development of a high-pressure liquid chromatographic (HPLC) method to determine trinitroglycerin as well as the primary isomeric dinitro- and mononitroglyceryl metabolites in whole blood. The application of this methodology to the blood of dogs orally dosed with trinitroglycerin is described.

EXPERIMENTAL

Reagents—Acetone[1] and ethyl acetate[1] were glass distilled. Trinitroglycerin[2] was used as a powder (10% trinitroglycerin in lactose). *N*-Nitrosodipropylamine[3] was supplied as a standard solution in isooctane. All other chemicals and solvents were standard reagent grade and were used without further purification. Authentic samples of 1,3- and 1,2-dinitroglycerols and 1- and 2-mononitroglycerols were obtained[4].

Apparatus—The chromatographic system consisted of a liquid

[1] Burdick & Jackson Laboratory, Muskegon, MI 49442.
[2] ICI United States, Wilmington, DE 19897.
[3] ITT Research Institute, Chicago, IL 60616.
[4] Midwest Research Institute, Kansas City, MO 64110.

0022-3549/80/0400-0444$01.00/0

© 1980, American Pharmaceutical Association

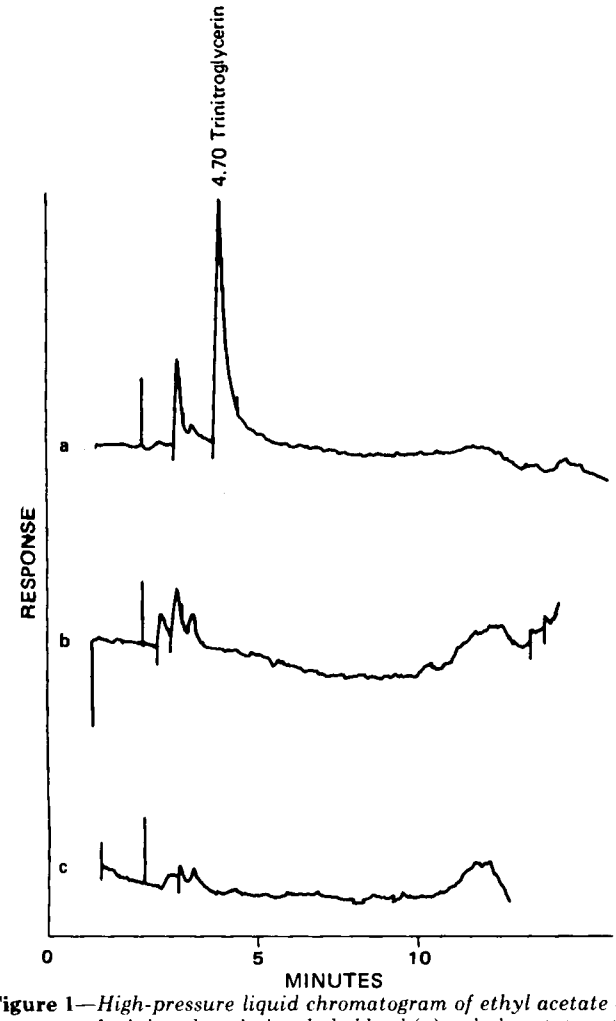

Figure 1—*High-pressure liquid chromatogram of ethyl acetate concentrates of trinitroglycerin in whole blood (a), ethyl acetate extract of whole blood (b), and ethyl acetate concentrate (c).*

chromatograph[5] with gradient elution capability. A 250 × 4.6-mm Lichrosorb Si-60[6] (5-μm) column was used. The solvent system was isooctane–ethyl acetate–acetone, 54:6:40 (v/v) for 10 min isocratically and programmed to 9:1:90 (v/v) over 5 min at a flow rate of 1.4 ml/min. The detection of trinitroglycerin was accomplished with a thermal energy analyzer[7] using the following parameters: furnace temperature, 450°; argon flow rate, 15 ml/min; and oxygen flow rate, 5 ml/min.

Extraction—Whole blood, 2 ml, was combined with 100 μl of 1 *M* $AgNO_3$. The silver nitrate was added to inhibit trinitroglycerin degradation before extraction (3). Extraction was achieved by rapid injection of ethyl acetate (2 ml, then 5 × 1 ml) into the whole blood solution. The organic layers were drawn off after each injection, combined, dried, and filtered through a short column of anhydrous sodium sulfate. The dried extract was concentrated to 500 μl using a gentle nitrogen stream. Then 500 μl of isooctane was added, and the solution was concentrated to 500 μl.

Dosing—A female beagle[8] dog (13.5 kg) was fasted overnight, with free access to water, and dosed by gavage over 10 min with 6.7 g of lactose containing 10% trinitroglycerin (670 mg) incorporated into canned dog food. At various times thereafter, blood (2 ml) was drawn from the cephalic vein into a heparin-containing syringe and then was placed in a vial containing silver nitrate.

Quantitation—Quantitation of the samples was achieved by the internal standard method; the internal standard was *N*-nitrosodipropylamine. A known amount of the internal standard was added to the sample before extraction. Peak areas were determined with the aid of an integrator–recorder[9].

[5] Model 3500B, Spectra-Physics, Santa Clara, Calif.
[6] E. Merck, Darmstadt, West Germany.
[7] Model 502/LC, Analytical Instrument Division, Thermo Electron Corp., Waltham, Mass.
[8] AKC registered, Marshall Research Animals, North Rose, N.Y.
[9] Hewlett-Packard model 3380A.

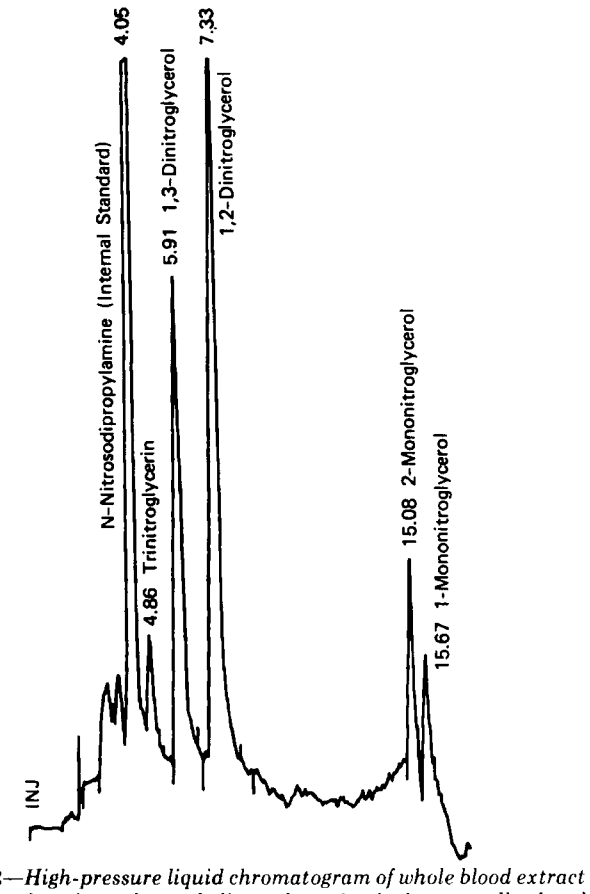

Figure 2—*High-pressure liquid chromatogram of whole blood extract of trinitroglycerin and metabolites after 10 min in an orally dosed dog.*

RESULTS AND DISCUSSION

HPLC was applied previously to the analysis of trinitroglycerin and the primary hydrolysis products, 1,3- and 1,2-dinitroglycerols, in wastewaters from trinitroglycerin production (5). The sensitivity and specificity of this technique were improved greatly when it was coupled to the thermal energy analyzer detector.

Figure 1 shows a normal-phase HPLC profile of an ethyl acetate extract of trinitroglycerin spiked in whole blood, an unspiked ethyl acetate extract of whole blood, and an ethyl acetate solvent control concentrate using the thermal energy analyzer detector. The relatively interference-free baseline of the spiked and unspiked whole blood extracts

Table I—Relative Responses and Detection Limits for Trinitroglycerin and Metabolites

Compound	Response Ratio, DPN[a]/compound	Lower Limit of Detection[b], ng
Trinitroglycerin	0.89	0.5
1,3-Dinitroglycerol	0.90	1.0
1,2-Dinitroglycerol	1.4	1.0
2-Mononitroglycerol	2.1	3.0
1-Mononitroglycerol	2.6	3.0

[a] *N*-Nitrosodipropylamine. [b] Per 100-μl injection.

Table II—Precision of the HPLC–Thermal Energy Analyzer Method for Trinitroglycerin [a]

Spiked	Observed (Mean ± *SD*)	Range[b]
13.2	12.5 ± 1.5	10.5–14.6
37.6	34.7 ± 2.0	32.2–37.0
75.2	73.1 ± 6.7	65.1–82.1

[a] Nanograms per milliliter of whole blood. [b] $n = 5$.

Table III—Quantitative Distribution of Trinitroglycerin and Metabolites (Micrograms per Milliliter) in Dog Blood after Oral Administration of Trinitroglycerin

Compound	Minutes										
	10	20	30	60	90	120	150	180	240	300	360
Trinitroglycerin	0.019	—	—	—	—	—	—	—	—	—	—
1,3-Dinitroglycerol	0.081	0.107	0.100	0.161	0.285	0.723	0.458	1.50	0.545	0.628	0.192
1,2-Dinitroglycerol	0.278	0.308	0.293	0.425	0.775	1.73	0.915	3.89	1.20	1.13	0.315
1-Mononitroglycerol	0.085	0.094	0.131	0.226	0.308	0.749	0.566	0.758	1.17	2.25	0.707
2-Mononitroglycerol	0.058	0.061	0.099	0.225	0.310	0.748	0.676	0.955	1.42	3.37	0.907

demonstrates the selectivity of the thermal energy analyzer detector for trinitroglycerin in the presence of numerous coextractants. Ethyl acetate was chosen as the extraction solvent because of its ability to extract the more polar mono- and dinitroglyceryl metabolites from whole blood; these metabolites also are responsive to the thermal energy analyzer detector. This selectivity for organonitrates permits the quantitative analysis of the 1,2- and 1,3-dinitroglyceryl and 1- and 2-mononitroglyceryl esters (Fig. 2), which could only be qualitatively estimated by previous GLC methods (2, 3). Linear gradient programming allows for the analysis of trinitroglycerin and its four nitro-containing metabolites in 17 min. This programming also flushes the column to remove nonresponsive polar materials and it prolongs column life.

Internal as well as external standard quantitation methods can be applied to the quantitative analysis of trinitroglycerin using the thermal energy analyzer. With *N*-nitrosodipropylamine as an internal standard, the relative responses of trinitroglycerin and its metabolites to this standard, along with the lower limits of detection for each compound, appear in Table I. For trinitroglycerin, a linear response was obtained over the 1–1000-ng range with a correlation coefficient of 0.99.

Ethyl acetate proved to be an efficient extraction solvent for trinitroglycerin and its metabolites in whole blood. Since ethyl acetate readily emulsifies with whole blood upon shaking, rapid injection of the ethyl acetate into the blood from a syringe and removal of the separated phases by syringe provided adequate extraction efficiency with little emulsion problem. Due to the partitioning of this solvent in whole blood, repeated injections were performed for quantitative removal. The precision of the HPLC–thermal energy analyzer method is shown in Table II, which gives recovery values for spiked blood samples.

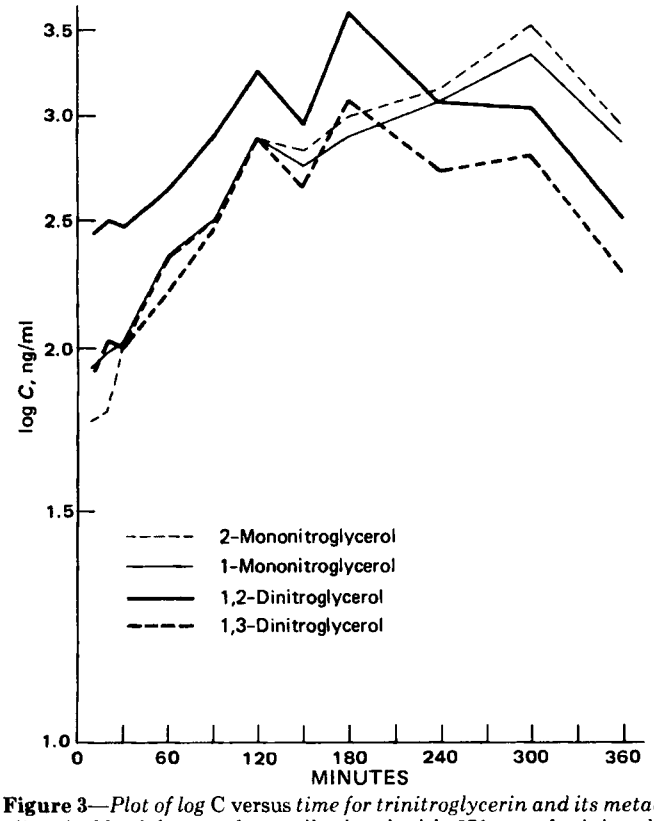

Figure 3—*Plot of log* C versus *time for trinitroglycerin and its metabolites in blood from a dog orally dosed with 670 mg of trinitroglycerin.*

The sensitivity of this method for whole blood was 0.5 ng (25% scale deflection) with the thermal energy analyzer detector at an attenuation of 8. The sensitivity of previously reported GLC methods using electron-capture detection was 0.5–0.1 ng in serum only after extensive cleanup and sample preparation (2, 3). The present method has the advantage of minimal sample preparation and is useful in situations where large samples of serum are not readily available (such as rat and mouse studies); it should be applicable to the study of therapeutic doses of trinitroglycerin in humans.

To test the applicability of the method, a beagle dog was dosed orally (force fed) with trinitroglycerin (49.6 mg/kg). Blood samples were removed at various times and analyzed over 6 hr. The quantitative distribution of trinitroglycerin and its metabolites appears in Table III. As reported previously (3, 6), trinitroglycerin is metabolized rapidly; no trinitroglycerin (<0.5 ng/ml) was detected 20 min after administration. However, the 1,2- and 1,3-dinitroglyceryl and the 1- and 2-mononitroglyceryl metabolites increased to high levels in a parallel fashion and started to decline 5 hr after administration. This finding is consistent with results reported by Hodgson and Lee (7), who found maximum carbon-14 activity in blood 4 hr after oral administration of [^{14}C]trinitroglycerin to rats. A plot of log *C versus* time appears in Fig. 3.

The relative distribution of metabolites in the blood observed in this study paralleled that found by DiCarlo *et al.* (8) in the urine of rats orally dosed with [^{14}C]trinitroglycerin, indicating similar disposition routes of trinitroglycerin for the two species. In both cases, the deesterification appeared to be stepwise.

The data show that there was a slight preference to deesterify at the primary carbon atom. In the early stages of metabolism, the 1,2-dinitroglycerol concentration was three times that of the 1,3-dinitroglycerol isomer. This ratio fell to <2.0 (the expected value if deesterification occurred equally at primary and secondary carbons) at 6 hr. At the same time, the ratio of 2-mononitroglycerol to 1-mononitroglycerol increased from an initial value of 0.68 to 1.5 over 5 hr. Since the source of 2-mononitroglycerol is 1,2-dinitroglycerol (assuming a stepwise process) and the source of 1-mononitroglycerol is both the 1,2- and 1,3-dinitroglycerols, the ratio increase of 2-mononitroglycerol to 1-mononitroglycerol indicates that the 2-position is less reactive to deesterification than is the 1-position.

The present study demonstrates the utility of the thermal energy analyzer detector in the analysis of organonitrates in blood. The application of this method to tissues and other complex matrixes should be useful in pharmacological studies.

REFERENCES

(1) M. T. Rossell and M. G. Bogaert, *J. Chromatogr.*, **64**, 364 (1972).

(2) M. T. Rossell and M. G. Bogaert, *J. Pharm. Sci.*, **62**, 754 (1973).

(3) P. S. K. Yap, E. F. McNiff, and H. Fung, *ibid.*, **67**, 582 (1978).

(4) T. S. Fan, R. Ross, D. H. Fine, L. H. Keith, and A. W. Garrison, *Environ. Sci. Technol.*, **12**, 692 (1978).

(5) C. D. Chandler, G. R. Gibson, and W. T. Bolleter, *J. Chromatogr.*, **100**, 185 (1974).

(6) F. J. DiCarlo, *Drug Metab. Rev.*, **4**, 1 (1975).

(7) J. R. Hodgson and C. C. Lee, *Toxicol. Appl. Pharmacol.*, **34**, 449 (1975).

(8) F. J. DiCarlo, M. C. Crew, L. J. Haynes, M. D. Melgar, and R. L. Gala, *Biochem. Pharmacol.*, **17**, 2179 (1968).

Use of Mannitol to Obviate Propranolol-Induced Myocardial Depression in Ischemic Canine Heart

GEORGE KYRIAKIDIS and MICHAEL BARLETTA ˣ

Received December 18, 1978, from the *Department of Pharmaceutical Sciences, College of Pharmacy and Allied Health Professions, St. John's University, Jamaica, NY 11439.* Accepted for publication November 16, 1979.

Abstract □ To obviate the myocardial depressant action of propranolol, the use of this drug in combination with a positive inotropic agent, mannitol, was studied in the ischemic heart of the dog. Mannitol (25%) administered prior to propranolol augmented myocardial contractility, as shown by an upward shift of the relationship between the pressure change with time and the mean left atrial pressure. Subsequent administration of propranolol did not offset the positive inotropic response to mannitol whereas it markedly reduced the heart rate from a control ischemic value of 127.8 ± 3.4 to 109 ± 4.0 beats/min. The myocardial oxygen requirement, as determined by the tension–time index per minute, decreased 26.3 ± 1.2% below the control ischemic value. These findings suggest that hypertonic mannitol augments contractility in the ischemic failing heart while sustaining the desirable negative chronotropic action of propranolol. This procedure may potentiate the beneficial effects of propranolol on the myocardial oxygen balance and serve as an effective therapeutic modality in the control of acute irreversible ischemia.

Keyphrases □ Propranolol—β-adrenergic blocking activity, effect on myocardial contractility, oxygen requirement, and heart rate, combined action of propranolol and hypertonic mannitol, hemodynamic changes in dogs □ β-Adrenergic blocking activity—effects of propranolol on ischemic failing heart, effects of hypertonic mannitol, dogs □ Myocardial depressants—propranolol, effects of hypertonic mannitol, β-adrenergic blocking activity, dogs

Propranolol, a β-adrenergic blocking agent, was introduced for clinical use in 1968. The value of this drug in the control of reversible ischemia (angina) has been established and reviewed extensively (1). Reversible myocardial ischemia suggests that there is a temporary imbalance between the myocardial oxygen supply and demand and the inability of the coronary vessels to provide adequate oxygenated blood. If the oxygen supply cannot be improved, the only way to establish the myocardial oxygen balance is to reduce the oxygen demands of the heart. Propranolol achieves this goal by reducing the heart rate and cardiac contractility.

The role of β-adrenergic blockade in the treatment of irreversible myocardial ischemia (acute myocardial infarction) has been controversial. β-Adrenergic blockade has been demonstrated to reduce the area of myocardial ischemia in the dog heart following experimental occlusion of the anterior descending coronary artery (2, 3). Studies in humans also have provided evidence that propranolol may reduce the area of ischemia, as evidenced by a reversal of the S-T segment elevation during acute myocardial infarction (4). Similar results were obtained using the cardioselective β-blocking drug practolol (5).

Nevertheless, most reports have implied that β-adrenergic blockade is contraindicated in acute myocardial infarction because it decreases myocardial contractility and may aggravate or precipitate heart failure (6–8). Accordingly, the present study was undertaken to determine whether administration of a nonadrenergic positive inotropic agent, such as hypertonic mannitol (9–11), in conjunction with propranolol may prevent myocardial depression. A second objective was to evaluate the combined effects of mannitol and propranolol in myocardial oxygen requirements during generalized left ventricular ischemia in the intact canine heart. To date, the combined administration of hypertonic mannitol to obviate propranolol-induced myocardial depression in the intact dog has not been investigated. The results of these experiments could have important therapeutic implications.

EXPERIMENTAL

Healthy male and female mongrel dogs, 16–21 kg, were anesthetized by intravenous administration of chloralose (60 mg/kg). The trachea was intubated, and ventilation was instituted with a respiratory pump. The heart was exposed through a left thoracotomy at the fifth intercostal space by pericardiotomy, and the left main coronary artery was dissected free from the adjacent connective tissue.

Left ventricular pressure was recorded with a transducer attached to a polyethylene catheter, which was introduced into the left ventricle through the apex. Mean systemic arterial and left atrial pressures were measured through polyethylene cannulas inserted *via* the carotid artery and left atrial appendage, respectively, and connected to transducers. The maximal rate of left ventricular pressure development was obtained with an R–C differentiator, the amplitude of which was a linear function of 70 Hz. All variables were recorded on a polygraph.

After all parameters had stabilized following the surgical procedures, the mean left atrial and mean systemic pressures, changes in the left ventricular pressure, and heart rates were obtained. Control coronary occlusions were performed to determine the effects of ischemia alone. Generalized left ventricular ischemia was produced by gradual closure of a coarse cotton snare surrounding the left main coronary artery. The magnitude of ischemia was monitored by assessing the left ventricular myocardial contractility, which was evaluated by relating the change in the left ventricular pressure to the mean left atrial pressure. The latter parameter is an approximation of the left ventricular end diastolic pressure (12), and it was selected to avoid the artifacts generated by undamped catheters. Alterations in contractility produced by various interventions were used to assess their effects on the severity of myocardial ischemia. It was assumed that changes in the myocardial oxygen requirements mediated by the infused drugs affected the magnitude of ischemia and, thereby, myocardial contractility.

Alterations in myocardial oxygen requirements were evaluated using the tension–time index, which was obtained by multiplying the mean aortic systolic pressure by the duration of the systole (13). Mean systolic arterial pressure was estimated by:

$$\text{mean systolic pressure} = a - (a - b/3) \qquad \text{(Eq. 1)}$$

where a represents the peak systolic pressure and b is the aortic valve closure pressure (14).

Twelve dogs were divided into two equal study groups. In the first group, the effects of propranolol (0.5 mg/kg iv) in the ischemic failing heart were studied. After the onset of ischemia in the second group, the dogs were treated with hypertonic mannitol (25 g/100 ml) infused through the cannulated femoral vein at 3.82 ml/min by an infusion pump, and the responses to mannitol alone were recorded. Following recovery, the effects of mannitol plus propranolol (0.5 mg/kg) were assessed.

Serum osmolality was checked before, during, and after mannitol infusion and was consistent with the expected level (17 mOsm above the control value). Each experimental animal was used as its own control before any intervention was made in each experiment. The control state was considered to be the ischemic stage before treatment. The magnitude of ischemia was monitored by the decline in myocardial contractility. The standard t test, as described by Snedecor and Cochran (15), was used for group comparisons; the t test for paired comparison was used as presented

0022-3549/80/0400-0447$01.00/0
© 1980, American Pharmaceutical Association

Table I—Effect of Partial Occlusion of the Main Left Coronary Artery on Left Ventricular Hemodynamics [a]

Parameter	Control	Ischemia	Change from Control, %
Heart rate, beats/min	106.5 ± 2.5	125.3 ± 3.0	16.8 ± 1.1
Mean systemic arterial pressure, mm Hg	105.6 ± 2.0	98.4 ± 2.3	6.8 ± 1.1
Mean systolic arterial pressure, mm Hg	117.8 ± 2.1	108.8 ± 2.0	−7.6 ± 0.7
Mean left atrial pressure, mm Hg	4.8 ± 0.7	10.7 ± 1.5	122.8 ± 3.3
Ventricular ejection time, msec	197.1 ± 3.4	221.7 ± 3.2	12.6 ± 1.5
Maximal rate of left ventricular pressure development (*dp/dt*), mm Hg/sec	2633 ± 108.3	2298 ± 109.4	14.5 ± 1.9

[a] All values are expressed as the mean ± *SEM* of 12 experiments, and $p < 0.001$ for each parameter.

Table II—Effect of Generalized Left Ventricular Ischemia on Tension-Time Index [a]

Parameter	Control	Ischemia	Change from Control, %	*p*
Tension-time index per beat, mm Hg sec	23.2 ± 0.6	24.2 ± 0.6	4.5 ± 1.1	<0.01
Tension-time index per min, mm Hg sec/min	2502 ± 114	3057 ± 117	22.7 ± 1.9	<0.001

[a] Each value is expressed as the mean ± *SEM* of 12 experiments.

by Hill (16). All results are expressed with their standard error of the mean.

RESULTS

Ischemia—After partial occlusion of the left main coronary artery, myocardial contractility showed a rapid and pronounced decline (Fig. 1). As shown in Fig. 2, concurrent with the rise in the mean left atrial pressure (122.8 ± 3.3%), the left ventricular pressure fell (14.5 ± 1.9%); the heart rate increased from 106.5 ± 2.5 to 125 ± 3 beats/min whereas the mean systemic arterial pressure exhibited a moderate fall (6.8 ± 1.1%). The data are summarized in Table I. Table II shows the effect of generalized left ventricular ischemia on the tension-time index.

Propranolol—The hemodynamic changes following propranolol administration during generalized left ventricular ischemia are illustrated in Fig. 3. The mean left atrial pressure rose from an average control level of 8.9 ± 1.6 to 14.7 ± 2.3 mm Hg whereas the change in the left ventricular pressure decreased by 21 ± 2.5%, indicating a decline in cardiac contractility (Table III). Figure 4 depicts the myocardial depressant effect of propranolol in the ischemic failing heart. Although the heart rate fell substantially (17.9 ± 1.4%), the myocardial oxygen requirements did not decrease significantly, as evidenced by the tension-time index per minute. Propranolol evidently raised the tension-time index per beat by lengthening the systolic ejection time, as a result of which the tension-time index per minute failed to decrease (Fig. 5).

Mannitol—As shown in Fig. 4, infusion of hypertonic mannitol enhanced myocardial contractility in the ischemic heart; the mean left atrial pressure fell from the control ischemia value of 15.3 ± 2.1 to 6.7 ± 1 mm Hg whereas the change in the left ventricular pressure increased by 18.1 ± 1% (Table III). No significant changes in the heart rate and the mean systemic arterial pressure were noted. Although the heart rate remained essentially unaltered, the tension-time index per minute fell substantially (Fig. 5). By decreasing the systolic ejection time (12 ± 0.4%) (Table III), mannitol lowered the tension-time index per beat, thereby reducing the tension-time index per minute (Table IV).

Mannitol plus Propranolol—Administration of propranolol subsequent to mannitol infusion produced a progressive rise in the change in the left ventricular pressure (18.7 ± 0.7% above the control ischemia level) accompanied by a fall in the mean left atrial pressure (41 ± 4.5% below the control ischemia value), indicating a rise in myocardial contractility (Fig. 4). The heart rate fell from an average control ischemia value of 127.8 ± 3.4 to 109 ± 4 beats/min whereas the mean systemic arterial pressure remained essentially unaltered (Table III). The results clearly show that hypertonic mannitol may prevent the myocardial depressant action of propranolol (Fig. 4) but not its negative chronotropic effect (Fig. 3).

Direct comparison of the effects of mannitol and of mannitol plus propranolol in myocardial oxygen requirements were made in the same animals (Fig. 5). Propranolol administration subsequent to mannitol infusion greatly decreased the tension-time index per minute (26.7 ± 1.2% below the control ischemic value); this decrease was much greater than that achieved when mannitol was administered alone (9.7 ± 1.2%).

DISCUSSION

The present investigation demonstrates the ability of hypertonic mannitol to prevent the myocardial depressant action of propranolol in the ischemic failing canine heart without increasing the myocardial oxygen requirements. These results are in accord with reported observations (9) that infusion of hypertonic mannitol markedly improved ventricular function in the failing heart–lung preparation following occlusion of the left anterior descending coronary artery. The fact that the increased myocardial contractility was not accompanied by ECG S-T segment elevation suggested that the positive inotropic effects of mannitol are not oxygen wasting (9).

The effect of hypertonic mannitol on myocardial contractility is indicated by the rate of rise of the left ventricular pressure, an index of vigor of the left ventricular contraction. The change in the left ventricular pressure is determined mainly by the ventricular end diastolic volume and myocardial contractility (17). The decrease in the left ventricular pressure changes and the rise of the mean left atrial pressure manifested after the induction of ischemia indicate a depression of cardiac contractility (Fig. 1). As shown in Fig. 3, the rise in the left ventricular pressure changes that occurred concurrently with a fall in the mean left atrial pressure after mannitol infusion clearly shows the cardiotonic effects of mannitol in the ischemic failing heart.

The possible mechanisms by which hypertonic mannitol exerts its positive inotropic effects in the ischemic tissue are not known at present. It has been postulated that its osmotic action may decrease cellular edema

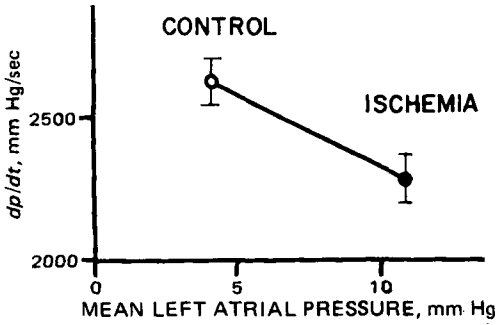

Figure 1—*Effect of partial occlusion of the main left coronary artery on myocardial contractility. The* x *axis shows the mean left atrial pressure, and the* y *axis shows the maximal rate of left ventricular pressure development* (dp/dt).

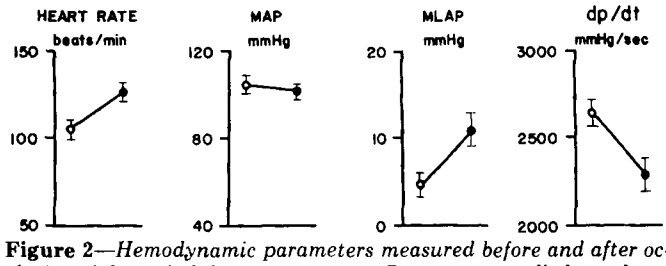

Figure 2—*Hemodynamic parameters measured before and after occlusion of the main left coronary artery. Parameters studied were heart rate, mean systemic arterial pressure (MAP), mean left atrial pressure (MLAP), and maximal rate of left ventricular pressure development* (dp/dt). *Key:* ○, *control; and* ●, *ischemia.*

Table III—Hemodynamic Changes [a] after Administration of Propranolol, Mannitol, and Propranolol plus Mannitol during Generalized Left Ventricular Ischemia

Condition	Heart Rate, beats/min	Mean Arterial Pressure, mm Hg	Mean Systolic Pressure, mm Hg	Mean Left Atrial Pressure, mm Hg	Ventricular Ejection Time, msec	*dp/dt*, mm Hg/sec
Control ischemia	122.7 ± 4.5	95.8 ± 3.0	106.8 ± 3.0	8.9 ± 1.6	220.8 ± 2.4	2086 ± 98.0
Ischemia plus propranolol	100.5 ± 3.1	92.3 ± 2.8	102.8 ± 2.7	14.7 ● 2.3	264.2 ± 3.0	1639 ± 60.2
Percent change from control	17.9 ± 1.4	3.6 ± 0.5	3.5 ± 0.6	74.3 ± 7.2	19.2 ± 1.8	21.0 ± 2.5
p	<0.005	<0.5	<0.2	<0.025	<0.001	<0.005
Control ischemia	128.0 ± 3.6	101.0 ± 2.9	107.2 ± 3.2	15.3 ± 2.1	222.0 ± 5.9	2510 ± 144.0
Ischemia plus mannitol	131.3 ± 4.5	99.8 ± 2.7	108.3 ± 3.0	6.7 ± 1.0	196.7 ± 5.9	2965 ± 177.0
Percent change from control	2.5 ± 1.3	1.1 ± 0.4	0.6 ± 0.3	46.0 ± 2.0	12.0 ± 0.4	18.1 ± 1.0
p	<0.5	<0.5	<0.5	<0.01	<0.001	<0.025
Postcontrol ischemia	127.7 ± 2.9	103.5 ± 3.3	111.0 ± 3.0	12.3 ± 1.7	227.0 ± 5.0	2554 ± 166
Control ischemia	127.8 ± 3.4	99.2 ± 2.5	109.0 ± 2.6	11.9 ± 1.9	220.0 ± 6.2	2534 ± 142
Ischemia plus propranolol plus mannitol	109.0 ± 4.0	97.0 ± 2.2	106.7 ± 2.2	6.7 ± 1.0	193.3 ± 4.9	3009 ± 170
Percent change from control	14.8 ± 1.4	2.1 ± 0.8	2.4 ± 0.6	41.0 ± 4.5	12.1 ± 0.5	187 ± 0.7
p	<0.005	<0.2	<0.2	<0.01	<0.005	<0.025
Postcontrol ischemia	129.3 ± 4.1	101.0 ± 2.2	109.0 ± 2.3	11.1 ± 1.9	222.0 ± 5.1	2515 ± 142

[a] Each value is expressed as the mean ± *SEM* of six experiments. [b] *dp/dt* = maximal rate of left ventricular pressure development.

and thereby enhance blood flow, which, in turn, may improve organ function (18). Ames *et al.* (19) stressed that edematous cells may impede blood flow within an organ and thus may impair nutritional circulation in the tissues. Summers and Jamison (20) used the silicone rubber technique to visualize the patency of the renal vasculature during ischemia to demonstrate, in the rat kidney, that cellular edema during transient ischemia may obstruct small vessels and thus intensify tissue damage. Apparently, the lumen of minute vessels, although narrowed by compression from the surrounding edematous cells, permitted the passage of the silicone rubber particles but not of the erythrocytes. Intravascular injection of hypertonic mannitol reestablished a normal vascular pattern, reduced tissue injury, and improved renal function (20). Osmotic shrinkage of the swollen cells presumably reduced the extravascular pressure exerted on the vascular bed, thus enhancing the blood flow.

Although hypertonic mannitol augmented collateral as well as total coronary blood flow in experimentally induced ischemia (9), the increase observed in myocardial contractility may not be totally dependent on changes in myocardial perfusion. It was demonstrated recently that hypertonic mannitol also exerts a positive inotropic effect in the isolated cat papillary muscle (11). The developed tension and the rate of tension rise were significantly greater when the papillary muscles were treated with mannitol regardless of whether mannitol was introduced before or later in the hypoxic period (11).

It has been postulated that a decrease in the intracellular volume produced by the osmotic action of hypertonic mannitol may increase the degree of activation of the myocardial contractile elements. This increased contractile activity may be a result of an increased calcium con-

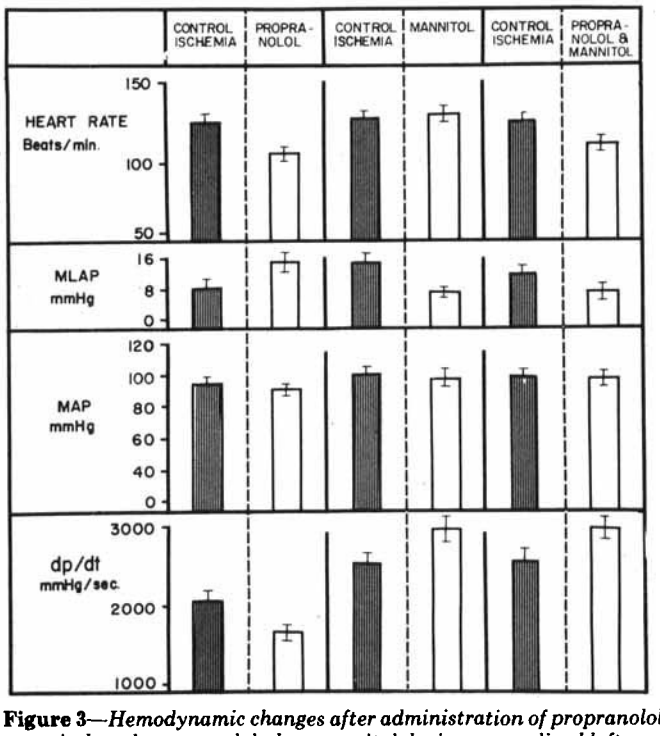

Figure 3—*Hemodynamic changes after administration of propranolol, mannitol, and propranolol plus mannitol during generalized left ventricular ischemia. Parameters measured are indicated on the y axis: heart rate, mean systemic arterial pressure (MAP), mean left atrial pressure (MLAP), and maximal rate of left ventricular pressure development* (dp/dt).

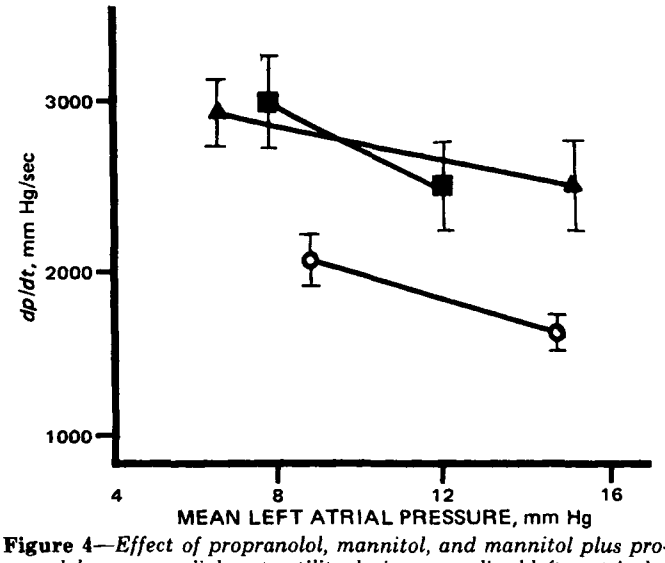

Figure 4—*Effect of propranolol, mannitol, and mannitol plus propranolol on myocardial contractility during generalized left ventricular ischemia. The x axis shows the mean left atrial pressure, and the y axis shows the maximal rate of left ventricular pressure development* (dp/dt). *Key:* ○, *ischemia plus propranolol* ($p < 0.005$); ▲, *ischemia plus mannitol* ($p < 0.025$); *and* ■, *ischemia plus propranolol plus mannitol* ($p < 0.025$).

Table IV—Effect of Propranolol, Mannitol, and Propranolol plus Mannitol during Generalized Left Ventricular Ischemia on Tension–Time Index [a]

Parameter	Control Ischemia	Ischemia plus Drug	Change, %	Level of Significance [b]	Postcontrol Ischemia
		Propranolol			
Tension–time index per beat, mm Hg sec	23.8 ± 0.5	27.2 ± 0.8	14.2 ± 2.1	**	—
Tension–time index per minute mm Hg sec/min	2953 ± 145	2738 ± 161	−7.3 ± 1.3	NS	—
		Mannitol			
Tension–time index per beat, mm Hg sec	24.7 ± 0.9	21.7 ± 0.9	−11.9 ± 0.6	**	24.6 ± 1.0
Tension–time index per minute, mm Hg sec/min	3163 ± 171	2862 ± 182	−9.7 ± 1.2	*	3192 ± 191
		Propranolol plus Mannitol			
Tension–time index per beat, mm Hg sec	24.1 ± 0.9	20.6 ± 0.7	−13.9 ± 1.1	**	23.9 ± 0.8
Tension–time index per minute mm Hg sec/min	3075 ± 177	2258 ± 146	−26.7 ± 1.2	**	3077 ± 173

[a] Each value is expressed as the mean ± *SEM* of six experiments. [b] *, $p < 0.05$; **, $p < 0.001$; and NS, not significant ($p > 0.05$).

centration in a superficial area of the muscle fiber (21). In contrast, Apstein *et al.* (22) were unable to observe any increase in contractility in the isolated hypoxic tissue by mannitol. However, this discrepancy may be explained by the fact that Apstein *et al.* used smaller concentrations of mannitol than those used by the other investigator.

The present study shows that hypertonic mannitol enhances myocardial contractility in the ischemic failing heart without raising myocardial oxygen demands. Although the mean arterial oxygen levels were not measured directly in this investigation, the changes in the tension–time index reflected alterations in the myocardial oxygen requirements (13). These observations were consistent with the findings of Sarnoff *et al.* (23), who showed that norepinephrine may exert a positive inotropic effect in the ischemic failing heart without augmenting mean arterial oxygen levels; the inotropic action of norepinephrine was associated with a marked decrease in the left ventricular end diastolic volume (23). This effect, according to the Laplace principle, tends to lower myocardial tension and offsets the rise in the mean arterial oxygen levels produced by increased contractility. A similar effect also was demonstrated in the pharmacologically depressed dog after ouabain administration (24).

Although the decrease in ventricular tension may prevent a rise in the mean arterial oxygen levels associated with augmentation of myocardial contractility, the present results suggest that the systolic ejection time also may be an important factor. Figure 4 and Tables III and IV show that mannitol augmented myocardial contractility whereas the heart rate and the mean systemic arterial pressure were not altered significantly. As contractility rose and the systolic ejection time decreased, the tension–time index per beat fell. The fact that the tension–time index per minute was lowered significantly, although neither the heart rate nor the mean systolic pressure was decreased, indicates that augmentation of myocardial contractility may diminish myocardial oxygen requirements in the failing heart by decreasing the systolic ejection time.

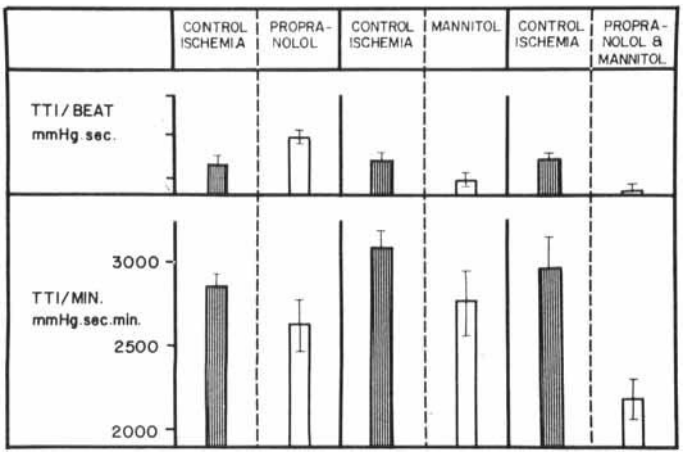

Figure 5—*Effect of propranolol, mannitol, and propranolol plus mannitol on the tension–time index during generalized ventricular ischemia. The* y *axis shows the tension–time index per beat (TTI/beat); the* x *axis shows the tension–time index per minute (TTI/min).*

In contrast, propranolol, through reduced contractility (Fig. 4) and a lowered heart rate (Table III), produced no significant decrease in myocardial oxygen requirements. Figure 5 demonstrates the effects of propranolol on the tension–time index; the tension–time index per minute was not altered significantly whereas the tension–time index per beat exhibited a pronounced increase. The results show that propranolol raised the myocardial oxygen demands by increasing the systolic ejection time (Table III), thereby offsetting the oxygen-sparing effect of its negative chronotropic action. This observation suggests that the principal benefit of β-adrenergic blocking drugs such as propranolol lies in their ability to lower the heart rate rather than to reduce myocardial contractility. Consistent with this view are the findings of Balcon (25), who showed that propranolol could not reduce the pain threshold in patients in whom angina was produced by electrical pacing of the heart. Evidently, the failure of the drug to exert its negative chronotropic activity prevented its beneficial effect. The most pronounced decreases in myocardial oxygen requirements were noted in this study when the myocardial depressant action of propranolol was prevented by administration of hypertonic mannitol (Fig. 5).

Furthermore, when the mean systolic pressure was multiplied by the heart rate, there was a significant drop in the tension–time index per minute after the combined administration of mannitol with propranolol (Fig. 5). The fall in this product was much greater than that achieved by mannitol or propranolol alone. This result was due largely to the fact that propranolol lowered the heart rate whereas the systolic ejection times and the mean systolic pressures, as compared to mannitol, were not very different.

The findings of the present investigation suggest that augmentation of contractility in the ischemic failing heart by a positive nonadrenergic agent may potentiate the beneficial effects of propranolol on the myocardial oxygen balance and prevent cardiac depression. Mannitol is an inotropic agent with highly desirable properties since it does not produce any unwanted hemodynamic or ECG changes. Finally, the ability of mannitol to augment myocardial perfusion (9) may be of great physiological importance. Although further studies are required, augmentation of myocardial contractility and the reduction in heart rate brought about by the combined action of mannitol and propranolol may prove to be an effective therapeutic modality in the control of acute irreversible ischemia.

REFERENCES

(1) T. C. Dollery, W. J. Paterson, and E. M. Connolly, *Clin. Pharmacol. Ther.*, **10**, 765 (1969).

(2) R. P. Maroko, K. J. Kjekshus, E. B. Sobel, T. Watanabe, W. J. Covell, J. Ross, and E. Braunwald, *Circulation*, **43**, 67 (1971).

(3) P. Libby, R. P. Maroko, W. J. Covell, I. C. Malloch, J. Ross, and E. Braunwald, *Clin. Res.*, **20**, 207 (1972).

(4) R. P. Maroko, P. Libby, W. J. Covell, E. B. Sobell, J. Ross, and E. Braunwald, *Am. J. Cardiol.*, **29**, 223 (1972).

(5) D. Reid, J. L. Pelides, M. Thomas, and P. J. Shillingford, *Br. Heart J.*, **33**, 609 (1971).

(6) M. Stannard, G. Sloman, and L. Sangster, *Med. J. Aust.*, **1**, 333 (1968).

(7) H. R. Helfant, V. M. Herman, and R. Gorlin, *Circulation*, **43**, 641 (1971).
(8) R. S. Ross, "Myocardial Ischemia," Excerpta Medica, Amsterdam, The Netherlands, 1971, p. 98.
(9) J. T. Willerson, W. J. Powell, T. E. Guiney, J. J. Stark, C. A. Sanders, and A. Leaf, *J. Clin. Invest.*, **51**, 2989 (1972).
(10) J. B. Caulfield, J. T. Willerson, M. L. Weisfeldt, and W. J. Powell, "Myocardial Metabolism," University Park Press, Baltimore, Md., 1972, p. 753.
(11) J. T. Willerson, M. L. Weisfeldt, C. A. Sanders, and W. J. Powell, *Cardiovas. Res.*, **8**, 8 (1974).
(12) E. Braunwald and C. J. Frahm, *Circulation*, **24**, 633 (1961).
(13) J. S. Arnoff, E. Braunwald, H. G. Welch, R. B. Case, N. W. Stainsby, and R. Macruz, *Am. J. Physiol.*, **192**, 148 (1958).
(14) A. A. Walker, J. S. Janicki, K. T. Weber, R. O. Russell, and C. E. Rackley, *Cardiovasc. Res.*, **7**, 567 (1973).
(15) G. W. Snedecor and W. G. Cochran, "Statistical Methods," Iowa State University Press, Ames, Iowa, 1967, p. 59.
(16) B. A. Hill, "Principles of Medical Statistics," Oxford University Press, New York, N.Y., 1961, p. 149.
(17) J. T. Reeves, L. L. Hefner, B. W. Jones, C. Coghlan, G. Prieto, and J. Carrol, *Am. Heart J.*, **60**, 745 (1960).
(18) J. Flores, D. R. Dibona, C. H. Beck, and A. Leaf, *J. Clin. Invest.*, **51**, 118 (1972).
(19) A. Ames, R. L. Wright, M. Kowada, J. M. Thurston, and G. Majno, *Am. J. Pathol.*, **52**, 437 (1968).
(20) K. W. Summers and R. L. Jamison, *Lab. Invest.*, **25**, 635 (1971).
(21) J. Koch-Weser, *Am. J. Physiol.*, **204**, 957 (1963).
(22) C. S. Apstein, O. L. Bing, and H. J. Levine, *J. Mol. Cell. Cardiol.*, **8**, 627 (1976).
(23) J. S. Sarnoff, J. P. Gilmore, and A. G. Wallace, "Nervous Control of the Heart," Williams & Wilkins, Baltimore, Md., 1965, pp. 54–129.
(24) T. Watanabe, J. W. Covell, P. R. Maroko, E. Braunwald, and J. Ross, *Am. J. Cardiol.*, **30**, 371 (1972).
(25) R. Balcon, *Postgrad. Med. J., Suppl.*, **47**, 53 (1971).

Synthesis and Cyclization of Dialkylmalonuric Esters

JAMES A. BERES ˣ, MAX G. VARNER, and CARMEN BRIA

Received September 10, 1979, from the *Department of Chemistry, Shippensburg State College, Shippensburg, PA 17257.* Accepted for publication November 26, 1979.

Abstract □ A novel method for the synthesis of methyl dialkylmalonuric esters was developed using the base-catalyzed ring opening of an isopropylidene malonic ester with urea as the key step. The rates of cyclization of these malonuric esters to the corresponding barbituric acids then were studied at buffer concentrations ranging from 0.01 to 1.00 *M*. The reaction was shown to be general base catalyzed, and the reaction rate was found to be subject to a deuterium isotope effect, $k_{H_2O}/k_{D_2O} = 1.3$. The thermodynamic activation parameters also were determined. A three-step mechanism for the conversion of malonuric esters to barbituric acids was proposed; it involved a rapid cyclization step, followed by proton removal by a general base catalyst and a rate-determining collapse of the resulting tetrahedral intermediate aided by a general acid.

Keyphrases □ Dialkylmalonuric esters—synthesis, cyclization to barbituric acids □ Barbituric acids—mechanism for formation by cyclization of malonuric acids □ Activation parameters—cyclization of dialkylmalonuric esters to barbituric acids

Numerous barbituric acids have been synthesized over the past 75 years, but the mechanism of the reaction has not been defined. Barbituric acids usually are prepared by reacting a malonic ester with urea in the presence of a basic catalyst. The mechanism proposed some years ago (1) involved the formation of an intermediate malonuric ester (I), followed by rapid ring closure to the barbituric acid product (Scheme I).

The fact that malonuric esters undergo facile cyclization in basic media was suggested in 1907 (2), and later these esters were shown to cyclize rapidly in weakly basic solution (1). In a continuing effort to elucidate the mechanism of the reaction between malonic esters and urea, the present study focuses on the cyclization step.

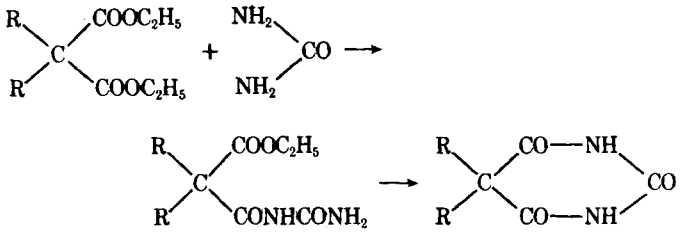

I

Scheme I

BACKGROUND

Although no kinetic studies on the cyclization of malonuric esters have been reported, hydrolysis of barbituric acids in alkaline solution has been investigated. Such hydrolyses produce various products, including the malonuric acid. A complete scheme for the alkaline decomposition of barbiturates was given by Aspelund (3), and a kinetic study on the hydrolysis rate of barbituric acid derivatives was reported by Garrett *et al.* (4). The latter report stated that malonuric acids are capable of hydrolysis to the barbituric acids at pH 7–10, and the enthalpy (ΔH^*) and entropy (ΔS^*) of activation were determined for the hydrolysis of numerous barbituric acids.

One facet of the present investigation involved determination of the mechanism of base catalysis in the cyclization of esters of diethylmalonuric acid. The classical experiment for distinguishing general base catalysis from specific base catalysis involves determining the reaction rate in a series of buffers of constant pH but with varying concentrations of total buffer species at constant ionic strength (5). General base catalysis, which requires catalysis by all bases present, is demonstrated if the reaction rate depends on the total absolute buffer concentration. Specific base catalysis is independent of the absolute buffer concentration.

UV spectrophotometry was employed to monitor the cyclization reaction of the malonuric esters. A pH 10 buffer system was chosen since at that pH the barbituric acid product exists as the monoanionic species (99+%), which absorbs strongly at 240 nm (6), facilitating easy assessment of its formation rate.

This method also was used to measure the reaction rates in deuterium oxide since a comparison of rates in heavy *versus* light water can be valuable in mechanism elucidation. Jencks (7) reported that because of zero-point energy differences and different stretching frequencies, rate constants for OH and OD bond cleavage can be 10-fold larger for hydrogen than for deuterium.

Determination of the thermodynamic activation parameters also was undertaken. The entropy and enthalpy of activation were obtained from plots of $\log k/T$ *versus* $1/T$ (8).

0022-3549/80/0400-0451$01.00/0
© 1980, American Pharmaceutical Association

(7) H. R. Helfant, V. M. Herman, and R. Gorlin, *Circulation*, **43**, 641 (1971).
(8) R. S. Ross, "Myocardial Ischemia," Excerpta Medica, Amsterdam, The Netherlands, 1971, p. 98.
(9) J. T. Willerson, W. J. Powell, T. E. Guiney, J. J. Stark, C. A. Sanders, and A. Leaf, *J. Clin. Invest.*, **51**, 2989 (1972).
(10) J. B. Caulfield, J. T. Willerson, M. L. Weisfeldt, and W. J. Powell, "Myocardial Metabolism," University Park Press, Baltimore, Md., 1972, p. 753.
(11) J. T. Willerson, M. L. Weisfeldt, C. A. Sanders, and W. J. Powell, *Cardiovas. Res.*, **8**, 8 (1974).
(12) E. Braunwald and C. J. Frahm, *Circulation*, **24**, 633 (1961).
(13) J. S. Arnoff, E. Braunwald, H. G. Welch, R. B. Case, N. W. Stainsby, and R. Macruz, *Am. J. Physiol.*, **192**, 148 (1958).
(14) A. A. Walker, J. S. Janicki, K. T. Weber, R. O. Russell, and C. E. Rackley, *Cardiovasc. Res.*, **7**, 567 (1973).
(15) G. W. Snedecor and W. G. Cochran, "Statistical Methods," Iowa State University Press, Ames, Iowa, 1967, p. 59.
(16) B. A. Hill, "Principles of Medical Statistics," Oxford University Press, New York, N.Y., 1961, p. 149.
(17) J. T. Reeves, L. L. Hefner, B. W. Jones, C. Coghlan, G. Prieto, and J. Carrol, *Am. Heart J.*, **60**, 745 (1960).
(18) J. Flores, D. R. Dibona, C. H. Beck, and A. Leaf, *J. Clin. Invest.*, **51**, 118 (1972).
(19) A. Ames, R. L. Wright, M. Kowada, J. M. Thurston, and G. Majno, *Am. J. Pathol.*, **52**, 437 (1968).
(20) K. W. Summers and R. L. Jamison, *Lab. Invest.*, **25**, 635 (1971).
(21) J. Koch-Weser, *Am. J. Physiol.*, **204**, 957 (1963).
(22) C. S. Apstein, O. L. Bing, and H. J. Levine, *J. Mol. Cell. Cardiol.*, **8**, 627 (1976).
(23) J. S. Sarnoff, J. P. Gilmore, and A. G. Wallace, "Nervous Control of the Heart," Williams & Wilkins, Baltimore, Md., 1965, pp. 54–129.
(24) T. Watanabe, J. W. Covell, P. R. Maroko, E. Braunwald, and J. Ross, *Am. J. Cardiol.*, **30**, 371 (1972).
(25) R. Balcon, *Postgrad. Med. J., Suppl.*, **47**, 53 (1971).

Synthesis and Cyclization of Dialkylmalonuric Esters

JAMES A. BERES ˣ, MAX G. VARNER, and CARMEN BRIA

Received September 10, 1979, from the *Department of Chemistry, Shippensburg State College, Shippensburg, PA 17257.* Accepted for publication November 26, 1979.

Abstract □ A novel method for the synthesis of methyl dialkylmalonuric esters was developed using the base-catalyzed ring opening of an isopropylidene malonic ester with urea as the key step. The rates of cyclization of these malonuric esters to the corresponding barbituric acids then were studied at buffer concentrations ranging from 0.01 to 1.00 *M*. The reaction was shown to be general base catalyzed, and the reaction rate was found to be subject to a deuterium isotope effect, $k_{H_2O}/k_{D_2O} = 1.3$. The thermodynamic activation parameters also were determined. A three-step mechanism for the conversion of malonuric esters to barbituric acids was proposed; it involved a rapid cyclization step, followed by proton removal by a general base catalyst and a rate-determining collapse of the resulting tetrahedral intermediate aided by a general acid.

Keyphrases □ Dialkylmalonuric esters—synthesis, cyclization to barbituric acids □ Barbituric acids—mechanism for formation by cyclization of malonuric acids □ Activation parameters—cyclization of dialkylmalonuric esters to barbituric acids

Numerous barbituric acids have been synthesized over the past 75 years, but the mechanism of the reaction has not been defined. Barbituric acids usually are prepared by reacting a malonic ester with urea in the presence of a basic catalyst. The mechanism proposed some years ago (1) involved the formation of an intermediate malonuric ester (I), followed by rapid ring closure to the barbituric acid product (Scheme I).

The fact that malonuric esters undergo facile cyclization in basic media was suggested in 1907 (2), and later these esters were shown to cyclize rapidly in weakly basic solution (1). In a continuing effort to elucidate the mechanism of the reaction between malonic esters and urea, the present study focuses on the cyclization step.

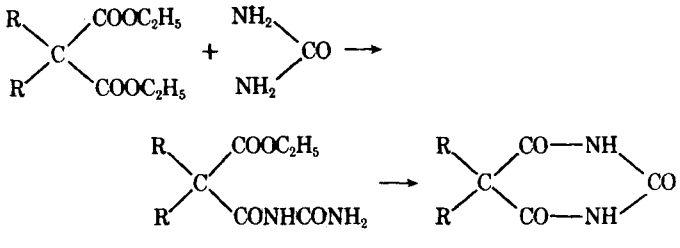

I

Scheme I

BACKGROUND

Although no kinetic studies on the cyclization of malonuric esters have been reported, hydrolysis of barbituric acids in alkaline solution has been investigated. Such hydrolyses produce various products, including the malonuric acid. A complete scheme for the alkaline decomposition of barbiturates was given by Aspelund (3), and a kinetic study on the hydrolysis rate of barbituric acid derivatives was reported by Garrett *et al.* (4). The latter report stated that malonuric acids are capable of hydrolysis to the barbituric acids at pH 7–10, and the enthalpy (ΔH^*) and entropy (ΔS^*) of activation were determined for the hydrolysis of numerous barbituric acids.

One facet of the present investigation involved determination of the mechanism of base catalysis in the cyclization of esters of diethylmalonuric acid. The classical experiment for distinguishing general base catalysis from specific base catalysis involves determining the reaction rate in a series of buffers of constant pH but with varying concentrations of total buffer species at constant ionic strength (5). General base catalysis, which requires catalysis by all bases present, is demonstrated if the reaction rate depends on the total absolute buffer concentration. Specific base catalysis is independent of the absolute buffer concentration.

UV spectrophotometry was employed to monitor the cyclization reaction of the malonuric esters. A pH 10 buffer system was chosen since at that pH the barbituric acid product exists as the monoanionic species (99+%), which absorbs strongly at 240 nm (6), facilitating easy assessment of its formation rate.

This method also was used to measure the reaction rates in deuterium oxide since a comparison of rates in heavy *versus* light water can be valuable in mechanism elucidation. Jencks (7) reported that because of zero-point energy differences and different stretching frequencies, rate constants for OH and OD bond cleavage can be 10-fold larger for hydrogen than for deuterium.

Determination of the thermodynamic activation parameters also was undertaken. The entropy and enthalpy of activation were obtained from plots of $\log k/T$ *versus* $1/T$ (8).

0022-3549/80/0400-0451$01.00/0
© 1980, American Pharmaceutical Association

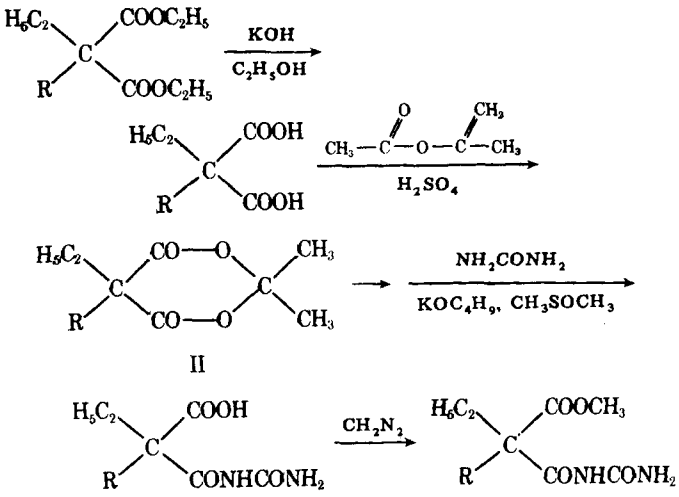

Scheme II—Synthesis of methyl esters of dialkylmalonuric acids

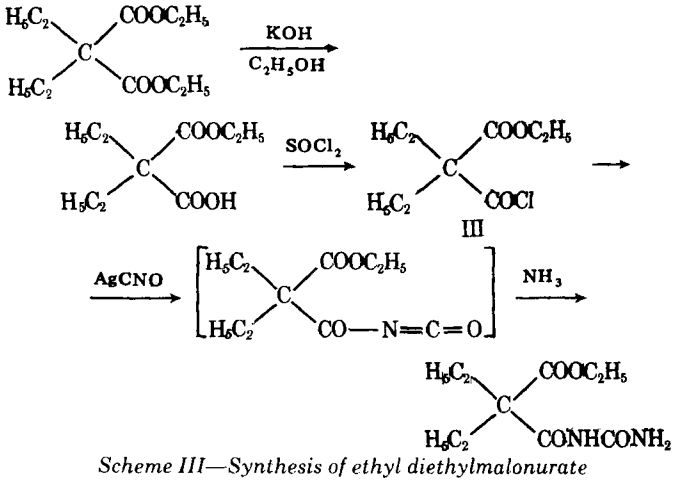

Scheme III—Synthesis of ethyl diethylmalonurate

EXPERIMENTAL

Synthesis of Reactants—The methyl esters of diethylmalonuric acid and ethylisoamylmalonuric acid were prepared by the sequence shown in Scheme II. This reaction represents a novel procedure for the preparation of various methyl dialkylmalonuric esters from the readily available malonic esters. The isopropylidene malonate (II), prepared by a modified method of Davidson and Bernhard (9), serves as a convenient intermediate for the base-catalyzed conversion to the malonuric acid. This reaction presumably occurs *via* a nucleophilic attack of urea on the carbonyl group of II with simultaneous ring opening and elimination of acetone.

The ethyl ester of diethylmalonuric acid was prepared by the sequence shown in Scheme III. Preparation of the intermediate diethylmalonyl chloride monoethyl ester (III) was accomplished using standard procedures, and its conversion into the malonuric ester was reported previously (1). In this instance, the acyl isocyanate was not isolated but was treated immediately upon generation with aqueous ammonia to give a mixture of the desired ethyl ester of diethylmalonuric acid and a substantial amount of the ethyl ester of diethylmalonamic acid, which was separated by fractional crystallization from ligroin.

Reagents—Ethanolamine was redistilled. Concentrated hydrochloric acid was refluxed until a constant vapor temperature of 107° was obtained, and then it was standardized as 6.36 *M* against tris(hydroxymethyl)aminomethane. Reagent grade potassium chloride, sodium bicarbonate, and sodium carbonate were used without further purification. The deuterium oxide, 99.8% pure, was used as received. Sodium deuteriocarbonate was prepared by dissolving 0.5 g of sodium bicarbonate in 10 ml of deuterium oxide and evaporating the solution to dryness (10).

Syntheses[1]—*Diethylmalonic Acid*—Diethyl diethylmalonate, 79.5 ml (0.37 mole), was added dropwise to a refluxing solution of 123 g (2.20 moles) of potassium hydroxide in 500 ml of ethanol. After the mixture was heated for 3–4 hr, a white solid began to separate. Then the mixture was cooled, and the precipitate was filtered off and washed once with cold ethanol.

The solid was purified by dissolving it in water, acidifying the solution, and collecting the crystalline free acid by filtration. The yield was 39.4 g (67%) of colorless crystals, mp 122–127° [lit. (11) mp 125°]; IR (KBr): 3440 (OH), 1700 (C=O), 1410, and 915 cm^{-1}.

Isopropylidene Diethylmalonate (II)—Sulfuric acid (0.5 ml) was added cautiously to a mixture of 10.0 g (62.5 mmoles) of diethylmalonic acid and 7.6 ml (70 mmoles) of isopropenyl acetate. Then a second equivalent (70 mmoles) of isopropenyl acetate was added, and the mixture was heated briefly to 40°. It then was stirred for 4–5 hr at room temperature. After removal of the volatiles at reduced pressure, the residue was dissolved in ether, washed with sodium bicarbonate and water, and dried over magnesium sulfate.

Removal of the ether left an orange oil. This oil was vacuum distilled to yield 2.9 g (23%) of a colorless liquid, bp 97–100° (0.3 mm), which crystallized on standing to a colorless solid, mp 35–37.5°; IR (KBr): 1785 and 1755 (C=O) cm^{-1}; NMR (acetone-d_6): δ 1.93 (q, 4H, CH_2), 1.66 [s, 6H, $C(CH_3)_2$], and 0.87 (t, 6H, CH_3).

Anal.—Calc. for $C_{10}H_{16}O_4$: C, 60.04; H, 8.06; saponification equivalent 200. Found: C, 60.16; H, 7.90; saponification equivalent 201.

Methyl Diethylmalonurate—A solution of isopropylidene diethylmalonate (2.00 g, 10 mmoles) and urea (0.90 g, 15 mmoles) in 20 ml of dry dimethyl sulfoxide was added slowly, with stirring, to a solution of 2.24 g (20 mmoles) of potassium *tert*-butoxide in 20 ml of dimethyl sulfoxide. Stirring was continued at room temperature for 4 hr. Then the mixture was poured into 100 ml of ice water and extracted once with 50 ml of ether.

The aqueous layer was acidified with hydrochloric acid and extracted three times with 50 ml of ether. These extracts were dried over magnesium sulfate, and the solvent was removed under vacuum, depositing a crystalline residue. This residue was recrystallized from water, yielding 0.47 g (25%) of diethylmalonuric acid as colorless platelets, mp 158–161° [lit. (12) mp 162°]; IR (KBr): 1710, 1650, and 1250 cm^{-1}.

An ethereal solution containing a three- to fivefold excess of diazomethane (generated from *N*-methyl-*N*-nitroso-*p*-toluenesulfonamide[2]) at 0° was added, with stirring, to an ether solution of 0.26 g (1.3 mmoles) of diethylmalonuric acid at 0°. The mixture was stirred for 1 hr at room temperature, and the ether then was evaporated under a nitrogen stream to yield an oil that solidified on cooling. The solid was recrystallized from ligroin to give 116 mg (42% yield) of colorless needles, mp 112–114.5°; IR (KBr): 3420, 1725, 1700, and 1585 cm^{-1}; NMR ($CDCl_3$): δ 3.70 (s, 3H, OCH_3), 1.90 (q, 4H, CH_2), and 0.78 (t, 6H, CH_3).

Anal.—Calc. for $C_9H_{16}N_2O_4$: C, 49.99; H, 7.46. Found: C, 50.04; H, 7.46.

Methyl Ethylisoamylmalonurate—Methyl ethylisoamylmalonurate was prepared from diethyl ethylisoamylmalonate by the same route as for methyl diethylmalonurate. It was obtained as colorless crystals from ligroin, mp 74–76° [lit. (13) mp 74–75°]; IR (KBr): 3410, 1740, 1715, 1690, and 1570 cm^{-1}; NMR ($CDCl_3$): δ 3.70 (s, 3H, OCH_3), 1.85 (m, CH_2), and 0.80 [d, 6H, $CH(CH_3)_2$].

General Buffer Preparation[3]—Buffers for the kinetic studies were prepared with ethanolamine in carbon dioxide-free distilled water and were adjusted to pH 10.0 with constant boiling hydrochloric acid. Potassium chloride was added when necessary to maintain the ionic strength. The buffers were prepared on a cold plate at the experimental temperature at concentrations of 0.011, 0.110, and 1.100 *M* with respect to ethanolamine so that, upon dilution with the malonuric ester solutions, the final concentrations for the kinetic studies were 0.010, 0.100, and 1.000 *M*, respectively.

For the deuterium oxide study, the buffers were prepared from sodium carbonate and sodium deuteriocarbonate to give a final concentration of 0.18 *M* total buffer at pH 10.0 and 15°.

General Spectrophotometric Method[4]—Malonuric ester solutions were prepared with either carbon dioxide-free distilled water or degassed deuterium oxide at 10^{-3} *M* and were used on the same day. The malonuric

[1] Melting points were determined with a Fisher Mel-Temp apparatus and are uncorrected. IR spectra were recorded on a Perkin-Elmer model 457 grating spectrophotometer, and NMR spectra were recorded on a Hitachi Perkin-Elmer R-20B spectrometer. Elemental analyses were performed by Galbraith Laboratories, Knoxville, Tenn.

[2] Diazald, Aldrich Chemical Co.

[3] All pH measurements were made with a Corning model 10 pH meter equipped with a glass electrode and a potassium chloride reference electrode. The meter was standardized with buffer solutions at the experimental temperature before use.

[4] UV spectral data were obtained on a Beckman DK-2A recording spectrophotometer.

Table I—First-Order Rate Constants for the Cyclization of Diethylmalonuric Esters

Medium	k, min^{-1} [a] Methyl Diethylmalonurate	Ethyl Diethylmalonurate
0.01 *M* Buffer[b,c]	0.61	0.28
0.10 *M* Buffer[b,c]	0.79	0.38
1.00 *M* Buffer[b,c]	1.07	0.51
Water[c,d]	0.93	0.43
Deuterium oxide[c,e]	0.70	0.33

[a] The k values represent an average of at least six determinations. [b] Ethanolamine–hydrochloric acid buffer; the ionic strength was maintained at 0.51 *M* with potassium chloride. [c] Reaction temperature of 15.0 ± 0.1°. [d] Buffered with sodium carbonate–sodium bicarbonate at 0.18 *M*. [e] Buffered with sodium carbonate–sodium deuteriocarbonate at 0.18 *M*.

ester solution, the appropriate buffer, and the cell compartment of the spectrophotometer were preequilibrated at the experimental temperature (±0.1°). The reactions were initiated by injecting 0.3 ml of the malonuric ester solution from a calibrated syringe into the spectrophotometer cell already containing 2.7 ml of buffer. The solution was agitated and placed quickly into the spectrophotometer cell compartment. Absorbance at 240 nm was recorded as a function of time compared to the pure buffer solution reference.

Data for the calculation of the rate constants were obtained directly from the absorbance plots and were treated by the Guggenheim method (14).

RESULTS

The cyclization of the dialkylmalonuric esters was studied in aqueous ethanolamine–hydrochloric acid buffers at pH 10.0 over total buffer concentrations ranging from 0.01 to 1.00 *M*. The rate constants for the methyl and ethyl esters of diethylmalonuric acid are given in Table I. The rates varied with total absolute buffer concentration, consistent with a mechanism involving general base catalysis. Since the reaction is an ester aminolysis, the mechanism proposed by Bunnett and Davis (15) implicating general base catalysis in the reaction of butylamine with ethyl formate might be expected to apply. In addition, general base catalysis in the aminolysis of phenyl acetate was observed (10), and susceptibility to general base catalysis appears to be a general characteristic of ester aminolysis reactions (15).

The thermodynamic activation parameters are shown in Table II for the same two esters and the methyl ester of ethylisoamylmalonuric acid. The values of the thermodynamic parameters indicate that the variation in overall cyclization rates was due largely to the ΔS^* term. The ΔH^* values were all close (<5% difference) and actually in reverse order to the measured rates. The methyl ester, which reacted fastest, had the highest ΔH^* value. However, the ΔS^* values were significantly different and closely paralleled the observed rates. In fact, a plot of ΔS^* *versus* k for the three esters was linear. Combining the ΔH^* and ΔS^* terms produced an overall ΔG^* that paralleled the observed rate differences.

The cyclization rates in water and deuterium oxide containing sodium carbonate–bicarbonate buffers also are shown in Table I. Both esters showed a rate decrease in deuterium oxide of approximately the same magnitude, $k_{H_2O}/k_{D_2O} = 1.3$.

DISCUSSION

A probable mechanism for the cyclization of malonuric esters, based on the general mechanism for ester aminolysis given by Bunnett and

Table II—First-Order Rate Constants and Activation Parameters for the Cyclization of Dialkylmalonuric Esters

Compound	k, min^{-1} [a,b] 10°	15°	20°	Activation Parameters ΔH^*, kcal/mole	ΔS^*, cal/K° mole	ΔG^*, kcal/mole
Methyl diethylmalonurate	0.59	1.06	1.91	18.8	−3.2	19.7
Methyl ethylisoamylmalonurate	0.47	0.80	1.49	18.4	−5.1	19.9
Ethyl diethylmalonurate	0.29	0.51	0.89	17.9	−7.8	20.1

[a] The k values represent an average of at least six determinations. [b] The buffer concentration was 1.00 *M*, and the ionic strength was 0.59 *M*.

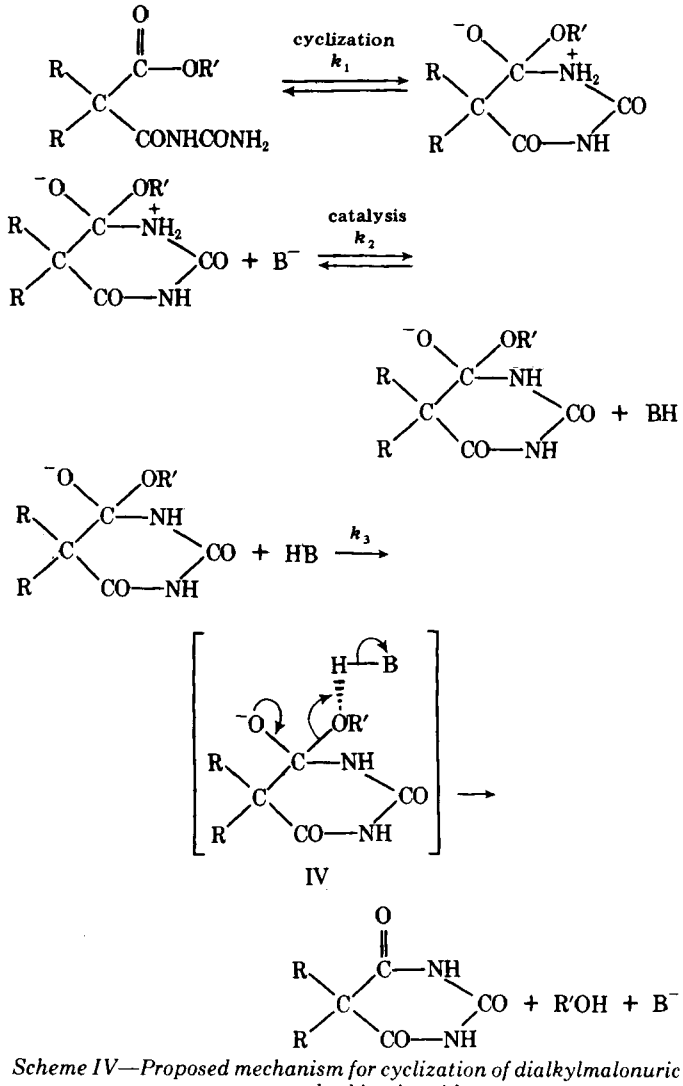

Scheme IV—Proposed mechanism for cyclization of dialkylmalonuric esters to barbituric acids

Davis (15), is shown in Scheme IV. Several kinetic pathways are possible, depending on which step is rate determining. If the cyclization step is slow (k_2 and $k_3 > k_1$), the reaction is subject to specific base catalysis since the strongest base in the medium, OH^-, should eliminate catalysis by the weaker bases once the cyclization occurs. However, if catalysis is rate limiting ($k_1 > k_2$ and k_3), then general base catalysis is observed since all basic species present should catalyze these steps at individual measurable rates.

Since the reaction rate of both the methyl and ethyl esters has been shown experimentally to decrease by a factor of 1.8 as the total buffer concentration is varied 100-fold, the reaction must be subject to general base catalysis, and the rate-determining step is either the catalytic step, k_2, or the collapse of the tetrahedral intermediate aided by the general acid (HB), k_3. The measured deuterium isotope effect, $k_H/k_D = 1.3$, tends to implicate k_3 as the limiting step. Even though the observed isotope effects are small compared to normal d^2 isotope effects, k_H/k_D values in the range of 1.1–1.5 have been reported for the general base-catalyzed reaction of phenyl acetate with glycine and ammonia (10).

The observations that substitution of an isoamyl group for an ethyl group in the acyl portion of the malonuric ester caused a rate decrease

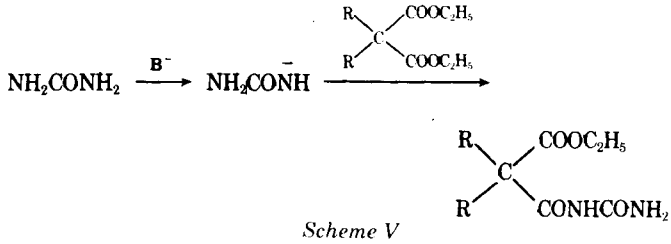

Scheme V

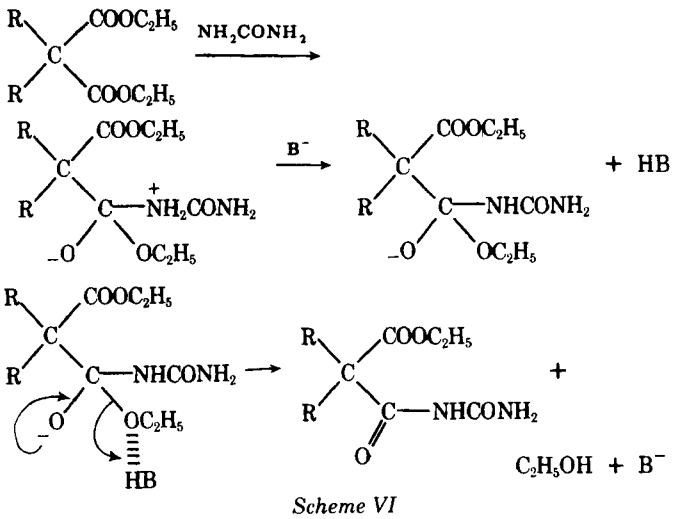

Scheme VI

by a factor of 1.3 and, more importantly, that substitution of the ethyl ester for the methyl ester decreased the rate by a factor of 2.1 also are consistent with a rate-limiting collapse of the tetrahedral intermediate. This dependence on the bulkiness of both the acyl substituents and the leaving alkoxy groups can be attributed to steric hindrance from formation of the hydrogen-bonded intermediate (IV). It also seems reasonable that the identity of the alkoxy group should play the greater role since it is closer to the reaction site. On the other hand, the identity of these groups should have little effect on the proton removal in the catalytic step (k_2).

In view of these findings, it also seems reasonable that the mechanism proposed for the formation of the malonuric ester from urea and the malonic ester needs to be revised (1). Rather than the base functioning to form urea anions, which subsequently attack the malonic ester (Scheme V), the base probably functions in proton removal from the dipolar tetrahedral intermediate that results from the initial attack of neutral urea on the malonic ester (Scheme VI).

REFERENCES

(1) J. A. Beres, D. E. Pearson, and M. T. Bush, *J. Med. Chem.*, **10,** 1078 (1967).

(2) C. F. Boeringer and Sons, German pat. 193 447 (1907); through *Chem. Zentralbl.*, **1908I,** 1000.

(3) H. Aspelund, *Acta Acad. Abo., Ser. B,* **20** (1955); through *Chem. Abstr.*, **50,** 11351f (1956).

(4) E. R. Garrett, J. T. Bojarski, and G. J. Yakatan, *J. Pharm. Sci.*, **60,** 1145 (1971).

(5) L. P. Hammett, "Physical Organic Chemistry," McGraw-Hill, New York, N.Y., 1940, p. 215.

(6) M. E. Krall, *J. Phys. Chem.*, **44,** 449 (1940). J. C. Butler, J. M. Ruth, and G. F. Tucker, *J. Am. Chem. Soc.*, **77,** 1486 (1955).

(7) W. P. Jencks, "Catalysis in Chemistry and Enzymology," McGraw-Hill, New York, N.Y., 1969, p. 247.

(8) J. A. Hirsch, "Concepts in Theoretical Organic Chemistry," Allyn and Bacon, Boston, Mass., 1974, p. 124.

(9) D. Davidson and S. A. Bernhard, *J. Am. Chem. Soc.*, **70,** 3426 (1948).

(10) W. P. Jencks and J. Carriuolo, *J. Am. Chem. Soc.*, **82,** 675 (1960). W. P. Jencks and M. Gilchrist, *ibid.*, **88,** 104 (1966).

(11) D. Heilbron and H. M. Bunbury, "Dictionary of Organic Compounds," vol. II, Eyre and Spottiswoode, London, England, 1953, p. 186.

(12) E. Fischer and A. Dilthey, *Ann.*, **335,** 334 (1904).

(13) E. W. Maynert and E. Washburn, *J. Org. Chem.*, **15,** 259 (1950).

(14) G. M. Fleck, "Chemical Reaction Mechanisms," Holt, Rinehart and Winston, New York, N.Y., 1971, p. 37.

(15) J. F. Bunnett and G. T. Davis, *J. Am. Chem. Soc.*, **82,** 665 (1960).

ACKNOWLEDGMENTS

Abstracted in part from a thesis submitted by M. G. Varner to Shippensburg State College in partial fulfillment of the Master of Science degree requirements.

Distribution of Tetracycline in Red Blood Cells

H. W. JUN ˣ and B. H. LEE

Received July 6, 1979, from the *Department of Pharmacy, School of Pharmacy, University of Georgia, Athens, GA 30602.* Accepted for publication October 15, 1979.

Abstract □ The distribution of tetracycline into human red blood cells was studied *in vitro* at 37°. The drug was taken up rapidly by the cells, and its distribution equilibrium was reached after ~10 min of incubation. The steady-state distribution ratio of the drug between the red cells and extracellular fluid of 0.9% NaCl solution was 2.84, while the distribution ratio between the cells and the plasma solution was 0.9. The reduced cellular uptake in plasma was due to binding of the drug to plasma components. Calcium ions in plasma appeared to reduce tetracycline uptake by the red cells. The red cell distribution of tetracycline in dogs was in close agreement with the *in vitro* data using the washed human red cells. A dog suffering from severe hypoalbuminemia showed greater uptake of the drug by the erythrocytes, while a normal healthy dog exhibited the red cell–plasma distribution ratio of 0.98. The release rate of tetracycline from the preloaded cells into normal saline solution indicated that the release was directly proportional to the cellular concentration of the drug; the first-order release rate was ~1.38 hr^{-1}.

Keyphrases □ Tetracycline—distribution in red blood cells □ Antibacterials—tetracycline, distribution in red blood cells □ Drug distribution—tetracycline, uptake by red blood cells

One important function of red blood cells is to store hemoglobin, which carries and supplies oxygen to various tissues in the body. Drugs can enter red blood cells and bind to the intracellular constituents (1–3). For many drugs, however, erythrocyte uptake means that less drug is available at the site of pharmacological action.

Plasma and serum concentrations have been monitored commonly to study the pharmacokinetics of drugs in the body, with the assumption that drug levels in the plasma and serum are linearly related to drug concentrations in whole blood. Although several drugs such as chlorthalidone (4) and salicylate (5) were shown to accumulate significantly in the red cells, several reports (6–8) indicated that extensive plasma protein binding lowers the red cell uptake of the drug by reducing the free plasma drug concentration. In patients suffering from hypoalbuminemia, the basic pharmacokinetic parameters of the drug thus can be different from those obtained in normal patients (9, 10).

This study was an attempt to elucidate the *in vitro* and *in vivo* distribution characteristics of tetracycline into red blood cells and to measure the effects of the normal plasma components on the red cell uptake of this drug.

EXPERIMENTAL

Materials and Equipment—Tetracycline hydrochloride[1], pentobarbital sodium[2], trichloroacetic acid[3], calcium chloride[3], and human serum albumin[2] were used as received. A rotating apparatus[4] with multiple sample holders was immersed in a water bath, which was kept at 37 ± 1° by a controlled-temperature circulating pump[5]. Fluorescence measurements were made using a spectrophotofluorometer[6] equipped with a 150-w xenon lamp and a R-447 photomultiplier tube.

Preparation of Red Cell Suspensions for *In Vitro* Distribution Studies—Human blood, obtained from either healthy young volunteers or a local blood bank[7], was centrifuged at 1200×*g* for 8 min. The packed red cells were obtained after removing the plasma water and buffy layer containing leukocytes. The cells then were washed three times with isotonic buffer solution (pH 7.4). After the final washing, the cells were suspended in either 0.9% NaCl solution or human plasma solution containing varying amounts of tetracycline (5, 10, 20, 30, and 50 μg/ml). These concentrations are slightly higher than normal clinical concentrations of the drug in patients (11).

Distribution of Tetracycline into Cells—The distribution of tetracycline into the red cells was measured by assaying the drug both in the extracellular fluid and in the cells after incubating the samples consisting of 5 ml of washed cells and 5 ml of 0.9% NaCl solution or human plasma containing 20 μg of tetracycline/ml in a rotating water bath (40 rpm) at 37 ± 1°. Following the incubation for different time intervals (3, 5, 10, 15, 20, and 30 min), the cells were separated by centrifugation at 1200×*g* for 8 min for the assay of the drug in the cells and in the medium.

Effect of pH on Cellular Uptake of Tetracycline—Five milliliters of red cells was suspended in 5 ml of phosphate buffer solution (pH 6.7, 7.4, or 8.0) containing 20 μg of tetracycline/ml. After incubation for 15 min in a rotating water bath at 37 ± 1°, the cells were separated by centrifugation. The concentration ratio of tetracycline between the medium and red cells was determined for each pH solution.

Drug Release Rate from Red Cells—The release rate of tetracycline from the preloaded cells into 0.9% NaCl solution was measured by assaying the drug in the extracellular fluid after incubation of the samples in a rotating water bath at 37 ± 1°. Initially, 5 ml of washed red cells, preequilibrated with 5 ml of tetracycline solution (20 μg/ml) in 0.9% NaCl solution for 15 min, was mixed with 5 ml of 0.9% NaCl solution; this mixture was subjected to incubation in a rotating water bath at 37 ± 1° for 10 min. After centrifugation at 1200×*g* for 8 min, the tetracycline concentration in the extracellular medium was measured. The remaining cells then were reequilibrated with an equal volume of fresh 0.9% NaCl solution for 10 min, followed by centrifugation and assay of the drug in the extracellular fluid. The procedure was repeated five times.

Effect of Plasma Albumin and Calcium Ion on Red Cell Uptake of Tetracycline—The cellular uptake of tetracycline was measured in the solutions containing plasma albumin (4%) and/or calcium chloride (2.5×10^{-5} *M*). The results then were compared with the distribution of tetracycline between the red cells and 0.9% NaCl solution.

Red Cell Uptake of Tetracycline in Dogs—*In vivo* distribution of tetracycline between the plasma and red cells was determined in a healthy beagle dog (Dog A) and in another beagle dog (Dog B) suffering from hypoalbuminemic conditions. The red cell counts for Dogs A and B were 5.59×10^6 and 5.48×10^6/ml, respectively. The normal ranges of the average red cell counts and albumin levels in dogs are 5.26×10^6–6.57×10^6/ml and 3.1–4.0%, respectively. The dogs received a bolus intravenous injection of 10 mg of tetracycline/kg, and the blood samples taken at different time intervals were assayed for the drug both in the cells and in the plasma.

Assay of Tetracycline in Cells and Extracellular Fluids—A spectrophotofluorometric method (12) was used. This method measures

[1] American Cyanamid Co., Pearl River, N.Y.
[2] Sigma Chemical Co., St. Louis, Mo.
[3] J. T. Baker Chemical Co., Phillipsburg, N.J.
[4] Menold, Lester, Pa.
[5] Haake E52, Berlin-Lichterfied, West Germany.
[6] Model MPF-4, Perkin-Elmer Corp., Norwalk, Conn.
[7] St. Mary's Hospital, Athens, Ga.

0022-3549/80/0400-0455$01.00/0
© 1980, American Pharmaceutical Association

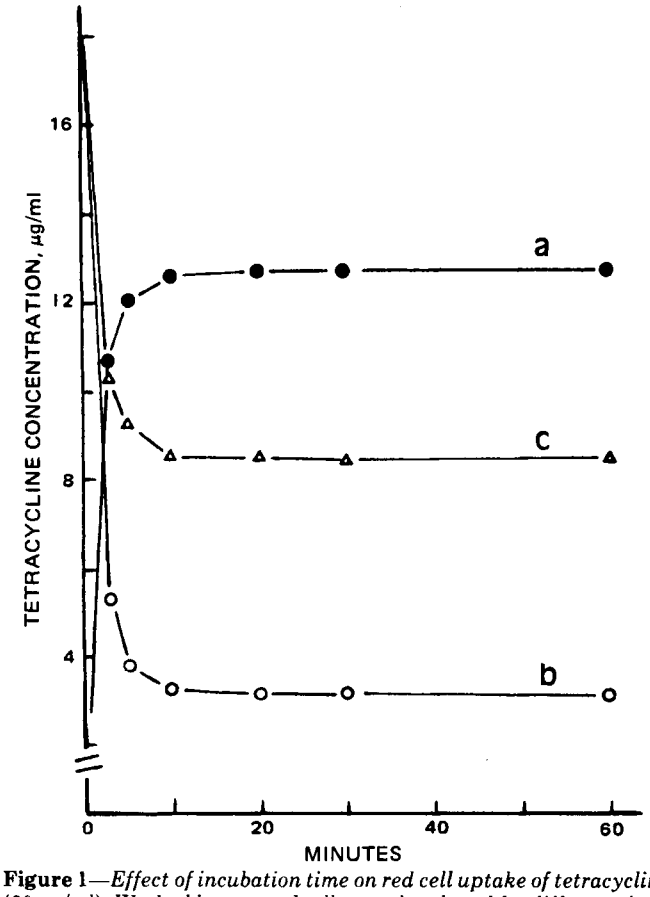

Figure 1—*Effect of incubation time on red cell uptake of tetracycline (20 μg/ml). Washed human red cells were incubated for different times in 0.9% NaCl solution (a, drug in red cells; and b, drug in extracellular fluid) and in human plasma (c, drug in extracellular fluid).*

the fluorescence intensity of the tetracycline–pentobarbital–calcium complex at 525 nm when it is activated at 390 nm.

RESULTS AND DISCUSSION

Figure 1 shows the distribution profile of tetracycline into the red cells as a function of time during the incubation of the washed cells in an equal volume of 0.9% NaCl solution containing 20 μg of tetracycline/ml. During the first 10 min of incubation, the drug was taken up rapidly by the cells, and the steady-state distribution ratio between the red cells and extracellular fluid was ~2.84. The large distribution into the cells probably was due to the significant binding of tetracycline to the intracellular components. However, when tetracycline was subjected to equilibration between the human plasma and erythrocytes, the distribution ratio between the red cells and plasma was 0.9 ± 0.12 (Fig. 1, curve c).

Since plasma contains various proteins and also divalent cations that form lipid-insoluble complexes with tetracycline (13), studies were done to identify the plasma components responsible for the lowered cellular uptake of the drug in the plasma as compared with that in 0.9% NaCl solution. Figure 2 compares the distribution ratios of tetracycline between the red cells and 0.9% NaCl solution (bar A) in the presence of various additives. When both calcium (2.5×10^{-5} *M*) and serum albumin (4%) were added to 0.9% NaCl solution, the steady-state distribution ratio of

Table I—Effect of pH on Steady-State Tetracycline Concentrations in Red Cells and Extracellular Fluid at 37° [a]

	Measured Tetracycline Concentration[b], μg/ml		
	pH 6.7	pH 7.4	pH 8.0
Red blood cells	14.78	14.72	14.79
Medium	5.14	5.24	5.27
Red cell-medium ratio	2.88	2.81	2.81

[a] Initial extracellular concentration was 20 μg/ml. [b] Average of three experiments.

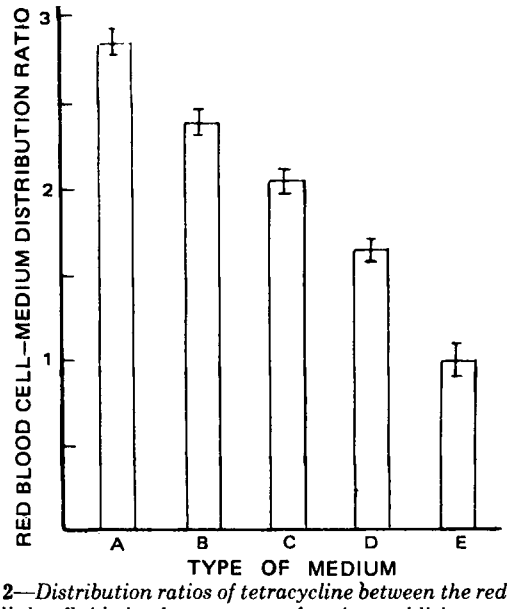

Figure 2—*Distribution ratios of tetracycline between the red cells and extracellular fluids in the presence of various additives at 37°. The extracellular fluids were 0.9% NaCl solution containing 20 μg of tetracycline/ml (A); 20 μg of tetracycline/ml and 2.5×10^{-5} M $CaCl_2$ (B); 20 μg of tetracycline/ml and 4% albumin (C); and 20 μg of tetracycline/ml, 2.5×10^{-5} M $CaCl_2$, and 4% albumin (D); and human plasma containing 20 μg of tetracycline/ml (E). The vertical bars* (I) *represent the standard error of the mean.*

tetracycline between the cells and medium was significantly lower (bar D) than that in the solution containing calcium (bar B) or albumin (bar C) alone. However, the cellular uptake of tetracycline in human plasma (bar E) was still lower than that in 0.9% NaCl solution containing calcium and albumin (bar D).

These results indicate that the components other than calcium and albumin in the plasma also were responsible for the lowered drug partitioning into the cells. Globulins in the plasma possibly may provide additional binding sites to tetracycline. Nevertheless, the distribution of tetracycline into the red cells observed in this study was somewhat similar to the rate of uptake of tetracycline by *Escherichia coli* cells. Franklin and Higginson (14) found that tetracycline rapidly entered the bacterial cells, and its distribution equilibrium between the cells and extracellular medium was reached within 10 min of incubation.

Figure 3 illustrates the effect of tetracycline concentration on the red cell uptake in 0.9% NaCl solution. The steady-state distribution ratio between the cells and extracellular fluid generally was the same among the different total tetracycline concentrations studied. When the concentration of tetracycline was increased from 5 to 50 μg/ml, the distribution of the drug into the cells also was increased while the steady-state distribution ratio between the red cell and the medium was maintained

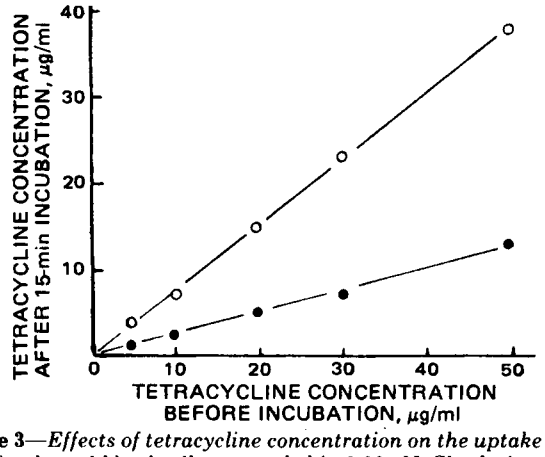

Figure 3—*Effects of tetracycline concentration on the uptake of tetracycline by red blood cells suspended in 0.9% NaCl solution at 37°. Key:* O, *red blood cells; and* ●, *0.9% NaCl solution.*

Table II—Distribution of Tetracycline into Red Blood Cells in Two Dogs

	Dog A	Dog B[a]	
Body weight, kg	24	16.5	16.6
Intravenous dose, mg/kg	10	10	10
Total protein, %	6.81	5.32	5.54
Albumin, %	2.98	1.52	1.84
Hematocrit, %	44.5	37.4	36.9
Red cell–plasma ratio	0.98	1.97	1.74

[a] The data were obtained 2 weeks apart.

at 2.84. This finding probably was due to the fact that a large amount of tetracycline could partition into the cellular components of the red cells.

Table I shows the effect of pH on the distribution of tetracycline into the red cells. Between pH 6.7 and 8.0, the steady-state distribution ratio of the drug remained nearly the same. Since tetracycline undergoes extensive ionization in this pH range, the transport of this drug across cellular membranes probably was mediated by facilitated diffusion as suggested previously (15).

Figure 4 shows the steady-state concentrations of tetracycline in the red cells and the medium after each successive 10-min equilibration with 0.9% NaCl solution. The rate of drug release apparently was an exponential function of the drug concentration in the cells, and the concentration-dependent release rate was $\sim 1.38\ hr^{-1}$. The large release rate constant of the drug from the red cells as compared to its relatively slow

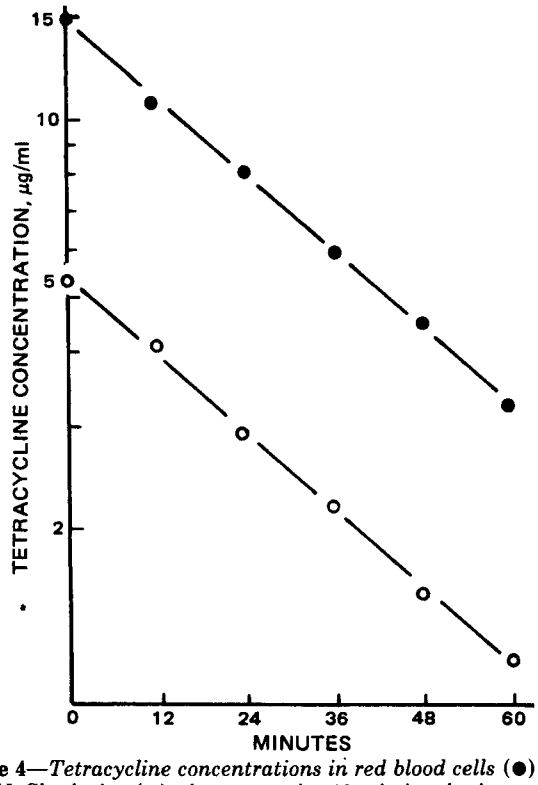

Figure 4—*Tetracycline concentrations in red blood cells (●) and in 0.9% NaCl solution (○) after successive 10-min incubations.*

elimination rate constant ($0.07\ hr^{-1}$) in humans (11) indicates that elimination of tetracycline from the body usually was not affected by the red cell uptake of the drug. Tetracycline will be released quickly from the erythrocytes as the drug in the blood disappears from the body by elimination.

It is generally recognized that the pharmacokinetic behavior of the drug in the normal healthy population may differ from that in patients suffering from chronic illness. Several investigators (9, 10, 16) showed that hypoalbuminemic patients tend to suffer more often than normal patients from adverse drug reactions. Table II compares the distribution of tetracycline in the blood of a dog suffering from severe hypoalbuminemia (1.68%) to that of a normal healthy dog. Dog A, with a normal albumin level (2.98%), had a cell–plasma distribution ratio of 0.98; Dog B, which suffered from hypoalbuminemia, showed a distribution ratio of 1.8, which was nearly two times higher than that in Dog A. These findings are in close agreement with the results obtained from the *in vitro* experiments using the human plasma and the solutions containing different additives.

In summary, tetracycline rapidly enters red blood cells, forming a steady-state distribution equilibrium with the extracellular fluid within 10 min of incubation. The steady-state distribution ratio of the drug between the red cells and extracellular fluid of 0.9% NaCl solution was 2.84, while the distribution ratio between the cells and the plasma solution was 0.9. The low cellular uptake in the plasma was due to binding of the drug to the plasma components. A dog suffering from severe hypoalbuminemia exhibited much greater red cell uptake of tetracycline. The large release rate of the drug from the cells found in this study indicates that the elimination rate of tetracycline from the body is not influenced by the cellular uptake of the drug.

REFERENCES

(1) I. E. Hughes, K. F. Ilett, and L. B. Jellett, *Br. J. Clin. Pharmacol.*, **2**, 521 (1975).

(2) S. M. Wallace and S. Riegelman, *J. Pharm. Sci.*, **66**, 729 (1977).

(3) B. Beerman, K. Hellstrom, B. Lindstrom, and A. Rosen, *Clin. Pharmacol. Ther.*, **17**, 424 (1975).

(4) M. G. Tweeddale and R. I. Ogilvie, *J. Pharm. Sci.*, **63**, 1065 (1974).

(5) J. N. McArthur, P. D. Dawkins, and J. H. Smith, *J. Pharm. Pharmacol.*, **23**, 32 (1971).

(6) D. Kurata and G. R. Wilkinson, *Clin. Pharmacol. Ther.*, **16**, 355 (1974).

(7) I. E. Hughes, L. B. Jellett, and K. F. Ilett, *Br. J. Clin. Pharmacol.*, **3**, 285 (1976).

(8) G. H. Evans and D. G. Shand, *Clin. Pharmacol. Ther.*, **14**, 494 (1973).

(9) W. J. Jusko, in "The Effect of Disease States on Drug Pharmacokinetics," L. Z. Benet, Ed., American Pharmaceutical Association, Washington, D.C., 1976, pp. 99–123.

(10) P. T. Schoenemann, D. W. Yesair, J. J. Coffey, and F. J. Bullock, *Ann. N.Y. Acad. Sci.*, **226**, 172 (1973).

(11) W. H. Barr, L. M. Gerbracht, K. Letcher, M. Plant, and N. Strahl, *Clin. Pharmacol. Ther.*, **13**, 97 (1972).

(12) K. W. Kohn, *Anal. Chem.*, **33**, 862 (1961).

(13) T. Higuchi and S. Bolton, *J. Am. Pharm. Assoc., Sci. Ed.*, **48**, 557 (1959).

(14) T. J. Franklin and B. Higginson, *Biochem. J.*, **116**, 287 (1970).

(15) J. W. Perrin and J. J. Vallner, *J. Pharm. Pharmacol.*, **22**, 758 (1970).

(16) W. J. Jusko and M. Gretch, *Drug Metab. Rev.*, **5**, 43 (1976).

Induced Resistance in *Staphylococcus aureus* for Assay of Antibiotic Mixtures in Pharmaceutical Preparations

DORA BALANDRANO ˣ **and RAMÓN VALLE**

Received February 5, 1979, from the *Department of Quality Control Assurance, S.A. Pharmaceutical Division, Syntex, Apdo. 10-821, México 10, D.F.* Accepted for publication October 15, 1979.

Abstract □ A new microbiological method was developed for the assay of neomycin and spiramycin. These antibiotics usually cannot be quantitated individually when they are combined in a pharmaceutical preparation since both act on the same test organism. By inducing resistance to each antibiotic in *Staphylococcus aureus*, two new strains were obtained. Quantitation can be accomplished easily with these strains.

Keyphrases □ Neomycin—microbiological determination with spiramycin □ Spiramycin—microbiological determination with neomycin □ *Staphylococcus aureus*—microbiological determination of antibiotic mixtures, induced resistance to neomycin and spiramycin

The combination of two or more antibiotics in a pharmaceutical preparation is used widely in the therapy of several infections to permit reduction of the dose of a potentially toxic drug, to prevent the development of bacterial resistance, and to develop a synergistic effect. The last of these uses probably is the most important.

However, these mixtures frequently create problems in the quantitation of their components by microbiological procedures. Arret *et al.* (see Ref. 1) prepared tables with which approximate results may be obtained. Similar tables should be prepared in each laboratory for every antibiotic combination.

BACKGROUND

Arret *et al.* demonstrated that if the test organism used for the assay of one antibiotic (A) is not affected by a second antibiotic (B), no problem results. However, if the test organism is affected by both antibiotics, erroneous high or low values are obtained. Therefore, more specific methods must be developed to eliminate the effect of B. Such methods could involve: (*a*) inactivation of B, (*b*) use of a different test organism that is sensitive to A and relatively resistant to B, (*c*) separation of the antibiotics by differential solubility techniques, and (*d*) compensation for the presence of B by its addition to every solution of A used for the standard response curve.

Grove and Randall (2) presented numerous applications of these possibilities. For instance, they discussed the use of specific enzymes or chemical inactivators to eliminate certain antibiotics from action and the extraction of one antibiotic with a solvent in which the other is not soluble. However, the preferred technique is to choose as the test organism a microorganism that is very sensitive to one antibiotic and is not sensitive to the other antibiotic.

An organism can be made resistant to an antibiotic by forcing its growth in media containing increasing amounts of the antibiotic until the desired resistance is attained. This organism then can be used as a test organism. This paper describes a microbiological method to quantitate two antibiotics mixed in a pharmaceutical dosage form.

EXPERIMENTAL

Materials—The equipment used was that required by the USP XIX (3) cylinder-plate assay, and the assay plates were prepared (3) using antibiotic medium No. 11 for the base layer and No. 1 for the inoculum layer. Sample and standard solutions were diluted in phosphate buffer solution No. 3 (pH 8).

Neomycin sulfate USP was used as the standard. The test organisms were *Staphylococcus aureus* (ATCC 6538P) and *Bacillus subtilis* (ATCC 6633).

Table I—Precision and Accuracy of the Determination of Neomycin and Spiramycin

Antibiotic	Precision at 95% Confidence Interval, % ± *SD*	Accuracy at 95% Confidence Interval, % ± *SD*
Neomycin	105 ± 2.8	98.6 ± 2.0
Spiramycin	95.4 ± 3.07	102 ± 1.6

Table II—Results for Neomycin and Spiramycin in Stability Samples

Sample	Neomycin, %	Spiramycin, %
6 months at room temperature	107, 106	105, 100
	100, 107	105, 100
	93, 104	107, 105
	107, 116	102, 106
6 months at 37°	97, 94	71, 69
	94, 93	78, 78
	97, 98	76, 74
	93, 93	69, 70
6 months at 45°	89, 87	66, 60
	82, 82	65, 66
	84, 88	62, 62
	92, 88	64, 66

Resistance to Spiramycin[1]—The test organism was inoculated successively in a series of tubes of medium No. 1 containing increasing amounts of the antibiotic. From 1 unit of spiramycin base/ml in the first tube, the concentration was increased until a strain was obtained that was able to grow in a medium containing 20 units of spiramycin base/ml. Assays by the cylinder-plate method were made to confirm that the microorganism was resistant to this spiramycin concentration.

Resistance to Neomycin—By following steps similar to those used for spiramycin, *S. aureus* was inoculated successively in tubes of medium No. 1 containing increasing amounts of the antibiotic, from 1 to 10 μg of neomycin base/ml of culture medium. Assays by the cylinder-plate method also were made to confirm the resistance of the strain obtained.

With this technique, two new strains were obtained. One strain was resistant to 20 IU of spiramycin base/ml of medium (for the determination of neomycin), and the other strain was resistant to 10 μg of neomycin base/ml of medium (for the determination of spiramycin).

Method—Analyses were performed as described in the USP under the cylinder-plate method (3). The basic steps of this method are: (*a*) inhibition of growth by different dilutions of the antibiotic placed in cylinders on agar plates inoculated with the test organism, (*b*) measurement of the zones of inhibition, and (*c*) quantitative estimation by interpolation of the values obtained in a standard curve.

Statistical Evaluation—To determine the precision of the method, repeated assays were carried out in a homogeneous sample of a topical solution for cattle containing, in 100 ml, 2.0 mg of neomycin base (as the sulfate), 2.0 mg of spiramycin base (as the adipate), and 2.5 mg of flumethasone with polyethylene glycol-water as the vehicle.

For accuracy, a placebo of the dosage form was dosed with known amounts of the antibiotics (5, 8, and 10 mg of neomycin base/g and 5, 8, and 10 IU of spiramycin/g), and recovery assays were done after homogenization. The results are given in Table I.

[1] The spiramycin was obtained from the World Health Organization.

0022-3549/80/0400-0458$01.00/0
© 1980, American Pharmaceutical Association

The specificity of the method was determined with dosage form samples maintained for 6 months at room temperature, 37°, and 45°. The results are given in Table II.

RESULTS AND DISCUSSION

A microbiological method for the determination of neomycin and spiramycin mixed in pharmaceutical preparations was developed. The initial plan was to develop a *Staphylococcus* strain that was resistant to spiramycin for the determination of neomycin and to develop a *Bacillus* strain that was resistant to neomycin for the determination of spiramycin.

Resistance to spiramycin in *S. aureus* was obtained easily. However, since the *B. subtilis* inoculum was a spore suspension, a strain resistant to neomycin was not obtained. Therefore, since *S. aureus* also is recommended for the evaluation of spiramycin (4), this microorganism was chosen for both antibiotics.

This method may be used as a quality control procedure for samples of production batches as well as in stability studies since substances produced by degradation products of excipients or other active ingredients do not interfere. The assay may be carried out without special preparation of the sample. This technique may be used in the assay of mixtures of other antibiotics by inducing resistance in the proper microorganisms.

REFERENCES

(1) F. Kavanagh, "Analytical Microbiology," Academic, New York, N.Y., 1963, pp. 252, 255.

(2) "Assay Methods of Antibiotics, a Laboratory Manual," Grove and Randall, Eds., Medical Encyclopedia, Inc., New York, N.Y., 1956, p. 124.

(3) "The United States Pharmacopeia," 19th rev., Mack Publishing Co., Easton, Pa., 1975, pp. 596, 598.

(4) "Pharmacopee Francaise. Codex Medicamentarius," Gallicus ed. VIII, Paris, France, 1965, p. 1102.

Determination of Dextro- and Levomethorphan Mixtures Using Chiral Lanthanide NMR Shift Reagents

IRVING W. WAINER ˣ, MARC A. TISCHLER, and ERIC B. SHEININ

Received August 20, 1979, from the *Division of Drug Chemistry, Food and Drug Administration, Washington, DC 20204.* Accepted for publication October 29, 1979.

Abstract □ Europium and praseodymium chiral NMR shift reagents were used to differentiate between dextro- and levomethorphan. The enantiomeric shift differences ($\Delta\Delta\delta$) demonstrated by the singlet associated with the methoxy protons were large enough to identify the *levo*- and *dextro*-isomers and to allow for the determination of as little as 10% of one enantiomer in the presence of the other in a prepared mixture. The analytical method is rapid and can analyze samples as small as 1 mg.

Keyphrases □ Dextromethorphan—NMR determination with levomethorphan □ Levomethorphan—NMR determination with dextromethorphan □ Enantiomers—NMR determination of dextromethorphan and levomethorphan mixtures, chiral lanthanide shift reagents □ NMR spectroscopy—determination of dextro- and levomethorphan mixtures, chiral lanthanide shift reagents □ Analgesics, narcotic—levomethorphan, NMR identification with dextromethorphan □ Antitussives, nonnarcotic—dextromethorphan, NMR identification with levomethorphan

The determination of the enantiomeric purity of a substance is an important aspect of the regulatory process. This determination is especially important in cases such as methorphan where the *levo*- and racemic forms of the drug are regulated narcotics while the *dextro*-isomer is a widely used nonnarcotic antitussive.

BACKGROUND

Specific rotation (1) is the standard method used to distinguish dextromethorphan from levomethorphan. This method is simple and accurate if there is an adequate amount of sample and if one can be reasonably certain that there are no interfering compounds. The hanging microdrop technique (2), which has a sensitivity of 0.2 μg, also is used. However, these approaches cannot serve as identification tests and they cannot accurately detect one enantiomer in the presence of the other.

Chiral lanthanide nuclear magnetic shift reagents may be utilized in the development of rapid, sensitive, and accurate assays of enantiomeric purity. Shaath and Soine (3) recently demonstrated the utility of this approach in the determination of the enantiomeric purity of isoquinoline alkaloids. By using a europium chiral shift reagent, they differentiated rapidly between the components of five enantiomeric pairs and accurately detected an enantiomeric mixture of 95:5.

This paper reports the application of the chiral lanthanide shift reagents to the identification of the methorphan enantiomers and the determination of one isomer in the presence of the other.

EXPERIMENTAL

Instrumentation—A 60-MHz NMR spectrometer[1] equipped with a Fourier transform system[2] was used for all spectra.

Reagents and Chemicals—Deuterated chloroform was used as purchased[3].

Dextro- and levomethorphan were supplied as their hydrobromide salts[4], and the free bases were prepared according to the NF procedure (1). Stock solutions (0.16 *M*) of the free bases were prepared by dissolving 220 mg of the respective enantiomer in 5.00 ml of deuterated chloroform. Enantiomeric mixtures were prepared from the two stock solutions.

The europium and praseodymium chiral shift reagents were used as purchased[5]. Stock solutions (0.2 *M* in deuterated chloroform) were prepared in a dry box under a nitrogen atmosphere before the start of each series of experiments. Each solution was stored in a sealed vial equipped with a septum and sampled using a microliter syringe.

Procedure—The appropriate methorphan solution (0.4 ml) was placed in an NMR tube equipped with a rubber septum. The shift reagent then was added sequentially in 20-μl increments. An NMR spectrum with 64 additive pulses was run after each addition, and the peak chemical shifts were computer recorded.

The peak height ratios associated with the various molar ratios of levo- and dextromethorphan were measured after the addition of 300 μl of the europium shift reagent or 260 μl of the praseodymium shift reagent.

RESULTS AND DISCUSSION

The effect of the europium shift reagent on the NMR spectrum of an equimolar mixture of dextro- and levomethorphan is shown in Fig. 1. The

[1] Model R12B, Perkin-Elmer Corp., Norwalk, CT 06856.
[2] TT7, Nicolet Instrument Corp., Madison, WI 53711.
[3] Aldrich Chemical Co., Milwaukee, WI 53233.
[4] Hoffmann-La Roche, Nutley, NJ 07110.
[5] Eu-Opt and Pra-Opt, Alfa Products, Ventron Corp., Danvers, MA 01923.

0022-3549/80/0400-0459$01.00/0
© 1980, American Pharmaceutical Association

The specificity of the method was determined with dosage form samples maintained for 6 months at room temperature, 37°, and 45°. The results are given in Table II.

RESULTS AND DISCUSSION

A microbiological method for the determination of neomycin and spiramycin mixed in pharmaceutical preparations was developed. The initial plan was to develop a *Staphylococcus* strain that was resistant to spiramycin for the determination of neomycin and to develop a *Bacillus* strain that was resistant to neomycin for the determination of spiramycin.

Resistance to spiramycin in *S. aureus* was obtained easily. However, since the *B. subtilis* inoculum was a spore suspension, a strain resistant to neomycin was not obtained. Therefore, since *S. aureus* also is recommended for the evaluation of spiramycin (4), this microorganism was chosen for both antibiotics.

This method may be used as a quality control procedure for samples of production batches as well as in stability studies since substances produced by degradation products of excipients or other active ingredients do not interfere. The assay may be carried out without special preparation of the sample. This technique may be used in the assay of mixtures of other antibiotics by inducing resistance in the proper microorganisms.

REFERENCES

(1) F. Kavanagh, "Analytical Microbiology," Academic, New York, N.Y., 1963, pp. 252, 255.

(2) "Assay Methods of Antibiotics, a Laboratory Manual," Grove and Randall, Eds., Medical Encyclopedia, Inc., New York, N.Y., 1956, p. 124.

(3) "The United States Pharmacopeia," 19th rev., Mack Publishing Co., Easton, Pa., 1975, pp. 596, 598.

(4) "Pharmacopee Francaise. Codex Medicamentarius," Gallicus ed. VIII, Paris, France, 1965, p. 1102.

Determination of Dextro- and Levomethorphan Mixtures Using Chiral Lanthanide NMR Shift Reagents

IRVING W. WAINER ˣ, MARC A. TISCHLER, and ERIC B. SHEININ

Received August 20, 1979, from the *Division of Drug Chemistry, Food and Drug Administration, Washington, DC 20204.* Accepted for publication October 29, 1979.

Abstract □ Europium and praseodymium chiral NMR shift reagents were used to differentiate between dextro- and levomethorphan. The enantiomeric shift differences ($\Delta\Delta\delta$) demonstrated by the singlet associated with the methoxy protons were large enough to identify the *levo*- and *dextro*-isomers and to allow for the determination of as little as 10% of one enantiomer in the presence of the other in a prepared mixture. The analytical method is rapid and can analyze samples as small as 1 mg.

Keyphrases □ Dextromethorphan—NMR determination with levomethorphan □ Levomethorphan—NMR determination with dextromethorphan □ Enantiomers—NMR determination of dextromethorphan and levomethorphan mixtures, chiral lanthanide shift reagents □ NMR spectroscopy—determination of dextro- and levomethorphan mixtures, chiral lanthanide shift reagents □ Analgesics, narcotic—levomethorphan, NMR identification with dextromethorphan □ Antitussives, nonnarcotic—dextromethorphan, NMR identification with levomethorphan

The determination of the enantiomeric purity of a substance is an important aspect of the regulatory process. This determination is especially important in cases such as methorphan where the *levo*- and racemic forms of the drug are regulated narcotics while the *dextro*-isomer is a widely used nonnarcotic antitussive.

BACKGROUND

Specific rotation (1) is the standard method used to distinguish dextromethorphan from levomethorphan. This method is simple and accurate if there is an adequate amount of sample and if one can be reasonably certain that there are no interfering compounds. The hanging microdrop technique (2), which has a sensitivity of 0.2 μg, also is used. However, these approaches cannot serve as identification tests and they cannot accurately detect one enantiomer in the presence of the other.

Chiral lanthanide nuclear magnetic shift reagents may be utilized in the development of rapid, sensitive, and accurate assays of enantiomeric purity. Shaath and Soine (3) recently demonstrated the utility of this approach in the determination of the enantiomeric purity of isoquinoline alkaloids. By using a europium chiral shift reagent, they differentiated rapidly between the components of five enantiomeric pairs and accurately detected an enantiomeric mixture of 95:5.

This paper reports the application of the chiral lanthanide shift reagents to the identification of the methorphan enantiomers and the determination of one isomer in the presence of the other.

EXPERIMENTAL

Instrumentation—A 60-MHz NMR spectrometer[1] equipped with a Fourier transform system[2] was used for all spectra.

Reagents and Chemicals—Deuterated chloroform was used as purchased[3].

Dextro- and levomethorphan were supplied as their hydrobromide salts[4], and the free bases were prepared according to the NF procedure (1). Stock solutions (0.16 *M*) of the free bases were prepared by dissolving 220 mg of the respective enantiomer in 5.00 ml of deuterated chloroform. Enantiomeric mixtures were prepared from the two stock solutions.

The europium and praseodymium chiral shift reagents were used as purchased[5]. Stock solutions (0.2 *M* in deuterated chloroform) were prepared in a dry box under a nitrogen atmosphere before the start of each series of experiments. Each solution was stored in a sealed vial equipped with a septum and sampled using a microliter syringe.

Procedure—The appropriate methorphan solution (0.4 ml) was placed in an NMR tube equipped with a rubber septum. The shift reagent then was added sequentially in 20-μl increments. An NMR spectrum with 64 additive pulses was run after each addition, and the peak chemical shifts were computer recorded.

The peak height ratios associated with the various molar ratios of levo- and dextromethorphan were measured after the addition of 300 μl of the europium shift reagent or 260 μl of the praseodymium shift reagent.

RESULTS AND DISCUSSION

The effect of the europium shift reagent on the NMR spectrum of an equimolar mixture of dextro- and levomethorphan is shown in Fig. 1. The

[1] Model R12B, Perkin-Elmer Corp., Norwalk, CT 06856.
[2] TT7, Nicolet Instrument Corp., Madison, WI 53711.
[3] Aldrich Chemical Co., Milwaukee, WI 53233.
[4] Hoffmann-La Roche, Nutley, NJ 07110.
[5] Eu-Opt and Pra-Opt, Alfa Products, Ventron Corp., Danvers, MA 01923.

0022-3549/80/0400-0459$01.00/0
© 1980, American Pharmaceutical Association

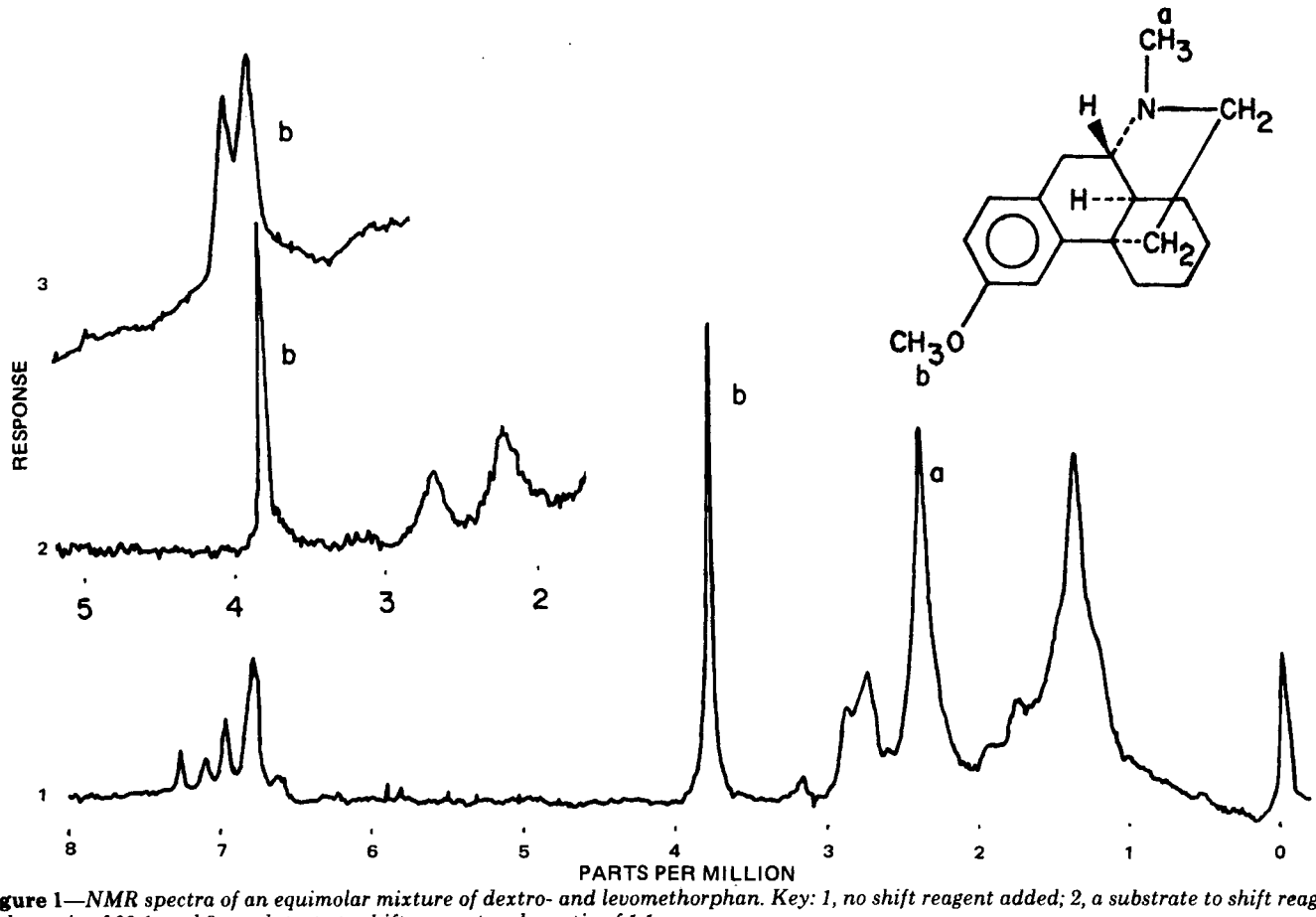

Figure 1—*NMR spectra of an equimolar mixture of dextro- and levomethorphan. Key: 1, no shift reagent added; 2, a substrate to shift reagent molar ratio of 80:1; and 3, a substrate to shift reagent molar ratio of 1:1.*

singlet associated with the N-methyl protons at 2.9 ppm broadened and disappeared at a substrate to reagent molar ratio of 80:1. This result suggests that the nitrogen atom is the site of pseudocontact or dipolar interaction between the methorphan and the shift reagent.

The induced shifts ($\Delta\delta$) and the enantiomeric shift differences ($\Delta\Delta\delta$) for the singlet due to the methoxy protons are shown in Figs. 2 and 3, respectively. The europium shift reagent had little effect on the spectra up to a substrate to shift reagent molar ratio of 8:3. Continued addition of the shift reagent shifted the signal associated with the *dextro*-isomer downfield while the signal associated with the *levo*-isomer remained relatively constant. The maximum resolution of the signals occurred at a substrate to reagent molar ratio of ~1:1. Beyond this point, peak broadening tended to collapse the peaks. The signal from the *dextro*-isomer was the one most affected by this broadening, with the result that the peak height associated with dextromethorphan was 85% of the corresponding peak height for levomethorphan at a 50:50 ratio of the two isomers.

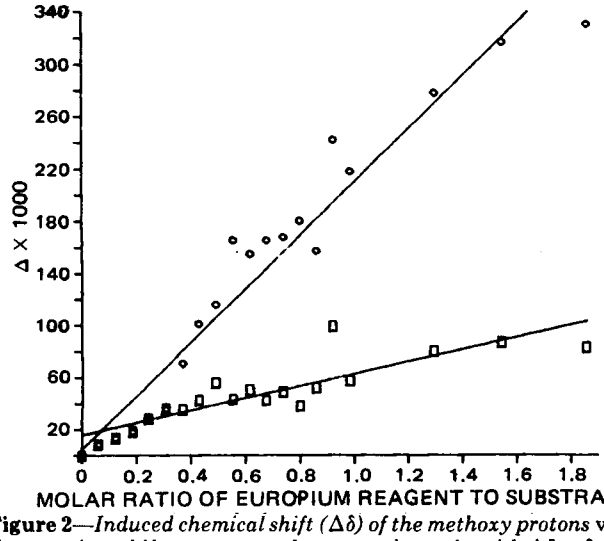

Figure 2—*Induced chemical shift ($\Delta\delta$) of the methoxy protons* versus *the europium shift reagent to substrate molar ratio, with $\Delta\delta = \delta t - \delta_0$, where δ_0 is the chemical shift of the initial signal and δt is the chemical shift of the signal after the addition of the shift reagent. Key:* ○, *dextromethorphan; and* □, *levomethorphan.*

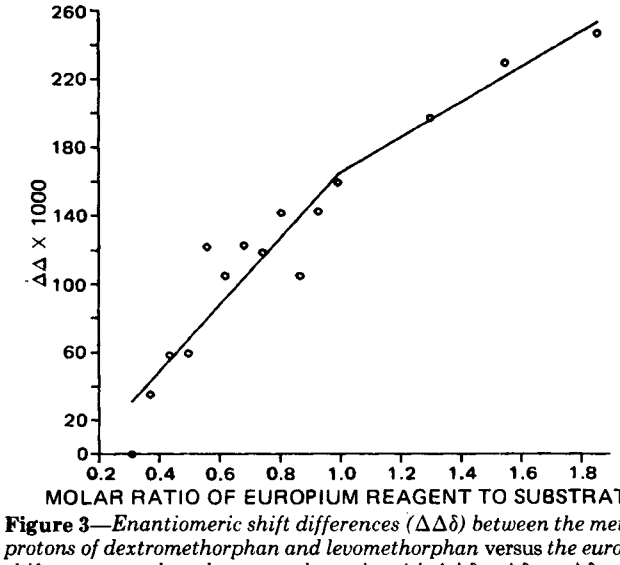

Figure 3—*Enantiomeric shift differences ($\Delta\Delta\delta$) between the methoxy protons of dextromethorphan and levomethorphan* versus *the europium shift reagent to the substrate molar ratio, with $\Delta\Delta\delta = \Delta\delta_D - \Delta\delta_L$, where $\Delta\delta_D$ is the induced chemical shift for the methoxy protons of dextromethorphan and $\Delta\delta_L$ is the induced chemical shift for the methoxy protons of levomethorphan.*

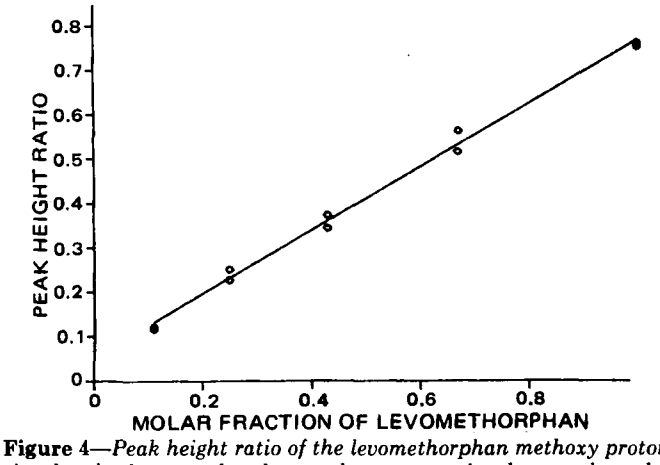

Figure 4—*Peak height ratio of the levomethorphan methoxy proton signal to the dextromethorphan methoxy proton signal* versus *the molar fraction of levomethorphan in dextromethorphan.*

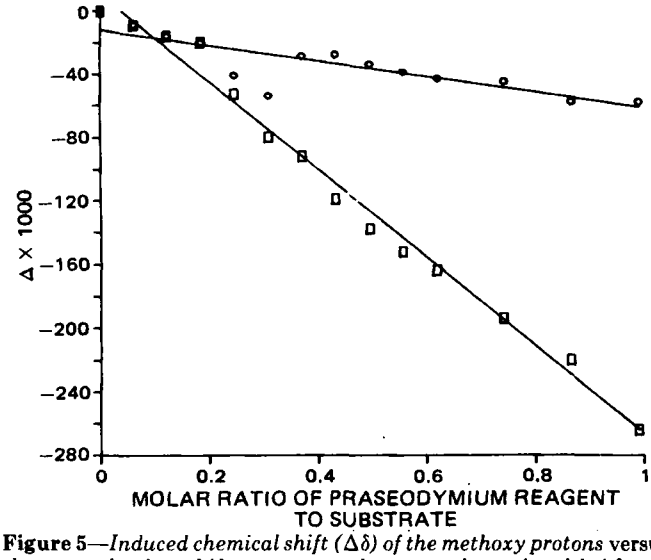

Figure 5—*Induced chemical shift ($\Delta\delta$) of the methoxy protons* versus *the praseodymium shift reagent to substrate molar ratio, with $\Delta\delta = \delta t - \delta_0$, where δ_0 is the chemical shift of the initial signal and δt is the chemical shift of the signal after the addition of the shift reagent. Key:* O, *levomethorphan; and* □, *dextromethorphan.*

The peak height ratios that correspond to prepared solutions of various molar ratios of the two enantiomers are shown in Fig. 4. The peak heights were determined by direct measurement to an adjusted baseline. The peak heights of shoulders were determined by dropping a vertical line to intersect the tangent of the slope of the larger peak. In this manner, as little as 10% of the *levo*-isomer could be estimated in the presence of the *dextro*-isomer. At this level, the signal associated with the *levo*-isomer appeared as a shoulder of the signal associated with the *dextro*-isomer, with a peak height of ~1:10.

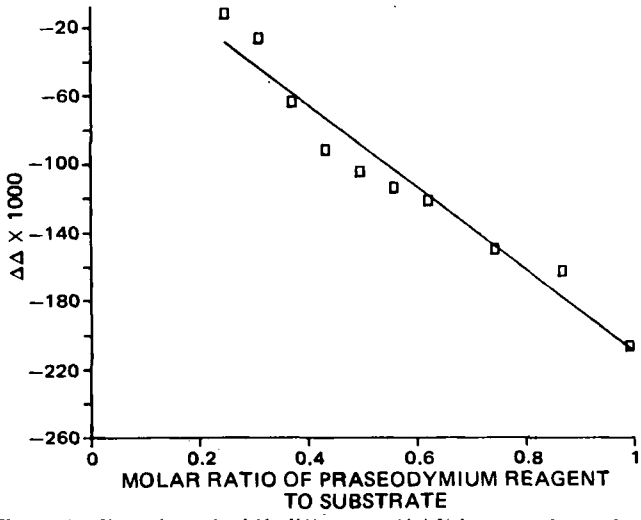

Figure 6—*Enantiomeric shift differences ($\Delta\Delta\delta$) between the methoxy protons of dextromethorphan and levomethorphan* versus *the praseodymium shift reagent to substrate molar ratio, with $\Delta\Delta\delta = \Delta\delta_D - \Delta\delta_L$, where $\Delta\delta_D$ is the induced chemical shift for the methoxy protons of dextromethorphan and $\Delta\delta_L$ is the induced chemical shift for the methoxy protons of levomethorphan.*

The induced shifts ($\Delta\delta$) and the enantiomeric shift differences ($\Delta\Delta\delta$) of the methoxy protons after the addition of the praseodymium reagent are shown in Figs. 5 and 6, respectively. The effects of this reagent on the spectra of the *dextro*- and *levo*-isomers were similar to those observed with the europium reagent, except that the signal associated with dextromethorphan was shifted upfield. The maximum resolution between the two methoxy signals occurred at a substrate to reagent molar ratio of 10:8. The peak height ratios associated with the various molar ratios of the two enantiomers also were similar to those determined with the europium shift reagent. However, the peak broadening associated with the praseodymium reagent was greater than that observed with the europium reagent, making the praseodymium reagent less sensitive as an analytical probe for the detection of one isomer in the presence of the other.

In conclusion, the chiral lanthanide shift reagents can be used to identify the enantiomers of methorphan. This method rapidly and accurately differentiates between dextromethorphan and levomethorphan, with detection and estimation of as little as 10% of one isomer in the presence of the other.

REFERENCES

(1) "The National Formulary," 14th ed., Mack Publishing Co., Easton, Pa., 1975, p. 192.

(2) E. G. C. Clarke, *J. Pharm. Pharmacol.*, **10**, 642 (1958).

(3) N. A. Shaath and T. O. Soine, *J. Org. Chem.*, **40**, 1987 (1975).

ACKNOWLEDGMENTS

The authors thank R. Venable for aid in analyzing the data and T. D. Doyle for editorial assistance.

Potent Inhibition of Oxidative Phosphorylation by Marine Natural Products

DANA D. JAMIESON ˣ, PAUL J. de ROME, and KENNETH M. TAYLOR

Received June 29, 1979, from the *Roche Research Institute of Marine Pharmacology, Dee Why, New South Wales, 2099 Australia.* Accepted for publication October 22, 1979.

Abstract □ Many lipid-soluble extracts from various marine organisms have a nonspecific depressant effect on smooth muscle contractions. Novel compounds isolated from such lipid-soluble extracts were tested for their effects on the respiration of rat liver mitochondria and produced potent stimulation or inhibition of oxygen uptake by the mitochondria.

Keyphrases □ Oxidative phosphorylation—effect of marine natural products on mitochondrial respiration □ Adenosine diphosphate—stimulating and inhibitory effects on mitochondrial respiration by compounds from marine organisms, oxidative phosphorylation □ Depressants, smooth muscle—novel marine compounds □ Respiration, mitochondrial—effect of marine natural products

Der Marderosian (1) observed that marine organisms offered enormous potential for the development of new and different pharmaceuticals, and he cited examples of the pharmacological activities from marine sources known at that time. In addition, Der Marderosian stressed the difficulties in handling the crude extracts for biological screening and the problems inherent in the extraction and characterization of the compounds responsible for the biological activity. While research of marine natural products in pharmacology and microbiology has continued since that time, there has been little biochemical experimentation, and marine natural products have not been tested yet in the field of energy metabolism.

During routine screening of compounds isolated from marine organisms in these laboratories, it was observed that many compounds obtained from organic solvent extraction depressed the contractile activity of mammalian smooth muscle preparations. The most sensitive tissue to the inhibitory action was the isolated guinea pig ileum. The inhibition was nonspecific in that the contractions produced by acetylcholine, histamine, nicotine, and 5-hydroxytryptamine were affected equally. One possible mode of action of the compounds was inhibition of energy metabolism. Therefore, in the present experiments, the compounds were tested for their effects on oxygen uptake by isolated rat liver mitochondria.

EXPERIMENTAL

Mitochondria were prepared by homogenizing rat liver in 20 volumes of solution (pH 7.0) containing 225 m*M* mannitol, 75 m*M* sucrose, and 0.5 m*M* ethylenediaminetetraacetic acid using a polytef pestle and a glass tube. From the supernate obtained after centrifugation at 500×*g* for 5 min, the mitochondria were precipitated by centrifugation at 9000×*g* for 5 min. The mitochondrial pellet was washed twice by resuspension in the described solution, followed by centrifugation at 9000×*g* for 5 min. The washed mitochondrial pellet was resuspended in 2 ml of the preparation medium.

Mitochondrial respiratory activity was measured in a medium containing 225 m*M* mannitol, 75 m*M* sucrose, 20 m*M* tromethamine hydrochloride, and 10 m*M* monobasic potassium phosphate adjusted to pH 7.4. The reaction vessel was a 4-ml glass cell, and oxygen uptake was measured with a polytef-covered oxygen electrode connected to a pO_2 module and a pen recorder. The temperature was 23.5°. Additions to the mitochondrial suspension (2.5–3 mg of protein) were made with microsyringes through a rubber seal in the sidearm of the reaction vessel in a manner essentially the same as that described by Estabrook (2).

Because the compounds tested had low water solubility, they were dissolved in dimethyl sulfoxide to suitable dilutions such that 1–10 μl of solution was added to the reaction vessel. Control experiments showed that <50 μl of dimethyl sulfoxide had no effect on the oxygen uptake of the rat liver mitochondria. Protein determinations were carried out according to Lowry *et al.* (3). Results are expressed as micromoles of oxygen consumed per minute per milligram of protein.

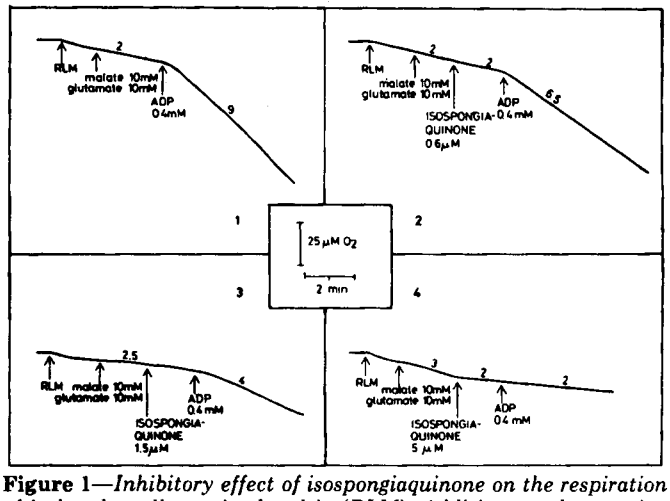

Figure 1—*Inhibitory effect of isospongiaquinone on the respiration of isolated rat liver mitochondria (RLM). Additions to the reaction vessel are as indicated, and numerals on the trace indicate micromoles of oxygen consumed per liter per minute per milligram of mitochondrial protein.*

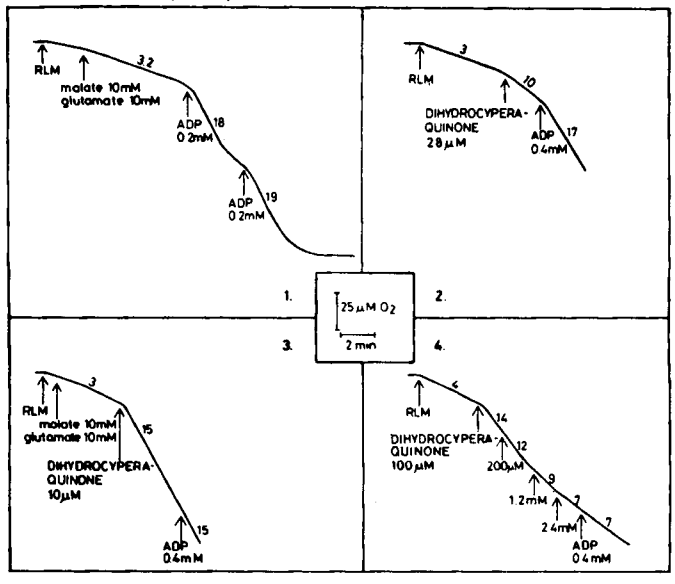

Figure 2—*Effect of dihydrocyperaquinone in stimulating the respiration of rat liver mitochondria (RLM). In Panel 4, increasing concentrations of dihydrocyperaquinone above 100 μM gradually decreased the initially stimulated respiration.*

0022-3549/80/0400-0462$01.00/0
© 1980, American Pharmaceutical Association

Table I—Effects on Respiration of Isolated Rat Liver Mitochondria by Novel Lipid-Soluble Compounds from Marine Organisms

Reference	Compound	Structure	Marine Organism	Concentration for 50% Inhibition of State 3 Respiration, μM	Concentration for 100% Increase of State 4 Respiration, μM
5	Isospongiaquinone	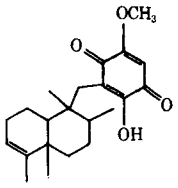	Sponge (Spongiidae)	1	—
5	Dihydroisospongiaquinone	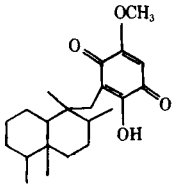	Sponge (Spongiidae)	1	—
6	Dihydrocyperaquinone	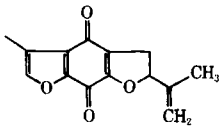	Cyperaceae (*Remirea martima*)	1000	4
7	Costatol	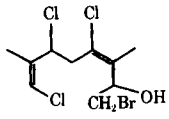	Red alga (*Plocamium costatum*)	20–30	6
8	13(*R*),14-Epoxy-6,10,14-trimethyl-5,9-pentadecadiene-2-one	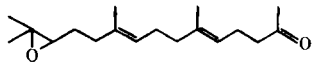	Brown alga (*Cystophora moniliformis*)	5	—
8	6,10,14-Trimethyl-5,9-pentadecadiene-2,13-dione	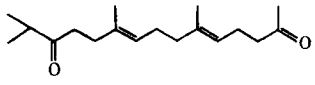	Brown alga (*Cystophora moniliformis*)	3	—
9	Furanoquinol	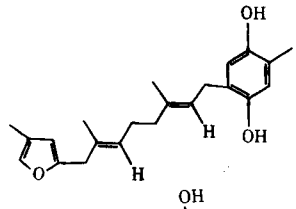	Soft coral	10	—
10	Furospongenol	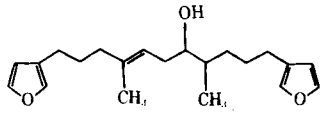	Sponge (Spongia)	20	—
11	—	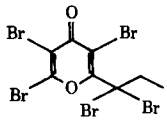	Red alga (*Ptilonia australasica*)	20	—
12	Plocamene E	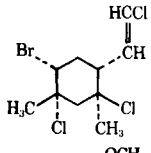	Red alga (*Plocamium cartilagineum*)	150–300	30
5	Dehydrocyclospongiaquinone	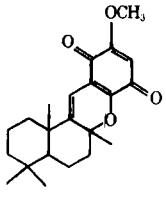	Sponge (Spongiidae)	30	—
13	Heterocladol	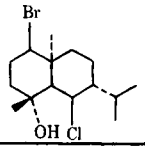	Red alga (*Laurencia filiformis*)	60	60

(*continued*)

Table I—*Continued*

Reference	Compound	Structure	Marine Organism	Concentration for 50% Inhibition of State 3 Respiration, μM	Concentration for 100% Increase of State 4 Respiration, μM
14	Filiformin	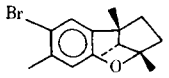	Red alga (*Laurencia filiformis*)	150	—
15	Acetoxyfimbrolide	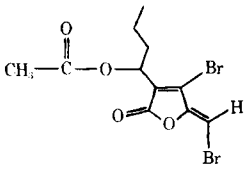	Red alga (*Delisea fimbriata*)	260	130
15	—	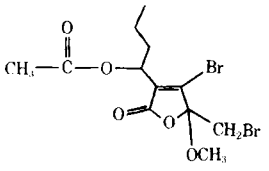	Red alga (*Delisea fimbriata*)	260	130
16	—	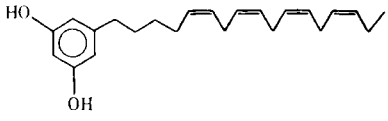	Brown alga (*Cystophora torulosa*)	300	—
17	—	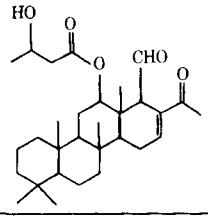	Sponge (*Phyllospongia dendyi*)	—	200

After a steady State 4 respiration (4) was established with substrates of 10 mM malate and 10 mM glutamate, the test compound was added to the reaction vessel; adenosine diphosphate was added ~5 min later. Thus, the effects on both State 4 (resting, adenosine diphosphate-limited) and State 3 (active, adenosine diphosphate-stimulated) respiration were assessed in each trial. Each compound was tested at three or more concentrations on three batches of mitochondria to estimate an accurate concentration for doubling of State 4 respiration (*i.e.*, uncoupling action) or inhibition of the adenosine diphosphate-stimulated respiration to one-half of its control value.

RESULTS AND DISCUSSION

The chemical isolation and structural determinations of the compounds isolated from marine organisms in these laboratories have been reported, and the references are given in Table I. The structures of the tested compounds, the organisms from which the compounds were extracted, and the mean compound concentration required to produce doubling of oxygen uptake in mitochondria in State 4 (uncoupling effect) or 50% inhibition of oxygen uptake in State 3 respiration are summarized in Table I. The estimated effective potencies for each compound were very similar in the different mitochondrial batches.

Several compounds were very potent in either stimulating or inhibiting respiration. The most potent compounds were two closely related substances, isospongiaquinone and dihydroisospongiaquinone, extracted from a sponge of the family Spongiidae (5). Both compounds produced ~50% inhibition of State 3 respiration at 1 μM; at 5 μM, considerable depression of State 4 respiration also was seen. The effect of isospongiaquinone is illustrated in Fig. 1.

The most potent stimulant of State 4 respiration was dihydrocyperaquinone (6), which approximately doubled State 4 respiration at 4 μM. As the dihydrocyperaquinone concentration was increased, State 3 respiration gradually decreased, as is usual with compounds that uncouple oxidative phosphorylation. However, concentrations of 1 mM were needed to produce 50% inhibition of the State 3 respiration (Fig. 2).

Several other compounds showed mixed effects. The halogenated compounds costatol (7), heterocladol (13), and acetoxyfimbrolide (15) all showed mixed stimulation of State 4 and inhibition of State 3 respiration such that, while State 4 respiration could be approximately doubled at the concentrations shown in Table I, there was little or no further stimulation of respiration by adenosine diphosphate. As the concentration of these compounds was increased further, decreased stimulation of State 4 respiration was observed. However, such mixed effects on mitochondrial respiration were not always apparent with halogenated compounds. Filiformin and the pentabromopyrone from *Ptilonia australasica* (11) produced only inhibition with no uncoupling action.

While the precise site of action of these novel marine compounds in the respiratory chain is unknown, their nonselective inhibitory effects on smooth muscle preparations may be explained largely by the inhibition of electron transport or the uncoupling of oxidative phosphorylation (18, 19). In addition, compounds that uncouple oxidative phosphorylation affect the permeability of many excitable cells (20). Other enzyme systems also may be inhibited by these compounds because it was shown recently that several halogenated compounds isolated from red algae and from the sea hare *Aplysia dactylomela* prolonged pentobarbital-induced sleeping times and blood pentobarbital levels in mice, probably by inhibiting pentobarbital metabolism (21, 22).

REFERENCES

(1) A. Der Marderosian, *J. Pharm. Sci.*, **58**, 1 (1969).

(2) R. W. Estabrook, in "Methods in Enzymology," vol. 10, R. W. Estabrook and M. E. Pullman, Eds., Academic, New York, N.Y., 1967, p. 41.

(3) O. H. Lowry, N. J. Rosebrough, A. L. Farr, and R. J. Randall, *J. Biol. Chem.*, **193**, 265 (1951).

(4) B. Chance and G. R. Williams, *ibid.*, **217**, 409 (1955).

(5) R. Kazlauskas, P. T. Murphy, R. G. Warren, R. J. Wells, and J. F. Blount, *Aust. J. Chem.*, **31**, 2685 (1978).

(6) R. D. Allan, R. L. Correll, and R. J. Wells, *Tetrahedron Lett.*, **1969**, 4669.

(7) R. Kazlauskas, P. T. Murphy, R. J. Quinn, and R. J. Wells, *ibid.*, **1976**, 4451.

(8) R. Kazlauskas, P. T. Murphy, and R. J. Wells, *Experientia*, **34**,

156 (1978).
(9) J. C. Coll, N. Liyanage, G. J. Stokie, I. Van Altena, J. N. E. Nemorin, S. Sternhell, and R. Kazlauskas, *Aust. J. Chem.*, **31**, 157 (1978).
(10) R. Kazlauskas, P. T. Murphy, R. J. Quinn, and R. J. Wells, *Tetrahedron Lett.*, **1976**, 1333.
(11) R. Kazlauskas, R. O. Lidgard, and R. J. Wells, *ibid.*, **1978**, 3165.
(12) R. S. Norton, R. G. Warren, and R. J. Wells, *ibid.*, **1977**, 3905.
(13) R. Kazlauskas, P. T. Murphy, R. J. Wells, J. J. Daly, and W. E. Oberhansli, *Aust. J. Chem.*, **30**, 2679 (1977).
(14) R. Kazlauskas, P. T. Murphy, R. J. Quinn, and R. J. Wells, *ibid.*, **29**, 2533 (1976).
(15) R. Kazlauskas, P. T. Murphy, R. J. Quinn, and R. J. Wells, *Tetrahedron Lett.*, **1977**, 37.
(16) R. P. Gregson, R. Kazlauskas, P. T. Murphy, and R. J. Wells, *Aust. J. Chem.*, **30**, 2527 (1977).
(17) R. J. Wells, *Pure Appl. Chem.*, **51**, 1829 (1979).
(18) T. C. West, G. Hadden, and A. Farah, *Am. J. Physiol.*, **164**, 565 (1951).
(19) G. V. R. Born and E. Bulbring, *J. Physiol. (London)*, **127**, 626 (1955).
(20) J. L. Barker and H. Levitan, *Membr. Biol.*, **25**, 361 (1975).
(21) P. N. Kaul, S. K. Kulkarni, and E. Kurosawa, *J. Pharm. Pharmacol.*, **30**, 589 (1978).
(22) P. N. Kaul and S. K. Kulkarni, *J. Pharm. Sci.*, **67**, 1293 (1978).

Inhibition of *In Vitro* Cytochrome P-450-Catalyzed Reactions by Substituted Pyridines

JERRY L. BORN ˣ and WILLIAM M. HADLEY

Received August 29, 1979, from the *College of Pharmacy, University of New Mexico, Albuquerque, NM 87131.* Accepted for publication October 25, 1979.

Abstract □ A series of substituted pyridines was investigated as inhibitors of cytochrome P-450-catalyzed reactions. The relative potencies for the *in vitro* inhibition of aminopyrine demethylation and aniline hydroxylation are reported for a series of 2-, 3-, and 4-substituted pyridines.

Keyphrases □ Oxidation—cytochrome P-450, inhibition of *in vitro* metabolism of aniline and aminopyrine, effect of substituted pyridines on inhibition □ Aniline—hydroxylase activity, effect of substituted pyridines on *in vitro* aniline metabolism, cytochrome P-450 oxidation reactions □ Aminopyrine—demethylation activity, effect of substituted pyridines on *in vitro* aminopyrine metabolism, cytochrome P-450 oxidation reactions

Cytochrome P-450 is the terminal oxygenase responsible for the metabolism of many drugs and xenobiotics. Numerous pyridine-containing compounds such as metyrapone and ellipticine are known to inhibit cytochrome P-450-catalyzed reactions (1,2). It has been suggested that potent inhibitors of cytochrome P-450-catalyzed oxidations may be useful therapeutically in the prevention of chemical-induced cancer (2). Another potential use of cytochrome P-450 inhibitors is to increase the half-lives for drugs, thus increasing their therapeutic effectiveness.

The nonselective nature of the known inhibitors of cytochrome P-450-mediated reactions limits their therapeutic application. For example, metyrapone is used to inhibits steroid 11-β-hydroxylase, but it also is a potent inhibitor of many other cytochrome P-450 transformations (1, 3).

To develop leads in designing potent substrate-selective inhibitors of hepatic cytochrome P-450-catalyzed reactions, the ability of some simple pyridine compounds to inhibit the metabolism of aniline and aminopyrine was investigated.

EXPERIMENTAL

Male Sprague–Dawley rats were sacrificed by cervical dislocation, and their livers were excised and placed in ice-cold isotonic 1.15% KCl–tromethamine [tris(hydroxymethyl)aminomethane] buffer (0.1 *M*, pH 7.4). The following steps were performed at 0–4°. The liver was pressed through a tissue press, and the mince was weighed and homogenized[1] in three volumes of ice-cold isotonic potassium chloride–tromethamine buffer.

The homogenate was centrifuged for 20 min at 9000×*g* in an ultracentrifuge[2] using a No. 30 rotor. The supernate was withdrawn and centrifuged at 78,000×*g* for 60 min. Then the supernate was decanted, and the pellet was resuspended in tromethamine buffer so that 1 ml of buffer contained microsomes from 250 mg of liver. The protein content was determined using the method of Lowry *et al.* (4).

Aniline hydroxylase activity was determined by the analysis for *p*-hydroxyaniline. Metabolic reactions were run in 25-ml erlenmeyer flasks. The 5-ml reaction volume contained microsomal protein (10 mg), glucose-6-phosphate (30 μM), nicotinamide adenine dinucleotide phosphate (4 μM), magnesium chloride (50 μM), glucose-6-phosphate dehydrogenase (2 units), inhibitor in tromethamine buffer (pH 7.4), and substrate (1.09 μM) in buffer (pH 7.4). The reaction components, except the substrate, were preincubated for 5 min at 37° in a metabolic incubator under oxygen (flow rate >1000 ml/min) at 100 oscillations/min. Substrate then was added, and the reaction was incubated for 30 min. The production of *p*-hydroxyaniline was analyzed as described by Netter and Seidel (5).

Aminopyrine demethylation was determined by the analysis of formaldehyde. The 5-ml reaction volume contained the same cofactors used for aniline hydroxylation. The aminopyrine concentration was 8 m*M*. Formaldehyde was analyzed by the method of McMahon and Easton (6).

All samples were run in duplicate, and each experiment was repeated. The I_{50} values were calculated from three inhibitor concentrations.

All compounds were prepared by literature methods, and their physical constants corresponded to the literature values (7–9).

RESULTS AND DISCUSSION

The inhibition of aniline and aminopyrine metabolism by the substituted pyridines is shown in Table I. Inhibition of aniline metabolism was highly dependent on the position of substitution on pyridine. The 4-substituted pyridines were the most potent inhibitors of aniline metabolism, and the 3-substituted pyridines were more potent inhibitors than the 2-substituted pyridines. The presence of a hydroxyl group in the inhibitors lowered their ability to inhibit aniline metabolism. The decreased lipid solubility of the hydroxyl-substituted pyridines may be involved in their lower inhibitory activity.

[1] Potter-Elvejhem-type homogenizer.
[2] Beckman L5-40.

0022-3549/80/0400-0465$01.00/0
© 1980, American Pharmaceutical Association

156 (1978).
(9) J. C. Coll, N. Liyanage, G. J. Stokie, I. Van Altena, J. N. E. Nemorin, S. Sternhell, and R. Kazlauskas, *Aust. J. Chem.*, **31**, 157 (1978).
(10) R. Kazlauskas, P. T. Murphy, R. J. Quinn, and R. J. Wells, *Tetrahedron Lett.*, **1976**, 1333.
(11) R. Kazlauskas, R. O. Lidgard, and R. J. Wells, *ibid.*, **1978**, 3165.
(12) R. S. Norton, R. G. Warren, and R. J. Wells, *ibid.*, **1977**, 3905.
(13) R. Kazlauskas, P. T. Murphy, R. J. Wells, J. J. Daly, and W. E. Oberhansli, *Aust. J. Chem.*, **30**, 2679 (1977).
(14) R. Kazlauskas, P. T. Murphy, R. J. Quinn, and R. J. Wells, *ibid.*, **29**, 2533 (1976).
(15) R. Kazlauskas, P. T. Murphy, R. J. Quinn, and R. J. Wells, *Tetrahedron Lett.*, **1977**, 37.
(16) R. P. Gregson, R. Kazlauskas, P. T. Murphy, and R. J. Wells, *Aust. J. Chem.*, **30**, 2527 (1977).
(17) R. J. Wells, *Pure Appl. Chem.*, **51**, 1829 (1979).
(18) T. C. West, G. Hadden, and A. Farah, *Am. J. Physiol.*, **164**, 565 (1951).
(19) G. V. R. Born and E. Bulbring, *J. Physiol. (London)*, **127**, 626 (1955).
(20) J. L. Barker and H. Levitan, *Membr. Biol.*, **25**, 361 (1975).
(21) P. N. Kaul, S. K. Kulkarni, and E. Kurosawa, *J. Pharm. Pharmacol.*, **30**, 589 (1978).
(22) P. N. Kaul and S. K. Kulkarni, *J. Pharm. Sci.*, **67**, 1293 (1978).

Inhibition of *In Vitro* Cytochrome P-450-Catalyzed Reactions by Substituted Pyridines

JERRY L. BORN ˣ and WILLIAM M. HADLEY

Received August 29, 1979, from the *College of Pharmacy, University of New Mexico, Albuquerque, NM 87131.* Accepted for publication October 25, 1979.

Abstract □ A series of substituted pyridines was investigated as inhibitors of cytochrome P-450-catalyzed reactions. The relative potencies for the *in vitro* inhibition of aminopyrine demethylation and aniline hydroxylation are reported for a series of 2-, 3-, and 4-substituted pyridines.

Keyphrases □ Oxidation—cytochrome P-450, inhibition of *in vitro* metabolism of aniline and aminopyrine, effect of substituted pyridines on inhibition □ Aniline—hydroxylase activity, effect of substituted pyridines on *in vitro* aniline metabolism, cytochrome P-450 oxidation reactions □ Aminopyrine—demethylation activity, effect of substituted pyridines on *in vitro* aminopyrine metabolism, cytochrome P-450 oxidation reactions

Cytochrome P-450 is the terminal oxygenase responsible for the metabolism of many drugs and xenobiotics. Numerous pyridine-containing compounds such as metyrapone and ellipticine are known to inhibit cytochrome P-450-catalyzed reactions (1,2). It has been suggested that potent inhibitors of cytochrome P-450-catalyzed oxidations may be useful therapeutically in the prevention of chemical-induced cancer (2). Another potential use of cytochrome P-450 inhibitors is to increase the half-lives for drugs, thus increasing their therapeutic effectiveness.

The nonselective nature of the known inhibitors of cytochrome P-450-mediated reactions limits their therapeutic application. For example, metyrapone is used to inhibits steroid 11-β-hydroxylase, but it also is a potent inhibitor of many other cytochrome P-450 transformations (1, 3).

To develop leads in designing potent substrate-selective inhibitors of hepatic cytochrome P-450-catalyzed reactions, the ability of some simple pyridine compounds to inhibit the metabolism of aniline and aminopyrine was investigated.

EXPERIMENTAL

Male Sprague–Dawley rats were sacrificed by cervical dislocation, and their livers were excised and placed in ice-cold isotonic 1.15% KCl–tromethamine [tris(hydroxymethyl)aminomethane] buffer (0.1 *M*, pH 7.4). The following steps were performed at 0–4°. The liver was pressed through a tissue press, and the mince was weighed and homogenized[1] in three volumes of ice-cold isotonic potassium chloride–tromethamine buffer.

The homogenate was centrifuged for 20 min at 9000×*g* in an ultracentrifuge[2] using a No. 30 rotor. The supernate was withdrawn and centrifuged at 78,000×*g* for 60 min. Then the supernate was decanted, and the pellet was resuspended in tromethamine buffer so that 1 ml of buffer contained microsomes from 250 mg of liver. The protein content was determined using the method of Lowry *et al.* (4).

Aniline hydroxylase activity was determined by the analysis for *p*-hydroxyaniline. Metabolic reactions were run in 25-ml erlenmeyer flasks. The 5-ml reaction volume contained microsomal protein (10 mg), glucose-6-phosphate (30 μM), nicotinamide adenine dinucleotide phosphate (4 μM), magnesium chloride (50 μM), glucose-6-phosphate dehydrogenase (2 units), inhibitor in tromethamine buffer (pH 7.4), and substrate (1.09 μM) in buffer (pH 7.4). The reaction components, except the substrate, were preincubated for 5 min at 37° in a metabolic incubator under oxygen (flow rate >1000 ml/min) at 100 oscillations/min. Substrate then was added, and the reaction was incubated for 30 min. The production of *p*-hydroxyaniline was analyzed as described by Netter and Seidel (5).

Aminopyrine demethylation was determined by the analysis of formaldehyde. The 5-ml reaction volume contained the same cofactors used for aniline hydroxylation. The aminopyrine concentration was 8 m*M*. Formaldehyde was analyzed by the method of McMahon and Easton (6).

All samples were run in duplicate, and each experiment was repeated. The I_{50} values were calculated from three inhibitor concentrations.

All compounds were prepared by literature methods, and their physical constants corresponded to the literature values (7–9).

RESULTS AND DISCUSSION

The inhibition of aniline and aminopyrine metabolism by the substituted pyridines is shown in Table I. Inhibition of aniline metabolism was highly dependent on the position of substitution on pyridine. The 4-substituted pyridines were the most potent inhibitors of aniline metabolism, and the 3-substituted pyridines were more potent inhibitors than the 2-substituted pyridines. The presence of a hydroxyl group in the inhibitors lowered their ability to inhibit aniline metabolism. The decreased lipid solubility of the hydroxyl-substituted pyridines may be involved in their lower inhibitory activity.

[1] Potter-Elvejhem-type homogenizer.
[2] Beckman L5-40.

0022-3549/80/0400-0465$01.00/0
© 1980, American Pharmaceutical Association

Table I—Inhibition of *In Vitro* Metabolism of Aniline and Aminopyrine by Substituted Pyridines

Inhibitor	I_{50} of Aniline[a], M	I_{50} of Aminopyrine[b], M	$\frac{I_{50} \text{ of Aminopyrine}^c}{I_{50} \text{ of Aniline}}$
4-(*n*-Pentoxy)pyridine (I)	4.9×10^{-6}	1.1×10^{-4}	22.4
1-(4-Pyridyl)pentane (II)	5.3×10^{-6}	1.0×10^{-4}	18.9
1-(4-Pyridyl)pentanol (III)	1.1×10^{-5}	1.3×10^{-4}	11.8
1-(3-Pyridyl)pentane (IV)	9.6×10^{-5}	1.0×10^{-4}	10.4
1-(3-Pyridyl)pentanol (V)	1.6×10^{-4}	1.35×10^{-4}	0.8
1-(2-Pyridyl)pentane (VI)	3.6×10^{-4}	1.8×10^{-4}	0.5
1-(2-Pyridyl)pentanol (VII)	1.35×10^{-3}	2.7×10^{-4}	0.2

[a] Aniline concentration = 1.09 μM. [b] Aminopyrine concentration = 8 mM. [c] A ratio of >1 indicates that the compound is a more potent inhibitor of aniline hydroxylation than of aminopyrine demethylation.

Aminopyrine demethylation showed much less sensitivity to inhibition by the 4-substituted pyridines than did aniline hydroxylation. In each case, the pyridine compounds that contained an alcohol functional group were less potent inhibitors than the corresponding alkylpyridines. The magnitude of this effect was significantly less than that observed for inhibition of aniline metabolism. The most potent inhibitors of aminopyrine demethylation, 1-(4-pyridyl)pentane (II) and 1-(3-pyridyl)pentane (IV), were only 2.7 times as active as the least potent compound, 1-(2-pyridyl)pentanol (VII). A similar comparison of the most potent inhibitor of aniline hydroxylation, 4-(*n*-pentoxy)pyridine (I), and VII reveals a 275-fold difference in potency.

The most selective inhibitors of this series were the 4-substituted pyridines. Compound I was 22 times more potent an inhibitor of aniline hydroxylation than it was an inhibitor of aminopyrine demethylation. The differential in potency of inhibitors for the two substrates suggests that appropriate molecular modifications on pyridine compounds may produce substrate-selective inhibitors of cytochrome P-450 reactions.

REFERENCES

(1) K. C. Leibman, *Mol. Pharmacol.*, **5**, 1 (1969).

(2) P. Lesca, P. Lecointe, C. Paoletti, and D. Mansay, *Biochem. Pharmacol.*, **27**, 1023 (1978).

(3) G. W. Liddle, D. Island, H. Ester, and G. M. Tomkins, *J. Clin. Invest.*, **37**, 912 (1958).

(4) O. H. Lowry, N. J. Rosebrough, A. L. Farr, and R. J. Randall, *J. Biol. Chem.*, **193**, 265 (1951).

(5) K. J. Netter and G. Seidel, *J. Pharmacol. Exp. Ther.*, **146**, 61 (1964).

(6) R. E. McMahon and N. R. Easton, *J. Pharmacol.*, **135**, 128 (1962).

(7) S. Rocal, French pat. 1,481,022; through *Chem. Abstr.*, **68**, P87188t (1968).

(8) E. Scozewinski and M. Bieganowska, *J. Chromatogr.*, **40**, 431 (1969).

(9) T. Cavigny and H. Normant, *Bull. Soc. Chim. Fr.*, **1965**, 1872.

ACKNOWLEDGMENTS

Supported by the Faculty Research Fund of the University of New Mexico.

Solid Dispersion of Morphine–Tristearin with Reduced Presystemic Inactivation in Rats

KEY S. CHANG and CHARLES I. JAROWSKI ˣ

Received June 15, 1979, from the *Department of Allied Health and Industrial Sciences, College of Pharmacy and Allied Health Professions, St. John's University, Jamaica, NY 11439.* Accepted for publication October 24, 1979.

Abstract □ Solid dispersions of morphine in tristearin, β-sitosterol, and cholesterol were prepared by evaporation of their ethanol solutions. Weight ratios of morphine–lipid of 1:1, 1:3, and 1:4.5 were prepared. Dissolution studies of the solid dispersions and morphine were conducted in a simulated GI medium at 37°. The release rates of morphine from the tristearin dispersions were the slowest. The 1:1 morphine–tristearin dispersion was administered orally to rats. Free and total morphine levels in rat urine were determined by spectrofluorometric and enzymatic immunoassay procedures, respectively. The morphine–tristearin dispersion yielded a higher percentage of free morphine after 24 and 48 hr as compared with morphine and its sulfate.

Keyphrases □ Morphine–tristearin—solid dispersion, reduced presystemic inactivation, rats □ Analgesics—morphine, solid dispersion containing tristearin, reduced presystemic inactivation, rats □ Dissolution—morphine–tristearin solid dispersion, *in vitro*

Orally administered morphine produces a poorer analgesic response as compared with the parenteral route (1). In addition, the LD_{50} of orally administered morphine in rats was 905 ± 144 mg/kg, whereas it was 237 ± 6 mg/kg with the intravenous dose.

In the past, the major organ responsible for first-pass metabolism has been assumed to be the liver. Incubation of morphine with liver tissue was shown to result in inactivation (2). Although the drug-metabolizing capacity of the gut mucosa has been known for many years (3), the involvement of the intestinal wall in the biotransformation of opiates has been observed only recently (4). By using tritium-labeled morphine in rats, approximately two-thirds of the overall first-pass effect (82%) of morphine was estimated to be due to extraction and/or metabolism in the intestine and the remaining one-third occurs in the liver (5).

It was of interest to determine if solid dispersions of morphine in lipids might reduce the extent of first-pass inactivation after oral administration. It was demonstrated previously (6) that orally administered progesterone gave higher blood levels when the hormone was solvent deposited on lactose as a solid solution with cholesterol or its acetate ester. Patel and Jarowski (7) reported that urinary excretion of unmetabolized salicylate was increased when

0022-3549/80/0400-0466$01.00/0

© 1980, American Pharmaceutical Association

Table I—Inhibition of *In Vitro* Metabolism of Aniline and Aminopyrine by Substituted Pyridines

Inhibitor	I_{50} of Aniline[a], M	I_{50} of Aminopyrine[b], M	$\frac{I_{50} \text{ of Aminopyrine}^c}{I_{50} \text{ of Aniline}}$
4-(*n*-Pentoxy)pyridine (I)	4.9×10^{-6}	1.1×10^{-4}	22.4
1-(4-Pyridyl)pentane (II)	5.3×10^{-6}	1.0×10^{-4}	18.9
1-(4-Pyridyl)pentanol (III)	1.1×10^{-5}	1.3×10^{-4}	11.8
1-(3-Pyridyl)pentane (IV)	9.6×10^{-5}	1.0×10^{-4}	10.4
1-(3-Pyridyl)pentanol (V)	1.6×10^{-4}	1.35×10^{-4}	0.8
1-(2-Pyridyl)pentane (VI)	3.6×10^{-4}	1.8×10^{-4}	0.5
1-(2-Pyridyl)pentanol (VII)	1.35×10^{-3}	2.7×10^{-4}	0.2

[a] Aniline concentration = 1.09 μM. [b] Aminopyrine concentration = 8 mM. [c] A ratio of >1 indicates that the compound is a more potent inhibitor of aniline hydroxylation than of aminopyrine demethylation.

Aminopyrine demethylation showed much less sensitivity to inhibition by the 4-substituted pyridines than did aniline hydroxylation. In each case, the pyridine compounds that contained an alcohol functional group were less potent inhibitors than the corresponding alkylpyridines. The magnitude of this effect was significantly less than that observed for inhibition of aniline metabolism. The most potent inhibitors of aminopyrine demethylation, 1-(4-pyridyl)pentane (II) and 1-(3-pyridyl)pentane (IV), were only 2.7 times as active as the least potent compound, 1-(2-pyridyl)pentanol (VII). A similar comparison of the most potent inhibitor of aniline hydroxylation, 4-(*n*-pentoxy)pyridine (I), and VII reveals a 275-fold difference in potency.

The most selective inhibitors of this series were the 4-substituted pyridines. Compound I was 22 times more potent an inhibitor of aniline hydroxylation than it was an inhibitor of aminopyrine demethylation. The differential in potency of inhibitors for the two substrates suggests that appropriate molecular modifications on pyridine compounds may produce substrate-selective inhibitors of cytochrome P-450 reactions.

REFERENCES

(1) K. C. Leibman, *Mol. Pharmacol.*, **5**, 1 (1969).

(2) P. Lesca, P. Lecointe, C. Paoletti, and D. Mansay, *Biochem. Pharmacol.*, **27**, 1023 (1978).

(3) G. W. Liddle, D. Island, H. Ester, and G. M. Tomkins, *J. Clin. Invest.*, **37**, 912 (1958).

(4) O. H. Lowry, N. J. Rosebrough, A. L. Farr, and R. J. Randall, *J. Biol. Chem.*, **193**, 265 (1951).

(5) K. J. Netter and G. Seidel, *J. Pharmacol. Exp. Ther.*, **146**, 61 (1964).

(6) R. E. McMahon and N. R. Easton, *J. Pharmacol.*, **135**, 128 (1962).

(7) S. Rocal, French pat. 1,481,022; through *Chem. Abstr.*, **68**, P87188t (1968).

(8) E. Scozewinski and M. Bieganowska, *J. Chromatogr.*, **40**, 431 (1969).

(9) T. Cavigny and H. Normant, *Bull. Soc. Chim. Fr.*, **1965**, 1872.

ACKNOWLEDGMENTS

Supported by the Faculty Research Fund of the University of New Mexico.

Solid Dispersion of Morphine–Tristearin with Reduced Presystemic Inactivation in Rats

KEY S. CHANG and CHARLES I. JAROWSKI ˣ

Received June 15, 1979, from the *Department of Allied Health and Industrial Sciences, College of Pharmacy and Allied Health Professions, St. John's University, Jamaica, NY 11439.* Accepted for publication October 24, 1979.

Abstract □ Solid dispersions of morphine in tristearin, β-sitosterol, and cholesterol were prepared by evaporation of their ethanol solutions. Weight ratios of morphine–lipid of 1:1, 1:3, and 1:4.5 were prepared. Dissolution studies of the solid dispersions and morphine were conducted in a simulated GI medium at 37°. The release rates of morphine from the tristearin dispersions were the slowest. The 1:1 morphine–tristearin dispersion was administered orally to rats. Free and total morphine levels in rat urine were determined by spectrofluorometric and enzymatic immunoassay procedures, respectively. The morphine–tristearin dispersion yielded a higher percentage of free morphine after 24 and 48 hr as compared with morphine and its sulfate.

Keyphrases □ Morphine–tristearin—solid dispersion, reduced presystemic inactivation, rats □ Analgesics—morphine, solid dispersion containing tristearin, reduced presystemic inactivation, rats □ Dissolution—morphine–tristearin solid dispersion, *in vitro*

Orally administered morphine produces a poorer analgesic response as compared with the parenteral route (1). In addition, the LD_{50} of orally administered morphine in rats was 905 ± 144 mg/kg, whereas it was 237 ± 6 mg/kg with the intravenous dose.

In the past, the major organ responsible for first-pass metabolism has been assumed to be the liver. Incubation of morphine with liver tissue was shown to result in inactivation (2). Although the drug-metabolizing capacity of the gut mucosa has been known for many years (3), the involvement of the intestinal wall in the biotransformation of opiates has been observed only recently (4). By using tritium-labeled morphine in rats, approximately two-thirds of the overall first-pass effect (82%) of morphine was estimated to be due to extraction and/or metabolism in the intestine and the remaining one-third occurs in the liver (5).

It was of interest to determine if solid dispersions of morphine in lipids might reduce the extent of first-pass inactivation after oral administration. It was demonstrated previously (6) that orally administered progesterone gave higher blood levels when the hormone was solvent deposited on lactose as a solid solution with cholesterol or its acetate ester. Patel and Jarowski (7) reported that urinary excretion of unmetabolized salicylate was increased when

0022-3549/80/0400-0466$01.00/0

© 1980, American Pharmaceutical Association

Table I—Dissolution of Morphine and Morphine–Lipid Solid Dispersions in Simulated GI Media at 37°

Sample	Weight Ratio	Percent Dissolved at 15 min	30 min	60 min	90 min	120 min	150 min
		Simulated Intestinal Fluid					
Morphine	1:0	53.9	70.4	81.6	88.2	92.9	96.8
Morphine–cholesterol	1:1	59.8	70.4	84.3	90.9	92.9	93.9
	1:3	69.7	79.7	91.2	94.5	95.9	96.8
	1:4.5	74.4	87.9	93.9	96.5	97.2	97.5
Morphine—β-sitosterol	1:1	48.9	65.4	71.4	77.7	81.3	83.3
	1:3	47.6	64.4	71.4	80.3	86.9	87.6
	1:4.5	47.9	64.8	77.3	87.9	92.9	95.5
Morphine–tristearin	1:1	7.6	15.2	23.8	29.4	33.1	37.0
	1:3	3.9	12.5	22.9	27.8	32.1	34.1
	1:4.5	1.9	6.6	9.5	12.2	13.6	16.5
		Simulated Gastric Fluid					
Morphine[a]	1:0	99.4	99.8	—	—	—	—
Morphine–tristearin[a]	1:1	50.2	57.8	66.1	76.7	83.3	88.3

[a] Morphine equivalent of 250 mg.

salicylic acid was given to humans as a solid solution in cholesteryl *n*-decylate.

This investigation concerned the *in vitro* dissolution rate of morphine (I) from solid dispersions containing cholesterol (II), β-sitosterol (III), or tristearin (IV). Based on the *in vitro* data, a candidate was selected for an *in vivo* study in rats. Measurement of the urinary excretion and its biologically inactive glucuronide showed whether first-pass inactivation was reduced.

EXPERIMENTAL

Materials—The following materials were obtained commercially: morphine[1], morphine sulfate pentahydrate[1], cholesterol[2], β-sitosterol[3], tristearin[4], absolute ethanol[5] (ACS), chloroform[5] (ACS), isopropanol[5] (ACS), hydrochloric acid[5] (ACS), sodium hydroxide[5] (ACS), citric acid monohydrate[6] (laboratory grade), potassium chloride[5] (ACS), monobasic potassium phosphate[5] (ACS), boric acid[5] (ACS), dibasic anhydrous sodium phosphate[5] (ACS), ammonium hydroxide[5] (ACS), opiate antibody reagent[7] (Reagent A), opiate enzyme immunoassay reagent[7] (Reagent B), bacterial suspension[7], buffer[7], and laboratory chow[8].

Equipment—The following equipment was used: a differential scanning calorimeter with a recorder[9], a turret spectrofluorometer with a Servo recorder[10], a dissolution basket stirrer[11], a grating spectrophotometer with digital display[12], a microsample spectrophotometer with thermal control[13], a gyrotory incubator shaker[14], a zeromatic pH meter[12], a polytherm water bath with thermal control[15], U.S. standard sieve No. 60[16], a Swinny adaptor[17] (13 mm), a filter disk[17] (13 mm, 0.45 μm), a medium porosity sintered-glass filter[18] (ASTM 10–15 M), and polycarbonate metabolism units[19].

Preparation of Morphine–Lipid Solid Dispersions—Powdered morphine base (1 g) was blended with powdered lipid (cholesterol, β-sitosterol, or tristearin) in drug–lipid ratios of 1:1, 1:3, and 1:4.5. The blend was dissolved in sufficient absolute ethanol (~300 ml). The solutions were magnetically stirred while the solvent was evaporated in a gentle stream of air. The residue was dried to constant weight at 37°, passed through a 60-mesh sieve, and manually bottle blended. Portions of the blended material were assayed for morphine. Only those samples assaying 100 ± 5% were used in the dissolution study.

Differential Scanning Calorimetry—Thermal analyses were performed on the 1:1 ratio of morphine–tristearin, morphine, and tristearin using a differential scanning calorimeter. Aluminum pans and lids were used for all samples. Studies were conducted from 20 to 300° with nitrogen as the effluent gas (20 ml/min). Temperature calibrations were made using indium (156.6°) and tin (231.9°) as standards with scanning speeds of 10°/10 mm/min (morphine–tristearin and morphine) and 10°/5 mm/min (tristearin). The transition temperature was determined by extrapolating a linear portion of the leading edge of the endothermic peak to the baseline.

Spectrophotometric Absorption and Calibration Curves for Morphine in Selected Solvent Systems—Absorption spectral curves for morphine base (100 μg/ml) in four solvent systems were drawn. The absorption maxima were 288 nm for ethanol and 286 nm for distilled water and simulated gastric and intestinal fluids. The morphine concentration in these solvent systems obeyed Beer's law. Incorporation of the three lipids did not alter the absorbance values for morphine.

Dissolution Studies—The dissolution procedure was described previously (8). It was established that 144 mg of morphine forms a saturated solution in 500 ml of distilled water at 37°. Consequently, sink conditions were maintained since only 30 mg of morphine equivalent was used in the dissolution studies in simulated gastric fluid (without pepsin) and simulated intestinal fluid (without pancreatin). A basket speed of 50 rpm was used for all samples.

Morphine stability in simulated gastric fluid was excellent for 72 hr at 37° (absorbance increase of 0.42%). However, in simulated intestinal fluid, a similar absorbance increase was seen after 2 hr; after 24 hr, the absorbance increase was 3.74%. Five-milliliter aliquots were withdrawn at 15, 30, 60, 90, 120, and 150 min by a pipet adapted with a sintered-glass filter (medium porosity). The dissolution medium volume (500 ml) was maintained by replacement of 5-ml aliquots of preheated simulated GI fluids.

The dissolution data are shown in Table I. Each data point represents the average of two readings. Concentrations were corrected by taking into account the amount of morphine discarded in prior 5-ml aliquots.

Morphine Bioavailability in Rats—Eight male Sprague–Dawley rats, 350–450 g, were allowed free access to water and laboratory food. An aqueous vehicle was used for the oral intubation of morphine, morphine sulfate, and morphine–tristearin (1:1). The aqueous vehicle contained methylcellulose 4000 (0.4%), benzyl alcohol (0.9%), polysorbate 80 (0.5%), and sodium chloride (0.9%). Each rat was placed in individual metabolism cages, and each animal served as its own control.

The dosing volume employed for the solution (morphine sulfate) or the suspensions (morphine or morphine–tristearin) was 3.5–4.5 ml/kg. The morphine equivalent administered was 15 mg/kg. Blank urine was collected for 24 hr after oral administration of the placebo vehicle. After oral administration of one morphine candidate, 24-hr urine samples were collected over 4 days. All samples were frozen immediately.

Aliquots of each 24-hr urinary collection were proportionally pooled and filtered through a 0.45-μm filter disk. Proportional pooling was necessary to provide adequate urine volumes for the assays. The filtered urine was diluted 1:10 with distilled water and assayed for free and total morphine. Weekly intervals were maintained between experiments.

Total Morphine Assay in Rat Urine (9)—The proportionally pooled

[1] S. B. Penick, Lyndhurst, N.J.
[2] K & K Laboratories, Plainview, N.Y.
[3] Amend Drug & Chemical Co., New York, N.Y.
[4] ICN Pharmaceuticals, Plainview, N.Y.
[5] J. T. Baker Chemical Co., Phillipsburg, N.J.
[6] Fisher Scientific Co., Fair Lawn, N.J.
[7] Syva Corp., Palo Alto, Calif.
[8] Ralston Purina Co., St. Louis, Mo.
[9] Model DSC-19, Perkin-Elmer, Norwalk, Conn.
[10] Farrand Optical Co., New York, N.Y.
[11] Models 53 and 48-158, Hanson Research Corp., Northridge, Calif.
[12] Model DB-GT, Beckman Instrument Co., Fullerton, Calif.
[13] Gilford Instrument Co., Oberlin, Ohio
[14] Model G-25, New Brunswick Scientific Co., New Brunswick, N.J.
[15] Bench Scale Equipment Co., Dayton, Ohio.
[16] Newark Wire Cloth Co., Newark, N.J.
[17] Millipore Corp., Bedford, Mass.
[18] Pyrex Laboratories, New York, N.Y.
[19] Econo-cage, Maryland Plastics Inc., New York, N.Y.

Table II—Percent of Free and Total Morphine Recovered from the Urine of Rats Given 15 mg of Morphine Equivalent/kg Orally

Drug	Percent Recovered in 24 hr		Percent Recovered in 48 hr		Percent Recovered in 72 hr	
	Free	Total	Free	Total	Free	Total
Morphine sulfate	23.80	40.46	39.66	61.71	—	71.07
Morphine	21.31	25.57	30.90	35.43	—	38.84
Morphine–tristearin (1:1)	32.45	36.35	45.82	51.63	—	55.44

urine from the eight rats that had been diluted with distilled water was treated with 1 *N* HCl or NaOH if the pH was outside the 5.5–8 range. Fifty microliters of the diluted urine sample was added to 250 μl of buffer. Fifty microliters of the morphine antibody (Reagent A) was added followed by 50 μl of the enzyme-labeled morphine (Reagent B).

The reaction mixture (1.1 ml) was aspirated into a spectrophotometer, which automatically activated the enzymatic immunoassay printer. After a 10-sec delay for thermal equilibration, the initial absorbance was printed. After an additional 40 sec, a second absorbance was measured and recorded, followed by a printing of the differences between these values. The amount of morphine in the urine sample was determined by reference to a standard curve. The data points in the standard curve were determined by applying the identical assay on pooled blank urines spiked with known quantities of morphine. The results are summarized in Table II.

Free Morphine Assay in Rat Urine (10)—Two milliliters of the diluted urine sample was transferred to a 15-ml borosilicate glass-stoppered centrifuge tube. The pH of the solution was adjusted between 9 and 10 with 3.7 *N* NH_4OH. Four milliliters of chloroform–isopropanol (3:1 v/v) was added, and the mixture was shaken manually for 60 sec. The organic layer was evaporated to dryness on a water bath at 85° under a stream of air, and the residue was dried in an oven at 100° for 10 min. Concentrated sulfuric acid (0.1 ml) was added to the residue and mixed. One milliliter of distilled water was added, followed by 1 ml of concentrated ammonium hydroxide. After thorough shaking, the samples were autoclaved for 15 min at 120° at 15–18 psi.

The solution was transferred to a 7 × 150-mm round, borosilicate glass cell, and its fluorescence was determined in an automated turret spectrofluorometer using a No. 4-77 filter in combination with a 410-nm interference filter. This filter combination provided an excitation wavelength maximum at 392 nm with an emission wavelength maximum at 425 nm.

The spectrofluorometer was equipped with an 85-w high-intensity mercury vapor lamp, quartz lenses, and 0.2-mm slits. Sample readings were recorded in 20 sec. The emission monochromator drum dial was set at 410 nm, and all samples were scanned to 510 nm.

The recorded curve was cut out and weighed. Its concentration then could be determined from a standard curve prepared by plotting concentration *versus* curve weight. The standard solutions were prepared by diluting a stock solution of morphine in pooled, blank rat urine (100 μg/ml) with distilled water. These solutions were assayed spectrofluorometrically as described, and the recorded curves were cut out and weighed.

RESULTS

The thermograms for morphine and morphine–tristearin revealed that the melting point of morphine base was not significantly lowered in the presence of an equal weight of tristearin. A similarity in the transition temperature of morphine–tristearin indicated the presence of crystalline morphine base in the solid dispersion. The slope ratios of the endothermic peaks for morphine and morphine–tristearin were coincident. This result indicates that essentially no morphine decomposition occurred during the preparation of the solid dispersion (11). The thermograms showed no evidence for the existence of polymorphic forms.

On the basis of the dissolution data in Table I, the solid dispersion of morphine–tristearin (1:1) was selected for the *in vivo* study in rats. Only 37% of the morphine in this solid dispersion had dissolved in 150 min, whereas 53.9% of morphine base alone had dissolved in 15 min. The more dilute dispersions (1:3 and 1:4.5) were not considered in the interest of using as little tristearin as possible.

Dissolution studies in simulated gastric fluid were conducted with a larger morphine equivalent (250 mg) since the 30-mg equivalent dissolved too rapidly. As expected, the dissolution of morphine base was essentially complete in 15 min. Solid dispersions of morphine in cholesterol or β-sitosterol were ineffective in altering the morphine dissolution rate.

The *in vivo* results in Table II indicate that a reduction in first-pass inactivation was achieved by the administration of morphine base or its 1:1 solid dispersion in tristearin. Thus, at the end of 24 hr, 58.8% of the total morphine recovered was unmetabolized when morphine sulfate was administered orally. After the base was administered, 83.3% of the total morphine recovered was unmetabolized. Oral administration of the 1:1 solid dispersion yielded 89.3% of unmetabolized morphine. The recovery data after 72 hr reveal that the rank order in free morphine collected was solid dispersion > morphine sulfate > morphine base. Oral administration of morphine sulfate yielded the largest values for total morphine at the three time intervals studied. On the other hand, the percentage of free morphine was highest at all time intervals after oral administration of the 1:1 solid dispersion.

Oguri *et al.* (12) reported that after 30 mg of morphine equivalent/kg was administered subcutaneously to rats, free urinary morphine recovered during 24 hr amounted to 19.5% of the dose; total morphine conjugate recovered during this time was 3.5% of the dose. The higher percentage of free morphine recovered by this administration route is not surprising since intestinal wall enzymatic inactivation is significantly bypassed. The reduced total recovery was attributed to biliary excretion of morphine and its conjugates by the rat.

Cochin *et al.* (13) reported that urinary free morphine recovered during 24 hr after an oral dose of morphine sulfate (30 mg/kg) was given to dogs ranged from 10 to 15%; morphine conjugates recovered during this period ranged from 60 to 70%. Yeh *et al.* (14) administered morphine hydrochloride subcutaneously to cats (morphine equivalent of 20 mg/kg). During the first 48 hr after dosing, urinary recovery of free morphine amounted to 19.2 ± 1.5%; morphine conjugates recovered during this period amounted to 48.4 ± 2.4% of the dose.

The following explanation is proposed for the interesting results obtained with the 1:1 morphine–tristearin dispersion. Release of morphine from the lipid dispersion occurs more efficiently beyond the pylorus where contact is made with the fat-emulsifying bile secretions. Inhibition of the intestinal wall enzymes by the emulsified lipid component permits a portion of the simultaneously released morphine molecules to evade inactivation partially. Two-thirds of the total morphine inactivation in rats occurs in the gut wall and one-third occurs in the liver (5).

The lesser recovery of total morphine from the morphine–tristearin solid dispersion as compared with morphine sulfate was not unexpected in view of the slow dissolution rate of the former substance in simulated GI media. The superior oral absorption efficiency of morphine from the solid dispersion as compared with morphine base may be the result of smaller drug particle size in the solid dispersion. The facile *in vivo* absorption of a neutral lipid molecule such as tristearin may expose finely divided morphine base molecules for rapid dissolution and absorption.

The reduction in first-pass inactivation should stimulate further research on the use of lipid dispersions with drugs enzymatically inactivated after oral administration.

REFERENCES

(1) J. K. Finnegan, H. B. Haag, P. S. Larson, and M. L. Dreyfuss, *J. Pharmacol. Exp. Ther.*, **92**, 269 (1948).

(2) M. H. Seevers, in "Pharmacologic Principles of Medical Practice," 7th ed., J. C. Krantz, Jr., and C. J. Carr, Eds., Williams & Wilkins, Baltimore, Md., p. 137.

(3) K. J. W. Hartiala, *Physiol. Rev.*, **53**, 4960 (1973).

(4) E. Del Villar, E. Sanchez, and T. R. Tephley, *Drug Metab. Disp.*, **2**, 443 (1974).

(5) K. Iwamoto and C. D. Klaassen, *J. Pharmacol. Exp. Ther.*, **200**, 236 (1977).

(6) H. Rudel, U.S. pat. 3,828,106 (Aug. 6, 1974).

(7) S. P. Patel and C. I. Jarowski, *J. Pharm. Sci.*, **64**, 869 (1975).

(8) D. C. Monkhouse and J. L. Lach, *ibid.*, **61**, 1430 (1972).

(9) "Technical Bulletin on the Enzymatic Immunoassay," Syva Corp.,

Palo Alto, Calif.
(10) S. J. Mule and P. L. Hushin, *Anal. Chem.*, **43**, 708 (1971).
(11) D. C. Monkhouse and J. L. Lach, *J. Pharm. Sci.*, **61**, 1435 (1972).
(12) K. Oguri, S. Ida, H. Yoshimura, and H. Tsukamoto, *Chem. Pharm. Bull.*, **18**, 2414 (1970).
(13) J. Cochin, J. Haggart, L. A. Woods, and M. H. Seevers, *J. Pharmacol. Exp. Ther.*, **111**, 74 (1954).
(14) S. Y. Yeh, H. I. Chernov, and L. A. Woods, *J. Pharm. Sci.*, **60**, 469 (1971).

Identification of Degradation Products in a Phenylbutazone Tablet Formulation

F. MATSUI ˣ, D. L. ROBERTSON, M. A. POIRIER, and E. G. LOVERING

Received April 27, 1979, from the *Drug Research Laboratories, Health Protection Branch, Tunney's Pasture, Ottawa, Ontario, Canada, K1A 0L2.* Accepted for publication October 24, 1979.

Abstract □ Two previously reported but unidentified phenylbutazone degradation products were isolated from a tablet that was stored at 60° for 203 days. The compounds, α-(*N*-phenylcarbamoyl)-*N*-caproylhydrazobenzene and α-hydroxy-α-(*N*-phenylcarbamoyl)-*N*-caproylhydrazobenzene, were isolated by chromatography, identified by mass and NMR spectrometry, and synthesized by the reaction of aniline with phenylbutazone or its hydroxy analog, respectively.

Keyphrases □ Phenylbutazone—tablets, identification of degradation products □ Anti-inflammatory agents—phenylbutazone, tablets, identification of degradation products □ Degradation products—phenylbutazone, tablets, identification

In a recent study on the stability of phenylbutazone formulations under stress conditions (1), one formulation (G) was found to contain one or more compounds previously unidentified in degradation of the drug. These compounds are α-(*N*-phenylcarbamoyl)-*N*-caproylhydrazobenzene (I) and α-hydroxy-α-(*N*-phenylcarbamoyl)-*N*-caproylhydrazobenzene (II). This paper describes the isolation, identification, and synthesis of I and II.

EXPERIMENTAL

Materials—Tablets of Formulation G (1) were obtained directly from the manufacturer. Phenylbutazone[1] (*III*), cyclohexane[2], chloroform[2], methanol[2], ethyl acetate[2], and acetic acid[3] were used as received. Phenyl phthalate[4] was recrystallized from acetone[2]–water, and 1,2-diphenyl-4-*n*-butyl-4-hydroxypyrazolidine-3,5-dione (IV) was prepared by the method described previously (1, 2). TLC plates[5] precoated with silica gel G-60 F-254, 60–200-mesh silica gel[6], diatomaceous earth[7], and nylon tubing[8] were used.

Equipment—The gas chromatograph[9] was equipped with a flame-ionization detector and a U-shaped glass column packed with 5% OV-7 on Gas Chrom Q[7] (100–120 mesh). NMR spectra were obtained on a 90-MHz instrument[10]; chemical shifts are reported in parts per million from tetramethylsilane, the internal standard. All spectra were recorded in deuterated chloroform[11] ($CDCl_3$). Mass spectra[12] were recorded at an ionizing potential of 70 ev, and the samples were introduced *via* the direct probe at 120 and 130°. Accurate mass measurements were made by the peak matching technique.

TLC Solvent System A (3) consisted of cyclohexane–chloroform–methanol–acetic acid (60:30:5:5), and Solvent System B was chloroform–ethyl acetate (80:20). Filter paper-lined TLC tanks were equilibrated with the solvent system for 30 min prior to use. Spots were visualized by UV light at 254 nm and by spraying with a solution of 0.5% potassium dichromate in 20% (v/v) H_2SO_4.

Isolation of Degradation Products from Formulation G—Five tablets (equivalent to 500 mg of phenylbutazone), which had been stored for 203 days at 60°, were finely powdered, wetted with ethyl acetate, and triturated with 2 g of diatomaceous earth until the mixture was uniform. The triturate was placed at the top of a nylon column containing 200 g of 60–200-mesh silica gel, which had been deactivated with 30 ml of water and dry packed into a 0.03 × 1-m nylon column. A 500-ml solution of Solvent System A was added until the solvent front reached the bottom of the column. The tube was incised into 5-cm sections, and the location of each compound on the column was established by removing small portions of the silica gel from the different incised sections of the nylon tube, extracting these portions with ethyl acetate, and spotting aliquots directly onto a TLC plate.

The spots were visualized with the potassium dichromate spray, and the spots containing the components of interest immediately developed a bright-purple color. The sections of interest then were cut; the degradation products were extracted from the silica gel with ethyl acetate, concentrated under nitrogen, and rechromatographed on a TLC plate using Solvent System A to remove residual phenylbutazone. The R_f values of I, II, and III in this system were 0.37, 0.37, and 0.43, respectively.

The band containing the mixture of I and II was visualized by spraying the edges of the TLC plate with dichromate spray. The band was scraped off and extracted with ethyl acetate, and the eluate was reduced to a small volume under nitrogen. Resolution of I and II was effected by TLC using Solvent System B. Isolation was carried out by elution with ethyl acetate and evaporation under nitrogen. The R_f values of I, II, and III using Solvent System B were 0.56, 0.50, and 0.58, respectively.

Syntheses—*Compound I*—A solution of 308 mg (1 mmole) of III and 180 mg of aniline (100% excess) in 15 ml of chloroform was heated under nitrogen at 45° for 48 hr in a culture tube. Compound I was separated from unreacted phenylbutazone by TLC (System A), and the spot was scraped from the plate and eluted with ethyl acetate. Traces of II were removed by subsequent TLC using Solvent System B. Crystallization from ethanol–water (90:10) gave pure I, mp 197–199°; NMR ($CDCl_3$): δ 8.9 (s, NH), 8.5 (s, CONH), 7.4–6.8 (m, 15H, aromatic), 4.2 (t, CH), 2.0, 1.5, and 0.87 (*n*-butyl) ppm; mass spectrum (70 ev, 120°): *m/e* 401 (M^+ 5.3%), 307 (7.1), 218 (12.5), 184 (48.1), 148 (13.1), 120 (18.1), 93 (100), and 77 (72.3). The GLC[13] retention time was 11.0 min or 0.92 relative to the internal standard, phenyl phthalate.

Compound II—Compound II was prepared from 1,2-diphenyl-4-*n*-butyl-4-hydroxypyrazoline-3,5-dione (IV) by the procedure described for the synthesis of I. Compound II also can be obtained from III by carrying out the reaction under an oxygen atmosphere. After purification by TLC, crystallization from ethanol–water (90:10) yielded II, mp

[1] Mount Royal Chemicals, Montreal, Quebec, Canada.
[2] Caledon Laboratories, Georgetown, Ontario, Canada.
[3] J. T. Baker Chemical Co., Phillipsburg, N.J.
[4] Aldrich Chemical Co., Milwaukee, Wis.
[5] Brinkmann Instruments, Toronto, Ontario, Canada.
[6] E. Merck, Darmstadt, West Germany.
[7] Celite 545, Chromatographic Specialties, Brockville, Ontario, Canada.
[8] ICN Pharmaceuticals, Cleveland, Ohio.
[9] Varian Aerograph 2100.
[10] Bruker HFX-90 spectrometer.
[11] Stohler isotope chemicals, Waltham, Mass.
[12] AEI MS-9 mass spectrometer.
[13] With 5% OV-7 on Gas Chrom Q (100–120 mesh) in a U-shaped glass column under isothermal conditions at 230°. All other conditions were described previously (4).

0022-3549/80/0400-0469$01.00/0
© 1980, American Pharmaceutical Association

Palo Alto, Calif.
(10) S. J. Mule and P. L. Hushin, *Anal. Chem.*, **43**, 708 (1971).
(11) D. C. Monkhouse and J. L. Lach, *J. Pharm. Sci.*, **61**, 1435 (1972).
(12) K. Oguri, S. Ida, H. Yoshimura, and H. Tsukamoto, *Chem. Pharm. Bull.*, **18**, 2414 (1970).
(13) J. Cochin, J. Haggart, L. A. Woods, and M. H. Seevers, *J. Pharmacol. Exp. Ther.*, **111**, 74 (1954).
(14) S. Y. Yeh, H. I. Chernov, and L. A. Woods, *J. Pharm. Sci.*, **60**, 469 (1971).

Identification of Degradation Products in a Phenylbutazone Tablet Formulation

F. MATSUI ˣ, D. L. ROBERTSON, M. A. POIRIER, and E. G. LOVERING

Received April 27, 1979, from the *Drug Research Laboratories, Health Protection Branch, Tunney's Pasture, Ottawa, Ontario, Canada, K1A 0L2.* Accepted for publication October 24, 1979.

Abstract □ Two previously reported but unidentified phenylbutazone degradation products were isolated from a tablet that was stored at 60° for 203 days. The compounds, α-(*N*-phenylcarbamoyl)-*N*-caproylhydrazobenzene and α-hydroxy-α-(*N*-phenylcarbamoyl)-*N*-caproylhydrazobenzene, were isolated by chromatography, identified by mass and NMR spectrometry, and synthesized by the reaction of aniline with phenylbutazone or its hydroxy analog, respectively.

Keyphrases □ Phenylbutazone—tablets, identification of degradation products □ Anti-inflammatory agents—phenylbutazone, tablets, identification of degradation products □ Degradation products—phenylbutazone, tablets, identification

In a recent study on the stability of phenylbutazone formulations under stress conditions (1), one formulation (G) was found to contain one or more compounds previously unidentified in degradation of the drug. These compounds are α-(*N*-phenylcarbamoyl)-*N*-caproylhydrazobenzene (I) and α-hydroxy-α-(*N*-phenylcarbamoyl)-*N*-caproylhydrazobenzene (II). This paper describes the isolation, identification, and synthesis of I and II.

EXPERIMENTAL

Materials—Tablets of Formulation G (1) were obtained directly from the manufacturer. Phenylbutazone[1] (*III*), cyclohexane[2], chloroform[2], methanol[2], ethyl acetate[2], and acetic acid[3] were used as received. Phenyl phthalate[4] was recrystallized from acetone[2]–water, and 1,2-diphenyl-4-*n*-butyl-4-hydroxypyrazolidine-3,5-dione (IV) was prepared by the method described previously (1, 2). TLC plates[5] precoated with silica gel G-60 F-254, 60–200-mesh silica gel[6], diatomaceous earth[7], and nylon tubing[8] were used.

Equipment—The gas chromatograph[9] was equipped with a flame-ionization detector and a U-shaped glass column packed with 5% OV-7 on Gas Chrom Q[7] (100–120 mesh). NMR spectra were obtained on a 90-MHz instrument[10]; chemical shifts are reported in parts per million from tetramethylsilane, the internal standard. All spectra were recorded in deuterated chloroform[11] ($CDCl_3$). Mass spectra[12] were recorded at an ionizing potential of 70 ev, and the samples were introduced *via* the direct probe at 120 and 130°. Accurate mass measurements were made by the peak matching technique.

TLC Solvent System A (3) consisted of cyclohexane–chloroform–methanol–acetic acid (60:30:5:5), and Solvent System B was chloroform–ethyl acetate (80:20). Filter paper-lined TLC tanks were equilibrated with the solvent system for 30 min prior to use. Spots were visualized by UV light at 254 nm and by spraying with a solution of 0.5% potassium dichromate in 20% (v/v) H_2SO_4.

Isolation of Degradation Products from Formulation G—Five tablets (equivalent to 500 mg of phenylbutazone), which had been stored for 203 days at 60°, were finely powdered, wetted with ethyl acetate, and triturated with 2 g of diatomaceous earth until the mixture was uniform. The triturate was placed at the top of a nylon column containing 200 g of 60–200-mesh silica gel, which had been deactivated with 30 ml of water and dry packed into a 0.03 × 1-m nylon column. A 500-ml solution of Solvent System A was added until the solvent front reached the bottom of the column. The tube was incised into 5-cm sections, and the location of each compound on the column was established by removing small portions of the silica gel from the different incised sections of the nylon tube, extracting these portions with ethyl acetate, and spotting aliquots directly onto a TLC plate.

The spots were visualized with the potassium dichromate spray, and the spots containing the components of interest immediately developed a bright-purple color. The sections of interest then were cut; the degradation products were extracted from the silica gel with ethyl acetate, concentrated under nitrogen, and rechromatographed on a TLC plate using Solvent System A to remove residual phenylbutazone. The R_f values of I, II, and III in this system were 0.37, 0.37, and 0.43, respectively.

The band containing the mixture of I and II was visualized by spraying the edges of the TLC plate with dichromate spray. The band was scraped off and extracted with ethyl acetate, and the eluate was reduced to a small volume under nitrogen. Resolution of I and II was effected by TLC using Solvent System B. Isolation was carried out by elution with ethyl acetate and evaporation under nitrogen. The R_f values of I, II, and III using Solvent System B were 0.56, 0.50, and 0.58, respectively.

Syntheses—*Compound I*—A solution of 308 mg (1 mmole) of III and 180 mg of aniline (100% excess) in 15 ml of chloroform was heated under nitrogen at 45° for 48 hr in a culture tube. Compound I was separated from unreacted phenylbutazone by TLC (System A), and the spot was scraped from the plate and eluted with ethyl acetate. Traces of II were removed by subsequent TLC using Solvent System B. Crystallization from ethanol–water (90:10) gave pure I, mp 197–199°; NMR ($CDCl_3$): δ 8.9 (s, NH), 8.5 (s, CONH), 7.4–6.8 (m, 15H, aromatic), 4.2 (t, CH), 2.0, 1.5, and 0.87 (*n*-butyl) ppm; mass spectrum (70 ev, 120°): *m/e* 401 (M^+ 5.3%), 307 (7.1), 218 (12.5), 184 (48.1), 148 (13.1), 120 (18.1), 93 (100), and 77 (72.3). The GLC[13] retention time was 11.0 min or 0.92 relative to the internal standard, phenyl phthalate.

Compound II—Compound II was prepared from 1,2-diphenyl-4-*n*-butyl-4-hydroxypyrazoline-3,5-dione (IV) by the procedure described for the synthesis of I. Compound II also can be obtained from III by carrying out the reaction under an oxygen atmosphere. After purification by TLC, crystallization from ethanol–water (90:10) yielded II, mp

[1] Mount Royal Chemicals, Montreal, Quebec, Canada.
[2] Caledon Laboratories, Georgetown, Ontario, Canada.
[3] J. T. Baker Chemical Co., Phillipsburg, N.J.
[4] Aldrich Chemical Co., Milwaukee, Wis.
[5] Brinkmann Instruments, Toronto, Ontario, Canada.
[6] E. Merck, Darmstadt, West Germany.
[7] Celite 545, Chromatographic Specialties, Brockville, Ontario, Canada.
[8] ICN Pharmaceuticals, Cleveland, Ohio.
[9] Varian Aerograph 2100.
[10] Bruker HFX-90 spectrometer.
[11] Stohler isotope chemicals, Waltham, Mass.
[12] AEI MS-9 mass spectrometer.
[13] With 5% OV-7 on Gas Chrom Q (100–120 mesh) in a U-shaped glass column under isothermal conditions at 230°. All other conditions were described previously (4).

0022-3549/80/0400-0469$01.00/0
© 1980, American Pharmaceutical Association

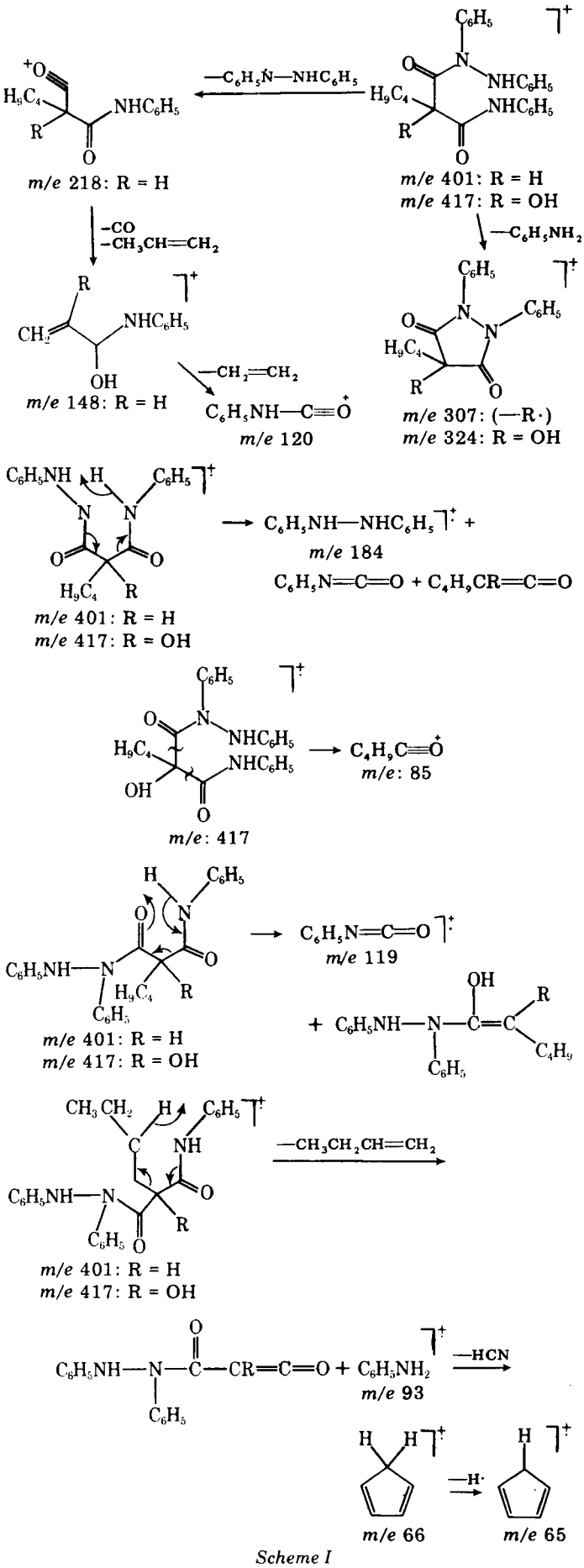

Scheme I

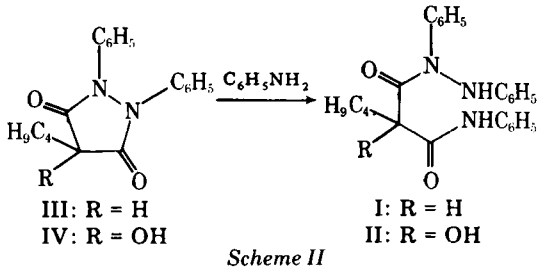

Scheme II

175–176°; NMR ($CDCl_3$): δ 9.4 (s, NH), 9.0 (s, CONH), 7.5–7.2 (m, 15H, aromatic), 5.4 (broad, OH), 2.0, 1.2, and 0.70 (*n*-butyl) ppm; mass spectrum (70 ev, 130°): *m/e* 417 (M^+ 10.3%), 324 (11.5), 207 (12.7), 184 (100), 164 (16.5), 119 (13.4), 93 (89.5), 85 (28.3), 81 (14.2), and 77 (77.3). The GLC[13] retention time was 11.0 min or 0.92 relative to the internal standard, phenyl phthalate.

RESULTS AND DISCUSSION

The mass spectra of I and II contained major peaks at *m/e* 401 (5.3%) and 417 (10.3), respectively, corresponding to their molecular ions. The possible fragmentation patterns of I and II are presented in Scheme I. The mass spectra of I and II differ from those of their respective precursors, III and IV (2, 5), in that they exhibit major losses of aniline at *m/e* 93 (100 and 90%, respectively), indicating the presence of open-ring compounds. The loss of aniline seems to occur with ring closure in the mass spectrometer, giving ions at *m/e* 307 (7.1%) and 324 (11.5). Most fragments in the mass spectrum can be rationalized by McLafferty rearrangements (5, 6).

The most common ions in the mass spectra of pyrazolidinediones are the series of peaks at 183, 184, and 185, which are characteristic of hydrazobenzene fragments. The ion at *m/e* 184 may originate from the molecular ions of I or II by a McLafferty rearrangement with a loss of phenyl isocyanate. A characteristic fragment in pyrazolidinediones is the loss of phenyl isocyanate as a neutral molecule or as an ion at *m/e* 119 (5.1% for I and 13.4% for II). The formation of the fragment at *m/e* 184 in the mass spectra of I and II is rationalized by a proton transfer from the anilide portion (2). The formation of the ion at *m/e* 85 in II, attributable to (C_4H_9–C≡O$^+$), indicates the presence of the hydroxyl group at carbon 4.

The NMR spectra of I and II in deuterochloroform showed two singlets due to NH protons at δ 8.9 and 8.5 and 9.4 and 9.0 ppm, respectively. One of these NH signals corresponds to an amide function. This assignment is supported by the chemical shifts and by the fact that one singlet disappears slowly when deuterated water is added, while the other disappears immediately. The chemical shifts of the methine proton in I (4.2 ppm, triplet, J = 8.0 Hz, HCCH) and 5.4 ppm for the hydroxylic proton in II are in agreement with the chemical shifts of the equivalent proton in the free α-carboxy compounds reported previously (7). Integration of the aromatic protons revealed the presence of three aromatic rings. The complexity of the aromatic pattern in the spectra of I and II, as compared to that of III, suggests that the plane of symmetry was destroyed, an observation that supports the proposed structure of I and II.

Compounds I and II may have formed in Formulation G by the reaction of aniline with III and IV, respectively (Scheme II). The source of the aniline required for the formation of these compounds is not known. It may originate from the degradation of III by an unusual excipient-induced mechanism. The presence of II in the tablets can be rationalized in terms of air oxidation of I at carbon 4 (2). On the basis of previous results (1), the ring opening of the lactam-type compounds by aniline seems to be more probable than hydrolysis of III and IV to α-carboxy-*N*-caproylhydrazobenzene and α-carboxy-α-hydroxy-*N*-caproylhydrazobenzene, respectively (2, 7), followed by combination with aniline. Antacid formulations would be expected to show degradation *via* hydrolysis, and the presence of relatively high concentrations of carboxy compounds in antacid formulations subjected to 60° storage for 18 months is in accord with this expectation. These antacid formulations showed only traces of the previously unidentified I and II, thus giving indirect evidence for the ring-opening reaction with aniline.

REFERENCES

(1) F. Matsui, D. L. Robertson, P. Lafontaine, H. Kolasinski, and E. G. Lovering, *J. Pharm. Sci.*, **67**, 646 (1978).

(2) D. V. C. Awang and A. Vincent, *ibid.*, **65**, 68 (1976).

(3) H. D. Beckstead, K. K. Kaistha, and S. J. Smith, *ibid.*, **57**, 1952 (1968).
(4) J. R. Watson, F. Matsui, R. C. Lawrence, and P. M. J. McConnell, *J. Chromatogr.*, **76**, 141 (1973).
(5) R. A. Locock, R. E. Moskalyk, L. G. Chatten, and L. M. Lundy, *J. Pharm. Sci.*, **63**, 1896 (1974).
(6) B. Unterhalt, *Arch. Pharm.*, **305**, 334 (1972).
(7) G. A. Neville and D. V. C. Awang, *Org. Mag. Res.*, **2**, 341 (1970).

Stability-Indicating Colorimetric Assay for Indicine *N*-Oxide Using TLC

JOSEPH B. D'SILVA and ROBERT E. NOTARI ˣ

Received May 18, 1979, from the *College of Pharmacy, Ohio State University, Columbus, OH 43210.* Accepted for publication October 31, 1979.

Abstract □ Aliquots of aqueous solutions in which indicine *N*-oxide may be degraded were mixed with 0.5 *M* formic acid (1:3) to adjust the pH to ~2–4 to quench the reaction and to ensure adequate TLC resolution. Silica-coated aluminum sheets were used to isolate indicine *N*-oxide by cutting the appropriate region from the chromatogram. By a modification of a known procedure, the silica gel then was treated with an acetic anhydride–diglyme mixture, and the mixture was heated to convert the drug to a pyrrole, which was then coupled with 4-dimethylaminobenzaldehyde to produce a color. The absorbance of the resulting solution was determined at 566 nm, and the apparent molar absorptivity, ϵ, based on the final indicine *N*-oxide concentration was 6.13×10^4. The recovery was ~92%, and the assays were readily reproducible with a coefficient of variation of 4.4%.

Keyphrases □ Indicine *N*-oxide—stability-indicating colorimetric assay using TLC □ Alkaloids—indicine *N*-oxide, stability-indicating colorimetric assay using TLC □ Antineoplastic agents, potential—indicine *N*-oxide, stability-indicating colorimetric assay using TLC

Indicine *N*-oxide[1] (I), an unsaturated pyrrolizidine alkaloid found in *Heliotropium indicum* Linn (Boraginaceae) (1), is undergoing clinical testing as an anticancer agent (2). While stability data have not been reported, alkaline ester hydrolysis is predicted from degradation studies of related alkaloids.

BACKGROUND

Approximate half-lives for the decomposition of 12 pyrrolizidines were estimated in 0.5 *N* aqueous or hydroalcoholic sodium hydroxide at room temperature (3). The relatively facile hydrolysis of esters of trachelanthic and viridifloric acids was attributed to their potential for β-hydroxyl participation, presumably *via* hydrogen bonding (3). This potential for intramolecular catalysis is present in I, which also is a trachelanthic acid ester (of retronecine *N*-oxide). The products obtained from the hydrolysis of indicine in 2 *N* NaOH at 100° for 2 hr were shown to be retronecine and a diastereoisomer of trachelanthic acid (4). It is not known whether the presence of the *N*-oxide in I gives rise to additional degradation pathways. Kugelman *et al.* (1) found that the properties of I extracted from *H. indicum* Linn (Boraginaceae) did not agree with those of synthesized I. Although these differences were ascribed to solvation problems, they also might reflect chemical instability.

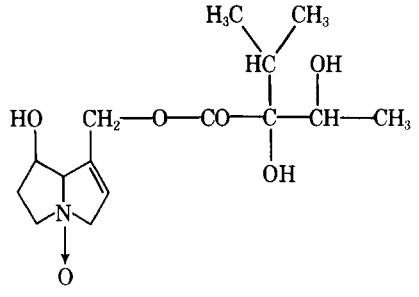

I

Two assays for I in biological samples have been reported (2, 5). An electron-capture GLC assay after formation of the pentafluoropropionic anhydride derivative of indicine was applied to the analysis of mixtures of indicine and I in plasma and urine (2). Prior to analysis, indicine was extracted selectively with chloroform; the I remaining in the raffinate then was reduced to indicine. A GLC–mass spectrometric method using selective-ion monitoring recently achieved nanogram sensitivity through formation of the trimethylsilyl derivative of I (5). Although the method is selective for I, the equipment required is sophisticated and expensive.

This study was undertaken to develop a simple, specific assay for I in the presence of its degradation products. A colorimetric assay for unsaturated pyrrolizidine alkaloids using modified Ehrlich reagent (6) was adapted to assay I under aqueous conditions, in which it was shown to be unstable. TLC on aluminum sheets was employed to isolate I from buffers and reaction products. After the appropriate region was cut and scraped, the silica gel mixture was treated to convert the pyrrolizidine structure to a pyrrole. The pyrrole then was coupled with 4-dimethylaminobenzaldehyde to produce a color which was measured spectrophotometrically.

EXPERIMENTAL

Materials and Chemicals—The TLC aluminum sheets were precoated with 0.2 mm of silica gel 60 F-254[2]. Ether[3], absolute ethanol[4], ammonium hydroxide solution[5], acetic anhydride[6], and acetone[3] were analytical reagent grade. The diglyme[7] was kept free of peroxides (6). Modified Ehrlich reagent was prepared by dissolving 2% (w/v) 4-dimethylaminobenzaldehyde[8] in an ethanolic solution containing 14% (w/v) boron trifluoride, which was incorporated as its etherate complex (6, 7).

pH Adjustment—The assay results, obtained from absorbance values, were consistent provided that the sample to be spotted had a pH of 2–4.5. At pH < 2, erratic absorbance values were obtained. The pH was maintained at <4.5 since I degraded in alkali but not in acid. One part of 0.5 *M* formic acid was effective in controlling the pH when it was mixed with three parts of simulated reaction solutions of pH 2–13. Indicine *N*-oxide solutions treated in this manner were stable for several weeks under refrigeration.

Optimum Conditions—The amount of acetic anhydride used in the conversion of I to the pyrrole was varied from 0.1 to 0.4 ml. The best results were obtained with 0.2 ml. The optimum heating time for this step was 3.5 min. An optimum heating period of 4.5 min was observed for the color-producing step using modified Ehrlich reagent.

Assay of I in Aqueous Solutions or Reaction Mixtures—An aliquot of ~0.01 *M* I solution or reaction mixture at pH 2–13 was mixed with

[1] NSC-132319.

[2] EM Laboratories, Elmsford, N.Y.
[3] Mallinckrodt, St. Louis, Mo.
[4] U.S. Industrial Chemicals Co., New York, N.Y.
[5] Allied Chemical Co., Morristown, N.J.
[6] Drake Brothers, Menomonee Falls, Wis.
[7] Aldrich Chemical Co., Milwaukee, Wis.
[8] J. T. Baker Chemical Co., Phillipsburg, N.J.

0022-3549/80/0400-0471$01.00/0
© 1980, American Pharmaceutical Association

(3) H. D. Beckstead, K. K. Kaistha, and S. J. Smith, *ibid.*, **57**, 1952 (1968).
(4) J. R. Watson, F. Matsui, R. C. Lawrence, and P. M. J. McConnell, *J. Chromatogr.*, **76**, 141 (1973).
(5) R. A. Locock, R. E. Moskalyk, L. G. Chatten, and L. M. Lundy, *J. Pharm. Sci.*, **63**, 1896 (1974).
(6) B. Unterhalt, *Arch. Pharm.*, **305**, 334 (1972).
(7) G. A. Neville and D. V. C. Awang, *Org. Mag. Res.*, **2**, 341 (1970).

Stability-Indicating Colorimetric Assay for Indicine *N*-Oxide Using TLC

JOSEPH B. D'SILVA and ROBERT E. NOTARI ˣ

Received May 18, 1979, from the *College of Pharmacy, Ohio State University, Columbus, OH 43210.* Accepted for publication October 31, 1979.

Abstract □ Aliquots of aqueous solutions in which indicine *N*-oxide may be degraded were mixed with 0.5 *M* formic acid (1:3) to adjust the pH to ~2–4 to quench the reaction and to ensure adequate TLC resolution. Silica-coated aluminum sheets were used to isolate indicine *N*-oxide by cutting the appropriate region from the chromatogram. By a modification of a known procedure, the silica gel then was treated with an acetic anhydride–diglyme mixture, and the mixture was heated to convert the drug to a pyrrole, which was then coupled with 4-dimethylaminobenzaldehyde to produce a color. The absorbance of the resulting solution was determined at 566 nm, and the apparent molar absorptivity, ϵ, based on the final indicine *N*-oxide concentration was 6.13×10^4. The recovery was ~92%, and the assays were readily reproducible with a coefficient of variation of 4.4%.

Keyphrases □ Indicine *N*-oxide—stability-indicating colorimetric assay using TLC □ Alkaloids—indicine *N*-oxide, stability-indicating colorimetric assay using TLC □ Antineoplastic agents, potential—indicine *N*-oxide, stability-indicating colorimetric assay using TLC

Indicine *N*-oxide[1] (I), an unsaturated pyrrolizidine alkaloid found in *Heliotropium indicum* Linn (Boraginaceae) (1), is undergoing clinical testing as an anticancer agent (2). While stability data have not been reported, alkaline ester hydrolysis is predicted from degradation studies of related alkaloids.

BACKGROUND

Approximate half-lives for the decomposition of 12 pyrrolizidines were estimated in 0.5 *N* aqueous or hydroalcoholic sodium hydroxide at room temperature (3). The relatively facile hydrolysis of esters of trachelanthic and viridifloric acids was attributed to their potential for β-hydroxyl participation, presumably *via* hydrogen bonding (3). This potential for intramolecular catalysis is present in I, which also is a trachelanthic acid ester (of retronecine *N*-oxide). The products obtained from the hydrolysis of indicine in 2 *N* NaOH at 100° for 2 hr were shown to be retronecine and a diastereoisomer of trachelanthic acid (4). It is not known whether the presence of the *N*-oxide in I gives rise to additional degradation pathways. Kugelman *et al.* (1) found that the properties of I extracted from *H. indicum* Linn (Boraginaceae) did not agree with those of synthesized I. Although these differences were ascribed to solvation problems, they also might reflect chemical instability.

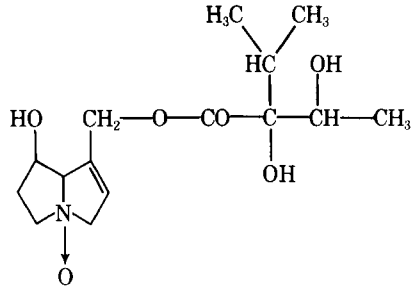

I

Two assays for I in biological samples have been reported (2, 5). An electron-capture GLC assay after formation of the pentafluoropropionic anhydride derivative of indicine was applied to the analysis of mixtures of indicine and I in plasma and urine (2). Prior to analysis, indicine was extracted selectively with chloroform; the I remaining in the raffinate then was reduced to indicine. A GLC–mass spectrometric method using selective-ion monitoring recently achieved nanogram sensitivity through formation of the trimethylsilyl derivative of I (5). Although the method is selective for I, the equipment required is sophisticated and expensive.

This study was undertaken to develop a simple, specific assay for I in the presence of its degradation products. A colorimetric assay for unsaturated pyrrolizidine alkaloids using modified Ehrlich reagent (6) was adapted to assay I under aqueous conditions, in which it was shown to be unstable. TLC on aluminum sheets was employed to isolate I from buffers and reaction products. After the appropriate region was cut and scraped, the silica gel mixture was treated to convert the pyrrolizidine structure to a pyrrole. The pyrrole then was coupled with 4-dimethylaminobenzaldehyde to produce a color which was measured spectrophotometrically.

EXPERIMENTAL

Materials and Chemicals—The TLC aluminum sheets were precoated with 0.2 mm of silica gel 60 F-254[2]. Ether[3], absolute ethanol[4], ammonium hydroxide solution[5], acetic anhydride[6], and acetone[3] were analytical reagent grade. The diglyme[7] was kept free of peroxides (6). Modified Ehrlich reagent was prepared by dissolving 2% (w/v) 4-dimethylaminobenzaldehyde[8] in an ethanolic solution containing 14% (w/v) boron trifluoride, which was incorporated as its etherate complex (6, 7).

pH Adjustment—The assay results, obtained from absorbance values, were consistent provided that the sample to be spotted had a pH of 2–4.5. At pH < 2, erratic absorbance values were obtained. The pH was maintained at <4.5 since I degraded in alkali but not in acid. One part of 0.5 *M* formic acid was effective in controlling the pH when it was mixed with three parts of simulated reaction solutions of pH 2–13. Indicine *N*-oxide solutions treated in this manner were stable for several weeks under refrigeration.

Optimum Conditions—The amount of acetic anhydride used in the conversion of I to the pyrrole was varied from 0.1 to 0.4 ml. The best results were obtained with 0.2 ml. The optimum heating time for this step was 3.5 min. An optimum heating period of 4.5 min was observed for the color-producing step using modified Ehrlich reagent.

Assay of I in Aqueous Solutions or Reaction Mixtures—An aliquot of ~0.01 *M* I solution or reaction mixture at pH 2–13 was mixed with

[1] NSC-132319.

[2] EM Laboratories, Elmsford, N.Y.
[3] Mallinckrodt, St. Louis, Mo.
[4] U.S. Industrial Chemicals Co., New York, N.Y.
[5] Allied Chemical Co., Morristown, N.J.
[6] Drake Brothers, Menomonee Falls, Wis.
[7] Aldrich Chemical Co., Milwaukee, Wis.
[8] J. T. Baker Chemical Co., Phillipsburg, N.J.

0022-3549/80/0400-0471$01.00/0
© 1980, American Pharmaceutical Association

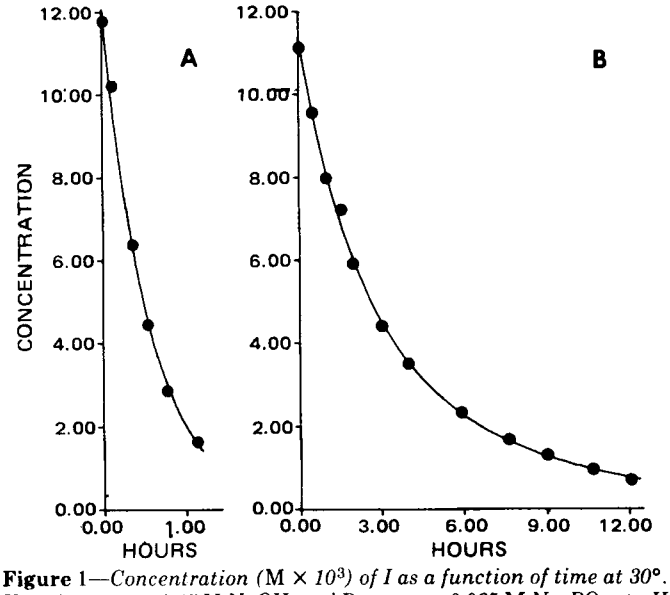

Figure 1—*Concentration (M × 10³) of I as a function of time at 30°. Key: A, aqueous 0.15 N NaOH; and B, aqueous 0.065 M Na_3PO_4 at pH 12.18.*

one-third of its volume of 0.5 *M* formic acid to adjust the pH to 2–4. An 8-μl sample was spotted on a TLC sheet, and the spot was air dried. Eight microliters of a reference solution consisting of I (~8×10^{-3} *M*) also was spotted on the same sheet. The sheet was developed (12 cm) with ether–ethanol–ammonium hydroxide solution–water (5:4:1:1) and air dried.

The entire channel containing the reference spot was cut out, sprayed with sulfuric acid–ether (1:4), and heated in an oven to locate I, which appeared at $R_f \sim 0.42$. The area in the sample channel corresponding to the I reference spot was scraped into a glass-stoppered test tube (12 × 1.5 cm). One milliliter of diglyme, followed by 0.2 ml of acetic anhydride, was added; the mixture was agitated thoroughly and heated in a boiling water bath for 3.5 min, during which it was agitated thoroughly at the end of 1 and 2 min. The tube was cooled to room temperature using a water bath (10–15°), and 1 ml of modified Ehrlich reagent was added.

The mixture then was agitated thoroughly and heated in a water bath at 57.5° for 4.5 min, during which it was agitated at the end of 100 and 200 sec. The tube was cooled, and 2 ml of acetone was added with thorough agitation followed by centrifugation at 3400 rpm for 1.5 min. The clear supernate was swirled carefully around the sides of the tube to wash down any silica gel particles. The tube was centrifuged a second time for 3.5 min, and the absorbance of the clear supernate was determined immediately at 566 nm against a similarly prepared blank.

The concentration of I in the initial solution may be calculated from:

$$[\mathrm{I}] = \frac{(A_{566})(R)}{\epsilon} \qquad \text{(Eq. 1)}$$

where A_{566} is the measured absorbance at 566 nm (λ_{max}), ϵ is the apparent molar absorptivity in the final solution (6.13×10^4), and R is the ratio of the final volume of the assayed solution to the sample volume spotted on the TLC sheet.

Beer's Law Plots—Aliquots of 2, 4, 6, 8, and 10 μl of a solution of I (8×10^{-3} *M*) in 0.125 *M* formic acid were chromatographed and assayed as described. A Beer's law plot was constructed using the absorbance data and the I concentration in the final assay solution.

Indicine *N*-oxide (8×10^{-3} *M*) was dissolved in a 3:1 mixture of phosphate buffer (pH 11.93, [Na_3PO_4] = 0.0328 *M*) and 0.5 *M* formic acid. Aliquots were chromatographed and used to prepare a Beer's law plot as described.

Percent Recovery—Aliquots of 2, 4, 6, 8, and 10 μl of an aqueous solution of I (8×10^{-3} *M*) were placed in glass-stoppered test tubes (12 × 1.5 cm) and dried under a dry nitrogen stream since water interferes with the assay (6). The residues were assayed without TLC separation. A Beer's law plot of absorbance at 566 nm *versus* the I concentration in the final assay solution was constructed.

RESULTS AND DISCUSSION

Beer's Law Plots—The apparent molar absorptivity, ϵ, from the Beer's law plot prepared by chromatographic assays of solutions of I in 0.125 *M* formic acid was 6.13×10^4 ($r^2 = 0.9996$). The molar absorptivity from the Beer's law plot prepared by assaying the I solution in the phosphate buffer–formic acid mixture was 6.37×10^4 ($r^2 = 0.9996$), which is within 4% of that obtained for I in 0.125 *M* formic acid alone. The Beer's law plots passed through the origin, and all experimental points were on the regression lines.

Assay reproducibility was assessed by estimating ϵ 18 times, each using two known concentrations of I in solutions simulating a variety of reaction conditions ($\bar{\epsilon} = 6.18 \times 10^4$, $s = 0.27 \times 10^4$).

TLC Assay Recovery of I—The percent recovery of I following chromatographic separation was evaluated relative to solutions that were not chromatographed by comparing their Beer's law plots. The ϵ value without chromatographic separation was 6.69×10^4 ($r^2 = 0.9990$). Therefore, the percent recovery of I in the TLC assay was 91.6% as calculated from:

$$\%\ \text{recovery} = \frac{(100)(6.13 \times 10^4)}{(6.69 \times 10^4)} \qquad \text{(Eq. 2)}$$

Application to Kinetics of I Degradation—Preliminary studies indicated that I was unstable in alkali. The assay successfully measured the decreasing concentration of I as a function of time under a wide variety of aqueous alkaline conditions. Figure 1 shows two examples that illustrate the stability-indicating efficacy of this assay. Detailed studies on the kinetics and mechanisms of I degradation are in progress.

REFERENCES

(1) M. Kugelman, W. C. Liu, M. Axelrod, T. J. McBride, and K. V. Rao, *Lloydia*, **39**, 125 (1976).

(2) M. M. Ames and G. Powis, *J. Chromatogr.*, **166**, 519 (1978).

(3) L. B. Bull, C. C. J. Culvenor, and A. T. Dick, "The Pyrrolizidine Alkaloids," North-Holland, Amsterdam, The Netherlands, 1968, p. 60.

(4) A. R. Mattocks, R. Schoental, H. C. Crowley, and C. C. J. Culvenor, *J. Chem. Soc.*, **1961**, 5400.

(5) J. V. Evans, A. Peng, and C. J. Nielsen, *Biomed. Mass Spectrum*, **6**, 38 (1979).

(6) A. R. Mattocks, *Anal. Chem.*, **39**, 443 (1967).

(7) *Ibid.*, **40**, 1749 (1968).

ACKNOWLEDGMENTS

Supported in part by National Cancer Institute Contract CM-53828, Division of Cancer Treatment, and Grant CA-16058 from the National Cancer Institute, National Institutes of Health.

The authors are grateful to the Drug Synthesis and Chemistry Branch, Division of Cancer Treatment, National Cancer Institute, for supplying indicine *N*-oxide.

Anticonvulsant Properties of Selected Pyrrolo[2,3-*d*]pyrimidine-2,4-diones and Intermediates

DEBRA L. POWERS *, J. WALTER SOWELL, Sr.‡, J. J. FREEMAN *, and J. W. KOSH *x

Received August 20, 1979, from the **Division of Pharmacology and the* ‡*Division of Medicinal Chemistry, College of Pharmacy, University of South Carolina, Columbia, SC 29208.* Accepted for publication October 16, 1979.

Abstract □ A series of pyrrolo[2,3-*d*]pyrimidine-2,4-diones and intermediates was tested for anticonvulsant activity in mice. Eleven of the 15 compounds possessed anticonvulsant activity against pentylenetetrazol-induced convulsions. One compound afforded more anticonvulsant protection against pentylenetetrazol than did trimethadione (67 and 50%, respectively). A suspension of this compound was found to be as effective as a solution in producing anticonvulsant activity. The results suggest that the nitrile analogs were more potent compared to the carbamyl analog due to higher lipid solubility.

Keyphrases □ Pyrrolo[2,3-*d*]pyrimidine-2,4-diones and intermediates—anticonvulsant activity, structure–activity relationships □ Anticonvulsant activity—pyrrolo[2,3-*d*]pyrimidine-2,4-diones and intermediates, structure–activity relationships □ Structure–activity relationships—pyrrolo[2,3-*d*]pyrimidine-2,4-diones and intermediates, anticonvulsant activity

Many clinically useful anticonvulsants such as the hydantoins (1), succinimides (2), oxazolidinediones (3), and barbiturates (4) incorporate a cyclic imide structure. A series of substituted pyrrolopyrimidinediones synthesized in this laboratory (5) also contain a cyclic imide structure and, therefore, were postulated to possess possible anticonvulsant activity. Preliminary information from this laboratory confirmed the hypothesis and demonstrated that several of the pyrrolopyrimidinediones possessed anticonvulsant activity against pentylenetetrazol-induced seizures in mice.

In addition, some clinically useful anticonvulsants such as the propanediol carbamates (6) and acetylureas (7) contain a linear carbamate or urea function. Since intermediates in the synthesis of pyrrolopyrimidinediones contained carbamate functions, these compounds also were predicted to possess anticonvulsant activity.

Johnson *et al.* (8) reported the synthesis of a series of 2-aminopyrrole analogs of lidocaine that possessed cardiovascular depressant properties devoid of central nervous system (CNS) motor stimulation (9,10). Since one compound appeared to possess CNS depressant properties, it also was predicted to possess anticonvulsant activity.

The purpose of this study was to examine the anticonvulsant activity and structure–activity relationship for selected pyrrolo[2,3-*d*]pyrimidine-2,4-diones and related intermediates.

EXPERIMENTAL[1]

The synthesis of the compounds (I*b*, Ic, IIc–II*i*, III*a*, and III*b*) (Table I) used in this study was reported previously (5). The intermediates (I*a*, II*a*, and II*b*) were synthesized by the following procedure.

Chemistry—*2-(2-Chlorocarbethoxyamido)-3-cyano-4-methyl-5-benzylpyrrole* (*Ia*)—A solution of 2-amino-3-cyano-4-methyl-5-benzylpyrrole (16.5 g, 0.078 mole) (11) in acetone (100 ml) and pyridine (6.8 g, 0.086 mole) was stirred in an ice bath with the dropwise addition of 2-chloroethyl chloroformate (12.3 g, 0.086 mole). After the addition was complete, the bath was removed, and the solution was stirred at room temperature for 30 min. The solution was diluted with ice water (400 ml), and the precipitate was collected and air dried. The crude carbamate was recrystallized from 300 ml of methanol–water (2:1) to yield beige crystals (22.2 g, 89.5%). Recrystallization from methanol yielded beige crystals that were homogeneous on TLC with ethyl acetate (R_f 0.55), mp 110–111°; IR (KBr): 3560, 3300, 2200, 1715, 1630, 1240, and 1020 cm^{-1}.

Anal.—Calc. for $C_{16}H_{16}ClN_3O_2$: C, 60.47; H, 5.08; Cl, 11.16; N, 13.22. Found: C, 60.58; H, 5.13; Cl, 11.05; N, 13.25.

2-(2-Chlorocarbethoxyamido) -3- carbamyl-4-methyl-5-benzylpyrrole (*IIa*)—The carbamate (I*a*) (20.0 g, 0.063 mole) was added to 85% phosphoric acid (300 ml) that was preheated to 110°. The resulting solution was stirred for 7 min at 110–130° and then was poured over ice (1000 g). Potassium hydroxide (100 g) dissolved in water was added, and the precipitate was collected, washed with water, and air dried. The crude product (14.0 g, 66.3% yield) was recrystallized from 95% ethanol (500 ml), followed by recrystallization from methanol to yield pale-pink crystals that were homogeneous on TLC with ethyl acetate (R_f 0.45), mp 172–173°; IR (KBr): 3500, 3420, 3340, 3300, 1715, 1640, 1600, 1580, 1560, 1390, and 1210 cm^{-1}.

Anal.—Calc. for $C_{16}H_{18}ClN_3O_3$: C, 57.23; H, 5.40; Cl, 10.56; N, 12.51. Found: C, 57.30; H, 5.44; Cl, 10.55; N, 12.51.

2-(2,2,2-Trichlorocarbethoxyamido) -3- carbamyl-4,5-dimethylpyrrole (*IIb*)—A solution of 2-(2,2,2-trichlorocarbethoxyamido)-3-cyano-4,5-dimethylpyrrole (23.4 g, 0.0753 mole) in concentrated sulfuric acid (50 ml) was stirred at 100° for 6 min and then was poured slowly into 800 g of ice water (1:1). The precipitate was collected, washed with water, and air dried. The product was recrystallized from methanol (800 ml) to yield pale-pink crystals (18.0 g, 72.7% yield) that were homogeneous on TLC with ethyl acetate (R_f 0.60), mp > 300°; IR (KBr): 3525, 3360, 3280, 1730, 1650, 1590, 1570, 1560, 1400, 1200, 810, 750, and 720 cm^{-1}.

Anal.—Calc. for $C_{10}H_{12}Cl_3N_3O_3$: C, 36.55; H, 3.68; N, 12.79. Found: C, 36.46; H, 3.72; N, 12.85.

Pharmacology—*Animal Preparation*—Male HA/ICR mice[2], 15–30 g, were used. Compounds tested for anticonvulsant activity were prepared as 3% suspensions containing polysorbate 80[3] (0.5%) and acacia (0.5%) in water and were injected intraperitoneally. Solutions for intravenous administration (6%) were prepared by dissolving the compound in 30% propylene glycol and adjusting the pH to 8.0 with sodium hydroxide. Intravenous injections were administered *via* the tail vein using a 27-gauge needle and a mouse holder.

Maximal Electroshock Seizure Test—Mice were administered 50 mamp of alternating current[4] (60 Hz) for 200 msec through corneal electrodes (12). Several drops of 0.9% NaCl were instilled in each eye prior to application of the electrodes. Abolition of the tonic hindlimb extensor component of the seizure was defined as anticonvulsant activity.

Phenytoin[5] was used as the reference anticonvulsant for maximal electroshock. Three-hour pretreatment with phenytoin (10 mg/kg sc) produced 100% protection against maximal electroshock seizures in mice (12). The procedure was modified by using a 45-min pretreatment with a dose of 30 mg/kg ip (suspension) to produce 100% protection.

Pentylenetetrazol Seizure Test—Pentylenetetrazol[6] was administered subcutaneously at a dose of 85 mg/kg (ED_{97}) to elicit a clonic seizure lasting at least 5 sec (12). Trimethadione[7] was used as the reference

[1] IR spectra were determined on a Beckman AccuLab 4 spectrophotometer using the potassium bromide technique. Melting points were obtained using a Thomas-Hoover capillary apparatus and are uncorrected. TLC was performed using Eastman chromatogram sheets, type 6060 (silica gel), and the sheets were developed in an iodine chamber. Carbon, hydrogen, chlorine, and nitrogen values were obtained from Atlantic Microlab, Atlanta, Ga.

[2] Sprague–Dawley, Madison, Wis.
[3] Tween 80, ICI Americas, Wilmington, Del.
[4] Wahlquist electroshock apparatus, Provo, Utah.
[5] Dilantin, Parke-Davis, Detroit, Mich.
[6] Metrazol, Sigma Chemical Co., St. Louis, Mo.
[7] Tridione, Abbott Laboratories, North Chicago, Ill.

0022-3549/80/0400-0473$01.00/0
© 1980, American Pharmaceutical Association

Table I—Anticonvulsant Activity and Rotorod Toxicity of Selected Pyrrolo[2,3-*d*]pyrimidine-2,4-diones and Intermediates [a]

Compound	R_1	R_2	R_3	Protection against Pentylenetetrazol-Induced Convulsions[b], %	Rotorod Toxicity[c], %
	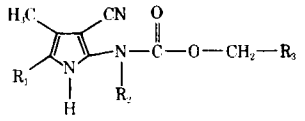				
I*a*	$CH_2C_6H_5$	H	CH_2Cl	33	0
I*b*	C_2H_5	H	CH_3	67	83
I*c*	$CH_2C_6H_5$	H	CH_3	17	0
	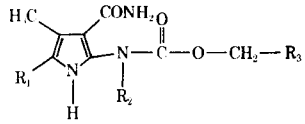				
II*a*	$CH_2C_6H_5$	H	CH_2Cl	17	0
II*b*	CH_3	H	CCl_3	0	0
II*c*	CH_3	H	CH_3	17	0
II*d*	CH_3	CH_3	CH_3	0	0
II*e*	C_2H_5	H	CH_3	33	33
II*f*	iso-C_4H_9	H	CH_3	17	0
II*g*	C_6H_5	H	CH_3	0	0
II*h*	$CH_2C_6H_4$-*p*-OH	H	CH_3	17	0
II*i*	$CH_2C_6H_5$	H	CH_3	0	0
	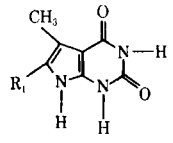				
III*a*	C_2H_5			17	0
III*b*	$CH_2C_6H_5$			17	0
IV[d]				17	0
Control[e]				0	0
Trimethadione (400 mg/kg)				50	0
Phenytoin (30 mg/kg)				—	0

[a] Male mice were injected with 30 mg/kg ip (suspension) of test compound and evaluated for maximal electroshock protection. All compounds were injected 45 min before administration of 50 mamp of alternating current for 200 msec. None of the compounds exhibited any protection against maximal electroshock-induced convulsions. Phenytoin, 30 mg/kg ip, provided 100% protection (n = 6). [b] Male mice were injected with 400 mg/kg ip of test compounds (suspension) 45 min before 85 mg of pentylenetetrazol/kg sc. Percent protection equals the percentage of animals protected against seizures induced by 85 mg of pentylenetetrazol/kg (ED_{97}) (n = 6). [c] Previously trained male mice received 400 mg/kg ip of test compounds (suspension) 45 min before placement on the rotorod for 90 sec. Rotorod toxicity is defined as the percentage of animals that did not remain on the rod for at least 90 sec (n = 6). [d] 2-Diethylaminoacetamido-3-carbamyl-4-methyl-5-benzylpyrrole hydrochloride (8, 9). [e] Control mice received 3.84 ml of suspension vehicle/kg (0.5% polysorbate 80 and 0.5% acacia in water).

Table II—Effect of Injection Route and Solubilization of I*b* on Anticonvulsant Activity

Convulsive Method[a]	Dose of I*b* and Route	Preparation[b]	Protection[c], %	Rotorod Toxicity[d], %
Electroshock	Control[e], ip	Solution	0	—
	30 mg/kg ip or iv	Solution	0	0
	30 mg/kg ip	Suspension	0	0
Pentylenetetrazol	Control, ip	Solution	0	—
	50 mg/kg ip or iv	Solution	0	0
	400 mg/kg ip	Solution	83	83
	400 mg/kg ip	Suspension	67	83

[a] Male mice were injected with 30 mg of I*b*/kg ip (suspension) and evaluated for maximal electroshock protection. Compound I*b* was injected 45 min before administration of 50 mamp of alternating current for 200 msec. Male mice were injected with I*b* 45 min before 85 mg of pentylenetetrazol/kg sc (ED_{97}) (n = 6). [b] Solution of I*b* was prepared in 30% propylene glycol. Suspension of I*b* was prepared as described in *Experimental* (n = 6). [c] Percent protection equals the percentage of animals protected against seizures induced by 85 mg of pentylenetetrazol/kg (ED_{99}) or electroshock (n = 6). [d] Rotorod toxicity is defined as the percentage of animals that did not remain on the rod for at least 90 sec (n = 6). [e] Control = 3.84 ml/kg of 30% propylene glycol (1.2 g/kg of propylene glycol).

pentylenetetrazol antagonist. At a pretreatment time of 45 min, 400 mg/kg of trimethadione suspension given intraperitoneally protected 50% of the animals against pentylenetetrazol-induced convulsion.

Test compounds were administered intravenously or intraperitoneally at a dose of 50 or 400 mg/kg 45 min before injection of pentylenetetrazol. Anticonvulsant activity was recorded if clonic spasms were not observed within 30 min after the pentylenetetrazol administration. The data were reported as the percentage of animals protected against seizures induced by 85 mg of pentylenetetrazol/kg given subcutaneously.

Rotorod Test—Previously trained mice were placed on a 2.54-cm diameter rubber-coated plastic rod (rotorod) rotating at 6 rpm before and 45 min after administration of the test compound. Rotorod toxicity was defined as the percentage of animals that did not remain on the rod for at least 90 sec.

RESULTS AND DISCUSSION

A test compound dose of 400 mg/kg was chosen for comparison with the anticonvulsant ED_{50} dose (400 mg/kg) of trimethadione (Table I). Suspensions of the test compounds were administered intraperitoneally due to solubility problems. At a dose of 400 mg/kg ip, 11 of the 15 test compounds protected against pentylenetetrazol-induced seizures (Table I). Compound I*b* was more active than trimethadione (67 *versus* 50% protection, respectively). Compounds II*e* and I*a* were slightly less active than trimethadione (33 *versus* 50% protection, respectively). Compounds I*c*, II*a*, II*c*, II*f*, II*h*, III*a*, III*b*, and IV exhibited slight anticonvulsant activity (17%).

Phenytoin at a dose of 30 mg/kg ip afforded 100% protection against maximal electroshock seizures. Since the test compounds were insoluble,

suspensions of the compounds including phenytoin were prepared. None of the test compounds exhibited any protection against maximal electroshock seizures at 40 mg/kg ip (suspension, footnote *a*, Table I). Compounds II*e* and I*b* produced definite signs of neurological toxicity (33 and 83%, respectively) as measured on the rotorod at 400 mg/kg (Table I). No CNS toxicity was observed with any other test compound.

The anticonvulsant evaluation indicated that compounds possessing a nitrile group at the 3-position (I*a*–I*c*) were more potent compared to compounds possessing a carbamyl group at that position (II*a*–II*i*). Introduction of the more polar carbamyl group (13) in II*a*–II*i* resulted in decreased lipid solubility compared to I*a*–I*c*, which contain the nitrile group. Decreased lipid solubility probably retards the passage of these compounds into the CNS.

The effect of the administration route and solubilization method on the most potent compound (I*b*) was examined further (Table II). Suspensions of I*b* were administered intraperitoneally due to solubility limitations. Suspensions then were compared to the anticonvulsant effects produced by propylene glycol solutions of I*b* when it was administered intraperitoneally or intravenously.

In the electroshock studies, 30 mg of I*b*/kg was chosen since phenytoin produced 100% protection against maximal electroshock seizures when it was administered as an intraperitoneal suspension. Variation in neither the injection route (intraperitoneal *versus* intravenous) nor the means of solubilization (suspension *versus* solution) was effective in producing anticonvulsant activity.

Compound I*b*, 75 mg/kg, was lethal following intravenous administration. Gross observation of the animals following this dose indicated that death was probably due to cardiovascular toxicity. Therefore, 50 mg/kg iv was selected as the maximum allowable dose for comparative purposes. Unfortunately, at 50 mg of I*b*/kg, variation in the administration route (intravenous *versus* intraperitoneal) was ineffective in producing protection against pentylenetetrazol-induced seizures.

Since 400 mg of I*b*/kg ip (suspension) afforded 67% protection in the pentylenetetrazol seizure test, 400 mg/kg ip of I*b* then was administered as a solution in propylene glycol for comparison (Table II). The completely dissolved solution of I*b* appeared to be slightly more effective than the intraperitoneally injected suspension of I*b* (83 *versus* 67% protection, respectively). However, the extent of rotorod toxicity appeared equivalent (83%). Therefore, complete solubilization of I*b* was concluded to be unnecessary for anticonvulsant activity.

Drugs that are useful in petit mal seizures are effective in elevating the threshold of electroshock- and drug-induced convulsions (14). Drugs used for grand mal epilepsy do not significantly affect the threshold of electrically induced seizures. None of the test compounds exhibited anticonvulsant activity against maximal electroshock but did block pentylenetetrazol-induced seizures. The active pyrrolopyrimidinediones and intermediates probably exert their activity through an elevation of the convulsive threshold, similar to trimethadione (14).

REFERENCES

(1) H. H. Merritt and T. J. Putnam, *Arch. Neurol. Psychiat. (Chicago)*, **39**, 1003 (1938).

(2) F. T. Zimmerman, *ibid.*, **66**, 156 (1951).

(3) W. G. Lennox, *J. Am. Med. Assoc.*, **129**, 1069 (1945).

(4) A. Hauptmann, *Muench. Med. Wochenschr.*, **59**, 1907 (1912).

(5) S. R. Etson, R. J. Mattson, and J. W. Sowell, Sr., *J. Heterocycl. Chem.*, **16**, 929 (1970).

(6) M. A. Perlstein, *J. Am. Med. Assoc.*, **161**, 1040 (1956).

(7) F. A. Gibbs, G. M. Everett, and R. K. Richards, *Dis. Nerv. Syst.*, **10**, 47 (1949).

(8) R. W. Johnson, T. H. Keenan, J. W. Kosh, and J. W. Sowell, Sr., *J. Pharm. Sci.*, **68**, 955 (1979).

(9) T. H. Keenan, MS thesis, University of South Carolina, Columbia, S.C., 1977.

(10) T. H. Keenan, J. J. Freeman, J. W. Sowell, and J. W. Kosh, *Pharmacology*, **19**, 36 (1979).

(11) R. W. Johnson, R. J. Mattson, and J. W. Sowell, Sr., *J. Heterocycl. Chem.*, **14**, 383 (1977).

(12) E. A. Swinyard, W. C. Brown, and L. S. Goodman, *J. Pharmacol. Exp. Ther.*, **106**, 319 (1952).

(13) "Remington's Pharmaceutical Sciences," 14th ed., J. E. Hoover, Ed., Mack Publishing Co., Easton, Pa., 1970, chap. 15.

(14) "Drill's Pharmacology in Medicine," 4th ed., J. R. DiPalma, Ed., McGraw-Hill, New York, N.Y., 1971, p. 306.

High-Pressure Liquid Chromatographic Analysis of Pramoxine Hydrochloride in High Lipoid Aerosol Foam Dosage Form

R. WEINBERGER ˣ, B. MANN, and J. POSLUSZNY

Received July 10, 1979, from *Reed & Carnrick Research Institute, Kenilworth, NJ 07033.* Accepted for publication November 1, 1979.

Abstract □ A rapid and quantitative method for the determination of pramoxine hydrochloride by high-pressure liquid chromatography is presented. The drug is extracted as the salt from a preparation with a high lipoid composition by partitioning it to the aqueous phase of an ether–methanol–water–acetic acid system. The extract is chromatographed on an octadecylsilane bonded packing with a methanol–water–acetic acid–methanesulfonic acid mobile phase. The time required for each separation is ~6 min. Analytical recoveries of 100.4 ± 1.5% were obtained.

Keyphrases □ Pramoxine hydrochloride—analysis, high-pressure liquid chromatography, high lipoid aerosol foam dosage form □ High-pressure liquid chromatography—analysis, pramoxine hydrochloride, high lipoid aerosol foam dosage form □ Anesthetics, topical—pramoxine hydrochloride, high-pressure liquid chromatographic analysis, high lipoid aerosol foam dosage form

Pramoxine hydrochloride, a widely used topical anesthetic, can present analytical difficulties due to its surfactant behavior. Its hydrophilic and lipophilic properties result in substantial matrix effects from common pharmaceutical excipients, particularly when the drug is incorporated into a high lipoid content base.

The conventional analytical method described in NF XIV (1) is based on nonspecific, nonaqueous titrimetry and spectrophotometric determinations. TLC[1] was used for qualitative analysis. Mario and Meehan (2) used the drug as an internal standard for a GLC assay of cough–cold preparations. Analysis of the high lipoid composition by GLC in this laboratory resulted in lengthy sample preparation and 30-min separations.

This study was undertaken to develop a rapid and reliable method for the determination of pramoxine hydrochloride in high lipoid preparations. The method was re-

[1] T. E. Rusch, Abbott Laboratories, Chicago, Ill., personal communication.

0022-3549/80/0400-0475$01.00/0

© 1980, American Pharmaceutical Association

suspensions of the compounds including phenytoin were prepared. None of the test compounds exhibited any protection against maximal electroshock seizures at 40 mg/kg ip (suspension, footnote *a*, Table I). Compounds II*e* and I*b* produced definite signs of neurological toxicity (33 and 83%, respectively) as measured on the rotorod at 400 mg/kg (Table I). No CNS toxicity was observed with any other test compound.

The anticonvulsant evaluation indicated that compounds possessing a nitrile group at the 3-position (I*a*–I*c*) were more potent compared to compounds possessing a carbamyl group at that position (II*a*–II*i*). Introduction of the more polar carbamyl group (13) in II*a*–II*i* resulted in decreased lipid solubility compared to I*a*–I*c*, which contain the nitrile group. Decreased lipid solubility probably retards the passage of these compounds into the CNS.

The effect of the administration route and solubilization method on the most potent compound (I*b*) was examined further (Table II). Suspensions of I*b* were administered intraperitoneally due to solubility limitations. Suspensions then were compared to the anticonvulsant effects produced by propylene glycol solutions of I*b* when it was administered intraperitoneally or intravenously.

In the electroshock studies, 30 mg of I*b*/kg was chosen since phenytoin produced 100% protection against maximal electroshock seizures when it was administered as an intraperitoneal suspension. Variation in neither the injection route (intraperitoneal *versus* intravenous) nor the means of solubilization (suspension *versus* solution) was effective in producing anticonvulsant activity.

Compound I*b*, 75 mg/kg, was lethal following intravenous administration. Gross observation of the animals following this dose indicated that death was probably due to cardiovascular toxicity. Therefore, 50 mg/kg iv was selected as the maximum allowable dose for comparative purposes. Unfortunately, at 50 mg of I*b*/kg, variation in the administration route (intravenous *versus* intraperitoneal) was ineffective in producing protection against pentylenetetrazol-induced seizures.

Since 400 mg of I*b*/kg ip (suspension) afforded 67% protection in the pentylenetetrazol seizure test, 400 mg/kg ip of I*b* then was administered as a solution in propylene glycol for comparison (Table II). The completely dissolved solution of I*b* appeared to be slightly more effective than the intraperitoneally injected suspension of I*b* (83 *versus* 67% protection, respectively). However, the extent of rotorod toxicity appeared equivalent (83%). Therefore, complete solubilization of I*b* was concluded to be unnecessary for anticonvulsant activity.

Drugs that are useful in petit mal seizures are effective in elevating the threshold of electroshock- and drug-induced convulsions (14). Drugs used for grand mal epilepsy do not significantly affect the threshold of electrically induced seizures. None of the test compounds exhibited anticonvulsant activity against maximal electroshock but did block pentylenetetrazol-induced seizures. The active pyrrolopyrimidinediones and intermediates probably exert their activity through an elevation of the convulsive threshold, similar to trimethadione (14).

REFERENCES

(1) H. H. Merritt and T. J. Putnam, *Arch. Neurol. Psychiat. (Chicago)*, **39**, 1003 (1938).

(2) F. T. Zimmerman, *ibid.*, **66**, 156 (1951).

(3) W. G. Lennox, *J. Am. Med. Assoc.*, **129**, 1069 (1945).

(4) A. Hauptmann, *Muench. Med. Wochenschr.*, **59**, 1907 (1912).

(5) S. R. Etson, R. J. Mattson, and J. W. Sowell, Sr., *J. Heterocycl. Chem.*, **16**, 929 (1970).

(6) M. A. Perlstein, *J. Am. Med. Assoc.*, **161**, 1040 (1956).

(7) F. A. Gibbs, G. M. Everett, and R. K. Richards, *Dis. Nerv. Syst.*, **10**, 47 (1949).

(8) R. W. Johnson, T. H. Keenan, J. W. Kosh, and J. W. Sowell, Sr., *J. Pharm. Sci.*, **68**, 955 (1979).

(9) T. H. Keenan, MS thesis, University of South Carolina, Columbia, S.C., 1977.

(10) T. H. Keenan, J. J. Freeman, J. W. Sowell, and J. W. Kosh, *Pharmacology*, **19**, 36 (1979).

(11) R. W. Johnson, R. J. Mattson, and J. W. Sowell, Sr., *J. Heterocycl. Chem.*, **14**, 383 (1977).

(12) E. A. Swinyard, W. C. Brown, and L. S. Goodman, *J. Pharmacol. Exp. Ther.*, **106**, 319 (1952).

(13) "Remington's Pharmaceutical Sciences," 14th ed., J. E. Hoover, Ed., Mack Publishing Co., Easton, Pa., 1970, chap. 15.

(14) "Drill's Pharmacology in Medicine," 4th ed., J. R. DiPalma, Ed., McGraw-Hill, New York, N.Y., 1971, p. 306.

High-Pressure Liquid Chromatographic Analysis of Pramoxine Hydrochloride in High Lipoid Aerosol Foam Dosage Form

R. WEINBERGER ˣ, B. MANN, and J. POSLUSZNY

Received July 10, 1979, from *Reed & Carnrick Research Institute, Kenilworth, NJ 07033.* Accepted for publication November 1, 1979.

Abstract □ A rapid and quantitative method for the determination of pramoxine hydrochloride by high-pressure liquid chromatography is presented. The drug is extracted as the salt from a preparation with a high lipoid composition by partitioning it to the aqueous phase of an ether–methanol–water–acetic acid system. The extract is chromatographed on an octadecylsilane bonded packing with a methanol–water–acetic acid–methanesulfonic acid mobile phase. The time required for each separation is ~6 min. Analytical recoveries of 100.4 ± 1.5% were obtained.

Keyphrases □ Pramoxine hydrochloride—analysis, high-pressure liquid chromatography, high lipoid aerosol foam dosage form □ High-pressure liquid chromatography—analysis, pramoxine hydrochloride, high lipoid aerosol foam dosage form □ Anesthetics, topical—pramoxine hydrochloride, high-pressure liquid chromatographic analysis, high lipoid aerosol foam dosage form

Pramoxine hydrochloride, a widely used topical anesthetic, can present analytical difficulties due to its surfactant behavior. Its hydrophilic and lipophilic properties result in substantial matrix effects from common pharmaceutical excipients, particularly when the drug is incorporated into a high lipoid content base.

The conventional analytical method described in NF XIV (1) is based on nonspecific, nonaqueous titrimetry and spectrophotometric determinations. TLC[1] was used for qualitative analysis. Mario and Meehan (2) used the drug as an internal standard for a GLC assay of cough–cold preparations. Analysis of the high lipoid composition by GLC in this laboratory resulted in lengthy sample preparation and 30-min separations.

This study was undertaken to develop a rapid and reliable method for the determination of pramoxine hydrochloride in high lipoid preparations. The method was re-

[1] T. E. Rusch, Abbott Laboratories, Chicago, Ill., personal communication.

0022-3549/80/0400-0475$01.00/0

© 1980, American Pharmaceutical Association

Table I—Recovery of Pramoxine Hydrochloride from a High Lipoid Composition at Different Potency Levels

Potency Level, %	Amount Added, mg	Amount Recovered, mg	Recovery, %	*RSD*	*n*[a]
75[b]	165.0	164.8	99.9	0.5	4
100	220.0	220.9	100.4	1.5	14
125[b]	275.0	276.4	100.5	2.0	4

[a] Number of assays. [b] An expanded standard curve (0.7–1.2 mg/ml) was used to bracket the expected range of potencies.

Table II—Analysis of the Commercial High Lipoid Preparation

Batch	Pramoxine Hydrochloride, mg/can[a]	Mean	*RSD*
7071	228, 230, 214, 225, 224, 219	223	2.4
8811	224, 229, 217, 211, 227, 222	222	2.6
8041	225, 223, 223, 223	224	0.4

[a] Single-can assays; theoretical amount = 220 mg/can.

quired to handle relatively large samples to accommodate a total contents assay for the aerosol dosage form. A practical requirement was that the technique not utilize large quantities of solvents or reagents.

EXPERIMENTAL[2]

Reagents and Chemicals—A commercial pramoxine hydrochloride sample[3] was used as the reference standard. Absolute methanol[4], ether[4], acetic acid[4], and deionized water were used for the extraction. The mobile phase contained 50% methanol[5], 48.9% deionized water, 1% acetic acid[4], and 0.1% methanesulfonic acid[6]. After mixing, the mobile phase was filtered through a 0.45-μm filter[7]. The solution was prepared fresh daily and was degassed prior to use.

Standard Solutions for Calibration Curves—Standard solutions of pramoxine hydrochloride (0.8, 0.9, and 1.0 mg/ml) were prepared in 50% methanol. The three standards were analyzed, and the results were subjected to regression analysis.

Sample Preparation—The contents of each aerosol unit were dispensed into a 500-ml separator. After expulsion of the foam, the unit was opened and the remainder of the contents was transferred to the separator with 100 ml of ether–methanol (5:1). The sample was extracted twice with 100- and 75-ml aliquots of 20% acetic acid, respectively. The aqueous extracts then were combined in a 250-ml volumetric flask and brought to volume with water.

Chromatographic Conditions—Octadecyltrichlorosilane was permanently bonded to 10-μm porous silica particles and packed into a 25-cm × 4-mm i.d. stainless steel column[8]. The mobile phase was pumped through the column at 2 ml/min at room temperature until a stable baseline was obtained. The variable-wavelength detector was set at 286 nm. A range of 0.1 aufs was used.

Replicate 15-μl injections were made using an autosampler[9]. The output of the spectrophotometer was monitored with a 10-mv strip-chart recorder[10]. Peak height measurements, determined electronically[11], were used for all calculations.

RESULTS AND DISCUSSION

The pharmaceutical aerosol foam dosage form presents a unique problem; it is difficult to analyze a portion of the aerosol content with precision because of the solubility of the propellant in the foam base. To circumvent this feature, the contents of an entire aerosol unit may be assayed, with the results reported in milligrams per can. The technique fits in well with the commercial production of pharmaceutical aerosols.

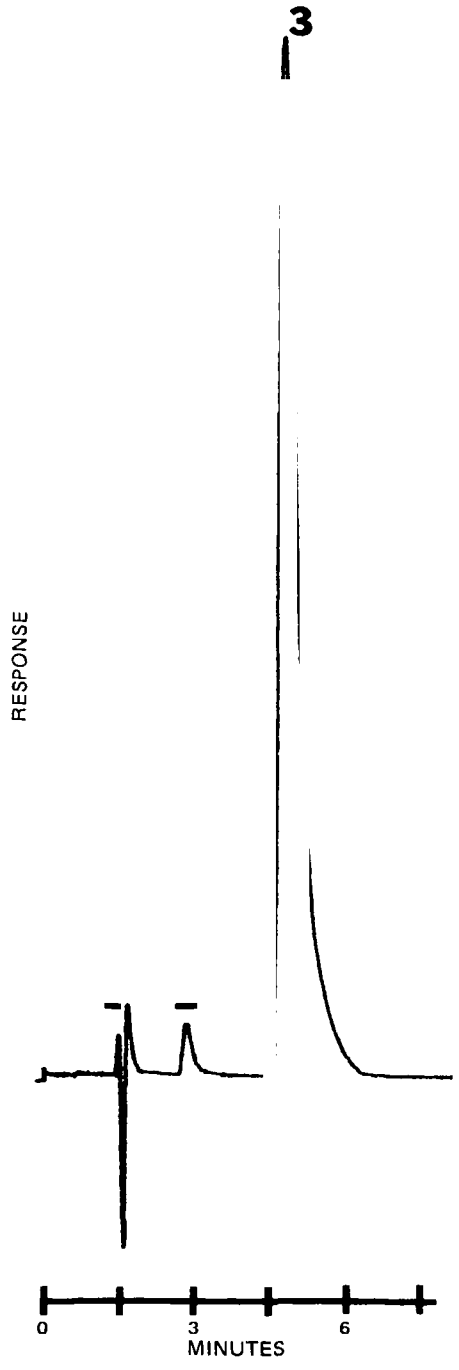

Figure 1—*Chromatogram of high lipoid extract obtained under the assay conditions. Key: 1 and 2, methylparaben; and 3, pramoxine hydrochloride.*

Information concerning potency, net content, and uniformity can be discerned simultaneously from the analytical data.

In this context, it became necessary to analyze 20–25-g high lipoid samples containing pramoxine hydrochloride, and several approaches were followed. Direct extraction with chloroform yielded substantial chromatographic interference. Dissolution of the sample required almost 1 liter of methanol–tetrahydrofuran (50:50).

The described extraction procedure required only 100 ml of ether–methanol and 175 ml of 20% acetic acid. The method had the advantage of partitioning the drug directly into the aqueous phase, which allowed determination by reversed-phase liquid chromatography without further manipulation.

To determine the accuracy and precision of the method, aerosol units were prepared quantitatively at three levels of potency, and these units were assayed. The average recovery at the 100% potency level was 100.4 ± 1.5 (*SD*)% (Table I). Recoveries at other potency levels were compa-

[2] A Waters Associates liquid chromatograph equipped with an M6000A pump and a Schoeffel variable-wavelength UV-visible detector were used.
[3] Abbott Laboratories, Chicago, Ill.
[4] Reagent grade.
[5] Burdick & Jackson, Muskegon, Mich.
[6] Pfaltz and Bauer, Stamford, Conn.
[7] FHUPO4700, Millipore Corp., Bedford, Mass.
[8] μBondapak C_{18}, Waters Associates, Milford, Mass.
[9] WISP, Waters Associates, Milford, Mass.
[10] Linear Instruments, Irvine, Calif.
[11] Minigrator, Spectra-Physics, Santa Clara, Calif.

rable. Analysis of the commercial preparation[12] gave results (Table II) that were consistent with the potency and the amount of the aerosol concentrate contained in each unit. Typical correlation coefficients for the standard curve were usually ≥0.999. Therefore, with the accuracy of the system established, the external standardization was considered satisfactory. A placebo preparation gave no interference.

The amount and concentration of the acetic acid solution were critical to the success of the extraction. If less than the prescribed amounts were used, difficulties with emulsification and incomplete recoveries resulted. A stronger acid such as hydrochloric acid could have been used at lower concentrations; but since the system was to be automated, a milder acid was preferred to preserve the instruments.

Prior to introduction into the high-pressure liquid chromatograph, good chromatographic practice generally requires filtering the analytical solutions through a fractional micrometer filter. This practice caused a 1–2% increase in recovery above that expected in the analytically prepared samples. Because of this feature, filtering samples is not recommended. The speed and accuracy of the method make occasional chromatograph filter and frit changes worthwhile.

A typical chromatogram of the high lipoid extract is shown in Fig. 1. The only excipient carried through the extraction and appearing on the chromatogram was methylparaben ($k' = 1$). Pramoxine hydrochloride ($k' = 2.2$) eluted in ~6 min.

The described method has general applicability to most pharmaceutical dosage forms containing pramoxine hydrochloride. In many cases, the drug can be extracted directly with the mobile phase or the entire composition can be dissolved. The high lipoid aerosol foam dosage form analysis was described because of the restrictions imposed on the analytical method.

[12] Non-Steroid Proctofoam, Reed & Carnrick, Kenilworth, N.J.

REFERENCES

(1) "The National Formulary," 14th ed., Mack Publishing Co., Easton, Pa., 1974, pp. 598, 599.

(2) E. Mario and L. G. Meehan, *J. Pharm Sci.*, **59**, 538 (1970).

Antileukemic Activity of 2-Bis(2-methylthio)vinyl-1-methylquinolinium Iodides

WILLIAM O. FOYE ˣ and JOEL M. KAUFFMAN

Received September 13, 1979, from the *Samuel M. Best Research Laboratory, Massachusetts College of Pharmacy, Boston, MA 02115.* Accepted for publication November 16, 1979.

Abstract □ Reaction of 1-methylquinolinium-2-dithioacetic acid zwitterions with excess methyl iodide in dimethylformamide gave the corresponding bis(2-methylthio)vinyl derivatives. These compounds were more soluble in both aqueous and organic media than the dithioacetic acid zwitterions but showed comparable antileukemic activity in mice. Reaction with morpholine converted a bis(2-methylthio)vinyl derivative almost quantitatively to the 2-mono(methylthio)-2-morpholino derivative. Leukemia cell culture studies of the 6-methyl derivative showed no effect on cell cycle processes.

Keyphrases □ Antileukemic activity—2-bis(2-methylthio)vinyl-1-methylquinolinium iodides, comparative testing in cell culture and mice □ 2-Bis(2-methylthio)vinyl-1-methylquinolinium iodides—NMR analysis and synthesis of bis(methylthio)vinyl derivatives, comparative testing for antileukemic activity in cell culture and mice □ NMR spectroscopy—analysis, synthesized bis(methylthio)vinyl derivatives

1,6-Dimethylquinolinium-2-dithioacetic acid zwitterion (III*b*) was found to have appreciable activity against P-388 lymphocytic leukemia in mice (1) and against CD_8F_1 mammary tumor in mice[1]. Other 6-substituted 1-methylquinolinium-2-dithioacetic acid zwitterions showed comparable antileukemic activity in mice (2), regardless of the electron-donating or electron-releasing ability of the 6-substituent. Since these zwitterions were amorphous and poorly soluble in both aqueous and organic media, more soluble derivatives were desired having potential chemical reactivity similar to that of the dithioacetic acid function. Accordingly, the bis(methylthio)vinyl derivatives were prepared (Scheme I), and their antileukemic activities were determined. These derivatives are crystalline and more soluble in both water and organic solvents.

[1] Screening results were obtained from the Division of Cancer Treatment, National Cancer Institute, National Institutes of Health.

DISCUSSION

Chemistry—Gompper *et al.* (3) reported the formation of the 2-bis(2-methylthio)vinyl compound (V*a*) by reaction of iodomethane with the dithioacetic acid zwitterion (III*a*). No reaction temperature or yield was stated. Mizuyama *et al.* (4) also reported the formation of a mono(methylthio) compound from the corresponding 1,2-dihydroquinoline analog and iodomethane, but no physical constants or experimental data were given. The procedure of Rosenhauer (5), in which the intermediate zwitterion (III*a*) was not isolated but was treated with excess iodomethane, was employed accordingly. The 6-unsubstituted bis(methylthio)vinyl compound and the corresponding 6-bromo derivative were reported previously (2).

Dilute sodium hydroxide generally sufficed for removal of the 2-methyl proton prior to condensation with carbon disulfide, but sodium hydride in 2-propanol was required for the 6-methoxy derivative. To obtain the bis(methylthio)vinyl derivatives, the methiodides (I) were treated with aqueous base, and the methylene derivatives (II) were extracted into toluene. The toluene solutions were treated with carbon disulfide, and the precipitated zwitterions (III) were taken up in dimethylformamide and were allowed to react with excess iodomethane. The 6-bromo and 6-unsubstituted analogs (3) were prepared by suspending the zwitterions (III) in dimethylformamide and adding iodomethane.

In the preparation of the methiodides (I), use of colored quinaldines gave impure methiodides, which could not be purified by recrystallization. Therefore, freshly distilled quinaldine was used. The methiodides were prepared with excess iodomethane without solvent. The quinaldines were prepared as described previously (2). The prepared bis(methylthio)vinyl compounds gave NMR spectra that agreed with the proposed structure (V). The *N*-methyl protons appeared at δ 4.4 ppm, and the aromatic protons appeared at δ 7.5–9.4 ppm. The 2-methyl protons of the methiodides at δ 3.1 ppm were absent in the bis(methylthio)vinyl derivatives; a methine proton appeared as a singlet at δ 6.6–6.8 ppm. The *S*-methyl protons were found as separate peaks at δ 2.5 and 2.7 ppm. The 6-methyl protons of V*b* appeared at δ 2.6 ppm, and the 6-methoxy protons (V*c*) were found at δ 4.0 ppm.

With the possible exception of the 6-bromo analog, none of the bis(methylthio)vinyl compounds was obtained in yields over 50%. The recrystallization liquors of the 6-methyl derivative were examined, and only one definable material was found, the original 1,2,6-trimethylqui-

0022-3549/80/0400-0477$01.00/0
© 1980, American Pharmaceutical Association

rable. Analysis of the commercial preparation[12] gave results (Table II) that were consistent with the potency and the amount of the aerosol concentrate contained in each unit. Typical correlation coefficients for the standard curve were usually ≥0.999. Therefore, with the accuracy of the system established, the external standardization was considered satisfactory. A placebo preparation gave no interference.

The amount and concentration of the acetic acid solution were critical to the success of the extraction. If less than the prescribed amounts were used, difficulties with emulsification and incomplete recoveries resulted. A stronger acid such as hydrochloric acid could have been used at lower concentrations; but since the system was to be automated, a milder acid was preferred to preserve the instruments.

Prior to introduction into the high-pressure liquid chromatograph, good chromatographic practice generally requires filtering the analytical solutions through a fractional micrometer filter. This practice caused a 1–2% increase in recovery above that expected in the analytically prepared samples. Because of this feature, filtering samples is not recommended. The speed and accuracy of the method make occasional chromatograph filter and frit changes worthwhile.

A typical chromatogram of the high lipoid extract is shown in Fig. 1. The only excipient carried through the extraction and appearing on the chromatogram was methylparaben ($k' = 1$). Pramoxine hydrochloride ($k' = 2.2$) eluted in ~6 min.

The described method has general applicability to most pharmaceutical dosage forms containing pramoxine hydrochloride. In many cases, the drug can be extracted directly with the mobile phase or the entire composition can be dissolved. The high lipoid aerosol foam dosage form analysis was described because of the restrictions imposed on the analytical method.

[12] Non-Steroid Proctofoam, Reed & Carnrick, Kenilworth, N.J.

REFERENCES

(1) "The National Formulary," 14th ed., Mack Publishing Co., Easton, Pa., 1974, pp. 598, 599.

(2) E. Mario and L. G. Meehan, *J. Pharm Sci.*, **59**, 538 (1970).

Antileukemic Activity of 2-Bis(2-methylthio)vinyl-1-methylquinolinium Iodides

WILLIAM O. FOYE ˣ and JOEL M. KAUFFMAN

Received September 13, 1979, from the *Samuel M. Best Research Laboratory, Massachusetts College of Pharmacy, Boston, MA 02115.* Accepted for publication November 16, 1979.

Abstract □ Reaction of 1-methylquinolinium-2-dithioacetic acid zwitterions with excess methyl iodide in dimethylformamide gave the corresponding bis(2-methylthio)vinyl derivatives. These compounds were more soluble in both aqueous and organic media than the dithioacetic acid zwitterions but showed comparable antileukemic activity in mice. Reaction with morpholine converted a bis(2-methylthio)vinyl derivative almost quantitatively to the 2-mono(methylthio)-2-morpholino derivative. Leukemia cell culture studies of the 6-methyl derivative showed no effect on cell cycle processes.

Keyphrases □ Antileukemic activity—2-bis(2-methylthio)vinyl-1-methylquinolinium iodides, comparative testing in cell culture and mice □ 2-Bis(2-methylthio)vinyl-1-methylquinolinium iodides—NMR analysis and synthesis of bis(methylthio)vinyl derivatives, comparative testing for antileukemic activity in cell culture and mice □ NMR spectroscopy—analysis, synthesized bis(methylthio)vinyl derivatives

1,6-Dimethylquinolinium-2-dithioacetic acid zwitterion (III*b*) was found to have appreciable activity against P-388 lymphocytic leukemia in mice (1) and against CD_8F_1 mammary tumor in mice[1]. Other 6-substituted 1-methylquinolinium-2-dithioacetic acid zwitterions showed comparable antileukemic activity in mice (2), regardless of the electron-donating or electron-releasing ability of the 6-substituent. Since these zwitterions were amorphous and poorly soluble in both aqueous and organic media, more soluble derivatives were desired having potential chemical reactivity similar to that of the dithioacetic acid function. Accordingly, the bis(methylthio)vinyl derivatives were prepared (Scheme I), and their antileukemic activities were determined. These derivatives are crystalline and more soluble in both water and organic solvents.

[1] Screening results were obtained from the Division of Cancer Treatment, National Cancer Institute, National Institutes of Health.

DISCUSSION

Chemistry—Gompper *et al.* (3) reported the formation of the 2-bis(2-methylthio)vinyl compound (V*a*) by reaction of iodomethane with the dithioacetic acid zwitterion (III*a*). No reaction temperature or yield was stated. Mizuyama *et al.* (4) also reported the formation of a mono(methylthio) compound from the corresponding 1,2-dihydroquinoline analog and iodomethane, but no physical constants or experimental data were given. The procedure of Rosenhauer (5), in which the intermediate zwitterion (III*a*) was not isolated but was treated with excess iodomethane, was employed accordingly. The 6-unsubstituted bis(methylthio)vinyl compound and the corresponding 6-bromo derivative were reported previously (2).

Dilute sodium hydroxide generally sufficed for removal of the 2-methyl proton prior to condensation with carbon disulfide, but sodium hydride in 2-propanol was required for the 6-methoxy derivative. To obtain the bis(methylthio)vinyl derivatives, the methiodides (I) were treated with aqueous base, and the methylene derivatives (II) were extracted into toluene. The toluene solutions were treated with carbon disulfide, and the precipitated zwitterions (III) were taken up in dimethylformamide and were allowed to react with excess iodomethane. The 6-bromo and 6-unsubstituted analogs (3) were prepared by suspending the zwitterions (III) in dimethylformamide and adding iodomethane.

In the preparation of the methiodides (I), use of colored quinaldines gave impure methiodides, which could not be purified by recrystallization. Therefore, freshly distilled quinaldine was used. The methiodides were prepared with excess iodomethane without solvent. The quinaldines were prepared as described previously (2). The prepared bis(methylthio)vinyl compounds gave NMR spectra that agreed with the proposed structure (V). The *N*-methyl protons appeared at δ 4.4 ppm, and the aromatic protons appeared at δ 7.5–9.4 ppm. The 2-methyl protons of the methiodides at δ 3.1 ppm were absent in the bis(methylthio)vinyl derivatives; a methine proton appeared as a singlet at δ 6.6–6.8 ppm. The *S*-methyl protons were found as separate peaks at δ 2.5 and 2.7 ppm. The 6-methyl protons of V*b* appeared at δ 2.6 ppm, and the 6-methoxy protons (V*c*) were found at δ 4.0 ppm.

With the possible exception of the 6-bromo analog, none of the bis(methylthio)vinyl compounds was obtained in yields over 50%. The recrystallization liquors of the 6-methyl derivative were examined, and only one definable material was found, the original 1,2,6-trimethylqui-

0022-3549/80/0400-0477$01.00/0
© 1980, American Pharmaceutical Association

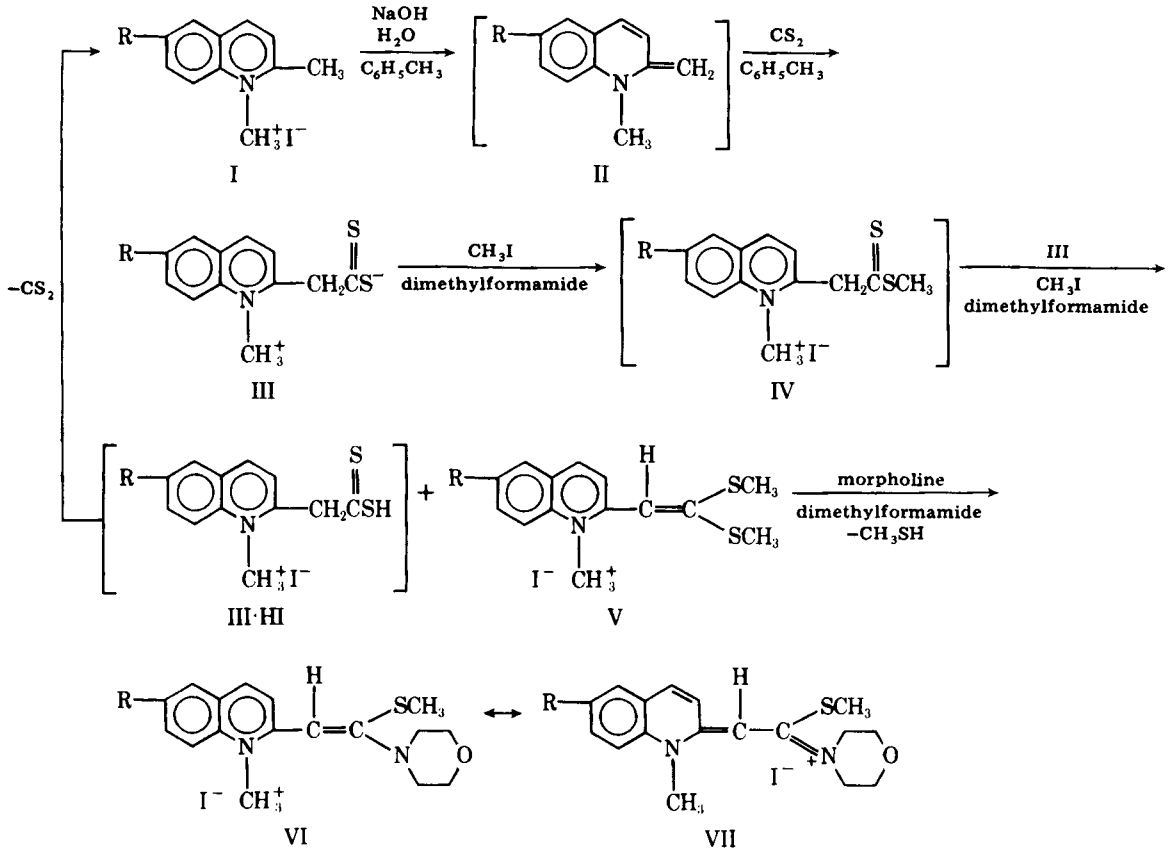

a: R = H
b: R = CH_3
c: R = OCH_3
d: R = Br

Scheme I

nolinium iodide. It is unlikely that this compound was unreacted starting material since it would not be soluble in the toluene extraction of the methylene base (II*b*). Instead, abstraction of one of the methylene protons of the mono(methylthio) derivative (IV*b*) by the intermediate zwitterion (III*b*) may have taken place to form a free dithioacetic acid (III*b*-HI), which lost carbon disulfide to give I*b*. The mono(methylthio) derivative then reacted with a second mole of iodomethane to give the bis(methylthio) compound (V*b*). The ease of abstraction of a methylene proton from quinolinium-2-acetate esters has been recorded (6).

An attempt was made to hydrolyze the 6-unsubstituted zwitterion (III*a*) with 3 *N* HCl. Hydrogen sulfide was evolved slowly at 25–35°, and the reaction still was incomplete after 10 days. Refluxing produced elemental sulfur. Evaporation of the resulting neutralized solution gave no organic products. A possible hydrolysis product, 1-methylquinolinium-2-acetate (VIII), was not found in the literature, and the ready decarboxylation of quinoline-2-acetic acids has been noted (7). Thus, with the synthesis of the quinoliniumdithioacetic acid zwitterions, it was possible to prepare stable sulfur analogs of acids that are not stable in the oxygen series. In addition, a recent attempt to prepare quinoline-2-acetic acid by carbonation of quinaldinyl lithium gave no identifiable acid (8).

As an indication of the reactivity of the bis(methylthio)vinyl compounds with amines, the 6-methyl derivative (III*b*) was reacted with morpholine in dimethylformamide at 35°. A 91% yield of the mono(methylthio)morpholino compound (VI*b*) was obtained over 5 days, with evolution of methanethiol. The 6-bromo analog (VI*d*) gave a comparable conversion to the mono(methylthio)morpholine derivative in a comparable period. Although these conditions were not physiological, the temperature was comparable; the mixture remained nearly neutral throughout the reaction. Evidently, the bis(methylthio)vinyl compounds may react readily with cellular amines.

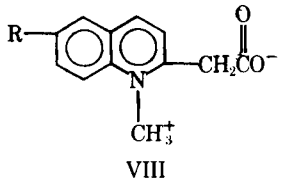

VIII

The NMR spectrum of VI*b* showed the remaining *S*-methyl protons as a singlet at δ 2.51 ppm. This finding allows the assignment of the *S*-methyl protons in the bis(methylthio) derivatives since the morpholine is assumed to be *trans* to the quinoline ring. The eight morpholine protons appeared as a broad singlet at δ 3.71 ppm. This observation can be explained by the existence of a partial positive charge on the morpholino nitrogen. The *N*-methyl peak at δ 4.09 ppm was shifted upfield from 4.41 ppm in the starting material, indicating decreased positive charge on the quinoline nitrogen. The vinyl proton, at δ 5.59 ppm, was shielded drastically compared with its position at δ 6.76 ppm in the bis(methylthio) compound. These facts, as well as the green color of the compound, indicate the contribution of resonance form VII to the structure and reinforce the assumption of the *trans* morpholine configuration.

Antileukemia Test Results—Antileukemia testing[2] of the bis(methylthio) compounds was performed in mice. The NCI protocol (9) and P-388 lymphocytic leukemia were used. Details regarding the dose and survival times of the treated animals are listed in Table I. No weight loss was found at the highest dose used, except with the 6-bromo derivative, which gave T/C (test/control) values of −0.3, −1.2, and −2.7 at 6.25, 12.5, and 25.0 mg/kg, respectively.

All tested compounds showed positive activity (a T/C × 100 ratio of 125 or better). Similar testing of the corresponding dithioacetic acid zwitterions (2) showed that the 6-unsubstituted derivative gave slightly less activity than the 6-substituted compounds. With the bis(methyl-

[2] Results were reported through the courtesy of Dr. Ralph G. Child, Lederle Laboratories; the 6-bromo derivative was tested at the National Cancer Institute (NCI).

Table I—Antileukemic Activities in Mice[a]

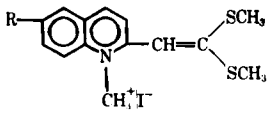

R	Dose, mg/kg[b]	Median Survival Time, T/C, %[c] Test 1	Test 2
H	25.0	115	
	12.5	120	130
	6.25	120	140
	3.12		125
	1.56		120
	0.78		110
CH_3	25.0	85	
	12.5	110	130
	6.25	120	130
	3.12		130
	1.56		120
	0.78		110
OCH_3	25.0	45	
	12.5	125	130
	6.25	125	110
	3.12		115
	1.56		110
	0.78		110
Br	25.0	107	
	12.5	125	127
	6.25	121	117
	3.12		110

[a] BDF_1 mice were inoculated with P-388 lymphocytic leukemia. [b] Drugs were administered intraperitoneally on Days 1, 5, and 9. [c] A T/C % value of ≥125 is considered a positive result.

thio)vinyl derivatives, the 6-unsubstituted compound was slightly more active than the 6-substituted derivatives, but the differences in both cases were small. Apparently, a 6-substituent is not required for antileukemic activity of the bis(methylthio)vinyl compounds.

Leukemic cell culture studies also were performed using the 6-methyl derivative[3]. Human leukemic lymphoblasts in culture were incubated with 10^{-4}, 10^{-5}, 10^{-6}, and 10^{-7} *M* test compound for 24 hr. Then the cells were harvested, stained with propidium iodide, and analyzed by flow cytometry. The flow cytometry data showed no accumulation of cells in any particular phase of the cell cycle at any drug concentration used. This negative result *in vitro* may indicate that a metabolic conversion of the bis(methylthio)vinyl compounds as well as their dithioacetic acid precursors, possibly to the reactive methylene intermediates (II), may be necessary for antileukemic activity.

EXPERIMENTAL[4]

2-Bis(2-methylthio)vinyl-1,6-dimethylquinolinium Iodide—A suspension of 22.44 g (0.075 mole) of 1,2,6-trimethylquinolinium iodide (1) and 100 ml of water was covered with 450 ml of toluene and stirred while 22 g of 50% NaOH solution was added quickly. Stirring was continued for 1 hr, and the toluene layer was decanted, dried with potassium carbonate for 5 min, decanted, and treated with 6.77 ml (0.1125 mole) of carbon disulfide. The mixture was swirled, capped, and allowed to stand overnight at 25°. The precipitated zwitterion was filtered, washed with toluene, suspended in 75 ml of dimethylformamide, and treated with 14.0 ml (0.225 mole) of iodomethane.

The mixture was kept overnight at 25°, and the yellow-green powder was filtered, washed with 50 ml of acetone, and dried at 80° (30 torr) for 4 hr. Recrystallization from water, with cooling only to 25°, gave 8.3 g (27% yield) of bronze needles, mp 205–207° dec.; NMR: δ 2.50 (s, 3H, SCH_3), 2.60 (s, 3H, 6-CH_3), 2.70 (s, 3H, SCH_3), 4.41 (s, 3H, NCH_3), 6.76 (s, 1H, vinyl), and 7.95–9.00 (m, 5H, aromatic) ppm.

Anal.—Calc. for $C_{15}H_{18}INS_2$: C, 44.66; H, 4.50; N, 3.47; S, 15.90. Found: C, 44.60; H, 4.46; N, 3.39; S, 16.10.

6-Methoxy-1-methyl-2-bis(2-methylthio)vinylquinolinium Iodide—Sodium hydride (2.1 g, 0.05 mole) (57% dispersion in oil)[5] was allowed to react with 150 ml of 2-propanol at 27–37°, and the flask then was packed in ice. 1,2-Dimethyl-6-methoxyquinolinium iodide (2) (15.76 g, 0.05 mole) was added below 10°, with stirring for 15 min after the addition. Carbon disulfide (11.7 g, 0.15 mole) was added dropwise over 60 min, and stirring was maintained for another 60 min. The resulting red zwitterion was filtered and washed with ether. The solid was suspended quickly in 50 ml of dimethylformamide and treated with iodomethane (21.29 g, 0.15 mole).

The mixture was kept overnight at 30°, diluted with 100 ml of ether, allowed to stand at 25° for 3 hr, and filtered. The crude product was washed with ether, dried at 20° (1 torr) for 16 hr, and recrystallized from water (cooling only to 20°) to give 2.12 g (10% yield) of brown needles, mp 222–225° dec.; NMR: δ 2.40 (s, 3H, SCH_3), 2.60 (s, 3H, SCH_3), 3.90 (s, 3H, OCH_3), 4.35 (s, 3H, NCH_3), 6.63 (s, 1H, vinyl), and 7.6–9.1 (m, 5H, aromatic) ppm.

Anal.—Calc. for $C_{15}H_{18}INOS_2$: C, 42.96; H, 4.33; N, 3.34. Found: C, 43.04; H, 4.26; N, 3.29.

Isolation of 1,2,6-Trimethylquinolinium Iodide in Preparation of 2-Bis(2-methylthio)vinyl-1,6-dimethylquinolinium Iodide—The aqueous mother liquor from which V*b* was crystallized deposited no solid on prolonged cooling at 1°. The liquid, 700 ml, was treated with 0.5 g of activated charcoal[6] at 20°, and water was removed with a rotary evaporator until a solid appeared. The yield was 0.3 g, mp 240–244° dec. Further evaporation and three recrystallizations from 95% ethanol gave 1.9 g, mp 252–252.5° dec.; mixed with a sample of I*b*, the melting point was 248–250° dec. The NMR spectrum was identical to that of I*b*.

1,6-Dimethyl-2-[2-methylthio -2- (1-morpholino)vinyl]quinolinium Iodide—A flask was charged with 7.26 g (0.018 mole) of 2-bis(2-methylthio)vinyl-1,6-dimethylquinolinium iodide, 80 ml of dimethylformamide, and 1.74 g (0.020 mole) of morpholine (redistilled after drying with a 3-Å molecular sieve). A drying tube containing 20 g of indicating calcium sulfate[7] was attached, and the reaction was stirred magnetically at 35° for 5.5 days. The reaction could be followed by the progression of brown coloration on the calcium sulfate and the detection of the odor of methanethiol. Toluene, 80 ml, was added, and the mixture was stored at 25° for 4 hr.

Following filtration, the filtrate was diluted with 350 ml of toluene and kept at −20° to give a first crop of 6.78 g (85% yield), mp 198–199° dec. A second crop was obtained by heating the filtrate to 90°, diluting with 250 ml of toluene, and cooling to −20°; 0.44 g was obtained (6% yield), mp 197–199° dec.; NMR: δ 2.51 (s, 3H, SCH_3), 2.57 (s, 3H, 6-CH_3), 3.71 (s, br, 8H, morpholine), 4.09 (s, 3H, NCH_3), 5.59 (s, 1H, vinyl), and 7.65–8.20 (m, 5H, aromatic) ppm.

Anal.—Calc. for $C_{18}H_{23}IN_2OS$: C, 48.87; H, 5.24; N, 6.33. Found: C, 48.77; H, 5.04; N, 5.93.

REFERENCES

(1) W. O. Foye, Y. J. Lee, K. A. Shah, and J. M. Kauffman, *J. Pharm. Sci.*, **67**, 962 (1978).

(2) W. O. Foye and J. M. Kauffman, *ibid.*, **68**, 336 (1979).

(3) R. Gompper, B. Wetzel, and W. Elser, *Tetrahedron Lett.*, **1968**, 5519.

(4) K. Mizuyama, Y. Tominaga, J. Matsuda, and G. Kobayashi, *Yakugaku Zasshi*, **94**, 702 (1974).

(5) E. Rosenhauer, *Chem. Ber.*, **57**, 1294 (1924).

(6) W. J. Irwin and D. G. Wibberley, *J. Chem. Soc.*, **1974**, 250.

(7) R. B. Woodward and E. C. Kornfeld, *J. Am. Chem. Soc.*, **70**, 2508 (1948).

(8) A. M. Jones, C. A. Russell, and S. Skidmore, *J. Chem. Soc.*, **1969**, 2245.

(9) R. I. Geran, N. H. Greenberg, M. M. MacDonald, A. M. Schumacher, and B. J. Abbott, *Cancer Chemother. Rep., Part 3*, **3**, 1 (1972).

ACKNOWLEDGMENTS

Presented at the 11th International Congress of Chemotherapy and the 19th Interscience Conference on Anti-Microbial Agents and Chemotherapy, Boston, Mass., October 1979.

[3] Testing was performed by Dr. Ram Ganapathi, University of Miami School of Medicine, Miami, Fla.

[4] Melting points were determined in capillaries with a Mel-Temp block and are uncorrected. PMR spectra were obtained with a Varian T-60 spectrometer using dimethyl sulfoxide-d_6 as the solvent and tetramethylsilane as the internal standard. Elemental analyses were done by F. B. Strauss, Oxford, England, and by Instranal Laboratory, Rensselaer, N.Y. TLC was carried out using silica gel plates, and the products were detected by exposure to iodine vapor. Organic reagents were supplied by Aldrich Chemical Co. and Eastman Organic Chemicals.

[5] Alfa-Ventron.

[6] Aqua Nuchar A.

[7] Drierite.

Supported by funds from the John R. and Marie K. Sawyer Memorial Fund, Massachusetts College of Pharmacy.

The authors are indebted to Dr. Ralph G. Child, Lederle Laboratories, and to the Division of Cancer Treatment, National Cancer Institute, for the antileukemia test results, and to Dr. Ram Ganapathi, University of Miami School of Medicine, for carrying out the cell culture studies.

COMMUNICATIONS

Hepatic Extraction of Endogenous Inhibitors of Plasma Protein Binding

Keyphrases □ Drug binding—plasma protein, hepatic extraction of endogenous inhibitors □ Pharmacokinetics—plasma protein binding, hepatic extraction of endogenous inhibitors □ Plasma protein binding—hepatic extraction of endogenous inhibitors

To the Editor:

Determination of the systemic intrinsic clearance of free (unbound) drug requires measurement of the drug's free fraction in blood, plasma, or serum. For drugs whose total clearance from the blood is much lower than the blood flow through the eliminating organ(s), the intrinsic clearance of the free drug is equal to the total clearance divided by the free fraction (1, 2). The use of free fraction values obtained in the usual manner (*i.e.*, by *in vitro* determinations of protein binding in plasma from peripheral venous blood) for intrinsic clearance calculations is based on the assumption that drug protein binding does not change as the blood passes through the liver or another drug-eliminating organ.

The free fraction value of many drugs in blood or plasma is reasonably constant over a wide drug concentration range. Consequently, it will not be affected by modest drug concentration changes during a single pass of blood through the liver. If, however, protein binding of the drug is affected by endogenous or exogenous (other drugs) inhibitors of binding, then the organ extraction ratio of these inhibitors must be considered. The potential consequences of hepatic extraction of binding inhibitors on the pharmacokinetics and pharmacological activity of a restrictively cleared drug can be appreciated by considering the following limiting cases.

If the extraction ratio [(concentration in inflowing blood − concentration in outflowing blood)/concentration in inflowing blood] of inhibitors of protein binding is close to zero (*i.e.*, there is very little extraction), then the inhibitors will cause an increase in the free fraction, a decrease in the steady-state total concentration, and *no change* in the steady-state free concentration of drug in peripheral blood or plasma (3). Since the pharmacological activity of a drug is usually a function of its free concentration (4), the intensity of pharmacological activity at steady state should not be affected by poorly extracted inhibitors of binding unless they have pharmacological effects of their own.

Conversely, if an inhibitor of protein binding is very rapidly and completely extracted from blood by the liver during a single pass (extraction ratio is near unity and the time for extraction of inhibitor from blood is much shorter than the transit time of that blood through the liver), then the inhibitor will have little or no effect on the steady-state concentration of total (free plus bound) drug, but it will cause the free fraction and the steady-state concentration of free drug in extrahepatic blood or plasma to be *increased*. This result would come about for two reasons:

1. Protein binding of the drug in blood is normal (rather than reduced) during most of the residence time of any one small portion of blood in the liver.
2. Protein binding of the drug leaving the liver is soon reduced as that blood mixes with inhibitor-containing blood in the vena cava, causing the free fraction and concentration of free drug to rise again.

Drug binding inhibitors with hepatic extraction ratios near unity may be cleared quite rapidly from the body. However, their concentration in blood can be quite stable if they are continuously formed endogenously, are continuously administered (other drugs or dietary components), or have a large apparent volume of distribution. Such inhibitors can be expected to increase the pharmacological activity of drugs that they displace by increasing the steady-state free concentration of these drug in extrahepatic blood. Since the steady-state concentration of total drug may be almost unchanged, the increased pharmacological activity may be unanticipated.

It is relatively easy to determine the hepatic extraction characteristics of drugs that act as displacers of other drugs from plasma protein binding sites; such a determination can be done by measuring the hepatic clearance of the displacer drugs. However, this approach is not possible (at least at this time) in the case of endogenous inhibitors associated with certain changes in the pathophysiological status of humans and animals. The hepatic extraction characteristics of binding inhibitors associated with pregnancy (5) and renal failure (6) are presently being investigated directly. To describe the method used for this investigation and to demonstrate in principle that certain endogenous inhibitors are indeed subject to considerable hepatic extraction, data on heparin-induced inhibitors of protein binding will be reported here. Since the composi-

0022-3549/80/0400-0480$01.00/0
© 1980, American Pharmaceutical Association

Supported by funds from the John R. and Marie K. Sawyer Memorial Fund, Massachusetts College of Pharmacy.

The authors are indebted to Dr. Ralph G. Child, Lederle Laboratories, and to the Division of Cancer Treatment, National Cancer Institute, for the antileukemia test results, and to Dr. Ram Ganapathi, University of Miami School of Medicine, for carrying out the cell culture studies.

COMMUNICATIONS

Hepatic Extraction of Endogenous Inhibitors of Plasma Protein Binding

Keyphrases □ Drug binding—plasma protein, hepatic extraction of endogenous inhibitors □ Pharmacokinetics—plasma protein binding, hepatic extraction of endogenous inhibitors □ Plasma protein binding—hepatic extraction of endogenous inhibitors

To the Editor:

Determination of the systemic intrinsic clearance of free (unbound) drug requires measurement of the drug's free fraction in blood, plasma, or serum. For drugs whose total clearance from the blood is much lower than the blood flow through the eliminating organ(s), the intrinsic clearance of the free drug is equal to the total clearance divided by the free fraction (1, 2). The use of free fraction values obtained in the usual manner (*i.e.*, by *in vitro* determinations of protein binding in plasma from peripheral venous blood) for intrinsic clearance calculations is based on the assumption that drug protein binding does not change as the blood passes through the liver or another drug-eliminating organ.

The free fraction value of many drugs in blood or plasma is reasonably constant over a wide drug concentration range. Consequently, it will not be affected by modest drug concentration changes during a single pass of blood through the liver. If, however, protein binding of the drug is affected by endogenous or exogenous (other drugs) inhibitors of binding, then the organ extraction ratio of these inhibitors must be considered. The potential consequences of hepatic extraction of binding inhibitors on the pharmacokinetics and pharmacological activity of a restrictively cleared drug can be appreciated by considering the following limiting cases.

If the extraction ratio [(concentration in inflowing blood − concentration in outflowing blood)/concentration in inflowing blood] of inhibitors of protein binding is close to zero (*i.e.*, there is very little extraction), then the inhibitors will cause an increase in the free fraction, a decrease in the steady-state total concentration, and *no change* in the steady-state free concentration of drug in peripheral blood or plasma (3). Since the pharmacological activity of a drug is usually a function of its free concentration (4), the intensity of pharmacological activity at steady state should not be affected by poorly extracted inhibitors of binding unless they have pharmacological effects of their own.

Conversely, if an inhibitor of protein binding is very rapidly and completely extracted from blood by the liver during a single pass (extraction ratio is near unity and the time for extraction of inhibitor from blood is much shorter than the transit time of that blood through the liver), then the inhibitor will have little or no effect on the steady-state concentration of total (free plus bound) drug, but it will cause the free fraction and the steady-state concentration of free drug in extrahepatic blood or plasma to be *increased*. This result would come about for two reasons:

1. Protein binding of the drug in blood is normal (rather than reduced) during most of the residence time of any one small portion of blood in the liver.
2. Protein binding of the drug leaving the liver is soon reduced as that blood mixes with inhibitor-containing blood in the vena cava, causing the free fraction and concentration of free drug to rise again.

Drug binding inhibitors with hepatic extraction ratios near unity may be cleared quite rapidly from the body. However, their concentration in blood can be quite stable if they are continuously formed endogenously, are continuously administered (other drugs or dietary components), or have a large apparent volume of distribution. Such inhibitors can be expected to increase the pharmacological activity of drugs that they displace by increasing the steady-state free concentration of these drug in extrahepatic blood. Since the steady-state concentration of total drug may be almost unchanged, the increased pharmacological activity may be unanticipated.

It is relatively easy to determine the hepatic extraction characteristics of drugs that act as displacers of other drugs from plasma protein binding sites; such a determination can be done by measuring the hepatic clearance of the displacer drugs. However, this approach is not possible (at least at this time) in the case of endogenous inhibitors associated with certain changes in the pathophysiological status of humans and animals. The hepatic extraction characteristics of binding inhibitors associated with pregnancy (5) and renal failure (6) are presently being investigated directly. To describe the method used for this investigation and to demonstrate in principle that certain endogenous inhibitors are indeed subject to considerable hepatic extraction, data on heparin-induced inhibitors of protein binding will be reported here. Since the composi-

0022-3549/80/0400-0480$01.00/0
© 1980, American Pharmaceutical Association

tion of these endogenously produced inhibitors is not established definitively, their activity in plasma was determined indirectly by measuring their effect on the protein binding of a suitable marker substance, bilirubin.

Intravenous injection of heparin causes a decrease in the plasma protein binding of bilirubin and certain drugs, apparently due to increased concentrations of fatty acids (7–9). In this study, male adult Sprague–Dawley rats had a cannula inserted in the femoral vein under ether anesthesia. A blood sample (~0.7 ml) was then collected. Immediately thereafter, the rats received an intravenous injection of heparin (500 units/kg) or an equal volume of normal saline solution. The liver was then exposed through a midline abdominal incision, a cannula was inserted in the hepatic vein of the left lobe (10), and the hepatic vein was clamped near its junction with the vena cava immediately before the hepatic vein blood sample was taken. These procedures were completed within 1–3 min.

Blood samples (0.7 ml) were obtained simultaneously from the femoral and hepatic veins from 3 to 5 min after heparin injection. Plasma was separated, bilirubin was added to yield a final concentration of ~10 mg/100 ml, and the free fraction of this substance was determined by a peroxidase-catalyzed reaction rate method (3, 11). Blood samples obtained before heparin or saline injection were treated in the same manner.

In the control (saline injection) experiments, the plasma bilirubin free fraction values (mean $\times 10^4 \pm SD$, $n = 6$) were 3.06 ± 0.63 before injection, 3.75 ± 1.05 in plasma from the femoral vein after injection, and 3.98 ± 0.87 in plasma from the hepatic vein after injection. The ratio of the bilirubin free fraction values, hepatic vein plasma: femoral vein plasma, was 1.08 ± 0.10 (mean ± SD, $n = 6$). Thus, perfusion through the liver had no apparent effect on the bilirubin binding characteristics of plasma in control animals.

Heparin injection caused a rapid and pronounced increase in the plasma free fraction of bilirubin as reported previously (7). Moreover, there was a pronounced difference between the protein binding of bilirubin in femoral vein and hepatic vein plasma. The ratio of the bilirubin free fraction values, hepatic vein plasma:femoral vein plasma, was 0.647 ± 0.192 (mean ± SD, $n = 11$).

The results of this investigation demonstrate that certain endogenous inhibitors of plasma protein binding are extracted quite efficiently by the liver. The plasma protein binding of drugs affected by these inhibitors is not the same in plasma obtained from a peripheral vein and in plasma obtained immediately after passage through the liver. Therefore, estimations of the intrinsic clearance of free drug in the presence of inhibitors of protein binding of that drug are incorrect if these inhibitors have large hepatic (or other eliminating organ) extraction ratios.

(1) G. Levy and A. Yacobi, *J. Pharm. Sci.*, **63**, 805 (1974).
(2) G. R. Wilkinson and D. G. Shand, *Clin. Pharmacol. Ther.*, **18**, 377 (1975).
(3) S. Øie and G. Levy, *J. Pharm. Sci.*, **68**, 1 (1979).
(4) G. Levy, *ibid.*, **65**, 1264 (1976).
(5) G. Levy, J. A. Procknal, and L. K. Garrettson, *Clin. Pharmacol. Ther.*, **18**, 210 (1975).
(6) G. Levy, T. Baliah, and J. A. Procknal, *ibid.*, **20**, 512 (1976).
(7) U. W. Wiegand and G. Levy, *J. Pharm. Sci.*, **68**, 1483 (1979).
(8) L. Storstein and H. Janssen, *Clin. Pharmacol. Ther.*, **20**, 15 (1976).
(9) M. Wood, D. G. Shand, and A. J. J. Wood, *ibid.*, **25**, 103 (1979).
(10) M. Yokota, T. Iga, S. Awazu, and M. Hanano, *J. Appl. Physiol.*, **41**, 439 (1976).
(11) J. Jacobsen and O. Fedders, *Scand. J. Clin. Lab. Invest.*, **26**, 237 (1970).

Ulf W. Wiegand
Gerhard Levy ˣ
Department of Pharmaceutics
School of Pharmacy
State University of New York at Buffalo
Amherst, NY 14260

Received October 22, 1979.
Accepted for publication January 4, 1980.
Supported in part by Grant GM 19568 from the National Institutes of Health.
The technical assistance of Mr. David M. Soda is gratefully acknowledged.

High-Pressure Liquid Chromatography of Triamcinolone Acetonide: Effect of Different Octadecylsilane Columns on Mobility

Keyphrases □ Triamcinolone acetonide—high-pressure liquid chromatographic analysis, effects of various octadecylsilane columns on mobility □ High-pressure liquid chromatography—analysis, triamcinolone acetonide, effects of various octadecylsilane columns on mobility □ Anti-inflammatory agents—triamcinolone acetonide, high-pressure liquid chromatographic analysis, effects of various octadecylsilane columns on mobility

To the Editor:

Triamcinolone acetonide[1], a topical anti-inflammatory agent, was assayed by high-pressure liquid chromatography (1) with fluoxymesterone as the internal standard. A reversed-phase octadecylsilane column was used with a mobile phase of acetonitrile–water (30:70) at a flow rate of 2 ml/min. Detection was at 254 nm.

With a column[2] packed with particles 10% covered by octadecylsilane, fluoxymesterone eluted in 10 min and triamcinolone acetonide eluted in 12 min. With a column[3] covered with 5% octadecylsilane, and under otherwise identical chromatographic conditions, fluoxymesterone eluted in 8 min and triamcinolone acetonide eluted in 6 min. The elution patterns were reversed, as also was shown by separate injections of the individual steroids and linearity studies using various concentrations of both steroids.

Both columns are ostensibly the same L-1 type (2). This reversal may be due to the difference in coverage of the particles by octadecylsilane[4] if no other proprietary differences are assumed. The former column separates primarily on the basis of partition, and the latter separates primarily by a combination of partition and adsorption. [The order of elution using the first column can be reversed by using a mobile phase of methanol–water (60:40) instead of acetonitrile–water (30:70).] Both columns gave similar values for triamcinolone acetonide.

[1] Kenalog, E. R. Squibb.
[2] μBondapak, Waters Associates.
[3] Partisil, Whatman.
[4] Manufacturers' literature.

0022-3549/80/0400-0481$01.00/0
© 1980, American Pharmaceutical Association

tion of these endogenously produced inhibitors is not established definitively, their activity in plasma was determined indirectly by measuring their effect on the protein binding of a suitable marker substance, bilirubin.

Intravenous injection of heparin causes a decrease in the plasma protein binding of bilirubin and certain drugs, apparently due to increased concentrations of fatty acids (7–9). In this study, male adult Sprague–Dawley rats had a cannula inserted in the femoral vein under ether anesthesia. A blood sample (~0.7 ml) was then collected. Immediately thereafter, the rats received an intravenous injection of heparin (500 units/kg) or an equal volume of normal saline solution. The liver was then exposed through a midline abdominal incision, a cannula was inserted in the hepatic vein of the left lobe (10), and the hepatic vein was clamped near its junction with the vena cava immediately before the hepatic vein blood sample was taken. These procedures were completed within 1–3 min.

Blood samples (0.7 ml) were obtained simultaneously from the femoral and hepatic veins from 3 to 5 min after heparin injection. Plasma was separated, bilirubin was added to yield a final concentration of ~10 mg/100 ml, and the free fraction of this substance was determined by a peroxidase-catalyzed reaction rate method (3, 11). Blood samples obtained before heparin or saline injection were treated in the same manner.

In the control (saline injection) experiments, the plasma bilirubin free fraction values (mean $\times 10^4 \pm SD$, $n = 6$) were 3.06 ± 0.63 before injection, 3.75 ± 1.05 in plasma from the femoral vein after injection, and 3.98 ± 0.87 in plasma from the hepatic vein after injection. The ratio of the bilirubin free fraction values, hepatic vein plasma: femoral vein plasma, was 1.08 ± 0.10 (mean ± SD, $n = 6$). Thus, perfusion through the liver had no apparent effect on the bilirubin binding characteristics of plasma in control animals.

Heparin injection caused a rapid and pronounced increase in the plasma free fraction of bilirubin as reported previously (7). Moreover, there was a pronounced difference between the protein binding of bilirubin in femoral vein and hepatic vein plasma. The ratio of the bilirubin free fraction values, hepatic vein plasma:femoral vein plasma, was 0.647 ± 0.192 (mean ± SD, $n = 11$).

The results of this investigation demonstrate that certain endogenous inhibitors of plasma protein binding are extracted quite efficiently by the liver. The plasma protein binding of drugs affected by these inhibitors is not the same in plasma obtained from a peripheral vein and in plasma obtained immediately after passage through the liver. Therefore, estimations of the intrinsic clearance of free drug in the presence of inhibitors of protein binding of that drug are incorrect if these inhibitors have large hepatic (or other eliminating organ) extraction ratios.

(1) G. Levy and A. Yacobi, *J. Pharm. Sci.*, **63**, 805 (1974).
(2) G. R. Wilkinson and D. G. Shand, *Clin. Pharmacol. Ther.*, **18**, 377 (1975).
(3) S. Øie and G. Levy, *J. Pharm. Sci.*, **68**, 1 (1979).
(4) G. Levy, *ibid.*, **65**, 1264 (1976).
(5) G. Levy, J. A. Procknal, and L. K. Garrettson, *Clin. Pharmacol. Ther.*, **18**, 210 (1975).
(6) G. Levy, T. Baliah, and J. A. Procknal, *ibid.*, **20**, 512 (1976).
(7) U. W. Wiegand and G. Levy, *J. Pharm. Sci.*, **68**, 1483 (1979).
(8) L. Storstein and H. Janssen, *Clin. Pharmacol. Ther.*, **20**, 15 (1976).
(9) M. Wood, D. G. Shand, and A. J. J. Wood, *ibid.*, **25**, 103 (1979).
(10) M. Yokota, T. Iga, S. Awazu, and M. Hanano, *J. Appl. Physiol.*, **41**, 439 (1976).
(11) J. Jacobsen and O. Fedders, *Scand. J. Clin. Lab. Invest.*, **26**, 237 (1970).

Ulf W. Wiegand
Gerhard Levy ˣ
Department of Pharmaceutics
School of Pharmacy
State University of New York at Buffalo
Amherst, NY 14260

Received October 22, 1979.
Accepted for publication January 4, 1980.
Supported in part by Grant GM 19568 from the National Institutes of Health.
The technical assistance of Mr. David M. Soda is gratefully acknowledged.

High-Pressure Liquid Chromatography of Triamcinolone Acetonide: Effect of Different Octadecylsilane Columns on Mobility

Keyphrases □ Triamcinolone acetonide—high-pressure liquid chromatographic analysis, effects of various octadecylsilane columns on mobility □ High-pressure liquid chromatography—analysis, triamcinolone acetonide, effects of various octadecylsilane columns on mobility □ Anti-inflammatory agents—triamcinolone acetonide, high-pressure liquid chromatographic analysis, effects of various octadecylsilane columns on mobility

To the Editor:

Triamcinolone acetonide[1], a topical anti-inflammatory agent, was assayed by high-pressure liquid chromatography (1) with fluoxymesterone as the internal standard. A reversed-phase octadecylsilane column was used with a mobile phase of acetonitrile–water (30:70) at a flow rate of 2 ml/min. Detection was at 254 nm.

With a column[2] packed with particles 10% covered by octadecylsilane, fluoxymesterone eluted in 10 min and triamcinolone acetonide eluted in 12 min. With a column[3] covered with 5% octadecylsilane, and under otherwise identical chromatographic conditions, fluoxymesterone eluted in 8 min and triamcinolone acetonide eluted in 6 min. The elution patterns were reversed, as also was shown by separate injections of the individual steroids and linearity studies using various concentrations of both steroids.

Both columns are ostensibly the same L-1 type (2). This reversal may be due to the difference in coverage of the particles by octadecylsilane[4] if no other proprietary differences are assumed. The former column separates primarily on the basis of partition, and the latter separates primarily by a combination of partition and adsorption. [The order of elution using the first column can be reversed by using a mobile phase of methanol–water (60:40) instead of acetonitrile–water (30:70).] Both columns gave similar values for triamcinolone acetonide.

[1] Kenalog, E. R. Squibb.
[2] μBondapak, Waters Associates.
[3] Partisil, Whatman.
[4] Manufacturers' literature.

0022-3549/80/0400-0481$01.00/0
© 1980, American Pharmaceutical Association

This striking difference between similarly designated columns may represent the possible extremes in retention. Columns should be tested for suitability prior to use for the official method (1). Alternatively, either the internal standard can be omitted (3) if a precision loop injector[5] is used or the mobile phase composition may be altered to change the elution order of the steroids.

(1) "The United States Pharmacopeia," 20th rev., Mack Publishing Co., Easton, Pa., 1980, p. 812.
(2) *Pharmaceutical Forum*, 4, 408 (1978).
(3) J. Kirschbaum, R. Poet, K. Bush, and G. Petrie, *J. Chromatogr.*, **190**, 481 (1980).

Joel Kirschbaum
Squibb Institute for Medical Research
New Brunswick, NJ 08903

Received December 17, 1979.
Accepted for publication February 22, 1980.
Presented at the 18th Annual Meeting on the Practice of Chromatography, American Society for Testing and Materials, Philadelphia, Pa., October 1979.

[5] Rheodyne model 7010 or equivalent.

Effect of Plasma Protein Binding on Renal Clearance of Drugs

Keyphrases □ Plasma protein binding—effect on renal clearance of drugs □ Drug clearance, renal—effect of plasma protein binding □ Renal clearance—effect of plasma protein binding

To the Editor:

The theoretical concepts of the relationships between plasma or serum protein binding and hepatic metabolic clearance of drugs are now reasonably well defined (1–3 and references cited therein). On the other hand, corresponding theory and experimental data concerning the effect of plasma protein binding on the renal excretion of drugs are quite limited (4–13). The purpose of this communication is to propose certain relationships between plasma protein binding and renal clearance of drugs that may be useful for the design and interpretation of experimental studies.

The renal excretion of drugs usually involves three processes: glomerular filtration, renal tubular secretion, and partial reabsorption from the renal tubular lumen. Glomerular filtration is a passive process and may be assumed to be a function of the free (unbound) concentration of drug in plasma (11) if the glomeruli are intact. Renal tubular secretion is a specialized process; it is saturable in principle but appears to be linear for most drugs under the usual clinical or experimental conditions. The rate of renal tubular secretion may be proportional to the concentration of free or total (free and bound) drug in plasma; it may or may not be affected by blood flow. Renal tubular reabsorption of most drugs involves passive diffusion of nonionized molecules from the renal tubular lumen. Therefore, the rate of reabsorption is proportional to the concentration gradient of diffusible (usually free and nonionized) drug across the renal tubular boundary. Consequently, reabsorption may be affected by the urine flow rate and by the urine pH if the drug is a weak acid or base. The concentration of diffusible drug on the tissue side of the renal tubule is likely to be negligible compared to that in the lumen of the tubule, except in some cases of pronounced diuresis or urine pH alteration. Drug in the urine exists in unbound form unless there is serious nephropathy with marked proteinuria[1]. Thus, if the glomerular excretion rate is proportional to and the renal tubular secretion rate is a function of the concentration of *free* drug in plasma:

$$\text{renal excretion rate} = k_g fC + \frac{Qfk_sC}{Q + fk_s} - F\left(k_g fC + \frac{Qfk_sC}{Q + fk_s}\right) \quad \text{(Eq. 1)}$$

where k_g is the glomerular filtration clearance and k_s is the intrinsic renal tubular secretion clearance (both clearances are referenced to the free drug concentration in plasma), Q is the flow rate of plasma perfusing the renal tubular secretion sites, f is the free fraction of drug in plasma (which is assumed to be independent of concentration in the usual therapeutic or experimental concentration range), C is the concentration of total drug in plasma, and F is a (possibly urine flow rate- and urine pH-dependent) dimensionless constant equal to the fraction of filtered and secreted drug that is reabsorbed.

Implied in the equation is the assumption that F for filtered and secreted drug is the same; this assumption is reasonable if secretion takes place in the proximal region of the tubules and reabsorption occurs mainly from the distal region of the renal tubules. If the concentration ratio, erythrocytes:plasma, of the drug is substantial and reequilibration of the drug between erythrocytes and plasma is very rapid, C may be designated as the concentration of drug in whole blood and k_g, k_s, Q, and f have to be defined accordingly. However, this approach may be complicated if, as was suggested (9), a proportion of the erythrocytes is separated off by "plasma skimming" and shunted into the renal veins without contacting the renal tubules.

The second term on the right side of Eq. 1 is analogous to, and derived in a similar manner as, the hepatic metabolic clearance equation (2). If $Q \gg fk_s$, that term reduces to fk_sC and Eq. 1 reduces to:

$$\text{renal excretion rate} = k_g fC + k_s fC - F(k_g fC + k_s fC) \quad \text{(Eq. 2)}$$

Since renal clearance equals excretion rate/C, division of both sides of Eq. 2 by C and rearrangement yield:

$$\text{renal clearance} = f[k_g + k_s - F(k_g + k_s)] \quad \text{(Eq. 3)}$$

Therefore, a plot of renal clearance *versus* f should be linear and intersect the origin. This situation appears to be the case with salicylic acid in rats, according to preliminary results obtained in this laboratory[2]. If tubular reabsorption is prevented (which can be done with certain weak acids or bases by changing the urine pH), $F = 0$ and the slope of a plot of renal clearance *versus* f increases to $(k_g + k_s)$. The value of $(k_g + k_s)$ should not exceed the renal blood flow unless the compound is formed entirely or in part in the kidneys.

[1] Another rare exception is the case in which a drug or endogenous substance and a complexing or chelating agent are excreted concurrently, separately and as the complex. Each of these species will exhibit distinct renal pharmacokinetic characteristics.
[2] To be published.

0022-3549/80/0400-0482$01.00/0
© 1980, American Pharmaceutical Association

This striking difference between similarly designated columns may represent the possible extremes in retention. Columns should be tested for suitability prior to use for the official method (1). Alternatively, either the internal standard can be omitted (3) if a precision loop injector[5] is used or the mobile phase composition may be altered to change the elution order of the steroids.

(1) "The United States Pharmacopeia," 20th rev., Mack Publishing Co., Easton, Pa., 1980, p. 812.
(2) *Pharmaceutical Forum*, 4, 408 (1978).
(3) J. Kirschbaum, R. Poet, K. Bush, and G. Petrie, *J. Chromatogr.*, **190**, 481 (1980).

Joel Kirschbaum
Squibb Institute for Medical Research
New Brunswick, NJ 08903

Received December 17, 1979.
Accepted for publication February 22, 1980.
Presented at the 18th Annual Meeting on the Practice of Chromatography, American Society for Testing and Materials, Philadelphia, Pa., October 1979.

[5] Rheodyne model 7010 or equivalent.

Effect of Plasma Protein Binding on Renal Clearance of Drugs

Keyphrases □ Plasma protein binding—effect on renal clearance of drugs □ Drug clearance, renal—effect of plasma protein binding □ Renal clearance—effect of plasma protein binding

To the Editor:

The theoretical concepts of the relationships between plasma or serum protein binding and hepatic metabolic clearance of drugs are now reasonably well defined (1–3 and references cited therein). On the other hand, corresponding theory and experimental data concerning the effect of plasma protein binding on the renal excretion of drugs are quite limited (4–13). The purpose of this communication is to propose certain relationships between plasma protein binding and renal clearance of drugs that may be useful for the design and interpretation of experimental studies.

The renal excretion of drugs usually involves three processes: glomerular filtration, renal tubular secretion, and partial reabsorption from the renal tubular lumen. Glomerular filtration is a passive process and may be assumed to be a function of the free (unbound) concentration of drug in plasma (11) if the glomeruli are intact. Renal tubular secretion is a specialized process; it is saturable in principle but appears to be linear for most drugs under the usual clinical or experimental conditions. The rate of renal tubular secretion may be proportional to the concentration of free or total (free and bound) drug in plasma; it may or may not be affected by blood flow. Renal tubular reabsorption of most drugs involves passive diffusion of nonionized molecules from the renal tubular lumen. Therefore, the rate of reabsorption is proportional to the concentration gradient of diffusible (usually free and nonionized) drug across the renal tubular boundary. Consequently, reabsorption may be affected by the urine flow rate and by the urine pH if the drug is a weak acid or base. The concentration of diffusible drug on the tissue side of the renal tubule is likely to be negligible compared to that in the lumen of the tubule, except in some cases of pronounced diuresis or urine pH alteration. Drug in the urine exists in unbound form unless there is serious nephropathy with marked proteinuria[1]. Thus, if the glomerular excretion rate is proportional to and the renal tubular secretion rate is a function of the concentration of *free* drug in plasma:

$$\text{renal excretion rate} = k_g fC + \frac{Qfk_sC}{Q + fk_s} - F\left(k_g fC + \frac{Qfk_sC}{Q + fk_s}\right) \quad \text{(Eq. 1)}$$

where k_g is the glomerular filtration clearance and k_s is the intrinsic renal tubular secretion clearance (both clearances are referenced to the free drug concentration in plasma), Q is the flow rate of plasma perfusing the renal tubular secretion sites, f is the free fraction of drug in plasma (which is assumed to be independent of concentration in the usual therapeutic or experimental concentration range), C is the concentration of total drug in plasma, and F is a (possibly urine flow rate- and urine pH-dependent) dimensionless constant equal to the fraction of filtered and secreted drug that is reabsorbed.

Implied in the equation is the assumption that F for filtered and secreted drug is the same; this assumption is reasonable if secretion takes place in the proximal region of the tubules and reabsorption occurs mainly from the distal region of the renal tubules. If the concentration ratio, erythrocytes:plasma, of the drug is substantial and reequilibration of the drug between erythrocytes and plasma is very rapid, C may be designated as the concentration of drug in whole blood and k_g, k_s, Q, and f have to be defined accordingly. However, this approach may be complicated if, as was suggested (9), a proportion of the erythrocytes is separated off by "plasma skimming" and shunted into the renal veins without contacting the renal tubules.

The second term on the right side of Eq. 1 is analogous to, and derived in a similar manner as, the hepatic metabolic clearance equation (2). If $Q \gg fk_s$, that term reduces to fk_sC and Eq. 1 reduces to:

$$\text{renal excretion rate} = k_g fC + k_s fC - F(k_g fC + k_s fC) \quad \text{(Eq. 2)}$$

Since renal clearance equals excretion rate/C, division of both sides of Eq. 2 by C and rearrangement yield:

$$\text{renal clearance} = f[k_g + k_s - F(k_g + k_s)] \quad \text{(Eq. 3)}$$

Therefore, a plot of renal clearance *versus* f should be linear and intersect the origin. This situation appears to be the case with salicylic acid in rats, according to preliminary results obtained in this laboratory[2]. If tubular reabsorption is prevented (which can be done with certain weak acids or bases by changing the urine pH), $F = 0$ and the slope of a plot of renal clearance *versus* f increases to $(k_g + k_s)$. The value of $(k_g + k_s)$ should not exceed the renal blood flow unless the compound is formed entirely or in part in the kidneys.

[1] Another rare exception is the case in which a drug or endogenous substance and a complexing or chelating agent are excreted concurrently, separately and as the complex. Each of these species will exhibit distinct renal pharmacokinetic characteristics.
[2] To be published.

0022-3549/80/0400-0482$01.00/0
© 1980, American Pharmaceutical Association

If tubular secretion is blocked ($k_s = 0$) and k_g is assumed to equal the glomerular filtration rate (GFR), Eq. 3 becomes:

$$F = 1 - (\text{renal clearance}/f\ \text{GFR}) \quad \text{(Eq. 4)}$$

A similar form of that equation was developed by Arita *et al.* (14); the inverse of the term in parentheses is the excretion ratio as defined by Fisher *et al.* (15). With F determined by means of Eq. 4, k_s can be calculated by a rearranged form of Eq. 3:

$$k_s = \frac{\text{renal clearance}}{f(1 - F)} - \text{GFR} \quad \text{(Eq. 5)}$$

It is reasonable to assume that k_g, being referenced to free drug and characterizing a physical rather than enzymatic or carrier process, is equal to the glomerular filtration rate, a constant that can be determined from the renal clearance of inulin or creatinine.

If the rate of renal tubular secretion is proportional to the concentration of *total* drug in plasma and if the previously stated assumptions apply:

$$\text{renal excretion rate} = k_g fC + k_s^* C - F(k_g fC + k_s^* C) \quad \text{(Eq. 6)}$$

where k_s^* is the renal secretion clearance referenced to the total drug concentration in plasma. Division of both sides of the equation by C and rearrangement yield:

$$\text{renal clearance} = fk_g(1 - F) + k_s^*(1 - F) \quad \text{(Eq. 7)}$$

In this case, a plot of renal clearance *versus* f should be linear and have a positive intercept. Such a relationship was observed recently by Yacobi and Levy (7) with respect to the renal clearance of sulfisoxazole in rats.

Dividing the slope of a plot of renal clearance *versus* f according to Eq. 7 by its intercept gives:

$$\frac{\text{slope}}{\text{intercept}} = \frac{k_g(1 - F)}{k_s^*(1 - F)} = \frac{k_g}{k_s^*} \quad \text{(Eq. 8)}$$

Consequently, inhibition of renal tubular secretion (for example, by administration of probenecid in the case of certain acidic drugs) should cause an increase of the slope:intercept ratio if the renal tubular secretion rate is proportional to the total drug concentration in plasma.

Inhibition or absence of renal tubular reabsorption ($F = 0$) reduces Eq. 7 to:

$$\text{renal clearance} = fk_g + k_s^* \quad \text{(Eq. 9)}$$

and, therefore, results in increased slope and intercept values but has no effect on the slope:intercept ratio. The slope should not exceed the glomerular filtration rate of a completely filtered substance such as inulin or creatinine, and k_s^* should not exceed the renal blood flow minus k_g unless the excreted substance is entirely or partly formed in the kidneys.

Equation 8 may be useful for estimating k_s^*, again with the assumption that k_g = GFR. Then, k_s^* = GFR (intercept/slope). Thus, it may be possible to estimate k_s^* under physiological conditions, *i.e.*, without changing the urine pH to prevent renal tubular reabsorption or administering a drug that blocks renal tubular secretion. Since the intercept of a plot of renal clearance *versus* f according to Eq. 7 is equal to $k_s^*(1 - F)$, F can be estimated if k_s^* is known.

Proportionality between the renal tubular secretion rate and the total rather than the free drug concentration in plasma may be a consequence of blood flow rate-limited secretion (12). Under these conditions, the sum of k_g and k_s^* may be equal to the renal blood flow or it may be less than that if part of the blood perfusing the kidneys bypasses the sites of renal secretion for a particular drug (12, 16). Thus, Eq. 6 may be a limiting case of Eq. 1 when $fk_s \gg Q$. Then the second term on the right side of Eq. 1 reduces to QC, and k_s^* in Eqs. 6–9 becomes Q.

(1) G. Levy and A. Yacobi, *J. Pharm. Sci.*, **63**, 805 (1974).

(2) G. Wilkinson and D. G. Shand, *Clin. Pharmacol. Ther.*, **18**, 377 (1975).

(3) P. J. McNamara, G. Levy, and M. Gibaldi, *J. Pharmacokinet. Biopharm.*, **7**, 195 (1979).

(4) R. Hori, K. Sunayashiki, and A. Kamiya, *J. Pharm. Sci.*, **65**, 463 (1976).

(5) E. R. Garrett, *Int. J. Clin. Pharmacol.*, **16**, 155 (1978).

(6) R. Runkel, E. Forchielli, H. Sevelius, M. Chaplin, and E. Segre, *Clin. Pharmacol. Ther.*, **15**, 261 (1974).

(7) A. Yacobi and G. Levy, *J. Pharm. Sci.*, **68**, 742 (1979).

(8) B. K. Ochwadt and R. F. Pitts, *Am. J. Physiol.*, **187**, 318 (1956).

(9) M. D. Milne, B. H. Scribner, and M. A. Crawford, *Am. J. Med.*, **24**, 709 (1958).

(10) A. H. Anton, *J. Pharmacol. Exp. Ther.*, **134**, 291 (1961).

(11) F. Portwich, H. Büttner, and K. Engelhardt, *Klin. Wochenschr.*, **41**, 447 (1963).

(12) I. M. Weiner, in "Handbook of Physiology, Renal Physiology Section," J. Orloff and R. W. Berliner, Eds., American Physiological Society, Washington, D.C., 1973, pp. 521–554.

(13) F. J. Koschier and M. Acara, *J. Pharmacol. Exp. Ther.*, **208**, 287 (1979).

(14) T. Arita, R. Hori, E. Owada, and K. Takahashi, *Chem. Pharm. Bull.*, **17**, 2526 (1969).

(15) S. H. Fisher, L. Troast, A. Waterhouse, and J. A. Shannon, *J. Pharmacol. Exp. Ther.*, **79**, 373 (1943).

(16) K. E. Britton, *Clin. Sci.*, **56**, 101 (1979).

Gerhard Levy

Department of Pharmaceutics
School of Pharmacy
State University of New York at Buffalo
Amherst, NY 14260

Received July 9, 1979.

Accepted for publication January 10, 1980.

Supported in part by Grant GM 20852 from the National Institute of General Medical Sciences, National Institutes of Health.

REVIEWS

Autonomic Pharmacology: Experimental and Clinical Aspects. By MICHAEL D. DAY. Churchill Livingstone, 19 West 44th St., New York, NY 10036. 1979. 255 pp. 14 × 21 cm. Price $15.00 (soft cover).

This excellent small book, in the words of the author, "is intended primarily for undergraduate students of medical sciences." Students of medicine, pharmacy, dentistry, nursing, and other health sciences also should be included. Written for British students, this book contains many drug names that are not familiar to American students. This is due mainly to the fact that the FDA considers some of these drugs neither safe nor effective, even though they have been used in England for many years. The fact that drugs available on this side of the Atlantic are not identified may be a slight handicap. However, by describing these foreign drugs, this book gives the American student a better and more complete view of autonomic drug development.

There are three chapters covering the anatomy, physiology, and chemistry of the autonomic motor system and neurohumoral transmission. Ten chapters cover adrenergic and cholinergic agonists and blocking agents. For each drug class, one or two prototype compounds are described in detail. Other drugs of the same category then are briefly compared clinically to the prototype. The historical aspects of autonomic physiology and pharmacology are well covered. As far as the drugs that are included and the mechanism of actions described are concerned, this work is up to date. The only thing missing is some mention of radioligand studies of receptors. This book is recommended for all biomedical students.

Reviewed by R. P. Ahlquist
Medical College of Georgia
Augusta, GA 30912

The Anticancer Drugs. By WILLIAM B. PRATT and RAYMOND W. RUDDON. Oxford University Press, 200 Madison Ave., New York, NY 10016. 1979. 323 pp. 15 × 23 cm. Price $18.95 hard cover or $12.95 soft cover.

The stated purpose of this text is to offer "a full, but concise description of anticancer drugs, both old and new." The authors have achieved their objective with respect to describing currently used agents for human neoplastic diseases. There is excellent integration of the proposed mechanism of action of the agent, its uses against specific tumor types, and toxicity of the agent in humans.

The first chapter is a cursory review of the incidence of cancer in the United States and the world, biochemical and genetic characteristics of malignant cells, and role of drugs in cancer therapy.

Historical milestones in the development of the major chemical categories of antineoplastic agents are dealt with in the second chapter.

The third chapter discusses Gompertizian cell growth of tumors, the cell cycle, fraction of cells in mitosis, development of drug-resistant states, and determinant factors of the host involved in drug response.

Chapter 4 reviews, as general concepts, the responsiveness of tumors to chemotherapy drugs, the choice of drugs for specific types of tumors, combination chemotherapy, adjuvant therapy, and toxicity of antineoplastics.

Individual alkylating agents, antimetabolites, antibiotics, hormones, plant alkaloids, enzymes, and miscellaneous drugs are delineated in Chapters 5–9. The chemical structure, mechanism of action, administration routes, absorption, bioactivation, metabolism, distribution, excretion, causes of resistant states, and toxicity are given.

The last chapter briefly describes how new drugs are established as antineoplastic agents in animal models. Thirteen new drugs are discussed that are currently in human clinical trials, potent in animal screens, or unique in structure as an approach to drug design. This chapter also includes a treatment of biological markers of neoplastic cells, *e.g.*, antigens or enzymes, which is more appropriately included in an earlier chapter.

There are several weaknesses of the book as a general text in academic instruction. There is no discussion of structure–activity relationships or the reasons some agents are restricted from use in this country. Only a limited conceptual discussion of immunotherapy agents and their uses in neoplastic therapy and the use of chemotherapy prior to and post-surgery and/or radiation is presented. Neither percentages of response in the clinic to a specific agent for a given tumor type nor the percentage of relapses from therapy is delineated in the text. Furthermore, no differentiation is made between singular and combination therapy in the discussion of the uses of an agent.

The primary emphasis of this book is on the mechanisms of action as seen from the viewpoint of both biochemistry and molecular biology. Few texts have achieved such a complete description of all major agents.

Received by Iris H. Hall
School of Pharmacy
University of North Carolina
Chapel Hill, NC 27514

Index of Antibiotics from Actinomycetes, Vol. 11. Edited by HAMAO UMEZAWA. University Park Press, 233 E. Redwood St., Baltimore, MD 21202. 1979. 1466 pp. 18 × 23 cm. Price $97.50.

This update of a 1966 index lists the antibiotics produced by Actinomycetes reported mainly between 1966 and 1976. Chapter I lists generic names, common names, trivial names, and selected trade names, including those from the previous volume, in alphabetical order followed by those antibiotics designated by letter and numerical arrangement. The group to which the antibiotic belongs and its synonyms are given along with a page reference to an entry in the previous or present volume.

Chapter II gives data on the antibiotics. A typical compound entry includes the antibiotic group, synonyms and similar compounds, molecular weight and formula, structure, isolation, physical properties such as melting point and solubility, elemental analysis, UV characteristics, IR spectrum, activity, LD_{50} value, and literature references.

Staff Review

Analytical Profiles of Drug Substances, Vol. 8. Edited by KLAUS FLOREY. Academic, 111 Fifth Ave., New York, NY 10003. 1979. 558 pp. 15.5 × 23.5 cm.

This ongoing series is concerned with reporting supplemental information on drug substances that are listed in the official compendia but for which the compendia do not provide detailed physical or chemical data, methods of synthesis, or pathways of physical or biological degradation and metabolism.

Volume 8 contains individual monographs for the following drugs: aspirin, bromocriptine methanesulphonate, calcitrol, chlortetracycline hydrochloride, dobutamine hydrochloride, erythromycin, gramicidin, griseofulvin, halcinonide, hydralazine hydrochloride, calcium leucovorin, methimazole, nalidixic acid, neomycin, pseudoephedrine hydrochloride, triprolidine hydrochloride, and sodium valproate and valproic acid. The monographs contain some or all of the general headings such as introductory information (*e.g.*, history, appearance, and odor), physicochemical properties (*e.g.*, elemental analysis, spectra, crystal properties, solubility, and partition coefficients), synthesis, stability and degradation, biopharmaceutics (*e.g.*, pharmacokinetics and metabolism), toxicology, analytical methods, and literature references. Most of the monographs seem to have surveyed the drug literature through 1977 or 1978. The spectra and other analytical curves in the book have been reproduced in a clear and uncluttered fashion.

The entire series should be available in libraries of drug firms, FDA laboratories, toxicology laboratories, and schools of medicine and pharmacy. The volumes are not organized for use as textbooks in courses such

REVIEWS

Autonomic Pharmacology: Experimental and Clinical Aspects. By MICHAEL D. DAY. Churchill Livingstone, 19 West 44th St., New York, NY 10036. 1979. 255 pp. 14 × 21 cm. Price $15.00 (soft cover).

This excellent small book, in the words of the author, "is intended primarily for undergraduate students of medical sciences." Students of medicine, pharmacy, dentistry, nursing, and other health sciences also should be included. Written for British students, this book contains many drug names that are not familiar to American students. This is due mainly to the fact that the FDA considers some of these drugs neither safe nor effective, even though they have been used in England for many years. The fact that drugs available on this side of the Atlantic are not identified may be a slight handicap. However, by describing these foreign drugs, this book gives the American student a better and more complete view of autonomic drug development.

There are three chapters covering the anatomy, physiology, and chemistry of the autonomic motor system and neurohumoral transmission. Ten chapters cover adrenergic and cholinergic agonists and blocking agents. For each drug class, one or two prototype compounds are described in detail. Other drugs of the same category then are briefly compared clinically to the prototype. The historical aspects of autonomic physiology and pharmacology are well covered. As far as the drugs that are included and the mechanism of actions described are concerned, this work is up to date. The only thing missing is some mention of radioligand studies of receptors. This book is recommended for all biomedical students.

Reviewed by R. P. Ahlquist
Medical College of Georgia
Augusta, GA 30912

The Anticancer Drugs. By WILLIAM B. PRATT and RAYMOND W. RUDDON. Oxford University Press, 200 Madison Ave., New York, NY 10016. 1979. 323 pp. 15 × 23 cm. Price $18.95 hard cover or $12.95 soft cover.

The stated purpose of this text is to offer "a full, but concise description of anticancer drugs, both old and new." The authors have achieved their objective with respect to describing currently used agents for human neoplastic diseases. There is excellent integration of the proposed mechanism of action of the agent, its uses against specific tumor types, and toxicity of the agent in humans.

The first chapter is a cursory review of the incidence of cancer in the United States and the world, biochemical and genetic characteristics of malignant cells, and role of drugs in cancer therapy.

Historical milestones in the development of the major chemical categories of antineoplastic agents are dealt with in the second chapter.

The third chapter discusses Gompertizian cell growth of tumors, the cell cycle, fraction of cells in mitosis, development of drug-resistant states, and determinant factors of the host involved in drug response.

Chapter 4 reviews, as general concepts, the responsiveness of tumors to chemotherapy drugs, the choice of drugs for specific types of tumors, combination chemotherapy, adjuvant therapy, and toxicity of antineoplastics.

Individual alkylating agents, antimetabolites, antibiotics, hormones, plant alkaloids, enzymes, and miscellaneous drugs are delineated in Chapters 5–9. The chemical structure, mechanism of action, administration routes, absorption, bioactivation, metabolism, distribution, excretion, causes of resistant states, and toxicity are given.

The last chapter briefly describes how new drugs are established as antineoplastic agents in animal models. Thirteen new drugs are discussed that are currently in human clinical trials, potent in animal screens, or unique in structure as an approach to drug design. This chapter also includes a treatment of biological markers of neoplastic cells, *e.g.*, antigens or enzymes, which is more appropriately included in an earlier chapter.

There are several weaknesses of the book as a general text in academic instruction. There is no discussion of structure–activity relationships or the reasons some agents are restricted from use in this country. Only a limited conceptual discussion of immunotherapy agents and their uses in neoplastic therapy and the use of chemotherapy prior to and post-surgery and/or radiation is presented. Neither percentages of response in the clinic to a specific agent for a given tumor type nor the percentage of relapses from therapy is delineated in the text. Furthermore, no differentiation is made between singular and combination therapy in the discussion of the uses of an agent.

The primary emphasis of this book is on the mechanisms of action as seen from the viewpoint of both biochemistry and molecular biology. Few texts have achieved such a complete description of all major agents.

Received by Iris H. Hall
School of Pharmacy
University of North Carolina
Chapel Hill, NC 27514

Index of Antibiotics from Actinomycetes, Vol. 11. Edited by HAMAO UMEZAWA. University Park Press, 233 E. Redwood St., Baltimore, MD 21202. 1979. 1466 pp. 18 × 23 cm. Price $97.50.

This update of a 1966 index lists the antibiotics produced by Actinomycetes reported mainly between 1966 and 1976. Chapter I lists generic names, common names, trivial names, and selected trade names, including those from the previous volume, in alphabetical order followed by those antibiotics designated by letter and numerical arrangement. The group to which the antibiotic belongs and its synonyms are given along with a page reference to an entry in the previous or present volume.

Chapter II gives data on the antibiotics. A typical compound entry includes the antibiotic group, synonyms and similar compounds, molecular weight and formula, structure, isolation, physical properties such as melting point and solubility, elemental analysis, UV characteristics, IR spectrum, activity, LD_{50} value, and literature references.

Staff Review

Analytical Profiles of Drug Substances, Vol. 8. Edited by KLAUS FLOREY. Academic, 111 Fifth Ave., New York, NY 10003. 1979. 558 pp. 15.5 × 23.5 cm.

This ongoing series is concerned with reporting supplemental information on drug substances that are listed in the official compendia but for which the compendia do not provide detailed physical or chemical data, methods of synthesis, or pathways of physical or biological degradation and metabolism.

Volume 8 contains individual monographs for the following drugs: aspirin, bromocriptine methanesulphonate, calcitrol, chlortetracycline hydrochloride, dobutamine hydrochloride, erythromycin, gramicidin, griseofulvin, halcinonide, hydralazine hydrochloride, calcium leucovorin, methimazole, nalidixic acid, neomycin, pseudoephedrine hydrochloride, triprolidine hydrochloride, and sodium valproate and valproic acid. The monographs contain some or all of the general headings such as introductory information (*e.g.*, history, appearance, and odor), physicochemical properties (*e.g.*, elemental analysis, spectra, crystal properties, solubility, and partition coefficients), synthesis, stability and degradation, biopharmaceutics (*e.g.*, pharmacokinetics and metabolism), toxicology, analytical methods, and literature references. Most of the monographs seem to have surveyed the drug literature through 1977 or 1978. The spectra and other analytical curves in the book have been reproduced in a clear and uncluttered fashion.

The entire series should be available in libraries of drug firms, FDA laboratories, toxicology laboratories, and schools of medicine and pharmacy. The volumes are not organized for use as textbooks in courses such

REVIEWS

Autonomic Pharmacology: Experimental and Clinical Aspects. By MICHAEL D. DAY. Churchill Livingstone, 19 West 44th St., New York, NY 10036. 1979. 255 pp. 14 × 21 cm. Price $15.00 (soft cover).

This excellent small book, in the words of the author, "is intended primarily for undergraduate students of medical sciences." Students of medicine, pharmacy, dentistry, nursing, and other health sciences also should be included. Written for British students, this book contains many drug names that are not familiar to American students. This is due mainly to the fact that the FDA considers some of these drugs neither safe nor effective, even though they have been used in England for many years. The fact that drugs available on this side of the Atlantic are not identified may be a slight handicap. However, by describing these foreign drugs, this book gives the American student a better and more complete view of autonomic drug development.

There are three chapters covering the anatomy, physiology, and chemistry of the autonomic motor system and neurohumoral transmission. Ten chapters cover adrenergic and cholinergic agonists and blocking agents. For each drug class, one or two prototype compounds are described in detail. Other drugs of the same category then are briefly compared clinically to the prototype. The historical aspects of autonomic physiology and pharmacology are well covered. As far as the drugs that are included and the mechanism of actions described are concerned, this work is up to date. The only thing missing is some mention of radioligand studies of receptors. This book is recommended for all biomedical students.

Reviewed by R. P. Ahlquist
Medical College of Georgia
Augusta, GA 30912

The Anticancer Drugs. By WILLIAM B. PRATT and RAYMOND W. RUDDON. Oxford University Press, 200 Madison Ave., New York, NY 10016. 1979. 323 pp. 15 × 23 cm. Price $18.95 hard cover or $12.95 soft cover.

The stated purpose of this text is to offer "a full, but concise description of anticancer drugs, both old and new." The authors have achieved their objective with respect to describing currently used agents for human neoplastic diseases. There is excellent integration of the proposed mechanism of action of the agent, its uses against specific tumor types, and toxicity of the agent in humans.

The first chapter is a cursory review of the incidence of cancer in the United States and the world, biochemical and genetic characteristics of malignant cells, and role of drugs in cancer therapy.

Historical milestones in the development of the major chemical categories of antineoplastic agents are dealt with in the second chapter.

The third chapter discusses Gompertizian cell growth of tumors, the cell cycle, fraction of cells in mitosis, development of drug-resistant states, and determinant factors of the host involved in drug response.

Chapter 4 reviews, as general concepts, the responsiveness of tumors to chemotherapy drugs, the choice of drugs for specific types of tumors, combination chemotherapy, adjuvant therapy, and toxicity of antineoplastics.

Individual alkylating agents, antimetabolites, antibiotics, hormones, plant alkaloids, enzymes, and miscellaneous drugs are delineated in Chapters 5–9. The chemical structure, mechanism of action, administration routes, absorption, bioactivation, metabolism, distribution, excretion, causes of resistant states, and toxicity are given.

The last chapter briefly describes how new drugs are established as antineoplastic agents in animal models. Thirteen new drugs are discussed that are currently in human clinical trials, potent in animal screens, or unique in structure as an approach to drug design. This chapter also includes a treatment of biological markers of neoplastic cells, *e.g.*, antigens or enzymes, which is more appropriately included in an earlier chapter.

There are several weaknesses of the book as a general text in academic instruction. There is no discussion of structure–activity relationships or the reasons some agents are restricted from use in this country. Only a limited conceptual discussion of immunotherapy agents and their uses in neoplastic therapy and the use of chemotherapy prior to and post-surgery and/or radiation is presented. Neither percentages of response in the clinic to a specific agent for a given tumor type nor the percentage of relapses from therapy is delineated in the text. Furthermore, no differentiation is made between singular and combination therapy in the discussion of the uses of an agent.

The primary emphasis of this book is on the mechanisms of action as seen from the viewpoint of both biochemistry and molecular biology. Few texts have achieved such a complete description of all major agents.

Received by Iris H. Hall
School of Pharmacy
University of North Carolina
Chapel Hill, NC 27514

Index of Antibiotics from Actinomycetes, Vol. 11. Edited by HAMAO UMEZAWA. University Park Press, 233 E. Redwood St., Baltimore, MD 21202. 1979. 1466 pp. 18 × 23 cm. Price $97.50.

This update of a 1966 index lists the antibiotics produced by Actinomycetes reported mainly between 1966 and 1976. Chapter I lists generic names, common names, trivial names, and selected trade names, including those from the previous volume, in alphabetical order followed by those antibiotics designated by letter and numerical arrangement. The group to which the antibiotic belongs and its synonyms are given along with a page reference to an entry in the previous or present volume.

Chapter II gives data on the antibiotics. A typical compound entry includes the antibiotic group, synonyms and similar compounds, molecular weight and formula, structure, isolation, physical properties such as melting point and solubility, elemental analysis, UV characteristics, IR spectrum, activity, LD_{50} value, and literature references.

Staff Review

Analytical Profiles of Drug Substances, Vol. 8. Edited by KLAUS FLOREY. Academic, 111 Fifth Ave., New York, NY 10003. 1979. 558 pp. 15.5 × 23.5 cm.

This ongoing series is concerned with reporting supplemental information on drug substances that are listed in the official compendia but for which the compendia do not provide detailed physical or chemical data, methods of synthesis, or pathways of physical or biological degradation and metabolism.

Volume 8 contains individual monographs for the following drugs: aspirin, bromocriptine methanesulphonate, calcitrol, chlortetracycline hydrochloride, dobutamine hydrochloride, erythromycin, gramicidin, griseofulvin, halcinonide, hydralazine hydrochloride, calcium leucovorin, methimazole, nalidixic acid, neomycin, pseudoephedrine hydrochloride, triprolidine hydrochloride, and sodium valproate and valproic acid. The monographs contain some or all of the general headings such as introductory information (*e.g.*, history, appearance, and odor), physicochemical properties (*e.g.*, elemental analysis, spectra, crystal properties, solubility, and partition coefficients), synthesis, stability and degradation, biopharmaceutics (*e.g.*, pharmacokinetics and metabolism), toxicology, analytical methods, and literature references. Most of the monographs seem to have surveyed the drug literature through 1977 or 1978. The spectra and other analytical curves in the book have been reproduced in a clear and uncluttered fashion.

The entire series should be available in libraries of drug firms, FDA laboratories, toxicology laboratories, and schools of medicine and pharmacy. The volumes are not organized for use as textbooks in courses such

REVIEWS

Autonomic Pharmacology: Experimental and Clinical Aspects. By MICHAEL D. DAY. Churchill Livingstone, 19 West 44th St., New York, NY 10036. 1979. 255 pp. 14 × 21 cm. Price $15.00 (soft cover).

This excellent small book, in the words of the author, "is intended primarily for undergraduate students of medical sciences." Students of medicine, pharmacy, dentistry, nursing, and other health sciences also should be included. Written for British students, this book contains many drug names that are not familiar to American students. This is due mainly to the fact that the FDA considers some of these drugs neither safe nor effective, even though they have been used in England for many years. The fact that drugs available on this side of the Atlantic are not identified may be a slight handicap. However, by describing these foreign drugs, this book gives the American student a better and more complete view of autonomic drug development.

There are three chapters covering the anatomy, physiology, and chemistry of the autonomic motor system and neurohumoral transmission. Ten chapters cover adrenergic and cholinergic agonists and blocking agents. For each drug class, one or two prototype compounds are described in detail. Other drugs of the same category then are briefly compared clinically to the prototype. The historical aspects of autonomic physiology and pharmacology are well covered. As far as the drugs that are included and the mechanism of actions described are concerned, this work is up to date. The only thing missing is some mention of radioligand studies of receptors. This book is recommended for all biomedical students.

Reviewed by R. P. Ahlquist
Medical College of Georgia
Augusta, GA 30912

The Anticancer Drugs. By WILLIAM B. PRATT and RAYMOND W. RUDDON. Oxford University Press, 200 Madison Ave., New York, NY 10016. 1979. 323 pp. 15 × 23 cm. Price $18.95 hard cover or $12.95 soft cover.

The stated purpose of this text is to offer "a full, but concise description of anticancer drugs, both old and new." The authors have achieved their objective with respect to describing currently used agents for human neoplastic diseases. There is excellent integration of the proposed mechanism of action of the agent, its uses against specific tumor types, and toxicity of the agent in humans.

The first chapter is a cursory review of the incidence of cancer in the United States and the world, biochemical and genetic characteristics of malignant cells, and role of drugs in cancer therapy.

Historical milestones in the development of the major chemical categories of antineoplastic agents are dealt with in the second chapter.

The third chapter discusses Gompertizian cell growth of tumors, the cell cycle, fraction of cells in mitosis, development of drug-resistant states, and determinant factors of the host involved in drug response.

Chapter 4 reviews, as general concepts, the responsiveness of tumors to chemotherapy drugs, the choice of drugs for specific types of tumors, combination chemotherapy, adjuvant therapy, and toxicity of antineoplastics.

Individual alkylating agents, antimetabolites, antibiotics, hormones, plant alkaloids, enzymes, and miscellaneous drugs are delineated in Chapters 5–9. The chemical structure, mechanism of action, administration routes, absorption, bioactivation, metabolism, distribution, excretion, causes of resistant states, and toxicity are given.

The last chapter briefly describes how new drugs are established as antineoplastic agents in animal models. Thirteen new drugs are discussed that are currently in human clinical trials, potent in animal screens, or unique in structure as an approach to drug design. This chapter also includes a treatment of biological markers of neoplastic cells, *e.g.*, antigens or enzymes, which is more appropriately included in an earlier chapter.

There are several weaknesses of the book as a general text in academic instruction. There is no discussion of structure–activity relationships or the reasons some agents are restricted from use in this country. Only a limited conceptual discussion of immunotherapy agents and their uses in neoplastic therapy and the use of chemotherapy prior to and post-surgery and/or radiation is presented. Neither percentages of response in the clinic to a specific agent for a given tumor type nor the percentage of relapses from therapy is delineated in the text. Furthermore, no differentiation is made between singular and combination therapy in the discussion of the uses of an agent.

The primary emphasis of this book is on the mechanisms of action as seen from the viewpoint of both biochemistry and molecular biology. Few texts have achieved such a complete description of all major agents.

Received by Iris H. Hall
School of Pharmacy
University of North Carolina
Chapel Hill, NC 27514

Index of Antibiotics from Actinomycetes, Vol. 11. Edited by HAMAO UMEZAWA. University Park Press, 233 E. Redwood St., Baltimore, MD 21202. 1979. 1466 pp. 18 × 23 cm. Price $97.50.

This update of a 1966 index lists the antibiotics produced by Actinomycetes reported mainly between 1966 and 1976. Chapter I lists generic names, common names, trivial names, and selected trade names, including those from the previous volume, in alphabetical order followed by those antibiotics designated by letter and numerical arrangement. The group to which the antibiotic belongs and its synonyms are given along with a page reference to an entry in the previous or present volume.

Chapter II gives data on the antibiotics. A typical compound entry includes the antibiotic group, synonyms and similar compounds, molecular weight and formula, structure, isolation, physical properties such as melting point and solubility, elemental analysis, UV characteristics, IR spectrum, activity, LD_{50} value, and literature references.

Staff Review

Analytical Profiles of Drug Substances, Vol. 8. Edited by KLAUS FLOREY. Academic, 111 Fifth Ave., New York, NY 10003. 1979. 558 pp. 15.5 × 23.5 cm.

This ongoing series is concerned with reporting supplemental information on drug substances that are listed in the official compendia but for which the compendia do not provide detailed physical or chemical data, methods of synthesis, or pathways of physical or biological degradation and metabolism.

Volume 8 contains individual monographs for the following drugs: aspirin, bromocriptine methanesulphonate, calcitrol, chlortetracycline hydrochloride, dobutamine hydrochloride, erythromycin, gramicidin, griseofulvin, halcinonide, hydralazine hydrochloride, calcium leucovorin, methimazole, nalidixic acid, neomycin, pseudoephedrine hydrochloride, triprolidine hydrochloride, and sodium valproate and valproic acid. The monographs contain some or all of the general headings such as introductory information (*e.g.*, history, appearance, and odor), physicochemical properties (*e.g.*, elemental analysis, spectra, crystal properties, solubility, and partition coefficients), synthesis, stability and degradation, biopharmaceutics (*e.g.*, pharmacokinetics and metabolism), toxicology, analytical methods, and literature references. Most of the monographs seem to have surveyed the drug literature through 1977 or 1978. The spectra and other analytical curves in the book have been reproduced in a clear and uncluttered fashion.

The entire series should be available in libraries of drug firms, FDA laboratories, toxicology laboratories, and schools of medicine and pharmacy. The volumes are not organized for use as textbooks in courses such

as drug analysis or pharmaceutics, although the information contained in each volume can be used as reference material.

The volumes are highly recommended to any scientist who is actively involved in drug research and development.

Reviewed by James T. Stewart
Department of Medicinal Chemistry
School of Pharmacy
University of Georgia
Athens, GA 30602

Handbook of U.S. Colorants for Foods, Drugs, and Cosmetics. By DANIEL M. MARMION. Wiley-Interscience, One Wiley Drive, Somerset, NJ 08873. 1979. 350 pp. 13.5 × 21 cm.

The purpose of this book is to give a general survey of the colorants used in the United States in foods, drugs, and cosmetics. The author divided his book into three approximately equal parts. The first one offers a concise, well-written summary of the regulations related to coloring agents. It deals with the permanent and temporary listing of the colorants and sums up their properties, specifications, permitted uses, and limitations.

The second part of the book is a useful survey of the qualitative and quantitative analytical procedures applied for the colorants and their impurities. The author describes a wide range of techniques such as column, paper, and thin-layer chromatography, thermal analytical methods [differential thermal analysis (DTA) and differential scanning calorimetry (DSC)], spectrophotometry, IR spectrometry, and NMR spectroscopy. Model spectra and thermograms help the reader to understand the interpretation of the plotted data. The selected examples are presented in simple, clear language with good diagrams where needed, and they can be followed easily by chemists or technicians with appropriate training in analytical laboratory techniques. A reasonably up-to-date bibliography in each chapter assists those who desire more theoretical background or technical details.

The last section of the book basically is an extended biography, with ample comments by the author, on the analysis of colorant mixtures and commercial products such as beverages, cosmetics, drugs, and meat. These chapters, of course, were not intended to cover every possible product or application; nevertheless, the selection is a good starting point for the analyst who has to solve problems in the analysis of color additives.

In summary, this book is a first in this area. While the scope is restricted to color additives used in the United States, the book also may help professionals in other countries who are manufacturing, controlling, or using colorants.

Reviewed by Paul Turi
Pharmaceutical Research and Development
Sandoz, Inc.
East Hanover, NJ 07936

CRC Handbook Series in Clinical Laboratory Science, Section B: Toxicology, Vol. 1. Edited by DAVID SELIGSON and IRVING SUNSHINE. CRC Press, 2255 Palm Beach Lakes Blvd., West Palm Beach, FL 33409. 1978. 414 pp. 19 × 26 cm. Price $54.95 ($62.95 outside the United States).

The preface states that "in the last few years, there has been a flood of scientific articles dealing with use and misuse of chemical agents. From this surfeit has come a plethora of data which need to be at the fingertips of many scientists." This volume is an attempt to fill that need.

The book consists of five chapters. The first and major chapter encompasses slightly over 300 pages or 75% of the book. This chapter is a detailed presentation of the chromatographic separation of drugs and chemicals. It is divided into several subsections including a basic introduction to chromatography, a presentation of GC, a presentation of TLC, and a final section on high-pressure liquid chromatography (HPLC). These sections include extensive tables on the methodology to be employed to separate hundreds of chemicals of interest to the analytical toxicologist. These tables include listings of numerous solvent systems, which are frequently indexed according to their R_f values. The section on HPLC is the least extensive of the sections on chromatography but is still a valuable introduction to the technology.

The second major chapter is on the immunoassay of drugs and includes a brief description of the development of radioimmunoassay. This chapter lists 70 drugs that can be quantitated by this technique and includes over 400 references.

The third chapter has microcrystalline tests for approximately 250 drugs and chemicals with references and explanations for each particular test.

The fourth chapter is a tabulation of solubilities of numerous antibiotics arranged in two tables. One table gives the solubility of 76 antibiotics in 24 solvents at 28°. The second table includes 53 additional antibiotics and their solubilities at 21° in 24 solvents.

The last chapter is a tabulation of approximately 600 chemicals arranged in ascending order of their melting points.

In summary, as stated in the preface, this book is a compilation of a large number of tables dealing with the separation and identification of toxic chemicals. The one drawback is that it takes a fair amount of time to become familiar with its organization since the tables frequently are extremely long. However, this book should be valuable to individuals involved with identifying chemicals in biological systems.

Reviewed by Gary L. Lage
Philadelphia College of Pharmacy and Science
Philadelphia, PA 19104

Sustained and Controlled Release Drug Delivery Systems, Vol. 6. Edited by JOSEPH R. ROBINSON. Dekker, 270 Madison Ave., New York, NY 10016. 1978. 773 pp. 15 × 23 cm. Price $59.75.

The book starts with a standard overview of controlled-release delivery systems, but the inclusion of the role of disease states and of circadian rhythm makes the chapter stimulating. Chapter 2 also gives standard material with a brief discussion of liposomes. Reference 200 in this chapter is cited incorrectly. Salicylate, not aspirin, has a biological half-life of 6 hr. Chapters 3 and 4 discuss physical methods of obtaining a sustained-release drug delivery system.

Chapter 5, as written, seems totally irrelevant to the rest of the book and should have been omitted. Chapters 6 and 7 give interesting accounts of the prodrug and biomedical engineering approach. Chapters 8 and 9 give the classical pharmacokinetic picture of sustained-release systems.

In general, the book provides a current and comprehensive picture of the sustained-release product area and is recommended to anyone interested in understanding the principles, technologies, and applications of controlled-release drug delivery systems.

Reviewed by John H. Perrin
College of Pharmacy
University of Florida
Gainesville, FL 32610

Microcapsule Processing and Technology. By ASAJI KONDO. Edited and revised by J. WADE VAN VALKENBURG. Dekker, 270 Madison Ave., New York, NY 10016. 1979. 182 pp. Price $22.50.

This hard-bound book represents an edited English revision of the original text published in Japanese by Asaji Kondo in 1970. The first four chapters provide an in-depth discussion into the history, general principles, and applications of microencapsulation. The remaining 14 chapters examine various methods of preparing microcapsules. In all cases, the author attempted to simplify each system, with detailed explanations of the various procedures employed to manufacture microcapsules. Schematic diagrams, tables, and scanning electron micrographs are scattered liberally throughout the text and adequately illustrate the concepts under discussion. The bulk of the book is devoted to explana-

as drug analysis or pharmaceutics, although the information contained in each volume can be used as reference material.

The volumes are highly recommended to any scientist who is actively involved in drug research and development.

Reviewed by James T. Stewart
Department of Medicinal Chemistry
School of Pharmacy
University of Georgia
Athens, GA 30602

Handbook of U.S. Colorants for Foods, Drugs, and Cosmetics. By DANIEL M. MARMION. Wiley-Interscience, One Wiley Drive, Somerset, NJ 08873. 1979. 350 pp. 13.5 × 21 cm.

The purpose of this book is to give a general survey of the colorants used in the United States in foods, drugs, and cosmetics. The author divided his book into three approximately equal parts. The first one offers a concise, well-written summary of the regulations related to coloring agents. It deals with the permanent and temporary listing of the colorants and sums up their properties, specifications, permitted uses, and limitations.

The second part of the book is a useful survey of the qualitative and quantitative analytical procedures applied for the colorants and their impurities. The author describes a wide range of techniques such as column, paper, and thin-layer chromatography, thermal analytical methods [differential thermal analysis (DTA) and differential scanning calorimetry (DSC)], spectrophotometry, IR spectrometry, and NMR spectroscopy. Model spectra and thermograms help the reader to understand the interpretation of the plotted data. The selected examples are presented in simple, clear language with good diagrams where needed, and they can be followed easily by chemists or technicians with appropriate training in analytical laboratory techniques. A reasonably up-to-date bibliography in each chapter assists those who desire more theoretical background or technical details.

The last section of the book basically is an extended biography, with ample comments by the author, on the analysis of colorant mixtures and commercial products such as beverages, cosmetics, drugs, and meat. These chapters, of course, were not intended to cover every possible product or application; nevertheless, the selection is a good starting point for the analyst who has to solve problems in the analysis of color additives.

In summary, this book is a first in this area. While the scope is restricted to color additives used in the United States, the book also may help professionals in other countries who are manufacturing, controlling, or using colorants.

Reviewed by Paul Turi
Pharmaceutical Research and Development
Sandoz, Inc.
East Hanover, NJ 07936

CRC Handbook Series in Clinical Laboratory Science, Section B: Toxicology, Vol. 1. Edited by DAVID SELIGSON and IRVING SUNSHINE. CRC Press, 2255 Palm Beach Lakes Blvd., West Palm Beach, FL 33409. 1978. 414 pp. 19 × 26 cm. Price $54.95 ($62.95 outside the United States).

The preface states that "in the last few years, there has been a flood of scientific articles dealing with use and misuse of chemical agents. From this surfeit has come a plethora of data which need to be at the fingertips of many scientists." This volume is an attempt to fill that need.

The book consists of five chapters. The first and major chapter encompasses slightly over 300 pages or 75% of the book. This chapter is a detailed presentation of the chromatographic separation of drugs and chemicals. It is divided into several subsections including a basic introduction to chromatography, a presentation of GC, a presentation of TLC, and a final section on high-pressure liquid chromatography (HPLC). These sections include extensive tables on the methodology to be employed to separate hundreds of chemicals of interest to the analytical toxicologist. These tables include listings of numerous solvent systems, which are frequently indexed according to their R_f values. The section on HPLC is the least extensive of the sections on chromatography but is still a valuable introduction to the technology.

The second major chapter is on the immunoassay of drugs and includes a brief description of the development of radioimmunoassay. This chapter lists 70 drugs that can be quantitated by this technique and includes over 400 references.

The third chapter has microcrystalline tests for approximately 250 drugs and chemicals with references and explanations for each particular test.

The fourth chapter is a tabulation of solubilities of numerous antibiotics arranged in two tables. One table gives the solubility of 76 antibiotics in 24 solvents at 28°. The second table includes 53 additional antibiotics and their solubilities at 21° in 24 solvents.

The last chapter is a tabulation of approximately 600 chemicals arranged in ascending order of their melting points.

In summary, as stated in the preface, this book is a compilation of a large number of tables dealing with the separation and identification of toxic chemicals. The one drawback is that it takes a fair amount of time to become familiar with its organization since the tables frequently are extremely long. However, this book should be valuable to individuals involved with identifying chemicals in biological systems.

Reviewed by Gary L. Lage
Philadelphia College of Pharmacy and Science
Philadelphia, PA 19104

Sustained and Controlled Release Drug Delivery Systems, Vol. 6. Edited by JOSEPH R. ROBINSON. Dekker, 270 Madison Ave., New York, NY 10016. 1978. 773 pp. 15 × 23 cm. Price $59.75.

The book starts with a standard overview of controlled-release delivery systems, but the inclusion of the role of disease states and of circadian rhythm makes the chapter stimulating. Chapter 2 also gives standard material with a brief discussion of liposomes. Reference 200 in this chapter is cited incorrectly. Salicylate, not aspirin, has a biological half-life of 6 hr. Chapters 3 and 4 discuss physical methods of obtaining a sustained-release drug delivery system.

Chapter 5, as written, seems totally irrelevant to the rest of the book and should have been omitted. Chapters 6 and 7 give interesting accounts of the prodrug and biomedical engineering approach. Chapters 8 and 9 give the classical pharmacokinetic picture of sustained-release systems.

In general, the book provides a current and comprehensive picture of the sustained-release product area and is recommended to anyone interested in understanding the principles, technologies, and applications of controlled-release drug delivery systems.

Reviewed by John H. Perrin
College of Pharmacy
University of Florida
Gainesville, FL 32610

Microcapsule Processing and Technology. By ASAJI KONDO. Edited and revised by J. WADE VAN VALKENBURG. Dekker, 270 Madison Ave., New York, NY 10016. 1979. 182 pp. Price $22.50.

This hard-bound book represents an edited English revision of the original text published in Japanese by Asaji Kondo in 1970. The first four chapters provide an in-depth discussion into the history, general principles, and applications of microencapsulation. The remaining 14 chapters examine various methods of preparing microcapsules. In all cases, the author attempted to simplify each system, with detailed explanations of the various procedures employed to manufacture microcapsules. Schematic diagrams, tables, and scanning electron micrographs are scattered liberally throughout the text and adequately illustrate the concepts under discussion. The bulk of the book is devoted to explana-

as drug analysis or pharmaceutics, although the information contained in each volume can be used as reference material.

The volumes are highly recommended to any scientist who is actively involved in drug research and development.

Reviewed by James T. Stewart
Department of Medicinal Chemistry
School of Pharmacy
University of Georgia
Athens, GA 30602

Handbook of U.S. Colorants for Foods, Drugs, and Cosmetics. By DANIEL M. MARMION. Wiley-Interscience, One Wiley Drive, Somerset, NJ 08873. 1979. 350 pp. 13.5 × 21 cm.

The purpose of this book is to give a general survey of the colorants used in the United States in foods, drugs, and cosmetics. The author divided his book into three approximately equal parts. The first one offers a concise, well-written summary of the regulations related to coloring agents. It deals with the permanent and temporary listing of the colorants and sums up their properties, specifications, permitted uses, and limitations.

The second part of the book is a useful survey of the qualitative and quantitative analytical procedures applied for the colorants and their impurities. The author describes a wide range of techniques such as column, paper, and thin-layer chromatography, thermal analytical methods [differential thermal analysis (DTA) and differential scanning calorimetry (DSC)], spectrophotometry, IR spectrometry, and NMR spectroscopy. Model spectra and thermograms help the reader to understand the interpretation of the plotted data. The selected examples are presented in simple, clear language with good diagrams where needed, and they can be followed easily by chemists or technicians with appropriate training in analytical laboratory techniques. A reasonably up-to-date bibliography in each chapter assists those who desire more theoretical background or technical details.

The last section of the book basically is an extended biography, with ample comments by the author, on the analysis of colorant mixtures and commercial products such as beverages, cosmetics, drugs, and meat. These chapters, of course, were not intended to cover every possible product or application; nevertheless, the selection is a good starting point for the analyst who has to solve problems in the analysis of color additives.

In summary, this book is a first in this area. While the scope is restricted to color additives used in the United States, the book also may help professionals in other countries who are manufacturing, controlling, or using colorants.

Reviewed by Paul Turi
Pharmaceutical Research and Development
Sandoz, Inc.
East Hanover, NJ 07936

CRC Handbook Series in Clinical Laboratory Science, Section B: Toxicology, Vol. 1. Edited by DAVID SELIGSON and IRVING SUNSHINE. CRC Press, 2255 Palm Beach Lakes Blvd., West Palm Beach, FL 33409. 1978. 414 pp. 19 × 26 cm. Price $54.95 ($62.95 outside the United States).

The preface states that "in the last few years, there has been a flood of scientific articles dealing with use and misuse of chemical agents. From this surfeit has come a plethora of data which need to be at the fingertips of many scientists." This volume is an attempt to fill that need.

The book consists of five chapters. The first and major chapter encompasses slightly over 300 pages or 75% of the book. This chapter is a detailed presentation of the chromatographic separation of drugs and chemicals. It is divided into several subsections including a basic introduction to chromatography, a presentation of GC, a presentation of TLC, and a final section on high-pressure liquid chromatography (HPLC). These sections include extensive tables on the methodology to be employed to separate hundreds of chemicals of interest to the analytical toxicologist. These tables include listings of numerous solvent systems, which are frequently indexed according to their R_f values. The section on HPLC is the least extensive of the sections on chromatography but is still a valuable introduction to the technology.

The second major chapter is on the immunoassay of drugs and includes a brief description of the development of radioimmunoassay. This chapter lists 70 drugs that can be quantitated by this technique and includes over 400 references.

The third chapter has microcrystalline tests for approximately 250 drugs and chemicals with references and explanations for each particular test.

The fourth chapter is a tabulation of solubilities of numerous antibiotics arranged in two tables. One table gives the solubility of 76 antibiotics in 24 solvents at 28°. The second table includes 53 additional antibiotics and their solubilities at 21° in 24 solvents.

The last chapter is a tabulation of approximately 600 chemicals arranged in ascending order of their melting points.

In summary, as stated in the preface, this book is a compilation of a large number of tables dealing with the separation and identification of toxic chemicals. The one drawback is that it takes a fair amount of time to become familiar with its organization since the tables frequently are extremely long. However, this book should be valuable to individuals involved with identifying chemicals in biological systems.

Reviewed by Gary L. Lage
Philadelphia College of Pharmacy and Science
Philadelphia, PA 19104

Sustained and Controlled Release Drug Delivery Systems, Vol. 6. Edited by JOSEPH R. ROBINSON. Dekker, 270 Madison Ave., New York, NY 10016. 1978. 773 pp. 15 × 23 cm. Price $59.75.

The book starts with a standard overview of controlled-release delivery systems, but the inclusion of the role of disease states and of circadian rhythm makes the chapter stimulating. Chapter 2 also gives standard material with a brief discussion of liposomes. Reference 200 in this chapter is cited incorrectly. Salicylate, not aspirin, has a biological half-life of 6 hr. Chapters 3 and 4 discuss physical methods of obtaining a sustained-release drug delivery system.

Chapter 5, as written, seems totally irrelevant to the rest of the book and should have been omitted. Chapters 6 and 7 give interesting accounts of the prodrug and biomedical engineering approach. Chapters 8 and 9 give the classical pharmacokinetic picture of sustained-release systems.

In general, the book provides a current and comprehensive picture of the sustained-release product area and is recommended to anyone interested in understanding the principles, technologies, and applications of controlled-release drug delivery systems.

Reviewed by John H. Perrin
College of Pharmacy
University of Florida
Gainesville, FL 32610

Microcapsule Processing and Technology. By ASAJI KONDO. Edited and revised by J. WADE VAN VALKENBURG. Dekker, 270 Madison Ave., New York, NY 10016. 1979. 182 pp. Price $22.50.

This hard-bound book represents an edited English revision of the original text published in Japanese by Asaji Kondo in 1970. The first four chapters provide an in-depth discussion into the history, general principles, and applications of microencapsulation. The remaining 14 chapters examine various methods of preparing microcapsules. In all cases, the author attempted to simplify each system, with detailed explanations of the various procedures employed to manufacture microcapsules. Schematic diagrams, tables, and scanning electron micrographs are scattered liberally throughout the text and adequately illustrate the concepts under discussion. The bulk of the book is devoted to explana-

as drug analysis or pharmaceutics, although the information contained in each volume can be used as reference material.

The volumes are highly recommended to any scientist who is actively involved in drug research and development.

Reviewed by James T. Stewart
Department of Medicinal Chemistry
School of Pharmacy
University of Georgia
Athens, GA 30602

Handbook of U.S. Colorants for Foods, Drugs, and Cosmetics. By DANIEL M. MARMION. Wiley-Interscience, One Wiley Drive, Somerset, NJ 08873. 1979. 350 pp. 13.5 × 21 cm.

The purpose of this book is to give a general survey of the colorants used in the United States in foods, drugs, and cosmetics. The author divided his book into three approximately equal parts. The first one offers a concise, well-written summary of the regulations related to coloring agents. It deals with the permanent and temporary listing of the colorants and sums up their properties, specifications, permitted uses, and limitations.

The second part of the book is a useful survey of the qualitative and quantitative analytical procedures applied for the colorants and their impurities. The author describes a wide range of techniques such as column, paper, and thin-layer chromatography, thermal analytical methods [differential thermal analysis (DTA) and differential scanning calorimetry (DSC)], spectrophotometry, IR spectrometry, and NMR spectroscopy. Model spectra and thermograms help the reader to understand the interpretation of the plotted data. The selected examples are presented in simple, clear language with good diagrams where needed, and they can be followed easily by chemists or technicians with appropriate training in analytical laboratory techniques. A reasonably up-to-date bibliography in each chapter assists those who desire more theoretical background or technical details.

The last section of the book basically is an extended biography, with ample comments by the author, on the analysis of colorant mixtures and commercial products such as beverages, cosmetics, drugs, and meat. These chapters, of course, were not intended to cover every possible product or application; nevertheless, the selection is a good starting point for the analyst who has to solve problems in the analysis of color additives.

In summary, this book is a first in this area. While the scope is restricted to color additives used in the United States, the book also may help professionals in other countries who are manufacturing, controlling, or using colorants.

Reviewed by Paul Turi
Pharmaceutical Research and Development
Sandoz, Inc.
East Hanover, NJ 07936

CRC Handbook Series in Clinical Laboratory Science, Section B: Toxicology, Vol. 1. Edited by DAVID SELIGSON and IRVING SUNSHINE. CRC Press, 2255 Palm Beach Lakes Blvd., West Palm Beach, FL 33409. 1978. 414 pp. 19 × 26 cm. Price $54.95 ($62.95 outside the United States).

The preface states that "in the last few years, there has been a flood of scientific articles dealing with use and misuse of chemical agents. From this surfeit has come a plethora of data which need to be at the fingertips of many scientists." This volume is an attempt to fill that need.

The book consists of five chapters. The first and major chapter encompasses slightly over 300 pages or 75% of the book. This chapter is a detailed presentation of the chromatographic separation of drugs and chemicals. It is divided into several subsections including a basic introduction to chromatography, a presentation of GC, a presentation of TLC, and a final section on high-pressure liquid chromatography (HPLC). These sections include extensive tables on the methodology to be employed to separate hundreds of chemicals of interest to the analytical toxicologist. These tables include listings of numerous solvent systems, which are frequently indexed according to their R_f values. The section on HPLC is the least extensive of the sections on chromatography but is still a valuable introduction to the technology.

The second major chapter is on the immunoassay of drugs and includes a brief description of the development of radioimmunoassay. This chapter lists 70 drugs that can be quantitated by this technique and includes over 400 references.

The third chapter has microcrystalline tests for approximately 250 drugs and chemicals with references and explanations for each particular test.

The fourth chapter is a tabulation of solubilities of numerous antibiotics arranged in two tables. One table gives the solubility of 76 antibiotics in 24 solvents at 28°. The second table includes 53 additional antibiotics and their solubilities at 21° in 24 solvents.

The last chapter is a tabulation of approximately 600 chemicals arranged in ascending order of their melting points.

In summary, as stated in the preface, this book is a compilation of a large number of tables dealing with the separation and identification of toxic chemicals. The one drawback is that it takes a fair amount of time to become familiar with its organization since the tables frequently are extremely long. However, this book should be valuable to individuals involved with identifying chemicals in biological systems.

Reviewed by Gary L. Lage
Philadelphia College of Pharmacy and Science
Philadelphia, PA 19104

Sustained and Controlled Release Drug Delivery Systems, Vol. 6. Edited by JOSEPH R. ROBINSON. Dekker, 270 Madison Ave., New York, NY 10016. 1978. 773 pp. 15 × 23 cm. Price $59.75.

The book starts with a standard overview of controlled-release delivery systems, but the inclusion of the role of disease states and of circadian rhythm makes the chapter stimulating. Chapter 2 also gives standard material with a brief discussion of liposomes. Reference 200 in this chapter is cited incorrectly. Salicylate, not aspirin, has a biological half-life of 6 hr. Chapters 3 and 4 discuss physical methods of obtaining a sustained-release drug delivery system.

Chapter 5, as written, seems totally irrelevant to the rest of the book and should have been omitted. Chapters 6 and 7 give interesting accounts of the prodrug and biomedical engineering approach. Chapters 8 and 9 give the classical pharmacokinetic picture of sustained-release systems.

In general, the book provides a current and comprehensive picture of the sustained-release product area and is recommended to anyone interested in understanding the principles, technologies, and applications of controlled-release drug delivery systems.

Reviewed by John H. Perrin
College of Pharmacy
University of Florida
Gainesville, FL 32610

Microcapsule Processing and Technology. By ASAJI KONDO. Edited and revised by J. WADE VAN VALKENBURG. Dekker, 270 Madison Ave., New York, NY 10016. 1979. 182 pp. Price $22.50.

This hard-bound book represents an edited English revision of the original text published in Japanese by Asaji Kondo in 1970. The first four chapters provide an in-depth discussion into the history, general principles, and applications of microencapsulation. The remaining 14 chapters examine various methods of preparing microcapsules. In all cases, the author attempted to simplify each system, with detailed explanations of the various procedures employed to manufacture microcapsules. Schematic diagrams, tables, and scanning electron micrographs are scattered liberally throughout the text and adequately illustrate the concepts under discussion. The bulk of the book is devoted to explana-

as drug analysis or pharmaceutics, although the information contained in each volume can be used as reference material.

The volumes are highly recommended to any scientist who is actively involved in drug research and development.

Reviewed by James T. Stewart
Department of Medicinal Chemistry
School of Pharmacy
University of Georgia
Athens, GA 30602

Handbook of U.S. Colorants for Foods, Drugs, and Cosmetics. By DANIEL M. MARMION. Wiley-Interscience, One Wiley Drive, Somerset, NJ 08873. 1979. 350 pp. 13.5 × 21 cm.

The purpose of this book is to give a general survey of the colorants used in the United States in foods, drugs, and cosmetics. The author divided his book into three approximately equal parts. The first one offers a concise, well-written summary of the regulations related to coloring agents. It deals with the permanent and temporary listing of the colorants and sums up their properties, specifications, permitted uses, and limitations.

The second part of the book is a useful survey of the qualitative and quantitative analytical procedures applied for the colorants and their impurities. The author describes a wide range of techniques such as column, paper, and thin-layer chromatography, thermal analytical methods [differential thermal analysis (DTA) and differential scanning calorimetry (DSC)], spectrophotometry, IR spectrometry, and NMR spectroscopy. Model spectra and thermograms help the reader to understand the interpretation of the plotted data. The selected examples are presented in simple, clear language with good diagrams where needed, and they can be followed easily by chemists or technicians with appropriate training in analytical laboratory techniques. A reasonably up-to-date bibliography in each chapter assists those who desire more theoretical background or technical details.

The last section of the book basically is an extended biography, with ample comments by the author, on the analysis of colorant mixtures and commercial products such as beverages, cosmetics, drugs, and meat. These chapters, of course, were not intended to cover every possible product or application; nevertheless, the selection is a good starting point for the analyst who has to solve problems in the analysis of color additives.

In summary, this book is a first in this area. While the scope is restricted to color additives used in the United States, the book also may help professionals in other countries who are manufacturing, controlling, or using colorants.

Reviewed by Paul Turi
Pharmaceutical Research and Development
Sandoz, Inc.
East Hanover, NJ 07936

CRC Handbook Series in Clinical Laboratory Science, Section B: Toxicology, Vol. 1. Edited by DAVID SELIGSON and IRVING SUNSHINE. CRC Press, 2255 Palm Beach Lakes Blvd., West Palm Beach, FL 33409. 1978. 414 pp. 19 × 26 cm. Price $54.95 ($62.95 outside the United States).

The preface states that "in the last few years, there has been a flood of scientific articles dealing with use and misuse of chemical agents. From this surfeit has come a plethora of data which need to be at the fingertips of many scientists." This volume is an attempt to fill that need.

The book consists of five chapters. The first and major chapter encompasses slightly over 300 pages or 75% of the book. This chapter is a detailed presentation of the chromatographic separation of drugs and chemicals. It is divided into several subsections including a basic introduction to chromatography, a presentation of GC, a presentation of TLC, and a final section on high-pressure liquid chromatography (HPLC). These sections include extensive tables on the methodology to be employed to separate hundreds of chemicals of interest to the analytical toxicologist. These tables include listings of numerous solvent systems, which are frequently indexed according to their R_f values. The section on HPLC is the least extensive of the sections on chromatography but is still a valuable introduction to the technology.

The second major chapter is on the immunoassay of drugs and includes a brief description of the development of radioimmunoassay. This chapter lists 70 drugs that can be quantitated by this technique and includes over 400 references.

The third chapter has microcrystalline tests for approximately 250 drugs and chemicals with references and explanations for each particular test.

The fourth chapter is a tabulation of solubilities of numerous antibiotics arranged in two tables. One table gives the solubility of 76 antibiotics in 24 solvents at 28°. The second table includes 53 additional antibiotics and their solubilities at 21° in 24 solvents.

The last chapter is a tabulation of approximately 600 chemicals arranged in ascending order of their melting points.

In summary, as stated in the preface, this book is a compilation of a large number of tables dealing with the separation and identification of toxic chemicals. The one drawback is that it takes a fair amount of time to become familiar with its organization since the tables frequently are extremely long. However, this book should be valuable to individuals involved with identifying chemicals in biological systems.

Reviewed by Gary L. Lage
Philadelphia College of Pharmacy and Science
Philadelphia, PA 19104

Sustained and Controlled Release Drug Delivery Systems, Vol. 6. Edited by JOSEPH R. ROBINSON. Dekker, 270 Madison Ave., New York, NY 10016. 1978. 773 pp. 15 × 23 cm. Price $59.75.

The book starts with a standard overview of controlled-release delivery systems, but the inclusion of the role of disease states and of circadian rhythm makes the chapter stimulating. Chapter 2 also gives standard material with a brief discussion of liposomes. Reference 200 in this chapter is cited incorrectly. Salicylate, not aspirin, has a biological half-life of 6 hr. Chapters 3 and 4 discuss physical methods of obtaining a sustained-release drug delivery system.

Chapter 5, as written, seems totally irrelevant to the rest of the book and should have been omitted. Chapters 6 and 7 give interesting accounts of the prodrug and biomedical engineering approach. Chapters 8 and 9 give the classical pharmacokinetic picture of sustained-release systems.

In general, the book provides a current and comprehensive picture of the sustained-release product area and is recommended to anyone interested in understanding the principles, technologies, and applications of controlled-release drug delivery systems.

Reviewed by John H. Perrin
College of Pharmacy
University of Florida
Gainesville, FL 32610

Microcapsule Processing and Technology. By ASAJI KONDO. Edited and revised by J. WADE VAN VALKENBURG. Dekker, 270 Madison Ave., New York, NY 10016. 1979. 182 pp. Price $22.50.

This hard-bound book represents an edited English revision of the original text published in Japanese by Asaji Kondo in 1970. The first four chapters provide an in-depth discussion into the history, general principles, and applications of microencapsulation. The remaining 14 chapters examine various methods of preparing microcapsules. In all cases, the author attempted to simplify each system, with detailed explanations of the various procedures employed to manufacture microcapsules. Schematic diagrams, tables, and scanning electron micrographs are scattered liberally throughout the text and adequately illustrate the concepts under discussion. The bulk of the book is devoted to explana-

tions of process applications for the manufacture of paper, adhesives, plasticizers, copying materials, pigments, perfumes, and many other substances including drugs.

My biggest criticism of the book is that the original text by Asaji Kondo is 10 years old. As a result, the English version by J. Wade Van Valkenburg contains reference material published prior to 1970. However, microencapsulation is a highly patented field and several patents discussed in the book will expire in the 1980's. Therefore, the text could prove to be of great assistance to scientists working in this field.

Reviewed by James W. McGinity
Drug Dynamics Institute
College of Pharmacy
University of Texas
Austin, TX 78712

Catecholamines: Basic and Clinical Frontiers, Vols. I and II. Edited by E. USDIN, I. J. KOPIN, and J. BARCHAS. Pergamon Press, Maxwell House, Fairview Park, Elmsford, NY 10523. 1979. Vol I: 1003 pp. Vol. II: 946 pp. 17 × 25 cm. Price $200.00 per volume.

The material in both volumes represents the phenomenal growth of research in catecholamines. Although the impact of catecholamine research in medicine has been universal, this international symposium represents research carried out mainly in the United States, France, Sweden, Britain, and Germany. The opening chapter presents a coherent, concise, and important summary by the internationally respected scientist–teacher, Arvid Carlsson, concerning the impact of catecholamine research on medical science and practices.

Compared to the previous symposium, a meaningful morphology appears on many pages. Dopamine occupies the central theme with which other endogenous substances such as enkephalins, substance P, and γ-aminobutyric acid (GABA) are intertwined. Drug-induced side effects and their influence on neurochemistry receive only limited attention. The value of genetics in relation to psychotropic illness with or without coherent neurochemical markers is included. One occasionally sees a marked overlap between the material published in these symposia and that published elsewhere. In the present era of rapid scientific communication, publishing the same material repeatedly should be discouraged. Catecholamine receptors occupy a large section in Vol. I.

The cost of both volumes may produce mental and neurochemical disturbances in the poor scientist who may want to buy them, so only departmental and institutional purchases are recommended.

Reviewed by P. N. Patil
College of Pharmacy
Ohio State University
Columbus, OH 43210

Introduction to Powder Surface Area. By S. LOWELL. Wiley, 605 Third Ave., New York, NY 10016. 1979. 199 pp. 15 × 23 cm. Price $17.95.

The subject of micromeritics should be important to pharmaceutical scientists. The features of a powder, *e.g.*, particle size, shape, and area, can greatly influence product development and processing as well as the properties of the finished product. However, the articles published about powders often present complicated dissolution equations derived for idealized situations. Thus, the important term for powder surface area in many pharmaceutical papers is calculated from assumed particle distributions for regularly shaped, isotropic particles. The assumption of no pores, no surface irregularities, and no interparticle forces leading to aggregation is far from reality. It should be of interest in pharmacy to characterize powders in regard to actual surface area and then to seek valid relationships between area and powder behaviors. This book may provide the proper introduction into this field for many pharmaceutical scientists.

Lowell treats powder surface area and pore-size distribution mostly as a subject of gas adsorption. However, mercury porosimetry is discussed. The book is relatively small (199 pages) and is divided into two parts. The author discusses the theoretical bases for surface area measurements in the first part. The topics discussed in these first 11 chapters also may be found in books on surface chemistry or particle-size measurement, but Lowell's presentation is clear and generally easy to follow. For example, in Chapter 5, he carefully leads the reader through the Brunauer, Emmett, and Teller theory using 25 equations.

The second section, the experimental section, should be quite helpful to those entering the field of surface area measurement. The basic techniques are described, but the narratives on vacuum volumetric methods (Chapter 13) and particularly on dynamic flow methods (Chapter 14) are somewhat less clear than the discussions in the first part of the book. Quick comparisons on various points (gas mixtures, calibration, speed, *etc.*) of the three important gas adsorption techniques (*i.e.*, vacuum volumetric, continuous flow, and gravimetric methods) are given in Chapter 17.

One frustrating feature of this book is the large number of typographical and content errors. These errors reduce reader confidence in the text. Many of these are immediately recognizable as errors but some are not. Thus, while trying to understand the vacuum volumetric method in Chapter 13, we depend on Eqs. 13.3–13.8 to help, not hinder, us. Here, a simple sign error can lead to considerable confusion.

The real advantage of this book may be psychological. The author has separated the topic from the generally larger subject of particle-size measurement. By limiting the topic, he has made it possible for us to become more immediately interested in surface area measurement and, perhaps, more willing to use such measurements.

Thus, this book should be worthwhile for self-study or as a basic reference and should be recommended to pharmaceutical scientists. Nevertheless, it is only an introduction. The implication given on the dust cover that meaningful measurements of powder surface areas will immediately result from study of this book is probably too optimistic.

Reviewed by Dana Brooke
Mead Johnson Pharmaceutical Division
Evansville, IN 47721

tions of process applications for the manufacture of paper, adhesives, plasticizers, copying materials, pigments, perfumes, and many other substances including drugs.

My biggest criticism of the book is that the original text by Asaji Kondo is 10 years old. As a result, the English version by J. Wade Van Valkenburg contains reference material published prior to 1970. However, microencapsulation is a highly patented field and several patents discussed in the book will expire in the 1980's. Therefore, the text could prove to be of great assistance to scientists working in this field.

Reviewed by James W. McGinity
Drug Dynamics Institute
College of Pharmacy
University of Texas
Austin, TX 78712

Catecholamines: Basic and Clinical Frontiers, Vols. I and II. Edited by E. USDIN, I. J. KOPIN, and J. BARCHAS. Pergamon Press, Maxwell House, Fairview Park, Elmsford, NY 10523. 1979. Vol I: 1003 pp. Vol. II: 946 pp. 17 × 25 cm. Price $200.00 per volume.

The material in both volumes represents the phenomenal growth of research in catecholamines. Although the impact of catecholamine research in medicine has been universal, this international symposium represents research carried out mainly in the United States, France, Sweden, Britain, and Germany. The opening chapter presents a coherent, concise, and important summary by the internationally respected scientist–teacher, Arvid Carlsson, concerning the impact of catecholamine research on medical science and practices.

Compared to the previous symposium, a meaningful morphology appears on many pages. Dopamine occupies the central theme with which other endogenous substances such as enkephalins, substance P, and γ-aminobutyric acid (GABA) are intertwined. Drug-induced side effects and their influence on neurochemistry receive only limited attention. The value of genetics in relation to psychotropic illness with or without coherent neurochemical markers is included. One occasionally sees a marked overlap between the material published in these symposia and that published elsewhere. In the present era of rapid scientific communication, publishing the same material repeatedly should be discouraged. Catecholamine receptors occupy a large section in Vol. I.

The cost of both volumes may produce mental and neurochemical disturbances in the poor scientist who may want to buy them, so only departmental and institutional purchases are recommended.

Reviewed by P. N. Patil
College of Pharmacy
Ohio State University
Columbus, OH 43210

Introduction to Powder Surface Area. By S. LOWELL. Wiley, 605 Third Ave., New York, NY 10016. 1979. 199 pp. 15 × 23 cm. Price $17.95.

The subject of micromeritics should be important to pharmaceutical scientists. The features of a powder, *e.g.*, particle size, shape, and area, can greatly influence product development and processing as well as the properties of the finished product. However, the articles published about powders often present complicated dissolution equations derived for idealized situations. Thus, the important term for powder surface area in many pharmaceutical papers is calculated from assumed particle distributions for regularly shaped, isotropic particles. The assumption of no pores, no surface irregularities, and no interparticle forces leading to aggregation is far from reality. It should be of interest in pharmacy to characterize powders in regard to actual surface area and then to seek valid relationships between area and powder behaviors. This book may provide the proper introduction into this field for many pharmaceutical scientists.

Lowell treats powder surface area and pore-size distribution mostly as a subject of gas adsorption. However, mercury porosimetry is discussed. The book is relatively small (199 pages) and is divided into two parts. The author discusses the theoretical bases for surface area measurements in the first part. The topics discussed in these first 11 chapters also may be found in books on surface chemistry or particle-size measurement, but Lowell's presentation is clear and generally easy to follow. For example, in Chapter 5, he carefully leads the reader through the Brunauer, Emmett, and Teller theory using 25 equations.

The second section, the experimental section, should be quite helpful to those entering the field of surface area measurement. The basic techniques are described, but the narratives on vacuum volumetric methods (Chapter 13) and particularly on dynamic flow methods (Chapter 14) are somewhat less clear than the discussions in the first part of the book. Quick comparisons on various points (gas mixtures, calibration, speed, *etc.*) of the three important gas adsorption techniques (*i.e.*, vacuum volumetric, continuous flow, and gravimetric methods) are given in Chapter 17.

One frustrating feature of this book is the large number of typographical and content errors. These errors reduce reader confidence in the text. Many of these are immediately recognizable as errors but some are not. Thus, while trying to understand the vacuum volumetric method in Chapter 13, we depend on Eqs. 13.3–13.8 to help, not hinder, us. Here, a simple sign error can lead to considerable confusion.

The real advantage of this book may be psychological. The author has separated the topic from the generally larger subject of particle-size measurement. By limiting the topic, he has made it possible for us to become more immediately interested in surface area measurement and, perhaps, more willing to use such measurements.

Thus, this book should be worthwhile for self-study or as a basic reference and should be recommended to pharmaceutical scientists. Nevertheless, it is only an introduction. The implication given on the dust cover that meaningful measurements of powder surface areas will immediately result from study of this book is probably too optimistic.

Reviewed by Dana Brooke
Mead Johnson Pharmaceutical Division
Evansville, IN 47721

tions of process applications for the manufacture of paper, adhesives, plasticizers, copying materials, pigments, perfumes, and many other substances including drugs.

My biggest criticism of the book is that the original text by Asaji Kondo is 10 years old. As a result, the English version by J. Wade Van Valkenburg contains reference material published prior to 1970. However, microencapsulation is a highly patented field and several patents discussed in the book will expire in the 1980's. Therefore, the text could prove to be of great assistance to scientists working in this field.

Reviewed by James W. McGinity
Drug Dynamics Institute
College of Pharmacy
University of Texas
Austin, TX 78712

Catecholamines: Basic and Clinical Frontiers, Vols. I and II. Edited by E. USDIN, I. J. KOPIN, and J. BARCHAS. Pergamon Press, Maxwell House, Fairview Park, Elmsford, NY 10523. 1979. Vol I: 1003 pp. Vol. II: 946 pp. 17 × 25 cm. Price $200.00 per volume.

The material in both volumes represents the phenomenal growth of research in catecholamines. Although the impact of catecholamine research in medicine has been universal, this international symposium represents research carried out mainly in the United States, France, Sweden, Britain, and Germany. The opening chapter presents a coherent, concise, and important summary by the internationally respected scientist–teacher, Arvid Carlsson, concerning the impact of catecholamine research on medical science and practices.

Compared to the previous symposium, a meaningful morphology appears on many pages. Dopamine occupies the central theme with which other endogenous substances such as enkephalins, substance P, and γ-aminobutyric acid (GABA) are intertwined. Drug-induced side effects and their influence on neurochemistry receive only limited attention. The value of genetics in relation to psychotropic illness with or without coherent neurochemical markers is included. One occasionally sees a marked overlap between the material published in these symposia and that published elsewhere. In the present era of rapid scientific communication, publishing the same material repeatedly should be discouraged. Catecholamine receptors occupy a large section in Vol. I.

The cost of both volumes may produce mental and neurochemical disturbances in the poor scientist who may want to buy them, so only departmental and institutional purchases are recommended.

Reviewed by P. N. Patil
College of Pharmacy
Ohio State University
Columbus, OH 43210

Introduction to Powder Surface Area. By S. LOWELL. Wiley, 605 Third Ave., New York, NY 10016. 1979. 199 pp. 15 × 23 cm. Price $17.95.

The subject of micromeritics should be important to pharmaceutical scientists. The features of a powder, *e.g.*, particle size, shape, and area, can greatly influence product development and processing as well as the properties of the finished product. However, the articles published about powders often present complicated dissolution equations derived for idealized situations. Thus, the important term for powder surface area in many pharmaceutical papers is calculated from assumed particle distributions for regularly shaped, isotropic particles. The assumption of no pores, no surface irregularities, and no interparticle forces leading to aggregation is far from reality. It should be of interest in pharmacy to characterize powders in regard to actual surface area and then to seek valid relationships between area and powder behaviors. This book may provide the proper introduction into this field for many pharmaceutical scientists.

Lowell treats powder surface area and pore-size distribution mostly as a subject of gas adsorption. However, mercury porosimetry is discussed. The book is relatively small (199 pages) and is divided into two parts. The author discusses the theoretical bases for surface area measurements in the first part. The topics discussed in these first 11 chapters also may be found in books on surface chemistry or particle-size measurement, but Lowell's presentation is clear and generally easy to follow. For example, in Chapter 5, he carefully leads the reader through the Brunauer, Emmett, and Teller theory using 25 equations.

The second section, the experimental section, should be quite helpful to those entering the field of surface area measurement. The basic techniques are described, but the narratives on vacuum volumetric methods (Chapter 13) and particularly on dynamic flow methods (Chapter 14) are somewhat less clear than the discussions in the first part of the book. Quick comparisons on various points (gas mixtures, calibration, speed, *etc.*) of the three important gas adsorption techniques (*i.e.*, vacuum volumetric, continuous flow, and gravimetric methods) are given in Chapter 17.

One frustrating feature of this book is the large number of typographical and content errors. These errors reduce reader confidence in the text. Many of these are immediately recognizable as errors but some are not. Thus, while trying to understand the vacuum volumetric method in Chapter 13, we depend on Eqs. 13.3–13.8 to help, not hinder, us. Here, a simple sign error can lead to considerable confusion.

The real advantage of this book may be psychological. The author has separated the topic from the generally larger subject of particle-size measurement. By limiting the topic, he has made it possible for us to become more immediately interested in surface area measurement and, perhaps, more willing to use such measurements.

Thus, this book should be worthwhile for self-study or as a basic reference and should be recommended to pharmaceutical scientists. Nevertheless, it is only an introduction. The implication given on the dust cover that meaningful measurements of powder surface areas will immediately result from study of this book is probably too optimistic.

Reviewed by Dana Brooke
Mead Johnson Pharmaceutical Division
Evansville, IN 47721

MAY 1980
VOLUME 69 NUMBER 5

JOURNAL OF PHARMACEUTICAL SCIENCES

MARY H. FERGUSON
Editor

SHELLY ELLIOTT
Production Editor

MARCIA GARTRELL
Copy Editor

NICOLETTE TRIANTAFELLU
Copy Editor

EDWARD G. FELDMANN
Contributing Editor

SAMUEL W. GOLDSTEIN
Contributing Editor

BELLE R. BECK
Editorial Secretary

DAVID BOHARDT
Director of Publications

L. LUAN CORRIGAN
Assistant Director of Publications

EDITORIAL ADVISORY BOARD

JOHN AUTIAN
HERBERT A. LIEBERMAN
NORMAN R. FARNSWORTH
DAVID E. MANN, JR.
WILLIAM O. FOYE
GERALD J. PAPARIELLO
WILLIAM J. JUSKO
EDWARD G. RIPPIE

The *Journal of Pharmaceutical Sciences* (ISSN 0022-3549) is published monthly by the American Pharmaceutical Association (APhA) at 2215 Constitution Ave., N.W., Washington, DC 20037. Second-class postage paid at Washington, D.C., and at additional mailing office.

All expressions of opinion and statements of supposed fact appearing in articles or editorials carried in this journal are published on the authority of the writer over whose name they appear and are not to be regarded as necessarily expressing the policies or views of APhA.

Offices—Editorial, Advertising, and Subscription: 2215 Constitution Ave., N.W., Washington, DC 20037. All Journal staff may be contacted at this address. Printing: 20th & Northampton Streets, Easton, PA 18042.

Annual Subscriptions—United States and foreign, industrial and government institutions $60, educational institutions $60, individuals *for personal use only* $30; single copies $5. All foreign subscriptions add $5 for postage. Subscription rates are subject to change without notice. Members of APhA may elect to receive the *Journal of Pharmaceutical Sciences* as a part of their annual $80 (foreign $85) APhA membership dues.

Claims—Missing numbers will not be supplied if dues or subscriptions are in arrears for more than 60 days or if claims are received more than 60 days after the date of the issue, or if loss was due to failure to give notice of change of address. APhA cannot accept responsibility for foreign delivery when its records indicate shipment was made.

Change of Address—Members and subscribers should notify at once both the Post Office and APhA of any change of address.

Photocopying—The code at the foot of the first page of an article indicates that APhA has granted permission for copying of the article beyond the limits permitted by Sections 107 and 108 of the U.S. Copyright Law provided that the copier sends the per copy fee stated in the code to the Copyright Clearance Center, Inc., P.O. Box 8891, Boston, MA 02114. Copies may be made for personal or internal use only and not for general distribution.

Microfilm—Available from University Microfilms International, 300 N. Zeeb Road, Ann Arbor, MI 48106.

© Copyright 1980, American Pharmaceutical Association, 2215 Constitution Ave., N.W., Washington, DC 20037; all rights reserved.

PR IN THE PHARMACEUTICAL SCIENCES

"Better Living Through Chemistry!"

For those readers who are in the same age bracket as this writer, there is no need to identify the slogan quoted above, or to tell when it was in wide, popular use. For our younger readers, however, we should explain that this was a theme that ran through the extensive advertising of the DuPont Chemical Company during and immediately following World War II.

Having developed artificial fibers, and nylon in particular, from a virtual nothing into a huge segment of American industrial production during the decade of the 1940's, the DuPont firm could truly boast of the wonderous changes that chemistry, nylon, and DuPont had worked for the citizens of this country in the span of a few short years.

But chemistry was responsible for more than just women's sheer stockings and Air Force pilots' parachutes. It also was the vehicle that brought us vitamins, miracle drugs, artificial rubber tires, sudsy detergents, and countless other consumer products that literally transformed the average person's daily life-style more dramatically than mankind had previously experienced in time periods covering hundreds or even thousands of years.

Consequently, to have grown up as a teenager during those fabulous late forties was to feel and share the excitement of breathtaking new discoveries and to marvel at the almost daily new products and conveniences.

And, at that time, to be able to tell friends, colleagues, and relatives that you were embarking on the study of science and chemistry was to feel the pride and to sense the adulation experienced more recently by moon-walking astronauts or Super Bowl quarterbacks.

But as time went on, the public began to hear about insecticide buildup in birds and fish, about waterways being fouled with nonbiodegradable detergents, about the cancer risk of certain food additives, about growth hormone residues in food animals, about the risk of nuclear power plant accidents, and about dozens of other problems associated with those wonderful products of the chemical age—and all of a sudden it wasn't too popular to be identified as a chemist or scientist.

Pharmacy and pharmacists shared to a great extent in these swings of public favor. After all, pharmacy and pharmacists most directly deal with the drugs, the vitamins, the hormones, the pharmaceutical excipients, the flavors, the artificial sweeteners, and so on that first appeared so attractive but later were looked upon with misgivings and fear. And aside from chemists *per se*, among the professions, pharmacists probably take more chemistry courses in their formal education than any other professionals with the possible exception of chemical engineers.

And naturally, within the community of pharmacy, pharmaceutical scientists probably felt the brunt of this fall from public popularity more severely than any other group. But, on the other hand, no group is more aware than pharmaceutical scientists of the many good things that science, chemistry, and more specifically the pharmaceutical sciences have done to contribute to better health and longer lives.

Consequently, it may be timely for some down-to-earth, grass-roots public relations in which we take the opportunity to talk at meetings of consumer groups, fraternal organizations, ladies' clubs, boy scouts, community associations, better business bureaus, or whatever and to provide a balanced picture of the benefits and risks of drugs as well as the special stories about timed-release preparations, about novel drug delivery systems, and about the development of prodrugs.

The key to success in such public relations efforts is that such presentations must be credible. The hazards of potent drugs, the unknown problems associated with all new products, and the difficulty of achieving zero defects in product quality must also be recognized in an honest and forthright manner.

Certainly, the "pill for every ill" approach is harmful and dangerous to society; as such, we must do what we can to reject such thinking. However, for the public to espouse an attitude of therapeutic nihilism would be at least equally unfortunate for society.

Pharmaceutical scientists have the information, background, and opportunity to influence public opinion to see that neither of these extremes is allowed to prevail. And, in speaking out with such a message, pharmaceutical scientists will enhance their own image in the area of public esteem.

—EGF

MAY 1980
VOLUME 69 NUMBER 5

JOURNAL OF PHARMACEUTICAL SCIENCES

MARY H. FERGUSON
Editor

SHELLY ELLIOTT
Production Editor

MARCIA GARTRELL
Copy Editor

NICOLETTE TRIANTAFELLU
Copy Editor

EDWARD G. FELDMANN
Contributing Editor

SAMUEL W. GOLDSTEIN
Contributing Editor

BELLE R. BECK
Editorial Secretary

DAVID BOHARDT
Director of Publications

L. LUAN CORRIGAN
Assistant Director of Publications

EDITORIAL ADVISORY BOARD

JOHN AUTIAN
HERBERT A. LIEBERMAN
NORMAN R. FARNSWORTH
DAVID E. MANN, JR.
WILLIAM O. FOYE
GERALD J. PAPARIELLO
WILLIAM J. JUSKO
EDWARD G. RIPPIE

The *Journal of Pharmaceutical Sciences* (ISSN 0022-3549) is published monthly by the American Pharmaceutical Association (APhA) at 2215 Constitution Ave., N.W., Washington, DC 20037. Second-class postage paid at Washington, D.C., and at additional mailing office.

All expressions of opinion and statements of supposed fact appearing in articles or editorials carried in this journal are published on the authority of the writer over whose name they appear and are not to be regarded as necessarily expressing the policies or views of APhA.

Offices—Editorial, Advertising, and Subscription: 2215 Constitution Ave., N.W., Washington, DC 20037. All Journal staff may be contacted at this address. Printing: 20th & Northampton Streets, Easton, PA 18042.

Annual Subscriptions—United States and foreign, industrial and government institutions $60, educational institutions $60, individuals *for personal use only* $30; single copies $5. All foreign subscriptions add $5 for postage. Subscription rates are subject to change without notice. Members of APhA may elect to receive the *Journal of Pharmaceutical Sciences* as a part of their annual $80 (foreign $85) APhA membership dues.

Claims—Missing numbers will not be supplied if dues or subscriptions are in arrears for more than 60 days or if claims are received more than 60 days after the date of the issue, or if loss was due to failure to give notice of change of address. APhA cannot accept responsibility for foreign delivery when its records indicate shipment was made.

Change of Address—Members and subscribers should notify at once both the Post Office and APhA of any change of address.

Photocopying—The code at the foot of the first page of an article indicates that APhA has granted permission for copying of the article beyond the limits permitted by Sections 107 and 108 of the U.S. Copyright Law provided that the copier sends the per copy fee stated in the code to the Copyright Clearance Center, Inc., P.O. Box 8891, Boston, MA 02114. Copies may be made for personal or internal use only and not for general distribution.

Microfilm—Available from University Microfilms International, 300 N. Zeeb Road, Ann Arbor, MI 48106.

© Copyright 1980, American Pharmaceutical Association, 2215 Constitution Ave., N.W., Washington, DC 20037; all rights reserved.

PR IN THE PHARMACEUTICAL SCIENCES

"Better Living Through Chemistry!"

For those readers who are in the same age bracket as this writer, there is no need to identify the slogan quoted above, or to tell when it was in wide, popular use. For our younger readers, however, we should explain that this was a theme that ran through the extensive advertising of the DuPont Chemical Company during and immediately following World War II.

Having developed artificial fibers, and nylon in particular, from a virtual nothing into a huge segment of American industrial production during the decade of the 1940's, the DuPont firm could truly boast of the wonderous changes that chemistry, nylon, and DuPont had worked for the citizens of this country in the span of a few short years.

But chemistry was responsible for more than just women's sheer stockings and Air Force pilots' parachutes. It also was the vehicle that brought us vitamins, miracle drugs, artificial rubber tires, sudsy detergents, and countless other consumer products that literally transformed the average person's daily life-style more dramatically than mankind had previously experienced in time periods covering hundreds or even thousands of years.

Consequently, to have grown up as a teenager during those fabulous late forties was to feel and share the excitement of breathtaking new discoveries and to marvel at the almost daily new products and conveniences.

And, at that time, to be able to tell friends, colleagues, and relatives that you were embarking on the study of science and chemistry was to feel the pride and to sense the adulation experienced more recently by moon-walking astronauts or Super Bowl quarterbacks.

But as time went on, the public began to hear about insecticide buildup in birds and fish, about waterways being fouled with nonbiodegradable detergents, about the cancer risk of certain food additives, about growth hormone residues in food animals, about the risk of nuclear power plant accidents, and about dozens of other problems associated with those wonderful products of the chemical age—and all of a sudden it wasn't too popular to be identified as a chemist or scientist.

Pharmacy and pharmacists shared to a great extent in these swings of public favor. After all, pharmacy and pharmacists most directly deal with the drugs, the vitamins, the hormones, the pharmaceutical excipients, the flavors, the artificial sweeteners, and so on that first appeared so attractive but later were looked upon with misgivings and fear. And aside from chemists *per se*, among the professions, pharmacists probably take more chemistry courses in their formal education than any other professionals with the possible exception of chemical engineers.

And naturally, within the community of pharmacy, pharmaceutical scientists probably felt the brunt of this fall from public popularity more severely than any other group. But, on the other hand, no group is more aware than pharmaceutical scientists of the many good things that science, chemistry, and more specifically the pharmaceutical sciences have done to contribute to better health and longer lives.

Consequently, it may be timely for some down-to-earth, grass-roots public relations in which we take the opportunity to talk at meetings of consumer groups, fraternal organizations, ladies' clubs, boy scouts, community associations, better business bureaus, or whatever and to provide a balanced picture of the benefits and risks of drugs as well as the special stories about timed-release preparations, about novel drug delivery systems, and about the development of prodrugs.

The key to success in such public relations efforts is that such presentations must be credible. The hazards of potent drugs, the unknown problems associated with all new products, and the difficulty of achieving zero defects in product quality must also be recognized in an honest and forthright manner.

Certainly, the "pill for every ill" approach is harmful and dangerous to society; as such, we must do what we can to reject such thinking. However, for the public to espouse an attitude of therapeutic nihilism would be at least equally unfortunate for society.

Pharmaceutical scientists have the information, background, and opportunity to influence public opinion to see that neither of these extremes is allowed to prevail. And, in speaking out with such a message, pharmaceutical scientists will enhance their own image in the area of public esteem.

—EGF

JOURNAL OF PHARMACEUTICAL SCIENCES

MAY 1980
VOLUME 69 NUMBER 5

RESEARCH ARTICLES

Extended Hildebrand Solubility Approach: Solubility of Theophylline in Polar Binary Solvents

A. MARTIN ˣ, J. NEWBURGER, and A. ADJEI

Received September 6, 1979, from the *Drug Dynamics Institute, College of Pharmacy, University of Texas, Austin, TX 78712.* Accepted for publication November 21, 1979.

Abstract □ A quantitative approach is presented for predicting solubilities of crystalline compounds in binary solvent systems. The solubility of theophylline in mixed solvents consisting of dioxane and water was determined at 25 ± 0.1°. The solubilities across this range of polar solvents were back-calculated using a technique involving an interaction energy term, W. This parameter is regressed against a polynomial expression in δ_1, the solubility parameter for the mixed solvents. Except for the end-points, solubilities were predicted within <12% and with considerably better accuracy in most cases. The new approach modifies the well-known Hildebrand solubility equation to make it applicable to polar systems. Although the method may be used with solutes in pure solvents, its greatest application appears to be the prediction of drug solubility in binary solvent mixtures.

Keyphrases □ Theophylline—solubility in polar binary solvents □ Solvent systems—solubility of theophylline in polar binary solvents

Solubility data on drugs and pharmaceutical adjuncts in mixed solvents have wide application in the drug sciences. Knowledge of interactive forces between solutes and solvents are of considerable theoretical and practical interest throughout the physical and biological sciences.

BACKGROUND

The term regular solution was introduced by Hildebrand (1) to describe solutions showing random molecular distribution and orientation as found in ideal solutions. There is no entropy change, but heat is absorbed when the components of a regular solution are mixed. Although these solutions are not ideal, they yield curves of log solubility *versus* $1/T$ that are quite regular. Other kinds of solutions, those that involve solvation or association, produce irregular solubility curves. Modifications of the Hildebrand approach for irregular solutions have been reported in the field of solution technology by various investigators (2–8).

The Hildebrand–Scatchard equation for the solubility of solids in a regular solution may be written as (9–13):

$$-\log X_2 = \frac{\Delta S_m^f}{R}\log\frac{T_m}{T} + \frac{V_2\phi_1^2}{2.303RT}(\delta_1 - \delta_2)^2 \qquad \text{(Eq. 1)}$$

where X_2 is the mole fraction solubility of the solute or drug (represented by subscript 2); ΔS_m^f is the entropy of fusion of the crystalline drug at its melting point, T_m, on the Kelvin scale; T is the temperature in degrees Kelvin at which the solubility is determined; R is the molar gas constant; V_2 is the molar volume of the drug; ϕ_1 is the volume fraction of the solvent (represented by subscript 1); δ_2 is the solubility parameter of the solute; and δ_1 is the solubility parameter of the solvent or mixed solvent. Solubility parameters also are referred to as delta values. The first right-hand term of Eq. 1 frequently is written as $(\Delta H_m^f/2.303RT)(1/T - 1/T_m)$, but the ΔS_m^f term of Eq. 1 is more correct, as will be discussed later.

The solubility parameter or delta value of the solvent, δ_1, is obtained as suggested by Hildebrand and Scott (10) using the relationship:

$$\delta_1 = \left(\frac{\Delta E_1^v}{V_1}\right)^{1/2} = \left(\frac{\Delta H_1^v - RT}{V_1}\right)^{1/2} \qquad \text{(Eq. 2)}$$

where ΔE_1^v is the molar energy of vaporization, ΔH_1^v is the heat of vaporization, and V_1 is the molar volume of the solvent. The square of δ_1, or $\Delta E_1^v/V_1$, is called the cohesive energy density of the solvent. Other methods for obtaining δ_1 were given by Hildebrand and Scott (10).

The solubility parameter of a solid compound is difficult to obtain, and few values are recorded in the literature. The δ^2 value for iodine is ~14.1 (10), and the value for naphthalene, phenanthrene, and anthrancene is ~9.8. Several investigators (12, 14) estimated the solubility parameters of benzoic acid and some *p*-hydroxybenzoic acid esters from the peak values obtained from a plot of mole fraction solubility *versus* delta values of solvents. The parameter for benzoic acid also was determined from the solubility data in hexane and was found to be 11.5. The solubility parameters for barbiturates have been determined (15, 16). Yalkowsky *et al.* (17) obtained the solubility parameters for *p*-aminobenzoate esters from their solubility in hexane. For example, the value for the ethyl ester was 12.05. James *et al.* (18) reported solubility parameters for some testosterone esters and related compounds.

The first term on the right side of Eq. 1, the ideal solubility term, is for the dissociation of the crystal lattice of a solid compound, rendering it in the liquid form. In the presence of solvents that form nearly ideal solutions, the second right-hand quantity, the regular solution term, is nearly zero and may be omitted.

The regular solution term, involving solubility parameters, is an activity coefficient, log α_v, used to represent nonideality due to the interaction of solute and solvent molecules in a regular solution where only nonpolar and weak polar forces exist:

$$\log \alpha_v = A(\delta_1 - \delta_2)^2 \qquad \text{(Eq. 3)}$$

where A represents $V_2\phi_1^2/2.303RT$ and the subscript v stands for van der Waals forces.

Following the suggestion by Crowley *et al.* (8), Hansen (5, 6) introduced a three-dimensional system of solubility parameters. The energy of va-

0022-3549/80/0500-0487$01.00/0
© 1980, American Pharmaceutical Association

porization in Eq. 2 was assumed to be an additive quantity composed of three energies representing London dispersion forces (ΔE_d^v), polar forces (ΔE_p^v), and hydrogen bonding (ΔE_h^v) in the solvent. Dividing each term by the molar volume of the solvent (V_1), the total cohesive energy density was obtained:

$$\frac{\Delta E^v}{V_1} = \frac{\Delta E_d^v}{V_1} + \frac{\Delta E_p^v}{V_1} + \frac{\Delta E_h^v}{V_1} \qquad \text{(Eq. 4)}$$

or, in terms of delta values:

$$\delta^2 = \delta_d^2 + \delta_p^2 + \delta_h^2 \qquad \text{(Eq. 5)}$$

where δ^2 is the total cohesive energy density for the liquid. Values for δ_d were determined by reference to a corresponding hydrocarbon called a homomorph, and δ_p and δ_h were estimated by empirical methods. Hoy *et al.* (19) developed extensive tables of three-dimensional delta values, which differ somewhat from the values of Hansen (5, 6). Hansen noted that there is yet no theoretical basis for the new three-dimensional solubility parameters, and he used them empirically to interpret the solubility of polymers and other solutes employed in industry and commerce.

Weimer and Prausnitz (20) calculated polar and nonpolar solubility parameters using the homomorph concept, and Blanks and Prausnitz (7) applied these values to the study of polymer solubility in polar solvents. These investigators did not consider hydrogen bonding systems.

The method presented here[1] allows calculation of the solubility of polar and nonpolar solutes in solvents ranging from nonpolar (hexane) to aprotic polar (*e.g.*, *N,N*-dimethylformamide) and highly polar protic solvents such as alcohols, acids, and water. Although formulated specifically in terms of the solubility of a nonelectrolytic solid in liquid solution, the technique should apply as well to liquid–liquid and other equilibrium systems.

Equation 1 ordinarily provides a poor prediction for the solubility of a drug or other crystalline compound in a polar solvent. These solutions are quite irregular, often involving self-association or solvation. The logarithm of the activity coefficient, calculated using Eq. 3, accounts for the nonideality of solutions resulting from the interaction of solute and solvent molecules of the physical or van der Waals type. Several investigators, including Hildebrand, have cautioned that expressions in the form of Eq. 3 are not good representations of nonideality in solutions of polymers and various polar and semipolar compounds in polar and hydrogen bonding solvents. For irregular solutions, a total activity coefficient, α_2, must be written consisting of the term (Eq. 3) representing physical or van der Waals forces and an additional term, $\log \alpha_R$, representing residual, presumably stronger, forces:

$$\log \alpha_2 = \log \alpha_v + \log \alpha_R \qquad \text{(Eq. 6)}$$

The total activity coefficient may be written as:

$$\log \alpha_2 = A(\delta_1^2 + \delta_2^2 - 2W) \qquad \text{(Eq. 7)}$$

where W is the interaction energy between the solute and solvent in an irregular solution.

Employing Eqs. 3, 6, and 7, one obtains for the residual term:

$$\log \alpha_R = 2A(\delta_1\delta_2 - W) \qquad \text{(Eq. 8)}$$

The logarithm of the total activity coefficient may be written for irregular solutions as:

$$\log \alpha_2 = A(\delta_1 - \delta_2)^2 + 2A(\delta_1\delta_2 - W) \qquad \text{(Eq. 9)}$$

and the modified Hildebrand solubility equation becomes:

$$-\log X_2 = \frac{\Delta S_m^f}{R} \log \frac{T_m}{T} + A(\delta_1^2 + \delta_2^2 - 2W) \qquad \text{(Eq. 10)}$$

EXPERIMENTAL

Materials—Anhydrous theophylline[2] and *p*-dioxane[3] were obtained commercially.

Solubility Determination—The solubility of theophylline ($\delta^2 = 14.0$) was determined in mixed solvents consisting of dioxane ($\delta_{1_a} = 10.01$) and water ($\delta_{1_b} = 23.45$). Glass-distilled deionized water was used to prepare mixtures with dioxane in concentrations of 0–100% by volume of dioxane. About 10 ml of the mixture was introduced into screw-capped vials containing excess theophylline. The vials were agitated for 96 hr in a shaker bath maintained at 25 ± 0.1°. Preliminary studies showed that this period was sufficient to ensure saturation at 25°.

After equilibrium was attained, vials were removed for analysis. The solutions were filtered, and aliquots were placed in volumetric flasks and brought to the final volume with the solvent mixture in which the drug was originally dissolved. The solutions were analyzed in a spectrophotometer[4] at 273.4 nm. Three samples were withdrawn from four separate vials and measured at each mixed solvent concentration. The standard error for the analysis of individual samples was $<\pm 0.7$ μg/ml.

The densities of the solvent mixtures and the filtrates of the saturated solutions of theophylline were determined in triplicate at 25 ± 0.1° using a pycnometer.

Heat of Fusion—The heat of fusion of crystalline theophylline was determined experimentally in a differential scanning calorimeter[5,6]. Thermograms were run at 100 psi to retard sublimation, and the heat of fusion was determined from the area under the curve, using indium metal as a standard. The equation employed in calculating the heats of fusion from differential scanning calorimetry is:

$$\Delta H_m^f = \Delta H_m^f \text{ (standard)} \times \text{standard weight} \times \text{sample peak area} \times \frac{\text{instrument range for sample} \times \text{sample mol. wt.}}{\text{instrument range for standard} \times \text{sample weight} \times \text{standard mol. wt.} \times \text{standard peak area}} \qquad \text{(Eq. 11)}$$

To obtain the ideal solubility, X_2^i, Hildebrand *et al.* (22) showed that entropy of fusion, ΔS_m^f, can replace heat of fusion to take into account the molar heat capacity change, ΔC_p, in going from a solid to a liquid solute. The equation for calculating the ideal solubility employing ΔS_m^f is (22):

$$\log X_2^i \cong \frac{\Delta S_m^f}{R} \log \frac{T}{T_m} \qquad \text{(Eq. 12)}$$

The entropy of fusion is obtained by plotting $\log X_2$ *versus* $\log T$ under ideal solution conditions. With solubility data, X_2, at three or four temperatures, a linear plot with a slope proportional to ΔS_m^f is obtained. However, the ΔH_m^f and T_m values may be determined more conveniently using a differential scanning calorimeter (23). Once these values are obtained, ΔS_m^f is calculated from:

$$\Delta S_m^f = \frac{\Delta H_m^f}{T_m} \qquad \text{(Eq. 13)}$$

Solubility Parameter of Mixed Solvents—The solubility parameter, δ_1, for a mixture of two solvents, a and b, is calculated (24, 25) using the expression:

$$\delta_1 = \frac{\phi_a\delta_a + \phi_b\delta_b}{\phi_a + \phi_b} \qquad \text{(Eq. 14)}$$

where:

$$\phi_1 = \phi_a + \phi_b \qquad \text{(Eq. 15)}$$

in which ϕ_1 is the total volume fraction of the two solvents and δ_1, the solubility parameter of solvents a and b, is averaged in terms of volume fractions.

Volume Fraction and Mean Molar Volume in Mixed Solvents—The total volume fraction, ϕ_1, of the solvent mixture is calculated using the expression:

$$\phi_1 = \frac{(1 - X_2)V_1}{(1 - X_2)V_1 + X_2V_2} \qquad \text{(Eq. 16)}$$

where X_2 is the mole fraction solubility of the drug in the mixed solvent and V_1 is the mean molar volume of the binary solvent. For each mixed solvent composed of solvents a and b in various proportions:

$$V_1 = \frac{X_aM_a + (1 - X_a)M_b}{\rho_1} \qquad \text{(Eq. 17)}$$

where X_i and M_i are the mole fraction and molecular weight of the par-

[1] The first report in this series is Ref. 21. It provides a sample calculation for the method described here and in subsequent papers.

[2] Knoll Chemicals.

[3] Mallinckrodt Chemical Works.

[4] Model 25 spectrophotometer, Beckman.

[5] Model 1B, Perkin-Elmer.

[6] L. T. Grady of the United States Pharmacopeia Laboratories, Rockville, Md., and S. H. Yalkowsky, The Upjohn Co., Kalamazoo, Mich., provided independent measurements of theophylline, theobromine, and caffeine in their laboratories.

Table I—Mole Fraction Solubility of Theophylline in Dioxane–Water Mixtures at 25°

Dioxane, %	V_1	δ_1	Solution Density	ϕ_1	X_2 (obs.)[a]	A	Log α_2	Log α_v	Log α_R	W (Eq. 7)
0	18.063	23.45	0.9988	0.99493	0.0007414	0.08997	1.40772	8.03426	−6.62654	365.128
5	21.577	22.78	0.9988	0.99390	0.0010668	0.08978	1.24969	6.92101	−5.67132	350.504
10	24.880	22.11	1.0058	0.99228	0.0015583	0.09849	1.08512	5.88581	−4.80069	336.363
15	28.232	21.43	1.0105	0.99082	0.0021046	0.08922	0.95460	4.92565	−3.97105	322.273
20	31.566	20.76	1.0148	0.98916	0.0027831	0.08925	0.83325	4.06366	−3.23041	308.804
25	34.875	20.09	1.0190	0.98761	0.0035158	0.08865	0.73175	3.28777	−2.55602	295.677
30	38.158	19.42	1.0232	0.98494	0.0046818	0.08817	0.60736	2.59010	−1.98274	283.124
35	41.450	18.75	1.0265	0.98320	0.0056783	0.08786	0.52356	1.98230	−1.45874	270.802
40	44.713	18.07	1.0300	0.98168	0.0066856	0.08759	0.45263	1.45084	−0.99821	258.679
45	48.018	17.40	1.0321	0.97877	0.0083295	0.08707	0.35716	1.00650	−0.64934	247.329
55	54.589	16.06	1.0362	0.97438	0.0114449	0.08629	0.21916	0.36617	−0.14701	225.692
60	57.907	15.39	1.0374	0.97352	0.0125411	0.08614	0.17944	0.16642	0.01302	215.384
62	59.228	15.12	1.0379	0.97287	0.0131436	0.08602	0.15906	0.10791	0.05115	211.383
66	64.630	14.58	1.0379	0.97277	0.0143803	0.08600	0.12001	0.02893	0.09108	203.590
70	64.630	14.04	1.0379	0.97293	0.0142926	0.08603	0.12266	0.00014	0.12252	195.848
75	68.011	13.37	1.0379	0.97428	0.0142711	0.08627	0.12332	0.03424	0.08908	186.664
77	69.385	13.10	1.0375	0.97480	0.0142592	0.08636	0.12368	0.06995	0.05373	183.089
80	71.464	12.70	1.0368	0.97617	0.0138736	0.08661	0.13559	0.14636	−0.01077	177.862
85	74.956	12.03	1.0352	0.97816	0.0331770	0.08696	0.15334	0.33748	−0.18414	169.479
90	78.459	11.35	1.0367	0.98162	0.0117074	0.08758	0.20931	0.61500	−0.40569	161.216
100	85.663	10.01	1.0286	0.99625	0.0025959	0.09020	0.86349	1.43607	−0.57258	143.314

[a] Mole fraction solubilities are obtained at best to five figures following the decimal point. Two additional positions have been retained to provide four to six significant figures and thus facilitate comparison with calculated solubility values and to compute percentage differences.

ticular solvent in the mixture, respectively, and ρ_1 is the density of the solvent mixture at the experimental temperature.

Molar Volume and Solubility Parameter for Solute—The molar volume of theophylline taken as a supercooled liquid at 25° is calculated using the group contribution approach of Fedors (26). The solubility parameter, δ_2, for theophylline is obtained at the peak solubility where the δ_1 value of the solvent should equal δ_2 as required by Eq. 1. This principle was discussed previously (12). The δ_2 value of theophylline also may be calculated by the Fedors method (26).

Calculations of Ideal Solubility, Activity Coefficients, and W—The method begins with a calculation of the ideal solubility, X_2^i, of theophylline, employing the first right-hand term of Eq. 1 or 10. The logarithmic ideal solubility, together with the logarithm of the experimentally determined solubility, yields the logarithm of the solute activity coefficient:

$$\log X_2^i - \log X_2 = \log \alpha_2 \qquad \text{(Eq. 18)}$$

Log α_v is obtained from the application of Eq. 3, and log α_R is obtained from Eq. 6 or 8. Values for W, the solute–solvent interaction energy, are calculated with Eq. 7.

RESULTS AND DISCUSSION

The experimentally determined solubilities of theophylline at 25° in dioxane–water mixtures are found in Table I together with the composition and densities of the solutions. The densities of solutions are included in reporting solubility data to allow conversion from mole fractions to molar concentrations, to assist in obtaining partial molar volumes, and to permit the calculation of other quantities. The calculated log α_2, log α_v, log α_R, and W values also are found in Table I.

By employing the procedure described under *Experimental* to yield ideal solubility, a ΔH_m^f value of 7097 cal/mole[7] and T_m value of 547.7°K were obtained. Then ΔS_m^f was calculated using Eq. 13 to yield a value of 12.96 cal/mole/degree and a mole fraction ideal solubility for theophylline of 0.01896 (log X_2^i = −1.7222). The molar volume of theophylline is 124.

The experimental solubilities, expressed as mole fractions, are plotted in Fig. 1 against the solubility parameter, δ_1, of the various mixed solvents. Also shown in Fig. 1 is the ideal solubility level (horizontal line at a mole fraction of 0.01896). The regular solution line of Fig. 1 is a curve expressing solubilities of theophylline, with the assumption that the mixtures follow regular solution theory. The solubility of theophylline (δ_2 = 14.0) in pure dioxane (δ_1 = 10.01), in pure water (δ_1 = 23.45), and in the binary solutions composed of these two solvents did not approach the level of ideality, namely X_2 = 0.019, and did not coincide with regular solution behavior except where the experimental curve, by chance, crossed the regular solution line.

[7] L. T. Grady and W. H. Yalkowsky (personal communications) obtained values of ΔH_m^f varying between 5940 and 7225 cal/mole.

The original Hildebrand equation for regular solution behavior cannot be used to represent solubility in these polar solvents. However, Eq. 10, which involves the interaction term, W, does reproduce exactly the solubility of theophylline in dioxane, water, and the mixed solvent systems. Figure 1 shows that the peak solubility, although lower than ideal, occurred at a δ_1 value of ~14.0, which was taken as the δ_2 value of theophylline. The Fedors method (26) of calculating δ values from molecular group and fragment constants gives essentially the same value (14.1).

When solubility was plotted as moles per liter instead of as mole fraction concentration, a slightly different shape than the curve of Fig. 1 was obtained. Peaks and valleys were not obtained in the curve of theophylline in dioxane–water mixture as reported by Paruta *et al.* (27). However, two small plateaus were found. These plateaus possibly were overlooked because the solubility measurements were not spaced as closely in the solvent composition as in the results of Paruta *et al.* Ongoing work in this laboratory with caffeine in dioxane–water has reproduced the two-peak maximum reported by Paruta *et al.* (27).

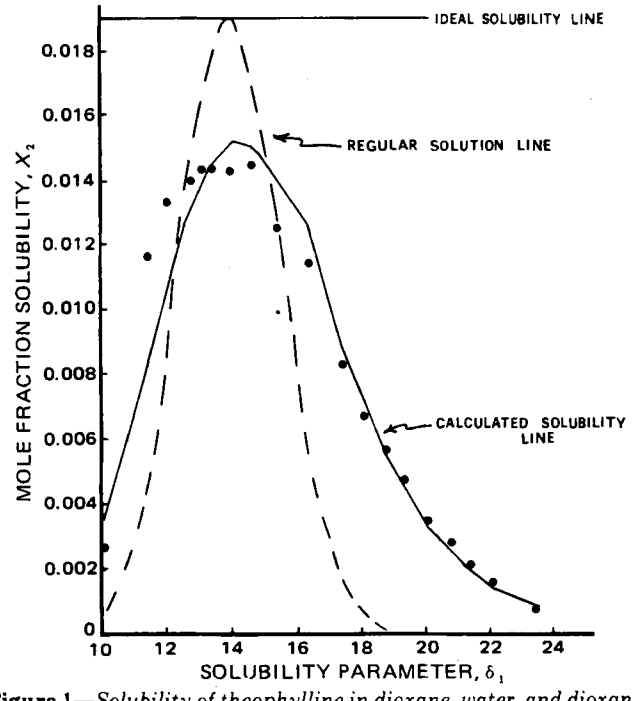

Figure 1—*Solubility of theophylline in dioxane, water, and dioxane–water mixtures at 25°. Key: ● experimental solubilities; and — back-calculated solubilities from Eq. 10.*

Table II—Calculated Solubilities of Theophylline in Dioxane–Water Systems at 25°

Dioxane, %	δ_1	W^a	Log α_2/A^b	X_2 (calc.)	X_2 (obs.) − X_2 (calc.) Difference
0	23.45	365.501	14.901	0.0008654	0.00012 (16.2%)
5	22.78	350.581	13.766	0.0011013	0.00003 (2.8%)
10	22.11	336.158	12.536	0.0014321	0.00013 (8.3%)
15	21.43	322.012	11.221	0.0018904	0.00021 (10.0%)
20	20.76	308.544	9.891	0.0025018	0.00028 (10.1%)
25	20.09	295.527	8.554	0.0033073	0.00021 (6.0%)
30	19.42	282.947	7.241	0.0043582	0.00032 (6.8%)
35	18.75	270.790	5.982	0.0056522	0.00003 (0.5%)
40	18.07	258.868	4.788	0.0072174	0.00053 (7.9%)
45	17.40	247.517	3.726	0.0089824	0.00065 (7.8%)
55	16.06	225.934	2.056	0.0126004	0.00116 (10.1%)
60	15.39	215.672	1.508	0.0140577	0.00152 (12.1%)
62	15.12	211.632	1.350	0.0145088	0.00137 (10.4%)
66	14.58	203.711	1.155	0.0150804	0.00070 (4.9%)
70	14.04	195.994	1.133	0.0151452	0.00085 (5.9%)
75	13.37	186.694	1.369	0.0144424	0.00017 (1.2%)
77	13.10	183.028	1.553	0.0139202	0.00034 (2.4%)
80	12.70	177.683	1.925	0.0129147	0.00096 (6.9%)
85	12.03	168.946	2.829	0.0107594	0.00256 (19.2%)
90	11.35	160.345	4.133	0.0082377	0.00347 (29.6%)
100	10.01	144.118	7.962	0.0036262	0.00103 (39.7%)

[a] Back-calculated by Eq. 19. [b] Back-calculated by Eq. 21.

Figure 2 shows the three activity coefficients, log α_v, log α_R, and log α_2, which represent the van der Waals interactions between the solute and solvent, the residual term that accounts for stronger interactions, and the total solute activity coefficient, respectively. As expressed by Eq. 6, log α_2 is the sum of log α_v and log α_R. As noted in Fig. 2, log α_v is plotted using a positive vertical axis (left side), while log α_R is plotted with reference to a negative (right) axis. The positive and negative values almost balance each other so that their composite values, represented by log α_2, yield only a moderately bowed curve across the range of δ_1 values (horizontal axis). This result demonstrates that the nonregularity in mixed solvents is not large and, when contrasted to individual solvents, provides a greater possibility of predicting solubilities by back-calculation as described.

The usefulness of a theoretical approach is the ability to calculate solubilities of a drug in mixed or pure solvents, using only fundamental physicochemical properties of the solute and solvent. Unfortunately, W is not a property that is readily and accurately back-calculated by independent means. The method could be useful for predicting solubilities, however, if a procedure were found for estimating W in this range of mixed solvents. Then, with Eq. 10, the solubility of theophylline could be estimated in pure dioxane, pure water, and mixed dioxane–water solvents for which the δ_1 values were known.

When W values, obtained from Eq. 7, are plotted against δ_1, a curved line results, as shown in Fig. 3 for theophylline in dioxane–water. This curve suggests that W should be regressed against a polynomial in δ_1 for as many solutions for which accurate experimental solubilities are available. With the data of Table I, the following third-degree (cubic) equation was obtained:

$$W = 42.121367 + 9.424012\delta_1 - 0.005242\delta_1^2 + 0.008163\delta_1^3 \quad \text{(Eq. 19)}$$

The W values calculated by the cubic expression (Eq. 19) are shown in Table II and are comparable to the original W values (Table I) calculated by Eq. 7. The W values obtained from the cubic polynomial are substituted into Eq. 10 to predict the solubility of theophylline in mixed solvents. The back-calculated solubilities are recorded in Table II.

The solid line, passing through the experimental points in Fig. 1, was obtained by this procedure. The solubilities are faithfully reproduced for solvent mixtures of high δ_1 values. At the peak of the curve, the experimental points fall below the solubility predicted by the theoretical line, but the error is not great (<~12%). Solubilities represented by the points to the left of the peak values are reproduced less well than to the right of the peak. The solubilities of theophylline in pure dioxane and in pure water are predicted within an error of <40% by this method. Solubilities in these pure solvents are quite small, and this percentage error is not excessive.

The drug solubility obtained by this method is expressed in mole fraction concentration. It can be converted to molal concentration or to grams of solute per gram of solvent. Since the various solution densities are known (Table I), solubility also may be expressed in molarity or in

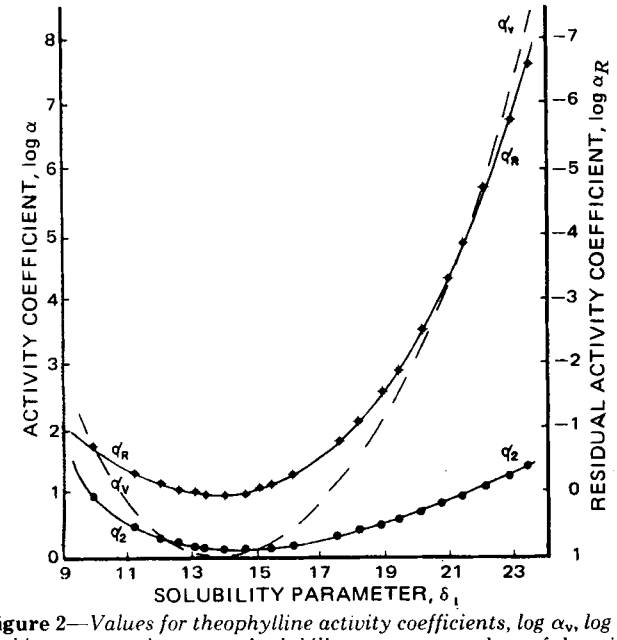

Figure 2—*Values for theophylline activity coefficients, log α_v, log α_R, and log α_2, over the range of solubility parameter values of the mixed dioxane–water solvent system. Log α_v and log α_2 are plotted with reference to the vertical axis on the left side of the figure; log α_R is plotted with reference to the right side.*

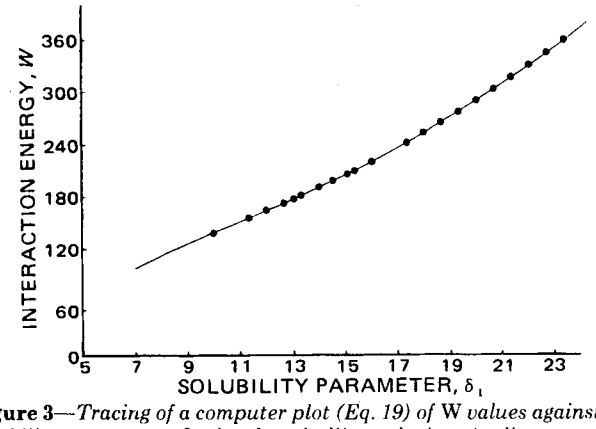

Figure 3—*Tracing of a computer plot (Eq. 19) of W values against the solubility parameter, δ_1, for theophylline solutions in dioxane–water mixtures. Points represent W values calculated from experimental solubility data using Eq. 7.*

grams of solute per liter or per milliliter of solution.

The interaction value, W, may be bypassed and log α_2/A may be back-calculated directly. The removal of W occurs by observing from Eq. 7 that:

$$2W = \delta_1^2 + \delta_2^2 - \log \alpha_2/A \qquad \text{(Eq. 20)}$$

Substituting Eq. 20 for W in Eq. 19 yields:

$$\log \alpha_2/A = 111.757266 - 18.848024\delta_1 + 1.010484\delta_1^2 - 0.016327\delta_1^3 \qquad \text{(Eq. 21)}$$

Equations 19 and 21 are analogous and yield identical results except for rounding-off errors. The back-calculated log α_2 values are found in Table II and may be compared with the original values obtained from experimental solubilities found in Table I.

This method for adapting the Hildebrand approach to polar systems has advantages and drawbacks, and certain precautions should be taken in its use. The best δ_1 values should be used for pure solvents and should be accurate to two decimal points where possible. Bagley *et al.* (28) and Nisbet (29) discussed methods for obtaining accurate solvent delta values.

Solute delta values, δ_2, and molar volumes, V_2, for solids ordinarily are not recorded in the literature and are difficult to determine. An interesting result of the new approach is that solubility predictions do not depend on the choice of δ or V of the solute. Whatever values for these quantities were used originally to obtain the W values will, of course, remain unchanged in the back-calculation and will not affect the accuracy of solubility predictions. However, the investigator must make every effort to obtain reasonable values for δ_2 and V_2 and to employ the same values each time a solubility analysis is conducted for a particular solute. The best possible δ_2 and V_2 values must be estimated and used uniformly from one laboratory to another if consistent and reproducible data are to be recorded in the literature.

CONCLUSION

The present technique is an extension of the Hildebrand method for expressing the solubility of solids in liquid solvents. It should also find use in related equilibria studies. The new method extends the Hildebrand approach from regular solutions, where van der Waals forces predominate, to irregular systems involving stronger solute–solvent interactions such as hydrogen bonding and other acid–base interactions.

The method is not a new physical theory but rather is a technique partly based on polynomial regression for back-calculating solubilities of drugs and other solutes in polar and nonpolar liquids. In a previous report (21) and in cases to be treated later, the procedure may be used to reproduce solubilities of drugs in a range of pure solvents, most satisfactorily in a particular class of solvents; however, it appears to be considerably more successful in predicting solubilities in mixed solvent systems.

REFERENCES

(1) J. H. Hildebrand, *J. Am. Chem. Soc.*, **51**, 66 (1929).

(2) H. Burrell, *Interchem. Rev.*, **14**, 31 (1955).

(3) H. Burrell, in "Polymer Handbook," J. Brandrup and E. H. Immergut, Eds., Wiley, New York, N.Y., 1975, p. IV-337.

(4) P. A. Small, *J. Appl. Chem.*, **71**, 1953.

(5) C. M. Hansen, *Ind. Eng. Chem., Prod. Res. Dev.*, **8**, 2 (1969).

(6) C. M. Hansen and A. Beerbower, in "Encyclopedia of Chemical Technology," suppl. vol., 2nd ed., A. Standen, Ed., Wiley, New York, N.Y., 1971.

(7) R. G. Blanks and J. M. Prausnitz, *Ind. Eng. Chem. Fund.*, **3**, 1 (1964).

(8) J. D. Crowley, G. S. Teague, and J. W. Lowe, *J. Paint Technol.*, **38**, 296 (1966).

(9) G. Scatchard, *Chem. Rev.*, **8**, 321 (1931).

(10) J. H. Hildebrand and R. L. Scott, "The Solubility of Nonelectrolytes," 3rd ed., Dover, New York, N.Y., 1964.

(11) J. H. Hildebrand, J. M. Prausnitz, and R. L. Scott, "Regular and Related Solutions," Van Nostrand Reinhold, New York, N.Y., 1970.

(12) M. J. Chertkoff and A. Martin, *J. Am. Pharm. Assoc., Sci. Ed.*, **49**, 444 (1960).

(13) A. Martin, J. Swarbrick, and A. Cammarata, "Physical Pharmacy," 2nd ed., Lea & Febiger, Philadelphia, Pa., 1969, chap. 12.

(14) F. A. Restaino and A. Martin, *J. Pharm. Sci.*, **53**, 636 (1964).

(15) S. A. Khalil and A. Martin, *ibid.*, **56**, 1225 (1967).

(16) S. A. Khalil, M. A. Moustafa, and O. Y. Abdullah, *Can. J. Pharm. Sci.*, **11**, 121 (1976).

(17) S. H. Yalkowsky, G. L. Flynn, and T. G. Slunick, *J. Pharm. Sci.*, **61**, 852 (1972).

(18) K. C. James, C. T. Ng, and P. R. Noyce, *ibid.*, **65**, 656 (1976).

(19) K. Hoy, B. A. Price, and R. A. Martin, "Tables of Solubility Parameters," Union Carbide, Tarrytown, N.Y., 1975.

(20) F. Weimer and J. M. Prausnitz, *Hydrocarbon Process.*, **44**, 237 (1965).

(21) A. Martin, J. Newburger, and A. Adjei, *J. Pharm. Sci.*, **68**, iv (Oct. 1979).

(22) J. H. Hildebrand, J. M. Prausnitz, and R. L. Scott, "Regular and Related Solutions," Van Nostrand Reinhold, New York, N.Y., 1970, p. 22.

(23) P. A. Schwartz and A. N. Paruta, *J. Pharm. Sci.*, **65**, 252 (1976).

(24) R. L. Scott and M. Magat, *J. Polym. Sci.*, **4**, 555 (1949).

(25) L. J. Gordon and R. L. Scott, *J. Am. Chem. Soc.*, **74**, 4138 (1952).

(26) R. F. Fedors, *Polym. Eng. Sci.*, **14**, 147 (1974).

(27) A. N. Paruta, B. J. Sciarrone, and N. G. Lordi, *J. Pharm. Sci.*, **54**, 838 (1965).

(28) E. B. Bagley, T. P. Nelson, J. W. Barlow, and S. A. Chen., *I.E.C. Fund.*, **9**, 93 (1970).

(29) K. D. Nisbet, in "Structure–Solubility Relationships in Polymers," F. W. Harris and R. B. Seymour, Eds., Academic, New York, N.Y., 1977, chap. 4.

ACKNOWLEDGMENTS

Supported in part by the endowed professorship provided to A. Martin by Mr. Coulter R. Sublett.

The authors are grateful to Dr. S. Yalkowsky, The Upjohn Co.; Dr. J. M. Prausnitz, University of California; Dr. A. Cammarata, Temple University; and P. W. M. John, University of Texas, for valuable suggestions.

Dissolution Studies of Povidone–Sulfathiazole Coacervated Systems

A. A. BADAWI ˣ and A. A. EL-SAYED

Received February 22, 1979, from the *Department of Pharmaceutics, Faculty of Pharmacy, Cairo University, Cairo, Egypt.* Accepted for publication November 20, 1979.

Abstract □ Sulfathiazole and povidone were coacervated by many methods, indicating complexation of the two compounds. The coacervated complex had a higher solubility and dissolution rate than did sulfathiazole. It resisted the action of dilute acids and alkalies, suggesting a helical structure with sulfathiazole situated between two povidone chains and a hydrogen bond linking the amino groups of the sulfathiazole to the oxygen of povidone. Upon addition of precipitants for sulfathiazole, the povidone portion attempted to compensate and to solubilize the whole complex; hence, partial precipitation or coacervation occurred. A model is given to describe the dissolution profile of the different coacervate systems prepared.

Keyphrases □ Povidone—coacervation with sulfathiazole, dissolution of coacervated system □ Sulfathiazole—coacervation with povidone, dissolution of coacervated system □ Coacervation—povidone and sulfathiazole, dissolution of coacervated system

The interaction of povidone with drugs is of theoretical and practical importance since it may influence their availability, efficacy, and transport (1).

Povidone reduced the dissolution rate of salicylic acid. This reduction was attributed to increased viscosity or to complex formation (2). When incorporated into compressed disks of ephedrine hydrochloride, potassium chloride, and sodium chloride, the polymer reduced their dissolution rates (3, 4).

However, several investigators described increases in solubility of various compounds by povidone (5, 6). A solid dispersion of reserpine, a poorly water-soluble drug, with the polymer enhanced its *in vitro* dissolution and absorption (7). A povidone–digitoxin coprecipitate exhibited enhanced dissolution and absorption, as indicated by a decrease in the LD_{50} value (8). Increased dissolution of hydroflumethiazide (9), hydrochlorothiazide (10), and ellipticine (11) was achieved by incorporation of the polymer into similar products.

Simonelli *et al.* (12, 13) described the preparation of a high energy form of sulfathiazole when it is dissolved in an alcoholic solution of povidone and evaporated to dryness or when an aqueous solution of its sodium salt and povidone is acidified. There was no explanation for the precipitation of the polymer along with the sulfathiazole, although the polymer by itself is not affected by acids. The nature of this high energy form and the mechanism of its formation were not given. Only the possible formation of a complex was reviewed.

The present study attempted to explain the coprecipitation from another viewpoint. The study was based on the facts that povidone is a linear polymer and that, when its complex with sulfathiazole is treated with acids that precipitate sulfathiazole, the whole molecule coils to form a coacervate. When dried, the coacervate droplets give colloidal particles of sulfathiazole complexed with the polymer, and a higher dissolution rate results.

In this study, sulfathiazole and povidone were mixed to form solutions. Different precipitants for sulfathiazole or for the polymer then were added separately. The products were examined microscopically to follow the development of the coacervate droplets and their transformation to solid colloidal particles.

EXPERIMENTAL

Interaction of Sulfathiazole and Povidone—*Method 1*—Sulfathiazole[1] and povidone[2] (mol. wt. 25,000), 5 g each, were dissolved in 25 ml of alcohol, which was evaporated on a water bath. When the volume was reduced to ~5 ml, a sample was taken and examined microscopically. Evaporation was continued, and a dried alcohol coacervate was obtained.

Method 2—Five grams of each of the two materials was dissolved by heating in 15 ml of alcohol. Water was added dropwise, the colloidal dispersion formed, and this precipitate coacervate was examined.

Method 3—Sulfathiazole, 5 g, was placed in a beaker, and 8 *N* NaOH was added until dissolution was complete. Povidone, 5 g, was added and dissolved by stirring. An equivalent quantity of 8 *N* HCl was added dropwise with continuous stirring to give the pH coacervate.

Method 4—Sulfathiazole, 5 g, was dissolved using an equivalent amount of 8 *N* NaOH. Povidone, 5 g, was added and dissolved by stirring. Resorcinol[1] solution, 20%, was added dropwise, and the colloidal dispersion obtained was investigated microscopically. This dispersion is referred to as the resorcinol coacervate.

Each process was repeated using different ratios of sulfathiazole and povidone. Each ratio will be described by its percent content of povidone.

Microencapsulation of Sulfathiazole—Sulfathiazole powder, 3 or 10 g, was suspended in 50 ml of 2% povidone solution. Resorcinol solution, 20%, was added dropwise with continuous stirring until complete phase separation was obtained. The microcapsules were filtered and air dried. The product was used without sieving because it was free flowing and very fine.

Separation of pH Coacervate into Its Components—Sulfathiazole, 7 g, was dissolved in 50 ml of water containing an equivalent quantity of sodium hydroxide. Povidone, 3 g, was added and dissolved by stirring. Hydrochloric acid, 5 *N*, was added dropwise with continuous stirring. When the povidone was consumed, the sticky mass that formed was withdrawn. The rest of the equivalent volume of the acid was added, and the fine particles that precipitated were filtered and dried.

Dissolution Study—Weighed quantities of each prepared sample were compressed into tablets using a single-stroke compression tablet machine[3] with a 1-cm die. The tablets were compressed to an average hardness of 5–6 kg. Each tablet was fixed to the top of a test tube with melted wax and placed at a constant level into a 600-ml beaker containing 400 ml of water as the dissolution medium.

Hydrodynamic equilibrium was established with a constant stirrer placed at a fixed distance from the tablet surface. At each time interval, a 0.5-ml aliquot was withdrawn, diluted suitably, and assayed spectrophotometrically at 283 nm.

Solubility Study—Weighed excesses of sulfathiazole and of each sample of the coacervated systems were placed in 25-ml ampuls containing 10 ml of water. The ampuls were sealed and placed on a rotating shaft (42 rpm) immersed in a water bath at 25 ± 1°. Duplicate samples were withdrawn, filtered, and assayed spectrophotometrically at 283 nm.

RESULTS AND DISCUSSION

Figure 1 shows the coacervate formed in all cases. These coacervates

[1] BP 1963.
[2] BASF (West Germany)
[3] Diaf, Copenhagen, Denmark.

0022-3549/80/0500-0492$01.00/0
© 1980, American Pharmaceutical Association

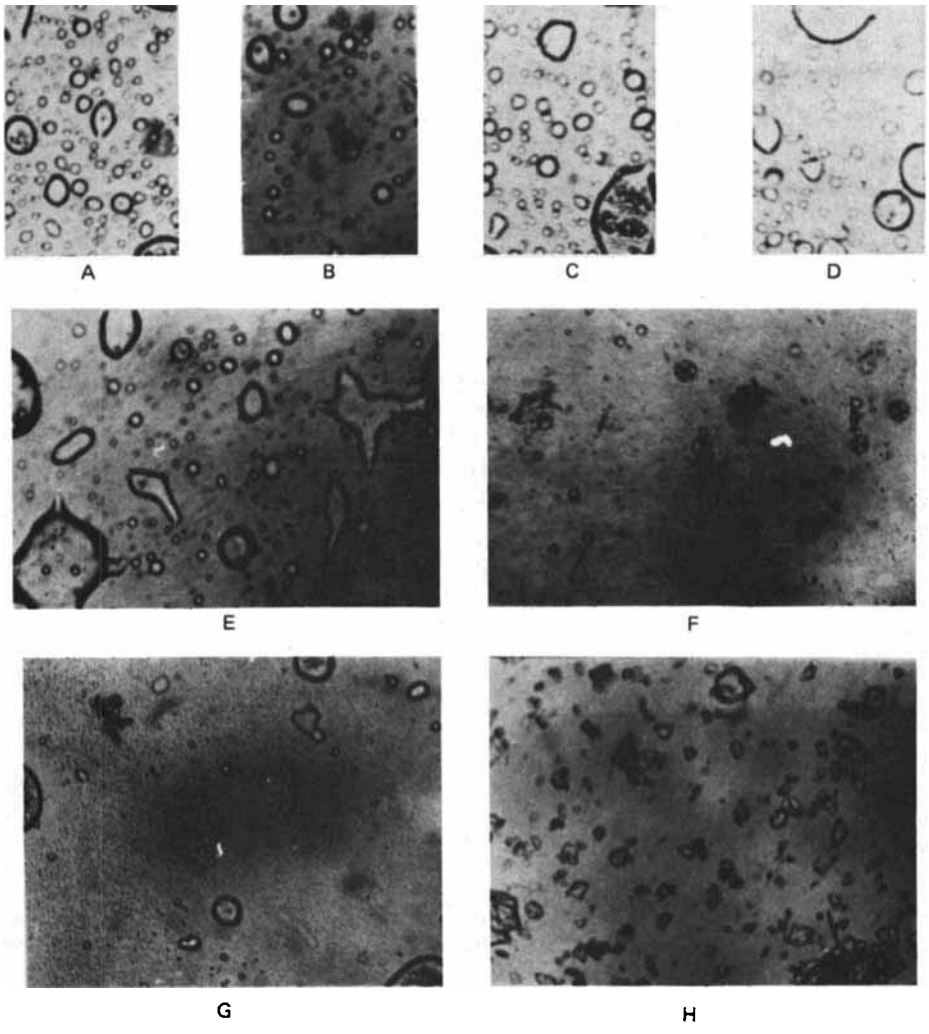

Figure 1—*Photographs (×40) of sulfathiazole–povidone coacervated systems. Key: A, alcohol coacervate; B, pH coacervate; C, precipitate coacervated; D, resorcinol coacervate; E, coalesced coacervate; F, dried coacervate; G, dried coacervate treated with water; and H, sulfathiazole precipitated with pH change.*

exhibited brownian motion. Upon continuous stirring, they coalesced into larger drops, which dried to give very fine particles. These particles were distributed in water to give spherical colloidal particles in the submicron range, which rapidly went into solution.

Coacervation can be considered as an intermediate state between true solution and complete precipitation, or it can be described as partial precipitation. When a solution of the sodium salt of sulfathiazole is treated with hydrochloric acid or when its hydrochloride salt solution is treated with sodium hydroxide, precipitation of amorphous or crystalline sulfathiazole normally occurs. On the other hand, povidone is not affected by acids or alkalis.

The coacervate formed when sulfathiazole and povidone both are present can be explained only by the interaction of povidone and sulfathiazole to form a complex with intermediate properties. Povidone retains its linear polymeric structure, which may be coacervated. Sulfathiazole still is affected by its precipitants. The povidone portion counteracts the precipitation of sulfathiazole and tries to solubilize the whole complex. The molecule thus is coiled around itself, thereby reducing its surface area that holds minimal water and reducing the total free energy of the coacervated system.

On the same basis, povidone is very soluble in both water and alcohol and does not precipitate if its solution in one solvent is treated with the other solvent. Sulfathiazole alone in its alcoholic solution precipitates as amorphous particles or as crystals when it is mixed with water. Again, the coacervate formed when the alcoholic solution of the two materials was mixed with water indicated the formation of a complex that was coacervated by the nonsolvent addition phase separation method. On the other hand, when the aqueous solution of sulfathiazole sodium and povidone was treated with resorcinol solution, which is a coacervating agent for povidone, a coacervate containing sulfathiazole was formed.

When sulfathiazole was suspended in the povidone solution and resorcinol solution was added, the coacervated povidone droplets microencapsulated the sulfathiazole particles, which, upon drying, were free flowing. The dissolution of the microcapsules was exactly the same as that of pure sulfathiazole when the coat to core ratio was 1:10 and slightly higher when the ratio was 1:3 (Fig. 2). This result indicated that the povidone did not interact with sulfathiazole when it was in the insoluble form and that the coacervated povidone microencapsulated the drug to form a protective layer. It rapidly went into solution to give sulfathiazole since the coacervation of povidone by resorcinol is reversible and since solvation of povidone occurs once the equilibrium is disturbed.

During the preparation of the pH coacervate, it was clear that the

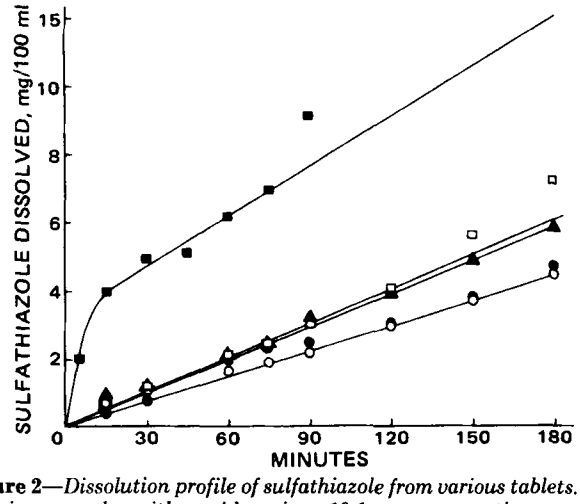

Figure 2—*Dissolution profile of sulfathiazole from various tablets. Key: ●, microcapsules with povidone in a 10:1 core-coat ratio; ▲, microcapsules of povidone in a 3:1 core-coat ratio; ■, alcohol coacervate with 20% povidone; ○, amorphous sulfathiazole; and □, physical mixture containing 20% povidone.*

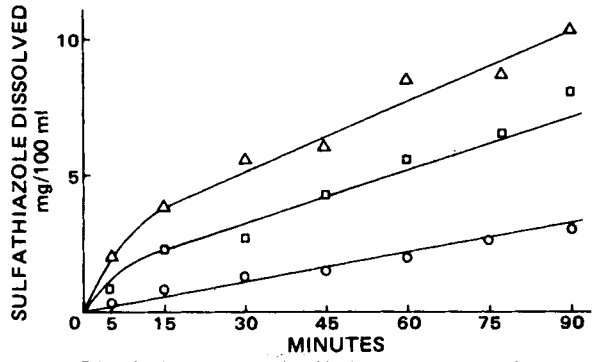

Figure 3—*Dissolution profile of sulfathiazole from a pH coacervate containing 40% povidone made with different volumes of equilibrium liquid. Key: ○, 100 ml; □, 50 ml; and △, 25 ml.*

volume of the equilibrium liquid greatly affected the product (Fig. 3). The large volume caused dissolution of the coacervated complex. Therefore, for preparation of samples for dissolution studies, 12 ml of liquid was used. However, to observe the process sequence, a volume of 50 ml was more suitable. Upon addition of hydrochloric acid by drops, coacervate droplets were formed; they coalesced into a sticky mass upon stirring. When the povidone was consumed, subsequent addition of acid caused the fine precipitated sulfathiazole particles to become enmeshed within the sticky mass. At a low povidone ratio, the sticky mass was small and the fine particles were large. With successive increases in the povidone ratio, the amount of fine particles precipitated was smaller; a homogeneous mass was obtained at 65%.

Figure 4 shows the release profile of sulfathiazole from the two components of the 30% povidone system. The fine particles gave almost the same profile as did sulfathiazole alone, and the sticky mass had a much higher dissolution rate. The mixture of the two compounds had a high initial rate and a slower terminal rate. On this basis, the release profile of sulfathiazole from its alcohol coacervates or its pH coacervates (Figs. 5–8) composed of different weight fractions of povidone could be explained easily.

This profile greatly resembled that of Simonelli *et al.* (12, 13), whose model was divided into five stages. For up to 25% povidone, amorphous

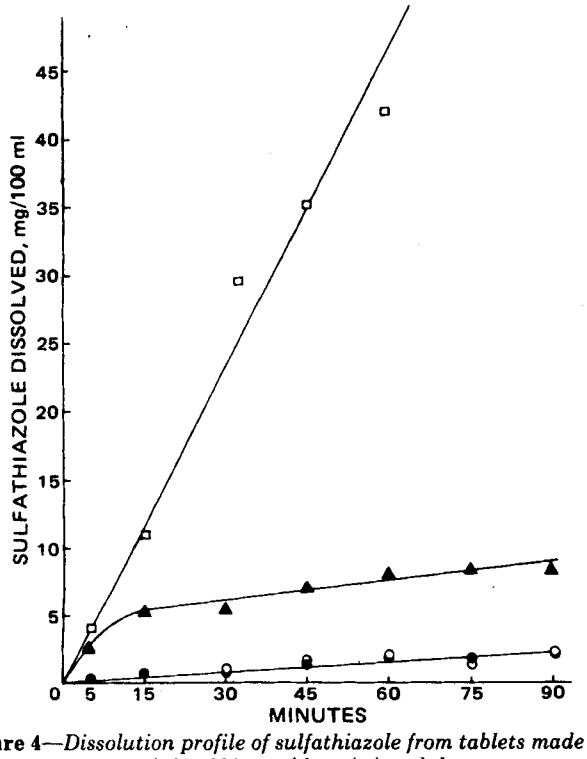

Figure 4—*Dissolution profile of sulfathiazole from tablets made of a pH coacervate containing 30% povidone (▲) and the same proportion separated into a fine powder (○) and a sticky mass (□). The dissolution profile of sulfathiazole is shown for comparison (●).*

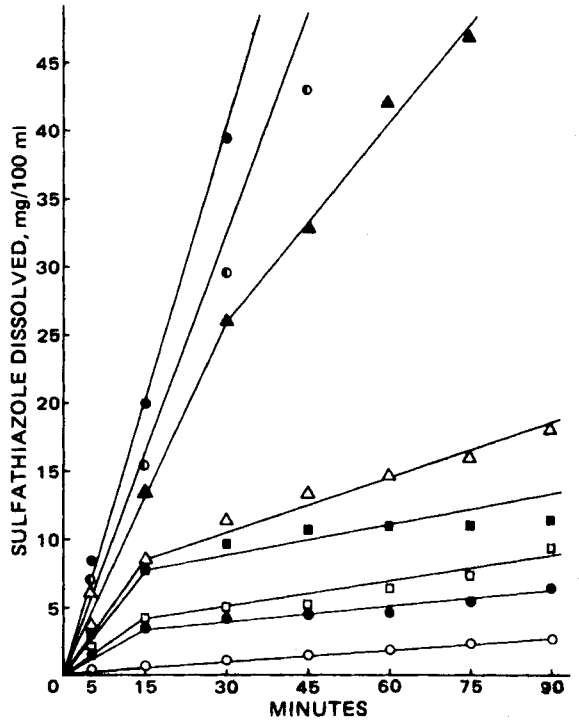

Figure 5—*Dissolution profile of sulfathiazole from tablets made of an alcohol coacervate containing low percentages of povidone. Key: ●, 10%; □, 20%; ■, 30%; △, 40%; ▲, 50%; ◐, 60%; and ⊙, 65%. The dissolution profile of sulfathiazole is shown for comparison (○).*

or unbound sulfathiazole was dissolved to leave an outer layer of crystalline Form I. From 25 to 50% povidone, amorphous sulfathiazole initially formed the outer layer, but a secondary layer of crystalline Form I eventually was formed in front of the previous amorphous layer. From

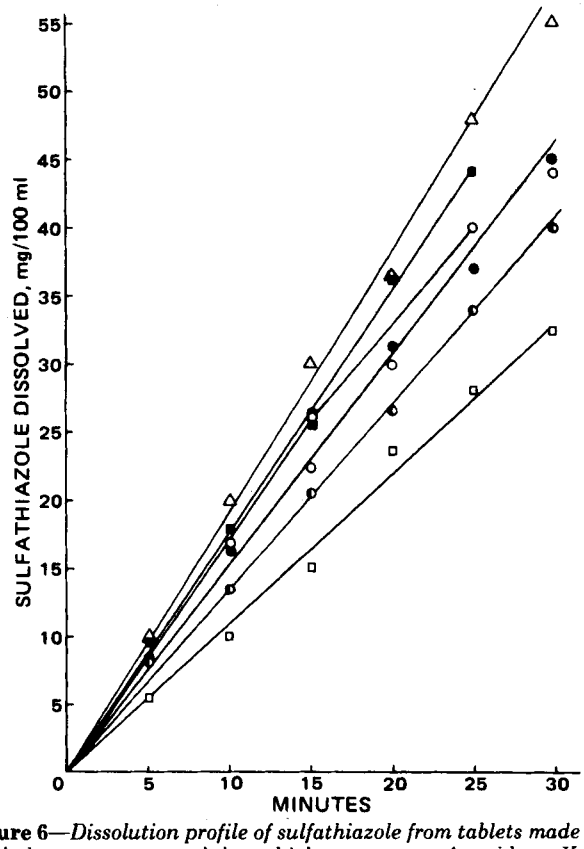

Figure 6—*Dissolution profile of sulfathiazole from tablets made of an alcohol coacervate containing a high percentage of povidone. Key: ◐, 65%; ●, 70%; ■, 75%; △, 80%; ○, 85%; and □, 90%.*

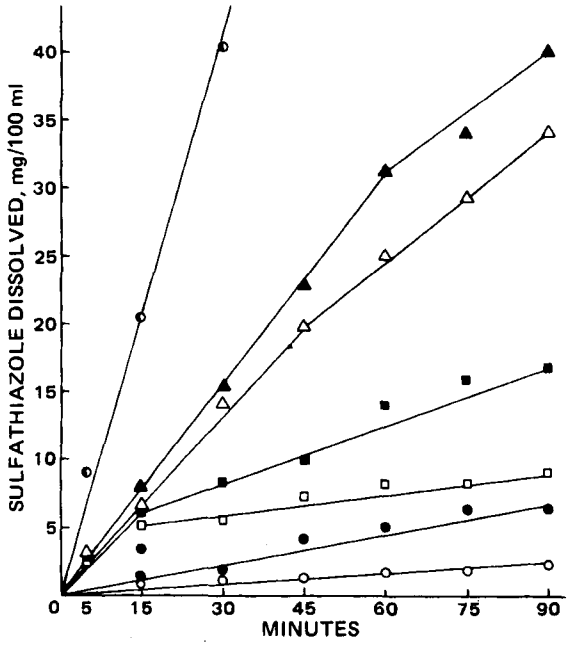

Figure 7—*Dissolution profile of sulfathiazole from tablets made of a pH coacervate containing low percentages of povidone. Key: ●, 20%; □, 30%; ■, 40%; △, 50%; ▲, 60%; and ◐, 70%. The dissolution profile of sulfathiazole is shown for comparison (○).*

50 to 77% povidone, the thickness of the amorphous sulfathiazole layer allowed the povidone to carry the sulfathiazole into solution. As the povidone weight fraction was increased from 78 to 80%, the thickness of the amorphous layer continued to decrease until it became zero. At this point, the sulfathiazole and povidone boundaries receded at the same rate, and the tablet retained the integrity of the original composition throughout the experiment. Above 80% povidone, the povidone boundary was in front and the sulfathiazole boundary moved behind.

In the present work, the dissolution medium was large enough to guard against the precipitation of crystalline Form I. However, the same stages

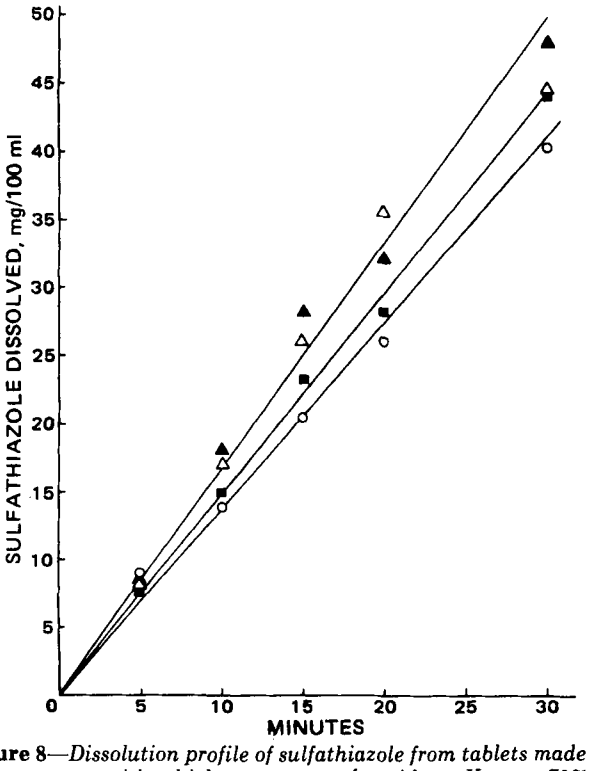

Figure 8—*Dissolution profile of sulfathiazole from tablets made of a pH coacervate with a high percentage of povidone. Key: ○, 70%; ■, 75%; △, 80%; and ▲, 85%.*

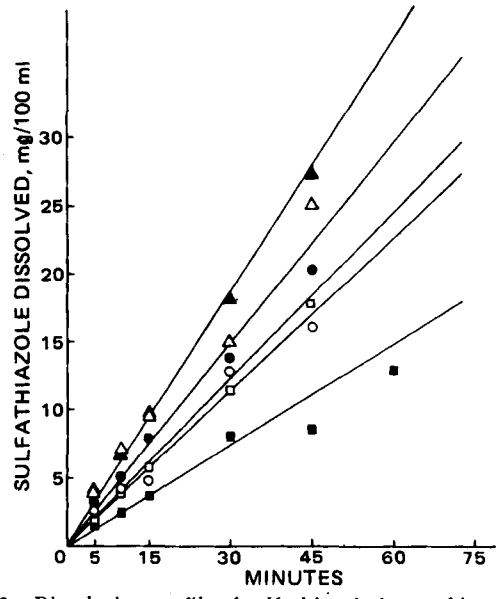

Figure 9—*Dissolution profile of sulfathiazole from tablets made of a resorcinol coacervate containing various percentages of povidone. Key: ○, 10%; ●, 20%; △, 30%; ▲, 40%; □, 50%; and ■, 60%.*

recognized in the dissolution profile (Fig. 9) can be explained by the formation of a highly soluble coacervated complex of sulfathiazole and povidone. At a low povidone content, the coacervated systems contained a lower percentage of the complex and a larger amount of free sulfathiazole. The complex rapidly went into solution, leaving behind the sulfathiazole, which was amorphous in the case of the pH coacervate and was Form I in the case of the alcohol coacervate. Table I shows good agreement between the percent content of the complex within the coacervate and its initial dissolution rate. Also, the solubility of the coacervates tested showed direct dependency on the ratio of the complex.

Increasing the ratio of povidone, *i.e.*, increasing the ratio of the complex, resulted in approachment of the initial and terminal rates. Above 60% povidone, the coacervates gave a line function whose slope increased with increasing povidone content.

From these findings, it was postulated that, in the presence of its excess, sulfathiazole interacted with povidone in the ratio of one molecule of sulfathiazole to four units of povidone; this ratio corresponded to 63.5% povidone. Above this ratio, a greater number of units of povidone participated in the interaction and many complexes were formed; the more polymer that was included, the more soluble was the coacervate. This region was described by Simonelli *et al.* (12) as the carrier region, and this description held well in the present model in which the povidone carried the complexed sulfathiazole to the dissolution medium.

Above 75% povidone, the alcohol coacervates showed a decrease in their dissolution rates, indicating that saturation of the povidone chain oc-

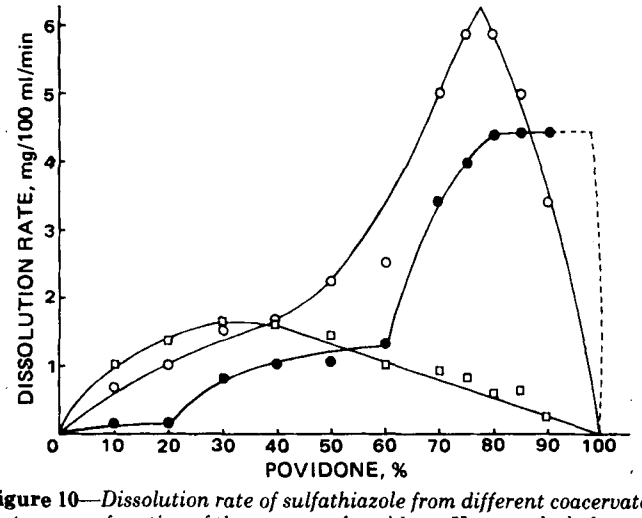

Figure 10—*Dissolution rate of sulfathiazole from different coacervate systems as a function of the percent of povidone. Key: ○, alcohol coacervate; ●, pH coacervate; and □, resorcinol coacervate.*

Table I—Relationship between the Amount of Povidone–Sulfathiazole Complex and the Initial Dissolution Rate and Solubilities of Alcohol Coacervates [a]

Amount of Povidone, %	Amount of Complexed Sulfathiazole, %	Amount of Complex (a), %	Dissolution Rate (b), mg/100 ml/min	Solubility (c) Expressed as Milligrams of Sulfathiazole per Milliliter of Water	a/b	a/c
10	5.74	15.74	0.65	—	24.22	
20	11.48	31.48	1.00	2.45	31.48	12.85
30	17.22	47.22	1.50	—	31.48	
40	22.96	62.96	1.60	5.02	39.35	12.54
50	28.70	78.70	2.25	—	34.98	
60	34.44	84.44	2.50	7.60	37.78	12.43
65	35.00	100.00	4.20	—	23.81	

[a] Solubility of sulfathiazole was 0.78 mg/ml.

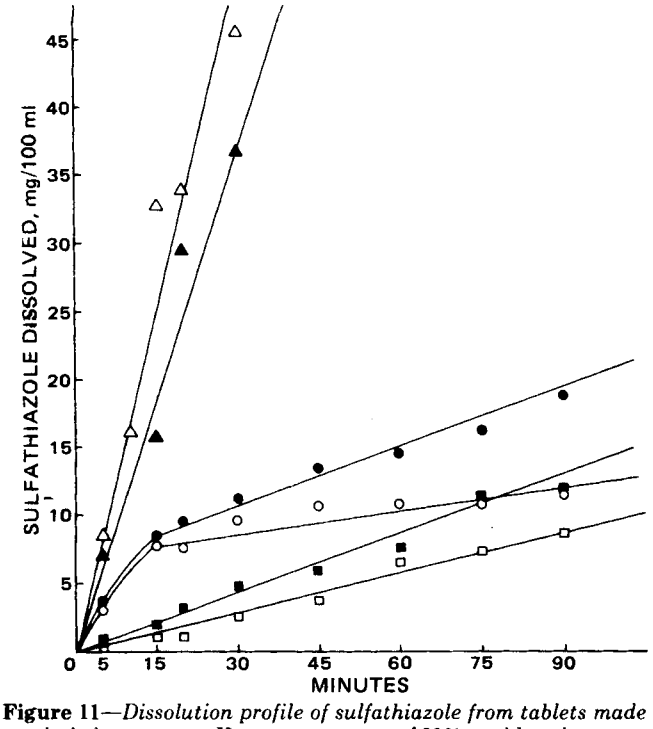

Figure 11—*Dissolution profile of sulfathiazole from tablets made of an alcohol coacervate. Key:* ○, *coacervate of 30% povidone in water;* □, *coacervate of 30% povidone in 0.05* N *HCl;* △, *coacervate of 30% povidone in 0.05* N *NaOH;* ●, *coacervate of 40% povidone in water;* ■, *coacervate of 40% povidone in 0.05* N *HCl; and* ▲, *coacervate of 40% povidone in 0.05* N *NaOH.*

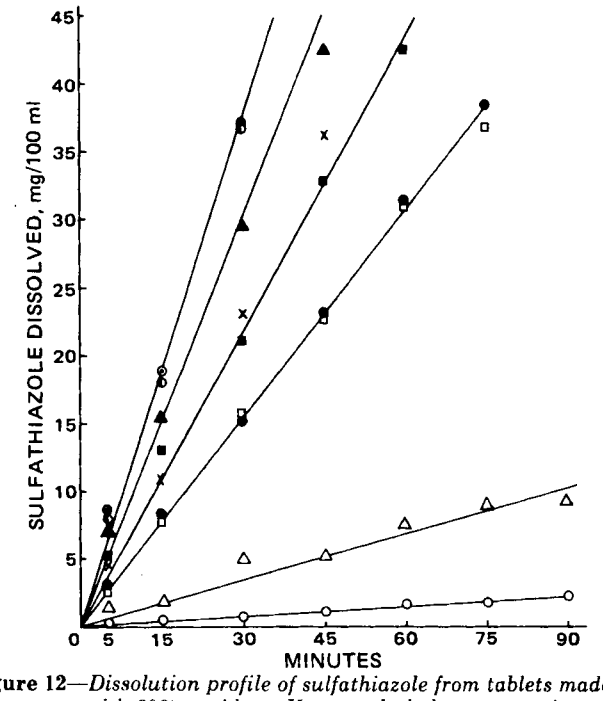

Figure 12—*Dissolution profile of sulfathiazole from tablets made of coacervates with 60% povidone. Key:* ▲, *alcohol coacervate in water;* ◐, *alcohol coacervate in 0.05* N *HCl;* ⊙, *alcohol coacervate in 0.05* N *NaOH;* ●, *pH coacervate in water;* ■, *pH coacervate in 0.05* N *HCl; and* x, *pH coacervate in 0.05* N *NaOH. The dissolution profiles for sulfathiazole tablets in water* (○), *hydrochloric acid* (△), *and sodium hydroxide* (□) *are included for comparison.*

curred at 77.7%, corresponding to eight units of povidone to each molecule of sulfathiazole. The tablet in this region was formed of two entities, the complex and excess povidone, which hindered the dissolution of the complex or its dissolution. With the pH coacervate, such a decline was not noticed. This finding was explained on the basis that the excess povidone was not precipitated with the coacervated complex.

With the resorcinol coacervate system (Fig. 10), a sudden and pronounced increase in the dissolution rate was noticed. A plateau was reached at 40% povidone, and then a linear decline occurred up to 100% povidone. This observation can be explained by the fact that, in the presence of a large excess of sulfathiazole, resorcinol coacervates a complex made of povidone with an equivalent amount of sulfathiazole, leaving its excess in solution as the sodium salt. With an increased povidone concentration, the amount of complexed sulfathiazole increases until the concentration of the two materials are equivalent; this effect yields a product with the maximal dissolution rate. With excess povidone, a mixture of the coacervated complex and coacervated povidone forms, and the access of sulfathiazole to the dissolution medium is hindered. Hence, the decline in the dissolution rate is observed.

Figure 11 shows that 0.05 *N* HCl gave slightly higher dissolution rates of pure sulfathiazole and of the alcohol coacervate containing 30 and 40% povidone. Sodium hydroxide at the same strength had a much higher effect, which was more pronounced in plain sulfathiazole than with the two coacervates. The coacervate with 30% povidone dissolved more rapidly than that with 40% povidone.

Both 60% alcohol and the pH coacervate (Fig. 12) greatly resisted the action of sodium hydroxide and hydrochloric acid. Both reagents had nearly the same dissolution rate, which was slightly higher than that of water. This result may suggest that sulfathiazole is linked by hydrogen bonds through its amino group to the oxygen of the povidone:

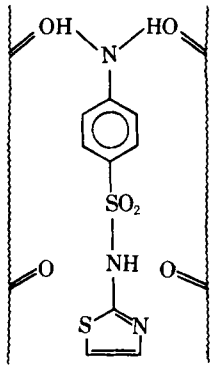

The polymer still retains its linearity; upon addition of any precipitant to sulfathiazole, the whole molecule is coiled and coacervated.

REFERENCES

(1) C. H. Hsiao, H. J. Rhodes, and M. I. Blake, *J. Pharm. Sci.*, **66**, 1157 (1977).

(2) M. Gibaldi and H. Weintraub, *ibid.*, **57**, 832 (1968).

(3) A. T. Florence and A. Rahman, *J. Pharm. Pharmacol., Suppl.*, **27**, 55 (1975).

(4) A. T. Florence, P. H. El-Worthy, and A. Rahman, *ibid.*, **25**, 779 (1973).

(5) T. Higuchi and R. J. Kuramoto, *J. Am. Pharm. Assoc., Sci. Ed.*, **43**, 393 (1954).

(6) D. Guttman and T. Higuchi, *ibid.*, **45**, 659 (1956).

(7) E. I. Stupak and T. R. Bates, *J. Pharm. Sci.*, **61**, 400 (1972).

(8) *Ibid.*, **62**, 1806 (1973).

(9) O. I. Corrigan and R. F. Timoney, *J. Pharm. Pharmacol.*, **27**, 759 (1975).

(10) O. I. Corrigan, R. F. Timoney, and M. J. Whelan, *ibid.*, **28**, 703 (1976).

(11) A. Rahman, J. C. Cradock, and J. P. Davignon, *J. Pharm. Sci.*, **67**, 611 (1978).

(12) A. P. Simonelli, S. C. Mehta, and W. I. Higuchi, *ibid.*, **65**, 355 (1976).

(13) *Ibid.*, **58**, 538 (1969).

Quantitative Structure–Activity Relationships in Drug Metabolism and Disposition: Pharmacokinetics of *N*-Substituted Amphetamines in Humans

BERNARD TESTA ˣ and BJARNE SALVESEN *

Received August 20, 1979, from the *School of Pharmacy, University of Lausanne, CH-1005 Lausanne, Switzerland.* Accepted for publication November 26, 1979. *Institute of Pharmacy, University of Oslo, Blindern, Oslo 3, Norway.

Abstract □ Pharmacokinetic data of 15 *N*-alkyl-substituted amphetamines in humans have been the object of a retrospective quantitative structure–activity relationship study. The urinary excretion of amphetamines was shown to decrease with increasing lipophilicity; the correlation equations revealed that, for identical lipophilicities, tertiary amines are excreted faster than secondary amines, which are excreted faster than primary amines. The apparent *n*-heptane–pH 7.4 buffer partition coefficient correlates better with urinary excretion than does the true *n*-octanol–water partition coefficient, probably because it includes a pKa term that accounts for the fraction of the drug present in the tubules as nonionic species. The *N*-dealkylation rate increases with increasing lipophilicity of the substrates (enhanced enzyme affinity) but decreases with increasing bulk of the *N*-substituent that is split off (steric hindrance of initial C_α-hydroxylation).

Keyphrases □ Quantitative structure–activity relationships—*N*-substituted amphetamines, pharmacokinetics, humans □ Amphetamines, *N*-substituted—pharmacokinetics, quantitative structure–activity relationships, humans □ Pharmacokinetics—*N*-substituted amphetamines, quantitative structure–activity relationships, humans

Quantitative structure–activity relationships have many pharmacological and toxicological applications. The correlation equations obtained in such studies often provide valuable steps in the rational design of improved drugs (1).

Suitable results of drug metabolism studies also can provide a valuable biological input to quantitative structure–activity relationship studies. While the results thus obtained could help in designing drugs with improved metabolic profiles, previous investigations (2–5) concentrated entirely on interpreting the correlation equations in terms of reaction mechanisms and of the structural factors influencing the biological response.

One prerequisite of any quantitative structure–activity relationship investigation is the need for quantitative and reliable biological data. This fact may help to explain why applications of quantitative structure–activity relationships to drug metabolism and disposition have been based almost exclusively on results from *in vitro* studies (*e.g.*, protein binding, drug–enzyme interactions, and parameters of *in vitro* biotransformation). In contrast, few, if any, *in vivo* studies have led to successful quantitative structure–activity relationship interpretations.

The present report describes the application of quantitative structure–activity relationship methodology to the results of a pharmacokinetic study of *N*-alkyl-substituted amphetamine derivatives in humans (6). The thoroughness of the work of the previous investigators, the quantitative nature of results, the number (15) of molecules investigated, and the large spread in the biological responses made this study an attractive candidate for a quantitative interpretation in terms of molecular properties. Furthermore, the previous investigators measured the apparent

Table I—Physicochemical and Structural Parameters of Amphetamine and Derivatives

	Compound	Log P_H[a]	$f_{RR'}$[b]	V_R[c]	NH[d]	$C_\alpha H$[e]
I	Amphetamine	−2.26	0.94	—	2	—
II	*N*-Methyl	−1.51	1.17	13.67	1	3
III	*N*-Ethyl	−0.92	1.69	23.90	1	2
IV	*N*-*n*-Propyl	−0.20	2.21	34.13	1	2
V	*N*-2-Propyl	−0.41	2.21	34.12	1	1
VI	*N*-*n*-Butyl	−0.32	2.73	44.36	1	2
VII	*N*-2-Butyl	0.07	2.73	44.35	1	1
VIII	*N*-Benzyl	3.18	2.83	56.07	1	2
IX	*N*,*N*-Dimethyl	−0.27	1.40	13.67	0	3
X	*N*,*N*-Diethyl	0.58	2.44	23.90	0	2
XI	*N*,*N*-Di-*n*-propyl	2.38	3.48	34.13	0	2
XII	*N*,*N*-Di-*n*-butyl	3.83	4.52	44.36	0	2
XIII	*N*-Ethyl-*N*-methyl	−0.09	1.92	13.67[f]	0	3[f]
				23.90[g]		2[g]
XIV	*N*-Methyl-*N*-*n*-propyl	0.45	2.44	13.67[f]	0	3[f]
				34.13[g]		2[g]
XV	*N*-*n*-Butyl-*N*-methyl	1.44	2.96	13.67[f]	0	3[f]
				44.36[g]		2[g]

[a] P_H is the apparent *n*-heptane–water partition coefficient measured at pH 7.4 (6). [b] Hydrophobic fragmental constant of the two nitrogen substituents (hydrogen and/or alkyl) (7). [c] Volume in milliliters per mole of substituent that is cleaved by *N*-dealkylation, calculated according to Bondi (9). [d] Number of hydrogen atoms on the nitrogen. [e] Number of hydrogen atoms on the α-carbon of substituent that is cleaved by *N*-dealkylation. [f] *N*-Methyl group. [g] *N*-Alkyl group.

0022-3549/80/0500-0497$01.00/0

© 1980, American Pharmaceutical Association

The polymer still retains its linearity; upon addition of any precipitant to sulfathiazole, the whole molecule is coiled and coacervated.

REFERENCES

(1) C. H. Hsiao, H. J. Rhodes, and M. I. Blake, *J. Pharm. Sci.*, **66**, 1157 (1977).

(2) M. Gibaldi and H. Weintraub, *ibid.*, **57**, 832 (1968).

(3) A. T. Florence and A. Rahman, *J. Pharm. Pharmacol., Suppl.*, **27**, 55 (1975).

(4) A. T. Florence, P. H. El-Worthy, and A. Rahman, *ibid.*, **25**, 779 (1973).

(5) T. Higuchi and R. J. Kuramoto, *J. Am. Pharm. Assoc., Sci. Ed.*, **43**, 393 (1954).

(6) D. Guttman and T. Higuchi, *ibid.*, **45**, 659 (1956).

(7) E. I. Stupak and T. R. Bates, *J. Pharm. Sci.*, **61**, 400 (1972).

(8) *Ibid.*, **62**, 1806 (1973).

(9) O. I. Corrigan and R. F. Timoney, *J. Pharm. Pharmacol.*, **27**, 759 (1975).

(10) O. I. Corrigan, R. F. Timoney, and M. J. Whelan, *ibid.*, **28**, 703 (1976).

(11) A. Rahman, J. C. Cradock, and J. P. Davignon, *J. Pharm. Sci.*, **67**, 611 (1978).

(12) A. P. Simonelli, S. C. Mehta, and W. I. Higuchi, *ibid.*, **65**, 355 (1976).

(13) *Ibid.*, **58**, 538 (1969).

Quantitative Structure–Activity Relationships in Drug Metabolism and Disposition: Pharmacokinetics of *N*-Substituted Amphetamines in Humans

BERNARD TESTA ˣ and BJARNE SALVESEN *

Received August 20, 1979, from the *School of Pharmacy, University of Lausanne, CH-1005 Lausanne, Switzerland.* Accepted for publication November 26, 1979. *Institute of Pharmacy, University of Oslo, Blindern, Oslo 3, Norway.

Abstract □ Pharmacokinetic data of 15 *N*-alkyl-substituted amphetamines in humans have been the object of a retrospective quantitative structure–activity relationship study. The urinary excretion of amphetamines was shown to decrease with increasing lipophilicity; the correlation equations revealed that, for identical lipophilicities, tertiary amines are excreted faster than secondary amines, which are excreted faster than primary amines. The apparent *n*-heptane–pH 7.4 buffer partition coefficient correlates better with urinary excretion than does the true *n*-octanol–water partition coefficient, probably because it includes a pKa term that accounts for the fraction of the drug present in the tubules as nonionic species. The *N*-dealkylation rate increases with increasing lipophilicity of the substrates (enhanced enzyme affinity) but decreases with increasing bulk of the *N*-substituent that is split off (steric hindrance of initial C_α-hydroxylation).

Keyphrases □ Quantitative structure–activity relationships—*N*-substituted amphetamines, pharmacokinetics, humans □ Amphetamines, *N*-substituted—pharmacokinetics, quantitative structure–activity relationships, humans □ Pharmacokinetics—*N*-substituted amphetamines, quantitative structure–activity relationships, humans

Quantitative structure–activity relationships have many pharmacological and toxicological applications. The correlation equations obtained in such studies often provide valuable steps in the rational design of improved drugs (1).

Suitable results of drug metabolism studies also can provide a valuable biological input to quantitative structure–activity relationship studies. While the results thus obtained could help in designing drugs with improved metabolic profiles, previous investigations (2–5) concentrated entirely on interpreting the correlation equations in terms of reaction mechanisms and of the structural factors influencing the biological response.

One prerequisite of any quantitative structure–activity relationship investigation is the need for quantitative and reliable biological data. This fact may help to explain why applications of quantitative structure–activity relationships to drug metabolism and disposition have been based almost exclusively on results from *in vitro* studies (*e.g.*, protein binding, drug–enzyme interactions, and parameters of *in vitro* biotransformation). In contrast, few, if any, *in vivo* studies have led to successful quantitative structure–activity relationship interpretations.

The present report describes the application of quantitative structure–activity relationship methodology to the results of a pharmacokinetic study of *N*-alkyl-substituted amphetamine derivatives in humans (6). The thoroughness of the work of the previous investigators, the quantitative nature of results, the number (15) of molecules investigated, and the large spread in the biological responses made this study an attractive candidate for a quantitative interpretation in terms of molecular properties. Furthermore, the previous investigators measured the apparent

Table I—Physicochemical and Structural Parameters of Amphetamine and Derivatives

	Compound	Log P_H[a]	$f_{RR'}$[b]	V_R[c]	NH[d]	$C_\alpha H$[e]
I	Amphetamine	−2.26	0.94	—	2	—
II	*N*-Methyl	−1.51	1.17	13.67	1	3
III	*N*-Ethyl	−0.92	1.69	23.90	1	2
IV	*N*-*n*-Propyl	−0.20	2.21	34.13	1	2
V	*N*-2-Propyl	−0.41	2.21	34.12	1	1
VI	*N*-*n*-Butyl	−0.32	2.73	44.36	1	2
VII	*N*-2-Butyl	0.07	2.73	44.35	1	1
VIII	*N*-Benzyl	3.18	2.83	56.07	1	2
IX	*N*,*N*-Dimethyl	−0.27	1.40	13.67	0	3
X	*N*,*N*-Diethyl	0.58	2.44	23.90	0	2
XI	*N*,*N*-Di-*n*-propyl	2.38	3.48	34.13	0	2
XII	*N*,*N*-Di-*n*-butyl	3.83	4.52	44.36	0	2
XIII	*N*-Ethyl-*N*-methyl	−0.09	1.92	13.67[f]	0	3[f]
				23.90[g]		2[g]
XIV	*N*-Methyl-*N*-*n*-propyl	0.45	2.44	13.67[f]	0	3[f]
				34.13[g]		2[g]
XV	*N*-*n*-Butyl-*N*-methyl	1.44	2.96	13.67[f]	0	3[f]
				44.36[g]		2[g]

[a] P_H is the apparent *n*-heptane–water partition coefficient measured at pH 7.4 (6). [b] Hydrophobic fragmental constant of the two nitrogen substituents (hydrogen and/or alkyl) (7). [c] Volume in milliliters per mole of substituent that is cleaved by *N*-dealkylation, calculated according to Bondi (9). [d] Number of hydrogen atoms on the nitrogen. [e] Number of hydrogen atoms on the α-carbon of substituent that is cleaved by *N*-dealkylation. [f] *N*-Methyl group. [g] *N*-Alkyl group.

0022-3549/80/0500-0497$01.00/0

© 1980, American Pharmaceutical Association

Table II—Percent of Amphetamine Derivatives Excreted Unchanged (PEU): Experimental *versus* Calculated Values

	Log PEU								
	Subject 1			Subject 2			Subject 3		
Derivative	Exp.[a]	Calc.[b]	Residual	Exp.[a]	Calc.[c]	Residual	Exp.[a]	Calc.[d]	Residual
I	1.78	1.82	−0.04	1.76	1.84	−0.08	1.79	2.11	−0.32
II	1.83	1.78	0.05	1.79	1.77	0.02	1.69	1.72	−0.03
III	1.68	1.68	0.00	1.66	1.66	0.00	1.16	1.42	−0.26
IV	1.51	1.50	0.01	1.49	1.47	0.02	1.08	1.05	0.03
V	1.59	1.56	0.03	1.60	1.53	0.07	1.35	1.15	0.20
VI	0.87	1.31[e]	−0.44	0.76	1.28[e]	−0.52	0.29	0.78	−0.49
VII	1.28	1.41	−0.13	1.34	1.38	−0.04	1.10	0.91	0.19
VIII	−0.23	−0.45	0.22	−0.27	−0.33	0.06	−0.78	−0.70	−0.08
IX	1.59	1.52	0.07	1.61	1.49	0.12	1.33	1.08	0.25
X	1.60	1.20	0.40	1.44	1.18	0.26	1.29	0.64[e]	0.65
XI	0.25	0.17	0.08	0.17	0.22	−0.05	−0.28	−0.29	0.01
XII	−1.16	−1.02	−0.14	−0.82	−0.85	0.03	−1.12	−1.04	−0.08
XIII	1.54	1.46	0.08	1.58	1.43	0.15	1.18	0.99	0.19
XIV	1.38	1.26	0.12	1.40	1.23	0.17	0.87	0.71	0.16
XV	0.47	0.77	−0.30	0.57	0.78	−0.21	−0.21	0.20	−0.41

[a] Data from Ref. 6. [b] Calculated according to Eq. 2. [c] Calculated according to Eq. 6. [d] Calculated according to Eq. 9. [e] Outlier (outside ±2 *SD*).

Table III—Rate Constant of Excretion (EXC) in Hours^{-1} of Amphetamine Derivatives: Experimental *versus* Calculated Values

	Log EXC								
	Subject 1			Subject 2			Subject 3		
Derivative	Exp.[a]	Calc.[b]	Residual	Exp.[a]	Calc.[c]	Residual	Exp.[a]	Calc.[d]	Residual
I	−1.17	−1.14	−0.03	−1.10	−1.00	−0.10	−1.09	−1.20	0.11
II	−1.15	−1.02	−0.13	−1.04	−0.93	−0.11	−1.14	−1.18	0.04
III	−1.15	−1.22	0.07	−1.12	−1.18	0.06	−1.55	−1.42	−0.13
IV	−1.31	−1.46	0.15	−1.28	−1.47	0.19	−1.86	−1.71	−0.15
V	−1.27	−1.39	0.12	−1.28	−1.39	0.11	−1.47	−1.63	0.16
VI	−1.75	−1.63	−0.12	−1.89	−1.69	−0.20	−2.33	−1.93	−0.40
VII	−1.59	−1.55	−0.04	−1.54	−1.58	0.04	−1.68	−1.82	0.14
VIII	−2.61	−2.58	−0.03	−2.76	−2.86	0.10	−3.07	−3.10	0.03
IX	−1.17	−1.07	−0.10	−1.16	−1.07	−0.09	−1.41	−1.36	0.05
X	−1.19	−1.35	0.16	−1.37	−1.42	0.05	−1.38	−1.71	0.33
XI	−2.36	−1.95[e]	−0.41	−1.55	−2.16[e]	0.61	−2.79	−2.44	−0.35
XII	—[f]	—	—	−3.20	−2.76	−0.44	—[f]	—	—
XIII	−1.28	−1.13	−0.15	−1.16	−1.15	−0.01	−1.55	−1.43	−0.12
XIV	−1.32	−1.31	−0.01	−1.34	−1.37	0.03	−1.79	−1.65	−0.14
XV	−2.04	−1.64[e]	−0.40	−2.03	−1.78	−0.25	−2.72	−2.06[e]	−0.66

[a] Data from Ref. 6. [b] Calculated according to Eq. 12. [c] Calculated according to Eq. 15. [d] Calculated according to Eq. 18. [e] Outlier (outside ±2 *SD*). [f] Data not available.

partition coefficient of their compounds and established graphical correlations for limited subsets of observations.

EXPERIMENTAL

Table I lists the 15 molecules investigated. Two parameters are used as a measure of lipophilicity: (*a*) the apparent *n*-heptane–water partition coefficient measured at pH 7.4 (6), and (*b*) the sum of the hydrophobic fragmental constants of the two nitrogen substituents (hydrogen and/or alkyl) (7). The latter parameter represents the incremental contributions of molecular fragments to the true *n*-octanol–water partition coefficient (8).

The degree of substitution on the nitrogen atom (primary, secondary, or tertiary) is taken into account by the structural descriptor NH, *i.e.*, the number of hydrogen atoms on the nitrogen. Two parameters specifically consider the *N*-alkyl substituent that is cleaved from the molecule: the volume of the substituent, calculated according to Bondi (9), and the number of hydrogen atoms on the α-carbon.

Donike *et al.* (6) determined three biological responses that are valuable parameters in this study. They are: (*a*) the cumulative urinary excretion of unchanged drug expressed as the percent of the administered dose [percent excreted unchanged (PEU)]; (*b*) the rate constant of urinary excretion, EXC, in hours^{-1}; and (*c*) the rate constant of the first *N*-dealkylation step, DEA, in hours^{-1}.

Three subjects were used in the study of Donike *et al.* (6). Subjects 1 and 2 were kept under acidic urinary control by ingestion of ammonium chloride (urinary pH values were 5.0–5.2 and 4.9–5.1, respectively). The urinary pH of Subject 3 was not controlled and was comparatively higher (5.4–5.7). The individual values of log PEU, log EXC, and log DEA for Subjects 1–3 are reported in Tables II–IV. These data provided the input for the dependent variables in the present calculations.

The multiple linear regression analyses were performed on a computer[1] using the SPSS program (10) with a stepwise method. The program calculates the regression coefficients of all independent variables and their standard deviation (given in parentheses) and the constant term (intercept). The statistics performed include the squared multiple correlation coefficient, r^2, the standard deviation of the equation, *s*, and the *F* test. Testing the null hypotheses for each regression coefficient individually is done by the Student *t* test; these values are not reported here, but all variables included in Eqs. 1–28 are significant at the probability level of 0.05 or better.

Table V gives the correlation matrixes for 15 observations (Eqs. 1–19) and for 17 observations (Eqs. 20–28).

RESULTS AND DISCUSSION

Cumulative Urinary Excretion of Unchanged Drugs—The significant correlation equations derived for log PEU are shown in Table VI, revealing that this biological response depends heavily on the lipophilicity of the molecules as assessed by the apparent *n*-heptane–water partition coefficient (Eqs. 1, 5, and 9). These equations indicate that the total excretion of unchanged drug increases with decreasing log P_H; *i.e.*, high hydrophilicity favors fast excretion and limited biotransformation. This linear correlation can be improved by the inclusion of a squared term to yield parabolic equations (Eqs. 2 and 6). The optimal log P_H value thus determined is that of amphetamine for Subject 1, while the value for Subject 2 is that of a hypothetical derivative somewhat more hydrophilic than amphetamine.

However, Eqs. 2 and 6 are not truly meaningful from a physical point of view. It is reasonable to expect that hypothetical derivatives that are

[1] Cyber, CDC, Federal Institute of Technology and the University of Lausanne

Table IV—Rate Constant of First *N*-Dealkylation Step (DEA) in Hours^{-1} of Amphetamine Derivatives: Experimental *versus* Calculated Values

	Log DEA								
	Subject 1			Subject 2			Subject 3		
Derivative	Exp.[a]	Calc.[b]	Residual	Exp.[a]	Calc.[c]	Residual	Exp.[a]	Calc.[d]	Residual
II	−2.07	−1.83	−0.24	−1.84	−1.97	0.14	−1.90	−1.62	−0.28
III	−1.76	−1.82	0.06	−1.69	−1.80	0.11	−1.94	−1.69	−0.25
IV	−1.69	−1.77	0.08	−1.51	−1.63	0.12	−1.69	−1.73	0.04
V	−1.69	−1.82	0.13	−1.66	−1.63	−0.03	−1.63	−1.80	0.17
VI	−1.45	−1.77[e]	0.32	−1.53	−1.46	−0.07	−1.70	−1.83	0.13
VII	−1.82	−1.84	0.02	−1.71	−1.46	−0.25	−1.58	−1.91	0.33
VIII	−1.15	−1.15	0.00	−1.49	−1.64	0.15	−1.25	−1.27	0.02
IX	−1.63	−1.48	−0.15	−1.57	−1.80	0.23	−1.34	−1.25	−0.09
X	−1.20	−1.39	0.19	−1.26	−1.24	−0.02	−0.81	−1.25[e]	0.44
XI	−0.78	−1.04	0.26	−0.74	−0.68	−0.06	−0.80	−0.96	0.16
XII	—[f]	—	—	0.30	−0.12[e]	0.42	—[f]	—	—
XIII[g]	−1.61	−1.43	−0.18	−1.52	−1.41	−0.11	−1.25	−1.19	−0.06
XIII[h]	−1.70	−1.58	−0.12	−1.55	−1.63	0.08	−1.56	−1.45	−0.11
XIV[g]	−1.04	−1.28	0.24	−1.16	−1.03	−0.13	−0.79	−1.03	0.24
XIV[h]	−1.50	−1.58	0.08	−1.53	−1.46	−0.07	−1.42	−1.54	0.12
XV[g]	−0.94	−1.00	0.06	−0.82	−0.64	−0.18	−0.80	−0.74	−0.06
XV[h]	−1.54	−1.46	−0.08	−1.64	−1.29	−0.35	−1.69	−1.50	−0.19

[a] Data from Ref. 6. [b] Calculated according to Eq. 20. [c] Calculated according to Eq. 24. [d] Calculated according to Eq. 26. [e] Outlier (outside ±2 *SD*). [f] Data not available. [g] *N*-Demethylation. [h] *N*-Dealkylation.

Table V—Correlation Matrix for 15 Observations[a] (Eqs. 1–19)

	$(\text{Log P}_H)^2$	Log P_H	$f_{RR'}$	V_R	$C_\alpha H$	NH	Log PEU_1	Log PEU_2	Log PEU_3	Log EXC_1	Log EXC_2	Log EXC_3	Log DEA_1	Log DEA_2
Log P_H	0.69	—	—	—	—	—	—	—	—	—	—	—	—	—
	0.84													
$f_{RR'}$	0.58	0.91	—	—	—	—	—	—	—	—	—	—	—	—
	0.71	*0.89*												
V_R	0.53	0.55	0.58	—	—	—	—	—	—	—	—	—	—	—
	0.49	*0.56*	*0.59*											
$C_\alpha H$	−0.08	−0.11	−0.32	−0.74	—	—	—	—	—	—	—	—	—	—
	−0.06	*−0.11*	*−0.30*	*−0.72*										
NH	−0.03	−0.54	−0.49	0.48	−0.53	—	—	—	—	—	—	—	—	—
	−0.07	*−0.33*	*−0.27*	*0.36*	*−0.43*									
Log PEU_1	−0.85	−0.93	−0.88	−0.58	0.11	0.33	–	–	–	–	–	–	–	–
	−0.90	*−0.95*	*−0.89*	*−0.59*	*0.10*	*0.19*								
Log PEU_2	−0.83	−0.94	−0.87	−0.62	0.13	0.31	0.99	—	—	—	—	—	—	—
	−0.89	*−0.96*	*−0.88*	*−0.62*	*0.11*	*0.16*	*0.99*							
Log PEU_3	−0.74	−0.95	−0.87	−0.56	0.06	0.38	0.97	0.98	—	—	—	—	—	—
	−0.81	*−0.94*	*−0.86*	*−0.59*	*0.06*	*0.21*	*0.97*	*0.98*						
Log EXC_1	−0.71	−0.88	−0.77	−0.58	0.13	0.14	0.99	0.99	0.96	—	—	—	—	—
	−0.82	*−0.91*	*−0.80*	*−0.60*	*0.12*	*0.01*	*0.99*	*0.97*	*0.96*					
Log EXC_2	−0.81	−0.88	−0.81	−0.65	0.16	0.21	0.95	0.94	0.92	0.88	—	—	—	—
	−0.86	*−0.89*	*−0.82*	*−0.65*	*0.15*	*0.06*	*0.95*	*0.95*	*0.92*	*0.88*				
Log EXC_3	−0.55	−0.90	−0.82	−0.52	0.05	0.25	0.97	0.96	0.99	0.95	0.87	—	—	—
	−0.70	*−0.90*	*−0.82*	*−0.56*	*0.05*	*0.08*	*0.98*	*0.96*	*0.99*	*0.96*	*0.88*			
Log DEA_1	0.45	0.83	0.78	0.06	0.17	−0.61	−0.71	−0.72	−0.75	−0.66	−0.53	−0.73	—	—
	0.46	*0.80*	*0.74*	*0.06*	*0.18*	*−0.48*	*−0.67*	*−0.69*	*−0.69*	*−0.63*	*−0.51*	*−0.67*		
Log DEA_2	0.73	0.80	0.86	0.17	0.07	−0.61	−0.81	−0.78	−0.76	−0.54	−0.70	−0.62	0.93	—
	0.73	*0.76*	*0.81*	*0.12*	*0.10*	*−0.47*	*−0.77*	*−0.74*	*−0.69*	*−0.47*	*−0.66*	*−0.52*	*0.92*	
Log DEA_3	0.23	0.65	0.58	−0.22	0.31	−0.84	−0.44	−0.43	−0.45	−0.39	−0.29	−0.41	0.88	0.86
	0.23	*0.58*	*0.50*	*−0.26*	*0.33*	*−0.65*	*−0.36*	*−0.37*	*−0.36*	*−0.32*	*−0.22*	*−0.32*	*0.87*	*0.87*

[a] The italicized numbers are the correlation matrix for 17 observations (Eqs. 20–28).

markedly more hydrophilic than amphetamine will simply be excreted totally unchanged (log PEU = 2.0); in this region, a plot of log P_H *versus* log PEU should be a horizontal line, and the true nature of the mathematical relationship can be envisioned as a bilinear function. However, testing of this hypothesis is not feasible due to a lack of suitable observations. In any case, extrapolation of Eqs. 2 and 6 to hypothetical compounds that are more hydrophilic than amphetamine is misleading.

For Subject 3, the inclusion of a squared term is not significant, indicating that the lack of urinary pH control alters not only the magnitude of excretion but apparently also the nature of the mathematical relationship between elimination and lipophilicity.

Equations 3 and 7 explore another aspect of the structure–activity relationships: total excretion of unchanged drug increases with the number of *N*-substituents once the lipophilicity of the molecules is accounted for by the log P_H term. The correlation between log PEU and NH alone is positive (Table V), but Eqs. 3 and 7 indicate that, for identical lipophilicities, tertiary amines are excreted faster and are less metabolized than are secondary amines. However, such a relationship holds only in the case of urinary pH control, with the inclusion of the NH parameter being nonsignificant for Subject 3.

Replacement of log P_H by $f_{RR'}$, a measure of the *n*-octanol–water partition coefficient of the nonprotonated bases, to yield Eqs. 4, 8, and 10 results in less favorable statistics, as evidenced by smaller r^2 values, and considerably larger standard deviations. Also, the inclusion of any other variable in Eqs. 4, 8, and 10 is nonsignificant.

The better correlations displayed by log P_H as compared to $f_{RR'}$ probably is due to the fact the log P_H includes a pKa term, thus accounting for the fraction of drug present in the tubules as nonionic species. This fraction is no less important than the lipophilicity of the neutral form in influencing the urinary excretion of amphetamines.

The best equations for log PEU_i are Eqs. 2, 6, and 9. A comparison of experimental and calculated log PEU_i values is given in Table II.

Rate Constant of Urinary Excretion—The significant correlation equations obtained for log EXC are given in Table VII. As with the previous examples, this biological response is mainly dependent on lipophilicity. Equations 11, 14, and 17 show that the rate of excretion increases with decreasing log P_H, confirming that high hydrophilicity favors fast excretion, presumably due to minimal tubular reabsorption. The relationship is linear, with the parabolic equations being nonsignificant.

Table VI—Correlation Equations for Log PEU (Percent Excreted Unchanged) in Subjects 1–3

Equation	Dependent Variable	$(\text{Log } P_H)^2$	Log P_H	NH	$f_{RR'}$	Intercept	n	r^2	s	F
1	Log PEU_1	—	−0.486 (±0.057)	—	—	1.28 (±0.09)	15	0.868	0.330	72.2
2[a]	Log PEU_1	−0.0771 (±0.0201)	−0.345 (±0.053)	—	—	1.43 (±0.07)	15	0.947	0.220	88.7
3	Log PEU_1	—	−0.556 (±0.058)	−0.342 (±0.153)	—	1.51 (±0.13)	15	0.912	0.283	51.7
4	Log PEU_1	—	—	—	−0.829 (±0.137)	3.04 (±0.35)	15	0.770	0.435	36.7
5	Log PEU_2	—	−0.458 (±0.050)	—	—	1.27 (±0.08)	15	0.886	0.286	85.3
6[b]	Log PEU_2	−0.0643 (±0.0184)	−0.341 (±0.048)	—	—	1.40 (±0.07)	15	0.949	0.201	92.5
7	Log PEU_2	—	−0.530 (±0.045)	−0.352 (±0.119)	—	1.52 (±0.10)	15	0.939	0.219	77.4
8	Log PEU_2	—	—	—	−0.769 (±0.130)	2.90 (±0.33)	15	0.761	0.414	35.1
9	Log PEU_3	—	−0.517 (±0.053)	—	—	0.943 (±0.088)	15	0.896	0.307	94.4
10	Log PEU_3	—	—	—	−0.865 (±0.145)	2.77 (±0.37)	15	0.764	0.461	35.6

[a] Optimal log $P_H = -2.24$. [b] Optimal log $P_H = -2.65$.

Table VII—Correlation Equations for Log EXC (Log Rate Constant of Excretion) in Subjects 1–3

Equation	Dependent Variable	Log P_H	NH	$f_{RR'}$	Intercept	n	r^2	s	F
11	Log EXC_1	−0.257 (±0.041)	—	—	−1.41 (±0.07)	14	0.781	0.237	39.2
12	Log EXC_1	−0.332 (±0.027)	−0.362 (±0.071)	—	−1.16 (±0.06)	14	0.940	0.130	78.1
13	Log EXC_1	—	—	−0.616 (±0.036)	—	14	0.960	0.332	288.0
14	Log EXC_2	−0.335 (±0.056)	—	—	−1.44 (±0.09)	15	0.767	0.321	36.2
15	Log EXC_2	−0.412 (±0.053)	−0.373 (±0.139)	—	−1.18 (±0.12)	15	0.864	0.257	31.8
16	Log EXC_2	—	—	−0.655 (±0.042)	—	15	0.953	0.384	243.0
17	Log EXC_3	−0.343 (±0.050)	—	—	−1.69 (±0.08)	14	0.813	0.286	47.8
18	Log EXC_3	−0.410 (±0.048)	−0.327 (±0.125)	—	−1.47 (±0.11)	14	0.888	0.232	39.9
19	Log EXC_3	—	—	−0.753 (±0.040)	—	14	0.967	0.368	350.0

Table VIII—Correlation Equations for Log DEA (Log Rate Constant of First Dealkylation) in Subjects 1–3

Equation	Dependent Variable	Log P_H	$f_{RR'}$	V_R	$C_\alpha H$	Intercept	n	r^2	s	F
20	Log DEA_1	0.280 (±0.031)	—	−0.0149 (±0.0032)	—	−1.20 (±0.09)	16	0.861	0.142	40.4
21	Log DEA_1	—	0.484 (±0.073)	−0.0152 (±0.0043)	—	−2.21 (±0.15)	16	0.770	0.183	21.8
22	Log DEA_1	—	0.390 (±0.067)	—	0.251 (±0.084)	−2.98 (±0.29)	16	0.729	0.198	17.5
23	Log DEA_2	0.371 (±0.065)	—	−0.0172 (±0.0068)	—	−1.06 (±0.20)	17	0.716	0.297	16.4
24	Log DEA_2	—	0.748 (±0.081)	−0.0213 (±0.0047)	—	−2.56 (±0.17)	17	0.868	0.203	42.8
25	Log DEA_2	—	0.606 (±0.086)	—	0.309 (±0.108)	−3.52 (±0.37)	17	0.793	0.254	24.8
26	Log DEA_3	0.299 (±0.039)	—	−0.249 (±0.0040)	—	−0.826 (±0.117)	16	0.832	0.176	32.3
27	Log DEA_3	—	0.500 (±0.093)	−0.0247 (±0.0054)	—	−1.88 (±0.19)	16	0.711	0.231	16.0
28	Log DEA_3	—	0.329 (±0.104)	—	0.331 (±0.130)	−2.92 (±0.44)	16	0.497	0.305	6.4

In contrast, the inclusion of the NH parameter markedly improves the statistics (Eqs. 12, 15, and 18). These equations confirm the conclusions obtained previously in that, for identical lipophilicities and when pKa is accounted for, tertiary amines undergo faster excretion than do secondary amines, which are excreted faster than primary amines. This structural influence has never been characterized, and no convincing physicochemical or biochemical explanation can be offered at present. Steric hindrance in the reabsorption process is a mere possibility.

Replacing log P_H with $f_{RR'}$ yields Eqs. 13, 16, and 19 in which the constant term is eliminated. The equations are less satisfactory than Eqs. 11, 14, and 17 due to larger standard deviations for reasons outlined earlier.

The best equations for log EXC_i are Eqs. 12, 15, and 18. Table III compares experimental and calculated log EXC_i values.

Rate Constant of First *N*-Dealkylation—For this biological response, 17 observations are available and consist of 14 compounds, three

of which bear two different N-substituents. From Table V, it is clear that log DEA is markedly dependent on lipophilicity, with log P_H and $f_{RR'}$ each accounting for ~50–60% of the variance (~30% for Subject 3). Equations based on log P_H or $f_{RR'}$ alone thus are below acceptable levels of significance and are not reported. The inclusion of quadratic terms or of NH did not improve the correlation.

Good levels of significance were obtained by including a second parameter that served as a descriptor of the N-substituent removed by dealkylation. This approach results in Eqs. 20–28 (Table VIII). Equations 20, 21, 23, 24, 26, and 27 indicate that the rate of the first dealkylation increases with increasing lipophilicity of the molecules (as assessed by log P_H or $f_{RR'}$) and with decreasing volume of the substituent that is split off. There is an apparent contradiction between these two trends, allowing an interesting insight into the molecular factors controlling N-dealkylation. The equations may mean that a high lipophilicity favors affinity to cytochrome P-450 and, hence, a fast reaction (2). On the other hand, the bulkier the substituent to be split off, the less favorable appears the initial C_α-hydroxylation ultimately leading to N-dealkylation.

Such an interpretation is strengthened by Eqs. 22, 25, and 28, which show that the rate of dealkylation increases with the number of hydrogen atoms on the α-carbon. In other words, increasing the steric bulk on the α-carbon being hydroxylated decreases the rate of N-dealkylation, suggesting that, in terms of the reaction mechanism, the C_α-hydroxylation by oxene transfer is the rate-limiting step in the overall N-dealkylation reaction.

Table VIII shows that the utility of the three sets of independent variables (log P_H and V_R, $f_{RR'}$ and V_R, and $f_{RR'}$ and $C_\alpha H$) varies from one subject to another. The set of log P_H and V_R yields the best correlations for Subjects 1 and 3 but not for Subject 2. This situation outlines the interest in quantitative structure–activity relationship studies of having a variety of parameters and descriptors available. The fourth possible set of variables, log P_H and $C_\alpha H$, does not yield significant equations, despite the orthogonality of the two variables (Table V).

Experimental log DEA_i values are compared in Table IV with the values calculated from the best equations in Table VIII.

CONCLUSION

The present study indicates that careful pharmacokinetic studies can yield biological data suitable for quantitative structure–activity relationship treatment and that following pharmacokinetic calculations with quantitative structure–activity relationship calculations can lead to new insights into, and a better understanding of, drug metabolism and disposition. This study also shows that the excretion of amphetamines decreases with increasing lipophilicity of the molecules and that, given the same lipophilicity, tertiary amines are excreted faster than secondary amines, which are excreted faster than primary amines. Also, the correlation equations indicate that the rate of N-dealkylation increases with increasing lipophilicity of the substrates (enhanced enzyme affinity) but decreases with increasing bulk of the N-substituent that is split off (steric hindrance of C_α-hydroxylation).

The quantitative nature of the correlations obtained will allow interesting comparisons with other series of drugs when data become available.

REFERENCES

(1) Y. C. Martin, "Quantitative Drug Design," Dekker, New York, N.Y., 1978.

(2) C. Hansch, *Drug. Metab. Rev.*, **1**, 1 (1972).

(3) G. L. Tong and E. J. Lien, *J. Pharm. Sci.*, **65**, 1651 (1976).

(4) B. Testa and P. Jenner, in "Concepts in Drug Metabolism," vol. 1, P. Jenner and B. Testa, Eds., Dekker, New York, N.Y., 1980, pp. 143–168.

(5) B. Testa, *Pharm. Acta Helv.*, **53**, 143 (1978).

(6) M. Donike, R. Iffland, and L. Jaenicke, *Arzneim.-Forsch.*, **24**, 556 (1974).

(7) R. F. Rekker and H. M. De Kort, *Eur. J. Med. Chem.*, in press.

(8) R. F. Rekker, "The Hydrophobic Fragmental Constant," Elsevier, Amsterdam, The Netherlands, 1977.

(9) A. Bondi, *J. Phys. Chem.*, **68**, 441 (1964).

(10) N. H. Nie, C. H. Hull, J. G. Jenkins, K. Steinbrenner, and D. H. Bent, "SPSS, Statistical Package for the Social Sciences," 2nd ed., McGraw-Hill, New York, N.Y., 1975.

ACKNOWLEDGMENTS

B. Salvesen is indebted to the University of Oslo for a sabbatical leave and to the Norwegian Research Council for a grant.

Interactions of Cephalosporins and Penicillins with Nonpolar Octadecylsilyl Stationary Phase

FRANCISCO SALTO ˣ, JULIO G. PRIETO, and MARY TERESA ALEMANY

Received June 18, 1979, from the *Departamento Interfacultativo de Bioquimica, Cátedra de Química, Facultad de Veterinaria, Leon, Spain.* Accepted for publication November 26, 1979.

Abstract □ The capacity factors of several penicillins and cephalosporins, as well as those of 7-aminocephalosporanic acid, 6-aminopenicillanic acid, and 7-aminodeacetoxycephalosporanic acid, were determined at pH 2.5–7.5 with different methanol concentrations in the mobile phase. The influence of ionic strength on activity factors also was studied. Some theoretical equations providing a quantitative description of the influence of the mobile phase pH on the retention of penicillins and cephalosporins by an octadecylsilyl stationary phase were established. The analysis of experimental data by a nonlinear least-squares fit to theoretically deduced equations permitted determination of the capacity factors of anionic, cationic, zwitterion, and undissociated forms of the substances studied.

Keyphrases □ Cephalosporins—interactions with a nonpolar octadecylsilyl stationary phase □ Penicillins—interactions with a nonpolar octadecylsilyl stationary phase □ Capacity factors—cephalosporins and penicillins, interactions with a nonpolar octadecylsilyl stationary phase □ Antibiotics—cephalosporins and penicillins, interactions with a nonpolar octadecylsilyl stationary phase, capacity factors

Penicillins and cephalosporins constitute a large family of antibiotics of generalized use and similar structure. All of these compounds have at least one carboxylic group, and some possess one or more amino groups. Therefore, depending on the medium, they can be in undissociated, anionic, cationic, or zwitterion form.

There have been several studies of nonpolar stationary phases for the separation of certain cephalosporins and penicillins (1–4). However, a more systematic study of the influence of the ionization of penicillins and cephalosporins on interactions with nonpolar octadecylsilyl stationary phases was desired to elucidate the factors in the chro-

0022-3549/80/0500-0501$01.00/0

© 1980, American Pharmaceutical Association

of which bear two different N-substituents. From Table V, it is clear that log DEA is markedly dependent on lipophilicity, with log P_H and $f_{RR'}$ each accounting for ~50–60% of the variance (~30% for Subject 3). Equations based on log P_H or $f_{RR'}$ alone thus are below acceptable levels of significance and are not reported. The inclusion of quadratic terms or of NH did not improve the correlation.

Good levels of significance were obtained by including a second parameter that served as a descriptor of the N-substituent removed by dealkylation. This approach results in Eqs. 20–28 (Table VIII). Equations 20, 21, 23, 24, 26, and 27 indicate that the rate of the first dealkylation increases with increasing lipophilicity of the molecules (as assessed by log P_H or $f_{RR'}$) and with decreasing volume of the substituent that is split off. There is an apparent contradiction between these two trends, allowing an interesting insight into the molecular factors controlling N-dealkylation. The equations may mean that a high lipophilicity favors affinity to cytochrome P-450 and, hence, a fast reaction (2). On the other hand, the bulkier the substituent to be split off, the less favorable appears the initial C_α-hydroxylation ultimately leading to N-dealkylation.

Such an interpretation is strengthened by Eqs. 22, 25, and 28, which show that the rate of dealkylation increases with the number of hydrogen atoms on the α-carbon. In other words, increasing the steric bulk on the α-carbon being hydroxylated decreases the rate of N-dealkylation, suggesting that, in terms of the reaction mechanism, the C_α-hydroxylation by oxene transfer is the rate-limiting step in the overall N-dealkylation reaction.

Table VIII shows that the utility of the three sets of independent variables (log P_H and V_R, $f_{RR'}$ and V_R, and $f_{RR'}$ and $C_\alpha H$) varies from one subject to another. The set of log P_H and V_R yields the best correlations for Subjects 1 and 3 but not for Subject 2. This situation outlines the interest in quantitative structure–activity relationship studies of having a variety of parameters and descriptors available. The fourth possible set of variables, log P_H and $C_\alpha H$, does not yield significant equations, despite the orthogonality of the two variables (Table V).

Experimental log DEA_i values are compared in Table IV with the values calculated from the best equations in Table VIII.

CONCLUSION

The present study indicates that careful pharmacokinetic studies can yield biological data suitable for quantitative structure–activity relationship treatment and that following pharmacokinetic calculations with quantitative structure–activity relationship calculations can lead to new insights into, and a better understanding of, drug metabolism and disposition. This study also shows that the excretion of amphetamines decreases with increasing lipophilicity of the molecules and that, given the same lipophilicity, tertiary amines are excreted faster than secondary amines, which are excreted faster than primary amines. Also, the correlation equations indicate that the rate of N-dealkylation increases with increasing lipophilicity of the substrates (enhanced enzyme affinity) but decreases with increasing bulk of the N-substituent that is split off (steric hindrance of C_α-hydroxylation).

The quantitative nature of the correlations obtained will allow interesting comparisons with other series of drugs when data become available.

REFERENCES

(1) Y. C. Martin, "Quantitative Drug Design," Dekker, New York, N.Y., 1978.

(2) C. Hansch, *Drug. Metab. Rev.*, **1**, 1 (1972).

(3) G. L. Tong and E. J. Lien, *J. Pharm. Sci.*, **65**, 1651 (1976).

(4) B. Testa and P. Jenner, in "Concepts in Drug Metabolism," vol. 1, P. Jenner and B. Testa, Eds., Dekker, New York, N.Y., 1980, pp. 143–168.

(5) B. Testa, *Pharm. Acta Helv.*, **53**, 143 (1978).

(6) M. Donike, R. Iffland, and L. Jaenicke, *Arzneim.-Forsch.*, **24**, 556 (1974).

(7) R. F. Rekker and H. M. De Kort, *Eur. J. Med. Chem.*, in press.

(8) R. F. Rekker, "The Hydrophobic Fragmental Constant," Elsevier, Amsterdam, The Netherlands, 1977.

(9) A. Bondi, *J. Phys. Chem.*, **68**, 441 (1964).

(10) N. H. Nie, C. H. Hull, J. G. Jenkins, K. Steinbrenner, and D. H. Bent, "SPSS, Statistical Package for the Social Sciences," 2nd ed., McGraw-Hill, New York, N.Y., 1975.

ACKNOWLEDGMENTS

B. Salvesen is indebted to the University of Oslo for a sabbatical leave and to the Norwegian Research Council for a grant.

Interactions of Cephalosporins and Penicillins with Nonpolar Octadecylsilyl Stationary Phase

FRANCISCO SALTO ˣ, JULIO G. PRIETO, and MARY TERESA ALEMANY

Received June 18, 1979, from the *Departamento Interfacultativo de Bioquimica, Cátedra de Química, Facultad de Veterinaria, Leon, Spain.* Accepted for publication November 26, 1979.

Abstract □ The capacity factors of several penicillins and cephalosporins, as well as those of 7-aminocephalosporanic acid, 6-aminopenicillanic acid, and 7-aminodeacetoxycephalosporanic acid, were determined at pH 2.5–7.5 with different methanol concentrations in the mobile phase. The influence of ionic strength on activity factors also was studied. Some theoretical equations providing a quantitative description of the influence of the mobile phase pH on the retention of penicillins and cephalosporins by an octadecylsilyl stationary phase were established. The analysis of experimental data by a nonlinear least-squares fit to theoretically deduced equations permitted determination of the capacity factors of anionic, cationic, zwitterion, and undissociated forms of the substances studied.

Keyphrases □ Cephalosporins—interactions with a nonpolar octadecylsilyl stationary phase □ Penicillins—interactions with a nonpolar octadecylsilyl stationary phase □ Capacity factors—cephalosporins and penicillins, interactions with a nonpolar octadecylsilyl stationary phase □ Antibiotics—cephalosporins and penicillins, interactions with a nonpolar octadecylsilyl stationary phase, capacity factors

Penicillins and cephalosporins constitute a large family of antibiotics of generalized use and similar structure. All of these compounds have at least one carboxylic group, and some possess one or more amino groups. Therefore, depending on the medium, they can be in undissociated, anionic, cationic, or zwitterion form.

There have been several studies of nonpolar stationary phases for the separation of certain cephalosporins and penicillins (1–4). However, a more systematic study of the influence of the ionization of penicillins and cephalosporins on interactions with nonpolar octadecylsilyl stationary phases was desired to elucidate the factors in the chro-

0022-3549/80/0500-0501$01.00/0

© 1980, American Pharmaceutical Association

Table I—Structure of Investigated Substances

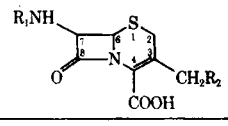

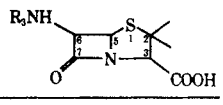

Compound	Substituents R_1	R_2	R_3
I 7-Aminodeacetoxycephalosporanic acid	H	H	—
II 7-Phenylacetamidodeacetoxycephalosporin	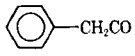	H	—
III Cephalexin	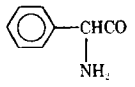	H	—
IV Cephradine	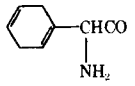	H	—
V 7-Aminocephalosporanic acid	H	$OCOCH_3$	—
VI Cephalosporin C	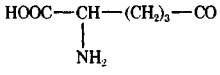	$OCOCH_3$	—
VII Cephalothin	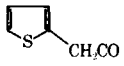	$OCOCH_3$	—
VIII Cephaloridine	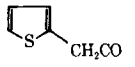		—
IX Cefazolin	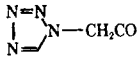	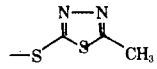	—
X 6-Aminopenicillanic acid	—	—	H
XI Ampicillin	—	—	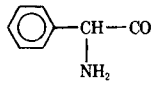
XII Penicillin G	—	—	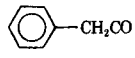
XIII Penicillin V	—	—	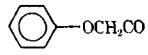
XIV Phenoxypropylpenicillin	—	—	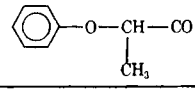

matographic process and to determine the conditions necessary for optimum separation. It also may help to define the hydrophobic properties of the various penicillins and cephalosporins and their possible relationships to pharmacological characteristics.

EXPERIMENTAL

Materials—The penicillins, cephalosporins, 7-aminocephalosporanic acid, 6-aminopenicillanic acid, and 7-aminodeacetoxycephalosporanic acid were used as supplied[1]. The chemicals were of the highest commercial grade available and were used without further purification.

Phosphate buffer solutions were used at a concentration of 0.05 *M*; sodium sulfate was used to obtain the desired ionic strength in each case. The mixtures of methanol and the buffer solution are expressed in volume percent.

Chromatographic Conditions—A 2.5 × 600-mm steel column, fitted with suitable adaptors and a 10-μm filter, was packed using a dry-packing technique with 30–70-μm silica with bonded octadecylsilane[2]. After packing, the column was conditioned with 200 ml of dimethylformamide at 40° followed immediately by 300 ml of methanol. The liquid chromatograph was fitted with a pump[3], a 20-μl sample valve injector[4], a 250-nm UV detector[5], and a strip-chart recorder[6].

[1] Courtsey of Antibióticos, S.A., Madrid, Spain.
[2] Bondapak C_{18}, Waters Associates, Milford, Mass.
[3] Constametrick II, Laboratory Data Control.
[4] Model 7120, Rheodyne.
[5] UV III monitor, Laboratory Data Control.
[6] Model XER, Sargent-Welch Scientific Co., Skokie, Ill.

The solutions of the chromatographed substances were prepared in the mobile phase at a concentration of 0.5 mg/ml, except for the penicillins, which were dissolved at a concentration of 3 mg/ml. In each case, 20 μl of a sample solution was injected. The flow rate was 1 ml/min, and the sensitivity of the UV detector was set between 0.004 and 0.128 aufs according to the coefficient of extinction of the analyzed product.

The capacity factors, k', were calculated using $k' = (V_R - V_0)/V_0$, where V_R is the elution volume of the chromatographic peak and V_0 is the column void volume, determined as the elution volume of a nonretained peak.

Determination of pKa—The literature does not contain pKa values of the drugs determined under appropriate conditions of the mobile phase. Therefore, the apparent pKa values were determined by a potentiometric method (5) for the ionic strength and methanol content of each mobile phase at room temperature.

Analysis of Experimental Data—The numerical analysis of the experimental data was carried out on a calculator[7] specially programmed for a nonlinear least-squares fit.

RESULTS AND DISCUSSION

The structures of the studied substances are given in Table I. The apparent pKa values, determined at room temperature at an ionic strength of 0.15 and at different methanol concentrations, are given in Table II.

Influence of pH—Due to the low stability of the penicillins, cephalosporins, and the stationary phase in strongly acidic or alkaline media, the studies were conducted within the pH 2.5–7.7 range.

[7] Texas Instruments TI-59.

Table II—Apparent pKa Values of Investigated Substances, Determined Potentiometrically at 20°, Ionic Strength of 0.15, and Various Methanol Concentrations

Compound	pKa_1 0% (v/v) Methanol	pKa_1 10% (v/v) Methanol	pKa_1 20% (v/v) Methanol	pKa_1 30% (v/v) Methanol	pKa_2 0% (v/v) Methanol	pKa_2 10% (v/v) Methanol	pKa_2 20% (v/v) Methanol	pKa_2 30% (v/v) Methanol
I	3.63	—	—	—	5.16	—	—	—
II	—	3.67	3.85	4.08	—	—	—	—
III	—	3.52	3.93	4.02	—	7.29	7.23	7.16
IV	—	4.00	4.17	4.37	—	7.56	7.56	7.54
V	3.49	—	—	—	4.71	—	—	—
VII	—	3.59	3.76	3.94	—	—	—	—
VIII	—	3.53	3.70	3.88	—	—	—	—
IX	—	3.03	3.18	3.38	—	—	—	—
X	3.04	—	—	—	4.90	—	—	—
XI	—	3.60	3.74	3.93	—	7.31	7.21	7.16
XII	—	—	3.82	4.10	—	—	—	—
XIII	—	—	—	4.00	—	—	—	—
XIV	—	—	—	4.21	—	—	—	—

Figure 1 shows the capacity coefficients for I, V, VI, and X at room temperature at different pH values and with a mobile phase of 0.05 *M* phosphate buffer at an ionic strength of 0.15. An octadecylsilyl stationary phase was used.

The capacity factors for II–IV, VI–IX, and XI at the various pH values are shown in Fig. 2. The mobile phase was a 10:90 mixture of methanol and the corresponding 0.05 *M* phosphate buffer at an ionic strength of 0.05. Figure 3 shows the capacity factors of the same substances as well as XII at different pH values when a mobile phase of 20 volumes of methanol and 80 volumes of 0.05 *M* phosphate buffer and an ionic strength of 0.15 was used. Figure 4 shows the capacity factors of the described penicillins and cephalosporins along with those of XII and XIV for different pH values with a mobile phase that was a 30:70 mixture of methanol and 0.05 *M* phosphate buffer at an ionic strength of 0.15. All tests were carried out at room temperature.

The physicochemical interactions between the solutes and the nonpolar stationary phase may be interpreted in accordance with the solvophobic theory (6); therefore, the influence of the solute ionization on chromatographic retention may be justified.

Depending on the pH of the medium, I, V, X, and penicillins and cephalosporins with amino and carboxyl groups may be found in solution in cationic ($^+H_3NPCOOH$), anionic (H_2NPCOO^-), or dipolar ($^+H_3NPCOO^-$) form. The dissociation equilibria are:

$$^+H_3NPCOOH \rightleftharpoons {}^+H_3NPCOO^- + H^+$$

Scheme I

$$K_{a_1} = \frac{[^+H_3NPCOO^-][H^+]}{[^+H_3NPCOOH]} \qquad \text{(Eq. 1)}$$

$$^+H_3NPCOO^- \rightleftharpoons H_2NPCOO^- + H^+$$

Scheme II

$$K_{a_2} = \frac{[H_2NPCOO^-][H^+]}{[^+H_3NPCOO^-]} \qquad \text{(Eq. 2)}$$

The chromatographic process may be considered as a reversible association of the solute, in any of its forms, with the ligand, L, formed by the octadecyl radical joined covalently to the surface of the silica. The process essentially is governed by solvophobic interactions, and no ionic or hydrogen bond is formed between the solute and the stationary phase. The equilibria governing these processes and their respective constants are:

$$^+H_3NPCOO^- + L \rightleftharpoons L^+H_3NPCOO^-$$

Scheme III

$$K_{L^+HP} = \frac{[L^+H_3NPCOO^-]}{[^+H_3NPCOO^-][L]} \qquad \text{(Eq. 3)}$$

$$H_2NPCOO^- + L \rightleftharpoons LH_2NPCOO^-$$

Scheme IV

$$K_{LP^-} = \frac{[LH_2NPCOO^-]}{[H_2NPCOO^-][L]} \qquad \text{(Eq. 4)}$$

$$^+H_3NPCOOH + L \rightleftharpoons L^+H_3NPCOOH$$

Scheme V

$$K_{L^+HP} = \frac{[L^+H_3NPCOOH]}{[^+H_3NPCOOH][L]} \qquad \text{(Eq. 5)}$$

The retention of a solute is expressed by the capacity factor, k', defined as the coefficient of distribution of the solute between the mobile and stationary phases. In a column where the relationship between the volume of the stationary phase and that of the mobile phase is constant and equal to ϕ, the distribution ratio is given by:

$$k' = \phi \frac{[L^+H_3NPCOOH] + [LH_2NPCOO^-] + [L^+H_3NPCOO^-]}{[^+H_3NPCOOH] + [H_2NPCOO^-] + [^+H_3NPCOO^-]} \qquad \text{(Eq. 6)}$$

The numerator of Eq. 6 is the sum of the concentrations of each solute form bound to the stationary phase; the denominator is the sum of the concentrations of each solute form in the mobile phase.

By substituting into Eq. 6 the values of the concentrations of each form found in Eqs. 1–4 and defining the capacity factor of the dipolar form, k'_0, as $k'_0 = \phi[L]K_{L^+HP^-}$, the capacity factor of the anionic form, k'_{-1}, as $k'_{-1} = \phi[L]K_{LP^-}$, and the capacity factor of the cationic form, k'_{+1}, as $k'_{+1} = \phi[L]K_{L^+HP}$, Eq. 6 finally may be transformed into:

$$k' = \frac{k'_0 + k'_{-1}\frac{K_{a_2}}{[H^+]} + k'_{+1}\frac{[H^+]}{K_{a_1}}}{1 + \frac{K_{a_2}}{[H^+]} + \frac{[H^+]}{K_{a_1}}} \qquad \text{(Eq. 7)}$$

Therefore, Eq. 7 should explain the influence of pH on the capacity factors of the amphoteric penicillins and cephalosporins as well as those of I, V, and X.

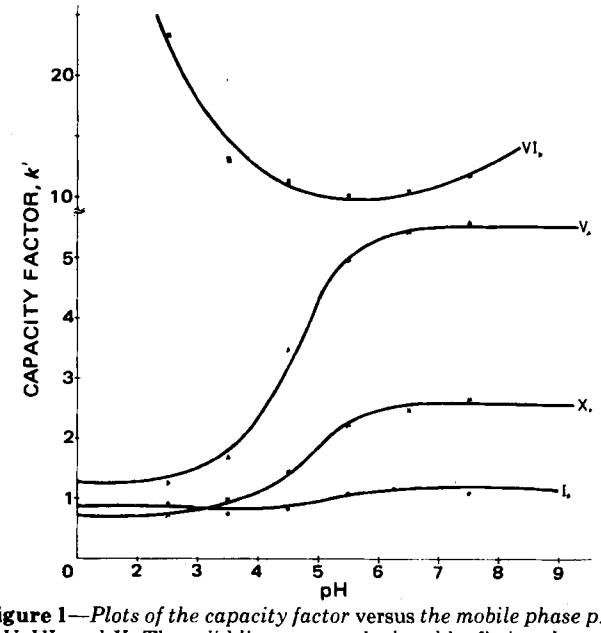

Figure 1—*Plots of the capacity factor* versus *the mobile phase pH for I, V, VI, and X. The solid lines were calculated by fitting the experimental data to Eq. 7.*

Table III—Capacity Factors of Molecular Forms

Compound	0% (v/v) Methanol			10% (v/v) Methanol			20% (v/v) Methanol			30% (v/v) Methanol		
	k'_0	k'_{-1}	k'_{+1}	k'_0	k'_{-1}	k'_{+1}	k'_0	k'_{-1}	k'_{+1}	k'_0	k'_{-1}	k'_{+1}
I	0.76	1.14	0.84									
X	0.95	2.58	0.69									
V	2.10	5.52	1.25									
III				6.40	20.3	18.6	2.10	7.70	6.10	0.70	1.90	2.00
XI				7.50	30.9	25.6	3.20	11.8	9.30	0.87	2.58	3.23
IV				9.40	35.3	27.3	3.70	10.9	9.20	1.00	3.40	3.00
VIII				11.4	—	10.3	4.10	—	3.80	1.30	—	1.40
IX				40.7	21.3	—	8.50	5.40	—	2.10	1.00	—
VII				83.7	63.7	—	27.2	20.3	—	7.60	4.20	—
II				111	31.1	—	38.6	13.1	—	9.90	3.10	—
XII							65.8	29.0	—	22.3	6.00	—
XIII										35.5	15.7	—
XIV										47.0	21.3	—

Each dissociated and undissociated form of penicillins and cephalosporins with only one ionizable group can interact with the stationary phase, giving rise to equilibria similar to those discussed previously.

By proceeding in the same way as for amphoteric penicillins and cephalosporins, the following is obtained:

$$k' = \frac{k'_0 + k'_{-1}\dfrac{K_a}{[H^+]}}{1 + \dfrac{K_a}{[H^+]}} \qquad \text{(Eq. 8)}$$

where k'_0 and k'_{-1} represent the capacity factors of the undissociated and anionic forms of the penicillins and cephalosporins, respectively.

The continuous lines in Figs. 1–4 were obtained by a nonlinear least-squares fit of the experimental data to Eq. 7 for I, V, and X as well as for the amphoteric penicillins and cephalosporins (III, IV, VIII, and XI). For penicillins and cephalosporins having only one carboxyl group (II, VII, IX, and XII–XIV), the lines were obtained with Eq. 8. The analysis of the experimental data by a nonlinear least-squares fit to Eq. 7 permitted calculation of the capacity factors for the zwitterion (k'_0), anionic (k'_{-1}), and cationic (k'_{+1}) forms of I, V, X, and amphoteric penicillins and cephalosporins (Table III). Similarly, a nonlinear least-squares fit to Eq. 8 was used to calculate the capacity factors of the undissociated (k'_0) and dissociated (k'_{-1}) forms of penicillins and cephalosporins with only one carboxyl group (Table III).

The acylation of the amino group of I, V, and X gave cephalosporins and penicillins that were retained more by the octadecylsilyl column. In general, cephalosporins were retained less than were penicillins.

For the nucleus of penicillins and cephalosporins, the hightest k' values were for V and the lowest ones were for I; X had intermediate values (Fig. 1). The greater retention of V may be attributed to its greater hydrophobicity due to the introduction of the acetoxy group in position 3.

For I, V, X, and the amphoteric penicillins and cephalosporins, the capacity factors of the anionic forms (k'_{-1}) (Table III) had the highest values, possibly due to the protective effect of the water molecules (7), which form hydrogen bonds with the protonated amino groups; this protection is smaller in the anionic forms, thus favoring hydrophobic interactions with the stationary phase. For I, V, and X, the capacity factors of the zwitterion form (k'_0) were similar to, but somewhat higher than, those of the cationic form (k'_{+1}). On the other hand, for amphoteric penicillins and cephalosporins, the capacity factors of the zwitterion form

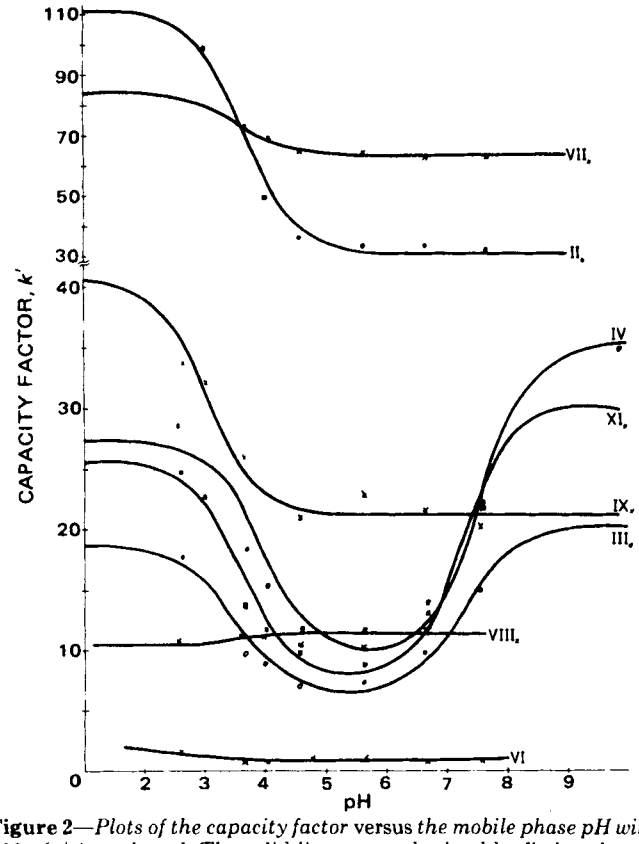

Figure 2—*Plots of the capacity factor* versus *the mobile phase pH with 10% (v/v) methanol. The solid lines were obtained by fitting the experimental data for III, IV, and XI to Eq. 7 and for II and VII–IX to Eq. 8.*

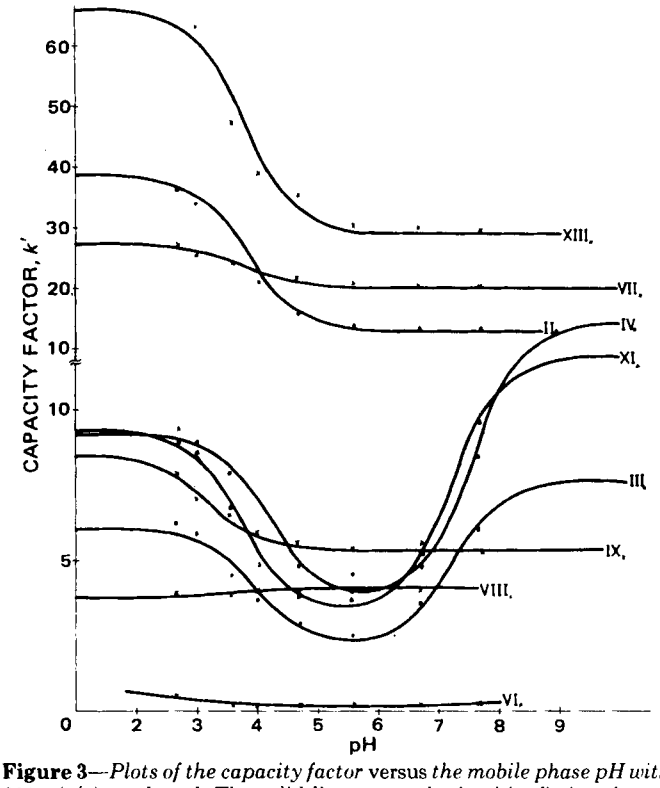

Figure 3—*Plots of the capacity factor* versus *the mobile phase pH with 20% (v/v) methanol. The solid lines were obtained by fitting the experimental data for II, IV, and XI to Eq. 7 and for II, VII–IX, and XII to Eq. 8.*

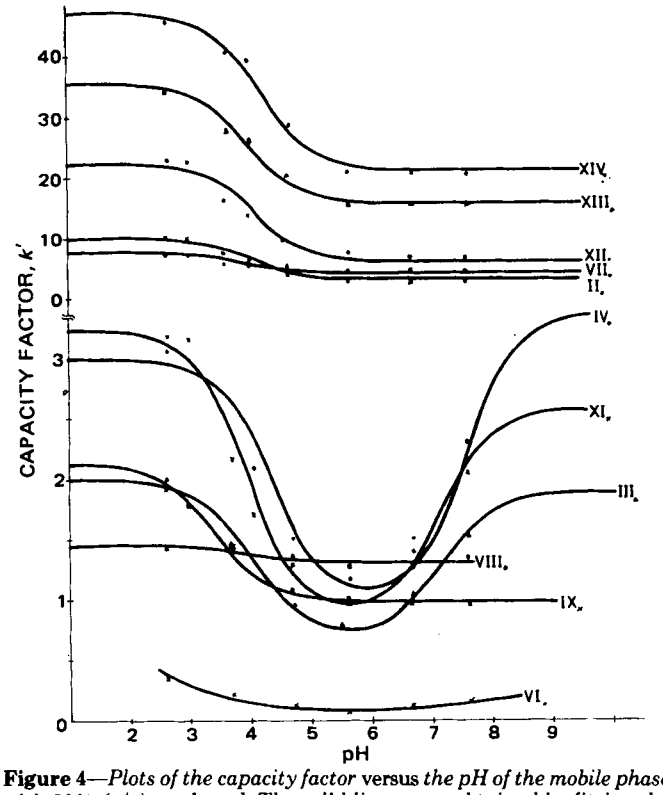

Figure 4—*Plots of the capacity factor* versus *the pH of the mobile phase with 30% (v/v) methanol. The solid lines were obtained by fitting the experimental data for III, IV, and XI to Eq. 7 and for II, VII–IX, and XII–XIV to Eq. 8.*

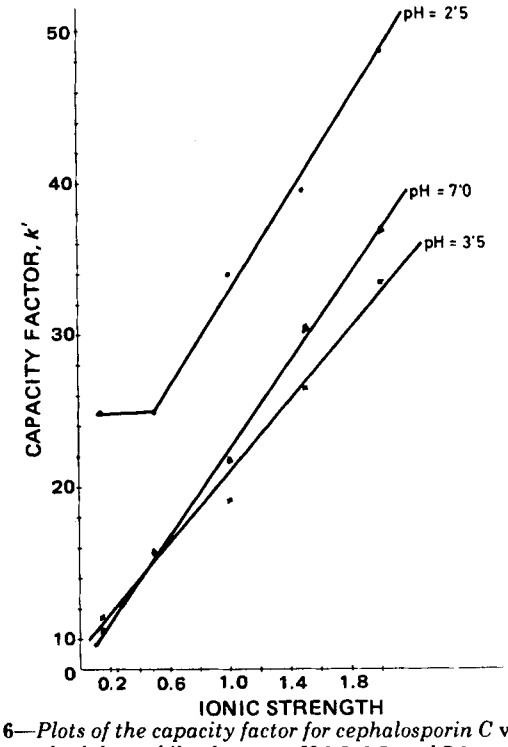

Figure 6—*Plots of the capacity factor for cephalosporin C* versus *the ionic strength of the mobile phase at pH 2.5, 3.5, and 7.0.*

(k'_0) were systematically lower than those of the other two (k'_{+1} and k'_{-1}). Therefore, in amphoteric cephalosporins and penicillins, the dipolar form interacts the least with the octadecylsilyl stationary phase, probably because although the form has no charge, there are a positive charge and a negative charge, which make the hydrophobic interaction with the stationary phase difficult.

In penicillins and cephalosporins with only one carboxyl group, as expected, the capacity factor of the undissociated acid form with no charge (k'_0) was greater than that of the negatively charged dissociated form (k'_{-1}).

Among cephalosporins, the influence of the nature of the lateral chain is remarkable. Of the cephalosporins studied, cephalothin had the highest capacity factor and cephalosporin C had the lowest.

Cephalothin (VII) was more retained by the nonpolar stationary phase than was cephaloridine (VIII). This result probably was a consequence of the substitution in position 3 of the cephalothin thiazine ring of a charged pyridino group by the acetoxy group, thus increasing the polarity and consequently decreasing cephaloridine retention.

For deacetoxycephalosporins, the capacity factor values decreased in the order 7-phenylacetamidoacetoxycephalosporin > cephradine >

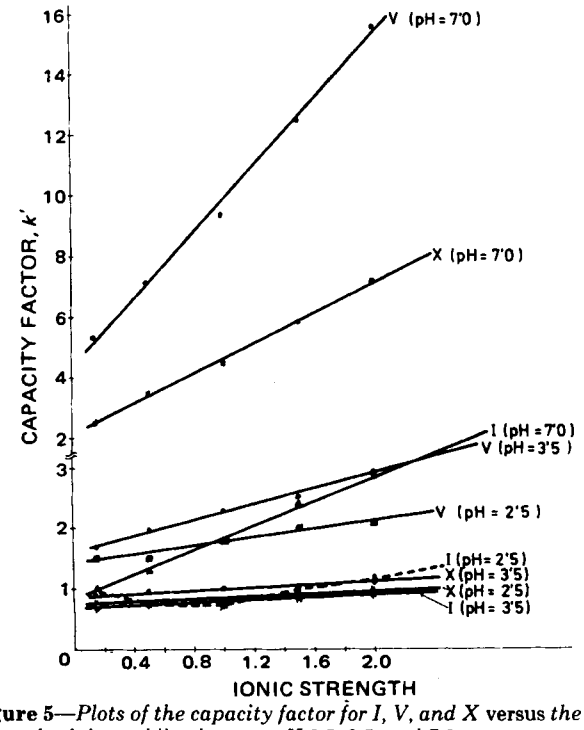

Figure 5—*Plots of the capacity factor for I, V, and X* versus *the ionic strength of the mobile phase at pH 2.5, 3.5, and 7.0.*

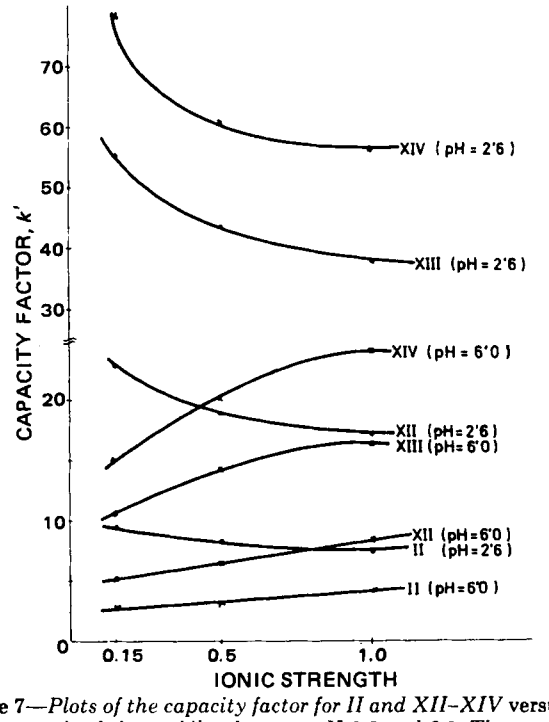

Figure 7—*Plots of the capacity factor for II and XII–XIV* versus *the ionic strength of the mobile phase at pH 2.6 and 6.0. The methanol content in the mobile phase was 20% (v/v).*

cephalexin. The introduction of an amino group in the lateral chain evidently reduced considerably the hydrophobicity of the molecule and, therefore, its retention by the octadecylsilyl column. In penicillins, capacity factors decreased in the order XIV > XIII > XII > XI.

Influence of Methanol Content in Mobile Phase—As expected, the retention of cephalosporins and penicillins by the nonpolar octadecylsilyl stationary phase decreased as the methanol concentration of the mobile phase increased. For the various penicillins and cephalosporins studied, the representation of $\log k'_0$, $\log k'_{-1}$, or $\log k'_{+1}$ *versus* the methanol concentration in the mobile phase, expressed in volume percent, shows a reasonable linear relationship with similar slopes.

Yamana *et al.* (8) used $\log k'$ as a lipophilic index for certain cephalosporins and penicillins, considering it to be analogous to the R_m index determined for cephalosporins and penicillins by means of reversed-phase TLC and comparable to $\log P$, the logarithm of the distribution ratio, determined in *n*-octanol–water systems, which is generally accepted as a lipophilic index. Similarly, $\log k'_0$, $\log k'_{-1}$, and $\log k'_{+1}$ could represent the lipophilic character of each form of penicillins and cephalosporins.

Influence of Salt Concentration—The effect of ionic strength on the capacity factor for I, V, and X was studied (Fig. 5). The mobile phases used were 0.05 *M* phosphate buffers at pH 2.5, 3.5, and 7.0; the ionic strength was varied from 0.51 to 2.0 for each pH value. The influence of the ionic strength on capacity factors at pH 2.5 and 3.5, where I, V, and X are in cationic or zwitterion forms, was very small. At pH 7.0, where these substances are in anionic form, this influence was important, especially for V; it decreased in the order V > X > I.

According to Horvath *et al.* (6), the increase in k' with ionic strength can be attributed to an increase in water surface tension when the salt concentration increases. On the contrary, the ionic form of cephalosporin C does not affect the influence of ionic strength on capacity factors. The k'/μ plots are straight lines of similar slope for each pH value studied, except at pH 2.5 and a very low ionic strength (Fig. 6).

The influence of ionic strength on the retention of II and XII–XIV also was studied at pH 2.6 and 6.0 (Fig. 7). The mobile phase was a mixture of 0.05 *M* phosphate buffer and methanol (2:1 v/v). Plotting k'/μ resulted in lines with negative slopes at the lowest acid pH, where the penicillins are in cationic or undissociated form. At pH 6, where the penicillins and the cephalosporins are in anionic form, the slopes of the k'/μ lines are positive.

It must be emphasized that the ionic strength of the mobile phase has a greater influence on the capacity factors of charged forms than on those of uncharged ones, and it is in the opposite direction. In fact, an increase of the ionic strength increases the retention of the charged forms while decreasing the retention of the uncharged acid forms.

CONCLUSION

The effect of cephalosporin and penicillin ionization on the chromatographic retention by nonpolar stationary phases can be interpreted in terms of hydrophobic interactions between the solute and the hydrocarbon function bound to the support surface. This quantitative study permitted determination of the capacity factors of each molecular form (k'_0, k'_{-1}, and k'_{+1}) of the investigated drugs.

The results given in this work will aid in the separation and analysis of some of the investigated substances.

The logarithms of the capacity factors of each molecular form, being independent of pH, probably will represent more adequately the lipophilic or hydrophobic characteristic of a compound having ionizable groups.

REFERENCES

(1) E. R. White, M. A. Carrol, J. E. Zarembo, and A. D. Bender, *J. Antibiot.*, **28**, 205 (1975).

(2) E. R. White, M. A. Carrol, and J. E. Zarembo, *ibid.*, **30**, 811 (1977).

(3) R. D. Miller and N. Neuss, *ibid.*, **29**, 902 (1975).

(4) F. Salto, *J. Chromatogr.*, **161**, 379 (1978).

(5) A. Albert and E. P. Serjeant, "The Determination of Ionization Constants," Chapman and Hall, London, England, 1971, chap. 2.

(6) C. Horvath, W. Melander, and I. Molnar, *Anal. Chem.*, **49**, 142 (1977).

(7) G. W.-K. Fong and E. Grushka, *ibid.*, **50**, 1154 (1978).

(8) T. Yamana, A. Tsusi, E. Miyamoto, and O. Kubo, *J. Pharm. Sci.*, **66**, 747 (1977).

Hypocholesterolemic Agents VII: Inhibition of β-Hydroxy-β-methylglutaryl-CoA Reductase by Monoesters of Substituted Glutaric Acids

MARVIN R. BOOTS ˣ, YEONG-MAW YEH, and SHARON G. BOOTS *

Received August 23, 1979, from the *Department of Pharmaceutical Chemistry, Medical College of Virginia, Health Sciences Division, Virginia Commonwealth University, Richmond, VA 23298.* Accepted for publication November 26, 1979.

*Present address: Department of Chemistry, Stanford University, Stanford, CA 94305.

Abstract □ A series of 1-(4-biphenylyl)pentyl hydrogen 3-alkylglutarates and 3-hydroxy-3-alkylglutarates was synthesized and assayed for inhibition of rat liver β-hydroxy-β-methylglutaryl-CoA reductase. Limited solubility of the monoesters in the enzyme assay system prevented the determination of the I_{50} values. However, the limited data indicated no significant changes in the activity of the analogs when they were assayed at identical concentrations.

Keyphrases □ Hypocholesterolemic agents—inhibition of β-hydroxy-β-methylglutaryl-CoA reductase, monoesters of substituted glutaric acids, rat liver microsomes □ Microsomes, rat liver—inhibition of cholesterol biosynthesis, monoesters of substituted glutaric acids □ Enzyme inhibition—effect of monoesters of glutaric acids on cholesterol biosynthesis, rat liver microsomes

An approach to the design of cholesterol biosynthesis inhibitors as potential hypocholesterolemic agents was discussed previously (1, 2). The rationale for the inhibition of the enzyme β-hydroxy-β-methylglutaryl-CoA reductase was presented (1). Structure–activity relationships indicated that maximum activity was observed when R_1 = biphenylyl, R_2 = *n*-butyl, and n = 1–4 in a series of arylalkyl hydrogen alkanedioates (I). In addition, the incorporation of a β-hydroxy-β-methyl moiety into the acid portion of the glutarate analog provided II, which was seven times more active than the glutarate analog of I.

This paper describes the synthesis and assay of a series of 1-(4-biphenylyl)-*n*-pentyl hydrogen 3-alkylglutarates (III) and 3-hydroxy-3-alkylglutarates (IV). The 3-alkyl series (III) was designed specifically to determine if there was a hydrophobic binding site on the enzyme where the 3-alkyl group of the glutaric acid moiety could bind. The

0022-3549/80/0500-0506$01.00/0

© 1980, American Pharmaceutical Association

cephalexin. The introduction of an amino group in the lateral chain evidently reduced considerably the hydrophobicity of the molecule and, therefore, its retention by the octadecylsilyl column. In penicillins, capacity factors decreased in the order XIV > XIII > XII > XI.

Influence of Methanol Content in Mobile Phase—As expected, the retention of cephalosporins and penicillins by the nonpolar octadecylsilyl stationary phase decreased as the methanol concentration of the mobile phase increased. For the various penicillins and cephalosporins studied, the representation of $\log k'_0$, $\log k'_{-1}$, or $\log k'_{+1}$ *versus* the methanol concentration in the mobile phase, expressed in volume percent, shows a reasonable linear relationship with similar slopes.

Yamana *et al.* (8) used $\log k'$ as a lipophilic index for certain cephalosporins and penicillins, considering it to be analogous to the R_m index determined for cephalosporins and penicillins by means of reversed-phase TLC and comparable to $\log P$, the logarithm of the distribution ratio, determined in *n*-octanol–water systems, which is generally accepted as a lipophilic index. Similarly, $\log k'_0$, $\log k'_{-1}$, and $\log k'_{+1}$ could represent the lipophilic character of each form of penicillins and cephalosporins.

Influence of Salt Concentration—The effect of ionic strength on the capacity factor for I, V, and X was studied (Fig. 5). The mobile phases used were 0.05 *M* phosphate buffers at pH 2.5, 3.5, and 7.0; the ionic strength was varied from 0.51 to 2.0 for each pH value. The influence of the ionic strength on capacity factors at pH 2.5 and 3.5, where I, V, and X are in cationic or zwitterion forms, was very small. At pH 7.0, where these substances are in anionic form, this influence was important, especially for V; it decreased in the order V > X > I.

According to Horvath *et al.* (6), the increase in k' with ionic strength can be attributed to an increase in water surface tension when the salt concentration increases. On the contrary, the ionic form of cephalosporin C does not affect the influence of ionic strength on capacity factors. The k'/μ plots are straight lines of similar slope for each pH value studied, except at pH 2.5 and a very low ionic strength (Fig. 6).

The influence of ionic strength on the retention of II and XII–XIV also was studied at pH 2.6 and 6.0 (Fig. 7). The mobile phase was a mixture of 0.05 *M* phosphate buffer and methanol (2:1 v/v). Plotting k'/μ resulted in lines with negative slopes at the lowest acid pH, where the penicillins are in cationic or undissociated form. At pH 6, where the penicillins and the cephalosporins are in anionic form, the slopes of the k'/μ lines are positive.

It must be emphasized that the ionic strength of the mobile phase has a greater influence on the capacity factors of charged forms than on those of uncharged ones, and it is in the opposite direction. In fact, an increase of the ionic strength increases the retention of the charged forms while decreasing the retention of the uncharged acid forms.

CONCLUSION

The effect of cephalosporin and penicillin ionization on the chromatographic retention by nonpolar stationary phases can be interpreted in terms of hydrophobic interactions between the solute and the hydrocarbon function bound to the support surface. This quantitative study permitted determination of the capacity factors of each molecular form (k'_0, k'_{-1}, and k'_{+1}) of the investigated drugs.

The results given in this work will aid in the separation and analysis of some of the investigated substances.

The logarithms of the capacity factors of each molecular form, being independent of pH, probably will represent more adequately the lipophilic or hydrophobic characteristic of a compound having ionizable groups.

REFERENCES

(1) E. R. White, M. A. Carrol, J. E. Zarembo, and A. D. Bender, *J. Antibiot.*, **28**, 205 (1975).

(2) E. R. White, M. A. Carrol, and J. E. Zarembo, *ibid.*, **30**, 811 (1977).

(3) R. D. Miller and N. Neuss, *ibid.*, **29**, 902 (1975).

(4) F. Salto, *J. Chromatogr.*, **161**, 379 (1978).

(5) A. Albert and E. P. Serjeant, "The Determination of Ionization Constants," Chapman and Hall, London, England, 1971, chap. 2.

(6) C. Horvath, W. Melander, and I. Molnar, *Anal. Chem.*, **49**, 142 (1977).

(7) G. W.-K. Fong and E. Grushka, *ibid.*, **50**, 1154 (1978).

(8) T. Yamana, A. Tsusi, E. Miyamoto, and O. Kubo, *J. Pharm. Sci.*, **66**, 747 (1977).

Hypocholesterolemic Agents VII: Inhibition of β-Hydroxy-β-methylglutaryl-CoA Reductase by Monoesters of Substituted Glutaric Acids

MARVIN R. BOOTS ˣ, YEONG-MAW YEH, and SHARON G. BOOTS *

Received August 23, 1979, from the *Department of Pharmaceutical Chemistry, Medical College of Virginia, Health Sciences Division, Virginia Commonwealth University, Richmond, VA 23298.* Accepted for publication November 26, 1979.

*Present address: Department of Chemistry, Stanford University, Stanford, CA 94305.

Abstract □ A series of 1-(4-biphenylyl)pentyl hydrogen 3-alkylglutarates and 3-hydroxy-3-alkylglutarates was synthesized and assayed for inhibition of rat liver β-hydroxy-β-methylglutaryl-CoA reductase. Limited solubility of the monoesters in the enzyme assay system prevented the determination of the I_{50} values. However, the limited data indicated no significant changes in the activity of the analogs when they were assayed at identical concentrations.

Keyphrases □ Hypocholesterolemic agents—inhibition of β-hydroxy-β-methylglutaryl-CoA reductase, monoesters of substituted glutaric acids, rat liver microsomes □ Microsomes, rat liver—inhibition of cholesterol biosynthesis, monoesters of substituted glutaric acids □ Enzyme inhibition—effect of monoesters of glutaric acids on cholesterol biosynthesis, rat liver microsomes

An approach to the design of cholesterol biosynthesis inhibitors as potential hypocholesterolemic agents was discussed previously (1, 2). The rationale for the inhibition of the enzyme β-hydroxy-β-methylglutaryl-CoA reductase was presented (1). Structure–activity relationships indicated that maximum activity was observed when R_1 = biphenylyl, R_2 = *n*-butyl, and n = 1–4 in a series of arylalkyl hydrogen alkanedioates (I). In addition, the incorporation of a β-hydroxy-β-methyl moiety into the acid portion of the glutarate analog provided II, which was seven times more active than the glutarate analog of I.

This paper describes the synthesis and assay of a series of 1-(4-biphenylyl)-*n*-pentyl hydrogen 3-alkylglutarates (III) and 3-hydroxy-3-alkylglutarates (IV). The 3-alkyl series (III) was designed specifically to determine if there was a hydrophobic binding site on the enzyme where the 3-alkyl group of the glutaric acid moiety could bind. The

0022-3549/80/0500-0506$01.00/0

© 1980, American Pharmaceutical Association

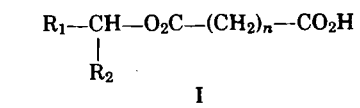

I

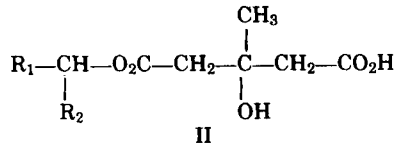

II

3-hydroxy-3-alkyl series (IV) was synthesized and evaluated to determine if binding to the hydrogen-bonding site *via* the hydroxyl group and to the hydrophobic site *via* the 3-alkyl group on the enzyme could occur simultaneously.

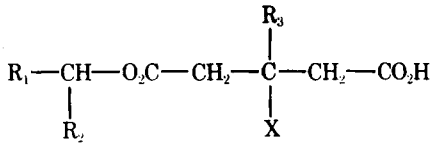

III: R_3 = alkyl, X = H
IV: R_3 = alkyl, X = OH

EXPERIMENTAL[1]

Chemistry—The desired monoesters (III and IV) were prepared from 1-(4-biphenylyl)-*n*-pentanol (1) and the appropriate substituted glutaric acid using the method of Büchi *et al.* (3). Synthesis of the required 3-alkylglutaric acids (VI) was performed *via* the pathway illustrated in Scheme I. Condensation of diethyl malonate with aliphatic aldehydes in the presence of potassium fluoride gave the alkylidenedimalonates (V) (4) in 25–85% yields. Acid hydrolysis and decarboxylation of V afforded the desired acids (VI) in 60–80% yields.

The 3-hydroxy-3-alkylglutaric acids (VIII) were synthesized using the pathway illustrated in Scheme II. Treatment of the appropriate ester with the allyl Grignard reagent, as described by Tschesche and Machleidt (5), gave the 4-hydroxy-4-alkyl-1,6-heptadienes (VII) in good yields (80–87%). Ozonolysis of VII followed by treatment with hydrogen peroxide gave the required hydroxy acids (VIII) in 70% yields.

1-(4-Biphenylyl)-n-pentyl Hydrogen 3-Alkyl- and 3-Hydroxy-3-alkylglutarates—The monoesters (IIIa–IIId and IVa–IVd) of the 3-alkylglutaric acids (VI) and 3-hydroxy-3-alkylglutaric acids (VIII) were prepared using the procedure of Büchi *et al.* (3) as described previously (2). The crude oily monoesters were chromatographed on silicic acid. Elution with 20% ether–petroleum ether (bp 60–75°) afforded colorless oily monoesters. The monoesters were characterized as their solid *S*-benzylthiuronium salts using the method of Donleavy (6) as described previously (1). Table I lists the analytical data.

3-Alkylglutaric Acids (VI)—The 3-*n*-propyl- (7), 3-isopropyl- (8), and 3-isobutyl- (9) glutaric acids were prepared by acid hydrolysis and decarboxylation of the appropriate tetraethyl alkylidenedimalonate (4). The preparation of 3-*n*-butylglutaric acid serves as an example.

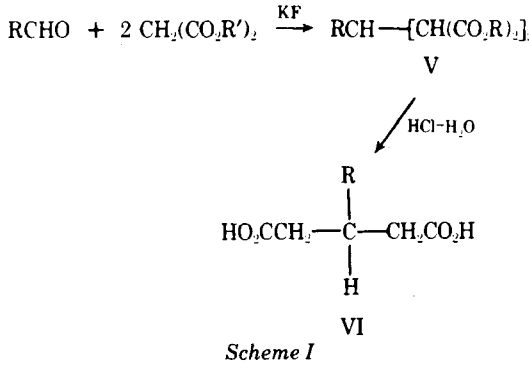

Scheme I

A mixture of 26.0 g (0.067 mole) of tetraethyl *n*-butylidenedimalonate (4), 250 ml of water, and 250 ml of concentrated hydrochloric acid was refluxed for 24 hr. The resulting solution was extracted with ethyl acetate. The organic phase was washed three times with water, washed with a saturated sodium chloride solution, and then dried over anhydrous sodium sulfate. The solvent was removed to give 9.9 g (78%) yield of a pale-yellow oil; NMR ($CDCl_3$): δ 0.35–0.82 (m, 9H, C_4H_9), 1.2 (s, 4H, CH_2CCH_2), 1.93–2.17 (m, 1H, CH), and 5.80 [s, 2H, $(CO_2H)_2$] ppm. The oil was characterized analytically as the white *S*-benzylthiuronium salt (1), mp 165–167°.

Anal.—Calc. for $C_{25}H_{36}N_4O_4S_2$: C, 57.7; H, 6.9; N, 10.8. Found: C, 57.8; H, 7.1; N, 10.8.

3-Hydroxy-3-alkylglutaric Acids (VIII)—The acids were prepared by ozonolysis followed by hydrogen peroxide oxidation of the appropriate 4-hydroxy-4-alkyl-1,6-heptadiene to afford the desired 3-hydroxy-3-alkylglutaric acid (VIII). The 4-hydroxy-4-alkyl-1,6-heptadienes were prepared using the method of Tschesche and Machleidt (5). The preparation of 4-hydroxy-4-isobutyl-1,6-heptadiene serves as an example.

To a stirred suspension of 4.62 g (0.19 g atom) of magnesium turnings in 8 ml of dry ether, 8 ml of dry tetrahydrofuran, and a crystal of iodine was added dropwise a solution of 6.5 g (0.05 mole) of ethyl isovalerate and 14 ml (0.16 mole) of allyl bromide in 19 ml of dry ether and 56 ml of dry tetrahydrofuran. The reaction mixture was maintained at a gentle reflux during the addition and was refluxed for 3 hr after the addition was complete. The resulting mixture was poured onto ice–hydrochloric acid and then extracted with ether.

The organic phase was washed with water, 5% NaOH, water, and finally saturated sodium chloride solution. It then was dried over anhydrous sodium sulfate and concentrated under reduced pressure to give 9.4 g of an orange liquid. Vacuum distillation afforded 7.8 g (81% yield) of a colorless liquid, bp 50–51° (0.65 mm Hg); NMR ($CDCl_3$): δ 0.95 [d, 6H, $C(CH_3)_2$], 1.39 (d, 2H, CH_2), 1.56 (s, 1H, OH), 1.69 (m, 1H, R_3CH), 2.25 [d, 4H, $(C{=}CCH_2)_2$], 4.89–5.43 [m, 4H, $(C{=}CH_2)_2$], and 5.54–6.31 [m, 2H, $(C{=}CH)_2$] ppm.

Anal.—Calc. for $C_{11}H_{20}O$: C, 78.5; H, 12.0. Found: C, 78.4; H, 12.0.

The following 4-hydroxy-4-alkyl-1,6-heptadienes were prepared using the described procedure: 4-hydroxy-4-*n*-propyl-1,6-heptadiene, bp 39–41° (2.0 mm Hg) [lit. (10) bp 70° (17 mm Hg)]; 4-hydroxy-4-isopropyl-1,6-heptadiene, bp 48–51° (1.5 mm Hg) [lit. (10) bp 43–45° (1.3 mm Hg)]; and 4-hydroxy-4-*n*-butyl-1,6-heptadiene, bp 93–95° (6 mm Hg) [lit. (10) bp 90–92° (6 mm Hg)].

3-Hydroxy-3-n-propylglutaric Acid—The method of Tschesche and Machleidt (5) was used. A solution containing 4.16 g (0.027 mole) of 4-hydroxy-4-*n*-propyl-1,6-heptadiene, 3.5 ml of acetic acid, and 43 ml of methylene chloride was cooled in an isopropanol–dry ice bath. Ozone was passed through the solution for 2 hr, and the resulting blue solution was allowed to warm to 25°. To the clear, colorless solution was added 25 ml of acetic acid, and the methylene chloride was removed under reduced pressure.

To the residue were added 25 ml of acetic acid and 25 ml of 30% H_2O_2. The solution was heated at reflux for 8 hr, and removal of the solvent under reduced pressure afforded 3.69 g of a colorless oil. Trituration with petroleum ether (bp 60–75°) afforded 3.6 g (70% yield) of a white solid, mp 90–94°. Two recrystallizations from ether–petroleum ether (bp 60–75°) afforded a white solid, mp 96–98°; NMR (dimethyl sulfoxide-d_6): δ 0.54–1.77 [m, 7H, $CH_3(CH_2)_2$], 2.51 [s, 4H, $(CH_2COO)_2$], and 6.11 [broad s, 3H, OH, $(COOH)_2$] ppm.

Anal.—Calc. for $C_8H_{14}O_5$: C, 50.5; H, 7.4. Found: C, 50.5; H, 7.4.

3-Hydroxy-3-isopropylglutaric Acid—The procedure described for

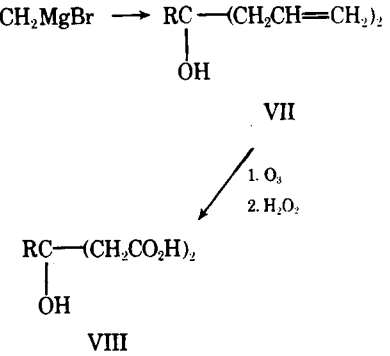

VII

VIII

Scheme II

[1] Melting points were determined with a Thomas-Hoover capillary apparatus and are uncorrected. Elemental analyses were carried out by Atlantic Microlaboratories, Atlanta, Ga. IR spectra were determined using a Perkin-Elmer model 257 spectrophotometer. NMR spectra were obtained using a Perkin-Elmer model R-24 spectrometer in the solvent specified with tetramethylsilane as the internal reference.

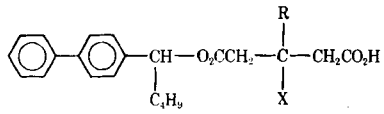

Table I—Properties of Monoesters of Substituted Glutaric Acids

Compound	R	X	Yield[a], %	Melting Point (Salt)	Formula	Analysis, %	Calc.	Found
III*a*	$CH_3(CH_2)_2$	H	35	116–117°	$C_{33}H_{42}N_2O_4S$	C	70.4	70.4
						H	7.5	7.5
						N	5.0	5.0
III*b*	$(CH_3)_2CH$	H	34	122–123°	$C_{33}H_{42}N_2O_4S$	C	70.4	70.5
						H	7.5	7.5
						N	5.0	5.0
III*c*	$CH_3(CH_2)_3$	H	38	106–108°	$C_{34}H_{44}N_2O_4S$	C	70.8	70.7
						H	7.7	7.7
						N	4.9	4.9
III*d*	$(CH_3)_2CHCH_2$	H	32	136–138°	$C_{34}H_{44}N_2O_4S$	C	70.8	70.6
						H	7.7	7.7
						N	4.9	4.8
IV*a*	$CH_3(CH_2)_2$	OH	20	110–112°	$C_{33}H_{42}N_2O_5S$	C	68.4	68.4
						H	7.3	7.3
						N	4.8	4.8
IV*b*	$(CH_3)_2CH$	OH	22	118–120°	$C_{33}H_{42}N_2O_5S$	C	68.4	68.2
						H	7.3	7.4
						N	4.8	4.9
IV*c*	$CH_3(CH_2)_3$	OH	17	101–103°	$C_{34}H_{44}N_2O_5S$	C	68.9	68.8
						H	7.5	7.5
						N	4.7	4.7
IV*d*	$(CH_3)_2CHCH_2$	OH	19	121–122°	$C_{34}H_{44}N_2O_5S$	C	68.9	68.7
						H	7.5	7.5
						N	4.7	4.7

[a] The monoesters were colorless, viscous oils. The IR (chloroform) and NMR (deuterochloroform) spectra were consistent with the assigned structures.

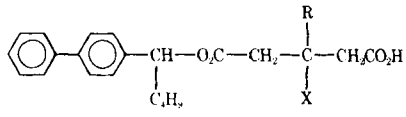

Table II—Inhibition of β-Hydroxy-β-methylglutaryl-CoA Reductase

Compound	R	X	Activity (I/S)[a] 0.5	1.0	2.0	2.5
IX	CH_3	H	—	—	50[b]	—
III*a*	$CH_3(CH_2)_2$	H	19	28	Insoluble	—
III*b*	$(CH_3)_2CH$	H	13	24	Insoluble	—
III*c*	$CH_3(CH_2)_3$	H	16	27	Insoluble	—
III*d*	$(CH_3)_2CHCH_2$	H	17	28	Insoluble	—
X	CH_3	OH	—	—	50[c]	—
IV*a*	$CH_3(CH_2)_2$	OH	—	17	52	Insoluble
IV*b*	$(CH_3)_2CH$	OH	—	15	43	Insoluble
IV*c*	$CH_3(CH_2)_3$	OH	17	22	28	Insoluble
IV*d*	$(CH_3)_2CHCH_2$	OH	—	22	36	Insoluble
XI	H	H	—	—	58[d]	—

[a] The inhibition index, I/S, equals the ratio of the micromolar concentration of the inhibitor to the micromolar concentration of the substrate required to give the percentage inhibition shown. At least two sets of duplicate determinations were used. [b] I/S = 9 as reported previously (2). [c] I/S = 1.5 as reported previously (2). [d] A standard inhibitor used routinely to provide comparability of each assay set (2); I/S = 7.

3-hydroxy-3-*n*-propylglutaric acid was used to give 3-hydroxy-3-isopropylglutaric acid (73% yield) as a white solid, mp 87–92°. Two recrystallizations from ethyl acetate–petroleum ether (bp 60–75°) afforded a white solid, mp 99–101°; NMR (dimethyl sulfoxide-d_6): δ 0.93 [d, 6H, $C(CH_3)_2$], 1.30–2.12 (m, 2H, OH, R_3CH), 2.63 [s, 4H, $(CH_2COO)_2$], and 8.00 [broad s, 3H, OH, $(COOH)_2$] ppm.

Anal.—Calc. for $C_8H_{14}O_5$: C, 50.5; H, 7.4. Found: C, 50.4; H, 7.4.

*3-Hydroxy-3-*n*-butylglutaric Acid*—The procedure described for 3-hydroxy-3-*n*-propylglutaric acid was used to give 3-hydroxy-3-*n*-butylglutaric acid (68% yield) as a white solid, mp 66–76°. Two recrystallizations from ethyl acetate–petroleum ether (bp 60–75°) afforded a white solid, mp 76–78°; NMR ($CDCl_3$): δ 0.67–2.23 [m, 9H, $CH_3(CH_2)_3$], 2.78 (s, 4H, $(CH_2COO)_2$], and 8.70 [broad s, 3H, OH, $(COOH)_2$] ppm.

Anal.—Calc. for $C_9H_{16}O_5$: C, 52.9; H, 7.9. Found: C, 53.0; H, 7.9.

3-Hydroxy-3-isobutylglutaric Acid—The procedure described for 3-hydroxy-3-*n*-propylglutaric acid was used to give 3-hydroxy-3-isobutylglutaric acid (70% yield) as a white solid, mp 90–98°. Recrystallization from ethyl acetate–petroleum ether (bp 60–75°) afforded a white solid, mp 106–108°; NMR (dimethyl sulfoxide-d_6): δ 0.93 [d, 6H, $C(CH_3)_2$], 1.49 (d, 2H, CH_2), 2.06 (m, 1H, R_3CH), 2.61 [s, 4H, $(CH_2COO)_2$], and 5.66 [broad s, 3H, OH, $(COOH)_2$] ppm.

Anal.—Calc. for $C_9H_{16}O_5$: C, 52.9; H, 7.9. Found: C, 52.8; H, 7.9.

Preparation of Rat Liver Microsomes—Rat liver microsomes containing β-hydroxy-β-methylglutaryl-CoA reductase activity were prepared according to the method of Shapiro and Rodwell (11) as described previously (2).

Enzyme Activity and Inhibition—The assay (2) was modified with regard to the isolation of mevalonolactone. The enzyme incubation mixture consisted of $NADP^+$ (9.7 μmoles)[2], glucose-6-phosphate[2] (59.7 μmoles), torula yeast glucose-6-phosphate dehydrogenase[2] (5 units), microsomal protein (2 mg) as determined by a modification of the method of Lowry *et al.* (2, 12), 0.1 ml of ethylene glycol monoethyl ether containing the inhibitor, and sufficient assay buffer [30 m*M* ethylenediaminetetraacetic acid, 70 m*M* NaCl, and 10 m*M* β-mercaptoethanol (pH 6.8)] to give a total volume of 2.9 ml.

Enzymatic activity was initiated by the addition of 0.1 ml of a solution containing 94 nmoles (31 μ*M*) of *dl*-β-hydroxy-β-methyl[3-^{14}C]glutaryl-CoA[3] (specific activity of 920 dpm/nmole). After 25 min of shaking incubation at 37°, the reaction was stopped by the addition of 0.2 ml of concentrated hydrochloric acid. Fifty microliters of an acetone solution containing 7×10^5 dpm (24 μmoles) of *dl*-4-[^{3}H]mevalonolactone[4] was added to the incubation mixture, and the mixture was incubated at 37°

[2] Sigma Chemical Co.
[3] P-L Biochemicals.
[4] Amersham Corp.

for 30 min. To the mixture was added 3.2 g of anhydrous sodium sulfite, and this mixture was extracted twice with 10-ml portions of benzene (13).

The benzene extract was evaporated to dryness in a liquid scintillation vial at 50° under a nitrogen stream. Twenty milliliters of Bray's scintillation solution (14) was added, and tritium and carbon 14 were determined simultaneously in a liquid scintillation counter[5]. Counting efficiency was determined by the external standard method. Some variability in the inhibition data was noted between tubes of microsomes (even from the same liver preparation). For this reason, a standard inhibitor, 1-(4-biphenylyl)pentyl hydrogen succinate (IX), was utilized routinely.

RESULTS AND DISCUSSION

The activity of IIIa–IIId and IVa–IVd as inhibitors of rat liver β-hydroxy-β-methylglutaryl-CoA reductase is shown in Table II. Unfortunately, the low solubility of these compounds in the enzyme assay prevented the determination of I/S values required for 50% inhibition. Thus, no definite conclusions can be made concerning the effect of increasing the size of the alkyl group at the C-3 position of the glutaric acid moiety with or without a C-3 hydroxyl group. However, the limited data do indicate that no substantial changes in inhibitory activity resulted from these modifications [compare 3-hydroxy-3-methyl (X) to 3-hydroxy-3-*n*-propyl (IVa) and the similar degree of inhibition shown by the analogs when assayed at identical I/S values].

REFERENCES

(1) M. R. Boots, S. G. Boots, C. M. Noble, and K. E. Guyer, *J. Pharm. Sci.*, **62**, 952 (1973).

(2) K. E. Guyer, S. G. Boots, P. E. Marecki, and M. R. Boots, *ibid.*, **65**, 548 (1976).

(3) H. Büchi, K. Steen, and A. Eschenmoser, *Angew. Chem. Int. Ed. Engl.*, **3**, 62 (1964).

(4) A. Sakurai, *Sci. Pap. Inst. Phys. Chem. Res. (Jpn.)*, **53**, 250 (1959).

(5) R. Tschesche and H. Machleidt, *Ann. Chem.*, **631**, 61 (1960).

(6) J. J. Donleavy, *J. Am. Chem. Soc.*, **58**, 1004 (1936).

(7) J. N. E. Day and J. F. Thorpe, *J. Chem. Soc.*, **117**, 1465 (1920).

(8) A. W. Crossley and W. R. Pratt, *ibid.*, **107**, 171 (1915).

(9) R. H. Curtis, J. N. E. Day, and L. G. Kimmins, *ibid.*, **123**, 3131 (1923).

(10) J. S. Baran and D. Langford (to G. D. Searle and Co.), U.S. pat. 3,818,080 (1974).

(11) D. J. Shapiro and V. W. Rodwell, *J. Biol. Chem.*, **246**, 3210 (1971).

(12) O. H. Lowry, N. J. Rosenbrough, A. L. Farr, and R. J. Randall, *ibid.*, **193**, 265 (1951).

(13) C. D. Goodwin and S. Margolis, *J. Lipid Res.*, **17**, 297 (1976).

(14) G. A. Bray, *Anal. Biochem.*, **1**, 279 (1960).

[5] Beckman LS-355.

ACKNOWLEDGMENTS

Presented at the Medical Sciences Section, Virginia Academy of Science, Richmond meeting, May 1979.

Abstracted in part from a dissertation submitted by Y.-M. Yeh to Virginia Commonwealth University in partial fulfillment of the Doctor of Philosophy degree requirements.

Comparison of Dye Dilution Method to Radionuclide Techniques for Cardiac Output Determination in Dogs

SAM SUN-CHONG ENG *x, JUAN R. ROBAYO ‡, WILLIAM PORTER §, and ROBERT E. SMITH ¶

Received July 2, 1979, from the **Faculty of Pharmacy, Wayne State University, and the Department of Pharmacy, Children's Hospital of Michigan, Detroit, MI 48201*, the ‡*College of Pharmacy, University of Oklahoma, Oklahoma City, OK 73190*, the §*Faculty of Pharmacy, Wayne State University, and the Department of Nuclear Medicine, William Beaumont Hospital, Royal Oak, MI 48072*, and the ¶*School of Pharmacy, Creighton University, Omaha, NE 68178.* Accepted for publication November 26, 1979.

Abstract □ A study was undertaken to identify the most accurate ^{99m}Tc-labeled radiopharmaceutical and to determine the accuracy of a noninvasive radionuclide technique (antecubital injection and precordial detection) for cardiac output determinations. Phase I employed sodium pertechnetate, stannous pyrophosphate with sodium pertechnetate, technetium-99*m* red blood cells, and technetium-99*m* human serum albumin as radionuclide tracers. Cardiac output was determined by the dye dilution method and then by the invasive radionuclide technique. The radiopharmaceutical was injected into the same intracardiac catheter used in the dye dilution method. Seven to 10 mongrel dogs were used to test the accuracy of each radiopharmaceutical. A paired *t* test and regression analysis indicated that technetium-99*m* human serum albumin was the most accurate radiopharmaceutical for cardiac output determinations, and the results compared favorably to those obtained by the dye dilution method. In Phase II, technetium-99*m* human serum albumin was used as the radionuclide tracer for cardiac output determinations with the noninvasive technique. The results compared favorably to those obtained by the dye dilution method. Regression analysis indicated a correlation coefficient of 0.91. A paired *t* test demonstrated that the difference between the two methods was not statistically significant ($p > 0.05$). The data suggest that a noninvasive radionuclide technique using an intravascular radiopharmaceutical may be safe and nontraumatic for cardiac output determinations in humans.

Keyphrases □ Cardiac output—determination, comparison of dye dilution method and radionuclide techniques, dogs □ Dye dilution method—determination of cardiac output, comparison to radionuclide techniques, dogs □ Radionuclides—use in determination of cardiac output, comparison to dye dilution method, dogs

Measurement of cardiac output using readily detectable tracers such as indocyanine green[1] or suitable radionuclides is based on the principle of conservation of mass (1–3). The direct Fick method involves measuring the amount of oxygen extracted from the inspired air by the lungs and the arteriovenous oxygen difference (4–6). The Stewart–Hamilton dye dilution method is analogous to the direct Fick method (7–9). The validity and reproducibility of this method were verified by several investigators (10–14). The relative ease of detection and quantitation of radioactive tracers have resulted in the use of radiopharmaceuticals for cardiac output determinations (15–29). However, the necessity for cardiac catheterization and cannulation usually limits their usefulness.

[1] Cardio-green, Hynson, Westcott and Dunning, Baltimore, Md.

0022-3549/80/0500-0509$01.00/0

© 1980, American Pharmaceutical Association

for 30 min. To the mixture was added 3.2 g of anhydrous sodium sulfite, and this mixture was extracted twice with 10-ml portions of benzene (13).

The benzene extract was evaporated to dryness in a liquid scintillation vial at 50° under a nitrogen stream. Twenty milliliters of Bray's scintillation solution (14) was added, and tritium and carbon 14 were determined simultaneously in a liquid scintillation counter[5]. Counting efficiency was determined by the external standard method. Some variability in the inhibition data was noted between tubes of microsomes (even from the same liver preparation). For this reason, a standard inhibitor, 1-(4-biphenylyl)pentyl hydrogen succinate (IX), was utilized routinely.

RESULTS AND DISCUSSION

The activity of IIIa–IIId and IVa–IVd as inhibitors of rat liver β-hydroxy-β-methylglutaryl-CoA reductase is shown in Table II. Unfortunately, the low solubility of these compounds in the enzyme assay prevented the determination of I/S values required for 50% inhibition. Thus, no definite conclusions can be made concerning the effect of increasing the size of the alkyl group at the C-3 position of the glutaric acid moiety with or without a C-3 hydroxyl group. However, the limited data do indicate that no substantial changes in inhibitory activity resulted from these modifications [compare 3-hydroxy-3-methyl (X) to 3-hydroxy-3-*n*-propyl (IVa) and the similar degree of inhibition shown by the analogs when assayed at identical I/S values].

REFERENCES

(1) M. R. Boots, S. G. Boots, C. M. Noble, and K. E. Guyer, *J. Pharm. Sci.*, **62**, 952 (1973).

(2) K. E. Guyer, S. G. Boots, P. E. Marecki, and M. R. Boots, *ibid.*, **65**, 548 (1976).

(3) H. Büchi, K. Steen, and A. Eschenmoser, *Angew. Chem. Int. Ed. Engl.*, **3**, 62 (1964).

(4) A. Sakurai, *Sci. Pap. Inst. Phys. Chem. Res. (Jpn.)*, **53**, 250 (1959).

(5) R. Tschesche and H. Machleidt, *Ann. Chem.*, **631**, 61 (1960).

(6) J. J. Donleavy, *J. Am. Chem. Soc.*, **58**, 1004 (1936).

(7) J. N. E. Day and J. F. Thorpe, *J. Chem. Soc.*, **117**, 1465 (1920).

(8) A. W. Crossley and W. R. Pratt, *ibid.*, **107**, 171 (1915).

(9) R. H. Curtis, J. N. E. Day, and L. G. Kimmins, *ibid.*, **123**, 3131 (1923).

(10) J. S. Baran and D. Langford (to G. D. Searle and Co.), U.S. pat. 3,818,080 (1974).

(11) D. J. Shapiro and V. W. Rodwell, *J. Biol. Chem.*, **246**, 3210 (1971).

(12) O. H. Lowry, N. J. Rosenbrough, A. L. Farr, and R. J. Randall, *ibid.*, **193**, 265 (1951).

(13) C. D. Goodwin and S. Margolis, *J. Lipid Res.*, **17**, 297 (1976).

(14) G. A. Bray, *Anal. Biochem.*, **1**, 279 (1960).

[5] Beckman LS-355.

ACKNOWLEDGMENTS

Presented at the Medical Sciences Section, Virginia Academy of Science, Richmond meeting, May 1979.

Abstracted in part from a dissertation submitted by Y.-M. Yeh to Virginia Commonwealth University in partial fulfillment of the Doctor of Philosophy degree requirements.

Comparison of Dye Dilution Method to Radionuclide Techniques for Cardiac Output Determination in Dogs

SAM SUN-CHONG ENG *x, JUAN R. ROBAYO ‡, WILLIAM PORTER §, and ROBERT E. SMITH ¶

Received July 2, 1979, from the **Faculty of Pharmacy, Wayne State University, and the Department of Pharmacy, Children's Hospital of Michigan, Detroit, MI 48201*, the ‡*College of Pharmacy, University of Oklahoma, Oklahoma City, OK 73190*, the §*Faculty of Pharmacy, Wayne State University, and the Department of Nuclear Medicine, William Beaumont Hospital, Royal Oak, MI 48072*, and the ¶*School of Pharmacy, Creighton University, Omaha, NE 68178.* Accepted for publication November 26, 1979.

Abstract □ A study was undertaken to identify the most accurate ^{99m}Tc-labeled radiopharmaceutical and to determine the accuracy of a noninvasive radionuclide technique (antecubital injection and precordial detection) for cardiac output determinations. Phase I employed sodium pertechnetate, stannous pyrophosphate with sodium pertechnetate, technetium-99*m* red blood cells, and technetium-99*m* human serum albumin as radionuclide tracers. Cardiac output was determined by the dye dilution method and then by the invasive radionuclide technique. The radiopharmaceutical was injected into the same intracardiac catheter used in the dye dilution method. Seven to 10 mongrel dogs were used to test the accuracy of each radiopharmaceutical. A paired *t* test and regression analysis indicated that technetium-99*m* human serum albumin was the most accurate radiopharmaceutical for cardiac output determinations, and the results compared favorably to those obtained by the dye dilution method. In Phase II, technetium-99*m* human serum albumin was used as the radionuclide tracer for cardiac output determinations with the noninvasive technique. The results compared favorably to those obtained by the dye dilution method. Regression analysis indicated a correlation coefficient of 0.91. A paired *t* test demonstrated that the difference between the two methods was not statistically significant ($p > 0.05$). The data suggest that a noninvasive radionuclide technique using an intravascular radiopharmaceutical may be safe and nontraumatic for cardiac output determinations in humans.

Keyphrases □ Cardiac output—determination, comparison of dye dilution method and radionuclide techniques, dogs □ Dye dilution method—determination of cardiac output, comparison to radionuclide techniques, dogs □ Radionuclides—use in determination of cardiac output, comparison to dye dilution method, dogs

Measurement of cardiac output using readily detectable tracers such as indocyanine green[1] or suitable radionuclides is based on the principle of conservation of mass (1–3). The direct Fick method involves measuring the amount of oxygen extracted from the inspired air by the lungs and the arteriovenous oxygen difference (4–6). The Stewart–Hamilton dye dilution method is analogous to the direct Fick method (7–9). The validity and reproducibility of this method were verified by several investigators (10–14). The relative ease of detection and quantitation of radioactive tracers have resulted in the use of radiopharmaceuticals for cardiac output determinations (15–29). However, the necessity for cardiac catheterization and cannulation usually limits their usefulness.

[1] Cardio-green, Hynson, Westcott and Dunning, Baltimore, Md.

0022-3549/80/0500-0509$01.00/0

© 1980, American Pharmaceutical Association

Table I—Data Pairs Obtained by the Radionuclide Method Using Sodium Pertechnetate as the Tracer and the Dye Dilution Method

Dog	Cardiac Output, liters/min: Dye Dilution Method	Cardiac Output, liters/min: Radionuclide Method (Sodium Pertechnetate)
1	2.27	1.51
2	1.62	1.37
3	2.83	1.98
4	1.91	1.32
5	3.94	2.64
6	2.02	1.14
7	1.68	1.41
8	2.39	1.88
Mean	2.33	1.66
SD	0.71	0.46
Paired *t* test		
mean of difference = 0.67		
standard deviation of difference = 0.35		
t test = 5.49 (statistically significant)		

BACKGROUND

Technetium-99*m* as the pertechnetate ion and ^{99m}Tc-labeled human serum albumin and red blood cells have been investigated as tracers for cardiac function determinations. Technetium-99*m* was used in its pertechnetate form for cardiac output studies (30). Invasive arterial cannulation was used to inject pertechnetate into the external jugular vein, and blood samples were drawn at a constant rate from the femoral artery. This technique may distort the radionuclide dilution curve and render the results inaccurate due to the distance between the injection and sampling sites.

Schelbert *et al.* (31) reported a correlation coefficient of 0.94 for the left ventricular ejection fraction between the radionuclide method and cineangiocardiography. Although precordial recording was utilized, technetium-99*m* human serum albumin was injected into a central venous catheter at the superior vena cava. Antecubital injection and precordial recording of dilution curves for cardiac function determinations have been studied (32–34); however, the validity of this technique has not been established.

In radionuclide cardioangiography, intravascular agents are preferred. Technetium-99*m* human serum albumin and technetium-99*m* red blood cells have been the two most commonly studied intravascular agents. In this study, sodium pertechnetate was used because the leakage of pertechnetate ions from the vascular compartment was not thought to be significant. Stannous pyrophosphate plus sodium pertechnetate was selected as a tracer following reports on the *in vivo* labeling of red blood cells (35, 36).

Four technetium-99*m* radiopharmaceuticals were studied to determine which one correlated best with the dye dilution method for cardiac output determination. The superior radiopharmaceutical, technetium-99*m* human serum albumin, then was used to determine the reliability of a relatively noninvasive radionuclide technique.

EXPERIMENTAL

Technetium-99*m* was eluted from a molybdenum-99–technetium-99*m* generator[2] as sodium pertechnetate. Technetium-99*m* human serum albumin was prepared by the electrolytic method (37, 38). Technetium-99*m* red blood cells were prepared by pretinning red blood cells with stannous glycoheptonate and then were mixed with technetium-99*m* as the pertechnetate (39).

In Phase I, 37 mongrel dogs were anesthetized with pentobarbital, 35 mg/kg, by intravenous bolus injection. The injection catheter was inserted *via* the right femoral vein to the right ventricle, and the sampling catheter was inserted *via* the right femoral artery to the aorta. Catheter placement was verified by radiological examination. A 25-mg vial of indocyanine green was reconstituted aseptically with 10 ml of diluent to yield a solution of 2.5 mg/ml.

The densitometer[3] was calibrated with a known concentration of indocyanine green in 10 ml of mongrel dog blood. After calibration, a bolus of 2.5 mg (1.0 ml) of indocyanine green was injected *via* the injection catheter using a 1.0-ml syringe[4], a three-way stopcock, and a 5-ml saline flush. The dilution was traced on the densitometer, and the computed cardiac output was displayed at the lighted digital window.

Table II—Cardiac Output Obtained by the Dye Dilution Method and the Radionuclide Method Using Stannous Pyrophosphate plus Sodium Pertechnetate for *In Vivo* Labeling of Red Blood Cells

Dog	Cardiac Output, liters/min: Dye Dilution Method	Cardiac Output, liters/min: Radionuclide Method (Stannous Pyrophosphate and Sodium Pertechnetate)
1	1.92	1.67
2	2.36	1.39
3	2.01	1.13
4	3.18	3.05
5	2.18	2.03
6	3.32	2.65
7	2.45	1.09
8	2.40	1.57
9	2.16	0.67
10	1.79	1.04
Mean	2.38	1.63
SD	0.48	0.71
Paired *t* test		
mean of difference = 0.75		
standard deviation of difference = 0.47		
t test = 0.53 (statistically significant)		

Immediately following the determination of cardiac output by the dye dilution method and while the animal was still anesthetized, the dog was placed in the supine position with its four extremities held toward the four corners of a stretcher. The detector of the mobile radioisotopic camera[5] was positioned at a left anterior oblique view with a 60° angle for proper recording of cardiac anatomy and bolus passage through the cardiopulmonary circulation. Before the radiopharmaceutical injection, the videotape system of the mobile camera was activated. A 5–10-mCi dose of a ^{99m}Tc-radiopharmaceutical was injected *via* the injection catheter in the identical manner as the dye dilution method.

The bolus passage, which gives the radionuclide dilution curve, was recorded by the videostorage system of the camera. Five minutes after the ^{99m}Tc-radiopharmaceutical bolus injection, an equilibrium count rate, C_e, was recorded. Then ^{125}I-radioiodinated serum albumin was injected *via* a peripheral vein for blood volume determination (40). The data from individual videotapes were transferred to a large magnetic storage tape through the computer-attached recording unit.

After individual animal data were fed to the computer[6] for analysis, the bolus passage through the cardiopulmonary circulation was framed by the computer into multiple 1-sec frames; the equilibrium study appeared as a single frame. For each set of animal data, four regions of interest were selected using a light pen and the oscilloscope of the computer. In the flow study and the equilibrium study, the left ventricle was labeled as Regions 1 and 3, respectively. The backgrounds surrounding the left ventricle in the flow study and in the equilibrium study were labeled Regions 2 and 4, respectively. The criteria for the selection were that there should be no overlap between regions of interest of the left ventricle and the background and that the point area of the background should be half that of the left ventricle on integration.

Once the four regions were selected and the data were entered into the computer, the computer utilized these data to calculate the area under the total dilution curve. The area of the background curve subsequently was subtracted from the total dilution curve to give the actual radionuclide dilution curve. The computer program excluded secondary recirculation from the primary dilution curve by extrapolation. It converted the points of the original curve to their semilog counterparts that were shown at the computer oscilloscope. The slope of each individual point was printed on a computer sheet. After the investigators selected the points that gave the best semilog extrapolation, the computer integrated the area under the radionuclide dilution curve. The blood volume was entered, and the offset for the curve was selected to eliminate interference by counts derived from the passage of radiopharmaceuticals through the injection catheter. The computer calculated the cardiac output of each animal using:

[2] Mallinckrodt, St. Louis, Mo.
[3] COR-100, Water Instruments, Rochester, Minn.
[4] Cornwall.
[5] Series 120, Ohio Nuclear Corp., Solon, Ohio.
[6] Model 5407A scintigraphic data analyzer, Hewlett-Packard, Palo Alto, Calif.

Table III—Cardiac Output Obtained by the Radionuclide Method Using Technetium-99*m* Red Blood Cells as the Tracer and the Dye Dilution Method

Dog	Cardiac Output, liters/min: Dye Dilution Method	Cardiac Output, liters/min: Radionuclide Method (Technetium-99*m* Red Blood Cells)
1	2.43	2.92
2	1.68	2.15
3	2.00	3.44
4	2.14	3.03
5	2.94	2.21
6	2.71	2.91
7	2.07	1.98
8	2.48	2.62
9	2.24	2.67
10	3.67	3.59
Mean	2.44	2.75
SD	0.54	0.51

Paired *t* test
mean of difference = 0.32
standard deviation of difference = 0.59
t test = −1.70

Table IV—Cardiac Output Obtained by the Radionuclide Method Using Technetium-99*m* Human Serum Albumin as the Tracer and the Dye Dilution Method

Dog	Cardiac Output, liters/min: Dye Dilution Method	Cardiac Output, liters/min: Noninvasive Radionuclide Method (Technetium-99*m* Human Serum Albumin)
1	2.96	2.49
2	1.89	1.80
3	2.02	2.34
4	1.99	2.18
5	2.97	2.85
6	2.21	2.51
7	2.43	2.39
8	2.20	1.97
9	1.48	1.25
Mean	2.24	2.20
SD	0.46	0.44

Paired *t* test
mean of difference = 0.04
standard deviation of difference = 0.26
t test = 0.48

$$Q_r = \frac{C_e BV}{A} \qquad \text{(Eq. 1)}$$

where A is the area under the radionuclide dilution curve, Q_r is the cardiac output in liters per minute, C_e is the equilibrium in counts per minute, and BV is the total blood volume.

Subsequent to the selection of the most appropriate radiopharmaceutical, seven mongrel dogs were anesthetized with pentobarbital, and the cardiac output was determined by the dye dilution method as in Phase I. Immediately following the determination of cardiac output by the dye dilution method, technetium-99*m* human serum albumin was injected *via* an antecubital vein, and the radionuclide dilution curve was traced precordially by the radionuclide camera and recorded onto the videotape. The data then were analyzed as described.

RESULTS AND DISCUSSION

In Phase I, cardiac output determinations were obtained in 37 mongrel dogs. In Group I, the cardiac output measurements determined by the dye dilution method had a mean of 2.33 ± 0.71 liters/min (mean ± *SD*); results of the pertechnetate radionuclide method had a mean of 1.66 ± 0.46 liters/min (Table I). For individual data pairs, the radionuclide cardiac output values were consistently lower than those obtained by the dye dilution method. This result might have been due to the rapid extravascularization of the pertechnetate ions after injection. On regression analysis, cardiac output data determined by the radionuclide method, Q_r, were assigned as the independent variable, and the data obtained by the dye dilution method, Q_d, were assigned as the dependent variable. The regression line of best fit was $Q_d = -0.08 + 1.46Q_r$. The correlation coefficient was 0.93, which may be due to the consistently lower radionuclide determinations. A paired *t* test indicated that the difference between the radionuclide method and the dye dilution method was statistically significant ($p < 0.05$).

In Group 2, stannous pyrophosphate was injected 10 min prior to the sodium pertechnetate injection to pretin the erythrocytes and to facilitate subsequent *in vivo* labeling of erythrocytes by the pertechnetate. The mean cardiac output value obtained by the radionuclide method (1.63 ± 0.71 liters/min) again was consistently lower than that obtained by the dye dilution method (2.38 ± 0.48 liters/min) (Table II). This result may have been due to the incomplete *in vivo* labeling of erythrocytes. Consequently, part of the injected sodium pertechnetate escaped to the extravascular compartments. This loss resulted in low equilibrium counts and low cardiac output determinations. The regression line of best fit was $Q_d = 1.51 + 0.53Q_r$. The correlation coefficient was lower ($F = 0.79$), possibly because of greater intrapair variations. A paired *t* test also indicated that the difference between the two methods was statistically significant ($p < 0.05$).

For Group 3, data obtained by using technetium-99*m* red blood cells as the tracer in the radionuclide method were compared to those obtained by the dye dilution method (Table III). Although there was a small difference between the mean cardiac output value determined by the radionuclide method (2.75 ± 0.51 liters/min) and the dye dilution method (2.44 ± 0.54 liters/min), individual data pairs varied greatly. Therefore, the correlation coefficient ($F = 0.43$) was significantly lower than that of the previous two groups, and the regression line of best fit was $Q_d = 1.19 + 0.45Q_r$. A paired *t* test indicated that the difference between the two methods was not statistically significant ($p > 0.05$).

In Group 4, the mean cardiac output obtained by using technetium-99*m* human serum albumin as a tracer in the radionuclide method (2.20 ± 0.44 liters/min) was close to the value of the dye dilution method (2.24 ± 0.46 liters/min). The difference between the individual data pairs also was very small (Table IV). Regression analysis gave a correlation coefficient of 0.85 and a regression line of best fit of $Q_d = 0.31 + 0.88Q_r$. The difference between the values in cardiac output by the two methods was not statistically significant ($p > 0.05$).

When all of the results from Phase I of the study were examined, cardiac output determinations using technetium-99*m* human serum albumin as the radionuclide tracer compared favorably to the dye dilution method. The correlation coefficient between the two methods was 0.85, and a paired *t* test indicated that the difference between these two methods was not statistically significant ($p > 0.05$). Sodium pertechnetate and stannous pyrophosphate plus sodium pertechnetate gave significantly different results when compared to the dye dilution method ($p < 0.05$). Even though cardiac output determinations using technetium-99*m* red blood cells were not significantly different from the cardiac output determined by the dye dilution method, regression analysis of the data gave a correlation coefficient of 0.43. Therefore, technetium-99*m* red blood cells appeared to be an inferior tracer.

In Phase II of the study, technetium-99*m* human serum albumin was injected antecubitally, and the dilution curve was recorded precordially. The mean cardiac output by the noninvasive radionuclide method was 2.22 ± 0.57 liters/min and that of the dye dilution method was 2.24 ± 0.54 liters/min. The intrapair differences (Table V) were small and could be explained as physiological occurrences.

Regression analysis gave a correlation coefficient of 0.91 and a regression line of best fit of $Q_d = 0.31 + 0.87Q_r$. A paired *t* test also revealed that the difference in cardiac output determinations between the noninvasive radionuclide method, using technetium-99*m* human serum albumin as the tracer, and the dye dilution method was not statistically significant ($p > 0.05$).

Various investigators reported favorable results using the radionuclide technique for cardiac flow studies when compared to the currently accepted methods. Zekert *et al.* (19) reported a correlation coefficient of 0.80 between the dye dilution method and the radionuclide method, and the difference between the pairs was not statistically significant. Campione and Steiner (20) observed good correlation between cardiac indexes determined simultaneously by the Fick method and the radionuclide technique after antecubital injections and precordial recording using ^{131}I-radioiodinated serum albumin as the tracer. Falch and Norman (28) reported a correlation coefficient of 0.96 between the dye dilution technique and the radionuclide technique using indium-113*m* as the tracer. Van Dyke *et al.* (41) also reported that cardiac output determined by the radionuclide method using technetium-99*m* human serum albumin showed good agreement with cardiac output determined by the Fick method. In the determination of the left ventricular ejection fraction, Strauss *et al.* (34) and Groch *et al.* (42) found that the correlation coef-

Table V—Cardiac Output Obtained by Noninvasive Radionuclide Technique Using Technetium-99*m* Human Serum Albumin as the Tracer and the Dye Dilution Method

Dog	Cardiac Output, liters/min: Dye Dilution Method	Cardiac Output, liters/min: Noninvasive Radionuclide Method (Technetium-99*m* Human Serum Albumin)
1	2.16	2.14
2	3.38	3.44
3	2.06	1.78
4	2.62	2.45
5	1.88	1.55
6	1.93	2.02
7	1.75	2.19
Mean	2.24	2.22
SD	0.54	0.57

Paired *t* test
mean of difference = 0.02
standard deviation of difference = 0.25
t test = 0.20

ficients between contrast angiocardiography and the radionuclide technique were 0.92 and 0.90, respectively.

The radionuclide technique employed by most of these investigators used intracardiac catheters for the injection of radiopharmaceuticals. The data from this animal model clearly demonstrated that noninvasive peripheral injection of an intravascular radiopharmaceutical yields results that are not significantly different from the widely used dye dilution method for cardiac output determinations. Although additional investigations are necessary, this study suggests that a noninvasive radionuclide technique may be safe, relatively nontraumatic, and accurate for cardiac output determinations in humans.

REFERENCES

(1) P. Kantrowitz and B. Kingley, *Med. Res. Eng.*, **10,** 12 (1971).

(2) J. B. Bassingthwaights and G. A. Holloway, Jr., *Sem. Nucl. Med.*, **6,** 141 (1976).

(3) J. S. Carey and R. K. Hughes, *Ann. Thorac. Surg.*, **7,** 150 (1969).

(4) A. C. Burton, "Physiology and Biophysics of Circulation—An Introduction Text," Year Book Publishers, Chicago, Ill., 1965, p. 167.

(5) A. Selzer and R. B. Sudrann, *Circulation*, **6,** 485 (1958).

(6) W. F. Hamilton, R. L. Riley, A. M. Attyah, A. Cousnand, D. M. Fowell, A. Himmelstein, R. P. Noble, J. W. Remington, D. W. Richards, Jr., N. C. Wheeler, and A. C. Witham, *Am. J. Physiol.*, **153,** 309 (1948).

(7) G. N. Stewart, *J. Physiol.*, **22,** 159 (1897–8).

(8) P. Dow, *Physiol. Rev.*, **36,** 77 (1956).

(9) W. F. Hamilton, J. W. Moore, J. M. Kinsman, and R. G. Spurling, *Am. J. Physiol.*, **99,** 534 (1932).

(10) K. L. Zierler, *Circ. Res.*, **10,** 393 (1962).

(11) J. M. Gonzalez-Fernandez, *ibid.*, **10,** 409 (1962).

(12) G. J. A. Cropp and A. C. Burton, *ibid.*, **18,** 26 (1966).

(13) J. C. Sleeper, H. K. Thompson, H. D. McIntosh, and R. C. Elston, *ibid.*, **11,** 712 (1962).

(14) E. V. Newman, M. Merrell, A. Genecin, C. Monge, W. R. Milnor, and W. P. McKeever, *Circulation*, **4,** 735 (1951).

(15) M. Prinzmetal, E. Corday, R. J. Spritzler, and W. Flieg, *J. Am. Med. Assoc.*, **139,** 617 (1949).

(16) R. J. Sanders and R. G. Sullivan, *J. Surg. Res.*, **8,** 522 (1968).

(17) H. M. Shizgal, M. Goldstein, P. F. Richard, and L. D. Maclean, *Surg. Gynecol. Obstet.*, **136,** 618 (1973).

(18) L. Donato, D. F. Rochester, M. L. Lewis, J. Durand, J. O. Parker, and R. M. Harvey, *Circulation*, **26,** 183 (1962).

(19) H. Zekert, F. Herbig, and T. Cooper, *J. Nucl. Med.*, **7,** 424 (1966).

(20) K. M. Campione and S. H. Steiner, *ibid.*, **9,** 630 (1968).

(21) F. E. Kloster, J. D. Bristow, and H. E. Griswold, *J. Appl. Physiol.*, **26,** 465 (1969).

(22) M. H. Lombardi, *Am. J. Vet. Res.*, **33,** 1825 (1972).

(23) M. Mariani, A. Maseri, and C. Giuntini, *J. Nucl. Biol. Med.*, **10,** 66 (1966).

(24) C. Giuntini, V. Oren, and E. Lubin, *ibid.*, **15,** 81 (1971).

(25) R. J. Gorten and J. C. Stauffer, *Am. J. Med. Sci.*, **238,** 274 (1959).

(26) B. F. Schreiner, F. W. Lovejoy, and P. N. Yu, *Circ. Res.*, **7,** 595 (1959).

(27) B. L. Carter, S. E. Johnsen, R. K. Loeffler, and M. E. Southard, *Am. J. Roentgenol. Rad. Ther.*, **82,** 618 (1959).

(28) D. Falch and N. Norman, *Scand. J. Clin. Lab. Invest.*, **2,** 207 (1974).

(29) T. Berndt, E. L. Alderman, and R. Wasnich, *J. Nucl. Med.*, **16,** 289 (1975).

(30) J. H. Meyers, R. E. Steadham, L. H. Blackwell, S. C. Hsieh, D. Van Dyke, and D. C. Harrison, *ibid.*, **12,** 591 (1971).

(31) H. R. Schelbert, J. W. Verba, A. D. Johnson, G. W. Brock, N. P. Alazraki, and F. J. Rose, *Circulation*, **51,** 902 (1975).

(32) V. L. Majano, E. Kaplan, and R. A. Rhodes, *Cor Vasa*, **13,** 124 (1971).

(33) M. J. Williams and T. Deegan, *Thorax*, **26,** 460 (1971).

(34) H. W. Strauss, B. L. Zaret, P. J. Hurley, T. K. Natarjan, and B. Pitt, *Am. J. Cardiol.*, **28,** 575 (1971).

(35) E. M. Stokely, R. W. Parkey, F. J. Bonte, K. D. Graham, M. J. Stone, and J. T. Willerson, *J. Nucl. Med.*, **17,** 565 (1976).

(36) A. M. Zimmer, D. G. Pavel, and V. N. Paterson, *ibid.*, **17,** 566 (1976).

(37) R. J. Callahan, K. A. McKusick, M. Lamson, III, F. P. Castronovo, and M. S. Potsaid, *ibid.*, **17,** 47 (1976).

(38) H. J. Dworkin and R. F. Gutkowski, *ibid.*, **12,** 562 (1971).

(39) R. F. Gutkowski and H. J. Dworkin, *ibid.*, **15,** 1187 (1974).

(40) W. H. Blahd, "Nuclear Medicine," 2nd ed., McGraw-Hill, New York, N.Y., 1971, p. 599.

(41) D. Van Dyke, H. O. Anger, R. W. Sullivan, W. R. Vetter, Y. Yano, and H. G. Baker, *J. Nucl. Med.*, **13,** 585 (1972).

(42) M. W. Groch, S. Gottlieb, S. M. Mallon, and A. Miale, *ibid.*, **17,** 930 (1976).

Micromeritic Properties of Sulfamethoxazole Microcapsules Prepared by Gelatin–Acacia Coacervation

H. TAKENAKA, Y. KAWASHIMA ˣ, and S. Y. LIN

Received December 14, 1978, from the *Gifu College of Pharmacy, Mitahora, Gifu 502, Japan.* Accepted for publication November 26, 1979.

Abstract □ Micronized sulfamethoxazole particles were microencapsulated using the gelatin–acacia complex coacervation method. The effects of the coacervation pH and the amount of formaldehyde used on the micromeritic parameters of the microcapsules were investigated. The particle-size and the wall thickness distributions were log-normal forms. As the pH was increased, the particle size decreased (8.5–28.5 μm). The porosity of various pH-adjusted microcapsules was between 0.158 and 0.277. The particle size of formalized microcapsules was larger than that of the unformalized microcapsules because formalization prevents shrinking of microcapsules during the dehydration and drying process. A smooth surface appeared on the unformalized microcapsule, but a net-like wrinkled structure was observed upon scanning the formalized one. Moreover, folding and invaginating structures were found on the spray-dried microcapsules. The optimum coacervation pH value was 3.5, at which the highest core content was obtained (77.5% w/w). Approximately 6.73 μg of formaldehyde remained in 1 g of the microcapsules formalized with 50 ml of formaldehyde. The crystalline sulfamethoxazole in the microcapsules prepared by spray drying the coacervate slurries was changed into the amorphous form, while the microcapsules dried in the conventional manner showed the same sulfamethoxazole form as the starting substance.

Keyphrases □ Sulfamethoxazole—microcapsules, prepared by gelatin–acacia coacervation □ Microencapsulation—sulfamethoxazole, gelatin–acacia coacervation □ Antibacterial agents—sulfamethoxazole, microencapsulation by gelatin–acacia coacervation

Microencapsulation is an attractive tool for the preparation of dosage forms to control the release rate, to separate incompatible materials in compounding, and to protect against moisture and oxidation. Many microencapsulation processes have been described (1). One accepted technique is gelatin–acacia complex coacervation, which was developed initially for processing carbonless copy paper (2–5). Various studies were reported later (6–8) on the effect of physical factors such as stirring speed, molecular weight of gelatin, and temperature on coacervation behavior. However, few studies have been published on the effects of the optimum coacervation pH and the amount of cross-linking agents used on the micromeritic parameters such as particle size, particle distribution, wall thickness, and porosity of the microcapsules.

The objective of the present study was to elucidate the effects of these factors on the preparation of sulfamethoxazole microcapsules. The effects of spray drying as an alternative to conventional drying of the coacervates on the surface characteristics and on the crystalline form of the microencapsulated sulfamethoxazole also were investigated. The remaining amounts of formaldehyde used as a hardening agent and the content of sulfamethoxazole in the microcapsules prepared under various conditions were determined.

EXPERIMENTAL

Materials—Gelatin[1] and acacia[2] were used as 3% (w/w) solutions. Micronized sulfamethoxazole[3] was used as a model drug. Acetic acid (10%), formaldehyde solution[4] (5, 15, 30, and 50 ml), isopropanol (70%), acetylacetone reagent solution[5], and formaldehyde standard solution[6] were JP grade and were used as received without further purification or recrystallization.

Microencapsulation—The microcapsules were prepared by the method of Green and Schleicher (2, 3) as modified by Luzzi and Gerraughty (8–10). In these experiments, gelatin and acacia solutions were prepared by dissolving 3.0 g of gelatin and 3.0 g of acacia each in 100 ml of purified distilled water. Five grams of micronized sulfamethoxazole was suspended in acacia solution at 50° for 5 min; an equal amount of gelatin solution, which was thermally controlled at 50°, was added gradually, with stirring at 620 rpm, to the acacia suspension. This suspension was maintained for 5 min, and the pH of the mixture was adjusted gradually by dropwise addition of diluted acetic acid with stirring. At the desired pH (2.5–4.0), the gelatin particles were positively charged and were attracted to the negatively charged acacia particles. Coacervation occurred, and a gelatin coating was formed (Fig. 1A). This mixture was cooled to 5° by immersion in a water bath.

A part of the mixture was withdrawn directly onto a slide glass for analysis of the particle size of the coacervate droplets. The rest of the coacervates was isolated from the equilibrium system and washed with 1 liter of distilled water to remove the excess colloid liquid. A part of the coacervated aggregates was retained for examination of the internal texture with a scanning electron microscope. Figure 1B shows the nest-like structure in which many crystals were encapsulated by a surrounding wall. The coacervates were hardened with formaldehyde solution (5, 15, 30, or 50 ml) for ~2 hr. Then the hardened coacervates were filtered and washed with distilled water. The wet mass was added, with stirring, to 70% isopropanol solution (11); stirring was continued for 30 min.

The sediments were filtered and dried at 40° by the conventional method for 2 hr to yield free-flowing discrete particles. The spray-drying technique (12) also was applied to prepare dried discrete microcapsule powders. The aqueous slurries containing the unformalized coacervates were atomized into a drying chamber at 140 ± 10° by a centrifugal wheel atomizer. Two batches for the preparation of microcapsules were run. The maximum batch-to-batch differences in the micromeritic properties of the microcapsules are indicated in Table I.

Measurement of Micromeritic Properties—Particle size was determined by a photographic counting method using a particle-size ana-

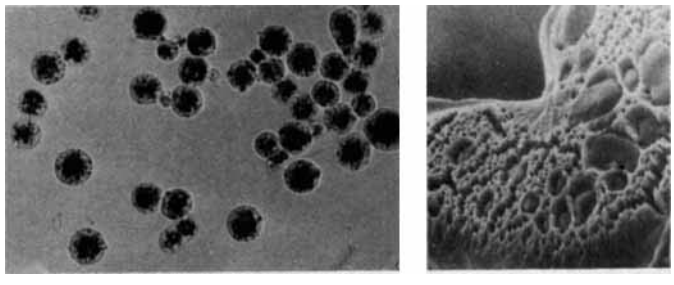

Figure 1—*Photomicrograph of sulfamethoxazole gelatin–acacia coacervates (left) and scanning electron microscopic photograph of the internal texture of coacervate aggregates (right).*

[1] Isoelectric point 4.9 and pH 6.3; the melting point of a 3% solution was 29° (Japan Leather Co., Japan).

[2] Kanto Chemical Co., Japan.

[3] Micronized to <6 μm by a jet micronizer (Shionogi Pharmaceuticals Co., Japan).

[4] Five, 15, 30, and 50 ml of 37% HCHO were added, respectively, to the coacervate suspension and diluted to a total volume of 200 ml.

[5] Ammonium acetate, 150 g, was dissolved in the proper volume of distilled water in a 1000-ml volumetric flask, 3 ml of acetic acid and 2 ml of acetylacetone were added, and the solution was diluted to 1000 ml (prepared just prior to use).

[6] Four micrograms of formaldehyde/ml of solution.

0022-3549/80/0500-0513$01.00/0
© 1980, American Pharmaceutical Association

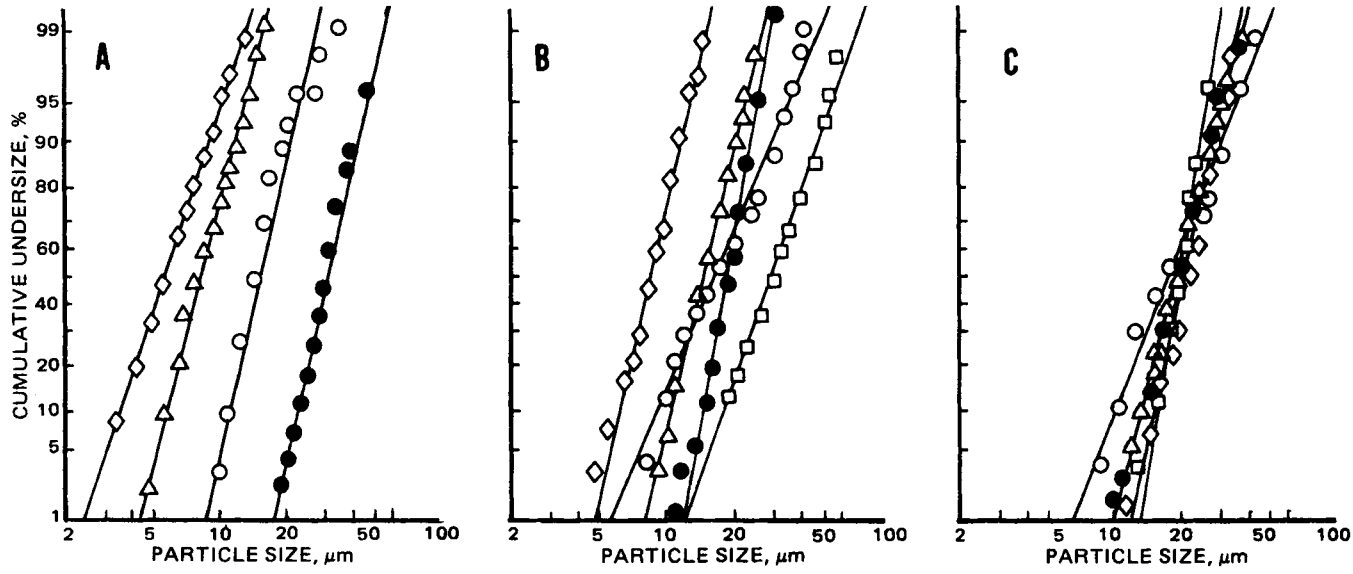

Figure 2—*Particle-size distribution of coacervates (A) and unformalized (B) and formalized (C) dried microcapsules. Key (for A and B): □, 2.5 adjusted pH; ●, 3.0 adjusted pH; ○, 3.5 adjusted pH; △, 3.7 adjusted pH; and ◇, 4.0 adjusted pH. Key (for C): ○, 0 ml of formaldehyde; ●, 5 ml of formaldehyde; △, 15 ml of formaldehyde; □, 30 ml of formaldehyde; and ◇, 50 ml of formaldehyde.*

lyzer[7]. Not less than 600 particles were measured for each batch. The coating thickness of the microcapsules was determined by direct measurement after microtome slicing of the microcapsules embedded in paraffin (mp 48–50°). The microcapsules were added to melted paraffin solution, and this mixture immediately was immersed into an ice bath and hardened. The paraffin masses subsequently were sliced with a congelation microtome. The slice thickness was ~10 μm. Each slice was placed on an object slide and mounted with liquid paraffin. Approximately 100 specimens were tested to measure the coating thickness, and the averaged value represented the wall thickness. The sections that came from the extremes of the microcapsules may have given somewhat high values for the wall thickness. However, comparison of the relative differences is valid.

The particle densities of various microcapsules and raw materials (*e.g.*, gelatin and micronized sulfamethoxazole) were measured with a helium–air comparison pycnometer[8].

The surface topography of the microcapsules was investigated by a scanning electron microscope[9]. The microcapsule samples were mounted on a sample stub with double-sided adhesive tape and were vacuum coated with carbon and gold.

The crystalline form of the microcapsulated sulfamethoxazole was determined with an X-ray diffractometer[10] with CuKα radiation (1.5418 Å). The IR spectrum was recorded with an IR spectrometer[11].

Assay of Sulfamethoxazole Content and Remaining Formaldehyde—The sulfamethoxazole content in the microcapsules was assayed by the following method. Approximately 100 mg of each sample was weighed accurately, extracted with pH 7.5 solution (simulated intestinal fluid of JP IX), and then determined spectrophotometrically at a suitable UV wavelength using a double-beam spectrophotometer. Ten 100-mg samples from two batches were tested, and the mean was obtained.

The remaining amount of hardening agent was determined by the modified acetylacetone method (13–15). One gram of each sample (*e.g.*, gelatin, acacia, sulfamethoxazole, and formalized microcapsules using 50 ml of formaldehyde) was extracted for ~2 hr with 100 ml of distilled water by shaking the sample at 40 ± 1° in a water bath, and the sample was filtered with a millipore filter (3 μm). Ten milliliters of the extracted sample solutions and of the formaldehyde standard solution were pipetted into separate 50-ml volumetric flasks containing 10 ml of acetylacetone reagent solution, and the flasks were shaken for 30 min at 40 ± 1° in a water bath. A blank test using 10 ml of distilled water instead of acetylacetone reagent solution also was undertaken. The absorbance of each extracted sample solution was determined at 415 nm by a spectrophotometer[12].

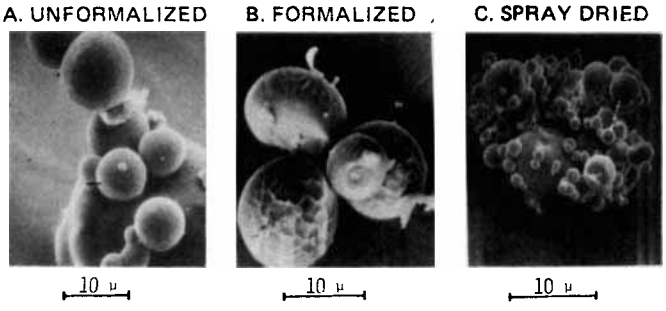

Figure 3—*Scanning electron microscopy photograph of dried sulfamethoxazole microcapsules prepared by complex coacervation.*

RESULTS AND DISCUSSION

Particle-Size Distribution of Gelatin–Acacia Coacervates and Dried Microcapsules Made Conventionally—The cooled coacervate droplets in equilibrium solution and the dried microcapsules prepared under the various pH adjustments without formalization were placed on a slide glass for particle-size measurements. These data are shown graphically in Figs. 2A and 2B, respectively. The sizes of the coacervates and the microcapsules followed a log-normal distribution. As the pH was increased from 3.3 to 4.2 in the equilibrium liquid, the geometric mean particle diameter of the microcapsules decreased (Table I). This result may have been due to the electrophoretic characteristic of gelatin–acacia coacervates. Electrophoretic data of coacervates obtained previously[13] showed that, at a pH above 3.5, the coacervates were electronegatively charged and the charges increased with increasing pH. This finding indicates that, at the higher pH range, the small coacervates could be formed due to the strong repulsive force between the coacervates. In addition, the reduced amounts of gelatin in the coacervates formed at the lower pH region enhanced the swelling of gelatin below pH 3.5–4.0 (16), leading to the formation of larger coacervates.

The unformalized microcapsules prepared at pH values higher than 3.5 were larger than the corresponding coacervates. The coacervates used for measuring the size were taken directly from the coacervation system prior to further processing. The rest of the coacervates were washed with 1 liter of distilled water, during which swelling occurred. The following drying process, *i.e.*, isopropanol treatment and air drying at 40°, contributed to the shrinkage of the microcapsules and offset the enlargement of the microcapsules caused by swelling. The coacervate with a thicker

[7] Karl Zeiss TGZ-3.
[8] Model 1302, Micromeritics Instrument Co.
[9] Nihon Denshi JDX.
[10] Nihon Denshi JSM-S1.
[11] Nihon Denshi DS-403G.
[12] Hitachi model 556.
[13] The original data for this study.

Table I—Micromeritic Properties of Dried Microcapsules by a Conventional Method [a]

Adjusted pH	D_g^1, μm	l, μm	ρ, g/cm³	ϵ (−)	Drug Content, %
4.0 (4.2)[b]	8.5 ± 0.3 (5.7 ± 0.3)[c]	1.31 ± 0.02	1.02 ± 0.01	0.270 ± 0.006	53.6 ± 0.6
3.7 (3.9)[b]	15.2 ± 0.4 (8.4 ± 0.3)[c]	1.15 ± 0.02	1.03 ± 0.01	0.277 ± 0.005	63.9 ± 0.5
3.5 (3.76)[b]	17.1 ± 0.4 (15.0 ± 0.4)[c]	1.00 ± 0.03	1.19 ± 0.03	0.186 ± 0.006	77.5 ± 0.8
3.0 (3.26)[b]	19.1 ± 0.5 (31.2 ± 0.6)[c]	0.87 ± 0.01	1.08 ± 0.01	0.217 ± 0.004	46.8 ± 0.4
2.5 (2.85)[b]	28.5 ± 0.5	0.75 ± 0.02	1.03 ± 0.00	0.264 ± 0.001	54.1 ± 0.5

Amount of Formaldehyde, ml	D_g^2, μm	ρ, g/cm³	ϵ (−)	Remaining Formaldehyde, μg/g	Drug Content, %
50	22.0 ± 0.4	1.17 ± 0.02	0.167 ± 0.004	6.73 ± 0.06	56.4 ± 0.5
30	20.1 ± 0.4	1.11 ± 0.02	0.203 ± 0.005		51.7 ± 0.5
15	19.0 ± 0.2	1.19 ± 0.03	0.158 ± 0.003		59.5 ± 0.4
5	19.1 ± 0.5	1.18 ± 0.02	0.161 ± 0.002		57.1 ± 0.6
0	17.1 ± 0.4	1.19 ± 0.03	0.186 ± 0.003		77.5 ± 0.8

[a] All data show the average values from two batches. Key: D_g^1, D_g^2, geometric mean diameter of unformalized and formalized dried microcapsules, respectively; ρ, particle density; l, wall thickness of unformalized dried microcapsules; and ϵ, porosity. [b] Final pH of equilibrium solution. [c] Geometric mean diameter of coacervates.

wall at the higher pH region (Table I) might retard shrinkage during the drying process, leading to the described results (Figs. 2A and 2B and Table I). For the microcapsule with a thinner wall at pH 3.0, the shrinking effects compared to the swelling might result in a size that is smaller than the coacervate (Table I). This expectation also was confirmed using a scanning electron microscope by the detection of a smooth surface on the microcapsule at the higher pH and a wrinkled surface at the lower pH.

The particle-size distributions of the unformalized and formalized microcapsules are seen in Figs. 2B and 2C, respectively. Upon formalizing the coacervates, some differences were observed in the particle-size distribution of microcapsules. An increase in the size of the microcapsules was found as more hardening agent was used (Table I). The hardened wall may prevent the shrinkage that occurs during the dehydration and drying process.

Microcapsule Wall Thickness and Porosity—The influence of pH on the wall thickness of dried microcapsules is shown in Table I. The wall of the dried microcapsules made at the higher pH was thicker than that of microcapsules made at the lower pH. Previous investigators (17–19) concluded that gelatin–acacia coacervates have a gelatin structure in which acacia is attracted by ionic bonds only and does not participate in the gel structure formation. At high pH values, NH_3^+ groups of gelatin are comparatively few but COO^- groups of acacia are numerous. To prepare coacervates, a larger amount of gelatin is required to interact with acacia, therefore leading to a thicker wall.

The particle densities (1.02–1.19) of the microcapsules, as measured by a helium–air comparison pycnometer, were smaller than those of the raw materials, *i.e.*, gelatin (1.27) and sulfamethoxazole (1.53). This result is reasonable because the microcapsule film may prevent helium penetration into the internal matrix of the microcapsule. If it is assumed that the microcapsule film is composed of gelatin alone (16, 17), the porosity, ϵ, of the microcapsule can be determined by inserting the density values into:

$$\epsilon = 1 - \frac{(C_g\rho_s + C_s\rho_g)\rho_m}{\rho_s\rho_g} \qquad \text{(Eq. 1)}$$

where C_g is the weight percent of gelatin, C_s is the weight percent of drug, ρ_s is the density of the drug particles, ρ_g is the density of the gelatin particles, and ρ_m is the density of the microcapsule particles. The porosity of the microcapsules was 0.158–0.277 (Table I).

Microcapsule Surface Topography—The surface of the unformalized microcapsules (Fig. 3A) was smooth and had no cracking or pore penetration. Evidence of folding and invagination was absent. The formalized microcapsules (Fig. 3B) also had a partially smooth surface and were free from structural defects. However, miscellaneous matter was seen occasionally on the capsule surface, which may have been due to crystals or polymer remaining in the medium during hardening. Another partial surface appearance showed a net-like wrinkled structure, which also was observed on the simple coacervated microcapsules during formalizing (23).

Adhesive sundries and crystals on the surface can be attributed to the soluble complex formed by the interaction between the formaldehyde and the primary amino groups of sulfamethoxazole, which was leached out to the surface during the washing process (24). These surface aberrations also may be the partially ruptured coacervates formed during hardening or dehydration, with the unencapsulated crystals adhering to the surface. The shrinking structure, which was not found on the unformalized microcapsules, may suggest that crossover linkage occurred during the formalizing procedure. Reaction of the gel with formaldehyde caused a high degree of insolubility as a result of intermolecular crosslinkage formation. Adhesive polymer sundries could be due to the ruptured fractions of coacervates or the remaining gelatin fractions that were crosslinked with formaldehyde upon hardening.

Drug Content and Remaining Amounts of Hardening Agents—The extraction of sulfamethoxazole microcapsules showed that >45% (w/w) of sulfamethoxazole was contained in the microcapsules (Table I). The microcapsules adjusted to pH 3.5 had the highest content. This result may have been due to the high volume of coacervates formed when the pH was adjusted to 3.5, at which point the positive and negative charges were equivalent (25). According to these data and those from a previous report (26), pH 3.5 is the optimum pH for coacervation in the present system where the acacia is strongly negative and the gelatin is strongly positive. Table I illustrates that the content of the unformalized microcapsules was higher than that of the formalized microcapsules. Because of the interaction between formaldehyde and sulfamethoxazole, this soluble complex was leached out and lost in the medium, resulting in a drug content of ~55% in the formalized microcapsules, which was 22% less than the unformalized content.

Approximately 6.73 μg of formaldehyde remained in 1 g of the formalized microcapsules prepared with 50 ml of formaldehyde. If 710 mg of these microcapsules (56.4%) is administered orally, according to the

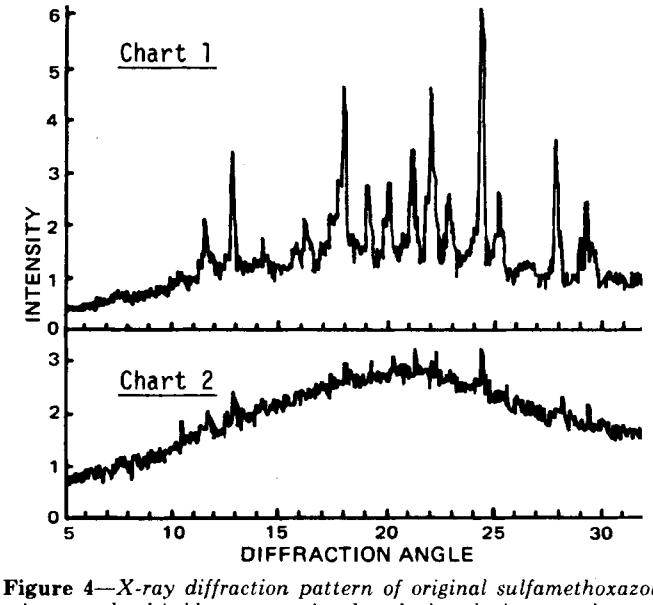

Figure 4—*X-ray diffraction pattern of original sulfamethoxazole, microcapsules dried by a conventional method, and microcapsules spray dried after coacervation. Key: Chart 1, original sulfamethoxazole or dried microcapsules by a conventional method; and Chart 2, spray-dried microcapsules. (Intensity scale: 1 = 10 Hz.)*

formulation of co-trimoxazole tablets[14] (BP 1973), it is predicted that no side effects would occur since only 4.75 μg of formaldehyde is contained in this formulation. The other formalized microcapsules may have a lower amount of remaining formaldehyde, although no such data are available. The method of removing the remaining formaldehyde from the formalized microcapsules also is important for microencapsulation if formaldehyde is applied as a hardening agent.

Effect of Spray-Drying Procedure on Microcapsule Surface Topography and Crystalline Drug Form—On the surface of the spray-dried microcapsules prepared from the unformalized coacervates (Fig. 3C), a smooth surface with some fissures of the coating was observed. Moreover, a few microcapsules possessed a characteristically folded and invaginated surface. This phenomenon may be deduced from a diagram (20–22) of a spray-dried slurry droplet.

X-ray diffraction patterns of the ground microcapsules were obtained to investigate the crystalline forms of sulfamethoxazole in the microcapsule prepared by conventional and spray-drying techniques. The intensities of the diffraction peaks of the spray-dried sulfamethoxazole were weaker than those of the original material. A rapid evaporation of solvent from spray droplets might change the crystalline form to the disordered form (Fig. 4). On the other hand, the intensities of the peaks found in the microcapsules dried by the conventional method coincided with those of the original sulfamethoxazole. This result may be explained in that, although the coacervation temperature was 50°, the crystalline forms could not be disordered due to the mild drying process employed. In addition, the IR spectrum of all of the microcapsules coincided with that of the original sulfamethoxazole, indicating that complexes between sulfamethoxazole and the polymers (gelatin or acacia) were not formed through spray drying and the complex coacervation processes.

REFERENCES

(1) L. A. Luzzi, *J. Pharm. Sci.*, **59**, 1367 (1970).

(2) B. K. Green and L. Schleicher, U.S. pats. 2,730,456 and 2,730,457 (1956).

(3) *Ibid.*, U.S. pats. 2,800,457 and 2,800,458 (1957).

(4) N. C. R. Co., *Sci. Dig.*, **44**, 66 (July 1958).

(5) N. C. R. Co., *Chem. Week*, **83** (Dec. 21), 43 (1963).

(6) J. W. McGinity, A. B. Combs, and A. N. Martin, "The Proceedings of Third International Symposium on Microencapsulation," Tokyo, Japan, 1976, p. 3.

(7) P. L. Madan, J. C. Price, and L. A. Luzzi, "Microencapsulation Process and Application," Plenum, New York, N.Y., 1974, p. 39.

(8) L. A. Luzzi and R. J. Gerraughty, *J. Pharm. Sci.*, **53**, 429 (1964).

(9) *Ibid.*, **56**, 643 (1967).

(10) *Ibid.*, **56**, 1174 (1967).

(11) P. L. Madan, L. A. Luzzi, and J. C. Price, *J. Pharm. Sci.*, **61**, 1586 (1972).

(12) H. Takenaka, Y. Kawashima, and R. Ishibashi, *Drug Dev. Ind. Pharm.*, **3**, 459 (1977).

(13) "TRS," Quality Control Department, Tolei Co., Tokyo, Japan, 1977.

(14) T. Nash, *Nature*, **170**, 976 (1952).

(15) T. Nash, *Biochem. J.*, **55**, 416 (1953).

(16) C. Thies, *J. Colloid Interface Sci.*, **44**, 133 (1973).

(17) Bungenberg de Jong and J. M. F. Landsmeer, *Proc. K. Ned. Akad. Wet., Amsterdam*, **51**, 137 (1948).

(18) *Ibid.*, **51**, 259 (1948).

(19) Bungenberg de Jong and J. M. F. Landsmeer, *Rec. Trav. Chim.*, **65**, 606 (1964).

(20) Y. Kawashima, *Powder Ind. (Jpn.)*, **4**, 32 (1972).

(21) Y. Kawashima, K. Matsuda, and H. Takenaka, *J. Pharm. Pharmacol.*, **24**, 505 (1972).

(22) W. R. Marshall and D. H. Charlesworth, *AIChE J.*, **6**, 9 (1960).

(23) J. R. Nixon and S. E. Walker, *J. Pharm. Pharmacol., Suppl.*, **23**, 147S (1971).

(24) J. R. Nixon, S. A. H. Khalil, and J. E. Carless, *ibid.*, **20**, 528 (1968).

(25) M. Glicksman and R. E. Sand, "Industrial Gums: Polysaccharides and Their Derivatives," Academic, New York, N.Y., 1973, p. 235.

(26) A. Kondo, *Surface (Jpn.)*, **7**, 23 (1969).

ACKNOWLEDGMENTS

The authors acknowledge the advice of Dr. B. A. Matthews, Ciba-Geigy Co., Jakarta, Indonesia, in the text preparation and also the use of a diffractometer through the courtesy of Professor A. Otsuka, Meijyo University, Nagoya, Japan.

[14] One tablet of co-trimoxazole contains 400 mg of sulfamethoxazole and 80 mg of trimethoprim.

Effects of Dansylated Acetylcholine Analogs on *Schistosoma mansoni*

G. R. HILLMAN *x, S.-H. CHU ‡, and M. J. DOTSON *

Received April 18, 1979, from the **Department of Pharmacology and Toxicology, University of Texas Medical Branch, Galveston, TX 77550,* and the ‡*Division of Biomedical Sciences, Brown University, Providence, RI 02912.* Accepted for publication December 3, 1979.

Abstract □ A series of dansylated fluorescent analogs was synthesized and tested for cholinergic and anticholinergic activity in *Schistosoma mansoni*. The compounds were compared with a previously reported analog, 5-(dimethylamino)-*N*-(2-dimethylaminoethyl)naphthalenesulfonamide hydrochloride (I). All of the compounds produced some fluorescent labeling of a structure in the head region of the worms. Major differences were not seen among the compounds. The compounds also were tested as antagonists of carbachol-induced paralysis in an activity monitor. Significant carbachol antagonism was seen for all compounds. Effects on the serotonin response also were recorded. Only one compound, a dibutylaminopropylamine derivative, produced striking antagonism of serotonin-induced motor activity.

Keyphrases □ Cholinergics—antagonists, dansylated acetylcholine analogs, *in vitro* scanning fluorescence method, neuroactive drugs in schistosomes □ Carbachol—effect on schistosomes, effect of anticholinergic agents, scanning fluorescence method, motility studies □ Serotonin—effect on schistosomes, anticholinergic agents, scanning fluorescence method □ Structure–activity relationships—dansylated acetylcholine analogs, effect on motility and neuroactivity in schistosomes, scanning fluorescence method, motility studies

Various cholinomimetic and anticholinergic drugs affect the nervous system of schistosomes. However, some drugs, such as muscarine, nicotine, and tubocurarine, which are highly active at mammalian cholinergic synapses, are conspicuously inactive in schistosomes (1), although acetylcholine and carbachol are effective immediately. This finding suggests that sensitivity to cholinergic drugs in schistosomes is different from that in nicotinic or muscarinic mammalian synapses.

Dimethylaminonaphthalene - 5 - sulfonamidoethyltri-

0022-3549/80/0500-0516$01.00/0

© 1980, American Pharmaceutical Association

formulation of co-trimoxazole tablets[14] (BP 1973), it is predicted that no side effects would occur since only 4.75 μg of formaldehyde is contained in this formulation. The other formalized microcapsules may have a lower amount of remaining formaldehyde, although no such data are available. The method of removing the remaining formaldehyde from the formalized microcapsules also is important for microencapsulation if formaldehyde is applied as a hardening agent.

Effect of Spray-Drying Procedure on Microcapsule Surface Topography and Crystalline Drug Form—On the surface of the spray-dried microcapsules prepared from the unformalized coacervates (Fig. 3C), a smooth surface with some fissures of the coating was observed. Moreover, a few microcapsules possessed a characteristically folded and invaginated surface. This phenomenon may be deduced from a diagram (20–22) of a spray-dried slurry droplet.

X-ray diffraction patterns of the ground microcapsules were obtained to investigate the crystalline forms of sulfamethoxazole in the microcapsule prepared by conventional and spray-drying techniques. The intensities of the diffraction peaks of the spray-dried sulfamethoxazole were weaker than those of the original material. A rapid evaporation of solvent from spray droplets might change the crystalline form to the disordered form (Fig. 4). On the other hand, the intensities of the peaks found in the microcapsules dried by the conventional method coincided with those of the original sulfamethoxazole. This result may be explained in that, although the coacervation temperature was 50°, the crystalline forms could not be disordered due to the mild drying process employed. In addition, the IR spectrum of all of the microcapsules coincided with that of the original sulfamethoxazole, indicating that complexes between sulfamethoxazole and the polymers (gelatin or acacia) were not formed through spray drying and the complex coacervation processes.

REFERENCES

(1) L. A. Luzzi, *J. Pharm. Sci.*, **59**, 1367 (1970).

(2) B. K. Green and L. Schleicher, U.S. pats. 2,730,456 and 2,730,457 (1956).

(3) *Ibid.*, U.S. pats. 2,800,457 and 2,800,458 (1957).

(4) N. C. R. Co., *Sci. Dig.*, **44**, 66 (July 1958).

(5) N. C. R. Co., *Chem. Week*, **83** (Dec. 21), 43 (1963).

(6) J. W. McGinity, A. B. Combs, and A. N. Martin, "The Proceedings of Third International Symposium on Microencapsulation," Tokyo, Japan, 1976, p. 3.

(7) P. L. Madan, J. C. Price, and L. A. Luzzi, "Microencapsulation Process and Application," Plenum, New York, N.Y., 1974, p. 39.

(8) L. A. Luzzi and R. J. Gerraughty, *J. Pharm. Sci.*, **53**, 429 (1964).

(9) *Ibid.*, **56**, 643 (1967).

(10) *Ibid.*, **56**, 1174 (1967).

(11) P. L. Madan, L. A. Luzzi, and J. C. Price, *J. Pharm. Sci.*, **61**, 1586 (1972).

(12) H. Takenaka, Y. Kawashima, and R. Ishibashi, *Drug Dev. Ind. Pharm.*, **3**, 459 (1977).

(13) "TRS," Quality Control Department, Tolei Co., Tokyo, Japan, 1977.

(14) T. Nash, *Nature*, **170**, 976 (1952).

(15) T. Nash, *Biochem. J.*, **55**, 416 (1953).

(16) C. Thies, *J. Colloid Interface Sci.*, **44**, 133 (1973).

(17) Bungenberg de Jong and J. M. F. Landsmeer, *Proc. K. Ned. Akad. Wet., Amsterdam*, **51**, 137 (1948).

(18) *Ibid.*, **51**, 259 (1948).

(19) Bungenberg de Jong and J. M. F. Landsmeer, *Rec. Trav. Chim.*, **65**, 606 (1964).

(20) Y. Kawashima, *Powder Ind. (Jpn.)*, **4**, 32 (1972).

(21) Y. Kawashima, K. Matsuda, and H. Takenaka, *J. Pharm. Pharmacol.*, **24**, 505 (1972).

(22) W. R. Marshall and D. H. Charlesworth, *AIChE J.*, **6**, 9 (1960).

(23) J. R. Nixon and S. E. Walker, *J. Pharm. Pharmacol., Suppl.*, **23**, 147S (1971).

(24) J. R. Nixon, S. A. H. Khalil, and J. E. Carless, *ibid.*, **20**, 528 (1968).

(25) M. Glicksman and R. E. Sand, "Industrial Gums: Polysaccharides and Their Derivatives," Academic, New York, N.Y., 1973, p. 235.

(26) A. Kondo, *Surface (Jpn.)*, **7**, 23 (1969).

ACKNOWLEDGMENTS

The authors acknowledge the advice of Dr. B. A. Matthews, Ciba-Geigy Co., Jakarta, Indonesia, in the text preparation and also the use of a diffractometer through the courtesy of Professor A. Otsuka, Meijyo University, Nagoya, Japan.

[14] One tablet of co-trimoxazole contains 400 mg of sulfamethoxazole and 80 mg of trimethoprim.

Effects of Dansylated Acetylcholine Analogs on *Schistosoma mansoni*

G. R. HILLMAN *x, S.-H. CHU ‡, and M. J. DOTSON *

Received April 18, 1979, from the **Department of Pharmacology and Toxicology, University of Texas Medical Branch, Galveston, TX 77550,* and the ‡*Division of Biomedical Sciences, Brown University, Providence, RI 02912.* Accepted for publication December 3, 1979.

Abstract □ A series of dansylated fluorescent analogs was synthesized and tested for cholinergic and anticholinergic activity in *Schistosoma mansoni*. The compounds were compared with a previously reported analog, 5-(dimethylamino)-*N*-(2-dimethylaminoethyl)naphthalenesulfonamide hydrochloride (I). All of the compounds produced some fluorescent labeling of a structure in the head region of the worms. Major differences were not seen among the compounds. The compounds also were tested as antagonists of carbachol-induced paralysis in an activity monitor. Significant carbachol antagonism was seen for all compounds. Effects on the serotonin response also were recorded. Only one compound, a dibutylaminopropylamine derivative, produced striking antagonism of serotonin-induced motor activity.

Keyphrases □ Cholinergics—antagonists, dansylated acetylcholine analogs, *in vitro* scanning fluorescence method, neuroactive drugs in schistosomes □ Carbachol—effect on schistosomes, effect of anticholinergic agents, scanning fluorescence method, motility studies □ Serotonin—effect on schistosomes, anticholinergic agents, scanning fluorescence method □ Structure–activity relationships—dansylated acetylcholine analogs, effect on motility and neuroactivity in schistosomes, scanning fluorescence method, motility studies

Various cholinomimetic and anticholinergic drugs affect the nervous system of schistosomes. However, some drugs, such as muscarine, nicotine, and tubocurarine, which are highly active at mammalian cholinergic synapses, are conspicuously inactive in schistosomes (1), although acetylcholine and carbachol are effective immediately. This finding suggests that sensitivity to cholinergic drugs in schistosomes is different from that in nicotinic or muscarinic mammalian synapses.

Dimethylaminonaphthalene - 5 - sulfonamidoethyltri-

0022-3549/80/0500-0516$01.00/0

© 1980, American Pharmaceutical Association

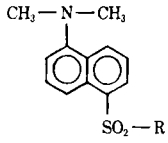

Table I—Analogs of I

Compound	R	Formula	Melting Point	Yield, %	Analysis, % Calc.	Found
II	$NH(CH_2)_2N(C_2H_5)_2$	$C_{18}H_{27}N_3SO_2 \cdot 2HCl \cdot H_2O$	140–142°	70	C 49.44 H 7.47 N 9.58	49.47 7.30 9.38
III	$NH(CH_2)_3N(CH_3)_2$	$C_{17}H_{25}N_3SO_2Cl \cdot 2HCl \cdot H_2O$	170°	70	C 47.88 H 6.86 N 9.85	48.14 7.25 9.75
IV	$NH(CH_2)_3N(C_2H_5)_2$	$C_{19}H_{29}N_3SO_2 \cdot HCl$	150°	73	C 57.08 H 7.51 N 10.51	57.03 7.46 10.17
V		$C_{17}H_{23}N_3SO_2 \cdot 0.75HCl \cdot 0.25H_2O$	200°	52	C 55.90 H 6.69 N 11.50	56.23 6.99 10.79
VI	$NH(CH_2)_3N(C_4H_9)_2$	$C_{23}H_{37}N_3SO_2 \cdot HCl \cdot 1.75H_2O$	124°	30	C 59.00 H 8.42 N —	59.03 8.47 —

methylammonium perchlorate, a dansylated choline derivative, acts as a fluorescent probe of acetylcholine receptors (2, 3). Related compounds having selective agonist or antagonist properties also have been studied (4), as has fluorescein-conjugated snake toxin (5). An analog of this compound, 5-(dimethylamino)-*N*-(2-dimethylaminoethyl)naphthalenesulfonamide hydrochloride (I), is a more effective labeling agent (6–8). For the present study, a series of dansylated fluorescent acetylcholine analogs was synthesized having systematic variations in the choline-like portions of the molecule.

A scanning fluorescence method and a technique for monitoring the movements of adult schistosomes *in vitro* (8, 9) are two approaches for assessing the effects of neuroactive drugs. With these methods, it was hypothesized (10) that hycanthone has selective anticholinergic action in schistosomes. This finding suggests that the cholinergic pharmacology of schistosomes may be important in chemotherapy, and the cholinomimetic or anticholinergic actions of structurally related compounds therefore are being studied. These structure–activity relationships are intended to suggest molecular variations that may lead to selective toxicity in schistosomes. This information will be used as a guide in the synthesis of other compounds.

EXPERIMENTAL[1]

Compound I and its analogs were synthesized by a method related to that reported previously (5, 7). 5-(Dimethylamino)-1-naphthalenesulfonyl (dansyl) chloride was refluxed with the appropriate *N,N*-dialkylethylenediamines, *N,N*-dialkylpropylenediamines, or 1-methylpiperazine in 50 ml of acetone for 1 hr. The acetone was evaporated to dryness at reduced pressure, and the resulting residue was washed with 100 ml of ether. The resulting hydrochloride was neutralized with 20 ml of 3% Na_2CO_3. Then it was repeatedly extracted with ether and dried over magnesium sulfate.

The solid was removed by filtration, and the filtrate was cooled in an ice bath and bubbled with excess hydrogen chloride gas. On cooling, it solidified slowly to yield analytically pure material. The product was highly hydroscopic and tended to form an oil on exposure to air. It was homogeneous by paper electrophoresis and had fluorescence excitation and emission spectra similar to those reported for dimethylaminonaphthalene-5-sulfonamidoethyltrimethylammonium perchlorate. The analyses and physical properties are given in Tables I and II.

Table II—Physical Properties of I Analogs

Compound	λ_{max}, nm (ϵ, 10^{-3}) pH 1	pH 11	Ethanol	R_f[a]
II	287 (12.6) 321 (3.8)	243 (18.4) 320 (6.0)	255 (19.8) 340 (4.0)	0.81
III	287 (11.6) 321 (2.6)	244 (15.8) 325 (4.4)	252 (13.0) 340 (3.8)	0.45
IV	289 (9.0) 322 (2.0)	244 (16.7) 323 (5.2)	254 (15.8) 340 (4.8)	0.31
V	292 (6.8) 321 (2.2)	249 (15.0) 330 (12.8)	254 (16.0) 345 (4.4)	0.79
VI	287 (7.3) 321 (1.3)	Low solubility	250 (10.7) 340 (3.2)	0.95

[a] TLC was run on silica gel and developed with ethanol.

Mice infested with *Schistosoma mansoni* were obtained from a mouse–snail cycle[2]. The adult, paired schistosomes were removed 45–60 days postinoculation. The infected mice were administered heparin and ether before being sacrificed by cervical dislocation. Using gentle-hook dissection, the adult, paired schistosomes were removed from the portal and mesenteric veins. The worms were maintained at 37° and pH 7.4 in cell culture medium[3] with added antibiotics and buffering (11). About 1 ml of culture medium was used per worm pair.

For scanning fluorescence measurements, the worm pairs from a mouse were divided into test and control groups and incubated at 37° for 60 min in a culture medium containing the appropriate compound. Each test group was paired with a control group of worms incubated in I. After incubation, the worms were rinsed with saline and placed under a cover slip on a microscope slide for evaluation of fluorescence as described previously (8).

The mounted schistosome was placed on the microscope[4] stage and aligned in the field of view. A small synchronous motor attached to the stage controlled the movement of the image of the worm across the light-sensitive spot of the photometer. As the microscope stage moved, the fluorescence (as a function of distance across the specimen) was recorded from the photometer output. The photometric information was entered directly into a computer for interpretation. The computer au-

[1] Melting points were determined on a Gallenkamp apparatus and are uncorrected. UV spectra were determined on a Perkin-Elmer model 402 spectrophotometer. Elemental analyses were performed by Baron Consulting Co., Orange, Conn. TLC was run on silica gel, and the plates were developed with ethanol.

[2] Obtained from Dr. S. File and Dr. J. Smith, University of Texas Medical Branch, Pathology Department, Galveston, Tex.

[3] Fischer, Grand Island Biological Co.

[4] Olympus model BMB with vertical fluorescence illumination. Emitted fluorescent light, returning through the microscope objective, was directed to the camera port at the top of the microscope. On the camera port, a Farrand MSA microscope spectrum analyzer was mounted. An Aminco potted 1P21 photomultiplier was adapted to the Farrand housing. The photomultiplier was connected to an Aminco J-22A photometer. The photometer output was directly connected to a Hewlett-Packard 9825A computer.

Table III—Specific Fluorescence and Partition Coefficients of the Compounds

Compound	Specific Fluorescence, % transmittance	Partition Coefficient (P)
I	26.0	0.0941
II	31.0	0.2374
III	40.0	0.0190
IV	46.5	0.0345
V	14.0	0.6108
VI	46.5	0.0676

tomatically recorded 250 fluorescence values for each scan, located the fluorescent peak, and determined the height and area of the scanned fluorescent region.

Schistosomes were routinely scanned twice: once across the esophageal region and once across the region of maximal brightness posterior to the esophagus (Fig. 1). Only male schistosomes were scanned due to the small size of the females. The data obtained included the peak height or maximum recorded fluorescence intensity at any point in the scanned region and the peak area or total fluorescence over the scanned region. Both parameters were used to evaluate the esophageal and central regions of the head.

The specific fluorescence of the compounds was compared by two methods. The fluorescence of a 10^{-6} M solution of each compound in pH 7.4 phosphate buffer was measured using a spectrophotofluorometer. The maximum excitation and emission wavelengths for each compound were used to determine the fluorescence. The compounds also were compared using the microfluorometer. A 2-mm thick plastic ring[5] was placed on a microscope slide, filled with drug solution, and covered with a cover slip; this procedure gave a reproducible depth of solution for observation. The specific fluorescence of each compound at 10^{-3} M in phosphate buffer (pH 7.4) was recorded and evaluated at an emission wavelength of 530 nm.

Figure 1—*Fluorescence micrograph of the head region of a male* S. mansoni *labeled with II. The worm was incubated for 1 hr in cell culture medium with* 1×10^{-5} M *II.*

[5] Delrin.

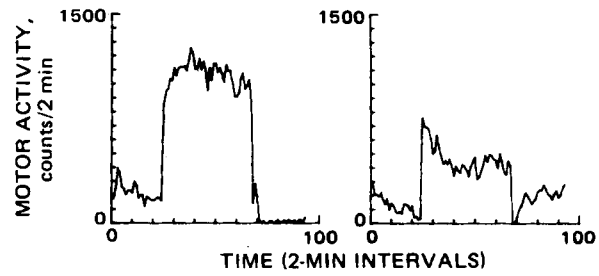

Figure 2—*Effects of IV on carbachol-induced paralysis. Serotonin (1* $\times 10^{-3}$ M*) was added after 18 intervals to produce stimulation. Carbachol (1* $\times 10^{-4}$ M*) was added later, producing paralysis in the control (left). Compound IV (1* $\times 10^{-4}$ M*) was present throughout the experiment (right).*

The motor response of paired *S. mansoni* to the compounds was measured in a specially constructed activity cage described previously (9, 11–13). The apparatus contained four chambers mounted in a temperature-regulated block. Two worm pairs were placed in each glass-bottom chamber, which was located directly above an array of fiberoptics connected to photocells. Movement of the worms in the chamber obscured a light beam, producing a change in the light intensity measured by the photocells. The resultant electronic changes registered by the photocells were translated into numerical counts that were proportional to the total amount of movement. The counts for each chamber were accumulated for 2 min, and the data were automatically transferred to a computer. The data were collected and plotted automatically by the computer.

Four experiments were run simultaneously in the presence and absence of the test compounds. The test compounds, serotonin and carbachol, in culture medium solution were perfused through the 37° chambers, and the response data were accumulated. The activity of the worm was plotted as a function of time.

The partition coefficient was determined for each compound. Equal amounts of pH 7.4 phosphate buffer and ether were shaken for 30 min and allowed to equilibrate. The equilibrated phosphate buffer was used to make a 10^{-4} M solution of each compound. The absorbance of these solutions at 350 nm was recorded. A combination of 4.5 ml of the drug solution and 0.5 ml of the buffer-saturated ether was vortexed for 3 min. The absorbance of the aqueous phase of the mixture was measured after mixing.

The partition coefficient was calculated from:

$$p = \frac{V_2(x - y)}{V_1 y} \qquad \text{(Eq. 1)}$$

where V_1 is the volume of the aqueous phase of the mixture, V_2 is the volume of ether, x is the absorbance of the compound in the buffer before partitioning, and y is the absorbance of the aqueous phase of the buffer

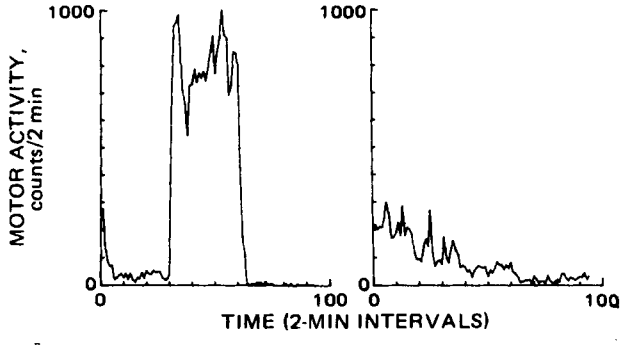

Figure 3—*Effects of VI on serotonin-induced motility. Serotonin (1* $\times 10^{-3}$ M*) was added to the basal medium at 30 intervals, and carbachol (3* $\times 10^{-4}$ M*) was added at 60 intervals. Key: left, normal response; and right, VI present throughout the experiment.*

Table IV—Relative Labeling Intensity of Schistosomes by Dansylated Choline Analogs

Compound	Region 1[a]								Region 2[a]							
	Peak Area				Peak Height				Peak Area				Peak Height			
	N_1[b]	N_2[c]	$\bar{F}$[d]	SE[e]	N_1	N_2	$\bar{F}$	SE	N_1	N_2	$\bar{F}$	SE	N_1	N_2	$\bar{F}$	SE
II	22	4	1.027	0.130	29	5	1.072	0.098	22	4	0.984	0.136	24	4	1.162	0.154
III	24	4	0.737	0.057	23	4	0.710	0.078	24	4	0.672	0.074	23	4	0.698	0.125
IV	51	9	0.772	0.051	54	9	0.730	0.038	55	7	0.727	0.059	54	5	0.901	0.098
V	27	4	1.004	0.114	27	4	0.981	0.110	23	3	1.096	0.118	21	3	0.925	0.035
VI	13	2	1.883	0.424	13	2	1.803	0.114	11	2	1.719	0.321	13	2	1.428	0.046

[a] Regions 1 and 2 represent the anterior and posterior fluorescently labeled areas in the head of the male schistosome, respectively. [b] N_1 is the total number of test worms in N_2 experiments; an equal number of control (I) worms were measured concurrently. [c] N_2 is the number of experiments, each involving about six test worms and controls. [d] $\bar{F}$ is the mean of the results for N_2 experiments. Values are normalized so that I = 1.000. [e] SE is the standard error of the mean $\bar{F}$.

Table V—Significance of Drug Effects on Carbachol Motility Response[a] for Several Drug to Carbachol Concentration Ratios

Compound	0.1 m*M*/0.1 m*M*			0.1 m*M*/0.3 m*M*			0.3 m*M*/0.3 m*M*		
	Percent Change			Percent Change			Percent Change		
	Drug, $\bar{x} \pm SD$	Control, $\bar{x} \pm SD$	p	Drug, $\bar{x} \pm SD$	Control, $\bar{x} \pm SD$	p	Drug, $\bar{x} \pm SD$	Control, $\bar{x} \pm SD$	p
I	75.6 ± 5.2	69.6 ± 22.63	NS	95.7 ± 3.69	82.13 ± 14.13	NS	76.80 ± 19.49	94.43 ± 4.40	<0.01
II	76.42 ± 13.93	78.52 ± 19.05	NS	81.90 ± 14.36	87.13 ± 13.57	NS	76.10 ± 12.01	96.13 ± 1.88	<0.01
III	51.52 ± 20.6	76.00 ± 19.60	<0.01	92.33 ± 10.51	94.25 ± 6.18	NS	91.33 ± 3.46	92.43 ± 4.38	NS
IV	52.58 ± 18.45	78.63 ± 10.77	<0.001	92.78 ± 6.73	97.32 ± 2.55	NS	46.45 ± 18.10	94.45 ± 1.99	<0.001
V	73.73 ± 13.69	87.63 ± 7.68	<0.05	93.87 ± 5.54	94.37 ± 3.11	NS	84.53 ± 11.08	95.48 ± 6.35	NS
VI	54.58 ± 15.55	87.32 ± 8.83	<0.001	57.73 ± 18.33	82.95 ± 19.13	<0.05	79.17 ± 8.39	89.30 ± 9.77	NS[b]

[a] Numbers are the mean and standard deviation of four or more experiments. Each experimental value is the percent change in average motor activity from 46 min before to 46 min after the addition of carbachol. [b] This value could not be determined since the activity of the worms had already been diminished such that a carbachol effect could not be measured.

after partitioning. The absorbance was assumed to be directly proportional to the compound concentration.

RESULTS

Specific Fluorescence—The relative fluorescences observed using the fluorescence microscope were in excellent agreement with those recorded using the spectrophotometer. However, due to the dependence of these measurements on variables such as microscope focus, the spectrophotofluorometric measurements were used for further calculations. The specific fluorescence measurements are shown in Table III.

Schistosome Fluorescence—Both test and control (I) schistosomes were from the same mouse and were measured in the same experiment. The fluorescence of the esophageal region and the region of maximal brightness posterior to the esophagus of the schistosome was measured with each fluorescent compound. The maximum fluorescence intensity (scanning peak height) and integrated total fluorescence (scanning peak area) were calculated for both regions. All fluorescence values then were corrected by the specific fluorescence of the tested compound. Each test value was compared to the corresponding mean value from a group of scanned I-labeled worms from the same host to determine a fluorescence intensity ratio. Table IV summarizes the ratios of the fluorescence intensity of the test compounds to that of I. All compounds fluorescently labeled specific regions in the schistosome in a manner similar to I (7).

The fluorescent labeling of worms by each compound relative to labeling by I was calculated according to:

$$\bar{F} = \frac{1}{N_2}\sum_{1}^{N_2}\left(\frac{1}{N_0}\sum_{1}^{N_0}\frac{F_{\text{compound}}}{\bar{F}_I}\right) \qquad \text{(Eq. 2)}$$

where N_0 is the number of test worms (*i.e.*, exposed to the compound being tested) in an experiment, F_{compound} is the fluorescence of a test worm adjusted for specific fluorescence of the compound, $\bar{F}_I$ is the mean fluorescence of all I-treated (control) worms in the same experiment adjusted for the specific fluorescence of I (usually equal in number to N_0), and N_2 is the number of experiments conducted with the same test compound.

Table IV gives the values for N_1 where $N_1 = \Sigma_1^{N_2} N_0$. The standard error of $\bar{F}$ for $n = N_2$ also is shown in Table IV.

Motility—The acetylcholine-like drug carbachol was used to evaluate the anticholinergic effect of the compounds on the schistosomes in the activity monitor (Table V). Carbachol has a paralytic effect on schistosomal movements (1). Worm pairs were exposed to a 1 m*M* solution of serotonin to stimulate the worm activity maximally (10). Carbachol at 10^{-4} or 3×10^{-4} *M* then was added, and the activity response of the schistosomes was recorded with and without the test compound.

The movement of the worms was monitored in 2-min intervals. The values for these intervals were averaged for each period (at least 36 min) of drug exposure. The percent decrease in movement due to carbachol administration was calculated from these means. This experiment was conducted in the presence and absence of the test drug on different worms from the same host. The effect of carbachol on motility with and without each test drug is shown in Table V. The difference between the carbachol effect with and without the test drug was tested for significance by the t test with n as the number of repetitions of the experiments. The p value derived from the t test also is shown in Table V.

All compounds were effective in blocking the carbachol action. Since VI had a strong paralytic action of its own, its effects on the carbachol response could not be assessed reliably at higher concentrations.

The effects of the drugs on the serotonin response could be assessed by the same technique. However, since the percent increase with serotonin was more variable (from 60 to 2000%, depending critically on the value of the motility rate before serotonin) than the decrease with carbachol (reliably about 90%), quantitation of drug effects on the serotonin response was difficult. However, it was clear that VI strongly blocked the response to serotonin. None of the other compounds had this effect.

Typical experiments are shown in Figs. 2 and 3. The reduction of the carbachol response by IV and the inhibition of the serotonin response by VI can be seen clearly.

Partition Coefficients—Table III shows the partition coefficients for each drug solution. Compound V demonstrated the highest lipid solubility. The lipid solubility was not related in any obvious way to the structure of the drugs.

DISCUSSION

Previous studies showed that a dansylated choline analog (I) fluorescently labels schistosomes in regions containing nerve endings and behaves as an antagonist at acetylcholine receptors. In view of the evidence that some antischistosomal drugs (*e.g.*, hycanthone and metrifonate) may act by affecting the cholinergic nervous system, this study was conducted to determine the structural requirements for anticholinergic activity in schistosomes. This problem was approached by the synthesis of structurally related analogs of I, with testing of the compounds in two independent schistosomal experimental systems.

The fluorescent labeling experiments were conducted on the premise that I and its analogs label the physiological acetylcholine binding sites. This hypothesis is supported by prior observations that dansylated compounds not resembling acetylcholine, such as dansyl glycine, do not label specific structures in schistosomes and that anticholinergic drugs

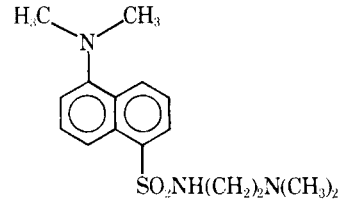

I

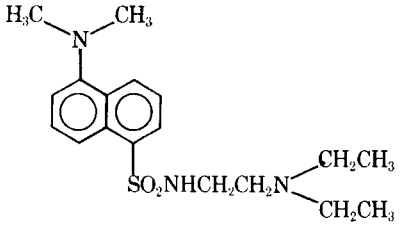

II

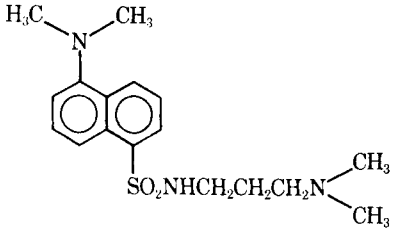

III

IV

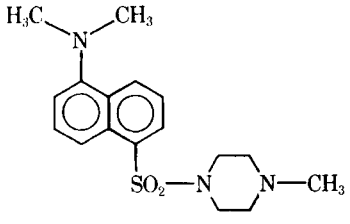

V

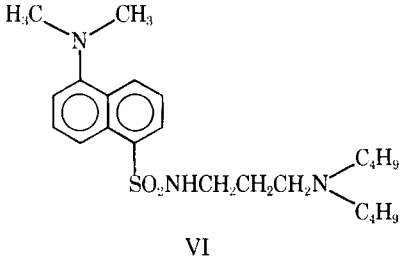

VI

such as atropine and mecamylamine block labeling of schistosomes by I. The results (Table IV) indicate that there were some differences among the compounds. Analogs with two-carbon chains (I and V, in which the chain is part of a piperazine ring) gave more effective labeling; the three-carbon analogs (III and IV) were less effective as labels.

Addition of larger groups to the terminal nitrogen produced some increase in labeling effectiveness. Compound VI shows that large *N*-substitutions result in increased labeling, even with a three-carbon aliphatic chain. The variations do not correlate in an obvious way with lipid solubility, as shown in Table III. It is suggested that the labeling site preferentially binds molecules with an aliphatic two-carbon side chain and may have a hydrophobic region near an anionic site; more extensive structure–activity studies are needed to characterize this site.

The motility (activity cage) studies provide an independent approach to measuring the neuroactivity of drugs by allowing observation of the antagonism of acetylcholine or serotonin responses. The ability of I to block carbachol-induced paralysis is reported in Table V. All compounds produced a significant block of the carbachol response under at least one set of conditions, indicating that the compounds do have anticholinergic activity. Compound IV had the most clearcut effect. Because IV was one of the less effective fluorescent labels, some of the sites involved in the control of body movements probably are not labeling sites. Only VI effectively blocked the serotonin response. This drug had strong paralytic effects of its own, which made it impossible to determine its ability to block carbachol paralysis.

The structural series reported here is too small to provide a full description of activity requirements in the schistosome system, particularly since several compounds had very similar activity. However, the results with VI suggest that the addition of bulkier groups on the amine nitrogen may be a useful modification. In future studies, similar compounds, with or without the fluorescent dansyl group, will be tested *in vivo* for toxicity to schistosomes within the host animal.

REFERENCES

(1) L. R. Barker, E. Bueding, and A. R. Timms, *Br. J. Pharmacol.*, **26,** 656 (1966).

(2) J. B. Cohen and J. P. Changeux, *Biochemistry,* **12,** 477 (1973).

(3) G. Waksman, M.-C. Fournié-Zaluski, B. Rouques, T. Heidmann, H.-H. Grünhagen, and J. P. Changeux, *FEBS Lett.*, **67,** 335 (1976).

(4) M. J. Anderson and M. W. Cohen, *J. Physiol. (London)*, **237,** 385 (1974).

(5) G. Weber, D. P. Borris, E. DeRobertis, F. J. Barrentes, J. L. La-Torre, and M. C. Llorente de Carlos, *Mol. Pharmacol.*, **7,** 530 (1971).

(6) G. R. Hillman and W. B. Gibler, *Biochem. Pharmacol.*, **24,** 1911 (1975).

(7) G. R. Hillman, W. B. Gibler, and S. Chu, *ibid.*, **25,** 2529 (1976).

(8) G. R. Hillman, A.-M. Gibler, and J. B. Anderson, *J. Pharmacol. Exp. Ther.*, **207,** 992 (1978).

(9) G. R. Hillman, *J. Pharmacol. Methods,* **2,** 21 (1979).

(10) G. R. Hillman and A. W. Senft, *Am. J. Trop. Med. Hyg.*, **24,** 827 (1975).

(11) G. R. Hillman and A. W. Senft, *J. Pharmacol. Exp. Ther.*, **185,** 177 (1973).

(12) A. W. Senft and G. R. Hillman, *Am. J. Trop. Med. Hyg.*, **22,** 734 (1973).

(13) G. R. Hillman, N. J. Olsen, and A. W. Senft, *J. Pharmacol. Exp. Ther.*, **188,** 529 (1974).

ACKNOWLEDGMENTS

Supported by U.S. Public Health Service Grant DHEW 5R22 AI 14103.

The authors are grateful to Dr. Sharon File and Dr. Jerome Smith for the schistosome materials.

Thermal Decomposition of Ibuproxam

S. CHIMICHI *, F. INNOCENTI ‡, and G. ORZALESI ‡x

Received July 5, 1979, from the *Instituto Medicina del Lavoro, University of Florence, Largo Palagi 1, Florence, Italy, and the ‡Società Italo-Britannica L. Manetti-H. Roberts, Florence, Italy. Accepted for publication November 26, 1979.

Abstract □ The thermal behavior of ibuproxam was studied at several temperatures, and the degradation products were separated by column chromatography and ethereal extractions. The resulting products were ibuprofen [2-(4-isobutylphenyl)propionic acid], 1-(4-isobutylphenyl)-ethylamine, 4-isobutylacetophenone, and 4-isobutylacetophenone oxime. The compounds were identified by IR, UV, and NMR spectroscopy and elemental analyses. 4-Isobutylacetophenone was treated with hydroxylamine to give 4-isobutylacetophenone oxime.

Keyphrases □ Thermal decomposition—ibuproxam, analysis of degradation products □ Ibuproxam—thermal decomposition, identification of thermal degradation products □ Anti-inflammatory agents—ibuproxam, identification of thermal degradation products

Ibuproxam [(*RS*)-2-(4-isobutylphenyl)propiohydroxamic acid, I] is a potent oral nonsteroidal anti-inflammatory agent (1, 2). The pharmacology of ibuproxam was described previously (3), and absorption, metabolism, and extraction patterns in animals (4) and humans (5–7) were reported. Ibuproxam is safe and effective in the treatment of rheumatic diseases. Preclinical pharmacology has indicated the utility of oral dosage forms; this paper identifies the compounds arising from thermal decomposition of ibuproxam.

RESULTS AND DISCUSSION

The stability studies showed that I was thermally unstable (Table I). This instability initially was ascribed to the impurities of the technical grade product, but further testing of the analytical grade substance led to the conclusion that the observed trend was characteristic of the compound (Fig. 1). Ibuproxam, heated over 70°, decomposed to give four products; during these preliminary tests, the presence of water and metals (particularly iron) due to the manufacturing process did not substantially alter the decomposition (Table II).

Table I—GLC Analysis of Thermal Decompostion of I at Different Temperatures [a]

Time	Degradation Products, %			
	40°	60°	80°	105°
10 min	0	0	0	2.4
20 min	0	0	2.7	49.5
40 min	0	0	30.0	67.0
1 hr	0	0	57.5	81.0
2 hr	0	1.2	76.0	87.5
4 hr	0	3.8	90.3	97.0
8 hr	0	7.4	96.7	—
12 hr	0	12.3	—	—
24 hr	0	48.2	—	—
2 days	0	81.3	—	—
4 days	0	91.3	—	—
8 days	0	98.5	—	—
16 days	0	—	—	—
1 month	1.7	—	—	—
2 months	1.9	—	—	—
4 months	4.8	—	—	—
8 months	7.9	—	—	—

[a] Samples were analyzed with a Perkin-Elmer 990 gas–liquid chromatograph on a 2-m × 6.35-mm 3% Dexil on Anachrom AB column at 180° with nitrogen as the carrier gas at 30 ml/min.

From a preliminary examination of the crude decomposition product, it was possible to separate two main products: a white sublimate (insoluble in most organic solvents but soluble in water) and a sticky yellow mass that still contained the nondecomposed product (TLC controls) (Fig. 2). Chemical and spectroscopic properties of the sublimate gave evidence of its saline structure, which was confirmed by isolation of II and III; further evidence (melting point and IR spectrum) was obtained by treatment of a commercial sample of II with III.

By column chromatography of the oily mass, IV and V were obtained together with a small amount of I. The structure of V was confirmed chemically by reaction of ketone IV with hydroxylamine (Scheme I).

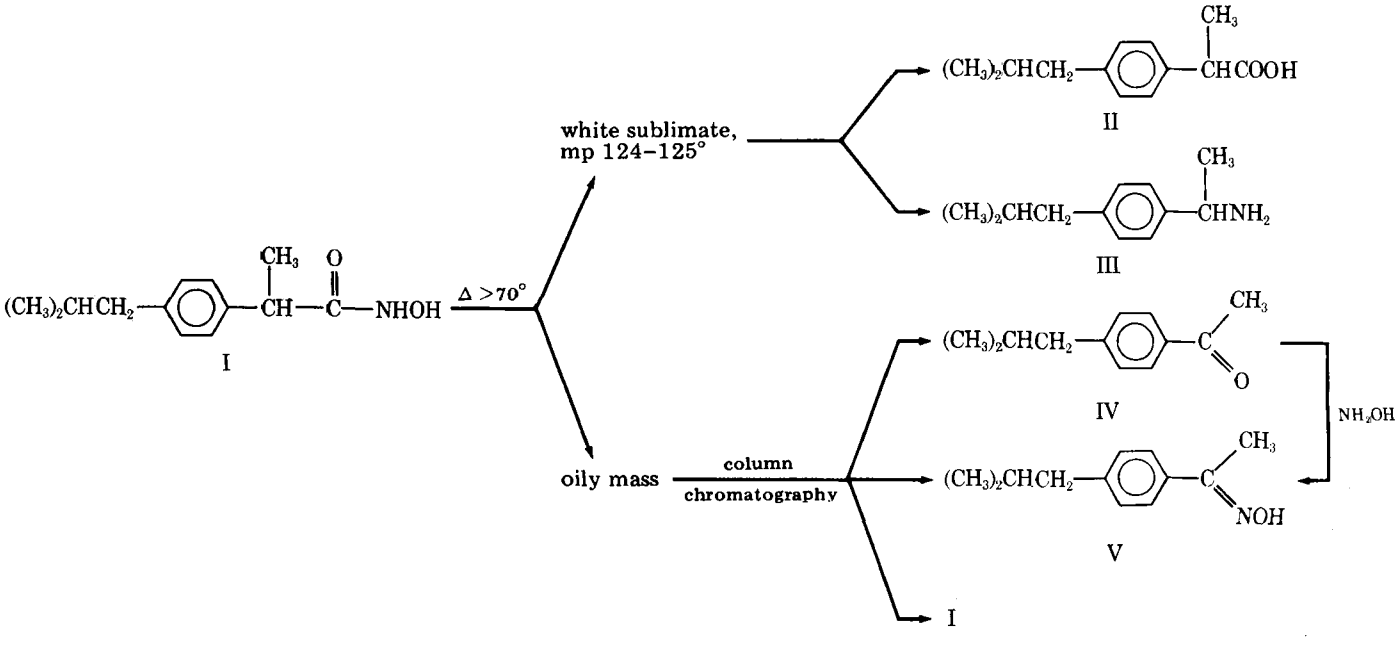

Scheme I

0022-3549/80/0500-0521$01.00/0
© 1980, American Pharmaceutical Association

Table II—^{1}H-NMR Spectra of Ibuproxam and Degradation Products [a]

Compound	Proton Resonance, ppm	Assignment
I	0.78 (d, J = 7 Hz)	6H, $(CH_3)_2CH$
	1.4 (d, J = 7 Hz)	3H, $CH_3CHCONHOH$
	1.65–2.05 (m)	1H, $CHCH_2$
	2.42 (d, J = 7 Hz)	2H, CH_2
	3.45 (q, J = 7 Hz)	1H, $COCHCH_3$
	6.9–7.3 (m)	4H, aromatic H_4
	8.8[b] (broad s)	1H, NH
III	0.88 (d, J = 7 Hz)	6H, $(CH_3)_2CH$
	1.33 (d, J = 7 Hz)	3H, CH_3CHNH_2
	1.47[b] (s)	2H, NH_2
	1.5–2.1 (m)	1H, $CHCH_2$
	2.42 (d, J = 7 Hz)	2H, CH_2
	4.03 (q, J = 7 Hz)	1H, CH_3CHNH_2
	7.0–7.3[c] (m)	4H, aromatic H_4
IV	0.88 (d, J = 7 Hz)	6H, $(CH_3)_2CH$
	1.5–2.1 (m)	1H, CH
	2.52 (s)	3H, CH_3CO
	7.2[c] (d)	2H, H-2, H-6
	7.87[c] (d)	2H, H-3, H-5
V	0.89 (d, J = 7 Hz)	6H, $(CH_3)_2$-CH
	1.5–2.1 (m)	1H, CH
	2.27 (s)	3H, CH_3CNOH
	2.47 (d, J = 7 Hz)	2H, CH_2
	7.14[c] (d)	2H, H-2, H-6
	7.54[c] (d)	2H, H-3, H-5
	9.52[b] (s)	1H, OH

[a] Obtained at 90 MHz; δ values are expressed in parts per million; tetramethylsilane was the internal reference, and deuterated chloroform was the solvent. [b] Signal disappears on deuteration. [c] For these signals, a progressive change was noted from a pattern type of *AA'BB'* to *AA'XX'*.

EXPERIMENTAL[1]

Thermal Degradation—Ibuproxam (I) (4 g) was sublimed at 110° and 760 mm Hg for 24 hr to yield a white product (1.5 g) and a pale-yellow residue. This residue was extracted with ether (50 ml), and evaporation of the extracts gave an oil (2.3 g).

Ibuprofen [2-(4-Isobutylphenyl)propionic Acid, II]—The sublimate (1 g), purified by several washings with ether (mp 124–125°), was dissolved in water (25 ml). Acidification with concentrated hydrochloric acid (pH 1–2) precipitated a white solid (0.48 g, 90% yield), mp 76–77° (after crystallization from ethyl acetate).

Anal.—Calc. for $C_{13}H_{18}O_2$: C, 75.73; H, 8.73. Found: C, 75.81; H, 8.75.

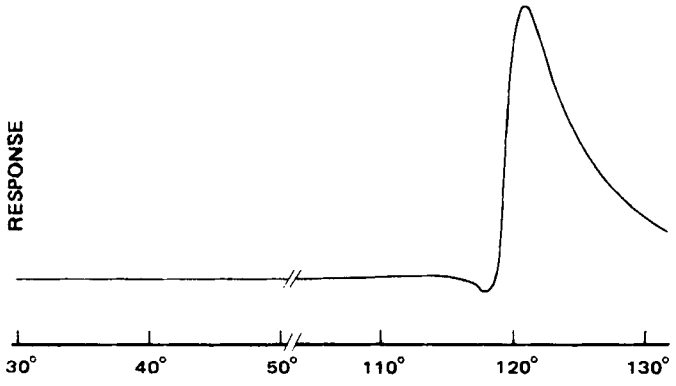

Figure 1—*Thermal decomposition of I. The scan speed was 4°/min, R = 500 μv, and the nitrogen gas flow rate was 20 ml/min.*

[1] Unless otherwise stated, IR spectra were measured for dispersions in Nujol with a Perkin-Elmer 457 spectrometer, and UV spectra were measured for solutions in ethanol with a Perkin-Elmer 124 recording spectrophotometer. ^{1}H-NMR spectra were recorded with a Perkin-Elmer R 32 instrument; chemical shifts are reported in parts per million downfield from the internal standard, tetramethylsilane. Thermal analysis was taken with a TA 2000 Mettler apparatus. Silica gel plates (Merck F_{254}) were used for analytical TLC, and the spots were detected by their UV absorption. Column chromatography was carried out with silica gel (Merck kieselgel 60, 70–230 mesh, ASTM). The extracts were dried over sodium sulfate, and the solvents were removed under reduced pressure. Melting points (uncorrected) were determined by the capillary method.

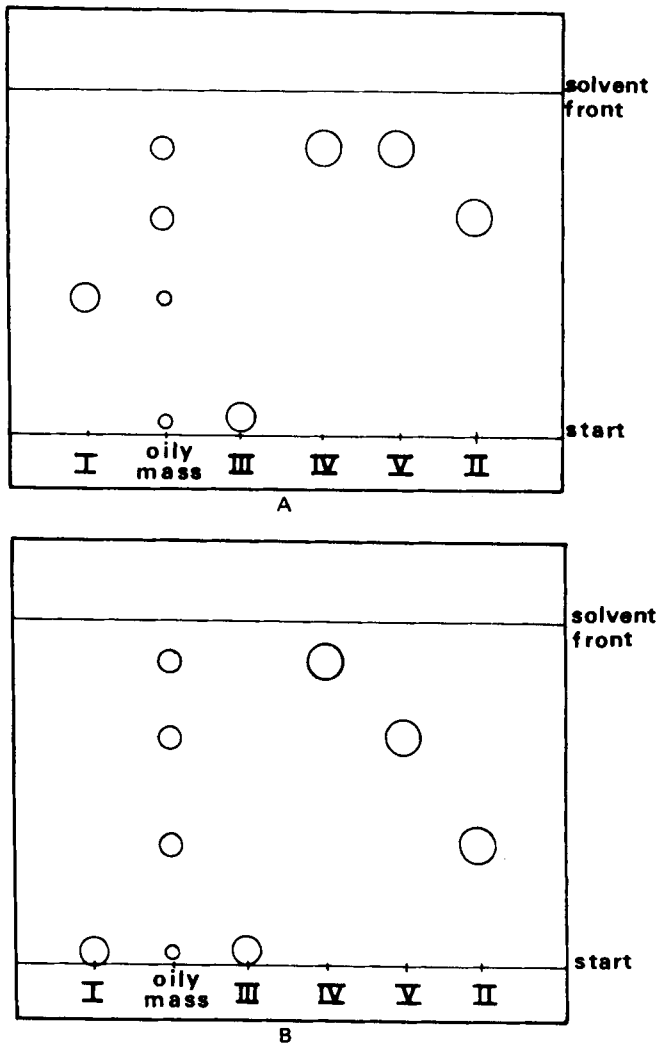

Figure 2—*TLC of the decomposition products of I. Key: A, eluent of benzene–ethyl acetate (1:1 v/v); and B, eluent of benzene–cyclohexane–ethyl acetate (5:5:1 v/v). The spot for I was detected best by spraying with sodium sulfate solution in methanol to give a characteristic green color.*

The product was identical to a commercial sample on the basis of mixed melting-point, IR, UV, and NMR analyses.

1-(4-Isobutylphenyl)ethylamine (III)—The sublimate (1 g), purified as described, was dissolved in water (25 ml); the solution was made alkaline with 10% NaOH and extracted with ether (3 × 30 ml). Removal of the solvent left an oil, which was purified by column chromatography with methanol as the eluent. Compound III (0.35 g, 75% yield) is a colorless liquid whose hydrochloride melts at 178–180°; IR: ν_{max} 3370, 3280, 2955, and 2860 cm^{-1}; UV: λ_{max} 263 (log ϵ 2.20), 272 sh (2.09), 252 (1.97), and 258 (2.12) nm.

Anal.—Calc. for $C_{12}H_{19}N$: C, 81.35; H, 10.73; N, 7.90. Found: C, 81.50; H, 10.95; N, 8.05.

4-Isobutylacetophenone (IV)—The oily residue (2 g) from thermal degradation was resolved into two products by column chromatography with benzene as the eluent. The first fractions gave IV (0.44 g, 50% yield) as a yellow liquid, bp 248°; IR: ν_{max} 2955, 2920, 2860, 1680, and 1608 cm^{-1}; UV: λ_{max} 254 nm (log ϵ 3.94).

Anal.—Calc. for $C_{12}H_{16}O$: C, 81.81; H, 9.09. Found: C, 82.05; H, 9.28.

4-Isobutylacetophenone Oxime (V)—*Method A*—The second product of the oily residue, treated as described, gave V as a white solid (0.57 g, 60% yield), mp 64–65° (after crystallization from *n*-hexane); IR: ν_{max} 3500–2800 br, 2955, 2920, and 2860 cm^{-1}; UV: λ_{max} 250 nm (log ϵ 3.86).

Anal.—Calc. for $C_{12}H_{17}NO$: C, 75.39; H, 11.80; N, 7.32. Found: C, 75.32; H, 11.60; N, 7.46.

Method B—A solution of IV (0.2 g) in methanol (20 ml) was treated with hydroxylamine (0.1 g) and refluxed gently for 6 hr. Removal of the solvent left a white solid (0.2 g, 90% yield), which was identical (melting point, IR, and NMR analyses) with the material obtained by Method A.

REFERENCES

(1) G. Orzalesi and R. Selleri, U.S. pat. 4,061,668 (Dec. 1977).

(2) G. Orzalesi and R. Selleri, U.S. pat. 4,082,707 (Apr. 1978).

(3) G. Orzalesi, R. Selleri, O. Caldini, I. Volpato, F. Innocenti, J. Colome, A. Sacristan, and G. Varez, *Arzneim.-Forsch.*, **27**, 1006 (1977).

(4) G. Orzalesi, R. Selleri, O. Caldini, I. Volpato, F. Innocenti, J. Colome, A. Sacristan, G. Varez, and G. Pisaturo, *ibid.*, **27**, 1012 (1977).

(5) T. Tuzi and P. Marroni, *Cl. Terap.*, in press.

(6) A. Debolini, R. Marcolongo, and G. Granelli, *ibid.*, **82**, 531 (1977).

(7) M. Ciarimboli, C. Guercello, M. Lingetti, G. Orzalesi, and D. Policicchio, *Eur. J. Rheum. Inflammation*, **1**, 337 (1978).

High-Performance Liquid Chromatographic Analysis of Griseofulvin in Drug Substance and Solid Dosage Forms: Separation of Impurities and Metabolites

EDWARD TOWNLEY * **and PAUL RODEN** *

Received July 30, 1979, from the *Physical and Analytical Chemical Research and Development Department, Schering-Plough Corporation, Bloomfield, NJ 07003.* Accepted for publication December 5, 1979.

*Present address: Duke University, Durham, NC 27706.

Abstract □ A high-performance liquid chromatographic (HPLC) system, consisting of a methanol–water (3:2 v/v) mobile phase and a Zorbax CN column with *m*-phenylphenol as the internal standard, was utilized to determine the purity of griseofulvin bulk drug substance, to assay griseofulvin in powders, tablets, capsules, and boluses, and to separate griseofulvin from its metabolites. The method was tested on commercial griseofulvin samples, griseofulvin tablets, and a mixture of griseofulvin and its metabolites. The HPLC method is compared to a GLC method.

Keyphrases □ Griseofulvin—high-performance liquid chromatographic analysis, purity and stability of drug substance, powders, tablets, capsules, and boluses, metabolites □ High-performance liquid chromatography—analysis, griseofulvin, purity and stability of griseofulvin dosage forms, metabolites □ Antifungal agents—griseofulvin, high-performance liquid chromatographic analysis of powders, tablets, capsules, and boluses

Griseofulvin has well-established fungistatic activity against various species of *Microsporum, Epidermophyton,* and *Trichophyton.* Usual dosage forms are powders, capsules, tablets, and boluses. Liquid–solid extraction methods for the preparation of griseofulvin for subsequent analysis include extraction of griseofulvin from tablets with boiling alcohol (1) and extraction from tablets with warm chloroform (2, 3).

The drug substance has been determined by several methods, the most common of which is a simple UV analysis (1, 4, 5). Other methods include polarography (6), GLC (2, 3), spectrofluorometry (7, 8), colorimetry (9–11), iodimetry (12), paper chromatography (13), and TLC (14–17). Liquid chromatography has been useful for the analysis of griseofulvin in crude mycelium (18) and in plasma (19).

This report describes a specific, simple, and robust high-performance liquid chromatographic (HPLC) procedure. It is applicable to the drug substance and solid dosage forms and to the separation of griseofulvin from its metabolites. The procedure is offered as an alternative to the GLC method (2), which suffers from the difficulty of drug analysis at high temperatures.

EXPERIMENTAL

Materials—*m*-Phenylphenol[1], reagent grade dichloromethane[2], sodium chloride[3], and anhydrous sodium sulfate[4] were obtained from commercial sources.

Apparatus—The modular high-pressure liquid chromatograph was equipped with a constant-flow pump[5], a valve-type injector[6], a fixed-wavelength (254-nm) UV detector[7], and a strip-chart recorder[8]. Stainless steel columns (4.6 mm × 30 cm) were packed with fully porous 10-μm silica particles to which a monomolecular layer of cyanopropylsilane[9] was chemically bonded. A rotating mixing wheel[10] and centrifuge tubes[11] were used to extract the samples. A data acquisition system[12] was used for both peak height and area measurements.

Chromatographic Conditions—The mobile phase was methanol–water (3:2). This solution was passed through a 0.45-μm filter[13], degassed, and then pumped through the HPLC system at a rate of 1 or 2 ml/min.

Table I—Analysis for Purity and Dechlorogriseofulvin Content in Griseofulvin Batches from Worldwide Sources

Batch	Purity[a], %	Dechlorogriseofulvin Content, %
0672-F2	100[b]	0.6
UGFP-1961	99.4	1.1
UGRB-505	96.6	2.0
GU-4830S	97.0	3.2
GU-4910S	97.0	2.8
26	99.7	0.9
5209	98.9	1.6
15 (805/7)	97.9	1.5

[a] Determined using USP XIX, p. 584. [b] USP reference standard.

[1] Eastman Organic Chemicals, Rochester, N.Y.
[2] Matheson, Coleman and Bell, Norwood, Ohio.
[3] NF grade, J. T. Baker Chemical Co., Phillipsburg, N.J.
[4] NF grade, Fisher Scientific Co., Fair Lawn, N.J.
[5] Model M-6000 A chromatography pump, Waters Associates, Milford, Mass.
[6] Universal injector model U6K, Waters Associates, Milford, Mass.
[7] Model 440 absorbance detector, Waters Associates, Milford, Mass.
[8] Class 19, No. 196711-008-000-506-01, Honeywell, Fort Washington, Pa.
[9] Zorbax CN column, E.I. duPont de Nemours & Co., Wilmington, Del.
[10] Rugged Rotator, Craft Apparatus, New York, N.Y.
[11] Bellco Glass Co., Vineland, N.J.
[12] PDP 11/34 minicomputer, Peak 11 Software Digital Electronics Corp., Maynard, Mass.
[13] Metricel membrane filter DM-450, Gelman Instrument Co., Andover, Mich.

0022-3549/80/0500-0523$01.00/0

© 1980, American Pharmaceutical Association

Method B—A solution of IV (0.2 g) in methanol (20 ml) was treated with hydroxylamine (0.1 g) and refluxed gently for 6 hr. Removal of the solvent left a white solid (0.2 g, 90% yield), which was identical (melting point, IR, and NMR analyses) with the material obtained by Method A.

REFERENCES

(1) G. Orzalesi and R. Selleri, U.S. pat. 4,061,668 (Dec. 1977).

(2) G. Orzalesi and R. Selleri, U.S. pat. 4,082,707 (Apr. 1978).

(3) G. Orzalesi, R. Selleri, O. Caldini, I. Volpato, F. Innocenti, J. Colome, A. Sacristan, and G. Varez, *Arzneim.-Forsch.*, **27**, 1006 (1977).

(4) G. Orzalesi, R. Selleri, O. Caldini, I. Volpato, F. Innocenti, J. Colome, A. Sacristan, G. Varez, and G. Pisaturo, *ibid.*, **27**, 1012 (1977).

(5) T. Tuzi and P. Marroni, *Cl. Terap.*, in press.

(6) A. Debolini, R. Marcolongo, and G. Granelli, *ibid.*, **82**, 531 (1977).

(7) M. Ciarimboli, C. Guercello, M. Lingetti, G. Orzalesi, and D. Policicchio, *Eur. J. Rheum. Inflammation*, **1**, 337 (1978).

High-Performance Liquid Chromatographic Analysis of Griseofulvin in Drug Substance and Solid Dosage Forms: Separation of Impurities and Metabolites

EDWARD TOWNLEY * **and PAUL RODEN** *

Received July 30, 1979, from the *Physical and Analytical Chemical Research and Development Department, Schering-Plough Corporation, Bloomfield, NJ 07003.* Accepted for publication December 5, 1979.

*Present address: Duke University, Durham, NC 27706.

Abstract □ A high-performance liquid chromatographic (HPLC) system, consisting of a methanol–water (3:2 v/v) mobile phase and a Zorbax CN column with *m*-phenylphenol as the internal standard, was utilized to determine the purity of griseofulvin bulk drug substance, to assay griseofulvin in powders, tablets, capsules, and boluses, and to separate griseofulvin from its metabolites. The method was tested on commercial griseofulvin samples, griseofulvin tablets, and a mixture of griseofulvin and its metabolites. The HPLC method is compared to a GLC method.

Keyphrases □ Griseofulvin—high-performance liquid chromatographic analysis, purity and stability of drug substance, powders, tablets, capsules, and boluses, metabolites □ High-performance liquid chromatography—analysis, griseofulvin, purity and stability of griseofulvin dosage forms, metabolites □ Antifungal agents—griseofulvin, high-performance liquid chromatographic analysis of powders, tablets, capsules, and boluses

Griseofulvin has well-established fungistatic activity against various species of *Microsporum, Epidermophyton,* and *Trichophyton.* Usual dosage forms are powders, capsules, tablets, and boluses. Liquid–solid extraction methods for the preparation of griseofulvin for subsequent analysis include extraction of griseofulvin from tablets with boiling alcohol (1) and extraction from tablets with warm chloroform (2, 3).

The drug substance has been determined by several methods, the most common of which is a simple UV analysis (1, 4, 5). Other methods include polarography (6), GLC (2, 3), spectrofluorometry (7, 8), colorimetry (9–11), iodimetry (12), paper chromatography (13), and TLC (14–17). Liquid chromatography has been useful for the analysis of griseofulvin in crude mycelium (18) and in plasma (19).

This report describes a specific, simple, and robust high-performance liquid chromatographic (HPLC) procedure. It is applicable to the drug substance and solid dosage forms and to the separation of griseofulvin from its metabolites. The procedure is offered as an alternative to the GLC method (2), which suffers from the difficulty of drug analysis at high temperatures.

EXPERIMENTAL

Materials—*m*-Phenylphenol[1], reagent grade dichloromethane[2], sodium chloride[3], and anhydrous sodium sulfate[4] were obtained from commercial sources.

Apparatus—The modular high-pressure liquid chromatograph was equipped with a constant-flow pump[5], a valve-type injector[6], a fixed-wavelength (254-nm) UV detector[7], and a strip-chart recorder[8]. Stainless steel columns (4.6 mm × 30 cm) were packed with fully porous 10-μm silica particles to which a monomolecular layer of cyanopropylsilane[9] was chemically bonded. A rotating mixing wheel[10] and centrifuge tubes[11] were used to extract the samples. A data acquisition system[12] was used for both peak height and area measurements.

Chromatographic Conditions—The mobile phase was methanol–water (3:2). This solution was passed through a 0.45-μm filter[13], degassed, and then pumped through the HPLC system at a rate of 1 or 2 ml/min.

Table I—Analysis for Purity and Dechlorogriseofulvin Content in Griseofulvin Batches from Worldwide Sources

Batch	Purity[a], %	Dechlorogriseofulvin Content, %
0672-F2	100[b]	0.6
UGFP-1961	99.4	1.1
UGRB-505	96.6	2.0
GU-4830S	97.0	3.2
GU-4910S	97.0	2.8
26	99.7	0.9
5209	98.9	1.6
15 (805/7)	97.9	1.5

[a] Determined using USP XIX, p. 584. [b] USP reference standard.

[1] Eastman Organic Chemicals, Rochester, N.Y.
[2] Matheson, Coleman and Bell, Norwood, Ohio.
[3] NF grade, J. T. Baker Chemical Co., Phillipsburg, N.J.
[4] NF grade, Fisher Scientific Co., Fair Lawn, N.J.
[5] Model M-6000 A chromatography pump, Waters Associates, Milford, Mass.
[6] Universal injector model U6K, Waters Associates, Milford, Mass.
[7] Model 440 absorbance detector, Waters Associates, Milford, Mass.
[8] Class 19, No. 196711-008-000-506-01, Honeywell, Fort Washington, Pa.
[9] Zorbax CN column, E.I. duPont de Nemours & Co., Wilmington, Del.
[10] Rugged Rotator, Craft Apparatus, New York, N.Y.
[11] Bellco Glass Co., Vineland, N.J.
[12] PDP 11/34 minicomputer, Peak 11 Software Digital Electronics Corp., Maynard, Mass.
[13] Metricel membrane filter DM-450, Gelman Instrument Co., Andover, Mich.

0022-3549/80/0500-0523$01.00/0

© 1980, American Pharmaceutical Association

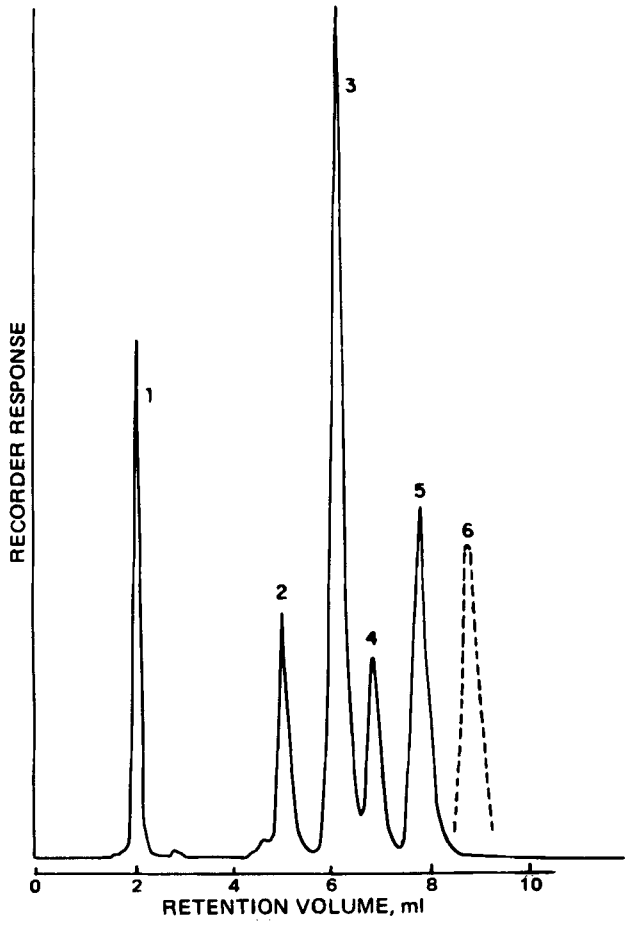

Figure 1—*HPLC separation of biosynthetic impurities (substances identified in the fermentation broth). Key: 1, griseofulvic acid; 2, dechlorogriseofulvin; 3, griseofulvin; 4, isogriseofulvin; 5, tetrahydrogriseofulvin; and 6,* m*-phenylphenol.*

Internal Standard Solution—The internal standard was *m*-phenylphenol prepared as a 1-mg/ml solution in methanol.

Standard Solution—Griseofulvin standard, ~60 mg, was weighed accurately into a 50-ml volumetric flask and was dissolved and diluted to 50 ml with methanol. Five milliliters of this solution was pipetted into a 50-ml volumetric flask. Four milliliters of the internal standard solution also was added by pipet, and the solution was diluted to 50 ml with methanol.

Standard Chromatogram—Twenty microliters of the standard solution was injected into the liquid chromatograph, and the chromatogram was recorded. The peak heights obtained were used in the calculations for griseofulvin.

Griseofulvin Samples—Griseofulvin samples were obtained from England[14] (Batches UGFP-1961 and UGRB-505), Japan[15] (Batches GU-4830S and GU-4910S), Rumania[16] (Batches 26 and 5209), Austria[17] [Batch 15 (805/7)], and the USP reference file[18] (Batch 0672-F2).

Impurities—Isogriseofulvin[14], dechlorogriseofulvin[14], griseofulvic acid[14], and tetrahydrogriseofulvin[19,20] were obtained. Dihydrogriseofulvin and additional tetrahydrogriseofulvin were synthesized[21] *via* the catalytic reduction of griseofulvin (19). The metabolites, 4-demethylgriseofulvin and 6-demethylgriseofulvin, were obtained as a result of previous research (20, 21). Identities were confirmed by comparison of the IR spectra to

[14] Glaxo Holdings Ltd., London, England.
[15] Nippon-Kayaku Co. Ltd., Chugai Boyeki (America) Corp. Importers and Exporters, New York, N.Y.
[16] Rumanian State Trading Agency; provided by the Jerdan Chemical Corp., Valley Stream, N.Y.
[17] Biochemi Gesmb H-Werk Kundl, Austria; provided by R. W. Greeff and Co., New York, N.Y.
[18] USP XIX, p. 584.
[19] Mr. T. Alexander, HFD-436, Food and Drug Administration, Washington, D.C.
[20] Dr. F. Bailey, I.C.I. Ltd. Pharmaceutical Division, Macclesfield, Great Britain.
[21] Schering-Plough Research, Bloomfield, N.J.

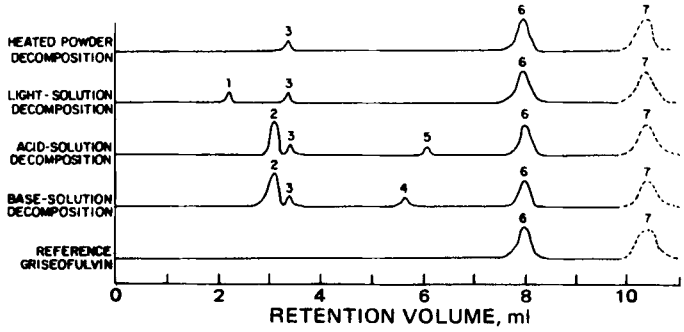

Figure 2—*Retention volume of decomposition impurities (substances resulting from extreme, accelerated decomposition studies). Key: 1, 3, 4, and 5, unknown minor decomposition products; 2, griseofulvic acid; 6, griseofulvin; and 7,* m*-phenylphenol.*

authentic references (isogriseofulvin, dechlorogriseofulvin, and griseofulvic acid) or by mass spectral studies (dihydrogriseofulvin, tetrahydrogriseofulvin, 4-demethylgriseofulvin, and 6-demethylgriseofulvin).

Accelerated Decomposition Studies—Accelerated, extreme degradation of griseofulvin was accomplished by several methods:

1. Griseofulvin drug substance was heated at 75° for 3 weeks.
2. Griseofulvin (0.25 mg/ml) was dissolved in methanol–0.1 *N* NaOH (4:1) and allowed to stand for 7 days.
3. Griseofulvin (0.25 mg/ml) was dissolved in methanol–0.1 *N* HCl (4:1) and allowed to stand for 7 days.
4. Griseofulvin was dissolved in methanol–water (4:1) in a Pyrex volumetric flask and exposed to daylight for 14 days through window glass.

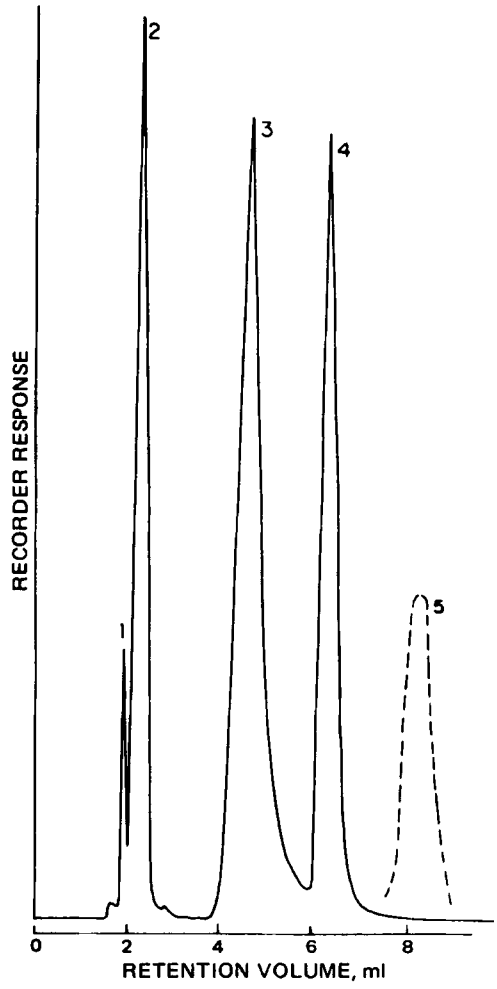

Figure 3—*HPLC separation of 4-demethylgriseofulvin and 6-demethylgriseofulvin metabolites. Key: 1, griseofulvic acid (impurity); 2, 6-demethylgriseofulvin; 3, 4-demethylgriseofulvin; 4, griseofulvin, and 5,* m*-phenylphenol.*

Griseofulvin Drug Substance Purity Determination—Approximately 60 mg of a griseofulvin test sample was weighed accurately into a 50-ml volumetric flask and dissolved and diluted to volume with methanol. Five milliliters of the sample solution was pipetted into a 50-ml volumetric flask. Four milliliters of the internal standard solution was added, and the solution was diluted to volume. Then 20 μl of the sample was injected into the liquid chromatograph operating at the described conditions. The percent purity was calculated from:

$$\text{percent griseofulvin} = \left(\frac{P'_{sple}}{P'_{is}}\right)\left(\frac{P_{is}}{P_{std}}\right)\left(\frac{W_{std}}{W_{sple}}\right) \times 100 \qquad \text{(Eq. 1)}$$

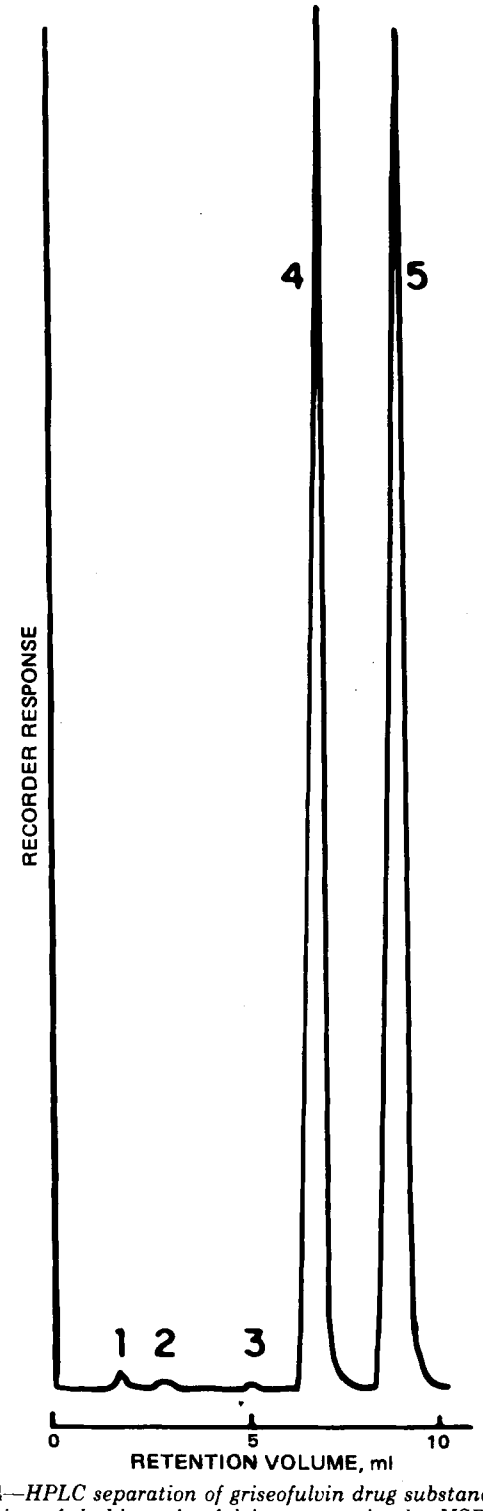

Figure 4—*HPLC separation of griseofulvin drug substance and demonstration of dechlorogriseofulvin content in the USP standard (Batch 0672-F2). Key: 1, solvent; 2, griseofulvic acid; 3, dechlorogriseofulvin; 4, griseofulvin; and 5,* m*-phenylphenol.*

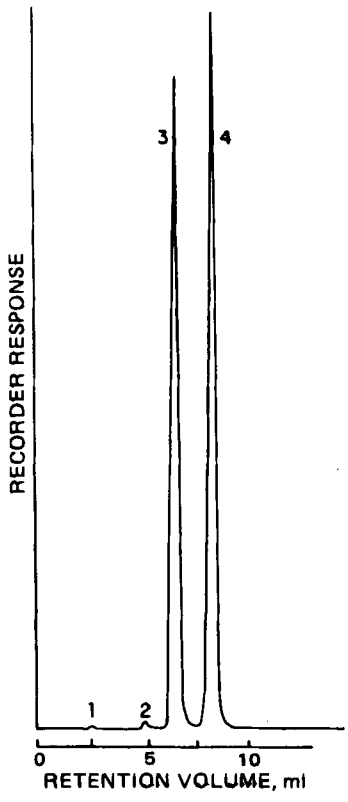

Figure 5—*High-performance liquid chromatogram of griseofulvin extracted from tablets (Batch 7934-45A). Key: 1, griseofulvic acid; 2, dechlorogriseofulvin; 3, griseofulvin; and 4,* m*-phenylphenol.*

where P'_{sple} is the peak height of the sample in the sample chromatogram, P'_{is} is the peak height of the internal standard in the sample chromatogram, P_{is} is the peak height of the internal standard in the standard chromatogram, P_{std} is the peak height of the standard in the standard chromatogram, W_{std} is the weight of the standard, and W_{sple} is the weight of the sample.

Griseofulvin in Solid Dosage Form Determination—A sample of well-mixed ground powder (from powders, tablets, capsules, or boluses) containing 250 mg of griseofulvin was weighed accurately into a 50-ml screw-capped centrifuge tube[11]. Then 20 ml of 10% aqueous sodium chloride solution and 20 ml of dichloromethane were added. Mixing resulted in extraction of the griseofulvin into the dichloromethane after the tube was placed on a rotating wheel[10] for 10 min.

The dichloromethane layer was transferred with a 20-ml syringe and a 16-gauge needle and filtered through ~200 mg of anhydrous sodium sulfate into a 200-ml volumetric flask. The extraction was performed three times and the extracts were combined (total of 60 ml) and diluted to volume. A 5.0-ml portion was transferred to a 50-ml volumetric flask and evaporated to dryness. The *m*-phenylphenol internal standard solution, 4.0 ml, was added, and the griseofulvin residue was dissolved in methanol and diluted to 50 ml. Then 20-μl portions were injected into the liquid chromatograph.

The griseofulvin content was calculated from:

$$\text{milligrams per unit} = \left(\frac{P'_{sple}}{P'_{is}}\right)\left(\frac{P_{is}}{P_{std}}\right)\left(\frac{W_{std}}{W_{sple}}\right)(W_{avg}) \times 4 \qquad \text{(Eq. 2)}$$

where W_{avg} is the average weight of the sample unit (gram, tablet, capsule, or bolus).

Table II—Comparison of the Accuracy of the HPLC and GLC (2) Methods for Griseofulvin Drug Substance

Batch	Mean Purity, %: HPLC Method (n = 4)	Mean Purity, %: GLC Method (n = 2)
S-03294	99.4 (99.3–99.6)	99.7 (99.6, 99.8)
3-2-58161	98.2 (97.9–98.4)	99.1 (98.9, 99.3)
UGRB-505	96.6 (96.3–96.9)	97.1 (96.8, 97.5)

Table III—Comparison of the Accuracy of the HPLC and GLC (2) Methods for Griseofulvin Tablets

Griseofulvin Tablets, mg	Content, mg/tablet	
	HPLC Method (n = 12)	GLC Method (n = 4)
125	125 (122–127)	126 (125–127)
250	247 (244–253)	250 (249–251)

Dechlorogriseofulvin Content Determination—The area under the dechlorogriseofulvin and griseofulvin peaks was obtained using a suitable area measurement integrator[12]. The percent dechlorogriseofulvin content was calculated according to:

$$\text{percent dechlorogriseofulvin} = \frac{\left[A_{DCG}\left(\frac{a_2}{a_1}\right)\right]}{\left[A_{DCG}\left(\frac{a_2}{a_1}\right)\right] + A_G} \times 100 \quad \text{(Eq. 3)}$$

where A_{DCG} is the area of the dechlorogriseofulvin peak, A_G is the area of the griseofulvin peak, a_2 is the absorptivity of griseofulvin at 254 nm, and a_1 is the absorptivity of dechlorogriseofulvin at 254 nm.

RESULTS AND DISCUSSION

The HPLC separation of biosynthetic impurities that were identified in the fermentation broths (18, 22) is demonstrated in Fig. 1. The HPLC separation of decomposition impurities that result when griseofulvin is subjected to accelerated, extreme decomposition is demonstrated in Fig. 2. The separation of 4-demethylgriseofulvin (23) and 6-demethylgriseofulvin (13) metabolites is shown in Fig. 3. The system is applicable to the determination of nonconjugated metabolites.

The data presented in Figs. 1–3 show that an internal standard eluting with a retention volume of ~10 ml will not interfere with a common biosynthetic impurity, decomposition product, or metabolite. *m*-Phenylphenol, whose retention is demonstrated in Figs. 1–3, meets this criterion.

To ascertain the purity of commercial griseofulvin, eight batches were obtained from worldwide sources and then were assayed by the described method. The purity data are given in Table I. The present study showed, as was reported previously (2, 18), that dechlorogriseofulvin was the major impurity and that it was common to all of the batches tested. The USP standard (Fig. 4) contained 0.6% of this impurity. Dechlorogriseofulvin also was separated by TLC using a silica gel adsorbent and ethyl acetate developing solvent. The absence of other significant impurities was confirmed. Table II compares the accuracy of the HPLC results to those of a GLC method (2) for griseofulvin drug substance.

The analysis of griseofulvin in both fresh and aged samples of powders, tablets, capsules, and boluses was performed by the extraction and HPLC procedures described previously. The analysis of griseofulvin tablets[22], 125 and 250 mg, serves as an example. The sample HPLC curve for griseofulvin extracted from griseofulvin tablets is given in Fig. 5. The extraction efficiency was 98% for a single extraction and 100% for the described method. A linear plot of peak height *versus* griseofulvin concentration response was obtained for griseofulvin in ground tablet powder from 62.5 to 500 mg of griseofulvin/sample. The least-squares coefficient was 0.99995. A system suitability test (reproducibility of six samples analyzed on the liquid chromatograph described) gave a relative standard deviation of ±0.3%.

The accuracy of the method was tested by the addition of griseofulvin to a placebo (procedural amount) and analysis by the described method. Recoveries were 100% with respect to a similarly chromatographed standard. The assay results are compared to those obtained by the GLC method of Margosis (2) in Table III.

[22] Fulvicin P/G griseofulvin ultramicrosize tablets, Schering.

REFERENCES

(1) "British Pharmacopoeia 1973," Her Majesty's Stationery Office, London, England, 1973, p. 221.

(2) M. Margosis, *J. Chromatogr.*, **70**, 73 (1972).

(3) M. Margosis, *J. Pharm. Sci.*, **64**, 1020 (1975).

(4) "European Pharmacopoeia," European Treaty Series No. 50, vol. 2, Maisonnmeuve S.A., Sainte-Ruffine, France, 1971, p. 234.

(5) "Code of Federal Regulations" Food and Drugs, Title 21, part 449.20, U.S. Government Printing Office, Washington, D.C., 1978.

(6) H. W. Unterman and A. Duca, *Isr. J. Chem.*, **12**, 985 (1974).

(7) W. C. Neely and J. R. McDuffie, *J. Assoc. Off. Anal. Chem.*, **55**, 1300 (1972).

(8) R. L. Nation, G. W. Peng, V. Smith, and W. L. Chiou, *J. Pharm. Sci.*, **67**, 805 (1978).

(9) H. W. Unterman, *Rev. Chim. (Bucharest)*, **16**, 286 (1965).

(10) H. W. Unterman and A. Duca, *Rev. Roum. Chim.*, **16**, 1077 (1971).

(11) H. W. Unterman and A. Duca, *Lucr. Conf. Nat. Chim. Anal., 3rd 1971*, **3**, 311 (Rom).

(12) H. W. Unterman and A. Duca, *Chim. Anal. (Bucharest)*, **2**, 196 (1972).

(13) S. Symchowicz and K. K. Wong, *Biochem. Pharmacol.*, **15**, 1595 (1966).

(14) R. J. Cole, J. W. Kirksey, and C. E. Holaday, *Appl. Microbiol.*, **19**, 106 (1970).

(15) C. Lin, R. Chang, C. Casmer, and S. Symchowicz, *Drug Metab. Dispos.*, **1**, 611 (1973).

(16) Z. Durackova, V. Betina, and P. Nemec, *J. Chromatogr.*, **116**, 141 (1976).

(17) H. J. Issaq, E. W. Barr, T. Wei, C. Meyers, and A. Aszalos, *ibid.*, **133**, 291 (1977).

(18) F. Bailey and P. N. Brittain, *ibid.*, **83**, 431 (1973).

(19) A. E. Oxford, H. Raistrick, and P. Simonart, *Biochem. J.*, **33**, 240, (1938).

(20) C. Lin, R. Chang, J. Magat, and S. Symchowicz, *J. Pharm. Pharmacol.*, **24**, 911 (1972).

(21) P. Kabasakalian, M. Katz, B. Rosenkrantz, and E. Townley, *J. Pharm. Sci.*, **59**, 595 (1970).

(22) A. Holbrook, F. Bailey, and G. M. Bailey, *J. Pharm. Pharmacol.*, **15**, 274T (1963).

(23) M. J. Barnes and B. Boothroyd, *Biochem. J.*, **78**, 41 (1961).

Calculation of Partition Coefficient of an Unstable Compound Using Kinetic Methods

PETER R. BYRON *, ROBERT E. NOTARI ˣ, and ERIC TOMLINSON

Received June 27, 1979, from the *College of Pharmacy, Ohio State University, Columbus, OH 43210.* Accepted for publication December 6, 1979. *Present address: Department of Pharmacy, University of Aston in Birmingham, Birmingham, B4 7ET, England.

Abstract □ A stirred transfer cell containing equal volumes of light liquid paraffin and an aqueous phase at 37° was used to demonstrate the feasibility of calculating the partition coefficient of an unstable compound by kinetic analysis. Cyclohept-2-enone was chosen since it is a neutral molecule and, therefore, should have a pH-independent oil–water partition coefficient, K_D. Moreover, this cyclic α,β-unsaturated ketone undergoes hydrogen-ion-catalyzed hydration but is sufficiently stable at neutral pH to determine K_D. The model system chosen represents first-order transfer between the aqueous (C_1) and organic (C_2) phases with simultaneous, reversible, first-order hydration. The transfer constants, k'_{12} and k'_{21}, were determined at 37° in the absence of degradation where asymptotic values for C_1 agreed with the observed equilibrium values in nonkinetic partitioning studies. The first-order rate constants for hydration in 0.1 *N* HCl were determined at 37° in the absence of the organic phase. Partitioning with simultaneous hydration then was studied using 0.1 *N* HCl and light liquid paraffin. Data were analyzed by nonlinear regression based on the equation for C_1 as a function of time. The values for k'_{12} and k'_{21} from these experiments were comparable to the estimates obtained under stable conditions. This agreement demonstrates that simultaneous degradation and partitioning can be analyzed for k'_{12} and k'_{21}, thus permitting calculation of the partition coefficient (*i.e.*, $K_D = k'_{12}/k'_{21}$) that would be observed if the drug were stable.

Keyphrases □ Partition coefficients—unstable compounds, cyclohept-2-enone, calculation by kinetic methods □ Cyclohept-2-enone—partition coefficient, calculation by kinetic methods □ Drug partitioning—unstable compounds, cyclohept-2-enone, calculation of partition coefficient by kinetic methods

The two-film theory proposed by Lewis and Whitman (1, 2) for the kinetics of solute transfer between two liquid phases was first experimentally verified by Gordon and Sherwood (3, 4) using a stirred transfer cell (Fig. 1). Since then, both the cell and the theory have been studied extensively and discussed (5–7). A transfer cell was employed to measure the rates of helium and isobutane mass transfer from water to toluene and decahydronaphthalene (8). The diffusion of salts across a butanol–water interface was studied at 13–40°, and the Arrhenius parameters were compared with those for uptake of ions by frog muscle (9). An interesting application of this cell to a drug involved a study that demonstrated ion-pair formation in the transfer of dextromethorphanium ions from water to chloroform (10). McNulty (11) employed a stirred transfer cell to study the effect of polysorbate 60 on the cholesterol uptake by vegetable oil from an aqueous solution containing 5% isopropanol.

The three-phase transfer cell of Rosano *et al.* (12) frequently has been applied to pharmaceutical problems. Lippold and Schneider (13–16) determined the forward (k_f; aqueous to organic) and reverse (k_r) rate constants for a homologous series of benzilic acid quaternary esters. Kubinyi (17) used these data to show that log k_f and log k_r can be defined as a function of the number (n) of CH_2 groups in a homologous series, provided that log K_D also is a simple function of n, where K_D is the partition coefficient.

This report demonstrates that the partition coefficient

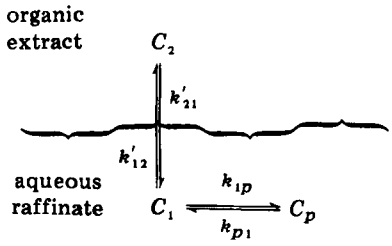

Scheme I

may be calculated from data representing the partitioning kinetics in a simple transfer cell (Fig. 1) when a drug undergoes simultaneous degradation in the aqueous phase. The two-phase cell was chosen to accommodate the added complexity introduced by drug instability in the aqueous phase. The model system (cyclohept-2-enone partitioning between liquid petrolatum and water or aqueous hydrochloric acid) chosen to test this theory allows independent evaluation of each rate constant in Scheme I, which represents partitioning in a stirred transfer cell with a competing reversible reaction in the aqueous phase. The concentration of cyclohept-2-enone in the extract (liquid petrolatum) is represented by C_2, and that in the raffinate (aqueous phase) is represented by C_1. The concentration of the degradation product, C_p, is limited to the aqueous phase, which is consistent with the experimental results. Rate constants are apparent first order, and the initial conditions are $C_1 = C_1^0$ with $C_2 = C_p = 0$.

THEORY

Partitioning Kinetics with Stable Drug—For the case where the partition coefficient, K_D, remains constant over the concentration range of the transfer experiment, the observed value may be defined by:

$$K_D = C_2^\infty / C_1^\infty \qquad \text{(Eq. 1)}$$

where C_2^∞ and C_1^∞ are the equilibrium concentrations in the raffinate (C_1) and the organic extract (C_2). At any time during a kinetic run (according to the two-film theory):

$$K_D = C_2^*/C_1 = C_{2i}/C_{1i} = C_2/C_1^* \qquad \text{(Eq. 2)}$$

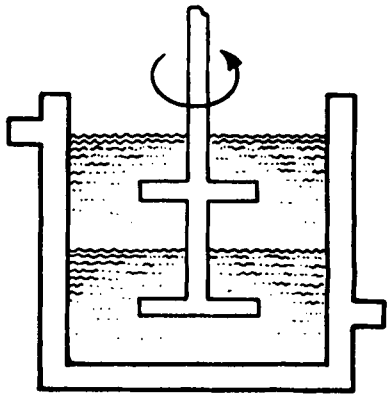

Figure 1—*Schematic diagram of a two-phase transfer cell with a jacketed beaker for constant-temperature control.*

0022-3549/80/0500-0527$01.00/0
© 1980, American Pharmaceutical Association

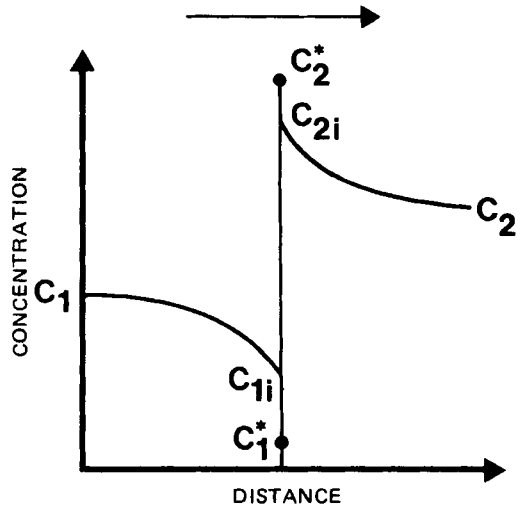

Figure 2—*Concentration gradients in a two-phase transfer cell. The arrow at the top indicates the direction of mass transfer. The concentration of diffusing solute in various regions is defined as: the average or mixed concentration in the stirred raffinate* (C_1) *and extract* (C_2); *at the interface on the raffinate side* (C_{1i}) *and extract side* (C_{2i}); $C_1^* = C_2/K_D$; *and* $C_2^* = C_1/K_D$.

The symbols are defined in Fig. 2. The solute transfer rate from the bulk of the raffinate to the interface through the diffusion layer is dependent on Fick's first law and may be written as:

$$J = -da/dt = V_1(-dC_1/dt) = (C_1 - C_{1i})(D_1A/h_1) \quad \text{(Eq. 3)}$$

where a is the amount of solute in the raffinate, V_1 is the volume of the raffinate, A is the interfacial area, and D_1 and h_1 are the diffusion coefficient and thickness of the diffusion layer in the raffinate, respectively. Similarly, the transfer rate from the interface to the bulk of the extract may be written as:

$$J = (C_{2i} - C_2)(D_2A/h_2) \quad \text{(Eq. 4)}$$

Provided that the interfacial barrier has no significant resistance and that thermal, electrical, and osmotic gradients are absent, then application of the two-film theory enables the *overall* transfer rate to be defined in terms of the overall concentration gradient $[C_1 - (C_2/K_D)]$ as:

$$J = k_{12}A(C_1 - C_1^*) \quad \text{(Eq. 5)}$$

since C_1^* is defined as (C_2/K_D) in Eq. 2. According to Flynn *et al.* (18), the *overall* rate constant for transfer from the raffinate to the extract, k_{12}, can be calculated from:

$$R_T = \frac{1}{k_{12}} = \frac{h_1}{D_1} + \frac{h_2}{D_2K_D} \quad \text{(Eq. 6)}$$

where R_T (the diffusional resistance) is the sum of the individual resistances. Equation 6 assumes the validity of the two-film theory and allows the derivation of Eq. 5 from Eqs. 2–4. Equation 5 is the form of the rate expression generally found in the literature (1–7). Its use requires analysis of both the raffinate and extract to determine $C_1 - C_1^*$ experimentally.

Since $C_1^* = C_2/K_D$ and the amount of solute in the extract, b, may be calculated from $b = a_0 - a$, Eq. 5 also may be written as:

$$J = \frac{-da}{dt} = k_{12}A\left[\left(\frac{a}{V_1}\right) - \left(\frac{(a_0 - a)}{K_DV_2}\right)\right] \quad \text{(Eq. 7)}$$

where V_2 is the volume of the extract, and the amount of solute in the interface is negligible. Integration of Eq. 7 from $t = 0$ to t and from $a = a_0$ to a, followed by substitution of a_∞ for $[a_0V_1/(K_DV_2 + V_1)]$, yields:

$$\ln(a - a_\infty) = \ln(a_0 - a_\infty) - St \quad \text{(Eq. 8)}$$

which also may be written as:

$$(a - a_\infty) = (a_0 - a_\infty)e^{-St} \quad \text{(Eq. 9)}$$

Dividing by V_1 allows conversion of Eq. 9 to concentration:

$$(C_1 - C_1^\infty) = (C_1^0 - C_1^\infty)e^{-St} \quad \text{(Eq. 10)}$$

Thus, a plot of $\ln(a - a_\infty)$ or $\ln(C_1 - C_1^\infty)$ *versus* time is linear with a negative slope, S, defined by:

$$S = \left[\frac{A(K_DV_2 + V_1)}{K_DV_1V_2}\right]k_{12} \quad \text{(Eq. 11)}$$

which may be used to calculate the *overall* rate constant for transfer from the raffinate to the extract. The S value is equivalent to the stirred cell transfer rate constant, S_{SC}, calculated by McNulty (11).

Solving for k_{12} in Eq. 6 and substituting in Eq. 11 yield:

$$S = \frac{D_1D_2A(K_DV_2 + V_1)}{V_1V_2(D_2K_Dh_1 + D_1h_2)} \quad \text{(Eq. 12)}$$

In a transfer cell, the interfacial area, phase volumes, and stirring rate may be kept constant throughout the experiment. In these studies, $V_1 = V_2 = V$, while D_1, D_2, h_1, h_2, and A remain constant, which leads to:

$$S = \left[\frac{A(K_D + 1)}{VK_D}\right]k_{12} = \frac{k'_{12}(K_D + 1)}{K_D} \quad \text{(Eq. 13)}$$

where k'_{12} is expressed in reciprocal time and is the apparent first-order forward rate constant for the partitioning process (Scheme I). Thus:

$$k'_{12} = D_1D_2AK_D/V(D_2K_Dh_1 + D_1h_2) = k_{12}A/V \quad \text{(Eq. 14)}$$

For data representing the extract, an equation similar to Eq. 5 may be written:

$$J = k_{21}A(C_2^* - C_2) \quad \text{(Eq. 15)}$$

Since $C_2^* = C_1K_D$ and $a = a_0 - b$, Eq. 15 may be rewritten as:

$$\frac{db}{dt} = k_{21}A\left[\frac{(a_0 - b)K_D}{V_1} - \left(\frac{b}{V_2}\right)\right] \quad \text{(Eq. 16)}$$

which, after integrating between the limits $t = 0$ to t and $b = 0$ to b and substituting b_∞ for $[a_0K_DV_2/(K_DV_2 + V_1)]$, yields:

$$\ln(b_\infty - b) = \ln b_\infty - S't \quad \text{(Eq. 17)}$$

Division of the exponential form of Eq. 17 by V_2 allows conversion to C_2. A plot of $\ln(b_\infty - b)$ or $\ln(C_2^\infty - C_2)$ *versus* time is linear with a negative slope, S', defined by:

$$S' = \left[\frac{A(K_DV_2 + V_1)}{V_1V_2}\right]k_{21} \quad \text{(Eq. 18)}$$

With the assumption that $V_1 = V_2 = V$, Eq. 18 reduces to:

$$S' = \left[\frac{A(K_D + 1)}{V}\right]k_{21} \quad \text{(Eq. 19)}$$

and the apparent first-order reverse rate constant for the partitioning process (Scheme I) is:

$$k'_{21} = \frac{S'}{(K_D + 1)} \quad \text{(Eq. 20)}$$

where $k'_{21} = k_{21}A/V$. Since mass balance requires that:

$$\frac{-da}{dt} = \frac{db}{dt} \quad \text{(Eq. 21)}$$

then $S = S'$, and the observed slopes of first-order plots based on Eqs. 8 and 17 are equal. Therefore, Eq. 13 equals Eq. 19 and:

$$S = S' = \left[\frac{A(K_D + 1)}{VK_D}\right]k_{12} = \left[\frac{A(K_D + 1)}{V}\right]k_{21} \quad \text{(Eq. 22)}$$

Therefore:

$$K_D = (k_{12}/k_{21}) = (k'_{12}/k'_{21}) \quad \text{(Eq. 23)}$$

Thus, the partition coefficient, K_D, is the ratio of the forward and reverse rate constants.

From Eqs. 13 and 20, it can be shown that:

$$(k'_{12} + k'_{21}) = S = S' \quad \text{(Eq. 24)}$$

Thus, the negative slope of a first-order plot for concentration in the raffinate (Eq. 10) or the extract (Eq. 17) equals the observed first-order rate constant, k_{obs}, which is the sum of the constants, $k'_{12} + k'_{21}$, whose ratio (k'_{12}/k'_{21}) is the partition coefficient, K_D.

Simultaneous Partitioning and Reversible Aqueous Degradation—Scheme I represents simultaneous first-order partitioning with reversible aqueous degradation to a nonpartitioning product. Solving (19) the corresponding equation for $-dC_1/dt$ and setting A constant and $V_1 = V_2$ yields:

$$C_1 = Xe^{-\gamma t} + Ye^{-\delta t} + Z \quad \text{(Eq. 25)}$$

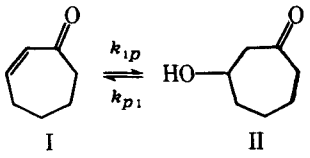

Scheme II

where $X = C_1^0(k'_{21} - \gamma)(k_{p1} - \gamma)/\gamma(\gamma - \delta)$, $Y = C_1^0(k'_{21} - \delta)(k_{p1} - \delta)/\delta(\delta - \gamma)$, $Z = C_1^0 k'_{21} k_{p1}/\gamma\delta$, $\gamma = 0.5(K_1 + \sqrt{K_1^2 - 4K_2})$, $\delta = 0.5(K_1 - \sqrt{K_1^2 - 4K_2})$, $K_1 = (k'_{12} + k'_{21} + k_{1p} + k_{p1})$, and $K_2 = (k'_{12}k_{p1} + k'_{21}k_{p1} + k'_{21}k_{1p})$. If partitioning of the product into the organic extract is significant, then Scheme I and Eq. 25 must be modified to include the additional compartment, C_{2p}. The aqueous degradation of drugs usually goes to completion (*i.e.*, apparent irreversibility), and the time course for C_1 therefore is independent of C_p. This case, in which the partitioning behavior of the product is immaterial, is discussed later.

Nonlinear regression of data for a system described by Scheme I using Eq. 25 with known values for k_{1p} and k_{p1} allows estimation of k'_{12} and k'_{21}. The ratio (k'_{12}/k'_{21}) should estimate the partition coefficient, K_D (Eq. 23).

EXPERIMENTAL

Ideal properties to test the theory were defined as follows. The solute should not contain any acidic or basic groups but should remain neutral throughout the pH range studied. (Alternatively, it should have a constant ionic form throughout the studies.) This condition eliminates the complication of a pH-dependent distribution coefficient. A simple stability-indicating assay is required. It must be possible to determine K_D, k'_{12}, and k'_{21} under conditions where the solute is stable. The value for K_D must be sufficiently small to allow accuracy in the estimation of both k'_{12} and k'_{21}. Sink conditions ($k'_{12} \gg k'_{21}$), which prevent the estimation of k'_{21}, eliminated the use of several nonaqueous solvents. The rate constants for degradation, k_{1p} and k_{p1}, must be on the same order of magnitude as k'_{12} and k'_{21} to prevent domination by either extraction or degradation. The solute should not undergo self-association so that K_D remains constant throughout the experiment.

UV absorption[1] was automatically recorded with a flowcell to monitor the C_1 time course continuously. Absorbance at a single wavelength was related directly to C_1 by selecting a solute whose degradation product did not interfere.

The α,β-unsaturated ketone, cyclohept-2-enone (I), was chosen since it was expected to undergo hydrogen-ion-catalyzed hydration to the nonchromophoric compound, 3-hydroxycycloheptanone (II). Previous studies indicated that the process is reversible and that some reaction conditions do not favor complete hydration (20, 21).

In Scheme II, the concentration of I is given by:

$$C_1 = \frac{C_1^0 k_{1p}}{(k_{1p} + k_{p1})} e^{-(k_{1p}+k_{p1})t} + \frac{C_1^0 k_{p1}}{(k_{1p} + k_{p1})} \qquad \text{(Eq. 26)}$$

The negative slope, k_{app}, of a plot of $\ln(C_1 - C_1^\infty)$ *versus* t, where $C_1^\infty = C_1^0 k_{p1}/(k_{1p} + k_{p1})$, is the sum of the first-order rate constants $(k_{1p} + k_{p1})$. The reverse and forward constants may be calculated from:

$$k_{p1} = k_{app} C_1^\infty / C_1^0 \qquad \text{(Eq. 27)}$$

and:

$$k_{1p} = k_{app} - k_{p1} \qquad \text{(Eq. 28)}$$

The 233-nm absorption maximum of cyclohept-2-enone decreased to <5% of its initial value in 1 *N* HCl at 37° within 24 hr. A similar trial using cyclohex-2-enone produced a 32% reduction in 60 hr. The percent residual absorption of cyclohept-2-enone increased with decreasing acid strength.

The theory relating to Scheme I indicates that nonlinear regression based on Eq. 25 can be used to estimate k'_{12} and k'_{21} if the values for k_{1p} and k_{p1} (which may be assessed independently) are known. Equation 23 shows that the partition coefficient may be calculated from the ratio of the distribution constants, $K_D = (k'_{12}/k'_{21})$.

Estimates for K_D were similar at three initial concentrations, representing the range observed in the aqueous phase during partitioning kinetics. Determinations were made by equilibration of cyclohept-2-enone between equal volumes of water and light liquid petrolatum at 37° using the UV absorbance of the solute in the aqueous phase (λ_{max} = 233 nm, ϵ = 10,182). Control experiments to determine the partitioning of the solute between potassium chloride solutions of varying ionic strength (μ = 0–1) and light liquid petrolatum at 37° showed that K_D was independent of μ. Prior to use, the light liquid petrolatum was extracted repeatedly with double-distilled water until the extracts showed no absorption at 233 nm and both phases were preequilibrated.

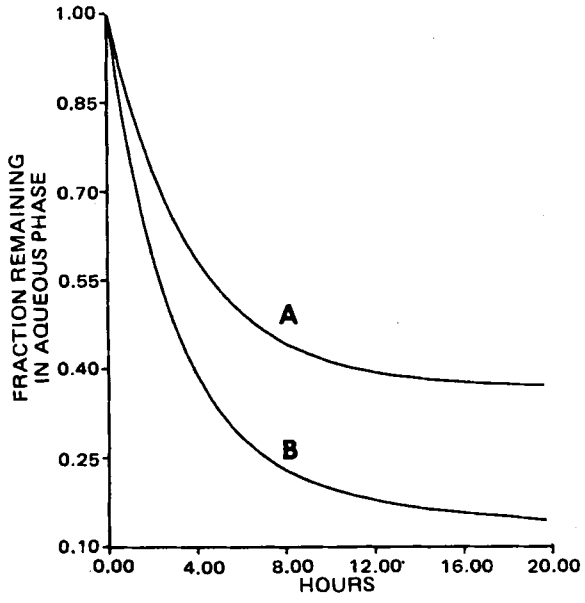

Figure 3—*Fraction of the initial concentration of cyclohept-2-enone remaining in the raffinate as a function of time at 37° under stable (curve A) and unstable (curve B; 0.1 N HCl at 37°) conditions at 50 rpm in the transfer cell. The continuous data presented in the figure are indistinguishable from the theoretical curves obtained using Eq. 10 (curve A) and Eq. 25 (curve B) when* k'_{12}, k'_{21}, k_{1p}, *and* k_{p1} *values are as given in Table I.*

Distribution rate constants were estimated by introducing the solute into the aqueous phase of a transfer cell (Fig. 1) containing 90 ml of each preequilibrated phase, stirred[2] at 50 or 100 rpm and maintained at 37°. The initial concentration in the aqueous phase was 1.4×10^{-4} *M*. The aqueous phase was pumped[3] through a flowcell in the thermally controlled spectrophotometer. The 233-nm absorbance was recorded automatically as a function of time until equilibrium was attained. Final values agreed with the nonkinetic partitioning studies. Cyclohept-2-enone underwent <3% hydration after 96 hr under the study conditions. First-order plots based on Eq. 10 were linear for >95% of the process; k'_{12} and k'_{21} were calculated from Eqs. 23 and 24.

The kinetics of cyclohept-2-enone hydration were studied as a function of the hydrochloric acid concentration at 37°. Rate constants, k_{1p} and k_{p1}, were calculated from Eqs. 27 and 28; those in 0.1 *N* HCl were considered best for the evaluation of k'_{12} and k'_{21} under competing conditions. The residual absorbance after equilibration in 0.1 *N* HCl was 10.3% and is attributed to I since the contribution by II is negligible (20, 21).

The kinetics of hydration in 0.1 *N* HCl with simultaneous partitioning into light liquid petrolatum were measured in a stirred transfer cell at 50 or 100 rpm at 37°. Absorbance data (A at λ_{max} = 233 nm) were analyzed by nonlinear regression (22) based on Eq. 25 where $C_1 = A/\epsilon$. Equilibration studies of I between 0.1 *N* HCl and light liquid petrolatum gave observed values for Z similar to those calculated from $Z = C_1^0 k'_{12} k_{p1}/\gamma\delta$ (Eq. 25). This agreement is consistent with the formation of a nonchromophoric product that does not partition significantly (Scheme I). The values for k'_{12} and k'_{21}, obtained in these experiments with simultaneous partitioning and hydration, were compared to those determined in the absence of hydration.

RESULTS AND DISCUSSION

Curve A in Fig. 3 shows a typical time course for the fraction of solute remaining in the aqueous phase of a stirred transfer cell containing equal volumes of water and light liquid petrolatum at 37° and 50 rpm. The

[1] Models 250 and 6051, Gilford Instruments, Oberlin, Ohio.

[2] Model 53 dissolution stirrer, Hanson Research Corp., Northridge, Calif.

[3] Model 396/2396 minipump, Milton Roy Co., Riviera Beach, Fla.

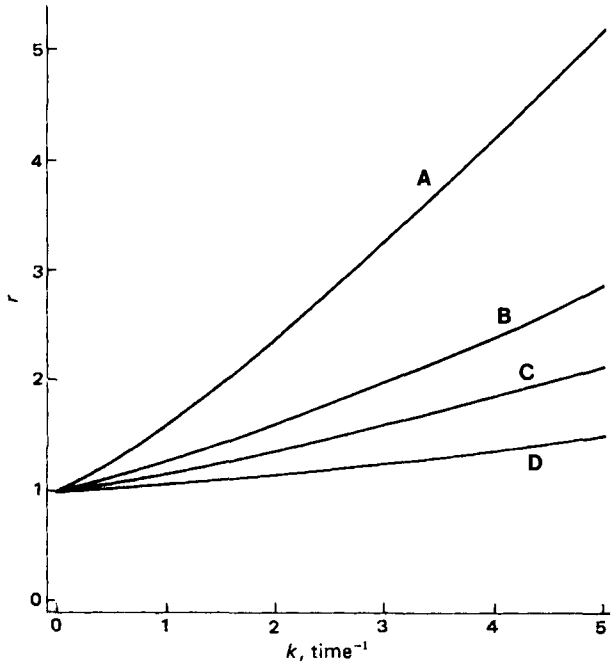

Figure 4—*Relationship between* r *(calculated from Eq. 32) and* K_D *(Eq. 1) as a function of the relative values of* k'_{12}, k'_{21}, *and* k. *In this illustration,* $k_{12} = k'_{21}$, *so that* $K_D = 1$, *which is the value for* r *when* k = 0. *The* k'_{12} *and* k'_{21} *values are 1 (curve A), 2 (curve B), 3 (curve C), and 6 (curve D).*

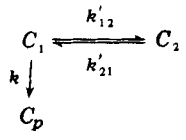

Scheme III

negative slope, S, of a first-order plot based on Eq. 10 was used to calculate k'_{12} and k'_{21} (Eqs. 23 and 24) from such data. Since cyclohept-2-enone is a neutral molecule, its K_D value should be independent of pH. Thus, the values determined for k'_{12} and k'_{21} under stable conditions should be the same as those determined in the presence of simultaneous degradation.

When the experiment was repeated with 0.1 *N* HCl as the aqueous phase, cyclohept-2-enone loss (Fig. 3, curve B) was described by Eq. 25 in accordance with Scheme I. Data were analyzed by nonlinear regression (22) of the entire time course to reiterate the values for k'_{12} and k'_{21} while assigning to k_{1p} and k_{p1} the values determined independently in 0.1 *N* HCl saturated with light liquid petrolatum at 37°. The agreement between the regression estimates and those determined independently (Table I) supports the proposed theory in which $K_D = k'_{12}/k'_{21}$.

The calculation of K_D under unstable conditions may be important to the chemist concerned with its modification. This approach can provide values that may be needed for structural correlations on partitioning. It may not be possible to determine K_D independently as was done with cyclohept-2-enone. For example, the solute may exist as a different charge species at pH values where it is stable, or conditions sufficiently stable for equilibration may not exist.

Partitioning Kinetics with Simultaneous Irreversible Loss of Drug—The present study demonstrated that biexponential loss from the aqueous phase of Scheme I can be analyzed for k'_{12} and k'_{21} whose ratio (k'_{12}/k'_{21}) is K_D. This theory can be extended to Scheme III, which shows the irreversible loss of drug competing with the process of distribution as discussed previously (23) in reference to apomorphine distribution into the brains of mice. This process is analogous to the reversible first-order transfer of a compound between the aqueous phase, C_1, and the organic phase, C_2, of a stirred transfer cell with simultaneous, irreversible, first-order degradation to the product, C_p, in the aqueous phase. Applying the initial conditions of $C_1 = C_1^0$ and $C_2 = C_p = 0$ and again assuming that $[A/V_1] = [A/V_2]$ remains constant provide:

$$C_1 = X'e^{-\alpha t} + Y'e^{-\beta t} \qquad \text{(Eq. 29)}$$

Table I—Comparison of the Rate Constants k'_{12} and k'_{21} for Distribution of Cyclohept-2-enone between Light Liquid Petrolatum and Water to the Estimates Obtained with Simultaneous Hydration and Partitioning (Light Liquid Petrolatum–0.1 *N* HCl) in a Stirred Transfer Cell at 37°

Revolutions per Minute	Stable Conditions			Simultaneous Loss[a]		
	k'_{12}	k'_{21}	K_D[b]	k'_{12}	k'_{21}	Percent Error[c]
50	0.168	0.098	1.7	0.163	0.105	−5.9
100	0.206	0.120	1.7	0.210	0.130	−5.9

[a] The k'_{12} and k'_{21} values were determined by nonlinear regression based on Eq. 25; k_{1p} and k_{p1} were held constant at 0.117 and 0.0134 hr^{-1}, respectively. [b] $K_D = C_2^\infty/C_1^\infty = k'_{12}/k'_{21}$. [c] $|[(k'_{12}/k'_{21})^a - K_D]/K_D{}^b| \times 100$ = percent error.

where $X' = C_1^0(\alpha - k'_{21})/(\alpha - \beta)$, $Y' = C_1^0(k'_{21} - \beta)/(\alpha - \beta)$, $\alpha = 0.5(K_3 + \sqrt{K_3^2 - 4k'_{21}k})$, $\beta = 0.5(K_3 - \sqrt{K_3^2 - 4k'_{21}k})$, and $K_3 = (k'_{12} + k'_{21} + k)$. The time course for solute concentration in the extract may be defined by:

$$C_2 = Z'(e^{-\beta t} - e^{-\alpha t}) \qquad \text{(Eq. 30)}$$

where $Z' = C_1^0 k'_{12}/(\alpha - \beta)$. Such a system, involving the simultaneous partitioning and hydrolysis of ampicillin and amoxicillin in isobutanol–aqueous hydrochloric acid, was investigated (24).

The observed phase ratio, C_2/C_1, will change as a function of time. The time required for this ratio to approach a constant value during an experiment depends on the values for k'_{12}, k'_{21}, and k. When the contribution of the first term in Eq. 29 ($X'e^{-\alpha t}$) becomes insignificant relative to the second term ($Y'e^{-\beta t}$), the ratio approaches a constant. The time required for this result to occur, t_d, may be estimated from:

$$t_d \approx [\ln(F/R)]/(\beta - \alpha) \qquad \text{(Eq. 31)}$$

where $R = (k'_{21} - \alpha)/(k'_{12} - \beta)$ and F is the fraction of C_1 (Eq. 29) at t_d that is due to $X'e^{-\alpha t}$ (25). If, for example, a contribution of 1% is considered insignificant, then $F = 0.01$. At $t > t_d$, C_2/C_1 (Scheme III) approaches a constant distribution ratio, which may be estimated from:

$$r = k'_{12}/(k'_{21} - \beta) \qquad \text{(Eq. 32)}$$

in the limit as $Xe^{-\alpha t}$ approaches zero. Provided that t_d is not too large, C_2/C_1 will approach r during the experiment. However, the value for r will not approximate K_D except under conditions in which the drug is relatively stable and $(k'_{21} - \beta) \to k'_{21}$.

The situation in which C_2/C_1 may be described by r rather than by K_D is referred to as kinetic control of distribution in contrast to thermodynamic control (23). Although many successful biological correlations have been achieved using K_D values, there may be situations where kinetic control dominates. It was noted (23) that the distribution of norapomorphine to the brain [reported by Burkman *et al.* (26)] might be an example where competing kinetic processes controlled the brain–blood ratios, r, due to simultaneous drug loss by glucuronidation. It was suggested that t_d was too large to allow the observation of a constant r value before complete loss of the drug from the animal.

Another example where r may be of greater value than K_D is in simultaneous first-order absorption and degradation. This situation might occur through chemical degradation caused by stomach acidity or metabolism by intestinal flora. Tomlinson *et al.* (24) compared r and K_D values for amoxicillin and ampicillin under unstable conditions and discussed the potential significance of kinetic control of the phase ratios.

Figure 4 illustrates the relationship between r and K_D as a function of selected relative values for k'_{12}, k'_{21}, and k (Scheme III). When $k = 0$, $r = K_D$. From a practical viewpoint, $r \approx K_D$ (within 5%) when $(k'_{12} + k'_{21}) \geq 20k$. As the k value increases, r increases relative to K_D, and kinetic control becomes increasingly significant.

Conclusion—A stirred transfer cell has been employed to calculate the partition coefficient, K_D, for a compound that is unstable in the aqueous phase. Equations for drugs that degrade *irreversibly* in one of the transfer cell phases (Scheme III) can simultaneously estimate the first-order rate constants for both degradation and distribution. This calculation, using kinetic methods, provides K_D values under conditions where equilibration experiments are not possible. These constants may be used to calculate K_D, r, and the time at which distribution is considered complete ($t > t_d$, $F = 0.01$) as simultaneous irreversible degradation competes with partitioning. The difference between r and K_D indicates the degree of kinetic control for the system.

REFERENCES

(1) W. G. Whitman, *Chem. Metall. Eng.*, **29**, 146 (1923)

(2) W. K. Lewis and W. G. Whitman, *Ind. Eng. Chem.*, **16**, 1215 (1924).

(3) K. F. Gordon and T. K. Sherwood, *Chem. Eng. Progr. (Symp. Ser.)*, **50**, 15 (1954).

(4) T. K. Sherwood and K. F. Gordon, *AIChE J.*, **1**, 129 (1955).

(5) R. E. Treybal, "Liquid Extraction," 2nd ed., McGraw-Hill, New York, N.Y., 1963, pp. 173–182.

(6) J. T. Davies and E. K. Rideal, "Interfacial Phenomena," Academic, New York, N.Y., 1961, pp. 311–321.

(7) T. K. Sherwood, R. L. Pigford, and C. R. Wilke, "Mass Transfer," McGraw-Hill, New York, N.Y., 1975, pp. 178–181.

(8) W. J. McManamey, J. T. Davies, J. M. Woollen, and J. R. Coe, *Chem. Eng. Sci.*, **28**, 1061 (1973).

(9) H. P. Ting, G. L. Bertrand, and D. F. Sears, *Biophys. J.*, **6**, 813 (1966).

(10) T. Higuchi and A. F. Michaelis, *Anal. Chem.*, **40**, 1925 (1968).

(11) P. B. McNulty, *J. Pharm. Sci.*, **64**, 1500 (1975).

(12) H. L. Rosano, P. Duby, and J. H. Schulman, *J. Phys. Chem.*, **65**, 1704 (1961), and references cited therein.

(13) B. C. Lippold and G. F. Schneider, *Arzneim.-Forsch.*, **25**, 843 (1975).

(14) *Ibid.*, **25**, 1683 (1975).

(15) *Ibid.*, **26**, 2202 (1976).

(16) B. C. Lippold and G. F. Schneider, *Pharmazie*, **31**, 237 (1976).

(17) H. Kubinyi, *J. Pharm. Sci.*, **67**, 262 (1978).

(18) G. L. Flynn, S. H. Yalkowsky, and T. J. Roseman, *ibid.*, **63**, 479 (1974).

(19) L. Benet, *ibid.*, **61**, 536 (1972).

(20) R. E. Notari and S. M. Caiola, *ibid.*, **58**, 1203 (1969).

(21) E. R. Garrett and R. E. Notari, *J. Org. Chem.*, **31**, 425 (1966).

(22) C. M. Metzler, G. L. Elfring, and A. J. McEwen, *Biometrics*, **30** (3) (1974).

(23) R. E. Notari, *Pharm. Weekbl.*, **110**, 577 (1975).

(24) E. Tomlinson, R. E. Notari, and P. R. Byron, *J. Pharm. Sci.*, in press.

(25) P. R. Byron and R. E. Notari, *ibid.*, **65**, 1140 (1976).

(26) A. M. Burkman, R. E. Notari, and W. K. Van Tyle, *J. Pharm. Pharmacol.*, **26**, 493 (1974).

2-^{14}C-1-(2′-Deoxy-β-D-ribofuranosyl)-5-ethyluracil: Synthesis and Biotransformation in Rats

RAVINDER KAUL ˣ, GEBHARD KIEFER, SIEGFRIED ERHARDT, and BERND HEMPEL

Received December 15, 1975, from the *Research Laboratories, Pharmaceuticals Robugen GmbH, Alleenstrasse 22, D-73 Esslingen-Zell, West Germany.* Accepted for publication November 29, 1978.

Abstract □ With ^{14}C-urea as the starting material, 2-^{14}C-1-(2′-deoxy-β-D-ribofuranosyl)-5-ethyluracil [2-^{14}C-β-5-ethyl-2′-deoxyuridine] was synthesized for metabolic studies. After intravenous administration in rats, the radioactivity disappeared in the blood within 72 hr, being eliminated primarily in the urine (97%). The major elimination took place in the first 24 hr (92%). Little radioactivity was detected in the organs and tissues after 3 days. Approximately 50% of the urine radioactivity probably was due to an unidentified conjugate, 30% was due to Metabolite II, and 20% was unchanged drug. Metabolite II was identified as 5-ethyluracil by mass and ^{1}H-NMR spectra and by comparison with an authentic sample.

Keyphrases □ Ethyldeoxyuridine—synthesis, biotransformation in rats, metabolites □ Antiviral agents—ethyldeoxyuridine, synthesis, biotransformation in rats, metabolites

1-(2′-Deoxy-β-D-ribofuranosyl)-5-ethyluracil (β-5-ethyl-2′-deoxyuridine[1], VIII) has shown promising therapeutic activity against herpes simplex and vaccina viruses (1, 2) and against herpes keratitis in rabbits (3). Due to its compatibility with the ophthalmic mucous membrane, VIII is particularly suitable for the treatment of herpetic eye disease (4–7). Its excretion, distribution, and biotransformation were studied in rats using ^{14}C-VIII.

EXPERIMENTAL[2]

Synthesis—For metabolic studies, ^{14}C-β-5-ethyl-2′-deoxyuridine (VIII), specific activity 0.168 mCi/mmole, was synthesized (Scheme I). The starting material was ^{14}C-urea[3], specific activity 5.13 mCi/mmole.

2-^{14}C-5-Ethylbarbituric Acid (III)—Diethyl ethylmalonate (II) (9.4 g, 0.05 mole) was added dropwise to 10 ml of a 30% methanolic sodium methoxide solution. The reaction mixture was refluxed for 30 min with constant stirring. Then the ^{14}C-urea solution (3 g, 0.05 mole) in 10 ml of methanol was added quickly. The reaction mixture was refluxed with stirring for 6 hr under anhydrous conditions.

After cooling, the solvent was evaporated to dryness, and the residue was dissolved in 30 ml of hot water. The solution was acidified to pH 1–2 with 10 ml of concentrated hydrochloric acid. Crystals that precipitated overnight under refrigeration were filtered off, washed with ice water, and dried to yield 6.1 g of 2-^{14}C-III (78.3% based on ^{14}C-urea), mp 195–197° [lit. (8) mp 194–195°, (9) mp 193–194°].

2-^{14}C-5-Ethyl-6-chlorouracil (IV)—Phosphoryl chloride (14 ml) was added dropwise into a mixture of III (6.1 g, 0.035 mole) and water (0.5 ml). The reaction mixture temperature was slowly raised to 100° with constant stirring. After heating on an oil bath for 90 min at 90–100°, the reaction mixture was cooled. The remaining phosphoryl chloride was decomposed carefully with 25 ml of water.

The cooled mixture was stirred for 1 hr and allowed to stand in the refrigerator overnight. The white crystalline precipitate was filtered off, washed with ice water, and dried to yield 6.1 g of 2-^{14}C-IV (70% based on ^{14}C-urea), mp 215–217° [lit. (10) mp 215–217°].

2-^{14}C-5-Ethyluracil (V)—The solution of IV (6.1 g, 0.035 mole) in 2 *N* NaOH (58 ml) and 1% palladium-on-charcoal was hydrogenated at 60°. The hydrogen uptake virtually ceased after 3 hr. The catalyst was filtered off, and the filtrate was acidified with concentrated hydrochloric acid. After cooling, the precipitated crystals were filtered off, washed with cold water, and dried to yield 3.6 g of 2-^{14}C-V (51.4% based on ^{14}C-urea), mp 308–309° [lit. (8) mp 302–303°, (11, 12) mp 300–303°, (13) mp 300°, (14, 15) mp 308–309°].

2-^{14}C-2,4-Bis-O-(trimethylsilyl)-5-ethylpyrimidine (VI)—Compound V (3.6 g, 25.5 mmoles), hexamethyldisilazane (21 ml), and dimethylformamide (1.8 ml) were heated on an oil bath for 12 hr at 160–170° with constant stirring under anhydrous conditions. After cooling, the solvent was removed under reduced pressure. The residue, an oily yellow liquid, was used without further purification in the next step.

2-^{14}C-1-(3′,5′-Di-O-p-chlorobenzoyl-2′-deoxy-α,β-D-ribofuranosyl)-5-ethyluracil (VIIa and VIIb)—The reaction of VI with 3,5-di-*O*-*p*-chlorobenzoyl-2′-deoxy-α,β-D-ribofuranosyl chloride (16) to produce 1-(3′,5′-di-*O*-*p*-chlorobenzoyl-2′-deoxy-α,β-D-ribofuranosyl)-5-substi-

[1] Edurid, Robugen GmbH, 7300 Esslingen/Neckar, West Germany.

[2] Melting points were taken on a Tottoli (Büchi, Switzerland) apparatus and are uncorrected. Mass spectra were measured at an ionizing potential of 70 ev with a CH-7 Varian MAT spectrometer using a direct evaporator inlet system. ^{1}H-NMR spectra were recorded on a Varian T-60 spectrometer using dimethyl sulfoxide-d_6 as the solvent and trimethylsilane as the internal standard.

[3] New England Nuclear Corp., Boston, Mass.

0022-3549/80/0500-0531$01.00/0

© 1980, American Pharmaceutical Association

REFERENCES

(1) W. G. Whitman, *Chem. Metall. Eng.*, **29**, 146 (1923)

(2) W. K. Lewis and W. G. Whitman, *Ind. Eng. Chem.*, **16**, 1215 (1924).

(3) K. F. Gordon and T. K. Sherwood, *Chem. Eng. Progr. (Symp. Ser.)*, **50**, 15 (1954).

(4) T. K. Sherwood and K. F. Gordon, *AIChE J.*, **1**, 129 (1955).

(5) R. E. Treybal, "Liquid Extraction," 2nd ed., McGraw-Hill, New York, N.Y., 1963, pp. 173–182.

(6) J. T. Davies and E. K. Rideal, "Interfacial Phenomena," Academic, New York, N.Y., 1961, pp. 311–321.

(7) T. K. Sherwood, R. L. Pigford, and C. R. Wilke, "Mass Transfer," McGraw-Hill, New York, N.Y., 1975, pp. 178–181.

(8) W. J. McManamey, J. T. Davies, J. M. Woollen, and J. R. Coe, *Chem. Eng. Sci.*, **28**, 1061 (1973).

(9) H. P. Ting, G. L. Bertrand, and D. F. Sears, *Biophys. J.*, **6**, 813 (1966).

(10) T. Higuchi and A. F. Michaelis, *Anal. Chem.*, **40**, 1925 (1968).

(11) P. B. McNulty, *J. Pharm. Sci.*, **64**, 1500 (1975).

(12) H. L. Rosano, P. Duby, and J. H. Schulman, *J. Phys. Chem.*, **65**, 1704 (1961), and references cited therein.

(13) B. C. Lippold and G. F. Schneider, *Arzneim.-Forsch.*, **25**, 843 (1975).

(14) *Ibid.*, **25**, 1683 (1975).

(15) *Ibid.*, **26**, 2202 (1976).

(16) B. C. Lippold and G. F. Schneider, *Pharmazie*, **31**, 237 (1976).

(17) H. Kubinyi, *J. Pharm. Sci.*, **67**, 262 (1978).

(18) G. L. Flynn, S. H. Yalkowsky, and T. J. Roseman, *ibid.*, **63**, 479 (1974).

(19) L. Benet, *ibid.*, **61**, 536 (1972).

(20) R. E. Notari and S. M. Caiola, *ibid.*, **58**, 1203 (1969).

(21) E. R. Garrett and R. E. Notari, *J. Org. Chem.*, **31**, 425 (1966).

(22) C. M. Metzler, G. L. Elfring, and A. J. McEwen, *Biometrics*, **30** (3) (1974).

(23) R. E. Notari, *Pharm. Weekbl.*, **110**, 577 (1975).

(24) E. Tomlinson, R. E. Notari, and P. R. Byron, *J. Pharm. Sci.*, in press.

(25) P. R. Byron and R. E. Notari, *ibid.*, **65**, 1140 (1976).

(26) A. M. Burkman, R. E. Notari, and W. K. Van Tyle, *J. Pharm. Pharmacol.*, **26**, 493 (1974).

2-^{14}C-1-(2′-Deoxy-β-D-ribofuranosyl)-5-ethyluracil: Synthesis and Biotransformation in Rats

RAVINDER KAUL ˣ, GEBHARD KIEFER, SIEGFRIED ERHARDT, and BERND HEMPEL

Received December 15, 1975, from the *Research Laboratories, Pharmaceuticals Robugen GmbH, Alleenstrasse 22, D-73 Esslingen-Zell, West Germany.* Accepted for publication November 29, 1978.

Abstract □ With ^{14}C-urea as the starting material, 2-^{14}C-1-(2′-deoxy-β-D-ribofuranosyl)-5-ethyluracil [2-^{14}C-β-5-ethyl-2′-deoxyuridine] was synthesized for metabolic studies. After intravenous administration in rats, the radioactivity disappeared in the blood within 72 hr, being eliminated primarily in the urine (97%). The major elimination took place in the first 24 hr (92%). Little radioactivity was detected in the organs and tissues after 3 days. Approximately 50% of the urine radioactivity probably was due to an unidentified conjugate, 30% was due to Metabolite II, and 20% was unchanged drug. Metabolite II was identified as 5-ethyluracil by mass and ^{1}H-NMR spectra and by comparison with an authentic sample.

Keyphrases □ Ethyldeoxyuridine—synthesis, biotransformation in rats, metabolites □ Antiviral agents—ethyldeoxyuridine, synthesis, biotransformation in rats, metabolites

1-(2′-Deoxy-β-D-ribofuranosyl)-5-ethyluracil (β-5-ethyl-2′-deoxyuridine[1], VIII) has shown promising therapeutic activity against herpes simplex and vaccina viruses (1, 2) and against herpes keratitis in rabbits (3). Due to its compatibility with the ophthalmic mucous membrane, VIII is particularly suitable for the treatment of herpetic eye disease (4–7). Its excretion, distribution, and biotransformation were studied in rats using ^{14}C-VIII.

EXPERIMENTAL[2]

Synthesis—For metabolic studies, ^{14}C-β-5-ethyl-2′-deoxyuridine (VIII), specific activity 0.168 mCi/mmole, was synthesized (Scheme I). The starting material was ^{14}C-urea[3], specific activity 5.13 mCi/mmole.

2-^{14}C-5-Ethylbarbituric Acid (III)—Diethyl ethylmalonate (II) (9.4 g, 0.05 mole) was added dropwise to 10 ml of a 30% methanolic sodium methoxide solution. The reaction mixture was refluxed for 30 min with constant stirring. Then the ^{14}C-urea solution (3 g, 0.05 mole) in 10 ml of methanol was added quickly. The reaction mixture was refluxed with stirring for 6 hr under anhydrous conditions.

After cooling, the solvent was evaporated to dryness, and the residue was dissolved in 30 ml of hot water. The solution was acidified to pH 1–2 with 10 ml of concentrated hydrochloric acid. Crystals that precipitated overnight under refrigeration were filtered off, washed with ice water, and dried to yield 6.1 g of 2-^{14}C-III (78.3% based on ^{14}C-urea), mp 195–197° [lit. (8) mp 194–195°, (9) mp 193–194°].

2-^{14}C-5-Ethyl-6-chlorouracil (IV)—Phosphoryl chloride (14 ml) was added dropwise into a mixture of III (6.1 g, 0.035 mole) and water (0.5 ml). The reaction mixture temperature was slowly raised to 100° with constant stirring. After heating on an oil bath for 90 min at 90–100°, the reaction mixture was cooled. The remaining phosphoryl chloride was decomposed carefully with 25 ml of water.

The cooled mixture was stirred for 1 hr and allowed to stand in the refrigerator overnight. The white crystalline precipitate was filtered off, washed with ice water, and dried to yield 6.1 g of 2-^{14}C-IV (70% based on ^{14}C-urea), mp 215–217° [lit. (10) mp 215–217°].

2-^{14}C-5-Ethyluracil (V)—The solution of IV (6.1 g, 0.035 mole) in 2 *N* NaOH (58 ml) and 1% palladium-on-charcoal was hydrogenated at 60°. The hydrogen uptake virtually ceased after 3 hr. The catalyst was filtered off, and the filtrate was acidified with concentrated hydrochloric acid. After cooling, the precipitated crystals were filtered off, washed with cold water, and dried to yield 3.6 g of 2-^{14}C-V (51.4% based on ^{14}C-urea), mp 308–309° [lit. (8) mp 302–303°, (11, 12) mp 300–303°, (13) mp 300°, (14, 15) mp 308–309°].

2-^{14}C-2,4-Bis-O-(trimethylsilyl)-5-ethylpyrimidine (VI)—Compound V (3.6 g, 25.5 mmoles), hexamethyldisilazane (21 ml), and dimethylformamide (1.8 ml) were heated on an oil bath for 12 hr at 160–170° with constant stirring under anhydrous conditions. After cooling, the solvent was removed under reduced pressure. The residue, an oily yellow liquid, was used without further purification in the next step.

2-^{14}C-1-(3′,5′-Di-O-p-chlorobenzoyl-2′-deoxy-α,β-D-ribofuranosyl)-5-ethyluracil (VIIa and VIIb)—The reaction of VI with 3,5-di-*O*-*p*-chlorobenzoyl-2′-deoxy-α,β-D-ribofuranosyl chloride (16) to produce 1-(3′,5′-di-*O*-*p*-chlorobenzoyl-2′-deoxy-α,β-D-ribofuranosyl)-5-substi-

[1] Edurid, Robugen GmbH, 7300 Esslingen/Neckar, West Germany.

[2] Melting points were taken on a Tottoli (Büchi, Switzerland) apparatus and are uncorrected. Mass spectra were measured at an ionizing potential of 70 ev with a CH-7 Varian MAT spectrometer using a direct evaporator inlet system. ^{1}H-NMR spectra were recorded on a Varian T-60 spectrometer using dimethyl sulfoxide-d_6 as the solvent and trimethylsilane as the internal standard.

[3] New England Nuclear Corp., Boston, Mass.

0022-3549/80/0500-0531$01.00/0

© 1980, American Pharmaceutical Association

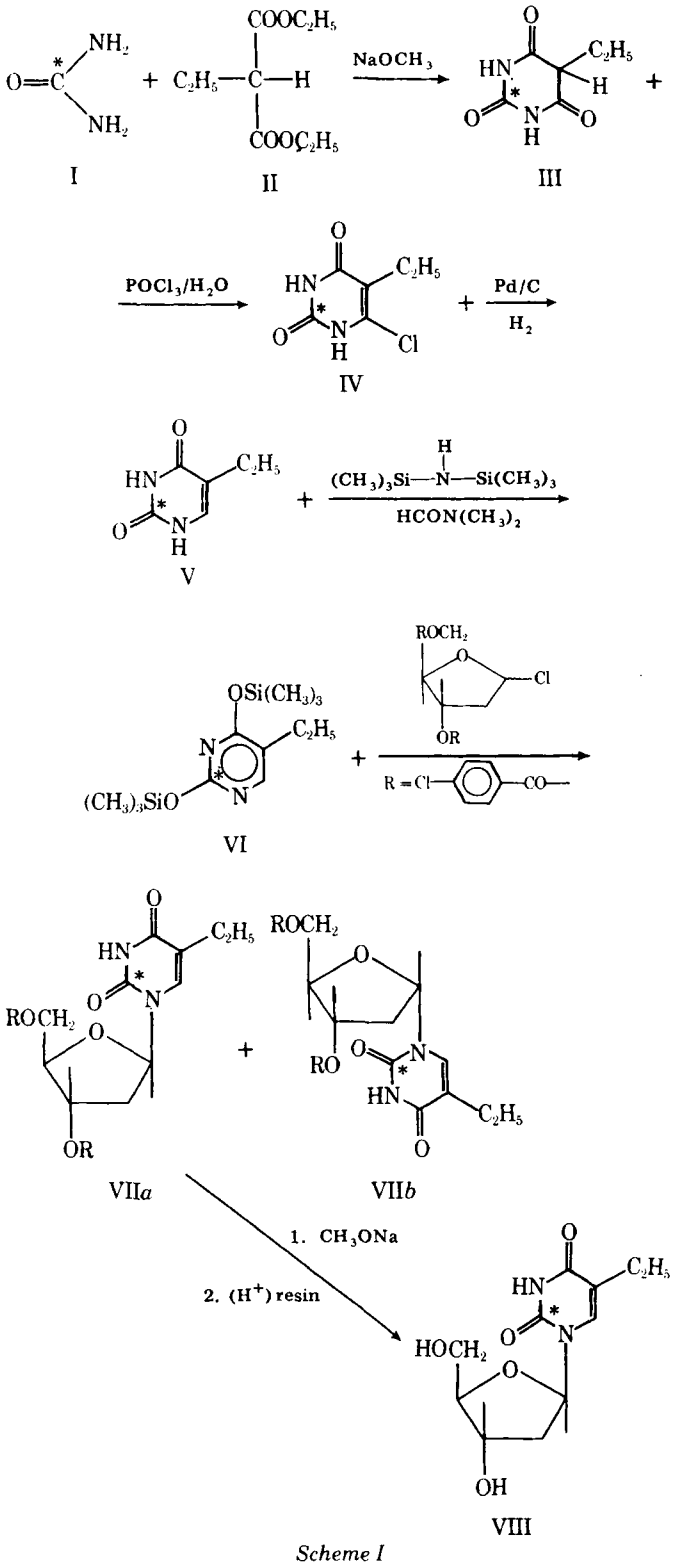

Scheme I

tuted pyrimidines is reported in the literature (17–21). With this method, ^{14}C-labeled VII*a* and VII*b* were synthesized in 43.4% yield based on ^{14}C-urea, mp 169–174°. The mixture of the blocked anomers was crystallized fractionally from toluene, yielding the pure α- and β-anomers: VII*a* (β-anomer), mp 196–197° [lit. (22) mp 195–196°]; and VII*b* (α-anomer), mp 186–188° [lit. (22) mp 186.5–187.5°].

2-^{14}C-1-(2′-Deoxy-β-D-ribofuranosyl)-5-ethyluracil (VIII)—To a suspension of the protected nucleoside VII*a* (3.6 g, 6.75 mmoles) in anhydrous methanol (35 ml), 30% methanolic sodium methoxide (0.65 ml) was added. The solution was stirred at room temperature for 4 hr, and methanol was evaporated under reduced pressure. Water (15 ml) was added to the oily residue. The formed ester was removed by extracting

Table I—Elimination of Radioactivity in Urine and Feces of Rats after 20 mg of 2-^{14}C-β-5-Ethyl-2′-deoxyuridine/kg iv

Sample	Hours	Radioactivity, % of applied dose
Urine	24	92
	48	5.1
	72	0.1
	96	—
Feces	24	0.5
	48	0.3
	72	0.1
	96	—

several times with methylene chloride. To the resulting solution an ion-exchange resin[4] (H^+), previously washed with methanol, was added. Stirring was continued for 5 min.

The solution was filtered from the resin, the filtrate was evaporated *in vacuo* to dryness, and acetone (25 ml) was added to the residue. After overnight refrigeration, the crystalline product was collected by filtration to yield 1.59 g of VIII (92% based on the blocked nucleoside VII*a*), mp 152–153° [lit. (22) mp 152–153°], specific activity 0.168 mCi/mmole. Radiochemical purity was checked by radioscanning of the TLC plates.

Radioactivity Measurements—The radioactive zones on TLC plates were located with a thin-layer scanner[5]. The radioassay in the solution was carried out in a two-canal liquid scintillation counter[6], using a scintillation solution of 1000 ml of dioxane, 180 g of naphthalene, 8 g of 2,5-diphenyloxazole, and 0.1 g of 1,4-bis[2-(4-methyl-5-phenyloxazolyl)]benzene. The external standardization technique was employed.

Application—A 1% solution of ^{14}C-VIII was made in normal saline. One-half milliliter was injected into the tail vein of 250-g male Wistar rats. The animals were kept in metabolic cages, which enabled collection of feces and urine separately. They were given free access to food[7] and water and were kept at 22° temperature and 55% humidity.

Sample Preparation—*Feces, Organs, and Tissues*—For qualitative and quantitative determination of the radioactivity, the fecal samples were dried at 60°, powdered, homogenized, and extracted with methanol in a soxhlet apparatus for 48 hr. The organs and tissues were cut into fine pieces and extracted with methanol for 72 hr. An aliquot (0.1 ml) of these samples was taken for required measurements.

Urine—An aliquot (0.1–0.2 ml) was mixed directly into the scintillation solution, and radioactivity was measured.

Chromatography—Analytical TLC was performed on 20 × 5-cm silica gel plates[8]. Solvent systems were (volume per volume): (*a*) chloroform–ether (8:2) for the blocked nucleoside, (*b*) chloroform–isopropanol (7:3) for the deblocked nucleoside, and (*c*) chloroform–isopropanol (5:5) for the metabolites.

Column chromatography was carried out on 0.05–0.2-mm silica gel with increasing proportions of isopropanol in chloroform.

Metabolite Isolation—The urine radioactivity could not be extracted with ether. The urine was evaporated to dryness, and the residue was extracted three times with isopropanol, yielding about 50% of the radioactivity (Extract A). The rest of the radioactivity could not be removed with organic solvents and possibly was due to conjugates (Extract B). The hydrolysis of the conjugate with β-glucuronidase and arylsulfatase[9] and subsequent isolation and identification of the fractions presented some difficulties and is in progress.

Extract A TLC showed radioactive peaks I and II in a 4:6 ratio, I being more polar than II. Extract A was concentrated to dryness and taken up in chloroform. It was loaded on a glass column (80 × 3 cm) filled with silica gel and eluted with increasing proportions of isopropanol in chloroform using a automatic fraction collector. Three hundred 20-ml fractions were collected. A radioassay was carried out with each fraction. The loaded radioactivity was recovered fully. Eluates 107–172 (7.5% isopropanol in chloroform) were pooled and concentrated to dryness, and the residue was recrystallized twice from methanol, mp 302–303°. It was designated Metabolite II.

Eluates 228–307 (20% isopropanol in chloroform) were concentrated, the solvent was removed, and the residue was recrystallized from toluene,

[4] Dowex 50 WX4, Dow Chemical Co., Midland, Mich.
[5] Prof. Dr. Rudolf Berthold Co., Wildbad, West Germany.
[6] Tri-Carb model 3950, Packard Instrument Co., La Grange, Ill.
[7] Altromin, Altromin, Lage/Lippe, West Germany.
[8] Silica gel HF_{254}, 0.25 mm, E. Merck AG, Darmstadt, West Germany.
[9] Glusulase, Boehringer, Mannheim, West Germany.

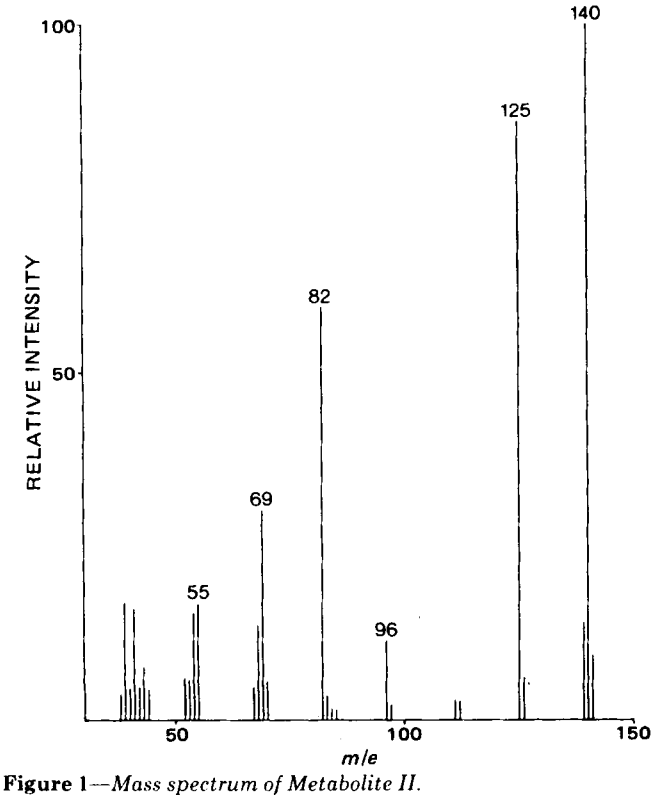

Figure 1—*Mass spectrum of Metabolite II.*

mp 152–153°. It was designated Metabolite I. By mixed melting-point determination and by comparison of the R_f values and mass spectra with an authentic VIII sample, Metabolite I could be identified as unchanged β-5-ethyl-2′-deoxyuridine (VIII).

RESULTS AND DISCUSSION

Excretion—Table I shows the elimination of urine and feces radioactivity up to 96 hr. Almost all of the radioactivity (98%) was extracted within 3 days. Moreover, the major part of the activity (92%) was excreted in the first 24 hr. Therefore, the kidneys are the main elimination organs in the excretion of β-5-ethyl-2′-deoxyuridine and its metabolites. Only a small amount of radioactivity could be found in the feces.

Distribution—In most organs and tissues as well as in the blood, <0.1% of the radioactivity could be found after 72 hr. After intravenous administration, VIII spontaneously disappeared from the blood and was completely eliminated.

Identification of Metabolite II—Metabolite II showed R_f values identical with those of 5-ethyluracil. In the mass spectrum (Fig. 1), the metastable peaks established the following fragmentation:

$$m/e\ 140 \xrightarrow{m^*\ 111.6} m/e\ 125 \xrightarrow{m^*\ 53.9} m/e\ 82$$

This pattern is characteristic of 5-ethyluracil, in which a methyl group is cleaved first. The hydrogen isocyanate (HCNO) loss in the final sequence is characteristic of uracil and barbituric acid derivatives in a retro-Diels-Alder fragmentation (23–25). For comparison, the mass spectrum of VIII was recorded (Fig. 2). The fragmentation of VIII can be formulated according to Scheme II.

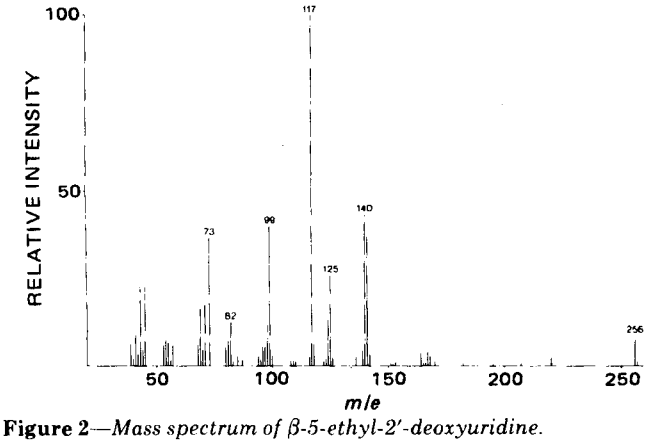

Figure 2—*Mass spectrum of β-5-ethyl-2′-deoxyuridine.*

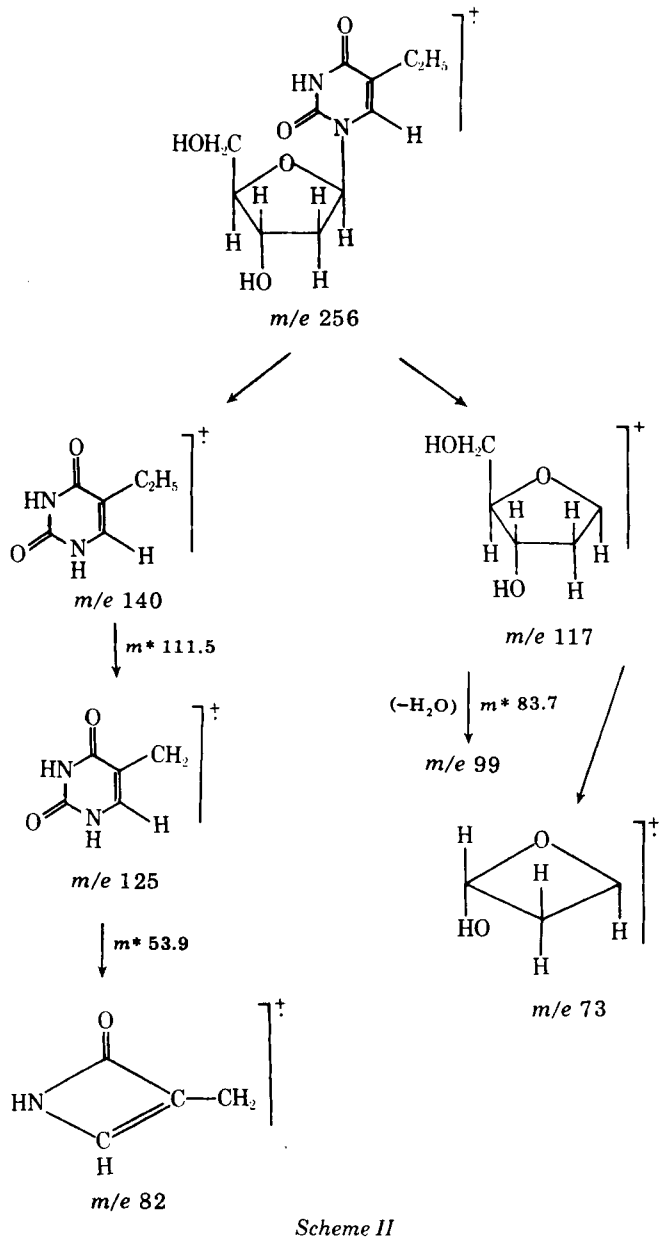

Scheme II

The ^{1}H-NMR spectrum of II in dimethyl sulfoxide-d_6 showed the presence of eight protons. Three protons appeared as a triplet at δ 1.02 ppm, and two protons appeared as a quadruplet at δ 2.2 ppm. The broad doublet (one proton) appeared at δ 7.17 ppm ($J_{6\text{-H/N}^1\text{-H}}$ = 6 Hz). The broad lower field signals at δ 10.26 and 10.66 ppm were in close agreement with the N^1- and N^3-protons of thymine (N^1-H 10.55 ppm, N^3-H 10.95 ppm, dimethyl sulfoxide-d_6), respectively.

These data establish Metabolite II as 5-ethyluracil. The metabolite structure was further confirmed by an independent synthesis; the synthetic 5-ethyluracil mass spectrum and ^{1}H-NMR data were identical with those of II.

REFERENCES

(1) K. K. Gauri and G. Malorny, *Naunyn-Schmiedebergs Arch. Pharmakol. Exp. Pathol.*, **257**, 21 (1967).

(2) T. Kulikowski and D. Shugar, *J. Med. Chem.*, **17**, 269 (1974).

(3) K. K. Gauri, *Klin. Monatsbl. Augenheilkd.*, **153**, 837 (1968).

(4) W. de Decker, *ibid.*, **157**, 487 (1968).

(5) K. K. Gauri, G. Malorny, and E. Riehm, *Albrecht Graefes Arch. Klin. Exp. Ophthalmol.*, **179**, 287 (1970).

(6) E. Riehm and K. K. Gauri, *Dtsch. Ophthalmol. Ges., Heidelberg*, **1968**, 69.
(7) W. Lerche and B. Schmolke, *Albrecht Graefes Arch. Klin. Exp. Ophthalmol.*, **184**, 193 (1972).
(8) J. Shapira, *J. Org. Chem.*, **27**, 1918 (1962).
(9) A. von Merkats, *Ber. Dtsch. Chem. Ges.*, **52**, 869 (1919).
(10) K. K. Gauri, Patent Robugen, DP 16 20 185 (1966).
(11) J. H. Burckhalter and H. C. Scarborough, *J. Am. Pharm. Assoc., Sci. Ed.*, **44**, 545 (1955).
(12) J. Tafeland and H. B. Thompson, *Ber. Dsch. Chem. Ges.*, **10**, 4498 (1907).
(13) T. B. Johnson and G. A. Menge, *J. Biol. Chem.*, **2**, 105 (1906).
(14) M. Shakun-Todorovic and V. Tezdic, *J. Labelled Compd.*, **9**, 475 (1973).
(15) A. Guyot, J. Chopin, and C. Mentzer, *Bull. Soc. Chim. Fr.*, **1960**, 1596.
(16) M. P. Kotick, C. Szantai, and T. J. Bardos, *J. Org. Chem.*, **34**, 3806 (1969).
(17) E. Wittenburg, *Z. Chem.*, **4**, 303 (1964).
(18) E. Wittenburg, *Chem. Ber.*, **101**, 1095 (1968).
(19) T. Nishimura and J. Iwai, *Chem. Pharm. Bull.*, **12**, 357 (1964); through *Chem. Abstr.*, **60**, 15968 (1964).
(20) T. Nishimura, B. Shimizu, and J. Iwai, *Chem. Pharm. Bull.*, **12**, 1471 (1964); through *Chem. Abstr.*, **62**, 12236 (1965).
(21) T. Nishimura and B. Shimizu, *Chem. Pharm. Bull.*, **13**, 803 (1965); through *Chem. Abstr.*, **63**, 13388 (1965).
(22) M. Swierkowski and D. Shugar, *J. Med. Chem.*, **12**, 533 (1969).
(23) T. Nishiwaki, *Tetrahedron*, **22**, 3117 (1966).
(24) J. M. Rice, G. O. Dudek, and M. Barber, *J. Am. Chem. Soc.*, **87**, 4569 (1965).
(25) R. F. Skinner, E. G. Gallaher, and D. B. Predmore, *Anal. Chem.*, **45**, 574 (1973).

ACKNOWLEDGMENTS

The authors thank Miss Silvia Müller for technical assistance.

Antimuscarinic Agents: Furan Analogs of Benzilate Esters

JAMES F. STUBBINS ˣ, PATRICIA M. HUDGINS *, and DAGMAR C. MURPHY

Received July 23, 1979, from the *Departments of Pharmaceutical Chemistry and Pharmacology, Medical College of Virginia, Virginia Commonwealth University, Richmond, VA 23298.* Accepted for publication November 29, 1979. *Present address: Department of Pharmacology, Kirksville College of Osteopathic Medicine, Kirksville, MO 63501.

Abstract □ The methiodide and ethiodide salts of 5-(dimethylaminomethyl)- and 5-(diethylaminomethyl)-α,α-diphenylfurfuryl alcohol were prepared. These compounds may be considered as furan analogs of dialkylaminoethyl benzilate alkiodides. The pA_2 values of these compounds as antagonists of acetylcholine were determined on rat jejunum preparation. All four compounds were significantly less potent than the analogous ester antimuscarinic lachesine. The furan ring cannot be substituted for the ester moiety of typical antimuscarinics. Possible modes of binding by antagonists to the receptor proposed previously are considered that might account for this less-than-expected antimuscarinic activity.

Keyphrases □ Antimuscarinic agents—furan analogs of benzilate esters, synthesis and activity □ Furan analogs—of benzilate esters, synthesis and antimuscarinic activity □ Benzilate esters, furan analogs—synthesis and antimuscarinic activity □ Structure-activity relationships—effect of furan analogs of benzilate esters on receptor binding activity, synthesis of antimuscarinic agents

A fundamental problem in medicinal chemistry is the determination of the topography of drug receptors, *i.e.*, the nature and relative position of groups (subsites) on the receptor that interact with groups on the drug molecule. Knowledge of receptor topography usually comes from the study of the relative activities of structurally different drugs that are used as probes of the receptor surface. In general, present knowledge of topography for the autonomic drug receptors is unsatisfactory.

BACKGROUND

An example is the muscarinic cholinergic receptor. For typical potent agonists such as acetylcholine, Bovet's acetal (I), and methylfurtrethonium (II), it usually is assumed that each compound combines with the same receptor site by interaction of the positive nitrogen with an anionic subsite and with the ester group, acetal group, or a portion of the furan ring interacting with an ester binding subsite.

Several investigators noted that extension of the carbon chain in potent muscarinic agonists caused a progressive decline in agonist potency and the appearance of competitive antagonist properties (1–3). It is uncertain just how the competitive antagonists combine with the muscarinic receptor relative to the acetylcholine receptor site. In the classical view, the competitive antagonists can bind to the anionic and ester binding subsites in the same manner as acetylcholine. The hydrocarbon rings then are believed to bind to a hydrophobic area located just beyond the ester binding subsite (Fig. 1).

Several discrepancies in the known structure–activity relationships are difficult to explain according to this classical view. Many potent antagonists do not contain an ester or comparable group between the nitrogen and the hydrophobic rings. The distance between the nitrogen and the rings is too short in many cases to bind as shown in Fig. 1. Even in ester-type antagonists, many changes in structure or stereochemistry cause changes in activity that do not parallel the effect of that change on agonist activity (4).

As a possible means of explaining the discrepancies between muscarinic agonist and antagonist structure–activity relationships, an alternative mode of binding for the antagonists was proposed (5, 6). In this view, the antagonist is believed to bind so that the cationic head overlaps the anionic subsite used by acetylcholine but the remainder of the molecule does

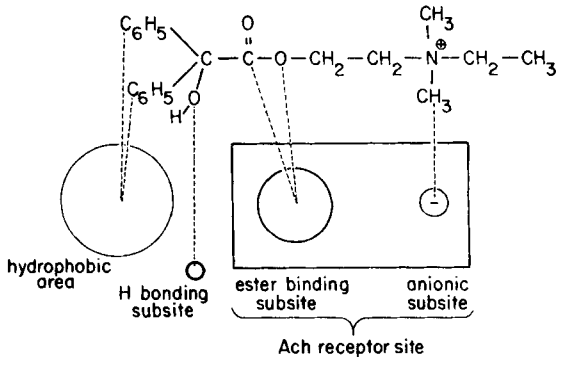

Figure 1—*Classical view of binding of lachesine to the muscarinic receptor (Ach = acetylcholine).*

0022-3549/80/0500-0534$01.00/0
© 1980, American Pharmaceutical Association

(6) E. Riehm and K. K. Gauri, *Dtsch. Ophthalmol. Ges., Heidelberg*, **1968**, 69.
(7) W. Lerche and B. Schmolke, *Albrecht Graefes Arch. Klin. Exp. Ophthalmol.*, **184**, 193 (1972).
(8) J. Shapira, *J. Org. Chem.*, **27**, 1918 (1962).
(9) A. von Merkats, *Ber. Dtsch. Chem. Ges.*, **52**, 869 (1919).
(10) K. K. Gauri, Patent Robugen, DP 16 20 185 (1966).
(11) J. H. Burckhalter and H. C. Scarborough, *J. Am. Pharm. Assoc., Sci. Ed.*, **44**, 545 (1955).
(12) J. Tafeland and H. B. Thompson, *Ber. Dsch. Chem. Ges.*, **10**, 4498 (1907).
(13) T. B. Johnson and G. A. Menge, *J. Biol. Chem.*, **2**, 105 (1906).
(14) M. Shakun-Todorovic and V. Tezdic, *J. Labelled Compd.*, **9**, 475 (1973).
(15) A. Guyot, J. Chopin, and C. Mentzer, *Bull. Soc. Chim. Fr.*, **1960**, 1596.
(16) M. P. Kotick, C. Szantai, and T. J. Bardos, *J. Org. Chem.*, **34**, 3806 (1969).
(17) E. Wittenburg, *Z. Chem.*, **4**, 303 (1964).
(18) E. Wittenburg, *Chem. Ber.*, **101**, 1095 (1968).
(19) T. Nishimura and J. Iwai, *Chem. Pharm. Bull.*, **12**, 357 (1964); through *Chem. Abstr.*, **60**, 15968 (1964).
(20) T. Nishimura, B. Shimizu, and J. Iwai, *Chem. Pharm. Bull.*, **12**, 1471 (1964); through *Chem. Abstr.*, **62**, 12236 (1965).
(21) T. Nishimura and B. Shimizu, *Chem. Pharm. Bull.*, **13**, 803 (1965); through *Chem. Abstr.*, **63**, 13388 (1965).
(22) M. Swierkowski and D. Shugar, *J. Med. Chem.*, **12**, 533 (1969).
(23) T. Nishiwaki, *Tetrahedron*, **22**, 3117 (1966).
(24) J. M. Rice, G. O. Dudek, and M. Barber, *J. Am. Chem. Soc.*, **87**, 4569 (1965).
(25) R. F. Skinner, E. G. Gallaher, and D. B. Predmore, *Anal. Chem.*, **45**, 574 (1973).

ACKNOWLEDGMENTS

The authors thank Miss Silvia Müller for technical assistance.

Antimuscarinic Agents: Furan Analogs of Benzilate Esters

JAMES F. STUBBINS ˣ, PATRICIA M. HUDGINS *, and DAGMAR C. MURPHY

Received July 23, 1979, from the *Departments of Pharmaceutical Chemistry and Pharmacology, Medical College of Virginia, Virginia Commonwealth University, Richmond, VA 23298.* Accepted for publication November 29, 1979. *Present address: Department of Pharmacology, Kirksville College of Osteopathic Medicine, Kirksville, MO 63501.

Abstract □ The methiodide and ethiodide salts of 5-(dimethylaminomethyl)- and 5-(diethylaminomethyl)-α,α-diphenylfurfuryl alcohol were prepared. These compounds may be considered as furan analogs of dialkylaminoethyl benzilate alkiodides. The pA_2 values of these compounds as antagonists of acetylcholine were determined on rat jejunum preparation. All four compounds were significantly less potent than the analogous ester antimuscarinic lachesine. The furan ring cannot be substituted for the ester moiety of typical antimuscarinics. Possible modes of binding by antagonists to the receptor proposed previously are considered that might account for this less-than-expected antimuscarinic activity.

Keyphrases □ Antimuscarinic agents—furan analogs of benzilate esters, synthesis and activity □ Furan analogs—of benzilate esters, synthesis and antimuscarinic activity □ Benzilate esters, furan analogs—synthesis and antimuscarinic activity □ Structure-activity relationships—effect of furan analogs of benzilate esters on receptor binding activity, synthesis of antimuscarinic agents

A fundamental problem in medicinal chemistry is the determination of the topography of drug receptors, *i.e.*, the nature and relative position of groups (subsites) on the receptor that interact with groups on the drug molecule. Knowledge of receptor topography usually comes from the study of the relative activities of structurally different drugs that are used as probes of the receptor surface. In general, present knowledge of topography for the autonomic drug receptors is unsatisfactory.

BACKGROUND

An example is the muscarinic cholinergic receptor. For typical potent agonists such as acetylcholine, Bovet's acetal (I), and methylfurtrethonium (II), it usually is assumed that each compound combines with the same receptor site by interaction of the positive nitrogen with an anionic subsite and with the ester group, acetal group, or a portion of the furan ring interacting with an ester binding subsite.

Several investigators noted that extension of the carbon chain in potent muscarinic agonists caused a progressive decline in agonist potency and the appearance of competitive antagonist properties (1–3). It is uncertain just how the competitive antagonists combine with the muscarinic receptor relative to the acetylcholine receptor site. In the classical view, the competitive antagonists can bind to the anionic and ester binding subsites in the same manner as acetylcholine. The hydrocarbon rings then are believed to bind to a hydrophobic area located just beyond the ester binding subsite (Fig. 1).

Several discrepancies in the known structure–activity relationships are difficult to explain according to this classical view. Many potent antagonists do not contain an ester or comparable group between the nitrogen and the hydrophobic rings. The distance between the nitrogen and the rings is too short in many cases to bind as shown in Fig. 1. Even in ester-type antagonists, many changes in structure or stereochemistry cause changes in activity that do not parallel the effect of that change on agonist activity (4).

As a possible means of explaining the discrepancies between muscarinic agonist and antagonist structure–activity relationships, an alternative mode of binding for the antagonists was proposed (5, 6). In this view, the antagonist is believed to bind so that the cationic head overlaps the anionic subsite used by acetylcholine but the remainder of the molecule does

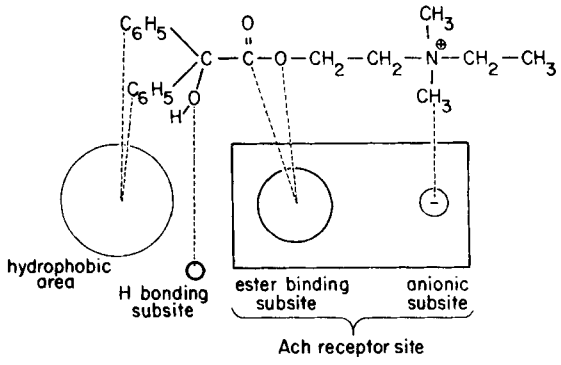

Figure 1—*Classical view of binding of lachesine to the muscarinic receptor (Ach = acetylcholine).*

0022-3549/80/0500-0534$01.00/0
© 1980, American Pharmaceutical Association

Table I—Properties of New 5-(Dialkylaminomethyl)-α,α-diphenyl-2-furfuryl Alcohol Alkiodides

Compound	Melting Point[a]	Yield, %[b]	Formula	Analysis, %[c]		pA₂ ± SE[d]
				Calc.	Found	
IV*a*	205–206°	41	$C_{21}H_{24}INO_2$	C 56.13	55.92	6.35 ± 0.13 (29)
				H 5.38	5.41	
				N 3.11	3.04	
IV*b*	193–194°	57	$C_{22}H_{26}INO_2$	C 57.02	57.20	6.24 ± 0.14 (31)
				H 5.65	5.69	
				N 3.02	2.98	
IV*c*	191–192°	70	$C_{23}H_{28}INO_2$	C 57.86	57.97	6.14 ± 0.12 (32)
				H 5.91	5.97	
				N 2.93	2.92	
IV*d*	184–186°	34	$C_{24}H_{30}INO_2$	C 58.66	58.77	5.75 ± 0.11 (26)
				H 6.15	6.29	
				N 2.85	2.79	
Lachesine						7.70 ± 0.17 (28)

[a] Melting points were determined on a Thomas-Hoover capillary apparatus and are uncorrected. [b] Reported yields are from single experiments with no attempt to recover additional compound from filtrates. [c] Elemental analyses were performed by Micro-Tech Laboratories, Skokie, Ill. [d] The $pA_2 + SE$ value is the negative log of the concentration causing a twofold shift in the response to acetylcholine plus or minus the standard error of the mean. The figure in parentheses is the number of points used in determining the pA_2 value.

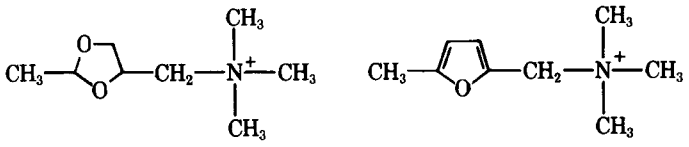

I

II

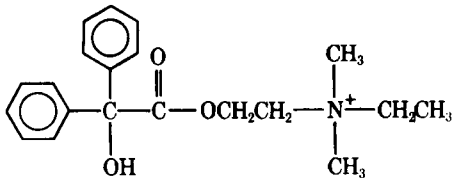

III

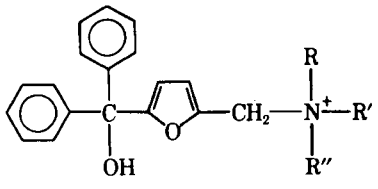

IV*a*: R = R′ = R″ = CH_3
IV*b*: R = R′ = CH_3, R″ = C_2H_5
IV*c*: R = CH_3, R′ = R″ = C_2H_5
IV*d*: R = R′ = R″ = C_2H_5

not cover the ester binding subsite. The lipophilic and hydrogen bonding moieties in the antagonist may bind to other subsites as shown in Fig. 2.

Moran and Triggle proposed a third possible view of the antagonist binding to the receptor (7). They proposed a distinct site on the receptor for the antagonists that is near but does not overlap the acetylcholine binding site. Occupation of the antagonist site results in a perturbation of the acetylcholine binding site so that the affinity is lowered and the antagonism is still competitive.

The most potent muscarinic antagonists derived from acetylcholine generally are obtained by replacement of the acetyl group by benzilyl or similar groups containing two hydrophobic rings and a hydroxyl group attached to the α-carbon atom such as is found in lachesine (III) (8). If methylfurtrethonium and lachesine both bind to the anionic and ester binding subsites utilized by acetylcholine, in accord with the classical view, then substitution of two phenyl groups and a hydroxyl group on the terminal carbon atom of methylfurtrethonium (II) to give Type IV compounds should produce potent antagonists. In the present study, a series of such compounds with different substituents on the cationic nitrogen was prepared and examined for antimuscarinic activity.

RESULTS AND DISCUSSION

Chemistry—The desired compounds were prepared by a method used (9) to prepare the bromide salt of IV*c* as illustrated in Scheme I, except that the methyl ester rather than the ethyl ester was the starting material. Chloromethylation of methyl 2-furoate (V) with paraformaldehyde, zinc chloride, and anhydrous hydrogen chloride yielded VI. Treatment of VI with dimethylamine or diethylamine gave VII*a* or VII*b*, respectively. An attempt to prepare VII*a* directly from V by a Mannich-type reaction, utilizing conditions employing 2-methylfuran (10), was unsuccessful. The ring-inactivating effect of the ester substituent apparently is too strong in this case.

Reaction of VII*a* or VII*b* with commercially prepared phenylmagnesium bromide gave the 5-(dialkylaminomethyl)-α,α-diphenyl-2-furfuryl alcohols (VIII*a* and VIII*b*). Alkylation of VIII*a* and VIII*b* with methyl iodide and ethyl iodide produced the desired alkiodide compounds. Properties of the new compounds are presented in Table I.

Pharmacology—To evaluate the affinity of the compounds for the muscarinic receptor, pA_2 values were measured by standard techniques. The method used was described previously in detail (11). Briefly, segments of rat jejunum were placed in an isolated organ bath containing Tyrode's solution at 25° and aerated with 95% oxygen–5% carbon dioxide. Cumulative dose–response curves to acetylcholine were obtained on each segment. These curves then were repeated in the presence of three or four different concentrations of the compound being evaluated. Segments of rat jejunum from six to eight animals were used with each compound. Linear regression analysis of the data according to the method of Arunlakshana and Schild (12) yielded the pA_2 values.

Because methylfurtrethonium is a more potent agonist than acetylcholine, it seems that the furan ring must bind well to a subsite on the receptor. If methylfurtrethonium binds to the same set of subsites as does acetylcholine, it would be reasonable to expect that the addition of two phenyl rings and a hydroxyl group to the terminal methyl group would produce a potent antagonist comparable to lachesine (III). An examination of Table I shows that the affinities of IV*a*–IV*d* are much less than those of lachesine; they are ~23–90-fold less potent as antagonists on rat

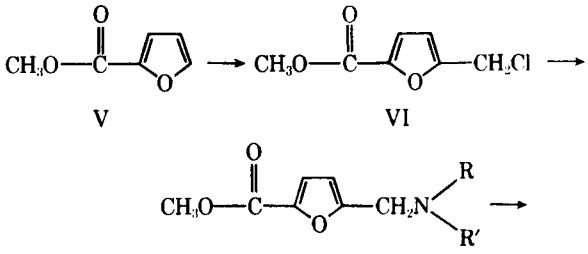

V VI

VII*a*: R = R′ = CH_3
VII*b*: R = R′ = C_2H_5

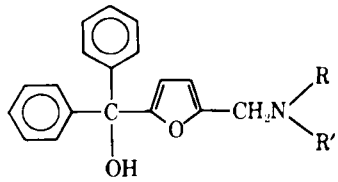

VIII*a*: R = R′ = CH_3
VIII*b*: R = R′ = C_2H_5

Scheme I

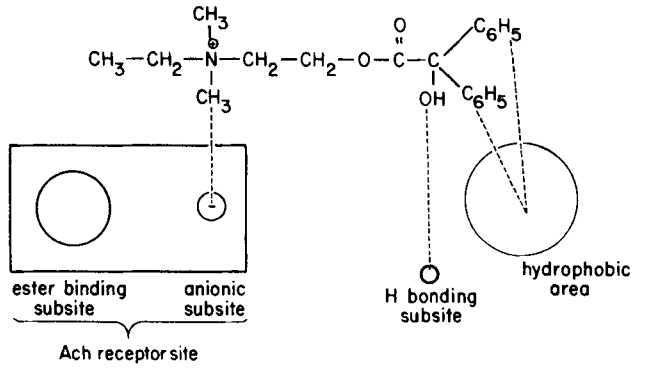

Figure 2—*Possible binding of lachesine to the muscarinic receptor according to Ariens' theory.*

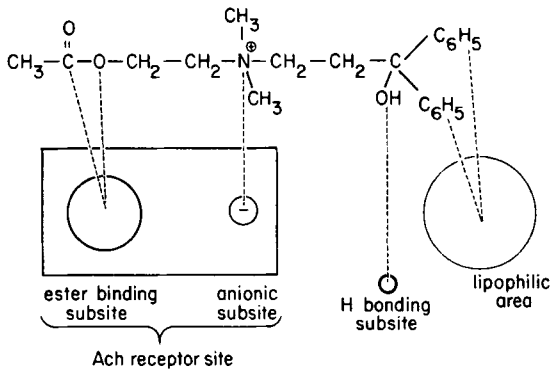

Figure 4—*Possible binding of nonester antagonist with an additional agonist moiety to the muscarinic receptor.*

jejunum. The furan ring clearly cannot be substituted for the ester group in the antagonists in the same manner as with the agonists. The classical view of antagonist binding to receptors does not explain the reason for this difference.

If antagonists bind in the manner proposed by Ariëns (5, 6) (Fig. 2), the relatively poor activity of the furan analogs could be explained. In such a case, the furan ring in the antagonists would not occupy a position on the receptor comparable to the furan ring in methylfurtrethonium. Earlier work by Stubbins and coworkers (11, 13, 14) was directed at finding evidence for the correctness of Ariëns' view. Since the ester binding subsite was not involved in binding antagonists according to this theory, it was proposed that addition of a properly placed agonist moiety on typical antagonists might increase the affinity and selectivity for the muscarinic receptor compared to antagonists lacking such a feature. A series of ester-type antagonists with moieties added to resemble acetylcholine, carbachol, or methylfurtrethonium was synthesized and compared in activity to lachesine. The binding of such compounds might be typified as shown in Fig. 3. In fact, the addition of the agonist moiety lowered the affinity in all compounds (13).

Ariëns' proposal might not apply to ester-type antagonists (which resemble acetylcholine more closely) but only to nonester antagonists. Therefore, a second series of 11 compounds having agonist moieties attached to typical nonester antagonist molecules was prepared and tested. A member of this series might bind as illustrated in Fig. 4. No consistent increase in affinity was found (14). Therefore, evidence in support of Ariëns' theory was not found, but this theory cannot be excluded.

Another possible way in which the difference could be explained is on the basis of the suggestion by Moran and Triggle (7) that methylfurtrethonium might bind to the receptor differently from acetylcholine. They suggested that the cationic head of all agonists binds to the anionic subsite but that the remainder of the molecule changes its position on the receptor depending on its relative lipophilic or hydrophilic character. According to this theory, methylfurtrethonium might bind as shown in Fig. 5. In this case, addition of two phenyl rings and a hydroxyl group to the two agonists would not be expected to affect affinity in the same way. Alternatively, the suggestion of Moran and Triggle that antagonists bind to entirely different sites than acetylcholine might account for the result.

In summary, the furan ring cannot replace the ester group in antimuscarinics without a significant loss in affinity for the receptor. The classical view of antagonist binding to the receptor is inadequate to explain this observation, but several alternative hypotheses might account for the results. More work is needed to determine the topography of the muscarinic receptor sites for agonists and antagonists.

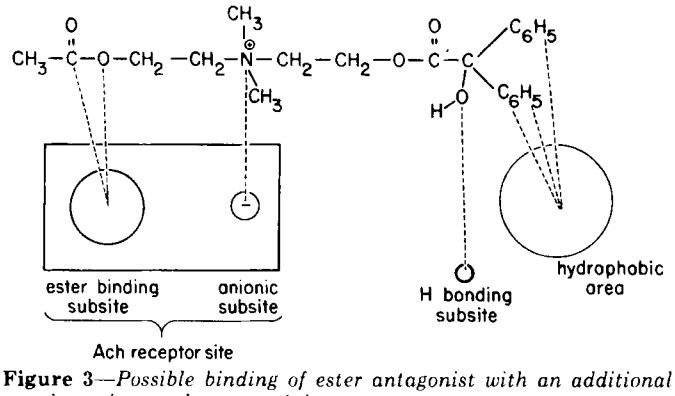

Figure 3—*Possible binding of ester antagonist with an additional agonist moiety to the muscarinic receptor.*

EXPERIMENTAL

Methyl 5-Chloromethyl-2-furoate (VI)—Methyl 2-furoate (17.6 g, 140 mmoles) was dissolved in 50 ml of methylene chloride. Paraformaldehyde (6.0 g, 200 mmoles of formaldehyde) and zinc chloride (5.0 g, 37 mmoles) were added, and the mixture was warmed to 35°. Anhydrous hydrogen chloride gas was passed through the mixture until the exothermic reaction subsided. The mixture was poured into 300 ml of water. The organic layer was separated, washed twice more with water, and dried over potassium carbonate. The solvent was removed *in vacuo*, and the residual oil was distilled to give 16.2 g (66% yield) of VI, bp 86–88°/0.2 mm [lit. (15) bp 116–117°/2 mm].

Methyl 5-Dimethylaminomethyl-2-furoate (VII*a*)—Dimethylamine gas was bubbled slowly through a solution containing 15.0 g (86 mmoles) of VI in 130 ml of dry benzene for 2 hr. The mixture was allowed to stand overnight and was filtered. The solvent was evaporated from the filtrate, and the residue was distilled. Compound VII*a*, 11.5 g (73% yield), was obtained, bp 72–78°/0.2 mm.

Methyl 5-Diethylaminomethyl-2-furoate (VII*b*)—A solution of 16.2 g (93 mmoles) of VI in 35 ml of benzene was added dropwise to a stirred solution, heated to reflux, of diethylamine (17.4 g, 238 mmoles) in 30 ml of benzene. Heating was continued for 5 hr after addition was completed, and the mixture was allowed to stand at room temperature overnight. The solid by-product was removed by filtration, and the filtrate was evaporated. The residual oil was distilled to obtain 15.8 g (81% yield) of VII*b*, bp 94–98°/0.2 mm.

5 - Dimethylaminomethyl - α,α - diphenylfurfuryl Alcohol (VIII*a*)—Methyl 5-dimethylaminomethyl-2-furoate (11.1 g, 61 mmoles) dissolved in 30 ml of ether was added dropwise to a 2.07 *M* ethereal solution of phenylmagnesium bromide (120 ml, 241 mmoles) with stirring. After the addition was completed, the mixture was allowed to stand at room temperature for 1 hr and was heated to reflux for 2 hr. The mixture then was poured slowly into 350 ml of water containing 214 g of ethylenediaminetetraacetic acid and 117 g of sodium hydroxide. The ether layer was separated, and the aqueous layer was extracted three times with ether. The ethereal solutions were combined and dried over magnesium

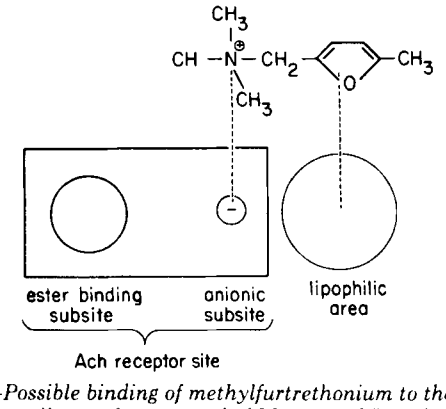

Figure 5—*Possible binding of methylfurtrethonium to the muscarinic receptor according to the proposal of Moran and Triggle (7).*

sulfate. Solvent removal left an oily residue, which crystallized upon trituration with petroleum ether. Recrystallization of the solid from benzene–petroleum ether yielded 7.6 g (41% yield) of VIII*a*, mp 122–124°.

5 - Diethylaminomethyl - α,α - diphenylfurfuryl Alcohol (VIII *b*)—Methyl 5-diethylaminomethyl-2-furoate (15.8 g, 75 mmoles) was reacted with phenylmagnesium bromide (300 mmoles) as in the preparation of VIII*a*. Compound VIII*b*, 10.0 g (40% yield), was obtained, mp 110–111.5° [lit. (9) mp 112–113°].

5-Dialkylaminomethyl-α,α-diphenylfurfuryl Alcohol Alkiodides (IV*a*–IV*d*)—Two grams of the tertiary amine (VIII*a* or VIII*b*) was dissolved in a minimum quantity of benzene. Methyl iodide or ethyl iodide (2 ml) was added, and the mixture was allowed to stand overnight. The product was removed by filtration and recrystallized from isopropanol. The physical properties of the compounds are given in Table I; NMR (dimethyl sulfoxide-d_6): 7.32–7.34 (s, 10H, phenyl), 6.83–6.88 (d, 1H, furan), 6.67–6.70 (s, 1H, OH), 6.17–6.27 (d, 1H, furan), and 4.59–4.68 (s, 2H, furfuryl methylene). In addition, the different compounds exhibited appropriate NMR peaks for the *N*-alkyl groups: 3.18–3.28 (m, NCH_2C), 2.91–3.04 (s, NCH_3), and 1.16–1.22 (t, CCH_3).

REFERENCES

(1) R. P. Stephenson, *Br. J. Pharmacol.*, **11**, 379 (1956).

(2) R. Schneider and A. R. Timms, *ibid.*, **12**, 30 (1957).

(3) J. M. van Rossum and E. J. Ariëns, *Arch. Int. Pharmacodyn. Ther.*, **110**, 349 (1957).

(4) E. J. Ariëns and A. M. Simonis, *Ann. N.Y. Acad. Sci.*, **144**, 842 (1967).

(5) E. J. Ariëns and A. M. Simonis, *J. Pharm. Pharmacol.*, **16**, 137 (1964).

(6) E. J. Ariëns, *Adv. Drug Res.*, **3**, 235 (1966).

(7) J. F. Moran and D. J. Triggle, in "Cholinergic Ligand Interactions," Academic, New York, N.Y., 1971, pp. 119–136.

(8) E. J. Ariëns and A. M. Simonis, *Arch. Int. Pharmacodyn. Ther.*, **127**, 479 (1960).

(9) C. L. Zirkle, U.S. pat. 3,097,206 (1963); through *Chem. Abstr.*, **59**, 13,950 (1963).

(10) R. F. Holdren and R. M. Hixon, *J. Am. Chem. Soc.*, **68**, 1198 (1946).

(11) J. F. Stubbins, P. M. Hudgins, J. Andrako, and A. J. Beebe, *J. Pharm. Sci.*, **57**, 534 (1968).

(12) O. Arunlakshana and H. O. Schild, *Br. J. Pharmacol.*, **14**, 48 (1959).

(13) P. M. Hudgins and J. F. Stubbins, *J. Pharmacol. Exp. Ther.*, **166**, 237 (1969).

(14) J. F. Stubbins, P. M. Hudgins, D. C. Murphy, and T. L. Dickerson, *J. Pharm. Sci.*, **61**, 470 (1972).

(15) British pat. 705,950 (1954); through *Chem. Abstr.*, **49**, 2233 (1955).

ACKNOWLEDGMENTS

Supported in part by National Institutes of Health Grant NS-07273.

The authors thank Ms. T. L. Dickerson for technical assistance.

Mode of Action of Sesquiterpene Lactones as Anti-Inflammatory Agents

I. H. HALL *x, C. O. STARNES, Jr. *, K. H. LEE *, and T. G. WADDELL ‡

Received July 29, 1979, from the **Division of Medicinal Chemistry, School of Pharmacy, University of North Carolina, Chapel Hill, NC 27514,* and the ‡*Department of Chemistry, University of Tennessee at Chattanooga, Chattanooga, TN 37401.* Accepted for publication December 7, 1979.

Abstract □ Sesquiterpene lactones containing an α-methylene-γ-lactone moiety were shown to be potent inhibitors of carrageenan-induced edema and chronic adjuvant-induced arthritis in rodents at 2.5 mg/kg/day. The mode of action of sesquiterpene lactones as anti-inflammatory agents appeared to be at multiple sites; for example, at 5×10^{-4} *M*, the sesquiterpene lactones effectively uncoupled the oxidative phosphorylation of human polymorphonuclear neutrophils and elevated the cyclic adenosine monophosphate levels of rat neutrophils and rat and mouse liver cells. Free and total lysosomal enzymatic activity was inhibited by these agents at 5×10^{-4} *M* in both rat and mouse liver and rat and human neutrophils. Furthermore, the structure–activity relationships for the stabilization of lysosomal membrane for rat liver cathepsin activity followed the same structural requirement necessary for anti-inflammatory activity; *i.e.*, the α-methylene-γ-lactone moiety contributed the most activity, whereas the β-unsubstituted cyclopentenone and α-epoxycyclopentanone contributed only minor activity. Human polymorphonuclear neutrophil chemotaxis was inhibited at low concentrations (*i.e.*, 5×10^{-5} and 5×10^{-6} *M*), whereas prostaglandin synthetase activity was inhibited at a higher concentration (*i.e.*, 10^{-3} *M*) by the sesquiterpene lactones.

Keyphrases □ Anti-inflammatory agents—sesquiterpene lactones, mode of action determined *in vitro* and *in vivo* □ Sesquiterpene lactones—anti-inflammatory agents, antiarthritic agents, mode of action determined in rat and human neutrophils and rat and mouse liver cells □ Oxidative phosphorylation—uncoupling effect of sesquiterpene lactones, mode of action determined in inflammation process □ Lysosomal membrane—effect of sesquiterpene lactones on membrane stability, hydrolytic enzyme release, mode of action in inflammation process □ Cyclic adenosine monophosphate—effect of sesquiterpene lactones on *in vitro* levels, role in inflammation process □ Structure–activity relationships—effect of sesquiterpene lactones on inflammation process, several modes of action determined *in vitro* and *in vivo*

The anti-inflammatory activity of sesquiterpene lactones in rodents was reported previously (1). An α-methylene-γ-lactone moiety within the structure of the pseudoguaianolide and germacranolide derivatives was required for activity against edema-induced carrageenan inflammation. Saturation of the 11,13-double bond of the methylene group of the lactone resulted in a loss of activity (1).

In the chronic adjuvant-induced arthritic screen, compounds containing the α-methylene-γ-lactone, the β-unsubstituted cyclopentenone, and α-epoxycyclopentanone afforded significant inhibitory activity at 2.5 mg/kg/day (1). In addition, these derivatives also suppressed the writhing reflex, induced pleurisy, delayed hypersensitivity, and passive cutaneous anaphylaxis and were mild immunostimulants of immunoglobulins (1). The effects of the

0022-3549/80/0500-0537$01.00/0

© 1980, American Pharmaceutical Association

sulfate. Solvent removal left an oily residue, which crystallized upon trituration with petroleum ether. Recrystallization of the solid from benzene–petroleum ether yielded 7.6 g (41% yield) of VIII*a*, mp 122–124°.

5 - Diethylaminomethyl - α,α - diphenylfurfuryl Alcohol (VIII *b*)—Methyl 5-diethylaminomethyl-2-furoate (15.8 g, 75 mmoles) was reacted with phenylmagnesium bromide (300 mmoles) as in the preparation of VIII*a*. Compound VIII*b*, 10.0 g (40% yield), was obtained, mp 110–111.5° [lit. (9) mp 112–113°].

5-Dialkylaminomethyl-α,α-diphenylfurfuryl Alcohol Alkiodides (IV*a*–IV*d*)—Two grams of the tertiary amine (VIII*a* or VIII*b*) was dissolved in a minimum quantity of benzene. Methyl iodide or ethyl iodide (2 ml) was added, and the mixture was allowed to stand overnight. The product was removed by filtration and recrystallized from isopropanol. The physical properties of the compounds are given in Table I; NMR (dimethyl sulfoxide-d_6): 7.32–7.34 (s, 10H, phenyl), 6.83–6.88 (d, 1H, furan), 6.67–6.70 (s, 1H, OH), 6.17–6.27 (d, 1H, furan), and 4.59–4.68 (s, 2H, furfuryl methylene). In addition, the different compounds exhibited appropriate NMR peaks for the *N*-alkyl groups: 3.18–3.28 (m, NCH_2C), 2.91–3.04 (s, NCH_3), and 1.16–1.22 (t, CCH_3).

REFERENCES

(1) R. P. Stephenson, *Br. J. Pharmacol.*, **11**, 379 (1956).

(2) R. Schneider and A. R. Timms, *ibid.*, **12**, 30 (1957).

(3) J. M. van Rossum and E. J. Ariëns, *Arch. Int. Pharmacodyn. Ther.*, **110**, 349 (1957).

(4) E. J. Ariëns and A. M. Simonis, *Ann. N.Y. Acad. Sci.*, **144**, 842 (1967).

(5) E. J. Ariëns and A. M. Simonis, *J. Pharm. Pharmacol.*, **16**, 137 (1964).

(6) E. J. Ariëns, *Adv. Drug Res.*, **3**, 235 (1966).

(7) J. F. Moran and D. J. Triggle, in "Cholinergic Ligand Interactions," Academic, New York, N.Y., 1971, pp. 119–136.

(8) E. J. Ariëns and A. M. Simonis, *Arch. Int. Pharmacodyn. Ther.*, **127**, 479 (1960).

(9) C. L. Zirkle, U.S. pat. 3,097,206 (1963); through *Chem. Abstr.*, **59**, 13,950 (1963).

(10) R. F. Holdren and R. M. Hixon, *J. Am. Chem. Soc.*, **68**, 1198 (1946).

(11) J. F. Stubbins, P. M. Hudgins, J. Andrako, and A. J. Beebe, *J. Pharm. Sci.*, **57**, 534 (1968).

(12) O. Arunlakshana and H. O. Schild, *Br. J. Pharmacol.*, **14**, 48 (1959).

(13) P. M. Hudgins and J. F. Stubbins, *J. Pharmacol. Exp. Ther.*, **166**, 237 (1969).

(14) J. F. Stubbins, P. M. Hudgins, D. C. Murphy, and T. L. Dickerson, *J. Pharm. Sci.*, **61**, 470 (1972).

(15) British pat. 705,950 (1954); through *Chem. Abstr.*, **49**, 2233 (1955).

ACKNOWLEDGMENTS

Supported in part by National Institutes of Health Grant NS-07273.

The authors thank Ms. T. L. Dickerson for technical assistance.

Mode of Action of Sesquiterpene Lactones as Anti-Inflammatory Agents

I. H. HALL *x, C. O. STARNES, Jr. *, K. H. LEE *, and T. G. WADDELL ‡

Received July 29, 1979, from the **Division of Medicinal Chemistry, School of Pharmacy, University of North Carolina, Chapel Hill, NC 27514,* and the ‡*Department of Chemistry, University of Tennessee at Chattanooga, Chattanooga, TN 37401.* Accepted for publication December 7, 1979.

Abstract □ Sesquiterpene lactones containing an α-methylene-γ-lactone moiety were shown to be potent inhibitors of carrageenan-induced edema and chronic adjuvant-induced arthritis in rodents at 2.5 mg/kg/day. The mode of action of sesquiterpene lactones as anti-inflammatory agents appeared to be at multiple sites; for example, at 5×10^{-4} *M*, the sesquiterpene lactones effectively uncoupled the oxidative phosphorylation of human polymorphonuclear neutrophils and elevated the cyclic adenosine monophosphate levels of rat neutrophils and rat and mouse liver cells. Free and total lysosomal enzymatic activity was inhibited by these agents at 5×10^{-4} *M* in both rat and mouse liver and rat and human neutrophils. Furthermore, the structure–activity relationships for the stabilization of lysosomal membrane for rat liver cathepsin activity followed the same structural requirement necessary for anti-inflammatory activity; *i.e.*, the α-methylene-γ-lactone moiety contributed the most activity, whereas the β-unsubstituted cyclopentenone and α-epoxycyclopentanone contributed only minor activity. Human polymorphonuclear neutrophil chemotaxis was inhibited at low concentrations (*i.e.*, 5×10^{-5} and 5×10^{-6} *M*), whereas prostaglandin synthetase activity was inhibited at a higher concentration (*i.e.*, 10^{-3} *M*) by the sesquiterpene lactones.

Keyphrases □ Anti-inflammatory agents—sesquiterpene lactones, mode of action determined *in vitro* and *in vivo* □ Sesquiterpene lactones—anti-inflammatory agents, antiarthritic agents, mode of action determined in rat and human neutrophils and rat and mouse liver cells □ Oxidative phosphorylation—uncoupling effect of sesquiterpene lactones, mode of action determined in inflammation process □ Lysosomal membrane—effect of sesquiterpene lactones on membrane stability, hydrolytic enzyme release, mode of action in inflammation process □ Cyclic adenosine monophosphate—effect of sesquiterpene lactones on *in vitro* levels, role in inflammation process □ Structure–activity relationships—effect of sesquiterpene lactones on inflammation process, several modes of action determined *in vitro* and *in vivo*

The anti-inflammatory activity of sesquiterpene lactones in rodents was reported previously (1). An α-methylene-γ-lactone moiety within the structure of the pseudoguaianolide and germacranolide derivatives was required for activity against edema-induced carrageenan inflammation. Saturation of the 11,13-double bond of the methylene group of the lactone resulted in a loss of activity (1).

In the chronic adjuvant-induced arthritic screen, compounds containing the α-methylene-γ-lactone, the β-unsubstituted cyclopentenone, and α-epoxycyclopentanone afforded significant inhibitory activity at 2.5 mg/kg/day (1). In addition, these derivatives also suppressed the writhing reflex, induced pleurisy, delayed hypersensitivity, and passive cutaneous anaphylaxis and were mild immunostimulants of immunoglobulins (1). The effects of the

0022-3549/80/0500-0537$01.00/0

© 1980, American Pharmaceutical Association

Table I—Anti-Inflammatory Activity of Sesquiterpene Lactones and Germacranolides in Sprague–Dawley Rats

Compound	Percent of Control: Anti-Inflammatory Screen[a], 2.5 mg/kg twice	Percent of Control: Antiarthritic Screen[b], 2.5 mg/kg/day
I Helenalin	25 ± 15[c]	23 ± 4[c]
II Tenulin	84 ± 18	47 ± 8[c]
III Isotenulin	84 ± 17	47 ± 10[c]
IV Aromaticin	65 ± 6[c]	—
V 2,3-Dihydrohelenalin	53 ± 19[c]	—
VI 2,3-Dihydrotenulin	93 ± 8	92 ± 5
VII 2,3-Dihydroisotenulin	92 ± 15	—
VIII 2,3-Epoxyhelenalin	54 ± 3[c]	54 ± 6[c]
IX 2,3-Epoxytenulin	57 ± 19[c]	33 ± 5[c]
X 2,3-Epoxyisotenulin	69 ± 9[c]	37 ± 3[c]
XI 2,3,11,13-Tetrahydrohelenalin	96 ± 15	—
XII α-Methylene-γ-lactone	64 ± 13[c]	17 ± 3[c]
XIII 2-Cyclopentenone	77 ± 13[d]	—
XIV Eupaformosanin	69 ± 8[c]	—
XV Eupahyssopin	43 ± 6[c]	34 ± 5[c]
XVI Molephantinin	68 ± 17[d]	—
XVII Molephantin	67 ± 8[c]	40 ± 6[c]
XVIII Deoxyelephantopin	49 ± 11[c]	31 ± 4[c]
XIX Phantomolin	54 ± 19[c]	—
XX Eupatolide	70 ± 12[d]	70 ± 7[c]
XXI Indomethacin (10 mg/kg)	27 ± 6[c]	55 ± 5[c]
XXII 0.05% Polysorbate 80	100 ± 12 (0.655 g)	100 ± 9 (0.830 g)

[a] Expressed as mean ± *SD*, $n = 8$. [b] Expressed as mean ± *SD*, $n = 6$. [c] $p \leq 0.001$. [d] $p \leq 0.010$.

sesquiterpene lactones on metabolic events associated with the inflammation process are reported here.

EXPERIMENTAL

Test Compounds—Twenty sesquiterpene lactones and related compounds were chosen. Some of the compounds were natural products isolated from plant species by literature techniques (2): helenalin (I) from *Balduina angustifolia* (3); tenulin (II) (4) and aromaticin (IV) (4, 5) from *Helenium amarum;* eupaformosanin (XIV) from *Eupatorium formosanum* (6); eupahyssopin (XV) from *E. hyssopifolium* (7); molephantinin (XVI) (8), molephantin (XVII) (9), and phantomolin (XIX) (10) from *Elephantopus mollis;* deoxyelephantopin (XVIII) from *El. carolinianus* (11); and eupatolide (XX) from *E. formosanum* (12).

2,3-Dihydrohelenalin (V), 2,3-epoxyhelenalin (VIII), and 2,3,11,13-tetrahydrohelenalin (XI) were modified chemically from helenalin (13). 2,3-Dihydrotenulin (VI), 2,3-epoxytenulin (IX), isotenulin (III), 2,3-dihydroisotenulin (VII), and 2,3-epoxyisotenulin (X) were prepared by a literature method (14), as was α-methylene-γ-lactone (XII) (15). The 2-cyclopentenone[1] and indomethacin[2] were purchased commercially.

Anti-Inflammatory Screen—Sprague–Dawley male rats (~160 g) were administered test compounds at 2.5 mg/kg ip in 0.05% polysorbate 80–water 3 hr and 30 min prior to injection of 0.2 ml of 1% carrageenan in 0.9% saline into the plantar surface of the right hindfoot. Isotonic saline was injected into the left hindfoot, which served as a baseline. After 3 hr, both feet were excised at the tibiotarsal (ankle) joint according to a modified method (16, 17), resulting in an average net increase of 0.655 g for the control animals.

Antiarthritic Screen—Male Sprague–Dawley rats (~160 g) were injected at the base of the tail with 0.2 ml of light mineral oil containing 1 mg of dried *Mycobacterium butyricum* and 0.4 mg of digitonin. The test drugs were administered on Days 3–20 at 2.5 mg/kg/day ip. Animals were sacrificed on Day 21, and the feet were excised and weighed (18). The control animals achieved an average net weight increase of 0.830 g.

Cell Preparation—Metabolic studies were conducted on CF_1 male mouse (~30 g) and Sprague–Dawley male rat (~180 g) liver homogenates (10%) in 0.25 *M* sucrose and 0.001 *M* ethylenediaminetetraacetic acid at pH 7.2. Polymorphonuclear neutrophils were collected from the peripheral blood of healthy human males (25–28 years) and separated by Ficol–Hypaque density gradient centrifugation by the technique of English and Anderson (19). The neutrophils were aspirated from the lower density gradient level; after water lysis of the red blood cells, the neutrophils constituted 99.9% of the cells.

Polymorphonuclear neutrophils were collected from the peritoneal cavity of male Sprague–Dawley rats (~280 g) ~4 hr after injection of 35 ml of 0.5% oyster glycogen in isotonic saline. The neutrophils were centrifuged at 800×*g* for 20 min, washed, and resuspended in pH 7.4 minimum essential medium and 10% fetal calf serum (20). The neutrophil concentration was ~80% of the cell content.

Oxidative Phosphorylation Studies—Basal and adenosine diphosphate-stimulated respiration of the 10% liver homogenates of rats and mice or 10^6 human polymorphonuclear neutrophils was measured using succinate or α-ketoglutarate as the substrate (21). The reaction vessel contained sucrose (55 μmoles), potassium chloride (22 μmoles), dibasic potassium phosphate (22 μmoles), sodium succinate (90 μmoles) or α-ketoglutarate (60 μmoles), and the test compounds at 5×10^{-4} *M* in 0.05% polysorbate 80–water in a total volume of 1.8 ml.

Oxygen consumption was measured using a Clark electrode connected to an oxygraph. After the basal metabolism (state 4) level was obtained, 0.257 μmole of adenosine diphosphate was added to obtain the adenosine diphosphate-stimulated respiration rate (state 3). The respiration rate was calculated in microliters of oxygen consumed per hour per milligram of wet weight of rat or mouse liver homogenates or 10^7 human polymorphonuclear neutrophils.

In vivo oxidative phosphorylation studies were conducted on mice and rats treated with helanalin (I) at 6 mg/kg or tenulin (II), eupahyssopin (XV), and deoxyelephantopin (XVIII) at 12.5 mg/kg for 3 days. Animals were sacrificed on Day 4, and liver homogenates were prepared for the respiration studies.

Lysosomal Hydrolytic Enzymatic Activities—Free and total acid phosphatase activities were studied using 0.1 *M* β-glycerol phosphate in pH 5.0, 0.1 *M* acetate buffer on CF_1 mouse liver homogenates for 20 min or rat polymorphonuclear neutrophils for 60 min (22). The test drugs were incubated *in vitro* at 5×10^{-4} *M* in 1% carboxymethylcellulose. The total enzymatic activity was obtained by treating the liver homogenates or neutrophils with 0.02% alkylphenoxypolyethoxyethanol 100 to release the bound hydrolytic enzymes from the lysosomal membrane. The reaction was terminated with 10% trichloroacetic acid, and the mixture was centrifuged.

Inorganic phosphate was determined by the method of Chen *et al.* (23). Free, total, and percent released acid phosphatase activities were calculated after correcting for the blank values. Free and total cathepsin activities were determined in an analogous manner on mouse and rat liver homogenates and on rat polymorphonuclear neutrophils with 2% azocasein as the substrate in pH 5.0, 0.1 *M* acetate buffer (24). The supernate was assayed for acid-soluble peptide fragments at 366 nm. Free, total, and percent released cathepsin activities were calculated after correcting for the blank values.

The effects of the drugs on lysosomal membrane stabilization were studied on rat liver homogenates by incubating the test drugs (5×10^{-4} *M*) for 20 min at 37° prior to measuring the enzymatic catalytic activity (25). Free and total aryl sulfatase activities were determined on mouse liver homogenates with 0.72 μmole of *p*-nitrocatechol sulfate as the substrate in pH 5.8, 0.2 *M* acetate buffer. The reaction was conducted for 20 min at 37° and terminated with 4 *N* NaOH. The formation of 4-nitrocatechol in the supernate was measured at 510 nm spectrophotometrically (25).

Cyclic Adenosine Monophosphate Levels—Isolated rat polymorphonuclear neutrophils were incubated with the test drugs at 5×10^{-4} *M* for 1 hr at 37° in pH 7.4 minimum essential medium. The reaction was stopped with 6% trichloroacetic acid, and the cyclic adenosine monophosphate levels were determined by radioimmunoassay[3] using ^{125}I-2-*O*-succinyl cyclic adenosine monophosphate tyrosine methyl ester and cyclic adenosine monophosphate antibody (26). Results were calculated in picomoles of cyclic adenosine monophosphate per 10^7 polymorphonuclear neutrophils.

Cyclic adenosine monophosphate levels also were determined after treating the mice or rats *in vivo* with helenalin (I) at 6 mg/kg or tenulin (II), eupahyssopin (XV), and deoxyelephantopin (XVIII) at 12.5 mg/kg for 3 days. The animals were sacrificed on the 4th day, and a 10% liver homogenate was prepared for the radioimmunoassay. Results were calculated as picomoles per milligram of wet liver.

Prostaglandin Synthetase Activity—The incubation medium of Tomlinson *et al.* (27) was used to determine the [^{3}H]prostaglandin for-

[1] Aldrich.
[2] Merck Sharp & Dohme.
[3] Becton Dickinson.

mation from [^{3}H](N)-arachidonic acid (86.2 Ci/mmole) and 10 mg of purified commercial prostaglandin synthetase from bovine seminal vesicles[4]. After 1 hr at 37°, the reaction was terminated with 1 *N* HCl, and the mixture was extracted with ether and evaporated. The residue was dissolved in ethyl acetate and spotted on silica gel TLC plates, which were eluted with chloroform–methanol–water–acetic acid (90:8:1:0.8) (28). The plates were dried and developed in iodine vapor; with the use of prostaglandin standards, the appropriate areas were scraped and counted for tritium content. Indomethacin was used as an internal standard at 10^{-4} and 10^{-6} *M*. Helenalin (I) and tenulin (II) were tested at 10^{-3} and 10^{-4} *M*.

Polymorphonuclear Neutrophil Chemotaxis—Isolated human polymorphonuclear neutrophils were utilized to measure the inhibition of chemotaxis and migration to *Escherichia coli* bacterial culture filtrate, as the chemotactant agent, by the method of Nelson *et al.* (29) on agarose tissue culture plates. The test drugs at 10^{-4}, 5×10^{-5}, and 10^{-6} *M* were incubated for 30 min at 37° with the neutrophils in pH 7.4 minimum essential medium prior to the assay. The plates were incubated in a carbon dioxide incubator at 37° for 2.5 hr and fixed in methanol overnight. After staining with Wright's stain, the migration from the wells was measured in micrometers. The migration for the control neutrophils was 991 ± 52 μm. Indomethacin was used as an internal standard at 10^{-3} *M*.

RESULTS

The sesquiterpene lactone analogs containing an α-methylene-γ-lactone moiety (I, IV, and V) possessed potent anti-inflammatory activity in rodents at a relatively low dose of 2.5 mg/kg (Table I); II, III, VI, VII, and XI were inactive. Administration of helenalin (I) resulted in the best inhibitory activity of the sesquiterpene lactones both in the carrageenan-induced screen (75%) and the chronic adjuvant-induced arthritic screen (77%). Compounds V, VIII, IX, XV, XVIII, and XIX caused 43–57% inhibition of the carrageenan-induced edema. In the chronic arthritic screen, treatment with the simple α-methylene-γ-lactone (XII) resulted in 83% inhibition. Compounds IX, X, XV, and XVIII resulted in 63–69% inhibition of induced arthritis; II, III, VIII, and indomethacin caused 45–53% inhibition of arthritis.

Representative compounds were selected for the biochemical studies. Helenalin (I) and tenulin (II) were selected from the pseudoguaianolides,

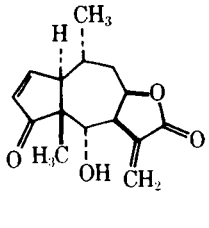

I

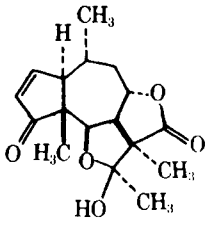

II

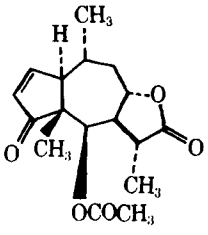

III

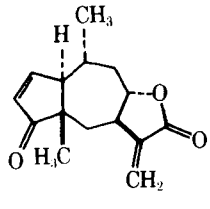

IV

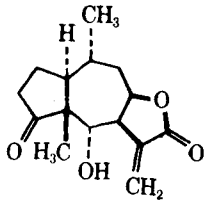

V

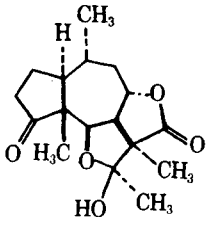

VI

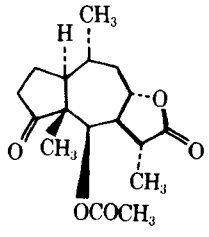

VII

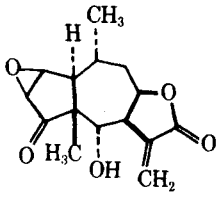

VIII

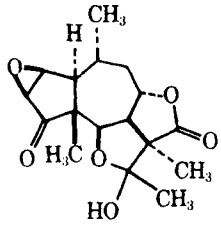

IX

[4] Miles Research Products.

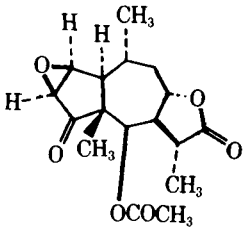

X

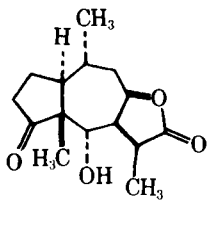

XI

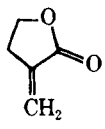

XII

XIII

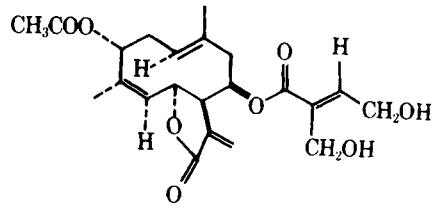

XIV

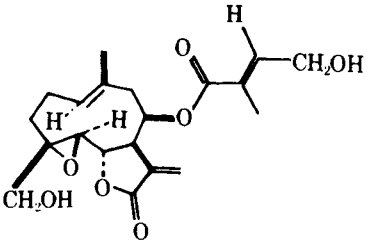

XV

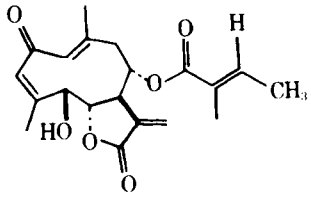

XVI

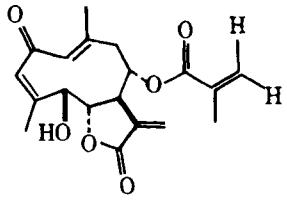

XVII

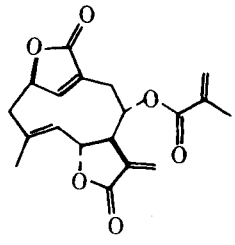

XVIII

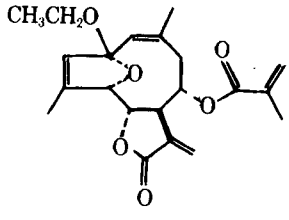

XIX

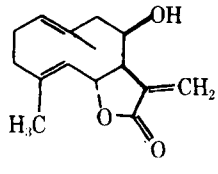

XX

and eupahyssopin (XV) and deoxyelephantopin (XVIII) were selected from the germacranolides. The *in vitro* mouse and rat liver oxidative phosphorylation studies demonstrated that these compounds at 5×10^{-4} *M* only marginally altered the basal respiration (state 4) and the adenosine monophosphate-stimulated respiration (state 3), utilizing as the substrates either succinate, a flavin adenine dinucleotide-linked dehydrogenase, or α-ketoglutarate, a nicotinic adenine dinucleotide-linked dehydrogenase (Table II).

In vivo administration of the sesquiterpene lactones for 3 days significantly increased rat and mouse basal respiration with succinate; although not significant, the trend followed the same pattern with α-ketoglutarate. Adenosine monophosphate-stimulated respiration was reduced drastically in mouse liver with I using succinate (Table III). Human polymorphonuclear neutrophil basal respiration (Table IV) was increased significantly with I, II, XV, and XVIII at 5×10^{-4} *M* using either succinate or α-ketoglutarate as the substrate, whereas the adenosine diphosphate-stimulated respiration was reduced significantly with both succinate and α-ketoglutarate as the substrate. These studies indicate that the respiration of human neutrophils was uncoupled by these four sesquiterpene lactones.

Table II—*In Vitro* Effects of Sesquiterpene Lactones on Rodent Liver Oxidative Phosphorylation

Compound (5×10^{-4} *M*)	Percent of Control[a]			
	Succinate		α-Ketoglutarate	
	State 4	State 3	State 4	State 3
		Mouse Liver[b]		
I	94.3 ± 7.1	98.3 ± 11.7	93.2 ± 17.3	85.6 ± 9.7
II	88.3 ± 7.0	98.5 ± 11.3	95.7 ± 21.3	98.6 ± 17.4
XV	95.7 ± 6.8	97.6 ± 12.1	101.3 ± 11.7	86.7 ± 10.3
XVIII	90.1 ± 4.2	98.7 ± 9.9	99.1 ± 16.2	89.2 ± 12.1
0.05% Polysorbate 80	100.0 ± 8.8	100.0 ± 17.5	100.0 ± 6.3	
		Rat Liver[c]		
I	96.4 ± 6.2	97.2 ± 7.9	94.6 ± 12.1	88.9 ± 9.2
II	92.3 ± 7.1	96.4 ± 8.1	93.3 ± 10.8	96.7 ± 12.2
XV	101.3 ± 5.8	85.6 ± 7.6	96.5 ± 11.1	88.2 ± 10.1
XVIII	97.5 ± 3.2	88.4 ± 5.8	103.2 ± 9.1	83.6 ± 9.8
0.05% Polysorbate 80	100.0 ± 7.6	100.0 ± 7.8	100.0 ± 8.9	100.0 ± 11.4

[a] See Table III for control values. [b] Expressed as mean ± *SD*, $n = 9$. [c] Expressed as mean ± *SD*, $n = 6$.

Table III—Oxidative Phosphorylation Respiration of Rodent Liver after 3 Days of Treatment with Sesquiterpene Lactones

Compound and Dose	Percent of Control			
	Succinate		α-Ketoglutarate	
	State 4	State 3	State 4	State 3
		Mouse Liver[a]		
I, 6 mg/kg/day	158 ± 21[b]	60 ± 15[b]	108 ± 12	84 ± 23
II, 12 mg/kg/day	143 ± 19[b]	118 ± 23	113 ± 25	132 ± 15[b]
XV, 12 mg/kg/day	138 ± 17[b]	82 ± 17[c]	115 ± 19	87 ± 19
XVIII, 12 mg/kg/day	127 ± 12[c]	89 ± 11	103 ± 10	86 ± 13
0.05% Polysorbate 80	100 ± 16[d]	100 ± 12[e]	100 ± 17[f]	100 ± 6[g]
		Rat Liver[h]		
I, 6 mg/kg/day	138 ± 11[b]	84 ± 7[c]	115 ± 13	83 ± 8[c]
II, 12 mg/kg/day	125 ± 9[c]	96 ± 8	110 ± 12	95 ± 12
XV, 12 mg/kg/day	132 ± 14[c]	82 ± 5[c]	119 ± 10	86 ± 7
XVIII, 12 mg/kg/day	128 ± 13[c]	93 ± 6	99 ± 9	84 ± 10
0.05% Polysorbate 80	100 ± 12[i]	100 ± 9[j]	100 ± 13[k]	100 ± 10[l]

[a] Expressed as mean ± *SD*, $n = 8$. [b] $p \leq 0.001$. [c] $p \leq 0.010$. [d] 5.92 μl of oxygen consumed/hr/mg of wet tissue. [e] 11.31 μl of oxygen consumed/hr/mg of wet tissue. [f] 3.51 μl of oxygen consumed/hr/mg of wet tissue. [g] 5.21 μl of oxygen consumed/hr/mg of wet tissue. [h] Expressed as mean ± *SD*, $n = 6$. [i] 4.52 μl of oxygen consumed/hr/mg of wet tissue. [j] 9.13 μl of oxygen consumed/hr/mg of wet tissue. [k] 3.42 μl of oxygen consumed/hr/mg of wet tissue. [l] 6.36 μl of oxygen consumed/hr/mg of wet tissue.

Table IV—*In Vitro* Effects of Sesquiterpene Lactones on Human Polymorphonuclear Neutrophil Oxidative Phosphorylation Processes

Compound	Percent of Control[a]			
	Succinate		α-Ketoglutarate	
	State 4	State 3	State 4	State 3
I	141 ± 15[b]	59 ± 12[b]	146 ± 14[c]	67 ± 8[c]
II	166 ± 24[c]	72 ± 8[b]	141 ± 13[b]	81 ± 15
XV	149 ± 14[c]	64 ± 6[c]	149 ± 23[b]	69 ± 9[c]
XVIII	139 ± 10[b]	64 ± 12[b]	140 ± 20[d]	60 ± 11[b]
0.05% Polysorbate 80	100 ± 19[e]	100 ± 16[f]	100 ± 17[g]	100 ± 15[h]

[a] Expressed as mean ± *SD*, $n = 9$. [b] $p \leq 0.005$. [c] $p \leq 0.001$. [d] $p \leq 0.010$. [e] 3.008 ± 0.562 μl of oxygen consumed/min/10^6 cells. [f] 4.545 ± 0.722 μl of oxygen consumed/min/10^6 cells. [g] 2.632 ± 0.460 μl of oxygen consumed/min/10^6 cells. [h] 3.487 ± 0.517 μl of oxygen consumed/min/10^6 cells.

Liver hydrolytic enzyme studies *in vitro* showed that the sesquiterpene lactones were potent inhibitors of lysosomal enzyme activities (Table V). Helenalin (I) and tenulin (II) suppressed mouse liver free acid phosphatase, cathepsin, and aryl sulfatase activities at pH 5.0 and 5×10^{-4} *M*. The total enzymatic activities were suppressed by I for acid phosphatase and cathepsin, whereas the total cathepsin activity was inhibited by II. Both I and II reduced the percent of cathepsin and aryl sulfatase enzymes released into the cytoplasm.

The structure–activity study of sesquiterpene lactones *in vitro* on rat liver free cathepsin and the percent of cathepsin released demonstrated that all of the sesquiterpene lactones tested were active at 5×10^{-4} *M* (Table VI). Helenalin caused a maximum inhibition of 92%, with IV, IX, X, XII, and XIV–XIX resulting in 64–88% inhibition. The internal standard, indomethacin, resulted in 33% inhibition of free cathepsin activity at 5×10^{-4} *M*. Masking of the α-methylene-γ-lactone (compare I to II) or alteration from the *cis*- to the *trans*-fused ring (compare I to IV) also resulted in loss of activity. The 2,3-epoxy derivatives (VIII–X) improved the ability to inhibit the free cathepsin activity, with the exception of the helenalin epoxy derivative (VIII). Loss or acetylation of the 6-hydroxyl group of the cycloheptane ring along with the *trans*-fused orientation of the α-methylene-γ-lactone moiety (III and IV) resulted in an even greater loss of activity. The effects of the sesquiterpene lactones on the precent release of the cathepsin enzyme from the bound lysosomal membrane demonstrated that the sesquiterpene lactones probably stabilized the membrane and reduced the release of the enzyme.

Helenalin (I) reduced the percent of lysosomal enzyme release from 24 to 2%; the reduction for XV was to 3%, and the reduction for IX, X, XIV, and XVI–XIX was to 6–8%. Compounds that were not active in the anti-inflammatory screen had minimal effects on reducing the lysosomal enzyme release (*e.g.*, II, III, VI, VII, XI, and XIII were essentially inactive). Compounds that demonstrated potent anti-inflammatory activity also significantly reduced the lysosomal enzyme release (*e.g.*, I, IV, V, VIII–X, XII, and XIV–XIX). The lysosomal enzymatic activities of rat polymorphonuclear neutrophils also were reduced by sesquiterpene lactones at 5×10^{-4} *M* (Table VII). Helenalin (I) demonstrated 93% inhibition of free acid phosphatase activity, 94% inhibition of total acid phosphatase activity, 84% inhibition of free cathepsin activity, and 73% inhibition of total cathepsin activity. Compounds III, IV, IX, X, and XIII–XVI caused 70–87% inhibition of the free acid phosphatase activity, whereas IV, VIII–X, XII, and XIV–XVIII caused 54–88% inhibition of the total acid phosphatase activity. Free cathepsin activity was suppressed 55–67% by II, IV, V, VIII, XII, XVI, XVII, XIX, and XX. Total cathepsin activity was inhibited 51–63% by IV, VIII, XIII, and XVII.

The inhibition of lysosomal enzymatic activities of rat polymorphonuclear neutrophils correlated more with the ability to inhibit chronic arthritis than the anti-inflammatory screen. Masking of the α-methylene-γ-lactone (compare I to II), loss of the free 6-hydroxyl group, or alteration from a *cis*- to a *trans*-fusion of the α-methylene-γ-lactone moiety to the cycloheptane backbone (compare I to III and IV) again reduced the ability to inhibit the free and total lysosomal enzymatic activity.

In vivo treatment with helenalin (I) at 6 mg/kg/day for 3 days resulted in a 61 and a 51% increase in mouse liver and in rat liver cyclic nucleotide levels, respectively. Tenulin (II) at 12.5 mg/kg had little effect in mouse

Table V—*In Vitro* Effects of Sesquiterpene Lactones on CF_1 Mouse Liver Lysosomal Enzymatic Activity at pH 5.0

Compound and Dose	Percent of Control[a]								
	Acid Phosphatase			Cathepsin			Aryl Sulfatase		
	Free	Total	Percent Released	Free	Total	Percent Released	Free	Total	Percent Released
I, 5×10^{-4} *M*	77 ± 10[b]	79 ± 6[c]	97 ± 18	0[c]	6 ± 4[c]	0[c]	24 ± 11[c]	100 ± 4	24 ± 4
II, 5×10^{-4} *M*	83 ± 4[b]	91 ± 8	93 ± 11	4 ± 2[c]	19 ± 4[c]	18 ± 3[c]	22 ± 9[c]	90 ± 5	25 ± 5[c]
1% Carboxymethylcellulose	100 ± 8[d]	100 ± 5[e]	100 ± 9[f]	100 ± 4[g]	100 ± 9[h]	100 ± 6[i]	100 ± 12[j]	100 ± 6[k]	100 ± 4[l]

[a] Expressed as mean ± *SD*, $n = 6$. [b] $p \leq 0.010$. [c] $p \leq 0.001$. [d] 0.753 mg of phosphate released/hr/g of wet tissue. [e] 1.701 mg of phosphate released/hr/g of wet tissue. [f] 44% released. [g] 2.688 mg of protein released/hr/g of wet tissue. [h] 7.384 mg of protein released/hr/g of wet tissue. [i] 36% released. [j] 2.237 mg of 4-nitrocatechol released/hr/g of wet tissue. [k] 12.229 mg of 4-nitrocatechol released/hr/g of wet tissue. [l] 19% released.

Table VI—Structure–Activity Relationship of Sesquiterpene Lactones on *In Vitro* Liver Cathepsin Activity of Sprague–Dawley Rats

Compound (5×10^{-4} *M*)	Cathepsin Activity[a]		
	Free Cathepsin	Percent Control Free	Percent Released
I	0.328 ± 0.068[b]	8.1 ± 1.7[b]	1.9 ± 0.4
II	2.528 ± 0.364[b]	62.5 ± 9.0[b]	15.0 ± 2.2
III	2.030 ± 0.211[b]	50.1 ± 8.5[b]	12.1 ± 1.3
IV	1.468 ± 0.154[b]	36.3 ± 3.8[b]	8.7 ± 0.9
V	1.610 ± 0.139[b]	39.8 ± 3.4[b]	9.6 ± 0.8
VI	2.879 ± 0.146[b]	71.2 ± 3.6[b]	17.1 ± 0.9
VII	2.394 ± 0.226[b]	59.2 ± 5.5[b]	14.2 ± 1.3
VIII	1.545 ± 0.198[b]	38.2 ± 4.9[b]	9.2 ± 1.2
IX	1.019 ± 0.169[b]	25.2 ± 4.2[b]	6.0 ± 1.0
X	0.966 ± 0.134[b]	23.9 ± 3.3[b]	5.7 ± 0.8
XI	2.833 ± 0.296[b]	71.3 ±7.3[b]	17.1 ± 1.8
XII	1.467 ± 0.174[b]	36.3 ± 4.3[b]	8.7 ± 1.0
XIII	2.559 ± 0.133[b]	63.3 ± 3.3[b]	15.1 ± 0.8
XIV	1.023 ± 0.190[b]	25.3 ± 4.7[b]	6.1 ± 1.1
XV	0.465 ± 0.067[c]	11.5 ± 1.7[b]	2.8 ± 0.3
XVI	1.217 ± 0.162[b]	30.1 ± 4.0[b]	7.2 ± 0.9
XVII	1.387 ± 0.254[b]	34.3 ± 6.3[b]	8.2 ± 1.5
XVIII	0.995 ± 0.123[b]	24.6 ± 3.0[b]	5.9 ± 0.7
XIX	1.266 ± 0.171[b]	31.3 ± 4.2[b]	7.5 ± 1.0
XX	2.378 ± 0.218[b]	58.8 ± 5.4[b]	14.1 ± 1.3
1% Carboxymethylcellulose	4.0439 ± 0.207[c]	100.0 ± 8.1	24.0[d] ± 1.2
Indomethacin	2.718 ± 0.246	67.2 ± 6.1	16.1 ± 1.5

[a] Expressed as mean ± *SD*, $n = 6$. [b] $p \leq 0.001$. [c] Free cathepsin = 4.0439 mg of protein released/hr/g of wet tissue. [d] Control total cathepsin = 16.845 mg of protein released/hr/g of wet tissue; therefore, percent free control = 24.

Table VII—Structure–Activity Relationship of Sesquiterpene Lactones on *In Vitro* Cathepsin and Acid Phosphatase Activities of Rat Polymorphonuclear Neutrophils at pH 5.0

Compound (5×10^{-4} *M*)	Percent of Control[a]			
	Acid Phosphatase		Cathepsin	
	Free	Total	Free	Total
I	7 ± 1[b]	6 ± 1[b]	16 ± 2[b]	27 ± 4[b]
II	41 ± 4[b]	62 ± 6[b]	45 ± 4[b]	59 ± 3[b]
III	22 ± 2[b]	57 ± 3[b]	67 ± 5[b]	65 ± 4[b]
IV	30 ± 5[b]	33 ± 6[b]	35 ± 3[b]	44 ± 2[b]
V	54 ± 4[b]	68 ± 7[b]	42 ± 5[b]	51 ± 3[b]
VI	41 ± 3[b]	82 ± 9[c]	62 ± 4[b]	59 ± 4[b]
VII	53 ± 4[b]	100 ± 5	62 ± 4[b]	71 ± 8[b]
VIII	43 ± 7[b]	46 ± 5[b]	38 ± 3[b]	48 ± 5[b]
IX	21 ± 5[b]	38 ± 5[b]	53 ± 3[b]	69 ± 6[b]
X	16 ± 2[b]	16 ± 2[b]	62 ± 4[b]	51 ± 4[b]
XI	69 ± 6[b]	77 ± 4[b]	74 ± 7[b]	72 ± 3[b]
XII	45 ± 7[b]	44 ± 2[b]	44 ± 5[b]	58 ± 4[b]
XIII	26 ± 9[b]	90 ± 7[b]	49 ± 4[b]	37 ± 5[b]
XIV	13 ± 2[b]	12 ± 3[b]	59 ± 5[b]	61 ± 3[b]
XV	17 ± 1[b]	16 ± 2[b]	51 ± 3[b]	59 ± 2[b]
XVI	21 ± 3[b]	26 ± 2[b]	33 ± 4[b]	53 ± 5[b]
XVII	32 ± 6[b]	40 ± 5[b]	42 ± 4[b]	49 ± 5[b]
XVIII	36 ± 5[b]	39 ± 3[b]	69 ± 6[b]	78 ± 6[b]
XIX	41 ± 3[b]	72 ± 3[b]	47 ± 2[b]	60 ± 4[b]
XX	47 ± 5[b]	75 ± 4[b]	42 ± 4[b]	50 ± 3[b]
1% Carboxymethylcellulose	100 ± 3[d]	100 ± 5[e]	100 ± 3[f]	100 ± 4[g]
Indomethacin	86 ± 8	100 ± 4	100 ± 1	100 ± 3

[a] Expressed as mean ± *SD*, $n = 6$. [b] $p \leq 0.001$. [c] $p \leq 0.010$. [d] 0.272 μg of phosphate released/hr/10^7 cells. [e] 0.347 μg of phosphate released/hr/10^7 cells. [f] 0.147 mg of protein released/hr/10^7 cells. [g] 0.183 mg of protein released/hr/10^7 cells.

or rat liver. Eupahyssopin (XV) and deoxyelephantopin (XVIII) followed essentially the same pattern as I but with a slightly lower magnitude (Table VIII). The cyclic adenosine monophosphate levels of rat polymorphonuclear neutrophils were elevated 158% by I (Table IX). Compounds II, IV, V, VIII, IX, and XIII elevated the cyclic nucleotide level significantly. The isotenulin series (III, VII, and X) and the germacranolides (XIV–XX) in general lowered the cyclic nucleotide levels in neutrophils.

Sesquiterpene lactones containing an α-methylene-γ-lactone or an α-epoxycyclopentanone ring successfully inhibited polymorphonuclear neutrophil chemotaxic migration (Table X). Compounds I, IV, VIII–X, XV, XVIII, and XX caused 100% inhibition or paralysis of neutrophil migration at 5×10^{-5} *M*. At a lower concentration—*viz.*, 10^{-6} *M*, I, X, XVIII, and, surprisingly, XX caused significant inhibition.

In vitro prostaglandin synthetase activity (Table XI) was suppressed 29% by I and 8% by II at 10^{-3} *M*. These two sesquiterpene lactones had no inhibitory effects at $^{-4}$ *M*. Indomethacin caused 38 and 24% inhibition at 10^{-4} and 10^{-6} *M*, respectively.

DISCUSSION

The pseudoguaianolide (I, IV, and V) and germacranolide (XIV–XX) sesquiterpene lactones at 2.5 mg/kg significantly suppressed induced inflammation in rats. In the carrageenan-induced edema screen, the α-methylene-γ-lactone moiety plays a major role in affording anti-inflammatory activity, demonstrated by these sesquiterpene lactones. In addition, the α-epoxycyclopentanone system contributed to the anti-inflammatory activity (VIII–X) of these compounds against the induced edema. In the chronic adjuvant-induced arthritic screen, not only did the α-methylene-γ-lactone moiety and the α-epoxycyclopentanone system contribute significantly to the antiarthritic activity, but the β-unsubstituted cyclopentenone ring (II and III) also instilled antiarthritic activity for the sesquiterpene lactones.

Sesquiterpene lactones affected a number of biochemical parameters that influence the inflammation process. The synthesis of the chemical mediator, prostaglandin, was suppressed in the presence of sesquiterpene lactones at 10^{-3} *M* compared to indomethacin at 10^{-4} *M* in this isolated enzyme system. Dithiothreitol and mercaptoethanol, thiol-blocking reagents, are known to inhibit prostaglandin synthesis from arachidonic acid (30). Sesquiterpene lactones have been shown to inhibit sulfhydryl-bearing enzymes, supposedly through a Michael addition of the cyclopentenone ring and the α-methylene-γ-lactone moiety (4). It was noted that saturation of the 2,3-double bond of the cyclopentenone and the 11,13-double bond of the α-methylene-γ-lactone of helenalin resulted in a loss of anti-inflammatory activity (1).

Whereas it was difficult to demonstrate the effects of sesquiterpene lactones on mouse and rat liver oxidative phosphorylation processes, these agents definitely uncoupled the *in vitro* oxidative phosphorylation respiration of polymorphonuclear neutrophils of humans. The concentration (5×10^{-4} *M*) of sesquiterpene lactones necessary to cause uncoupling compared favorably with standard anti-inflammatory agents, *e.g.*, salicylates at 10^{-3} *M* (31) and phenylbutazone at 10^{-4} *M* (32). Suppression of oxidative phosphorylation processes of neutrophils may be associated with the lack of an efficient energy-generating system necessary for leukocyte chemotaxis, microtubular contraction, and migration to the inflammation site. A relatively low concentration of sesquiterpene lactones, *i.e.*, 5×10^{-5} and 10^{-6} *M*, was required to inhibit neutrophil chemotaxis and migration to the chemoattractant *E. coli* bacterial culture filtrate. Bryant *et al.* (33) demonstrated that sodium arsenite, which uncoupled oxidative phosphorylation at 2.5×10^{-4} *M*, also inhibited neutrophil migration. Likewise, the uncouplers iodoacetamide and dinitrophenol blocked chemotaxis partially at 10^{-4} *M* (34).

Standard anti-inflammatory drugs have been shown to inhibit liver

Table VIII—Cyclic Adenosine Monophosphate Levels [a] of Rodent Liver after 3 Days of Treatment with Sesquiterpene Lactones

Compound and Dose	Mouse, pmoles/mg of wet tissue	Percent Control	Rat, pmoles/mg of wet tissue	Percent Control
I, 6 mg/kg/day	1.94 ± 0.34[b]	161 ± 28	1.12 ± 0.21[b]	151 ± 28
II, 12.5 mg/kg/day	1.35 ± 0.35	112 ± 26	0.87 ± 0.16	118 ± 22
XV, 12.5 mg/kg/day	1.66 ± 0.28[b]	137 ± 23	1.06 ± 0.19[b]	143 ± 26
XVIII, 12.5 mg/kg/day	1.52 ± 0.24[c]	126 ± 20	0.93 ± 0.14[c]	127 ± 19
0.05% Polysorbate 80	1.21 ± 0.18	100 ± 15	0.74 ± 0.12	100 ± 16

[a] Expressed as mean ± *SD*, $n = 6$. [b] $p \leq 0.01$. [c] $p \leq 0.03$.

Table IX—Cyclic Adenosine Monophosphate Levels [a] of Rat Polymorphonuclear Neutrophils 1 hr after Incubation with Sesquiterpene Lactones

Compound (5×10^{-4} *M*)	Picomoles/10^7 cells	Percent Control
I	44.0 ± 0.5	258 ± 2.8
II	24.2 ± 0.3	142 ± 1.7
III	0.5 ± 0.1	3 ± 0.5
IV	33.0 ± 0.5	194 ± 2.8
V	34.0 ± 0.3	200 ± 1.7
VI	19.2 ± 0.4	113 ± 2.2
VII	16.0 ± 0.2	94 ± 1.1
VIII	34.0 ± 0.3	200 ± 1.7
IX	29.0 ± 0.2	171 ± 1.1
X	7.8 ± 0.1	46 ± 0.5
XI	6.5 ± 0.2	38 ± 1.1
XII	19.2 ± 0.2	113 ± 1.1
XIII	29.5 ± 0.2	174 ± 1.1
XIV	12.5 ± 0.2	74 ± 1.1
XV	9.9 ± 0.1	58 ± 0.5
XVI	15.6 ± 0.2	87 ± 1.1
XVII	18.9 ± 0.2	111 ± 1.1
XVIII	10.0 ± 0.3	57 ± 1.7
XIX	0.8 ± 0.2	5 ± 1.1
XX	11 5 ± 0.3	68 ± 1.7
0.05% Polysorbate 80	17.6 ± 0.2	100 ± 1.1
Indomethacin	17.7 ± 0.3	100 ± 1.7

[a] Expressed as mean ± *SD*, $n = 4$.

Table X—*In Vitro* Effects of Sesquiterpene Lactones in Human Polymorphonuclear Neutrophil Chemotaxic Migration

Compound	Percent Inhibition[a] 10^{-6} *M*	5×10^{-5} *M*	10^{-4} *M*
I	54 ± 4	100 ± 3	100 ± 5
II	1 ± 1	39 ± 2	100 ± 4
III	—	55 ± 3	—
IV	0	100 ± 6	—
V	—	20 ± 2	—
VI	—	0	—
VII	—	0	—
VIII	0	100 ± 5	—
IX	7 ± 2	100 ± 3	—
X	39 ± 4	100 ± 5	—
XI	—	18 ± 1	—
XII	—	4 ± 1	—
XIII	—	8 ± 3	—
XIV	—	0	—
XV	—	100 ± 4	—
XVIII	46 ± 2	100 ± 6	—
XX	58 ± 3	100 ± 4	—
0.05% Polysorbate 80	0	0	0
Indomethacin[b]	—	—	—

[a] Expressed as mean ± *SD*, $n = 4$. [b] Inhibition of indomethacin at 10^{-3} *M* is 31%.

Table XI—Effects of Helenalin and Tenulin on Prostaglandin Synthetase Activity [a]

Compound and Dose	dpm[b] per Milligram of Enzyme per Hour	Percent Control
0.05% Polysorbate 80	65,640[c] ± 3938	100 ± 6
Indomethacin (10^{-4} *M*)	40,670 ± 5694[d]	62 ± 9
I, 10^{-3} *M*	46,604 ± 2064[d]	71 ± 3
II, 10^{-3} *M*	60,389 ± 5908	92 ± 8

[a] $n = 6$. [b] Disintegrations per minute. [c] 75% conversion from [^{3}H](N)-arachidonic acid. [d] $p = 0.001$.

lysosomal aryl sulfatase enzymatic activity and lysosomal rupture; *e.g.*, at 10^{-3} *M*, indomethacin, acetyl salicylate, and phenylbutazone caused 18, 13, and 42% inhibition, respectively (25). The sesquiterpene lactones, helenalin and tenulin, at 5×10^{-4} *M* suppressed liver lysosomal aryl sulfatase enzymatic activity and rupture by 75%. Higher magnitudes of inhibition were observed with helenalin and tenulin on mouse liver cathepsin activity and rupture of lysosomes. Structure–activity studies on rat liver free cathepsin activity correlated positively with the anti-inflammatory activity of the sesquiterpene lactones. Furthermore, cathepsin D enzymatic activity has been implicated in the inflammation process as causing the release of vasoamine peptides and chemotactic factors, which are chemical mediators that can attract phagocytic cells to the site of inflammation (35). Rupture of the lysosomal membrane to release hydrolytic enzymes, *i.e.*, cathepsin, appeared to be retarded drastically by the sesquiterpene lactones. Again, there was a strong positive correlation between lysosomal membrane stabilization and the anti-inflammatory activity of the sesquiterpene lactones.

A similar pattern was observed with the incubation of sesquiterpene lactones with polymorphonuclear neutrophils. Free and total acid phosphatase and cathepsin activities were inhibited significantly following generally the same structural requirements for inhibition. The neutrophils (leukocytes) supposedly contain high concentrations of hydrolytic enzymes that are released at the sites of inflammation, causing the spread of infection and digestion of tissue cellular components. Inhibition of lysosomal release and catalytic activity will reduce the spread of inflammation and tissue damage. Both acid phosphatase (36) and crude cathepsin (37) enzymatic activities can be blocked by thiol-blocking reagents.

Elevated levels of cyclic adenosine monophosphate have been correlated with the stabilization of lysosomal membranes; *e.g.*, 10^{-6} *M* cyclic adenosine monophosphate inhibited the release of β-glucuronidase from human neutrophils (38). High cyclic adenosine monophosphate levels inhibited rabbit (39) and human (40) polymorphonuclear neutrophil chemotaxis and migration. In addition, elevated levels of cyclic adenosine monophosphate or its derivatives were associated with the blockage of allergen-mediated immunoglobulin E hypersensitivity, T-cell-mediated cytolysis, formation of migration inhibitory factor, activation of phagocytic cell function, and release of histamine, slow-reacting substances, and prostaglandins (38, 41–43). Furthermore, induced chronic arthritis was related to decreased cyclic adenosine monophosphate levels, increased lysosomal enzymatic activity, and release in the paw (44).

Helenalin, the most potent sesquiterpene lactone anti-inflammatory agent, as well as eupahyssopin and deoxyelephantopin, was observed to elevate the cyclic adenosine monophosphate level of mouse and rat liver significantly after *in vivo* administration whereas tenulin had little effect. The pseudoguaianolide sesquiterpene lactones, except the isotenulin series, significantly elevated the cyclic adenosine monophosphate levels of polymorphonuclear neutrophils whereas the germacranolide sesquiterpene lactones either had no effect or the opposite effect.

The mode of action of sesquiterpene lactones as anti-inflammatory agents appeared to be similar to commercially available agents. These agents were shown to be potent inhibitors of neutrophil migration, lysosomal rupture and enzymatic activity, and prostaglandin synthesis, which was linked to elevated cyclic adenosine monophosphate levels.

REFERENCES

(1) I. H. Hall, K. H. Lee, C. O. Starnes, Y. Sumida, R. Y. Wu, T. G. Waddell, J. W. Cochran, and K. G. Gerhart, *J. Pharm. Sci.*, **68**, 537 (1979).

(2) K. H. Lee and T. A. Geissman, *Phytochemistry*, **9**, 403 (1970).

(3) K. H. Lee, D. C. Anuforo, E. S. Huang, and C. Piantadosi, *J. Pharm. Sci.*, **61**, 626 (1972).

(4) I. H. Hall, K. H. Lee, E. C. Mar, C. O. Starnes, and T. G. Waddell, *J. Med. Chem.*, **20**, 333 (1971).

(5) R. A. Lucas, S. Rovinski, R. J. Kiesel, L. Dortman, and H. B. Mac Phillamy, *J. Org. Chem.*, **29**, 1549 (1964).
(6) K. H. Lee, T. Kimura, M. Haruna, A. T. McPhail, K. D. Onan, and H. C. Huang, *Phytochemistry*, **16**, 1068 (1977).
(7) K. H. Lee, T. Kimura, M. Okamoto, C. M. Cowherd, A. T. McPhail, and K. D. Onan, *Tetrahedron Lett.*, **14**, 1051 (1976).
(8) K. H. Lee, T. Ibuka, H. C. Huang, and D. L. Harris, *J. Pharm. Sci.*, **64**, 1077 (1975).
(9) K. H. Lee, H. Furukawa, M. Kozuka, H. C. Huang, P. A. Luchan, and A. T. McPhail, *J. Chem. Soc., Chem. Commun.*, **1973**, 476.
(10) A. T. McPhail, K. D. Onan, K. H. Lee, T. Ibuka, M. Kozuka, T. Shingu, and H. C. Huang, *Tetrahedron Lett.*, **1974**, 2739.
(11) K. H. Lee, C. M. Cowherd, and M. T. Walo, *J. Pharm. Sci.*, **64**, 1572 (1975).
(12) K. H. Lee, H. C. Huang, E. S. Huang, and H. Furukawa, *ibid.*, **61**, 629 (1972).
(13) K. H. Lee, T. Ibuka, A. T. McPhail, K. D. Onan, T. A. Geissman, and T. G. Waddell, *Tetrahedron Lett.*, **1974**, 1149.
(14) T. G. Waddell, A. M. Austin, J. W. Cochran, K. G. Gerhart, I. H. Hall, and K. H. Lee, *J. Pharm. Sci.*, **68**, 715 (1979).
(15) G. M. Ksander, J. E. McMurry, and M. Johnson, *J. Org. Chem.*, **42**, 1180 (1977).
(16) A. P. Roszkowski, W. H. Rooks, A. Tomolonis, and L. M. Miller, *J. Pharmacol. Exp. Ther.*, **179**, 114 (1971).
(17) C. A. Winter, E. A. Risley, and G. W. Nuss, *Proc. Soc. Exp. Biol. Med.*, **111**, 544 (1962).
(18) B. H. Waksman, C. M. Pearson, and J. T. Sharp, *J. Immunol.*, **85**, 403 (1960).
(19) D. English and B. R. Anderson, *J. Immunol. Methods*, **5**, 249 (1974).
(20) R. P. Orange, M. D. Valentine, and K. F. Austen, *J. Exp. Med.*, **127**, 767 (1968).
(21) I. H. Hall and G. L. Carlson, *J. Med. Chem.*, **19**, 1257 (1976).
(22) R. Gianetto and C. deDuve, *Biochem. J.*, **59**, 433 (1955).
(23) P. S. Chen, T. Y. Toribara, and H. Warner, *Anal. Chem.*, **28**, 1756 (1956).
(24) W. D. Schleuning and H. Fritz, *Methods Enzymol.*, **XLV**, 330 (1976).
(25) R. J. Smith, C. Sabin, H. Gilchrest, and S. Williams, *Biochem. Pharmacol.*, **25**, 2171 (1976).
(26) A. L. Steiner, D. M. Kipnis, R. Utiger, and C. Parker, *Proc. Natl. Acad. Sci. USA*, **64**, 367 (1969).
(27) R. V. Tomlinson, H. J. Ringold, M. C. Qureshi, and E. Forchielli, *Biochem. Biophys. Res. Commun.*, **46**, 552 (1972).
(28) M. Glatt, H. Kälin, K. Watner, and K. Borene, *Agents Action*, **7**, 321 (1977).
(29) R. D. Nelson, P. G. Quie, and R. L. Simmons, *J. Immunol.*, **115**, 1650 (1975).
(30) C. Deby, Z. M. Bacq, and P. Van Cuneghem, in "Perspectives in Inflammation;" D. A. Willoughby, J. P. Givoud, and G. P. Velo, Eds., University Park Press, Baltimore, Md., 1977, p. 339.
(31) M. W. Whitehouse and P. D. G. Dean, *Biochem. Pharmacol.*, **14**, 557 (1965).
(32) M. W. Whitehouse and J. M. Haslam, *Nature*, **196**, 1323 (1962).
(33) R. E. Bryant, R. M. de Prez, M. H. Van Way, and D. E. Roger, *J. Exp. Med.*, **124**, 483 (1966).
(34) P. C. Wilkinson, "Chemotaxis and Inflammation," Churchill and Livingstone, London, England, 1974, pp. 62, 63.
(35) O. Rojas-Espinosa and A. M. Dannenberg, in "Inflammation and Anti-inflammatory Therapy," G. Katona and J. R. Blengio, Eds., Spectrum, New York, N.Y., 1974, p. 31.
(36) M. A. Verity and W. J. Brown, *Biochim. Biophys. Acta*, **151**, 289 (1968).
(37) E. M. Press, R. R. Porter, and J. Cebra, *Biochem. J.*, **74**, 501 (1960).
(38) E. Arrigoni-Martelli, "Inflammation and Anti-inflammatories," Spectrum, New York, N.Y., 1977, pp. 85–98.
(39) I. Rivikin and E. L. Becker, *Fed. Proc. Fed. Am. Soc. Exp. Biol.*, **31**, 657 (1972).
(40) R. L. Tse, P. Phelps, and D. Urban, *J. Lab. Clin. Med.*, **80**, 264 (1972).
(41) H. R. Borene, L. M. Lichtenstein, K. L. Melmon, C. S. Henney, Y. Weinstein, and G. M. Shearer, *Science*, **184**, 19 (1974).
(42) M. Kalimer and K. F. Austin, *Biochem. Pharmacol.*, **23**, 763 (1974).
(43) C. W. Parker, T. J. Sullivan, and H. J. Wedner, *Adv. Cycl. Nucleotides*, **4**, 1 (1974).
(44) M. J. Parnhem, I. L. Bonta, and M. J. P. Adolfs, in "Perspectives in Inflammation," D. A. Willoughby, J. P. Giroud, and G. P. Velo, Eds., University Park Press, Baltimore, Md., 1977, pp. 279–287.

ACKNOWLEDGMENTS

Supported by University of North Carolina Research Council Grant VF 475 (awarded to I. H. Hall); National Institutes of Health Grant CA-17625 and American Cancer Society Grants CH-19A, CH-19B, and CH-19C (awarded to K. H. Lee); and a Research Corporation of America grant and an American Chemical Society grant (awarded to T. G. Waddell).

Aspirin—A National Survey I: Semiautomated Determination of Aspirin in Bulk and Tablet Formulations and Salicylic Acid in Tablet Formulations

WILLIAM E. JUHL ˣ **and ROSS D. KIRCHHOEFER**

Received October 29, 1979, from the *National Center for Drug Analysis, Food and Drug Administration, St. Louis, MO 63101.* Accepted for publication December 14, 1979.

Abstract □ A semiautomated assay to determine aspirin (acetylsalicylic acid) in aspirin tablets, powdered tablet composites, and pure drug substances is presented. The sample was dissolved in alcoholic buffer, diluted, and extracted with chloroform. The absorbance of the chloroform solution was read at 280 nm. Results obtained by the USP XIX and semiautomated methods are compared. The proposed method is accurate and precise, and common excipients do not interfere. Recoveries of 100% were obtained. A semiautomated assay for salicylic acid in aspirin tablets also is presented. The sample was dissolved in alcoholic buffer, ferric nitrate was added, and the absorbance of the resulting purple color was read at 532 nm. The method is suitable as a rapid screening procedure for testing the salicylic acid content of aspirin products. Results obtained by the USP XIX and semiautomated methods are compared, and the accuracy and precision of the proposed method are given. One hundred seventy tablet samples and 34 bulk drug substances were analyzed for aspirin and salicylic acid content. Approximately 5% of the tablet samples failed to meet the USP XIX limits for aspirin content, and 10% failed to meet the limits for salicylic acid.

Keyphrases □ Salicylic acid—semiautomated colorimetric determination in tablet formulations □ Analgesics—determination of aspirin and salicylic acid □ Aspirin—semiautomated UV determination in bulk and tablet formulations

A national survey of aspirin products and formulations was conducted in this laboratory. The survey consisted of the analysis of 170 samples of tablets, representing 58 formulations from 38 manufacturers, and 34 samples of bulk aspirin from 12 manufacturers. The purpose was to evaluate the quality of aspirin products on the market and the adequacy of present standards. Methodology was developed in these laboratories for the semiautomated analysis of the content uniformity test for aspirin (acetylsalicylic acid) and the limit test for salicylic acid, for the determination of impurities (1) and salicylic acid by high-pressure liquid chromatography (HPLC) (2), and for the determination of dissolution rates using semiautomated procedures (3). This paper presents the data on the determination of aspirin and salicylic acid.

Previously developed methods (4–11), including semiautomated procedures for the determination of aspirin (4, 5), were rejected for various reasons. The method of Hubin and Ganshirt (4) was not suitable because it involves the hydrolysis of aspirin itself. The method of Oydvin and Sapiraa (5) was not tried because it involves the use of chloroform, which is not a practical solvent to use in a semiautomated system with a liquid sampler. The Clayton and Thiers (6) manual spectrophotometric procedure determines up to five compounds simultaneously and thus appeared to be too complicated to automate. Other methods were eliminated because of the described problems or other practical considerations.

This paper describes a semiautomated UV method for the determination of aspirin and a semiautomated colorimetric method for the determination of salicylic acid. The aspirin method is applicable to plain and buffered tablets, powdered composites, and bulk drug substances and is free from the influence of excipient interferences. The salicylic acid procedure is based on the method of Cullen *et al.* (12) and can be used as a rapid screening assay. This method is applicable to plain, buffered, and pediatric aspirin tablets. Results are compared with the official USP XIX (13) procedures.

EXPERIMENTAL

Aspirin

Apparatus—An automatic analyzer with a sampler[1], pump[2], manifold, and timer[3] was used. The manifold was connected to a spectrophotometer[4] equipped with a quartz flowcell[5]. A 100-mv recorder[6] was connected to the spectrophotometer.

Reagents—Ethanol, 95%, was used. Chloroform, ACS grade, was washed with water and filtered through paper on the day of use. The pH 2.2 buffer solution was prepared by diluting 250.0 ml of 0.2 *M* KCl and 39.0 ml of 0.2 *M* HCl to 1 liter with water. The 0.2 *M* KCl was prepared by dissolving 14.911 g of potassium chloride in water and diluting to 1 liter with water. The 0.2 *M* HCl was prepared by diluting 17.0 ml of concentrated hydrochloric acid to 1 liter with water. The buffer–ethanol solution was prepared by mixing equal volumes of pH 2.2 buffer solution and ethanol.

Standard Preparation—About 324 mg of USP aspirin reference standard was weighed accurately and dissolved in 50.0 ml of buffer–ethanol (1:1). It was prepared fresh daily.

Sample Preparation—*324-mg Tablets*—One tablet was placed in a snap-cap vial or erlenmeyer flask. Three or four drops of water were placed on each tablet, and 50.0 ml of buffer–ethanol (1:1) was added. The solution was shaken or treated ultrasonically until the tablet disintegrated. Samples were analyzed within 6 hr of preparation. For buffered tablets, 1 ml of dilute hydrochloric acid (15:85 v/v) was added.

Powdered Composites or Bulk Drug Substances—An amount equivalent to 325 mg of aspirin was dissolved in 50.0 ml of buffer–ethanol (1:1). The sample was shaken mechanically or placed in an ultrasonic generator for ~5 min.

Semiautomated Determination—The automated system was assembled as shown in Fig. 1. The solutions were sampled at a rate of 30 cups/hr with a sample-to-wash ratio of 2:1. A sampling pattern of three standards, five samples, one standard, five samples, *etc.*, was used. Two cups of standard were placed at the end. The first two standards and the last standard were not included in the calculations. A polytetrafluoroethylene[7] strip was inserted into the BO fitting to direct the organic phase downward.

To start the system, ethanol was pumped through the chloroform pump tube for 5 min and then the tube was pumped dry. The chloroform line

[1] AutoAnalyzer sampler II, 127A000, Technicon Instruments Corp., Tarrytown, NY 10591.

[2] AutoAnalyzer proportioning pump III, 133-A014-04, Technicon Instruments Corp., Tarrytown, NY 10591.

[3] Flexopulse, model HG93A603, Eagle Signal Timer Division, Gulf Western Industries, Davenport, IA 52803 (14).

[4] Model DBGT, Beckman Instruments, Fullerton, CA 92634.

[5] The length was 10 mm and the capacity was 0.25 ml; model 8495-L10, Arthur H. Thomas Co., Philadelphia, PA 19105.

[6] Servo-Riter II, PS01W6A, Texas Instruments Inc., Houston, TX 77001.

[7] Teflon.

0022-3549/80/0500-0544$01.00/0
© 1980, American Pharmaceutical Association

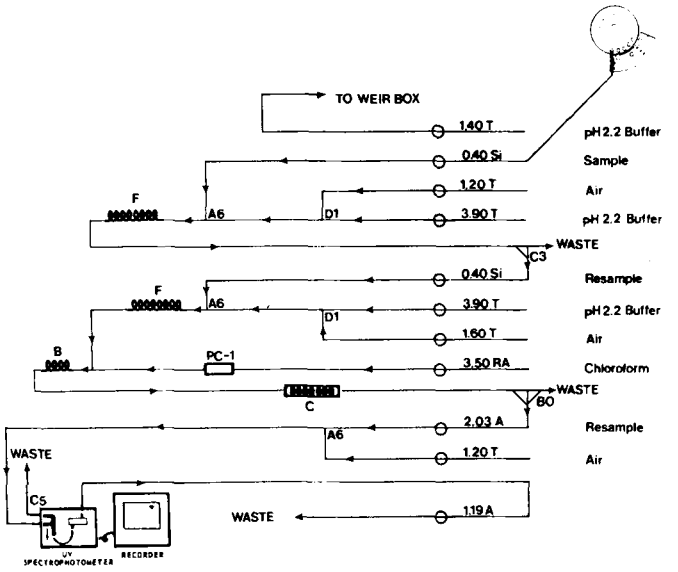

Figure 1—*Flow diagram of an automated system for aspirin. Key: Si, silicon pump tube; T, Tygon pump tube; RA, red Acidflex pump tube; A, Acidflex pump tube; F, 28-turn × 2.4-mm i.d. mixing coil; B, 28-turn × 2.4-mm i.d. mixing coil with one double end; and C, 5.5-turn settling coil.*

was placed in its solution and pumped until the solution reached the spectrophotometer cell. The pH 2.2 buffer line was placed in its solution, and the system was allowed to equilibrate. In the manifold, the sample stream was diluted twice with pH 2.2 buffer and chloroform was added. The chloroform containing the extracted drug was pumped through a flowcell, and the absorbance of the drug was read at 280 nm.

Salicylic Acid

Apparatus—The same type of automatic analyzer was connected to a spectrophotometer[8] equipped with a quartz flowcell[9] and a 100-mv recorder[6].

Reagents—Ethanol, 95%, was used. The pH 2.2 buffer solution was prepared as described. The ferric nitrate hexahydrate was prepared by adding 10 g of ferric nitrate and 5.0 ml of concentrated nitric acid to a 1-liter volumetric flask and diluting to volume with water.

Standard Preparation—*Plain Tablets*—About 20 mg of salicylic acid standard was weighed accurately and dissolved in 100 ml of pH 2.2 buffer–ethanol (3:1).

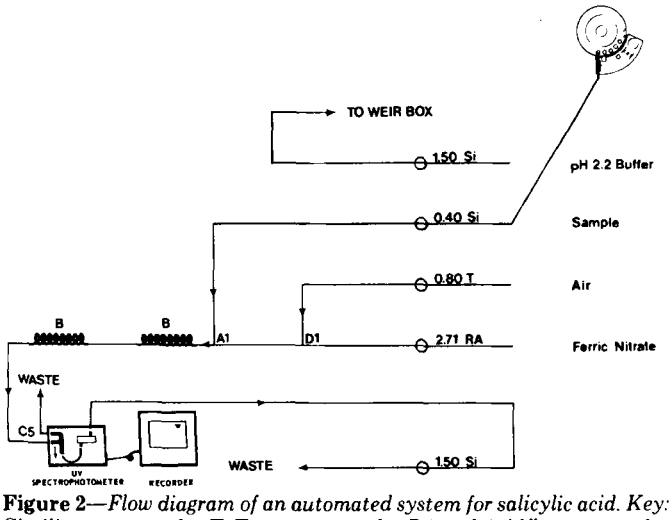

Figure 2—*Flow diagram of an automated system for salicylic acid. Key: Si, silicon pump tube; T, Tygon pump tube; RA, red Acidflex pump tube; and B, 28-turn × 2.4-mm i.d. mixing coil.*

[8] Model PM2DL, Carl Zeiss, Oberkochen, West Germany.

[9] The length was 10 mm and the capacity was 18 μl (model 886881), or the length was 10 mm and the capacity was 80 μl (model 886878); Beckman Instruments, Fullerton, CA 92634.

Table I—Comparison of Results (Percent of Label Claim) Obtained by USP XIX and Automated Procedures for Aspirin in Aspirin Tablets

Tablet	USP[a]	Automated[b]
324 mg, plain	101.2	101.5 (1.11, 1.09)[c]
324 mg, plain	97.9	99.0 (0.69, 0.70)
324 mg, buffered	98.2	100.1 (1.36, 1.36)
324 mg, buffered	95.3	94.2 (0.75, 0.79)
81 mg, pediatric	103.3	103.3 (0.75, 0.73)
81 mg, pediatric	105.4	106.1 (1.08, 1.01)

[a] Average of four results. [b] Average of 10 results. [c] Values in parentheses are standard deviations and coefficients of variation, respectively.

Buffered Tablets—About 200 mg of salicylic acid standard was weighed accurately and dissolved in 100 ml of pH 2.2 buffer–ethanol (3:1).

Sample Preparation—*Plain Tablets*—Ten tablets were placed in an erlenmeyer flask, 25 ml of buffer–ethanol (1:1) was added, and the flask was shaken for 5 min. Then 25 ml of pH 2.2 buffer was added and mixed. The solution was filtered through paper, and the first 10 ml was discarded.

Buffered Tablets—Ten tablets were placed in an erlenmeyer flask, 10 ml of ethanol was added, and the flask was shaken for 5 min. Then 40 ml of pH 2.2 buffer was added and mixed. The solution was filtered through paper, and the first 10 ml was discarded.

Semiautomated Determination—The automated system was assembled as shown in Fig. 2. The solutions were sampled at a rate of 30 cups/hr with a sample-to-wash ratio of 2:1. A sampling pattern of three standards, two samples, and two standards was used. The first two standards and the last standard were not included in the calculation.

To start the system, the pH 2.2 buffer and ferric nitrate reagent lines were placed in their respective solutions and the pump was started. The sample stream was introduced and then segmented with air, and ferric nitrate reagent was added. The absorbance of the colored solution was read at 532 nm.

RESULTS AND DISCUSSION

Aspirin—*Validation Tests*—A series of validation tests was performed on the automated system. A linear response was obtained when four standard solutions containing 3–13 mg of aspirin/ml (corresponding to 50–200% of declaration) were tested. A standard solution containing 6.5 mg of aspirin/ml gave reproducible peaks whose heights reached ~95% of the steady state. The assay of 20 individual cups of solution exhibited a relative standard deviation of 1.0%.

Hydrolysis—There was concern that the aspirin might hydrolyze to salicylic acid in the solvent, thus giving erroneous results. A sample solution of powdered aspirin tablet composite was prepared and assayed with freshly prepared aspirin standard solutions for 6 hr, and the assay results did not change significantly.

Composite Assays—Portions of tablet composites equivalent to single tablets were analyzed by the proposed method and the USP XIX (13) method. The ground tablet composites were prepared from available commercial samples. Table I shows the close agreement between the two methods and the precision of the automated procedure.

Interferences—Separate tests were performed to check for interferences from impurities, dyes, and common excipients. Two known impurities and one postulated impurity from aspirin formulations were tested: acetylsalicylsalicylic acid, acetylsalicylic anhydride, and *O*-salicylsalicylic acid. The interferences by impurities were measured by spiking standard solutions of aspirin with weighed amounts of each im-

Table II—Comparison of Results (Percent of Label Claim) Obtained by USP XIX and Automated Procedures for Salicylic Acid in Aspirin Tablets

Tablet	USP[a]	Automated[a,b]
324 mg, plain	0.073	0.089 (0.01)
324 mg, plain	0.036	0.050 (0.01)
324 mg, buffered	0.580	0.420 (0.05)
324 mg, buffered	3.400	3.480 (0.14)
81 mg, pediatric	0.230	0.620 (0.02)
81 mg, pediatric	0.264	0.421 (0.01)

[a] Average of three or more determinations. [b] Values in parentheses are standard deviations.

Table III—National Survey Results (Percent of Label Claim) for Aspirin and Salicylic Acid Determined by Automated and USP XIX Procedures

Manufacturer[a]	Type of Sample	Aspirin		Salicylic Acid	
		Automated[b]	USP	Automated[c]	USP
A	324-mg tablet	100.2 (2.2)		0.06	
	324-mg tablet	99.7 (2.3)		0.08	
	324-mg tablet	99.4 (2.2)		0.08	
	324-mg tablet	100.3 (2.2)		0.09	
	Bulk (10% starch)	89.5		—[d]	
B	Bulk (10% starch)	90.1		—[d]	
	324-mg tablet	100.1 (1.1)		0.16	
	324-mg tablet	102.0 (2.2)		0.22	
	421-mg tablet	101.5 (2.7)		0.14	
	421-mg tablet	100.3 (1.9)		0.19	
C	Bulk	99.7		—[d]	
	Bulk (10% starch)	90.3		—[d]	
	81-mg tablet	104.0 (2.9)		1.23	0.6
	324-mg tablet	98.7 (2.1)		0.07	
	324-mg tablet	100.5 (1.1)		0.04	
	324-mg tablet	98.6 (3.1)		0.07	
	324-mg tablet	102.0 (1.2)		0.05	
	160-mg tablet	100.6 (4.1)		0.78	
	324-mg tablet	97.2 (2.4)		0.05	
	324-mg tablet	101.4 (2.1)		0.15	
D	486-mg tablet[e]	99.1 (2.8)		0.24	
	486-mg tablet[e]	96.6 (3.0)		0.22	
	486-mg tablet[e]	94.4 (2.5)	92.0	0.33	
	486-mg tablet[e]	94.4 (3.6)	90.5	0.43	
	486-mg tablet[e]	98.1 (2.4)		0.32	
	324-mg tablet	95.8 (2.4)		0.35	
	324-mg tablet	101.4 (3.0)		0.46	
	324-mg tablet	97.6 (2.3)		0.42	
	324-mg tablet	97.8 (2.7)		0.36	
	Bulk	100.0		—[d]	
E	324-mg tablet	98.4 (4.2)		3.30	
F	Bulk (10% starch)	89.5		—[d]	
	324-mg tablet[e]	95.8 (2.3)		5.30	7.8
	324-mg tablet[e]	95.0 (4.3)	94.6	5.00	4.0
	324-mg tablet[e]	94.9 (3.1)	94.5	4.30	3.2
G	324-mg tablet	98.4 (2.1)		0.03	
	324-mg tablet	99.4 (1.7)		0.04	
	324-mg tablet	99.4 (2.2)		0.04	
H	81-mg tablet	99.2 (4.5)		0.54	
	Bulk	100.0		—[d]	
	Bulk	99.8		—[d]	
	324-mg tablet	100.5 (2.4)		0.03	
	324-mg tablet	100.4 (3.8)		0.03	
	324-mg tablet	98.2 (2.6)		0.03	
	324-mg tablet	97.0 (2.9)		0.03	
	324-mg tablet	99.7 (5.0)		0.03	
	81-mg tablet	99.9 (4.7)		0.24	
	81-mg tablet	104.6 (3.2)		0.40	1.0
I	81-mg tablet	99.6 (2.9)		2.70	2.5
	324-mg tablet	100.2 (1.3)		0.10	
	324-mg tablet	100.7 (2.9)		0.09	
	324-mg tablet	100.8 (1.8)		0.05	
	324-mg tablet	100.0 (1.3)		0.07	
J	324-mg tablet	100.1 (2.4)		2.07	
	Bulk (10% starch)	90.4		0.46	
K	Bulk	100.3		—[d]	
	324-mg tablet	101.6 (1.1)		0.04	
	324-mg tablet	100.7 (1.4)		1.87	
	81-mg tablet	80.4 (3.6)	79.4	2.07	1.5
	81-mg tablet	104.1 (4.2)		0.46	0.5
L	324-mg tablet[e]	101.4 (5.4)		2.20	
	324-mg tablet[e]	97.8 (3.1)		1.51	
	324-mg tablet[e]	97.2 (2.7)		1.68	
M	324-mg tablet	98.6 (2.0)		0.04	
N	324-mg tablet	97.9 (2.9)		0.06	
	324-mg tablet	97.9 (1.9)		0.05	
	324-mg tablet	97.0 (2.1)		0.04	
	Bulk	100.3		—[d]	
	324-mg tablet	96.7 (2.2)		0.05	
O	324-mg tablet	99.3 (2.7)		0.07	
	Bulk (10% starch)	89.5		0.28	
	324-mg tablet[e]	97.4 (1.8)		0.28	
	Bulk (10% starch)	90.0		—[d]	
P	324-mg tablet	98.1 (2.3)		0.07	
Q	Bulk	99.8		—[d]	
	324-mg tablet	97.7 (1.6)		0.40	0.3
	324-mg tablet	99.3 (1.9)		0.10	
	324-mg tablet	98.1 (1.8)		0.33	
R	324-mg tablet	100.6 (3.0)		0.07	
	324-mg tablet	99.4 (3.0)		0.08	
	324-mg tablet	103.1 (3.6)		0.14	
	324-mg tablet	101.8 (1.6)		0.06	
	324-mg tablet	101.3 (1.8)		0.10	
	Bulk	99.5		—[d]	
S	Bulk	99.5		—[d]	
	324-mg tablet	98.8 (2.1)		0.08	
	324-mg tablet	103.1 (3.3)		0.07	
	324-mg tablet	100.5 (1.8)		0.06	
	324-mg tablet	101.1 (3.2)		0.07	
	324-mg tablet	100.3 (2.0)		0.06	
	324-mg tablet	100.2 (1.9)		0.08	
	324-mg tablet	100.2 (1.9)		0.09	
	324-mg tablet	99.1 (2.2)		0.07	
	324-mg tablet	101.8 (2.0)		0.08	
	324-mg tablet	100.7 (2.1)		0.06	
T	81-mg tablet	102.3 (1.9)		0.26	0.5
	Bulk	99.8		—[d]	
	324-mg tablet[e]	96.9 (2.9)		2.00	
	324-mg tablet[e]	98.1 (3.2)		1.60	
	324-mg tablet[e]	97.9 (3.8)		1.13	
	Bulk (10% starch)	90.9		—[d]	
	324-mg tablet	97.8 (3.9)		—[f]	
	81-mg tablet	103.5 (2.0)		0.36	
U	324-mg tablet[e]	98.7 (3.7)		2.10	
	324-mg tablet[e]	99.6 (3.0)		3.70	4.1
	324-mg tablet[e]	99.0 (3.3)		3.10	
	324-mg tablet[e]	105.4 (3.9)	104.8	1.10	
	324-mg tablet[e]	101.2 (3.4)		1.80	
	81-mg tablet	100.7 (3.1)		0.40	0.6
	81-mg tablet	103.1 (4.8)		0.50	0.5
	81-mg tablet	104.5 (5.0)	100.4	0.50	0.4
	81-mg tablet	100.9 (3.8)		0.50	0.4
V	324-mg tablet[e]	97.5 (2.3)		0.77	
	324-mg tablet[e]	96.7 (2.5)		0.44	
	324-mg tablet[e]	96.6 (2.3)		0.68	
	324-mg tablet[e]	96.7 (2.3)		0.61	
	324-mg tablet[e]	98.4 (2.0)		0.50	
	81-mg tablet	102.8 (3.2)		0.62	0.6
	81-mg tablet	101.0 (3.0)		0.64	0.6
	81-mg tablet	99.3 (2.1)		0.59	0.6
	81-mg tablet	102.1 (2.4)		0.58	0.6
	Bulk (10% starch)	89.8		—[d]	
	Bulk	100.4		—[d]	
W	324-mg tablet	95.3 (5.2)		0.99	1.2
	324-mg tablet	103.0 (3.2)		0.09	
	Bulk	99.7		—[d]	
	324-mg tablet	98.0 (1.3)		0.05	
X	324-mg tablet	100.7 (1.4)		0.04	
	324-mg tablet	100.9 (1.6)		0.03	
	324-mg tablet	100.9 (1.5)		0.04	
	324-mg tablet	101.8 (1.4)		0.04	
	81-mg tablet	100.7 (2.4)		0.21	
	81-mg tablet	101.1 (2.6)		0.20	
	81-mg tablet	100.5 (2.8)		0.21	
	81-mg tablet	98.2 (2.6)		0.21	
	81-mg tablet	98.2 (2.1)		0.20	
	Bulk	99.5		—[d]	
	Bulk	99.5		—[d]	
Y	81-mg tablet	97.9 (2.5)		0.30	
	648-mg tablet	100.8 (2.0)		0.14	
	324-mg tablet	99.6 (1.6)		0.19	
	Bulk	99.8		—[d]	
	648-mg tablet	99.6 (1.4)		0.14	
	324-mg tablet	98.9 (1.9)		0.11	
	486-mg tablet	95.8 (2.0)		—[f]	
	324-mg tablet	98.3 (2.2)		0.12	
Z	Bulk	99.9		—[d]	
	324-mg tablet	96.2 (3.2)		0.08	
	486-mg tablet	98.4 (3.4)		0.03	
	486-mg tablet	98.8 (3.8)		0.07	
AA	Bulk (10% starch)	89.3		—[d]	
	300-mg tablet	101.9 (2.6)		0.24	0.2
	81-mg tablet	97.8 (3.3)		0.31	
BB	324-mg tablet	101.6 (2.1)		0.40	
	Bulk	99.9		—[d]	
CC	Bulk (10% starch)	88.0		—[d]	
	324-mg tablet[e]	99.3 (4.7)		0.90	
	324-mg tablet[e]	97.7 (3.0)		1.20	

(continued)

Table III—*Continued*

Manufacturer[a]	Type of Sample	Aspirin Automated[b]	Aspirin USP	Salicylic Acid Automated[c]	Salicylic Acid USP
DD	324-mg tablet[e]	98.9 (2.2)		2.03	
	324-mg tablet[e]	96.6 (3.2)		1.23	
	324-mg tablet[e]	98.1 (2.4)		2.90	
EE	81-mg tablet	100.7 (1.8)		0.14	
	81-mg tablet	100.6 (4.0)		0.15	
	81-mg tablet	100.9 (2.7)		0.19	
	81-mg tablet	100.8 (2.3)		0.18	
	325-mg tablet	101.6 (1.7)		0.06	
	325-mg tablet	101.9 (1.4)		0.06	
	325-mg tablet	101.2 (1.5)		0.05	
	325-mg tablet	100.6 (2.0)		0.04	
	325-mg tablet	100.0 (1.8)		0.05	
	Bulk	100.4		—[d]	
FF	324-mg tablet	100.0 (2.0)		0.08	
	324-mg tablet	100.2 (2.2)		0.06	
	324-mg tablet	97.8 (2.5)		0.06	
	324-mg tablet	98.9 (2.1)		0.09	
	Bulk (10% starch)	91.4		—[d]	
GG	324-mg tablet[e]	97.9 (3.1)		1.34	
	324-mg tablet[e]	97.0 (3.7)		2.03	
	81-mg tablet	104.0 (3.5)		0.27	
	Bulk	78.3		—[d]	
	324-mg tablet[e]	97.9 (1.9)		1.13	
	81-mg tablet	97.8 (2.7)		0.61	
	324-mg tablet	97.2 (2.0)		0.35	
HH	320-mg tablet	99.4 (2.0)		0.04	
	320-mg tablet	98.6 (2.0)		0.05	
	65-mg tablet	99.9 (2.5)		0.32	
	Bulk (10% starch)	89.5		—[d]	
II	324-mg tablet	97.4 (2.5)		0.51	
	324-mg tablet	99.8 (3.1)		0.65	
	Bulk	80.7		—[d]	
JJ	324-mg tablet	98.5 (2.3)		0.07	
	81-mg tablet	97.0 (1.8)		0.28	
	81-mg tablet	97.7 (1.8)		0.29	
	324-mg tablet	101.9 (3.0)		0.04	
	324-mg tablet[e]	99.4 (1.9)		0.04	
KK	486-mg tablet[e]	102.4 (3.4)		0.87	
	486-mg tablet[e]	101.7 (3.1)		0.96	
	486-mg tablet[e]	100.0 (2.0)		0.45	
	486-mg tablet[e]	99.4 (2.8)		0.71	
	486-mg tablet[e]	100.4 (2.6)		0.84	
LL	325-mg tablet[e]	95.9 (3.5)		1.13	
	Bulk	100.3		—[d]	
	325-mg tablet[e]	97.3 (2.4)		1.22	
	325-mg tablet[e]	97.4 (3.4)		1.03	

[a] A = Bell Pharmacal, Greenville, S.C.; B = Block Drug Co., Memphis, Tenn.; C = Bowman Pharmaceuticals, Canton, Ohio; D = Bristol-Myers Co., New York, N.Y.; E = Chromalloy American Corp., Culver City, Calif.; F = Otis Clapp & Sons, Boston, Mass.; G = Cord Laboratories, Detroit, Mich.; H = Davis Manufacturing Co., Knoxville, Tenn.; I = Dewey Products Co., Grand Rapids, Mich.; J = Ferndale Laboratories, Ferndale, Mich.; K = Freeda Vitamins, New York, N.Y.; L = ICN Pharmaceuticals, Cincinnati, Ohio; M = Lannett Co., Philadelphia, Pa.; N = Eli Lilly & Co., Indianapolis, Ind.; O = Mallard, Detroit, Mich.; P = Manhattan Drug Co., Hillside, N.J.; Q = Marshall Pharmacal Corp., South Hackensack, N.J.; R = McKesson Laboratories, Fairfield, Conn.; S = Norwich-Eaton Pharmaceuticals, Norwich, N.Y.; T = Oak Park Pharmaceuticals, Fredonia, Wis.; U = Pennex Products Co., Pittsburg, Pa.; V = L. Perrigo Co., Allegan, Mich.; W = Pill Mill, Grand Rapids, Mich.; X = Plough, Memphis, Tenn.; Y = Rexall Drug Co., St. Louis, Mo.; Z = Richlyn Laboratories, Philadelphia, Pa.; AA = Sein-Mendez Labs, Rio Piedas, Puerto Rico; BB = Stanback Co., Salisbury, N.C.; CC = Standard Pharmacal Co., Chicago, Ill.; DD = Stanley Laboratories, Portland, Ore.; EE = Sterling Drug, New York, N.Y.; FF = E. R. Squibb & Sons, New York, N.Y.; GG = Sun Laboratories, Portland, Ore.; HH = Vale Chemical Co., Allentown, Pa.; II = Walgreen Co., Chicago, Ill.; JJ = West-Ward, Eatontown, N.J.; KK = Whitehall Laboratories, New York, N.Y.; and LL = Zenith Laboratories, Hoboken, N.J. [b] Average of 30 results for tablets and one assay for bulk formulations. Numbers in parentheses are standard deviations. [c] Composite assays, 10 tablets. [d] Not determined by automated method. [e] Buffered tablets. [f] No result obtained.

purity and comparing the response with that from the standard solution. No interferences were found.

Colorimetric interference from the dye in a manufactured tablet was checked by adding chloroform to an aqueous sample solution of the tablet in a separator and shaking manually. All of the color from the dye remained in the aqueous layer. Since the drug is extracted into the chloroform layer on the automated system, there is no interference from the dye at 280 nm.

Common excipients were examined and found not to interfere. A recovery of 99.9% was obtained with a mixture of 90% aspirin and 10% starch. A mixture of aspirin, cornstarch, lactose, and magnesium stearate gave a recovery of 99.8%. With a mixture of aspirin and magnesium carbonate, the recovery was 101.0%.

Evaporation Test—Since 50% ethanol was the sample solvent, the possibility of evaporation during the time required to analyze a number of solutions on the automated system was investigated. Twenty cups of a sample solution were loaded on the system and analyzed, and then three fresh cups were loaded just after sampling the 20th cup. There was no difference in absorbance between the first 20 cups and the last three cups. Thus, there was little evaporation over a 1-hr period.

Solvent Selection—Several solvents were tested for this method, including 95% ethanol, pH 2.2 buffer–ethanol (1:1), and buffer–ethanol (3:1). Results indicated that the buffer–ethanol (1:1) was the best solvent. If the alcohol concentration was too low, the aspirin did not completely dissolve. If the pH of the sample solution was too high, aspirin was hydrolyzed to salicylic acid.

Buffered Aspirin Preparation—With some buffered aspirin formulations, it was necessary to add acid to decrease the pH of the solution to that of the standard solution to prevent low recoveries. Usually 1 ml of dilute hydrochloric acid was sufficient.

Salicylic Acid—*Validation Tests*—A series of validation tests was performed on the automated system. A linear response was obtained when solutions of salicylic acid standard containing 0.1–0.4 and 1.0–4.0 mg/ml were tested. The absorbance of 30 individual cups of solution exhibited a relative standard deviation of 1.4%.

Composite Assays—Portions of tablet composites equivalent to 10 tablets were analyzed by the proposed method and the USP XIX method. The ground tablet composites were prepared from available commercial samples. Table II shows the results obtained by both methods and the precision of the automated procedure.

Recovery of Standards—Recovery assays, using the proposed method, were made on simulated mixtures of aspirin based on the manufacturers' formulations. Recoveries were obtained by spiking standard solutions of salicylic acid with weighed amounts of excipient materials and comparing the results with those from the standard solution. A recovery of 101.0% salicylic acid was obtained from a mixture of 90% aspirin and 10% starch. A mixture of aspirin, cornstarch, lactose, and magnesium stearate gave a recovery of 100.7% salicylic acid.

Interferences—Interference from the impurities acetylsalicylsalicylic acid, acetylsalicylic anhydride, and *O*-salicylsalicylic acid was measured by spiking standard solutions of salicylic acid with weighed amounts of each impurity and comparing the response with that of the standard solution. No impurity interference was found.

Solvent Selection—Aspirin is stable at pH 2.2 but is not very soluble in a pH 2.2 buffer; ethanol is needed to increase the solubility. When a solvent containing >25% ethanol was used, a brown hazy solution resulted when the ferric nitrate reagent was added. Cullen *et al.* (12) reported that a violet color resulted with the addition of ferric nitrate. A series of tests using different percentages of ethanol was performed to obtain the violet color. As a result, 25% ethanol in pH 2.2 buffer was selected as the solvent. Buffered tablets first were dissolved in 95% ethanol. When they were dissolved in 50% ethanol, a mass of undissolved flocculent material formed, which made it difficult to obtain sufficient filtered solution for analysis on the automated system.

Sensitivity Adjustment—Different levels of salicylic acid were found in plain as opposed to buffered tablets. Therefore, it was necessary to use a spectrophotometer with adjustable sensitivity.

Filtering—All solutions of plain or buffered tablets were filtered through paper since insoluble excipient materials present in the sample solutions interfered with the automated procedure.

Hydrolysis—Because of possible hydrolysis of the aspirin to salicylic acid in the solvent, tests were performed to check the hydrolysis. Aspirin was added to a standard salicylic acid solution, and this solution was compared to the unspiked standard solution. There was no detectable hydrolysis on the automated system. To limit the hydrolysis that would occur with time, all solutions were analyzed within 30 min after the solvent addition to the tablets.

Table III lists the results obtained from the national survey by the automated methods for aspirin and salicylic acid. It also shows comparisons with the USP methods for some samples. One hundred seventy tablet samples were analyzed for aspirin and salicylic acid content, and 34 bulk drug substances were analyzed for aspirin content. Four tablet samples failed to meet the USP XIX limits for aspirin content. Eighteen tablet samples failed to meet the USP XIX limits for salicylic acid content.

REFERENCES

(1) R. D. Kirchhoefer, J. C. Reepmeyer, and W. E. Juhl, *J. Pharm. Sci.*, **69**, 550 (1980).

(2) R. D. Kirchhoefer and W. E. Juhl, *ibid.*, **69**, 548 (1980).
(3) W. E. Juhl and R. D. Kirchhoefer, *ibid.*, in press.
(4) V. H. Hubin and H. Ganshirt, *Pharm. Ind.*, **38**, 224 (1976).
(5) H. Oydvin and O. E. Sapiraa, *Medd. Nor. Farm. Selsk.*, **37**, 115 (1975).
(6) A. W. Clayton and R. E. Thiers, *J. Pharm. Sci.*, **55**, 404 (1966).
(7) G. H. Schenk, F. H. Boyer, C. I. Miles, and D. R. Wirtz, *Anal. Chem.*, **44**, 1593 (1972).
(8) R. D. Deodhar, M. R. Shastri, and R. C. Mehta, *Indian J. Pharm.*, **38**, 18 (1975).
(9) C. I. Miles and G. H. Schenk, *Anal. Chem.*, **42**, 650 (1970).
(10) N. Shane and R. Stillman, *J. Pharm. Sci.*, **60**, 114 (1971).
(11) N. Shane and D. Meele, *ibid.*, **59**, 397 (1970).
(12) L. F. Cullen, D. L. Packman, and G. J. Papariello, *Ann. N.Y. Acad. Sci.*, **153**, 525 (1968).
(13) "The United States Pharmacopeia," 19th rev., Mack Publishing Co., Easton, Pa., 1975, p. 39.
(14) J. W. Myrick and W. B. Furman, Laboratory Information Bulletin No. 1640, Food and Drug Administration, Washington, D.C., 1974.

ACKNOWLEDGMENTS

The authors thank Margaret Randall, John Gleason, Rudolph Kulousek, Everett Jefferson, and Brian Keller for technical assistance and Donald P. Page and William B. Furman for editorial assistance.

Aspirin—A National Survey II: Determination of Salicylic Acid in Bulk Aspirin and Aspirin Formulations by High-Pressure Liquid Chromatography Using a Fluorescence Detector

ROSS D. KIRCHHOEFER ˣ **and WILLIAM E. JUHL**

Received October 29, 1979, from the *National Center for Drug Analysis, Food and Drug Administration, St. Louis, MO 63101.* Accepted for publication December 14, 1979.

Abstract □ A quantitative high-pressure liquid chromatographic method, using a reversed-phase column coupled to a fluorescence detector, was developed to determine salicylic acid in bulk aspirin and plain and buffered aspirin tablets. The aspirin was dissolved, filtered, and injected into the chromatograph; the fluorescence of the salicylic acid was measured at ~425 nm. Excipients and impurities did not interfere, and recoveries of 100% were obtained. The method was used to analyze 84 aspirin samples.

Keyphrases □ Salicylic acid—high-pressure liquid chromatography, fluorescence detection and measurement □ Analgesics—determination of salicylic acid in aspirin by high-pressure liquid chromatography □ Aspirin—determination of salicylic acid by high-pressure liquid chromatography □ High-pressure liquid chromatography—determination of salicylic acid in aspirin

The nonaspirin salicylate test in USP XIX (1) is required for the assay of bulk aspirin and plain and buffered aspirin tablets. The official monograph test for salicylic acid in bulk aspirin is a tube comparison based on the color of the complex formed by ferric ion and salicylic acid and has only a pass–fail requirement at a limit of 0.1%. The plain tablet test, based on the method of Weber and Levine (2), uses a ferric chloride–urea trap of the salicylic acid on a diatomaceous earth[1] column with subsequent elution and measurement of salicylic acid at ~306 nm. The absorbance of the standard is only ~0.1 absorbance unit; samples with low levels of salicylic acid give very low absorbance readings, making accurate measurements difficult. The limit for salicylic acid in plain tablets is 0.3%. The buffered tablet assay, based on the method of Guttman and Salomon (3), uses the same column but can accommodate higher concentrations of salicylic acid. The limit in buffered tablets is 3.0%.

[1] Celite.

Salicylic acid and other impurities in aspirin products have been determined by high-pressure liquid chromatography (HPLC) (4, 5). As part of a national survey, the screening of many aspirin samples for salicylic acid was desired; therefore, a suitable HPLC procedure was needed. The method of Jansson and Andersson (5) was not suitable because of the *in situ* column preparation, which could cause reproducibility problems. The method of Ali (4) was chosen because of the commercial availability of the reversed-phase column and because the solvent system was compatible with aspirin solubility. However, preliminary experiments showed that salicylic acid was not easily determined at 254 nm at levels of 0.3% or lower in aspirin products.

Shane and Stillman (6) determined salicylic acid in the presence of aspirin by fluorescence in chloroform solution. The work of Shane and Miele (7) indicated that salicylic acid could be determined fluorometrically in the presence of aspirin using a pH 4 aqueous buffer solution.

An aqueous–alcoholic solvent of pH 3.4 is obtained when acetic acid is added to the HPLC mobile phase used by Ali (4). This solvent causes salicylic acid to fluoresce and is an excellent solvent for aspirin formulations.

The procedure described in this paper combines HPLC with a fluorescence detector and accurately measures the salicylic acid content of bulk, plain, and buffered aspirin formulations. The samples were prepared in methanol–water–acetic acid and injected into the chromatograph, and the salicylic acid was measured by the fluorescence detector. The results were compared with those obtained using the official USP XIX procedure and a semiautomated colorimetric procedure (8). The procedure was used successfully to analyze 34 bulk and 50 tablet aspirin formulations.

0022-3549/80/0500-0548$01.00/0
© 1980, American Pharmaceutical Association

(2) R. D. Kirchhoefer and W. E. Juhl, *ibid.*, **69**, 548 (1980).
(3) W. E. Juhl and R. D. Kirchhoefer, *ibid.*, in press.
(4) V. H. Hubin and H. Ganshirt, *Pharm. Ind.*, **38**, 224 (1976).
(5) H. Oydvin and O. E. Sapiraa, *Medd. Nor. Farm. Selsk.*, **37**, 115 (1975).
(6) A. W. Clayton and R. E. Thiers, *J. Pharm. Sci.*, **55**, 404 (1966).
(7) G. H. Schenk, F. H. Boyer, C. I. Miles, and D. R. Wirtz, *Anal. Chem.*, **44**, 1593 (1972).
(8) R. D. Deodhar, M. R. Shastri, and R. C. Mehta, *Indian J. Pharm.*, **38**, 18 (1975).
(9) C. I. Miles and G. H. Schenk, *Anal. Chem.*, **42**, 650 (1970).
(10) N. Shane and R. Stillman, *J. Pharm. Sci.*, **60**, 114 (1971).
(11) N. Shane and D. Meele, *ibid.*, **59**, 397 (1970).
(12) L. F. Cullen, D. L. Packman, and G. J. Papariello, *Ann. N.Y. Acad. Sci.*, **153**, 525 (1968).
(13) "The United States Pharmacopeia," 19th rev., Mack Publishing Co., Easton, Pa., 1975, p. 39.
(14) J. W. Myrick and W. B. Furman, Laboratory Information Bulletin No. 1640, Food and Drug Administration, Washington, D.C., 1974.

ACKNOWLEDGMENTS

The authors thank Margaret Randall, John Gleason, Rudolph Kulousek, Everett Jefferson, and Brian Keller for technical assistance and Donald P. Page and William B. Furman for editorial assistance.

Aspirin—A National Survey II: Determination of Salicylic Acid in Bulk Aspirin and Aspirin Formulations by High-Pressure Liquid Chromatography Using a Fluorescence Detector

ROSS D. KIRCHHOEFER ˣ **and WILLIAM E. JUHL**

Received October 29, 1979, from the *National Center for Drug Analysis, Food and Drug Administration, St. Louis, MO 63101.* Accepted for publication December 14, 1979.

Abstract □ A quantitative high-pressure liquid chromatographic method, using a reversed-phase column coupled to a fluorescence detector, was developed to determine salicylic acid in bulk aspirin and plain and buffered aspirin tablets. The aspirin was dissolved, filtered, and injected into the chromatograph; the fluorescence of the salicylic acid was measured at ~425 nm. Excipients and impurities did not interfere, and recoveries of 100% were obtained. The method was used to analyze 84 aspirin samples.

Keyphrases □ Salicylic acid—high-pressure liquid chromatography, fluorescence detection and measurement □ Analgesics—determination of salicylic acid in aspirin by high-pressure liquid chromatography □ Aspirin—determination of salicylic acid by high-pressure liquid chromatography □ High-pressure liquid chromatography—determination of salicylic acid in aspirin

The nonaspirin salicylate test in USP XIX (1) is required for the assay of bulk aspirin and plain and buffered aspirin tablets. The official monograph test for salicylic acid in bulk aspirin is a tube comparison based on the color of the complex formed by ferric ion and salicylic acid and has only a pass–fail requirement at a limit of 0.1%. The plain tablet test, based on the method of Weber and Levine (2), uses a ferric chloride–urea trap of the salicylic acid on a diatomaceous earth[1] column with subsequent elution and measurement of salicylic acid at ~306 nm. The absorbance of the standard is only ~0.1 absorbance unit; samples with low levels of salicylic acid give very low absorbance readings, making accurate measurements difficult. The limit for salicylic acid in plain tablets is 0.3%. The buffered tablet assay, based on the method of Guttman and Salomon (3), uses the same column but can accommodate higher concentrations of salicylic acid. The limit in buffered tablets is 3.0%.

[1] Celite.

Salicylic acid and other impurities in aspirin products have been determined by high-pressure liquid chromatography (HPLC) (4, 5). As part of a national survey, the screening of many aspirin samples for salicylic acid was desired; therefore, a suitable HPLC procedure was needed. The method of Jansson and Andersson (5) was not suitable because of the *in situ* column preparation, which could cause reproducibility problems. The method of Ali (4) was chosen because of the commercial availability of the reversed-phase column and because the solvent system was compatible with aspirin solubility. However, preliminary experiments showed that salicylic acid was not easily determined at 254 nm at levels of 0.3% or lower in aspirin products.

Shane and Stillman (6) determined salicylic acid in the presence of aspirin by fluorescence in chloroform solution. The work of Shane and Miele (7) indicated that salicylic acid could be determined fluorometrically in the presence of aspirin using a pH 4 aqueous buffer solution.

An aqueous–alcoholic solvent of pH 3.4 is obtained when acetic acid is added to the HPLC mobile phase used by Ali (4). This solvent causes salicylic acid to fluoresce and is an excellent solvent for aspirin formulations.

The procedure described in this paper combines HPLC with a fluorescence detector and accurately measures the salicylic acid content of bulk, plain, and buffered aspirin formulations. The samples were prepared in methanol–water–acetic acid and injected into the chromatograph, and the salicylic acid was measured by the fluorescence detector. The results were compared with those obtained using the official USP XIX procedure and a semiautomated colorimetric procedure (8). The procedure was used successfully to analyze 34 bulk and 50 tablet aspirin formulations.

0022-3549/80/0500-0548$01.00/0
© 1980, American Pharmaceutical Association

Table I—Comparison of Results (Percent of Label Claim) Obtained by USP XIX and Fluorometric HPLC Methods for Salicylic Acid in Aspirin Tablets

Tablet	USP[a]	Fluorometric HPLC[a]
324 mg, plain	0.073	0.088
324 mg, plain	0.036	0.048
324 mg, buffered	0.580	0.420
81 mg, pediatric	0.230	0.492[b]
81 mg, pediatric	0.264	0.372[b]

[a] Average of four determinations. [b] Average of five to seven determinations.

EXPERIMENTAL

Apparatus—The high-pressure liquid chromatograph[2] was coupled to a ratio fluorometer[3] equipped with a quartz flowcell[4], a primary 5 × 5-cm glass filter[5], and a secondary 5 × 5-cm glass filter[6]. A 100-mv recorder[7] was connected to the fluorometer. Standard 0.2-cm small-bore polytetrafluoroethylene[8] tubing connected the liquid chromatograph to the fluorometer.

A 250 × 4.6-mm column, packed with octadecylsilane bonded to 10-μm silica[9], was used at ambient temperature. The flow rate was 1.5 ml/min, and column pressure was ~1600 psi. The volume of the sample and standard solutions introduced on the column was 40 μl. Methanol was used to rinse the column.

Reagents—Methanol and acetic acid were ACS reagent grade. The methanol and deionized water were filtered with suction through 0.6[10]- and 0.45[11]-μm filters, respectively, before use. The mobile phase, consisting of 54% methanol and 46% water that contained 2.5% acetic acid, was degassed on the instrument at 40° for 20 min before use.

The mobile phase for the liquid chromatograph can be made independently from the sample solvent. The mobile phase should not be left on the column overnight.

The same batch of mobile phase was used to dilute the sample and standard.

Standard Salicylic Acid Solutions—*Stock Solution*—Approximately 100 mg of salicylic acid[12] of known purity was weighed accurately, transferred to a 100-ml volumetric flask, and dissolved in and diluted to volume with methanol.

Working Solution—A 1.0-ml aliquot of the stock solution was transferred to a 50-ml volumetric flask and diluted to volume with the mobile phase. This concentration should be 0.972 mg/50 ml to be equivalent to the 0.3% limit for salicylic acid in plain 324-mg tablets.

Sample Solution—*Bulk and Plain Tablets*—An amount of aspirin or ground composite equivalent to 324 mg of aspirin was transferred to a 50-ml volumetric flask, and 25–30 ml of the mobile phase was added. Then the solution was either treated ultrasonically for 30–90 sec or shaken vigorously for 60–120 sec, diluted to volume with the mobile phase, mixed, and filtered[13,14]. After the first 5 ml was discarded, the HPLC vial was filled and capped, and the solution was injected. The total time for manipulation should be <3 min.

Buffered Tablets—An amount of aspirin formulation equivalent to 324 mg of aspirin was transferred to a 100-ml volumetric flask. Fifty milliliters of the mobile phase was added, and the sample was treated as outlined under *Bulk and Plain Tablets*. Then a 10.0-ml aliquot was transferred to a 100-ml volumetric flask, diluted to volume with the mobile phase, and mixed. The solution was filtered and injected as outlined under *Bulk and Plain Tablets*. The total time for manipulation should be <4 min.

The fluorometer response and/or the standard concentration were adjusted when salicylic acid levels greatly exceeded 0.3% for plain tablets or 3.0% for buffered tablets.

[2] Model 1084A, Hewlett-Packard Co., Avondale, PA 19311.
[3] Farrand Optical Co., Valhalla, NY 10595.
[4] No. 124374, 300 μl, 10 mm, Farrand Optical Co., Valhalla, NY 10595.
[5] No. UG-11, 325-nm peaking, Beckman Instrument Co., Fullerton, CA 92634.
[6] No. 3389, 80% transmission at 425 nm, Corning Glass Co., Corning, NY 14830.
[7] Servo-Riter II, Texas Instruments Inc., Houston, TX 77001.
[8] Teflon.
[9] Reversed-phase C_{18}, E. Merck, Darmstadt, West Germany; available as No. 906046-94 from Alltech Associates, Arlington Heights, IL 60004.
[10] BDWP04700, Millipore Corp., Bedford, MA 01730.
[11] HAWP04700, Millipore Corp., Bedford, MA 01730.
[12] Sigma Chemical Co., St. Louis, MO 63178.
[13] BDWP02500, 0.6-μm pore size, Millipore Corp., Bedford, MA 01730.
[14] BSWP02500, 2.0-μm pore size, Millipore Corp., Bedford, MA 01730.

Table II—Comparison of Results (Percent of Label Claim) Obtained by Fluorometric HPLC, USP XIX, and Semiautomated Colorimetric Methods for Salicylic Acid

Manufacturer[a]	Type of Sample	HPLC	USP	Colorimetric
AA	300-mg tablet	0.270	0.248	0.245
BB	324-mg tablet	0.350	0.307[b]	0.396
C	81-mg tablet	1.200	1.270[b]	1.230
H	81-mg tablet	0.456	0.410	0.540
H	81-mg tablet	0.240	0.197	0.239
E	324-mg tablet (buffered)	4.400	3.360	3.400
EE	324-mg tablet	0.048[c]	0.030[c]	0.050[c]
JJ	81-mg tablet	0.129	0.149	0.292
JJ	81-mg tablet	0.148	0.142	0.275
II	324-mg tablet (buffered)	0.428[c]	0.581[c]	0.420[c]
Q	324-mg tablet	0.375	0.370	0.330
Q	324-mg tablet	0.461	0.511	0.400
S	324-mg tablet	0.088[c]	0.072[c]	0.089[c]
T	81-mg tablet	0.350	0.240	0.262
U	81-mg tablet	0.495	0.520	0.500
U	81-mg tablet	0.400	0.400	0.500
K	81-mg tablet[d]	2.245	4.400	2.100, 4.160, 2.160, 2.310, 3.790
K	81-mg tablet	0.500	0.534[e]	0.500
V	81-mg tablet	0.600	0.524[b]	0.600
V	81-mg tablet	0.645	0.520[b]	0.625
V	81-mg tablet	0.580	0.520[b]	0.629
SM	Bulk	0.020	—[f]	—[g]
MA	Bulk	0.020	—[f]	—[g]
MA	Bulk (10% starch mix)	0.320	0.300	—[g]

[a] C = Bowman Pharmaceuticals, Canton, Ohio; E = Chromalloy American Corp., Culver City, Calif.; H = Davis Manufacturing Co., Knoxville, Tenn.; K = Freeda Vitamins, New York, N.Y.; Q = Marshall Pharmacal Corp., South Hackensack, N.J.; S = Norwich-Eaton Pharmaceuticals, Norwich, N.Y.; T = Oak Park Pharmaceuticals, Fredonia, Wis.; U = Pennex Products Co., Pittsburgh, Pa.; V = L. Perrigo Co., Allegan, Mich.; AA = Sein-Mendez Labs, Rio Piedas, Puerto Rico; BB = Stanback Co., Salisbury, N.C.; EE = Sterling Drug, New York, N.Y.; II = Walgreen Co., Chicago, Ill.; JJ = West-Ward, Eatontown, N.J.; SM = Sigma Chemical Co., St. Louis, Mo.; and MA = Monsanto Chemical Co., St. Louis, Mo. [b] USP XIX modified; tablet material was mixed for 10 min with chloroform before being poured onto column. [c] Average of four or more results. [d] Results due to difference in salicylic acid content of individual tablets. Results reported are from separate prepared composites. [e] USP modified; formic acid was used to free salicylic acid from the formulation (see Ref. 11). [f] Method lacked sensitivity for proper analysis. [g] Passed USP XIX limit test of 0.1%.

Quantitation—Quantitation was achieved by measuring peak height with the 100-mv recorder. The column and detector were primed with two or three injections of a salicylic acid solution before a standard was injected. The first injection of the standard and sample was used to calculate the salicylic acid content.

RESULTS AND DISCUSSION

Salicylic acid can be determined even if the HPLC column does not separate salicylic acid and aspirin. When the HPLC column fails to separate these compounds, any interference with the salicylic acid peak height due to aspirin should be checked. This problem did not arise in this study since the C_{18} reversed-phase column separated the salicylic acid from aspirin; the retention times of aspirin and salicylic acid were 3.9 and 5.0 min, respectively.

Salicylic acid was detected at 40 pg/40-μl injection at a signal-to-noise ratio of 100:1, indicating a detection limit of ~1 pg/40 μl. This procedure is at least 100 times more sensitive than the procedures of Peng *et al.* (9) and Terweij-Groen *et al.* (10), who determined salicylic acid in plasma and deproteinized serum, respectively, by the use of HPLC with UV detectors at 237 and 235 nm.

Salicylic acid gave a linear response over almost the full range of the fluorometer, *i.e.*, 0–9 mg/50 ml. The fluorometer was normally operated on midrange with the salicylic acid peak height adjusted to ~75% full scale. Since the relative fluorescence of salicylic acid is pH dependent (6), the standard and samples must be prepared with the same mobile phase solution. The reproducibility of 11 salicylic acid standard injections calculated from the peak heights was ±1.2 fluorescence units with an average peak height of 67.3 fluorescence units. Recoveries of salicylic acid in the presence of aspirin from simulated formulations ranged from 101.0 to 105.5%. Recoveries of salicylic acid from buffered aspirin samples ranged from 100.0 to 117.0%. With some buffered tablet formulations,

it may be necessary to add a small amount of formic acid to the tablet material to release salicylic acid into the solution (3, 11).

The average result for 10 individual weighings from a prepared 325-mg commercial sample composite was 0.048% salicylic acid with a relative standard deviation of 3.9%.

Table I shows a comparison of the results of the fluorometric HPLC procedure with the official USP XIX procedure. The samples are the same as those reported in Table II in Ref. 8. The results were obtained on composites prepared from commercial tablet samples.

Table II shows a comparison of the fluorometric HPLC procedure with the USP XIX method and with a semiautomated colorimetric procedure (8) for samples collected during the aspirin survey. The results listed for each manufacturer were not determined on the same composite.

Baum and Cantwell (12) recently reported the simultaneous determination of salicylic acid in aspirin formulations by HPLC with UV detection. The Baum and Cantwell method was noted only after the HPLC procedure was being used routinely on manufactured formulations in this laboratory.

The hydrolysis of aspirin to salicylic acid (12) is well recognized. For this reason, a time limit was placed on the sample preparation in the procedure. Sample preparation times exceeding 10 min were unsatisfactory for accurate and precise recoveries.

REFERENCES

(1) "The United States Pharmacopeia," 19th rev., Mack Publishing Co., Easton, Pa., 1975, pp. 38, 39.

(2) J. D. Weber and J. Levine, *J. Pharm. Sci.*, **55**, 78 (1966).

(3) D. E. Guttman and G. W. Salomon, *ibid.*, **58**, 120 (1969).

(4) S. L. Ali, *J. Chromatogr.*, **126**, 651 (1976).

(5) S. Jansson and I. Andersson, *Acta Pharm. Suec.*, **14**, 161 (1977).

(6) N. Shane and R. Stillman, *J. Pharm. Sci.*, **60**, 114 (1971).

(7) N. Shane and D. Miele, *ibid.*, **59**, 397 (1970).

(8) W. E. Juhl and R. D. Kirchhoefer, *ibid.*, **69**, 544 (1980).

(9) G. W. Peng, M. A. F. Gadalla, V. Smith, A. Peng, and W. L. Chiou, *ibid.*, **67**, 710 (1978).

(10) C. P. Terweij-Groen, T. Vahlkamp, and J. C. Korak, *J. Chromatogr.*, **145**, 115 (1978).

(11) J. Levine and J. D. Weber, *J. Pharm. Sci.*, **57**, 631 (1968).

(12) R. G. Baum and F. F. Cantwell, *ibid.*, **67**, 1066 (1978).

ACKNOWLEDGMENTS

The authors thank John Gleason and Everett Jefferson for technical assistance and Donald P. Page and William B. Furman for editorial assistance.

Aspirin—A National Survey III: Determination of Impurities in Bulk Aspirin and Aspirin Formulations by High-Pressure Liquid Chromatography and Spectrophotometry

ROSS D. KIRCHHOEFER ˣ, JOHN C. REEPMEYER, and WILLIAM E. JUHL

Received October 29, 1979, from the *National Center for Drug Analysis, Food and Drug Administration, St. Louis, MO 63101.* Accepted for publication December 14, 1979.

Abstract □ A quantitative high-pressure liquid chromatographic method, using a reversed-phase column and an aqueous acetic acid–methanol solution as the mobile phase, was employed for the determination of *O*-acetyl-*O*-salicylsalicylic acid and *O*-salicylsalicylic acid in pharmaceutical aspirin preparations. The aspirin was dissolved, filtered, and injected into the chromatograph. The absorbance of the impurities was measured at 254 nm. Acetylsalicylic anhydride was determined by a spectrophotometric method. The aspirin was dissolved in pH 11.3 buffer and extracted with benzene. An aliquot of the benzene was evaporated, and the residue was dissolved in α-benzamidocinnamate–pyridine reagent. The acetylsalicylic anhydride was measured using the difference between the absorbance at 362 and 372 nm. Possible interference of aspirin with the procedure is discussed. Thirty-four bulk aspirin and 172 tablet formulations were examined. Results for *O*-acetyl-*O*-salicylsalicylic acid, *O*-salicylsalicylic acid, and acetylsalicylic anhydride are given.

Keyphrases □ *O*-Acetyl-*O*-salicylsalicylic acid—high-pressure liquid chromatographic determination □ Analgesics—determination of impurities in aspirin □ Aspirin—determination of impurities □ *O*-Salicylsalicylic acid—high-pressure liquid chromatographic determination □ Acetylsalicylic anhydride—spectrophotometric determination

Acetylsalicylic anhydride (I), *O*-acetyl-*O*-salicylsalicylic acid (II), and salicylic acid have been determined in aspirin tablets by high-pressure liquid chromatography (HPLC) (1–5), GLC (1, 3, 6–9), TLC (10, 11), and spectrophotometry (12, 13).

The HPLC procedure of Ali (1) was used in these laboratories to determine impurities in aspirin products. However, certain reversed-phase HPLC columns did not separate I from another impurity, which was isolated and identified as *O*-salicylsalicylic acid (III) (14). Compound I also is decomposed rapidly while in contact with the mobile phase. Therefore, this procedure was used only for the measurement of II and III. Additional impurities were found in commercial samples but have not been identified.

Bundgaard (5) postulated the presence of III and *p*-acetoxybenzoic acid in aspirin formulations based on their HPLC retention times. Bundgaard indicated that these

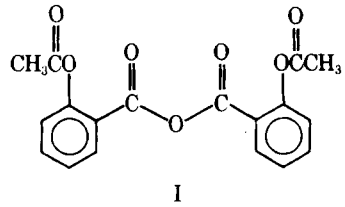

I

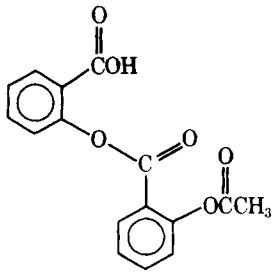

II

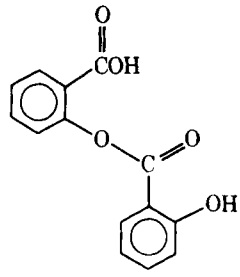

III

0022-3549/80/0500-0550$01.00/0

© 1980, American Pharmaceutical Association

it may be necessary to add a small amount of formic acid to the tablet material to release salicylic acid into the solution (3, 11).

The average result for 10 individual weighings from a prepared 325-mg commercial sample composite was 0.048% salicylic acid with a relative standard deviation of 3.9%.

Table I shows a comparison of the results of the fluorometric HPLC procedure with the official USP XIX procedure. The samples are the same as those reported in Table II in Ref. 8. The results were obtained on composites prepared from commercial tablet samples.

Table II shows a comparison of the fluorometric HPLC procedure with the USP XIX method and with a semiautomated colorimetric procedure (8) for samples collected during the aspirin survey. The results listed for each manufacturer were not determined on the same composite.

Baum and Cantwell (12) recently reported the simultaneous determination of salicylic acid in aspirin formulations by HPLC with UV detection. The Baum and Cantwell method was noted only after the HPLC procedure was being used routinely on manufactured formulations in this laboratory.

The hydrolysis of aspirin to salicylic acid (12) is well recognized. For this reason, a time limit was placed on the sample preparation in the procedure. Sample preparation times exceeding 10 min were unsatisfactory for accurate and precise recoveries.

REFERENCES

(1) "The United States Pharmacopeia," 19th rev., Mack Publishing Co., Easton, Pa., 1975, pp. 38, 39.

(2) J. D. Weber and J. Levine, *J. Pharm. Sci.*, **55**, 78 (1966).

(3) D. E. Guttman and G. W. Salomon, *ibid.*, **58**, 120 (1969).

(4) S. L. Ali, *J. Chromatogr.*, **126**, 651 (1976).

(5) S. Jansson and I. Andersson, *Acta Pharm. Suec.*, **14**, 161 (1977).

(6) N. Shane and R. Stillman, *J. Pharm. Sci.*, **60**, 114 (1971).

(7) N. Shane and D. Miele, *ibid.*, **59**, 397 (1970).

(8) W. E. Juhl and R. D. Kirchhoefer, *ibid.*, **69**, 544 (1980).

(9) G. W. Peng, M. A. F. Gadalla, V. Smith, A. Peng, and W. L. Chiou, *ibid.*, **67**, 710 (1978).

(10) C. P. Terweij-Groen, T. Vahlkamp, and J. C. Korak, *J. Chromatogr.*, **145**, 115 (1978).

(11) J. Levine and J. D. Weber, *J. Pharm. Sci.*, **57**, 631 (1968).

(12) R. G. Baum and F. F. Cantwell, *ibid.*, **67**, 1066 (1978).

ACKNOWLEDGMENTS

The authors thank John Gleason and Everett Jefferson for technical assistance and Donald P. Page and William B. Furman for editorial assistance.

Aspirin—A National Survey III: Determination of Impurities in Bulk Aspirin and Aspirin Formulations by High-Pressure Liquid Chromatography and Spectrophotometry

ROSS D. KIRCHHOEFER ˣ, JOHN C. REEPMEYER, and WILLIAM E. JUHL

Received October 29, 1979, from the *National Center for Drug Analysis, Food and Drug Administration, St. Louis, MO 63101.* Accepted for publication December 14, 1979.

Abstract □ A quantitative high-pressure liquid chromatographic method, using a reversed-phase column and an aqueous acetic acid–methanol solution as the mobile phase, was employed for the determination of *O*-acetyl-*O*-salicylsalicylic acid and *O*-salicylsalicylic acid in pharmaceutical aspirin preparations. The aspirin was dissolved, filtered, and injected into the chromatograph. The absorbance of the impurities was measured at 254 nm. Acetylsalicylic anhydride was determined by a spectrophotometric method. The aspirin was dissolved in pH 11.3 buffer and extracted with benzene. An aliquot of the benzene was evaporated, and the residue was dissolved in α-benzamidocinnamate–pyridine reagent. The acetylsalicylic anhydride was measured using the difference between the absorbance at 362 and 372 nm. Possible interference of aspirin with the procedure is discussed. Thirty-four bulk aspirin and 172 tablet formulations were examined. Results for *O*-acetyl-*O*-salicylsalicylic acid, *O*-salicylsalicylic acid, and acetylsalicylic anhydride are given.

Keyphrases □ *O*-Acetyl-*O*-salicylsalicylic acid—high-pressure liquid chromatographic determination □ Analgesics—determination of impurities in aspirin □ Aspirin—determination of impurities □ *O*-Salicylsalicylic acid—high-pressure liquid chromatographic determination □ Acetylsalicylic anhydride—spectrophotometric determination

Acetylsalicylic anhydride (I), *O*-acetyl-*O*-salicylsalicylic acid (II), and salicylic acid have been determined in aspirin tablets by high-pressure liquid chromatography (HPLC) (1–5), GLC (1, 3, 6–9), TLC (10, 11), and spectrophotometry (12, 13).

The HPLC procedure of Ali (1) was used in these laboratories to determine impurities in aspirin products. However, certain reversed-phase HPLC columns did not separate I from another impurity, which was isolated and identified as *O*-salicylsalicylic acid (III) (14). Compound I also is decomposed rapidly while in contact with the mobile phase. Therefore, this procedure was used only for the measurement of II and III. Additional impurities were found in commercial samples but have not been identified.

Bundgaard (5) postulated the presence of III and *p*-acetoxybenzoic acid in aspirin formulations based on their HPLC retention times. Bundgaard indicated that these

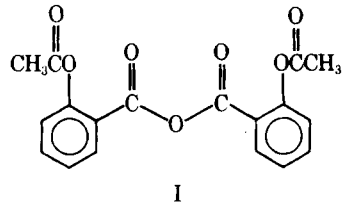

I

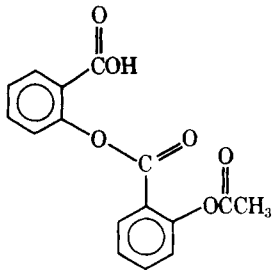

II

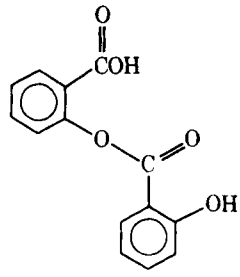

III

0022-3549/80/0500-0550$01.00/0

© 1980, American Pharmaceutical Association

Table I—Amounts of I–III as Percent of Declared Aspirin in Aspirin Tablets

Tablet[a]	Tablet Dosage	I	II	III
A	324 mg	0.004	0.148	0.02
	324 mg	0.005	0.175	0.01
	324 mg	0.004	0.193	0.02
	324 mg	0.007	0.170	0.02
B	421 mg	0.075	0.210	0.02
	421 mg	0.067	0.506	0.03
	421 mg	—[b]	0.358	0.04
	421 mg	—[b]	0.247	0.02
C	324 mg	0.006	0.131	Trace[c]
	324 mg	0.036	0.065	Trace
	81 mg	0.036	0.037	0.02
	324 mg	0.009	1.057	0.02
	324 mg	0.002	0.046	Trace
	324 mg	0.003	0.269	—[d]
	324 mg	0.007	0.041	0.01
	160 mg	—[b]	0.036	Trace
D	486 mg[e]	0.006	0.141	0.01
	486 mg[e]	0.043	0.415	0.02
	324 mg	0.011	0.346	0.01
	324 mg	—[b]	0.301	0.01
	324 mg	0.018	0.237	0.01
	324 mg	0.026	0.223	0.02
	486 mg[e]	0.004	0.142	—[d]
	486 mg[e]	0.006	0.128	0.01
	486 mg[e]	0.003	0.173	0.01
E	324 mg[e]	—[b]	0.610	0.06
F	324 mg[e]	0.015	0.241	0.06
	324 mg[e]	—[b]	0.506	0.06
	324 mg[e]	—[b]	0.247	0.03
G	324 mg	0.018	0.099	—[d]
	324 mg	0.011	0.169	Trace
	324 mg	0.012	0.029	—[d]
H	81 mg	0.033	0.051	—[d]
	81 mg	0.050	0.068	—[d]
	81 mg	0.004	0.018	—[d]
	324 mg	0.005	0.022	—[d]
	324 mg	0.006	0.020	—[d]
	324 mg	0.008	0.029	—[d]
	324 mg	0.005	0.089	—[d]
	81 mg	—[b]	0.054	Trace
I	324 mg	0.002	0.092	0.01
	81 mg	—[b]	0.097	0.03
	324 mg	0.003	0.147	0.02
	324 mg	0.001	0.095	0.01
	324 mg	0.003	0.991	0.02
J	324 mg	0.022	0.109	0.01
K	324 mg	0.012	0.097	0.02
	81 mg	0.034	0.418	0.04
	81 mg	0.011	0.083	0.01
	324 mg	0.001	0.065	0.01
L	324 mg[e]	0.038	1.040	0.03
	324 mg[e]	0.039	0.540	0.03
	324 mg[e]	0.040	0.371	0.02
M	324 mg	0.006	0.230	0.01
N	324 mg	0.023	0.173	—[d]
	324 mg	0.014	0.165	—[d]
	324 mg	0.022	0.079	—[d]
	324 mg	0.003	0.094	0.01
O	324 mg[e]	0.002	0.155	0.01
	324 mg	0.023	0.199	0.02
P	324 mg	0.001	0.056	Trace
Q	324 mg	—[b]	0.013	—[d]
	324 mg	0.014	0.033	Trace
	324 mg	0.024	0.088	0.01
R	324 mg	0.007	0.016	—[d]
	324 mg	0.004	0.027	—[d]
	324 mg	0.030	0.055	Trace
	324 mg	0.006	0.060	Trace
	324 mg	0.005	0.091	—[d]
S	324 mg	0.003	0.419	0.08
	324 mg	—[b]	0.094	0.01
	324 mg	0.007	0.872	0.16
	324 mg	0.004	0.548	0.09
	324 mg	0.004	0.490	0.08
	324 mg	0.004	0.493	0.08
	324 mg	0.008	0.418	0.09
	324 mg	0.012	0.492	0.08
	324 mg	0.007	0.518	0.10
	324 mg	—[b]	0.513	0.09
	324 mg	0.018	0.470	0.11[f]
T	81 mg	0.044	0.166	Trace
	81 mg	0.006	0.106	0.01
	324 mg[e]	0.007	0.383	0.25
	324 mg[e]	—[b]	0.513	0.04
	324 mg[e]	0.001	0.355	0.04
	324 mg[e]	0.004	0.202	0.03
U	81 mg	0.015	0.124	0.02
	81 mg	0.008	0.099	0.02
	81 mg	0.012	0.107	0.02
	324 mg[e]	0.005	0.231	0.04
	324 mg[e]	0.005	0.199	—[d]
	324 mg[e]	0.004	0.193	0.01
	324 mg[e]	0.012	0.137	0.02
	81 mg	0.010	0.140	0.01
	324 mg[e]	—[b]	0.219	0.03
V	81 mg	0.008	0.090	0.01
	81 mg	0.003	0.125	0.01
	81 mg	0.003	0.092	0.01
	81 mg	0.003	0.147	0.02
	324 mg[e]	0.008	0.197	0.02
	324 mg[e]	0.005	0.171	0.02
	324 mg[e]	0.007	0.202	0.02
	324 mg[e]	0.004	0.215	0.02
	324 mg[e]	0.004	0.188	0.02
W	324 mg	0.004	0.026	—[d]
	324 mg	0.012	0.152	0.09
	324 mg	0.002	0.067	0.01
X	81 mg	0.013	0.140	Trace
	81 mg	0.012	0.116	0.01
	81 mg	0.028	0.117	Trace
	324 mg	0.012	0.142	0.001
	324 mg	0.004	0.094	—[d]
	324 mg	0.001	0.071	0.01
	81 mg	0.021	0.207	0.03
	81 mg	0.022	0.207	0.02
	324 mg	0.002	0.054	Trace
Y	324 mg	0.006	0.012	Trace
	648 mg	0.007	0.094	Trace
	324 mg	0.009	0.060	0.01
	486 mg[e]	0.014	0.286	0.02
	81 mg	0.008	0.041	—[d]
	648 mg	0.001	0.108	0.01
	324 mg	0.001	0.077	0.01
Z	324 mg	0.001	0.031	—[d]
	486 mg	0.001	0.077	0.01
	486 mg	0.001	0.129	0.01
AA	81 mg	0.015	0.308	0.03
	300 mg	0.288	0.177	0.02
BB	324 mg	0.001	0.028	—[d]
CC	324 mg[e]	0.010	0.598	0.06
	324 mg[e]	0.019	0.480	0.07
DD	324 mg[e]	—[b]	0.285	Trace
	324 mg[e]	—[b]	0.682	0.05
	324 mg[e]	—[b]	0.276	0.02
EE	325 mg	0.003	0.331	—[d]
	81 mg	—[b]	0.027	0.01
	325 mg	0.002	0.281	0.01
	81 mg	—[b]	0.194	0.01
	81 mg	—[b]	0.229	Trace
	81 mg	0.022	0.212	—[d]
	325 mg	0.003	0.296	—[d]
	325 mg	0.002	0.319	—[d]
	325 mg	0.002	0.336	—[d]
FF	324 mg	0.013	0.276	0.03
	324 mg	0.010	0.231	0.01
	324 mg	0.024	0.190	0.02
	324 mg	0.012	0.195	0.02
GG	81 mg	0.010	0.120	Trace
	324 mg	0.244	0.028	—[d]
	324 mg[e]	0.019	1.358	0.05
	324 mg	0.012	0.026	—[d]
	324 mg[e]	—[b]	0.833	0.04
	324 mg[e]	0.027	0.499	0.02
HH	65 mg	—[b]	0.081	0.02
	320 mg	0.003	0.036	Trace
	320 mg	0.002	0.027	—[d]
II	324 mg[e]	—[b]	0.253	0.01
	324 mg[e]	—[b]	0.340	0.02
JJ	81 mg	0.010	0.120	Trace
	81 mg	0.005	0.175	Trace
	324 mg[e]	0.014	0.241	0.02

(continued)

Table I—*Continued*

Tablet[a]	Tablet Dosage	I	II	III
	324 mg	0.002	0.052	—[d]
	324 mg	0.001	0.093	—[d]
KK	486 mg[e]	0.010	0.231	0.02
	486 mg[e]	0.038	0.337	0.01
	486 mg[e]	—[b]	0.339	0.02
	486 mg[e]	0.008	0.346	0.02
	486 mg	0.044	0.306	0.02
LL	325 mg[e]	—[b]	0.140	0.02
	325 mg[e]	—[b]	0.217	0.04
	325 mg[e]	—[b]	0.185	0.02

[a] A = Bell Pharmacal, Greenville, S.C.; B = Block Drug Co., Memphis, Tenn.; C = Bowman Pharmaceuticals, Canton, Ohio; D = Bristol-Myers Co., New York, N.Y.; E = Chromalloy American Corp., Culver City, Calif.; F = Otis Clapp & Sons, Boston, Mass.; G = Cord Laboratories, Detroit, Mich.; H = Davis Manufacturing Co., Knoxville, Tenn.; I = Dewey Products Co., Grand Rapids, Mich.; J = Ferndale Laboratories, Ferndale, Mich.; K = Freeda Vitamins, New York, N.Y.; L = ICN Pharmaceuticals, Cincinnati, Ohio; M = Lannett Co., Philadelphia, Pa; N = Eli Lilly & Co., Indianapolis, Ind.; O = Mallard, Detroit, Mich.; P = Manhattan Drug Co., Hillside, N.J.; Q = Marshall Pharmacal Corp., Hackensack, N.J.; R = McKesson Laboratories, Fairfield, Conn.; S = Norwich-Eaton Pharmaceuticals, Norwich, N.Y.; T = Oak Park Pharmaceuticals, Fredonia, Wis.; U = Pennex Products Co., Pittsburgh, Pa; V = L. Perrigo Co., Allegan, Mich.; W = Pill Mill, Grand Rapids, Mich.; X = Plough, Memphis, Tenn.; Y = Rexall Drug Co., St. Louis, Mo; Z = Richlyn Laboratories, Philadelphia, Pa; AA = Sein-Mendez Labs, Rio Piedas, Puerto Rico; BB = Stanback Co., Salisbury, N.C.; CC = Standard Pharmacal Co., Chicago, Ill.; DD = Stanley Laboratories, Portland, Ore.; EE = Sterling Drug, New York, N.Y.; FF = E. R. Squibb & Sons, New York, N.Y.; GG = Sun Laboratories, Portland, Ore.; HH = Vale Chemical Co., Allentown, Pa.; II = Walgreen Co., Chicago, Ill.; JJ = West-Ward, Eatontown, N.J.; KK = Whitehall Laboratories, New York, N.Y.; and LL = Zenith Laboratories, Hoboken, N.J. [b] No valid reading was obtained. [c] Trace = <0.003% of II or <0.01% of III. [d] Not detected. [e] Buffered tablet formulation. [f] Sample from which *O*-salicylsalicylic acid was isolated and identified.

impurities were present in salicylic acid, the starting material for aspirin. The presence of III in aspirin formulations was confirmed in this laboratory and was determined to be a commonly occurring impurity in commercial aspirin preparations. This paper presents the first procedure for the quantitation of III in aspirin and its formulations.

The spectrophotometric procedure of Bundgaard and Bundgaard (13) was modified and used to determine I in bulk aspirin and in plain and buffered tablets, and an HPLC method was used to determine II and III in these products. Thirty-four bulk aspirin products, representing 12 foreign and domestic bulk drug suppliers, and 172 tablet formulations, representing 38 manufacturers, were analyzed for I–III.

EXPERIMENTAL

Chromatographic Method—*Apparatus*—A high-pressure liquid chromatograph[1] with a single-wavelength 254-nm detector was used. The operating conditions, column, and reagents were as described previously (15), except that the flow rate was 1.5 ml/min and the amount of acetic acid was increased to 2.5%.

Standard Stock Solution—Approximately 10 mg of *O*-acetyl-*O*-salicylsalicylic acid, synthesized according to the general method of Chattaway (16), and 10 mg of *O*-salicylsalicylic acid[2] were weighed accurately, transferred to a 10-ml volumetric flask, and dissolved in and diluted to volume with methanol.

Standard Working Solution—A 1.0-ml aliquot of the stock solution was transferred to a 10-ml volumetric flask and diluted to volume with the mobile phase. This solution was transferred to the HPLC vial, the vial was capped, and 40 μl of the solution was injected.

Sample Preparation—An amount of powder equivalent to 324 mg of aspirin for tablet formulations or 700 mg for bulk aspirin was transferred to a 25-ml erlenmeyer flask. The mobile phase (10.0 ml) was added, and the solution was shaken or treated ultrasonically for 2–3 min. The solution was filtered, if needed, through a 0.6-μm filter[3]. After the first milliliter was discarded, the HPLC vial was filled and capped, and 40 μl of the solution was injected.

[1] Model 1084A, Hewlett-Packard Co., Avondale, PA 19311.
[2] K&K Laboratories, Plainview, NY 11803.
[3] BDWP01300, Millipore Corp., Bedford, MA 01730.

Table II—Amounts of I–III (Percent of Assay) in Bulk Aspirin

Tablet[a]	Bulk Drug[b]	I	II	III
A	ZZ	0.026	0.906	0.05
B	MA	0.014	0.123	Trace[c]
C	MA	0.003	0.042	—[d]
C	MA	0.024	0.148	—[d]
D	ZZ	0.044	0.210	Trace
F	MA	0.005	0.730	0.02
H	MA	0.004	0.065	—[d]
H	XX	0.007	Trace	—[d]
J	MA	0.007	0.088	Trace
K	MA	0.003	0.050	—[d]
N	ZZ	0.009	0.063	Trace
O	MA	0.020	0.058	Trace
O	MA	0.011	0.088	Trace
Q	WW	0.012	0.029	—[d]
R	VV	0.010	0.022	—[d]
S	S	0.016	0.229	0.03
T	MA	0.010	0.065	—[d]
T	MA	0.028	0.130	—[d]
V	ZZ	0.026	0.236	0.02
V	MA	0.002	0.032	—[d]
W	MA	0.005	0.023	—[d]
X	MA	0.012	0.049	—[d]
X	ZZ	0.015	0.107	Trace
Y	ZZ	0.020	0.097	Trace
Z	UU	0.320	0.073	Trace
AA	MA	0.014	0.122	0.12[e]
BB	MA	0.009	0.049	Trace
CC	TT	—[f]	0.188	Trace
EE	EE	0.068	0.345	0.02
FF	RR	0.043	0.122	0.02
GG	QQ	0.019	0.035	—[d]
HH	MA	0.019	0.455	—[d]
II	MA	0.012	0.040	0.01
LL	SS	—[f]	Trace	—[d]

[a] See Table I, footnote *a*. [b] MA = Monsanto Chemical Co., St. Louis, Mo.; QQ = Polfa-Starogard, Poland; RR = Schering AG, West Germany; SS = Kim, Romania; TT = McKesson and Robbins Co., Oak Lawn, Ill.; UU = Flavine International, Northvale, N.J.; VV = Polfa Pharmaceutical Works, Warsaw, Poland; WW = unknown, Romania; XX = Graynor Chemical Co., Pine Brook, N.J., supplier Poland; and ZZ = Dow Chemical Co., Midland, Mich. [c] Trace = <0.003% of II or <0.01% of III. [d] Not detected. [e] Salicylic acid content of 0.30%. [f] No valid reading was obtained.

Quantitation—The concentration of each impurity was determined by comparing its peak area, as measured by the data system integrator, with that of its standard.

Spectrophotometric Method—The method of Bundgaard and Bundgaard (13) was modified for determining I. Compound I was ex-

Table III—Amounts of I–III (Percent of Declared Aspirin) and Correlation of Bulk Aspirin with Manufactured Tablets

Tablet[a]	Bulk Drug[b]	Type of Sample	I	II	III
H	XX	Bulk	0.007	Trace[c]	—[d]
		324-mg tablet	0.007	Trace	—[d]
		324-mg tablet	0.005	0.089	—[d]
		324-mg tablet	0.006	0.020	—[d]
		324-mg tablet	0.004	0.018	—[d]
		324-mg tablet	0.005	0.022	—[d]
H	MA	Bulk	0.004	0.065	—[d]
		81-mg tablet	0.050	0.068	—[d]
		81-mg tablet	0.033	0.051	—[d]
T	MA	Bulk	0.028	0.130	—[d]
		324-mg tablet[e]	0.007	0.383	0.25[f]
		324-mg tablet[e]	—[g]	0.513	0.04
		324-mg tablet[e]	0.001	0.355	0.04
		Bulk	0.010	0.065	—[d]
		81-mg tablet	0.044	0.539	Trace
W	MA	Bulk	0.005	0.023	—[d]
		324-mg tablet	0.004	0.026	—[d]
O	MA	Bulk	0.020	0.058	Trace
		324-mg tablet[e]	—[g]	0.155	0.01
J	MA	Bulk	0.07	0.088	Trace
		324-mg tablet	0.022	0.109	0.01

[a] See Table I, footnote *a*. [b] MA = Monsanto Chemical Co., St. Louis, Mo.; and XX = Graynor Chemical Co., Pine Brook, N.J., supplier Poland. [c] Trace = <0.003% of II or <0.01% of III. [d] Not detected. [e] Buffered formulation. [f] Salicylic acid content of 2.1%, limit 3.0%. [g] No valid reading was obtained.

tracted from a powdered sample containing 500 mg of aspirin. To an evaporated portion of the benzene extract was added 3 ml of α-benzamidocinnamate–pyridine reagent, producing an azlactone. The solution was read in the UV region after 25 and 60 min.

The method of calculation was changed from the given procedure by subtracting the absorbance of the minimum at 372 nm from the absorbance of the maximum at 362 nm and using this net absorbance. The standard was synthesized according to Bundgaard and Bundgaard (13).

RESULTS AND DISCUSSION

Compounds II and III were stable in the chromatographic solvents and were determined by this procedure; I was unstable in the mobile phase and decomposed rapidly during analysis. Therefore, I could not be determined by HPLC. While attempting to measure I, it was found that some C_{18} reversed-phase HPLC columns would not separate I from III. However, the column (15) used in the present work separated I and III. Compound III has not previously been identified in aspirin formulations, but its presence was postulated by Bundgaard (5) based on its retention time on silica gel HPLC. Compound III has been identified in these laboratories by IR, UV, and mass spectrometry and TLC after isolation (14).

The original spectrophotometric procedure (13) gave results that indicated that aspirin did not interfere with the determination of I. However, aspirin itself will react with the reagent but at a much slower rate than I. When as little as 0.044% (0.22 mg) aspirin was extracted with I, it contributed to an artificially high value of I by 0.004% (additive with the percentage of I present) after a 30-min reaction period and by 0.008% after 60 min. During the survey, results for I averaged ~0.015%.

Aspirin interference in this analysis can be determined by following the reaction over a period of time. Absorbance readings were taken at 25 and 60 min. A continual increase in absorbance indicated the presence of aspirin, and the quantitation was considered invalid. Thorough shaking of the pH 11.3 buffer solution with benzene, followed by centrifugation, usually removed the aspirin to permit determination of I.

Table I lists the amounts of I–III found in a national survey of aspirin formulations, and Table II lists the amounts found in bulk aspirin. The levels of I–III listed for bulk aspirin from the same bulk drug suppliers sometimes were different, presumably because they were from different lots.

Linearity for II and III was established at levels down to 0.003 and 0.01% (0.01 and 0.03 mg/10 ml) of declared aspirin, respectively. A recovery (from a synthetic starch–lactose formulation) of 100% for II and III was obtained at the 0.03% level relative to aspirin.

Table III shows the only correlations available to match the same lot of bulk aspirin to the finished tablets. Bundgaard (5) stated that the levels of I and II found in tablets originate from the starting bulk aspirin. In general, the level of II was lower in bulk aspirin than in tablets manufactured from that bulk, indicating that aspirin is converted to II during or after tablet manufacture (Table III).

REFERENCES

(1) S. L. Ali, *J. Chromatogr.*, **126**, 651 (1976).

(2) S. O. Jansson and I. Andersson, *Acta Pharm. Suec.*, **14**, 161 (1977).

(3) S. L. Ali, *Pharm. Ztg.*, **121**, 201 (1976).

(4) K. Harzer and R. Barchet, *Dtsch. Apoth. Ztg.*, **116**, 1229 (1967).

(5) H. Bundgaard, *Arch. Pharm. Chem. Sci. Ed.*, **4**, 103 (1976).

(6) S. L. Ali, *Chromatographia*, **7**, 655 (1974).

(7) *Ibid.*, **6**, 478 (1973).

(8) S. L. Ali, *Fresenius Z. Anal. Chem.*, **278**, 365 (1976).

(9) S. Patel, J. H. Perrin, and J. J. Windheuser, *J. Pharm. Sci.*, **61**, 1794 (1972).

(10) A. L. DeWeck, *Int. Arch. Allergy Appl. Immunol.*, **41**, 393 (1971).

(11) H. D. Spitz, *J. Chromatogr.*, **140**, 131 (1977).

(12) P. D. Sethi, *Indian J. Pharm.*, **37**, 65 (1975).

(13) H. Bundgaard and C. Bundgaard, *J. Pharm. Pharmacol.*, **25**, 593 (1973).

(14) J. C. Reepmeyer and R. D. Kirchhoefer, *J. Pharm. Sci.*, **68**, 1167 (1979).

(15) R. D. Kirchhoefer and W. E. Juhl, *ibid.*, **69**, 548 (1980).

(16) F. D. Chattaway, *J. Chem. Soc.*, **1931**, 2495.

ACKNOWLEDGMENTS

The authors acknowledge the technical assistance of John Gleason, Everett Jefferson, Rudolph Kulousek, and Brian Keller and the editorial assistance of Donald P. Page and William B. Furman.

Synthesis and Anticancer Activity of Asparagine Analogs

MICHAEL J. MURPHY and JAMES F. STUBBINS ˣ

Received August 31, 1979, from the *Department of Pharmaceutical Chemistry, School of Pharmacy, Medical College of Virginia, Virginia Commonwealth University, Richmond, VA 23298.* Accepted for publication December 12, 1979.

Abstract □ A series of 11 asparagines substituted on N^4 was prepared and evaluated for their ability to inhibit the growth of L5178Y leukemia cell cultures. These cells require an exogenous source of L-asparagine and should be sensitive to an asparagine antimetabolite. The compounds were prepared by reaction of phthalylaspartic anhydride with a primary or secondary amine, followed by removal of the phthalyl group with hydrazine. One compound, *N,N*-dibenzylasparagine, showed significant activity. Additional study of asparagine derivatives bearing large, lipophilic groups at N^4 is warranted.

Keyphrases □ Asparagine analogs—synthesis and anticancer activity □ Anticancer activity—asparagine analogs □ Antileukemic activity—asparagine analogs

There has been great interest in the enzyme L-asparaginase (L-asparagine amidohydrolase, E.C. 3.5.1.1) since it was shown (1) to be the active antitumor agent found in guinea pig serum. Several tumor cell types are sensitive to L-asparaginase treatment, including some human leukemias (2–4). Dramatic remissions were obtained with sensitive tumors, but resistance to the L-asparaginase treatment developed rapidly (4).

BACKGROUND

L-Asparaginase acts on sensitive tumors by removing the required exogenous supply of L-asparagine (I), whereas most normal cells and resistant tumors can synthesize L-asparagine (5). Large doses of injected L-asparaginase rapidly reduced L-asparagine below detectable levels in the plasma, but extracellular fluid concentrations were reduced by only 70% (6). Thus, leukemic cells in the bloodstream generally are killed, but some inaccessible cells have a good chance of survival on the remaining tissue levels of L-asparagine. Furthermore, those cells that survive long

0022-3549/80/0500-0553$01.00/0

© 1980, American Pharmaceutical Association

tracted from a powdered sample containing 500 mg of aspirin. To an evaporated portion of the benzene extract was added 3 ml of α-benzamidocinnamate–pyridine reagent, producing an azlactone. The solution was read in the UV region after 25 and 60 min.

The method of calculation was changed from the given procedure by subtracting the absorbance of the minimum at 372 nm from the absorbance of the maximum at 362 nm and using this net absorbance. The standard was synthesized according to Bundgaard and Bundgaard (13).

RESULTS AND DISCUSSION

Compounds II and III were stable in the chromatographic solvents and were determined by this procedure; I was unstable in the mobile phase and decomposed rapidly during analysis. Therefore, I could not be determined by HPLC. While attempting to measure I, it was found that some C_{18} reversed-phase HPLC columns would not separate I from III. However, the column (15) used in the present work separated I and III. Compound III has not previously been identified in aspirin formulations, but its presence was postulated by Bundgaard (5) based on its retention time on silica gel HPLC. Compound III has been identified in these laboratories by IR, UV, and mass spectrometry and TLC after isolation (14).

The original spectrophotometric procedure (13) gave results that indicated that aspirin did not interfere with the determination of I. However, aspirin itself will react with the reagent but at a much slower rate than I. When as little as 0.044% (0.22 mg) aspirin was extracted with I, it contributed to an artificially high value of I by 0.004% (additive with the percentage of I present) after a 30-min reaction period and by 0.008% after 60 min. During the survey, results for I averaged ~0.015%.

Aspirin interference in this analysis can be determined by following the reaction over a period of time. Absorbance readings were taken at 25 and 60 min. A continual increase in absorbance indicated the presence of aspirin, and the quantitation was considered invalid. Thorough shaking of the pH 11.3 buffer solution with benzene, followed by centrifugation, usually removed the aspirin to permit determination of I.

Table I lists the amounts of I–III found in a national survey of aspirin formulations, and Table II lists the amounts found in bulk aspirin. The levels of I–III listed for bulk aspirin from the same bulk drug suppliers sometimes were different, presumably because they were from different lots.

Linearity for II and III was established at levels down to 0.003 and 0.01% (0.01 and 0.03 mg/10 ml) of declared aspirin, respectively. A recovery (from a synthetic starch–lactose formulation) of 100% for II and III was obtained at the 0.03% level relative to aspirin.

Table III shows the only correlations available to match the same lot of bulk aspirin to the finished tablets. Bundgaard (5) stated that the levels of I and II found in tablets originate from the starting bulk aspirin. In general, the level of II was lower in bulk aspirin than in tablets manufactured from that bulk, indicating that aspirin is converted to II during or after tablet manufacture (Table III).

REFERENCES

(1) S. L. Ali, *J. Chromatogr.*, **126**, 651 (1976).

(2) S. O. Jansson and I. Andersson, *Acta Pharm. Suec.*, **14**, 161 (1977).

(3) S. L. Ali, *Pharm. Ztg.*, **121**, 201 (1976).

(4) K. Harzer and R. Barchet, *Dtsch. Apoth. Ztg.*, **116**, 1229 (1967).

(5) H. Bundgaard, *Arch. Pharm. Chem. Sci. Ed.*, **4**, 103 (1976).

(6) S. L. Ali, *Chromatographia*, **7**, 655 (1974).

(7) *Ibid.*, **6**, 478 (1973).

(8) S. L. Ali, *Fresenius Z. Anal. Chem.*, **278**, 365 (1976).

(9) S. Patel, J. H. Perrin, and J. J. Windheuser, *J. Pharm. Sci.*, **61**, 1794 (1972).

(10) A. L. DeWeck, *Int. Arch. Allergy Appl. Immunol.*, **41**, 393 (1971).

(11) H. D. Spitz, *J. Chromatogr.*, **140**, 131 (1977).

(12) P. D. Sethi, *Indian J. Pharm.*, **37**, 65 (1975).

(13) H. Bundgaard and C. Bundgaard, *J. Pharm. Pharmacol.*, **25**, 593 (1973).

(14) J. C. Reepmeyer and R. D. Kirchhoefer, *J. Pharm. Sci.*, **68**, 1167 (1979).

(15) R. D. Kirchhoefer and W. E. Juhl, *ibid.*, **69**, 548 (1980).

(16) F. D. Chattaway, *J. Chem. Soc.*, **1931**, 2495.

ACKNOWLEDGMENTS

The authors acknowledge the technical assistance of John Gleason, Everett Jefferson, Rudolph Kulousek, and Brian Keller and the editorial assistance of Donald P. Page and William B. Furman.

Synthesis and Anticancer Activity of Asparagine Analogs

MICHAEL J. MURPHY and JAMES F. STUBBINS ˣ

Received August 31, 1979, from the *Department of Pharmaceutical Chemistry, School of Pharmacy, Medical College of Virginia, Virginia Commonwealth University, Richmond, VA 23298.* Accepted for publication December 12, 1979.

Abstract □ A series of 11 asparagines substituted on N^4 was prepared and evaluated for their ability to inhibit the growth of L5178Y leukemia cell cultures. These cells require an exogenous source of L-asparagine and should be sensitive to an asparagine antimetabolite. The compounds were prepared by reaction of phthalylaspartic anhydride with a primary or secondary amine, followed by removal of the phthalyl group with hydrazine. One compound, *N,N*-dibenzylasparagine, showed significant activity. Additional study of asparagine derivatives bearing large, lipophilic groups at N^4 is warranted.

Keyphrases □ Asparagine analogs—synthesis and anticancer activity □ Anticancer activity—asparagine analogs □ Antileukemic activity—asparagine analogs

There has been great interest in the enzyme L-asparaginase (L-asparagine amidohydrolase, E.C. 3.5.1.1) since it was shown (1) to be the active antitumor agent found in guinea pig serum. Several tumor cell types are sensitive to L-asparaginase treatment, including some human leukemias (2–4). Dramatic remissions were obtained with sensitive tumors, but resistance to the L-asparaginase treatment developed rapidly (4).

BACKGROUND

L-Asparaginase acts on sensitive tumors by removing the required exogenous supply of L-asparagine (I), whereas most normal cells and resistant tumors can synthesize L-asparagine (5). Large doses of injected L-asparaginase rapidly reduced L-asparagine below detectable levels in the plasma, but extracellular fluid concentrations were reduced by only 70% (6). Thus, leukemic cells in the bloodstream generally are killed, but some inaccessible cells have a good chance of survival on the remaining tissue levels of L-asparagine. Furthermore, those cells that survive long

0022-3549/80/0500-0553$01.00/0

© 1980, American Pharmaceutical Association

Table I—N^2-Phthalyl-N^4-substituted Asparagines (VI)

Compound	R_1	R_2	Yield, %	Melting Point	Recrystallization Solvent	Formula	Analysis, % Calc.	Found
VI*a*	$CH_3(CH_2)_3$	H	62	192–193°	Water–ethanol	$C_{16}H_{18}N_2O_5$	C 60.37	59.99
							H 5.70	5.99
							N 8.80	8.89
VI*b*	$CH_3(CH_2)_7$	H	26	>300°	Water–ethanol	$C_{20}H_{26}N_2O_5$	C 64.16	64.44
							H 7.00	6.73
							N 7.48	7.11
VI*c*	C_6H_5	H	56	207–209°	Water–ethanol	$C_{18}H_{14}N_2O_5$	C 63.90	64.16
							H 4.17	4.39
							N 8.28	8.16
VI*d*	$C_6H_5CH_2$	H	51	220–222°	Water–acetone	$C_{19}H_{16}N_2O_5$	C 64.77	65.01
							H 4.58	4.62
							N 7.95	7.69
VI*e*	$C_6H_5(CH_2)_2$	H	45	179–180°	Water–ethanol	$C_{20}H_{18}N_2O_5$	C 65.57	65.51
							H 4.95	4.83
							N 7.65	7.92
VI*f*	$C_6H_5(CH_2)_3$	H	37	165–167°	Water–ethanol	$C_{21}H_{20}N_2O_5$	C 66.31	66.49
							H 5.30	5.11
							N 7.36	7.24

enough produce asparagine synthetase and are resistant to subsequent treatment with L-asparaginase (7).

To circumvent the development of resistance with L-asparaginase, an asparagine analog given concomitantly might be of value if the analog would distribute throughout the body fluid and act as an antimetabolite. Cultured asparagine-requiring tumor cells have been shown (8) to possess an active uptake system that might be inhibited by such an analog without affecting normal cells. An antimetabolite also might block the incorporation of asparagine into protein. Although such an action also might affect normal cells, cells that require an exogenous metabolite generally are more susceptible to an antimetabolite. Nonrequiring cells generally can overcome a competitive block simply by increasing their synthesis of the metabolite (9).

Several simple analogs of asparagine have been reported to possess some *in vivo* antitumor activity. L-Aspartic acid β-hydrazide (II), for example, showed weak activity (10). It was shown (11) that 5-diazo-4-oxo-L-norvaline (III) has an irreversible inhibitory effect against L5178Y tumor cells requiring L-asparagine, but it also inhibits the nonrequiring cells, probably by blocking asparagine synthesis.

In the present study, a series of substituted asparagines (IV) was prepared as an initial approach to finding selective inhibitors of asparagine-requiring cancers that will be minimally toxic to normal cells.

$HOOCCH(NH_2)CH_2COX$

I: X = NH_2
II: X = $NHNH_2$
III: X = CHN_2
IV: X = NR_1R_2

RESULTS AND DISCUSSION

Chemistry—The desired mono- and disubstituted asparagines were prepared by a modification of the method of Tanenbaum (12). L-Aspartic acid was heated with phthalic anhydride in pyridine to give the phthalyl-blocked derivative. The aspartic acid was not isolated but was converted to the N^2-phthalylaspartic anhydride (V) by treatment with acetic anhydride. The product had racemized completely, and no optical rotation was observable.

The direction of ring opening of V with ammonia was shown to be dependent on the solvent polarity (12). Only the N^2-phthalylasparagine and none of the isomeric α-amides were obtained in ether. When V was treated with a series of primary amines, the substituted N^2-phthalylasparagines (VI) were prepared in a similar fashion. The properties of the compounds are listed in Table I. The compounds displayed IR absorption bands near 1160, 1630, and 1560 cm^{-1}, indicative of the secondary amide structure, and the bands at 1780 and 1710 cm^{-1} indicated the presence of imide carbonyl groups. The NMR spectra were consistent with the assigned structure and included a doublet near 3.5 ppm and a triplet near 5.7 ppm associated with the asparagine moiety.

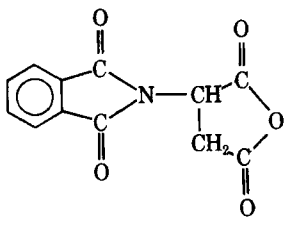

V

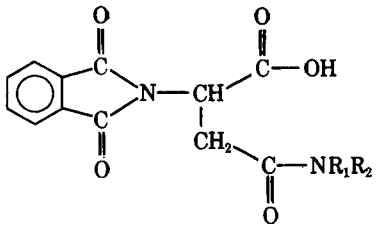

VI

Treatment of the phthalylasparagines (VI) with hydrazine removed the phthalyl group to give the N^4-substituted asparagines (IV) in reasonable yield. For preparation of the tertiary amides, the intermediate phthalylasparagines were not isolated; the crude products were treated directly with hydrazine. The properties of the compounds are given in Table II. The products all displayed NMR signals at ~4.50 and 3.30 ppm for the asparagine methine and methylene protons, respectively; otherwise, the spectra were consistent with the assigned structures. The considerably higher melting point of IV*d* compared to that reported previously (13) could not be explained.

Biology—The compounds were tested for their ability to inhibit the growth of L5178Y cells grown in McCoy's 5A medium. The desired quantity of each compound was dissolved in ethanol and diluted with sterile distilled water. A portion of this solution, 0.1 ml, was added to 5 ml of cell suspension containing ~2.5×10^5 leukemic cells. Duplicate tubes were used with a final compound concentration of 10 or 100 μg/ml and an ethanol concentration of <1%.

The tubes were placed in a carbon dioxide incubator at 36–38° for 96 hr. The contents of the tubes were counted[1] to determine inhibition of cell growth. Under the experimental conditions, L-asparaginase at a concentration of 1×10^{-3} μg/ml gave 100% inhibition.

Only one test compound had significant activity. At a concentration of 100 μg/ml, *N,N*-dibenzylasparagine (IV*k*) inhibited growth by 96%. The ID_{50} value was estimated to be 55 μg/ml. The drug concentration needed for appreciable inhibition was rather high; however, the culture medium contained 45 μg of L-asparagine/ml. Therefore, if the drug were acting as a competitive antimetabolite of L-asparagine, there was considerable metabolite with which to compete. Furthermore, the analog is racemic, and only the enantiomer with the L-configuration probably is an effective inhibitor.

Since the initiation of this study, Uren *et al.* (14) reported the testing of 19 asparagine analogs for inhibition of growth of a subline of L5178Y capable of asparagine synthesis and for inhibition of isolated asparagine synthetase. Of the 19 analogs studied, four were *N*-alkylasparagines. *N*-Methylasparagine was the most active inhibitor of asparagine synthetase and also actively inhibited L5178Y cell growth in the absence of asparagine. Inhibition was reversed completely in the presence of 1 m*M* asparagine. The *N*-ethyl, *N*-isopropyl, and *N,N*-dimethyl (IV*g*) analogs were completely inactive.

Inhibition of asparagine synthetase seems limited to analogs that have no more bulk than one methyl group on the amide nitrogen. The activity found in the present study of the dibenzyl analog (IV*k*) was not an inhibition of asparagine synthetase since these cells lack this synthetic capability. The analog must be interfering with asparagine uptake or utilization.

The only distinctive structural feature of IV*k* that might account for its activity is the dibenzyl moiety, which provides the highest lipophilicity of any of the analogs examined. Therefore, other asparagine derivatives

[1] Coulter counter.

Table II—N^4-Substituted Asparagines (IV)

Compound	R_1	R_2	Yield, %	Melting Point	Recrystallization Solvent	Formula	Analysis, % Calc.	Found
IV*a*	$CH_3(CH_2)_3$	H	62[a]	276–278°[b]	Water	$C_8H_{16}N_2O_3$	C 51.05	51.00
							H 8.57	8.60
							N 14.88	14.65
IV*b*	$CH_3(CH_2)_7$	H	72[a]	238–240°	Water–ethanol	$C_{12}H_{24}N_2O_3$	C 64.16	64.44
							H 7.00	6.73
							N 7.48	7.11
IV*c*	C_6H_5	H	87[a]	248–249°[c]	Water	$C_{10}H_{12}N_2O_3$	C 63.90	64.16
							H 4.17	4.39
							N 8.28	8.16
IV*d*	$C_6H_5CH_2$	H	79[a]	305–309°[d]	Water–ethanol	$C_{11}H_{14}N_2O_3$	C 59.45	59.16
							H 6.35	6.07
							N 12.60	12.49
IV*e*	$C_6H_5(CH_2)_2$	H	73[c]	251–253°	Water–ethanol	$C_{12}H_{16}N_2O_3$	C 61.00	60.67
							H 6.83	6.84
							N 11.86	11.62
IV*f*	$C_6H_5(CH_2)_3$	H	46[a]	248–250°	Water–ethanol	$C_{13}H_{18}N_2O_3$	C 62.38	62.15
							H 7.25	7.38
							N 11.19	11.17
IV*g*	CH_3	CH_3	64[e]	314–317°	Water–ethanol	$C_6H_{12}N_2O_3$	C 44.99	45.31
							H 7.55	7.16
							N 17.49	17.45
IV*h*	C_6H_5	CH_3	46[e]	>310°	Water–ethanol	$C_{11}H_{14}N_2O_3$	C 59.45	59.13
							H 6.35	6.47
							N 12.60	12.71
IV*i*	$C_6H_5CH_2$	CH_3	48[e]	>310°	Water–ethanol	$C_{12}H_{16}N_2O_3$	C 61.00	60.73
							H 6.83	6.89
							N 11.86	11.99
IV*j*	$CH_3(CH_2)_3$	$CH_3(CH_2)_3$	34[e]	>310°	Water–ethanol	$C_{12}H_{24}N_2O_3$	C 58.99	58.97
							H 9.90	9.85
							N 11.47	11.44
IV*k*	$C_6H_5CH_2$	$C_6H_5CH_2$	57[e]	243–245°	Water–ethanol	$C_{18}H_{20}N_2O_3$	C 69.21	69.50
							H 6.45	6.61
							N 9.31	9.31

[a] Yields are based on the purified N^2-phthalylasparagines. [b] Lit. (15) mp 265° (crude material). [c] Lit. (16) mp 255°. [d] Lit. (13) mp 265°. [e] Yields are based on N^2-phthalylaspartic anhydride.

with large lipophilic substituents on the amide nitrogen should be prepared. By testing these additional compounds in a medium deficient in L-asparagine, it might be possible to find a prospective anticancer agent for use in combination with L-asparaginase.

EXPERIMENTAL[2]

N^2-Phthalylaspartic Anhydride (V)—L-Aspartic acid (13.3 g, 100 mmoles) and phthalic anhydride (14.8 g, 100 mmoles) were heated under reflux in 200 ml of pyridine for 2 hr. The mixture was cooled to room temperature, and the undissolved solids were removed by filtration. The filtrate was concentrated under reduced pressure to a yellow oil. Acetic anhydride (50 ml) was added to the oil with vigorous agitation, and the mixture was chilled at 0° for 2 hr. The resulting precipitate was collected, washed with anhydrous ether, and recrystallized from *p*-dioxane to give 17.1 g (70% yield) of V, mp 224–226° [lit. (12) mp 224–225°]; IR: 1875, 1210, 932 (COOCO), 1795 (C=O), 1785, and 1705 (CONRCO) cm^{-1}; NMR (dimethyl sulfoxide-d_6): 3.53 (d, 2H, CH_2), 5.77 (t, 1H, CH), and 8.00 (s, 4H, C_6H_4).

N^2-Phthalyl-*N*-substituted Asparagines (VI)—N^2-Phthalylaspartic anhydride (3.0 g, 12 mmoles) was suspended in 75 ml of anhydrous ether. Then 25 mmoles of the appropriate amine was added, and the mixture was stirred at room temperature for 24 hr. The solvent was evaporated under reduced pressure. The residue was dissolved in water, and the solution was acidified with 6 *N* HCl to pH 2. The resulting precipitate was removed by filtration. The compounds derived from primary amines were recrystallized from aqueous ethanol (Table I). For compounds derived from secondary amines, the crude product was used directly in the succeeding step.

N^4-Substituted Asparagines (IV)—Either the purified or crude preparation of N^2-phthalyl-N^4-substituted asparagine was dissolved in 25 ml of 20% aqueous hydrazine hydrate solution. The solution was stirred at room temperature for 24 hr. The reaction mixture was acidified with dilute hydrochloric acid to pH 5–6. The resulting precipitate was collected and recrystallized to give the pure product (Table II).

[2] Melting points were obtained with a Thomas-Hoover capillary apparatus and are uncorrected. Combustion analyses were performed using a Perkin-Elmer 240 elemental analyzer. IR spectra were obtained using a Perkin-Elmer model 257 grating spectrophotometer on samples prepared in a potassium bromide pellet. NMR spectra were obtained using a Hitachi Perkin-Elmer R-24 high-resolution spectrometer. Compounds were dissolved in deuterated solvents from commercial sources with tetramethylsilane as the internal standard.

REFERENCES

(1) J. D. Broome, *Nature*, **191**, 1114 (1961).

(2) E. A. Boyse, L. J. Old, H. A. Campbell, and L. T. Mashburn, *J. Exp. Med.*, **125**, 17 (1967).

(3) R. H. Adamson and S. Fabro, *Cancer Chemother. Rep.*, **52**, 617 (1968).

(4) N. Jaffe, D. Traggis, L. Das, W. C. Maloney, H. W. Hann, B. S. Kim, and R. Nair, *Cancer Res.*, **31**, 942 (1971).

(5) J. D. Broome and J. H. Schwartz, *Biochim. Biophys. Acta*, **138**, 637 (1967).

(6) D. H. W. Ho, B. Thetford, C. J. K. Carter, and E. Frei, *Clin. Pharmacol. Ther.*, **11**, 408 (1970).

(7) C. M. Haskell and G. P. Canellos, *Biochem. Pharmacol.*, **18**, 2578 (1969).

(8) J. D. Broome, *J. Exp. Med.*, **227**, 1055 (1968).

(9) D. W. Woolley, "A Study of Antimetabolites," Wiley, New York, N.Y., 1952, p. 28.

(10) T. Ohnuma, F. Bergel, and R. C. Bray, *Biochem. J.*, **103**, 238 (1967).

(11) W. P. Summers and R. E. Handschumacher, *Biochem. Pharmacol.*, **20**, 2213 (1971).

(12) S. W. Tanenbaum, *J. Am. Chem. Soc.*, **75**, 1754 (1953).

(13) F. H. McMillan and N. F. Albertson, *ibid.*, **70**, 3778 (1948).

(14) J. R. Uren, P. K. Chang, and R. E. Handschumacher, *Biochem. Pharmacol.*, **26**, 1405 (1977).

(15) Y. Liwschitz, Y. Edlitz-Pfeffermann, and Y. Lapidoth, *J. Am. Chem. Soc.*, **78**, 3069 (1956).

(16) Y. Liwschitz, A. Zilka, and E. Nemes, *Bull. Res. Counc. Isr. Sect. A*, **10**, 107 (1961).

ACKNOWLEDGMENTS

Supported in part by National Institutes of Health Training Grant GM-484 from the National Institute of General Medical Sciences.

The authors thank Ms. Kathleen Kalaher and Dr. J. H. Burchenal of Memorial Sloan-Kettering Cancer Center for evaluation of the antileukemic activity.

Mercapto Steroids in Protection against Mercury and Lead Poisoning

ROBERT T. BLICKENSTAFF *§x, BRIAN COX ‡, EMERSON FOSTER §, LESLIE ROBERTS *, and LARRY K. STEINRAUF *‡

Received October 10, 1979, from the *Department of Biochemistry and the ‡Department of Biophysics, Indiana University School of Medicine, and the §Veterans Administration Hospital, Indianapolis, IN 46202. Accepted for publication December 18, 1979.

Abstract □ When thiocholesterol is administered as liposomes, it provides significant protection against methylmercuric chloride in mice when given in three intraperitoneal injections, 0.5 hr before and 2 and 8 hr after the methylmercuric chloride. Thiositosterol, 5α-cholestane-2β,3α-dithiol, and 5β-cholane-3β,24-dithiol also are active, but 3α-mercapto-5α-pregnan-20-one, 6β-mercapto-5α-cholestane-3β,5α-diol, 3β-mercapto-5β-cholanic acid, and adamantanethiol are ineffective under these conditions. Adamantanethiol is somewhat effective when administered in soybean oil. Cholestanyl amine was treated with acetylthiosuccinic anhydride to give the half amide; cleavage with hydroxylamine liberated the thiol group. This product is active against both methylmercuric chloride and lead nitrate.

Keyphrases □ Methylmercuric chloride toxicity—protection by mercapto steroids □ Steroids—mercapto compounds, protection against mercury and lead poisoning □ Heavy metal poisoning—protection by mercapto steroids

In a study to identify lipophilic therapeutic agents for heavy metal poisoning that would minimize the burden placed on the kidney, thiocholesterol was found to be superior to dimercaprol and penicillamine in protecting mice against methylmercuric chloride toxicity (1). An investigation of how alterations in the structure of the molecule might alter activity then was desired. Compounds were synthesized containing, in addition to the thiol group, a hydroxyl, a carboxyl, or a second thiol group. A thiosemicarbazone, synthesized in connection with another problem and lacking a mercapto group, was included because it forms a precipitate with methylmercuric chloride *in vitro*. Several nonsteroidal mercaptans also were studied.

EXPERIMENTAL[1]

Thiositosterol (II)—Tosylation of 20.0 g of β-sitosterol[2] in 140 ml of pyridine[3] with 20 g of *p*-toluenesulfonyl chloride in the refrigerator overnight gave 28.7 g of crude product, mp 130°. Recrystallization from 2-butanone–acetone–water gave β-sitosteryl *p*-toluenesulfonate[4], 24.0 g (89% yield), mp 130–132°; IR: 1601 (benzene ring), 1198 and 1180 (SO_3), 950, 900, 878, 820, and 675 cm^{-1}.

Anal.—Calc. for $C_{36}H_{50}O_3S$: C, 76.00; H, 9.92; S, 5.64. Found: C, 76.24; H, 10.19; S, 5.64.

The tosylate (24.0 g) was treated with thiourea (24.0 g) in 248 ml of 95% alcohol and 25 ml of pyridine at reflux for 4.5 hr. Water precipitated the crude product, 22.8 g (82% yield), mp 233–239°. Two recrystallizations from methanol gave β-sitosteryl isothiouronium tosylate, mp 238–239°; IR: 3300–3000 (NH), 1675, 1230, 1181 (SO_3), 1139, 1050, 1025, 822, and 698 cm^{-1}.

Anal.—Calc. for $C_{37}H_{60}N_2O_3S_2$: C, 68.90; H, 9.38; N, 4.34; S, 9.94. Found: C, 68.60; H, 9.61; N, 4.14; S, 9.72.

Hydrolysis of 7.753 g of the isothiouronium salt in alcoholic sodium hydroxide (2.46 g/180 ml, 5 hr reflux) followed by precipitation with cold water and dilute hydrochloric acid gave the crude product, 4.594 g (89% yield), mp 61–65°. Two crystallizations from acetone–water gave II, mp 70–71°; IR: 1200, 968, and 802 cm^{-1}.

Anal.—Calc. for $C_{29}H_{50}S$: C, 80.86; H, 11.70; S, 7.44. Found: C, 80.59; H, 11.95; S, 7.29.

3α-Mercapto-5α-pregnan-20-one (V)—A comparable reaction of 3β-tosyloxy-5α-pregnan-20-one, mp 131.5–133° [lit. (4) mp 132–135°], with thiourea gave the corresponding isothiouronium tosylate, mp 270–272°; IR: 3275 (NH), 1701 (C=O), 1180 (SO_3), 1090, 1041, 1005, and 819 cm^{-1}.

Anal.—Calc. for $C_{29}H_{44}N_2O_4S_2$: C, 63.47; H, 8.08; N, 5.10; S, 11.67. Found: C, 63.73; H, 8.31; N, 4.90; S, 11.82.

Alkaline hydrolysis of the isothiouronium salt gave V in an 89% yield, mp 123–125° (methanol–water); IR: 1710 (C=O), 1208, 1160, and 978 cm^{-1}.

Anal.—Calc. for $C_{21}H_{34}OS$: C, 75.39; H, 10.24; S, 9.58. Found: C, 75.59; H, 10.34; S, 9.36.

***N*-(5α-Cholestan-3α-yl)mercaptosuccinic Acid Monoamide (VIII)**—A solution of 16.0 g of 5α-cholestan-3α-yl amine and 14.2 g of *S*-acetylmercaptosuccinic anhydride in acetic acid was held under nitrogen at 90–100° for 15 min. The solution was cooled to 35° and poured onto ice. The solid was filtered, the filtrate was extracted with ether, and the ethereal solution and solid were combined and evaporated. The solid residue was dissolved in 75 ml of tetrahydrofuran, 30 ml of methanol, and 10 ml of water. Hydroxylamine hydrochloride was added, and the solution was saturated with gaseous ammonia.

After standing at room temperature for 1.5 hr, the solution was made acidic with cold dilute hydrochloric acid. The precipitate was filtered, washed with water, and dried to give 20.0 g (93% yield), mp 113–118°. The analytical sample was precipitated from acidic methanol–water to yield VIII, mp 117–121°; IR: 3300 and 3170 (NH), 1710 (acid C=O), 1635 (amide C=O), 1540, 1220, and 1175 cm^{-1}.

Anal.—Calc. for $C_{31}H_{53}NO_3S$: C, 71.61; H, 10.28; N, 2.60; S, 6.16. Found: C, 71.26, 71.92; H, 10.46, 10.84; N, 2.48; S, 5.74.

3β-Hydroxy-5-androstene-16,17-dione 16-Oxime 17-Thiosemicarbazone (XI)—3β-Hydroxy-5-androsten-17-one tetrahydropyranyl ether (5, 6) (IX, 23.40 g) was added to a stirred solution of 5.89 g of potassium in 262 ml of *tert*-butanol under nitrogen. The mixture was stirred 1 hr, and 22.0 ml of isopentyl nitrite was added. The contents of the flask solidified within 2 min. After standing overnight at room temperature, the solid mass was dissolved in 1300 ml of cold water and extracted three times with ether.

Table I—Effect of Timing on Intraperitoneal Thiocholesterol Therapy for Methylmercuric Chloride Toxicity

Steroid[a]	Hours before First Injection[b]	Hours after Second Injection[b]	Hours after Third Injection[b]	Survivors	p^c
Cholesterol	24	24	48	3/20, 15%	—
Thiocholesterol	24	24	48	3/16, 19%	—
Thiocholesterol	2	24	48	9/16, 56%	<0.0093
Thiocholesterol	0.5	24	48	8/16, 50%	<0.0278
Cholesterol	0.5	2	8	1/15, 7%	—
Thiocholesterol	0.5	2	8	13/16, 81%	<0.0001
Thiocholesterol	0.25	2	4	0/16, 0%	—
Thiocholesterol	0.25	2	8	0/16, 0%	—

[a] Steroids were administered as liposomes with 400 mg of steroid/kg of body weight. [b] Before and after intraperitoneal injection of 25 mg of methylmercuric chloride/kg of body weight. [c] Normal difference test as compared to appropriate cholesterol control (13).

[1] Melting points were obtained on a Thomas-Hoover melting point apparatus and are corrected. IR spectra were taken as smears or mineral oil mulls on a Perkin-Elmer 247 spectrophotometer. Microanalyses were performed by Galbraith Laboratories, Knoxville, Tenn.

[2] Mann, dried by benzene azeotropy.

[3] Dried over molecular sieve.

[4] Reported without the melting point by Stoll (2) and possibly the same as the compound with a melting point of 123–124.5° reported by Rathmann and Morrow (3).

0022-3549/80/0500-0556$01.00/0
© 1980, American Pharmaceutical Association

Table II—Activity of Compounds against Methylmercuric Chloride Toxicity [a]

	Compound [b]	Survivors	p [c]
	Cholesterol	15/78, 19%	—
I	Thiocholesterol	16/22, 73%	<0.0001
II	Thiositosterol	13/30, 43%	<0.0124
III	5α-Cholestane-2β,3α-dithiol	17/22, 77%	<0.0001
IV	6β-Mercapto-5α-cholestane-3β,5α-diol	0/10, 0%	—
V	3α-Mercapto-5α-pregnan-20-one	3/10, 30%	—
VIII	*N*-(5α-Cholestan-3α-yl)mercaptosuccinic acid monoamide	16/36, 44%	<0.0069
XI	3β-Hydroxy-5-androstene-16,17-dione 16-oxime 17-thiosemicarbazone	2/9, 22%	—
XII	3β-Mercapto-5β-cholanic acid	4/10, 40%	<0.1936
XIII	5β-Cholane-3β,24-dithiol	6/10, 60%	<0.0001
XIV	1-Adamantanethiol	1/10, 10%	—

[a] All mice received 20 mg of methylmercuric chloride/kg of body weight by intraperitoneal injection. [b] Administered as liposomes injected intraperitoneally 0.5 hr before and 2 and 8 hr after methylmercuric chloride injection at the level of 400 mg of steroid or 170 mg of adamantanethiol/kg of body weight. [c] Normal difference test (13) as compared to the control group.

The combined ethereal layer was washed with water; the water wash was added to the original alkaline layer, which then was cooled and acidified with acetic acid. Filtration of the mixture after several hours of refrigeration gave 22.36 g of crude product, mp 161–166° (88% yield). Three recrystallizations in methanol–water gave 3β-hydroxy-5-androstene-16,17-dione 16-oxime 3-tetrahydropyranyl ether (X), mp 176–191°; IR: 3245 (OH), 1735 (C=O), 1632, 1135, 1112, 1058, 1022, 974, 940, 908, and 868 cm^{-1}.

Anal.—Calc. for $C_{24}H_{35}NO_4$: C, 71.79; H, 8.79; N, 3.49. Found: C, 71.69; H, 8.78; N, 3.64.

The thiosemicarbazone was prepared in the usual way with 5 ml of concentrated hydrochloric acid, 2.00 g of the oxime (X), and 1.50 g of thiosemicarbazide in 39 ml of boiling 95% ethanol and 6 ml of water. Two recrystallizations from methanol–dimethylformamide–water gave XI[5], mp 296–298° dec.; *IR*: 3408 (OH), 3230 (OH), 3145 (NH), 1580, 1300, 1080, and 968 cm^{-1}.

Anal.—Calc. for $C_{20}H_{30}N_4O_2S$: C, 61.51; H, 7.74; N, 14.35; S, 8.21. Found: C, 61.32; H, 7.91; N, 14.37; S, 8.10.

Assays—Assays were conducted with male, Swiss–Webster mice, 22–25 g. Liposomes were prepared as described previously (1); with VIII and XI, cholesterol was added (compound to cholesterol, 4:1) to obtain stable liposomes. 1-Dodecanethiol was tested in cottonseed oil because it would not form liposomes under these conditions. Methylmercuric chloride was dissolved in warm water at a concentration of 1 mg/ml, and lead nitrate was dissolved at a concentration of 20 mg/ml. Mice were injected with test compounds in the left groin and with mercury or lead in the right groin.

RESULTS AND DISCUSSION

Thiositosterol (II) was synthesized from sitosterol and 3α-mercapto-5α-pregnan-20-one (V) was synthesized from 3β-hydroxy-5α-pregnan-20-one *via* the corresponding tosylates and isothiouronium salts in a sequence comparable to the synthesis of thiocholesterol (7). Cholestane-2β,3α-dithiol (III) (8), 6β-mercapto-5α-cholestane-3β,5α-diol (IV) (9), and 1-adamantanethiol (XIV) (10) were synthesized by literature methods. 5α-Cholestan-3α-yl amine (VI) reacted with *S*-acetylmercaptosuccinic anhydride to give the corresponding hemiamide (VII) following a reported method (11). The product was deacylated with hydroxylamine to give the mercapto compound (VIII). The mercapto group may be on the carbon adjacent to either the carboxyl or the amide group, and, although the product exhibited a single spot by TLC, it may be a mixture of the two isomers. The tetrahydropyranyl ether (IX) of androstenolone was oximated with isopentyl nitrite and potassium *tert*-butoxide (12). When the intermediate (X) was converted to the corresponding thiosemicarbazone (XI), the tetrahydropyranyl ether group was cleaved, giving the 3-hydroxy derivative. Compounds XII and XIII were reported previously.

[5] Mixing equal volumes of 0.01 *N* mercuric acetate in 70% alcohol and 0.01 *N* XI in alcohol caused a rapid precipitation.

Table III—Activity against Methylmercuric Chloride of Compounds Tested in Vegetable Oil [a]

Compound [b]	Survivors	p [c]
Soybean oil	2/20, 10%	—
III	5/10, 50%	<0.0594
XIV	5/10, 50%	<0.0594
1-Dodecanethiol	0/13, 0%	—

[a] All mice received 20 mg of methylmercuric chloride/kg of body weight by intraperitoneal injection. [b] Administered in soybean oil solution by intraperitoneal injection 0.5 hr before and 2 and 8 hr after the methylmercuric chloride injection at the level of 400 mg (of steroid or 1-dodecanethiol) or 170 mg (of adamantanethiol)/kg of body weight. [c] Normal difference test (13) as compared to the control group.

Table IV—Activity of VIII against Lead Nitrate Toxicity [a]

Compound	Dose [b], mg/kg	Survivors	p [c]
Cholesterol	400	2/10, 20%	—
VIII	292	9/10, 90%	<0.0019

[a] All mice received 180 mg of lead nitrate/kg of body weight by intraperitoneal injection. [b] Administered as liposomes injected 0.5 hr before and 2 and 8 hr after lead acetate injection. [c] Normal difference test (13) as compared to the control group.

The desirability of having an assay in which the test compound is administered only following administration of the toxic dose of the heavy metal, thereby mimicking real life conditions, is obvious. However, in earlier work (1), thiocholesterol was an effective protective agent when given 24 and 48 hr *before* methylmercuric chloride but not when given 0, 12, 24, and 36 hr *after* methylmercuric chloride. To decrease the time between pretreatment and the toxic dose, the comparisons in Table I were carried out. Significant protection was afforded when the first of three injections of thiocholesterol was given 0.5 or 2 hr before the methylmercuric chloride but not when given 0.25 or 24 hr before. The highest survival rate was obtained with the sequence 0.5 hr before and 2 and 8 hr after the toxic dose, and this regimen was used in subsequent assays.

The results reported in Table II are composites of a series of assays and illustrate that II, III, VIII, and XIII are active in addition to thiocholesterol. 3β-Mercapto-5β-cholanoic acid (XII) was active when tested under a less stringent protocol (1). Adamantanethiol, inactive under these conditions, exhibited some activity when administered in soybean oil (Table III), but 1-dodecanethiol was totally inactive.

The hemisuccinamide (VIII) exhibited high protective activity when tested against lead nitrate (Table IV).

While there are too few examples for extensive structure–activity generalizations, it is useful to note that 3-mercapto (but not 6-mercapto) steroids were active against methylmercuric chloride. The 2,3- and 3,24-dithiols also were active. The high activity of the hemisuccinamide against lead may be the result of coordination of the lead to both carboxyl and thiol groups. These observations provide leads for the synthesis of other mercapto steroids for heavy metal therapy.

REFERENCES

(1) L. K. Steinrauf, B. Cox, E. Foster, A. Sattar, and R. T. Blickenstaff, *J. Pharm. Sci.*, **67**, 1739 (1978).

(2) A. Stoll, *Z. Physiol. Chem.*, **246**, 1 (1937).

(3) D. M. Rathmann and L. R. Morrow, *J. Am. Chem. Soc.*, **72**, 5647 (1950).

(4) A. Ruff and T. Reichstein, *Helv. Chim. Acta*, **34**, 70 (1951).

(5) A. C. Ott, M. F. Murray, and R. L. Pederson, *J. Am. Chem. Soc.*, **74**, 1239 (1952).

(6) A. Bowers and R. Becerra, *ibid.*, **82**, 4007 (1960).

(7) L. C. King, R. M. Dodson, and L. A. Subluskey, *ibid.*, **70**, 1176 (1948).

(8) K. Takeda, *Tetrahedron*, **21**, 329 (1965).

(9) T. Komeno, *Chem. Pharm. Bull.*, **8**, 672 (1960).

(10) D. D. Tanner and B. G. Brownlee, *Can. J. Chem.*, **51**, 3366 (1973).

(11) Imperial Chemical Industries, British pat. 858,482 (Jan. 11, 1961); through *Chem. Abstr.*, **55**, 17318f (1961).

(12) F. H. Stodola, E. C. Kendall, and B. F. McKenzie, *J. Org. Chem.*, **6**, 841 (1941).

(13) A. K. Bahn, "Basic Medical Statistics," Grune and Stratton, New York, N.Y., 1972, pp. 52–55.

ACKNOWLEDGMENTS

Presented at the American Chemical Society–Chemical Society of Japan Chemical Congress, Honolulu meeting, April 1979 (Abs. MEDI 79).

Supported by Public Health Service Grant R01-ES-942-03 and by Veterans Administration Research Project 8-583.

The technical assistance of Donna Stolz, Peter Craig, and Bob Shepard is greatly appreciated.

Application of Queueing Theory to Pharmacokinetics

P. H. BRILL *x **and R. E. MOON** ‡

Received October 30, 1978, from the *Department of Quantitative Methods, University of Illinois at Chicago Circle, Chicago, IL 60680, and the ‡Institute of Biomedical Engineering and Department of Medicine, University of Toronto, Toronto, Canada. Accepted for publication December 20, 1979.

Abstract □ This paper considers the steady-state plasma drug concentration in a one-compartment, open pharmacokinetic model with multiple doses and first-order kinetics using a classical deterministic technique as well as a queueing theoretical stochastic analysis. The stochastic analysis employs a new method for obtaining the steady-state probability distribution of the content of a dam with compound Poisson input and a general release rule. It is shown that if the deterministic steady-state average concentration exists, it is equal to the mean value of the steady-state concentration, the probability distribution of which is obtained using the stochastic model. Moreover, the steady-state probability distribution of the concentration and its mean always exist in the stochastic model. Ramifications of the stochastic method of analysis are discussed.

Keyphrases □ Pharmacokinetics—steady-state plasma drug concentration, queueing theory □ Models, pharmacokinetic—steady-state plasma drug concentration, queueing theory □ Queueing theory—application to pharmacokinetics, steady-state plasma drug concentration

This paper introduces a method of analyzing drug accumulation based on a stochastic model of multiple-dosing regimens. In classical pharmacokinetic theory, transient and steady-state drug concentrations in the blood for multiple-dosing regimens are derived from knowledge of the deterministic dose sizes, intervals between doses, volumes of distribution, and kinetics of elimination and transfer between body compartments (1–4). This analysis may be clinically useful only if two major conditions are true: (*a*) the dosage intervals are known, and (*b*) the amount of drug absorbed as a consequence of each dose is known.

These conditions rarely are met in practice. As noted previously (2), nonstandard definitions of *bid*, *tid*, and *qid* may lead to varying dosage intervals. Family physicians and drug package inserts often direct that drugs should be taken near meal times, bed time, or three or four times daily without defining these terms specifically (2). Patients rarely take drugs on schedule unless they are in the hospital. Furthermore, dose size may vary because the initial dose or other doses may be different from the usual maintenance dose. The fractional absorption of oral drugs depends on several factors. For drugs administered intramuscularly, the fractional absorption partially depends on the injection site (1). Moreover, completeness of drug absorption always is clinically important (1, 5).

These observations suggest the desirability of obtaining the drug concentration in the plasma when the dose intervals, doses, or absorption fractions are subject to random fluctuations and must be considered random variables. Accounting for such random variations in these parameters leads to the consideration of a stochastic analysis of pharmacokinetic models. This paper emphasizes the new technique itself rather than its application to general multiple-dosing models. The model presented is a one-compartment, open model with instantaneous input and first-order elimination. A classical, well-known deterministic method of analysis is presented for convenience of reference, and a stochastic, queueing theoretical approach for studying the same model then is given. The latter technique is based on a new method of analyzing the model of a dam with a general release rule[1], which was studied previously in stochastic processes using other approaches.

THEORETICAL

The Model—The model treated is a one-compartment, open model with multiple dosing and first-order kinetics (1–4, 6). For clarity and to focus attention on the new technique, very rapid administration of each dose directly into and instantaneous distribution throughout the compartment is assumed. This assumption is a good approximation for intravenous bolus dosing. For outpatient oral dosing (to which the stochastic technique is more applicable), first-order absorption may be a more appropriate assumption. However, for many drugs in common clinical use, the absorption constant is appreciably larger than the elimination constant. Examples are digoxin, sublingually administered nitrites, salicylates, and phenylbutazone. For such drugs, the assumption of instantaneous absorption, although only approximate, is not entirely unreasonable.

The following notations are used in both the deterministic and stochastic analyses:

V = volume of compartment
K_e = elimination rate constant (time^{-1})
$t_{1/2e}$ = elimination half-life; $1/k_e = t_{1/2e}/\ln 2 = 1.44t_{1/2e}$
τ_n = administration time of nth dose, $n = 1, 2, 3, \ldots$; $\tau_1 = 0$
T_n = nth dosage interval; $T_n = \tau_{n+1} - \tau_n$
D_n = amount of nth dose
F_n = fraction of D_n distributed throughout V
E_n = effective increase in drug concentration at time τ_n; $E_n = F_nD_n/V$
$C(t)$ = drug concentration at time t; $t \geq 0$
C_n = drug concentration at time τ_n; $C_1 = C(0) = 0$
λ = rate of administration of doses
B = common distribution function of effective increases in concentration, E_n, independent of n; $B(0) = 0$
$r(x)$ = drug elimination rate when the concentration is x (mass times volume^{-1} times time^{-1})

Deterministic Analysis—The following well-known deterministic analysis is presented for comparison with the stochastic analysis. Vari-

[1] P. H. Brill, unpublished data.

0022-3549/80/0500-0558$01.00/0
© 1980, American Pharmaceutical Association

ACKNOWLEDGMENTS

Presented at the American Chemical Society–Chemical Society of Japan Chemical Congress, Honolulu meeting, April 1979 (Abs. MEDI 79).

Supported by Public Health Service Grant R01-ES-942-03 and by Veterans Administration Research Project 8-583.

The technical assistance of Donna Stolz, Peter Craig, and Bob Shepard is greatly appreciated.

Application of Queueing Theory to Pharmacokinetics

P. H. BRILL *x **and R. E. MOON** ‡

Received October 30, 1978, from the *Department of Quantitative Methods, University of Illinois at Chicago Circle, Chicago, IL 60680, and the ‡Institute of Biomedical Engineering and Department of Medicine, University of Toronto, Toronto, Canada. Accepted for publication December 20, 1979.

Abstract □ This paper considers the steady-state plasma drug concentration in a one-compartment, open pharmacokinetic model with multiple doses and first-order kinetics using a classical deterministic technique as well as a queueing theoretical stochastic analysis. The stochastic analysis employs a new method for obtaining the steady-state probability distribution of the content of a dam with compound Poisson input and a general release rule. It is shown that if the deterministic steady-state average concentration exists, it is equal to the mean value of the steady-state concentration, the probability distribution of which is obtained using the stochastic model. Moreover, the steady-state probability distribution of the concentration and its mean always exist in the stochastic model. Ramifications of the stochastic method of analysis are discussed.

Keyphrases □ Pharmacokinetics—steady-state plasma drug concentration, queueing theory □ Models, pharmacokinetic—steady-state plasma drug concentration, queueing theory □ Queueing theory—application to pharmacokinetics, steady-state plasma drug concentration

This paper introduces a method of analyzing drug accumulation based on a stochastic model of multiple-dosing regimens. In classical pharmacokinetic theory, transient and steady-state drug concentrations in the blood for multiple-dosing regimens are derived from knowledge of the deterministic dose sizes, intervals between doses, volumes of distribution, and kinetics of elimination and transfer between body compartments (1–4). This analysis may be clinically useful only if two major conditions are true: (*a*) the dosage intervals are known, and (*b*) the amount of drug absorbed as a consequence of each dose is known.

These conditions rarely are met in practice. As noted previously (2), nonstandard definitions of *bid*, *tid*, and *qid* may lead to varying dosage intervals. Family physicians and drug package inserts often direct that drugs should be taken near meal times, bed time, or three or four times daily without defining these terms specifically (2). Patients rarely take drugs on schedule unless they are in the hospital. Furthermore, dose size may vary because the initial dose or other doses may be different from the usual maintenance dose. The fractional absorption of oral drugs depends on several factors. For drugs administered intramuscularly, the fractional absorption partially depends on the injection site (1). Moreover, completeness of drug absorption always is clinically important (1, 5).

These observations suggest the desirability of obtaining the drug concentration in the plasma when the dose intervals, doses, or absorption fractions are subject to random fluctuations and must be considered random variables. Accounting for such random variations in these parameters leads to the consideration of a stochastic analysis of pharmacokinetic models. This paper emphasizes the new technique itself rather than its application to general multiple-dosing models. The model presented is a one-compartment, open model with instantaneous input and first-order elimination. A classical, well-known deterministic method of analysis is presented for convenience of reference, and a stochastic, queueing theoretical approach for studying the same model then is given. The latter technique is based on a new method of analyzing the model of a dam with a general release rule[1], which was studied previously in stochastic processes using other approaches.

THEORETICAL

The Model—The model treated is a one-compartment, open model with multiple dosing and first-order kinetics (1–4, 6). For clarity and to focus attention on the new technique, very rapid administration of each dose directly into and instantaneous distribution throughout the compartment is assumed. This assumption is a good approximation for intravenous bolus dosing. For outpatient oral dosing (to which the stochastic technique is more applicable), first-order absorption may be a more appropriate assumption. However, for many drugs in common clinical use, the absorption constant is appreciably larger than the elimination constant. Examples are digoxin, sublingually administered nitrites, salicylates, and phenylbutazone. For such drugs, the assumption of instantaneous absorption, although only approximate, is not entirely unreasonable.

The following notations are used in both the deterministic and stochastic analyses:

V = volume of compartment
K_e = elimination rate constant (time^{-1})
$t_{1/2e}$ = elimination half-life; $1/k_e = t_{1/2e}/\ln 2 = 1.44t_{1/2e}$
τ_n = administration time of nth dose, $n = 1, 2, 3, \ldots$; $\tau_1 = 0$
T_n = nth dosage interval; $T_n = \tau_{n+1} - \tau_n$
D_n = amount of nth dose
F_n = fraction of D_n distributed throughout V
E_n = effective increase in drug concentration at time τ_n; $E_n = F_nD_n/V$
$C(t)$ = drug concentration at time t; $t \geq 0$
C_n = drug concentration at time τ_n; $C_1 = C(0) = 0$
λ = rate of administration of doses
B = common distribution function of effective increases in concentration, E_n, independent of n; $B(0) = 0$
$r(x)$ = drug elimination rate when the concentration is x (mass times volume^{-1} times time^{-1})

Deterministic Analysis—The following well-known deterministic analysis is presented for comparison with the stochastic analysis. Vari-

[1] P. H. Brill, unpublished data.

0022-3549/80/0500-0558$01.00/0
© 1980, American Pharmaceutical Association

ations and generalizations of this analysis were given previously (1–4, 6). Equations 1–9 in the present discussion parallel formulas presented previously. All of the parameters are considered deterministic so that T_n, D_n, F_n, E_n, and C_n are real nonnegative constants for $n = 1, 2, 3, \ldots$. The deterministic differential equations of elimination are:

$$\frac{dC(t)}{dt} = -K_e C(t) \qquad \tau_n < t \leq \tau_{n+1} \qquad \text{(Eq. 1)}$$

with initial conditions $C(\tau_n^+) = C_n + E_n$, $n = 1, 2, 3, \ldots$ (3). It then follows that:

$$C(t) = (C_n + E_n) \exp[-K_e(t - \tau_n)] \qquad \tau_n < t \leq \tau_{n+1},\ n = 1, 2, 3, \ldots \qquad \text{(Eq. 2)}$$

and thus:

$$C_{n+1} = C(\tau_{n+1}) = (C_n + E_n) \exp(-K_e T_n) \qquad n = 1, 2, 3, \ldots \qquad \text{(Eq. 3)}$$

Three sequences are of interest in pharmacokinetics: minimum (or infimum), maximum (or supremum), and average concentrations during each dosage interval, which are C_n, $C_n + E_n$, and $\overline{C}_n = (1/T_n) \int_{t=\tau_n}^{\tau_{n+1}} C(t)\, dt$, respectively. Consideration of general constraints on the parameters E_n and T_n that are necessary and sufficient for the convergence of these sequences to limiting values is outside the scope of this paper. However, a sufficient (but not necessary) condition for any of these sequences to converge is monotonicity (*i.e.*, always increasing or always decreasing) after some finite value of n. For different dosing regimens, the limits of all three, any two, only one, or none of these sequences may exist. In the remainder of this section, all limits are taken as $n \to \infty$.

If $\lim C_n$ exists, Eq. 3 yields:

$$\lim C_n = \lim\{E_n/[\exp(K_e T_n) - 1]\} \qquad \text{(Eq. 4)}$$

If $\lim (C_n + E_n)$ exists, Eq. 3 yields:

$$\lim (C_n + E_n) = \lim\{E_{n+1}/[1 - \exp(-K_e T_n)]\} \qquad \text{(Eq. 5)}$$

Using Eq. 2 and substituting from Eq. 3 result in:

$$\overline{C}_n = (1/T_n) \int_{t=\tau_n}^{\tau_{n+1}} C(t)\, dt = (1/K_e)(C_n + E_n - C_{n+1})/T_n \qquad \text{(Eq. 6a)}$$

and, hence, if $\lim \overline{C}_n$ exists:

$$\lim \overline{C}_n = (1/K_e) \lim [(C_n + E_n - C_{n+1})/T_n] \qquad \text{(Eq. 6b)}$$

With the assumption that $\lim \overline{C}_n$ and $\lim C_n$ exist, it follows from Eq. 6*b* that:

$$\lim \overline{C}_n = (1/K_e) \lim (E_n/T_n) = (1/K_e) \lim (F_n D_n/T_n) \qquad \text{(Eq. 7)}$$

If both $\lim \overline{C}_n$ and $\lim (C_n + E_n)$ exist, then:

$$\lim \overline{C}_n = (1/K_e) \lim (E_{n+1}/T_n) = (1/K_e) \lim (F_{n+1} D_{n+1}/T_n) \qquad \text{(Eq. 8)}$$

In Eqs. 4–8, E_n and T_n must be known to predict whether the sequences will converge or oscillate. Knowledge of these parameters rarely is obtainable, except possibly in controlled hospital situations or laboratory studies. In pharmacokinetic literature, analytical results for these limits usually are derived by assuming uniform dosing, *i.e.*, $F_n = F$, $D_n = D$, and $T_n = T$, so that the E_n values all are equal. The condition of uniform dosing is sufficient but not necessary for the limits in Eqs. 4–8 to exist. Under uniform dosing, the steady-state average concentration is given by:

$$\lim \overline{C}_n = 1.44 t_{1/2e} E/T = 1.44 t_{1/2e} FD/(VT) \qquad \text{(Eq. 9)}$$

Since actual dosing rarely is uniform in ambulatory patients, even when it is the intended therapy, nonuniform dosing must be considered. A generalization of Eq. 9 holds for nonuniform dosing of the following type. Both $\lim C_n$ and $\lim \overline{C}_n$ are assumed to exist, so Eq. 7 holds. In addition, let the average increase in drug concentration per dose after n intervals, which is given by $(\sum_{i=1}^n E_i)/n$ (or equivalently by $\sum_{i=1}^n F_i D_i/n$), and the average dose interval after n intervals, $(\sum_{i=1}^n T_i)/n$, tend to the limits E' $[\equiv (FD)']$ and T', respectively, as $n \to \infty$. Then, with Eq. 7 and the fact that both E_n and T_n are bounded away from zero and also bounded above, the following is obtained:

$$\lim \overline{C}_n = (1/K_e) \lim (E_n/T_n) \qquad \text{(Eq. 10a)}$$

$$\lim \overline{C}_n = (1/K_e) E'/T' \qquad \text{(Eq. 10b)}$$

$$\lim \overline{C}_n = 1.44 t_{1/2e} E'/T' \qquad \text{(Eq. 10c)}$$

$$\lim \overline{C}_n = 1.44 t_{1/2e} (FD)'/T' \qquad \text{(Eq. 10d)}$$

The introduction of this type of nonuniform dosing model serves a dual purpose. First, it leads to Eqs. 10*c* and 10*d*, which demonstrate that the limiting average concentration depends on the effective increases in concentration and the dose intervals only through their respective limiting average values. Second, it links the deterministic models of this section to the stochastic model. The latter model also possesses the property established in Eqs. 10*c* and 10*d*.

Stochastic Analysis—In this section, a completely different method for analyzing the present model is introduced. The parameters T_n, D_n, and F_n, $n = 1, 2, \ldots$, are considered to be sequences of independently, identically distributed, random variables, so that $E_n = F_n D_n/V$ is a random variable. Hence, $\{C_n, n \geq 1\}$ and $\{C(t), t \geq 0\}$ are stochastic processes.

Furthermore, it is assumed that $\{N(t), t \geq 0\}$ is a Poisson process with arrival rate λ, where $N(t)$ denotes the number of doses in the time interval $[0, t]$. Note that $P[N(t) = k] = [e^{-\lambda t}(\lambda t)^k]/k!$, $k = 0, 1, 2, \ldots$. Thus, $\{T_n, n \geq 1\}$ is a sequence of exponentially distributed random variables with the common probability distribution function $1 - \exp(-\lambda x)$, $x \geq 0$. The sequence $\{E_n, n \geq 1\}$ is assumed to have common probability distribution, B, with $B(0) = 0$. The mean value of the random variable with distribution B is denoted by $E'' = \int_{z=0}^{\infty} z\, dB(z)$. The drug elimination is described by a general release function, r, with $r(c) > 0$ for $c > 0$ and $r(0) = 0$, where c denotes the concentration level. Therefore, the pharmacokinetic system previously modeled deterministically is modeled stochastically as a dam with a general release rule[1] (7–9). Hence, in general, the following analysis is not constrained to first-order kinetics of elimination. Sample functions of the process $\{C(t), t \geq 0\}$ satisfy the differential equations:

$$dC(t)/dt = -r[C(t)] \qquad \tau_n < t \leq \tau_{n+1} \qquad \text{(Eq. 11)}$$

with initial conditions $C(\tau_n^+) = C_n + E_n$, $n = 1, 2, 3, \ldots$.

The relation $\lim_{c \to \infty} r(c) > \lambda \int_0^\infty z B(dz) = \lambda E''$ guarantees the existence of the steady-state probability distribution function of the drug concentration (8). This result implies, as will be seen following Eq. 15, that for first-order kinetics the steady-state concentration, its probability distribution, and its average always exist. This probability distribution function is denoted by G having the probability density function g. An equation for G that is well known in the literature of stochastic processes (7–9) now is derived by a new method[1]. The present investigators believe that this method has strong intuitive appeal as well as other desirable properties that are outside the scope of this paper. This method differs from one given previously (9), which counts crossings of levels during regenerative cycles of the process rather than during time intervals of the form $(0, t]$, as is done here. Let $E[D_t(c)]$ and $E[U_t(c)]$ denote the expected values of the number of times that a sample function of the process $\{C(t), t \geq 0\}$ downcrosses and upcrosses level c, respectively, during time interval $(0, t]$. The theorems given previously[1] state that:

$$\lim_{t \to \infty} E[D_t(c)]/t = r(c) g(c) \qquad c > 0 \qquad \text{(Eq. 12)}$$

and:

$$\lim_{t \to \infty} E[U_t(c)]/t = \lambda \int_{z=0}^{c} \overline{B}(c - z) G(dz) \qquad \text{(Eq. 13)}$$

where $\overline{B}(x) = 1 - B(x)$, $x \geq 0$. Since the number of downcrossings and upcrossings cannot differ by more than one during any time interval, it follows that the right sides of Eqs. 12 and 13 must be equal, so that[1] Eq. 14 holds:

$$r(c) g(c) = \lambda \int_{z=0}^{c} \overline{B}(c - z) G(dz) \qquad \text{(Eq. 14)}$$

This relation is the well-known equation in stochastic processes referred to previously (7–9). Up to this point, the release function, r, has not been specified so that Eq. 14 holds for non-first-order kinetics of elimination. At this stage, Eq. 14 is specialized to first-order kinetics of elimination by assuming that:

$$r(c) = K_e c \qquad c \geq 0 \qquad \text{(Eq. 15)}$$

Notice that $\lim_{c \to \infty} K_e c = \infty$, which is greater than $\lambda E''$ since E'' is finite. Therefore, with first-order elimination, the limiting probability distribution and its average always exist (8). This property of the stochastic model obviates the need to consider the convergence properties of the sequences in Eqs. 4–8. The actual observed increases in concentration per dose and actual observed dosage intervals encountered in any particular therapy will vary in accordance with sampling from distribution B and from an exponential distribution, respectively. Due to the law

of large numbers, their averages will tend to E'' and $1/\lambda$, respectively, as the number of doses increases. Therefore, this model is the stochastic analog of a deterministic model with the type of nonuniform dosing considered preceding Eq. 10*a*. Thus, the stochastic model does not assume that the intended therapy must involve uniform dosing, but it also applies if the intended therapy actually happens to comprise uniform dosing. This result follows since uniform dosing is just a special type of deterministic nonuniform dosing considered following Eq. 9. To apply the stochastic model for drug management in a given therapy, it must be established that there is a known probability distribution, B, and that the number of doses in any time interval has a Poisson distribution.

With Eq. 15, Eq. 14 reduces to:

$$K_e c g(c) = \lambda \int_{z=0}^{c} \overline{B}\,(c - z) g(z)\, dz \qquad \text{(Eq. 16)}$$

whose tractability without using integral transforms depends on the nature of the function B. Even if Eq. 16 is not readily solvable for g, the steady-state mean value of the concentration with probability density g can be found immediately by integrating both sides of Eq. 16 with respect to the variable c over the range $(0, \infty)$. This integration leads to:

$$\overline{C} = \lambda E''/K_e = 1.44 t_{1/2e} E'' \lambda \qquad \text{(Eq. 17)}$$

where $\overline{C}$ is the mean value of the steady-state probability distribution of the drug concentration. If D_n and F_n are completely independent sequences of random variables, then $E'' = F''D''/V$, where F'' and D'' are the mean fractional absorption and mean dosage, respectively. In this case, setting $\lambda = 1/T''$ transforms Eq. 17 into:

$$\overline{C} = 1.44 t_{1/2e} F''D''/(VT'') \qquad \text{(Eq. 18)}$$

Comparison of Eqs. 9, 10*c*, and 10*d* with Eqs. 17 and 18 demonstrates that $\lim \overline{C}_n = \overline{C}$, provided $\lim \overline{C}_n$ exists. A complete solution of Eq. 16 is given when the effective increases in concentration at dose times are exponentially distributed with the mean $1/\mu$, *i.e.*, $B(x) = 1 - \exp(-\mu x), x \geq 0$. Substitution of this B into Eq. 16 yields:

$$K_e c g(c) = \lambda \int_{z=0}^{c} \exp[-\mu(c - z)] g(z)\, dz \qquad \text{(Eq. 19)}$$

Operating on Eq. 19 with differential operator $\langle D + \mu \rangle$, solving the resulting differential equation, and using the normalizing condition $\int_{z=0}^{\infty} G(dz) = 1$ (or proceeding as in Example 1 of Ref. 7) result in the following solution:

$$g(c) = \exp(-\mu c)(\mu c)^{(\lambda/K_e - 1)}\, \mu/\Gamma(\lambda/K_e) \qquad c > 0 \quad \text{(Eq. 20)}$$

where Γ denotes the gamma function. This result was obtained previously by several investigators (8, 10). In this example, Eq. 17 becomes $\overline{C} = 1.44 t_{1/2e} \lambda/\mu = 1.44 t_{1/2e} F''D''/(VT'')$ as in Eq. 18. This relation expresses the fact that $\overline{C}$ is exactly the same as the classical steady-state average concentration in Eq. 9 or its generalization in Eq. 10*d*, if the latter limits exist.

DISCUSSION

The steady-state probability distribution function of drug concentration and its average always exist and have been calculated under the assumptions that dose administrations occur in a Poisson process, fractional absorptions and dose amounts are independent random variables, the common probability distribution of the resulting drug concentration increases at dose times is known, and elimination is first order. The probabilistic approach presented might be used to predict the percentage of the time that a patient's drug concentration will be below or above any level in the steady state. Imprecise knowledge of the deterministic sequences of doses, dosage intervals, and the resulting limiting behavior of the concentration in the compartment is quantified by exact knowledge of the steady-state probability distribution function.

Using classical theory, one simply predicts a patient's minimum, maximum, or average drug concentration; in addition, it is assumed that the dosage intervals and absorption characteristics are precisely known constants. In classical theory, one can predict, for example, that if a patient takes 500 mg of procainamide every 4 hr, his or her serum level will "likely" be therapeutic because these constants are rarely known exactly. It would be more informative and useful to know that if the patient takes the drug *approximately* every 4 hr and if drug absorption is subject to chance variations, then the serum will contain an established therapeutic concentration 95% of the time.

The latter type of prediction might allow more rational therapy with drugs taken by ambulatory patients for which the therapeutic effect is close to toxicity or for which it is essential to maintain a therapeutic serum level. Digoxin, antiarrhythmics, anticonvulsants, certain antibiotics, antineoplastics, aminophylline, salicylates in the therapy of rheumatic disorders, antihypertensives, and corticosteroids are examples of medications belonging to this class. The particular stochastic analysis presented here may be directly applicable to some of these agents, particularly those with relatively rapid absorption and first-order elimination kinetics.

Similarly, the stochastic approach can be used to predict caffeine levels in coffee and tea drinkers since these beverages usually are imbibed at random intervals and by sipping random amounts. Carbon monoxide and nicotine levels in tobacco users and ethanol levels in partygoers might be predicted in the same manner. The exponential dam described by Eq. 19 might be a good model for these situations, and Eq. 20 then would be an exact analytical solution for the steady-state probability distribution of the serum concentration. The dosage rate, λ, and the average increase in concentration, $1/\mu$, would have to be determined experimentally.

Extension of the present analysis to include first-order absorption would make the probabilistic technique applicable to a broader class of drugs. Moreover, development of similar queueing theoretical methods for multicompartment models with more general dosing regimens is of interest.

REFERENCES

(1) D. J. Greenblatt and J. Koch-Weser, *N. Engl. J. Med.*, **293,** 702, 964 (1975).

(2) P. J. Niebergall, E. T. Sugita, and R. L. Schnaare, *J. Pharm. Sci.*, **63,** 100 (1974).

(3) K. H. Norwich, "Molecular Dynamics in Biosystems," Pergamon, Oxford, England, 1977, pp. 97–129.

(4) J. G. Wagner and C. M. Metzler, *J. Pharm. Sci.*, **58,** 87 (1969).

(5) J. Koch-Weser, *N. Engl. J. Med.*, **291,** 233, 503 (1974).

(6) J. M. Van Rossum, *J. Pharm. Sci.*, **57,** 2162 (1968).

(7) P. H. Brill, *J. Appl. Probability*, **16,** 174 (1979).

(8) D. P. Gaver and R. G. Miller, in "Studies in Applied Probability and Management Science," K. J. Arrow, S. Karlin, and H. Searf, Eds., Stanford University Press, Stanford, Calif., 1962.

(9) J. W. Cohen, *J. Appl. Probability*, **14,** 405 (1977).

(10) J. Keilson and N. D. Mermin, *Trans. Inst. Radio Eng.*, **5,** 75 (1959).

ACKNOWLEDGMENTS

Supported in part by University of Manitoba Grant 431-2013-20.

This work was partially performed while P. H. Brill was visiting the Department of Industrial Engineering, University of Toronto, Toronto, Canada.

The authors appreciated the pertinent comments of the referee.

TLC Determination of Griseofulvin in Plasma and 6-Demethylgriseofulvin in Urine

Y. GARCEAU, J. BRISSON, I. DAVIS, R. L. DeANGELIS *, and J. HASEGAWA ˣ

Received February 26, 1979, from the *Biopharmacy Section, Pharmacy Research and Development Division, Ayerst Laboratories, Inc., Rouses Point, NY 12979.* Accepted for publication December 21, 1979. *Present address: Wellcome Research Laboratories, Research Triangle Park, NC 27709.

Abstract □ Fluorometric TLC procedures are described for the determination of griseofulvin in human plasma and 6-demethylgriseofulvin in human urine. Griseofulvin is extracted from plasma with ether, and its metabolite, 6-demethylgriseofulvin, is extracted from urine with benzene. Both compounds are subjected to TLC on silica gel plates. The plates are scanned using the fluorescent mode of a spectrodensitometer. For griseofulvin, the quantitation limit is 20 ng/ml of plasma and the recovery is 100%; for 6-demethylgriseofulvin, the limit is 1 μg/ml of urine and the recovery is 96%. The methods were used to determine the plasma levels of griseofulvin and the amount of 6-demethylgriseofulvin excreted in the urine of human volunteers after a single oral dose of griseofulvin.

Keyphrases □ Griseofulvin—TLC determination in plasma □ 6-Demethylgriseofulvin—TLC determination in urine □ TLC—determination of griseofulvin in plasma and 6-demethylgriseofulvin in urine □ Antifungal agents—TLC determination of griseofulvin in plasma and 6-demethylgriseofulvin in urine

The antifungal agent griseofulvin is metabolized mainly to 6-demethylgriseofulvin and 6-demethylgriseofulvin glucuronide in humans (1–3). Following oral griseofulvin administration to human volunteers, intact griseofulvin and 6-demethylgriseofulvin were measured in plasma (3). In urine, <0.2% of an oral dose was excreted as unchanged griseofulvin (3); the main urinary metabolites were 6-demethylgriseofulvin and its glucuronide, and together they accounted for 65% of an intravenous dose and 34–64% of an oral dose (4).

Plasma levels of unchanged griseofulvin and the urinary excretion of 6-demethylgriseofulvin have been used to estimate griseofulvin bioavailability (4–7). Griseofulvin has been measured in plasma using spectrophotofluorometry (8), GLC (9, 10), and high-pressure liquid chromatography (11, 12). The metabolite 6-demethylgriseofulvin has been measured in urine using UV spectrophotometry (13) and GLC (5, 14). A qualitative TLC procedure also was described and used to identify griseofulvin and its metabolites in urine (15).

This paper describes quantitative fluorometric TLC procedures that have the simplicity of a spectrophotometric method as well as the sensitivity and specificity of a GLC assay.

EXPERIMENTAL

Materials—All reagents and solvents were analytical reagent grade. Commercial silica gel TLC plates[1], 20 × 20 cm (without fluorescent indicator), were used. The plates were divided into 20 channels of 1-cm width with a scoring device[2].

Solutions of griseofulvin and 6-demethylgriseofulvin were prepared in methanol. Acetate buffer (0.1 *M*, pH 4.7) was prepared by dissolving 0.37 g of sodium acetate in 100 ml of distilled water and adjusting to pH 4.7 with acetic acid. Enzyme solutions of β-glucuronidase[3] from beef liver were prepared in this acetate buffer. 6-Demethylgriseofulvin was obtained by extraction from dog urine according to a published procedure (15).

Determination of Plasma Griseofulvin—One milliliter of human plasma was shaken with 5 ml of ether for 15 min to extract the drug. After centrifugation, a 3-ml aliquot of the ether phase was transferred to a clean centrifuge tube and evaporated to dryness under nitrogen[4] at 40–45°. The residue was dissolved in 100 μl of chloroform, and a 40-μl aliquot from this solution was spotted on a TLC plate along with standard griseofulvin solutions.

The plate was developed to a height of 10 cm in a saturated tank containing 100 ml of the ether–acetone (80:20) solvent system. Then the plate was air dried and scanned in a spectrodensitometer[5] containing a 200-w xenon–mercury lamp[6] and coupled to a density computer[7]. The instrument was operated in the fluorescence mode with excitation at 305 nm and emission at 650 nm. Quantitation was achieved by a computing digital integrator[8].

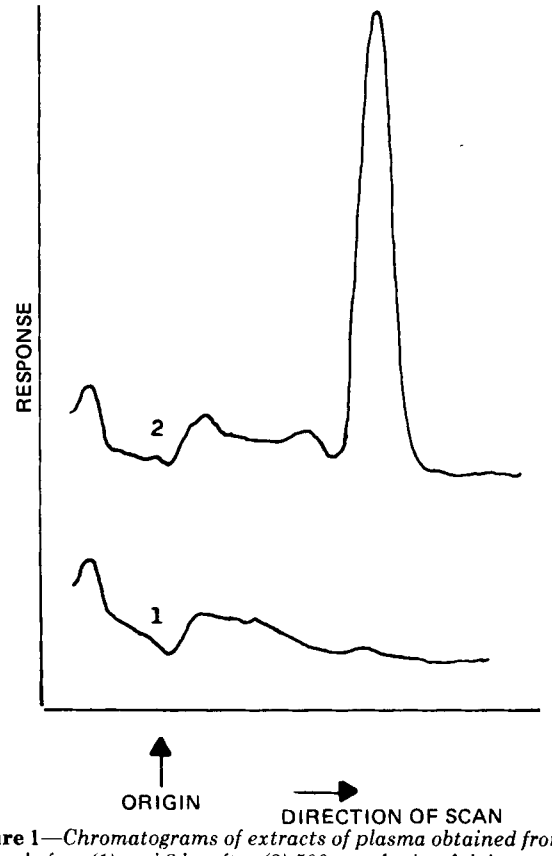

Figure 1—*Chromatograms of extracts of plasma obtained from a volunteer before (1) and 3 hr after (2) 500 mg of griseofulvin po.*

[1] Silplate-22, Brinkmann Instruments.
[2] SDA 320, Schoeffel Instrument Corp.
[3] Worthington Biochemical Corp.
[4] N-Evap, Organomation Associates.
[5] Model SD 3000, Schoeffel Instrument Corp.
[6] Hanovia Lamp Division, Comrand Precision Industries.
[7] Model SDC 300, Schoeffel Instrument Corp.
[8] Autolab System I, Spectra-Physics Corp.

0022-3549/80/0500-0561$01.00/0
© 1980, American Pharmaceutical Association

Table I—Recovery of Griseofulvin from Human Plasma

Amount Spiked, ng/ml	Amount Recovered, ng/ml	Percent Recovery
20	20	100.0
30	30	100.0
40	41	102.5
100	93	93.0
100	100	100.0
100	103	103.0
200	210	105.0
200	217	108.5
300	303	101.0
300	296	98.7
300	297	99.0
300	290	96.7
400	383	95.8
400	379	94.8
400	380	95.0
400	383	95.8
500	500	100.0
1000	1050	105.0
1000	1000	100.0
1000	980	98.0
1000	1020	102.0
1500	1570	104.6
Mean		99.9
SD		3.9

Determination of 6-Demethylgriseofulvin in Urine—For the determination of free 6-demethylgriseofulvin, 1 ml of urine was acidified with 0.1 ml of 1 *N* HCl and shaken with 2 ml of benzene for 15 min. The mixture was centrifuged to obtain a clear benzene phase. Ten-microliter aliquots of the benzene solution were spotted on a TLC plate along with standard solutions of 6-demethylgriseofulvin. The plate was developed to 10 cm in a saturated tank containing 100 ml of the chloroform–ether–acetone–acetic acid (65:20:15:0.5) solvent system. Then the plate was air dried and read in the fluorescence mode of a spectrodensitometer as described.

To assay conjugated 6-demethylgriseofulvin, 1 ml of urine was mixed with 0.5 ml of 0.1 *M* acetate buffer containing 430 units of β-glucuronidase. The solution was incubated at 37° for 90 min. After incubation, 0.1 ml of 1 *N* HCl was added, and the sample was shaken with 10 ml of benzene for 15 min. The mixture was centrifuged to obtain a clear benzene phase, and 20-μl aliquots of this phase were analyzed as described for the determination of free 6-demethylgriseofulvin. This procedure measures total (free and conjugated) 6-demethylgriseofulvin. To determine the amount of conjugated 6-demethylgriseofulvin, the free metabolite is subtracted from the total.

Recovery Experiments—Samples of human plasma were spiked with solutions of various griseofulvin concentrations, and urine samples were spiked with 6-demethylgriseofulvin. The spiked samples were assayed by the described procedure and compared to absolute standards.

Linearity of Response and Quantitation Limit of Absolute Standards—Solutions with different concentrations of griseofulvin and 6-demethylgriseofulvin were spotted on TLC plates and chromatographed to determine the linear ranges of instrument response. The quantitation limit was set as an "area under the peak" of 25,000 units,

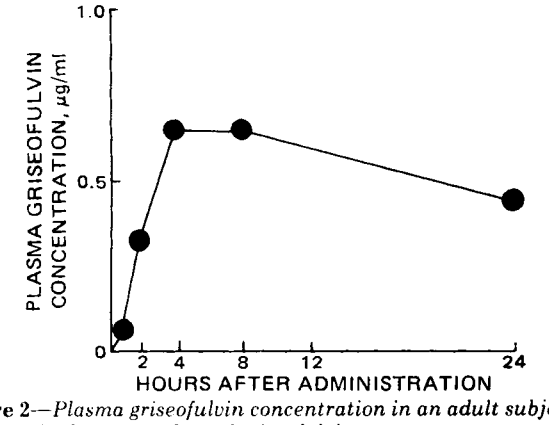

Figure 2—*Plasma griseofulvin concentration in an adult subject following a single 250-mg dose of griseofulvin.*

Table II—Recovery of 6-Demethylgriseofulvin from Human Urine

Amount Spiked, μg/ml	Amount Recovered, μg/ml	Percent Recovery
10	11	110.0
10	10	100.0
20	21	105.0
20	20	100.0
20	20	100.0
40	35	87.5
40	35	87.5
40	44	110.0
60	59	98.3
60	52	86.7
60	62	103.3
80	68	85.0
80	66	82.5
80	69	86.3
Mean		95.9
SD		9.6

which corresponded to 5 ng of griseofulvin or 6-demethylgriseofulvin/spot.

***In Vivo* Experiment**—To demonstrate the applicability of the methods, a plasma level profile of griseofulvin and a urinary excretion profile of 6-demethylgriseofulvin were obtained in human volunteers. One volunteer received 250 mg of griseofulvin[9], and blood samples were drawn before and 1, 2, 4, 8, and 24 hr after medication. Blood was transferred to tubes containing ethylenediaminetetraacetic acid, and the contents were mixed and centrifuged. Plasma was kept frozen until it was analyzed. A second volunteer received griseofulvin as one 500-mg tablet[10], and urine was collected for 72 hr after drug administration in pools at 24,

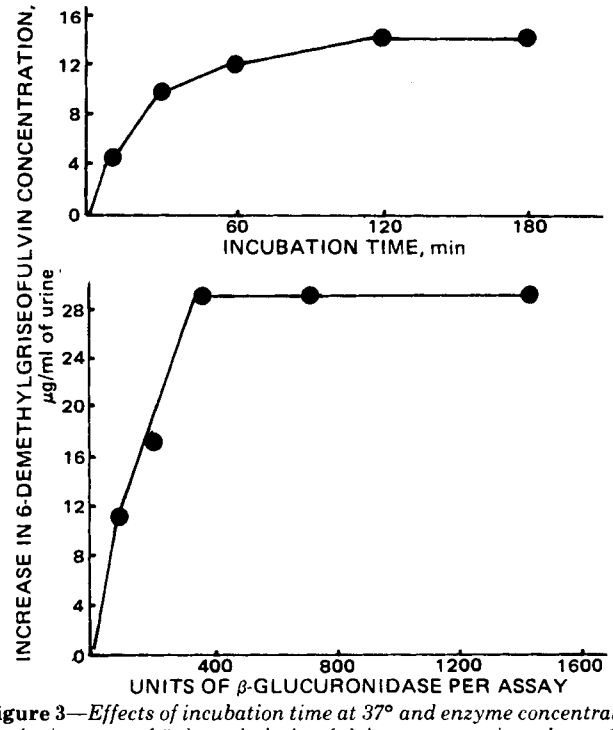

Figure 3—*Effects of incubation time at 37° and enzyme concentration on the increase of 6-demethylgriseofulvin concentration when a 1-ml urine sample was subjected to hydrolysis by β-glucuronidase. Top: time of incubation of urine sample in the presence of 430 units of β-glucuronidase. The urine specimen (0–24 hr) was collected from a volunteer receiving a daily dose of 125 mg of griseofulvin. Bottom: incubation of urine sample at 37° for 90 min in the presence of various concentrations of β-glucuronidase. Enzyme activity is expressed in Fishman units. The urine specimen (0–24 hr) was obtained from a volunteer who had received one oral dose of 450 mg of griseofulvin.*

[9] Grisactin 250, Ayerst Laboratories.
[10] Grisactin 500, Ayerst Laboratories.

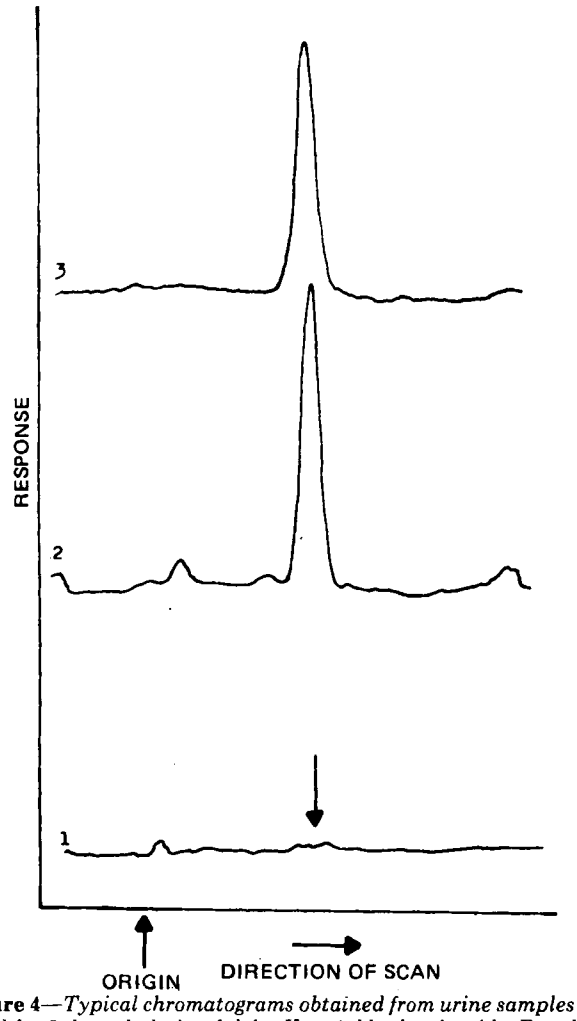

Figure 4—*Typical chromatograms obtained from urine samples analyzed for 6-demethylgriseofulvin. Key: 1, blank urine (the R_f value of 6-demethylgriseofulvin is indicated by the arrow); 2, pooled urine (0–24 hr) from a volunteer who received one single oral 500-mg dose of griseofulvin; and 3, standard of 6-demethylgriseofulvin with 100 ng/spot.*

48, and 72 hr. A preadministration urine sample also was obtained. The samples were kept frozen until they were analyzed.

RESULTS AND DISCUSSION

Plasma Griseofulvin—Griseofulvin had an R_f value of 0.25 in the TLC system and could be quantitated to 5 ng/spot. In terms of assay sensitivity in plasma, the limit of reliable quantitation was set at 20 ng/ml. Instrument response, as determined by the area under the peak, was linear from 0 to at least 300 ng/spot. In terms of concentrations in plasma, linearity was observed from 10 to at least 1000 ng/ml. The assay was free of interference from extractable plasma impurities and from the metabolite 6-demethylgriseofulvin (R_f 0.05).

Chromatograms of extracts from human plasma obtained before and after griseofulvin administration are shown in Fig. 1. Recoveries obtained from plasma samples spiked with griseofulvin over the 20–1500-ng/ml range varied between 93 and 109%, with a mean of 99.9% (Table I). The reproducibility was ±3.9% (*SD*), n = 22. The absolute accuracy of the mean was calculated using the expression $\overline{X} - \hat{X}$, where $\overline{X}$ is the mean of the set and $\hat{X}$ is the true value, defined here as 100% recovery. Therefore, the absolute accuracy of the mean was 99.9% − 100.0% = −0.1%. A plasma griseofulvin concentration–time curve obtained in a volunteer following oral administration of a single 250-mg dose is shown in Fig. 2.

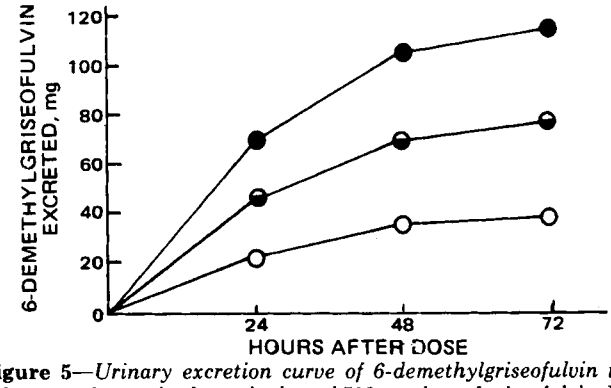

Figure 5—*Urinary excretion curve of 6-demethylgriseofulvin in a volunteer who received one single oral 500-mg dose of griseofulvin. Key: ●, total 6-demethylgriseofulvin; ⊖, free 6-demethylgriseofulvin; and ○, conjugated 6-demethylgriseofulvin.*

6-Demethylgriseofulvin in Urine—In the system used, 6-demethylgriseofulvin (R_f 0.26) was well separated from urine impurities and from the parent drug, griseofulvin (R_f 0.47). Instrument response, as measured by the areas under the peaks, was linear over the range tested, 0–600 ng/spot or 0–120 μg/ml of urine when expressed in concentration units. The detection limit was 5 ng/spot or 1 μg/ml. Recoveries obtained from urine samples spiked with 6-demethylgriseofulvin over the 10–80-μg/ml range varied between 88 and 108%, with a mean of 95.9% (Table II). The reproducibility was ±9.6% (*SD*), n = 14. The absolute accuracy of the mean was −4.1%.

In the determination of total (free and conjugated) 6-demethylgriseofulvin, it was essential to establish that the incubation period and the enzyme concentration used were adequate to hydrolyze all glucuronide present. Since no standard material of 6-demethylgriseofulvin glucuronide was available, urine samples from volunteers dosed with griseofulvin were subjected to hydrolysis using various β-glucuronidase concentrations and incubation times. As seen in Fig. 3, a glucuronidase concentration of 370 units in the 1.5-ml incubation mixture and an incubation time of 1.5 hr were sufficient to liberate the maximum amount of free 6-demethylgriseofulvin from the sample.

Chromatograms of a blank human urine sample and of a postdosing urine sample are shown in Fig. 4.

Figure 5 shows the 72-hr urinary excretion profile of 6-demethylgriseofulvin of a volunteer following oral administration of a single 500-mg dose of griseofulvin.

The described methods are sensitive, specific, and reproducible. In addition, they are simple, relatively rapid, and especially useful when a large number of samples must be analyzed.

REFERENCES

(1) M. J. Barnes and B. Boothroyd, *Biochem. J.*, **78**, 41 (1961).

(2) M. Rowland and S. Riegelman, *J. Pharm. Sci.*, **62**, 2030 (1973).

(3) C. C. Lin, J. Margat, R. Chang, J. McGlotten, and S. Symchowicz, *J. Pharmacol. Exp. Ther.*, **187**, 415 (1973).

(4) W. L. Chiou and S. Riegelman, *J. Pharm. Sci.*, **60**, 1376 (1971).

(5) P. Kabasakalian, M. Katz, B. Rosenkrantz, and E. Townley, *ibid.*, **59**, 595 (1970).

(6) W. E. Barrett and J. J. Hanigan, *Curr. Ther. Res.*, **18**, 491 (1975).

(7) W. E. Barrett and J. R. Bianchine, *ibid.*, **18**, 501 (1975).

(8) M. Rowland, S. Riegelman, and W. L. Epstein, *J. Pharm. Sci.*, **57**, 984 (1968).

(9) V. P. Shah, S. Riegelman, and W. L. Epstein, *ibid.*, **61**, 634 (1972).

(10) H. J. Schwarz, B. A. Waldman, and V. Madrid, *ibid.*, **65**, 370 (1976).

(11) L. P. Hackett and L. J. Dusci, *J. Chromatogr.*, **155**, 206 (1978).

(12) R. L. Nation, G. W. Peng, V. Smith, and W. L. Chiou, *J. Pharm. Sci.*, **67**, 805 (1978).

(13) M. Rowland and S. Riegelman, *ibid.*, **62**, 2030 (1973).

(14) E. Papp, K. Magyar, and H. J. Schwarz, *ibid.*, **65**, 441 (1976).

(15) P. A. Harris and S. Riegelman, *ibid.*, **58**, 93 (1969).

Stoichiometric Model of α-Cyclodextrin Complex Formation

THOMAS W. ROSANSKE and KENNETH A. CONNORS ˣ

Received October 9, 1979, from the *School of Pharmacy, University of Wisconsin, Madison, WI 53706.* Accepted for publication January 7, 1980.

Abstract □ The solubility, spectral, and kinetic methods were used to study complexing between α-cyclodextrin (ligand, L) and 3,5-dimethoxycinnamic acid, benzalacetone, and methyl cinnamate (substrates, S). In aqueous solution at 25° and with an ionic strength of 0.01 *M*, the following stability constants were found (K_{11} for SL and K_{12} for SL_2): 3,5-dimethoxycinnamic acid, $K_{11} = 1965\ M^{-1}$ and $K_{12} = 0$; benzalacetone, $K_{11} = 105\ M^{-1}$ and $K_{12} = 15\ M^{-1}$; and methyl cinnamate, $K_{11} = 1200\ M^{-1}$ and $K_{12} = 50\ M^{-1}$. A model of complex formation is proposed that can account for the observed stoichiometry and that yields stability estimates for two isomeric 1:1 complexes in the systems in which a 1:2 complex forms. For cinnamic acid, benzalacetone, and methyl cinnamate, stability constants are inversely correlated with the substrate dipole moment.

Keyphrases □ α-Cyclodextrin—complexation with 3,5-dimethoxycinnamic acid, benzalacetone, and methyl cinnamate, stoichiometric model □ Stability constants—complexes of α-cyclodextrin with cinnamic acid, benzalacetone, and methyl cinnamate □ Complexation—α-cyclodextrin, stoichiometric model

A previous study (1) showed that *trans*-cinnamic acid forms 1:1 (SL) and 1:2 (SL_2) complexes[1] with α-cyclodextrin (cyclohexaamylose) in aqueous solution. Therefore, knowledge of the factors that influence the stoichiometric relationships in such a system and that control the magnitudes of the complex stability constants was desired. For this purpose, the complexing of several substrates structurally related to cinnamic acid was studied in aqueous α-cyclodextrin solutions. These substrates are 3,5-dimethoxy-*trans*-cinnamic acid (I), benzalacetone (*trans*-4-phenyl-3-buten-2-one, II), and methyl *trans*-cinnamate (III). The complexing behavior was studied by the solubility, spectral, and kinetic techniques.

EXPERIMENTAL

Materials—3,5-Dimethoxy-*trans*-cinnamic acid[2] was recrystallized twice from water, mp 174.6–175°. Benzalacetone[2] was recrystallized twice from *n*-hexane, mp 39.7–40.7° [lit. (2) mp 41–42°]. Methyl *trans*-cinnamate[3] was distilled under reduced pressure, bp 95–97° (10–12 mm Hg), mp 32.9–33.9° [lit. (3) mp 33.5–34.5°]. α-Cyclodextrin[4] was used directly; drying to constant weight at 90° indicated 9.77% water content, corresponding closely to the hexahydrate (9.99% water); $[\alpha]_D^{25}$ +150.4 ± 2.2° (10 measurements) [lit. (4) $[\alpha]_D^{25}$ +150.5°].

Procedures—The solubility and spectral studies were carried out as described for cinnamic acid (1), except that in the solubility technique the supernatant solution was analyzed spectrophotometrically after appropriate dilution. For the 3,5-dimethoxycinnamic acid, this dilution was made a basic pH to minimize spectral perturbations caused by complexing since it is known (5) that acid anions complex less strongly than the parent carboxylic acid.

A kinetic method was used to study methyl cinnamate. Increasing amounts of α-cyclodextrin were weighed accurately into a series of 10-ml volumetric flasks and were dissolved in pH 10.36 carbonate buffer. To each flask, 0.2 ml of a saturated aqueous solution of methyl cinnamate was added. The solutions were brought to volume with the carbonate buffer. At recorded times, samples were analyzed spectrophotometrically at 295 nm. The kinetics were apparent first order.

All studies were carried out at 25.0° and an ionic strength of 0.01 *M*. The stability constants are defined by:

$$K_{11} = \frac{[SL]}{[S][L]} \qquad \text{(Eq. 1)}$$

$$K_{12} = \frac{[SL_2]}{[SL][L]} \qquad \text{(Eq. 2)}$$

RESULTS

3,5-Dimethoxycinnamic Acid—UV spectra of 3,5-dimethoxycinnamic acid with varying concentrations of α-cyclodextrin revealed isosbestic points at 231, 240, and 300 nm; these isosbestic points were preserved even at high ligand concentrations. This behavior is consistent with 1:1 stoichiometry, and the Benesi–Hildebrand double-reciprocal plot is shown in Fig. 1. Least-squares analysis gave $K_{11} = 1970\ M^{-1}$.

Figure 2 is the solubility diagram for this system. The linear rise in total solubility is consistent with 1:1 complexing, and the stability constant evaluated from the line (excluding the three highest points) was $K_{11} = 1960\ M^{-1}$, in excellent agreement with the result from the spectral study. (The deviation of the three terminal points is attributed to a small spectral perturbation caused by complexation in the analytical solution.) The well-behaved isosbestic points, the linear spectral and solubility plots, and the agreement of K_{11} values from the independent spectral and solubility studies all indicate that this system is described fully by 1:1 stoichiometry.

Benzalacetone—Figure 3 shows the solubility diagram for the benzalacetone system. The initial rising portion is followed by a plateau region, and then a decrease in S_t occurs with a shoulder unusual in such diagrams. The shape of this curve will be discussed. Analysis of the solid phases gave the following results for $10^2 L_t$ and x_L, where x_L is the mole fraction of cyclodextrin in the solid: 2.90, 0.26; 4.90, 0.60; 6.01, 0.61; 6.90, 0.65; 8.02, 0.66; and 10.1, 0.67. These data show that at least one complex with a stoichiometric L to S ratio of greater than unity must be present.

Interpretation of the initial rising portion in terms of 1:1 plus 1:2 complexes, as described previously (1, 6), shows that the slope of the line is 0.50, which implies that $K_{11} = 1/s_0$, where s_0 is the solubility at $L_t = 0$. This relationship gives $K_{11} = 105\ M^{-1}$; with $K_{11} = 1/s_0$, the data can be fitted regardless of the value of K_{12}. Thus, the solubility study showed that a complex of higher L to S stoichiometry must be present and yielded an estimate of K_{11}.

The spectral data showed isosbestic points at 241 and 304 nm; these points were lost at cyclodextrin concentrations of greater than ~0.007

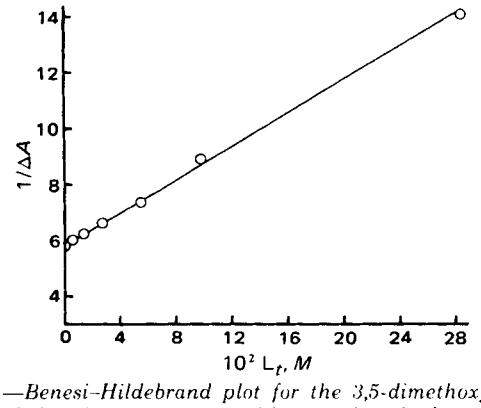

Figure 1—*Benesi–Hildebrand plot for the 3,5-dimethoxycinnamic acid–α-cyclodextrin system at 25° with a wavelength of 291 nm, a path length of 1 cm, a total substrate concentration of 4.54 × 10⁻⁵ M, and a pH of 2.3; L_t represents the total ligand concentration (moles per liter), and ΔA is the change in absorbance.*

[1] The substrate (cinnamic acid in this example) is represented by S, and the ligand (cyclodextrin) is represented by L.

[2] Aldrich.

[3] Eastman.

[4] Sigma lot 106C-0046-1.

0022-3549/80/0500-0564$01.00/0
© 1980, American Pharmaceutical Association

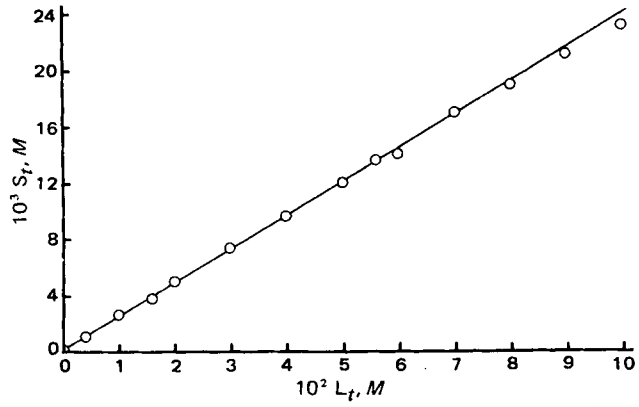

Figure 2—*Solubility study of the 3,5-dimethoxycinnamic acid–α-cyclodextrin system at 25°. The substrate solubility at $L_t = 0$ is 1.51×10^{-4} M; S_t represents the total substrate concentration.*

M, indicating the presence of at least two complexes. The spectral results at 291 nm are given in Fig. 4. The smooth curve was calculated by assuming 1:1 and 1:2 complexes, fixing K_{11} at 105 M^{-1} (from the solubility data), and allowing K_{12} and the complex molar absorptivities to function as adjustable parameters, as described previously (1). The resulting values were $K_{11} = 105\ M^{-1}$, $K_{12} = 15\ M^{-1}$, $\Delta a_{11} = 4500$, and $\Delta a_{12} = 6600$, where $\Delta a_{11} = a_S - a_{11}$, *etc.*, with *a* representing the designated molar absorptivity.

Methyl Cinnamate—The solubility plot for methyl cinnamate (Fig. 5) is qualitatively similar to that of benzalacetone. The solid phase analysis again gave evidence of a 1:2 complex ($10^2 L_t$ and x_L): 2.00, 0.17; 4.01, 0.56; 4.90, 0.60; 6.01, 0.62; 6.80, 0.66; and 10.1, 0.67. Treatment of the initial rising portion in terms of SL and SL_2 complexes gives $K_{11} = 1200\ M^{-1}$ and $K_{12} = 50\ M^{-1}$.

The kinetic method used to study this system is based on the inhibitory effect of cyclodextrin on the rate of alkaline hydrolysis of methyl cinnamate. Scheme I shows the assumed kinetics.

$$S + OH^- \xrightarrow{k_S} \text{products}$$

$$SL + OH^- \xrightarrow{k_{11}} \text{products}$$

$$SL_2 + OH^- \xrightarrow{k_{12}} \text{products}$$

Scheme I

The following equations then are readily derived, as was shown previously (6, 7):

$$L_t = [L] + \frac{S_t(K_{11}[L] + 2K_{11}K_{12}[L]^2)}{1 + K_{11}[L] + K_{11}K_{12}[L]^2} \qquad \text{(Eq. 3)}$$

$$\frac{k_S - k'_S}{k_S} = \frac{q_{11}K_{11}[L] + q_{12}K_{11}K_{12}[L]^2}{1 + K_{11}[L] + K_{11}K_{12}[L]^2} \qquad \text{(Eq. 4)}$$

where L_t is the total ligand concentration, [L] is the free (uncomplexed) ligand concentration, k'_S is the apparent second-order rate constant in the presence of ligand, $q_{11} = 1 - k_{11}/k_S$, and $q_{12} = 1 - k_{12}/k_S$. It is not practical to obtain an expression for k'_S as an explicit function of L_t, so a curve-fitting procedure is used. Figure 6 shows the kinetic data; the smooth line was calculated with Eqs. 3 and 4, taking $K_{11} = 1200\ M^{-1}$ and $K_{12} = 50\ M^{-1}$ (from the solubility study) and treating q_{11} and q_{12} as adjustable parameters. The method is used to assign reasonable values to [L] and to calculate corresponding values for L_t and k'_S for comparison with the experimental results. The line in Fig. 6 was obtained using $q_{11} = 0.75$ and $q_{12} = 0.86$.

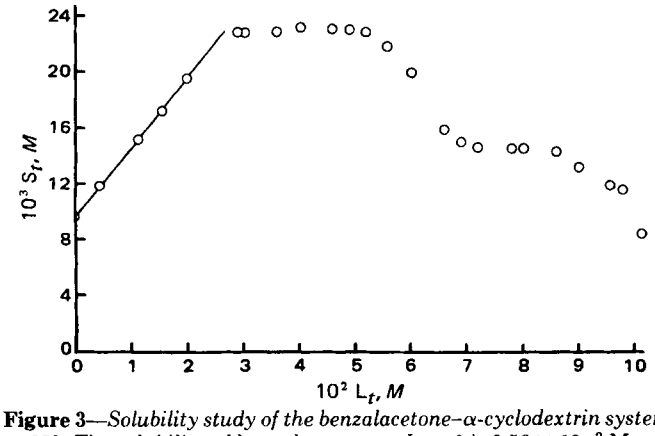

Figure 3—*Solubility study of the benzalacetone–α-cyclodextrin system at 25°. The solubility of benzalacetone at $L_t = 0$ is 9.56×10^{-3} M.*

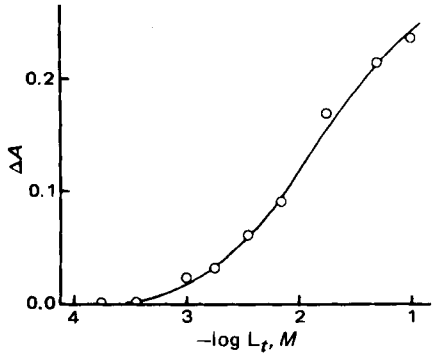

Figure 4—*Change in absorbance at 291 nm in the benzalacetone–α-cyclodextrin system with a path length of 1 cm, a total substrate concentration of 4.39×10^{-5} M, and a pH of 2.3.*

DISCUSSION

Complex Stoichiometry and Stability—Each substrate was investigated by two experimental techniques because such comparative studies have been effective in elucidating stoichiometric relationships (1, 7). The important pieces of information are the isosbestic point behavior, the solid phase compositions, and the quantitative consistency between the two methods. The essential conclusion is that solutions of α-cyclodextrin with 3,5-dimethoxycinnamic acid can be described fully in terms of 1:1 complex formation whereas the benzalacetone and methyl cinnamate systems require 1:1 and 1:2 stoichiometries for their description.

The shapes of the solubility curves for benzalacetone and methyl cinnamate have not been explained fully. In systems containing 1:1 and 1:2 complexes, there are several possibilities for solubility behavior: (*a*) the solubility of SL will be reached first, (*b*) the solubility of SL_2 will be reached first, (*c*) the solubilities of SL and SL_2 will be reached essentially simultaneously, and (*d*) SL and SL_2 will form solid solutions. Case *a* is observed with cinnamic acid and apparently does not apply here (1). Cases *b* and *c* both require, as argued previously (6), that $x_L = 0.67$ at the point terminating the plateau; hence, these cases do not account for the solid phase analyses. The formation of a solid solution from solid SL and SL_2 does not seem unlikely if these are inclusion complexes; X-ray evidence for solid cyclodextrin complexes with channel-like structures was reported (8, 9). This reaction decreases the number of solid phases by one; then upon depletion of solid S, only one solid phase remains (the solid solution), and the constraint on S_t is removed.

The q_{11} and q_{12} values obtained from the kinetic analysis may be interpreted as the fractional decrease in reactivity of the complexed substrate relative to the uncomplexed substrate. If the system actually contains two isomeric 1:1 complexes, then q_{11} is a weighted average of the corresponding quantities for the individual complexes (7). It is quite possible for one of these quantities to be positive ($k_{11} < k_S$) while the other is negative ($k_{11} > k_S$). The value of q_{12} seems somewhat low

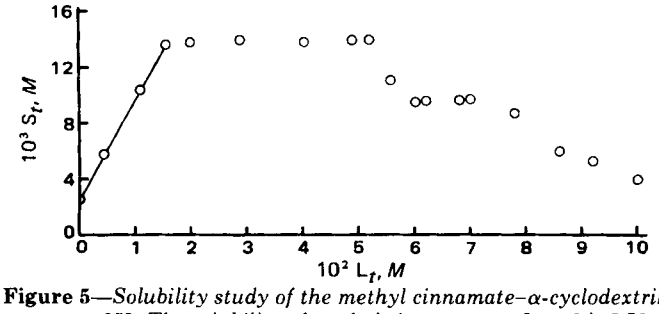

Figure 5—*Solubility study of the methyl cinnamate–α-cyclodextrin system at 25°. The solubility of methyl cinnamate at $L_t = 0$ is 2.50×10^{-3} M.*

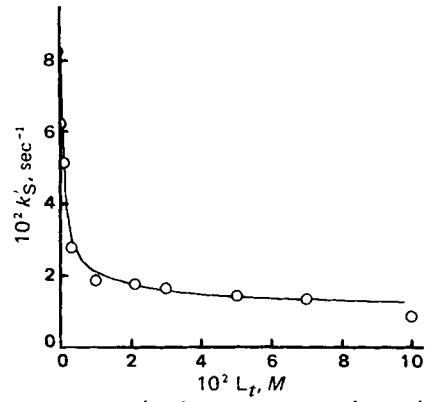

Figure 6—*Apparent second-order rate constants for methyl cinnamate hydrolysis as a function of the α-cyclodextrin concentration; the rate constant at* $L_t = 0$ *was* 8.33×10^{-2} M^{-1} sec^{-1}.

(complete inhibition, $q_{12} = 1$, is anticipated for the fully included substrate); however, as Fig. 6 shows, considerable uncertainty (at least 10%) may be associated with this value because of imprecision in the rate data. Table I summarizes the stability constant findings for these substrates.

Stoichiometric Model of Complexing—As a framework for describing and explaining complex stoichiometry and stability in these systems, the following argument may be useful. Let h-H represent the cyclodextrin (host) molecule, the lower and upper case letters indicating that the two ends of the cavity are structurally different, and let g-G represent a linear nonsymmetrical substrate (guest) molecule. Then all possible 1:1 inclusion complexes may be represented as follows, where it is assumed that, within each orientation, the energy distribution of positional isomers is narrow so that only a single complex need be considered:

1:1 complexes	symbol
g-G h-H	gH
g-G H-h	gh
G-g h-H	GH
G-g H-h	Gh

It also is possible, in principle, to form 2:1 and 1:2 inclusion complexes:

2:1 complexes	symbol
g-G G-g H-h	HGGh
g-G g-G H-h	HGgh
G-g g-G H-h	Hggh
G-g G-g H-h	HgGh

1:2 complexes	symbol
g-G h-H h-H	gHhG
g-G H-h h-H	ghhG
G-g h-H H-h	GHHg
G-g H-h H-h	GhHg

Now suppose that, for the systems being considered, no 2:1 complexes exist. In the present study, there was no necessity to invoke S_2L complexes, and there appears to be no literature report of S_2L complexes with α-cyclodextrin. Then it is reasonable to infer that the guest molecule can enter only one end of the host. As a consequence of this inference, there can be only two 1:1 complexes and only one 1:2 complex. For example, suppose only the H end of the host can be entered. In this case, the only possible complexes are gH, GH, and GHHg. The model thus has led, for this experimental case, to a great simplification of the stoichiometric possibilities. Other special cases of the general model can be described but are not required in this treatment.

Table I—Stability Constants for α-Cyclodextrin Complexes at 25°

Substrate	K_{11}, M^{-1}	K_{12}, M^{-1}
Cinnamic acid[a]	2260	60
Cinnamate ion[a]	110	15
3,5-Dimethoxycinnamic acid	1965	0
Benzalacetone	105	15
Methyl cinnamate	1200	50

[a] From Ref. 1.

It is known (7) that the observed K_{11} value obtained from any experimental technique is the sum of the stability constants for all isomeric 1:1 complexes; hence, for the case being considered:

$$K_{11} = K_{gH} + K_{GH} \qquad \text{(Eq. 5)}$$

To carry the analysis further, the assumption is made that the 1:2 complex is formed by adding a host molecule to a 1:1 complex without perturbing the structure (or energy) of the 1:1 complex. The 1:2 complex can be formed *via* the gH route (Scheme II) or the GH route (Scheme III).

$$gH + h\text{-}H \overset{K'}{\rightleftharpoons} GHHg$$

Scheme II

$$GH + h\text{-}H \overset{K''}{\rightleftharpoons} GHHg$$

Scheme III

The observed stability constant for 1:2 complex formation therefore is given by:

$$K_{12} = \frac{[GHHg]}{([gH] + [GH])[h\text{-}H]} \qquad \text{(Eq. 6)}$$

which becomes:

$$K_{12} = \frac{K'K''}{K' + K''} \qquad \text{(Eq. 7)}$$

The assumption that addition of the second host molecule does not perturb the preformed 1:1 complex structure is equivalent to assuming $K' = K_{GH}$ and $K'' = K_{gH}$; thus:

$$K_{12} = \frac{K_{gH}K_{GH}}{K_{gH} + K_{GH}} \qquad \text{(Eq. 8)}$$

With Eqs. 5 and 8, K_{gH} and K_{GH} can be evaluated[5].

Table II lists K_{gH} and K_{GH} values for the substrates of Table I. The assignment of symbols is arbitrary. Because of the structural likenesses among the members of this series of substrates, it seems reasonable to attribute all larger values to one mode (K_{GH}) and the smaller constants to the other (K_{gH}).

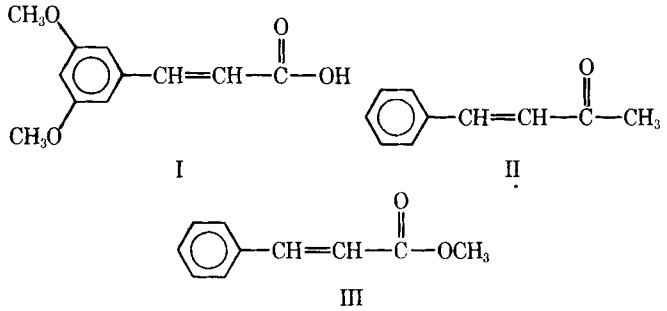

Interpretation of the data for these substrates (I–III) in terms of the model suggests that the two isomeric 1:1 complexes are formed by inclusion of either the side chain or the phenyl ring in the cyclodextrin cavity. Molecular models indicate that the disubstituted phenyl ring of I cannot penetrate the ligand cavity; hence, the stoichiometric model predicts that one of the isomeric 1:1 constants will be zero and, therefore, that $K_{12} = 0$. This behavior is observed; therefore, the assignments in Table II signify that K_{GH} describes binding of the side chain whereas K_{gH} describes binding of the phenyl ring. A further prediction is that K_{GH} for I should be very similar to that for cinnamic acid, as is seen.

[5] Equation 8 can be written as $1/K_{12} = 1/K_{gH} + 1/K_{GH}$; *i.e.*, the 1:2 dissociation constant is equal to the sum of the 1:1 dissociation constants.

Table II—Calculated Isomeric 1:1 Stability Constants [a]

Substrate	K_{GH}, M^{-1}	K_{gH}, M^{-1}
Cinnamic acid	2199	61.5
Cinnamate ion	92.1	17.9
3,5-Dimethoxycinnamic acid	1965	0
Benzalacetone	86.9	18.1
Methyl cinnamate	1148	52.3

[a] Calculated with Eqs. 5 and 8 from the data in Table I.

All substrates in Table II other than I evidently offer the possibility of binding at both sites, so significant values of both K_{11} and K_{12} are anticipated and observed. Since the model has no provision for substituent effects, it does not provide quantitative predictions for these substrates. The advantages of the model are in transforming a potentially very complicated system into a fairly simple one on the basis of experimental observation and reasonable approximations and in providing qualitative stoichiometric predictive ability and a means for deriving quantitative estimates of isomeric stability constants when certain assumptions are met.

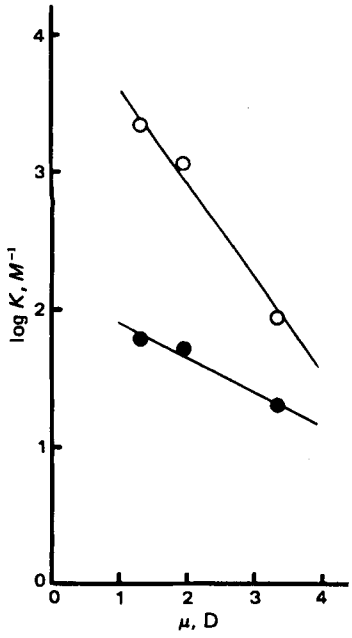

Figure 7—*Plot of log* K_{GH} (○) *and log* K_{gH} (●) *against the substrate dipole moment for II (μ = 3.34 D), III (μ = 1.95 D), and cinnamic acid (μ = 1.31 D). Dipole moments are from Ref. 10. The lines have no theoretical significance.*

Dipole Moment Correlation—The stability constants for the substrates in Table II, particularly K_{GH}, vary more than might be expected based on the apparent structural similarity of these compounds. The behavior of benzalacetone, in particular, seems anomalous. However, the constants in Table II for II, III, and cinnamic acid correlate well with the substrate dipole moment, as shown in Fig. 7; the larger the dipole moment, the smaller is the stability constant. This behavior is consistent with the view that the interior of the cyclodextrin cavity is less polar than the surrounding aqueous medium; hence, the more polar the substrate, the less is its tendency to partition into the ligand cavity.

The relative slopes of the plots for K_{GH} and K_{gH} in Fig. 7 substantiate the structural assignments of these quantities, the more sensitive quantity (K_{GH}) representing the side chain upon which the structural change is made and, therefore, responding more to the change than does K_{gH}, which describes binding far removed from the structural alteration. That the constant assigned to the side chain, which is the more polar end of the substrate molecule, is larger than that for the phenyl ring may seem inconsistent, but the comparison overlooks other factors, particularly the sizes of these two binding sites.

The cinnamate-ion system is qualitatively consistent with this interpretation. The essentially identical stability constants for cinnamate and benzalacetone suggest that a methyl ketone may be a good model for the polarity of a carboxylate ion.

REFERENCES

(1) K. A. Connors and T. W. Rosanske, *J. Pharm. Sci.*, **69,** 173 (1980).

(2) A. L. Wilds, L. W. Beck, W. J. Close, C. Djerassi, J. A. Johnson, Jr., T. L. Johnson, and C. H. Shunk, *J. Am. Chem. Soc.*, **69,** 1985 (1947).

(3) M. L. Bender and B. Zerner, *ibid.*, **84,** 2550 (1962).

(4) D. French, M. L. Levine, J. H. Pazur, and E. Norberg, *ibid.*, **71,** 353 (1949).

(5) K. A. Connors and J. M. Lipari, *J. Pharm. Sci.*, **65,** 379 (1976).

(6) T. W. Rosanske, Ph.D. thesis, University of Wisconsin, Madison, Wis., 1979.

(7) K. A. Connors and J. A. Mollica, *J. Pharm. Sci.*, **55,** 772 (1966).

(8) P. C. Manor and W. Saenger, *Nature*, **237,** 392 (1972).

(9) M. Noltemeyer and W. Saenger, *ibid.*, **259,** 629 (1977).

(10) A. L. McClellan, "Tables of Experimental Dipole Elements," W. H. Freeman, San Francisco, Calif., 1963.

ACKNOWLEDGMENTS

Supported in part by National Science Foundation Grant GP-36567 and in part by a grant from The Upjohn Co.

Rate and Pattern of Gastric Emptying in Humans Using ^{99m}Tc-Labeled Triethylenetetraamine–Polystyrene Resin

MICHAEL C. THEODORAKIS *x, GEORGE A. DIGENIS ‡, ROBERT M. BEIHN ‡, MANVENDRA B. SHAMBHU ‡, and FRANK H. DeLAND ‡

Received September 17, 1979, from the **Department of Veterinary Biosciences, Division of Nuclear Medicine, College of Veterinary Medicine, University of Illinois at Urbana–Champaign, Urbana, IL 61801,* and the ‡*Divisions of Medicinal Chemistry and Nuclear Medicine, Colleges of Pharmacy and Medicine, University of Kentucky, Lexington, KY 40506.* Accepted for publication December 26, 1979.

Abstract □ The preparation and application of a new radiopharmaceutical used in the investigation of the rate and pattern of gastric emptying by external scintigraphy are described. Triethylenetetraamine was bound covalently to cross-linked chloromethylated polystyrene. The triethylenetetraamine–polystyrene resin tenaciously and rapidly bound technetium 99*m*. The gastric emptying rate was evaluated in normal adult volunteers and patients by serially recording the gastric radioactivity after ingestion of a test meal mixed with ^{99m}Tc-labeled triethylenetetraamine–polystyrene resin. The data indicated that ^{99m}Tc-labeled triethylenetetraamine–polystyrene resin was an ideal agent for assessing the rate and pattern of gastric emptying in humans. The gastric emptying half-time ($t_{1/2}$GE) in normal subjects ranged from 25 to 75 min.

Keyphrases □ Radiopharmaceuticals—^{99m}Tc-labeled triethylenetetraamine–polystyrene resin, determination of gastric emptying rate and pattern, humans □ GI motility—determination of gastric emptying rate and pattern, radionuclide imaging, humans □ Triethylenetetraamine–polystyrene resin, ^{99m}Tc-labeled—determination of gastric emptying rate and pattern, humans

The introduction of γ-emitting short-lived radionuclides and the development of the scintillation camera connected to a fast-acquisition digital data processor, multimode analyzer, and videotape recorder permit the noninvasive investigation of the rate and pattern of gastric emptying by external scintigraphy. Quantitative dynamic data and excellent scintigraphic images of the stomach, intestines, and colon can be obtained without physical or physiological influences on the GI tract.

BACKGROUND

In several clinical situations, detailed information about abnormalities in the pattern and rate of gastric emptying would be helpful. Such abnormalities already are recognized as being concomitant with certain diseases. For instance, hypermotility has been associated with duodenal ulcers, while diminished gastric peristalsis has been associated with gastric ulcers (1, 2). Furthermore, delayed gastric emptying has been observed in malignant diseases of the stomach and in pyloric stenosis (3, 4).

Measurement of gastric emptying is not only an important aid to the clinician studying gastroduodenal disease, dumping syndrome, and postvagotomy disturbances but also is a major determinant in the absorption rate of drugs. Individual variations in the drug absorption rate from any dosage form may be due largely to differences in the rate of gastric emptying (5, 6).

Since sodium [^{51}Cr]chromate and a rectilinear scanner first were used to measure the gastric emptying rate (7), several other radiopharmaceutical preparations have been used for the same purpose, including: ^{113m}In- and ^{99m}Tc-labeled diethylenetriaminepentaacetic acid (8, 9), a ^{113m}In-labeled microcolloid (10), a ^{99m}Tc-labeled colloid of antimony sulfide (11), ^{99m}Tc-labeled human albumin microspheres (12), cesium 129 adsorbed onto a suspension of zirconium phosphate (13), and their combinations (8, 13).

The disadvantages of these radiopharmaceutical preparations are well known. For instance, ^{113m}In- and ^{99m}Tc-labeled diethylenetriaminepentaacetic acid are water soluble and remain in the liquid phase of the gastric content, which is discharged through the pylorus more rapidly than the solid phase, and thus lower half-time values of gastric emptying result. Colloidal preparations are difficult to prepare, and their physicochemical properties offer disadvantages such as the formation of micelles and coagulation. The adsorption or absorption of the radiopharmaceutical by the stomach walls also provides an opportunity for error.

The recently introduced radiopharmaceutical ^{99m}Tc-labeled triethylenetetraamine–polystyrene resin (I) (14, 15) is free of these shortcomings and approximates the characteristics of an ideal radiopharmaceutical for assessing the rate and pattern of gastric emptying. These characteristics are: (*a*) not to influence the osmolality of the stomach content, (*b*) to be nonabsorbable and nonadsorbable, (*c*) to bind the radionuclide tenaciously and not to exchange it with food particles or the stomach wall, (*d*) to possess ideal food-mixing characteristics and have a particle size comparable to that of foods, and (*e*) to be nontoxic and inert and give reproducible and noninvasive estimates of the gastric emptying time without exposing the patient to a high radiation dose.

EXPERIMENTAL

Preparation of Popcorn Polystyrene—The polymer was prepared according to the procedure described by Letsinger *et al.* (16). It was washed three times with chloroform, dried, and broken down in a blender.

Preparation of Chloromethylated Polystyrene—Popcorn polystyrene (70 g, 40–100 mesh) was allowed to swell in 550 ml of chloroform for 1 hr. A mixture of 100 ml of chloromethyl methyl ether and 40 ml of stannic chloride was added to the polystyrene, and the contents were stirred at 25° for 2 hr. After filtration, the resin was washed with chloroform, dioxane, dioxane–water, water, and acetone. The product was dried at 60° under vacuum for 24 hr, yielding 86 g.

Anal.—Calc. for chloromethyl groups on 50% of the resin rings: Cl, 13.4%. Found: Cl, 13.3%.

Preparation of Triethylenetetraamine–Polystyrene Resin (I)—Chloromethylated polystyrene (10 g) was added to 30 ml of pyridine. After 30 min, a 10-fold excess of the amine was added; the mixture was maintained at 95° in an oil bath under a calcium chloride drying tube. The resin was recovered by filtration and washed with pyridine, water, and methanol. It was dried at 60° under vacuum.

Anal.—Calc. for: N, 14.87; Cl, 0.0. Found: N, 9; Cl, 0.08.

Uptake of Sodium [^{99m}Tc]Pertechnetate by Triethylenetetraamine–Polystyrene Resin—Triethylenetetraamine–polystyrene resin (0.20 g), with a bead size ranging between 0.16 and 0.4 mm, was placed in a 150-ml beaker, and 50 ml of double-distilled water was added. The pH was adjusted to a predetermined value with 0.1 *N* HCl. A 50-ml aliquot of sodium [^{99m}Tc]pertechnetate (52 μCi) in distilled water was added. The mixture was stirred magnetically, and the pH was kept constant and monitored by a pH meter[1]. The temperature was maintained at 23–25°. At the appropriate time intervals, 1-ml samples were withdrawn and counted by a γ-ray well counter[2].

Preparation of ^{99m}Tc-Labeled Triethylenetetraamine–Polystyrene Resin—Triethylenetetraamine–polystyrene resin (0.25 g, 40–100 mesh) was placed in a 50-ml beaker with 20 ml of distilled water and stirred for 1 min. A solution of sodium pertechnetate[3] (20 μCi–1 mCi) was added. The mixture was stirred for 10 min, and the labeled resin was

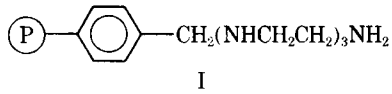

I

[1] Beckman Zeromatic SS-3.
[2] Picker Spector Scaler-4.
[3] Technetium 99*m*, obtained from a ^{99}Mo-generator (E. R. Squibb and Sons, Princeton, NJ 08540), as sodium [^{99m}Tc]pertechnetate in saline.

0022-3549/80/0500-0568$01.00/0
© 1980, American Pharmaceutical Association

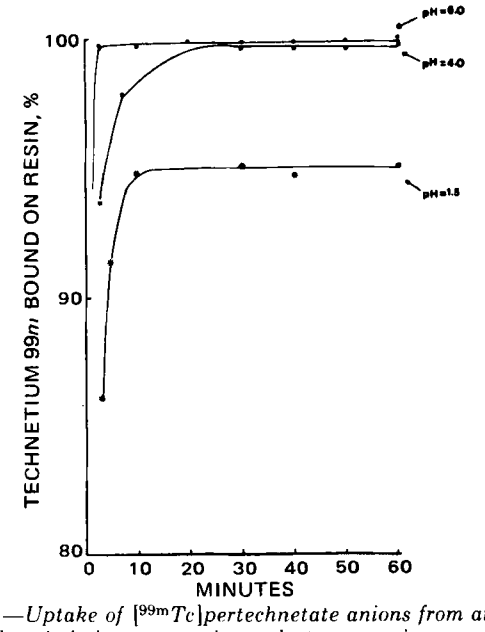

Figure 1—*Uptake of [^{99m}Tc]pertechnetate anions from an aqueous solution by triethylenetetraamine–polystyrene resin.*

recovered by filtration. The resin was washed with two 50-ml aliquots of distilled water and subsequently was counted to determine the specific activity.

Stability of ^{99m}Tc-Labeled Triethylenetetraamine–Polystyrene Resin in Simulated Gastric Juice—The ^{99m}Tc-labeled triethylenetetraamine–polystyrene resin (0.4 g, 2 μCi/g) was introduced in a beaker containing 50 ml of simulated gastric juice[4] (pH 1.4). The mixture was stirred magnetically, and the temperature was maintained at 25°. Samples of 0.5 ml were withdrawn at predetermined time intervals.

Human Testing—To evaluate the new radiodiagnostic agent, 20 adult male and female hospital patients were studied. Normal subjects who had never undergone GI tract surgery and subjects who had had surgery of the upper GI tract participated in the study. None of the subjects was treated with anticholinergic drugs prior to or during the study. No special preparation of the subject was needed. Two reference points were drawn on the abdominal skin of the subject and on the oscilloscope by the radioactive marker, cobalt 57, to ensure reproducibility of the position of the subject relative to the camera.

The ^{99m}Tc-labeled triethylenetetraamine–polystyrene resin was mixed with a test meal consisting of 33.3 g of cream of wheat and 2.4 g of sodium chloride in 235 ml of water. After the subject ingested the labeled test meal, the time was recorded and the subject was placed under the γ-camera[5,6] in the supine position. The positions of the γ-camera and the subject were adjusted so that the entire stomach appeared in the center of the monitoring oscilloscope. Several scintiphotographs of the stomach were obtained at certain time intervals.

In each time interval, four to nine points were collected. Each point represented the integrated relative radioactivity per minute of the desired flagged area of the stomach. The data were stored on a magnetic tape for future reference. The logarithm of the relative radioactivity of the stomach was plotted against time. From the slope of the graph, the half-time of the gastric emptying ($t_{1/2}$GE) of the test meal and the ^{99m}Tc-labeled triethylenetetraamine–polystyrene resin beads was determined. A whole-body survey at the end of each study failed to show any detectable activity outside of the GI tract.

RESULTS

Popcorn polystyrene, an opaque, low-density polymer, was prepared by copolymerization of styrene and divinylbenzene (99.8:0.2) according to a literature procedure (16). The particle size was reduced after a chloroform wash, and 40–100-mesh beads were used.

[4] USP.

[5] Baird atomic system 77 (Baird Atomic Nuclear Division, Bedford, MA 01730) equipped with a computer and magnetic tape and possessing storage and replay capability.

[6] Pho-Hp camera interfaced with a Nuclear data 50/50 computer, Nuclear of Chicago, Des Plaines, Ill.

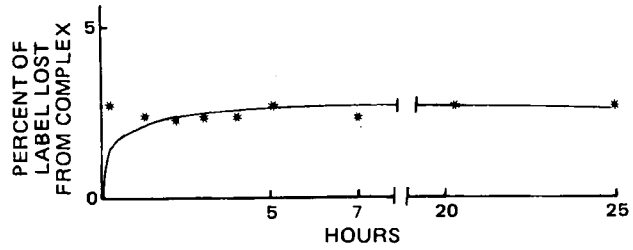

Figure 2—*Percent of radioactivity lost from ^{99m}Tc-labeled triethylenetetraamine–polystyrene in simulated gastric juice (pH 1.4).*

Introduction of chloromethyl functions into the insoluble polymer was carried out by reaction with chloromethyl methyl ether in the presence of anhydrous stannic chloride. The degree of chloromethylation of popcorn polystyrene was controlled by the amounts of stannic chloride and chloromethyl methyl ether and the reaction time. Chloromethyl groups were introduced in 50% of the polystyrene rings, producing a resin with 3.6 mEq of chloride/g.

Attachment of triethylenetetraamine was performed by swelling of the chloromethylated resin beads (40–100 mesh) in pyridine, followed by treatment with a 10-fold excess of triethylenetetraamine at 95°. Elemental analysis for nitrogen and chlorine indicated that triethylenetetraamine was bound to polystyrene by more than one attachment (17).

Triethylenetetraamine–polystyrene resin beads (40–100 mesh) efficiently and quantitatively bound the [^{99m}Tc]pertechnetate anions from aqueous solutions of ~10^{-9} *M* sodium [^{99m}Tc]pertechnetate. The anion uptake at three pH values (1.4, 4.0, and 6.0) was complete in 10 min (Fig. 1). When the popcorn polystyrene and chloromethylated polystyrene resins were used, the uptake of pertechnetate anions was 8.4 and 8.6%, respectively, after 60 min.

The ^{99m}Tc-labeled resin was stable in simulated gastric juice, releasing only 2.0% of the radioactivity in 25 hr at 37° (Fig. 2). The results of experiments in humans showed that <0.2% of the ingested radioactivity appeared in the blood and urine during the passage of the resin throughout the entire GI tract. A whole-body survey at the end of each study failed to show any detectable activity outside of the GI tract.

Twenty healthy adult volunteers were studied to establish a normal range of the gastric emptying rate (Table I). Invariably, the subjects exhibited a monoexponential pattern of gastric emptying. A typical curve is shown in Fig. 3. The ordinate represents the logarithm of relative radioactivity (expressed as counts per minute) and the abscissa denotes the time (minutes). The relative radioactivity was determined by selecting, with an electronic cursor, a region of interest over the whole gastric area excluding the pylorus and intestines. The slope of the curve was equal to $-\lambda\text{eff}/2.303$.

The observed constant, λeff, was equal to the sum of the technetium 99*m* decay constant, λ, and the rate constant of gastric emptying, λGE, where $\lambda\text{eff} = 0.693/t_{1/2}\text{eff}$, $\lambda = 0.693/t_{1/2}$, and $\lambda\text{GE} = 0.693/t_{1/2}\text{GE}$. The half-time of gastric emptying, $t_{1/2}$GE, was calculated from the following equation: $t_{1/2}\text{eff} = (t_{1/2}t_{1/2}\text{GE})/(t_{1/2} + t_{1/2}\text{GE})$. With this technique, the $t_{1/2}$GE for normal individuals ranged from 25 to 75 min (Table I). This

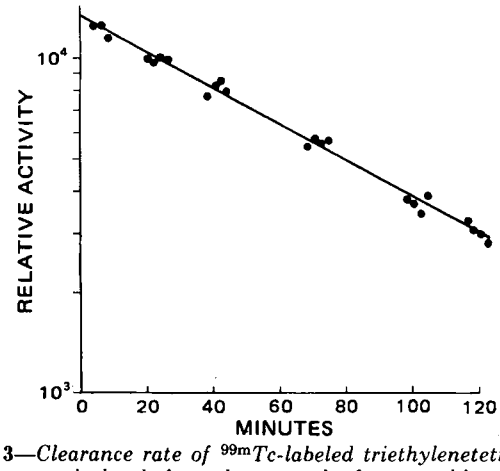

Figure 3—*Clearance rate of ^{99m}Tc-labeled triethylenetetraamine–polystyrene resin beads from the stomach of a normal human male, $t_{1/2}GE$ = 58 min.*

Table I—Gastric Emptying Half-Time in Normal Volunteers

Patient (Sex)	$t_{1/2}$GE, min
KM (M)	63
TF (M)	57
LW (M)	75
AM (M)	25
RB (M)	43
FD (M)	63
MS (F)	34
MT (F)	41
HF (M)	60
AM (M)	37
RL (F)	39
BM (F)	58
JW (M)	35
NF (F)	41
CE (F)	39
MV (F)	55
VS (F)	45
WG (M)	51
GD (M)	57
MM (M)	62

range was in agreement with results obtained using other radiopharmaceuticals (11). The $t_{1/2}$eff was not affected by the duodenal or jejunal overlap with the stomach (9). The gradual movement of radioactivity from the stomach through the pylorus into the intestines was indicated by a series of sequential scintigraphic images (Fig. 4). The entire stomach and the intestines were visualized. The absorbed radiation dose by the stomach was 102 mrads/250 μCi.

A second group of three individuals suffering from various disorders of the GI tract was used to demonstrate the difference in gastric emptying rates between normals and patients. Two patients suffering from pyloric stenosis exhibited a monoexponential pattern of gastric emptying with half-times of 115 and 136 min, respectively. A third patient with a 70% gastric resection and gastrojejunostomy exhibited a gastric emptying pattern consisting of two components: a component with a high rate of decrease, $t_{1/2}$GE = 5 min, representing dumping, and a component with a low rate of decrease, $t_{1/2}$GE = 91 min (Fig. 5).

DISCUSSION

The purpose of this study was to demonstrate the suitability of ^{99m}Tc-labeled triethylenetetraamine–polystyrene resin as an agent for investigating the pattern and rate of gastric emptying in humans. This study ascertained that the ^{99m}Tc-labeled resin was an ideal agent for measuring the gastric emptying rate of a solid meal in normal subjects and patients. The agent fulfilled the criteria of an ideal agent. It tenaciously bound [^{99m}Tc]pertechnetate anions; it was not absorbed or adsorbed on the gastric mucosa; the polystyrene beads had a particle size comparable to that of solid food and mixed homogeneously with the solid phase of the gastric content; it was nontoxic; it was an easily prepared radiopharmaceutical with the ideal radiation characteristics of technetium 99*m*; and, finally, the technique was noninvasive and comfortable to the patient. The use of the γ-camera coupled with a fast data-acquisition device allowed rapid and convenient observation of second-by-second alterations in the pattern and rate of gastric emptying.

Two fundamental assumptions were made in using this technique: the stomach was presumed to remain in the same position and retain the same shape throughout the study, and no correction was made for changes of depth of the radioisotope below the abdominal wall. The error that was

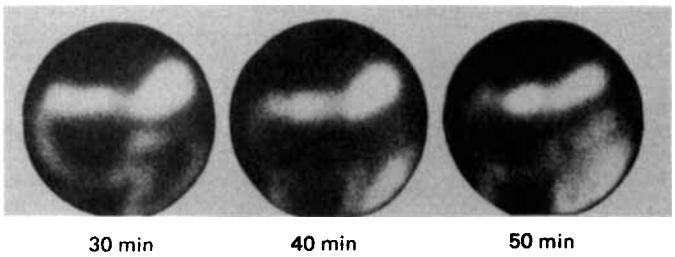

Figure 4—*Anterior scintigraphic series at 10-min intervals illustrating the gastric elimination and bowel distribution of the ^{99m}Tc-labeled triethylenetetraamine–polystyrene resin, $t_{1/2}GE$ = 36 min.*

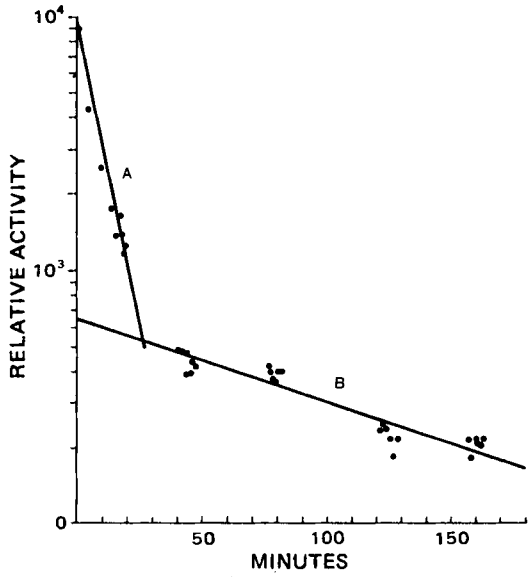

Figure 5—*Clearance rate of ^{99m}Tc-labeled triethylenetetraamine–polystyrene from the stomach of a male patient with Billroth II. Key: A, $t_{1/2}GE$ = 5 min; and B, $t_{1/2}GE$ = 99 min.*

introduced by these assumptions was minimal (13). Another source of error was the variations in tissue absorption of the γ-rays and the overlap of the duodenal–jejunal flexure with the gastric antrum, which tended to increase the count when, at the time of reading, the labeled gastric contents went through the duodenum or jejunum. However, this error did not change the slope of the linear logarithmic equation that described the gastric emptying process (3).

This study demonstrated that the gastric emptying of the solid phase of the ^{99m}Tc-labeled triethylenetetraamine–polystyrene gastric content can be described by a monoexponential function, at least for the first 120 min for normal subjects and patients suffering from pyloric stenosis. Moreover, it was shown that GI surgery, such as gastrojejunostomy, may drastically change the pattern and rate of gastric emptying (Fig. 5). Since the gastric emptying rate was affected by various factors, the position of the patient, the test meal, the position of camera, and the administered radioactivity dose were kept as constant as possible.

The use of ^{99m}Tc-labeled triethylenetetraamine–polystyrene in combination with a scintillation camera is a better technique than the isotopic and nonisotopic techniques that have been used for the investigation of the pattern and rates of gastric emptying of the solid phase of the gastric content. The disadvantages of the previous techniques and agents were discussed extensively elsewhere (9). Clinicians may use this technique to study GI diseases such as gastric and duodenal ulcers, gastric neoplasms, pyloric stenosis, dumping syndrome, and postsurgical status of gastrectomy, gastrojejunostomy, vagotomy, and pyloroplasty.

REFERENCES

(1) D. Bromster, *Scand. J. Gastroenterol.*, **4**, 193 (1969).

(2) G. H. Griffith, G. M. Owen, P. H. Campbell, and R. Shields, *Gastroenterology*, **54**, 1 (1968).

(3) M. C. Theodorakis, Ph.D. thesis, University of Kentucky, Lexington, Ky., 1975.

(4) T. K. Chaudhuri, A. J. Greenwald, R. C. Heading, and T. K. Chaudhuri, *Dig. Dis.*, **20**, 1063 (1975).

(5) R. C. Heading, J. Nimmo, L. F. Prescott, and P. Tothill, *Br. J. Pharmacol.*, **47**, 415 (1973).

(6) J. B. Houston and G. Levy, *J. Pharm. Sci.*, **64**, 1504 (1975).

(7) G. H. Griffith, G. M. Owen, S. Kirkman, and R. Shields, *Lancet*, **1**, 1244 (1966).

(8) R. C. Heading, P. Tothill, A. J. Laidlaw, and D. J. Shearman, *Gut*, **12**, 611 (1971).

(9) T. K. Chaudhuri, *J. Nucl. Med.*, **15**, 391 (1974).

(10) E. Signer and R. Fridrich, *Acta Paediatr. Scand.*, **64**, 525 (1975).

(11) A. P. M. van Dam, *Radiology*, **110**, 155 (1974).

(12) M. Calderon, R. E. Sonnemaker, T. Herch, and J. A. Burdine, *ibid.*, **101**, 371 (1971).

(13) T. Jones, J. C. Clark, N. Kocak, A. G. Cox, and H. I. Glass, *Br. J.*

Radiol., **43**, 537 (1970).
(14) G. A. Digenis, M. B. Shambhu, and M. C. Theodorakis, U.S. pat. 4,115,540 (1978).
(15) G. A. Digenis, R. M. Beihn, M. C. Theodorakis, and M. B. Shambhu, *J. Pharm. Sci.*, **66**, 442 (1977).
(16) R. L. Letsinger, M. J. Kornet, V. Macadevan, and D. M. Jerina, *J. Am. Chem. Soc.*, **86**, 5163 (1964).
(17) M. B. Shambhu, M. C. Theodorakis, and G. A. Digenis, *J. Polym. Sci., Polym. Chem. Ed.*, **15**, 525 (1977).

ACKNOWLEDGMENTS

The authors thank Ms. S. Yonts for assistance.

Preliminary Evaluation of Furosemide–Probenecid Interaction in Humans

DAVID E. SMITH *, WINNIE LIANG GEE *, D. CRAIG BRATER ‡§, EMIL T. LIN *, and LESLIE Z. BENET *x

Received October 5, 1979, from the **Department of Pharmacy, School of Pharmacy, and the* ‡*Division of Clinical Pharmacology, School of Medicine, University of California, San Francisco, CA 94143.* Accepted for publication December 28, 1979. §Present address: Department of Pharmacology, Division of Clinical Pharmacology, University of Texas Health Science Center at Dallas, Southwestern Medical School, Dallas, TX 75235.

Abstract □ The pharmacokinetics and pharmacodynamics of intravenous furosemide, 40 mg, were studied in four healthy male subjects in a crossover fashion with and without probenecid pretreatment. In each study, 16 plasma and 10 urine samples were collected over 24 hr. Fluid and electrolyte urinary losses were replaced orally throughout the study. Unchanged furosemide and probenecid were measured using high-pressure liquid chromatography; urinary sodium was measured by flame photometry. Although probenecid caused marked changes in the pharmacokinetic parameters of furosemide (increased area under the curve, decreased plasma and renal clearance, increased half-life, and decreased fraction excreted unchanged in the urine), there was no significant difference in its gross 8-hr natriuretic and diuretic effect. However, analysis of the time course of natriuresis showed a pattern similar to that of the urinary furosemide excretion rate, whereas the plasma concentration was poorly correlated over the entire dose–response curve.

Keyphrases □ Furosemide—pharmacokinetics and pharmacodynamics with and without probenecid pretreatment, humans □ Probenecid—pharmacokinetics and pharmacodynamics of furosemide with and without probenecid pretreatment, humans □ Drug–drug interactions—pharmacokinetics and pharmacodynamics of furosemide with and without probenecid pretreatment, humans □ Pharmacokinetics—furosemide with and without probenecid pretreatment, humans

Furosemide is an anthranilic acid derivative used to treat edematous states of hepatic, cardiac, and renal origin (1–3). It is believed to act at the luminal surface of the nephron where it inhibits the active reabsorption of chloride in the ascending limb of the loop of Henle (4–7). Since furosemide is highly protein bound (8, 9), access to the lumen occurs primarily through active secretion *via* the nonspecific organic acid secretory pathway (5, 6, 10). Thus, any drug or chemical substance that competes for this pathway could prevent furosemide from reaching its site of action and thereby attenuate its diuretic response.

Probenecid is a weak organic acid that competes with furosemide for active secretion into the kidney lumen. This competition can prevent furosemide from achieving an adequate cellular or luminal concentration and thereby diminish its natriuretic and diuretic response. Previous studies in experimental animals supported this hypothesis and showed that probenecid can decrease the natriuretic action of furosemide (10, 11). Studies in humans evaluating the effect of probenecid on the pharmacokinetics and pharmacodynamics of furosemide are limited and less clear (12–14).

The present investigation was undertaken to clarify the mechanism by which probenecid alters the diuretic response of furosemide. An additional objective was to define, in humans, a relationship between the dose of furosemide, its concentration or amount in a measurable sampling compartment, and its diuretic effect.

EXPERIMENTAL

Materials and Methods—Four males, 21–33 years and 65–77 kg, participated as outpatients in this study. Each subject had a normal medical history, physical examination, and standard laboratory tests. Each subject received 40 mg of furosemide alone and after pretreatment with probenecid. An interval of at least 1 week elapsed between studies. Subjects fasted the night before and until at least 2 hr after administration of the diuretic. Identical lot numbers for each drug were used throughout the study.

Furosemide was administered intravenously over ~3 min, with the midpoint of the infusion considered as time zero. Probenecid (1 g) was ingested at bedtime the night before and on arising the morning of the study (30–60 min prior to furosemide administration). Blood samples (3 ml) to determine the drug concentration were obtained with an indwelling heparinized scalp vein needle at 0, 5, 10, 20, 30, 45, 60, 80, 100, 120, 180, 240, 300, 360, and 480 min and ~24 hr.

Voided urine was collected at 0, 0.5, 1.0, 1.5, 2.0, 3.0, 4.0, 5.0, 6.0, 8.0, and 24 hr and at two times of spontaneous voiding at home between the 8- and 24-hr collections. After each voiding, subjects drank a volume of balanced electrolyte solution flavored with fruit syrup equal to their urinary volume to avoid dehydration and electrolyte depletion.

All 24-hr blood samples showed normal electrolytes, urea nitrogen, and creatinine. Sodium concentrations were measured with a flame photometer[1]. Statistical differences were determined using a paired t test.

Plasma samples of furosemide, with and without probenecid pretreatment, were analyzed using a rapid, sensitive, and specific high-pressure liquid chromatographic[2] (HPLC) assay developed in this laboratory (15). Samples were run on a μBondapak C_{18} reversed-phase column[3] (30 cm × 3.9 mm i.d.) using dual-channel UV detection[4] (0.01 aufs). A 20-μl aliquot containing the internal standard, phenobarbital sodium (0.25 mg/ml), was added to 0.20-ml plasma furosemide samples. The mixture was vortexed, and 0.40 ml of acetonitrile was added. The mixture was vortexed again and then centrifuged for 10 min. The supernate was transferred to a clean test tube and evaporated under nitrogen gas until ~0.15 ml of the solution remained. A solvent system of 25% acetonitrile in 0.01 *M* acetic acid, adjusted to pH 5.0 with sodium hydroxide, was employed to measure furosemide at 280 nm and pheno-

[1] Model 450, Corning Scientific Instruments, Medfield, Mass.
[2] Model 6000A, Waters Associates, Milford, Mass.
[3] Waters Associates, Milford, Mass.
[4] Model 440 absorbance detector, Waters Associates, Milford, Mass.

0022-3549/80/0500-0571$01.00/0
© 1980, American Pharmaceutical Association

Radiol., **43**, 537 (1970).
(14) G. A. Digenis, M. B. Shambhu, and M. C. Theodorakis, U.S. pat. 4,115,540 (1978).
(15) G. A. Digenis, R. M. Beihn, M. C. Theodorakis, and M. B. Shambhu, *J. Pharm. Sci.*, **66**, 442 (1977).
(16) R. L. Letsinger, M. J. Kornet, V. Macadevan, and D. M. Jerina, *J. Am. Chem. Soc.*, **86**, 5163 (1964).
(17) M. B. Shambhu, M. C. Theodorakis, and G. A. Digenis, *J. Polym. Sci., Polym. Chem. Ed.*, **15**, 525 (1977).

ACKNOWLEDGMENTS

The authors thank Ms. S. Yonts for assistance.

Preliminary Evaluation of Furosemide–Probenecid Interaction in Humans

DAVID E. SMITH *, WINNIE LIANG GEE *, D. CRAIG BRATER ‡§, EMIL T. LIN *, and LESLIE Z. BENET *x

Received October 5, 1979, from the **Department of Pharmacy, School of Pharmacy, and the* ‡*Division of Clinical Pharmacology, School of Medicine, University of California, San Francisco, CA 94143.* Accepted for publication December 28, 1979. §Present address: Department of Pharmacology, Division of Clinical Pharmacology, University of Texas Health Science Center at Dallas, Southwestern Medical School, Dallas, TX 75235.

Abstract □ The pharmacokinetics and pharmacodynamics of intravenous furosemide, 40 mg, were studied in four healthy male subjects in a crossover fashion with and without probenecid pretreatment. In each study, 16 plasma and 10 urine samples were collected over 24 hr. Fluid and electrolyte urinary losses were replaced orally throughout the study. Unchanged furosemide and probenecid were measured using high-pressure liquid chromatography; urinary sodium was measured by flame photometry. Although probenecid caused marked changes in the pharmacokinetic parameters of furosemide (increased area under the curve, decreased plasma and renal clearance, increased half-life, and decreased fraction excreted unchanged in the urine), there was no significant difference in its gross 8-hr natriuretic and diuretic effect. However, analysis of the time course of natriuresis showed a pattern similar to that of the urinary furosemide excretion rate, whereas the plasma concentration was poorly correlated over the entire dose–response curve.

Keyphrases □ Furosemide—pharmacokinetics and pharmacodynamics with and without probenecid pretreatment, humans □ Probenecid—pharmacokinetics and pharmacodynamics of furosemide with and without probenecid pretreatment, humans □ Drug–drug interactions—pharmacokinetics and pharmacodynamics of furosemide with and without probenecid pretreatment, humans □ Pharmacokinetics—furosemide with and without probenecid pretreatment, humans

Furosemide is an anthranilic acid derivative used to treat edematous states of hepatic, cardiac, and renal origin (1–3). It is believed to act at the luminal surface of the nephron where it inhibits the active reabsorption of chloride in the ascending limb of the loop of Henle (4–7). Since furosemide is highly protein bound (8, 9), access to the lumen occurs primarily through active secretion *via* the nonspecific organic acid secretory pathway (5, 6, 10). Thus, any drug or chemical substance that competes for this pathway could prevent furosemide from reaching its site of action and thereby attenuate its diuretic response.

Probenecid is a weak organic acid that competes with furosemide for active secretion into the kidney lumen. This competition can prevent furosemide from achieving an adequate cellular or luminal concentration and thereby diminish its natriuretic and diuretic response. Previous studies in experimental animals supported this hypothesis and showed that probenecid can decrease the natriuretic action of furosemide (10, 11). Studies in humans evaluating the effect of probenecid on the pharmacokinetics and pharmacodynamics of furosemide are limited and less clear (12–14).

The present investigation was undertaken to clarify the mechanism by which probenecid alters the diuretic response of furosemide. An additional objective was to define, in humans, a relationship between the dose of furosemide, its concentration or amount in a measurable sampling compartment, and its diuretic effect.

EXPERIMENTAL

Materials and Methods—Four males, 21–33 years and 65–77 kg, participated as outpatients in this study. Each subject had a normal medical history, physical examination, and standard laboratory tests. Each subject received 40 mg of furosemide alone and after pretreatment with probenecid. An interval of at least 1 week elapsed between studies. Subjects fasted the night before and until at least 2 hr after administration of the diuretic. Identical lot numbers for each drug were used throughout the study.

Furosemide was administered intravenously over ~3 min, with the midpoint of the infusion considered as time zero. Probenecid (1 g) was ingested at bedtime the night before and on arising the morning of the study (30–60 min prior to furosemide administration). Blood samples (3 ml) to determine the drug concentration were obtained with an indwelling heparinized scalp vein needle at 0, 5, 10, 20, 30, 45, 60, 80, 100, 120, 180, 240, 300, 360, and 480 min and ~24 hr.

Voided urine was collected at 0, 0.5, 1.0, 1.5, 2.0, 3.0, 4.0, 5.0, 6.0, 8.0, and 24 hr and at two times of spontaneous voiding at home between the 8- and 24-hr collections. After each voiding, subjects drank a volume of balanced electrolyte solution flavored with fruit syrup equal to their urinary volume to avoid dehydration and electrolyte depletion.

All 24-hr blood samples showed normal electrolytes, urea nitrogen, and creatinine. Sodium concentrations were measured with a flame photometer[1]. Statistical differences were determined using a paired t test.

Plasma samples of furosemide, with and without probenecid pretreatment, were analyzed using a rapid, sensitive, and specific high-pressure liquid chromatographic[2] (HPLC) assay developed in this laboratory (15). Samples were run on a μBondapak C_{18} reversed-phase column[3] (30 cm × 3.9 mm i.d.) using dual-channel UV detection[4] (0.01 aufs). A 20-μl aliquot containing the internal standard, phenobarbital sodium (0.25 mg/ml), was added to 0.20-ml plasma furosemide samples. The mixture was vortexed, and 0.40 ml of acetonitrile was added. The mixture was vortexed again and then centrifuged for 10 min. The supernate was transferred to a clean test tube and evaporated under nitrogen gas until ~0.15 ml of the solution remained. A solvent system of 25% acetonitrile in 0.01 *M* acetic acid, adjusted to pH 5.0 with sodium hydroxide, was employed to measure furosemide at 280 nm and pheno-

[1] Model 450, Corning Scientific Instruments, Medfield, Mass.
[2] Model 6000A, Waters Associates, Milford, Mass.
[3] Waters Associates, Milford, Mass.
[4] Model 440 absorbance detector, Waters Associates, Milford, Mass.

0022-3549/80/0500-0571$01.00/0
© 1980, American Pharmaceutical Association

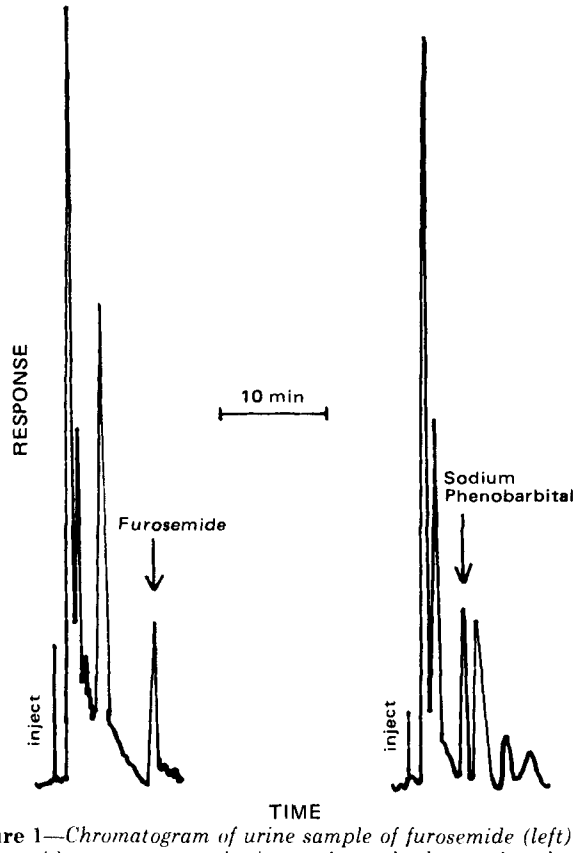

Figure 1—*Chromatogram of urine sample of furosemide (left) with probenecid pretreatment; the internal standard was phenobarbital sodium (right).*

barbital sodium at 254 nm. Urine samples of furosemide administered alone were prepared in a similar fashion, except that the addition of acetonitrile and the evaporation step were omitted.

During the assay of urine furosemide samples obtained following probenecid pretreatment, interfering peaks (possibly from probenecid metabolites) occurred in both the 280- and 254-nm detection channels. Therefore, it was necessary to develop a new assay system to separate the interfering peaks from those of furosemide and the internal standard, phenobarbital sodium. These urine samples were assayed for furosemide by HPLC[5] on a C_{18} reversed-phase column[3] using fluorescence detection[6]. The excitation and emission wavelengths of furosemide were set at 345 and 405 nm, respectively. The photomultiplier gain was set at 4, and the sensitivity range was set at 10. A 20-μl aliquot of the internal standard, phenobarbital sodium (2.5 mg/ml), still was measured by UV detection[7] at 254 nm (0.05 aufs).

With a solvent system of 30% acetonitrile in 0.015 *M* aqueous phosphoric acid solution at a flow rate of 2.0 ml/min, furosemide and phenobarbital sodium had retention times of 9.0 and 5.0 min, respectively (Fig. 1). A typical standard curve of the peak height ratio of furosemide to phenobarbital sodium over the concentration range of 0.82–20.50 μg/ml resulted in a linear least-squares regression equation of $y = 0.205x + 0.008$ ($r^2 = 0.999$). With fluorescent detection, concentrations as low as 8.20 ng/ml were measured.

Plasma samples of probenecid were prepared in a similar fashion to furosemide. A 40-μl aliquot of phenobarbital sodium (4 mg/ml) was used as the internal standard, and the solvent system (30% acetonitrile in 0.01 *M* acetic acid, adjusted to pH 5.0 with sodium hydroxide) had a flow rate of 2.0 ml/min. Both probenecid and phenobarbital sodium were measured using UV detection[7] at 254 nm. Plasma probenecid concentrations were fairly constant during the entire study and ranged from 100 to 165 μg/ml (Fig. 2).

Calculations—The half-life of furosemide, $t_{1/2}$, was determined by linear regression from the terminal portion of the urinary excretion rate *versus* midpoint time plots. The area under the plasma concentration–time curve, *AUC*, was calculated using the trapezoidal rule, extrapolated to infinity from the last measured concentration.

The volume of distribution at steady state, Vd_{ss}, was determined by the compartment-independent method of Benet and Galeazzi (16):

$$Vd_{ss} = \text{dose } (AUMC)/(AUC)^2 \qquad \text{(Eq. 1)}$$

where *AUMC* is the area under the curve of the first moment of the concentration–time curve, *i.e.*, $\int_0^\infty tC_p\,dt$. The total plasma clearance of furosemide, Cl_p, was calculated from:

$$Cl_p = \text{dose}/AUC \qquad \text{(Eq. 2)}$$

The total renal clearance, Cl_r, was estimated from:

$$Cl_r = Ae_\infty/AUC \qquad \text{(Eq. 3)}$$

where the amount of unchanged drug recovered in the urine at time infinity is represented by Ae_∞. The fraction of furosemide excreted unchanged in the urine, f_e, was calculated by dividing Ae_∞ by the intravenous dose. Nonrenal plasma clearance, Cl_{nr}, was calculated as the difference between the plasma and renal clearances. The fraction excreted by nonrenal routes, f_{nr}, was calculated by dividing the nonrenal clearance by the total plasma clearance.

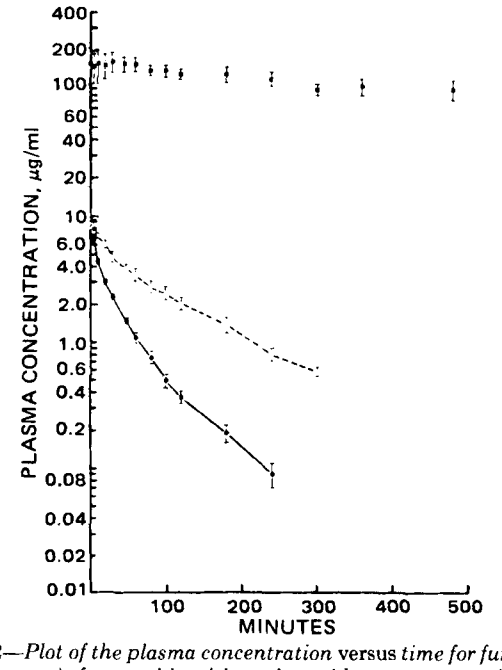

Figure 2—*Plot of the plasma concentration* versus *time for furosemide alone (●——●), furosemide with probenecid pretreatment (○- - -○), and probenecid (■). Data are expressed as the mean ± SEM (n = 4).*

RESULTS

The effects of probenecid on the pharmacokinetics of furosemide were analyzed in both plasma and urine (Table I). Mean plasma concentrations of furosemide with probenecid pretreatment were significantly increased at all time points except at 5 min (Fig. 2). The significant increase in *AUC* supports this observation [252 ± 24 (μg min)/ml for furosemide alone (Treatment I) and 785 ± 87 (μg min)/ml for furosemide with probenecid pretreatment (Treatment II); $p < 0.001$]. In addition, the total plasma clearance of furosemide was decreased significantly in the presence of probenecid (160 ± 15 ml/min for Treatment I and 51.4 ± 5.3 ml/min for Treatment II; $p < 0.001$). This difference in total plasma clearance was reflected by the significant increase in the half-life of furosemide (82 ± 5 min for Treatment I and 175 ± 17 min for Treatment II; $p < 0.001$) since the Vd_{ss} value was not altered significantly (8.44 ± 0.93 liters for Treatment I and 6.66 ± 1.78 liters for Treatment II; $p > 0.20$).

The total renal clearance of furosemide was reduced markedly with probenecid pretreatment (118 ± 17 ml/min for Treatment I and 23.1 ± 1.0 ml/min for Treatment II; $p < 0.002$), while the nonrenal plasma clearance did not change significantly (42 ± 12 ml/min for Treatment I and 28.3 ± 4.9 ml/min for Treatment II; $p > 0.10$). In addition, the fraction of furosemide excreted unchanged in the urine in the presence of probenecid was reduced significantly (0.74 ± 0.07 for Treatment I and 0.46 ± 0.05 for Treatment II; $p < 0.01$) with a corresponding increase in

[5] Perkin-Elmer Series 2, Norwalk, Conn.
[6] Fluorescence spectrophotometer 204-A, Perkin-Elmer, Norwalk, Conn.
[7] LC 250, Perkin-Elmer, Norwalk, Conn.

Table I—Pharmacokinetic Effects of Probenecid on Furosemide

Subject	Treatment	AUC, (μg min)/ml	Cl_p, ml/min	Vd_{ss}, liters	$t_{1/2}$, min	Cl_r, ml/min	Cl_{nr}, ml/min	f_e	f_{nr}
TP	Furosemide	225	178	8.85	85	122	56	0.68	0.31
	Furosemide with probenecid	723	55.3	6.00	185	22.8	32.5	0.41	0.59
RP	Furosemide	280	143	9.55	85	101	42	0.71	0.29
	Furosemide with probenecid	907	44.1	5.50	193	22.7	21.4	0.52	0.49
TT	Furosemide	242	165	7.62	75	139	26	0.84	0.16
	Furosemide with probenecid	787	50.9	5.81	160	22.3	28.6	0.44	0.56
DH	Furosemide	261	153	7.73	82	109	44	0.71	0.29
	Furosemide with probenecid	724	55.3	9.31	161	24.6	30.7	0.45	0.56
Mean ± *SD*	Furosemide	252 ± 24	160 ± 15	8.44 ± 0.93	82 ± 5	118 ± 17	42 ± 12	0.74 ± 0.07	0.26 ± 0.07
	Furosemide with probenecid	785 ± 87	51.4 ± 5.3	6.66 ± 1.78	175 ± 17	23.1 ± 1.0	28.3 ± 4.9	0.46 ± 0.05	0.55 ± 0.04
Level of significance		S ($p < 0.001$)	S ($p < 0.001$)	NS ($p > 0.20$)	S ($p < 0.001$)	S ($p < 0.002$)	NS ($p > 0.10$)	S ($p < 0.01$)	S ($p < 0.01$)

the fraction excreted by nonrenal routes (0.26 ± 0.07 for Treatment I and 0.55 ± 0.04 for Treatment II; $p < 0.01$).

Analysis of the urinary excretion rate of furosemide, with and without probenecid pretreatment, is shown in Fig. 3. Initially, the urinary excretion rate of furosemide with probenecid was significantly lower than that of furosemide when administered alone. However, after ~125 min, the two curves (Treatments I and II) intersect; at subsequent times, probenecid caused a significant increase in the furosemide excretion rate. This result was primarily due to the large difference in plasma furosemide concentrations at subsequent times between Treatments I and II (Fig. 2) since the renal clearance was reduced but was constant throughout each study.

The effect of probenecid on furosemide-induced natriuresis is shown in Fig. 4. The initial natriuretic response to furosemide when it was given concomitantly with probenecid was reduced compared to that of furosemide administered alone. The two curves (Treatments I and II) intersect at 100 min; at subsequent times, probenecid caused an increase in furosemide-induced natriuresis, similar to that seen for the urinary excretion rate of furosemide. Although differences in the sodium excretion rate were seen with and without probenecid pretreatment, they did not appear to be statistically different. Table II shows that the 8-hr sodium excretion (milliequivalents) was 291 ± 53 for Treatment I and 323 ± 106 for Treatment II ($p > 0.50$). The diuretic response (milliliters per 8 hr) was 2257 ± 422 for Treatment I and 2637 ± 632 for Treatment II ($p > 0.20$).

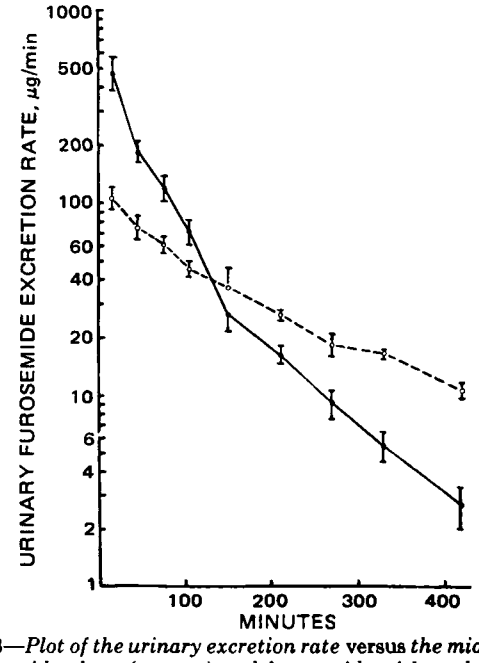

Figure 3—*Plot of the urinary excretion rate* versus *the midpoint time for furosemide alone (●—●) and furosemide with probenecid pretreatment (○---○). Data are expressed as the mean* ± SEM (n = *4).*

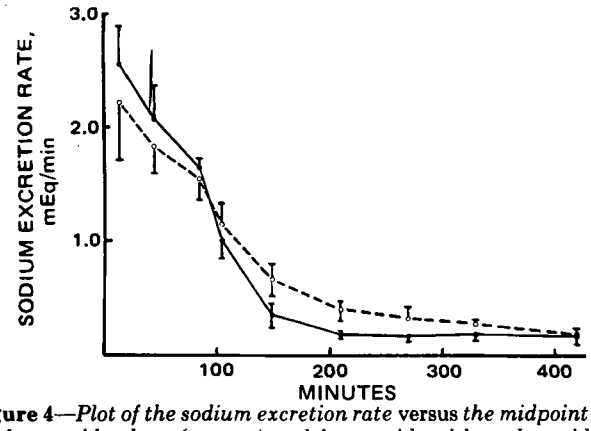

Figure 4—*Plot of the sodium excretion rate* versus *the midpoint time for furosemide alone (●—●) and furosemide with probenecid pretreatment (○---○). Data are expressed as the mean* ± SEM (n = *4).*

DISCUSSION

Experiments in animals suggested that the luminal concentration or amount of furosemide rather than its plasma concentration may be the critical determinant with respect to its natriuretic and diuretic effect (10, 11, 17, 18). Hook and Williamson (10) and Friedman and Roch-Ramel (11) demonstrated in the dog and cat, respectively, that probenecid (50 mg/kg iv) significantly inhibited furosemide-induced natriuresis. Since probenecid is highly secreted (19), it can compete for active transport and prevent furosemide from reaching the tubular fluid, thereby attenuating its natriuretic effect. However, human studies (12–14) do not

Table II—Effects of Probenecid on Furosemide Diuresis and Natriuresis

Subject	Treatment	Urine Volume, ml/8 hr	Sodium Excretion, mEq/8 hr
TP	Furosemide	2451	328
	Furosemide with probenecid	2117	232
RP	Furosemide	2251	262
	Furosemide with probenecid	2555	288
TT	Furosemide	1674	232
	Furosemide with probenecid	2329	296
DH	Furosemide	2653	343
	Furosemide with probenecid	3546	477
Mean ± *SD*	Furosemide	2257 ± 422	291 ± 53
	Furosemide with probenecid	2637 ± 632	323 ± 106
Level of significance		NS ($p > 0.20$)	NS ($p > 0.50$)

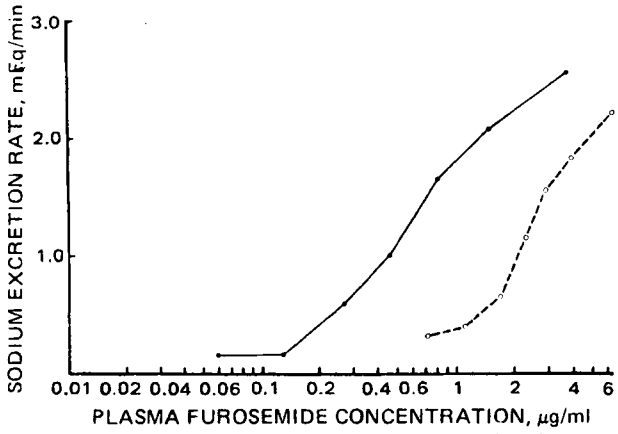

Figure 5—*Plot of the sodium excretion rate* versus *the plasma concentration for furosemide alone (●—●) and furosemide with probenecid pretreatment (O---O) (n = 4).*

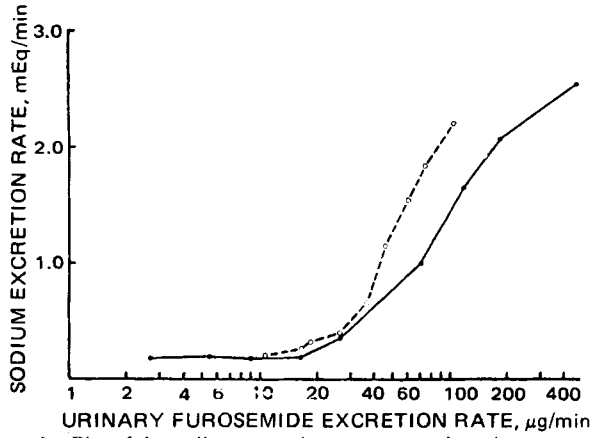

Figure 6—*Plot of the sodium excretion rate* versus *the urinary excretion rate for furosemide alone (●—●) and furosemide with probenecid pretreatment (O---O) (n = 4).*

corroborate these findings in animals. In contrast, probenecid caused either no change or a significant increase in the natriuretic response to furosemide.

The first study of the effect of probenecid on furosemide kinetics and natriuretic response in humans showed that probenecid significantly decreased the total plasma clearance (155 ml/min for Treatment I and 85 ml/min for Treatment II) and the total renal clearance (134 ml/min for Treatment I and 63 ml/min for Treatment II) of furosemide, and significantly increased the furosemide half-life (35.8 min for Treatment I and 60.8 min for Treatment II) (12). However, the 6-hr urine volume (5098 ml for Treatment I and 6164 ml for Treatment II) and the sodium excretion (578 mEq for Treatment I and 694 mEq for Treatment II) were not significantly different between treatments. In addition, the fraction of the dose excreted unchanged in the urine was not statistically altered with probenecid pretreatment, although three of the four subjects studied did excrete a smaller percentage. Therefore, the investigators (12) concluded that their results were consistent with the findings of a previous study (10), which suggested that the amount of furosemide in the tubular fluid is the main determinant of furosemide diuresis. Although we do not disagree with their conclusions, the previous investigators did not fully characterize the mechanism of this interaction between furosemide and probenecid. Since the time course of the natriuretic and diuretic response was not described, the previous investigators were considering only gross effects.

Homeida *et al.* (13) also demonstrated marked changes in furosemide pharmacokinetics with probenecid pretreatment. Similarly, these investigators noted that since the total proportion of unchanged drug reaching the renal tubule was not changed markedly, the total diuretic effect remained unaltered. However, this conclusion is suspect since our calculations of their data show an approximate 41% decrease in the fraction of the furosemide dose excreted unchanged in the urine (from 0.34 to 0.20) when the subjects were pretreated with probenecid. In addition, furosemide was assayed spectrofluorometrically, which is rather nonspecific, especially in urine. This method may account for the unusual values for the total, renal, and nonrenal plasma clearances reported in their control subjects, as suggested by Benet (20).

In a more recent study, the pharmacodynamic effect of probenecid on the response to furosemide in humans was quantified (14). Analysis of the time course of natriuresis and diuresis showed that probenecid actually decreased the response of furosemide for the first 60–90 min but increased the subsequent response sufficiently to result in a statistically greater overall effect. However, it was noted (14) that since the concentrations or amounts of furosemide in the urine were not compared with the response, a unifying hypothesis to explain the mechanism of a furosemide–probenecid interaction was not possible[8].

In the present investigation, the time course of furosemide in plasma and urine was compared with that of the natriuretic effect in an attempt to explain the mechanism for a furosemide–probenecid interaction. Although probenecid caused marked changes in the pharmacokinetic parameters of furosemide (Table I), there was no significant difference in its gross natriuretic and diuretic effect (Table II). Analysis of the time course for natriuresis (Fig. 4) shows that probenecid actually decreased the response for the first 100 min after furosemide administration. However, the subsequent response was increased sufficiently to result in no statistical difference in the mean 8-hr value for sodium excretion. Although a similar pattern was seen with respect to the urinary excretion of furosemide, the magnitude of this difference between treatments was statistically significant (Fig. 3).

Figure 5 shows that probenecid caused a significant shift to the right in the relationship between the plasma concentration of furosemide and its natriuretic effect. This observation suggests that higher plasma furosemide concentrations are needed in the presence of probenecid to produce a natriuretic response equivalent to that produced by lower concentrations when probenecid is absent. Figure 6 shows the relationship between the urinary furosemide excretion rate and the natriuretic effect. Although Treatments I and II were not parallel over the entire dose–response curve, the amount of furosemide excreted into the urine was better correlated with response than was the plasma furosemide concentration.

The shift to the left between the urinary excretion rate of furosemide and the effect (upper portion of Fig. 6) may be real or may be an artifact due to the limited number of subjects. However, a possible explanation for this finding may involve an interaction between probenecid and prostaglandins. Previous investigators hypothesized that prostaglandins mediate the natriuretic–diuretic effect of furosemide (21–25). Renal prostaglandins are synthesized primarily in the medulla (24, 26–28) and are released into the extracellular fluids (29). *In vitro* studies showed that prostaglandins accumulate in several tissues, including the renal cortex, as a result of an active transport mechanism (30, 31). In addition, it was shown that probenecid can inhibit the renal tubular transport of prostaglandins, presumably by competing for active transport into the urine (32, 33). Although this conclusion is speculation, this inhibition by probenecid of prostaglandin transport may result in a tubule that is more responsive to smaller amounts of furosemide in the urine and thus account for the shift to the left as described.

CONCLUSIONS

The mechanism by which probenecid alters furosemide-induced natriuresis is consistent with *in vitro* studies (6) indicating that furosemide acts at the luminal surface of the nephron. This study in humans, as well as previous animal studies (18), demonstrates that the urinary excretion rate of furosemide is a better indicator of natriuresis and diuresis than is the plasma concentration.

REFERENCES

(1) W. B. Stason, P. J. Cannon, H. O. Heinemann, and J. H. Laragh, *Circulation*, **34**, 910 (1966).

(2) W. M. Kirkendall and J. H. Stein, *Am. J. Cardiol.*, **22**, 162 (1968).

(3) K. E. Kim, G. Onesti, J. H. Moyer, and C. Swartz, *ibid.*, **27**, 407 (1971).

(4) H. R. Jacobson and J. P. Kokko, *Ann. Rev. Pharmacol. Toxicol.*, **16**, 201 (1976).

(5) M. B. Burg, *Kidney Int.*, **9**, 189 (1976).

(6) M. Burg, L. Stoner, J. Cardinal, and N. Green, *Am. J. Physiol.*, **225**, 119 (1973).

[8] The data presented here describe the kinetics of furosemide in patients for whom the diuretic effects were reported previously (14).

(7) J. F. Seely and J. H. Dirks, *Kidney Int.*, **11**, 1 (1977).
(8) F. Andreasen, H. E. Hansen, and E. Mikkelsen, *Eur. J. Clin. Pharmacol.*, **13**, 41 (1978).
(9) A. Rane, J. P. Villeneuve, W. J. Stone, A. S. Nies, G. R. Wilkinson, and R. A. Branch, *Clin. Pharmacol. Ther.*, **24**, 199 (1978).
(10) J. B. Hook and H. E. Williamson, *J. Pharmacol. Exp. Ther.*, **149**, 404 (1965).
(11) P. A. Friedman and F. Roch-Ramel, *ibid.*, 203, 82 (1977).
(12) J. Honari, A. D. Blair, and R. E. Cutler, *Clin. Pharmacol. Ther.*, **22**, 395 (1977).
(13) M. Homeida, C. Roberts, and R. A. Branch, *ibid.*, **22**, 402 (1977).
(14) D. C. Brater, *ibid.*, **24**, 548 (1978).
(15) E. T. Lin, D. E. Smith, L. Z. Benet, and B. A. Hoener, *J. Chromatogr.*, **163**, 315 (1979).
(16) L. Z. Benet and R. L. Galeazzi, *J. Pharm. Sci.*, **68**, 1071 (1979).
(17) H. J. Rose, A. W. Pruitt, P. G. Dayton, and J. L. McNay, *J. Pharmacol. Exp. Ther.*, **199**, 490 (1976).
(18) D. E. Smith and L. Z. Benet, *Pharmacology*, in press.
(19) I. M. Weiner, in "Handbook of Physiology," Section 8, J. Orloff and R. W. Berliner, Eds., American Physiological Society, Washington, D.C., 1973, p. 521.
(20) L. Z. Benet, *J. Pharmacokinet. Biopharm.*, **7**, 1 (1979).
(21) B. Scherer and P. C. Weber, *Clin. Sci.*, **56**, 77 (1979).
(22) R. V. Patak, B. K. Mookerjee, C. J. Bentzel, P. E. Hysert, M. Babej, and J. B. Lee, *Prostaglandins*, **10**, 649 (1975).
(23) J. C. Frolich, J. W. Hollifield, J. C. Dormois, B. L. Frolich, H. Seyberth, A. M. Michelakid, and J. A. Oates, *Circ. Res.*, **39**, 447 (1976).
(24) J. B. Lee, R. V. Patak, and B. K. Mookerjee, *Am. J. Med.*, **60**, 798 (1976).
(25) D. E. Smith, D. C. Brater, E. T. Lin, and L. Z. Benet, *J. Pharmacokinet. Biopharm.*, **7**, 265 (1979).
(26) G. R. Zins, *Am. J. Med.*, **58**, 14 (1975).
(27) J. C. McGiff, K. Crowshaw, and H. D. Itskovitz, *Fed. Proc., Fed. Am. Soc. Exp. Biol.*, **33**, 39 (1974).
(28) J. C. Frolich, T. W. Wilson, B. J. Sweetman, M. Smigel, A. S. Nies, K. Carr, T. Watson, and J. A. Oates, *J. Clin. Invest.*, **55**, 763 (1975).
(29) L. Z. Bito, *Prostaglandins*, **9**, 851 (1975).
(30) L. Z. Bito, M. Wallerstein, and R. Baroody, in "Advances in Prostaglandin and Thromboxane Research," vol. 1, B. Samuelsson and R. Paoletti, Eds., Raven, New York, N.Y., 1976, p. 297.
(31) L. Z. Bito, *J. Physiol.*, **221**, 371 (1972).
(32) L. Z. Bito, *Prostaglandins*, **12**, 639 (1976).
(33) B. R. Rennick, *Pharmacologist*, **18**, 162 (1976).

ACKNOWLEDGMENTS

Presented in part at the APhA Academy of Pharmaceutical Sciences, Montreal meeting, May 1978.

Supported in part by National Institutes of Health Grant AM 20884.

D. E. Smith was supported as a National Institutes of Health Predoctoral Scholar on Training Grant GM 07175.

Syntheses and Evaluation of Ketals, Hemithioketals, and Dithioketals of Conjugated Styryl Ketones Principally for Antineoplastic Activity

J. R. DIMMOCK ˣ and L. M. SMITH

Received November 6, 1979, from the *College of Pharmacy, University of Saskatchewan, Saskatoon, Saskatchewan, S7N OWO, Canada.* Accepted for publication January 7, 1980.

Abstract □ Ketals, hemithioketals, and dithioketals of nuclear-substituted styryl ketones were prepared as latentiated forms of the ketones. This undertaking was based on the premise that there is increased acidity in tumors compared to normal tissue, and thus preferential regeneration of the ketone in neoplastic tissue may occur. Attempts to form 1,3-dioxolans of Mannich bases were unsuccessful. The prepared compounds did not possess significant anticancer properties, but analgesic, anti-inflammatory, antihistaminic, and antimicrobial activities were found in the prepared Mannich bases.

Keyphrases □ Antineoplastic activity—ketals, hemithioketals, and dithioketals of conjugated styryl ketones, synthesis and evaluation of activity □ Styryl ketones, conjugated—synthesis of ketals, hemithioketals, and dithioketals, evaluation for antineoplastic activity □ Mannich bases—synthesized from conjugated styryl ketones and acetophenones, evaluation for antineoplastic activity

A recurrent problem in the design of compounds for cancer chemotherapy is the synthesis of derivatives possessing selective toxicity for tumors. Biochemical differences between cancerous and normal cells have been claimed (1), including the increased acidity of certain malignant cells compared to normal tissue (2–4). The increased acidity of tumors has been ascribed to the greater rate of aerobic glycolysis in neoplastic tissue (5), which leads to increased lactic acid production. The pH of a number of tumors has been reported to be ~7.0 (2–4), although such measurements probably recorded the extracellular pH. Therefore, the pH of the intracellular fluid probably is even lower (6), and an average pH value for a number of tumorous tissues has been considered to be ~6.5 (7). Hence, a prodrug permitting the release of a cytotoxic agent under acidic conditions may afford selective lethality of tumors with ameliorated toxicity for normal tissue. Only a few attempts have been made to design compounds based on this pH differential (8–11).

Several investigations in this laboratory involved the preparation of some nuclear-substituted styryl ketones (I) and related Mannich bases (II) for evaluation as anticancer agents (12–14) and in other screens (15–17). While the ketones have not been evaluated against P-388 lymphocytic leukemia, some of the Mannich bases showed promising levels of activity in this screen (12); one compound (IIe) increased the mean survival time in mice by >40% (12). However, murine toxicity was found in II due at least partially to interference with mitochondrial function (18, 19). Therefore, prodrugs of both I and II were prepared, and both I and the prodrugs were evaluated in the P-388 screen so that anticancer activities and murine toxicities of the ketones (I and II) and their latentiated precursors could be compared. Since ketals, hemithioketals, and dithioketals are known to hydrolyze under acidic conditions but are stable in neutral or alkaline media (20), the preparation of these derivatives from I and II may

0022-3549/80/0500-0575$01.00/0
© 1980, American Pharmaceutical Association

(7) J. F. Seely and J. H. Dirks, *Kidney Int.*, **11**, 1 (1977).
(8) F. Andreasen, H. E. Hansen, and E. Mikkelsen, *Eur. J. Clin. Pharmacol.*, **13**, 41 (1978).
(9) A. Rane, J. P. Villeneuve, W. J. Stone, A. S. Nies, G. R. Wilkinson, and R. A. Branch, *Clin. Pharmacol. Ther.*, **24**, 199 (1978).
(10) J. B. Hook and H. E. Williamson, *J. Pharmacol. Exp. Ther.*, **149**, 404 (1965).
(11) P. A. Friedman and F. Roch-Ramel, *ibid.*, 203, 82 (1977).
(12) J. Honari, A. D. Blair, and R. E. Cutler, *Clin. Pharmacol. Ther.*, **22**, 395 (1977).
(13) M. Homeida, C. Roberts, and R. A. Branch, *ibid.*, **22**, 402 (1977).
(14) D. C. Brater, *ibid.*, **24**, 548 (1978).
(15) E. T. Lin, D. E. Smith, L. Z. Benet, and B. A. Hoener, *J. Chromatogr.*, **163**, 315 (1979).
(16) L. Z. Benet and R. L. Galeazzi, *J. Pharm. Sci.*, **68**, 1071 (1979).
(17) H. J. Rose, A. W. Pruitt, P. G. Dayton, and J. L. McNay, *J. Pharmacol. Exp. Ther.*, **199**, 490 (1976).
(18) D. E. Smith and L. Z. Benet, *Pharmacology*, in press.
(19) I. M. Weiner, in "Handbook of Physiology," Section 8, J. Orloff and R. W. Berliner, Eds., American Physiological Society, Washington, D.C., 1973, p. 521.
(20) L. Z. Benet, *J. Pharmacokinet. Biopharm.*, **7**, 1 (1979).
(21) B. Scherer and P. C. Weber, *Clin. Sci.*, **56**, 77 (1979).
(22) R. V. Patak, B. K. Mookerjee, C. J. Bentzel, P. E. Hysert, M. Babej, and J. B. Lee, *Prostaglandins*, **10**, 649 (1975).
(23) J. C. Frolich, J. W. Hollifield, J. C. Dormois, B. L. Frolich, H. Seyberth, A. M. Michelakid, and J. A. Oates, *Circ. Res.*, **39**, 447 (1976).
(24) J. B. Lee, R. V. Patak, and B. K. Mookerjee, *Am. J. Med.*, **60**, 798 (1976).
(25) D. E. Smith, D. C. Brater, E. T. Lin, and L. Z. Benet, *J. Pharmacokinet. Biopharm.*, **7**, 265 (1979).
(26) G. R. Zins, *Am. J. Med.*, **58**, 14 (1975).
(27) J. C. McGiff, K. Crowshaw, and H. D. Itskovitz, *Fed. Proc., Fed. Am. Soc. Exp. Biol.*, **33**, 39 (1974).
(28) J. C. Frolich, T. W. Wilson, B. J. Sweetman, M. Smigel, A. S. Nies, K. Carr, T. Watson, and J. A. Oates, *J. Clin. Invest.*, **55**, 763 (1975).
(29) L. Z. Bito, *Prostaglandins*, **9**, 851 (1975).
(30) L. Z. Bito, M. Wallerstein, and R. Baroody, in "Advances in Prostaglandin and Thromboxane Research," vol. 1, B. Samuelsson and R. Paoletti, Eds., Raven, New York, N.Y., 1976, p. 297.
(31) L. Z. Bito, *J. Physiol.*, **221**, 371 (1972).
(32) L. Z. Bito, *Prostaglandins*, **12**, 639 (1976).
(33) B. R. Rennick, *Pharmacologist*, **18**, 162 (1976).

ACKNOWLEDGMENTS

Presented in part at the APhA Academy of Pharmaceutical Sciences, Montreal meeting, May 1978.

Supported in part by National Institutes of Health Grant AM 20884.

D. E. Smith was supported as a National Institutes of Health Predoctoral Scholar on Training Grant GM 07175.

Syntheses and Evaluation of Ketals, Hemithioketals, and Dithioketals of Conjugated Styryl Ketones Principally for Antineoplastic Activity

J. R. DIMMOCK ˣ and L. M. SMITH

Received November 6, 1979, from the *College of Pharmacy, University of Saskatchewan, Saskatoon, Saskatchewan, S7N OWO, Canada.* Accepted for publication January 7, 1980.

Abstract □ Ketals, hemithioketals, and dithioketals of nuclear-substituted styryl ketones were prepared as latentiated forms of the ketones. This undertaking was based on the premise that there is increased acidity in tumors compared to normal tissue, and thus preferential regeneration of the ketone in neoplastic tissue may occur. Attempts to form 1,3-dioxolans of Mannich bases were unsuccessful. The prepared compounds did not possess significant anticancer properties, but analgesic, anti-inflammatory, antihistaminic, and antimicrobial activities were found in the prepared Mannich bases.

Keyphrases □ Antineoplastic activity—ketals, hemithioketals, and dithioketals of conjugated styryl ketones, synthesis and evaluation of activity □ Styryl ketones, conjugated—synthesis of ketals, hemithioketals, and dithioketals, evaluation for antineoplastic activity □ Mannich bases—synthesized from conjugated styryl ketones and acetophenones, evaluation for antineoplastic activity

A recurrent problem in the design of compounds for cancer chemotherapy is the synthesis of derivatives possessing selective toxicity for tumors. Biochemical differences between cancerous and normal cells have been claimed (1), including the increased acidity of certain malignant cells compared to normal tissue (2–4). The increased acidity of tumors has been ascribed to the greater rate of aerobic glycolysis in neoplastic tissue (5), which leads to increased lactic acid production. The pH of a number of tumors has been reported to be ~7.0 (2–4), although such measurements probably recorded the extracellular pH. Therefore, the pH of the intracellular fluid probably is even lower (6), and an average pH value for a number of tumorous tissues has been considered to be ~6.5 (7). Hence, a prodrug permitting the release of a cytotoxic agent under acidic conditions may afford selective lethality of tumors with ameliorated toxicity for normal tissue. Only a few attempts have been made to design compounds based on this pH differential (8–11).

Several investigations in this laboratory involved the preparation of some nuclear-substituted styryl ketones (I) and related Mannich bases (II) for evaluation as anticancer agents (12–14) and in other screens (15–17). While the ketones have not been evaluated against P-388 lymphocytic leukemia, some of the Mannich bases showed promising levels of activity in this screen (12); one compound (IIe) increased the mean survival time in mice by >40% (12). However, murine toxicity was found in II due at least partially to interference with mitochondrial function (18, 19). Therefore, prodrugs of both I and II were prepared, and both I and the prodrugs were evaluated in the P-388 screen so that anticancer activities and murine toxicities of the ketones (I and II) and their latentiated precursors could be compared. Since ketals, hemithioketals, and dithioketals are known to hydrolyze under acidic conditions but are stable in neutral or alkaline media (20), the preparation of these derivatives from I and II may

0022-3549/80/0500-0575$01.00/0
© 1980, American Pharmaceutical Association

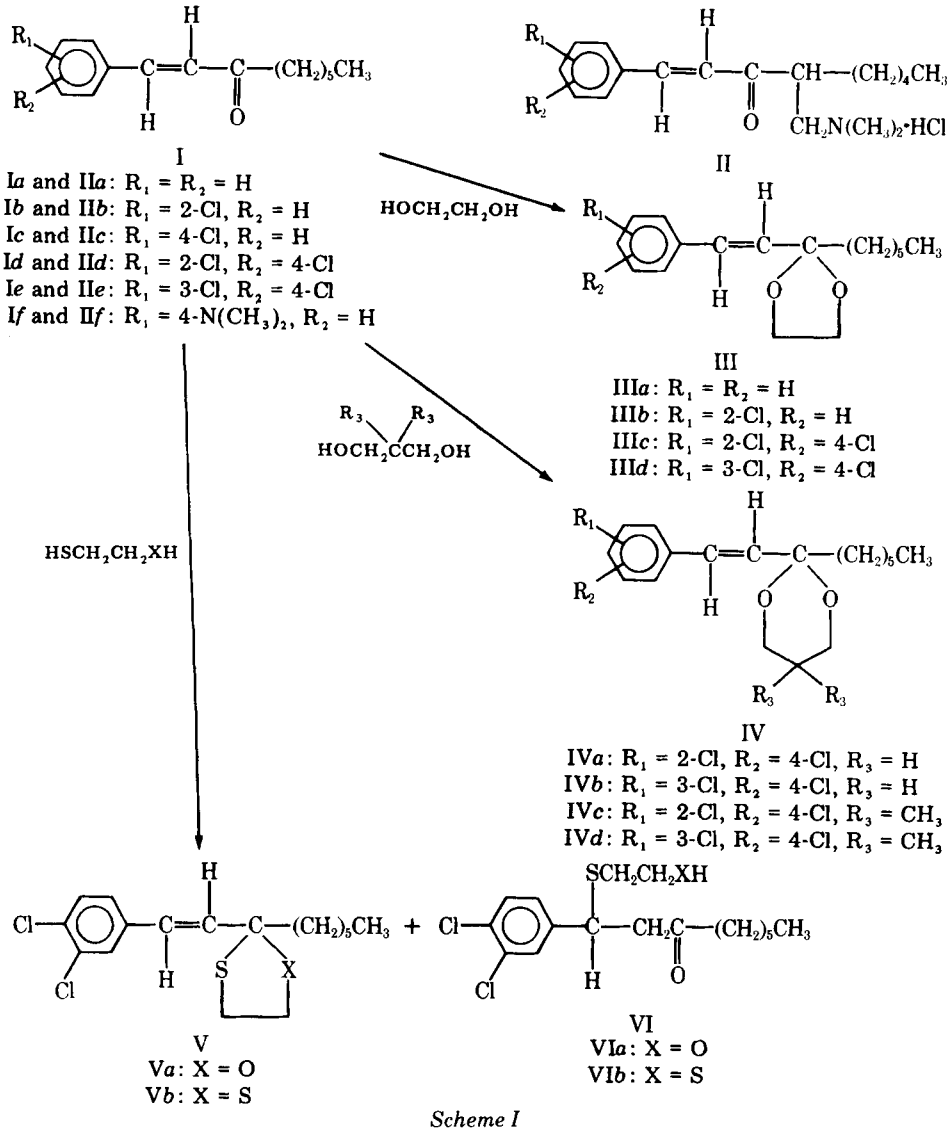

Scheme I

permit selective regeneration of these ketones in neoplastic tissue.

DISCUSSION

A review of synthetic methods available for preparing ketals, hemithioketals, and dithioketals, including the synthesis of these heterocycles derived from α,β-unsaturated ketones (20), outlined various reaction conditions that may be employed.

Initially, several abortive attempts were made to prepare the ketal IIIa from ethylene glycol and 1-phenyl-1-nonen-3-one (Ia) using different catalysts, solvents, and reaction times. However, prolonged heating of the reactants in benzene or toluene using *p*-toluenesulfonic acid as the catalyst led to the successful preparation of III–V, although there occasionally were low yields (Scheme I). The preparation of VII also was undertaken to examine the effect on biological activity of replacing the *n*-hexyl chain by a methyl group. Preliminary attempts to prepare Va and Vb by using milder reaction conditions and piperidine as the catalyst led to the Michael adducts (VIa and VIb) in low yields.

Attempts to react 4-dimethylaminomethyl-1-phenyl-1-nonen-3-one with ethylene glycol to produce the desired ketal were unsuccessful. The only product found on some occasions was the diolefin, 4-methylene-1-phenyl-1-nonen-3-one, which must have originated by the loss of dimethylamine hydrochloride from the Mannich base IIa. To eliminate this deamination process, the Mannich bases IXa and IXb were prepared as shown in Scheme II, but no reaction between IXa and ethylene glycol occurred under the conditions employed.

The antineoplastic evaluation of I and III–IX is shown in Table I. Unless otherwise stated, none of the compounds caused mortalities to mice at a dose of 200 mg/kg. Therefore, the styryl ketones (I) do not have marked murine toxicity, unlike the Mannich bases (II) (12), but only marginal levels of anticancer activity were seen. However, modification of the *n*-hexyl group of Ia led to the analogs VIIa and VIIIa with perceptible beneficial responses in the P-388 lymphocytic leukemia screen.

The lack of antineoplastic activity of the heterocycles III–V and VIIb is not surprising if reversion to the ketones (I) occurs. But the question may be posited as to whether these compounds are stable under neutral or acid conditions and if this is the case, any biological response or lack of activity may be due to the heterocycles *per se*. Seven representative compounds (IIIa, IIId, IVb, IVd, Va, Vb, and VIIa) were hydrolyzed to only a minute extent in buffer solutions of pH 7.0 and 6.4 for 20 hr at 37°; therefore, reversion of these compounds to the precursor ketones may not occur.

Compounds III–IX, with the exception of those indicated under *Experimental*, were evaluated for analgesic, anti-inflammatory, antidepressant, and antihistaminic properties. Of the 15 compounds examined, four met the criterion for analgesic activity, defined as protection of 50% or more in the phenylquinone writhing test (Table I). Compound Va displayed algesic properties. The unsubstituted 1,3-dioxolan (IIIa) showed higher activity than the chlorinated analogs (IIIb–IIId). However, expansion of the dioxolan ring of IIIc and IIId to the 1,3-dioxan heterocycles (IVa and IVb) led to compounds with improved analgesic activities, although insertion of geminal dimethyl groups onto the heterocyclic rings led to virtually inactive compounds, IVc and IVd.

The most active analgesic was the Mannich base IXa; it had an ED_{50} of 20 mg/kg. The analgesic activity of codeine, expressed as an ED_{50} value, is 14.2 mg/kg in the hot plate test (21); although the compounds listed

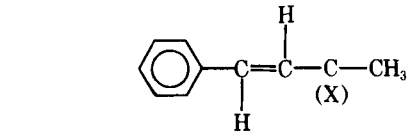

VII

VII*a*: X = =O

VII*b*: X = OCH_2CH_2O

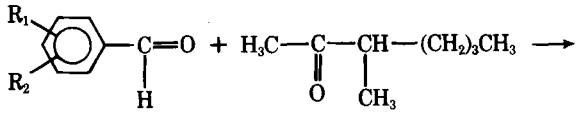

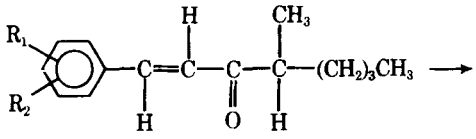

VIII

VIII*a*: $R_1 = R_2 = H$

VIII*b*: R_1 = 3-Cl, R_2 = 4-Cl

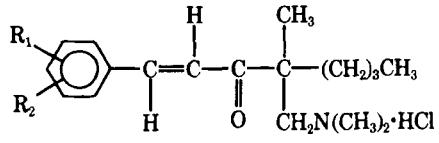

IX

IX*a*: $R_1 = R_2 = H$

IX*b*: R_1 = 3-Cl, R_2 = 4-Cl

Scheme II

in Table I were evaluated differently, it appears that IX*a* and codeine have comparable potencies. As noted previously for III, the presence of chlorine atoms in the aromatic ring reduced analgesic potency, and the dichlorinated analog of IX*a*, IX*b*, did not have analgesic activity. It is conceivable that the bulky chlorine atoms hinder alignment of the aromatic ring at a nonpolar area of a receptor.

In certain pathological conditions, an analgesic possessing anti-inflammatory properties can be a useful therapeutic agent. However, III–IX were inactive in the anti-inflammatory screen except for the Mannich base IX*b*, which at a dose of 120 mg/kg showed antagonism to carrageenan-induced rat paw edema of 100 and 17% at 3 and 5 hr, respectively, after treatment[1]. In addition, IX*b* was the only compound that met the criterion for activity[2] in the antidepressant screen, showing antagonism to tetrabenazine-induced ptosis in mice of 50 and 63% at the end of 0.5 and 1 hr, respectively, at a dose of 120 mg/kg. The only other compound with slight activity was IV*c*, which showed antagonism of 54 and 11% at the end of 0.5 and 1 hr, respectively.

All compounds examined in the antihistaminic screen showed activity (Table I), with the two Mannich bases IX*a* and IX*b* showing the greatest potencies. These two derivatives may be regarded as substituted propylamines, which is a class of compounds known to possess antihistaminic activity. Halogenation in the aromatic ring in the antihistaminic propylamines generally enhances activity (22), as was observed with these two compounds.

Some of the series III–IX compounds were examined for antimicrobial activity and were shown to be inactive with the exception of III*a*, which inhibited the growth of *Trichophyton mentagrophytes* at 10 μg/ml, and the Mannich bases IX*a* and IX*b*. Certain Mannich bases display antimicrobial activities (23), and this class of compounds is known to undergo facile deamination (24, 25). Therefore, the antimicrobial activities of Mannich bases may be due to the compound *per se* or to the corresponding deaminated product, *i.e.*, the analogous α,β-unsaturated ketone (26). The Mannich bases IX*a* and IX*b* are incapable of undergoing deamination. Evaluation of simpler Mannich bases (X) in this screen

[1] The reference compound, indomethacin, showed antagonism of 17 and 83% at the end of 3 and 5 hr, respectively, at a dose of 32 mg/kg. Values obtained in excess of 30% are considered to indicate anti-inflammatory activity.

[2] The reference compound was amitriptyline, which showed antagonism at 8 mg/kg of 90 and 49% at the end of 0.5 and 1 hr, respectively. A compound is considered active if it shows an antagonistic effect to tetrabenazine in excess of 50 and 25% after 0.5 and 1 hr, respectively.

Table I—Evaluation of the Styryl Ketones (I) and Related Derivatives (III–IX) for Antineoplastic, Analgesic, and Antihistaminic Activities

Compound	Maximum Increase in Mean Survival Time[a] (Dose, mg/kg)	Analgesic Activity[b] Dose, mg/kg	Analgesic Activity[b] Percentage Protection	Antihistaminic Activity[c]
I*a*	106 (200)	—	—	—
I*b*	118 (200)	—	—	—
I*c*	100 (400)	—	—	—
I*d*	109 (100)	—	—	—
I*e*	106 (75)	—	—	—
I*f*	97 (200)	—	—	—
III*a*	110 (100)	256	71	15
III*b*	108 (200)	256	44	2
III*c*	110 (100)	256	37	23
III*d*	108 (100)	256	14	3
IV*a*	97 (200)	100	55	15
IV*b*	98 (200)	ED_{50} = 62 mg/kg		19
IV*c*	102 (200)	100	16	16
IV*d*	100 (50)	120	12	28
V*a*	104 (25)	120	Algesic[e]	—
V*b*	113 (50)[d]	—	—	—
VI*a*	104 (200)	—	—	—
VI*b*	102 (50)[f]	120	10	9
VII*a*	126 (400)	—	—	—
VII*b*	102 (200)	120	34	46
VIII*a*	120 (200)	120	23	26
VIII*b*	115 (100)[f]	120	17	20
IX*a*	105 (50)[f]	ED_{50} = 20 mg/kg[g]		50
IX*b*	113 (12.5)[h]	120	1[g]	100

[a] The figures are the ratios of the survival time of treated animals to control animals expressed as a percentage. A compound should increase the mean survival time by 20% to be considered active. [b] Analgesic activity was measured by the percentage protection in the phenylquinone writhing test in mice. Protection in excess of 50% indicates an active compound. [c] The figures indicate the percentage protection of a compound at a concentration of 0.1 mg/ml against a standard dose of histamine. A compound is considered active if 50% or more protection is found. [d] There were 1/6 and 6/6 survivors on Day 5 at dose levels of 200 and 100 mg/kg, respectively. [e] The percentage increase in writhes for this compound was 58%. [f] There were 5/6 and 6/6 survivors on Day 5 at dose levels of 200 and 100 mg/kg, respectively. [g] This compound elicited a Straub tail response. [h] There were 0/6, 1/6, 5/6, and 6/6 survivors on Day 5 at dose levels of 200, 100, 50, and 25 mg/kg, respectively.

where deamination could occur was desired, and it has been claimed that antimicrobial activity is increased as the facility for deamination is enhanced (27). Table II shows that IX and X showed both antibacterial and antifungal activities; while the unsubstituted Mannich bases IX*a* and X*a* had similar activity, the chlorinated compounds in series X showed lower potency than IX*b*.

The levels of analgesic, anti-inflammatory, antidepressant, and antihistaminic activities displayed by IX*a* and IX*b* also were found in X (Table III). All of the series X derivatives showed anti-inflammatory and analgesic properties and, as noted in series IX, X*a*, which has no nuclear halogen, was more potent as an analgesic than were the chlorinated analogs X*b*–X*d*. Series X compounds, like IX, showed antidepressant and antihistaminic activities, but unlike the IX derivatives, the chlorinated compounds, X*b*–X*d*, had lower antihistaminic activity than the unsubstituted compound, X*a*.

In conclusion, this study outlined a synthetic route for the preparation of some potential prodrugs of certain nuclear-substituted styryl ketones and recorded some of the failures to synthesize 1,3-dioxolan derivatives from Mannich bases. The prepared heterocycles did not show improved antineoplastic activity over the precursor α,β-unsaturated ketones, probably due to the inactivity of the compounds *per se* or to the lack of activity of the ketones. Some of the heterocyclic compounds displayed analgesic and antihistaminic activities, although these were of a lower magnitude than some Mannich bases synthesized in this study. While

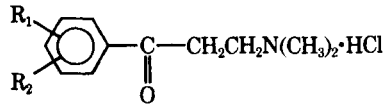

X

X*a*: $R_1 = R_2 = H$

X*b*: R_1 = 4-Cl, R_2 = H

X*c*: R_1 = 2-Cl, R_2 = 4-Cl

X*d*: R_1 = 3-Cl, R_2 = 4-Cl

Table II—Evaluation of the Mannich Bases (IX and X) for Antimicrobial Activity[a]

Microorganism	IX*a*	IX*b*	X*a*	X*b*	X*c*	X*d*
Escherichia coli (ATCC 8739)	>500	<100	>500	>500	>500	>500
Pseudomonas aeruginosa (ATCC 10145)	>500	>500	>500	>500	>500	>500
Klebsiella pneumoniae (ATCC 4352)	>100	>500	>500	>500	>500	>500
Salmonella typhimurium (G46)	>500	>500	>500	>500	>500	>500
Bordetella bronchiseptica (ATCC 4617)	>500	>500	>500	>500	>500	>500
Staphylococcus aureus (ATCC 6538)	<100	<100	>100	<100	<100	<100
Streptococcus pyogenes (hospital isolate)	>500	<100	>500	<100	>100	<100
Sarcina lutea (ATCC 9341)	>500	<100	>100	<100	<100	<100
Streptococcus faecalis (ATCC 8030)	<100	<100	>500	>500	<100	>100
Bacillus subtilis (ATCC 6633)	>500	<100	>500	>100	<100	<100
Trichophyton mentagrophytes (ATCC 9533)	<100	<10	<10	<10	<10	<100
Microsporum gypseum (ATCC 14683)	<100	<100	>500	<10	<10	<100
Aspergillus niger (ATCC 10535)	>500	<10	>500	>500	>500	>500
Candida albicans (ATCC 10231)	<100	<10	>500	>500	>500	>500
Saccharomyces carlsbergenis (ATCC 9080)	>500	>500	>500	>500	>500	>500
Average antimicrobial activity[b]	183	733	200	467	483	217

[a] The values are the minimum inhibitory concentrations of the compounds in micrograms per milliliter. [b] Figures were calculated from (combined antimicrobial activity × 100)/number of microorganisms in the screen. The combined antimicrobial activity was determined by giving the following scores at the highest potency of the compound against the microorganism: >100 = 2.5, <100 = 5, and <10 = 25.

Table III—Evaluation of the Mannich Bases (IX and X) for Analgesic, Anti-Inflammatory, Antidepressant, and Antihistaminic Activities

	Analgesic Activity[a]		Anti-Inflammatory Activity[b]			Antidepressant Activity[c]			
				Percentage Protection			Percentage Protection		Anti-histaminic
Compound	Dose, mg/kg	Percentage Protection	Dose, mg/kg	3 hr	5 hr	Dose, mg/kg	0.5 hr	1 hr	Activity[d]
IX*a*	ED_{50} = 20 mg/kg[e]		100	17	17	30	25	13	50
IX*b*	120	1[e]	120	100	17	120	50	63	100
X*a*	30	91	120	100	33	60	52	52	83
X*b*	60	91	120	100	87	120	43	48	45
X*c*	120	30	120	100	50	120	33	14	67
X*d*	120	85[e]	120	100	50	120	5	9	43
Reference compound[f]	50	50	32	17	83	8	90	49	100

[a] Analgesic activity was measured by the percentage protection in the phenylquinone writhing test using mice. Protection in excess of 50% indicates an active compound. [b] The anti-inflammatory activity was measured by the percentage protection afforded by the compound to carrageenan-induced edema in rats. Compounds showing greater than 30% protection are considered active. [c] The antidepressant screen measured the antagonism of a compound to tetrabenazine-induced ptosis in mice. A compound is considered active if >50 and >25% protection are obtained at the end of 0.5 and 1 hr, respectively. [d] The antihistaminic screen was undertaken by measuring the effect of the compound (0.1 mg/ml) on a guinea pig ileum preparation. A compound is considered active if 50% protection or more to a standard dose of histamine (0.5 mg/ml) is obtained. The reference compound, diphenhydramine, gives 100% protection at a dose of 0.01 mg/ml. [e] These compounds elicited a Straub tail response. [f] The reference compounds in the analgesic, anti-inflammatory, antidepressant, and antihistaminic screens were aspirin, indomethacin, amitriptyline, and diphenhydramine, respectively.

little antimicrobial activity was found in the nonnitrogenous derivatives, some of the Mannich bases displayed activity against certain pathogenic bacteria and fungi.

EXPERIMENTAL[3]

Melting points and boiling points are uncorrected. Organic extracts were washed with water and dried over anhydrous magnesium sulfate. The solvent was removed using a water aspirator. The boiling point of the petroleum ether was 30–60°. TLC was carried out on all of the compounds, which were purified by column chromatography using aluminum oxide sheets[4] and petroleum ether as the solvent to confirm the homogeneity of the product. The 60-MHz NMR spectra[5] were determined in deuterochloroform with tetramethylsilane as the internal standard. Mass spectra[6] were run at 70 ev, and IR spectra[7] were determined as films.

Syntheses of Compounds—Compounds I*a*–I*f* (28) and II*a* (29) were prepared by literature methods.

*Ketals, Hemithioketals, and Dithioketals (III–V and VII*b)—The general synthetic procedure was as follows. A mixture of the ketone (I) (0.1 mole), the appropriate alcohol or thiol (0.125 mole), and a catalytic quantity of *p*-toluenesulfonic acid (0.1 g) in benzene (200 ml) was heated under reflux for 48 hr. A Dean-Stark trap attached to the apparatus collected the water formed during the reaction. Upon cooling, the mixture was extracted with ether to give viscous yellow oils.

Modifications of this general synthetic route were employed in the preparation of IV, for which toluene was used as the solvent in place of benzene, and for V, for which the length of time of heating under reflux in benzene was reduced to 24 hr. The ketals III and VII*b* derived from ethylene glycol were purified by distillation, while attempts to effect purification in this manner with some of the other compounds (IV and V) invariably led to decomposition to the starting reactants.

The boiling points of III*a*–III*d* and VII*b* were 151°/0.1 mm, 155°/0.15 mm, 161°/0.1 mm, 167°/0.1 mm, and 133°/0.1 mm, respectively. Compounds IV and V were purified by column chromatography using neutral aluminum oxide[8] and eluting the compounds with petroleum ether to give viscous yellow oils. For IV*d*, colorless granular crystals, mp 65–67°, were obtained after chromatography. Attempts to use basic aluminum oxide[9] followed by elution with petroleum ether led to the decomposition of the dioxolan on the column.

NMR and IR spectroscopy and mass spectrometry were carried out on III–V and VII*b*, and the spectra obtained were consistent with the proposed structures. The NMR spectroscopy data found for five representative compounds are: III*a*: δ 7.23 (m, 5, C_6H_5), 6.68 (d, 1, C_1H), 6.02 (d, 1, C_2H), 3.85 (s, 4, OC_2H_4O), 2.12–1.08 [m, 10, $(CH_2)_5$], and 0.88 (t, 3, C_9H_3); IV*b*: δ 7.38–6.78 (m, 3, C_6H_3), 6.45 (d, 1, C_1H), 5.95 (d, 1, C_2H), 3.92 (m, 2, $OCH_2CH_2CH_2O$), 3.78 (t, 4, $OCH_2CH_2CH_2O$), 2.35–1.05 [m, 10, $(CH_2)_5$], and 0.88 (t, 3, C_9H_3); IV*d*: δ 7.48–6.91 (m, 3, C_6H_3), 6.48 (d, 1, C_1H), 5.94 (d, 1, C_2H), 3.48 [q, 4, $OCH_2C(CH_3)_2CH_2O$], 2.04–1.04 [m, 10, $(CH_2)_5$], 1.21 (s, 3, $OCH_2CH_3(-C-)CH_3-CH_2O$), 0.88 (t, 3, C_9H_3), and 0.68 (s, 3, $OCH_2CH_3(-C-)CH_3-CH_2O$); V*a*: δ 7.51–6.91 (m, 3, C_6H_3), 6.44 (d, 1, C_1H), 6.04 (d, 1, C_2H), 4.11 (octet, 2, OCH_2CH_2S), 3.01 (t, 2, OCH_2CH_2S), 2.21–1.08 [m, 10, $(CH_2)_5$], and 0.88 (t, 3, C_9H_3); V*b*: δ 7.45–6.97 (m, 3, C_6H_3), 6.60 (d, 1, C_1H), 6.20 (d, 1, C_2H), 3.25 (s, 4, SCH_2CH_2S), 2.27–1.05 [m, 10, $(CH_2)_5$], and 0.90 (t, 3, C_9H_3). The coupling constant for the olefinic protons in these five compounds was 16 Hz.

[3] Elemental analyses were carried out by Mr. R. E. Teed, Department of Chemistry and Chemical Engineering, University of Saskatchewan.
[4] Eastman-Kodak Co.
[5] Varian T 60 spectrophotometer, Varian Associates of Canada Ltd.
[6] AEI MS-12 mass spectrometer, Picker X-Ray Engineering Ltd.
[7] Beckman IR8 spectrophotometer, Beckman Instruments Inc.
[8] Neutral aluminum oxide (Brockman activity 1.0, 80–200 mesh), Fisher Scientific Co.
[9] Alcoa Chemicals aluminum oxide (F-20), Aluminum Company of Canada.

IR spectroscopy of the ketals III and IV showed loss of the α,β-unsaturated carbonyl peak of I in the region of 1700–1600 cm^{-1}, while the strong absorption at ~965 cm^{-1} due to the out-of-plane methine deformation band of the olefinic group (30) was present. Peaks at ~1190 (w), 1170 (s), and 1095 (w) cm^{-1} were assigned to the carbon–oxygen stretching vibrations associated with the ketal group (31). In the sulfur analogs (V), the absence of carbonyl absorption was noted and the peak at 965 cm^{-1}, while retained, was of diminished intensity compared to III and IV. The sulfur–carbon absorption in the region of 700–590 cm^{-1} (32) was not observed.

Examination of the mass spectrum of a representative ketal (IV*a*) showed that loss of the *n*-hexyl group occurred, producing an ion (A) at *m/e* 175 that was derived from the molecular ion (*m/e* 260). Ion A lost 44 mass units and yielded an ion (B) at *m/e* 131, whose structure was considered to be $C_6H_5CH{=}CHC{\equiv}O^+$. Ion B lost carbon monoxide to form the styrenoid ion $C_6H_5CH{=}C^+H$. Metastable peaks were observed, which supported this fragmentation pathway, and all of the ketals fragmented to give analogous ions. The analytical data and the yields of these compounds are summarized in Table IV.

Initial attempts to prepare the ketal III*a* were either unsuccessful or unsatisfactory. When the reactants were heated in benzene for 4 or 8 hr, little or no reaction product was obtained. When either stannic chloride or boron trifluoride etherate replaced *p*-toluenesulfonic acid (heating under reflux for 48 hr in benzene), no product was obtained. When the reactants were heated under reflux for 48 hr in methanol or chloroform in place of benzene, no reaction occurred, even if anhydrous magnesium sulfate or anhydrous sodium sulfate was added to the reaction mixture. When toluene replaced benzene as the solvent, III*a* was formed in greater yield than when benzene was used as the solvent, but there was an increase in tar formation.

Adducts (VI)—A mixture of 1-(3,4-dichlorophenyl)-1-nonen-3-one (0.1 mole), 2-mercaptoethanol (0.25 mole), and 2 or 3 drops of piperidine in ethanol (100 ml) was heated at 40° for 24 hr. The solvent was removed to give a pale-yellow oil, which was purified by chromatography using aluminum oxide[8]. Elution with petroleum ether gave 1-(3,4-dichlorophenyl)-1-(2-hydroxyethylthio)-3-nonanone (VI*a*) as a colorless oil in a 13% yield; mass spectrum: *m/e* 362 (M^+).

Anal.—Calc. for $C_{17}H_{24}Cl_2O_2S$: C, 56.20; H, 6.66. Found: C, 55.10; H, 6.57.

The thio analog (VI*b*) was prepared in a similar fashion, except that a colorless solid was obtained after completion of the reaction and removal of the solvent. Recrystallization of the solid from acetone produced 1-(3,4-dichlorophenyl)-1-(2-mercaptoethylthio)-3-nonanone (VI*b*) as fluffy, colorless crystals, mp 84–85°, in an 18% yield.

Anal.—Calc. for $C_{17}H_{24}Cl_2OS_2$: C, 53.82: H, 6.38. Found: C, 54.03; H, 6.43.

Styryl Ketones (VIII) and Related Mannich Bases (IX)—1-Phenyl-4-methyl-1-octen-3-one (VIII*a*) was prepared by the literature method (28) as a pale-yellow oil, bp 132°/0.8 mm, in a 64% yield.

Anal.—Calc. for $C_{15}H_{20}O$: C, 83.28; H, 9.32. Found: C, 83.42; H, 9.53.

1-(3,4-Dichlorophenyl)-4-methyl-1-octen-3-one (VIII*b*) was prepared in a similar fashion as a pale-yellow oil, bp 151–153°/0.75 mm, in a 52% yield; mass spectrum: *m/e* 284 (M^+).

Anal.—Calc. for $C_{15}H_{18}Cl_2O$: C, 63.17; H, 6.36. Found: C, 62.35; H, 6.42.

4-Dimethylaminomethyl-4-methyl-1-phenyl-1-octen-3-one hydrochloride (IX*a*) was prepared from VIII*a* by the literature procedure (29) with crystallization from acetone to give fluffy, colorless crystals, mp 153.5–154°, in a 53% yield.

Anal.—Calc. for $C_{18}H_{28}ClNO$: C, 69.77; H, 9.11; N, 4.52. Found: C, 70.12; H, 9.08; N, 4.58.

The corresponding 3,4-dichloro analog (IX*b*), prepared in a similar fashion from VIII*b*, crystallized from acetone as fluffy, colorless crystals, mp 126.5–127°, in a 56% yield.

Anal.—Calc. for $C_{18}H_{26}Cl_3NO$: C, 57.07; H, 6.92; N, 3.70. Found: C, 56.61; H, 6.94; N, 3.67.

Dioxolan Derivative of 4-Dimethylaminomethyl-1-phenyl-1-nonen-3-one—A mixture of 4-dimethylaminomethyl-1-phenyl-1-nonen-3-one hydrochloride (II*a*, 0.1 mole), ethylene glycol (0.125 mole), and a catalytic quantity of *p*-toluenesulfonic acid in benzene (200 ml) was heated under reflux for 48 hr. Water did not appear to collect in a Dean-Stark trap attached to the reaction vessel but the pH of the benzene in the trap was ~1 after 4 hr of heating. After the solvent was removed, a mixture of equal volumes of water and ether was added to the reaction product.

The organic extract was separated and revealed the presence of a compound whose mass spectral, NMR, IR, and TLC characteristics were identical with those of an authentic specimen of 4-methylene-1-phenyl-1-nonen-3-one (29). The aqueous layer was cooled in ice, made basic with aqueous sodium hydroxide solution (10% w/v), and extracted with ether; the product that was isolated was shown by mass spectrometry and IR and NMR spectroscopy to be an unreacted Mannich base.

Other attempts to prepare this ketal used ratios of the Mannich base hydrochloride (II*a*), ethylene glycol, and solvent similar to those described; unless otherwise stated, the reaction proceeded for 24 hr.

1. A catalytic quantity of anhydrous stannic chloride in dry chloroform was used, and the reaction mixture was kept at 40° overnight, from which only unreacted starting material was isolated.

2. The previous experiment was repeated, except that anhydrous magnesium sulfate was added as a drying agent. No reaction occurred.

3. When the reactants were heated under reflux in benzene with anhydrous stannic chloride, the olefin 4-methylene-1-phenyl-1-nonen-3-one and a viscous oil were found.

4. A mixture of Mannich base hydrochloride (0.1 mole), ethylene glycol (0.125 mole), and anhydrous stannic chloride (0.1 g) was heated under reflux in benzene (20 ml) and produced a tarry oil.

5. The reactants were heated under reflux in chloroform containing a catalytic quantity of anhydrous zinc chloride in the presence of molecular sieves[10], from which only unreacted material was isolated.

6. When the previous reaction was repeated using benzene as the solvent and eliminating the molecular sieves, 4-methylene-1-phenyl-1-nonen-3-one was isolated.

7. When boron trifluoride etherate in dry ether was employed and the reaction mixture was heated overnight at 30°, no reaction occurred.

8. The reactants were heated overnight under reflux in chloroform to which adipic acid has been added as the catalyst. The isolated product was 4-methylene-1-phenyl-1-nonen-3-one.

9. Instead of the hydrochloride salt, the free Mannich base was used; the same results were produced.

Dioxolan Derivative of 4-Dimethylaminomethyl-4-methyl-1-phenyl-1-octen-3-one—A mixture of IX*a* (0.1 mole), ethylene glycol (0.125 mole), and a catalytic quantity of *p*-toluenesulfonic acid in benzene (200 ml) was heated under reflux for 48 hr. The mixture was treated as described previously, and only unreacted materials were isolated.

Mannich Bases (X)—The Mannich bases (X) were prepared by the literature method (29) and gave the required derivatives as fluffy, colorless crystals, which were recrystallized from acetone. 3-Dimethylamino-1-phenyl-1-propanone hydrochloride (X*a*) was prepared in a 41% yield, mp 159–160° [lit. (33) mp 160°]. The *p*-chloro analog (X*b*) was obtained in a 43% yield, mp 171–173° [lit. (34) mp 170°]. Compound X*c* was synthesized in a 15% yield, mp 193–195° [lit. (35) mp 193–195°]. Compound X*d* was prepared in a 22% yield, mp 138–139° [lit. (35) mp 138–139°].

Table IV—Ketals, Hemithioketals, and Dithioketals of Conjugated Styryl Ketones

Compound	Yield, %	Formula		Analysis, % Calc.	Found
III*a*	68	$C_{17}H_{24}O_2$	C	78.46	78.56
			H	9.23	9.23
III*b*	62	$C_{17}H_{23}ClO_2$	C	69.27	69.26
			H	7.81	7.81
III*c*	56	$C_{17}H_{22}Cl_2O_2$	C	62.01	62.07
			H	6.69	6.75
III*d*	58	$C_{17}H_{22}Cl_2O_2$	C	62.01	62.16
			H	6.69	6.79
IV*a*	14	$C_{18}H_{24}Cl_2O_2$	C	62.98	63.02
			H	7.05	6.98
IV*b*	16	$C_{18}H_{24}Cl_2O_2$	C	62.98	63.11
			H	7.05	6.92
IV*c*	17	$C_{20}H_{28}Cl_2O_2$	C	64.69	64.45
			H	7.60	7.65
IV*d*	5	$C_{20}H_{28}Cl_2O_2$	C	64.69	63.92
			H	7.60	7.49
V*a*	11	$C_{17}H_{22}Cl_2OS$	C	59.13	59.05
			H	6.42	6.51
V*b*	6	$C_{17}H_{22}Cl_2S_2$	C	56.50	54.54
			H	6.14	6.19
VII*b*	73	$C_{12}H_{14}O_2$	C	75.76	75.51
			H	7.42	7.43

[10] Molecular sieves (type 4A, grade 514, 8–12 mesh), Fisher Scientific Co.

Hydrolyses of the Ketals (IIIa, IIId, IVb, IVd, Va, Vb, and VIIb)—The acetonitrile–buffer solutions were prepared as follows. A solution of monobasic sodium phosphate monohydrate (9.30 g) in double-distilled water was adjusted to 1000 ml (Solution A), and a solution of dibasic sodium phosphate heptahydrate was prepared by dissolving the salt (17.88 g) in water and diluting to 1000 ml (Solution B). A mixture of acetonitrile (500.0 ml) and Solution A (389.0 ml) was placed in a 1000-ml volumetric flask, and Solution B was added to 1000 ml. The pH of the resultant solution was 7.00. The acetonitrile–buffer solution of pH 6.40 was prepared in a similar manner, except that the amount of Solution A was 464.0 ml.

The appropriate ketal (10^{-3} g) was dissolved in acetonitrile–buffer (100.0 ml) at pH 7.00 and 6.40 and heated in a constant-temperature bath at 37° for 20 hr. At the commencement of the experiment and also at the end of 20 hr, 1.0-ml aliquots were withdrawn and diluted to 10.0 ml with the same solvent. The UV spectrum[11] was observed at the λ_{max} of both the ketal and the corresponding ketone. The percentage hydrolysis was obtained by noting the ketone absorption (A), and since there is some end-absorption of the ketal in the region of the λ_{max} of the ketone, the extent of the hydrolyses was obtained from:

$$\% \text{ hydrolysis} = \frac{A_{obs} - A_{\text{end-absorption of ketal}}}{A_{\text{pure ketone}}} \qquad \text{(Eq. 1)}$$

The percentage hydrolyses of IIIa, IIId, IVb, IVd, Va, Vb, and VIIb at pH 7.00 were 3.53, 4.29, 2.23, 1.30, 0.21, 0, and 3.81, respectively. At pH 6.40, the percentage hydrolyses of the same compounds were 1.68, 3.07, 0.13, 0, 0, 0, and 2.75, respectively.

Screening of Compounds—The anticancer screening was carried out by the Drug Research and Development Division of the National Cancer Institute, Bethesda, Md., using their protocols (36). In the P-388 screen, the compounds were administered by the intraperitoneal route into either male or female CD_2F_1 mice, although on rare occasions the $B_6D_2F_1$ strain was employed. The compounds were administered for 9 consecutive days, except for Ia and VIa, for which injections were made every 4 days with a total of two and three injections, respectively. The derivatives were administered in saline (Va, VIb, VIIIb, and IXb), saline with polysorbate 80[12] (Ia–If, IIIa, IVd, VIIa, VIIb, VIIIa, and IXa), saline with alcohol (IVa–IVc), or hydroxypropylcellulose (IIIb–IIId) or as a suspension in saline (VIa). Compound Vb was administered either in saline or in saline containing polysorbate 80.

All of the series III–X compounds, except where noted, were evaluated[13] for analgesic, anti-inflammatory, antidepressant, and antihistaminic activities by previously reported procedures (37). Compounds Vb, VIa, and VIIa were not included in any of these screens; IIIc and Va were not assessed for antidepressant and antihistaminic activities, respectively. The antimicrobial screen[13] was performed by the literature method (37) on the series III–IX compounds with the exception of IVa and VIIa.

REFERENCES

(1) L. N. Ferguson, *Chem. Soc. Rev.*, **4**, 289 (1975).

(2) M. Eden, B. Haines, and H. Kahler, *J. Natl. Cancer Inst.*, **16**, 541 (1955).

(3) H. Kahler and W. v B. Robertson, *ibid.*, **3**, 495 (1943).

(4) K. A. Meyer, E. M. Kammerling, L. Amtman, M. Koller, and S. J. Hoffman, *Cancer Res.*, **8**, 513 (1948).

(5) E. Racker, *J. Cell. Physiol.*, **89**, 697 (1976).

(6) W. C. J. Ross, *Biochem. Pharmacol.*, **8**, 235 (1961).

(7) G. Abel, T. A. Connors, P. Goddard, H. Hoellinger, Nguyen-Hoang-Nam, L. Pichat, W. C. J. Ross, and D. E. V. Wilman, *Eur. J. Cancer*, **11**, 787 (1975).

(8) M. J. Kornet, A. P. Thio, and J. H. Thorstenson, *J. Pharm. Sci.*, **66**, 1022 (1977).

(9) Z. B. Papanastassiou, R. J. Bruni, E. White, V, and P. L. Levins, *J. Med. Chem.*, **9**, 725 (1966).

(10) J. H. Billman, F. Koehler, and R. May, *J. Pharm. Sci.*, **58**, 767 (1969).

(11) Y. F. Shealy, J. A. Montgomery, and W. R. Laster, Jr., *Biochem. Pharmacol.*, **11**, 674 (1962).

(12) J. R. Dimmock and W. G. Taylor, *J. Pharm. Sci.*, **64**, 241 (1975).

(13) J. R. Dimmock, G. B. Baker, and R. G. Sutherland, *Can. J. Pharm. Sci.*, **10**, 53 (1975).

(14) J. R. Dimmock, C. B. Nyathi, and P. J. Smith, *J. Pharm. Sci.*, **67**, 1543 (1978).

(15) J. R. Dimmock, N. W. Hamon, L. M. Noble, and D. E. Wright, *ibid.*, **68**, 1033 (1979).

(16) J. R. Dimmock, D. K. Kowal, W. A. Turner, P. J. Smith, L. M. Noble, and W. J. Pannekoek, *ibid.*, **67**, 401 (1978).

(17) J. R. Dimmock, A. M. Qureshi, L. M. Noble, P. J. Smith, and H. A. Baker, *ibid.*, **65**, 38 (1976).

(18) J. R. Dimmock, N. W. Hamon, K. W. Hindmarsh, D. G. Mills, L. E. Negrave, G. H. Rank, and A. J. Robertson, *ibid.*, **65**, 482 (1976).

(19) N. W. Hamon, D. L. Bassendowski, D. E. Wright, J. R. Dimmock, and L. M. Noble, *ibid.*, **67**, 1539 (1978).

(20) H. J. E. Loewenthal, in "Protective Groups in Organic Chemistry," J. F. W. McOmie, Ed., Plenum, London, England, 1973, p. 323 seq.

(21) N. B. Eddy and D. Leimback, *J. Pharmacol. Exp. Ther.*, **107**, 385 (1953).

(22) O. L. Salerni, "Natural and Synthetic Organic Medicinal Compounds," C. V. Mosby, St. Louis, Mo., 1976, p. 87.

(23) J. R. Dimmock and M. C. L. Wong, *Can. J. Pharm. Sci.*, **11**, 35 (1976).

(24) F. F. Blicke, in "Organic Reactions," vol. 1, R. Adams, Ed., Wiley, New York, N.Y., 1942, p. 318.

(25) H. Riviere, *Ann. Chim. (Paris)*, **5**, 1273 (1960).

(26) P. N. Gordon, J. D. Johnston, and A. R. English, in "Antimicrobial Agents and Chemotherapy," G. L. Hobby, Ed., American Society for Microbiology, Ann Arbor, Mich., 1965, p. 165.

(27) H. Schönenberger, T. Bastug, L. Bindl, A. Adam, D. Adam, A. Petter, and W. Zwez, *Pharm. Acta Helv.*, **44**, 691 (1969).

(28) P. J. Smith, J. R. Dimmock, and W. G. Taylor, *Can. J. Chem.*, **50**, 871 (1972).

(29) J. R. Dimmock and W. G. Taylor, *J. Pharm. Sci.*, **63**, 69 (1974).

(30) A. D. Cross, "An Introduction to Practical Infra-red Spectroscopy," Butterworths Scientific Publications, London, England, 1960, p. 58.

(31) R. T. Conley, "Infrared Spectroscopy," Allyn and Bacon, Boston, Mass., 1966, p. 128.

(32) *Ibid.*, p. 179.

(33) C. Mannich and F. T. Chang, *Ber.*, **66B**, 418 (1933); through *Chem. Abstr.*, **27**, 2940 (1933).

(34) J. Dhont and J. P. Wibaut, *Rec. Trav. Chim.*, **63**, 81 (1944).

(35) Italian pat. 637,371 (Mar. 29, 1962); through *Chem. Abstr.*, **60**, 479c (1964).

(36) R. I. Geran, N. H. Greenberg, M. M. MacDonald, A. M. Schumacher, and B. J. Abbott, *Cancer Chemother. Rep. (Part 3)*, **3** (Sept. 1972).

(37) J. R. Dimmock, P. J. Smith, and S. K. Tsui, *J. Pharm. Sci.*, **68**, 866 (1979).

[11] Model 250 spectrophotometer, Gilford Instrument Laboratories.

[12] Tween 80, Atlas Chemical Industries.

[13] Bio-Research Laboratories Ltd., Montreal, Quebec, Canada. It is recognized that the evaluation of the series X compounds against different microorganisms has been discussed in the literature and that the efficacy of Xa and Xb as analgesics has been assessed. They were included in this work for comparative purposes under identical screening conditions as the novel compounds described herein.

ACKNOWLEDGMENTS

The authors thank the Medical Research Council of Canada for the award of an operating grant (MA 5538) to J. R. Dimmock. The authors also thank the Drug Research and Development Division of the National Cancer Institute, Bethesda, Md., and Bio-Research Laboratories, Montreal, Quebec, Canada, who undertook the screening of the compounds.

Localization of Technetium 99m–Ethylenediamine-*N,N'*-bis(α-2-hydroxy-5-bromophenyl)acetic Acid and Technetium 99m–*N*-(2-Mercapto-1-oxopropyl)glycine in Hepatobiliary System

MICHAEL C. THEODORAKIS *x, WILLIAM C. GROUTAS ‡, ALEX J. BERMUDEZ *, DAVID MAGNIN ‡, and STAVROULA-VANI S. STEFANAKOU *

Received September 17, 1979, from the *Division of Nuclear Medicine and Radiopharmacology, College of Veterinary Medicine, University of Illinois at Urbana-Champaign, Urbana, IL 61801, and the ‡College of Chemistry, University of Wisconsin at Eau Claire, Eau Claire, WI 54701. Accepted for publication January 4, 1980.

Abstract □ Two radiopharmaceuticals, technetium 99m–*N*-(2-mercapto-1-oxopropyl)glycine (^{99m}Tc-I) and technetium 99m–ethylenediamine-*N,N'*-bis(α-2-hydroxy-5-bromophenyl)acetic acid (^{99m}Tc-II), were prepared and evaluated in dogs, rabbits, and rats. Both agents gave good scintigraphic images of the liver and gallbladder in dogs. The cumulative amount of ^{99m}Tc-I and ^{99m}Tc-II excreted in the bile of dogs and the physiological disposition data in rats revealed slight, inconclusive differences in their distributions. However, the scintigraphic images and physiological disposition data in rabbits revealed gross differences in the distribution pattern of the two agents. The observed similarities in the biliary excretion of both agents in dogs and rats were attributed to the fact that these species are relatively good biliary excretors, and both agents therefore were excreted extensively. However, rabbits, which are poor biliary excretors relative to dogs and rats, excreted ^{99m}Tc-II more extensively than ^{99m}Tc-I because of the favorable molecular characteristics of ^{99m}Tc-II.

Keyphrases □ Radiopharmaceuticals—technetium 99m complexes of *N*-(2-mercapto-1-oxopropyl)glycine and ethylenediamine-*N,N'*-bis(α-2-hydroxy-5-bromophenyl)acetic acid, localization in hepatobiliary system □ Technetium 99m—complexes with *N*-(2-mercapto-1-oxopropyl)glycine and ethylenediamine-*N,N'*-bis(α-2-hydroxy-5-bromophenyl)acetic acid, localization in hepatobiliary system □ Scintigraphic imaging agents—complexes of technetium 99m with *N*-(2-mercapto-1-oxopropyl)glycine and ethylenediamine-*N,N'*-bis(α-2-hydroxy-5-bromophenyl)acetic acid, localization in hepatobiliary system

External scintigraphic diagnosis of gallbladder pathology has been the subject of several investigations. Application of the intravenous radionuclide cholangiogram has saved time in routine hepatobiliary function tests, demonstrating the patency of the cystic duct in patients with suspected acute cholecystitis, and also in evaluating the patency of surgically devised drainage pathways of the biliary system, particularly after liver transplantation and after the Kusai procedure for biliary atresia (1).

Complexes of technetium 99m with mercaptoisobutyric acid (2), dihydrothioctic acid (3), pyridoxylidene glutamate (4), pyridoxal phenylalanine (5), methyliminodiacetic acid (6), and *N*-[[(2,6-dimethyl)phenylcarbamoyl]-methyl]iminodiacetic acid (6) have been used for the intravenous radionuclide cholangiogram in humans and for replacing [^{131}I]rose bengal, which has undesirable radiation characteristics. Complexes of technetium 99m with *N*-(2-mercapto-1-oxopropyl)glycine (7) and ethylenediamine-*N,N'*-bis(α-2-hydroxy-5-bromophenyl)acetic acid (8) have been proposed as possible agents for the intravenous radionuclide cholangiogram.

The purpose of this study was to use animals to explore the relative merit of technetium 99m–*N*-(2-mercapto-1-oxopropyl)glycine (^{99m}Tc-I) and technetium 99m–ethylenediamine-*N,N'*-bis(α-2-hydroxy-5-bromophenyl)acetic acid (^{99m}Tc-II) as diagnostic radiopharmaceuticals in humans. The criteria for selecting the best agent were the quality of the scintigraphic images of the hepatobiliary system in dogs and rabbits and the tissue distribution of both agents in rats and rabbits.

EXPERIMENTAL

***N*-(2-Mercapto-1-oxopropyl)glycine[1] (I)**—Compound I was used without further purification.

Ethylenediamine-*N,N'*-bis(α-2-hydroxy-5-bromophenyl)acetic Acid[2] (II)—A solution of *p*-bromophenol (22.82 g, 0.1319 mole), sodium dichloroacetate (19.92 g, 0.1319 mole), and ethylenediamine (3.96 g, 0.066 mole) in 10 ml of methanol and 6 ml of water was heated to 85° and stirred for 24 hr under nitrogen. The reaction mixture pH was maintained at 9.5 by adding 6 *N* NaOH. After cooling to room temperature, the pH was adjusted carefully to 6.0 with 6 *N* HCl. The precipitated *p*-bromophenol was removed by extraction with ether (3 × 35 ml).

The aqueous solution pH was lowered to 4.0 with 6 *N* HCl, whereupon an orange solid precipitated. The dark supernate was carefully decanted, and the residue was washed repeatedly with methanol and acetone. The solvent finally was removed *in vacuo*, leaving a yellow solid (9.57 g, 30% yield), mp 245° dec. The compound could be purified further by column chromatography with silica gel and methanol–ammonium hydroxide as the eluent; IR (KBr): 3400–2400 (hydrogen-bonded OH) and 1660 (C=O) cm^{-1}; NMR (CF_3COOH–tetramethylsilane): δ 10.56 (s, 4H), 7.0 (s, 4H), 6.34–6.48 (d, 2H), 4.75 (s, 2H), and 3.4 (m, 4H).

Anal.—Calc. for $C_{18}H_{18}Br_2N_2O_6$: C, 41.72; H, 3.50; Br, 30.84; N, 5.4. Found: C, 41.72; H, 3.52; Br, 28.17; N, 6.18.

Technetium 99m-*N*-(2-Mercapto-1-oxopropyl)glycine (^{99m}Tc-I)—The technetium 99m complex of I was prepared by a modification of a reported method (7). Three milliliters of a saline eluate of sodium pertechnetate (III) (1–5 mCi), received from a molybdenum 99-technetium 99m generator[3], was mixed with 0.5 ml of a stock solution of stannous chloride–I, followed by 5–10 min of incubation at room temperature under a nitrogen atmosphere. The stock solution was prepared by mixing 40 ml of 0.15 *M* I in 1 *M* $NaHCO_3$ with 40 ml of 8.4×10^{-3} *M* $SnCl_2 \cdot 2H_2O$ in 0.1 *M* HCl. The stock solution pH was adjusted

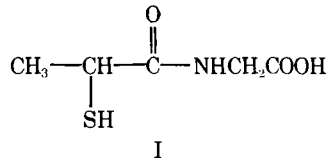

I

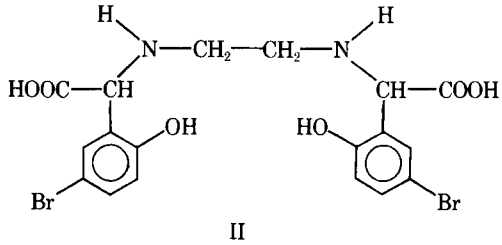

II

[1] A D and L mixture, Calbiochem, La Jolla, Calif.
[2] A D, L, and *meso* mixture.
[3] Mallinckrodt Chemical, St Louis, Mo.

0022-3549/80/0500-0581$01.00/0
© 1980, American Pharmaceutical Association

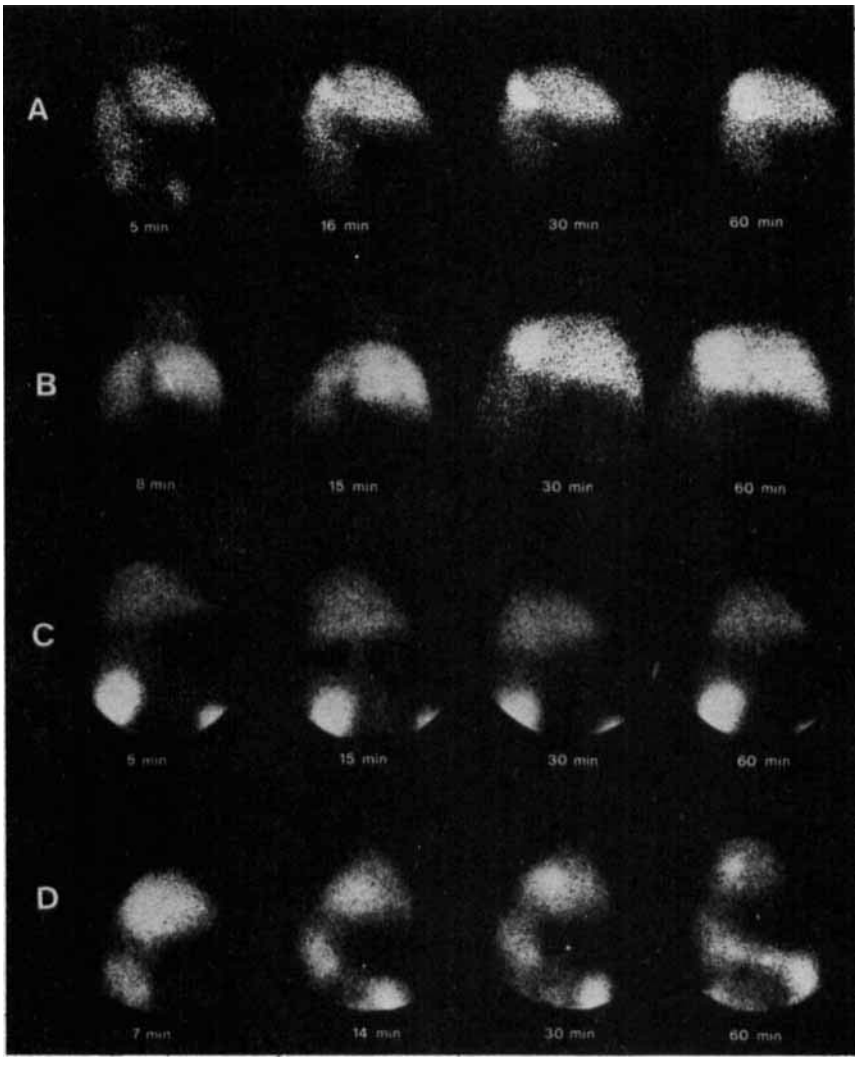

Figure 1—*Successive scintigraphic ventral images of the liver and gallbladder of* ^{99m}*Tc-I (A and C) and* ^{99m}*Tc-II (B and D) in beagles (A and B) and rabbits (C and D).*

to 7.0 with 5 *M* HCl, and it then was filtered through a 0.22-μm membrane filter into a sterile glass container.

All solutions were purged with nitrogen and were prepared fresh prior to each experiment. The molar ratio of I to tin was 18:1.

Technetium 99m-Ethylenediamine-*N,N'*-bis(*α*-2-hydroxy-5-bromophenyl)acetic Acid (^{99m}Tc-II)—The technetium 99m complex of II was prepared under a nitrogen atmosphere by mixing 2 ml of III (1–5 mCi) with 1 ml of a stock solution of stannous chloride–II, followed by 5–10 min of incubation at room temperature. The stock solution was prepared by mixing 100 ml of 2.5×10^{-2} *M* II in 0.1 *M* NaOH with 2.0×10^{-4} mole of stannous chloride dihydrate. After the stannous chloride was dissolved completely, the pH was adjusted to 8.8 with 1 *M* HCl, and the solution was filtered through a 0.22-μm membrane filter into a sterile glass container.

All solutions were purged with nitrogen and were prepared fresh prior to each experiment. The molar ratio of II to tin was 12.5:1.

Labeling Efficiency of ^{99m}Tc-I and ^{99m}Tc-II—Prior to administration, ^{99m}Tc-I was analyzed for unreacted III by TLC on cellulose plates[4] with acetone as the developing solvent. The carrier I and the complex ^{99m}Tc-I remained at the origin, while the unreacted III moved with the solvent front. The unreacted III was always <3%.

The ^{99m}Tc-II was chromatographed on cellulose TLC plates[4] sprayed with 1% (w/v) $BaCl_2$. The developing solvent was prepared by mixing five parts of *n*-butanol with four parts of water and one part of acetic acid in a separator and retaining the organic layer. The R_f values of III and ^{99m}Tc-II were 0.43 and 0.94, respectively. The labeling efficiency was higher than 95%.

Distribution Studies in Animals—An 8-kg fasted beagle was injected intravenously with ^{99m}Tc-I (5×10^{-4} mmole of I, 1 mCi). The same beagle was injected intravenously 15 days later with ^{99m}Tc-II (6.6×10^{-4} mmole of II, 1 mCi). In both instances, the animal was anesthetized with an intramuscular dose of the dissociative anesthetic fentanyl and droperidol[5] (0.12 cm^3/kg); the animal was immobilized on a restrainer and placed under a γ-camera[6]. A series of ventral scintigraphic images was taken using a high-resolution pinhole collimator (Fig. 1).

Table I—Percent of Injected Dose Recovered in Dog Bile[a]

^{99m}Tc-I	^{99m}Tc-II
70.1[a]	48.6
55.9	64.1

[a] Obtained 75 min postinjection; result of one measurement.

For the bile recovery studies, two groups of two beagles each were injected in the forelimb vein with ^{99m}Tc-I (1×10^{-3} mmole, 1 mCi) and ^{99m}Tc-II (1×10^{-3} mmole, 1 mCi), respectively. The animals were anesthetized with pentobarbital sodium (30 mg/kg), the common bile duct was catheterized with a polyethylene catheter, and bile was collected for 75 min (Table I). The cystic duct was ligated.

Two groups, each containing 21 albino New Zealand rabbits (2–3 kg), received by injection into the ear vein freshly prepared ^{99m}Tc-I (6.6×10^{-4} mmole of I/kg, 1 mCi) and ^{99m}Tc-II[7] (6.6×10^{-4} mmole of II/kg, 1 mCi), respectively. Groups of three animals were sacrificed at 0.25, 0.5, 1, 2, 3, 5, and 24 hr after injection of a lethal dose of pentobarbital. Blood samples were obtained by cardiac puncture immediately after death. The blood weight was considered to be 7% of the body weight. Certain organs were excised, wet weighed, and counted by a shielded scintillation crystal

[4] No. 6064, Eastman Kodak.

[5] Innovar, Pitman-Moore, Washington Crossing, N.J.

[6] Model II C, Picker Dyna camera.

[7] Reconstituted from lyophilized II provided by R. E. Boyd, Australian AEC.

Table II—Distribution of Technetium 99m–*N*-(2-Mercapto-1-oxopropyl)glycine in Rabbits [a]

Organ	0.25 hr	0.50 hr	1.00 hr	2.00 hr	3.00 hr	5.00 hr	24.00 hr
Liver	0.07 ± 0.01[a]	0.08 ± 0.02	0.09 ± 0.01	0.07 ± 0.02	0.08 ± 0.00	0.06 ± 0.02	0.03 ± 0.00
Kidneys	0.79 ± 0.27	1.23 ± 0.04	1.29 ± 0.09	1.19 ± 0.04	1.08 ± 0.19	0.68 ± 0.21	0.25 ± 0.03
Gallbladder	0.10 ± 0.06	0.14 ± 0.06	0.41 ± 0.03	0.37 ± 0.06	0.25 ± 0.13	0.09 ± 0.07	0.00 ± 0.01
Blood	1.34 ± 0.19	0.69 ± 0.10	0.89 ± 0.09	0.50 ± 0.04	0.29 ± 0.03	0.25 ± 0.02	0.02 ± 0.04
Intestines	0.03 ± 0.02	0.04 ± 0.00	0.04 ± 0.01	0.03 ± 0.01	0.02 ± 0.00	0.03 ± 0.01	0.02 ± 0.00
Urine and bladder	0.71 ± 0.13	3.50 ± 3.53	3.69 ± 1.70	4.21 ± 1.59	3.10 ± 1.90	2.58 ± 1.25	5.35 ± 3.57

[a] Percent of dose per gram of organ (±*SD*); average results from three replications.

Table III—Distribution of Technetium 99m–Ethylenediamine-*N,N'*-bis(α-2-hydroxy-5-bromophenyl)acetic Acid in Rabbits [a]

Organ	0.25 hr	0.50 hr	1.00 hr	2.00 hr	3.00 hr	5.00 hr	24.00 hr
Liver	0.32 ± 0.05[a]	0.18 ± 0.02	0.17 ± 0.01	0.12 ± 0.02	0.13 ± 0.01	0.09 ± 0.02	0.04 ± 0.00
Kidneys	0.72 ± 0.11	0.63 ± 0.05	0.61 ± 0.10	0.64 ± 0.17	0.61 ± 0.17	0.33 ± 0.03	0.20 ± 0.05
Gallbladder	0.57 ± 0.46	0.30 ± 0.23	1.23 ± 0.92	0.94 ± 0.28	0.92 ± 0.50	0.86 ± 0.39	0.00 ± 0.00
Blood	0.53 ± 0.09	0.30 ± 0.00	0.30 ± 0.04	0.31 ± 0.02	0.35 ± 0.08	0.27 ± 0.09	0.10 ± 0.06
Intestines	0.07 ± 0.00	0.09 ± 0.02	0.08 ± 0.00	0.11 ± 0.00	0.13 ± 0.04	0.13 ± 0.02	0.13 ± 0.01
Urine and bladder	1.34 ± 1.00	1.14 ± 0.20	1.49 ± 0.07	1.40 ± 0.57	1.20 ± 0.34	1.51 ± 0.70	4.63 ± 2.4

[a] Percent of dose per gram of organ (±*SD*); average results from three replications.

Table IV—Distribution of Technetium 99m–*N*-(2-Mercapto-1-oxopropyl)glycine in Rats [a]

Organ	0.50 hr	1.00 hr	2.00 hr	3.00 hr	5.00 hr	24.00 hr
Liver	15.1 ± 1.1[a]	12.5 ± 2.0	9.3 ± 0.5	6.8 ± 1.0	4.9 ± 0.3	1.1 ± 0.7
Kidneys	11.5 ± 0.6	16.0 ± 2.0	15.1 ± 0.3	14.7 ± 2.3	16.1 ± 3.1	7.7 ± 2.6
Blood	9.0 ± 0.8	8.0 ± 0.8	4.8 ± 0.7	3.2 ± 0.9	1.3 ± 0.3	0.7 ± 0.4
Urine and bladder	15.9 ± 3.0	16.1 ± 3.0	18.1 ± 2.5	15.9 ± 3.3	23.4 ± 2.5	38.0 ± 3.7
GI tract and feces	30.1 ± 4.0	35.1 ± 2.0	40.1 ± 3.6	48.4 ± 2.7	52.1 ± 3.9	49.3 ± 6.1

[a] Percent of total (±*SD*); average results from three replications.

Table V—Distribution of Technetium 99m–Ethylenediamine-*N,N'*-bis(α-2-hydroxy-5-bromophenyl)acetic Acid in Rats [a]

Organ	0.50 hr	1.00 hr	2.00 hr	3.00 hr	5.00 hr	24.00 hr
Liver	20.5 ± 1.3	15.6 ± 2.0	13.5 ± 0.9	10.9 ± 0.8	6.7 ± 1.0	2.9 ± 0.7
Kidneys	8.9 ± 0.3	7.0 ± 0.1	7.7 ± 0.3	5.9 ± 0.4	4.7 ± 0.7	3.1 ± 0.1
Blood	5.7 ± 0.5	3.0 ± 0.3	3.2 ± 0.2	1.9 ± 0.3	1.5 ± 0.0	1.0 ± 0.0
Urine and bladder	4.4 ± 0.3	5.5 ± 1.0	5.9 ± 0.7	8.1 ± 1.2	8.4 ± 0.9	10.9 ± 3.9
GI tract and feces	45.9 ± 3.7	49.7 ± 4.3	59.7 ± 2.8	61.3 ± 5.0	74.9 ± 3.9	80.6 ± 5.4

[a] Percent of total (±*SD*); average results from three replications.

of fixed geometry linked to a counter[8,9]. The results were reported as the percent of total injected radioactivity per gram of organ (Tables II and III). Prior to sacrifice, several scintigraphic images of the abdominal area were taken with a γ-camera[6] shielded with a pinhole collimator (Fig. 1).

Two groups, each containing 18 white rats, received by injection into the tail vein freshly prepared ^{99m}Tc-I (1.3×10^{-3} mmole of I, 0.5 mCi) and ^{99m}Tc-II[10] (1.3×10^{-3} mmole of II, 0.5 mCi), respectively. Prior to experimentation, the animals were housed in groups of three for 3 days. They were allowed free access to food and tap water. The animals were sacrificed in groups of three at 0.5, 1, 2, 3, 5, and 24 hr postinjection. Certain organs were excised and counted in a well counter[9]. The results are reported as the percent of total injected radioactivity (Tables IV and V).

RESULTS AND DISCUSSION

The radioactive sodium pertechnetate (III) reacted with an excess of I. The complexation took place at room temperature in the presence of the oxidizable salt stannous chloride and under a nitrogen atmosphere. Since trace quantities of cations could interfere with the stability of the thiol (I), highly pure reagents and diluents were used. Although the ligand (I) to tin ratio varied from 9:1 to 18:1, this variation did not affect the extent of the complexation with III, as was evident from TLC–radiochromatographic monitoring of the extent of chelation of III.

Ligand II was soluble at pH values lower than 4.0 and higher than 8.0. The complex was formed by reducing III with stannous chloride in the presence of II at pH 8.5. The solutions were purged thoroughly with nitrogen to avoid oxidation of the phenol rings. Although the ligand to tin ratio ranged from 10:1 to 16:1, this variation did not affect the extent of complexation of the reduced technetium with the ligand II.

In both instances, the exact nature of the technetium complexes (^{99m}Tc-I and ^{99m}Tc-II) was uncertain. The presence of a thiol and a carboxyl group in I and the carboxyl, secondary amine, and hydroxyl groups in II were necessary for the formation of stable chelates. The high molecular weight (mol. wt. 518) of ligand II and the presence of two bromophenolic rings rendered the molecule susceptible to extensive biliary excretion. In contrast, ligand I had a lower molecular weight (mol. wt. 163) and lacked lipophilic groups. Therefore, it was expected to be less suitable than II for hepatobiliary excretion.

The sequential scintigraphic images (Fig. 1) of the liver and gallbladder of a beagle indicated that both ^{99m}Tc-I and ^{99m}Tc-II had a similar distribution pattern. Specifically, ^{99m}Tc-I started accumulating in the liver 5 min following intravenous administration. During the same period, the gallbladder became visible, and it was delineated clearly 30 min postinjection. When ^{99m}Tc-II was administered, the gallbladder was clearly delineated in the first 30 min postinjection, and the quality of the scintigraphic images was the same as that received with ^{99m}Tc-I. Upon intravenous administration of 50 μg of cerulein, the gallbladder in both cases contracted and enabled visualization of the common bile duct as the radioactivity was excreted into the intestines. A slight kidney uptake was noted with ^{99m}Tc-I.

The scintigraphic images taken following intravenous administration of ^{99m}Tc-I in rabbits (Fig. 1) indicated rapid accumulation of the radioactivity in the liver 5–15 min postinjection. During the same period, the gallbladder became slightly visible but never was clearly delineated

[8] Logic model 111, Abbott Laboratories, North Chicago, Ill.
[9] Picker Spectro Scaler-4, North Haven, Conn.
[10] Compound II was obtained by the described synthetic process.

Table VI—Target to Nontarget Ratios for ^{99m}Tc-I and ^{99m}Tc-II in Rabbits

	0.25 hr	0.50 hr	1.00 hr	2.00 hr	3.00 hr	5.00 hr	24.00 hr
			Gallbladder to Liver Ratio[a]				
^{99m}Tc-II	1.8	1.7	7.2	7.8	7.1	9.6	0.0
^{99m}Tc-I	1.4	1.8	4.5	5.3	3.1	1.5	0.0
			Gallbladder to Blood Ratio[a]				
^{99m}Tc-II	1.1	1.0	4.1	3.0	2.6	3.2	0.0
^{99m}Tc-I	0.1	0.2	0.5	0.7	0.9	0.4	0.0

[a] Ratio of percent of dose per gram of tissue to percent of dose per gram of tissue.

during the experiment. The visualization of the kidneys, urinary bladder, and small intestine indicated that part of the radioactivity was shunted through the urinary system and part was excreted through the intestines. The scintigraphic images (Fig. 1) taken when ^{99m}Tc-II was administered indicated a similar distribution pattern, except that the gallbladder was clearly visible and delineated 30 min postinjection and remained as such throughout the experiment.

The distribution of the radioactivity as a function of time in rabbits (Tables II and III) indicated that ^{99m}Tc-II cleared from the blood more rapidly than ^{99m}Tc-I and was accumulated rapidly in the liver. For instance, at 30 min postinjection, the radioactivity levels of ^{99m}Tc-I in the liver and blood were 0.08 and 0.69% of the dose/g, respectively; the corresponding levels for ^{99m}Tc-II were 0.18 and 0.30%, respectively. On the other hand, the urinary excretion, as denoted by the kidney, urine, and bladder levels, was higher for ^{99m}Tc-I than for ^{99m}Tc-II during the same period. In contrast, the levels of the gallbladder and intestines were higher for ^{99m}Tc-II than for ^{99m}Tc-I throughout the testing period. Furthermore, the target organ to nontarget organ ratio, which is the parameter for assessing the imaging capability of any diagnostic radiopharmaceutical, was higher for ^{99m}Tc-II than for ^{99m}Tc-I (Table VI). In particular, the gallbladder to blood ratio of ^{99m}Tc-II was five to 10 times higher than that of ^{99m}Tc-I during the first 30 or 60 min postinjection. The gallbladder to liver ratio of ^{99m}Tc-II was higher than that of ^{99m}Tc-I and remained as such up to 5 hr postinjection.

The distribution of ^{99m}Tc-I and ^{99m}Tc-II in rats (Tables IV and V) indicated that a good portion of ^{99m}Tc-I was excreted through the kidneys while the urinary excretion of ^{99m}Tc-II was lower. The high urinary excretion component of ^{99m}Tc-I was in agreement with observations made by previous investigators that low molecular weight mercaptans are retained in the kidneys and excreted through the urine in rats (9). Liver uptake was appreciable for ^{99m}Tc-II.

The scintigraphic images in dogs (Fig. 1) of both ^{99m}Tc-I and ^{99m}Tc-II were of equivalent quality. In both instances, the liver and gallbladder were delineated clearly and rapidly. The bile collection during the first 75 min postinjection did not reveal appreciable differences in the bile excretion of the two compounds (Table I). The tissue levels in rats revealed certain differences in the distribution of both ^{99m}Tc-I and ^{99m}Tc-II; however, the tissue levels in rabbits revealed gross differences, as was corroborated by the target to nontarget ratios (Table VI) and the differences in the quality of scintigraphic images (Fig. 1).

The *in vivo* distribution data agree with certain observations of previous investigators concerning the hepatobiliary excretion of substances as affected by the species of the experimental animal and the molecular characteristics of the compound. According to one investigator (10), hepatobiliary excretion in both dogs and rats is extensive. These species are classified as good hepatobiliary excretors, while rabbits, humans, and primates are classified relative to dogs and rats as poor hepatobiliary excretors. Furthermore, high lipophilicity and high molecular weight are factors that favor hepatobiliary excretion, while low molecular weight hydrophilic substances are shunted through the urinary pathway of excretion (10).

The exact reason for the higher biliary excretion of ^{99m}Tc-I in dogs and rats is not known. It may be the result of increased lipophilicity and increased molecular weight due to the formation of ^{99m}Tc-I or due to the formation of a complex with two ligands (^{99m}Tc-I_2). Further studies are in progress to investigate the complex. In rabbits, which like humans and primates are poor biliary excretors relative to dogs and rats (10), ^{99m}Tc-II, due to its favorable molecular characteristics, was a better hepatobiliary scintigraphic agent than ^{99m}Tc-I. Finally, in light of the presented data, it is concluded that rabbits are a better model than dogs or rats for evaluating hepatobiliary scintigraphic agents for use in humans.

REFERENCES

(1) P. M. Ronai, *J. Nucl. Med.*, **18**, 488 (1977).

(2) T. H. Lin, A. Khentigan, and H. S. Winchell, *ibid.*, **15**, 613 (1974).

(3) A. K. Tonkin and F. H. DeLand, *ibid.*, **15**, 539 (1974).

(4) R. J. Baker, J. C. Bellen, and P. M. Ronai, *ibid.*, **16**, 720 (1975).

(5) A. Fotopoulos, E. Chiotelis, C. Koutoudis, A. Dassiou, and J. Papadimitriou, *ibid.*, **18**, 1189 (1977).

(6) M. D. Loberg, M. Cooper, E. Harvey, P. Callery, and W. Faith, *ibid.*, **17**, 633 (1976).

(7) G. P. Basmadjian, M. Fitzgerald, and K. R. Hetzel, *ibid.*, **18**, 635 (1977).

(8) F. C. Hunt, J. G. Wilson, D. J. Maddalena, G. J. Bautovich, and R. Hutcherson, "Proceedings, First Asia and Oceania Congress of Nuclear Medicine," Sydney, Australia, 1976, pp. 140–143.

(9) D. O. Kubiatowicz, T. F. Bolles, J. C. Nord, and D. S. Ithakissios, *J. Pharm. Sci.*, **68**, 621 (1979).

(10) R. L. Smith, in "The Excretory Function of Bile," Chapman and Habl, London, England, 1973, pp. 77, 82.

Binding of Gold to Bovine Serum Albumin Using Flameless Atomic Absorption

SRIKUMARAN MELETHIL *§x, ALPHONSE POKLIS ‡¶, and VIDYA A. SAGAR ‡

Received August 23, 1978, from the *Departments of *Pharmaceutics and Pharmacy Practice and ‡Pharmacology and Toxicology, College of Pharmacy, North Dakota State University, Fargo, ND 58105. Accepted for publication December 3, 1979. §Present address: Division of Pharmaceutical Sciences, Schools of Pharmacy and Medicine, University of Missouri-Kansas City, Kansas City, MO 64111. ¶Present address: Department of Pathology, School of Medicine, St. Louis University, St. Louis, MO 63104.

Abstract □ A graphite furnace atomic absorption spectrophotometric assay capable of accurately determining nanogram amounts of gold in biological fluids was developed. The presence of bovine serum albumin and/or phosphate in the sample reduced the method sensitivity without affecting the linear response. Binding of gold was studied by ultrafiltration using cones with a molecular weight cutoff of 25,000. The binding of gold at various concentrations to 2 and 4% bovine serum albumin in 0.1 *M* phosphate buffer, pH 7.4, was independent of the gold and protein concentrations. In the 2–10-μg/ml range, the overall binding values (mean ± *SD*) of gold to 2 and 4% bovine serum albumin were 98 ± 1.6 (n = 35) and 99 ± 1.0% (n = 15), respectively. When ultrafiltration cones with a molecular weight cutoff of 50,000 were used, the extent of binding to 2% bovine serum albumin was 85.4 ± 1.6% (n = 11). This statistically significant difference ($p < 0.001$) was due to variations in the protein retention of the two cone types. Interaction studies showed that gold was not displaced from the binding sites by salicylic acid (200 μg/ml) or vice versa.

Keyphrases □ Antiarthritis agents—gold, effect of plasma protein and gold concentrations on gold binding, flameless atomic absorption determination of gold in biological fluids □ Aspirin—effect of salicylic acid on binding of gold to bovine serum albumin, flameless atomic absorption determination □ Protein binding—gold to bovine serum albumin, effect of plasma protein and gold concentration on gold binding, effect of salicylic acid on gold bound to albumin, flameless atomic absorption determination □ Salicylic acid—effect on gold bound to serum albumin, flameless atomic absorption determination

Gold salts are widely used in rheumatoid arthritis treatment (1). Although gold has a high affinity for plasma proteins (2–10), the specific protein to which it is bound most extensively is a matter of controversy. Some reports indicated that gold is bound exclusively to albumin (2, 3, 9), while others implicated fibrinogen (5) and α- and β-globulins (8). No data currently are available on the effect of protein concentration on the extent of gold binding. This aspect has important therapeutic implications since hypoalbuminemia often is encountered in arthritic patients (11). The recent observation (12) that aspirin hepatotoxicity increased in patients who were treated simultaneously with gold raises questions about competition for binding sites between salicylic acid and gold.

BACKGROUND

Several analytical methods have been used to determine gold in biological fluids. They include colorimetry (13), neutron activation analysis (14), polarography (15), and flame and carbon rod atomic absorption spectrophotometric techniques (4, 11, 16–21). Colorimetry and polarography require extensive sample manipulation, are time consuming, and suffer from low sensitivity. These disadvantages make these methods inapplicable to the routine determination of therapeutic gold concentrations (1–10 μg/ml). While neutron activation analysis has high sensitivity (0.01 μg/ml), the cost of instrumentation is prohibitive to most clinical laboratories.

Atomic absorption spectrophotometry has greatly facilitated the detection of minute concentrations of metals in biological fluids. Earlier procedures for gold estimation in biological fluids were conducted using flame atomic absorption spectrophotometric techniques (4, 6, 17). However, the required dilution, digestion, and extraction steps resulted in a loss of sensitivity and time. New atomic absorption spectrophotometric techniques using a carbon rod or a graphite furnace atomizer have overcome these problems (18–21). The advantages of these new techniques are high absolute sensitivity, microliter sample size, the potential for analyzing samples without pretreatment, speed of analysis, freedom from introduction of contaminants, and low background noise.

The first objective of this study was to develop a sensitive flameless atomic absorption spectrophotometric assay to determine gold in biological fluids. The second objective was to study the extent of the binding of gold to bovine serum albumin and the effect of salicylate on this interaction.

EXPERIMENTAL

Materials—Graphite tubes[1] for sample atomization, gold standards[2], ultrafiltration membrane cones[3], bovine serum albumin[4], and salicylic acid[5] were obtained commercially. Distilled, deionized water was prepared by passing distilled water through an ion-exchange system[6]. To avoid possible loss of gold by binding to glass, plastic laboratoryware was used.

Instrumentation—An atomic absorption spectrophotometer[7] equipped with a graphite furnace atomizer[8], a deuterium-arc background corrector[9], and an automatic injector system[10] was used for gold determination. A gold hollow cathode lamp[11] was the light source. Atomization peak heights of gold were recorded on a strip-chart recorder[12] at a chart speed of 10 mm/min and a recorder current of 10 mamp.

Operating Conditions—The optimum parameters for gold determination in the test solutions were: drying cycle, 100° for 20 sec with a temperature ramp of 30 sec; charring cycle, 800° for 60 sec with a temperature ramp of 30 sec; and atomization cycle, 2200° for 5 sec. The ramp setting permits gradual rise in the furnace temperature during each run. The carrier gas was argon at a flow rate of 30 ml/min. Atomization peak heights were recorded at 242.8 nm.

Calibration Curves for Gold—A working standard, 100 μg/ml, was prepared by diluting commercially obtained gold solution with distilled, deionized water. This working standard was diluted further with 0.1 *M* phosphate buffer, pH 7.4, to give solutions containing 0.1, 0.2, 0.3, and 0.4 μg of gold/ml. Twenty-microliter aliquots of each solution were in-

[1] Part 290-1633, Perkin-Elmer Corp., Norwalk, Conn.
[2] Harelco, Gibbstown, N.J.
[3] Centriflo membrane cones, types CF25 and CF50A, Amicon Corp., Lexington, Mass.
[4] Sigma Chemical Corp., St. Louis, Mo.
[5] Fisher Scientific Corp., Springfield, N.J.
[6] Model D-0800 Barnstead demineralizer with D-0809 cartridge.
[7] Perkin-Elmer model 403.
[8] Perkin-Elmer model HGA-2100.
[9] Perkin-Elmer deuterium-arc power supply.
[10] Perkin-Elmer model AS-1
[11] Perkin-Elmer intensitron 303-6031.
[12] Perkin-Elmer model 56.

0022-3549/80/0500-0585$01.00/0
© 1980, American Pharmaceutical Association

Table I—Effect of Bovine Serum Albumin Concentration on Binding of Gold

Gold Concentration, μg/ml	Percent Bound[a]	
	2% Bovine Serum Albumin[b]	4% Bovine Serum Albumin[c]
2	100 ± 0.5	99 ± 1.4
4	98 ± 1.8	99 ± 0.5
6	99 ± 1.0	99 ± 1.1
8	97 ± 0.9	98 ± 0.9
10	99 ± 1.5	98 ± 1.1

[a] Expressed as mean ± *SD*. [b] Number of samples was seven. [c] Number of samples was three.

Table II—Effect of Salicylic Acid [a] on Binding of Gold to 2% Bovine Serum Albumin

Gold Concentration, μg/ml	Percent Bound[b]	
	Salicylic Acid Added 24 hr after Gold	Salicylic Acid Added 24 hr before Gold
2	100 ± 0.0	100 ± 0.3
4	99 ± 0.0	100 ± 0.5
6	99 ± 0.2	100 ± 0.3
8	98 ± 0.2	98 ± 0.8
10	98 ± 0.2	99 ± 0.3

[a] Concentration of 200 μg/ml. [b] Expressed as mean ± *SD*; $n = 3$.

Table III—Results from Linear Regression of Atomization Peak Heights [a] *versus* Gold Concentrations [b] in Various Media

Medium	Slope	Intercept	r[c]
Distilled, deionized water	193	1.5	0.997
0.1 *M* Phosphate buffer, pH 7.4	138	1.5	0.999
0.2% Bovine serum albumin in 0.1 *M* phosphate buffer, pH 7.4	77	1.0	0.996

[a] Expressed in arbitrary units. [b] Gold concentration ranged from 0.1 to 0.4 μg/ml. [c] Correlation coefficient.

jected into the atomic absorption spectrophotometer, and the atomization peak heights were recorded. Calibration plots were prepared on all days of sample analysis using the same graphite tube used for the samples.

Matrix Effects—Gold solutions of 0.1–0.4 μg/ml were prepared by diluting the working standard with (*a*) distilled, deionized water, (*b*) 0.1 *M* phosphate buffer, pH 7.4, or (*c*) 0.2% bovine serum albumin in 0.1 *M* phosphate buffer, pH 7.4. The atomization peak heights of 20-μl aliquots of these gold solutions were obtained as described earlier.

Binding Studies—The binding of gold to bovine serum albumin was studied using a previously reported ultrafiltration technique (22) with minor modifications. The membrane cones, after pretreatment as recommended by the manufacturer, were dried by centrifugation at 2000 rpm (484×*g*) for 25 min. A comparison of cone weights before and after soaking and centrifugation showed that <0.06 ml of distilled, deionized water remained in the cones.

Bovine serum albumin solutions, 2 and 4%, containing various concentrations of gold (2–10 μg/ml) were prepared in 0.1 *M* phosphate buffer, pH 7.4. Following equilibration for 16–24 hr (overnight), 5-ml aliquots were transferred to pretreated cones and centrifuged for 30 sec at 2000 rpm. The filtrate, ~0.1 ml, was discarded to minimize dilution errors that can be expected from the residual water in the cones. A second 0.4-ml aliquot of filtrate was collected, and a 20-μl portion was injected into the atomic absorption spectrophotometer. The atomization peaks at 242.8 nm were recorded and converted into concentrations using calibration plots prepared with standard gold solutions in 0.1 *M* phosphate buffer, pH 7.4.

To determine the nonspecific loss of gold due to binding to the ultrafiltration cones and/or the apparatus, gold solutions in phosphate buffer (2–4 μg/ml) were filtered through the cones in the absence of bovine serum albumin. Gold concentrations in the filtrates were compared to the corresponding concentrations prior to filtration.

Displacement Studies with Salicylic Acid—The procedure was identical to that described under *Binding Studies*, except for the addition of salicylic acid. These studies were conducted with the 2% bovine serum albumin solution. In one set of experiments, salicylic acid was added to bovine serum albumin 24 hr prior to the addition of gold. In the second set, salicylic acid was added 24 hr after the addition of gold to bovine serum albumin.

While gold concentrations varied from 2 to 10 μg/ml, the salicylic acid concentration was 200 μg/ml in all trials. Following the addition of gold in the first set of experiments and salicylic acid in the second set, the solutions were equilibrated overnight. Binding studies then were performed. Salicylate concentrations in the ultrafiltrates were determined by UV spectrophotometry at 295 nm.

RESULTS AND DISCUSSION

Analytical—Atomization peak heights for gold at 242.8 nm were linearly related to concentration in the 0.1–0.4-μg/ml range. Peak heights varied considerably among the graphite tubes. For instance, the slope of the peak height (arbitrary units) *versus* gold concentration (micrograms per milliliter) ranged from 139 to 240 during a 2-month period when most of the samples were analyzed. However, the correlation coefficients of calibration plots obtained during this period were better than 0.990, with very small intercept values that were not statistically significant.

Visual examination of the graphite tubes revealed differences in their thickness. The "thicker" tubes gave erratic results and were not used in the analyses. In view of these problems, the peak heights obtained with test solutions were converted to gold concentrations using calibration plots prepared using the same graphite tube. Under such controlled conditions, the overall coefficient of variation of the technique was <2% (Tables I and II). The life of a tube ranged from 50 to 60 determinations under the conditions used.

Matrix Effects—The medium or matrix in which the gold solutions were prepared also affected the method sensitivity (Table III). A decrease in the slope of the regression line corresponded to a decrease in the peak height. Based on the slope values in Table III, a gold solution prepared in 0.1 *M* phosphate buffer was expected to have a peak height that was ~25% lower than that obtained with an aqueous gold solution of equal concentration. The presence of even small amounts of bovine serum albumin in the buffer resulted in a further decrease in peak heights to ~40% of those obtained in water.

The reasons for these effects remain unclear. However, they emphasize the need to recognize that electrolytes and other normal constituents of biological fluids can interfere with atomic absorption measurements. The interference may be due to molecular absorption of electrolytes at the wavelength of gold absorption or to the physical occlusion of gold in a host of condensing interferent atoms.

While this work was in progress, Kamel *et al.* (11) reported a similar method to determine gold in blood. They reported that the organic matrix of blood reduced the sensitivity of the technique. It was speculated that a stable protein complex that was not destroyed during the charring cycle may have prevented the complete atomization of gold. However, such an explanation does not fit the interference observed with phosphate.

Binding Studies—Small amounts of protein escaped through the ultrafiltration cones used in this study. Depending on this amount and the affinity of the drug for the macromolecule, the values obtained for the extent of binding may have been underestimated. The manufacturer specifies that cones with molecular weight cutoffs of 25,000 (Type 1)[13] and 50,000 (Type 2)[14] retain >95 and 90% of albumin, respectively. For five randomly chosen Type 2 cones, the mean protein leakage was determined to be 11% (range 9–12.5%); these values were obtained by expressing the protein concentration in the filtrate as a fraction of that placed in the cone (2%) prior to ultrafiltration. Protein concentrations were measured by the biuret method (23). In a similar study with Type 1 cones, four cones showed no detectable leak and one had a leak of 5.8%.

The extent of gold binding to 2% bovine serum albumin was 85 ± 1.6% ($n = 11$) with Type 2 cones. The corresponding value with Type 1 cones was 98 ± 1.0% ($n = 15$), which is significantly higher ($p < 0.001$) than the value obtained with the Type 2 cones. The extent of underestimation (13%) is in good agreement with the differences in protein leakage (11%) between these two cone varieties. Therefore, all binding studies used Type 1 cones. Although each cone was not tested for protein leakage, suspiciously low values for binding were always associated with cones that were found to leak, as indicated by the presence of protein in the ultrafiltrate. Such cases were repeated.

A paired *t* test showed that, in the absence of bovine serum albumin,

[13] Centriflo membrane cones, type CF25, Amicon Corp., Lexington, Mass.
[14] Centriflo membrane cones, type CF50, Amicon Corp., Lexington, Mass.

gold concentrations in the ultrafiltrates were not statistically different ($p > 0.05$) from the corresponding concentrations prior to filtration. Hence, no corrections for nonspecific binding were warranted. Gold was almost 100% bound to bovine serum albumin (Table I). These results indicate that gold may be bound exclusively to the albumin fraction of plasma, as was reported earlier (2, 3, 9). However, more definite conclusions can be made only after studies in the presence of other plasma proteins. The overall values for the percent of gold bound to 2 ($n = 35$) and 4% ($n = 15$) bovine serum albumin were 98 ± 1.6 and 99 ± 1.0% (mean ± *SD*), respectively.

Two factors that often determine the extent of binding are the concentrations of the drug and of the protein. The gold concentrations studied were selected to include the plasma concentrations of the drug encountered in chrysotherapy (2, 6, 16, 24, 25). While there is a paucity of data regarding the extent of hypoalbuminemia in arthritis patients, a recent study observed serum albumin levels as low as 2.47 g/100 ml (11). The results of the present work show that, in the clinically important range, the extent of gold binding was independent of gold and bovine serum albumin concentrations. The validity of these results in the *in vivo* situation in humans remains to be examined.

Interaction with Salicylic Acid—Salicylic acid did not compete with gold for binding sites on bovine serum albumin (Table II). Since the sequence of addition of salicylic acid had no significant effect on the affinity of gold for bovine serum albumin, inhibition of a noncompetitive nature also can be ruled out. Similarly, gold did not interfere with salicylate binding; salicylate was 62–70% bound to bovine serum albumin in the absence and presence of gold (2–10-μg/ml range). During aspirin therapy, plasma concentrations of salicylate range from 50 to 200 μg/ml (26). The *in vitro* results suggest that mutual displacement of gold and salicylic acid from plasma proteins may not be a serious drug interaction in arthritis management.

The results of this study show that clinically encountered plasma concentrations of gold, salicylate, and albumin are unlikely to cause statistically significant alterations in the extent of protein binding of these two drugs. However, for drugs that are bound extensively to plasma protein as is gold, minor binding alterations may be clinically significant due to the resulting dramatic changes in the free concentration. For instance, a 1% decrease in the binding of gold (assumed to be 99% bound) results in a twofold (1–2%) increase in the free concentration of gold. Such changes, although extremely difficult to document experimentally, could cause gold toxicity in arthritic patients.

REFERENCES

(1) "The Pharmacological Basis of Therapeutics," 5th ed., L. S. Goodman and A. Gilman, Eds., Macmillan, New York, N.Y., 1975, p. 931.

(2) B. R. Mascarenhas, J. L. Granda, and R. H. Freyberg, *Arthritis Rheum.*, **15**, 391 (1972).

(3) E. G. McQueen and P. W. Dykes, *Ann. Rheum. Dis.*, **28**, 437 (1969).

(4) M. Harth, D. S. M. Haines, and D. C. Bondy, *Am. J. Clin. Pathol.*, **59**, 423 (1973).

(5) J. S. Lawrence, *Ann. Rheum. Dis.*, **20**, 341 (1961).

(6) A. Lorber, R. A. Bovy, and C. C. Chang, *Nature (New Biol.)*, **236**, 250 (1972).

(7) P. M. Smith, E. M. Smith, and N. L. Gottilieb, *J. Lab. Clin. Med.*, **82**, 930 (1973).

(8) N. Simon, *Science*, **119**, 95 (1954).

(9) D. S. Campion, R. Olsen, A. Bohan, and R. Bluestone, *J. Rheumatol. (Suppl. 1)*, **1**, 112 (1974).

(10) R. W. Mason, *Pharmacology*, **15**, 536 (1974).

(11) H. Kamel, D. H. Brown, J. M. Ottaway, and W. E. Smith, *Analyst*, **101**, 790 (1976).

(12) J. D. Davis, R. A. Turner, R. L. Collins, I. R. Ruchte, and J. S. Kaufmann, *Clin. Pharm. Ther.*, **21**, 52 (1977).

(13) J. F. Goodwin and A. J. Bollet, *J. Lab. Clin. Med.*, **55**, 965 (1960).

(14) A. A. Dietz and H. M. Rubinstein, *Ann. Rheum. Dis.*, **32**, 124 (1973).

(15) G. D. Christian, *Clin. Chem.*, **11**, 459 (1965).

(16) A. Lorber, R. L. Cohen, C. C. Chang, and H. E. Anderson, *Arthritis Rheum.*, **11**, 170 (1968).

(17) J. V. Dunckley, *Clin. Chem.*, **17**, 992 (1971).

(18) F. J. M. J. Maessen, F. D. Posma, and J. Balke, *Anal. Chem.*, **46**, 1445 (1974).

(19) J. Agget and T. S. West, *Anal. Chim. Acta*, **55**, 349 (1971).

(20) J. Agget, *ibid.*, **63**, 473 (1973).

(21) J. P. Matousek and B. J. Stevens, *Clin. Chem.*, **17**, 636 (1971).

(22) S. M. Singhvi, A. F. Heald, H. H. Gadenbusch, M. E. Resnick, L. T. Difazio, and M. A. Leitz, *J. Lab. Clin. Med.*, **89**, 414 (1977).

(23) D. T. Plummer, "An Introduction to Practical Biochemistry," McGraw-Hill, Berkshire, England, 1971, p. 156.

(24) A. Lorber, *Clin. Pharmacokinet.*, **2**, 127 (1977).

(25) J. T. Sharp, M. D. Lidsky, J. Duffy, H. K. Thompson, Jr., B. D. Person, A. F. Masri, and A. A. Andrianakos, *Arthritis Rheum.*, **20**, 1179 (1977).

(26) M. Mayersohn, *J. Am. Pharm. Assoc.*, **NS 17**, 107 (1977).

ACKNOWLEDGMENTS

Presented at the Basic Pharmaceutics Section, APhA Academy of Pharmaceutical Sciences, Phoenix meeting, November 1977.

Supported in part by Program 821, Veterans Administration Center, Fargo, ND 58102.

GLC Analysis of Poison Ivy and Poison Oak Urushiol Components in Vegetable Oil Preparations

MAHMOUD A. ELSOHLY ˣ and CARLTON E. TURNER

Received August 6, 1979, from the *Research Institute of Pharmaceutical Sciences, School of Pharmacy, University of Mississippi, University, MS 38677.* Accepted for publication November 26, 1979.

Abstract □ A procedure is described for the analysis of urushiol content of pharmaceutical preparations containing extracts of poison ivy (*Toxicodendron radicans*) and poison oak (*T. diversilobum*) in vegetable oils. The procedure involves extraction of the urushiols from the oily solutions using 90% methanol in water followed by GLC analysis of the extracts. Recoveries of both poison ivy and poison oak urushiols from solutions in corn oil, olive oil, sesame seed oil, and cottonseed oil were calculated. Correlation coefficients (r^2) ranged from 0.97 to 1.00, and the coefficients of variations ranged from 3.08 to 7.90%.

Keyphrases □ Urushiols—GLC analysis, pharmaceutical preparations containing poison ivy and poison oak extracts in vegetable oils □ GLC—analysis, urushiols in pharmaceutical preparations containing poison ivy and poison oak extracts in vegetable oils □ Poison ivy—urushiol components in vegetable oil preparations, GLC analysis

Contact dermatitis due to poison ivy (*Toxicodendron radicans*) and other related *Anacardiaceae* species [*e.g.*, poison oak (*T. diversilobum*) and poison sumac (*T. vernix*)] is a major problem among outdoor workers in the

0022-3549/80/0500-0587$01.00/0

© 1980, American Pharmaceutical Association

gold concentrations in the ultrafiltrates were not statistically different ($p > 0.05$) from the corresponding concentrations prior to filtration. Hence, no corrections for nonspecific binding were warranted. Gold was almost 100% bound to bovine serum albumin (Table I). These results indicate that gold may be bound exclusively to the albumin fraction of plasma, as was reported earlier (2, 3, 9). However, more definite conclusions can be made only after studies in the presence of other plasma proteins. The overall values for the percent of gold bound to 2 ($n = 35$) and 4% ($n = 15$) bovine serum albumin were 98 ± 1.6 and 99 ± 1.0% (mean ± *SD*), respectively.

Two factors that often determine the extent of binding are the concentrations of the drug and of the protein. The gold concentrations studied were selected to include the plasma concentrations of the drug encountered in chrysotherapy (2, 6, 16, 24, 25). While there is a paucity of data regarding the extent of hypoalbuminemia in arthritis patients, a recent study observed serum albumin levels as low as 2.47 g/100 ml (11). The results of the present work show that, in the clinically important range, the extent of gold binding was independent of gold and bovine serum albumin concentrations. The validity of these results in the *in vivo* situation in humans remains to be examined.

Interaction with Salicylic Acid—Salicylic acid did not compete with gold for binding sites on bovine serum albumin (Table II). Since the sequence of addition of salicylic acid had no significant effect on the affinity of gold for bovine serum albumin, inhibition of a noncompetitive nature also can be ruled out. Similarly, gold did not interfere with salicylate binding; salicylate was 62–70% bound to bovine serum albumin in the absence and presence of gold (2–10-μg/ml range). During aspirin therapy, plasma concentrations of salicylate range from 50 to 200 μg/ml (26). The *in vitro* results suggest that mutual displacement of gold and salicylic acid from plasma proteins may not be a serious drug interaction in arthritis management.

The results of this study show that clinically encountered plasma concentrations of gold, salicylate, and albumin are unlikely to cause statistically significant alterations in the extent of protein binding of these two drugs. However, for drugs that are bound extensively to plasma protein as is gold, minor binding alterations may be clinically significant due to the resulting dramatic changes in the free concentration. For instance, a 1% decrease in the binding of gold (assumed to be 99% bound) results in a twofold (1–2%) increase in the free concentration of gold. Such changes, although extremely difficult to document experimentally, could cause gold toxicity in arthritic patients.

REFERENCES

(1) "The Pharmacological Basis of Therapeutics," 5th ed., L. S. Goodman and A. Gilman, Eds., Macmillan, New York, N.Y., 1975, p. 931.

(2) B. R. Mascarenhas, J. L. Granda, and R. H. Freyberg, *Arthritis Rheum.*, **15**, 391 (1972).

(3) E. G. McQueen and P. W. Dykes, *Ann. Rheum. Dis.*, **28**, 437 (1969).

(4) M. Harth, D. S. M. Haines, and D. C. Bondy, *Am. J. Clin. Pathol.*, **59**, 423 (1973).

(5) J. S. Lawrence, *Ann. Rheum. Dis.*, **20**, 341 (1961).

(6) A. Lorber, R. A. Bovy, and C. C. Chang, *Nature (New Biol.)*, **236**, 250 (1972).

(7) P. M. Smith, E. M. Smith, and N. L. Gottilieb, *J. Lab. Clin. Med.*, **82**, 930 (1973).

(8) N. Simon, *Science*, **119**, 95 (1954).

(9) D. S. Campion, R. Olsen, A. Bohan, and R. Bluestone, *J. Rheumatol. (Suppl. 1)*, **1**, 112 (1974).

(10) R. W. Mason, *Pharmacology*, **15**, 536 (1974).

(11) H. Kamel, D. H. Brown, J. M. Ottaway, and W. E. Smith, *Analyst*, **101**, 790 (1976).

(12) J. D. Davis, R. A. Turner, R. L. Collins, I. R. Ruchte, and J. S. Kaufmann, *Clin. Pharm. Ther.*, **21**, 52 (1977).

(13) J. F. Goodwin and A. J. Bollet, *J. Lab. Clin. Med.*, **55**, 965 (1960).

(14) A. A. Dietz and H. M. Rubinstein, *Ann. Rheum. Dis.*, **32**, 124 (1973).

(15) G. D. Christian, *Clin. Chem.*, **11**, 459 (1965).

(16) A. Lorber, R. L. Cohen, C. C. Chang, and H. E. Anderson, *Arthritis Rheum.*, **11**, 170 (1968).

(17) J. V. Dunckley, *Clin. Chem.*, **17**, 992 (1971).

(18) F. J. M. J. Maessen, F. D. Posma, and J. Balke, *Anal. Chem.*, **46**, 1445 (1974).

(19) J. Agget and T. S. West, *Anal. Chim. Acta*, **55**, 349 (1971).

(20) J. Agget, *ibid.*, **63**, 473 (1973).

(21) J. P. Matousek and B. J. Stevens, *Clin. Chem.*, **17**, 636 (1971).

(22) S. M. Singhvi, A. F. Heald, H. H. Gadenbusch, M. E. Resnick, L. T. Difazio, and M. A. Leitz, *J. Lab. Clin. Med.*, **89**, 414 (1977).

(23) D. T. Plummer, "An Introduction to Practical Biochemistry," McGraw-Hill, Berkshire, England, 1971, p. 156.

(24) A. Lorber, *Clin. Pharmacokinet.*, **2**, 127 (1977).

(25) J. T. Sharp, M. D. Lidsky, J. Duffy, H. K. Thompson, Jr., B. D. Person, A. F. Masri, and A. A. Andrianakos, *Arthritis Rheum.*, **20**, 1179 (1977).

(26) M. Mayersohn, *J. Am. Pharm. Assoc.*, **NS 17**, 107 (1977).

ACKNOWLEDGMENTS

Presented at the Basic Pharmaceutics Section, APhA Academy of Pharmaceutical Sciences, Phoenix meeting, November 1977.

Supported in part by Program 821, Veterans Administration Center, Fargo, ND 58102.

GLC Analysis of Poison Ivy and Poison Oak Urushiol Components in Vegetable Oil Preparations

MAHMOUD A. ELSOHLY ˣ and CARLTON E. TURNER

Received August 6, 1979, from the *Research Institute of Pharmaceutical Sciences, School of Pharmacy, University of Mississippi, University, MS 38677.* Accepted for publication November 26, 1979.

Abstract □ A procedure is described for the analysis of urushiol content of pharmaceutical preparations containing extracts of poison ivy (*Toxicodendron radicans*) and poison oak (*T. diversilobum*) in vegetable oils. The procedure involves extraction of the urushiols from the oily solutions using 90% methanol in water followed by GLC analysis of the extracts. Recoveries of both poison ivy and poison oak urushiols from solutions in corn oil, olive oil, sesame seed oil, and cottonseed oil were calculated. Correlation coefficients (r^2) ranged from 0.97 to 1.00, and the coefficients of variations ranged from 3.08 to 7.90%.

Keyphrases □ Urushiols—GLC analysis, pharmaceutical preparations containing poison ivy and poison oak extracts in vegetable oils □ GLC—analysis, urushiols in pharmaceutical preparations containing poison ivy and poison oak extracts in vegetable oils □ Poison ivy—urushiol components in vegetable oil preparations, GLC analysis

Contact dermatitis due to poison ivy (*Toxicodendron radicans*) and other related *Anacardiaceae* species [*e.g.*, poison oak (*T. diversilobum*) and poison sumac (*T. vernix*)] is a major problem among outdoor workers in the

0022-3549/80/0500-0587$01.00/0

© 1980, American Pharmaceutical Association

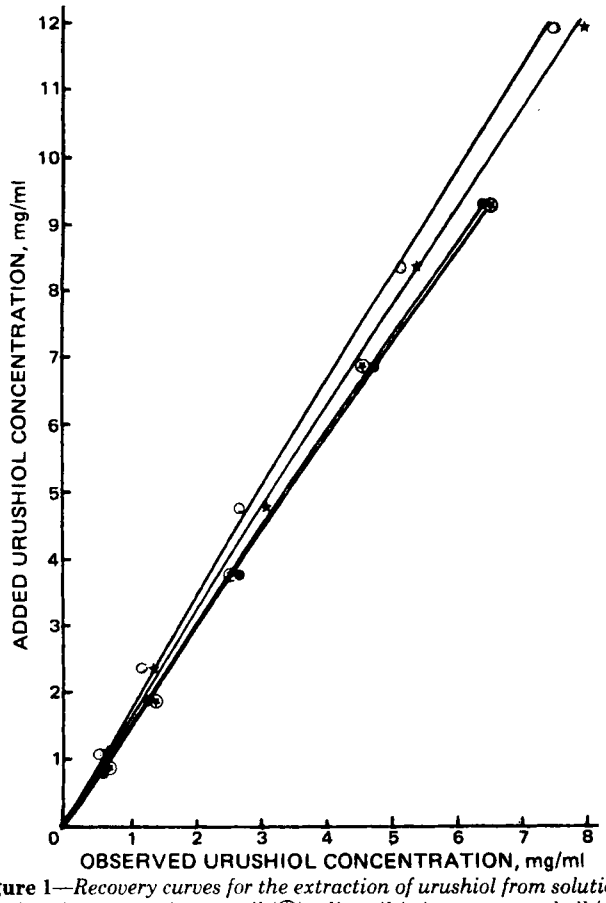

Figure 1—*Recovery curves for the extraction of urushiol from solutions of poison ivy extract in corn oil (⊛), olive oil (●), sesame seed oil (★), and cottonseed oil (○) using a methanol–water (9:1) mixture.*

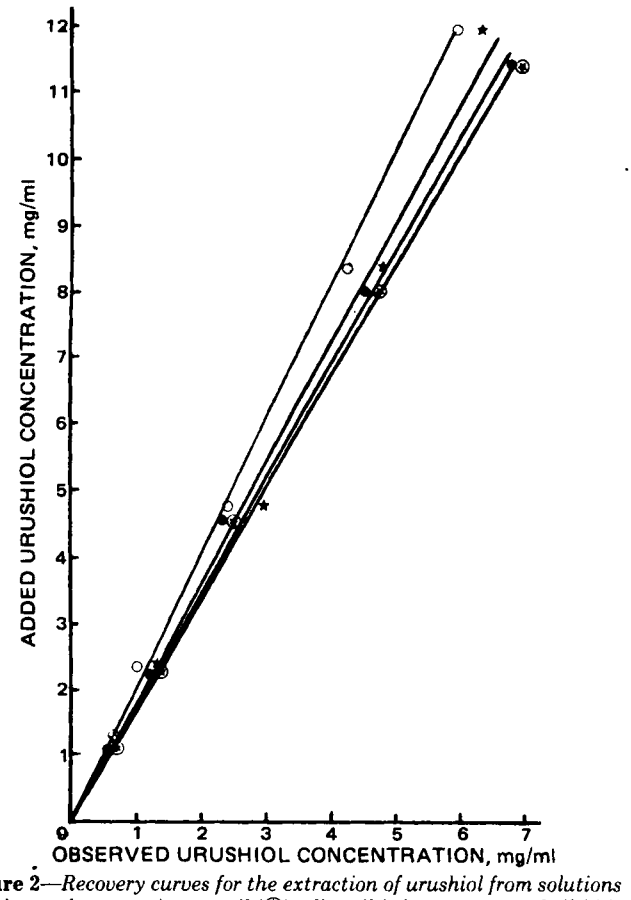

Figure 2—*Recovery curves for the extraction of urushiol from solutions of poison oak extract in corn oil (⊛), olive oil (●), seasame seed oil (★), and cottonseed oil (○) using a methanol–water (9:1) mixture.*

United States. Urushiol, the constituent in these plants that causes dermatitis, has been shown to be a mixture of 3-*n*-alk(en)yl catechols with zero, one, two, or three double bonds in the C_{15}-side chain of poison ivy (1–4) and the C_{17}-side chain of poison oak (5, 6).

Extracts of poison ivy and poison oak have been used in the detection and prophylactic treatment of sensitivity (7–9). Solutions of these extracts are provided mainly in vegetable oils, *e.g.*, corn oil (poison ivy–poison oak extract capsules[1]) and olive oil (injection[2]) (10). Although these preparations have been in use for a long time, no procedure is available to determine the concentration of the active component (urushiol) in these formulations. This report describes a simple GLC procedure for the determination of the total urushiol content of preparations containing poison ivy or poison oak extracts in vegetable oils such as corn oil, cottonseed oil, olive oil, and sesame seed oil.

EXPERIMENTAL

Plant Extracts—Poison ivy (*T. radicans*) and poison oak (*T. diversilobum*) extracts were prepared as described previously (6) or were obtained commercially[1]. The extracts were analyzed for urushiol content following the literature procedure (6).

Preparation of Oil Solutions of Poison Ivy and Poison Oak Extracts—Commercially available corn oil, cottonseed oil, olive oil, and sesame seed oil were used for the preparation of the solutions. For each oil, two sets of solutions were prepared containing 1, 2, 4, 7, or 10% of either poison ivy or poison oak extracts corresponding to 0.96–12.0 mg of urushiol/ml. The actual urushiol content of each solution (milligrams per milliliter) was based on the preanalysis of the extracts.

Extraction of Urushiol from Oil Solutions—One-milliliter aliquots of each solution were transferred to 15-ml screw-capped centrifuge tubes. To each oil solution was added 5 ml of methanol–water (9:1). The tubes were capped and vortexed for 20 sec or shaken vigorously for ~1 min and then centrifuged for 5 min. The top layer from each tube was withdrawn carefully into a 10-ml round-bottom flask, and the solvent was evaporated under vacuum at 40°.

The extraction was repeated twice using 5 ml of the same solvent each time. In each case, the top layer was added to the respective flask and the solvent was evaporated. Complete evaporation of the small amount of water remaining in the evaporation flask was achieved by adding ~2 ml each of absolute ethanol and benzene, followed by evaporation. This step was done twice to ensure complete dryness of the extract.

Preparation of Samples for GLC Analysis—*Dilute Samples*—Samples obtained from oil solutions containing <2 mg of urushiol/ml were prepared directly for GLC analysis by the addition of 0.25 ml of pyridine and 0.5 ml of bis(trimethylsilyl)trifluoroacetamide[3] containing 1% trimethylchlorosilane to the residue in the round-bottom flask. Then 0.5 ml of internal standard (dotriacontane, 5 mg/ml in isooctane) was added.

Concentrated Samples—Samples expected to contain >2 mg of urushiol/ml were treated in the following manner. The residue obtained after evaporation of the methanol–water extract was transferred quantitatively to a 5- or 10-ml volumetric flask with chloroform, and the volume was adjusted with the same solvent. A 1-ml aliquot then was withdrawn from the chloroform solution and evaporated, and the residue was treated as described for the dilute samples. The dilution factor was considered in the calculations.

GLC Analysis—The samples were analyzed using a gas–liquid chromatograph[4] and a 5% OV-225 column under the conditions reported previously (6).

[1] Supplied by Hollister-Stier Laboratories, Spokane, Wash.
[2] Ivyol injection, Merck Sharp & Dohme.
[3] Pierce Chemical Co., Rockford, Ill.
[4] Beckman GC-65.

Table I—Recovery of Urushiols from Vegetable Oil Solutions of Poison Ivy and Poison Oak Extracts Using 90% Methanol–Water [a]

	Recovery, % [b]	Correlation [b] Coefficient (r^2)	Coefficient of Variation [c], %
Corn oil			
Poison ivy	66.6	1.00	3.55
Poison oak	60.2	0.99	3.70
Olive oil			
Poison ivy	69.3	0.99	4.01
Poison oak	59.6	0.99	3.22
Sesame oil			
Poison ivy	68.4	0.99	3.50
Poison oak	52.0	0.98	3.30
Cottonseed oil			
Poison ivy	64.1	0.97	7.90
Poison oak	49.9	0.99	3.08

[a] The urushiol concentration in the different oils ranged from 0.96 to 12 mg/ml. [b] Calculated from the least-squares line. The correction factor is the reciprocal of the recovery. [c] Mean coefficient of variation of all extractions over the concentration range used.

RESULTS AND DISCUSSION

GLC procedures were described previously for the identification of urushiol (11, 12), and the use of GLC–mass spectrometry for the quantitative determination of the different congeners also was reported (13). A new GLC procedure was reported previously for the quantitation of the different components of poison ivy and poison oak urushiols as their trimethylsilyl derivatives using a 5% OV-225 column (6). The separation of the different congeners allowed the quantitation of each. The procedure was applied for the analysis of poison ivy and poison oak urushiol components in extracts obtained from different plant parts.

Extracts of poison ivy, poison oak, and, in some cases, poison sumac in vegetable oil solutions have been used for prophylactic treatment of Rhus dermatitis. The lack of an analytical procedure to determine the concentration of the active constituent, urushiol, in these preparations prompted the present study.

Corn oil, olive oil, sesame seed oil, and cottonseed oil were selected as representatives of vegetable oils. Solutions of poison ivy and poison oak extracts were made in each oil to contain different amounts of the extracts corresponding to concentrations of 0.94–12.0 mg of urushiol/ml. The extracts were analyzed for urushiol content prior to mixing.

Different cleanup procedures were investigated to separate the urushiol components from the oils prior to analysis. These procedures included column chromatography, TLC, and solvent partitioning. Due to on-column decomposition, column chromatography on silica gel 60 resulted in a loss of a significant amount of the urushiols. The loss was maximized when a large enough column was used (20 g) to permit the clean separation of the urushiol from the oil. Aluminum oxide adsorbents could not be used since urushiol binds irreversibly to alumina. Other chromatographic materials also were tried including polyamide, cellulose, cellulose acetate, and diethylaminoethylcellulose with no success.

Different solvents then were investigated for the extraction of urushiol from the oil solutions of the extracts. These solvents included methanol, ethanol, methanol–butanol mixtures (5–20% butanol), and methanol–water mixtures (2–20% water). A methanol–water mixture (9:1) was the best solvent for extraction since it gave a high percentage recovery of urushiol with the least contamination of the extracts with the oil components. GLC analysis (6) of the 90% methanol–water extracts of the pure vegetable oils showed virtually no peaks that might interfere with the urushiol peaks. Thus, the previously outlined procedure (6) was applicable to the analysis of urushiols in the methanol–water (9:1) extracts of poison ivy and poison oak preparations in vegetable oils. The extraction efficiency of this solvent mixture was determined for each oil by plotting the actual concentration of urushiol (milligrams per milliliter *versus* the observed concentration).

Figure 1 shows the recovery curves for the extraction of urushiol from solutions of poison ivy extract in different vegetable oils; Fig. 2 shows the same curves for poison oak. Each point in these curves is the average of triplicate analyses. The coefficient of variation (CV) for each point was calculated, and a mean CV value was given for each curve (Table I). A linear relationship was shown between the added and observed concentrations in each case with correlation coefficients (r^2) ranging between 0.97 and 1.00 (Table I). This result makes it possible to use this extraction procedure and to compensate for the recovery percentage. The slope of each curve (Figs. 1 and 2) thus represents the correction factor used to compensate for the extraction efficiency in each case. The same correction factors were found when preparations containing a mixture of poison ivy and poison oak extracts were formulated.

The reported procedure can be used for the analysis of the total urushiols content as well as for the percentage of each individual congener.

REFERENCES

(1) G. A. Hill, V. Mattacotti, and W. D. Grahan, *J. Am. Chem. Soc.*, **56**, 3736 (1934).

(2) W. F. Symes and C. R. Dawson, *ibid.*, **76**, 2959 (1954).

(3) S. V. Sunthankar and C. R. Dawson, *ibid.*, **76**, 5070 (1954).

(4) K. H. Markiewitz and C. R. Dawson, *J. Org. Chem.*, **30**, 1610 (1965).

(5) M. D. Corbett and S. Billets, *J. Pharm. Sci.*, **64**, 1715 (1975).

(6) J. C. Craig, C. W. Waller, S. Billets, and M. A. Elsohly, *ibid.*, **67**, 483 (1978).

(7) C. H. Ducan, *N.Y. Med. J.*, **104**, 901 (1976).

(8) G. A. Gellin, D. R. Wolf, and H. Milby, *Arch. Environ. Health*, **2**, 280 (1971).

(9) H. S. Mason and A. Lada, *J. Invest. Dermatol.*, **22**, 457 (1975).

(10) "Facts and Comparisons," Facts and Comparisons Inc., St. Louis, Mo., 1978, p. 565.

(11) H. Baer, S. Srinivasan, R. T. Bowser, and A. Karmen, *J. Allergy*, **34**, 221 (1963).

(12) S. Srinivasan, H. Baer, R. Bowser, and A. Karmen, *Anal. Biochem.*, **6**, 234 (1963).

(13) M. Gross, H. Baer, and H. M. Fales, *Phytochemistry*, **14**, 2263 (1975).

ACKNOWLEDGMENTS

Supported in part by Hollister-Stier Laboratories, Spokane, Washington, and the Research Institute of Pharmaceutical Sciences.

The authors thank Ms. Julie Crocker and Mr. William Torres for technical assistance.

High-Pressure Liquid Chromatographic Identification of Drugs Used in Management of Arthritis

JOHN K. BAKER ˣ **and E. KIM FIFER**

Received March 19, 1979, from the *Department of Medicinal Chemistry, School of Pharmacy, University of Mississippi, University, MS 38677.* Accepted for publication November 26, 1979.

Abstract □ A screening procedure was developed for the identification of drugs used in the clinical treatment of arthritis. Each glucocorticoid, nonsteroidal anti-inflammatory agent, or tranquilizer was characterized by its retention on a reversed-phase high-pressure liquid chromatographic column and by the ratio of the response of dual UV detectors (254 and 280 nm). Although the retention times of all 14 drugs examined were <4 min, each drug could be distinguished easily from the other drugs in the series.

Keyphrases □ Antiarthritis agents—glucocorticoids, nonsteroidal anti-inflammatory agents, tranquilizers, high-pressure liquid chromatographic identification □ High-pressure liquid chromatography—identification of glucocorticoids, nonsteroidal anti-inflammatory agents, and tranquilizers used in arthritis treatment □ Glucocorticoids—identification by high-pressure liquid chromatography, arthritis treatment □ Anti-inflammatory agents, nonsteroidal—identification by high-pressure liquid chromatography, arthritis treatment □ Tranquilizers—identification by high-pressure liquid chromatography, arthritis treatment

Solid dosage forms obtained from patients who received treatment in specialized arthritis clinics in Mexico have been analyzed in these laboratories. In many cases, the patients were told that these drugs were vitamins or natural products and were given a large supply of two or three different tablets to continue taking on their return to the United States. GLC (1) and standard spectroscopic analyses (2) showed that many of these tablets were a tranquilizer (*e.g.*, diazepam or chlordiazepoxide) and an anti-inflammatory steroid or a tranquilizer and a nonsteroidal anti-inflammatory drug (*e.g.*, phenylbutazone or indomethacin). Although there are many qualitative and quantitative analytical methods reported in the literature for individual drugs, a single analytical method for the screening of such samples has not been reported.

BACKGROUND

Since both types of anti-inflammatory agents require different derivatization methods for GLC analysis, high-pressure liquid chromatography (HPLC) was investigated for the identification of the tranquilizers, steroids, and nonsteroidal anti-inflammatory agents.

One major limitation of any chromatographic method for identifying drugs is that many compounds have identical retention times if a fairly large population of compounds is examined. In a recent study (3) of a diverse group of only 101 narcotics, amphetamines, barbiturates, and tranquilizers, only 9% of the drugs could be identified uniquely by HPLC retention times. In that study, if dual UV detectors were used to measure accurately the absorbance of each chromatographic peak at 254 and 280 nm, 95% of the drugs could be characterized uniquely. Moreover, HPLC retention times and A_{254}/A_{280} ratios as paired discriminators were more useful than HPLC retention times on a silica column and on a reversed-phase column as paired discriminators (3). Because of the utility, speed, and low cost of the technique, its usefulness in aiding in the identification of the present group of drugs was investigated.

It is generally recognized that the utility of HPLC retention times is limited because of the small variations that occur with time when the same column is used and because of the large variations that occur with a new column. Relative retention times are considerably more reproducible, but this measurement also has limitations. For example, when reversed-phase HPLC columns are used and the alcohol content of the mobile phase is increased inadvertently or a new column with a lower percent of the stationary phase is used, the observed relative retention time generally increases.

Many of these problems can be reduced or eliminated through the use of a retention index scale based on the relative retention of a homologous series of C_3–C_{23} 2-ketoalkanes and the drug in question (4). The retention index of a given drug is fairly independent of the mobile phase composition, even when the drug retention time varies by several orders of magnitude. The retention index of many drugs also was found to be nearly the same when a bonded cyanoalkyl reversed-phase column was substituted for a C_{18} reversed-phase column (4). Although the retention index measurements were slightly more time consuming than the conventional relative retention time measurements, the former method was selected for this study because of the greater potential for laboratory-to-laboratory reproducibility of the data.

EXPERIMENTAL

Chromatographic Conditions—A 30-cm × 3.9-mm i.d. octadecyl reversed-phase column[1] with a 10-μm particle size was used. The mobile phase was prepared using 3.3 g of dibasic potassium phosphate, 4.2 g of monobasic potassium phosphate, 2.8 liters of methanol, and 1.2 liters of water. The flow rate was 2.0 ml/min, and the column was operated at room temperature.

An HPLC pump[2] and a microsyringe-loaded loop injector[3] also were used. Two UV detectors[4] were used in series (254-nm detector followed by a 280-nm detector), and they were calibrated with a morphine reference standard (3).

Measurement of Retention Indexes—The method used in this study was essentially the same as that reported previously (4). The retention index scale was based on the relative retention of the drug in question and a series (C_3–C_{23}) of 2-ketoalkanes[5]. The capacity factor, k', of the drugs and the standards was determined from the retention time observed for the compound, t_R, and the retention time of the solvent front, t_0, using Eq. 1:

$$k' = \frac{t_R - t_0}{t_0} \qquad \text{(Eq. 1)}$$

The retention index of a given 2-keto alkane standard was, by definition, equal to 100 times the number of carbons in the compound. Thus, 2-butanone was assigned a value of 400. The retention index, I, of a given drug was calculated from the observed capacity factor for the drug, k'_D, the capacity factor for the standard eluting just before the test compound, k'_N, and the capacity factor for the next higher homolog, k'_{N+1}, using Eq. 2:

$$I = 100\,\frac{\log k'_D - \log k'_N}{\log k'_{N+1} - \log k'_N} + 100N \qquad \text{(Eq. 2)}$$

Each drug was chromatographed as a mixture with the 2-ketoalkane reference compounds to minimize the effect of retention time variations on the precision of the retention index measurements. If the chromatographic peak for the drug could not be resolved from the peaks of the standards, the mixture of the standards was chromatographed immediately after the drug. Because of the much smaller molar absorptivity of the 2-ketoalkane standards, a larger quantity of the ketones (~50 μg each) was injected with the drugs (~1 μg) to obtain comparable peak heights.

Preparation of Solid Dosage Forms for HPLC—The tablets were crushed to a fine powder. Approximately 100 mg of the powder was mixed with 1.0–2.0 ml of methanol, and the mixture was then filtered through

[1] μBondapak C_{18} column, Waters Associates, Milford, Mass.
[2] Model M-6000, Waters Associates, Milford, Mass.
[3] Model U6-K, Waters Associates, Milford, Mass.
[4] Model 440, Waters Associates, Milford, Mass.
[5] Analabs Inc., North Haven, Conn.

0022-3549/80/0500-0590$01.00/0
© 1980, American Pharmaceutical Association

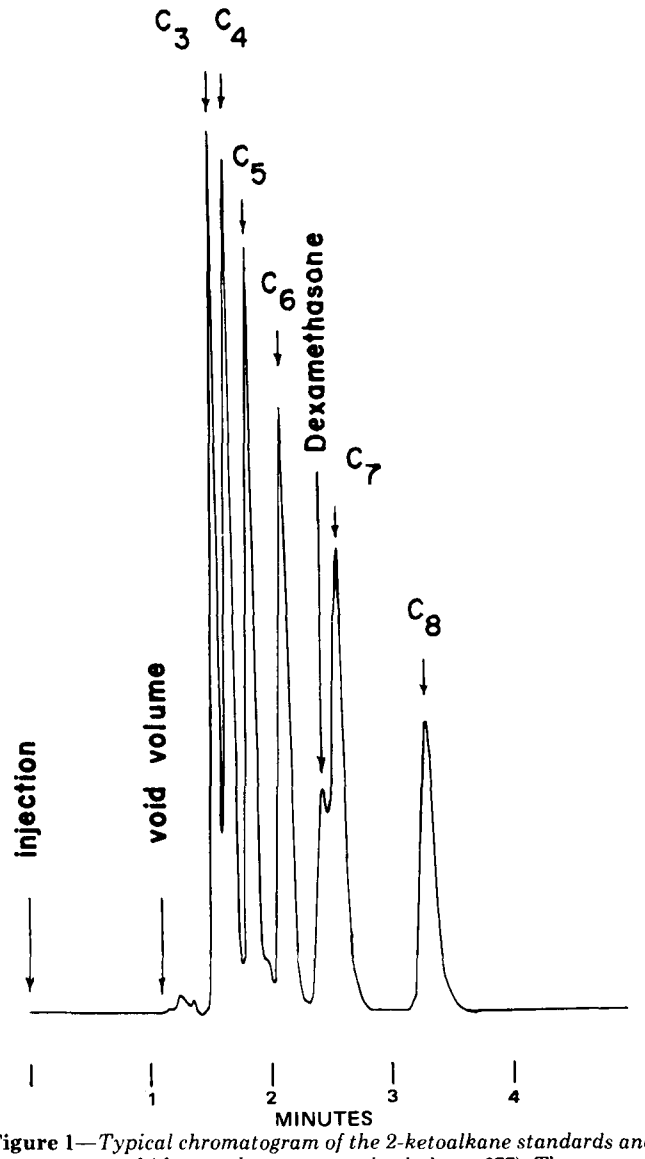

Figure 1—*Typical chromatogram of the 2-ketoalkane standards and a test compound (dexamethasone, retention index = 677). The response of only the 280-nm detector is shown.*

a disposable Pasteur pipet containing a small, tightly packed plug of cotton. Then 0.1–2.0 μl of the methanolic extract was injected into the chromatograph along with the 2-ketoalkane standards mixture.

RESULTS AND DISCUSSION

The chromatogram shown in Fig. 1 for dexamethasone and the 2-ketoalkanes is typical of the results obtained, except that the 254-nm detector response is not shown to simplify the figure. Although the retention times of all of the drugs were fairly short, the drugs were sufficiently removed from the solvent front to obtain precise retention index and absorbance ratio measurements. The longest retention tine was observed for diazepam (3.43 min), the shortest time was observed for naproxen (1.56 min), and the retention time of the solvent front was 1.12 min.

The drugs are listed in Table I in order of increasing retention index, and there is an apparent discrepancy between the retention index and the retention time measurements. Although the short-term reproducibility of the retention time generally was ±0.01 min, the long-term variations were greater. The retention index measurements are considerably more reliable than the retention time measurements (4), and more emphasis was placed on this measurement in the present study.

Although the retention indexes of many drugs in the series were fairly close, each compound could be distinguished from the others if the A_{254}/A_{280} values also were utilized. For example, the retention indexes of fenoprofen and triamcinolone were very close, but the two drugs could be readily distinguished using the absorbance ratio measurements. With

Table I—HPLC Characterization of Various Drugs Used in Management of Arthritis

Drug	Retention Index	A_{254}/A_{280}	Retention Time, min
Naproxen	304	1.61	1.56[a]
Phenylbutazone	363	1.27	1.56
Fenoprofen	439	1.09	1.78
Triamcinolone	463	6.23	1.74
Prednisone	550	6.86	1.97
Ibuprofen	566	6.55	2.03
Mefenamic acid	598	0.51	2.07
Indomethacin	621	1.46	2.16
Prednisolone	625	4.97	2.22
Dexamethasone	677	5.91	2.48
Methylprednisolone	707	5.12	2.64
Chlordiazepoxide	750	1.85	2.91
Methylprednisolone acetate	786	5.06	3.20
Diazepam	812	4.64	3.43

[a] The void volume was 2.24 ml (1.12 min).

methylprednisolone acetate and diazepam, both the retention index and the absorbance ratio measurements were fairly close, but even these two drugs could be differentiated if care was taken in making the measurements. The retention index and absorbance ratio of prednisone and ibuprofen also were grouped closely, but these compounds could be differentiated. The precision of the A_{254}/A_{280} measurements previously was ±1.9% (1), and essentially the same precision was observed in the present study. The short-term precision of the retention index measurements was typically ±5 units. Thus, if the retention index and A_{254}/A_{250} values were used as paired discriminators, all of the drugs in Table I could be distinguished from each other.

All of the steroids had similar absorbance ratio values. The highest value was observed for prednisone (6.86), and the lowest value was observed for prednisolone (4.97). Since all of the steroids in the study had essentially the same chromophore, it was expected that the absorbance ratio also would be similar.

Naproxen, fenoprofen, ibuprofen, mefenamic acid, and indomethacin all contain a carboxylic acid group that is completely ionized at the pH of the mobile phase (7.0). Thus, it was not unexpected that even drugs with a very lipophilic naphthyl group, such as naproxen, had a small retention index. Because of the diversity of the chromophores in this group of drugs, the A_{254}/A_{280} ratios varied greatly.

Although each drug in Table I can be distinguished from the others, other steroids that occasionally were used should have similar indexes and absorbance ratios. The relationship between the drug retention on reversed-phase columns and the lipophilicity of the drug was investigated previously (3, 5–8). Hansch substituent constants, π values, have been used to estimate the lipophilicity of the drugs (9), and these estimates have been used to estimate their HPLC retention indexes (10). The HPLC retention index of a given drug, I_x, could be estimated using the sum of the Hansch substituent values for the drug, π_x, and the experimentally observed index for the reference or parent drug for the series, I_{ref}, by (10):

$$I_x = 200\pi_x + I_{\text{ref}} \qquad \text{(Eq. 3)}$$

With Eq. 3, it is possible to predict other clinically used steroids that might be misidentified as one of the drugs in Table I. It is expected that both the retention index and the absorbance ratio of triamcinolone and meprednisone would be very close. Similarly, there is a potential for interference between dexamethasone (I = 677) and its isomer, betamethasone. Other interferences might be observed between methylprednisolone and triamcinolone diacetate and between methylprednisolone acetate and triamcinolone acetonide.

Other compounds that were not examined in this study also might be misidentified as one of the drugs listed in Table I. Although the absorbance ratio technique greatly reduces the probability of error in the identification of drugs based on retention times alone (3), the methods presented in this study are simple and rapid. As with any analytical method, good laboratory procedures dictate that the initial results should be confirmed by an independent method.

REFERENCES

(1) J. K. Baker, *Anal. Chem.*, **49**, 906 (1977).

(2) E. G. C. Clarke, "Isolation and Identification of Drugs," The

Pharmaceutical Press, London, England, 1969.
(3) J. K. Baker, R. E. Skelton, and C. Y. Ma, *J. Chromatogr.*, **168**, 417 (1979).
(4) J. K. Baker and C. Y. Ma, *ibid.*, **169**, 107 (1979).
(5) J. M. McCall, *J. Med. Chem.*, **18**, 549 (1975).
(6) M. S. Mirrlees, S. J. Moulton, C. T. Murphy, and P. J. Taylor, *ibid.*, **19**, 615 (1976).
(7) D. Henry, J. H. Black, J. L. Anderson, and G. R. Carlson, *ibid.*, **19**, 619 (1976).
(8) K. Miyake and H. Terada, *J. Chromatogr.*, **157**, 386 (1978).
(9) M. S. Tute, *Adv. Drug Res.*, **6**, 1 (1971).
(10) J. K. Baker, *Anal. Chem.*, **51**, 1693 (1979).

ACKNOWLEDGMENTS

Supported in part by a faculty research grant from the University of Mississippi and in part by the Research Institute of Pharmaceutical Sciences, School of Pharmacy, University of Mississippi.

Chemotherapy of Neuroblastoma in Mice with Anticancer Agents

GEORGE C. Y. CHIOU ˣ **and MARILYN K. MARTIN**

Received August 20, 1979, from the *Department of Medical Pharmacology & Toxicology, College of Medicine, Texas A&M University, College Station, TX 77843.* Accepted for publication December 4, 1979.

Abstract □ Neuroblastoma-inoculated A/J mice were treated with various anticancer chemotherapeutic agents, including cyclophosphamide, daunorubicin, vincristine, α-bungarotoxin, dihydroxytryptamine, and diaminopropane. Cyclophosphamide and diaminopropane inhibited neuroblastoma as effectively as bromoacetylcholine and bromoacetate. The effectiveness of these drugs could be related to the inhibition of ornithine decarboxylase, a rate-limiting enzyme for the synthesis of polyamines.

Keyphrases □ Anticancer agents—chemotherapy of neuroblastoma in mice □ Ornithine decarboxylase—inhibition by anticancer agents, chemotherapy of neuroblastoma □ Cyclophosphamide—chemotherapy of neuroblastoma in mice □ Diaminopropane—chemotherapy of neuroblastoma in mice

Despite many efforts, the prognosis of the clinical treatment of neuroblastoma in patients over the age of 1 year is very poor (1). Since the A/J mouse inoculated with C-1300 neuroblastoma cells is considered to be a model of the neuroblastoma disease of humans (2), various anticancer drugs were tested on this animal model to determine an effective way to treat the neuroblastoma disease. Bromoacetylcholine and bromoacetate recently were reported to be effective in inhibiting the neuroblastoma growth *in vivo* (3–6). Therefore, a combination of bromoacetylcholine and other anticancer drugs also was tested in this neuroblastoma mouse model.

METHODS

Adult male A/J mice[1] were inoculated subcutaneously in the interscapular area with 1×10^6 cells of murine C-1300 neuroblastoma cells. Ten days was allowed for a measurable tumor to develop. Drug injections began on the 10th day after neuroblastoma inoculation, and this time was designated as Day 0 of drug treatment. Identical conditions were maintained for the control groups, except that saline was injected instead of drug solutions. Drug treatment was continued for 6 weeks unless otherwise specified. For all injections, the volume of the drug solutions was <50 μl.

Bromoacetylcholine percholate was synthesized by a previously described method (7). Sodium bromoacetate, cyclophosphamide, 1,3-diaminopropane, 5,6-dihydroxytryptamine, α-bungarotoxin, and vincristine were purchased commercially. All drug solutions were freshly prepared at the time of injection.

[1] Jackson Laboratory, Bar Harbor, Me.

RESULTS

It has been established that bromoacetylcholine (30 mg/kg) injected intratumorly one to three times per day and bromoacetate (12 mg/kg) injected intratumorly twice per day inhibit neuroblastoma growth in A/J mice efficiently and prolong the lifespan of these animals by >200% (4, 5). The only anticancer agent that was able to produce an effectiveness equivalent to bromoacetylcholine and bromoacetate was cyclophosphamide (100 mg/kg) injected only once intraperitoneally (Table I). A higher dose (200 mg/kg) of cyclophosphamide reduced its effectiveness due to toxicity. Combination of cyclophosphamide with bromoacetylcholine or bromoacetate did not additionally prolong the lifespan. On the contrary, the lifespan was shortened somewhat as compared to the lifespan of mice receiving the optimal doses of bromoacetylcholine, bromoacetate, and cyclophosphamide administered individually (Table I).

Daunorubicin[2] at a dose of 2 mg/kg injected intravenously twice per week worsened the disease as compared to the control. Combined use of daunorubicin and bromoacetylcholine prolonged the lifespan by only 33%, which was much shorter than the result with bromoacetylcholine alone (Table I).

Vincristine (1 mg/kg) injected intraperitoneally three times daily did not improve the neuroblastoma disease and did not potentiate the effect of bromoacetylcholine (Table I). On the contrary, it shortened the mean lifespan of bromoacetylcholine-treated animals from 73.4 (207% change of lifespan) (5) to 52.1 (129% change of lifespan) days (Table I).

Table II shows the effects of various agents known to inhibit neuroblastoma growth in cell culture on the neuroblastoma growth in A/J mice. α-Bungarotoxin is an inhibitor of neuroblastoma in cell culture (8) but is too toxic to be used *in vivo*. The mice survival rate was shorter than that of the untreated controls (Table II).

5,6-Dihydroxytryptamine has degenerated serotonergic neurons (9, 10) and inhibited gliomas in cell culture (11). However, it did not prolong the lifespan of neuroblastoma-inoculated A/J mice and did not enhance the inhibition of neuroblastoma growth when used in combination with bromoacetylcholine (Table II).

1,3-Diaminopropane was shown to inhibit ornithine decarboxylase, a rate-limiting enzyme for the synthesis of polyamines, which in turn suppressed neuroblastoma growth in cell culture (6). It also produced a significant improvement in mice inoculated with neuroblastoma cells when injected intratumorly twice per day for 6 weeks at a dose of 110 mg/kg (Table II). The combination of diaminopropane and bromoacetylcholine was even more instrumental in prolonging the lifespan of neuroblastoma-inoculated mice.

Various routes of administration were used to find an effective alternative to the intratumor route. Bromoacetylcholine and bromoacetate were ineffective with intraperitoneal administration (Table III), mainly because bromoacetylcholine has a permanent positive charge at the

[2] Obtained from the Drug Liaison and Distribution Section, Division of Cancer Treatment, National Cancer Institute.

0022-3549/80/0500-0592$01.00/0
© 1980, American Pharmaceutical Association

Pharmaceutical Press, London, England, 1969.
(3) J. K. Baker, R. E. Skelton, and C. Y. Ma, *J. Chromatogr.*, **168**, 417 (1979).
(4) J. K. Baker and C. Y. Ma, *ibid.*, **169**, 107 (1979).
(5) J. M. McCall, *J. Med. Chem.*, **18**, 549 (1975).
(6) M. S. Mirrlees, S. J. Moulton, C. T. Murphy, and P. J. Taylor, *ibid.*, **19**, 615 (1976).
(7) D. Henry, J. H. Black, J. L. Anderson, and G. R. Carlson, *ibid.*, **19**, 619 (1976).
(8) K. Miyake and H. Terada, *J. Chromatogr.*, **157**, 386 (1978).
(9) M. S. Tute, *Adv. Drug Res.*, **6**, 1 (1971).
(10) J. K. Baker, *Anal. Chem.*, **51**, 1693 (1979).

ACKNOWLEDGMENTS

Supported in part by a faculty research grant from the University of Mississippi and in part by the Research Institute of Pharmaceutical Sciences, School of Pharmacy, University of Mississippi.

Chemotherapy of Neuroblastoma in Mice with Anticancer Agents

GEORGE C. Y. CHIOU ˣ **and MARILYN K. MARTIN**

Received August 20, 1979, from the *Department of Medical Pharmacology & Toxicology, College of Medicine, Texas A&M University, College Station, TX 77843.* Accepted for publication December 4, 1979.

Abstract □ Neuroblastoma-inoculated A/J mice were treated with various anticancer chemotherapeutic agents, including cyclophosphamide, daunorubicin, vincristine, α-bungarotoxin, dihydroxytryptamine, and diaminopropane. Cyclophosphamide and diaminopropane inhibited neuroblastoma as effectively as bromoacetylcholine and bromoacetate. The effectiveness of these drugs could be related to the inhibition of ornithine decarboxylase, a rate-limiting enzyme for the synthesis of polyamines.

Keyphrases □ Anticancer agents—chemotherapy of neuroblastoma in mice □ Ornithine decarboxylase—inhibition by anticancer agents, chemotherapy of neuroblastoma □ Cyclophosphamide—chemotherapy of neuroblastoma in mice □ Diaminopropane—chemotherapy of neuroblastoma in mice

Despite many efforts, the prognosis of the clinical treatment of neuroblastoma in patients over the age of 1 year is very poor (1). Since the A/J mouse inoculated with C-1300 neuroblastoma cells is considered to be a model of the neuroblastoma disease of humans (2), various anticancer drugs were tested on this animal model to determine an effective way to treat the neuroblastoma disease. Bromoacetylcholine and bromoacetate recently were reported to be effective in inhibiting the neuroblastoma growth *in vivo* (3–6). Therefore, a combination of bromoacetylcholine and other anticancer drugs also was tested in this neuroblastoma mouse model.

METHODS

Adult male A/J mice[1] were inoculated subcutaneously in the interscapular area with 1×10^6 cells of murine C-1300 neuroblastoma cells. Ten days was allowed for a measurable tumor to develop. Drug injections began on the 10th day after neuroblastoma inoculation, and this time was designated as Day 0 of drug treatment. Identical conditions were maintained for the control groups, except that saline was injected instead of drug solutions. Drug treatment was continued for 6 weeks unless otherwise specified. For all injections, the volume of the drug solutions was <50 μl.

Bromoacetylcholine percholate was synthesized by a previously described method (7). Sodium bromoacetate, cyclophosphamide, 1,3-diaminopropane, 5,6-dihydroxytryptamine, α-bungarotoxin, and vincristine were purchased commercially. All drug solutions were freshly prepared at the time of injection.

[1] Jackson Laboratory, Bar Harbor, Me.

RESULTS

It has been established that bromoacetylcholine (30 mg/kg) injected intratumorly one to three times per day and bromoacetate (12 mg/kg) injected intratumorly twice per day inhibit neuroblastoma growth in A/J mice efficiently and prolong the lifespan of these animals by >200% (4, 5). The only anticancer agent that was able to produce an effectiveness equivalent to bromoacetylcholine and bromoacetate was cyclophosphamide (100 mg/kg) injected only once intraperitoneally (Table I). A higher dose (200 mg/kg) of cyclophosphamide reduced its effectiveness due to toxicity. Combination of cyclophosphamide with bromoacetylcholine or bromoacetate did not additionally prolong the lifespan. On the contrary, the lifespan was shortened somewhat as compared to the lifespan of mice receiving the optimal doses of bromoacetylcholine, bromoacetate, and cyclophosphamide administered individually (Table I).

Daunorubicin[2] at a dose of 2 mg/kg injected intravenously twice per week worsened the disease as compared to the control. Combined use of daunorubicin and bromoacetylcholine prolonged the lifespan by only 33%, which was much shorter than the result with bromoacetylcholine alone (Table I).

Vincristine (1 mg/kg) injected intraperitoneally three times daily did not improve the neuroblastoma disease and did not potentiate the effect of bromoacetylcholine (Table I). On the contrary, it shortened the mean lifespan of bromoacetylcholine-treated animals from 73.4 (207% change of lifespan) (5) to 52.1 (129% change of lifespan) days (Table I).

Table II shows the effects of various agents known to inhibit neuroblastoma growth in cell culture on the neuroblastoma growth in A/J mice. α-Bungarotoxin is an inhibitor of neuroblastoma in cell culture (8) but is too toxic to be used *in vivo*. The mice survival rate was shorter than that of the untreated controls (Table II).

5,6-Dihydroxytryptamine has degenerated serotonergic neurons (9, 10) and inhibited gliomas in cell culture (11). However, it did not prolong the lifespan of neuroblastoma-inoculated A/J mice and did not enhance the inhibition of neuroblastoma growth when used in combination with bromoacetylcholine (Table II).

1,3-Diaminopropane was shown to inhibit ornithine decarboxylase, a rate-limiting enzyme for the synthesis of polyamines, which in turn suppressed neuroblastoma growth in cell culture (6). It also produced a significant improvement in mice inoculated with neuroblastoma cells when injected intratumorly twice per day for 6 weeks at a dose of 110 mg/kg (Table II). The combination of diaminopropane and bromoacetylcholine was even more instrumental in prolonging the lifespan of neuroblastoma-inoculated mice.

Various routes of administration were used to find an effective alternative to the intratumor route. Bromoacetylcholine and bromoacetate were ineffective with intraperitoneal administration (Table III), mainly because bromoacetylcholine has a permanent positive charge at the

[2] Obtained from the Drug Liaison and Distribution Section, Division of Cancer Treatment, National Cancer Institute.

0022-3549/80/0500-0592$01.00/0
© 1980, American Pharmaceutical Association

Table I—Inhibition of Neuroblastoma Growth in A/J Mice by Cyclophosphamide, Daunorubicin, and Vincristine

Drug	Dose (mg/kg) and Route	Frequency per Day	*n*	Range, days	Mean ± *SE*, days	Change of Lifespan[a], %	Median, days
Saline	— it	2	10	13–63	33.0 ± 5.1	—	29
Cyclophosphamide	100 ip	Once only	10	34–150[b]	108.2 ± 17.2[c]	227	150
Cyclophosphamide	200 ip	Once only	9	9–150[b]	66.4 ± 29.0	101	26
Cyclophosphamide + bromoacetylcholine	100 ip 30 it	Once only 2	10	11–150[b]	73.6 ± 17.2[c]	124	56
Cyclophosphamide + bromoacetylcholine	200 ip 30 it	Once only 3	10	5–86	21.7 ± 9.0	−34	10
Cyclophosphamide + bromoacetate	100 ip 12 it	Once only 2	10	34–150[b]	78.5 ± 15.8[c]	138	56
Daunorubicin	2 iv	Twice per week	10	11–34	25.1 ± 2.4	−24	27
Daunorubicin + bromoacetylcholine	2 iv 30 it	Twice per week 2	10	18–150[b]	52.7 ± 16.6	60	32
Saline	— it	3	10	11–38	22.8 ± 3.4	—	18
Vincristine	1 ip	3	8	8–43	23.9 ± 4.4	5	25
Vincristine + bromoacetylcholine	1 ip 30 it	3 3	8	29–150[b]	52.1 ± 14.6	129	34

[a] Calculated from the mean lifespan of the control. [b] Many mice survived beyond 150 days after drug treatment began; 150 days was chosen arbitrarily as the cut-off date for the statistical analysis. [c] $p < 0.05$ as compared to the control.

Table II—Effects of Various Agents, Administered Intratumorly, that Suppressed Neuroblastoma in Tissue Culture on Neuroblastoma Growth in A/J Mice

Drug	Dose, mg/kg	Frequency per Day	*n*	Range, days	Mean ± *SE*, days	Change of Lifespan[a], %	Median, days
Saline	—	3	8	27–55	40.3 ± 3.4	—	43
α-Bungarotoxin	0.03	1	10	20–48	31.8 ± 3.1	−21	31
α-Bungarotoxin	0.1	1	9	16–16	16.0 ± 0	−60	16
α-Bungarotoxin	0.3	1	7	14–14	14.0 ± 0	−65	14
Saline	—	2	6	33–43	36.8 ± 1.6	—	36
Dihydroxytryptamine	50	2	8	29–68	43.1 ± 4.7	17	47
Dihydroxytryptamine + bromoacetylcholine	50 30	2 2	8	3–63	32.6 ± 7.8	−11	40
Dihydroxytryptamine + bromoacetylcholine	50 30	1 1	7	22–43	30.4 ± 3.1	−17	29
Dihydroxytryptamine + bromoacetate	50 12	1 1	6	15–150[b]	50.1 ± 17.1	36	38
Saline	—	2	6	33–43	36.8 ± 1.6	—	36
Diaminopropane	110	2	8	31–150[b]	68.8 ± 24.3[c]	87	50
Diaminopropane	220	2	8	29–58	44.3 ± 4.1	20	50
Diaminopropane + bromoacetylcholine	110 30	2 2	8	26–150[b]	81.1 ± 20.4[c]	120	50

[a,b,c] See Table I.

Table III—Inhibition of Neuroblastoma Growth in A/J Mice by Bromoacetylcholine and Bromoacetate with Various Routes of Administration

Drug	Dose (mg/kg) and Route[a]	*n*	Range, days	Mean ± *SE*, days	Change of Life-span[b], %	Median, days
Saline	— ip	10	9–42	28.5 ± 2.8	—	32
Bromoacetyl-choline	30 ip	8	26–38	29.1 ± 1.4	2	30
Bromoacetate	12 ip	8	26–40	32.3 ± 1.6	13	32
Bromoacetate	6 im	10	9–32	21.3 ± 2.1	−25	21
Bromoacetate	12 im	10	11–35	22.9 ± 2.7	−20	25
Bromoacetate	24 im	10	4–35	17.3 ± 2.9	−39	18
Bromoacetate	12 sc	10	11–35	24.1 ± 2.5	−14	28
Bromoacetate	24 sc	10	4–37	18.3 ± 3.3	−36	18

[a] The drug was administered three times daily. [b] See footnote[a], Table I.

quaternary nitrogen group of the molecule and bromoacetate has a negative charge in the molecule, which hinders absorption from the GI system. Intramuscular and subcutaneous injections of bromoacetate also were ineffective in suppressing neuroblastoma growth (Table III). Intratumor injection is the only viable route at this time. Intravenous administration was not tried because the mouse tail vein cannot withstand multiple daily injections for 6 weeks. Larger animal models are sought for experimentation to solve this problem.

DISCUSSION

Neuroblastoma is a cancer that cannot be treated well with current medical knowledge and methodology (1). After unsuccessful attempts to treat neuroblastoma surgically, with immunotherapy, and by radiation therapy, partial success was achieved with chemotherapy (1). Chemotherapy should be explored further.

Among the drugs tested, bromoacetylcholine, bromoacetate, cyclophosphamide, and 1,3-diaminopropane effectively inhibited neuroblastoma growth and prolonged the lifespan of A/J mice inoculated with neuroblastoma cells. Bromoacetylcholine, bromoacetate, and 1,3-diaminopropane are potent inhibitors of ornithine decarboxylase, a rate-limiting enzyme for the synthesis of polyamines. Since cellular levels of polyamines are closely related to cell proliferation and growth (12–17), it is highly possible that neuroblastoma growth is suppressed *via* the inhibition of ornithine decarboxylase (6). The only agent that is not clearly known to inhibit ornithine decarboxylase is cyclophosphamide, because cyclophosphamide must be activated *in vivo* while ornithine decarboxylase activity can only be determined *in vitro* with tissue culture experiments. The effect of cyclophosphamide also may possibly be manifested through the ornithine decarboxylase inhibition *in vivo*. Daunorubicin is an antibiotic that binds tightly with DNA (18) but has no inhibiting action on neuroblastoma growth.

Vincristine inhibits cell mitosis at the metaphase and dissolves the microtubule structures (18). However, it has little effect on ornithine decarboxylase activity, and this fact could be why it is ineffective in the inhibition of neuroblastoma growth.

Although bromoacetylcholine binds to the nicotinic receptor at the neuromuscular junction irreversibly (19), as does α-bungarotoxin (20), the latter compound produced little effect on neuroblastoma growth, indicating that bromoacetylcholine inhibits neuroblastoma growth through an action mechanism that differs from α-bungarotoxin, similar to action at cholinergic receptors. Neuroblastoma cells possess adrenergic, cholinergic, and nonspecific receptors but very few serotonergic receptors. It thus is understandable that neuroblastoma cell growth was not inhibited by a serotonergic neuron degenerator, 5,6-dihydroxytryptamine.

Among the routes of administration studied, intratumor administration for bromoacetylcholine, bromoacetate, and 1,3-diaminopropane and intraperitoneal administration for cyclophosphamide were the best.

In summary, it seems that drugs capable of inhibiting ornithine decarboxylase can suppress the cell growth of neuroblastoma. A more potent ornithine decarboxylase inhibitor that produces few side effects may be developed as an effective weapon to treat neuroblastoma.

REFERENCES

(1) C. Pochedly, "Neuroblastoma," Publ. Sci. Group, Inc., Acton, Mass., 1976.

(2) J. Z. Finklestein, E. Arima, P. E. Byfield, J. E. Byfield, and E. W. Fonkalsrud, *Cancer Chemother. Rep.*, **57**, 405 (1973).

(3) C. Y. Chiou, *J. Pharm. Sci.*, **64**, 469 (1975).

(4) *Ibid.*, **66**, 837 (1977).

(5) *Ibid.*, **67**, 331 (1978).

(6) S. K. Chapman, M. K. Martin, M. S. Hoover, and C. Y. Chiou, *Biochem. Pharmacol.*, **27**, 717 (1978).

(7) C. Y. Chiou and B. V. R. Sastry, *ibid.*, **17**, 805 (1968).

(8) C. Y. Chiou, N. E. Liddell, M. K. Martin, and C. J. Chu, *Arch. Int. Pharmacodyn. Ther.*, **233**, 235 (1978).

(9) A. Bjorklund, H. G. Baumgarten, and A. Nobin, *Adv. Biochem. Psychopharmacol.*, **10**, 13 (1974).

(10) K. Fuxe and G. Jonsson, *ibid.*, **10**, 1 (1974).

(11) C. Y. Chiou, C. J. Chu, and N. E. Liddell, *Arch. Int. Pharmacodyn. Ther.*, **235**, 35 (1978).

(12) U. Bachrach, *Proc. Natl. Acad. Sci. USA*, **72**, 3087 (1975).

(13) J. L. Clark and P. Duffy, *Arch. Biochem. Biophys.*, **172**, 551 (1976).

(14) Z. N. Canellakis and T. C. Theoharides, *J. Biol. Chem.*, **251**, 4436 (1976).

(15) T. C. Theoharides and Z. N. Canellakis, *Nature (London)*, **255**, 733 (1975).

(16) P. P. McCann, C. Tardiff, P. S. Mamont, and F. Schuber, *Biochem. Biophys. Res. Commun.*, **64**, 336 (1975).

(17) K. J. Lembeck, *Biochim. Biophys. Acta*, **354**, 88 (1974).

(18) P. Calabres and R. E. Parks, in "The Pharmacological Basis of Therapeutics," L. S. Goodman and A. Gilman, Eds., Macmillan, New York, N.Y., 1975, p. 1284.

(19) C. Y. Chiou, *Eur. J. Pharmacol.*, **26**, 268 (1974).

(20) C. C. Chang, *J. Formosan Med. Assoc.*, **59**, 315 (1960).

ACKNOWLEDGMENTS

Supported in part by American Cancer Society Grant CH-81.

Effect of pH, Chlorobutanol, Cysteine Hydrochloride, Ethylenediaminetetraacetic Acid, Propylene Glycol, Sodium Metabisulfite, and Sodium Sulfite on Furosemide Stability in Aqueous Solutions

KIRIT A. SHAH *, V. DAS GUPTA ˣ, and KENNETH R. STEWART ‡

Received November 2, 1979, from the *College of Pharmacy, University of Houston, Houston, TX 77004.* Accepted for publication December 20, 1979.

*Present address: College of Pharmacy, Texas Southern University, Houston, TX 77004. ‡Ben Taub Hospital Pharmacy, Houston, TX 77030.

Abstract □ A study was conducted to determine the effects of pH, two antioxidants, a chelating agent, a preservative, and propylene glycol on furosemide stability. Aqueous solutions of furosemide containing 10% alcohol (v/v) were prepared in phosphate buffers with various pH values (5, 6, and 9) whose ionic strength was adjusted to 0.1 *M* with potassium chloride. Some solutions contained chlorobutanol, ethylenediaminetetraacetic acid, or sodium metabisulfite. Another set of aqueous solutions contained phosphate buffer (0.1 *M*), alcohol (10% v/v), and propylene glycol (40% v/v) with or without cysteine hydrochloride, ethylenediaminetetraacetic acid, and sodium sulfite. The solutions were divided into two parts, stored at 24 and 50°, and assayed frequently using a previously developed high-pressure liquid chromatographic procedure. At the lowest pH value (pH 5), furosemide appeared to be very unstable. Cysteine hydrochloride, ethylenediaminetetraacetic acid, and sodium sulfite failed to improve the stability of furosemide. Chlorobutanol and sodium metabisulfite had an adverse effect on the stability, probably due to the fact that they decreased the pH of the solution. The pH value appears to be the only critical factor for the stability of furosemide. Buffered solutions containing propylene glycol were very stable at both temperatures for 170 days, and they tasted good.

Keyphrases □ Furosemide—stability in aqueous solutions, effect of formulation factors □ Diuretics—furosemide, stability in aqueous solutions, effect of formulation factors □ Stability—furosemide in aqueous solutions, effect of formulation factors

Furosemide (I) is a widely used diuretic, but little information is available concerning the stability of this drug in dosage forms. Rowbotham *et al.* (1) reported that aqueous furosemide solutions undergo hydrolysis and photochemical degradation. Quantification of photochemical degradation products of furosemide by the USP XIX (2) UV assay procedures was not successful. A stability-indicating assay for furosemide using high-pressure liquid chromatography (HPLC) was developed by Ghanekar *et al.* (3). It also was reported that an aqueous furosemide solution containing sorbitol and 10% alcohol (v/v) had limited stability. The pH of the solution was adjusted to ~8.5. However, it was difficult to maintain the pH value of the solution, which caused rapid decomposition.

The objectives of the present investigation were to study

0022-3549/80/0500-0594$01.00/0

© 1980, American Pharmaceutical Association

Vincristine inhibits cell mitosis at the metaphase and dissolves the microtubule structures (18). However, it has little effect on ornithine decarboxylase activity, and this fact could be why it is ineffective in the inhibition of neuroblastoma growth.

Although bromoacetylcholine binds to the nicotinic receptor at the neuromuscular junction irreversibly (19), as does α-bungarotoxin (20), the latter compound produced little effect on neuroblastoma growth, indicating that bromoacetylcholine inhibits neuroblastoma growth through an action mechanism that differs from α-bungarotoxin, similar to action at cholinergic receptors. Neuroblastoma cells possess adrenergic, cholinergic, and nonspecific receptors but very few serotonergic receptors. It thus is understandable that neuroblastoma cell growth was not inhibited by a serotonergic neuron degenerator, 5,6-dihydroxytryptamine.

Among the routes of administration studied, intratumor administration for bromoacetylcholine, bromoacetate, and 1,3-diaminopropane and intraperitoneal administration for cyclophosphamide were the best.

In summary, it seems that drugs capable of inhibiting ornithine decarboxylase can suppress the cell growth of neuroblastoma. A more potent ornithine decarboxylase inhibitor that produces few side effects may be developed as an effective weapon to treat neuroblastoma.

REFERENCES

(1) C. Pochedly, "Neuroblastoma," Publ. Sci. Group, Inc., Acton, Mass., 1976.

(2) J. Z. Finklestein, E. Arima, P. E. Byfield, J. E. Byfield, and E. W. Fonkalsrud, *Cancer Chemother. Rep.*, **57**, 405 (1973).

(3) C. Y. Chiou, *J. Pharm. Sci.*, **64**, 469 (1975).

(4) *Ibid.*, **66**, 837 (1977).

(5) *Ibid.*, **67**, 331 (1978).

(6) S. K. Chapman, M. K. Martin, M. S. Hoover, and C. Y. Chiou, *Biochem. Pharmacol.*, **27**, 717 (1978).

(7) C. Y. Chiou and B. V. R. Sastry, *ibid.*, **17**, 805 (1968).

(8) C. Y. Chiou, N. E. Liddell, M. K. Martin, and C. J. Chu, *Arch. Int. Pharmacodyn. Ther.*, **233**, 235 (1978).

(9) A. Bjorklund, H. G. Baumgarten, and A. Nobin, *Adv. Biochem. Psychopharmacol.*, **10**, 13 (1974).

(10) K. Fuxe and G. Jonsson, *ibid.*, **10**, 1 (1974).

(11) C. Y. Chiou, C. J. Chu, and N. E. Liddell, *Arch. Int. Pharmacodyn. Ther.*, **235**, 35 (1978).

(12) U. Bachrach, *Proc. Natl. Acad. Sci. USA*, **72**, 3087 (1975).

(13) J. L. Clark and P. Duffy, *Arch. Biochem. Biophys.*, **172**, 551 (1976).

(14) Z. N. Canellakis and T. C. Theoharides, *J. Biol. Chem.*, **251**, 4436 (1976).

(15) T. C. Theoharides and Z. N. Canellakis, *Nature (London)*, **255**, 733 (1975).

(16) P. P. McCann, C. Tardiff, P. S. Mamont, and F. Schuber, *Biochem. Biophys. Res. Commun.*, **64**, 336 (1975).

(17) K. J. Lembeck, *Biochim. Biophys. Acta*, **354**, 88 (1974).

(18) P. Calabres and R. E. Parks, in "The Pharmacological Basis of Therapeutics," L. S. Goodman and A. Gilman, Eds., Macmillan, New York, N.Y., 1975, p. 1284.

(19) C. Y. Chiou, *Eur. J. Pharmacol.*, **26**, 268 (1974).

(20) C. C. Chang, *J. Formosan Med. Assoc.*, **59**, 315 (1960).

ACKNOWLEDGMENTS

Supported in part by American Cancer Society Grant CH-81.

Effect of pH, Chlorobutanol, Cysteine Hydrochloride, Ethylenediaminetetraacetic Acid, Propylene Glycol, Sodium Metabisulfite, and Sodium Sulfite on Furosemide Stability in Aqueous Solutions

KIRIT A. SHAH *, V. DAS GUPTA ˣ, and KENNETH R. STEWART ‡

Received November 2, 1979, from the *College of Pharmacy, University of Houston, Houston, TX 77004.* Accepted for publication December 20, 1979.

*Present address: College of Pharmacy, Texas Southern University, Houston, TX 77004. ‡Ben Taub Hospital Pharmacy, Houston, TX 77030.

Abstract □ A study was conducted to determine the effects of pH, two antioxidants, a chelating agent, a preservative, and propylene glycol on furosemide stability. Aqueous solutions of furosemide containing 10% alcohol (v/v) were prepared in phosphate buffers with various pH values (5, 6, and 9) whose ionic strength was adjusted to 0.1 *M* with potassium chloride. Some solutions contained chlorobutanol, ethylenediaminetetraacetic acid, or sodium metabisulfite. Another set of aqueous solutions contained phosphate buffer (0.1 *M*), alcohol (10% v/v), and propylene glycol (40% v/v) with or without cysteine hydrochloride, ethylenediaminetetraacetic acid, and sodium sulfite. The solutions were divided into two parts, stored at 24 and 50°, and assayed frequently using a previously developed high-pressure liquid chromatographic procedure. At the lowest pH value (pH 5), furosemide appeared to be very unstable. Cysteine hydrochloride, ethylenediaminetetraacetic acid, and sodium sulfite failed to improve the stability of furosemide. Chlorobutanol and sodium metabisulfite had an adverse effect on the stability, probably due to the fact that they decreased the pH of the solution. The pH value appears to be the only critical factor for the stability of furosemide. Buffered solutions containing propylene glycol were very stable at both temperatures for 170 days, and they tasted good.

Keyphrases □ Furosemide—stability in aqueous solutions, effect of formulation factors □ Diuretics—furosemide, stability in aqueous solutions, effect of formulation factors □ Stability—furosemide in aqueous solutions, effect of formulation factors

Furosemide (I) is a widely used diuretic, but little information is available concerning the stability of this drug in dosage forms. Rowbotham *et al.* (1) reported that aqueous furosemide solutions undergo hydrolysis and photochemical degradation. Quantification of photochemical degradation products of furosemide by the USP XIX (2) UV assay procedures was not successful. A stability-indicating assay for furosemide using high-pressure liquid chromatography (HPLC) was developed by Ghanekar *et al.* (3). It also was reported that an aqueous furosemide solution containing sorbitol and 10% alcohol (v/v) had limited stability. The pH of the solution was adjusted to ~8.5. However, it was difficult to maintain the pH value of the solution, which caused rapid decomposition.

The objectives of the present investigation were to study

0022-3549/80/0500-0594$01.00/0

© 1980, American Pharmaceutical Association

Table I—Prepared Solutions[a] (0.5 mg of Furosemide/ml)

Solution	Buffer Solution (±0.1) pH	Other Ingredients
1	5	None
2	5	0.2% Chlorobutanol
3	5	0.05% III
4–6	5	0.1, 0.2, and 0.4% V, respectively
7–9	6	0.1, 0.2, and 0.4% V, respectively
10–12	9	0.1, 0.2, and 0.4% V, respectively
13	8.4	None
14	8.2	0.02% II
15	8.4	0.05% IV
16	8.3	0.05% II and 0.05% IV
17	8.0	0.05% II, 0.05% IV, and 0.05% III

[a] All solutions contained 10% alcohol (v/v) since the stock solution was made in alcohol; Solutions 13–17 contained propylene glycol, and the pH values of the final solutions were those obtained after diluting 1:10 with water.

Table II—Assay Results at Room Temperature

Solution	Percent of Label Claim					pH_f (±0.1)
	35 Days	90 Days	152 Days	170 Days	240 Days	
1	—	100.0	—	95.9	96.2	5.2
2	97.7	—	—	96.9	96.5	5.1
3	96.4	93.3	—	—	94.7	5.2
4	5.2[a]	—	—	—	—	3.3
5	15.1[a]	—	—	—	—	2.9
6	44.8[a]	—	—	—	—	2.8
7	91.8	—	81.1[b]	—	—	5.0
8	94.7	—	15.9[c]	—	—	4.5
9	98.3	—	93.0[b]	—	—	5.4
10	98.1	—	98.0	82.1	—	7.5
11	95.2	—	78.6[b]	—	—	6.9
12	91.7	—	60.5[b]	—	—	5.7
13	—	100.6	—	99.7	—	8.4
14	—	100.7[b]	—	100.8	—	8.2
15	—	99.5	—	99.5	—	8.4
16	—	100.8	—	100.4	—	8.3
17	—	100.9	—	100.2	—	8.0

[a] Crystals were found in the solution, so it was not reassayed. [b] Color had changed to light yellow (from colorless). [c] Fungus.

the effect of pH, chlorobutanol, cysteine hydrochloride monohydrate (II), ethylenediaminetetraacetic acid (III), sodium sulfite (IV), and sodium metabisulfite (V) on the stability of furosemide in aqueous solutions and to develop an appropriate buffering system to maintain the adjusted pH value.

EXPERIMENTAL

Chemicals and Reagents—All chemicals and reagents were USP, NF, or ACS grade and were used without further purification. Furosemide[1] powder was used as received.

Apparatus—The apparatus was the same as that reported previously (3), except that a variable-wavelength detector[2] set at 254 nm was used. The column also was the same as that reported previously (3).

Preparation of Solutions—A stock solution of furosemide was prepared by dissolving 1.25 g of furosemide in enough alcohol to make 250 ml. The solutions for stability studies were prepared by diluting an appropriate quantity of the stock solution with a buffer of an appropriate pH value (0.05 *M* phosphate buffers of pH 5, 6, and 9 whose ionic strength was adjusted to 0.1 *M* with potassium chloride). The phosphate buffers were prepared according to the USP procedure (4). Before the solutions were diluted to volume, additional ingredients, if any, were added.

Another set of solutions was prepared by dissolving an appropriate quantity of furosemide in 50.0 ml of 0.2 *M* aqueous dibasic potassium phosphate solution and then adding 10 ml of ethanol and bringing the solution to volume (100.0 ml) with propylene glycol. Additional ingredients, if any, were dissolved before bringing the solution to volume. The pH values of these solutions were determined after diluting 5.0 ml to 50.0 ml with water and are reported in Table I. All of the solutions prepared are listed in Table I.

The solutions were divided into two portions, stored at 24 and 50°, and assayed frequently using the HPLC method reported previously (3), except that the absorbance unit for full-scale deflection was 0.1 instead of 0.16 and the injection volume was 20.0 instead of 40.0 μl. The results, which were calculated as previously reported (3), are presented in Tables II and III. Sample chromatograms are presented in Figs. 1 and 2.

[1] Generously supplied by Hoechst-Roussel Pharmaceuticals, Somerville, N.J.
[2] Spectroflow monitor 770, Schoeffel Instrument Corp., Westwood, N.J.

Table III—Assay Results at 50°

Solution	Percent of Label Claim				pH_f (±0.1)
	35 Days	90 Days	170 Days	240 Days	
1	94.7	—	93.5	94.5	5.2
2	80.9	—	51.8	3.5[c]	3.3
3	94.8	—	88.7	79.3	5.2
4	15.3[a]	—	—	—	3.0
5–12[b]					
13	—	100.1	99.5	—	8.4
14	—	100.1[c]	99.2	—	8.2
15	—	99.4	99.4	—	8.4
16	—	100.7	100.0	—	8.3
17	—	101.1	100.5	—	8.0

[a] Crystals were found in the solution, so it was not reassayed. [b] Not studied at 50° since they were not stable even at room temperature. [c] Color had changed to light yellow.

RESULTS AND DISCUSSION

For convenience, the results from Solutions 1–12 (Table I), which did not contain any propylene glycol, will be discussed first, followed by the results from Solutions 13–17 (Table I), which contained 40% (v/v) propylene glycol.

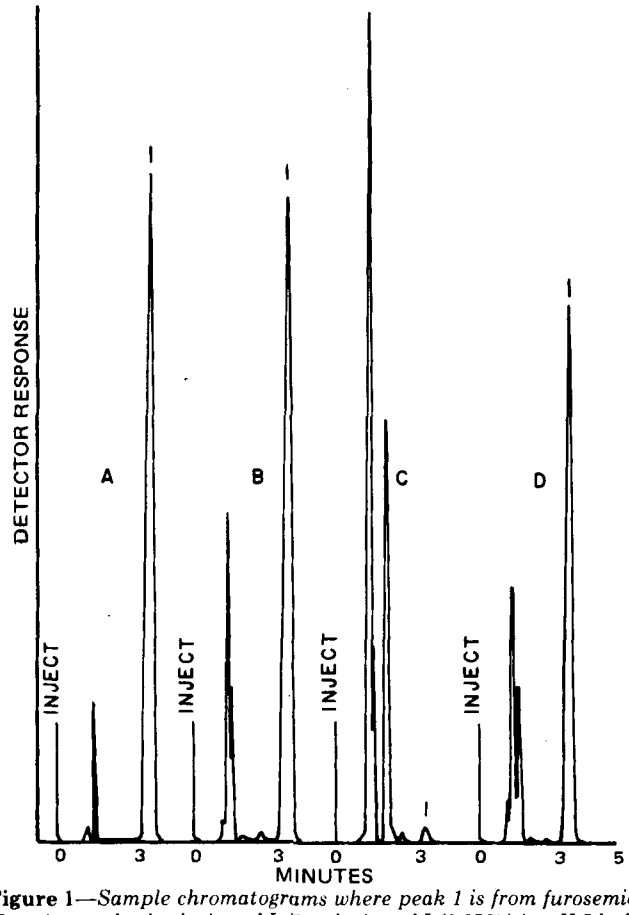

Figure 1—*Sample chromatograms where peak 1 is from furosemide. Key: A, standard solution of I; B, solution of I (0.05%) in pH 5 buffer after 240 days of storage at 50°; C, same as B except that it also contained 0.2% chlorobutanol; and D, same as B except that it also contained 0.05% III.*

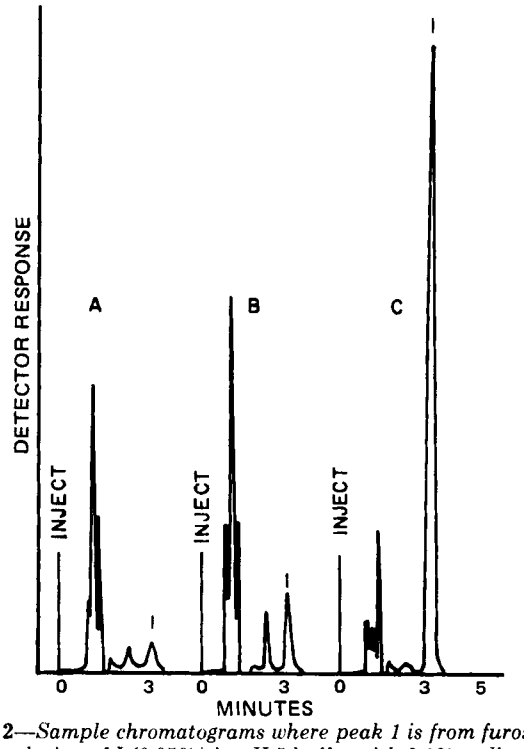

Figure 2—*Sample chromatograms where peak 1 is from furosemide. Key: A, solution of I (0.05%) in pH 5 buffer with 0.1% sodium metabisulfite after 170 days of storage at room temperature; B, same as A except that pH 6 buffer was used; and C, same as A except that pH 9 buffer was used.*

Solutions 1–12 (without Propylene Glycol)—The results indicate that Solutions 1–12 were not very stable for 170 days either at room temperature or at 50° (Tables II and III). Furthermore, the additional ingredients, ethylenediaminetetraacetic acid, chlorobutanol, or sodium metabisulfite, did not improve furosemide stability. In fact, chlorobutanol and sodium metabisulfite had an adverse effect on its stability, especially when added with pH 5 buffers. This effect may be due to a decrease in the pH of the solutions (Table III). Furosemide is known to be unstable at lower pH values (3). The pH values of most solutions changed after storage (Tables II and III).

The effect of sodium metabisulfite (as the concentration was raised from 0.1 to 0.4%) on furosemide stability is interesting. In Solutions 4–6 and 7–9 (Table II), the stability of furosemide improved as the concentration of sodium metabisulfite was increased, perhaps due to initial oxidation of metabisulfite to sulfate by the oxygen present. The sulfate ion increased the rate of decomposition (oxidation) of furosemide. A similar scheme using epinephrine has been reported (5).

Furthermore, the additional amount of sodium metabisulfite, after all of the oxygen was consumed, protected furosemide from the oxidation effect of the sulfate ion. This effect also has been reported (5).

The described effects were not found in Solutions 10–12, probably due to their high pH values (Table II). In these solutions, the effect of pH appears to be more prominent. Moreover, in solutions with basic pH values, furosemide does not appear to be susceptible to oxidation. The same may be true of solutions with pH values above 5.5.

Crystals of furosemide were found in several solutions after 35 days, especially in those kept at room temperature (Table II, Solutions 4–6). Furosemide is known to be poorly soluble in aqueous systems, especially acidic ones.

Several other solutions (Solutions 7, 9, 11, and 12) became discolored after 152 days (Table II). The cause of this discoloration was not determined.

It was not possible to treat the data mathematically because of very little decomposition (Solutions 1–3) or changes in pH values (Solutions 4–12).

Solutions 13–17 (with Propylene Glycol)—Solutions 13–17 proved to be very stable at both 24 and 50°. Considering experimental errors, the results of both temperatures were almost 100% for all solutions at 170 days (Tables II and III). Furthermore, the pH values of the solutions did not change (Tables II and III). However, the addition of cysteine hydrochloride monohydrate (II), ethylenediaminetetraacetic acid, sodium sulfite, or their combinations did not improve furosemide stability. Although the solution containing II became discolored, the loss in furosemide potency was negligible. Compound II apparently was oxidized in this solution. This discoloration did not occur when II was present in combination with sodium sulfite due to the protection provided by the sodium sulfite. Nevertheless, the addition of these ingredients is not desirable. In weakly basic solutions, furosemide does not appear to be susceptible to oxidation.

The only critical factor in furosemide stability is the pH of the solution, which must be slightly basic and not change on storage. A stable liquid dosage form of furosemide can be prepared by dissolving an appropriate quantity of furosemide powder in 0.2 *M* aqueous dibasic potassium phosphate solution (50% of the total volume), adding alcohol (10% v/v), and bringing the solution to volume with propylene glycol. Since the solution did not lose potency at 50° for ~6 months, it should be stable for at least 2 years at room temperature. A panel of three persons approved the taste of the product.

REFERENCES

(1) P. C. Rowbotham, J. B. Standrod, and J. K. Sugden, *Pharm. Acta Helv.*, **51**, 305 (1976).

(2) "The United States Pharmacopeia," 19th rev., Mack Publishing Co., Easton, Pa., 1975, p. 213.

(3) A. G. Ghanekar, V. D. Gupta, and C. W. Gibbs, *J. Pharm. Sci.*, **67**, 808 (1978).

(4) "The United States Pharmacopeia," 19th rev., Mack Publishing Co., Easton, Pa., 1975, pp. 653, 654.

(5) R. Bonevski, J. M. Culjat, and L. Balint, *J. Pharm. Sci.*, **67**, 1474 (1978).

Colorimetric and Spectrophotometric Determinations of Hydrastis Alkaloids in Pharmaceutical Preparations

SAWSAN EL-MASRY ˣ, M. A. KORANY, and A. H. A. ABOU-DONIA

Received October 9, 1979, from the *Faculty of Pharmacy, University of Alexandria, Alexandria, Egypt.* Accepted for publication December 19, 1979.

Abstract □ Hydrastine, canadine, and berberine were determined by the acid-dye technique. At pH 5.6, both the tertiary and the quaternary hydrastis alkaloids formed ion-pairs with bromcresol purple. The liberated hydrastine and canadine from the alkaloid–dye complexes were determined spectrophotometrically in the presence of berberine by the three-wavelength method of analysis. However, berberine could not be assayed successfully by this method due to significant partitioning in the aqueous phase during extraction. At pH 7.2, only berberine could ion-pair with bromcresol purple to form a chloroform-extractable complex. Consequently, the berberine content was analyzed selectively through the colorimetric determination of the combined dye at 580 nm. The suitability of the proposed methods was examined through the analyses of synthetic mixtures of hydrastis alkaloids and samples of hydrastis tincture and liquid extract. Percentage recoveries were 98.2–101.4 for the synthetic mixtures and 98.4–101.7 for the tincture and liquid extract spiked with berberine.

Keyphrases □ Colorimetry—analysis, berberine in pharmaceutical preparations and synthetic mixtures of hydrastis alkaloids, effect of pH on alkaloid–dye complex formation □ Spectrophotometry—analyses, hydrastine and canadine in pharmaceutical preparations and synthetic mixtures of hydrastis alkaloids, effect of pH on alkaloid–dye complex formation □ Hydrastis alkaloids—spectrophotometric and colorimetric determinations of alkaloid–dye complexes, effect of pH on complex formation □ Berberine—hydrastis alkaloid, colorimetric determination, effect of pH on alkaloid–dye complex formation □ Canadine—hydrastis alkaloid, spectrophotometric determination, effect of pH on alkaloid–dye complex formation □ Hydrastine—hydrastis alkaloid, spectrophotometric determination of alkaloid–dye complex, effect of pH on complex formation

The active ingredients and therapeutic uses of hydrastis were reviewed previously (1). The drug and its preparations are official in several pharmacopeias (2). Pharmacopeial assay methods for hydrastis rhizome or its liquid extract determine the hydrastine content while neglecting other alkaloids (3, 4).

BACKGROUND

The BPC (3) assays for hydrastine involve either a gravimetric step (for the liquids) or a titrimetric end-point (for powdered hydrastis). As with most gravimetric methods, the residue obtained was found to be impure since more than one spot was revealed by TLC. The titrimetric assay suffers from the disadvantage that the end-point is masked by the color of the extract.

The procedure of the French Pharmacopoeia (4) depends on the selective extraction by ether of hydrastine from the powdered drug after alkalinization with ammonia. Stanislas *et al.* (5) suggested a modification of the method in which the extracted hydrastine was determined spectrophotometrically at 295 and 313 nm. However, this modified method is relatively time consuming; it requires at least 7 hr.

Paper chromatography followed by colorimetric or spectrofluorometric determination was suggested (6, 7) for the assay of hydrastis. Direct spectrofluorometric determination of berberine, hydrastine, and canadine in synthetic mixtures was attempted by Gaille *et al.* (8). However, when applied to the hydrastis extract, only berberine and canadine could be determined by this method.

Column chromatography followed by spectrophotometric determination of hydrastine and berberine in liquid extracts of hydrastis also was suggested (9). Berberine and coptisine in coptis rhizome were separated by constant-potential electrophoresis followed by fluorescence densitometry at 550 nm (10). TLC was used to separate berberine prior to its determination as the tetrabromophenolphthalein ethyl ester ion-pair (11). Sakai *et al.* (12) determined berberine in pharmaceutical preparations as an ion-pair using 2,6-dichloroindophenol sodium. The ion-pair complex was stable for only 30 min.

The objective of the present work was to devise a simple and sensitive method for the determination of hydrastis alkaloids without chromatographic separation. Although the UV spectra of berberine, hydrastine, and canadine suggest that they can be determined spectrophotometrically by applying the three-wavelength method, it was possible to estimate only hydrastine and canadine in preparations of hydrastis. Because berberine is water soluble (1 in 4.5), it could not be determined by this method due to its incomplete recovery during extraction. Alternatively, berberine was selectively assayed colorimetrically using the acid-dye technique since, at pH 7.2, neither hydrastine nor canadine formed chloroform-extractable complexes with bromcresol purple.

EXPERIMENTAL

Materials—McIlvain buffers of pH 5.6 and 7.2 were prepared by mixing the required volumes of 0.1 *M* citric acid and 0.2 *M* dibasic sodium phosphate. Hydrastis liquid extract BPC, hydrastis tincture BPC, and analytical reagent grade sodium chloride were used. Hydrastine[1], canadine[2], and berberine acid sulfate[1] were used as received.

Solution Preparation—A berberine stock solution was prepared by dissolving 0.25 g of berberine acid sulfate in 100 ml of water. A berberine reference solution (1.25 mg %) was prepared by diluting 0.5 ml of the stock solution to 100 ml with 1 *N* HCl.

The canadine and hydrastine stock solutions were prepared by dissolving 0.2 g of either alkaloidal base in 100 ml of 1 *N* HCl. The canadine and hydrastine reference solutions were prepared by diluting 2 ml of the respective stock solution to 100 ml with 1 *N* HCl. Each reference solution contained 4 mg % of the alkaloidal base.

The bromcresol purple solution was prepared by dissolving 50 mg of the dye[3] in a few drops of 0.1 *N* NaOH and bringing the solution to 100 ml with water.

Methods—*Berberine Content of Hydrastis Tincture and Liquid Extract*—A 5-ml aliquot of hydrastis tincture (or 0.5 ml of hydrastis liquid extract diluted to 5 ml with 60% ethanol) was diluted to 1 liter with pH 7.2 buffer. A 10-ml aliquot (containing 0.05–0.2 mg of berberine) was transferred to a 50-ml separator containing 10 ml of chloroform and 1 ml of the dye solution. After shaking for 1 min, the layers were allowed to separate completely (15 min).

The chloroform layer was transferred to a second separator, and the aqueous layer was reextracted with another 10 ml of chloroform. The combined chloroform extracts were shaken for 15 sec with 10 ml of 0.1 *N* NaOH to liberate the combined dye. The aqueous layer was transferred to a 25-ml volumetric flask. After adjustment to volume, the intensity of the color of the solution was measured at 590 nm. The berberine content was determined by assaying a standard berberine solution concomitantly.

Hydrastine and Canadine Content of Hydrastis Tincture and Liquid Extract—Five milliliters of the tincture (or 0.5 ml of the liquid extract diluted to 5 ml with 60% ethanol) was diluted to 500 ml with pH 5.6 buffer. A 10-ml aliquot (containing 0.2–0.6 mg of total hydrastis alkaloids) was transferred to a 50-ml separator containing 1 ml of the dye solution and 10 ml of chloroform. After shaking for 1 min, the layers were allowed to separate completely.

The chloroform layer was transferred to a second separator, and the extraction was repeated with 2 × 10 ml of chloroform. The combined chloroform layers were extracted with 10 ml of 0.1 *N* NaOH for 15 sec,

[1] Merck, Darmstadt, West Germany.
[2] Provided by Dr. Peter W. Jeffs, Chemistry Department, Duke University, Durham, N.C.
[3] British Drug Houses Ltd., Poole, England.

0022-3549/80/0500-0597$01.00/0
© 1980, American Pharmaceutical Association

Table I—Results of Replicate Assays of Hydrastine, Canadine, and Berberine in Hydrastis Tincture

Assay	Alkaloid Concentration, g % (w/v)		
	Hydrastine[a]	Canadine	Berberine
1	0.229	0.054	0.265
2	0.227	0.050	0.261
3	0.218	0.077	0.262
4	0.223	0.052	0.266
5	0.218	0.054	0.265
6	0.223	0.052	0.262
Mean	0.223	0.056	0.263

[a] The hydrastine content found by the BPC method was 0.21 g % (w/v).

followed by 5 ml of saturated sodium chloride solution. The chloroform layer was evaporated on a water bath just to dryness. The residue was dissolved in 1 *N* HCl, transferred to a 25-ml volumetric flask, and brought to volume. The absorbances of the final solution together with the canadine, hydrastine, and berberine reference solutions were measured concomitantly in 1-cm cells at 285, 295, and 345 nm with a suitable spectrophotometer[4] using 1 *N* HCl as the blank.

The concentrations of canadine, C_a, and hydrastine, C_b, expressed in gram percent (w/v), were calculated from:

$$C_a = \frac{\left(A_1 - A_3\frac{\gamma_1}{\gamma_3}\right)\beta_2 - \left(A_2 - A_3\frac{\gamma_2}{\gamma_3}\right)\beta_1}{\alpha_1\beta_2 - \alpha_2\beta_1} \times \frac{1}{4} \times \frac{500}{10} \times \frac{100}{5} \quad \text{(Eq. 1)}$$

$$C_b = \frac{\left(A_2 - A_3\frac{\gamma_2}{\gamma_3}\right)\alpha_1 - \left(A_1 - A_3\frac{\gamma_1}{\gamma_3}\right)\alpha_2}{\alpha_1\beta_2 - \alpha_2\beta_1} \times \frac{1}{4} \times \frac{500}{10} \times \frac{100}{5} \quad \text{(Eq. 2)}$$

where:

$$A_1 = C_a\alpha_1 + C_b\beta_1 + C_c\gamma_1$$
$$A_2 = C_a\alpha_2 + C_b\beta_2 + C_c\gamma_2$$
$$A_3 = C_c\gamma_3$$

and where A_1, A_2, and A_3 are the absorbances of the final solution at 285, 295, and 345 nm, respectively, and α, β, and γ are the absorptivities of canadine, hydrastine, and berberine, respectively. The subscripts 1, 2, and 3 refer to the respective wavelengths at 285, 295, and 345 nm.

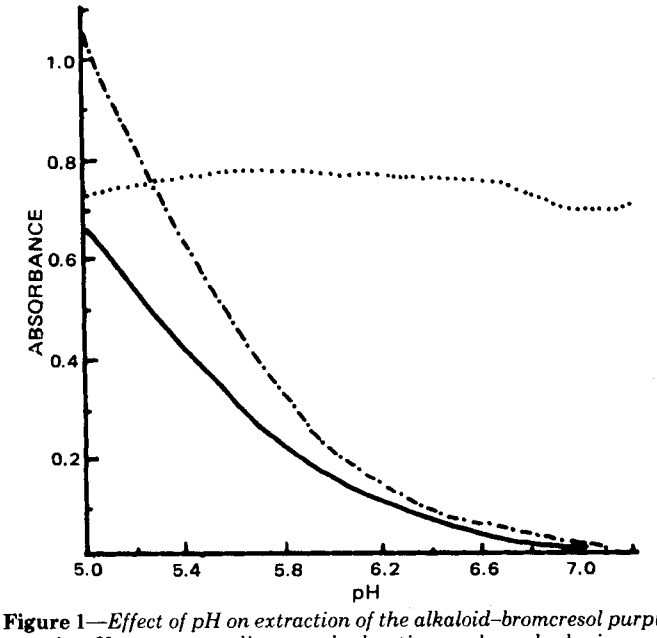

Figure 1—*Effect of pH on extraction of the alkaloid–bromcresol purple complex. Key: —, canadine; -·-, hydrastine; and ·····, berberine.*

[4] Beckman model 24 spectrophotometer.

RESULTS AND DISCUSSION

The λ_{max} values were 230 and 345 (berberine), 285 (canadine), and 295 (hydrastine) nm. Analysis of a synthetic mixture containing 0.2% (w/v) hydrastine, 0.05% (w/v) canadine, and 0.25% (w/v) berberine by the proposed method gave percentage recoveries of 98.2 and 101.4 for canadine and hydrastine, respectively. Direct UV estimation was successful for berberine in synthetic mixtures. However, in preparations where an extraction step was involved, berberine could not be determined successfully (<80% recovery). This result was due mainly to its partitioning between the aqueous and organic phases.

Table I shows the results of replicate assays of hydrastis tincture for hydrastine and canadine by the suggested method. The mean gram percent of hydrastine found (±*SD*) was 0.223 (±0.004). This result compares favorably with the result obtained by the BPC method (0.21% w/v). The slightly lower percentage recovery found by the BPC method might be attributed to incomplete extraction of hydrastine during the assay. For canadine, which oftens represents one-third to one-fourth of the hydrastine content, the results showed more scattering (Table I).

Figure 1 shows the effect of pH on the extractability of alkaloid–bromcresol purple complexes for berberine, canadine, and hydrastine. The formation of the complexes was strongly pH dependent for canadine and hydrastine, with an optimum pH range of 5–5.6. At pH values above 7, any complexes formed between canadine and hydrastine and the dye were not recovered in the chloroform phase. For berberine, the alkaloid–dye complex apparently was formed within the whole pH range studied (5.0–7.2), with the complex extractability being only slightly pH dependent.

The selective formation of the berberine–bromcresol purple complex at pH 7.2 was applied to the assay of this alkaloid in the presence of canadine and hydrastine. Replicate assays for berberine in a synthetic mixture containing the three alkaloids gave a mean percentage recovery (±*SD*) of 100.7 (± 0.31) for six determinations. Results of the berberine assay in the hydrastis tincture are shown in Table I. Recovery experiments made for hydrastis tincture spiked with various berberine concentrations gave a percentage recovery of 98.4–101.7.

The proposed procedures have the advantage of being less time consuming, with the assay requiring an average of 1 hr. The BPC procedure requires >5 hr and 100 ml of the tincture whereas 0.1 ml is required in the proposed method. This paper also presents a sensitive method for the assay of berberine in the presence of other tertiary hydrastis alkaloids.

REFERENCES

(1) K. Genest and D. W. Hughes, *Can. J. Pharm. Sci.*, 4 (1969).

(2) "Martindale The Extra Pharmacopoeia," 27th ed, Pharmaceutical Press, London, England, 1977, p. 1768.

(3) "British Pharmaceutical Codex," Pharmaceutical Press, London, England, 1949, pp. 1124, 1360.

(4) "French Pharmacopoeia," Ministere de la Santé Publique et de la Securité Sociale, Paris, France, 1965, p. 590.

(5) E. Stanislas, J. Gleye, and R. Rouffiac, *Ann. Pharm. Fr.*, **29**, 27 (1971).

(6) W. Wisniewski and T. Gorta, *Acta Pol. Pharm.*, **25**, 427 (1968).

(7) W. Wisniewski, Z. Furmanczyk, and M. Zapasnik, *ibid.*, **27**, 487 (1970).

(8) G. Gaille, D. Leclerc-Chevalier, and J. A. Mockle, *Can. J. Pharm. Sci.*, **5**, 55 (1970).

(9) M. S. El-Ridi, K. Khalifa, and A. Mamoon, *J. Pharm. Pharmacol.*, **8**, 602 (1956).

(10) M. Noguchi and K. Mochida, *Shoyakugaku Zasshi*, **30**, 47 (1976).

(11) T. Hattori, M. Inoue, and M. Hayakawa, *Yakugaku Zasshi*, **97**, 1263 (1977).

(12) T. Sakai, I. Hara, and M. Tsubouchi, *Chem. Pharm. Bull.*, **25**, 2451 (1977).

Effect of Etidronate Disodium on Filterability of Sickle Cell Erythrocytes

B. F. VAN DUZEE ˣ, R. J. SUNBERG, and J. J. BENEDICT

Received October 4, 1979, from the *Miami Valley Laboratories, Procter & Gamble Company, Cincinnati, OH 45247.* Accepted for publication December 19, 1979.

Abstract □ The effect of etidronate disodium on the deformability of human sickle cell erythrocytes was determined. A filtration process that demonstrated changes in trapping of ^{51}Cr-tagged sickle cells in the filtration apparatus was used to evaluate drug effects. Compared to the nontreated control, etidronate disodium [disodium dihydrogen (1-hydroxyethylidene)diphosphonate] reduced the trapping of sickled cells at low concentrations and increased trapping at high concentrations. These results indicate that etidronate disodium alters the deformability of sickled erythrocytes.

Keyphrases □ Etidronate disodium—effect on filterability of sickle cell erythrocytes □ Erythrocytes—sickle cell, effect of etidronate disodium on filterability □ Blood cell membrane—deformability of sickled erythrocytes, effect of etidronate disodium □ Sickle cell anemia—deformability of erythrocytes, effect of etidronate disodium

Sickle cell anemia has been studied intensively for the last decade. It is a unique disease in that its etiology is well known. The link between the genetically determined structural defect in the hemoglobin molecule and the clinical manifestations of the disease make it an excellent system for study by molecular biologists.

BACKGROUND

Despite the well-understood cause of the disease, some details about the sickling process are poorly understood. For example, it was shown only recently that the erythrocyte membrane may play an important role in the sickling process (1). Measurements of the deformability of erythrocytes as a function of time after deoxygenation showed that erythrocytes containing sickle cell hemoglobin became less deformable before any appreciable gelation of the sickle cell hemoglobin occurred. This finding is taken as evidence that the erythrocyte membrane is not only abnormal but that it also contributes significantly to the rigidity of the sickled erythrocyte.

One factor considered to be responsible for the abnormal membrane rigidity of the sickled erythrocyte is the presence of a high level of calcium in the cell (2). This calcium is expected to bind to the erythrocyte membrane, altering its deformability much as it does in normal erythrocytes (3). Another factor involved in the process is hemoglobin binding to the erythrocyte membrane. It was shown that the extent of hemoglobin binding to the membrane influences membrane rigidity and that normal hemoglobin binds to the sickled erythrocyte membrane to a greater extent than to the normal erythrocyte membrane (4).

Knowledge of the role of the erythrocyte membrane in deformability and its association with abnormally high levels of calcium has led to a new approach in the search for agents useful for therapeutic treatment of sickle cell disease. Investigators have begun looking for compounds that alter the calcium content of membranes (1). Anesthetics perform this function, and at least one, procaine hydrochloride, was shown to improve the filterability (deformability) of sickled erythrocytes (5). This approach has the potential of producing new and useful compounds for the treatment of sickle cell disease.

During early clinical trials of a diphosphonate-based bone scanning agent[1], patients with sickle cell disease had a high soft tissue uptake of the scanning agent in their extremities. Since diphosphonates adsorb strongly to calcium salts, it was suggested that this uptake might be due to the adsorption of the scanning agent to calcium in the erythrocytes trapped in the extremities. If this adsorption did occur, the deformability of the erythrocyte might perhaps be altered by etidronate disodium, which was the diphosphonate used in the scanning agent. Consequently, an investigation was initiated to determine if etidronate disodium alters sickle cell erythrocyte deformability.

EXPERIMENTAL

The filterability of erythrocyte suspensions generally is accepted as a measure of the deformability of the erythrocytes (6). Consequently, filterability was chosen as the parameter to determine the effects of etidronate disodium on deformability. The specific technique was adapted from the method of Wagner *et al.* (4).

Approximately 10 ml of blood was obtained from individual patients with sickle cell anemia whose hematology was well characterized. The samples were washed three times in an isotonic buffer solution containing 107 m*M* NaCl, 6 m*M* glucose, 400 mg of albumin/ml, and pH 7.4, 30 m*M* phosphate. The cells were tagged with sodium [^{51}Cr]chromate and treated with either etidronate disodium[2] or potassium cyanate.

The tagging was accomplished by splitting the sample in thirds. One-third of the sample (the negative control) was suspended in the isotonic buffer with 50 μCi of sodium [^{51}Cr]chromate and incubated for 1 hr at 37°. Another third (the positive control) (2) was suspended in a solution containing sodium [^{51}Cr]chromate as described and the same concentrations of glucose, albumin, and phosphate as the standard buffer but also containing potassium cyanate. The potassium cyanate concentration was varied from one experiment to the next, with the isotonicity of the solutions maintained by addition of sodium chloride to the buffer. The remaining one-third of the sample was suspended in buffer and treated in the same manner as the positive control, except that etidronate disodium was substituted for potassium cyanate.

The suspensions then were incubated for 1 hr at 37°. After incubation, the cell suspensions were washed three times with the isotonic buffer and were suspended in a ratio of 1:9 with unlabeled washed cells from a normal healthy donor to a final hematocrit of 1%. At this point, cell suspensions were stored overnight at 4°. The cells were equilibrated the next day to a partial pressure of oxygen of 26 mm Hg at 37° and filtered through 5-μm

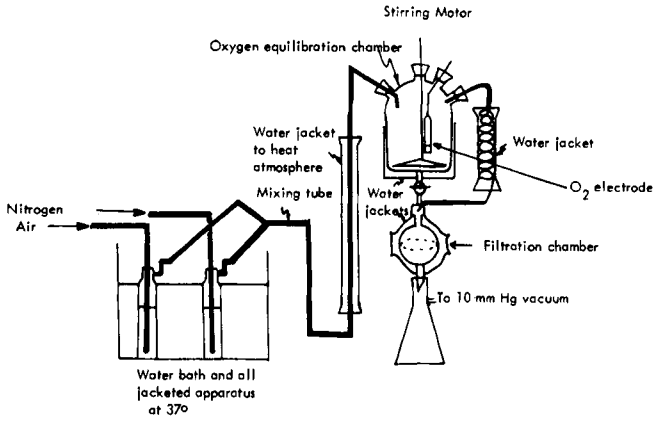

Figure 1—*Schematic diagram of the filtration apparatus. The erythrocyte suspension is introduced into the oxygen equilibration chamber where the partial pressure of oxygen and temperature are monitored. The air–nitrogen mixture is saturated with water and heated to 37° before it is introduced into the equilibration chamber. When the system is equilibrated (partial pressure of oxygen of 26 mm Hg and temperature of 37°), ~5 ml of suspension is transferred directly to the filtration chamber. Then a 10-mm Hg vacuum differential is applied to the filtration system, and the suspension passes through the filter.*

[1] Osteoscan.

[2] Procter & Gamble.

0022-3549/80/0500-0599$01.00/0
© 1980, American Pharmaceutical Association

Table I—Filtration Data for Untreated and Potassium Cyanate-Treated Controls and Etidronate Disodium-Treated Cells

Treatment	Treatment, m*M*	Percent of Cells Trapped ± *SD*	*p*[a]
Control		10.8 ± 3.9	
Potassium cyanate	107	0.88 ± 0.13	<0.01
Etidronate disodium	107	18.7 ± 4.5	<0.01
Control		44.3 ± 11.4	
Potassium cyanate	107	13.9 ± 0.8	<0.01
Etidronate disodium	10.7	36.4 ± 6.7	<0.11
Control		31.4 ± 5.8	
Potassium cyanate	1.0	20.2 ± 4.8	<0.01
Etidronate disodium	1.0	20.6 ± 6.8	<0.025
Control		58.2 ± 3.5	
Potassium cyanate	1.0	50.5 ± 11.1	<0.10
Etidronate disodium	0.10	44.4 ± 5.8	<0.001
Control		33.6 ± 4.5	
Potassium cyanate	107	5.1 ± 0.5	<0.001
Etidronate disodium	0.001	35.5 ± 11.0	NS

[a] The *p* values were determined using a single-tailed Student *t* test.

polycarbonate filter disks with a 10-mm Hg pressure differential. The filtration apparatus is described in Fig. 1. Following filtration, the filter paper and filtrate were counted in a well-type scintillation counter, and the percentage of cells that were not deformable enough to pass through the 5-μm pores of the filter disk were determined as:

$$\% \text{ trapping} = \frac{\text{number of trapped cells}}{\text{total number of cells}} \times 100 - \frac{\text{cpm from filter disk}}{\text{cpm from filter disk + cpm from filtrate}} \times 100 \quad \text{(Eq. 1)}$$

The percent trapping is taken as a measure of deformability. The larger the trapping, the lower is the deformability.

RESULTS AND DISCUSSION

The results from five filtration experiments are shown in Table I. The values reported are the means (±*SD*) of five filtrations per treatment group. The filtrations for all three treatments in each experiment were completed on the same day.

The average trapping for the controls in each experiment varied from 10.8 to 58.2%. Since the blood samples each came from different donors, this variability was not unexpected. It may have been due to the difference in the sickle cell hemoglobin content or the oxygen affinity of the erythrocytes from individual to individual.

Cyanate is effective in increasing the deformability of sickled erythrocytes and was included in these experiments as a positive control on the procedure (4). The average trapping for the cyanate-treated samples was significantly less than the control trapping in each experiment over the range of 1.0–107 m*M* cyanate. Consequently, it is believed that this apparatus and these procedures were capable of detecting changes in deformability.

In these experiments, etidronate disodium altered the deformability of the sickled erythrocytes. At high concentrations (107 m*M*), the deformability of the erythrocytes was decreased; at lower concentrations

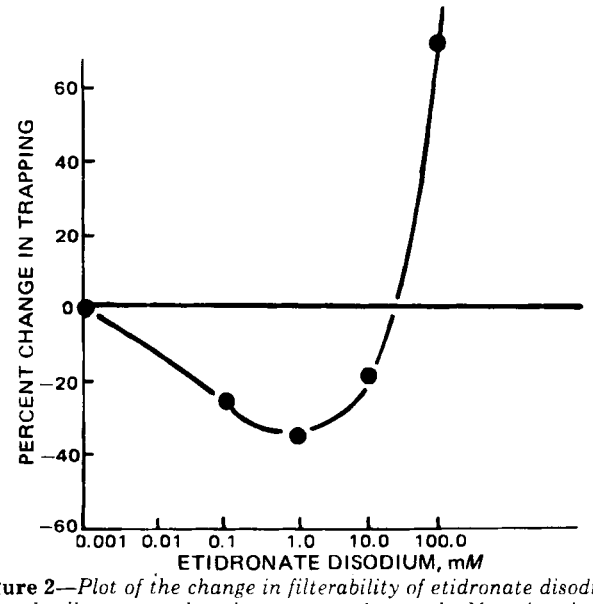

Figure 2—*Plot of the change in filterability of etidronate disodium-treated cells compared to the nontreated controls. Negative changes in trapping indicate increased cell (membrane) deformability, whereas positive changes indicate decreased deformability.*

(0.10–10 m*M*), the deformability of the cells was increased significantly. This biphasic response is quite obvious in Fig. 2, although the position of the minimum is subject to some uncertainty since different blood samples were used at each concentration. This type of biphasic effect is unusual but not unique. For example, isoproterenol and the prostaglandins exhibit a biphasic response on erythrocyte deformability. It is believed that this type of response is produced by the action of the drug on specific membrane receptors (7).

Since filtration experiments generally are considered to be a measure of membrane deformability (6), and since etidronate disodium produces an effect similar to that produced by the membrane actions of prostaglandin and isoproterenol, it is tempting to conclude that the filterability changes seen with etidronate disodium result from an interaction of etidronate disodium and the erythrocyte membrane. However, since sickle cell hemoglobin gelation is known to influence sickle cell erythrocyte filterability, such a conclusion cannot be reached from this work alone.

REFERENCES

(1) G. J. Brewer, *Am. J. Hematol.*, 1, 121 (1976).

(2) J. W. Eaton, T. D. Skelton, H. S. Swofford, C. E. Kolpin, and H. S. Jacob, *Nature*, **246**, 105 (1973).

(3) M. Chau-Wong and P. Seeman, *Biochim. Biophys. Acta*, **241**, 473 (1971).

(4) S. M. Wagner, J. Bishop, P. Flanigan, P. A. Bromberg, and S. P. Balcerzak, *J. Lab. Clin. Med.*, **85**, 445 (1975).

(5) R. Baker, D. Powars, and L. J. Haywood, *Progr. Clin. Biol. Res.*, 1, 437 (1975).

(6) D. Braasch, *Physiol. Rev.*, **51**, 679 (1971).

(7) J. E. Allen and H. Rasmussen, *Science*, **174**, 512 (1971).

Radioimmunoassay of Flurazepam in Human Plasma

WILLIAM GLOVER ˣ, JAMES EARLEY, MICHAEL DELANEY, and ROSS DIXON

Received August 22, 1979, from the *Research Division, Hoffmann-La Roche Inc., Nutley, NJ 07110.* Accepted for publication December 12, 1979.

Abstract □ A radioimmunoassay for the determination of the hypnotic flurazepam in plasma was developed. Plasma levels of intact flurazepam were measured following oral administration of therapeutic doses to humans. The procedure employs an antiserum obtained from a rabbit immunized with 3-hemisuccinyloxyflurazepam covalently coupled to bovine serum albumin and tritium-labeled flurazepam as the radioligand. Assay specificity was achieved by chromatographic isolation of flurazepam from plasma extracts on Sephadex LH-20 prior to analysis. The method has a sensitivity limit of 0.1 ng of flurazepam/ml using a 1-ml plasma sample, and the intra- and interassay coefficients of variation did not exceed 9% over a range of 0.1–5 ng/ml. In eight subjects who received a single 30-mg dose of flurazepam, peak plasma concentrations of 0.5–3.0 ng of intact drug/ml were reached after 0.5–1 hr, except in one subject where the peak occurred at 4 hr. The plasma concentrations of flurazepam declined with a harmonic mean apparent half-life of 2.3 hr.

Keyphrases □ Flurazepam—radioimmunoassay, plasma levels in humans □ Radioimmunoassay—flurazepam, plasma levels in humans □ Hypnotic agents—flurazepam, radioimmunoassay, human plasma

Flurazepam hydrochloride[1] (Table I) was synthesized by Sternbach *et al.* (1) and now is the most widely prescribed hypnotic agent for the treatment of insomnia in the United States (2). Studies on the biotransformation of flurazepam in humans and dogs have shown that the drug is metabolized extensively (3). The major metabolite in human plasma is *N*-1-desalkylflurazepam (Table I). Intravenous studies (3) of the elimination of flurazepam in dogs showed that the blood levels of the intact drug disappeared rapidly (half-life of 1.4 hr).

BACKGROUND

Kaplan *et al.* (4) used a fluorometric assay to study the blood level profile of the major flurazepam metabolites in humans following chronic dosage. This procedure requires a two-stage derivatization process involving acid hydrolysis of flurazepam and its metabolites to their respective benzophenones followed by cyclization to the 9-acridinone derivatives. The derivatives then are separated by TLC and are analyzed by a spectrofluorometric procedure. However, the levels of the intact drug were below the assay sensitivity and could not be measured.

More recently, an electron-capture GLC assay was developed by de Silva *et al.* (5) with sufficient sensitivity to measure the intact *N*-1-desalkyl metabolite. While this method is useful for toxicological work and measurement of the major metabolite present in plasma, it lacks sufficient sensitivity to measure the intact drug after administration of therapeutic doses. Thus, the plasma level profile and the apparent half-life of flurazepam in humans have not been established.

The present report describes the development of a radioimmunoassay to determine the plasma levels of intact flurazepam in humans following a single 30-mg oral dose.

EXPERIMENTAL

Preparation of Immunogen—3-Hydroxyflurazepam (Table I) was refluxed with succinic anhydride in dichloromethane containing triethylamine to yield the desired hapten, 3-hemisuccinyloxyflurazepam (Table I), which was coupled covalently to bovine serum albumin by the mixed anhydride procedure of Erlanger *et al.* (6). The resulting conjugate was dialyzed against 0.05 *M* $NaHCO_3$ followed by dialysis against distilled water and isolated by lyophilization. UV analysis of the immunogen (6) indicated that ~18 moles of the hapten was covalently linked to 1 mole of albumin.

Table I—Flurazepam, the Hapten 3-Hemisuccinyloxyflurazepam, and the Cross-Reactivity of Metabolites Present in Plasma

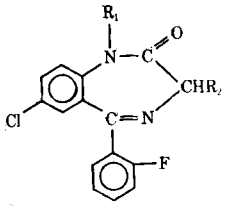

Compound	R_1	R_2	Cross-Reactivity, %
Flurazepam	$(CH_2)_2N(C_2H_5)_2$	H	100
3-Hydroxyflurazepam	$(CH_2)_2N(C_2H_5)_2$	OH	—
3-Hemisuccinyloxyflurazepam	$(CH_2)_2N(C_2H_5)_2$	$OCO(CH_2)_2COOH$	—
Monodesethylflurazepam	$(CH_2)_2NHC_2H_5$	H	17.0
Didesethylflurazepam	$(CH_2)_2NH_2$	H	3.5
N-1-Hydroxyethylflurazepam	$(CH_2)_2OH$	H	<1.0
N-1-Desalkylflurazepam	H	H	<1.0

Immunization and Antibody Production—A female New Zealand White rabbit was immunized intradermally and boosted intravenously as described previously (7). Serum was collected at monthly intervals and stored at −20°. The antiserum obtained following the second booster immunization was used throughout this study. The antiserum was diluted 1:2000 with assay buffer[2] prior to use.

Extraction of Flurazepam from Plasma—Plasma (1 ml) was buffered to pH 9 with 1 ml of 1 *M* borate buffer and extracted twice with 5 ml of hexane[3] on a reciprocating shaker for 15 min. The combined hexane extracts were evaporated to dryness in a 15-ml conical tube at 40° under nitrogen, and the inside wall of each tube was rinsed down with 1 ml of hexane. Duplicate control plasma samples and internal standards containing 0.125, 0.5, and 1 ng of flurazepam/ml were processed along with the unknowns.

Column Chromatography of Plasma Extracts—Prepacked columns containing 1 g of Sephadex LH-20[4] were washed first with methanol and then equilibrated with hexane–benzene–methanol (95:5:4).

Each plasma extract was dissolved in 0.2 ml of the solvent system, applied to the top of column, and allowed to percolate into the bed. The tube was rinsed with another 0.5-ml portion of the solvent and transferred to the column. The column was developed using the solvent system, and the first 3.5 ml of eluate (which previously was shown to be devoid of flurazepam) was discarded. The next 5 ml of eluate containing the flurazepam was collected in a 20-ml glass scintillation vial and evaporated to dryness under nitrogen at 40°. The residue was dissolved in 0.5 ml of the assay buffer, and the vial was capped and incubated for 1 hr at 37° to obtain maximum dissolution of flurazepam prior to radioimmunoassay.

[1] Flurazepam hydrochloride is the active drug substance in Dalmane. Its chemical structure is 7-chloro-1-[2-(diethylamino)ethyl]-5-(*o*-fluorophenyl)-1,3-dihydro-2*H*-1,4-benzodiazepin-2-one dihydrochloride.

[2] Assay buffer is Dulbecco phosphate-buffered saline (GIBCO, Grand Island, NY 14072).

[3] Hexane is UV grade, Burdick & Jackson Laboratories, Muskegan, Mich.

[4] Isolab, Akron, OH 44321.

0022-3549/80/0500-0601$01.00/0
© 1980, American Pharmaceutical Association

Table II—Plasma Concentrations[a] (Nanograms per Milliliter) of Flurazepam in Eight Human Subjects following a 30-mg Oral Dose

Hour	Subject 1	2	3	4	5	6	7	8
0.0	NM	NM	NM	NM	NM	NM	NM	NM
0.5	1.00	0.30	0.15	1.00	0.14	1.80	0.24	NM
1.0	0.80	1.10	0.80	1.40	0.75	3.00	0.50	NM
							0.30[b]	
2.0	0.70	0.50	0.40	0.75	0.40	0.60	0.24	NM
3.0	0.50	0.40	0.30	0.45	0.30	0.80	0.20	0.35
4.0	0.30	0.25	0.20	0.40	0.20	0.30	0.19	0.61
							0.12[c]	0.27[c]
6.0	0.17	NM	0.10	0.28	0.17	0.20	0.12	0.27
								0.14[d]
8.0	NM	NM	NM	0.16	NM	0.16	NM	NM

[a] The reported concentrations are based on duplicate analyses of each plasma sample. NM = not measurable. [b] At 1.5 hr. [c] At 5 hr. [d] At 7 hr.

Radioimmunoassay—A calibration curve was generated by adding [^{3}H]flurazepam[5] (15,000 dpm) in 0.1 ml of buffer to duplicate 12 × 75-mm disposable glass culture tubes containing 0.03–2 ng of flurazepam in 0.2 ml of buffer. Following preparation of the standards, duplicate 0.2-ml aliquots of the reconstituted unknown flurazepam fractions were added to tubes containing 0.1 ml of the [^{3}H]flurazepam. Then the diluted antiserum (0.2 ml) was added to all tubes, except the nonspecific-binding control specimen to which was added 0.4 ml of buffer.

Each tube was mixed gently on a vortex mixer and allowed to stand at room temperature for 1 hr. Following the incubation, the antibody-bound radioligand was separated from the unbound fraction by precipitation with saturated ammonium sulfate (7). After the pellet was dissolved in 0.4 ml of water and 3 ml of scintillator[6] to give a clear solution, radioactivity in each tube was quantified in a modified liquid scintillation counter as described previously (8).

The calculation of the unknown flurazepam levels was performed by interpolation from a logit–log standard curve.

Determination of Assay Blank—One-milliliter aliquots of pooled normal human control plasma were extracted and chromatographed as described previously on eight separate columns. A separate control column was developed in the absence of any plasma extract. The fraction containing flurazepam eluate from each column was reconstituted with 0.5 ml of buffer and then analyzed by the radioimmunoassay.

Recovery of Flurazepam from Human Plasma—Various concentrations (0.125–5 ng) of unlabeled flurazepam were added to the control human plasma, incubated for 30 min at 37° and then stored at −20° until they were assayed. Then 1 ml of each plasma standard was extracted and chromatographed as described previously and analyzed by the radioimmunoassay.

RESULTS AND DISCUSSION

Radioimmunoassay Characteristics—The antiserum bound 50% of the radioligand at a final dilution of 1:5000 in a 0.5-ml incubation volume. A logit–log plot of B/B_0 (percent) *versus* concentration of unlabeled flurazepam gave a linear response between 0.03 and 2 ng, where B and B_0 are the amounts of antibody-bound radioligand in the presence and absence of the unlabeled drug, respectively, following correction for nonspecific binding. A typical calibration curve had a slope of −0.98 with a correlation coefficient of 0.99. Repeated analyses of the 0.03-ng standard gave a B/B_0 value of 87%; the working sensitivity of the procedure was ~0.1 ng of flurazepam/ml using a 1-ml plasma sample.

Blank values for eight 1-ml aliquots of control plasma following the extraction and chromatographic procedures were well below (mean B/B_0 = 95 ± 2%) the detection limit while the recovery of internal standards over the range of 0.1–5 ng of flurazepam/ml averaged 82.5 ± 3%.

The intra- and interassay coefficients of variation were determined by repeated analysis of six randomly selected plasma samples from subjects who had received a single 30-mg oral dose of flurazepam over a 6-week period. The coefficients of variation did not exceed 9% over a range of 0.1–1.6 ng of flurazepam/ml.

[5] [^{3}H]Flurazepam, with a specific activity of 27 Ci/mmole, was stored as the free base in toluene at −20°.

[6] Aquasol, New England Nuclear, Boston, MA 02118.

Radioimmunoassay Specificity—The specificity of the antiserum initially was evaluated by cross-reactivity studies involving all of the flurazepam metabolites known to be present in plasma (3). The mono- and didesethyl metabolites exhibited a cross-reactivity of 17 and 3.7%, respectively, while the other possible competitors cross-reacted less than 1% (Table I). As the large substituent at the N-1 position of flurazepam was progressively metabolized to the N-desalkyl metabolite, cross-reactivity decreased, indicating that the substituent at N-1 on the hapten is a major antigenic determinant.

In view of the cross-reactivity of both the mono- and didesethyl metabolites, a specific assay for flurazepam in plasma could not be developed without first separating it from its metabolites. Therefore, column chromatography on Sephadex LH-20 was employed. The elution profile of flurazepam was determined as described previously. Under these conditions, the plasma metabolites are not eluted from the column, thus providing a rapid and reproducible procedure for separating flurazepam from its interfering metabolites.

Plasma Flurazepam Levels in Humans—The method was applied to the analysis of plasma samples from eight subjects who received single 30-mg doses of the drug. Peak plasma concentrations of intact flurazepam were reached after 0.5–1 hr in seven subjects and at 4 hr in one subject (Table II). Although the data could not be used for detailed pharmacokinetic analysis, the intact drug had a harmonic mean apparent half-life in plasma of 2.3 hr.

This study demonstrates that, although orally administered flurazepam undergoes extensive first-pass metabolism to yield N-1-desalkylflurazepam as its major metabolite in plasma, some intact flurazepam does reach the peripheral circulation. The extent to which intact flurazepam contributes to the hypnotic activity of the drug is unknown.

REFERENCES

(1) L. H. Sternbach, G. A. Archer, J. V. Earley, R. I. Fryer, E. Reeder, N. Wasyliw, L. O. Randall, and R. Banziger, *J. Med. Chem.*, **8**, 815 (1965).

(2) "Drug Store and Hospital Purchases In America," Ambler, Pa., Category 67220, 1976–1977, p. 940.

(3) M. A. Schwartz and E. Postma, *J. Pharm. Sci.*, **59**, 1800 (1970).

(4) S. A. Kaplan, J. A. F. de Silva, M. L. Jack, K. Alexander, N. Strojny, R. E. Weinfeld, C. V. Puglisi, and L. Weissman, *ibid.*, **62**, 1932 (1973).

(5) J. A. F. de Silva, C. V. Puglisi, M. A. Brooks, and M. R. Hackman, *J. Chromatogr.*, **99**, 461 (1974).

(6) B. F. Erlanger, F. Borek, S. M. Beiser, and S. Lieberman, *J. Biol. Chem.*, **234**, 1090 (1957).

(7) W. R. Dixon, J. Earley, and E. Postma, *J. Pharm. Sci.*, **64**, 927 (1975).

(8) R. Dixon and E. Cohen, *Clin. Chem.*, **22**, 1746 (1976).

ACKNOWLEDGMENTS

The authors are grateful to Dr. Peter Blumenthal for supplying the plasma samples and to Mrs. Peggy Althoff for manuscript preparation.

Analysis of Mepivacaine, Bupivacaine, Etidocaine, Lidocaine, and Tetracaine

GEORGE B. PARK, PAUL E. ERDTMANSKY, RICHARD R. BROWN, M. PETER KULLBERG, and JEROME EDELSON ˣ

Received August 20, 1979, from the *Department of Drug Metabolism and Disposition, Sterling-Winthrop Research Institute, Rensselaer, NY 12144.* Accepted for publication December 4, 1979.

Abstract □ A GLC method, employing a nitrogen–phosphorus-sensitive detector, is described for the analysis of mepivacaine, bupivacaine, etidocaine, lidocaine, and tetracaine in biological fluids. The method is simple, reliable, and sensitive, with a practical limit of sensitivity of ~2.5 ng/ml, well below therapeutic plasma levels. Extensive start-up procedures and sample preparation are not required.

Keyphrases □ GLC—analysis, mepivacaine, bupivacaine, etidocaine, lidocaine, and tetracaine in biological fluids □ Anesthetics, local—simultaneous GLC analysis of mepivacaine, bupivacaine, etidocaine, lidocaine, and tetracaine in biological fluids □ Mepivacaine—simultaneous GLC analysis with bupivacaine, etidocaine, lidocaine, and tetracaine in biological fluids □ Bupivacaine—simultaneous GLC analysis with mepivacaine, etidocaine, lidocaine, and tetracaine in biological fluids □ Etidocaine—simultaneous GLC analysis with mepivacaine, bupivacaine, lidocaine, and tetracaine in biological fluids □ Lidocaine—simultaneous GLC analysis with mepivacaine, bupivacaine, etidocaine, and tetracaine in biological fluids □ Tetracaine—simultaneous GLC analysis with mepivacaine, bupivacaine, etidocaine, and lidocaine in biological fluids

GLC has been the method of choice for the quantitative analysis of basic drugs in biological media for many years. Goehl and Davison (1) reported a method, developed in these laboratories, for the analysis of meperidine by GLC with flame-ionization detection; an improved, general flame-ionization GLC method for basic drugs was described by Mather and Tucker (2). Other methods for basic drugs, based on GLC with various detectors, have been published (3–10). The most sensitive methods utilize GLC–mass spectrometry (11, 12).

This paper describes a GLC method, employing a nitrogen–phosphorus-sensitive detector, that was used to determine mepivacaine, bupivacaine, etidocaine, lidocaine, and tetracaine in various biological fluids including plasma, cerebrospinal fluid, placental blood, and umbilical cord blood. It has proven to be facile, dependable, and equally applicable to a single sample or a large number of samples. Start-up time is minimal, and the sensitivity of the assay is several times greater than that of other reported GLC methods and is comparable to reported GLC–mass spectrometry methods.

EXPERIMENTAL

Reagents—Bupivacaine hydrochloride[1], mepivacaine hydrochloride[2], etidocaine hydrochloride[3], reagent grade ether, methanol, hydrochloric acid, and sodium hydroxide were used as received.

Apparatus—The gas–liquid chromatograph[4] was fitted with a nitrogen–phosphorus detector. Columns (122 and 183 cm) packed with OV-1 or OV-17 on 100–120-mesh Ultrabond[5] or on 100–120-mesh Gas Chrom Q[6] were used, depending on the resolution required. Typical operating parameters were: column temperature, 200 or 250°; injector temperature, 300°; detector temperature, 350°; helium carrier gas flow, 35 ml/min; hydrogen detector gas flow, 5 ml/min; air detector gas flow, 50 ml/min; and detector bead voltage, 20 v.

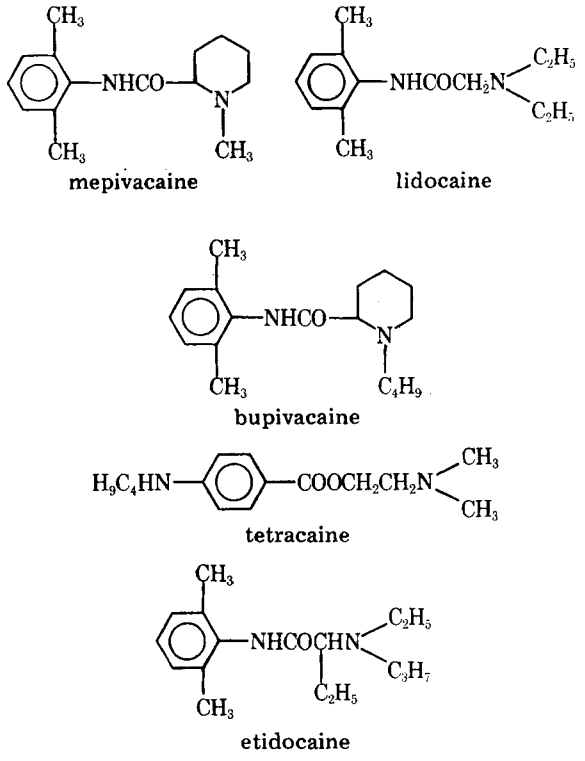

Procedure—To a 12-ml, round-bottom centrifuge tube fitted with a fluoroplastic-lined screw cap were added 1.0 ml of plasma, 25 μl of the internal standard solution (10 μg/ml in methanol), and 5.0 ml of ether. The tube was shaken on a horizontal shaker for 10 min and centrifuged. After the aqueous layer was frozen in a dry ice–acetone bath, the ether layer was transferred to a clean 12-ml centrifuge tube and treated with 0.2 ml of 1.0 *N* HCl. The tube was shaken, centrifuged, and frozen as before, and the ether phase was discarded.

Following the addition of 0.2 ml of 2.0 *N* NaOH, the aqueous phase was extracted with 5.0 ml of ether and frozen. The ether phase was decanted into a 6-ml, glass-stoppered conical tube and dried at 50° with a gentle stream of dry air. The residue was dissolved in 50 μl of methanol, and 1.0 μl of the solution was analyzed by GLC.

For the analysis of related esters, such as tetracaine, hydrolysis of the ester function must be prevented (13) by: (*a*) utilizing sodium arsenite (50 mg/ml of blood) as an esterase inhibitor, and (*b*) eliminating the back-extraction step.

RESULTS AND DISCUSSION

Figure 1 is a chromatogram, obtained with 3% OV-17 on Ultrabond, of a sample containing equal amounts of etidocaine, bupivacaine, and mepivacaine. Figure 2 shows chromatograms, obtained with 10% OV-1 on Gas Chrom Q, of a blank plasma standard, a 0.2-μg/ml plasma standard, and a clinical plasma sample using bupivacaine as an internal

[1] Marcaine Hydrochloride, Sterling-Winthrop Research Institute, Rensselaer, N.Y.
[2] Carbocaine Hydrochloride, A. B. Bofors, Nobelkrut, Sweden.
[3] Duranest Hydrochloride, Astra Pharmaceutical Products, Worchester, Mass.
[4] Model 5710A, Hewlett-Packard, Palo Alto, Calif.
[5] RFR Corp., Hope, R.I.
[6] Applied Science Laboratories, State College, Pa.

0022-3549/80/0500-0603$01.00/0
© 1980, American Pharmaceutical Association

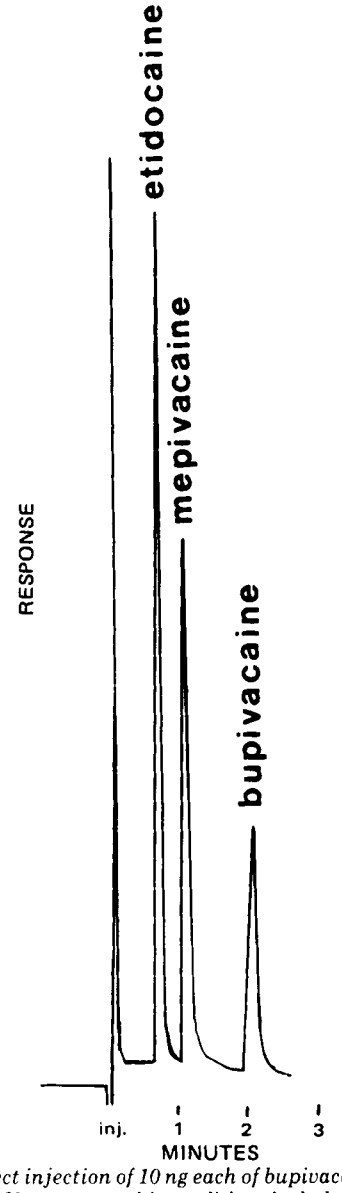

Figure 1—*Direct injection of 10 ng each of bupivacaine, mepivacaine, and etidocaine. Chromatographic conditions included a 122-cm × 2-mm (i.d.) column packed with 3% OV-17 on 100–120-mesh Ultrabond, an injector temperature of 300°, a column temperature of 200°, a detector temperature of 350°, a carrier gas flow rate of 35 ml/min, and detector gases of hydrogen and air at flow rates of 5 and 50 ml/min, respectively.*

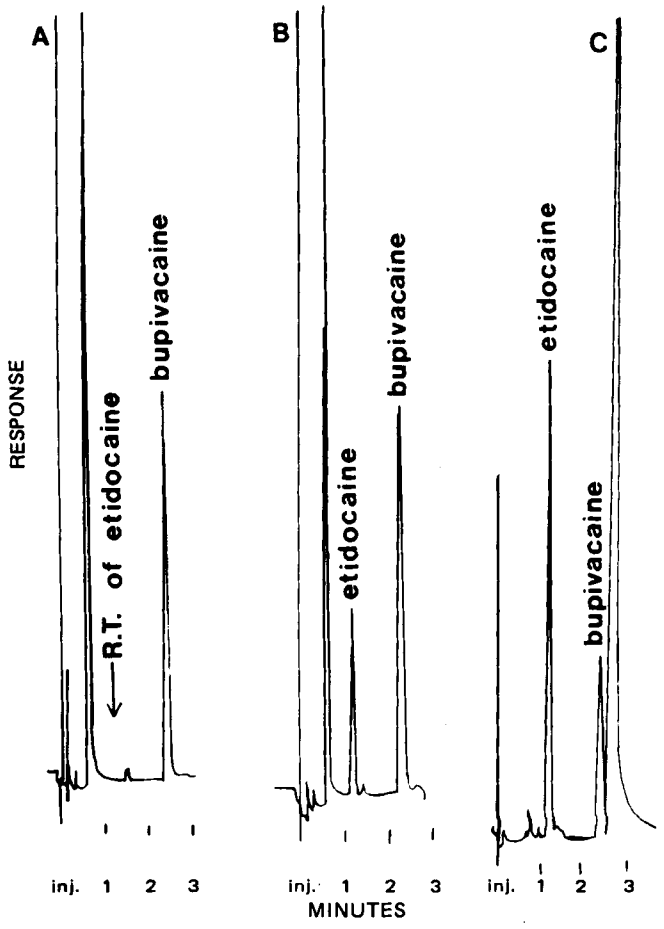

Figure 2—*Analysis of etidocaine extracted from plasma with bupivacaine (250 ng/ml) as the internal standard. Key: A, plasma blank (attenuation 128); B, 200 ng/ml of plasma standard (attenuation 128); and C, clinical sample (attenuation 256). Chromatographic conditions included a 183-cm × 2-mm (i.d.) column packed with 10% OV-1 on 100–120-mesh Gas Chrom Q, an injector temperature of 300°, a column temperature of 250°, a detector temperature of 350°, a carrier gas (helium) flow rate of 35 ml/min, and detector gases of hydrogen and air at flow rates of 5 and 50 ml/min, respectively.*

standard for etidocaine. The resolution obtained from the different columns is more of a function of the efficiency of the column, the carrier gas flow rate, and the temperature than of the stationary phase used. This effect is an added advantage since a particular column is not required, depending on the resolution requirements.

The plasma sample represented in Fig. 2C was one of 72 samples in a study involving anephric patients. The large peak eluting just after bupivacaine in this chromatogram was seen in the plasma of all of the patients studied but was not observed in the standards. Similar peaks, observed in samples collected in tubes with rubber stoppers, were identified by mass spectral analysis as the plasticizer tributoxyethyl phosphate. This phenomenon was reported by previous investigators (14), and it did not interfere with the analysis. By avoiding this plasticizer, the analysis time can be shortened; if high sensitivity is not required, the back-extraction step in sample preparation can be eliminated.

The analytical method works equally well for mepivacaine, bupivacaine, etidocaine, lidocaine, and tetracaine. However, tetracaine is hydrolyzed rapidly by plasma pseudocholinesterase, making its detection after normal doses extremely difficult (13). The minimum quantifiable level, defined as the concentration whose lower 80% confidence limit just encompasses zero[7], was ~20 ng/ml for each of the five drugs when duplicate standards of 0 and 50–500 ng/ml of the drug were used to produce the calibration curve. The minimum quantifiable level is dependent on the concentrations of the standards used, and lower values can be generated by using lower concentration standards. For example, a minimum quantifiable level of 0.8 ng/ml was calculated using duplicate mepivacaine standards of 0 and 2.5–20 ng/ml in plasma with bupivacaine as an internal standard. The practical limit of sensitivity is 2.5 ng/ml, with the size of the solvent front as the limiting factor. The standard error of the assay, calculated from the pure error term of the least-squares fit of the standards for three assays, using standards of 0 and 50–500 ng/ml was ±2 ng/ml.

The described method has proven to be simple, reliable, and sensitive, giving a linear response in the analysis of mepivacaine, bupivacaine, etidocaine, lidocaine, and tetracaine. Any of these compounds can be used as an internal standard for one or all of the others. Except for tetracaine, the sensitivity of the assay is well below that required to determine therapeutic levels and, for specific applications, can be extended to somewhat lower levels. Previously, this sensitivity was possible only through GLC–mass spectrometry. Since extensive start-up procedures and sample pretreatment are not required, the method is equally applicable to a single sample or numerous samples. It has been used to analyze plasma, cerebrospinal fluid, placental blood, and umbilical cord blood for drug concentrations.

[7] R. W. Ross, Jr., and H. Stander, paper presented at the Princeton Conference on Applied Statistics, Dec. 1975.

REFERENCES

(1) T. J. Goehl and C. Davison, *J. Pharm. Sci.*, **62**, 907 (1973).
(2) L. E. Mather and G. T. Tucker, *ibid.*, **63**, 306 (1974).
(3) B. J. Kline and M. F. Martin, *ibid.*, **67**, 887 (1978).
(4) G. T. Tucker, *Anesthesiology*, **32**, 255 (1970).
(5) N. Benowitz and M. Rowland, *ibid.*, **39**, 639 (1973).
(6) J. D. Cameron, *Clin. Chim. Acta*, **56**, 307 (1974).
(7) T. R. Irgins, W. M. Henderson, and W. H. Shelver, *J. Pharm. Sci.*, **65**, 608 (1976).
(8) H. B. Hucker and S. C. Stauffer, *ibid.*, **65**, 926 (1976).
(9) K. K. Adjepon-Yamoak and L. F. Prescott, *J. Pharm. Pharmacol.*, **26**, 889 (1974).
(10) R. F. Adams, F. C. Vandemark, and G. J. Schmidt, *Clin. Chim. Acta*, **69**, 515 (1976).
(11) E. C. Todd and D. T. Stafford, "Abstracts of the 1979 Pittsburgh Conference on Analytical Chemistry and Applied Spectroscopy," No. 710, Pittsburgh, Pa., Mar. 1979.
(12) C. Lindberg, M. Berg, L. O. Boreus, P. Hartvicj, K. E. Karlsson, C. Palmer, and A. M. Thoenblad, *Biomed. Mass Spectrom.*, **5**, 540 (1978).
(13) G. T. Mather and L. E. Tucker, *Clin. Pharmacokinet.*, **4**, 241 (1979).
(14) C. J. Dusci and L. P. Hackett, *Clin. Chem.*, **22**, 1236 (1976).

Dependence of Area under the Curve on Proquazone Particle Size and *In Vitro* Dissolution Rate

FRITZ NIMMERFALL and JOACHIM ROSENTHALER ˣ

Received November 14, 1979, from the *Pharmaceutical Department, Sandoz Ltd., Basel, Switzerland.* Accepted for publication January 11, 1980.

Abstract □ The *in vitro* dissolution and GI absorption of various sieve fractions of proquazone were studied (particle-size ranges of 45–74, 160–300, and 500–1000 μm). The dissolution rates of preparations F45, F160, and F500 were determined *in vitro* in a flow-through assembly in artificial gastric juice at 37°. The time required for 63% of the maximum amount of soluble drug to pass into solution was characterized by the dissolution variable τ_D. The *in vitro* dissolution rates for the preparations differed significantly in the order $\tau_{D,F45} < \tau_{D,F160} < \tau_{D,F500}$. After oral administration of 300 mg of the fractions to each of eight rhesus monkeys, the area under the plasma level–time curve (AUC) differed significantly in the order $AUC_{F45} > AUC_{F160} > AUC_{F500}$. The dissolution rate increased with decreasing particle size. The AUC increased with decreasing particle size and with increasing dissolution rate. These results indicate that the dissolution rate probably determines the extent of absorption when dissolution is rate limiting.

Keyphrases □ Proquazone—effect of particle size on area under the curve □ Dissolution rate, *in vitro*—proquazone, dependence on particle size □ Particle size—proquazone, effect on *in vitro* dissolution rate

After oral administration of solid dosage forms, absorption from the GI tract can be described as a sum of two consecutive transport processes: (*a*) dissolution of the drug from the dosage form (which produces a solution, micelles, or a solubilized entity), characterized by the dissolution rate constant k_1 for dissolution *in vivo;* and (*b*) transport of the drug to and through the intestinal membranes and its penetration into the general circulation, characterized by the total absorption rate constant k_2.

It is possible to distinguish between two fundamentally different cases (1): either the dissolution proceeds more slowly than the absorption ($k_1 < k_2$), or the absorption proceeds more slowly than the dissolution ($k_1 > k_2$). When $k_1 < k_2$, it should be possible to increase the absorption rate by increasing k_1 through a reduction in the particle size (2). When $k_1 > k_2$, a reduction in the particle size cannot affect the absorption rate.

The effect of particle size on relative absorbability has been demonstrated for several drugs, *e.g.*, griseofulvin (3), tetracycline (4), tolbutamide (5), and benoxaprofen (6). There also have been reviews on this subject (7–9). The relationship between particle surface area and GI absorption holds when absorption is dissolution rate limited, *i.e.*, when $k_1 < k_2$. For example, for proquazone, with a saturation solubility of 0.1% in artificial gastric juice, the area under the curve as a function of particle size and as a function of the *in vitro* dissolution rate was investigated. Proquazone[1] (I) is a quinazolidine anti-inflammatory drug.

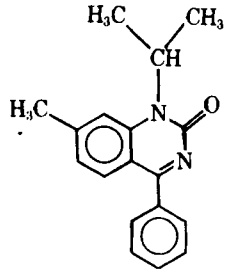

I

EXPERIMENTAL

The experimental preparation was crystallized from ethyl acetate. A sonic sifter[2] followed by an air-jet sieve[3] was used to fractionate the product into the following ranges: 45–74 μm (F45), 160–300 μm (F160), and 500–1000 μm (F500). Care was taken to ensure that the particle-size ranges did not overlap. The experimental fractions were packed by hand in hard gelatin capsules for oral administration. The packing appeared to be very loose when the content was inspected.

The measurement of the dissolution rate was carried out in a flow-through assembly at a rate of 33 ml/min and at 37° (10). The solvent consisted of 0.082 *N* HCl and 0.034 *M* NaCl at pH 1.2. Samples were drawn after 5, 10, 15, 20, 25, 30, 45, 60, 90, 120, 180, and 240 min. The concentration of free drug was determined spectrophotometrically at 232 nm.

Male rhesus monkeys (*Macaca mulatta*), ~3 years old and 8–10 kg, received no food for a period extending from 20 hr before administration to 4 hr after it, but they had free access to water. A 300-mg proquazone

[1] Biarison, Sandoz Ltd.
[2] Allen Bradley, Fisher Scientific Co.
[3] Alpine, Augsburg, West Germany.

0022-3549/80/0500-0605$01.00/0

© 1980, American Pharmaceutical Association

REFERENCES

(1) T. J. Goehl and C. Davison, *J. Pharm. Sci.*, **62**, 907 (1973).
(2) L. E. Mather and G. T. Tucker, *ibid.*, **63**, 306 (1974).
(3) B. J. Kline and M. F. Martin, *ibid.*, **67**, 887 (1978).
(4) G. T. Tucker, *Anesthesiology*, **32**, 255 (1970).
(5) N. Benowitz and M. Rowland, *ibid.*, **39**, 639 (1973).
(6) J. D. Cameron, *Clin. Chim. Acta*, **56**, 307 (1974).
(7) T. R. Irgins, W. M. Henderson, and W. H. Shelver, *J. Pharm. Sci.*, **65**, 608 (1976).
(8) H. B. Hucker and S. C. Stauffer, *ibid.*, **65**, 926 (1976).
(9) K. K. Adjepon-Yamoak and L. F. Prescott, *J. Pharm. Pharmacol.*, **26**, 889 (1974).
(10) R. F. Adams, F. C. Vandemark, and G. J. Schmidt, *Clin. Chim. Acta*, **69**, 515 (1976).
(11) E. C. Todd and D. T. Stafford, "Abstracts of the 1979 Pittsburgh Conference on Analytical Chemistry and Applied Spectroscopy," No. 710, Pittsburgh, Pa., Mar. 1979.
(12) C. Lindberg, M. Berg, L. O. Boreus, P. Hartvicj, K. E. Karlsson, C. Palmer, and A. M. Thoenblad, *Biomed. Mass Spectrom.*, **5**, 540 (1978).
(13) G. T. Mather and L. E. Tucker, *Clin. Pharmacokinet.*, **4**, 241 (1979).
(14) C. J. Dusci and L. P. Hackett, *Clin. Chem.*, **22**, 1236 (1976).

Dependence of Area under the Curve on Proquazone Particle Size and *In Vitro* Dissolution Rate

FRITZ NIMMERFALL and JOACHIM ROSENTHALER ˣ

Received November 14, 1979, from the *Pharmaceutical Department, Sandoz Ltd., Basel, Switzerland.* Accepted for publication January 11, 1980.

Abstract □ The *in vitro* dissolution and GI absorption of various sieve fractions of proquazone were studied (particle-size ranges of 45–74, 160–300, and 500–1000 μm). The dissolution rates of preparations F45, F160, and F500 were determined *in vitro* in a flow-through assembly in artificial gastric juice at 37°. The time required for 63% of the maximum amount of soluble drug to pass into solution was characterized by the dissolution variable τ_D. The *in vitro* dissolution rates for the preparations differed significantly in the order $\tau_{D,F45} < \tau_{D,F160} < \tau_{D,F500}$. After oral administration of 300 mg of the fractions to each of eight rhesus monkeys, the area under the plasma level–time curve (AUC) differed significantly in the order $AUC_{F45} > AUC_{F160} > AUC_{F500}$. The dissolution rate increased with decreasing particle size. The AUC increased with decreasing particle size and with increasing dissolution rate. These results indicate that the dissolution rate probably determines the extent of absorption when dissolution is rate limiting.

Keyphrases □ Proquazone—effect of particle size on area under the curve □ Dissolution rate, *in vitro*—proquazone, dependence on particle size □ Particle size—proquazone, effect on *in vitro* dissolution rate

After oral administration of solid dosage forms, absorption from the GI tract can be described as a sum of two consecutive transport processes: (*a*) dissolution of the drug from the dosage form (which produces a solution, micelles, or a solubilized entity), characterized by the dissolution rate constant k_1 for dissolution *in vivo;* and (*b*) transport of the drug to and through the intestinal membranes and its penetration into the general circulation, characterized by the total absorption rate constant k_2.

It is possible to distinguish between two fundamentally different cases (1): either the dissolution proceeds more slowly than the absorption ($k_1 < k_2$), or the absorption proceeds more slowly than the dissolution ($k_1 > k_2$). When $k_1 < k_2$, it should be possible to increase the absorption rate by increasing k_1 through a reduction in the particle size (2). When $k_1 > k_2$, a reduction in the particle size cannot affect the absorption rate.

The effect of particle size on relative absorbability has been demonstrated for several drugs, *e.g.*, griseofulvin (3), tetracycline (4), tolbutamide (5), and benoxaprofen (6). There also have been reviews on this subject (7–9). The relationship between particle surface area and GI absorption holds when absorption is dissolution rate limited, *i.e.*, when $k_1 < k_2$. For example, for proquazone, with a saturation solubility of 0.1% in artificial gastric juice, the area under the curve as a function of particle size and as a function of the *in vitro* dissolution rate was investigated. Proquazone[1] (I) is a quinazolidine anti-inflammatory drug.

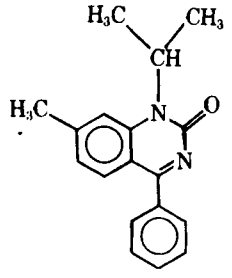

I

EXPERIMENTAL

The experimental preparation was crystallized from ethyl acetate. A sonic sifter[2] followed by an air-jet sieve[3] was used to fractionate the product into the following ranges: 45–74 μm (F45), 160–300 μm (F160), and 500–1000 μm (F500). Care was taken to ensure that the particle-size ranges did not overlap. The experimental fractions were packed by hand in hard gelatin capsules for oral administration. The packing appeared to be very loose when the content was inspected.

The measurement of the dissolution rate was carried out in a flow-through assembly at a rate of 33 ml/min and at 37° (10). The solvent consisted of 0.082 *N* HCl and 0.034 *M* NaCl at pH 1.2. Samples were drawn after 5, 10, 15, 20, 25, 30, 45, 60, 90, 120, 180, and 240 min. The concentration of free drug was determined spectrophotometrically at 232 nm.

Male rhesus monkeys (*Macaca mulatta*), ~3 years old and 8–10 kg, received no food for a period extending from 20 hr before administration to 4 hr after it, but they had free access to water. A 300-mg proquazone

[1] Biarison, Sandoz Ltd.
[2] Allen Bradley, Fisher Scientific Co.
[3] Alpine, Augsburg, West Germany.

0022-3549/80/0500-0605$01.00/0

© 1980, American Pharmaceutical Association

Table I—*In Vitro* Dissolution Rate (Percent Dissolved) at a Given Time

Minutes	F45 Mean[a]	F45 SD[b]	F160 Mean	F160 SD	F500 Mean	F500 SD
5	8.6	4.4	4.2	1.2	2.5	0.6
10	43.1	2.9	13.1	1.4	6.8	0.7
15	68.6	4.1	21.9	2.0	10.8	0.7
20	81.5	4.0	30.5	2.2	14.9	1.1
25	85.5	3.7	38.3	2.0	18.9	1.3
30	88.6	3.2	45.4	2.5	22.9	1.5
45	93.2	2.4	61.9	2.2	33.0	1.9
60	95.6	2.3	73.9	1.8	46.9	10.2
90	97.6	2.0	88.2	1.3	60.7	8.5
120	97.7	2.7	94.8	1.0	68.5	2.6
180	97.6	2.3	98.7	0.6	83.8	1.8
240	96.7	2.6	99.2	1.0	91.7	2.3
τ_D, min[c]	8.5	1.2	42.8	2.9	93.1	9.8

[a] Three determinations. [b] Standard deviation. [c] Values for the time where 63% of the maximum amount of soluble drug passes into solution were obtained using the Weibull distribution. This distribution is a general linearization function that was described for dissolution rate curves (17). The τ_D values were estimated according to a plot that was obtained using the published empirical function (14) and, therefore, may not necessarily correspond to the experimental timing where 63% of the drug was dissolved.

capsule was administered to each animal orally by provoking a swallowing reflex with the finger. The capsule was rinsed down with 5 ml of tap water. Blood, 2.5 ml, was drawn at 0, 0.33, 0.66, 1, 1.5, 2, 2.5, 3, 4, 6, 8, and 24 hr.

The fluorometric method detected the unchanged compound and the 7-hydroxymethyl metabolite in the plasma. The plasma concentration is expressed in nanogram equivalents of proquazone per milliliter. By the addition of 2 *N* sodium carbonate, the alkaline plasma sample (1 ml) was extracted into *n*-heptane. This sample was reextracted into 5 *N* aqueous HCl. The compound was excited at 326 nm, and its emission was measured at 510 nm.

For the *in vitro* dissolution experiments, the homogeneity of the mean values was tested by simple analysis of variance and the differences between mean values were tested by the Student–Newman–Keuls test (11).

The plan for the experiments in laboratory animals was arranged according to two independent random designs based on 4 × 4 Latin squares. Since another proquazone preparation had to be tested, it was included in the experimental design but was not evaluated further. The homogeneity of the mean values was tested by analysis of variance for repeated Latin squares (12), and the distinction between mean values was verified by Tukey's test (13).

RESULTS AND DISCUSSION

The experiments on the dissolution rate were evaluated by means of the dissolution variable τ_D (14). The τ_D value is the time in minutes during which 63% of the maximum amount of soluble drug passes into solution.

Table II—Mean Plasma Level Data[a] (Nanogram Equivalents per Milliliter) for Proquazone

Hours	F45 Mean	F45 SD[b]	F160 Mean	F160 SD	F500 Mean	F500 SD
0	0		0		0	
0.33	229	266	41	80	11	15
0.66	834	727	84	125	66	60
1	1191	798	106	146	83	61
1.5	1217	820	116	141	76	47
2	830	563	122	127	62	40
2.5	601	297	101	107	57	41
3	509	238	125	109	56	71
4	357	185	159	165	64	87
6	231	118	149	98	61	88
8	152	71	75	36	56	59
24	153	182	105	97	43	24
AUC[c]	6156	3159	1966	674	986	499

[a] Experiments were conducted in eight rhesus monkeys after oral gavage of various sieve fractions of the drug: F45 (45–74 μm), F160 (160–300 μm), and F500 (500–1000 μm). [b] Standard deviation. [c] The area under the plasma level–time curve (*AUC*) (nanogram equivalents per milliliter per hour) was estimated by an approximate integration formula, the trapezoidal rule.

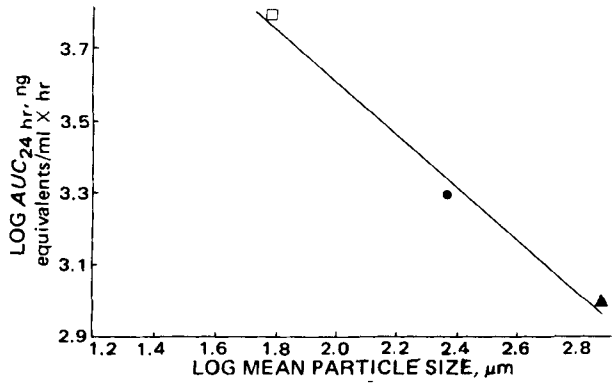

Figure 1—*Linear relationship between the logarithm of the mean value of the area under the plasma level–time curve* (AUC) *and the logarithm of the mean value of the particle size for preparations F45 (45–74 μm, □), F160 (160–300 μm, ●), and F500 (500–1000 μm, ▲).*

In the experiments in rhesus monkeys, three of the animals had to be replaced. The influence of the particular animal was negligible in comparison with the clearly significant effect of the product; *i.e.*, the variance component caused by the animals was about three times less than that caused by the product. Blood samples could only be obtained up to a maximum period of 24 hr because of sampling difficulties. Therefore, the area under the plasma concentration–time curve (*AUC*) was integrated up to 24 hr employing the trapezoidal rule.

The fluorometric analysis was carried out on plasma samples on the assumption that there was a constant distribution of the drug and metabolites between plasma and blood cells. From *in vitro* binding experiments using human blood, the quantity of drug and metabolites bound to blood cells was known to amount to ~20%. To comply with the conditions necessary for the analysis of variance, the figures for the *AUC* were submitted to a logarithmic transformation. Because of the small number of particle-size ranges investigated, no attempt was made to establish quantitative correlative equations. Nalimov's test was applied to the measurements to detect outliers before statistical analysis (15). Significant outliers ($p < 0.01$) were replaced by the next highest or the next lowest value (16).

Table I shows that the *in vitro* dissolution rate increased with decreasing particle size. The statistical analysis of the dissolution variable, τ_D, of preparations F45, F160, and F500 yielded the following significant series ($p = 0.01$): $\tau_{D,F45} < \tau_{D,F160} < \tau_{D,F500}$. By calculation, log τ_D for F45, F160, and F500 for the particle-size ranges investigated was a linear function of the logarithm of the mean particle size.

The mean plasma level–time profile (Table II) shows characteristic differences. Preparation F45 yielded a peak value (1217 ng equivalents/ml) at 1.5 hr, and this value was much higher than those obtained for F160 and F500, which were 159 ng equivalents/ml at 4 hr and 83 ng equivalents/ml at 1 hr, respectively. From this result, it can be concluded that the relationship between the plasma level and particle size is particularly

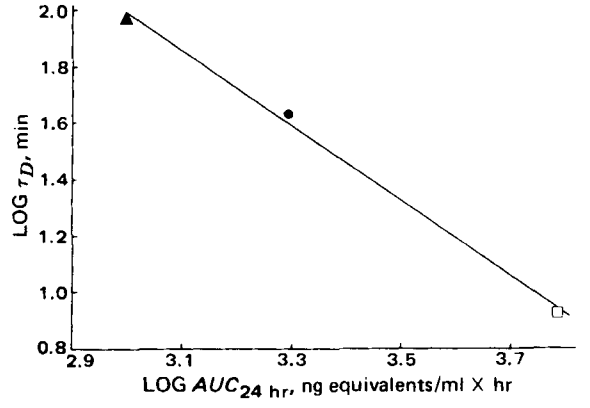

Figure 2—*Linear relationship between the logarithm of the area under the plasma level–time curve* (AUC) *and the logarithm of the mean value of the dissolution variable, τ_D, of proquazone for preparations F45 (45–74 μm, □), F160 (160–300 μm, ●), and F500 (500–1000 μm, ▲).*

critical when it exceeds a certain range, *i.e.*, 45–74 μm. The statistical analysis of the area under the curve (Table II) yielded the following sequence: $AUC_{F45} > AUC_{F160} > AUC_{F500}$. Figure 1 shows that for these preparations, there was a nearly linear relationship between the logarithm of the area under the curve and the logarithm of the mean particle size in the particle-size range investigated. Therefore, the dissolution of the drug in the intestines appears to constitute the rate-limiting step for the whole process of intestinal absorption; *i.e.*, $k_1 < k_2$.

Figure 2 shows a clear linear relationship between the logarithm of the area under the curve and log τ_D. The statistically significant difference between the area under the curve and τ_D for the preparations suggests that there is a genuine correlation between the *AUC* and the *in vitro* dissolution rate.

These results indicate that it may be possible, in principle, to estimate the *AUC* from the *in vitro* dissolution rate. The same correlation probably is obtained for any drug where dissolution is the rate-limiting step in absorption.

REFERENCES

(1) R. R. Levine, in "Topics in Medicinal Chemistry," vol. 4, J. L. Rabinowitz and R. M. Myerson, Eds., Wiley–Interscience, New York, N.Y., 1971, p. 58.

(2) W. A. Ritschel, in "Angewandte Biopharmazie," Wissenschaftliche Verlagsgesellschaft, Stuttgart, West Germany, 1973, p. 297.

(3) R. M. Atkinson, C. Bedford, K. J. Child, and E. G. Tomich, *Nature*, **193**, 588 (1962).

(4) E. Nelson, *J. Am. Pharm. Assoc., Sci. Ed.*, **48**, 96 (1959).

(5) E. Nelson, S. Long, and J. G. Wagner, *J. Pharm. Sci.*, **53**, 1224 (1964).

(6) A. S. Ridolfo, L. Thompkins, L. D. Bechtol, and R. H. Carmichael, *ibid.*, **68**, 850 (1979).

(7) G. Levy, *Am. J. Pharm.*, **135**, 78 (1963).

(8) J. H. Fincher, *J. Pharm. Sci.*, **57**, 1825 (1968).

(9) J. Blanchard, *Am. J. Pharm.*, **150**, 132 (1978).

(10) C. Cakiryildiz, P. J. Metha, W. Rahmen, and D. Schoenleber, *J. Pharm. Sci.*, **64**, 1692 (1975).

(11) L. Sachs, "Statistische Auswertungsmethoden," 2nd ed., Springer-Verlag, Berlin, Germany, 1969, p. 512.

(12) E. Walter, "Statistische Methoden, Teil 1: Grundlagen und Versuchsplanung," Springer-Verlag, Berlin, Germany, 1970, p. 256.

(13) E. Weber, "Grundriss der Biologischen Statistik," 7th ed., VEB Gustav Fischer-Verlag, Jena, East Germany, 1972, p. 262.

(14) F. Langenbucher, *Pharm. Ind.*, **38**, 472 (1976).

(15) R. Kaiser, *Chromatographia*, **4**, 126 (1971).

(16) L. Sachs, "Statistische Auswertungsmethoden," 2nd ed., Springer-Verlag, Berlin, Germany, 1969, p. 281.

(17) F. Langenbucher, *J. Pharm. Pharmacol.*, **24**, 979 (1972).

ACKNOWLEDGMENTS

The authors thank Mrs. C. Adas for the *in vitro* dissolution experiments, Dr. D. Schoenleber for the sieve fractions, and Dr. W. Pacha for the fluorometric analysis.

COMMUNICATIONS

Correlation between Porosity and Dissolution Rate Constants for Disintegrating Tablets

Keyphrases □ Correlation coefficients—disintegrating tablets, relationship between porosity and dissolution rate □ Disintegration—tablets, correlation between porosity and dissolution rate □ Dissolution rate—correlation with porosity for disintegrating tablets □ Tablet disintegration—correlation between porosity and dissolution rate

To the Editor:

The importance of tablet porosity from a mechanical point of view has been discussed extensively (1, 2). Porosity also has been linked to the release characteristics of drugs from dosage forms and enters directly into the Higuchi square root law for dissolution (3). In the latter case, both penetration and diffusion characteristics are important.

There are cases in which tablets disintegrate and where the dissolution is relatively rapid so that the dissolution is a function of the disintegration (4, 5). However, there are cases in which tablets disintegrate fairly rapidly and where the dissolution is dictated by the rapid penetration of water into the granule. If the dissolution of the active ingredient and its diffusion out through the granule are rapid in relation to the penetration, then the dissolution is given by the amount of water that penetrates, *i.e.*, by an equation of the type described by Jost (6, 7):

$$\ln (m/m_0) = -k(t - t_i) \qquad \text{(Eq. 1)}$$

where m is the undissolved mass at time t, t_i is the disintegration time, and k is the dissolution constant (in reciprocal time units). Since the penetration rate is expected to be a function of the porosity, ϵ, of the tablet, then k also should be a function of ϵ. This argument assumes that the granules after disintegration have the same porosity as did the tablet before disintegration (8).

In a recent study in these laboratories, tablets were formed from granulations made by several processes: (*a*) fluid bed granulation[1], (*b*) chopper–ribbon blender[2], (*c*) chopper–ribbon blender followed by an oscillating granulator, and (*d*) chopper–ribbon blender followed by a rotating granulator[3]. The formula used was equal parts of dibasic calcium phosphate (anhydrous) and sulfanilamide granulated with 0.7 parts of 5% cornstarch paste. Drying was carried out to 1% loss on drying. Several differences were observed among these processes, and the phenomena related to dissolution and porosity will be discussed.

The granulations were screened and separated into four size fractions (<315, 315–400, 400–630, and >630 μm). Each fraction was compressed at three machine pressures (1200, 2400, and 3600 kg), and the resulting 12 batches of tablets from the four manufacturing procedures were subjected to dissolution tests by the beaker method (9). The porosities were measured using a mercury porosimeter.

The dissolution tests followed the relationship expressed in Eq. 1, and the prepared tablets had dissolution rate constants described by:

$$k = a_i + b_i\epsilon \qquad \text{(Eq. 2)}$$

[1] Glatt Lufttechnische Apparate, Maltingen, Binzen/Baden, West Germany.
[2] Lödige Maschinen Bau, GmBH, 479 Paderborn, West Germany.
[3] Erweka Apparatebau, GmBH, 6056 Heusenstamm, West Germany.

0022-3549/80/0500-0607$01.00/0

© 1980, American Pharmaceutical Association

critical when it exceeds a certain range, *i.e.*, 45–74 μm. The statistical analysis of the area under the curve (Table II) yielded the following sequence: $AUC_{F45} > AUC_{F160} > AUC_{F500}$. Figure 1 shows that for these preparations, there was a nearly linear relationship between the logarithm of the area under the curve and the logarithm of the mean particle size in the particle-size range investigated. Therefore, the dissolution of the drug in the intestines appears to constitute the rate-limiting step for the whole process of intestinal absorption; *i.e.*, $k_1 < k_2$.

Figure 2 shows a clear linear relationship between the logarithm of the area under the curve and log τ_D. The statistically significant difference between the area under the curve and τ_D for the preparations suggests that there is a genuine correlation between the *AUC* and the *in vitro* dissolution rate.

These results indicate that it may be possible, in principle, to estimate the *AUC* from the *in vitro* dissolution rate. The same correlation probably is obtained for any drug where dissolution is the rate-limiting step in absorption.

REFERENCES

(1) R. R. Levine, in "Topics in Medicinal Chemistry," vol. 4, J. L. Rabinowitz and R. M. Myerson, Eds., Wiley–Interscience, New York, N.Y., 1971, p. 58.

(2) W. A. Ritschel, in "Angewandte Biopharmazie," Wissenschaftliche Verlagsgesellschaft, Stuttgart, West Germany, 1973, p. 297.

(3) R. M. Atkinson, C. Bedford, K. J. Child, and E. G. Tomich, *Nature*, **193**, 588 (1962).

(4) E. Nelson, *J. Am. Pharm. Assoc., Sci. Ed.*, **48**, 96 (1959).

(5) E. Nelson, S. Long, and J. G. Wagner, *J. Pharm. Sci.*, **53**, 1224 (1964).

(6) A. S. Ridolfo, L. Thompkins, L. D. Bechtol, and R. H. Carmichael, *ibid.*, **68**, 850 (1979).

(7) G. Levy, *Am. J. Pharm.*, **135**, 78 (1963).

(8) J. H. Fincher, *J. Pharm. Sci.*, **57**, 1825 (1968).

(9) J. Blanchard, *Am. J. Pharm.*, **150**, 132 (1978).

(10) C. Cakiryildiz, P. J. Metha, W. Rahmen, and D. Schoenleber, *J. Pharm. Sci.*, **64**, 1692 (1975).

(11) L. Sachs, "Statistische Auswertungsmethoden," 2nd ed., Springer-Verlag, Berlin, Germany, 1969, p. 512.

(12) E. Walter, "Statistische Methoden, Teil 1: Grundlagen und Versuchsplanung," Springer-Verlag, Berlin, Germany, 1970, p. 256.

(13) E. Weber, "Grundriss der Biologischen Statistik," 7th ed., VEB Gustav Fischer-Verlag, Jena, East Germany, 1972, p. 262.

(14) F. Langenbucher, *Pharm. Ind.*, **38**, 472 (1976).

(15) R. Kaiser, *Chromatographia*, **4**, 126 (1971).

(16) L. Sachs, "Statistische Auswertungsmethoden," 2nd ed., Springer-Verlag, Berlin, Germany, 1969, p. 281.

(17) F. Langenbucher, *J. Pharm. Pharmacol.*, **24**, 979 (1972).

ACKNOWLEDGMENTS

The authors thank Mrs. C. Adas for the *in vitro* dissolution experiments, Dr. D. Schoenleber for the sieve fractions, and Dr. W. Pacha for the fluorometric analysis.

COMMUNICATIONS

Correlation between Porosity and Dissolution Rate Constants for Disintegrating Tablets

Keyphrases □ Correlation coefficients—disintegrating tablets, relationship between porosity and dissolution rate □ Disintegration—tablets, correlation between porosity and dissolution rate □ Dissolution rate—correlation with porosity for disintegrating tablets □ Tablet disintegration—correlation between porosity and dissolution rate

To the Editor:

The importance of tablet porosity from a mechanical point of view has been discussed extensively (1, 2). Porosity also has been linked to the release characteristics of drugs from dosage forms and enters directly into the Higuchi square root law for dissolution (3). In the latter case, both penetration and diffusion characteristics are important.

There are cases in which tablets disintegrate and where the dissolution is relatively rapid so that the dissolution is a function of the disintegration (4, 5). However, there are cases in which tablets disintegrate fairly rapidly and where the dissolution is dictated by the rapid penetration of water into the granule. If the dissolution of the active ingredient and its diffusion out through the granule are rapid in relation to the penetration, then the dissolution is given by the amount of water that penetrates, *i.e.*, by an equation of the type described by Jost (6, 7):

$$\ln (m/m_0) = -k(t - t_i) \qquad \text{(Eq. 1)}$$

where m is the undissolved mass at time t, t_i is the disintegration time, and k is the dissolution constant (in reciprocal time units). Since the penetration rate is expected to be a function of the porosity, ϵ, of the tablet, then k also should be a function of ϵ. This argument assumes that the granules after disintegration have the same porosity as did the tablet before disintegration (8).

In a recent study in these laboratories, tablets were formed from granulations made by several processes: (*a*) fluid bed granulation[1], (*b*) chopper–ribbon blender[2], (*c*) chopper–ribbon blender followed by an oscillating granulator, and (*d*) chopper–ribbon blender followed by a rotating granulator[3]. The formula used was equal parts of dibasic calcium phosphate (anhydrous) and sulfanilamide granulated with 0.7 parts of 5% cornstarch paste. Drying was carried out to 1% loss on drying. Several differences were observed among these processes, and the phenomena related to dissolution and porosity will be discussed.

The granulations were screened and separated into four size fractions (<315, 315–400, 400–630, and >630 μm). Each fraction was compressed at three machine pressures (1200, 2400, and 3600 kg), and the resulting 12 batches of tablets from the four manufacturing procedures were subjected to dissolution tests by the beaker method (9). The porosities were measured using a mercury porosimeter.

The dissolution tests followed the relationship expressed in Eq. 1, and the prepared tablets had dissolution rate constants described by:

$$k = a_i + b_i\epsilon \qquad \text{(Eq. 2)}$$

[1] Glatt Lufttechnische Apparate, Maltingen, Binzen/Baden, West Germany.
[2] Lödige Maschinen Bau, GmBH, 479 Paderborn, West Germany.
[3] Erweka Apparatebau, GmBH, 6056 Heusenstamm, West Germany.

0022-3549/80/0500-0607$01.00/0

© 1980, American Pharmaceutical Association

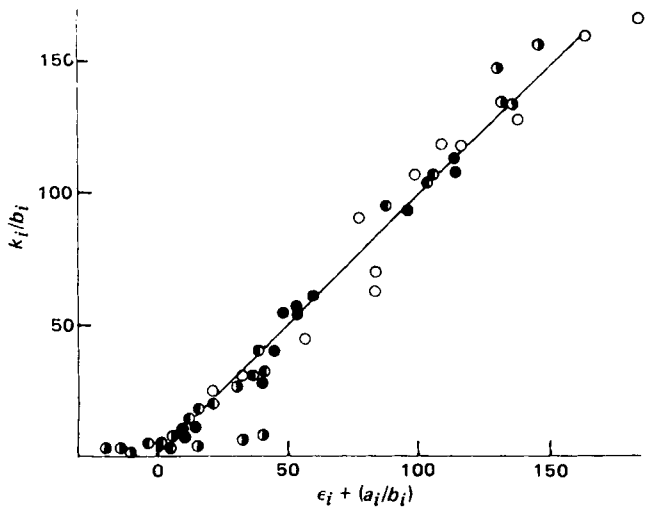

Figure 1—*Plot of* k_i/b_i versus $\epsilon_i + (a_i/b_i)$ *according to Eq. 3. Key:* ○, *chopper–ribbon blender;* ●, *chopper–ribbon blender followed by an oscillating granulator;* ◐, *chopper–ribbon blender followed by a rotating granulator; and* ◑, *fluid bed granulation.*

where a_i and b_i are constants and the subscript i refers to the ith condition (sieve fraction, manufacturing method, or compression pressure). The constants a and b are functions of these variables. Therefore, there are 48 lines corresponding to Eq. 1. The correlation coefficients generally were >0.94, and it is possible to tabulate all 48 values or draw 48 regression lines on one graph. For graphical presentation, a method (10) was used for which the data for each condition were recast in the following form:

$$k/b_i = \epsilon + (a_i/b_i) \qquad \text{(Eq. 3)}$$

where k/b_i and $\epsilon + (a_i/b_i)$ are dimensionless parameters. When one parameter is plotted as a function of the other, a straight line with a unity slope and a zero intercept should result. The 48 data points are plotted in Fig. 1 (the origin is offset), which shows visual agreement with the statements. The treatment is not statistical since the two variables (the left- and right-hand expressions in Eq. 3) are not independent. If a least-squares fit is drawn, the following relationship is obtained:

$$k/b_i = (0.98 \pm 0.05)[\epsilon + (a_i/b_i)] + (0.22 \pm 0.30) \qquad \text{(Eq. 4)}$$

in accordance with a unity slope and a zero intercept.

Equation 3 includes all of the data points, but Fig. 1 shows that the relationship fails at very low porosity values (high compression pressures). The four cases where $-a_i/b_i > \epsilon_i$ [*i.e.*, where values of $\epsilon_i + (a_i/b_i)$ are negative] do not seem to be part of the line. In these four cases, the adherence to Eq. 1 also was marginal (the correlation coefficients for these four points were 0.85–0.91), whereas the agreement was good to excellent in all of the other cases (*i.e.*, correlation coefficients of >0.94).

The data and the treatment show that there is a correlation between the dissolution constants, k, and the porosity, ϵ, in the case where a tablet disintegrates into porous granules and the limiting process is the penetration of water into the dislodged granule.

(1) T. Higuchi, R. D. Arnold, S. J. Tucker, and L. W. Busse, *J. Am. Pharm. Assoc., Sci. Ed.*, **41**, 93 (1952).
(2) J. B. Schwartz, *J. Pharm. Sci.*, **63**, 774 (1974).
(3) T. Higuchi, *ibid.*, **52**, 1145 (1963).
(4) J. T. Carstensen, J. L. Wright, K. W. Blessel, and J. Sheridan, *ibid.*, **67**, 48 (1978).
(5) *Ibid.*, **67**, 982 (1978).
(6) J. T. Carstensen, in "Dissolution Technology," L. Leeson and J. T. Carstensen, Eds., APhA Academy of Pharmaceutical Sciences, Washington, D.C., 1974, p. 189.
(7) W. Jost, "Diffusion in Solids, Liquids and Gases," Academic, New York, N.Y., 1952, pp. 45–47.
(8) A. B. Selkirk, *J. Pharm. Pharmacol.*, **25**, 258 (1973).
(9) G. Levy and B. Hayes, *N. Engl. J. Med.*, **262**, 1053 (1960).
(10) J. T. Carstensen, R. Kothari, V. K. Prasad, and J. Sheridan, *J. Pharm. Sci.*, **69**, 290 (1980).

Odile Cruaud
Dominique Duchêne
Francis Puisieux
J. T. Carstensen *x
Faculte de Pharmacie
Laboratoire Galenique
Universite de Paris-Sud
92290, Chatenay-Malabry, France

Received August 4, 1978.
Accepted for publication December 21, 1979.
* Sabbatical year. Current address: School of Pharmacy, University of Wisconsin, Madison, WI 53706.

Identification of Subvisible Barium Sulfate Crystals in Parenteral Solutions

Keyphrases □ Barium sulfate—crystal formation in commercial parenteral solutions, identification by polarizing microscopy, scanning electron microscopy, micro X-ray powder diffraction, and micro Raman spectroscopy □ Parenteral solutions, commercial—barium sulfate crystal formation, identification by polarizing microscopy, scanning electron microscopy, micro X-ray powder diffraction, and micro Raman spectroscopy □ Crystals—barium sulfate formation in commercial parenteral solutions, characterization by polarizing microscopy, scanning electron microscopy, micro X-ray powder diffraction, and micro Raman spectroscopy

To the Editor:

Concern about the presence of particulate matter in parenteral products is increasing, and certain harmful effects when such contamination is introduced into the body during intravenous therapy have been described (1–4). Additionally, studies in our laboratory implicated particulate contamination in infusion fluids as a cause of phlebitis (5–7).

To gain insight into the nature and clinical significance of particulate matter in intravenous solutions, an extensive research program has been undertaken in cooperation with the Food and Drug Administration, which includes the identification of particulate matter in parenteral products. During this investigation, barium sulfate crystals were isolated and identified in six parenteral solutions packaged both in sealed glass ampuls and in glass vials with rubber stoppers. The conclusive identification of barium sulfate crystals was achieved through the correlation of analytical data from polarizing microscopy, scanning electron microscopy with energy-dispersive X-ray analysis capability, micro X-ray powder diffraction, and micro Raman spectroscopy.

With the polarizing microscope, barium sulfate crystals isolated from the parenteral solutions appeared as single or agglomerated, well-formed, birefringent crystals, 8–30

0022-3549/80/0500-0608$01.00/0
© 1980, American Pharmaceutical Association

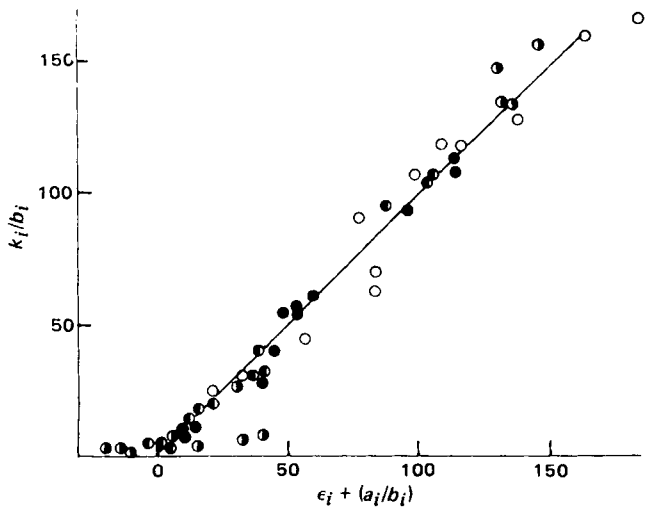

Figure 1—*Plot of* k_i/b_i versus $\epsilon_i + (a_i/b_i)$ *according to Eq. 3. Key:* ○, *chopper–ribbon blender;* ●, *chopper–ribbon blender followed by an oscillating granulator;* ◐, *chopper–ribbon blender followed by a rotating granulator; and* ◑, *fluid bed granulation.*

where a_i and b_i are constants and the subscript i refers to the ith condition (sieve fraction, manufacturing method, or compression pressure). The constants a and b are functions of these variables. Therefore, there are 48 lines corresponding to Eq. 1. The correlation coefficients generally were >0.94, and it is possible to tabulate all 48 values or draw 48 regression lines on one graph. For graphical presentation, a method (10) was used for which the data for each condition were recast in the following form:

$$k/b_i = \epsilon + (a_i/b_i) \qquad \text{(Eq. 3)}$$

where k/b_i and $\epsilon + (a_i/b_i)$ are dimensionless parameters. When one parameter is plotted as a function of the other, a straight line with a unity slope and a zero intercept should result. The 48 data points are plotted in Fig. 1 (the origin is offset), which shows visual agreement with the statements. The treatment is not statistical since the two variables (the left- and right-hand expressions in Eq. 3) are not independent. If a least-squares fit is drawn, the following relationship is obtained:

$$k/b_i = (0.98 \pm 0.05)[\epsilon + (a_i/b_i)] + (0.22 \pm 0.30) \qquad \text{(Eq. 4)}$$

in accordance with a unity slope and a zero intercept.

Equation 3 includes all of the data points, but Fig. 1 shows that the relationship fails at very low porosity values (high compression pressures). The four cases where $-a_i/b_i > \epsilon_i$ [*i.e.*, where values of $\epsilon_i + (a_i/b_i)$ are negative] do not seem to be part of the line. In these four cases, the adherence to Eq. 1 also was marginal (the correlation coefficients for these four points were 0.85–0.91), whereas the agreement was good to excellent in all of the other cases (*i.e.*, correlation coefficients of >0.94).

The data and the treatment show that there is a correlation between the dissolution constants, k, and the porosity, ϵ, in the case where a tablet disintegrates into porous granules and the limiting process is the penetration of water into the dislodged granule.

(1) T. Higuchi, R. D. Arnold, S. J. Tucker, and L. W. Busse, *J. Am. Pharm. Assoc., Sci. Ed.*, **41**, 93 (1952).
(2) J. B. Schwartz, *J. Pharm. Sci.*, **63**, 774 (1974).
(3) T. Higuchi, *ibid.*, **52**, 1145 (1963).
(4) J. T. Carstensen, J. L. Wright, K. W. Blessel, and J. Sheridan, *ibid.*, **67**, 48 (1978).
(5) *Ibid.*, **67**, 982 (1978).
(6) J. T. Carstensen, in "Dissolution Technology," L. Leeson and J. T. Carstensen, Eds., APhA Academy of Pharmaceutical Sciences, Washington, D.C., 1974, p. 189.
(7) W. Jost, "Diffusion in Solids, Liquids and Gases," Academic, New York, N.Y., 1952, pp. 45–47.
(8) A. B. Selkirk, *J. Pharm. Pharmacol.*, **25**, 258 (1973).
(9) G. Levy and B. Hayes, *N. Engl. J. Med.*, **262**, 1053 (1960).
(10) J. T. Carstensen, R. Kothari, V. K. Prasad, and J. Sheridan, *J. Pharm. Sci.*, **69**, 290 (1980).

Odile Cruaud
Dominique Duchêne
Francis Puisieux
J. T. Carstensen *x
Faculte de Pharmacie
Laboratoire Galenique
Universite de Paris-Sud
92290, Chatenay-Malabry, France

Received August 4, 1978.
Accepted for publication December 21, 1979.
* Sabbatical year. Current address: School of Pharmacy, University of Wisconsin, Madison, WI 53706.

Identification of Subvisible Barium Sulfate Crystals in Parenteral Solutions

Keyphrases □ Barium sulfate—crystal formation in commercial parenteral solutions, identification by polarizing microscopy, scanning electron microscopy, micro X-ray powder diffraction, and micro Raman spectroscopy □ Parenteral solutions, commercial—barium sulfate crystal formation, identification by polarizing microscopy, scanning electron microscopy, micro X-ray powder diffraction, and micro Raman spectroscopy □ Crystals—barium sulfate formation in commercial parenteral solutions, characterization by polarizing microscopy, scanning electron microscopy, micro X-ray powder diffraction, and micro Raman spectroscopy

To the Editor:

Concern about the presence of particulate matter in parenteral products is increasing, and certain harmful effects when such contamination is introduced into the body during intravenous therapy have been described (1–4). Additionally, studies in our laboratory implicated particulate contamination in infusion fluids as a cause of phlebitis (5–7).

To gain insight into the nature and clinical significance of particulate matter in intravenous solutions, an extensive research program has been undertaken in cooperation with the Food and Drug Administration, which includes the identification of particulate matter in parenteral products. During this investigation, barium sulfate crystals were isolated and identified in six parenteral solutions packaged both in sealed glass ampuls and in glass vials with rubber stoppers. The conclusive identification of barium sulfate crystals was achieved through the correlation of analytical data from polarizing microscopy, scanning electron microscopy with energy-dispersive X-ray analysis capability, micro X-ray powder diffraction, and micro Raman spectroscopy.

With the polarizing microscope, barium sulfate crystals isolated from the parenteral solutions appeared as single or agglomerated, well-formed, birefringent crystals, 8–30

0022-3549/80/0500-0608$01.00/0
© 1980, American Pharmaceutical Association

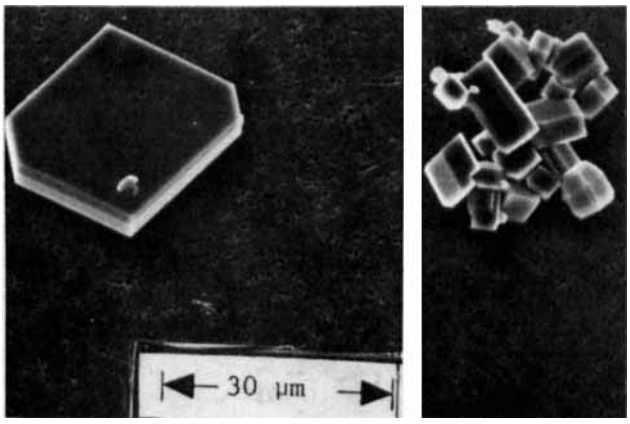

a b

Figure 1—*Scanning electron micrographs of barium sulfate crystals isolated from procaine hydrochloride* (a) *and atropine sulfate* (b) *(1000×, 20 kv).*

μm in maximum linear dimension with symmetrical edges and smooth surfaces. Under crossed polars, the crystals were birefringent and had symmetrical extinction. The high melting point (>300°) is indicative of the inorganic nature of the particles. Following characterization by polarizing microscopy, the crystals were examined by scanning electron microscopy and analyzed by energy-dispersive X-ray analysis to obtain the elemental composition. Under scanning electron microscopy, the crystals appeared as perfect rhombohedra with smooth surfaces (Fig. 1). The energy-dispersive X-ray analysis spectrum (Fig. 2), monitored for 40 sec, indicated strong signals of sulfur (2.31 kev) and barium (4.47, 4.83, 5.13, and 5.45 kev) (8).

To identify the crystals conclusively, micro X-ray powder diffraction was employed. A 57.3-mm diameter X-ray Phillips camera was used with the diameter reduced to 28.98 mm by means of a brass insert, which shortens the exposure time and reduces the dark film background (9). Eight to 10 crystals were subjected to X-rays under vacuum for 12–16 hr. By adjusting the energy output to 35 kv and 15 mamp and using a CuKα radiation source and a nickel filter, a diffraction pattern was obtained. The *d* spacings calculated from the diffraction pattern using the

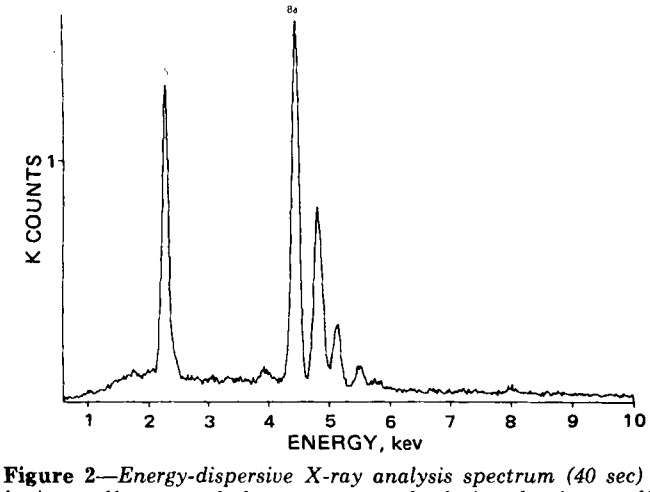

Figure 2—*Energy-dispersive X-ray analysis spectrum (40 sec) of barium sulfate crystals from a parenteral solution showing a sulfur signal at 2.3 kev and barium signals at 4.5, 4.8, 5.1, and 5.5 kev.*

Table I—Comparison of *d* Spacings of Particles from a Commercial Product with Reported Values for Barium Sulfate [a]

d Spacing for Sample Particles	Reported *d* Spacing for Barium Sulfate
3.864 (50)	3.900 (57)
3.559 (10)	3.576 (31)
3.424 (100)	3.442 (100)
3.300 (50)	3.317 (67)
3.077 (100)	3.101 (97)
2.812 (50)	2.834 (50)
2.710 (50)	2.726 (47)
2.466 (10)	2.444 (2)
2.319 (10)	2.303 (6)
2.210 (10)	2.209 (27)
2.111 (100)	2.120 (80)
2.056 (10)	2.056 (23)
1.865 (10)	1.857 (16)

[a] The values in parentheses indicate the percent relative intensity of diffraction lines corresponding to various *d* spacings.

Table II—Parenteral Solutions Containing Barium Sulfate Crystals

Product	Type of Glass Container	Source of Sulfate or Bisulfite Ions
Procaine hydrochloride, 2%	30-ml vial	Antioxidant
Kanamycin sulfate, 0.5 g/2 ml	2-ml vial	Drug
Meperidine hydrochloride, 100 mg/ml	1-ml vial	Antioxidant
Magnesium sulfate, 5 g/10 ml	10-ml vial (plunger) and rubber closure	Drug
Atropine sulfate, 0.5 mg/ml	1-ml ampul	Drug
Promethazine hydrochloride, 25 mg/ml	1-ml ampul	Antioxidant

Bragg equation show maximum relative intensities at 3.42, 3.08, and 2.11 Å, which match well with those reported for barium sulfate (10) (Table I).

Barium sulfate crystals in parenteral solutions also were identified by micro Raman spectroscopy[1]. An instrument for this technique became available recently and provides the composition of the particulate sample on the molecular scale. The sample is mounted on an ordinary microscope slide, the laser beam is focused on the crystal to be analyzed, and a Raman spectrum is obtained. The spectrum of particles isolated from a parenteral product (Fig. 3) compares well with the reference spectrum of known barium sulfate crystals (Fig. 4). The spectrum of sample particles exhibited peaks at 455, 988, and 1135 cm^{-1}, and the reference particles exhibited peaks at 450, 988, and 1135 cm^{-1}.

Using the described microanalytical techniques, crystals detected in six commercial parenteral solutions were identified as barium sulfate. The solutions are listed in Table II; on the basis that barium sulfate forms *in situ*[2], the sulfate ions appear to originate from the anion of the drug and/or the bisulfite ion of the antioxidant. The barium ions appear to come from the borosilicate glass, which contains up to 5% BaO (11).

[1] Microprobe MOLE, Instruments SA, Metuchen, NJ 08840.

[2] $BaO + H_2O \rightarrow Ba(OH)_2$.

$Ba^{2+} + SO_4^{2-} \rightarrow BaSO_4 \downarrow$.

$2SO_3^{2-} + O_2 \rightarrow 2SO_4^{2-}$.

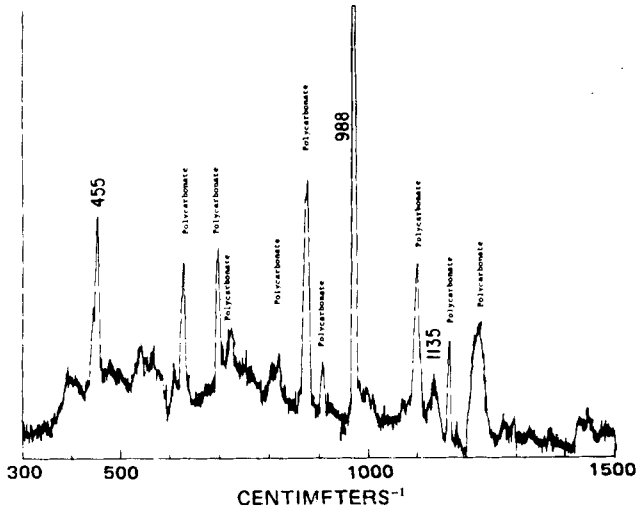

Figure 3—*Raman spectrum of barium sulfate crystal isolated from a parenteral product on a 0.45-μm polycarbonate filter (Nuclepore Corp., Pleasanton, Calif.). Peaks due to the crystal appear at 455, 988, and 1135 cm^{-1}.*

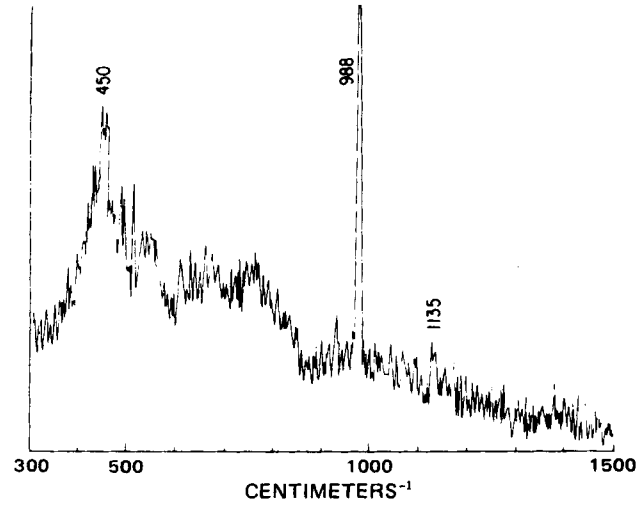

Figure 4—*Raman spectrum of reference barium sulfate crystals on a glass slide showing peaks at 450, 988, and 1135 cm^{-1}.*

In a preliminary experiment, we were able to generate barium sulfate crystals in 10-ml ampuls containing particulate-free solutions of either 0.2% sodium sulfate or 0.2% sodium bisulfite. These ampuls were autoclaved for 2 hr and stored at room temperature for 30 days. Ampuls containing particulate-free water treated identically did not produce any crystals.

Barium sulfate is so insoluble that it can be tolerated orally since it is the barium ion that is highly toxic. However, crystals injected intravenously will lodge in various tissues, depending on their size, and can cause irritation. Therefore, it is important to define the conditions under which barium sulfate crystals form in parenteral products and to devise a means for preventing their formation, such as siliconizing the glass surface or adding either a complexing agent (*i.e.*, ethylenediaminetetraacetic acid) or a nucleation inhibitor (*i.e.*, polyvinylpyrrolidone).

(1) E. J. Bruning, *Virchows Arch.*, **327**, 460 (1955).
(2) S. Sarrut and C. Nezelof, *Presse Med.*, **68**, 375 (1960).
(3) J. M. Garvan and B. W. Gunner, *Med. J. Aust.*, **2**, 140 (1963).
(4) *Ibid.*, **2**, 1 (1964).
(5) P. P. DeLuca, R. Rapp, B. Bivins, H. McKean, and W. Griffen, *Am. J. Hosp. Pharm.*, **32**, 1001 (1975).
(6) H. G. Schroeder and P. P. DeLuca, *ibid.*, **33**, 543 (1976).
(7) S. Rusmin, R. Rapp, B. Bivins, and P. P. DeLuca, *Bull. Parent. Drug Assoc.*, **31**, 1 (1977).
(8) W. C. McCrone and J. G. Delly, "The Particle Atlas, Edition II," vol. III, Ann Arbor Science Publishers, Ann Arbor, Mich., 1973, p. 747.
(9) *Ibid.*, pp. 119–129.
(10) "X-Ray Powder Data File No. 5-0488," ASTM Special Technical Publication 48-J, American Society for Testing and Materials, Philadelphia, Pa., 1960, p. 622.
(11) S. V. Sanga, *J. Parent. Drug Assoc.*, **33**, 61 (1979).

Sam Boddapati
L. David Butler
Sophann Im
Patrick P. DeLuca ˣ
College of Pharmacy
University of Kentucky
Lexington, KY 40506

Received October 9, 1979.
Accepted for publication February 21, 1980.
Supported by FDA Contract 223-77-3001.

Prediction of Steady-State Behavior of Metabolite from Dosing of Parent Drug

Keyphrases □ Metabolism—prediction of steady-state metabolite concentration, cinromide and carbamazepine, monkeys □ Steady-state concentration—prediction of metabolite and parent drug concentrations, metabolism, cinromide and carbamazepine, monkeys □ Cinromide—prediction of steady-state metabolite concentration, monkeys □ Carbamazepine—prediction of steady-state metabolite concentration, monkeys

To the Editor:

It has become apparent that the metabolites of many drugs contribute to the observed clinical efficacy and/or toxicity (1). In assessing the contribution of a given metabolite during chronic dosing, the relative steady-state concentrations of the metabolite and the parent drug (as well as the relative potencies) must be determined. This steady-state ratio was shown to be dependent only on the formation and elimination clearances of the metabolite (2, 3):

$$\frac{C^*_m}{C^*_p} = \frac{Cl_f}{Cl_m} = \frac{f_m Cl_p}{Cl_m} \qquad \text{(Eq. 1)}$$

where C^*_m and C^*_p represent the steady-state plasma concentrations of the metabolite and the parent drug, respectively; Cl_f and Cl_m represent the formation clearance and intrinsic clearance (4) of the metabolite, respectively; f_m is the fraction of the parent drug metabolized to this metabolite; and Cl_p is the systemic clearance of the parent drug.

From Eq. 1, it appears that knowledge of the metabolite clearance and the fraction metabolized (or formation clearance) is necessary to calculate this ratio. The purpose of the present report is to show that the steady-state metabolite to parent drug ratio, as well as the actual steady-state metabolite concentration, can be determined from administration of a single dose of the parent drug without administration of the metabolite. A change in the admin-

0022-3549/80/0500-0610$01.00/0
© 1980, American Pharmaceutical Association

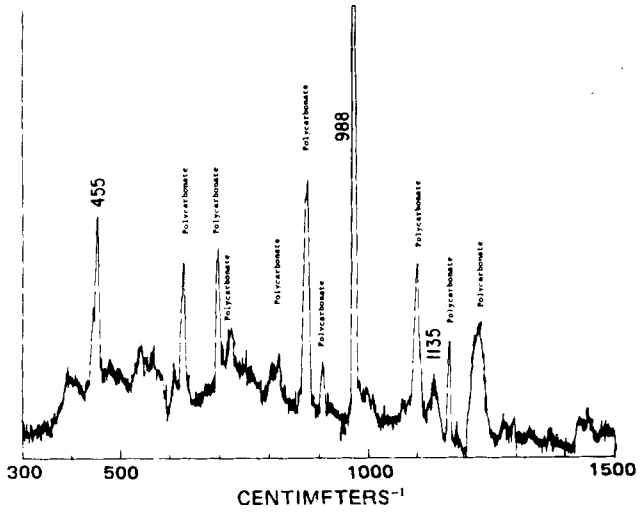

Figure 3—*Raman spectrum of barium sulfate crystal isolated from a parenteral product on a 0.45-μm polycarbonate filter (Nuclepore Corp., Pleasanton, Calif.). Peaks due to the crystal appear at 455, 988, and 1135 cm^{-1}.*

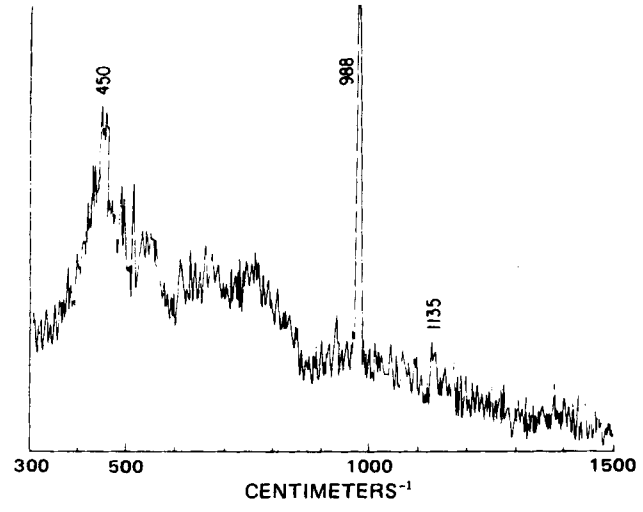

Figure 4—*Raman spectrum of reference barium sulfate crystals on a glass slide showing peaks at 450, 988, and 1135 cm^{-1}.*

In a preliminary experiment, we were able to generate barium sulfate crystals in 10-ml ampuls containing particulate-free solutions of either 0.2% sodium sulfate or 0.2% sodium bisulfite. These ampuls were autoclaved for 2 hr and stored at room temperature for 30 days. Ampuls containing particulate-free water treated identically did not produce any crystals.

Barium sulfate is so insoluble that it can be tolerated orally since it is the barium ion that is highly toxic. However, crystals injected intravenously will lodge in various tissues, depending on their size, and can cause irritation. Therefore, it is important to define the conditions under which barium sulfate crystals form in parenteral products and to devise a means for preventing their formation, such as siliconizing the glass surface or adding either a complexing agent (*i.e.*, ethylenediaminetetraacetic acid) or a nucleation inhibitor (*i.e.*, polyvinylpyrrolidone).

(1) E. J. Bruning, *Virchows Arch.*, **327**, 460 (1955).
(2) S. Sarrut and C. Nezelof, *Presse Med.*, **68**, 375 (1960).
(3) J. M. Garvan and B. W. Gunner, *Med. J. Aust.*, **2**, 140 (1963).
(4) *Ibid.*, **2**, 1 (1964).
(5) P. P. DeLuca, R. Rapp, B. Bivins, H. McKean, and W. Griffen, *Am. J. Hosp. Pharm.*, **32**, 1001 (1975).
(6) H. G. Schroeder and P. P. DeLuca, *ibid.*, **33**, 543 (1976).
(7) S. Rusmin, R. Rapp, B. Bivins, and P. P. DeLuca, *Bull. Parent. Drug Assoc.*, **31**, 1 (1977).
(8) W. C. McCrone and J. G. Delly, "The Particle Atlas, Edition II," vol. III, Ann Arbor Science Publishers, Ann Arbor, Mich., 1973, p. 747.
(9) *Ibid.*, pp. 119–129.
(10) "X-Ray Powder Data File No. 5-0488," ASTM Special Technical Publication 48-J, American Society for Testing and Materials, Philadelphia, Pa., 1960, p. 622.
(11) S. V. Sanga, *J. Parent. Drug Assoc.*, **33**, 61 (1979).

Sam Boddapati
L. David Butler
Sophann Im
Patrick P. DeLuca ˣ
College of Pharmacy
University of Kentucky
Lexington, KY 40506

Received October 9, 1979.
Accepted for publication February 21, 1980.
Supported by FDA Contract 223-77-3001.

Prediction of Steady-State Behavior of Metabolite from Dosing of Parent Drug

Keyphrases □ Metabolism—prediction of steady-state metabolite concentration, cinromide and carbamazepine, monkeys □ Steady-state concentration—prediction of metabolite and parent drug concentrations, metabolism, cinromide and carbamazepine, monkeys □ Cinromide—prediction of steady-state metabolite concentration, monkeys □ Carbamazepine—prediction of steady-state metabolite concentration, monkeys

To the Editor:

It has become apparent that the metabolites of many drugs contribute to the observed clinical efficacy and/or toxicity (1). In assessing the contribution of a given metabolite during chronic dosing, the relative steady-state concentrations of the metabolite and the parent drug (as well as the relative potencies) must be determined. This steady-state ratio was shown to be dependent only on the formation and elimination clearances of the metabolite (2, 3):

$$\frac{C^*_m}{C^*_p} = \frac{Cl_f}{Cl_m} = \frac{f_m Cl_p}{Cl_m} \qquad \text{(Eq. 1)}$$

where C^*_m and C^*_p represent the steady-state plasma concentrations of the metabolite and the parent drug, respectively; Cl_f and Cl_m represent the formation clearance and intrinsic clearance (4) of the metabolite, respectively; f_m is the fraction of the parent drug metabolized to this metabolite; and Cl_p is the systemic clearance of the parent drug.

From Eq. 1, it appears that knowledge of the metabolite clearance and the fraction metabolized (or formation clearance) is necessary to calculate this ratio. The purpose of the present report is to show that the steady-state metabolite to parent drug ratio, as well as the actual steady-state metabolite concentration, can be determined from administration of a single dose of the parent drug without administration of the metabolite. A change in the admin-

0022-3549/80/0500-0610$01.00/0
© 1980, American Pharmaceutical Association

istration route from systemic to oral results in a first-pass effect for drugs with medium or high extraction ratios. Methods for such corrections are provided. Preliminary experimental data with two drugs support the proposed theoretical approaches.

Equation 1 was derived assuming one-compartmental distribution and first-order elimination for the parent drug and the metabolite. It also is valid if either species (or both) exhibits multicompartmental behavior (mamillary model), as long as elimination occurs from the central compartment.

In Eq. 1, Cl_p and f_m can be expressed in a model-independent manner using areas under the curve (5):

$$Cl_p = \frac{D_p}{(AUC_p)_p} \qquad \text{(Eq. 2)}$$

$$f_m = \left(\frac{(AUC_m)_p}{D_p}\right)\left(\frac{D_m}{(AUC_m)_m}\right) = \left(\frac{(AUC_m)_p}{D_p}\right)Cl_m \qquad \text{(Eq. 3)}$$

where AUC is the area under the plasma concentration (molar)–time curve from zero to infinity; $(AUC_c)_b$ represents the AUC of c after a single dose of b; the subscripts m and p refer to the metabolite and the parent drug, respectively; and D refers to the dose in molar units.

The formation clearance, Cl_f, then is given by the product of Eqs. 2 and 3:

$$Cl_f = \left(\frac{(AUC_m)_p}{(AUC_p)_p}\right)Cl_m \qquad \text{(Eq. 4)}$$

Substitution of Eq. 4 into Eq. 1 shows that the steady-state ratio, C^*_m/C^*_p, becomes equal to the ratio of the areas of the metabolite and the parent drug after a single dose:

$$\frac{C^*_m}{C^*_p} = \frac{(AUC_m)_p}{(AUC_p)_p} \qquad \text{(Eq. 5)}$$

Equation 5 shows that the ratio of the steady-state concentrations of the metabolite and the parent drug can be predicted from concentration–time data obtained after a single intravenous dose of the parent drug. This relationship assumes linearity (with respect to dose and time) for the parent drug and the metabolite. This prediction requires the monitoring of metabolite and parent drug levels but does not require administration of the metabolite.

Equation 5 also can be used to calculate the actual steady-state concentration of the metabolite achieved by a given infusion rate, R_0, of the parent drug:

$$C^*_m = \left(\frac{(AUC_m)_p}{(AUC_p)_p}\right)C^*_p \qquad \text{(Eq. 6)}$$

With Eq. 2, C^*_p can be expressed as:

$$C^*_p = \frac{R_0}{Cl_p} = \frac{R_0(AUC_p)_p}{D_p} \qquad \text{(Eq. 7)}$$

Substitution of C^*_p from Eq. 7 into Eq. 6 yields:

$$C^*_m = \frac{R_0}{D_p}(AUC_m)_p \qquad \text{(Eq. 8)}$$

From a practical point of view, Eq. 8 implies that the steady-state metabolite concentration can be calculated by monitoring only metabolite levels without knowledge of parent drug levels (following administration of a single dose of the parent drug).

Equations 5 and 8 are directly applicable to the multiple dosing situation without any modifications as long as the multiple doses are given by the same route as the single dose (*i.e.*, the same dosage form). When there is a change in the administration route, Eqs. 5 and 8 must be modified. For instance, to estimate the C^*_m/C^*_p ratio after multiple oral doses from areas under the curve obtained after a single intravenous dose, a correction for any first-pass effect of the parent drug must be included so that Eq. 5 becomes:

$$\frac{\overline{C}^*_m}{\overline{C}^*_p} = \left[\frac{(AUC_m)_p}{(AUC_p)_p}\right]_{iv}\frac{1}{F_p} \qquad \text{(Eq. 9)}$$

where F_p represents the fraction of the dose of the parent drug systemically available, and $\overline{C}^*_m$ and $\overline{C}^*_p$ refer to the average concentrations during a dosing interval (a fixed-dose, fixed-time schedule).

Similarly, to estimate the average steady-state concentration of the metabolite after multiple oral doses from the area under the curve obtained after a single intravenous dose, Eq. 8 becomes:

$$\overline{C}^*_m = \left[\frac{(AUC_m)_p}{D_p}\right]_{iv} f_a \times \text{dose rate} \qquad \text{(Eq. 10)}$$

where f_a represents the dose fraction absorbed into the portal circulation; no correction for the first-pass effect of the parent drug is necessary. The applicability of Eqs. 5 and 8 was verified using data obtained during the pharmacokinetic characterization of cinromide and carbamazepine in rhesus monkeys.

Cinromide [(*E*)-*m*-bromo-*N*-ethylcinnamamide], a new antiepileptic drug[1], is metabolized by *N*-deethylation to 3-bromocinnamamide (6, 7). Short-term (not to steady state) and long-term (to steady state) infusions of the parent drug were administered to two monkeys. The C^*_m/C^*_p ratios and C^*_m values for the long-term infusions were predicted from the short infusion studies. Table I shows the agreement between the predicted and experimental values.

Carbamazepine is metabolized to a 10,11-epoxide, and the kinetics of the parent drug and the metabolite were elucidated (2). Single-dose intravenous studies with the parent drug in two monkeys enabled a prediction of C^*_m/C^*_p and C^*_m. These values compared favorably with the corresponding values obtained during a zero-order intravenous infusion of carbamazepine to the steady state (Table I).

The proposed theoretical approach has applications in drug development and in therapeutics. In the preclinical evaluation of new drugs, prediction of steady-state metabolite concentrations is useful in planning efficacy and toxicity studies. Furthermore, clinical monitoring of me-

Table I—Comparison of Predicted and Observed Metabolite to Parent Drug Ratio (C^*_m/C^*_p) and Metabolite Concentration (C^*_m) at Steady State

Monkey	C^*_m/C^*_p Predicted	C^*_m/C^*_p Observed	C^*_m, μg/ml Predicted	C^*_m, μg/ml Observed
	Cinromide and 3-Bromocinnamamide			
184	4.1 ± 0.55[a]	4.5	14.5 ± 2.0	12.3
336	2.9 ± 0.6	3.5	10.6 ± 1.8	10.6
	Carbamazepine and Carbamazepine-10,11-epoxide			
346	0.12	0.15	0.26	0.30
336	0.08	0.08	0.15	0.19

[a] Mean and standard deviation of prediction.

[1] Developed by Burroughs-Wellcome Laboratories, Research Triangle Park, N.C.

tabolites is becoming necessary with several pharmacological classes of drugs (antidepressants, antiarrhythmics, antiepileptics, and steroids).

(1) D. E. Drayer, *Clin. Pharmacokinet.*, 1, 426 (1976).
(2) I. H. Patel, R. H. Levy, and W. F. Trager, *J. Pharmacol. Exp. Ther.*, **206**, 607 (1978).
(3) A. A. Lai, B. H. Min, W. A. Garland, and R. H. Levy, *J. Pharm. Biopharm.*, 7, 87 (1979).
(4) K. S. Pang and J. R. Gillette, *J. Pharmacokinet. Biopharm.*, 7, 275 (1979).
(5) S. A. Kaplan, M. L. Jack, S. Cotler, and K. Alexander, *ibid.*, 1, 201 (1973).
(6) J. S. Lockard, R. H. Levy, L. L. Ducharme, and W. C. Congdon, *Epilepsia*, **20**, 339 (1979).
(7) E. A. Lane and R. H. Levy, "Epilepsy: Vancouver International Symposium," Raven, New York, N.Y., in press.

E. A. Lane
R. H. Levy ˣ
Departments of Pharmaceutical Sciences and Neurological Surgery
Schools of Pharmacy and Medicine
University of Washington
Seattle, WA 98195

Received January 7, 1980.
Accepted for publication February 22, 1980.
Supported by National Institutes of Health Research Contract NO1-NS-1-2282.

Glass Transition Temperature of Citric Acid

Keyphrases □ Glass transition temperature—citric acid, glass formation, temperature variations due to water loss variations □ Citric acid—glass formation, glass transition temperature, comparison of anhydrous and monohydrate forms of citric acid □ Glass formation—citric acid, glass transition temperature

To the Editor:

A recent publication (1) examined solid dispersion systems using techniques similar to those we described previously (2, 3). Discrepancies between the glass transition temperature observed by the two groups of investigators (33–36°) have been explained as being due to an artifact. We hope the present observations will clarify the matter.

The glass transition temperature cannot be given an absolute value other than that extrapolated to a zero heating rate (4), because it is dependent on the rate of quenching of the glass and the heating rate employed to measure the transition. This was shown clearly by Rötger (5), who characterized the glass transition temperature by two rate indexes applicable to the quenching and heating rates of the sample. One immediate difference between the two reported studies (1, 3) was the heating rate employed during the measurement of the glass transition. Timko and Lordi (1) used 10°/min, whereas we used 2°/min (3). We also quoted the glass transition temperature as the onset of the transition (first deviation from the thermogram[1] baseline) rather than the extrapolated onset of Timko and Lordi (1), because this approach appeared to give better precision with different sample sizes. At 2°/min, the difference between the extrapolated onset and the initial deviation is only ~0.5–1°.

[1] D.S.B.1B, Perkin-Elmer, Beaconsfield, England.

Table I—Effect of Water on Glass Transition Temperature

Water Added to Melt, % (w/w)	Glass Transition Temperature
3	−8–−13°
4	−13–−18°
5	−23–−26°

However, these two differences do not account for the large discrepancy reported in the two studies. For example, with our methods, the glass transition temperature of anhydrous citric acid was 7°, rather than 10° as quoted by Timko and Lordi (1).

The second difference in the two studies was the use of citric acid monohydrate (2, 3) rather than anhydrous citric acid. We believe that the discrepancy in the glass transition temperature of the two materials is due to the water bound in the glass of the monohydrate, which is difficult to remove from the melt at 150° (the temperature used in our method). This concept is in agreement with our previous suggestion (2) that using the monohydrate is advantageous because of the formation of a citric acid solution.

Since the devitrified glasses contain anhydrous citric acid, water probably is lost during crystallization of the melt and should be detectable as a weight loss. We measured the weight loss on devitrification and drying at 60° after heating the monohydrate melt for varying periods at 140–150°. After 4 min of heating, the weight loss was 4.8–5.6% (w/w); after 10 min of heating, it was reduced only to 4.3–5.3% (w/w).

The effect of water on the glass transition temperature can be shown by incorporating water into a melt of anhydrous citric acid produced by the method outlined previously (2) and above and measuring the glass transition temperature as described previously (3). The results are shown in Table I. There is some variation in the glass transition temperature due to variation in water loss on its addition to the melt. However, if the water is added when the melt is relatively cool, it induces crystallization; therefore, the system has to be reheated, resulting again in loss of water. These results are consistent with the reported weight losses and suggest that ~4.5% moisture is in the glass. If 9% (w/w) water (the amount present in the monohydrate) is added to anhydrous citric acid before melting and the glass preparation method is repeated, the glass transition temperature is −23–−24°, which is consistent with our previous results.

The results suggest that when the monohydrate is used, an unavoidable amount of water is present in the glass, which affects the glass transition temperature. This effect is reproducible, suggesting a consistent amount of entrapment in the melt. Furthermore, the properties of the anhydrous and monohydrate glasses are similar because, as a continuation of previous work (6), we found that the effect of phenobarbital on the citric acid (monohydrate) transition temperature was similar to that reported by Timko and Lordi (1).

(1) R. J. Timko and N. G. Lordi, *J. Pharm. Sci.*, **68**, 601 (1979).
(2) M. P. Summers and R. P. Enever, *ibid.*, **65**, 1613 (1976).
(3) *Ibid.*, **66**, 825 (1977).
(4) J. P. Mercier and J. J. Aklonis, *J. Paint Technol.*, **43**, 44 (1974).
(5) H. Rötger, in "Amorphous Materials," R. W. Douglas and B. Ellis, Eds., Wiley-Interscience, London, England, 1972.

0022-3549/80/0500-0612$01.00/0
© 1980, American Pharmaceutical Association

tabolites is becoming necessary with several pharmacological classes of drugs (antidepressants, antiarrhythmics, antiepileptics, and steroids).

(1) D. E. Drayer, *Clin. Pharmacokinet.*, 1, 426 (1976).
(2) I. H. Patel, R. H. Levy, and W. F. Trager, *J. Pharmacol. Exp. Ther.*, **206**, 607 (1978).
(3) A. A. Lai, B. H. Min, W. A. Garland, and R. H. Levy, *J. Pharm. Biopharm.*, 7, 87 (1979).
(4) K. S. Pang and J. R. Gillette, *J. Pharmacokinet. Biopharm.*, 7, 275 (1979).
(5) S. A. Kaplan, M. L. Jack, S. Cotler, and K. Alexander, *ibid.*, 1, 201 (1973).
(6) J. S. Lockard, R. H. Levy, L. L. Ducharme, and W. C. Congdon, *Epilepsia*, **20**, 339 (1979).
(7) E. A. Lane and R. H. Levy, "Epilepsy: Vancouver International Symposium," Raven, New York, N.Y., in press.

E. A. Lane
R. H. Levy ˣ
Departments of Pharmaceutical Sciences and Neurological Surgery
Schools of Pharmacy and Medicine
University of Washington
Seattle, WA 98195

Received January 7, 1980.
Accepted for publication February 22, 1980.
Supported by National Institutes of Health Research Contract NO1-NS-1-2282.

Glass Transition Temperature of Citric Acid

Keyphrases □ Glass transition temperature—citric acid, glass formation, temperature variations due to water loss variations □ Citric acid—glass formation, glass transition temperature, comparison of anhydrous and monohydrate forms of citric acid □ Glass formation—citric acid, glass transition temperature

To the Editor:

A recent publication (1) examined solid dispersion systems using techniques similar to those we described previously (2, 3). Discrepancies between the glass transition temperature observed by the two groups of investigators (33–36°) have been explained as being due to an artifact. We hope the present observations will clarify the matter.

The glass transition temperature cannot be given an absolute value other than that extrapolated to a zero heating rate (4), because it is dependent on the rate of quenching of the glass and the heating rate employed to measure the transition. This was shown clearly by Rötger (5), who characterized the glass transition temperature by two rate indexes applicable to the quenching and heating rates of the sample. One immediate difference between the two reported studies (1, 3) was the heating rate employed during the measurement of the glass transition. Timko and Lordi (1) used 10°/min, whereas we used 2°/min (3). We also quoted the glass transition temperature as the onset of the transition (first deviation from the thermogram[1] baseline) rather than the extrapolated onset of Timko and Lordi (1), because this approach appeared to give better precision with different sample sizes. At 2°/min, the difference between the extrapolated onset and the initial deviation is only ~0.5–1°.

[1] D.S.B.1B, Perkin-Elmer, Beaconsfield, England.

Table I—Effect of Water on Glass Transition Temperature

Water Added to Melt, % (w/w)	Glass Transition Temperature
3	−8–−13°
4	−13–−18°
5	−23–−26°

However, these two differences do not account for the large discrepancy reported in the two studies. For example, with our methods, the glass transition temperature of anhydrous citric acid was 7°, rather than 10° as quoted by Timko and Lordi (1).

The second difference in the two studies was the use of citric acid monohydrate (2, 3) rather than anhydrous citric acid. We believe that the discrepancy in the glass transition temperature of the two materials is due to the water bound in the glass of the monohydrate, which is difficult to remove from the melt at 150° (the temperature used in our method). This concept is in agreement with our previous suggestion (2) that using the monohydrate is advantageous because of the formation of a citric acid solution.

Since the devitrified glasses contain anhydrous citric acid, water probably is lost during crystallization of the melt and should be detectable as a weight loss. We measured the weight loss on devitrification and drying at 60° after heating the monohydrate melt for varying periods at 140–150°. After 4 min of heating, the weight loss was 4.8–5.6% (w/w); after 10 min of heating, it was reduced only to 4.3–5.3% (w/w).

The effect of water on the glass transition temperature can be shown by incorporating water into a melt of anhydrous citric acid produced by the method outlined previously (2) and above and measuring the glass transition temperature as described previously (3). The results are shown in Table I. There is some variation in the glass transition temperature due to variation in water loss on its addition to the melt. However, if the water is added when the melt is relatively cool, it induces crystallization; therefore, the system has to be reheated, resulting again in loss of water. These results are consistent with the reported weight losses and suggest that ~4.5% moisture is in the glass. If 9% (w/w) water (the amount present in the monohydrate) is added to anhydrous citric acid before melting and the glass preparation method is repeated, the glass transition temperature is −23–−24°, which is consistent with our previous results.

The results suggest that when the monohydrate is used, an unavoidable amount of water is present in the glass, which affects the glass transition temperature. This effect is reproducible, suggesting a consistent amount of entrapment in the melt. Furthermore, the properties of the anhydrous and monohydrate glasses are similar because, as a continuation of previous work (6), we found that the effect of phenobarbital on the citric acid (monohydrate) transition temperature was similar to that reported by Timko and Lordi (1).

(1) R. J. Timko and N. G. Lordi, *J. Pharm. Sci.*, **68**, 601 (1979).
(2) M. P. Summers and R. P. Enever, *ibid.*, **65**, 1613 (1976).
(3) *Ibid.*, **66**, 825 (1977).
(4) J. P. Mercier and J. J. Aklonis, *J. Paint Technol.*, **43**, 44 (1974).
(5) H. Rötger, in "Amorphous Materials," R. W. Douglas and B. Ellis, Eds., Wiley-Interscience, London, England, 1972.

0022-3549/80/0500-0612$01.00/0
© 1980, American Pharmaceutical Association

(6) M. P. Summers and R. P. Enever, *J. Pharm. Sci.*, **67**, 1606 (1978).

M. P. Summers ˣ
R. P. Enever *
Department of Pharmaceutics
School of Pharmacy
University of London
London, WC1N 1AX England

Received January 4, 1979.
Accepted for publication January 25, 1980.
*Present address: Department of Pharmaceutics, University of Minnesota, Minneapolis, MN 35455.

Charge Transfer Effect through Hydrogen Bonding in Caffeine–*p*-Cresol and Theophylline–*p*-Cresol Complexes

Keyphrases □ Charge transfer effect—hydrogen bonding in caffeine–*p*-cresol and theophylline–*p*-cresol complexes □ Caffeine—hydrogen bonding in complex with *p*-cresol □ Theophylline—hydrogen bonding in complex with *p*-cresol

To the Editor:

Charge transfer transitions were detected in the UV absorption spectra of mixtures containing caffeine–*p*-cresol and theophylline–*p*-cresol in chloroform (1). To gain more information about the bonding mechanism and the various geometries of the complexes that may exist in solution, we conducted an IR study of the two combinations.

Changes can be detected in the IR absorption bands of the compounds mixed in chloroform. [The frequencies, expressed in reciprocal centimeters, were assigned according to Cross (2) and Silverstein and Bassler (3).]

Caffeine–*p*-Cresol (Fig. 1)—p-*Cresol*—The intensity of the free OH stretching vibration of *p*-cresol at 3590 decreased. The intensity of the intermolecular hydrogen-bonded OH stretching vibration increased appreciably, with a slight shift toward a longer wavelength (~5). A measurable increase in the intensity of the in-plane skeletal stretching vibrations was detected at 1615, 1595, and 1502.

Caffeine—The intensity of the CH stretching vibrations of the caffeine methyl groups at 2980 and 2945 decreased slightly. A decrease in the intensity of the carbonyl groups at C_2 (1700) and C_6 (1655) was found, with the stretching vibration at C_6 affected more.

Theophylline–*p*-Cresol (Fig. 2)—p-*Cresol*—The intensity of the free OH stretching vibration at 3590 decreased considerably. An appreciable increase in the intensity of the hydrogen-bonded OH stretching vibration at 3370 of the self-associated species was observed, with a considerable shift toward a longer wavelength (3320). The intensity of the aromatic CH stretching vibration at 2990 decreased noticeably, while a slight decrease was observed in the bands of the CH stretching vibrations of the methyl group at 2920 and 2860. The intensity at 1615 and 1502 of the in-plane skeletal stretching vibrations decreased slightly.

Theophylline—An increase in the free NH stretching vibration at 3425 was observed. The broad band of the hydrogen-bonded NH overlapping the CH stretching vibration at 3300–3000 seemed to be affected to a different extent; the maximum percentage increase was at 3260, while the minimum increase was at 3150. At 3060, a noticeable decrease was found. The intensity of the bands at 2990 and 2952, representing the CH methyl stretching vibrations, was decreased. A considerable decrease was found in the intensity of the C_2=O band at 1700, while a smaller decrease was found for the C_6=O band at 1655. A decrease was observed at 1551 of the C=C and C=N stretching vibrations of the ring.

Based on theory and experimental observations (4–7), changes in the IR spectra may be explained as being due to the formation of heterogeneous complexes or to the formation of self-associated species.

Calculation of dilution effects on *p*-cresol in chloroform

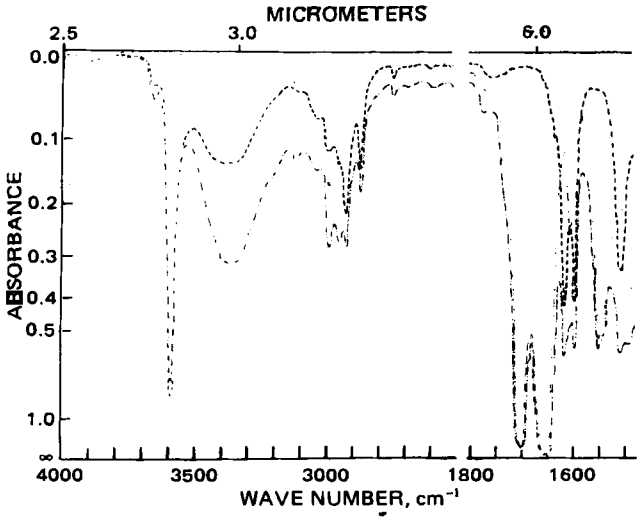

Figure 1—*IR spectra of chloroform solutions containing 4 × 10^{-2} M caffeine (–·–·–), 1.5 × 10^{-1} M p-cresol (- - -), and an equimolar mixture of the pure components (——). The baseline of the solvent is represented by the dotted line. Measurements were taken in the sodium chloride cells with a 0.05-cm path length at ~22°. The materials and methods used were those given by Al-Ani and Borazan (1).*

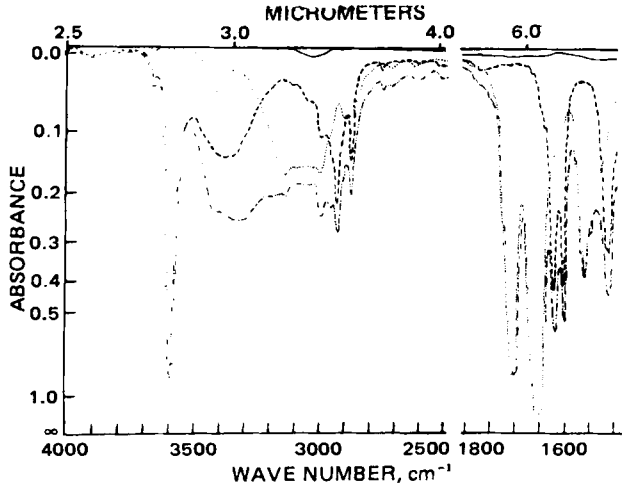

Figure 2—*IR spectra of chloroform solution containing 2 × 10^{-2} M theophylline (. . .), 1.5 × 10^{-1} M p-cresol (- - -), and an equimolar mixture of the pure components (——). The baseline of the solvent is represented by the solid line. Measurements were taken in sodium chloride cells with a 0.05-cm path length at ~22°.*

0022-3549/80/0500-0613$01.00/0
© 1980, American Pharmaceutical Association

(6) M. P. Summers and R. P. Enever, *J. Pharm. Sci.*, **67**, 1606 (1978).

M. P. Summers ˣ
R. P. Enever *
Department of Pharmaceutics
School of Pharmacy
University of London
London, WC1N 1AX England

Received January 4, 1979.
Accepted for publication January 25, 1980.
*Present address: Department of Pharmaceutics, University of Minnesota, Minneapolis, MN 35455.

Charge Transfer Effect through Hydrogen Bonding in Caffeine–*p*-Cresol and Theophylline–*p*-Cresol Complexes

Keyphrases □ Charge transfer effect—hydrogen bonding in caffeine–*p*-cresol and theophylline–*p*-cresol complexes □ Caffeine—hydrogen bonding in complex with *p*-cresol □ Theophylline—hydrogen bonding in complex with *p*-cresol

To the Editor:

Charge transfer transitions were detected in the UV absorption spectra of mixtures containing caffeine–*p*-cresol and theophylline–*p*-cresol in chloroform (1). To gain more information about the bonding mechanism and the various geometries of the complexes that may exist in solution, we conducted an IR study of the two combinations.

Changes can be detected in the IR absorption bands of the compounds mixed in chloroform. [The frequencies, expressed in reciprocal centimeters, were assigned according to Cross (2) and Silverstein and Bassler (3).]

Caffeine–*p*-Cresol (Fig. 1)—p-*Cresol*—The intensity of the free OH stretching vibration of *p*-cresol at 3590 decreased. The intensity of the intermolecular hydrogen-bonded OH stretching vibration increased appreciably, with a slight shift toward a longer wavelength (~5). A measurable increase in the intensity of the in-plane skeletal stretching vibrations was detected at 1615, 1595, and 1502.

Caffeine—The intensity of the CH stretching vibrations of the caffeine methyl groups at 2980 and 2945 decreased slightly. A decrease in the intensity of the carbonyl groups at C_2 (1700) and C_6 (1655) was found, with the stretching vibration at C_6 affected more.

Theophylline–*p*-Cresol (Fig. 2)—p-*Cresol*—The intensity of the free OH stretching vibration at 3590 decreased considerably. An appreciable increase in the intensity of the hydrogen-bonded OH stretching vibration at 3370 of the self-associated species was observed, with a considerable shift toward a longer wavelength (3320). The intensity of the aromatic CH stretching vibration at 2990 decreased noticeably, while a slight decrease was observed in the bands of the CH stretching vibrations of the methyl group at 2920 and 2860. The intensity at 1615 and 1502 of the in-plane skeletal stretching vibrations decreased slightly.

Theophylline—An increase in the free NH stretching vibration at 3425 was observed. The broad band of the hydrogen-bonded NH overlapping the CH stretching vibration at 3300–3000 seemed to be affected to a different extent; the maximum percentage increase was at 3260, while the minimum increase was at 3150. At 3060, a noticeable decrease was found. The intensity of the bands at 2990 and 2952, representing the CH methyl stretching vibrations, was decreased. A considerable decrease was found in the intensity of the C_2=O band at 1700, while a smaller decrease was found for the C_6=O band at 1655. A decrease was observed at 1551 of the C=C and C=N stretching vibrations of the ring.

Based on theory and experimental observations (4–7), changes in the IR spectra may be explained as being due to the formation of heterogeneous complexes or to the formation of self-associated species.

Calculation of dilution effects on *p*-cresol in chloroform

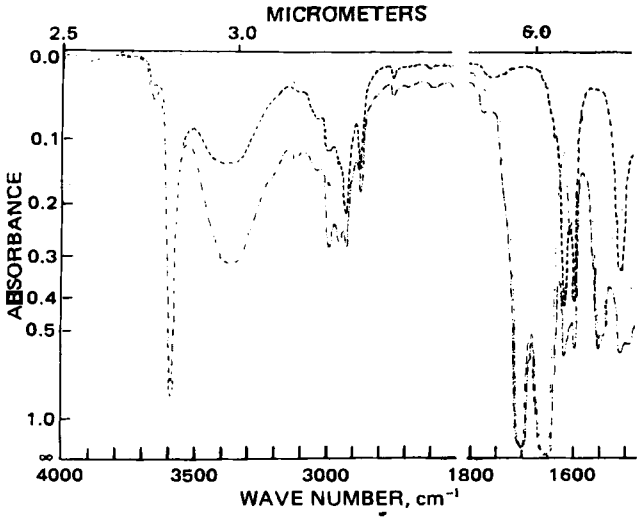

Figure 1—*IR spectra of chloroform solutions containing 4 × 10^{-2} M caffeine (–·–·–), 1.5 × 10^{-1} M p-cresol (- - -), and an equimolar mixture of the pure components (——). The baseline of the solvent is represented by the dotted line. Measurements were taken in the sodium chloride cells with a 0.05-cm path length at ~22°. The materials and methods used were those given by Al-Ani and Borazan (1).*

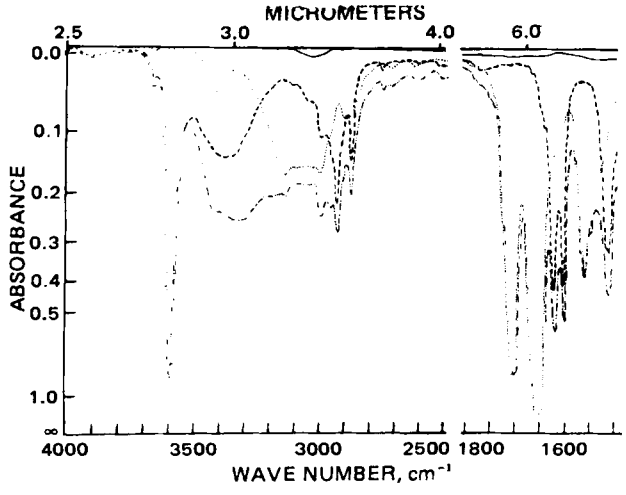

Figure 2—*IR spectra of chloroform solution containing 2 × 10^{-2} M theophylline (. . .), 1.5 × 10^{-1} M p-cresol (- - -), and an equimolar mixture of the pure components (——). The baseline of the solvent is represented by the solid line. Measurements were taken in sodium chloride cells with a 0.05-cm path length at ~22°.*

0022-3549/80/0500-0613$01.00/0
© 1980, American Pharmaceutical Association

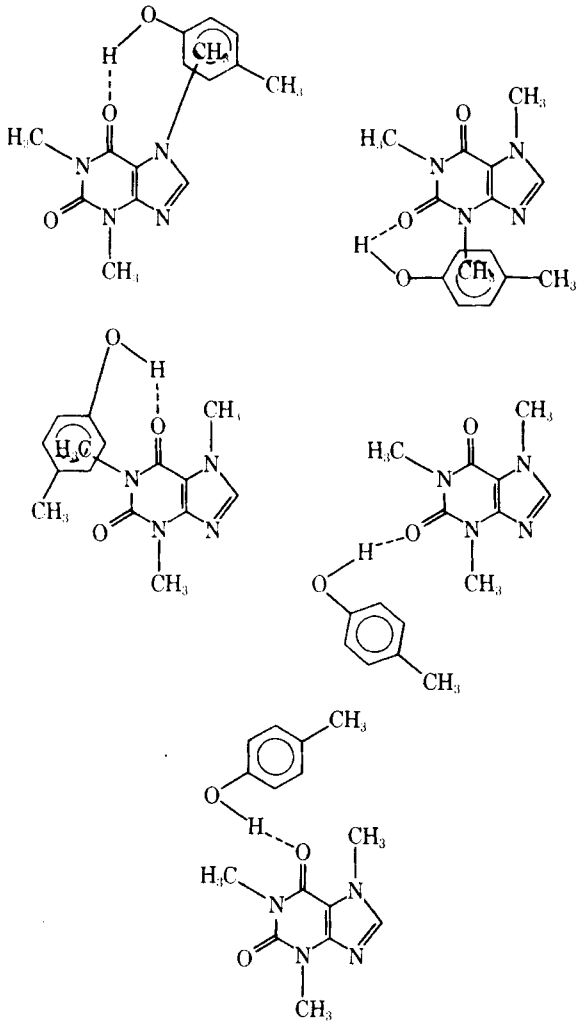

Proposed models for 1:1 caffeine–p-cresol complex in chloroform

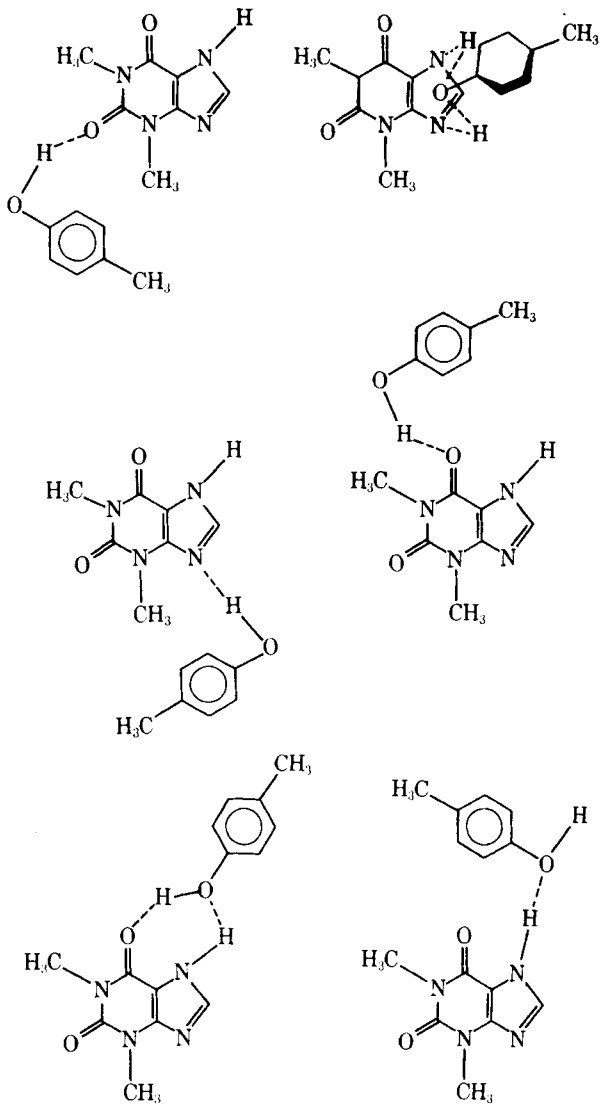

Proposed models 1:1 theophylline–p-cresol complex in chloroform

indicated that the band at 3590 increased while the band at 3370 decreased. These results are further evidence that the first band can be attributed to the free OH stretching vibration while the second one can be assigned to the hydrogen-bonded OH of the self-associated species. The band at 2990 of the aromatic CH stretching vibration also increased. However, bands belonging to the CH stretching vibrations of the methyl groups (2920 and 2860) were unaffected; those of the in-plane skeletal stretching vibrations (1615, 1595, and 1502) all increased. The band at 1502 was shifted toward shorter wavelength (1512) with a drastic increase in absorption.

All of these results indicate the presence of self-associated molecules. The groups involved in bonding are the hydroxyl group and the benzene ring. However, it is difficult to propose an exact geometry or a stoichiometry of such self-associated species. Nevertheless, the following geometries of the self-associated aggregates may be proposed: hydrogen-bonded dimers, stacks of hydrogen-bonded dimers with methyl groups projected away from each other, stacked hydrogen-bonded dimers, and spherically oriented polymers with the OH groups projected inward and the nonpolar methyl groups oriented outside.

It is evident from changes in the IR spectrum (Fig. 1) of the solution containing caffeine–*p*-cresol that the areas that contribute most to the formation of the complex are the OH group and the skeletal carbons of *p*-cresol and the $C_2{=}O$, $C_6{=}O$, and CH_3 groups of caffeine. The models proposed for the geometry of a 1:1 complex are presented.

When theophylline is mixed with *p*-cresol, a complex appears to be formed (Fig. 2). The groups predominantly involved in formation of such a complex are the OH group and the aromatic CH group of *p*-cresol and the NH, aromatic CH, methyl CH, $C_2{=}O$, and $C_6{=}O$ groups of theophylline. The formation of a planar complex where hydrogen bonding is the dominant attractive force contributing to its formation may be proposed.

The increase in the intensity of the band corresponding to the free NH stretching vibration at 3425 may be due to overlapping with the hydrogen-bonded hydroxyl group of *p*-cresol or may result because dimers and polymers of theophylline, held together through hydrogen bonds with their NH groups, dissociate to interact with molecules of *p*-cresol and to free some of the bonded NH groups.

The equilibrium constants, calculated at 22°, of both

complexes were 0.22 and 0.16 M^{-1} for caffeine–*p*-cresol and theophylline–*p*-cresol, respectively, at 308 nm (1). On the other hand, the molar absorptivities of these complexes at the intermolecular hydrogen-bonded OH stretching vibration band, 3370 cm^{-1}, were $\sim 3 \times 10^3$ and $\sim 4.3 \times 10^3$ for caffeine–*p*-cresol and theophylline–*p*-cresol, respectively.

The present work supported the theory that hydrogen bonding is a type of charge transfer phenomenon (8–10).

(1) N. I. Al-Ani and H. N. Borazan, *J. Pharm. Sci.*, **67**, 1381 (1978).

(2) A. D. Cross, "Introduction to Practical Infra-Red Spectroscopy," 2nd ed., Butterworths, London, England, 1964, pp. 63–79.

(3) R. M. Silverstein and G. C. Bassler, "Spectroscopic Identification of Organic Compounds," 2nd ed., Wiley, New York, N.Y., 1967, pp. 64–109.

(4) W. B. Person, R. E. Humphrey, W. A. Deskin, and A. I. Popov, *J. Am. Chem. Soc.*, **80**, 2049 (1958).

(5) W. B. Person, R. E. Humphrey, and A. I. Popov, *ibid.*, **81**, 273 (1959).

(6) E. E. Ferguson and F. A. Matsen, *ibid.*, **82**, 3268 (1960).

(7) P. C. McKinney and G. M. Barrow, *J. Chem. Phys.*, **31**, 294 (1959).

(8) R. S. Mulliken, *J. Am. Chem. Soc.*, **74**, 811 (1952).

(9) R. S. Mulliken, *J. Chem. Phys.*, **23**, 397 (1955).

(10) R. S. Mulliken, *Rec. Trav. Chim.*, **75**, 845 (1956).

Hanna N. Borazan ˣ
Nadhim I. Al-Ani
Department of Pharmaceutical Chemistry
College of Pharmacy
University of Baghdad
Baghdad, Republic of Iraq

Received August 27, 1979.
Accepted for publication December 3, 1979.
The authors thank Professor Hatif H. Al-Jalil for encouragement.

Pilocarpine Ocular Distribution Volume

Keyphrases □ Pilocarpine—ocular volume of distribution □ Volumes of distribution—ocular distribution of pilocarpine □ Ophthalmic drugs—pilocarpine, ocular volume of distribution

To the Editor:

It is well established that drugs introduced into the body by various routes distribute to and equilibrate with the blood as well as numerous body tissues. Thus, the apparent volume of distribution has become a useful parameter in explaining the drug concentrations achieved in the blood after dosing and for determining the extent of absorption of various agents administered in different formulations or dosage forms.

Similarly, apparent distribution volumes also are useful in describing the ocular disposition characteristics of drugs administered topically to the eye. To make meaningful statements regarding the bioavailability of an ophthalmic preparation, it is necessary to know the apparent volume of distribution for that drug in the eye.

As with volumes of distribution obtained for drugs administered by other routes, various factors can affect apparent volumes of distribution of ocular drugs. These factors include protein binding, tissue distribution, pigmentation of the eye, and, of course, any pharmacological action the drug itself might exert. Therefore, the following discussion is limited to pharmacokinetic data obtained in albino rabbits of approximately the same weight.

Conrad and Robinson (1) developed a method of quantitating apparent ocular drug distribution volumes in experimental animals by injecting drug directly into the anterior chamber and monitoring the decline in the aqueous humor concentration as a function of time. The data from the study were used subsequently[1] (2, 3) to quantitate and describe the disposition of drugs in the eye.

Conrad and Robinson (1) determined the apparent volumes of distribution and elimination rate constants for both a therapeutically active substance (pilocarpine) and a nondistributing species (inulin). From the relationship:

$$Cl = V_d K \qquad \text{(Eq. 1)}$$

and the values obtained for inulin, a clearance of 4.59 μl/min from the aqueous humor was obtained. Since inulin neither binds nor distributes into the tissues and exits the anterior chamber solely *via* aqueous humor drainage, this value should represent normal aqueous humor turnover. The calculated value is consistent with values reported by other investigators (4, 5) for aqueous humor turnover in rabbits. Similarly, unless an agent is known to decrease aqueous humor turnover, the value of 4.59 μl/min also should represent the slowest possible clearance of any compound from the aqueous humor.

Following intracameral injection, the aqueous humor concentration of pilocarpine declined monoexponentially with an apparent first-order elimination rate constant of 0.059 min^{-1}. Based on the reported volume of distribution of 575 μl, a clearance value of 33.9 μl/min was obtained for pilocarpine. Since pilocarpine is known to facilitate aqueous humor outflow, it is not surprising that the elimination rate constant for pilocarpine and, in turn, the clearance were greater than those observed for inulin.

In a recent study by Makoid and Robinson (6), the decline of pilocarpine concentration in the aqueous humor following topical dosing was multiexponential when followed for 12 hr. Conrad and Robinson (1) only followed the aqueous humor concentration of pilocarpine for 1 hr after direct intracameral injection. The effect that this apparent discrepancy might have in determining the ocular volume of distribution for pilocarpine led us to examine further the decline in the aqueous humor concentration following direct injection into the aqueous humor.

For this study, the experimental procedure of Conrad and Robinson was repeated with pilocarpine of a higher specific activity (19.7 mCi/mg). In the original study, Conrad and Robinson (1) measured aqueous humor levels of pilocarpine at 5, 10, 15, 20, 30, and 60 min after injection, but they stated that the accuracy of their 60-min time point was in doubt. In our study, the 30-min point was excluded; however, a 25-min point was added, and sampling was extended to include 45-, 60-, 90-, and 120-min points.

Figure 1 shows the results of this study when 10 μl of 1×10^{-4} *M* pilocarpine was injected intracamerally. The

[1] M. C. Makoid and J. Cobby, presented at the APhA Academy of Pharmaceutical Sciences, Anaheim meeting, April 1979.

0022-3549/80/0500-0615$01.00/0
© 1980, American Pharmaceutical Association

complexes were 0.22 and 0.16 M^{-1} for caffeine–*p*-cresol and theophylline–*p*-cresol, respectively, at 308 nm (1). On the other hand, the molar absorptivities of these complexes at the intermolecular hydrogen-bonded OH stretching vibration band, 3370 cm^{-1}, were $\sim 3 \times 10^3$ and $\sim 4.3 \times 10^3$ for caffeine–*p*-cresol and theophylline–*p*-cresol, respectively.

The present work supported the theory that hydrogen bonding is a type of charge transfer phenomenon (8–10).

(1) N. I. Al-Ani and H. N. Borazan, *J. Pharm. Sci.*, **67**, 1381 (1978).

(2) A. D. Cross, "Introduction to Practical Infra-Red Spectroscopy," 2nd ed., Butterworths, London, England, 1964, pp. 63–79.

(3) R. M. Silverstein and G. C. Bassler, "Spectroscopic Identification of Organic Compounds," 2nd ed., Wiley, New York, N.Y., 1967, pp. 64–109.

(4) W. B. Person, R. E. Humphrey, W. A. Deskin, and A. I. Popov, *J. Am. Chem. Soc.*, **80**, 2049 (1958).

(5) W. B. Person, R. E. Humphrey, and A. I. Popov, *ibid.*, **81**, 273 (1959).

(6) E. E. Ferguson and F. A. Matsen, *ibid.*, **82**, 3268 (1960).

(7) P. C. McKinney and G. M. Barrow, *J. Chem. Phys.*, **31**, 294 (1959).

(8) R. S. Mulliken, *J. Am. Chem. Soc.*, **74**, 811 (1952).

(9) R. S. Mulliken, *J. Chem. Phys.*, **23**, 397 (1955).

(10) R. S. Mulliken, *Rec. Trav. Chim.*, **75**, 845 (1956).

Hanna N. Borazan ˣ
Nadhim I. Al-Ani
Department of Pharmaceutical Chemistry
College of Pharmacy
University of Baghdad
Baghdad, Republic of Iraq

Received August 27, 1979.
Accepted for publication December 3, 1979.
The authors thank Professor Hatif H. Al-Jalil for encouragement.

Pilocarpine Ocular Distribution Volume

Keyphrases □ Pilocarpine—ocular volume of distribution □ Volumes of distribution—ocular distribution of pilocarpine □ Ophthalmic drugs—pilocarpine, ocular volume of distribution

To the Editor:

It is well established that drugs introduced into the body by various routes distribute to and equilibrate with the blood as well as numerous body tissues. Thus, the apparent volume of distribution has become a useful parameter in explaining the drug concentrations achieved in the blood after dosing and for determining the extent of absorption of various agents administered in different formulations or dosage forms.

Similarly, apparent distribution volumes also are useful in describing the ocular disposition characteristics of drugs administered topically to the eye. To make meaningful statements regarding the bioavailability of an ophthalmic preparation, it is necessary to know the apparent volume of distribution for that drug in the eye.

As with volumes of distribution obtained for drugs administered by other routes, various factors can affect apparent volumes of distribution of ocular drugs. These factors include protein binding, tissue distribution, pigmentation of the eye, and, of course, any pharmacological action the drug itself might exert. Therefore, the following discussion is limited to pharmacokinetic data obtained in albino rabbits of approximately the same weight.

Conrad and Robinson (1) developed a method of quantitating apparent ocular drug distribution volumes in experimental animals by injecting drug directly into the anterior chamber and monitoring the decline in the aqueous humor concentration as a function of time. The data from the study were used subsequently[1] (2, 3) to quantitate and describe the disposition of drugs in the eye.

Conrad and Robinson (1) determined the apparent volumes of distribution and elimination rate constants for both a therapeutically active substance (pilocarpine) and a nondistributing species (inulin). From the relationship:

$$Cl = V_d K \qquad \text{(Eq. 1)}$$

and the values obtained for inulin, a clearance of 4.59 μl/min from the aqueous humor was obtained. Since inulin neither binds nor distributes into the tissues and exits the anterior chamber solely *via* aqueous humor drainage, this value should represent normal aqueous humor turnover. The calculated value is consistent with values reported by other investigators (4, 5) for aqueous humor turnover in rabbits. Similarly, unless an agent is known to decrease aqueous humor turnover, the value of 4.59 μl/min also should represent the slowest possible clearance of any compound from the aqueous humor.

Following intracameral injection, the aqueous humor concentration of pilocarpine declined monoexponentially with an apparent first-order elimination rate constant of 0.059 min^{-1}. Based on the reported volume of distribution of 575 μl, a clearance value of 33.9 μl/min was obtained for pilocarpine. Since pilocarpine is known to facilitate aqueous humor outflow, it is not surprising that the elimination rate constant for pilocarpine and, in turn, the clearance were greater than those observed for inulin.

In a recent study by Makoid and Robinson (6), the decline of pilocarpine concentration in the aqueous humor following topical dosing was multiexponential when followed for 12 hr. Conrad and Robinson (1) only followed the aqueous humor concentration of pilocarpine for 1 hr after direct intracameral injection. The effect that this apparent discrepancy might have in determining the ocular volume of distribution for pilocarpine led us to examine further the decline in the aqueous humor concentration following direct injection into the aqueous humor.

For this study, the experimental procedure of Conrad and Robinson was repeated with pilocarpine of a higher specific activity (19.7 mCi/mg). In the original study, Conrad and Robinson (1) measured aqueous humor levels of pilocarpine at 5, 10, 15, 20, 30, and 60 min after injection, but they stated that the accuracy of their 60-min time point was in doubt. In our study, the 30-min point was excluded; however, a 25-min point was added, and sampling was extended to include 45-, 60-, 90-, and 120-min points.

Figure 1 shows the results of this study when 10 μl of 1×10^{-4} *M* pilocarpine was injected intracamerally. The

[1] M. C. Makoid and J. Cobby, presented at the APhA Academy of Pharmaceutical Sciences, Anaheim meeting, April 1979.

0022-3549/80/0500-0615$01.00/0
© 1980, American Pharmaceutical Association

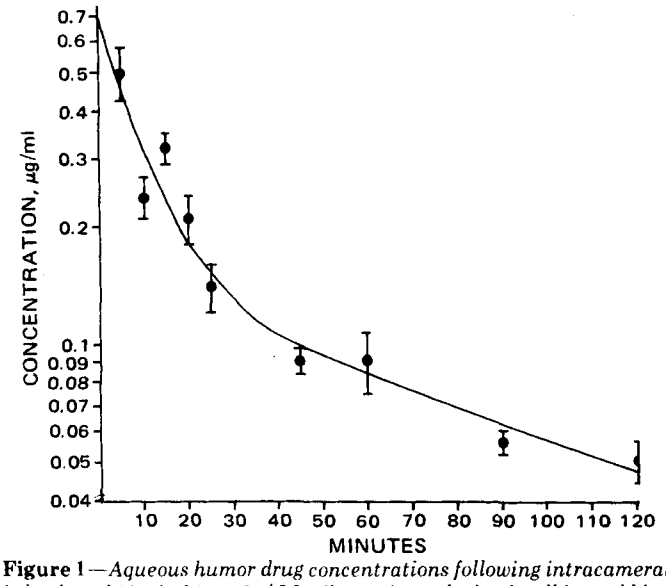

Figure 1—*Aqueous humor drug concentrations following intracameral injection of 10 μl of 1 × 10^{-4} M pilocarpine solution in albino rabbits. Points represent the mean of at least seven determinations. Bars represent the standard error of the mean. The solid line is the nonlinear regression line of the data fitted to a biexponential equation using the NONLIN program.*

absolute pilocarpine levels obtained are in reasonable agreement with those of Conrad and Robinson for the first 25 min. However, when later time points are considered, the curve clearly is not monoexponential. When the data reported here for the first 25 min are fitted to a monoexponential equation, an apparent volume of distribution and an elimination rate similar to those of Conrad and Robinson are obtained. However, due to the curvature noted at later time points, the short sampling period reported by Conrad and Robinson evidently resulted in an underestimation of the apparent ocular distribution volume for pilocarpine and represents a nonequilibrium apparent volume of distribution. This interpretation was mentioned by Conrad and Robinson but was rejected by reference to unpublished data.

The concept of a changing volume of distribution with time is, of course, not new and is expected with tissues that equilibrate slowly (7). Preliminary studies in this laboratory indicate that the partitioning of pilocarpine between aqueous humor and some ocular tissues is, in fact, a slow process. In addition, due to the effect of pilocarpine on aqueous humor turnover, it is to be expected that the slope of the pilocarpine decline from aqueous humor following intracameral injection would not remain constant over time. Ongoing experiments in this laboratory indicate that if pilocarpine levels are followed for times longer than those shown in Fig. 1, the slope becomes even more shallow. Therefore, a combination of factors, slow equilibration along with pilocarpine's pharmacological effect, makes it difficult to assign precise values to the ocular volume of distribution or, in turn, to the clearance of pilocarpine.

From a practical standpoint, apparent volumes of distribution obtained in short-term studies such as those of Conrad and Robinson may suffice for some drugs in describing aqueous humor drug levels in single-dose situations since most of the drug is eliminated quite rapidly. However, such studies usually will not suffice to predict aqueous humor drug levels over a long time or in steady-state situations. Therefore, pharmacokinetic data obtained during ocular multiple dosing or steady-state conditions may require a somewhat different interpretation than those obtained during short duration, single-dose studies.

(1) J. M. Conrad and J. R. Robinson, *J. Pharm. Sci.*, **66**, 219 (1977).
(2) T. F. Patton, *ibid.*, **66**, 1058 (1977).
(3) V. H. Lee and J. R. Robinson, *ibid.*, **68**, 673 (1979).
(4) V. E. Kinsey and D. V. N. Reddy, in "The Rabbit in Eye Research," J. H. Prince, Ed., Charles C Thomas, Springfield, Ill., 1964, p. 235.
(5) D. M. Maurice, *Am. J. Ophthalmol.*, **47**, 361 (1958).
(6) M. C. Makoid and J. R. Robinson, *J. Pharm. Sci.*, **68**, 435 (1979).
(7) S. Niazi, *ibid.*, **65**, 452 (1976).

Susan C. Miller *
Rajeev D. Gokhale
Thomas F. Patton ˣ
Department of Pharmaceutical Chemistry
University of Kansas
Lawrence, KS 66044

Kenneth J. Himmelstein
Department of Chemical and Petroleum Engineering
University of Kansas
Lawrence, KS 66045

Received July 5, 1979.
Accepted for publication February 7, 1980.
Supported in part by Grant EY 01945 from the National Institutes of Health.
*William E. Weiss Memorial Fellow of the American Foundation for Pharmaceutical Education.

Applications of TLC and Bioautography to Detect Contaminated Antibiotic Residues: Tetracycline Identification Scheme

Keyphrases □ Cephalosporins—TLC–bioautographic analysis as contaminants in various tetracyclines □ Penicillin—TLC–bioautographic analysis as contaminant in erythromycin □ Tetracyclines, various—TLC–bioautographic analysis of four cephalosporins as contaminants □ Erythromycin—TLC–bioautographic analysis of penicillin and ampicillin as contaminants

To the Editor:

A method to detect penicillin and ampicillin as contaminants in various tetracyclines and penicillamine was reported previously (1). The method utilizes TLC followed by bioautography and has been applied to other contamination situations and antibiotic standard problems. The cephalosporins are related closely to penicillin in chemical structure, antimicrobial activity, and allergenicity. In addition to the occurrence of allergenic cross-reactivity with penicillin, several cases of apparent primary allergy to cephalosporins in patients not known to be hypersensitive have been reported (2). Minor modification of the assay permitted the separation of four cephalosporin contaminants from seven tetracyclines: demeclocycline, methacycline, minocycline, chlortetracycline, oxytetracycline, doxycycline, and tetracycline.

The original method was followed with several excep-

0022-3549/80/0500-0616$01.00/0
© 1980, American Pharmaceutical Association

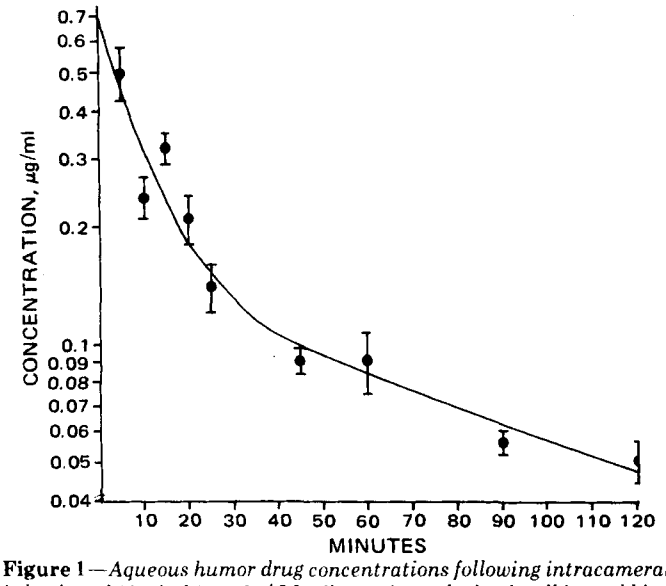

Figure 1—*Aqueous humor drug concentrations following intracameral injection of 10 μl of 1 × 10^{-4} M pilocarpine solution in albino rabbits. Points represent the mean of at least seven determinations. Bars represent the standard error of the mean. The solid line is the nonlinear regression line of the data fitted to a biexponential equation using the NONLIN program.*

absolute pilocarpine levels obtained are in reasonable agreement with those of Conrad and Robinson for the first 25 min. However, when later time points are considered, the curve clearly is not monoexponential. When the data reported here for the first 25 min are fitted to a monoexponential equation, an apparent volume of distribution and an elimination rate similar to those of Conrad and Robinson are obtained. However, due to the curvature noted at later time points, the short sampling period reported by Conrad and Robinson evidently resulted in an underestimation of the apparent ocular distribution volume for pilocarpine and represents a nonequilibrium apparent volume of distribution. This interpretation was mentioned by Conrad and Robinson but was rejected by reference to unpublished data.

The concept of a changing volume of distribution with time is, of course, not new and is expected with tissues that equilibrate slowly (7). Preliminary studies in this laboratory indicate that the partitioning of pilocarpine between aqueous humor and some ocular tissues is, in fact, a slow process. In addition, due to the effect of pilocarpine on aqueous humor turnover, it is to be expected that the slope of the pilocarpine decline from aqueous humor following intracameral injection would not remain constant over time. Ongoing experiments in this laboratory indicate that if pilocarpine levels are followed for times longer than those shown in Fig. 1, the slope becomes even more shallow. Therefore, a combination of factors, slow equilibration along with pilocarpine's pharmacological effect, makes it difficult to assign precise values to the ocular volume of distribution or, in turn, to the clearance of pilocarpine.

From a practical standpoint, apparent volumes of distribution obtained in short-term studies such as those of Conrad and Robinson may suffice for some drugs in describing aqueous humor drug levels in single-dose situations since most of the drug is eliminated quite rapidly. However, such studies usually will not suffice to predict aqueous humor drug levels over a long time or in steady-state situations. Therefore, pharmacokinetic data obtained during ocular multiple dosing or steady-state conditions may require a somewhat different interpretation than those obtained during short duration, single-dose studies.

(1) J. M. Conrad and J. R. Robinson, *J. Pharm. Sci.*, **66**, 219 (1977).
(2) T. F. Patton, *ibid.*, **66**, 1058 (1977).
(3) V. H. Lee and J. R. Robinson, *ibid.*, **68**, 673 (1979).
(4) V. E. Kinsey and D. V. N. Reddy, in "The Rabbit in Eye Research," J. H. Prince, Ed., Charles C Thomas, Springfield, Ill., 1964, p. 235.
(5) D. M. Maurice, *Am. J. Ophthalmol.*, **47**, 361 (1958).
(6) M. C. Makoid and J. R. Robinson, *J. Pharm. Sci.*, **68**, 435 (1979).
(7) S. Niazi, *ibid.*, **65**, 452 (1976).

Susan C. Miller *
Rajeev D. Gokhale
Thomas F. Patton ˣ
Department of Pharmaceutical Chemistry
University of Kansas
Lawrence, KS 66044

Kenneth J. Himmelstein
Department of Chemical and Petroleum Engineering
University of Kansas
Lawrence, KS 66045

Received July 5, 1979.
Accepted for publication February 7, 1980.
Supported in part by Grant EY 01945 from the National Institutes of Health.
*William E. Weiss Memorial Fellow of the American Foundation for Pharmaceutical Education.

Applications of TLC and Bioautography to Detect Contaminated Antibiotic Residues: Tetracycline Identification Scheme

Keyphrases □ Cephalosporins—TLC–bioautographic analysis as contaminants in various tetracyclines □ Penicillin—TLC–bioautographic analysis as contaminant in erythromycin □ Tetracyclines, various—TLC–bioautographic analysis of four cephalosporins as contaminants □ Erythromycin—TLC–bioautographic analysis of penicillin and ampicillin as contaminants

To the Editor:

A method to detect penicillin and ampicillin as contaminants in various tetracyclines and penicillamine was reported previously (1). The method utilizes TLC followed by bioautography and has been applied to other contamination situations and antibiotic standard problems. The cephalosporins are related closely to penicillin in chemical structure, antimicrobial activity, and allergenicity. In addition to the occurrence of allergenic cross-reactivity with penicillin, several cases of apparent primary allergy to cephalosporins in patients not known to be hypersensitive have been reported (2). Minor modification of the assay permitted the separation of four cephalosporin contaminants from seven tetracyclines: demeclocycline, methacycline, minocycline, chlortetracycline, oxytetracycline, doxycycline, and tetracycline.

The original method was followed with several excep-

0022-3549/80/0500-0616$01.00/0
© 1980, American Pharmaceutical Association

Table I—R_f Values and Detection Limits of Cephalosporins

Antibiotic	R_f	Detection Limit, μg
Cephalothin	0.65	0.01
Cephaloridine	0.41	0.01
Cephalexin	0.59	0.005
Cephaloglycin	0.38	0.01

tions. The standard solutions of the cephalosporins were prepared at concentrations of 1.0, 0.5, 0.25, and 0.125 μg/ml, and the mobile phase composition was adjusted to a barbital acetate buffer (pH 7.4) to acetone ratio of 80:20 (v/v). The tetracyclines remained near the starting point; the cephalosporins migrated with the R_f values indicated in Table I.

Similarly, erythromycin is administered frequently to patients sensitive to penicillin. Thus, any contamination of erythromycin by penicillin is particularly undesirable for such patients. The existing conventional methods to detect penicillin in erythromycin are extraction procedures followed by cylinder–plate assay or direct cylinder–plate assay. These methods are time consuming and require much more sample handling than does this TLC method. Again, the same methodology was followed except that the mobile phase composition ratio was changed to 90:10 (v/v). Erythromycin base, erythromycin stearate, and erythromycin stearate tablets were assayed. The erythromycin remained at the spotting point, whereas the R_f value for penicillin G was 0.24 and that for ampicillin was 0.47.

The original system has been helpful in assessing the purity of some antibiotic standards. UV spectrophotometry is the official identity test for many antibiotics, including penicillin V. When a proposed standard of penicillin V potassium was assayed, the spectrum showed an additional peak. The following solutions were chromatographed in this system: penicillin V potassium, the proposed standard; penicillin V potassium, the working standard; a mixture of penicillin G potassium and penicillin V potassium; penicillin G potassium, the working standard; and *p*-hydroxypenicillin V potassium. The results are shown in Fig. 1. Carbenicillin, amoxicillin, neomycin, and cyclacillin were assayed using this system.

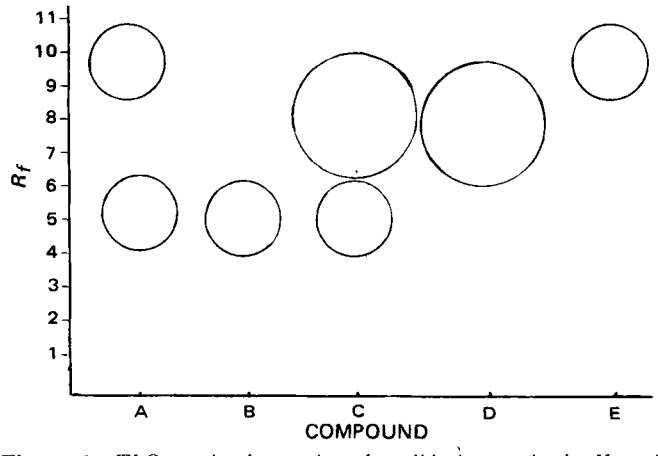

Figure 1—*TLC results for purity of antibiotic standards. Key: A, penicillin V potassium, proposed standard, 0.1 μg; B, penicillin V potassium, working standard, 0.1 μg; C, penicillin G potassium, 0.005 μg, and penicillin V potassium, 0.1 μg; D, penicillin G potassium, working standard, 0.005 μg; and E, p-hydroxypenicillin V potassium, 0.01 μg.*

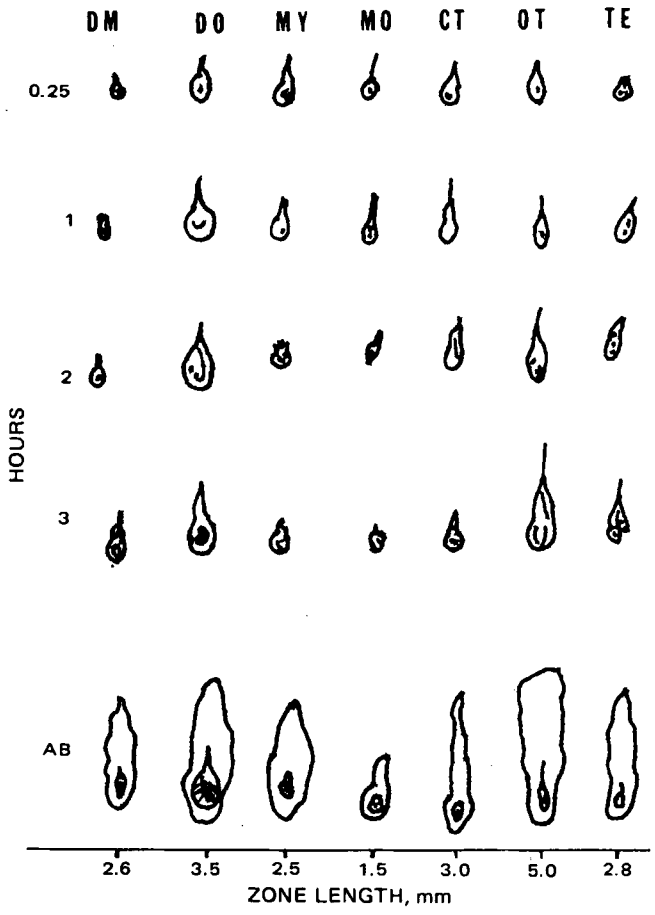

Figure 2—*Bioautography of seven antibiotic standards (left to right): DM, demeclocycline; DO, doxycycline; MY, methacycline; MO, minocycline; CT, chlortetracycline; OT, oxytetracycline; and TE, tetracycline. Top to bottom and left to right: 0.25 hr—yellow, pale yellow with pink tint, pale yellow, yellow, yellow, yellow, and yellow; 1 hr—yellow circle with purple beard, yellow center with pink outline, pale yellow, yellow, yellow, yellow, and yellow with pink beard; 2 hr—yellow center with purple beard, yellow center with rose outline, yellow center with pink outline, yellow, yellow center with gray beard, pale yellow, and orange center with purple beard; 3 hr—light brown, dark brown with yellow center, pale-orange outline with gray beard, bright yellow, bright yellow with tan beard, pale yellow, and gray. The spots obtained after the bioautograph are denoted by AB.*

The method described in the *Code of Federal Regulations* (paragraph 436.308) to identify the tetracyclines is a paper chromatographic technique in which individual tetracyclines are identified presumptively when the R_f value of the unknown matches the R_f value of a known tetracycline. During the development of this thin-layer technique, it was noted that, after the chromatographic procedure, a series of color changes takes place that is unique for each tetracycline spot. Each spot develops in an individual manner with regard to shape and color so that no two give the exact same pictures. After the bioautograph, no two zones have identical configurations. The combination of shape and color at the point of origin and individual shapes of the zones of inhibition can serve as a means of identification. As in the paper chromatographic method, an unknown sample can be run with the seven known standards and readily identified (Fig. 2).

Since this TLC system is quite adaptable and the biological phase is readily adjusted for particular needs, variations of the basic system should be applied success-

fully to other contamination problems and other areas of interest.

(1) D. V. Herbst, *J. Pharm. Sci.*, **66**, 1646 (1977).
(2) H. Bundgaard, *Arch. Pharm. Chem. Sci. Ed.*, **3**, 74 (1975).

Doris V. Herbst

National Center for
Antibiotics Analysis
Food and Drug Administration
Washington, DC 20204

Received November 8, 1979.
Accepted for publication February 6, 1980.

BOOKS

REVIEWS

Drug Design, Vol. VIII. Edited by E. J. ARIENS. Academic, 111 Fifth Ave., New York, NY 10003. 1979. 420 pp. 15 × 23 cm. $42.00.

This book is the eighth member of a continuing set, which collectively comprises Volume 11 of the series of monographs entitled "Medicinal Chemistry." Dr. Ariens has produced another valuable book. As stated in the preface of this volume, the term "drug" is to be interpreted in the widest sense. Indeed, this volume includes such diverse agents as synthetic sweeteners, ionophores, and potential environmental pollutants.

In the first chapter, Martin discusses "Advances in the Methodology of Quantitative Drug Design." This chapter is a systematic survey of the approaches available for finding the substituent group giving optimum activity from a lead compound either by batch or stepwise selection of new derivatives. The parameters for describing electronic, steric, and, particularly, lipophilic effects of substituents are considered. Considerable attention is devoted to theoretical models for the distribution of drugs into different compartments depending on their physicochemical properties. Finally, the information that can be obtained by regression and discriminate analyses is discussed. The most valuable aspect of the chapter probably is the many caveats concerning the limitations and pitfalls of quantitative structure–activity relationship methods.

In the second chapter, Kirschner and Kowalski deal with the "Application of Pattern Recognition to Drug Design." The first portion covers the general methodology of pattern recognition, and the second portion covers applications to drugs. Although development of this powerful mathematical tool has been initiated, much more work is needed.

In Chapter 3, the design of drug delivery systems that will release a constant amount of drug over a long period is discussed by Chandrasekaran, Theeuwes, and Yum. This chapter primarily describes the features and theory behind three currently available systems; OROS Theophyllin for oral use, a transdermal scopolamine system, and the Alzet osmotic minipump. Chapter 4 is an excellent discussion of the use of receptor binding data for the design of steroid hormones by Raynaud, Ojasoo, Bouton, and Philibert. The general techniques of receptor isolation and displacement of bound, radiolabeled ligands for various hormonal activities are presented. Then, the specific structure–activity relationships for receptor binding of estrogens, progestins, androgens, and mineralcorticoid and glucocorticoid hormones are considered. The relationship between receptor binding and *in vivo* activity is discussed last.

The fifth chapter, authored by Crosby, DuBois, and Wingard, covers synthetic sweeteners. There is an interesting discussion of the theory of taste and the known structure–activity relationships for sweet substances; however, too much basic material on molecular interactions, Hansch treatment, *etc.*, is included that is covered elsewhere in the series and detracts from this chapter. Chapter 6, "Prospective Assessment of Environmental Effects of Chemicals," by Hueck-van der Plas and Hueck is concerned with the test systems that can be used to predict the environmental impact of chemicals. This chapter probably will be of more interest to researchers dealing with agricultural chemicals rather than to those concerned with drugs for human use.

The final chapter is fascinating; it describes the "Design of Selective Ion Binding Macrocyclic Compounds and Their Biological Applications" and was authored by Izatt, Lamb, Eatough, Christensen, and Rytting. The factors affecting the selective-ion complexation by crown ethers and derivatives are discussed in detail.

This volume generally is well written and free from typographical errors. Every medicinal chemist should find something of interest.

Reviewed by James F. Stubbins
Department of Pharmaceutical Chemistry
Medical College of Virginia
Virginia Commonwealth University
Richmond, VA 23298

Foreign Compound Metabolism in Mammals, Vol. 5. A Review of the Literature Published During 1976 and 1977. Senior Reporter, D. E. HATHWAY. The Chemical Society, Burlington House, London W1V OBN, England. 1979. 567 pp. 13 × 22 cm. Price $70.00. (Available from the American Chemical Society, 1155 16th St., N.W., Washington, DC 20036.)

This volume is an organized condensation of almost 3000 major metabolism–pharmacokinetics papers published in 1976 and 1977. The first half of the volume consists of five subject-oriented chapters, which are followed by eight product-oriented chapters.

Chapter 1, Drug Kinetics by P. G. Wellington, is the longest chapter (86 pages) and has the highest density of references (758 total references for a mean of 8.6 references/page). This chapter has 20 well-selected sections and deals with prostaglandins, ethanol, inorganic ions, and diagnostic agents in addition to a wide variety of drug classes. Chapter 2, Enzymic Mechanisms of Oxidation, Reduction, and Hydrolysis by P. Bentley and F. Oesch, interestingly covers the assigned terrain. Many readers will appreciate the subsection on epoxide hydratase for its inclusion of topics such as control and induction and occurrence in extrahepatic tissues.

P. C. Hirom and P. Millburn cover Enzymic Mechanisms of Conjugation (Chapter 3) in a fairly lively fashion. They briefly discuss new conjugation reactions and amino acid conjugations, and they animate their treatment of "the usual suspects" by reporting the tissue distribution of the enzymes responsible for conjugations with glucuronic acid, sulfate, and glutathione. In Chapter 4, J. D. Baty deals selectively and well with Species, Strain, and Sex Differences in Metabolism. Beside discussing comparative catabolic and conjugation reactions, Baty focuses on comparative differences in biliary excretion. The final subject-oriented chapter, Mechanisms of Chemical Carcinogenesis by D. E. Hathway, has this reviewer's enthusiastic endorsement for its interesting, valuable, and topical content. Its 54 pages utilize 358 well-chosen references that are integrated superbly.

The first product-oriented chapter has a more pharmacological orientation than do the others. This chapter, the Effect of Drugs on the Central Nervous System by B. E. Leonard, integrates mechanisms of action with biotransformations. C. Rhodes divides his report on Cardiovascular Drugs into sections dealing with thrombosis, hypertension, and cardiac disorders and summarizes some particularly interesting interspecies differences in biotransformation pathways of numerous drugs. L. G. Dring and P. Millburn address the metabolism of Sympathomimetic Amines and Bronchodilators and underscore many differences between *in vivo* and *in vitro* biotransformation routes.

fully to other contamination problems and other areas of interest.

(1) D. V. Herbst, *J. Pharm. Sci.*, **66**, 1646 (1977).
(2) H. Bundgaard, *Arch. Pharm. Chem. Sci. Ed.*, **3**, 74 (1975).

Doris V. Herbst

National Center for
Antibiotics Analysis
Food and Drug Administration
Washington, DC 20204

Received November 8, 1979.
Accepted for publication February 6, 1980.

BOOKS

REVIEWS

Drug Design, Vol. VIII. Edited by E. J. ARIENS. Academic, 111 Fifth Ave., New York, NY 10003. 1979. 420 pp. 15 × 23 cm. $42.00.

This book is the eighth member of a continuing set, which collectively comprises Volume 11 of the series of monographs entitled "Medicinal Chemistry." Dr. Ariens has produced another valuable book. As stated in the preface of this volume, the term "drug" is to be interpreted in the widest sense. Indeed, this volume includes such diverse agents as synthetic sweeteners, ionophores, and potential environmental pollutants.

In the first chapter, Martin discusses "Advances in the Methodology of Quantitative Drug Design." This chapter is a systematic survey of the approaches available for finding the substituent group giving optimum activity from a lead compound either by batch or stepwise selection of new derivatives. The parameters for describing electronic, steric, and, particularly, lipophilic effects of substituents are considered. Considerable attention is devoted to theoretical models for the distribution of drugs into different compartments depending on their physicochemical properties. Finally, the information that can be obtained by regression and discriminate analyses is discussed. The most valuable aspect of the chapter probably is the many caveats concerning the limitations and pitfalls of quantitative structure–activity relationship methods.

In the second chapter, Kirschner and Kowalski deal with the "Application of Pattern Recognition to Drug Design." The first portion covers the general methodology of pattern recognition, and the second portion covers applications to drugs. Although development of this powerful mathematical tool has been initiated, much more work is needed.

In Chapter 3, the design of drug delivery systems that will release a constant amount of drug over a long period is discussed by Chandrasekaran, Theeuwes, and Yum. This chapter primarily describes the features and theory behind three currently available systems; OROS Theophyllin for oral use, a transdermal scopolamine system, and the Alzet osmotic minipump. Chapter 4 is an excellent discussion of the use of receptor binding data for the design of steroid hormones by Raynaud, Ojasoo, Bouton, and Philibert. The general techniques of receptor isolation and displacement of bound, radiolabeled ligands for various hormonal activities are presented. Then, the specific structure–activity relationships for receptor binding of estrogens, progestins, androgens, and mineralcorticoid and glucocorticoid hormones are considered. The relationship between receptor binding and *in vivo* activity is discussed last.

The fifth chapter, authored by Crosby, DuBois, and Wingard, covers synthetic sweeteners. There is an interesting discussion of the theory of taste and the known structure–activity relationships for sweet substances; however, too much basic material on molecular interactions, Hansch treatment, *etc.*, is included that is covered elsewhere in the series and detracts from this chapter. Chapter 6, "Prospective Assessment of Environmental Effects of Chemicals," by Hueck-van der Plas and Hueck is concerned with the test systems that can be used to predict the environmental impact of chemicals. This chapter probably will be of more interest to researchers dealing with agricultural chemicals rather than to those concerned with drugs for human use.

The final chapter is fascinating; it describes the "Design of Selective Ion Binding Macrocyclic Compounds and Their Biological Applications" and was authored by Izatt, Lamb, Eatough, Christensen, and Rytting. The factors affecting the selective-ion complexation by crown ethers and derivatives are discussed in detail.

This volume generally is well written and free from typographical errors. Every medicinal chemist should find something of interest.

Reviewed by James F. Stubbins
Department of Pharmaceutical Chemistry
Medical College of Virginia
Virginia Commonwealth University
Richmond, VA 23298

Foreign Compound Metabolism in Mammals, Vol. 5. A Review of the Literature Published During 1976 and 1977. Senior Reporter, D. E. HATHWAY. The Chemical Society, Burlington House, London W1V OBN, England. 1979. 567 pp. 13 × 22 cm. Price $70.00. (Available from the American Chemical Society, 1155 16th St., N.W., Washington, DC 20036.)

This volume is an organized condensation of almost 3000 major metabolism–pharmacokinetics papers published in 1976 and 1977. The first half of the volume consists of five subject-oriented chapters, which are followed by eight product-oriented chapters.

Chapter 1, Drug Kinetics by P. G. Wellington, is the longest chapter (86 pages) and has the highest density of references (758 total references for a mean of 8.6 references/page). This chapter has 20 well-selected sections and deals with prostaglandins, ethanol, inorganic ions, and diagnostic agents in addition to a wide variety of drug classes. Chapter 2, Enzymic Mechanisms of Oxidation, Reduction, and Hydrolysis by P. Bentley and F. Oesch, interestingly covers the assigned terrain. Many readers will appreciate the subsection on epoxide hydratase for its inclusion of topics such as control and induction and occurrence in extrahepatic tissues.

P. C. Hirom and P. Millburn cover Enzymic Mechanisms of Conjugation (Chapter 3) in a fairly lively fashion. They briefly discuss new conjugation reactions and amino acid conjugations, and they animate their treatment of "the usual suspects" by reporting the tissue distribution of the enzymes responsible for conjugations with glucuronic acid, sulfate, and glutathione. In Chapter 4, J. D. Baty deals selectively and well with Species, Strain, and Sex Differences in Metabolism. Beside discussing comparative catabolic and conjugation reactions, Baty focuses on comparative differences in biliary excretion. The final subject-oriented chapter, Mechanisms of Chemical Carcinogenesis by D. E. Hathway, has this reviewer's enthusiastic endorsement for its interesting, valuable, and topical content. Its 54 pages utilize 358 well-chosen references that are integrated superbly.

The first product-oriented chapter has a more pharmacological orientation than do the others. This chapter, the Effect of Drugs on the Central Nervous System by B. E. Leonard, integrates mechanisms of action with biotransformations. C. Rhodes divides his report on Cardiovascular Drugs into sections dealing with thrombosis, hypertension, and cardiac disorders and summarizes some particularly interesting interspecies differences in biotransformation pathways of numerous drugs. L. G. Dring and P. Millburn address the metabolism of Sympathomimetic Amines and Bronchodilators and underscore many differences between *in vivo* and *in vitro* biotransformation routes.

fully to other contamination problems and other areas of interest.

(1) D. V. Herbst, *J. Pharm. Sci.*, **66**, 1646 (1977).
(2) H. Bundgaard, *Arch. Pharm. Chem. Sci. Ed.*, **3**, 74 (1975).

Doris V. Herbst

National Center for
Antibiotics Analysis
Food and Drug Administration
Washington, DC 20204

Received November 8, 1979.
Accepted for publication February 6, 1980.

BOOKS

REVIEWS

Drug Design, Vol. VIII. Edited by E. J. ARIENS. Academic, 111 Fifth Ave., New York, NY 10003. 1979. 420 pp. 15 × 23 cm. $42.00.

This book is the eighth member of a continuing set, which collectively comprises Volume 11 of the series of monographs entitled "Medicinal Chemistry." Dr. Ariens has produced another valuable book. As stated in the preface of this volume, the term "drug" is to be interpreted in the widest sense. Indeed, this volume includes such diverse agents as synthetic sweeteners, ionophores, and potential environmental pollutants.

In the first chapter, Martin discusses "Advances in the Methodology of Quantitative Drug Design." This chapter is a systematic survey of the approaches available for finding the substituent group giving optimum activity from a lead compound either by batch or stepwise selection of new derivatives. The parameters for describing electronic, steric, and, particularly, lipophilic effects of substituents are considered. Considerable attention is devoted to theoretical models for the distribution of drugs into different compartments depending on their physicochemical properties. Finally, the information that can be obtained by regression and discriminate analyses is discussed. The most valuable aspect of the chapter probably is the many caveats concerning the limitations and pitfalls of quantitative structure–activity relationship methods.

In the second chapter, Kirschner and Kowalski deal with the "Application of Pattern Recognition to Drug Design." The first portion covers the general methodology of pattern recognition, and the second portion covers applications to drugs. Although development of this powerful mathematical tool has been initiated, much more work is needed.

In Chapter 3, the design of drug delivery systems that will release a constant amount of drug over a long period is discussed by Chandrasekaran, Theeuwes, and Yum. This chapter primarily describes the features and theory behind three currently available systems; OROS Theophyllin for oral use, a transdermal scopolamine system, and the Alzet osmotic minipump. Chapter 4 is an excellent discussion of the use of receptor binding data for the design of steroid hormones by Raynaud, Ojasoo, Bouton, and Philibert. The general techniques of receptor isolation and displacement of bound, radiolabeled ligands for various hormonal activities are presented. Then, the specific structure–activity relationships for receptor binding of estrogens, progestins, androgens, and mineralcorticoid and glucocorticoid hormones are considered. The relationship between receptor binding and *in vivo* activity is discussed last.

The fifth chapter, authored by Crosby, DuBois, and Wingard, covers synthetic sweeteners. There is an interesting discussion of the theory of taste and the known structure–activity relationships for sweet substances; however, too much basic material on molecular interactions, Hansch treatment, *etc.*, is included that is covered elsewhere in the series and detracts from this chapter. Chapter 6, "Prospective Assessment of Environmental Effects of Chemicals," by Hueck-van der Plas and Hueck is concerned with the test systems that can be used to predict the environmental impact of chemicals. This chapter probably will be of more interest to researchers dealing with agricultural chemicals rather than to those concerned with drugs for human use.

The final chapter is fascinating; it describes the "Design of Selective Ion Binding Macrocyclic Compounds and Their Biological Applications" and was authored by Izatt, Lamb, Eatough, Christensen, and Rytting. The factors affecting the selective-ion complexation by crown ethers and derivatives are discussed in detail.

This volume generally is well written and free from typographical errors. Every medicinal chemist should find something of interest.

Reviewed by James F. Stubbins
Department of Pharmaceutical Chemistry
Medical College of Virginia
Virginia Commonwealth University
Richmond, VA 23298

Foreign Compound Metabolism in Mammals, Vol. 5. A Review of the Literature Published During 1976 and 1977. Senior Reporter, D. E. HATHWAY. The Chemical Society, Burlington House, London W1V OBN, England. 1979. 567 pp. 13 × 22 cm. Price $70.00. (Available from the American Chemical Society, 1155 16th St., N.W., Washington, DC 20036.)

This volume is an organized condensation of almost 3000 major metabolism–pharmacokinetics papers published in 1976 and 1977. The first half of the volume consists of five subject-oriented chapters, which are followed by eight product-oriented chapters.

Chapter 1, Drug Kinetics by P. G. Wellington, is the longest chapter (86 pages) and has the highest density of references (758 total references for a mean of 8.6 references/page). This chapter has 20 well-selected sections and deals with prostaglandins, ethanol, inorganic ions, and diagnostic agents in addition to a wide variety of drug classes. Chapter 2, Enzymic Mechanisms of Oxidation, Reduction, and Hydrolysis by P. Bentley and F. Oesch, interestingly covers the assigned terrain. Many readers will appreciate the subsection on epoxide hydratase for its inclusion of topics such as control and induction and occurrence in extrahepatic tissues.

P. C. Hirom and P. Millburn cover Enzymic Mechanisms of Conjugation (Chapter 3) in a fairly lively fashion. They briefly discuss new conjugation reactions and amino acid conjugations, and they animate their treatment of "the usual suspects" by reporting the tissue distribution of the enzymes responsible for conjugations with glucuronic acid, sulfate, and glutathione. In Chapter 4, J. D. Baty deals selectively and well with Species, Strain, and Sex Differences in Metabolism. Beside discussing comparative catabolic and conjugation reactions, Baty focuses on comparative differences in biliary excretion. The final subject-oriented chapter, Mechanisms of Chemical Carcinogenesis by D. E. Hathway, has this reviewer's enthusiastic endorsement for its interesting, valuable, and topical content. Its 54 pages utilize 358 well-chosen references that are integrated superbly.

The first product-oriented chapter has a more pharmacological orientation than do the others. This chapter, the Effect of Drugs on the Central Nervous System by B. E. Leonard, integrates mechanisms of action with biotransformations. C. Rhodes divides his report on Cardiovascular Drugs into sections dealing with thrombosis, hypertension, and cardiac disorders and summarizes some particularly interesting interspecies differences in biotransformation pathways of numerous drugs. L. G. Dring and P. Millburn address the metabolism of Sympathomimetic Amines and Bronchodilators and underscore many differences between *in vivo* and *in vitro* biotransformation routes.

The short chapter on Anti-Infective Agents by P. Johnson and J. D. Coombes deals with the biotransformation of some unusual structures while covering antiparasitics, antibiotics, antimycotic agents, antidiarrheals, antitubercular drugs, antivirals, and sulfonamides. Interesting interspecies and *in vivo–in vitro* comparisons pervade the coverage of Prostaglandins and Steroids by G. R. Bourne and D. E. Hathway. In the chapter on Food Constituents, D. E. Hathway objectively evaluates the saccharin and cyclamate problems under the heading of sweetening agents and deals with single-cell proteins, flour, vitamins, urethane and diethyl dicarbonate, food colorants, flavoring principles, and natural constituents.

C. T. Bedford reviews Agricultural Chemicals in sections on animal health products, rodenticides, insecticides, herbicides, and fungicides. This chapter is enlivened by descriptions of an anticoagulant with selective toxicity for vampire bats, an anthelmintic that is degraded to benzene, and an ususual example of *N*-dearylation. C. T. Bedford also contributed the final chapter, Industrial Chemicals and Miscellaneous Organic Compounds, which contains sections on aliphatic compounds, aromatic compounds, heteroaromatic compounds, and organometallic and inorganic compounds. Like the previous chapter, this chapter summarizes the biotransformation of many important environmental contaminants. Some of the more interesting reactions involve the formation of a metabolite of 4-dimethylaminophenol, which contains three glutathione residues attached to a single aromatic ring, and the formation of phosgene and carbon monoxide as metabolites.

The few typographical errors in this book are readily understood, as are the misspellings of the names of some prominent scientists in the author index. The compound index lists only substrates, not metabolites. More unfortunate is the absence of a comprehensive subject index that would enable readers to use the volume cross-sectionally; for example, to collect valuable information on studies performed in the wide variety of species covered in the volume (including humans, subhuman primates, sheep, cattle, lambs, pigs, tree shrews, and insects) or on reaction types or sites of biotransformation.

Overall, this volume is recommended highly as an organized source of metabolism–pharmacokinetics literature on important xenobiotics of many kinds. One of its major achievements is that it demonstrates the richness of opportunities for valuable future investigations.

Reviewed by Frederick J. Di Carlo
Office of Toxic Substances
U.S. Environmental Protection Agency
Washington, DC 20460

Quality Control in the Pharmaceutical Industry, Vol. 3. Edited by M. S. COOPER. Academic, 111 Fifth Ave., New York, NY 10003. 1979. 292 pp. 15.5 × 22.5 cm. Price $29.50.

Volume 3 of this series consists of six chapters covering the interpretation of current good manufacturing practice regulations, the auditing function in the total control of quality, filtrative sterilization with porous membranes, bioavailability standards for pharmaceutical products, quality control of poliomyelitis vaccines, and quality control of ophthalmic products.

The chapter by A. S. Arambulo on "Interpretation of Current Good Manufacturing Practice Regulations" exceeds 100 pages and presents an excellent comprehensive review. The concept and parts of the regulations are discussed and illustrated by examples. This chapter should be of special interest to graduate students and recent graduates who are joining the pharmaceutical industry and to management personnel who have not been trained as physical or biological scientists.

The chapter on "Auditing Function in the Total Control of Quality" by A. J. Schmitz, Jr., reviews the quality control of the product and the quality control of operations and control techniques. Auditing includes managerial review of quality assurance to a firm to procure, produce, distribute, and control all phases of the function of a firm including facilities, personnel, standards, and the auditing method.

The chapter on "Filtrative Sterilization with Porous Membranes" by T. H. Meltzer and R. C. Lukaszewicz is concerned with the technology of porous membranes. It does not discuss sterility testing, but it does discuss pore properties, manufacture, filter rating, retentivity, and types of filters used. Prefilters and filter construction, design, preparation for use, and usage are discussed.

The chapter on "Bioavailability Standards for Pharmaceutical Products" by R. V. Smith and G. J. Yakatan is the shortest chapter. It presents elemental remarks on bioequivalency and gives an overview of analytical methods and their selection in bioavailability studies.

The chapter on "Quality Control of Poliomyelitis Vaccines" is by P. B. Stone. A review is given of tissue culture and animal testing of inactivated polio vaccine and the testing of live polio vaccine for adventitious agents, mycoplasma, and identity.

The chapter on "Quality Control of Ophthalmic Products" by J. D. Mullins and T. C. Fleming presents an elemental review of the anatomy of the eye, absorption, ophthalmic dosages, formulation, and processing.

This volume presents useful information for those seeking an overview of quality control in the specific areas covered; however, pharmaceutical scientists currently involved in quality assurance may find the treatment too cursory.

Reviewed by Eugene L. Parrott
College of Pharmacy
University of Iowa
Iowa City, IA 52242

Handbook of Analytical Derivatization Reactions. By DANIEL R. KNAPP. Wiley, One Wiley Drive, Somerset, NJ 08873. 1979. 741 pp. 15 × 23 cm. Price $34.95.

This book presents a collection of analytical derivatization methods for gas chromatographic, liquid chromatographic, and mass spectral analysis. The reactions involve only the covalent derivatives of organic compounds formed prior to analysis. Part I briefly discusses the uses of analytical derivatization, the types of derivatives formed, and a typical apparatus employed in such reactions.

Part II features 15 sections concerning the derivatization of particular compound types. Among the classes considered are steroids, prostaglandins, and drugs. An overview of derivatization for the sample type is given along with specific derivatization methods. For each major compound type, the derivatization reactions are organized further into subsections of the compound type and within each subsection according to the type of derivative formed. Each method description includes structural formulas for the reaction, experimental directions, and references to the original literature. Sections on derivatives for substituent location by mass spectrometry and derivatives for chromatographic separation of optical isomers also are included.

Part III contains author and general subject indexes along with appendixes listing the composition of brand name reagents and U.S. and foreign suppliers of reagents and apparatuses used for analytical derivatization. An index of the derivatives and reagents discussed in Part II also is included.

This book should serve both as a self-contained methodology reference and as an introduction to the literature on analytical derivatization.

Staff Review

Pharmacognosy, 11th ed. By G. E. TREASE and W. C. EVANS. Cassell and Collier Macmillan Publishers Ltd., 35 Red Lion Square, London WC1R 49G, England. 1978. 784 pp. 16 × 23 cm. Price $32.50.

This is the 11th edition of a longstanding series of revisions that trace their origin to the original work in 1934. The latest revision reflects the increasing awareness and knowledge of the active constituents of natural, particularly vegetable, drugs. The book has been partially rearranged from the 10th edition with lengthy revisions in the parts dealing with drug sources, including production and quality control and the consideration of the various classes of drugs of biological origin.

The book is composed of eight parts with a total of 41 chapters, including an index. It is liberally filled with numerous structural formulas, pictures (none in color), tables, and illustrations. Part 1 (Chapters 1–3) deals with drug classification, the literature of pharmacognosy, and plant nomenclature and taxonomy. Part 2 (Chapters 4–7) covers plant morphology, anatomy, histology, and cellular content. Part 3 (Chapters 8–12) discusses the botanical and chemical characteristics of the more important orders and families of both nonflowering and flowering plants with references taken from Volumes 74–84 of *Chemical Abstracts*. Part 4 (Chapters 13–18) includes a discussion of the sources of crude drugs, drug production, quality control, drug deterioration, and plant growth regu-

The short chapter on Anti-Infective Agents by P. Johnson and J. D. Coombes deals with the biotransformation of some unusual structures while covering antiparasitics, antibiotics, antimycotic agents, antidiarrheals, antitubercular drugs, antivirals, and sulfonamides. Interesting interspecies and *in vivo–in vitro* comparisons pervade the coverage of Prostaglandins and Steroids by G. R. Bourne and D. E. Hathway. In the chapter on Food Constituents, D. E. Hathway objectively evaluates the saccharin and cyclamate problems under the heading of sweetening agents and deals with single-cell proteins, flour, vitamins, urethane and diethyl dicarbonate, food colorants, flavoring principles, and natural constituents.

C. T. Bedford reviews Agricultural Chemicals in sections on animal health products, rodenticides, insecticides, herbicides, and fungicides. This chapter is enlivened by descriptions of an anticoagulant with selective toxicity for vampire bats, an anthelmintic that is degraded to benzene, and an ususual example of *N*-dearylation. C. T. Bedford also contributed the final chapter, Industrial Chemicals and Miscellaneous Organic Compounds, which contains sections on aliphatic compounds, aromatic compounds, heteroaromatic compounds, and organometallic and inorganic compounds. Like the previous chapter, this chapter summarizes the biotransformation of many important environmental contaminants. Some of the more interesting reactions involve the formation of a metabolite of 4-dimethylaminophenol, which contains three glutathione residues attached to a single aromatic ring, and the formation of phosgene and carbon monoxide as metabolites.

The few typographical errors in this book are readily understood, as are the misspellings of the names of some prominent scientists in the author index. The compound index lists only substrates, not metabolites. More unfortunate is the absence of a comprehensive subject index that would enable readers to use the volume cross-sectionally; for example, to collect valuable information on studies performed in the wide variety of species covered in the volume (including humans, subhuman primates, sheep, cattle, lambs, pigs, tree shrews, and insects) or on reaction types or sites of biotransformation.

Overall, this volume is recommended highly as an organized source of metabolism–pharmacokinetics literature on important xenobiotics of many kinds. One of its major achievements is that it demonstrates the richness of opportunities for valuable future investigations.

Reviewed by Frederick J. Di Carlo
Office of Toxic Substances
U.S. Environmental Protection Agency
Washington, DC 20460

Quality Control in the Pharmaceutical Industry, Vol. 3. Edited by M. S. COOPER. Academic, 111 Fifth Ave., New York, NY 10003. 1979. 292 pp. 15.5 × 22.5 cm. Price $29.50.

Volume 3 of this series consists of six chapters covering the interpretation of current good manufacturing practice regulations, the auditing function in the total control of quality, filtrative sterilization with porous membranes, bioavailability standards for pharmaceutical products, quality control of poliomyelitis vaccines, and quality control of ophthalmic products.

The chapter by A. S. Arambulo on "Interpretation of Current Good Manufacturing Practice Regulations" exceeds 100 pages and presents an excellent comprehensive review. The concept and parts of the regulations are discussed and illustrated by examples. This chapter should be of special interest to graduate students and recent graduates who are joining the pharmaceutical industry and to management personnel who have not been trained as physical or biological scientists.

The chapter on "Auditing Function in the Total Control of Quality" by A. J. Schmitz, Jr., reviews the quality control of the product and the quality control of operations and control techniques. Auditing includes managerial review of quality assurance to a firm to procure, produce, distribute, and control all phases of the function of a firm including facilities, personnel, standards, and the auditing method.

The chapter on "Filtrative Sterilization with Porous Membranes" by T. H. Meltzer and R. C. Lukaszewicz is concerned with the technology of porous membranes. It does not discuss sterility testing, but it does discuss pore properties, manufacture, filter rating, retentivity, and types of filters used. Prefilters and filter construction, design, preparation for use, and usage are discussed.

The chapter on "Bioavailability Standards for Pharmaceutical Products" by R. V. Smith and G. J. Yakatan is the shortest chapter. It presents elemental remarks on bioequivalency and gives an overview of analytical methods and their selection in bioavailability studies.

The chapter on "Quality Control of Poliomyelitis Vaccines" is by P. B. Stone. A review is given of tissue culture and animal testing of inactivated polio vaccine and the testing of live polio vaccine for adventitious agents, mycoplasma, and identity.

The chapter on "Quality Control of Ophthalmic Products" by J. D. Mullins and T. C. Fleming presents an elemental review of the anatomy of the eye, absorption, ophthalmic dosages, formulation, and processing.

This volume presents useful information for those seeking an overview of quality control in the specific areas covered; however, pharmaceutical scientists currently involved in quality assurance may find the treatment too cursory.

Reviewed by Eugene L. Parrott
College of Pharmacy
University of Iowa
Iowa City, IA 52242

Handbook of Analytical Derivatization Reactions. By DANIEL R. KNAPP. Wiley, One Wiley Drive, Somerset, NJ 08873. 1979. 741 pp. 15 × 23 cm. Price $34.95.

This book presents a collection of analytical derivatization methods for gas chromatographic, liquid chromatographic, and mass spectral analysis. The reactions involve only the covalent derivatives of organic compounds formed prior to analysis. Part I briefly discusses the uses of analytical derivatization, the types of derivatives formed, and a typical apparatus employed in such reactions.

Part II features 15 sections concerning the derivatization of particular compound types. Among the classes considered are steroids, prostaglandins, and drugs. An overview of derivatization for the sample type is given along with specific derivatization methods. For each major compound type, the derivatization reactions are organized further into subsections of the compound type and within each subsection according to the type of derivative formed. Each method description includes structural formulas for the reaction, experimental directions, and references to the original literature. Sections on derivatives for substituent location by mass spectrometry and derivatives for chromatographic separation of optical isomers also are included.

Part III contains author and general subject indexes along with appendixes listing the composition of brand name reagents and U.S. and foreign suppliers of reagents and apparatuses used for analytical derivatization. An index of the derivatives and reagents discussed in Part II also is included.

This book should serve both as a self-contained methodology reference and as an introduction to the literature on analytical derivatization.

Staff Review

Pharmacognosy, 11th ed. By G. E. TREASE and W. C. EVANS. Cassell and Collier Macmillan Publishers Ltd., 35 Red Lion Square, London WC1R 49G, England. 1978. 784 pp. 16 × 23 cm. Price $32.50.

This is the 11th edition of a longstanding series of revisions that trace their origin to the original work in 1934. The latest revision reflects the increasing awareness and knowledge of the active constituents of natural, particularly vegetable, drugs. The book has been partially rearranged from the 10th edition with lengthy revisions in the parts dealing with drug sources, including production and quality control and the consideration of the various classes of drugs of biological origin.

The book is composed of eight parts with a total of 41 chapters, including an index. It is liberally filled with numerous structural formulas, pictures (none in color), tables, and illustrations. Part 1 (Chapters 1–3) deals with drug classification, the literature of pharmacognosy, and plant nomenclature and taxonomy. Part 2 (Chapters 4–7) covers plant morphology, anatomy, histology, and cellular content. Part 3 (Chapters 8–12) discusses the botanical and chemical characteristics of the more important orders and families of both nonflowering and flowering plants with references taken from Volumes 74–84 of *Chemical Abstracts*. Part 4 (Chapters 13–18) includes a discussion of the sources of crude drugs, drug production, quality control, drug deterioration, and plant growth regu-

The short chapter on Anti-Infective Agents by P. Johnson and J. D. Coombes deals with the biotransformation of some unusual structures while covering antiparasitics, antibiotics, antimycotic agents, antidiarrheals, antitubercular drugs, antivirals, and sulfonamides. Interesting interspecies and *in vivo–in vitro* comparisons pervade the coverage of Prostaglandins and Steroids by G. R. Bourne and D. E. Hathway. In the chapter on Food Constituents, D. E. Hathway objectively evaluates the saccharin and cyclamate problems under the heading of sweetening agents and deals with single-cell proteins, flour, vitamins, urethane and diethyl dicarbonate, food colorants, flavoring principles, and natural constituents.

C. T. Bedford reviews Agricultural Chemicals in sections on animal health products, rodenticides, insecticides, herbicides, and fungicides. This chapter is enlivened by descriptions of an anticoagulant with selective toxicity for vampire bats, an anthelmintic that is degraded to benzene, and an ususual example of *N*-dearylation. C. T. Bedford also contributed the final chapter, Industrial Chemicals and Miscellaneous Organic Compounds, which contains sections on aliphatic compounds, aromatic compounds, heteroaromatic compounds, and organometallic and inorganic compounds. Like the previous chapter, this chapter summarizes the biotransformation of many important environmental contaminants. Some of the more interesting reactions involve the formation of a metabolite of 4-dimethylaminophenol, which contains three glutathione residues attached to a single aromatic ring, and the formation of phosgene and carbon monoxide as metabolites.

The few typographical errors in this book are readily understood, as are the misspellings of the names of some prominent scientists in the author index. The compound index lists only substrates, not metabolites. More unfortunate is the absence of a comprehensive subject index that would enable readers to use the volume cross-sectionally; for example, to collect valuable information on studies performed in the wide variety of species covered in the volume (including humans, subhuman primates, sheep, cattle, lambs, pigs, tree shrews, and insects) or on reaction types or sites of biotransformation.

Overall, this volume is recommended highly as an organized source of metabolism–pharmacokinetics literature on important xenobiotics of many kinds. One of its major achievements is that it demonstrates the richness of opportunities for valuable future investigations.

Reviewed by Frederick J. Di Carlo
Office of Toxic Substances
U.S. Environmental Protection Agency
Washington, DC 20460

Quality Control in the Pharmaceutical Industry, Vol. 3. Edited by M. S. COOPER. Academic, 111 Fifth Ave., New York, NY 10003. 1979. 292 pp. 15.5 × 22.5 cm. Price $29.50.

Volume 3 of this series consists of six chapters covering the interpretation of current good manufacturing practice regulations, the auditing function in the total control of quality, filtrative sterilization with porous membranes, bioavailability standards for pharmaceutical products, quality control of poliomyelitis vaccines, and quality control of ophthalmic products.

The chapter by A. S. Arambulo on "Interpretation of Current Good Manufacturing Practice Regulations" exceeds 100 pages and presents an excellent comprehensive review. The concept and parts of the regulations are discussed and illustrated by examples. This chapter should be of special interest to graduate students and recent graduates who are joining the pharmaceutical industry and to management personnel who have not been trained as physical or biological scientists.

The chapter on "Auditing Function in the Total Control of Quality" by A. J. Schmitz, Jr., reviews the quality control of the product and the quality control of operations and control techniques. Auditing includes managerial review of quality assurance to a firm to procure, produce, distribute, and control all phases of the function of a firm including facilities, personnel, standards, and the auditing method.

The chapter on "Filtrative Sterilization with Porous Membranes" by T. H. Meltzer and R. C. Lukaszewicz is concerned with the technology of porous membranes. It does not discuss sterility testing, but it does discuss pore properties, manufacture, filter rating, retentivity, and types of filters used. Prefilters and filter construction, design, preparation for use, and usage are discussed.

The chapter on "Bioavailability Standards for Pharmaceutical Products" by R. V. Smith and G. J. Yakatan is the shortest chapter. It presents elemental remarks on bioequivalency and gives an overview of analytical methods and their selection in bioavailability studies.

The chapter on "Quality Control of Poliomyelitis Vaccines" is by P. B. Stone. A review is given of tissue culture and animal testing of inactivated polio vaccine and the testing of live polio vaccine for adventitious agents, mycoplasma, and identity.

The chapter on "Quality Control of Ophthalmic Products" by J. D. Mullins and T. C. Fleming presents an elemental review of the anatomy of the eye, absorption, ophthalmic dosages, formulation, and processing.

This volume presents useful information for those seeking an overview of quality control in the specific areas covered; however, pharmaceutical scientists currently involved in quality assurance may find the treatment too cursory.

Reviewed by Eugene L. Parrott
College of Pharmacy
University of Iowa
Iowa City, IA 52242

Handbook of Analytical Derivatization Reactions. By DANIEL R. KNAPP. Wiley, One Wiley Drive, Somerset, NJ 08873. 1979. 741 pp. 15 × 23 cm. Price $34.95.

This book presents a collection of analytical derivatization methods for gas chromatographic, liquid chromatographic, and mass spectral analysis. The reactions involve only the covalent derivatives of organic compounds formed prior to analysis. Part I briefly discusses the uses of analytical derivatization, the types of derivatives formed, and a typical apparatus employed in such reactions.

Part II features 15 sections concerning the derivatization of particular compound types. Among the classes considered are steroids, prostaglandins, and drugs. An overview of derivatization for the sample type is given along with specific derivatization methods. For each major compound type, the derivatization reactions are organized further into subsections of the compound type and within each subsection according to the type of derivative formed. Each method description includes structural formulas for the reaction, experimental directions, and references to the original literature. Sections on derivatives for substituent location by mass spectrometry and derivatives for chromatographic separation of optical isomers also are included.

Part III contains author and general subject indexes along with appendixes listing the composition of brand name reagents and U.S. and foreign suppliers of reagents and apparatuses used for analytical derivatization. An index of the derivatives and reagents discussed in Part II also is included.

This book should serve both as a self-contained methodology reference and as an introduction to the literature on analytical derivatization.

Staff Review

Pharmacognosy, 11th ed. By G. E. TREASE and W. C. EVANS. Cassell and Collier Macmillan Publishers Ltd., 35 Red Lion Square, London WC1R 49G, England. 1978. 784 pp. 16 × 23 cm. Price $32.50.

This is the 11th edition of a longstanding series of revisions that trace their origin to the original work in 1934. The latest revision reflects the increasing awareness and knowledge of the active constituents of natural, particularly vegetable, drugs. The book has been partially rearranged from the 10th edition with lengthy revisions in the parts dealing with drug sources, including production and quality control and the consideration of the various classes of drugs of biological origin.

The book is composed of eight parts with a total of 41 chapters, including an index. It is liberally filled with numerous structural formulas, pictures (none in color), tables, and illustrations. Part 1 (Chapters 1–3) deals with drug classification, the literature of pharmacognosy, and plant nomenclature and taxonomy. Part 2 (Chapters 4–7) covers plant morphology, anatomy, histology, and cellular content. Part 3 (Chapters 8–12) discusses the botanical and chemical characteristics of the more important orders and families of both nonflowering and flowering plants with references taken from Volumes 74–84 of *Chemical Abstracts*. Part 4 (Chapters 13–18) includes a discussion of the sources of crude drugs, drug production, quality control, drug deterioration, and plant growth regu-

The short chapter on Anti-Infective Agents by P. Johnson and J. D. Coombes deals with the biotransformation of some unusual structures while covering antiparasitics, antibiotics, antimycotic agents, antidiarrheals, antitubercular drugs, antivirals, and sulfonamides. Interesting interspecies and *in vivo–in vitro* comparisons pervade the coverage of Prostaglandins and Steroids by G. R. Bourne and D. E. Hathway. In the chapter on Food Constituents, D. E. Hathway objectively evaluates the saccharin and cyclamate problems under the heading of sweetening agents and deals with single-cell proteins, flour, vitamins, urethane and diethyl dicarbonate, food colorants, flavoring principles, and natural constituents.

C. T. Bedford reviews Agricultural Chemicals in sections on animal health products, rodenticides, insecticides, herbicides, and fungicides. This chapter is enlivened by descriptions of an anticoagulant with selective toxicity for vampire bats, an anthelmintic that is degraded to benzene, and an ususual example of *N*-dearylation. C. T. Bedford also contributed the final chapter, Industrial Chemicals and Miscellaneous Organic Compounds, which contains sections on aliphatic compounds, aromatic compounds, heteroaromatic compounds, and organometallic and inorganic compounds. Like the previous chapter, this chapter summarizes the biotransformation of many important environmental contaminants. Some of the more interesting reactions involve the formation of a metabolite of 4-dimethylaminophenol, which contains three glutathione residues attached to a single aromatic ring, and the formation of phosgene and carbon monoxide as metabolites.

The few typographical errors in this book are readily understood, as are the misspellings of the names of some prominent scientists in the author index. The compound index lists only substrates, not metabolites. More unfortunate is the absence of a comprehensive subject index that would enable readers to use the volume cross-sectionally; for example, to collect valuable information on studies performed in the wide variety of species covered in the volume (including humans, subhuman primates, sheep, cattle, lambs, pigs, tree shrews, and insects) or on reaction types or sites of biotransformation.

Overall, this volume is recommended highly as an organized source of metabolism–pharmacokinetics literature on important xenobiotics of many kinds. One of its major achievements is that it demonstrates the richness of opportunities for valuable future investigations.

Reviewed by Frederick J. Di Carlo
Office of Toxic Substances
U.S. Environmental Protection Agency
Washington, DC 20460

Quality Control in the Pharmaceutical Industry, Vol. 3. Edited by M. S. COOPER. Academic, 111 Fifth Ave., New York, NY 10003. 1979. 292 pp. 15.5 × 22.5 cm. Price $29.50.

Volume 3 of this series consists of six chapters covering the interpretation of current good manufacturing practice regulations, the auditing function in the total control of quality, filtrative sterilization with porous membranes, bioavailability standards for pharmaceutical products, quality control of poliomyelitis vaccines, and quality control of ophthalmic products.

The chapter by A. S. Arambulo on "Interpretation of Current Good Manufacturing Practice Regulations" exceeds 100 pages and presents an excellent comprehensive review. The concept and parts of the regulations are discussed and illustrated by examples. This chapter should be of special interest to graduate students and recent graduates who are joining the pharmaceutical industry and to management personnel who have not been trained as physical or biological scientists.

The chapter on "Auditing Function in the Total Control of Quality" by A. J. Schmitz, Jr., reviews the quality control of the product and the quality control of operations and control techniques. Auditing includes managerial review of quality assurance to a firm to procure, produce, distribute, and control all phases of the function of a firm including facilities, personnel, standards, and the auditing method.

The chapter on "Filtrative Sterilization with Porous Membranes" by T. H. Meltzer and R. C. Lukaszewicz is concerned with the technology of porous membranes. It does not discuss sterility testing, but it does discuss pore properties, manufacture, filter rating, retentivity, and types of filters used. Prefilters and filter construction, design, preparation for use, and usage are discussed.

The chapter on "Bioavailability Standards for Pharmaceutical Products" by R. V. Smith and G. J. Yakatan is the shortest chapter. It presents elemental remarks on bioequivalency and gives an overview of analytical methods and their selection in bioavailability studies.

The chapter on "Quality Control of Poliomyelitis Vaccines" is by P. B. Stone. A review is given of tissue culture and animal testing of inactivated polio vaccine and the testing of live polio vaccine for adventitious agents, mycoplasma, and identity.

The chapter on "Quality Control of Ophthalmic Products" by J. D. Mullins and T. C. Fleming presents an elemental review of the anatomy of the eye, absorption, ophthalmic dosages, formulation, and processing.

This volume presents useful information for those seeking an overview of quality control in the specific areas covered; however, pharmaceutical scientists currently involved in quality assurance may find the treatment too cursory.

Reviewed by Eugene L. Parrott
College of Pharmacy
University of Iowa
Iowa City, IA 52242

Handbook of Analytical Derivatization Reactions. By DANIEL R. KNAPP. Wiley, One Wiley Drive, Somerset, NJ 08873. 1979. 741 pp. 15 × 23 cm. Price $34.95.

This book presents a collection of analytical derivatization methods for gas chromatographic, liquid chromatographic, and mass spectral analysis. The reactions involve only the covalent derivatives of organic compounds formed prior to analysis. Part I briefly discusses the uses of analytical derivatization, the types of derivatives formed, and a typical apparatus employed in such reactions.

Part II features 15 sections concerning the derivatization of particular compound types. Among the classes considered are steroids, prostaglandins, and drugs. An overview of derivatization for the sample type is given along with specific derivatization methods. For each major compound type, the derivatization reactions are organized further into subsections of the compound type and within each subsection according to the type of derivative formed. Each method description includes structural formulas for the reaction, experimental directions, and references to the original literature. Sections on derivatives for substituent location by mass spectrometry and derivatives for chromatographic separation of optical isomers also are included.

Part III contains author and general subject indexes along with appendixes listing the composition of brand name reagents and U.S. and foreign suppliers of reagents and apparatuses used for analytical derivatization. An index of the derivatives and reagents discussed in Part II also is included.

This book should serve both as a self-contained methodology reference and as an introduction to the literature on analytical derivatization.

Staff Review

Pharmacognosy, 11th ed. By G. E. TREASE and W. C. EVANS. Cassell and Collier Macmillan Publishers Ltd., 35 Red Lion Square, London WC1R 49G, England. 1978. 784 pp. 16 × 23 cm. Price $32.50.

This is the 11th edition of a longstanding series of revisions that trace their origin to the original work in 1934. The latest revision reflects the increasing awareness and knowledge of the active constituents of natural, particularly vegetable, drugs. The book has been partially rearranged from the 10th edition with lengthy revisions in the parts dealing with drug sources, including production and quality control and the consideration of the various classes of drugs of biological origin.

The book is composed of eight parts with a total of 41 chapters, including an index. It is liberally filled with numerous structural formulas, pictures (none in color), tables, and illustrations. Part 1 (Chapters 1–3) deals with drug classification, the literature of pharmacognosy, and plant nomenclature and taxonomy. Part 2 (Chapters 4–7) covers plant morphology, anatomy, histology, and cellular content. Part 3 (Chapters 8–12) discusses the botanical and chemical characteristics of the more important orders and families of both nonflowering and flowering plants with references taken from Volumes 74–84 of *Chemical Abstracts*. Part 4 (Chapters 13–18) includes a discussion of the sources of crude drugs, drug production, quality control, drug deterioration, and plant growth regu-

lators and a summary of the pharmacological actions of plant drugs.

Part 5 (Chapters 19–22) discusses phytochemistry, biogenesis, and basic and secondary phytometabolism with a small section on microbial conversions and aberrant syntheses in higher plants. Part 6 (Chapters 23–35) constitutes the bulk of the book and is a discussion of the drugs of biological origin, organized by chemical class (*e.g.*, carbohydrates and alkaloids) or by biological activity (plant tumor inhibitors, hallucinogens, and pesticides). Part 7 (Chapters 36 and 37) concerns genetics and comparative phytochemistry, while Part 8 (Chapters 38–41) finishes the book with a discussion of microscopy.

One can find some inconsistencies in this book, as in any text. For instance, the stereochemistry of the cardiac steroid glycosides is not illustrated in Chapter 27 (although these features are discussed), while the stereochemistry of the tropane alkaloids hyoscyamine and hyoscine is nicely illustrated in Chapter 30. A somewhat disturbing feature is that the authors chose to discuss the pharmacological activities of plant-derived drugs in one specific chapter instead of with the specific compound in the appropriate chapter. To my knowledge, there is little or no mention of the commonly occurring adverse effects associated with therapy with plant-derived drugs. There is no discussion of immunizing biologicals nor of antibiotics as therapeutic agents. Finally, the chapter on tumor inhibitors from plants seems weak and is particularly lacking in structural illustrations.

The writing of a textbook on pharmacognosy is a labor of love in many ways. It is a particularly broad subject and it is difficult to be "all things to all people." The authors have worked diligently to "marry" biology, biochemistry, chemistry, plant histology/anatomy, and pharmacology into one voluminous work. As the authors state: "The new edition has the same purpose as its predecessors, namely to give a comprehensive presentation of pharmacognosy which complements the very varied treatments which the subject receives in schools of pharmacy throughout the world." Despite some shortcomings, the book adequately fulfills its broad-based mission, and I recommend that anyone involved in the broad discipline of pharmacognosy should obtain a copy. Furthermore, libraries of pharmacy schools and institutions interested in natural products should be interested in this work.

Reviewed by Paul L. Schiff, Jr.
Department of Pharmacognosy
School of Pharmacy
University of Pittsburgh
Pittsburgh, PA 15261

NOTICES

The Heritage of Nuclear Medicine. Edited by MARSHALL BRUCER, C. CRAIG HARRIS, WILLIAM J. MacINTYRE, and GEORGE V. TAPLIN. Society of Nuclear Medicine, 475 Park Ave. S., New York, NY 10016. 1979. 191 pp. 21 × 27 cm. Price $14.50.

Connective Tissue Change in Rheumatoid Arthritis and the Use of Penicillamine. Edited by I. L. BONTA and A. CATS. (Agents and Actions Supplement 5.) Birkhäuser Boston Inc., 380 Green St., P.O. Box 2007, Cambridge, MA 02139. 1979. 190 pp. 16 × 24 cm. Price $29.00.

Behavior Analysis and Treatment of Substance Abuse. Edited by NORMAN A. KRASNEGOR. (NIDA Research Monograph 25.) National Institute on Drug Abuse. 1979. 256 pp. 14 × 23 cm. (Available from Superintendent of Documents, U.S. Government Printing Office, Washington, DC 20402.)

The Behavioral Aspects of Smoking. Edited by NORMAN A. KRASNEGOR. (NIDA Research Monograph 26.) National Institute on Drug Abuse. 1979. 192 pp. 14 × 23 cm. (Available from Superintendent of Documents, U.S. Government Printing Office, Washington, DC 20402.)

Handbook of Biological Psychiatry, Part I: Disciplines Relevant to Biological Psychiatry. Edited by HERMAN M. VAN PRAAG. Dekker, 270 Madison Ave., New York, NY 10016. 1979. 429 pp. 15 × 23 cm. Price $45.00.

Recent Advances in Drug Research. By M. J. CLEARE, C. R. GANELLIN, D. HARTLEY, W. J. ROSS, M. S. TUTE, and K. R. H. WOOLDRIDGE. Symposium Press, 3/4 St. Andrews Hill, London EC4V 5BY, England. 1979. 169 pp. 15 × 22 cm. Price $23.00.

Drugs and Immune Responsiveness. Edited by J. L. TURK and DARIEN PARKER. University Park Press, 233 E. Redwood St., Baltimore, MD 21202. 1979. 254 pp. 15 × 24 cm. Price $44.50.

Carcinogens and Related Substances: Analytical Chemistry for Toxicological Research. By MALCOLM C. BOWMAN. Dekker, 270 Madison Ave., New York, NY 10016. 1979. 316 pp. 15 × 23 cm. Price $34.50.

Plant Organelles. Edited by ERIC REID. (Methodological Surveys Biochemistry Subseries, Vol. 9.) Wiley, 605 Third Ave., New York, NY 10016. 1979. 232 pp. 15 × 23 cm.

Quantitative Mass Spectrometry in Life Sciences II. Edited by A. P. De LEENHEER, R. R. RONCUCCI, and C. VAN PETEGHEM. Elsevier/North-Holland Inc., 52 Vanderbilt Ave., New York, NY 10017. 1978. 501 pp. 16 × 25 cm. Price $48.45.

Foundations of Molecular Pharmacology, Vol. 2: The Chemical Basis of Drug Action. By J. B. STENLAKE. Athlone Press, University of London, 4 Gower St., London WC1, England. 1979. 318 pp. 15 × 23 cm. Price $46.25.

Advances in Chromatography, Vol. 17. Edited by J. CALVIN GIDDINGS, ELI GRUSHKA, JACK CAZES, and PHYLLIS R. BROWN. Dekker, 270 Madison Ave., New York, NY 10016. 1979. 352 pp. 15 × 23 cm. Price $36.50.

Maternal Recognition of Pregnancy. (Ciba Foundation Symposium 64.) Elsevier/North-Holland Inc., 52 Vanderbilt Ave., New York, NY 10017. 1979. 425 pp. 16 × 24 cm.

Oxygen Free Radicals and Tissue Damage. (Ciba Foundation Symposium 65.) Elsevier/North-Holland Inc., 52 Vanderbilt Ave., New York, NY 10017. 1979. 381 pp. 16 × 24 cm.

Human Genetics: Possibilities and Realities. (Ciba Foundation Symposium 66.) Elsevier/North-Holland, Inc., 52 Vanderbilt Ave., New York, NY 10017. 1979. 425 pp. 16 × 24 cm.

Submolecular Biology and Cancer. (Ciba Foundation Symposium 67.) Elsevier/North-Holland Inc., 52 Vanderbilt Ave., New York, NY 10017. 1979. 349 pp. 16 × 24 cm.

Studies in Drug Utilization: Methods and Applications. Edited by U. BERGMAN, A. H. W. WAHBA, A. GRIMSSON, and B. WESTERHOLM. (WHO Regional Publications European Series No. 8.) World Health Organization, 1211 Geneva 27, Switzerland. 1979. 185 pp. 15 × 24 cm. Price 20 Sw.fr.

Nutrition and Cancer. Edited by JAN VAN EYS, MILDRED S. SEELIG, and BUFORD L. NICHOLS, Jr. Spectrum Publications, 175–20 Wexford Terrace, Jamaica, NY 11432. 1979. 297 pp. 15 × 23 cm. Price $25.00.

Synthetic Aspects of Biologically Active Cyclic Peptides—Gramicidin S and Tyrocidines. By NOBUO IZUMIYA, TETSUO KATO, HARUHIKO AOYAGI, MICHINORI WAKI, and MICHIO KONDO. Wiley, One Wiley Dr., Somerset, NJ 08873. 1979. 166 pp. 14 × 23 cm. Price $29.95.

Terpenoids and Steroids, Vol. 9. Senior Reporter, J. R. HANSON. (A Specialist Periodical Report.) The Chemical Society. 1979. 352 pp. 14 × 22 cm. Price $72.00. (Available from Special Issue Sales, American Chemical Society, 1155 16th St., N. W., Washington, DC 20036.)

Aromatic and Heteroaromatic Chemistry, Vol. 7. Senior Reporters, H. SUSCHITZKY and O. METH-COHN. (A Specialist Periodical Report.) The Chemical Society. 1979. 368 pp. 13 × 23 cm. Price $72.50. (Available from Special Issue Sales, American Chemical Society, 1155 16th St., N. W., Washington, DC 20036.)

Recent Development in Mass Spectrometry in Biochemistry and Medicine, Vol. 2. Edited by ALBERTO FRIGERIO. Plenum, 227 W. 17th St., New York, NY 10011. 1979. 492 pp. 16 × 25 cm. Price $45.00.

Vitamin K Metabolism and Vitamin K-Dependent Proteins. Edited by J. W. SUTTIE. University Park Press, 233 E. Redwood St., Baltimore, MD 21202. 1980. 592 pp. 15 × 23 cm. Price $39.50.

The Nature of Enzymology. By R. L. FOSTER. Wiley, One Wiley Dr., Somerset, NJ 08873. 1980. 383 pp. 13 × 22 cm. Price $39.95.

Selected Methods in Cellular Immunology. Edited by BARBARA B. MISHELL and STANLEY M. SHOIGI. W. H. Freeman and Co., 660 Market St., San Francisco, CA 94104. 1980. 486 pp. 16 × 23 cm. Price $29.95.

Essays on the Anatomy and Physiology of Lymphoid Tissues. Edited by Z. TRNKA and R. N. P. CAHILL. (Monographs in Allergy, Vol. 16.) S. Karger AG, Arnold-Böcklin-Strasse 25, CH-4011 Basel, Switzerland. 1980. 262 pp. 15 × 23 cm. Price $94.50.

The short chapter on Anti-Infective Agents by P. Johnson and J. D. Coombes deals with the biotransformation of some unusual structures while covering antiparasitics, antibiotics, antimycotic agents, antidiarrheals, antitubercular drugs, antivirals, and sulfonamides. Interesting interspecies and *in vivo–in vitro* comparisons pervade the coverage of Prostaglandins and Steroids by G. R. Bourne and D. E. Hathway. In the chapter on Food Constituents, D. E. Hathway objectively evaluates the saccharin and cyclamate problems under the heading of sweetening agents and deals with single-cell proteins, flour, vitamins, urethane and diethyl dicarbonate, food colorants, flavoring principles, and natural constituents.

C. T. Bedford reviews Agricultural Chemicals in sections on animal health products, rodenticides, insecticides, herbicides, and fungicides. This chapter is enlivened by descriptions of an anticoagulant with selective toxicity for vampire bats, an anthelmintic that is degraded to benzene, and an ususual example of *N*-dearylation. C. T. Bedford also contributed the final chapter, Industrial Chemicals and Miscellaneous Organic Compounds, which contains sections on aliphatic compounds, aromatic compounds, heteroaromatic compounds, and organometallic and inorganic compounds. Like the previous chapter, this chapter summarizes the biotransformation of many important environmental contaminants. Some of the more interesting reactions involve the formation of a metabolite of 4-dimethylaminophenol, which contains three glutathione residues attached to a single aromatic ring, and the formation of phosgene and carbon monoxide as metabolites.

The few typographical errors in this book are readily understood, as are the misspellings of the names of some prominent scientists in the author index. The compound index lists only substrates, not metabolites. More unfortunate is the absence of a comprehensive subject index that would enable readers to use the volume cross-sectionally; for example, to collect valuable information on studies performed in the wide variety of species covered in the volume (including humans, subhuman primates, sheep, cattle, lambs, pigs, tree shrews, and insects) or on reaction types or sites of biotransformation.

Overall, this volume is recommended highly as an organized source of metabolism–pharmacokinetics literature on important xenobiotics of many kinds. One of its major achievements is that it demonstrates the richness of opportunities for valuable future investigations.

Reviewed by Frederick J. Di Carlo
Office of Toxic Substances
U.S. Environmental Protection Agency
Washington, DC 20460

Quality Control in the Pharmaceutical Industry, Vol. 3. Edited by M. S. COOPER. Academic, 111 Fifth Ave., New York, NY 10003. 1979. 292 pp. 15.5 × 22.5 cm. Price $29.50.

Volume 3 of this series consists of six chapters covering the interpretation of current good manufacturing practice regulations, the auditing function in the total control of quality, filtrative sterilization with porous membranes, bioavailability standards for pharmaceutical products, quality control of poliomyelitis vaccines, and quality control of ophthalmic products.

The chapter by A. S. Arambulo on "Interpretation of Current Good Manufacturing Practice Regulations" exceeds 100 pages and presents an excellent comprehensive review. The concept and parts of the regulations are discussed and illustrated by examples. This chapter should be of special interest to graduate students and recent graduates who are joining the pharmaceutical industry and to management personnel who have not been trained as physical or biological scientists.

The chapter on "Auditing Function in the Total Control of Quality" by A. J. Schmitz, Jr., reviews the quality control of the product and the quality control of operations and control techniques. Auditing includes managerial review of quality assurance to a firm to procure, produce, distribute, and control all phases of the function of a firm including facilities, personnel, standards, and the auditing method.

The chapter on "Filtrative Sterilization with Porous Membranes" by T. H. Meltzer and R. C. Lukaszewicz is concerned with the technology of porous membranes. It does not discuss sterility testing, but it does discuss pore properties, manufacture, filter rating, retentivity, and types of filters used. Prefilters and filter construction, design, preparation for use, and usage are discussed.

The chapter on "Bioavailability Standards for Pharmaceutical Products" by R. V. Smith and G. J. Yakatan is the shortest chapter. It presents elemental remarks on bioequivalency and gives an overview of analytical methods and their selection in bioavailability studies.

The chapter on "Quality Control of Poliomyelitis Vaccines" is by P. B. Stone. A review is given of tissue culture and animal testing of inactivated polio vaccine and the testing of live polio vaccine for adventitious agents, mycoplasma, and identity.

The chapter on "Quality Control of Ophthalmic Products" by J. D. Mullins and T. C. Fleming presents an elemental review of the anatomy of the eye, absorption, ophthalmic dosages, formulation, and processing.

This volume presents useful information for those seeking an overview of quality control in the specific areas covered; however, pharmaceutical scientists currently involved in quality assurance may find the treatment too cursory.

Reviewed by Eugene L. Parrott
College of Pharmacy
University of Iowa
Iowa City, IA 52242

Handbook of Analytical Derivatization Reactions. By DANIEL R. KNAPP. Wiley, One Wiley Drive, Somerset, NJ 08873. 1979. 741 pp. 15 × 23 cm. Price $34.95.

This book presents a collection of analytical derivatization methods for gas chromatographic, liquid chromatographic, and mass spectral analysis. The reactions involve only the covalent derivatives of organic compounds formed prior to analysis. Part I briefly discusses the uses of analytical derivatization, the types of derivatives formed, and a typical apparatus employed in such reactions.

Part II features 15 sections concerning the derivatization of particular compound types. Among the classes considered are steroids, prostaglandins, and drugs. An overview of derivatization for the sample type is given along with specific derivatization methods. For each major compound type, the derivatization reactions are organized further into subsections of the compound type and within each subsection according to the type of derivative formed. Each method description includes structural formulas for the reaction, experimental directions, and references to the original literature. Sections on derivatives for substituent location by mass spectrometry and derivatives for chromatographic separation of optical isomers also are included.

Part III contains author and general subject indexes along with appendixes listing the composition of brand name reagents and U.S. and foreign suppliers of reagents and apparatuses used for analytical derivatization. An index of the derivatives and reagents discussed in Part II also is included.

This book should serve both as a self-contained methodology reference and as an introduction to the literature on analytical derivatization.

Staff Review

Pharmacognosy, 11th ed. By G. E. TREASE and W. C. EVANS. Cassell and Collier Macmillan Publishers Ltd., 35 Red Lion Square, London WC1R 49G, England. 1978. 784 pp. 16 × 23 cm. Price $32.50.

This is the 11th edition of a longstanding series of revisions that trace their origin to the original work in 1934. The latest revision reflects the increasing awareness and knowledge of the active constituents of natural, particularly vegetable, drugs. The book has been partially rearranged from the 10th edition with lengthy revisions in the parts dealing with drug sources, including production and quality control and the consideration of the various classes of drugs of biological origin.

The book is composed of eight parts with a total of 41 chapters, including an index. It is liberally filled with numerous structural formulas, pictures (none in color), tables, and illustrations. Part 1 (Chapters 1–3) deals with drug classification, the literature of pharmacognosy, and plant nomenclature and taxonomy. Part 2 (Chapters 4–7) covers plant morphology, anatomy, histology, and cellular content. Part 3 (Chapters 8–12) discusses the botanical and chemical characteristics of the more important orders and families of both nonflowering and flowering plants with references taken from Volumes 74–84 of *Chemical Abstracts*. Part 4 (Chapters 13–18) includes a discussion of the sources of crude drugs, drug production, quality control, drug deterioration, and plant growth regu-

lators and a summary of the pharmacological actions of plant drugs.

Part 5 (Chapters 19–22) discusses phytochemistry, biogenesis, and basic and secondary phytometabolism with a small section on microbial conversions and aberrant syntheses in higher plants. Part 6 (Chapters 23–35) constitutes the bulk of the book and is a discussion of the drugs of biological origin, organized by chemical class (*e.g.*, carbohydrates and alkaloids) or by biological activity (plant tumor inhibitors, hallucinogens, and pesticides). Part 7 (Chapters 36 and 37) concerns genetics and comparative phytochemistry, while Part 8 (Chapters 38–41) finishes the book with a discussion of microscopy.

One can find some inconsistencies in this book, as in any text. For instance, the stereochemistry of the cardiac steroid glycosides is not illustrated in Chapter 27 (although these features are discussed), while the stereochemistry of the tropane alkaloids hyoscyamine and hyoscine is nicely illustrated in Chapter 30. A somewhat disturbing feature is that the authors chose to discuss the pharmacological activities of plant-derived drugs in one specific chapter instead of with the specific compound in the appropriate chapter. To my knowledge, there is little or no mention of the commonly occurring adverse effects associated with therapy with plant-derived drugs. There is no discussion of immunizing biologicals nor of antibiotics as therapeutic agents. Finally, the chapter on tumor inhibitors from plants seems weak and is particularly lacking in structural illustrations.

The writing of a textbook on pharmacognosy is a labor of love in many ways. It is a particularly broad subject and it is difficult to be "all things to all people." The authors have worked diligently to "marry" biology, biochemistry, chemistry, plant histology/anatomy, and pharmacology into one voluminous work. As the authors state: "The new edition has the same purpose as its predecessors, namely to give a comprehensive presentation of pharmacognosy which complements the very varied treatments which the subject receives in schools of pharmacy throughout the world." Despite some shortcomings, the book adequately fulfills its broad-based mission, and I recommend that anyone involved in the broad discipline of pharmacognosy should obtain a copy. Furthermore, libraries of pharmacy schools and institutions interested in natural products should be interested in this work.

Reviewed by Paul L. Schiff, Jr.
Department of Pharmacognosy
School of Pharmacy
University of Pittsburgh
Pittsburgh, PA 15261

NOTICES

The Heritage of Nuclear Medicine. Edited by MARSHALL BRUCER, C. CRAIG HARRIS, WILLIAM J. MacINTYRE, and GEORGE V. TAPLIN. Society of Nuclear Medicine, 475 Park Ave. S., New York, NY 10016. 1979. 191 pp. 21 × 27 cm. Price $14.50.

Connective Tissue Change in Rheumatoid Arthritis and the Use of Penicillamine. Edited by I. L. BONTA and A. CATS. (Agents and Actions Supplement 5.) Birkhäuser Boston Inc., 380 Green St., P.O. Box 2007, Cambridge, MA 02139. 1979. 190 pp. 16 × 24 cm. Price $29.00.

Behavior Analysis and Treatment of Substance Abuse. Edited by NORMAN A. KRASNEGOR. (NIDA Research Monograph 25.) National Institute on Drug Abuse. 1979. 256 pp. 14 × 23 cm. (Available from Superintendent of Documents, U.S. Government Printing Office, Washington, DC 20402.)

The Behavioral Aspects of Smoking. Edited by NORMAN A. KRASNEGOR. (NIDA Research Monograph 26.) National Institute on Drug Abuse. 1979. 192 pp. 14 × 23 cm. (Available from Superintendent of Documents, U.S. Government Printing Office, Washington, DC 20402.)

Handbook of Biological Psychiatry, Part I: Disciplines Relevant to Biological Psychiatry. Edited by HERMAN M. VAN PRAAG. Dekker, 270 Madison Ave., New York, NY 10016. 1979. 429 pp. 15 × 23 cm. Price $45.00.

Recent Advances in Drug Research. By M. J. CLEARE, C. R. GANELLIN, D. HARTLEY, W. J. ROSS, M. S. TUTE, and K. R. H. WOOLDRIDGE. Symposium Press, 3/4 St. Andrews Hill, London EC4V 5BY, England. 1979. 169 pp. 15 × 22 cm. Price $23.00.

Drugs and Immune Responsiveness. Edited by J. L. TURK and DARIEN PARKER. University Park Press, 233 E. Redwood St., Baltimore, MD 21202. 1979. 254 pp. 15 × 24 cm. Price $44.50.

Carcinogens and Related Substances: Analytical Chemistry for Toxicological Research. By MALCOLM C. BOWMAN. Dekker, 270 Madison Ave., New York, NY 10016. 1979. 316 pp. 15 × 23 cm. Price $34.50.

Plant Organelles. Edited by ERIC REID. (Methodological Surveys Biochemistry Subseries, Vol. 9.) Wiley, 605 Third Ave., New York, NY 10016. 1979. 232 pp. 15 × 23 cm.

Quantitative Mass Spectrometry in Life Sciences II. Edited by A. P. De LEENHEER, R. R. RONCUCCI, and C. VAN PETEGHEM. Elsevier/North-Holland Inc., 52 Vanderbilt Ave., New York, NY 10017. 1978. 501 pp. 16 × 25 cm. Price $48.45.

Foundations of Molecular Pharmacology, Vol. 2: The Chemical Basis of Drug Action. By J. B. STENLAKE. Athlone Press, University of London, 4 Gower St., London WC1, England. 1979. 318 pp. 15 × 23 cm. Price $46.25.

Advances in Chromatography, Vol. 17. Edited by J. CALVIN GIDDINGS, ELI GRUSHKA, JACK CAZES, and PHYLLIS R. BROWN. Dekker, 270 Madison Ave., New York, NY 10016. 1979. 352 pp. 15 × 23 cm. Price $36.50.

Maternal Recognition of Pregnancy. (Ciba Foundation Symposium 64.) Elsevier/North-Holland Inc., 52 Vanderbilt Ave., New York, NY 10017. 1979. 425 pp. 16 × 24 cm.

Oxygen Free Radicals and Tissue Damage. (Ciba Foundation Symposium 65.) Elsevier/North-Holland Inc., 52 Vanderbilt Ave., New York, NY 10017. 1979. 381 pp. 16 × 24 cm.

Human Genetics: Possibilities and Realities. (Ciba Foundation Symposium 66.) Elsevier/North-Holland, Inc., 52 Vanderbilt Ave., New York, NY 10017. 1979. 425 pp. 16 × 24 cm.

Submolecular Biology and Cancer. (Ciba Foundation Symposium 67.) Elsevier/North-Holland Inc., 52 Vanderbilt Ave., New York, NY 10017. 1979. 349 pp. 16 × 24 cm.

Studies in Drug Utilization: Methods and Applications. Edited by U. BERGMAN, A. H. W. WAHBA, A. GRIMSSON, and B. WESTERHOLM. (WHO Regional Publications European Series No. 8.) World Health Organization, 1211 Geneva 27, Switzerland. 1979. 185 pp. 15 × 24 cm. Price 20 Sw.fr.

Nutrition and Cancer. Edited by JAN VAN EYS, MILDRED S. SEELIG, and BUFORD L. NICHOLS, Jr. Spectrum Publications, 175–20 Wexford Terrace, Jamaica, NY 11432. 1979. 297 pp. 15 × 23 cm. Price $25.00.

Synthetic Aspects of Biologically Active Cyclic Peptides—Gramicidin S and Tyrocidines. By NOBUO IZUMIYA, TETSUO KATO, HARUHIKO AOYAGI, MICHINORI WAKI, and MICHIO KONDO. Wiley, One Wiley Dr., Somerset, NJ 08873. 1979. 166 pp. 14 × 23 cm. Price $29.95.

Terpenoids and Steroids, Vol. 9. Senior Reporter, J. R. HANSON. (A Specialist Periodical Report.) The Chemical Society. 1979. 352 pp. 14 × 22 cm. Price $72.00. (Available from Special Issue Sales, American Chemical Society, 1155 16th St., N. W., Washington, DC 20036.)

Aromatic and Heteroaromatic Chemistry, Vol. 7. Senior Reporters, H. SUSCHITZKY and O. METH-COHN. (A Specialist Periodical Report.) The Chemical Society. 1979. 368 pp. 13 × 23 cm. Price $72.50. (Available from Special Issue Sales, American Chemical Society, 1155 16th St., N. W., Washington, DC 20036.)

Recent Development in Mass Spectrometry in Biochemistry and Medicine, Vol. 2. Edited by ALBERTO FRIGERIO. Plenum, 227 W. 17th St., New York, NY 10011. 1979. 492 pp. 16 × 25 cm. Price $45.00.

Vitamin K Metabolism and Vitamin K-Dependent Proteins. Edited by J. W. SUTTIE. University Park Press, 233 E. Redwood St., Baltimore, MD 21202. 1980. 592 pp. 15 × 23 cm. Price $39.50.

The Nature of Enzymology. By R. L. FOSTER. Wiley, One Wiley Dr., Somerset, NJ 08873. 1980. 383 pp. 13 × 22 cm. Price $39.95.

Selected Methods in Cellular Immunology. Edited by BARBARA B. MISHELL and STANLEY M. SHOIGI. W. H. Freeman and Co., 660 Market St., San Francisco, CA 94104. 1980. 486 pp. 16 × 23 cm. Price $29.95.

Essays on the Anatomy and Physiology of Lymphoid Tissues. Edited by Z. TRNKA and R. N. P. CAHILL. (Monographs in Allergy, Vol. 16.) S. Karger AG, Arnold-Böcklin-Strasse 25, CH-4011 Basel, Switzerland. 1980. 262 pp. 15 × 23 cm. Price $94.50.

JUNE 1980
VOLUME 69 NUMBER 6

JOURNAL OF PHARMACEUTICAL SCIENCES

MARY H. FERGUSON
Editor

SHELLY ELLIOTT
Production Editor

MARCIA GARTRELL
Copy Editor

NICOLETTE TRIANTAFELLU
Copy Editor

EDWARD G. FELDMANN
Contributing Editor

SAMUEL W. GOLDSTEIN
Contributing Editor

BELLE R. BECK
Editorial Secretary

DAVID BOHARDT
Director of Publications

L. LUAN CORRIGAN
Assistant Director of Publications

EDITORIAL ADVISORY BOARD

JOHN AUTIAN
HERBERT A. LIEBERMAN
NORMAN R. FARNSWORTH
DAVID E. MANN, JR.
WILLIAM O. FOYE
GERALD J. PAPARIELLO
WILLIAM J. JUSKO
EDWARD G. RIPPIE

The *Journal of Pharmaceutical Sciences* (ISSN 0022-3549) is published monthly by the American Pharmaceutical Association (APhA) at 2215 Constitution Ave., N.W., Washington, DC 20037. Second-class postage paid at Washington, D.C., and at additional mailing office.

All expressions of opinion and statements of supposed fact appearing in articles or editorials carried in this journal are published on the authority of the writer over whose name they appear and are not to be regarded as necessarily expressing the policies or views of APhA.

Offices—Editorial, Advertising, and Subscription: 2215 Constitution Ave., N.W., Washington, DC 20037. All Journal staff may be contacted at this address. Printing: 20th & Northampton Streets, Easton, PA 18042.

Annual Subscriptions—United States and foreign, industrial and government institutions $60, educational institutions $60, individuals *for personal use only* $30; single copies $5. All foreign subscriptions add $5 for postage. Subscription rates are subject to change without notice. Members of APhA may elect to receive the *Journal of Pharmaceutical Sciences* as a part of their annual $80 (foreign $85) APhA membership dues.

Claims—Missing numbers will not be supplied if dues or subscriptions are in arrears for more than 60 days or if claims are received more than 60 days after the date of the issue, or if loss was due to failure to give notice of change of address. APhA cannot accept responsibility for foreign delivery when its records indicate shipment was made.

Change of Address—Members and subscribers should notify at once both the Post Office and APhA of any change of address.

Photocopying—The code at the foot of the first page of an article indicates that APhA has granted permission for copying of the article beyond the limits permitted by Sections 107 and 108 of the U.S. Copyright Law provided that the copier sends the per copy fee stated in the code to the Copyright Clearance Center, Inc., 21 Congress St., Salem, MA 01970. Copies may be made for personal or internal use only and not for general distribution.

Microfilm—Available from University Microfilms International, 300 N. Zeeb Road, Ann Arbor, MI 48106.

© Copyright 1980, American Pharmaceutical Association, 2215 Constitution Ave., N.W., Washington, DC 20037; all rights reserved.

WHERE HAVE ALL THE RESEARCHERS GONE?

The "researchers" referred to in the title of this editorial are the clinical research people who conduct the studies concerning safety and effectiveness of new drugs using human volunteers as test subjects.

Twenty-five years ago, it seemed that people conducting clinical trials were the proverbial "a-dime-a-dozen." Today, however, they are few and far between; and their number keeps shrinking at an alarming pace.

What has happened? What has caused this major shift? Is the net effect good or bad? And what impact will this have for the future of new drug development? A brief recapitulation and examination of this general phenomenon would appear to be in order.

Drug testing was an extremely lax business back in the 1950s. Furthermore, not only was it simple and easy for virtually any medical practitioner to begin conducting clinical experiments using human subjects—without their consent or even their knowledge—but it was also glamorous, exciting, and the "in thing" among many physicians. Not surprisingly, abuses were commonplace and the results and findings of these pseudoscientific studies by mostly untrained researchers were frequently of questionable validity and doubtful value.

Reform in the shape of the 1962 amendments to the Federal Food, Drug, and Cosmetic Act, coupled with related FDA regulations, changed this situation very abruptly by the mid-60s. "Experts qualified by scientific training and experience," "submission of preclinical test" protocols, "signed agreements from each such investigator," "the establishment and maintenance of records," "making of reports to the Secretary of HEW," certification of "informed human consent," and granting general authority for FDA inspectors to have "access to, to copy, and to verify all such records," were some of the new provisions of that legislation which directly related to the future operation of clinical investigators and their work.

In retrospect, that new law and its associated regulations had a very salutory effect. Most of the abuses were curbed, the amateur researchers were effectively weeded out, and the remaining people constituted a largely conscientious, qualified, and professional core of medical scientists. Indeed, almost overnight, clinical pharmacology came into its own, and this cadre of clinical investigators became regarded as a highly respectable sort of subdiscipline or specialty group.

But because some abuses continued, and because a few investigators were dishonest and got caught at it, increasingly stringent rules and regulations were subsequently promulgated to govern the operation of clinical investigators. Concurrently, other forces were at play that also impacted on the area of clinical investigations and on those who conduct such studies.

One of these was concern over the use of prisoners in human drug trials and the question of whether prisoners could participate in a truly voluntary fashion. A second development was the surge of malpractice cases and the soaring costs of settling liability claims and judgments. A third development was our growing sophistication as to what is needed to produce a valid drug investigation—including, for example, larger and better selected patient populations, adequate controls, and double-blind study designs.

More recently, there have been some other changes. Institutional review boards, or IRBs, have been established and have become a formal part of the clinical investigation process. They provide a broad perspective in reviewing the drug investigator's study plan, the suitability of its design, and the protection offered the patients participating. All of this is good, but it greatly lessens the feeling of freedom and hence the challenge that once attracted clinical investigators to such work.

The same can be said of FDA inspections which now are both more frequent and more thorough. They, too, give society greater confidence that patients' rights are protected and that society is being properly served; but concurrently, they also add greatly to the annoyance and frustration level of the clinical investigator who is subjected to this often intense scrutiny.

Increasingly, we are hearing reports that good people are dropping out of the pool of clinical researchers and that new people are reluctant to embark on careers in that field. Consequently, the field is giving signs that it is beginning to dry up, at least in this country. Partially, the impact has been dulled because many drug firms are now drawing upon foreign data to support their new drug applications. But that is no real or long-term solution for the problem.

If this country is to continue to benefit from the introduction of important new drugs, we need to find an answer that will somehow rejuvenate clinical testing in the United States, while continuing to afford reasonable protection for those who participate as test subjects in such studies. And the importance of this problem is such that it calls for prompt attention and serious consideration.

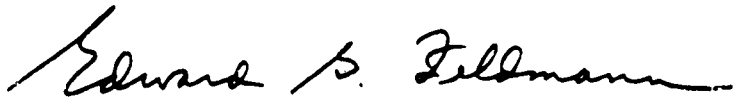

JUNE 1980
VOLUME 69 NUMBER 6

JOURNAL OF PHARMACEUTICAL SCIENCES

MARY H. FERGUSON
Editor

SHELLY ELLIOTT
Production Editor

MARCIA GARTRELL
Copy Editor

NICOLETTE TRIANTAFELLU
Copy Editor

EDWARD G. FELDMANN
Contributing Editor

SAMUEL W. GOLDSTEIN
Contributing Editor

BELLE R. BECK
Editorial Secretary

DAVID BOHARDT
Director of Publications

L. LUAN CORRIGAN
Assistant Director of Publications

EDITORIAL ADVISORY BOARD

JOHN AUTIAN
HERBERT A. LIEBERMAN
NORMAN R. FARNSWORTH
DAVID E. MANN, JR.
WILLIAM O. FOYE
GERALD J. PAPARIELLO
WILLIAM J. JUSKO
EDWARD G. RIPPIE

The *Journal of Pharmaceutical Sciences* (ISSN 0022-3549) is published monthly by the American Pharmaceutical Association (APhA) at 2215 Constitution Ave., N.W., Washington, DC 20037. Second-class postage paid at Washington, D.C., and at additional mailing office.

All expressions of opinion and statements of supposed fact appearing in articles or editorials carried in this journal are published on the authority of the writer over whose name they appear and are not to be regarded as necessarily expressing the policies or views of APhA.

Offices—Editorial, Advertising, and Subscription: 2215 Constitution Ave., N.W., Washington, DC 20037. All Journal staff may be contacted at this address. Printing: 20th & Northampton Streets, Easton, PA 18042.

Annual Subscriptions—United States and foreign, industrial and government institutions $60, educational institutions $60, individuals *for personal use only* $30; single copies $5. All foreign subscriptions add $5 for postage. Subscription rates are subject to change without notice. Members of APhA may elect to receive the *Journal of Pharmaceutical Sciences* as a part of their annual $80 (foreign $85) APhA membership dues.

Claims—Missing numbers will not be supplied if dues or subscriptions are in arrears for more than 60 days or if claims are received more than 60 days after the date of the issue, or if loss was due to failure to give notice of change of address. APhA cannot accept responsibility for foreign delivery when its records indicate shipment was made.

Change of Address—Members and subscribers should notify at once both the Post Office and APhA of any change of address.

Photocopying—The code at the foot of the first page of an article indicates that APhA has granted permission for copying of the article beyond the limits permitted by Sections 107 and 108 of the U.S. Copyright Law provided that the copier sends the per copy fee stated in the code to the Copyright Clearance Center, Inc., 21 Congress St., Salem, MA 01970. Copies may be made for personal or internal use only and not for general distribution.

Microfilm—Available from University Microfilms International, 300 N. Zeeb Road, Ann Arbor, MI 48106.

© Copyright 1980, American Pharmaceutical Association, 2215 Constitution Ave., N.W., Washington, DC 20037; all rights reserved.

WHERE HAVE ALL THE RESEARCHERS GONE?

The "researchers" referred to in the title of this editorial are the clinical research people who conduct the studies concerning safety and effectiveness of new drugs using human volunteers as test subjects.

Twenty-five years ago, it seemed that people conducting clinical trials were the proverbial "a-dime-a-dozen." Today, however, they are few and far between; and their number keeps shrinking at an alarming pace.

What has happened? What has caused this major shift? Is the net effect good or bad? And what impact will this have for the future of new drug development? A brief recapitulation and examination of this general phenomenon would appear to be in order.

Drug testing was an extremely lax business back in the 1950s. Furthermore, not only was it simple and easy for virtually any medical practitioner to begin conducting clinical experiments using human subjects—without their consent or even their knowledge—but it was also glamorous, exciting, and the "in thing" among many physicians. Not surprisingly, abuses were commonplace and the results and findings of these pseudoscientific studies by mostly untrained researchers were frequently of questionable validity and doubtful value.

Reform in the shape of the 1962 amendments to the Federal Food, Drug, and Cosmetic Act, coupled with related FDA regulations, changed this situation very abruptly by the mid-60s. "Experts qualified by scientific training and experience," "submission of preclinical test" protocols, "signed agreements from each such investigator," "the establishment and maintenance of records," "making of reports to the Secretary of HEW," certification of "informed human consent," and granting general authority for FDA inspectors to have "access to, to copy, and to verify all such records," were some of the new provisions of that legislation which directly related to the future operation of clinical investigators and their work.

In retrospect, that new law and its associated regulations had a very salutory effect. Most of the abuses were curbed, the amateur researchers were effectively weeded out, and the remaining people constituted a largely conscientious, qualified, and professional core of medical scientists. Indeed, almost overnight, clinical pharmacology came into its own, and this cadre of clinical investigators became regarded as a highly respectable sort of subdiscipline or specialty group.

But because some abuses continued, and because a few investigators were dishonest and got caught at it, increasingly stringent rules and regulations were subsequently promulgated to govern the operation of clinical investigators. Concurrently, other forces were at play that also impacted on the area of clinical investigations and on those who conduct such studies.

One of these was concern over the use of prisoners in human drug trials and the question of whether prisoners could participate in a truly voluntary fashion. A second development was the surge of malpractice cases and the soaring costs of settling liability claims and judgments. A third development was our growing sophistication as to what is needed to produce a valid drug investigation—including, for example, larger and better selected patient populations, adequate controls, and double-blind study designs.

More recently, there have been some other changes. Institutional review boards, or IRBs, have been established and have become a formal part of the clinical investigation process. They provide a broad perspective in reviewing the drug investigator's study plan, the suitability of its design, and the protection offered the patients participating. All of this is good, but it greatly lessens the feeling of freedom and hence the challenge that once attracted clinical investigators to such work.

The same can be said of FDA inspections which now are both more frequent and more thorough. They, too, give society greater confidence that patients' rights are protected and that society is being properly served; but concurrently, they also add greatly to the annoyance and frustration level of the clinical investigator who is subjected to this often intense scrutiny.

Increasingly, we are hearing reports that good people are dropping out of the pool of clinical researchers and that new people are reluctant to embark on careers in that field. Consequently, the field is giving signs that it is beginning to dry up, at least in this country. Partially, the impact has been dulled because many drug firms are now drawing upon foreign data to support their new drug applications. But that is no real or long-term solution for the problem.

If this country is to continue to benefit from the introduction of important new drugs, we need to find an answer that will somehow rejuvenate clinical testing in the United States, while continuing to afford reasonable protection for those who participate as test subjects in such studies. And the importance of this problem is such that it calls for prompt attention and serious consideration.

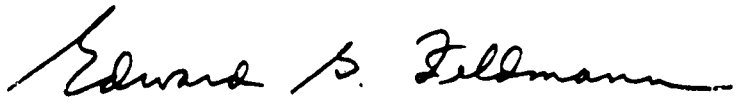

Suspension Theory—Psychological/ Physiological States

The tissues composing the body can be viewed as cell suspension systems. The various individual tissues organize and coordinate to function as a whole system.

The cells of each local tissue continuously fluctuate between the coagulated and flocculated aggregation states. In addition, blood cells can exist in the dispersed state as separate entities.

By flocculated is meant an aggregation of cells held together by bridging macromolecules in an open network structure. Entrapped in the openings of the network is polar bulk water.

By coagulated is meant an aggregation held together by films of macromolecules that cover the adhering surfaces of closely adjacent cells. The water in which the cells are suspended is bound and forms part of an interstitial structured matrix, which is nonpolar in its solvent properties[1,2].

It was postulated[1] and then shown[3,4] that a direct correlation exists between psychological states and erythrocyte sedimentation rates and, thereby, between psychological states and the red blood cell aggregation state producing the erythrocyte sedimentation rate[5]. The normal emotional state exists with a dynamic equilibrium among the dispersed, coagulated, and flocculated suspension states. Increasing emotional agitation up to the manic state shifts the aggregation equilibrium to a predominately flocculated state. Conversely, the depressed state (manic-depressive) shifts the suspension states to predominately a coagulated aggregation.

If it is assumed that the normal emotional state is the ground state with respect to free energy content, any increase in stress, psychological or physical, produces an increase in matrix structure breakers (catecholamines, *etc.*), which is accompanied by liberation of metabolic energy, *i.e.*, a decrease in enthalpy. There is a corresponding increase in the entropy as reflected in the shift toward a flocculated and dispersed system. Thus, fuel for responding to the stress is at the expense of the free energy content of the total body as well as the local tissues involved. Countervailing conditions toward normal and depressive states are initiated by removal of the stress or prolonged presence of stress with excessive expenditure of the free energy.

The presence of stress is accompanied by rising levels of macromolecules, chiefly albumin, along with the catecholamines.

Removal of stress lowers catecholamine as well as other energy-stimulating hormone production, thereby permitting excess macromolecules to layer out on cell surfaces. Sufficient film production on cell surfaces results in a shift toward coagulation.

Prolonged presence of stress results in depletion of local tissue free energy. The liberation of chemical energy decreases and then ceases. The entropy of the tissue cellular suspensions then becomes increasingly more negative as the cells begin to pack closely together and to form the more structured coagulated state. The coagulated state permits regeneration of free energy and eventually the metabolic processes that start the cycle toward the flocculated state.

In summary, as the manic stage is approached, the change in entropy of the cell suspensions becomes increasingly positive as the change in enthalpy becomes increasingly negative. As the depressed stage is approached, the entropy becomes increasingly negative. With time, the local tissue enthalpy becomes increasingly positive. The local tissue free energy is increased as the by-product of the metabolic processes occurring in the other tissues.

The coagulated state is the state of energy regeneration, growth, and division. Its organization is controlled by the external environment. The flocculated state is the state of energy expenditure and internal control of tissue organization (contact inhibition)[6]. In the extreme case, depression is an energy-rich state, energy that the body cannot liberate. The energy is expended on the tissues of the internal environment. In the manic state, excessive amounts of energy are being expended on the external environment. The body is continually responding to stress with psychological–physiological buffering processes.

Accordingly, after a period of stress, sleep is a process for regenerating reversible thermodynamic states under optimum conditions. In sleep, there is a minimum of external energy-stimulating signals.

In aging, the reversible coagulation–flocculation process proceeds with a slow loss of entropy regeneration and reversibility and, thereby, a loss of ability to organize cell tissue aggregates. The final result is the loss of internal control of body organization and finally death, although individual cells might still live.

The immortality of cancer cells, an irreversible coagulated state, is obtained at the loss of the ability to go to an organized state, *e.g.*, the flocculated state[6].

Bernard Ecanow
University of Illinois
at the Medical Center
Chicago, IL 60612

Received March 31, 1980.

[1] B. Ecanow, "Aggregation of Biological Suspension Systems," U.S. copyright registration A825763 Ecanow, Skokie, Ill., 1966.

[2] B. Ecanow, R. Balagots, B. Gold, and C. Ecanow, *J. Soc. Cosmet. Chem.*, **23**, 679 (1972).

[3] B. Ecanow, B. Gold, S. Touguan, and W. Stanaszek, *Dis. Nerv. Syst.*, **30**, 1072 (1969).

[4] B. Ecanow, B. Gold, and P. Tunkunas, in "Application of Physical Chemistry Principles to the Study of Anxiety and Depression; Psychotherapy and Psychosomatic," J. Ruesch, Ed., S. Karger, Basel, Switzerland, 1972.

[5] B. Ecanow and H. Klawans, in "Models of Human Neurological Disease," H. Klawans, Ed., Excerpta Medica, Amsterdam, The Netherlands, 1974.

[6] B. Ecanow, B. H. Gold, D. Kohn, and C. Ecanow, *Physiol. Chem. Phys.*, **11**, 97 (1979).

JOURNAL OF PHARMACEUTICAL SCIENCES

JUNE 1980
VOLUME 69 NUMBER 6

RESEARCH ARTICLES

Cost Evaluation of Alternative Pharmaceutical Tableting Processes by Simulation

R. M. FRANZ, G. S. BANKER, J. R. BUCK *, and G. E. PECK x

Received August 20, 1979, from the *Department of Industrial and Physical Pharmacy, Purdue University, School of Pharmacy and Pharmacal Sciences, West Lafayette, IN 47907.* Accepted for publication January 18, 1980. *School of Industrial Engineering, Purdue University, West Lafayette, IN 47907.

Abstract □ A simulation model and a subsequent computer program were developed as experimentation methods for evaluating tableting processes with respect to cost. These methods also allow estimation of the various times involved in a tableting operation (*e.g.*, the processing time). The model was programmed in FORTRAN using the GASP IV simulation language. After verification of the program, experiments were run that involved comparing different levels of specific input variables to determine which variable had an effect on the cost–time relationships of a particular processing method. Among the possible input variables chosen for evaluation were the drying method, the type of tableting machine, the batch size, the labor rate, and the operation of the equipment in the process. An analysis of variance was made, and three separate regression equations were developed that described the relationship between the input variables and the dependent variables of processing cost and time. Graphs were developed from the regression equations by manipulating them through series of different independent variables. These graphs then were used in determining minimum costs and times, breakeven points, and rates of change, as well as in simple evaluation of processes through graphic representation. By using the simulation program to run experiments and then by analyzing them, results can be obtained to help in making intelligent decisions about the cost–time relationships of a particular tableting procedure before it is implemented.

Keyphrases □ Tableting processes—cost evaluation, simulation model □ Models, simulation—cost evaluation of tableting processes □ Cost evaluation—tableting processes, simulation model □ Processing formulations—tableting procedures, cost evaluation, simulation model

The effects of alternative processing methods and formulations on the physical, chemical, and biological characteristics of tablet dosage forms (1, 2) have been discussed extensively. Although these alternative processes and formulations can affect the time and cost for tablet production, little information has been published on these time–cost effects. This paper describes a method for assessing various processing time and cost effects with specific alternative formulations and processing techniques. The general implications of these effects also are shown.

The basic element of this method is a computer simulation encompassing the various tablet-processing techniques. Although simulation has been used in the pharmaceutical industry for the development of a completely computerized tableting plant (3) and for various chemical and business operations, these simulations are specific for a particular company and application. Also, these simulations have been employed to answer specific questions.

The approach illustrated here is generalized to simulate virtually any tableting operation, and it is coupled with an example of an experimental design so that inferences can be made over numerous factors that change from one tableting operation to another. In this way, the individual simulation serves as a basic experimental unit, much as would an individual laboratory experiment. Results from such simulations thus can be used in process analysis, design, and performance evaluation with respect to cost–time information.

MODEL

Development—A general simulation model for the tableting of pharmaceutical products was developed. The model was constructed so that any of the three basic tableting methods (wet granulation, direct compression, and slugging) as well as variations in these methods could be simulated. The basic unit operations employed by these methods were arranged in linear fashion as shown in Part A of Fig. 1. To simulate a particular tablet processing technique, unit operations that are not part of the technique are excluded by having a zero time interval. In this way, a single model can simulate two or more tableting methods where any differences in the methods are inputted explicitly in the program.

General unit operation input variables are included in every step of the model (Fig. 1, Part B). The times involved in each unit operation are determined by the type of equipment used in that particular step. These times reflect the cost involved per unit operation. Power and depreciation are other cost components. Only linear depreciation is used in the model,

0022-3549/80/0600-0621$01.00/0
© 1980, American Pharmaceutical Association

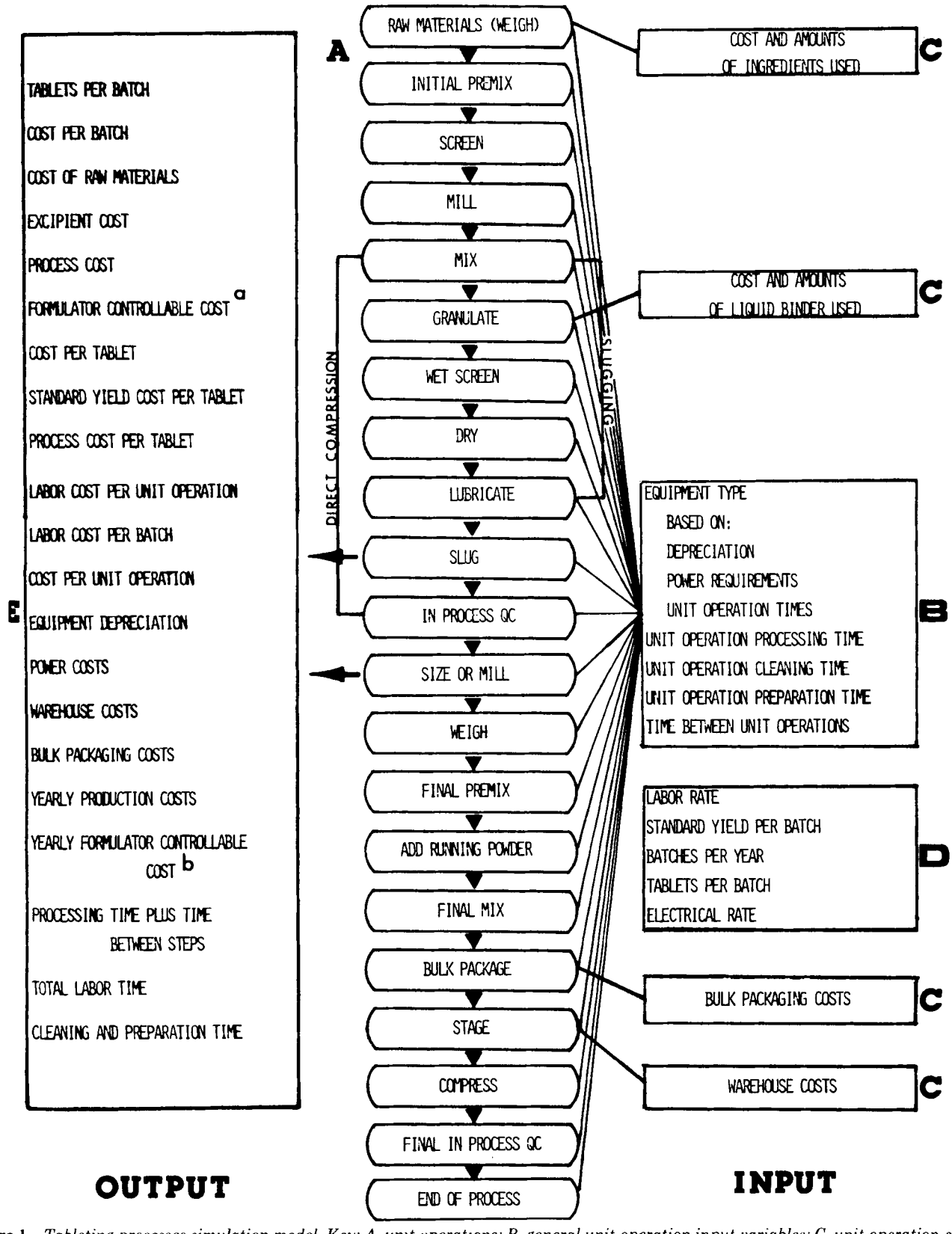

Figure 1—*Tableting processes simulation model. Key: A, unit operations; B, general unit operation input variables; C, unit operation-specific input variables; D, batch-specific input variables; and E, final cost–time output. [a]Process and formulation controllable cost. [b]Yearly process and formulation controllable cost.*

as noted in Table I, which also includes some of the important equations used in the model (4, 5). The utilization factor used here is unity minus the fraction of time the equipment is idle. The utilization factor adjusts the actual batch time to account for a proportional amount of the idle time for the equipment.

Unit operation-specific input variables that are used in only certain operations are given in Part C of Fig. 1. These variables include warehousing costs, but only those incurred during the staging operations before the final product is complete.

Batch-specific input variables that are used throughout the entire

Table I—Partial List of Basic Equations Used in the Model [a]

Computed Output	Equations	Variables
Power consumption cost per unit operation (PCC)	PCC = (HP) (UOPT) (ER) (0.012426432)	HP = Horsepower of the equipment in the unit operation UOPT = Unit operation processing time (minutes) ER = Electrical rate (dollars per kilowatt hour) 0.012426432 = Conversion factor
Labor cost per unit operation (LC)	LC = (PT + CT + UOPT + TBUO) (LR)	PT = Unit operation preparation time CT = Unit operation cleaning time UOPT = Unit operation processing time TBUO = Time between unit operations LR = Labor rate (dollars per hour)
Total cost per unit operation (TCUO)	TCUO = PCC + LED + LC + AC	PCC = Power consumption cost per unit operation LED = Linear equipment depreciation per unit operation LC = Labor cost per unit operation AC = Additional costs (*i.e.*, raw materials, bulk packaging costs, and warehouse cost)
Total cost per batch (TCB)	TCB = $\Sigma_{i=1}^{x}$TCUO, where x is the total number of unit operations in the process	TCUO = Total cost per unit operation
Processing cost per batch (PC)	PC = TCB − CRM	TCB = Total cost per batch CRM = Cost of raw materials
Process and formulation controllable cost (FCC)	FCC = (EC − PC)/SY	EC = Excipient cost PC = Processing cost SY = Standard yield per batch
Standard yield cost per tablet (SYCT)	SYCT = TCPT/SY	TCPT = Theoretical cost per tablet SY = Standard yield per batch
Linear equipment depreciation per unit operation (LED)	LED = [(IC − SV)/(SL × 525,960 × UF)] (UOPT + PT + CT)	IC = Initial cost of each piece of equipment in the process SV = Salvage value of each piece of equipment in the process SL = Service life of each piece of equipment in the process UF = Utilization of each piece of equipment in the process 525,960 = Conversion factor UOPT = Unit operation processing time PT = Unit operation preparation time CT = Unit operation cleaning time

[a] All times are in minutes.

simulation are given in Part D of Fig. 1.

The final cost–time output needed for process analysis and evaluation is denoted as Part E in Fig. 1. The *Appendix* gives detailed information regarding this output. In addition, various histograms and tables that show the cost breakdowns for individual unit operations are provided by the basic program to aid in specific process verifications and corrections.

The basic simulation model was kept simple to reduce computer costs and to make it easier for users to adjust to specific operational variations. Adjustments to the input data will be needed when the operation being simulated deviates from the assumptions made in constructing the basic model. These assumptions and some of the required adjustments include the following:

1. The time "between" unit operations is included in the cost of the successive operation.

2. If a unit operation is skipped, then the time between it and the successive unit operation is uniform. The time "between" unit operations is dictated by the unit operation being left, *not* by the next unit operation in the process. This convention allows variations in the sequences of unit operations.

3. Equipment depreciation for each unit operation in a process is based on the unit operation processing time, cleaning time, and preparation time. The batch depreciation is the sum of the individual depreciations of the unit operations.

4. Labor cost for a unit operation includes the time between the current and the previous unit operation, cleaning time, preparation time, and unit operation processing time multiplied by a single labor rate. If multiple labor rates are involved, then a single composite labor rate can be used.

5. The unit operation processing labor time is equal to the unit operation processing time, except in the drying step (tray drying only) and the staging step. In the drying and staging steps, the unit operation processing labor time is much less than the unit operation processing time.

6. Costs are assigned only to the particular batch being processed. Accordingly, the time a laborer works on more than one batch during any particular processing step is not included in the final cost estimates.

7. The laborer can do only one thing at a time. For example, if the mixing unit operation lasted 15 min, the laborer would be at this step for 15 min and would *not* be starting the next unit operation in advance. The only exceptions are the drying and staging unit operations, where the unit operation processing labor time differs from the unit operation processing time.

8. All equipment used is powered by electricity; or if it is powered by some alternative form of energy, it can be converted into equivalent electrical units (kilowatt hours).

Data—Data were collected from various pharmaceutical manufac-

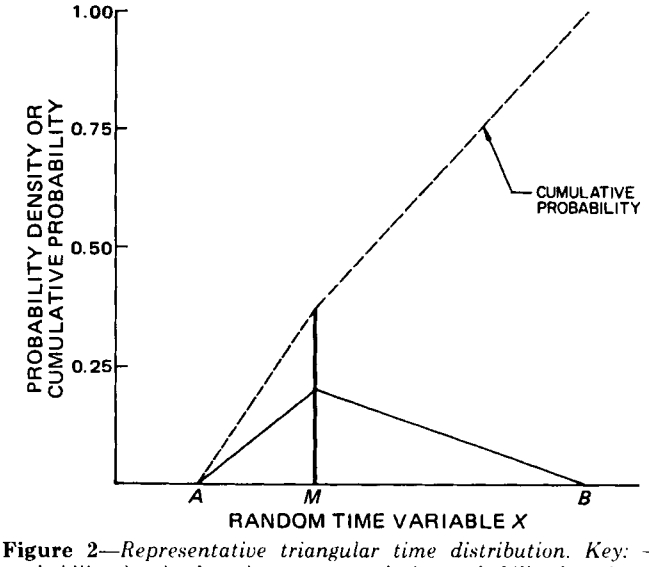

Figure 2—*Representative triangular time distribution. Key:* —, *probability density function;* - - -, *cumulative probability function;* A, *minimum;* B, *maximum; and* M, *mode.*

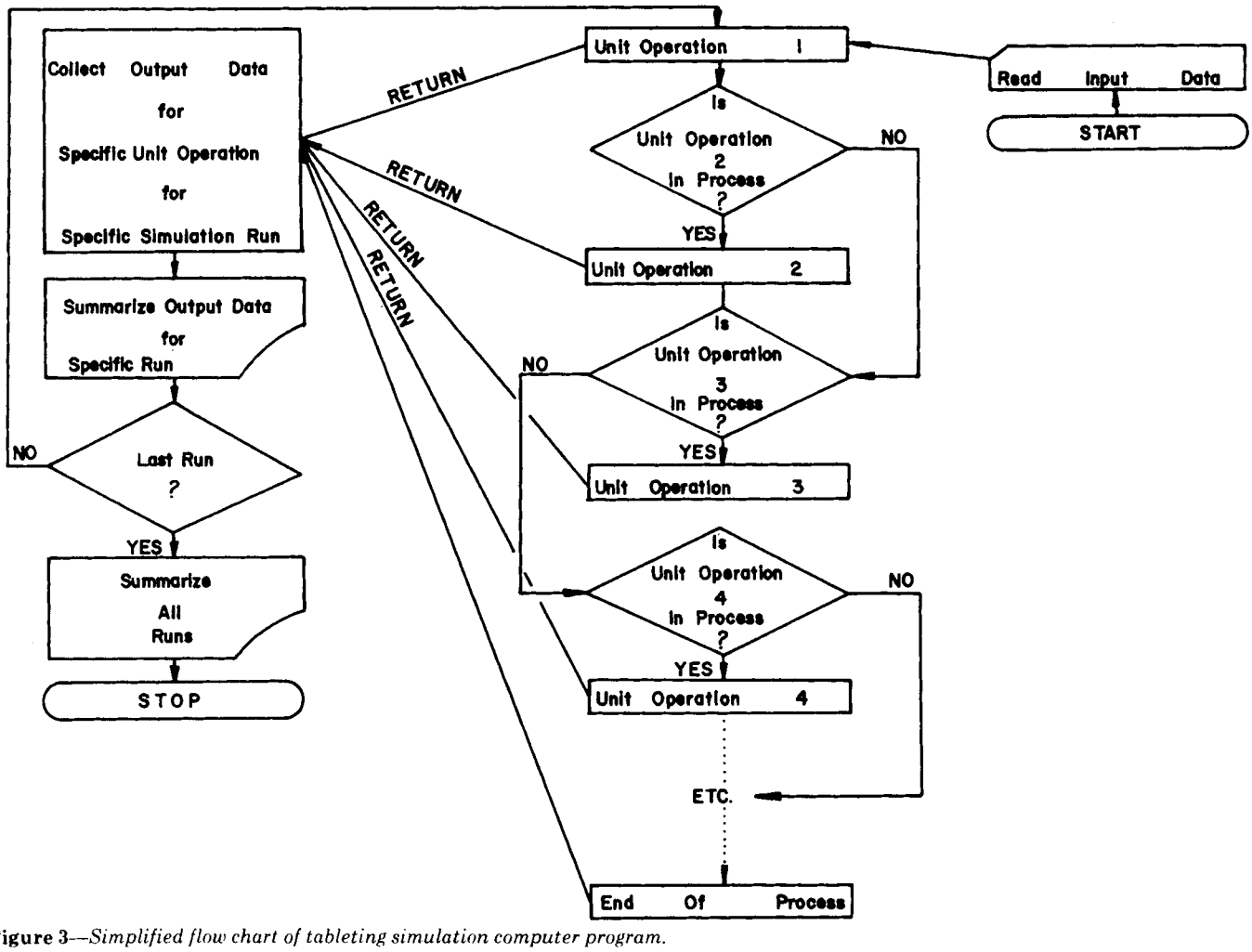

Figure 3—*Simplified flow chart of tableting simulation computer program.*

turing firms on specific operations performed, sequences of operations, equipment specifications and layouts, products made, manpower requirements, approximate time requirements, and other relevant features to assure reasonable generality of the model and to provide reasonable values and ranges for various parameters and coefficients.

Time and cost variations occur randomly in the unit operations, and an allowance was made in the basic model to include these uncertainties. Time data were collected in triangular distribution form to provide users with a consistent and highly intuitive method for including these uncertainties (6). With the triangular distribution, users must specify the minimum value, the most likely or modal value, and the maximum value for the random time variable being described. Distributions representative of the data collected were used in the program, but other distributions can be incorporated, if necessary, with a minimum of programming effort. Figure 2 shows the probability density and cumulative probability functions of the triangular distribution.

The probability density function is described by:

$$F(X) = \frac{2(X - A)}{(M - A)(B - A)} \qquad A \le X \le M \qquad \text{(Eq. 1}a\text{)}$$

$$F(X) = \frac{2(B - X)}{(B - M)(B - A)} \qquad M \le X \le B \qquad \text{(Eq. 1}b\text{)}$$

$$F(X) = 0 \qquad \text{otherwise} \qquad \text{(Eq. 1}c\text{)}$$

The cumulative probability function is described by:

$$F^*(X) = \frac{(X - A)^2}{(M - A)(B - A)} \qquad A \le X \le M \qquad \text{(Eq. 2}a\text{)}$$

$$F^*(X) = \frac{(M - A)}{(B - A)} + \frac{(B - M)^2 - (B - X)^2}{(B - M)(B - A)} \qquad M \le X \le B \qquad \text{(Eq. 2}b\text{)}$$

where X is the random time variable, A is the minimum value, B is the maximum value, and M is the modal (most likely) value. This distribution allows for asymmetry in the random variable, which often occurs in processing time requirements. In the computer program, a uniform random deviate is called and converted to a value of X through the cumulative probability function described by Eqs. 2*a* and 2*b*.

Programming—The model was programmed in FORTRAN with the

Table II—Example of the Printout Produced by the FORTRAN Simulation Program

Average Results of All Runs	Average	*SD*
Tablets per batch	250,000.00	
Cost per batch	$6,293.00	4.108
Cost of raw materials	$5,879.76	
Excipient cost	$59.13	
Process cost	$413.24	4.108
Process and formulation controllable cost	$476.18	4.141
Cost per tablet	$0.025172	0.00001643
Standard yield cost per tablet	$0.025375	0.00001656
Process cost per tablet	$0.001653	0.00001643
Labor cost per step	$25.73	0.270
Labor cost per batch	$385.98	4.047
Cost per step	$419.53	0.274
Equipment depreciation	$4.42	0.075
Power costs	$2.84	0.065
Warehouse costs	$0.00	
Package costs	$20.00	
Yearly production cost	$1,132,739.82	739.415
Yearly process and formulation controllable cost	$85,712.12	745.378
Processing time plus time between steps	46.999 hr	0.755
Total labor time	70.951 hr	0.744
Cleaning and preparation time	41.057 hr	0.850

Table III—Comparison of Actual *versus* Simulated Average Total Processing Time plus Time between Unit Operations

Product	Actual Time from Manufacturer, hr	Simulated Time from Program, hr	Percent Difference from Actual Time
1	5.12	5.57	8.79
2	33.0	36.7	11.2
3	17.0	16.0	5.88
4	26.5	27.2	2.64
5	39.5	33.4	15.4
7	28.5	29.3	2.81
7	41.0	37.0	9.76
8	39.5	36.4	7.85

aid of a computer simulation package called GASP IV (7). GASP IV allows users to build computer simulations with a minimum of effort. The programmer develops subroutines that interact with various GASP IV subroutines. Subroutines in the GASP IV package provide much of the statistical analysis used in the simulation and in creating the cost–time histograms in the program output. Each unit operation in the model was programmed as a separate subroutine so that users could incorporate additional cost–time features into any unit operation with a minimum of difficulty.

By using different initial uniform random deviates, a different stream of random numbers are generated with each simulation run and are converted to random variations in time and cost output through the specific forms of the triangular distributions. These variations take the form of an average and a standard deviation for each cost–time output of the model. This result is indicated in the simplified flow diagram of the computer program shown in Fig. 3.

Table II shows a sample of the output averages and standard deviations to illustrate the management information provided by the basic simulation program.

Verification—The model verification was accomplished in two steps. The first step involved inspection by pharmaceutical processing personnel, including tableting operation supervisors and directors of pharmaceutical manufacturing departments, of the model concept, assumptions, and variable values to assure that they were representative of actual tableting processes.

The second step involved taking various tablet products from different companies, running the simulation on them as specified by their processing sheets, and then comparing the average simulated processing times with the average time reported in the company's records. Table III shows the results of these comparisons and the percentage differences between the simulation and the actual processing times. No relationships between simulation errors and actual processing times were evident from these data when they were plotted on a scattergram. Final cost data comparisons could not be obtained for proprietary reasons.

Model Application—Numerous experiments were run using the simulation, especially those involving interprocess analysis. The experiment illustrated here is an example of an intraprocess analysis. The goal was to determine how different levels of specific processing variables affect the final processing time and processing cost of a particular wet granulation tableting technique.

Numerous variables affect the processing time and cost. The variables chosen for investigation were the type of drying (tray or fluid bed), the type of tableting machine, the batch size, the average utilization of all equipment in the process, and the labor rate.

Except for the variable of the type of drying, there are many options for each variable, so the number of combinations possible is extremely large. Consequently, investigation of even a small fraction of these combinations is economically unfeasible in a search for more economical

Table IV—Fixed Unit Operation Input [a]

Unit Operations in Process	Equipment Used in Unit Operation	Cost of Equipment in Unit Operation[b]	Horsepower of Equipment
1. Raw materials	Scales	$7,000.00	0.1
2. Premix	Small blender[c]	$20,000.00	3.0
3. Screen	Screens	$50.00	0.0
4. Mix	Mixer[d]	$30,000.00	2.0
5. Granulate	Mixer	$30,000.00	2.0
6. Wet screen	Screens	$50.00	0.0
7. Dry	—[e]	—[e]	—[e]
8. Dry screen or size	Hammer mill[f]	$10,000.00	10.0
9. Weigh	Scales	$7,000.00	0.1
10. Add running powder or lubricant	Scoop	$5.00	0.0
11. Final mix	Large mixer[g]	$43,000.00	15.0
12. Bulk package	Scoop	$5.00	0.0
13. Compress	—[e]	—[e]	—[e]
14. Final in-process quality control	Quality control	$2,000.00	0.1

[a] The additional inputs were: bulk packaging costs = $20.00; electrical rate = $0.025/kw hr; standard yield = 0.992; and batches per year = 100. [b] Service life of equipment is 15 years. [c] Patterson Kelly Co., Division of Harsco Corp., East Stroudsburg, PA 18301. [d] Day Mixing, Cincinnati, OH 45212. [e] Variable level input. [f] Fitzpatrick Co., Elmhurst, IL 60126. [g] General Machine Co. of New Jersey, Newark, NJ 97114.

Table V—Variable Unit Operation Input [a]

Levels	Drying Method	Tableting Machine	Utilization of All Equipment in Process, %	Batch Size, tablets	Labor Rate per Hour
1	Tray dried (stainless steel tray dryer) Horsepower = 3.0 Cost = $20,000.00 Tray drying processing time: mode = 1080.0, minimum = 960.0, and maximum = 1200.0 Tray drying labor time: mode = 60.0, minimum = 50.0, and maximum = 70.0	Tablet machine A Horsepower = 3.0 Cost = $43,000.00 Tablets per minute: mode = 2800.0, minimum = 1500.0, and maximum = 4100.0	100	500,000	$5.50
2	Fluid bed dried Horsepower = 25.0 Cost = $100,000.00 Fluid bed drying processing and labor time: mode = 32.5, minimum = 20.0, and maximum = 45.0	Tablet machine B Horsepower = 15.0 Cost = $90,000.00 Tablets per minute: mode = 7608.0, minimum = 4347.0, and maximum = 10,869.0	50	1,000,000	$11.00
3	—	—	—	1,500,000	$16.50

[a] All times are in minutes.

Table VI—Results of Analysis of Variance [a]

Processing Cost Model ANOVA Results	Processing Time Model ANOVA Results	
	Fluid Bed Dried	Tray Dried
B (Batch size)	B (Batch size)	B (Batch size)
L (Labor rate)	T (Tableting	T (Tableting
U Utilization factor	machine)	machine)
T (Tableting machine	BT (B–T	BT (B–T
D (Drying method)	interaction)	interaction)
LU (L–U interaction)		
BT (B–T interaction)		
LT (L–T interaction)		
UT (U–T interaction)		
LUT (L–U–T interaction)		

[a] Tested at 0.01 level of significance with pooled error term. Certain interactions were determined to be poolable into an error term after testing indirectly across the restriction error with the residual error at a 0.25 level of significance.

tableting methods. An alternative approach is to use an experimental design that analyzes the effect of entire variables and their interactions to identify those that affect the processing time and cost. This approach allows identification of those variables and interactions where processing times and costs do change significantly, thereby reducing the number of variables to be considered.

Once the significant variables and interactions are identified, a formula for describing the processing time and cost can be devised through regression methods to show the magnitude of these time and cost effects. Various decision rules then can be developed with these formulas to aid in the management of the tableting process, the potential purchase of new equipment, or the design of a new tableting process. Some of these features will be demonstrated here. In addition, optimization methods may be employed to find the most economic processing method following the concepts discussed previously (8–10). A variety of experimental designs, regression procedures, and optimization techniques can be employed in this conceptual approach, but the choice among these alternatives is beyond the scope of this investigation.

EXPERIMENTAL

The particular tableting technique being investigated, as well as the fixed unit operation input, is shown in Table IV. The levels of the fixed input remain the same throughout the entire experiment. Salvage values for all equipment were estimated to be zero at the end of the service life of 15 years.

The different levels of the variables of the drying method, tableting machine, utilization factor, batch size, and labor rate used in the experimental design approach are noted in Table V. All of the variables in Table V were assumed to be continuous between the levels tested, except for the drying method, which was considered discrete.

A five-way split–split plot experimental design was employed. This design allows the experimental conditions to be run twice using two separate sets of initial uniform random deviates, which are used to obtain random time variables from the different triangular time distributions. It was assumed that the effect of the two different sets of initial uniform random deviates would be statistically insignificant; consequently, the interactions involving this effect could be pooled together as an error term. This error term then could be used in an analysis of variance. A test was made on this assumption by rerunning the simulation strictly at the model value for all of the triangular time distributions and comparing the average processing time and cost output without variability to that obtained from the results using the different sets of initial uniform random deviates. Since there was an insignificant difference, this assumption was partially verified.

Before running an analysis of variance, the generated processing cost and time outputs were checked to assure homogeneous variances. Since the processing cost means were proportional to the cost variances, a logarithmic transformation of these data was made, and the Burr–Foster Q test (11) assured homogeneity at a 0.01 level of significance. Mean processing time data were separated into tray drying and fluid bed drying categories due to trends in the data within each method. The need for this separation was expected since drying method levels were considered discrete. Logarithmic and fourth-root logarithmic transformations on the tray drying and fluid bed drying processing time data, respectively, gave homogeneous variances at the 0.01 level of significance as confirmed by the Burr–Foster Q test.

An analysis of variance was performed separately on each of three data sets: (*a*) the processing cost with both drying methods, (*b*) the processing time using tray drying, and (*c*) the processing time using fluid bed drying. The results showed that the effects of the two different sets of initial uniform random deviates were insignificant. The main effects and interactions that were statistically significant in the analysis of variance are listed in Table VI.

A second-order stepwise regression analysis was performed on those variables found to be statistically significant in the analysis of variance. The equations developed by this analysis, as well as the squared correlation coefficients, are given in Table VII.

Table VII—Results of Regression Analysis [a]

Processing Cost Regression Equation		Processing Time Regression Equations	
Variable	B (Coefficent)	Variable	B (Coefficient)
L	0.781*e*-01	Tray Drying	
L^2	−0.179*e*-02	T	−0.146*e*-05
B	0.982*e*-07	B	0.126*e*-06
UT	−0.608*e*-05	BT	−0.106*e*-10
B^2T	0.161*e*-17	B^2	−0.500*e*-14
U	−0.411*e*-01	Constant	1.464
LU	0.245*e*-02	R^2 = 0.9999	
D	−0.555*e*-02	Fluid Bed Drying	
LUT	0.620*e*-06	T	−0.153*e*-05
B^2	−0.128*e*-13	B	0.585*e*-07
T	0.117*e*-04	BT	−0.374*e*-11
BT	−0.101*e*-10	B^2	−0.600*e*-14
LT	−0.922*e*-06	Constant	1.021
L^2T	0.302*e*-07	R^2 = 0.9998	
L^2UT	−0.243*e*-07		
Constant	2.146		
R^2 = 0.9998			

[a] B = batch size, L = labor rate, U = utilization factor, T = tablet machine, and D = drying method. Minimum F value for variable entry = 0.01, maximum F value for variable removal = 0.005, and tolerance = 0.001.

RESULTS AND DISCUSSION

Graphical Development—The regression equations in Table VII were programmed on a digital computer and manipulated through a series of over 100 points between the high and low levels of the factors tested. The graphs shown in Figs. 4–7 were selected for discussion from among the many that were developed using a computer plotting technique and the points generated from the regression equations.

Processing Time Analysis—The processing time increased as a function of increasing batch size (between 0.5×10^6 and 1.5×10^6 tablets/batch), as expected, but the rate of increase always was greater with tablet machine A[1]. The reason for this greater rate of increase was that tablet machine A had a lower speed than tablet machine B[2], so it took longer for tablet machine A to produce a fixed batch size of tablets than tablet machine B. Tray-dried batches made with tablet machine A always had longer processing times than fluid bed-dried and tablet machine B-produced batches. The most interesting feature of this test was that processing times were almost linear functions of the batch size, even though there were interactions and higher order terms in the regression equation.

Another test was made on the processing time as a function of the mean tableting rate for different batch sizes with different drying methods as shown in Fig. 4. The tray-dried processing time for a fixed batch size was offset by a constant processing time of ~27.8 hr more per batch than the fluid bed-dried[3] processing time. Beside the decrease of the batch processing time with increased tableting rates, the processing time effects also were marginally decreased (Fig. 4).

Although the effects of the examples follow the form of intuitive expectations, the magnitude of these effects would be difficult to anticipate without considerable data. However, use of the graph allows easy visual understanding of the trends caused by these effects as well as computation of their magnitude.

Processing Cost Analysis—Figure 5 illustrates how the processing cost decreases with increasing mean tableting rate using different combinations of drying methods and batch sizes. The processing cost change over the limits of the tableting rate (mean tablets per minute) becomes

[1] Model 541, Stokes Division, Pennwalt Corp., Philadelphia, Pa.
[2] Model M75MKIII, Manesty Machines Ltd., Speke, Liverpool, England.
[3] Model AG100, Aeromatic Inc., Bernardsville, NJ 07924.

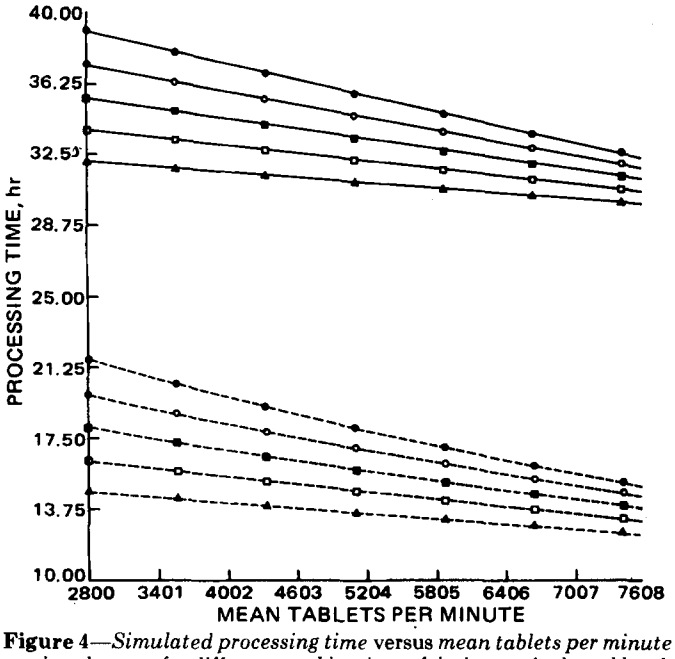

Figure 4—*Simulated processing time* versus *mean tablets per minute produced curves for different combinations of drying methods and batch sizes. Key: -●-, tray dried, 1,500,000 tablets; -○-, tray dried, 1,250,000 tablets; -■-, tray dried, 1,000,000 tablets; -□-, tray dried, 750,000 tablets; -▲-, tray dried, 500,000 tablets; --●--, fluid bed dried, 1,500,000 tablets; --○--, fluid bed dried, 1,250,000 tablets; --■--, fluid bed dried, 1,000,000 tablets; --□--, fluid bed dried, 750,000 tablets; and --▲--, fluid bed dried, 500,000 tablets.*

less as the batch size decreases. Breakeven points normally are observed when only one factor is changing, but the breakeven points shown here are between different batch sizes as well as between different drying methods. For example, at a production rate of ~7207 tablets/min, the processing cost per 1000 tablets is about 24¢ for a 1,500,000-tablet batch that is fluid bed dried compared to 28¢/1000 tablets for a 1,250,000-tablet tray-dried batch. To find a true cost breakeven point between these two curves, the mean tablets per minute *versus* the processing cost per fixed number of tablets (*i.e.*, per thousand) has to be plotted. This can be done easily using Fig. 5.

Figure 6 shows how the processing cost per batch increases with increasing batch size using different combinations of tableting machines, utilization factors, and drying methods. Processing costs with tablet

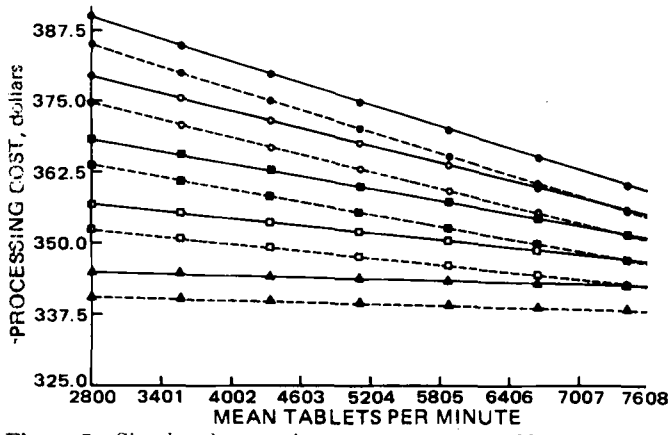

Figure 5—*Simulated processing cost* versus *mean tablets per minute produced curves for different combinations of drying methods and batch sizes at a fixed labor rate of $5.50/hr and utilization factor (UF) of 1.0. Key: -●-, tray dried, 1,500,000 tablets; --●--, fluid bed dried, 1,500,000 tablets; -○-, tray dried, 1,250,000 tablets; --○--, fluid bed dried, 1,250,000 tablets; -■-, tray dried, 1,000,000 tablets; --■--, fluid bed dried, 1,000,000 tablets; -□-, tray dried, 750,000 tablets; --□--, fluid bed dried, 750,000 tablets; -▲-, tray dried, 500,000 tablets; and --▲--, fluid bed dried, 500,000 tablets.*

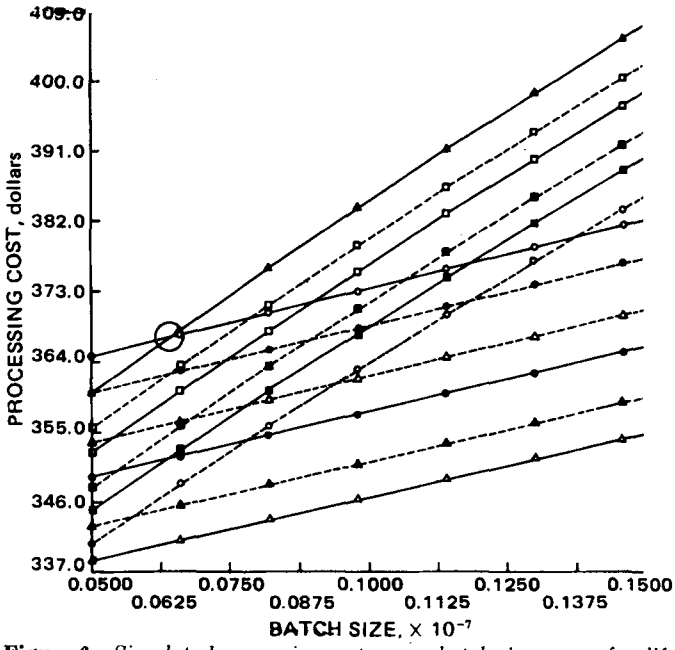

Figure 6—*Simulated processing cost* versus *batch size curves for different combinations of tableting machines, utilization factors (UF), and drying methods at a fixed labor rate of $5.50/hr. Key: -▲-, tablet machine A, UF = 0.5, tray dried; --□--, tablet machine A, UF = 0.5, fluid bed dried; -□-, tablet machine A, UF = 0.75, tray dried; --■--, tablet machine A, UF = 0.75, fluid bed dried; -■-, tablet machine A, UF = 1.0, tray dried; --○--, tablet machine A, UF = 1.0, fluid bed dried; -○-, tablet machine B, UF = 0.5, tray dried; --●--, tablet machine B, UF = 0.5, fluid bed dried; --△--, tablet machine B, UF = 0.75, tray dried; -●-, tablet machine B, UF = 0.75, fluid bed dried; --▲--, tablet machine B, UF = 1.0, tray dried; and -△-, tablet machine B, UF = 1.0, fluid bed dried.*

machine A are lower than tablet machine B with small batch sizes, but these costs increase at a greater rate with increasing batch sizes. As a result, there is a breakeven point with the batch size. For example at ~640,625 tablets/batch, the curves for tray-dried tablets with a utilization factor of 0.5 intersect. This breakeven point can be seen in the encircled area of Fig. 6. The only difference in these two curves is the type of tableting machine used. Tablet machine A is less expensive to operate at small batch sizes due to its smaller power cost and equipment depreciation charged per batch. However, as the batch size increases, tablet machine B becomes less expensive to operate due to its high production output and, thus, minimal tableting unit operation processing labor cost. The cleaning and preparation time for both tablet machines were assumed to be approximately the same. For a constant utilization factor, Fig. 6 shows that the breakeven batch size is the same for tray drying or fluid bed drying. As the utilization factor increases, the breakeven batch sizes decrease. Increases in processing cost with larger batch sizes are approximately linear with tablet machine B, but those with tablet machine A tend to be slightly marginally decreasing.

Figure 7 illustrates how the processing cost changes with increasing labor rate up to $8.25/hr using all combinations of drying methods, tableting machines, and utilization factors at a fixed batch size of 1,000,000 tablets. The processing costs increase with labor rate in a marginally increasing manner up to $8.25/hr. Figure 7 also shows that for a given utilization factor and a given tableting machine, fluid bed drying has a lower processing cost than tray drying. Figure 7 may be useful in evaluating processes as labor rates become inflated.

Processing Time–Processing Cost Interaction—By comparing the graphs where the dependent variable is processing time with graphs where the dependent variable is processing cost, it is evident that the drying method affects the processing time to a greater extent than does the tableting rate while the tableting rate affects the processing cost more than the drying method. This observation indicates that while the cost of either drying method varies little per batch, the time difference between the two is great. The time saved by using fluid bed drying over tray drying could be used for increased production of other product batches. Since the simulation only represents the cost–time variables for a single batch of a single product, multiple-batch and multiple-product considerations should be kept in mind.

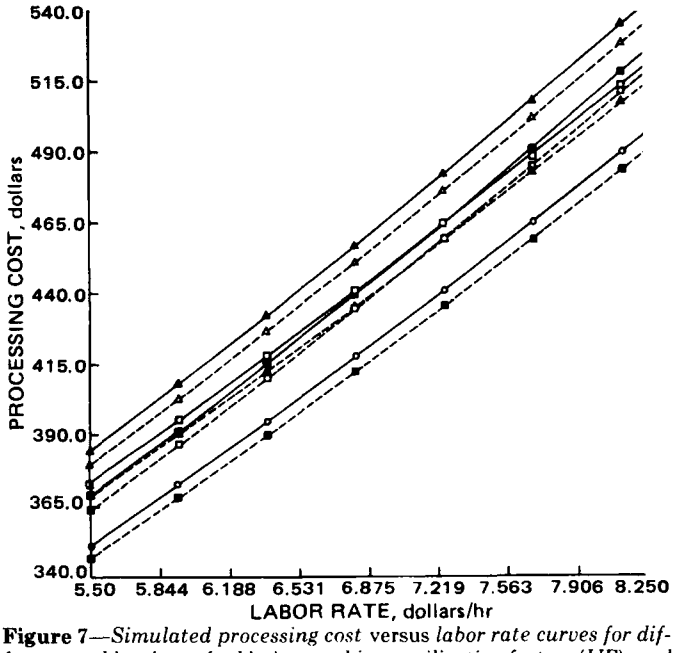

Figure 7—*Simulated processing cost* versus *labor rate curves for different combinations of tableting machines, utilization factors (UF), and drying methods at a fixed batch size of 1,000,000 tablets. Key: –▲–, tablet machine A, UF = 0.5, tray dried; --△--, tablet machine A, UF = 0.5, fluid bed dried; –■–, tablet machine A, UF = 1.0, tray dried; –□–, tablet machine B, UF = 0.5, tray dried; --□--, tablet machine A, UF = 1.0, fluid bed dried; --▲--, tablet machine B, UF = 0.5, fluid bed dried; –○–, tablet machine B, UF = 1.0, tray dried; and --■--, tablet machine B, UF = 1.0, fluid bed dried.*

CONCLUSIONS

1. The model and simulation program shown here can be used in intraprocess as well as interprocess cost and time evaluations.

2. The simulation program itself can be used as an experimentation method, with an almost unlimited number of experiments and manipulations possible at a fraction of the cost and time of the actual processing experiments.

3. Statistical methods as well as optimization techniques can be applied to the experimental simulation output to make optimal decisions about the results.

4. The model and simulation can be a tool in making management and process-engineering decisions concerning tableting cost and time considerations, especially with processes that are new or being updated.

APPENDIX

The following cost–time outputs for each run of the simulation program may be defined:

1. Tablets per batch—the number of tablets produced in a batch. It is the theoretical yield rather than the standard yield of tablets.

2. Cost per batch—the total cost per batch, including raw material cost, labor cost, equipment depreciation, power consumption costs, warehouse costs, and bulk packaging costs.

3. Cost of raw materials—the cost of both active and inactive ingredients in the formulation.

4. Excipient cost—the cost of the raw materials *minus* the cost of the active ingredients in the formulation.

5. Process cost—the total cost minus the cost of the raw materials.

6. Process and formulation controllable cost—the processing cost plus the excipient cost divided by the standard yield per batch. This cost will change if one uses a different process or a different formulation.

7. Cost per tablet—the total cost divided by the theoretical number of tablets.

8. Standard yield cost per tablet—the cost per tablet divided by the standard yield per batch.

9. Process cost per tablet—the process cost divided by the theoretical number of tablets produced.

10. Labor cost per unit operation—the average labor cost per step including the end-of-process step.

11. Labor cost per batch—the total labor cost per batch.

12. Cost per unit operation—the same explanation as in the section on labor cost per step applies here. This cost is the total *average* cost per step. It includes raw material costs.

13. Equipment depreciation—the total equipment depreciation that can be assigned to this particular batch.

14. Power costs—the cost of the energy consumed by the equipment during the process.

15. Warehouse costs—the total cost of using warehouse space to store a batch of unfinished product.

16. Package costs—the cost of bulk packaging the unfinished product to be stored or bulk packaging the final product to be stored. It is a fixed number in that the formulator must know the cost.

17. Yearly production cost—the total cost per batch multiplied by the number of batches produced per year.

18. Yearly process and formulation controllable cost—the per batch formulator controllable cost multiplied by the number of batches per year.

19. Processing time plus time between steps—the total time it takes to process a batch. This time does not include cleaning or preparation time; it only includes the time it takes to produce a batch if everything is prepared and cleaned.

20. Total labor time—the total labor time spent in producing a batch. It is the time that a laborer is paid for that can be assigned to a particular batch.

21. Cleaning and preparation time—the total cleaning and preparation time spent during the production of a batch.

REFERENCES

(1) J. Cooper and J. E. Rees, *J. Pharm. Sci.*, **61**, 1511 (1972).

(2) H. Gucluyildiz, G. S. Banker, and G. E. Peck, *ibid.*, **66**, 407 (1977).

(3) "Innovation in Pharmaceutical Manufacturing; Compounding a Prescription Medicine by Computer Control," Merck Sharp and Dohme, West Point, Pa., Oct. 1977.

(4) J. R. Buck and T. W. Hill, *Eng. Economist*, **16** (4), 247 (1971).

(5) R. H. Perry and C. H. Chilton, "Chemical Engineers' Handbook," 5th ed., McGraw-Hill, New York, N.Y., 1973, section 25, pp. 1–44.

(6) J. R. Buck and J. M. Tanchoco, "Research Memorandum on Triangular Distributions, School of Industrial Engineering," Purdue University, West Lafayette, Ind.

(7) A. A. B. Pritsker, "The GASP IV Simulation Language," Wiley, New York, N.Y., 1974.

(8) D. E. Fonner, J. R. Buck, and G. S. Banker, *J. Pharm. Sci.*, **59**, 1587 (1970).

(9) J. B. Schwartz, T. R. Flamholz, and R. H. Press, *ibid.*, **62**, 1165 (1973).

(10) H. M. Wagner, "Principles of Operations Research," 2nd ed., Prentice-Hall, Englewood Cliffs, N.J., 1975.

(11) I. W. Burr and L. A. Foster, "A Test for Equality of Variances," Department of Statistics Mimeo Series No. 282, Purdue University, West Lafayette, Ind., 1972.

ACKNOWLEDGMENTS

Presented at the Industrial Pharmaceutical Technology Section, APhA Academy of Pharmaceutical Sciences, Anaheim meeting, April 1979.

Supported by a grant from FMC Corp., Philadelphia, PA 19103.

Derivative and Graphical Procedures for Correction of Irrelevant UV Spectrophotometric Absorption in Changeable Matrixes

J. TRAVESET *, V. SUCH *, R. GONZALO *, and E. GELPI ‡x

Received December 10, 1979, from the *Departamento de Análisis y Control, Lácer S.A., Cerdeña 350, Barcelona-25, Spain, and the ‡Instituto de Química Bio-orgánica, CSIC, Jorge Girona Salgado s/n, Barcelona-34, Spain. Accepted for publication January 15, 1980.

Abstract □ The application of direct zero-order UV spectrophotometric and graphical or derivative background correction methods to selected pharmaceutical preparations shows their relative advantages in different situations. The assay of the active components in a changeable matrix is a problem with formulations having a limited shelflife. Although the standard three-point correction procedures can provide accurate data, there are practical problems if the irrelevant absorption band is such that only the derivative approach gives enough resolving power for reliable qualitative and quantitative determinations.

Keyphrases □ Excipients—solutions, suspensions, and suppositories, changeable matrixes and their effect on UV absorbance spectra, comparison of three background correction methods □ Spectroscopy, UV—changeable matrixes of pharmaceutical preparations, comparison of three background correction methods, interference by excipients or degradation products □ Degradation—pharmaceutical preparations, effect on UV absorbance spectra, comparison of three background correction methods, changeable matrixes

The assay of certain drugs or natural products by classical UV spectroscopic techniques usually can be accomplished by simple and direct procedures. These procedures generally involve reading the absorbance of the sample *versus* that of a standard at selected wavelengths, except where the analyte is part of a complex matrix containing other UV-absorbing degradation products and chemicals (1). In such a situation, the spectral overlapping of the irrelevant absorption bands produced by the interfering components can be so strong as to mask completely the band of the compound, making it difficult or impossible to determine not only its concentration but also its presence. Since the irrelevant absorption of multicomponent samples cannot be suppressed efficiently due to the inherent lack of resolution of the classical UV spectroscopic techniques, its effects must be compensated for by often cumbersome sample cleanup and separation procedures. Thus, the convenience of the direct UV readings using a conventional spectrophotometer is lost.

BACKGROUND

The practical limitation derived from variable and nonspecific spectral interferences has been treated by mathematical and graphical methods, ranging from very simple to tedious and lengthy procedures, according to the shape of the irrelevant absorption spectrum (2). The Morton–Stubbs (3) three-point correction method has been used extensively where there is an unknown or variable contribution to the measured absorption. However, the method assumes that the irrelevant absorption is linear over the working wavelength range (4).

Background interferences also have been corrected by the application of absorbance ratios and orthogonal function coefficients (5, 6), which are sensitive to instrumental parameters and difficult to apply if the irrelevant background absorption is similar to the spectral band of the analyte (4). The method of Glenn (5) was applied and evaluated by Wahbi and Abdine (7), who, in spite of considering it useful in many cases, acknowledged that it may give unsatisfactory results if the polynomial, number of points, and wavelength range and intervals are not selected properly. Furthermore, many of these methods require special attention to operational parameters, which detracts from their applicability to many practical problems in pharmaceutical analyses.

On the other hand, the recently introduced commercial systems that can produce a graphic display of the derivative ($dA/d\lambda$ or $d^2A/d\lambda^2$) of the analog signal given by the spectrophotometer provide a different approach to these problems. In many cases, the derivative techniques allow resolution of two spectral bands of very close wavelength so they can be used in the quantitative spectrophotometric assay of complex mixtures of spectrally interfering substances (8).

The derivative spectroscopy technique was introduced (9) as a means of resolving two overlapping spectral bands of almost coincident wavelength. However, the potential of this technique for pharmaceutical analysis has not been studied in detail, although it could be easily inferred from the small, though significant, body of data reported by different laboratories. For instance, derivative recording of UV spectra was applied successfully to steroid structure determination (10) and to the quantitation of mutually interfering rare earth elements and dyes (11) and gases (12, 13). The quantitation of pyrene in the presence of excess anthracene by derivative luminescence also was reported (14), and more recently, the technique was used in biology to determine total urinary porphyrins (15) as well as phenylalanine residues in proteins (16).

A recent communication discussed second derivative UV–visible spectrophotometry for the quantitation of drugs in their dosage forms (17) and reported coefficients of variation of better than 2% for routine quality control. A general review of derivative and wavelength modulation spectroscopy appeared recently, which mentioned other selected applications (18). All of these data support the idea that derivative spectroscopy may have considerable potential in routine quantitative measurements (18, 19).

Thus, considering the present state of the art with regard to UV determinations of a complex matrix in pharmaceutical preparations, comparative assessment was desired for the applicability of simple, direct, graphical–algebraical and derivative UV measurements in cases where: (*a*) the background absorption of excipients or other products may not be constant due to manual batch-to-batch variations, and (*b*) the corresponding excipient absorbance is either strong (samples with large excipient concentrations) or weak compared to that of the substance assayed (samples with few excipients and a large amount of active drug). Four examples representative of the various cases usually encountered in pharmaceutical analysis were considered.

EXPERIMENTAL

Apparatus—A double-beam ratio recording, scanning, grating spectrophotometer[1] with a variable bandpass from 0.2 to 4.0 nm was used. This spectrophotometer was equipped with a derivative spectrum attachment[2] consisting of an analog differentiating circuit that can record optionally the first or second derivative spectrum and the original (zero-order) spectrum.

The spectra were obtained at a bandpass of 1 nm and a scanning speed of 240 nm/min. The recorder response was set at medium, and the scan speed was set to 12 cm/min at a span of 1 or 2 and a mode of 0.5.

Pharmaceutical Preparations—*Suppositories*—The active ingredients in the suppositories were: dipyrone (1 g), anisotropine methylbromide (0.020 g), and phenobarbital (0.015 g). The suppositories also contained 2.204 g of saturated fatty acid glycerides as excipients and had a total weight of 3.24 g.

Solutions—One solution contained 1.58 g of oxyfedrine hydrochloride (a sympathomimetic agent) and 113.2 g of excipients brought to a total volume of 150 ml with distilled water. Estradiol benzoate (10 mg/ml) was

[1] Perkin-Elmer model 200.
[2] Perkin-Elmer model 200-0628.

0022-3549/80/0600-0629$01.00/0
© 1980, American Pharmaceutical Association

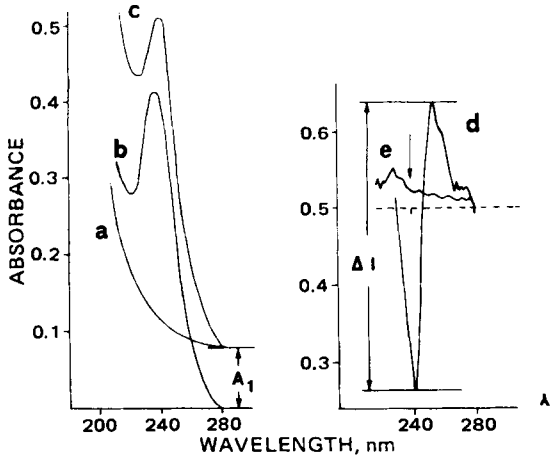

Figure 1—*Curve a, zero-order UV spectrum of a sample containing all of the pharmaceutical preparation components, except phenobarbital; curve b, zero-order UV spectrum of a phenobarbital standard; curve c, zero-order UV spectrum of an extract of the commercial formula; curve d, second derivative UV spectrum of the extract of the commercial formula; and curve e, second derivative UV spectrum of the extract of the excipients without phenobarbital.*

contained in a suspension of lecithin (8 mg/ml) and chlorobutanol (3 mg/ml). An excipient solution (100 ml) contained 0.2 g of progesterone.

All preparations except the progesterone-containing formula were commercial preparations. For the three solutions, the only sample preparation needed prior to the actual determinations was simple dilution to a predetermined volume with a suitable solvent. However, since phenobarbital was present in a ratio of 1 part to 216 parts of excipients, the suppositories first were subjected to a cleanup procedure to remove a significant proportion of the unwanted materials.

Cleanup Procedure for Phenobarbital in Suppositories—The sample to be assayed (three suppositories, equivalent to 45 mg of phenobarbital) was placed in a 250-ml erlenmeyer flask and dissolved in ~200 ml of ether. The solution was filtered[3], and the filtrate was collected in a 500-ml volumetric flask and taken to dryness on a rotary-film evaporator.

The dry residue was extracted with 200 ml of 10% NH_4OH in ethanol at ~50°. The filtrate was cooled in an ice bath under agitation, filtered[3] again under vacuum, and collected in a 250-ml flask. The residue on the filter paper was washed, and the filtrate was brought to volume with the ammonium hydroxide–ethanol solution. A 5-ml aliquot was diluted to 100 ml with ammonium hydroxide in ethanol to obtain a final phenobarbital concentration of 9 μg/ml.

RESULTS AND DISCUSSION

Phenobarbital in Suppositories—Standard solutions of phenobarbital and of the excipient mixture of the commercial preparations were run individually on the UV spectrophotometer and gave the absorption spectra shown in Fig. 1 (peaks a and b). The corresponding absorption spectrum of a commercial product extract (phenobarbital plus excipients) is also illustrated in Fig. 1 (peak c). In this case, the spectral band was displaced upward due to the background interference of the coextracted excipients, which was clearly reflected in the absorbance value (A_1) at 280 nm (Fig. 1, peak c). Quantitatively, this spectral interference significantly affected the direct measurement of the absorbance value at the peak maximum. Consequently, the relative error obtained by direct UV determinations of the known phenobarbital amounts added to the residual excipient matrix remaining after extraction of the suppositories was +14.3% (Table I).

In contrast, the peak-to-peak (ΔI) measurement of the second derivative spectra of the same samples (Fig. 1, peak d) reduced the relative error to −4.2%. Accordingly, the dispersion of these comparative data indicates that the applicability of the procedure is neither dependent on nor limited by the extraction efficiency of the active drug but instead by the method used to quantitate the UV absorbance curves. As will be demonstrated with other examples, this case is often true in the application of UV spectrophotometric techniques for the quantitation of pharmaceutical preparations.

[3] W-41 filter paper, Whatman Inc., Clifton, N.J.

Table I—Determination of Phenobarbital Content of Standard Solutions [a]

	Direct Reading of UV Absorbance	Second Derivative Readings (ΔI)
Average, %[b]	114.3	95.8
Relative error,	+14.3	−4.2
SD, %	4.0	0.6

[a] Heavy spectral interferences, due to relatively large quantities of excipients, were removed partially by preextraction of reconstituted samples (n = 5) lacking phenobarbital but prepared according to the manufacturing process. These excipient samples were extracted according to the procedure outlined in the text. A known amount of phenobarbital (equivalent to that contained in the commercial formulas) was next added to the extracts, which thus were certified to contain the specified amount of active drug. [b] n = 5.

Table II—Determination of Phenobarbital Content in Suppositories [a]

	UV Absorbance			
	Direct Reading		Second Derivative	
Sample	A_{242}	Found, mg	ΔI (n = 5)	Found, mg
1	0.486	17.81	9.33	14.99
2	0.454	16.63	8.97	14.43
3	0.455	16.67	8.76	14.10
4	0.457	16.74	8.74	14.07
5	0.506	18.54	9.75	15.66
6	0.454	16.63	8.59	13.83
$\bar{x}$		17.17		14.51
SD, %		4.73		4.75
Relative error, %		+14.46		−3.2

[a] Recently prepared commercial suppositories with a declared value of 15 mg/suppository.

The experimental data proved that phenobarbital was extracted efficiently from the suppositories in a 97% yield (average of five derivative determinations, *SD* 1.6%). Nevertheless, to discard the possibility of a loss due to faulty extraction or to any other unexplained causes, the active drug was added to the final ethanol solution of the extract, thus ensuring that each test sample contained exactly the specified amount of phenobarbital. By removing this possible sampling error, it was expected that the values obtained from the different spectroscopic measurements would allow for a true and representative assessment of the UV background correction methods.

An application of the direct UV reading and second derivative procedures (Fig. 1, peak d) to the control assay of suppositories randomly selected from a single recent batch gave the results shown in Table II. The relative errors from both methods represent the kind of data consistently obtained in this laboratory since the introduction of second derivative UV spectroscopic methods for routine control work on complex changeable matrixes. Moreover, the −3–−4% error of these second derivative determinations could be a consequence of the second derivative UV absorption band of the blank sample (no phenobarbital added) (Fig. 1, peak e).

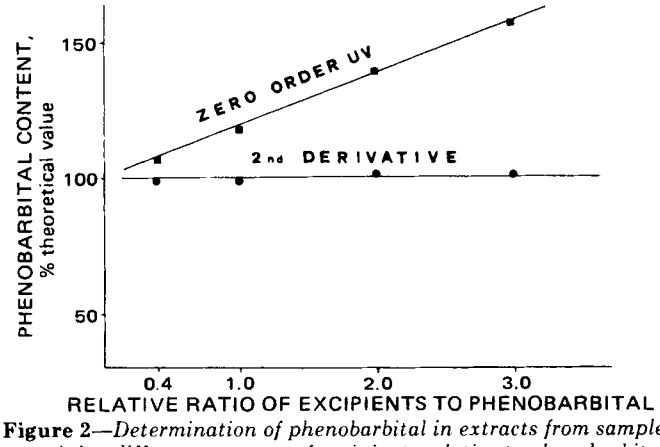

Figure 2—*Determination of phenobarbital in extracts from samples containing different amounts of excipients relative to phenobarbital.*

Table III—Comparison of Phenobarbital Content (Percent) in Aged Commercial Preparations by Different Methods

Sample	HPTLC	Direct UV[a]	Second Derivative UV	UV with Morton–Stubbs Three-Point Correction[a]
D-1 (1969)	79	108.0 (29)	79.3 (0.3)	82.5 (3.5)
D-2 (1969)	91.1	127.7 (36.6)	88.3 (−1.8)	90.7 (−0.4)
F-1 (1971)	94.7	115.9 (21.2)	94.8 (0.1)	—
F-2 (1971)	84.2	106.8 (22.6)	79.7 (−4.5)	82.3 (−1.9)

[a] The differences relative to the HPTLC determinations are given in parentheses (8).

The small positive signal at 242 nm (indicated by the arrow) has a subtracting effect on the total amplitude of the ΔI measured. These results are in agreement with the errors calculated theoretically for a similar case. According to the data reported previously (20) using the same peak-to-peak (ΔI) measurement of the second derivative band, theoretical systematic errors of −2–−4.3% and a random error of 1.8% were found, which compare favorably with the data in this report.

The potential of the derivative data for quantitation is demonstrated in Fig. 2, which shows that the increase in the excipient concentration relative to that of phenobarbital affected the zero-order UV determinations of this active drug with relative errors of up to 58%, without much effect on the derivative measurements.

Although the example given proves in principle the higher reliability of the derivative UV data, it also could be argued that a three-point Morton–Stubbs (3) background correction often still could compete favorably with the derivative procedures. In pharmaceutical product analysis, the procedure is applicable, providing that the excipients give a uniform background and can be used as a kind of "blank" (1). However, even in such a case, the irrelevant background absorption should be constant in each sample, which may be difficult to achieve due to the usual variations between excipient batches. This factor is especially important in aged commercial preparations that also contain undefined amounts of unknown degradation products. Furthermore, the operating conditions must remain perfectly reproducible. And the corresponding absorbance must be weak in comparison to that of the active drug (1), a condition that often cannot be met without lengthy concentration or cleanup procedures (4), as was done in this study to increase the ratio of phenobarbital to excipients (initially, 1:216).

For these reasons, the results of the direct, derivative, and three-point UV methods were compared for the quantitative determination of phenobarbital in aged commercial preparations. These samples were considered to be representative of cases in which the background absorption changes with time due to the formation of unknown degradation products (*i.e.*, no reference samples available as "blanks"). The results (Table III) demonstrate that when a derivative UV spectrophotometer is unavailable, the Morton–Stubbs correction provides comparable data; in this case, the amount of phenobarbital remaining undegraded in the four samples was determined by separating it from the excipients and degradation products using high-performance TLC (HPTLC). These samples then were quantitated spectrophotometrically (8).

Oxyfedrine Hydrochloride Solution—The UV absorption spectrum of a standard oxyfedrine solution as the hydrochloride (Fig. 3a) showed two maxima in the 350–220 range, one centered at 310 nm and the other at 252 nm. The absorption spectrum of the excipient mixture was characterized by a peak at 270 nm with an appreciable shoulder at 310 nm (Fig. 3b). This comparison represents an interesting practical case since the difference in absorption maxima of the active drug and the excipient blank (252 *versus* 270 nm) was such that the inflection point in the composite spectrum (at the position indicated by the arrow in Fig. 3c) in many cases was obliterated completely. The result was a continuous straight slope that precluded any meaningful qualitative or quantitative work without isolation of the active product from the excipient mixture or the application of background correction methods.

Furthermore, the inapplicability of the uncorrected measurements for quantitative purposes is demonstrated in the plot of Fig. 4, where even at a low ratio of excipients to oxyfedrine (0.5), the zero-order data included a 20% error. This situation deteriorated further as the matrix changed due to increased concentrations of those excipients responsible for the irrelevant background absorption relative to the concentration of the active drug. As shown, at a relative ratio of two, the uncorrected error was 70% relative to the true 100% value. The corresponding values obtained with UV derivative techniques or the Morton–Stubbs three-point correction (Fig. 4) stayed within a 12% margin of error. A good

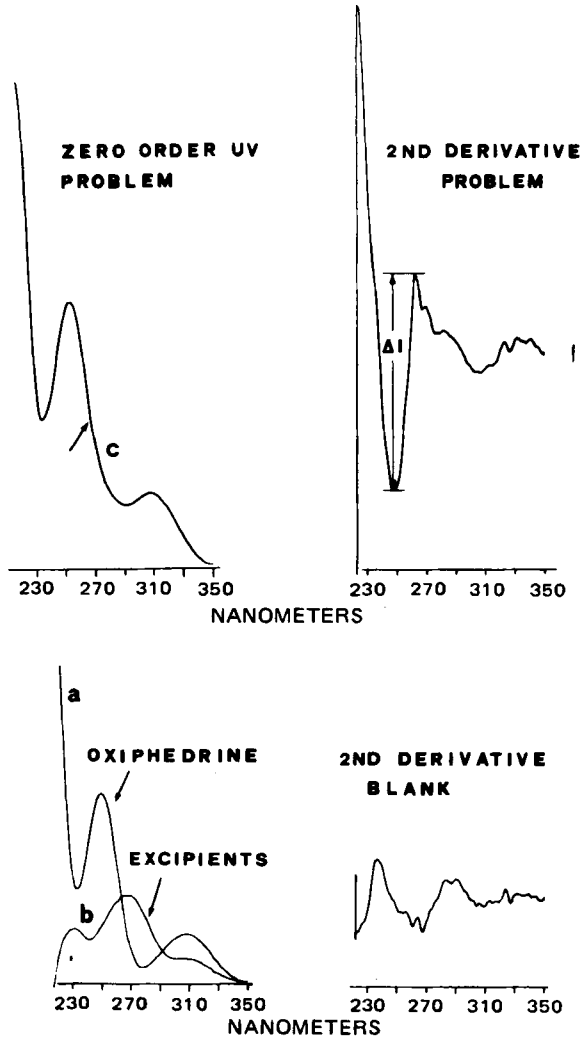

Figure 3—*Zero-order and second derivative UV spectra of oxyfedrine-containing formulation. Key: a, UV spectrum of oxyfedrine alone; b, UV spectrum of the excipients; and c, UV spectrum of the mixture.*

correlation between both correction methods thus is illustrated by this practical application. However, as the next two examples indicate, this case is not always true.

Progesterone in Solution—Figure 5 shows the results obtained with a noncommercial progesterone-containing product according to the zero-order and second derivative UV spectroscopic methods. The UV determination of progesterone alone does not pose any special difficulties. However, in these mixtures, it gave a spectrum in which the absorbance

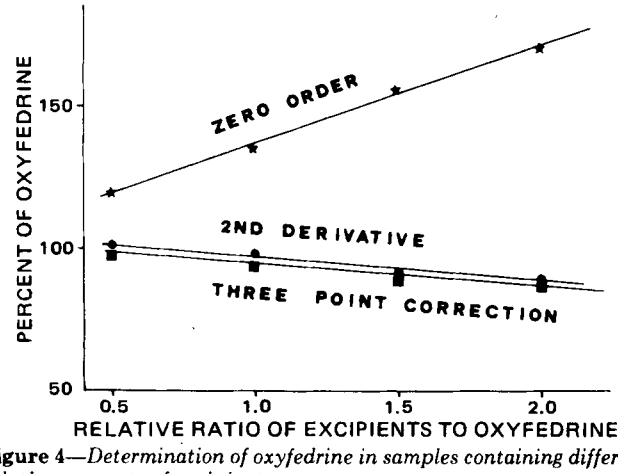

Figure 4—*Determination of oxyfedrine in samples containing different relative amounts of excipients.*

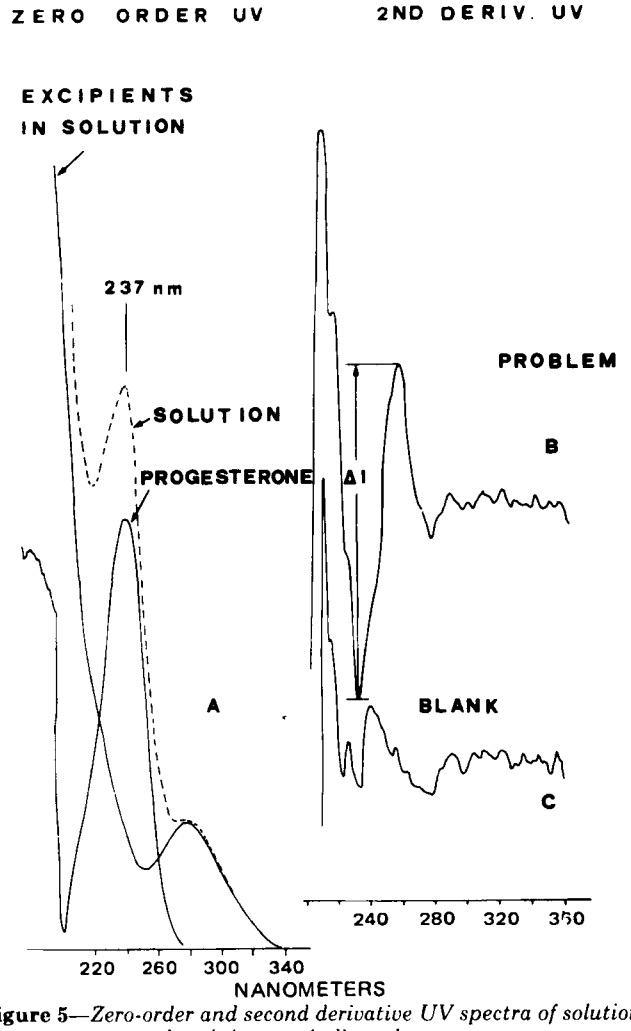

Figure 5—*Zero-order and second derivative UV spectra of solutions of progesterone and excipients as indicated.*

band with its characteristic 237-nm maximum became a shoulder. On the first determinations carried out on this preparation, it was observed that at a progesterone concentration of 10 μg/ml, corresponding to a progesterone to excipients ratio of one, the direct zero-order UV measurements produced relative errors of +37 and 45% for replicate sample determinations while the second derivative and three-point correction methods gave errors of −5.4 and +11.9%, respectively. In contrast with the previous two cases, the relative error calculated by the three-point method was significantly higher than the value computed from the second derivative (ΔI in Fig. 5). Therefore, it was necessary to analyze different solutions characterized by values of the progesterone to excipients below or above the usual ratio of one. The results obtained are plotted in Fig. 6. In this case, since the level of the irrelevant background absorption was kept constant while the amount of the active drug was increased, the points on the graph were distributed, as expected, along curves asymptotically approaching the theoretical value.

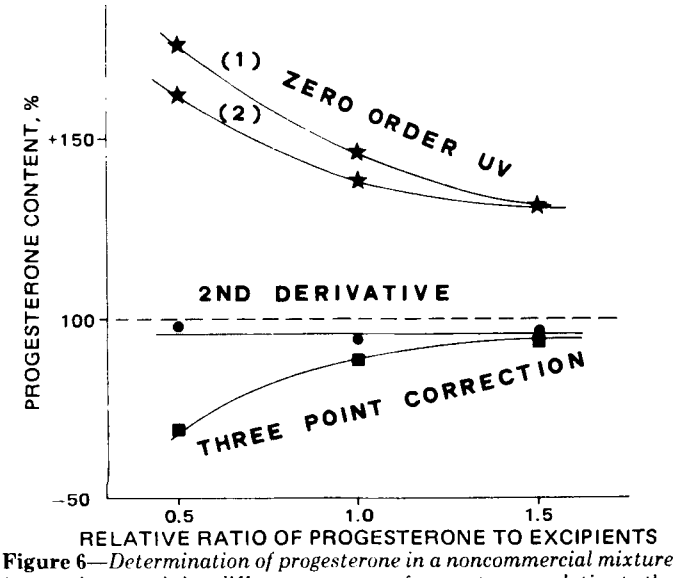

Figure 6—*Determination of progesterone in a noncommercial mixture in samples containing different amounts of progesterone relative to the excipients. The two zero-order UV curve determinations were carried out on different samples. As indicated in Table IV, the points of curve 2 are the average values obtained from the UV readings of two solutions from the same sample.*

Table IV—Replicate Determination of Progesterone in Samples with a Progesterone to Excipient Ratio of 1:2

Method	Solution A, %	Solution B, %
Direct UV	162.8	160.8
Derivative UV	99.0	98.2
Three-point correction	71.4 68.4	63.9
$\frac{A_{\lambda_{max}}}{A_{\lambda_1}} = \frac{A_{\lambda_{max}}}{A_{\lambda_2}}$	1.174 1.076	1.130

The results demonstrate that the only points not seriously affected by the changing interference due to the background absorption were those of the derivative determinations. Also, as expected, when the relative amount of the active drug in the preparation increased, the relative error given by the three-point correction approached the value obtained by derivative analysis, fulfilling the requirement that the background absorbance must be weak relative to that of the substance being determined (1). The points represented for the three-point correction curve in Fig. 6 are the average values of two determinations on the same solution carried out at different absorbance ratios, as indicated in Table IV (Solution A). Solution B (Table IV), determined at a different $A_{\lambda_{max}}/A_{\lambda_1}$ ratio, gave a similar value. From a consideration of the absorption spectrum, slightly different wavelengths were selected on each side of the peak maximum at 241 nm to give different absorbance ratios (Table IV). Nevertheless, the results were comparable.

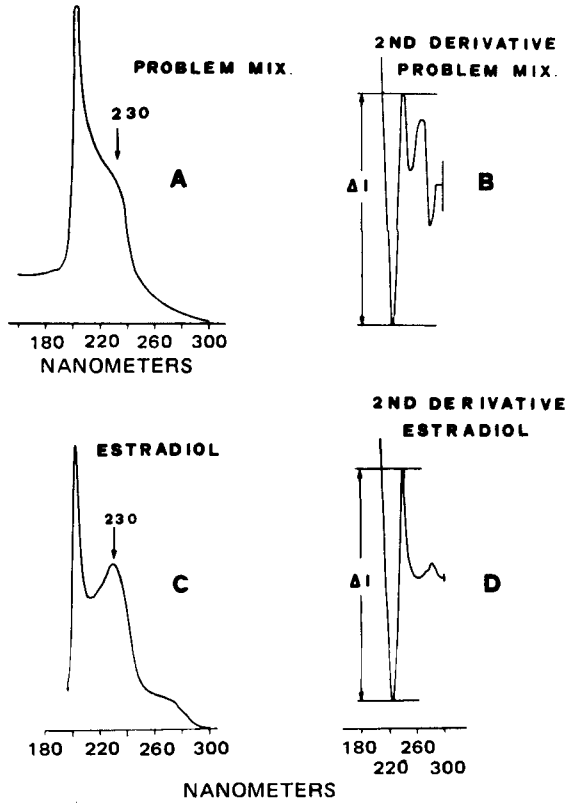

Figure 7—*Curve A, zero-order UV spectrum of an estradiol benzoate suspension in lecithin; curve B, second derivative UV spectrum of the same; curve C, UV spectrum of estradiol benzoate; and curve D, second derivative UV spectrum of estradiol benzoate.*

Table V—Estradiol Benzoate Determination in the Presence of Lecithin in Different Proportions

Method	Estradiol Benzoate–Lecithin Ratio		
	1:0.8	1:5	1:10
Direct UV reading	103	121.8	143.6
Derivative UV	101.2	105	108.8
Three-point correction[a]	96.8	111.3	115.0

[a] $A_{\lambda_{max}}/A_{\lambda_1}$ = 1152. Absorbances were read at 221.6, 231, and 237.6 nm for the three-point correction.

Estradiol Benzoate in Suspension—A final representative case where the derivative techniques demonstrated their superiority over other background-correction methods is illustrated by the assay of estradiol in a pharmaceutical suspension with lecithin. At the usual concentrations in the pharmaceutical preparation analyzed (1:0.8), the characteristic 230-nm spectrum of estradiol benzoate (Fig. 7C) was masked by the spectrum of the problem mixture (Fig. 7A). Under these conditions (*e.g.*, relatively high active drug to lecithin ratio), the three methods gave values that fit within a 3.5% margin of error, with the second derivative determination being the most accurate (Table V). However, when this ratio was diminished, the relative error increased proportionally, representing a case where the three-point correction cannot cope with the level of irrelevant background interference. Evidently, this method requires a cleanup procedure to remove as much of the interfering compound as possible, thus increasing the relative concentration ratio to more amenable values. The more simple approach is to cancel as much of this background effect as possible by the application of second derivative UV spectroscopic techniques.

Conclusions—An appraisal of the UV assay of active drugs in pharmaceutical preparations illustrates the kind of results that can be expected by application of graphical and derivative background correction procedures to samples whose background absorption characteristics preclude a direct reading of the UV spectra.

Depending on the ratio of the active drug to the rest of the components in a given formulation (excipients and degradation products), the direct quantitation of the uncorrected UV absorption spectra may lead to significant errors relative to the formulated values. These values, allowing for factors such as extraction efficiency whenever applicable, are well established by the formulation of the commercial product, except products with a limited shelflife.

By working with changeable matrixes (varying the active drug to excipient ratio), it also was shown that the derivative and three-point correction techniques provide comparable results in some cases. In general, both can compensate for the irrelevant UV absorption from the secondary sample ingredients, as long as it is within reasonable limits. However, the graphical Morton–Stubbs three-point correction procedure sometimes cannot cope with the level of interference, leaving the derivative spectroscopic procedure as the only method giving reliable results over a relatively wide span of drug to excipient ratios.

Likewise, the three-point or other related correction methods (3–7) are applicable qualitatively as long as there is an identifiable, though distorted, UV profile characteristic of the product assayed. On the other hand, there are situations where it becomes difficult, if not impossible, to infer the presence of the active product, because its characteristic UV pattern may be masked totally by the background. One such situation is the assay of estradiol.

REFERENCES

(1) M. Pesez, in "The Quality Control of Medicines," P. B. Deasy and R. F. Timoney, Eds., Elsevier, Amsterdam, The Netherlands, 1976, pp. 321–335.

(2) H. Abdine, A. M. Wahbi, and M. A. Korany, *J. Pharm. Pharmacol.*, **23**, 444 (1971).

(3) R. A. Morton and A. L. Stubbs, *Analyst*, **71**, 348 (1946).

(4) W. D. Williams, in "Practical Pharmaceutical Chemistry," part 2, A. H. Beckett and J. B. Stenlake, Eds., Athlone Press, University of London, London, England, 1976, pp. 250–252.

(5) A. L. Glenn, *J. Pharm. Pharmacol., Suppl.*, **15**, 123T (1963).

(6) I. V. Agwu and A. L. Glenn, *ibid.*, **19**, 765 (1967).

(7) A. M. Wahbi and H. Abdine, *ibid.*, **25**, 69 (1973).

(8) V. Such, J. Traveset, R. Gonzalo, and E. Gelpi, *Anal. Chem.*, in press.

(9) A. T. Giese and C. S. French, *Appl. Spectrosc.*, **9**, 78 (1955).

(10) E. C. Olson and D. C. Alway, *Anal. Chem.*, **32**, 370 (1960).

(11) Technical memos 5 and 44, Perkin-Elmer Corp., Norwalk, Conn., 1970.

(12) R. N. Hager, *Anal. Chem.*, **45**, 1131 A (1973).

(13) J. W. Strojek, D. Yates, and T. Kuwana, *ibid.*, **47**, 1050 (1975).

(14) G. L. Green and T. C. O'Haver, *ibid.*, **46**, 2191 (1974).

(15) V. A. Schmitt, *J. Clin. Chem. Clin. Biochem.*, **15**, 303 (1977).

(16) T. Ichikawa and H. Terada, *Biochim. Biophys. Acta*, **494**, 267 (1977).

(17) A. F. Fell, *Proc. Anal. Div. Chem. Soc.*, **15**, 260 (1978).

(18) T. C. O'Haver, *Anal. Chem.*, **51**, 91A (1979).

(19) T. C. O'Haver and G. L. Green, *Int. Lab.*, **May/June 1975**, 11–18.

(20) T. C. O'Haver and G. L. Green, *Anal. Chem.*, **48**, 312 (1976).

Comparative Pharmacokinetics of Coumarin Anticoagulants XLVI: Effect of Treatment with Phenobarbital on Pharmacokinetics of (S)-(−)-Warfarin in Rats

AVRAHAM YACOBI, JOHN T. SLATTERY, and GERHARD LEVY ˣ

Received December 17, 1979, from the *Department of Pharmaceutics, School of Pharmacy, State University of New York at Buffalo, Amherst, NY 14260.* Accepted for publication January 22, 1980.

Abstract □ This investigation was carried out (*a*) to determine if the enzyme inductive effect produced by phenobarbital reduces the interindividual variability in the biotransformation of a drug, as suggested in the literature; (*b*) to test whether the intrinsic clearance of free drug, for drugs exhibiting restrictive clearance, reflects the activity of drug-metabolizing enzyme systems; and (*c*) to determine if enzyme induction affects the apparent volume of distribution of a drug that tends to concentrate in the liver. Twelve pairs of adult male rats, matched with respect to their serum warfarin free fraction, received an intravenous injection of (*S*)-(−)-warfarin, 0.6 mg/kg, after four daily injections of either saline solution or phenobarbital (75 mg/kg). Phenobarbital treatment increased both the total and intrinsic clearance of (*S*)-(−)-warfarin almost threefold but did not reduce the coefficient of variation of the intrinsic clearance. Serum protein binding of (*S*)-(−)-warfarin was not affected by phenobarbital treatment. The biological half-life of warfarin and the duration of its anticoagulant effect were reduced substantially by treatment with phenobarbital. Consistent with pharmacokinetic theory, the relationship between total clearance and the free fraction of warfarin in serum remained approximately linear, but the slope of the regression line was increased for the animals treated with phenobarbital.

Keyphrases □ Warfarin—pharmacokinetics, effect of phenobarbital on drug biotransformation and enzyme induction, rats □ Pharmacokinetics—warfarin biotransformation, inductive enzyme effect of phenobarbital, rats □ Phenobarbital—effect on enzyme induction, effect on warfarin biotransformation, pharmacokinetics, intersubject variability determination, rats □ Anticoagulants—warfarin, effect of phenobarbital on warfarin biotransformation, rats

It is well known that treatment with phenobarbital enhances the elimination of warfarin in both humans and rats (1–7). *In vitro* studies indicated that phenobarbital causes induction of the enzyme system(s) responsible for the biotransformation of warfarin (6), but these studies failed to test for variability in the degree of induction (as measured by the enhancement of warfarin elimination) as a function of the elimination kinetics of warfarin prior to enzyme induction. This question is important because there are pronounced interindividual differences in the elimination kinetics of warfarin in humans as well as in animals (8, 9).

BACKGROUND

Intersubject variability in antipyrine half-life decreased when subjects were treated with phenobarbital, and it was suggested that treatment with phenobarbital (or another enzyme inducer) might have a similar effect on the variability in the elimination kinetics of other drugs (10). In the cited study, the relative decrease in the half-life of antipyrine after phenobarbital administration was proportional to the prephenobarbital half-life.

Previous reports in this series showed that the total body clearance of warfarin is highly dependent on the serum protein binding of the drug, specifically on its free fraction in serum (9, 11). Recent studies revealed a 15-fold range in the serum free fraction of warfarin in rats (8, 12) and an approximately fourfold variation in humans (9, 13–15).

The proportionality constant between the total clearance and the free fraction for nonperfusion rate-limited systems is the intrinsic clearance k''. Thus, $k'' = TC/f_p$, where TC is the total body clearance and f_p is the free fraction of drug in serum or plasma (11). An essentially linear relationship between TC and f_p of warfarin has been observed in both humans and rats (9, 11). This relationship permits isolation of the effects of certain treatments or procedures on the protein binding of a drug from the effects on the activity of enzymes responsible for the biotransformation of that drug. This ability should help to determine the reasons for a change in the total clearance of a drug.

If enzyme induction leads to a decrease of the intersubject variability in the biotransformation kinetics of a drug, then a decrease in the coefficient of variation of k'' should be observed. Furthermore, if the relative degree of enhancement of drug elimination caused by induction of an enzyme system is proportional to the preinduction activity of the enzyme system, then the relative increase in intrinsic clearance caused by induction should be proportional to its preinduction (control) value.

Treatment of rats with phenobarbital produces an increase in their relative liver weight (16). Since the liver contains a large fraction of the amount of warfarin in the body of a rat (8, 17), treatment of rats with phenobarbital might increase the apparent volume of distribution of warfarin. This possibility has not been explored to date.

The purposes of this investigation were (*a*) to determine if the enzyme inductive effect produced by phenobarbital reduces the interindividual variability in the biotransformation of (*S*)-(−)-warfarin; (*b*) to test whether the intrinsic clearance of free (*S*)-(−)-warfarin reflects the activity of drug-metabolizing enzyme systems; and (*c*) to determine if enzyme induction affects the apparent volume of distribution of (*S*)-(−)-warfarin. (*S*)-(−)-Warfarin rather than racemic warfarin was used to decrease the complexity of the experiment since the metabolism of the individual enantiomers might be induced to a different extent. Since the (*S*)-(−)-enantiomer of warfarin is a more potent anticoagulant and has a longer biological half-life than the (*R*)-(+)-enantiomer in rats (18), experiments with (*S*)-(−)-warfarin are easier to perform.

EXPERIMENTAL

Seventy-two adult male Sprague–Dawley rats[1], 250–300 g initially and 320–400 g during the study, were screened to obtain two groups of rats matched individually with respect to their free fraction of warfarin in serum.

For screening purposes, 3 ml of blood was taken from the tail artery of the rats and the serum was separated. Approximately 1 μg/ml of racemic [^{14}C]warfarin[2] (specific activity 76 μCi/mg) was added to the serum, and its free fraction was determined by equilibrium dialysis for 20 hr against isotonic pH 7.4 phosphate buffer at 37° (8). Twenty-four rats were paired according to their free fraction of warfarin in serum. One member of each pair was assigned to the group to be treated with phenobarbital, and the other served as a control. The free fraction values ranged from 0.00296 to 0.0158.

Two weeks after the screening experiment, the rats in the group designated for phenobarbital treatment received 75 mg of phenobarbital/kg ip daily for 4 days, while the control group received injections of a comparable volume of normal saline for the same period. The rats had unrestricted access to food[3] and water throughout the study.

On Day 5, the rats in both groups received a single dose of [^{3}H](*S*)-(−)-warfarin[4] (0.578 mg/kg, specific activity 0.943 mCi/mg, in isotonic

[1] Blue Spruce Farms, Altamont, N.Y.
[2] Amersham-Searle Corp., Arlington Heights, Ill.
[3] Charles River formula 4RF.
[4] Research Triangle Inc., Research Triangle Park, N.C.

0022-3549/80/0600-0634$01.00/0
© 1980, American Pharmaceutical Association

Table I—Effect of Phenobarbital on Pharmacokinetics of (*S*)-(−)-Warfarin in Matched Pairs of Rats [a]

Parameter	Control	Phenobarbital	Ratio of Phenobarbital to Control
Serum free fraction × 100	0.266–1.29[b]	0.315–1.42	1.04 ± 0.14[b]
Half-life, hr	10.6–47.2	3.28–30.1	0.409 ± 0.114
Volume of distribution, ml/kg	103–155	112–185	1.13 ± 0.08
Total clearance, ml/(hr kg)	1.56–9.62	2.58–35.5	2.95 ± 0.78
Intrinsic clearance of free drug, [ml/(hr kg)] × 100	7.00 ± 1.65[b]	19.9 ± 5.07[c]	2.85 ± 0.80[b]
Duration of anticoagulant effect[d], hr	62–124	25–75	0.469 ± 0.079

[a] Twelve pairs of rats matched with respect to their serum free fraction of racemic warfarin. Results are shown as ranges of values for those parameters that are not normally distributed due to the intentional selection of animals with a wide range of free fraction values. Ratio and intrinsic clearance data are reported as the mean ± *SD*. [b] Data from 11 animals or animal pairs only due to loss of the blood sample for the serum free fraction determination from one rat. [c] Statistically significantly different from control (*t* test, $p < 0.001$). [d] Time required for prothrombin complex activity to return to 60% of normal after intravenous injection of 0.6 mg/kg.

saline adjusted to pH 7.4) *via* the tail vein. Blood samples (0.27 ml) were obtained at ~2–6-hr intervals from the tail artery (19). The plasma was separated, and the warfarin concentration in 0.1 ml of plasma was determined by TLC and scintillation counting as described previously (8, 20). Tritium exchange has been shown to be negligible under these experimental conditions (21). Prothrombin complex activity in plasma was measured (19) to determine the duration of the anticoagulant effect.

At the completion of the study, the rats were sacrificed by removing as much blood as possible from the abdominal aorta under ether anesthesia. The serum was separated, 0.5 μg/ml of [^{3}H](*S*)-(−)-warfarin (specific activity 3.77 mCi/mg) was added, and the free fraction was determined by equilibrium dialysis as described. The total intrinsic clearances, half-life, and apparent volume of distribution were determined as described previously (18, 20).

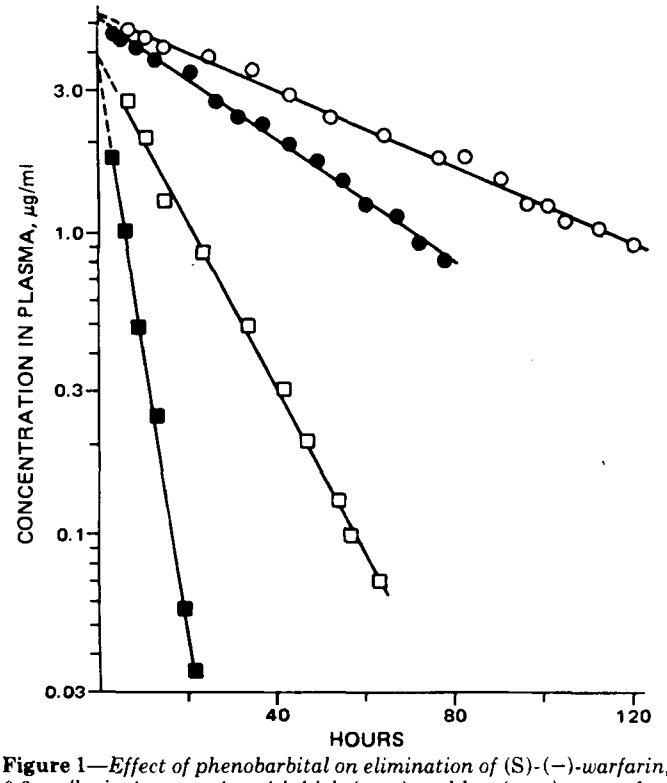

Figure 1—*Effect of phenobarbital on elimination of* (S)-(−)-*warfarin, 0.6 mg/kg iv, in rat pairs with high* (□,■) *and low* (○,●) *serum free fraction values of the drug. Key: solid symbols, phenobarbital-treated animals; and open symbols, control animals.*

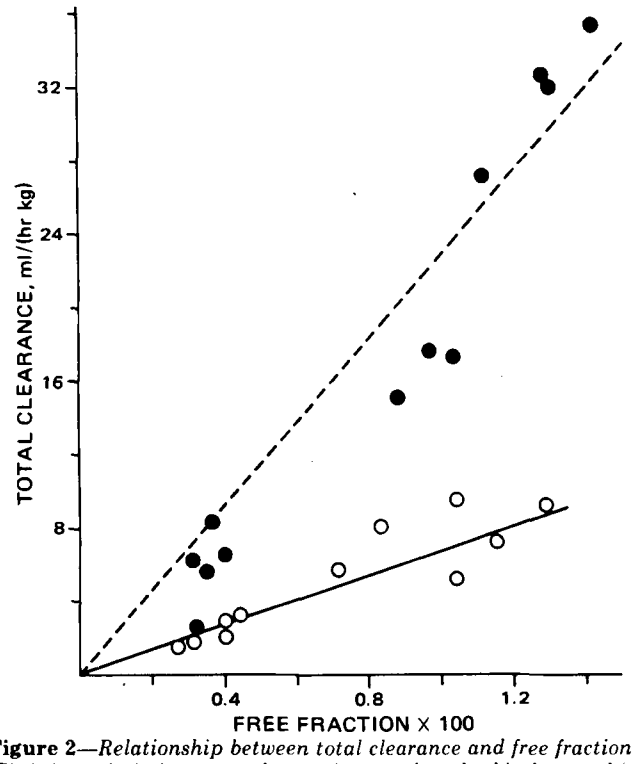

Figure 2—*Relationship between total clearance and free fraction of* (S)-(−)-*warfarin in serum of rats. Key:* ●, *phenobarbital treated* ($r = 0.968$, $p < 0.001$); *and* ○, *control* ($r = 0.902$, $p < 0.001$). *Regression lines were forced through the origin.*

RESULTS

The initial screening study permitted the selection of well-matched pairs of rats over a wide range of serum racemic warfarin free fraction values. The mean ± *SD* of the free fraction ratios of the 12 pairs was 1.00 ± 0.05. The correlation coefficient of the free fraction values for the two members of each pair in the entire group was 0.995 ($p < 0.001$).

In agreement with previous observations (18), the free fraction value of racemic warfarin determined in the screening study correlated strongly with that of the free fraction of (*S*)-(−)-warfarin determined at the end of the experiment ($r = 0.982$, $p < 0.001$), indicating the suitability of the racemic warfarin free fraction for screening purposes. The ratio of racemic to (*S*)-(−)-warfarin free fraction values (mean ± *SD*) was 1.12 ± 0.068 for the control rats and 1.10 ± 0.18 for the phenobarbital-treated rats, showing that phenobarbital treatment had no apparent effect on the free fraction of warfarin in serum. This lack of effect is consistent with previous observations (22).

The similarity of warfarin free fraction values in the rat pairs was maintained throughout the study (Table I). The correlation coefficient of the free fraction value of (*S*)-(−)-warfarin within pairs at the end of the study was 0.984 ($p < 0.001$).

The time course of the (*S*)-(−)-warfarin concentration in serum after intravenous injection in individual members of two pairs of rats (those with the highest and lowest mean free fraction values, respectively) is shown in Fig. 1. A summary of the pharmacokinetic data obtained in the study is presented in Table I. The biological half-life of (*S*)-(−)-warfarin and the duration of the anticoagulant effect in rats treated with phenobarbital were ~ 50–60% shorter on the average than those of the control member of each pair. On the other hand, the apparent volume of distribution showed no statistically significant change by the Wilcoxon test, even though it was larger in 11 of 12 phenobarbital-treated animals than in their controls. A strong correlation was observed in both groups between the first-order elimination rate constant and the free fraction of (*S*)-(−)-warfarin in serum ($r = 0.983$ and $r = 0.938$ for phenobarbital-treated and control groups, respectively; $p < 0.001$ for both groups). As observed previously (8), the apparent volume of distribution also correlated with the free fraction of warfarin in serum based on combined results from both groups ($r = 0.713$, $p < 0.001$).

On the average, the total clearance of (*S*)-(−)-warfarin was almost three times higher in rats treated with phenobarbital than in their respective controls (Table I). The intrinsic clearance in the phenobarbital-treated rats also was approximately three times higher on the average than that

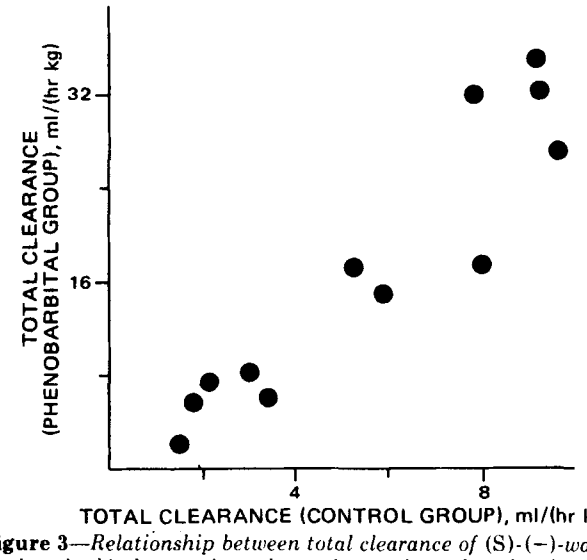

Figure 3—*Relationship between total clearance of* (S)-(−)-*warfarin in phenobarbital-treated member and control member of each matched pair of rats* ($r = 0.931$, $p < 0.001$).

of the control member of each pair. Treatment with phenobarbital did not decrease the coefficient of variation of the intrinsic clearance; it was 24% in the control group and 26% in the phenobarbital group.

The relationship between the free fraction of (*S*)-(−)-warfarin in serum and the total clearance for control and phenobarbital-treated animals is shown in Fig. 2. Essentially linear relationships were obtained in each case. The slope of a plot of the relative increase (expressed in percent) in the intrinsic clearance caused by phenobarbital treatment (comparing members of matched rat pairs) *versus* the control intrinsic clearance was not significantly different from zero. There was a strong and apparently linear relationship between the total clearance of (*S*)-(−)-warfarin in the control member and phenobarbital-treated member of each rat pair (Fig. 3).

DISCUSSION

The dose and the duration of phenobarbital administration used in this study were sufficient to produce a pronounced enzyme inductive effect as reflected by an almost threefold increase in the intrinsic clearance of (*S*)-(−)-warfarin. However, enzyme induction did not decrease the interindividual variability of the intrinsic clearance; there was essentially no difference in the coefficient of variation of the intrinsic clearance between the control and treated animals. Since phenobarbital treatment had no effect on the serum protein binding of (*S*)-(−)-warfarin, and since the relative effect of enzyme induction was independent of the normal intrinsic clearance value, the relationship between the total clearance and the serum free fraction remained essentially linear as predicted by theory (11). Thus, the slope of such a plot, *i.e.*, the intrinsic clearance of free drug, does reflect the effect of enzyme induction.

In a recent study, it was found that the liver contains about 44% of the total amount of warfarin in normal (not phenobarbital-treated) rats (8). The phenobarbital treatment regimen used in this study increased the relative liver weight of rats by ~22% (16). This increase suggests that the apparent volume of distribution of warfarin should increase by ~10% in phenobarbital-treated rats. The results of the present study show that the apparent volume of distribution of (*S*)-(−)-warfarin was increased by 13% on the average, but this increase was not statistically significant. Statistical analysis of the data for the probability of a type II error strongly suggests ($P_B \simeq 0.4$) that a real difference of 10% would not be detected in our study at $\alpha = 0.05$ (23).

Branch and Shand (24) recently reevaluated previously published data on the effect of enzyme induction on antipyrine elimination kinetics in humans. Rather than basing their analysis on the biological half-life as did Vesell and Page (10), they used the clearance value as a more appropriate index of the activity of antipyrine-metabolizing enzyme systems. They found that the intersubject variability of antipyrine clearance by nine normal subjects was as large after phenobarbital treatment as in the noninduced state. The results of the present study with warfarin are consistent with these conclusions and are particularly noteworthy because the degree of enzyme induction was more pronounced than in the antipyrine study.

REFERENCES

(1) S. A. Cucinell, A. H. Conney, M. Sansur, and J. J. Burns, *Clin. Pharmacol. Ther.*, **6**, 420 (1965).

(2) M. Corn, *Thromb. Diath. Haemorrh.*, **16**, 606 (1966).

(3) M. G. MacDonald, D. S. Robinson, D. Sylwester, and J. J. Jaffe, *Clin. Pharmacol. Ther.*, **10**, 80 (1969).

(4) P. M. Aggeler and R. A. O'Reilly, *J. Lab. Clin. Med.*, **74**, 229 (1969).

(5) A. H. Conney, C. Davidson, R. Gastel, and J. J. Burns, *J. Pharmacol. Exp. Ther.*, **130**, 1 (1960).

(6) M. Ikeda, A. H. Conney, and J. J. Burns, *ibid.*, **162**, 338 (1968).

(7) C. W. T. Pilcher, R. P. H. Thompson, and R. Williams, *Biochem. Pharmacol.*, **21**, 129 (1972).

(8) A. Yacobi and G. Levy, *J. Pharm. Sci.*, **64**, 1660 (1975).

(9) A. Yacobi, J. A. Udall, and G. Levy, *Clin. Pharmacol. Ther.*, **19**, 552 (1976).

(10) E. S. Vesell and J. G. Page, *J. Clin. Invest.*, **48**, 2202 (1969).

(11) G. Levy and A. Yacobi, *J. Pharm. Sci.*, **63**, 805 (1974).

(12) J. T. Slattery, A. Yacobi, and G. Levy, *Life Sci.*, **19**, 447 (1976).

(13) A. Yacobi, R. G. Stoll, A. R. DiSanto, and G. Levy, *Res. Commun. Chem. Pathol. Pharmacol.*, **14**, 743 (1976).

(14) A. Yacobi, J. A. Udall, and G. Levy, *Clin. Pharmacol. Ther.*, **20**, 300 (1976).

(15) A. Yacobi, T. Lampman, and G. Levy, *ibid.*, **21**, 283 (1977).

(16) C.-M. Lai, A. Yacobi, and G. Levy, *J. Pharmacol. Exp. Ther.*, **199**, 74 (1976).

(17) K. Takada and G. Levy, *J. Pharm. Sci.*, **68**, 1569 (1979).

(18) A. Yacobi and G. Levy, *J. Pharmacokinet. Biopharm.*, **2**, 239 (1974).

(19) L. B. Wingard, Jr., and G. Levy, *J. Pharmacol. Exp. Ther.*, **184**, 253 (1973).

(20) A. Yacobi, L. B. Wingard, Jr., and G. Levy, *J. Pharm. Sci.*, **63**, 868 (1974).

(21) A. Yacobi and G. Levy, *ibid.*, **66**, 1275 (1977).

(22) A. Yacobi, J. T. Slattery, and G. Levy, *ibid.*, **66**, 941 (1977).

(23) A. R. Feinstein, *Clin. Pharmacol. Ther.*, **18**, 491 (1975).

(24) R. A. Branch and D. G. Shand, *Clin. Pharmacokinet.*, **4**, 104 (1979).

ACKNOWLEDGMENTS

Supported in part by Grant 20852 from the National Institute of General Medical Sciences, National Institutes of Health.

Previous paper in this series: A. Yacobi, C.-M. Lai, and G. Levy, *J. Pharm. Sci.*, **69**, 14 (1980).

Stability of Brompton Mixtures: Determination of Heroin (Diacetylmorphine) and Cocaine in Presence of Their Hydrolysis Products

G. K. POOCHIKIAN ˣ and J. C. CRADOCK

Received October 12, 1979, from the *Analytical and Product Development Section, Pharmaceutical Resources Branch, National Cancer Institute, Bethesda, MD 20205.* Accepted for publication January 23, 1980.

Abstract □ The application of a rapid, selective, and sensitive reversed-phase high-performance liquid chromatographic method to the separation of the hydrochloride salts of heroin (diacetylmorphine) and cocaine and their hydrolysis products is described. The method was used to study the stability of heroin and cocaine in Brompton mixtures in pharmaceutically useful pH range and vehicles at different temperatures. The pH range of optimal stability for both heroin and cocaine was 3.0–3.5. The disappearance of heroin and cocaine in Brompton mixtures followed pseudo-first-order kinetics in buffered solutions. Increased alcohol and decreased syrup concentrations diminished heroin hydrolysis but did not influence cocaine stability. Substitution of morphine for heroin in Brompton mixtures markedly increased the rate of cocaine hydrolysis.

Keyphrases □ Cocaine—high-performance liquid chromatographic analysis with heroin and hydrolysis products, Brompton mixtures □ Heroin—high-performance liquid chromatographic analysis with cocaine and hydrolysis products, Brompton mixtures □ High-performance liquid chromatography—analysis, cocaine and heroin with hydrolysis products, Brompton mixtures □ Brompton mixtures—stability, high-performance liquid chromatographic analysis of cocaine and heroin with hydrolysis products □ Diacetylmorphine—high-performance liquid chromatographic analysis with cocaine and hydrolysis products, Brompton mixtures

The treatment of patients with chronic severe pain has triggered interest in the use of morphine and heroin (diacetylmorphine) in popular oral formulations, namely Haustus elixir and diacetylmorphine and cocaine elixir, respectively (1). The latter formulation, referred to as a Brompton mixture, has been in use in Great Britain and Canada. Since heroin is a Schedule I narcotic in the United States, morphine frequently is substituted for this agent. There is no set composition for Brompton mixture. However, most variations contain salts of morphine or heroin combined with cocaine hydrochloride (hereafter referred to as their respective bases), alcohol, and a sweetening agent in an aqueous medium. Varying degrees of effectiveness have been reported for these analgesic mixtures (2–4).

The hydrolysis of diacetylmorphine to morphine *via* 6-monoacetylmorphine has been confirmed qualitatively (5, 6) and quantitatively (7). Furthermore, numerous methods have been published for the stability determination of cocaine (8–10). Several methods include the determination of one or more of its hydrolysis products, mainly benzoylecgonine, ecgonine, and benzoic acid (10–12). However, no single system has been used for both of these substances in the presence of their decomposition products.

Separation and quantitation of these components in such a complex mixture by TLC (12–14) is laborious and quantitatively imprecise. GLC requires extraction and derivatization and suffers from thermal degradation limitations (8, 9, 12). On the other hand, the reversed-phase high-performance liquid chromatographic (HPLC) method described here allows the simultaneous quantitation of heroin and cocaine in the presence of their hydrolytic products, an internal standard, and "inert" components by a simple, direct isocratic elution on a single analytical column. The separation was carried out in aqueous solution at a pH that showed minimal degradation of heroin and cocaine and eliminated preparatory procedures. The HPLC–UV method was applied to evaluate the stability of morphine or heroin plus cocaine at various temperatures and pH levels. The influence of alcohol and sucrose concentrations on heroin and cocaine stability was studied also.

EXPERIMENTAL

Reagents—Hydrochloride salts of heroin, 6-monoacetylmorphine, morphine, cocaine, and benzoylecgonine were used as received[1]. Benzoic acid, 2-chloro-3-nitropyridine, and the internal standard, 4-chloropyridine hydrochloride, were obtained commercially[2]. Acetonitrile[3] (HPLC grade) and distilled water were filtered through 0.45-μm solvent-resistant filters[4]. All other chemicals were reagent grade and were used without further purification.

Equipment—A modular high-pressure liquid chromatograph equipped with a constant-flow pump[5] was used to deliver the eluent to a stainless steel column packed with fully porous 10-μm silica particles bonded with a monomolecular layer of octadecylsilane[6]. Injections were made with a rotary valve injector equipped with a 10-μl injection loop[7]. No attempt was made to control the column temperature. A variable-wavelength UV detector[8] set at 235 nm was operated at an attenuation of 0.02 aufs, and the integrator output to the recorder was attenuated ×4 to detect the eluted compounds. The output signals were recorded with a strip-chart recorder[9].

Peak retention times and peak areas were monitored and quantitated automatically relative to the internal standard by area measurements using a computing integrator[10].

Chromatographic Conditions—The chromatographic mobile phase consisted of one volume of acetonitrile and three volumes of 0.015 *M* monobasic potassium phosphate adjusted to pH 3.0 with 2 *N* phosphoric acid[11]. The apparent pH of the eluent mixture was 3.30. The column pressure at a flow rate of 0.8 ml/min was ~620 psi. Separations were effected isocratically at ambient temperature. The chromatographic parameters, *i.e.*, capacity factors (k'), separation factors (relative retention, α), and resolution (R_s), of various solutes were calculated from the adjusted retention times (15).

Preparation of Solutions—Heroin and cocaine were dissolved in appropriate media (Table I) to yield concentrations of 1 and 0.5 mg/ml, respectively. Morphine–cocaine solutions at respective concentrations of 1 and 0.5 mg/ml were prepared only in the "standard vehicle" (II).

The solutions were filtered[4] through solvent-resistant filters and dispensed promptly (1.0 ml) in 2-ml flint ampuls. These ampuls were sealed

[1] National Institute on Drug Abuse, Rockville, Md.
[2] Aldrich Chemical Co., Milwaukee, Wis.
[3] Fisher Scientific Co., Fair Lawn, N.J.
[4] Millipore, Bedford, Mass.
[5] Model 3500B, Spectra-Physics, Santa Clara, Calif.
[6] μBondapak C_{18}, Waters Associates, Milford, Mass.
[7] Valco Instruments Co., Houston, Tex.
[8] Model SP 770, Spectra-Physics, Santa Clara, Calif.
[9] OmniScribe, Houston Instruments, Austin, Tex.
[10] System I, Spectra-Physics, Santa Clara, Calif.
[11] Beckman Zeromatic pH meter, Beckman Instruments, Irvine, Calif.

0022-3549/80/0600-0637$01.00/0
© 1980, American Pharmaceutical Association

Table I—Composition of Various Vehicles

Vehicle	Alcohol, % (v/v)	Syrup (16), % (v/v)	Distilled Water, % (v/v)	0.05 *M* Citrate Buffer, % (v/v)
I	0	25	75	—
II	12.5	25	62.5	—
III	25	25	50	—
IV	40	25	35	—
V	100	—	—	—
VI	12.5	12.5	75	—
VII	12.5	40	47.5	—
VIII	25	75	—	—
IX	12.5	25	—	62.5 (2.30)[a]
X	12.5	25	—	62.5 (3.00)
XI	12.5	25	—	62.5 (3.50)
XII	12.5	25	—	62.5 (4.50)
XIII	12.5	25	—	62.5 (5.25)

[a] The pH values are given in parentheses.

and stored at 5 ± 0.1, 25 ± 0.1, and 50 ± 0.1°. Periodically, 300-μl samples were removed and diluted to 2.0 ml with the mobile phase containing 85 μg/ml of the internal standard, 4-chloropyridine hydrochloride. The stability of heroin, morphine, and cocaine in these mixtures was monitored over a period not exceeding 65 days.

RESULTS AND DISCUSSION

Chromatographic Behavior—The hydrochlorides of morphine, 6-monoacetylmorphine, benzoylecgonine, 4-chloropyridine, heroin, and cocaine were eluted in that order. Figure 1 illustrates the separation of a synthetic mixture of these substances and benzoic acid. The chromatographic retention data for each substance are listed in Table II. At a flow rate of 0.8 ml/min, the analysis time was ~22 min, and baseline resolution was achieved in nearly every case. The retention times (T_R in seconds), k', α, and R_s for all of these substances in hydrolyzed samples were identical to those determined for the synthetic mixture. During the 2-month study, there was no noticeable loss in column performance.

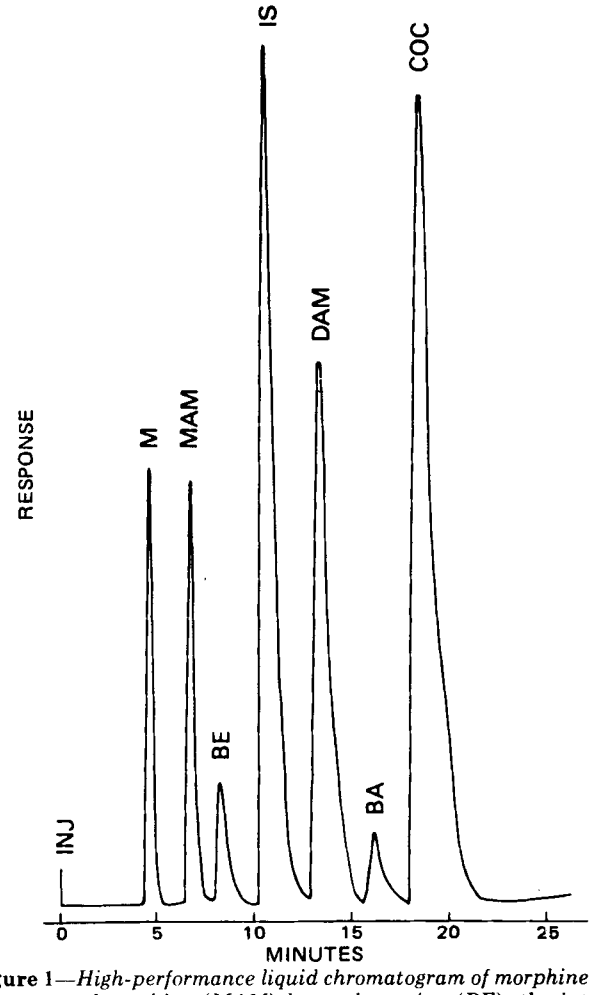

Figure 1—*High-performance liquid chromatogram of morphine (M), 6-monoacetylmorphine (MAM) benzoylecgonine (BE), the internal standard (IS), diacetylmorphine (DAM), benzoic acid (BA), and cocaine (COC).*

Table II—Retention Times (T_R), Capacity Factors (k'), Separation Factors (α), and Resolution (R_s) of Various Solutes[a]

Compound	T_R, sec	k'	α	R_s
Morphine	270	0.42	2.88	4.89
6-Monoacetylmorphine	420	1.21	1.35	2.19
Benzoylecgonine	500	1.63	1.48	3.12
4-Chloropyridine	648	2.41	1.38	2.87
Diacetylmorphine	820	3.32	1.24	2.14
Benzoic acid	972	4.12	1.22	2.02
Cocaine	1140	5.00	1.26	2.46
2-Chloro-3-nitropyridine	1390	6.32		

[a] Retention data of various solutes from a 300 × 4.6-mm i.d. μBondapak C_{18} (10 μm) column. The mobile phase was acetonitrile–monobasic potassium phosphate (0.015 *M*) (pH 3.0), the flow rate was 0.8 ml/min, and UV detection was at 235 nm.

Table III—Effect of Alcohol Concentration on the Stability of Heroin and Cocaine in the Brompton Mixture at Various Temperatures

Alcohol, % (v/v)	t_{90} at 5 ± 0.1°, days		t_{90} at 25 ± 0.1°, days		t_{90} at 50 ± 0.1°, days	
	Heroin	Cocaine	Heroin	Cocaine	Heroin	Cocaine
0 (I)	16	>60	6	>60	1.5	5
12.5 (II)	25	>60	10	>60	2	5
25 (III)	40	>60	15	>60	4	5
40 (IV)	75	>60	30	>60	8	7
100[a] (V)	—	—	—	—	50	48

[a] Contains heroin (1 mg/ml) and cocaine (0.5 mg/ml).

Table IV—Effect of Syrup Concentration on Heroin and Cocaine Stability in the Brompton Mixture at 50 ± 0.1°

Simple Syrup, % (v/v)	t_{90}, days	
	Heroin	Cocaine
12.5 (VI)	4	5
25 (II)	2	5
40 (VII)	1.5	5

The HPLC system may be used to quantitate every component in solution when desired. In this study, only the disappearance of heroin and cocaine was followed. The chromatographic responses for these compounds were linear ($r > 0.999$) in the working concentration range (20–200 μg/ml). The sensitivity limits were 10 ng for heroin and 3 ng for cocaine with a signal-to-noise ratio of better than five. To reduce the duration of each analysis, 4-chloropyridine hydrochloride was selected as the internal standard on the basis of its shorter retention time. However, 2-chloro-3-nitropyridine may be used instead (Table II).

Effects of Alcohol and Syrup Concentrations—The disappearance rates of heroin and cocaine as a function of the alcohol content in the mixture containing a fixed concentration of simple syrup were evaluated at various temperatures (5 ± 0.1, 25 ± 0.1, and 50 ± 0.1°) (Table III). Cocaine was stable at 25 and 5° and did not approach the t_{90} values (time for 10% disappearance of original concentration) during the 2-month observation period. However, heroin was markedly less stable at all temperatures studied. Thus, recommendations are based on the stability of heroin in these mixtures.

Hydrolysis of heroin was diminished with increasing proportions of alcohol, while the disappearance rate of cocaine was unaffected. Under the usual alcohol concentrations found in Brompton mixtures (12.5–25%), these solutions had a useful life of 10–14 days at 25°. However, the stability of diacetylmorphine was markedly enhanced in alcohol. The t_{90} of either heroin or cocaine in ethanol was >45 days at 50°. When stored at 5°, such a mixture may be used as a stock solution to facilitate preparation of Brompton mixtures at the time of dispensing.

Unlike alcohol, decreasing the syrup content at a fixed alcohol concentration in the mixture had a less pronounced effect on diacetylmorphine and no effect on cocaine stability (Table IV).

Effects of pH and Temperature—The influence of the Brompton mixture pH on the stability of heroin and cocaine was of interest since

Table V—Disappearance Rates of Heroin and Cocaine in Various Brompton Mixtures

Vehicle	k_1 at 5 ± 0.1°, day^{-1}		k_1 at 50 ± 0.1°, day^{-1}	
	Heroin	Cocaine	Heroin	Cocaine
I	6.56×10^{-3}	0.42×10^{-3}	—	—
II	4.20×10^{-3}	0.42×10^{-3}	—	—
III	2.62×10^{-3}	0.35×10^{-3}	—	—
IV	1.40×10^{-3}	0.31×10^{-3}	—	—
V	—	—	2.10×10^{-3} (50)[a]	2.20×10^{-3} (48)
IX	—	—	146×10^{-3} (0.7)	1.75×10^{-3} (60)
X	—	—	70.0×10^{-3} (1.5)	2.15×10^{-3} (49)
XI	—	—	39.5×10^{-3} (2.7)	4.25×10^{-3} (24)
XII	—	—	36.2×10^{-3} (2.9)	16.15×10^{-3} (6.5)
XIII	—	—	105×10^{-3} (1)	70.0×10^{-3} (1.5)

[a] Period (days) for 10% disappearance of original concentration is given in parentheses.

Table VI—Effects of Morphine and Heroin on Cocaine in Brompton Mixture

Vehicle	t_{90} at 25 ± 0.1°, days		t_{90} at 50 ± 0.1°, days	
	Heroin	Cocaine	Heroin	Cocaine
II	10	>60	2	5
IIa[a]	—	—	1.75	—
IIb[b]	—	10	—	1.5
XII	—	—	2.9	6.5
XIIa[c]	—	>60	—	11

[a] Contains only heroin (1 mg/ml) in standard vehicle II. [b] Contains morphine (1 mg/ml) and cocaine (0.5 mg/ml) in vehicle II. [c] Contains only cocaine (0.5 mg/ml) in vehicle XII.

the optimal pH values for minimal degradation of diacetylmorphine (7) and cocaine (11, 17) were shown separately to be 4.0–4.5 and 2.5–3.0, respectively. Hence, the pH range of 2.30–5.25 was chosen. The results (Table V) indicate that the optimal pH is between 3.0 and 3.5 for the overall minimal hydrolysis of heroin and cocaine in such a mixture.

The available data show the predominant influence of temperature on the rate of diacetylmorphine and, particularly, of cocaine hydrolysis in the Brompton mixture (Tables III and VI). A 10-fold decrease in temperature of the Brompton mixture diminished the rate of hydrolysis of heroin by ~10-fold and that of cocaine by at least 50-fold.

Kinetic Evaluations—Semilog plots of heroin or cocaine concentrations in the Brompton mixture *versus* time exhibited excellent linearity ($r > 0.99$) in 95% ethanol or buffered solutions (V and IX–XIII). Thus, the disappearance of heroin and cocaine followed pseudo-first-order kinetics under the conditions studied. Table V presents the calculated pseudo-first-order rate constants and t_{90} values at 50 ± 0.1° for heroin (2.36×10^{-3} *M*) and cocaine (1.47×10^{-3} *M*) in 0.05 *M* citrate buffers (18) or in 95% ethanol.

However, the disappearance rates of both diacetylmorphine and cocaine in unbuffered solutions (common in Brompton mixtures) at 25 ± 0.1 and 50 ± 0.1° were biphasic. A rapid change was followed by a more gradual one, with the final phase being linear on a semilogarithmic plot ($r > 0.99$). The extent of the initial change and the terminal phase slope of each solution were temperature dependent and were more dominant at high temperature. The t_{90} values of heroin and cocaine in these solutions were determined from the respective plots of concentration *versus* time. At 5 ± 0.1°, the hydrolysis rates of heroin and cocaine in unbuffered Brompton mixtures followed pseudo-first-order kinetics over the period studied (Table V). However, the amount of hydrolysis was minimal and did not approach t_{90} values.

Effects of Heroin, Cocaine, and Morphine—The results (Table VI) indicated that although cocaine had no effect on the heroin decomposition rate in the Brompton mixture (II *versus* IIa), the presence of diacetylmorphine increased the cocaine decomposition rate in the mixture (XII *versus* XIIa).

The frequent substitution of morphine for heroin in the Brompton mixture in the United States warranted a study to determine the effect of this substitution on the stability of cocaine and morphine in 12.5% alcohol and 25% simple syrup USP. Morphine appeared to be stable, but such a replacement adversely affected the cocaine hydrolysis rate at all temperatures studied (II *versus* IIb). In fact, the t_{90} value (10 days) was essentially the same as that observed in the diacetylmorphine–cocaine mixture at 25°. This acceleration of cocaine hydrolysis is of special concern. Cocaine hydrolyzes to pharmacologically inactive substances (19), whereas the diacetylmorphine decomposition products, 6-monoacetylmorphine and morphine, retain analgesic activity. The chemical stability of both cocaine and diacetylmorphine was enhanced by adjustment to pH 3.0–3.5. However, the biological effects of this pH adjustment have not been evaluated.

REFERENCES

(1) "Martindale: The Extra Pharmacopoeia," 27th ed., A. Wade, Ed., Pharmaceutical Press, London, England, 1977, pp. 960, 973.

(2) R. G. Twycross, *Int. J. Clin. Pharmacol.*, **9**, 184 (1974).

(3) B. M. Mount, I. Ajemian, and J. F. Scott, *Can. Med. Assoc. J.*, **115**, 122 (1976).

(4) R. Melzack, B. M. Mount, and J. M. Gordon, *ibid.*, **120**, 435 (1979).

(5) E. A. Davey, J. B. Murray, and A. R. Rogers, *J. Pharm. Pharmacol., Suppl.*, **20**, 515 (1968).

(6) P. E. Kamp and R. A. Van Welsum, *Pharm. Weekbl.*, **108**, 987 (1973).

(7) G. K. Poochikian and J. C. Cradock, *J. Chromatogr.*, **171**, 371 (1979).

(8) D. L. Von Minden and N. A. D'Amato, *Anal. Chem.*, **49**, 1974 (1977).

(9) M. J. Prager, S. M. Harrington, and T. F. Governo, *J. Assoc. Off. Anal. Chem.*, **62**, 304 (1979).

(10) O. A. Akopyan, *Farm. Zh. Kiev*, **20**, 59 (1965); through *Chem. Abstr.*, **64**, 5428f (1966).

(11) J. B. Murray and H. Al-Sheura, *J. Pharm. Pharmacol., Suppl.*, **28**, 24p (1976).

(12) F. K. Rafla and R. L. Epstein, *J. Anal. Toxicol.*, **3**, 59 (1979).

(13) D. J. Stewart, T. Inaba, M. Lucassen, and W. Kalow, *Clin. Pharmacol. Ther.*, **25**, 464 (1979).

(14) R. G. Twycross, *Pharm. J.*, **212**, 153 (1974).

(15) L. R. Snyder and J. J. Kirkland, "Introduction to Modern Liquid Chromatography," Wiley, New York, N.Y., 1974, p. 35.

(16) "The United States Pharmacopeia," 19th rev., Mack Publishing Co., Easton, Pa., 1975, p. 578.

(17) M. D. Denisov, *Farm. Zh. Kiev*, **22**, 74 (1967); through *Chem. Abstr.*, **68**, 33158q (1968).

(18) R. D. Lillie, "Histopathologic Technique," Blakiston, Philadelphia, Pa., 1948.

(19) A. L. Misra, P. K. Nayak, R. Block, and S. J. Mulé, *J. Pharm. Pharmacol.*, **27**, 784 (1975).

ACKNOWLEDGMENTS

The authors thank Mrs. Shirely Swindell for assistance in the preparation of this manuscript.

GLC–Mass Spectrometric Procedure with Selected-Ion Monitoring for Determination of Plasma Concentrations of Unlabeled and Labeled Barbital following Simultaneous Oral and Intravenous Administration

F. VARIN *, C. MARCHAND *†, P. LAROCHELLE *, and K. K. MIDHA ‡§x

Received September 26, 1979, from the **Department of Pharmacology, University of Montreal, Montreal, Quebec H3C 3J7, Canada,* and the ‡*Drug Research Laboratories, Health Protection Branch, Health and Welfare Canada, Ottawa, Ontario K1A 0L2, Canada.* Accepted for publication January 7, 1980. §Present address: College of Pharmacy, University of Saskatchewan, Saskatoon, Saskatchewan S7N 0W0, Canada. †Deceased.

Abstract □ A GLC–mass spectrometric method employing specific-ion monitoring was developed for the determination of plasma concentrations of labeled ($^{15}N_{1,3}$, $^{13}C_2$) and unlabeled barbital following simultaneous intravenous and oral administration. This method proved to be more sensitive and precise than the method employing GLC with flame-ionization detection or GLC with alkali flame-ionization detection. After extraction of [$^{15}N_{1,3}$, $^{13}C_2$]barbital, barbital, and the internal standard, butalbital, from plasma with ether, the organic solvent is evaporated, and the labeled and unlabeled drug as well as the internal standard are converted into their *N,N*-dimethyl derivatives by treatment with diazomethane. The excess reagent is evaporated, and the resulting methyl derivatives are analyzed by GLC–mass spectrometry with selected-ion monitoring. The method is sufficiently sensitive to determine 0.5 μg of the labeled and unlabeled drug/ml with a relative standard deviation of <5%. The application of the method to the determination of the plasma concentration of labeled and unlabeled drug over 6 days following simultaneous oral and intravenous administration of a single dose is demonstrated.

Keyphrases □ Barbital—plasma concentrations of unlabeled and labeled drug following simultaneous oral and intravenous administration, GLC–mass spectrometric analysis □ GLC–mass spectrometry—analysis of plasma concentrations of unlabeled and labeled barbital following simultaneous oral and intravenous administration, specific-ion monitoring □ Pharmacokinetics—barbital, plasma concentrations of unlabeled and labeled drug following simultaneous oral and intravenous administration, GLC–mass spectrometric analysis

Barbiturates have been investigated extensively. GLC procedures employing flame-ionization detection have been preferred for the quantitative determination of barbiturates in biological fluids and tissues (1–5). GLC techniques using newer and more sensitive detectors than flame-ionization detectors, such as alkali flame-ionization detectors and electron-capture detectors, also have been explored (6, 7). Analysis of barbiturates by high-pressure liquid chromatography was reported (8). More recently, barbiturates have been analyzed by rapid and specific radioimmunoassay (9, 10) and by GLC–mass spectrometric procedures (11–13).

To study the effect of congestive heart failure on drug disposition, a procedure capable of simultaneously and separately quantitating the amounts of drug in plasma originating from oral as well as intravenous dosing was required. Simultaneous quantitation of the two fractions in the same plasma sample was essential because congestive heart failure is not easily stabilized and pharmacokinetic parameters may differ in successive studies.

Barbital was chosen as the model drug for this study since it is not metabolized; the determination of pharmacokinetic parameters therefore is simplified. Stable isotopically labeled barbital was given intravenously at the same time that unlabeled barbital was administered orally. A GLC–mass spectrometric method employing a specific-ion monitoring technique was developed for the simultaneous quantitation of barbital given by the two routes.

EXPERIMENTAL

Reagents—Barbital sodium[1], ether[2], hydrochloric acid[3], sodium sulfate[4], methanol[5], and butalbital[6] were used. [$^{15}N_{1,3}$, $^{13}C_2$]Barbital sodium[7] was specified to contain at least 90 atom % of carbon 13 and 95 atom % of nitrogen 15. Diazomethane was generated using a commercially available kit[8]. Plasma was obtained from the Red Cross Blood Bank.

Animals—Male Sprague–Dawley rats were assigned randomly to two groups. The first group (276 ± 2 g, n = 5) was administered 25 mg of barbital sodium/kg iv. The second group (271 ± 7 g, n = 5) was treated similarly with [$^{15}N_{1,3}$, $^{13}C_2$]barbital sodium. Two hours after treatment, rats were sacrificed by decapitation; their blood was collected in a heparinized[9] centrifuge tube (50 IU/ml of 0.9% NaCl solution). Plasma obtained after centrifugation for 20 min was frozen until it was assayed.

Standards—Stock solutions equivalent to 1 mg of the acid form/ml were prepared by dissolving the appropriate amounts of the sodium salts of both labeled and unlabeled barbital in methanol. Appropriate dilutions were prepared as required. Aliquots of the stock solution containing 1 mg/ml of butalbital in methanol were diluted before assay with 0.25 *N* HCl to obtain the working internal standard solution (10 μg/ml).

Extraction from Plasma—To 1 ml of a human or rat plasma sample (spiked or from dosed animals) in screw-capped[10] culture tubes was added 1 ml of the internal standard solution. The samples were mixed[11] and then extracted with 10 ml of anhydrous ether by mixing[12] for 10 min. After separation by centrifugation[13] for 10 min, the organic phase was transferred with a pipet and desiccated with anhydrous sodium sulfate. After further centrifugation for 10 min, the organic phase was decanted into an evaporating tube[14] and evaporated[15] to dryness at 50° under a dry nitrogen stream. The samples then were frozen until analysis.

Methylation was carried out immediately before the GLC–mass spectrometric analysis to avoid any breakdown and formation of side products. The dried extract was dissolved in 50 μl of methanol by mixing, and 1 ml of ethereal diazomethane was added. The sample was mixed and allowed to react at room temperature for 5 min. The excess diazomethane

[1] Reagent grade, BDH Chemicals, Toronto, Ontario, Canada.
[2] Diethyl ether (anhydrous), Baker Analyzed Reagent, Canlab, Montreal, Quebec, Canada.
[3] Baker Analyzed Reagent, Canlab, Montreal, Quebec, Canada.
[4] Anhydrous, Baker Analyzed Reagent, Canlab, Montreal, Quebec, Canada.
[5] Burdick & Jackson Laboratories, Muskegon, Mich.
[6] Provided by Sandoz Pharmaceuticals, Dorval, Quebec, Canada.
[7] Merck Sharp and Dohme Canada Ltd., Montreal, Quebec, Canada.
[8] Diazald, Aldrich Chemical Co., Milwaukee, Wis.
[9] Heparin sodium, Fisher Scientific Co., Montreal, Quebec, Canada.
[10] Kimak with Teflon liner.
[11] Vortex Genie, Fisher Scientific Co., Montreal, Quebec, Canada.
[12] Eberbach reciprocating shaker, Ann Arbor, Mich.
[13] IEC International Centrifuge, Boston, Mass.
[14] Custom made, Montreal Glass Blowing Registered, Montreal, Quebec, Canada.
[15] Thermolyne Dri Bath, Thermolyne Corp., Dubuque, Iowa.

0022-3549/80/0600-0640$01.00/0
© 1980, American Pharmaceutical Association

Table I—Recovery of Barbital and [$^{15}N_{1,3}$, $^{13}C_2$]Barbital from Plasma Determined by the GLC–Mass Spectrometric Assay

Micrograms Added[a] to 1 ml of Plasma	Mean Micrograms Recovered	Mean Percent Recovery ± *SD*
Barbital		
0.3	0.302	100.56 ± 5.16
4.0	3.36	84.00 ± 3.56
10.0	8.50	84.97 ± 1.47
Mean		89.84 ± 8.61
[$^{15}N_{1,3}$, $^{13}C_2$]Barbital		
0.5	0.560	112.08 ± 2.50
2.0	1.90	95.21 ± 6.19
10.0	8.98	89.80 ± 2.74
Mean		99.00 ± 10.56

[a] $n = 4$.

was removed by evaporation at 50°, leaving a methanolic solution that was injected in aliquots of 1–2 μl into the gas–liquid chromatograph.

GLC with Flame-Ionization Detection—The gas–liquid chromatograph[16] was equipped with a flame-ionization detector. The column was coiled glass tubing, 1.83 m long × 2 mm i.d., packed with 3% phenylmethylsilicone[17] on acid-washed, dimethylchlorosilane-treated, flux-calcined diatomite support[18] (80–100 mesh). The operating temperatures were: injection port, 250°; column, 225°; and detector, 275°. The carrier gas was nitrogen at a 35-ml/min flow rate. The hydrogen and compressed air flow rates were adjusted to give the maximum response. Pentobarbital[19] (30 μg/ml of plasma) was the internal standard. Flash-heater methylation was carried out with trimethylanilinium hydroxide in methanol[20].

GLC with Alkali Flame-Ionization Detection—The gas–liquid chromatograph[16] was equipped with an alkali flame-ionization detector. The operating temperatures were: injection port, 275°; column, 170°; and detector, 300°. The internal standard was aminopyrine[21] (10 μg/ml of plasma). The column was the same as that described for the method with flame-ionization detection.

GLC–Mass Spectrometry—The gas–liquid chromatograph–mass spectrometer[22] was operated in the electron-impact mode with 70 ev as the ionization beam energy. The source was maintained at 200°. The chromatographic column was a coiled glass tube, 1.22 m long × 2 mm i.d., packed with 3% cyanopropylmethyl phenylmethylsilicone[23] on acid-washed, dimethylchlorosilane-treated, flux-calcined diatomite support[24] (100–120 mesh). The injection port, the column, and the interface temperatures were 250, 150, and 275°, respectively. The carrier gas was helium at a 35-ml/min flow rate.

Reference Samples for Recovery—The acid form of barbital was obtained by successive extractions of an acidified aqueous solution of barbital sodium with ether. The combined extracts were evaporated and dried at 80° overnight. The reference solution of barbital (1 mg/ml) was prepared by dissolving appropriate amounts of the drug in methanol. Different volumes of this solution were added to each evaporating tube to obtain four solutions at each of three concentrations (Table I). The external standard (10 μg of butalbital) and 10 ml of anhydrous ether then were added. The mixture was evaporated to dryness at 55° under a dry nitrogen stream. Methylation was carried out as described, and aliquots (1–2 μl) were injected into the gas–liquid chromatograph–mass spectrometer. The mean of the peak area ratio thus obtained was designated as the 100% value.

For the recovery experiments for barbital sodium, amounts equivalent to the acid form added to plasma (1.0 ml) were extracted with ether as described. Then 10 μg of butalbital was added to the organic extract and the procedure was followed. The recovery of barbital was calculated from the peak ratio thus obtained (mean ± *SD*) compared to the value designated as 100%. The same procedure was followed for the recovery of [$^{15}N_{1,3}$, $^{13}C_2$]barbital sodium.

Calibration Curve—Calibration curves were assembled from the results of spiked control plasma by plotting the peak area ratios *versus* the concentration of the drug (Tables II and III). Peak area ratios were calculated by dividing the peak area under each ion investigated (*e.g.*, *m/e* 169 for barbital and *m/e* 172 for labeled barbital) by the peak area under the ion (*m/e* 196) monitored for the internal standard.

[16] Model 5830A, Hewlett-Packard, Montreal, Quebec, Canada.
[17] OV-17, Chromatographic Specialties, Brockville, Ontario, Canada.
[18] Gas Chrom Q, Chromatographic Specialties, Brockville, Ontario, Canada.
[19] Abbott Laboratories Ltd., Montreal, Quebec, Canada.
[20] Methelute, Chromatographic Specialties, Brockville, Ontario, Canada.
[21] Casgrain et Charbonneau, Montreal, Quebec, Canada.
[22] Model 5985 data system, Hewlett-Packard, Avondale, Pa.
[23] OV-225, Chromatographic Specialties, Brockville, Ontario, Canada.
[24] Chromosorb W (HP), Chromatographic Specialties, Brockville, Ontario, Canada.

Table II—GLC–Mass Spectrometric Estimation of Barbital Added to Plasma

Barbital[a] Added, μg	*n*	Mean Peak Area Ratio ± *SD*	*CV*, %
0.5	6	0.059 ± 0.003	4.55
2.0	5	0.252 ± 0.010	3.84
4.0	5	0.445 ± 0.019	4.31
6.0	5	0.660 ± 0.037	5.59
10.0	6	1.081 ± 0.038	3.49

[a] Mean *CV* was 4.36% for $y = mx$, where $m = 0.109 \pm 0.002$; $r^2 = 0.998$.

Table III—GLC–Mass Spectrometric Estimation of [$^{15}N_{1,3}$, $^{13}C_2$]Barbital Added to Plasma

[$^{15}N_{1,3}$, $^{13}C_2$]-Barbital[a] Added, μg	*n*	Mean Peak Area Ratio ± *SD*	*CV*, %
0.3	6	0.030 ± 0.001	4.71
1.0	5	0.160 ± 0.004	4.08
2.0	5	0.197 ± 0.008	4.06
3.0	6	0.299 ± 0.010	3.23
6.0	6	0.590 ± 0.015	2.57

[a] Mean *CV* was 3.73% for $y = mx$, where $m = 0.099 \pm 0.001$; $r^2 = 0.999$.

RESULTS AND DISCUSSION

Methylation of barbital with diazomethane gave a major peak (99% by the peak area on the total-ion monitor) when it was analyzed under the described conditions. GLC–mass spectrometric analysis of the eluted compound did not show a molecular ion (*m/e* 212); however, other diagnostic ions at *m/e* 184, 183, 169, 126, and 112 supported identification of the compound as N_1,N_3-dimethylbarbital. Similarly, methylation of [$^{15}N_{1,3}$, $^{13}C_2$]barbital gave a peak with the same retention time (1.1 min) with major ions at *m/e* 187, 186, 172, 127, and 113 (Fig. 1). The ions were consistent with the fragmentation pattern reported (14) for N_1,N_3-dimethylbarbital. The isotopic purity of the labeled compound is demonstrated by the absence of an ion at *m/e* 169 (Fig. 1).

Mass spectral analysis of the methylated internal standard, butalbital, suggested that the N_1,N_3-dimethylated derivative was formed (99% by the peak area). The mass spectrum showed no molecular ion; however, characteristic ions at *m/e* 209, 196, 195, 181, and 74 were consistent with identification of the compound as the N_1,N_3-dimethyl derivative.

The use of diazomethane as a suitable methylating agent for barbiturates was reported previously (15). Dried extracts of samples are stable for periods of months when kept at −20°. However, when diazomethane is added to them, analysis must be completed within 12 hr. In preliminary studies, flash-heater methylation with the safer reagent, trimethylanilinium hydroxide, was tried; however, because of the decomposition of the barbital derivative, it was abandoned. Diazomethane methylation of barbital and bultalbital gave the desired N_1,N_3-dimethyl derivative of the compounds with negligible amounts of by-products (methyl enol ethers).

Single-ion chromatograms obtained after methylation of a reference sample containing [$^{15}N_{1,3}$, $^{13}C_2$]barbital and butalbital in methanol are

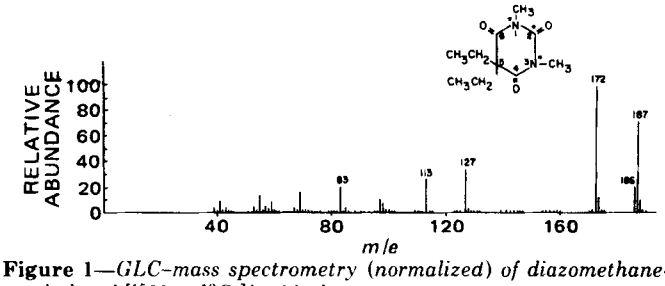

Figure 1—*GLC–mass spectrometry (normalized) of diazomethane-methylated* [$^{15}N_{1,3}$, $^{13}C_2$]*barbital.*

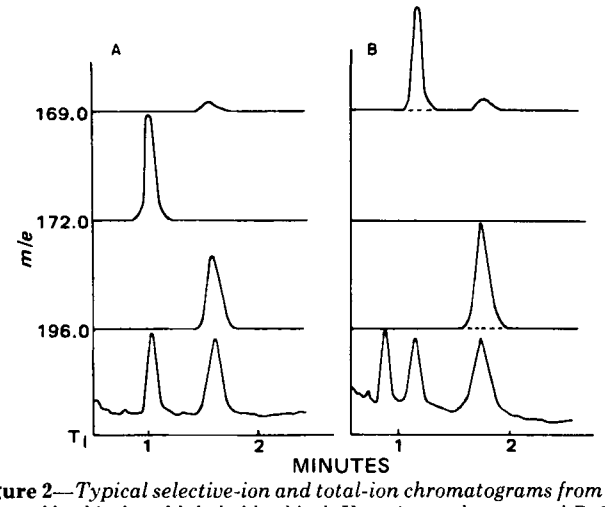

Figure 2—*Typical selective-ion and total-ion chromatograms from the assay of barbital and labeled barbital. Key: A, no plasma; and B, 2-hr plasma sample from a barbital-treated rat. The ions at* m/e *169, 172, and 196 represent barbital, [$^{15}N_{1,3}$, $^{13}C_2$]barbital, and the internal standard, butalbital, respectively.*

shown in Fig. 2*a*. The isotopic purity of the labeled compound is established further by the absence of a signal due to the *m/e* 169 ion (relative abundance <0.2%). Figure 2*b* shows a typical single-ion chromatogram obtained from a 2-hr plasma sample of a barbital-treated rat. The plasma had to be diluted with Red Cross Blood Bank plasma to fit the peak in the linear portion of the detector response curve. To rule out the possibility of any difference between the plasma disposition of barbital and [$^{15}N_{1,3}$, $^{13}C_2$]barbital, two groups of rats were treated with each drug respectively as described under *Experimental*. Comparison of 2-hr plasma concentrations in treated rats is illustrated in Table IV. Results are expressed as the mean for five rats. Results were compared using the Student *t* test, and no statistical difference could be found. Therefore, it was concluded that there was no isotopic effect in the plasma disposition of [$^{15}N_{1,3}$, $^{13}C_2$]barbital sodium in rats.

The overall recoveries of barbital and labeled barbital from plasma are summarized in Table I. Mean percent recoveries of 89 and 99% were considered satisfactory. Recoveries of slightly over 100% sometimes were observed at very low concentrations. This artifact probably is due to background noise.

The accuracy and precision of the GLC–mass spectrometric assay are demonstrated in Tables II and III. Results from at least five determinations of each barbital concentration, ranging from 0.3 to 10 μg/ml of plasma, were obtained as described under *Experimental*. The overall coefficients of variation for barbital and [$^{15}N_{1,3}$, $^{13}C_2$]barbital were 4.36 and 3.73%, respectively. The GLC–mass spectrometric response was linear for both compounds within this concentration range. The detection limit was 1 ng on-column (3× noise). The calibration curves for barbital and labeled barbital were straight lines with an intercept of 0.020 and 0.003, respectively, when they were not forced through the origin. Mean slopes of 0.109 ± 0.002 and 0.099 ± 0.001 for the two compounds were obtained when linear regression without the intercept program was applied.

The sensitivity of the GLC–mass spectrometric detection using single-ion monitoring was compared against GLC with flame-ionization detection and GLC with alkali flame-ionization detection when the same

Table IV—Comparison of 2-hr Plasma Concentrations in Treated Rats

Compound	Plasma Concentration, μg/ml	Mean ± *SD*
[$^{15}N_{1,3}$, $^{13}C_2$]Barbital sodium	25.03	
	24.81	
	24.04	25.13 ± 0.88
	26.47	
	25.29	
Barbital sodium	24.95	
	24.42	
	24.13	24.81 ± 0.61
	25.73	
	24.82	

Table V—Estimation of Barbital Added to Plasma by GLC with Flame-Ionization Detection

Barbital[a] Added, μg	*n*	Mean Peak Area Ratio ± *SD*	*CV*, %
5.0	12	0.13 ± 0.015	11.8
8.0	14	0.227 ± 0.031	13.7
15.0	8	0.414 ± 0.012	2.83
30.0	12	0.765 ± 0.016	2.09
50.0	10	1.309 ± 0.036	2.77

[a] Mean *CV* was 6.64% with $y = mx + b$, where $m = 0.025 \pm 0.012$ and $b = 0.027$; $r^2 = 0.995$.

Table VI—Estimation of Barbital Added to Plasma by GLC with Alkali Flame-Ionization Detection

Barbital[a] Added, μg	*n*	Mean Peak Area Ratio ± *SD*	*CV*, %
1.0	6	0.132 ± 0.024	18.41
5.0	8	0.543 ± 0.036	6.78
10.0	8	1.028 ± 0.059	5.71
20.0	6	2.168 ± 0.087	3.87
30.0	8	3.257 ± 0.212	6.53

[a] Mean *CV* was 8.26% with $y = mx + b$, where $m = 0.107 \pm 0.050$ and $b = 0.008$; $r^2 = 0.993$.

extraction procedure was employed (see *Experimental*). As shown in Tables V and VI, both methods are applicable when plasma barbital concentrations of >5 μg/ml are expected. However, the GLC–mass spectrometric method offers the greatest sensitivity and precision and is more suited to quantitation in the therapeutic range, *e.g.*, <5 μg/ml.

Figure 3*a* shows selective-ion and total-ion chromatograms obtained from control plasma processed as described under *Experimental* but with the internal standard omitted. Most of the endogenous plasma constituents were eluted at 0.86 min. No extraneous peaks that interfered with the selected ions for labeled (*m/e* 172) and unlabeled (*m/e* 169) barbital or butalbital (*m/e* 196) were observed over 20 min (2 min shown). Figure 3*b* shows typical selective-ion and total-ion chromatograms from a 2-hr plasma sample collected from a human volunteer treated with [$^{15}N_{1,3}$, $^{13}C_2$]barbital sodium intravenously and barbital sodium orally at the same time. The signals at *m/e* 169 and 172 represent 7.62 μg of unlabeled barbital/ml and 2.51 μg of labeled barbital/ml, respectively.

Application of the GLC–mass spectrometric procedure to the determination of plasma levels of both labeled and unlabeled barbital is shown in Fig. 4. A dose of 1.5 mg of [$^{15}N_{1,3}$, $^{13}C_2$]barbital sodium/kg was injected intravenously (within 20 sec) into a healthy female volunteer (65 kg); at the same time, she swallowed a capsule containing 4.5 mg of barbital

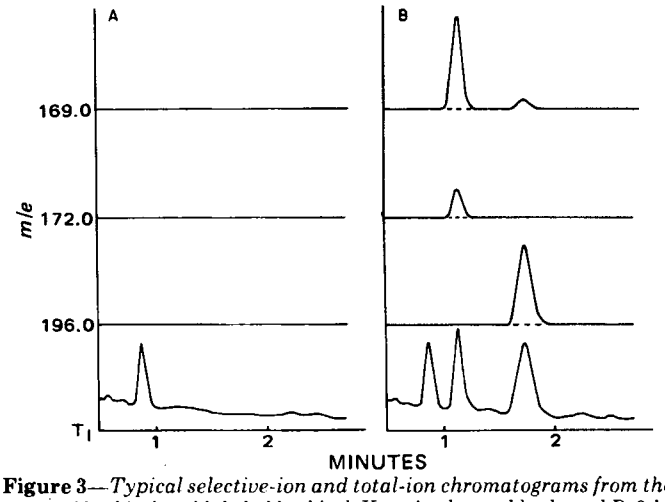

Figure 3—*Typical selective-ion and total-ion chromatograms from the assay of barbital and labeled barbital. Key: A, plasma blank; and B, 2-hr plasma sample from the same volunteer (65 kg) who received* [$^{15}N_{1,3}$, $^{13}C_2$]*barbital sodium intravenously and barbital sodium orally at the same time. The signals at* m/e *169 and 172 represent 7.62 μg of barbital/ml and 2.51 μg of labeled barbital/ml, respectively. The signal at* m/e *196 is that for the internal standard, butalbital.*

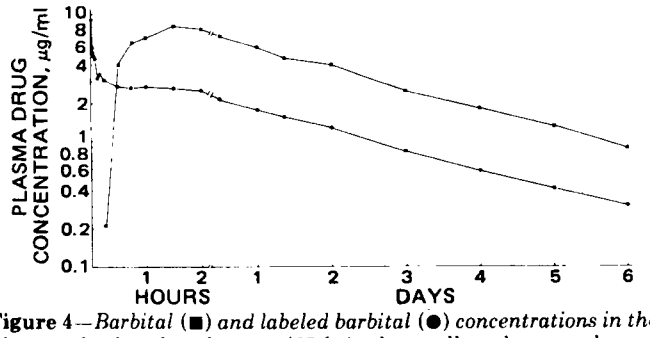

Figure 4—*Barbital (■) and labeled barbital (●) concentrations in the plasma of a female volunteer (65 kg) who swallowed a capsule containing 4.5 mg of barbital sodium/kg and simultaneously received 1.5 mg of [$^{15}N_{1,3}$, $^{13}C_2$]barbital sodium/kg iv (within 20 sec).*

sodium/kg. Blood (7 ml) was withdrawn at intervals over 6 days, and aliquots of plasma (1.0 ml) were assayed for barbital. Concentration–time curves of both isotopes in plasma are illustrated in Fig. 4, and the parallelism observed between their elimination phases strongly supports the evidence that both isotopes behave similarly in the organism.

In conclusion, the described GLC–mass spectrometric procedure is sensitive and specific and should be applicable to studies on the effect of congestive heart failure on barbital disposition.

REFERENCES

(1) D. J. Berry, *J. Chromatogr.*, **86**, 89 (1973).

(2) J. DeGraeve and J. Vanroy, *ibid.*, **129**, 171 (1976).

(3) K. Schweizer, H. Wick, and T. Brechbühler, *Clin. Chim. Acta*, **90**, 203 (1978).

(4) W. Dünges, E. Bergheim-Irps, H. Straub, and R. E. Kaiser, *J. Chromatogr.*, **145**, 265 (1978).

(5) N. Elahi, *J. Anal. Toxicol.*, **3**, 35 (1979).

(6) M. Riedmann, *J. Chromatogr.*, **92**, 55 (1974).

(7) S. Dilli and D. N. Phillai, *ibid.*, **137**, 111 (1977).

(8) U. R. Tjaden, J. C. Kraak, and J. F. K. Huber, *ibid.*, **143**, 183 (1977).

(9) A. Castro and H. Malkus, *Res. Commun. Chem. Pathol. Pharmacol.*, **16**, 291 (1977).

(10) A. Castro and R. Mittleman, *Clin. Biochem.*, **11**, 103 (1978).

(11) R. F. Skinner, E. G. Gallaher, and D. B. Predmore, *Anal. Chem.*, **45**, 574 (1973).

(12) R. Saferstein, J. J. Manura, and P. K. De, *J. Forensic Sci.*, **23**, 29 (1978).

(13) M. G. Horning, W. G. Stillwell, J. Nowlin, K. Lertratanangkoon, D. Carroll, I. Dzidic, R. N. Stillwell, E. C. Horning, and R. M. Hill, *J. Chromatogr.*, **91**, 413 (1974).

(14) J. N. T. Gilbert, B. J. Millard, and J. W. Powell, *J. Pharm. Pharmacol.*, **22**, 897 (1974).

(15) J. D. Nicholson, *Analyst*, **103**, 1 (1978).

ACKNOWLEDGMENTS

The authors are grateful to Dr. I. J. McGilveray, Dr. Keith Bailey, and Mr. A. G. Butterfield for helpful discussions and Mr. J.-C. Ethier for mass spectral assistance. They also thank Mrs. Lucie Nantel for blood sampling at the Hotel-Dieu de Montreal Hospital and Dr. G. Caillé for analytical advice. The Medical Research Council of Canada is acknowledged for studentship assistance to F. Varin.

Permeability of Everted Rat Small Intestine to Lidocaine and Derivatives

PETER J. CASCELLA * and STUART FELDMAN ‡x

Received June 11, 1979, from the **College of Pharmacy, South Dakota State University, Brookings, SD 57006*, and the ‡*Department of Pharmaceutics, University of Houston, Houston, TX 77004.* Accepted for publication January 8, 1980.

Abstract □ The transfer rates of lidocaine and five derivatives were measured across the everted rat intestine. No obvious relationship was observed between the first-order rate constants for transfer and the lipophilicity of the compounds as measured by their apparent partition coefficients. The intestinal mucosal epithelium also did not appear to be the rate-limiting barrier for the passage of these agents across the intestinal membrane regardless of the respective clearance of the compound. It is suggested that the ionized form of these agents may be capable of crossing the intestinal barrier at substantial rates, although it is not known if a similar situation exists *in vivo*. The transfer rate is believed to be due to the passage of intact drug and not the metabolite.

Keyphrases □ Lidocaine—determination of transfer and clearance rates of parent drug and analogs across everted rat intestinal mucosa, mucosal concentrations and pH, *in vitro* absorption □ Absorption—lidocaine and derivatives, determination of transfer rates across everted rat intestinal mucosa, *in vitro* □ Permeability—lidocaine and derivatives across everted rat intestinal mucosa, *in vitro* absorption

The *in vitro* everted rat small intestine is a technique that has been utilized as a biological screen for the assessment of drug permeability and may be indicative of *in vivo* absorption problems. Feldman *et al.* (1) found a rank-order agreement between the *in vitro* transfer of prednisolone across the everted rat small intestine in the presence of various substituted propionamides with that reported for *in situ* experiments in the rat. Kaplan and Cotler (2) used the everted rat intestine as a biological screen to assess permeability characteristics of numerous compounds and concluded that this technique, employed along with a dissolution screen, allows evaluation of potential problems in the initial stages of product development.

The nature of the mechanical separation of the intestine from the intact animal imparts inherent advantages and disadvantages to the technique. Separation enables the investigator to control the physical environment of the intestinal preparation and to study some effects of the physicochemical properties of the drugs on the transfer of these agents across the intestinal preparation. However, separation of the intestinal preparation may alter or obliterate some important influencing factors present in the absorption of a compound *in vivo*. Concern has been expressed over viability (2–5), structural integrity (6), and the presence of unnatural absorption barriers.

This study concerned the transfer rates of lidocaine (I) and five experimental derivatives across the everted rat intestine. These compounds were chosen because they represent minor molecular modifications of the parent

0022-3549/80/0600-0643$01.00/0
© 1980, American Pharmaceutical Association

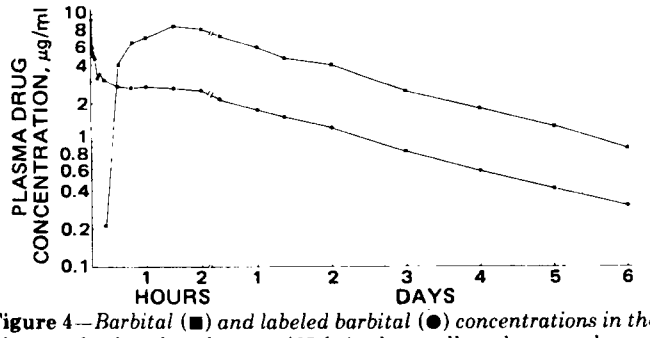

Figure 4—*Barbital (■) and labeled barbital (●) concentrations in the plasma of a female volunteer (65 kg) who swallowed a capsule containing 4.5 mg of barbital sodium/kg and simultaneously received 1.5 mg of [$^{15}N_{1,3}$, $^{13}C_2$]barbital sodium/kg iv (within 20 sec).*

sodium/kg. Blood (7 ml) was withdrawn at intervals over 6 days, and aliquots of plasma (1.0 ml) were assayed for barbital. Concentration–time curves of both isotopes in plasma are illustrated in Fig. 4, and the parallelism observed between their elimination phases strongly supports the evidence that both isotopes behave similarly in the organism.

In conclusion, the described GLC–mass spectrometric procedure is sensitive and specific and should be applicable to studies on the effect of congestive heart failure on barbital disposition.

REFERENCES

(1) D. J. Berry, *J. Chromatogr.*, **86**, 89 (1973).

(2) J. DeGraeve and J. Vanroy, *ibid.*, **129**, 171 (1976).

(3) K. Schweizer, H. Wick, and T. Brechbühler, *Clin. Chim. Acta*, **90**, 203 (1978).

(4) W. Dünges, E. Bergheim-Irps, H. Straub, and R. E. Kaiser, *J. Chromatogr.*, **145**, 265 (1978).

(5) N. Elahi, *J. Anal. Toxicol.*, **3**, 35 (1979).

(6) M. Riedmann, *J. Chromatogr.*, **92**, 55 (1974).

(7) S. Dilli and D. N. Phillai, *ibid.*, **137**, 111 (1977).

(8) U. R. Tjaden, J. C. Kraak, and J. F. K. Huber, *ibid.*, **143**, 183 (1977).

(9) A. Castro and H. Malkus, *Res. Commun. Chem. Pathol. Pharmacol.*, **16**, 291 (1977).

(10) A. Castro and R. Mittleman, *Clin. Biochem.*, **11**, 103 (1978).

(11) R. F. Skinner, E. G. Gallaher, and D. B. Predmore, *Anal. Chem.*, **45**, 574 (1973).

(12) R. Saferstein, J. J. Manura, and P. K. De, *J. Forensic Sci.*, **23**, 29 (1978).

(13) M. G. Horning, W. G. Stillwell, J. Nowlin, K. Lertratanangkoon, D. Carroll, I. Dzidic, R. N. Stillwell, E. C. Horning, and R. M. Hill, *J. Chromatogr.*, **91**, 413 (1974).

(14) J. N. T. Gilbert, B. J. Millard, and J. W. Powell, *J. Pharm. Pharmacol.*, **22**, 897 (1974).

(15) J. D. Nicholson, *Analyst*, **103**, 1 (1978).

ACKNOWLEDGMENTS

The authors are grateful to Dr. I. J. McGilveray, Dr. Keith Bailey, and Mr. A. G. Butterfield for helpful discussions and Mr. J.-C. Ethier for mass spectral assistance. They also thank Mrs. Lucie Nantel for blood sampling at the Hotel-Dieu de Montreal Hospital and Dr. G. Caillé for analytical advice. The Medical Research Council of Canada is acknowledged for studentship assistance to F. Varin.

Permeability of Everted Rat Small Intestine to Lidocaine and Derivatives

PETER J. CASCELLA * and STUART FELDMAN ‡x

Received June 11, 1979, from the **College of Pharmacy, South Dakota State University, Brookings, SD 57006*, and the ‡*Department of Pharmaceutics, University of Houston, Houston, TX 77004.* Accepted for publication January 8, 1980.

Abstract □ The transfer rates of lidocaine and five derivatives were measured across the everted rat intestine. No obvious relationship was observed between the first-order rate constants for transfer and the lipophilicity of the compounds as measured by their apparent partition coefficients. The intestinal mucosal epithelium also did not appear to be the rate-limiting barrier for the passage of these agents across the intestinal membrane regardless of the respective clearance of the compound. It is suggested that the ionized form of these agents may be capable of crossing the intestinal barrier at substantial rates, although it is not known if a similar situation exists *in vivo*. The transfer rate is believed to be due to the passage of intact drug and not the metabolite.

Keyphrases □ Lidocaine—determination of transfer and clearance rates of parent drug and analogs across everted rat intestinal mucosa, mucosal concentrations and pH, *in vitro* absorption □ Absorption—lidocaine and derivatives, determination of transfer rates across everted rat intestinal mucosa, *in vitro* □ Permeability—lidocaine and derivatives across everted rat intestinal mucosa, *in vitro* absorption

The *in vitro* everted rat small intestine is a technique that has been utilized as a biological screen for the assessment of drug permeability and may be indicative of *in vivo* absorption problems. Feldman *et al.* (1) found a rank-order agreement between the *in vitro* transfer of prednisolone across the everted rat small intestine in the presence of various substituted propionamides with that reported for *in situ* experiments in the rat. Kaplan and Cotler (2) used the everted rat intestine as a biological screen to assess permeability characteristics of numerous compounds and concluded that this technique, employed along with a dissolution screen, allows evaluation of potential problems in the initial stages of product development.

The nature of the mechanical separation of the intestine from the intact animal imparts inherent advantages and disadvantages to the technique. Separation enables the investigator to control the physical environment of the intestinal preparation and to study some effects of the physicochemical properties of the drugs on the transfer of these agents across the intestinal preparation. However, separation of the intestinal preparation may alter or obliterate some important influencing factors present in the absorption of a compound *in vivo*. Concern has been expressed over viability (2–5), structural integrity (6), and the presence of unnatural absorption barriers.

This study concerned the transfer rates of lidocaine (I) and five experimental derivatives across the everted rat intestine. These compounds were chosen because they represent minor molecular modifications of the parent

0022-3549/80/0600-0643$01.00/0
© 1980, American Pharmaceutical Association

compound lidocaine and have some similar physicochemical properties, such as molecular weight and size, but a relatively wide degree of difference in their lipophilicity. Previous studies (7) in these laboratories showed that the effect of lidocaine and these derivatives on the pharmacological end-points of overturn and death in goldfish was related to the lipophilicity of these compounds and the effect on the absorption rate.

EXPERIMENTAL

Determination of Transfer Rates of Drugs across Everted Rat Intestine—Sprague–Dawley rats[1], 200–300 g, were fasted 24 hr prior to the experiment. Water was allowed *ad libitum*. The animals were anesthetized with ether, a midline abdominal incision was made, and the intestine was cut at the ileo–cecal junction. The intestine also was cut at the pyloric junction and removed from the animal. The first 15 cm proximal to the pyloric junction was discarded, and the remaining intestinal segment was rinsed inside and out with normal saline.

The proximal portion of the intestine was fastened to a glass rod, and the intestine was everted. Two consecutive 10-cm everted intestinal segments were attached to cannulas, placed in 60 ml of mucosal solution in a test tube, suspended in a constant-temperature water bath[2] at 37°, and oxygenated with 95% oxygen–5% carbon dioxide. The mucosal solution was modified Krebs bicarbonate buffer (8) of either pH 6.4 or 7.4 containing various concentrations of lidocaine or its derivatives[3]. Two milliliters of serosal solution consisting of the modified Krebs bicarbonate buffer without any drug present was introduced into the everted segment *via* a syringe and polyethylene tubing. At the end of the predetermined sampling time, the serosal solution was removed and the serosa was rinsed with 2 ml of the modified Krebs bicarbonate buffer. This rinse was combined with the initial sample and was retained for analysis. Two milliliters of fresh serosal solution then was added to the everted segment for the next sampling interval.

Stripping Experiments—The procedure for the preparation of the segments was modified as follows. Either the proximal or distal segment was stripped of its epithelial layer after eversion by running forceps up and down the length of the segment until the epithelial tissue was sloughed off about the tips of the forceps. The experiment then was performed as described previously.

Assay—The samples were alkalinized by the addition of 1 ml of 2 *N* NaOH and extracted into 10 ml of carbon tetrachloride by shaking[4] for 5 min. The aqueous layer was aspirated, and 8 ml of the organic phase was shaken with 10 ml of 0.004% bromthymol blue in pH 6.0, 0.05 *M* phosphate buffer for 5 min. Following centrifugation[5] for 6 min at 4000 rpm, the bromthymol blue layer was removed by aspiration. Five milliliters of the organic layer and 5 ml of 0.1 *N* NaOH solution were shaken for 5 min, and the samples were centrifuged[6] at 2000 rpm for 5 min. The aqueous supernate was read at 615 nm on a double-beam spectrophotometer[7].

The drug concentration in each sample was determined using absorbance *versus* concentration plots obtained in the described manner which were linear over the concentration range studied.

Qualitative Assay for Metabolites—Everted sacs were attached to cannulas and placed in 60 ml of bathing mucosal solutions consisting of pH 7.4 modified Krebs bicarbonate buffer containing 400 μg of lidocaine/ml. Two milliliters of the buffer was placed on the serosal side of the membrane. A 10-cm long segment of intestine was used as a blank and was placed in an erlenmeyer flask containing the pH 7.4 buffer. All solutions were placed in a constant-temperature water bath at 37° and oxygenated with 95% oxygen–5% carbon dioxide.

At the end of 1 hr, the sacs were removed from the bath and serosal samples were placed in glass bottles. Sacs were washed with 2 ml of the pH 7.4 buffer, which was added to serosal samples. Two milliliters of mucosal solution was taken and added to bottles containing 2 ml of the buffer. To the serosal and mucosal samples, 1 ml of 2 *N* NaOH was added. The treated and untreated sacs were rinsed with distilled water and added to bottles containing 4 ml of the buffer and 1 ml of 2 *N* NaOH.

[1] TIMCO Breeding Laboratories, Houston, Tex.
[2] Thermomix 1420, B Braun Melsungen AG.
[3] Generously supplied by Astra Pharmaceuticals, Worcester, Mass.
[4] Eberbach shaker power unit, No. 6000.
[5] Damon/IEC Division model HN-S centrifuge.
[6] Clay Adams Dynac centrifuge.
[7] Perkin-Elmer model 124.

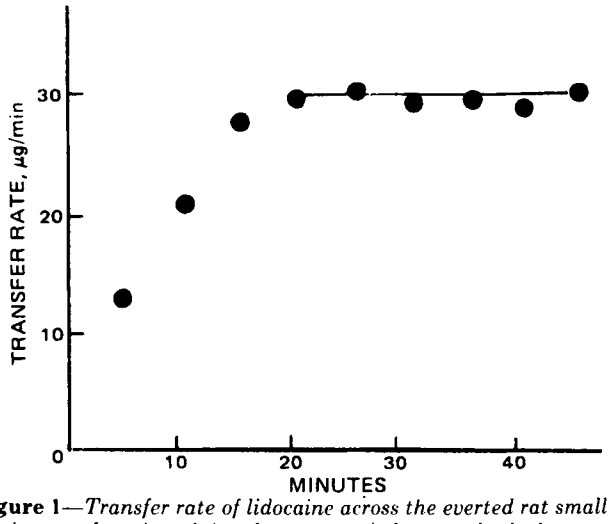

Figure 1—*Transfer rate of lidocaine across the everted rat small intestine as a function of time for a 400-μg/ml mucosal solution.*

Sacs were homogenized[8] and centrifuged[9] at 10,000 rpm for 10 min. The supernate was added to 5 ml of benzene. The serosal and mucosal samples also were added to 5 ml of benzene. All samples then were shaken and centrifuged[6] at 2000 rpm for 5 min. The supernatant benzene then was drawn off and placed in test tubes immersed in a constant-temperature water bath[2], which was maintained at 50° under a continuous-flow air hood until the benzene was evaporated completely.

The evaporated samples were reconstituted with 100 μl of benzene of which 5 μl was injected into a gas–liquid chromatograph[10] equipped with a flame-ionization detector. A 198-cm × 3.2-mm column, packed with 3% OV-17 coated onto 100–120-mesh Gas Chrom Q, was utilized. The

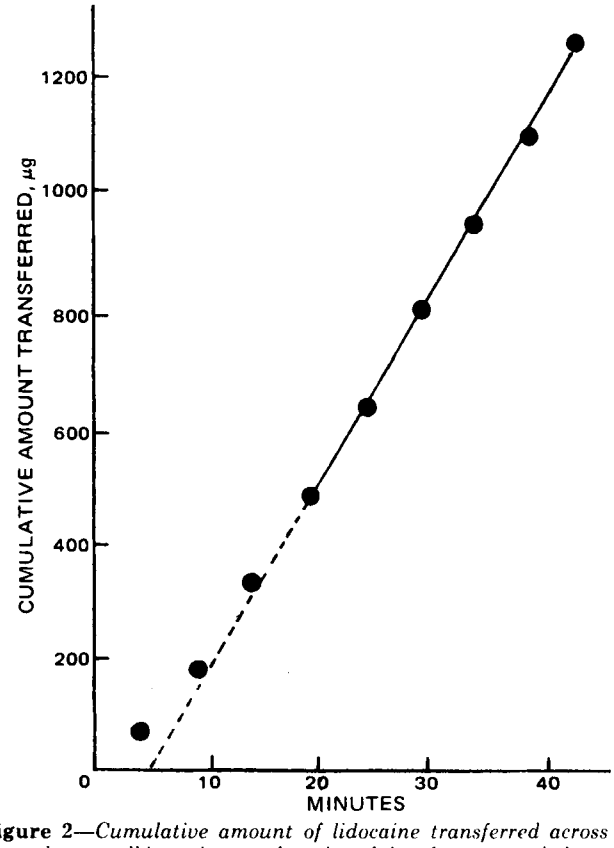

Figure 2—*Cumulative amount of lidocaine transferred across the everted rat small intestine as a function of time for a 400-μg/ml mucosal solution.*

[8] Brinkmann Polytron type PT 10 10 20 3500.
[9] Sorvall RC-5 superspeed refrigerated centrifuge.
[10] Shimadzu GC-4BPTF.

Table I—Average Rates of Transfer and Clearances for Lidocaine at Different Mucosal Concentrations at pH 7.4

Mucosal Concentation, μg/ml	Number of Segments	Slope, μg/min	Clearance, ml/min
200	7	11.64 ± 1.00	0.0582 ± 0.0050
400	12	27.34 ± 2.84	0.0684 ± 0.0071
700	3	40.73 ± 4.84	0.0582 ± 0.0069

Table II—Transfer Rates of Lidocaine for a 200-μg/ml Mucosal Solution

	Transfer Rate, μg/min		
	Proximal Segment		Distal Segment
	11.85		13.30
	11.11		10.16
	11.27		12.39
	11.41		—[a]
Mean	11.41		11.64
SD	0.31		1.61
t		−0.6726	
		$p > 0.05$	

[a] Intestinal preparation was torn

operating temperatures were: injection port, 250°; detector, 260°; and column, 180°. Nitrogen was used as the carrier gas at a flow rate of 42 ml/min.

RESULTS AND DISCUSSION

Drug concentrations in each sample were converted into amounts of the drug, which then were divided by the sampling time to give the average transfer rate (micrograms per minute). The time at which the transfer rate plateaus can be considered as the start of steady-state transfer of drug. A typical plot of the transfer rate as a function of time is illustrated in Fig. 1 for lidocaine. In this example, the time to reach steady state is ~20 min. The cumulative amount of drug transferred as a function of time for each drug was plotted, and a representative plot is illustrated in Fig. 2 for lidocaine. The slope of the line calculated from the values obtained after steady state is achieved represents the transfer rate (micrograms per minute) for the respective compound and was obtained by linear least-squares analysis.

The average transfer rates for lidocaine were determined for 200-, 400-, and 700-μg/ml mucosal concentrations of the drug at pH 7.4. The slopes (transfer rate) of the cumulative amount *versus* time plots as determined by linear least-squares analyses are listed in Table I. The drug clearance is defined as the milliliters of drug solution completely cleared of drug per unit time and can be obtained from:

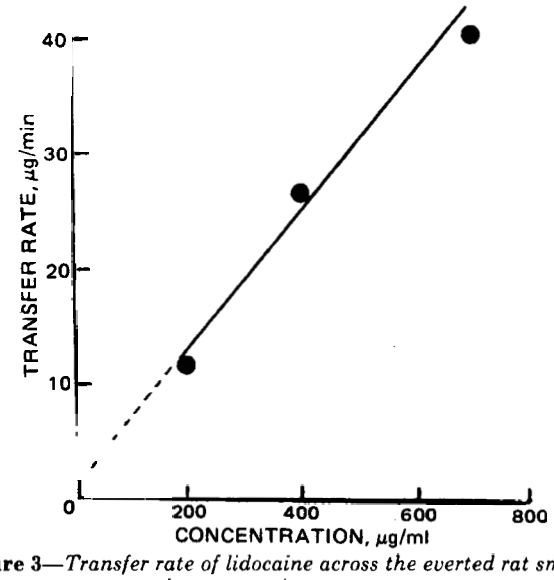

Figure 3—*Transfer rate of lidocaine across the everted rat small intestine* versus *mucosal concentration.*

Table III—Chemical Structure and Physicochemical Parameters

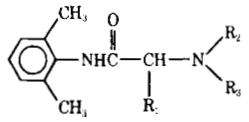

	I	II[a]	III[a]	IV[a]	V[a]	VI[a]
R_1	H	H	CH_3	H	CH_3	CH_3
R_2	C_2H_5	CH_3	CH_3	CH_3	C_2H_5	C_2H_5
R_3	C_2H_5	CH_3	CH_3	C_2H_5	C_2H_5	C_3H_7
pKa	7.72	7.22	7.26	7.53	7.98	7.88
$PC_{hept-buf}$[b]	3.59	0.27	0.79	1.55	9.60	54.56
$PC_{oct-buf}$[c]	68.66	8.75	16.99	19.35	125.86	244.90

[a] Compounds II–VI have the following Astra Pharmaceuticals code numbers: II, W36017; III, W36024; IV, W36004; V, W36023; and VI, W36032. [b] Partition coefficient between *n*-heptane–pH 7.4 buffer. [c] Partition coefficient between *n*-octanol–pH 7.4 buffer.

Table IV—Average Rates of Transfer and Clearances for Local Anesthetic Agents at a 400-μg/ml Mucosal Concentration at pH 7.4

Compound	Number of Segments	Slope, μg/min	Clearance, ml/min	K, min^{-1}
I	12	27.34 ± 2.84	0.0684 ± 0.0071	0.00114
II	7	17.59 ± 1.76	0.0440 ± 0.0044	0.00073
III	4	15.03 ± 0.70	0.0376 ± 0.0018	0.00063
IV	4	23.42 ± 3.49	0.0585 ± 0.0087	0.00098
V	4	22.83 ± 1.48	0.0571 ± 0.0037	0.00095
VI	4	19.60 ± 1.99	0.0490 ± 0.0050	0.00082

$$Cl = \frac{\Delta x/\Delta t}{C} \qquad \text{(Eq. 1)}$$

where Cl is the clearance of the respective compound, $\Delta x/\Delta t$ is the rate of drug transferred from the driving-force compartment (mucosal solution), and C is the drug concentration in the driving-force compartment. If one assumes that the transfer of drug occurs *via* a passive first-order process, then the drug clearance would be expected to be identical at the different concentrations since the clearances are reflective of a rate of transfer per unit concentration. Inspection of Table I shows no obvious trend of clearance with respect to drug concentration in the mucosal solution. A linear relationship is observed between the average transfer rates and the drug concentration in the mucosal solution (Fig. 3). The average clearance of lidocaine obtained from the slope of the transfer rate *versus* concentration plot was 0.0571 ml/min.

Since the experiments used two segments from the same intestinal preparation of each rat, a statistical analysis was performed to determine whether selection of one segment over another led to significant differences in the observed rates. In general, the selection of one segment over another probably is of greater concern for a drug transported by an active process due to site specificity of the carrier. However, if the size or composition of the intestinal barrier were to change dramatically from one segment to another, changes in the transfer rates reflecting these alterations might be observed.

A *t* test was utilized to determine if any significant differences existed between the proximal and distal segments of the intestinal preparations in terms of transfer rates for the 200-μg/ml mucosal solution (Table II). No differences were found for transfer rates with regard to the segment of the intestinal preparation used. Therefore, no distinction will be made between the proximal and distal segments employed in this study.

Table III includes the structural formulas for lidocaine and the five derivatives. Molecular modification of the lidocaine molecule involves the substitution of methyl, ethyl, and propyl groups at the R_1, R_2, and R_3 positions of the lidocaine molecule. The pKa values of the compounds ranged from 7.22 for II to 7.98 for V. The partition coefficients between *n*-heptane–pH 7.4 buffer[11] and *n*-octanol–pH 7.4 buffer[12] also are listed in Table III.

The transfer rates and clearances for the lidocaine derivatives also were determined utilizing a 400-μg/ml mucosal concentration (Table IV). The

[11] Reported by Astra Pharmaceuticals.
[12] Determined in this laboratory.

Table V—Rank-Order Relationship for Lidocaine and Five Derivatives

Rank	Partition Coefficient (*n*-heptane–pH 7.4 buffer)	Partition Coefficient (*n*-octanol–pH 7.4 buffer)	Rate Constant
1[a]	VI	VI	I
2	V	V	IV
3	I	I	V
4	IV	IV	VI
5	III	III	II
6	II	II	III

[a] The largest value.

apparent rates ranged from 15.03 ± 0.70 μg/min for III (clearance of 0.0380 ml/min) to 27.34 ± 2.84 μg/min for lidocaine (I) (clearance of 0.68 ml/min). Dividing the rate (micrograms per minute) by the total amount of drug (micrograms) in the mucosal solution or dividing the clearance by the volume of mucosal solution yields the apparent first-order rate constant (Table IV).

Table V gives the rank ordering of lidocaine and the five derivatives in terms of the apparent rate constant and partition coefficient. No apparent relationship appears to exist between the first-order rate constants for transfer and the partition coefficients. Kakemi *et al.* (9) demonstrated a rather good logarithmic relationship between the gastric absorption rate constants for numerous barbiturate derivatives and their corresponding partition coefficients. Plots of the logarithm of the apparent rate constant as a function of the logarithm of the partition coefficient between *n*-heptane–pH 7.4 buffer and *n*-octanol–pH 7.4 buffer are illustrated in Figs. 4 and 5. No relationship appears to exist between the observed transfer rate constants and the partition coefficient regardless of which partition coefficient is used.

To determine if the ionized form of the drug moiety also is capable of being transferred across the everted rat intestine, experiments were performed using lidocaine at pH 6.4 and a mucosal concentration of 400 μg/ml. Figure 6 is a representative plot of the transfer rate of lidocaine as a function of time. The transfer rates were obtained from the cumulative amount *versus* time plots, and the average transfer rates of lidocaine are listed in Table VI. The average transfer rate at pH 7.4 was ~27 μg/min; at pH 6.4, it was ~22 μg/min. A Student *t* test showed that the difference in rates at the two different pH values was significant ($p < 0.001$). It is possible, by using simultaneous equations, to calculate the approximate transfer rates for the unionized and ionized species. The transfer rate is given by:

$$R_t = f_i R_i + f_u R_u \qquad \text{(Eq. 2)}$$

where R_t is the total transfer rate, f is the fraction of drug that exists as a specific species, and R_i and R_u are the respective transfer rates of the ionized and unionized species. Substituting the average transfer rate and the drug fraction that exists as each respective species yields at pH 7.4:

$$27.34 = 0.68R_i + 0.32R_u \qquad \text{(Eq. 3)}$$

and at pH 6.4:

$$22.16 = 0.95R_i + 0.05R_u \qquad \text{(Eq. 4)}$$

Multiplying Eq. 3 by 1.39706 and subtracting from Eq. 4 yield:

$$-16.036 = -0.397R_u \qquad \text{(Eq. 5)}$$

Multiplying both sides of Eq. 5 by −1 and solving for R_u yield:

$$40.39\ \mu g/min = R_u \qquad \text{(Eq. 6)}$$

Substituting 40.39 back into Eq. 3 and solving for R_i yield:

$$21.20\ \mu g/min = R_i \qquad \text{(Eq. 7)}$$

It appears that the ionized species is capable of crossing the everted rat small intestine at a relatively high rate. Whether the same situation exists *in vivo* is not known. The ability of the ionized species to cross the *in vitro* intestinal preparation may be a manifestation of the mechanical process of everting the intestine as well as a loss of structural integrity with time.

Since the *in vitro* everted rat intestine includes the presence of unnatural absorption barriers, evaluation of whether differences in the transfer rates would occur if the intestinal mucosal epithelium was

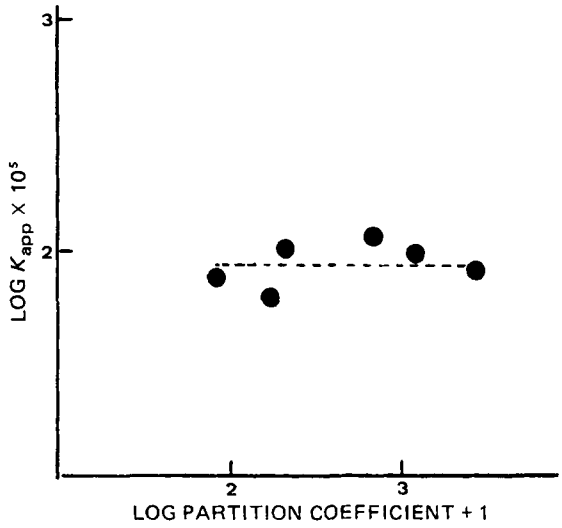

Figure 5—*Log–log plot of apparent transfer rate constants for anesthetic agents across the everted rat small intestine as a function of the partition coefficient* (n-*octanol–pH 7.4 buffer*).

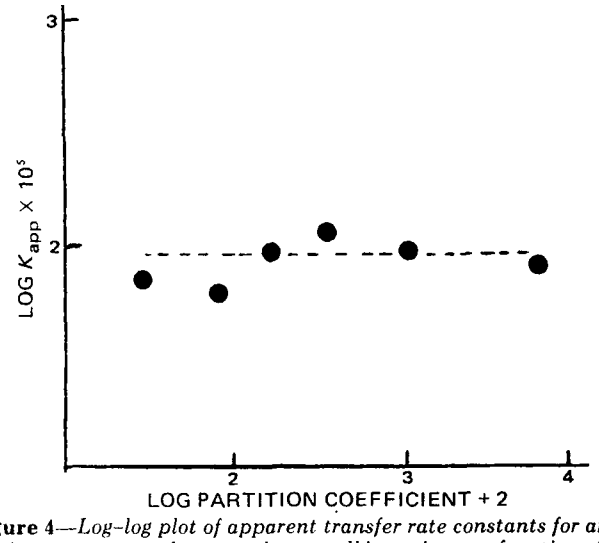

Figure 4—*Log–log plot of apparent transfer rate constants for anesthetic agents across the everted rat small intestine as a function of the partition coefficient* (n-*heptane–pH 7.4 buffer*).

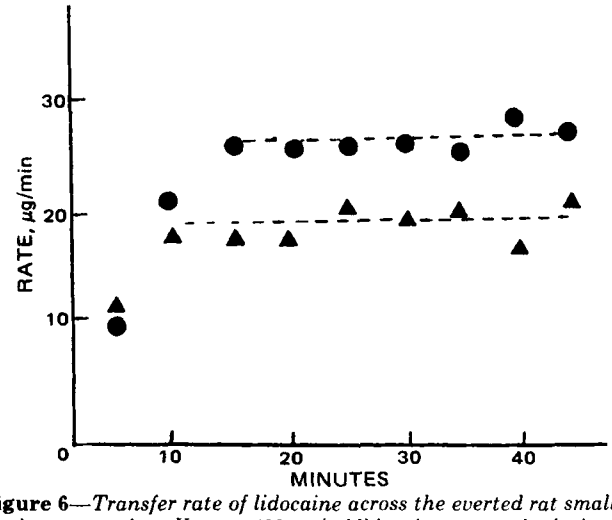

Figure 6—*Transfer rate of lidocaine across the everted rat small intestine* versus *time. Key:* ▲, *400-μg/ml lidocaine mucosal solution, pH 6.4; and* ●, *400-μg/ml lidocaine mucosal solution, pH 7.4.*

Table VI—Average Rates of Transfer and Clearance of Lidocaine (400 μg/ml) at pH 6.4 and 7.4

pH	Number of Segments	Rate, μg/min	Clearance, ml/min
7.4	12	27.34 ± 2.84	0.0684 ± 0.0071
6.4	7	22.15 ± 1.98	0.0554 ± 0.0050

Table VII—Average Transfer Rates for Lidocaine and II across Stripped and Unstripped Intestinal Segments at pH 7.4 and 6.4

Compound	Intestinal Segment[a]	pH	Transfer Rate, μg/min
I	Stripped	7.4	25.70 ± 2.84
I	Unstripped	7.4	26.79 ± 4.22
I	Stripped	6.4	21.27 ± 2.57
I	Unstripped	6.4	22.62 ± 1.36
II	Stripped	7.4	17.64 ± 2.80
II	Unstripped	7.4	16.66 ± 1.72

[a] Three segments were used.

stripped from the intestinal segments was desired. In the *in vitro* model, the intestinal mucosal epithelium represents a distinct barrier that may be rate limiting *in vivo*. Experiments were performed utilizing a 400-μg/ml mucosal concentration of lidocaine at pH 7.4 and 6.4. Stripping was performed alternately on the proximal and distal segments of the intestinal preparations. A representative plot of the cumulative amount transferred as a function of time is illustrated in Fig. 7. The rates for the stripped and unstripped segments at pH 7.4 and 6.4 are listed in Table VII. Statistical analysis using the Student t test showed that the transfer rates of lidocaine were not significantly ($p > 0.05$) different between the stripped and unstripped segments at either pH studied. Since the fraction of unionized and ionized species changed dramatically between the two pH values studied and the rates for the stripped and unstripped were the same, the intestinal mucosal epithelium apparently is not the rate-limiting barrier for either species.

Since previous studies (10, 11) suggested that the intestinal mucosal epithelium may be rate limiting for compounds with low clearances and not for compounds with high clearances, it was decided to evaluate whether the intestinal mucosal epithelium was rate limiting for one compound with a lower clearance than lidocaine. Compound III would have been the ideal selection, but lack of a sufficient quantity prohibited its use. Therefore, II was chosen. It has a clearance of 0.0439 ml/min and was utilized with stripping again performed alternately on the proximal and distal segments. The results are listed in Table VII, with the statistical analysis using the Student t test showing no significant difference ($p > 0.05$) between the transfer rates of the stripped and unstripped intestinal segments. Therefore, II, which has the next to lowest clearance value of the drugs investigated, also does not appear to be rate limited in its transfer by the intestinal mucosal membrane.

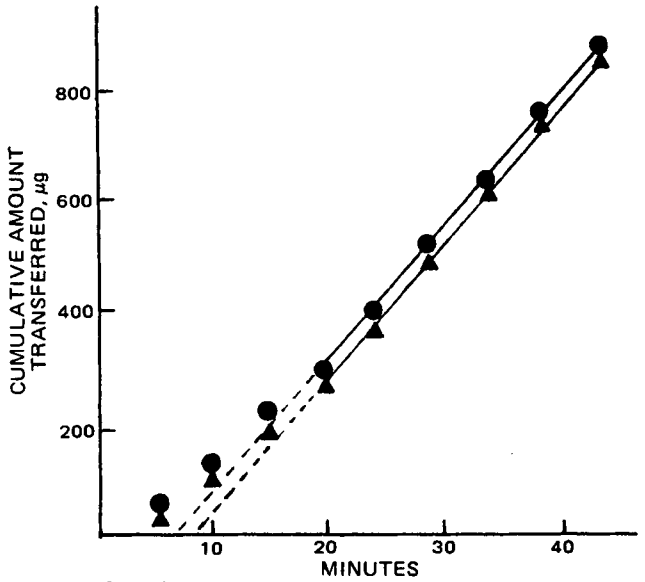

Figure 7—*Cumulative amount of lidocaine transferred across the everted rat small intestine as a function of time from a 400-μg/ml mucosal solution. Key: ●, unstripped intestinal preparation; and ▲, stripped intestinal preparation.*

Since the absorption rate of a drug *in vivo* can be defined as the rate of appearance of free unchanged drug, a qualitative evaluation was performed to determine if the transfer rate of the drug *in vitro* represents the transfer rate of the parent molecule and not the metabolite formed by a first-pass intestinal metabolic phenomenon. Everted sacs were suspended in mucosal solutions containing 400 μg of lidocaine/ml in the pH 7.4 buffer. The inside of the sac (serosa) also was filled with 2 ml of the same solutions. At the end of the predetermined incubation time, the mucosal solution, serosal solution, and tissue homogenates were assayed by GLC.

Only one peak was evident in all of the samples for the mucosal and serosal solutions and for the proximal or distal tissue homogenates. These samples all had the same retention time (10 min) as the control lidocaine samples. No peaks indicative of a lidocaine metabolite were observed[13]. Since amide-linked local anesthetics are metabolized almost completely by the liver in both humans (12) and rats (13), it appears reasonable to conclude that the transfer rates of the compounds across the everted rat small intestine are reflective of the transfer of intact drug.

From these results, it appears that the anesthetic agents are absorbed across the everted rat small intestine by a passive process with no apparent metabolism. The ionized drug molecule also is capable of crossing the membrane at appreciable rates, although it is somewhat lower than the unionized species. No apparent relationship was found between the rate constants and their respective lipophilicity. This result is in contrast to previous studies in goldfish (7). Removal of the epithelial layer by stripping did not appear to affect the transfer rates significantly, regardless of the clearance of the compound or the pH of the bathing solution. Thus, the intestinal mucosal epithelium apparently is not the rate-limiting barrier for the transfer of these compounds across the everted rat small intestine. The relationship between the parameters obtained in the present *in vitro* study and absorption of these agents in an intact animal remains to be evaluated.

REFERENCES

(1) S. Feldman, J. Richardson, C. Freeman, S. Pollock, J. Berger, F. Kaplan, and G. Rhoa, *J. Pharm. Sci.*, **63**, 454 (1974).

(2) S. A. Kaplan and S. Cotler, *ibid.*, **61**, 1361 (1972).

(3) J. W. L. Robinson and J. P. Felber, *Gastroenterologia*, **105**, 17 (1966).

(4) D. R. Branford, *Proc. R. Soc., Ser. B*, **166**, 30 (1966).

(5) R. Jordana and F. Ponz, *Rev. Esp. Fisiol.*, **25**, 225 (1969).

(6) R. R. Levine, W. F. McNary, P. J. Kornguth, and R. LeBlanc, *Eur. J. Pharmacol.*, **9**, 211 (1970).

(7) P. J. Cascella and S. Feldman, *J. Pharm. Sci.*, **68**, 401 (1979).

(8) H. A. Krebs, *Biochim. Biophys. Acta*, **4**, 249 (1950).

(9) K. Kakemi, T. Arita, R. Hori, and R. Konishi, *Chem. Pharm. Bull.*, **15**, 1534 (1967).

(10) M. Gibaldi and B. Grundhofer, *J. Pharm. Sci.*, **61**, 116 (1972).

(11) M. Gibaldi and B. Grundhofer, *Proc. Soc. Exp. Biol. Med.*, **141**, 564 (1972).

(12) R. H. deJong, "Physiology and Pharmacology of Local Anesthesia," Charles C Thomas, Springfield, Ill., 1970, chap. 12.

(13) E. Hansson, in "International Encylopedia of Pharmacology and Therapeutics," vol. I, section 8, P. Lechat, Ed., Pergamon, Oxford, England, 1971, chap. 6.

[13] Further work showed that known lidocaine metabolites do not interfere with the assay for lidocaine.

Lipophilicity, Molecular Weight, and Drug Action: Reexamination of Parabolic and Bilinear Models

ERIC J. LIEN ˣ **and P. H. WANG**

Received October 4, 1979, from the *Section of Biomedicinal Chemistry, School of Pharmacy, University of Southern California, Los Angeles, CA 90033.* Accepted for publication January 7, 1980.

Abstract □ The effect of molecular weight on drug diffusion and drug action has been described based on the relation $D = (RT/6\pi\eta N)(\sqrt[3]{4\pi N/3M\bar{v}})$, an inverse relation between the clearance of drugs through artificial membranes and molecular weights, and apparent correlations between log (1/dose) and log mol. wt. for various central nervous system-acting drugs, anticancer drugs, and water-soluble vitamins. *In situ* rat jejunum permeability data of various drugs were correlated with log P (octanol–buffer) and log mol. wt. A parabolic equation of log P combined with log mol. wt. proposed previously was shown to give significant correlations for hydrolysis data of amides and antifungal data of amines. This model is mathematically simpler and easier to interpret than the more complex curvilinear and bilinear models.

Keyphrases □ Molecular weight—effect on drug diffusion and activity, parabolic model □ Diffusion—effect of molecular weight, parabolic model □ Structure–activity relationships—effect of molecular weight, parabolic model

While the importance of lipophilicity (partition coefficient) in drug action has been well recognized (1, 2), the effect of molecular weight on the biological activity of drugs has not been appreciated fully. This report discusses the rationale of including a log mol. wt. term in quantitative structure–activity correlations by using specific examples of drug absorption data and *in vitro* biological data. Statistical analysis is employed to assess the significant contribution of the log mol. wt. term above and beyond the contribution from lipophilicity (log P).

MATHEMATICAL MODELS

Few of the various mathematical models developed (3–12) include the effect of the change in molecular weight among homologs, analogs, or congeners (13, 14). Several of these models are discussed here.

Model A—A parabolic model based on a nonsteady-state theory (3–5):

$$\log 1/C = -k(\log P)^2 + k' \log P + k'' \qquad \text{(Eq. 1)}$$

where C is the drug concentration required to produce a standard biological response (*e.g.*, ED_{50} and I_{50}), P is the 1-octanol–water partition coefficient, and k, k', and k'' are derived by the least-squares method.

Model B—The curvilinear model of Franke and Oehme (7):

$$\log 1/C = a \log P + b \qquad \text{for } \log P < \log P_x \qquad \text{(Eq. 2a)}$$

$$\log 1/C = \alpha(\log P)^2 + \beta(\log P) + \gamma \qquad \text{for } \log P > \log P_x \qquad \text{(Eq. 2b)}$$

where α, β, and γ are derived by least-squares fit and P_x is the limit of the straight line.

Model C—A bilinear model (8, 9):

$$\log 1/C = a \log P - b \log(\beta P + 1) + c \qquad \text{(Eq. 3)}$$

where a, b, β, and c are coefficients derived from the regression analysis.

Model D—The Hyde model (10):

$$\log C = \text{constant} + \log(a + 10^{-\pi}) \qquad \text{(Eq. 4)}$$

where π is the Hansch π constant.

Model E—The Higuchi–Davis model (equilibrium model) (11):

$$D = C_w V_w + \sum_{i=1}^{i=t} C_i V_i \qquad \text{(Eq. 5)}$$

$$C_w = \frac{D}{V_{aq} + P_i V_i} \qquad \text{(Eq. 6)}$$

$$C_r = C_w P_r = \frac{DP_r}{V_w + \sum_{i=1}^{i=t} P_i V_i} \qquad \text{(Eq. 7)}$$

where D is the amount of drug, C_w is the concentration in the water phase, C_r is the drug concentration on the receptor, and $P_i = C_i/C_w$.

Model F—The asymptotic model of Ho *et al.* (12):

$$P^*_{app} = \frac{1}{\frac{1}{P^*_{aq}} + \frac{1}{P^*_p + P^*_{e,lipid}}} \qquad \text{(Eq. 8)}$$

where P^*_{app} is the predicted apparent permeability coefficient; P^*_{aq}, P^*_p, and $P^*_{e,lipid}$ are the permeability coefficients of the aqueous diffusion layer, aqueous pores, and lipid membrane diffusion–bioconversion pathway, respectively; and $P^*_{e,lipid} = (10^{n\pi}/X_s)$, where X_s is the fraction of the undissociated form.

Model G—The Lien model (13):

$$\log \%\,\text{Abs. or } \log k = -k_1(\log P)^2 + k_2(\log P) + m[\log(U/D)] + n(\log \text{mol. wt.}) + q(\log \chi) + k_3 \qquad \text{(Eq. 9)}$$

where U/D = (pKa − pH) for acids and χ is a parameter to account for branching or stereochemical factors.

Regardless of the fact that in many instances there is a high degree of covariance between the partition coefficient (log P) and the molecular weight (log mol. wt.) while in other cases there may not be a wide spread in the molecular weight, the molecular weight may affect both *in vitro* drug diffusion and *in vivo* drug action in the following ways:

1. An inverse relationship exists between the diffusion coefficient (D) and the molecular weight [(mol. wt.)$^{1/3}$] according to the Sutherland and Einstein equation:

$$D = \frac{RT}{6\pi\eta r N} = \frac{RT}{6\pi\eta N}\sqrt[3]{\frac{4\pi N}{3M\bar{v}}} \qquad \text{(Eq. 10)}$$

where η is the viscosity of the solution, r is the radius of the spherical particle, N is Avogadro's number, $\bar{v}$ is the partial specific volume in cubic centimeters per gram of the solute, and M is the molecular weight (15, 16).

2. An inverse relationship exists between log clearance and log mol. wt. for clearance through artificial membranes and possibly through biological membranes and the kidneys as well according to (17):

$$\log \text{clearance} = -0.432 \log \text{mol. wt.} + 2.701 \qquad n = 6 \quad r = 0.997 \quad s = 0.016 \qquad \text{(Eq. 11)}$$

for drugs with molecular weights less than 1000.

3. Direct apparent correlations appear to exist between log (1/dose) and log mol. wt. of various central nervous system-acting drugs, anticancer drugs, and water-soluble vitamins (14).

Accumulated data have shown that in many cases where a bilinear model gives a better correlation than a parabolic model, one can obtain equally good correlation simply by including a log mol. wt. term in the equation. Furthermore, when log $1/C$ or log K is corrected for the difference in log mol. wt., a bilinear dependence on log P usually is restored to a parabolic dependence (or only part of a parabola) (Eqs. 12–21 and Figs. 1–3).

RESULTS AND DISCUSSION

The biological data and the physicochemical constants used in the regression analysis are summarized in Tables I–III.

Equations 12–17 were derived from the data of Ho *et al.* (12). Since

0022-3549/80/0600-0648$01.00/0
© 1980, American Pharmaceutical Association

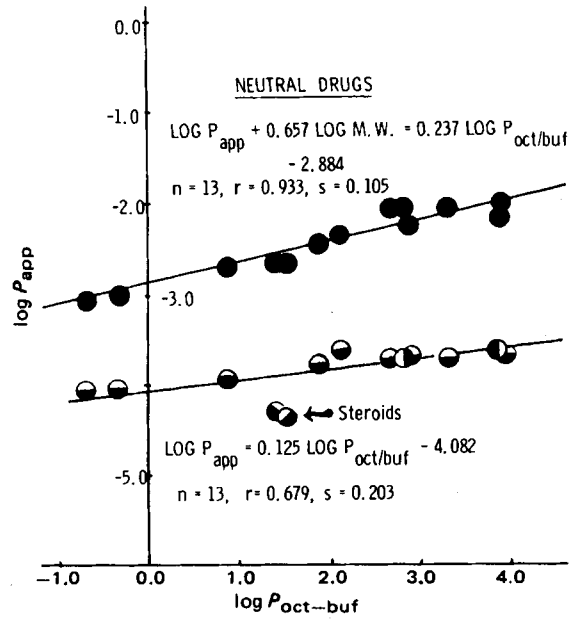

Figure 1—*Linear dependence of the apparent permeability coefficient on the uncorrected octanol–buffer (pH 6.0) partition coefficient for 13 neutral compounds. Lower permeability coefficients (log P_{app}) for the steroids result when the log mol. wt. term is not included.*

the uncorrected octanol–buffer (pH 6.0) partition coefficients were used, no apparent correlation could be obtained when both neutral and acidic drugs were included. When these two groups were separated, statistically highly significant correlations were obtained, as judged from the correlation coefficient r and the standard deviation s of the regression for permeability (log P_{app}) through the rat jejunum with high stirring (12).

For both neutral and acidic drugs, the equations are:

$$\log P_{app} = 0.090 \log P_{(oct\text{-}buf)} - 3.967$$
$$n = 24 \quad r = 0.407 \quad s = 0.258 \qquad \text{(Eq. 12)}$$

$$\log P_{app} = 0.183 \log P_{(oct\text{-}buf)} - 0.689 \log \text{mol. wt.} - 2.627$$
$$n = 24 \quad r = 0.740 \quad s = 0.195 \qquad \text{(Eq. 13)}$$

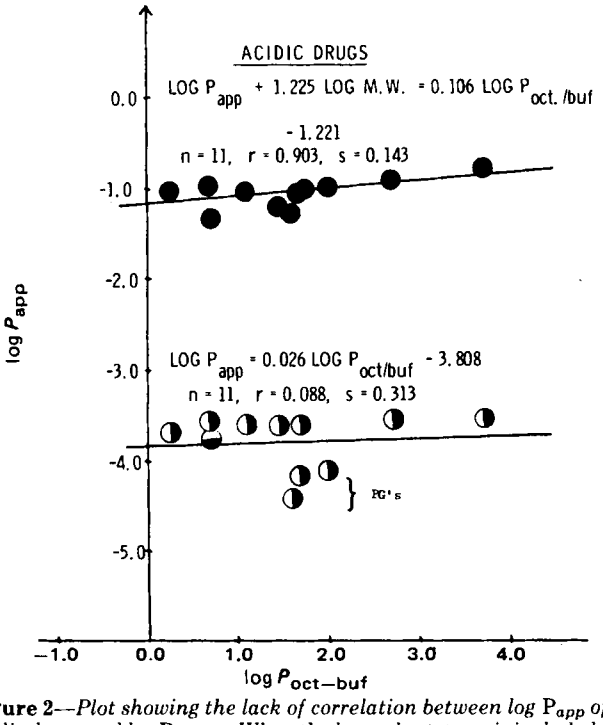

Figure 2—*Plot showing the lack of correlation between log P_{app} of 11 acidic drugs and log $P_{oct\text{-}buf}$. When the log mol. wt. term is included, the correlation becomes statistically significant.*

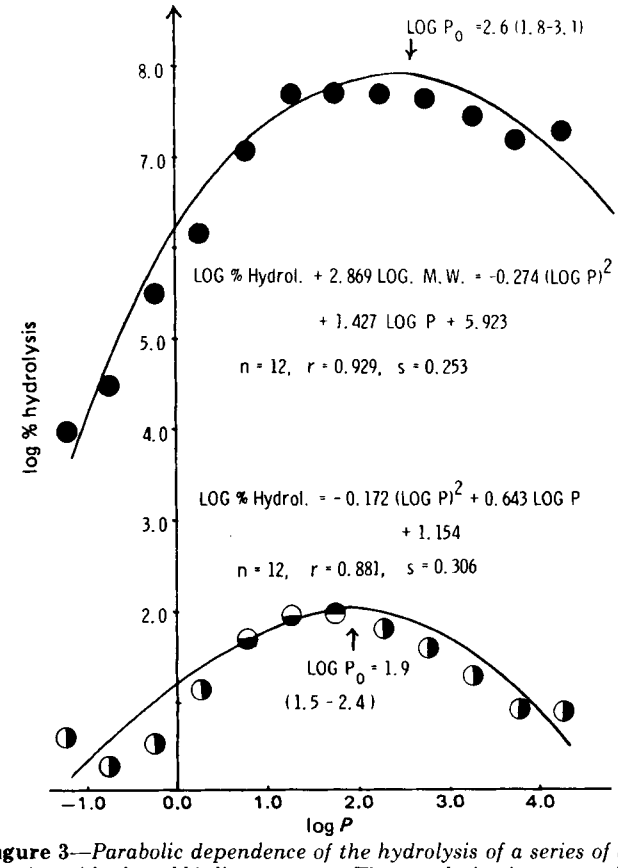

Figure 3—*Parabolic dependence of the hydrolysis of a series of aliphatic amides by rabbit liver extracts. The correlation improves when the log mol. wt. term is included.*

For neutral drugs only, they are:

$$\log P_{app} = 0.125 \log P_{(oct\text{-}buf)} - 4.082$$
$$n = 13 \quad r = 0.679 \quad s = 0.203 \qquad \text{(Eq. 14)}$$

$$\log P_{app} = 0.237 \log P_{(oct\text{-}buf)} - 0.657 \log \text{mol. wt.} - 2.884$$
$$n = 13 \quad r = 0.933 \quad s = 0.105 \qquad \text{(Eq. 15)}$$

For acidic drugs only, they are:

$$\log P_{app} = 0.026 \log P_{(oct\text{-}buf)} - 3.808$$
$$n = 11 \quad r = 0.088 \quad s = 0.313 \qquad \text{(Eq. 16)}$$

$$\log P_{app} = 0.106 \log P_{(oct\text{-}buf)} - 1.225 \log \text{mol. wt.} - 1.221$$
$$n = 11 \quad r = 0.903 \quad s = 0.143 \qquad \text{(Eq. 17)}$$

The log mol. wt. term is significant at the 99.95 percentile level in Eqs. 15 and 17 as indicated by an F test ($F_{1,10} = 31.4$ and $F_{1,8} = 35.1$, respectively).

For the limited data available, addition of the $(\log P)^2$ term did not result in significant improvement in the correlation.

Equations 18 and 19 were derived from the data of Bray *et al.* (18) on the hydrolysis of aliphatic amides by amidase from rabbit liver extract:

$$\log \% \text{ hydrolysis} = -0.172 (\log P)^2 + 0.643 \log P + 1.154$$
$$n = 12 \quad r = 0.881 \quad s = 0.306 \qquad \text{(Eq. 18)}$$

$$\log \% \text{ hydrolysis} = -0.274 (\log P)^2 + 1.427 \log P - 2.869 \log \text{mol. wt.} + 5.923$$
$$n = 12 \quad r = 0.929 \quad s = 0.253 \qquad \text{(Eq. 19)}$$

The addition of the log mol. wt. term to the parabolic equation of log P again significantly improves the correlation at the 90 percentile level ($F_{1,8} = 5.12$).

Equations 20 and 21 were derived from the antifungal data of a series of aliphatic amines against *Rhinocladium beurmanni* (19):

$$\log 1/C = -0.199 (\log P)^2 + 2.119 \log P - 1.382$$
$$n = 15 \quad r = 0.967 \quad s = 0.354 \qquad \text{(Eq. 20)}$$

Table I—*In Situ* Permeability Coefficients and Physicochemical Constants Used in the Regression Analysis for Rat Jejunum Data

Compound	log P_{app}, cm/sec Exp.[a]	log P_{app}, cm/sec Calc.[b]	log mol. wt.	log P (oct–buf)[a]
Neutral				
Methanol	−4.036	−4.029	1.506	−0.66
Ethanol	−4.081	−4.052	1.663	−0.32
Butanol	−3.896	−3.904	1.870	0.88
Hexanol	−3.726	−3.758	2.009	1.88
Octanol	−3.609	−3.591	2.115	2.88
Decanol	−3.597	−3.414	2.205	3.88
Hydrocortisone	−4.310	−4.202	2.559	1.53
Prednisolone	−4.292	−4.227	2.557	1.42
Progesterone	−3.635	−3.601	2.498	3.90
Benzene	−3.558	−3.623	1.893	2.13
Acidic				
Prostaglandin F_2	−4.377	−4.175[c]	2.550	1.60
Prostaglandin E_2	−4.167	−4.162	2.547	1.69
Prostaglandin E_1	−4.081	−4.133	2.550	2.00
Butyric acid	−3.726	−3.525	1.945	0.74
Hexanoic acid	−3.578	−3.566	2.065	1.74
Octanoic acid	−3.530	−3.575	2.159	2.74
Decanoic acid	−3.506	−3.564	2.236	3.74
Phenol	−3.616	−3.484	1.974	1.46
Benzoic acid	−3.587	−3.660	2.087	1.11
Phenylacetic acid	−3.585	−3.761	2.134	0.70
Salicylic acid	−3.668	−3.813	2.140	0.28

[a] Taken from Ref. 12. [b] Calculated from Eq. 15. [c] Calculated from Eq. 17.

Table II—Hydrolysis of Aliphatic Amides by Rabbit-Liver Extracts and Physicochemical Parameters Used in the Regression Analysis

Amide	log % Hydrolysis Exp.[a]	log % Hydrolysis Calc.[b]	log mol. wt.	log P (oct–water)[c]
CH_3	0.602	0.418	1.177	−1.21
C_2H_5	0.301	0.574	1.463	−0.71
C_3H_7	0.544	0.617	1.741	−0.21[d]
C_4H_9	1.114	1.273	1.757	0.29
C_5H_{11}	1.748	1.566	1.852	0.79
C_6H_{13}	1.964	1.605	1.988	1.29
C_7H_{15}	1.964	1.873	1.996	1.79
C_8H_{17}	1.806	1.860	2.054	2.29
C_9H_{19}	1.597	1.731	2.105	2.79
$C_{10}H_{21}$	1.255	1.481	2.150	3.29
$C_{11}H_{23}$	0.903	1.106	2.191	3.79
$C_{12}H_{25}$	0.903	0.602	2.229	4.29

[a] Taken from Ref. 18. [b] Calculated from Eq. 19. [c] Calculated from the value of $C_3H_7CONH_2$ by subtracting or adding 0.50 for each CH_2 unit. [d] Experimentally determined value taken from A. Leo, C. Hansch, and D. Elkins, *Chem. Rev.*, **71**, 525 (1971).

$$\log 1/C = -0.499 (\log P)^2 + 8.010 \log P - 42.691 \log \text{mol. wt.} + 74.281$$
$$n = 15 \quad r = 0.994 \quad s = 0.161 \qquad \text{(Eq. 21)}$$

The log mol. wt. term in Eq. 21 is significant at the 99.95 percentile level ($F_{1,11} = 46.7$). The relatively large coefficient associated with the log mol. wt. term and the large constant term in Eq. 21 probably are due to the fact that the log mol. wt. values range only from 1.864 to 2.431. Similarly, high coefficients were obtained for many other sets of antimicrobial data from the same and other sources. In some cases when the parabolic equation of log P gave an almost perfect correlation ($r \geq 0.97$), the addition of the log mol. wt. term did not further improve the correlation. In reality, when one considers the experimental errors involved, a correlation coefficient of ~0.95–0.97 (r^2 of ~0.90–0.94) probably is the maximum limit one should expect.

The data suggest that the semiempirical model of Lien (13) can be used when there is a fairly wide spread in the molecular weights of the drug molecules. The advantages of this model are the simplicity of the mathematical equation (one can use any standard linear or nonlinear regression programs) and the more understandable physical meaning linking diffusion and molecular weight.

Table III—Antifungal Activities of Aliphatic Amines against *Rhinocladium beurmanni* and Physicochemical Constants Used in the Correlation

Amine	log 1/C, M Exp.[a]	log 1/C, M Calc.[b]	log mol. wt.	log P (oct–water)[c]
C_4H_9	0.663	0.866	1.864	0.81
C_5H_{11}	1.190	1.098	1.940	1.31
C_6H_{13}	1.675	1.551	2.005	1.81
C_7H_{15}	2.151	2.095	2.062	2.31
C_8H_{17}	2.621	2.732	2.111	2.81
C_9H_{19}	3.075	3.290	2.156	3.31
$C_{10}H_{21}$	3.536	3.770	2.197	3.81
$C_{11}H_{23}$	3.983	4.171	2.234	4.31
$C_{12}H_{25}$	4.388	4.451	2.268	4.81
$C_{13}H_{27}$	4.629	4.567	2.300	5.31
$C_{14}H_{29}$	4.709	4.562	2.329	5.81
$C_{15}H_{31}$	4.397	4.350	2.357	6.31
$C_{16}H_{33}$	3.882	3.974	2.383	6.81
$C_{17}H_{35}$	3.307	3.434	2.407	7.31
$C_{18}H_{37}$	2.530	2.645	2.431	7.81

[a] Taken from Ref. 19. [b] Calculated from Eq. 21. [c] Taken from E. J. Lien, C. Hansch, and S. M. Anderson, *J. Med. Chem.*, **11**, 430 (1968); higher homologs were calculated by adding 0.50 for each CH_2 unit.

REFERENCES

(1) E. Overton, "Studien über Narkose," Fisher, Jena, East Germany, 1901.

(2) H. Meyer, *Arch. Exp. Pathol. Pharmakol.*, **42**, 109 (1899). *Ibid.*, **46**, 338 (1901).

(3) C. Hansch, A. R. Steward, S. M. Anderson, and D. Bentley, *J. Med. Chem.*, **11**, 1 (1968).

(4) E. J. Lien, C. Hansch, and S. M. Anderson, *ibid.*, **11**, 430 (1968).

(5) J. T. Penniston, L. Beckett, D. L. Bentley, and C. Hansch, *Mol. Pharmacol.*, **5**, 333 (1969).

(6) C. Hansch and J. M. Clayton, *J. Pharm. Sci.*, **62**, 1 (1973).

(7) R. Franke and P. Oehme, *Pharmazie*, **28**, 489 (1973).

(8) H. Kubinyi, *Arzneim.-Forsch.*, **26**, 1991 (1976).

(9) H. Kubinyi and O.-H. Kehrhahn, *ibid.*, **28**, 598 (1978).

(10) R. M. Hyde, *J. Med. Chem.*, **18**, 231 (1975).

(11) T. Higuchi and S. S. Davis, *J. Pharm. Sci.*, **59**, 1376 (1970).

(12) N. F. H. Ho, J. Y. Park, W. Morozowich, and W. I. Higuchi, in "Design of Biopharmaceutical Properties through Prodrugs and Analogs," E. B. Roche, Ed., APhA Academy of Pharmaceutical Sciences, Washington, D.C., 1977, pp. 136–227.

(13) E. J. Lien, in "Medicinal Chemistry IV, Proceedings of the 4th International Symposium on Medicinal Chemistry," Elsevier, Amsterdam, The Netherlands, 1974, pp. 319–342.

(14) E. J. Lien, "Molecular Weight and Therapeutic Dose of Drugs," presented at the APhA Academy of Pharmaceutical Sciences, Orlando meeting, Nov. 1976.

(15) A. N. Martin, J. Swarbrick, and A. Cammarata, "Physical Pharmacy," 2nd ed., Lea & Febiger, Philadelphia, Pa., 1970, pp. 451, 452.

(16) E. L. Parrott, "Pharmaceutical Technology—Fundamental Pharmaceutics," Burgess, Minneapolis, Minn., 1970, pp. 299, 300.

(17) E. J. Lien, *J. Clin. Pharm.*, **4**, 133 (1979).

(18) H. G. Bray, S. P. James, W. V. Thorpe, and M. R. Wasdell, *Biochem. J.*, **47**, 294 (1950).

(19) V. P. Koelzer and J. Büchi, *Arzneim.-Forsch.*, **21**, 1721 (1971).

ACKNOWLEDGMENTS

Presented in part at the APhA Academy of Pharmaceutical Sciences, Washington, D.C. meeting, April 1980.

Supported in part by National Institutes of Health Biomedical Research Support Grant 5 S07 RR05792 03.

Particle-Size Analysis of Pharmaceutical Powders

L. J. BEAUBIEN and A. J. VANDERWIELEN ˣ

Received October 29, 1979, from *Product Control II, The Upjohn Company, Kalamazoo, MI 49001.* Accepted for publication January 17, 1980.

Abstract □ An automated electrolytic sensing zone (electrozone) method was developed to determine the particle-size distribution of milled and micronized pharmaceutical powders. The powdered drugs obeyed log-normal statistics, and the distributions were well defined by their geometric volume mean diameter and the geometric standard deviation. The results show that accurate data can be obtained between 2 and 80 μm with a precision of ~0.5 μm. Pulse-width analyses were performed to determine the feasibility of using a pulse-width discrimination program. However, in this case, the program discriminates against real particles and, therefore, its usefulness is limited. Milled and micronized materials are described adequately by a spherical diameter, and the automated electrozone system described is an excellent method for quality control purposes.

Keyphrases □ *Particle-size distribution*—milled and micronized pharmaceutical powders, geometric volume mean diameter, electrolytic sensing zone method with and without a pulse-width discriminator □ Distribution, particle size—milled and micronized pharmaceutical powders, geometric volume mean diameter, electrolytic sensing zone method with and without a pulse-width discriminator □ Powders—milled and micronized, particle-size distribution, geometric volume mean diameter, electrolytic sensing zone method with and without a pulse-width discriminator.

The physical properties of pharmaceutical powders are as important to an acceptable drug formulation as are its chemical properties (1). For example, the solubility, dissolution rate, and processing characteristics often depend on the particle size of the powders. Furthermore, the particle size can influence the bioavailability of poorly soluble drugs (2).

The growing need for particulate analyses and determination of particulate-size distributions in the quality control of pharmaceutical products emphasizes the need for efficient and reproducible methods. The popular microscopic method has several disadvantages for use in a quality control laboratory operation. It is time consuming, the counting and sizing results are subject to the judgment and experience of the microscopist, and the analyst cannot readily discern particles that are <5 μm long.

Other methods are available for the particle-size analysis of powdered drugs (1, 3). One method that overcomes the disadvantages of the microscopic determinations utilizes the Coulter or electrozone principle (electrolytic sensing). This electrical sensing zone method is capable of detecting and sizing small particles and counting a statistically significant number of particles.

The present study is part of a continuing project to automate the particle-size analysis of powdered drugs used for formulating suspensions, capsules, and tablets. Milled and micronized materials were studied since these particle reduction methods create particles that are well suited for particle sizing by an electrical sensing zone.

EXPERIMENTAL

Materials—The micronized steroids and spectinomycin hydrochloride were commercially available[1]. Research grade sodium chloride, lithium chloride, and 3A ethanol (contains 5% methanol) were used in the electrolytic solutions. Polysorbate 80 (polyoxyethylene 20 sorbitan monooleate) was used as a wetting agent. Polystyrene spheres of 2.0, 3.5, 5.2, 8.0, 9.8, 10.3, 17.7, 20.0, 32.0, 40.0, and 80.0 μm^2 were used to calibrate the instrument. Neomycin sulfate was selected as a mold inhibitor[1].

Equipment—The particle-size analyses were carried out using a multichannel electrozone particle-size analyzer interfaced to a digital minicomputer[3]. The system is depicted graphically in Fig. 1. Orifice tubes with diameters of 48, 76, 120, and 190 μm were used. The depths of the orifices were between 75 and 100% of the diameter.

Electrolyte—The aqueous electrolyte consisted of 0.9% NaCl, 0.1% polysorbate 80, and neomycin sulfate (4 g/liter) in water saturated with the bulk drug to be analyzed. The solution was prepared by stirring the powdered drug into the aqueous solution for 20 min and filtering once through a 0.22-μm filter. The alcoholic electrolyte was made in a similar manner using lithium chloride and 3A ethanol.

Sample Preparation—About 100 mg of the steroid was placed in ~25 ml of the saturated electrolyte. The vial containing the powdered drug and the electrolyte then was immersed in an ultrasonic bath for a time sufficient to disperse the sample and break up the agglomerated particles. The required time varied from 2 to 10 min, depending on the material. No prior sample preparation was required for spectinomycin hydrochloride.

Particle-Size Determination—For the steriods, a few (1–4) drops of the sonicated suspension were added to the counting cell until the count was between 10 and 100 times greater than the background at the most sensitive current setting. Care also was taken to ensure that the coincident count (*i.e.*, two particles counted as one) was <10%. The background count should be maintained at a level of ~5% of the sample count in the lowest channel. The analysis then was performed under computer control until 2000 counts were accumulated in one of the 128 raw data channels. The particle size in each channel then was calculated by the computer using the calibration tables stored on the flexible disk

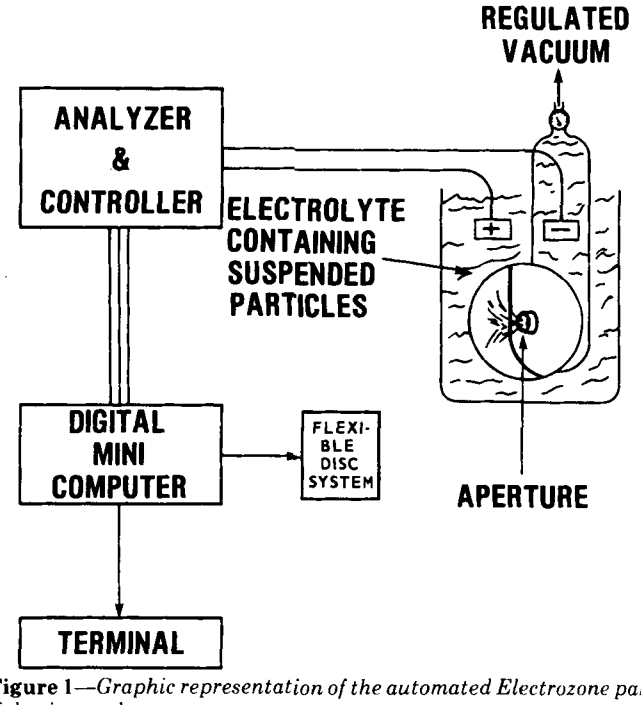

Figure 1—*Graphic representation of the automated Electrozone particle-size analyzer.*

[1] The Upjohn Co.

[2] Duke Standards, Inc.

[3] Celloscope model 112 LTSA/ADCW, Particle Data Inc.

0022-3549/80/0600-0651$01.00/0
© 1980, American Pharmaceutical Association

Table I—Resistivity Measurements

Electrolyte	Resistivity, ohm-cm
0.9% LiCl in 3A ethanol with 0.1% polysorbate 80	316
0.9% LiCl in methanol with 0.1% polysorbate 80	123
0.9% NaCl in water with 0.1% polysorbate 80	62
4% Ammonium thiocyanate in isopropanol with 0.14% polysorbate 80	398
Methanol[a]	>50,000
Distilled water	>50,000
Tap water	1,280

[a] Research grade.

system. This operation was repeated at several current settings until a complete distribution was obtained.

The analyses of spectinomycin hydrochloride were performed in a similar manner, except that a small amount of powder (~9 mg) was introduced directly into the saturated 3A ethanolic electrolyte solution that had been normalized previously. This suspension was stirred vigorously for 15–30 sec before proceeding with the particle-size analysis.

RESULTS AND DISCUSSION

Spectinomycin Hydrochloride—During this investigation, the resistivities of several electrolytes were measured using a conductivity bridge (Table I). Resistivity is important because it limits the maximum

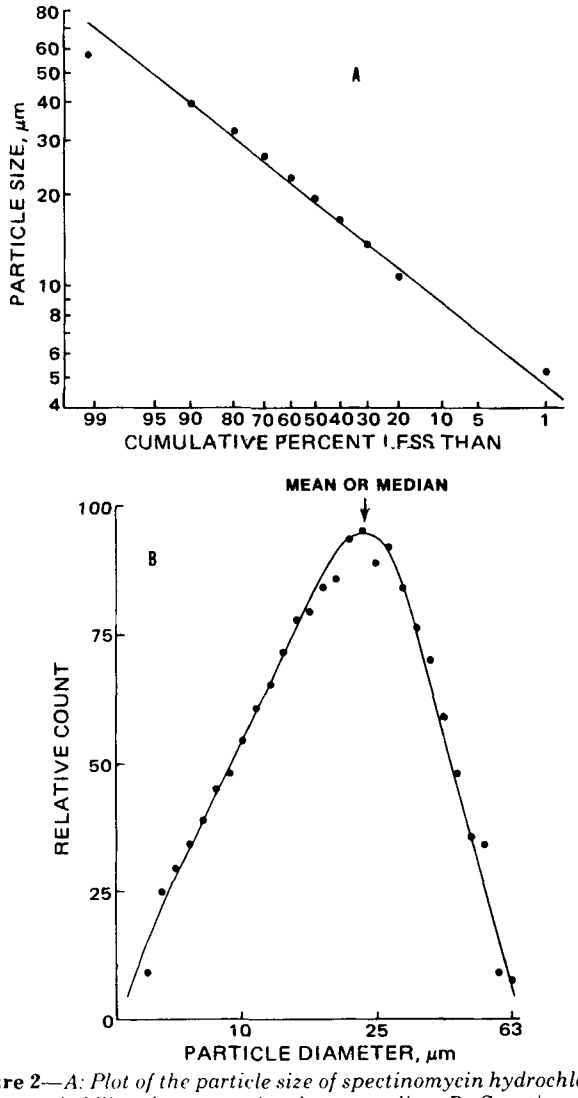

Figure 2—*A: Plot of the particle size of spectinomycin hydrochloride versus probability demonstrating log-normality. B: Spectinomycin hydrochloride particle-size distribution on a volume or mass basis.*

Table II—Calibration and Linearity Data for the Orifice Tubes

Tube Size, μm	Observed Count Diameter, μm	Microscopic Count Diameter, μm[a]
76	1.9	2.0
48	4.2	3.5
120	5.2	5.2
48, 190	8.9, 7.9	8.0
76	9.8	10.3
120	10.5	10.4
48, 76	18.2, 17.7	17.7
120, 190	19.9, 19.7	20.0
76, 120	31.3, 32.3	32.0
120	40.4	40.0
190	83.0	80.0

[a] The relative standard deviation as listed by Duke Standards was 10%.

usable current through the appearance of thermal noise. Thermal noise occurs due to power dissipation at the orifice (*e.g.*, released bubbles of dissolved gases). This effect is observed as ragged baseline grass on the display scope or is viewed microscopically as a grayish stream line trailing from the orifice.

Power dissipation and hence thermal noise are inversely proportional to the orifice size. Consequently, an electrolyte of low resistivity is required when a small orifice is used. A resistivity in the range of 10–100 ohm-cm is considered optimum, although solutions having a resistivity between 1 and 1000 ohm-cm are usable. Spectinomycin hydrochloride is an electrical nonconductor that is soluble in water and methanol but is only slightly soluble in 3A ethanol. Therefore, even though the lithium chloride–3A solution has a conductivity that is outside the optimum range, it was the electrolyte of choice because of the low solubility of spectinomycin hydrochloride in this solution.

The measured primary spectinomycin particles obeyed log-normal statistics when the data were converted to a volume or mass basis as shown in Fig. 2A (4). A typical volume distribution is depicted in Fig. 2B. For a log-normal distribution, only the geometric mean and the standard deviation are needed to define the whole distribution function. These values can be calculated from a log-normal plot of the cumulative data. A computer program was used to calculate the geometric volume mean (mass median) diameter ($\overline{M}v$) and the geometric standard deviation (σ) defined by:

$$\overline{M}v = \exp\left(\frac{\sum_{i=1}^{n} N_i \ln M_i}{\sum N_i}\right) \qquad \text{(Eq. 1)}$$

and:

$$\sigma = \exp\left(\sqrt{\frac{\sum_{i=1}^{n} N_i(\ln M_i - \ln \overline{M}v)}{\sum_{i=1}^{n} N_i}}\right) \qquad \text{(Eq. 2)}$$

where M is the particle diameter on the volume or mass basis, and N is the number of particles. The geometric count mean diameter, $\overline{M}c$, was derived from the geometric volume mean diameter by the relation:

$$\overline{M}c = \exp\left[\ln \overline{M}v - 3.0\,(\ln \sigma)^2\right] \qquad \text{(Eq. 3)}$$

The orifice tubes were calibrated using polystyrene spheres of known

Table III—Precision of Spectinomycin Hydrochloride Particle-Size Analyses

Sample	Geometric Mean Diameter, μm	
	Volume	Count
1	18.5	4.9
2	18.2	4.9
3	18.9	5.4
4	18.7	5.7
5	18.9	5.4
6	19.2	6.1
7	19.5	5.8
8	18.8	5.5
9	18.2	4.9
Mean	18.8	5.4
SD	0.4	0.4

Table IV—Results of Milling Effects

Sample	Millfeed Rate	Geometric Volume Mean Diameter, μm	Geometric *SD*
1	Unmilled	47.0	1.88
2	Fast feed	18.5	1.85
3	Slow feed	16.6	1.86
4	Blocked feed	13.0	1.62

Table V—Pulse-Width Analyses

Sample	Current, mamp[a]	Mode, μsec	*SD*[b], μsec
Spectinomycin	1/16	33	10
Spectinomycin	$\sqrt{2}$	31	13
Spectinomycin	1/16	34	10
Spectinomycin	$\sqrt{2}$	29	13
32-μm Polystyrene	1/16	63	7
32-μm Polystyrene	1/2	116	13

[a] Log = 8 and gain = 2⅛ for all analyses. [b] *SD* = 0.425 × (full width at half maximum).

diameter. The data (Table II) show that there was good agreement between the present results and the microscopic results of the manufacturer. A linear regression of the data for the observed size *versus* the microscopic size showed that the method was linear with little or no bias (slope 0.97, intercept 0.3, and correlation coefficient 0.999). The precision (Table III) of the method was excellent for the volume mean diameter (*RSD* 2.3%) and adequate for calculating the count mean diameter (*RSD* 8.0%).

Spectinomycin hydrochloride is formulated as a powder for resuspension. It is injected into muscle tissue as a saturated aqueous suspension, and the particle size must be controlled for patient comfort and good injection properties (*i.e.*, the suspension should not block the injection needle). The results in Table IV show that different size particles were created by different milling speeds. This observation indicates that the method is capable of determining the effectiveness of particle reduction during the milling operation and, therefore, makes an excellent quality control method.

Pulse-Width Analysis—There is a direct relationship between the basic transit time of small spheres flowing through the center of the orifice tube aperture and the width of the electrical pulse produced (5). The pulse-width overlay for the analysis program allows the analyzer to provide data on typical transit times for solid particles. The results of the pulse-width analysis are listed in Table V, and typical distribution curves are illustrated in Figs. 3 and 4. It took a normal particle of spectinomycin hydrochloride 32 μsec to travel through an orifice that was 90–120 μm deep. Prolonged transit times result if the particles are near the aperture wall where the fluid velocity is less or if they are prolate or oblate ellipsoids or flexible structures (5). The results indicate that particle size also has an important effect. This effect is well illustrated by the fact that the apparent transit time was almost twice as long (63 μsec) for the 32-μm

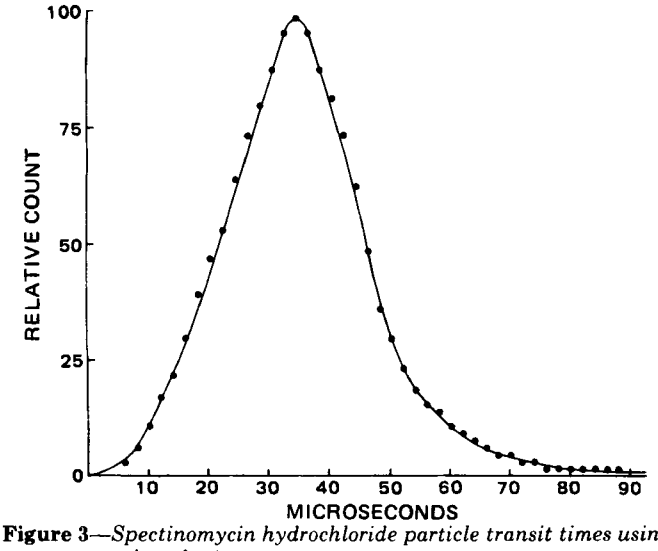

Figure 3—*Spectinomycin hydrochloride particle transit times using a current setting of 1.414 mamp.*

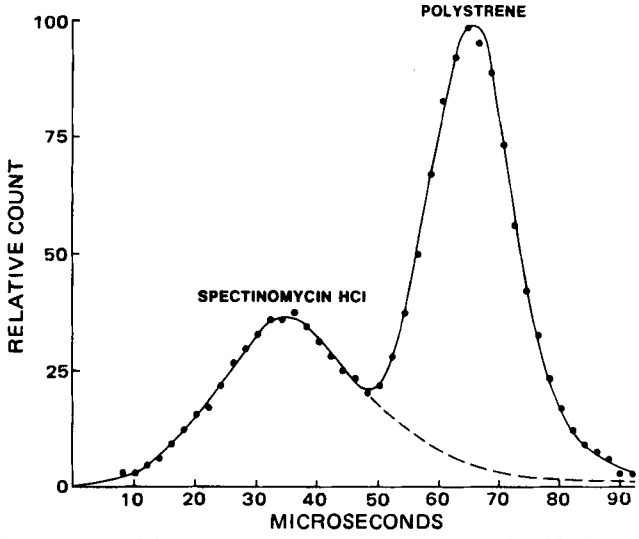

Figure 4—*Particle transit times of spectinomycin hydrochloride and 32-μm polystyrene spheres using a current setting of 0.062 mamp.*

reference than for the spectinomycin whose average particle size was 19 μm (Table III).

It has been suggested that since pulses produced by particles traveling along the orifice walls have correspondingly longer durations than pulses produced by particles passing along the orifice axis, the undesirable pulses may be eliminated by pulse-width discrimination. However, as noted earlier, this effect also would discriminate against the larger particles present. The effect of using a pulse-width discrimination of 79 μsec (pulses greater than 79 μsec are not counted) can be demonstrated by comparing the results listed in Tables III and VI. These data were obtained on the same sample of material. The apparent smaller geometric volume mean diameter (12.8 *versus* 18.8 μm) can only be the result of the computer ignoring the larger particles. It is suggested that pulse-width discrimination is a viable technique only if all of the particles are much smaller (≤10%) than the orifice length and diameter.

Steroids—The aqueous saline solution was chosen as the electrolyte and saturated with bulk drug even though the steroids are rather insoluble in water. This precaution controls the nonproportional dissolution of the smaller particles relative to the larger ones. As a further check on dissolution, the number of particles in 100 μl of prepared sample was counted before and after the determination at a fixed current. Comparison of these counts indicated that sample dissolution (or decomposition) was negligible.

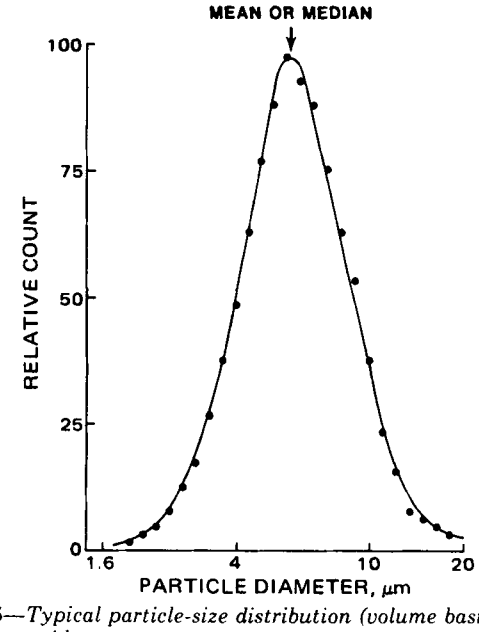

Figure 5—*Typical particle-size distribution (volume basis) of a micronized steroid.*

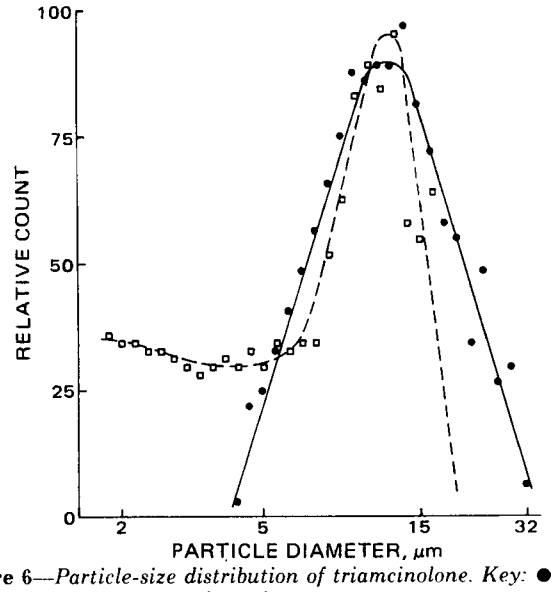

Figure 6—*Particle-size distribution of triamcinolone. Key: ●, nonsonicated; and □, sonicated 10 min.*

One basic objective of particle-size determinations is to measure the size of primary particles rather than the size of agglomerates or fractured primary particles. In general, samples routinely are sonicated to break up agglomerates into primary particles prior to obtaining particle-size distributions. Since extended sonication can reduce the size of polyethylene spheres (6), the effects of sonication on steroid particle size was examined.

The effect of sonication time on the agglomerate and primary particle size indicated that optimum times exist for each of these steroids. Samples were prepared as described under *Experimental*, except that the time of sample sonication was varied. All steroids displayed a rapid initial decrease in their volume mean and in the cumulative percent of observed particles with a diameter greater than 10 or 20 μm. This apparent decrease in size with sonication leveled off within the optimum times listed in Table VII. The appearance of the size distribution remained smooth and log-normal for all of the micronized steroids (Fig. 5). However, for triamcinolone (not micronized), the ratio of small to large particles increased with sonication time (Fig. 6).

The effect of sample dispersion also was studied using microscopic methods. The results (Fig. 7) confirm that sample sonication disperses the agglomerates into single crystals for counting and sizing. This observation was true for all of the steroids except triamcinolone. This steroid exists as individual crystals with very few agglomerates. The deterioration (Fig. 6) of the triamcinolone particle-size distribution upon sonication observed with the celloscope and the fact that sonication is known to fracture particles (6) suggest that sonication results in primary particle breakdown for this steroid.

The case of triamcinolone is important because it points out that, although dispersion of samples by ultrasonication works well, it should not be used without examining the effects on the material to be dispersed. This consideration is important for any analytical measurement made directly on the solid material. The distributions depicted in Fig. 6 show that a significant number of small particles are created by sonication. It is clear that a sample sonicated for 10 min does not represent the actual particle size of triamcinolone. As shown by the unsonicated sample in Fig. 6 and the results listed in Table VIII, it is possible to obtain a rea-

Table VI—Particle Size of Spectinomycin Hydrochloride Determined Using Pulse-Width Discrimination [a]

	Geometric Mean, μm	
	Volume	Derived Count
	14.5	5.0
	14.5	4.9
	14.8	5.1
	10.8	5.2
	11.6	5.4
	10.3	5.2
Mean	12.8	5.1
RSD, %	16.4	3.9

[a] Pulse-width discrimination set at 79 μsec.

Table VII—Optimum Sample Dispersion Time Using Ultrasonic Mixing

Steroid	Sonication Time, min
Hydrocortisone	1–2
Hydrocortisone acetate	1–2
Methylprednisolone	1–2
Methylprednisolone acetate	1–2
Medroxyprogesterone acetate	2–5
Prednisolone anhydrous	1–2
Prednisolone acetate	1–2
Prednisone	2–5
Prednisone acetate	5–10
Progesterone	5–10

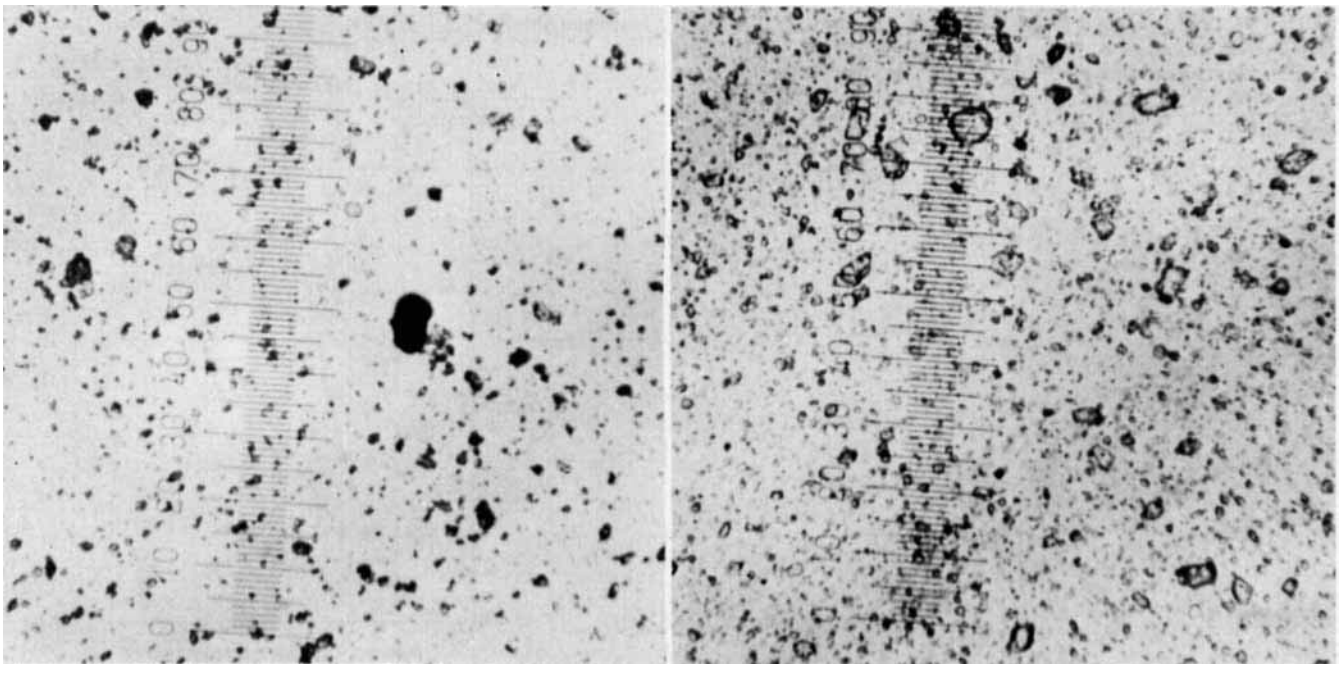

Figure 7—*Photomicrographs of hydrocortisone acetate; magnification is 125×. Key: left, sample not sonicated; and right, sample sonicated 10 min.*

Table VIII—Particle-Size Results for Triamcinolone

Sample	Geometric Volume Mean Diameter, μm	Geometric *SD*
A	9.5	1.7
B	8.5	1.8
C	9.2	1.7
D	10.3	1.8
E	10.8	1.8
F	9.3	1.9
G	8.3	1.8
H	8.7	1.8

sonable measure of the particle size for triamcinolone by shaking the sample vial gently to disperse the powder. The results presented for triamcinolone indicate that the method of sampling and dispersion is as important to the particle-size measurement as the parameters relating directly to the measurement. In fact, it was found previously that the error in counting particles by the electrozone method is less than the error due to sampling (3).

CONCLUSIONS

Experience has shown that, for pharmaceutical powders, the volume or mass basis (identical to volume if the measured particles have equal densities) is the most useful way of representing particle diameters for milled and micronized powders. These powders usually have log-normal particle distributions (7) that can be described completely by the geometric median or mean diameter and the geometric standard deviation. In addition, milled and micronized materials are described adequately by a spherical diameter; therefore, the automated electrozone system described in this paper is excellent for quality control purposes.

The electrolytic sensing zone method does have some limitations. The particles must be relatively insoluble in a solvent that has a moderate dielectric constant. Unusually shaped particles (*i.e.*, long rods or platelets) are converted to a mean diameter that is considerably less than the longest dimension of the actual particle. For example, a sphere of 4-μm diameter would have approximately the same volume as a cylinder of diameter 2.5 μm and length 7.5 μm. Thus, the method is relatively insensitive to particle shape. However, the advantages clearly outnumber the disadvantages. The method is highly sensitive, fast, and generally applicable. Sample preparation and data reduction are simple. The operator-fatigue factor is much less than for microscopy.

REFERENCES

(1) L. Lachman, H. A. Lieberman, and J. L. Kanig, "The Theory and Practice of Industrial Pharmacy," Lea & Febiger, Philadelphia, Pa., 1970.

(2) N. Kitamori, S. Kawajiri, and T. Matsuzawa, *Chem. Pharm. Bull.*, **24**, 2597 (1976).

(3) M. J. Groves, "Particle Size Analysis," Heyden, Philadelphia, Pa., 1978.

(4) R. R. Irani and C. F. Callis, "Particle Size: Measurement, Interpretation and Application," Wiley, New York, N.Y., 1963.

(5) D. R. Komiwz, *Biophys. J.*, **11**, 47 (1971).

(6) M. A. Sheikh, J. C. Price, and R. J. Gerraughty, *J. Pharm. Sci.*, **55**, 1048 (1966).

(7) J. T. Carstensen and M. Patel, *ibid.*, **63**, 1494 (1974).

ACKNOWLEDGMENTS

The authors thank D. S. Aldrich for the excellent microscopy work and acknowledge the assistance of W. C. Laughlin and P. V. Allen.

Simultaneous Partitioning and Hydrolysis Kinetics of Amoxicillin and Ampicillin

ERIC TOMLINSON, ROBERT E. NOTARI ˣ, and PETER R. BYRON *

Received June 27, 1979, from the *College of Pharmacy, Ohio State University, Columbus, OH 43210.* Accepted for publication January 16, 1980. *Present address: Department of Pharmacy, University of Aston in Birmingham, Birmingham, B4 7ET, England.

Abstract □ The kinetics of ampicillin and amoxicillin partitioning with simultaneous acid-catalyzed hydrolysis were studied in a stirred transfer cell containing isobutanol as the extract and aqueous hydrochloric acid (0.1–0.5 *N*) as the raffinate at 37°. Biexponential data for the concentration in both the raffinate (C_1) and the extract (C_2) as a function of time were analyzed simultaneously by nonlinear regression to estimate the apparent first-order rate constant for transfer from hydrochloric acid to isobutanol (k'_{12}), the reverse transfer constant (k'_{21}), and the hydrolysis rate constant (k). Agreement between k values determined in the presence of simultaneous partitioning and those determined in the absence of partitioning (k_{app}) verified the nonlinear estimates. Apparent partition coefficients, which represent the values that would be obtained in the absence of hydrolysis ($K'_D = C_1^\infty/C_2^\infty$), were estimated from $K'_D = k'_{12}/k'_{21}$. During terminal monoexponential loss, where $C_1 \simeq Y'e^{-\beta t}$ and $C_2 \simeq Z'e^{-\beta t}$, the kinetically controlled C_2/C_1 ratio (r) is described by $[k'_{12}/(k'_{21} - \beta)]$, which decreases with decreasing k values until r approaches K'_D. The difference between the terminal concentration ratio, r, and its corresponding partition coefficient, K'_D, is a measure of the degree to which kinetic processes control distribution. Both ampicillin and amoxicillin showed kinetic control of the distribution ratios in 0.5 *N* HCl, where the hydrolysis rate constant was significant relative to the distribution rate constants. Ampicillin had $r \simeq 1.74$ and $K'_D \simeq 0.92$; amoxicillin had $r \simeq 0.95$ and $K'_D \simeq 0.65$. As the $(k'_{12} + k'_{21})/k$ ratio increased, the r values approached K'_D so that in 0.1 *N* HCl, $r \approx K'_D = 0.33$ for amoxicillin and $r \approx 0.6$ and $K'_D \approx 0.56$ for ampicillin. In general, amoxicillin distribution rate constants ($k'_{12} + k'_{21}$) were roughly twice those of ampicillin, whereas ampicillin K'_D and r values were nearly double those of amoxicillin. Thus, the kinetic and thermodynamic rank orders are opposite. This result may have implications in drug design *via* molecular modification.

Keyphrases □ Amoxicillin—kinetics of simultaneous partitioning and hydrolysis □ Ampicillin—kinetics of simultaneous partitioning and hydrolysis □ Hydrolysis kinetics—amoxicillin and ampicillin, simultaneous partitioning □ Partitioning kinetics—amoxicillin and ampicillin, simultaneous hydrolysis □ Kinetics—amoxicillin and ampicillin, simultaneous partitioning and hydrolysis

A stirred transfer cell can be used to determine the rate constants for distribution between partially miscible phases with simultaneous degradation in the aqueous phase (1). This technique is potentially useful for comparing the partitioning of closely related drugs under conditions where they are not stable. The method allows calculation of the apparent partition coefficient, K'_D, that would be observed if the drug were stable. It also allows estimation of the concentration ratio, r, of the two phases at a time sufficiently long for r to approach a constant value. Thus, the calculated equilibrium value, K'_D, and the kinetic value, r, can be compared. If these values vary

0022-3549/80/0600-0655$01.00/0

© 1980, American Pharmaceutical Association

Table VIII—Particle-Size Results for Triamcinolone

Sample	Geometric Volume Mean Diameter, μm	Geometric *SD*
A	9.5	1.7
B	8.5	1.8
C	9.2	1.7
D	10.3	1.8
E	10.8	1.8
F	9.3	1.9
G	8.3	1.8
H	8.7	1.8

sonable measure of the particle size for triamcinolone by shaking the sample vial gently to disperse the powder. The results presented for triamcinolone indicate that the method of sampling and dispersion is as important to the particle-size measurement as the parameters relating directly to the measurement. In fact, it was found previously that the error in counting particles by the electrozone method is less than the error due to sampling (3).

CONCLUSIONS

Experience has shown that, for pharmaceutical powders, the volume or mass basis (identical to volume if the measured particles have equal densities) is the most useful way of representing particle diameters for milled and micronized powders. These powders usually have log-normal particle distributions (7) that can be described completely by the geometric median or mean diameter and the geometric standard deviation. In addition, milled and micronized materials are described adequately by a spherical diameter; therefore, the automated electrozone system described in this paper is excellent for quality control purposes.

The electrolytic sensing zone method does have some limitations. The particles must be relatively insoluble in a solvent that has a moderate dielectric constant. Unusually shaped particles (*i.e.*, long rods or platelets) are converted to a mean diameter that is considerably less than the longest dimension of the actual particle. For example, a sphere of 4-μm diameter would have approximately the same volume as a cylinder of diameter 2.5 μm and length 7.5 μm. Thus, the method is relatively insensitive to particle shape. However, the advantages clearly outnumber the disadvantages. The method is highly sensitive, fast, and generally applicable. Sample preparation and data reduction are simple. The operator-fatigue factor is much less than for microscopy.

REFERENCES

(1) L. Lachman, H. A. Lieberman, and J. L. Kanig, "The Theory and Practice of Industrial Pharmacy," Lea & Febiger, Philadelphia, Pa., 1970.

(2) N. Kitamori, S. Kawajiri, and T. Matsuzawa, *Chem. Pharm. Bull.*, **24**, 2597 (1976).

(3) M. J. Groves, "Particle Size Analysis," Heyden, Philadelphia, Pa., 1978.

(4) R. R. Irani and C. F. Callis, "Particle Size: Measurement, Interpretation and Application," Wiley, New York, N.Y., 1963.

(5) D. R. Komiwz, *Biophys. J.*, **11**, 47 (1971).

(6) M. A. Sheikh, J. C. Price, and R. J. Gerraughty, *J. Pharm. Sci.*, **55**, 1048 (1966).

(7) J. T. Carstensen and M. Patel, *ibid.*, **63**, 1494 (1974).

ACKNOWLEDGMENTS

The authors thank D. S. Aldrich for the excellent microscopy work and acknowledge the assistance of W. C. Laughlin and P. V. Allen.

Simultaneous Partitioning and Hydrolysis Kinetics of Amoxicillin and Ampicillin

ERIC TOMLINSON, ROBERT E. NOTARI ˣ, and PETER R. BYRON *

Received June 27, 1979, from the *College of Pharmacy, Ohio State University, Columbus, OH 43210.* Accepted for publication January 16, 1980. *Present address: Department of Pharmacy, University of Aston in Birmingham, Birmingham, B4 7ET, England.

Abstract □ The kinetics of ampicillin and amoxicillin partitioning with simultaneous acid-catalyzed hydrolysis were studied in a stirred transfer cell containing isobutanol as the extract and aqueous hydrochloric acid (0.1–0.5 *N*) as the raffinate at 37°. Biexponential data for the concentration in both the raffinate (C_1) and the extract (C_2) as a function of time were analyzed simultaneously by nonlinear regression to estimate the apparent first-order rate constant for transfer from hydrochloric acid to isobutanol (k'_{12}), the reverse transfer constant (k'_{21}), and the hydrolysis rate constant (k). Agreement between k values determined in the presence of simultaneous partitioning and those determined in the absence of partitioning (k_{app}) verified the nonlinear estimates. Apparent partition coefficients, which represent the values that would be obtained in the absence of hydrolysis ($K'_D = C_1^\infty/C_2^\infty$), were estimated from $K'_D = k'_{12}/k'_{21}$. During terminal monoexponential loss, where $C_1 \simeq Y'e^{-\beta t}$ and $C_2 \simeq Z'e^{-\beta t}$, the kinetically controlled C_2/C_1 ratio (r) is described by $[k'_{12}/(k'_{21} - \beta)]$, which decreases with decreasing k values until r approaches K'_D. The difference between the terminal concentration ratio, r, and its corresponding partition coefficient, K'_D, is a measure of the degree to which kinetic processes control distribution. Both ampicillin and amoxicillin showed kinetic control of the distribution ratios in 0.5 *N* HCl, where the hydrolysis rate constant was significant relative to the distribution rate constants. Ampicillin had $r \simeq 1.74$ and $K'_D \simeq 0.92$; amoxicillin had $r \simeq 0.95$ and $K'_D \simeq 0.65$. As the $(k'_{12} + k'_{21})/k$ ratio increased, the r values approached K'_D so that in 0.1 *N* HCl, $r \approx K'_D = 0.33$ for amoxicillin and $r \approx 0.6$ and $K'_D \approx 0.56$ for ampicillin. In general, amoxicillin distribution rate constants ($k'_{12} + k'_{21}$) were roughly twice those of ampicillin, whereas ampicillin K'_D and r values were nearly double those of amoxicillin. Thus, the kinetic and thermodynamic rank orders are opposite. This result may have implications in drug design *via* molecular modification.

Keyphrases □ Amoxicillin—kinetics of simultaneous partitioning and hydrolysis □ Ampicillin—kinetics of simultaneous partitioning and hydrolysis □ Hydrolysis kinetics—amoxicillin and ampicillin, simultaneous partitioning □ Partitioning kinetics—amoxicillin and ampicillin, simultaneous hydrolysis □ Kinetics—amoxicillin and ampicillin, simultaneous partitioning and hydrolysis

A stirred transfer cell can be used to determine the rate constants for distribution between partially miscible phases with simultaneous degradation in the aqueous phase (1). This technique is potentially useful for comparing the partitioning of closely related drugs under conditions where they are not stable. The method allows calculation of the apparent partition coefficient, K'_D, that would be observed if the drug were stable. It also allows estimation of the concentration ratio, r, of the two phases at a time sufficiently long for r to approach a constant value. Thus, the calculated equilibrium value, K'_D, and the kinetic value, r, can be compared. If these values vary

0022-3549/80/0600-0655$01.00/0

© 1980, American Pharmaceutical Association

Table I—Apparent First-Order Rate Constants (10^3 k in minutes^{-1}) for the Transfer and Hydrolysis (k'_{12}, k'_{21}, and k) of Ampicillin in an Isobutanol–Aqueous Hydrochloric Acid Stirred Transfer Cell at 37° [a]

Revolutions per Minute	[HCl][b]	k'_{12}	k'_{21}	k	K'_D	r
75	0.5	7.57	8.03	10.5	0.94	1.78
	0.3	6.66	7.46	5.78	0.89	1.34
	0.2	6.09	7.35	3.53	0.83	1.08
	0.1	4.69	8.28	1.53	0.57	0.64
120	0.5	8.71	9.05	10.7	0.96	1.71
	0.3	7.46	8.29	6.09	0.90	1.32
	0.3[c]	8.14	8.68	5.56	0.94	1.30
	0.2	6.41	7.80	3.60	0.82	1.06
	0.1	5.00	9.04	1.51	0.55	0.62

[a] The apparent partition coefficient ($K'_D = k'_{12}/k'_{21}$) is compared to the distribution ratio according to Eq. 5, where $r = [AMP]_i/[AMP]_w = k'_{12}/(k'_{21} - \beta)$. [b] Concentration prior to equilibration with isobutanol. [c] Initial ampicillin concentration of 2.4×10^{-3} M. The other concentrations were 4.0×10^{-3} M.

widely, *e.g.*, $r > K'_D$, then the phase ratio is controlled by the rate constants. This observation may be important for molecular modification.

BACKGROUND

Ampicillin and amoxicillin were studied because of their molecular similarity and the dramatic increase in the oral absorption of amoxicillin compared to ampicillin (2). The kinetics of acid-catalyzed hydrolysis and partitioning into isobutanol are represented in Scheme I:

$$C_{1p} \xleftarrow{k} C_1 \underset{k'_{21}}{\overset{k'_{12}}{\rightleftharpoons}} C_2$$

Scheme I

where k represents the apparent first-order hydrolysis constant; the distribution constants, k'_{12} and k'_{21}, were described previously (1). The penicillin concentration in the raffinate is represented by C_1 and that in the extract is represented by C_2. The hydrolysis product concentration in the raffinate is represented by C_{1p}. According to theory (1), the concentration in the raffinate (aqueous hydrochloric acid) is described by:

$$C_1 = X'e^{-\alpha t} + Y'e^{-\beta t} \qquad \text{(Eq. 1)}$$

where $X' = C_1^0(\alpha - k'_{21})/(\alpha - \beta)$, $Y' = C_1^0(k'_{21} - \beta)/(\alpha - \beta)$, C_1^0 is the initial concentration in the raffinate, and α and β are as defined previously (1). The concentration in the extract (isobutanol) is described by:

$$C_2 = Z'(e^{-\beta t} - e^{-\alpha t}) \qquad \text{(Eq. 2)}$$

where $Z' = C_1^0 k'_{12}/(\alpha - \beta)$. In agreement with theory, both penicillins illustrate kinetic control of the phase ratios when hydrolysis is significant.

Table II—Apparent First-Order Rate Constants (10^3 k in minutes^{-1}) for the Transfer and Hydrolysis (k'_{12}, k'_{21}, and k) of Amoxicillin [a] in an Isobutanol–Aqueous Hydrochloric Acid Stirred Transfer Cell at 37° [b]

Revolutions per Minute	[HCl][c]	k'_{12}	k'_{21}	k	K'_D	r
75	0.5	10.7	16.4	11.1	0.65	0.99
	0.3	9.17	16.3	5.37	0.56	0.70
	0.2	7.39	16.6	3.04	0.44	0.51
	0.1	6.22	18.8	1.03	0.33	0.34
120	0.5	14.2	21.4	10.9	0.66	0.91
	0.3	10.4	18.9	5.71	0.55	0.67
	0.2	10.3	23.2	3.16	0.44	0.49
	0.1	6.87	20.9	1.03	0.33	0.34

[a] The apparent partition coefficient ($K'_D = k'_{12}/k'_{21}$) is compared to the distribution ratio according to Eq. 5, where $r = [AMOX]_i/[AMOX]_w = k'_{12}/(k'_{21} - \beta)$. [b] Initial concentration of 4.4×10^{-2} M. [c] Concentration prior to equilibration with isobutanol.

Table III—Apparent First-Order Rate Constants (k_{app} at 37°) for Hydrolysis in Aqueous Hydrochloric Acid Saturated with Isobutanol

[HCl][a], N	10^3 k_{app}, min^{-1} Ampicillin[b]	10^3 k_{app}, min^{-1} Amoxicillin[b]
0.1	1.32	1.25
0.2	2.82	3.21
0.3	4.89	4.83
0.4	8.44	7.89
0.5	10.5	10.9
0.7	18.1	18.0

[a] Concentration prior to equilibration with isobutanol. [b] Initial concentration of $4.4–4.5 \times 10^{-2}$ M.

EXPERIMENTAL

Analytical Methods—Amoxicillin trihydrate[1] (85.0% amoxicillin) and ampicillin trihydrate[1] (83.7% ampicillin) were 97% pure after accounting for the water of hydration when they were assayed by the acid degradation method. All other materials were analytical grade.

Both penicillins were assayed by a literature method that involves reaction with hydroxylamine and subsequent complexation with a ferric reagent (3). Absorbance was measured at 486 nm against appropriate blanks that were modified to accommodate aqueous acid or isobutanol samples.

Kinetics of Simultaneous Partitioning and Hydrolysis of Ampicillin and Amoxicillin—Aqueous hydrochloric acid (0.1–0.5 N) and isobutanol were equilibrated by shaking at 37°. The phases then were separated and kept at 37°. A stirred transfer cell containing 100 ml of each of the previously equilibrated phases was used to study the kinetics of simultaneous partitioning and hydrolysis at 37°. This system was described previously (1).

Samples of ampicillin or amoxicillin were introduced into the aqueous phase. Aliquots (0.25 or 0.5 ml) were withdrawn simultaneously from both phases as a function of time and assayed. The phase volume ratio thus was kept constant. The number of samples withdrawn was limited to provide a maximum decrease in the total volume of ~5%. Experimental conditions are listed in Tables I and II.

Control Experiments for Kinetics of Degradation in Separated Phases—Experimental controls were designed to take into account both the miscibility of phases and the partitioning of hydrochloric acid into isobutanol during the equilibration step. Aqueous hydrochloric acid (0.1–0.7 N) and isobutanol were equilibrated by shaking at 37°. The phases were separated, and the aqueous acid was kept at 37°. A penicillin sample then was dissolved in the acid to provide an initial concentration of $\sim 4.5 \times 10^{-2}$ M. Aliquots were assayed as a function of time. Experimental conditions are listed in Table III. Apparent first-order rate constants, k_{app}, were obtained from the negative slopes of linear plots of ln [concentration] *versus* time.

Degradation in the isobutanol phase was shown to be insignificant by the following technique. Experiments were initiated as described for the simultaneous partitioning and hydrolysis with the 0.5 N HCl system. After the isobutanol phase had achieved a peak penicillin concentration, the phases were separated; the isobutanol phase was maintained at 37°. Aliquots were assayed as a function of time for 24 hr. The apparent first-order rate constants were negligible relative to those for hydrolysis in the aqueous controls. The rate constant for amoxicillin was 1% of the control, and that for ampicillin was 2% of the control. Therefore, Scheme I is adequate to describe the simultaneous partitioning and hydrolysis experiments.

RESULTS AND DISCUSSION

Kinetics of Hydrolysis of Amoxicillin and Ampicillin—In aqueous solutions, aminopenicillins can undergo hydrolysis with simultaneous polymerization. Bundgaard (4, 5) demonstrated both ampicillin and amoxicillin dimerization *via* nucleophilic attack by the free side-chain amino group in one molecule on the β-lactam of a second molecule. The percentage of total degradation attributed to dimerization ranged from 98% at pH 8.10 (0.673 M) to 13% at pH 9.10 (0.054 M) for ampicillin and from 93% at pH 8.6 (0.477 M) to 9% at pH 10 (0.024 M) for amoxicillin. Under the conditions in Table III, both penicillins are in the cationic form (AH^+) since, in both cases, the pKa (35°) of the carboxylic acid is ~2.6

[1] Beecham Pharmaceuticals, Sussex, England.

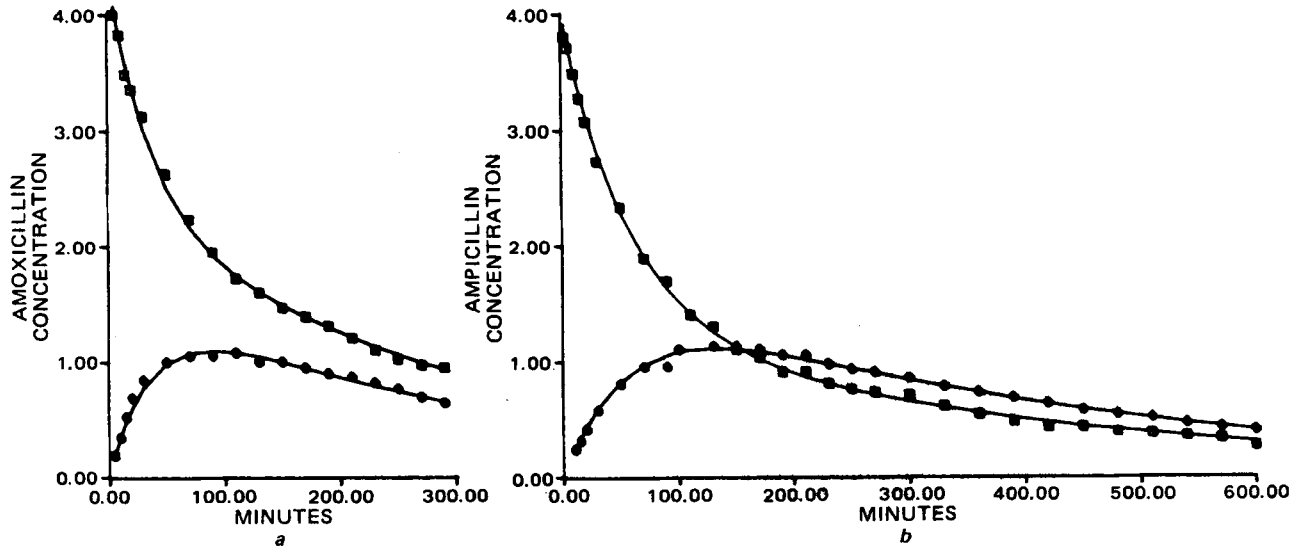

Figure 1—*Data representing the simultaneous determination of* C_1 (□) *and* C_2 (○) *in Scheme I using a stirred transfer cell containing 0.3* N *HCl and isobutanol (preequilibrated) at 37° at 75 rpm. The curves were obtained by simultaneous nonlinear regression based on Eqs. 1 and 2. The resulting estimates for the rate constants are given in Tables I and II.*

and that of the side-chain protonated amine is ~7.2 (4, 5). The lack of unprotonated amine to act as the nucleophile together with the dilute solutions (~0.04 *M*) makes self-association unlikely. Hou and Poole (6) reported simple first-order hydrolysis in the presence of 0.04–0.20 *N* HCl at 35°.

The precise degradation mechanism is not critical to this study since identical conditions were employed for both the simultaneous partitioning and hydrolysis kinetics (Tables I and II) and the controls (Table III). Furthermore, it is not necessary to determine the exact content of the two phases since hydrolysis in the aqueous phase is carried out as a control in which phase separation represents the sole difference between the experiments. At 37°, the solubility of isobutanol in water is ~7.4% (w/w) and that of water in isobutanol is ~18% (w/w) (7). Miscibility of the solvents, while significant, was kept constant throughout all experiments by preequilibration. Therefore, the reported rate constants are associated with water–isobutanol–hydrochloric acid mixtures. This technique provides a simple control experiment without requiring an exact definition of the phases.

Kinetics of Simultaneous Partitioning and Hydrolysis of Ampicillin and Amoxicillin—A previous report (1) demonstrated that the apparent partition coefficient, K'_D, defined by:

$$K'_D = C_2^\infty / C_1^\infty \qquad \text{(Eq. 3)}$$

where, at constant pH, C_2^∞ is the equilibrium concentration in the extract and C_1^∞ is the equilibrium concentration in the raffinate, may be calculated from:

$$K'_D = k'_{12}/k'_{21} \qquad \text{(Eq. 4)}$$

where k'_{12} and k'_{21} are the observed first-order rate constants for transfer from the raffinate to the extract and from the extract to the raffinate, respectively. Data for both phases (such as those shown in Fig. 1) were analyzed simultaneously using nonlinear regression (8) for the best estimates of k'_{12}, k'_{21}, and k based on Eqs. 1 and 2, which are derived from Scheme I.

According to theory, the rate constants for hydrolysis (k in Scheme I) should agree with those determined without partitioning under the same aqueous conditions (1). Thus, a plot of the k values *versus* the k_{app} values (Table II) should be linear with a slope of unity and an intercept of zero. Figure 2 shows good agreement with this prediction. Figure 2*a*, for ampicillin, has a slope of 0.97 and an intercept of 0.6×10^{-3}. Figure 2*b*, for amoxicillin, has a slope of 1.0 and an intercept of -0.05×10^{-3}. In both cases, the correlation coefficient exceeds 0.996. The hydrolysis rate constant also should be independent of the stirring rate. Tables I and II show good agreement between the k values determined with different stirring rates.

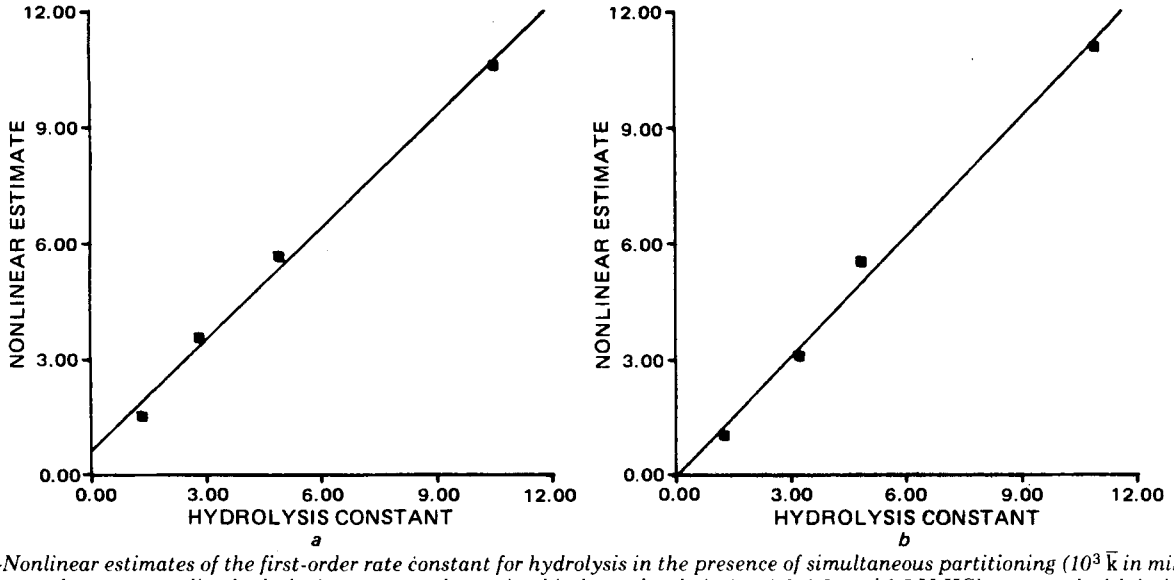

Figure 2—*Nonlinear estimates of the first-order rate constant for hydrolysis in the presence of simultaneous partitioning (10^3 $\bar{k}$ in min^{-1}, Tables I and II)* versus *the corresponding hydrolysis constants determined independently in 0.1, 0.2, 0.3, and 0.5* N *HCl saturated with isobutanol (10^3 k_{app} in min^{-1}; Table III) for ampicillin* (a) *and amoxicillin* (b). *In each case, the correlation coefficient of the regression line exceeds 0.996 and the slope is ~1.*

The apparent partition coefficient that would be obtained for the penicillin if it were stable in aqueous hydrochloric acid may be calculated from Eq. 4. Estimates for k'_{12}, k'_{21}, and K'_D are given in Tables I and II. Contrary to the values for hydrolysis, k, the distribution constants increase with increased stirring rate, as expected. However, the partition coefficient, K'_D, should be independent of the stirring rate. Comparison of the K'_D values at a fixed hydrochloric acid concentration but with different stirring rates shows good agreement between the estimates.

There also is evidence for an increase in K'_D with increasing hydrochloric acid concentration. Since the pKa values are ~2.6 (carboxylic acid) and ~7.2 (protonated amine), both penicillins exist in the cationic form (AH^+) under these conditions. [The pKa of the phenolic hydroxyl group on amoxicillin is 9.5 at 35° (5)]. Therefore, it is not likely that the increase in K'_D is due to any pH effect on the ionic species. Examination of the values for k'_{12} and k'_{21} reveals that k'_{21} is relatively independent of the hydrochloric acid concentration but that k'_{12} increases with increased hydrochloric acid concentration. Therefore, the observed increase is due to an effect in the aqueous phase since the rate constant for transfer from isobutanol to aqueous hydrochloric acid is relatively constant. This should not be due to the increase in ionic strength in going from 0.1 to 0.5 N HCl. Since the aqueous solutes are in the form of cations (AH^+), increased ionic strength would be expected to decrease the activity coefficient, thus decreasing the apparent K'_D value since the latter is based on concentration measurements.

A second and more likely possibility is the increased rate of diffusion of the neutral ion-pair (AH^+, Cl^-), as reported previously for bromide on the dextromethorphanium ion (9). This effect appears to be very likely based on the work of Hurwitz and Carney (10), who enhanced the apparent partition coefficients for ampicillin using several ion-pair or adduct-forming additives. At pH 7, quaternary compounds were the most effective, but the results also were dependent on the anion. For example, the chloroform–water K'_D values using tetraheptylammonium with various anions were: acetate, 4.78; hydroxide, 1.74; chloride, 1.80; bromide, 0.46; and iodide, 0.016. At pH 3, the anions trichloroacetate (added as the carboxylic acid, pKa = 0.70) and picric acid (as the phenol, pKa = 0.38) increased the K'_D value in octanol by ~30 and ~250 times, respectively. Thus, chloride was effective as the counteranion at pH 7. At pH 3, where ampicillin exists in the AH^+ form, K'_D was increased by the addition of anions without the quaternary cations. These observations support the suggestion that the increase in k'_{12} values with increased hydrochloric acid may be due to the formation of the neutral ion-pair (AH^+, Cl^-).

Both penicillins illustrate the difference between the observed phase ratios, r, and the apparent partition coefficients, K'_D. This difference was most pronounced with 0.5 N HCl. When a constant r value was observed, the values agreed with those calculated from Eq. 5 (11):

$$r = k'_{12}/(k'_{21} - \beta) \qquad \text{(Eq. 5)}$$

For example, with 0.5 N HCl, where β is most significant relative to k'_{12} and k'_{21}, the ampicillin r value was 1.78, while K'_D was 0.94. This result illustrates how kinetic control can reverse the expected results based on partition coefficients. Here, the K'_D value predicts that the aqueous concentration should be greater than that in the isobutanol phase. However, the concentration in isobutanol was 1.78 times that of the aqueous phase. As the hydrochloric acid concentration decreased, r approached K'_D. This result is due to the decreasing significance of the competing hydrolysis process.

The observed rate constant for the partitioning between the phases is the sum of the forward and reverse constants, k'_{12} and k'_{21} (1). If this sum becomes large enough relative to the hydrolysis constant, k, then r approaches K'_D. This effect has been referred to as preequilibrium, and a first approximation that $(k'_{12} + k'_{21}) \geq 20k$ will provide $r \approx K'_D$ has been suggested (11). In both cases (Tables I and II), k decreased nearly 10-fold as the hydrochloric acid concentration was decreased from 0.5 to 0.1 N. At the same time, k'_{21} remained nearly constant, while k'_{12} only decreased to about 60% of its value using 0.5 N HCl. Therefore, the $(k'_{12} + k'_{21})/k$ ratio increased 10-fold (75 rpm) and eight-fold (120 rpm) for amoxicillin and six-fold (75 rpm) and 5.6-fold (120 rpm) for ampicillin. The r values for amoxicillin at 0.1 N HCl were the same as its K'_D values since the $(k'_{12} + k'_{21})/k$ ratios were 24 (75 rpm) and 27 (120 rpm).

Although the K'_D and r values were larger for ampicillin than for amoxicillin, the rate constants for distribution $(k'_{12} + k'_{21})$ were nearly twice as large for amoxicillin. Amoxicillin thus distributed more rapidly but showed a lower isobutanol concentration for any given C_1 value. With significant hydrolysis, neither drug distribution ratio (C_2/C_1) was reflected by the K'_D values.

These observations illustrate one potential limitation in the application of partition coefficients to biological systems. The use of partition coefficients to predict the biological activity of structurally nonspecific drugs has received much attention since its inception (Meyer–Overton law). These well-accepted concepts are included in most undergraduate textbooks on medicinal chemistry. Further quantitation of these principles uses linear free energy relationships of the type known to chemists as Hammett $\sigma\rho$ functions. Since K'_D values are thermodynamic parameters, they describe equilibrium ratios rather than distribution rates. For systems that do not achieve equilibrium, such as an intravenous injection of a rapidly metabolized drug, the apparent distribution ratio may be predicted better from kinetic parameters. Comparisons of the type reported here for ampicillin and amoxicillin may be useful in drug design *via* molecular modification.

Conclusion—Ampicillin and amoxicillin both illustrated a difference between the observed isobutanol–aqueous phase concentration ratio, r, and that predicted by the partition coefficient value, K'_D, when 0.5 N HCl was used. This difference diminished as the hydrochloric acid concentration (and, therefore, the hydrolysis rate) was decreased. Both the r and K'_D values were roughly twice as large for ampicillin compared to amoxicillin. However, the sums of the distribution rate constants for amoxicillin were larger than those for ampicillin. There was no significant difference between the hydrolysis rate constants for the compounds. The estimates for the hydrolysis rate constants in the presence of partitioning were in good agreement with those determined independently.

REFERENCES

(1) P. R. Byron, R. E. Notari, and E. Tomlinson, *J. Pharm. Sci.*, **69**, 527 (1980).

(2) D. Zarowny, R. Ogilvie, D. Tamblyn, C. MacLeod, and J. Ruedy, *Clin. Pharmacol. Ther.*, **16**, 1045 (1974).

(3) J. W. Dale and J. T. Smith, *Biochem. J.*, **123**, 493 (1971).

(4) H. Bundgaard, *Acta Pharm. Suec.*, **13**, 9 (1976).

(5) *Ibid.*, **14**, 47 (1977).

(6) J. P. Hou and J. W. Poole, *J. Pharm. Sci.*, **58** 447 (1969).

(7) A. P. Colburn and D. G. Welsh, *Trans. Am. Inst. Chem. Eng.*, **33**, 197 (1942).

(8) C. M. Metzler, G. L. Elfring, and A. J. McEwen, *Biometrics*, **30**, No. 3 (1974).

(9) T. Higuchi and A. F. Michaelis, *Anal. Chem.*, **40**, 1925 (1968).

(10) A. R. Hurwitz and C. F. Carney, *J. Pharm. Sci.*, **67**, 138 (1978).

(11) R. E. Notari, "Biopharmaceutics and Clinical Pharmacokinetics," 3rd ed., Dekker, New York, N.Y. 1980, pp. 27, 102, 344.

Extended Hildebrand Approach: Solubility of Caffeine in Dioxane–Water Mixtures

A. ADJEI, J. NEWBURGER, and A. MARTIN ˣ

Received November 19, 1979, from the *Drug Dynamics Institute, College of Pharmacy, University of Texas, Austin, TX 78712.* Accepted for publication January 18, 1980.

Abstract □ The solubility of caffeine in various dioxane–water mixtures was analyzed in terms of solute–solvent interactions using a modified version of the Hildebrand treatment for regular solutions. The solubility equation employs a term (W) to replace the geometric mean $(c_1c_2)^{1/2}$, where c_1 and c_2 are the cohesive energy densities for the solvent and solute, respectively. The new equation provides an accurate prediction of solubility once the interaction energy, W, is obtained. In this case, the energy term is regressed against a polynomial in δ_1 of the binary mixture. A quartic expression of W in terms of the solvent solubility parameter was found for predicting the solubility of caffeine in dioxane–water mixtures. The expression yields an error in mole fraction solubility of <3%, a value approximating that of the experimentally determined solubility. The one exception to a good fit is near the maximum solubility, where a depression or valley occurs between the two peaks in solubility data; at this point, the theoretical equation predicts the solubility within ~9%. The new model also may be used to estimate the solubility of drug molecules employing the volume fraction of water in the solvent mixture instead of the composite solubility parameter, δ_1. The method has potential usefulness in preformulation and formulation studies during which solubility determination is important for drug design.

Keyphrases □ Caffeine—solubility in water–dioxane mixtures, extended Hildebrand approach, mathematical prediction of solute–solvent solubilities □ Solubility—caffeine in water–dioxane mixtures, prediction of solubility, extended Hildebrand approach □ Hildebrand solubility equation, modified—caffeine in water–dioxane mixtures, solubility predictions

In previous reports (1, 2), the Hildebrand–Scatchard solubility approach (3) to the prediction of solubility was extended to semipolar crystalline drugs in pure solvents and in polar binary solvent mixtures. The equation for calculating the solubility of drug molecules in polar and nonpolar solvents is (2):

$$-\log X_2 = \frac{\Delta S_m^f}{R}\log\frac{T_m}{T} + \frac{V_2\phi_1^2}{2.303RT}(\delta_1^2 + \delta_2^2 - 2\delta_1\delta_2) + \frac{V_2\phi_1^2}{2.303RT}(2\delta_1\delta_2 - 2W) \quad \text{(Eq. 1}a\text{)}$$

or:

$$-\log X_2 = \frac{\Delta S_m^f}{R}\log\frac{T_m}{T} + \frac{V_2\phi_1^2}{2.303RT}(\delta_1^2 + \delta_2^2 - 2W) \quad \text{(Eq. 1}b\text{)}$$

where X_2 is the mole fraction solubility of the crystalline solute at temperature T on the Kelvin scale; ΔS_m^f is the entropy of fusion of the crystalline drug molecule at its melting point, T_m; R is the molar gas constant; V_2 is the molar volume of the solute, and ϕ_1 is the volume fraction of the pure or mixed solvent. The solubility parameters for the solvent (subscript 1) and the solute (subscript 2) are δ_1 and δ_2, respectively. The W expression is an interaction term which, in regular solution theory, is taken to be equal to a geometric mean, $(c_1c_2)^{1/2}$, where c_1 is the cohesive energy density of the solvent (δ_1^2) and c_2 is the cohesive energy density of the solute (δ_2^2).

The first right-hand term of Eq. 1b is the negative logarithm of the ideal solubility ($-\log X_2^i$), and the second term is the logarithmic solute activity coefficient ($\log \alpha_2$). In Eq. 1a, $\log \alpha_2$ is divided into the regular solution term for van der Waals interaction energies ($\log \alpha_v$) and a final term ($\log \alpha_R$) representing residual solute–solvent interactions (2). The quantities $V_2\phi_1^2/(2.303RT)$ will be represented by A.

In the present approach, W is evaluated from knowledge of the other terms in Eq. 1, obtained experimentally or found in the literature. In polar systems, W equals the geometric mean $(c_1c_2)^{1/2}$ only at points A and B along the solubility profile (Fig. 1) where the real solubility line crosses the regular solution line. This fact emphasizes that the Hildebrand–Scatchard equation (3), written in terms of cohesive energy densities:

$$-\log X_2 = \frac{\Delta S_m^f}{R}\log\frac{T_m}{T} + \frac{V_2\phi_1^2}{2.303RT}\{c_1 + c_2 + 2(c_1c_2)^{1/2}\} \quad \text{(Eq. 2)}$$

correctly calculates the solubility of drugs in mixed polar solvents only at these two points in Fig. 1.

A better approach is not to restrict the interaction term W to a geometric mean but rather to evaluate it experimentally from the solubility of the solute in various solvent concentrations in a binary mixture employing Eq. 1b. An empirical equation for W as a function of solubility parameters of the solvent mixture remains to be discovered. Then, back-calculating W and substituting into Eq. 1 permit the mole fraction solubility of a drug (solute) to be predicted in essentially any solvent mixture.

EXPERIMENTAL

The solubility of crystalline caffeine[1] in dioxane, water, and mixtures of dioxane and water was determined as described for theophylline solutions (2). The other quantities required for predicting drug solubility in mixed solvents also were discussed (2). The solubility parameter, δ_2, for caffeine may be obtained from the peak solubility (Fig. 1), where the solvent δ_1 value should approximate the δ_2 value as required by Eq. 2. A more accurate determination (4) may be obtained by a differential method, plotting $\Delta X_2/\Delta\delta_1$ *versus* δ_1 (Fig. 2) and reading δ_2 as the δ_1 value at the apex of this curve.

RESULTS AND DISCUSSION

To obtain the ideal solubility of caffeine, the procedures described under *Experimental* were employed; the following values were obtained: ΔH_m^f, 5044 cal/mole; T_m, 512°K; and $\Delta S_m^f = \Delta H_m^f/T_m$, 9.85 cal/mole/degree. The ideal mole fraction solubility of caffeine was calculated from these values: $X_2^i = 0.06845$ ($\log X_2^i = -1.1646$). The molar volume of caffeine is 144 cm³/mole, which may be obtained as an average of the apparent molar volume in the mixtures (5). It also may be estimated by the group contribution method of Fedors (6).

The experimental solubility of caffeine at 25 ± 0.1° in dioxane–water mixtures is plotted in Fig. 1 *versus* the solubility parameter, δ_1, of the various mixed solvent systems. Also shown in Fig. 1 are the ideal solubility ($X_2^i = 0.06845$) and the regular solution curve (Eq. 2). The solubility of caffeine ($\delta_2 = 13.8$) in pure dioxane ($\delta_1 = 10.0$), pure water ($\delta_1 = 23.5$), and in the mixture of the two solvents is represented by the solid circles in Fig. 1. The maximum solubility of caffeine in the mixture is X_2 =

[1] Knoll Chemicals.

0022-3549/80/0600-0659$01.00/0
© 1980, American Pharmaceutical Association

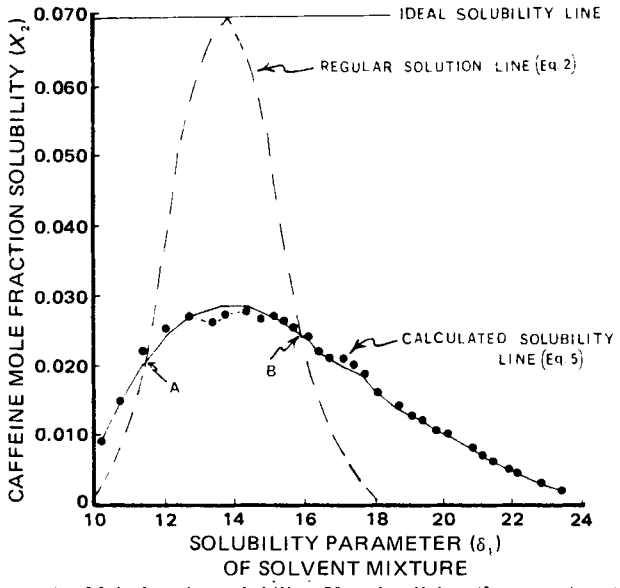

Figure 1—*Mole fraction solubility, X_2, of caffeine (δ_2 = 13.8) at 25° in dioxane, water, and dioxane–water mixtures. Key: A and B, points where real solubility equals regular solution solubility and $W = (c_1c_2)^{1/2} = \delta_1\delta_2$; ●, experimental points; and ··· ● ···, valley between two peaks in the caffeine solubility profile.*

0.0282 and occurs at δ_1 = 13.8. This value is well below the ideal solubility, X_2^i = 0.06845, as predicted from regular solution theory. The discrepancy between the results using the original Hildebrand equation and the experimental points demonstrates that Eq. 2 cannot be used to predict drug solubility in polar solvent systems.

Solubility Prediction Using Regression of *W versus* δ_1—Equation 1, differing from Eq. 2 in that the geometric mean is not used, provides an accurate prediction of solubility once W is obtained. Although W presently cannot be estimated based on fundamental physicochemical properties of the solute and solvent, W may be regressed against a polynomial in δ_1 of the solvent mixtures as described previously (1, 2). The following quadratic, cubic, and quartic equations were obtained using the experimental solubility data for caffeine in dioxane–water mixtures:

$$W = 79.4113802 + 1.8685725\delta_1 + 0.4356481\delta_1^2 \quad \text{(Eq. 3)}$$

$$W = 66.3515007 + 4.3901982\delta_1 + 0.2792065\delta_1^2 + 0.0031281\delta_1^3 \quad \text{(Eq. 4)}$$

$$W = 15.0752785 + 17.6279025\delta_1 - 0.9668266\delta_1^2 + 0.0539120\delta_1^3 - 0.0007578\delta_1^4 \quad \text{(Eq. 5)}$$

The W values calculated using these expressions compared favorably

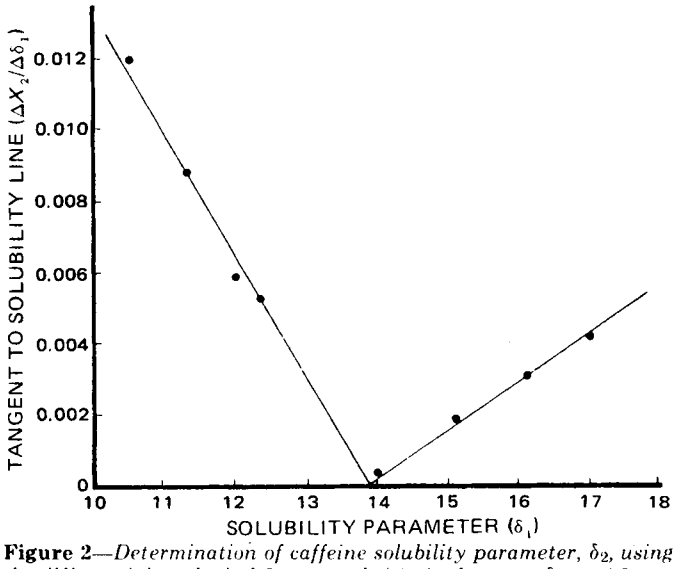

Figure 2—*Determination of caffeine solubility parameter, δ_2, using the differential method of James* et al. *(4). At the apex, δ_2 = 13.8.*

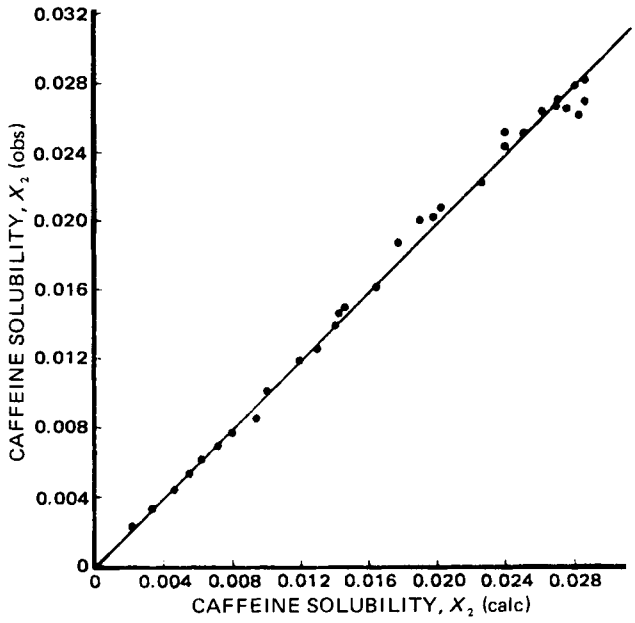

Figure 3—*Comparison of 31 observed caffeine solubilities in dioxane–water systems at 25° with solubilities predicted by the extended Hildebrand approach. The intercept of the line is 0.001, and the slope is 0.999. The correlation coefficient, r^2, is 0.989 for* n = 31.

with the original W values computed using Eq. 1. The solid line plotted in Fig. 1 was obtained employing the quartic expression (Eq. 5). This calculated solubility curve fits the experimental data points quite well (Figs. 1 and 3), predicting the solubility of caffeine in dioxane–water mixtures at most points within an error of ~3%, a value approximating the error in experimentally determined solubility values.

One notable exception to the fit is near the peak solubility where a depression or valley occurs between two peaks in the solubility data. Here the theoretical equation cannot reproduce the exact solubility and results in an error of 8.6%. Paruta *et al.* (7) first reported the peaks and valleys in solubility data and demonstrated essentially the same profile for caffeine as shown in Fig. 1. These workers (7) attributed the decreased solubility of caffeine in the dioxane–water mixture at this solvent composition to solvation or to the possible self-association of caffeine into polymeric forms as reported previously (8).

Equations 3–5 are empirical expressions and cannot be expected to reproduce the acute change in solubility represented by small peaks and

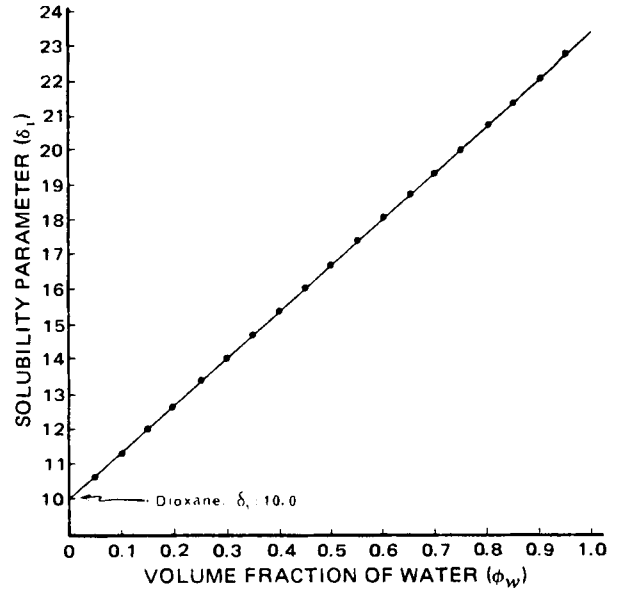

Figure 4—*Solvent solubility parameter, δ_1, in relation to the composition, ϕ, of the dioxane–water mixture as calculated from Eq. 6. The intercept of the line is 10.00, and the slope is 23.45. The number of data sets,* n, *is 31.*

Table I—Comparisons of Observed [a] and Calculated Solubilities of Caffeine (δ_2 = 13.8) in Dioxane–Water Systems at 25° ($-\log X_2^i$ = 1.1646); X_2^i = 0.06845; V_2 = 144 cm³/mole

Volume Percent of Water ($100\phi_w$)	Solution Density	A [b]	δ_1	X_2 (obs)	X_2 (calc)	Percent Solubility Difference
0	1.0337	0.10257	10.01	0.00849	0.00939	10.6
10	1.0440	0.09714	11.33	0.02255	0.01976	12.4
20	1.0516	0.09467	12.70	0.02698	0.02696	0.1
25	1.0532	0.09454	13.37	0.02605	0.02830	8.6
30	1.0542	0.09310	14.04	0.02823	0.02866	1.5
35	1.0556	0.09323	14.71	0.02647	0.02762	4.3
40	1.0542	0.09269	15.39	0.02628	0.02606	0.8
45	1.0516	0.09294	16.06	0.02429	0.02388	1.7
50	1.0506	0.09369	16.73	0.02137	0.02138	0.0
55	1.0481	0.09374	17.40	0.01997	0.01904	4.7
60	1.0443	0.09520	18.07	0.01617	0.01641	1.5
65	1.0399	0.09543	18.75	0.01465	0.01420	3.1
70	1.0346	0.09653	19.42	0.01195	0.01194	0.1
80	1.0254	0.09837	20.76	0.00780	0.00796	2.1
90	1.0095	0.10020	22.11	0.00453	0.00466	2.9
100	1.0024	0.10179	23.45	0.00229	0.00222	3.1

[a] Data selected from the 31 solubility points shown in Fig. 1. Calculated solubilities were obtained with the help of Eq. 8 as described in the text. [b] $A = V_2\phi_1^2/(2.303RT)$ in Eqs. 1 and 2.

valleys in a solubility profile. The calculated solubility line (solid line of Fig. 1), representing the quartic expression (Eq. 5), passes smoothly through the points about the peak solubility, ignoring the slight depression (dotted line at the peak in Fig. 1) at the maximum solubility. This kind of second-order deviation in drug solubility in polar solvents requires additional investigation and a considerably refined model for its characterization.

Predicting Drug Solubility from Solvent Concentration—The solubility parameter, δ_1, against which W is regressed to calculate solubility is calculated for a mixture of two solvents, a and b, using:

$$\delta_1 = \frac{\phi_a\delta_a + \phi_b\delta_b}{\phi_a + \phi_b} \quad \text{(Eq. 6)}$$

where the total volume fraction of the two solvents is given by:

$$\phi_1 = \phi_a + \phi_b \quad \text{(Eq. 7)}$$

Therefore, it is possible to express δ_1 in terms of the volume fraction (or volume percent) of either binary solvent species. The solubility parameter, δ_1, is plotted in Fig. 4 against the volume fraction of water in the mixture. A straight line is obtained, which suggests the possibility of bypassing W and δ_1 and back-calculating $\log \alpha_2/A$ by regressing it directly against the volume fraction of water, ϕ_w, in the solvent mixture. The quartic regression equation becomes:

$$\log \alpha_2/A = 8.409751 - 38.419518\phi_w + 109.607554\phi_w^2 - 114.353521\phi_w^3 + 49.383099\phi_w^4 \quad \text{(Eq. 8)}$$

Equation 8 yields the calculated solubility data found in Table I. For example, at 65% water, a volume fraction, ϕ_w, of 0.65 is substituted in Eq. 8, which yields 7.157 for $\log \alpha_2/A$. This value is multiplied by A to obtain $\log \alpha_2$ or 0.68299. Log α_2 then is added to $-\log X_2^i$, which is 1.1646, to obtain the negative logarithm of the solubility, $-\log X_2$. The sign is changed and the antilog is calculated to obtain X_2 = 0.01420. This result is within 3.1% of X_2 (obs) = 0.01465. The procedure is shown more clearly as:

$$\log \alpha_2 - \log X_2^i = -\log X_2 \quad \text{(Eq. 9a)}$$

$$0.68299 + 1.1646 = 1.84759 = -\log X_2 \quad \text{(Eq. 9b)}$$

$$\text{antilog}\,(-1.84759) = X_2 = 0.01420 \quad \text{(Eq. 9c)}$$

CONCLUSIONS

The extended Hildebrand approach to solubility employs a power series (quartic) equation in δ_1 to back-calculate W, which reproduces the solubility of caffeine in dioxane–water mixtures within the accuracy ordinarily achieved in experimental solubility results.

Hildebrand *et al.* (9) made the following observations: "Plato asserted that heavenly bodies move in circles because a circle is the most perfect geometrical figure. He was wrong: the most perfect geometrical construct is a straight line between two axes; one which expresses theory, the other which states the facts" (9). To test this Hildebrand hypothesis, Fig. 3 was drawn, and an almost straight line of zero intercept was obtained, r^2 = 0.989.

The close correlation of calculated results with experimental solubility is gratifying, although the extended method cannot be called a theory. At best, the method is semiempirical, because one uses solubilities originally to obtain the W values. Then W (or $\log \alpha_2/A$) is regressed in terms of solvent δ values or volume fractions of a solvent in the mixture to back-calculate solubilities. It is surprising that such good fits of the data have been obtained both with theophylline (2) and with caffeine in binary solvent systems. However, dioxane–water mixtures are relatively well behaved, producing fairly uniform bell-shaped solubility profiles; other solvent pairs may not perform as well. Limited experience with the solubility of drugs in pure solvents shows that the extended Hildebrand approach will prove useful for pure solvent systems only if a technique more fundamental than power series regression on δ_1 is found.

REFERENCES

(1) A. Martin, J. Newburger, and A. Adjei, *J. Pharm. Sci.*, **68**(10), IV (1979).

(2) *Ibid.*, **69**, 487 (1980).

(3) J. H. Hildebrand and R. L. Scott, "The Solubility of Nonelectrolytes," 3rd ed., Dover, New York, N.Y., 1964.

(4) K. C. James, C. T. Ng, and P. R. Noyce, *J. Pharm. Sci.*, **65**, 656 (1976).

(5) F. T. Gucker, Jr., W. I. Ford, and C. E. Moser, *J. Phys. Chem.*, **43**, 153 (1939).

(6) R. F. Fedors, *Polym. Eng. Sci.*, **14**, 147 (1974).

(7) A. N. Paruta, B. J. Sciarrone, and N. G. Lordi, *J. Pharm. Sci.*, **54**, 838 (1965).

(8) T. Higuchi and D. Guttmann, *J. Am. Pharm. Assoc., Sci. Ed.*, **46**, 4 (1957).

(9) J. H. Hildebrand, J. M. Prausnitz, and R. L. Scott, "Regular and Related Solutions," Van Nostrand Reinhold, New York, N.Y., 1970, p. 141.

ACKNOWLEDGMENTS

Supported in part by the endowed professorship provided to A. Martin by Mr. Coulter R. Sublett.

Effects of Different Buffer Species on Partition Coefficients of Drugs Used in Quantitative Structure–Activity Relationships

POU-HSIUNG WANG and ERIC J. LIEN ˣ

Received December 10, 1979, from the *Section of Biomedicinal Chemistry, School of Pharmacy, University of Southern California, Los Angeles, CA 90033.* Accepted for publication January 29, 1980.

Abstract □ A study was conducted in which the same organic solvent, 1-octanol, and different buffer systems were used to obtain intercorrelations among log P_{corr} values given by log P (octanol–water) = a log P (octanol–buffer) + b, where a and b are different constants for the different systems used. The range of a was 0.418–1.156 and that of b was −1.962–1.176 for the four buffer systems examined. Only with neutral drugs was the slope (a) close to 1.0 and the intercept (b) close to 0.0 for the three buffer systems studied. For acidic drugs, only 1-octanol–phosphate buffer gave a 1:1 correlation with 1-octanol–water partition coefficients. Acetate and bicarbonate buffer systems gave different correlations. For basic drugs, none of the three systems examined gave a 1:1 correlation with 1-octanol–water partition coefficients.

Keyphrases □ Partition coefficients—acidic, basic, and neutral drugs, effects of various octanol–buffer systems □ Solvents—various octanol–buffer systems, effects on partitioning of acidic, basic, and neutral drugs □ Buffers—various octanol–buffer systems, effects on partitioning of acidic, basic, and neutral drugs

The distribution of a drug or chemical compound between two phases in which it is soluble is an important topic. Nernst (1) emphasized that the partition coefficient is constant only if a single molecular species is distributed between two immiscible phases. Therefore, partitioning can be considered as classical thermodynamics in an equilibrium process. Pharmacologists became interested in the partition coefficient following the work of Meyer (2) and Overton (3), who first showed the parallel relationship between the nonspecific narcotic activity of drugs and their oil–water partition coeffients. In biochemical and pharmacological systems, the partition coefficient is an extrathermodynamic property and is a useful parameter for hydrophobic interactions with macromolecules, membranes, enzymes, and drug receptors.

BACKGROUND

There has been a recent rapid development in correlation studies of molecular structure with biological activity based on a model that utilizes the partition coefficient of the active compound in a reference partition system as a major parameter in the correlation equation. Hansch and coworkers (4–9) successfully used the linear free energy approach to establish quantitative structure–activity relationships for many biological systems. Lien and coworkers (10–18) studied the quantitative structure–activity relationships of various derivatives of drugs having a high correlation of biological activity with lipophilicity. The linear free energy relationship approach still has limitations due to the nonadditivity of the partition coefficients of some organic compounds (19, 20).

Among the many solvent systems studied, 1-octanol–water has been used most for quantitative structure–activity relationship studies (21, 22). The possible intermolecular interactions of solute molecules have not been studied systematically. Purcell *et al.* (23) stated that the behavior of aliphatic acids can be complex but can be controlled by proper buffering. Several investigators (24–26) recently used phosphate buffer systems in which the ionic strength was adjusted by inorganic compounds (*i.e.*, sodium chloride, potassium chloride, *etc.*); the pKa values of the drug were determined using the Debye–Hückel equation. This factor then was used to calculate the degree of ionization (α) in the measurement of the partition coefficient.

Ballard (27), who has done extensive work in this field, recently studied the carbonic acid system. He suggested that the pKa value of carbonic acid is a mixed constant involving the pKa of carbonic acid, the hydration of carbon dioxide in solution to form carbonic acid, and the activity and degree of dissociation of bicarbonate ion. He concluded that the thermodynamic pKa value of carbonic acid probably is not as affected by pH as is pKa′. However, both pKa and pKa′ are affected by temperature.

Other investigators (27–31) used phosphate buffers without adjusting the ionic strength. Rouot *et al.* (32) used a combined buffer system such as 0.067 M KH_2PO_4 mixed with 0.067 M Na_2HPO_4, while Moore and Koreeda (33) used citric acid (pH 1.8) and sodium bicarbonate (pH 9.0) in addition to phosphate buffer (pH 7.00). Marco *et al.* (34) used a pH 7.4 tris(hydroxymethyl)aminomethane hydrochloride buffer system. The pKa′ values were ignored in all of these investigations.

Each buffer species has its optimum pH range. It is questionable whether only one buffer can be utilized for a wide range of pH values. Moser *et al.* (35) suggested that the measurement of the partition coefficient of many weak acids is valid only within a pH range of about three units above the pKa. Above this range, they showed that such effects as ion-pair extraction of some species with buffer counterions can cause extreme deviations from the straight line described by the log P *versus* pH plot.

Dearden and George (36) criticized the assumption that the ionized fractions of an ionizable drug are insoluble in the lipid phases. It generally is assumed that the partition coefficient of the unionized species may be measured from the experimental apparent distribution coefficient at a pH giving a significant degree of ionization and the pKa of the solute. However, when octanol is saturated with water, the small amount of water in the octanol layer may be expected to dissolve some ionized species. It was concluded that differences in log P values between unionized and ionized species decreased steadily as log P was increased due to ion-pair formation with buffer counterions (36). Thus, the extraction of such ion-pairs into the nonaqueous phase should be related directly to the lipophilicity of the drug. The buffer system still retains a certain complexity when it comes to the measurement of the partition coefficient of a drug. There are some advantages in using a particular buffer system since it may increase the solubility of a drug, keep the pH of the medium constant, and/or retain the neutral form of the drug to avoid intermolecular interaction.

In measuring the partition coefficient, the ratio of the concentrations of the solute in two immiscible solvents is determined after equilibrium is reached. Mathematically, it may be defined as $C_{organic}/C_{aqueous}$. The 1-octanol–water system is a system of two immiscible solvents that has been used extensively. In the Pomona College data bank, Hansch and coworkers collected several thousand compounds for which the partition coefficients were measured in 1-octanol–water. Therefore, 1-octanol–water is the most frequently used system for comparative correlation studies. In addition, many diverse immiscible systems have been employed to avoid hydrogen bonding, solubility problems, *etc.* These systems have parallel relationships with the 1-octanol–water system and with each other. Examples of other organic solvents are chloroform, heptane, cyclohexane, butanol, and oil.

In the measurement of the partition coefficient of a drug, one considers the species that distributes to the binary phases, a water-saturated organic solvent phase and an organic solvent-saturated water phase; the partition coefficient should not be mistaken as arising from a system composed of simply one pure solvent phase and one pure water phase. The true (corrected) partition coefficient, P_{corr}, should characterize the transfer of only an undissociated molecular species. It generally is assumed that the true or corrected partition coefficient of a drug is independent of the pH and the buffer species used. In other words, one can use different buffer systems and a given organic solvent (*e.g.*, 1-octanol) in measuring the partition coefficient of an acidic or basic drug as long

0022-3549/80/0600-0662$01.00/0
© 1980, American Pharmaceutical Association

as one considers the degree of ionization. The true partition coefficient of the undissociated form then is obtained from $P_{corr} = P_{app}/(1 - \alpha)$, where α is the degree of ionization. The α value can be readily calculated from $\alpha = 1/[1 + \text{antilog (pKa} - \text{pH)}]$ for acids and $\alpha = 1/[1 + \text{antilog (pH} - \text{pKa)}]$ for bases; these expressions are obtained from buffer equations.

The validity of the assumption that only the pH of the buffer system will affect the apparent partition coefficient, but not the pH of the buffer species, has been questioned but has never been proven or disproven. The major objectives of this study were to explore whether this assumption is valid and to ascertain how the results obtained may affect quantitative structure–activity relationship studies.

EXPERIMENTAL[1]

pKa Values—The pKa values of the drugs studied were obtained from the literature (38, 39). The pKa values of several drugs were estimated from homologs or analogs (Table I).

Purification of 1-Octanol—Recent grade 1-octanol was purified by shaking with 1 *N* NaOH, shaking with 1 *N* H_2SO_4, shaking with 5% $NaHCO_3$, drying with excess anhydrous magnesium sulfate, and fractional distillation with collection of the fraction at the boiling range of 192–194° (23, 40). The purified solvent did not show any UV-absorbing contaminant.

Buffer Preparation—Buffer systems such as acetate, phosphate, tris(hydroxymethyl)aminomethane, and bicarbonate were prepared as stock solutions according to a literature procedure (41) and then were diluted to 0.01 *M*. The pH values were adjusted by adding 0.1 *N* HCl or NaOH and were checked with a digital pH meter[2]. Each buffer was within the appropriate pH range for its own optimum buffer capacity.

The acetate buffer pH was adjusted to 4.00. Both the phosphate buffer and the tris(hydroxymethyl)aminomethane buffer were adjusted to pH 7.40. The pH value of the bicarbonate buffer was 9.20. The pH value of the deionized, distilled water was 6.90 ± 0.05. The pH value always changed when acidic or basic drugs were dissolved in water saturated with 1-octanol, so the final pH value of the water layer was measured after partitioning.

Determination of Apparent and True (or Corrected) Partition Coefficients—The drugs were partitioned between 1-octanol saturated with buffer (or distilled water) and the same aqueous phase saturated with 1-octanol. In most cases, a 1:1 (v/v) ratio (*i.e.*, 25 ml:25 ml) of 1-octanol to buffer (or water) was used. The drug was dissolved first in the aqueous phase and then equilibrated with gentle shaking for 3–4 hr at room temperature (25 ± 1°) followed by centrifugation for 30 min. A standard curve was obtained from six or eight points of the drug solution by the UV or visible spectrophotometric method[3] to give an absorbance of 0.2–0.9 in a 3-ml cell. The concentration of the sample in the aqueous phase after equilibrium and separation was determined from the absorbance and the standard curve. The absorbance of the sample was adjusted to 0.2–0.9 by dilution.

The apparent partition coefficient was calculated from $P_{app} = C_{1\text{-octanol}}/C_{aqueous}$. Each determination was done at least in quadruplicate using different amounts of the sample, and the mean and standard deviation were determined ($SD \leq 0.03$). Values with a deviation of >0.03 were remeasured. The true or corrected partition coefficient (log P_{corr} value) was calculated from $P_{corr} = P_{app}/(1 - \alpha)$, where α is the degree of drug ionization at the given pH. The problem of the low solubility of benzoic acid, hydrocortisone, and 5-methyl-5-phenylhydantoin was circumvented by using <2% absolute methanol.

Regression Analysis—For the regression analysis, a least-squares program was used to derive the equations listed in Table II and run on a computer through a remote terminal[4].

RESULTS AND DISCUSSION

The apparent and corrected partition coefficients of various drugs measured in this study are summarized in Tables I, III, and IV.

Bonner and Woolsey (42) showed that different solutes and temperature may affect the structure of water (*i.e.*, the percentage of unbonded water molecules and the number of water molecules on different solutes), which undoubtedly affects the solubility of a drug in the aqueous phase and the organic–aqueous partition coefficient. The buffer and water may form a complex structure, and since the buffer has a counterion function (ion-pair function), it may affect the physicochemical properties of the drug. The pH value of distilled water changes by ~2.5 when a certain amount of acidic drug is dissolved in the water layer. Therefore, after partitioning, the final pH value of the water layer has to be determined by a pH meter. Equations correlating the log P_{corr} values obtained from different systems with those from 1-octanol–water are summarized in Tables II and V and Figs. 1–3.

In Table II, according to the slopes and intercepts in the equations, acidic, basic, and neutral drugs should not be grouped together in a single equation in most cases. The correlation coefficients and standard deviations of separate equations are much better than those of the composite equation (compare Eqs. 1–3 with Eqs. 5–7, 8–10, and 11–13). Several basic drugs such as propanolol and labetalol were not soluble enough in an alkaline pH (9.2). Hence, the partition coefficients could not be determined by the conventional methodology; consequently, Eq. 7 has only six data points. For a basic drug with Eqs. 5, 6, and 7, the slopes are 0.870, 0.421, and 0.496, respectively; they are all less then one, and the intercepts are −1.253, 1.143, and 1.137, which do not approach zero. If the slope of an equation is approximately one and the intercept approaches zero, it may be interpreted that the ratio of the true partition coefficient of the drug in octanol–water and in octanol–buffer is 1:1. In this case, the true partition coefficient, which was measured in octanol–buffer, is equivalent to that obtained in octanol–water. These values could be utilized in quantitative structure–activity relationship studies without correction.

It may be seen from Eqs. 5–7 that no 1:1 ratio exists between the three systems examined. Equation 5 has a higher slope and a lower intercept compared to Eqs. 6 and 7. It is suggested that the acetate buffer interacts with the protonated form of basic drug molecules and increases their lipophilicity. On the other hand, phosphate buffer and bicarbonate buffer attract basic drug molecules in the aqueous layer. For acidic drugs, according to the slope (0.984) and the intercept (0.081) from Eq. 9, the measured partition coefficients of acidic drugs in phosphate buffer as well as in octanol–water can be combined in the quantitative structure–activity relationship work. The partition coefficient of the acidic drug measured in acetate buffer or in bicarbonate buffer must be corrected with the necessary equations before extrapolation to octanol–water.

For neutral drugs, the slopes of Eqs. 11, 12, and 13 are 0.988, 0.992, and 0.997, respectively, all of which are very close to one, and the intercepts are −0.020, −0.045, and −0.025, respectively, which are nearly zero. The measured partition coefficients of neutral drugs in any of the three buffer systems will give similar results to the octanol–water system. The slope of Eq. 4 is 0.985, which is close to unity, and the intercept is 0.015, which approaches zero. Therefore, the partitioning behavior of the drugs analyzed in octanol–tris(hydroxymethyl)aminomethane is the same as in octanol–phosphate.

The ability of counterions in different buffers to affect the mechanism of intermolecular or intramolecular bonding forces in the partitioning behavior presents a complex problem. In the measurement of the partition coefficients of drugs, many different solvent systems have been used to ensure proper solubility of the drug. Equations for various organic solvent systems were published by Hansch and Leo (21, 22). It is proposed that the equations obtained from this study, as outlined in Table II, be used to correct for different buffer systems. These equations should be important in quantitative structure–activity relationship studies since no previous systematic study with different buffers has been reported.

Salicylic acid may be used to illustrate the complex phenomenon of molecular interaction in partitioning. According to the Debye–Hückel equation (43), the errors in the measurement of the partition coefficient of salicylic acid and phenformin might be attributed to the difference between pKa and pKa′ due to the ionic strength of the electrolytes.

[1] Phenolsulfonphthalein, 1-octanol (reagent grade), and salicylic acid were purchased from Fisher Scientific Co. Atropine sulfate and hydrocortisone were purchased from Sigma Chemical Co. Benzoic acid was purchased from Pfizer, Inc. 3,5-Diamino-1,2,4-triazole was purchased from Aldrich Chemical Co. Thiosemicarbazide was purchased from Eastman Organic Chemicals. Phthalimide potassium was purchased from Matheson, Coleman & Bell. Theobromine and ephedrine hydrochloride were purchased from Merck & Co. Thiourea and sulfanilamide were purchased from Mallinckrodt Chemical Works. Procainamide hydrochloride was purchased from Pfaltz & Bauer. Sulfadiazine sodium was purchased from City Chemical Corp. Diphenhydramine, propranolol, labetalol, atenolol, metoprolol, and methapyrilene hydrochloride were kindly provided by Dr. S. H. Wan, School of Pharmacy, University of Southern California. 5-Methyl-5-phenylhydantoin was kindly provided by Dr. J. Cohen, School of Pharmacy, University of Southern California. Trimethylene thiourea, *N,N′*-diethylethylene thiourea, butylene thiourea, and ethylene thiourea were synthesized by Lien (37).

[2] Beckman 3500.

[3] Perkin-Elmer double-beam spectrophotometer or Coleman 124.

[4] IBM 370/155 computer *via* an IBM 4012 RJE terminal.

Table I—log P_{app} and log P_{corr} of Various Drugs in Octanol–Phosphate and in Octanol–Bicarbonate

Drug	pKa	1-Octanol–Phosphate Buffer (pH 7.4)			1-Octanol–Bicarbonate Buffer (pH 9.2)		
		$1-\alpha$	log P_{app}	log P_{corr} ($\pm SD$)	$1-\alpha$	log P_{app}	log P_{corr} ($\pm SD$)
Diphenhydramine	8.98	0.025640	1.60	3.20 (0.02)	—	—[a]	—[a]
Propranolol	9.45	0.008836	1.24	3.29 (0.01)	—	—[a]	—[a]
Phenformin	11.80	0.000040	−1.47	2.94 (0.02)	0.002562	−0.96	1.64 (0.02)
Labetalol	9.45	0.008836	1.13	3.18 (0.01)	—	—[a]	—[a]
Atropine sulfate	9.25	0.013933	−0.06	1.24 (0.01)	0.471500	0.08	1.14 (0.02)
Metoprolol	9.68	0.005223	−0.25	2.04 (0.02)	0.248700	1.62	2.22 (0.02)
Atenolol	9.45	0.008836	−1.62	0.43 (0.01)	0.360205	−0.37	0.08 (0.01)
Methapyrilene	8.90	0.030679	1.29	2.81 (0.02)	—	—[a]	—[a]
Procainamide	9.24	0.014254	−1.33	0.51 (0.01)	0.476985	0.37	0.65 (0.01)
Ephedrine	9.63	0.005989	−1.35	0.87 (0.02)	0.271191	0.46	1.02 (0.02)
Phenolsulfonphthalein	7.90	0.759927	−1.60	−1.45 (0.03)	0.047727	−2.15	−0.83 (0.03)
Salicylic acid	2.75	0.000447	−1.62	1.73 (0.03)	0.00000036	−1.27	(5.18)[b] (0.02)
Sulfanilamide	10.43	0.999068	−0.73	−0.73 (0.03)	0.944439	−0.74	−0.71 (0.01)
Benzoic acid	4.34	0.000863	−1.34	1.72 (0.03)	0.000014	−2.46	2.43 (0.03)
Theobromine	10.05	0.997741	−0.72	−0.72 (0.01)	0.875001	−0.81	−0.75 (0.03)
Phthalimide	8.30	0.984078	−1.47	−1.47 (0.02)	0.112045	−2.57	−1.60 (0.01)
5-Methyl-5-phenylhydantoin	8.33	0.999226	1.01	1.01 (0.01)	0.119040	0.51	1.44 (0.03)
Sulfadiazine sodium	6.48	0.107342	−1.00	−0.03 (0.02)	0.001902	−2.12	0.06 (0.02)
N,N'-Trimethylene thiourea	—	1.00	−0.65	−0.66 (0.02)	1.00	−0.71	−0.72 (0.02)
N,N'-Diethylethylene thiourea	—	1.00	1.16	1.17 (0.01)	1.00	1.11	1.11 (0.01)
N,N'-Ethylene thiourea	—	1.00	−0.65	−0.65 (0.01)	1.00	−0.65	−0.65 (0.02)
Thiourea	—	1.00	−0.97	−0.97 (0.02)	1.00	−0.98	−0.98 (0.02)
Thiosemicarbazide	—	1.00	−1.26	−1.26 (0.02)	1.00	−1.25	−1.25 (0.01)
N,N'-Butylene thiourea	—	1.00	−0.09	−0.09 (0.01)	1.00	−0.10	−0.10 (0.01)
Hydrocortisone	—	1.00	1.53	1.53 (0.01)	1.00	1.51	1.51 (0.01)

[a] Not determined due to limited solubility. [b] This was probably due to the error in high α and low $1-\alpha$; see *Discussion*.

Table II—Equations Correlating log P_{corr} in 1-Octanol–Water with that in 1-Octanol–Buffer

Equation	n[a]	r[b]	s[c]
All Drugs Pooled Together			
(1) log P (octanol–water) = −0.260 + 0.685 log P (octanol–acetate buffer, pH 4.0)	23	0.941	0.541
(2) log P (octanol–water) = 0.122 + 0.892 log P (octanol–phosphate buffer, pH 7.4)	24	0.947	0.504
(3) log P (octanol–water) = 0.037 + 1.029 log P (octanol–bicarbonate buffer, pH 9.2)	20	0.939	0.480
(4) log P (octanol–phosphate buffer, pH 7.4) = 0.015 + 0.985 log P [octanol–tris(hydroxymethyl)aminomethane buffer, pH 7.4]	12	0.997	0.109
For Basic Drugs			
(5) log P (octanol–water) = −1.253 + 0.870 log P (octanol–acetate buffer, pH 4.0)	9	0.901	0.257
(6) log P (octanol–water) = 1.143 + 0.421 log P (octanol–phosphate buffer, pH 7.4)	10	0.954	0.167
(7) log P (octanol–water) = 1.137 + 0.496 log P (octanol–bicarbonate buffer, pH 9.2)	6	0.870	0.235
For Acidic Drugs			
(8) log P (octanol–water) = −0.217 + 1.156 log P (octanol–acetate buffer, pH 4.0)	7	0.989	0.292
(9) log P (octanol–water) = 0.081 + 0.984 log P (octanol–phosphate buffer, pH 7.4)	7	0.980	0.291
(10) log P (octanol–water) = −0.304 + 0.895 log P (octanol–bicarbonate buffer, pH 9.2)	7	0.967	0.375
For Neutral Drugs			
(11) log P (octanol–water) = −0.020 + 0.988 log P (octanol–acetate buffer, pH 4.0)	7	0.998	0.070
(12) log P (octanol–water) = −0.045 + 0.992 log P (octanol–phosphate buffer, pH 7.4)	7	0.999	0.061
(13) log P (octanol–water) = −0.025 + 0.997 log P (octanol–bicarbonate buffer, pH 9.2)	7	0.999	0.052

[a] Number of data points used in the regression analysis. [b] Correlation coefficient. [c] Standard deviation of regression (standard error of estimate).

Table III—log P_{app} and log P_{corr} of Various Drugs in Octanol–Acetate and in Octanol–Water

Drug	pKa	1-Octanol–Acetate Buffer (pH 4.0)			1-Octanol–Water		
		$1-\alpha$	log P_{app}	log P_{corr} ($\pm SD$)	$1-\alpha$	log P_{app}	log P_{corr} ($\pm SD$)
Diphenhydramine	8.98	0.000010	−0.61	4.37 (0.01)	0.000926	−0.27	2.76 (0.02)
Phenformin	11.80	0.00000008	−0.95	(6.12)[a] (0.01)	0.000140	0.03	2.43 (0.02)
Atenolol	9.45	0.000035	−1.84	2.62 (0.02)	0.002812	−0.05	1.21 (0.03)
Atropine sulfate	9.25	0.000006	−1.83	3.42 (0.02)	0.003970	−0.59	1.81 (0.02)
Propranolol	9.45	0.000035	−0.23	4.22 (0.01)	0.002812	−1.40	2.41 (0.03)
Metoprolol	9.68	0.000002	−1.72	3.96 (0.02)	0.001857	−0.71	2.01 (0.02)
Labetalol	9.45	0.000035	−0.42	4.03 (0.01)	0.002812	−1.27	2.51 (0.02)
Procainamide	9.24	0.000006	−2.18	3.06 (0.02)	0.005104	−1.11	1.19 (0.01)
Methapyriline	8.90	0.000013	−1.10	3.80 (0.01)	0.011115	0.22	2.17 (0.01)
Ephedrine	9.63	0.000002	−1.71	3.93 (0.01)	0.000229	−1.96	1.70 (0.02)
Salicylic acid	2.75	0.053240	1.60	2.87 (0.01)	0.025626	1.10	3.10 (0.02)
Phenolsulfonphthalein	7.90	—	—	−1.16[b] (0.04)	0.788070	−1.77	−1.66 (0.03)
Sulfadiazine sodium	6.48	—	—[c]	—[c]	0.705874	−0.27	−0.08 (0.01)
Sulfanilamide	10.43	0.999963	−0.70	−0.70 (0.02)	0.999898	−0.75	−0.75 (0.02)
Benzoic acid	4.34	0.685211	1.82	1.98 (0.02)	0.369592	1.61	2.04 (0.02)
5-Methyl-5-phenylhydantoin	8.33	0.999953	1.03	1.03 (0.03)	0.999226	1.01	1.01 (0.01)
Theobromine	10.05	0.9999991	−0.68	−0.68 (0.01)	0.999985	−0.69	−0.69 (0.02)
Phthalimide	8.30	0.999950	−0.66	−0.66 (0.03)	0.984078	−1.47	−1.47 (0.02)
N,N′-Trimethylene thiourea	—	1.00	−0.74	−0.74 (0.02)	1.00	−0.76	−0.76 (0.02)
Thiourea	—	1.00	−0.96	−0.96 (0.02)	1.00	−1.09	−1.09 (0.01)
N,N′-Diethylethylene thiourea	—	1.00	1.14	1.14 (0.01)	1.00	1.11	1.11 (0.01)
N,N′-Ethylene thiourea	—	1.00	−0.65	−0.65 (0.02)	1.00	−0.65	−0.65 (0.01)
Hydrocortisone	—	1.00	1.52	1.52 (0.02)	1.00	1.48	1.48 (0.01)
N,N′-Butylene thiourea	—	1.00	−0.09	−0.09 (0.01)	1.00	−0.09	−0.09 (0.01)
Thiosemicarbazide	—	1.00	−1.31	−1.31 (0.01)	1.00	−1.22	−1.22 (0.01)

[a] This was probably due to the error in high α and low $1-\alpha$; see *Discussion*. [b] E. J. Lien, *Drug Intell.*, **4**, 7 (1970). [c] Not determined due to limited solubility.

Table IV—log P_{app} and log P_{corr} of Various Drugs in Octanol–Tris(hydroxymethyl)aminomethane

Drug	pKa	1-Octanol–Tris(hydroxymethyl)aminomethane (pH 7.4)		
		$1-\alpha$	log P_{app}	log $P_{corr} \pm SD$
Propranolol	9.45	0.008836	1.33	3.39 ± 0.01
Atropine sulfate	9.25	0.013933	−0.05	1.31 ± 0.01
Labetalol	9.45	0.008836	1.08	3.13 ± 0.01
Diphenhydramine	8.98	0.025640	1.61	3.20 ± 0.02
Metoprolol	9.68	0.005223	−0.25	2.04 ± 0.01
Atenolol	9.45	0.008836	−1.78	0.27 ± 0.03
Methapyrilene	8.90	0.030679	1.35	2.87 ± 0.02
Procainamide	9.24	0.014254	−1.09	0.76 ± 0.01
Ephedrine	9.63	0.005989	−1.48	0.75 ± 0.02
Sulfadiazine sodium	6.48	0.107352	−1.00	−0.03 ± 0.02
N,N′-Trimethylene thiourea	—	1.00	−0.68	−0.68 ± 0.02
N,N′-Diethylethylene thiourea	—	1.00	1.13	1.13 ± 0.01

Therefore, pKa′ is introduced to correct for the ionic strength of electrolytes according to:

$$pKa' = pKa + \frac{0.51(2Z-1)\sqrt{\mu}}{1+\sqrt{\mu}}$$

where μ is the ionic strength of the electrolytes. In this study, the concentration of the buffer solution was 0.01 *M*. The second term in the equation contributed to the increase in the pKa′ value by ~0.05. However, the corrected value of α was not altered substantially. The value of pKa′ did not affect log P_{corr} of the drug in this study. The salicylic acid was dissolved in water, which resulted in a pH change of the solution from 6.8 to 4.33. According to $\alpha = 1/[1 + \text{antilog}(pKa - pH)]$, α is 0.9744. Therefore, it may be assumed that most of the drug molecules have ionized and subsequently are concentrated in the aqueous layer. This effect

Table V—Intercorrelation between log P_{corr} in Octanol–Water and log P_{corr} in Octanol–Buffer

			log P (octanol–water) = a log P (octanol–buffer) + b	
			a	b
Drug	Buffer	pH	(slope)	(intercept)
Basic	Acetate	4.0	0.870	−1.253
	Phosphate	7.4	0.421	1.143
	Bicarbonate	9.2	0.496	1.137
Acidic	Acetate	4.0	1.156	−0.217
	Phosphate	7.4	0.984	0.081
	Bicarbonate	9.2	0.895	−0.304
Neutral	Acetate	4.0	0.988	−0.020
	Phosphate	7.4	0.992	−0.045
	Bicarbonate	9.2	0.997	−0.025

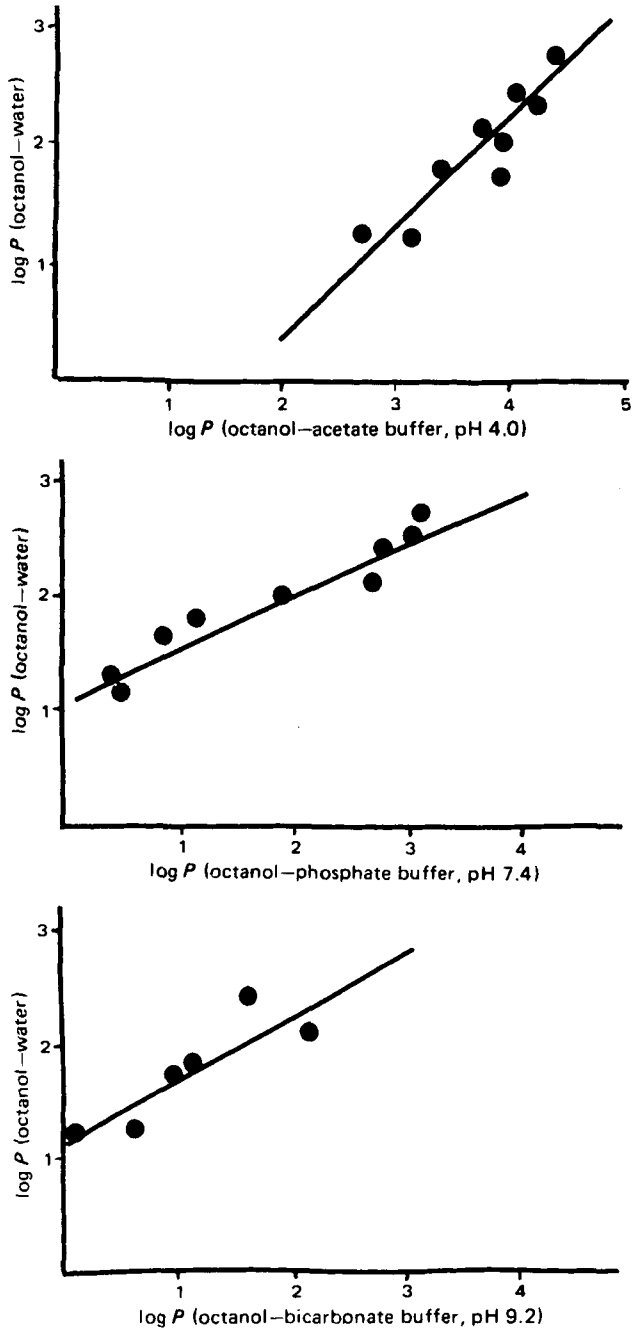

Figure 1—*Linear relationships between the corrected (true) partition coefficient in 1-octanol–water and that in 1-octanol–buffer for basic drugs.*

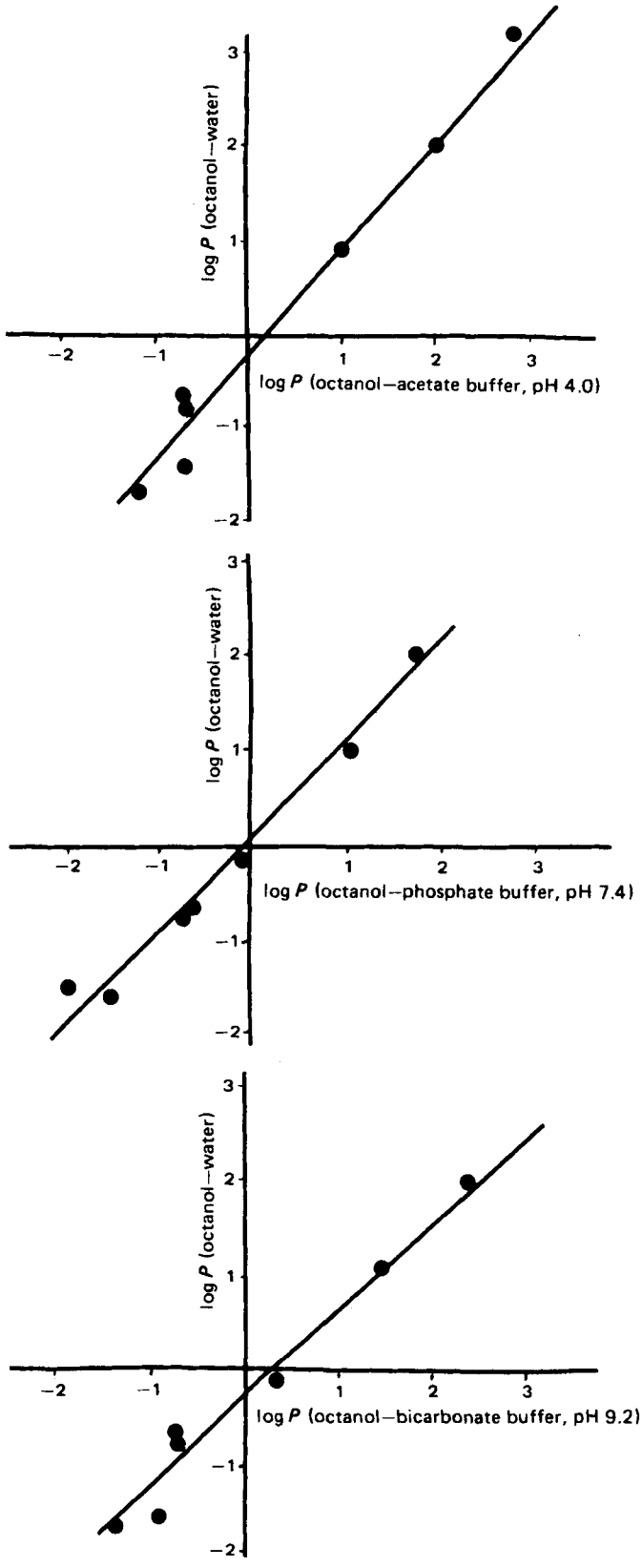

Figure 2—*Linear relationships between the corrected (true) partition coefficient in 1-octanol–water and that in 1-octanol–buffer for acidic drugs.*

would result in a very low value for the apparent partition coefficient. Consequently, the $1 - \alpha$ value is very small. A small error in $1 - \alpha$ will result in a large difference in log P_{corr}. If one utilizes π constants or fragment constants, f (44, 45), to calculate log P_{corr} of salicylic acid, the value appears to be much lower than that obtained in Table I. It appears

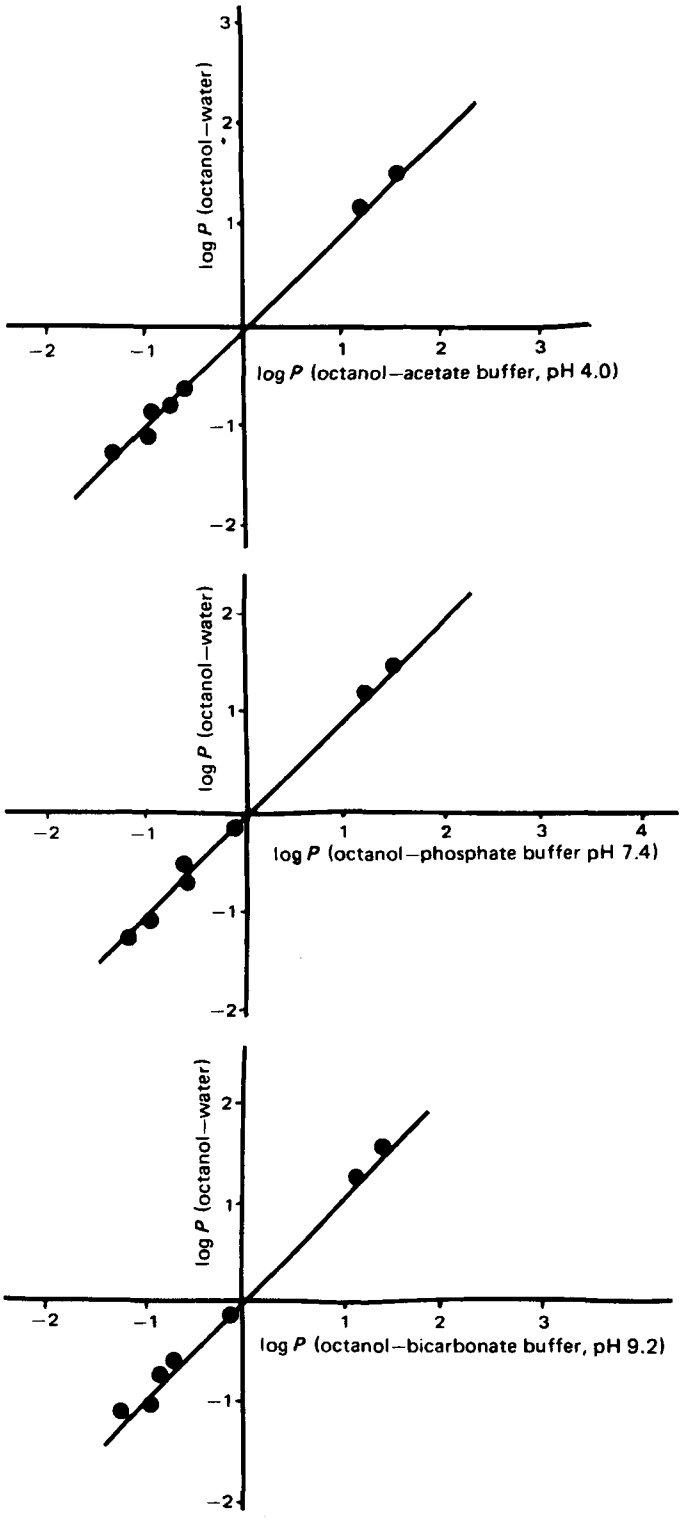

Figure 3—*Linear relationships between the corrected (true) partition coefficient in 1-octanol–water and that in 1-octanol–buffer for neutral drugs.*

to be an outlier on the statistical line. This result may be attributed to entrapment of the ionized species by the small amount of the buffer solution dissolved in the octanol phase. Phenformin, a basic drug highly ionized at low pH, presents the same problem. Consequently, both of these outliers were deleted from the appropriate equations.

Both water and buffer species have their own intrinsic capacity, which may affect the partitioning behavior of the drug. A comparison of acetate buffer, tris(hydroxymethyl)aminomethane buffer, phosphate buffer, and bicarbonate buffer reveals that the phosphate buffer is similar to water, according to Eqs. 6, 9, and 12. All of these equations have high correlation coefficients. It may be concluded that phosphate buffer (pH 7.4) is appropriate to keep the constant pH in the measurement of the partition coefficient of neutral and acidic drugs as long as they are soluble enough in the system.

CONCLUSION

These findings have significant bearing on quantitative structure–activity relationship studies; *i.e.*, the true partition coefficients (log P_{corr}) of acidic and basic drugs obtained from different buffer systems may not be suitable for regression analysis without correction. For acidic and neutral drugs, the phosphate buffer (pH 7.4) appears to give log P_{corr} values closer to those obtained from octanol–water than acetate and bicarbonate buffers. Therefore, the phosphate buffer system probably is the most suitable system for measuring true (or corrected) partition coefficients for quantitative structure–activity relationship work as long as the drug is soluble enough in this system. For basic drugs, any discrepancies must be corrected when different buffer systems are used in the measurement of partition coefficients.

REFERENCES

(1) W. Nernst, *Z. Phys. Chem.*, **8**, 110 (1891).

(2) H. Meyer, *ibid.*, **7**, 477 (1891).

(3) E. Overton, "Studien über die Narkose," Fischer, Jena, East Germany, 1901.

(4) C. Hansch, S. H. Unger, and A. B. Forsythe, *J. Med. Chem.*, **16**, 1217 (1973).

(5) C. Hansch, M. Yoshimoto, and M. H. Doll, *ibid.*, **19**, 1089 (1976).

(6) C. Hansch and D. F. Calef, *J. Org. Chem.*, **41**, 1240 (1976).

(7) C. Hansch and W. J. Dunn, III, *J. Pharm. Sci.*, **61**, 1 (1972).

(8) C. Hansch, R. M. Mair, T. Fujita, and P. P. Maloney, *J. Am. Chem. Soc.*, **85**, 2817 (1963).

(9) J. M. Blaney, S. W. Dietrich, M. A. Reynolds, and C. Hansch, *J. Med. Chem.*, **22**, 614 (1979).

(10) F. M. Plakogiannis and E. J. Lien, *Acta Pharm. Suec.*, **2**, 1917 (1974).

(11) E. J. Lien, *Agr. Food Chem.*, **17**, 1265 (1969).

(12) E. J. Lien, M. Hassain, and M. P. Golden, *J. Med. Chem.*, **13**, 623 (1970).

(13) E. J. Lien and C. Hansch, *Adv. Chem. Ser.*, **11**, 155 (1973).

(14) E. J. Lien, *J. Med. Chem.*, **13**, 1189 (1970).

(15) E. J. Lien, K. Mayer, P. H. Wang, and G. L. Tong, *Acta Pharm. Jugosl.*, **29** (4) (1979).

(16) E. J. Lien, J. Kuwahara, and R. T. Koda, *Drug Intell. Clin. Pharm.*, **8**, 470 (1979).

(17) E. J. Lien, *J. Clin. Pharm.*, **4**, 133 (1979).

(18) E. J. Lien and P. H. Wang, *J. Pharm. Sci.*, **69**, 648 (1980).

(19) R. Collonder, *Physiol. Plant*, **7**, 420 (1954).

(20) E. Cohen and J. Edsal, "Protein, Amino Acids and Peptides," Reinhold, New York, N.Y., 1943, p. 200.

(21) A. Leo, C. Hansch, and D. Elkins, *Chem. Rev.*, **71**, 525 (1971).

(22) C. Hansch and A. J. Leo, "Substituent Constants for Correlation Analysis in Chemistry and Biology," Wiley, New York, N.Y., 1979, Appendix II.

(23) W. P. Purcell, G. E. Bass, and J. M. Clayton, "Strategy of Drug Design: A Guide to Biological Activity," Wiley, New York, N.Y., 1973, p. 126.

(24) D. T. Cooke and I. Gonda, *Commun. J. Pharm. Pharmacol.*, **29**, 190 (1977).

(25) J. L. Colaizzi and P. R. Klink, *J. Pharm. Sci.*, **58**, 1184 (1969).

(26) W. J. Welbter, M. A. Johnson, M. Hall, D. T. Warner, A. E. Berger, A. H. Wenzel, D. T. Gish, and G. L. Neil, *J. Med. Chem.*, **18**, 339 (1975).

(27) B. E. Ballard, *J. Pharm. Sci.*, **63**, 1345 (1974).

(28) J. Watanabe and A. Kozaki, *Chem. Pharm. Bull.*, **26**, 3463 (1978).

(29) J. K. Seydel, H. Abrens, and W. Losert, *J. Med. Chem.*, **18**, 234 (1975).

(30) K. Korfen and K. W. Miller, *Can. J. Physiol. Pharmacol.*, **57**, 325 (1979).

(31) V. D. Moore and M. Koreeda, *Biochem. Biophys. Res. Commun.*, **73**, 459 (1976).

(32) B. Rouot, G. Uclere, C. G. Wemuth, F. Miesch, and J. Schwarts, *J. Med. Chem.*, **19**, 1049 (1976).

(33) P. D. Moore and M. Koreeda, *Biochem. Biophys. Res. Commun.*, **73**, 459 (1976).
(34) A. D. Marco, A. M. Casazza, and Pratesi, *Can. Tred. Rep.*, **61**, 893 (1977).
(35) P. Moser, K. Jakel, P. Krupp, R. Menassa, and A. Sallmann, *Eur. J. Med. Chem.*, **10**, 613 (1975).
(36) J. C. Dearden and E. George, *J. Pharm. Pharmacol.*, **30**, 49p (1978).
(37) E. J. Lien, Ph.D. thesis, University of California Medical Center, San Francisco, Calif., 1966.
(38) D. W. Newton and R. B. Kenza, *Drug Intell. Clin. Pharm.*, **12**, 546 (1978).
(39) "The Merck Index," 9th ed., Merck & Co., Rahway, N.J., 1976.
(40) R. N. Smith, C. Hansch, and M. M. Arres, *J. Pharm. Sci.*, **64**, 599 (1975).
(41) G. Gomori, in "Methods in Enzymology," S. P. Colowick and W. O. Kaplan, Eds., Academic, New York, N.Y., 1955.
(42) O. D. Bonner and G. B. Woolsey, *J. Phys. Chem.*, **72**, 899 (1968).
(43) A. N. Martin, J. Swarbrick, and A. Cammarata, "Physical Pharmacy," 2nd ed., Lea & Febiger, Philadelphia, Pa., 1969, pp. 181–186.
(44) C. Hansch, A. Leo, S. H. Unger, K. H. Kim, D. Nikaitani, and E. J. Lien, *J. Med. Chem.*, **16**, 1207 (1973).
(45) R. F. Rekker, in "Biological Activity and Chemical Structure," J. A. Keverling Buisman, Ed., Elsevier, Amsterdam, The Netherlands, 1977, pp. 231–238.

ACKNOWLEDGMENTS

Presented in part at the APhA Academy of Pharmaceutical Sciences, Kansas City meeting, November 1979.

Adapted in part from a thesis submitted by P.-H. Wang to the University of Southern California in partial fulfillment of the Master of Science degree requirements.

Effect of Polybasic Acids on Structure of Aluminum Hydroxycarbonate Gel

MING K. WANG *, JOE L. WHITE *, and STANLEY L. HEM ‡x

Received September 24, 1979, from the **Department of Agronomy and the* ‡*Department of Industrial and Physical Pharmacy, Purdue University, West Lafayette, IN 47907.* Accepted for publication January 11, 1980.

Abstract □ The effect of oxalic acid, citric acid, and their sodium salts on the structure of aluminum hydroxycarbonate gel was studied to illustrate the various mechanisms by which polybasic acids interact with aluminum hydroxycarbonate gel. Analysis of changes in the pH-stat titrigram, the carbonate to aluminum ratio, the aluminum content of the supernate following centrifugation, and the adsorption of the organic solute indicates that polybasic acids may: (*a*) partially neutralize the aluminum hydroxycarbonate gel by a general acid effect, (*b*) modify the aluminum hydroxycarbonate surface by adsorption of the anionic form of the polybasic acid, (*c*) extract aluminum by the formation of a soluble complex, and (*d*) lead to the precipitation of a new crystalline phase.

Keyphrases □ Polybasic acids—oxalic acid, citric acid, and their sodium salts, effect on aluminum hydroxycarbonate gel structure, complexation of polybasic acids with aluminum, adsorption of polybasic anion, acid neutralization □ Complexation—polybasic acids and their sodium salts with aluminum hydroxycarbonate gel, acid neutralization, structural changes in aluminum hydroxycarbonate gel □ Acid neutralization—complex formation with polybasic acids and aluminum hydroxycarbonate gel □ Aluminum hydroxycarbonate—complexation with polybasic acids and their sodium salts, structural changes, acid neutralization

Citric acid, oxalic acid, and other polybasic acids can inhibit the crystallization of aluminum hydroxide and form complexes with aluminum (1–3). Gibaldi and Mufson (4) found that the neutralization of dried aluminum hydroxide gel was inhibited when sodium citrate or sodium tartrate was added to the 0.1 *N* HCl used as the reaction medium. It was concluded that dried aluminum hydroxide gel reacts with sodium citrate or sodium tartrate to produce a water-soluble complex as well as to reduce surface area by flocculation.

Polybasic acids are important in soil-weathering reactions due to their role in complexing and solubilizing aluminum (5, 6). In addition, it was found that the edge faces of gibbsite (7), as well as synthetic goethite (8), can adsorb oxalate anion.

The nature of the interaction of polybasic acids with the surface of aluminum hydroxycarbonate has not been examined in detail. This study describes the mechanisms by which polybasic acids interact with aluminum hydroxycarbonate and the effect of these interactions on the acid reactivity of aluminum hydroxycarbonate gel.

EXPERIMENTAL

An aluminum hydroxycarbonate gel that exhibited a moderate rate of acid neutralization was selected so that any increase or decrease in the acid neutralization rate would be observed easily. The gel was amorphous to X-rays and had an IR spectrum characteristic of aluminum hydroxycarbonate gel (9).

Mixtures containing 0.2 *M* equivalent aluminum oxide and either 0.1 or 0.2 *M* polybasic acid or salt were prepared by dissolving the polybasic acid or salt in water and adding the solution to an appropriate quantity of aluminum hydroxycarbonate gel with mixing.

The acid neutralization reaction was monitored by an automated pH-stat titration at pH 3.0 and 25° (10).

The carbonate content was determined by gasometric displacement using the Chittick apparatus[1] (11) and is expressed as the molar ratio of carbonate to aluminum.

The aluminum content of the supernate was determined by centrifuging at 15,000 rpm (27,000×*g*) for 30 min and measuring the aluminum content of the supernate by atomic absorption spectroscopy. The result represents the aluminum-ion content as well as the aluminum content of hydroxyaluminum polymers that remain in the supernate after centrifugation. The aluminum content of the supernate depended on the conditions of centrifugation, and all results reported were obtained under carefully standardized conditions.

The distribution of the organic solute was monitored by analyzing both the supernate and the solid phase for organic carbon content by the Walkley–Black method (12). In every case, the sum of the organic carbon in solution and in the solid phase was 82–101% of the theoretical carbon content.

The solid phase that formed when 0.2 *M* citric acid was added to the aluminum hydroxycarbonate gel was analyzed by X-ray diffraction[2] and IR spectroscopy. A sample of the solid phase was vacuum dried over phosphorus pentoxide and ground to a fine powder with an agate mortar

[1] Sargent-Welch Scientific Co., Skokie, Ill.
[2] Siemens AG Kristalloflex 4 generator, type F diffractometer, Karlsruhe, West Germany.

0022-3549/80/0600-0668$01.00/0
© 1980, American Pharmaceutical Association

(33) P. D. Moore and M. Koreeda, *Biochem. Biophys. Res. Commun.*, **73**, 459 (1976).
(34) A. D. Marco, A. M. Casazza, and Pratesi, *Can. Tred. Rep.*, **61**, 893 (1977).
(35) P. Moser, K. Jakel, P. Krupp, R. Menassa, and A. Sallmann, *Eur. J. Med. Chem.*, **10**, 613 (1975).
(36) J. C. Dearden and E. George, *J. Pharm. Pharmacol.*, **30**, 49p (1978).
(37) E. J. Lien, Ph.D. thesis, University of California Medical Center, San Francisco, Calif., 1966.
(38) D. W. Newton and R. B. Kenza, *Drug Intell. Clin. Pharm.*, **12**, 546 (1978).
(39) "The Merck Index," 9th ed., Merck & Co., Rahway, N.J., 1976.
(40) R. N. Smith, C. Hansch, and M. M. Arres, *J. Pharm. Sci.*, **64**, 599 (1975).
(41) G. Gomori, in "Methods in Enzymology," S. P. Colowick and W. O. Kaplan, Eds., Academic, New York, N.Y., 1955.
(42) O. D. Bonner and G. B. Woolsey, *J. Phys. Chem.*, **72**, 899 (1968).
(43) A. N. Martin, J. Swarbrick, and A. Cammarata, "Physical Pharmacy," 2nd ed., Lea & Febiger, Philadelphia, Pa., 1969, pp. 181–186.
(44) C. Hansch, A. Leo, S. H. Unger, K. H. Kim, D. Nikaitani, and E. J. Lien, *J. Med. Chem.*, **16**, 1207 (1973).
(45) R. F. Rekker, in "Biological Activity and Chemical Structure," J. A. Keverling Buisman, Ed., Elsevier, Amsterdam, The Netherlands, 1977, pp. 231–238.

ACKNOWLEDGMENTS

Presented in part at the APhA Academy of Pharmaceutical Sciences, Kansas City meeting, November 1979.

Adapted in part from a thesis submitted by P.-H. Wang to the University of Southern California in partial fulfillment of the Master of Science degree requirements.

Effect of Polybasic Acids on Structure of Aluminum Hydroxycarbonate Gel

MING K. WANG *, JOE L. WHITE *, and STANLEY L. HEM ‡x

Received September 24, 1979, from the **Department of Agronomy and the* ‡*Department of Industrial and Physical Pharmacy, Purdue University, West Lafayette, IN 47907.* Accepted for publication January 11, 1980.

Abstract □ The effect of oxalic acid, citric acid, and their sodium salts on the structure of aluminum hydroxycarbonate gel was studied to illustrate the various mechanisms by which polybasic acids interact with aluminum hydroxycarbonate gel. Analysis of changes in the pH-stat titrigram, the carbonate to aluminum ratio, the aluminum content of the supernate following centrifugation, and the adsorption of the organic solute indicates that polybasic acids may: (*a*) partially neutralize the aluminum hydroxycarbonate gel by a general acid effect, (*b*) modify the aluminum hydroxycarbonate surface by adsorption of the anionic form of the polybasic acid, (*c*) extract aluminum by the formation of a soluble complex, and (*d*) lead to the precipitation of a new crystalline phase.

Keyphrases □ Polybasic acids—oxalic acid, citric acid, and their sodium salts, effect on aluminum hydroxycarbonate gel structure, complexation of polybasic acids with aluminum, adsorption of polybasic anion, acid neutralization □ Complexation—polybasic acids and their sodium salts with aluminum hydroxycarbonate gel, acid neutralization, structural changes in aluminum hydroxycarbonate gel □ Acid neutralization—complex formation with polybasic acids and aluminum hydroxycarbonate gel □ Aluminum hydroxycarbonate—complexation with polybasic acids and their sodium salts, structural changes, acid neutralization

Citric acid, oxalic acid, and other polybasic acids can inhibit the crystallization of aluminum hydroxide and form complexes with aluminum (1–3). Gibaldi and Mufson (4) found that the neutralization of dried aluminum hydroxide gel was inhibited when sodium citrate or sodium tartrate was added to the 0.1 *N* HCl used as the reaction medium. It was concluded that dried aluminum hydroxide gel reacts with sodium citrate or sodium tartrate to produce a water-soluble complex as well as to reduce surface area by flocculation.

Polybasic acids are important in soil-weathering reactions due to their role in complexing and solubilizing aluminum (5, 6). In addition, it was found that the edge faces of gibbsite (7), as well as synthetic goethite (8), can adsorb oxalate anion.

The nature of the interaction of polybasic acids with the surface of aluminum hydroxycarbonate has not been examined in detail. This study describes the mechanisms by which polybasic acids interact with aluminum hydroxycarbonate and the effect of these interactions on the acid reactivity of aluminum hydroxycarbonate gel.

EXPERIMENTAL

An aluminum hydroxycarbonate gel that exhibited a moderate rate of acid neutralization was selected so that any increase or decrease in the acid neutralization rate would be observed easily. The gel was amorphous to X-rays and had an IR spectrum characteristic of aluminum hydroxycarbonate gel (9).

Mixtures containing 0.2 *M* equivalent aluminum oxide and either 0.1 or 0.2 *M* polybasic acid or salt were prepared by dissolving the polybasic acid or salt in water and adding the solution to an appropriate quantity of aluminum hydroxycarbonate gel with mixing.

The acid neutralization reaction was monitored by an automated pH-stat titration at pH 3.0 and 25° (10).

The carbonate content was determined by gasometric displacement using the Chittick apparatus[1] (11) and is expressed as the molar ratio of carbonate to aluminum.

The aluminum content of the supernate was determined by centrifuging at 15,000 rpm (27,000×*g*) for 30 min and measuring the aluminum content of the supernate by atomic absorption spectroscopy. The result represents the aluminum-ion content as well as the aluminum content of hydroxyaluminum polymers that remain in the supernate after centrifugation. The aluminum content of the supernate depended on the conditions of centrifugation, and all results reported were obtained under carefully standardized conditions.

The distribution of the organic solute was monitored by analyzing both the supernate and the solid phase for organic carbon content by the Walkley–Black method (12). In every case, the sum of the organic carbon in solution and in the solid phase was 82–101% of the theoretical carbon content.

The solid phase that formed when 0.2 *M* citric acid was added to the aluminum hydroxycarbonate gel was analyzed by X-ray diffraction[2] and IR spectroscopy. A sample of the solid phase was vacuum dried over phosphorus pentoxide and ground to a fine powder with an agate mortar

[1] Sargent-Welch Scientific Co., Skokie, Ill.
[2] Siemens AG Kristalloflex 4 generator, type F diffractometer, Karlsruhe, West Germany.

0022-3549/80/0600-0668$01.00/0
© 1980, American Pharmaceutical Association

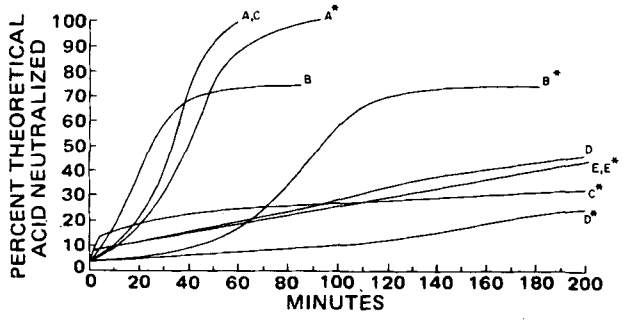

Figure 1—*The pH-stat titrigrams at pH 3.0 and 25° for aluminum hydroxycarbonate gel equivalent to 0.2 M Al_2O_3 with 0.1 M polybasic acids. Key: A, control; B, oxalic acid; C, sodium oxalate; D, citric acid; E, sodium citrate; and *, aged at 40° for 2 weeks.*

and pestle. Powder mounts for X-ray diffraction were prepared using McCreery mounts. The diffraction pattern was recorded from 6 to 55° 2θ under the following conditions: CuK_γ radiation, 40 kv, 20 mamp, 500 cps full scale, and 2°/min scan speed. IR spectra[3] were obtained by pressing a disk containing 0.5 mg of the dried powder with 300 mg of potassium bromide.

RESULTS

Figure 1 shows the pH-stat titrigrams of aluminum hydroxycarbonate gel immediately following the addition of 0.1 *M* oxalic acid, citric acid, sodium oxalate, or sodium citrate and after aging for 2 weeks at 40°. As expected, the acid neutralization rate decreased slightly during aging of the control aluminum hydroxycarbonate gel (Fig. 1A).

Oxalic acid (Fig. 1B) caused an initial decrease in the total amount of neutralized acid that was related directly to the oxalic acid concentration. In addition, a more rapid acid neutralization rate was observed immediately following oxalic acid addition. However, the acid neutralization rate decreased much more rapidly with aging (Fig. 1B*) than did the rate for the control aluminum hydroxycarbonate gel.

Sodium oxalate initially did not affect the pH-stat titrigram (Fig. 1C). However, a totally different acid neutralization profile was observed upon aging; it was characterized by a two-phase titrigram in which ~15% of the acid was neutralized immediately and the major portion followed a slow, zero-order reaction (Fig. 1C*).

The addition of citric acid substantially decreased the acid neutralization rate (Fig. 1D), which decreased further upon aging (Fig. 1D*). However, the pH-stat titrigram still shows evidence of the three-phase titrigram that characterized aluminum hydroxycarbonate gel (9).

The addition of sodium citrate resulted in a slow, two-phase neutralization reaction, which did not change during aging (Fig. 1E).

The polybasic acids caused a decrease in pH accompanied by a decrease in the carbonate to aluminum ratio (Table I). This effect also was observed when 0.1 *M* HCl was added to the aluminum hydroxycarbonate gel. The carbonate to aluminum ratio was not affected by the addition of sodium oxalate or sodium citrate.

Oxalic acid caused an initial increase in the aluminum content of the supernate, which decreased slowly during aging. Citric acid initially produced a high level of aluminum in the supernate, which dropped significantly during aging. The addition of 0.2 *M* citric acid converted the liquid gel into a solid within 30 min of mixing. Hydrochloric acid increased the aluminum content in the supernate, which increased further upon aging.

Sodium oxalate caused a small increase in the aluminum content of the supernate, which did not change during aging. A substantial increase in the aluminum content of the supernate occurred following the addition of sodium citrate, with approximately half of the aluminum in the gel solubilized by the addition of 0.2 *M* sodium citrate.

The adsorption of the polybasic acid or its salt was measured by determining the carbon content of the supernate and the solid phase (Table I). Approximately 40% of the added oxalic acid was in solution immediately following the addition of oxalic acid. The oxalic acid concentration in solution slowly decreased during aging. Sodium oxalate showed the same pattern, except that higher levels of oxalate ion were found in solution.

[3] Model 180, Perkin-Elmer Corp., Norwalk, Conn.

Table I—Effect of Polybasic Acids and Their Salts on the Composition of Aluminum Hydroxycarbonate Gel[a]

Polybasic Acid or Salt Added	pH			Molar Ratio of Carbonate to Aluminum			Total Aluminum in Supernate, %			Total Carbon in Supernate, %		
	Initial	1 Week	2 Weeks	Initial	1 Week	2 Weeks	Initial	1 Week	2 Weeks	Initial	1 Week	2 Weeks
Control	6.5	6.4	6.1	0.36	0.34	0.33	0.3	0.3	0.3	—	—	—
0.1 *M* Oxalic acid	4.6	5.1	5.2	0.21	0.08	0.08	3.8	2.2	1.4	41.3	30.8	21.6
0.2 *M* Oxalic acid	4.1	4.4	4.3	0.15	0.03	0.02	11.5	9.0	7.8	37.5	24.1	25.0
0.1 *M* Sodium oxalate	9.3	8.8	8.8	0.36	0.32	0.31	2.3	2.3	2.3	53.6	46.2	36.4
0.2 *M* Sodium oxalate	9.6	8.9	8.9	0.36	0.32	0.33	2.4	2.8	2.3	61.5	52.6	41.7
0.1 *M* Citric acid	4.0	4.6	4.7	0.26	0.10	0.10	28.0	5.1	2.3	44.3	8.4	6.2
0.2 *M* Citric acid[b]	—	—	—	—	—	—	—	—	—	—	—	—
0.1 *M* Sodium citrate	10.0	10.1	10.2	0.36	0.33	0.33	15.7	19.2	22.6	64.2	66.2	56.3
0.2 *M* Sodium citrate	10.5	10.3	10.3	0.35	0.34	0.34	34.0	57.5	62.1	79.0	71.0	87.7
0.1 *M* Hydrochloric acid	4.2	4.6	4.4	0.24	0.07	0.07	13.9	15.3	17.2	—	—	—

[a] Samples were maintained at 40°. [b] Sample turned solid within 30 min of preparation.

Table II—X-Ray Powder Diffraction Pattern of the New Phase Formed when 0.2 *M* Citric Acid Was Added to Aluminum Hydroxycarbonate Gel Equivalent to 0.2 *M* Al_2O_3 Compared to the 10 Most Intense Peaks for Citric Acid, Sodium Citrate, and Aluminum Citrate[a]

New Phase		Citric Acid Monohydrate[b]		Sodium Citrate Dihydrate[c]	
Interplanar Spacing, Å	Relative Intensity, %	Interplanar Spacing, Å	Relative Intensity, %	Interplanar Spacing, Å	Relative Intensity, %
14.26	100	5.82	100	7.86	100
7.63	10	4.87	90	3.70	35
7.20	10	3.980	65	5.05	30
6.92	16	3.849	55	5.49	18
6.66	21	2.741	40	3.01	14
6.28	12	4.94	25	2.438	14
6.19	12	3.639	25	9.54	12
5.64	10	3.045	25	3.258	12
5.10	6	2.684	18	2.742	12
5.01	6	4.66	16	4.83	10
3.82	9	3.744	16	3.23	10
3.65	22	3.025	16	2.964	10
3.49	16	2.913	16	2.414	10
3.47	16				
3.35	16				
3.29	20				
3.13	14				
3.10	14				
3.02	7				
2.93	10				
2.15	7				

[a] Sample obtained from Pfaltz and Bauer, Stamford, Conn., was amorphous to X-rays. [b] Data from A.S.T.M. Card 15-985. [c] Data from A.S.T.M. Card 16-1170.

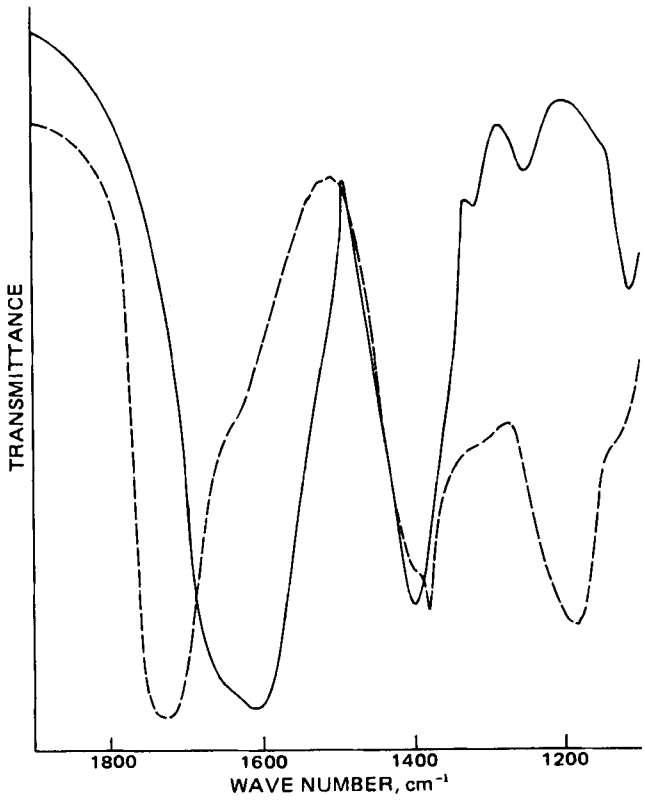

Figure 2—*IR spectra of citric acid (- -) and the solid phase that formed from a mixture of 0.2* M *citric acid and aluminum hydroxycarbonate gel equivalent to 0.2* M Al_2O_3 *(—).*

A high citric acid level was seen in solution initially but dropped sharply during aging. Most of the added sodium citrate was present in solution both initially and during aging.

The X-ray diffractogram and IR spectrum of the solid that formed upon the addition of 0.2 *M* citric acid are shown in Table II and Fig. 2, respectively. The appearance of a new phase is indicated by the peaks in the X-ray diffractogram, which differ from that of citric acid, sodium citrate, or aluminum citrate. The reaction of citric acid with aluminum to form citrate anion in the new phase was confirmed by the shift of the carbonyl stretching band of citric acid at 1730 cm^{-1} to an unresolved doublet with maxima at 1615 and 1640 cm^{-1}.

DISCUSSION

Polybasic acids and their salts cause significant changes in the structure of aluminum hydroxycarbonate gel that affect both acid reactivity and stability, and several mechanisms may be responsible for these changes.

Oxalic acid appears to act by a general acid effect, which causes partial neutralization of the aluminum hydroxycarbonate gel. This effect is suggested by the decrease in the total amount of acid neutralized, the loss of carbonate from the gel structure, and the increased aluminum content of the supernate.

The increased acid neutralization rate following the addition of oxalic acid agrees with the previous observation (13) that the reaction of structural carbonate with acid disrupts the gel structure and increases the porosity. This effect facilitates diffusion of acid into the gel and leads to an accelerated acid neutralization rate. However, the gel is expected to polymerize more rapidly upon aging in the absence of structural carbonate. This behavior was confirmed by the large decrease in the acid neutralization rate upon aging (Fig. 1B*).

Adsorption of the oxalate anion produced in the neutralization reaction of oxalic acid and aluminum hydroxycarbonate gel may occur, as suggested by the decreased concentration of organic carbon in solution. Evidence for the adsorption of oxalate anion also was seen when sodium oxalate was added to the aluminum hydroxycarbonate gel. No immediate effect was observed on the pH-stat titrigram, but the slow, constant rate of acid neutralization observed after aging (Fig. 1C*) suggests that oxalate anion is adsorbed by the aluminum hydroxycarbonate surface and that the acid neutralization rate is controlled by the diffusion of protons through the adsorbed oxalate layer to the aluminum hydroxycarbonate gel surface.

The carbonate to aluminum ratio was not affected by sodium oxalate. However, the amount of oxalate anion in solution decreased during aging, and only a relatively small increase in the aluminum content of the supernate was observed. This behavior supports the proposed surface adsorption mechanism.

The addition of sodium citrate to aluminum hydroxycarbonate gel also produced a pH-stat titrigram consisting primarily of a slow, zero-order acid neutralization reaction, which did not change during aging.

It is hypothesized that citrate anion is adsorbed by the aluminum hydroxycarbonate surface, producing the same type of diffusion-controlled acid neutralization as was seen in the aged sodium oxalate sample.

Adsorption of citrate anion occurs immediately in contrast to oxalate anion. The increase in the aluminum content of the supernate to ~60% following aging of the 0.2 *M* sodium citrate sample and the high levels of citrate anion in solution suggest that, following citrate anion adsorption, aluminum is extracted from the aluminum hydroxycarbonate through the formation of a soluble complex.

Citric acid caused the greatest decrease in the acid neutralization rate. After aging for 2 weeks at 40°, only 30% of the theoretical amount of acid was neutralized in 200 min (Fig. 1D*).

The decrease in the carbonate to aluminum ratio and the high initial aluminum content of the supernate suggest that citric acid acts by a general acid effect to neutralize partially the aluminum hydroxycarbonate gel. However, the mechanism by which citric acid affects the gel structure appears to be more complex than that observed for oxalic acid.

The sharp decrease in both aluminum in the supernate and organic carbon in solution during aging suggests the precipitation of a new phase containing aluminum and citrate. When 0.2 *M* citric acid was added, the aluminum hydroxycarbonate gel turned solid within 30 min. The structure of the solid phase that formed is not known; the new phase contained citrate anion, but the X-ray diffractogram differed from that for sodium or aluminum citrate.

Although the crystalline phase was not identified, its formation rate is dependent on the citric acid concentration. The crystalline phase does not exhibit acid neutralization properties when measured by pH-stat titration at pH 3, and its formation destroys the antacid properties of aluminum hydroxycarbonate gel.

REFERENCES

(1) K. F. NyKee Kwong and P. M. Huang, *Clays Clay Miner.*, **23**, 164 (1975).

(2) K. F. NyKee Kwong and P. M. Huang, *Soil Sci. Soc. Am. J.*, **41**, 692 (1977).

(3) K. F. NyKee Kwong and P. M. Huang, *Nature*, **271**, 336 (1978).

(4) M. Gibaldi and D. Mufson, *J. Pharm. Sci.*, **56**, 46 (1967).

(5) C. J. Lind and J. D. Hem, "Effects of Organic Solutes on Chemical Reactions of Aluminum," U.S. Geological Survey Water-Supply Paper 1827-G, U.S. Government Printing Office, Washington, D.C., 1975.

(6) W. H. Huang and W. D. Keller, *Clays Clay Miner.*, **20**, 69 (1972).

(7) R. L. Parfitt, A. R. Fraser, J. D. Russell, and V. C. Farmer, *J. Soil Sci.*, **28**, 40 (1977).

(8) R. L. Parfitt, V. C. Farmer, and J. D. Russell, *ibid.*, **28**, 29 (1977).

(9) C. J. Serna, J. L. White, and S. L. Hem, *J. Pharm. Sci.*, **67**, 324 (1978).

(10) N. J. Kerkhof, R. K. Vanderlaan, J. L. White, and S. L. Hem, *ibid.*, **66**, 1528 (1977).

(11) "Official Methods of Analysis of the Association of Official Analytical Chemists," 12th ed., W. Horwitz, Ed., Association of Official Analytical Chemists, Washington, D.C., 1975, p. 147.

(12) A. Walkley and I. A. Black, *Soil Sci.*, **37**, 29 (1934).

(13) N. J. Kerkhof, J. L. White, and S. L. Hem, *J. Pharm. Sci.*, **66**, 1533 (1977).

ACKNOWLEDGMENTS

Supported in part by the Barcroft Co.

This report is Journal Paper 7798, Purdue University Agricultural Experiment Station, West Lafayette, IN 47907.

Deiodination Kinetics of Water-Soluble Radiopaques

YU-CHANG JOHN WANG

Received July 29, 1979, from *Pharmaceutical R & D, Squibb Institute for Medical Research, New Brunswick, NJ 08903.* Accepted for publication January 16, 1980.

Abstract □ Deiodination of diatrizoic acid, an anionic radiopaque, was found to be catalyzed by Cu(II). Through a detailed study of *o*-iodobenzoic acid, a model compound, the copper-catalyzed S_N1 mechanism was established based on observations of common ion, salt, and pH effects. *Meta*- and *para*-iodobenzoic acids were unreactive. Deiodination thus was facilitated by a neighboring carboxylate that attracted copper. Iopamidol, a nonionic radiopaque, also underwent deiodination. At pH 7 or above, the hydroxide-ion substitution predominated. At pH below 7, the reaction is in favor of the copper-catalyzed S_N1 mechanism.

Keyphrases □ Diatrizoic acid—radiopaque, deiodination kinetics □ *o*-Iodobenzoic acid—deiodination, metal-catalyzed S_N1 mechanism □ Iopamidol—radiopaque, deiodination mechanism □ Kinetics—aromatic S_N1 deiodination of radiopaques □ Radiopaques—diatrizoic acid and iopamidol, deiodination kinetics □ Metal catalysis—neighboring carboxylate deiodination

The most important radiopaques are the water-soluble, anionic compounds such as diatrizoic acid (I), iothalamic acid, and iodipamide. These compounds are benzoic acid derivatives with two or three iodines attached to the benzene ring. There appears to be no evidence in the literature that appreciable deiodination occurs in products containing any of these compounds (1). However, experiments in these laboratories showed that significant deiodination took place in the absence of chelating agents.

Since the mechanism of this reaction was not established, this paper will discuss the deiodination kinetics of diatrizoic acid as a representative of anionic radiopaques. A model compound, *o*-iodobenzoic acid, was studied to support the proposed mechanism. A new nonionic radiopaque, iopamidol (II) (2), also was examined, and its deiodination kinetics were compared with those of diatrizoic acid.

EXPERIMENTAL

Materials—Diatrizoic acid[1], iopamidol[2], 8-hydroxyquinoline[3], and

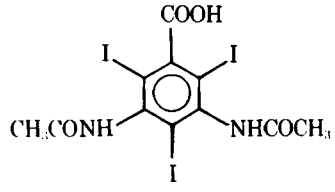

I

m- and *p*-iodobenzoic acids[3] were used without further purification; *o*-iodobenzoic acid[3] was recrystallized twice from ethanol–water. All other chemicals were reagent grade. The water used complied with the USP specifications for purified water.

Deiodination of Diatrizoic Acid—Diatrizoic acid was dissolved in water with a stoichiometric amount of sodium hydroxide. Sørensen phosphate buffer (3) was added to bring the final phosphate concentration to 0.0067 *M*. The chelating agent employed was edetate disodium USP at 0.04% (w/v). The amount of iodide produced after stressed conditions was determined by the USP method (4), which specifies the measurement of the absorbance of iodine in a toluene extract at 495 nm[4] after the iodide has been oxidized to iodine. The concentration was calculated from a standard curve obtained from potassium iodide solutions. Similar to the USP specification, the amount of iodide found was expressed as the percentage of the weight of iodide with respect to the weight of radiopaque in the same solution.

Kinetic Studies for *o*-Iodobenzoic Acid—*o*-Iodobenzoic acid was dissolved in water with a stoichiometric amount of sodium hydroxide. Sørensen phosphate buffer at 0.0067 *M* and cupric sulfate at 0.5 ppm of Cu(II) were used unless stated otherwise. Solutions were immersed in a constant-temperature (±0.1°) oil bath[5], and samples were removed periodically for UV assay. Absorbances of the samples at 295 nm were used

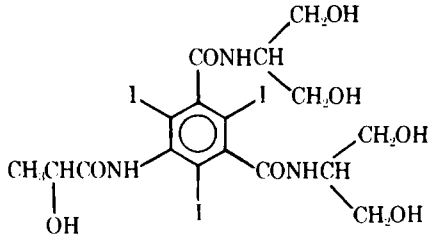

II

[1] Renografin, E. R. Squibb & Sons, New Brunswick, N.J.

[2] $C_{17}H_{22}I_3N_3O_8$, *N,N'*-bis[2-hydroxy-1-(hydroxymethyl)ethyl]-5-[(2-hydroxy-1-oxopropyl)amino]-2,4,6-triiodo-1,3-benzenedicarboxamide (Bracco 15,000, SQ 13,396), E. R. Squibb & Sons, New Brunswick, N.J.

[3] Eastman Kodak Co., Rochester, N.Y.

[4] Model 25 spectrophotometer, Beckman Instruments, Irvine, Calif.

[5] Constant-temperature circulator model FJ, Haake Inc., Saddle Brook, N.J.

0022-3549/80/0600-0671$01.00/0

© 1980, American Pharmaceutical Association

REFERENCES

(1) K. F. NyKee Kwong and P. M. Huang, *Clays Clay Miner.*, **23**, 164 (1975).

(2) K. F. NyKee Kwong and P. M. Huang, *Soil Sci. Soc. Am. J.*, **41**, 692 (1977).

(3) K. F. NyKee Kwong and P. M. Huang, *Nature*, **271**, 336 (1978).

(4) M. Gibaldi and D. Mufson, *J. Pharm. Sci.*, **56**, 46 (1967).

(5) C. J. Lind and J. D. Hem, "Effects of Organic Solutes on Chemical Reactions of Aluminum," U.S. Geological Survey Water-Supply Paper 1827-G, U.S. Government Printing Office, Washington, D.C., 1975.

(6) W. H. Huang and W. D. Keller, *Clays Clay Miner.*, **20**, 69 (1972).

(7) R. L. Parfitt, A. R. Fraser, J. D. Russell, and V. C. Farmer, *J. Soil Sci.*, **28**, 40 (1977).

(8) R. L. Parfitt, V. C. Farmer, and J. D. Russell, *ibid.*, **28**, 29 (1977).

(9) C. J. Serna, J. L. White, and S. L. Hem, *J. Pharm. Sci.*, **67**, 324 (1978).

(10) N. J. Kerkhof, R. K. Vanderlaan, J. L. White, and S. L. Hem, *ibid.*, **66**, 1528 (1977).

(11) "Official Methods of Analysis of the Association of Official Analytical Chemists," 12th ed., W. Horwitz, Ed., Association of Official Analytical Chemists, Washington, D.C., 1975, p. 147.

(12) A. Walkley and I. A. Black, *Soil Sci.*, **37**, 29 (1934).

(13) N. J. Kerkhof, J. L. White, and S. L. Hem, *J. Pharm. Sci.*, **66**, 1533 (1977).

ACKNOWLEDGMENTS

Supported in part by the Barcroft Co.

This report is Journal Paper 7798, Purdue University Agricultural Experiment Station, West Lafayette, IN 47907.

Deiodination Kinetics of Water-Soluble Radiopaques

YU-CHANG JOHN WANG

Received July 29, 1979, from *Pharmaceutical R & D, Squibb Institute for Medical Research, New Brunswick, NJ 08903.* Accepted for publication January 16, 1980.

Abstract □ Deiodination of diatrizoic acid, an anionic radiopaque, was found to be catalyzed by Cu(II). Through a detailed study of *o*-iodobenzoic acid, a model compound, the copper-catalyzed S_N1 mechanism was established based on observations of common ion, salt, and pH effects. *Meta*- and *para*-iodobenzoic acids were unreactive. Deiodination thus was facilitated by a neighboring carboxylate that attracted copper. Iopamidol, a nonionic radiopaque, also underwent deiodination. At pH 7 or above, the hydroxide-ion substitution predominated. At pH below 7, the reaction is in favor of the copper-catalyzed S_N1 mechanism.

Keyphrases □ Diatrizoic acid—radiopaque, deiodination kinetics □ *o*-Iodobenzoic acid—deiodination, metal-catalyzed S_N1 mechanism □ Iopamidol—radiopaque, deiodination mechanism □ Kinetics—aromatic S_N1 deiodination of radiopaques □ Radiopaques—diatrizoic acid and iopamidol, deiodination kinetics □ Metal catalysis—neighboring carboxylate deiodination

The most important radiopaques are the water-soluble, anionic compounds such as diatrizoic acid (I), iothalamic acid, and iodipamide. These compounds are benzoic acid derivatives with two or three iodines attached to the benzene ring. There appears to be no evidence in the literature that appreciable deiodination occurs in products containing any of these compounds (1). However, experiments in these laboratories showed that significant deiodination took place in the absence of chelating agents.

Since the mechanism of this reaction was not established, this paper will discuss the deiodination kinetics of diatrizoic acid as a representative of anionic radiopaques. A model compound, *o*-iodobenzoic acid, was studied to support the proposed mechanism. A new nonionic radiopaque, iopamidol (II) (2), also was examined, and its deiodination kinetics were compared with those of diatrizoic acid.

EXPERIMENTAL

Materials—Diatrizoic acid[1], iopamidol[2], 8-hydroxyquinoline[3], and

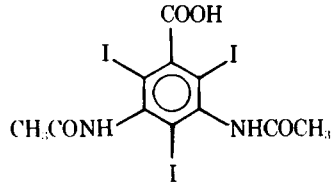

I

m- and *p*-iodobenzoic acids[3] were used without further purification; *o*-iodobenzoic acid[3] was recrystallized twice from ethanol–water. All other chemicals were reagent grade. The water used complied with the USP specifications for purified water.

Deiodination of Diatrizoic Acid—Diatrizoic acid was dissolved in water with a stoichiometric amount of sodium hydroxide. Sørensen phosphate buffer (3) was added to bring the final phosphate concentration to 0.0067 *M*. The chelating agent employed was edetate disodium USP at 0.04% (w/v). The amount of iodide produced after stressed conditions was determined by the USP method (4), which specifies the measurement of the absorbance of iodine in a toluene extract at 495 nm[4] after the iodide has been oxidized to iodine. The concentration was calculated from a standard curve obtained from potassium iodide solutions. Similar to the USP specification, the amount of iodide found was expressed as the percentage of the weight of iodide with respect to the weight of radiopaque in the same solution.

Kinetic Studies for *o*-Iodobenzoic Acid—*o*-Iodobenzoic acid was dissolved in water with a stoichiometric amount of sodium hydroxide. Sørensen phosphate buffer at 0.0067 *M* and cupric sulfate at 0.5 ppm of Cu(II) were used unless stated otherwise. Solutions were immersed in a constant-temperature (±0.1°) oil bath[5], and samples were removed periodically for UV assay. Absorbances of the samples at 295 nm were used

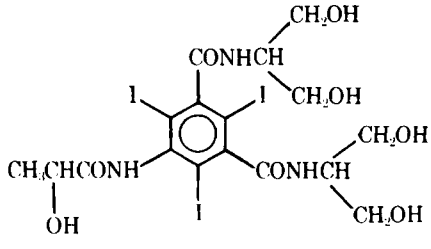

II

[1] Renografin, E. R. Squibb & Sons, New Brunswick, N.J.

[2] $C_{17}H_{22}I_3N_3O_8$, *N,N'*-bis[2-hydroxy-1-(hydroxymethyl)ethyl]-5-[(2-hydroxy-1-oxopropyl)amino]-2,4,6-triiodo-1,3-benzenedicarboxamide (Bracco 15,000, SQ 13,396), E. R. Squibb & Sons, New Brunswick, N.J.

[3] Eastman Kodak Co., Rochester, N.Y.

[4] Model 25 spectrophotometer, Beckman Instruments, Irvine, Calif.

[5] Constant-temperature circulator model FJ, Haake Inc., Saddle Brook, N.J.

0022-3549/80/0600-0671$01.00/0

© 1980, American Pharmaceutical Association

Table I—Production of Iodide from Diatrizoic Acid Solutions [a] at Various pH Values

pH	Iodide Found[b], % [c]
7.8	0.371
7.4	0.388
7.0	0.333
6.6	0.227
6.2	0.150

[a] Solutions contained 20% (w/v) diatrizoic acid and 0.0067 *M* Sørensen phosphate buffer and were assayed after autoclaving at 120° for 30 min. [b] Unautoclaved samples and samples containing 0.04% (w/v) edetate disodium autoclaved at 120° for 30 min showed undetectable amounts of iodide (<0.0001%). [c] The weight percent of iodide with respect to the weight of diatrizoic acid in the same solution.

to calculate the amount of salicylic acid produced in the reaction. The residual amount of *o*-iodobenzoic acid, employed in the semilogarithmic plot, was obtained by subtracting the concentration of salicylic acid produced from the initial concentration of *o*-iodobenzoic acid. The reaction rates were calculated graphically from the initial slopes.

In one experiment, deiodination was followed simultaneously by three assay methods: the iodine assay, which was the same as for diatrizoic acid; the colorimetric assay, which measures the violet color produced by salicylic acid in the presence of ferric chloride; and the UV assay.

In another experiment, samples were analyzed by high-pressure liquid chromatography (HPLC) to identify the degradants produced in the kinetic study. The column was prepacked with reversed-phase Partisil ODS-2[6]. The mobile phase was methanol–water–phosphoric acid (48:52:0.04). The UV detector[7] was operated at 240 nm. The flow rate[8] was 2 ml/min, and the volume of the injector[9] loop was 20 μl.

Deiodination of *o*-, *m*-, and *p*-Iodobenzoic Acids—Solutions of these compounds at 0.5 *M* were prepared by the addition of a stoichiometric amount of sodium hydroxide, 0.0067 *M* phosphate buffer, and 0.04 m*M* of Cu(II). After autoclave sterilization, the iodide content in these solutions was determined by the method described for diatrizoic acid.

Deiodination of Iopamidol—The reaction kinetics were followed by monitoring the iodide content. The solution pH values were maintained by 0.0067 *M* Sørensen phosphate buffer, and the iodide concentration was assayed by the procedure described for diatrizoic acid solutions.

Since the iodide ion produced by deiodination was much less than 1% of the iopamidol, a typical equation for first-order kinetics can be simplified (5) through approximation in an infinite series:

$$k_0 = \frac{1}{t}\log_e \frac{[\text{iopamidol}]}{[\text{iopamidol}] - [I_t]} = \left(\frac{1}{t}\right)\frac{[I_t]}{[\text{iopamidol}]} \qquad \text{(Eq. 1)}$$

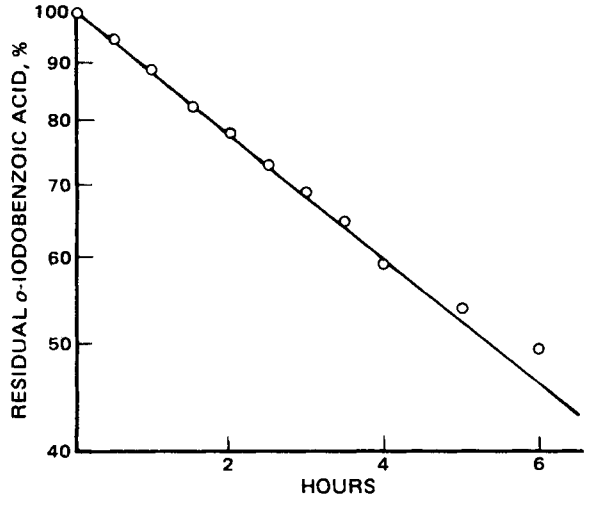

Figure 1—*Production of iodide (M) at 90° in 0.01 M diatrizoic acid solution containing 0.0067 M, pH 7 phosphate buffer and 4 ppm of Cu(II).*

[6] Whatman, Clifton, N.J.
[7] Model 1201 SpectroMonitor 1, Laboratory Data Control, Riviera Beach, Fla.
[8] Model 110A solvent metering pump, Altex, Berkeley, Calif.
[9] Model 7010 injection valve, Rheodyne, Berkeley, Calif.

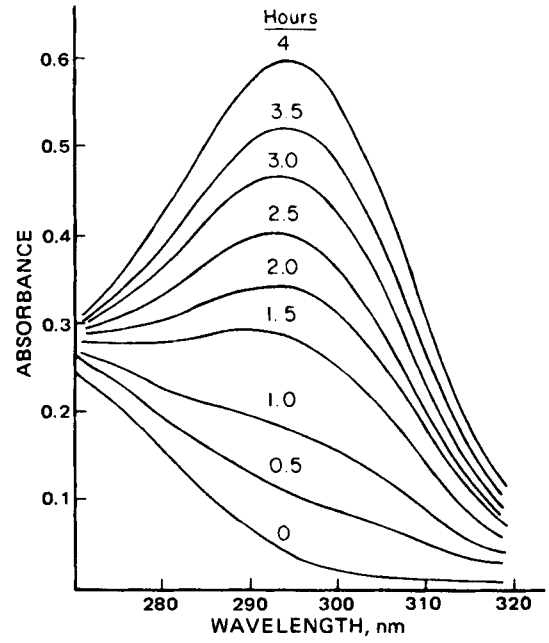

Figure 2—*UV spectral changes due to the formation of salicylic acid from o-iodobenzoic acid (0.002 M). The numbers shown by the curves are the times elapsed in hours when the solution was studied at 90° and pH 7.*

where [iopamidol] is the initial concentration of iopamidol, $[I_t]$ is the iodide concentration at time t, and k_0 is the initial rate constant expressed in reciprocal time.

RESULTS AND DISCUSSION

Deiodination of Diatrizoic Acid—To examine the effect of chelating agents, 20% diatrizoic acid solutions at various pH values were autoclaved at 120° for 30 min. Table I shows the production of the iodide content in solutions without a chelating agent. The iodide content, although small, exceeded the USP limit of 0.02%. Under the same conditions, preparations containing edetate disodium (0.04%) yielded undetectable amounts of iodide (<0.0001%). Therefore, it was concluded that in solutions without edetate, the trace amounts of heavy metals catalyzed the liberation of iodine from diatrizoic acid.

A spectrochemical analysis of water from the same source revealed a heavy metal content at the parts-per-billion level: Fe, 16; Cu, 9; Pb, 3; Ni, 1.4; and Zn, 37. The 0.0067 *M* phosphate buffer may contribute ~6 ppb or less of heavy metals. Since the USP limit for heavy metals for radiopaque compounds is 20 ppm, the majority of the heavy metal in the diatrizoic acid solution probably comes from the bulk compound; therefore, a heavy metal concentration in the parts-per-million range results.

To identify the metal responsible for catalysis, solutions of low metal content were obtained by extracting the same 20% diatrizoic acid solution at pH 7 with chloroform containing 0.1% 8-hydroxyquinoline. This solution was subdivided and spiked with 1 ppm each of Cu(II), Fe(III), and Fe(II) as the sulfate salt, Co(II), Zn(II), and Ag(I) as the nitrate salt, or Pb(II) as lead acetate. After autoclaving for 30 min, only the solution

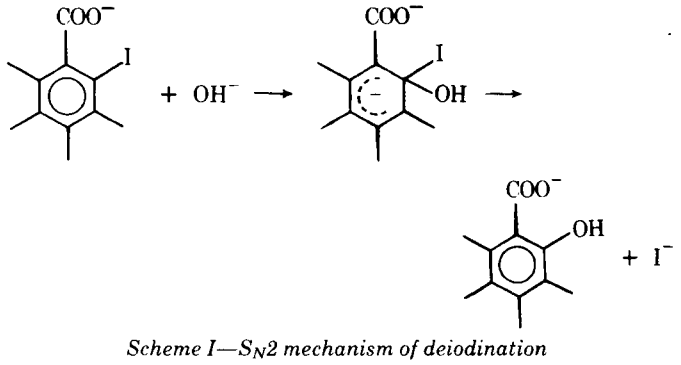

Scheme I—S_N2 mechanism of deiodination

Table II—Deiodination Rate Constants for *o*-Iodobenzoic Acid

Experiment	Iodobenzoic Concentration, m*M*	[Cu(II)], ppm[a]	pH	Other Additives[b]	Temperature	k_0, hr^{-1}
1	2	0.5	7.0		90°	0.127[c]
2	1	0.5	7.0		90°	0.121
3	0.4	0.5	7.0		90°	0.131
4	4	0.5	7.6	1.45 m*M* salicylic acid	90°	0.127
5	4	0.5	7.6		90°	0.127
6	4	0.5	8.0		90°	0.129
7	4	0.5	6.5		90°	0.118
8	2	5.08	7.0		90°	0.117
9	2	2.54	7.0		90°	0.116
10	2	1.27	7.0		90°	0.122
11	2	0.25	7.0		90°	0.127
12	2	0.2	7.0		90°	0.134
13	2	0.5	7.0	0.6 m*M* KI	90°	0.112
14	2	0.5	7.0	1.2 m*M* KI	90°	0.844
15	2	0.5	7.0	2.4 m*M* KI	90°	0.0739
16	2	0.5	7.0	20 m*M* NaBr	90°	0.126
17	2	0.5	7.0	100 m*M* KNO_3	90°	0.174
18	2	0.5	7.0		85.5°	0.0589
19	2	0.5	7.0		81°	0.0462
20	2	0.5	7.0		75.5°	0.0165
21	2	0.5	7.0		68°	0.0054

[a] For Cu(II), 1 ppm is equivalent to 0.015 m*M*. [b] All solutions included 0.0067 *M* Sørensen phosphate buffer and a stoichiometric amount of sodium hydroxide. [c] The standard deviation of k_0 for Experiments 1–12 is 0.00577.

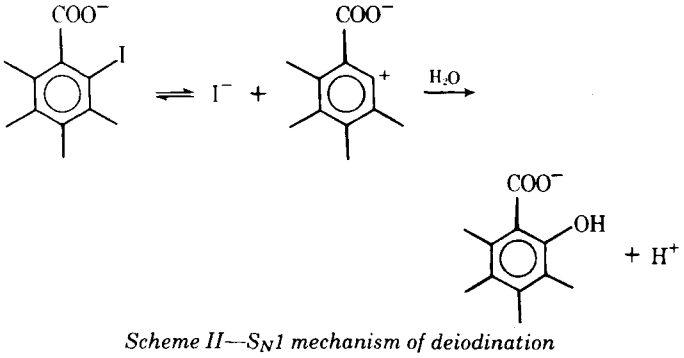

Scheme II—S_N1 mechanism of deiodination

spiked with Cu(II) yielded a detectable iodide content. From these results, it is evident that Cu(II) catalyzed the deiodination of diatrizoic acid. By using a chelating agent such as edetate disodium, this reaction can be retarded.

To investigate the Cu(II)-catalyzed deiodination further, production of iodide in a diatrizoic acid solution was monitored as a function of time. Figure 1 shows the increasing iodide content as the solution was heated at 90°. By assuming that each diatrizoic acid molecule produces only one iodide ion, a semilogarithmic first-order plot (not shown) of the diatrizoic acid concentration *versus* time resulted in a significant curvature. To explain this deviation from first-order kinetics, the two possible mechanisms (6) for deiodination were examined.

The S_N2 Mechanism—At constant pH, the S_N2 mechanism (Scheme I) cannot explain the curvature observed in the first-order plot of diatrizoic acid. In addition, the deiodination of diatrizoic acid is independent of the pH between pH 6 and 8 (Table I), and that observation does not support a bimolecular reaction in which the hydroxide ion takes part in the rate-determining step.

The S_N1 Mechanism—The first step in the S_N1 mechanism (Scheme II), the rate-determining step, is the formation of carbonium ion. The iodide produced in the first step can inhibit further deiodination through the reversible reaction and thus accounts for the curvature observed in the semilog plot. In addition, this mechanism requires pH independence, which is consistent with the observed results. The aromatic S_N1 mechanism is well established for the dissociation of diazonium salts. However, for aromatic halides, even active ones, a unimolecular S_N1 mechanism has not been observed with certainty (7).

To obtain further support that an S_N1 mechanism is operative in deiodination, a simple model compound was studied because a diatrizoic acid contains other labile moieties such as anilide linkages that may perturb the reactivity of the molecule and complicate the mechanism. *o*-Iodobenzoic acid was selected for its structural similarity to radiopaque compounds in general. Furthermore, deiodination kinetics can be followed by a simple UV assay of its deiodination product, salicylic acid, rather than by the more time-consuming iodide assay.

Deiodination of *o*-Iodobenzoic Acid—At neutral pH, *o*-iodobenzoic acid hydrolyzes to yield equal moles of salicylic acid, iodide, and the hydronium ion. Typical UV spectral changes are illustrated in Fig. 2. In one experiment, the reaction was followed by UV, colorimetric, and iodine assays, and the consistent results verified that deiodination of *o*-iodobenzoic acid, within experimental errors, produced only salicylic acid and iodide. This fact also was supported by the HPLC evidence shown in Fig. 3, in which only iodide and salicylic acid could be identified on the chromatogram. Figure 3 also shows that salicylic acid was stable under the conditions of the kinetic study, with decarboxylation, in particular, not taking place.

A semilogarithmic plot of the *o*-iodobenzoic acid concentration *versus* time shows that a typical reaction initially is rectilinear and finally exhibits definite exponential decline (Fig. 4). The pseudo-first-order rate constants, k_0, were calculated graphically from the initial slopes from:

$$\log_e \frac{A_0}{A_t} = -k_0 t \qquad \text{(Eq. 2)}$$

where A_0 and A_t are the *o*-iodobenzoic acid concentrations at times zero and t, respectively. The time was measured in hours. Rate constants under various conditions are shown in Table II. In Experiments 1–3 and 5 in Table II, in which the initial concentration of *o*-iodobenzoic acid was varied, consistent rate constants further demonstrated that the reaction is first order with respect to the *o*-iodobenzoic acid concentration.

Since deiodination required Cu(II) as a catalyst, the reaction product, salicylic acid, might chelate copper, affect reaction rates, and thus cause a curvature in the semilog plot. Experiments 4 and 5 (Table II) showed that the reaction rate remained constant with excess salicylic acid. A Cu(II)–salicylate complex probably still is capable of catalyzing deiodination. The fact that deiodination is independent of pH between pH 6 and 8, as demonstrated with diatrizoic acid (Table I), also was shown by Experiments 5–8 (Table II).

The effect of the Cu(II) concentration was illustrated by Experiments 8–11 (Table II), which showed that the reaction seemed to be independent of the Cu(II) concentration between 0.25 and 5.08 ppm. Solutions spiked with Cu(II) in this concentration range resulted in essentially constant reaction rates. Without spiking, the reactions rates often were scattered, perhaps due to various amounts of Cu(II) introduced as impurities in water, buffer, or bulk compounds.

Addition of a small amount of potassium iodide greatly retarded deiodination. For the deiodination of *o*-iodobenzoic acid, iodide is the common ion. The magnitude of the common ion effect (8), α[10], can be

[10] The common ion effect can be used as strong evidence for a carbonium-ion intermediate. In deiodination reactions, the α value measures the relative reactivities of iodide and water to the carbonium ion. Generally, the more stable the intermediate carbonium is, the larger α is.

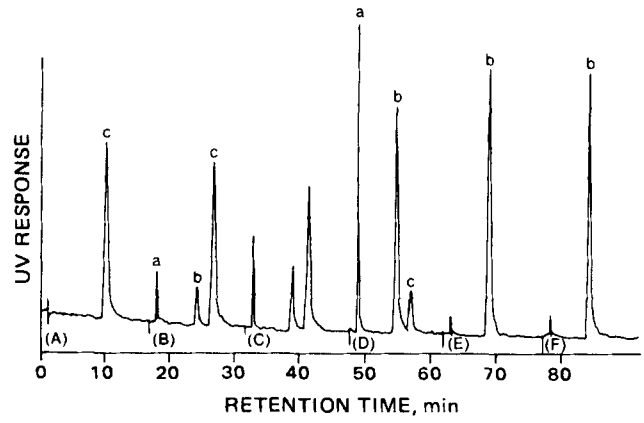

Figure 3—*High-pressure liquid chromatograms from kinetic studies of o-iodobenzoic acid (0.002 M) in pH 7 phosphate buffer and 4 ppm of Cu(II) at 90° for 0 hr (A), 1 hr (B), 2 hr (C), and 24 hr (D) and for salicylic acid under the same conditions for 0 hr (E) and 24 hr (F). Key: a, iodide; b, salicylic acid; and c, o-iodobenzoic acid.*

calculated from:

$$\alpha = \frac{1}{[I^-]}\left(\frac{k_0}{k_1} - 1\right) \qquad \text{(Eq. 3)}$$

where k_1 is the initial rate constant with an added iodide concentration of $[I^-]$ and k_0 is the rate constant at $[I^-] = 0$.

The α values for deiodination were 400 and 517 when the iodide concentrations were 1.2 and 2.4 mM, respectively. These values are on the same order of magnitude as the α values for the S_N1 hydrolysis of triphenylmethyl chloride (9). Such large α values for iodobenzoic acid lend strong support to the proposed S_N1 mechanism.

Addition of other halide ions, such as sodium bromide, did not affect reaction rates (Experiment 16). Increasing the ionic strength by adding large amounts of salt, such as potassium nitrate, enhanced deiodination (Experiment 17). These observations support an S_N1 mechanism. From an Arrhenius plot (Fig. 5) of the rate constants at five temperatures (Experiments 1 and 18–21), the heat of activation was calculated graphically to be 34 kcal/mole, which is comparable to many unimolecular S_N1 reactions (10).

Deiodination of *m*- and *p*-Iodobenzoic Acids—Apart from Cu(II) catalysis, deiodination is clearly of the S_N1 type for o-iodobenzoic acid. This reaction could be a unique instance of unimolecular aromatic substitutions in addition to the decomposition of diazonium ions. In the S_N1 mechanism, the neighboring carboxylate can function in either of two ways to facilitate the reaction. First, through electronic resonance effects, the negative carboxylate moiety could stabilize the formation of positive carbonium intermediates. If this were the case, *p*-iodobenzoic acid should undergo a reaction similar to o-iodobenzoic acid. Second, through a chelation effect, the carboxylate moiety could associate with copper ions, bringing them close to the reaction site and, perhaps, assisting the copper ion in polarizing the carbon–iodine bond. If this were the case, only o-iodobenzoic acid would be reactive and the *m*- and *p*-analogs would not be.

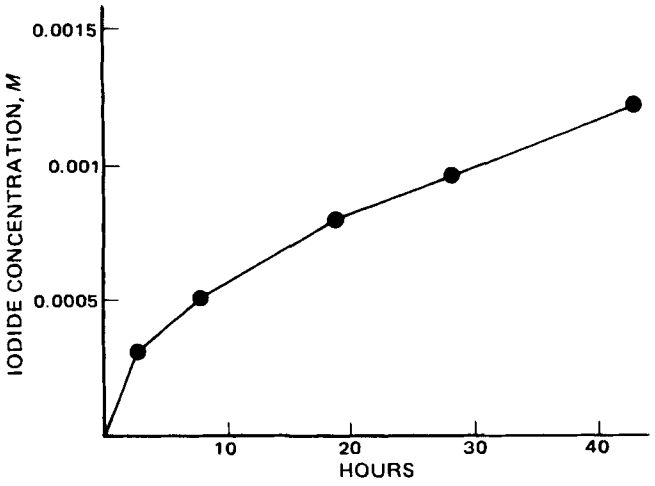

Figure 4—*First-order plot of deiodination of o-iodobenzoic acid.*

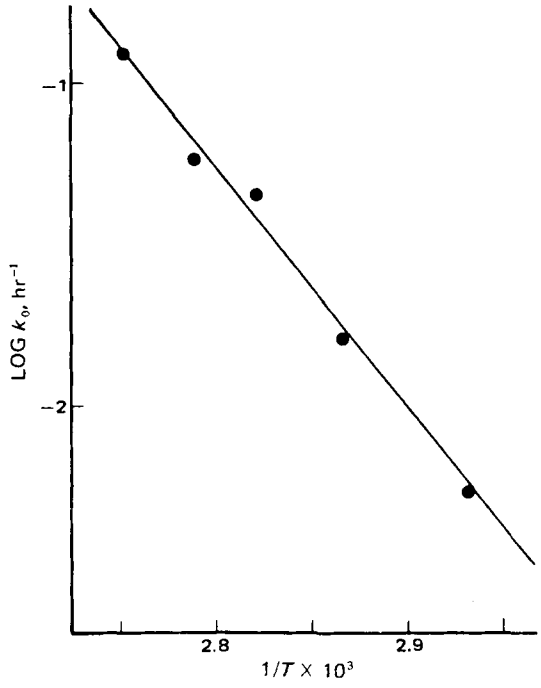

Figure 5—*Arrhenius plot of deiodination of o-iodobenzoic acid at pH 7.0 with Cu(II) catalysis.*

Table III demonstrates that *m*- and *p*-analogs of iodobenzoic acid produced almost negligible amounts of iodide. The reaction rates of *o*-iodobenzoic acid and diatrizoic acid were comparable. These results ruled out any possible effect from electronic resonance and favored the second alternative of copper complexation by the *ortho*-carboxylate. This result also indicated that the two iodines adjacent to carboxylate in diatrizoic acid are most vulnerable to deiodination.

Deiodination of Iopamidol—The anionic radiopaque benzoic acid derivatives were examined in the previous sections. However, the newly developed nonionic radiopaques, due to a lack of negatively charged carboxylate moieties, tend to undergo deiodination *via* other mechanisms.

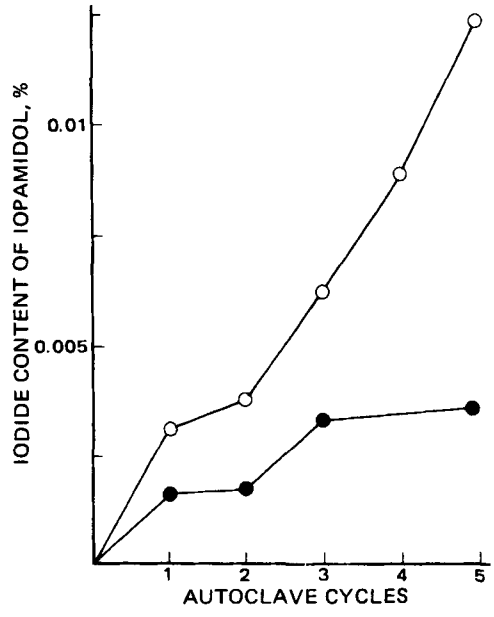

Figure 6—*Amount of iodide found in 20% iopamidol solution (pH 7, 0.0067 M phosphate buffer) subjected to various numbers of autoclave cycles. Each cycle was 90 min at 120°. Key: ○, without chelating agent; and ●, with 0.04% edetate disodium.*

Table III—Deiodination of Diatrizoic Acid and *o*-, *m*-, and *p*-Iodobenzoic Acids upon Autoclaving [a,b]

Compound	Iodide Produced, *M*
Diatrizoic acid	0.0397
o-Iodobenzoic acid	0.0452
m-Iodobenzoic acid	0.00001
p-Iodobenzoic acid	0.00003

[a] Solutions contained 0.5 *M* compound, 0.04 m*M* $CuSO_4$, and 0.0067 *M* Sørensen phosphate buffer to maintain the pH at 7.6. [b] Samples were subjected to 30 min of autoclave sterilization at 120°.

An understanding of deiodination of this class of compounds is beneficial.

Deiodination of iopamidol was found to be extremely slow. To study the mechanism, samples had to be subjected to more drastic conditions, *i.e.*, 90 min of 120° autoclave treatment. The production of iodide was plotted against the number of 90-min cycles (Fig. 6). In the range of ~0.01% or less, the iodide content could be considered rectilinear with respect to the number of cycles. The reaction rate can be calculated directly from the iodide content and reaction time. Figure 7 shows the semilogarithmic plot of the reaction rate constants at various pH values. In the absence of a chelating agent, thus probably causing the reaction to be catalyzed by copper, a plateau on the rate–pH profile suggests a predominant S_N1 mechanism that would be similar to the S_N1 mechanism already described.

In the presence of a chelating agent, such as edetate disodium, a unit slope on the pH–rate profile indicates that the reaction is dependent on the hydroxide-ion concentration and clearly suggests an S_N2 mechanism. The S_N2 mechanism becomes more important as the pH increases due to the increase of the hydroxide concentration. At pH values above 7.5, the S_N2 mechanism overshadows the S_N1 mechanism. The deiodination is predominantly a substitution of hydroxide ion and occurs regardless of the presence of a chelating agent.

The different behavior of diatrizoic acid and iopamidol can be summarized as follows. In diatrizoic acid, the carboxylate group promoted the S_N1 mechanism by drawing the copper ion closer to the reaction center or by stabilizing the carbonium charge. The S_N2 mechanism was completely inoperative because of the repulsion of hydroxide ion by the same negative charge. In iopamidol, the absence of carboxylate eased the attack by hydroxide ion, and thus the S_N2 mechanism was operable, although only in barely detectable rates. The Cu(II) ions catalyzed the deiodination of iopamidol; however, the S_N1 reaction was much slower than that of diatrizoic acid.

CONCLUSION

This investigation was undertaken to determine the deiodination mechanism of certain water-soluble radiopaques. For the benefit of formulating injectable radiopaques, deiodination was examined only at neutral pH values. Evidence has been presented to show that, in anionic radiopaques, deiodination proceeds by an S_N1 mechanism, which also requires the assistance of neighboring carboxylate groups and Cu(II) ion. By studying a model compound, *o*-iodobenzoic acid, the high magnitude of the common ion effect, salt effect, pH independency, and high activation energy, characteristics of an S_N1 reaction, were observed. In nonionic radiopaques, because of the absence of negatively charged carboxylate, deiodination is facilitated by hydroxide ion. With trace metal, S_N1 deiodination of a nonionic radiopaque remains operative, although at a much slower rate than an anionic radiopaque.

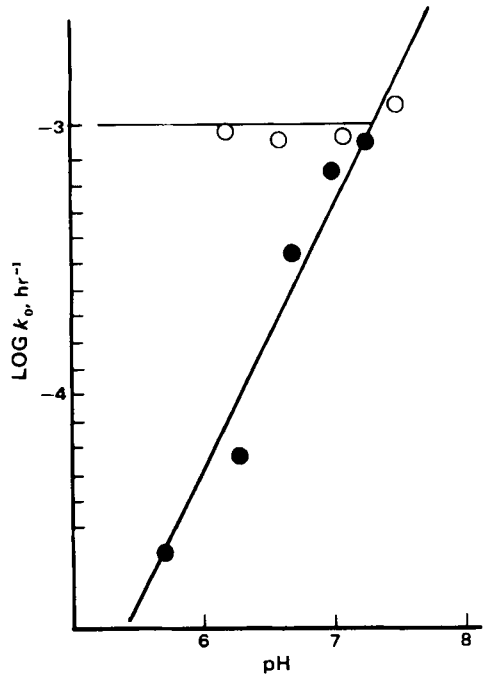

Figure 7—*Deiodination rate–pH profile for iopamidol in 0.0067* M *phosphate buffer at autoclave temperature. Key:* ○, *without chelating agent; and* ●, *with 0.04% edetate disodium.*

REFERENCES

(1) A. Burger, "Medicinal Chemistry," 3rd ed., Wiley-Interscience, New York, N.Y., 1970, p. 1686.

(2) E. Felder and D. E. Pitre, U.S. pat. 4,001,323 (Jan. 4, 1977).

(3) "Documenta Geigy," 6th ed., Geigy Pharmaceuticals, Ardsley, N.Y., 1962, p. 314.

(4) "The United States Pharmacopeia," 19th rev., Mack Publishing Co., Easton, Pa., 1975, p. 130.

(5) J. T. Carstensen, "Pharmaceutics of Solids and Solid Dosage Forms," 1st ed., Wiley, New York, N.Y., 1977, pp. 182–206.

(6) J. March, "Advanced Organic Chemistry—Reaction Mechanism and Structure," 2nd ed., McGraw-Hill, New York, N.Y., 1977, chap. 13.

(7) *Ibid.*, p. 587.

(8) C. A. Bunton, "Nucleophilic Substitution at a Saturated Carbon Atom," American Elsevier, New York, N.Y., 1963, pp. 129–132.

(9) C. G. Swain, C. B. Scott, and R. H. Lohmann, *J. Am. Chem. Soc.*, **75**, 136 (1953).

(10) D. R. Flanagan and A. P. Simonelli, *J. Org. Chem.*, **41**, 3114 (1976).

ACKNOWLEDGMENTS

The author thanks Dr. D. R. Flanagan for valuable suggestions.

Solubility of Polar Organic Solutes in Nonaqueous Systems: Role of Specific Interactions

BRADLEY D. ANDERSON, J. HOWARD RYTTING ˣ, and TAKERU HIGUCHI

Received February 26, 1979, from the *Department of Pharmaceutical Chemistry, University of Kansas, Lawrence, KS 66045.* Accepted for publication January 10, 1980.

Abstract □ The changes in solubility of several polar organic solutes when polar organic solvents are added to a relatively inert solvent such as isooctane were determined. The relative changes in solubility predicted from regular solution theory using solubility parameters often did not agree with the observed results. However, the solubilities could be rationalized mathematically by assuming the formation of specific solute–solvent complexes. Agreement of the thermodynamic data reported here with such models provides further evidence that specific interactions, when they occur, are more important than the bulk properties of the pure components in determining drug solubilities in nonaqueous systems. Specific examples demonstrate the relationship between the solubility and molecular structure of the solute and solvent. For example, solubility can be related to the hydrogen-donating and hydrogen-accepting abilities of the solute and solvent. Steric factors also appear to play a role in solubility, while structural modifications in a solute or solvent molecule far removed from the interactive functional group have little influence on molar solubility changes with the added polar cosolvent.

Keyphrases □ Solubility—polar organic solutes in nonaqueous systems, role of specific interactions □ Solute–solvent interactions—polar organic solutes in nonaqueous systems, role of specific interactions □ Solvents, nonaqueous—solubility of polar organic solutes, role of specific interactions

The solubility of a drug in a given solvent is an important property in pharmaceutical chemistry. Much work in drug design and drug product formulation stems from a need to achieve higher or lower solubilities to promote drug stability and bioavailability, to obtain controlled release rates, to avoid unpleasant side effects, and to optimize drug delivery to a target site. Consequently, the ability to predict drug solubility from molecular structure would be useful.

Current methods of solubility prediction often rely on the premise that the solubility of a solute in a given solvent is related simply to the bulk properties of the pure components. Such expressions as "polar solutes dissolve in polar solvents" or "like dissolves like" are based on this approach. This assumption also is the basis of a popular predictive method derived from regular solution theory, in which solubility is predicted from the solubility parameters of the pure components (1). Although this approach originally was intended strictly for systems involving only London dispersion forces, its use has been extended to include quite polar solution components in some cases (2, 3).

Recent studies indicated that the relative solubilities of polar solutes in both polar and nonpolar organic solvents often may be unrelated to the bulk properties of the pure components but are highly sensitive to the functional groups of the interacting molecules (4–9). One study suggested that specific intermolecular interactions, when they occur, often are the dominant factors in determining solubility, with corrections based on regular solution theory being unnecessary (4).

In the present study, the relative solubilities of several organic substances in various solvents or cosolvent mixtures were compared with predicted solubilities from regular solution theory and from a model assuming the existence of stoichiometric solvate species. The results indicate that the relative solubilities of polar substances in solvents that interact specifically with the solute are determined largely by these specific interactions.

EXPERIMENTAL

Reagents—Isooctane[1], with a stated purity of ≥99 mole %, was used without further purification. *n*-Butyl ether[2] was purified by slow shaking with an alkaline-saturated potassium permanganate solution followed by repeated washing with distilled water, concentrated sulfuric acid, and water. It was dried with calcium chloride overnight. This liquid then was distilled from sodium, and the middle fraction was collected and stored under nitrogen in an amber glass bottle.

n-Butyl ether[3], with a stated purity of 99%, was used without further purification. *n*-Pentyl ether[4] was treated similarly to *n*-butyl ether. *n*-Butyl *n*-butyrate[5] was shaken with 2 *N* NaOH, washed repeatedly with distilled water, dried over anhydrous magnesium sulfate, and then distilled under reduced pressure. The middle fraction was collected for use. Chloroform[6] was purified by washing with water to remove the ethanol preservative, dried over calcium chloride, and distilled. All solvents were stored over 4-Å molecular sieves[7] to remove possible trace amounts of water.

The solutes selected had relatively low isooctane solubilities and a minimum number of hydrogen donor or acceptor functional groups available for interaction with solvent molecules. Anthracene[3] had a claimed purity of 99.7% and was used without further purification. Anthraquinone[2], *p*-iodophenol[3], and *p*-nitrophenol[8] were recrystallized from chloroform–isooctane. Carbazole[3] and *p*-phenylphenol[3], with an indicated purity of 99+ and 97%, respectively, were recrystallized further from acetone–isooctane. 2,4,6-Triiodophenol[3] was recrystallized from methanol.

Solubility Determination—Solubilities of the solutes were determined in a series of solvents or cosolvent mixtures ranging from 100% isooctane to 100% ether, ester, or chloroform. Isooctane–interactive cosolvent mixtures were prepared by weight. Cosolvent molarities were calculated from the densities of the pure components. A series of vials was prepared, each containing an amount of solid well in excess of its estimated saturation solubility and ~5 ml of one of the described solvents or cosolvent mixtures. The vials were sealed[9] and brought to equilibrium by rotating in a constant-temperature bath at 25° for at least 2 days. Random duplicate samples were allowed to equilibrate for longer periods, but no significant differences in saturation solubility were observed.

The molar concentration of solute in solution was determined spectrophotometrically[10] by filtering[11] a portion of the solution and diluting a known aliquot as required. The filter assemblies, pipets, and other materials used in transferring the original sample were maintained at a temperature equal to the sample equilibration temperature prior to sampling. The solvent used as a diluent in the spectrophotometric de-

[1] Phillips Petroleum Co.
[2] Baker grade, J. T. Baker Chemical Co.
[3] Aldrich Chemical Co.
[4] Pfaltz and Bauer.
[5] Eastman.
[6] Reagent grade, Fisher Scientific Co.
[7] Linde.
[8] Matheson, Coleman and Bell.
[9] Teflon cap liners were used.
[10] Cary 14, 15, 16, or 118 spectrophotometer.
[11] Millipore filters BDWP 01300 or FHLP 01300.

0022-3549/80/0600-0676$01.00/0
© 1980, American Pharmaceutical Association

Table I—Molar Solubilities of Various Organic Solutes in Organic Solvents at 25°

Solute	Structure	Isooctane ($\times 10^4$)	Butyl Butyrate	Butyl Ether	Pentyl Ether	Chloroform
p-Nitrophenol	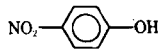	3.3	—	1.27	—	—
p-Iodophenol	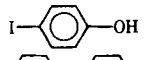	150	—	3.39	—	—
p-Phenylphenol	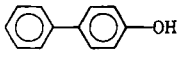	12.4	0.62	0.21	0.12	0.10
2,4,6-Triiodophenol	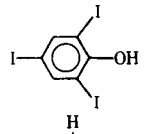	50	—	0.10	—	—
Carbazole	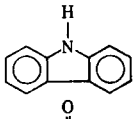	7.7	0.099	0.029	0.018	0.047
Anthraquinone	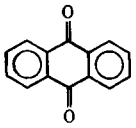	2.8	0.0038	—	—	0.044
Anthracene	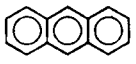	66	—	0.021	0.016	—

terminations was methanol or methanol containing 0.1 *N* HCl. While the nonphenolic compounds obeyed Beer's law in methanol, the phenols followed Beer's law more closely at low concentrations when the solvent was acidified.

RESULTS AND DISCUSSION

The molar solubilities determined in this study for various organic substances in several organic solvents are listed in Table I. Compounds expected to be strong hydrogen donors (phenols), weak hydrogen donors (chloroform and carbazole), and hydrogen acceptors (ethers, butyl butyrate, and anthraquinone) are included. Table II lists the molar solubility of carbazole in various interactive and inert solvents.

Comparison of Experimental Data with Regular Solution Theory Predictions—The term regular solution as proposed by Hildebrand in 1929 refers to solutions in which the entropy change is the same as for an ideal solution of the same composition but where the heat content increases with mixing (1). Regular solution theory gave rise to the now familiar solubility equation, expressed here in terms of the activity coefficient of the solute, γ_2:

$$\gamma_2 = \exp \frac{V_2\phi_1^2(\delta_1 - \delta_2)^2}{RT} \qquad \text{(Eq. 1)}$$

where δ_1 and δ_2 are the solubility parameters or cohesive energy densities [$\delta = (\Delta E/V)^{1/2}$] of the solute and solvent, respectively (12). Equation 1 involves an important assumption, the geometric mean rule, that frequently has been incorrectly taken for granted. In using solubility parameters, it is assumed that the energy of interaction of unlike molecules is given by the geometric mean of the interaction of like pairs ($\epsilon_{12} = [\epsilon_{11}\epsilon_{22}]^{1/2}$). This assumption is strictly true only for nonpolar molecules interacting *via* London dispersion forces (13). The geometric mean rule should not be presumed to be valid for either polar solutes or solvents.

The failure of simple one-component solubility parameter theory in systems of polar or interactive components has been recognized (14). However, since this approach still is widely used and recommended, several additional examples may illustrate the inadequacy of regular solution theory for predicting the solubilities of substances considered in this study.

The solubility parameters for various solvents are listed in Table II along with the molar solubility of carbazole in those solvents. The solubility parameter of carbazole is estimated as ~10, and its molar volume is ~150 cm^3. By comparing the solubility parameters of the hydrocarbon solvents in Table II, the solubility of carbazole predicted from regular solution theory should be five times higher in hexadecane and cyclohexane than in isooctane. The actual solubilities are relatively constant in these hydrocarbon solvents, which is intuitively satisfying considering the chemical similarity of these solvent molecules. Also, previous studies showed that the molar solubilities of several other polar solutes are relatively independent of the alkane reference solvent chosen (4, 5). Although molar volume corrections may be a factor, these errors apparently are compensated for by using molarity as the concentration unit. In addition, recent work suggested that even for systems involving components of markedly different molal volumes, the assumption of ideal entropy of mixing gives more satisfactory agreement with observed results than do theories considering molal volume differences (15).

From a comparison of solubility parameters in Table II, the solubility of carbazole in some hydrocarbon solvents should be roughly equal to or higher than its solubility in ethyl ether (δ = 7.4), butyl ether (δ = 7.5), pentyl ether (δ = 7.9), and butyl butyrate (δ = 8.0). However, the observed solubilities are 20–100 times higher in the hydrogen-accepting solvents than in the relatively inert alkane solvents, a result that cannot be accounted for by regular solution theory but is readily explainable from a consideration of the specific interactions occurring.

In general, one would predict from regular solution theory that, for all solutes in this study, the order of solubility should be chloroform > butyl butyrate > ethers ≃ hydrocarbons. These predictions obviously are not confirmed in Table II or by the relevant data for phenylphenol in Table I. Only for anthraquinone (and perhaps anthracene) is the solubility highest in chloroform, which also would be predicted from the knowledge that anthraquinone is a hydrogen acceptor and chloroform is a weak hydrogen donor.

In some instances, it may be possible to rationalize a particular change in solubility between two solvents using solubility parameters, even though the molecules involved would be expected to interact through hydrogen bonding. For example, the ratio of the solubility of anthraquinone in chloroform to its solubility in isooctane is 77 (using mole fractions) and is consistent with a solubility parameter of ~11.8, assuming

Table II—Molar Solubility of Carbazole at 25° in Several Solvents with Various Solubility Parameters (δ)

Solvent	δ	Solubility, *M*
Isooctane	6.9[a]	1.1×10^{-3} [a]
n-Hexane	7.3[a]	1.3×10^{-3} [a]
n-Heptane	7.4[a]	1.6×10^{-3} [a]
Ethyl ether	7.4[a]	1.25×10^{-1} [a]
Butyl ether	7.6[b]	2.9×10^{-2} [c]
Decane	7.8[a]	1.5×10^{-3} [a]
Dodecane	7.9[a]	1.4×10^{-3} [a]
Pentyl ether	7.9[d]	1.8×10^{-2} [c]
Butyl butyrate	8.0	1.0×10^{-1} [c]
Hexadecane	8.0[a]	1.7×10^{-3} [a]
Chloroform	9.2[a]	4.5×10^{-2} [a]

[a] From Ref. 4. [b] Calculated from heat of vaporization (Ref. 10). [c] Data from this study. [d] Estimated from Ref. 11.

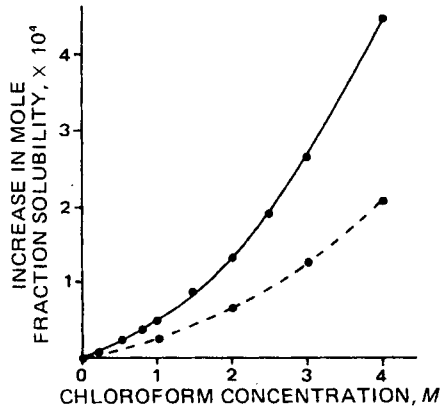

Figure 1—*Solubility of anthraquinone* versus *molarity of chloroform* (●) *in isooctane at 25°. The solid line was calculated from the equilibrium constants in Table III. The dashed line represents predicted solubilities using solubility parameters described from solubility data in the pure solvents.*

a molar volume of 150 cm^3 for anthraquinone. A further test of this solubility parameter is to determine whether the theory can reliably predict solubilities between these two solvent extremes, that is, in mixed solvents. From regular solution theory, the solubility parameter of a mixed solvent is the weighted average (based on volume fractions) of the solubility parameters of the pure components (1):

$$\delta = \phi_1\delta_1 + \phi_2\delta_2 \qquad \text{(Eq. 2)}$$

With Eq. 2, the predicted solubility values for anthraquinone in chloroform–isooctane cosolvent mixtures can be represented by the dashed line in Fig. 1. In comparison to the experimental points, the predicted solubilities increase much too gradually at low chloroform concentrations, illustrating the failure of the solubility parameter approach to predict the shape of the solubility profile for this example.

The inadequacy of the simple one-component solubility parameter approach has led to many more or less empirical multicomponent solubility parameters to incorporate the effects of specific interactions (13, 16). Although such attempts generally lack a firm theoretical foundation, they demonstrate that specific interactions are of great importance in many cases.

Specific Interactions and Solubility—Much early criticism of the specific interaction theory was based on the difficulty in proving the existence of "species" from thermodynamic data alone (1). However, a wealth of spectroscopic data now documents the formation of stoichiometric species through hydrogen-bonding interactions. Abundant evidence, based on IR frequency shifts (17), ^{1}H-NMR data (18, 19), and ^{13}C-NMR studies (20), supports the existence of molecular complexes between various hydrogen donors [including phenols (21) and chloroform (22)] and hydrogen acceptors [even for such a weak hydrogen acceptor as benzene (23)].

It would be unreasonable to assume that hydrogen-bonding interactions are not an important contribution to the solubilities of interest in the present study, based on the available spectroscopic data. Additional features supporting the contention that specific interactions such as hydrogen bonding are reflected in the solubility data reported here will be discussed later.

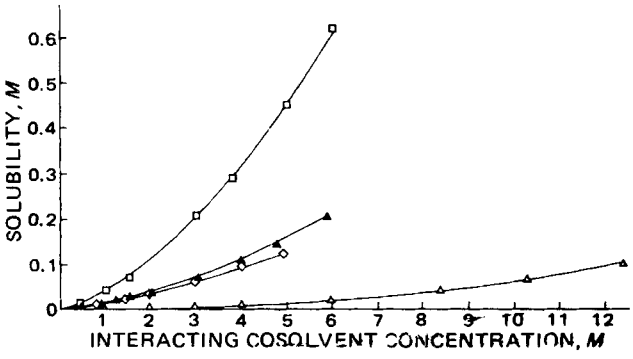

Figure 2—*Solubility of* p-*phenylphenol* versus *molarity of various interacting cosolvents in isooctane at 25°. The lines represent the calculated solubilities based on the equilibrium constants in Table III. Key:* □, *butyl butyrate;* ▲, *butyl ether;* ◇, *pentyl ether; and* △, *chloroform. The final point in each case represents the solubility in the pure cosolvent.*

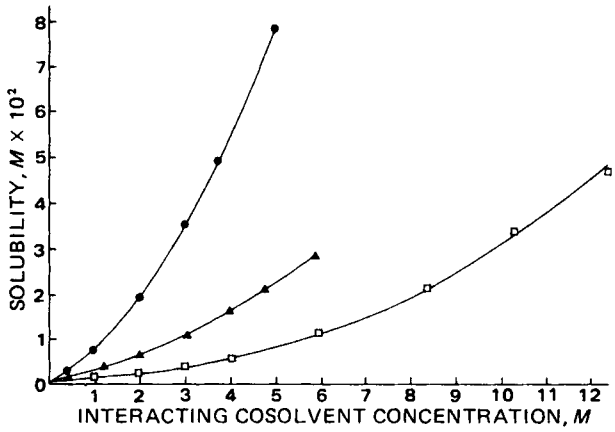

Figure 3—*Solubility of carbazole* versus *molarity of various interacting cosolvents in isooctane at 25°. The lines represent the calculated solubilities based on the equilibrium constants in Table III. Key:* ●, *butyl butyrate;* ▲, *butyl ether; and* □, *chloroform. The final point in each case represents the solubility in the pure cosolvent.*

Mathematical Treatment of Solubility Data in Terms of Solute–Solvent Species Formation—Typical diagrams of solubility *versus* molarity of the interactive cosolvent are shown in Figs. 2 and 3 for *p*-phenylphenol and carbazole in the presence of various complexing agents. A plot of the solubility of anthraquinone *versus* chloroform molarity was shown in Fig. 1. The solubility curves generally are parabolic. These curves can be fitted mathematically using a model that assumes solvate species formation.

Solubility in Unassociated Solvents—It is assumed that the following equilibria hold between the solute, S, and the complexing agents or interacting cosolvents, L:

$$S + L \rightleftharpoons SL \overset{+L}{\rightleftharpoons} SL_2 \overset{+L}{\rightleftharpoons} \ldots SL_n$$

Scheme I

Each reaction is defined by an equilibrium constant for formation of the complex:

$$K_{1:1} = \frac{[SL]}{[S_0][L_f]} \qquad \text{(Eq. 3)}$$

$$K_{1:n} = \frac{[SL_n]}{[SL_{n-1}][L_f]} \qquad \text{(Eq. 4)}$$

where the concentrations are expressed as molarities; S_0 is the saturation solubility of solute in isooctane, which is assumed to represent the free solute concentration in the cosolvent mixtures; and L_f is the free (uncomplexed) ligand. It also is assumed that a single solute molecule is present in each complex, but the mathematical form of the resulting equation is not changed by allowing more than one solute per complex. Throughout this discussion, it is assumed that the activity coefficients of all species are one where the standard state in every case is a 1 M solution of solute behaving as if it were completely surrounded by isooctane solvent. The total solubility of solute in any system can be expressed as:

$$S_T = [S_0] + K_{1:1}[S_0][L_f] + K_{1:2}K_{1:1}[S_0][L_f]^2 + \ldots \qquad \text{(Eq. 5)}$$

and L_T, the total complexing agent added, is:

$$L_T = [L_f] + K_{1:1}[S_0][L_f] + 2K_{1:2}K_{1:1}[S_0][L_f]^2 + \ldots \qquad \text{(Eq. 6)}$$

The total concentration of interactive cosolvent, L_T, is equal to L_f in the absence of solute. This relationship is true only when the extent of self-association of cosolvent is negligible, and it cannot be assumed for alcohol cosolvents.

As is evident from Eq. 5, the shape of the plots of solubility *versus* cosolvent added should be concave upward in unassociated solvents, in agreement with the data in Figs. 1–3.

Estimation of Equilibrium Constants—If S_0, the solubility of the solute in isooctane, is very low, the amount of ligand in complexes is small

Table III—Solvate Equilibrium Constants (Liters per Mole) of Various Solutes with Polar Solvents at 25°

Solute	Butyl Ether			Pentyl Ether			Butyl Butyrate			Chloroform			
	$K_{1:1}$	$K_{1:2}$	$\sigma\%$[a]	$K_{1:1}$	$K_{1:2}$	$\sigma\%$	$K_{1:1}$	$K_{1:2}$	$\sigma\%$	$K_{1:1}$	$K_{1:2}$	$K_{1:3}$	$\sigma\%$
p-Nitrophenol	102.5	0.56	2.2[b]	—	—	—	—	—	—	—	—	—	—
p-Iodophenol	26.0	—	0.5[c]	—	—	—	—	—	—	—	—	—	—
p-Phenylphenol	8.9	0.42	2.7	8.3	0.27	2.1	21.2	0.78	3.3	0.73	0.25	0.15	2.8
Carbazole	2.5	0.25	1.1	1.9	0.23	1.9	6.5	0.44	3.3	0.68	0.30	0.06	4.3
2,4,6-Triiodophenol	1.1	0.33	1.4	—	—	—	—	—	—	—	—	—	—
Anthraquinone	—	—	—	—	—	—	—	—	—	0.96	0.39	0.15	2.5

[a] The $\sigma\%$ value is the square root of the sum of the squares of the percent deviation between the calculated and observed solubilities divided by the degrees of freedom. [b] Fit of data below 0.1 *M*. [c] Fit of data in 1:1 region only.

and $[L_T] \simeq [L_f]$. Also, at low concentrations of L, only 1:1 complexes are important, and a plot of the fractional change in solubility *versus* ligand added gives a straight line at low cosolvent concentrations with a slope of $K_{1:1}$:

$$\text{fractional change in solubility} = \frac{[S_T] - [S_0]}{[S_0]} = K_{1:1}[L_T] \qquad \text{(Eq. 7)}$$

Such plots are shown in Fig. 4 for several substances in butyl ether. At higher cosolvent molarities, two-parameter equations containing terms for 1:1 and 1:2 complexes were needed to describe the data adequately. Only two parameters were necessary to describe completely the entire solubility curve in all solvents except chloroform, where three parameters often were required (Table III).

Graphical methods are quite cumbersome when an appreciable amount of the added cosolvent exists in complexed form, because L_T then does not equal the free ligand concentration. Therefore, a computer program using the simplex method of least squares (24, 25) was written to solve Eqs. 5 and 6 simultaneously, optimizing the variables $K_{1:1}$, $K_{1:2}$, and $K_{1:3}$. The sum of squares of the percent deviation of the experimental solubilities from the calculated solubilities was minimized to give equal weight to each point. The computer-calculated complexation constants for those instances where specific interactions can reasonably be assumed are listed in Table III. Constants determined graphically (Fig. 4) usually were within 10% of the computer-optimized values.

Choices of Most Important Factors in Predicting Solubility—Nonaqueous systems of pharmaceutical interest generally involve polar solutes in polar, interactive solvents. Therefore, predictive relationships between solubility and one or more independent variables that express the interactive tendencies of the molecules involved would be valuable. It was shown in the preceding discussion that solubility parameters, which reflect bulk properties of the pure components, often are not related to the observed relative solubilities. However, specific solvation models can readily account for the solubility behavior.

By first determining the solubilities in an alkane solvent, an estimate of factors that are not related to specific interactions in solution is obtained. Differences in alkane solubilities largely reflect differences in solute crystalline energies, although dispersion interactions between the solute and solvent also may vary with molecular structure. In interactive solvents, the specific interaction component, which is of primary interest here, is reflected by the change in solubility from that in isooctane.

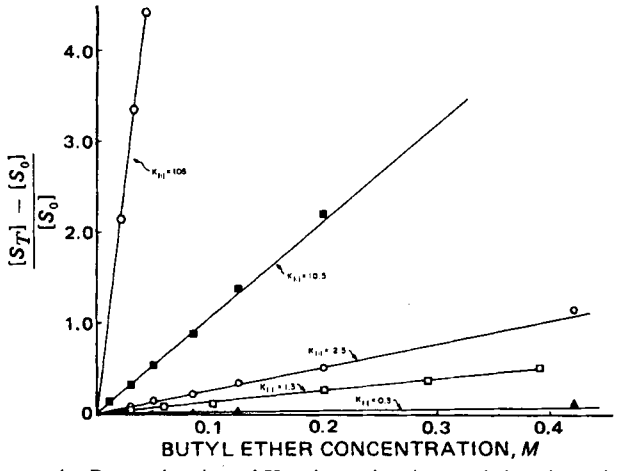

Figure 4—*Determination of* $K_{1:1}$ *from the slopes of the plots of the fractional change in solubility* versus *butyl ether molarity in isooctane at 25° (see Eq. 7). Key:* ○, p-*nitrophenol;* ■, p-*phenylphenol;* ○, *carbazole;* □, *2,4,6-triiodophenol; and* ▲, *anthracene.*

While the fact that these systems can be fit with solvation models does not prove conclusively that the solubility changes are due largely to specific interactions, the $K_{1:1}$ values obtained from the solubility data are consistent with what is expected from a consideration of the relative hydrogen-donating and hydrogen-accepting abilities of the respective molecules (8). A brief comparison of the solubility data in Table I provides a qualitative indication of the importance of hydrogen bonding in determining relative solubilities. The solubility of the strong hydrogen donor *p*-nitrophenol increases by almost 4000-fold in going from isooctane to the hydrogen-acceptor solvent butyl ether. The solubility of the weaker hydrogen donor carbazole increases by ~38 times in going from isooctane to butyl ether; anthracene, which has no donatable hydrogens, differs by a factor of only three in the two solvents.

These large differences cannot be accounted for by solubility parameters since the solubility parameter of butyl ether is quite similar to that of isooctane. However, they are quite consistent with specific interaction theory.

It also is instructive to compare the butyl ether–isooctane solubility ratios for *p*-nitro-, *p*-iodo-, and *p*-phenylphenols, which are 3850, 226, and 169, respectively. These phenols are listed in order of decreasing acidity and also decreasing hydrogen-donating ability based on literature data (8).

Empirical correlations of equilibrium data based on linear free energy relationships were applied previously in hydrogen-bonded systems (8, 26), usually taking the form of the Hammett equation (27, 28), $\log (K/K_0) = \rho\sigma$, where K and K_0 are the equilibrium constants of a substituted and an unsubstituted solute species, respectively; ρ reflects the sensitivity of the reaction to solute substituent changes; and σ represents the Hammett substituent constant. Higuchi *et al.* (8) derived a similar equation, $\log (K/K_0) = h_d h_a$, and calculated h_d and h_a values for donors and acceptors in nonpolar solvents, where h_d is a measure of the effect of change in the hydrogen donor on hydrogen bonding and h_a measures the influence of the acceptor on the interaction.

Figure 5 is a plot of $\log K_{1:1}$ derived from the solubility data of the *para*-substituted phenols in butyl ether *versus* the Hammett σ_p substituent constant obtained from the effect of these *para*-substituents on the ionization of benzoic acids in water[12] (29). Because the ionization

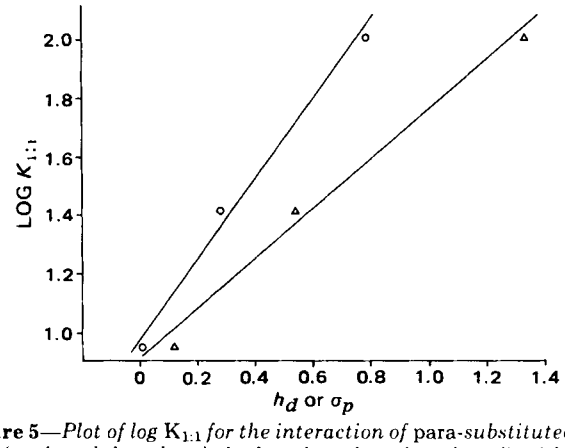

Figure 5—*Plot of log* $K_{1:1}$ *for the interaction of* para-*substituted phenols* (p-*phenylphenol,* p-*iodophenol, and* p-*nitrophenol) with butyl ether in isooctane at 25°* versus *the Hammett* σ_p *substituent* (●) *constant and* versus *Higuchi* h_d *values* (△).

[12] Resonance effects are less important in hydrogen bonding than in Brönsted acidity and basicity, so poor correlations of hydrogen bonding with acidity are obtained with σ^- values, which reflect the substituent effect on phenol ionization (14).

Table IV—Standard Free Energies of Transfer of Solute ($\Delta G°$) from Isooctane to Various Interactive Solvents and the Calculated Hydrogen-Bonding Contribution to the Free Energy from $K_{1:1}$ Values ($\Delta G°_{HB}$)

Solute	Butyl Ether		Pentyl Ether		Butyl Butyrate		Chloroform	
	$\Delta G°$[a]	$\Delta G°_{HB}$[a]	$\Delta G°$[a]	$\Delta G°_{HB}$[a]	$\Delta G°$[a]	$\Delta G°_{HB}$[a]	$\Delta G°$[a]	$\Delta G°_{HB}$[a]
p-Nitrophenol	−4.90	−3.6	—	—	—	—	—	—
p-Iodophenol	−3.2	−2.5	—	—	—	—	—	—
p-Phenylphenol	−3.0	−2.3	−2.7	−2.2	−3.7	−2.8	−2.6	−1.4
Carbazole	−2.1	−1.6	−1.9	−1.4	−2.9	−2.2	−2.4	−1.3
2,4,6-Triiodophenol	−1.8	−1.2	—	—	—	—	—	—
Anthraquinone	—	—	—	—	—	—	−3.0	−1.5

[a] Units are kilocalories per mole.

constants in nonpolar media have not been determined, a direct correlation with acidity under the same solvent conditions is impossible. Figure 5 also shows the plot of the same values of log $K_{1:1}$ *versus* Higuchi's h_d values (8), which were derived from both thermodynamic and spectroscopic data. This correlation clearly suggests that the $K_{1:1}$ values reflect hydrogen-bonding interactions.

Steric effects also come into play in solubility, as demonstrated by the relatively low $K_{1:1}$ and low solubility for 2,4,6-triiodophenol in butyl ether, a hydrogen-accepting solvent (Table III). This effect presumably is due to the steric hindrance to hydrogen bonding by the *ortho*-iodo groups.

While solubility is quite sensitive to the solute and solvent functional group composition, structural alterations that are not in the vicinity of an interacting functional group and do not alter the acidity or basicity of the functional group have little influence on solubility differences in organic solvents. For example, $K_{1:1}$ values for the interaction of carbazole with ethers varying in alkyl chain length are 3.53 M^{-1} for ethyl ether (5), 2.5 M^{-1} for butyl ether, and 1.9 M^{-1} for pentyl ether. Furthermore, $K_{1:1}$ for the interaction of *p*-phenylphenol with butyl ether is 8.9 M^{-1}; with pentyl ether, it is 8.3 M^{-1}. Solubilities in the pure ethers differ by a much larger amount (Table II), due in part to the greater concentration of ether oxygens in pure ethers of shorter chain length.

The $K_{1:2}$ values listed in Table III are very small and relatively insensitive to the molecular structure of the solute or solvent. These constants cannot justifiably be called specific interaction constants. The much smaller magnitudes of $K_{1:2}$ suggest that the 1:1 solute–solvent interactions are saturable, a characteristic of specific interactions. For instance, for the nitrophenol–butyl ether system, $K_{1:1}$ = 102.5 liters/mole and $K_{1:2}$ = 0.56 liter/mole. The strong hydrogen-bonding tendency between these two species does not carry over into the 1:2 interaction since the hydrogen-donating tendency of *p*-nitrophenol is "saturated" in forming the 1:1 complex.

If it is assumed that the $K_{1:1}$ values obtained in dilute solutions of the interactive cosolvents represent specific interactions, one can calculate the contribution of this specific interaction to the overall transfer free energy from isooctane to pure solvent (Table IV). This comparison ignores the likelihood that complexes larger than 1:1 may exist in the pure interactive solvent. For example, 1:2 complexes are expected to be quite important in chloroform solutions of anthraquinone since anthraquinone has two hydrogen-acceptor sites. Therefore, the specific interaction contributions to solubility expressed in Table IV probably are minimum estimates. However, nonspecific contributions to the $K_{1:1}$ values in dilute solution also may be a factor, particularly when the $K_{1:1}$ values are small.

In most cases, the specific interaction contribution to the overall free energy of transfer is the major factor, as is evident from Table IV. The differences may be composed of higher order molecular complexes or nonspecific effects, but these differences generally are small compared to the overall transfer free energy. Clearly, the specific interaction tendency should receive the greatest emphasis in attempts to predict solubility in similar systems.

CONCLUSION

It was shown that solubilities of polar organic substances in polar organic solvents can be rationalized quantitatively by assuming the formation of stoichiometric solvate species. Additional evidence also supports the contention that specific interactions are more important than bulk properties of the pure components in determining relative solubilities.

REFERENCES

(1) J. H. Hildebrand and R. L. Scott, "The Solubility of Nonelectrolytes," Reinhold, New York, N.Y., 1950.

(2) C. Sunwoo and H. Eisen, *J. Pharm. Sci.*, **60,** 238 (1971).

(3) D. B. Bowen and K. C. James, *J. Pharm. Pharmacol.*, **22,** 104S (1970).

(4) H. L. Fung and T. Higuchi, *J. Pharm. Sci.*, **60,** 1782 (1971).

(5) H. L. Fung, Ph.D. thesis, University of Kansas, Lawrence, Kans., 1970.

(6) S. Chulkaratana, M. S. thesis, University of Wisconsin, Madison, Wis., 1961.

(7) S. Chulkaratana, Ph.D. thesis, University of Wisconsin, Madison, Wis., 1964.

(8) T. Higuchi, J. H. Richards, S. S. Davis, A. Kamada, J. P. Hou, M. Nakano, N. I. Nakano, and I. H. Pitman, *J. Pharm. Sci.*, **58,** 661 (1969).

(9) T. Higuchi and K. A. Connors, *Adv. Anal. Chem. Instr.*, **4,** 117 (1965).

(10) J. A. Riddick and W. B. Bunger, "Techniques in Chemistry, Vol. II. Organic Solvents: Physical Properties and Methods of Purification," 3rd ed., Wiley–Interscience, New York, N.Y., 1970.

(11) R. F. Fedors, *Polym. Eng. Sci.*, **14,** 147 (1974).

(12) K. Shinoda, "Principles of Solution and Solubility," Dekker, New York, N.Y., 1978, p. 61.

(13) A. F. M. Barton, *Chem. Rev.*, **75,** 735 (1975).

(14) *Ibid.*, **75,** 737 (1975).

(15) K. Shinoda, "Principles of Solution and Solubility," Dekker, New York, N.Y., 1978, pp. 111–116.

(16) J. D. Crowley, G. S. Teague, Jr., and J. W. Lowe, Jr., *J. Paint Technol.*, **38,** 269 (1966).

(17) C. S. Chamberlain and R. S. Drago, *J. Am. Chem. Soc.*, **98,** 6142 (1976).

(18) J. P. Sheridan, D. E. Martire, and Y. B. Tewari, *ibid.*, **94,** 3294 (1972).

(19) D. E. Martire, J. P. Sheridan, J. W. King, and S. E. O'Donnell, *ibid.*, **98,** 3101 (1976).

(20) T. T. Nakashima, D. D. Traficante, and G. E. Maciel, *J. Phys. Chem.*, **78,** 124 (1974).

(21) T. Gramstad and O. Mundheim, *Spectrochim. Acta, Part A*, **28,** 1405 (1972).

(22) C. J. Creswell and A. L. Allred, *J. Phys. Chem.*, **66,** 1469 (1962).

(23) K. M. Baker and R. G. Wilson, *J. Chem. Soc. B*, **1970,** 236.

(24) S. N. Deming and S. L. Morgan, *Anal. Chem.*, **45,** 278A (1973).

(25) S. L. Morgan and S. N. Deming, *ibid.*, **46,** 1170 (1974).

(26) J. Hine, "Structural Effects on Equilibria in Organic Chemistry," Wiley, New York, N.Y., 1975, pp. 200–205.

(27) L. P. Hammett, *J. Am. Chem. Soc.*, **59,** 96 (1937).

(28) L. P. Hammett, "Physical Organic Chemistry," McGraw-Hill, New York, N.Y., 1940, chap. 7.

(29) J. Hine, "Structural Effects on Equilibria in Organic Chemistry," Wiley, New York, N.Y., 1975, p. 66.

GLC Determination of Bretylium in Biological Fluids

CHII-MING LAI, BURDE L. KAMATH, JAMES E. CARTER, PAUL ERHARDT, ZEE M. LOOK, and AVRAHAM YACOBI ×

Received November 16, 1979, from the *Department of Pharmaceutical Development, Research and Development Department, Arnar-Stone Laboratories Inc., McGaw Park, IL 60085.* Accepted for publication January 9, 1980.

Abstract □ Bretylium [(*o*-bromobenzyl)ethyldimethylamine] is a quaternary ammonium compound used as the tosylate salt for treatment of ventricular fibrillation in humans. A sensitive assay was developed for the determination of low bretylium concentrations in plasma and urine. The internal standards were (*p*-bromobenzyl)ethyldimethylammonium *p*-toluenesulfonate and (*o*-methoxybenzyl)ethyldimethylammonium *p*-toluenesulfonate. Samples were deproteinized with acetonitrile and extracted with methylene chloride. After the evaporation of the organic phase, the residue was reacted with sodium 2,4,5,-trichlorothiophenolate in methanol. This procedure yielded volatile compounds with excellent electron-capture capabilities for the GLC analysis. The assay sensitivity is 5 ng/ml. The extraction recovery of bretylium as determined by a direct radioactivity measurement was 90 and 97% for plasma and urine, respectively. The method is highly reproducible with no significant day-to-day variations. Comparisons of 60 standard plasma samples, 25 standard urine samples, and plasma samples from a dog that received [^{14}C]bretylium showed excellent agreement between the GLC method and direct radioactivity measurement of bretylium.

Keyphrases □ Bretylium—determination in biological fluids by GLC and direct radioactivity measurement, humans □ GLC—analysis of bretylium in biological fluids, humans □ Radiochemistry—analysis of bretylium in biological fluids, compared to GLC determination, humans

Bretylium [(*o*-bromobenzyl)ethyldimethylamine] is a quaternary ammonium compound used as the tosylate salt for the treatment of ventricular fibrillation in humans (1, 2). Various methods for its determination have been reported (3–7). The most promising method is a GLC analysis (6) utilizing sodium thiophenolate to react with bretylium to produce *o*-bromobenzyl phenylthio ether. However, it is tedious and lacks sufficient sensitivity.

This paper reports a simplified and sensitive GLC method for the determination of bretylium in small plasma and urine samples. The new extraction procedure minimizes the variability in assay recovery and reproducibility. To validate this method, the results of the GLC method were compared with direct radioactivity measurement of [^{14}C]bretylium in standard samples as well as in samples collected from a dog that received the labeled drug.

EXPERIMENTAL

Materials and Methods—A stock solution of bretylium tosylate[1] (I) (10 mg/ml as a quaternary ammonium compound) was prepared in purified water. This solution was used to prepare standard plasma and urine samples containing 5–250 ng of bretylium/ml. The stock solutions of the internal standards, (*p*-bromobenzyl)ethyldimethylammonium *p*-toluenesulfonate[2] (II) and (*o*-methoxybenzyl)ethyldimethylammonium *p*-toluenesulfonate[2] (III) (each containing 1 μg/ml as the quaternary ammonium compound), were prepared in purified water. The glassware used in solution preparation and in the assay was washed with soap, soaked in 4 *N* HNO_3 for 24 hr, rinsed with purified water, and finally rinsed with methanol.

Sodium 2,4,5-trichlorothiophenolate (IV) was used as a reacting agent. It was synthesized by a method similar to that described previously for the preparation of sodium thiophenolate (6, 8). The reagent was only moderately hygroscopic and, when stored in a drying oven, was stable for at least 6 months.

Table I—Recovery of [^{14}C]Bretylium from Plasma and Urine

[^{14}C]Bretylium Added[a], ng/ml	Percent Recovery from Plasma[a]	Percent Recovery from Urine
4.75	90.8 (3.68)	
9.33	89.2 (1.03)	97.3
24.10	90.2 (1.23)	96.3
49.8	89.3 (1.56)	97.4
73.7	90.3 (1.30)	96.1
98.7	92.7 (1.07)	99.3
Mean	90.4 (1.66)	97.2
CV	1.41 —	1.17

[a] Mean of five determinations. The [^{14}C]bretylium concentration was determined by direct scintillation counting of each sample. The numbers in parentheses are the coefficients of variation in percent.

Assay—*Method I*—To 1 ml of plasma or urine was added 0.1 ml of the internal standard solution containing 100 ng of II and 1 ml of acetonitrile[3]. The sample was vortexed for 10 sec and centrifuged at 4000 rpm for 5 min. The supernate was transferred into a 155 × 13-mm polytef-lined screw-capped culture tube[4], extracted with 5 ml of methylene dichloride[5] by gentle shaking for 30 min, and centrifuged at 4000 rpm for 5 min. Five milliliters of the organic layer was evaporated to dryness in a new culture tube. The residue was dissolved in 3 ml of methanol containing 1.0 μg of IV and allowed to react and evaporate to dryness at 60° with vigorous shaking in a vacuum. The same reaction procedure was repeated twice using 1 ml of the substituted thiophenolate solution. The residue was reconstituted with 200 ml of methanol from which 2 μl was injected into the gas–liquid chromatograph.

Method II—To 0.25 ml of plasma or urine was added 0.1 ml of the internal standard solution containing 100 ng of III, 0.5 ml of 0.1 *N* NaCl solution, and 1 ml of acetonitrile. The sample was vortexed for 10 sec and centrifuged at 4000 rpm for 5 min. The supernate was transferred into a culture tube to which 0.2 ml of 1 *N* NaOH was added. The mixture was extracted with 5 ml of methylene dichloride by gentle shaking for 30 min and was centrifuged at 4000 rpm for 5 min. The samples then were treated as in Method I, except that they were reacted only once with 3 ml of methanolic solution containing 1.0 μg of IV.

GLC Procedure—Analysis was performed on a gas–liquid chromatograph[6] equipped with a 2.08-m × 4-mm i.d. silanized glass column (coiled) packed with 3% OV-225 on 100–120-mesh Supelcoport and a ^{63}Ni-electron-capture detector. The injection port, column, and detector temperatures were maintained isothermally at 270, 250, and 300°, respectively. Argon–methane (95:5 v/v) was used as the carrier gas at a flow rate of 50 ml/min (30 ml/min through the column, 20 ml/min directly to the detector as a scavenger gas).

Data acquisition was performed on a laboratory minicomputer[7]. The peak heights of the derivatized bretylium were divided by the peak heights of the derivatized internal standard, and the ratios were used to construct the standard curve and to determine its linearity.

Animal Study—One male beagle dog[8], 13.1 kg, received [^{14}C]bretylium tosylate[9] ([*benzyl*-7-^{14}C], 0.512 μCi/mg), 10 mg/kg iv. Food was withheld for 4 hr after drug administration. Blood samples (5 ml each) were drawn in heparinized vacutainers through the jugular vein at 4, 6, 8, 12, 16, 20, and 24 hr after dosing. The plasma samples were kept frozen until they

[1] Ganes Chemical Co., New York, N.Y.
[2] Synthesized by the method of Jenden *et al.* (8), Arnar-Stone Laboratories, McGaw Park, Ill.
[3] HPLC grade, E. M. Laboratories, Cincinnati, Ohio.
[4] No. 2511-B3, Wheaton Tubing Products, Millville, N.J.
[5] Nanograde, Burdick & Jackson Laboratories, Muskegon, Mich.
[6] Model 428, Packard Instruments, Downers Grove, Ill.
[7] Model 3352D, Hewlett-Packard, Avondale, Pa.
[8] Laboratory Research Enterprises, Kalamazoo, Mich.
[9] New England Nuclear, Boston, Mass.

0022-3549/80/0600-0681$01.00/0
© 1980, American Pharmaceutical Association

Table II—Reproducibility, Day-to-Day Variations, and Recovery of the GLC Method for Determination of Bretylium in Plasma and Urine

Actual Concentration[a], ng/ml	Plasma Assay[b]			Urine Assay[b]	
	Mean Concentration in Plasma, ng/ml		Mean Overall Percent of Added Concentration[e]	Mean Concentration in Urine[f], ng/ml	Mean Overall Percent of Added Concentration[e]
	Day 1[c]	Day 5[d]			
4.75	4.50 (4.47)	4.81 (4.14)	98.0 (5.37)	—	—
9.33	9.10 (11.6)	9.61 (2.85)	99.7 (9.09)	10.8 (3.87)	115.8 (4.84)
24.1	24.6 (11.5)	25.8 (3.01)	104.0 (9.01)	23.8 (3.81)	98.9 (3.82)
49.8	53.7 (4.66)	51.1 (1.38)	105.7 (4.47)	46.4 (2.97)	93.2 (2.97)
73.7	75.1 (6.06)	72.8 (3.16)	100.7 (5.28)	74.5 (4.50)	101.1 (4.49)
98.7	98.3 (6.46)	101.0 (4.98)	100.7 (5.94)	102.3 (2.22)	103.6 (2.25)
Mean	— (7.45)	— (3.25)	101.5 (6.52)	— (3.47)	102.5 (3.67)
CV			2.8		8.15

[a] [^{14}C]Bretylium added to plasma and urine samples. [b] The numbers in parentheses are the coefficients of variation in percent. [c] $n = 6$. [d] $n = 4$. [e] $n = 10$. [f] $n = 5$.

were assayed. Plasma samples were analyzed by direct counting of the radioactivity *via* a scintillation counter[10] and by the GLC method described under *Method II*.

RESULTS AND DISCUSSION

Bretylium, a quaternary ammonium compound, can be extracted from biological samples by an ion-pair extraction procedure, a complicated and tedious method described previously (6). In the present study, the use of acetonitrile as a deproteinization agent served to remove the proteins, to purify the biological sample, and to enhance the partitioning of bretylium into methylene dichloride, which was used as the extraction solvent. Although acetonitrile is fully miscible with the aqueous solution, it was almost completely partitioned in the organic layer. The recovery of [^{14}C]bretylium from plasma and urine was 90.4 and 97.2%, respectively (Table I). The coefficient of variation for five samples at each concentration (range 4.8–98.7 ng/ml) ranged from 1.0 to 3.7%. There was no correlation between the extraction recovery and plasma concentrations. This approach simplified the previous procedures for bretylium extraction from plasma and may be useful for extracting other quaternary amines from biological fluids.

To determine bretylium by GLC, Kuntzman *et al.* (6) used sodium thiophenolate, which reacts with the quaternary ammonium compound and yields a volatile derivative, *o*-bromobenzylphenylthio ether. The use of this reagent resulted in a sensitivity of ~70 ng/ml when a large volume (3 ml) of the sample was used. To improve this sensitivity, sodium

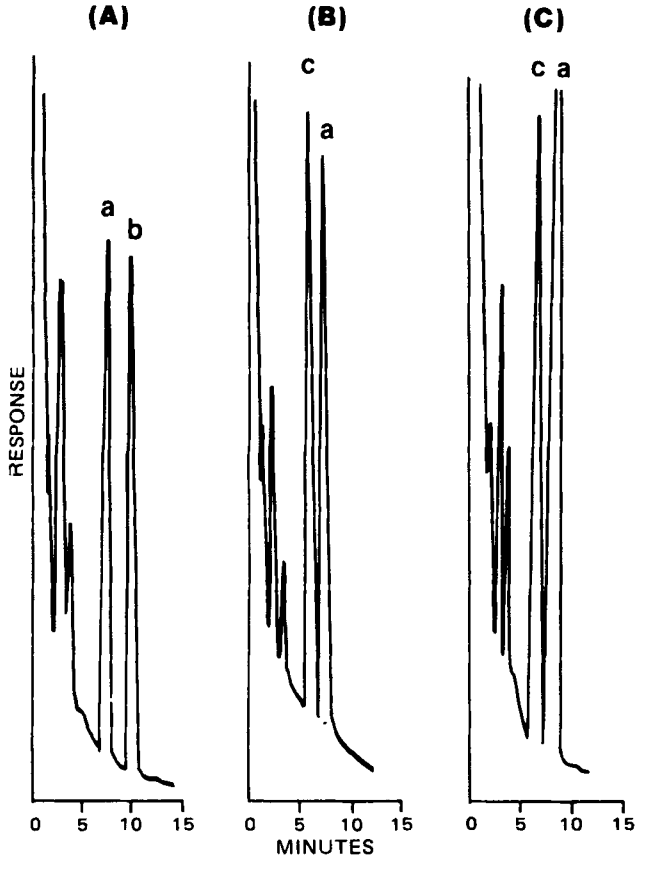

Figure 1—*Typical chromatograms for a blank standard sample spiked with the internal standard for Method I (A) and Method II (B), and a sample from a patient who received bretylium (C), where a, b, and c are the thiophenylether derivatives of bretylium, (p-bromobenzyl)ethyldimethylamine, and (o-methoxybenzyl)ethyldimethylamine, respectively.*

[10] Model 2425, Packard Instruments, Downers Grove, Ill.

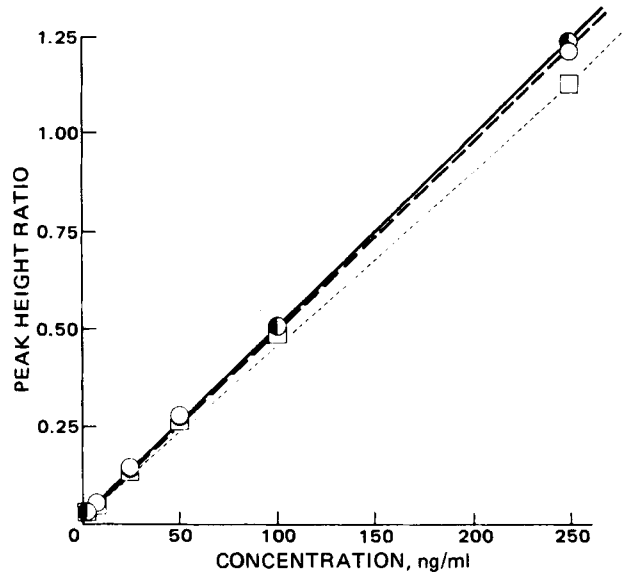

Figure 2—*Reproducibility of the assay of three sets of standard plasma samples determined on Days 1 (●), 3 (○), and 8 (□) by Method II.*

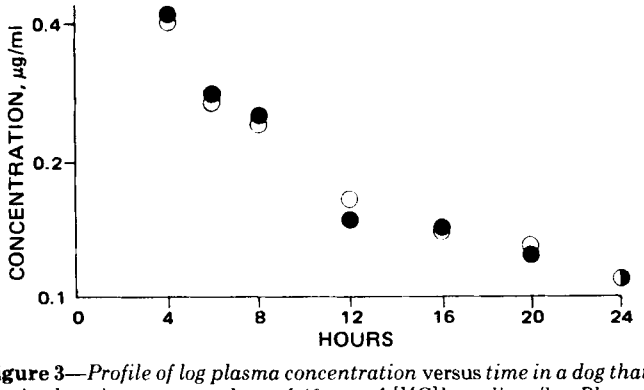

Figure 3—*Profile of log plasma concentration* versus *time in a dog that received an intravenous dose of 10 mg of [^{14}C]bretylium/kg. Plasma samples were assayed by direct radioactivity measurement (○) and by the GLC method (Method II, ●).*

Table III—Precision of the GLC Method for Determination of Bretylium in Plasma

Actual Concentration[a], ng/ml	Concentration Found[b], ng/ml					
	Sample 1	Sample 2	Sample 3	Sample 4	Sample 5	Sample 6
4.75	4.49	4.73	4.24	4.52		
9.33	9.38	9.38	7.00	10.00	9.41	9.41
24.1	22.6	27.1	26.1	19.8	26.7	25.3
49.8	51.4	53.6	56.4	57.1	52.2	51.5
73.7	74.9	70.7	68.6	80.1	70.0	78.0
98.7	95.5	103.2	97.9	92.3	108.4	92.7

[a] [^{14}C]Bretylium was used. [b] See mean and coefficient of variation values in Table II.

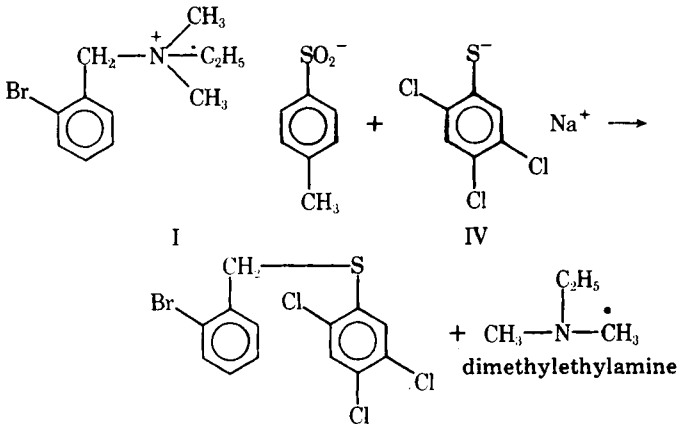

o-bromobenzyl 2,4,5-trichlorothiophenyl ether

Scheme I

thiophenolate was replaced by IV, which also readily reacts with bretylium and its congeners to produce derivatives extremely sensitive to electron-capture detection. Scheme I shows the derivative. Although the thiophenolate anion can attack at any of the four amine substituents by an S_N2 process, attack at the *o*-bromobenzyl group, as depicted, is preferred due to resonance stabilization of the reaction transition state (9).

In this study, two internal standards, II (Method I) and III (Method II), were used. Compound III reacts more readily with sodium thiophenolate and makes the assay less time consuming. Figure 1 shows typical chromatograms from the assay. The retention times of the phenylthio ether derivatives were 6.1, 7.4, and 9.4 min. Bretylium usually is given with other drugs that may interfere with the assay. To minimize such interference, one of the two internal standards may be selected, depending on the desired retention time.

Under the assay conditions, there were observable impurity peaks at retention times of 2.7 and 3.4 min that did not interfere with the drug or internal standard peak. As expected, qualitative and quantitative GLC showed that the corresponding primary, secondary, and tertiary amines of bretylium do not react with the thiophenolate and have very poor intrinsic electron-capturing ability. The GLC chromatograms showed symmetrical peaks for bretylium and the internal standards, and there were no indications of interference from those amines.

Figure 2 and Table II show the linearity, reproducibility, day-to-day variation, and recovery data of the assay. Table III lists the precision data of the GLC method for the determination of bretylium in plasma. The slopes of the plots of the peak height ratio of bretylium to that of the internal standard *versus* bretylium concentrations in the range of 5–250 ng/ml were 0.00409, 0.00476, and 0.00449 as determined on Days 1, 3, and 8, respectively (10). There was no statistically significant difference in the slopes, intercepts, and individual concentrations determined on two or three occasions during an 8-day period.

In this study, plasma and urine concentrations of 5 ng/ml were determined easily using a 0.25-ml sample. However, the sensitivity can be improved by simple modifications. The GLC assay was compared with a direct radioactivity measurement in 60 standard plasma samples and 25 standard urine samples (Table II). The correlation coefficients between the results of the two methods were 0.999 for plasma and 0.998 for urine samples. Similarly, plasma samples from a dog that received an intravenous dose of 10 mg of [^{14}C]bretylium tosylate/kg were assayed by both the GLC and the direct radioactivity measurement methods. Figure 3 shows the plasma bretylium concentration *versus* time profile. There was excellent correlation between the results of the two procedures, and there was no significant difference between the data (paired *t* test).

A series of standard plasma samples with concentrations ranging from 5 to 250 ng/ml was kept at ambient temperature for 4 days. The GLC determinations showed results of 102.2 ± 10.5% of the corresponding concentrations of controls that were kept frozen during the same period. These data indicate that bretylium is stable in plasma. This result also is consistent with data reported previously on bretylium stability (7).

The proposed procedure is sensitive and requires a single extraction step without any back-extraction or cleaning procedure. This method offers the distinct advantage of requiring very small biological samples. The choice of the internal standard depends on the individual case and drugs involved. Although both internal standards give essentially the same results, the use of the *o*-methoxy congener is less time consuming. This GLC method may be used in single-dose pharmacokinetic studies in humans and animals. It also may be applicable to quality control tests and drug compatibility studies. Other quaternary amines may be extracted and derivatized in a similar manner.

REFERENCES

(1) M. B. Bacaner, *Am. J. Cardiol.*, **21**, 530 (1968).

(2) A. R. Castaneda and M. Bacaner, *ibid.*, **23**, 107 (1969).

(3) C. D. Johnson and J. P. Revill, *Acta Pharmacol. Toxicol.*, **22**, 112 (1965).

(4) W. G. Duncombe and A. McCoubrey, *Br. J. Pharmacol.*, **15**, 260 (1960).

(5) S. L. Tompsett, W. Forshall, and D. C. Smith, *Acta Pharmacol. Toxicol.*, **18**, 75 (1961).

(6) R. Kuntzman, I. Tsai, R. Chang, and A. H. Conney, *Clin. Pharmacol. Ther.*, **11**, 829 (1970).

(7) C. M. Lai, Z. M. Look, P. K. Lai, and A. Yacobi, *J. Liquid Chromatogr.*, **3**, 93 (1980).

(8) D. J. Jenden, I. Hanin, and S. I. Lamb, *Anal. Chem.*, **40**, 125 (1968).

(9) R. Breslow, "Organic Reaction Mechanisms," W. A. Benjamin, New York, N.Y., 1969, p. 82.

(10) A. Goldstein, "Biostatistics: An Introductory Test," Macmillan, New York, N.Y., 1971, p. 144.

GLC–Mass Spectrometric Determination of Maprotiline and Its Major Metabolite Using Stable Isotope-Labeled Analog as Internal Standard

SATYA P. JINDAL ˣ, THERESA LUTZ, and PER VESTERGAARD

Received June 14, 1979, from the *Rockland Research Institute, Orangeburg, NY 10962.* Accepted for publication January 18, 1980.

Abstract □ A quantitative GLC–mass spectrometric assay was developed for the determination of maprotiline and its major metabolite, desmethylmaprotiline, in animal and human plasma. The assay utilizes selective-ion focusing to monitor, in a GLC effluent, the fragment ions and the base peaks of maprotiline and desmethylmaprotiline trifluoroacetamides generated by electron-impact ionization. Maprotiline-d_3 was the internal standard. The assay can measure 2 ng of maprotiline (and the metabolite)/ml of plasma with ~5% precision. The curves relating the amounts of maprotiline and the metabolite added *versus* the amounts experimentally found over a large concentration range were linear with nearly zero intercepts and slopes of 0.99 ± 0.01 and 0.98 ± 0.02, respectively. The method was used to study the pharmacokinetic pattern of the drug in rabbits as well as to analyze intact maprotiline and the metabolite in patients maintained on therapeutic doses of maprotiline. Assay specificity was confirmed by complete consistency of the mass spectra of maprotiline and desmethylmaprotiline with those of the authentic materials.

Keyphrases □ Maprotiline—GLC–mass spectrometric analysis, human and animal plasma □ Desmethylmaprotiline—GLC–mass spectrometric analysis, human and animal plasma □ GLC–mass spectrometry—stable isotope-labeled maprotiline, selected-ion monitoring, pharmacokinetics □ Antidepressants—maprotiline, GLC–mass spectrometric analysis, human and animal plasma

Maprotiline, 1-(3-methylaminopropyl)dibenzo[*b,e*]-bicyclo[2,2,2]octadiene[1,2], is a tetracyclic drug with sedative, antiaggressive, and antidepressant effects. In contrast to the tricyclic antidepressants, it has no influence on the central metabolism of 5-hydroxytryptamine and has weak anticholinergic actions (1). As an antidepressant, it has shown equal therapeutic efficacy but fewer side effects compared to tricyclic antidepressants (2–4); it also is less toxic (5, 6) and has less of an effect on the cardiovascular system (7, 8). Maprotiline has been used in Europe for the treatment of patients who had severe side effects with other antidepressants and for depressed patients with cardiovascular symptomatology. It is under evaluation for clinical use in the United States.

A precise and specific assay for maprotiline and its major metabolites in biological fluids and tissues is needed. Assays based on the double radioisotope derivative technique (9), electron-capture detection (10), and specific nitrogen detection (11) have been reported. This report describes a GLC–mass spectrometric assay for the intact drug and its major metabolite, desmethylmaprotiline, in the plasma of rabbits and humans.

GLC–mass spectrometry in the selected-ion monitoring (12–14) mode was used to quantitate plasma levels of the drug and its major metabolite, *N*-desmethylmaprotiline, in rabbits after maprotiline administration. The methodology also was applied to measure steady-state levels of the free drug and the metabolite in the plasma of patients on therapeutic doses. Stable isotope-labeled maprotiline, maprotiline-d_3 ([*N*-*methyl*-^{3}H]maprotiline), was synthesized and used as an internal standard for the estimation of both maprotiline and desmethylmaprotiline.

EXPERIMENTAL

Materials—Analytical grade maprotiline hydrochloride[1], desmethylmaprotiline methanesulfonate[2], trifluoroacetic anhydride[3], ethyl chloroformate[3], and lithium aluminum deuteride[4] were used without further purification. All solvents were analytical grade[5]. Silanized tubes[6] (10 ml) with screw caps[7] were used for extraction; final solvent evaporation was performed in 5-ml glass-stoppered centrifuge tubes[8]. Pasteur pipets with hand-drawn constricted tips were utilized for all solution transfers. Plasma samples were stored frozen at −10° until they were analyzed.

Maprotiline-d_3—Desmethylmaprotiline, upon treatment with ethyl chlorocarbonate, gave the corresponding carbonate (15) in a 78% yield. The carbonate was reduced with lithium aluminum deuteride in tetrahydrofuran to maprotiline-d_3 (16). The material showed satisfactory mass spectral (electron-impact ionization) characteristics. A selective-ion detection analysis of maprotiline-d_3 showed the presence of an ion equivalent to 99 ± 0.2% (n = 5) maprotiline-d_3.

Extraction from Plasma—To 1 ml of plasma was added an appropriate amount of maprotiline-d_3 (typically 70 ng/ml) as an internal standard. The plasma was diluted to 5 ml with borate buffer and sonicated for 0.5 min while keeping the temperature at ~6°. The homogenized material was adjusted to pH 9.5 with 0.1 *N* NH_4OH and extracted twice with 5 ml of benzene. The organic fractions were combined, 1 ml of 0.1 *N* HCl was added, and the solution was shaken for 15 min and centrifuged.

The organic layer was discarded, and the aqueous phase was adjusted to pH 9.5 with 1 *N* NH_4OH and extracted twice with 3 ml of benzene. The organic fractions were combined and dried, and the solvent was evaporated at 50° under a gentle nitrogen stream. Recovery of maprotiline and desmethylmaprotiline added to control plasma was studied at the 10-ng/ml level.

Formation of Derivatives—The dried extract was taken up in 100 μl of ethyl acetate, and 50 μl of trifluoroacetic anhydride was added. The material then was heated in an oil bath at 80° for 45 min. The solution was cooled to room temperature, and the solvents were evaporated at 40° under a gentle nitrogen stream. The dried extract was reconstituted in 50 μl of chloroform, and ~1 μl was injected into the gas–liquid chromograph–mass spectrometer for mass fragmentographic assay.

Instrumentation—The magnetic sector, single-focusing mass spectrometer[9] was interfaced with a gas chromatograph and equipped with a multiple-ion detector–peak matcher accessory (14, 17). GLC was performed on a 1.8-m × 2-mm i.d. glass column silanized with 5% dimethyldichlorosilane in toluene and packed with 1% OV-17 on 100–200-mesh Gas Chrom Q. The column was conditioned for 24 hr at 280° with a flow rate of 20 ml of helium/min. The column temperature was 225°, the flash heater was at 240°, the separator was at 250°, and the ion source was at 275°.

The accelerating voltage was 3.5 kv in the scan mode and 3.0 kv in the multiple-ion detection mode, the ionization potential was 70 ev, and the trap current was set at 60 μamp. The magnetic field was kept constant

[1] Ciba 34,276-Ba, Ludiomil, Ciba-Geigy AG, Basel, Switzerland.
[2] Kindly provided by Dr. W. Riess of Ciba-Geigy, Basel, Switzerland.
[3] Aldrich Chemical Co., Milwaukee, Wis.
[4] Isotopic purity of 99 atom % deuterium, Merck Sharp & Dohme, Canada Ltd., Montreal, Quebec, Canada.
[5] Fisher Scientific Co., Pittsburg, Pa.
[6] Kimble Owens, Illinois, Toledo, Ohio.
[7] Lined with Teflon, DuPont.
[8] Pyrex 8084.
[9] LKB 9000, LKB, Stockholm, Sweden.

0022-3549/80/0600-0684$01.00/0
© 1980, American Pharmaceutical Association

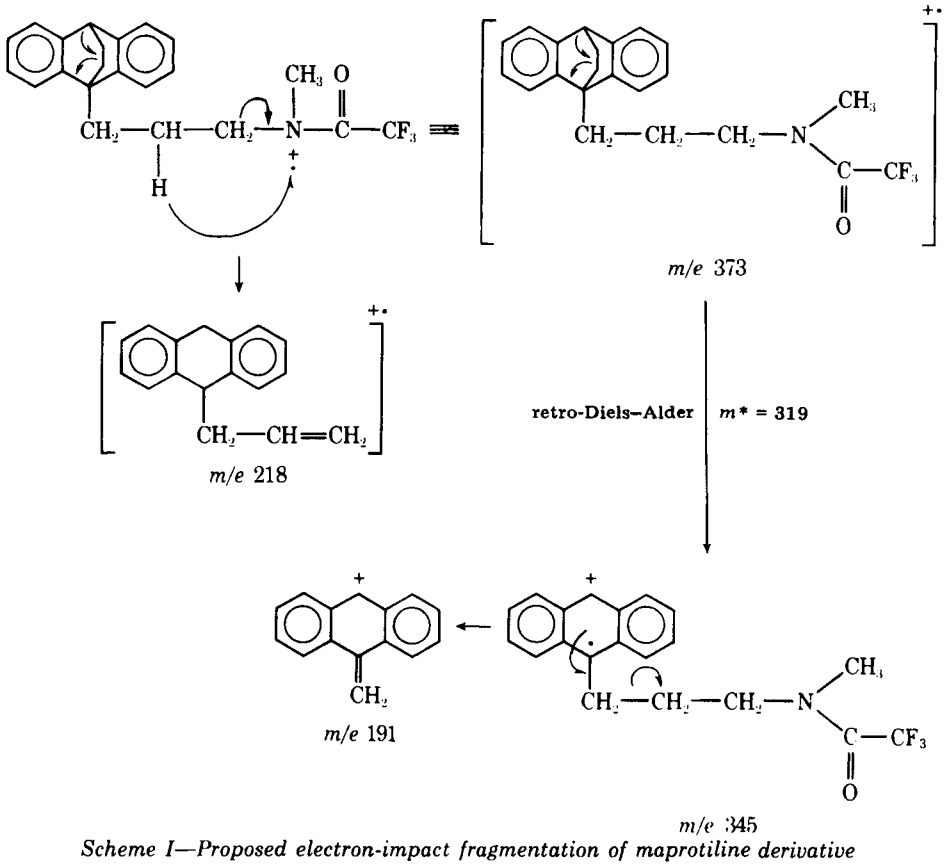

Scheme I—Proposed electron-impact fragmentation of maprotiline derivative

by focusing the background ion (column bleed) at *m/e* 355, and the additional voltages were 752, 600, and 569 v for measuring ion intensities at *m/e* 331, 345, and 348, respectively. The retention times of desmethylmaprotiline and maprotiline trifluoroacetamides were 2.0 and 3.0 min, respectively.

Experiments with Animals—Experiments were performed on rabbits to determine the time course of maprotiline and desmethylmaprotiline in plasma after the intravenous administration of varying drug doses. In a typical experiment, a 6-kg rabbit was given a single intravenous dose of 2.7 mg of maprotiline hydrochloride in water.

Blood samples were drawn and collected in heparinized tubes. The plasma was prepared as usual. An appropriate amount of the internal standard (typically 70 ng) was added to the plasma samples (1.0 ml), and the samples were processed as described. The amounts of endogenous maprotiline and desmethylmaprotiline were calculated from the ratio of ion intensities at *m/e* 345, 331, and 348, respectively.

Human Studies—Plasma of several patients on a normal therapeutic dose of maprotiline was analyzed for maprotiline and the metabolite. An appropriate amount of the internal standard was added to the plasma samples (0.25 ml), and the samples were processed as described. The amounts of endogenous maprotiline and desmethylmaprotiline were calculated from the ratio of ion intensities at *m/e* 345, 331, and 348, respectively.

RESULTS AND DISCUSSION

The mass spectrum of maprotiline trifluoroacetamide (Table I) shows a molecular ion at *m/e* 373, a base peak at *m/e* 345, an intense peak at *m/e* 191, and a peak of modest intensity at *m/e* 218. A reasonable mechanism for the fragmentation is presented in Scheme I. The molecular ion underwent a typical retro-Diels–Alder process (18, 19) to give a radical ion at *m/e* 345, the base peak. The driving force for this reaction must be the expulsion of a stable neutral ethylene molecule and the formation of an unusually stable radical ion at *m/e* 345. Since both the radical site and the cationic site are benzylic in this ion, obviously this very stable ion results in a base peak at *m/e* 345.

This interpretation is substantiated further by the presence of a metastable ion at *m/e* 319. The mass spectrum of maprotiline-d_3 trifluoroacetamide (Table I) confirms this interpretation, since in this case the molecular ion and the base peak, as expected, are shifted to a higher mass by 3 amu. The mass spectrum of desmethylmaprotiline trifluoroacetamide (Table I) shows a molecular ion at *m/e* 359, a base peak at *m/e* 331 as a result of a retro-Diels–Alder process, and a metastable ion at *m/e* 305. The ions at *m/e* 218 and 191 are the common fragment ions appearing in the spectra of maprotiline, maprotiline-d_3, and desmethylmaprotiline trifluoroacetamides.

GLC–Mass Spectrometric Quantitation—The ions at *m/e* 345 and 331 are specific for maprotiline and desmethylmaprotiline (*m/e* 348 for maprotiline-d_3) trifluoroacetamides and are not observed in the electron-impact ionization spectra of other tricyclic antidepressants (20, 21) and known metabolites of maprotiline (22). Consequently, the biological extract along with maprotiline-d_3 was treated with trifluoroacetic anhydride at 80°, the excess reagents were evaporated, and an aliquot of the reconstituted solution was injected into the gas–liquid chromatograph–mass spectrometer; maprotiline was quantitated by measuring the ion intensities at *m/e* 345 and 348 while desmethylmaprotiline was assayed by measuring the ion intensities at *m/e* 331 and 348.

Control plasma samples subjected to the described procedure showed no significant background ions at *m/e* 345, 348, and 331. Known amounts of maprotiline and desmethylmaprotiline and a fixed amount of the isotopic analog (maprotiline-d_3) were added to control plasma and processed as described. Maprotiline and desmethylmaprotiline were quantitated from the ratios of ion intensities at *m/e* 345/348 and 331/348, respectively. Analysis of the data for maprotiline (Fig. 1) gave a slope of 0.99 ± 0.01 and an intercept of 0.15 ± 0.1 ng. Similarly, the data for

Table I—Mass Spectral Analysis [a] of Trifluoroacetamides of Maprotiline, Maprotiline-d_3, and Desmethylmaprotiline

Presumed Fragmentation	*m/e* [b] Maprotiline	Maprotiline-d_3	Desmethylmaprotiline
M	373 (6)	376 (6)	359 (4)
M − 28	345 (100)	348 (100)	331 (100)
M − 28 part side chain	218 (11)	218 (11)	218 (6)
M − 28 side chain	191 (82)	191 (82)	191 (82)

[a] Only common major fragments are presented. [b] The values in parentheses represent the percent relative intensity.

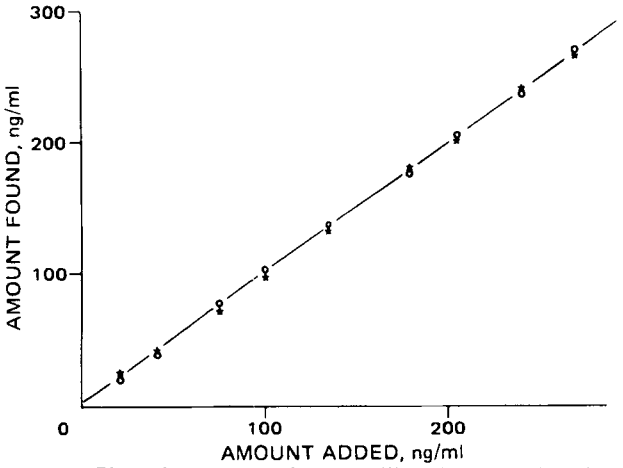

Figure 1—*Plot of amounts of maprotiline (0–285 ng) (O) and desmethylmaprotiline (0–285 ng) (×) added to control plasma versus the amounts found using the described method. Maprotiline-d_3 (70 ng/ml) was added as the internal standard.*

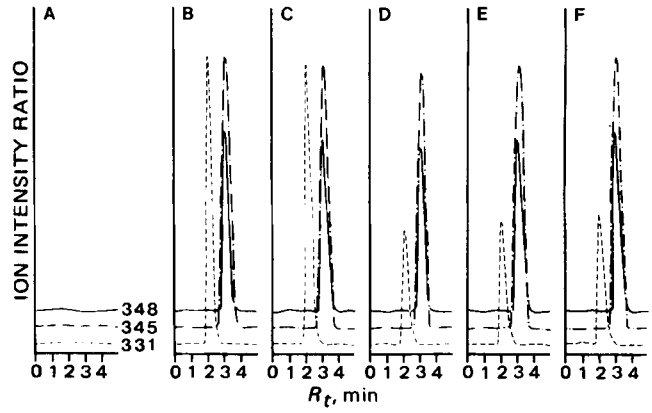

Figure 2—*Selective-ion chromatograms for maprotiline (m/e 345), desmethylmaprotiline (m/e 331), and maprotiline-d_3 (m/e 348). Key: A, control human plasma; B, control human plasma (1 ml) spiked with 10 ng each of maprotiline and desmethylmaprotiline and 7 ng of maprotiline-d_3; C, control rabbit plasma (1 ml) spiked as in B; and D, E, and F, typical rabbit and human plasma.*

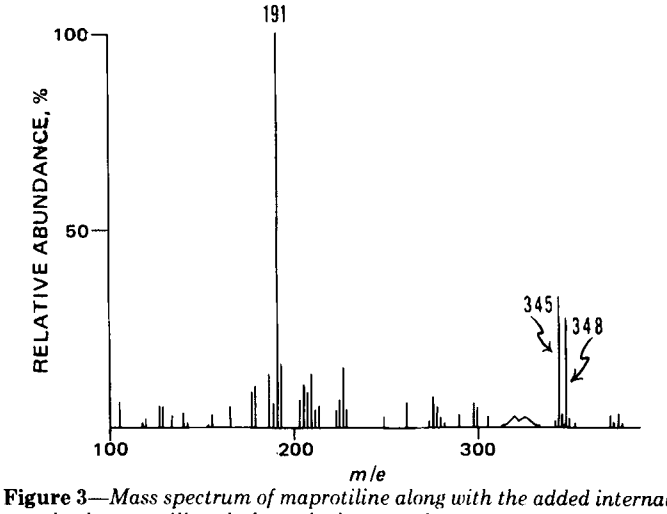

Figure 3—*Mass spectrum of maprotiline along with the added internal standard maprotiline-d_3 from the human plasma extract.*

desmethylmaprotiline (Fig. 1) gave a slope of 0.98 ± 0.01 and an intercept of 0.2 ± 0.11 ng. These data affirm a simple linear relationship between the ion intensity ratios and concentrations of maprotiline and desmethylmaprotiline and exclude any isotopic fractionation in the fragmentation process as well as in the physicochemical steps in the assay.

Six samples containing 10 ng each of maprotiline and desmethylmaprotiline/ml were analyzed using 7.0 ng of maprotiline-d_3/ml as the internal standard. The results were 9.91 ± 0.15 ng/ml for maprotiline and 9.87 ± 0.16 ng/ml for desmethylmaprotiline. These samples were assayed in duplicate; in this set, exactly the same amounts were taken as before, but the internal standard was added after the extraction. The recoveries for these samples, based on comparison of the ion intensity ratios of the two sets, were 82 ± 7% for maprotiline (*m/e* 345/348) and 85 ± 6% for desmethylmaprotiline (*m/e* 331/348). The variability in recoveries is to be expected in trace analysis and is attributed to variable glassware and GLC column adsorption.

Table II shows the concentration of intact drug and its major metabolite in rabbit plasma after a single intravenous dose. The decline of maprotiline concentration in plasma exhibited a typical fast absorption phase (α) followed by a slow disposition phase (β), while desmethylmaprotiline peaked out at ~50 hr after maprotiline administration.

The plasma levels of maprotiline and the metabolite varied considerably in different patients maintained on a normal therapeutic dose. More extensive data are needed for assessment of steady-state concentrations of these materials in human plasma.

Sensitivity and Specificity—The assay for maprotiline and its major metabolite presented here is sensitive, specific, and applicable to other body fluids and tissues. The assay sensitivity is a function of extraction efficiencies, GLC column conditions, and the ion source and cannot be quoted in absolute terms. With good mass spectrometer performance, a clean ion source, a freshly silanized GLC column and glassware, and >50% recoveries, an assay sensitivity of ~2 ng each of maprotiline and desmethylmaprotiline/ml of plasma is possible.

The results from the control plasma and plasma of patients show good specificity of the assay. The mass chromatograms obtained from biological extracts (Fig. 2) show clean and symmetrical peaks. Furthermore, these biological extracts were pure enough so that the entire mass spectra of maprotiline and desmethylmaprotiline trifluoroacetamides could be recorded. The mass spectrum of maprotiline trifluoroacetamide with added maprotiline-d_3 (Fig. 3) shows expected doublets at *m/e* 345–348. Also significant was a singlet of increased relative ion intensity at *m/e* 191, a common fragment ion from the two isotopic species. The mass spectrum of desmethylmaprotiline trifluoroacetamide in the biological extract was identical to that of the authentic material.

Table II—Analyses [a] of Maprotiline and Desmethylmaprotiline in the Plasma of Rabbits and Patients on Maprotiline Therapy

Sample	Hours	Desmethylmaprotiline	Maprotiline
		Rabbit Plasma[b], ng/ml	
1	1.25	6.3 ± 0.34	2320.0 ± 22
2	2.25	27.4 ± 1.1	1096.0 ± 13
3	5	46.0 ± 1.3	95.2 ± 2.8
4	18	120.0 ± 2.2	38.6 ± 2.6
5	48	280.0 ± 4.5	30.2 ± 2.1
6	68	35.4 ± 1.7	17.6 ± 0.9
7	97	14.0 ± 0.61	9.8 ± 0.28
		Human Plasma[c], ng/ml	
Patient 1		179.6 ± 3.1	1558.3 ± 14
Patient 2		88.1 ± 2.8	1160.6 ± 12
Patient 3		179.2 ± 3.4	677.6 ± 7.2
Patient 4		140.2 ± 3.3	353.4 ± 4.9

[a] Mean of duplicate determinations. [b] Analysis of maprotiline and desmethylmaprotiline in rabbits as a function of time after the administration of a single dose. [c] Steady-state plasma levels of maprotiline and desmethylmaprotiline in patients.

REFERENCES

(1) L. Maitre, P. C. Waldmeier, P. M. Greengrass, J. Jaekel, S. Sedlacek, and A. Delini-Stula, *J. Int. Med Res., Suppl.* (2), **3**, 2 (1975).

(2) A. Balestrieri, P. Benassi, G. B. Cassano, P. Castrogiovanni, A. Catalano, A. Colombi, C. Contorto, G. Del Soldato, F. Giberti, P. E. Lucchelli, A. Muratorio, M. Nistri, and P. Sarteschi, *Int. Pharmacopsychiatry*, **6**, 236 (1971).

(3) J. N. Logue, B. A. Sachais, and J. P. Feighner, *J. Clin. Pharmacol.*, **19**, 64 (1979).

(4) B. J. Lauritsen and H. Madsen, *Acta Psychiatr. Scand.*, **50**, 192 (1974).

(5) H. Tanaka, M. Furast, and S. Takasaki, *Acta Pathol.*, **25**, 413 (1975).
(6) S. Szeless, G. Kleinberger, R. Kotzaurek, H. Pall, M. Pichler, and G. Raberger, *Wien. Klin. Wochenschr.*, **87**, 254 (1975).
(7) A. Reale and M. Motolese, "Haemodynamic Studies with CIBA 34,276 BA in Depressive Illness, Diagnosis, Assessment, Treatment," Hans Huber, Bern, Switzerland, 1972, p. 161.
(8) H. Madsen and B. J. Lauritsen, *Ugeskr. Laeg.*, **138**, 992 (1976).
(9) W. Riess, *Anal. Chim. Acta*, **68**, 363 (1974).
(10) U. P. Geiger, T. G. Rajagopalan, and W. Riess, *J. Chromatogr.*, **114**, 167 (1975).
(11) R. N. Gupta, G. Molnar, and M. L. Gupta, *Clin. Chem.*, **23**, 1849 (1977).
(12) C. C. Fenselau, *Appl. Spectrosc. Rev.*, **28**, 305 (1974).
(13) S. D. Nelson and L. R. Pohl, *Ann. Rep. Med. Chem.*, **12**, 319 (1977).
(14) C. G. Hammar, B. Holmstedt, and R. Ryhage, *Anal. Biochem.*, **25**, 53e (1968).
(15) F. J. Marshall and R. E. McMahon, *J. Labeled Compd.*, **6**, 261 (1970).
(16) V. A. Fung and J. I. Degraw, *Synthesis*, **1976**, 311.
(17) B. Holmstedt and L. Palmer, *Adv. Biochem. Psychopharmacol.*, **7**, 1 (1973).
(18) F. W. McLafferty, "Interpretation of Mass Spectra," Benjamin, Reading, Mass., 1977, p. 49.
(19) D. M. S. Wheeler, T. H. Kinstel, and K. L. Rinehart, Jr., *J. Am. Chem. Soc.*, **89**, 4494 (1967).
(20) B. S. Finkel, R. L. Foltz, and D. M. Taylor, *J. Chromatogr. Sci.*, **12**, 304 (1974).
(21) B. J. Gudzinowicz and M. J. Gudzinowicz, "Analysis of Drugs and Metabolites by Gas Chromatography-Mass Spectrometry," Dekker, New York, N.Y., 1977, pp. 3, 125.
(22) W. Riess, L. Dubey, E. W. Funfgeld, P. Imhof, H. Hurzeler, N. Matussek, T. G. Rajagopalan, J. Raschdorf, and K. Schmidt, *J. Int. Med. Res., Suppl. (2)*, **3**, 16 (1975).

ACKNOWLEDGMENTS

Supported by the Office of Research, Department of Mental Hygiene, State of New York.

Dr. R. N. Gupta and Dr. M. L. Gupta of St. Joseph's Hospital, Hamilton, Ontario, Canada, are gratefully acknowledged for providing the plasma samples of maprotiline.

Identification and Analysis of Persistent Contaminants Associated with Gemcadiol

J. PHILIP and D. H. SZULCZEWSKI ˣ

Received August 6, 1979, from *Analytical Research, Warner-Lambert Company, Morris Plains, NJ 07950.* Accepted for publication January 17, 1980.

Abstract □ Application of several analytical probes indicated that certain batches of the investigational new drug gemcadiol (2,2,9,9-tetramethyl-1,10-decanediol) were contaminated with impurities whose nature and source were unknown. Subsequent study showed that these impurities consisted of polymeric material formed by self-condensation of the dialdehyde precursor. Gel permeation chromatographic techniques were found to be useful in the analysis of polymers present in both the aldehyde precursor and the finished drug.

Keyphrases □ Gemcadiol—identification and analysis of persistent contaminants □ Drug impurities—gemcadiol, identification and analysis of persistent contaminants □ Cholesterol-lowering agents, potential—gemcadiol, identification and analysis of persistent contaminants

Gemcadiol (2,2,9,9-tetramethyl-1,10-decanediol, I) is an investigational new drug that is being evaluated as a triglyceride- and cholesterol-lowering agent (1). This drug may be synthesized by a process whose last step involves sodium borohydride reduction of 2,2,9,9-tetramethyl-1,10-decanedial (II) (2).

When various batches of I were analyzed, it became apparent that significant interbatch variation existed for which the cause was not known. This study was conducted to determine the reason for the observed inconsistencies and to provide a more definitive method of analysis.

EXPERIMENTAL

Reagents—The solvents were analytical reagent grade. The sodium borohydride[1] was used as received.

Apparatus—IR spectra were obtained using a grating IR spectrophotometer[2]. GLC was done on a programmable research chromatograph[3] equipped with a flame-ionization detector and an electronic integrator[4]. NMR spectra were obtained on a 90-MHz instrument[5] with deuterochloroform as the solvent and tetramethylsilane as the internal standard.

GLC Studies—GLC studies were performed using 183 × 0.64-cm stainless steel columns packed with 5% silicone gum rubber[6] on silanized diatomaceous earth[7]. Chromatograms were obtained under isothermal conditions (225°) after injection of 2 μl of a 10% solution of the sample in methanol. In certain cases, the solution injected was acidified by adding 1 drop of 3 *N* HCl to 1 ml of the methanolic sample solution.

Liquid Chromatography of I—Liquid chromatographic separation of the components present in impure samples of I was accomplished using modified dextran beads[8] packed in a 40 × 3-cm glass chromatographic column. Methanol (25% v/v) in benzene was the mobile phase. The column was charged with a sample of ~500 mg dissolved in 5 ml of the mobile

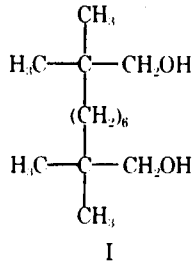

I

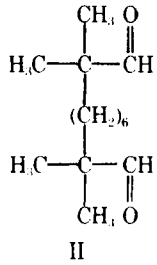

II

[1] Alfa Inorganics, Ventron Corp.

[2] Model 457, Perkin-Elmer Corp.
[3] Model 5750, F & M Scientific Corp.
[4] Model 3370A, Hewlett-Packard Corp.
[5] Bruker WH 90.
[6] OV-17, Hewlett-Packard.
[7] Chromasorb G, Hewlett-Packard.
[8] Sephadex LH-20, Pharmacia Fine Chemicals.

0022-3549/80/0600-0687$01.00/0
© 1980, American Pharmaceutical Association

(5) H. Tanaka, M. Furast, and S. Takasaki, *Acta Pathol.*, **25**, 413 (1975).
(6) S. Szeless, G. Kleinberger, R. Kotzaurek, H. Pall, M. Pichler, and G. Raberger, *Wien. Klin. Wochenschr.*, **87**, 254 (1975).
(7) A. Reale and M. Motolese, "Haemodynamic Studies with CIBA 34,276 BA in Depressive Illness, Diagnosis, Assessment, Treatment," Hans Huber, Bern, Switzerland, 1972, p. 161.
(8) H. Madsen and B. J. Lauritsen, *Ugeskr. Laeg.*, **138**, 992 (1976).
(9) W. Riess, *Anal. Chim. Acta*, **68**, 363 (1974).
(10) U. P. Geiger, T. G. Rajagopalan, and W. Riess, *J. Chromatogr.*, **114**, 167 (1975).
(11) R. N. Gupta, G. Molnar, and M. L. Gupta, *Clin. Chem.*, **23**, 1849 (1977).
(12) C. C. Fenselau, *Appl. Spectrosc. Rev.*, **28**, 305 (1974).
(13) S. D. Nelson and L. R. Pohl, *Ann. Rep. Med. Chem.*, **12**, 319 (1977).
(14) C. G. Hammar, B. Holmstedt, and R. Ryhage, *Anal. Biochem.*, **25**, 53e (1968).
(15) F. J. Marshall and R. E. McMahon, *J. Labeled Compd.*, **6**, 261 (1970).
(16) V. A. Fung and J. I. Degraw, *Synthesis*, **1976**, 311.
(17) B. Holmstedt and L. Palmer, *Adv. Biochem. Psychopharmacol.*, **7**, 1 (1973).
(18) F. W. McLafferty, "Interpretation of Mass Spectra," Benjamin, Reading, Mass., 1977, p. 49.
(19) D. M. S. Wheeler, T. H. Kinstel, and K. L. Rinehart, Jr., *J. Am. Chem. Soc.*, **89**, 4494 (1967).
(20) B. S. Finkel, R. L. Foltz, and D. M. Taylor, *J. Chromatogr. Sci.*, **12**, 304 (1974).
(21) B. J. Gudzinowicz and M. J. Gudzinowicz, "Analysis of Drugs and Metabolites by Gas Chromatography-Mass Spectrometry," Dekker, New York, N.Y., 1977, pp. 3, 125.
(22) W. Riess, L. Dubey, E. W. Funfgeld, P. Imhof, H. Hurzeler, N. Matussek, T. G. Rajagopalan, J. Raschdorf, and K. Schmidt, *J. Int. Med. Res., Suppl. (2)*, **3**, 16 (1975).

ACKNOWLEDGMENTS

Supported by the Office of Research, Department of Mental Hygiene, State of New York.

Dr. R. N. Gupta and Dr. M. L. Gupta of St. Joseph's Hospital, Hamilton, Ontario, Canada, are gratefully acknowledged for providing the plasma samples of maprotiline.

Identification and Analysis of Persistent Contaminants Associated with Gemcadiol

J. PHILIP and D. H. SZULCZEWSKI ˣ

Received August 6, 1979, from *Analytical Research, Warner-Lambert Company, Morris Plains, NJ 07950.* Accepted for publication January 17, 1980.

Abstract □ Application of several analytical probes indicated that certain batches of the investigational new drug gemcadiol (2,2,9,9-tetramethyl-1,10-decanediol) were contaminated with impurities whose nature and source were unknown. Subsequent study showed that these impurities consisted of polymeric material formed by self-condensation of the dialdehyde precursor. Gel permeation chromatographic techniques were found to be useful in the analysis of polymers present in both the aldehyde precursor and the finished drug.

Keyphrases □ Gemcadiol—identification and analysis of persistent contaminants □ Drug impurities—gemcadiol, identification and analysis of persistent contaminants □ Cholesterol-lowering agents, potential—gemcadiol, identification and analysis of persistent contaminants

Gemcadiol (2,2,9,9-tetramethyl-1,10-decanediol, I) is an investigational new drug that is being evaluated as a triglyceride- and cholesterol-lowering agent (1). This drug may be synthesized by a process whose last step involves sodium borohydride reduction of 2,2,9,9-tetramethyl-1,10-decanedial (II) (2).

When various batches of I were analyzed, it became apparent that significant interbatch variation existed for which the cause was not known. This study was conducted to determine the reason for the observed inconsistencies and to provide a more definitive method of analysis.

EXPERIMENTAL

Reagents—The solvents were analytical reagent grade. The sodium borohydride[1] was used as received.

Apparatus—IR spectra were obtained using a grating IR spectrophotometer[2]. GLC was done on a programmable research chromatograph[3] equipped with a flame-ionization detector and an electronic integrator[4]. NMR spectra were obtained on a 90-MHz instrument[5] with deuterochloroform as the solvent and tetramethylsilane as the internal standard.

GLC Studies—GLC studies were performed using 183 × 0.64-cm stainless steel columns packed with 5% silicone gum rubber[6] on silanized diatomaceous earth[7]. Chromatograms were obtained under isothermal conditions (225°) after injection of 2 μl of a 10% solution of the sample in methanol. In certain cases, the solution injected was acidified by adding 1 drop of 3 *N* HCl to 1 ml of the methanolic sample solution.

Liquid Chromatography of I—Liquid chromatographic separation of the components present in impure samples of I was accomplished using modified dextran beads[8] packed in a 40 × 3-cm glass chromatographic column. Methanol (25% v/v) in benzene was the mobile phase. The column was charged with a sample of ~500 mg dissolved in 5 ml of the mobile

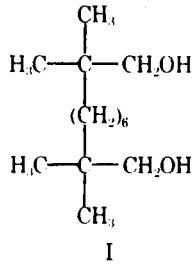

I

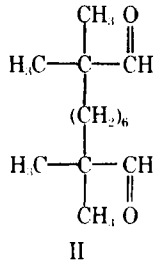

II

[1] Alfa Inorganics, Ventron Corp.

[2] Model 457, Perkin-Elmer Corp.
[3] Model 5750, F & M Scientific Corp.
[4] Model 3370A, Hewlett-Packard Corp.
[5] Bruker WH 90.
[6] OV-17, Hewlett-Packard.
[7] Chromasorb G, Hewlett-Packard.
[8] Sephadex LH-20, Pharmacia Fine Chemicals.

0022-3549/80/0600-0687$01.00/0
© 1980, American Pharmaceutical Association

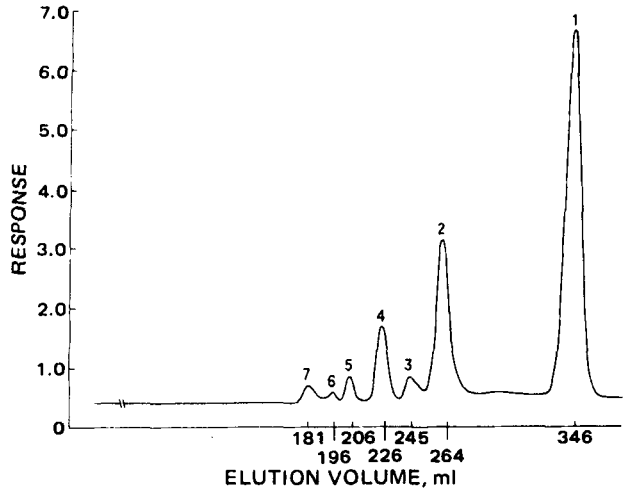

Figure 1—*Liquid chromatogram of polymerized II obtained on a column packed with Bio Beads SX-2 using benzene as the eluent. Elution volumes of each peak are indicated. The indicated molecular weights are: peak 2, 610–690; peak 3, 750–840; peak 4, 940–1060; peak 5, 1200–1400; and peak 6, 1300–1600.*

phase; it was operated at a flow rate of 1 ml/min, and 10-ml fractions were collected. The fractions were transferred to tared aluminum weighing pans[9] (70 mm), the eluent was allowed to evaporate, and the pans were brought to constant weight under a vacuum. The weight of nonvolatile material in each pan then was plotted *versus* the eluent volume to obtain the chromatogram.

Liquid Chromatography of II—The chromatographic system employed for II was essentially the same as that developed by Mulder and Buytenhuys (3). Glass columns (90 × 2.4 cm) packed with porous styrenedivinylbenzene beads[10] were employed with benzene as the mobile phase. The columns were attached to a commercial high-efficiency liquid chromatographic system[11] equipped with a refractive index detector[12]. Five milliliters of a 5% sample solution in benzene was introduced to the column with a sample injection valve[13]. The columns were operated at a flow rate of 20 ml/hr at ambient temperature.

Estimation of Molecular Weights of Components Present in Partially Polymerized II—A mixture containing known compounds of relatively high molecular weights was prepared by dissolving 100 mg of II and 50 mg each of tristearin[14] (mol. wt. 891), trimyristin[14] (mol. wt. 723), and trilaurin[14] (mol. wt. 639) in 5 ml of benzene. A chromatogram was obtained for this mixture using the chromatographic system and conditions described for the liquid chromatography of II. The elution volumes of the known components were noted, and a plot of log mol. wt. *versus* elution volume was constructed.

Although the plot was linear, its slope caused the anticipated molecular weights to be underestimated (specific adsorption effects). Nevertheless, these estimates are the basis for the lower molecular weights of the molecular weight estimate given in Fig. 1. By assuming that the lowest polymeric contaminant of the aldehyde mixture, Component 2, had a molecular weight of 678 and by calibrating the column with this compound and II (mol. wt. 226), the estimates for the upper limit of the range estimate were obtained.

Reduction of Samples of II—In general, 1 g of II was dissolved in 5 ml of 2-propanol and placed in a small beaker containing a magnetic stirring bar. A solution of sodium borohydride (176 mg/g of II) in distilled water was added dropwise with stirring. The resulting mixture was stirred for an additional 30 min.

After the reaction was complete, the mixture was poured into excess water and ice, and this mixture was stirred. The final mixture was extracted with three equal volumes of chloroform, and the chloroform extract was dried over anhydrous magnesium sulfate. After the magnesium sulfate was separated by filtration, the chloroform was evaporated and and the residue was brought to constant weight under vacuum.

Reduction of Components in Impure Samples of II—Each component found in polymerized samples of II was reduced immediately following elution from the chromatographic column by piping the column eluate into separate receivers, each containing 100 mg of sodium borohydride dissolved in water–methanol (10:40). The methanol was evaporated in a rotary evaporator, and excess water was added.

The aqueous mixture was extracted three times with 25-ml portions of chloroform, and the chloroform extracts were pooled. The combined chloroform extracts were back-washed with water until they were neutral to litmus paper and then they were dried over anhydrous magnesium sulfate. After freeing the extract of solid magnesium sulfate, the chloroform was evaporated and the residue was collected.

Preparation and Characterization of 10-Hydroxy-2,2,9,9-tetramethyldecanal (III)—Compound II, 100 g, was dissolved in 128 ml of 2-propanol and was kept stirring in a beaker. A solution of 8.3 g of sodium borohydride in 109 ml of water was added dropwise. At the end of this addition, the reaction mixture was analyzed by GLC and found to be a mixture of 80% I and 20% III. The solvent was evaporated, and the residue was dissolved in warm acetonitrile. Upon cooling, some I crystallized, leaving a supernate containing 32% I and 68% III. Compound III was isolated from the mother liquor as follows.

The solvent was evaporated, and 50 g of the residue was refluxed for 2 hr with 50 g of Girard's Reagent T[15], 50 ml of acetic acid, and 500 ml of 95% ethanol. The alcohol then was evaporated, and the residue was washed three times with 200-ml portions of ether. It then was dissolved in 300 ml of water, and 60 ml of 5 *N* HCl was added. The mixture was heated on the steam bath for 1 hr. The formed oil was separated and dissolved in ether. The ether solution was washed with a dilute potassium bicarbonate solution and then with water. The ether solution was dried over anhydrous magnesium sulfate, and the ether was evaporated.

The residue was free of I and was identified as 10-hydroxy-2,2,9,9-tetramethyldecanal (III). The mass spectrum exhibited a molecular ion

Table I—NMR (Deuterochloroform) Data for III

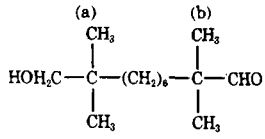

Functional Group	Chemical Shift, ppm	Relative Area
CH_3 (a)	0.82	6
CH_3 (b)	1.0	6
CH_2 (alkyl)	1.21	12
CH	1.74	1
CH_2 (CH_2OH)	3.27	2
CHO	9.40	1

Table II—Results from Analysis of Various Batches of I by Differential Scanning Calorimetry (DSC) and GLC

Batch	Percent I	
	DSC	GLC
A	99.6	98.0
B	97.4	92.4
C	98.9	97.8
D	—[a]	86.9

[a] Thermogram was excessively distorted so calculation was not possible.

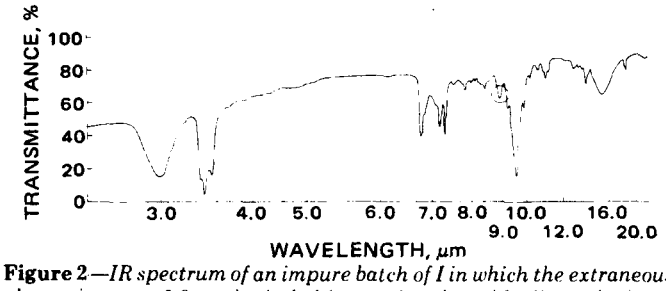

Figure 2—*IR spectrum of an impure batch of I in which the extraneous absorption near 9.0 μm is circled (potassium bromide dispersion).*

[9] Arthur H. Thomas Co.
[10] Bio Beads SX-2, Bio Rad Laboratories.
[11] Series 4100, Varian Aerograph.
[12] Varian Aerograph.
[13] SV-8031, Chromatronix.
[14] Nu Chek Prep, Elysian, Minn.
[15] Aldrich Chemical Co., Milwaukee, Wis.

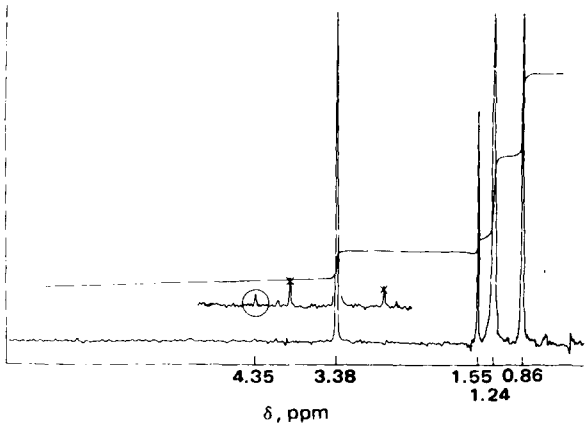

Figure 3—*NMR spectrum of impure I (1% in deuterochloroform) in which the extraneous absorption at 4.35 ppm is circled and where × denotes side bands.*

at *m/e* 228. IR analysis gave a strong band at 5.78 μm due to C=O. GLC gave only one peak. The NMR data are given in Table I.

Anal.—Calc. for $C_{14}H_{28}O$: C, 73.68; H, 12.28. Found: C, 73.60; H, 12.20.

Determination of Amount of Polymeric Contaminants in I—Approximately 10 g of Sephadex LH-20 was conditioned by stirring with benzene–methanol (75:25) for several hours. The solvated beads were packed into a 45 × 2-cm glass column. The height of the resin bed was 42 cm. Approximately 200 mg of the sample was weighed accurately and dissolved in 5 ml of the eluent (benzene–methanol). The solution then was introduced into the column, and the column was eluted with benzene–methanol (75:25).

Fractions of 30, 35, and 40 ml were collected and transferred into three tared aluminum pans. The solvent was evaporated, and the pans were dried under vacuum to constant weight. Fractions 2 and 3 contained the total polymeric impurities and the drug, respectively. These fractions were weighed, and the amount of polymeric contaminants in I was calculated from their weights.

RESULTS AND DISCUSSION

Purity estimates of various batches of I, obtained by differential calorimetry[16] (4), are shown in Table II; significant interbatch variation was observed. IR spectra obtained from these batches differed in that the spectrum of the less pure material had extraneous absorption near 9 μm (Fig. 2). The NMR spectra of high and low quality drug were similar (Fig. 3), except for a barely perceptible peak near 4.35 ppm.

Gas–liquid chromatograms obtained from impure batches (Fig. 4, left) were characterized by a large symmetrical peak preceded by a small distorted peak or shoulder. The relative area of the distorted peak or shoulder varied from batch to batch, and its shape suggested it could have arisen from partial thermal decomposition of I itself or associated contaminants. When the methanolic sample solution used for injection was acidified prior to injection, relatively impure samples gave a chromatogram like that shown in Fig. 4 (right). The retention time of two of the observed small peaks corresponded to II and III. The presence of these compounds was confirmed through mass spectrometry and the coincidence of the retention time with authentic samples.

Since the chromatographic behavior of the vapor phase indicated thermal decomposition, other means of separation were investigated. It was determined that extraneous material could be separated from the

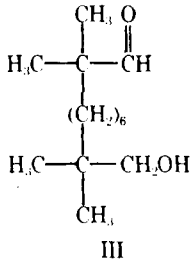

III

[16] Model DSC 1B differential scanning calorimeter, Perkin-Elmer.

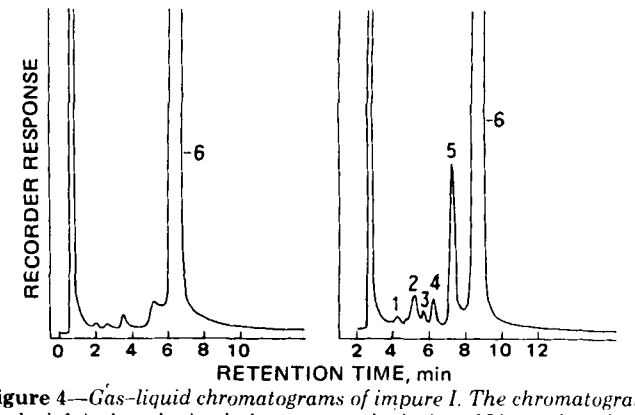

Figure 4—*Gas–liquid chromatograms of impure I. The chromatogram on the left is that obtained when a neutral solution of I in methanol was injected. The chromatogram on the right was obtained when an acidic solution of I in methanol was injected. Peaks 5, 4, and 6 represent III, II, and I, respectively.*

drug through gel permeation chromatography using Sephadex LH-20 with methanol–benzene as the eluent[17]. A typical chromatogram obtained on an impure batch of drug is shown in Fig. 5. IR spectra obtained on the material responsible for the various peaks showed strong absorption at ~9 μm for peaks 1–3, whereas the spectrum of peak 4 had no extraneous absorption and was consistent with the pure drug.

More of the major contaminant (peak 3) was obtained[18] for characterization, and the NMR spectrum was informative (Fig. 6). While the spectrum of the contaminant was similar to that of the drug, the details differed. A significant difference was that the signal from the methyl protons occurred at more than one chemical shift, and there was a small but real peak near 4.4 ppm. The complete NMR data obtained on this sample are summarized in Table III.

Structures A and B are consistent with the NMR data and are chemically reasonable (5–8).

Anal.—Calc. for Structure A or B: C, 73.68; H, 12.28. Found: C, 73.70; H, 12.19.

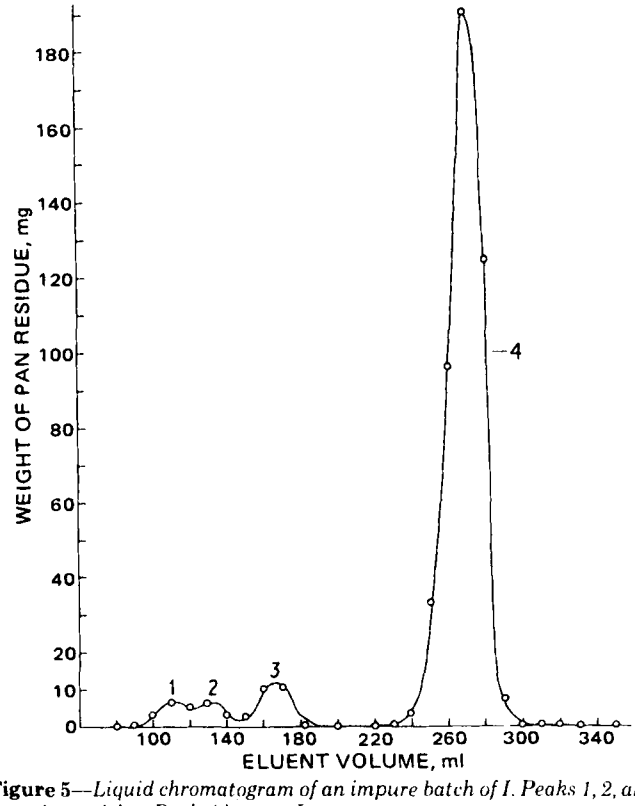

Figure 5—*Liquid chromatogram of an impure batch of I. Peaks 1, 2, and 3 are impurities. Peak 4 is pure I.*

[17] See *Experimental.*

[18] Preparative chromatography using a 45 × 6-cm glass column.

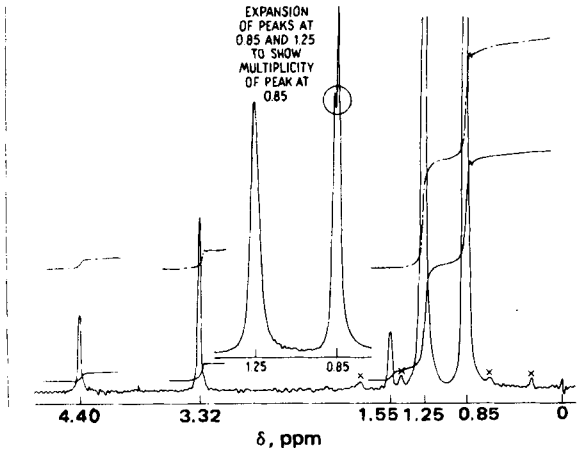

Figure 6—*NMR spectrum of material corresponding to peak 3 in Fig. 5 (2% in deuterochloroform).*

The IR spectrum showed a strong band at 9 μm, suggesting the presence of C—O—C. GLC of an acidified methanolic solution gave only one peak corresponding to 10-hydroxy-2,2,9,9-tetramethyldecanal (III). The molecular weight determined by the Rast procedure (9) was 611 ± 10%. This result and its behavior on the gel permeation column[19] indicate that its molecular weight cannot be 228, so Structure B is favored.

Examination of the IR spectrum of various batches of the dialdehyde precursor (II) revealed that relatively strong absorption near 9 μm existed in some batches but not in others. A sample of dialdehyde giving an IR spectrum that had strong absorption near 9 μm and a sample not having this extraneous absorption were reduced, and the reduction products were chromatographed. The chromatograms obtained showed that impurities were formed only in the case where the dialdehyde gave an IR spectrum with significant absorption near 9 μm.

Since further information regarding the nature of the contaminants in the dialdehyde was desirable, a liquid chromatographic system suitable for their separation was developed and chromatograms were obtained. A chromatogram representative of the dialdehyde with strong 9-μm absorption is shown in Fig. 1. The system employed provided near baseline separation of at least six contaminants.

A range estimate of molecular weights of the various components obtained on the basis of elution volume are included in Fig. 1. Attempts were made to obtain definitive NMR data directly on these contaminants; although peaks were present that could be assigned to ring and aldehyde protons (Table IV), spurious peaks also were observed. These peaks,

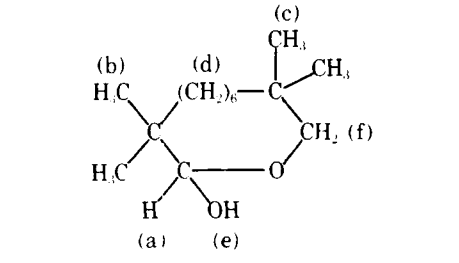

A

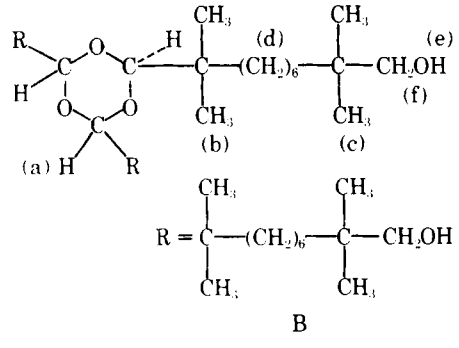

B

[19] The elution volume of this material is much less than that of II, whose molecular weight is 228.

Table III—NMR Data Obtained from Material Corresponding to Peak 3 in Fig. 5

Functional Group	Chemical Shift, ppm	Relative Area
CH (a)	4.4	1
CH_3 (b,c)	0.85	12.6
CH_2 (alkyl) (d)	1.25	12.6
OH (e)	1.57	1
CH_2 (CH_2OH) (f)	3.3	2

Table IV—NMR Data Obtained from Material Corresponding to Peak 4 in Fig. 1

Functional Group	Chemical Shift, ppm	Relative Area
CH	4.4	7.5
CH_3	(0.90) −(1.05)	72
CH_2	1.21 1.23 1.29 1.49	122
?	8.04	2
CHO	9.48	3

Table V—NMR Data Obtained from Material Corresponding to Peak 4 in Fig. 1 after Reduction with Sodium Borohydride

Functional Group	Chemical Shift, ppm	Proton Ratio
CH	4.37	1.44
CH_3	0.86	14.2
CH_2 (alkyl)	1.23	14.6
OH	1.67	1.0
CH_2 (CH_2OH)	3.29	1.85

which resulted from oxidation, precluded clear definition of proton ratios.

Since the components of the impure dialdehyde were well separated, they were reduced concurrently with elution, and an impure drug sample was spiked with the reduced aldehyde impurities. Liquid chromatograms then were obtained, which indicated that the material responsible for peak 2 (Fig. 1) corresponded to drug contaminant 3 (Fig. 5) and that aldehyde contaminant 4 (Fig. 1) corresponded to drug contaminant 2 (Fig. 5). Since components of the impure dialdehyde were better separated than their reduced counterparts, a sufficient sample of a minor drug contaminant, peak 2 (Fig. 5), was obtained by chromatographing partially polymerized dialdehyde and providing concurrent reduction. This material was a viscous clear liquid.

Anal.—Calc. for $C_{70}H_{138}O_{10}$ (Structure C): C, 73.81; H, 12.13. Found: C, 73.50; H, 12.09.

The molecular weight calculated for Structure C was 1138; the range indicated by gel permeation chromatography was 940–1060.

GLC of the acidic methanolic solution gave both the monoaldehyde monoalcohol (III) and the dialdehyde in a molar ratio of 4:1. The presence of the dialdehyde is significant and indicates that this higher molecular weight impurity contains a dialdehyde bridge incorporated so as to protect both potential aldehyde groups from reduction. The NMR data are presented in Table V.

These properties are consistent with and indicative of Structure C as the structure of the next most abundant drug contaminant.

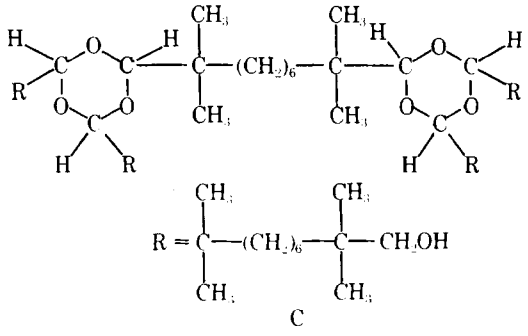

C

Table VI—Theoretical Proton Ratios for Various Protons Involved in Polymeric Alcohols Containing Various Numbers of Trioxane Rings

Protons	Proton Ratios (Group per OH)			
	1 Ring	2 Rings	3 Rings	4 Rings
Ring CH	1.0	1.5	1.8	2.0
Aliphatic CH_2	12.0	15.0	16.8	18.0
Methyl	12.0	15.0	16.8	18.0

The ratio of various protons having different chemical shifts would be expected to vary as polymerization continued. In particular, the ratio of ring CH, aliphatic CH_2, and methyl protons to hydroxyl protons would increase as the number of bridged trioxane rings increased (Table VI).

While it was important to separate individual components for characterization, this need does not apply for the establishment of drug purity. The gel permeation technique was modified to allow analysis of the total polymeric material in drug samples. To validate this method of analysis, mixtures having known compositions were analyzed. The results (percent impurity added: 0, 5.2, and 9.4; found: 0, 5.1, and 9.4) indicate that the method described under *Experimental* is sufficiently accurate for use.

CONCLUSIONS

Available information indicates that contaminants present in certain batches of I consist of polymeric alcohols characterized by at least one trioxane ring. These contaminants originate in the dialdehyde precursor, which may polymerize to form corresponding compounds. Reduction of polymers present in the dialdehyde yields the alcohol polymers, which may persist throughout purification and contaminate the finished drug. Analysis *via* gel permeation liquid chromatography provides a useful means to analyze the degree of contamination by these polymeric compounds.

REFERENCES

(1) H. P. Blumenthal, J. R. Ryan, and F. G. McMahon, *Clin. Pharmacol. Ther.*, **17**, 229 (1975).

(2) O. P. Goel, *Chem. Ind. (London)*, **16**, 665 (1974).

(3) J. L. Mulder and F. A. Buytenhuys, *J. Chromatogr.*, **51**, 459 (1970).

(4) *Thermal Analysis Newsletter*, vols. 5 and 6, Perkin-Elmer Corp., Norwalk, Conn.

(5) J. March, "Advanced Organic Chemistry: Reactions, Mechanisms, and Structure," McGraw-Hill, New York, N.Y., 1968, p. 717.

(6) J. D. Roberts and M. C. Caserio, "Basic Principles of Organic Chemistry," W. A. Benjamin, New York, N.Y., 1965, pp. 448, 449.

(7) J. C. Bevington, *Q. Rev. (London)*, **6**, 141 (1952).

(8) M. Baron, D. B. Mandirola, and J. F. Westerkamp, *Can. J. Chem.*, **41**, 1893 (1963).

(9) K. Rast, *Chem. Ber.*, **55**, 1051, 3727 (1922).

ACKNOWLEDGMENTS

The authors are indebted to Dr. O. Goel, who synthesized most of the materials used in this study, to Mr. B. Scott, who determined the NMR spectra, and to Dr. L. M. Wheeler for encouragement and support.

Preliminary Model for Streptozocin Metabolism in Mice

JONAS M. WEISSBROD * and RAKESH K. JAIN ‡x

Received June 25, 1979, from the **Department of Chemical Engineering, Columbia University, New York, NY 10027*, and the ‡*Department of Chemical Engineering, Carnegie-Mellon University, Pittsburgh, PA 15213.* Accepted for publication January 18, 1980.

Abstract □ A mathematical model for streptozocin metabolism in mice is presented. By using the available bioassay and chemical assay data for a 300-mg/kg ip injection and the principles of physiologically based pharmacokinetics, a membrane-limited transport model with first-order kinetics was found to simulate the data adequately (average error of <20%). Furthermore, the first-order reaction constant derived in analyzing the bioassay data (0.009 min^{-1}) was in close agreement with the half-life of streptozocin (1 hr) reported previously.

Keyphrases □ Streptozocin—drug metabolism and distribution, mathematical model based on bioassay and chemical assay, mice □ Metabolism—streptozocin distribution and transport, mice, mathematical model □ Diabetes—streptozocin induced, pharmacokinetic model, mice □ Pharmacokinetic models—streptozocin metabolism, bioassay and chemical assay, mice, membrane-limited transport

Streptozocin (NSC-85998), the 2-deoxy-D-glucose derivative of 1-methylnitrosourea (1), has been shown to inhibit primary DNA synthesis in mammalian cells (2, 3). Due to its selective toxicity for pancreatic β-cells, streptozocin has been used to induce diabetes in a variety of animals (4–6). In addition, it has been useful in the treatment of metastatic insulinoma (7, 8).

BACKGROUND

Previous kinetic studies showed that streptozocin degradation obeys first-order reaction kinetics. These studies also indicated the presence of at least two pathways for streptozocin degradation, one involving the *N*-nitroso group and the other involving another portion of the molecule, probably the glucose moiety (9). While chromatography has been used to isolate several streptozocin metabolites (10, 11), their molecular structures have not been identified precisely.

In addition, data for streptozocin concentrations in various tissues of mice as a function of time were obtained previously (10) using three assay methods: bioassay and chemical and radiochemical assays. The bioassay is the closest indicator of the actual streptozocin content, but this method does not preclude the possibility that some drug metabolites also may be bioactive. The chemical assay measures the *N*-nitroso group of streptozocin and its metabolites. The radiochemical assay measures a tritiated hydrogen atom that originally was at the C-6 position of the glucose moiety of streptozocin and must be accounted for either as part of the streptozocin molecule or as part of the several streptozocin metabolites known to exist.

The objective of this study was to utilize these data along with the present knowledge of streptozocin metabolism to develop mathematical models for the distribution, transport, and metabolism of streptozocin in mice.

THEORETICAL

In recent years, physiologically based pharmacokinetic modeling (12, 13) has been applied extensively to predict drug distributions in plasma and various tissues of mammalian systems (14, 15). A pharmacokinetic model is a simplified representation of a real physical system (Scheme I) derived from experimental observations, previous knowledge, and a number of assumptions. It is based on relevant physical and biochemical parameters such as plasma flow rates, tissue volumes, tissue binding constants, mass transfer coefficients, and, when necessary, chemical reaction constants to account for drug metabolism. The validity of the model as a means of predicting tissue drug distributions and excretion rates is tested by comparing model predictions with data. Plasma flow rates and tissue volumes for most species and tissues are readily available in the literature. Mass transfer, binding, and metabolism parameters for a given drug must be estimated from the available data.

0022-3549/80/0600-0691$01.00/0

© 1980, American Pharmaceutical Association

Table VI—Theoretical Proton Ratios for Various Protons Involved in Polymeric Alcohols Containing Various Numbers of Trioxane Rings

Protons	Proton Ratios (Group per OH)			
	1 Ring	2 Rings	3 Rings	4 Rings
Ring CH	1.0	1.5	1.8	2.0
Aliphatic CH_2	12.0	15.0	16.8	18.0
Methyl	12.0	15.0	16.8	18.0

The ratio of various protons having different chemical shifts would be expected to vary as polymerization continued. In particular, the ratio of ring CH, aliphatic CH_2, and methyl protons to hydroxyl protons would increase as the number of bridged trioxane rings increased (Table VI).

While it was important to separate individual components for characterization, this need does not apply for the establishment of drug purity. The gel permeation technique was modified to allow analysis of the total polymeric material in drug samples. To validate this method of analysis, mixtures having known compositions were analyzed. The results (percent impurity added: 0, 5.2, and 9.4; found: 0, 5.1, and 9.4) indicate that the method described under *Experimental* is sufficiently accurate for use.

CONCLUSIONS

Available information indicates that contaminants present in certain batches of I consist of polymeric alcohols characterized by at least one trioxane ring. These contaminants originate in the dialdehyde precursor, which may polymerize to form corresponding compounds. Reduction of polymers present in the dialdehyde yields the alcohol polymers, which may persist throughout purification and contaminate the finished drug. Analysis *via* gel permeation liquid chromatography provides a useful means to analyze the degree of contamination by these polymeric compounds.

REFERENCES

(1) H. P. Blumenthal, J. R. Ryan, and F. G. McMahon, *Clin. Pharmacol. Ther.*, **17**, 229 (1975).

(2) O. P. Goel, *Chem. Ind. (London)*, **16**, 665 (1974).

(3) J. L. Mulder and F. A. Buytenhuys, *J. Chromatogr.*, **51**, 459 (1970).

(4) *Thermal Analysis Newsletter*, vols. 5 and 6, Perkin-Elmer Corp., Norwalk, Conn.

(5) J. March, "Advanced Organic Chemistry: Reactions, Mechanisms, and Structure," McGraw-Hill, New York, N.Y., 1968, p. 717.

(6) J. D. Roberts and M. C. Caserio, "Basic Principles of Organic Chemistry," W. A. Benjamin, New York, N.Y., 1965, pp. 448, 449.

(7) J. C. Bevington, *Q. Rev. (London)*, **6**, 141 (1952).

(8) M. Baron, D. B. Mandirola, and J. F. Westerkamp, *Can. J. Chem.*, **41**, 1893 (1963).

(9) K. Rast, *Chem. Ber.*, **55**, 1051, 3727 (1922).

ACKNOWLEDGMENTS

The authors are indebted to Dr. O. Goel, who synthesized most of the materials used in this study, to Mr. B. Scott, who determined the NMR spectra, and to Dr. L. M. Wheeler for encouragement and support.

Preliminary Model for Streptozocin Metabolism in Mice

JONAS M. WEISSBROD * and RAKESH K. JAIN ‡x

Received June 25, 1979, from the **Department of Chemical Engineering, Columbia University, New York, NY 10027*, and the ‡*Department of Chemical Engineering, Carnegie-Mellon University, Pittsburgh, PA 15213.* Accepted for publication January 18, 1980.

Abstract □ A mathematical model for streptozocin metabolism in mice is presented. By using the available bioassay and chemical assay data for a 300-mg/kg ip injection and the principles of physiologically based pharmacokinetics, a membrane-limited transport model with first-order kinetics was found to simulate the data adequately (average error of <20%). Furthermore, the first-order reaction constant derived in analyzing the bioassay data (0.009 min^{-1}) was in close agreement with the half-life of streptozocin (1 hr) reported previously.

Keyphrases □ Streptozocin—drug metabolism and distribution, mathematical model based on bioassay and chemical assay, mice □ Metabolism—streptozocin distribution and transport, mice, mathematical model □ Diabetes—streptozocin induced, pharmacokinetic model, mice □ Pharmacokinetic models—streptozocin metabolism, bioassay and chemical assay, mice, membrane-limited transport

Streptozocin (NSC-85998), the 2-deoxy-D-glucose derivative of 1-methylnitrosourea (1), has been shown to inhibit primary DNA synthesis in mammalian cells (2, 3). Due to its selective toxicity for pancreatic β-cells, streptozocin has been used to induce diabetes in a variety of animals (4–6). In addition, it has been useful in the treatment of metastatic insulinoma (7, 8).

BACKGROUND

Previous kinetic studies showed that streptozocin degradation obeys first-order reaction kinetics. These studies also indicated the presence of at least two pathways for streptozocin degradation, one involving the *N*-nitroso group and the other involving another portion of the molecule, probably the glucose moiety (9). While chromatography has been used to isolate several streptozocin metabolites (10, 11), their molecular structures have not been identified precisely.

In addition, data for streptozocin concentrations in various tissues of mice as a function of time were obtained previously (10) using three assay methods: bioassay and chemical and radiochemical assays. The bioassay is the closest indicator of the actual streptozocin content, but this method does not preclude the possibility that some drug metabolites also may be bioactive. The chemical assay measures the *N*-nitroso group of streptozocin and its metabolites. The radiochemical assay measures a tritiated hydrogen atom that originally was at the C-6 position of the glucose moiety of streptozocin and must be accounted for either as part of the streptozocin molecule or as part of the several streptozocin metabolites known to exist.

The objective of this study was to utilize these data along with the present knowledge of streptozocin metabolism to develop mathematical models for the distribution, transport, and metabolism of streptozocin in mice.

THEORETICAL

In recent years, physiologically based pharmacokinetic modeling (12, 13) has been applied extensively to predict drug distributions in plasma and various tissues of mammalian systems (14, 15). A pharmacokinetic model is a simplified representation of a real physical system (Scheme I) derived from experimental observations, previous knowledge, and a number of assumptions. It is based on relevant physical and biochemical parameters such as plasma flow rates, tissue volumes, tissue binding constants, mass transfer coefficients, and, when necessary, chemical reaction constants to account for drug metabolism. The validity of the model as a means of predicting tissue drug distributions and excretion rates is tested by comparing model predictions with data. Plasma flow rates and tissue volumes for most species and tissues are readily available in the literature. Mass transfer, binding, and metabolism parameters for a given drug must be estimated from the available data.

0022-3549/80/0600-0691$01.00/0

© 1980, American Pharmaceutical Association

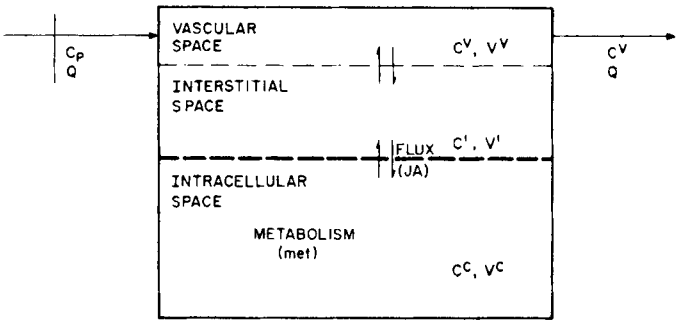

Scheme I—Schematic representation of a typical model compartment where Q is the plasma perfusion rate; C_p is the afferent plasma concentration; V^v, V^i, and V^c are the volumes of the vascular, interstitial, and intracellular spaces, respectively; C^v, C^i, and C^c are the drug concentrations in the vascular, interstitial, and intracellular spaces, respectively; jA is the net flux of drug to the intracellular space; and met is the rate of drug disappearance via metabolism. The vascular and interstitial spaces are combined into a single extracellular subcompartment, and the efferent plasma concentration is assumed to be equal to the extracellular drug concentration.

As shown in Scheme I, a tissue compartment can be divided into three subcompartments: the vascular, interstitial, and intracellular spaces. Drug concentrations in each subcompartment are assumed to be uniform, and the effluent plasma concentration is assumed to be equal to the drug concentration of the vascular subcompartment.

For most drugs and tissues, the vessel wall is more permeable than the cellular membrane, and the vascular and interstitial subcompartments can be combined into a single subcompartment, the extracellular space. Therefore, in the present study, transport in all of the compartments was modeled according to a membrane-limited model, which is similar to models applied previously to methotrexate uptake into the bone marrow, spleen, and intestine of rats (13), dactinomycin (actinomycin D) uptake into the testes of beagle dogs (16), and methotrexate uptake into several types of tumors (17, 18).

With these assumptions and definitions, two nonsteady-state material balance equations for a particular body (or tissue) compartment may be derived:

$$V_i^e \frac{dC_i^e}{dt} = Q_i(C_p - C_i^e) - (jA)_i - q_i C_i^e \qquad \text{(Eq. 1)}$$

$$V_i^c \frac{dC_i^c}{dt} = (jA)_i - (\text{met})_i \qquad \text{(Eq. 2)}$$

where the subscript i refers to the ith body compartment; V_i^e and V_i^c are the volumes of the extracellular and intracellular spaces (milliliters), respectively; C_i^e and C_i^c are the total drug concentrations in the extracellular and intracellular spaces (micrograms per milliliter), respectively; Q_i is the plasma perfusion rate (milliliters per minute); q_i is the drug clearance rate (zero for compartments other than the kidneys and liver) that accounts for drug elimination *via* the urine and bile (milliliters per minute); C_p is the afferent plasma concentration (micrograms per milliliter); $(jA)_i$ is the net flux of drug into the intracellular subcompartment (micrograms per minute); and $(\text{met})_i$ is the rate of drug metabolism in the ith compartment (micrograms per minute).

The net flux $(jA)_i$ between the extracellular and intracellular subcompartments and the relationship between free and bound drug are defined by:

$$(jA)_i = V_i h_i (C_i^e - C_i^c/R_i) \qquad \text{(Eq. 3)}$$

where h_i and R_i are apparent first-order diffusion constants and tissue equilibrium partition coefficients into which the effect of drug binding in the extracellular fluid has been incorporated, respectively. The use of a first-order diffusion constant, h_i, assumes that the transport mechanism across the cell membrane is linear and nonsaturable.

The drug metabolism rate, $(\text{met})_i$, in the intracellular subcompartment is defined by:

$$(\text{met})_i = k_i V_i C_i^c \qquad \text{(Eq. 4)}$$

where k_i is the first-order reaction constant for streptozocin degradation. The use of first-order kinetics to describe streptozocin degradation was verified by previous kinetic studies (9).

Previous pharmacokinetic studies illustrated the applicability of a nonlinear regression analysis to the available plasma data to obtain an exponential equation for plasma concentrations as a function of time (15, 17, 18). This approach was utilized in the present study. Thus, once the parameter values and plasma exponential equations are known, Eqs. 1 and 2 are solved to obtain predictions for streptozocin concentrations in a given tissue as a function of time.

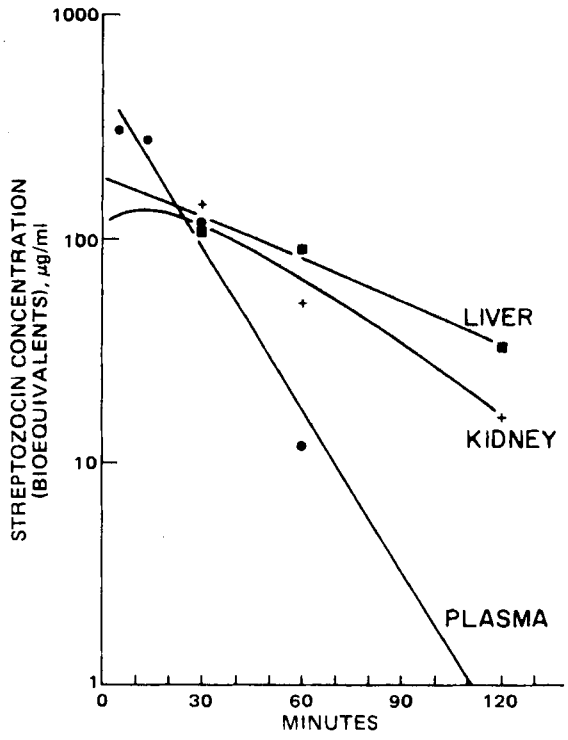

Figure 1—*Streptozocin bioequivalents* versus *time in plasma, liver, and kidneys of mice following an injection of 300 mg/kg ip. Points represent the experimental data of Bhuyan* et al. *(10) for plasma (●), liver (■); and kidneys (+). The curves represent model predictions. The parameters of Table I (bioassay values) and an exponential equation for the plasma concentration ($494.53e^{-0.0549t}$) were used to obtain the simulations.*

To compare model predictions with the data, the average drug concentration in a tissue must be defined as:

$$C_i = (C_i^e V_i^e + C_i^c V_i^c)/V_i \qquad \text{(Eq. 5)}$$

where C_i is the overall drug concentration of the ith compartment (micrograms per milliliter).

EXPERIMENTAL

Data for streptozocin concentrations as a function of time were obtained by Bhuyan *et al.* (10) using three independent assay methods: bioassay, chemical assay, and radiochemical assay. In these experiments, streptozocin (tritiated or unlabeled) was dissolved in phosphate buffer and was administered intraperitoneally to 20-g female BDF_1 (C57BL/6 × DBA/2) mice[1]. At various postinjection times up to 2 hr, groups of mice (four or five per group) were sacrificed; blood samples were collected, tissues were excised, and all were assayed for streptozocin.

The experimental procedures used were those described by Bhuyan *et al.* (10).

RESULTS AND DISCUSSION

Values for the compartmental volumes and tissue flow rates (V_i and Q_i, respectively) for each tissue were obtained from the literature (19). The binding, diffusion, and metabolism constants (R_i, h_i, and k_i) were determined by applying parameter estimation methods (18, 20) to the data of Bhuyan *et al.* (10). With these parameter values (Table I), the chemical and bioassay data for the liver, kidneys, and pancreas were modeled by first obtaining exponential fits for the plasma data and then solving Eqs. 1 and 2 for each tissue. The results are shown in Figs. 1 and

[1] Jackson Memorial Laboratory, Bal Harbor, Me.

Table I—Model Parameters [a] for Streptozocin Distribution in Mice [b]

Tissue	Tissue Volume (V), ml	Extracellular Volume (V^e), ml[d]	Plasma Flow Rate (Q), ml/min	Partition[c] Coefficient (R) Bio	Partition[c] Coefficient (R) Chem	Diffusion Constant[c] (h), min^{-1} Bio	Diffusion Constant[c] (h), min^{-1} Chem	Reaction Constant[c] (k), min^{-1} Bio	Reaction Constant[c] (k), min^{-1} Chem
Liver[e]	1.30[f]	0.5	1.1[f]	23.6	19.7	0.0164	0.1392	0.0086	0.0041
Kidneys[g]	0.34	0.13	0.8[f]	5.6	7.7	0.0305	0.1625	0.0096	0.0041[h]
Pancreas	0.09[b]	0.04	0.048[b]	—	15.8	—	0.0063	—	0.0041[h]

[a] Data were obtained by bioassay and chemical assay methods. [b] Mice weighed 20 g. [c] Obtained by parameter estimation using the bioassay and chemical assay data of Bhuyan *et al.* (10) for an injection of 300 mg/kg ip. [d] Estimated. [e] Bile clearance, q_1, is negligible (10). [f] Taken from Ref. 19. [g] Kidney clearance, q_k, was estimated from the data of Bhuyan *et al.* (10) to be 0.42 ml/min. [h] Assumed.

2. The average error between the data and the model predictions was 18.3% for the bioassay data (Fig. 1) and 15.1% for the chemical assay data (Fig. 2). The model also was applied to obtain fits for the radiochemical assay data (20). Since the parameter values obtained from the radioassay data are of limited value because of the rapid metabolism of streptozocin, these results are not given here.

The models presented in this report utilize data for an intraperitoneal injection of 300 mg/kg. They also provide a quantitative basis for the prediction of drug distributions at other doses and for other modes of injection. Such extensions were discussed previously for other drugs (16–18). In addition, the development of membrane-limited models for drug transport and the inclusion of terms to account for tissue binding and drug metabolism are emphasized here.

The bioassay is the best available measure of the whole streptozocin molecule. In modeling the bioassay data, a reaction constant of ~0.009 min^{-1} was determined for both the kidneys and the liver. This value is in good agreement with a half-life of ~1 hr, which was reported previously (9).

As stated previously, the chemical assay is a measure of the *N*-nitroso group of streptozocin and its metabolites. Previous investigators related the mode of action of streptozocin and other nitrosoureas to the alkylation of various cell components (*i.e.*, DNA, RNA, nucleic acid precursors, and proteins) and the subsequent inhibition of cell division and other critical biochemical processes (21, 22). The observed suppression of NAD^+ and inhibition of pyridine synthesis (23–27) also may be explained within the context of this mode of action.

The degradation pattern of streptozocin to yield a methyl carbonium ion capable of alkylating various cell constituents can be envisioned as a two-step process with methyldiazonium ion as an intermediate. This process is consistent with the known biological degradation patterns for *N*-nitrosoureido compounds (28) and illustrates the importance of the chemical assay in measuring drug activity relative to the proposed mode of drug action.

While the present analysis describes the available data in mice adequately, more data are needed to characterize the transport and metabolism more precisely. Chromatography has isolated several streptozocin metabolites (10, 11), but further work is needed for their identification. As those findings become available, they can be incorporated into a more complex pharmacokinetic model to describe the drug metabolism. In addition, detailed drug distribution data at different dose levels and for different species should be collected and compared with the present pharmacokinetic model as has been done for other drugs (14). Finally, pharmacokinetic studies on other nitrosoureas and glucose-like drugs would provide quantitative information about their transport, mode of action, and metabolism and additional insights into streptozocin pharmacokinetics.

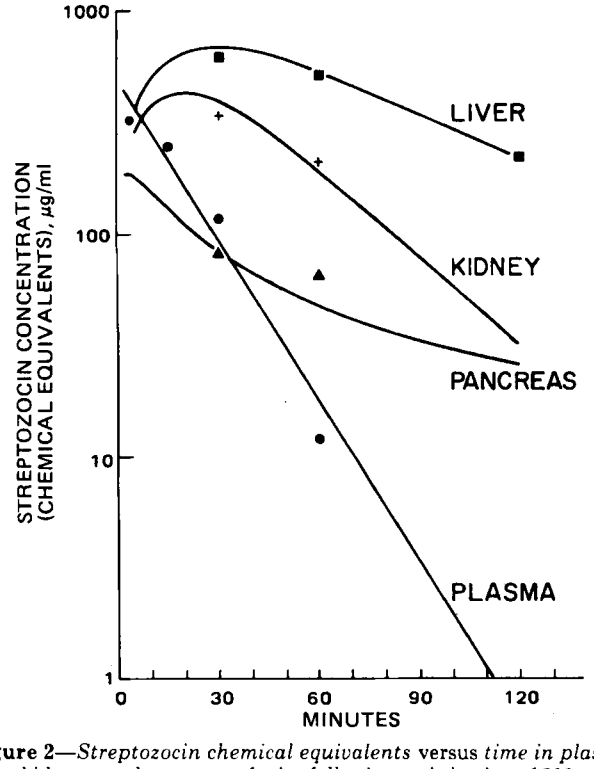

Figure 2—*Streptozocin chemical equivalents* versus *time in plasma, liver, kidneys, and pancreas of mice following an injection of 300 mg/kg ip. Points represent the experimental data of Bhuyan* et al. *(10) for plasma (●), liver (■), kidneys (+), and pancreas (▲). The curves represent model predictions. The parameters from Table I (chemical assay values) and an exponential equation for the plasma concentration ($494.53e^{-0.0549t}$) were used to obtain the simulations.*

REFERENCES

(1) R. R. Herr, J. K. Jahnke, and A. D. Argoudelis, *J. Am. Chem. Soc.*, **89**, 4808 (1967).

(2) B. K. Bhuyan, *Cancer Res.*, **30**, 2017 (1970).

(3) F. R. Reusser, *J. Bacteriol.*, **105**, 580 (1971).

(4) N. Rakienten, M. L. Rakienten, and M. V. Nadkarni, *Cancer Chemother. Rep.*, **29**, 91 (1963).

(5) J. S. Evans, G. C. Gerritsen, K. M. Mann, and S. P. Owen, *ibid.*, **48**, 1 (1965).

(6) A. Junod, A. E. Lambert, L. Orci, R. Pictet, A. E. Gonet, and A. E. Renold, *Proc. Soc. Exp. Biol. Med.*, **126**, 201 (1967).

(7) I. M. Murray-Lyon, A. L. Eddleston, R. Williams, M. Brown, B. M. Hogbin, A. Bennett, J. C. Edwards, and K. W. Taylor, *Lancet*, **2**, 895 (1968).

(8) L. E. Broder and S. K. Carter, *Ann. Intern. Med.*, **79**, 108 (1973).

(9) E. R. Garrett, *J. Am. Pharm. Assoc., Sci. Ed.*, **49**, 767 (1960).

(10) B. K. Bhuyan, S. L. Kuentzel, L. G. Gray, T. J. Fraser, D. Wallach, and G. L. Neil, *Cancer Chemother. Rep.*, **58**, 157 (1974).

(11) E. H. Karunanayake, D. J. Hearse, and G. Mellows, *Biochem. J.*, **142**, 673 (1974).

(12) R. L. Dedrick and K. B. Bischoff, *Chem. Eng. Prog. Symp. Ser.*, **64**, 32 (1968).

(13) R. L. Dedrick, D. S. Zaharko, and R. J. Lutz, *J. Pharm. Sci.*, **62**, 882 (1973).

(14) K. J. Himmelstein and R. J. Lutz, *J. Pharmacokinet. Biopharm.*, **7**, 127 (1979).

(15) R. K. Jain, J. Wei, and P. M. Gullino, *ibid.*, **7**, 181 (1979).

(16) R. J. Lutz, W. M. Galbraith, R. L. Dedrick, R. Shrager, and L. B. Mellett, *J. Pharmacol. Exp. Ther.*, **200**, 469 (1977).

(17) R. J. Lutz, R. L. Dedrick, J. A. Straw, M. M. Hart, P. Klubes, and D. S. Zaharko, *J. Pharmacokinet. Biopharm.*, **3**, 77 (1975).

(18) J. M. Weissbrod, R. K. Jain, and F. M. Sirotnak, *ibid.*, **6**, 487 (1978).

(19) K. B. Bischoff, R. L. Dedrick, D. S. Zaharko, and J. A. Longstreth, *J. Pharm. Sci.*, **60**, 1128 (1971).

(20) J. M. Weissbrod, D. E. S. dissertation, Columbia University, New York, N.Y., 1979 (obtainable from University Microfilms, Ann Arbor, Mich.).

(21) P. N. Magee and J. M. Barnes, *Adv. Cancer Res.*, **10**, 163 (1967).
(22) P. D. Lawley and S. A. Shah, *Biochem. J.*, **128**, 117 (1972).
(23) P. S. Schein and S. Loftus, *Cancer Res.*, **28**, 1501 (1968).
(24) P. S. Schein, D. A. Cooney, M. G. McMenamin, and T. Anderson, *Biochem. Pharmacol.*, **22**, 2625 (1973).
(25) S. S. Lazarus and S. H. Shapiro, *Diabetes*, **22**, 499 (1973).
(26) A. Junod, A. E. Lambert, W. Stauffacher, and A. E. Renold, *J. Clin. Invest.*, **48**, 2129 (1969).
(27) C. K. Ho and S. A. Hashim, *Diabetes*, **21**, 789 (1972).
(28) P. D. Lawley, *Nature*, **218**, 580 (1968).

ACKNOWLEDGMENTS

Supported in part by a grant from the National Science Foundation.

The authors thank Dr. B. K. Bhuyan and Dr. G. L. Neil of The Upjohn Co., Kalamazoo, Mich., for providing information about their data. They also are grateful to Mr. Charles Maldarelli and Mr. Walter Bartynski who participated in the early phase of this work.

Antihyperlipidemic Activity of Sesquiterpene Lactones and Related Compounds

I. H. HALL *x, K. H. LEE *, C. O. STARNES *, O. MURAOKA *, Y. SUMIDA *, and T. G. WADDELL ‡

Received September 28, 1979, from the **Division of Medicinal Chemistry, School of Pharmacy, University of North Carolina, Chapel Hill, NC 27514*, and the ‡*Department of Chemistry, University of Tennessee at Chattanooga, Chattanooga, TN 37401.* Accepted for publication January 23, 1980.

Abstract □ Some naturally occurring pseudoguaianolides and germacranolides as well as synthetic related compounds were observed to be antihyperlipidemic agents in mice. Several of these compounds at a dose of 20 mg/kg/day resulted in lowering of serum cholesterol by ~30% and of serum triglycerides by ~25%. Thiol-bearing enzymes of lipid synthesis, *i.e.*, acetyl-CoA, citrate-lyase, acetyl-CoA synthetase, and β-hydroxy-β-methylglutaryl-CoA reductase, were inhibited by these agents *in vitro*, supporting the premise that these agents alkylate thiol nucleophiles by a Michael-type addition. The α-methylene-γ-lactone moiety, the β-unsubstituted cyclopentenone ring, and the α-epoxycyclopentanone system of these compounds appeared to be responsible for the lowering of serum lipids.

Keyphrases □ Lactones, sesquiterpene—antihyperlipidemic activity, structure–activity relationships, serum levels of cholesterol and triglycerides, mice □ Structure–activity relationships—sesquiterpene lactones, antihyperlipidemic activity, effect on serum levels of cholesterol and triglycerides, mice □ Antihyperlipidemic activity—sesquiterpene lactones, structure–activity relationships, serum levels of cholesterol and triglycerides, mice

Pseudoguaianolide (I, III, IV, V, X, and XI) and germacranolide (XII and XIII) sesquiterpene lactones and related compounds (XIV and XV) are potent antineoplastic agents, effective against Walker 256 carcinosarcoma, Lewis lung carcinoma, P-388 lymphocytic leukemia, and Ehrlich ascites carcinoma in rodents (1). Furthermore, these agents significantly inhibited induced inflammation and arthritic states in rats (2).

In a study of the effects of sesquiterpene lactones on cellular metabolism as antineoplastics, these agents inhibited β-hydroxy-β-methylglutaryl-CoA reductase activity of 10-day-old Ehrlich ascites tumor cells. For example, helenalin (I) at 7 μmoles caused 67% inhibition. Compound I also lowered the elevated serum cholesterol level of tumor-bearing mice by 39% (3). These observations suggested that the sesquiterpene lactones should be tested as antihyperlipidemic agents.

EXPERIMENTAL

Source of Test Compounds—Some of the test compounds are natural products and were isolated from plant species by literature techniques (4). Helenalin (I) was isolated from *Balduina angustifolia*[1] (5); tenulin (V) (6) and aromaticin (XI) (6, 7) were isolated from *Helenium amarum*[2]; deoxyelephantopin (XII) was obtained from *Elephantopus carolinianus*[3] (8); and eupahyssopin (XIII) was isolated from *Eupatorium hyssopifolium*[4] (9).

Plenolin (III) was obtained by hydrogenation of helenalin to give the identical compound as the naturally occurring product (10). 2,3-Dihydrohelenalin (II) and 2,3-epoxyhelenalin (IV) were chemically modified from helenalin (11). Dihydrotenulin (VI), 2,3-epoxytenulin (VII), isotenulin (VIII), 2,3-epoxyisotenulin (X), and dihydroisotenulin (IX) were prepared by the methods of Waddell *et al.* (11). Thymine α-methylene-γ-lactone (XIV) (12), α-methylene-γ-lactone (XVIII) (13), and 2,3-epoxycyclopentan-1-one (XVI) (14) were prepared by literature methods. 2-Cyclopentenone[5] (XV), maleic anhydride[5] (XVII), clofibrate[6] (XIX), and acetazolamide[7] (XX) were obtained commercially.

Serum Hypolipidemic Activity—CF_1 male mice (~30 g) were fed food[8] with water *ad libitum* for the duration of the experiment. The drugs were suspended in 1% carboxymethylcellulose–water and homogenized. The doses were based on the weekly weights of the mice (15). The compounds were tested at 20 mg/kg/day ip.

On Days 9 and 16, blood was collected by tail vein bleeding in alkali-free nonheparinized microcapillary tubes, which then were centrifuged 3 min to obtain the serum. Duplicate 30-μl samples of nonhemolyzed serum were used to determine the serum cholesterol levels in milligram percent by a modification of the Liebermann–Burchard reaction (16). A separate group of mice were bled on Day 14, and their serum triglyceride levels (milligram percent) were determined using duplicate 25-μl samples (17).

Enzymatic Assays—Compounds were tested *in vitro* at 1 μmole for their effects on the enzymatic activity of a 10% liver homogenate prepared in 0.25 *M* sucrose and 0.001 *M* ethylenediaminetetraacetic acid at pH 7.2. Adenosine triphosphate citrate-lyase activity was measured by the method of Hoffmann *et al.* (18). Acetyl-CoA synthetase activity was determined by the method of Goodridge (19). The acetyl-CoA formed

[1] Obtained from Dr. M. E. Wall and H. L. Taylor, Research Triangle Institute, N.C. (No. R.T. 4147); Dr. R. E. Perdue, Jr., U.S. Department of Agriculture, Beltsville, Md., provided the identification number NO PR8878.
[2] Identified by Dr. G. S. Van Horn, Department of Biology, University of Tennessee at Chattanooga, Chattanooga, Tenn. Voucher specimen CAM-81775-FAR-TW is available from Dr. T. G. Waddell for inspection.
[3] Identified by S. W. Leonard, Coastal Zone Resources Corp., Wilmington, N.C. A voucher specimen has been placed in the herbarium of the Department of Botany, University of North Carolina at Chapel Hill, Chapel Hill, N.C.
[4] Obtained from Dr. M. E. Wall and H. L. Taylor, Research Triangle Institute, N.C. Voucher specimen NO PR21478 is available.
[5] Aldrich Chemical Co.
[6] Ayerst Laboratories.
[7] Sigma Chemical Co.
[8] Rodent lab chow, Wayne Blox.

0022-3549/80/0600-0694$01.00/0
© 1980, American Pharmaceutical Association

(21) P. N. Magee and J. M. Barnes, *Adv. Cancer Res.*, **10**, 163 (1967).
(22) P. D. Lawley and S. A. Shah, *Biochem. J.*, **128**, 117 (1972).
(23) P. S. Schein and S. Loftus, *Cancer Res.*, **28**, 1501 (1968).
(24) P. S. Schein, D. A. Cooney, M. G. McMenamin, and T. Anderson, *Biochem. Pharmacol.*, **22**, 2625 (1973).
(25) S. S. Lazarus and S. H. Shapiro, *Diabetes*, **22**, 499 (1973).
(26) A. Junod, A. E. Lambert, W. Stauffacher, and A. E. Renold, *J. Clin. Invest.*, **48**, 2129 (1969).
(27) C. K. Ho and S. A. Hashim, *Diabetes*, **21**, 789 (1972).
(28) P. D. Lawley, *Nature*, **218**, 580 (1968).

ACKNOWLEDGMENTS

Supported in part by a grant from the National Science Foundation.

The authors thank Dr. B. K. Bhuyan and Dr. G. L. Neil of The Upjohn Co., Kalamazoo, Mich., for providing information about their data. They also are grateful to Mr. Charles Maldarelli and Mr. Walter Bartynski who participated in the early phase of this work.

Antihyperlipidemic Activity of Sesquiterpene Lactones and Related Compounds

I. H. HALL *x, K. H. LEE *, C. O. STARNES *, O. MURAOKA *, Y. SUMIDA *, and T. G. WADDELL ‡

Received September 28, 1979, from the **Division of Medicinal Chemistry, School of Pharmacy, University of North Carolina, Chapel Hill, NC 27514*, and the ‡*Department of Chemistry, University of Tennessee at Chattanooga, Chattanooga, TN 37401.* Accepted for publication January 23, 1980.

Abstract □ Some naturally occurring pseudoguaianolides and germacranolides as well as synthetic related compounds were observed to be antihyperlipidemic agents in mice. Several of these compounds at a dose of 20 mg/kg/day resulted in lowering of serum cholesterol by ~30% and of serum triglycerides by ~25%. Thiol-bearing enzymes of lipid synthesis, *i.e.*, acetyl-CoA, citrate-lyase, acetyl-CoA synthetase, and β-hydroxy-β-methylglutaryl-CoA reductase, were inhibited by these agents *in vitro*, supporting the premise that these agents alkylate thiol nucleophiles by a Michael-type addition. The α-methylene-γ-lactone moiety, the β-unsubstituted cyclopentenone ring, and the α-epoxycyclopentanone system of these compounds appeared to be responsible for the lowering of serum lipids.

Keyphrases □ Lactones, sesquiterpene—antihyperlipidemic activity, structure–activity relationships, serum levels of cholesterol and triglycerides, mice □ Structure–activity relationships—sesquiterpene lactones, antihyperlipidemic activity, effect on serum levels of cholesterol and triglycerides, mice □ Antihyperlipidemic activity—sesquiterpene lactones, structure–activity relationships, serum levels of cholesterol and triglycerides, mice

Pseudoguaianolide (I, III, IV, V, X, and XI) and germacranolide (XII and XIII) sesquiterpene lactones and related compounds (XIV and XV) are potent antineoplastic agents, effective against Walker 256 carcinosarcoma, Lewis lung carcinoma, P-388 lymphocytic leukemia, and Ehrlich ascites carcinoma in rodents (1). Furthermore, these agents significantly inhibited induced inflammation and arthritic states in rats (2).

In a study of the effects of sesquiterpene lactones on cellular metabolism as antineoplastics, these agents inhibited β-hydroxy-β-methylglutaryl-CoA reductase activity of 10-day-old Ehrlich ascites tumor cells. For example, helenalin (I) at 7 μmoles caused 67% inhibition. Compound I also lowered the elevated serum cholesterol level of tumor-bearing mice by 39% (3). These observations suggested that the sesquiterpene lactones should be tested as antihyperlipidemic agents.

EXPERIMENTAL

Source of Test Compounds—Some of the test compounds are natural products and were isolated from plant species by literature techniques (4). Helenalin (I) was isolated from *Balduina angustifolia*[1] (5); tenulin (V) (6) and aromaticin (XI) (6, 7) were isolated from *Helenium amarum*[2]; deoxyelephantopin (XII) was obtained from *Elephantopus carolinianus*[3] (8); and eupahyssopin (XIII) was isolated from *Eupatorium hyssopifolium*[4] (9).

Plenolin (III) was obtained by hydrogenation of helenalin to give the identical compound as the naturally occurring product (10). 2,3-Dihydrohelenalin (II) and 2,3-epoxyhelenalin (IV) were chemically modified from helenalin (11). Dihydrotenulin (VI), 2,3-epoxytenulin (VII), isotenulin (VIII), 2,3-epoxyisotenulin (X), and dihydroisotenulin (IX) were prepared by the methods of Waddell *et al.* (11). Thymine α-methylene-γ-lactone (XIV) (12), α-methylene-γ-lactone (XVIII) (13), and 2,3-epoxycyclopentan-1-one (XVI) (14) were prepared by literature methods. 2-Cyclopentenone[5] (XV), maleic anhydride[5] (XVII), clofibrate[6] (XIX), and acetazolamide[7] (XX) were obtained commercially.

Serum Hypolipidemic Activity—CF_1 male mice (~30 g) were fed food[8] with water *ad libitum* for the duration of the experiment. The drugs were suspended in 1% carboxymethylcellulose–water and homogenized. The doses were based on the weekly weights of the mice (15). The compounds were tested at 20 mg/kg/day ip.

On Days 9 and 16, blood was collected by tail vein bleeding in alkali-free nonheparinized microcapillary tubes, which then were centrifuged 3 min to obtain the serum. Duplicate 30-μl samples of nonhemolyzed serum were used to determine the serum cholesterol levels in milligram percent by a modification of the Liebermann–Burchard reaction (16). A separate group of mice were bled on Day 14, and their serum triglyceride levels (milligram percent) were determined using duplicate 25-μl samples (17).

Enzymatic Assays—Compounds were tested *in vitro* at 1 μmole for their effects on the enzymatic activity of a 10% liver homogenate prepared in 0.25 *M* sucrose and 0.001 *M* ethylenediaminetetraacetic acid at pH 7.2. Adenosine triphosphate citrate-lyase activity was measured by the method of Hoffmann *et al.* (18). Acetyl-CoA synthetase activity was determined by the method of Goodridge (19). The acetyl-CoA formed

[1] Obtained from Dr. M. E. Wall and H. L. Taylor, Research Triangle Institute, N.C. (No. R.T. 4147); Dr. R. E. Perdue, Jr., U.S. Department of Agriculture, Beltsville, Md., provided the identification number NO PR8878.
[2] Identified by Dr. G. S. Van Horn, Department of Biology, University of Tennessee at Chattanooga, Chattanooga, Tenn. Voucher specimen CAM-81775-FAR-TW is available from Dr. T. G. Waddell for inspection.
[3] Identified by S. W. Leonard, Coastal Zone Resources Corp., Wilmington, N.C. A voucher specimen has been placed in the herbarium of the Department of Botany, University of North Carolina at Chapel Hill, Chapel Hill, N.C.
[4] Obtained from Dr. M. E. Wall and H. L. Taylor, Research Triangle Institute, N.C. Voucher specimen NO PR21478 is available.
[5] Aldrich Chemical Co.
[6] Ayerst Laboratories.
[7] Sigma Chemical Co.
[8] Rodent lab chow, Wayne Blox.

0022-3549/80/0600-0694$01.00/0
© 1980, American Pharmaceutical Association

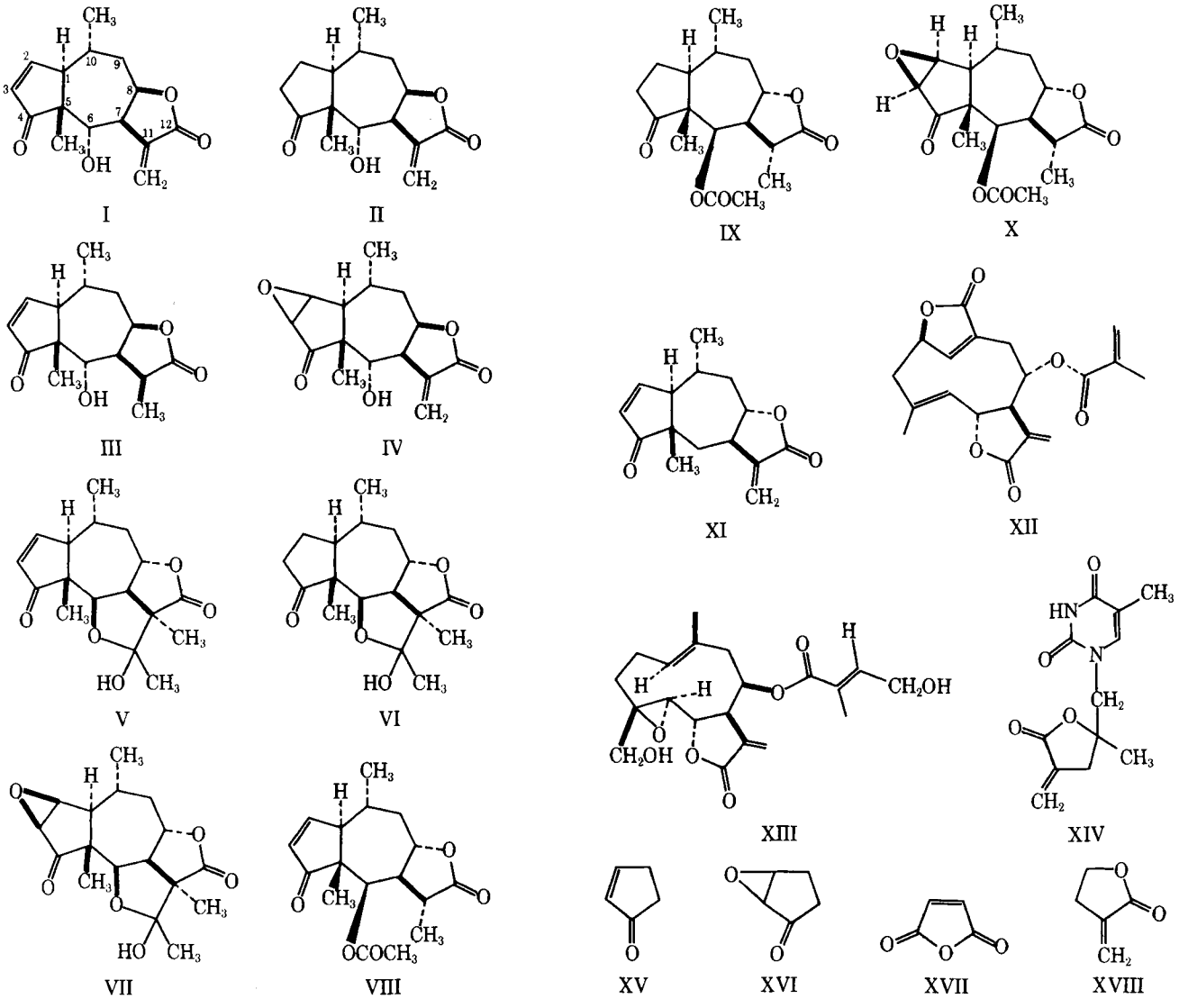

from both enzymatic assays was coupled with hydroxylamine to produce acetyl hydroxylmate, which was measured at 540 nm.

Acetyl-CoA carboxylase activity was measured by a method (20) utilizing sodium [^{3}H]bicarbonate (6.2 mCi/mmole) after 30 min of incubation at 37° for enzyme polymerization (21). Fatty acid synthetase was determined by the method of Brady *et al.* (22) utilizing incorporation of [2′-^{14}C]malonyl-CoA (37.5 mCi/mmole) into fatty acids. [^{14}C]Acetate (57.8 mCi/mmole) incorporated into cholesterol (β-hydroxy-β-methylglutaryl-CoA reductase activity) was extracted by the method of Wada *et al.* (23) and measured as described by Haven *et al.* (24).

RESULTS

The sesquiterpene lactones and germacranolides significantly lowered serum cholesterol levels in mice (Table I). Helenalin (I), tenulin (V), 2,3-epoxytenulin (VII), isotenulin (VIII), 2,3-epoxyisotenulin (X), deoxyelephantopin (XII), eupahyssopin (XIII), and thymine lactone (XIV) treatment *in vivo* resulted in >30% reduction in the serum cholesterol levels of mice after 16 days.

Helenalin at 6 mg/kg/day and tenulin at 20 mg/kg/day reduced serum triglyceride levels by 24 and 28%, respectively, after 2 weeks of dosing. 2-Cyclopentenone (XV) and eupahyssopin were essentially inactive, causing 2 and 6% reduction of serum triglyceride levels, respectively. Helenalin, tenulin, deoxyelephantopin, eupahyssopin, and 2-cyclopentenone *in vitro* at 1 μmole suppressed the enzymes that regulate acetyl-CoA availability for triglyceride and cholesterol synthesis, *i.e.*, acetyl-CoA synthetase and citrate-lyase activity. The sesquiterpene lactones tested suppressed acetyl-CoA synthetase activity by 41–49% and citrate-lyase activity by 25–39%. The regulatory enzyme of fatty acid synthesis, acetyl-CoA carboxylase, was inhibited 66–84% in the presence of sesquiterpene lactones. Fatty acid synthetase activity also was inhibited 40–52% by these agents. β-Hydroxy-β-methylglutaryl-CoA reductase activity of the liver was inhibited 21–28% by the sesquiterpene lactones tested.

Table I—Serum Cholesterol Levels in CF$_1$ Male Mice after Intraperitoneal Dosing at 20 mg/kg/day

Compound	Percent of Control Day 9	Percent of Control Day 16
I Helenalin (6 mg/kg/day)	60 ± 3[a]	63 ± 4[a]
II 2,3-Dihydrohelenalin	99 ± 5	77 ± 7[a]
III Plenolin	89 ± 6[b]	85 ± 5[c]
IV 2,3-Epoxyhelenalin	85 ± 7[c]	72 ± 3[a]
V Tenulin	76 ± 5[a]	65 ± 4[a]
VI 2,3-Dihydrotenulin	79 ± 9	89 ± 7[d]
VII 2,3-Epoxytenulin	86 ± 5[c]	65 ± 4[a]
VIII Isotenulin	81 ± 6[a]	65 ± 5[a]
IX 2,3-Dihydroisotenulin	79 ± 4[a]	79 ± 4[a]
X 2,3-Epoxyisotenulin	101 ± 7[a]	69 ± 6[a]
XI Aromaticin	82 ± 6[a]	71 ± 5[a]
XII Deoxyelephantopin	83 ± 7[c]	68 ± 4[a]
XIII Eupahyssopin	65 ± 5[a]	64 ± 4[a]
XIV Thymine lactone	93 ± 5	66 ± 3[a]
XV 2-Cyclopentenone	72 ± 4[a]	73 ± 6[a]
XVI 2,3-Epoxycyclopentan-1-one	77 ± 8[a]	74 ± 6[a]
XVII Maleic anhydride	84 ± 7[c]	78 ± 7[a]
XVIII α-Methylene-γ-lactone	87 ± 5[c]	73 ± 4[a]
XIX Clofibrate	98 ± 7	96 ± 5
1% Carboxymethylcellulose	100 ± 5[e]	100 ± 6[f]

[a] $p = 0.001$. [b] $p = 0.010$. [c] $p = 0.005$. [d] $p = 0.025$. [e] 115 mg %. [f] 119 mg %.

Table II—Effects of Sesquiterpene Lactones on Liver Regulatory Enzymes for Cholesterol and Triglyceride Synthesis

	Percent of Control, $\bar{x} \pm SD$				
	Acetyl-CoA Synthetase Activity	Citrate-Lyase Activity	Acetyl-CoA Carboxylase Activity	Fatty Acid Synthetase Activity	β-Hydroxy-β-Methyl-glutaryl-CoA Reductase Activity
I (1 μmole)	57 ± 3[a]	75 ± 3[a]	16 ± 2[a]	53 ± 4[a]	72 ± 3
V (1 μmole)	59 ± 4[a]	68 ± 3[a]	26 ± 4[a]	49 ± 6[a]	72 ± 4
XII (1 μmole)	51 ± 2[a]	66 ± 4[a]	28 ± 6[a]	60 ± 3[a]	79 ± 7
XIII (1 μmole)	52 ± 6[a]	61 ± 2[a]	34 ± 3[a]	48 ± 5[a]	77 ± 5
XV (1 μmole)	51 ± 3[a]	63 ± 3[a]	17 ± 4[a]	49 ± 3[a]	73 ± 4
XIX (41 μmoles)	—	—	—	—	77 ± 5
XX	66 ± 4[a]	66 ± 7[a]	13 ± 2[a]	82 ± 6	—
1% Carboxymethylcellulose	100 ± 5[b]	100 ± 4[c]	100 ± 7[d]	100 ± 7[e]	100 ± 4[f]

[a] $p = 0.001$. [b] 28.5 mg of acetyl-CoA formed/g of wet tissue/30 min. [c] 30.5 mg of citrate hydrolyzed/g of wet tissue/30 min. [d] 32,010 dpm/g of wet tissue/30 min. [e] 37,656 dpm/g of wet tissue/30 min. [f] 1,142,065 dpm/g of wet tissue/60 min.

DISCUSSION

The sesquiterpene lactones were effective antihyperlipidemic agents in rodents. The α-methylene-γ-lactone moiety, the β-unsubstituted cyclopentenone ring, and the α-epoxycyclopentanone system contributed to the antihyperlipidemic activity of the sesquiterpene lactones and related compounds. Saturation of the 2,3-double bond of the cyclopentenone ring led to a loss of antihyperlipidemic activity, as was seen with II, VI, and IX. The α-epoxycyclopentanone ring system retained the antihyperlipidemic activity regardless of whether the α-methylene group of the γ-lactone ring (11,13-double bond) was reduced (*i.e.*, IV, VII, and X). Compounds containing the α-methyl-γ-lactone group (V and VIII) as opposed to the α-methylene-γ-lactone moiety (I) were equally active, because in both cases the essential cyclopentenone ring was retained (with the exception of III, in which case the 11-methyl group was β-oriented). The configuration of the γ-lactone ring did not appear to play an important role in the ability of the pseudoguaianolides to lower serum cholesterol levels, because the *cis*-fused lactones I and IV were approximately as potent as the *trans*-fused V, VII, VIII, and XI.

Germacranolides that contain the α-methylene-γ-lactone moiety had significant antihypercholesterolemic activity, *e.g.*, deoxyelephantopin (XII) and eupahyssopin (XIII). In addition to the essential α-methylene-γ-lactone moiety, XIII contains an ester side chain, a primary hydroxyl group, and an epoxy ring, which may contribute to the pharmacological activity. Compound XII, in addition to the α-methylene-γ-lactone, contains an α,β-unsaturated-γ-lactone ring and an ester side chain. The simple 2-cyclopentenone (XV), 2,3-epoxycyclopentan-1-one (XVI), maleic anhydride (XVII), and α-methylene-γ-lactone (XVIII) were not as active in lowering serum cholesterol, indicating that some other steric, configurational, or conformational arrangement was required for potent activity. The sesquiterpene lactones also were observed to lower serum triglycerides.

The proposed mechanism of action of the sesquiterpene lactones is the formation of adducts with the thiol groups of enzymes by a rapid Michael-type addition of the α-methylene-γ-lactone moiety or cyclopentenone ring system to the thiol nucleophile, thereby inactivating the enzyme (25, 26). Helenalin and tenulin block cellular metabolism by inhibiting key regulatory thiol-bearing enzymes, *e.g.*, DNA polymerase (6, 27) and phosphofructokinase (25). The β-hydroxy-β-methylglutaryl-CoA reductase, acetyl-CoA carboxylase, and fatty acid synthetase reportedly contain exposed thiol groups (28, 29). Further elevated cyclic adenosine monophosphate levels, which helenalin elevated by 194% (30), were related to the reduction of β-hydroxy-β-methylglutaryl-CoA reductase activity (31) and fatty acid synthesis by modulating acetyl-CoA carboxylase, fatty acid synthetase, and cytosol pyruvate levels for acetyl-CoA generation (32). For these reasons, several key regulatory enzymes in the genesis of fatty acid and cholesterol synthesis were measured to evaluate the effects of sesquiterpene lactones *in vivo*.

Studies on the generation of acetyl-CoA for fatty acid and cholesterol synthesis from cytosol acetate and citrate showed that the pseudoguaianolides (helenalin and tenulin) and the germacranolides (deoxyelephantopin and eupahyssopin) equally suppressed the activities of these two enzymes. Acetyl-CoA carboxylase activity, the regulatory enzyme of fatty acid synthesis, was reduced drastically in the presence of the sesquiterpene lactones, with helenalin being the most potent agent. Fatty acid synthetase activity also was reduced in the presence of the sesquiterpene lactones by ~50%. β-Hydroxy-β-methylglutaryl-CoA reductase activity was inhibited equally by the sesquiterpene lactones. The commercially available clofibrate, present at 41 μmoles, resulted in 23% inhibition, indicating that the sesquiterpene lactones were far more potent in inhibiting this enzyme that regulates cholesterol synthesis. Clofibrate required a dose of 300 mg/kg/day in rodents to reduce serum cholesterol levels and had no effect at 20 mg/kg/day. Thus, it can be concluded that the sesquiterpene lactones possess sufficient ability to block lipogenesis to warrant further investigation as antihyperlipidemic agents.

REFERENCES

(1) I. H. Hall, K. H. Lee, C. O. Starnes, S. A. ElGebaly, T. Ibuka, Y. S. Wu, T. Kimura, and M. Haruna, *J. Pharm. Sci.*, **67**, 1235 (1978).

(2) I. H. Hall, K. H. Lee, C. O. Starnes, Y. Sumida, R. Y. Wu, T. G. Waddell, J. W. Cochran, and K. G. Gerhart, *ibid.*, **68**, 537 (1979).

(3) K. H. Lee, I. H. Hall, E. C. Mar, C. O. Starnes, S. A. ElGebaly, T. G. Waddell, R. I. Hadgraft, C. G. Ruffner, and I. Weidner, *Science*, **196**, 533 (1977).

(4) K. H. Lee and T. A. Geissman, *Phytochemistry*, **9**, 403 (1970).

(5) K. H. Lee, D. C. Anuforo, E. S. Huang, and C. Piantadosi, *J. Pharm. Sci.*, **61**, 626 (1972).

(6) I. H. Hall, K. H. Lee, E. C. Mar, C. O. Starnes, and T. G. Waddell, *J. Med. Chem.*, **20**, 333 (1977).

(7) R. A. Lucas, S. Rovinski, R. J. Kiesel, L. Dorfman, and H. B. MacPhillamy, *J. Org. Chem.*, **29**, 1549 (1964).

(8) K. H. Lee, C. M. Cowherd, and M. T. Wolo, *J. Pharm. Sci.*, **64**, 1572 (1975).

(9) K. H. Lee, T. Kimura, M. Okamoto, C. M. Cowherd, A. T. McPhail, and K. D. Onan, *Tetrahedron Lett.*, **14**, 1051 (1976).

(10) K. H. Lee, T. Kimura, D. Sims, A. T. McPhail, and K. D. Onan, *Phytochemistry*, **16**, 393 (1977).

(11) T. G. Waddell, A. M. Austin, J. W. Cochran, K. G. Gerhart, I. H. Hall, and K. H. Lee, *J. Pharm. Sci.*, **68**, 715 (1979).

(12) K. H. Lee, Y. S. Wu, and I. H. Hall, *J. Med. Chem.*, **20**, 911 (1977).

(13) G. M. Ksander, J. E. McMurry, and M. Johnson, *J. Org. Chem.*, **42**, 1180 (1977).

(14) R. G. Salomon and M. F. Salomon, *J. Am. Chem. Soc.*, **99**, 3501 (1977).

(15) I. H. Hall and G. L. Carlson, *J. Med. Chem.*, **19**, 1257 (1976).

(16) A. T. Ness, J. V. Pastewka, and A. C. Peacock, *Clin. Chim. Acta*, **10**, 229 (1964).

(17) J. M. Chapman, G. H. Cocolas, and I. H. Hall, *J. Med. Chem.*, **22**, 1399 (1979).

(18) G. Hoffmann, L. Weiss, and O. H. Wieland, *Anal. Biochem.*, **84**, 441 (1978).

(19) A. G. Goodridge, *J. Biol. Chem.*, **248**, 4318 (1973).

(20) M. D. Greenspan and J. M. Lowenstein, *ibid.*, **243**, 6273 (1968).

(21) T. P. Cao and S. Rous, *Life Sci.*, **22**, 2067 (1978).

(22) R. O. Brady, R. M. Bradley, and E. G. Trams, *J. Biol. Chem.*, **235**, 3093 (1960).

(23) F. Wada, K. Hirata, and Y. Sakamoto, *J. Biochem.*, **65**, 171 (1969).

(24) G. T. Haven, J. R. Krzemien, and T. T. Nguyen, *Res. Commun. Chem. Pathol. Pharmacol.*, **6**, 253 (1973).

(25) R. L. Hanson, H. A. Lardy, and S. M. Kupchan, *Science*, **168**, 378 (1970).

(26) C. H. Smith, J. Larner, A. M. Thomas, and S. M. Kupchan, *Biochim. Biophys. Acta*, **276**, 94 (1972).

(27) I. H. Hall, K. H. Lee, and S. A. ElGebaly, *J. Pharm. Sci.*, **67**, 1232 (1978).

(28) P. H. E. Groot, H. R. Scholte, and W. C. Hulsmann, *Adv. Lipid Res.*, **14**, 75 (1976).
(29) A. White, P. Handler, E. L. Smith, R. L. Hill, and I. R. Lehman, "Principles of Biochemistry," 6th ed., McGraw-Hill, New York, N.Y., 1978, pp. 584–589, 620.
(30) I. H. Hall, C. O. Starnes, Jr., K. H. Lee, and T. G. Waddell, *J. Pharm. Sci.*, **69**, 537 (1980).
(31) V. W. Rodwell, J. L. Nordstrom, and J. J. Mitschelen, *Adv. Lipid Res.*, **14**, 1 (1976).
(32) R. A. Harris, J. P. Mapes, R. S. Ochs, D. W. Crabb, and L. Stropes, *Adv. Exp. Med. Biol.*, **111**, 17 (1979).

ACKNOWLEDGMENTS

Supported by American Cancer Society Grant CH-19 and in part by National Cancer Institute Grant CA 17625 to K. H. Lee.

Evaluation of Nystatin Stability Using Tristimulus Colorimetry

JOHN E. FAIRBROTHER *, WILLIAM F. HEYES ˣ, GEOFFREY CLARKE, and PETER R. WOOD ‡

Received May 7, 1979, from the *Squibb Institute for Medical Research, International Development Laboratory, Moreton, Merseyside L46 1QW, United Kingdom.* Accepted for publication January 22, 1980. *Present address: School of Pharmacy, Nottingham University, United Kingdom. ‡Present address: Syntex Research Centre, Heriot Watt University, Edinburgh, United Kingdom.

Abstract □ A tristimulus reflectance spectrophotometer was used to examine the color changes of nystatin during accelerated stability studies, and a relationship was observed between the loss of microbiological potency and the change in color during thermal degradation. By substitution of the measured tristimulus values in the Kubelka–Munk equation, the remission function was calculated and resulted in a linear response with time. Application of the technique to bulk raw materials and formulated products is demonstrated, and uses of the technique are discussed.

Keyphrases □ Colorimetry—nystatin, thermal degradation, relationship between loss of microbiological potency and color change □ Degradation, thermal—nystatin, colorimetry, relationship between loss of microbiological potency, and color change □ Nystatin—thermal degradation, colorimetry, relationship between loss of microbiological potency and color change □ Antifungal agents—nystatin, thermal degradation colorimetry, relationship between loss of microbiological potency and color change

The most frequent use of surface color measurements in the pharmaceutical industry has been the monitoring of color stability of coated tablets (1). Alternative uses of the procedure have been described, particularly in preformulation and stability studies. These applications generally involve the determination of the discoloration exhibited by a particular drug–excipient mixture or formulation. By this means, the incompatibility of various mixtures was reported (2–6), and the stability of active ingredients in formulated products was determined (7). Prediction of the shelflife of tablets also may be assessed by this technique (8, 9). A comprehensive review of the pharmaceutical applications of tristimulus colorimetry and diffuse reflectance spectroscopy was published recently (10). The stability of the polyene antibiotic nystatin was evaluated in these laboratories by monitoring the color change at elevated temperatures. The color change at a solid surface is measured quantitatively by diffuse reflectance spectrometry, and monochromatic light generally is used to illuminate the sample. Alternatively, illumination may be by a white light source, and the values of each of the three primary color components (the tristimulus values) of the reflected light are determined. This technique usually is referred to as tristimulus colorimetry.

For nystatin, a visual relationship between the degree of browning observed and the loss of microbiological potency was demonstrated previously[1]. Therefore, tristimulus colorimetry was used to quantitate the observed color changes since the measurement of the tristimulus values closely parallels the color discrimination obtained with the human eye.

THEORY

To quantitate the observed degradation of nystatin, it was necessary to derive a suitable equation so that a relationship between the color and intensity of the reflected light, as described by the tristimulus values, and the concentration of colored material in the reflecting surface was defined. Kubelka and Munk (11, 12) derived an equation to describe the phenomenon of diffuse reflectance. For the special case of an infinitely thick opaque layer, it is:

$$f(R_\infty) = \frac{(1 - R_\infty)^2}{2R_\infty} = \frac{k}{s} \qquad \text{(Eq. 1)}$$

where R_∞ is the diffuse reflectance of the layer relative to a nonabsorbing standard, k is the molar absorption coefficient, s is the scattering coefficient, and $f(R_\infty)$ is the remission function. In practice, this requirement will be satisfied by a layer of material several millimeters deep.

The color of light reflected from the sample surface is described by the measured tristimulus values X, Y, and Z. The Y value corresponds to the Munsell value, which measures the degree of sample darkening, without regard to hue or chroma. The tristimulus values are used to calculate the chromaticity coordinates x, y, and z according to $x = X/(X + Y + Z)$, $y = Y/(X + Y + Z)$, and $z = Z/(X + Y + Z)$.

Tristimulus values are measured relative to a nonabsorbing standard, usually a white ceramic tile. For this study, the color of a sample before and after degradation was compared. This comparison may be achieved if the color of the degraded material is determined using the material prior to degradation as the standard. However, this procedure introduces practical difficulties and necessitates a large supply of original material. To overcome these difficulties, all materials were measured against a white tile as the standard, and the relative color change was calculated from the expression x_0/x_t, where x_0 is the initial chromaticity coordinate of the sample and x_t is the chromaticity coordinate at time t.

Substitution of these values into the Kubelka–Munk equation gives:

$$f(R_\infty) = \frac{(1 - x_0/x_t)^2}{2x_0/x_t} \qquad \text{(Eq. 2)}$$

[1] U. Nager, unpublished data.

0022-3549/80/0600-0697$01.00/0
© 1980, American Pharmaceutical Association

(28) P. H. E. Groot, H. R. Scholte, and W. C. Hulsmann, *Adv. Lipid Res.*, **14**, 75 (1976).
(29) A. White, P. Handler, E. L. Smith, R. L. Hill, and I. R. Lehman, "Principles of Biochemistry," 6th ed., McGraw-Hill, New York, N.Y., 1978, pp. 584–589, 620.
(30) I. H. Hall, C. O. Starnes, Jr., K. H. Lee, and T. G. Waddell, *J. Pharm. Sci.*, **69**, 537 (1980).
(31) V. W. Rodwell, J. L. Nordstrom, and J. J. Mitschelen, *Adv. Lipid Res.*, **14**, 1 (1976).
(32) R. A. Harris, J. P. Mapes, R. S. Ochs, D. W. Crabb, and L. Stropes, *Adv. Exp. Med. Biol.*, **111**, 17 (1979).

ACKNOWLEDGMENTS

Supported by American Cancer Society Grant CH-19 and in part by National Cancer Institute Grant CA 17625 to K. H. Lee.

Evaluation of Nystatin Stability Using Tristimulus Colorimetry

JOHN E. FAIRBROTHER *, WILLIAM F. HEYES ˣ, GEOFFREY CLARKE, and PETER R. WOOD ‡

Received May 7, 1979, from the *Squibb Institute for Medical Research, International Development Laboratory, Moreton, Merseyside L46 1QW, United Kingdom.* Accepted for publication January 22, 1980. *Present address: School of Pharmacy, Nottingham University, United Kingdom. ‡Present address: Syntex Research Centre, Heriot Watt University, Edinburgh, United Kingdom.

Abstract □ A tristimulus reflectance spectrophotometer was used to examine the color changes of nystatin during accelerated stability studies, and a relationship was observed between the loss of microbiological potency and the change in color during thermal degradation. By substitution of the measured tristimulus values in the Kubelka–Munk equation, the remission function was calculated and resulted in a linear response with time. Application of the technique to bulk raw materials and formulated products is demonstrated, and uses of the technique are discussed.

Keyphrases □ Colorimetry—nystatin, thermal degradation, relationship between loss of microbiological potency and color change □ Degradation, thermal—nystatin, colorimetry, relationship between loss of microbiological potency, and color change □ Nystatin—thermal degradation, colorimetry, relationship between loss of microbiological potency and color change □ Antifungal agents—nystatin, thermal degradation colorimetry, relationship between loss of microbiological potency and color change

The most frequent use of surface color measurements in the pharmaceutical industry has been the monitoring of color stability of coated tablets (1). Alternative uses of the procedure have been described, particularly in preformulation and stability studies. These applications generally involve the determination of the discoloration exhibited by a particular drug–excipient mixture or formulation. By this means, the incompatibility of various mixtures was reported (2–6), and the stability of active ingredients in formulated products was determined (7). Prediction of the shelflife of tablets also may be assessed by this technique (8, 9). A comprehensive review of the pharmaceutical applications of tristimulus colorimetry and diffuse reflectance spectroscopy was published recently (10). The stability of the polyene antibiotic nystatin was evaluated in these laboratories by monitoring the color change at elevated temperatures. The color change at a solid surface is measured quantitatively by diffuse reflectance spectrometry, and monochromatic light generally is used to illuminate the sample. Alternatively, illumination may be by a white light source, and the values of each of the three primary color components (the tristimulus values) of the reflected light are determined. This technique usually is referred to as tristimulus colorimetry.

For nystatin, a visual relationship between the degree of browning observed and the loss of microbiological potency was demonstrated previously[1]. Therefore, tristimulus colorimetry was used to quantitate the observed color changes since the measurement of the tristimulus values closely parallels the color discrimination obtained with the human eye.

THEORY

To quantitate the observed degradation of nystatin, it was necessary to derive a suitable equation so that a relationship between the color and intensity of the reflected light, as described by the tristimulus values, and the concentration of colored material in the reflecting surface was defined. Kubelka and Munk (11, 12) derived an equation to describe the phenomenon of diffuse reflectance. For the special case of an infinitely thick opaque layer, it is:

$$f(R_\infty) = \frac{(1 - R_\infty)^2}{2R_\infty} = \frac{k}{s} \qquad \text{(Eq. 1)}$$

where R_∞ is the diffuse reflectance of the layer relative to a nonabsorbing standard, k is the molar absorption coefficient, s is the scattering coefficient, and $f(R_\infty)$ is the remission function. In practice, this requirement will be satisfied by a layer of material several millimeters deep.

The color of light reflected from the sample surface is described by the measured tristimulus values X, Y, and Z. The Y value corresponds to the Munsell value, which measures the degree of sample darkening, without regard to hue or chroma. The tristimulus values are used to calculate the chromaticity coordinates x, y, and z according to $x = X/(X + Y + Z)$, $y = Y/(X + Y + Z)$, and $z = Z/(X + Y + Z)$.

Tristimulus values are measured relative to a nonabsorbing standard, usually a white ceramic tile. For this study, the color of a sample before and after degradation was compared. This comparison may be achieved if the color of the degraded material is determined using the material prior to degradation as the standard. However, this procedure introduces practical difficulties and necessitates a large supply of original material. To overcome these difficulties, all materials were measured against a white tile as the standard, and the relative color change was calculated from the expression x_0/x_t, where x_0 is the initial chromaticity coordinate of the sample and x_t is the chromaticity coordinate at time t.

Substitution of these values into the Kubelka–Munk equation gives:

$$f(R_\infty) = \frac{(1 - x_0/x_t)^2}{2x_0/x_t} \qquad \text{(Eq. 2)}$$

[1] U. Nager, unpublished data.

0022-3549/80/0600-0697$01.00/0
© 1980, American Pharmaceutical Association

Table I—Reproducibility of Nystatin Preparations

Sample	Cream			Powder		
	X	*Y*	*Z*	*X*	*Y*	*Z*
1	64.2	67.5	56.3	82.4	86.8	74.1
2	64.4	67.5	56.5	82.4	86.8	73.8
3	64.2	67.4	56.2	81.8	86.4	73.6
4	64.3	67.5	56.7	82.3	86.7	74.0
5	64.2	67.3	56.3	81.9	86.6	73.8
6	64.3	67.5	56.9			
7	64.1	67.5	56.8			
8	64.4	68.0	56.1			
9	63.9	67.5	56.4			
10	64.2	67.5	56.4			
Mean	64.2	67.5	56.5	82.2	86.6	73.8
SD	0.14	0.18	0.26	0.28	0.18	0.19
CV	0.21	0.26	0.46	0.34	0.20	0.25
95% Confidence limit	64.1–64.3	67.4–67.6	56.3–56.7	81.9–82.5	86.4–86.8	73.6–74.1

Similar equations may be written involving the *y* and *z* chromaticity coordinates.

EXPERIMENTAL

Tristimulus Value Measurements—*Powders*—To determine the tristimulus values of degraded nystatin powder, it was necessary to devise a sample holder. A nickel crucible cover[2] proved to be suitable. The recess in the cover was filled loosely with powder and leveled off with a spatula. The powder then was compressed into the recess by pressing a similar cover on top, resulting in a powder bed that was ~2 mm thick. The underside of this second cover was highly polished so that a smooth powder surface remained after compression.

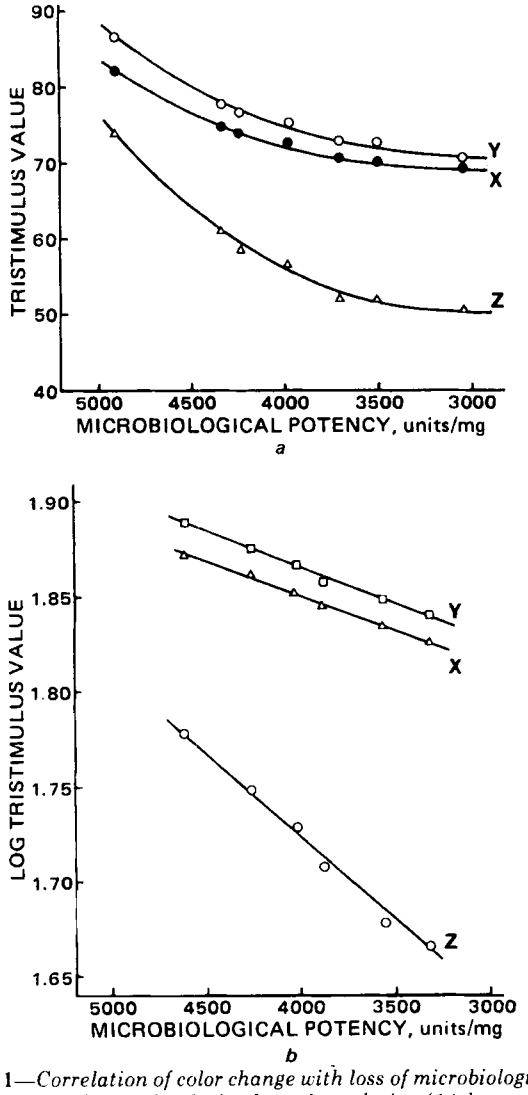

Figure 1—*Correlation of color change with loss of microbiological potency for nystatin powder during heat degradation (14 days at 75°).*

[2] Catalog item 3328-M10, A. H. Thomas, Philadelphia, Pa.

Ointments and Creams—For these formulations, a suitable sample holder consisted of a 3-mm thick polytef spacer, with a hole 30 mm in diameter, sandwiched between two clear glass microscope slides. To prepare a sample for color measurement, one microscope slide was placed beneath the spacer, and the 30-mm orifice was overfilled slightly with the ointment or cream to be tested. The second microscope slide then was placed on top, and the sandwich was gently squeezed together. By this means, all air bubbles were eliminated from the sample surface.

Measurement of the tristimulus values was accomplished by clipping either sample holder over the sample port of the colorimeter[3]. All measurements were made against a standard white tile[4] as the reference and with the nonspecular insert fitted.

Correlation of Potency with Color Change—Nystatin powder was heated at 75 and 85° in open dishes and in sealed screw-top bottles. Stored material was sampled at 24-hr intervals for 14 days. The color of the samples was determined as already described. The microbiological potencies of the same samples were determined by the agar-plate procedure using *Saccharomyces cereviseae*[5] (SQ 1600) and referenced against the current nystatin reference standard.

Degradation of Nystatin Powder and Formulations—Ointment and cream formulations were filled into Araldite-lined aluminum tubes and stored in thermostatically controlled environments at 20, 32, and 40°. The color of samples was assessed after 3, 6, and 12 months of storage. Additional examination of the samples at 40° was undertaken after 1 and 2 months of storage.

Powders were stored in humidity ovens[6] under ambient and 75% relative humidity (RH); 75% RH was achieved with a saturated aqueous solution of sodium chloride in contact with excess solid phase. Degradation was studied at 75, 85, and 100° by withdrawal of samples at 24-hr intervals for color determination.

RESULTS AND DISCUSSION

Before proceeding with the experimental work, the reproducibility of the proposed methods for tristimulus value determination was appraised. Tristimulus value measurements on representative fractions from the same batch of ointment or raw material (Table I) demonstrated good reproducibility for both sample types. A direct comparison of the tristimulus values with microbiological potency (Fig. 1*a*) demonstrated that an unprecedented quantitative relationship existed between the two parameters during the heat degradation of nystatin. The results represent the observed degradation over 14 days at 75°. Similar curves were obtained at higher temperatures. Furthermore, a linear correlation was obtained when the tristimulus values were plotted as logarithmic functions (Fig. 1*b*). Therefore, quantitation of the color change of the antibiotic is an alternative method of assessing the microbiological stability of nystatin.

Further examination of the heat-degraded nystatin by reversed-phase

[3] Color-Eye (Signature model), Instrument Development Laboratory.
[4] Reference Standard Daylight C, Instrument Development Laboratory.
[5] Squibb culture collection.
[6] Laboratory Thermal Equipment, Oldham, United Kingdom.

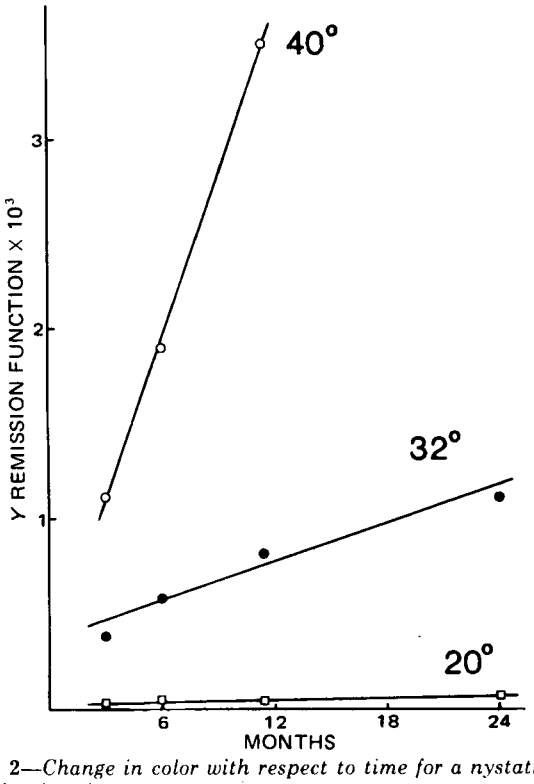

Figure 2—*Change in color with respect to time for a nystatin–steroid–lidocaine ointment.*

high-performance liquid chromatography[7] indicated that the observed color change also was related to the chemical decomposition of nystatin. A chemical decomposition of 13% was observed during the 14-day degradation period.

Ointments and Creams—To determine the applicability of the method to ointment and cream formulations, nystatin–steroid preparations were examined at intervals throughout the normal stability program, and the Kubelka–Munk functions were calculated from the tristimulus values obtained. A plot of the Kubelka–Munk remission function *versus* time (Fig. 2) for a nystatin–steroid–lidocaine ointment demonstrates a linear response over the time period considered. Either the X or Y function may be used with essentially similar results. The slope of the remission function *versus* time graph represents the degradation rate constant k. The k values obtained for the degradation of the ointment at 20, 32, and 40° were evaluated in accordance with the Arrhenius equation. A plot of log k *versus* $1/T$ resulted in a linear graph, thus suggesting that accelerated stability evaluations at 40° are valid for the prediction of room temperature stability (Fig. 3).

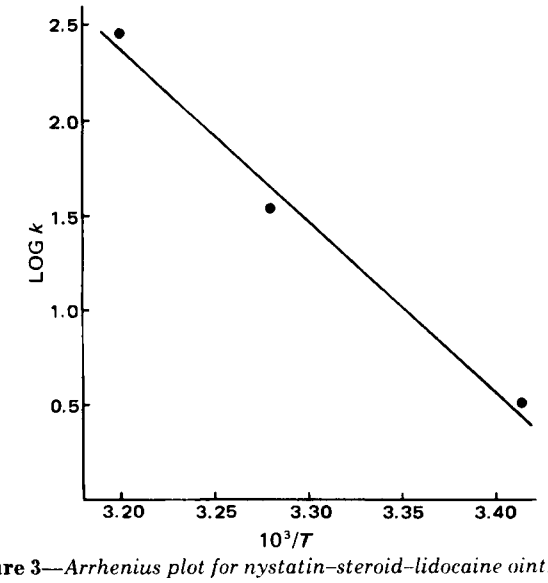

Figure 3—*Arrhenius plot for nystatin–steroid–lidocaine ointment.*

[7] P. R. Wood and J. R. Salmon, presented at the 35th International Congress of Pharmaceutical Sciences (F.I.P.), Dublin, Ireland, 1975.

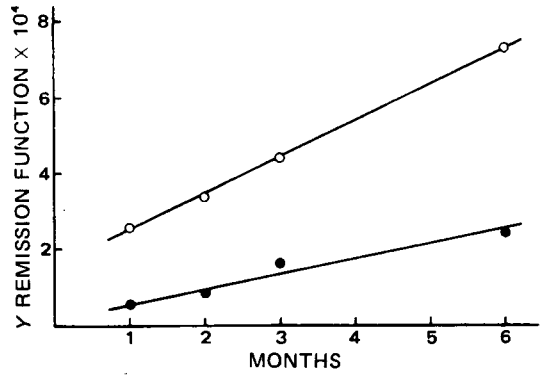

Figure 4—*Comparison of the color change of two nystatin creams. Key:* ●, *with added antioxidant; and* ○, *without antioxidant.*

Discoloration of the antibiotic in two cream formulations is shown in Fig. 4, and a linear response with time again is apparent. The difference in the slope values indicates the difference in stability of the two formulations (one contained an antioxidant) and confirmed data previously obtained in these laboratories using microbiological assays.

Accelerated stability testing of creams and ointments at temperatures higher than 40° has not been attempted.

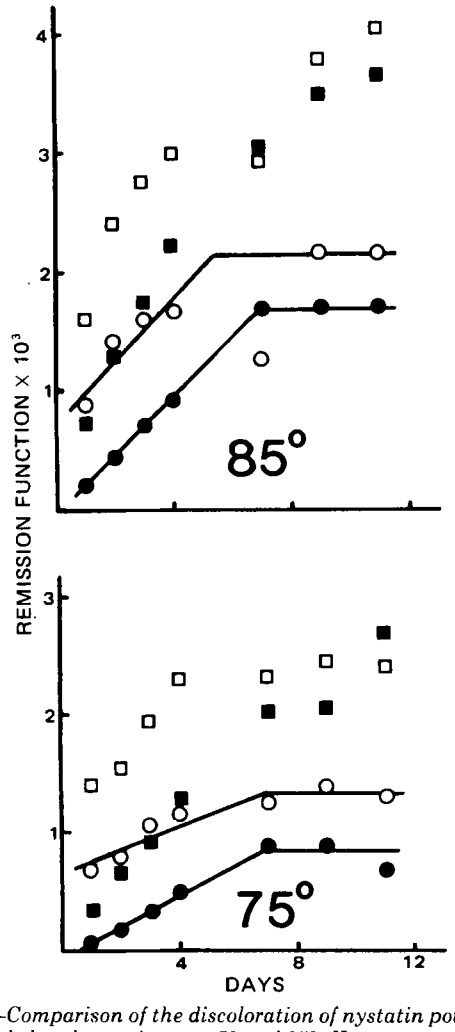

Figure 5—*Comparison of the discoloration of nystatin powder stored in open and closed containers at 75 and 85°. Key:* □, *open dish,* X *remission function;* ■, *closed container,* X *remission function;* ○, *open dish,* Y *remission function; and* ●, *closed container,* Y *remission function.*

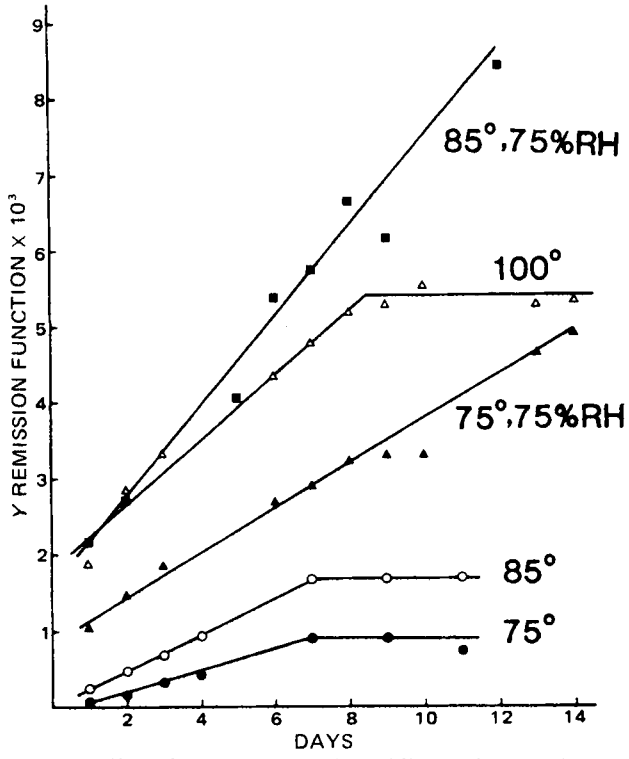

Figure 6—*Effect of temperature and humidity on the rate of nystatin powder discoloration.*

Bulk Raw Material—With the ointment and cream formulations, which are stored in sealed containers during stability monitoring, only one variable (temperature) is possible. However, with solids, the material may be stored in open or closed systems; with open containers, humidity may be included as another variable parameter. Bashkovich *et al.* (13) reported an increase in the rate of nystatin inactivation in a humid atmosphere.

To assess the effect of these variables on the discoloration of nystatin, the antibiotic was stored in open dishes and in sealed screw-top vials at

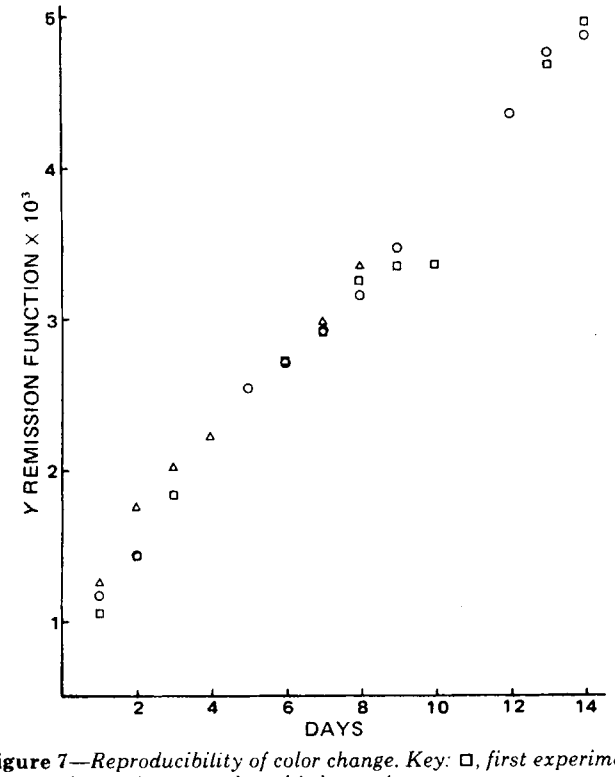

Figure 7—*Reproducibility of color change. Key:* □, *first experiment;* ○, *second experiment; and* ●, *third experiment.*

Table II—Reproducibility of Technique

Assay	Slope × 10^4	Correlation Coefficient
1	4.57	0.9935
2	4.79	0.9964
3	5.23	0.9928

a series of temperatures. In additional experiments, the powder was stored in an atmosphere of 75% RH in open dishes at elevated temperatures. The color change was determined daily, and the Kubelka–Munk remission functions were calculated from the results.

The use of open and closed containers is compared in Fig. 5, which shows the change in remission function with time. The plots for each type of container demonstrate that essentially similar results were obtained regardless of the temperature. Comparison of the tristimulus values of the degraded nystatin samples, determined before and after thorough mixing of the material, showed little difference, indicating that the color change was not a surface phenomenon but instead took place throughout the entire material.

The effect of moisture on nystatin degradation is demonstrated in Fig. 6. Not only was the degradation rate increased, but the plateau effect, noted with samples stored at ambient relative humidity, was eliminated under humid conditions. The nature of the plateau effect is not understood fully, but it is thought to be due in part to a loss of moisture from the nystatin samples, all of which contained about 5% moisture prior to degradation. This moisture level is normal in the manufactured product.

Only samples stored under humid conditions resulted in a linear change of the Kubelka–Munk remission function throughout the 14-day period. The most satisfactory correlation coefficient was obtained for the nystatin degraded at 75° and 75% RH. To assess the reproducibility of the degradation rate under these conditions, one batch of nystatin was degraded on three separate occasions during 3 months. The results (Fig. 7) show little scatter and indicate the robustness of the procedure. Calculation of the respective slopes and correlation coefficients for each set of points (Table II) demonstrated the reproducibility of the technique.

The linear response thus allows calculation of an actual degradation rate, which is advantageous when comparing factors affecting nystatin stability, as in preformulation studies, or when comparing the stability of bulk nystatin from different sources. Previous investigations were accomplished microbiologically (13–15). However, the decrease in potency observed during the degradation period was nonlinear and allowed only qualitative comparisons. With the alternative procedure described in this paper, it is possible to compare materials and formulations quantitatively, an objective previously unattainable.

If the application of this novel technique to other antibiotics proves successful, the tristimulus colorimetric technique should be established firmly in pharmaceutical analysis.

REFERENCES

(1) F. M. Bogdansky, *J. Pharm. Sci.*, **64**, 323 (1975).

(2) D. G. Pope and J. L. Lach, *Pharm. Acta Helv.*, **50**, 165 (1975).

(3) S. M. Blaug and W. Huang, *J. Pharm. Sci.*, **61**, 1770 (1972).

(4) J. T. Carstensen, J. B. Johnson, W. Valentine, and J. J. Vance, *ibid.*, **53**, 1050 (1964).

(5) D. G. Pope and J. L. Lach, *Can. J. Pharm. Sci.*, **10**, 126 (1975).

(6) *Ibid.*, **10**, 114 (1975).

(7) *Ibid.*, **10**, 109 (1975).

(8) F. Ebel and O. Mastilovic, *Acta Pharm. Jugosl.*, **24**, 37 (1974).

(9) F. Ebel and O. Mastilovic, *Hem. Ind.*, **30**, 449 (1976).

(10) J. E. Fairbrother, *Pharm. J.*, **220**, 261 (1978).

(11) P. Kubelka and E. Munk, *Z. Tech. Phys.*, **12**, 593 (1931).

(12) P. Kubelka, *J. Opt. Soc. Am.*, **38**, 448 (1948).

(13) A. P. Bashkovich, Y. D. Shenin, T. V. Kotenko, U. Y. Raigordskaya, M. P. Karpenko, N. A. Krasnobaeva, N. G. Vasil'eva, N. P. Bogdanova, and O. N. Ekyemphyarov, *Khim.-Farm. Zh.*, **1**, 31 (1967).

(14) S. Boteanu, S. Balliu-Mutu, E. Aiteanu, and O. Ludu, *Farmacia (Bucharest)*, **17**, 681 (1969).

(15) D. M. Trakhtenberg, E. I. Rodionovskaya, Z. V. Gordina, L. I. Rostovtseva, G. I. Kleiner, and A. M. Nagle, *Antibiotiki*, **5**, 9 (1960).

ACKNOWLEDGMENTS

Presented in part at the APhA Academy of Pharmaceutical Sciences, New York meeting, May 1977.

The authors thank Mr. K. Simpson for assistance in determining microbiological potencies and Miss F. Watson for determining the tristimulus values of the ointments.

High-Pressure Liquid Chromatographic Determination of Sulfamethazine Residues in Beef Tissues

DAVID SEYMOUR ˣ **and B. DEAN RUPE**

Received November 8, 1979, from *Jensen-Salsbery Laboratories, Division of Burroughs Wellcome Co., Kansas City, MO 64108.* Accepted for publication January 24, 1980.

Abstract □ A high-pressure liquid chromatographic procedure for the determination of sulfamethazine residues in beef tissues is presented. Tissue samples are extracted and analyzed utilizing normal-phase chromatography and a UV detector at 254 nm. Primary and confirmatory identification and quantitative determination are provided at the tolerance limit of 0.1 ppm of sulfamethazine in tissues. Recoveries obtained from liver, fat, kidney, and muscle tissues were 69, 82, 77, and 76%, respectively, when spiked at the tolerance limit.

Keyphrases □ Sulfamethazine—high-pressure liquid chromatographic determination, beef tissues □ High-pressure liquid chromatography—analysis, sulfamethazine, beef tissues □ Chemotherapeutic agents—sulfamethazine, high-pressure liquid chromatographic determination, beef tissues

Sulfamethazine (I), a chemotherapeutic agent, has been used successfully for more than 30 years in the treatment of infectious diseases in cattle. A tolerance limit of 0.1 ppm has been established for the drug residues in uncooked edible tissues of cattle[1]. The Bratton–Marshall (1) procedure and subsequent modifications (2, 3) were used to indicate the residue levels of I but, due to nonspecificity (4), these procedures no longer meet the rigorous requirements recently established by the regulatory agencies for residue assay procedures.

Several procedures that provide improved specificity for sulfamethazine residues in tissues using TLC (4), GLC (5), and high-pressure liquid chromatography (HPLC) (6) were reported recently. However, no procedure has been approved by the regulatory agencies for use in a tissue residue study. A study was conducted in this laboratory to develop a procedure that could be approved for the determination of sulfamethazine residues in beef tissues. The method employs HPLC to provide a qualitative (both primary and confirmatory) and quantitative assay of I in tissues at the tolerance limit.

EXPERIMENTAL

Materials—Methylene chloride[2], chloroform[2], methanol[3], isooctane[3], and acetic acid[3] were analytical reagent grade and were used as received. Sulfamethazine[4] (I), sulfadimethoxine[5] (III), sulfadiazine[6] (VI), and sulfachlorpyridazine[2] (V) were used as received. Sulfabromomethazine[7] (II) was dissolved in water, buffered to pH 5–6, and extracted into methylene chloride prior to chromatography. Sulfaethoxypyridazine[4] (IV) was obtained by direct dissolution of an equivalent amount of a bolus[8] into methylene chloride.

Apparatus and Chromatographic Parameters—A high-pressure liquid chromatograph[9] was equipped with a septumless injector, a normal-phase 25-cm column[10], a UV detector set at 254 nm, and a strip-chart recorder. Unless otherwise noted, a mobile phase of 65% chloroform, 30.5% isooctane, 4.0% methanol, and 0.5% acetic acid was used. The flow rate was 20 ml/hr, and the UV detector was operated at 0.002 aufs.

Working Standards—Solutions of each sulfonamide were prepared at 8 μg/ml in methylene chloride.

Analytical Standards—Standards equivalent to 0.1, 0.2, and 0.4 ppm of I in tissues were prepared by pipetting 0.5, 1.0, and 2.0 ml, respectively, of a 4-ppm solution of I in methylene chloride into tared 30-ml beakers. The weight of each solution was adjusted to 1 ± 0.02 g by evaporation or addition of methylene chloride immediately prior to injection of a 10-μl aliquot into the liquid chromatograph. *Standards were not allowed to evaporate to dryness.*

Acetylation Technique—One milliliter of methanol and 2 drops of acetic anhydride were added to each sample to be acetylated. The samples then were heated on a hot plate at 80–90° until acetic acid fumes could not be detected. The residue was dissolved in 1 g of methylene chloride, and 10-μl aliquots were injected.

Residue Assay Procedure—The tissues were cut into small pieces (200–300 mg), and 20 ± 0.1 g was weighed into 100-ml beakers. Following the addition of 25 ml of methylene chloride, the samples were mixed with a glass stirring rod and allowed to stand for 20–30 min with frequent stirring. The methylene chloride was decanted into 125-ml separators through a funnel plugged with glass wool. The tissues were extracted with two additional 25-ml portions of methylene chloride, and the aliquots were pooled in their respective separators.

After the addition of 10 ml of 3 *N* H_2SO_4, the samples were extracted for 15 min, and the lower phase was discarded completely. The remaining aqueous phase was washed twice by adding 10 ml of methylene chloride, shaking for 10 min, and discarding the lower phase.

One milliliter of 10% K_2HPO_4 and 3 ml of 40% NaOH were added to each separator. The samples were mixed well and allowed to cool, and the pH was measured with pH paper. A pH of 5–6 was obtained by dropwise addition of 3 *N* H_2SO_4 or 40% NaOH. The final pH was measured potentiometrically.

After the addition of 5 ml of methylene chloride, the samples were extracted for 15 min. The lower phase was dried by draining through a bed of anhydrous sodium sulfate and collected in previously weighed 50-ml beakers. The extraction was repeated, and the extracts were collected in their respective beakers.

The samples were placed on a hot plate at 60–70°, and the weight of the solution was adjusted to 1 ± 0.02 g by evaporation immediately prior to injecting 10 μl into the liquid chromatograph.

Evaporation to dryness of either samples or standards was avoided because of resulting sulfamethazine losses.

After the samples were chromatographed satisfactorily, the samples were acetylated and reinjected.

RESULTS AND DISCUSSION

Qualitative Assay—Ten-microliter samples of each working standard were injected into the liquid chromatograph stabilized at the specified parameters. Retention times of each sample are given in Table I. Primary identification of an unknown sulfonamide can be made by comparison of retention times for the sample to those of authentic standards.

Table I—Sulfonamide Retention Times

Sulfonamide	Retention Time, min
Sulfabromomethazine	3.56
Sulfadimethoxine	3.99
Sulfamethazine	4.34
Sulfaethoxypyridazine	4.60
Sulfachlorpyridazine	5.60
Sulfadiazine	5.55

[1] 21 CFR 556.670.
[2] Mallinckrodt Chemical Co., St. Louis, Mo.
[3] J. T. Baker Chemical Co., Phillipsburg, N.J.
[4] American Cyanamid Co., Princeton, N.J.
[5] Hoffmann-La Roche Inc., Nutley, N.J.
[6] K & K Laboratories, Plainview, N.Y.
[7] Merck and Co., Rahway, N.J.
[8] SEZ C-R bolus, American Cyanamid Co., Princeton, N.J.
[9] Aerograph 4100 series, Varian Associates, Palo Alto, Calif.
[10] MicroPak CN-10, Varian Associates, Palo Alto, Calif.

0022-3549/80/0600-0701$01.00/0
© 1980, American Pharmaceutical Association

Table II—Acetylated Sulfonamide Retention Times

Acetylated Sulfonamide	Retention Time, min
Acetylsulfabromomethazine	4.16
Acetylsulfadimethoxine	4.70
Acetylsulfamethazine	5.34
Acetylsulfaethoxypyridazine	5.23
Acetylsulfachlorpyridazine	6.68
Acetylsulfadiazine	6.78

Table III—Retention Times of Sulfadimethoxine, Sulfamethazine, Sulfaethoxypyridazine, and Their Acetylated Derivatives Using the Alternative Solvent System of 97% Chloroform, 2% Acetic Acid, and 1% Ethanol

Sulfonamide	Retention Time, min
Sulfadimethoxine	3.5
Sulfamethazine	4.4
Sulfaethoxypyridazine	5.3
Acetylsulfadimethoxine	8.0
Acetylsulfamethazine	10.2
Acetylsulfaethoxypyridazine	13.5

One-milliliter portions of each working standard were acetylated, and 10-μl aliquots were injected as described. Retention times of each acetylated sulfonamide are given in Table II. Confirmatory identification of an unknown sulfonamide can be made by comparison of its retention time after acetylation to that of acetylated authentic standards.

Improved resolution of I, III, and IV was obtained using an alternative solvent system of 97% chloroform, 2% acetic acid, and 1% ethanol (Fig. 1). Retention times of these three sulfonamides and their acetylated derivatives are given in Table III.

Solutions containing mixtures of sulfamethazine and any of the other sulfonamides examined could be resolved completely with the two solvent systems. Due to column variation, slight adjustment of the mobile phases may be necessary for adequate resolution.

The specificity of the technique, primarily due to the retention times of sulfamethazine and its acetylated derivative, is increased by the tissue extraction procedure. Only compounds possessing amphoteric properties very similar to I are recovered to any significant degree. Many potentially interfering, naturally occurring components of tissue and nearly all drugs other than sulfonamides currently being used in cattle are eliminated prior to chromatography. Although recoveries of sulfonamides other than I have not been confirmed, the potential interference of many compounds (II–VI) is eliminated by the resolutions obtained with the technique. Sulfonamides other than the ones mentioned previously that have been examined and found not to interfere include sulfamerazine, sulfathiazole, sulfanilamide, sulfapyridine, and sulfaquinoline. No compound has been found to date that interferes with the identification of residues of I in tissues using this method.

Quantitative Assay—Analytical standards containing amounts of I equivalent to 0.1, 0.2, and 0.4 ppm in tissues were prepared. Ten-microliter injections of these standards after weight adjustment of the solution to 1 ± 0.02 g gave peak heights proportional to the amounts of I injected. Reproducibility and linearity of the technique are shown by replicate injections of standards at the various concentrations (Table IV). Unknown amounts of I in solution are determined by comparison of sample and standard peak heights obtained from 10-μl injections after weight adjustment to 1 ± 0.02 g.

Residues of I in tissues are calculated from:

$$\frac{\text{sample peak height}}{\text{standard peak height}} \times \frac{\text{micrograms of I in standard}}{\text{weight of sample, g}} = \text{ppm of I} \quad \text{(Eq. 1)}$$

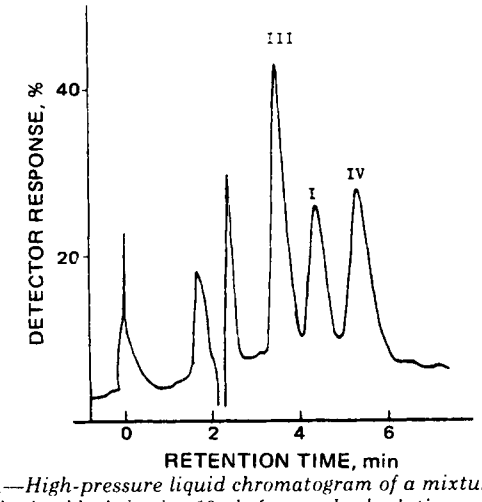

Figure 1—*High-pressure liquid chromatogram of a mixture of I, III, and IV obtained by injecting 10 µl of a standard solution equivalent to 0.1 ppm of each in tissue. The solvent system was 97% chloroform, 2% acetic acid, and 1% ethanol.*

Table IV—Reproducibility and Linearity of the Quantitative Technique

Concentration, ppm	Peak Height[a] (±*SD*)
0.1	29.2 (±1.16)
0.2	56.6 (±0.58)
0.4	103.4 (±3.3)

[a] Average of four injections.

Table V—Percent Recovery Data[a] Obtained by Applying the Residue Assay Procedure to Spiked Beef Tissues

Concentration Added, ppm	Percent Recovered			
	Liver	Kidneys	Muscle	Fat
0.1	73, 71	84, 91	76, 83	80, 87
0.1	66, 66	73, 71	76, 76	80, 86
0.1	59, 65	67, 75	76, 79	84, 83
0.1	75, 74	69, 73	65, 65	80, —[b]
0.1	73, —[b]	83, 81	81, 81	75, 83
Average	69.1	76.7	75.8	82.0
SD	5.4	7.7	6.2	3.7
0.2	68, 69	87, 84	61, 96	81, 83
0.2	64, 71	81, 78	76, 73	82, 87
0.2	68, 67	72, 72	76, 77	86, 80
0.2	68, 69	66, 74	67, 68	77, —[b]
0.2	68, 70	82, 79	79, 86	—[b], 76
Average	68.2	77.5	75.9	81.5
SD	1.9	6.4	9.9	3.9
0.4	82, 82	84, —[b]	91, 86	74, 83
0.4	72, 76	79, 79	87, 82	82, 72
0.4	71, 69	78, 78	79, 85	75, 81
0.4	63, 70	65, 72	70, 68	61, 86
0.4	74, —[b]	80, 82	90, 100	81, 86
Average	73.2	77.4	83.8	78.1
SD	6.1	5.7	9.6	7.7

[a] Duplicate samples. [b] Sample lost.

Recovery of I from Tissues—Percent recovery data (Table V) were obtained by taking beef tissues spiked at 0.1, 0.2, and 0.4 ppm of I through the tissue assay procedure and comparing the peak heights obtained to those of the appropriate analytical standards. These data were obtained from five samples of each tissue, in duplicate, at each concentration. Analyses of the data showed >70% average recovery in every tissue at the

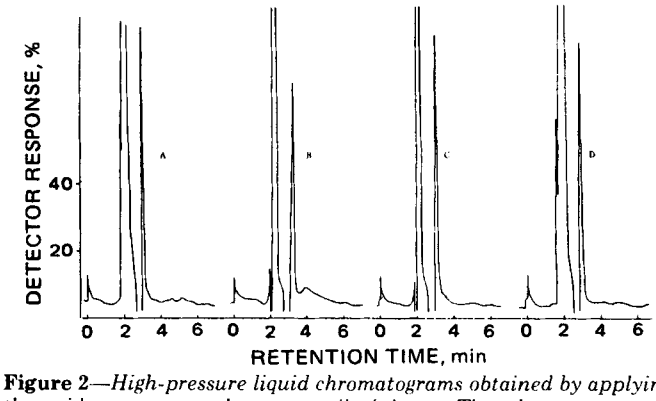

Figure 2—*High-pressure liquid chromatograms obtained by applying the residue assay procedure to unspiked tissues. The solvent system was 65% chloroform, 30.5% isooctane, 4.0% methanol, and 0.5% acetic acid. Key: A, liver; B, kidneys; C, muscle; and D, fat.*

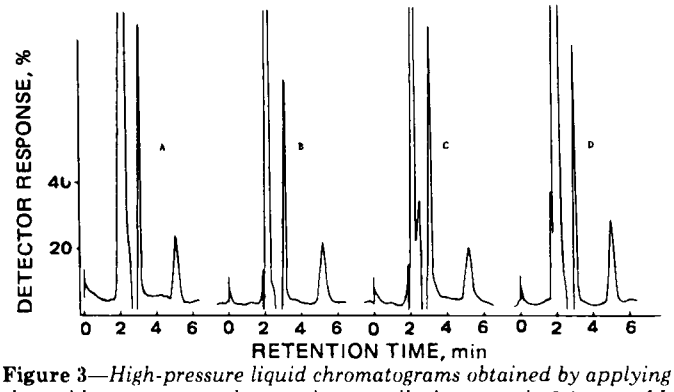

Figure 3—*High-pressure liquid chromatograms obtained by applying the residue assay procedure to tissues spiked to contain 0.1 ppm of I. The solvent system was 65% chloroform, 30.5% isooctane, 4.0% methanol, and 0.5% acetic acid. Key: A, liver; B, kidneys; C, muscle; and D, fat.*

tolerance level except liver, which had a recovery of 69% and a relative standard deviation of ~10% (Table V).

Unspiked tissues typically showed no peak other than random baseline noise in the region where I eluted (Fig. 2). The magnitude of the sulfamethazine signal obtained from tissues spiked at the tolerance limit was ~20% of full scale (Fig. 3). A favorable signal-to-blank ratio at the tolerance limit was obtained with this procedure, allowing low detection limits. The tolerance limit of 0.1 ppm of I in tissues was approximately five times the detection limit of the method.

With slight modifications, the method should be applicable to several sulfonamides currently used in veterinary medicine. Recoveries of sulfamethazine only have been demonstrated to date.

REFERENCES

(1) A. C. Bratton and E. K. Marshall, *J. Biol. Chem.*, **128**, 537 (1939).

(2) F. Tishler, J. L. Sutter, J. N. Bathish, and H. E. Hgman, *J. Agr. Food Chem.*, **16**, 50 (1968).

(3) J. Fellig and J. Westheimer, *ibid.*, 16, 738 (1968).

(4) W. F. Phillips and J. E. Trafton, *J. Assoc. Off. Anal. Chem.*, **58**, 44 (1975).

(5) D. P. Goodspeed, R. M. Simpson, R. B. Ashworth, J. W. Shafer, and H. R. Cook, "A Sensitive and Specific GLC–Spectrophotometric Screening Procedure for Trace Levels of Five Sulfonamides in Liver, Muscle and Kidney Tissue," Methods Development Laboratory, Animal and Plant Health Inspection Service, U.S. Department of Agriculture, Beltsville, Md.

(6) K. L. Johnson, D. T. Jeter, and K. C. Clairborne, *J. Pharm. Sci.*, **64**, 1657 (1975).

Teratogenic Potential of Cocaine Hydrochloride in CF-1 Mice

MICHAEL P. MAHALIK, RONALD F. GAUTIERI ˣ, and DAVID E. MANN, Jr.

Received December 20, 1979, from the *Department of Pharmacology, School of Pharmacy, Temple University, Philadelphia, PA 19140.* Accepted for publication January 30, 1980.

Abstract □ This investigation revealed that cocaine hydrochloride was teratogenic when administered in nontoxic doses to gravid CF-1 mice on Days 7–12 of gestation. The teratogenic susceptibility of the CF-1 mouse fetus to cocaine hydrochloride was evident throughout this portion of the gestation period. The early appearance of eye defects and the occurrence of skeletal defects later in gestation after cocaine hydrochloride challenge paralleled the sequence of ontogenesis.

Keyphrases □ Cocaine hydrochloride—evaluation as potential teratogen, effect on catecholamine levels in placenta, skeletal and soft tissue malformations in fetal mice □ Teratogenic drugs—cocaine hydrochloride, effect on fetal mice □ Inhibition, competitive—cocaine hydrochloride and norepinephrine, effect on fetal mice

Cocaine (benzoylmethylecgonine), the first local anesthetic discovered, not only inhibits nerve conduction but also prevents norepinephrine reuptake at nerve terminals (1). Because of the latter action, norepinephrine levels are augmented and vasoconstriction occurs (1).

BACKGROUND

Previous studies detected catecholamines in human amniotic fluid (2) and placenta (3). If the mechanisms for storage and release of norepinephrine in the placenta are comparable to those at nerve terminals, increased catecholamine levels induced by cocaine could cause placental vasoconstriction.

A relationship between placental vasoconstriction and fetal anomalies was demonstrated in studies involving mechanical obstruction of uterine and placental vascular flow by clamping, which probably causes fetal malformations through decreased oxygen availability (4–7), and by drugs such as serotonin (8) and morphine (9), which accomplish similar effects pharmacodynamically.

With respect to the autonomic neural involvement of cocaine as a potential teratogen, Furchgott *et al.* (10) detected a specific transfer site with which norepinephrine molecules combine before being transferred to storage or enzymatic inactivation loci. According to Johnson and Kahn (11), the potentiation of norepinephrine responses by cocaine results from competitive inhibition between the local anesthetic and norepinephrine molecules at these transfer sites. Thus, in pregnant mice, cocaine conceivably could induce fetal malformations by raising catecholamine levels which, in turn, cause placental vasoconstriction *via* competitive inhibition.

The purpose of this study was twofold: (*a*) to test the hypothesis that cocaine is a potential teratogen in mice, and (*b*) if the results were affirmative, to ascertain the precise days of gestation when fetal susceptibility to the teratogen is evident.

EXPERIMENTAL

Animals—The test animals were CF-1 mice[1], 25–30 g. Females were placed in aggregate cages, each holding 10 animals. Two weeks after their arrival, the mice were bred if they weighed at least 25 g. Males were placed individually in metal cages (12.5 × 15 × 10 cm) with a wire-mesh front and floor[2]. All animals were maintained on laboratory food[3] and tap water *ad libitum*.

The room housing the animals was protected from exposure to natural sunlight and was equipped with an electrical lighting system[4], which al-

[1] Charles River Breeding Laboratories, Wilmington, Mass.
[2] RD-T unit, Norwich Wire Works, Norwich, N.Y.
[3] Purina Laboratory Chow, Ralston Purina Co., St. Louis, Mo.
[4] Model V-45073 astronomic dial time switch with "skipper," International Register Co., Spring Grove, Ill.

0022-3549/80/0600-0703$01.00/0
© 1980, American Pharmaceutical Association

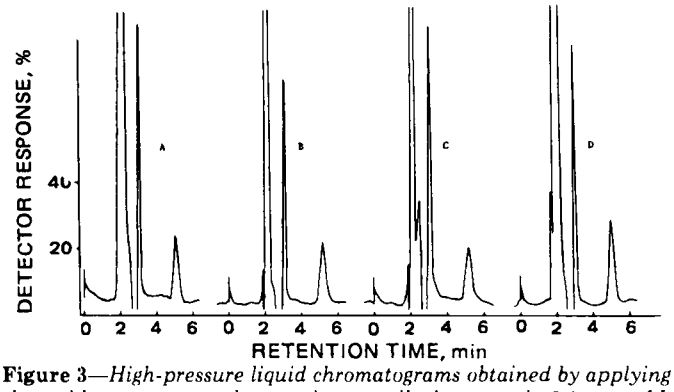

Figure 3—*High-pressure liquid chromatograms obtained by applying the residue assay procedure to tissues spiked to contain 0.1 ppm of I. The solvent system was 65% chloroform, 30.5% isooctane, 4.0% methanol, and 0.5% acetic acid. Key: A, liver; B, kidneys; C, muscle; and D, fat.*

tolerance level except liver, which had a recovery of 69% and a relative standard deviation of ~10% (Table V).

Unspiked tissues typically showed no peak other than random baseline noise in the region where I eluted (Fig. 2). The magnitude of the sulfamethazine signal obtained from tissues spiked at the tolerance limit was ~20% of full scale (Fig. 3). A favorable signal-to-blank ratio at the tolerance limit was obtained with this procedure, allowing low detection limits. The tolerance limit of 0.1 ppm of I in tissues was approximately five times the detection limit of the method.

With slight modifications, the method should be applicable to several sulfonamides currently used in veterinary medicine. Recoveries of sulfamethazine only have been demonstrated to date.

REFERENCES

(1) A. C. Bratton and E. K. Marshall, *J. Biol. Chem.*, **128**, 537 (1939).

(2) F. Tishler, J. L. Sutter, J. N. Bathish, and H. E. Hgman, *J. Agr. Food Chem.*, **16**, 50 (1968).

(3) J. Fellig and J. Westheimer, *ibid.*, 16, 738 (1968).

(4) W. F. Phillips and J. E. Trafton, *J. Assoc. Off. Anal. Chem.*, **58**, 44 (1975).

(5) D. P. Goodspeed, R. M. Simpson, R. B. Ashworth, J. W. Shafer, and H. R. Cook, "A Sensitive and Specific GLC–Spectrophotometric Screening Procedure for Trace Levels of Five Sulfonamides in Liver, Muscle and Kidney Tissue," Methods Development Laboratory, Animal and Plant Health Inspection Service, U.S. Department of Agriculture, Beltsville, Md.

(6) K. L. Johnson, D. T. Jeter, and K. C. Clairborne, *J. Pharm. Sci.*, **64**, 1657 (1975).

Teratogenic Potential of Cocaine Hydrochloride in CF-1 Mice

MICHAEL P. MAHALIK, RONALD F. GAUTIERI ˣ, and DAVID E. MANN, Jr.

Received December 20, 1979, from the *Department of Pharmacology, School of Pharmacy, Temple University, Philadelphia, PA 19140.* Accepted for publication January 30, 1980.

Abstract □ This investigation revealed that cocaine hydrochloride was teratogenic when administered in nontoxic doses to gravid CF-1 mice on Days 7–12 of gestation. The teratogenic susceptibility of the CF-1 mouse fetus to cocaine hydrochloride was evident throughout this portion of the gestation period. The early appearance of eye defects and the occurrence of skeletal defects later in gestation after cocaine hydrochloride challenge paralleled the sequence of ontogenesis.

Keyphrases □ Cocaine hydrochloride—evaluation as potential teratogen, effect on catecholamine levels in placenta, skeletal and soft tissue malformations in fetal mice □ Teratogenic drugs—cocaine hydrochloride, effect on fetal mice □ Inhibition, competitive—cocaine hydrochloride and norepinephrine, effect on fetal mice

Cocaine (benzoylmethylecgonine), the first local anesthetic discovered, not only inhibits nerve conduction but also prevents norepinephrine reuptake at nerve terminals (1). Because of the latter action, norepinephrine levels are augmented and vasoconstriction occurs (1).

BACKGROUND

Previous studies detected catecholamines in human amniotic fluid (2) and placenta (3). If the mechanisms for storage and release of norepinephrine in the placenta are comparable to those at nerve terminals, increased catecholamine levels induced by cocaine could cause placental vasoconstriction.

A relationship between placental vasoconstriction and fetal anomalies was demonstrated in studies involving mechanical obstruction of uterine and placental vascular flow by clamping, which probably causes fetal malformations through decreased oxygen availability (4–7), and by drugs such as serotonin (8) and morphine (9), which accomplish similar effects pharmacodynamically.

With respect to the autonomic neural involvement of cocaine as a potential teratogen, Furchgott *et al.* (10) detected a specific transfer site with which norepinephrine molecules combine before being transferred to storage or enzymatic inactivation loci. According to Johnson and Kahn (11), the potentiation of norepinephrine responses by cocaine results from competitive inhibition between the local anesthetic and norepinephrine molecules at these transfer sites. Thus, in pregnant mice, cocaine conceivably could induce fetal malformations by raising catecholamine levels which, in turn, cause placental vasoconstriction *via* competitive inhibition.

The purpose of this study was twofold: (*a*) to test the hypothesis that cocaine is a potential teratogen in mice, and (*b*) if the results were affirmative, to ascertain the precise days of gestation when fetal susceptibility to the teratogen is evident.

EXPERIMENTAL

Animals—The test animals were CF-1 mice[1], 25–30 g. Females were placed in aggregate cages, each holding 10 animals. Two weeks after their arrival, the mice were bred if they weighed at least 25 g. Males were placed individually in metal cages (12.5 × 15 × 10 cm) with a wire-mesh front and floor[2]. All animals were maintained on laboratory food[3] and tap water *ad libitum*.

The room housing the animals was protected from exposure to natural sunlight and was equipped with an electrical lighting system[4], which al-

[1] Charles River Breeding Laboratories, Wilmington, Mass.
[2] RD-T unit, Norwich Wire Works, Norwich, N.Y.
[3] Purina Laboratory Chow, Ralston Purina Co., St. Louis, Mo.
[4] Model V-45073 astronomic dial time switch with "skipper," International Register Co., Spring Grove, Ill.

0022-3549/80/0600-0703$01.00/0
© 1980, American Pharmaceutical Association

Table I—Mean Values of the Test Groups

Treatment[a]	Day	Maternal Weight Ratio, S/T[b]	Fetal Ratio, Right Horn/ Left Horn	Resorption Ratio, Right Horn/ Left Horn	Mean Fetal Weight, g	Sex Ratio, M/F	Soft Tissue Abnormalities	Skeletal Abnormalities
Untreated	—	28.2/50.9	5.6/5.3	0.3/0.2	1.13	4.7/6.2	0.0	1.3
Saline	7	30.2/56.3	6.1/5.6	0.0/0.2	1.16	8.0/3.7	0.1	3.5
	8	28.1/54.2	6.3/5.3	0.2/0.2	1.14	7.0/4.7	0.2	1.7
	9	28.4/53.3	6.3/5.1	0.3/0.0	1.17	8.3/3.1	0.1	1.6
	10	30.7/55.6	5.7/5.7	0.0/0.6	1.15	6.8/4.6	0.0	4.0
	11	30.6/53.0	5.8/5.5	0.0/0.5	1.11	6.1/5.2	0.0	2.6
	12	27.4/52.1	6.5/4.6	0.5/0.0	1.15	7.1/4.0	0.0	3.8
Cocaine	7	29.5/54.8	5.5/6.2	0.2/0.3	1.14	5.6/6.1	6.0[c]	7.7[c]
	8	28.6/50.9	5.7/5.0	0.5/0.2	1.10	6.2/4.5	2.1[c]	7.3[c]
	9	29.8/54.4	6.7/4.7	0.7/0.2	1.12	6.3[c]/5.1[c]	2.2[c]	8.6[c]
	10	30.1/52.0	5.7/4.3	1.1[c]/1.0	1.13	6.2/3.8	2.1[c]	5.2
	11	30.4/53.6	6.5/4.3	0.6/0.7	1.13	6.6/4.2	2.6[c]	6.0
	12	28.6/53.3	5.8/5.2	0.1/0.2	1.19	6.0/5.0	1.0[c]	8.1

[a] The dose of saline was 0.3 ml sc, and the dose of cocaine was 60 mg/kg sc. [b] S = starting weight, and T = terminal weight. [c] Statistically significant in comparison with respective saline controls, $p < 0.05$.

Table II—Occurrence of Exencephaly, Cryptorchidism, and Hydronephrosis on Day of Treatment (Compared with Saline)

		Exencephaly				Cryptorchidism				Hydronephrosis			
		Litters		Fetuses		Litters		Fetuses		Litters		Fetuses	
Treatment[a]	Day	Normal	Abnormal	Normal	Abnormal	Normal	Abnormal	Normal	Abnormal	Normal	Abnormal	Normal	Abnormal
Untreated	—	8	0	43	0	8	0	43	0	8	0	43	0
Saline	7	8	0	45	0	7	1	44	1	8	0	45	0
	8	8	0	46	0	7	1	45	1	8	0	46	0
	9	8	0	44	0	7	1	43	1	8	0	44	0
	10	8	0	44	0	8	0	44	0	8	0	44	0
	11	8	0	44	0	8	0	44	0	8	0	44	0
	12	8	0	43	0	8	0	43	0	8	0	43	0
Cocaine	7	7	1	44	1	6	2	42	3	4	4[b]	37	8[b]
	8	7	1	39	2	4	4	35	6[b]	7	1	40	1
	9	4	4[b]	41	5[b]	5	3	42	4	4	4[b]	41	5[b]
	10	7	1	39	1	4	4[b]	33	7[b]	6	2	37	3
	11	8	0	44	0	5	3	39	5[b]	6	2	41	3
	12	8	0	44	0	6	2	42	2	7	1	43	1

[a] The dose of saline was 0.3 ml sc, and the dose of cocaine was 60 mg/kg sc. [b] Statistically significant in comparison with respective saline controls, $p < 0.05$.

lowed 12 hr of light (7:00 am–7:00 pm) and 12 hr of darkness. The temperature was maintained at 22–26°.

Determination of Teratogenic Dose—The teratogenic dose of a suspected teratogen is based on its relationship to its toxic dose (LD_{50}). To ascertain the LD_{50} of cocaine hydrochloride, 40 female nongravid mice were selected randomly and assigned to one of five groups of eight animals each. Dosage levels for the five groups were 75, 100, 125, 150, and 175 mg/kg, respectively. Each mouse was weighed to the nearest 0.1 g, caged individually, and injected subcutaneously with a freshly prepared cocaine hydrochloride solution into the right side of the abdomen. After each injection, the mice were observed for behavioral changes and fatalities.

The estimated LD_{50} of cocaine hydrochloride in nongravid mice was 113 mg/kg (12). Nongravid animals are acceptable substitutes for gravid animals because the LD_{50} of a drug in gravid mice generally is equivalent to that in nongravid mice (13). Because a dose that produces severe toxicity and behavioral changes in female mice also will exert devastating effects on developing fetuses, the teratogenic dose should be nonlethal and elicit only minimal pharmacological responses.

Stimulation followed by depression and eventual recovery occurred in most animals receiving doses of 100 mg/kg or higher, but deaths also were noted at these levels. At the lowest dose (75 mg/kg), four animals showed no apparent effects; four became excited, developed a Straub tail, and bit the cage, and one convulsed. Although this dosage produced no deaths, it was not regarded as optimal because of excessive stimulation of the central nervous system. Therefore, another randomly selected group of animals was given a 70-mg/kg dose by the same route and procedure. At this level (below the LD_1), no deaths were noted, although convulsions still persisted. A 60-mg/kg dose was given to another group, which showed mild excitatory responses and a Straub tail in the absence of convulsions. Therefore, this dose (60 mg/kg) was selected as the teratogenic dose for this study.

Breeding Procedure and Treatment Regimen—Timed pregnancies were accomplished by placing two females in a cage with a male from 3:00 pm until 7:00 am, whereupon they were removed and examined for vaginal plugs. Animals with plugs were termed gravid, and the day of gestation coincident with their appearance was designated as Day 0. The pregnant mice then were weighed to the nearest 0.1 g[5], and each weight was recorded as the maternal starting weight.

Gravid animals were placed in individual cages identical to those of the males, where they remained undisturbed until the morning of Day 7 of gestation when they were reweighed. A weight gain of 2 g or more confirmed pregnancy. These animals then were assigned randomly to one of 13 groups of eight mice each. Six groups received single injections of cocaine hydrochloride (60 mg/kg) on Day 7, 8, 9, 10, 11, or 12, respectively; six groups received 0.3 ml of normal saline as a single injection on Days 7–12 of gestation (trauma controls). The final group represented untreated controls.

Preparation of Cocaine Hydrochloride Solution—Cocaine hydrochloride solution[6] (2%) was prepared by dissolving the drug in double-distilled water. The sodium chloride solution[7] was prepared commercially. All injections were made subcutaneously with a glass syringe[8].

Examination of Fetuses—Following treatment, each mouse was permitted to proceed to Day 18, the day prior to the termination of gestation, whereupon the terminal maternal weight was recorded. The animal then was sacrificed by cervical dislocation, and its abdomen was opened to expose the peritoneal cavity. The uterine horns were examined grossly for fetal swellings and resorption sites, appearing as small dark nodules, which were counted and recorded.

Following incision of the uterine horns, the exposed fetuses were removed, blotted dry, and weighed to the nearest 0.01 g on a torsion balance[9]. Each fetus was examined grossly for external soft tissue defects and sexed. Viability was determined by reflex movement of the limbs in response to mechanical stimulation with a blunt probe. Every other fetus

[5] Model 700 triple-beam balance, Ohaus.
[6] Merck 2209, lot L3506, Merck and Co., Rahway, N.J.
[7] Sodium chloride USP (code 2A1302), Travenol Laboratories, Deerfield, Ill.
[8] B-D 1-ml tuberculin syringe with a 1.27-cm, 26-gauge needle.
[9] Model PL-800, Torbal.

Table III—Occurrence of Anophthalmia, Malformed Lenses, and Missing Lenses on Day of Treatment (Compared with Saline)

		Anophthalmia				Malformed Lenses				Missing Lenses			
		Litters		Fetuses		Litters		Fetuses		Litters		Fetuses	
Treatment[a]	Day	Normal	Abnormal	Normal	Abnormal	Normal	Abnormal	Normal	Abnormal	Normal	Abnormal	Normal	Abnormal
Untreated	—	8	0	43	0	8	0	43	0	8	0	43	0
Saline	7	8	0	45	0	8	0	45	0	8	0	45	0
	8	8	0	46	0	8	0	46	0	8	0	46	0
	9	8	0	44	0	8	0	44	0	8	0	44	0
	10	8	0	44	0	8	0	44	0	8	0	44	0
	11	8	0	44	0	8	0	44	0	8	0	44	0
	12	8	0	43	0	8	0	43	0	8	0	43	0
Cocaine	7	5	3	41	4[b]	3	5[b]	31	14[b]	4	4[b]	39	6[b]
	8	6	2	39	2	5	3	38	3	6	2	39	2
	9	6	2	44	2	6	2	44	2	8	0	46	0
	10	5	3	37	3	7	1	39	1	7	1	39	1
	11	5	3	40	4[b]	6	2	42	2	5	3	41	3
	12	6	2	42	2	8	0	44	0	5	3	41	3

[a] The dose of saline was 0.3 ml sc, and the dose of cocaine was 60 mg/kg sc. [b] Statistically significant in comparison with respective saline controls, $p < 0.05$.

Table IV—Occurrence of Delayed Ossification of the Skull, Paws, and Centrum on Day of Treatment (Compared with Saline)

		Delayed Ossification Skull				Delayed Ossification Paws				Delayed Ossification Centrum			
		Litters		Fetuses		Litters		Fetuses		Litters		Fetuses	
Treatment[a]	Day	Normal	Abnormal	Normal	Abnormal	Normal	Abnormal	Normal	Abnormal	Normal	Abnormal	Normal	Abnormal
Untreated	—	8	0	45	0	3	5	36	9	8	0	45	0
Saline	7	8	0	50	0	3	5	34	16	8	0	50	0
	8	8	0	48	0	4	4	41	7	8	0	48	0
	9	8	0	48	0	7	1	43	5	8	0	48	0
	10	8	0	48	0	2	6	32	16	8	0	48	0
	11	8	0	47	0	4	4	33	14	8	0	47	0
	12	7	1	45	1	2	6	32	14	8	0	46	0
Cocaine	7	8	0	49	0	2	6	26	23	8	0	49	0
	8	7	1	42	3	2	6	22	23[b]	8	0	45	0
	9	7	1	45	1	1	7[b]	16	30[b]	7	1	45	1
	10	7	1	40	1	1	7	20	21	8	0	41	0
	11	6	2	38	5[b]	2	6	24	19	8	0	43	0
	12	2	5[b]	34	10[b]	0	7	19	25[b]	6	1	40	4[b]

[a] The dose of saline was 0.3 ml sc, and the dose of cocaine was 60 mg/kg sc. [b] Statistically significant in comparison with respective saline controls, $p < 0.05$.

Table V—Occurrence of Split Sternebrae, Malformed Sternebrae, and Crankshaft Sternebrae on Day of Treatment (Compared with Saline)

		Split Sternebrae				Malformed Sternebrae				Crankshaft Sternebrae			
		Litters		Fetuses		Litters		Fetuses		Litters		Fetuses	
Treatment[a]	Day	Normal	Abnormal	Normal	Abnormal	Normal	Abnormal	Normal	Abnormal	Normal	Abnormal	Normal	Abnormal
Untreated	—	7	1	44	1	8	0	45	0	7	1	44	1
Saline	7	3	5	40	10	8	0	50	0	7	1	49	1
	8	5	3	43	5	8	0	48	0	7	1	47	1
	9	5	3	44	4	6	2	46	2	6	2	46	2
	10	3	5	41	7	4	4	43	5	7	1	47	1
	11	6	2	45	2	8	0	47	0	6	2	45	2
	12	4	4	41	5	4	4	41	5	6	2	43	3
Cocaine	7	2	6	39	10	2	6[b]	35	14[b]	6	2	46	3
	8	4	4	38	7	4	4[b]	37	8[b]	4	4	39	6[b]
	9	1	7[b]	33	13[b]	5	3	39	7	3	5	37	9[b]
	10	5	3	37	4	1	7	29	12[b]	7	1	40	1
	11	5	3	38	5	3	5[b]	35	8[b]	6	2	41	2
	12	3	4	34	10	2	5	38	6	6	1	43	1

[a] The dose of saline was 0.3 ml sc, and the dose of cocaine was 60 mg/kg sc. [b] Statistically significant in comparison with respective saline controls, $p < 0.05$.

was immersed in either a bone-staining solution or Bouin's fixative and processed for skeletal or soft tissue examination, respectively.

Fetuses destined for soft tissue examination were fixed and decalcified in Bouin's fixative for at least 2 weeks, whereupon they were reexamined for external anomalies with a low power binocular dissecting microscope[10] and sectioned according to a literature method (14). Fetuses designated for skeletal examination were processed according to the technique of Staples and Schnell (15). The significance of observed variations among the experimental groups was determined by the Student t test and the uncorrected χ^2 test for binomial populations (16).

RESULTS AND DISCUSSION

The results of this study support the hypothesis that cocaine possesses teratogenic potential. Significant occurrences of soft tissue abnormalities, as compared with those of the controls, were observed on each day of cocaine treatment. Significant skeletal anomalies were observed on Days 7–9 of cocaine treatment as compared with the controls (Table I). Following the subcutaneous administration of cocaine hydrochloride (2%) at 60 mg/kg, a significant incidence of fetuses with exencephaly, cryptorchidism, hydronephrosis, anophthalmia, malformed or missing lenses, delayed ossification of the skull, paws (17), or centrum, extra ribs, malformed or crankshaft sternebrae (18), and split or butterfly xiphoid processes occurred when compared with those observed in the respective control groups (Tables II–VI).

Significant differences also were noted in the resorption (Day 10) and sex ratio (Day 9) when compared with those of the controls (Table I). Data in Table I indicate that cocaine did not alter the maternal mean terminal weights when compared to those of the controls, nor did the maternal weight gain during gestation appear to indicate fetal size or development. Furthermore, the initial starting weight of gravid mice was not responsible for any changes in the mean fetal weight (*i.e.*, there was no apparent

[10] Model ASZ30L2, Bausch & Lomb.

Table VI—Occurrence of Split Xiphoid, Butterfly Xiphoid, and Extra Ribs on Day of Treatment (Compared with Saline)

		Split Xiphoid				Butterfly Xiphoid				Extra Ribs			
		Litters		Fetuses		Litters		Fetuses		Litters		Fetuses	
Treatment[a]	Day	Normal	Abnormal	Normal	Abnormal	Normal	Abnormal	Normal	Abnormal	Normal	Abnormal	Normal	Abnormal
Untreated	—	8	0	45	0	8	0	45	0	8	0	45	0
Saline	7	8	0	50	0	8	0	50	0	8	0	50	0
	8	8	0	48	0	8	0	48	0	7	1	47	1
	9	8	0	48	0	8	0	48	0	8	0	48	0
	10	8	0	48	0	8	0	48	0	7	1	45	3
	11	8	0	47	0	8	0	47	0	6	2	44	3
	12	7	1	45	1	8	0	46	0	8	0	46	0
Cocaine	7	6	2	47	2	6	2	47	2	6	2	45	4[b]
	8	6	2	40	5[b]	6	2	42	3	6	2	42	3
	9	5	3	43	3	6	2	44	2	7	1	45	1
	10	8	0	41	0	8	0	41	0	6	2	39	2
	11	7	1	42	1	6	2	40	3	5	3	40	3
	12	7	0	44	0	4	3[b]	40	4[b]	3	4[b]	40	4[b]

[a] The dose of saline was 0.3 ml sc, and the dose of cocaine was 60 mg/kg sc. [b] Statistically significant in comparison with respective saline controls, $p < 0.05$.

correlation between fetal growth retardation and increased susceptibility to teratogenesis).

The central stimulatory effects of cocaine hydrochloride observed in the dams were minimal, and no fatalities occurred in the treated groups. These results agree with those of previous studies in which other teratogenic drugs also were nonlethal (19). Because of the mild excitability and nonlethality observed with the dose of cocaine hydrochloride employed in this study, there appears to be no correlation between the production of fetal malformations and increased maternal toxicity.

A critical period exists when a maximum frequency of teratogenic insults occurs. Although these periods overlap for different organs and structures, there is a definite time of susceptibility to teratogens, as was confirmed by this investigation. Interference with developmental or biochemical processes at a specific time during ontogenesis by either drug treatment or hypoxia causes defects that parallel the development period of the affected organ or structure. For example, the days of gestation during which the most prominent occurrence of defects was noted in this study corresponded to those reported previously (6, 8, 9, 19).

In addition, there was a correlation between cocaine hydrochloride and other specific treatments and conditions with respect to the production of comparable anomalies on similar days of gestation. For example, the most prominent day for the occurrence of exencephaly and sternebrae defects in this study was Day 9. Previous studies with different agents (8, 19) and hypoxic conditions (6, 20) also found maximum responses for exencephaly and vertebral defects on Day 9 of gestation. It appears that cocaine may decrease placental transfer of oxygen as a contributing factor to its teratogenicity, because hypoxic conditions elicit similar anomalies (*i.e.*, exencephaly) at similar times of the gestation period (6, 8, 19, 20).

A significant incidence of skeletal abnormalities appeared late in gestation whereas eye defects occurred early, paralleling closely the period of ontogenesis for these structures (21, 22) (Tables III and IV). The period of susceptibility of the CF-1 mouse fetus to the teratogenic effects of cocaine hydrochloride was evident throughout the range of drug administration in this study (Days 7–12) and was not confined to any particular day.

REFERENCES

(1) "The Pharmacological Basis of Therapeutics," 5th ed., L. S. Goodman and A. Gilman, Eds., Macmillan, New York, N.Y., 1975, p. 387.

(2) G. Cessian, *C. R. Soc. Biol.*, **157**, 2123 (1963).

(3) W. T. Sherman and R. F. Gautieri, *J. Pharm. Sci.*, **61**, 878 (1972).

(4) R. L. Brent and J. B. Franklin, *Science*, **132**, 89 (1960).

(5) C. T. Grabowski, *ibid.*, **134**, 1359 (1961).

(6) T. H. Ingalls, F. J. Curley, and R. A. Prindle, *N. Engl. J. Med.*, **247**, 758 (1952).

(7) T. H. Ingalls and F. J. Curley, *ibid.*, **257**, 1121 (1957).

(8) R. S. Thompson and R. F. Gautieri, *J. Pharm. Sci.*, **58**, 406 (1969).

(9) P. A. Arcuri and R. F. Gautieri, *ibid.*, **62**, 1626 (1973).

(10) R. F. Furchgott, S. M. Kirpekar, M. Rieker, and A. Schwab, *J. Pharmacol. Exp. Ther.*, **142**, 39 (1963).

(11) G. L. Johnson and J. B. Kahn, *ibid.*, **152**, 458 (1966).

(12) J. T. Litchfield and F. Wilcoxon, *ibid.*, **96**, 99 (1949).

(13) J. A. Russell, M. P. Mahalik, J. M. McDevitt, and R. F. Gautieri, *J. Pharm. Sci.*, **69**, 214 (1980).

(14) "Teratology Principles and Techniques," 3rd ed., J. G. Wilson and J. Warkany, Eds., University of Chicago, Chicago, Ill., 1965, p. 267.

(15) R. E. Staples and V. L. Schnell, *Stain Technol.*, **39**, 61 (1964).

(16) "Quantitative Zoology," G. G. Simpson, A. Roe, and R. C. Lewontin, Eds., Harcourt, Brace, New York, N.Y., 1960, pp. 176–186.

(17) J. E. Zellers and R. F. Gautieri, *J. Pharm. Sci.*, **66**, 1727 (1977).

(18) C. Chang, D. E. Mann, Jr., and R. F. Gautieri, *ibid.*, **66**, 1755 (1977).

(19) J. D. Iuliucci, Ph.D. thesis, Temple University, Philadelphia, Pa., 1971.

(20) U. Murakami and Y. Kameyama, *J. Embryol. Exp. Morphol.*, **11**, 107 (1963).

(21) "Bailey's Textbook of Histology," 17th ed., W. M. Copenhaver, D. E. Kelly, and R. L. Wood, Eds., Williams & Wilkins, Baltimore, Md., 1978, pp. 94–184, 731.

(22) "Foundations of Embryology," 3rd ed., B. M. Patten and B. M. Carlson, Eds., McGraw-Hill, New York, N.Y., 1974, p. 352.

ACKNOWLEDGMENTS

Abstracted in part from a thesis submitted by M. P. Mahalik to Temple University in partial fulfillment of the Master of Science degree requirements.

Sensitive GLC–Mass Spectrometric Determination of Chlorpheniramine in Serum

JOHN A. THOMPSON *x and FRED H. LEFFERT ‡

Received December 24, 1979, from the *School of Pharmacy, University of Colorado, Boulder, CO 80309, and the ‡National Jewish Hospital, Denver, CO 80206. Accepted for publication January 30, 1980.

Abstract □ A new method was developed for the quantitative analysis of chlorpheniramine in serum using the high sensitivity and selectivity of GLC–mass spectrometry with selected-ion monitoring. Intense fragment ions at *m/e* 203 and 207 from the drug and a tetradeuterated analog, respectively, are monitored continuously. The deuterated quantitation standard can be prepared by a simple exchange reaction. A linear calibration curve was obtained over the range of 0–160 ng/ml of serum using 85 ng of the standard/ml. The sensitivity limit is 1–2 ng/ml, and each serum extract can be analyzed in <2 min. The method was applied to a clinical pharmacokinetic investigation and was sufficiently sensitive to measure chlorpheniramine concentrations through at least 1.5 biological half-lives.

Keyphrases □ Chlorpheniramine—GLC–mass spectrometric analysis, pharmacokinetics, human serum □ GLC–mass spectrometry—analysis, chlorpheniramine, pharmacokinetics, human serum □ Pharmacokinetics—chlorpheniramine, GLC–mass spectrometric analysis, human serum □ Antihistaminics—chlorpheniramine, GLC–mass spectrometric analysis, human serum

Chlorpheniramine is an alkylamine antihistamine widely used to alleviate symptoms of the common cold and of allergic reactions. Despite the importance of this drug, little pharmacokinetic data have been published. In three studies using oral dosing with four to six adult subjects, biological half-lives of 12–15 hr (1), 24.5–36.3 hr (2), and 20.6–42.5 hr (3) were reported. The inconsistencies in the available pharmacokinetic data and the unavailability of data in subjects from different age groups with intravenous dosing established the need for further investigation in this area.

BACKGROUND

Chlorpheniramine is a potent antihistamine recommended for use in relatively small doses (4). Previous studies established the need for assay methods that are sufficiently sensitive to measure ~2 ng of drug/ml of serum (1, 2), a fact that contributed to the paucity of pharmacokinetic data. Although several analytical procedures are available to measure chlorpheniramine (1, 2, 5–10), most of the methods were developed to assay the drug in dosage forms or in urine; only a few of these methods have the necessary sensitivity to measure normal serum levels throughout a kinetic investigation.

TLC with liquid scintillation counting (1) cannot be used routinely because it requires administration of radiolabeled drug to human subjects. TLC followed by chemical conversion to an azo dye and subsequent colorimetric analysis (2) is a laborious procedure. The GLC procedure using electron-capture detection is also complicated (9). This method requires the liquid chromatographic separation of the drug from its metabolites and an oxidation reaction as preliminary steps.

Perhaps the best assay available with regard to sensitivity and analysis time involves GLC–mass spectrometry in the selected-ion mode (10). Disadvantages of this procedure for general application include the necessity to synthesize a deuterium-labeled analog of chlorpheniramine for use as the internal standard and the use of chemical-ionization techniques with trimethylamine as the reagent gas. Many analytical facilities are not equipped for chemical-ionization mass spectrometry.

The assay described in this report utilizes the high sensitivity and selectivity of GLC–mass spectrometry operated in the selected-ion mode with electron-impact ionization. A deuterium-labeled internal standard was prepared by a simple exchange reaction. Serum extracts can be analyzed in <2 min to a level of <2 ng of chlorpheniramine/ml. This method was applied to a clinical pharmacokinetic investigation.

EXPERIMENTAL

Materials—Chlorpheniramine[1], monodemethylchlorpheniramine[2], and didemethylchlorpheniramine[2] were obtained as maleate salts. The tetradeuterated analog of chlorpheniramine was prepared by dissolving 50 mg of the free base in 0.5 ml of 98% deuterosulfuric acid in deuterium oxide[3] (99.5 atom % deuterium) and heating the solution in a sealed glass tube at 120° for 6 hr. The contents were cooled and added slowly to 0.5 ml of deuterium oxide[4] (99.8 atom % deuterium).

Exchanged chlorpheniramine was isolated by adding the acidic solution dropwise to 4.2 ml of 5 *N* NaOH with ice bath cooling followed by extraction with ethyl acetate. The extract was washed with water and dried over anhydrous magnesium sulfate, and the solvent was evaporated. The resulting product was analyzed by TLC[5], GLC[6], high-performance liquid chromatography[7], PMR[8], and mass spectrometry[9] and was found to be chemically homogeneous. Deuterium was incorporated specifically in the *p*-chlorophenyl ring to >98% of the theoretical amount. Overall yields of tetradeuterated chlorpheniramine (chlorpheniramine-d_4) averaged 50%.

Instrumentation—A gas–liquid chromatograph–quadrupole mass spectrometer–computer system[9] was used. The gas–liquid chromatograph was equipped with a glass column (2 mm × 1.8 m) packed with 3% OV-22 on 80–100-mesh Supelcoport[10] and operated at a helium carrier gas flow rate of 30 ml/min. The injection port was maintained at 250°, the column oven was at 270°, the jet separator interface was at 270°, and the ion source was at 180°. The mass spectrometer was operated in the electron-impact mode with an electron energy of 70 ev.

Analytical Procedure—Serum samples, 1 or 2 ml, were placed in 16 × 125-mm disposable glass culture tubes, and 85 ng of chlorpheniramine-d_4 dissolved in 20 μl of methanol was added with vortex mixing. A 1-ml volume of saturated sodium borate solution and 8 ml of hexane[11] were added to each tube. The serum was extracted on a mechanical mixer[12] for 20 min and centrifuged at 2000 rpm for 3 min. The hexane layer was transferred to another tube and concentrated under a nitrogen stream at 40° to ~1 ml. To this solution was added 0.5 ml of 0.1 *N* HCl, the tubes were vortexed for 2 min and centrifuged, and the hexane layer was discarded.

The aqueous solution was brought to pH >9 with a saturated sodium borate solution and was extracted with 1 ml of ethyl acetate[13] by vortex mixing for 2 min. The mixture was centrifuged, and the ethyl acetate layer was transferred to a 1-ml vial[14]. The solvent was evaporated under a nitrogen stream with warming at 40°. The inner surface of the vial was rinsed with 100 μl of methanol[11] and evaporated to concentrate chlorpheniramine at the bottom. The residue was redissolved in 50 μl of acetonitrile[11], and the volume was reduced again under nitrogen to <5 μl.

Analyses were performed by injecting the entire sample (volumes of

[1] Courtesy of Cord Laboratories, Broomfield, Colo.
[2] Courtesy of Smith Kline and French Laboratories, Philadelphia, Pa.
[3] Merck and Co., Rahway, N.J.
[4] Norell Chemical Co., Landing, N.J.
[5] Silica gel G plates, Analtech, Newark, Del. The solvent system was ethyl acetate–methanol–ammonium hydroxide (45:4:1).
[6] Model 5710 with flame-ionization detector, Hewlett-Packard, Palo Alto, Calif. The column and column packing are described later and were operated at 180° with programming to 260° at 4°/min.
[7] Model 332 with 4.6 × 250-mm Partisil PAC column, Altex Scientific, Berkeley, Calif. The mobile phase was methanol.
[8] Model EM390, Varian, Sunnyvale, Calif.
[9] Model 5984A, Hewlett-Packard, Palo Alto, Calif.
[10] Supelco, Bellefonte, Pa.
[11] HPLC grade, Fisher Scientific Co., St. Louis, Mo.
[12] Labindustries, Berkeley, Calif.
[13] Spectranalyzed, Fisher Scientific Co., St. Louis, Mo.
[14] Reactivial, Pierce Chemical Co., Rockford, Ill.

0022-3549/80/0600-0707$01.00/0
© 1980, American Pharmaceutical Association

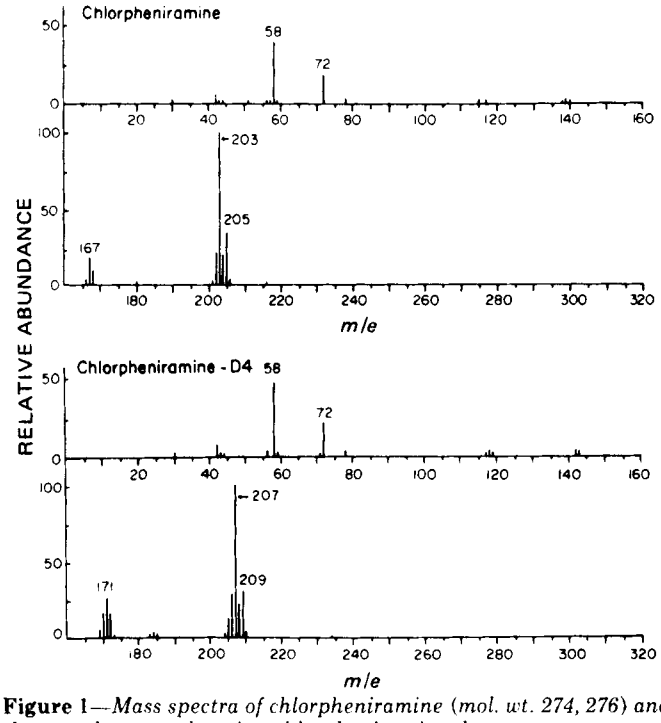

Figure 1—*Mass spectra of chlorpheniramine (mol. wt. 274, 276) and the tetradeuterated analog, chlorpheniramine-*d_4.

2–4 μl) into the gas–liquid chromatograph. After a 30-sec delay, the column effluent was directed into the mass spectrometer, which was operated under computer control in the selected-ion mode. Ions at *m/e* 203 and 207 were monitored continuously with 100-msec dwell times. The chlorpheniramine retention time was 50–60 sec under the conditions employed. Peak areas were determined with the standard system software[9]. Recoveries of chlorpheniramine consistently were in the range from 55 to 70%.

Standard Calibration Curve—Chlorpheniramine maleate was converted to the free base and purified by distillation under reduced pressure. A standard solution was prepared in methanol at a concentration of 1.0 mg/ml. Solutions in methanol were stable for at least 3 months when stored at −20°. Dilutions of the standard solution were prepared at 10, 1.0, and 0.10 μg/ml. Serum samples obtained from a drug-free volunteer were spiked with volumes of the appropriate solution so that no more than 20 μl was added to each milliliter of serum. Chlorpheniramine concentrations were 0, 3, 6, 10, 15, 20, 40, 60, 90, 120, and 160 ng/ml, and each sample contained 85 ng of chlorpheniramine-d_4. Extractions and analyses were performed as described using three or four samples at each concentration. Ratios of *m/e* 203 to 207 peak areas were plotted against known chlorpheniramine concentrations.

Pharmacokinetic Study—A 12-year-old male subject[15] with a history of allergic rhinitis was administered intravenously a 0.01-mg/kg dose of chlorpheniramine maleate over 5 min after removal of a control blood

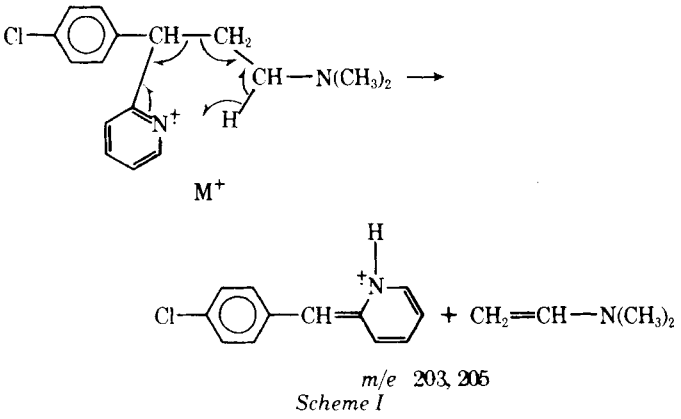

Scheme I

[15] Treated in the Clinical Research Unit of the National Jewish Hospital, Denver, CO 80206.

Table I—Hydrogen–Deuterium Exchange in the *p*-Chlorophenyl Group of Chlorpheniramine at 100°

Reaction Time, hr	Deuterium Incorporation[a], % of theoretical
0.17	28
0.33	43
1.0	58
4.0	74
8.5	86
14.6	94
24.0	96
48.0	>98

[a] Determined by PMR spectroscopy.

sample. Blood samples (5–8 ml) were drawn periodically, and the serum was prepared immediately and stored at −70° until it was analyzed. It was established that chlorpheniramine is stable under these conditions for at least 1 year. Analyses were performed as described, and peak ratios were converted to chlorpheniramine concentrations with reference to the standard curve. The plasma concentration *versus* time data were computer fitted (11) to a biexponential equation. After correction for the 5-min infusion period, pharmacokinetic parameters were calculated using standard methods (12).

RESULTS

The electron-impact mass spectrum of chlorpheniramine (Fig. 1) reveals an intense ion at *m/e* 203, which probably is formed by fragmentation of the molecular ion (Scheme I). A complementary ion containing chlorine 37 occurs at *m/e* 205. The relatively high mass and intensity of the *m/e* 203 ion provide an excellent opportunity for quantitation by GLC–mass spectrometry with selected-ion monitoring. The preferred internal standards for this technique are isotopic variants of the compounds to be measured (13). Inspection of the chlorpheniramine spectrum reveals no ions with *m/e* values higher than 206 (except for a small *m/e* 216 ion). Therefore, a deuterated analog should contain at least four deuterium atoms in the part of the molecule that is retained in the fragment ion.

Conditions have been developed for the efficient exchange of the four *p*-chlorophenyl hydrogens for deuterium atoms. The progress of this exchange reaction is shown in Table I. Two hydrogens are exchanged in less than 1 hr at 100°, and the reaction is >98% complete after 48 hr. At 120°, exchange is virtually complete after only 6 hr. A mass spectrum of the tetradeuterated analog of chlorpheniramine (chlorpheniramine-d_4) is shown in Fig. 1. The base peak is shifted to *m/e* 207, and no peak occurs at *m/e* 203 that would interfere with chlorpheniramine quantitation.

The brominated analog of chlorpheniramine is another useful antihistamine that can be quantitated by a similar procedure involving preparation of a tetradeuterated internal standard. Fragmentation of brompheniramine produces a mass spectrum with intense ions at *m/e* 247 and 249 (containing bromine 79 and bromine 81, respectively) with no ions of *m/e* higher than 250. The exchange reaction proceeds in a similar manner to yield brompheniramine-d_4 with intense ions at *m/e* 251 and 253.

A standard calibration curve was developed by adding chlorpheniramine in amounts from 0 to 160 ng together with 85 ng of chlorpheniramine-d_4 to 1.0-ml serum samples and extracting these samples as described under *Experimental*. Extracts were analyzed by monitoring the ion currents for ions at *m/e* 203 and 207. A background signal normally is observed at *m/e* 207 due to bleeding of the silicone rubber septum and of the GLC stationary liquid phase. This relatively small and constant signal easily can be subtracted from the signal of chlorpheniramine-d_4.

With the chromatographic conditions used, the retention time of the drug is 50–60 sec. Typical ion-current profiles obtained with a serum extract containing only the internal standard and with an extract containing both the drug and the internal standard are shown in Fig. 2. Analyses of serum samples yielded data for calculation of a regression line with a correlation coefficient of 0.998. Chlorpheniramine was added to four serum samples (2.0 ml each) at 4.0 ng/ml together with the internal standard. These samples were determined to contain 4.2 ± 0.2 ng of drug/ml (mean ± *SD*). The maximum sensitivity of the method is 1–2 ng/ml using 2 ml of serum.

The principal metabolites of chlorpheniramine that could interfere with the analysis are the products of mono- and di-*N*-demethylation (14,

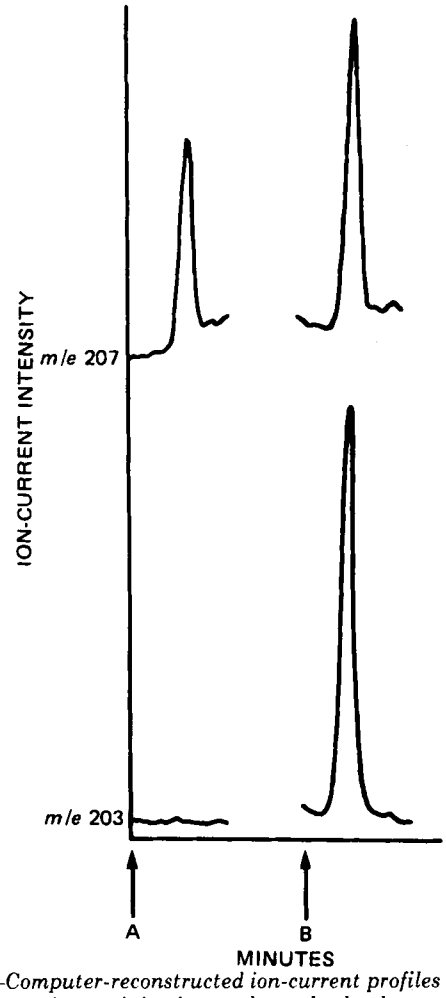

Figure 2—*Computer-reconstructed ion-current profiles of serum extracts. Extract A containing internal standard only was injected at* t = 0. *Extract B containing the internal standard and 10 ng of chlorpheniramine was injected at* t = 2 *min.*

15). The *m/e* 203 ion formed by fragmentation and loss of the amino group appears in the mass spectra of both metabolites. However, with the GLC conditions used in this work, the drug is well separated from its metabolites. The ion-current profiles of chlorpheniramine and monodemethylchlorpheniramine are shown in Fig. 3. The retention time of didemethylchlorpheniramine is greater than that of the metabolite shown, eliminating the possibility of interference with the drug.

The quantitative procedure described here was applied to a pharmacokinetic study of chlorpheniramine in a 12-year-old male subject. The plasma concentration *versus* time curve is shown in Fig. 4, and the selected pharmacokinetic parameters calculated from these data are summarized in Table II.

DISCUSSION

Pharmacokinetic studies of chlorpheniramine require methods capable of producing reliable quantitative data over the range of 2–100 ng/ml of serum. The high sensitivity of the technique involving GLC–mass spectrometry with selected-ion monitoring is particularly well suited to this analysis because of the favorable fragmentation pattern of chlorpheniramine. A high percentage of the total ion current of the compound is due to the *m/e* 203 ion. The selective nature of this analytical technique allows the use of chromatographic conditions with which analyses can be completed rapidly and without interferences from other compounds.

Table II—Pharmacokinetic Parameters for Chlorpheniramine Administered Intravenously to a 12-Year-Old Male Subject

Parameter	Value
Initial dilution volume (V_c)	298.2 ml/kg
Volume of distribution during postdistribution phase (V_β)	562.8 ml/kg
Total body clearance	0.415 ml/min/kg
$t_{1/2}, \alpha$	0.53 hr
$t_{1/2}, \beta$	15.6 hr

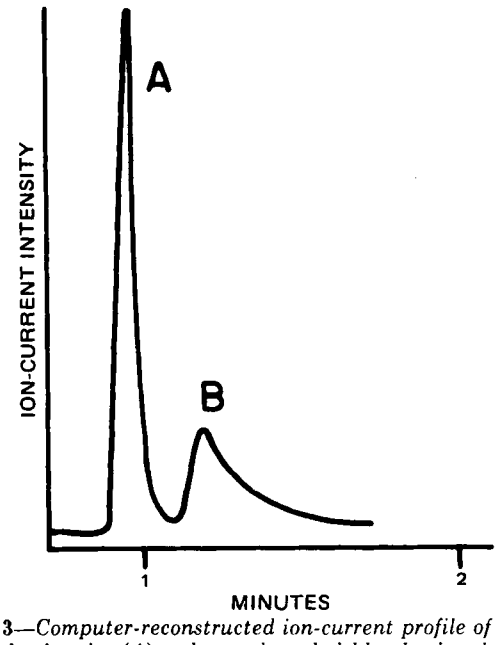

Figure 3—*Computer-reconstructed ion-current profile of a mixture of chlorpheniramine (A) and monodemethylchlorpheniramine (B). The ion current at* m/e *203 was monitored.*

The assay reported here is sufficiently sensitive to measure serum levels 24 hr after a single intravenous dose of 0.01 mg/kg. Each extract can be analyzed in <2 min. The chlorpheniramine assay using GLC–mass spectrometry that was published previously (10) involved the use of chemical-ionization conditions. However, the present results show that

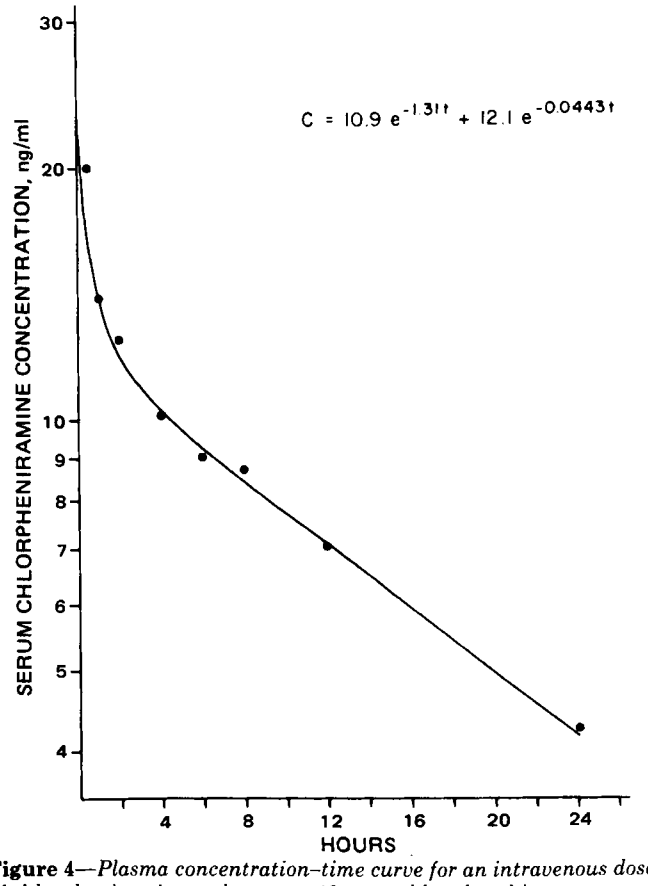

Figure 4—*Plasma concentration–time curve for an intravenous dose of chlorpheniramine maleate to a 12-year-old male subject.*

the more common method of electron-impact ionization is suitable. In addition, the previous investigators used a deuterated analog of chlorpheniramine that must be synthesized. The standard used in the present work can be prepared by a simple exchange reaction and without purification of the deuterated product.

The pharmacokinetic study conducted with one patient demonstrates the utility of the assay. Drug levels during the elimination (β) phase were in the range of 4–10 ng/ml of serum through 24 hr after dosing. These data demonstrate sufficient sensitivity to measure serum levels for a period in excess of 1.5 half-lives of the drug. Biological half-lives reported recently for adults after oral dosing are somewhat higher (2, 3) than the half-life determined in the present study. The young age of the patient and the drug administration route could explain the difference. Work is in progress using the assay described here to obtain pharmacokinetic data for a large group of subjects.

REFERENCES

(1) E. A. Peets, M. Jackson, and S. Symchowicz, *J. Pharmacol. Exp. Ther.*, **180,** 464 (1972).

(2) P. Haefelfinger, *J. Chromatogr.*, **124,** 351 (1976).

(3) W. L. Chiou, N. K. Athanikar, and S.-M. Huang, *N. Engl. J. Med.*, **300,** 501 (1979).

(4) "The Pharmacological Basis of Therapeutics," 5th ed., L. S. Goodman and A. Gilman, Eds., Macmillan, New York, N.Y., 1975, p. 609.

(5) S. Hanna and A. Tang, *J. Pharm. Sci.*, **63,** 1954 (1974).

(6) A. Cometti, G. Bagnasco, and N. Maggi, *ibid.*, **60,** 1074 (1971).

(7) H. Kinsun, M. A. Moulin, and E. C. Savini, *ibid.*, **67,** 118 (1978).

(8) C. M. Lai, R. G. Stoll, Z. M. Look, and A. Yacobi, *ibid.*, **68,** 1243 (1979).

(9) J. W. Barnhart and J. D. Johnson, *Anal. Chem.*, **49,** 1085 (1977).

(10) H. Miyazaki and H. Abuki, *Chem. Pharm. Bull.*, **24,** 2572 (1976).

(11) C. M. Metzler, G. L. Elfring, and A. J. McEwen, *Biometrics*, **30,** 562 (1974).

(12) M. Gibaldi and D. Perrier, "Pharmacokinetics," Dekker, New York, N.Y., 1975.

(13) B. J. Millard, "Quantitative Mass Spectrometry," Heyden and Sons, London, England, 1978, pp. 26–28, 60.

(14) P. Kabasakalian, M. Taggart, and E. Townley, *J. Pharm. Sci.*, **57,** 856 (1968).

(15) E. A. Peets, R. Weinstein, W. Bullard, and S. Symchowicz, *Arch. Int. Pharmacodyn. Ther.*, **199,** 172 (1972).

ACKNOWLEDGMENTS

Supported in part by the Council for Research and Creative Work of the University of Colorado.

The authors thank Dr. Duane Bloedow for assistance with the pharmacokinetic calculations.

Determination of Chlorambucil in Plasma by GLC with Selected-Ion Monitoring

HANS EHRSSON *x, STAFFAN EKSBORG *, INGER WALLIN *, YVONNE MÅRDE ‡, and BO JOANSSON §

Received September 5, 1979, from the **Karolinska Pharmacy, the* ‡*Laboratory for Mass Spectrometry, Karolinska Institut, and the* §*Department of Oncology, Karolinska Hospital, Box 60024, S-104 01 Stockholm, Sweden.* Accepted for publication January 25, 1980.

Abstract □ A GLC technique with selected-ion monitoring is described for chlorambucil determination in plasma using [^{2}H]chlorambucil as the internal standard. Chlorambucil is extracted from plasma with methylene chloride at pH 3 and converted to a thiazane derivative by reaction with 0.1 *M* sodium sulfide at 80°. The carboxylic group of the chlorambucil derivative is derivatized with allyl bromide using extractive alkylation. Analysis by selected-ion monitoring was performed by focusing at *m/e* 305 (M) and 313. The relative standard deviation was ±5% (n = 5) at the 10-ng/ml level.

Keyphrases □ Chlorambucil—GLC determination with selected-ion monitoring, plasma □ GLC—analysis, chlorambucil, selected-ion monitoring, plasma □ Antineoplastics—chlorambucil, GLC determination with selected-ion monitoring, plasma

Chlorambucil, a nitrogen mustard drug, is used for the treatment of neoplastic diseases. The fate of the drug in humans is partially unknown since analytical methods with sufficient sensitivity and selectivity have not been available. A mass fragmentographic method involving derivatization of the carboxylic group of chlorambucil by methylation was published recently (1). However, large variations in the GLC yield were observed in these laboratories after a derivatization involving alkylation, probably as a result of degradation of the nitrogen mustard group in the GLC system.

This paper presents a GLC technique using selected-ion monitoring for the determination of chlorambucil in plasma. The nitrogen mustard group is converted to a thiazane by reaction with sodium sulfide, followed by extractive alkylation of the carboxylic group.

EXPERIMENTAL

Synthesis of 4-[4-(Thiazane-4-yl)phenyl]butyric Acid (I)—Chlorambucil (25 mg) was dissolved in 10 ml of 0.1 *M* sodium sulfide and heated for 1 hr at 80°. The solution was cooled, acidified (pH ~3) with phosphoric acid, and extracted with methylene chloride (10 ml). The organic phase was separated and evaporated to dryness. The residue was recrystallized from methylene chloride–*n*-hexane (mp 81–82°). The purity (~97%) was established by TLC[1] and potentiometric titration with sodium hydroxide.

The mass spectrum[2] was consistent with the expected structure. There were prominent peaks at *m/e* 266 (20%), 265 (100), 218 (13), 193 (14), 192 (77), 191 (59), 132 (24), 131 (52), 130 (14), 118 (52), 117 (13), and 91 (11). No peak was observed at *m/e* 297, thus establishing that no dithiazane was formed (*cf.*, Ref. 2).

Reaction of Chlorambucil with Sodium Sulfide—Chlorambucil in methanol (0.5 ml) was mixed with an aqueous sodium sulfide solution (10 ml), giving a final chlorambucil concentration of 4 μg/ml. The yield of I was established by liquid chromatography[3] after acidifying part of the solution. The derivatization yields were calculated using the synthetically prepared I as a reference compound.

[1] Silica 60, F_{254}, 0.25 mm, Merck, Darmstadt, West Germany; the eluting solvent was methylene chloride–ethyl acetate (8:2).

[2] LKB 2091 with direct inlet; the ionizing energy was 70 ev.

[3] The chromatographic equipment used was described in Ref. 3. The mobile phase was methanol–water–acetic acid (0.1 *M*) (70:20:10). The support was LiChrosorb RP-18 from Merck, Darmstadt, West Germany.

0022-3549/80/0600-0710$01.00/0

© 1980, American Pharmaceutical Association

the more common method of electron-impact ionization is suitable. In addition, the previous investigators used a deuterated analog of chlorpheniramine that must be synthesized. The standard used in the present work can be prepared by a simple exchange reaction and without purification of the deuterated product.

The pharmacokinetic study conducted with one patient demonstrates the utility of the assay. Drug levels during the elimination (β) phase were in the range of 4–10 ng/ml of serum through 24 hr after dosing. These data demonstrate sufficient sensitivity to measure serum levels for a period in excess of 1.5 half-lives of the drug. Biological half-lives reported recently for adults after oral dosing are somewhat higher (2, 3) than the half-life determined in the present study. The young age of the patient and the drug administration route could explain the difference. Work is in progress using the assay described here to obtain pharmacokinetic data for a large group of subjects.

REFERENCES

(1) E. A. Peets, M. Jackson, and S. Symchowicz, *J. Pharmacol. Exp. Ther.*, **180,** 464 (1972).

(2) P. Haefelfinger, *J. Chromatogr.*, **124,** 351 (1976).

(3) W. L. Chiou, N. K. Athanikar, and S.-M. Huang, *N. Engl. J. Med.*, **300,** 501 (1979).

(4) "The Pharmacological Basis of Therapeutics," 5th ed., L. S. Goodman and A. Gilman, Eds., Macmillan, New York, N.Y., 1975, p. 609.

(5) S. Hanna and A. Tang, *J. Pharm. Sci.*, **63,** 1954 (1974).

(6) A. Cometti, G. Bagnasco, and N. Maggi, *ibid.*, **60,** 1074 (1971).

(7) H. Kinsun, M. A. Moulin, and E. C. Savini, *ibid.*, **67,** 118 (1978).

(8) C. M. Lai, R. G. Stoll, Z. M. Look, and A. Yacobi, *ibid.*, **68,** 1243 (1979).

(9) J. W. Barnhart and J. D. Johnson, *Anal. Chem.*, **49,** 1085 (1977).

(10) H. Miyazaki and H. Abuki, *Chem. Pharm. Bull.*, **24,** 2572 (1976).

(11) C. M. Metzler, G. L. Elfring, and A. J. McEwen, *Biometrics*, **30,** 562 (1974).

(12) M. Gibaldi and D. Perrier, "Pharmacokinetics," Dekker, New York, N.Y., 1975.

(13) B. J. Millard, "Quantitative Mass Spectrometry," Heyden and Sons, London, England, 1978, pp. 26–28, 60.

(14) P. Kabasakalian, M. Taggart, and E. Townley, *J. Pharm. Sci.*, **57,** 856 (1968).

(15) E. A. Peets, R. Weinstein, W. Bullard, and S. Symchowicz, *Arch. Int. Pharmacodyn. Ther.*, **199,** 172 (1972).

ACKNOWLEDGMENTS

Supported in part by the Council for Research and Creative Work of the University of Colorado.

The authors thank Dr. Duane Bloedow for assistance with the pharmacokinetic calculations.

Determination of Chlorambucil in Plasma by GLC with Selected-Ion Monitoring

HANS EHRSSON *x, STAFFAN EKSBORG *, INGER WALLIN *, YVONNE MÅRDE ‡, and BO JOANSSON §

Received September 5, 1979, from the **Karolinska Pharmacy, the* ‡*Laboratory for Mass Spectrometry, Karolinska Institut, and the* §*Department of Oncology, Karolinska Hospital, Box 60024, S-104 01 Stockholm, Sweden.* Accepted for publication January 25, 1980.

Abstract □ A GLC technique with selected-ion monitoring is described for chlorambucil determination in plasma using [^{2}H]chlorambucil as the internal standard. Chlorambucil is extracted from plasma with methylene chloride at pH 3 and converted to a thiazane derivative by reaction with 0.1 *M* sodium sulfide at 80°. The carboxylic group of the chlorambucil derivative is derivatized with allyl bromide using extractive alkylation. Analysis by selected-ion monitoring was performed by focusing at *m/e* 305 (M) and 313. The relative standard deviation was ±5% (n = 5) at the 10-ng/ml level.

Keyphrases □ Chlorambucil—GLC determination with selected-ion monitoring, plasma □ GLC—analysis, chlorambucil, selected-ion monitoring, plasma □ Antineoplastics—chlorambucil, GLC determination with selected-ion monitoring, plasma

Chlorambucil, a nitrogen mustard drug, is used for the treatment of neoplastic diseases. The fate of the drug in humans is partially unknown since analytical methods with sufficient sensitivity and selectivity have not been available. A mass fragmentographic method involving derivatization of the carboxylic group of chlorambucil by methylation was published recently (1). However, large variations in the GLC yield were observed in these laboratories after a derivatization involving alkylation, probably as a result of degradation of the nitrogen mustard group in the GLC system.

This paper presents a GLC technique using selected-ion monitoring for the determination of chlorambucil in plasma. The nitrogen mustard group is converted to a thiazane by reaction with sodium sulfide, followed by extractive alkylation of the carboxylic group.

EXPERIMENTAL

Synthesis of 4-[4-(Thiazane-4-yl)phenyl]butyric Acid (I)—Chlorambucil (25 mg) was dissolved in 10 ml of 0.1 *M* sodium sulfide and heated for 1 hr at 80°. The solution was cooled, acidified (pH ~3) with phosphoric acid, and extracted with methylene chloride (10 ml). The organic phase was separated and evaporated to dryness. The residue was recrystallized from methylene chloride–*n*-hexane (mp 81–82°). The purity (~97%) was established by TLC[1] and potentiometric titration with sodium hydroxide.

The mass spectrum[2] was consistent with the expected structure. There were prominent peaks at *m/e* 266 (20%), 265 (100), 218 (13), 193 (14), 192 (77), 191 (59), 132 (24), 131 (52), 130 (14), 118 (52), 117 (13), and 91 (11). No peak was observed at *m/e* 297, thus establishing that no dithiazane was formed (*cf.*, Ref. 2).

Reaction of Chlorambucil with Sodium Sulfide—Chlorambucil in methanol (0.5 ml) was mixed with an aqueous sodium sulfide solution (10 ml), giving a final chlorambucil concentration of 4 μg/ml. The yield of I was established by liquid chromatography[3] after acidifying part of the solution. The derivatization yields were calculated using the synthetically prepared I as a reference compound.

[1] Silica 60, F_{254}, 0.25 mm, Merck, Darmstadt, West Germany; the eluting solvent was methylene chloride–ethyl acetate (8:2).

[2] LKB 2091 with direct inlet; the ionizing energy was 70 ev.

[3] The chromatographic equipment used was described in Ref. 3. The mobile phase was methanol–water–acetic acid (0.1 *M*) (70:20:10). The support was LiChrosorb RP-18 from Merck, Darmstadt, West Germany.

0022-3549/80/0600-0710$01.00/0

© 1980, American Pharmaceutical Association

Table I—Acid Dissociation Constants and Partition Coefficients of Chlorambucil and I

Compound	Dissociation Constants[a]				log Partition Coefficient to Methylene Chloride
	pK_1	pK_2	pK_{12}	pK_{21}	
Chlorambucil[b]	—	2.49 ± 0.02	—	4.46 ± 0.04	4.45 ± 0.04
I	3.68 ± 0.02	4.12 ± 0.02	4.45 ± 0.03	4.00 ± 0.02	3.47 ± 0.04

[a] For definition, see Ref. 3. [b] Microscopic constants from Ref. 3.

Alkylation of I—A solution of the alkylating reagent (I) and the internal standard (decachlorobiphenyl) in methylene chloride (2 ml) was mixed with a solution (2 ml) of 0.1 *M* tetrabutylammonium in 0.1 *M* NaOH. The mixture was shaken at 25°. Part of the organic phase (0.1 ml) was separated and mixed with pH 4 phosphate buffer. The organic phase was analyzed by GLC with flame-ionization detection[4].

Extraction of Chlorambucil from Plasma—Plasma (2.00 ml) containing 8 μg of chlorambucil/ml was mixed with hydrochloric acid, phosphoric acid, or phosphate buffer (0.2 ml). The mixture was extracted with methylene chloride (2.00 ml) for 30 min. An aliquot of the organic phase was separated and evaporated to dryness with nitrogen gas. The residue was dissolved in methanol–water–acetic acid (0.1 *M*) (75:15:10) and analyzed by liquid chromatography[5].

Determination of Chlorambucil in Plasma—Plasma (2.00 ml) was mixed with 0.100 ml of [^{2}H]chlorambucil[6] in ethanol (2.00 μg/ml)[7] and 0.2 ml of 1 *M* phosphoric acid (final pH of ~3) and extracted with 5.00 ml of methylene chloride for 30 min. The organic phase was separated and extracted with 0.5 ml of 0.1 *M* sodium sulfide for 5 min. The aqueous phase was separated and heated for 15 min at 80°. Concentrated phosphoric acid (0.01 ml) was added, and hydrogen sulfide was removed with nitrogen for 5 min. Sodium hydroxide (12 *M*, 0.05 ml), 0.5 *M* tetrabutylammonium (0.2 ml), methylene chloride (0.2 ml), and allyl bromide (0.05 ml) were added, and then the mixture was shaken for 30 min at 25°. The organic phase (1–2 μl) was analyzed by GLC–mass spectrometry[8].

Handling of Blood Samples—Blood samples were obtained by venous puncture using 10-ml glass tubes containing 250 IU of lyophilized heparin. The plasma fraction was separated immediately, and an aliquot was mixed with the internal standard and frozen until it was assayed. Chlorambucil was stable for at least 2 weeks at −20°.

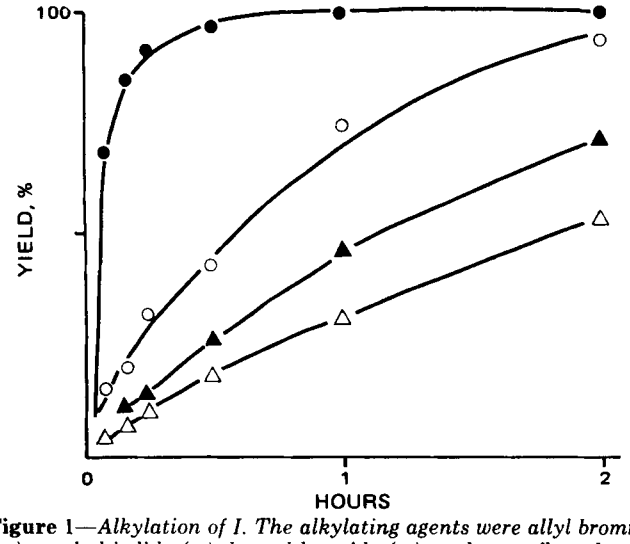

Figure 1—*Alkylation of I. The alkylating agents were allyl bromide (△), methyl iodide (▲), benzyl bromide (○), and pentafluorobenzyl bromide (●); the organic phase was 0.05* M *alkylating agent in methylene chloride; the aqueous phase was 0.100* M *tetrabutylammonium in 0.100* M *NaOH (equal phase volumes); and the temperature was 25.0°.*

[4] Varian 1400 gas–liquid chromatograph. The 1.5-m column was packed with 3% OV-17 on Gas Chrom Q and was operated at 275°.

[5] For the chromatographic equipment and conditions, see Ref. 3.

[6] Kindly supplied by AB Leo, Helsingborg, Sweden. The deuterium labeling was in the bis(2-chloroethyl)amino group.

[7] The internal standard was stable for at least 6 hr at 4° in ethanol.

[8] LKB 2091 with an ionizing energy of 70 ev. The 1.5-m column was packed with 5% OV-17 on Gas Chrom Q and was operated at 250°.

Table II—Extraction of Chlorambucil from Human Plasma

pH	log Distribution Ratio (Yield, %)	
	Calculated	Found
1	2.94 (99.9)	0.18 (60 ± 4)
3.2	4.35 (100.0)	>2 (102 ± 4)
7.0	1.91 (98.8)	0.10 (56 ± 2)

RESULTS AND DISCUSSION

Extraction from Plasma—A quantitative extraction of chlorambucil (log $D \sim 2$) theoretically should be obtained within the pH range of 1–7, as revealed by calculations based on the partition coefficient and the acid dissociation constants (Table I). However, the extraction of chlorambucil from plasma was quantitative only at pH ~3, while the yields at pH 1 and 7 were considerably lower (Table II). The extraction yields were unaffected by extraction times of 10–60 min. Obviously, a considerably higher extraction capacity is needed to obtain a quantitative recovery from plasma as compared to pure aqueous solutions. This effect might be due to the fact that chlorambucil is bound extensively to plasma albumin (4), giving a concomitant reduction in the partitioning to the organic phase.

Thiazane Formation—Nitrogen mustards previously were converted to thiazanes by reaction with sodium [^{35}S]sulfide for qualitative metabolic studies (2), but so far the reaction has not been studied quantitatively. The influence of the sodium sulfide concentration on the yield of thiazane was studied by liquid chromatography (Table III). The reaction was complete within 15 min at 80°. Hydrolysis of chlorambucil to 4-[*p*-[di(2-hydroxyethyl)amino]phenyl]butyric acid [*cf.*, Ref. 3] was insignificant, at least in 0.1 or 1 *M* sodium sulfide, reflecting the high nucleophilicity of the sulfide ion. The thiazane yield was only ~25% with a reaction time of 1 hr at 25° (0.10 *M* sodium sulfide).

Protolytic and Partition Properties of I—The protolytic properties of I were evaluated by a photometric technique described previously (3). The base strength of the amino group was considerably higher for I compared to chlorambucil (pK_2 = 4.12 and 2.49, respectively, Table I).

The lipophilic character of chlorambucil was decreased by the thiazane formation, as revealed by a decrease in the partition coefficient to methylene chloride by ~1 log unit (Table I).

Extractive Alkylation of I—The extractive alkylation of I was performed using methylene chloride as the organic phase and 0.1 *M* tetrabutylammonium in 0.1 *M* NaOH as the aqueous phase. More than 90% of I was extracted as an ion-pair into the organic phase, as calculated from the extraction constant ($\log E = 2.17 \pm 0.02$ and $-\log k_{diss} = 4.19 \pm 0.04$, determined according to Ref. 5). Therefore, an increase in the lipophilic character or concentration of the counterion should only slightly affect the reaction rate (6).

The alkylation rates using different alkylating agents are given in Fig. 1. Pentafluorobenzyl bromide showed the highest reactivity, while the lowest one was obtained with allyl bromide. By increasing the concen-

Table III—Influence of Sodium Sulfide Concentration on Yield of I[a]

Minutes	Sodium Sulfide Concentration, *M*		
	0.01	0.10	1.00
	Yield of I, %		
1	46	44	60
5	82	90	94
15	84	92	97
30	87	99	93
60	87	95	97

[a] The temperature was 80°.

Table IV—Relative Retention of Alkyl Derivatives of I [a]

Derivative	Relative Retention
Methyl	1.00
Allyl	1.46
Pentafluorobenzyl	3.50
Benzyl	7.25

[a] The column was packed with 3% OV-17 and was operated at 275°.

tration of allyl bromide to 1 *M*, a quantitative reaction was obtained within 30 min.

GLC Properties of Alkyl Derivatives of I—All of the alkyl derivatives chromatographed with excellent peak symmetry on an OV-17 column. The relative retentions of the derivatives are given in Table IV. The retention increased in the order methyl, allyl, pentafluorobenzyl, and benzyl. Due to their higher volatility, the methyl and allyl derivatives were selected for further studies regarding their selected-ion monitoring properties.

Selected-Ion Monitoring Properties of Methyl and Allyl Derivatives of I—The mass spectra of the allyl and methyl derivatives of I are given in Fig. 2. By focusing the mass spectrometer at the molecular ions of the compounds, a higher selectivity was obtained with respect to the metabolites formed by enzymatic transformation of the butyric acid side chain of chlorambucil as compared to focusing at *m/e* 192 [4-(thiazane-4-yl)benzyl fragment]. Derivatization with allyl bromide and focusing at *m/e* 305 were used in the analytical method since derivatization of plasma blanks with methyl iodide and detection at *m/e* 279 gave an interfering peak with a retention time close to that of the methyl derivative of I.

Internal Standard—Chlorambucil labeled with eight deuterium atoms in the nitrogen mustard moiety was used as the internal standard. It contained <1% of the unlabeled compound. The degradation rate of the internal standard did not differ significantly from that of chlorambucil.

Selectivity—No peaks interfering with the determination of chlorambucil or the internal standard were observed with blank plasma. The thiazane derivative of chlorambucil theoretically could be formed by the reaction of chlorambucil with endogenous sulfur-containing compounds and, if present, be codetermined with chlorambucil. Plasma samples (1, 2, 5, and 6 hr after an oral dose of 10 mg of chlorambucil) were analyzed according to the described procedure, except that the sodium sulfide extraction step was substituted with extraction with 0.1 *M* NaOH. In all cases, the thiazane concentration was below the detection limit (<1 ng/ml of plasma).

Precision—The standard curve obtained from plasma samples was linear in the range studied (10–640 ng/ml). A least-squares analysis gave a correlation coefficient of 0.9999, a slope of $7.96 \times 10^{-3} \pm 2.19 \times 10^{-5}$, and an intercept of $6.00 \times 10^{-2} \pm 7.36 \times 10^{-3}$. The relative standard deviation was ±5% ($n = 5$) at the 10-ng/ml level. A chromatogram obtained from the analysis of a sample containing 30 ng/ml is shown in Fig. 3.

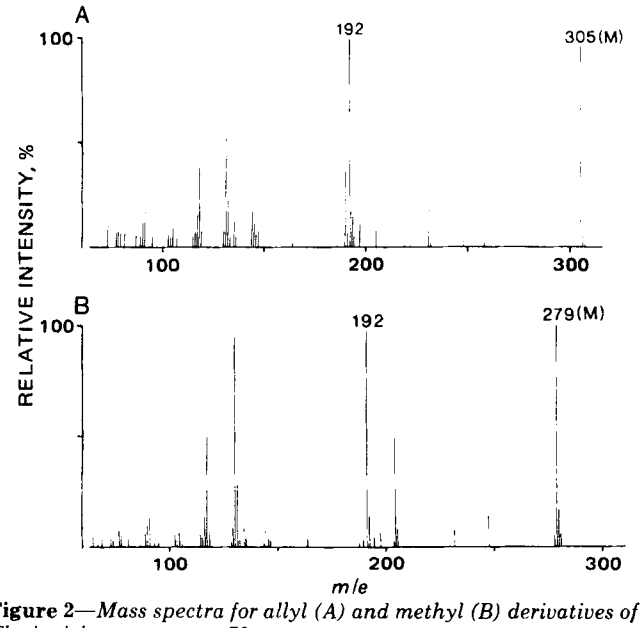

Figure 2—*Mass spectra for allyl (A) and methyl (B) derivatives of I. The ionizing energy was 70 ev.*

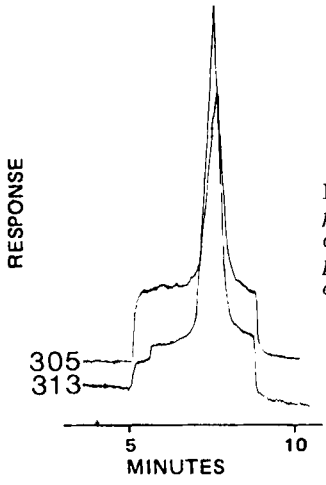

Figure 3—*Chromatogram obtained from patient plasma containing 30 ng of chlorambucil/ml. The chlorambucil peak was at* m/e *305, and the [²H]-chlorambucil was at* m/e *313.*

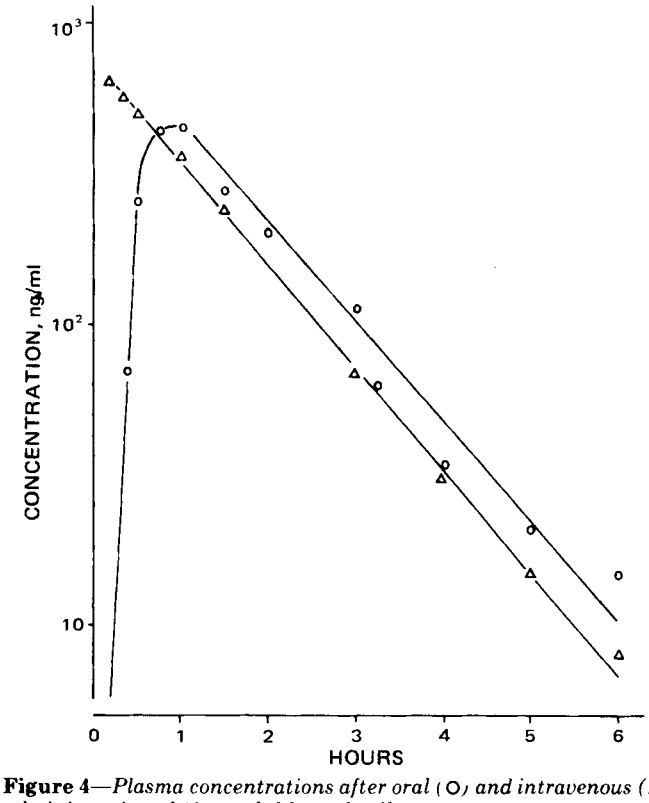

Figure 4—*Plasma concentrations after oral (○) and intravenous (△) administration of 10 mg of chlorambucil.*

Analysis of Plasma from Patients Undergoing Chlorambucil Treatment—The plasma concentration–time profile from a patient receiving 10 mg of chlorambucil orally and intravenously is shown in Fig. 4. A detailed study on the pharmacokinetics of chlorambucil will be published later.

REFERENCES

(1) T. Jakhammer, A. Olsson, and L. Svensson, *Acta Pharm. Suec.*, **14**, 485 (1977).

(2) A. B. Foster, A. M. Gilsenan, I. P. Horváth, M. Jarman, and M. J. Tisdale, *Biochem. Pharmacol.*, **24**, 71 (1975).

(3) H. Ehrsson, S. Eksborg, I. Wallin, and S. O. Nilsson, *J. Pharm. Sci.*, in press.

(4) J. H. Linford, *Biochem. Pharmacol.*, 8, 343 (1961).

(5) K. Gustavii and G. Schill, *Acta Pharm. Suec.*, **3**, 259 (1966).

(6) A. M. Tivert and K. Gustavii, *ibid.*, **16**, 1 (1979).

Video Characterization of Flume Patterns of Inhalation Aerosols

S. MISZUK *x, B. M. GUPTA ‡, F. C. CHEN *, C. CLAWANS ‡, and J. Z. KNAPP *

Received October 4, 1979, from **R&D Engineering Department and ‡Pharmaceutical Research and Development, Schering-Plough Corporation, Bloomfield, NJ 07003.* Accepted for publication January 30, 1980.

Abstract □ An *in vitro* technique was developed to characterize the intermittent flume patterns associated with the short bursts of metered-dose aerosols. Two orthogonal video images are utilized to describe the complex shape and direction of the flume pattern. This technique facilitates the evaluation of components manufactured by different suppliers.

Keyphrases □ Aerosols, inhalation—characterization of flume pattern, video technique compared with chemical analysis, delivery systems analyzed □ Delivery systems—inhalation aerosols, flume pattern characterized by video technique □ Distribution—of drug in lung alveoli, analysis of delivery systems, inhalation aerosols, flume patterns characterized by video technique

Various test procedures have been developed to evaluate aerosol products (1). The test methods for delivery rate, pressure measurement, unit spray sampling, container sampling, and propellents analysis are included in NF XIV (2). Particle-size analysis and spray patterns are among several tests that should be performed on inhalation aerosols to ensure their therapeutic effectiveness.

BACKGROUND

Extensive research (3) has been conducted on the relationship of the particle size of an active drug to its distribution and retention in the lungs. The conflict of theories and experimental results has been attributed to such variables as the species of animal used, nonuniform breathing rates, methods of measuring the particle-size distribution, methods of administering the agents used, and the effects of lung moisture content on the size of the inhaled particles (4–6). However, it generally is agreed that the depth of penetration increases with decreasing particle size while the whole lung retention increases with increasing particle size (7, 8). The optimum particle-size range for inhalation of medicinals into the lungs currently is accepted as 0.5–5 μm (9, 10).

While the importance of particle size in inhalation therapy has been well documented, other parameters affecting deposition and retention of inhaled matter have received less attention. Hayton (11) pointed out that, in many instances, a fairly high percentage of the formulation dispensed is retained in the oral adapter, the mouth, and the back of the throat instead of obtaining the desired deep penetration into the bronchi. Various methods have been useful for determining the aerosol dose delivered through an oral adapter to the desired portions of the lungs. Karig *et al.* (12) developed a compartmentalized lung chamber for the evaluation of oral inhalation aerosols. An *in vitro* method was established for evaluating the penetration of solid particles in the lungs using several aerosol generators. Sciarra and Cutie (13) developed a simulated respiratory system for the *in vitro* evaluation of two differently designed oral inhalation delivery systems and demonstrated that the deposition properties of the dose may be a function of the oral inhalation adapter.

The interest in therapeutic and diagnostic uses of inhalation aerosols can be directed at particles within the aerodynamic size range of 1–10 μm in diameter. When the alveolated regions of the lungs are the desired site of therapeutic action, the size is limited to 1–5 μm in diameter. The deposition of particles in the 1–10-μm aerodynamic diameter range is governed by inertial impaction and gravitational settling (14).

With the foregoing discussion, it can be concluded that the particle size and particle distribution within the aerosol cloud are the major factors affecting the site and mass of drug deposition in the airways. Other factors influencing aerosol penetration and deposition in the airways include the synchronization of the aerosol administration with inhalation and the aerosol mist characteristics. The spray pattern at different distances from the mouthpiece of the inhalation adapter can influence the penetration and deposition of particles in the desired portions of the lung. The nature of the flume pattern from an inhalation aerosol will be indicative of spray patterns at different distances.

The purpose of this study was to develop an *in vitro* technique to characterize the flume patterns to demonstrate physical equivalence of valve and actuator performance. With the same inhalation product, the technique also was used to screen actuators by studying their flume patterns. Manufacturers of inhalation aerosols must have alternative suppliers of package components, and this technique can be used as one criterion to demonstrate the equivalent performance of these alternative package components.

EXPERIMENTAL

Materials—The inhalation aerosol contained a suspension of a micronized corticosteroid in a fluorochlorocarbon propellent. The contents were packaged in a 16-ml aluminum can. Sixty-three-microliter valves and inhalation adapters from two suppliers (A and B) were used.

Video Systems—A high-resolution video camera[1] coupled with a macro lens[2] was used to capture the flume patterns of emitted sprays. These patterns were recorded on a 2.54-cm video tape recorder[3] (Fig. 1). This 2.5-cm broadcast quality video tape system provided a higher resolution of the flume patterns that the 1.3-cm video tape system in usual hobby use.

During playback, these flume patterns were displayed on a television monitor[4] from which the desired individual frames of flume pattern were photographed using a view camera[5]. Since video tape resolution is degraded by 50% whenever an individual frame is viewed, an accessory digital image enhancer[6] was employed to improve image contrast by gray-scale adjustment. The benefit of this adjustment was most visible along the fringe area of the aerosol flume. Image enhancement was applied only to the flume display on the video monitor. All of the original video data on the tape remained unchanged.

Imaging Requirements—Since the flume pattern is three dimensional, a single two-dimensional image cannot completely characterize

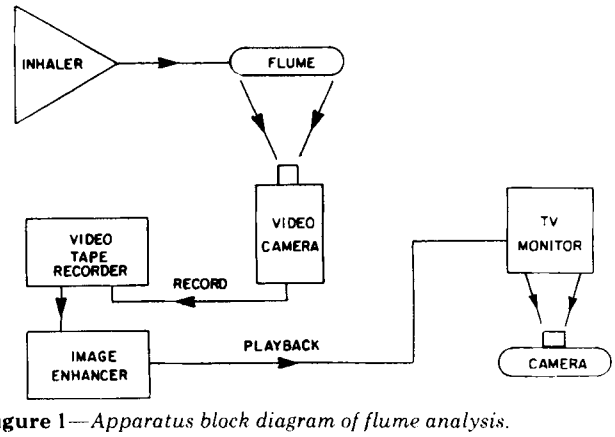

Figure 1—*Apparatus block diagram of flume analysis.*

[1] Model AVC 3200, Sony Corp., Tokyo, Japan.
[2] Cosmicar 25MM, Fl. 4 television lens, Cosmicar Corp., Tokyo, Japan.
[3] Model AV 3650, Sony Corp., Tokyo, Japan.
[4] Model TW19VL, Shiba Electric Corp., Tokyo, Japan.
[5] Model CC404, Calumet Corp., Elk Grove, Ill.
[6] Model 832, Dynasciences Corp., Chatsworth, Calif.

0022-3549/80/0600-0713$01.00/0
© 1980, American Pharmaceutical Association

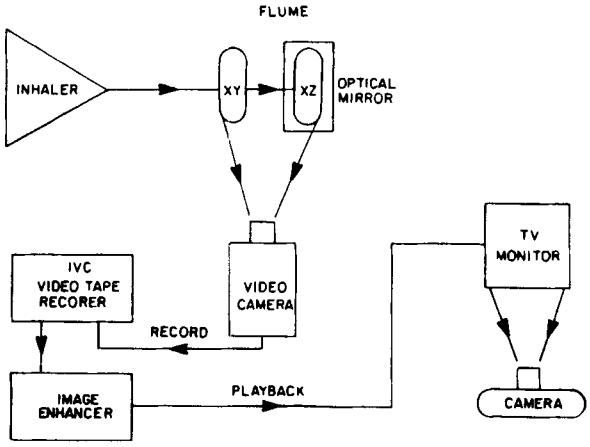

Figure 2—*Apparatus block diagram of flume analysis for orthogonal views.*

its complex shape and direction unless the pattern is symmetrical. When the flume pattern is asymmetric, a combination of two simultaneous orthogonal views is required to describe the character and direction of the flume pattern adequately.

In metered-dose aerosols, the total duration of the burst can be as short as 50 msec, so image delays between the two orthogonal views should be minimized. To achieve minimum delay, the same scan line was utilized for the corresponding image positions. This objective was accomplished by rotating the camera 90° from its usual viewing position. This action reduced the delay from milliseconds to microseconds for equivalent image portions, which was a prerequisite for accurate three-dimensional analysis.

For adequate visualization of the micrometer-sized aerosol droplets, a high-intensity light source was adjusted to deliver the scattered light from the flume droplets forward to the viewing lens (Fig. 2). For optimum contrast in orthogonal views, two flexible fiber optic bundles were used to ensure uniformity of the scattered light intensity in both views. A high quality optical front surface mirror, having a flatness of 0.5 λ, was positioned at a 45° angle to provide simultaneous images in the two orthogonal views of the video camera.

System Operation—Video and optical systems were assembled and arranged as shown in Figs. 2, 3, and 4 for orthogonal, side, and top views, respectively. A black screen was placed parallel to the flume as a background to achieve proper contrast.

The product to be tested, *i.e.*, an inhaler in its respective actuator, was placed in a fixed position (Fig. 4). An operator placed the recording system into the recording mode and subsequently actuated the product to emit a spray. After a single trial spray was emitted, flume patterns of the subsequent two sprays from that product were recorded by the video system. These series of sprays were identified on the video tape by an alphanumeric light-emitting diode configuration, which was recorded simultaneously during each spray burst. In the playback mode, the

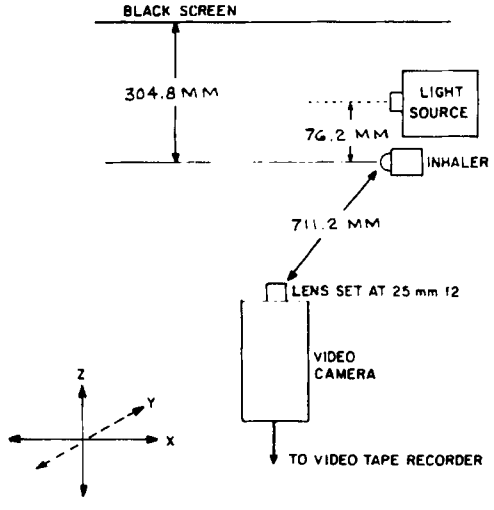

Figure 3—*Apparatus block diagram of flume analysis for side view.*

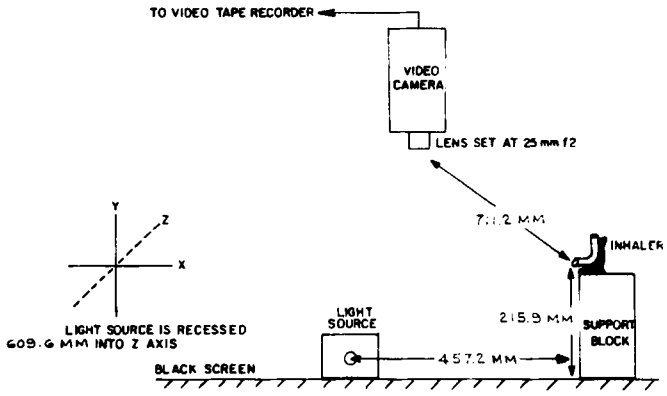

Figure 4—*Apparatus block diagram of flume analysis for top view.*

light-emitting diodes clearly identified the particular spray pattern being tested.

System Output—The output is a video image of the aerosol flume pattern that can be viewed on a video field basis (each field is spaced 16.7 msec apart). The total life of the flume pattern is available from the time it passes from the actuator until it is dissipated in the atmosphere. When flume patterns were observed on a frame-to-frame basis, flume size increased progressively up to the fourth frame (66.7 msec after flume commencement) and thereafter started dissipating. Therefore, the flume pattern in the fourth frame was selected to be photographed for comparison.

RESULTS AND DISCUSSION

Videotapes of flume patterns of the corticosteroid oral inhalers A and B were played and examined. Flume patterns were observed individually on a frame-to-frame basis; flume size increased progressively up to the fourth frame and thereafter started dissipating. For package components A and B, no significant difference was noticed in flume patterns of Sprays 1 and 2. Photographs of these flume patterns in the fourth frame for the top and side view are shown in Figs. 5 and 6, respectively. The similar shape and size of flume patterns for package components A and B indicate equivalent physical performance. This result suggests that the spray emitted from package components A and B will have a similar projectile and force to enter the throat and lung, suggesting equivalent dispensing of the drug by two different actuators to different parts of the respiratory system.

Application of this video system for screening actuators was extended to a nasal inhaler. Figures 7–9 are flume patterns of the orthogonal view of a nasal inhaler obtained using three actuators from the same lot. Each photograph also was taken during the fourth frame of a video field to establish a common basis for analysis.

A typical example for a good flume pattern is shown in Fig. 7. The aerosol spray patterns are symmetrical; if a line were drawn through the center of each flume, each half would be equal and that line would intersect the center of the actuator nozzle. This result indicates that the center of the aerosol spray pattern is at the center of the actuator. Moreover, the exit angles of the spray pattern in both views are parallel to the axis of the actuator nozzle in their respective views.

Marginal actuators yield poor flume patterns with one or more discrepancies with the described criteria for a good flume pattern as illustrated in Fig. 8. The flume patterns in both views exhibit a large displacement from the center of the actuator nozzle. This condition generally yields a poor or marginal delivery of product since a portion of the product is trapped on the inner wall of the nozzle and remains as a residue. In fact, with some actuators, the second burst showed streaking lines in the flume patterns. These lines were the corticosteroid, which was left as a residue in the nozzle and was evacuated with the second burst of propellent. Erratic delivery can be attributed to this actuator, *e.g.*, the first burst is low on product, and the second burst is much higher.

Figure 9 shows the flume pattern from an actuator with a defective nozzle; there is a slight burr around the exit jet of the nozzle. The right portion of the figure (the side view of the actuator) exhibits a very poor flume pattern with heavy streaking lines about the nozzle. These lines indicate a misdirection of the spray inside the nozzle piece. The other orthogonal view lacks these lines, which strongly suggests that two views are necessary for a proper flume definition.

Since the three actuators had a common canister of propellent and were evaluated at a similar video field, one actuator can be accepted as good,

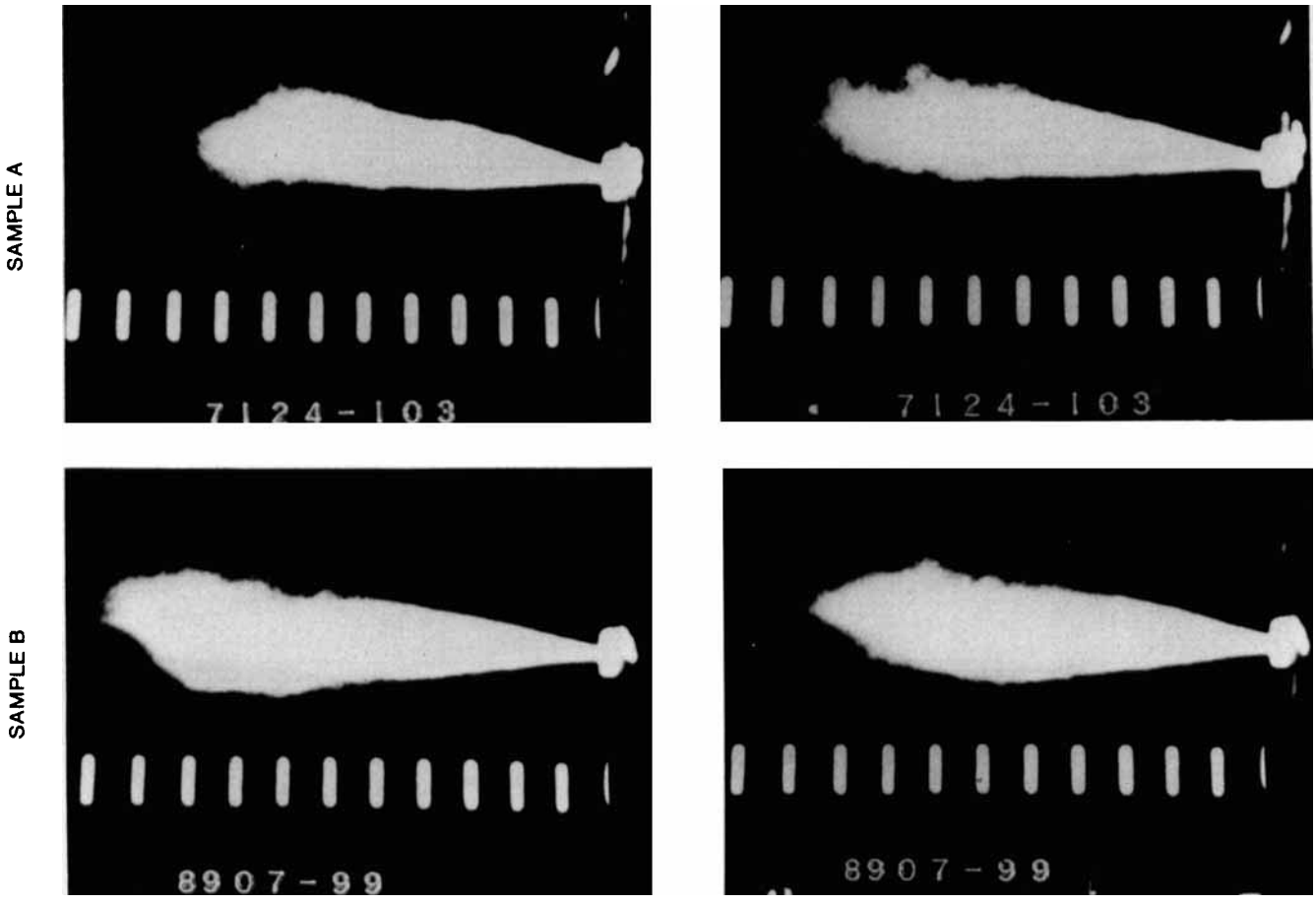

Figure 5—*Series of typical flume patterns that are shown in the top view.*

one as marginal, and one as bad. This video technique can be used to screen potentially bad actuators. To establish a comparison between the video technique and chemical analysis, 20 actuators were studied by both techniques. In the video technique, based on the described criteria, the quality of actuators was rated good (G), fair (F), and poor (P) (Table I).

The total amount of drug delivered from an actuator and the amount retained on the actuator were determined for 20 actuators by liquid chromatography. The ratio of B to A was calculated for each actuator, where A is the total amount of drug delivered through the actuator and B is the total amount of drug retained on the actuator. The smaller the ratio, the better is the rating. Actuators were rated from one to 20 based on the ratio. A rating of one was given to the actuator with the lowest ratio. Table I lists the ratings obtained by chemical analysis and the video technique. On the basis of these chemical analysis data, five actuators were rated as good, 10 as fair, and five as poor. These results compared very well with the results obtained by the video technique (Table II).

To increase the average amount of drug delivered through an actuator, the following two steps are necessary. First, the use of defective actuators should be eliminated by improving the incoming inspection of these units. Second, the design of the actuators should be modified to improve drug delivery.

The five actuators rated as good by the chemical test had an average delivery of 82%. However, the average yield of the five actuators rated as poor by the chemical test was 69%. To locate the defective parts of the actuators, the following experiments were performed.

The plastic inserts were replaced with machined-steel inserts, and the flume patterns were studied before and after the replacements. The replaced plastic inserts were inspected visually. These steel inserts gave an improved flume pattern after replacing plastic inserts with burrs inside

Table I—Comparison of Results Obtained by Chemical Analysis and the Video Technique

Actuator	B/A[a]	Analysis Ratings	
		Chemical	Video
I	0.185	2	G
II	0.636	20	P
III	0.515	18	P
IV	0.173	1	—[b]
V	0.224	6	F
VI	0.557	19	P
VII	0.345	13	P
VIII	0.229	8	F
IX	0.272	9	F
X	0.487	17	—[b]
XI	0.332	12	P
XII	0.199	4	G
XIII	0.214	5	G
XIV	0.307	11	P
XV	0.225	7	—[b]
XVI	0.467	16	P
XVII	0.304	10	G
XVIII	0.465	15	P
XIX	0.455	14	F
XX	0.197	3	G

[a] A is the amount of drug delivered through the actuator, and B is the amount of drug retained on the actuator. [b] Not available for video test.

Table II—Number of Actuators within Ratings According to Chemical Analysis and Video Technique

Rating Chemical Number	Number of Actuators within Rating Range	Video Ratings and Number of Actuators within Range		
		G[a]	F[a]	P[a]
1–5	5[b]	4	0	0
6–15	10[b]	1	4	4
16–20	5[b]	0	0	4

[a] G = good, F = fair, and P = poor. [b] One actuator not available for video test.

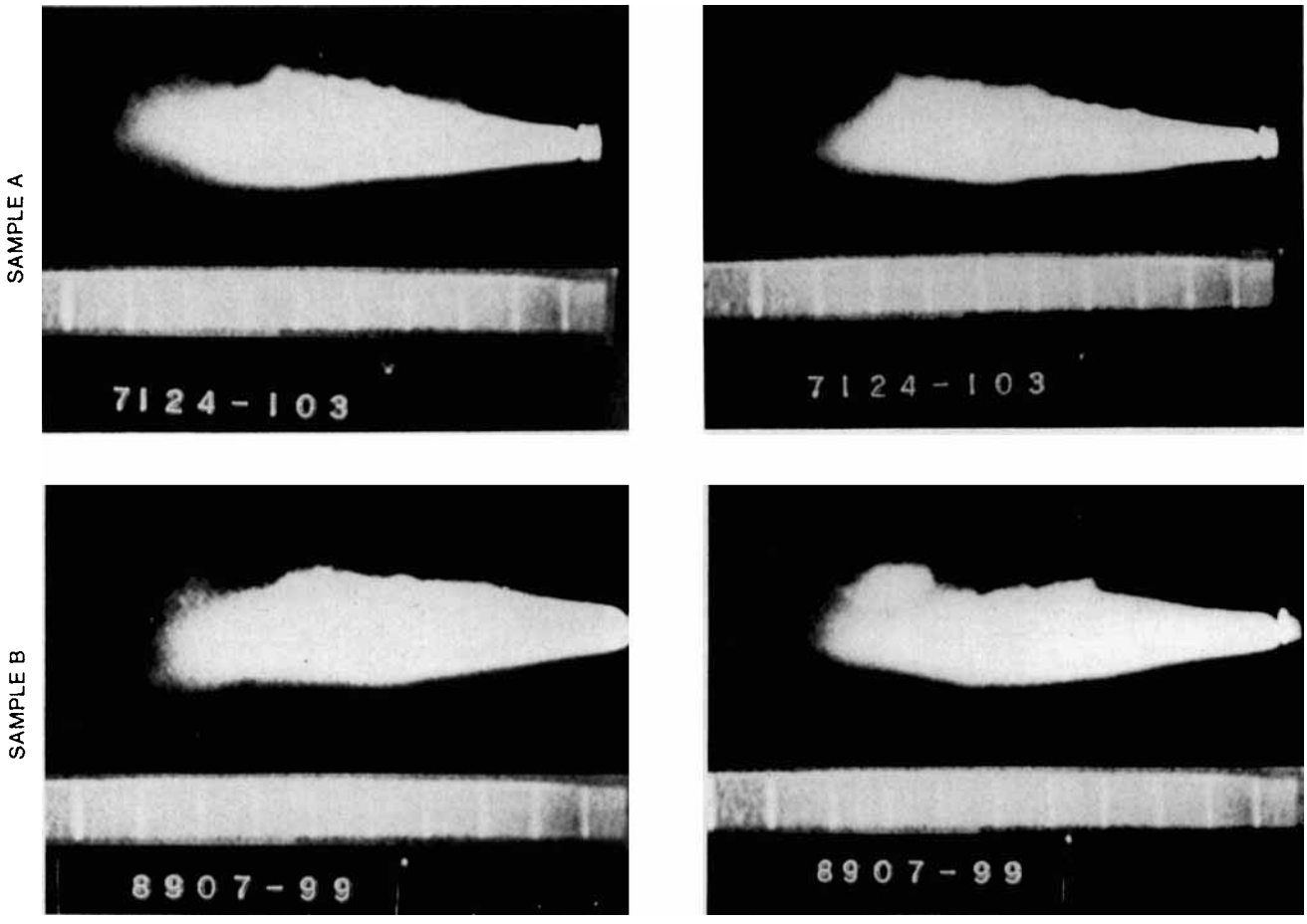

Figure 6—*Flume patterns in the side view of the same samples used in Fig. 5.*

the orifice or with irregular orifice shape. Otherwise, the flume patterns remained unchanged. This result shows that the aerosol ejected through the orifice with a nonzero exit angle with respect to the axis of the delivery tube was caused by skewed seating of the plastic insert. If the plastic inserts are inspected carefully before mounting in the actuators to eliminate those units showing burrs or other nonuniformity in either the rear or the insert tip, the yield of acceptable actuators can be improved.

The flume pattern of the vaporized liquid propellent shows that its spread was wider along the y axis than along the z axis because the propellent was accelerated first in the x–y plane and then along the x axis

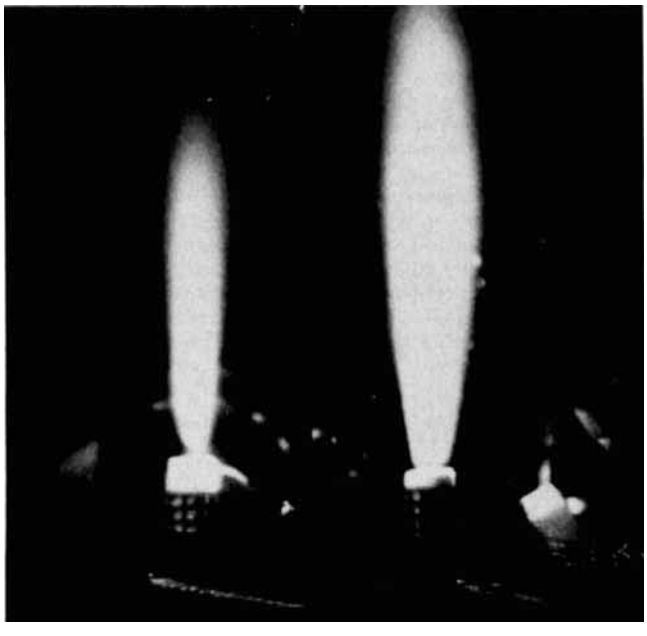

Figure 7—*Typical example of a good flume pattern in the orthogonal view.*

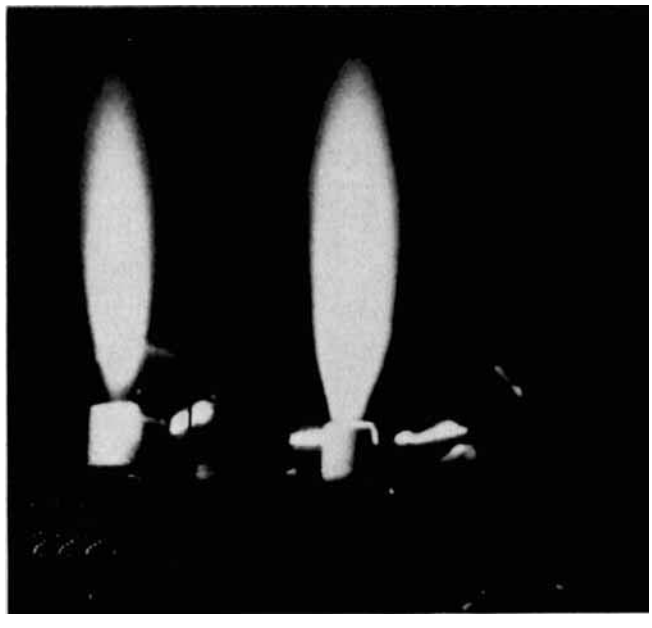

Figure 8—*Typical example of a marginal flume pattern in the orthogonal view.*

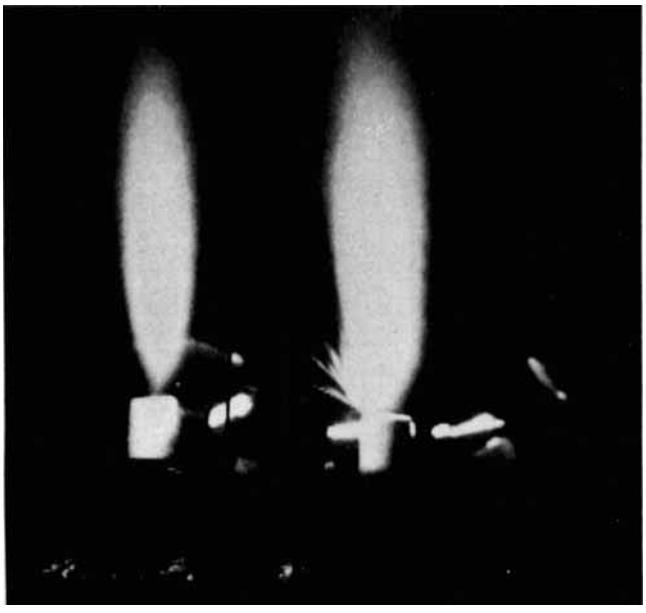

Figure 9—*Flume pattern from an actuator with a defect on its nozzle.*

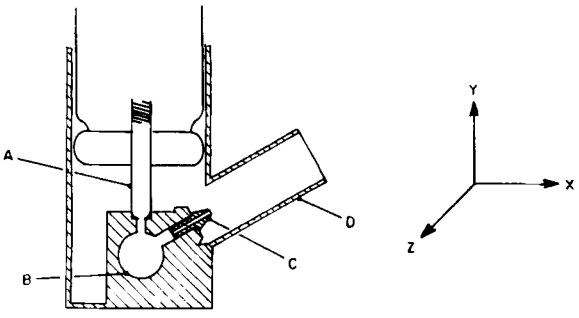

Figure 10—*Cross-sectional view of an actuator and product delivery system.*

(Fig. 10). Since the flume pattern was not cylindrically symmetrical, changing the cross section of the delivery tube from a circular to an elliptical shape with the major axis along the y axis can reduce the amount of drug trapped on the inner surface wall. The video technique also was used to study the flume patterns of an aerosol spray by varying the length of the discharging tip; as expected, the longer the tip, the narrower was the spread of the flume pattern. If the amount of drug retained inside the plastic insert is small compared with that retained on the inner wall of the delivery tube, the path length of the plastic insert could be increased.

After the propellent has been discharged and before it reaches Chamber B, the direction of acceleration has a negative component along the x axis. Thus, if one increases the angle between the axis of the plunger and the axis of the delivery tube, one can increase the drug delivery yield through the actuators.

REFERENCES

(1) "Aerosol Guide," Chemical Specialties Manufacturers Association, Washington, D.C., 1971.

(2) "The National Formulary," 14th ed., Mack Publishing Co., Easton, Pa., 1975, p. 849.

(3) L. Silverman, C. Billings, and H. W. First, "Particle Size Analysis in Industrial Hygiene," Academic, New York, N.Y., 1971.

(4) J. J. Sciarra and V. Lynch, *Aerosol Age*, **5**, 34 (1960).

(5) L. Dautrebande and W. Walkenhorst, *Arch. Int. Pharmacodyn. Ther.*, **162**, 194 (1966).

(6) J. L. Kanig, *J. Pharm. Sci.*, **52**, 513 (1963).

(7) L. Dautrebande, "Microaerosols," Academic, New York, N.Y., 1964.

(8) J. L. Kanig, *J. Pharm. Sci.*, **52**, 522 (1963).

(9) J. J. Sciarra, "International Encyclopedia of Pressurized Packaging Aerosols," Pergamon, New York, N.Y., 1966.

(10) A. B. Dobkin, "Ventilators and Inhalation Therapy," 2nd ed., Little, Brown, Boston, Mass., 1972.

(11) W. L. Hayton, *J. Am. Pharm. Assoc.*, **NS 16**, 201 (1976).

(12) A. W. Karig, G. E. Peck, and G. J. Sperandio, *J. Pharm. Sci.*, **62**, 811 (1973).

(13) J. J. Sciarra and A. Cutie, *ibid.*, **67**, 1428 (1978).

(14) P. E. Morrow, *Am. Rev. Resp. Dis.*, **110**, 88 (1974).

ACKNOWLEDGMENTS

The authors acknowledge Mr. Raymond Scharmach of the Food and Drug Administration for suggesting that flume patterns could serve as one way to show functional similarity between inhalation aerosol delivery systems.

Microcolumn Chromatographic Cleanup and GLC Determination of 11-Methyl-16,16-dimethylprostaglandin E_2 in Polyethylene Glycol 400 Solutions

RONALD F. QUADREL ˣ, SOOHEE LEE, and FRANCES M. BOGDANSKY

Received December 20, 1979, from the *Quality Control Department, Hoffmann-La Roche Inc., Nutley, NJ 07110.* Accepted for publication January 31, 1980.

Abstract □ An analytical procedure is described for the GLC determination of 11-methyl-16,16-dimethylprostaglandin E_2 in aqueous polyethylene glycol 400 solutions. Because of the nature of the carrier matrix, sample cleanup was required prior to GLC separation. Separation was achieved using a diethylaminoethylcellulose microcolumn. This procedure has proven to be amenable to routine analysis.

Keyphrases □ Prostaglandin analogs—GLC analysis, pre-GLC sample cleanup procedure, polyethylene glycol carrier matrix □ GLC—prostaglandin analog determination, sample cleanup prior to GLC, polyethylene glycol carrier matrix □ Polyethylene glycol—carrier matrix in aqueous prostaglandin analog solutions, GLC analysis, pre-GLC sample cleanup procedure

Research into the synthesis of prostaglandin analogs that provide increased metabolic and chemical stability over naturally occurring prostaglandins has focused on the prostanoid 11-methyl-16,16-dimethylprostaglandin E_2[1] (I), the structure of which differs only slightly from that of natural prostaglandin E_2 (II). Previous studies (1, 2) showed that I is a potent inhibitor of gastric acid secretion in humans and dogs with no appreciable side effects.

In compliance with the Good Laboratory Practices (GLP) regulations, aqueous solutions of I were analyzed as part of an analytical monitoring program for rat and dog toxicity studies. Many GLC and high-performance liquid chromatographic procedures have been published for the analysis of prostaglandin E_2 (3–13), but none was suitable for the present application because of interferences from excipients in the sample solutions.

This paper describes a sensitive and specific procedure for the analysis of I in aqueous media containing polyethylene glycol 400, butylated hydroxyanisole, and ascorbyl palmitate (III). The procedure involves the elimination of water and polyethylene glycol 400 by utilizing a diethylaminoethylcellulose microcolumn, conversion of I to the trimethylsilyl derivative, and GLC determination.

EXPERIMENTAL

Reagents—All solvents and chemicals were reagent grade unless otherwise specified.

Instrumentation—The gas chromatograph[2] was equipped with a hydrogen flame-ionization detector connected to an electronic chromatographic automation system[3] for peak area integration. The stainless steel column, 2.5 m × 2 mm i.d., was packed with 3% OV-1 on Chromosorb W-HP[4] (80–100 mesh) and conditioned at 320° for 24 hr under nitrogen at a flow rate of 30 ml/min. The instrument parameters were: injector temperature, 280°; detector temperature, 300°; carrier gas (nitrogen) flow rate, 30 ml/min; hydrogen flow rate, 30 ml/min; and air flow rate, 300 ml/min.

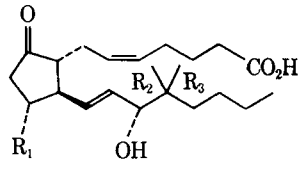

I: $R_1 = R_2 = R_3 = CH_3$
II: $R_1 = OH$, $R_2 = R_3 = H$

The column temperature was programmed stepwise isothermally from 0 to 12.5 min at 290°, followed by flash heating to 310° to elute III. Electrometer sensitivity was adjusted to give ~60% full-scale deflection for 8 μl of injected standard solution.

Sample Preparation—Aliquots of the sample solution (2.0 ml for I concentrations of >0.005% and 5.0 ml for those having <0.005%) were diluted to 50 ml with methanol.

Standard Preparation—Standard solutions were prepared by diluting I in methanol to give a final concentration of 8×10^{-3} mg/ml.

Internal Standard Preparation—Stock solutions of *n*-triacontane (IV), the internal standard, were prepared by dissolving 6 mg of IV in 50 ml of hexane. A 1.0-ml aliquot of this solution was added to a 12-ml conical flask and evaporated to dryness under a dry nitrogen stream. The residue was dissolved in 10 ml of trimethylsilylating reagent, which was a mixture of 60% hexamethyldisilazane[5] and 10% trimethylchlorosilane[5] in acetonitrile.

Microcolumn Cleanup Procedure—A diethylaminoethylcellulose[6] slurry was prepared by adding 300 ml of methanol to ~6.0 g of the ion-exchange medium. The slurry was degassed under vacuum for 30 min and transferred to a glass-stoppered solution bottle.

A glass column (15 cm × 6 mm i.d.) was used for the pre-GLC cleanup. The column, fitted with a hydrophilic polyethylene disk tapered to 1.65 mm i.d., was filled with the cellulose slurry to a gel height of 8 ± 1 mm (Fig. 1).

The column bed was washed with 2 ml of methanol, and the effluent was discarded. Based on the concentration of I, various volumes of the sample or standard solution (standard solution, 2.0 ml; samples with I concentrations of >0.02%, 2.0 ml; samples with I concentrations of <0.005%, 4.0 ml; and placebo, 4.0 ml) were applied to the top of the gel and allowed to absorb into the bed; the resulting effluent was discarded.

Interfering excipient substances were washed from the column with 4.0 ml of distilled water applied to the top of the gel bed, and the effluent was discarded. Residual water was removed from the gel by applying a

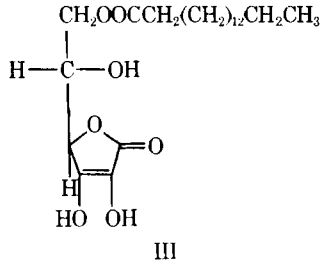

III

[1] Hoffmann-La Roche Inc., Nutley, N.J.
[2] Varian Aerograph model 3700, Varian Associates, Walnut Creek, Calif.
[3] Model 3385A, Hewlett-Packard, Palo Alto, Calif.
[4] Alltech Associates, Arlington Heights, Ill.
[5] Aldrich Chemical Co., Milwaukee, Wis.
[6] Preswollen DE-52, Whatman Inc., Clifton, N.J.

0022-3549/80/0600-0718$01.00/0
© 1980, American Pharmaceutical Association

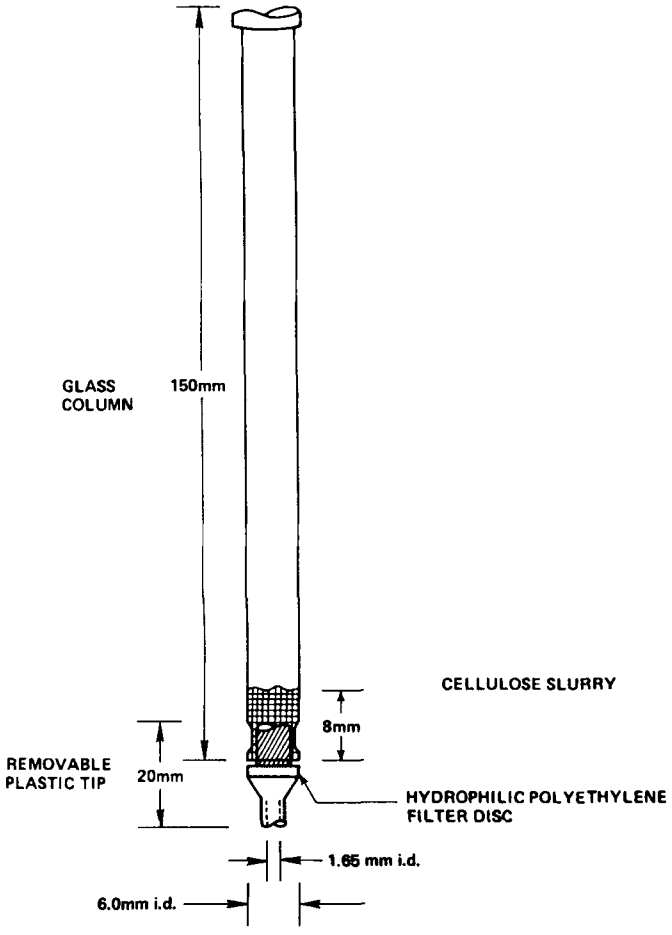

Figure 1—*Diethylaminoethylcellulose microcolumn utilized in pre-GLC sample cleanup procedure.*

gentle nitrogen stream to the top of the column for ~1 min. Compound I was eluted from the column with 7.0 ml of anhydrous ether, and the eluate was evaporated to dryness at room temperature under a nitrogen stream.

Preparation of Trimethylsilyl Derivatives—After the eluate was evaporated carefully to dryness, 400 μl of the trimethylsilylating reagent containing the internal standard (IV) was added, and the solution was left for 30 min at room temperature. This solution was injected onto the GLC column.

Calculations—The concentration of I in 40% polyethylene glycol 400 solutions was determined from:

$$\frac{\text{milligrams of I}}{\text{milliliters of solution}} = \left(\frac{X_{spl}}{Y_{spl}}\right)\left(\frac{Y_{std}}{X_{std}}\right)(C_{std})\left(\frac{DF}{V_I}\right) \qquad \text{(Eq. 1)}$$

where X_{spl} and X_{std} are the peak areas of I in the sample and standard preparations, respectively; Y_{spl} and Y_{std} are the peak areas of IV for the sample and standard, respectively; V_I is the volume of the initial sample aliquot (milliliters); DF is the sample dilution factor; and C_{std} is the concentration of I in the standard solution (milligrams per milliliter).

RESULTS AND DISCUSSION

The samples studied were aqueous solutions containing 40% polyethylene glycol 400, 0.05% ascorbyl palmitate, 0.02% butylated hydroxyanisole, and 0.001–0.02% (0.01–0.2 mg/ml) of I. In all cases, pre-GLC sample cleanup was necessary to eliminate sample matrix interferences.

Column chromatographic techniques have been used widely for sample preparation and cleanup procedures, but few applications employing ion-exchange resins have been reported where the adsorptive properties of the resin matrix were a factor in the separation. By utilizing ion-exchange resins and either nonpolar solvents or electrolyte-free water–alcohol mixtures as eluents, separations have been achieved for sugars (14), alcohols (15), organic acids (16), analgesics (17), and benzene derivatives (18, 19). In each of these applications, the dominant mechanism was adsorption onto the resin matrix with little or no ion exchange occurring.

With this technique, a microcolumn sample cleanup procedure was developed that eliminated matrix interferences in aqueous solutions of I. It was found that I could be separated selectively from polyethylene glycol 400 and isolated from water (water had to be eliminated before silylation reagents could be used) using a microcolumn containing diethylaminoethylcellulose (free base form). Columns were prepared by adding a degassed methanolic slurry of diethylaminoethylcellulose to a gel height of 8 ± 1 mm to a 15-cm × 6-mm i.d. glass column outfitted with a fritted disk. The small void volume of this column, a departure from most conventional procedures, was especially advantageous since only a small volume of solvent was needed for complete elution of I.

Aliquots of sample solutions of I were diluted with methanol and applied onto the microcolumns. Polyethylene glycol 400, I, and III were retained on the diethylaminoethylcellulose due to a combination of adsorption onto the cellulose matrix backbone and ion exchange with the diethylaminoethyl functional groups bound to the cellulose. The ion-exchange interaction was confirmed by attempting the same separation using cellulose without the diethylaminoethyl functional groups. With this medium, definitive separation of polyethylene glycol 400 and I was not accomplished, and the results were not reproducible.

With diethylaminoethylcellulose, solvent systems were investigated

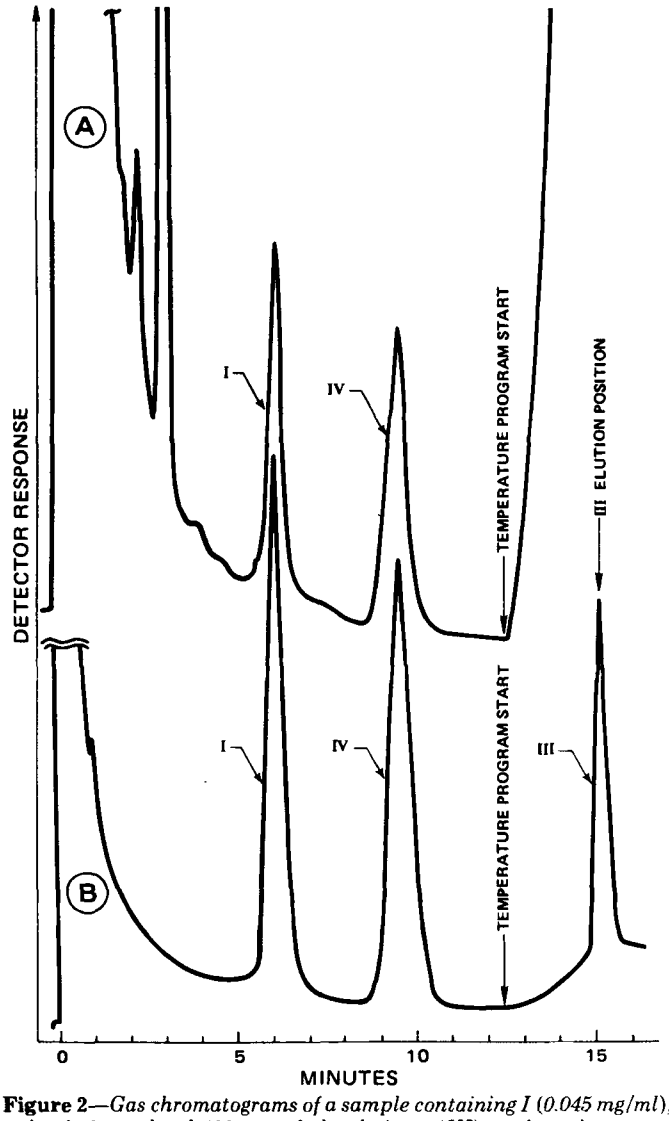

Figure 2—*Gas chromatograms of a sample containing I (0.045 mg/ml), polyethylene glycol 400, ascorbyl palmitate (III), and n-triacontane (IV) as the internal standard after pre-GLC sample cleanup for which detector response was 2 × 10^{-11} amp/sec full scale (A); and a standard stock solution containing I, ascorbyl palmitate (III), and n-triacontane (IV) for which the detector response was 16 × 10^{-11} amp/sec full scale (B).*

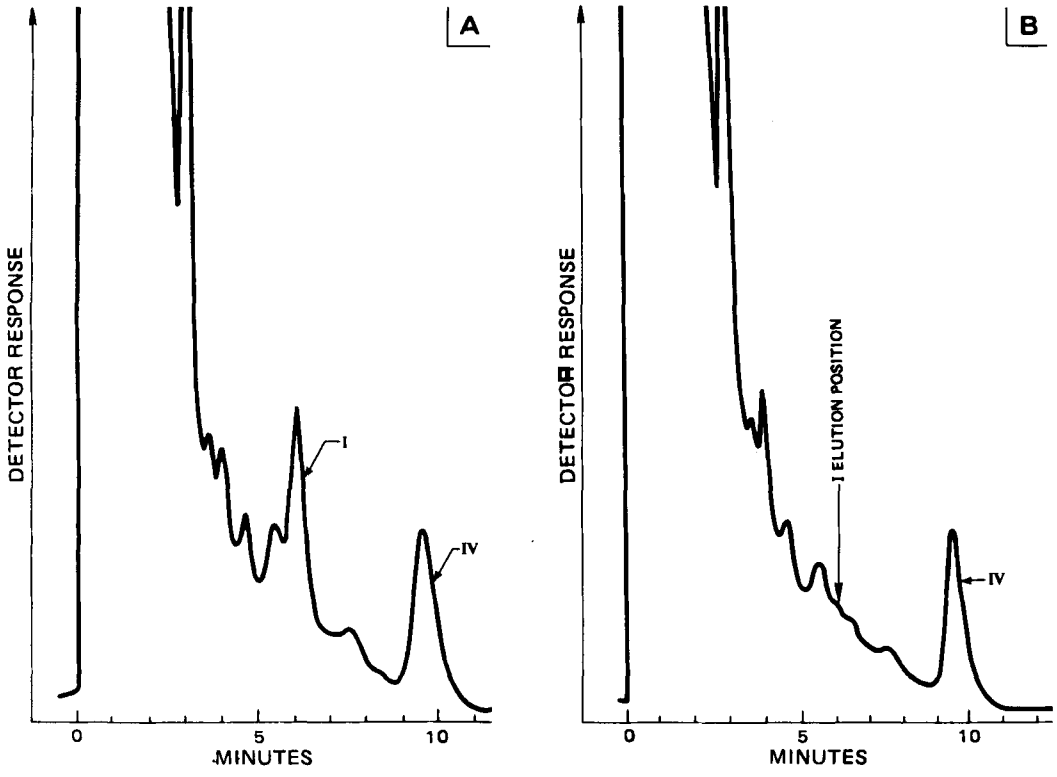

Figure 3—*Gas chromatograms of a sample containing I (0.01 mg/ml), polyethylene glycol 400, and* n*-triacontane (IV) as the internal standard after pre-GLC sample cleanup (A); and a placebo containing* n*-triacontane (IV) as the internal standard, after pre-GLC sample cleanup, prepared at the same excipient concentration level as Sample A (B). The detector response was 2 × 10^{-11} amp/sec full scale.*

Table I—Assay Results for Samples Containing I, Polyethylene Glycol 400, Ascorbyl Palmitate, and Butylated Hydroxyanisole

Sample Claim of I, mg/ml	*n*	Average Result ± *SD*, mg/ml	Percent of Claim	*RSD*, %
0.200	6	0.207 ± 0.00115	103	5.6
0.044	5	0.0469 ± 0.00530	106	11.3
0.010	3	0.00974 ± 0.00042	97.4	4.3

in which I would be retained on the column while polyethylene glycol 400 and III would be eluted; however, no system could be found with these properties that also would provide 100% recovery of I. For this reason, efforts were directed to the development of a system to remove polyethylene glycol 400 and water, leaving the separation of I and III by GLC as the next step.

Polyethylene glycol 400 was removed during the wash step by partitioning with water; I and III, having little affinity for water, remained bound to the column. The latter compounds then were eluted with anhydrous ether. The resulting eluate was evaporated to dryness under a nitrogen stream, and the residue was reacted with silylating reagent.

Baseline separation of I and III was achieved in 16 min by GLC using a 2.5-m × 2-mm i.d., 3% OV-1 on Chromosorb W-HP column for samples containing >0.045 mg of I/ml (Fig. 2). However, artifacts of polyethylene glycol 400 were found in those samples having <0.045 mg of I/ml because of the need to apply significantly more sample to the microcolumn for quantitative detection. Even at low levels, quantitation of I was not affected (Fig. 3).

The trimethylsilyl derivative of I was formed by reaction with a hexamethyldisilazane–trimethylchlorosilane mixture in acetonitrile, with no loss in potency of I detected after 24 hr. In earlier studies with stronger silylating reagents, I degradation was observed by GLC as a peak eluting prior to I.

Results of validation studies have shown that the procedure is accurate, precise, and suitable for routine analysis. The loading capacity of the microcolumns was linear over a range of 7.50–22.5 μg of I, with a least-squares correlation coefficient of 0.997. Results of a recovery study using the standard addition method yielded a mean value of 101%. A method precision study, conducted with 15 replicate samples, yielded a coefficient of variation of 7.3%. The analysis of actual samples over a concentration range of 0.01–0.2 mg of I/ml yielded results with acceptable variation (Table I).

REFERENCES

(1) D. E. Wilson and S. L. Winter, *Prostaglandins*, **16**, 127 (1978).

(2) D. E. Wilson, I. W. Chang, J. Paulsrud, and G. Holland, *ibid.*, **16**, 121 (1978).

(3) F. A. Fitzpatrick, *Anal. Chem.*, **50**, 47 (1978).

(4) W. C. Hubbard and J. T. Watson, *Prostaglandins*, **12**, 21 (1976).

(5) R. W. Kelly, *Proc. Anal. Div. Chem. Soc.*, **14**, 208 (1977).

(6) M. Korteweg, G. Verdonk, P. Sandra, and M. Verzale, *Prostaglandins*, **13**, 1221 (1977).

(7) D. L. Perry and D. M. Desiderio, *ibid.*, **14**, 745 (1977).

(8) I. Alam, K. Ohuchi, and L. Leving, *Anal. Biochem.*, **93**, 339 (1979).

(9) K. Carr, B. J. Sweetman, and J. C. Froelich, *Prostaglandins*, **11**, 3 (1976).

(10) F. A. Fitzpatrick, *J. Pharm. Sci.*, **65**, 1609 (1976).

(11) R. K. Lustgarten, *ibid.*, **65**, 1533 (1976).

(12) J. Turk, S. J. Weiss, J. E. Davis, and P. Needleman, *Prostaglandins*, **16**, 291 (1978).

(13) "The Identification and Quantitative Determination of Synthetic Prostaglandins by HPLC," Applications Bulletin AN 146, Waters Associates, Milford, Mass., 1974.

(14) O. Samuelson and B. Swenson, *Anal. Chim. Acta*, **28**, 426 (1963).

(15) C. Wu and R. M. McCready, *J. Chromatogr.*, **57**, 424 (1971).

(16) T. Seki, *ibid.*, **22**, 498 (1966).

(17) P. Larson, E. Murgia, T. Hsu, and H. F. Walton, *Anal. Chem.*, **45**, 2306 (1973).

(18) N. Nomura, S. Hiraki, M. Yamada, and D. Shiho, *J. Chromatogr.*, **59**, 373 (1971).

(19) W. Funasaka, T. Hanai, K. Fujimura, and T. Ando, *ibid.*, **72**, 187 (1972).

Production and Characterization of Specific Antibody for Radioimmunoassay of Procainamide

P. MOJAVERIAN ˣ **and G. D. CHASE**

Received June 21, 1979, from the *Department of Chemistry, Philadelphia College of Pharmacy and Science, Philadelphia, PA 19104.*
Accepted for publication February 1, 1980.

Abstract □ The production and characterization of a specific antibody for use in the radioimmunoassay of procainamide are described. Cross-reactivity was measured by a nonequilibrium competitive procedure. Procainamide analog concentrations resulting in 50% inhibition were: procainamide, 1.59 nmoles/ml; *N*-acetylprocainamide, 3.55 nmoles/ml; a propyl analog of procainamide, 398 nmoles/ml; procaine, 316 nmoles/ml; lidocaine, >8000 nmoles/ml; and practolol, >16,000 nmoles/ml. Variations in the ability to inhibit binding of labeled procainamide were related to structural similarities and differences. The affinity constant of the antibody for procainamide was 2.9×10^8 liters/mole as measured from a Scatchard plot. The assay allows the direct measurement of procainamide in a 0.1-ml aliquot of diluted serum. The advantages of this method over currently available techniques are its sensitivity, specificity, and simplicity. Furthermore, prior extraction of serum samples is not required. As little as 1 ng of drug/ml of serum can be detected by this method. The accuracy and precision were determined by adding known amounts of procainamide to human serum and then assaying five replicates of each concentration. The within-day and between-day coefficients of variation were 2 and 5%, respectively. The proposed method was used to determine the serum concentration after an intravenous dose of procainamide. A comparison of the radioimmunoassay results with values obtained by a GLC procedure showed excellent agreement.

Keyphrases □ Procainamide—radioimmunoassay in human serum □ Radioimmunoassay—procainamide in human serum □ Antiarrhythmic activity—procainamide, specific antibody production and characterization

Procainamide (I) is a widely used antiarrhythmic with a narrow therapeutic range (1). Since procainamide is very potent, the choice of the proper dosage is critical. Variation in the dose requirement of patients appears to be due mainly to individual differences in procainamide absorption, distribution, and elimination (2, 3).

Determination of plasma concentrations of I has been studied using spectrometric (4), GLC (5), and high-pressure liquid chromatographic (6) procedures. However, various shortcomings exist. A radioimmunoassay for I could provide more than a 1000-fold increase in sensitivity as well as much greater specificity over those levels offered by existing procedures. Radioimmunoassay is based on competition between antigenic determinants of the labeled and unlabeled antigens for a limited number of specific antibody binding sites. Anything that competes for such sites, or in any other way affects the binding of labeled antigen, will influence the results.

The establishment of a practical radioimmunoassay procedure for a particular compound of clinical significance depends, among other factors, on the production of a high affinity antiserum with little cross-reactivity with compounds of similar structure. An ideal antibody is one that reacts with only one species of the molecule (*i.e.*, the antigen). However, antibodies tend to cross-react with compounds other than the specific antigen if there are certain structural similarities. The greater the ability of an antibody to distinguish between minute structural differences, the less is the tendency to cross-react and the greater is the specificity of the antibody. A radioimmunoassay for I is described, with particular emphasis on antibody specificity.

EXPERIMENTAL

Hapten–Protein Condensation—Three drug–protein derivatives were prepared by coupling I[1] to bovine serum albumin[2], egg albumin[3], and rabbit serum albumin[2], respectively. Procainamide was conjugated mainly through the tyrosyl residues of bovine serum albumin *via* a diazotization and condensation procedure (7, 8). Compound I (150 mg) was dissolved in 2 ml of distilled water at 2°, and the pH was adjusted to 9 with 1 *N* NaOH.

Nitrous acid was prepared by mixing 40 mg of sodium nitrite, in 5 ml of ice-cold distilled water, with 1 ml of 1 *N* HCl. This solution was added immediately to the solution of I, and diazotization was allowed to proceed for 15 min with occasional stirring. The diazotized drug solution was added in 1-ml increments to the protein solution (1 g of protein in 50 ml of ice-cold 0.04 *N* NaOH), and the pH was adjusted to 8.5. The mixture was stirred to eliminate any local excess of acid. The pH of this mixture was checked at 15-min intervals for 2 hr and was finally adjusted to 8.5 with 0.1 *N* NaOH. The solution was incubated overnight at 5° to allow completion of the coupling reaction.

The conjugation mixture was dialyzed against distilled water over 2–3 days, thus allowing for the removal of unreacted low molecular weight materials. The purified drug–protein solution was lyophilized and stored frozen in small quantities. The spectrometric analysis of the conjugate (I–bovine serum albumin) indicated that the molar ratio of procainamide to bovine serum albumin was between 20 and 22.

Radioiodination—Radioiodinated antigen was prepared by conjugation of I to rabbit serum albumin with subsequent iodination of the complex by the chloramine-T procedure (9) using 2 mCi of carrier-free sodium [^{125}I]iodide[4]. The I–rabbit serum albumin (2 mg in 0.5 ml of phosphate buffer, pH 7.5) was added to 2 mCi of sodium [^{125}I]iodide (in 0.5 ml of phosphate buffer) and mixed with 2 mg of chloramine-T[5] in 0.5 ml of iodination buffer. After 2 min of incubation, 4 mg of sodium metabisulfite in 0.5 ml of phosphate buffer was added to reduce both chloramine-T and any unreacted iodine. Carrier potassium iodide (5 mg in 0.5 ml of buffer) then was added.

This mixture was incubated at room temperature for 2 min and then was purified by gel filtration in a 0.9 × 15-cm G-25 Sephadex column[6] equilibrated with the iodination buffer. The total iodination mixture (2.5 ml) was added to the column with a plastic disposable syringe, and the column eluate was collected in 0.5-ml fractions, which were counted to determine the radioactivity profile. The radiochemical purity and percent labeling yield were measured, and the specific activity of ^{125}I-labeled I–rabbit serum albumin was calculated (1.90 Ci/mmole of I).

Preparation of Anti-I Serum—The drug–protein conjugate (I–bovine serum albumin) was antigenic when female albino rabbits were given several injections of 0.5–2 mg of complex dissolved in phosphate-buffered saline (pH 7.5) emulsified in a 1:2 ratio of Freund's complete adjuvant[7].

Booster shots were given at 4–5 week intervals, and blood samples were collected 10 days after each booster *via* the marginal ear vein. Development of the drug-specific antibody was followed qualitatively and quantitatively by use of a microgel immunodiffusion technique (10, 11). After 5–6 months, antiserum dilutions of 1:500 and 1:1000 yielded 50% binding of 4 ng of I.

[1] E. R. Squibb & Sons, Princeton, N.J.
[2] Sigma Chemical Co., St. Louis, Mo.
[3] Fisher Scientific Co., Fair Lawn, N.J.
[4] New England Nuclear, Boston, Mass.
[5] J. T. Baker Chemical Co., Phillipsburg, N.J.
[6] Pharmacia Laboratories, Piscataway, N.J.
[7] Difco Laboratories, Detroit, Mich.

0022-3549/80/0600-0721$01.00/0
© 1980, American Pharmaceutical Association

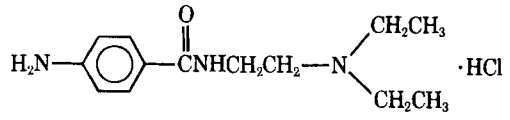

I

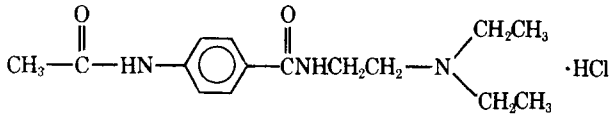

II

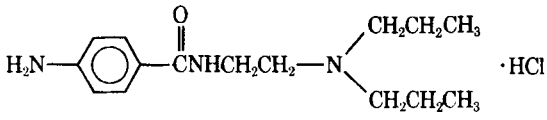

III

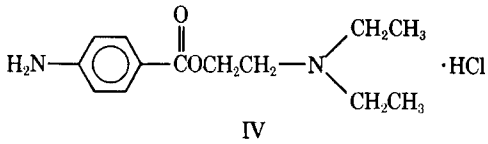

IV

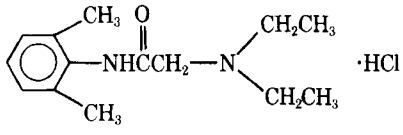

V

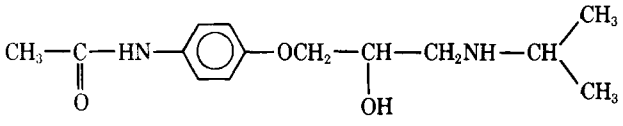

VI

Specificity Analysis—Several antiarrhythmic and cardiac depressants were selected as potential cross-reacting compounds on the basis of their structural similarity with I or because they are coprescribed with I. The compounds selected (shown as their hydrochlorides for I–V) were: *N*-acetylprocainamide[8] (II), a propyl analog of procainamide[1] (III), procaine[2] (IV), lidocaine[9] (V), and practolol[10] (VI).

Cross-reactivity of the antibody was measured by a nonequilibrium competitive procedure: 100 μl of the cross-reacting antigen in the range of 10^{-8}–10^{-3} *M* was mixed with 50 μl of the properly diluted antiserum in a 0.5-ml disposable polypropylene test tube[11] and incubated for 0.5 hr at 5°. Then 10 μl of the radioiodinated antigen (equivalent to 4 ng of the tracer) was added, and the mixture was incubated for 1 hr at 5°. Finally, 100 μl of the second antibody[12] (goat anti-rabbit immunoglobulin G) was added and the tubes were incubated for an additional hour at 5°.

The tubes then were centrifuged for 15 min at 3000 rpm, and the free (supernatant) and bound (precipitated) fractions were separated. The percentage of the iodinated antigen bound to the antibody was calculated in the presence (% B_p) and absence (% B_0) of the unlabeled cross-reacting molecules (12). The percentage of inhibition was calculated from:

$$\text{percentage of inhibition} = \left(\frac{\%\ B_0 - \%\ B_p}{\%\ B_0}\right) \times 100 \qquad \text{(Eq. 1)}$$

The percentage of inhibition was plotted as a function of the logarithm of the cross-reactant concentration (Figs. 1 and 2). The concentration resulting in 50% inhibition of binding with 4 ng of the radiolabeled antigen in a total volume of 260 μl was measured from the graph.

Radioimmunoassay—Procainamide standards were prepared by dilution of a 0.2-mg/ml stock solution in 0.05 *M* phosphate-buffered saline, pH 7.5. Duplicate standards, 0–200 ng, were prepared in the phosphate-buffered saline.

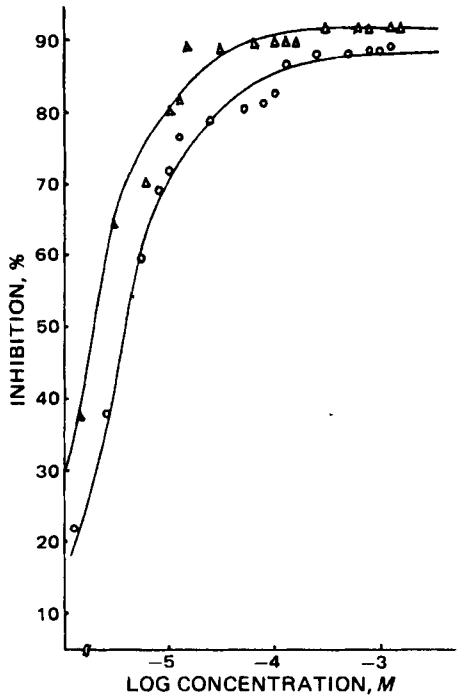

Figure 1—*Competitive inhibition of binding of 4 ng of radioiodinated procainamide by the prior addition of an increasing concentration of unlabeled I (△) or II (○).*

Antiserum was diluted (1:500–1:1000) with the assay buffer to yield 40–60% binding with labeled hapten. Then a 0.1-ml aliquot of diluted antibody was used per tube for the assay. The radioiodinated antigen also was diluted in 0.05 *M* phosphate-buffered saline so that a 0.05-ml aliquot had an activity of 35,000–40,000 cpm. Radioisotopic purity was checked periodically by paper chromatography, using 75% methanol for development. An appropriate dilution of goat anti-rabbit immunoglobulin G was used as the precipitating antibody (0.15 ml/tube). An equilibrium assay procedure was used.

Table I is an outline of the radioimmunoassay protocol. The procedure was as follows. The standards and unknowns were mixed with the radioiodinated antigen, buffer, and the antiserum in 6 × 50-mm disposable culture tubes[13], which were placed inside regular 12 × 75-mm disposable

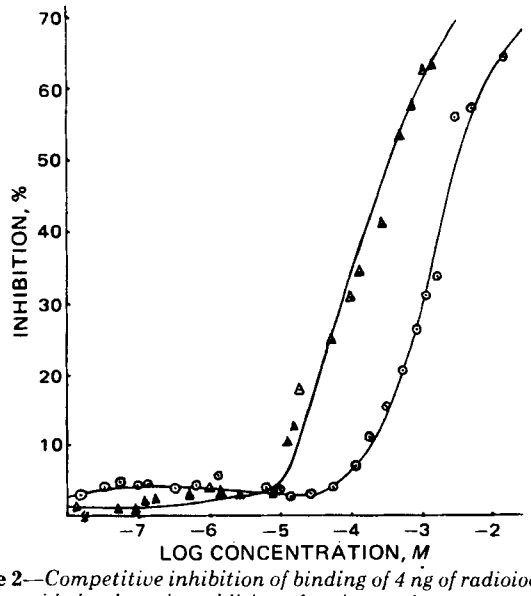

Figure 2—*Competitive inhibition of binding of 4 ng of radioiodinated procainamide by the prior addition of an increasing concentration of unlabeled III (△) or IV (⊙).*

[8] Arnar-Stone Laboratory, Mount Prospect, Ill.
[9] Astra Pharmaceutical Products, Worcester, Mass.
[10] Stuart Pharmaceutical Co., Wilmington, Del.
[11] Brinkmann Instruments, Westbury, N.Y.
[12] Miles Research Products, Elkhart, Ind.
[13] Corning Glass Works, Corning, N.Y.

Table I—Procainamide Radioimmunoassay Protocol and Volumes of Reagents Used

Tube Number	Description	Cold Procainamide, ml	Buffer, ml	Iodinated Procainamide, ml	Antiserum, ml	Second Antibody, ml	Total Volume, ml
1, 2	Zero standard	0.1	0.1	0.05	0.1	0.15	0.4
3, 4	10-ng standard	0.1	—	0.05	0.1	0.15	0.4
5, 6	20-ng standard	0.1	—	0.05	0.1	0.15	0.4
7, 8	40-ng standard	0.1	—	0.05	0.1	0.15	0.4
9, 10	60-ng standard	0.1	—	0.05	0.1	0.15	0.4
11, 12	80-ng standard	0.1	—	0.05	0.1	0.15	0.4
13, 14	100-ng standard	0.1	—	0.05	0.1	0.15	0.4
15, 16	120-ng standard	0.1	—	0.05	0.1	0.15	0.4
17, 18	140-ng standard	0.1	—	0.05	0.1	0.15	0.4
19, 20	160-ng standard	0.1	—	0.05	0.1	0.15	0.4
21, 22	200-ng standard	0.1	—	0.05	0.1	0.15	0.4
23, 24	Total count	—	0.350	0.05	—	—	0.4
25, 26	"Nonspecific binding"	—	0.200	0.05	—	0.15	0.4
27, 28	Unknowns (0.1 ml)	—	—	0.05	0.1	0.15	0.4

culture tubes for convenience in handling and centrifugation. All tubes were vortexed for 2–3 sec and then incubated for 3 hr at 25°. Then 0.15 ml of the second antibody was added to all tubes, which were vortexed again for 3 sec.

After centrifugation of the tubes at 3000 rpm for 20 min, the supernate (free fraction) was separated from the precipitate (bound fraction) using a disposable pasteur pipet[14]. The activity of the free and bound fractions was counted using a γ-scintillation spectrometer[15]. The procainamide concentration was plotted as a function of the total-to-bound radioactivity ratio. However, the data also can be processed by use of a computer program (13). The unknown concentrations were measured by interpolation.

Sensitivity and Detectability—Sensitivity was defined by Horwitz (14) as the amount of measured response per unit of stimulus (*i.e.*, the slope of the response curve). Sensitivity should be evaluated from a linear response plot, because a linear dose–response curve gives a constant value for sensitivity. Sensitivity of the procainamide radioimmunoassay system was calculated as the reciprocal of the slope of the dose–response plot (Fig. 3). The detectability or detection limit of a radioimmunoassay procedure is defined as the minimum concentration of the unlabeled antigen that provides a measurable response under defined conditions (14). The detection limit of the system, estimated as the reciprocal of the affinity constant, was 4.8×10^{-9} *M*.

Precision—The precision of the system was determined by addition of known amounts of I to procainamide-free human serum and then assay of five replicates of each concentration (Table II).

Human Study—A healthy, 26-year-old male subject was given an intravenous dose of I (461 mg/30 ml) over 10 min by use of an infusion pump[16]. Blood samples were collected at several postinfusion intervals (Table III). The serum was separated and kept frozen until it was analyzed.

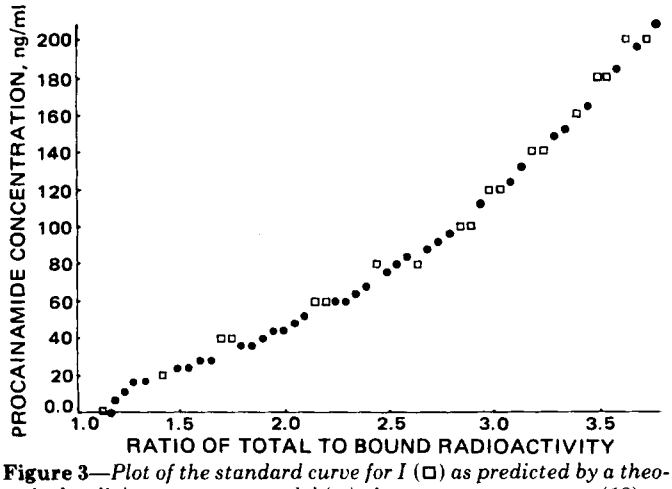

Figure 3—*Plot of the standard curve for I* (□) *as predicted by a theoretical radioimmunoassay model* (●) via *a computer program* (*13*).

[14] Fisher Scientific Co., Pittsburgh, Pa.
[15] Model 5220, Packard Instrument Co., Downers Grove, Ill.
[16] Harvard Apparatus, Hillis, Mass.

Table II—Estimation of Procainamide in Human Serum by Radioimmunoassay

Procainamide Added, ng	Procainamide Measured, ng	Mean ± *SE*	Ratio of Assayed to Added
5.00	4.85	4.92 ± 0.063	0.984
	4.72		
	4.96		
	5.10		
	4.95		
10.0	9.82	9.96 ± 0.102	0.996
	10.2		
	9.65		
	10.2		
	9.96		
15.0	14.5	14.9 ± 0.102	0.993
	15.1		
	14.9		
	14.9		
	15.0		
20.0	20.1	19.9 ± 0.081	0.998
	19.8		
	19.9		
	20.2		
	19.8		
25.0	24.8	24.8 ± 0.136	0.992
	25.1		
	24.5		
	24.6		
	25.2		

GLC Assay—Procainamide was extracted from the serum with methylene chloride as described by Elson *et al.* (15) and was analyzed by the GLC[17] method of Simons and Levy (16). Each serum sample then was analyzed for procainamide concentration by the radioimmunoassay. The results were compared with values obtained from the GLC procedure (Table III).

RESULTS AND DISCUSSION

The results of the cross-reactivity analysis of the procainamide antibody are summarized in Table IV. Inhibition plots of the cross-reacting analogs are shown in Figs. 1 and 2.

Since procainamide is a low molecular weight drug, *i.e.*, <500, the antiserum usually recognizes the whole structure rather than parts of it. Therefore, the antibody can detect slight changes in molecular structure from that of the immunizing antigen (I). This characteristic of the antibody is more pronounced in the nonequilibrium competitive procedure (Table IV). The results of the cross-reactivity experiments indicate that any modifications in the basic benzamide structure of I (*i.e.*, procaine and lidocaine) diminish the antibody binding stimulated by the I–bovine serum albumin complex. Also, the presence of the tertiary nitrogen and the carbon chain length on this nitrogen influence the immunoreactivity of the molecule.

[17] Series 2400, Varian Aerograph, Palo Alto, Calif. The gas chromatograph was equipped with a flame-ionization detector and had a 0.914-m glass column packed with 10% OV-7 on 100–120-mesh WH-P. The temperatures of the injector, column, and detector were 260, 245, and 280°, respectively.

Table III—Comparison of Procainamide Levels as Measured by Radioimmunoassay and GLC

Postinfusion Time, min	Serum Procainamide Levels, μg/ml	
	Radioimmunoassay	GLC
3	6.95	6.9
11	5.61	5.3
43	4.22	4.4
53	3.98	3.8
68	3.76	4.2
82	3.70	3.6
97	3.55	3.5
112	3.42	3.8
142	3.35	3.3
290	1.69	1.6

Table IV—Summary of Nonequilibrium Competitive Cross-Reactivity of Procainamide Antibody [a] with Structurally Related Compounds

Compound	Concentration for 50% Inhibition of Binding, $M \times 10^{-5}$	Concentration Ratio[b]	Molecular Weight
I	0.159	1.00	272.0
II	0.355	2.30	313.5
III	39.8	250	300.0
IV	316	1987	273.0
V	>800	>5000	272.0
VI	>1600	>10000	266.0

[a] Antibody raised against I-bovine serum albumin. [b] Compared to I.

Differences in 50% inhibition values for the cross-reacting compounds were indicated by inhibition curves with differing slopes. The antibody developed against the hapten differentiates between the antigen and its *N*-acetyl metabolite (II). Although the values of 50% inhibition for these two compounds differ only slightly, twice the concentration of II is required to compete equally with I for the antibody binding sites. In addition, the antibody recognizes the molecular differences between the immunizing antigen and its propyl analog. This analog concentration must be 250 times that of I to inhibit binding by 50%. In the case of procaine, this value is ~2000. The antibody appears to be very sensitive to changes in molecular structure.

The increasing value of 50% inhibition of II–VI parallels the degree of difference between the molecular structure of these compounds and I. Furthermore, the antibody was characterized with respect to its affinity constant by a Scatchard analysis. The calculated value was 2.9×10^8 liters/mole. The radioimmunoassay parameters were adjusted to optimum values. The standard curve showed excellent linearity over the range of 0–100 ng of I/ml. Therefore, patient samples should be diluted properly (about 100-fold) to fall within this concentration range. Dilution also reduces the degree of nonspecific binding. Correction for nonspecific binding was made by subtracting the activity of a nonspecific binding blank from both standards and unknowns.

The proposed method was characterized by evaluation of the sensitivity and detectability of the system, which were 0.04 division/ng of I and 1.3 ng of I/ml, respectively. The precision of the assay is good since the standard error of replicates was ≤1% of the mean value for each concentration measured (Table II). The ratios of the assayed procainamide to that added indicate an acceptable recovery.

The within-day and between-day precision were evaluated by duplicate measurements of identical samples on the same day and on consecutive days. The coefficient of variation, *CV*, was estimated from (17):

$$CV = \sqrt{\frac{\sum d^2}{2n}} \qquad \text{(Eq. 2)}$$

where:

$$d = \left[\frac{\text{highest value of each duplicate}}{\text{lowest value of each duplicate}} - 1\right] \times 100 \qquad \text{(Eq. 3)}$$

and n is the number of duplicate determinations. For the procainamide antibody, the within-day coefficient of variation ranged from 1.4 to 4.2% with a mean of 2.2%. The between-day coefficient of variation ranged from 2.9 to 9.1% with a mean of 5.6%. The coefficient of variation was measured over the concentration range of 0–200 ng/ml.

The validity of the assay was established further by comparing the values obtained by radioimmunoassay to values obtained from a GLC assay. The results (Table III) showed excellent agreement.

In summary, the described method is a sensitive and relatively simple microanalytical procedure, which can be performed directly on an aliquot of serum without prior extraction or purification. This radioimmunoassay procedure permits the simultaneous analysis of a large number of samples.

REFERENCES

(1) J. Koch-Weser and S. W. Klein, *J. Am. Med. Assoc.*, **215**, 1454 (1971).

(2) J. Koch-Weser, S. W. Klein, and L. Foo-Canto, *N. Engl. J. Med.*, **281**, 1253 (1969).

(3) E. Karlsson, L. Molin, B. Norlander, and S. F. Sojoquist, *Br. J. Clin. Pharmacol.*, **1**, 467 (1974).

(4) D. S. Sitar, D. N. Graham, and R. E. Rango, *Clin. Chem.*, **22**, 379 (1976).

(5) A. J. Atkinson, Jr., M. Parker, and G. Strong, *ibid.*, **18**, 643 (1972).

(6) R. F. Adams, F. L. Vandemark, and G. Schmidt, *Clin. Chim. Acta*, **69**, 515 (1976).

(7) G. E. Means and R. E. Feeney, "Chemical Modification of Proteins," Holden-Day, San Francisco, Calif., 1977, pp. 144–186.

(8) E. A. Kabat and M. M. Mayer, "Experimental Immunology," Charles C Thomas, Springfield, Ill., 1971, pp. 789–802.

(9) M. W. Hunter, in "Handbook of Experimental Immunology," D. M. Weir, Ed., Lippincott, Philadelphia, Pa., 1978, pp. 14.1–14.7.

(10) Ö. Ouchterlony, in "Immunological Method," J. F. Ackroyd, Ed., F. A. Davis Co., Philadelphia, Pa., 1964, pp. 55–91.

(11) G. Mancini and A. O. Carbonara, *Immunochemistry*, **2**, 235 (1965).

(12) G. H. Wainer, F. W. Fitch, and R. M. Rothberg, *J. Immunol.*, **110**, 667 (1973).

(13) G. D. Chase, "A Theoretical Approach to Radioimmunoassay Data Analysis," presented at Clinical Radioassay Society, 2nd Annual Meeting, New York, N.Y., 1976.

(14) W. Horwitz, "FDA By-Lines," No. 6, Washington, D.C., 1976, pp. 305–310.

(15) J. Elson, J. M. Strong, W. K. Lee, and A. J. Atkinson, *Clin. Pharmacol. Ther.*, **17**, 134 (1975).

(16) K. J. Simons and R. H. Levy, *J. Pharm. Sci.*, **64**, 1967 (1975).

(17) G. W. Snedecor, *Biometrics*, **8**, 85 (1952).

ACKNOWLEDGMENTS

Presented in part at the 30th Pittsburgh Conference on Analytical Chemistry and Applied Spectroscopy, Division of Clinical Chemistry, Cleveland, Ohio, March 1979, and in part at the Pharmaceutical Analysis and Control Section, APhA Academy of Pharmaceutical Sciences, Kansas City meeting, November 1979.

Abstracted in part from a thesis submitted by P. Mojaverian to the Philadelphia College of Pharmacy and Science in partial fulfillment of the Doctor of Philosophy degree requirements.

The authors thank Dr. K. Iqbal for the GLC studies of human samples.

Hydrolysis of Tetrakis-μ-acetylsalicylato-dicopper(II)

A. A. ALICH *x **and L. E. WITTMERS** ‡

Received October 22, 1979, from the *Department of Chemistry, College of St. Scholastica, Duluth, MN 55811, and the ‡Department of Physiology, School of Medicine, University of Minnesota-Duluth, Duluth, MN 55812. Accepted for publication February 4, 1980.

Abstract □ Hydrolysis rates of acetylsalicylate in the free acid and anion forms and in the dilute solution of the copper complex, tetrakis-μ-acetylsalicylato-dicopper(II), were compared. The hydrolysis rate was unaffected by the presence of copper(II). The pH-dependent rate was 3.64×10^{-4} mmole/liter/min per pH unit at 37° in Ringer's solution. The synthetic procedures commonly used for the preparation of this compound yield a product contaminated with salicylate. This contamination is avoided by synthesis of the compound in methanol, which yields a complex containing no measurable salicylate.

Keyphrases □ Anti-inflammatory agents—aspirin, comparison of hydrolysis rate with that of tetrakis-μ-acetylsalicylato-dicopper(II), pH dependency □ Aspirin—comparison of hydrolysis rate with that of tetrakis-μ-acetylsalicylato-dicopper(II), pH dependency □ Hydrolysis rates—aspirin and tetrakis-μ-acetylsalicylato-dicopper(II), pH dependency

The use of a mixture of copper and salicylate in the treatment of arthritis has been discussed (1–3). Sorenson (4) recently reported that tetrakis-μ-acetylsalicylato-dicopper(II) has greater anti-inflammatory properties than does aspirin (acetylsalicylic acid) alone and suggested that this complex might be the pharmacologically active form of aspirin. This hypothesis generated considerable testing and discussion of the copper complex (5–15), a review of which was given by Sorenson (16, 17).

The evidence presented in the literature concerning Sorenson's hypothesis that the copper complex is the pharmacologically active form of aspirin is limited to observations of the effect of the complex on induced inflammations in laboratory animals (*i.e.*, measurements of paw thickness and volume). It seemed important to assess the relationship between the chemistry of the copper complex and the pharmacological activity of aspirin. The first experiments undertaken involved the hydrolysis of the copper complex to salicylic acid and acetic acid.

The complex was first prepared in 1962 (18), and the X-ray structure was published in 1966 (19). The method used by Manojlovic-Muir (19) yielded a product containing a significant amount of salicylate, so other preparations were sought. This report compares the hydrolysis rates for the complex prepared by three published methods to that for aspirin alone.

EXPERIMENTAL

Materials—The chemicals were reagent grade and were used as obtained with several exceptions. Butyl ether (practical grade) was purified by a literature method (20) and refrigerated in brown glass. Tetrakis-μ-acetylsalicylato-dicopper(II) was prepared by three methods.

Sample B was prepared based on a statement that the complex can be formed in methanol (21). A solution of 25.0 g (0.129 mole) of aspirin in 200 ml of methanol was added to a solution of 13.85 g (0.0694 mole of copper) of copper(II) acetate in 1 liter of methanol. Crystallization of the complex occurred very slowly, and three successive crops of crystals were separated out (53% yield).

Anal.—Calc.: C, 51.25; H, 3.34; Cu, 15.07; O, 30.34. Found[1]: C, 51.04; H, 3.53; Cu, 14.95; O, 30.33.

Sample C was prepared by the method of Sorenson (4), which involves the addition of an aqueous solution of aspirin (pH adjusted to ~11 with 50% NaOH) to an aqueous solution of copper(II) chloride (68% yield).

Found: C, 50.94; H, 3.43; Cu, 14.94; O, 29.96.

Sample D was prepared by the method of Manojlovic-Muir (19) in which stoichiometric amounts of aspirin and copper(II) salicylate are heated in 50% aqueous ethanol to 50° (45% yield).

Found: C, 51.11; H, 3.50; Cu, 15.02; O, 29.90.

Mammalian Ringer's solutions were buffered with acetate to produce solutions of pH 5.8 and with tris(hydroxymethyl)aminomethane to produce solutions of pH 7.5 and 8.8. All solutions were prepared with deionized, glass-distilled water.

Procedures—Hydrolysis was carried out with 2.775 m*M* solutions of aspirin or 0.6953 m*M* solutions of tetrakis-μ-acetylsalicylato-dicopper(II) in the appropriately buffered Ringer's solution at 37° (each mole of complex has 4 moles of acetylsalicylate). Both aspirin and the complex dissolved very slowly. Time zero was taken as the time at which the solid compound was added to the Ringer's solution.

Analysis of salicylic acid (due to hydrolysis) was carried out with the following modifications of a published procedure (20). A 300-μl aliquot of the reaction mixture was extracted into 3.00 ml of butyl ether with shaking at 250 rpm for 10 min. The butyl ether contained 4.0 g of malonic acid/liter to facilitate separation and to prevent further hydrolysis. The two-phase mixture was centrifuged at 2500 rpm for 5 min, the ether layer was drawn off, and the UV spectrum was scanned between 330 and 275 nm[2]. The salicylic acid concentration was determined from a standard curve calculated from absorbances at 307 nm by linear regression analysis. The coefficient of determination (22) for standard curves was ≥0.99. Hydrolysis rates were determined by plotting the appearance of salicylic acid with respect to time over at least 4 hr. Slopes were calculated by linear regression analysis.

Samples for thermal analysis were placed in quartz or platinum crucibles and heated from 0 to 1000° over 20 hr in nitrogen or air at a flow rate of ~1 ml/min[3].

RESULTS

The hydrolyses of acetylsalicylate in aspirin and in the three preparations of tetrakis-μ-acetylsalicylato-dicopper(II) in dilute solution at an acidic pH appear in Fig. 1 as a series of nearly parallel lines. The hydrolysis rates were similar at a given pH (Table I), although the *y* intercepts differ. Table I also gives comparable data for the other pH values at which the experiment was performed.

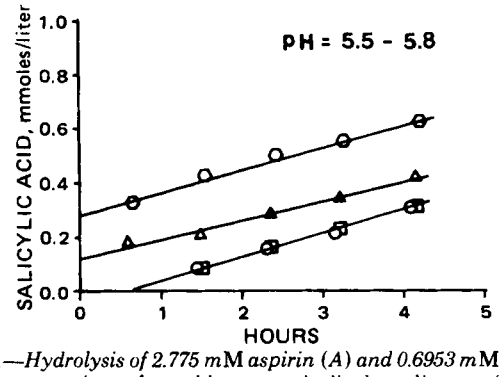

Figure 1—*Hydrolysis of 2.775 m*M *aspirin (A) and 0.6953 m*M *solutions of three preparations of tetrakis-μ-acetylsalicylato-dicopper(II) (B–D) at 37°. Key: ○, Sample A; □, Sample B; △, Sample C; and ○, Sample D.*

[1] All microanalyses for carbon, hydrogen, copper, and oxygen were done by Galbraith Laboratories, Knoxville, TN 37921.

[2] Beckman DB-G spectrophotometer, Beckman Instruments, Fullerton, CA 92634.

[3] Setaram thermoanalyzer G-70 and DTA-80, Marche Instruments, Waco, TX 76710.

0022-3549/80/0600-0725$01.00/0
© 1980, American Pharmaceutical Association

Table I—Hydrolysis Rates of 2.775 m*M* Aspirin (A) and 0.6953 m*M* Solutions of Three Preparations of Tetrakis-μ-acetylsalicylato-dicopper(II) (B–D) at 37° and Three pH Values

Sample	pH Range	pH Mean ± *SD*	Hydrolysis Rate, mmoles/liter/min × 10^3	r^2 [a]	Buffer
A	5.50–5.60	5.56 ± 0.055	1.394	0.9993	Acetate
B	5.75–5.80	5.78 ± 0.027	1.425	0.9956	Acetate
C	5.75–5.85	5.81 ± 0.042	1.155	0.9752	Acetate
D	5.65–5.75	5.71 ± 0.042	1.322	0.9904	Acetate
A	6.95–7.10	7.01 ± 0.065	1.580	0.9967	I[b]
B	6.78–6.90	6.83 ± 0.052	1.963	0.9989	I
C	6.80–6.95	6.83 ± 0.067	1.803	0.9983	I
D	6.75–6.95	6.82 ± 0.076	1.849	0.9906	I
A	8.65–8.80	8.69 ± 0.065	2.528	0.9933	I
B	8.62–8.70	8.65 ± 0.029	2.583	0.9948	I
C	8.55–8.70	8.61 ± 0.055	2.373	0.9868	I
D	8.55–8.70	8.61 ± 0.065	2.111	0.9448	I

[a] Coefficient of determination = $r^2 = \left[\Sigma x_i y_i - \frac{\Sigma x_i \Sigma y_i}{n}\right]^2 \Big/ \left[\Sigma x_i^2 - \frac{(\Sigma x_i)^2}{n}\right]\left[\Sigma y_i^2 - \frac{(\Sigma y_i)^2}{n}\right]$. [b] I = Tris(hydroxymethyl)aminomethane.

If the hydrolysis rates from Table I are plotted *versus* pH (nullifying the effect of any initial salicylate present), they fall on a single line, indicating that aspirin in the free form and in the copper complex hydrolyze at a rate of 3.64×10^{-4} mmole/liter/min per unit of pH increase at 37° (Fig. 2). The coefficient of determination (22) for all of these points was 0.878.

Purity assessment of synthesized compounds usually includes melting-point data. All samples of tetrakis-μ-acetylsalicylato-dicopper(II) decomposed without melting. Samples B and C turned from the original blue to green to brown between 220 and 235°. Sample D began to turn green at 180°. Thermal analysis in either air or nitrogen indicated an endothermic reaction at ~240° for all of the samples, which did not correspond to any weight loss. When heated in air, all samples decomposed in three exothermic steps between 250 and 370° to a weight corresponding to copper(II) oxide. Sample D slowly lost ~5% of its weight prior to the onset of the described reactions.

DISCUSSION

Hydrolysis rates of free and bound acetylsalicylate are nearly identical at a given pH, but the curves in Fig. 1 are not superimposable. Extrapolation of hydrolysis curves to zero time in Fig. 1 indicates the initial presence of salicylic acid in Samples C and D. Melting-point and thermal analysis data indicate an impurity in Sample D but not in Sample C. The *y* intercepts in Fig. 1 indicate approximately twice as much salicylate in Sample D as in Sample C. The contamination of Samples C and D with salicylic acid undoubtedly is due to the preparation methods. At the high pH used in the preparation of Sample C (4), hydrolysis occurs rapidly, causing the product to be contaminated with salicylate. Copper(II) salicylate was used in the reaction mixture for the preparation of Sample D (19) and probably contaminated the product. Recrystallization was not mentioned in the original literature for either procedure and was not used in the preparations made in this study.

The solubility of the complex is very slight in any common solvents (23). Thus, contamination by salicylate in the methods used for Samples C and D would be difficult if not impossible to avoid. Furthermore, contamination was not apparent from IR spectra or elemental analysis (nor was such a problem mentioned in the original literature). The *y* intercept for Sample B in Fig. 1 coincides with that of aspirin, indicating that Sample B does not contain salicylate. The data presented here appear to indicate that tetrakis-μ-acetylsalicylato-dicopper(II) should not be prepared in a solution of basic pH and perhaps should be prepared in a nonaqueous solvent such as methanol to prevent contamination with salicylate. This precaution is especially important in experiments concerning the pharmacological activity of the copper complex since salicylate also is pharmacologically active.

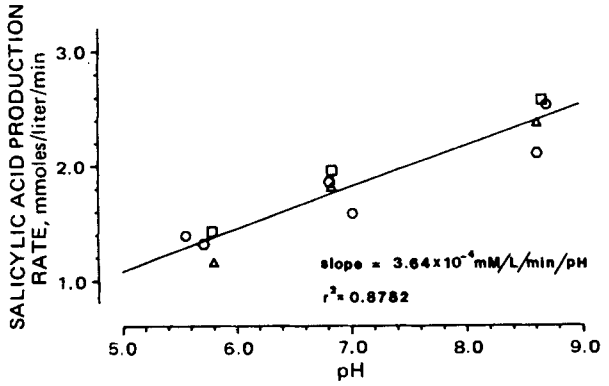

Figure 2—*Hydrolysis rate of aspirin in the free form (A) and in three preparations of tetrakis-μ-acetylsalicylato-dicopper(II) (B–D) as a function of pH. Key: ○, Sample A; □, Sample B; △, Sample C; and ○, Sample D.*

For aspirin alone as well as for Sample B of tetrakis-μ-acetylsalicylato-dicopper(II), Fig. 1 shows an induction period before the appearance of the hydrolysis product, salicylic acid. This induction period would not be present if zero time had been set when all compounds had dissolved (*i.e.*, the vertical axis would be moved to the right by ~30 min). However, the resulting plots would show some salicylic acid in all of the complex preparations and in the aspirin itself (as was the case in preliminary experiments), because hydrolysis begins as soon as any compound is present in solution. To show unambiguously that some salicylate contaminates two of the complex preparations, zero time was taken as described. Use of a sonicator to speed dissolution decreased the length of this period, so it was assumed that the time lag before the appearance of salicylate represents the time required to dissolve the compound.

As observed from Fig. 2, the hydrolysis rate of aspirin, measured by the appearance of salicylic acid, increases with increasing pH and is the same in the complex solutions as in the free form under the experimental conditions. Some inferences concerning the structure in solution may be drawn from this and other information. The crystal structure of the complex has binuclear units of tetrakis-μ-acetylsalicylato-dicopper(II) in which each of the four carboxyl groups is attached to both copper ions. The binuclear units are interconnected into a polymeric structure by a fifth copper–oxygen bond from the acetyl group of a neighboring residue. This bond is nearly 0.3 Å longer than the carboxyl copper–oxygen bonds (19).

Bose and Patel (21) modified this complex, substituting dimethylformamide or dimethyl sulfoxide in the terminal positions for the bond from the acetyl group. They reported that the copper–ligand (dimethylformamide or dimethyl sulfoxide ligand) bond was unusually weak for copper(II) complexes of these ligands. Kato *et al.* (24) reported evidence indicating that the copper(II) complexes of several carboxylic acids that are dimeric in crystalline form are monomeric in aqueous solution. If, in dilute solution, a monomer exists rather than a polymerized dimer, then solvent molecules will occupy the terminal positions and the acetyl group will not be bonded to copper. Thus, hydrolysis would occur at a rate similar to that in free aspirin.

There also is the possibility that the complex is completely dissociated. Sorenson was critical of several experiments on the pharmacological effectiveness of tetrakis-μ-acetylsalicylato-dicopper(II), in which the complex was administered orally in water solution, and suggested that in water the complex probably was dissociated (6, 17), especially at the stomach pH. It has not been possible to determine the extent of complexation under the conditions of this experiment due to the complexity of the solutions.

The stability constant of a 1:1 complex of copper and acetylsalicylate determined polarographically in phosphate buffer at pH 7.4 was 1000

(25). Gaur and Palrecha (26) also determined the stability constants polarographically with a sodium perchlorate supporting electrolyte (no buffer given) and found that 1:1, 1:2, and 1:3 species were formed, having stability constants of 80, 540, and 1610, respectively. Williams *et al.* (10) attempted to determine a stability constant potentiometrically but were unable to do so due to the rapid hydrolysis of acetylsalicylate. It is possible that at the concentrations employed and in the absence of excess acetylsalicylate ion, little complexed species exists. In this case, hydrolysis rates should not be different for solutions made from the copper complex than for those of aspirin.

In summary, the pH-dependent hydrolysis of aspirin was found to occur at the same rate in the free form as in a dilute solution of the tetrakis-μ-acetylsalicylato-dicopper(II) complex. Preparation of this complex in aqueous solution, especially a basic solution, yielded a compound contaminated with significant amounts of salicylic acid.

REFERENCES

(1) W. Hangarter and A. Lubke, *Dtsch. Med. Wochenschr.*, **77**, 870 (1952).

(2) W. Hangarter, *Z. Rheum.*, **25**, 289 (1966).

(3) J. Schubert, *Chimia*, **11**, 113 (1957).

(4) J. R. J. Sorenson, *J. Med. Chem.*, **19**, 135 (1976).

(5) J. R. J. Sorenson, *Inflammation*, **1**, 317 (1976).

(6) J. R. J. Sorenson, *J. Pharm. Pharmacol.*, **29**, 450 (1977).

(7) K. D. Rainsford and M. W. Whitehouse, *ibid.*, **28**, 83 (1976).

(8) K. D. Rainsford and M. W. Whitehouse, *Specialia*, **32**, 1172 (1976).

(9) K. D. Rainsford and M. W. Whitehouse, *Life Sci.*, **21**, 371 (1977).

(10) D. A. Williams, D. T. Walz, and W. O. Foye, *J. Pharm. Sci.*, **65**, 126 (1976).

(11) E. Boyle, P. C. Freeman, A. C. Goudie, F. R. Mangan, and M. Thomson, *J. Pharm. Pharmacol.*, **28**, 865 (1976).

(12) M. W. Whitehouse and W. R. Walker, *Agents Actions*, **8**, 85 (1978).

(13) V. Weser, L. Richter, A. Wendel, and M. Younes, *Bioinorg. Chem.*, **8**, 201 (1978).

(14) A. J. Lewis, *Agents Actions*, **8**, 244 (1978).

(15) A. J. Lewis, *Br. J. Pharmacol.*, **63**, 413p (1978).

(16) J. R. J. Sorenson and W. Hangarter, *Inflammation*, **2**, 217 (1977).

(17) J. R. J. Sorenson. *Prog. Med. Chem.*, **15**, 211 (1978).

(18) D. A. Williams, MsC thesis, Massachusetts College of Pharmacy, Boston, Mass., 1962.

(19) L. Manojlovic-Muir, *J. Chem. Soc., Chem. Commun.*, **1967**, 1057.

(20) G. W. Stevenson, *Anal. Chem.*, **32**, 1522 (1960).

(21) K. S. Bose and C. C. Patel, *Ind. J. Chem.*, **8**, 840 (1970).

(22) A. L. Edwards, "Statistical Methods for the Behavioral Sciences," Rinehart, New York, N.Y., 1955.

(23) W. R. Walker and S. J. Beveridge, *Inorg. Perspect. Biol. Med.*, **2**, 93 (1979).

(24) M. Kato, H. B. Jonassen, and J. C. Fanning, *Chem. Rev.*, **64**, 99 (1964).

(25) P. A. Pella and W. C. Purdy, *J. Electroanal. Chem.*, **10**, 51 (1965).

(26) J. N. Gaur and M. M. Palrecha, *J. Inst. Chem. (India)*, **41**, 25 (1969).

ACKNOWLEDGMENTS

Supported by the Miller-Dwan Medical Center Foundation and the Faculty Development Fund of the College of St. Scholastica.

NOTES

Quantitation of the Antineoplastic Agent Indicine-*N*-oxide in Human Plasma by Differential Pulse Polarography

MADELINE McCOMISH, ITAMAR BODEK, and ALAN R. BRANFMAN ˣ

Received September 27, 1979, from *Arthur D. Little, Inc., Acorn Park, Cambridge, MA 02140.* Accepted for publication January 14, 1980.

Abstract □ A sensitive and reproducible differential pulse polarographic method of analysis was developed for indicine-*N*-oxide (NSC 132319) in human plasma. Lyophilized plasma is extracted with methanol, and the extract is chromatographed over partially deactivated aluminum oxide and reversed-phase silica gel columns. Indicine-*N*-oxide is eluted from the silica gel column with 25% aqueous methanol and quantitated by differential pulse polarography by measurement of the peak current at -0.72 ± 0.03 v (*versus* the saturated calomel electrode). Recovery of indicine-*N*-oxide from plasma was $88 \pm 7\%$ (*SD*) in the 1–20-μg/ml range. The method was linear over the range of 0.5–10 μg/ml of pH 4.6 buffer.

Keyphrases □ Indicine-*N*-oxide—quantitation by differential pulse polarography, human plasma □ Antineoplastics—indicine-*N*-oxide, quantitation by differential pulse polarography, human plasma □ Polarography, differential pulse—indicine-*N*-oxide, quantitation in human plasma

Indicine-*N*-oxide (I) (NSC 132319) is an antineoplastic agent (1) that recently entered clinical trials. The purpose of this investigation was to develop a polarographic method of analysis for use in clinical studies on the physiological disposition of the drug. Assays based on GLC (2) and GLC–mass spectrometry (3–5) have been reported. These assays required derivatization of either indicine-*N*-oxide or its reduced form to a volatile species prior to analysis. The method reported here for the analysis of the drug in biological samples does not require derivatization and is not subject to interference from the reduced form.

With recent advances in instrumentation (6), differential pulse polarography has become a rapid and inexpensive technique. A quantitative polarographic assay was developed in these laboratories for indicine-*N*-oxide in human plasma that combines sufficient sensitivity, reproducibility, and ease of operation for the potential routine analysis of suitable clinical samples (7).

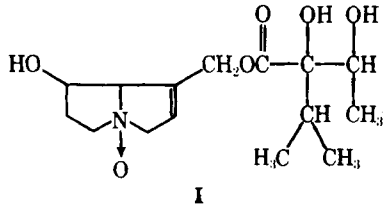

I

0022-3549/80/0600-0727$01.00/0

© 1980, American Pharmaceutical Association

(25). Gaur and Palrecha (26) also determined the stability constants polarographically with a sodium perchlorate supporting electrolyte (no buffer given) and found that 1:1, 1:2, and 1:3 species were formed, having stability constants of 80, 540, and 1610, respectively. Williams *et al.* (10) attempted to determine a stability constant potentiometrically but were unable to do so due to the rapid hydrolysis of acetylsalicylate. It is possible that at the concentrations employed and in the absence of excess acetylsalicylate ion, little complexed species exists. In this case, hydrolysis rates should not be different for solutions made from the copper complex than for those of aspirin.

In summary, the pH-dependent hydrolysis of aspirin was found to occur at the same rate in the free form as in a dilute solution of the tetrakis-μ-acetylsalicylato-dicopper(II) complex. Preparation of this complex in aqueous solution, especially a basic solution, yielded a compound contaminated with significant amounts of salicylic acid.

REFERENCES

(1) W. Hangarter and A. Lubke, *Dtsch. Med. Wochenschr.*, **77**, 870 (1952).

(2) W. Hangarter, *Z. Rheum.*, **25**, 289 (1966).

(3) J. Schubert, *Chimia*, **11**, 113 (1957).

(4) J. R. J. Sorenson, *J. Med. Chem.*, **19**, 135 (1976).

(5) J. R. J. Sorenson, *Inflammation*, **1**, 317 (1976).

(6) J. R. J. Sorenson, *J. Pharm. Pharmacol.*, **29**, 450 (1977).

(7) K. D. Rainsford and M. W. Whitehouse, *ibid.*, **28**, 83 (1976).

(8) K. D. Rainsford and M. W. Whitehouse, *Specialia*, **32**, 1172 (1976).

(9) K. D. Rainsford and M. W. Whitehouse, *Life Sci.*, **21**, 371 (1977).

(10) D. A. Williams, D. T. Walz, and W. O. Foye, *J. Pharm. Sci.*, **65**, 126 (1976).

(11) E. Boyle, P. C. Freeman, A. C. Goudie, F. R. Mangan, and M. Thomson, *J. Pharm. Pharmacol.*, **28**, 865 (1976).

(12) M. W. Whitehouse and W. R. Walker, *Agents Actions*, **8**, 85 (1978).

(13) V. Weser, L. Richter, A. Wendel, and M. Younes, *Bioinorg. Chem.*, **8**, 201 (1978).

(14) A. J. Lewis, *Agents Actions*, **8**, 244 (1978).

(15) A. J. Lewis, *Br. J. Pharmacol.*, **63**, 413p (1978).

(16) J. R. J. Sorenson and W. Hangarter, *Inflammation*, **2**, 217 (1977).

(17) J. R. J. Sorenson. *Prog. Med. Chem.*, **15**, 211 (1978).

(18) D. A. Williams, MsC thesis, Massachusetts College of Pharmacy, Boston, Mass., 1962.

(19) L. Manojlovic-Muir, *J. Chem. Soc., Chem. Commun.*, **1967**, 1057.

(20) G. W. Stevenson, *Anal. Chem.*, **32**, 1522 (1960).

(21) K. S. Bose and C. C. Patel, *Ind. J. Chem.*, **8**, 840 (1970).

(22) A. L. Edwards, "Statistical Methods for the Behavioral Sciences," Rinehart, New York, N.Y., 1955.

(23) W. R. Walker and S. J. Beveridge, *Inorg. Perspect. Biol. Med.*, **2**, 93 (1979).

(24) M. Kato, H. B. Jonassen, and J. C. Fanning, *Chem. Rev.*, **64**, 99 (1964).

(25) P. A. Pella and W. C. Purdy, *J. Electroanal. Chem.*, **10**, 51 (1965).

(26) J. N. Gaur and M. M. Palrecha, *J. Inst. Chem. (India)*, **41**, 25 (1969).

ACKNOWLEDGMENTS

Supported by the Miller-Dwan Medical Center Foundation and the Faculty Development Fund of the College of St. Scholastica.

NOTES

Quantitation of the Antineoplastic Agent Indicine-*N*-oxide in Human Plasma by Differential Pulse Polarography

MADELINE McCOMISH, ITAMAR BODEK, and ALAN R. BRANFMAN ˣ

Received September 27, 1979, from *Arthur D. Little, Inc., Acorn Park, Cambridge, MA 02140.* Accepted for publication January 14, 1980.

Abstract □ A sensitive and reproducible differential pulse polarographic method of analysis was developed for indicine-*N*-oxide (NSC 132319) in human plasma. Lyophilized plasma is extracted with methanol, and the extract is chromatographed over partially deactivated aluminum oxide and reversed-phase silica gel columns. Indicine-*N*-oxide is eluted from the silica gel column with 25% aqueous methanol and quantitated by differential pulse polarography by measurement of the peak current at -0.72 ± 0.03 v (*versus* the saturated calomel electrode). Recovery of indicine-*N*-oxide from plasma was $88 \pm 7\%$ (*SD*) in the 1–20-μg/ml range. The method was linear over the range of 0.5–10 μg/ml of pH 4.6 buffer.

Keyphrases □ Indicine-*N*-oxide—quantitation by differential pulse polarography, human plasma □ Antineoplastics—indicine-*N*-oxide, quantitation by differential pulse polarography, human plasma □ Polarography, differential pulse—indicine-*N*-oxide, quantitation in human plasma

Indicine-*N*-oxide (I) (NSC 132319) is an antineoplastic agent (1) that recently entered clinical trials. The purpose of this investigation was to develop a polarographic method of analysis for use in clinical studies on the physiological disposition of the drug. Assays based on GLC (2) and GLC–mass spectrometry (3–5) have been reported. These assays required derivatization of either indicine-*N*-oxide or its reduced form to a volatile species prior to analysis. The method reported here for the analysis of the drug in biological samples does not require derivatization and is not subject to interference from the reduced form.

With recent advances in instrumentation (6), differential pulse polarography has become a rapid and inexpensive technique. A quantitative polarographic assay was developed in these laboratories for indicine-*N*-oxide in human plasma that combines sufficient sensitivity, reproducibility, and ease of operation for the potential routine analysis of suitable clinical samples (7).

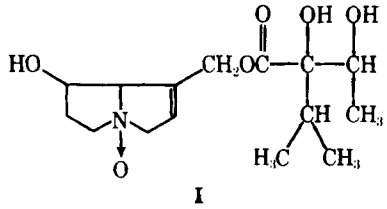

I

0022-3549/80/0600-0727$01.00/0

© 1980, American Pharmaceutical Association

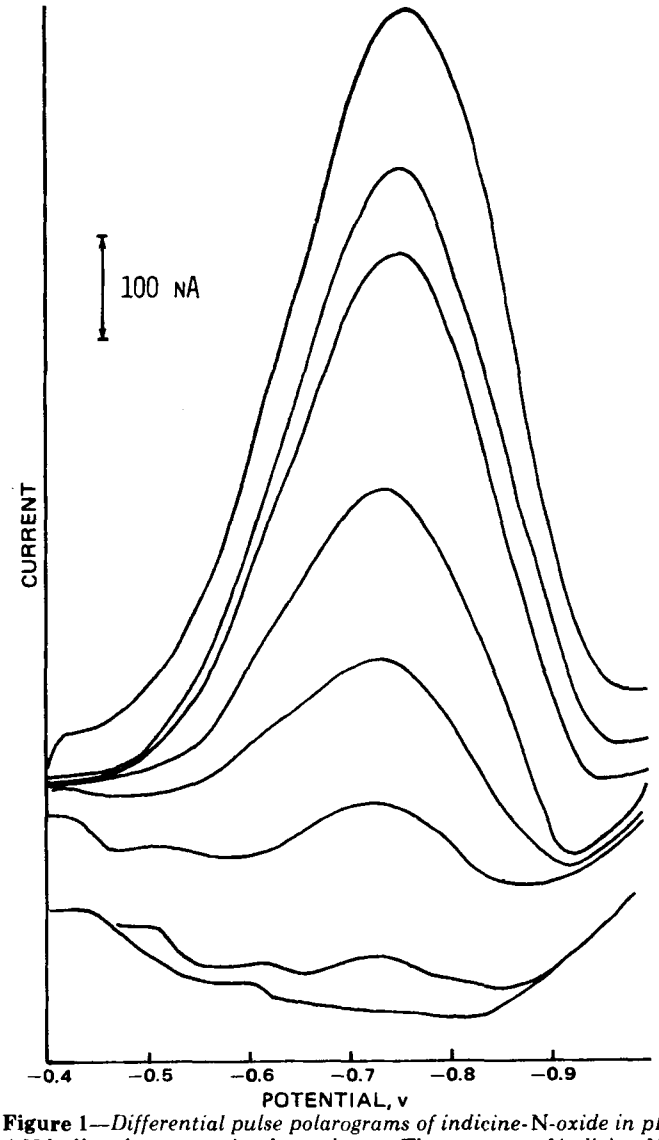

Figure 1—*Differential pulse polarograms of indicine-N-oxide in pH 4.63 buffer after extraction from plasma. The amounts of indicine-N-oxide added to 1 ml of plasma were 0 (plasma blank), 1, 3, 6, 9, 13, 15, 17, and 20 μg. A scale change to 2 μamp was necessary to record the 20-μg samples.*

EXPERIMENTAL

Conditions for Polarographic Analysis—Differential pulse polarograms were run on a polarographic analyzer[1] equipped with a drop timer and used in conjunction with a three-electrode polarographic cell comprised of a dropping mercury electrode, a saturated calomel electrode, and a platinum wire as the auxiliary electrode. The mercury drop time was 0.5 sec using a mercury column 70 cm in height. The current range typically was 1–2 μamp for a peak response of full-scale deflection, and the scan rate was 5 mv/sec.

Argon, cleansed of oxygen by passage through an acidic chromium(II) chloride solution, was used to deoxygenate the sample solutions. While polarograms were recorded, argon was passed continually over the surface of the solution. Samples were scanned from −0.4 to −1.3 v *versus* the saturated calomel electrode, and the differential pulse polarograms were recorded on an *x*–*y* recorder[2].

Reagents and Other Equipment—Indicine-*N*-oxide[3] and indicine[3] were used without further purification. The human plasma used contained the anticoagulant citrate dextrose. All other reagents were analytical grade and were used without further purification. Glass-distilled methanol[4] and deionized water[5] were used in the extraction. Standard buffer solutions[6] (pH 4.63, 5, 6, 7, and 8) were made with distilled water.

Table I—Effect of pH on the Position and Intensity of the Differential Pulse Polarographic Maxima of Indicine-*N*-oxide

pH	E_p[a], v	Intensity at E_p, μamp/μg/ml
1.65[b]	−0.70	0.133
4.63[c]	−0.735	0.141
5.00[d]	−0.775	0.141
5.60[d]	−0.830	0.097
6.00[d]	−0.860	0.091
7.00[e]	−1.08	0.050
8.00[e]	—[f]	~0

[a] Reduction peak potential. [b] 0.05 *M* HCl. [c] 0.05 *M* Sodium acetate–acetic acid. [d] 0.05 *M* Potassium biphthalate. [e] 0.05 *M* Monobasic potassium phosphate–dibasic potassium phosphate. [f] No wave detected.

Standard Solutions—Stock solutions for the preliminary work and standard curves were prepared containing indicine-*N*-oxide in water at 15.8 (5×10^{-2} *M*) and 0.15 (4.8×10^{-4} *M*) mg/ml. Aliquots of the stock solutions (10–200 μl) were added to 15 ml of the appropriate buffers. Most quantitative work was done in the pH 4.63 buffer and with a 2-ml cell. Biological samples were prepared by the addition of suitable aliquots of drug from an aqueous stock solution containing 0.5 mg/ml. Standard curves were prepared by plotting the peak current, corrected for the blank, at −0.72 ± 0.03 v (saturated calomel electrode) *versus* concentration.

Procedure for Analysis in Human Plasma—A known concentration of indicine-*N*-oxide was added to 1 ml of human plasma contained in a 15-ml glass-stoppered centrifuge tube, and the mixture was vortexed for 30 sec. The glass stopper was removed, the tube was covered with a thin film of silanized glass wool, and the mixture was lyophilized[7] overnight. After lyophilization, 3 ml of methanol was passed through the glass wool cover. The glass wool cover then was discarded, the glass stopper was replaced, and the mixture was vortexed for 30 sec. After centrifugation at 700×*g* for 10 min, the supernate was drawn off and set aside.

Methanol (3 ml) was added to the residue, and the mixture again was vortexed and centrifuged as described. The resulting supernate was combined with that from the previous extraction and evaporated under a nitrogen stream to ~1 ml. This 1-ml volume was loaded onto a 3.5-cm column of partially deactivated aluminum oxide[8] (94.5% aluminum oxide–5.5% water, w/w) packed in methanol in a disposable Pasteur pipet. The column was eluted with an additional 10 ml of methanol, and the eluate was evaporated to dryness under a nitrogen stream. This residue was dissolved in 1 ml of water, and the container was washed with an additional 1 ml of water.

Both samples were loaded onto a C_{18} bonded silica gel column[9]. The water effluent was discarded, and 10 ml of 25% aqueous methanol was used to elute the indicine-*N*-oxide from this column. The aqueous methanol eluate was collected and concentrated to 3 ml under a nitrogen stream, and the concentrate was lyophilized overnight. The residue from lyophilization was dissolved in 2 ml of pH 4.6 buffer containing 0.01 *M* KCl. The sample was deoxygenated for 5–10 min and analyzed by differential pulse polarography using the previously described conditions. The final concentrations of indicine-*N*-oxide in the plasma samples used to determine drug recovery were 0, 1, 3, 6, 9, 13, 15, 17, and 20 μg/ml of plasma.

pKa Determinations—The pKa of indicine-*N*-oxide was determined (in duplicate) by titration with 1 *N* HCl at 23°. The *N*-oxide (120 mg) was dissolved in 10 ml of 0.05 *M* KCl (freed of carbon dioxide by bubbling argon through the reagent for 15 min). Hydrochloric acid (1 *N*) was added in 25-μl increments, and the pH was recorded with each increment. The pKa was determined at the point where half-neutralization occurred. The method was checked by determining the pKa of tris(hydroxymethyl)-aminomethane, which has a value of 8.07 at 25° (8) (found 8.04 at 25°).

TLC—TLC was carried out on precoated silica gel plates[10] (20 cm × 20 cm × 0.25 mm) with chloroform–methanol–ammonium hydroxide

[1] PAR model 174A, Princeton Applied Research Corp., Princeton, N.J.
[2] Hewlett-Packard model 7044A.
[3] Obtained from Drug Research and Development, Division of Cancer Treatment, National Cancer Institute (indicine-*N*-oxide was lot 76-08-12-01).
[4] Burdick & Jackson, Muskegon, Mich.
[5] Milli-RO4 purification system, Millipore Corp., Bedford, Mass.
[6] Fisher Scientific Co., Medford, Mass.
[7] Model 10-100, The Virtis Co., Gardiner, N.Y.
[8] W200, neutral, supergrade 1, ICN Pharmaceuticals, Cleveland, Ohio.
[9] C_{18} Sep Pak, Waters Associates, Milford, Mass.
[10] EM Laboratories, Elmsford, N.Y.

Table II—Recovery of Indicine-*N*-oxide from Plasma Samples

Amount Added, μg	Amount Found[a], μg	Recovery, %
1	0.78 ± 0.04	78
3	3.07 ± 0.04	102
6	5.33 ± 0.07	89
9	7.99 ± 0.04	89
13	11.7 ± 0.1	90
15	12.9 ± 0.1	86
17	15.2 ± 0.1	90
20	16.1	81
Average		88 ± 7

[a] Average of duplicate samples.

(10:9:1) as the developing solvent. Components were visualized with Dragendorff's spray reagent (9).

RESULTS AND DISCUSSION

Solutions of indicine-*N*-oxide in pH 4.6 buffer exhibited a differential pulse polarographic maximum at −0.72 ± 0.03 v (saturated calomel electrode) (Fig. 1). The potential for this maximum was pH dependent, becoming more negative at higher pH values (Table I). Since similar reduction peak potentials and pH dependencies have been observed for other *N*-oxides (10–12), these data are consistent with reduction of an *N*-oxide moiety. In support of this reduction, no wave was detected for indicine (NSC 136052), the reduced form of indicine-*N*-oxide, under similar polarographic conditions. The pKa of indicine-*N*-oxide was 4.25 ± 0.02 at 23°. This value is consistent with values of other *N*-oxides, which are typically in the 4.3–5.4 range (10–12). The average purity of the drug was 95.9 ± 3% based on the number of millimoles of hydrogen ion added at the equivalence point to the millimoles of *N*-oxide added (based on the weight).

A pH of 4.63 was chosen for the analysis medium because the effect of pH on the peak potential in this region was minimal and the intensity of response was the greatest (Table I). A linear polarographic response was observed over a range of 0.5–10 μg/ml of pH 4.6 buffer. The standard curve parameters determined by a least-squares fit of the data indicated a response of 0.122 ± 0.002 μamp/μg/ml and a correlation coefficient of 0.9997.

Extraction of indicine-*N*-oxide from plasma samples was possible only after lyophilization. Both normal aluminum oxide and reversed-phase (C_{18} bonded silica gel) chromatographic columns were needed to remove other chemical species that gave polarographic responses in the same region as the drug. Qualitative confirmation of the drug in the methanolic extract of the lyophilized residue, the methanolic eluate from the aluminum oxide column, and the methanol–water eluate from the reversed-phase silica gel column was determined by TLC (R_f 0.41). Indicine-*N*-oxide was not retained to any significant extent by either column, as indicated by the recovery data.

Analysis of plasma spiked with known concentrations of indicine-*N*-oxide gave an overall recovery of 88 ± 7% (*SD*) (Table II) over a concentration range of 1–20 μg/ml of plasma. The plasma assay presented here is a reliable, sensitive method that is applicable for clinical use. The method is suitable for the analysis of the parent *N*-oxide in the presence of the known metabolic reduction product, indicine (2).

REFERENCES

(1) M. Kugelman, W. C. Liu, M. Axelrod, T. J. McBride, and K. V. Rao, *Lloydia*, **39**, 125 (1976).

(2) M. M. Ames and G. Powis, *J. Chromatogr.*, **166**, 519 (1978).

(3) J. V. Evans, A. Peng, and C. J. Nielsen, "26th Annual Conference on Mass Spectrometry and Allied Topics," American Society for Mass Spectrometry, 1978, abstr. MC3.

(4) J. V. Evans, S. K. Daley, and C. J. Nielsen, "27th Annual Conference on Mass Spectrometry and Allied Topics," American Society for Mass Spectrometry, 1979, abstr. WAMOA4.

(5) J. V. Evans, A. Peng, and C. J. Nielsen, *Biomed. Mass Spectrom.*, **6**, 38 (1979).

(6) J. H. Christie, J. Osteryoung, and R. A. Osteryoung, *Anal. Chem.*, **45**, 210 (1973).

(7) A. R. Branfman, I. Bodek, and M. McComish, "177th National Meeting of the American Chemical Society," Abstr. Anal. 022 (1979).

(8) "Handbook of Analytical Chemistry," L. Meites, Ed., McGraw-Hill, New York, N.Y., 1963, pp. 1–27.

(9) "Handbook of Chromatography," vol. II, CRC Press, Cleveland, Ohio, 1972, p. 113.

(10) A. H. Beckett, E. E. Essien, and W. F. Smyth, *J. Pharm. Pharmacol.*, **26**, 399 (1974).

(11) H. Hoffmann, *Arch. Pharm.*, **304**, 741 (1971).

(12) P. Jenner, *Xenobiotica*, **1**, 399 (1971).

ACKNOWLEDGMENTS

Supported by Contract NO1-CM-87163 from the Division of Cancer Treatment, National Cancer Institute, National Institutes of Health.

The authors thank Dr. C. J. Nielsen of the National Cancer Institute Frederick Cancer Research Center for helpful advice concerning the extraction of indicine-*N*-oxide from biological fluids and Dr. E. Modest of the Sidney Farber Cancer Institute for supplying the human plasma. Discussions with J. Valentine and T. Gilbert are gratefully acknowledged.

Synthesis of Phenylurethans of 1,2-Dialkyl-4-pyrazolidinols as Anticonvulsant Agents

MILTON J. KORNET

Received December 10, 1979, from the *College of Pharmacy, University of Kentucky, Lexington, KY 40506.* Accepted for publication January 18, 1980.

Abstract □ Twelve phenylurethans of 1,2-dialkyl-4-pyrazolidinols were synthesized and tested for anticonvulsant activity. Several compounds exhibited activity.

Keyphrases □ Phenylurethans—synthesized from 1,2-dialkyl-4-pyrazolidinols, evaluation as anticonvulsant agents □ Anticonvulsant activity—phenylurethans of 1,2-dialkyl-4-pyrazolidinols, synthesis and evaluation for activity □ 1,2-Dialkyl-4-pyrazolidinols—phenylurethan derivatives, synthesis and testing for anticonvulsant activity

4-Pyrazolidinyl benzoates, ester derivatives of 1,2-dialkyl-4-pyrazolidinols (I), reportedly possess local anesthetic activity (1). Since lidocaine (2) and many urethans (3) show anticonvulsant properties, synthesis and testing of a series of phenylurethans (III*a*–III*l*) of 1,2-dialkyl-4-pyrazolidinols as potential anticonvulsant agents were desired.

DISCUSSION

The necessary 1,2-dialkyl-4-pyrazolidinols (I) were obtained from the reaction of epichlorohydrin and 1,2-dialkylhydrazines according to a reported procedure (4). Hydrazinoalcohols possessing methyl (I*a*), ethyl (I*b*), and *n*-propyl (I*c*) substituents were prepared. The 1,2-dialkyl-4-

0022-3549/80/0600-0729$01.00/0

© 1980, American Pharmaceutical Association

Table II—Recovery of Indicine-*N*-oxide from Plasma Samples

Amount Added, μg	Amount Found[a], μg	Recovery, %
1	0.78 ± 0.04	78
3	3.07 ± 0.04	102
6	5.33 ± 0.07	89
9	7.99 ± 0.04	89
13	11.7 ± 0.1	90
15	12.9 ± 0.1	86
17	15.2 ± 0.1	90
20	16.1	81
Average		88 ± 7

[a] Average of duplicate samples.

(10:9:1) as the developing solvent. Components were visualized with Dragendorff's spray reagent (9).

RESULTS AND DISCUSSION

Solutions of indicine-*N*-oxide in pH 4.6 buffer exhibited a differential pulse polarographic maximum at −0.72 ± 0.03 v (saturated calomel electrode) (Fig. 1). The potential for this maximum was pH dependent, becoming more negative at higher pH values (Table I). Since similar reduction peak potentials and pH dependencies have been observed for other *N*-oxides (10–12), these data are consistent with reduction of an *N*-oxide moiety. In support of this reduction, no wave was detected for indicine (NSC 136052), the reduced form of indicine-*N*-oxide, under similar polarographic conditions. The pKa of indicine-*N*-oxide was 4.25 ± 0.02 at 23°. This value is consistent with values of other *N*-oxides, which are typically in the 4.3–5.4 range (10–12). The average purity of the drug was 95.9 ± 3% based on the number of millimoles of hydrogen ion added at the equivalence point to the millimoles of *N*-oxide added (based on the weight).

A pH of 4.63 was chosen for the analysis medium because the effect of pH on the peak potential in this region was minimal and the intensity of response was the greatest (Table I). A linear polarographic response was observed over a range of 0.5–10 μg/ml of pH 4.6 buffer. The standard curve parameters determined by a least-squares fit of the data indicated a response of 0.122 ± 0.002 μamp/μg/ml and a correlation coefficient of 0.9997.

Extraction of indicine-*N*-oxide from plasma samples was possible only after lyophilization. Both normal aluminum oxide and reversed-phase (C_{18} bonded silica gel) chromatographic columns were needed to remove other chemical species that gave polarographic responses in the same region as the drug. Qualitative confirmation of the drug in the methanolic extract of the lyophilized residue, the methanolic eluate from the aluminum oxide column, and the methanol–water eluate from the reversed-phase silica gel column was determined by TLC (R_f 0.41). Indicine-*N*-oxide was not retained to any significant extent by either column, as indicated by the recovery data.

Analysis of plasma spiked with known concentrations of indicine-*N*-oxide gave an overall recovery of 88 ± 7% (*SD*) (Table II) over a concentration range of 1–20 μg/ml of plasma. The plasma assay presented here is a reliable, sensitive method that is applicable for clinical use. The method is suitable for the analysis of the parent *N*-oxide in the presence of the known metabolic reduction product, indicine (2).

REFERENCES

(1) M. Kugelman, W. C. Liu, M. Axelrod, T. J. McBride, and K. V. Rao, *Lloydia*, **39**, 125 (1976).

(2) M. M. Ames and G. Powis, *J. Chromatogr.*, **166**, 519 (1978).

(3) J. V. Evans, A. Peng, and C. J. Nielsen, "26th Annual Conference on Mass Spectrometry and Allied Topics," American Society for Mass Spectrometry, 1978, abstr. MC3.

(4) J. V. Evans, S. K. Daley, and C. J. Nielsen, "27th Annual Conference on Mass Spectrometry and Allied Topics," American Society for Mass Spectrometry, 1979, abstr. WAMOA4.

(5) J. V. Evans, A. Peng, and C. J. Nielsen, *Biomed. Mass Spectrom.*, **6**, 38 (1979).

(6) J. H. Christie, J. Osteryoung, and R. A. Osteryoung, *Anal. Chem.*, **45**, 210 (1973).

(7) A. R. Branfman, I. Bodek, and M. McComish, "177th National Meeting of the American Chemical Society," Abstr. Anal. 022 (1979).

(8) "Handbook of Analytical Chemistry," L. Meites, Ed., McGraw-Hill, New York, N.Y., 1963, pp. 1–27.

(9) "Handbook of Chromatography," vol. II, CRC Press, Cleveland, Ohio, 1972, p. 113.

(10) A. H. Beckett, E. E. Essien, and W. F. Smyth, *J. Pharm. Pharmacol.*, **26**, 399 (1974).

(11) H. Hoffmann, *Arch. Pharm.*, **304**, 741 (1971).

(12) P. Jenner, *Xenobiotica*, **1**, 399 (1971).

ACKNOWLEDGMENTS

Supported by Contract NO1-CM-87163 from the Division of Cancer Treatment, National Cancer Institute, National Institutes of Health.

The authors thank Dr. C. J. Nielsen of the National Cancer Institute Frederick Cancer Research Center for helpful advice concerning the extraction of indicine-*N*-oxide from biological fluids and Dr. E. Modest of the Sidney Farber Cancer Institute for supplying the human plasma. Discussions with J. Valentine and T. Gilbert are gratefully acknowledged.

Synthesis of Phenylurethans of 1,2-Dialkyl-4-pyrazolidinols as Anticonvulsant Agents

MILTON J. KORNET

Received December 10, 1979, from the *College of Pharmacy, University of Kentucky, Lexington, KY 40506.* Accepted for publication January 18, 1980.

Abstract □ Twelve phenylurethans of 1,2-dialkyl-4-pyrazolidinols were synthesized and tested for anticonvulsant activity. Several compounds exhibited activity.

Keyphrases □ Phenylurethans—synthesized from 1,2-dialkyl-4-pyrazolidinols, evaluation as anticonvulsant agents □ Anticonvulsant activity—phenylurethans of 1,2-dialkyl-4-pyrazolidinols, synthesis and evaluation for activity □ 1,2-Dialkyl-4-pyrazolidinols—phenylurethan derivatives, synthesis and testing for anticonvulsant activity

4-Pyrazolidinyl benzoates, ester derivatives of 1,2-dialkyl-4-pyrazolidinols (I), reportedly possess local anesthetic activity (1). Since lidocaine (2) and many urethans (3) show anticonvulsant properties, synthesis and testing of a series of phenylurethans (III*a*–III*l*) of 1,2-dialkyl-4-pyrazolidinols as potential anticonvulsant agents were desired.

DISCUSSION

The necessary 1,2-dialkyl-4-pyrazolidinols (I) were obtained from the reaction of epichlorohydrin and 1,2-dialkylhydrazines according to a reported procedure (4). Hydrazinoalcohols possessing methyl (I*a*), ethyl (I*b*), and *n*-propyl (I*c*) substituents were prepared. The 1,2-dialkyl-4-

0022-3549/80/0600-0729$01.00/0

© 1980, American Pharmaceutical Association

Table I—Physical Properties of Hydrochlorides of Phenylurethans of 1,2-Dialkyl-4-pyrazolidinols

Compound	X	R	Melting Point	Yield, %	Formula	Analysis, % Calc.	Found
IIIa	o-CH_3	CH_3	208–209°	72	$C_{13}H_{19}N_3O_2$·HCl	C 54.64	54.67
						H 7.05	6.96
						N 14.70	14.80
IIIb	p-C_2H_5O	CH_3	176–179°	75	$C_{14}H_{21}N_3O_3$·HCl	C 53.25	53.29
						H 7.02	7.02
						N 13.31	13.28
IIIc	2-Cl,6-CH_3	CH_3	226–227°	75	$C_{13}H_{18}ClN_3O_2$·HCl	C 48.76	49.25
						H 5.98	6.33
						N 13.12	13.24
IIId	2,6-$(CH_3)_2$	CH_3	234–235° dec.	77	$C_{14}H_{21}N_3O_2$·HCl	C 56.09	56.23
						H 7.40	7.43
						N 14.02	14.07
IIIe	H	C_2H_5	135–136°	64	$C_{14}H_{21}N_3O_2$·HCl	C 56.09	56.18
						H 7.40	7.48
						N 14.02	14.05
IIIf	p-CH_3	C_2H_5	135–137°	32	$C_{15}H_{23}N_3O_2$·HCl	C 57.41	57.59
						H 7.71	7.59
						N 13.39	13.48
IIIg	2-Cl,6-CH_3	C_2H_5	212–213°	66	$C_{15}H_{22}ClN_3O_2$·HCl	C 51.73	52.22
						H 6.66	6.88
						N 12.07	12.19
IIIh	2,6-$(CH_3)_2$	C_2H_5	219–220°	69	$C_{16}H_{25}N_3O_2$·HCl	C 58.62	58.66
						H 7.99	7.88
						N 12.82	12.81
IIIi	m-Cl	$CH_3(CH_2)_2$	157–159°	68	$C_{16}H_{24}ClN_3O_2$·HCl	C 53.04	53.40
						H 6.96	7.36
						N 11.60	11.60
IIIj	p-CH_3O	$CH_3(CH_2)_2$	168–171°	74	$C_{17}H_{27}N_3O_3$·HCl	C 57.05	57.01
						H 7.89	7.77
						N 11.74	11.64
IIIk	p-CH_3	$CH_3(CH_2)_2$	157.5–160°	74	$C_{17}H_{27}N_3O_2$·HCl	C 59.72	59.77
						H 8.26	8.34
						N 12.29	12.26
IIIl	m-CF_3	$CH_3(CH_2)_2$	143–146°	30	$C_{17}H_{24}F_3N_3O_2$·HCl	C 51.58	51.41
						H 6.37	6.88
						N 10.61	10.54

Table II—Anticonvulsant and Toxic Effects

Compound	MES Activity[a] 0.5 hr	MES Activity[a] 4 hr	sc Met Activity[a] 0.5 hr	sc Met Activity[a] 4 hr	Toxicity[a] 0.5 hr	Toxicity[a] 4 hr
IIIa	–	–	–	–	–	–
IIIb	–	–	+	–	+	–
IIIc	+	–	+	–	+	–
IIId	+	–	+	–	+	–
IIIe	–	–	–	–	–	–
IIIf	–	[b]	–	–	–	–
IIIg	–	–	–	–	+	–
IIIh	+	–	++	–	+	–
IIIi	–	–	+	+	+	–
IIIj	–	–	–	–	+	–
IIIk	+	–	–	++[c]	+	–
IIIl	+	–	+	–	+	–

[a] Activity and toxicity at 30, 100, and 300 mg/kg are represented by +++, ++, and +, respectively; – denotes no activity or toxicity observed at 300 mg/kg. [b] No activity observed at 100 mg/kg. [c] Rescreening gave inconsistent results; activity was observed at 30 and 100 but not at 300 mg/kg; no toxicity at all three doses.

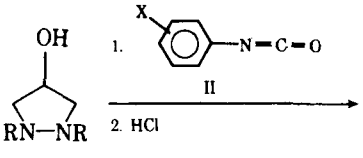

Ia: R = CH_3
Ib: R = CH_3CH_2
Ic: R = $CH_3(CH_2)_2$

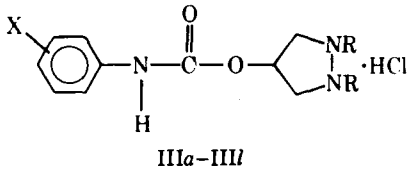

IIIa–IIIl

Scheme I

pyrazolidinols added readily to aryl substituted isocyanates (II) to give the adducts IIIa–IIIl (Scheme I). The latter compounds were isolated uniformly as their hydrochloride salts, and their physical properties are given in Table I.

Compounds IIIa–IIIl were examined in the maximal electroshock seizure (MES) and subcutaneous pentylenetetrazol seizure threshold (sc Met) tests for anticonvulsant activity and neurotoxicity in male mice[1] by reported procedures (5). Seven of the 12 compounds tested showed some degree of anticonvulsant activity (Table II). The most promising compound, IIIh, was evaluated further. The values for MES ED_{50}, sc Met ED_{50}, and TD_{50} (median toxic dose in the rotorod test) for IIIh were 193 (163–218), 336 (234–495), and 414 (353–499) mg/kg, respectively. Because of the moderate activity in this series of compounds, further work appears to be unwarranted.

EXPERIMENTAL[2]

A typical reaction for preparing the hydrochlorides of phenylurethans of 1,2-dialkyl-4-pyrazolidinols (IIIa–IIIl) is described using IIIk as the example. A mixture of 3.48 g (0.03 mole) of Ic (4), 3.99 g (0.03 mole) of p-tolyl isocyanate, and 45 ml of dry toluene was refluxed for 22 hr. The mixture was cooled and extracted twice with 50-ml portions of 2 *N* HCl. The combined acidic extract was washed with 50 ml of benzene, filtered through a sintered-glass funnel, and made basic with solid sodium carbonate. The separated oil was extracted into methylene chloride and dried over magnesium sulfate. Evaporation of the solution under reduced pressure gave an oily residue.

The oily free base was dissolved in absolute ethanol and acidified to pH ~2–3 by dropwise addition of concentrated hydrochloric acid. Upon cooling, a white solid precipitated, which was filtered and washed with cold absolute ethanol. Drying afforded 7.59 g (74% yield) of the hydrochloride salt, mp 156–159°. Recrystallization from absolute ethanol–ether gave analytically pure material, mp 157.5–160°; IR (KBr): 1720 (C=O) cm^{-1}.

[1] No. 1, Carworth Farms.

[2] Melting points were determined on a Thomas-Hoover apparatus and are uncorrected. IR spectra were taken on a Perkin-Elmer 700 spectrophotometer as either liquid films or as potassium bromide pellets. Elemental analyses were performed by Dr. Kurt Eder, Geneva, Switzerland.

REFERENCES

(1) R. Daniels, Ger. offen. 1,923,850; through *Chem. Abstr.*, **72**, 31787c (1970).

(2) J. Mercier, in "Anticonvulsant Drugs," vol. 1, J. Mercier, Section Ed., Pergamon, Elmsford, N.Y., 1973, p. 228.

(3) W. J. Murray and L. B. Kier, in "Anticonvulsants," J. A. Vida, Ed., Academic, New York, N.Y., 1977, p. 589.

(4) M. J. Kornet, *J. Heterocycl. Chem.*, **16**, 1485 (1979).

(5) M. J. Kornet, *J. Pharm. Sci.*, **67**, 1471 (1978).

ACKNOWLEDGMENTS

The author thanks Mr. Gill D. Gladding and the Antiepileptic Drug Development Program, National Institutes of Health, for providing the anticonvulsant activity data. He also is grateful to Mrs. Kelly Filo for technical assistance in the preparation of some compounds.

Evaluation of ^{99m}Tc-Labeled Iminodiacetic Acid Derivatives of Substituted 2-Aminopyrroles as Hepatobiliary Imaging Agents I

CARL M. DeJULIIS, BERNARD W. GRAHAM ˣ, RONALD J. MATTSON, and J. WALTER SOWELL, Sr.

Received November 5, 1979, from the *College of Pharmacy, University of South Carolina, Columbia, SC 29208.* Accepted for publication January 14, 1980.

Abstract □ *N*-(3-Cyano-4,5-dimethyl-2-pyrrylcarbamoylmethyl)iminodiacetic acid (II*a*) and *N*-(3-cyano-4-methyl-5-benzyl-2-pyrrylcarbamoylmethyl)iminodiacetic acid (II*b*) were synthesized, labeled with technetium 99*m*, and compared with ^{99m}Tc-labeled *p*-isopropylacetanilidoiminodiacetic acid (I) for hepatobiliary activity in rats. All three compounds showed similar clearance of radioactivity from the blood. Comparison of the amount of radioactivity in various organs 1 hr after injection showed no significant difference between I and II*b*. Compound II*a* showed significantly less radioactivity in the GI tract and a higher amount in the kidneys and bladder.

Keyphrases □ Iminodiacetic acid—^{99m}Tc-labeled, derivatives of 2-aminopyrroles, evaluation as hepatobiliary imaging agents, rats □ Lidocaine, 2-aminopyrrole analogs—^{99m}Tc-labeled iminodiacetic acid derivatives, evaluation as hepatobiliary imaging agents, rats □ Radiopharmaceuticals—^{99m}Tc-labeled iminodiacetic acid derivatives of 2-aminopyrroles, evaluation as hepatobiliary imaging agents, rats

Efforts have been made in recent years to formulate ^{99m}Tc-labeled radiopharmaceuticals for use in hepatobiliary scintigraphic imaging. Many lidocaine analogs with an iminodiacetic acid functional group capable of forming a stable complex with technetium 99*m* have been evaluated (1). Most lidocaine derivatives were synthesized by altering the lipophilic substituents on the benzene ring. One compound, *p*-isopropylacetanilidoiminodiacetic acid (I), has shown desirable characteristics and now is available commercially.

Johnson *et al.* (2) recently synthesized a series of 2-diethylaminoacetamido-3-cyano-4-methyl-5-substituted pyrrole analogs of lidocaine. These compounds compared favorably with lidocaine in local anesthetic and antiarrhythmic activities. The iminodiacetic acid derivatives of the methyl- (II*a*) and benzyl- (II*b*) substituted compounds were prepared. These two compounds were labeled with technetium 99*m* and compared with ^{99m}Tc-labeled I for hepatobiliary activity in rats.

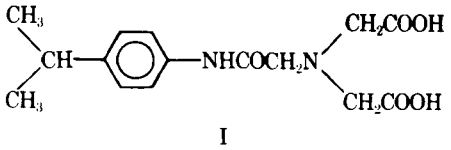

I

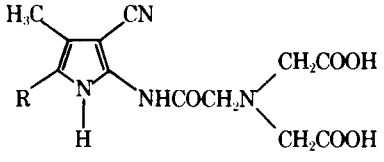

II

II*a*: R = CH_3
II*b*: R = $CH_2C_6H_5$

EXPERIMENTAL

Chemistry[1]—*N-(3-Cyano-4,5-dimethyl-2-pyrrylcarbamoylmethyl)-iminodiacetic Acid (II*a*)*—A modified procedure of Callery *et al.* (3) was used. A mixture of 2-chloroacetamido-3-cyano-4,5-dimethylpyrrole (5.72 g, 0.027 mole) (2), disodium iminodiacetic acid monohydrate (5.44 g, 0.027 mole), and sodium hydroxide (1.10 g, 0.027 mole) in 100 ml of methanol–water (3:1) was refluxed for 24 hr. The methanol was removed *in vacuo*, 100 ml of water was added to the residue, the suspension was filtered, and the pH of the filtrate was adjusted to 3 by the dropwise addition of concentrated hydrochloric acid. The precipitate was collected and air dried.

The crude product (6.2 g, 76.8% yield) was washed several times with boiling water to yield a brown powder (homogeneous on TLC in methanol, R_f 0.55), mp 203–204.5° dec.; IR (KBr): 3610, 3330, 2210, 1675, 1640, 1430, 1400, 1220, and 725 cm^{-1}; NMR (dimethyl sulfoxide-d_6): δ 1.92 (s, 3H, CH_3 at C-4), 2.03 (s, 3H, CH_3 at C-5), 3.47 (s, 6H, CH_2), 10.75 (s, 1H, N_1H), and 10.3–12.8 (broad s, 3H, NHCO, COOH, and $^+$NH) ppm.

Anal.—Calc. for $C_{13}H_{16}N_4O_5$: C, 50.64; H, 5.23; N, 18.17. Found: C, 50.53; H, 5.23; N, 18.16.

*N-(3-Cyano-4-methyl-5-benzyl -2- pyrrylcarbamoylmethyl)iminodiacetic Acid (II*b*)*—A mixture of 2-chloroacetamido-3-cyano-4-methyl-5-benzylpyrrole (7.77 g, 0.027 mole) (2), disodium iminodiacetic acid monohydrate (5.44 g, 0.027 mole), and sodium hydroxide (1.10 g, 0.027 mole) was condensed according to the procedure described for II*a*. A brown powder was obtained (6.5 g, 62.6% yield) (homogeneous on TLC in methanol, R_f 0.51), mp 190–192° dec.; IR (KBr): 3400, 3330, 2210, 1675, 1620, 1250, 1215, 950, and 710 cm^{-1}; NMR (dimethyl sulfoxide-d_6): δ 1.96 (s, 3H, CH_3 at C-4), 3.79 (s, 2H, CH_2 at C-5), 4.2 (broad s, 6H, CH_2), 7.07 (s, 5H, C_6H_5), 11.25 (broad s, 3H, NHCO, COOH, and $^+$NH), and 11.5 (broad s, 1H, N_1H) ppm.

Anal.—Calc. for $C_{19}H_{20}N_4O_5$: C, 59.37; H, 5.24; N, 14.58. Found: C, 59.23; H, 5.26; N, 14.53.

[1] IR spectra were determined on a Beckman Acculab 4 spectrophotometer using the potassium bromide technique. NMR spectra were determined on a Hitachi Perkin-Elmer R24 high-resolution spectrometer with tetramethylsilane as the internal reference. Melting points were obtained using a Thomas-Hoover capillary apparatus and are uncorrected. TLC was performed using Eastman type 6060 chromatogram sheets (silica gel), and the sheets were developed in an iodine chamber. Carbon, hydrogen, and nitrogen values were obtained from analyses performed by Atlantic Microlabs., Atlanta, Ga.

0022-3549/80/0600-0731$01.00/0

© 1980, American Pharmaceutical Association

REFERENCES

(1) R. Daniels, Ger. offen. 1,923,850; through *Chem. Abstr.*, **72**, 31787c (1970).

(2) J. Mercier, in "Anticonvulsant Drugs," vol. 1, J. Mercier, Section Ed., Pergamon, Elmsford, N.Y., 1973, p. 228.

(3) W. J. Murray and L. B. Kier, in "Anticonvulsants," J. A. Vida, Ed., Academic, New York, N.Y., 1977, p. 589.

(4) M. J. Kornet, *J. Heterocycl. Chem.*, **16**, 1485 (1979).

(5) M. J. Kornet, *J. Pharm. Sci.*, **67**, 1471 (1978).

ACKNOWLEDGMENTS

The author thanks Mr. Gill D. Gladding and the Antiepileptic Drug Development Program, National Institutes of Health, for providing the anticonvulsant activity data. He also is grateful to Mrs. Kelly Filo for technical assistance in the preparation of some compounds.

Evaluation of ^{99m}Tc-Labeled Iminodiacetic Acid Derivatives of Substituted 2-Aminopyrroles as Hepatobiliary Imaging Agents I

CARL M. DeJULIIS, BERNARD W. GRAHAM ˣ, RONALD J. MATTSON, and J. WALTER SOWELL, Sr.

Received November 5, 1979, from the *College of Pharmacy, University of South Carolina, Columbia, SC 29208.* Accepted for publication January 14, 1980.

Abstract □ *N*-(3-Cyano-4,5-dimethyl-2-pyrrylcarbamoylmethyl)iminodiacetic acid (II*a*) and *N*-(3-cyano-4-methyl-5-benzyl-2-pyrrylcarbamoylmethyl)iminodiacetic acid (II*b*) were synthesized, labeled with technetium 99*m*, and compared with ^{99m}Tc-labeled *p*-isopropylacetanilidoiminodiacetic acid (I) for hepatobiliary activity in rats. All three compounds showed similar clearance of radioactivity from the blood. Comparison of the amount of radioactivity in various organs 1 hr after injection showed no significant difference between I and II*b*. Compound II*a* showed significantly less radioactivity in the GI tract and a higher amount in the kidneys and bladder.

Keyphrases □ Iminodiacetic acid—^{99m}Tc-labeled, derivatives of 2-aminopyrroles, evaluation as hepatobiliary imaging agents, rats □ Lidocaine, 2-aminopyrrole analogs—^{99m}Tc-labeled iminodiacetic acid derivatives, evaluation as hepatobiliary imaging agents, rats □ Radiopharmaceuticals—^{99m}Tc-labeled iminodiacetic acid derivatives of 2-aminopyrroles, evaluation as hepatobiliary imaging agents, rats

Efforts have been made in recent years to formulate ^{99m}Tc-labeled radiopharmaceuticals for use in hepatobiliary scintigraphic imaging. Many lidocaine analogs with an iminodiacetic acid functional group capable of forming a stable complex with technetium 99*m* have been evaluated (1). Most lidocaine derivatives were synthesized by altering the lipophilic substituents on the benzene ring. One compound, *p*-isopropylacetanilidoiminodiacetic acid (I), has shown desirable characteristics and now is available commercially.

Johnson *et al.* (2) recently synthesized a series of 2-diethylaminoacetamido-3-cyano-4-methyl-5-substituted pyrrole analogs of lidocaine. These compounds compared favorably with lidocaine in local anesthetic and antiarrhythmic activities. The iminodiacetic acid derivatives of the methyl- (II*a*) and benzyl- (II*b*) substituted compounds were prepared. These two compounds were labeled with technetium 99*m* and compared with ^{99m}Tc-labeled I for hepatobiliary activity in rats.

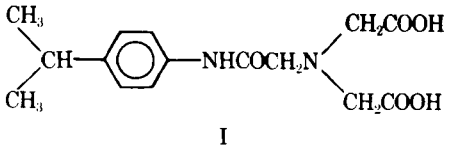

I

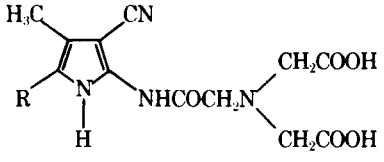

II

II*a*: R = CH_3
II*b*: R = $CH_2C_6H_5$

EXPERIMENTAL

Chemistry[1]—*N-(3-Cyano-4,5-dimethyl-2-pyrrylcarbamoylmethyl)-iminodiacetic Acid (II*a*)*—A modified procedure of Callery *et al.* (3) was used. A mixture of 2-chloroacetamido-3-cyano-4,5-dimethylpyrrole (5.72 g, 0.027 mole) (2), disodium iminodiacetic acid monohydrate (5.44 g, 0.027 mole), and sodium hydroxide (1.10 g, 0.027 mole) in 100 ml of methanol–water (3:1) was refluxed for 24 hr. The methanol was removed *in vacuo*, 100 ml of water was added to the residue, the suspension was filtered, and the pH of the filtrate was adjusted to 3 by the dropwise addition of concentrated hydrochloric acid. The precipitate was collected and air dried.

The crude product (6.2 g, 76.8% yield) was washed several times with boiling water to yield a brown powder (homogeneous on TLC in methanol, R_f 0.55), mp 203–204.5° dec.; IR (KBr): 3610, 3330, 2210, 1675, 1640, 1430, 1400, 1220, and 725 cm^{-1}; NMR (dimethyl sulfoxide-d_6): δ 1.92 (s, 3H, CH_3 at C-4), 2.03 (s, 3H, CH_3 at C-5), 3.47 (s, 6H, CH_2), 10.75 (s, 1H, N_1H), and 10.3–12.8 (broad s, 3H, NHCO, COOH, and $^+$NH) ppm.

Anal.—Calc. for $C_{13}H_{16}N_4O_5$: C, 50.64; H, 5.23; N, 18.17. Found: C, 50.53; H, 5.23; N, 18.16.

*N-(3-Cyano-4-methyl-5-benzyl -2- pyrrylcarbamoylmethyl)iminodiacetic Acid (II*b*)*—A mixture of 2-chloroacetamido-3-cyano-4-methyl-5-benzylpyrrole (7.77 g, 0.027 mole) (2), disodium iminodiacetic acid monohydrate (5.44 g, 0.027 mole), and sodium hydroxide (1.10 g, 0.027 mole) was condensed according to the procedure described for II*a*. A brown powder was obtained (6.5 g, 62.6% yield) (homogeneous on TLC in methanol, R_f 0.51), mp 190–192° dec.; IR (KBr): 3400, 3330, 2210, 1675, 1620, 1250, 1215, 950, and 710 cm^{-1}; NMR (dimethyl sulfoxide-d_6): δ 1.96 (s, 3H, CH_3 at C-4), 3.79 (s, 2H, CH_2 at C-5), 4.2 (broad s, 6H, CH_2), 7.07 (s, 5H, C_6H_5), 11.25 (broad s, 3H, NHCO, COOH, and $^+$NH), and 11.5 (broad s, 1H, N_1H) ppm.

Anal.—Calc. for $C_{19}H_{20}N_4O_5$: C, 59.37; H, 5.24; N, 14.58. Found: C, 59.23; H, 5.26; N, 14.53.

[1] IR spectra were determined on a Beckman Acculab 4 spectrophotometer using the potassium bromide technique. NMR spectra were determined on a Hitachi Perkin-Elmer R24 high-resolution spectrometer with tetramethylsilane as the internal reference. Melting points were obtained using a Thomas-Hoover capillary apparatus and are uncorrected. TLC was performed using Eastman type 6060 chromatogram sheets (silica gel), and the sheets were developed in an iodine chamber. Carbon, hydrogen, and nitrogen values were obtained from analyses performed by Atlantic Microlabs., Atlanta, Ga.

0022-3549/80/0600-0731$01.00/0

© 1980, American Pharmaceutical Association

Table I—Parameters for the Blood Elimination Equation of Technetium 99*m* in Rats following Intravenous Injection of ^{99m}Tc-Labeled I, II*a*, and II*b*[a]

Parameter	I	II*a*	II*b*
A	0.76 (0.05)	0.73 (0.04)	0.81 (0.03)
α	0.40 (0.06)	0.52 (0.04)	0.69 (0.05)
B	0.24 (0.03)	0.27 (0.02)	0.19 (0.01)
β	0.030 (0.005)	0.023 (0.003)	0.027 (0.002)
R_2	91.8	98.2	97.8

[a] Standard errors are given in parentheses.

Labeling with Technetium 99*m*—Technetium 99*m* labeling of I was achieved by adding 7 mCi (1.0 ml) of sodium [^{99m}Tc]pertechnetate (III) eluate from a molybdenum 99–technetium 99*m* generator[2] to a vial containing a lyophilized preparation of 20 mg of I and 0.2 mg of stannous chloride[3].

Preparation of ^{99m}Tc-labeled II*a* and II*b* was accomplished by stannous chloride reduction of III in aqueous solution. Ten milligrams of pure compound was dissolved in 0.3 ml of 0.1 *N* NaOH. This solution was back-titrated with 0.05 *N* HCl to pH 7. Seven millicuries of III in 0.2 ml was added, and the resulting solution was purged with nitrogen for 5 min. After purging, 0.1 ml of freshly prepared stannous chloride (1 mg/ml in 0.05 *N* HCl) was added, and the mixture was kept at room temperature for 20 min. The final solution then was passed through a Millipore filter into a sterile evacuated vial.

The radiochemical purity of the ^{99m}Tc-labeled I was determined using instant TLC[4] with a chloroform–acetone (70:30) solvent system. The radiochemical purity of ^{99m}Tc-labeled II*a* and II*b* was determined using instant TLC with a methyl ethyl ketone solvent system. Examination of the chromatographic strips revealed the bound fraction to be 93% or greater for all of the radiopharmaceuticals.

***In Vivo* Studies**—Fasting, nonhydrated, male Sprague–Dawley[5] rats, 175–240 g, were used. The left jugular vein was exposed and cannulated for each animal after anesthesia was achieved with pentobarbital sodium (30 mg/kg). The animal then was positioned over a rectilinear scanner[6] modified to record the counts arising from the cardiac pool. Following the injection of 0.25 mCi of the ^{99m}Tc-labeled compound into the cannula, sequential counts were obtained for the duration of the study. These counts were used to model the disappearance of the radioactivity from the blood.

Each animal was killed 1 hr after injection of the radiopharmaceutical by overanesthesia with ether. Selected organs were removed from the animal and assayed for radioactivity. The results are reported as the percentage of the total injected radioactivity.

RESULTS

The disappearance of the radioactivity from the blood is described by a two-compartment open model. The computer-fitted equation[7] used to describe the data is:

$$C_B = A \exp(-\alpha t) + B \exp(-\beta t) \qquad \text{(Eq. 1)}$$

where C_B refers to the fraction of the dose retained in the blood (biological) and t is time (minutes). The parameters for Eq. 1 and the correlation coefficient (R^2) for each parameter are listed in Table I. Examination of these data reveals that there was no significant difference among the drugs for the β-phase of the elimination equation; the half-life for the β-phase ranged from 20 to 30 min.

Table II—Percent of Administered Radioactivity at 1 hr after Intravenous Injection of ^{99m}Tc-Labeled I, II*a*, and II*b* in Rat Organs[a]

Rat Organ	I	II*a*	II*b*
GI tract	78.7 (3.3)	38.0 (2.4)	81.5 (2.4)
Liver	2.6 (0.4)	8.0 (0.2)	6.7 (0.9)
Spleen	0.09 (0.03)	0.07 (0.05)	0.15 (0.08)
Kidneys	2.5 (0.2)	11.1 (3.4)	2.3 (0.3)
Lungs	0.17 (0.05)	0.30 (0.18)	0.20 (0.03)
Heart	0.02 (0.01)	0.02 (0.01)	0.07 (0.02)
Carcass	16.2 (3.0)	44.0 (2.8)	9.9 (0.9)

[a] Standard errors are given in parentheses.

Table II shows the distribution of technetium 99*m* in selected organs and tissues of the rat 1 hr after intravenous injection. The data are expressed as the percent of the injected dose and represent the average of three rats for each compound. The carcass values represent the remainder after the removal of the other organs and include the bladder, which accounted for much of the activity.

The organ data following injection of I or II*b* are indistinguishable except for the liver. Excretion into the GI tract accounted for almost 80% of the activity for both compounds. The kidneys retained about 2% of the injected dose, and the carcass contained about 10%. The content of technetium 99*m* in the liver at necropsy was significantly higher for the benzyl compound as compared to I.

The methyl derivative (II*a*) showed significantly less activity in the GI tract than either of the other compounds. Higher amounts of the injected activity were noted in the kidneys and remaining carcass.

REFERENCES

(1) G. Subramanian, J. G. McAfee, R. W. Henderson, M. Rosentreich, and L. Krokenberger, *J. Nucl. Med.*, **18**, 624 (1977).

(2) R. W. Johnson, T. H. Keenan, J. W. Kosh, and J. W. Sowell, Sr., *J. Pharm. Sci.*, **68**, 317 (1979).

(3) P. S. Callery, W. C. Faith, M. D. Loberg, A. T. Fields, E. G. Harvey, and M. D. Cooper, *J. Med. Chem.*, **19**, 962 (1976).

ACKNOWLEDGMENTS

Adapted in part from a thesis to be submitted by C. M. DeJuliis to the University of South Carolina in partial fulfillment of the Master of Science degree requirements.

[2] CintiChem, Union Carbide Corp., Tuxedo, N.Y.
[3] Diagnostic Isotopes Inc., Bloomfield, N.J.
[4] ITLC SG, Gelman Instrument Co., Ann Arbor, Mich.
[5] GIBCO Animal Research Laboratories, Madison, Wis.
[6] Magnascanner 500, Picker Instruments, Cleveland, Ohio.
[7] NLIN, SAS 76, Raleigh, N.C.

Antiproliferative Effects of Inhibitors of Polyamine Synthesis in Tumors of Neural Origin

SHARON K. CHAPMAN ˣ and SUSAN K. GLANT

Received October 22, 1979, from the *Department of Pharmacology and Therapeutics, College of Medicine, University of Florida, Gainesville, FL 32610.* Accepted for publication January 30, 1980.

Abstract □ The antiproliferative properties of inhibitors of polyamine synthesis were evaluated in cultured neuroblastoma and glioma cells. The diamines (1,3-propanediamine, 1,5-pentanediamine, and 1,6-hexanediamine) dramatically decreased neuroblastoma replication and inhibited the rate-limiting enzyme, ornithine decarboxylase. Glioma cells were less sensitive to the diamines in spite of significant drug-induced decreases in enzyme activity. The fact that ornithine decarboxylase was inhibited in both cell lines with different effects on proliferation suggests that the activity of other enzymes in polyamine biosynthesis may be altered selectively by these inhibitors.

Keyphrases □ Polyamines—inhibition of synthesis, effects of inhibitors on tumor cell growth, *in vitro* testing □ Ornithine carboxylase activity—inhibition of polyamine synthesis, effects of inhibitors on tumor cell growth, *in vitro* testing □ Antitumor activity—inhibition of polyamine synthesis, *in vitro* testing of ornithine carboxylase activity

Many chemotherapeutic agents that are effective in tumor treatment have had limited success in the treatment of malignant gliomas and neuroblastomas (1–4). Results have not been satisfactory due to drug toxicity, low tumor remission rates, and short durations of drug effectiveness.

Data have been obtained showing the presence of high levels of ornithine decarboxylase activity in tumor cells of neural origin (5–8). This enzyme catalyzes the rate-limiting reaction in the synthesis of putrescine, spermidine, and spermine (9); its basal activity is the lowest of the enzymes engaged in the synthesis of these polyamines (9, 10).

BACKGROUND

Several studies suggested that polyamine synthesis may be obligatory for tumor proliferation. Heby *et al.* (8) found a positive correlation between the growth rate of a rat brain tumor cell line and ornithine decarboxylase activity; the pattern of fluctuation in spermidine content correlated in a likewise manner (11). In cell-free systems, polyamines influence nearly every aspect of the formation and turnover of DNA, RNA, and protein (12–14). The relationship of polyamine synthesis to rapid growth has been reviewed extensively (10, 15–18).

Since ornithine decarboxylase activity is associated with rapid growth (16), ornithine decarboxylase inhibitors may find application as antiproliferative agents. Results obtained in these laboratories show that the cytolytic effects of bromoacetylcholine and bromoacetate in neuroblastoma are associated with decreased ornithine decarboxylase activity (5). However, recent studies suggested that a similar relationship may not be true in gliomas (20). Bromoacetylcholine and bromoacetate are potent antiproliferative agents in cultured cells of both experimental tumors (19), but ornithine decarboxylase is not inhibited in glioma cells by these agents (20). Although neuroblastoma and glioma have a common embryonic origin, these results suggest that differences may exist in the control mechanisms of polyamine synthesis.

Neuroblastoma cells are sensitive to numerous analogs of the substrate, ornithine, and of the product, putrescine (20). In this cell line, a correlation exists between the antiproliferative effects of these agents and their ability to decrease the activity of ornithine decarboxylase (20). To define further the relationship between polyamine deficiency and decreases in neuronal tumor growth rates, the effects of selective inhibitors of ornithine decarboxylase in cultured neuroblastoma and glioma cells were compared.

EXPERIMENTAL

Tumor Maintenance—Mouse neuroblastoma cells[1] were grown as described previously (5). Rat glioma cells[2] were cultivated in Ham's F-10 nutrient medium[3] supplemented with 50 units of penicillin/ml, 50 mEq of streptomycin/ml, 0.125 μg of amphotericin B/ml, 2% fetal calf serum, and 18% horse serum. Incubation was maintained at 37° with 10% CO_2–90% air and 100% humidity.

Drug Treatment—1,3-Propanediamine dihydrochloride[4], 1,6-hexanediamine[4], 1,5-pentanediamine[4], and α-methylornithine[5] were dissolved in glass-distilled water, neutralized, filter sterilized, and added in 50-μl quantities to 10 ml of the medium at time zero. For assays of ornithine decarboxylase activity, 1×10^6 cells were seeded in 100-mm tissue culture dishes; for cell counting experiments, 5×10^4 cells were seeded in 35-mm tissue culture dishes. Cells were grown for 24 hr after seeding, at which time drugs and fresh medium were added (time zero). Tumor growth was measured by counting the cells in a hemocytometer; viability was determined by trypan blue exclusion.

Ornithine Decarboxylase Assay—Enzyme assays were performed as described previously (5). After the growth medium was removed from the cells, the cells were washed with ice-cold phosphate–saline buffer (0.8% NaCl, 0.02% KCl, 0.115% Na_2HPO_4, and 0.05% KH_2PO_4 at pH 7.2) and suspended in 1.0 ml of assay buffer (0.05 *M* sodium phosphate–potassium phosphate at pH 7.2 containing 1 m*M* 1,4-dithiothreitol, 0.25 m*M* ethylenediaminetetraacetic acid, and 3 μ*M* pyridoxal 5-phosphate). Cells then were scraped off the plate with a rubber policeman and homogenized (20 strokes) with a glass homogenizer. After centrifugation at 4500×*g*, 0.2-ml portions of the supernatant fractions were incubated for 15 min in 15 × 85-mm centrifuge tubes equipped with rubber stoppers that supported polyethylene center wells[6]. Supernatant fractions that were heated at 65° for 10 min before incubation served as controls.

The reaction was initiated when 0.05 ml of 9.5 m*M* [1-^{14}C]L-ornithine[7] (10 Ci/mole) was added. After incubation at 37° for 30 min, 0.2 ml of benzetronium[8] hydroxide was injected into each center well and the reaction was continued for 30 min. To stop the reaction, 1 *M* citric acid (0.3 ml) was injected into the incubation mixture. To release the dissolved carbon dioxide, the tubes were agitated for another 30 min. The center wells then were removed from the tubes and placed into scintillation vials, and the radioactivity was determined with a scintillation counter. Protein was determined with an assay kit[9].

RESULTS

The antiproliferative effects of the ornithine decarboxylase inhibitors are shown in Fig. 1. Neuroblastoma cell growth appeared to be more sensitive than glioma cell growth to all of the agents over the period studied. The diamine inhibitors (1,3-propanediamine, 1,5-pentanediamine, and 1,6-hexanediamine) markedly inhibited neuroblastoma replication; 1,5-pentanediamine and 1,3-propanediamine were effective as early as 24 hr after their addition. These cells were less sensitive to the competitive inhibitor α-methylornithine; a delay of one generation was required before a decrease in cell proliferation was observed using this agent.

In contrast to the neuroblastoma results, normal growth was observed in cultured glioma cells over a 48-hr period in the presence of the inhibitors. After a lag of at least two generations, a notable decrease in tumor

[1] C1300, American Type Culture Collection.
[2] Clone C6, American Type Culture Collection.
[3] Grand Island Biological Co., Grand Island, NY 14072.
[4] Aldrich Chemical Co., Milwaukee, WI 53233.
[5] Calbiochem-Behring Corp., San Diego, CA 92112.
[6] Kontes Glass Co., Vineland, NJ 08360.
[7] New England Nuclear, Boston, MA 02118.
[8] Hyamine.
[9] Bio-Rad Laboratories, Rockville Centre, NY 11570.

0022-3549/80/0600-0733$01.00/0
© 1980, American Pharmaceutical Association

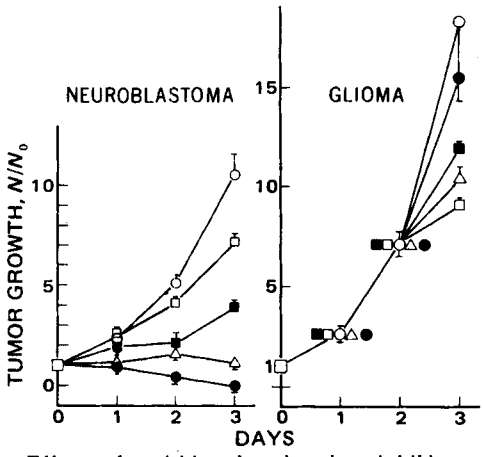

Figure 1—*Effects of ornithine decarboxylase inhibitors on neuroblastoma and glioma cell division. Key:* ○, *control;* □, *5 mM α-methylornithine;* ●, *5 mM 1,3-propanediamine;* △, *5 mM 1,5-pentanediamine; and* ■, *5 mM 1,6-hexanediamine. Results are expressed as the ratio* N/N_0, *where* N = *number of viable cells per dish at Day 1, 2, or 3 and* N_0 = *number of viable cells at time zero. Bars represent standard errors of the mean of six to 10 values.*

growth was apparent. At this time, α-methylornithine appeared to be slightly more effective than the diamines.

In experiments in which ornithine decarboxylase activity was measured, the antiproliferative effects of the diamines in neuroblastoma correlated with the decrease in enzyme activity (Fig. 2). Similarly, 1,3-propanediamine had no effect on glioma cell proliferation or on inhibition of ornithine decarboxylase activity. There were two exceptions to these parallel relationships:

1. Tumor growth was inhibited by α-methylornithine, but increases in enzyme activity were observed in both cell lines.
2. 1,5-Pentanediamine and 1,6-hexanediamine notably inhibited ornithine decarboxylase activity in glioma cells at a time when normal cell growth was observed.

DISCUSSION

An extensive amount of evidence has led to the concept that continuous polyamine synthesis is required to maintain maximum cell proliferation rates. An increase in ornithine decarboxylase activity is one of the earliest events to occur when cells are transformed from the resting to the growing state (5–7). It still is uncertain whether increases in polyamine synthesis are the cause or the consequence of rapid growth. However, a causal relationship between polyamine depletion and the inhibition of DNA synthesis has been suggested by results showing that exogenous ornithine or polyamines reversed the inhibition of DNA synthesis in tumor cells (21–24).

Most experimental efforts to deplete cellular polyamines have focused on the development of inhibitors of the rate-limiting enzyme, ornithine decarboxylase. Among these are competitive inhibitors such as α-methylornithine (22, 25, 26) and diamines such as 1,3-propanediamine, 1,5-pentanediamine, and 1,6-hexanediamine. The diamines have been shown to act by inducing the formation of macromolecular inhibitors of ornithine decarboxylase (27, 28) and by repressing the induction of the enzyme (28–32). The repression of enzyme synthesis has a relatively selective effect on ornithine decarboxylase; however, *S*-adenosylmethionine decarboxylase activity is inhibited slightly (33). A nonspecific inhibition of protein synthesis or a repression of other enzymes with short half-lives (*e.g.*, tyrosine aminotransferase) has not been demonstrated (33). The diamines are not inhibitory when added to cell-free assays (27–33).

In neuroblastoma, the diamines produced a dramatic decrease in both tumor growth and ornithine decarboxylase activity. In contrast, glioma cells continued to proliferate in the presence of the diamines. Differences in sensitivity probably are not due to drug accessibility since the enzyme was inhibited in both cell lines. These results may be explained by the interactions of the diamines with other enzymes in the polyamine biosynthetic pathway. Recent work with rat ventral prostate extracts (34) and Ehrlich ascites carcinoma cells (29) showed that diamines exert different inhibitory effects on the spermidine and spermine synthetases, regardless of their action on ornithine decarboxylase. Since a functional relationship between spermidine levels and growth rates has been confirmed in some cell lines (8, 11), these higher polyamines may be required for the expression of ornithine decarboxylase activity in proliferation (35).

In glioma cells, spermidine and spermine synthetases may be less sensitive to the diamine inhibitors and/or the half-life of endogenous spermidine may be quite long. In the latter case, the delay before the antiproliferative effects may correspond to the greater time required for spermidine depletion in this cell line. It also is possible that in glioma cells, these nonphysiological amines may be utilized to take over many of the metabolic functions of spermidine or spermine. The requirements for specific polyamines during rapid growth are being investigated.

In the present work, ornithine decarboxylase activity was increased in both neuroblastoma and glioma after treatment with α-methylornithine; competitive inhibition was observed only when the drug was added to cell-free assays (results not shown). This rise in the activity of the target enzyme in intact cells was reported for other cell lines (35) and may result either from a drug-induced increase in the apparent half-life of the enzyme (26, 36) or from a reversal of end-product inhibition of ornithine decarboxylase (24). Theoretically, an increased half-life could result from the ability of α-methylornithine to bind to the enzyme and protect it from degradation (37). However, in rat hepatoma cells, α-methylornithine increased the activities of ornithine decarboxylase as well as *S*-adenosylmethionine decarboxylase (24). This increase in an enzyme for which α-methylornithine is not a substrate is of concern. Reports that competitive ornithine decarboxylase inhibitors cause decreases in putrescine and spermidine levels (22) and that polyamines exert multiple negative feedback controls over both ornithine decarboxylase and *S*-adenosylmethionine decarboxylase (35) collectively favor the interpretation that increases in enzyme activity observed *in vivo* result from a reversal of end-product inhibition.

In summary, antiproliferative effects are achievable in tumors of neural origin using ornithine decarboxylase inhibitors. Some problems with this approach may be overcome by the design of more specific inhibitors of spermidine and spermine synthetases. The fact that ornithine decarboxylase was inhibited in both cell lines with vastly different effects on proliferation suggests that neuroblastoma and glioma cells may provide interesting model systems for drug development.

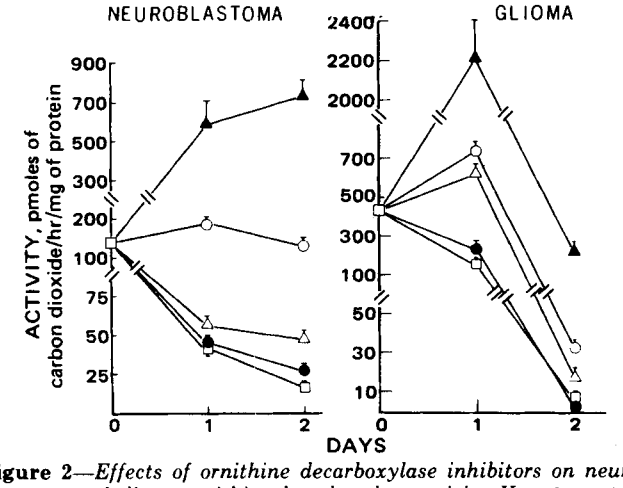

Figure 2—*Effects of ornithine decarboxylase inhibitors on neuroblastoma and glioma ornithine decarboxylase activity. Key:* ○, *control;* ▲, *0.5 mM α-methylornithine;* △, *0.5 mM 1,3-propanediamine;* ●, *0.5 mM 1,5-pentanediamine; and* □, *0.5 mM 1,6-hexanediamine. Bars represent standard errors of the mean of four to six values.*

REFERENCES

(1) D. H. James, Jr., O. Histu, E. L. Wren, Jr., and D. Pinkel, *J. Am. Med. Assoc.*, **194**, 123 (1965).

(2) A. E. Evans, R. M. Heyn, W. A. Newton, Jr., and S. L. Leiken, *ibid.*, **207**, 1325 (1967).

(3) M. P. Sullivan, A. H. Nora, P. Kulapongs, D. M. Lane, J. Windmiller, and W. G. Thurman, *Pediatrics*, **44**, 685 (1969).

(4) A. Shaw, in "Neuroblastoma," C. Pochedly, Ed., Publishing Sciences Group, Acton, Mass., 1976, p. 237.

(5) S. K. Chapman, M. Martin, M. S. Hoover, and C. Y. Chiou, *Biochem. Pharmacol.*, **27**, 717 (1978).

(6) U. Bachrach, *Proc. Natl. Acad. Sci. USA*, **72**, 3087 (1975).

(7) U. Bachrach, *FEBS Lett.*, **68**, 63 (1976).
(8) O. Heby, L. J. Marton, C. B. Wilson, and H. M. Martinez, *J. Cell Physiol.*, **86**, 511 (1975).
(9) A. Raina, R. L. Pajula, and T. Eloranta, *FEBS Lett.*, **67**, 252 (1976).
(10) J. Jänne, H. Pösö, and A. Raina, *Biochim. Biophys. Acta*, **473**, 241 (1978).
(11) O. Heby, L. J. Marton, C. B. Wilson, and H. M. Martinez, *FEBS Lett.*, **50**, 1 (1975).
(12) L. Stevens, *Biol. Rev.*, **45**, 1 (1970).
(13) A. Raina and J. Jänne, *Med. Biol.*, **53**, 121 (1975).
(14) C. M. Caldarera, C. Rossoni, and A. Casti, *Ital. J. Biochem.*, **25**, 33 (1976).
(15) U. Bachrach, "Function of Naturally Occurring Polyamines," Academic, New York, N.Y., 1973.
(16) D. H. Russell and B. G. M. Durie, *Prog. Cancer Res. Ther.*, **8**, 1 (1978).
(17) C. Clo, G. C. Orlandini, A. Casti, and C. Guarnieri, *Ital. J. Biochem.*, **25**, 94 (1976).
(18) H. G. Williams-Ashman and Z. N. Canellakis, *Perspec. Biol. Med.*, **22**, 421 (1979).
(19) C. Y. Chiou, C. J. Chu, and N. E. Liddell, *Arch. Int. Pharmacodyn. Ther.*, **235**, 35 (1978).
(20) S. K. Chapman, R. L. Hawke, S. K. Glant, S. S. Mann, K. S. Hwang, and J. W. Doyle, *Pharmacology*, **21**, 233 (1979).
(21) R. H. Fillingame, C. M. Jorstad, and D. R. Morris, *Proc. Natl. Acad. Sci. USA*, **72**, 4042 (1975).
(22) P. S. Mamont, P. Bohlen, P. McCann, P. Bey, F. Schuber, and C. Tardif, *ibid.*, **73**, 1626 (1976).
(23) J. E. Kay and A. E. Pegg, *FEBS Lett.*, **29**, 301 (1973).
(24) E. Hölttä, P. Pohjanpelto, and J. Jänne, *ibid.*, **97**, 9 (1979).
(25) M. M. Abdel-Monem, N. E. Newton, and C. E. Weeks, *J. Med. Chem.*, **17**, 447 (1974).
(26) P. P. McCann, C. Tardif, M. C. Duchesne, and P. S. Mamont, *Biochem. Biophys. Res. Commun.*, **76**, 893 (1977).
(27) W. F. Fong, J. S. Heller, and E. S. Canellakis, *Biochim. Biophys. Acta*, **428**, 456 (1976).
(28) A. Kallio, *Acta Chem. Scand.*, **32**, 759 (1978).
(29) A. Kallio, H. Pösö, G. Scalabrino, and J. Jänne, *FEBS Lett.*, **73**, 229 (1977).
(30) A. Kallio, H. Pösö, S. K. Guha, and J. Jänne, *Biochem. J.*, **166**, 89 (1977).
(31) H. Pösö, *Acta Chem. Scand. B*, **31**, 71 (1977).
(32) A. E. Pegg, C. Conover, and A. Wrona, *Biochem. J.*, **170**, 651 (1978).
(33) H. Pösö, A. Kallio, G. Scalabrino, and J. Jänne, *Biochim. Biophys. Acta*, **497**, 288 (1977).
(34) H. Hibasami and A. E. Pegg, *Biochem. Biophys. Res. Commun.*, **81**, 1398 (1978).
(35) P. S. Mamont, M. C. Duchesne, A. J. Joder-Ohlenbusch, and J. Grove, in "Enzyme-Activated Irreversible Inhibitors," Elsevier/North-Holland Biomedical Press, Amsterdam, The Netherlands, 1978, pp. 43–53.
(36) S. I. Harik, M. C. Hollenberg, and S. H. Snyder, *Mol. Pharmacol.*, **10**, 41 (1974).
(37) R. T. Schimke, *Adv. Enzymol.*, **37**, 135 (1973).

ACKNOWLEDGMENTS

The authors thank Ms. S. S. Mann and Mr. K. S. Hwang for their assistance.

Antineoplastic Evaluation of Pacific Basin Marine Algae

M. KASHIWAGI *x, J. S. MYNDERSE ‡, R. E. MOORE ‡, and T. R. NORTON *

Received October 18, 1979, from the **Department of Pharmacology, University of Hawaii, Leahi Hospital, Honolulu, HI 96816*, and the ‡*Department of Chemistry, University of Hawaii, Honolulu, HI 96822.* Accepted for publication January 24, 1980.

Abstract □ Extracts of 107 marine alga specimens from Pacific islands were tested for P-388 lymphocytic leukemia and Ehrlich ascites tumor in mice. Several specimens showed high antitumor activity in both systems, with some featuring a notable lack of toxicity.

Keyphrases □ Antineoplastic activity—marine algae from Pacific islands, testing against P-388 lymphocytic leukemia and Ehrlich ascites tumor □ Marine algae—antineoplastic evaluation against P-388 lymphocytic leukemia and Ehrlich ascites tumor □ Antitumor activity—marine algae from Pacific islands, testing against P-388 lymphocytic leukemia and Ehrlich ascites tumor

There have been numerous reports of antitumor substances obtained from terrestrial plants, but no information on antitumor agents from marine plants was published prior to 1977 when Mynderse *et al.* (1) reported that chloroform extracts of some marine blue-green algae showed activity against P-388 lymphocytic leukemia in mice. A P-388 active compound was isolated from one alga, *Lyngbya majuscula* Gomont, and shown to be debromoaplysiatoxin. This finding prompted screening of other marine algae from the Pacific basin for activity against P-388 lymphocytic leukemia and Ehrlich ascites tumor in mice.

The 107 alga specimens were collected from Palau (Western Caroline Islands), Fanning Island (Line Islands), Enewetak Atoll (Marshall Islands), Johnston Island, and the Hawaiian Islands. Voucher samples were retained for most specimens, and the collection site of each sample was recorded carefully.

This paper is a preliminary report of the antitumor activity of crude extracts and some partially purified fractions from these algae.

EXPERIMENTAL

Most algal samples were refrigerated or frozen soon after collection. When refrigerator or freezer facilities were not available, the samples were air dried. The frozen samples were freed from extraneous matter and freeze dried before extraction. The dried samples were powdered in a mortar or blender[1].

There were two general extraction procedures. In Method I, the dried alga was extracted initially with a succession of organic solvents of increasing polarity followed by a final extraction with water. In Method II, the sample was subjected to extraction with 30% ethanol followed by extractions (liquid–liquid) with a succession of organic solvents of the aqueous concentrate.

In Method I, the sample was homogenized in a blender[1] for 5 min with a volume of organic solvent weighing five to 10 times the sample weight. The mixture then was allowed to stand for 24 hr or was stirred for 4–5 hr. The resultant homogenate was centrifuged, and the supernate was

[1] Waring.

0022-3549/80/0600-0735$01.00/0
© 1980, American Pharmaceutical Association

(7) U. Bachrach, *FEBS Lett.*, **68**, 63 (1976).
(8) O. Heby, L. J. Marton, C. B. Wilson, and H. M. Martinez, *J. Cell Physiol.*, **86**, 511 (1975).
(9) A. Raina, R. L. Pajula, and T. Eloranta, *FEBS Lett.*, **67**, 252 (1976).
(10) J. Jänne, H. Pösö, and A. Raina, *Biochim. Biophys. Acta*, **473**, 241 (1978).
(11) O. Heby, L. J. Marton, C. B. Wilson, and H. M. Martinez, *FEBS Lett.*, **50**, 1 (1975).
(12) L. Stevens, *Biol. Rev.*, **45**, 1 (1970).
(13) A. Raina and J. Jänne, *Med. Biol.*, **53**, 121 (1975).
(14) C. M. Caldarera, C. Rossoni, and A. Casti, *Ital. J. Biochem.*, **25**, 33 (1976).
(15) U. Bachrach, "Function of Naturally Occurring Polyamines," Academic, New York, N.Y., 1973.
(16) D. H. Russell and B. G. M. Durie, *Prog. Cancer Res. Ther.*, **8**, 1 (1978).
(17) C. Clo, G. C. Orlandini, A. Casti, and C. Guarnieri, *Ital. J. Biochem.*, **25**, 94 (1976).
(18) H. G. Williams-Ashman and Z. N. Canellakis, *Perspec. Biol. Med.*, **22**, 421 (1979).
(19) C. Y. Chiou, C. J. Chu, and N. E. Liddell, *Arch. Int. Pharmacodyn. Ther.*, **235**, 35 (1978).
(20) S. K. Chapman, R. L. Hawke, S. K. Glant, S. S. Mann, K. S. Hwang, and J. W. Doyle, *Pharmacology*, **21**, 233 (1979).
(21) R. H. Fillingame, C. M. Jorstad, and D. R. Morris, *Proc. Natl. Acad. Sci. USA*, **72**, 4042 (1975).
(22) P. S. Mamont, P. Bohlen, P. McCann, P. Bey, F. Schuber, and C. Tardif, *ibid.*, **73**, 1626 (1976).
(23) J. E. Kay and A. E. Pegg, *FEBS Lett.*, **29**, 301 (1973).
(24) E. Hölttä, P. Pohjanpelto, and J. Jänne, *ibid.*, **97**, 9 (1979).
(25) M. M. Abdel-Monem, N. E. Newton, and C. E. Weeks, *J. Med. Chem.*, **17**, 447 (1974).
(26) P. P. McCann, C. Tardif, M. C. Duchesne, and P. S. Mamont, *Biochem. Biophys. Res. Commun.*, **76**, 893 (1977).
(27) W. F. Fong, J. S. Heller, and E. S. Canellakis, *Biochim. Biophys. Acta*, **428**, 456 (1976).
(28) A. Kallio, *Acta Chem. Scand.*, **32**, 759 (1978).
(29) A. Kallio, H. Pösö, G. Scalabrino, and J. Jänne, *FEBS Lett.*, **73**, 229 (1977).
(30) A. Kallio, H. Pösö, S. K. Guha, and J. Jänne, *Biochem. J.*, **166**, 89 (1977).
(31) H. Pösö, *Acta Chem. Scand. B*, **31**, 71 (1977).
(32) A. E. Pegg, C. Conover, and A. Wrona, *Biochem. J.*, **170**, 651 (1978).
(33) H. Pösö, A. Kallio, G. Scalabrino, and J. Jänne, *Biochim. Biophys. Acta*, **497**, 288 (1977).
(34) H. Hibasami and A. E. Pegg, *Biochem. Biophys. Res. Commun.*, **81**, 1398 (1978).
(35) P. S. Mamont, M. C. Duchesne, A. J. Joder-Ohlenbusch, and J. Grove, in "Enzyme-Activated Irreversible Inhibitors," Elsevier/North-Holland Biomedical Press, Amsterdam, The Netherlands, 1978, pp. 43–53.
(36) S. I. Harik, M. C. Hollenberg, and S. H. Snyder, *Mol. Pharmacol.*, **10**, 41 (1974).
(37) R. T. Schimke, *Adv. Enzymol.*, **37**, 135 (1973).

ACKNOWLEDGMENTS

The authors thank Ms. S. S. Mann and Mr. K. S. Hwang for their assistance.

Antineoplastic Evaluation of Pacific Basin Marine Algae

M. KASHIWAGI *x, J. S. MYNDERSE ‡, R. E. MOORE ‡, and T. R. NORTON *

Received October 18, 1979, from the **Department of Pharmacology, University of Hawaii, Leahi Hospital, Honolulu, HI 96816*, and the ‡*Department of Chemistry, University of Hawaii, Honolulu, HI 96822.* Accepted for publication January 24, 1980.

Abstract □ Extracts of 107 marine alga specimens from Pacific islands were tested for P-388 lymphocytic leukemia and Ehrlich ascites tumor in mice. Several specimens showed high antitumor activity in both systems, with some featuring a notable lack of toxicity.

Keyphrases □ Antineoplastic activity—marine algae from Pacific islands, testing against P-388 lymphocytic leukemia and Ehrlich ascites tumor □ Marine algae—antineoplastic evaluation against P-388 lymphocytic leukemia and Ehrlich ascites tumor □ Antitumor activity—marine algae from Pacific islands, testing against P-388 lymphocytic leukemia and Ehrlich ascites tumor

There have been numerous reports of antitumor substances obtained from terrestrial plants, but no information on antitumor agents from marine plants was published prior to 1977 when Mynderse *et al.* (1) reported that chloroform extracts of some marine blue-green algae showed activity against P-388 lymphocytic leukemia in mice. A P-388 active compound was isolated from one alga, *Lyngbya majuscula* Gomont, and shown to be debromoaplysiatoxin. This finding prompted screening of other marine algae from the Pacific basin for activity against P-388 lymphocytic leukemia and Ehrlich ascites tumor in mice.

The 107 alga specimens were collected from Palau (Western Caroline Islands), Fanning Island (Line Islands), Enewetak Atoll (Marshall Islands), Johnston Island, and the Hawaiian Islands. Voucher samples were retained for most specimens, and the collection site of each sample was recorded carefully.

This paper is a preliminary report of the antitumor activity of crude extracts and some partially purified fractions from these algae.

EXPERIMENTAL

Most algal samples were refrigerated or frozen soon after collection. When refrigerator or freezer facilities were not available, the samples were air dried. The frozen samples were freed from extraneous matter and freeze dried before extraction. The dried samples were powdered in a mortar or blender[1].

There were two general extraction procedures. In Method I, the dried alga was extracted initially with a succession of organic solvents of increasing polarity followed by a final extraction with water. In Method II, the sample was subjected to extraction with 30% ethanol followed by extractions (liquid–liquid) with a succession of organic solvents of the aqueous concentrate.

In Method I, the sample was homogenized in a blender[1] for 5 min with a volume of organic solvent weighing five to 10 times the sample weight. The mixture then was allowed to stand for 24 hr or was stirred for 4–5 hr. The resultant homogenate was centrifuged, and the supernate was

[1] Waring.

0022-3549/80/0600-0735$01.00/0
© 1980, American Pharmaceutical Association

Table I—Active Materials

Alga Sample	Location	Extracting Solvent and Purity of Fraction[a]	P-388 Lymphocytic Leukemia[b]				Ehrlich Ascites[c]		
			Dose, mg/kg	Percent Activity[d]	Number of Mice	Toxicity, deaths[e]	Survivors at 30 Days		
							Dose, mg/kg	Percent Alive	Nonascitic
Aphanococcus biformis A. Br., 30% *Chroococcus minor* (Kütz.) Nag., 30% *Oscillatoria foreaui* Fremy, 30%	Palau	*n*-Butanol, I	29.0	125	5	0	23.2	0	0
Bangia sp.	Palau	30% ethanol, I	17.5	230	4	0	14.0	100	100
		30% ethanol, II	21.8	224	5	0	12.4	80	80
		30% ethanol, II	12.4	196	5	0	11.9	100	100
		30% ethanol, III	<0.5	186	5	0	<0.5	100	100
Caulerpa racemosa var. *peltata* Lam.	Palau	30% ethanol, I	50.0	151	4	2	40.0	100	80
		30% ethanol, II	—	—	—	—	1.3	100	80
		30% ethanol, III	—	—	—	—	0.8	80	80
Crinalium sp.	Fanning Island	Ethyl acetate, I	—	—	—	—	6.0	50	50
		Ethyl acetate, I	17.5	178	6	1	14.0	80	80
		Water, III	0.5	210	4	0	—	—	—
Cryptonemia crenulata J. Ag.	Palau	30% ethanol, I	100	129	4	0	80.0	0	0
Dictyota crenulata J. Ag.	Oahu, Hawaii	Methylene chloride, I	153	129	4	0	122	0	0
		Methylene chloride, I	265	135	4	0	212	0	0
		Methylene chloride, I	—	—	—	—	68	80	80
Ectocarpus breviarticulatus J. Ag.	Fanning Island	Ethyl acetate, I	25	170	5	1	20	0	0
Gracilaria salicornia (C. Ag.) Dawson	Palau	30% ethanol, I	0.5	137	3	0	0.4	0	0
Halimeda sp.	Palau	Butanol, I	21.5	154	4	0	17.2	0	0
		Hexane, I	26.0	131	4	0	20.8	0	0
Herposiphonia arcuata Hollenberg	Fanning Island	30% ethanol, I	—	—	—	—	120	100	100
		30% ethanol, II	—	—	—	—	10	80	60
Lobophora variegata (Lamx.) Wom.	Palau	Butanol, I	21.5	127	4	0	17.2	0	0
		Hexane, I	10.0	127	5	0	8.0	0	0
		Chloroform, I	11.0	144	5	0	8.8	0	0
Lyngbya convervoides C. Ag.	Palau	30% ethanol, I	—	—	—	—	20	100	100
Lyngbya majuscula Gomont	Palau	Water, I	25.0	166	5	1			
		Water, II	10.0	164	5	0	8	60	40
		Water, III	<0.5	166	5	0	<0.4	100	100
	Oahu, Hawaii	Chloroform, I	4.2	134	5	1	3.2	20	20
		Chloroform, I	0.5	144	5	0	0.4	0	0
Lyngbya sp.	Hawaii, Hawaii	Methanol, I	—	—	—	—	27.2	100	100
		Methanol, II	150	182	5	0	—	—	—
		Methanol, III	—	—	—	—	1.6	100	100
Oscillatoria annae van Goor	Palau	30% ethanol, I	415	125	5	3	332	0	0
Oscillatoria sp.	Palau	30% ethanol, I	5.0	205	5	0	4.0	100	100
		30% ethanol, III	—	—	—	—	0.4	100	100
Phormidium crosbyanum Tilden	Johnston Island	Methylene chloride, I	7.5	134	5	3	6.0	0	0
Phormidium sp.	Molokai, Hawaii	Methanol, I	12.5	210	5	0	10	100	100
Sargassum polycystum C. Ag.	Palau	30% ethanol, I	250	129	4	0	200	0	0
Schizothrix calcicola (Ag.) Gomont	Fanning Island	Ethyl acetate, I	25	255	5	3	2.5	100	100
		Water, II	2.5	209	5	1	3.6	100	80
Rivularia atra Born. + Fla. *Entophysalis deusta* (J. Ag.) Dr. + Dail. *Anacystis dimidata* (Kütz.) Dr. + Dail.	Enewetak	Methanol, I	22	125	5	1	—	—	—
Schizothrix sp.	Enewetak	Methanol, I	—	—	—	—	8.0	40	40
Spyridia filamentosa (Wulfen) Harvey	Oahu, Hawaii	Methylene chloride, I	90	128	5	1	—	—	—
Tolypothrix conglutinata var. *clorata* Ghose	Fanning Island	Ethyl acetate, I	13.5	233	5	3	10.8	0	0

Table I—*Continued*

Alga Sample	Location	Extracting Solvent and Purity of Fraction[a]	P-388 Lymphocytic Leukemia[b] Dose, mg/kg	Percent Activity[d]	Number of Mice	Toxicity, deaths[e]	Ehrlich Ascites[c] Dose, mg/kg	Survivors at 30 Days Percent Alive	Nonascitic
Tydemannia expeditionis Weber van Bosse	Palau	30% ethanol, I	250	130	4	0	200	0	0
	Enewetak	Chloroform, I	19	156	5	3	15.2	0	0
Udotea geppii Yamada	Enewetak	Methylene chloride, I	—	—	—	—	47.6	100	100

[a] I = crude; II = fraction chromatographed through Sephadex G-25; and III = fraction chromatographed through CM Sephadex C-25. [b] Standard screening procedure used in this laboratory (2). [c] Procedure used in this laboratory described by Tabrah *et al.* (3). [d] Mean survival time as percent of untreated, diseased controls. [e] Number of mice that died within 7 days after tumor cell inoculation.

Table II—Nonactive Samples

Sample	Location	Sample	Location
Amphiroa fragilissima (L.) Lamour.	Palau	*Halophila ovata* Gaud.	Palau
Aphanocapsa biformis A. Br.	Palau	*Halymenia maculata* J. Ag.	Palau
Asparagopsis taxiformis (Del.) Coll. + Herr.	Enewetak	*Herposiphonia arcuata* Hollenberg	Fanning Island
Boodlea composita (Harv.) Brand.	Palau	*Hyella caespitosa* Born. et Flah.	Fanning Island
Bornetella nitida (Harv.) Mun.	Palau	*Hypnea nidifica* J. Ag.	Palau
Bryopsis sp.	Fanning Island	*Hypnea pannosa* J. Ag.	Palau
Calothrix crustacea Born. + Fla.	Enewetak	*Liagora farinosa* Lamour.	Enewetak
Caulerpa racemosa var. *laetevirens* (Mont.) Weber van Bosse	Palau	*Liagora maxima* Butters	Oahu, Hawaii
Caulerpa racemosa var. *occidentalis* (J. Ag.) Boerg.	Palau	*Lobophora* sp.	Enewetak
Caulerpa racemosa var. *peltata* Lam.	Palau	*Lobophora variegata* (Lamx.) Wom.	Palau
Caulerpa urvilliana Mont.	Fanning Island	*Lyngbya convervoides* C. Ag.	Palau
Centroceras clavulatum (C. Ag.) Mont.	Fanning Island	*Lyngbya majuscula* Gomont	Palau
Centroceras minimum Yamada	Enewetak	*Lyngbya porphyrosiphonis* Fremy	Palau
Chlorodesmis hildebrandtii Gepp et Gepp	Palau	*Lyngbya semiplena* (C. Ag.) J. Ag.	Palau
Chondrococcus hornemanni (Lyng.) Kütz.	Palau	*Martensia fragilis* Harvey	Oahu, Hawaii
Codium geppei Schmidt	Enewetak	*Microcoleus acutissimus* Gardner	Fanning Island
Crinalium sp.	Palau	*Microcoleus* sp.	Fanning Island
Dactylococcopsis raphidioides Hansg.	Fanning Island	*Microcoleus tenerrimus* Gomont	Enewetak
Derbesia sp.	Palau	*Microcoleus vaginatus* (Vaucher) Gomont	Palau
Dictyopteris repens (Okamura) Boerg.	Palau	*Nostoc calcicola* Born. et Flah.	Palau
Dictyosphaeria sp.	Oahu, Hawaii	*Oscillatoria hamelii* Fremy	Palau
Dictyota acutiloba J. Ag.	Oahu, Hawaii	*Oscillatoria nigroviridis* Gomont	Enewetak
Dictyota divariacata Lamour.	Enewetak	*Oscillatoria* sp.	Fanning Island
Dictyota friabilis Setchell	Fanning Island	*Padina commersonii* Bory	Palau
Dictyota patens J. Ag.	Palau	*Polysiphonia quadrata* Hollenberg	Fanning Island
Enteromorpha sp.	Oahu, Hawaii	*Pterocladia* sp.	Oahu, Hawaii
Eucheuma striatum Schmidt	Oahu, Hawaii	*Rhipilia orientalis* A. + E. Gepp	Enewetak
Falkenbergia rufanolosa Harvey	Enewetak	*Scytonema pascheri* Bharaduaja	Fanning Island
Gloeocapsa decorticans (A. Br.) Richter	Fanning Island	*Spyridia filamentosa* (Wulfen) Harvey	Oahu, Hawaii
Gracilaria salicornia (C. Ag.) Dawson	Palau	*Symploca hydnoides* Kütz.	Palau
Halimeda cylindracea Decaisne	Palau	*Symploca* sp.	Palau
Halimeda discoidea Decaisne	Palau	*Turbinaria ornata* (Turn.) J. Ag.	Palau
Halimeda macrophysa Barton	Enewetak	*Tydemannia expeditionis* Weber van Bosse	Palau
Halimeda monile (Sol.) Lamour.	Enewetak	*Valonia aegagropila* C. Ag.	Fanning Island
Halimeda opuntia (L.) Lamx.	Palau	*Valonia ventricosa* J. Ag.	Palau

evaporated *in vacuo* to yield the crude lipophilic extract. The marc was dried and then soaked in a volume of water weighing five to 10 times the marc weight for 4–5 hr with stirring and for an additional 24 hr or more without stirring. After centrifugation, the supernate was freeze dried to give the water-soluble extract. For initial fractionation, the water-soluble extract was subjected to gel filtration[2] with 0.1 *M* ammonium bicarbonate as the eluent. This procedure was followed by cation-exchange chromatography[3] with a gradient elution of the active compound with 0.03–3.0 *M* ammonium acetate. All column separations were monitored by UV spectroscopy at 280 nm[4].

In Method II, a sample was extracted initially with 30% ethanol in the same manner as described for Method I for the extraction of water-soluble constituents from the marc. After the ethanol was eliminated from the supernate by flash evaporation, this crude extract was extracted further with either *n*-butanol or chloroform to remove lipophilic constituents. The water-soluble fraction then was purified by procedures similar to those described for Method I for the water-soluble crude extract.

The isolation of the purified lipophilic antitumor agents will be reported later.

RESULTS AND DISCUSSION

The results of the screening tests are listed in Tables I and II. Table I shows that eight marine algal extracts had T/C (test/control) values of ≥170% in the P-388 lymphocytic leukemia test. Of these extracts, six species showed T/C activity of >200%. In the Ehrlich ascites tumor system, nine species of algae showed a 100% survival rate at 30 days with no ascitic condition. Several of the groups of mice that survived for 30 days with a nonascitic condition were kept alive for an additional 30 days with no tumor recurrence at the end of the 60-day period.

[2] Sephadex G-25, Pharmacia Fine Chemicals, Piscataway, NJ 08854.
[3] CM Sephadex C-25, Pharmacia Fine Chemicals, Piscataway, NJ 08854.
[4] Model UA-5 absorbance monitor, Instrument Specialties Co., Lincoln, NE 68505.

Some of the algal extracts active against both P-388 leukemia and Ehrlich ascites tumor were subjected to preliminary isolation work (Table I). The finding that some of these crude extracts as well as partially purified fractions showed excellent activity at relatively low dosages with no evidence of toxicity is most encouraging.

Table II lists the marine algae that showed a T/C activity of <125% against P-388 lymphocytic leukemia and <20% survivors at 30 days in the Ehrlich ascites tumor system.

REFERENCES

(1) J. S. Mynderse, R. E. Moore, M. Kashiwagi, and T. R. Norton, *Science*, **196**, 538 (1977).

(2) D. F. Dunn, M. Kashiwagi, and T. R. Norton, *Comp. Biochem. Physiol.*, **50C**, 133 (1975).

(3) F. L. Tabrah, M. Kashiwagi, and T. R. Norton, *Int. J. Clin. Pharmacol.*, **5**, 420 (1972).

ACKNOWLEDGMENTS

Supported by National Institutes of Health Grant CA 12623-06 from the National Cancer Institute, the George F. Straub Trust Estate and the Atherton Family Foundation, both of Honolulu, Hawaii, and the Elsa U. Pardee Foundation, Midland, Mich.

The authors thank Dr. Dennis J. Russell for identifying the algae and Dr. John Cardellina and Dennis Mead for technical assistance.

COMMUNICATIONS

Ocular Absorption of Propranolol in Rabbits

Keyphrases □ Propranolol—ocular absorption in rabbits □ β-Adrenergic blocking agents—propranolol, ocular absorption in rabbits □ Absorption, ocular—propranolol in rabbits

To the Editor:

The topical application of β-adrenergic blocking agents to the eye has been found to be effective in the control of glaucoma (1). However, the precise rate and extent of disposition of these compounds in the various ocular tissues have not been fully established. The purpose of this report is to compare and contrast the ocular absorption of a model β-blocking agent, propranolol, to what is known about the widely used miotic pilocarpine.

Male New Zealand albino rabbits, 3.0–3.6 kg, were minimally restrained in wooden boxes; topical and local anesthetics were not used. A 50-μl dose of 0.5% propranolol hydrochloride in isotonic buffer (pH 7.4) was instilled onto the cornea and allowed to distribute normally within the cul-de-sac. All tissue sampling procedures were performed as outlined previously (2, 3). The tissue samples collected were the whole intact cornea, aqueous humor, iris, and lens. The amount and concentration of propranolol in these tissues were determined spectrophotofluorometrically (4). The minimum detection limit for the drug was ~5 ng.

Figure 1 shows the propranolol concentration in ocular tissues as a function of time. The data indicate that propranolol reached a peak concentration in the aqueous humor at ~30 min. This result corresponds well with previous data for pilocarpine, which has a peak time of 20–30 min. This peak time was anticipated in the current studies since it was shown previously that the apparent ocular pharmacokinetic parameters are largely determined by the parallel first-order loss process in the precorneal area, so that most drugs show similar peak times in the aqueous humor (2, 5). The elimination characteristics of propranolol also are very similar to pilocarpine and suggest that both drugs are lost from the eye *via* the same mechanism, namely, aqueous humor turnover. The rate constant associated with this process for pilocarpine in rabbits is 0.017 min^{-1} (2), and this value is nearly identical to the elimination rate of propranolol from the aqueous humor in the present studies (0.019 min^{-1}).

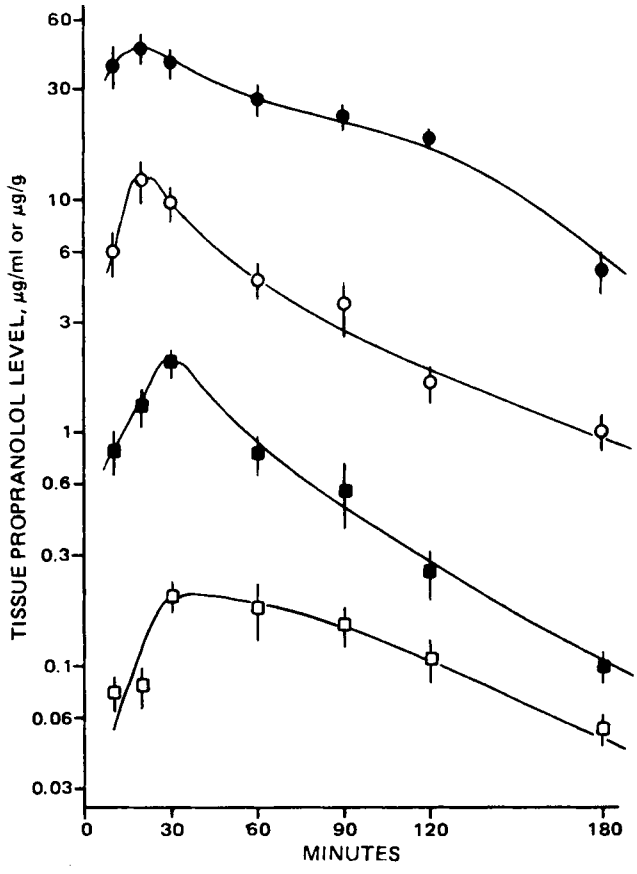

Figure 1—*Concentration of propranolol in various ocular tissues after topical application of propranolol solution. Key:* ●, *cornea;* ○, *iris;* ■, *aqueous humor; and* □, *lens.*

Concentration–time profiles such as those depicted in Fig. 1 can be somewhat misleading in ocular studies of this type which deal with tissues of greatly different distribution volumes. For this reason, it often is useful to consider the amount of drug represented by the peak drug concentration for each tissue. These data are presented in Table I. The rank order for tissue concentration was cornea > iris > aqueous humor > lens, whereas the rank order for tissue amounts was cornea > aqueous humor > iris > lens. The change in rank order for the iris and aqueous humor was due to the 12-fold difference in the wet weights of these

0022-3549/80/0600-0738$01.00/0

© 1980, American Pharmaceutical Association

Some of the algal extracts active against both P-388 leukemia and Ehrlich ascites tumor were subjected to preliminary isolation work (Table I). The finding that some of these crude extracts as well as partially purified fractions showed excellent activity at relatively low dosages with no evidence of toxicity is most encouraging.

Table II lists the marine algae that showed a T/C activity of <125% against P-388 lymphocytic leukemia and <20% survivors at 30 days in the Ehrlich ascites tumor system.

REFERENCES

(1) J. S. Mynderse, R. E. Moore, M. Kashiwagi, and T. R. Norton, *Science*, **196**, 538 (1977).

(2) D. F. Dunn, M. Kashiwagi, and T. R. Norton, *Comp. Biochem. Physiol.*, **50C**, 133 (1975).

(3) F. L. Tabrah, M. Kashiwagi, and T. R. Norton, *Int. J. Clin. Pharmacol.*, **5**, 420 (1972).

ACKNOWLEDGMENTS

Supported by National Institutes of Health Grant CA 12623-06 from the National Cancer Institute, the George F. Straub Trust Estate and the Atherton Family Foundation, both of Honolulu, Hawaii, and the Elsa U. Pardee Foundation, Midland, Mich.

The authors thank Dr. Dennis J. Russell for identifying the algae and Dr. John Cardellina and Dennis Mead for technical assistance.

COMMUNICATIONS

Ocular Absorption of Propranolol in Rabbits

Keyphrases □ Propranolol—ocular absorption in rabbits □ β-Adrenergic blocking agents—propranolol, ocular absorption in rabbits □ Absorption, ocular—propranolol in rabbits

To the Editor:

The topical application of β-adrenergic blocking agents to the eye has been found to be effective in the control of glaucoma (1). However, the precise rate and extent of disposition of these compounds in the various ocular tissues have not been fully established. The purpose of this report is to compare and contrast the ocular absorption of a model β-blocking agent, propranolol, to what is known about the widely used miotic pilocarpine.

Male New Zealand albino rabbits, 3.0–3.6 kg, were minimally restrained in wooden boxes; topical and local anesthetics were not used. A 50-μl dose of 0.5% propranolol hydrochloride in isotonic buffer (pH 7.4) was instilled onto the cornea and allowed to distribute normally within the cul-de-sac. All tissue sampling procedures were performed as outlined previously (2, 3). The tissue samples collected were the whole intact cornea, aqueous humor, iris, and lens. The amount and concentration of propranolol in these tissues were determined spectrophotofluorometrically (4). The minimum detection limit for the drug was ~5 ng.

Figure 1 shows the propranolol concentration in ocular tissues as a function of time. The data indicate that propranolol reached a peak concentration in the aqueous humor at ~30 min. This result corresponds well with previous data for pilocarpine, which has a peak time of 20–30 min. This peak time was anticipated in the current studies since it was shown previously that the apparent ocular pharmacokinetic parameters are largely determined by the parallel first-order loss process in the precorneal area, so that most drugs show similar peak times in the aqueous humor (2, 5). The elimination characteristics of propranolol also are very similar to pilocarpine and suggest that both drugs are lost from the eye *via* the same mechanism, namely, aqueous humor turnover. The rate constant associated with this process for pilocarpine in rabbits is 0.017 min^{-1} (2), and this value is nearly identical to the elimination rate of propranolol from the aqueous humor in the present studies (0.019 min^{-1}).

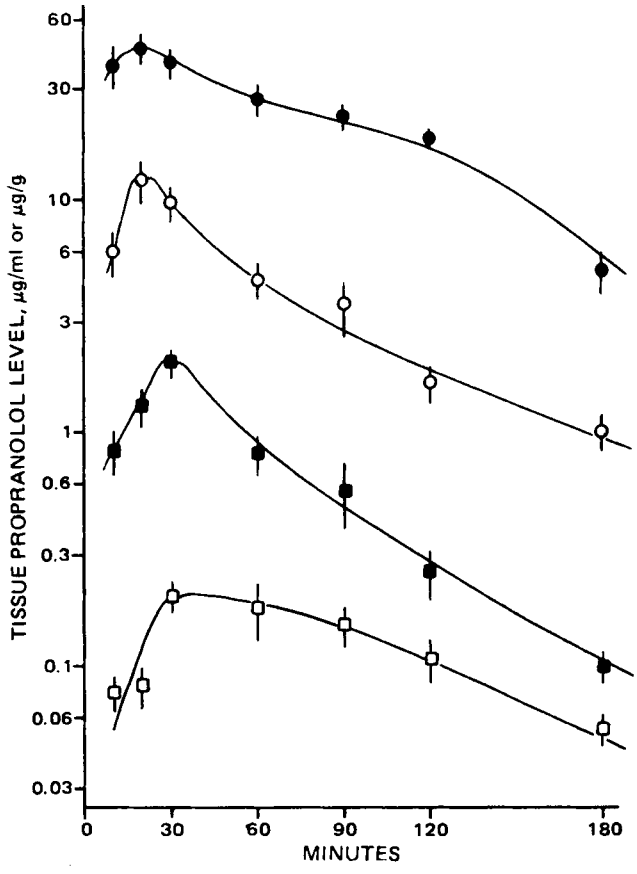

Figure 1—*Concentration of propranolol in various ocular tissues after topical application of propranolol solution. Key:* ●, *cornea;* ○, *iris;* ■, *aqueous humor; and* □, *lens.*

Concentration–time profiles such as those depicted in Fig. 1 can be somewhat misleading in ocular studies of this type which deal with tissues of greatly different distribution volumes. For this reason, it often is useful to consider the amount of drug represented by the peak drug concentration for each tissue. These data are presented in Table I. The rank order for tissue concentration was cornea > iris > aqueous humor > lens, whereas the rank order for tissue amounts was cornea > aqueous humor > iris > lens. The change in rank order for the iris and aqueous humor was due to the 12-fold difference in the wet weights of these

0022-3549/80/0600-0738$01.00/0

© 1980, American Pharmaceutical Association

Table I—Amount of Propranolol Represented by the Peak Concentration in Various Ocular Tissues [a]

Tissue	Peak Concentration, μg/g or μg/ml	Amount of Drug Present in Tissue, μg
Cornea	45.90	3.21
Aqueous humor	2.02	0.61
Iris	12.32	0.31
Lens	0.21	0.06

[a] The weights of the tissues are given in the text.

tissues. The approximate wet weight averages for the cornea, iris, aqueous humor, and lens in the current studies were 70, 25, 300, and 300 mg, respectively.

The relative disposition of propranolol in the various ocular tissues also was different than that of pilocarpine. There was a sixfold difference in peak concentration between the iris and the aqueous humor for propranolol, whereas the two tissues were virtually identical with pilocarpine (3). Furthermore, the penetration into the lens relative to other ocular tissues was greater for propranolol than for pilocarpine. Propranolol is known to act as a local anesthetic and as such may influence membrane permeability. It is unclear whether the differences in tissue distribution for propranolol and pilocarpine can be ascribed wholly, or in part, to this effect.

(1) R. L. Radius, G. R. Diamond, I. P. Pollack, and M. E. Langham, *Arch. Ophthalmol.*, **96**, 1003 (1978).
(2) J. W. Sieg and J. R. Robinson, *J. Pharm. Sci.*, **65**, 1816 (1976).
(3) M. C. Makoid and J. R. Robinson, *ibid.*, **68**, 435 (1979).
(4) D. G. Shand, E. M. Nuckolls, and J. A. Oates, *Clin. Pharmacol. Ther.*, 11, 112 (1970).
(5) J. W. Sieg, M. C. Makoid, and J. R. Robinson, *J. Pharm. Sci.*, **65**, 150 (1976).

A. Hussain ˣ
S. Hirai
J. Sieg
College of Pharmacy
University of Kentucky
Lexington, KY 40506

Received January 16, 1980.
Accepted for publication March 7, 1980.

Comparative *In Vitro* and *In Vivo* Antifungal Activity of Tolnaftate and Various Undecylenates

Keyphrases □ Antifungal activity—tolnaftate and various undecylenates, comparison *in vitro* and *in vivo* □ Tolnaftate—antifungal activity *in vitro* and *in vivo*, comparison with various undecylenates □ Undecylenates—antifungal activity *in vitro* and *in vivo*, comparison with tolnaftate

To the Editor:

Amsel *et al.* (1) compared the *in vitro* antifungal activity of undecylenic acid and tolnaftate and drew several conclusions. Among these conclusions were: (*a*) the undecylenate product killed the test organisms more rapidly than the tolnaftate-containing product; (*b*) undecylenates possibly are more effective in *in vitro* killing time than tolnaftate alone, and this finding probably applies to the commercial powders; and (*c*) although the concentrations of active ingredients varied in the commercial products tested, the undecylenates probably are more effective (as determined by killing time) than tolnaftate.

Table I—Agar Diffusion Study of Commercial Solutions T [a] and D [a] against Three Dermatophytes

Organism	Contact Time [b]	Zone Size, mm [c] T	D
T. mentagrophytes	1 min	30	0
	5 min	33	10
	15 min	31	11
	30 min	33	11
	1 hr	30	12
	4 hr	33	22
T. rubrum	1 min	42	± [d]
	5 min	20	±
	15 min	35	±
	30 min	41	±
	1 hr	37	±
	4 hr	38	17
E. floccosum	1 min	48	0
	5 min	50	0
	15 min	46	0
	30 min	50	5
	1 hr	47	10
	4 hr	45	10

[a] Commercial solution T contains 1% tolnaftate; commercial solution D contains 10% undecylenic acid. [b] Values between compounds were statistically significant ($p < 0.0001$) at all time points. [c] Using 6-mm disk. [d] These areas showed decreased mycelial growth but were not completely free of growth.

Table II—Agar Diffusion Study of Tolnaftate, Undecylenic Acid, and Zinc Undecylenate against Three Dermatophytes

Organism	Contact Time [b]	Zone Size after Incubation for 96 hr, mm [a] Tolnaftate Solution (0.1%)	Undecylenic Acid [c] Solution (0.1%)	Zinc Undecylenate [c] Suspension (0.1%)
T. mentagrophytes	1 min	29	± [d]	3
	5 min	34	±	8
	30 min	39	13	11
	1 hr	39	18	9
	3 hr	39	27	16
	6 hr	39	30	20
T. rubrum	1 min	43	±	±
	5 min	43	±	9
	30 min	44	18	9
	1 hr	47	25	15
	3 hr	47	33	26
	6 hr	47	>35 [e]	28
M. gypseum	1 min	28	0	0
	5 min	30	±	±
	30 min	37	±	6
	1 hr	38	14	±
	3 hr	39	23	17
	6 hr	39	25	20

[a] Using 6-mm disk. [b] Values between tolnaftate and undecylenates were statistically significant ($p < 0.0001$) at each time point. [c] Average of two disks. [d] These areas showed decreased mycelial growth but were not completely free of growth. [e] Too near edge of plate.

These conclusions were based on the methods, materials, and results of experiments presented in their paper. We have several concerns regarding their unusual methodology, and we therefore question their results and conclusions. We also wish to present *in vitro* and *in vivo* data using standard methods, which show, in contrast to the Amsel *et al.* (1) report, that tolnaftate is superior to the undecylenates. All data were submitted for statistical analysis using an appropriate analysis of variance, Duncan's multiple statistic test, and Fisher's exact test (2).

Our criticisms of the Amsel *et al.* (1) report are as follows:

0022-3549/80/0600-0739$01.00/0
© 1980, American Pharmaceutical Association

Table I—Amount of Propranolol Represented by the Peak Concentration in Various Ocular Tissues [a]

Tissue	Peak Concentration, μg/g or μg/ml	Amount of Drug Present in Tissue, μg
Cornea	45.90	3.21
Aqueous humor	2.02	0.61
Iris	12.32	0.31
Lens	0.21	0.06

[a] The weights of the tissues are given in the text.

tissues. The approximate wet weight averages for the cornea, iris, aqueous humor, and lens in the current studies were 70, 25, 300, and 300 mg, respectively.

The relative disposition of propranolol in the various ocular tissues also was different than that of pilocarpine. There was a sixfold difference in peak concentration between the iris and the aqueous humor for propranolol, whereas the two tissues were virtually identical with pilocarpine (3). Furthermore, the penetration into the lens relative to other ocular tissues was greater for propranolol than for pilocarpine. Propranolol is known to act as a local anesthetic and as such may influence membrane permeability. It is unclear whether the differences in tissue distribution for propranolol and pilocarpine can be ascribed wholly, or in part, to this effect.

(1) R. L. Radius, G. R. Diamond, I. P. Pollack, and M. E. Langham, *Arch. Ophthalmol.*, **96**, 1003 (1978).
(2) J. W. Sieg and J. R. Robinson, *J. Pharm. Sci.*, **65**, 1816 (1976).
(3) M. C. Makoid and J. R. Robinson, *ibid.*, **68**, 435 (1979).
(4) D. G. Shand, E. M. Nuckolls, and J. A. Oates, *Clin. Pharmacol. Ther.*, 11, 112 (1970).
(5) J. W. Sieg, M. C. Makoid, and J. R. Robinson, *J. Pharm. Sci.*, **65**, 150 (1976).

A. Hussain ˣ
S. Hirai
J. Sieg
College of Pharmacy
University of Kentucky
Lexington, KY 40506

Received January 16, 1980.
Accepted for publication March 7, 1980.

Comparative *In Vitro* and *In Vivo* Antifungal Activity of Tolnaftate and Various Undecylenates

Keyphrases □ Antifungal activity—tolnaftate and various undecylenates, comparison *in vitro* and *in vivo* □ Tolnaftate—antifungal activity *in vitro* and *in vivo*, comparison with various undecylenates □ Undecylenates—antifungal activity *in vitro* and *in vivo*, comparison with tolnaftate

To the Editor:

Amsel *et al.* (1) compared the *in vitro* antifungal activity of undecylenic acid and tolnaftate and drew several conclusions. Among these conclusions were: (*a*) the undecylenate product killed the test organisms more rapidly than the tolnaftate-containing product; (*b*) undecylenates possibly are more effective in *in vitro* killing time than tolnaftate alone, and this finding probably applies to the commercial powders; and (*c*) although the concentrations of active ingredients varied in the commercial products tested, the undecylenates probably are more effective (as determined by killing time) than tolnaftate.

Table I—Agar Diffusion Study of Commercial Solutions T [a] and D [a] against Three Dermatophytes

Organism	Contact Time [b]	Zone Size, mm [c] T	D
T. mentagrophytes	1 min	30	0
	5 min	33	10
	15 min	31	11
	30 min	33	11
	1 hr	30	12
	4 hr	33	22
T. rubrum	1 min	42	± [d]
	5 min	20	±
	15 min	35	±
	30 min	41	±
	1 hr	37	±
	4 hr	38	17
E. floccosum	1 min	48	0
	5 min	50	0
	15 min	46	0
	30 min	50	5
	1 hr	47	10
	4 hr	45	10

[a] Commercial solution T contains 1% tolnaftate; commercial solution D contains 10% undecylenic acid. [b] Values between compounds were statistically significant ($p < 0.0001$) at all time points. [c] Using 6-mm disk. [d] These areas showed decreased mycelial growth but were not completely free of growth.

Table II—Agar Diffusion Study of Tolnaftate, Undecylenic Acid, and Zinc Undecylenate against Three Dermatophytes

Organism	Contact Time [b]	Zone Size after Incubation for 96 hr, mm [a] Tolnaftate Solution (0.1%)	Undecylenic Acid [c] Solution (0.1%)	Zinc Undecylenate [c] Suspension (0.1%)
T. mentagrophytes	1 min	29	± [d]	3
	5 min	34	±	8
	30 min	39	13	11
	1 hr	39	18	9
	3 hr	39	27	16
	6 hr	39	30	20
T. rubrum	1 min	43	±	±
	5 min	43	±	9
	30 min	44	18	9
	1 hr	47	25	15
	3 hr	47	33	26
	6 hr	47	>35 [e]	28
M. gypseum	1 min	28	0	0
	5 min	30	±	±
	30 min	37	±	6
	1 hr	38	14	±
	3 hr	39	23	17
	6 hr	39	25	20

[a] Using 6-mm disk. [b] Values between tolnaftate and undecylenates were statistically significant ($p < 0.0001$) at each time point. [c] Average of two disks. [d] These areas showed decreased mycelial growth but were not completely free of growth. [e] Too near edge of plate.

These conclusions were based on the methods, materials, and results of experiments presented in their paper. We have several concerns regarding their unusual methodology, and we therefore question their results and conclusions. We also wish to present *in vitro* and *in vivo* data using standard methods, which show, in contrast to the Amsel *et al.* (1) report, that tolnaftate is superior to the undecylenates. All data were submitted for statistical analysis using an appropriate analysis of variance, Duncan's multiple statistic test, and Fisher's exact test (2).

Our criticisms of the Amsel *et al.* (1) report are as follows:

0022-3549/80/0600-0739$01.00/0
© 1980, American Pharmaceutical Association

Table III—*In Vitro* Activity of Tolnaftate, Undecylenic Acid, and Zinc Undecylenate against Six Fungi in Sabouraud Dextrose Broth

Organism	Minimal Inhibitory Concentration, μg/ml					
	Tolnaftate[a]		Undecylenic Acid[b]		Zinc Undecylenate[a]	
	48 hr[c]	72 hr[c]	48 hr	72 hr	48 hr	72 hr
M. canis	0.055	0.3	7.5	7.5	7.5	7.5
M. gypseum	0.055	0.055	7.5	7.5	7.5	>10[e]
T. rubrum	0.055	0.055	3.75	7.5	3.75	7.5
T. mentagrophytes	<1.0[d]	<1.0	8.5	8.5	—	—
E. floccosum	<1.0	<1.0	8.5	8.5	—	—
A. niger	0.055	0.3	>10	>10	>10	>10

[a] Suspension in ethanol. [b] Solution in ethanol. [c] Values between tolnaftate and undecylenates were statistically significant ($p < 0.0001$) at 48 and 72 hr. [d] Lower levels not tested. [e] Higher levels not tested.

Table IV—Effect of Commercial Powders A[a] and C[a] against Topical *T. mentagrophytes* Infection in Guinea Pigs[b]

Compound	Number of Animals	Percentage of Cultures Negative		Average Lesion Score		Average Time until Animals Became Negative	
		During Treatment (10 days)	After Treatment (7 days)	During Treatment (10 days)	After Treatment (7 days)	Number of Animals	Day[c]
Commercial powder A	7	100[d]	100[e]	16.4[f]	3.9[g]	7	2[h]
Commercial powder C	7	0	33	18.2	6.1	4	15.5
						3	>17
Commercial talc	7	0	29	19.1	7.9	4	16
						3	>17
Untreated	5	0	7	18.1	7.0	1	17
						4	>17

[a] Commercial powder A contains 1% tolnaftate; commercial powder C contains 10% calcium undecylenate. [b] Treatment twice daily for 10 days. [c] First day of culture was Day 2. [d] Statistically significant ($p < 0.002$). [e] Statistically significant until Day 15 ($p < 0.05$). [f] Not statistically different. [g] Statistically significant ($p < 0.05$). [h] Statistically significant ($p < 0.002$).

1. Standard procedures for determination of the minimum fungicidal concentration in broth or agar were not used. In addition, the minimum inhibitory concentration for the various preparations used was not given for the test organisms, and the killing time results showed tremendous variation (up to 50%). If this new method is more reproducible than standard ones, all replicates should be the same since death was used as the end-point.

2. Tolnaftate was used as a suspension even though it is readily soluble (polyethylene glycol 400 or acetone) and solutions give more reproducible results than suspensions. In addition, the use of commercial powder A[1] as an aqueous suspension clearly is a weakly active mode of application that was never intended.

3. Polysorbate 20 is a surfactant used for emulsification, dispersion, and solubilization of lipids. Therefore, use of this substance makes the undecylenates more bioavailable since they are fatty acids, but it certainly is not useful for tolnaftate.

4. No evidence is presented that the complex rinsing solution and the washing procedure (only three washes) used for 2% undecylenic acid and 1% tolnaftate (where no differences were seen between the two drugs) were sufficient to wash out both the 20% zinc undecylenate and 2% undecylenic acid in commercial powder D[2] (in contrast to the 1% tolnaftate in commercial powder A) to bring the concentration below the minimum inhibitory concentration.

5. The mycelium remained in the first wash for 1 hr, thereby increasing contact time with the drugs. This situation gives an advantage to the less potent drug.

6. In their Table IV, where clinical isolates were used, differences were significant only one of 15 times. In Table II, seven of 15 contacts were significant. Nevertheless, the authors claimed that the results again were essentially equivalent. Furthermore, Amsel *et al.* made their conclusion on a "global basis" based on six organisms tested *in vitro*.

We compared commercial solution D (Lot 18048, May 1980) with commercial solution T[3] (Lot 7AKU2, April 1982) in a conventional agar diffusion study (3). In our studies, 5 μl of each solution was pipetted onto disks that had been placed on 23 × 23-cm plastic plates containing Sabouraud dextrose agar seeded with *Trichophyton rubrum, T. mentagrophytes,* and *Epidermophyton floccosum* (clinical isolates). Fungi were grown in Sabouraud dextrose broth on a rotary shaker at 28°. After 72 hr, the mycelia were ground into a homogeneous suspension[4]. Four milliliters of the suspension was added to 200 ml of agar and shaken, and the agar was poured and allowed to harden. Disks were removed after 1, 5, 15, and 30 min and 1 and 4 hr, and the plates were incubated at 28°. Activity (measured as zone sizes of inhibition in millimeters) against *T. mentagrophytes* was measured after 72 hr; against *T. rubrum* and *E. floccosum,* it was measured after 6 days. With all three organisms and at all times, the T solution gave much larger zones of inhibition than the D solution, even after only 1 min of contact (Table I). These differences all were highly significant.

We also compared tolnaftate (USP M.I. No. P-03411) to undecylenic acid (M.I. No. P-07413) and zinc undecylenate[5] (Lot 47E343) in minimum inhibitory concentration and agar diffusion test systems against *Microsporum canis, M. gypseum, T. rubrum, T. mentagrophytes, E. floccosum,* and *Aspergillus niger* (clinical isolates). Methods for the agar diffusion tests were as already

[1] Aftate (contains 1% tolnaftate), Plough Corp., Memphis, Tenn.
[2] Desenex (contains 10% undecylenic acid), Pharmacraft, Pennwalt Corp., Rochester, N.Y.
[3] Tinactin (contains 1% tolnaftate), Schering Corp., Kenilworth, N.J.
[4] A Brinkmann Polytron was used.
[5] City Chemical Corp., New York, N.Y.

described with several exceptions. The compounds were solubilized or suspended in acetone (0.1%). Paper disks were dipped into the acetone solution or suspensions, allowed to dry, and then placed on the agar. Disks were removed after 1, 5, and 30 min and 1, 3, and 6 hr, and zone sizes were measured after incubation for 96 hr. As in the previous experiment, tolnaftate gave larger zones of inhibition than undecylenic acid and zinc undecylenate, even after only 1 min of contact (Table II). These differences again were highly significant, with the greatest differences occurring at the early time points.

The minimum inhibitory concentration was obtained in the conventional manner (2) using Sabouraud dextrose broth (Table III). Tolnaftate again was far more active than the two undecylenates in this second model of *in vitro* testing. The minimum inhibitory concentration values for tolnaftate all were <1.0 μg/ml, while the values for the undecylenates ranged from 7.5 to >10 μg/ml after 72 hr of incubation. These differences again were highly significant.

Since our data indicated *in vitro* superiority for tolnaftate over undecylenates and since efficacy *in vivo* certainly is more meaningful, it was of interest to determine if this superiority would be seen with formulated material. Results of a double-blind study comparing commercial powder A (Lot 7A503), commercial powder C[6] (Lot 14765), and commercial talc (USP M.I. No. N-03294) against a topical *T. mentagrophytes* infection in guinea pigs are shown in Table IV. Treatment was topical (powder liberally sprinkled on infected area) twice daily for 10 days. Hair and scales were removed from the infection site and plated onto Mycosel agar every other day. In addition, animals were scored for lesion appearance every day.

Procedures for establishing, culturing, and scoring the infection were described previously (4). All animals treated with commercial powder A were negative (as measured by lack of growth of the infecting organisms) throughout the treatment period (first culture taken after 2 days of treatment), and all remained negative up to 7 days posttreatment, at which time the experiment was terminated. These results were highly significant when compared with commercial powder C. Culture results seen with commercial powder C were similar to those seen with the talc controls. During treatment, all animals treated with commercial powder C remained positive; after treatment, 33% of the cultures obtained from animals treated with commercial powder C and 29% from animals treated with talc were negative. In both groups, no negative cultures were obtained until 15 days after treatment began. In addition, the average lesion scores both during and after treatment were lower with commercial powder A than with commercial powder C, and there was no statistical difference between commercial powder C and untreated controls.

Our results with this guinea pig model are similar to those reported by other investigators using similar procedures (5). In those experiments, 1% tolnaftate powder was compared to commercial powder D to determine the activity of both substances as prophylactic agents. The results showed that 1% tolnaftate powder was far more effective than commercial powder D.

[6] Cruex (contains 10% calcium undecylenate), Pharmacraft, Pennwalt Corp., Rochester, N.Y.

In the 15 years since the guinea pig model was described, the relationship between this model and clinical effectiveness has been demonstrated for many antifungal agents. Tolnaftate (4), clotrimazole (6), and miconazole (7) all were very active in the guinea pig model, and all are presently recommended for clinical use against dermatophytes (8).

Our *in vitro* and *in vivo* data obtained following conventional testing methodology clearly indicate that tolnaftate, commercial solution T, and commercial powder A are far more active than undecylenic acid, zinc undecylenate, commercial powder C, and commercial solution D.

(1) L. P. Amsel, L. Cravitz, R. VanderWyk, and S. Zahry, *J. Pharm. Sci.*, **68**, 384 (1979).

(2) B. J. Winer, "Statistical Principles in Experimental Design," McGraw-Hill, New York, N.Y., 1962.

(3) A. I. Barry, in "Infectious Diseases," 2nd ed., P. D. Hoeprich, Ed., Harper & Row, New York, N.Y., 1977.

(4) M. J. Weinstein, E. M. Oden, and E. L. Moss, Jr., *Antimicrob. Agents Chemother.*, **1964**, 595 (1965).

(5) J. A. Waitz and E. L. Moss, Jr., *Chemotherapy*, **14**, 170 (1969).

(6) J. A. Waitz, E. L. Moss, Jr., and M. J. Weinstein, *Appl. Microbiol.*, **22**, 891 (1971).

(7) J. M. VanCutsem and D. Thienpoint, *Chemotherapy*, **17**, 392 (1972).

(8) *Med. Lett.*, **18**, 101 (1976).

David Loebenberg ˣ
Raulo Parmegiani
Margaret Hanks
J. Allan Waitz

Chemotherapy, Antibiotic and Statistics Departments
Schering Corporation
Bloomfield, NJ 07003

Received August 20, 1979.
Accepted for publication February 29, 1980.

Comparative *In Vitro* and *In Vivo* Antifungal Activity of Tolnaftate and Various Undecylenates: A Rebuttal

Keyphrases □ Antifungal activity—tolnaftate and various undecylenates, comparison *in vitro* and *in vivo* □ Tolnaftate—antifungal activity *in vitro* and *in vivo*, comparison with various undecylenates □ Undecylenates—antifungal activity *in vitro* and *in vivo*, comparison with tolnaftate

To the Editor:

When different groups of scientists perform studies using differing techniques, one may expect somewhat different results, as evidenced by the work of Amsel *et al.* (1) and Loebenberg *et al.* (2). A rebuttal to the Loebenberg *et al.* communication (2) is clearly in order. The stress of Loebenberg *et al.* on our "unusual" methodology seems to hint that the use of a new or nonstandard method may be unacceptable. Our method (1) was reproducible by different investigators, rapid, and equivalent to older "standard" methods.

The following comments are presented in reply to the criticisms of Loebenberg *et al.* (2).

1. Their comment that minimum fungicidal concen-

0022-3549/80/0600-0741$01.00/0
© 1980, American Pharmaceutical Association

described with several exceptions. The compounds were solubilized or suspended in acetone (0.1%). Paper disks were dipped into the acetone solution or suspensions, allowed to dry, and then placed on the agar. Disks were removed after 1, 5, and 30 min and 1, 3, and 6 hr, and zone sizes were measured after incubation for 96 hr. As in the previous experiment, tolnaftate gave larger zones of inhibition than undecylenic acid and zinc undecylenate, even after only 1 min of contact (Table II). These differences again were highly significant, with the greatest differences occurring at the early time points.

The minimum inhibitory concentration was obtained in the conventional manner (2) using Sabouraud dextrose broth (Table III). Tolnaftate again was far more active than the two undecylenates in this second model of *in vitro* testing. The minimum inhibitory concentration values for tolnaftate all were <1.0 μg/ml, while the values for the undecylenates ranged from 7.5 to >10 μg/ml after 72 hr of incubation. These differences again were highly significant.

Since our data indicated *in vitro* superiority for tolnaftate over undecylenates and since efficacy *in vivo* certainly is more meaningful, it was of interest to determine if this superiority would be seen with formulated material. Results of a double-blind study comparing commercial powder A (Lot 7A503), commercial powder C[6] (Lot 14765), and commercial talc (USP M.I. No. N-03294) against a topical *T. mentagrophytes* infection in guinea pigs are shown in Table IV. Treatment was topical (powder liberally sprinkled on infected area) twice daily for 10 days. Hair and scales were removed from the infection site and plated onto Mycosel agar every other day. In addition, animals were scored for lesion appearance every day.

Procedures for establishing, culturing, and scoring the infection were described previously (4). All animals treated with commercial powder A were negative (as measured by lack of growth of the infecting organisms) throughout the treatment period (first culture taken after 2 days of treatment), and all remained negative up to 7 days posttreatment, at which time the experiment was terminated. These results were highly significant when compared with commercial powder C. Culture results seen with commercial powder C were similar to those seen with the talc controls. During treatment, all animals treated with commercial powder C remained positive; after treatment, 33% of the cultures obtained from animals treated with commercial powder C and 29% from animals treated with talc were negative. In both groups, no negative cultures were obtained until 15 days after treatment began. In addition, the average lesion scores both during and after treatment were lower with commercial powder A than with commercial powder C, and there was no statistical difference between commercial powder C and untreated controls.

Our results with this guinea pig model are similar to those reported by other investigators using similar procedures (5). In those experiments, 1% tolnaftate powder was compared to commercial powder D to determine the activity of both substances as prophylactic agents. The results showed that 1% tolnaftate powder was far more effective than commercial powder D.

[6] Cruex (contains 10% calcium undecylenate), Pharmacraft, Pennwalt Corp., Rochester, N.Y.

In the 15 years since the guinea pig model was described, the relationship between this model and clinical effectiveness has been demonstrated for many antifungal agents. Tolnaftate (4), clotrimazole (6), and miconazole (7) all were very active in the guinea pig model, and all are presently recommended for clinical use against dermatophytes (8).

Our *in vitro* and *in vivo* data obtained following conventional testing methodology clearly indicate that tolnaftate, commercial solution T, and commercial powder A are far more active than undecylenic acid, zinc undecylenate, commercial powder C, and commercial solution D.

(1) L. P. Amsel, L. Cravitz, R. VanderWyk, and S. Zahry, *J. Pharm. Sci.*, **68**, 384 (1979).

(2) B. J. Winer, "Statistical Principles in Experimental Design," McGraw-Hill, New York, N.Y., 1962.

(3) A. I. Barry, in "Infectious Diseases," 2nd ed., P. D. Hoeprich, Ed., Harper & Row, New York, N.Y., 1977.

(4) M. J. Weinstein, E. M. Oden, and E. L. Moss, Jr., *Antimicrob. Agents Chemother.*, **1964**, 595 (1965).

(5) J. A. Waitz and E. L. Moss, Jr., *Chemotherapy*, **14**, 170 (1969).

(6) J. A. Waitz, E. L. Moss, Jr., and M. J. Weinstein, *Appl. Microbiol.*, **22**, 891 (1971).

(7) J. M. VanCutsem and D. Thienpoint, *Chemotherapy*, **17**, 392 (1972).

(8) *Med. Lett.*, **18**, 101 (1976).

David Loebenberg ˣ
Raulo Parmegiani
Margaret Hanks
J. Allan Waitz

Chemotherapy, Antibiotic and Statistics Departments
Schering Corporation
Bloomfield, NJ 07003

Received August 20, 1979.
Accepted for publication February 29, 1980.

Comparative *In Vitro* and *In Vivo* Antifungal Activity of Tolnaftate and Various Undecylenates: A Rebuttal

Keyphrases □ Antifungal activity—tolnaftate and various undecylenates, comparison *in vitro* and *in vivo* □ Tolnaftate—antifungal activity *in vitro* and *in vivo*, comparison with various undecylenates □ Undecylenates—antifungal activity *in vitro* and *in vivo*, comparison with tolnaftate

To the Editor:

When different groups of scientists perform studies using differing techniques, one may expect somewhat different results, as evidenced by the work of Amsel *et al.* (1) and Loebenberg *et al.* (2). A rebuttal to the Loebenberg *et al.* communication (2) is clearly in order. The stress of Loebenberg *et al.* on our "unusual" methodology seems to hint that the use of a new or nonstandard method may be unacceptable. Our method (1) was reproducible by different investigators, rapid, and equivalent to older "standard" methods.

The following comments are presented in reply to the criticisms of Loebenberg *et al.* (2).

1. Their comment that minimum fungicidal concen-

0022-3549/80/0600-0741$01.00/0
© 1980, American Pharmaceutical Association

trations as well as minimum inhibitory concentrations for products used were not presented is irrelevant. Our purpose was not to compare the potency of undecylenic acid and tolnaftate (studied at 20–21°) but rather to show differences in their activity (*i.e.*, killing time).

2. Loebenberg *et al.* (2) questioned the use of suspensions *versus* solutions. Suspensions of active ingredients as well as finished products were used to eliminate, as much as possible, problems that frequently occur in *in vitro* testing (*e.g.*, differences in diffusion due to different vehicles). Thus, the use of polyethylene glycol 400 as a solvent for tolnaftate and of ethanol for undecylenic acid (both would be in solution) was, in our opinion, less justified and might have introduced more error into the results than the use of an aqueous suspension for both. Diffusional differences due to the solvent could well overshadow any antifungal action. Also, an "in-use" condition would be mimicked most closely by having the products in aqueous suspension (as might be expected in the humid cutaneous environment).

3. Certainly no claim for "more bioavailability" of undecylenic acid over tolnaftate was made based on an *in vitro* study (1), as suggested by Loebenberg *et al.* (2). We are unaware of any selectivity of polysorbate in aiding dispersion or wetting of any particular product.

4. Preliminary experimentation indicated that rinsing in simple peptone solution did not remove all active drug from the cultures. To ensure complete removal of the active ingredients, the rinsing solutions and procedures described (1) were utilized.

5. It appears to us that if the contact time between the drug and organism were increased, any benefit would be reaped by both compounds and not by one exclusively. The longest contact time was 240 min.

6. Loebenberg *et al.* (2) noted wide variation in our results (1). Although the differences in Table IV are less often significant, the trend is in the same direction as in Table II. Statistical procedures were employed and presented to substantiate the conclusions.

While Loebenberg *et al.* (2) criticized our use of suspensions of commercial powders[1,2], they did not present data on these commercial powders to refute our *in vitro* results. Instead, they compared solutions[1,3] *in vitro*. The vehicles of these products differ markedly (propanol and polyethylene glycol 400, respectively). Therefore, we used an aqueous powder suspension to eliminate vehicle differences and, hence, possible differences in diffusion. Even though lower minimum inhibitory concentrations were noted for tolnaftate, concentration obviously is not the sole criterion of an effective drug.

The introduction by Loebenberg *et al.* (2) of a guinea pig study into a discussion of *in vitro* results is perplexing; here, also, different commercial products were compared[2,4]. Loebenberg *et al.* (2) noted that the average lesion score for one product[2] (16.4) was lower than that for the other[4] (18.2). Whether a difference in scores of 1.8 is significant or of clinical importance is doubtful. Moreover, the guinea pig test system referred to (3) is of limited use. Weinstein *et al.* (3) noted that the system "can have suggestive value only" and that: "The absolute relationship between guinea pig efficacy and clinical utility in acute and particularly chronic human infections has not been established." These investigators (3) also noted that the *in vivo* test can act only as a guide to suggest possible clinical usefulness.

[1] Desenex.
[2] Aftate.
[3] Tinactin.
[4] Cruex.

(1) L. P. Amsel, L. Cravitz, R. VanderWyk, and S. Zahry, *J. Pharm. Sci.*, **68**, 384 (1979).
(2) D. Loebenberg, R. Parmegiani, M. Hanks, and J. A. Waitz, *ibid.*, **69**, 739 (1980).
(3) M. J. Weinstein, E. M. Oden, and E. L. Moss, *Antimicrob. Agents Chemother.*, **1964**, 595 (1965).

Lewis P. Amsel
Pharmaceutical Division
Pennwalt Corporation
Rochester, NY 14623

Received October 4, 1979.
Accepted for publication February 29, 1980.

Hygroscopicity of Poorly Soluble Porous Substances

Keyphrases □ Hygroscopicity—poorly soluble and insoluble substances, correlation between pore structure and equilibrium moisture content □ Pore-size distribution—overall porosity of poorly soluble substances, effect on hygroscopicity, equilibrium moisture content □ Equilibrium moisture content—poorly soluble substances, effect of overall porosity on hygroscopicity

To the Editor:

The general problem of hygroscopicity of soluble compounds has been defined (1, 2) and was reviewed recently (3). However, the hygroscopicity of poorly soluble compounds has attracted little attention. El-Sabaawi and Pei (4) showed that a correlation exists between pore structure and equilibrium moisture content for insoluble substances. This report extends this principle to insoluble substances with log-normally distributed pore spaces and shows that the equilibrium moisture curves obtained are of a traditional contour. It is presumed that this principle also extends to poorly soluble substances, as defined in the USP.

A liquid with zero contact angle exerts a vapor pressure when confined in a capillary pore of diameter d which is given by the modified Kelvin equation (5):

$$\ln(P/P^*) = -4\gamma V/[RT(d-t)] \qquad \text{(Eq. 1)}$$

where P is the vapor pressure over the liquid in the pore, P^* is the vapor pressure of pure water at the given temperature T, γ is the interfacial tension between the solid and liquid (water), V is the molar volume of the liquid (water), R is the gas constant, and t is the correction factor for the sorbed layer *in* the pore.

For the purpose of the example and for simplicity, t is neglected in the following equation, so Eq. 1 becomes:

$$\ln(P/P^*) = -4\gamma V/RTd \qquad \text{(Eq. 2)}$$

The hygroscopicity of a compound or powder mixture often is studied by means of equilibrium moisture curves. To obtain these curves, a given amount (W_0, expressed in

0022-3549/80/0600-0742$01.00/0
© 1980, American Pharmaceutical Association

trations as well as minimum inhibitory concentrations for products used were not presented is irrelevant. Our purpose was not to compare the potency of undecylenic acid and tolnaftate (studied at 20–21°) but rather to show differences in their activity (*i.e.*, killing time).

2. Loebenberg *et al.* (2) questioned the use of suspensions *versus* solutions. Suspensions of active ingredients as well as finished products were used to eliminate, as much as possible, problems that frequently occur in *in vitro* testing (*e.g.*, differences in diffusion due to different vehicles). Thus, the use of polyethylene glycol 400 as a solvent for tolnaftate and of ethanol for undecylenic acid (both would be in solution) was, in our opinion, less justified and might have introduced more error into the results than the use of an aqueous suspension for both. Diffusional differences due to the solvent could well overshadow any antifungal action. Also, an "in-use" condition would be mimicked most closely by having the products in aqueous suspension (as might be expected in the humid cutaneous environment).

3. Certainly no claim for "more bioavailability" of undecylenic acid over tolnaftate was made based on an *in vitro* study (1), as suggested by Loebenberg *et al.* (2). We are unaware of any selectivity of polysorbate in aiding dispersion or wetting of any particular product.

4. Preliminary experimentation indicated that rinsing in simple peptone solution did not remove all active drug from the cultures. To ensure complete removal of the active ingredients, the rinsing solutions and procedures described (1) were utilized.

5. It appears to us that if the contact time between the drug and organism were increased, any benefit would be reaped by both compounds and not by one exclusively. The longest contact time was 240 min.

6. Loebenberg *et al.* (2) noted wide variation in our results (1). Although the differences in Table IV are less often significant, the trend is in the same direction as in Table II. Statistical procedures were employed and presented to substantiate the conclusions.

While Loebenberg *et al.* (2) criticized our use of suspensions of commercial powders[1,2], they did not present data on these commercial powders to refute our *in vitro* results. Instead, they compared solutions[1,3] *in vitro*. The vehicles of these products differ markedly (propanol and polyethylene glycol 400, respectively). Therefore, we used an aqueous powder suspension to eliminate vehicle differences and, hence, possible differences in diffusion. Even though lower minimum inhibitory concentrations were noted for tolnaftate, concentration obviously is not the sole criterion of an effective drug.

The introduction by Loebenberg *et al.* (2) of a guinea pig study into a discussion of *in vitro* results is perplexing; here, also, different commercial products were compared[2,4]. Loebenberg *et al.* (2) noted that the average lesion score for one product[2] (16.4) was lower than that for the other[4] (18.2). Whether a difference in scores of 1.8 is significant or of clinical importance is doubtful. Moreover, the guinea pig test system referred to (3) is of limited use. Weinstein *et al.* (3) noted that the system "can have suggestive value only" and that: "The absolute relationship between guinea pig efficacy and clinical utility in acute and particularly chronic human infections has not been established." These investigators (3) also noted that the *in vivo* test can act only as a guide to suggest possible clinical usefulness.

[1] Desenex.
[2] Aftate.
[3] Tinactin.
[4] Cruex.

(1) L. P. Amsel, L. Cravitz, R. VanderWyk, and S. Zahry, *J. Pharm. Sci.*, **68**, 384 (1979).
(2) D. Loebenberg, R. Parmegiani, M. Hanks, and J. A. Waitz, *ibid.*, **69**, 739 (1980).
(3) M. J. Weinstein, E. M. Oden, and E. L. Moss, *Antimicrob. Agents Chemother.*, **1964**, 595 (1965).

Lewis P. Amsel
Pharmaceutical Division
Pennwalt Corporation
Rochester, NY 14623

Received October 4, 1979.
Accepted for publication February 29, 1980.

Hygroscopicity of Poorly Soluble Porous Substances

Keyphrases □ Hygroscopicity—poorly soluble and insoluble substances, correlation between pore structure and equilibrium moisture content □ Pore-size distribution—overall porosity of poorly soluble substances, effect on hygroscopicity, equilibrium moisture content □ Equilibrium moisture content—poorly soluble substances, effect of overall porosity on hygroscopicity

To the Editor:

The general problem of hygroscopicity of soluble compounds has been defined (1, 2) and was reviewed recently (3). However, the hygroscopicity of poorly soluble compounds has attracted little attention. El-Sabaawi and Pei (4) showed that a correlation exists between pore structure and equilibrium moisture content for insoluble substances. This report extends this principle to insoluble substances with log-normally distributed pore spaces and shows that the equilibrium moisture curves obtained are of a traditional contour. It is presumed that this principle also extends to poorly soluble substances, as defined in the USP.

A liquid with zero contact angle exerts a vapor pressure when confined in a capillary pore of diameter d which is given by the modified Kelvin equation (5):

$$\ln(P/P^*) = -4\gamma V/[RT(d-t)] \qquad \text{(Eq. 1)}$$

where P is the vapor pressure over the liquid in the pore, P^* is the vapor pressure of pure water at the given temperature T, γ is the interfacial tension between the solid and liquid (water), V is the molar volume of the liquid (water), R is the gas constant, and t is the correction factor for the sorbed layer *in* the pore.

For the purpose of the example and for simplicity, t is neglected in the following equation, so Eq. 1 becomes:

$$\ln(P/P^*) = -4\gamma V/RTd \qquad \text{(Eq. 2)}$$

The hygroscopicity of a compound or powder mixture often is studied by means of equilibrium moisture curves. To obtain these curves, a given amount (W_0, expressed in

0022-3549/80/0600-0742$01.00/0
© 1980, American Pharmaceutical Association

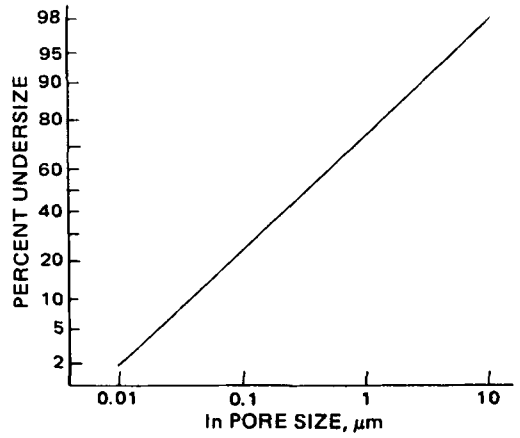

Figure 1—*Example of a log-normal pore-size distribution as used in Table I.*

grams) of a solid substance is exposed in a desiccator to the atmosphere of a saturated salt solution. The relative humidity of the atmosphere is a function of the particular salt used. The experiment is carried out until no more moisture is taken up by the solid, *i.e.*, until its weight, W_f, is constant. The amount $x = (W_f - W_0)100/W_f$ is the moisture content of the solid corresponding to the relative humidity, H, in question. The plot of x *versus* H or of H *versus* x is denoted as the equilibrium moisture curve. An excellent example of this type of experiment that allows interpretation is the work of Sangekar *et al.* (6). However, usually only the apparent kinetics of moisture adsorption are studied and only at one relative humidity (RH).

For an insoluble substance with known pore-size distribution, the equilibrium moisture curve can be deduced from this distribution. This distribution gives the volume fraction of pores with diameters below a certain size. These pores will not allow evaporation of water at pressures above a P value given by Eq. 2. The volume percent of pores (based on the pore volume) can be converted to the volume percent of solids since the total pore volume is known. The pressure, P, can be converted to relative humidity by multiplication by $100/P^*$.

This determination is best illustrated by example. Figure 1 gives an example of a log-normal pore-size distribution with 2% of the pore volume being of diameters below 0.01 μm and 98% being below 10 μm. If the vapor pressure

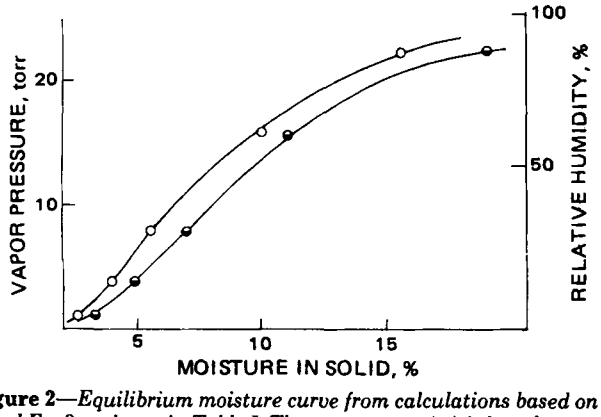

Figure 2—*Equilibrium moisture curve from calculations based on Fig. 1 and Eq. 3 as shown in Table I. The upper curve (○) is based on a solids density of 1.0 g/cm³, and the lower curve (◒) is based on a solids density of 1.25 g/cm³.*

Table I—Calculation of Critical Vapor Pressures from Pore-Size Distribution [a]

Volume Percent of Pores	Pore Diameter, μm	P, torr	Pore Volume[b], %	Moisture Content[c], %
2	<0.01	0.0002	0.4	0.62
11	<0.04	1.24	2.2	3.32
16.5	<0.063	3.78	3.3	4.90
24	<0.1	7.62	4.8	6.98
45	<0.25	15.6	9	12.3
75	<1.0	22.4	15	19.0

[a] Calculated from Fig. 1 and Eq. 3. [b] Assuming 1 cm³ of pores/5 cm³ of solid. [c] Using a true solids density of 1.25 g/cm³ and unit density for water.

above a pore of diameter 10 μm is 25 torr and the vapor pressure of water at the temperature in question is 25.3 torr, then it follows from Eq. 2 that:

$$\ln(P/25.3) = -0.12/d \qquad \text{(Eq. 3)}$$

where P is expressed in torr and d is expressed in micrometers.

A selected number of diameters calculated according to Eq. 3 are shown in Table I. The first column gives the volume percent of pores below the diameter shown in the second column. The vapor pressure corresponding to this diameter is calculated according to Eq. 3 and is shown in the third column. If the overall porosity is 20%, *i.e.*, if there is 1 cm³ of pore space in 5 cm³ of solid volume (*i.e.*, 4 cm³ of actual solid), then the percent of pore volume is as shown in the fourth column. This value is converted to percent moisture content as follows. If, as shown in line 2 of Table I, there is 2.2% of pore volume below 1.24 torr and if the solid has a true density of ρ, then the amount of solid (4 cm³) is $(4/\rho)$ g and the amount of water is 11% of 1 cm³ (1 g), *i.e.*, 0.11 g. Hence, the percent of moisture is $11/[(4/\rho) + 0.11]$.

Figures calculated for a value of $\rho = 1.25$ g/cm³ are shown in the fifth column of Table I and in Fig. 2. Figure 3 is an example taken from the literature (6). The slightly sigmoid nature of the curve in Fig. 2 may not be present in data reported in the literature since, in most cases, the equilibrium moisture curves are not precise below ~35% RH. Furthermore, for the example in Fig. 2, if the solid in a somewhat moist state was prepared for the experiment

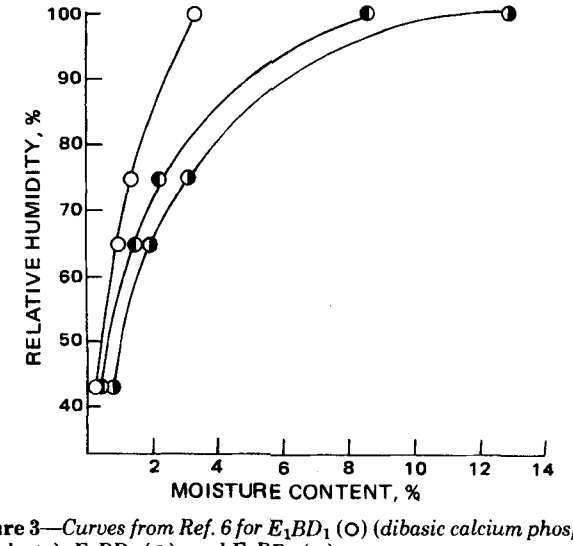

Figure 3—*Curves from Ref. 6 for E_1BD_1 (○) (dibasic calcium phosphate dihydrate), E_6BD_3 (◐), and E_8BD_2 (◑).*

by drying at 26° at a pressure of >3 torr (13% RH) or the equivalent at a higher temperature, then only the last five points would be involved and the shape would lose the initial sigmoid nature.

These comments are confined to situations where no gross swelling or pore-size distortion occurs during moisture uptake (7, 8). Furthermore, the solubility must be sufficiently low so that no significant volume changes or vapor pressure changes can result from dissolution.

(1) J. T. Carstensen, "Pharmaceutics of Solids and Solid Dosage Forms," Wiley, New York, N.Y., 1977, p. 15.

(2) R. Yamamoto and T. Takahashi, *J. Pharm. Soc. Jpn.*, **76**, 7 (1956).

(3) L. Van Campen, G. Zografi, and J. T. Carstensen, *Int. J. Pharm.*, in press.

(4) M. El-Sabaawi and D. C. T. Pei, *Ind. Eng. Chem. Fund.*, **16**, 321 (1977).

(5) P. W. M. Jacobs and F. C. Tompkins, in "Chemistry of the Solid State," W. E. Garner, Ed., Butterworths, London, England, 1955, p. 102.

(6) S. A. Sangekar, M. Sarli, and P. R. Sheth, *J. Pharm. Sci.*, **61**, 939 (1972).

(7) K. Marshall and D. Sixsmith, *Drug Dev. Commun.*, **1**, 51 (1974/75).

(8) K. G. Hollenbeck, G. E. Peck, and D. O. Kildsig, *J. Pharm. Sci.*, **67**, 1599 (1978).

J. T. Carstensen ˣ
P. Touré *
L. Van Campen
G. Zografi
School of Pharmacy
University of Wisconsin
Madison, WI 53706

Received November 16, 1979.
Accepted for publication March 12, 1980.

* On leave from Faculté de Pharmacie, Université de Paris-Sud, Châtenay-Malabry, France (February and March 1979).

L. Van Campen is an American Foundation for Pharmaceutical Education E. Mead Johnson Memorial Fellow.

Enhancement of Rectal Absorption of Drugs by Adjuvants

Keyphrases □ Absorption, rectal—enhancement by certain adjuvants □ Salicylate—enhancement of rectal absorption of theophylline and lidocaine □ Theophylline—enhancement of rectal absorption by salicylate □ Lidocaine—enhancement of rectal absorption by salicylate

To the Editor:

Rectal drug administration has the potential of overcoming some limitations encountered with other dosage forms. In this communication, we report that the rectal absorption of many drugs is facilitated markedly in the presence of certain adjuvants.

Although specific surfactants were shown to promote drug absorption from the rectum (1), their use seems to damage the rectal mucosa, reducing their suitability as absorption promoters. The adjuvants described in this report appear to function differently.

These observations were made using an *in situ* perfusion method of the rectum similar to that reported by Crommelin *et al.* (2). Six milliliters of drug solution was circulated at a rate of 2 ml/min at 38° through an ~2-cm section of the rectum of male Sprague–Dawley rats weighing 275–300 g. The amount of drug remaining in the perfusate was analyzed by high-pressure liquid chromatography as a function of time. Blood levels also were measured in blood samples taken from a vein in the leg of a rat.

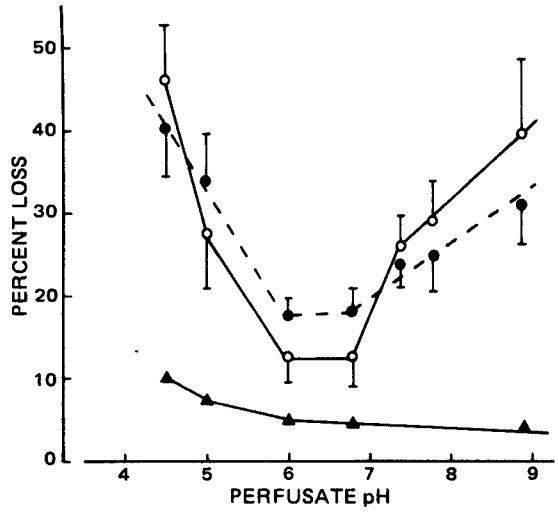

Figure 1—*Percent loss of salicylate or its acidic form (--●--) and theophylline (—○— and —▲—) after 1 hr from the perfusate in the rat rectum. Initial concentrations were 0.5% sodium salicylate (--●--), 0.5% sodium salicylate and 200 μg of theophylline/ml (—○—), and 200 μg of theophylline/ml (—▲—).*

Figure 1 shows the effect of salicylate at various pH values on the disappearance of theophylline from the perfusate in the rat rectum after 60 min of perfusion. The loss of theophylline from the perfusate in the absence of salicylic acid or salicylate was small at all pH values. However, in the presence of 0.5% salicylate at various pH values, the disappearance of theophylline was enhanced greatly, especially below pH 5 and above pH 7.4.

As shown in Fig. 1, the loss of theophylline paralleled the loss of salicylate from the perfusing solution; the greater the disappearance of salicylate from the perfusate, the greater was the loss of theophylline. Furthermore, contrary to the situation with some surfactants, the promotive effect of salicylate did not reflect a permanent change in the rectal membrane, because the effect of salicylate was eliminated by washing the rectum with buffer for 5 min at

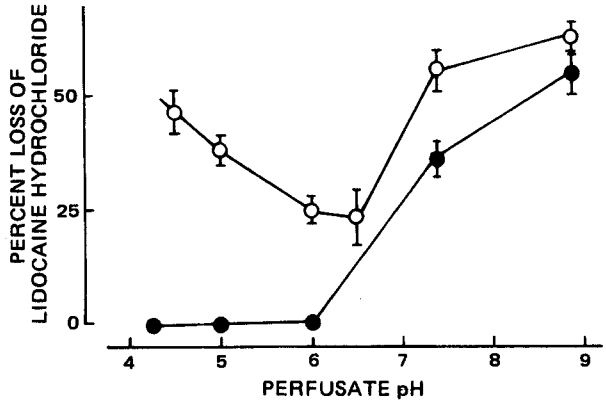

Figure 2—*Effect of pH and salicylate on the disappearance of lidocaine hydrochloride from a perfusate in the rat rectum after 1 hr. The initial lidocaine hydrochloride concentration was 500 μg/ml (○ and ●), and the sodium salicylate concentration was 0.5% (○).*

0022-3549/80/0600-0744$01.00/0
© 1980, American Pharmaceutical Association

by drying at 26° at a pressure of >3 torr (13% RH) or the equivalent at a higher temperature, then only the last five points would be involved and the shape would lose the initial sigmoid nature.

These comments are confined to situations where no gross swelling or pore-size distortion occurs during moisture uptake (7, 8). Furthermore, the solubility must be sufficiently low so that no significant volume changes or vapor pressure changes can result from dissolution.

(1) J. T. Carstensen, "Pharmaceutics of Solids and Solid Dosage Forms," Wiley, New York, N.Y., 1977, p. 15.

(2) R. Yamamoto and T. Takahashi, *J. Pharm. Soc. Jpn.*, **76**, 7 (1956).

(3) L. Van Campen, G. Zografi, and J. T. Carstensen, *Int. J. Pharm.*, in press.

(4) M. El-Sabaawi and D. C. T. Pei, *Ind. Eng. Chem. Fund.*, **16**, 321 (1977).

(5) P. W. M. Jacobs and F. C. Tompkins, in "Chemistry of the Solid State," W. E. Garner, Ed., Butterworths, London, England, 1955, p. 102.

(6) S. A. Sangekar, M. Sarli, and P. R. Sheth, *J. Pharm. Sci.*, **61**, 939 (1972).

(7) K. Marshall and D. Sixsmith, *Drug Dev. Commun.*, **1**, 51 (1974/75).

(8) K. G. Hollenbeck, G. E. Peck, and D. O. Kildsig, *J. Pharm. Sci.*, **67**, 1599 (1978).

J. T. Carstensen ˣ
P. Touré *
L. Van Campen
G. Zografi
School of Pharmacy
University of Wisconsin
Madison, WI 53706

Received November 16, 1979.
Accepted for publication March 12, 1980.

* On leave from Faculté de Pharmacie, Université de Paris-Sud, Châtenay-Malabry, France (February and March 1979).

L. Van Campen is an American Foundation for Pharmaceutical Education E. Mead Johnson Memorial Fellow.

Enhancement of Rectal Absorption of Drugs by Adjuvants

Keyphrases □ Absorption, rectal—enhancement by certain adjuvants □ Salicylate—enhancement of rectal absorption of theophylline and lidocaine □ Theophylline—enhancement of rectal absorption by salicylate □ Lidocaine—enhancement of rectal absorption by salicylate

To the Editor:

Rectal drug administration has the potential of overcoming some limitations encountered with other dosage forms. In this communication, we report that the rectal absorption of many drugs is facilitated markedly in the presence of certain adjuvants.

Although specific surfactants were shown to promote drug absorption from the rectum (1), their use seems to damage the rectal mucosa, reducing their suitability as absorption promoters. The adjuvants described in this report appear to function differently.

These observations were made using an *in situ* perfusion method of the rectum similar to that reported by Crommelin *et al.* (2). Six milliliters of drug solution was circulated at a rate of 2 ml/min at 38° through an ~2-cm section of the rectum of male Sprague–Dawley rats weighing 275–300 g. The amount of drug remaining in the perfusate was analyzed by high-pressure liquid chromatography as a function of time. Blood levels also were measured in blood samples taken from a vein in the leg of a rat.

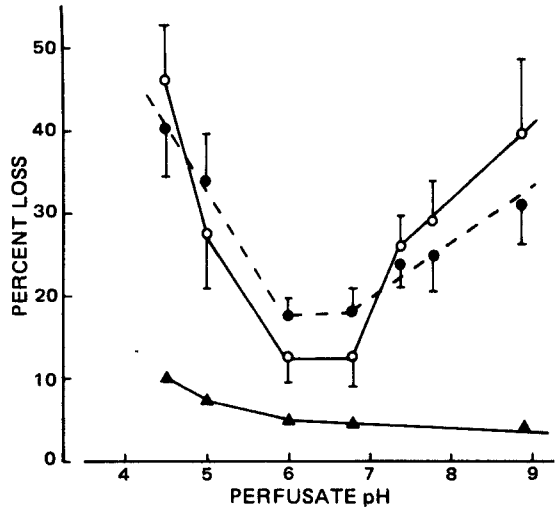

Figure 1—*Percent loss of salicylate or its acidic form (--●--) and theophylline (—○— and —▲—) after 1 hr from the perfusate in the rat rectum. Initial concentrations were 0.5% sodium salicylate (--●--), 0.5% sodium salicylate and 200 μg of theophylline/ml (—○—), and 200 μg of theophylline/ml (—▲—).*

Figure 1 shows the effect of salicylate at various pH values on the disappearance of theophylline from the perfusate in the rat rectum after 60 min of perfusion. The loss of theophylline from the perfusate in the absence of salicylic acid or salicylate was small at all pH values. However, in the presence of 0.5% salicylate at various pH values, the disappearance of theophylline was enhanced greatly, especially below pH 5 and above pH 7.4.

As shown in Fig. 1, the loss of theophylline paralleled the loss of salicylate from the perfusing solution; the greater the disappearance of salicylate from the perfusate, the greater was the loss of theophylline. Furthermore, contrary to the situation with some surfactants, the promotive effect of salicylate did not reflect a permanent change in the rectal membrane, because the effect of salicylate was eliminated by washing the rectum with buffer for 5 min at

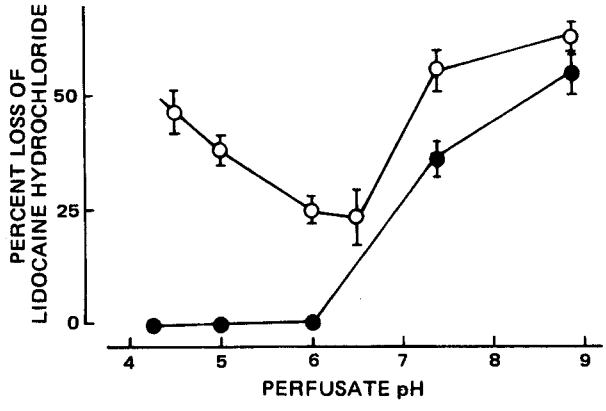

Figure 2—*Effect of pH and salicylate on the disappearance of lidocaine hydrochloride from a perfusate in the rat rectum after 1 hr. The initial lidocaine hydrochloride concentration was 500 μg/ml (○ and ●), and the sodium salicylate concentration was 0.5% (○).*

0022-3549/80/0600-0744$01.00/0
© 1980, American Pharmaceutical Association

a rate of 2 ml/min after pretreatment with salicylate; the effect of pretreatment with sodium lauryl sulfate was not eliminated by washing.

After rectal administration of 0.3 ml of theophylline solution (pH 7.4, 15 mg/ml) in the presence of salicylate (15 mg/ml), the blood levels of theophylline and salicylate increased rapidly and simultaneously, reaching maximum levels (41.2 ± 15.9 μg/ml for theophylline and 41.1 ± 14.3 μg/ml for salicylate; $n = 6$) 30 min after administration. The amounts of theophylline and salicylate remaining in the solution were 25.6 ± 4.7 and 30.3 ± 7.2%, respectively. Without salicylate, maximum blood levels of theophylline were <5 μg/ml ($n = 6$).

The presence of salicylate in the perfusate (pH 4.5 or 5.0) also enhanced the disappearance of lidocaine, which is a basic drug and is not absorbed below pH 6.0, from the perfusate in the rat rectum. The effects of salicylate on the disappearance of lidocaine at various pH values are presented in Fig. 2. Thirty minutes after rectal administration of 0.3 ml of lidocaine solution (pH 4.5, 15 mg/ml) in the presence of salicylate (15 mg/ml), lidocaine and salicylate reached maximum levels in the blood (43.3 ± 4.7 μg/ml for lidocaine and 48.5 ± 6.9 μg/ml for salicylate; $n = 6$).

These results indicate that salicylate and/or its acidic form markedly enhance the absorption of various compounds from the rectum. This effect appears to be general for other drugs including cefmetazole and levodopa. Furthermore, three isomers of sodium dihydroxybenzoate (3,4-, 2,5-, and 3,5-dihydroxybenzoates) and homovanillic acid were studied as adjuvants and found to enhance the rectal absorption of both theophylline and lidocaine. These and similar compounds have significant potential as adjuvants for enhancing rectal drug absorption. Studies are continuing on the mechanism of their action.

(1) Y. Nishioka and T. Kawamura, *Yakuzaigaku*, 37, 88 (1977).

(2) D. J. A. Crommelin, J. Modderkolk, and C. J. deBlaey, *Int. J. Pharm.*, 3, 299 (1979).

Toshiaki Nishihata
J. Howard Rytting ˣ
Takeru Higuchi

Department of Pharmaceutical Chemistry
University of Kansas
Lawrence, KS 66045

Received February 8, 1980.

Accepted for publication March 18, 1980.

Supported in part by a grant from INTERx Research Corp., Lawrence, Kans., and R. P. Scherer, North America, Detroit, Mich.

Kinetic Characterization of Liposomes

Keyphrases □ Liposomes—base-catalyzed hydrolysis of *p*-nitrophenyl acetate in liposomal suspensions □ *p*-Nitrophenyl acetate—base-catalyzed hydrolysis in liposomal suspensions □ Hydrolysis—base-catalyzed degradation of *p*-nitrophenyl acetate in liposomal suspensions

To the Editor:

Liposomes have been investigated extensively for possible use as novel drug carriers for therapeutic purposes (1, 2). From a drug stability viewpoint, we studied the hydrolysis of procaine and 2-diethylaminoethyl *p*-nitrobenzoate in liposomal suspensions and compared it with spontaneous hydrolysis in aqueous bulk solutions (3, 4). The base-catalyzed hydrolysis of procaine was retarded by liposomes; with 2-diethylaminoethyl *p*-nitrobenzoate, both retardation and enhancement were observed, depending on the pH of the dispersed medium.

These ester degradations followed first-order kinetics in the liposomal suspension as well as in the corresponding aqueous bulk solution, regardless of whether retardation or enhancement was observed. This finding indicates that the substrates added in the liposomal medium partitioned into the lipid phase at so fast a rate that it was undetectable, and this partitioning was followed by quasi-first-order degradation, which can be represented by the first-order rate constants defined in the aqueous bulk and lipid phases. Consequently, the partition model was applicable for degradation of these esters.

This communication discusses the base-catalyzed hydrolysis of *p*-nitrophenyl acetate in liposomal suspensions. This compound frequently is used as a substrate in studies of micellar catalysis (5, 6) and of esterase activity of bovine serum albumin and human serum albumin (7, 8).

Figure 1 indicates that the reaction followed first-order kinetics with the ester remaining in the aqueous solution. The reaction clearly was not a continuous process in liposomal suspensions. It was enhanced in the early stage and proceeded in a manner parallel to the spontaneous degradation. The degradation rate was dependent on the lecithin concentration; the more lecithin that was present, the faster was the hydrolysis. Furthermore, enhancement was accelerated more in the unilamellar dispersion system than in the multilamellar one when the lecithin content in

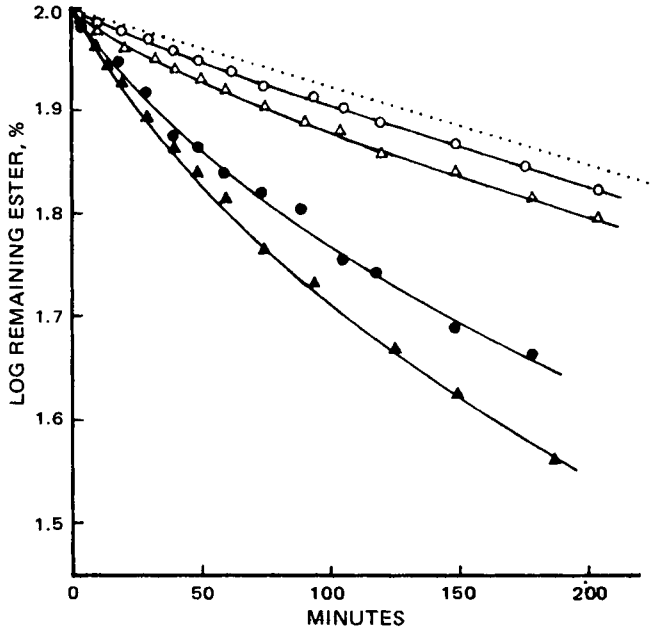

Figure 1—*First-order plots for hydrolysis of* p*-nitrophenyl acetate in aqueous solution and in liposomal suspensions. Tris(hydroxymethyl)-aminomethane buffer at pH 8.0 was used (μ = 0.3, 25°). The initial* p*-nitrophenyl acetate concentration was 5.92 × 10⁻⁴ M. The lecithin concentrations were 2.40 × 10⁻³ M (○ and △) and 8.67 × 10⁻³ M (● and ▲). Key: . . . , spontaneous degradation in water; ○ and ●, multilamellar liposome system; and △ and ▲, unilamellar liposome system. Liposomes were prepared from egg yolk lecithin as described previously (3).*

0022-3549/80/0600-0745$01.00/0
© 1980, American Pharmaceutical Association

a rate of 2 ml/min after pretreatment with salicylate; the effect of pretreatment with sodium lauryl sulfate was not eliminated by washing.

After rectal administration of 0.3 ml of theophylline solution (pH 7.4, 15 mg/ml) in the presence of salicylate (15 mg/ml), the blood levels of theophylline and salicylate increased rapidly and simultaneously, reaching maximum levels (41.2 ± 15.9 μg/ml for theophylline and 41.1 ± 14.3 μg/ml for salicylate; $n = 6$) 30 min after administration. The amounts of theophylline and salicylate remaining in the solution were 25.6 ± 4.7 and 30.3 ± 7.2%, respectively. Without salicylate, maximum blood levels of theophylline were <5 μg/ml ($n = 6$).

The presence of salicylate in the perfusate (pH 4.5 or 5.0) also enhanced the disappearance of lidocaine, which is a basic drug and is not absorbed below pH 6.0, from the perfusate in the rat rectum. The effects of salicylate on the disappearance of lidocaine at various pH values are presented in Fig. 2. Thirty minutes after rectal administration of 0.3 ml of lidocaine solution (pH 4.5, 15 mg/ml) in the presence of salicylate (15 mg/ml), lidocaine and salicylate reached maximum levels in the blood (43.3 ± 4.7 μg/ml for lidocaine and 48.5 ± 6.9 μg/ml for salicylate; $n = 6$).

These results indicate that salicylate and/or its acidic form markedly enhance the absorption of various compounds from the rectum. This effect appears to be general for other drugs including cefmetazole and levodopa. Furthermore, three isomers of sodium dihydroxybenzoate (3,4-, 2,5-, and 3,5-dihydroxybenzoates) and homovanillic acid were studied as adjuvants and found to enhance the rectal absorption of both theophylline and lidocaine. These and similar compounds have significant potential as adjuvants for enhancing rectal drug absorption. Studies are continuing on the mechanism of their action.

(1) Y. Nishioka and T. Kawamura, *Yakuzaigaku*, 37, 88 (1977).

(2) D. J. A. Crommelin, J. Modderkolk, and C. J. deBlaey, *Int. J. Pharm.*, 3, 299 (1979).

Toshiaki Nishihata
J. Howard Rytting ˣ
Takeru Higuchi

Department of Pharmaceutical Chemistry
University of Kansas
Lawrence, KS 66045

Received February 8, 1980.

Accepted for publication March 18, 1980.

Supported in part by a grant from INTERx Research Corp., Lawrence, Kans., and R. P. Scherer, North America, Detroit, Mich.

Kinetic Characterization of Liposomes

Keyphrases □ Liposomes—base-catalyzed hydrolysis of *p*-nitrophenyl acetate in liposomal suspensions □ *p*-Nitrophenyl acetate—base-catalyzed hydrolysis in liposomal suspensions □ Hydrolysis—base-catalyzed degradation of *p*-nitrophenyl acetate in liposomal suspensions

To the Editor:

Liposomes have been investigated extensively for possible use as novel drug carriers for therapeutic purposes (1, 2). From a drug stability viewpoint, we studied the hydrolysis of procaine and 2-diethylaminoethyl *p*-nitrobenzoate in liposomal suspensions and compared it with spontaneous hydrolysis in aqueous bulk solutions (3, 4). The base-catalyzed hydrolysis of procaine was retarded by liposomes; with 2-diethylaminoethyl *p*-nitrobenzoate, both retardation and enhancement were observed, depending on the pH of the dispersed medium.

These ester degradations followed first-order kinetics in the liposomal suspension as well as in the corresponding aqueous bulk solution, regardless of whether retardation or enhancement was observed. This finding indicates that the substrates added in the liposomal medium partitioned into the lipid phase at so fast a rate that it was undetectable, and this partitioning was followed by quasi-first-order degradation, which can be represented by the first-order rate constants defined in the aqueous bulk and lipid phases. Consequently, the partition model was applicable for degradation of these esters.

This communication discusses the base-catalyzed hydrolysis of *p*-nitrophenyl acetate in liposomal suspensions. This compound frequently is used as a substrate in studies of micellar catalysis (5, 6) and of esterase activity of bovine serum albumin and human serum albumin (7, 8).

Figure 1 indicates that the reaction followed first-order kinetics with the ester remaining in the aqueous solution. The reaction clearly was not a continuous process in liposomal suspensions. It was enhanced in the early stage and proceeded in a manner parallel to the spontaneous degradation. The degradation rate was dependent on the lecithin concentration; the more lecithin that was present, the faster was the hydrolysis. Furthermore, enhancement was accelerated more in the unilamellar dispersion system than in the multilamellar one when the lecithin content in

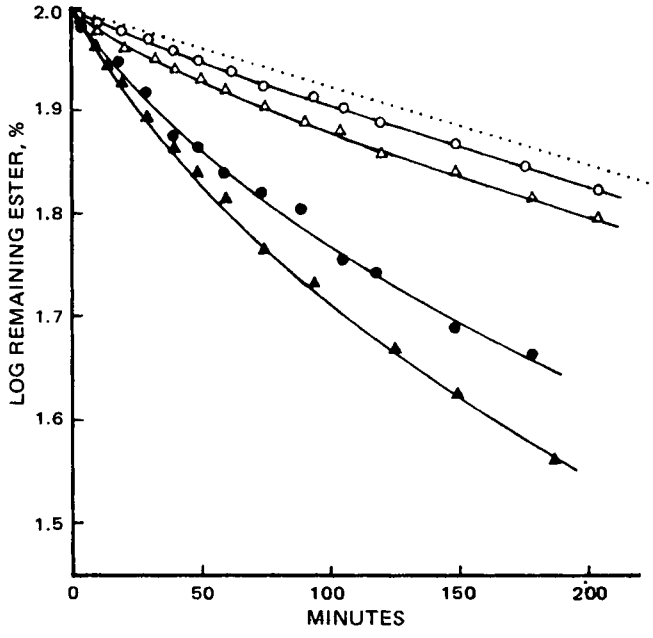

Figure 1—*First-order plots for hydrolysis of* p*-nitrophenyl acetate in aqueous solution and in liposomal suspensions. Tris(hydroxymethyl)-aminomethane buffer at pH 8.0 was used (μ = 0.3, 25°). The initial* p*-nitrophenyl acetate concentration was 5.92 × 10⁻⁴ M. The lecithin concentrations were 2.40 × 10⁻³ M (○ and △) and 8.67 × 10⁻³ M (● and ▲). Key: . . . , spontaneous degradation in water; ○ and ●, multilamellar liposome system; and △ and ▲, unilamellar liposome system. Liposomes were prepared from egg yolk lecithin as described previously (3).*

0022-3549/80/0600-0745$01.00/0
© 1980, American Pharmaceutical Association

the medium was equal in both cases.

These results suggest that partition theory, which was applied to procaine and 2-diethylaminoethyl *p*-nitrobenzoate and for the evaluation of drug entrapment in liposomes, may not apply to the present case because the liposomes appear to be exhausted by the degradation of *p*-nitrophenyl acetate. The exhaustion may be due to acetylation of the phosphate group of the lecithin molecule, which prevents further orientation of the substrate on the surface of the vesicles from being favorable for the hydroxide-ion attack. Furthermore, as seen in the difference between the rates for unilamellar and multilamellar liposomes, the effective surface area of the vesicles plays a key role, and the reaction occurring on the surface is much more predominant than that in the interior lipid phase.

Binding of *p*-nitrophenyl acetate by liposomes appears to be important at the first stage of the reaction to facilitate hydrolysis. The whole reaction can be treated in a manner analogous to that used for enzymatic catalysis:

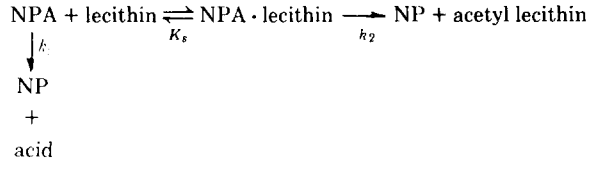

Scheme I

where NPA and NP are *p*-nitrophenyl acetate and the product, *p*-nitrophenol, respectively; NPA · lecithin is the substrate–lecithin complex; k_1 and k_2 are the rate constants for the spontaneous and facilitated reactions, respectively; and K_s is the dissociation constant of the complex.

According to Scheme I, the apparent first-order rate constant, k_{obs}, for the appearance of NP can be expressed under the condition of an excess lecithin concentration:

$$k_{obs} = \frac{k_1 K_s + k_2 [\text{lecithin}]}{K_s + [\text{lecithin}]} \qquad \text{(Eq. 1)}$$

By converting Eq. 1 to the double-reciprocal form, a Lineweaver–Burk plot makes it possible to determine K_s and k_2 values. However, since lecithin does not exist as a molecular form in water, k_{obs} does not depend on the practical lecithin concentration but instead on the effective surface area of the vesicles formed, which could be converted to the effective concentration of the lipid based on the ratio of the k_{obs} values of unilamellar and multilamellar liposomes prepared under various conditions with an equal lecithin content.

When the lecithin concentration is moderate, k_{obs} is no longer a constant but becomes a function of the effective concentration of the lipid changing with time. Therefore, the effective concentration is an adjustable parameter that is fitted best by a nonlinear optimization procedure in addition to the k_2 value.

Thus, the surface properties of liposomes, if they are prepared under the same conditions except for size reduction procedures, may greatly affect the stability of a drug, especially when the enhancement of degradation is involved.

(1) B. E. Ryman, in "Proceedings of the Sixth International Congress of Pharmacology," vol. 5, J. Tuomisto and M. K. Paasonen, Eds., Helsinki, Finland, 1975, p. 91.

(2) G. Gregoriadis, *Ann. N.Y. Acad. Sci.*, **308**, 343 (1978).

(3) T. Yotsuyanagi, T. Hamada, H. Tomida, and K. Ikeda, *Acta Pharm. Suec.*, **16**, 271 (1979).

(4) *Ibid.*, **16**, 325 (1979).

(5) V. Gani and C. Lapinte, *Tetrahedron Lett.*, **1973**, 2775.

(6) F. M. Menger and M. J. McCreery, *J. Am. Chem. Soc.*, **96**, 121 (1974).

(7) J. T. Tildon and J. W. Ogilvie, *J. Biol. Chem.*, **247**, 1265 (1972).

(8) K. Ikeda, Y. Kurono, Y. Ozeki, and T. Yotsuyanagi, *Chem. Pharm. Bull.*, **27**, 80 (1979).

Toshihisa Yotsuyanagi ˣ
Ken Ikeda

Faculty of Pharmaceutical Sciences
Nagoya City University
Nagoya 467, Japan

Received January 15, 1980.
Accepted for publication March 24, 1980.

Quantitative Change in Metabolic Fate of Drug Related to Serum Protein Binding

Keyphrases □ Protein binding, serum—effect on drug metabolism □ Drug metabolism—effect of serum protein binding □ Biotransformation—effect of serum protein binding on drug metabolism

To the Editor:

If a drug is eliminated by renal excretion and by biotransformation, then the fraction of the dose that is metabolized, F_m, is equal to the ratio of the metabolic formation clearance to the total clearance. Thus:

$$F_m = Cl_m/Cl_T \qquad \text{(Eq. 1)}$$

If clearance is not limited or affected by the organ blood perfusion rate and the rates of the clearance processes are proportional to the concentration of free (unbound) drug in serum:

$$F_m = \frac{fCl_{m\ \text{intrinsic}}}{fCl_{T\ \text{intrinsic}}} \qquad \text{(Eq. 2)}$$

where f is the free fraction of drug in serum and the clearance terms represent intrinsic clearances of free drug (1–3). Since f cancels out, F_m is independent of serum protein binding under the stated conditions.

If the renal clearance of a drug involves glomerular filtration (the rate of which usually is proportional to the concentration of free drug in serum) as well as renal tubular secretion and if the rate of tubular secretion is proportional to the concentration of total (free plus bound) drug in serum (3), then F_m is affected by f. Specifically:

$$\text{renal clearance} = fk_g(1 - F) + k_s^*(1 - F) \qquad \text{(Eq. 3)}$$

where k_g is the glomerular filtration clearance referenced to the free drug concentration, k_s^* is the apparent renal secretion clearance referenced to the total drug concentration, and F is a dimensionless constant representing the fraction of filtered and secreted drug that is reabsorbed (3). Proportionality between the renal tubular secretion rate and the total rather than free drug concentration in plasma or serum may occur if the true renal secretion clearance is much higher than the effective renal blood flow (4).

Since total clearance is the sum of the renal and metabolic clearances for drugs eliminated entirely by those two

0022-3549/80/0600-0746$01.00/0
© 1980, American Pharmaceutical Association

the medium was equal in both cases.

These results suggest that partition theory, which was applied to procaine and 2-diethylaminoethyl *p*-nitrobenzoate and for the evaluation of drug entrapment in liposomes, may not apply to the present case because the liposomes appear to be exhausted by the degradation of *p*-nitrophenyl acetate. The exhaustion may be due to acetylation of the phosphate group of the lecithin molecule, which prevents further orientation of the substrate on the surface of the vesicles from being favorable for the hydroxide-ion attack. Furthermore, as seen in the difference between the rates for unilamellar and multilamellar liposomes, the effective surface area of the vesicles plays a key role, and the reaction occurring on the surface is much more predominant than that in the interior lipid phase.

Binding of *p*-nitrophenyl acetate by liposomes appears to be important at the first stage of the reaction to facilitate hydrolysis. The whole reaction can be treated in a manner analogous to that used for enzymatic catalysis:

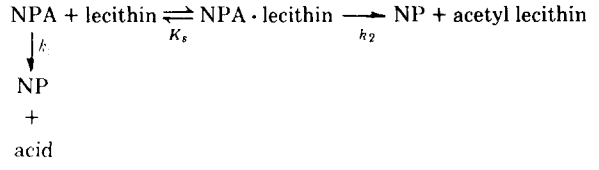

Scheme I

where NPA and NP are *p*-nitrophenyl acetate and the product, *p*-nitrophenol, respectively; NPA · lecithin is the substrate–lecithin complex; k_1 and k_2 are the rate constants for the spontaneous and facilitated reactions, respectively; and K_s is the dissociation constant of the complex.

According to Scheme I, the apparent first-order rate constant, k_{obs}, for the appearance of NP can be expressed under the condition of an excess lecithin concentration:

$$k_{obs} = \frac{k_1 K_s + k_2 [\text{lecithin}]}{K_s + [\text{lecithin}]} \qquad \text{(Eq. 1)}$$

By converting Eq. 1 to the double-reciprocal form, a Lineweaver–Burk plot makes it possible to determine K_s and k_2 values. However, since lecithin does not exist as a molecular form in water, k_{obs} does not depend on the practical lecithin concentration but instead on the effective surface area of the vesicles formed, which could be converted to the effective concentration of the lipid based on the ratio of the k_{obs} values of unilamellar and multilamellar liposomes prepared under various conditions with an equal lecithin content.

When the lecithin concentration is moderate, k_{obs} is no longer a constant but becomes a function of the effective concentration of the lipid changing with time. Therefore, the effective concentration is an adjustable parameter that is fitted best by a nonlinear optimization procedure in addition to the k_2 value.

Thus, the surface properties of liposomes, if they are prepared under the same conditions except for size reduction procedures, may greatly affect the stability of a drug, especially when the enhancement of degradation is involved.

(1) B. E. Ryman, in "Proceedings of the Sixth International Congress of Pharmacology," vol. 5, J. Tuomisto and M. K. Paasonen, Eds., Helsinki, Finland, 1975, p. 91.

(2) G. Gregoriadis, *Ann. N.Y. Acad. Sci.*, **308**, 343 (1978).

(3) T. Yotsuyanagi, T. Hamada, H. Tomida, and K. Ikeda, *Acta Pharm. Suec.*, **16**, 271 (1979).

(4) *Ibid.*, **16**, 325 (1979).

(5) V. Gani and C. Lapinte, *Tetrahedron Lett.*, **1973**, 2775.

(6) F. M. Menger and M. J. McCreery, *J. Am. Chem. Soc.*, **96**, 121 (1974).

(7) J. T. Tildon and J. W. Ogilvie, *J. Biol. Chem.*, **247**, 1265 (1972).

(8) K. Ikeda, Y. Kurono, Y. Ozeki, and T. Yotsuyanagi, *Chem. Pharm. Bull.*, **27**, 80 (1979).

Toshihisa Yotsuyanagi ˣ
Ken Ikeda

Faculty of Pharmaceutical Sciences
Nagoya City University
Nagoya 467, Japan

Received January 15, 1980.
Accepted for publication March 24, 1980.

Quantitative Change in Metabolic Fate of Drug Related to Serum Protein Binding

Keyphrases □ Protein binding, serum—effect on drug metabolism □ Drug metabolism—effect of serum protein binding □ Biotransformation—effect of serum protein binding on drug metabolism

To the Editor:

If a drug is eliminated by renal excretion and by biotransformation, then the fraction of the dose that is metabolized, F_m, is equal to the ratio of the metabolic formation clearance to the total clearance. Thus:

$$F_m = Cl_m/Cl_T \qquad \text{(Eq. 1)}$$

If clearance is not limited or affected by the organ blood perfusion rate and the rates of the clearance processes are proportional to the concentration of free (unbound) drug in serum:

$$F_m = \frac{fCl_{m\ \text{intrinsic}}}{fCl_{T\ \text{intrinsic}}} \qquad \text{(Eq. 2)}$$

where f is the free fraction of drug in serum and the clearance terms represent intrinsic clearances of free drug (1–3). Since f cancels out, F_m is independent of serum protein binding under the stated conditions.

If the renal clearance of a drug involves glomerular filtration (the rate of which usually is proportional to the concentration of free drug in serum) as well as renal tubular secretion and if the rate of tubular secretion is proportional to the concentration of total (free plus bound) drug in serum (3), then F_m is affected by f. Specifically:

$$\text{renal clearance} = fk_g(1 - F) + k_s^*(1 - F) \qquad \text{(Eq. 3)}$$

where k_g is the glomerular filtration clearance referenced to the free drug concentration, k_s^* is the apparent renal secretion clearance referenced to the total drug concentration, and F is a dimensionless constant representing the fraction of filtered and secreted drug that is reabsorbed (3). Proportionality between the renal tubular secretion rate and the total rather than free drug concentration in plasma or serum may occur if the true renal secretion clearance is much higher than the effective renal blood flow (4).

Since total clearance is the sum of the renal and metabolic clearances for drugs eliminated entirely by those two

0022-3549/80/0600-0746$01.00/0
© 1980, American Pharmaceutical Association

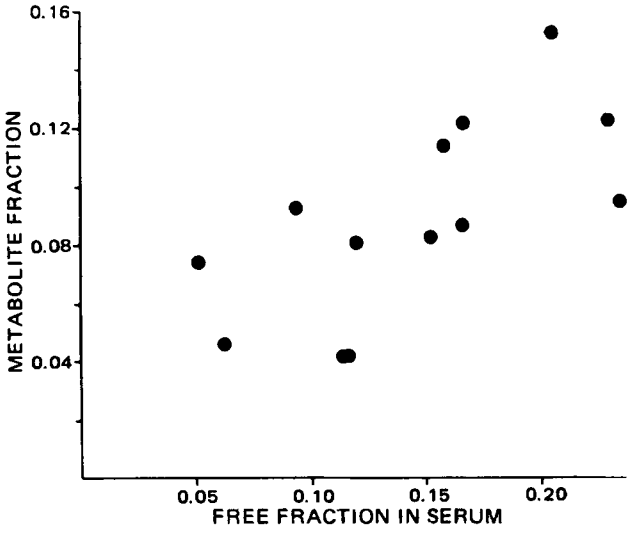

Figure 1—*Relationship between the fraction of a 20-mg/kg iv dose of sulfisoxazole excreted in the urine as metabolites and the free fraction of sulfisoxazole in serum. Data were obtained from 13 rats (6). The correlation coefficient is 0.68;* $p < 0.02$.

types of processes:

$$Cl_T = fk_g(1 - F) + k_s^*(1 - F) + fCl_{m\ \text{intrinsic}} \qquad \text{(Eq. 4)}$$

and the fraction of a dose metabolized is equal to $fCl_{m\ \text{intrinsic}}$ divided by all of the terms on the right side of Eq. 4. Dividing the numerator and denominator of that ratio by f yields:

$$F_m = \frac{Cl_{m\ \text{intrinsic}}}{k_g(1 - F) + Cl_{m\ \text{intrinsic}} + \frac{k_s^*(1 - F)}{f}} \qquad \text{(Eq. 5)}$$

Examination of Eq. 5 reveals that as f increases, F_m also increases. Thus, the fraction of a dose of drug converted to metabolite(s) increases if the serum protein binding of that drug is decreased in blood flowing through the eliminating organs (5)[1]. This conclusion applies only to drugs that are excreted in part by a process whose rate is proportional to the total rather than the free drug concentration in plasma or serum while the rates of other, parallel elimination processes are proportional to the free drug concentration. Sulfisoxazole appears to exhibit such characteristics in rats (6).

In 13 male Sprague–Dawley rats receiving a single intravenous injection of 20 mg of sulfisoxazole/kg, the fraction of the dose recovered in the urine as metabolites ranged from 0.042 to 0.152 and f ranged from 0.0518 to 0.235 (6). Drug concentrations in serum declined biexponentially with no downward curvature, which would occur if renal excretion, the major pathway of elimination, were saturable in the concentration range studied. Reexamination of the experimental data revealed a significant positive correlation between F_m and f (Fig. 1), as predicted by Eq. 5.

One important implication of these findings relates to the mechanism of certain drug interactions. Increased conversion of a drug (A) to its metabolite(s) caused by prior or concomitant administration of another drug (B) usually will be interpreted as resulting from either induction of biotransformation or inhibition of the renal clearance of A. However, if Drug B displaces Drug A from plasma protein binding sites, then the increased biotransformation of Drug A also could occur by the mechanism described in this communication. Another implication concerns the effect of the dose or dosing rate on the metabolic fate of a drug. For drugs that exhibit significant concentration dependence of plasma protein binding (f increases with increasing drug concentration), F_m may increase with increasing dose or dosing rate due to decreased protein binding.

(1) G. Levy and A. Yacobi, *J. Pharm. Sci.*, **63**, 805 (1974).
(2) G. Levy, in "The Effect of Disease States on Drug Pharmacokinetics," L. Z. Benet, Ed., American Pharmaceutical Association, Washington, D.C., 1976, chap. 9.
(3) G. Levy, *J. Pharm. Sci.*, **69**, 482 (1980).
(4) I. M. Weiner, in "Handbook of Physiology, Renal Physiology Section," J. Orloff and R. W. Berliner, Eds., American Physiological Society, Washington, D.C., 1973, pp. 521–554.
(5) U. W. Wiegand and G. Levy, *J. Pharm. Sci.*, **69**, 480 (1980).
(6) A. Yacobi and G. Levy, *ibid.*, **68**, 742 (1979).

Gerhard Levy
Department of Pharmaceutics
School of Pharmacy
State University of New York at Buffalo
Amherst, NY 14260

Received January 14, 1980.
Accepted for publication March 21, 1980.
Supported in part by Grant GM 20852 from the National Institute of General Medical Sciences, National Institutes of Health.

[1] The opposite would occur if biotransformation is blood flow rate limited while the renal excretion rate is proportional to the free drug concentration in plasma.

Polyethylene Glycols as Solvents in Implantable Osmotic Pumps

Keyphrases □ Polyethylene glycols—use as solvents in implantable osmotic pumps □ Solvents—polyethylene glycols, use in implantable osmotic pumps □ Drug delivery systems—implantable osmotic pumps, use of polyethylene glycols as solvents

To the Editor:

Implantable osmotic pumps[1] are useful for short-term delivery of water-soluble drugs and hormones (1–4). However, many compounds such as steroids are too insoluble in water to be administered as aqueous solutions (5). Although 5% ethanol and 5% dimethyl sulfoxide increase the concentration range over which lipophilic molecules can be delivered (6), the maximum dose still is quite low. Polyethylene glycols 400 and 600 are excellent solvents for many steroids (Table I) (1,5) and also are useful *in vivo* since they have very low toxicities (7). The objective of these experiments was to evaluate the suitability of polyethylene glycols as solvents with implantable pumps *in vivo*. Since the polyethylene glycols are known to influence fluid balance *in vivo*, the potential effects of the solvents and the pumps also were examined.

The ability of the pumps to function *in vivo* with polyethylene glycols as solvents was evaluated in two ways. Mineralocorticoids are known to induce the amiloride-

[1] Model 1701, Alza Corp., Palo Alto, CA 94304.

© 1980, American Pharmaceutical Association

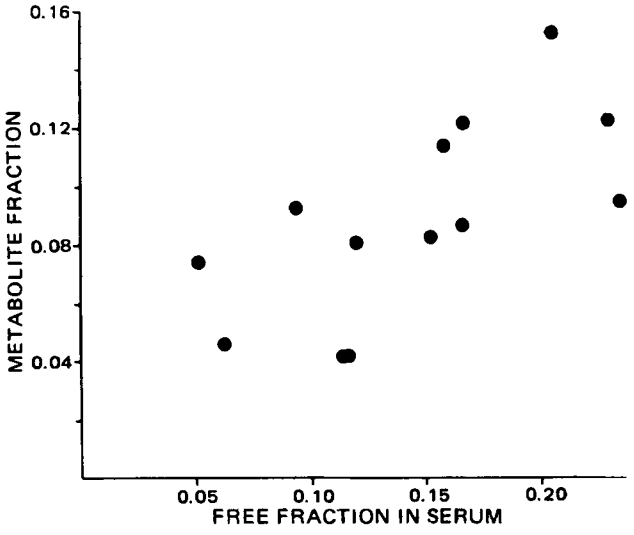

Figure 1—*Relationship between the fraction of a 20-mg/kg iv dose of sulfisoxazole excreted in the urine as metabolites and the free fraction of sulfisoxazole in serum. Data were obtained from 13 rats (6). The correlation coefficient is 0.68;* $p < 0.02$.

types of processes:

$$Cl_T = fk_g(1 - F) + k_s^*(1 - F) + fCl_{m\ \text{intrinsic}} \qquad \text{(Eq. 4)}$$

and the fraction of a dose metabolized is equal to $fCl_{m\ \text{intrinsic}}$ divided by all of the terms on the right side of Eq. 4. Dividing the numerator and denominator of that ratio by f yields:

$$F_m = \frac{Cl_{m\ \text{intrinsic}}}{k_g(1 - F) + Cl_{m\ \text{intrinsic}} + \frac{k_s^*(1 - F)}{f}} \qquad \text{(Eq. 5)}$$

Examination of Eq. 5 reveals that as f increases, F_m also increases. Thus, the fraction of a dose of drug converted to metabolite(s) increases if the serum protein binding of that drug is decreased in blood flowing through the eliminating organs (5)[1]. This conclusion applies only to drugs that are excreted in part by a process whose rate is proportional to the total rather than the free drug concentration in plasma or serum while the rates of other, parallel elimination processes are proportional to the free drug concentration. Sulfisoxazole appears to exhibit such characteristics in rats (6).

In 13 male Sprague–Dawley rats receiving a single intravenous injection of 20 mg of sulfisoxazole/kg, the fraction of the dose recovered in the urine as metabolites ranged from 0.042 to 0.152 and f ranged from 0.0518 to 0.235 (6). Drug concentrations in serum declined biexponentially with no downward curvature, which would occur if renal excretion, the major pathway of elimination, were saturable in the concentration range studied. Reexamination of the experimental data revealed a significant positive correlation between F_m and f (Fig. 1), as predicted by Eq. 5.

One important implication of these findings relates to the mechanism of certain drug interactions. Increased conversion of a drug (A) to its metabolite(s) caused by prior or concomitant administration of another drug (B) usually will be interpreted as resulting from either induction of biotransformation or inhibition of the renal clearance of A. However, if Drug B displaces Drug A from plasma protein binding sites, then the increased biotransformation of Drug A also could occur by the mechanism described in this communication. Another implication concerns the effect of the dose or dosing rate on the metabolic fate of a drug. For drugs that exhibit significant concentration dependence of plasma protein binding (f increases with increasing drug concentration), F_m may increase with increasing dose or dosing rate due to decreased protein binding.

(1) G. Levy and A. Yacobi, *J. Pharm. Sci.*, **63**, 805 (1974).
(2) G. Levy, in "The Effect of Disease States on Drug Pharmacokinetics," L. Z. Benet, Ed., American Pharmaceutical Association, Washington, D.C., 1976, chap. 9.
(3) G. Levy, *J. Pharm. Sci.*, **69**, 482 (1980).
(4) I. M. Weiner, in "Handbook of Physiology, Renal Physiology Section," J. Orloff and R. W. Berliner, Eds., American Physiological Society, Washington, D.C., 1973, pp. 521–554.
(5) U. W. Wiegand and G. Levy, *J. Pharm. Sci.*, **69**, 480 (1980).
(6) A. Yacobi and G. Levy, *ibid.*, **68**, 742 (1979).

Gerhard Levy
Department of Pharmaceutics
School of Pharmacy
State University of New York at Buffalo
Amherst, NY 14260

Received January 14, 1980.
Accepted for publication March 21, 1980.
Supported in part by Grant GM 20852 from the National Institute of General Medical Sciences, National Institutes of Health.

[1] The opposite would occur if biotransformation is blood flow rate limited while the renal excretion rate is proportional to the free drug concentration in plasma.

Polyethylene Glycols as Solvents in Implantable Osmotic Pumps

Keyphrases □ Polyethylene glycols—use as solvents in implantable osmotic pumps □ Solvents—polyethylene glycols, use in implantable osmotic pumps □ Drug delivery systems—implantable osmotic pumps, use of polyethylene glycols as solvents

To the Editor:

Implantable osmotic pumps[1] are useful for short-term delivery of water-soluble drugs and hormones (1–4). However, many compounds such as steroids are too insoluble in water to be administered as aqueous solutions (5). Although 5% ethanol and 5% dimethyl sulfoxide increase the concentration range over which lipophilic molecules can be delivered (6), the maximum dose still is quite low. Polyethylene glycols 400 and 600 are excellent solvents for many steroids (Table I) (1,5) and also are useful *in vivo* since they have very low toxicities (7). The objective of these experiments was to evaluate the suitability of polyethylene glycols as solvents with implantable pumps *in vivo*. Since the polyethylene glycols are known to influence fluid balance *in vivo*, the potential effects of the solvents and the pumps also were examined.

The ability of the pumps to function *in vivo* with polyethylene glycols as solvents was evaluated in two ways. Mineralocorticoids are known to induce the amiloride-

[1] Model 1701, Alza Corp., Palo Alto, CA 94304.

© 1980, American Pharmaceutical Association

Table I—Solubility of Selected Steroids in Polyethylene Glycols and Soybean Oil [a]

Compound	Solubility at 37°, g/liter: Polyethylene Glycol 400	Polyethylene Glycol 600	Soybean Oil
Aldosterone	83 ± 4 (2)	ND[b]	ND
Corticosterone	26 ± 2 (3)	26 ± 2 (3)	3.0
Desoxycorticosterone acetate	24 ± 2 (3)	28 ± 2 (3)	14
Dexamethasone acetate	45 ± 2 (4)	42 ± 2 (3)	1.4
17β-Estradiol	116 ± 4 (3)	97 ± 4 (3)	1.6
Hydrocortisone	15 ± 2 (3)	24 ± 2 (3)	0.9
Progesterone	27 ± 2 (3)	32 ± 2 (4)	19
Spironolactone	46 ± 3 (4)	44 ± 2 (3)	8
Testosterone	39 ± 2 (4)	42 ± 2 (3)	10

[a] The steroids and the polyethylene glycol solvents were obtained from Sigma Chemical Co., St. Louis, MO 63178. The steroids were suspended in the solvent, warmed to ~80°, and sonicated for dissolution. After storage in sealed vials at 37° for >72 hr, samples were centrifuged at 12,000×*g* for 20 min to pellet any insoluble drug. If insoluble drug was detected, additional solvent was added and the process of warming the solution, sonication, and prolonged storage was repeated until solubility was obtained. Since most values were determined only by approaching apparent equilibrium from a supersaturated solution rather than from both sides, the solubilities cannot be considered as rigorously established equilibrium values. Data with soybean oil (Wesson Oil, Hunt Wesson Foods Inc., Fullerton, CA 92634) are shown for comparison only. Results are given as the mean ± *SEM*; the number in parentheses is the number of independent determinations. [b] ND = not determined.

Table II—Ability of Polyethylene Glycol-Solubilized Steroids to Induce Amiloride-Sensitive Sodium Transport in the Rat Colon [a]

Animals	Treatment	Average Dose, μg/kg/hr	Amiloride-Sensitive Sodium Transport, % total
Control	Untreated	—	9.0 ± 2.8 (8)
Control	Glass rod	—	7.2 ± 1.3 (3)
Control	Pumps with solvent	—	22.6 ± 5.8 (5)
Control	Aldosterone	5.7	76.6 ± 6.4 (4)
Control	Aldosterone + spironolactone	6.0 + 193	36.3 ± 15.8 (3)
Control	Spironolactone	164	15.3 ± 6.6 (3)
ADX	Untreated	—	1.9 ± 1.9 (5)
ADX	Glass rod	—	2.6 ± 0.8 (5)
ADX	Pumps with solvent	—	3.6 ± 0.7 (4)
ADX	Aldosterone	4.3	74.1 ± 15.4 (3)

[a] Male Sprague–Dawley rats with intact adrenal glands (controls) and male bilaterally adrenalectomized rats were maintained on Purina Formulab Chow 5008 (Ralston Purina Co., Richmond, IN 47374) *ad libitum*. The control rats were given 150 m*M* NaCl and 29 m*M* sucrose to drink *ad libitum*. The adrenalectomized animals were given the same solution with 5 m*M* KCl. Drugs were dissolved in polyethylene glycol (Table I) and loaded into osmotic pumps (6). The pumps were placed in the peritoneal cavity of ~150-g rats under ether anesthesia. Glass rods used as sham pumps were 5 × 24-mm pieces of fire-polished soft glass. The descending colon was removed under pentobarbital anesthesia (~75 mg/kg ip) and mounted in a 0.28-cm² Schultz chamber perfused with Krebs–Henseleit balanced salt solution containing 5 m*M* D-glucose (Sigma Chemical Co., St. Louis, MO 63178). The short-circuit current was measured with a conventional circuit using calomel electrodes (catalog No. 13-639-79, Fisher Scientific Co., Pittsburgh, PA 15219) (10) and was displayed on a strip-chart recorder (Brush model 110, Instrument Division, Gould Inc., Cleveland, OH 44114). The amiloride sensitivity of the short-circuit current was the portion of the short-circuit current that was sensitive to 25 μ*M* amiloride added to the mucosal surface of the tissue. Results are shown as the mean ± *SEM*; the number in parentheses is the number of animals.

sensitive sodium transport system in the luminal membrane of the rat colon (8–10). The ability of aldosterone administered by the osmotic pumps to induce the amiloride-sensitive sodium transport system was examined initially. Sodium transport was estimated *in vitro* as the short-circuit current, and amiloride sensitivity was judged by the ability of 25 μ*M* amiloride[2] to inhibit the observed short-circuit current when added to the mucosal side of the tissue (10).

After 3–7 days of aldosterone[3] infusion (Table II), 77% of the short-circuit current was inhibited by amiloride while only 7% of the short-circuit current was sensitive to amiloride in the untreated animals. This effect was due to aldosterone since it could be suppressed by the aldosterone antagonist spironolactone. Since the half-time of the amiloride-sensitive sodium transport system in the absence of aldosterone is ~12 hr (10), aldosterone must have been released from the pumps for the entire infusion period (up to 7 days).

The effectiveness of the pumps also was tested by measuring the weight change of male rats during the administration of 17β-estradiol[3]. Estrogens are known to cause a weight reduction in male rats (11–13). Adrenalectomized (ADX) rats[4] treated for 6 days with pumps containing only polyethylene glycol gained 32.2 ± 6.6 g (mean ± *SEM*, $n = 3$); the adrenalectomized rats treated with 145 μg of 17β-estradiol/kg/hr lost 22.3 ± 5.8 g ($n = 3$).

These results indicate that polyethylene glycols are effective solvents for use with osmotic pumps *in vivo*.

Although relatively large volumes of polyethylene glycol (~3 ml/kg) may perturb the fluid balance when injected into the peritoneal cavity (14, 15), the quantity of polyethylene glycol delivered by the pumps (5–10 μl/kg/hr) (1) probably is too low for this problem to be significant. The slight elevation of amiloride-sensitive sodium transport observed with control animals[4] with intact adrenal glands when compared to control animals with sham pumps (glass rods) (Table II) is due to effects of the pumps. The pumps probably act as fluid sinks, reducing the extracellular volume, stimulating the renin–angiotensin system, and causing a slight elevation of the endogenous aldosterone levels. This increase in the circulating aldosterone concentration causes the amiloride sensitivity of the colon to be elevated over that of the sham pump-treated controls (23 *versus* 7%). The renin–angiotensin–aldosterone system probably is responsible for this effect since it was reduced by treatment with spironolactone (Table II) and was abolished in the adrenalectomized animals. Although the pump-mediated increase in the activity of the renin–angiotensin–aldosterone system is small, these results serve to advise potential users of osmotic pumps that sufficient controls are important.

Osmotic pumps are useful for studies of drug efficacy *in vivo* where the actual rate of drug treatment must be maintained over a relatively long period to compare the potency of different compounds adequately. When utilized with appropriate controls, polyethylene glycols greatly expand the usefulness of these pumps to otherwise insoluble lipophilic compounds.

[2] Obtained as amiloride hydrochloride as a gift from Merck Sharp & Dohme Research Laboratories, Rahway, NJ 07065.
[3] Sigma Chemical Co., St. Louis, MO 63178.
[4] Zivic Miller Laboratories, Allison Park, PA 15101.

(1) F. E. Yates, Ed., *Special Delivery*, **3**(1), 2 (1979).
(2) E. Wei and H. Loh, *Science*, **193**, 1262 (1976).
(3) C. Y. Bowers and K. Folkers, *Biochem. Biophys. Res. Commun.*, **72**, 1003 (1976).
(4) H. M. Pinedo, D. S. Zaharko, J. Bull, and B. A. Chadner, *Cancer Res.*, **37**, 445 (1977).
(5) B. W. Barry and D. I. D. El Eini, *J. Pharm. Pharmacol.*, **28**, 210 (1976).
(6) Alzet Osmotic Minipump Instruction Manual, Alza Corp., Palo Alto, Calif., 1976.
(7) W. Bartsch, G. Sponer, K. Dietmann, and G. Fuchs, *Arzneim.-Forsch.*, **26**, 1581 (1976).
(8) P. C. Will and U. Hopfer, *Fed. Proc. Fed. Am. Soc. Exp. Biol.*, **38**, 1240 (1979).

(9) U. Hopfer and P. C. Will, *ibid.*, **38**, 1060 (1979).
(10) P. C. Will, J. L. Lebowitz, and U. Hopfer, *Am. J. Physiol.*, in press.
(11) J. Menard, A. Malmejac, and P. Milliez, *Endocrinology*, **86**, 774 (1970).
(12) O. M. Helmer and R. S. Griffith, *ibid.*, **51**, 421 (1952).
(13) H. Burrows, "Biological Actions of Sex Hormones," 2nd ed., Cambridge University Press, Cambridge, England, 1949, pp. 160, 354, 443–445.
(14) A. E. Abdelaal, P. F. Mercer, and G. J. Mogenson, *Can. J. Physiol. Pharmacol.*, **52**, 362 (1974).
(15) J. T. Fitzsimons, *J. Physiol.*, **159**, 297 (1961).

Peter C. Will
Ronald N. Cortright
Ulrich Hopfer ˣ
Department of Anatomy and Developmental Biology Center
Case Western Reserve University
Cleveland, OH 44106

Received October 29, 1979.
Accepted for publication March 24, 1980.
Supported by Grant AM-08305 from the U.S. Public Health Service.

Disintegration Test for Hard Gelatin Capsules

Keyphrases □ Disintegration—hard gelatin capsules, modification of USP and NF tests for tablet disintegration □ Dosage forms—hard gelatin capsules, disintegration test, modification of USP and NF tests for tablet disintegration

To the Editor:

A proposed disintegration test procedure for capsules was published in the USP XX Comment Proof (Vol. 3, No. 56) dated August 14, 1978. This procedure was based on a series of collaborative studies conducted by the Disintegration Test Review Committee of the Pharmaceutical Manufacturers Association (PMA) Quality Control Section. Highlights of these studies are presented in this communication.

The USP and NF describe disintegration tests for five tablet categories. The PMA project was aimed at developing a similar test for hard gelatin capsule products using the apparatus and methodology for tablet disintegration with as few changes as necessary. Three test samples (No. 2 hard gelatin capsules containing 0.5, 1.0, and 1.5% magnesium stearate in lactose) were used in the studies to evaluate procedure variables. Comments on each variable follow.

A cross section of disintegration baskets used in industry was examined. The baskets generally fell into two categories: those with notched shafts and those having shafts equipped with hooks. The former type provides a rigid mounting to the motorized device, and the motion is primarily vertical; the latter basket type provides a nonrigid attachment where the motion is both vertical and rotational. Studies showed that the mounting mode had no influence on the test results. Disintegration times were identical, within normal variation, regardless of the type of mounting used.

The disintegration time of the three test samples could not be differentiated when the plastic disks described in the USP and NF were placed into the basket-rack assembly. The disintegration time for each sample was ~3 min. By eliminating the disks and placing a 10-mesh wire screen on top of the baskets to retain the capsules within the tubes, the disintegration times for the 0.5, 1.0, and 1.5% samples were 12, 25, and 39 min, respectively.

The compendia are not specific about the disintegration test vessel. Committee members reported that both the size of the vessel and the volume of the test vehicle affected the hydrodynamics of the system, thereby influencing the disintegration rate. A 1000-ml, low-form beaker containing ~900 ml of medium was the most convenient and compatible with the dimensions of the basket-rack assembly.

Purified water was a satisfactory test vehicle for the three samples. Reproducibility in disintegration time was improved by the addition of 0.1% benzalkonium chloride. The use of simulated gastric fluid was investigated, but it was reported that hydrogen chloride vapors emanating from the fluid slowly corrode the equipment. Because of variation in the composition of compendial capsule products, collaborators recommended that both the test medium and the disintegration time limit be specified in the individual monographs.

The Committee observed that the longer the path through which the basket travels in its vertical motion, the more rapid is the disintegration time. The USP and NF specify a stroke length of 5–6 cm. In a study involving one test specimen (1.0% magnesium stearate in lactose with an average disintegration time of 25 min), the disintegration time decreased by almost 6 min when the stroke was adjusted from the lower limit, 5 cm, to the upper limit, 6 cm. Therefore, a stroke length of 5.3–5.7 cm was recommended.

The final procedure was submitted to the USP after it was found to be workable in the laboratories of 13 PMA-member companies.

Jerry Polesuk, Chairman
Disintegration Test Review Committee
PMA Quality Control Section

Received August 20, 1979.
Accepted for publication March 14, 1980.
Inquiries may be directed to the author at the Quality Assurance Department, Sandoz Pharmaceuticals, East Hanover, NJ 07936.

Effect of Smoking on Binding of Lidocaine to Human Serum Proteins

Keyphrases □ Lidocaine—effect of smoking on binding to human serum proteins □ Protein binding—lidocaine, effect of smoking, human serum □ Smoking—effect on binding of lidocaine to human serum proteins

To the Editor:

Cigarette smoking can have striking effects on the disposition of theophylline (1, 2), propranolol (3), and other drugs (4, 5). These changes generally have been ascribed to increased intrinsic hepatic clearance secondary to enzyme induction. However, other mechanisms may be operative. This communication describes the apparent effect

0022-3549/80/0600-0749$01.00/0
© 1980, American Pharmaceutical Association

(9) U. Hopfer and P. C. Will, *ibid.*, **38**, 1060 (1979).
(10) P. C. Will, J. L. Lebowitz, and U. Hopfer, *Am. J. Physiol.*, in press.
(11) J. Menard, A. Malmejac, and P. Milliez, *Endocrinology*, **86**, 774 (1970).
(12) O. M. Helmer and R. S. Griffith, *ibid.*, **51**, 421 (1952).
(13) H. Burrows, "Biological Actions of Sex Hormones," 2nd ed., Cambridge University Press, Cambridge, England, 1949, pp. 160, 354, 443–445.
(14) A. E. Abdelaal, P. F. Mercer, and G. J. Mogenson, *Can. J. Physiol. Pharmacol.*, **52**, 362 (1974).
(15) J. T. Fitzsimons, *J. Physiol.*, **159**, 297 (1961).

Peter C. Will
Ronald N. Cortright
Ulrich Hopfer ˣ
Department of Anatomy and Developmental Biology Center
Case Western Reserve University
Cleveland, OH 44106

Received October 29, 1979.
Accepted for publication March 24, 1980.
Supported by Grant AM-08305 from the U.S. Public Health Service.

Disintegration Test for Hard Gelatin Capsules

Keyphrases □ Disintegration—hard gelatin capsules, modification of USP and NF tests for tablet disintegration □ Dosage forms—hard gelatin capsules, disintegration test, modification of USP and NF tests for tablet disintegration

To the Editor:

A proposed disintegration test procedure for capsules was published in the USP XX Comment Proof (Vol. 3, No. 56) dated August 14, 1978. This procedure was based on a series of collaborative studies conducted by the Disintegration Test Review Committee of the Pharmaceutical Manufacturers Association (PMA) Quality Control Section. Highlights of these studies are presented in this communication.

The USP and NF describe disintegration tests for five tablet categories. The PMA project was aimed at developing a similar test for hard gelatin capsule products using the apparatus and methodology for tablet disintegration with as few changes as necessary. Three test samples (No. 2 hard gelatin capsules containing 0.5, 1.0, and 1.5% magnesium stearate in lactose) were used in the studies to evaluate procedure variables. Comments on each variable follow.

A cross section of disintegration baskets used in industry was examined. The baskets generally fell into two categories: those with notched shafts and those having shafts equipped with hooks. The former type provides a rigid mounting to the motorized device, and the motion is primarily vertical; the latter basket type provides a nonrigid attachment where the motion is both vertical and rotational. Studies showed that the mounting mode had no influence on the test results. Disintegration times were identical, within normal variation, regardless of the type of mounting used.

The disintegration time of the three test samples could not be differentiated when the plastic disks described in the USP and NF were placed into the basket-rack assembly. The disintegration time for each sample was ~3 min. By eliminating the disks and placing a 10-mesh wire screen on top of the baskets to retain the capsules within the tubes, the disintegration times for the 0.5, 1.0, and 1.5% samples were 12, 25, and 39 min, respectively.

The compendia are not specific about the disintegration test vessel. Committee members reported that both the size of the vessel and the volume of the test vehicle affected the hydrodynamics of the system, thereby influencing the disintegration rate. A 1000-ml, low-form beaker containing ~900 ml of medium was the most convenient and compatible with the dimensions of the basket-rack assembly.

Purified water was a satisfactory test vehicle for the three samples. Reproducibility in disintegration time was improved by the addition of 0.1% benzalkonium chloride. The use of simulated gastric fluid was investigated, but it was reported that hydrogen chloride vapors emanating from the fluid slowly corrode the equipment. Because of variation in the composition of compendial capsule products, collaborators recommended that both the test medium and the disintegration time limit be specified in the individual monographs.

The Committee observed that the longer the path through which the basket travels in its vertical motion, the more rapid is the disintegration time. The USP and NF specify a stroke length of 5–6 cm. In a study involving one test specimen (1.0% magnesium stearate in lactose with an average disintegration time of 25 min), the disintegration time decreased by almost 6 min when the stroke was adjusted from the lower limit, 5 cm, to the upper limit, 6 cm. Therefore, a stroke length of 5.3–5.7 cm was recommended.

The final procedure was submitted to the USP after it was found to be workable in the laboratories of 13 PMA-member companies.

Jerry Polesuk, Chairman
Disintegration Test Review Committee
PMA Quality Control Section

Received August 20, 1979.
Accepted for publication March 14, 1980.
Inquiries may be directed to the author at the Quality Assurance Department, Sandoz Pharmaceuticals, East Hanover, NJ 07936.

Effect of Smoking on Binding of Lidocaine to Human Serum Proteins

Keyphrases □ Lidocaine—effect of smoking on binding to human serum proteins □ Protein binding—lidocaine, effect of smoking, human serum □ Smoking—effect on binding of lidocaine to human serum proteins

To the Editor:

Cigarette smoking can have striking effects on the disposition of theophylline (1, 2), propranolol (3), and other drugs (4, 5). These changes generally have been ascribed to increased intrinsic hepatic clearance secondary to enzyme induction. However, other mechanisms may be operative. This communication describes the apparent effect

0022-3549/80/0600-0749$01.00/0
© 1980, American Pharmaceutical Association

(9) U. Hopfer and P. C. Will, *ibid.*, **38**, 1060 (1979).
(10) P. C. Will, J. L. Lebowitz, and U. Hopfer, *Am. J. Physiol.*, in press.
(11) J. Menard, A. Malmejac, and P. Milliez, *Endocrinology*, **86**, 774 (1970).
(12) O. M. Helmer and R. S. Griffith, *ibid.*, **51**, 421 (1952).
(13) H. Burrows, "Biological Actions of Sex Hormones," 2nd ed., Cambridge University Press, Cambridge, England, 1949, pp. 160, 354, 443–445.
(14) A. E. Abdelaal, P. F. Mercer, and G. J. Mogenson, *Can. J. Physiol. Pharmacol.*, **52**, 362 (1974).
(15) J. T. Fitzsimons, *J. Physiol.*, **159**, 297 (1961).

Peter C. Will
Ronald N. Cortright
Ulrich Hopfer ˣ
Department of Anatomy and Developmental Biology Center
Case Western Reserve University
Cleveland, OH 44106

Received October 29, 1979.
Accepted for publication March 24, 1980.
Supported by Grant AM-08305 from the U.S. Public Health Service.

Disintegration Test for Hard Gelatin Capsules

Keyphrases □ Disintegration—hard gelatin capsules, modification of USP and NF tests for tablet disintegration □ Dosage forms—hard gelatin capsules, disintegration test, modification of USP and NF tests for tablet disintegration

To the Editor:

A proposed disintegration test procedure for capsules was published in the USP XX Comment Proof (Vol. 3, No. 56) dated August 14, 1978. This procedure was based on a series of collaborative studies conducted by the Disintegration Test Review Committee of the Pharmaceutical Manufacturers Association (PMA) Quality Control Section. Highlights of these studies are presented in this communication.

The USP and NF describe disintegration tests for five tablet categories. The PMA project was aimed at developing a similar test for hard gelatin capsule products using the apparatus and methodology for tablet disintegration with as few changes as necessary. Three test samples (No. 2 hard gelatin capsules containing 0.5, 1.0, and 1.5% magnesium stearate in lactose) were used in the studies to evaluate procedure variables. Comments on each variable follow.

A cross section of disintegration baskets used in industry was examined. The baskets generally fell into two categories: those with notched shafts and those having shafts equipped with hooks. The former type provides a rigid mounting to the motorized device, and the motion is primarily vertical; the latter basket type provides a nonrigid attachment where the motion is both vertical and rotational. Studies showed that the mounting mode had no influence on the test results. Disintegration times were identical, within normal variation, regardless of the type of mounting used.

The disintegration time of the three test samples could not be differentiated when the plastic disks described in the USP and NF were placed into the basket-rack assembly. The disintegration time for each sample was ~3 min. By eliminating the disks and placing a 10-mesh wire screen on top of the baskets to retain the capsules within the tubes, the disintegration times for the 0.5, 1.0, and 1.5% samples were 12, 25, and 39 min, respectively.

The compendia are not specific about the disintegration test vessel. Committee members reported that both the size of the vessel and the volume of the test vehicle affected the hydrodynamics of the system, thereby influencing the disintegration rate. A 1000-ml, low-form beaker containing ~900 ml of medium was the most convenient and compatible with the dimensions of the basket-rack assembly.

Purified water was a satisfactory test vehicle for the three samples. Reproducibility in disintegration time was improved by the addition of 0.1% benzalkonium chloride. The use of simulated gastric fluid was investigated, but it was reported that hydrogen chloride vapors emanating from the fluid slowly corrode the equipment. Because of variation in the composition of compendial capsule products, collaborators recommended that both the test medium and the disintegration time limit be specified in the individual monographs.

The Committee observed that the longer the path through which the basket travels in its vertical motion, the more rapid is the disintegration time. The USP and NF specify a stroke length of 5–6 cm. In a study involving one test specimen (1.0% magnesium stearate in lactose with an average disintegration time of 25 min), the disintegration time decreased by almost 6 min when the stroke was adjusted from the lower limit, 5 cm, to the upper limit, 6 cm. Therefore, a stroke length of 5.3–5.7 cm was recommended.

The final procedure was submitted to the USP after it was found to be workable in the laboratories of 13 PMA-member companies.

Jerry Polesuk, Chairman
Disintegration Test Review Committee
PMA Quality Control Section

Received August 20, 1979.
Accepted for publication March 14, 1980.
Inquiries may be directed to the author at the Quality Assurance Department, Sandoz Pharmaceuticals, East Hanover, NJ 07936.

Effect of Smoking on Binding of Lidocaine to Human Serum Proteins

Keyphrases □ Lidocaine—effect of smoking on binding to human serum proteins □ Protein binding—lidocaine, effect of smoking, human serum □ Smoking—effect on binding of lidocaine to human serum proteins

To the Editor:

Cigarette smoking can have striking effects on the disposition of theophylline (1, 2), propranolol (3), and other drugs (4, 5). These changes generally have been ascribed to increased intrinsic hepatic clearance secondary to enzyme induction. However, other mechanisms may be operative. This communication describes the apparent effect

0022-3549/80/0600-0749$01.00/0
© 1980, American Pharmaceutical Association

of tobacco smoking on the binding of lidocaine to human serum proteins. Furthermore, we report a significant increase in the lidocaine free fraction as the concentration was increased through the range usually observed in the treatment of ventricular arrhythmias. This observation is consistent with the data reported by Tucker *et al.* (6) and is inconsistent with other reports (7, 8).

Serum samples were obtained from 16 volunteers, eight smokers and eight nonsmokers. Seven of the eight smokers stated that they smoked between 0.88 and 1.25 packs/day, while the other subject smoked either one cigar or one pipeful of tobacco/day (the data from this individual are specifically identified in Fig. 1). The nonsmoking and smoking groups were well matched with respect to sex (six males and two females in each group), age (45 ± 20 *versus* 42 ± 12 years, mean ± *SD*), concurrent medication (none except diuretic therapy for hypertension), serum albumin concentration (4.9 ± 0.5 *versus* 4.7 ± 0.3 g/100 ml), and total serum protein concentration (7.5 ± 0.3 *versus* 7.2 ± 0.4 g/100 ml). All subjects had normal renal and liver function as assessed by an automatic analyzer[1], and all were apparently free of malignant or inflammatory disease.

Venous blood collected into glass syringes after an overnight fast was allowed to clot at room temperature for ~2 hr and then was centrifuged for ~20 min at 1000×*g*. The serum was removed and stored at −20°. The protein binding of lidocaine was determined by equilibrium dialysis using a dialysis membrane[2] in Plexiglas cells. Lidocaine was added to the buffer solution (0.134 *M* phosphate buffer at pH 7.4) to achieve concentrations of 2.0 and 14.0 μg/ml. A trace amount of radiolabeled drug (30 mCi of [*carbonyl*-^{14}C]lidocaine[3] hydrochloride/mmole obtained commercially with >98% radiochemical purity) also was added to the buffer. Serum aliquots were dialyzed in duplicate against an equal volume of buffer for 5 hr at 37°. Final (postdialysis) lidocaine concentrations in all samples were quantitated by liquid scintillation counting.

Substantial intersubject variability of lidocaine free fraction values was observed; at a final concentration of 1.4 μg/ml, the free fraction ranged from 0.208 to 0.342 (mean of 0.280). Little of the variability can be explained by the reproducibility of the method since the relative standard deviation of the determination of the free fraction was 5.6% (n = 22). However, part of this variability appeared to be related to the smoking status of the subjects. The data in Fig. 1 show that at a final lidocaine concentration of 1.4 μg/ml (left panel), smokers had a significantly lower free fraction than nonsmokers (0.258 ± 0.039 *versus* 0.307 ± 0.030; $p < 0.02$). Although there was a trend toward a lower free fraction at a final concentration of 9.0 μg/ml (right panel), the difference between serum binding in smokers and nonsmokers was not statistically significant ($p > 0.15$).

There are several possible explanations for the increased protein binding of lidocaine in the serum of smokers. An exogenous substance contained in tobacco smoke could cause a cooperative interaction between lidocaine and at least one of the binding proteins. However, a more plausible explanation is that the concentration of at least one

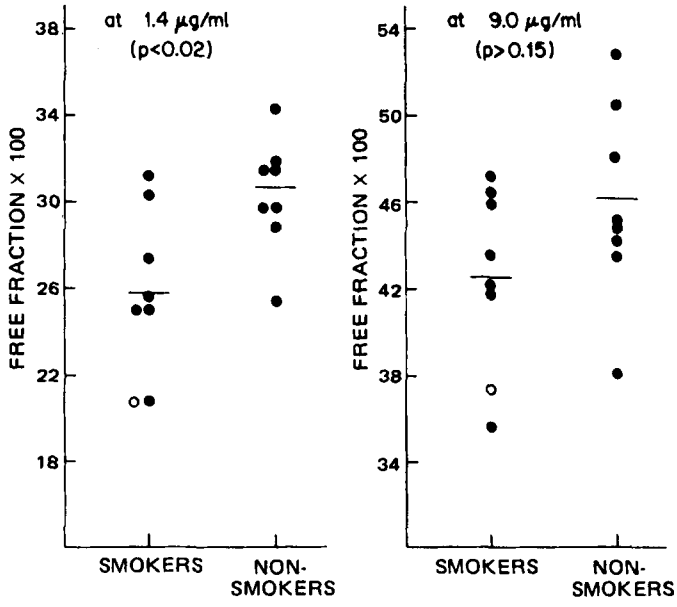

Figure 1—*Effect of smoking on the lidocaine free fraction in volunteers. Serum binding results at final lidocaine concentrations of 1.4 (left) and 9.0 (right) μg/ml are shown. The horizontal bar equals the mean free fraction value. The open symbol represents the data from the one smoker who did not smoke cigarettes.*

protein to which lidocaine binds is elevated in the serum of smokers. Some evidence suggests that the serum concentration of α_1-acid glycoprotein is elevated in smokers (9), and it is known that lidocaine binds to this acute phase reactant protein (10). Thus, the increased binding of lidocaine to the serum proteins of smokers at 1.4 μg/ml could be the result of elevated concentrations of α_1-acid glycoprotein. The failure to achieve statistical significance at a final lidocaine concentration of 9.0 μg/ml probably is related to the facts that, at this concentration, binding to albumin has greater importance (11, 12) than does binding to the glycoprotein (the 50% increase in the free fraction at 9.0 μg/ml suggests saturation of at least one class of binding sites) and, as stated earlier, albumin concentrations were nearly identical in our two populations.

Since increased binding of drugs to serum proteins is known to influence drug disposition and since increased binding of drugs to serum proteins of smokers has not been reported previously, our data may represent a significant new observation for an understanding of the effects of environmental factors on drug disposition. Furthermore, our data support the findings of Tucker *et al.* (6), who reported a lidocaine free fraction of ~0.30 at a serum drug concentration of 2 μg/ml. Finally, we confirmed the striking concentration dependence of lidocaine binding reported by Tucker *et al.* (6).

(1) J. W. Jenne, H. Nagasawa, R. Moltugh, F. McDonald, and E. Wyze, *Life Sci.*, **17**, 195 (1975).

(2) S. N. Hunt, W. J. Jusko, and A. M. Yurchak, *Clin. Pharmacol. Ther.*, **19**, 546 (1976).

(3) R. E. Vestal, A. J. J. Wood, R. A. Branch, D. G. Shand, and G. R. Wilkinson, *ibid.*, **26**, 8 (1979).

(4) W. J. Jusko, *J. Pharmacokinet. Biopharm.*, **6**, 7 (1978).

(5) A. J. J. Wood, R. E. Vestal, G. R. Wilkinson, R. A. Branch, and D. G. Shand, *Clin. Pharmacol. Ther.*, **26**, 16 (1979).

(6) G. T. Tucker, R. N. Boyes, P. O. Bridenbaugh, and D. C. Moore, *Anesthesiology*, **33**, 287 (1970).

(7) S. M. Shnider and E. L. Way, *ibid.*, **29**, 944 (1968).

[1] SMA 12/6.
[2] Spectrapor No. 2, Spectrum Medical Industries.
[3] New England Nuclear Corp.

(8) R. G. Burney, C. A. DiFazio, and J. A. Foster, *Anesth. Analg.*, **57**, 478 (1978).
(9) A. C. Hollinshead, C. H. Chuang, E. G. Cooper, and W. J. Catalona, *Cancer*, **40**, 2993 (1977).
(10) K. M. Piafsky and D. Knoppert, *Clin. Res.*, **26**, 836A (1979).
(11) P. J. McNamara, Ph.D. thesis, State University of New York at Buffalo, Buffalo, N.Y., 1979.
(12) V. J. Sawinski and G. W. Rapp, *J. Dent. Res.*, **42**, 1429 (1963).

P. J. McNamara
R. L. Slaughter
J. P. Visco
C. M. Elwood
J. H. Siegel
D. Lalka ˣ

Departments of Pharmaceutics and Pharmacy
School of Pharmacy
State University of New York at Buffalo
Buffalo, NY 14260, and the
Departments of Cardiology,
Nephrology, and Surgery, and the
Clinical Pharmacokinetics Laboratory
Buffalo General Hospital
Buffalo, NY 14203

Received December 24, 1979.
Accepted for publication March 18, 1980.
Supported in part by Grant GM 20852 from the Institute of General Medical Sciences, National Institutes of Health.

Effect of Changes in Plasma Protein Binding on Half-Life of Drugs

Keyphrases □ Pharmacokinetics—effect of changes in plasma protein binding on biological half-life of drugs □ Protein binding—effect of changes in plasma protein binding on biological half-life of drugs □ Half-life—effect of changes in plasma protein binding on biological half-life of drugs

To the Editor:

The binding of drugs to plasma proteins and extravascular tissues affects their distribution, elimination, and overall pharmacological activity. If the extent of such binding is altered by the presence of other drugs or the accumulation of certain endogenous compounds in various disease states, subsequent changes in the pharmacokinetic characteristics of the drug may be anticipated. Gibaldi *et al.* (1) suggested that the biological half-life of a drug bound to plasma proteins and tissues in a drug concentration-independent manner is a function largely of tissue binding but is independent of changes in binding to plasma proteins. However, they pointed out that this phenomenon generally is true only for drugs with apparent distribution volumes substantially larger than the plasma space. These drugs include those that distribute throughout the total body water and, more commonly, those that demonstrate extensive tissue binding as well.

The present discussion focuses on situations where the drug is bound to plasma proteins and the unbound drug is excluded from intracellular fluids. While these conditions may apply to only a few drugs, they can be important. A good example is the antibacterial agent sulfisoxazole. This compound is ~86% bound to plasma proteins after therapeutic doses (2) and is distributed only in extracellular fluids (3, 4). Since the drug does not enter the cells, it exhibits a slightly diminished toxicity while producing higher blood levels at lower doses as compared with sulfanilamide and sulfadiazine, both of which distribute throughout body water. Another example is streptomycin, which is distributed in the extracellular fluids and also is bound to plasma proteins, although to a lesser extent than sulfisoxazole (5).

Based on the physiological approach to drug distribution originally developed by Gillette (6), Øie and Tozer (7) recently proposed the following expression for the apparent volume of distribution, V:

$$V = V_P(1 + R_{E/I}) + f_P V_P(V_E/V_P - R_{E/I}) + \frac{V_T f_P}{f_T} \quad \text{(Eq. 1)}$$

where V_P is the plasma volume; V_E is the extracellular space minus the plasma volume; V_T is the physical volume into which the drug distributes minus the extracellular space; $R_{E/I}$ is the ratio of the amount of protein to which the drug binds in extracellular fluids outside the plasma to that in the plasma; and f_P and f_T are the drug fractions unbound in the spaces V_P and V_T, respectively. Furthermore, by assuming the extracellular fluid volume outside the plasma to be 12 liters and the plasma volume to be 3 liters and by assuming that the total extracellular drug-binding protein is distributed so that $R_{E/I}$ is ~1.4, Eq. 1 can be approximated as:

$$V = 7 + 8f_P + V_T\left(\frac{f_P}{f_T}\right) \quad \text{(Eq. 2)}$$

It then was pointed out (7) that if the distribution of a drug is restricted to the extracellular fluid, its apparent volume of distribution becomes:

$$V = 7 + 8f_P \quad \text{(Eq. 3)}$$

It has been shown (8) that the total clearance, Cl, of a drug whose elimination is linear and not perfusion rate limited in the organ of elimination is directly proportional to its free fraction in plasma, *i.e.*:

$$Cl = f_P Cl^* \quad \text{(Eq. 4)}$$

where Cl^* represents the intrinsic clearance. Moreover, since:

$$Cl = V\beta \quad \text{(Eq. 5)}$$

it follows that:

$$\beta = \frac{f_P Cl^*}{V} \quad \text{(Eq. 6)}$$

where, for a drug obeying two-compartment model kinetics, V is V_{area} and β equals ln 2 divided by the terminal half-life, $t_{1/2}$. Substituting Eq. 3 into Eq. 6 gives:

$$\beta = \frac{f_P Cl^*}{7 + 8f_P} \quad \text{(Eq. 7a)}$$

or:

$$t_{1/2} = \frac{\ln 2(7 + 8f_P)}{f_P Cl^*} \quad \text{(Eq. 7b)}$$

Equation 7*b* describes the effect of plasma protein binding on drug biological half-lives. When the fraction of drug unbound in plasma is changed to f'_P and the new β and $t_{1/2}$ are designated as β' and $t'_{1/2}$, respectively, then:

$$\frac{\beta'}{\beta} = \frac{t_{1/2}}{t'_{1/2}} = \frac{f'_P(7 + 8f_P)}{f_P(7 + 8f'_P)} \quad \text{(Eq. 8)}$$

or:

$$\frac{\beta'}{\beta} = \frac{7f'_P + 8f_P f'_P}{7f_P + 8f_P f'_P} \quad \text{(Eq. 9)}$$

0022-3549/80/0600-0751$01.00/0
© 1980, American Pharmaceutical Association

(8) R. G. Burney, C. A. DiFazio, and J. A. Foster, *Anesth. Analg.*, **57**, 478 (1978).
(9) A. C. Hollinshead, C. H. Chuang, E. G. Cooper, and W. J. Catalona, *Cancer*, **40**, 2993 (1977).
(10) K. M. Piafsky and D. Knoppert, *Clin. Res.*, **26**, 836A (1979).
(11) P. J. McNamara, Ph.D. thesis, State University of New York at Buffalo, Buffalo, N.Y., 1979.
(12) V. J. Sawinski and G. W. Rapp, *J. Dent. Res.*, **42**, 1429 (1963).

P. J. McNamara
R. L. Slaughter
J. P. Visco
C. M. Elwood
J. H. Siegel
D. Lalka ˣ

Departments of Pharmaceutics and Pharmacy
School of Pharmacy
State University of New York at Buffalo
Buffalo, NY 14260, and the
Departments of Cardiology,
Nephrology, and Surgery, and the
Clinical Pharmacokinetics Laboratory
Buffalo General Hospital
Buffalo, NY 14203

Received December 24, 1979.
Accepted for publication March 18, 1980.
Supported in part by Grant GM 20852 from the Institute of General Medical Sciences, National Institutes of Health.

Effect of Changes in Plasma Protein Binding on Half-Life of Drugs

Keyphrases □ Pharmacokinetics—effect of changes in plasma protein binding on biological half-life of drugs □ Protein binding—effect of changes in plasma protein binding on biological half-life of drugs □ Half-life—effect of changes in plasma protein binding on biological half-life of drugs

To the Editor:

The binding of drugs to plasma proteins and extravascular tissues affects their distribution, elimination, and overall pharmacological activity. If the extent of such binding is altered by the presence of other drugs or the accumulation of certain endogenous compounds in various disease states, subsequent changes in the pharmacokinetic characteristics of the drug may be anticipated. Gibaldi *et al.* (1) suggested that the biological half-life of a drug bound to plasma proteins and tissues in a drug concentration-independent manner is a function largely of tissue binding but is independent of changes in binding to plasma proteins. However, they pointed out that this phenomenon generally is true only for drugs with apparent distribution volumes substantially larger than the plasma space. These drugs include those that distribute throughout the total body water and, more commonly, those that demonstrate extensive tissue binding as well.

The present discussion focuses on situations where the drug is bound to plasma proteins and the unbound drug is excluded from intracellular fluids. While these conditions may apply to only a few drugs, they can be important. A good example is the antibacterial agent sulfisoxazole. This compound is ~86% bound to plasma proteins after therapeutic doses (2) and is distributed only in extracellular fluids (3, 4). Since the drug does not enter the cells, it exhibits a slightly diminished toxicity while producing higher blood levels at lower doses as compared with sulfanilamide and sulfadiazine, both of which distribute throughout body water. Another example is streptomycin, which is distributed in the extracellular fluids and also is bound to plasma proteins, although to a lesser extent than sulfisoxazole (5).

Based on the physiological approach to drug distribution originally developed by Gillette (6), Øie and Tozer (7) recently proposed the following expression for the apparent volume of distribution, V:

$$V = V_P(1 + R_{E/I}) + f_P V_P(V_E/V_P - R_{E/I}) + \frac{V_T f_P}{f_T} \quad \text{(Eq. 1)}$$

where V_P is the plasma volume; V_E is the extracellular space minus the plasma volume; V_T is the physical volume into which the drug distributes minus the extracellular space; $R_{E/I}$ is the ratio of the amount of protein to which the drug binds in extracellular fluids outside the plasma to that in the plasma; and f_P and f_T are the drug fractions unbound in the spaces V_P and V_T, respectively. Furthermore, by assuming the extracellular fluid volume outside the plasma to be 12 liters and the plasma volume to be 3 liters and by assuming that the total extracellular drug-binding protein is distributed so that $R_{E/I}$ is ~1.4, Eq. 1 can be approximated as:

$$V = 7 + 8f_P + V_T\left(\frac{f_P}{f_T}\right) \quad \text{(Eq. 2)}$$

It then was pointed out (7) that if the distribution of a drug is restricted to the extracellular fluid, its apparent volume of distribution becomes:

$$V = 7 + 8f_P \quad \text{(Eq. 3)}$$

It has been shown (8) that the total clearance, Cl, of a drug whose elimination is linear and not perfusion rate limited in the organ of elimination is directly proportional to its free fraction in plasma, *i.e.*:

$$Cl = f_P Cl^* \quad \text{(Eq. 4)}$$

where Cl^* represents the intrinsic clearance. Moreover, since:

$$Cl = V\beta \quad \text{(Eq. 5)}$$

it follows that:

$$\beta = \frac{f_P Cl^*}{V} \quad \text{(Eq. 6)}$$

where, for a drug obeying two-compartment model kinetics, V is V_{area} and β equals ln 2 divided by the terminal half-life, $t_{1/2}$. Substituting Eq. 3 into Eq. 6 gives:

$$\beta = \frac{f_P Cl^*}{7 + 8f_P} \quad \text{(Eq. 7a)}$$

or:

$$t_{1/2} = \frac{\ln 2(7 + 8f_P)}{f_P Cl^*} \quad \text{(Eq. 7b)}$$

Equation 7*b* describes the effect of plasma protein binding on drug biological half-lives. When the fraction of drug unbound in plasma is changed to f'_P and the new β and $t_{1/2}$ are designated as β' and $t'_{1/2}$, respectively, then:

$$\frac{\beta'}{\beta} = \frac{t_{1/2}}{t'_{1/2}} = \frac{f'_P(7 + 8f_P)}{f_P(7 + 8f'_P)} \quad \text{(Eq. 8)}$$

or:

$$\frac{\beta'}{\beta} = \frac{7f'_P + 8f_P f'_P}{7f_P + 8f_P f'_P} \quad \text{(Eq. 9)}$$

0022-3549/80/0600-0751$01.00/0
© 1980, American Pharmaceutical Association

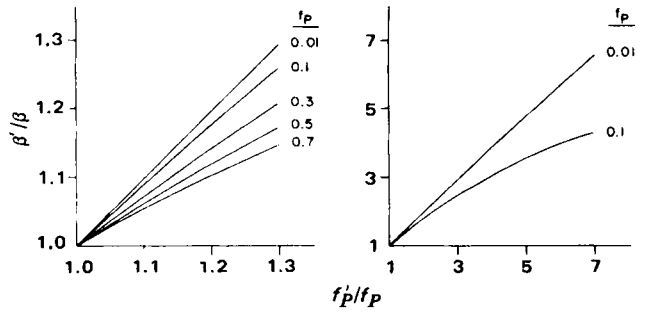

Figure 1—*Relationship between β'/β and f'_P/f_P for drugs with varying degrees of plasma protein binding.*

For the case where the binding of a drug is decreased (*i.e.*, $f'_P > f_P$), it is clear from Eq. 9 that β'/β (or $t_{1/2}/t'_{1/2}$) is smaller than f'_P/f_P but approaches f'_P/f_P as f_P approaches zero or as f'_P approaches f_P. These latter conditions apply to drugs that normally are bound to a large extent or to situations where the decrease in binding is slight.

To illustrate the relationship between relative changes in the drug half-life and plasma protein binding, Fig. 1 was constructed based on Eq. 9 using different f_P values.

From Fig. 1, it is obvious that the relationship between β'/β and f'_P/f_P is almost linear, especially when the change in f_P is relatively small. For drugs that are predominantly plasma protein bound (*e.g.*, $f_P = 0.01$), the slope of the plot is approximately one, indicating that $t_{1/2}$ is inversely proportional to f_P. Although this simple, inverse proportionality vanishes with less extensively bound drugs, the almost linear relationship between β'/β and f'_P/f_P offers a means of rapid estimation of half-life changes as a result of altered plasma protein binding.

When the percentage change in f_P is relatively large, a more rapid loss of linearity in the curves is observed with increasing f_P. Fortunately, for drugs that initially are predominantly unbound, such large percentage increases in f_P are not possible. Furthermore, the β or half-life values of these drugs are relatively insensitive to changes in binding (Fig. 1), and adjustments in the dosage regimen to correct for binding changes may not be necessary.

(1) M. Gibaldi, G. Levy, and P. J. McNamara, *Clin. Pharmacol. Ther.*, **24**, 1 (1978).

(2) W. A. Ritschel, "Handbook of Basic Pharmacokinetics," Drug Intelligence Publications, Hamilton, Ill., 1976, p. 324.

(3) E. K. Marshall, Jr., *Proc. Soc. Exp. Biol. Med.*, **68**, 472 (1948).

(4) L. Weinstein, M. A. Madoff, and C. M. Samet, *N. Engl. J. Med.*, **263**, 793 (1960).

(5) "The Pharmacological Basis of Therapeutics," 5th ed., L. S. Goodman and A. Gilman, Eds., Macmillan, New York, N.Y., 1975, p. 1169.

(6) J. R. Gillette, *Ann. N.Y. Acad. Sci.*, **179**, 43 (1971).

(7) S. Øie and T. N. Tozer, *J. Pharm. Sci.*, **68**, 1203 (1979).

(8) G. Levy and A. Yacobi, *ibid.*, **63**, 805 (1974).

Francis L. S. Tse
College of Pharmacy
Rutgers—The State University
Piscataway, NJ 08854

Received November 5, 1979.
Accepted for publication February 29, 1980.
Supported in part by a grant from the Rutgers Research Council.
The author thanks Dr. John L. Colaizzi for helpful suggestions.

BOOKS

REVIEWS

Foundations of Molecular Pharmacology, Vol. 1: Medicinal and Pharmaceutical Chemistry. By J. B. STENLAKE. The Athlone Press, University of London, Four Gower St., London WC1, England. 1979. 936 pp. 15 × 23 cm. Price $90.00.

It is easy to be enthusiastic about this well-crafted and scholarly book. The author skillfully leads us through a treatment of principles of organic chemistry applied to pharmaceutical agents. The organizational approach and its careful implementation consistently afford interesting reading.

The book is organized similar to an organic chemistry text. The medicinal agents are organized into 23 chapters by their organic chemical class; such groups as the alkanes, alkenes, benzenoid aromatic hydrocarbons, alkynes, and monohydric alcohols are included. Each chapter discusses the organic chemistry of the particular chemical class. The discussions generally are clear and succinct. The immediate pharmaceutical significance of the particular chemical property is illustrated by one or more examples from the pharmaceutical sciences. For example, following an explanation for the acidic nature of the acetylenic hydrogen atom, it is noted that the formation of a silver acetylide by the addition of silver nitrate is used as a test for identity and is the basis for the assay of some acetylenic pharmaceutical products such as ethclorvynol. Also, after a discussion of hydride reduction of aldehydes and ketones by lithium aluminum hydride and sodium borohydride, there ensues an account of the enzymatic reduction of these functional groups involving hydride donation from NADPH.

Almost all of the transitions from the general organic chemical discussion to the pharmaceutical application are made easily. Additionally, the particular pharmaceutical example usually is appropriate. One effect of this approach is to make the point repeatedly, without ever explicitly stating so, that knowledge of fundamental chemical properties is mandatory for an understanding of pharmaceutical procedures and pharmacological activities.

This reviewer has two minor criticisms relative to the author's pharmaceutical examples. There are several occasions when more appropriate pharmaceutical examples could have been presented. Also, the examples chosen could have been treated more in proportion to their importance. The following are instances in which these criticisms apply.

1. The decarboxylation of salicylic acid on bromination is discussed, but the decarboxylation of *p*-aminosalicylic acid in an acidic aqueous medium is not mentioned.
2. The structures of the amino acids GABA and taurine are given, but only GABA is cited as being an important transmitter.
3. Carbonic anhydrase-inhibiting sulfonamides are treated in detail, but benzothiazides are treated briefly.
4. The importance of ylids in synthesis is not developed.

However, these criticisms are minor, especially considering the great range of the book and the usually impressive appropriateness of the examples.

Medicinal and pharmaceutical chemists and many others in the pharmaceutical sciences should find this book to be an interesting and thought-provoking source of information. Additionally, teachers of medicinal and pharmaceutical chemistry may find that the volume is useful as a supplemental reference for both graduate and undergraduate students. Where the curriculum allows room for a course based on a format similar to that of the book (chemical class → chemical properties → pharmaceutical application), the book can serve as a textbook, although the cost is high.

Reviewed by Eugene I. Isaacson
College of Pharmacy
Idaho State University
Pocatello, ID 83209

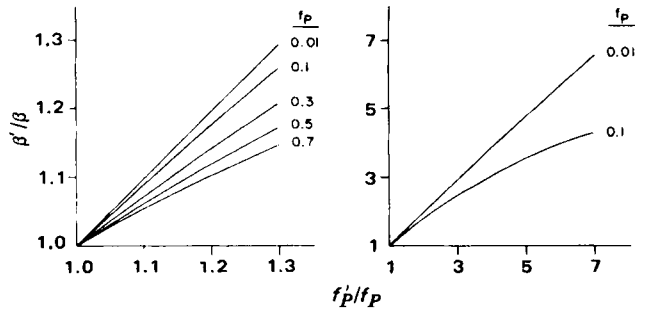

Figure 1—*Relationship between β'/β and f'_P/f_P for drugs with varying degrees of plasma protein binding.*

For the case where the binding of a drug is decreased (*i.e.*, $f'_P > f_P$), it is clear from Eq. 9 that β'/β (or $t_{1/2}/t'_{1/2}$) is smaller than f'_P/f_P but approaches f'_P/f_P as f_P approaches zero or as f'_P approaches f_P. These latter conditions apply to drugs that normally are bound to a large extent or to situations where the decrease in binding is slight.

To illustrate the relationship between relative changes in the drug half-life and plasma protein binding, Fig. 1 was constructed based on Eq. 9 using different f_P values.

From Fig. 1, it is obvious that the relationship between β'/β and f'_P/f_P is almost linear, especially when the change in f_P is relatively small. For drugs that are predominantly plasma protein bound (*e.g.*, $f_P = 0.01$), the slope of the plot is approximately one, indicating that $t_{1/2}$ is inversely proportional to f_P. Although this simple, inverse proportionality vanishes with less extensively bound drugs, the almost linear relationship between β'/β and f'_P/f_P offers a means of rapid estimation of half-life changes as a result of altered plasma protein binding.

When the percentage change in f_P is relatively large, a more rapid loss of linearity in the curves is observed with increasing f_P. Fortunately, for drugs that initially are predominantly unbound, such large percentage increases in f_P are not possible. Furthermore, the β or half-life values of these drugs are relatively insensitive to changes in binding (Fig. 1), and adjustments in the dosage regimen to correct for binding changes may not be necessary.

(1) M. Gibaldi, G. Levy, and P. J. McNamara, *Clin. Pharmacol. Ther.*, **24**, 1 (1978).

(2) W. A. Ritschel, "Handbook of Basic Pharmacokinetics," Drug Intelligence Publications, Hamilton, Ill., 1976, p. 324.

(3) E. K. Marshall, Jr., *Proc. Soc. Exp. Biol. Med.*, **68**, 472 (1948).

(4) L. Weinstein, M. A. Madoff, and C. M. Samet, *N. Engl. J. Med.*, **263**, 793 (1960).

(5) "The Pharmacological Basis of Therapeutics," 5th ed., L. S. Goodman and A. Gilman, Eds., Macmillan, New York, N.Y., 1975, p. 1169.

(6) J. R. Gillette, *Ann. N.Y. Acad. Sci.*, **179**, 43 (1971).

(7) S. Øie and T. N. Tozer, *J. Pharm. Sci.*, **68**, 1203 (1979).

(8) G. Levy and A. Yacobi, *ibid.*, **63**, 805 (1974).

Francis L. S. Tse
College of Pharmacy
Rutgers—The State University
Piscataway, NJ 08854

Received November 5, 1979.
Accepted for publication February 29, 1980.
Supported in part by a grant from the Rutgers Research Council.
The author thanks Dr. John L. Colaizzi for helpful suggestions.

BOOKS

REVIEWS

Foundations of Molecular Pharmacology, Vol. 1: Medicinal and Pharmaceutical Chemistry. By J. B. STENLAKE. The Athlone Press, University of London, Four Gower St., London WC1, England. 1979. 936 pp. 15 × 23 cm. Price $90.00.

It is easy to be enthusiastic about this well-crafted and scholarly book. The author skillfully leads us through a treatment of principles of organic chemistry applied to pharmaceutical agents. The organizational approach and its careful implementation consistently afford interesting reading.

The book is organized similar to an organic chemistry text. The medicinal agents are organized into 23 chapters by their organic chemical class; such groups as the alkanes, alkenes, benzenoid aromatic hydrocarbons, alkynes, and monohydric alcohols are included. Each chapter discusses the organic chemistry of the particular chemical class. The discussions generally are clear and succinct. The immediate pharmaceutical significance of the particular chemical property is illustrated by one or more examples from the pharmaceutical sciences. For example, following an explanation for the acidic nature of the acetylenic hydrogen atom, it is noted that the formation of a silver acetylide by the addition of silver nitrate is used as a test for identity and is the basis for the assay of some acetylenic pharmaceutical products such as ethclorvynol. Also, after a discussion of hydride reduction of aldehydes and ketones by lithium aluminum hydride and sodium borohydride, there ensues an account of the enzymatic reduction of these functional groups involving hydride donation from NADPH.

Almost all of the transitions from the general organic chemical discussion to the pharmaceutical application are made easily. Additionally, the particular pharmaceutical example usually is appropriate. One effect of this approach is to make the point repeatedly, without ever explicitly stating so, that knowledge of fundamental chemical properties is mandatory for an understanding of pharmaceutical procedures and pharmacological activities.

This reviewer has two minor criticisms relative to the author's pharmaceutical examples. There are several occasions when more appropriate pharmaceutical examples could have been presented. Also, the examples chosen could have been treated more in proportion to their importance. The following are instances in which these criticisms apply.

1. The decarboxylation of salicylic acid on bromination is discussed, but the decarboxylation of *p*-aminosalicylic acid in an acidic aqueous medium is not mentioned.
2. The structures of the amino acids GABA and taurine are given, but only GABA is cited as being an important transmitter.
3. Carbonic anhydrase-inhibiting sulfonamides are treated in detail, but benzothiazides are treated briefly.
4. The importance of ylids in synthesis is not developed.

However, these criticisms are minor, especially considering the great range of the book and the usually impressive appropriateness of the examples.

Medicinal and pharmaceutical chemists and many others in the pharmaceutical sciences should find this book to be an interesting and thought-provoking source of information. Additionally, teachers of medicinal and pharmaceutical chemistry may find that the volume is useful as a supplemental reference for both graduate and undergraduate students. Where the curriculum allows room for a course based on a format similar to that of the book (chemical class → chemical properties → pharmaceutical application), the book can serve as a textbook, although the cost is high.

Reviewed by Eugene I. Isaacson
College of Pharmacy
Idaho State University
Pocatello, ID 83209

Chlorophyll Organization and Energy Transfer in Photosynthesis. (Ciba Foundation Symposium 61.) Elsevier/North-Holland Inc., 52 Vanderbilt Ave., New York, NY 10017. 1979. 374 pp. 16 × 24 cm.

This symposium on chlorophyll organization and energy transfer in photosynthesis is a timely update of the basic processes through which plants and microorganisms contribute to the supply of nutritious food, high-quality feed, and fiber. This subject is especially important when one considers that the world population in 1930 reached 3 billion people and that by the year 2000, there will be about 7 billion people in the world. The projected increase underscores the need for a detailed understanding of the conversion of sun energy for sustaining the population growth.

On a more basic level, this symposium covers an important developing area of multidisciplinary science, yielding an updated concept of photosynthetic chemistry and mechanisms. Although many gaps remain in the isolation and characterization of chlorophyll–protein complexes, the symposium addresses itself to the more recent advances in this field.

The topics of the symposium include structure and function in photoreaction-center chlorophyll, properties of chlorophyll on plasticized polyethylene particles, the preparation and characterization of different types of light-harvesting pigment–protein complexes from certain purple bacteria, chlorophyll–protein complexes of brown algae, P700 reaction center and light-harvesting complexes, resonance Raman spectroscopy of chlorophyll–protein complexes, possible structures for chlorophyll, a diamer in Photosystem I of green plants delineated by polarized photochemistry, effects of ions and gravitational forces on the supramolecular organization and excitation energy distribution in chloroplast membranes, fluorescence of light-harvesting chlorophyll a/b–protein complexes, implications for the photosynthetic unit, energy transfer in a model of the photosynthetic unit, dynamics of excitons created by a single picosecond pulse, chlorophyll orientation and exciton migration in the photosynthetic membrane, tripartite and bipartite models of the photochemical apparatus of photosynthesis, picosecond fluorescence from photosynthetic systems *in vivo*, energy transfer and its dependence on membrane properties, quenching of chlorophyll fluorescence and photochemical activity of chloroplasts at low temperature, and transfer and trapping of excitation energy in Photosystem II.

Each topic is followed by an in-depth discussion by the participants, and the symposium is concluded with a general discussion which includes manganese and the evolution of oxygen; the state of chlorophyll in Photosystem I, Photosystem II, and the light-harvesting unit; the Grosser structure of chlorophyll–protein complexes; and comparison of the Paillotin–Swenberg kinetic theory and the Searle–Treswell empirical treatment.

For the most part, the chapters are well balanced and contain a wealth of information. I recommend this book for serious professionals concerned with basic aspects of chlorophyll organization and energy transfer in photosynthesis.

Reviewed by P. G. Vincent
Agricultural Environmental Quality Institute
Agricultural Research
Science and Education Administration
U.S. Department of Agriculture
Beltsville, MD 20705

Drug Toxicity. Edited by J. W. GORROD. Taylor and Francis Ltd., 10–14 Macklin St., London WC2B 5WF, England. 1979. 326 pp. 15 × 23 cm.

This volume was compiled from lectures presented at the Aspects of Drug Toxicity Session of the Pharmaceutical Society of Great Britain's Easter School in April 1978. The book is a broad-based basic text in toxicology and is a companion volume to another text, Drug Metabolism in Man.

The opening chapter covers the production of toxic substances from the metabolic conversion of drugs and other foreign substances. This discussion is followed by three chapters indicating how these metabolic processes can be modified by physiological and pharmacological factors. Among the topics discussed are age- and species-specific developmental factors, genetics, and dietary factors, with emphasis placed on pharmacokinetic and metabolic considerations.

The theme of proprietary drug toxicity is introduced with a chapter on the influence of formulations on drug-induced side effects and potential toxic manifestations. This discussion is followed by a consideration of generalized toxicological consequences resulting from drug-induced enzyme induction and enzyme inhibition. Another generalized topic is found in a survey of possible neoplasia induction occurring as a consequence of drug therapy.

These organism-directed discussions are complemented by a series of papers dealing with the effects of drugs and other biologically active substances on specific organs and organ systems. The systems covered include the liver, the lungs, blood and blood-forming organs, the nervous system, the fetus, the optic system, and the skin. Two final chapters cover the development of potentially useful drugs from chemicals toxic to connective tissue and the development of untoward effects during treatment with radiopharmaceuticals.

This text is a balanced blend of the theoretical and practical aspects of drug toxicity. Each chapter is adequately referenced to provide interested individuals with sources of more detailed information. This book provides a well-organized introductory approach for newcomers to the field of toxicology and points them in the direction in which this field is moving.

Reviewed by Anthony T. Dren
Medical Division
Burroughs Wellcome Co.
Research Triangle Park, NC 27709

Comprehensive Organic Chemistry. (A series of six volumes.) Edited by Sir D. BARTON and W. D. OLLIS. Pergamon, Oxford, England. 1979. 18.5 × 27.5 cm. Price $1250. Vol. 1: edited by J. F. STODDART, xiii + 1227 pp. Vol. 2: edited by I. O. SUTHERLAND, xiii + 1329 pp. Vol. 3: edited by D. N. JONES, xv + 1323 pp. Vol. 4: edited by P. G. SAMMES, xiii + 1228 pp. Vol. 5: edited by E. HASLAM, xv + 1205 pp. Vol 6: edited by C. J. DRAYTON, xv + 1628 pp.

The intent for publishing a work of this magnitude, encompassing over 8000 pages, was to provide a comprehensive and readable "work reflecting the current rapid development of modern organic chemistry." The result was perhaps not so much a comprehensive treatment of organic chemistry, as one would find in an encyclopedic series, as it is a comprehensible one, as hopefully stated by the volume editors. In addition to the anticipated treatment of the synthesis and reactions of organic compounds, the series attempts to relate the present development of organic chemistry to such developing subjects as biochemistry, inorganic chemistry, molecular biology, medicinal chemistry, and pharmacology. In this regard, the series was intended to be useful to those who employ the methods of organic chemistry in the study of both natural and synthetic compounds and their function in biological reactions. However, the presentation of organic chemistry as an intrinsic science also has been accomplished, and those facets of the subject that are essential to its present level of development are emphasized and adequately covered. E. Haslam states that the strength of organic chemistry does not lie in its naivete but in its rich diversity; this aspect of the science certainly is evident from the scope of topics selected for treatment.

An enumeration of the contents of the series should be of value to specialists and generalists alike. The treatment is based primarily on functional group chemistry but is presented throughout with the underlying mechanistic considerations. No separate section is devoted to theory, which the editors feel will "age" perhaps more quickly than the facts. The topics covered are arranged in 30 parts. Volume 1 includes a brief treatment of nomenclature and stereochemistry, followed by detailed discussions of hydrocarbons, halogen compounds, alcohols, phenols, ethers and related compounds, and aldehydes and ketones. The second volume is concerned with nitrogen-containing compounds, carboxylic acids and derivatives, and phosphorus compounds. Volume 3 treats organic compounds of sulfur, selenium, tellurium, silicon, and boron and organometallics.

Volume 4 involves heterocyclic compounds and gives a well-selected coverage of both common and uncommon heterocycles. Volume 5 is concerned mainly with compounds of biological importance: nucleic acids, amino acids, proteins, β-lactam antibiotics, enzyme catalysis, lipids, carbohydrates, synthesis of macromolecules, bioorganic chemistry including photosynthesis, and biosynthetic pathways. Volume 6 consists of formula, subject, author, reaction, and reagent indexes. This volume includes additional references, not specified in the text, for some of the subjects. About 20,000 references are cited in Volumes 1–5, and the literature up to mid 1978 generally is covered.

For a contemporary coverage of the entire subject of organic chemistry

Chlorophyll Organization and Energy Transfer in Photosynthesis. (Ciba Foundation Symposium 61.) Elsevier/North-Holland Inc., 52 Vanderbilt Ave., New York, NY 10017. 1979. 374 pp. 16 × 24 cm.

This symposium on chlorophyll organization and energy transfer in photosynthesis is a timely update of the basic processes through which plants and microorganisms contribute to the supply of nutritious food, high-quality feed, and fiber. This subject is especially important when one considers that the world population in 1930 reached 3 billion people and that by the year 2000, there will be about 7 billion people in the world. The projected increase underscores the need for a detailed understanding of the conversion of sun energy for sustaining the population growth.

On a more basic level, this symposium covers an important developing area of multidisciplinary science, yielding an updated concept of photosynthetic chemistry and mechanisms. Although many gaps remain in the isolation and characterization of chlorophyll–protein complexes, the symposium addresses itself to the more recent advances in this field.

The topics of the symposium include structure and function in photoreaction-center chlorophyll, properties of chlorophyll on plasticized polyethylene particles, the preparation and characterization of different types of light-harvesting pigment–protein complexes from certain purple bacteria, chlorophyll–protein complexes of brown algae, P700 reaction center and light-harvesting complexes, resonance Raman spectroscopy of chlorophyll–protein complexes, possible structures for chlorophyll, a diamer in Photosystem I of green plants delineated by polarized photochemistry, effects of ions and gravitational forces on the supramolecular organization and excitation energy distribution in chloroplast membranes, fluorescence of light-harvesting chlorophyll a/b–protein complexes, implications for the photosynthetic unit, energy transfer in a model of the photosynthetic unit, dynamics of excitons created by a single picosecond pulse, chlorophyll orientation and exciton migration in the photosynthetic membrane, tripartite and bipartite models of the photochemical apparatus of photosynthesis, picosecond fluorescence from photosynthetic systems *in vivo*, energy transfer and its dependence on membrane properties, quenching of chlorophyll fluorescence and photochemical activity of chloroplasts at low temperature, and transfer and trapping of excitation energy in Photosystem II.

Each topic is followed by an in-depth discussion by the participants, and the symposium is concluded with a general discussion which includes manganese and the evolution of oxygen; the state of chlorophyll in Photosystem I, Photosystem II, and the light-harvesting unit; the Grosser structure of chlorophyll–protein complexes; and comparison of the Paillotin–Swenberg kinetic theory and the Searle–Treswell empirical treatment.

For the most part, the chapters are well balanced and contain a wealth of information. I recommend this book for serious professionals concerned with basic aspects of chlorophyll organization and energy transfer in photosynthesis.

Reviewed by P. G. Vincent
Agricultural Environmental Quality Institute
Agricultural Research
Science and Education Administration
U.S. Department of Agriculture
Beltsville, MD 20705

Drug Toxicity. Edited by J. W. GORROD. Taylor and Francis Ltd., 10–14 Macklin St., London WC2B 5WF, England. 1979. 326 pp. 15 × 23 cm.

This volume was compiled from lectures presented at the Aspects of Drug Toxicity Session of the Pharmaceutical Society of Great Britain's Easter School in April 1978. The book is a broad-based basic text in toxicology and is a companion volume to another text, Drug Metabolism in Man.

The opening chapter covers the production of toxic substances from the metabolic conversion of drugs and other foreign substances. This discussion is followed by three chapters indicating how these metabolic processes can be modified by physiological and pharmacological factors. Among the topics discussed are age- and species-specific developmental factors, genetics, and dietary factors, with emphasis placed on pharmacokinetic and metabolic considerations.

The theme of proprietary drug toxicity is introduced with a chapter on the influence of formulations on drug-induced side effects and potential toxic manifestations. This discussion is followed by a consideration of generalized toxicological consequences resulting from drug-induced enzyme induction and enzyme inhibition. Another generalized topic is found in a survey of possible neoplasia induction occurring as a consequence of drug therapy.

These organism-directed discussions are complemented by a series of papers dealing with the effects of drugs and other biologically active substances on specific organs and organ systems. The systems covered include the liver, the lungs, blood and blood-forming organs, the nervous system, the fetus, the optic system, and the skin. Two final chapters cover the development of potentially useful drugs from chemicals toxic to connective tissue and the development of untoward effects during treatment with radiopharmaceuticals.

This text is a balanced blend of the theoretical and practical aspects of drug toxicity. Each chapter is adequately referenced to provide interested individuals with sources of more detailed information. This book provides a well-organized introductory approach for newcomers to the field of toxicology and points them in the direction in which this field is moving.

Reviewed by Anthony T. Dren
Medical Division
Burroughs Wellcome Co.
Research Triangle Park, NC 27709

Comprehensive Organic Chemistry. (A series of six volumes.) Edited by Sir D. BARTON and W. D. OLLIS. Pergamon, Oxford, England. 1979. 18.5 × 27.5 cm. Price $1250. Vol. 1: edited by J. F. STODDART, xiii + 1227 pp. Vol. 2: edited by I. O. SUTHERLAND, xiii + 1329 pp. Vol. 3: edited by D. N. JONES, xv + 1323 pp. Vol. 4: edited by P. G. SAMMES, xiii + 1228 pp. Vol. 5: edited by E. HASLAM, xv + 1205 pp. Vol 6: edited by C. J. DRAYTON, xv + 1628 pp.

The intent for publishing a work of this magnitude, encompassing over 8000 pages, was to provide a comprehensive and readable "work reflecting the current rapid development of modern organic chemistry." The result was perhaps not so much a comprehensive treatment of organic chemistry, as one would find in an encyclopedic series, as it is a comprehensible one, as hopefully stated by the volume editors. In addition to the anticipated treatment of the synthesis and reactions of organic compounds, the series attempts to relate the present development of organic chemistry to such developing subjects as biochemistry, inorganic chemistry, molecular biology, medicinal chemistry, and pharmacology. In this regard, the series was intended to be useful to those who employ the methods of organic chemistry in the study of both natural and synthetic compounds and their function in biological reactions. However, the presentation of organic chemistry as an intrinsic science also has been accomplished, and those facets of the subject that are essential to its present level of development are emphasized and adequately covered. E. Haslam states that the strength of organic chemistry does not lie in its naivete but in its rich diversity; this aspect of the science certainly is evident from the scope of topics selected for treatment.

An enumeration of the contents of the series should be of value to specialists and generalists alike. The treatment is based primarily on functional group chemistry but is presented throughout with the underlying mechanistic considerations. No separate section is devoted to theory, which the editors feel will "age" perhaps more quickly than the facts. The topics covered are arranged in 30 parts. Volume 1 includes a brief treatment of nomenclature and stereochemistry, followed by detailed discussions of hydrocarbons, halogen compounds, alcohols, phenols, ethers and related compounds, and aldehydes and ketones. The second volume is concerned with nitrogen-containing compounds, carboxylic acids and derivatives, and phosphorus compounds. Volume 3 treats organic compounds of sulfur, selenium, tellurium, silicon, and boron and organometallics.

Volume 4 involves heterocyclic compounds and gives a well-selected coverage of both common and uncommon heterocycles. Volume 5 is concerned mainly with compounds of biological importance: nucleic acids, amino acids, proteins, β-lactam antibiotics, enzyme catalysis, lipids, carbohydrates, synthesis of macromolecules, bioorganic chemistry including photosynthesis, and biosynthetic pathways. Volume 6 consists of formula, subject, author, reaction, and reagent indexes. This volume includes additional references, not specified in the text, for some of the subjects. About 20,000 references are cited in Volumes 1–5, and the literature up to mid 1978 generally is covered.

For a contemporary coverage of the entire subject of organic chemistry

Chlorophyll Organization and Energy Transfer in Photosynthesis. (Ciba Foundation Symposium 61.) Elsevier/North-Holland Inc., 52 Vanderbilt Ave., New York, NY 10017. 1979. 374 pp. 16 × 24 cm.

This symposium on chlorophyll organization and energy transfer in photosynthesis is a timely update of the basic processes through which plants and microorganisms contribute to the supply of nutritious food, high-quality feed, and fiber. This subject is especially important when one considers that the world population in 1930 reached 3 billion people and that by the year 2000, there will be about 7 billion people in the world. The projected increase underscores the need for a detailed understanding of the conversion of sun energy for sustaining the population growth.

On a more basic level, this symposium covers an important developing area of multidisciplinary science, yielding an updated concept of photosynthetic chemistry and mechanisms. Although many gaps remain in the isolation and characterization of chlorophyll–protein complexes, the symposium addresses itself to the more recent advances in this field.

The topics of the symposium include structure and function in photoreaction-center chlorophyll, properties of chlorophyll on plasticized polyethylene particles, the preparation and characterization of different types of light-harvesting pigment–protein complexes from certain purple bacteria, chlorophyll–protein complexes of brown algae, P700 reaction center and light-harvesting complexes, resonance Raman spectroscopy of chlorophyll–protein complexes, possible structures for chlorophyll, a diamer in Photosystem I of green plants delineated by polarized photochemistry, effects of ions and gravitational forces on the supramolecular organization and excitation energy distribution in chloroplast membranes, fluorescence of light-harvesting chlorophyll a/b–protein complexes, implications for the photosynthetic unit, energy transfer in a model of the photosynthetic unit, dynamics of excitons created by a single picosecond pulse, chlorophyll orientation and exciton migration in the photosynthetic membrane, tripartite and bipartite models of the photochemical apparatus of photosynthesis, picosecond fluorescence from photosynthetic systems *in vivo*, energy transfer and its dependence on membrane properties, quenching of chlorophyll fluorescence and photochemical activity of chloroplasts at low temperature, and transfer and trapping of excitation energy in Photosystem II.

Each topic is followed by an in-depth discussion by the participants, and the symposium is concluded with a general discussion which includes manganese and the evolution of oxygen; the state of chlorophyll in Photosystem I, Photosystem II, and the light-harvesting unit; the Grosser structure of chlorophyll–protein complexes; and comparison of the Paillotin–Swenberg kinetic theory and the Searle–Treswell empirical treatment.

For the most part, the chapters are well balanced and contain a wealth of information. I recommend this book for serious professionals concerned with basic aspects of chlorophyll organization and energy transfer in photosynthesis.

Reviewed by P. G. Vincent
Agricultural Environmental Quality Institute
Agricultural Research
Science and Education Administration
U.S. Department of Agriculture
Beltsville, MD 20705

Drug Toxicity. Edited by J. W. GORROD. Taylor and Francis Ltd., 10–14 Macklin St., London WC2B 5WF, England. 1979. 326 pp. 15 × 23 cm.

This volume was compiled from lectures presented at the Aspects of Drug Toxicity Session of the Pharmaceutical Society of Great Britain's Easter School in April 1978. The book is a broad-based basic text in toxicology and is a companion volume to another text, Drug Metabolism in Man.

The opening chapter covers the production of toxic substances from the metabolic conversion of drugs and other foreign substances. This discussion is followed by three chapters indicating how these metabolic processes can be modified by physiological and pharmacological factors. Among the topics discussed are age- and species-specific developmental factors, genetics, and dietary factors, with emphasis placed on pharmacokinetic and metabolic considerations.

The theme of proprietary drug toxicity is introduced with a chapter on the influence of formulations on drug-induced side effects and potential toxic manifestations. This discussion is followed by a consideration of generalized toxicological consequences resulting from drug-induced enzyme induction and enzyme inhibition. Another generalized topic is found in a survey of possible neoplasia induction occurring as a consequence of drug therapy.

These organism-directed discussions are complemented by a series of papers dealing with the effects of drugs and other biologically active substances on specific organs and organ systems. The systems covered include the liver, the lungs, blood and blood-forming organs, the nervous system, the fetus, the optic system, and the skin. Two final chapters cover the development of potentially useful drugs from chemicals toxic to connective tissue and the development of untoward effects during treatment with radiopharmaceuticals.

This text is a balanced blend of the theoretical and practical aspects of drug toxicity. Each chapter is adequately referenced to provide interested individuals with sources of more detailed information. This book provides a well-organized introductory approach for newcomers to the field of toxicology and points them in the direction in which this field is moving.

Reviewed by Anthony T. Dren
Medical Division
Burroughs Wellcome Co.
Research Triangle Park, NC 27709

Comprehensive Organic Chemistry. (A series of six volumes.) Edited by Sir D. BARTON and W. D. OLLIS. Pergamon, Oxford, England. 1979. 18.5 × 27.5 cm. Price $1250. Vol. 1: edited by J. F. STODDART, xiii + 1227 pp. Vol. 2: edited by I. O. SUTHERLAND, xiii + 1329 pp. Vol. 3: edited by D. N. JONES, xv + 1323 pp. Vol. 4: edited by P. G. SAMMES, xiii + 1228 pp. Vol. 5: edited by E. HASLAM, xv + 1205 pp. Vol 6: edited by C. J. DRAYTON, xv + 1628 pp.

The intent for publishing a work of this magnitude, encompassing over 8000 pages, was to provide a comprehensive and readable "work reflecting the current rapid development of modern organic chemistry." The result was perhaps not so much a comprehensive treatment of organic chemistry, as one would find in an encyclopedic series, as it is a comprehensible one, as hopefully stated by the volume editors. In addition to the anticipated treatment of the synthesis and reactions of organic compounds, the series attempts to relate the present development of organic chemistry to such developing subjects as biochemistry, inorganic chemistry, molecular biology, medicinal chemistry, and pharmacology. In this regard, the series was intended to be useful to those who employ the methods of organic chemistry in the study of both natural and synthetic compounds and their function in biological reactions. However, the presentation of organic chemistry as an intrinsic science also has been accomplished, and those facets of the subject that are essential to its present level of development are emphasized and adequately covered. E. Haslam states that the strength of organic chemistry does not lie in its naivete but in its rich diversity; this aspect of the science certainly is evident from the scope of topics selected for treatment.

An enumeration of the contents of the series should be of value to specialists and generalists alike. The treatment is based primarily on functional group chemistry but is presented throughout with the underlying mechanistic considerations. No separate section is devoted to theory, which the editors feel will "age" perhaps more quickly than the facts. The topics covered are arranged in 30 parts. Volume 1 includes a brief treatment of nomenclature and stereochemistry, followed by detailed discussions of hydrocarbons, halogen compounds, alcohols, phenols, ethers and related compounds, and aldehydes and ketones. The second volume is concerned with nitrogen-containing compounds, carboxylic acids and derivatives, and phosphorus compounds. Volume 3 treats organic compounds of sulfur, selenium, tellurium, silicon, and boron and organometallics.

Volume 4 involves heterocyclic compounds and gives a well-selected coverage of both common and uncommon heterocycles. Volume 5 is concerned mainly with compounds of biological importance: nucleic acids, amino acids, proteins, β-lactam antibiotics, enzyme catalysis, lipids, carbohydrates, synthesis of macromolecules, bioorganic chemistry including photosynthesis, and biosynthetic pathways. Volume 6 consists of formula, subject, author, reaction, and reagent indexes. This volume includes additional references, not specified in the text, for some of the subjects. About 20,000 references are cited in Volumes 1–5, and the literature up to mid 1978 generally is covered.

For a contemporary coverage of the entire subject of organic chemistry

and its interrelations with biochemistry, this series perhaps should be the first source consulted. Further detail may be located in monographs on specific topics; but for a comprehensive view of any general topic in organic chemistry, this series should be quite useful. Although the authors were faced with a formidable problem of selecting the most important topics, the series overall has a sufficient balance of new and old information to be of value for some time. For a relatively complete treatment of developments during the past two decades, this series probably is unchallenged by any single work; it represents a reasonable compromise between specialization and encyclopedism.

To the medicinal chemist, the extensive treatment of the newer methods of organic synthesis will be of great interest. Volume 5, which comprises naturally occurring compounds, enzyme catalysis, and biosynthetic pathways, should be of interest to all pharmaceutical scientists. Although relatively few examples of detailed mechanisms of enzyme catalysis are included, or known, the present understanding of the underlying factors is discussed well. The coverage of sulfur chemistry (vol. 3), usually deficient in most general texts on organic chemistry, is remarkably complete. The nitrogen heterocycles (vol. 4) also are given a more extensive treatment than some topics.

This series can be recommended for libraries in pharmacy colleges and in the pharmaceutical industry; the cost of the volumes, of course, would deter the individual purchaser. It is hoped that revisions of this series will be made, retaining the stated goal of keeping the science of organic chemistry comprehensible to those who use it.

Reviewed by William O. Foye
Massachusetts College of Pharmacy and Allied Health Sciences
Boston, MA 02115

Computer Assisted Studies of Chemical Structure and Biological Function. By A. J. STUPER, W. E. BRÜGGER, and P. C. JURS. Wiley, One Wiley Drive, Somerset, NJ 08873. 1979. xi + 220 pp. 16 × 23 cm. Price $23.50.

This book provides a convenient introduction to pattern recognition techniques. It is very well written and sufficiently referenced to allow interested persons access to pertinent literature for more in-depth studies. Preprocessing and classification methods are summarized. Various means of generating molecular descriptions also are described. The methods are applied to tranquilizers and sedatives and to musk and trigeminally active odorants.

This book describes some of the methods used in pattern recognition studies. However, it is inappropriate to view the book as a "how-to-do-it" introduction to pattern recognition. While the algorithms are available, the most appropriate application of these algorithms to biological data still is a developing area. This book should stimulate additional research in this regard.

Reviewed by Arthur Cammarata
School of Pharmacy
Temple University
Philadelphia, PA 19140

Antibiotics: Isolation, Separation, and Purification. Edited by MARVIN J. WEINSTEIN and GERALD H. WAGMAN. (Journal of Chromatography Library, Vol. 15.) Elsevier/North-Holland Inc., 52 Vanderbilt Ave., New York, NY 10017. 1978. 769 pp. 16 × 24 cm. Price $84.75.

At first glance, this 15th volume of the Journal of Chromatography Library appears to be an ambitious attempt to describe the isolation, separation, and purification of most of the known antibiotics. The publication contains 17 chapters, each of which is devoted to a group of chemically related antibiotics. Each chapter was written by a different contributor. The editors selected the authors for their competence and knowledge in their respective areas.

The book covers therapeutically useful drugs such as the penicillins, cephalosporins, griseofulvins, lincomycins, macrolide antibiotics, peptide antibiotics, tetracyclines, 2-deoxystreptamine-containing antibiotics, and actinomycins, as well as groups of less well-known antibiotics such as the ansamycins, siderchromes, streptothricins, polyethers, and marine and plant-derived antibiotics.

The contribution by scientists who are knowledgeable in their respective fields is the strength of this publication. However, multiple authorship often leads to variations in the format of the chapters and to unevenness in the depth of the discussions of the antibiotic groups. All of the authors cover in one form or another the subject matter of this volume; in many cases, useful additional information concerning the chemistry, physical characteristics, and therapeutic uses of the antibiotics is included.

The book is not encyclopedic in its coverage; although the naturally occurring penicillins are described, the semisynthetic penicillins are not included. The antitumor drugs, which are considered to be antibiotics in this country, also are not included. Discussions of polymyxin and bacitracin are not among the polypeptide antibiotics. Coverage in some areas appears to be sparse. The contributor for the tetracycline antibiotics included only 52 references for this important class of antibiotics, whereas the author of the streptothricins chapter made reference to 225 publications.

Overall, the publication brings together a lot of useful information, especially in the areas of the less well-known antibiotic groups.

Reviewed by George B. Selzer
National Center for Antibiotics Analysis
Bureau of Drugs
Food and Drug Administration
Washington, DC 20204

The price indicated in the April 1980 issue for Catecholamines: Basic and Clinical Frontiers, Vols. I and II (Pergamon Press) was $200.00 per volume. It should have been $200.00 per two-volume set.

and its interrelations with biochemistry, this series perhaps should be the first source consulted. Further detail may be located in monographs on specific topics; but for a comprehensive view of any general topic in organic chemistry, this series should be quite useful. Although the authors were faced with a formidable problem of selecting the most important topics, the series overall has a sufficient balance of new and old information to be of value for some time. For a relatively complete treatment of developments during the past two decades, this series probably is unchallenged by any single work; it represents a reasonable compromise between specialization and encyclopedism.

To the medicinal chemist, the extensive treatment of the newer methods of organic synthesis will be of great interest. Volume 5, which comprises naturally occurring compounds, enzyme catalysis, and biosynthetic pathways, should be of interest to all pharmaceutical scientists. Although relatively few examples of detailed mechanisms of enzyme catalysis are included, or known, the present understanding of the underlying factors is discussed well. The coverage of sulfur chemistry (vol. 3), usually deficient in most general texts on organic chemistry, is remarkably complete. The nitrogen heterocycles (vol. 4) also are given a more extensive treatment than some topics.

This series can be recommended for libraries in pharmacy colleges and in the pharmaceutical industry; the cost of the volumes, of course, would deter the individual purchaser. It is hoped that revisions of this series will be made, retaining the stated goal of keeping the science of organic chemistry comprehensible to those who use it.

Reviewed by William O. Foye
Massachusetts College of Pharmacy and Allied Health Sciences
Boston, MA 02115

Computer Assisted Studies of Chemical Structure and Biological Function. By A. J. STUPER, W. E. BRÜGGER, and P. C. JURS. Wiley, One Wiley Drive, Somerset, NJ 08873. 1979. xi + 220 pp. 16 × 23 cm. Price $23.50.

This book provides a convenient introduction to pattern recognition techniques. It is very well written and sufficiently referenced to allow interested persons access to pertinent literature for more in-depth studies. Preprocessing and classification methods are summarized. Various means of generating molecular descriptions also are described. The methods are applied to tranquilizers and sedatives and to musk and trigeminally active odorants.

This book describes some of the methods used in pattern recognition studies. However, it is inappropriate to view the book as a "how-to-do-it" introduction to pattern recognition. While the algorithms are available, the most appropriate application of these algorithms to biological data still is a developing area. This book should stimulate additional research in this regard.

Reviewed by Arthur Cammarata
School of Pharmacy
Temple University
Philadelphia, PA 19140

Antibiotics: Isolation, Separation, and Purification. Edited by MARVIN J. WEINSTEIN and GERALD H. WAGMAN. (Journal of Chromatography Library, Vol. 15.) Elsevier/North-Holland Inc., 52 Vanderbilt Ave., New York, NY 10017. 1978. 769 pp. 16 × 24 cm. Price $84.75.

At first glance, this 15th volume of the Journal of Chromatography Library appears to be an ambitious attempt to describe the isolation, separation, and purification of most of the known antibiotics. The publication contains 17 chapters, each of which is devoted to a group of chemically related antibiotics. Each chapter was written by a different contributor. The editors selected the authors for their competence and knowledge in their respective areas.

The book covers therapeutically useful drugs such as the penicillins, cephalosporins, griseofulvins, lincomycins, macrolide antibiotics, peptide antibiotics, tetracyclines, 2-deoxystreptamine-containing antibiotics, and actinomycins, as well as groups of less well-known antibiotics such as the ansamycins, siderchromes, streptothricins, polyethers, and marine and plant-derived antibiotics.

The contribution by scientists who are knowledgeable in their respective fields is the strength of this publication. However, multiple authorship often leads to variations in the format of the chapters and to unevenness in the depth of the discussions of the antibiotic groups. All of the authors cover in one form or another the subject matter of this volume; in many cases, useful additional information concerning the chemistry, physical characteristics, and therapeutic uses of the antibiotics is included.

The book is not encyclopedic in its coverage; although the naturally occurring penicillins are described, the semisynthetic penicillins are not included. The antitumor drugs, which are considered to be antibiotics in this country, also are not included. Discussions of polymyxin and bacitracin are not among the polypeptide antibiotics. Coverage in some areas appears to be sparse. The contributor for the tetracycline antibiotics included only 52 references for this important class of antibiotics, whereas the author of the streptothricins chapter made reference to 225 publications.

Overall, the publication brings together a lot of useful information, especially in the areas of the less well-known antibiotic groups.

Reviewed by George B. Selzer
National Center for Antibiotics Analysis
Bureau of Drugs
Food and Drug Administration
Washington, DC 20204

The price indicated in the April 1980 issue for Catecholamines: Basic and Clinical Frontiers, Vols. I and II (Pergamon Press) was $200.00 per volume. It should have been $200.00 per two-volume set.

and its interrelations with biochemistry, this series perhaps should be the first source consulted. Further detail may be located in monographs on specific topics; but for a comprehensive view of any general topic in organic chemistry, this series should be quite useful. Although the authors were faced with a formidable problem of selecting the most important topics, the series overall has a sufficient balance of new and old information to be of value for some time. For a relatively complete treatment of developments during the past two decades, this series probably is unchallenged by any single work; it represents a reasonable compromise between specialization and encyclopedism.

To the medicinal chemist, the extensive treatment of the newer methods of organic synthesis will be of great interest. Volume 5, which comprises naturally occurring compounds, enzyme catalysis, and biosynthetic pathways, should be of interest to all pharmaceutical scientists. Although relatively few examples of detailed mechanisms of enzyme catalysis are included, or known, the present understanding of the underlying factors is discussed well. The coverage of sulfur chemistry (vol. 3), usually deficient in most general texts on organic chemistry, is remarkably complete. The nitrogen heterocycles (vol. 4) also are given a more extensive treatment than some topics.

This series can be recommended for libraries in pharmacy colleges and in the pharmaceutical industry; the cost of the volumes, of course, would deter the individual purchaser. It is hoped that revisions of this series will be made, retaining the stated goal of keeping the science of organic chemistry comprehensible to those who use it.

Reviewed by William O. Foye
Massachusetts College of Pharmacy and Allied Health Sciences
Boston, MA 02115

Computer Assisted Studies of Chemical Structure and Biological Function. By A. J. STUPER, W. E. BRÜGGER, and P. C. JURS. Wiley, One Wiley Drive, Somerset, NJ 08873. 1979. xi + 220 pp. 16 × 23 cm. Price $23.50.

This book provides a convenient introduction to pattern recognition techniques. It is very well written and sufficiently referenced to allow interested persons access to pertinent literature for more in-depth studies. Preprocessing and classification methods are summarized. Various means of generating molecular descriptions also are described. The methods are applied to tranquilizers and sedatives and to musk and trigeminally active odorants.

This book describes some of the methods used in pattern recognition studies. However, it is inappropriate to view the book as a "how-to-do-it" introduction to pattern recognition. While the algorithms are available, the most appropriate application of these algorithms to biological data still is a developing area. This book should stimulate additional research in this regard.

Reviewed by Arthur Cammarata
School of Pharmacy
Temple University
Philadelphia, PA 19140

Antibiotics: Isolation, Separation, and Purification. Edited by MARVIN J. WEINSTEIN and GERALD H. WAGMAN. (Journal of Chromatography Library, Vol. 15.) Elsevier/North-Holland Inc., 52 Vanderbilt Ave., New York, NY 10017. 1978. 769 pp. 16 × 24 cm. Price $84.75.

At first glance, this 15th volume of the Journal of Chromatography Library appears to be an ambitious attempt to describe the isolation, separation, and purification of most of the known antibiotics. The publication contains 17 chapters, each of which is devoted to a group of chemically related antibiotics. Each chapter was written by a different contributor. The editors selected the authors for their competence and knowledge in their respective areas.

The book covers therapeutically useful drugs such as the penicillins, cephalosporins, griseofulvins, lincomycins, macrolide antibiotics, peptide antibiotics, tetracyclines, 2-deoxystreptamine-containing antibiotics, and actinomycins, as well as groups of less well-known antibiotics such as the ansamycins, siderchromes, streptothricins, polyethers, and marine and plant-derived antibiotics.

The contribution by scientists who are knowledgeable in their respective fields is the strength of this publication. However, multiple authorship often leads to variations in the format of the chapters and to unevenness in the depth of the discussions of the antibiotic groups. All of the authors cover in one form or another the subject matter of this volume; in many cases, useful additional information concerning the chemistry, physical characteristics, and therapeutic uses of the antibiotics is included.

The book is not encyclopedic in its coverage; although the naturally occurring penicillins are described, the semisynthetic penicillins are not included. The antitumor drugs, which are considered to be antibiotics in this country, also are not included. Discussions of polymyxin and bacitracin are not among the polypeptide antibiotics. Coverage in some areas appears to be sparse. The contributor for the tetracycline antibiotics included only 52 references for this important class of antibiotics, whereas the author of the streptothricins chapter made reference to 225 publications.

Overall, the publication brings together a lot of useful information, especially in the areas of the less well-known antibiotic groups.

Reviewed by George B. Selzer
National Center for Antibiotics Analysis
Bureau of Drugs
Food and Drug Administration
Washington, DC 20204

The price indicated in the April 1980 issue for Catecholamines: Basic and Clinical Frontiers, Vols. I and II (Pergamon Press) was $200.00 per volume. It should have been $200.00 per two-volume set.

JULY 1980
VOLUME 69 NUMBER 7

JOURNAL OF PHARMACEUTICAL SCIENCES

MARY H. FERGUSON
Editor

SHELLY ELLIOTT
Production Editor

MARCIA GARTRELL
Copy Editor

NICOLETTE TRIANTAFELLU
Copy Editor

EDWARD G. FELDMANN
Contributing Editor

SAMUEL W. GOLDSTEIN
Contributing Editor

BELLE R. BECK
Editorial Secretary

DAVID BOHARDT
Director of Publications

L. LUAN CORRIGAN
Assistant Director of Publications

EDITORIAL ADVISORY BOARD

JOHN AUTIAN
HERBERT A. LIEBERMAN
NORMAN R. FARNSWORTH
DAVID E. MANN, JR.
WILLIAM O. FOYE
GERALD J. PAPARIELLO
WILLIAM J. JUSKO
EDWARD G. RIPPIE

The *Journal of Pharmaceutical Sciences* (ISSN 0022-3549) is published monthly by the American Pharmaceutical Association (APhA) at 2215 Constitution Ave., N.W., Washington, DC 20037. Second-class postage paid at Washington, D.C., and at additional mailing office.

All expressions of opinion and statements of supposed fact appearing in articles or editorials carried in this journal are published on the authority of the writer over whose name they appear and are not to be regarded as necessarily expressing the policies or views of APhA.

Offices—Editorial, Advertising, and Subscription: 2215 Constitution Ave., N.W., Washington, DC 20037. All Journal staff may be contacted at this address. Printing: 20th & Northampton Streets, Easton, PA 18042.

Annual Subscriptions—United States and foreign, industrial and government institutions $60, educational institutions $60, individuals *for personal use only* $30; single copies $5. All foreign subscriptions add $5 for postage. Subscription rates are subject to change without notice. Members of APhA may elect to receive the *Journal of Pharmaceutical Sciences* as a part of their annual $80 (foreign $85) APhA membership dues.

Claims—Missing numbers will not be supplied if dues or subscriptions are in arrears for more than 60 days or if claims are received more than 60 days after the date of the issue, or if loss was due to failure to give notice of change of address. APhA cannot accept responsibility for foreign delivery when its records indicate shipment was made.

Change of Address—Members and subscribers should notify at once both the Post Office and APhA of any change of address.

Photocopying—The code at the foot of the first page of an article indicates that APhA has granted permission for copying of the article beyond the limits permitted by Sections 107 and 108 of the U.S. Copyright Law provided that the copier sends the per copy fee stated in the code to the Copyright Clearance Center, Inc., 21 Congress St., Salem, MA 01970. Copies may be made for personal or internal use only and not for general distribution.

Microfilm—Available from University Microfilms International, 300 N. Zeeb Road, Ann Arbor, MI 48106.

© Copyright 1980, American Pharmaceutical Association, 2215 Constitution Ave., N.W., Washington, DC 20037; all rights reserved.

AN EFFORT TO CREATE NEW UNDERSTANDINGS

This month, from July 20–24, many of our pharmacy school educators will be gathering in Boston, Massachusetts, to attend and to participate in the annual meeting of the American Association of Colleges of Pharmacy.

What makes this meeting noteworthy, in our opinion, is the theme topic that will be featured at this year's conference. The AACP utilizes a three-year sequence in issues for policy consideration. This process entails, in turn, (*a*) introducing for review, (*b*) subjecting to study, and (*c*) adopting a position or making a decision regarding each particular issue.

The theme topic for intensive consideration at this 1980 session is entitled "Bridging the Gap Between the Basic Sciences and Clinical Practice: Teaching, Research, and Service." Because of the interest of our readership—as well as our own personal interest—in the basic sciences, we are gratified that the AACP has chosen this theme for current intensive review and study.

Over the years, the respective educational elements of teaching, research, and service have been accorded varying degrees of emphasis in pharmacy academic circles. Indeed, this has happened to the extent that one or the other of the three elements has been given short-shrift in the process, while one of the other two elements has been lavished with attention, funds, and other scarce resources.

Such imbalance has prompted the more observant and concerned pharmacy leaders to voice some alarm and to suggest that, as in the case of a tripod or a three-legged stool, it is critical that all three supporting legs are of relatively equivalent strength if the load is to be properly held in place.

But despite recognizing this need, and despite apparent attempts to provide the desired equilibrium of support, a decided gap has developed between the basic sciences educators and clinical practice educators. The gap seems to have begun to form many years ago when some pharmacy schools began offering advanced degrees; in the process, at least a number of them began to neglect their first mission of undergraduate education. An attitude of disdain even became evident on the part of some faculty members—they wished to have as little as possible to do with the teaching of undergraduate students. In turn, this attitude seemed to evolve into a somewhat comparable but broader disdain for pharmacy practitioners and pharmacy practice, because these were equated with undergraduate—rather than graduate—training and education.

However, about 15 years ago, the pendulum began to swing back as clinical pharmacy first made its appearance in our pharmacy schools and as it subsequently proceeded to spread nationally within just a few short years.

Depending upon the particular pharmacy school, and depending upon the views of the particular people involved, one now hears that in many cases the basic sciences have been drastically downgraded to the point that students at those schools are receiving very inferior training in the sciences. And conversely, others will describe the reverse situation, claiming that too much emphasis is still being accorded the basic sciences and not sufficient attention is devoted to the clinical aspects.

In the competition for resources and the jockeying for position that have ensued, a very unfortunate further development has occurred within many pharmacy school faculties. Basically, a virtual schism has been created between the respective groups of faculty personnel. This split goes beyond the traditional fierce but good-natured rivalry. It appears to be a growing and deeply felt resentment of each group for the other. Moreover, it shows signs of increasing rather than diminishing in its intensity.

Perhaps for this reason, the fact that the AACP meeting in Boston will focus on bridging the science–practice gap becomes all the more important. If open study, debate, and discussion can be successful in bridging this professional strife among our faculty people, such will be a most significant accomplishment. Otherwise, if this schism—with its associated jealousy, back-biting, and squabbling—continues and escalates, we are faced with the eventual prospect that our educational system will literally tear itself apart. Needless to say, that would be tragic for the future of pharmacy in America.

—EGF

JULY 1980
VOLUME 69 NUMBER 7

JOURNAL OF PHARMACEUTICAL SCIENCES

MARY H. FERGUSON
Editor

SHELLY ELLIOTT
Production Editor

MARCIA GARTRELL
Copy Editor

NICOLETTE TRIANTAFELLU
Copy Editor

EDWARD G. FELDMANN
Contributing Editor

SAMUEL W. GOLDSTEIN
Contributing Editor

BELLE R. BECK
Editorial Secretary

DAVID BOHARDT
Director of Publications

L. LUAN CORRIGAN
Assistant Director of Publications

EDITORIAL ADVISORY BOARD

JOHN AUTIAN
HERBERT A. LIEBERMAN
NORMAN R. FARNSWORTH
DAVID E. MANN, JR.
WILLIAM O. FOYE
GERALD J. PAPARIELLO
WILLIAM J. JUSKO
EDWARD G. RIPPIE

The *Journal of Pharmaceutical Sciences* (ISSN 0022-3549) is published monthly by the American Pharmaceutical Association (APhA) at 2215 Constitution Ave., N.W., Washington, DC 20037. Second-class postage paid at Washington, D.C., and at additional mailing office.

All expressions of opinion and statements of supposed fact appearing in articles or editorials carried in this journal are published on the authority of the writer over whose name they appear and are not to be regarded as necessarily expressing the policies or views of APhA.

Offices—Editorial, Advertising, and Subscription: 2215 Constitution Ave., N.W., Washington, DC 20037. All Journal staff may be contacted at this address. Printing: 20th & Northampton Streets, Easton, PA 18042.

Annual Subscriptions—United States and foreign, industrial and government institutions $60, educational institutions $60, individuals *for personal use only* $30; single copies $5. All foreign subscriptions add $5 for postage. Subscription rates are subject to change without notice. Members of APhA may elect to receive the *Journal of Pharmaceutical Sciences* as a part of their annual $80 (foreign $85) APhA membership dues.

Claims—Missing numbers will not be supplied if dues or subscriptions are in arrears for more than 60 days or if claims are received more than 60 days after the date of the issue, or if loss was due to failure to give notice of change of address. APhA cannot accept responsibility for foreign delivery when its records indicate shipment was made.

Change of Address—Members and subscribers should notify at once both the Post Office and APhA of any change of address.

Photocopying—The code at the foot of the first page of an article indicates that APhA has granted permission for copying of the article beyond the limits permitted by Sections 107 and 108 of the U.S. Copyright Law provided that the copier sends the per copy fee stated in the code to the Copyright Clearance Center, Inc., 21 Congress St., Salem, MA 01970. Copies may be made for personal or internal use only and not for general distribution.

Microfilm—Available from University Microfilms International, 300 N. Zeeb Road, Ann Arbor, MI 48106.

© Copyright 1980, American Pharmaceutical Association, 2215 Constitution Ave., N.W., Washington, DC 20037; all rights reserved.

AN EFFORT TO CREATE NEW UNDERSTANDINGS

This month, from July 20–24, many of our pharmacy school educators will be gathering in Boston, Massachusetts, to attend and to participate in the annual meeting of the American Association of Colleges of Pharmacy.

What makes this meeting noteworthy, in our opinion, is the theme topic that will be featured at this year's conference. The AACP utilizes a three-year sequence in issues for policy consideration. This process entails, in turn, (*a*) introducing for review, (*b*) subjecting to study, and (*c*) adopting a position or making a decision regarding each particular issue.

The theme topic for intensive consideration at this 1980 session is entitled "Bridging the Gap Between the Basic Sciences and Clinical Practice: Teaching, Research, and Service." Because of the interest of our readership—as well as our own personal interest—in the basic sciences, we are gratified that the AACP has chosen this theme for current intensive review and study.

Over the years, the respective educational elements of teaching, research, and service have been accorded varying degrees of emphasis in pharmacy academic circles. Indeed, this has happened to the extent that one or the other of the three elements has been given short-shrift in the process, while one of the other two elements has been lavished with attention, funds, and other scarce resources.

Such imbalance has prompted the more observant and concerned pharmacy leaders to voice some alarm and to suggest that, as in the case of a tripod or a three-legged stool, it is critical that all three supporting legs are of relatively equivalent strength if the load is to be properly held in place.

But despite recognizing this need, and despite apparent attempts to provide the desired equilibrium of support, a decided gap has developed between the basic sciences educators and clinical practice educators. The gap seems to have begun to form many years ago when some pharmacy schools began offering advanced degrees; in the process, at least a number of them began to neglect their first mission of undergraduate education. An attitude of disdain even became evident on the part of some faculty members—they wished to have as little as possible to do with the teaching of undergraduate students. In turn, this attitude seemed to evolve into a somewhat comparable but broader disdain for pharmacy practitioners and pharmacy practice, because these were equated with undergraduate—rather than graduate—training and education.

However, about 15 years ago, the pendulum began to swing back as clinical pharmacy first made its appearance in our pharmacy schools and as it subsequently proceeded to spread nationally within just a few short years.

Depending upon the particular pharmacy school, and depending upon the views of the particular people involved, one now hears that in many cases the basic sciences have been drastically downgraded to the point that students at those schools are receiving very inferior training in the sciences. And conversely, others will describe the reverse situation, claiming that too much emphasis is still being accorded the basic sciences and not sufficient attention is devoted to the clinical aspects.

In the competition for resources and the jockeying for position that have ensued, a very unfortunate further development has occurred within many pharmacy school faculties. Basically, a virtual schism has been created between the respective groups of faculty personnel. This split goes beyond the traditional fierce but good-natured rivalry. It appears to be a growing and deeply felt resentment of each group for the other. Moreover, it shows signs of increasing rather than diminishing in its intensity.

Perhaps for this reason, the fact that the AACP meeting in Boston will focus on bridging the science–practice gap becomes all the more important. If open study, debate, and discussion can be successful in bridging this professional strife among our faculty people, such will be a most significant accomplishment. Otherwise, if this schism—with its associated jealousy, back-biting, and squabbling—continues and escalates, we are faced with the eventual prospect that our educational system will literally tear itself apart. Needless to say, that would be tragic for the future of pharmacy in America.

—EGF

JOURNAL OF PHARMACEUTICAL SCIENCES

JULY 1980
VOLUME 69 NUMBER 7

RESEARCH ARTICLES

Clearance of ^{141}Ce-Labeled Microspheres from Blood and Distribution in Specific Organs following Intravenous and Intraarterial Administration in Beagle Dogs

MOTOKO KANKE *, GUY H. SIMMONS, DANIEL L. WEISS ‡, BRACK A. BIVINS, and PATRICK P. DeLUCA ˣ

Received July 26, 1979, from the *College of Pharmacy, University of Kentucky, Lexington, KY 40506.* Accepted for publication March 3, 1980. *Present address: Kitasato University, Yokahama, Japan. ‡National Research Council, National Academy of Sciences, Washington, DC 20418.

Abstract □ The clearance of ^{141}Ce-labeled polystyrene divinylbenzene microspheres in the 3–12-μm diameter size range following intravascular administration was found to be size dependent, with the larger spheres clearing the circulation most rapidly. With spheres of high specific activity, dynamic distribution in various organs was determined by continuous whole-body scanning for the 1st hr after administration and by static imaging at selected times thereafter up to 4 weeks. The 7- and 12-μm spheres were filtered mechanically and retained for prolonged periods in the lungs, while the 3- and 5-μm spheres localized and were retained in the liver and spleen. Localization of these smaller spheres appeared to be due to phagocytosis by cells of the reticuloendothelial system; with the 12-μm spheres, there was no evidence of phagocytosis by the pulmonary macrophages of the reticuloendothelial system within 4 weeks postadministration. Intraarterially administered larger microspheres did not show any significantly different distribution patterns from those administered intravenously. Histological examination revealed occasional vascular engorgement about the site of multiple-sphere lodgment, but no destructive tissue phenomenon was apparent in relation to the lodgment of the microspheres.

Keyphrases □ Microspheres—cerium 141 labeled, clearance from blood and distribution in specific organs following intravenous and intraarterial administration, dogs □ Clearance—^{141}Ce-labeled microspheres, clearance from blood following intravenous and intraarterial administration, dogs □ Distribution—^{141}Ce-labeled microspheres, distribution in specific organs following intravenous and intraarterial administration, dogs

Particulate matter found in injectable fluids and drugs has been a cause of concern to both the pharmaceutical industry and the medical practitioner (1–9). Until recently, most research efforts were directed at the amounts, origins, and physical properties of the particulates in parenteral drugs (10–15). Removal of these contaminants with final filters significantly reduces the incidence of infusion phlebitis, a local inflammatory process associated with intravenous fluid administration (16–20). Although some reports suggested that foreign particulates in parenteral fluids may be hazardous, relatively little is known about distribution, relocation, and tissue effects of particulates entering the vascular system.

The possible effects and fate of injected model particulate matter recently were evaluated methodically as a function of the size and number administered intravenously to beagle dogs (21, 22). Of the size ranges chosen for these studies (microspheres of 3, 8, 15, and 25 μm in diameter), only the 3-μm model particles appeared to clear the lung capillary bed after an initial retention period and eventually relocated in the liver and spleen where they remained indefinitely. Although the studies yielded useful information about the ultimate fate of the microspheres, no definitive information concerning the dynamics of this relocation was obtained.

Since the previous study showed that relocation was limited to the smaller spheres, the purpose of this investigation was to obtain a clearer understanding of the time dependency of the observed relocation of a narrower range of microspheres injected intravenously and intraarterially. Four microsphere sizes in the 3–12-μm range were selected and were of higher specific activity than the ones used previously. Additionally, a more intensive histological examination was conducted on specific tissues at various intervals to assess the location of spheres, tissue loads, and possible tissue damage.

EXPERIMENTAL

Microspheres—Polystyrene divinylbenzene microspheres[1] labeled with cerium 141 were obtained as suspensions in normal saline. These

[1] Nuclear Products Division, 3M Co., St. Paul, Minn.

0022-3549/80/0700-0755$01.00/0
© 1980, American Pharmaceutical Association

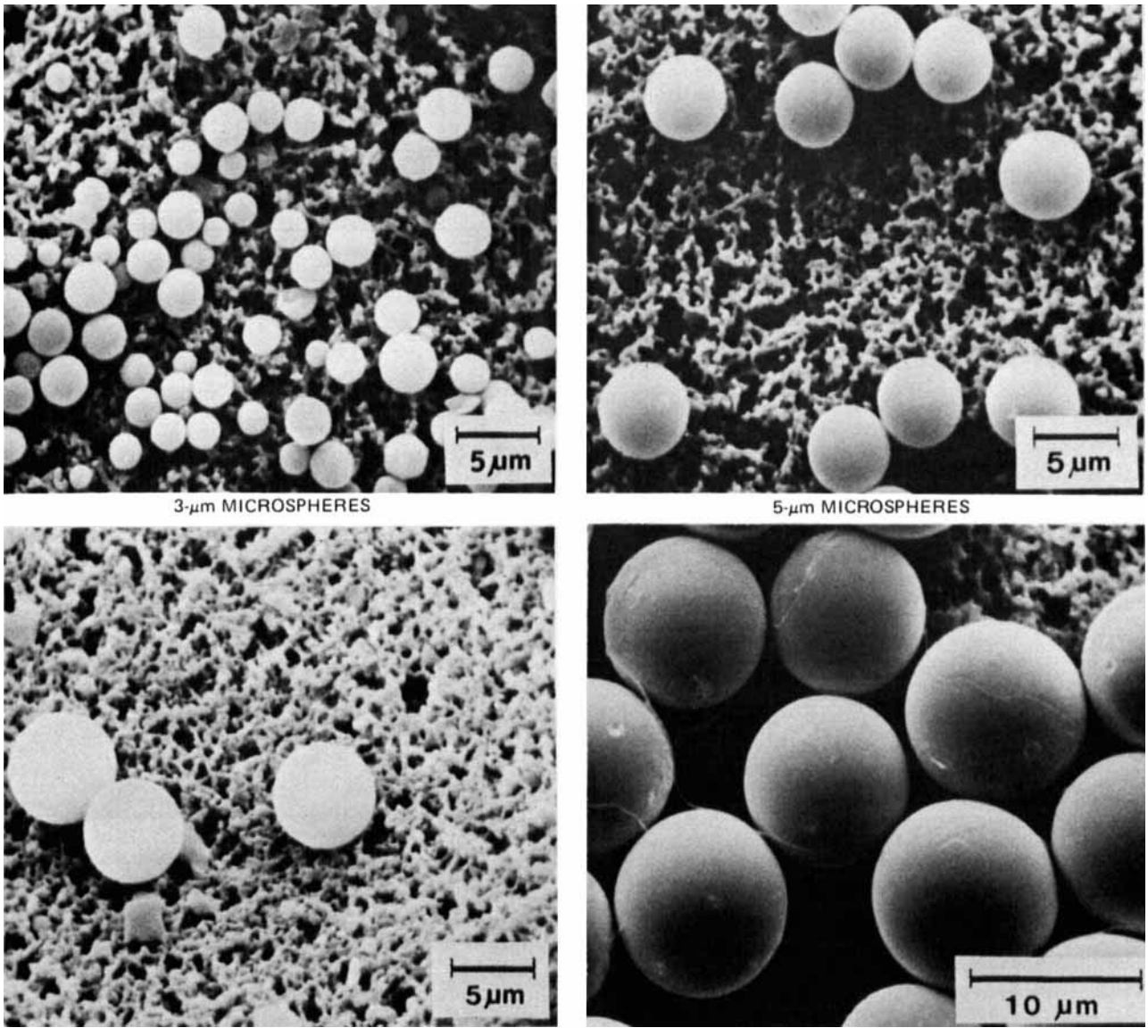

Figure 1—*Scanning electron micrographs of polystyrene divinylbenzene microspheres labeled with cerium 141 at 20 kv (2400× magnification).*

microspheres are shown in the scanning electron microscope photomicrographs in Fig. 1. The specific activity was ~50 mCi/g, five times higher than that used previously (21) to allow for more frequent scanning as well as blood level determinations using small blood samples. The size and number of spheres were controlled using an electronic particle counter[2] and microscopic[3] monitoring.

The permanency of the radioactive tag was checked by filtration of a sample using a 0.45-μm filter and monitoring of the filtrate for activity. Additionally, urine and feces excreted from the first dog of each sphere-size group were collected during the 1st day and analyzed for radioactivity. Analysis of the filtrate and excreta confirmed the permanency of the radioactive tag.

Dose Preparation—Following ultrasonic treatment of the spheres for at least 5 min as well as occasional agitation by hand, doses were drawn into a syringe; the radioactivity was checked with a radioisotope calibrator[4] prior to administration.

Preparation of Experimental Animals—The beagle dogs were 2–3-year-old purebred females weighing 8.1–12.5 kg. The dogs were anesthetized with pentobarbital sodium at a dose of 30 mg/kg iv, and a 20-gauge needle equipped with a three-way stopcock was inserted into the radial veins of the left and right forelegs for intravenous dosing and blood sampling, respectively. For intraarterial administration, a cannula was threaded from the common carotid artery into the left ventricle. The placement of the cannula was verified by demonstration of a left ventricular pressure curve *via* a transducer–recorder hookup.

Each dog was restrained in a supine position on a hard board, placed under a scintillation camera[5], and positioned to align the chest and abdomen for imaging. After completion of imaging, the dogs that had a cannula inserted were given antibiotic prophylaxis with penicillin G procaine at 400,000–1,000,000 units/day im for 1–3 days.

Dose Administration—The size and number of microspheres administered to the beagle dogs are listed in Table I. The prepared dose of microspheres was administered directly from the syringe through the stopcock over 2 min. The syringe and cannula were flushed with 20 ml of sterile water for injection through the stopcock, completing the injection.

Animals were sacrificed at 20 min, 1 hr, 24 hr, or 4 weeks after administration.

Mode of Imaging—For whole-body scanning, the scintillation camera was interfaced to a digital computer[6]. Immediately following dosing, serial images of the chest and abdomen were recorded at the rate of 12 frames/min for the first 2 min followed by 2 frames/min for the next 58 min. Delayed static images were recorded at 2 and 24 hr and 1, 2, and 4

[2] Coulter counter model TAII, Coulter Electronics, Hialeah, Fla.
[3] Zetopan Universal Research Microscope, Riechert, Austria.
[4] Model CRC-6A, E. R. Squibb & Sons, East Brunswick, N.J.
[5] Pho/Gamma LFOV, Searle Radiographics, Des Plaines, Ill.
[6] PDP-1140, Digital Equipment Corp., Maynard, Mass.

Table I—Size of Microspheres Administered and Dosage Range

Number of Dogs	Sphere Size, μm	Dosage Range: Radioactivity, μCi	Dosage Range: Number of Spheres[a], × 10^6
9	3.4 ± 0.7	244–838	253–890
8	5.4 ± 0.5	505–806	73–101
5	7.4 ± 0.5	571–1192	46–93
5	11.6 ± 0.5	409–538	8.6–10

[a] Number of spheres per milligram = $(1.55 \times 10^9)/D^3$, where D is the mean sphere diameter in microns.

weeks following microsphere administration. All data were stored on magnetic tapes for review and analysis.

Determination of Distribution—Microsphere distributions were determined externally by flagging individual organs using computer-generated images and integrating the counts within each flagged area.

Specific intact organs, including the lungs, liver, spleen, heart, kidneys, brain, and tongue, were removed following sacrifice and scanned individually with the scintillation camera to quantitate the distribution at specific times. Efficiency values with units of counts per minute per microcurie were determined for each organ by adding a known amount of radioactivity to a plastic bag filled with an amount of water equivalent to the mass of the organ. The bag was shaped to simulate the shape of the organ and scanned in the same geometry as the excised organ.

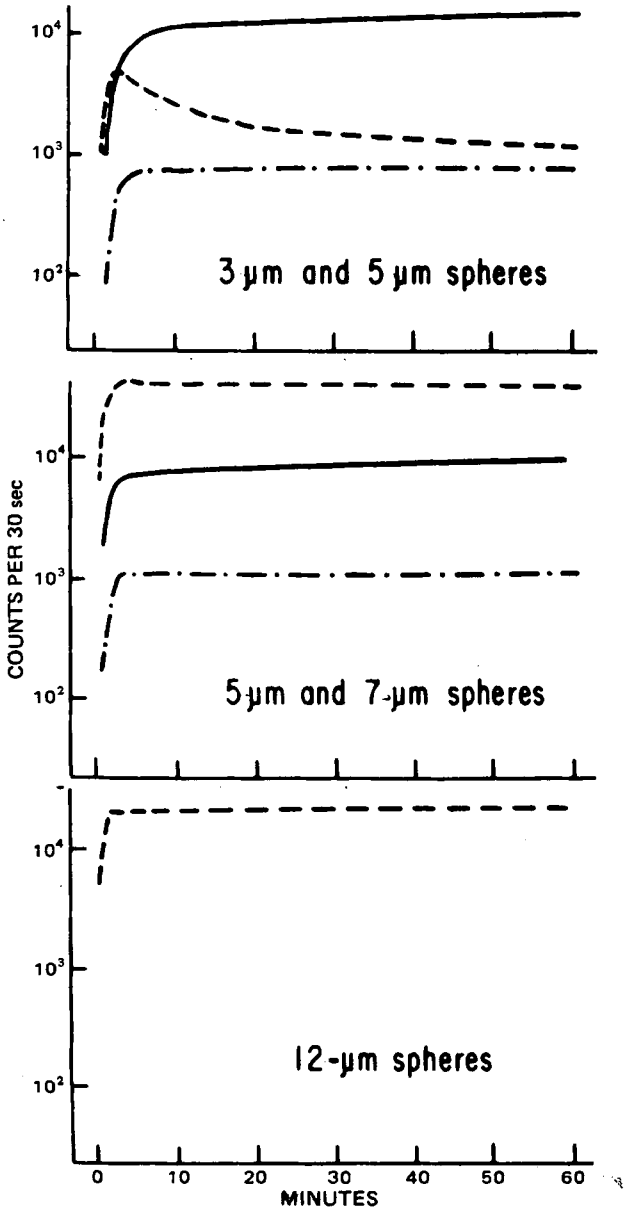

Figure 2—*Distribution patterns of microspheres obtained by rapid frame sequential scanning during the first 60 min following administration. Count rates were corrected for differences in administered activity. Key: —, liver; – –, lung; and · – ·, spleen.*

Table II—Tissues for Histological Study

Organ	Specific Tissue
Heart	Right ventricle, left ventricle
Lungs	Right middle lobe, right lower lobe, left lower lobe, left upper lobe
Liver	Right lobe, left lobe
Spleen	Including capsule
Kidneys	Right including capsule and pelvis, left including capsule and pelvix
Bone marrow	Squeezing of one rib for marrow sample
Brain	Left cortex
Peripheral blood	Direct blood smear immediately after injection, direct blood smear immediately before sacrifice, buffy coat immediately after injection, buffy coat immediately before sacrifice
Tongue	

Following the intact organ scanning, small specimens were removed from each organ for histological examination, and the remainder of the organ then was homogenized with a known amount of distilled water in a blender[7]. A 5-ml rubber-top container[8] was 70% filled with an aliquot of the homogenized sample and weighed. One to five samples were prepared for each organ and analyzed using a well-type γ-counter[9]. The counter efficiency was determined beforehand utilizing a known amount of radioactivity.

Blood Level Determination—Approximately 1–2 ml of venous blood was removed immediately after dose administration and at frequent intervals during the initial stage of each run. Total emissions of a weighed

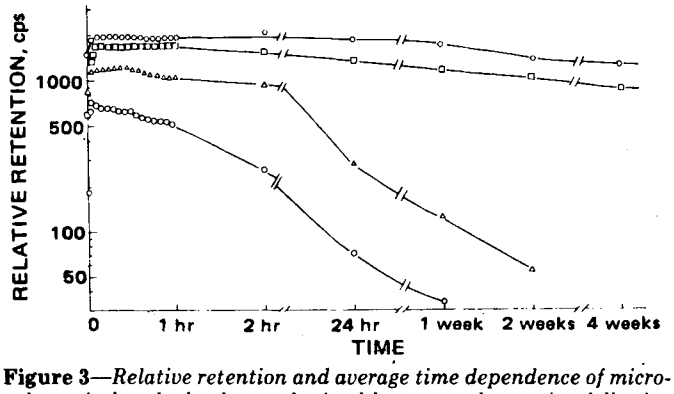

Figure 3—*Relative retention and average time dependence of microspheres in beagle dog lungs obtained by external scanning following intravenous administration based on a 500-μCi dose. Key: ○, 3-μm spheres; △, 5-μm spheres; □, 7-μm spheres; and ○, 12-μm spheres.*

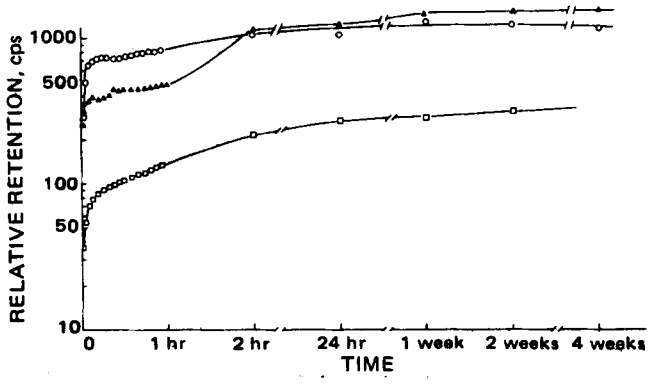

Figure 4—*Relative retention and average time dependence of microspheres in beagle dog liver obtained by external imaging following intravenous administration based on a 500-μCi dose. Key: ○, 3-μm spheres; △, 5-μm spheres; and □, 7-μm spheres.*

[7] Waring model 5011.
[8] Vacutainer.
[9] Model 4 spectroscaler, Picker Nuclear Corp., Northford, Conn.

Table III—Quantitative Recovery of Radioactivity (Percent) in Individually Scanned Intact Organs following Intravenous (IV) and Intraarterial (IA) Administration

Organ	3-μm Spheres		5-μm Spheres		7-μm Spheres		12-μm Spheres	
	IV	IA	IV	IA	IV	IA	IV	IA
			Sacrificed 20 min after Administration					
Heart	0	0.1		0.6				
Lungs	23.7	22.7		49.4				
Liver	54.6	49.2		7.8				
Spleen	14.3	9.3		1.6				
Kidneys	0	1.9		0.6				
Brain	0	0.1		0.1				
Total recovery	92.6	83.3		60.1				
			Sacrificed 1 hr after Administration					
Heart	0.3	0.3	0.9	0.9				
Lungs	21.1	9.4	47.6	43.0				
Liver	60.1	69.7	21.9	25.9				
Spleen	8.2	7.0	4.7	4.3				
Kidneys	0.2	1.7	0.6	1.5				
Brain	0.1	0.1	0.1	0.4				
Total recovery	90.0	88.2	75.8	76.0				
			Sacrificed 24 hr after Administration					
Heart	0	2.6[a]	0.6	0.7	1.0	0.6	0	0
Lungs	1.4	4.2	14.3	2.0	55.7	26.2	98.3	51.6
Liver	70.5	72.7	55.4	60.6	7.0	32.1	0.1	0
Spleen	7.4	8.3	5.0	6.8	0.9	3.1	0	0
Kidneys	0	0.3	0.1	0.2	0.2	1.4	0	0
Brain	0	0.4	0	0.2	0	0.7	0	6.9
Tongue							0.1	0.8
Total recovery	79.3	88.5	75.4	70.5	64.8	64.1	98.5	59.3
			Sacrificed 4 Weeks after Administration					
Heart	0	0.1		0.4	0.8	5.7	0	0.5
Lungs	5.0	1.1		0.6	36.9	10.3	106.4	56.4
Liver	69.2	74.8		81.4	28.3	27.7	0	0.6
Spleen	13.6	8.4		8.3	1.6	2.3	0	0.6
Kidneys	0	0		0.2	0.1	0.2	0	0.6
Brain	0	0		0.3	0.1	0.1	0	2.2
Tongue								3.1
Total recovery	87.8	84.4		91.2	67.8	46.3	106.4	64.0

[a] Obtained at 14 hr.

blood sample were counted by a well-type γ-counter for 10 min.

Histological Evaluation—Specific tissue specimens, ~10 × 20 × 3 mm, were cut from the organs listed in Table II. The tissues were processed through formaldehyde fixation, paraffin embedding, and staining with hematoxylin and eosin. Slide preparations 5–14 μm thick were prepared, depending on the size of the microspheres. Direct blood smears and buffy coat smears were prepared with blood samples obtained immediately after dose administration and immediately before sacrifice.

Table IV—Quantitative Recovery of Radioactivity (Percent) in Homogenized Organs following Intravenous (IV) and Intraarterial (IA) Administration

Organ	3-μm Spheres		5-μm Spheres		7-μm Spheres		12-μm Spheres	
	IV	IA	IV	IA	IV	IA	IV	IA
			Sacrificed 20 min after Administration					
Heart	0.3	0.1		0.5				
Lungs	15.9	19.3		42.5				
Liver	41.6	38.0		8.6				
Spleen	10.8	6.6		1.4				
Kidneys	0.1	1.5		0.6				
Total recovery	68.7	65.5		53.6				
			Sacrificed 1 hr after Administration					
Heart	0.2	0.2	0.7	0.4				
Lungs	15.5	9.5	32.9	28.9				
Liver	49.0	61.6	23.0	19.8				
Spleen	7.3	7.1	3.7	2.9				
Kidneys	0.1	0.6	0.6	1.1				
Total recovery	72.1	79.0	60.9	53.1				
			Sacrificed 24 hr after Administration					
Heart	0.1	1.8[a]	0.6	0.5	0.9	0.4	0	0
Lungs	1.2	3.5	12.4	1.6	42.8	15.9	58.5	37.6
Liver	62.5	52.9	50.9	54.8	6.5	28.8	0	0
Spleen	6.0	5.4	4.9	6.7	0.8	2.6	0.1	0
Kidneys	0	0.2	0.1	0.2	0.3	1.1	0	0
Total recovery	69.8	63.8	68.9	63.8	51.3	48.8	58.6	37.6
			Sacrificed 4 Weeks after Administration					
Heart	0	0.1		0.1	0.6	5.2	0	0
Lungs	4.4	0.9		0.2	26.3	8.1	75.7	54.0
Liver	52.1	68.0		79.5	20.1	34.9	0	0
Spleen	10.5	7.4		7.3	1.5	1.9	0	0
Kidneys	0	0.6		0	0.1	0.1	0	0
Total recovery	67.0	77.0		87.1	48.6	50.2	75.7	54.0

[a] Obtained at 14 hr.

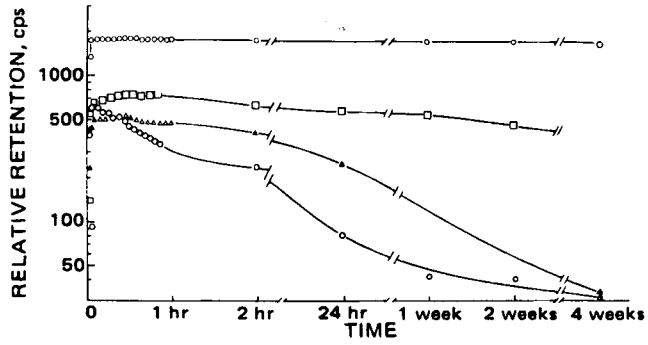

Figure 5—*Relative retention and average time dependence of microspheres in beagle dog lungs obtained by external scanning following intraarterial administration based on a 500-μCi dose. Key: ○, 3-μm spheres; △, 5-μm spheres; □, 7-μm spheres; and ○, 12-μm spheres.*

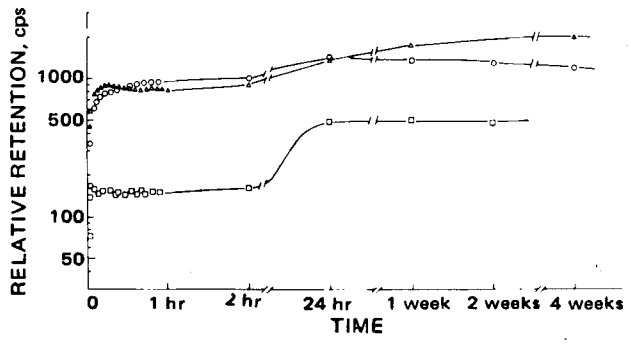

Figure 6—*Relative retention and average time dependence of microspheres in beagle dog liver obtained by external scanning following intraarterial administration based on a 500-μCi dose. Key: ○, 3-μm spheres; △, 5-μm spheres; and □, 7-μm spheres.*

RESULTS

Distribution Patterns—Whole-body scanning showed that almost all of the radioactivity was localized in the central region, with especially high concentrations in the lungs, liver, and spleen. A set of typical temporal distribution curves for these three organs obtained from rapid frame sequential scanning for the first 60 min is shown in Fig. 2. Although the curves were corrected for differences in administered activity, due to the

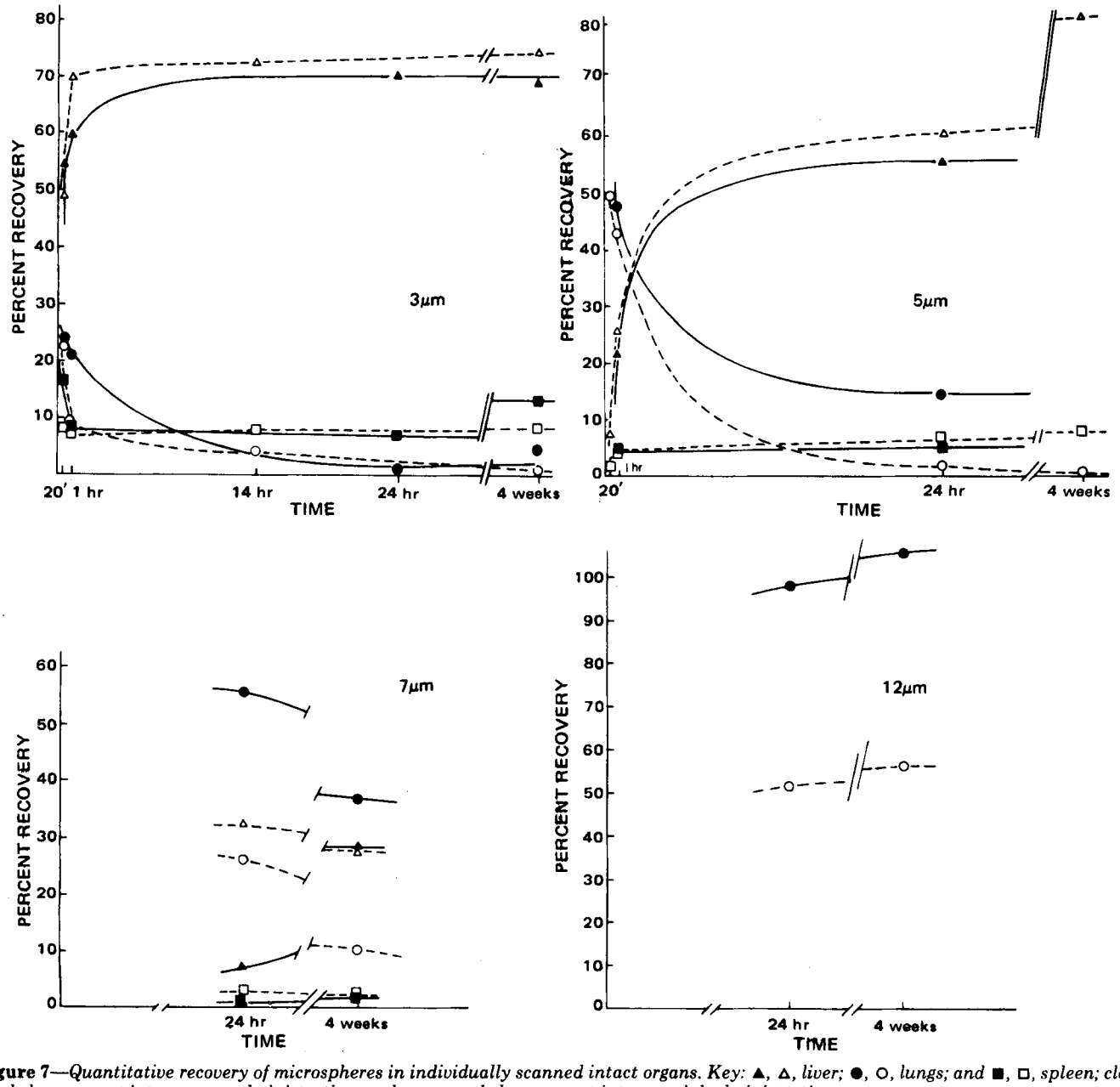

Figure 7—*Quantitative recovery of microspheres in individually scanned intact organs. Key: ▲, △, liver; ●, ○, lungs; and ■, □, spleen; closed symbols represent intravenous administration, and open symbols represent intraarterial administration.*

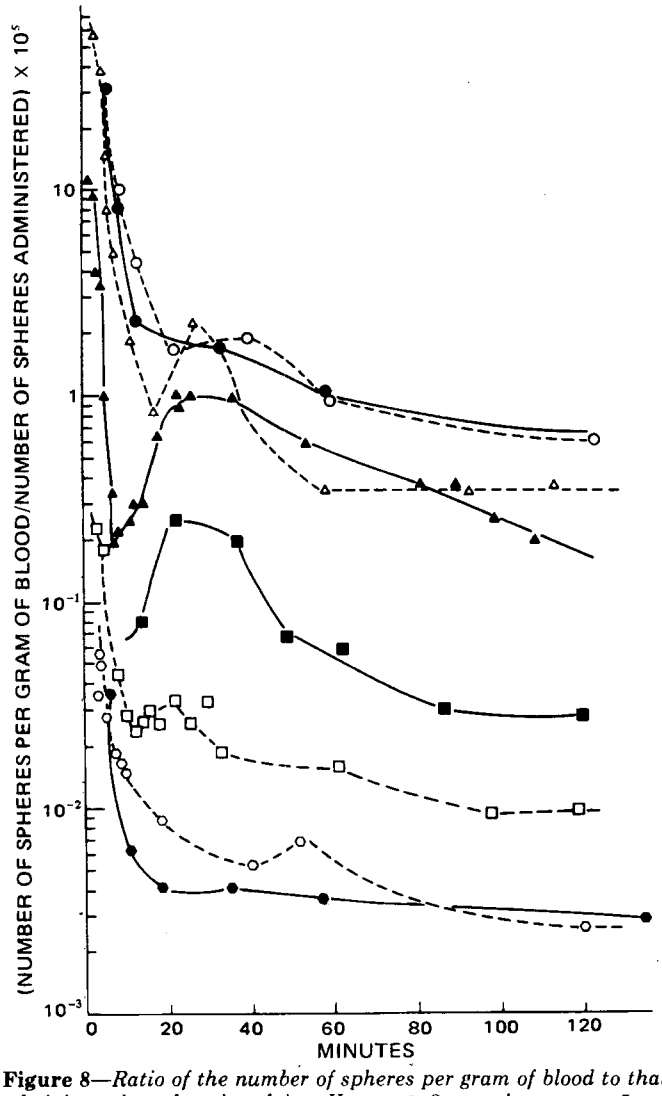

Figure 8—*Ratio of the number of spheres per gram of blood to that administered as a function of time. Key: ●, ○, 3-μm spheres; ▲, △, 5-μm spheres; ■, □, 7-μm spheres; and ◆, ◇, 12-μm spheres; closed figures and solid lines represent intravenous administration, and open figures and broken lines represent intraarterial administration.*

difficulty in isolating entire organ profiles resulting from organ overlap, only relative counts and not absolute uptake values are shown. However, the curves demonstrate the general distribution over the first 60 min.

No clearcut difference in distribution patterns was observed between intravenous and intraarterial administration of microspheres. With the 3-μm microspheres injected in nine dogs, there was an initial distribution to the lungs followed by rapid clearance from the lungs and localization in the liver and spleen. Six of eight dogs injected with 5-μm spheres exhibited similar lung patterns. With the 7-μm microspheres, retention in the lungs was greater and clearance was more gradual in all five dogs injected. On the other hand, all of the 12-μm microspheres were retained in the lungs.

Following the dynamic imaging for the initial 60 min, static images were recorded from the live animal at 2 and 24 hr and 1, 2, and 4 weeks after dose administration. The relative retention curves for the lungs and liver following either intravenous or intraarterial administration obtained by such external imaging are shown in Figs. 3–6. The 12-μm microspheres distributed only to the lungs regardless of the administration route and were retained in the lung area even at 4 weeks after administration.

Quantitative Determination of Distribution—Following sacrifice, specific organs including the lungs, liver, spleen, heart, kidneys, brain, and tongue were removed and scanned by the scintillation camera. The results are listed in Table III and plotted in Fig. 7. The analyzed data of uniformly homogenized organs are listed in Table IV.

The 3-μm spheres were cleared from the lungs and localized in the liver much more readily than the 5-μm spheres. Within 24 hr, >95% of the 3- and 5-μm spheres appeared to have passed from the lungs of all dogs except one of the 5-μm group, where 12–14% of the microsphere dose was retained in the lungs. Clearance of the 7-μm spheres from the lungs following intravenous administration was much slower than that with the smaller sizes. After 24 hr, over 43% of the dose was still in the lungs and only 7% had localized in the liver. However, after 4 weeks, only 26–37% of the microspheres administered intravenously remained in the lungs, and the level in the liver increased to 20–28%. The 12-μm spheres were not detected outside of the lungs after 24 hr following intravenous administration in dogs that were followed for up to 4 weeks.

There were no significant differences in distribution of the 3- and 5-μm spheres between intravenous and intraarterial administration, but some differences were observed with larger spheres. The 12-μm spheres administered intraarterially were retained in the lungs for at least 4 weeks. A major difference between the intravenous and intraarterial administration with the 12-μm size was that some spheres were detected in the brain and tongue after intraarterial administration.

The results obtained from the two quantitative recovery methods were reasonably close to each other. Therefore, the quantitative determination by imaging the intact organs was chosen as being easier and quicker than the homogenized method.

Blood Levels—Figure 8 shows the typical blood levels of the microspheres over a 2-hr period following intravenous or intraarterial administration. Elimination of spheres from the circulating blood pool appeared to be size dependent and more rapid with larger sizes. The blood levels of 12-μm spheres were essentially the same as background levels within 2 hr after administration, while the 3-μm spheres recirculated longer and maintained higher blood levels than did the larger sizes. The number of spheres administered within the size and volume ranges tested appeared to have no effect on the elimination rate from the blood.

Most curves in Fig. 8 show an increase in blood activity between 10 and 30 min after administration. This phenomenon is not explained easily, and more frequent blood sampling is required to define this portion of the curves.

Histology Data—A histological study of representative tissue samples from multiple organs was undertaken (Table II). Identification of microspheres was facilitated by examination under green and red filtered light. Under these conditions (Fig. 9), the microspheres appear as dense black spheres of smooth regular outline. Therefore, the spheres may be distinguished from cell nuclei, even when samples containing smaller spheres of approximately the same diameter as cell nuclei are evaluated.

Individual 3- and 5-μm microspheres were found consistently in vascular channels, Kupffer cells, and the sinusoids of the liver, spleen, and bone marrow within phagocytizing cells. The cells were vascular endothelium, monocytoid phagocytes, or cells of the reticuloendothelial system. There was moderate engorgement of the sinusoids, which were slightly distended and congested. No multinucleated giant cells appeared to participate in the phagocytic activity.

Larger microspheres and clusters of smaller spheres generally lay free in vascular and sinusoidal channels. A few 7-μm microspheres were phagocytized, but these microspheres represented <10% of the total tissue loads. Figure 9*c* shows three single spheres within slightly distended Kupffer cells. The histology of the liver is inconspicuous except for mild congestion. Figure 9*d* shows a single 12-μm sphere lodged in the pulmonary capillary, and slight engorgement of pulmonary vasculature is evident. The buffy coat smears were all negative, with two exceptions: one dog administered 3-μm spheres and one administered 5-μm spheres showed one and two spheres, respectively, in their buffy coats obtained immediately after injection. While this finding attests to the validity of the procedure, it does not provide information on the subsequent distribution characteristics.

Although occasional vascular engorgement was present around the site of multiple-sphere lodgment and may represent a local hemodynamic response to partial blockage of the vascular channels, destructive tissue phenomena were not seen in relation to the lodgment of the microspheres.

DISCUSSION

These studies confirm that clearance of microspheres from the blood following intravascular injection is size dependent, with the larger diameter spheres clearing most rapidly (Fig. 8). The initial clearance appears to be due to a simple filter effect of the pulmonary capillary beds, although vascular constriction and venous sphincters may play some role in the trapping process. Spheres of 7-μm diameter and larger initially were retained in the lungs, while large numbers of the 3- and 5-μm spheres

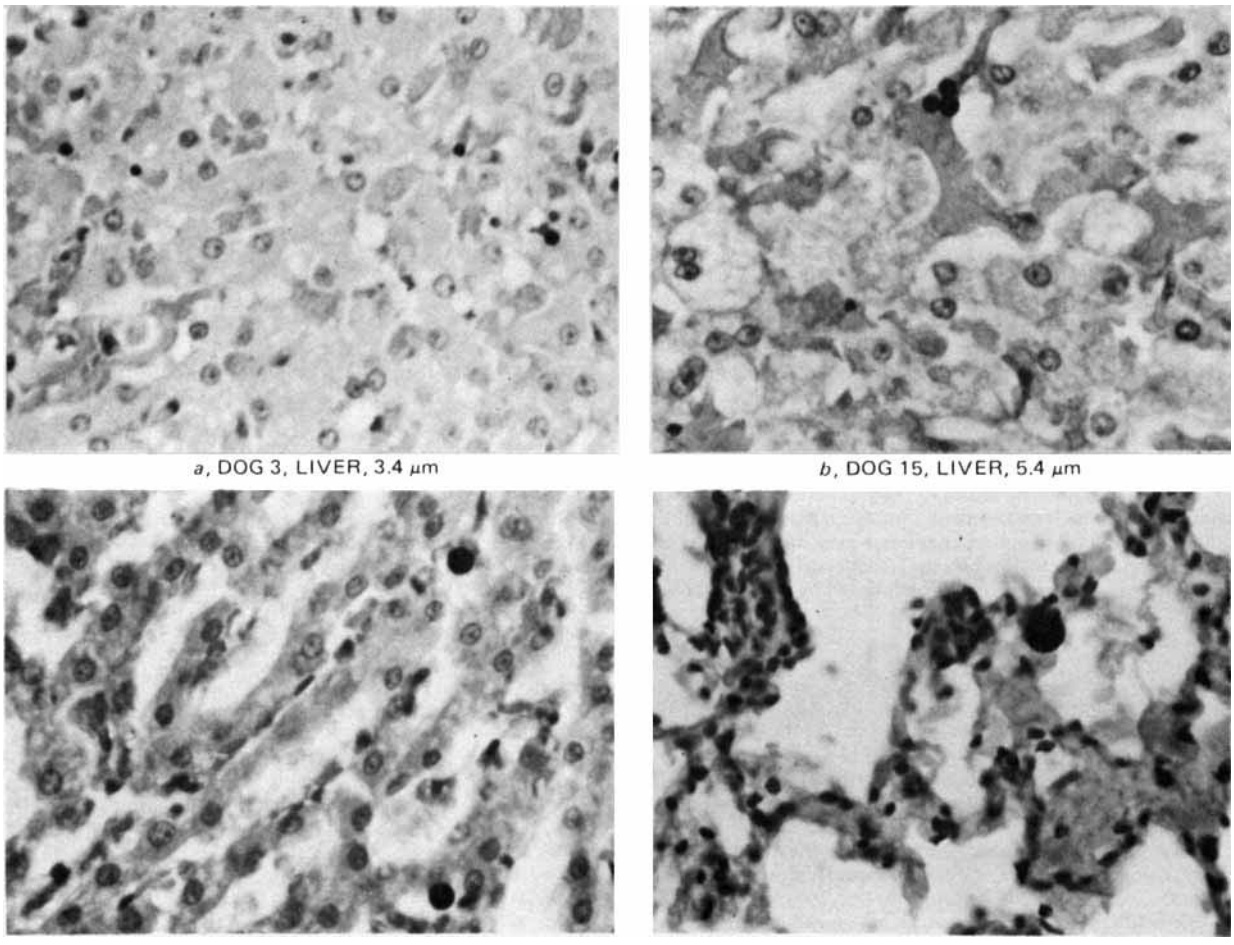

Figure 9—*Photomicrographs of tissue samples. Key:* a, *3-μm spheres in liver;* b, *5-μm spheres in liver;* c, *7-μm spheres in liver; and* d, *12-μm spheres in lungs. Obtained with hematoxylin and eosin stain (160×).*

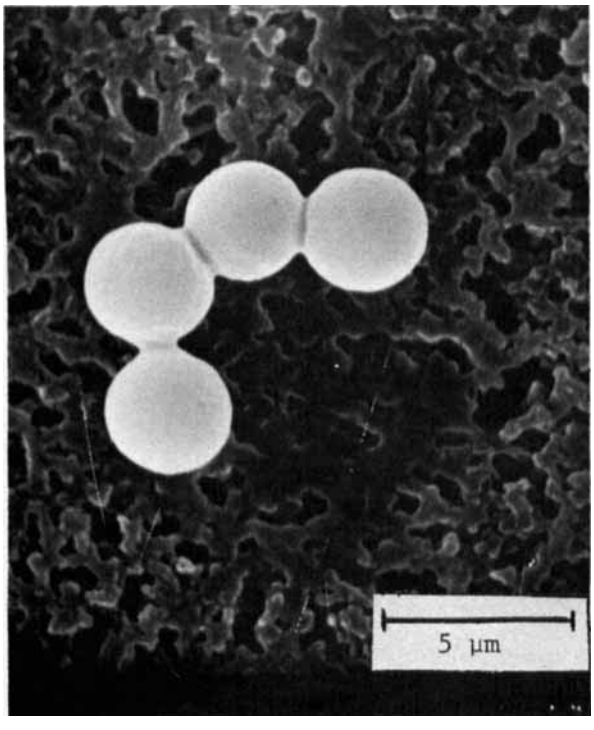

Figure 10—*Scanning electron photomicrograph of 3-μm microspheres from a venous blood sample 1 hr following administration at 20 kv (5000× magnification).*

passed through, implying a critical circulation diameter for nondeformable particles reaching the pulmonary vascular bed.

The increase in blood activity seen between 10 and 30 min following administration of the spheres may be due to washout within the lungs so that spheres initially trapped are washed through opening arteriovenous shunts to recirculate in the bloodstream (Fig. 8). Although 98–99% of the spheres were cleared from the circulation in 10–30 min, blood sampling over the first 2 hr following administration revealed concentrations of 10^4 3-μm spheres, 100–1000 5-μm spheres, 10–100 7-μm spheres, and less than one 12-μm sphere/g of blood. The possible association of the spheres with circulating blood cells warrants further attention and will be undertaken with more sophisticated scanning electron microscopic procedures.

Distribution patterns varied with the sphere size studied and became complex over time. With the 3-μm spheres and in six of eight dogs with the 5-μm spheres, there was initial distribution to the lungs followed by rapid clearance, with localization and retention in the liver and spleen peaking within 20 min of administration for the 3-μm spheres and within 24 hr for the 5-μm spheres (Tables III and IV). This retention is explained by the histological observation of phagocytosis of the 3- and 5-μm spheres by the Kupffer cells of the liver and the sinusoidal lining of the spleen (23, 24).

Clearance of the 7-μm spheres from the lungs to the liver and spleen occurred much more slowly, with 26–37% remaining in the lungs at 4 weeks. This slow migration may be due to retention in the lungs with phagocytosis by pulmonary macrophages and subsequent migration to the reticuloendothelial system. The 12-μm spheres were retained in the lungs from the initial injection throughout the study. Failure of the 12-μm spheres to undergo phagocytosis and relocation may indicate a size limit for phagocytosis of inert particles (25).

No clearcut differences in the clearance or distribution of the 3- and 5-μm spheres were observed between intraarterial and intravenous administration (Fig. 8 and Tables III and IV). For reasons that are not clear, these spheres either passed through or did not enter muscular or visceral

beds following intraarterial administration and recirculated as if they had been injected into the venous system. Minimal differences were seen between intravenous and intraarterial administration of the larger spheres, but 12-μm spheres were detected in the brain and tongue following intraarterial administration. These observations were contrary to expectations and suggest that the flow characteristics of the spheres are such that distribution to peripheral and visceral capillary beds is limited.

In many cases, the 3-μm spheres were seen microscopically to lodge in the studied tissues as agglomerated masses of three to 10 spheres. This property was observed less frequently with the 5-μm spheres and not at all with the 7- and 12-μm spheres. The light microscopy observations did not indicate any significant damage of cells containing the spheres at the substructural or functional levels. Progress in answering these questions will depend on enzyme biochemistry and electron microscopy studies.

Figure 10 shows a cluster of 3-μm microspheres from a venous blood sample obtained 1 hr after administration. Although further investigation is required to clarify this clustering phenomenon, the microspheres may become coated with blood proteins with sticky characteristics and may adsorb platelets on their surface (26–28)[10]. Clustering by surface to surface protein adhesion would be facilitated by slow flow through the capillary and sinusoidal beds and by the high surface to mass ratio of the smaller spheres. Contact among larger spheres may be limited by the diameter of the vascular channels, while the smaller surface to mass ratio may limit the mutual adherence potential exhibited by the 3- and 5-μm spheres.

CONCLUSIONS

1. Elimination of microspheres from the circulation following intravascular administration is size dependent, with the larger diameter spheres clearing most rapidly.

2. Mechanical filtration and prolonged retention of 7-μm and larger spheres in the lungs imply a critical size for passage through the pulmonary vascular bed.

3. Retention of small microspheres (3 and 5 μm) in the liver and spleen for prolonged periods appears to be due to phagocytosis of the spheres by cells of the reticuloendothelial system.

4. Small microspheres (3 μm) tend to agglomerate when administered intravascularly, presumably due to protein adherence and a large surface to mass ratio.

5. Intraarterially administered larger microspheres do not distribute to peripheral and visceral beds differently from the intravenous administration, presumably because of flow characteristics inhibiting peripheral distribution.

6. Large microspheres (12 μm) are not phagocytized by pulmonary macrophages or the reticuloendothelial system within 4 weeks of intravascular administration as are smaller sphere sizes, implying a size limit for phagocytosis of inert particles.

REFERENCES

(1) B. E. Konwaler, *Am. J. Clin. Pathol.*, **20**, 385 (1950).

(2) E. J. Bruning, *Virchovs Arch.*, **327**, 460 (1955).

(3) S. Sarrut and C. Nezelof, *Presse Med.*, **68**, 375 (1960).

(4) J. M. Garvan and B. W. Gunner, *Med. J. Aust.*, **2**, 140 (July 22, 1963).

(5) *Ibid.*, **2**, 1 (July 4, 1964).

(6) W. C. Walter, presented at the Food and Drug Administration Symposium on Safety of Large Volume Parenteral Solutions, Washington, D.C., July 1966.

(7) M. J. Groves, *J. Hosp. Pharm.*, **25**, 17 (1968).

(8) N. M. Davis, S. Turco, and E. Sivelly, *Am. J. Hosp. Pharm.*, **27**, 822 (1970).

(9) S. Turco and N. M. Davis, *Hosp. Pharm.*, **8**, 137 (1973).

(10) M. Sokol and J. Boyd, *Bull. Parenter. Drug Assoc.*, **22**, 9 (1968).

(11) B. Trasen, *ibid.*, **22**, 1 (1968).

(12) M. J. Groves and J. F. Major, *Pharm. J.*, **193**, 227 (1964).

(13) Y. S. Lim, S. Turco, and N. M. Davis, *Am. J. Hosp. Pharm.*, **30**, 518 (1973).

(14) J. Y. Masuda and J. H. Beckerman, *ibid.*, **30**, 72 (1973).

(15) P. P. DeLuca, R. P. Rapp, B. A. Bivins, and T. Rebagay, *ibid.*, **33**, 433 (1976).

(16) D. W. Wilmore and S. J. Dudrick, *Arch. Surg.*, **99**, 462 (1969).

(17) P. B. Ryan, R. P. Rapp, P. P. DeLuca, W. O. Griffen, J. D. Clark, and D. Cloys, *Bull. Parenter. Drug Assoc.*, **27**, 1 (1973).

(18) P. P. DeLuca, R. P. Rapp, B. A. Bivins, H. E. McKean, and W. O. Griffen, *Am. J. Hosp. Pharm.*, **32**, 1001 (1975).

(19) H. G. Schroeder and P. P. DeLuca, *ibid.*, **33**, 543 (1976).

(20) B. A. Bivins, R. P. Rapp, P. P. DeLuca, H. McKean, and W. O. Griffen, *Surgery*, **85**, 388 (1979).

(21) H. G. Schroeder, G. H. Simmons, and P. P. DeLuca, *J. Pharm. Sci.*, **67**, 504 (1978).

(22) H. G. Schroeder, B. A. Bivins, G. P. Sherman, and P. P. DeLuca, *ibid.*, **67**, 508 (1978).

(23) M. D. Schoenberg, P. A. Gilman, V. R. Mumaw, and R. D. Moore, *Br. J. Exp. Pathol.*, **42**, 486 (1961).

(24) J. M. Singer, L. Adlersberg, E. M. Hoenig, E. Ende, and Y. Tchorsch, *J. Reticuloendothel. Soc.*, **6**, 561 (1969).

(25) B. Holma, *Acta Med. Scand.*, **473**, 1 (1967).

(26) R. E. Baier and R. C. Dutton, *J. Biomed. Mater. Res.*, **3**, 43 (1969).

(27) D. E. Scarborough, R. G. Mason, T. G. Galldoxt, and K. M. Brinkhaus, *Lab. Invest.*, **20**, 164 (1969).

(28) M. A. Packhan, G. Evans, M. F. Glynn, and J. F. Mustard, *J. Lab. Clin. Med.*, **73**, 686 (1969).

[10] Confirmed by S. W. Kim, College of Pharmacy, University of Utah, personal communication.

ACKNOWLEDGMENTS

Presented at the Basic Pharmaceutics Section, APhA Academy of Pharmaceutical Sciences, Hollywood, Fla. meeting, November 1978.

Supported by Contract 223-77-3018 from the Public Health Service, Food and Drug Administration, Department of Health, Education, and Welfare.

The authors thank Dr. Irena Sniecinski for assistance and consultation with the histological evaluation and Mr. C. Cheng for assistance with the animal studies.

Determination of Ketoprofen in Biological Fluids by Reversed-Phase Chromatography

A. BANNIER ˣ, J. L. BRAZIER, B. RIBON, and C. QUINCY

Received November 27, 1978, from the *Département de Chimie Analytique, Faculté de Pharmacie, 8, Avenue Rockefeller, 69373 Lyon Cedex 2, France.* Accepted for publication February 1, 1980.

Abstract □ A sensitive and specific high-performance liquid chromatographic method was developed for the determination of ketoprofen [2-(3-benzoylphenyl)propionic acid] in plasma and urine. The method includes an extraction of the drug and the internal standard [2-(4-benzoylphenyl)butyric acid] into ether from acidified plasma. The organic phase is evaporated, and the residue is dissolved in the mobile phase (acetonitrile–0.02 *M* phosphate buffer, pH 3) (45:55). A 20-μl aliquot is analyzed on a reversed-phase column. The accuracy is within 1.5% for therapeutic concentrations, and the coefficients of variation are 5.5 and 3.4% for 2 and 10 μg/ml, respectively. For the urine assay, the accuracy is within 3%, and the coefficients of variation are 1.9 and 1.7% for 3 and 50 μg/ml, respectively. This method was applied successfully to the determination of ketoprofen in humans for pharmacokinetic studies.

Keyphrases □ Ketoprofen—high-performance liquid chromatographic analysis, human plasma and urine □ Anti-inflammatory agents—ketoprofen, high-performance liquid chromatographic analysis, human plasma and urine □ High-performance liquid chromatography—analysis, ketoprofen, human plasma and urine

Ketoprofen [2-(3-benzoylphenyl)propionic acid, I] is a benzophenone derivative with anti-inflammatory activity (1). Clinical proof of its therapeutic efficacy (2) has resulted in its wide use in rheumatology, leading to numerous clinical (3–5) and pharmacokinetic (6–9) studies.

Several methods for the determination of ketoprofen in biological fluids have been reported. Colorimetry and polarography (10) are simple but cannot be applied easily to plasma or serum. TLC (11) is rapid but lacks sensitivity. Methyl (10) and trimethylsilyl esters of ketoprofen (12) can be separated using GLC, and this method can be considered as a reference due to its sensitivity. However, the technique is relatively complex and time consuming, and the resulting precision is only ~10%.

A new rapid and accurate analytical method for ketoprofen was described recently, which involves the determination of its methyl ester by high-performance liquid chromatography (HPLC) (13). This report describes the development of a precise and rapid HPLC assay for determining ketoprofen in biological fluids without derivatization.

EXPERIMENTAL

Reagents and Solvents—Acetonitrile[1], phosphoric acid[1], monobasic potassium phosphate[2], sodium hydroxide[2], acetone[2], sodium sulfate[2] (anhydrous), hydrochloric acid[2], sodium nitrate[1], and ether[2] were analytical grade and were used without further purification. Water was deionized. Ketoprofen and the internal standard [2-(4-benzoylphenyl)-butyric acid, II] were synthesized[3].

HPLC mobile phases of pH 3, 4, 5, 6, and 7 were made from phosphoric acid–monobasic potassium phosphate or monobasic potassium phosphate–dibasic sodium phosphate aqueous buffer solutions diluted with various volumes of acetonitrile (30–70%). The pH of the resulting solutions was adjusted with either 10% NaOH or 10% phosphoric acid. The final phosphate-ion concentration was 0.02 *M*.

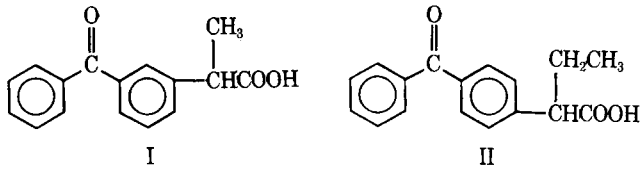

I II

Apparatus—The liquid chromatograph[4], equipped with a 254-nm UV detector[5], was operated at ambient temperature. The output of the detector was displayed on a recorder[6] having 10-mv full-scale deflection. The output signal also was fed to an electronic integrator[7] for quantification.

The 10-cm × 4.6-mm i.d. stainless steel columns were packed with Lichrosorb RP 18[2] (5 μm) or RP 8[2] (5 μm) by a balanced-density slurry technique (14). A 20-μl loop injection valve[8] was used to introduce samples into the chromatographic system. The efficiency of newly made columns was tested with a standard mixture using sodium nitrate as an unretained marker. The solvent system was methanol–water (80:20). Under these conditions, the column efficiency was 24,000 theoretical plates for benzene and 21,000 for anthracene.

Stock Solutions—The ketoprofen stock solution (10 mg/100 ml) was prepared by dissolving I in acetone. The internal standard stock solution (10 mg/100 ml) was prepared by dissolving II in acetone. A 10-fold dilution of these two solutions was made before use.

Calculations—The plasma and urine concentrations were calculated using the internal standard method.

Chromatographic Conditions—Columns were preconditioned with the mobile phase until a stable recorder baseline was obtained. The flow rate then was adjusted to 1 ml/min, generating a pressure of nearly 1000

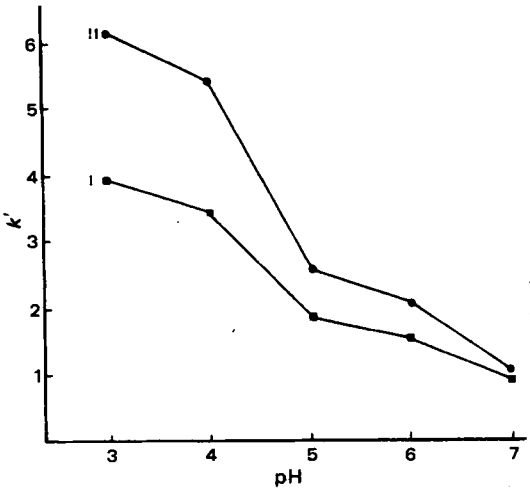

Figure 1—*Effect of variation of the solvent pH on the capacity factors, k', of ketoprofen (I) and the internal standard (II) on a Lichrosorb RP 18 column; the mobile phase was acetonitrile–0.020 M phosphate buffer (40:60).*

[1] Prolabo, Paris, France.
[2] E. Merck, Darmstadt, West Germany.
[3] Specia, Paris, France.
[4] Chromatem 38, Touzart and Matignon, Paris, France.
[5] Model 153, Altex, Berkeley, Calif.
[6] Model PE 1286, Sefram, Paris, France.
[7] Model 3385 A, Hewlett-Packard, Orsay, France.
[8] Model 70-10, Rheodyne, Berkeley, Calif.

0022-3549/80/0700-0763$01.00/0
© 1980, American Pharmaceutical Association

Table I—Chromatographic Parameters of I and II on Lichrosorb RP 18 and Lichrosorb RP 8 [a]

Compound	Lichrosorb RP 18		Lichrosorb RP 8	
	I	II	I	II
Retention time (T_R)	5.2	7	4.2	5.65
Capacity factor[b] (k')	3.3	4.83	3.2	4.65
Theoretical plates[b] (N)	1260	1380	2940	3200
Resolution[b] (R)	2.42		3.72	
Selectivity[b] (α)	1.46		1.45	

[a] Chromatographic conditions included a mobile phase of 45% acetonitrile–55% phosphate buffer (0.02 M, pH 3), a flow rate of 1 ml/min, and a pressure of 1100 psi. [b] For calculations, see C. F. Simpson, "Practical High Performance Liquid Chromatography," Heyden & Son, Philadelphia, Pa., 1976, pp. 7–12.

Table II—Reproducibility and Accuracy [a] for the Plasma Assay [b]

I Added, μg/ml	I Measured, μg/ml	Mean Error	Relative Error, %	CV, %
2	1.98 ± 0.11	0.02	1.01	5.5
5	5.13 ± 0.21	0.13	2.60	4.2
10	10.15 ± 0.34	0.15	1.50	3.4

[a] For chromatographic conditions, see Table I. [b] n = 10.

psi. The mobile phase solutions were prepared daily and degassed by sonification.

Plasma Extraction—One milliliter of plasma, 1 ml of diluted internal standard, and 1 ml of 1 N HCl were transferred to a 35-ml screw-capped centrifuge tube and extracted by shaking with 25 ml of ether for 5 min.

The organic and aqueous phases were separated by centrifugation for 3 min at 2000 rpm. The ether layer was then pipetted carefully into a 35-ml conical centrifuge tube, dried over anhydrous sodium sulfate, and evaporated to dryness under a nitrogen stream at 40°. The sample residue was reconstituted with various volumes of the mobile phase (200–500 μl), depending on the drug concentration. Aliquots of 20 μl then were injected onto the column.

Urine Extraction—To determine the total ketoprofen excreted in urine, any conjugated drug first was hydrolyzed in an alkaline medium (12). Then, 0.1–0.5 ml of urine, 1 ml of 1 N NaOH, 1 ml of the internal standard stock solution (10 mg/100 ml), and 25 ml of ether were transferred to a 35-ml screw-capped centrifuge tube. The sample was agitated for 5 min, and the organic phase was discarded. The aqueous phase, after acidification with 2 ml of 1 N HCl, was treated similarly to the plasma. The sample residue then was reconstituted with 1–2 ml of the mobile phase, and 20-μl aliquots were injected into the chromatograph.

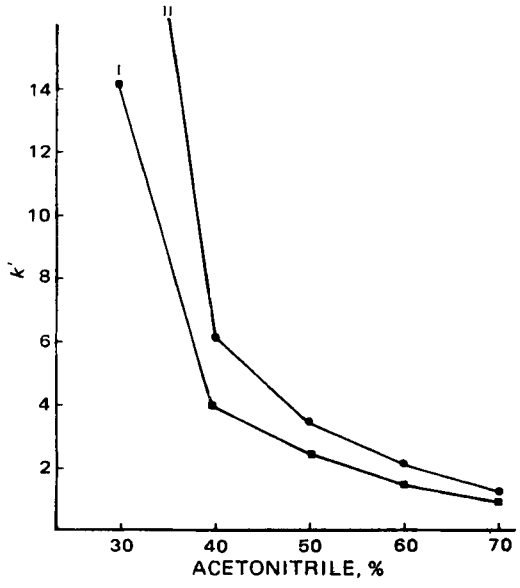

Figure 2—*Effect of the acetonitrile content at pH 3 upon the capacity factors, k', of ketoprofen (I) and the internal standard (II) on a Lichrosorb RP 18 column.*

Table III—Urine Assay Precision Data [a]

I Added, μg/ml	n	I Measured, μg/ml	Mean Error	Relative Error, %	CV, %
3	5	3.09 ± 0.06	0.09	3	1.94
9	6	8.87 ± 0.31	0.13	2.6	3.49
30	5	29.03 ± 0.72	0.97	3.23	2.48
50	5	48.99 ± 0.85	1.00	2.00	1.79

[a] For chromatographic conditions, see Table I.

Table IV—Retention Times and Column Efficiency of I, II, and Selected Drugs [a]

Compound	Retention Time, min	N^b
Aspirin	2.5	1860
I	4.2	2940
II	5.6	3200
Fenoprofen	7.6	2770
Metiazinic acid	8.6	2340
Indomethacin	9.1	3180
Niflumic acid	9.4 (tailing)	1640
Ibuprofen	10.7	2800
Protizinic acid	11.2	2570
Mefenamic acid[c]	15.8 (tailing)	1790
Flufenamic acid[c]	18.30	2010

[a] For chromatographic conditions, see Table I. [b] Theoretical plates. [c] The detection wavelength was 280 nm.

RESULTS AND DISCUSSION

Reversed-phase chromatography on modified silica (C_{18} or C_8) has replaced ion-exchange chromatography for the separation of many polar ionogenic compounds. The technique, called solvophobic chromatography, was developed by Horváth *et al.* (15, 16). Ketoprofen, a drug with a polar carboxylic functional group, can be determined by such a method.

The internal standard for this determination was proposed by Populaire *et al.* (10). Its structure is very close to that of I, and its physicochemical properties also are similar. Preliminary studies showed that separation of I and II in biological fluids was possible with a mixture of methanol–acetonitrile–0.025 M phosphate buffer (30:15:45) at pH 3 on a 5-μm Lichrosorb RP 18 column. However, under such conditions, retention times were long (8 and 12.8 min, respectively), and the peaks were unacceptably broad.

To determine the optimum chromatographic conditions, variation of the capacity factor, k', with pH was measured on 5-μm Lichrosorb RP

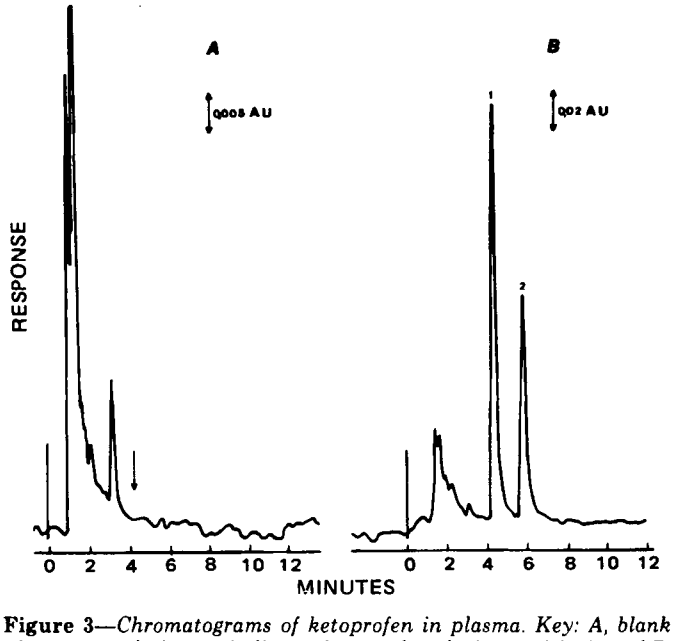

Figure 3—*Chromatograms of ketoprofen in plasma. Key: A, blank plasma sample (arrow indicates ketoprofen elution position); and B, plasma sample with 8.53 μg of ketoprofen/ml (peak 1) and 5 μg of the internal standard/ml (peak 2).*

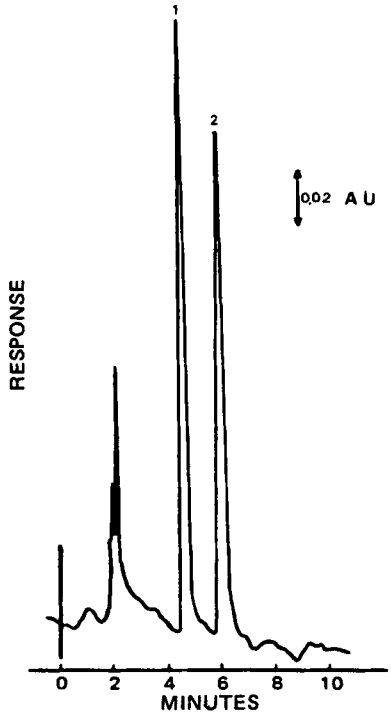

Figure 4—*Chromatogram of ketoprofen in urine for the 0–6-hr collection. The ketoprofen (peak 1) concentration was 189 μg/ml, and the internal standard (peak 2) concentration was 250 μg/ml.*

18 columns with an acetonitrile–phosphate buffer mobile phase. Figure 1 shows that the best separation was obtained at pH 3 ($k_I' = 3.89$, $k_{II}' = 6.10$, $R_S = 3.03$, and $\alpha = 1.57$). At pH 3, I and II were not ionized and thus showed a maximum affinity for the stationary phase. Moreover, Twitchett and Moffat (17) demonstrated that k' is influenced strongly by liposolubility. Figure 2 shows that an increase in the proportion of acetonitrile in the mobile phase decreases k'.

Results for the determination of I on Lichrosorb RP 18 under these conditions are summarized in Table I. Optimization of pH and liposolubility led to a shorter analysis time and better resolution. However, the efficiency of this column still was not sufficient and the peaks remained rather broad. A better separation subsequently was obtained using a 5-μm Lichrosorb RP 8 column. The right side of Table I shows that the chromatographic parameters for I and II were nearly the same for the two stationary phases, but resolution and efficiency were increased because of peak sharpness. Consequently, 5-μm Lichrosorb RP 8 was chosen as the stationary phase for the final determination.

Ether extracts of control plasma were free of endogenous UV (254-nm) absorbing peaks liable to interfere with the assay (Fig. 3). Figure 4, representing the chromatogram of a urine extract under these conditions, shows that ketoprofen and the internal standard were well resolved.

To verify the linearity of the chromatographic response, a plasma calibration curve was run in which the concentration of II was maintained at 5 μg/ml while that of I was varied from 1 to 10 μg/ml. A linear regression analysis of the data resulted in a good linear fit ($r^2 = 0.998$, intercept = 0.027, and slope = 0.200). For the calibration for urine, the concentration of I was varied from 10 to 150 μg/ml. Good linearity was observed ($r^2 = 0.999$, intercept = 0.04, and slope = 0.097).

Reproducibility and Accuracy—Reproducibility and accuracy of the HPLC method were studied by measuring the concentration of I in plasma samples spiked at 2, 5, and 10 μg/ml. The results (Table II) show that accuracy was within 4%. The assay precision for urine was determined for various ketoprofen concentrations (Table III). The lower limit of sensitivity was 0.04 μg/ml for plasma samples and 0.05 μg/ml for urine samples, both measured at a signal-to-noise ratio of 3:1.

Potential Interfering Substances—Retention times for several compounds that might potentially interfere with ketoprofen are shown in Table IV. The chromatographic system provided good specificity, and the column efficiency for these compounds was good. Moreover, no interference was found between ketoprofen and its hydroxylated metabolites since they were not extracted in the acidic medium.

Clinical Study—Figure 5 shows the plasma level in a human subject

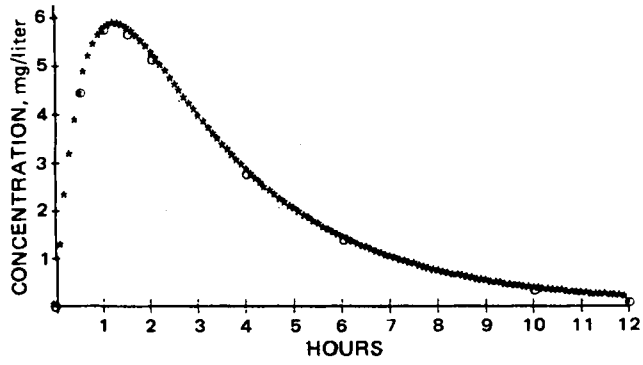

Figure 5—*Plasma decay for ketoprofen after a single oral dose of 100 mg ($K_e = 0.354\ hr^{-1}$ and $K_a = 1.54\ hr^{-1}$).*

following a single oral dose of 100 mg of I in tablet form. Blood samples were collected before medication and after 30 min and 1, 1.5, 2, 4, 6, 10, and 12 hr. The plasma levels of I were measured as described.

In this subject, a peak plasma level of 5.8 μg/ml was reached at 1 hr. The decrease in the plasma level followed a monoexponential decline with an elimination rate constant of 0.354 hr^{-1} and a half-life of 1.97 hr.

The urinary excretion levels of ketoprofen also were determined for the same subject. Urine was collected at intervals of 0–6, 6–12, and 12–24 hr during the first 24 hr following oral administration. A total of 61.2 ± 5.8% of the dose was excreted in 24 hr. These results agree closely with the data reported previously (5, 6, 18) and indicate that the method is well suited for the determination of plasma and urine levels of I in bioavailability and pharmacokinetic studies.

REFERENCES

(1) L. Julou, J. C. Guyonnet, R. Ducrot, C. Ducrot, C. Garret, M. C. Bardonne, G. Maignan, and J. Pasquet, *J. Pharmacol. (Paris)*, **2**, 259 (1971).

(2) B. Amor, A. de Gery, and F. Delbarre, *Rev. Rhum. Mal. Osteo-Articulaires*, **40**, 451 (1973).

(3) J. Fossgreen, *Scand. J. Rheum.*, **5**, 7 (1976).

(4) J. Sany and H. Serre, *Rheumatol. Rehabil., Suppl.: Symposium on Ketoprofen*, **1976**, 67.

(5) P. Coupron, J. L. Brazier, P. Meunier, B. Ribon, and A. Bannier, in "XIV International Congress of Rheumatology," J. R. Rice, Ed., Bethesda, Md., 1977, pp. 23, 24.

(6) P. Populaire, B. Terlain, S. Pascal, B. Decoulevaere, A. Renard, and J. P. Thomas, *Ann. Pharm. Fr.*, **31**, 735 (1973).

(7) A. Castegnaro, F. Annotta, and C. Pollini, *Farmaco Sci.*, **29**, 520 (1976).

(8) O. R. W. Lewellen and R. Templeton, *Scand. J. Rheum.*, **5**, 53 (1976).

(9) P. Meunier, R. Coupron, J. L. Brazier, B. Ribon, and A. Bannier, *Rev. Rhum. Mal. Osteo-Articulaires*, **44**, 519 (1977).

(10) P. Populaire, B. Terlain, S. Pascal, B. Decoulevaere, G. Lebreton, A. Renard, and J. P. Thomas, *Ann. Pharm. Fr.*, **31**, 679 (1973).

(11) R. Ballerini, A. Cambi, and P. Del Soldato, *J. Pharm. Sci.*, **66**, 281 (1977).

(12) N. Blazevic, M. Zinic, T. Kovac, V. Sunjic, and F. Kajfez, *Acta Pharm. Jugosl.*, **25**, 155 (1975).

(13) A. Bannier, J. L. Brazier, and B. Ribon, *J. Chromatogr.*, **155**, 371 (1978).

(14) B. Coq, C. Gonnet, and J. L. Rocca, *ibid.*, **106**, 249 (1975).

(15) C. Horváth, W. Melander, and J. Molnar, *Anal. Chem.*, **49**, 142 (1977).

(16) C. Horváth and W. Melander, *J. Chromatogr. Sci.*, **15**, 393 (1977).

(17) P. J. Twitchett and A. C. Moffat, *J. Chromatogr.*, **111**, 149 (1975).

(18) G. Caille, J. G. Besner, J. Brodeur, and M. Vezina, *Ann. Pharm. Fr.*, **36**, 243 (1978).

ACKNOWLEDGMENTS

The authors thank Dr. M. Friesen for assistance.

High-Performance Liquid Chromatographic Determination of Epimers, Impurities, and Content of the Glucocorticoid Budesonide and Preparation of Primary Standard

G. ROTH ˣ, A. WIKBY, L. NILSSON, and A. THALÉN

Received October 19, 1979, from the *Research and Development Laboratories, AB Draco (Subsidiary to AB Astra), Box 1707, S-221 01 Lund, Sweden.* Accepted for publication February 1, 1980.

Abstract □ The new glucocorticoid budesonide, a 1:1 mixture of two epimers, was evaluated analytically with respect to drug content, impurities, and epimer distribution in the drug substance. Reversed-phase high-performance liquid chromatographic (HPLC) systems using octadecylsilane columns with different ethanol–water mixtures as eluents were used. Budesonide and its epimers were determined with recoveries of 100.3% (±0.16 *SD*) and 99.7% (±0.27 *SD*), respectively. Individual foreign steroids in the ranges of 0.05–0.2 and 0.2–2% were determined with mean recoveries of 93% (±7.6 *SD*) and 97% (±2.5 *SD*), respectively. Analysis of eight small-scale production batches of budesonide gave a recovery of 99.9% (±0.39 *SD*) for the sum of budesonide and impurities. Analytical data and the procedure for preparation of a budesonide primary standard are given. The proposed HPLC procedure is faster, more accurate, more precise, and more selective than the usual pharmacopeial methods for corticosteroids.

Keyphrases □ Budesonide—high-performance liquid chromatographic analysis of drug content, impurities, and epimer distribution, preparation of primary standard □ Anti-inflammatory agents—budesonide, high-performance liquid chromatographic analysis of drug content, impurities, and epimer distribution, preparation of primary standard □ High-performance liquid chromatography—analysis, budesonide, determination of drug content, impurities, and epimer distribution

The new nonhalogenated glucocorticoid budesonide with high anti-inflammatory activity was synthesized by Thalén and coworkers (1–3). Evidence was given for the formation of two epimers in a 50:50 ratio. The epimers were isolated by chromatography on Sephadex LH-20 and studied by NMR spectroscopy and mass spectrometry (2, 3). An X-ray study of the molecular structures of the two epimers also was reported (4, 5).

The high-performance liquid chromatographic (HPLC) properties of budesonide and homologous corticosteroids were studied using both normal-phase (6) and reversed-phase (6, 7) systems. Optimal resolution of the budesonide epimers was obtained with octadecylsilane as the support and ethanol in the aqueous mobile phase.

For the assay of several steroid drugs, the USP proposes the separation of the drug substance from impurities by TLC and the final determination of the drug content by the blue tetrazolium method (8). Preliminary work indicated that this procedure was too laborious, time consuming, and not selective enough for accurate evaluation of budesonide batches with respect to drug content and impurities. Furthermore, the epimer distribution could not be determined by this method. The purpose of the present work was to develop HPLC methods for the quantitative evaluation of all of these parameters. This report also deals with the problem of preparing a reliable primary standard substance since an absolute assay for steroids is not available.

EXPERIMENTAL

Chemicals and Solvents—*Budesonide Drug Substance*—Budesonide (I) is a mixture of two epimers, 16α,17α-(22*S*)- and 16α,17α-(22*R*)-propylmethylenedioxypregna-1,4-diene-11β,21-diol-3,20-dione (A and B, respectively). The different solubilities of the epimers result in more Epimer B during purification of the crude substance, which is considered by specifying the limits for the epimer ratio of the drug substance.

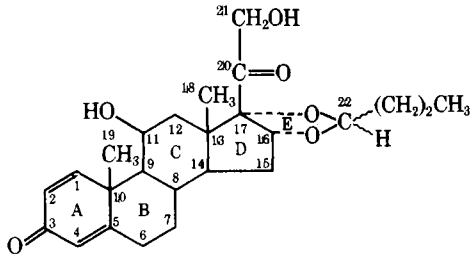

I

Flucloronide[1]—Flucloronide was used as the internal standard in the assay of budesonide. The HPLC purity was >99.8%.

Impurity 1—Impurity 1 was 16α-hydroxyprednisolone, the starting material in the synthesis of budesonide. The HPLC purity (254 nm) of the substance[2] was >98%. 16α-Hydroxyprednisolone appeared only in a few budesonide batches.

Impurity 2—Impurity 2 was a 1:1 mixture of two epimers, 16α,17α-(22*S*)- and 16α,17α-(22*R*)-methylmethylenedioxypregna-1,4-diene-11β,21-diol-3,20-dione (the propyl group of budesonide is replaced by a methyl group). The epimers were isolated by column chromatography and identified by NMR spectroscopy and mass spectrometry. Their HPLC purity was >99%.

Impurities 3 and 4—Impurities 3 and 4 were isolated by column chromatography. Work is now in progress[3] to identify them. Their HPLC purity was >99%.

Epimers A and B of Budesonide—Epimers A and B were isolated by column chromatography (2, 3), and the HPLC purity was >99.8%.

Solvents—Analytical or spectroscopic (for ethanol) grade solvents were used.

Apparatus—The liquid chromatograph was equipped with a pump[4], a high-pressure injector[5], and a 254-nm detector[6]. Peak areas were determined with an electronic digital integrator[7].

The columns (3.9 mm i.d. and 300 mm long) were prepacked with porous siliceous microbeads to which stationary phases of octadecylsilane or aminopropylsilane were chemically bonded[8].

Preparation of Budesonide Primary Standard—Budesonide was synthesized according to the method described previously (1, 3). Its purification was divided into seven steps.

The crude product was recrystallized three times from methanol–water (Steps 1–3). Since the repeated recrystallizations led to a significant change in the epimeric distribution, the product was partially resolved by chromatography on Sephadex LH-20, using chloroform as the eluent. Two fractions with different epimeric ratios were collected and evaporated to dryness, dissolved in methylene chloride, and precipitated with petroleum ether. Calculated amounts of the two precipitates were mixed to give budesonide with an epimeric ratio near 50:50 (Step 4). This

[1] Astra Syntex.
[2] Lark, Italy.
[3] A. Thalén, unpublished data.
[4] Model M 6000 solvent delivery system, Waters Associates.
[5] Model CV-6-UHPa-N60, Valco.
[6] Model M 440 UV detector, Waters Associates.
[7] Autolab System IV computing integrator, Spectra-Physics.
[8] μBondapak C_{18} and μBondapak NH_2, Waters Associates.

0022-3549/80/0700-0766$01.00/0
© 1980, American Pharmaceutical Association

Table I—Analytical Data of the Budesonide Primary Standard

Test for	Analytical Method	Content, %
Epimer A of budesonide	HPLC (reversed phase)	46.8
Epimer B of budesonide	HPLC (reversed phase)	53.0
Impurities	HPLC (reversed phase)	0.1
Impurities[a]	HPLC (normal phase)	0.1
Methylene chloride	GLC	<0.05
Petroleum ether	GLC	<0.02
Methanol	GLC	0.01
Water	Coulometric Karl Fischer titration	0.05

[a] The impurities obtained by normal-phase HPLC were identical to those detected by reversed-phase HPLC.

product was purified further by repeated recrystallizations from methanol–water (Step 5), ethanol–water (Step 6), and methanol–water (Step 7). A portion of the substance was dried *in vacuo* to constant weight and then was used for an assay of budesonide. The product was analyzed for foreign steroids and epimeric distribution by HPLC (System 2).

Analytical Procedures—*HPLC Conditions*—The mobile phase for reversed-phase chromatography (on μBondapak C_{18}) was ethanol–water in a 48:52 ratio (v/v) in the assay of budesonide (System 1) or in a 43:57 ratio (v/v) for determination of the epimer ratio and foreign steroids (System 2). Five microliters of the sample or of the standards was injected.

The mobile phase for normal-phase chromatography (on μBondapak NH_2) was heptane–ethanol (91:9 v/v). Five microliters of the samples dissolved in ethanol was injected.

HPLC Assay of Budesonide—For the assay of budesonide drug substance, samples of 14.00–16.00 mg were weighed into 25-ml volumetric flasks. The samples were dissolved and diluted to volume with a flucloronide internal standard solution. The latter was prepared by dissolving 35 mg of flucloronide in 100 ml of ethanol.

The samples were compared with a budesonide primary standard, from which solutions were prepared as for the samples.

Standard Addition Experiments—About 0.2 mg of each of the four impurities was weighed with a precision of 0.2% and dissolved together in 25.00 ml of ethanol. A second stock solution was prepared in the same way with 2 mg of the impurities. Aliquots of these solutions were transferred into flasks containing 14.00–16.00 mg of the budesonide primary standard substance. In this way, seven samples with known contents were prepared. They contained impurities in the range of 0.2–7.5%; *i.e.*, the budesonide content was 92.5–99.8%.

The samples were analyzed for their content of budesonide and impurities by reversed-phase HPLC.

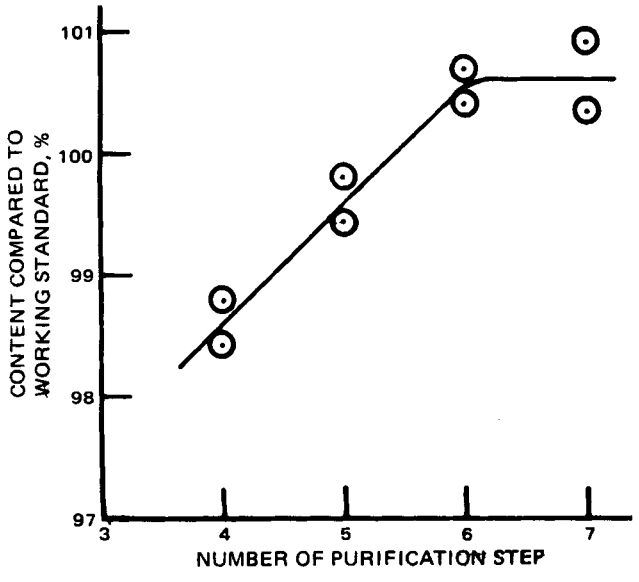

Figure 1—*Content* versus *number of purification step for preparation of budesonide primary standard. Purification step numbers correspond to the steps described in the text.*

Table II—Molar Absorptivities (254 nm), Absorbance (*A*) (1%, 1 cm) Values (254 nm), and Detector Response Factors for Epimers and Impurities of Budesonide

Compound	Molar Absorptivity	*A*	*A* (Relative)[a]	Response Factor (*R*)[b] Determined by HPLC
Budesonide primary standard	1.26×10^4	292	1.00	1.00
Epimer A of budesonide	1.26×10^4	292	1.00	0.99
Epimer B of budesonide	1.26×10^4	292	1.00	0.99
Impurity 1	1.26×10^4	334	1.14	1.14
Impurity 2	1.22×10^4	303	1.04	1.07
Impurity 3	1.21×10^4	282	0.97	—
Impurity 4	1.18×10^4	275	0.94	0.92

[a] Ratio of *A* (compound) to *A* (budesonide). [b] See text for definition.

Ethanolic solutions of Epimer A (0.103 mg/ml) and Epimer B (0.104 mg/ml) also were prepared. Aliquots of the two solutions were mixed to obtain samples with known epimeric distributions. These samples were used to evaluate the accuracy of the HPLC determination of the epimer distribution.

Detector Response Experiments—Four ethanolic solutions of budesonide were prepared. Each solution contained a known content of Impurity 1, 2, 3, or 4. Five microliters was injected in reversed-phase HPLC System 2. The peak areas of the impurity and of budesonide were determined for each sample. The relative detector response, *R*, was calculated according to:

$$R = \frac{\text{peak area of impurity}}{\text{concentration of impurity}} \times \frac{\text{concentration of budesonide}}{\text{peak area of budesonide}} \quad \text{(Eq. 1)}$$

From spectrophotometric measurements, absorbance (*A*) (1%, 1 cm) values and molar absorptivities were calculated for budesonide, Epimers A and B, and the four impurities.

Analysis of Solvent Residues—The water content of budesonide was analyzed by the coulometric Karl Fischer titration method (9). Organic solvent residues in budesonide originating from the synthesis were analyzed by GLC. The gas–liquid chromatograph[9] was equipped with a flame-ionization detector and a 1.5-m × 1.3-mm Porapak Q glass column. Nitrogen was the carrier gas at a flow rate of 20 ml/min. The injector temperature was 220°, and the oven temperature was 150°.

Two samples were prepared by dissolving 20.0–30.0 mg of budesonide bulk substance in 1.0 ml of absolute methanol and 1.0 ml of ethanol, respectively; 0.02% methanolic solutions of methylene chloride and petroleum ether and 0.02% ethanolic solutions of methanol were prepared and used as standards. One microliter of the samples and standards was injected. Solvent residues of >0.01% could be detected. Corrections for trace impurities in methanol and ethanol were made.

RESULTS AND DISCUSSION

Like other diastereoisomers, Epimers A and B of budesonide differ in solubility. This fact had to be considered in the preparation of the primary standard. During the recrystallizations (Steps 1–3), the ratio of Epimer A to B changed from about 50:50 to about 40:60. In purification Step 4, the epimeric distribution was adjusted back to 49.9:50.1. The final recrystallizations (Steps 5–7) resulted in 46.9% Epimer A and 53.1% Epimer B. The changes in epimeric distribution with the number of recrystallizations limit the purification procedure if the requirements for the epimer ratio in the drug substance specifications are to be fulfilled.

Figure 1 shows a plot of the budesonide content relative to a budesonide working standard *versus* the number of purification step. The content increased with purification to a constant value. The substance obtained in the ethanol–water recrystallization (Step 6) could not be purified further and, therefore, was defined as the primary standard. Reversed-phase HPLC with System 2 revealed a few traces of foreign steroids, and no further impurities were detected by normal-phase HPLC. Traces of methanol and water were detected by GLC and coulometric Karl Fischer titration, but no other chemicals used in purification could be traced. These results are summarized in Table I.

[9] Model 1400, Varian.

Table III—Recovery for Budesonide and Impurities in HPLC Analysis

Sample	Budesonide, %		Impurity 1, %		Impurity 2, %		Impurity 3, %		Impurity 4, %		Sum of Detected Impurities, %		Total Sum, %	
	Added	Found	Added	Found	Added	Found	Added	Found	Added	Found	Added	Found	Added	Found
1	99.78	99.89	0.06	0.05	0.05	0.05	0.05	0.04	0.05	—	0.16	0.14	99.99	100.05
2	99.60	100.06	0.11	0.10	0.11	0.10	0.10	0.07	0.10	—	0.32	0.27	100.02	100.33
3	99.18	99.45	0.21	0.20	0.21	0.19	0.20	0.17	0.20	—	0.62	0.56	100.00	100.01
Recovery, %				101.7		100.2		78.3		—		92.8		
SD				7.55		9.75		7.64		—		5.39		
4	99.01	99.07	0.25	0.25	0.23	0.21	0.26	0.26	0.25	—	0.74	0.72	100.00	99.79
5	97.93	98.26	0.53	0.51	0.48	0.45	0.54	0.55	0.52	0.52	2.07	2.03	100.00	100.29
6	96.03	96.50	1.02	0.96	0.92	0.85	1.04	1.08	0.98	0.89	3.96	3.78	99.99	100.28
7	92.42	92.70	1.95	1.86	1.77	1.62	1.98	2.04	1.88	1.78	7.58	7.30	100.00	100.00
Recovery, %				96.4		92.3		102.2		95.2		96.8		
SD				2.54		1.14		1.65		4.62		1.14		
Recovery, %		100.29												100.11
SD		0.162												0.197

Known detector response factors are necessary for a correct evaluation of foreign steroids and epimer distribution. Such factors are listed in Table II. They were used for all of the reported content determinations of the four impurities and the two epimers. These factors are close to one since the molar absorptivities of the impurities and of Epimers A and B are similar to that of budesonide. This result is due to the fact that the UV absorption originates from ring A in the steroid nucleus. This structure probably is common to each of the four impurities.

The HPLC assay for budesonide using System 1 was tested by a standard addition procedure (Table III). Known samples containing 92–100% of the budesonide primary standard were assayed with a mean recovery of 100.3% and a standard deviation of 0.16. In the same experiment, the four impurities were evaluated analytically (Table III). In the range of 0.05–0.2% of individual foreign steroids, recoveries of 78–102% were obtained. The corresponding standard deviations were 7.6–9.8. For samples with individual impurities between 0.2 and 2%, the recoveries were 92–102% with standard deviations of 1.1–4.6.

Even in the low impurity range (0.05–0.2%), quantification gives fairly good accuracy and precision. This result is possible since the detection limit, 0.005%, is below this range and since the chromatographic system works linearly and is stable down to the highest sensitivity, *i.e.*, 0.005 absorbance unit full scale. For Impurity 4, the analytical evaluation depends on its concentration; in the range of 0.05–0.25%, the impurity could not be separated chromatographically from the budesonide Epimer B. Therefore, the impurity peak is added to the budesonide peaks. This addition results in a slightly higher recovery for budesonide. However, if Impurity 4 has to be determined in the range of 0.05–0.25%, System 2 can be used since it results in larger retention times and, thus, in higher separation efficiency.

Mixtures with a known content of Epimers A and B were investigated with ethanol–water in ratios of 43:57 (v/v) (System 2) and 48:52 (v/v) (System 1) as the mobile phases. For the control of the epimer distribution of budesonide batches, System 2 was used since it was optimal with respect to the epimer separation. The effect of increasing the water content in the mobile phase to improve the epimer separation was due to increased retention and to an increase in the separation factor (7).

Figures 2 and 3 show chromatographic separations of the impurities and the epimers of budesonide using Systems 1 and 2. The resolution was improved significantly by increasing the mobile phase water content from 52 to 57%. This change in resolution had little effect on the quantification of the epimers. Although no baseline separation was obtained, System

Table IV—Recovery for Individual Epimers of Budesonide in HPLC Analysis

Sample	Percent of Epimer A in Standard Mixtures of Epimers A and B[a]		
	Added	Found[b]	Found[c]
1	62.41	62.16	62.41
2	55.46	55.30	55.72
3	49.90	49.62	49.95
4	44.34	44.20	44.58
5	37.50	37.56	37.75
Recovery, %		99.7	100.3
SD		0.27	0.29

[a] Since the standard mixtures contained only Epimers A and B, the percentage of Epimer B was obtained from 100% − % of Epimer A. [b] Mobile Phase System 1 was ethanol–water in a ratio of 48:52 (v/v). [c] Mobile Phase System 2 was ethanol–water in a ratio of 43:57 (v/v).

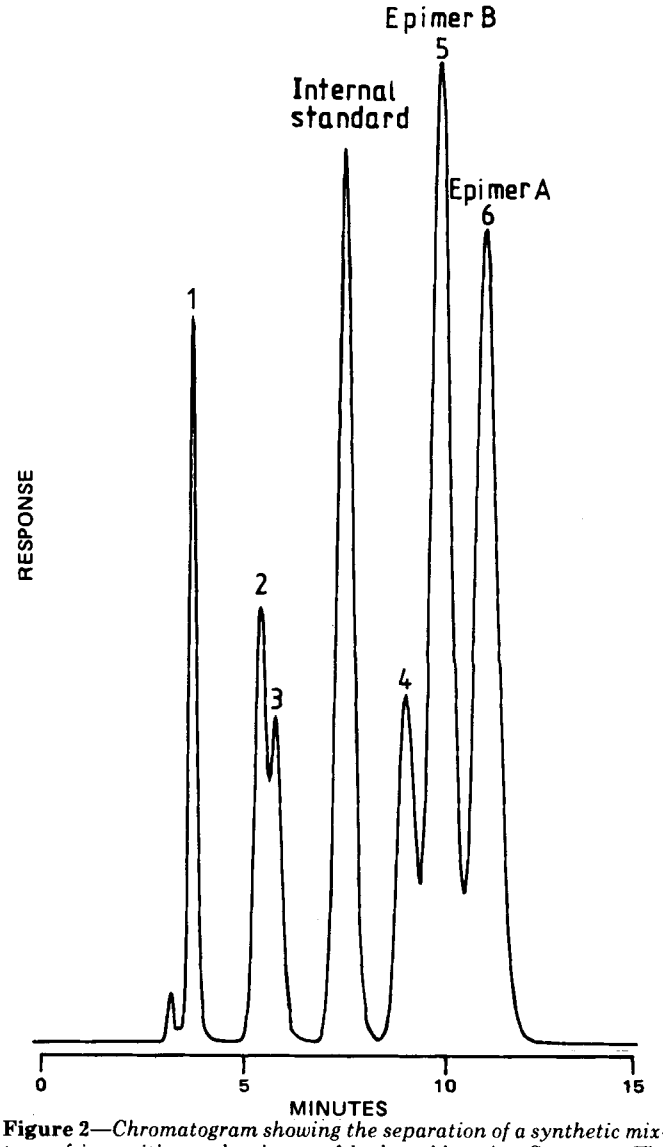

Figure 2—*Chromatogram showing the separation of a synthetic mixture of impurities and epimers of budesonide using System 1. The support was μBondapak C_{18}, the mobile phase was ethanol–water (48:52 v/v), and the flow rate was 1.0 ml/min. Key: 1, Impurity 1 (16α-hydroxyprednisolone); 2, Impurity 2 (homolog of budesonide; see text); 3, Impurity 3 (unknown); 4, Impurity 4 (unknown); 5, Epimer B of budesonide; and 6, Epimer A of budesonide.*

Table V—Analytical Data of Budesonide Batches

	Batch							
	372-40	2/76	22/77	23/77	24/77	33/77	34/77	35/77
Budesonide, %	97.6	98.6	99.2	98.7	98.6	98.5	98.4	98.7
Epimer A of budesonide, %	49.3	48.4	46.4	46.5	46.7	47.2	47.0	47.4
Impurities by HPLC (reversed phase), %	0.9	0.9	0.8	0.7	0.7	0.9	0.9	0.7
Impurities by HPLC (normal phase), %	0.0	0.1	0.4	0.4	0.3	0.4	0.3	0.3
Methylene chloride by GLC, %	0.6	0.0	0.0	—	—	—	—	—
Petroleum ether by GLC, %	0.1	0.0	0.0	—	—	—	—	—
Loss on drying, %	0.1	0.2	0.3	0.2	0.4	0.2	0.3	0.1
Total sum[a], %	99.3	99.8	100.7	100.0	100.0	100.0	99.9	99.8

[a] Mean of total sum is 99.9%. Standard deviation of total sum is 0.39.

1 gave similar accuracy in the epimer distribution determination to that of System 2 (Table IV). This result must be a consequence of the ideal behavior of the chromatographic system; *i.e.*, symmetrical peaks were obtained. As for the epimeric resolution, the separation of impurities was improved by changing from System 1 to System 2. Several tests showed that even the quantification of individual foreign steroids was not significantly affected by the differences in resolution.

The ratio between the peak area of budesonide and the peak area of the flucloronide internal standard was plotted *versus* the concentration of budesonide between 0 and 0.6 mg/ml. The result was a straight line with an intercept of 0.096, a slope of 6.01 ml/mg, and a correlation coefficient of 0.999989. The data indicate that the chromatographic system behaves properly and that the detector responds with high linearity. The use of an internal standard is necessary to minimize the injection error. Repeated injections gave a relative standard deviation of ~0.1% for the peak area ratio. Furthermore, the internal standard must not interfere with budesonide or impurity peaks. This condition is satisfied by flucloronide (Fig. 2).

In all budesonide batches analyzed, Impurities 1–4 represented ~75% of the total foreign steroids found by reversed-phase liquid chromatography. The remaining content (*i.e.*, traces of other impurities in budesonide) was quantified by calculation of the area under the chromatographic peaks since the detector response factors are unknown. The same procedure was used for traces of several nonpolar impurities, which could not be eluted by reversed-phase chromatography but were eluted and detected by normal-phase chromatography on μBondapak NH_2. In general, impurities that eluted before budesonide in the reversed-phase system eluted after the drug substance in the normal-phase system, as illustrated for the four impurities in Fig. 4. Figure 4 also shows the separation of the two epimers of Impurity 2, in contrast to the reversed-phase systems where they were not separated (Figs. 2 and 3).

Analytical results from eight small-scale production batches of budesonide (Table V) gave a mean for the sum of budesonide and impurities of 99.9% with a standard deviation of 0.39. This result suggests that the detector response factors are similar for budesonide and for all unknown impurities.

The results show that the necessary prerequisites for an accurate evaluation of budesonide substance by HPLC are fullfilled. The proposed analysis method is highly selective, linear, precise, and sensitive. Another advantage of the method is its high analytical capacity. The budesonide content, the impurity content, and the epimer distribution can be evaluated accurately by one chromatographic system. Comparison of retention times in sample and standard chromatograms may serve as an identity test for budesonide. The proposed HPLC method meets the main points in monographs for steroid substances and seems analytically superior to the usual procedures suggested in pharmacopeias.

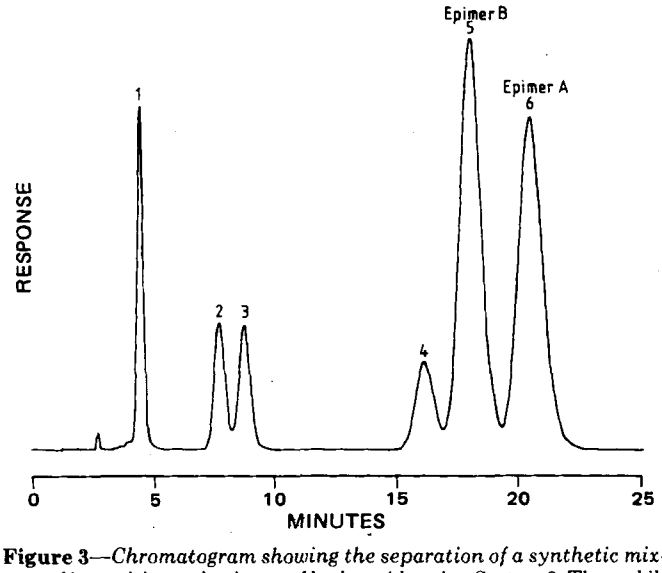

Figure 3—*Chromatogram showing the separation of a synthetic mixture of impurities and epimers of budesonide using System 2. The mobile phase was ethanol–water (43:57 v/v). The other conditions were the same as those described for Fig. 2.*

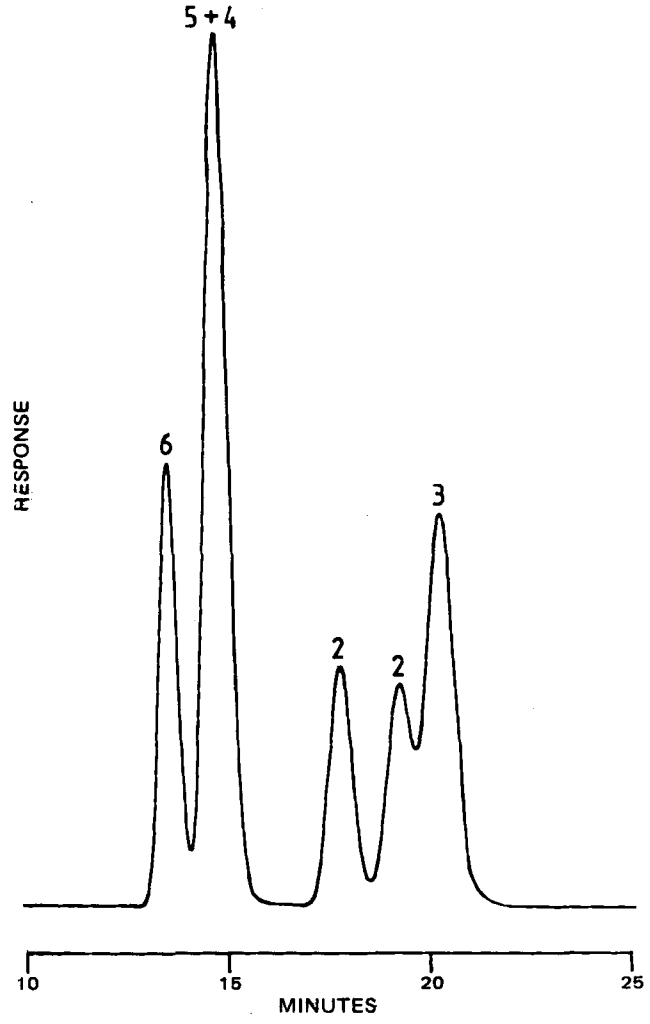

Figure 4—*Chromatogram showing the separation of a synthetic mixture of impurities and epimers of budesonide using a normal-phase system. The support was μBondapak NH_2, the mobile phase was heptane–ethanol (91:9 v/v), and the flow rate was 1.0 ml/min. The peak designations are the same as in Fig. 2. Impurity 2 (a mixture of two epimers; see text) appeared in this system as two peaks. Impurity 1 was not eluted.*

REFERENCES

(1) R. L. Brattsand, B. Thuresson af Ekenstam, K. G. Claesson, and A. Thalén, U.S. pat. 3,929,768 (1975).

(2) R. L. Brattsand, B. Thuresson af Ekenstam, K. G. Claesson, and A. Thalén, U.S. pat. 3,928,326 (1975).

(3) A. Thalén and R. L. Brattsand, *Arzneim.-Forsch.*, **29**, 1687 (1979).

(4) J. Albertsson, Å. Oskarsson, and C. Svensson, *Acta Crystallogr.*, **B34**, 3027 (1978).

(5) C. Svensson, PhD dissertation, University of Lund, Lund, Sweden, 1978.

(6) A. Wikby, A. Thalén, and G. Oresten, *J. Chromatogr.*, **157**, 65 (1978).

(7) A. Wikby, L. Nilsson, and G. Hällsås, *ibid.*, **157**, 51 (1978).

(8) "The United States Pharmacopeia," 19th rev., Mack Publishing Co., Easton, Pa., 1975.

(9) A. Cedergren, *Talanta*, **21**, 367 (1974).

ACKNOWLEDGMENTS

The authors thank Mr. Lars-Inge Wickström for technical assistance in the synthesis work.

Physical Model Evaluation of Topical Prodrug Delivery—Simultaneous Transport and Bioconversion of Vidarabine-5′-valerate III: Permeability Differences of Vidarabine and *n*-Pentanol in Components of Hairless Mouse Skin

CHENG DER YU *, WILLIAM I. HIGUCHI ˣ, NORMAN F. H. HO, JEFFREY L. FOX, and GORDON L. FLYNN

Received August 2, 1979, from the *College of Pharmacy, University of Michigan, Ann Arbor, MI 48109.* Accepted for publication December 13, 1979. *Present address: Syntex Research, Stanford Industrial Park, Palo Alto, CA 94304.

Abstract □ The permeation behavior of ^{3}H-vidarabine (^{3}H-9-β-D-arabinofuranosyladenine) and ^{14}C-*n*-pentanol through different strata of hairless mouse skin was studied using a diffusion cell at 37° under steady-state conditions. Partition coefficients for the skin components *versus* 0.9% aqueous NaCl solution also were obtained. Various skin preparations including full-thickness skin, cellophane-stripped skin, and dermis membranes of different thicknesses were employed. The dermis membranes were considered to be diffusionally homogeneous, and the product of the permeability coefficient and the thickness was taken as the apparent diffusivity. The apparent diffusivities for both compounds investigated were independent of thickness. Therefore, it was concluded that the molecular diffusivity is constant throughout the dermis. Comparisons of permeability coefficients in various strata of the skin revealed that, while the stratum corneum is the major diffusional barrier, the epidermis appears to be significantly less permeable than the dermis.

Keyphrases □ Vidarabine valerate prodrug—topical dosage forms, permeability differences through various mouse skin strata □ Prodrugs, topical—based on simultaneous transport and bioconversion of vidarabine, permeability differences in various components of mouse skin □ Diffusivity—vidarabine and *n*-pentanol, effect of skin strata and thickness on diffusivity □ Models, physical—based on simultaneous transport and bioconversion, effect of homogeneous distribution on prodrug evaluation

The basic experimental methods for determining key parameters and evaluating the transport and metabolism of a prodrug of vidarabine (9-β-D-arabinofuranosyladenine, I) in hairless mouse skin were discussed previously (1). Among the parameters needed for the mechanistic quantification of the problem are the transport parameters, the permeability coefficients, and the diffusivities in the various components of the skin. These parameters and the metabolizing enzyme constants, k_1 and k_2, permit a quantitative analysis of the prodrug delivery behavior in the skin.

The barrier nature of the various skin components is not fully understood. Several studies concerned the possible differences between the diffusional resistances of the epidermis and the dermis (2, 3). The purposes of this investigation were to study mechanistically the barrier nature of the various components of the hairless mouse skin using membrane preparations of different strata of the skin and to investigate the possible variations in the diffusivity with respect to position in the dermis component.

Studies were conducted on the permeabilities of I in various membrane preparations of the hairless mouse skin

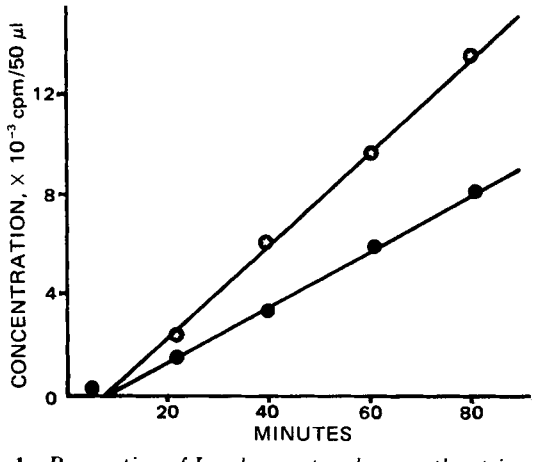

Figure 1—*Permeation of I and* n*-pentanol across the stripped skin. Key:* ●, ^{3}*H-2-I; and* ✪, ^{14}*C-*n*-pentanol. Both permeants were run concurrently, and the* Δ*C values were* 6.68×10^{5} *and* 2.55×10^{5} *cpm/50 µl for I and* n*-pentanol, respectively. The fluxes may be calculated according to flux = (slope) (volume/area), where the volume is 3.0 ml and the area is 1.767 cm^{2}.*

0022-3549/80/0700-0770$01.00/0

© 1980, American Pharmaceutical Association

REFERENCES

(1) R. L. Brattsand, B. Thuresson af Ekenstam, K. G. Claesson, and A. Thalén, U.S. pat. 3,929,768 (1975).

(2) R. L. Brattsand, B. Thuresson af Ekenstam, K. G. Claesson, and A. Thalén, U.S. pat. 3,928,326 (1975).

(3) A. Thalén and R. L. Brattsand, *Arzneim.-Forsch.*, **29**, 1687 (1979).

(4) J. Albertsson, Å. Oskarsson, and C. Svensson, *Acta Crystallogr.*, **B34**, 3027 (1978).

(5) C. Svensson, PhD dissertation, University of Lund, Lund, Sweden, 1978.

(6) A. Wikby, A. Thalén, and G. Oresten, *J. Chromatogr.*, **157**, 65 (1978).

(7) A. Wikby, L. Nilsson, and G. Hällsås, *ibid.*, **157**, 51 (1978).

(8) "The United States Pharmacopeia," 19th rev., Mack Publishing Co., Easton, Pa., 1975.

(9) A. Cedergren, *Talanta*, **21**, 367 (1974).

ACKNOWLEDGMENTS

The authors thank Mr. Lars-Inge Wickström for technical assistance in the synthesis work.

Physical Model Evaluation of Topical Prodrug Delivery—Simultaneous Transport and Bioconversion of Vidarabine-5′-valerate III: Permeability Differences of Vidarabine and *n*-Pentanol in Components of Hairless Mouse Skin

CHENG DER YU *, WILLIAM I. HIGUCHI ˣ, NORMAN F. H. HO, JEFFREY L. FOX, and GORDON L. FLYNN

Received August 2, 1979, from the *College of Pharmacy, University of Michigan, Ann Arbor, MI 48109.* Accepted for publication December 13, 1979. *Present address: Syntex Research, Stanford Industrial Park, Palo Alto, CA 94304.

Abstract □ The permeation behavior of ^{3}H-vidarabine (^{3}H-9-β-D-arabinofuranosyladenine) and ^{14}C-*n*-pentanol through different strata of hairless mouse skin was studied using a diffusion cell at 37° under steady-state conditions. Partition coefficients for the skin components *versus* 0.9% aqueous NaCl solution also were obtained. Various skin preparations including full-thickness skin, cellophane-stripped skin, and dermis membranes of different thicknesses were employed. The dermis membranes were considered to be diffusionally homogeneous, and the product of the permeability coefficient and the thickness was taken as the apparent diffusivity. The apparent diffusivities for both compounds investigated were independent of thickness. Therefore, it was concluded that the molecular diffusivity is constant throughout the dermis. Comparisons of permeability coefficients in various strata of the skin revealed that, while the stratum corneum is the major diffusional barrier, the epidermis appears to be significantly less permeable than the dermis.

Keyphrases □ Vidarabine valerate prodrug—topical dosage forms, permeability differences through various mouse skin strata □ Prodrugs, topical—based on simultaneous transport and bioconversion of vidarabine, permeability differences in various components of mouse skin □ Diffusivity—vidarabine and *n*-pentanol, effect of skin strata and thickness on diffusivity □ Models, physical—based on simultaneous transport and bioconversion, effect of homogeneous distribution on prodrug evaluation

The basic experimental methods for determining key parameters and evaluating the transport and metabolism of a prodrug of vidarabine (9-β-D-arabinofuranosyladenine, I) in hairless mouse skin were discussed previously (1). Among the parameters needed for the mechanistic quantification of the problem are the transport parameters, the permeability coefficients, and the diffusivities in the various components of the skin. These parameters and the metabolizing enzyme constants, k_1 and k_2, permit a quantitative analysis of the prodrug delivery behavior in the skin.

The barrier nature of the various skin components is not fully understood. Several studies concerned the possible differences between the diffusional resistances of the epidermis and the dermis (2, 3). The purposes of this investigation were to study mechanistically the barrier nature of the various components of the hairless mouse skin using membrane preparations of different strata of the skin and to investigate the possible variations in the diffusivity with respect to position in the dermis component.

Studies were conducted on the permeabilities of I in various membrane preparations of the hairless mouse skin

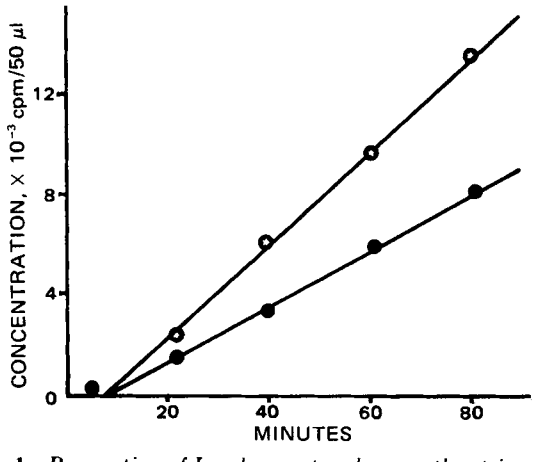

Figure 1—*Permeation of I and* n*-pentanol across the stripped skin. Key:* ●, ^{3}*H-2-I; and* ✪, ^{14}*C-*n*-pentanol. Both permeants were run concurrently, and the* Δ*C values were* 6.68×10^{5} *and* 2.55×10^{5} *cpm/50 µl for I and* n*-pentanol, respectively. The fluxes may be calculated according to flux = (slope) (volume/area), where the volume is 3.0 ml and the area is 1.767 cm^{2}.*

0022-3549/80/0700-0770$01.00/0

© 1980, American Pharmaceutical Association

Table I—Permeability Coefficients of I and *n*-Pentanol for Full-Thickness Skin

Mouse	Permeability Coefficients, × 10^8 cm/sec	
	I	*n*-Pentanol
A	1.87	—
B	2.33	—
C	2.96	—
D	4.76	331
E	—	315
—	—	408[a]

[a] From Ref. 2.

Table II—Permeability Coefficients of I and *n*-Pentanol for Stripped Skin

Mouse	Permeability Coefficients, × 10^6 cm/sec	
	I	*n*-Pentanol
F	2.12	22.6
G	4.72	19.8
H	4.37	17.4
—	—	40.1[a]

[a] From Ref. 3.

from which the permeability coefficients for the stratum corneum, the epidermis, and the dermis were calculated. Experiments with *n*-pentanol were included to determine any possible effects of molecular size.

EXPERIMENTAL

The experimental procedures for the permeation studies were described previously (1). The materials were the same as those used previously (1), except ^{14}C-*n*-pentanol[1] was diluted with saline to give a 1-μCi/μl solution. As described previously (1), full-thickness skin, cellophane[2]-stripped skin, and dermatome-planed dermis preparations were the membranes used.

RESULTS AND DISCUSSION

Figure 1 shows raw data obtained from a typical permeation experiment. The accumulation of I or *n*-pentanol in the receiver chamber increased linearly after a short lag time. The slopes gave the fluxes, F, for the permeants. The permeability coefficients, P, then were calculated from the slope and the concentration differential, ΔC, for each species from:

$$P = \frac{F}{\Delta C} = \frac{\left(\frac{V}{A}\right)\text{slope}}{\Delta C} \qquad \text{(Eq. 1)}$$

where V is the volume of the receiver solution and A is the diffusional area of the membrane. The permeability coefficients of I and *n*-pentanol for the full-thickness skin, stripped skin, and dermis membranes are shown in Tables I–IV. The apparent diffusivity[3], D, which is determined from the lag time, also is listed in Tables III and IV. Experimental reproducibility was satisfactory and consistent with previous experiments (1). Repeated permeation experiments showed an animal-to-animal variation of approximately a factor of two. Also, the stabilities of the various membrane preparations were satisfactory up to ~2–3 days.

Comparison of the permeability coefficients of I in the various membrane preparations (Table V) revealed that stripped skin was ~100 times more permeable than full-thickness skin, while the dermis was >1000 times more permeable. A similar relationship also existed for the permeation of *n*-pentanol, but the permeability differences were much smaller (Table V). This evidence suggests that, while the stratum corneum is the major diffusional barrier, the epidermis may be significantly less permeable than the dermis.

It was noted previously that the epidermis may be significantly less permeable than the dermis and that it may be a biopharmaceutically important barrier. Feldmann and Maibach (2) reported that both the stratum corneum and the Malpighian–basal layers serve as skin barriers for the penetration of hydrocortisone through normal human skin. The anatomy of the skin reveals a significant structural difference between the epidermis[4] and the dermis: the former consists of highly packed, well-aligned epithelial cells, whereas the latter is composed of cells loosely scattered throughout a gel-like interstitial matter. Therefore, epidermis may be less permeable than the dermis for some molecules having low overall skin permeabilities such as those that are simultaneously large and polar.

The diffusivities (both D_{app} and D) of I and *n*-pentanol were relatively constant with respect to position in the dermis membrane. The permeation data on the dermis membranes of different thicknesses (Tables III and IV) show a random scattering around a constant value when D_{app} is plotted *versus* the membrane thickness (Fig. 2).

Table VI presents the calculated permeability coefficients for the stratum corneum and the epidermis. The permeability coefficients for

Table III—Permeation Data for I with Dermis Membranes of Different Thicknesses

Mouse	h, μm	P, × 10^5 cm/sec	D_{app}[a], × 10^6 cm^2/sec	t_l, min	D[b], × 10^6 cm^2/sec
I	277	5.28	1.46	1.47	1.45
J	292	4.34	1.27	2.87	0.83
K	320	4.43	1.42	2.74	1.04
L	336	2.90	0.97	4.73	0.66
M	341	2.79	0.95	6.27	0.52
N	351	4.60	1.61	2.82	1.21
O	371	4.40	1.63	4.17	0.92
P	400	2.59	1.42	—	—
Average	—	—	1.34	—	0.95

[a] $D_{app} = P \times h$. [b] $D = h^2/6t_l$.

Table IV—Permeation Data for *n*-Pentanol with Dermis Membranes of Different Thicknesses

Mouse	h, μm	P, × 10^5 cm/sec	D_{app}[a], × 10^6 cm^2/sec	t_l, min	D[b], × 10^6 cm^2/sec
J	292	10.26	3.00	1.57	1.51
Q	312	6.61	2.06	3.61	0.75
L	336	6.92	2.33	2.86	1.10
N	351	8.91	3.13	2.21	1.55
Average	—	—	2.63	—	1.23

[a] $D_{app} = P \times h$. [b] $D = h^2/6t_l$.

Table V—Permeability Differences of I and *n*-Pentanol in Various Components of Hairless Mouse Skin

Membrane	Average Permeability Coefficients, cm/sec		Ratio[a]	
	I	*n*-Pentanol	I	*n*-Pentanol
Full-thickness skin	2.98×10^{-8}	3.23×10^{-6}	1.0	1.0
Stripped skin	3.74×10^{-6}	1.99×10^{-5}	125.5	6.2
Dermis[b]	3.83×10^{-5}	7.51×10^{-5}	1285.2	23.3

[a] The ratios were referred to a unity full-thickness permeability coefficient. [b] Average permeability coefficients in the dermis were calculated from $P = D_{app}/h$, with the assumption that the average thickness of the intact dermis is 350 μm.

Table VI—Permeability Coefficients of I and *n*-Pentanol in Various Components of Hairless Mouse Skin

Stratum	Permeability Coefficients, cm/sec	
	I	*n*-Pentanol
Stratum corneum[a]	3.00×10^{-8}	3.85×10^{-6}
Epidermis[b]	4.14×10^{-6}	2.71×10^{-5}
Dermis	3.83×10^{-5}	7.51×10^{-5}

[a] Calculated from the data in Table V using Eq. 2. [b] Calculated from the data in Table V using Eq. 3.

[1] California Bionuclear Co., Sun Valley, CA 91352.

[2] Scotch tape, Commercial Tape Division, 3M Corp., St. Paul, MN 55101.

[3] By definition, $D_{app} = P \times h$; therefore, it also can be related to D and the membrane–water partition coefficient, $K_{m/w}$, by $D_{app} = D \times K_{m/w}$ since $P = (D/h)K_{m/w}$.

[4] The epidermis includes the stratum granulosa and the basal layer, *i.e.*, the epidermal layer excluding the stratum corneum.

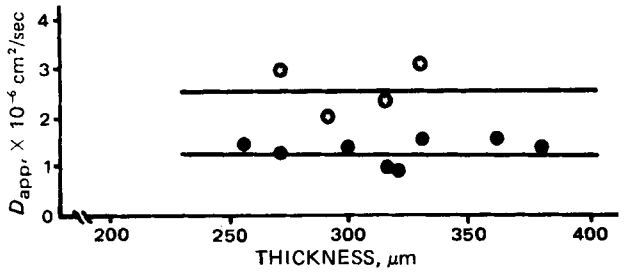

Figure 2—*Plot of the apparent diffusivities* versus *the thickness of the dermis. Key: see Fig. 1.*

the stratum corneum were calculated from the permeation data on whole skin and stripped skin from:

$$\frac{1}{P_{sc}} = \frac{1}{P_{ws}} - \frac{1}{P_{ss}} \qquad \text{(Eq. 2)}$$

where P_{sc}, P_{ws}, and P_{ss} are the permeability coefficients for the stratum corneum, the whole skin, and the stripped skin, respectively. Similarly, the permeability coefficients for the epidermis may be calculated from:

$$\frac{1}{P_e} = \frac{1}{P_{ss}} - \frac{1}{P_d} \qquad \text{(Eq. 3)}$$

where P_e and P_d are the permeability coefficients for the epidermis and dermis, respectively.

REFERENCES

(1) C. D. Yu, J. L. Fox, N. F. H. Ho, and W. I. Higuchi, *J. Pharm. Sci.*, **68**, 1347 (1979).

(2) R. J. Feldmann and H. I. Maibach, *Arch. Dermatol.*, **91**, 661 (1965).

(3) G. L. Flynn, H. H. Durrheim, and W. I. Higuchi, presented at the APhA Academy of Pharmaceutical Sciences, New York meeting, May 1977, Abstract 11.

ACKNOWLEDGMENTS

Abstracted in part from a thesis submitted by C. D. Yu to the University of Michigan in partial fulfillment of the Doctor of Philosophy degree requirements.

Supported by National Institutes of Health Research Grant AI14987 and Training Grant DE00204.

The authors thank Dr. D. C. Baker, University of Alabama, and Dr. A. J. Glazko and Dr. T. H. Haskell, Warner-Lambert/Parke-Davis, for supplying ^{3}H-labeled and nonlabeled vidarabine-5′-valerate ester.

Physical Model Evaluation of Topical Prodrug Delivery—Simultaneous Transport and Bioconversion of Vidarabine-5′-valerate IV: Distribution of Esterase and Deaminase Enzymes in Hairless Mouse Skin

CHENG DER YU *, JEFFREY L. FOX, WILLIAM I. HIGUCHI ˣ, and NORMAN F. H. HO

Received August 2, 1979, from the *College of Pharmacy, University of Michigan, Ann Arbor, MI 48109.* Accepted for publication December 13, 1979. *Present address: Syntex Research, Stanford Industrial Park, Palo Alto, CA 94304.

Abstract □ A semiquantitative assessment of esterase and deaminase distributions in hairless mouse skin was performed *in vitro*. The enzyme activities were quantified using ^{3}H-vidarabine and its 5′-valerate as the substrates. Full-thickness skin of the hairless mouse was cut into two halves, and each half was homogenized in pH 7.4 buffer. Both the supernate and the residue of the homogenate were assayed for esterase and deaminase activities. Results show that the outer half-thickness of the skin contained more esterase but slightly less deaminase than the other half. The characteristics of the esterase and the deaminase reactions also were studied employing the crude enzyme extract; these reactions were essentially irreversible. The deaminase reaction was in the linear region of Michaelis–Menten kinetics for substrate concentrations up to 4.5×10^{-5} *M*.

Keyphrases □ Vidarabine valerate prodrug—topical dosage forms, distribution of adenosine deaminase and esterase enzymes in various mouse skin strata □ Prodrugs, topical—simultaneous transport and bioconversion of vidarabine, distribution of adenosine deaminase and esterase enzymes in mouse skin, pharmacokinetics □ Enzyme distribution studies—location and nature of adenosine deaminase and esterase in mouse skin, pharmacokinetic parameters of deaminase and esterase □ Models, physical—based on simultaneous transport and metabolism, effect of nonhomogeneous distribution on prodrug evaluation

A physical model for the evaluation of a topical prodrug of vidarabine (9-β-D-arabinofuranosyladenine, I) was presented previously (1). The activity of the esterase that converts vidarabine-5′-valerate (III) to I and the activity of the deaminase that converts I to 9-β-D-arabinofuranosylhypoxanthine (II) were potentially capable of influencing the efficacy of the prodrug according to the model. For mathematical simplicity, the model assumed that the enzyme reactions were irreversible and within the linear range of Michaelis–Menten kinetics and that the distributions of both enzymes were homogeneous throughout the viable cutaneous tissue.

Subsequent experiments and data analysis using the model revealed some inconsistencies. Experiments conducted under two different boundary conditions yielded significantly different *in situ* enzyme rate constants. This result raised questions concerning the validity of the homogeneous enzyme distribution assumption employed in the calculations and the need for a more detailed study of the enzyme distribution in the membrane. Thus, the purpose of the present investigation was to study the distributions of the two enzymes in hairless mouse skin as well as the nature of the enzyme reactions.

EXPERIMENTAL

Materials—All materials used were described previously (2), except

0022-3549/80/0700-0772$01.00/0
© 1980, American Pharmaceutical Association

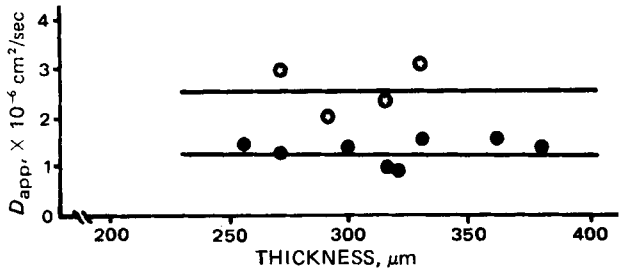

Figure 2—*Plot of the apparent diffusivities* versus *the thickness of the dermis. Key: see Fig. 1.*

the stratum corneum were calculated from the permeation data on whole skin and stripped skin from:

$$\frac{1}{P_{sc}} = \frac{1}{P_{ws}} - \frac{1}{P_{ss}} \qquad \text{(Eq. 2)}$$

where P_{sc}, P_{ws}, and P_{ss} are the permeability coefficients for the stratum corneum, the whole skin, and the stripped skin, respectively. Similarly, the permeability coefficients for the epidermis may be calculated from:

$$\frac{1}{P_e} = \frac{1}{P_{ss}} - \frac{1}{P_d} \qquad \text{(Eq. 3)}$$

where P_e and P_d are the permeability coefficients for the epidermis and dermis, respectively.

REFERENCES

(1) C. D. Yu, J. L. Fox, N. F. H. Ho, and W. I. Higuchi, *J. Pharm. Sci.*, **68**, 1347 (1979).

(2) R. J. Feldmann and H. I. Maibach, *Arch. Dermatol.*, **91**, 661 (1965).

(3) G. L. Flynn, H. H. Durrheim, and W. I. Higuchi, presented at the APhA Academy of Pharmaceutical Sciences, New York meeting, May 1977, Abstract 11.

ACKNOWLEDGMENTS

Abstracted in part from a thesis submitted by C. D. Yu to the University of Michigan in partial fulfillment of the Doctor of Philosophy degree requirements.

Supported by National Institutes of Health Research Grant AI14987 and Training Grant DE00204.

The authors thank Dr. D. C. Baker, University of Alabama, and Dr. A. J. Glazko and Dr. T. H. Haskell, Warner-Lambert/Parke-Davis, for supplying ^{3}H-labeled and nonlabeled vidarabine-5′-valerate ester.

Physical Model Evaluation of Topical Prodrug Delivery—Simultaneous Transport and Bioconversion of Vidarabine-5′-valerate IV: Distribution of Esterase and Deaminase Enzymes in Hairless Mouse Skin

CHENG DER YU *, JEFFREY L. FOX, WILLIAM I. HIGUCHI ˣ, and NORMAN F. H. HO

Received August 2, 1979, from the *College of Pharmacy, University of Michigan, Ann Arbor, MI 48109.* Accepted for publication December 13, 1979. *Present address: Syntex Research, Stanford Industrial Park, Palo Alto, CA 94304.

Abstract □ A semiquantitative assessment of esterase and deaminase distributions in hairless mouse skin was performed *in vitro*. The enzyme activities were quantified using ^{3}H-vidarabine and its 5′-valerate as the substrates. Full-thickness skin of the hairless mouse was cut into two halves, and each half was homogenized in pH 7.4 buffer. Both the supernate and the residue of the homogenate were assayed for esterase and deaminase activities. Results show that the outer half-thickness of the skin contained more esterase but slightly less deaminase than the other half. The characteristics of the esterase and the deaminase reactions also were studied employing the crude enzyme extract; these reactions were essentially irreversible. The deaminase reaction was in the linear region of Michaelis–Menten kinetics for substrate concentrations up to 4.5×10^{-5} *M*.

Keyphrases □ Vidarabine valerate prodrug—topical dosage forms, distribution of adenosine deaminase and esterase enzymes in various mouse skin strata □ Prodrugs, topical—simultaneous transport and bioconversion of vidarabine, distribution of adenosine deaminase and esterase enzymes in mouse skin, pharmacokinetics □ Enzyme distribution studies—location and nature of adenosine deaminase and esterase in mouse skin, pharmacokinetic parameters of deaminase and esterase □ Models, physical—based on simultaneous transport and metabolism, effect of nonhomogeneous distribution on prodrug evaluation

A physical model for the evaluation of a topical prodrug of vidarabine (9-β-D-arabinofuranosyladenine, I) was presented previously (1). The activity of the esterase that converts vidarabine-5′-valerate (III) to I and the activity of the deaminase that converts I to 9-β-D-arabinofuranosylhypoxanthine (II) were potentially capable of influencing the efficacy of the prodrug according to the model. For mathematical simplicity, the model assumed that the enzyme reactions were irreversible and within the linear range of Michaelis–Menten kinetics and that the distributions of both enzymes were homogeneous throughout the viable cutaneous tissue.

Subsequent experiments and data analysis using the model revealed some inconsistencies. Experiments conducted under two different boundary conditions yielded significantly different *in situ* enzyme rate constants. This result raised questions concerning the validity of the homogeneous enzyme distribution assumption employed in the calculations and the need for a more detailed study of the enzyme distribution in the membrane. Thus, the purpose of the present investigation was to study the distributions of the two enzymes in hairless mouse skin as well as the nature of the enzyme reactions.

EXPERIMENTAL

Materials—All materials used were described previously (2), except

0022-3549/80/0700-0772$01.00/0
© 1980, American Pharmaceutical Association

Table I—Distributions of the Esterase and the Deaminase in Hairless Mouse Skin [a]

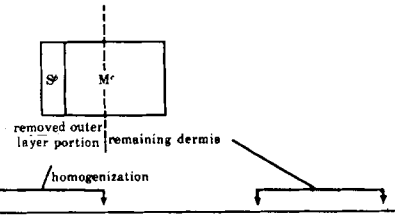

Enzyme	Extract	Residue	Extract	Residue
Deaminase	1.95×10^{-2}	0.10×10^{-2}	3.59×10^{-2}	0.18×10^{-2}
Esterase[d]	21.7×10^{-3}	7.93×10^{-3}	6.46×10^{-3}	0

[a] Values are in reciprocal seconds. [b] S is the stratum corneum. [c] M is the cutaneous tissue. [d] Raw data are shown in Figs. 1 and 2.

for a 0.01 *M* 4-(2-hydroxyethyl)-1-piperazineethanesulfonic acid[1] buffer solution (adjusted with 10 *N* NaOH to pH 7.4).

Enzyme Distribution Studies—Although extraction of enzymes from tissue homogenates may not reach 100%, useful data for comparing the relative enzyme content of tissue of the same mass may be obtained. Full-thickness skin may be planed into two halves, and each half may be extracted for its enzyme content. A comparison of enzyme activities in the extracts then may provide some measure of the relative enzyme distribution in the whole skin.

Hairless mice were sacrificed by snapping the neck. After sacrifice, the abdominal skin was planed with a dermatome[2] to remove a top layer (including the stratum corneum, the epidermis, and part of the dermis) about 150–200 μm thick. The remaining dermis then was excised from the animal. The two pieces, after weighing, were homogenized separately in a centrifuge-type tissue grinder[3] with 1 ml each of the buffer. The tissue grinder was immersed in an ice–water mixture during the grinding.

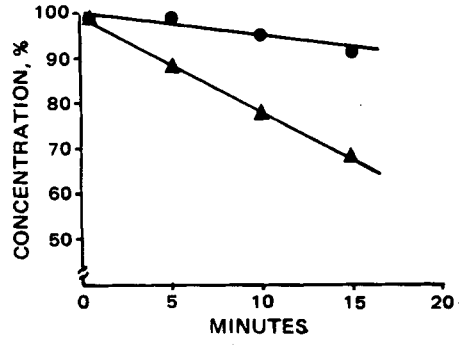

Figure 1—*Esterase activities in the supernates of the homogenates. Key: ●, supernate of the remaining dermis; and ▲, supernate of the dermatomed outer layer of the skin.*

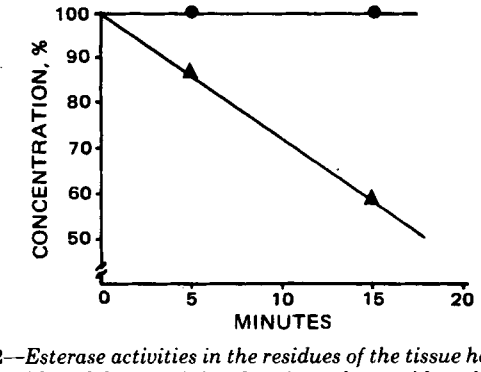

Figure 2—*Esterase activities in the residues of the tissue homogenate. Key: ●, residue of the remaining dermis; and ▲, residue of the dermatomed outer layer of the skin.*

[1] Calbiochem, San Diego, Calif.
[2] Castroviejo, a small electrical dermatome, Storz Instrument Co., St. Louis, MO 63110.
[3] Bellco Glass Inc., Vineland, NJ 08360.

Table II—Esterase and Deaminase Activities in Tissue Homogenate of Hairless Mouse Skin [a]

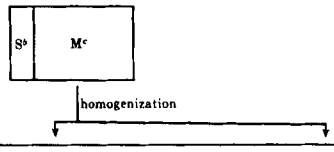

Enzyme	Extract	Residue
Deaminase	2.28×10^{-2}	0.15×10^{-2}
Esterase	5.78×10^{-3}	1.9×10^{-3}

[a] Values are in reciprocal seconds. [b] S is the stratum corneum. [c] M is the cutaneous tissue.

For each homogenate, the supernate was separated from the residue by centrifugation at 3000 rpm for 5 min. A 0.5-ml aliquot of the supernate then was divided into two aliquots. One aliquot was incubated with 5 μCi (specific activity of 41.7 μCi/μg) of ^{3}H-2-I and the other with ^{3}H-2-III at 37°. The residues were redispersed in 1 ml of buffer after washing several times by redispersion and centrifugation. The redispersed residues were divided into aliquots and incubated with ^{3}H-2-I and ^{3}H-2-III, as were the supernates. Samples were analyzed by TLC and scintillation counting as described previously (2). The initial rates were obtained from the substrate concentration–time curve.

Studies of Irreversible Nature of Enzyme Reactions—Two methods were employed to study the irreversibility of the esterase and deaminase enzyme reactions. One method involved the crude extracts; the other was based on the in-and-out method with intact full-thickness skin. The procedure for the in-and-out experiments was described previously (2), and the homogenization procedure for obtaining the enzyme extracts was the same as that given under *Enzyme Distribution Studies*, except that full-thickness abdominal skin (0.334 g) was homogenized without dermatome planing.

Determination of Linear Region of Enzyme Reaction—The spectrophotometric assay of Kalckar (3–5) for adenosine deaminase was employed. The skin homogenate (1.6 g from three mice of the same age in 5 ml of buffer) was obtained as described. After centrifugation, 0.05 ml of the supernate was diluted to 20 ml with buffer. A different enzyme concentration was prepared by diluting 0.5 ml of the supernate to 40 ml with the buffer.

To determine the reaction rate for a given substrate concentration, 2 ml of one enzyme solution was transferred into a cell of which 50 μl then was replaced with the appropriate solution of I at zero time. The change in absorbance at 265 μm (ΔA_{265}) was measured with a spectrophotometer[4] for 1 hr at 5-min intervals. A background reading was taken before

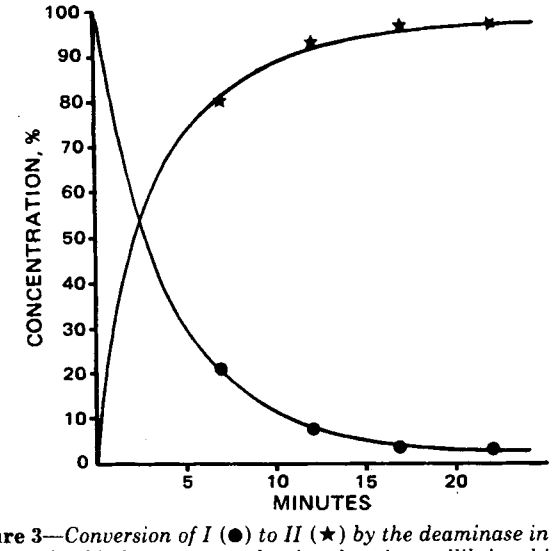

Figure 3—*Conversion of I (●) to II (★) by the deaminase in the supernate of a skin homogenate, showing that the equilibrium highly favors the formation of II.*

[4] Beckman DB, Beckman Instruments, Fullerton, Calif.

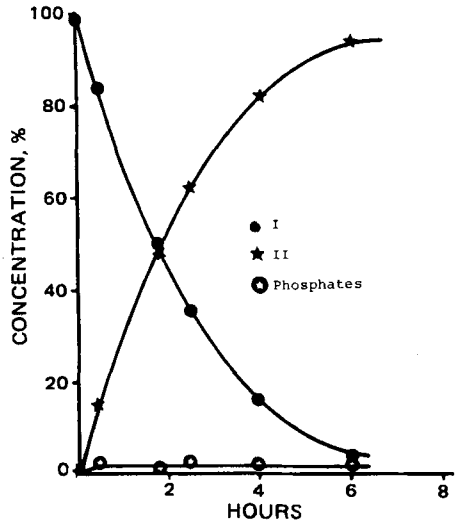

Figure 4—*Deamination of I by the deaminase in an in-and-out experiment, showing that the equilibrium highly favors the formation of II. Corresponding nucleotides formed from I and II are assayed as total phosphates.*

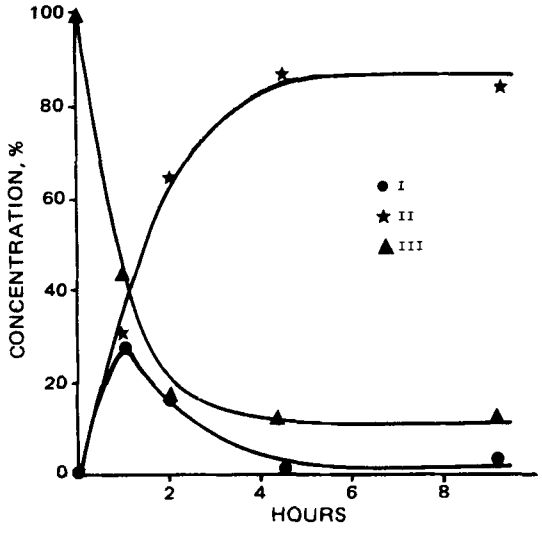

Figure 5—*Bioconversions of III to I and further to II by the esterase and the deaminase in an in-and-out experiment, showing that the equilibria highly favor formation of the products.*

introduction of the substrate, and the zero-time reading was taken 20 sec after the substrate was mixed well with enzyme solution in the cell.

RESULTS AND DISCUSSION

Esterase and Deaminase Distributions in Hairless Mouse Skin—Figures 1 and 2 show the esterase activities in the supernate and the residues of the homogenates prepared from the outer layer of skin and from the remaining dermis. The initial rates of the esterase and deaminase reactions obtained from these substrate concentration–time curves are tabulated in Table I. The esterase activity was much higher in the outer layer half than in the other half of the skin, whereas the deaminase distribution was in the reverse order but with less difference between the two halves. Table II shows the results of similar studies with a whole skin sample. These results have significant consequences in the physical model analysis of the transport and metabolism problem.

Because of the nonhomogeneous distribution of these enzymes, the analytical solutions describing the simultaneous diffusion and metabolism (1) based on the homogeneous enzyme distribution assumption may serve only as a first approximation in the evaluation of a prodrug. A more rigorous analysis that considers the effects of nonhomogeneous enzyme distributions may be carried out with a numerical computational procedure. A computer program for handling any possible enzyme distri-

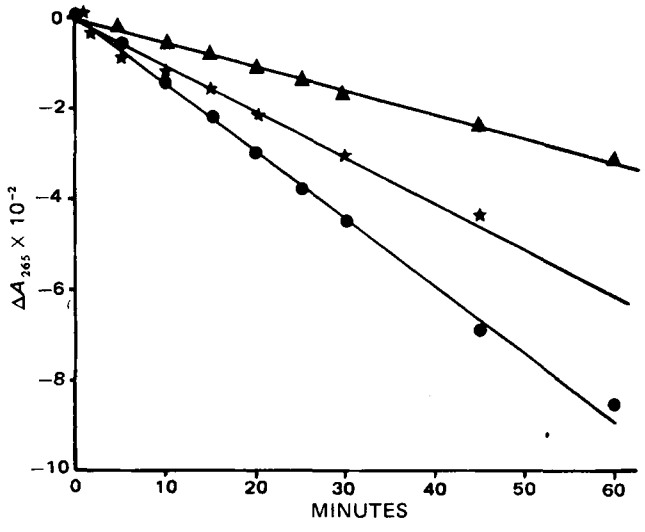

Figure 6—*Time curves showing the decrease in absorbance (ΔA_{265}) resulting from incubation of various concentrations of I with a crude extract of skin deaminase. Key: ▲, 3.1 μg/ml; ★, 6.5 μg/ml; and ●, 12.0 μg/ml.*

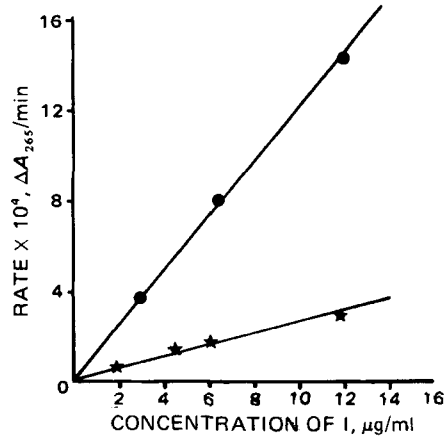

Figure 7—*Linear range of the deaminase activity, showing that the first-order enzyme kinetics hold up to a substrate concentration of 12 μg/ml (or 4.5 × 10^{-5} M). Key: ●, high enzyme concentration; and ★, low enzyme concentration.*

bution was developed by Fox *et al.* (6), and the rigorous evaluation of III as a potential prodrug using this approach will be presented later.

Irreversibility of Enzyme Reactions—Figure 3 shows the conversion of I to II by the deaminase in the supernate of a skin homogenate. The reaction is essentially complete in 20 min. Thus, the reaction is essentially irreversible from a practical standpoint. Similar results were obtained for the deaminase reaction in the intact skin with the in-and-out experiment. Figure 4 shows that the conversion of I to II by the deaminase in the intact skin experiment was almost complete in 6 hr. In the in-and-out experiment involving an intact skin incubated with ^{3}H-2-III, a typical A → B → C reaction pattern was observed (Fig. 5).

Linear Region of Michaelis–Menten Kinetics for Deaminase Reaction—Figure 6 shows the ΔA_{265} *versus* time curve for three different concentrations of I incubated at room temperature with the enzyme solution. The initial rates obtained from the slopes were plotted *versus* the substrate concentration (Fig. 7). Results of similar experiments with a different enzyme concentration also were plotted (Fig. 7). The deaminase enzyme reaction was in the linear region of Michaelis–Menten kinetics for substrate concentrations up to 12 μg/ml or 4.5 × 10^{-5} *M* for I. This result is in good agreement with reported K_m values (7–9) for purified adenosine deaminase (using I as the substrate) obtained from calf intestine mucosa, which range from 7 to 14 × 10^{-5} *M*.

REFERENCES

(1) C. D. Yu, J. L. Fox, N. F. H. Ho, and W. I. Higuchi, *J. Pharm. Sci.*, **68**, 1341 (1979).

(2) *Ibid.*, **68**, 1347 (1979).
(3) H. M. Kalckar, *J. Biol. Chem.*, **167**, 429 (1947).
(4) *Ibid.*, **167**, 445 (1947).
(5) *Ibid.*, **167**, 461 (1947).
(6) J. L. Fox, C. D. Yu, W. I. Higuchi, and N. F. H. Ho, *Int. J. Pharm.*, **2**, 41 (1979).
(7) S. Frederiksen, *Arch. Biochem. Biophys.*, **113**, 383 (1966).
(8) R. A. Lipper, S. M. Machkovech, J. C. Drach, and W. I. Higuchi, *Mol. Pharmacol.*, **14**, 366 (1978).
(9) J. L. York and G. A. LePage, *Can. J. Biochem.*, **44**, 331 (1966).

ACKNOWLEDGMENTS

Abstracted in part from a thesis submitted by C. D. Yu to the University of Michigan in partial fulfillment of the Doctor of Philosophy degree requirements.

Supported by National Institutes of Health Research Grant AI14987 and Training Grant DE00204.

The authors thank Dr. D. C. Baker, University of Alabama, and Dr. A. J. Glazko and Dr. T. H. Haskell, Warner-Lambert/Parke-Davis, for supplying ^{3}H-labeled and nonlabeled vidarabine-5′-valerate ester.

Physical Model Evaluation of Topical Prodrug Delivery—Simultaneous Transport and Bioconversion of Vidarabine-5′-valerate V: Mechanistic Analysis of Influence of Nonhomogeneous Enzyme Distributions in Hairless Mouse Skin

CHENG DER YU *, NEAL A. GORDON, JEFFREY L. FOX, WILLIAM I. HIGUCHI ˣ, and NORMAN F. H. HO

Received August 2, 1979, from the *College of Pharmacy, University of Michigan, Ann Arbor, MI 48109.* Accepted for publication December 13, 1979. *Present address: Syntex Research, Stanford Industrial Park, Palo Alto, CA 94304.

Abstract □ The mathematical problem of simultaneous transport and metabolism in the case of nonuniform enzyme distributions in the skin was solved, and the solutions were used for analyzing experimental data. Experimental data were obtained from permeation experiments with ^{3}H-vidarabine and its 5′-valerate using cellophane tape-stripped hairless mouse skin. Results of the analyses revealed that the esterase activity was four to nine times higher in the epidermis than in the dermis, whereas the deaminase activity was about the same in the two strata. These results were in good agreement with independent experiments using tissue homogenates. The enzyme distributions and the previously reported diffusivities were employed in generating concentration profiles for the prodrug and the drug in the skin. These results may be used in predicting the possible therapeutic effect of the prodrug when it is topically applied.

Keyphrases □ Vidarabine valerate prodrug—topical dosage forms, physical models employing homogeneous and nonhomogeneous enzyme distributions, various mouse skin strata, mathematical analysis □ Prodrugs, topical—simultaneous transport and bioconversion of vidarabine valerate, effect of enzyme distribution and diffusivities on bioavailability, various mouse skin strata, mathematical analysis □ Models, physical—homogeneous and nonhomogeneous enzyme distributions, various mouse skin strata, vidarabine valerate prodrug, topical dosage forms, mathematical analysis

A physicochemical method was developed to determine the *in situ* enzyme rate constants in hairless mouse skin (1, 2). Because of the lack of specific information, preliminary analyses of the experimental data were conducted based on the assumptions of uniform enzyme distribution and constant membrane diffusivities for the substrate and metabolite. It was believed then that when appropriate data became available, a more comprehensive analysis should be conducted based on the possible nonuniform enzyme distributions and the possible variations in diffusivity with respect to position in the membrane.

Subsequent studies were conducted to assess the possible variations in diffusivities and enzyme rate constants. Permeability coefficients of vidarabine (9-β-D-arabinofuranosyladenine, I) in various components of hairless mouse skin were factored out, and the dermis permeability of I was found to be constant throughout the whole stratum (3). Experiments using tissue homogenates revealed (4) that the outer half-thickness of the skin (*i.e.*, the stratum corneum, the epidermis, and part of the dermis) contained more esterase but slightly less deaminase than the remainder of the skin. These data now form the basis for a more comprehensive analysis.

The purposes of the present study were to solve the mathematical problem involved in the simultaneous diffusion and metabolism in the case of the nonuniform enzyme distributions and to analyze the experimental data using these mathematical solutions. The enzyme distributions together with the diffusivities then were employed to generate concentration profiles for the prodrug and the drug in the skin from which the behavior, including the efficacy, of the prodrug may be predicted.

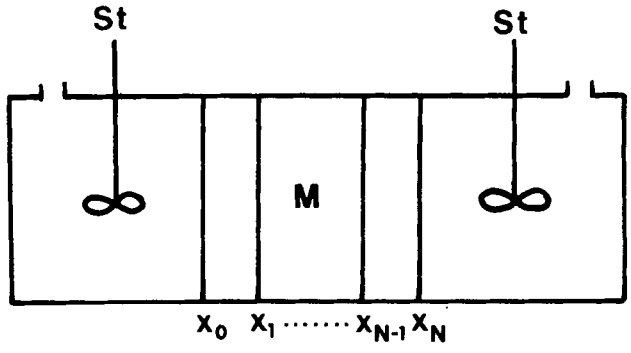

Figure 1—*Multilayer model for simultaneous diffusion and metabolism. Key: M, cutaneous membrane that consists of* N *layers; and St, stirrer.*

0022-3549/80/0700-0775$01.00/0
© 1980, American Pharmaceutical Association

(2) *Ibid.*, **68**, 1347 (1979).
(3) H. M. Kalckar, *J. Biol. Chem.*, **167**, 429 (1947).
(4) *Ibid.*, **167**, 445 (1947).
(5) *Ibid.*, **167**, 461 (1947).
(6) J. L. Fox, C. D. Yu, W. I. Higuchi, and N. F. H. Ho, *Int. J. Pharm.*, **2**, 41 (1979).
(7) S. Frederiksen, *Arch. Biochem. Biophys.*, **113**, 383 (1966).
(8) R. A. Lipper, S. M. Machkovech, J. C. Drach, and W. I. Higuchi, *Mol. Pharmacol.*, **14**, 366 (1978).
(9) J. L. York and G. A. LePage, *Can. J. Biochem.*, **44**, 331 (1966).

ACKNOWLEDGMENTS

Abstracted in part from a thesis submitted by C. D. Yu to the University of Michigan in partial fulfillment of the Doctor of Philosophy degree requirements.

Supported by National Institutes of Health Research Grant AI14987 and Training Grant DE00204.

The authors thank Dr. D. C. Baker, University of Alabama, and Dr. A. J. Glazko and Dr. T. H. Haskell, Warner-Lambert/Parke-Davis, for supplying ^{3}H-labeled and nonlabeled vidarabine-5′-valerate ester.

Physical Model Evaluation of Topical Prodrug Delivery—Simultaneous Transport and Bioconversion of Vidarabine-5′-valerate V: Mechanistic Analysis of Influence of Nonhomogeneous Enzyme Distributions in Hairless Mouse Skin

CHENG DER YU *, NEAL A. GORDON, JEFFREY L. FOX, WILLIAM I. HIGUCHI ˣ, and NORMAN F. H. HO

Received August 2, 1979, from the *College of Pharmacy, University of Michigan, Ann Arbor, MI 48109.* Accepted for publication December 13, 1979. *Present address: Syntex Research, Stanford Industrial Park, Palo Alto, CA 94304.

Abstract □ The mathematical problem of simultaneous transport and metabolism in the case of nonuniform enzyme distributions in the skin was solved, and the solutions were used for analyzing experimental data. Experimental data were obtained from permeation experiments with ^{3}H-vidarabine and its 5′-valerate using cellophane tape-stripped hairless mouse skin. Results of the analyses revealed that the esterase activity was four to nine times higher in the epidermis than in the dermis, whereas the deaminase activity was about the same in the two strata. These results were in good agreement with independent experiments using tissue homogenates. The enzyme distributions and the previously reported diffusivities were employed in generating concentration profiles for the prodrug and the drug in the skin. These results may be used in predicting the possible therapeutic effect of the prodrug when it is topically applied.

Keyphrases □ Vidarabine valerate prodrug—topical dosage forms, physical models employing homogeneous and nonhomogeneous enzyme distributions, various mouse skin strata, mathematical analysis □ Prodrugs, topical—simultaneous transport and bioconversion of vidarabine valerate, effect of enzyme distribution and diffusivities on bioavailability, various mouse skin strata, mathematical analysis □ Models, physical—homogeneous and nonhomogeneous enzyme distributions, various mouse skin strata, vidarabine valerate prodrug, topical dosage forms, mathematical analysis

A physicochemical method was developed to determine the *in situ* enzyme rate constants in hairless mouse skin (1, 2). Because of the lack of specific information, preliminary analyses of the experimental data were conducted based on the assumptions of uniform enzyme distribution and constant membrane diffusivities for the substrate and metabolite. It was believed then that when appropriate data became available, a more comprehensive analysis should be conducted based on the possible nonuniform enzyme distributions and the possible variations in diffusivity with respect to position in the membrane.

Subsequent studies were conducted to assess the possible variations in diffusivities and enzyme rate constants. Permeability coefficients of vidarabine (9-β-D-arabinofuranosyladenine, I) in various components of hairless mouse skin were factored out, and the dermis permeability of I was found to be constant throughout the whole stratum (3). Experiments using tissue homogenates revealed (4) that the outer half-thickness of the skin (*i.e.*, the stratum corneum, the epidermis, and part of the dermis) contained more esterase but slightly less deaminase than the remainder of the skin. These data now form the basis for a more comprehensive analysis.

The purposes of the present study were to solve the mathematical problem involved in the simultaneous diffusion and metabolism in the case of the nonuniform enzyme distributions and to analyze the experimental data using these mathematical solutions. The enzyme distributions together with the diffusivities then were employed to generate concentration profiles for the prodrug and the drug in the skin from which the behavior, including the efficacy, of the prodrug may be predicted.

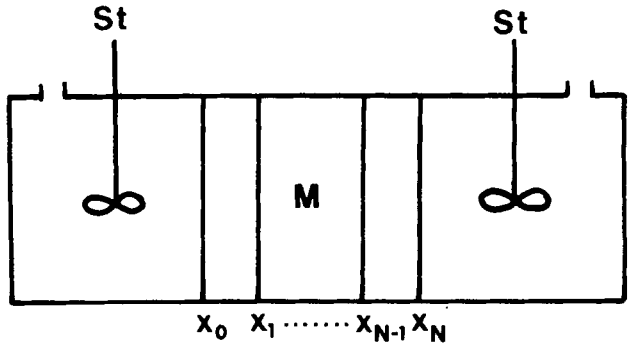

Figure 1—*Multilayer model for simultaneous diffusion and metabolism. Key: M, cutaneous membrane that consists of* N *layers; and St, stirrer.*

0022-3549/80/0700-0775$01.00/0
© 1980, American Pharmaceutical Association

Table I—Effect of Enzyme Leaching on Observed Fluxes in In-and-Out Experiments with III

Mouse	Pretreatment of Skin Preparation	Flux/Initial Donor Concentration, × 10^6 cm/sec
A	No pretreatment	57.17
B	No pretreatment	66.17
C	Soaking and rinsing for 80 min	29.33
D	Soaking and rinsing for 3 hr	33.67
E	Soaking and rinsing for 3 hr	29.50

Table II—Observed Fluxes in Go-Through Experiments with III Using a Stripped Skin [a]

Running Order[b]	Direction[c]	Flux/Initial Donor Concentration, × 10^6 cm/sec: Donor III	Donor I	Receiver III	Receiver I
Second	Dermis → epidermis	—	17.2	1.20	2.53
First	Epidermis → dermis	—	10.5	1.02	3.01

[a] From a 5-week-old mouse (F). [b] Indicates the first run or the second run with the given skin preparation. [c] Indicates the permeation direction, *i.e.*, from the donor side to the receiver side.

THEORY

General Multilayer Model for Analysis of Simultaneous Diffusion and Metabolism of a Compound—A physical model derived previously (Fig. 2 in Ref. 1) was modified to involve a membrane consisting of N layers (Fig. 1) in which the ith layer has the following properties:

1. Thickness is given by $h_i = x_i - x_{i-1}$.
2. A first-order reaction occurs in this layer, which converts A to B with a rate constant, k_i.
3. Diffusivities of A and B are given by $D_{A,i}$ and $D_{B,i}$.
4. Partition coefficients of A and B are $K_{A,i}$ and $K_{B,i}$.

For generality, aqueous diffusional layers will be considered in a manner similar to the other layers.

Mathematical Solution to Simultaneous Diffusion and Metabolism Problem of Multiple-Layer Model—The differential equations for the steady-state concentrations of A and B in the ith layer are:

$$D_{A,i}\frac{d^2[A]}{dx^2} - k_i[A] = 0 \qquad \text{(Eq. 1)}$$

$$D_{B,i}\frac{d^2[B]}{dx^2} + k_i[A] = 0 \qquad \text{(Eq. 2)}$$

Some new variables may be defined:

$$U_A(x) = \frac{[A]}{K_{A,i}} \qquad \text{(Eq. 3)}$$

$$U_B(x) = \frac{[B]}{K_{B,i}} \qquad \text{(Eq. 4)}$$

$$F_A(x) = -D_{A,i}\frac{d[A]}{dx} \qquad \text{(Eq. 5)}$$

$$F_B(x) = -D_{B,i}\frac{d[B]}{dx} \qquad \text{(Eq. 6)}$$

where $F_A(x)$ and $F_B(x)$ are the fluxes of A and B at x.

Some new constants may be defined:

$$a_i = \sqrt{\frac{k_i}{D_{A,i}}} \qquad \text{(Eq. 7)}$$

$$P_{A,i} = (K_{A,i})(D_{A,i}) \qquad \text{(Eq. 8)}$$

$$P_{B,i} = (K_{B,i})(D_{B,i}) \qquad \text{(Eq. 9)}$$

$$\Delta x = x_i - x_{i-1} \qquad \text{(Eq. 10)}$$

where $P_{A,i}$ and $P_{B,i}$ are the permeability coefficients of A and B, respectively.

The solution of the system in terms of these new variables in the ith layer can be written in matrix form as:

$$\begin{bmatrix} U_A(x) \\ F_A(x) \\ U_B(x) \\ F_B(x) \end{bmatrix} = \begin{bmatrix} \cosh a_i\,\Delta x & \frac{-\sinh a_i\,\Delta x}{P_{A,i}a_i} & 0 & 0 \\ -P_{A,i}a_i \sinh a_i\,\Delta x & \cosh a_i\,\Delta x & 0 & 0 \\ \frac{P_{A,i}}{P_{B,i}}(1-\cosh a_i\,\Delta x) & \frac{\sinh a_i x - a_i\,\Delta x}{P_{B,i}a_i} & 1 & \frac{-\Delta x}{P_{B,i}} \\ P_{A,i}a_i \sinh a_i\,\Delta x & 1-\cosh a_i\,\Delta x & 0 & 1 \end{bmatrix} \cdot \begin{bmatrix} U_A(x_{i-1}) \\ F_A(x_{i-1}) \\ U_B(x_{i-1}) \\ F_B(x_{i-1}) \end{bmatrix} \qquad \text{(Eq. 11)}$$

Table III—Observed Fluxes in Go-Through Experiments with III Using a Stripped Skin [a]

Running Order[b]	Direction[c]	Flux/Initial Donor Concentration, × 10^6 cm/sec: Donor III	Donor I	Receiver III	Receiver I
First	Dermis → epidermis	—	44.6	0.60	0.80
Second	Epidermis → dermis	—	2.59	1.01	1.06

[a] From a 5-week-old mouse (G). [b] Indicates the first run or the second run with the given skin preparation. [c] Indicates the permeation direction, *i.e.*, from the donor side to the receiver side.

Table IV—Observed Fluxes in Go-Through Experiments with III Using a Stripped Skin [a]

Running Order[b]	Direction[c]	Flux/Initial Donor Concentration, × 10^6 cm/sec: Donor III	Donor I	Receiver III	Receiver I
First	Dermis → epidermis	—	41.7	1.64	2.73
Second	Dermis → epidermis	—	18.9	1.82	2.43
Third	Epidermis → dermis	—	2.68	1.50	2.30

[a] From a 5-week-old mouse (H). [b] Indicates the sequence of the runs with the given skin preparation. [c] Indicates the permeation direction, *i.e.*, from the donor side to the receiver side.

Note that if $a_i = 0$, then:

$$-\frac{\sinh a_i\,\Delta x}{P_{A,i}a_i} = -\frac{\Delta x}{P_{A,i}} \qquad \text{(Eq. 12)}$$

and:

$$\frac{\sinh a_i\,\Delta x - a_i\,\Delta x}{P_{A,i}a_i} = 0 \qquad \text{(Eq. 13)}$$

Evaluation of the other terms is straightforward.

Since at $x = x_i$, $\Delta x = h_i$, by denoting the matrix evaluated for $\Delta x = h_i$ by M_i and $U_A(x_i)$ by $U_{A,i}$ and likewise for the other variables, the following is obtained:

$$\begin{bmatrix} U_{A,i} \\ F_{A,i} \\ U_{B,i} \\ F_{B,i} \end{bmatrix} = M_i \cdot \begin{bmatrix} U_{A,i-1} \\ F_{A,i-1} \\ U_{B,i-1} \\ F_{B,i-1} \end{bmatrix} \qquad \text{(Eq. 14)}$$

By applying this relationship repeatedly for $i = 1, \ldots, N$, it follows that:

$$\begin{bmatrix} U_{A,N} \\ F_{A,N} \\ U_{B,N} \\ F_{B,N} \end{bmatrix} = [M_N M_{N-1} \cdots M_2 M_1] \begin{bmatrix} U_{A,0} \\ F_{A,0} \\ U_{B,0} \\ F_{B,0} \end{bmatrix} \qquad \text{(Eq. 15)}$$

where the matrix, $M_N \cdots M_1$, can be shown to have the form:

$$m = \begin{bmatrix} m_{11} & m_{12} & 0 & 0 \\ m_{21} & m_{22} & 0 & 0 \\ m_{31} & m_{32} & m_{33} & m_{34} \\ m_{41} & m_{42} & m_{43} & m_{44} \end{bmatrix} \qquad \text{(Eq. 16)}$$

The solution now is straightforward. From the parameters for each layer, the matrixes, M_i, are evaluated and their product, m, is formed. This matrix then gives the relationship between the steady-state concentrations and fluxes at the two faces of the composite membrane. Determination of fluxes for the go-through and in-and-out experimental conditions is quite simple.

For the go-through experiment where $U_{A,0}$, $U_{A,N}$, $U_{B,0}$, and $U_{B,N}$ are given, it follows from Eqs. 15 and 16 that:

Table V—Least-Squares Fit of Calculated Fluxes to Experimental Data for Determination of Esterase Rate Constants in the Epidermis and the Dermis

		Experimentally Determined[a]	Homogeneous		Nonhomogeneous	
			Two Layer	Three Layer	Two Layer	Three Layer
Iteration parameters[b]						
k_{1e}, $\times 10^3$ sec^{-1}		—	3.35	3.39	9.02	9.27
k_{1d}, $\times 10^3$ sec^{-1}		—	3.35	3.39	1.09	1.06
D_{epi}, $\times 10^9$ cm^2/sec		—	4.55	4.15	4.23	4.40
P_{sc}, $\times 10^3$ cm/sec		—	—	1.28	—	1.80
(Flux/initial donor concentration), $\times 10^6$ cm/sec						
Dermis → epidermis	I (D)[c]	18.9	45.4	45.9	19.2	18.9
	I (R)[c]	2.43	2.43	2.18	2.38	2.36
	III (R)	1.82	1.82	1.70	1.62	1.65
Epidermis → dermis	I (D)	2.68	1.17	1.16	2.77	2.68
	I (R)	2.30	2.43	2.18	2.38	2.36
	III (R)	1.50	1.82	1.70	1.62	1.65
Reflection boundary experiment		19.4[d]	48.5	48.9	22.4	22.1
Σ dev.^{2}		—	2.24	2.23	0.03	0.03

[a] From Table IV. [b] The dermis diffusivity is 1.34×10^{-6} cm^2/sec; the thicknesses of the epidermis and the dermis are 10 and 190 μm, respectively; the aqueous permeability coefficient is 1.08×10^{-3} cm/sec; and the partition coefficient is 1.0. [c] D is the donor chamber and R is the receiver chamber. [d] Average value of the second and third runs from Fig. 2.

$$F_{A,0} = \frac{U_{A,N} - m_{11}U_{A,0}}{m_{12}} \quad \text{(Eq. 17)}$$

$$F_{A,N} = m_{21}U_{A,0} + m_{22}F_{A,0} \quad \text{(Eq. 18)}$$

$$F_{B,0} = \frac{U_{B,N} - m_{31}U_{A,0} - m_{32}F_{A,0} - m_{33}U_{B,0}}{m_{34}} \quad \text{(Eq. 19)}$$

$$F_{B,N} = m_{41}U_{A,0} + m_{42}F_{A,0} + m_{43}U_{B,0} + m_{44}F_{B,0} \quad \text{(Eq. 20)}$$

For the in-and-out experiment where $U_{A,0}$, $U_{B,0}$, $F_{A,N}$, and $F_{B,N}$ are given, it follows from Eqs. 15 and 16 that:

$$F_{A,0} = \frac{F_{A,N} - m_{21}U_{A,0}}{m_{22}} \quad \text{(Eq. 21)}$$

$$U_{A,N} = m_{11}U_{A,0} + m_{21}F_{A,0} \quad \text{(Eq. 22)}$$

$$F_{B,0} = \frac{F_{B,N} - m_{41}U_{A,0} - m_{42}F_{A,0} - m_{43}U_{B,0}}{m_{44}} \quad \text{(Eq. 23)}$$

$$U_{B,N} = m_{31}U_{A,0} + m_{32}F_{A,0} + m_{33}U_{B,0} + m_{34}F_{B,0} \quad \text{(Eq. 24)}$$

In both the go-through and in-and-out experiments, the boundary conditions require that several of the given quantities equal zero so that the equations are somewhat simpler. The matrixes, m, for the two situations are not identical because the go-through experiment has an aqueous diffusional layer on both sides as opposed to only one such layer for the in-and-out experiment.

EXPERIMENTAL

Stripped skin membranes were used for the go-through experiments, and full-thickness skin membranes were used for the in-and-out experiments. Procedures for preparing these skin specimens were described previously (2). The experimental arrangement and procedures for the go-through studies also were described previously (2). The materials were the same as those used previously. 2′-Deoxycoformycin (covidarabine) was used to inhibit the conversion of I to 9-β-D-arabinofuranosylhypoxanthine (II) by adenosine deaminase during the study of esterase activity.

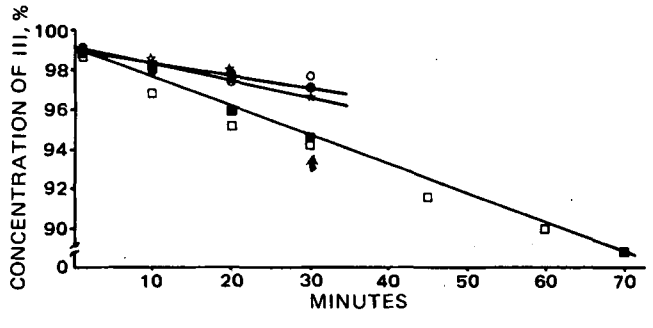

Figure 2—*Consecutive runs of the reflection boundary experiment with III using the same piece of full-thickness skin. The solid symbols are data from Mouse I; the open symbols are data from Mouse J. Lines are the linear regression of data of solid marks. Key:* ■, □, *the first run, which started immediately after preparation, where the arrow indicates the time when the bulk solution was separated from the skin;* ★, ☆, *the second run, which started 2 hr after the zero time of the first run; and* ●, ○, *the third run, which started 1 hr after the zero time of the second run. The system was soaked and rinsed thoroughly with saline between runs.*

RESULTS AND DISCUSSION

Since preliminary data (2) indicated that esterase leaches out from the dermis side of skin, it was desirable to determine if there is a steady level of remaining esterase activity. Therefore, consecutive runs of the reflection boundary experiment with vidarabine-5′-valerate (III) were carried out using a single piece of full-thickness skin (Fig. 2). After 2 hr of leaching, the remaining esterase activity reduced to about one-half of the activity of nonleached skin. An additional hour of leaching did not

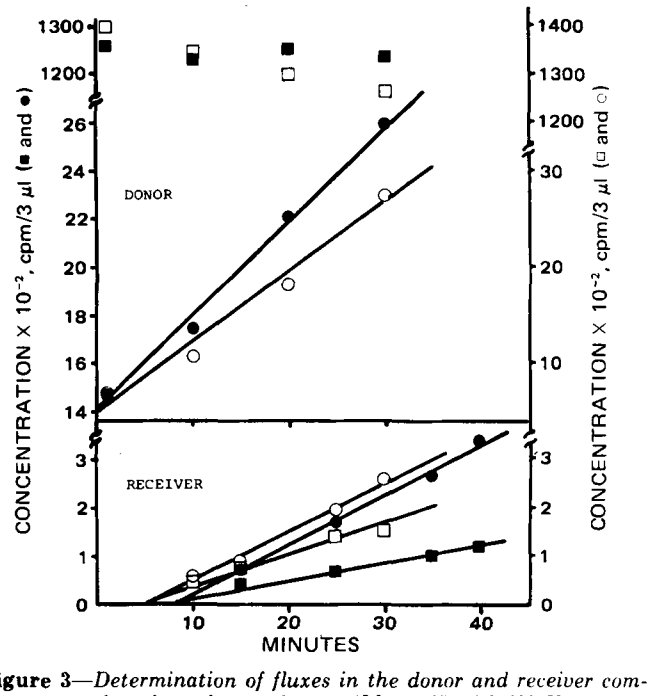

Figure 3—*Determination of fluxes in the donor and receiver compartments of go-through experiments (Mouse F) with III. Key:* ●, ○, *I; and* ■, □, *III. Flux = slope (volume per area), where volume = 1.5 ml and area = 0.713 cm^2. The solid symbols are data of the epidermis → dermis run; the open symbols are data of the dermis → epidermis run. The system was soaked and rinsed thoroughly with saline between runs. Lines are the linear regression of data points.*

Table VI—Least-Squares Fit of Calculated Fluxes to Experimental Data for Determination of Esterase Rate Constants in the Epidermis and the Dermis

		Experimentally Determined[a]	Homogeneous		Nonhomogeneous	
			Two Layer	Three Layer	Two Layer	Three Layer
Iteration parameters[b]						
k_{1e}, $\times 10^3$ sec^{-1}		—	2.07	2.07	3.57	3.56
k_{1d}, $\times 10^3$ sec^{-1}		—	2.07	2.07	1.06	1.11
D_{epi}, $\times 10^9$ cm^2/sec		—	2.36	2.22	2.37	2.36
P_{sc}, $\times 10^3$ cm/sec		—	—	3330	—	23.7
(Flux/initial donor concentration), $\times 10^6$ cm/sec						
Dermis → epidermis	I (D)[c]	21.2	31.6	31.8	18.3	19.0
	I (R)[c]	1.56	1.48	1.38	1.52	1.50
	III (R)	0.87	0.80	0.76	0.76	0.77
Epidermis → dermis	I (D)	1.41	0.68	0.68	1.12	1.11
	I (R)	1.66	1.48	1.38	1.52	1.50
	III (R)	0.49	0.80	0.76	0.76	0.77
Reflection boundary experiment		19.4[d]	33.2	33.2	19.9	20.6
Σ dev.^{2}		—	1.19	1.21	0.30	0.30

[a] Raw data are shown in Fig. 5. [b] The dermis diffusivity is 1.34×10^{-6} cm^2/sec; the thicknesses of the epidermis and the dermis are 10 and 190 μm, respectively; the aqueous permeability coefficient is 1.08×10^{-3} cm/sec; and the partition coefficient is 1.0. [c] D is the donor chamber and R is the receiver chamber. [d] Average value of the second and third runs from Fig. 2.

further reduce the remaining esterase activity. Moreover, as indicated in Fig. 2, the bulk solution after separation from the skin continued to show esterase activity. All of these observations strongly indicate that the leaching of esterase is essentially completed within the first 2 hr. The viability of the skin esterase essentially remains the same for at least 3 hr. Additional data from in-and-out experiments using skin preparations from different mice of the same age gave similar results (Table I).

The leaching effect also was clearly seen in the go-through experiment with nonleached stripped skin. Figure 3 shows the results of two go-through experimental runs carried out consecutively using a single stripped skin preparation (Mouse F). In the first run, the epidermis was in contact with the donor chamber; in the second run, after the system was rinsed thoroughly with saline, the donor and the receiver compartments were reversed so that the dermis side was in contact with the donor chamber. The fluxes[1] for these experiments are given in Table II. Similar experiments with reversed running order (*i.e.*, first run, dermis → epidermis; second run, epidermis → dermis) used stripped skin from another mouse (Mouse G) (Fig. 4 and Table III).

Comparison of Tables II and III reveals that the back-diffusion flux of I was larger when it was obtained from the first run than when it was obtained from the second run, especially for the dermis → epidermis case. The phenomenon was quite reproducible, as was observed in repeat experiments (5). To demonstrate the effect of leaching on the flux determination in a go-through experiment in another manner, a fresh piece of skin (Mouse H) was used for the go-through experiment, as usual, and then, after the system was rinsed thoroughly with saline, the same piece of skin was used for a repeat run (Table IV). Again, there was a twofold difference in the backflow fluxes before and after leaching.

Because of the profound effect of the esterase leaching on the determination of the fluxes, only experimental runs using a preleached skin may give meaningful data for esterase activity determination. Figures 5 and 6 show the results of duplicate runs with preleached skin preparations from the same mouse (Mouse K) conducted by two persons at the

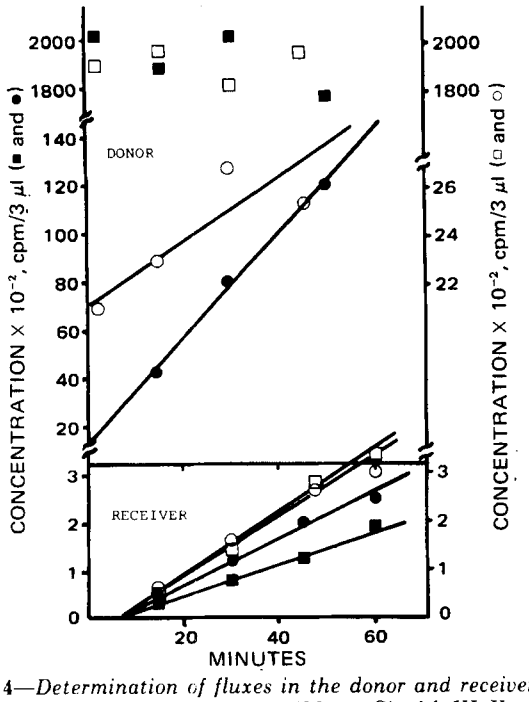

Figure 4—*Determination of fluxes in the donor and receiver compartments of go-through experiments (Mouse G) with III. Key: ●, ○, I; and ■, □, III. Flux = slope (volume per area), where volume = 1.5 ml and area = 0.713 cm^2. The solid symbols are data of the dermis → epidermis run; the open symbols are data of the epidermis → dermis run. The system was soaked and rinsed thoroughly with saline between runs. Lines are the linear regressions of data points.*

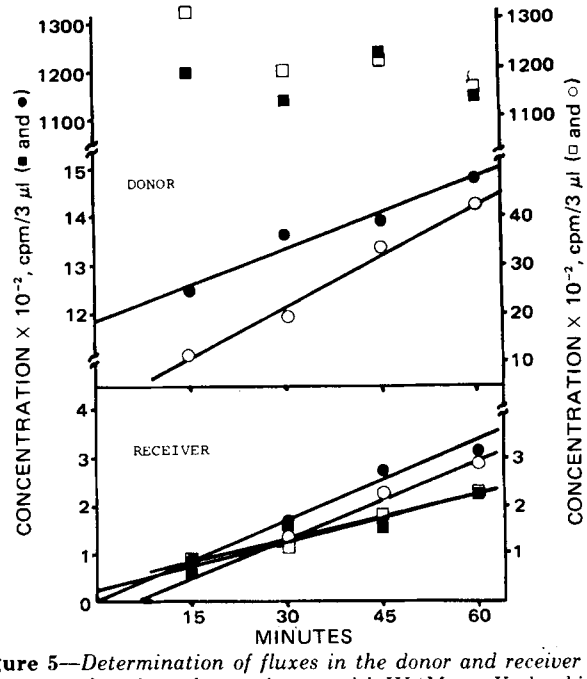

Figure 5—*Determination of fluxes in the donor and receiver compartments of go-through experiments with III (Mouse K; the skin was soaked and rinsed for 3 hr). Key: ■, □, III; and ●, ○, I. Flux = slope (volume per area), where volume = 1.5 ml and area = 0.713 cm^2. The solid symbols are data of the epidermis → dermis run; the open symbols are data of the dermis → epidermis run. The epidermis → dermis run preceded the dermis → epidermis run. The system was soaked and rinsed thoroughly between runs. Lines are the linear regressions of data points.*

[1] All fluxes discussed in this paper are normalized fluxes, *i.e.*, the ratios of fluxes to the initial donor concentration.

Table VII—Least-Squares Fit of Calculated Fluxes to Experimental Data for Determination of Esterase Rate Constants in the Epidermis and the Dermis

		Experimentally Determined[a]	Homogeneous		Nonhomogeneous	
			Two Layer	Three Layer	Two Layer	Three Layer
Iteration parameters[b]						
k_{1e}, $\times 10^3$ sec^{-1}		—	2.14	2.12	4.04	3.92
k_{1d}, $\times 10^3$ sec^{-1}		—	2.14	2.12	0.97	1.02
D_{epi}, $\times 10^9$ cm^2/sec		—	2.24	2.13	2.24	2.23
P_{sc}, $\times 10^3$ cm/sec		—	—	0.59	—	31.8
(Flux/initial donor concentration), $\times 10^6$ cm/sec						
Dermis → epidermis	I (D)[c]	21.2	32.7	32.5	17.0	17.8
	I (R)[c]	1.56[d]	1.37	1.30	1.39	1.39
	III (R)	0.87[d]	0.79	0.76	0.77	0.76
Epidermis → dermis	I (D)	1.90	0.70	0.68	1.24	1.20
	I (R)	1.60	1.37	1.30	1.39	1.39
	III (R)	0.38	0.79	0.76	0.77	0.76
Reflection boundary experiment		19.4[e]	34.2	33.9	18.6	19.3
Σ dev.^{2}		—	2.04	2.06	0.78	0.78

[a] Raw data are shown in Fig. 6. [b] The dermis diffusivity is 1.34×10^{-6} cm^2/sec; the thicknesses of the epidermis and the dermis are 10 and 190 μm, respectively; the aqueous permeability coefficient is 1.08×10^{-3} cm/sec; and the partition coefficient is 1.0. [c] D is the donor chamber and R is the receiver chamber. [d] From Table VI instead of Table VIII because of the unreasonably small permeability in that particular experimental run. [e] Average value of the second and third runs from Fig. 2.

same time. One person conducted experiments in which the epidermis → dermis permeation was run first (Fig. 5), and the other person ran the experiments with dermis → epidermis permeation first (Fig. 6).

The results of the go-through experiments with I using preleached skin (Mouse L) in the deaminase activity determination are shown in Fig. 7. Of the two experiments, the epidermis → dermis permeation preceded the dermis → epidermis permeation.

The following conclusions may be reached from the results using preleached skin:

1. The total fluxes as well as the flux ratio of the two species entering the receiver compartment are independent of direction (*i.e.*, from epidermis side to dermis side or from dermis side to epidermis side).
2. The backflow of metabolite into the donor compartment in the epidermis → dermis run is smaller than that in the reversed direction run.
3. The percentage rates of change in the donor concentrations of III are small. Consequently, these data were not used in the analysis.

Table V lists the results of computer iterations using Eqs. 17–20 to fit the calculated fluxes to the experimental data shown in Table IV. Nonlinear least-squares regression was employed for the best-fit procedure. The analyses were conducted for the nonhomogeneous case in which an epidermis layer was distinguishable from the dermis layer (from the standpoint of diffusivity and esterase activity), in contrast to the homogeneous case in which the two layers were different only in diffusivity and not in esterase activity. In addition to the two-layer model, a three-layer model, taking into account the possible presence of the residual stratum corneum due to incomplete stripping, also was considered.

Three adjustable parameters were involved in the fitting: the epidermis diffusivity, D_{epi}, and the esterase rate constants in the epidermis and the dermis, k_{1e} and k_{1d}, respectively. In the three-layer model, the residual (*i.e.*, if the skin was incompletely stripped) stratum corneum permeability, P_{sc}, is an additional adjustable parameter. The rest of the parameters required for the calculation of fluxes were predetermined experimentally, except for the thickness of the epidermis that was approximated anatomically to be 10 μm.

As seen in Table V, the best-fit iteration parameters under the nonhomogeneous column give calculated fluxes much closer to the experi-

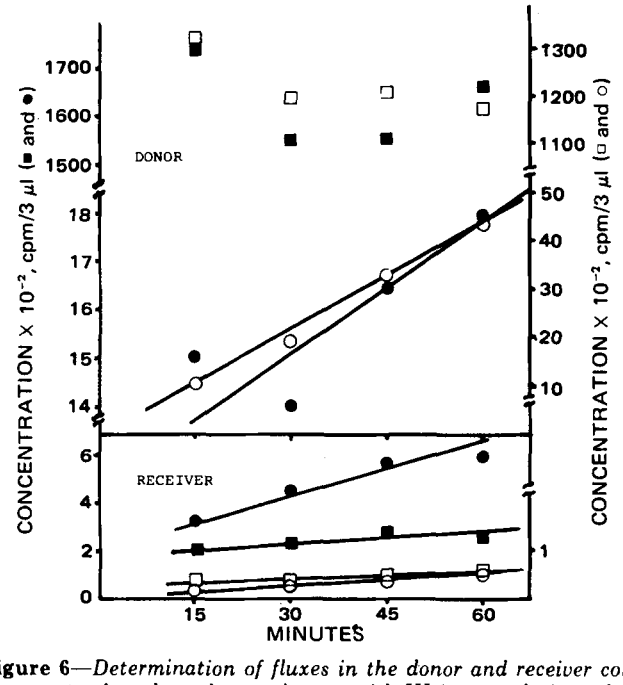

Figure 6—*Determination of fluxes in the donor and receiver compartments of go-through experiments with III (a second piece of abdominal skin from Mouse K; the skin was soaked and rinsed for 3 hr). Key: ■, □, III; and ●, ○, I. Flux = slope (volume per area), where volume = 1.5 ml and area = 0.713 cm². The solid symbols are data of the epidermis → dermis run; the open symbols are data of the dermis → epidermis run. The dermis → epidermis run preceded the epidermis → dermis run. The system was soaked and rinsed thoroughly between runs. Lines are the linear regressions of data points.*

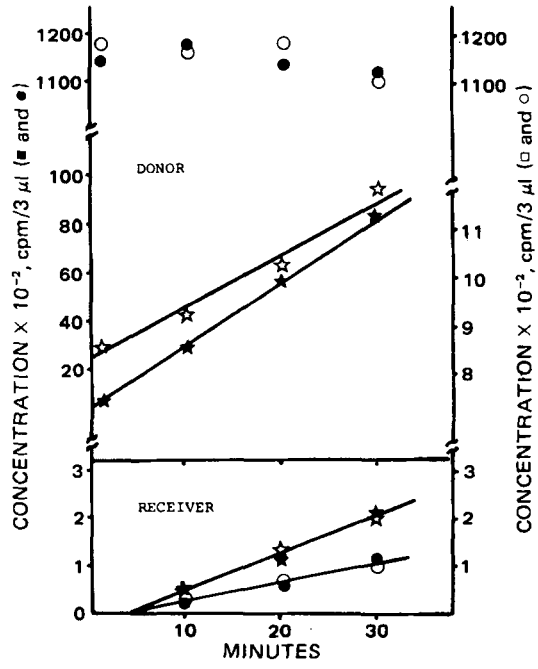

Figure 7—*Determination of fluxes in the donor and receiver compartments of go-through experiments (Mouse L) with I. Key: ★, ☆, II; and ●, ○, I. Flux = slope (volume per area), where volume = 1.5 ml and area = 0.713 cm². The solid symbols are data of the dermis → epidermis run; the open symbols are the data of the epidermis → dermis run. The system was soaked and rinsed thoroughly between runs. Lines are the linear regression of data points.*

Table VIII—Least-Squares Fit of Calculated Fluxes to Experimental Data for Determination of Deaminase Rate Constants in the Epidermis and the Dermis

		Experimentally Determined[a]	Homogeneous		Nonhomogeneous	
			Two Layer	Three Layer	Two Layer	Three Layer
Iteration parameters[b]						
k_{1e}, $\times 10^3$ sec^{-1}		—	7.14	—	7.14	—
k_{1d}, $\times 10^3$ sec^{-1}		—	7.14	—	7.14	—
D_{epi}, $\times 10^9$ cm^2/sec		—	3.00	—	3.00	—
P_{sc}, $\times 10^3$ cm/sec		—	—	—	—	—
(Flux/initial donor concentration), $\times 10^6$ cm/sec						
Dermis → epidermis	II (D)[c]	2.22	2.22	—	2.19	—
	I (R)[c]	1.10	1.13	—	1.12	—
	II (R)	2.30	2.40	—	2.40	—
Epidermis → dermis	II (D)	81.2	77.7	—	78.2	—
	I (R)	1.17	1.13	—	1.12	—
	II (R)	2.42	2.40	—	2.40	—
Reflection boundary experiment		114[d]	90.1	—	90.5	—
Σ dev.^{2}		—	1.16	—	1.17	—

[a] Raw data are shown in Fig. 7. [b] The dermis diffusivity is 1.34×10^{-6} cm^2/sec; the thicknesses of the epidermis and the dermis are 10 and 190 μm, respectively; the aqueous permeability coefficient is 1.08×10^{-3} cm/sec; and the partition coefficient is 1.0. [c] D is the donor chamber and R is the receiver chamber. [d] From Ref. 2.

mental values than do those under the homogeneous column. Thus, the nonhomogeneous model clearly is superior to the homogeneous model. The resultant esterase rate constants, k_{1e} and k_{1d}, reveal an esterase activity that is nine times higher in the epidermis than in the dermis. This result is in good agreement with the previous observation from tissue homogenates (4).

Table V also reveals that the best-fit parameters and calculated fluxes are only slightly different between the two-layer and the three-layer models for both the homogeneous and nonhomogeneous cases. The additional freedom for interaction contributes very little to the goodness of fit as seen from the statistics (Σ dev.^{2}). Moreover, the best-fit values of P_{sc} are on the order of 10^{-3} cm/sec, which is negligible compared to the overall permeability. In other words, the three-layer model essentially regresses to the two-layer model when applied to the present data. The effect of residual stratum corneum is negligible.

Similar analyses for the data shown in Figs. 5 and 6 are given in Tables VI and VII. These analyses lead to the same conclusion.

Results of the deaminase analyses are shown in Table VIII. The analysis based on nonhomogeneous deaminase distribution gave essentially the same results as those based on homogeneous deaminase distribution. The best-fit fluxes gave $k_{2e} = k_{2d} = 7.14 \times 10^{-3}$ sec^{-1}, which is in good agreement with previous observations (4).

The enzyme rate constants thus obtained, together with the transport parameters determined previously (3), give, according to the proposed physical model, the detailed description of concentration profiles of all three species in the viable cutaneous tissue. Figure 8 shows such plots generated from the computer simulation using $k_{1e} = 4.04 \times 10^{-3}$ sec^{-1}, $k_{1d} = 0.97 \times 10^{-3}$ sec^{-1}, $k_{2e} = k_{2d} = 7.14 \times 10^{-3}$ sec^{-1}, and the other required parameters as specified in the legend.

The bioavailability of the topically applied prodrug may be readily assessed quantitatively based on the concentration profiles. The area under the curve of the active parent drug species is ~25% of that of the prodrug species (Fig. 8) in the epidermis where the herpes virus is believed to proliferate. The somewhat low availability of the parent drug in this investigation is primarily due to the relatively slow conversion rate of the prodrug by the esterase. In a theoretical study reported previously (1), the parent drug was ~10 times more abundant than its prodrug when the esterase rate constant was nine times the value of the deaminase rate constant. A high esterase activity becomes a prerequisite in the search for promising prodrug candidates.

Recent studies (6) in this laboratory revealed that the esterase rate constant for the 5-monoesters of I with different chain lengths varies significantly in cultured KB cell suspension systems. The relative rate constants in that study were 22:3:1 for octanoate, valerate, and acetate, respectively. The chain length effect of these esters on the esterase activity of the hairless mouse skin is under investigation.

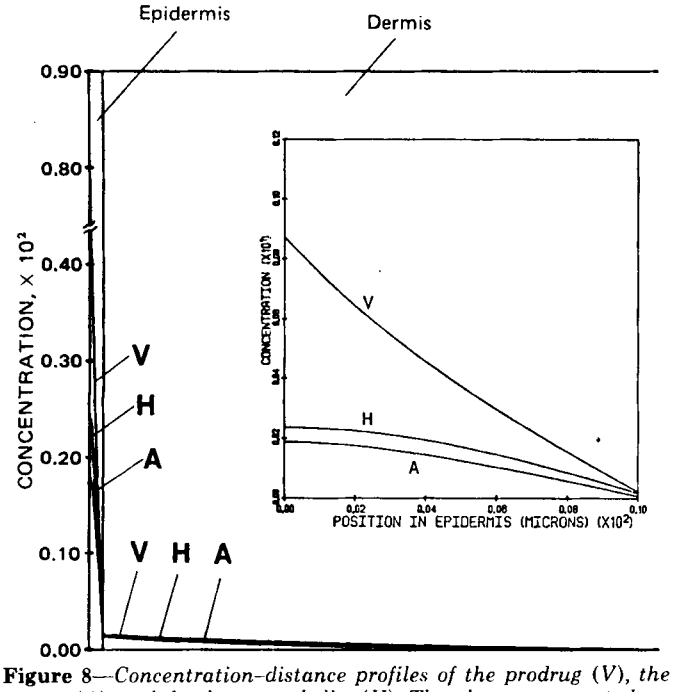

Figure 8—*Concentration-distance profiles of the prodrug (V), the parent (A), and the drug metabolite (H). The plot was generated according to the model using the following parameters: dose on the stratum corneum side of the skin was 1.0 M; diffusivities in the stratum corneum, the epidermis, and the dermis were 1.2×10^{-10}, 2.24×10^{-9}, and 1.34×10^{-6} cm^2/sec, respectively; and thicknesses of the stratum corneum, the epidermis, and the dermis were 40, 10, and 200 μm, respectively. The enzyme rate constants used were described in the text.*

REFERENCES

(1) C. D. Yu, J. L. Fox, N. F. H. Ho, and W. I. Higuchi, *J. Pharm. Sci.*, **68**, 1341 (1979).

(2) *Ibid.*, **68**, 1347 (1979).

(3) C. D. Yu, W. I. Higuchi, N. F. H. Ho, J. L. Fox, and G. L. Flynn, *J. Pharm. Sci.*, **69**, 770 (1980).

(4) C. D. Yu, J. L. Fox, W. I. Higuchi, and N. F. H. Ho, *ibid.*, **69**, 772 (1980).

(5) C. D. Yu, Ph.D. thesis, University of Michigan, Ann Arbor, Mich., 1978.

(6) S. M. Machkovech, W. I. Higuchi, R. A. Lipper, and J. C. Drach, presented at the APhA Academy of Pharmaceutical Sciences, Kansas City meeting, Nov. 1979, Abstract 107.

ACKNOWLEDGMENTS

Abstracted in part from a thesis submitted by C. D. Yu to the University of Michigan in partial fulfillment of the Doctor of Philosophy degree requirements.

Supported by National Institutes of Health Research Grant AI14987 and Training Grant DE00204.

The authors thank Dr. D. C. Baker, University of Alabama, and Dr. A. J. Glazko and Dr. T. H. Haskell, Warner-Lambert/Parke-Davis, for supplying ^{3}H-labeled and nonlabeled vidarabine-5′-valerate ester.

Permeation of Hairless Mouse Skin I: Experimental Methods and Comparison with Human Epidermal Permeation by Alkanols

HUGO DURRHEIM, GORDON L. FLYNN ˣ, WILLIAM I. HIGUCHI, and CHARAN R. BEHL

Received July 31, 1979, from the *College of Pharmacy, University of Michigan, Ann Arbor, MI 48109.* Accepted for publication February 1, 1980.

Abstract □ The permeation of intact hairless mouse skin by alkanols was studied. The method is described, and data for the quasi-steady-state and nonstationary-state aspects of mass transfer are given. Partitioning data also are presented. The permeability coefficients increased exponentially up to a carbon chain length of about eight (octanol). There was a marked temperature dependency ($E_a \simeq 19$ kcal for the series), and the partitioning was biphasic, increasing exponentially for alkanols larger than butanol. These data are compared with literature data on human skin tissues, and great similarity in all facets of behavior is noted.

Keyphrases □ Permeation—*n*-alkanols through intact hairless mouse skin and human skin, effect of temperature and carbon chain length, biphasic partitioning □ Partition coefficients—*n*-alkanols in intact hairless mouse skin and human skin, effect of temperature and carbon chain length, biphasic partitioning □ Alcohols, normal—permeability coefficients in hairless mouse skin and human skin, effect of temperature and carbon chain length, biphasic partitioning

The present studies were initiated to answer questions about the usefulness of the hairless mouse for developing clinically relevant insights into percutaneous absorption and for evaluating topical products intended for humans. Scattered reports allude to a barrier property similarity between hairless animal skins, particularly porcine and mouse, and the human integument. However, a high degree of sameness in permeability with respect to human skin has yet to be substantiated for any animal skin, although close parallelism in the permeation of select drugs between human and hairless mouse skin has been reported (1). More data are needed to generalize such unrelated observations into a broad conclusion.

A second, narrower basis for this work was the establishment of permeation baselines for the hairless mouse in preparation for the evaluation of the general consequences of burning and other traumatizing treatments on the permeation of skin tissue. Therefore, the present studies represent the development of analytical procedures suitable for studying mass transport through mechanically, chemically, and physically processed skins aimed at the quantitative definition of the effects of injury on percutaneous absorption. The permeation of select homologous *n*-alkanols (methanol through octanol) through intact hairless mouse skin is reported since these results can be compared with literature data on human epidermal permeation of the same compounds (2–6).

EXPERIMENTAL

Chemicals—The following homologous *n*-alkanols were used: [^{14}C]-methanol[1], [^{3}H]ethanol[1], [^{14}C]*n*-propanol[2], [^{3}H]*n*-butanol[1], [^{14}C]*n*-pentanol[2], [^{14}C]*n*-hexanol[1], [^{14}C]*n*-heptanol[2], [^{14}C]*n*-octanol[1], [^{14}C]*n*-nonanol[2], and [^{14}C]*n*-decanol[1].

The alkanols were diluted in 0.9% NaCl for irrigation[3], henceforth referred to as normal saline, and the actual permeation solutions were prepared from these stock solutions. The preparation of a stock solution was individualized to each alkanol since each compound was received with a different radioactivity. In every case, the stock solution was brought to ~50 μCi/ml. The alcohol concentrations were $\leq 10^{-4}$ *M*, precluding any direct effect of the alcohols on the membrane.

Diffusion—Small diffusion cells were machined from a polycarbonate plastic or were prepared from tempered glass in local shops. These cells were in the form of two cylindrical half-cells that had an inside diameter of ~1.0 cm and were ~2.5 cm deep, yielding a half-cell volume of ~1.5 ml. Each half-cell was equipped with two ports; one, ~2.5 cm long, was to accommodate the shaft of the stirring device; and the other, 1 cm long, was used for sampling and filling of the compartments. One half-cell contained a solid plastic or glass cylindrical extension of ~2.5 cm, which allowed it to be clamped rigidly in place in the constant-temperature bath. Each half-cell also was fitted with a flange at the open end to allow tight sealing of the membrane (Fig. 1*a*).

The cell halves were assembled, with the full-thickness, freshly excised, abdominal mouse skin between the half-cells, using a No. 18 ball-joint clamp (Fig. 1*b*). The assembled cell then was immersed in a constant-temperature bath, with the cell ports being the only components above the surface. The cell contents were stirred by motors mounted above the cell system[4]. The stirrers were small propellers placed in close proximity to the membrane surface. The stirring propeller was mounted on the end of the stirring shaft prior to clamping the half-cells since the propeller diameter was larger than the porthole. The stirrer shaft was attached to the motor by tightly fitting pieces of polymeric tubing. Care was taken to center the stirrer exactly in the cell to keep it from contact with the walls. The stirring speed of 150 rpm was checked after each assembly. By using a drop of dye solution, it was found that the mixing was gentle but adequate to distribute the color homogeneously in <2 min.

The diffusion cell was designed to have a large membrane surface area to half-cell volume ratio (~0.5) and also to have a small half-cell volume so that a minimal amount of radiolabeled compound was needed for each experiment. Construction materials were selected that had little tendency to adsorb the alkanol permeants but that also would allow viewing of the events inside the cell compartments. The cells were tested for tightness of the seal around the membranes, and no leakage was observed.

Membrane—The membranes were full-thickness skin taken from the abdominal surface of the hairless mouse, HRS/J strain[5]. Hairless mice (males), 4–6 weeks old, were sacrificed by snapping the spinal cord at the neck. A rectangular section of abdominal skin, several centimeters in each dimension (Fig. 2), was excised from the animal with surgical scissors. Since the skin was not firmly attached to the viscera, it was lifted easily from the animal after the incision was made. Adhering fat and other visceral debris were removed carefully from the undersurface with tweezers.

Prior to skin removal, a uniform circle was made on the abdomen marking the precise skin section to be positioned between the half-cells. After the excised skin was trimmed into an oversized, rough circle, it was mounted between the half-cells with the marked section centered. Stretching of the skin, as evidenced by distortion or expansion of the circular outline, was corrected, and the cell halves were held fast by a spring clamp. The dotted circular section in Fig. 2 indicates the area of skin used. The cell compartments then were filled with normal saline to keep the membrane moist. The areas available for diffusion between

[1] International Chemical and Nuclear Corp., Irvine, CA 92664.
[2] California Bionuclear Corp., Sun Valley, CA 91352.
[3] Abbott Laboratories, North Chicago, IL 60064.
[4] Model CA115V constant-speed motor (150 rpm), Hurst Manufacturing Co., Princeton, Ind.
[5] Jackson Laboratories, Bar Harbor, ME 04609.

0022-3549/80/0700-0781$01.00/0
© 1980, American Pharmaceutical Association

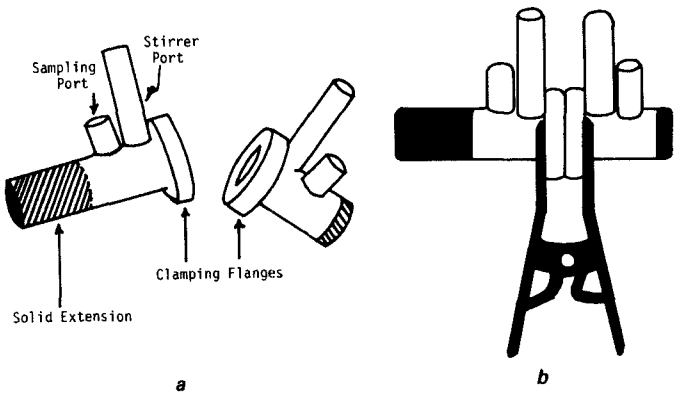

Figure 1—*Sketches of the unassembled and assembled diffusion cell showing the stirring ports, sampling ports, and other essential details.*

compartments were 0.713 cm^2 for the plastic cell and 1.094 cm^2 for the glass cell.

Permeation—The assembled saline-filled cell was immersed in a constant-temperature bath, the stirrer shafts were attached to the motor, and stirring was commenced. The contents were mixed for 30 min, at which time the compartments were evacuated with a syringe and refilled with fresh saline. Then the compartments were evacuated a second time, refilled, evacuated a third time, and finally refilled with normal saline preequilibrated to the experimental temperature. After mixing for 2 min, a sample of saline was withdrawn from the receptor compartment and counted to ensure that there was no residual activity from previous runs.

At this point, the donor compartment was charged with radioactive alkanol or alkanols (dual-absorption procedure), and the runs were commenced. Fifty microliters of concentrated solutions of the labeled alkanols in normal saline constituted the charge. The cell contents were stirred and, at predetermined times, samples were withdrawn from the respective compartments and transferred immediately using disposable Eppendorff[6] pipets to vials containing 10 ml of scintillation cocktail[7] for radiochemical assay[8].

In one set of experiments, aimed at determining the influence of pH on the permeation rate, isotonic buffers were used instead of normal saline (Table I). In the pH dependency experiments, the half-cells were rinsed with buffer in the final two rinses and filled with buffer prior to charging the donor compartment and initiating a run.

The moment of charging the donor half-cell marked the beginning of the diffusion run, and the receptor samples were referenced to this time. However, to allow for mixing to a uniform concentration, a minimum of 2 min was allowed to elapse before the initial donor sample was withdrawn. This sample was used as a close estimate of the initial donor cell concentration.

The overall procedure was designed such that depletion of the donor phase concentration was never an appreciable fraction of the donor concentration. There was no problem meeting this condition for water or the alkanols up to a chain length of seven. However, because partitioning from the aqueous medium into the lipoid phase of the tissue grows exponentially, a point is reached for longer chain length alkanols where the amount of alkanol retained in the membrane is a significant fraction of the total amount that has entered the membrane during the entire experiment. This problem is more acute when small donor and receiver volumes are involved, as is the case here, and a necessary condition for "stripping" the permeability coefficient from pseudo-steady-state slopes is violated.

The problem began with octanol in these studies, but the error induced was estimated not to be large enough to warrant discarding octanol results from the overall trend[9]. However, under the specified appropriate circumstances, the permeation enters a pseudo-steady state from which the permeability coefficient of each alkanol can be ascertained readily. If the concentration in the donor compartment changed significantly during the 2-hr run, as occurred for alkanols above a chain length of six, the donor compartment contents were replaced totally with fresh permeant solution periodically, as necessary, to maintain the concentration as essentially invariant.

Table I—Buffer Compositions [a]

Buffer Component	pH 3	pH 6	pH 8
$NaH_2PO_4 \cdot H_2O$	13.8 g	13.8 g	0.7 g
1.0 *N* HCl	11.7 ml	—	—
1.0 *N* NaOH	—	16.0 ml	—
NaCl	2.9 g	3.2 g	2.0 g
Na_2HPO_4	—	—	13.5 g

[a] All buffers were brought to a volume of 1000 ml with water.

In the initial experiments, the permeability of a membrane remained essentially unchanged for up to 12 hr using the lower molecular weight alkanols (*i.e.*, methanol and ethanol). Therefore, as many as four or five runs could be accomplished on a given piece of skin as long as the residual radioactive species from previous runs were fully washed out. Between runs on a given piece of skin, the cell volume was exchanged 12 times on each side with fresh saline. The skin, still mounted in the diffusion cell, was kept in contact with fresh saline for 45 min and then rinsed twice more with saline solution. The entire cleanup operation involved 14 rinses with an intermittent 45-min period of equilibration. The compartments then were refilled, the donor compartment was recharged, and a new run was commenced.

In subsequent extensive work (to be reported later), it was observed that invariant permeability as a function of the duration of skin immersion in the saline medium was strictly true only for water and the most polar alkanols, methanol and ethanol. For the higher homologs, there was up to a twofold change in the permeability coefficients over the initial 10 hr of skin hydration. Invariance was seen for all compounds after 10 hr of immersion. Partly because of the order of sequencing runs (lower alkanols preceding higher) and because of the small magnitude of change within compounds as compared to between compounds, these hydration-induced permeability alterations had no significant effect on the actual values or on the conclusions presented in this paper.

In the present studies, the permeation rates were assessed for selected *n*-alkanols through octanol at 20, 25, and 37°. The 20 and 25° data represent individual runs on each even-numbered alkanol. The 37° data represent averages of multiple runs for each alkanol on the uninterrupted homologous series from C_1 to C_8. The permeability data were plotted as counts (amount of permeant) collected in the receptor compartment as

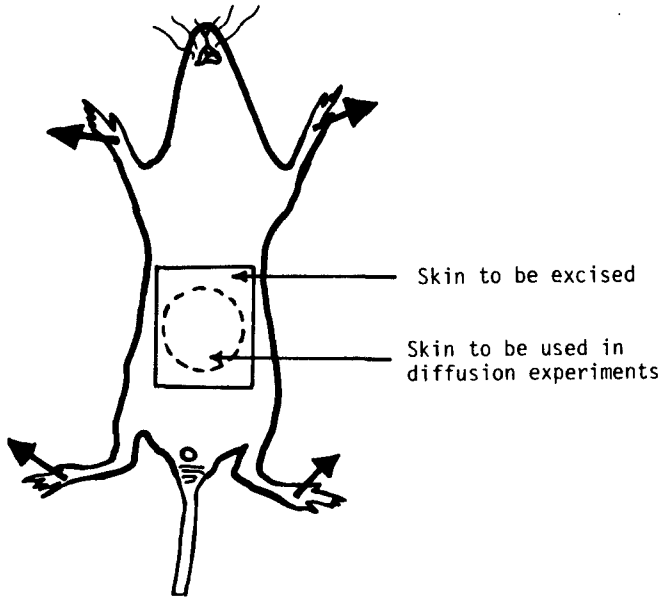

Figure 2—*Sketch of the hairless mouse indicating the exact section of skin excised for the diffusion cell studies.*

[6] Brinkmann Instruments, Westbury, NY 11590.
[7] Aquasol, New England Nuclear, Boston, MA 02118.
[8] Model LS 200 liquid scintillation counter, Beckman Instruments, Fullerton, Calif.
[9] Techniques were used to check the validity of this procedure and will be reported later. It was found that for octanol and above, the pseudo-steady-state procedure introduced an error, but this error was <15% with octanol, so these data are reported. The influence of membrane retention will be discussed quantitatively and theoretically in future reports.

Table II—Partitioning of the *n*-Alkanols into Full-Thickness Hairless Mouse Skin and Human Stratum Corneum

Alkanol	Partition Coefficient, cm^3/g: Hairless Mouse[a], 37°	Human Stratum Corneum[b], 25°
Methanol	5.5	0.6
Ethanol	5.4	0.9
n-Propanol	6.0	1.1
n-Butanol	6.6	2.5
n-Pentanol	7.7	5.0
n-Hexanol	10.7	10 0
n-Heptanol	24.0	30.0
n-Octanol	40.8	50.0
n-Nonanol	86.7	—

[a] Based on the weight of the full-thickness tissue and distribution from normal saline. [b] Obtained from Ref. 2. These data are for human stratum corneum and were obtained using dilute aqueous solutions rather than dilute saline solutions of the alkanols.

Table III—Permeability Coefficients of Full-Thickness Hairless Mouse Skin at 20, 25, and 37° and Human Epidermis at 25°

Alkanol	$P \times 10^3$, cm/hr: Hairless Mouse Skin 20°	37°	25°[a]	Human Epidermis[b], 25°[a]
Methanol	0.41	2.6 (0.46)[c]	0.93	0.5
Ethanol	0.72	4.8 (0.43)	1.23	0.8
n-Propanol	—	5.4	—	1.2
n-Butanol	2.9	14.6 (0.81)	4.4	2.5
Butanol, pH 3	—	10.23	—	—
Butanol, pH 6	—	10.66	—	—
Butanol, pH 8	—	11.75	—	—
n-Pentanol	—	22.0	—	6.0
n-Hexanol	5.25	48.0 (1.2)	8.6	13.0
n-Heptanol	—	92.9	—	32.0
n-Octanol	18.9	97.2 (2.4)	31.5	52.0
n-Nonanol	—	—	—	60.0
n-Decanol	—	—	—	80.0

[a] The 25° data were placed side by side for comparison. The hairless mouse permeation solutions were made in normal saline. [b] Obtained from Refs. 2 and 4. These data were obtained using dilute aqueous solutions. [c] Standard deviations of multiple runs.

a function of time. Correction was made for sampling, which was done by replacement using normal saline. The permeability coefficient for a given run was calculated from:

$$J_T = PA\,\Delta C \qquad \text{(Eq. 1)}$$

where J_T is the total flux and also the slope of plots of the amount penetrated *versus* time (counts per minute); P is the permeability coefficient (centimeters per hour); A is the diffusional area (square centimeters); and ΔC is the concentration differential across the membrane, which was taken to be equal to the donor phase concentration (counts per cubic centimeter).

The concentrations were expressed in terms of counts from a 50-μl sample. Thus, the permeability coefficient is calculated from:

$$P = \frac{J_T}{A\,\Delta C} \qquad \text{(Eq. 2)}$$

and since $J_T = dM/dt = V(dC/dt)$:

$$P = \frac{V\left(\frac{dC}{dt}\right)}{A\,\Delta C} \qquad \text{(Eq. 3)}$$

where V is the half-cell volume and the volume of the receptor compartment (cubic centimeters) and dC/dt is the steady-state slope in counts per minute per cubic centimeter. The computed permeability coefficients were converted to centimeters per hour by multiplying by 60.

Skin Partitioning—The skin–water partition coefficients of the alkanols also were assessed. These values were evaluated crudely by equilibrating the alkanol solutions with a known mass of skin, 20–50 mg, weighed immediately after removal from the animal. These skin pieces were immersed in 2 ml of normal saline containing the radiolabeled alkanol. The samples were equilibrated in a shaker bath at 37° overnight, which was sufficient to attain equilibrium.

Distribution of the alkanols between the aqueous phase of the tissue was estimated by the method of Scheuplein (2) as the difference between the initial aqueous phase concentration and the aqueous phase concentration at equilibrium. The relationship used was:

$$K = \frac{(C_0 - C_e)/W_T}{C_0/V_{aq}} \qquad \text{(Eq. 4)}$$

where C_0 is the initial alkanol solution concentration, C_e is the solution concentration at equilibrium, W_T is the tissue weight in grams, and V_{aq} is the solution phase volume (2 ml) in milliliters. Therefore, the partition coefficients are in cubic centimeters per gram. Given the obvious heterogeneity (multiphasic nature) of the tissue, no attempt was made to factor in density to obtain unitless values.

RESULTS

The data for the partitioning of the *n*-alkanols at 37° between full-thickness hairless mouse skin and saline are tabulated in Table II. The partition coefficients appeared to increase only slightly up to a chain length of five but then increased exponentially from pentanol to nonanol. The slope of the plot in the exponential growth region was ~0.285, corresponding to an increase in the partition coefficient by an average factor of 1.9 per chain unit (per methylene unit) past an alkyl chain length of five. Straightforward attempts to obtain a partition coefficient for decanol were unsuccessful since the small skin pieces absorbed essentially all of the C_{10} compound, making the estimate unreliable. The exponential trend was presumed to continue to C_{10}, and the experimental procedure was not adjusted to obtain a firm value for this compound.

Raw permeation profiles of the receptor phase concentration in moles per liter as a function of time for *n*-butanol are displayed in Fig. 3 for runs carried out at 20, 25, and 37°. Similar data were collected at 20 and 25° for select, mostly even homologs through *n*-octanol and at 37° for the uninterrupted homologous series from C_1 to C_8. Permeability coefficients were calculated from the terminal slopes of such plots, and lag times also were estimated graphically. The estimated permeability coefficients at each temperature are summarized in Table III, which also includes *n*-butanol data at 37° obtained using isotonic buffers at pH 3, 6, and 8.

An Arrhenius-like plot of the permeability coefficients is given in Fig. 4, where log P is plotted *versus* the reciprocal of temperature. In Fig. 5, the permeability data are plotted as log P *versus* alcohol chain length. Several significant trends are immediately evident from these data. There was a dramatic temperature dependency for the permeation process. Within the accuracy of the data, the apparent activation energy did not appear to vary among the homologs and was ~19 kcal/mole based on the slopes of statistically fitted lines through the data in Fig. 4. In both Figs.

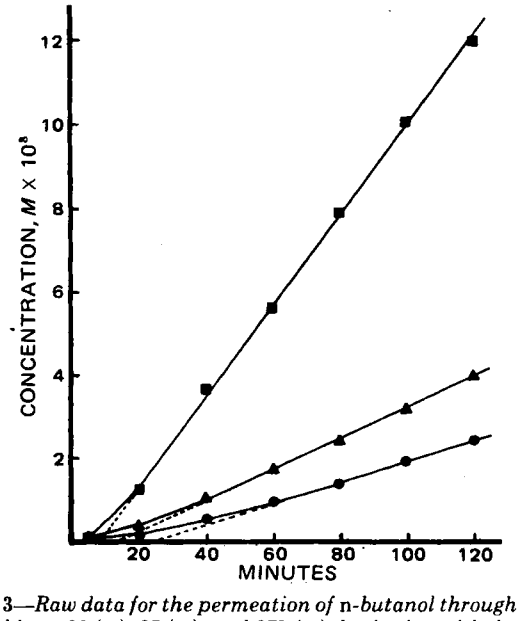

Figure 3—*Raw data for the permeation of* n-*butanol through hairless mouse skin at 20* (●), *25* (▲), *and 37°* (■), *beginning with donor solutions at* ~10^{-5} M. *Changes in diffusivity through the tissue as a function of temperature are indicated by shortened lag times (dotted extrapolations to the time axis) and increased slopes with increased temperature.*

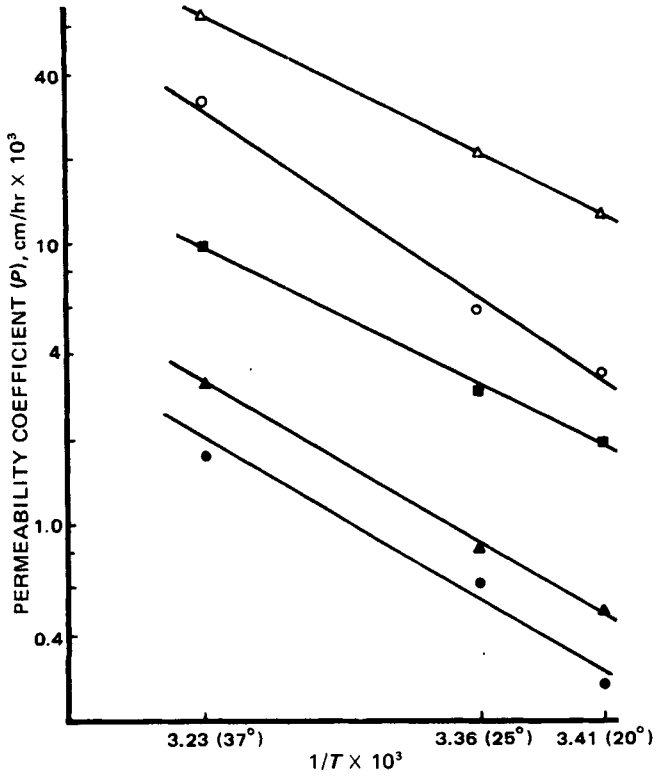

Figure 4—*Arrhenius plot of permeability coefficients for select (mostly even) alkanols. These data indicate an activation energy for the permeation process on the order of 19 kcal/mole. Key: ●, methanol; ▲, ethanol; ■, butanol; ○, hexanol; and △, octanol.*

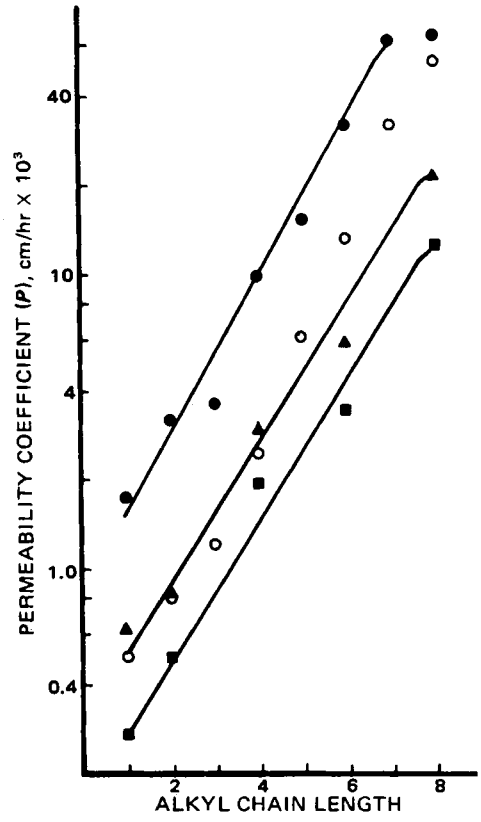

Figure 5—*Semilogarithmic plot of hairless mouse skin permeability coefficients against alkyl chain length for the alkanols at 20 (■), 25 (▲), and 37° (●) and human epidermis permeability coefficients (2, 4) at 25° (○). A general exponential increase in the permeation rate is evident from C_1 to C_8 in both hairless mice and humans, and the 25° data for the two species are in surprisingly close agreement.*

3 and 6, the lag times appear to shorten with increasing temperature, which is consistent with increasing diffusivity in the tissues. The lag times are considered as rough estimates since they are sensitive to placement of the steady-state line through the data. Nevertheless, the expectation that the lag times will be shorter at higher temperatures is supported by the data, even with this uncertainty. It also appears that the lag times tend to increase with increasing length of the alkyl chain (Fig. 6).

DISCUSSION

A nonhuman skin membrane that is sufficiently similar to the human integument is needed so that it can be substituted for human skin in *in vitro* percutaneous absorption and topical bioavailability studies. The human membrane is not procured as easily as an animal membrane, and its properties vary from sample to sample due to differences in the age, sex, race, and health of its donor (generally a cadaver) even if it is removed from the same anatomical site (7). It is not available on demand and must be stored frozen for variable periods (2), a condition that probably induces some physicochemical alteration. Furthermore, preparation of the excised human membrane for permeability studies is relatively complicated, requiring special equipment and demanding skill because the prepared membrane must be of uniform thickness and free of holes and other defects (2, 8, 9). These are surmountable but difficult experimental problems.

Alternatives to using excised human skin for percutaneous absorption assessment are *in vivo* studies in humans, such as the vasoconstriction assay for steroids, and the use of excised animal skins in *in vitro* diffusional systems. Studies on living human subjects are costly and time consuming due to the necessary safeguards, including approved clinical protocols that must be processed through local human use committees and the Food and Drug Administration. Thus, an animal membrane that behaves like human skin and is easily obtainable and relatively invariant from animal to animal could simplify the process of screening topical drugs. The development of critical structure–permeation relationships and of operationally superior drug delivery systems would be forwarded.

Montagna (10) pointed out that no animal skins sufficiently resemble human skin to serve as a general model. Instead, the skins of animals exhibit extraordinary variation and specialization. However, certain animal skins may be likened to human skin in one specific property or another, and an animal may prove suitable for a particular type of study. In terms of anatomical features that contribute to the unique chemical barrier properties of human skin, such as sparse hair distribution and a thickened epidermis with a highly cornified outer layer, the skins of essentially nude mammalian species have been suggested as suitable approximations. The pig, minipig, and hairless mouse are among the useful species; of these, only the latter is sufficiently small and inexpensive to make animal sacrifice for individual experiments practical.

The hairless mouse has another important and experimentally exploitable feature. The skin over both the dorsal and abdominal surfaces is loose and nonadhering to the viscera, making it possible to remove skin membranes of uniform thickness (several square centimeters in area) without recourse to microtomy. Thus, the hairless mouse has distinct advantages as an experimental animal for skin permeation studies *in vitro*. However, to be useful in research and development, it must behave at least qualitatively and, ideally, quantitatively like human skin as a chemical barrier.

The present studies deal with the question of similarity by comparing the permeabilities of hairless mouse skin and human skin to a homologous series of compounds, the *n*-alkanols, between 20 and 37°. These compounds were studied previously over a similar temperature span in human skin (2–6). The extent of barrier parallelism should be evident in permeability coefficients at a given temperature, in temperature dependency, and in partitioning.

Partitioning—In Table II, the partitioning of the alkanols into full-thickness hairless mouse skin is compared with the most recent literature values for humans (5). The comparison is made between the 37° distribution coefficients in mouse skin and the 25° distribution coefficients in human stratum corneum free of epidermal cells. Thus, the tissues are substantially different, with the mouse skin containing a significant living volume fraction (the living epidermis, the full dermis, and a subdermal basement membrane). Also, the literature values were obtained with water as the bathing medium, while the present data were obtained using normal saline. Nevertheless, the comparison is useful, particularly when considered along with permeation data.

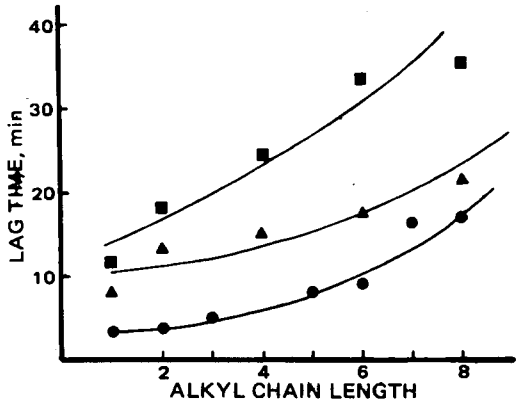

Figure 6—*Plot of lag times against alkyl chain length for data obtained at 20 (■), 25 (▲), and 37° (●). Both temperature and molecular size (alkyl chain length) effects are apparent. Lines through the data serve only to draw attention to the temperature groups and do not represent a best fit.*

In each case, the lower alkanols, methanol through propanol or butanol, did not exhibit a marked chain length sensitivity in phase distribution, with a value of slightly less than 1 for the human stratum corneum and a value of somewhat less than 6 for the hairless mouse tissue. The insensitivity suggests that the lower alkanols distribute into a polar phase in the tissue. One might speculate that this phase is imbibed water in human callus, which hydrates and swells up to 30% when immersed, and imbibed, cellular, intercellular, and interstitial water in the hairless mouse skin. Values greater than unity in the hairless mouse indicate that the tissue fluids or other tissue components have a greater affinity for the alkanols than the bathing saline phase. Whether the increased affinity is due to an actual solubility difference, adsorptive tissue binding, or another manner of tissue incorporation is unclear. What is clear is that the phenomenon responsible is not energetically dependent on hydrophobic factors since there is no chain-length effect (11, 12).

Partition coefficients above C_4 tended to increase rapidly; for the *n*-hexanol through *n*-nonanol homologs, the increase was exponential. Table II indicates that human data for the stratum corneum behave similarly; in each tissue, an approximately twofold increase in the partition coefficient per methylene group was experienced in the exponential region. The overall pattern of behavior (little or no chain-length effect for short homologs and an exponential growth with chain length for long homologs) is characteristic of a bi- or multiphasic tissue, with one phase (or collection of phases) polar and essentially aqueous and the other phase (or collection of phases) hydrophobic. In the intact hairless mouse skin, the hydrophobic phases would include the nonpolar elements of the stratum corneum and the Malpighian layer cell membranes, nonpolar elements of the dermis, fatty subdermal deposits, and, possibly, elements of the basement membrane.

Not only are the overall data trends for partitioning similar between human stratum corneum and full-thickness hairless mouse skin, but there also is an order of magnitude agreement in the values, despite the obvious differences in the tissues. In fact, at middle to long chain lengths, the agreement between the tissues is surprisingly close. Thus, the physicochemical natures of the tissue components apparently are similar.

Steady-State Permeability—The partitioning data suggest some gross physicochemical parallel between human stratum corneum and hairless mouse skin. However, this similarity need not correspond to a similarity in membrane barrier properties. Therefore, studies were begun to evaluate the permeability of hairless mouse skin to the alkanols. In Table III, permeability coefficient data are given as a function of temperature and pH for the various homologs studied. Also included are the 25° permeability coefficients obtained for heat-separated human epidermis (2). The hairless mouse data at 25° are tabulated immediately to the left of the human data for comparative purposes.

From the 37° data on butanol in isotonic buffers at pH 3, 6, and 8, it can be seen that pH had essentially no effect on membrane permeation over the wide pH range studied. Therefore, strict pH control (buffers) was not necessary in the remaining studies since the pH of saline solutions bathing the mouse skin for extended periods always was well within the specified pH range (the measured values were about pH 5 on both sides of the membrane).

In Fig. 4, the permeability coefficients for the C_1, C_2, C_4, C_6, and C_8 homologs are plotted semilogarithmically against the reciprocal of temperature. The average activation energy for these compounds based on the statistically evaluated slopes is ~19 kcal/mole with an uncertainty of several kilocalories per mole. This average activation energy is somewhat larger than the values obtained by Blank *et al.* (4) for the heat-separated human epidermis. Their average value for the alcohols ethanol through pentanol was 16.4 ± 2 kcal/mole and, above 25°, was comparably larger for hexanol through octanol. For the more nonpolar alkanols, biphasic temperature dependency was noted; below 25°, the activation energy was estimated to be about 10 kcal (4). In the present studies, this low temperature region was not investigated. Generally, the temperature dependencies for human epidermis and hairless mouse skin exhibited a marked similarity, with the animal membrane appearing slightly more temperature sensitive.

The data from Table III are treated graphically in Fig. 5 to illustrate the alkyl chain length dependency of the permeation process. At each temperature, the permeability coefficient initially increased exponentially as the alkyl chain was extended, except at 37° where octanol appeared to enter boundary layer control. The latter behavior is consistent with a series barrier consisting of a lipid or nonpolar phase of high diffusional resistance, presumably the stratum corneum, in series with an essentially aqueous phase or phases. At short chain length, the nonpolar barrier (stratum corneum) is rate determining, and the differences from compound to compound reflect differences in partitioning into this rate-limiting membrane phase. The permeability coefficient equation takes the following general form in this region (12, 13):

$$P = \frac{D_{sc}(K_{sc/aq})_0\, 10^{\pi n}}{h_{sc}} \qquad \text{(Eq. 5)}$$

which recognizes the exponentially increasing nature of the stratum corneum–water partition coefficient. Here D_{sc} is the effective stratum corneum diffusivity, $(K_{sc/aq})_0$ is a hypothetical zero chain length partition coefficient, h_{sc} is the tissue thickness, and n is the alkyl chain length. The π value in the exponent is the incremental increase in log P per unit increase in alkyl chain length. The slope of the plot at 37° indicates that the π_{CH_2} value (or incremental partitioning constant value) is ~0.263, and it appears to be of similar magnitude at 20 and 25°. The π_{CH_2} value for human stratum corneum may be obtained similarly from the data given previously (2–6) and is about 0.333, higher than but in reasonable agreement with that for the mouse skin. Values of π_{CH_2} can be expected to range to 0.62, the specified value for perfectly nonpolar, water-immiscible phases such as heptane or carbon tetrachloride (11).

The alkanol range where partition coefficients seemingly are invariant with chain length is a range where an exponential increase in permeability due to partitioning phenomena is observed. At first appearance, this finding may seem incongruent, but the respective observations in fact are internally consistent. Whereas the relative solubility in the stratum corneum and other lipid phases is small, the amounts partitioning into aqueous phases will determine the apparent partition coefficient. However, where the relative solubility in the stratum corneum is small, the molecular diffusional current across this stratum will be small and the stratum corneum will be the rate-determining tissue in the series. The limiting slope of the partitioning on the semilog plot, 0.285 (Fig. 5), is in very close agreement with the value of 0.263 obtained as the π_{CH_2} value for the permeability experiments. The difference is in the direction of an expected slight diffusion coefficient effect due to the increased molecular volume as the alkyl chain becomes longer.

Nonstationary State—The nonstationary-state data obtained in the present studies were crude. Slight differences in estimating the steady-state slopes led to large differences in estimating the lag time intercepts, particularly at short chain lengths where the slopes were relatively shallow. Nevertheless, several important patterns of behavior may be noted. The lag time for a given compound was dependent on temperature; lag times decreased as temperature was increased. This trend is consistent with a significant activation energy for the effective diffusivity in the membrane. The temperature dependency of the permeability coefficient seen in Fig. 4 is largely dependent on the temperature dependency of the diffusion coefficient, which directly affects the lag times. The increasing lag time with increasing molecular size may be a size effect on diffusivity or may be the result of increasing membrane binding (13).

CONCLUSIONS

The hairless mouse skin is an easily prepared membrane for permeation studies. Moreover, based on the permeability of homologous alcohols, the barrier properties are qualitatively and in some regards quantitatively similar to those of human epidermis. The membrane behaves as a complex barrier with a highly impermeable lipid phase (the stratum cor-

neum), in series with the viable tissues of the epidermis and connective tissue of the dermis. On the basis of this evidence, the hairless mouse might prove generally useful in sorting out membrane contributions to the relative activities of topical drugs and in evaluating the influence of formulation on the activity of a given topical therapeutic compound.

REFERENCES

(1) R. B. Stronghton, in "Animal Models in Dermatology," H. I. Maibach, Ed., Churchill Livingstone, New York, N.Y., 1975, p. 121.

(2) R. J. Scheuplein, *J. Invest. Dermatol.*, **45**, 334 (1965).

(3) *Ibid.*, **48**, 79 (1967).

(4) I. H. Blank, R. J. Scheuplein, and D. J. MacFarlane, *J. Invest. Dermatol.*, **49**, 582 (1967).

(5) R. J. Scheuplein and I. H. Blank, *ibid.*, **60**, 286 (1973).

(6) I. H. Blank, *ibid.*, **43**, 415 (1964).

(7) R. J. Tregear, "Physical Functions of Skin," Academic, London, England, 1966.

(8) M. Katz and B. J. Poulson, *Handbook Exp. Pharmacol.*, **28**, 103 (1971).

(9) R. J. Scheuplein and I. H. Blank, *Physiol. Rev.*, **51**, 702 (1971).

(10) W. Montagna, *Arch. Dermatol.*, **104**, 577 (1971).

(11) S. S. Davis, T. Higuchi, and J. M. Rytting, *Adv. Pharm. Sci.*, **4**, 73 (1974).

(12) G. L. Flynn and S. H. Yalkowsky, *J. Pharm. Sci.*, **61**, 838 (1972).

(13) G. L. Flynn, S. H. Yalkowsky, and T. J. Roseman, *ibid.*, **63**, 479 (1974).

Pharmacokinetic Studies of Propoxyphene I: Effect of Portacaval Shunt on Systemic Availability in Dogs

KATHLEEN M. GIACOMINI *, SHAHEEN M. NAKEEB ‡, and GERHARD LEVY *x

Received August 20, 1979, from the **Department of Pharmaceutics and the* ‡*Department of Laboratory Animal Science, State University of New York at Buffalo, Amherst, NY 14260.* Accepted for publication February 6, 1980.

Abstract □ The elimination kinetics and systemic availability of *d*-propoxyphene were determined in dogs before and after construction of a portacaval shunt. For this purpose, the drug was administered intravenously and orally, in aqueous solution, according to a balanced experimental design. The total plasma clearance of propoxyphene ranged from 14.4 to 31.8 ml/min/kg before the shunt and decreased appreciably in two of four dogs after shunting. There was no significant change in the serum protein binding of the drug. The systemic availability increased from an average of 25% before to an average of 54% after shunting ($p < 0.05$). The ratio of areas under the plasma concentration–time curve of norpropoxyphene to propoxyphene was not significantly affected by the shunt when propoxyphene was administered intravenously; it decreased substantially after shunting when the drug was administered orally. Pharmacokinetic analysis indicates that orally administered propoxyphene is subject to prehepatic as well as hepatic first-pass elimination in dogs. The magnitude of the first-pass effect is similar to that in humans. These results suggest that the dosage of orally administered propoxyphene should be reduced in patients with portacaval shunt or with cirrhosis of the liver.

Keyphrases □ Pharmacokinetics—propoxyphene, effect of portacaval shunt on systemic availability, dogs □ Propoxyphene—pharmacokinetics, effect of portacaval shunt on systemic availability, dogs □ Systemic availability—propoxyphene, effect of portacaval shunt, dogs

The analgesic propoxyphene (*d*-propoxyphene) is one of the most frequently prescribed drugs in the United States. About 31 million prescriptions for it were issued in 1978 (1). Large doses can be fatal and often have been used to commit suicide. Propoxyphene also has been implicated in accidental deaths. A number of these deaths apparently occurred as a result of the consumption of propoxyphene in quantities only slightly larger than the upper limit of the recommended dosage, usually together with alcohol and/or other central nervous system (CNS) depressants (1).

BACKGROUND

Propoxyphene is subject to a pronounced first-pass effect in that only a small fraction of the absorbed dose enters the general circulation in unmetabolized form (2–4). Moreover, there are very large and apparently relatively consistent interindividual differences in the systemic availability of propoxyphene in humans (2–6). This fact suggests that certain accidental (as opposed to suicidal) poisonings due to propoxyphene may result from an unfortunate coincidence of a large (probably larger than prescribed) dose, an unusually small first-pass effect relative to the population average, and ingestion of one or more CNS depressants. For this and other obvious reasons, it is important to determine the factors responsible for interindividual differences in the first-pass effect on propoxyphene.

An orally administered drug may be subject to hepatic as well as prehepatic (intestinal) first-pass effects. The relative contribution of these two sites of biotransformation is important in assessing the reasons for interindividual differences in the systemic availability and for predicting the possible effect of surgically induced or endogenous portacaval shunts (*i.e.*, shunts due to hepatic cirrhosis). There are indirect indications, based on pharmacokinetic analysis of systemic availability relative to total clearance, that propoxyphene may be subject to some prehepatic biotransformation in humans (3, 4).

It is not possible to determine the magnitude of the prehepatic biotransformation of a drug such as propoxyphene by comparing its systemic availability in normal subjects and in patients with surgically constructed portacaval shunts. Such shunts are used to relieve variceal bleeding secondary to portal hypertension caused by hepatic cirrhosis and other pathological conditions associated with obstruction of portal blood flow. Liver disease and the drugs taken by the recipients of a portacaval shunt may modify the metabolic clearance of propoxyphene and thereby introduce an additional variable that cannot be controlled or defined readily because propoxyphene is not available for intravenous injection. Moreover, patients with portacaval shunts can develop various degrees of collateral circulation. Therefore, it is necessary to conduct studies on a suitable animal model.

Some published evidence suggested that the dog, like humans, exhibits a pronounced first-pass effect on orally administered propoxyphene (7). Demethylation to norpropoxyphene is a major elimination pathway of propoxyphene in both species (8). The dog is large enough for the convenient surgical construction of a portacaval shunt. Other investigators successfully used dogs to study the first-pass effect on orally administered drugs before and after a portacaval shunt (9).

In the present investigation, propoxyphene was administered both orally and intravenously to dogs before and after a portacaval shunt, according to a balanced experimental design. Propoxyphene was administered intravenously before and after surgery because the shunt may affect the plasma clearance of a drug (9). There is conflicting evidence concerning the dose dependence of the first-pass effect on propoxyphene in humans (2–4, 10, 11). The intravenous dose in this study was lower than the oral dose so that the areas under the concentration–time curve produced by both routes of drug administration would be similar.

0022-3549/80/0700-0786$01.00/0
© 1980, American Pharmaceutical Association

neum), in series with the viable tissues of the epidermis and connective tissue of the dermis. On the basis of this evidence, the hairless mouse might prove generally useful in sorting out membrane contributions to the relative activities of topical drugs and in evaluating the influence of formulation on the activity of a given topical therapeutic compound.

REFERENCES

(1) R. B. Stronghton, in "Animal Models in Dermatology," H. I. Maibach, Ed., Churchill Livingstone, New York, N.Y., 1975, p. 121.

(2) R. J. Scheuplein, *J. Invest. Dermatol.*, **45**, 334 (1965).

(3) *Ibid.*, **48**, 79 (1967).

(4) I. H. Blank, R. J. Scheuplein, and D. J. MacFarlane, *J. Invest. Dermatol.*, **49**, 582 (1967).

(5) R. J. Scheuplein and I. H. Blank, *ibid.*, **60**, 286 (1973).

(6) I. H. Blank, *ibid.*, **43**, 415 (1964).

(7) R. J. Tregear, "Physical Functions of Skin," Academic, London, England, 1966.

(8) M. Katz and B. J. Poulson, *Handbook Exp. Pharmacol.*, **28**, 103 (1971).

(9) R. J. Scheuplein and I. H. Blank, *Physiol. Rev.*, **51**, 702 (1971).

(10) W. Montagna, *Arch. Dermatol.*, **104**, 577 (1971).

(11) S. S. Davis, T. Higuchi, and J. M. Rytting, *Adv. Pharm. Sci.*, **4**, 73 (1974).

(12) G. L. Flynn and S. H. Yalkowsky, *J. Pharm. Sci.*, **61**, 838 (1972).

(13) G. L. Flynn, S. H. Yalkowsky, and T. J. Roseman, *ibid.*, **63**, 479 (1974).

Pharmacokinetic Studies of Propoxyphene I: Effect of Portacaval Shunt on Systemic Availability in Dogs

KATHLEEN M. GIACOMINI *, SHAHEEN M. NAKEEB ‡, and GERHARD LEVY *x

Received August 20, 1979, from the **Department of Pharmaceutics and the* ‡*Department of Laboratory Animal Science, State University of New York at Buffalo, Amherst, NY 14260.* Accepted for publication February 6, 1980.

Abstract □ The elimination kinetics and systemic availability of *d*-propoxyphene were determined in dogs before and after construction of a portacaval shunt. For this purpose, the drug was administered intravenously and orally, in aqueous solution, according to a balanced experimental design. The total plasma clearance of propoxyphene ranged from 14.4 to 31.8 ml/min/kg before the shunt and decreased appreciably in two of four dogs after shunting. There was no significant change in the serum protein binding of the drug. The systemic availability increased from an average of 25% before to an average of 54% after shunting ($p < 0.05$). The ratio of areas under the plasma concentration–time curve of norpropoxyphene to propoxyphene was not significantly affected by the shunt when propoxyphene was administered intravenously; it decreased substantially after shunting when the drug was administered orally. Pharmacokinetic analysis indicates that orally administered propoxyphene is subject to prehepatic as well as hepatic first-pass elimination in dogs. The magnitude of the first-pass effect is similar to that in humans. These results suggest that the dosage of orally administered propoxyphene should be reduced in patients with portacaval shunt or with cirrhosis of the liver.

Keyphrases □ Pharmacokinetics—propoxyphene, effect of portacaval shunt on systemic availability, dogs □ Propoxyphene—pharmacokinetics, effect of portacaval shunt on systemic availability, dogs □ Systemic availability—propoxyphene, effect of portacaval shunt, dogs

The analgesic propoxyphene (*d*-propoxyphene) is one of the most frequently prescribed drugs in the United States. About 31 million prescriptions for it were issued in 1978 (1). Large doses can be fatal and often have been used to commit suicide. Propoxyphene also has been implicated in accidental deaths. A number of these deaths apparently occurred as a result of the consumption of propoxyphene in quantities only slightly larger than the upper limit of the recommended dosage, usually together with alcohol and/or other central nervous system (CNS) depressants (1).

BACKGROUND

Propoxyphene is subject to a pronounced first-pass effect in that only a small fraction of the absorbed dose enters the general circulation in unmetabolized form (2–4). Moreover, there are very large and apparently relatively consistent interindividual differences in the systemic availability of propoxyphene in humans (2–6). This fact suggests that certain accidental (as opposed to suicidal) poisonings due to propoxyphene may result from an unfortunate coincidence of a large (probably larger than prescribed) dose, an unusually small first-pass effect relative to the population average, and ingestion of one or more CNS depressants. For this and other obvious reasons, it is important to determine the factors responsible for interindividual differences in the first-pass effect on propoxyphene.

An orally administered drug may be subject to hepatic as well as prehepatic (intestinal) first-pass effects. The relative contribution of these two sites of biotransformation is important in assessing the reasons for interindividual differences in the systemic availability and for predicting the possible effect of surgically induced or endogenous portacaval shunts (*i.e.*, shunts due to hepatic cirrhosis). There are indirect indications, based on pharmacokinetic analysis of systemic availability relative to total clearance, that propoxyphene may be subject to some prehepatic biotransformation in humans (3, 4).

It is not possible to determine the magnitude of the prehepatic biotransformation of a drug such as propoxyphene by comparing its systemic availability in normal subjects and in patients with surgically constructed portacaval shunts. Such shunts are used to relieve variceal bleeding secondary to portal hypertension caused by hepatic cirrhosis and other pathological conditions associated with obstruction of portal blood flow. Liver disease and the drugs taken by the recipients of a portacaval shunt may modify the metabolic clearance of propoxyphene and thereby introduce an additional variable that cannot be controlled or defined readily because propoxyphene is not available for intravenous injection. Moreover, patients with portacaval shunts can develop various degrees of collateral circulation. Therefore, it is necessary to conduct studies on a suitable animal model.

Some published evidence suggested that the dog, like humans, exhibits a pronounced first-pass effect on orally administered propoxyphene (7). Demethylation to norpropoxyphene is a major elimination pathway of propoxyphene in both species (8). The dog is large enough for the convenient surgical construction of a portacaval shunt. Other investigators successfully used dogs to study the first-pass effect on orally administered drugs before and after a portacaval shunt (9).

In the present investigation, propoxyphene was administered both orally and intravenously to dogs before and after a portacaval shunt, according to a balanced experimental design. Propoxyphene was administered intravenously before and after surgery because the shunt may affect the plasma clearance of a drug (9). There is conflicting evidence concerning the dose dependence of the first-pass effect on propoxyphene in humans (2–4, 10, 11). The intravenous dose in this study was lower than the oral dose so that the areas under the concentration–time curve produced by both routes of drug administration would be similar.

0022-3549/80/0700-0786$01.00/0
© 1980, American Pharmaceutical Association

Table I—Experimental Design Indicating the Order of Intravenous and Oral Propoxyphene Administration [a]

Dog	Before Shunt		After Shunt	
	Intravenous	Oral	Intravenous	Oral
1	1	2	3	4
2	1	2	4	3
3	2	1	3	4
4	2	1	4	3

[a] Intravenous and oral doses of *d*-propoxyphene hydrochloride were 2.0 and 7.5 mg/kg, respectively.

Norpropoxyphene, a major metabolite of propoxyphene, is eliminated from the body much more slowly than its precursor and appears prominently in the circulation following propoxyphene administration (12, 13). The formation and elimination kinetics of norpropoxyphene are of clinical interest because this metabolite, like propoxyphene, can depress cardiac conduction and may contribute to the cardiac toxicity produced by ingestion of large amounts of propoxyphene (14–16). Therefore, norpropoxyphene concentrations also were determined in this investigation.

EXPERIMENTAL

Four male mongrel dogs, 14–27 kg, received *d*-propoxyphene hydrochloride intravenously (cephalic vein of the foreleg) in saline solution (0.5 ml/kg) at a dose of 2 mg/kg and orally in 100 ml of water *via* a stomach tube at a dose of 7.5 mg/kg. The dogs were fasted overnight and during the study. The doses were administered according to a crossover design (Table I) at 1-week intervals. Prior to each dose, a heparin trap was placed in a cephalic vein and 10 ml of blood was withdrawn. After drug administration, 10-ml blood samples were withdrawn serially for 8 hr.

One week after administration of the second dose, a modified side-to-side portacaval shunt was constructed under pentobarbital sodium anesthesia (30 mg/kg). The technique employed was that of a straight Eck fistula (17). Basically, this technique involved anastomosing the side of the portal vein to the side of the vena cava and then tying off the portal vein just proximal to the liver. Thus, a complete shunt of blood from the portal vein to the vena cava was produced.

One to 2 weeks after construction of the shunt, the dogs again received propoxyphene orally and intravenously (same dose per kilogram as before the shunt). As before, 1 week elapsed between administration of the two doses. Blood samples were collected as described.

Plasma was assayed simultaneously for propoxyphene and norpropoxyphene by the GLC method of Verebely and Inturrisi (18) with the following minor modifications. The gas chromatograph[1] had a 182.9-cm long × 2-mm i.d. glass spiral column. The column, detector, and injector port temperatures were 220, 240, and 230°, respectively. The carrier gas flow was 40 ml/min. The internal standard was trifluperazine. Under these conditions, the retention times for propoxyphene, norpropoxyphene, and trifluperazine were 2.5, 7.0, and 10 min, respectively. The assay is sensitive to 50 ng of propoxyphene and 100 ng of norpropoxyphene. The volume of plasma used for the assay was adjusted to yield amounts of the drug and the metabolite in the 500–3500-ng range. The coefficient of variation of the assay in this range was 6.3% for propoxyphene and 7.0% for norpropoxyphene.

The plasma protein binding of propoxyphene in each dog before and after portacaval anastamosis was determined by equilibrium dialysis. Two 1.5-ml predose plasma samples from each dog were dialyzed at 37° against an equal volume of pH 7.4 Sorensen phosphate buffer (0.13 *M*) containing *d*-propoxyphene hydrochloride (1.2 μg/ml), using Plexiglas cells separated by a cellophane membrane[2]. The dialysis time was 12 hr.

The total protein concentrations in the plasma of each dog before and after portacaval shunt were determined by the method of Gornall *et al.* (19) with crystalline dog albumin as the standard. The albumin fractions were determined by electrophoresis[3], and albumin concentrations were obtained by multiplying the total protein concentration by the fraction of albumin.

The area under the plasma concentration–time curve (*AUC*) after oral drug administration was calculated by the trapezoidal method for the first 8 hr and then extrapolated to infinity according to $AUC_{t-\infty} = C_t/\beta$, where $AUC_{t-\infty}$ is the area under the plasma concentration–time curve from the last observed plasma concentration (obtained at 8 hr) to infinity, C_t is the plasma concentration at 8 hr, and β is the terminal disposition rate constant (determined after intravenous injection). The $AUC_{t-\infty}$ was ~20% of $AUC_{0-\infty}$ before the shunt and ~28% after the bypass.

The plasma propoxyphene concentrations obtained after intravenous injection were fitted to the equation $C = Ae^{-\alpha t} + Be^{-\beta t}$ by a nonlinear least-squares regression procedure (20). The data were weighted by use of their reciprocal. The $AUC_{0-\infty}$ value was determined as the sum of A/α and B/β.

The total clearance, *Cl*, was calculated according to $Cl = D_{iv}/AUC_{iv}$, where D_{iv} is the intravenous dose of the free base and AUC_{iv} is the area under the intravenous plasma concentration–time curve from time zero to infinity.

The systemic availability, *F*, was calculated from $F = (100 \times D_{iv} \times AUC_{po})/(D_{po} \times AUC_{iv})$, where D_{iv} and D_{po} are the respective intravenous and oral doses and AUC_{po} and AUC_{iv} are the respective total areas under the plasma concentration–time curves following the oral and intravenous doses.

Table II—Pharmacokinetics of Propoxyphene in Dogs before and after Portacaval Shunt

Parameter[a]	Before	After
A, ng/ml	1360 ± 390[b]	1530 ± 435
B, ng/ml	237 ± 70	425 ± 30
α, hr^{-1}	4.13 ± 1.22	5.48 ± 1.30
β, hr^{-1}	0.202 ± 0.033	0.223 ± 0.032
Free fraction in plasma[c]	0.129 ± 0.037	0.159 ± 0.031

[a] Based on the relationship $C = Ae^{-\alpha t} + Be^{-\beta t}$, where *C* is the drug concentration in plasma at time *t* after intravenous injection of 1.81 mg (expressed as the base)/kg of body weight. [b] Mean ± *SEM*, $n = 4$. [c] At a total drug concentration at equilibrium of ~1000 ng/ml.

RESULTS

The propoxyphene concentrations in plasma declined biexponentially after intravenous injection. The drug was absorbed very rapidly after oral administration (Figs. 1 and 2). The pharmacokinetic constants for the elimination of injected propoxyphene are listed in Table II. The plasma total protein and albumin concentrations were 6.5 ± 0.2 and 3.0 ± 0.1 g/100 ml before the shunt and 6.0 ± 0.6 and 2.6 ± 0.2 g/100 ml after the shunt (mean ± *SEM*, differences not significant), respectively. The free fraction values of propoxyphene in plasma were similar before and after shunting (Table II).

The plasma clearance of injected propoxyphene was high (Table III) and comparable in magnitude to the hepatic plasma flow rate in dogs (21). It decreased appreciably after the portacaval shunt in the two dogs that exhibited the highest clearance values before the shunt (Dogs 2 and 3). The systemic availability of orally administered propoxyphene increased substantially after shunt construction in all of the animals; the average increase was from 25% before to 54% of the dose after the shunt (Table III). The areas under the concentration–time curve, time zero to infinity, following oral administration of propoxyphene increased even more, changing from 1470 ± 450 (ng hr)/ml before to 4390 ± 645 (ng hr)/ml after the bypass (mean ± *SEM*, $p < 0.025$).

Pertinent information concerning the norpropoxyphene concentrations in plasma is summarized in Table IV. The delayed occurrence of maxi-

Table III—Systemic Availability and Total Clearance of Propoxyphene in Dogs before and after Portacaval Shunt

Dog	Before		After	
	Availability[a], %	Clearance[b], ml/min/kg	Availability[a], %	Clearance[b], ml/min/kg
1	24.9	14.4	72.6	15.8
2	16.2	25.8	25.1	11.0
3	20.3	31.8	59.1	12.3
4	39.7	17.9	60.1	15.7
Mean	25.3	22.5	54.2[c]	13.7
SEM	5.1	3.9	10.2	1.2

[a] Systemic availability of an oral dose of 6.79 mg (base)/kg. [b] Total plasma clearance of a 1.81-mg (base)/kg intravenous dose. [c] Significantly different from availability before shunt ($p < 0.05$ by paired *t* test).

[1] Hewlett-Packard model 5830.
[2] Cut from dialysis tubing having an average pore radius of 24 Å, VWR Scientific, Rochester, N.Y.
[3] Serum protein electrophoresis system, Gelman Instrument Co., Ann Arbor, Mich.

Table IV—Concentrations of Norpropoxyphene in Plasma of Dogs following Intravenous and Oral Administration of Propoxyphene before and after Portacaval Shunt

	Intravenous[a]		Oral[b]	
	Before	After	Before	After
Maximum concentration, ng/ml	459 ± 152[c]	462 ± 67	2310 ± 1040	1820 ± 775
Time of maximum concentration, hr	0.8 ± 0.2	3.6 ± 1.0	1.8 ± 0.8	3.5 ± 1.0
Area under 0–8-hr curve, (ng hr)/ml	2440 ± 855	3380 ± 795	12,600 ± 5700	11,000 ± 5300
Ratio of areas[d] of norpropoxyphene to propoxyphene	1.87 ± 0.46	1.90 ± 0.47	10.4 ± 3.1	3.34 ± 1.14[e]

[a] 1.81 mg (base)/kg. [b] 6.79 mg (base)/kg. [c] Mean ± *SEM*, $n = 4$. [d] Areas under 0–8-hr plasma concentration curve. [e] Significantly different from ratio value before shunt ($p < 0.05$ by paired t test).

mum concentrations and apparently increased areas under the 0–8-hr concentration–time curve after intravenous injection of propoxyphene suggest decreased clearance of the metabolite after the shunt, but the differences were not statistically significant. The ratio of areas under the concentration–time curve (*AUC* ratio) of norpropoxyphene to propoxyphene after intravenous injection of propoxyphene was not affected by the portacaval shunt. The *AUC* ratio after oral administration of the drug was much higher than after intravenous injection and decreased appreciably after construction of the portacaval shunt (Table IV).

DISCUSSION

The dogs in this study received oral propoxyphene as an aqueous solution. Consistent with the results of clinical studies (2, 4–6, 8, 11–13), the drug was absorbed rapidly after oral administration. A clinical study showed that there is no apparent difference in the systemic availability of propoxyphene administered in capsules and in solution (11). The urinary recovery of radioactivity following oral and intravenous administration of [^{14}C]propoxyphene is not significantly different (4). On the basis of this information, it is reasonable to conclude that the incomplete systemic availability of propoxyphene observed in this study is due to presystemic biotransformation rather than incomplete absorption.

Gram *et al.* (4) found that the systemic availability of orally administered propoxyphene hydrochloride in humans was independent of the dose in the 65–195-mg dose range. The use of oral to intravenous *AUC* ratios in the present study to determine the systemic availability of orally administered propoxyphene in dogs was based on the assumption that the kinetics were linear under the experimental conditions. Moreover, the oral and intravenous doses were chosen to produce similar *AUC* values to minimize the effect of possible nonlinearity on the systemic availability determinations.

As in humans, the plasma clearance of injected propoxyphene in dogs is high and comparable in magnitude to the hepatic plasma flow rate. Since the renal clearance of propoxyphene is very low (8, 12), the plasma clearance of the drug is due almost entirely to metabolism. Therefore, propoxyphene should be subject to a large first-pass effect, based on theoretical pharmacokinetic considerations (3). Its plasma clearance after intravenous injection should be affected by the activity of drug-metabolizing enzyme systems and by hepatic blood flow (3), both of which may be reduced following the portacaval shunt (9, 22). Indeed, the plasma clearance of propoxyphene was substantially decreased in two of four dogs after the shunt. The two affected animals had the highest propoxyphene clearance before surgery and, therefore, were most sensitive to a reduction of hepatic blood flow. Other investigators reported reduction of lidocaine and antipyrine clearance after portacaval shunting in dogs (9).

The systemic availability of propoxyphene increased, but was not complete, after the portacaval shunt. This result suggests that the drug is subject to a prehepatic first-pass effect, which is consistent with the tentative conclusions of investigators who noted that the observed first-pass effect on propoxyphene in humans is larger than the magnitude of the hepatic first-pass effect predicted on the basis of pharmacokinetic considerations (3, 4).

If a drug is subject to prehepatic as well as hepatic first-pass biotransformation, then the fraction of the dose available systemically, F,

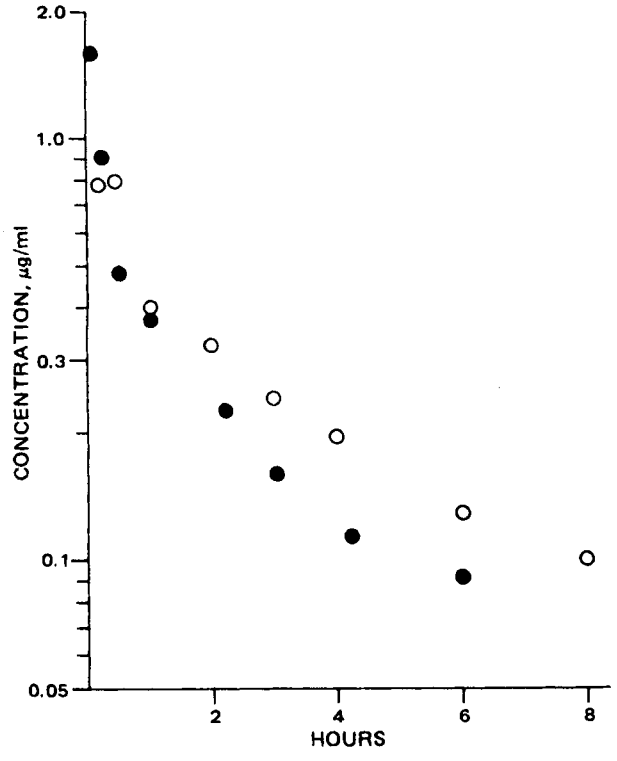

Figure 1—*Concentrations of* d-*propoxyphene in plasma of Dog 4 after oral administration of 7.5 mg/kg* (○) *and intravenous injection of 2.0 mg/kg* (●) *of propoxyphene hydrochloride in separate experiments before portacaval shunt.*

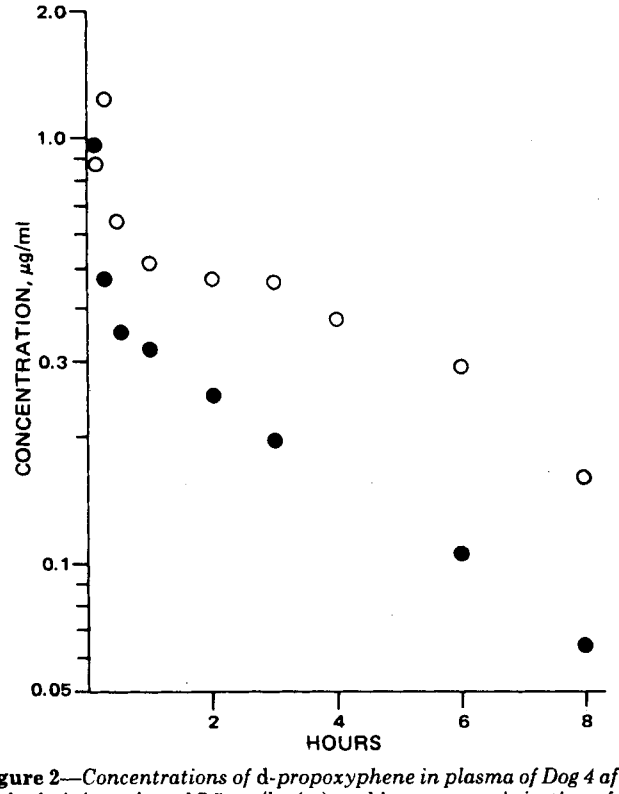

Figure 2—*Concentrations of* d-*propoxyphene in plasma of Dog 4 after oral administration of 7.5 mg/kg* (○) *and intravenous injection of 2.0 mg/kg* (●) *of propoxyphene hydrochloride in separate experiments after portacaval shunt.*

is $F_{PH}F_H$, where F_{PH} is the fraction of the dose reaching the liver as intact drug and F_H is the fraction of the drug reaching the liver intact that enters the systemic circulation in unmetabolized form. If $F_{PH} = F$ after portacaval shunt (assuming that F_{PH} was not affected by the surgery and that there was no significant development of collateral circulation after the surgery), then F_H before surgery was 0.253/0.542 or 0.47 (based on the average systemic availability values from Table III). Thus, the prehepatic and hepatic first-pass effects on propoxyphene appear to be of similar magnitude in the dog.

Hepatic cirrhosis often is associated with the formation of portacaval shunts and reduction of drug-metabolizing enzyme activity (23, 24). These changes should increase the systemic availability of a drug with the pharmacokinetic characteristics of propoxyphene. This increase should be less pronounced if a substantial part of the first-pass effect is due to prehepatic biotransformation, provided that liver disease does not affect the prehepatic metabolism of propoxyphene. Unfortunately, the effect of liver disease on the prehepatic biotransformation of drugs is not known. However, it appears prudent to reduce the dosage of propoxyphene in patients with portacaval shunt or with cirrhosis of the liver.

REFERENCES

(1) *Fed. Regist.*, **44**, 11837 (1979).

(2) R. L. Wolen, C. M. Gruber, Jr., G. F. Kiplinger, and N. E. Scholz, *Toxicol. Appl. Pharmacol.*, **19**, 480 (1971).

(3) D. Perrier and M. Gibaldi, *J. Clin. Pharmacol.*, **12**, 449 (1972).

(4) L. F. Gram, J. Schou, W. L. Way, J. Heltberg, and N. O. Bodin, *Clin. Pharmacol. Ther.*, **26**, 473 (1979).

(5) G. W. A. Slywka, A. P. Melikian, P. L. Whyatt, and M. C. Meyer, *J. Clin. Pharmacol.*, **15**, 598 (1975).

(6) A. Melander, A. Berlin-Wahlen, N. O. Bodin, K. Danielson, G. Gustafsson, L. Lindgren, and D. Westerlund, *Acta Med. Scand.*, **202**, 119 (1977).

(7) R. E. McMahon and H. R. Sullivan, *Res. Commun. Chem. Pathol. Pharmacol.*, **14**, 631 (1976).

(8) R. E. McMahon, A. S. Ridolfo, H. W. Culp, R. L. Wolen, and F. J. Marshall, *Toxicol. Appl. Pharmacol.*, **19**, 427 (1971).

(9) R. Gugler, P. Lain, and D. L. Azarnoff, *J. Pharmacol. Exp. Ther.*, **195**, 416 (1975).

(10) R. L. Wolen, E. A. Ziege, and C. M. Gruber, *Clin. Pharmacol. Ther.*, **17**, 15 (1975).

(11) J. G. Wagner, P. G. Welling, S. B. Roth, E. Sakmar, K. P. Lee, and J. E. Walker, *Int. J. Clin. Phdrmacol.*, **5**, 371 (1972).

(12) K. Verebely and C. E. Inturrisi, *Clin. Pharmacol. Ther.*, **15**, 302 (1973).

(13) R. L. Wolen, B. D. Obermeyer, E. A. Ziege, H. R. Black, and C. M. Gruber, in "Stable Isotopes. Applications in Pharmacology, Toxicology, and Clinical Research," T. A. Baille, Ed., University Park Press, Dallas, Tex., 1978, p. 113.

(14) R. Nickander, S. E. Smits, and M. I. Steinberg, *J. Pharmacol. Exp. Ther.*, **200**, 245 (1977).

(15) H. Lund-Jacobsen, *Acta Pharmacol. Toxicol.*, **42**, 171 (1978).

(16) D. R. Holland and M. I. Steinberg, *Toxicol. Appl. Pharmacol.*, **47**, 123 (1979).

(17) J. Markowitz, J. Archibald, and H. G. Downie, "Experimental Surgery," Williams & Wilkins, Baltimore, Md., 1964, p. 542.

(18) K. Verebely and C. E. Inturrisi, *J. Chromatogr.*, **75**, 195 (1973).

(19) A. C. Gornall, C. J. Bardawill, and M. M. David, *J. Biol. Chem.*, **177**, 751 (1949).

(20) C. M. Metzler, "NONLIN, A Computer Program for Parameter Estimation in Nonlinear Situations," Upjohn Co., Kalamazoo, Mich., 1969.

(21) P. L. Altman and D. S. Dittmer, "Biological Data Book," vol. III, 2nd ed., Federation of American Societies for Experimental Biology, Bethesda, Md., 1974, p. 1701.

(22) R. Kato, *Xenobiotica*, **7**, 25 (1977).

(23) E. A. Neal, P. J. Meffin, P. B. Gregory, and T. F. Blaschke, *Gastroenterology*, **77**, 96 (1979).

(24) D. G. Shand, *ibid.*, **77**, 184 (1979).

ACKNOWLEDGMENTS

Supported in part by Grant GM 20852 from the National Institute of General Medical Sciences, National Institutes of Health.

Anti-Inflammatory and Analgesic Profile of Amidines of 3-Amino-1,2,4-benzotriazine and 3-Amino-1,2,4-benzotriazine-1-oxide

B. A. REGAN, J. W. HANIFIN, M. J. LANDES, A. C. OSTERBERG, G. J. PATEL, D. N. RIDGE, A. E. SLOBODA, and S. A. LANG, Jr. ˣ

Received March 19, 1979, from the *Medical Research Division, American Cyanamid Company, Pearl River, NY 10965.* Accepted for publication February 6, 1980.

Abstract □ Several formamidine and acetamidine derivatives prepared from 3-amino-1,2,4-benzotriazine and 3-amino-1,2,4-benzotriazine-1-oxide displayed an aspirin-like anti-inflammatory and analgesic profile. The test systems included adjuvant-induced arthritis in rats, carrageenan-induced edema in rats, UV-induced erythema in guinea pigs, the analgesic gait test, the antipyretic test, and GI ulcer studies.

Keyphrases □ Anti-inflammatory activity—amidine derivatives of 3-amino-1,2,4-benzotriazines and their 1-oxides, synthesis and testing, rats □ Analgesic activity—amidine derivatives of 3-amino-1,2,4-benzotriazines and their 1-oxides, synthesis and testing, rats □ 3-Amino-1,2,4-benzotriazines—amidine derivatives, synthesis and testing for anti-inflammatory and analgesic activity, rats

Various new, nonsteroidal, anti-inflammatory agents such as ibuprofen, tolmetin, fenoprofen, naproxen, and sulindac have been introduced to the medical community in the past several years (1). Although these agents ameliorate the arthritic condition, they are not curative and have adverse effects, largely GI disturbances (1).

The continuing interest and need for more efficacious and safe anti-inflammatory agents prompted the synthesis of various formamidine and acetamidine derivatives of 3-amino-1,2,4-benzotriazine and 3-amino-1,2,4-benzotriazine-1-oxide. These agents were tested for analgesic, anti-inflammatory, and antipyretic properties in a battery of tests including adjuvant-induced arthritis, carrageenan-induced edema, and UV-induced guinea pig erythema (2, 3). Particular emphasis was placed on GI toxicity. The results are presented, and the potential of the active series is discussed.

RESULTS AND DISCUSSION

Chemistry—The amidines were prepared by the reaction of the

0022-3549/80/0700-0789$01.00/0

© 1980, American Pharmaceutical Association

is $F_{PH}F_H$, where F_{PH} is the fraction of the dose reaching the liver as intact drug and F_H is the fraction of the drug reaching the liver intact that enters the systemic circulation in unmetabolized form. If $F_{PH} = F$ after portacaval shunt (assuming that F_{PH} was not affected by the surgery and that there was no significant development of collateral circulation after the surgery), then F_H before surgery was 0.253/0.542 or 0.47 (based on the average systemic availability values from Table III). Thus, the prehepatic and hepatic first-pass effects on propoxyphene appear to be of similar magnitude in the dog.

Hepatic cirrhosis often is associated with the formation of portacaval shunts and reduction of drug-metabolizing enzyme activity (23, 24). These changes should increase the systemic availability of a drug with the pharmacokinetic characteristics of propoxyphene. This increase should be less pronounced if a substantial part of the first-pass effect is due to prehepatic biotransformation, provided that liver disease does not affect the prehepatic metabolism of propoxyphene. Unfortunately, the effect of liver disease on the prehepatic biotransformation of drugs is not known. However, it appears prudent to reduce the dosage of propoxyphene in patients with portacaval shunt or with cirrhosis of the liver.

REFERENCES

(1) *Fed. Regist.*, **44**, 11837 (1979).

(2) R. L. Wolen, C. M. Gruber, Jr., G. F. Kiplinger, and N. E. Scholz, *Toxicol. Appl. Pharmacol.*, **19**, 480 (1971).

(3) D. Perrier and M. Gibaldi, *J. Clin. Pharmacol.*, **12**, 449 (1972).

(4) L. F. Gram, J. Schou, W. L. Way, J. Heltberg, and N. O. Bodin, *Clin. Pharmacol. Ther.*, **26**, 473 (1979).

(5) G. W. A. Slywka, A. P. Melikian, P. L. Whyatt, and M. C. Meyer, *J. Clin. Pharmacol.*, **15**, 598 (1975).

(6) A. Melander, A. Berlin-Wahlen, N. O. Bodin, K. Danielson, G. Gustafsson, L. Lindgren, and D. Westerlund, *Acta Med. Scand.*, **202**, 119 (1977).

(7) R. E. McMahon and H. R. Sullivan, *Res. Commun. Chem. Pathol. Pharmacol.*, **14**, 631 (1976).

(8) R. E. McMahon, A. S. Ridolfo, H. W. Culp, R. L. Wolen, and F. J. Marshall, *Toxicol. Appl. Pharmacol.*, **19**, 427 (1971).

(9) R. Gugler, P. Lain, and D. L. Azarnoff, *J. Pharmacol. Exp. Ther.*, **195**, 416 (1975).

(10) R. L. Wolen, E. A. Ziege, and C. M. Gruber, *Clin. Pharmacol. Ther.*, **17**, 15 (1975).

(11) J. G. Wagner, P. G. Welling, S. B. Roth, E. Sakmar, K. P. Lee, and J. E. Walker, *Int. J. Clin. Phdrmacol.*, **5**, 371 (1972).

(12) K. Verebely and C. E. Inturrisi, *Clin. Pharmacol. Ther.*, **15**, 302 (1973).

(13) R. L. Wolen, B. D. Obermeyer, E. A. Ziege, H. R. Black, and C. M. Gruber, in "Stable Isotopes. Applications in Pharmacology, Toxicology, and Clinical Research," T. A. Baille, Ed., University Park Press, Dallas, Tex., 1978, p. 113.

(14) R. Nickander, S. E. Smits, and M. I. Steinberg, *J. Pharmacol. Exp. Ther.*, **200**, 245 (1977).

(15) H. Lund-Jacobsen, *Acta Pharmacol. Toxicol.*, **42**, 171 (1978).

(16) D. R. Holland and M. I. Steinberg, *Toxicol. Appl. Pharmacol.*, **47**, 123 (1979).

(17) J. Markowitz, J. Archibald, and H. G. Downie, "Experimental Surgery," Williams & Wilkins, Baltimore, Md., 1964, p. 542.

(18) K. Verebely and C. E. Inturrisi, *J. Chromatogr.*, **75**, 195 (1973).

(19) A. C. Gornall, C. J. Bardawill, and M. M. David, *J. Biol. Chem.*, **177**, 751 (1949).

(20) C. M. Metzler, "NONLIN, A Computer Program for Parameter Estimation in Nonlinear Situations," Upjohn Co., Kalamazoo, Mich., 1969.

(21) P. L. Altman and D. S. Dittmer, "Biological Data Book," vol. III, 2nd ed., Federation of American Societies for Experimental Biology, Bethesda, Md., 1974, p. 1701.

(22) R. Kato, *Xenobiotica*, **7**, 25 (1977).

(23) E. A. Neal, P. J. Meffin, P. B. Gregory, and T. F. Blaschke, *Gastroenterology*, **77**, 96 (1979).

(24) D. G. Shand, *ibid.*, **77**, 184 (1979).

ACKNOWLEDGMENTS

Supported in part by Grant GM 20852 from the National Institute of General Medical Sciences, National Institutes of Health.

Anti-Inflammatory and Analgesic Profile of Amidines of 3-Amino-1,2,4-benzotriazine and 3-Amino-1,2,4-benzotriazine-1-oxide

B. A. REGAN, J. W. HANIFIN, M. J. LANDES, A. C. OSTERBERG, G. J. PATEL, D. N. RIDGE, A. E. SLOBODA, and S. A. LANG, Jr. ˣ

Received March 19, 1979, from the *Medical Research Division, American Cyanamid Company, Pearl River, NY 10965.* Accepted for publication February 6, 1980.

Abstract □ Several formamidine and acetamidine derivatives prepared from 3-amino-1,2,4-benzotriazine and 3-amino-1,2,4-benzotriazine-1-oxide displayed an aspirin-like anti-inflammatory and analgesic profile. The test systems included adjuvant-induced arthritis in rats, carrageenan-induced edema in rats, UV-induced erythema in guinea pigs, the analgesic gait test, the antipyretic test, and GI ulcer studies.

Keyphrases □ Anti-inflammatory activity—amidine derivatives of 3-amino-1,2,4-benzotriazines and their 1-oxides, synthesis and testing, rats □ Analgesic activity—amidine derivatives of 3-amino-1,2,4-benzotriazines and their 1-oxides, synthesis and testing, rats □ 3-Amino-1,2,4-benzotriazines—amidine derivatives, synthesis and testing for anti-inflammatory and analgesic activity, rats

Various new, nonsteroidal, anti-inflammatory agents such as ibuprofen, tolmetin, fenoprofen, naproxen, and sulindac have been introduced to the medical community in the past several years (1). Although these agents ameliorate the arthritic condition, they are not curative and have adverse effects, largely GI disturbances (1).

The continuing interest and need for more efficacious and safe anti-inflammatory agents prompted the synthesis of various formamidine and acetamidine derivatives of 3-amino-1,2,4-benzotriazine and 3-amino-1,2,4-benzotriazine-1-oxide. These agents were tested for analgesic, anti-inflammatory, and antipyretic properties in a battery of tests including adjuvant-induced arthritis, carrageenan-induced edema, and UV-induced guinea pig erythema (2, 3). Particular emphasis was placed on GI toxicity. The results are presented, and the potential of the active series is discussed.

RESULTS AND DISCUSSION

Chemistry—The amidines were prepared by the reaction of the

0022-3549/80/0700-0789$01.00/0

© 1980, American Pharmaceutical Association

Table I—Amidine Derivatives Prepared from 3-Amino-1,2,4-benzotriazines and Their 1-Oxides

Compound	R_1	R_2	Melting Point	Yield, %	Molecular Formula	Analysis, %	Calc.	Found
Ia	F	H	106–109°	48	$C_{10}H_{10}FN_5$	C	54.78	54.62
						H	4.60	4.56
						F	8.67	8.77
						N	31.95	32.03
Ib	CH_3	H	98–101°	75	$C_{11}H_{13}N_5$	C	61.37	61.28
						H	6.09	6.18
						N	32.24	32.03
Ic	H	H	100–103°	65	$C_{10}H_{11}N_5$	C	59.68	59.53
						H	5.51	5.45
						N	34.81	34.77
Id	Cl	H	135–137°	84	$C_{10}H_{10}ClN_5$	C	50.96	50.93
						H	4.28	4.36
						Cl	16.05	15.91
						N	29.72	29.95
Ie	F	CH_3	125–126.5°	31	$C_{11}H_{12}FN_5$	C	56.74	56.65
						H	5.37	5.19
						F	8.06	8.15
						N	30.21	30.03
If	Cl	CH_3	141.5–143°	68	$C_{11}H_{12}ClN_5$	C	52.91	52.98
						H	4.84	4.69
						Cl	14.20	13.89
						N	28.05	28.11
IIa	F	H	188–190°	72	$C_{10}H_{10}FN_5O$	C	51.06	51.07
						H	2.48	4.12
						F	8.08	8.28
						N	29.78	30.03
IIb	CH_3	H	148–150°	61	$C_{11}H_{13}N_5O$	C	57.10	56.96
						H	5.66	5.83
						N	30.29	30.36
IIc	H	H	156–158°	58	$C_{10}H_{11}N_5O$	C	55.29	55.28
						H	5.10	5.22
						N	32.24	32.35
IId	Cl	H	177–178°	64	$C_{10}H_{10}ClN_5O$	C	47.72	47.95
						H	4.00	3.95
						Cl	14.09	14.06
						N	27.83	27.75
IIe	Br	H	162–164°	35	$C_{16}H_{10}BrN_5O$	C	40.56	40.24
						H	3.40	3.23
						Br	26.99	26.90
						N	23.65	23.90
IIf	F	CH_3	158–160°	19	$C_{11}H_{12}FN_5O$	C	52.77	53.01
						H	4.86	4.86
						F	7.48	7.62
						N	28.22	28.11

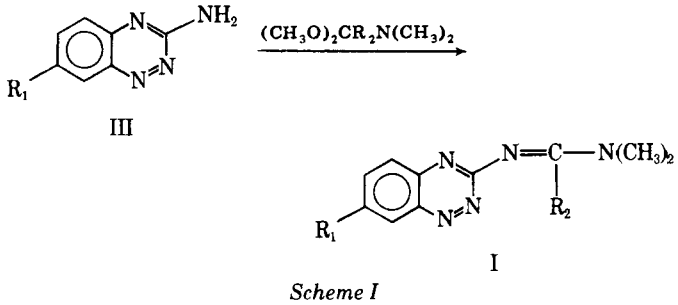

Scheme I

aminobenzotriazines (III) and their 1-oxides (IV) with excess dimethylformamide dimethylacetal or dimethylacetamide dimethylacetal (Schemes I and II).

Workup gave the derivatives of III (I) and the derivatives of IV (II) in 20–85% yields. Table I lists the 12 synthesized amidines.

Biological—Amidines Ia–If and IIa–IIf were first evaluated for activity against adjuvant-induced arthritis in rats (4). Groups of three Royal Hart Wistar rats, 200 ± 10 g, were injected intradermally in the right hindpaw with dried human tubercle bacilli in a mineral oil vehicle[1] at 2 mg/kg. The test compounds were administered orally in a 1.5% starch vehicle at the indicated dosage (Table II) once daily on Days 0–13 postchallenge. Control rats were treated similarly but were given the starch vehicle instead of the test compound.

On Days 14 and 21 postchallenge, the diameter of the injected paw (primary lesion) was measured with a micrometer caliper (6), the volumes of the inflamed paws were estimated from these measurements, and the results were expressed as percent inhibition of swelling as compared to 12 controls. If the percent inhibition was ≥24%, the compound was tested again. After the second test, the mean inhibition of swelling for both tests was calculated; if it was ≥26%, the compound was tested a third time. If the mean inhibition of all three tests was ≥25%, the compound was accepted as active. Such compounds were completely retested again in the same manner to confirm activity. Thus, no compound was considered to have confirmed activity until the test was repeated a minimum of six times (total of 18 rats).

In the dose–response experiments, the other inflamed sites such as the ears, paws, and tail (secondary lesions) were observed and graded. The mean grade was calculated and similarly expressed as the percent inhibition as compared to controls.

The active compounds (those showing at least 25% mean inhibition

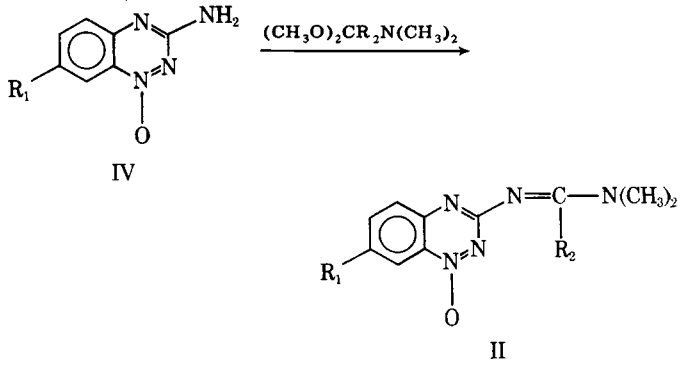

Scheme II

[1] Freund's adjuvant.

Table II—Pooled Data [a] for Adjuvant-Induced Arthritis

Compound	Oral Dose[b], mg/kg	Dead/Treated at 21 Days	Percent Inhibition of Swelling (Primary Lesion) Day 14	Percent Inhibition of Swelling (Primary Lesion) Day 21	Percent Inhibition of Control Grade (Secondary Lesion) Day 14	Percent Inhibition of Control Grade (Secondary Lesion) Day 21
Indomethacin[c]	2	8/57	51[d]	24[d]	38[d]	25[d]
	1	9/54	46[d]	19[d]	34[d]	20[d]
	0.5	5/54	40[d]	20[d]	25[d]	17[d]
	0.25	0/9	30[d]	4[d]	22[d]	4[d]
Aspirin[c]	400	18/57	73[d]	48[d]	58[d]	45[d]
	200	10/66	48[d]	27[d]	26[d]	17[d]
	100	18/63	36[d]	13	19[d]	8
	50	2/21	23[d]	3	12	9
I*a*	100	6/18	54[d]	44[d]	73[d]	48[d]
	50	6/33	51[d]	26[d]	69[d]	49[d]
	25	2/18	49[d]	24[d]	31[d]	0
I*d*	100	1/18	66[d]	24	83[d]	54[d]
	50	2/36	46[d]	15	36[d]	20[d]
	25	1/18	41	16	30[d]	18
II*a*	100	12/18	77[d]	76[d]	97[d]	82[d]
	50	5/36	51[d]	31[d]	65[d]	40[d]
	25	3/18	29[d]	19	35[d]	24[d]
I*b*	50	5/36	0	0	—	—
I*c*	50	0/3	27	5	—	—
I*e*	50	3/6	17	0	—	—
I*f*	50	2/18	59[d]	29[d]	—	—
II*b*	50	0/3	0	0	—	—
II*c*	50	0/3	0	0	—	—
II*d*	50	1/18	46[d]	13	—	—
II*e*	50	1/3	24	0	—	—
II*f*	50	0/3	12	32	—	—

[a] There were 12 control arthritic rats in each experiment with six treated rats per group in dose–response experiments and three treated rats per group in screening tests. Each experiment was repeated several times, as reflected by the total number of animals shown. Statistical comparisons were performed using paw diameters or arthritic grades, although results were expressed as percent inhibition. The statistical significance of each test result also was determined by a *t* test. Since the data from all available testing were pooled, the probabilities obtained in the individual Student *t* test analysis were combined as described by Snedecor and Cochran (5). For the control rats, eight of 186 had died by Day 21. [b] By gavage. [c] Historical data. [d] Statistically significant activity ($p < 0.05$) by the Student *t* test).

of swelling based on a total of 18 rats) then were tested against acute inflammatory conditions in carrageenan-induced edema in rats and UV-induced erythema in guinea pigs.

The method for the carrageenan-induced edema assay used was similar to that described by Winter *et al.* (7). Royal Hart Wistar rats, 80–90 g, were fasted overnight prior to dosing but had free access to water. Drugs in an aqueous suspension were administered by gavage in a volume of 1.7 ml/50 g of body weight (corresponding to the hydration volume used by Winter *et al.*).

The phlogistic agent, carrageenan[2], was prepared as a sterile 1% suspension in 0.9% NaCl for routine testing. A volume of 0.05 ml was injected through a 26-gauge needle into the plantar tissue of the right hindpaw. Measurements were made 5 hr after drug administration (4 hr after carrageenan challenge) unless otherwise indicated.

Volumes of both the normal and carrageenan-inflamed feet were determined, and the difference between the two measurements was considered to be the increased edema due to carrageenan administration. Results were expressed as a C/T efficacy ratio (mean edema of control animals/mean edema of treated animals). Each screening test had eight control rats and two treated rats. If the C/T ratio was ≥1.41, the test was repeated. If the mean ratio for Tests 1 and 2 was >1.43, the compound was considered active and the procedure was repeated for confirmation. Thus, no compound was considered to have confirmed activity until each test was repeated four times (32 controls, eight treated rats). The results for the amidines along with several reference agents are listed in Table III.

The method used to determine erythema in guinea pigs was similar to that of Winder *et al.* (8). Albino guinea pigs[3] were depilitated on their flanks the evening before testing with a standard mixture of barium sulfide and gum acacia. On the morning of testing, groups of four guinea pigs were dosed by gavage 1 hr prior to UV exposure (−1 hr). At 0 hr, they were restrained in a plastic container, which allowed exposure of three circular spots. They then were exposed to UV irradiation[4] for 60 sec. At +1 and +4 hr, the degree of erythema for each of the three sites was assessed according to the following scoring system: 0 = no erythema, 0.5 = incomplete circle or faint erythema, and 1.0 = complete circle of distinct erythema. Thus, the maximum score for each animal was 3.0. The results for a select group of amidines and reference drugs are shown in Table IV.

A modification of the method described by Atkinson and Cowan (9) was used to assess analgesic activity. A 40% suspension of Brewer's yeast in normal saline (0.25 ml/rat) was injected into the plantar surface of the left hindpaw of each rat. After 3 hr, predrug assessment of walking gait on a wire-mesh platform was made for each rat according to the following scoring system: 0 = normal gait, 0.5 = intermittent mild limp, 1 = constant limp with continuous use of foot pad, 1.5 = limping with occasional three-legged gait or intermittent use of digits in combination with foot pad, and 2 = continuous three-legged gait or continuous use of only the tips of the digits without any use of the inflamed foot pad.

Rats with a score of <2 were excluded from the experiment. The test compounds or vehicle then were administered orally to groups of six rats, and postdrug assessments were recorded after 90 min. A positive analgesic response was considered to be a ≥50% reversal of the pretreatment score (*i.e.*, posttreatment score of ≤1).

For selected compounds, subsequent experiments were performed with at least three graded dosage levels and five rats per group. Pre- and postdrug assessments were made as described.

The dose estimated to cause a positive analgesic response in 50% of the rats (ED_{50}) was calculated according to the arc-sine linear transformation method of Finney (10). The ED_{50} values for the remaining compounds were approximated.

The effect of the amidines on experimental elevated temperatures was examined during the analgesic gait test. The body temperature of rats increases after the plantar injection of Brewers' yeast, thus providing a good experimental model for studying antipyresis.

The rectal temperature of each rat was measured immediately after pretreatment scoring of abnormal gait by a rectal probe[5]. Ninety minutes after treatment with the compounds, the temperature was recorded again. The average change of each group of rats was calculated from the difference of the pretreatment and posttreatment temperatures.

The antipyretic and analgesic data are summarized in Table V.

GI ulcer studies were conducted in male Royal Hart Wistar rats weighing 190–210 g. The rats were distributed among control and treatment groups (five rats per group) and housed with one rat per cage. During the 52-hr test period, the rats were permitted free access to food and drinking water for the first 33 hr but were fasted overnight prior to

[2] Viscarin, obtained from Marine Colloids.
[3] Lederle breeding colony.
[4] Model 10 "Hanovia" Kromayer lamp.
[5] Yellow Springs telethermometer.

Table III—Pooled Data [a] of Carrageenan-Induced Edema of Rat Paws

Compound	Oral Dose, mg/kg	Number of Rats	C/T[b]
Controls		64	1.0
Aspirin[c]	250	32	2.8[d]
	83	32	1.4[d]
Phenylbutazone[c]	250	32	2.3[d]
	83	32	2.4[d]
	27	32	1.7[d]
Indomethacin[c]	250	32	2.9[d]
	83	32	2.3[d]
	27	32	2.2[d]
	9	32	2.0[d]
	3	32	1.5[d]
Ia	250	12	3.1[d]
	83	12	3.0[d]
	27	12	1.6[d]
Id	250	12	2.5[d]
	83	12	2.1[d]
IIa	250	12	3.4[d]
	83	12	2.8[d]
	27	12	1.6[d]
Ib	250	2	1.0
Ic	250	8	3.6[d]
Ie	250	2	2.4[d]
If	125	8	3.4[d]
IIc	250	8	2.7[d]
IId	250	8	2.6[d]
IIf	60	2	1.2

[a] There were eight control edematous rats in each experiment with four rats per treated group in dose–response experiments and three rats per treated group in screening tests. Each experiment was repeated several times, as reflected by the total number of rats shown. Statistical comparisons were performed using rat paw edema volumes, although the results were expressed as control/treated ratios. The statistical significance of each test result was determined by the Student *t* test. Since all available data were pooled, the probabilities obtained in each individual Student *t* test were combined as described by Snedecor and Cochran (5). [b] Edema of control animals/edema of treated animals. [c] Historical data. [d] Active ($p < 0.05$ by the Student *t* test).

Table IV—Effects on UV-Induced Erythema in Guinea Pigs [a]

Compound	Average Score 1 hr	Average Score 4 hr	Number of Guinea Pigs
Control[b]	2.1	2.8	364
Aspirin[b]	0.1[c]	2.0	16
Phenylbutazone[b]	0.1[c]	1.1[c]	16
Indomethacin[b]	0.1[c]	1.3[c]	12
Ia	0.2[c]	1.6	8
Ib	1.0[c]	2.3	4
If	0.4[c]	2.6	8
IIa	0.2[c]	1.7	8
IId	0.9[c]	2.2	8

[a] The dose was 125 mg/kg po. [b] Historical data. [c] Active ($p < 0.05$ by the Student *t* test).

Table V—Analgesic and Antipyretic Activity

Compound	Reversal of Abnormal Gait, ED_{50}, mg/kg po (95% confidence limit)	Inhibition of Yeast-Induced Pyresis Temperature Change, °F (dose, mg/kg po)
Ia	20 (4–91)	−2.7 (100)
Ic	~100	−4.1 (200)
Id	79 (52–120)	−1.5 (100)
IIb	~200	+0.9 (200)[a]
IIc	107 (58–202)	−1.5 (200)
IIe	~150	−0.1 (200)[a]
IIa	35 (10–120)	−3.0 (100)
Aspirin	93 (53–163)	−1.3 (200)
Vehicle	—[b]	+0.2[a]

[a] Inactive. [b] No reversal of abnormal gait.

sacrifice. Drugs were suspended in a 1.5% starch–phosphate buffer solution and injected by gavage or subcutaneously twice daily on Days 0 and 1. The rats received only one injection on Day 2, and 6 hr later they were killed with chloroform.

The stomachs were dissected, opened along the greater curvature, and rinsed briefly in tap water. They then were spread with the mucosal surface facing upward and were pinned onto corks (6.35-cm diameter) individually numbered on the back. The identification number for each stomach was not known to the investigator, and the stomachs were randomly graded according to the following scheme (11): 0 = normal; 1 = petechial hemorrhage or pinpoint ulcers; 2 = one or two small ulcers or hemorrhagic erosions; 3 = many areas of hemorrhagic erosion or ulcers, a few large; and 4 = massive areas of hemorrhagic erosion or many ulcers, mainly large.

The intestines also were removed and examined for ulcers. The intensity of intestinal ulceration was graded according to the following scheme: 0 = normal intestine; 1 = mucosa thin, petechial hemorrhage; 2 = "blow-outs" (intestine inflated with air); 3 = few ulcers—gut more fragile than normal and tears along line of mesentery attachments when removed; and 4 = many large perforating lesions, adhesions, gut hemorrhage (very fragile and tears readily and cannot be removed intact; *graded in situ*).

The results of two amidines and reference drugs are shown in Table VI.

Of the amidines reported in Table I, Ia, Id, IIa, and IId had the broadest scope of anti-inflammatory and analgesic activity, showing that the 3-amino-1,2,4-benzotriazines and 3-amino-1,2,4-benzotriazine-1-oxides with a fluorine or chlorine in the 7-position were the most active. The difference between the activity of the parent and the *N*-oxide in pairs Ia and IIa and Id and IId was marginal. Of the nonhalogenated compounds, Ib, featuring a methyl group at C-7, possessed significant activity in most tests.

The acetamidines Ie, If, and IIf were active, but If and IIf were significantly lower in overall activity than their formamidine counterparts. 7-Fluoroacetamidine (Ie) was slightly less active than Ia overall.

Many of the amidines tested in the anti-inflammatory and analgesic tests possessed an acceptable therapeutic index. However, one serious side effect involves ulceration or hemorrhaging in the GI tract. Two of the most interesting compounds, Ia and IId, were administered to rats, and the GI tracts were examined (Table VI). Both compounds exhibited severe GI problems in the form of gastric ulceration and hemorrhaging. At doses of 200 and 100 mg/kg, respectively, both exhibited a gastric ulcer grade of 3.6–4.0 out of a possible 4.0. The severe GI ulceration and hemorrhaging problem precludes further development of amidines of 3-amino-1,2,4-benzotriazines and their 1-oxides.

EXPERIMENTAL[6]

Preparation of Amidines (12, 13)—A suspension of the aminobenzotriazine or *N*-oxide in dimethylformamide dimethylacetal or dimethylacetamide dimethylacetal was stirred and heated under reflux for 5 hr. If solution was not attained, 10–20 ml of dimethylformamide or dimethylacetamide was added at the 2-hr point. The excess acetal was removed *in vacuo*, and the residue was recrystallized directly or chromatographed and recrystallized.

***N'*-(7-Fluoro-1,2,4-benzotriazin-3-yl)-*N,N*-dimethylformamidine (Ia)**—A suspension of 10 g (0.06 mole) of 3-amino-7-fluoro-1,2,4-benzotriazine in 20 ml of dimethylformamide dimethylacetal was refluxed for 5 hr. On cooling, the solution was evaporated to dryness *in vacuo*. The residue was recrystallized twice from chloroform–hexane, giving yellow-orange plates, mp 106–109° (6.3 g, 48% yield); NMR ($CDCl_3$): 3.15 (s, 3), 3.20 (s, 3), 7.5 (m, 1), 7.7 (m, 1), 7.95 (m, 1), and 8.95 (s, 1).

***N'*-(7-Chloro-1,2,4-benzotriazin-3-yl)-*N,N*-dimethylformamidine (IId)**—A suspension of 10 g of 3-amino-7-chloro-1,2,4-benzotriazine in 20 ml of dimethylformamide dimethylacetal was refluxed for 5 hr. On cooling, the solution was evaporated *in vacuo*. The residue was recrystallized from chloroform–hexane, giving 10.1 g (84% yield) of orange needles, mp 135–137°; NMR ($CDCl_3$): 3.3 and 3.5 (s, 6), 7.6 (aryl, 2), 8.21 (aryl, 1), and 8.88 (s, 1).

[6] All melting points were taken on a Mel-Temp apparatus. Samples for elemental analyses were dried at 55° for 5–24 hr. NMR spectra were determined with a Varian model HA-100 spectrometer; chemical shifts are reported in parts per million relative to the internal standard tetramethylsilane.

Table VI—GI Ulcer Studies

Compound	Oral Dose[a], mg/kg	Dead/Treated	Grade of Gastric Ulcer[b] (95% confidence limits)	Grade of Intestinal Ulcer (95% confidence limits)
Aspirin[c]	250	0/9	2.7 (1.8–3.6)	0.6 (0–1.5)
	83	0/10	1.7 (0.9–2.5)	0
	27	0/10	1.1 (0.5–1.7)	0
Indomethacin[c]	27	2/10	2.0 (1.6–2.4)	3.5[d] (3.1–3.9)
	9	0/10	2.2 (1.0–3.4)	3.4[d] (2.6–4.0)
	3	5/10	1.1 (0.4–1.8)	1.1 (0.4–1.8)
Phenylbutazone[c]	150	2/10	2.0 (1.4–2.6)	0.6 (0–1.2)
	50	0/10	0.3 (0–0.8)	0
	12	0/10	0.5 (0–1.1)	0
Ia	200	4/5	3.6[d] (2.8–4.0)	1.0 (0–2.4)
	100	0/5	3.8[d] (3.2–4.4)	0
Id	200	0/5	4.0[d] (3.2–4.5)	0
	100	0/5	3.6[d] (2.8–4.0)	0
Controls	—	0/25	0.2 (0–0.4)	0

[a] Twice daily for 2 days and once on the 3rd day for a total of five doses. [b] Both the stomach and the intestines were removed during the autopsy and inspected for lesions. The severity of lesions was expressed by a grading system ranging from 4 (many large ulcers or severe hemorrhagic erosion) to 0 (normal). [c] Historical data. [d] Severe GI hemorrhaging.

***N'*-(7-Bromo -1,2,4- benzotriazin-3-yl-1-oxide) -*N,N*- dimethylformamidine (IIe)**—A suspension of 10 g of 3-amino-7-bromo-1,2,4-benzotriazine-1-oxide was refluxed in 20 ml of dimethylformamide dimethylacetal. At 2 hr, a suspension still was evident; 10 ml of dimethylformamide was added, and reflux was resumed for 3 hr more. After cooling, the excess acetal was removed *in vacuo*. The residue was dissolved in chloroform, filtered through a silica gel plug, and heated to reflux. Hexane was added to induce cloudiness, and the solution was cooled, giving 5.1 g (35% yield) of yellow-brown cubes, mp 162–164°; NMR ($CDCl_3$): 3.26 and 3.29 (s, 6), 7.7 (d, 1, J = 8 Hz), 7.7 (d of d, 1, J = 1.0 and 8.1 Hz), 8.5 (d, 1, J = 1 Hz), and 8.8 (s, 1).

***N'*-(7-Fluoro - 1,2,4 - benzotriazin - 3-yl-1-oxide)-*N,N*-dimethylacetamidine (IIf)**—A solution of 10 g (0.056 mole) of 3-amino-7-fluoro-1,2,4-benzotriazine-1-oxide in 22 ml of dimethylacetamide dimethylacetal was refluxed for 5 hr and cooled, and the excess acetal was evaporated to dryness under vacuum. The residue was eluted through a short silica gel column with 20% ethyl acetate in hexane to provide 2.6 g (19% yield) of II*f*, mp 158–160°; NMR ($CDCl_3$): 2.24 (s, 3), 3.18 (s, 6), and 7.3–8 (m, 3).

***N'*-(7-Chloro-1,2,4-benzotriazin-3-yl) -*N,N*- dimethylacetamidine If)**—A solution of 5.0 g (0.03 mole) of 3-amino-7-chloro-1,2,4-benzotriazine in 11 ml of dimethylacetamide dimethylacetal was refluxed for 4 hr. The solution then was cooled, and the excess acetal was removed under vacuum. The residue was recrystallized from chloroform–hexane to yield 4.7 g of I*f* (58% yield), mp 141.5–143°; NMR ($CDCl_3$): 2.28 (s, 3), 3.26 (s, 6), 7.72 (m, 2), and 8.30 (m, 1).

***N'*-(7-Fluoro-1,2,4-benzotriazin-3-yl) -*N,N*- dimethylacetamidine (Ie)**—A solution of 10 g (0.06 mole) of 3-amino-7-fluoro-1,2,4-benzotriazine in 20 ml of dimethylacetamide dimethylacetal was refluxed for 5 hr. On cooling, the solution was evaporated to dryness under vacuum. The residue was dissolved in chloroform, eluted through a pad of silica gel, and concentrated. Trituration of the concentrate with petroleum ether (bp 30–60°) produced 9.4 g of a crystalline product (31% yield), mp 125–126.5°; NMR ($CDCl_3$): 2.24 (s, 3), 3.24 (s, 6), and 7.4–8.1 (m, 3).

REFERENCES

(1) R. C. Williams, Jr., *Hosp. Pract.*, **June**, 57 (1979).

(2) A. E. Sloboda and A. C. Osterberg, *Inflammation*, 1, 415 (1976).

(3) A. P. Roszkowski, W. H. Rooks, II, A. J. Tomolonis, and L. M. Miller, *J. Pharmacol. Exp. Ther.*, **179**, 114 (1979).

(4) S. A. Lang, Jr., B. D. Johnson, E. Cohen, A. E. Sloboda, and E. Greenblatt, *J. Med. Chem.*, **19**, 1404 (1976).

(5) G. W. Snedecor and W. G. Cochran, "Statistical Methods," Iowa State College Press, Ames, Iowa, 1967, pp. 216, 217.

(6) B. B. Newbould, *Br. J. Pharmacol. Chemother.*, **21**, 127 (1963).

(7) C. A. Winter, F. A. Risley, and G. W. Nuss, *Proc. Soc. Exp. Biol. Med.*, **111**, 544 (1962).

(8) C. A. Winder, J. Waz, V. Burr, M. Been, and C. E. Rosiere, *Arch. Int. Pharmacodyn. Ther.*, **116**, 261 (1958).

(9) D. C. Atkinson and A. Cowan, *J. Pharm. Pharmacol.*, **26**, 727 (1974).

(10) D. J. Finney, "Statistical Methods in Biological Assay," 2nd ed., Hafner, New York, N.Y., 1964, 456ff.

(11) A. A. A. Abdel-Galil and P. B. Marshall, *Br. J. Pharmacol. Chemother.*, **33**, 1 (1968).

(12) H. Meerwein, W. Florian, N. Schan, and G. Stopp, *Justus Liebigs Ann. Chem.*, **641**, 1 (1961).

(13) P. F. Fabio, T. L. Fields, Y. Lin, E. J. Burden, S. Carvajal, K. C. Murdock, and S. A. Lang, Jr., *J. Med. Chem.*, **21**, 273 (1978).

ACKNOWLEDGMENTS

The authors are grateful to Mr. W. Fulmor, Mr. L. Brancone, and their associates for their technical assistance in obtaining spectral and microanalytical data. They also thank Ms. L. Harten for synthetic support.

Macro- and Micromethods for High-Performance Liquid Chromatographic Analysis of Oxaprozin in Plasma

SUZANNE L. McHUGH, SANDRA K. KIRKMAN, and JOHN A. KNOWLES ˣ

Received December 6, 1979, from *Wyeth Laboratories, Philadelphia, PA 19101.* Accepted for publication February 7, 1980.

Abstract □ A high-performance liquid chromatographic method for the analysis of oxaprozin in the presence of ketoprofen (the internal standard) was developed. Sample preparation involved macro- and microextraction procedures. An octadecylsilane reversed-phase system with an acetonitrile–phosphate buffer (pH 3.9) mobile phase was used to separate the compounds from the extracted plasma components and the oxaprozin metabolites. Linear UV detector response over a wide concentration range resulted in rapid and reproducible quantitation.

Keyphrases □ Oxaprozin—high-performance liquid chromatographic analysis with macro- and microextraction methods, comparison with GLC, human and rat plasma □ High-performance liquid chromatography—analysis, oxaprozin, macro- and microextraction methods, comparison with GLC, human and rat plasma □ Anti-inflammatory agents—oxaprozin, high-performance liquid chromatographic analysis, comparison with GLC

Oxaprozin (4,5-diphenyl-2-oxazolepropionic acid), a nonsteroidal, anti-inflammatory compound (1), was analyzed previously in plasma using GLC (2). This paper describes both macro- and micromethods for the high-performance liquid chromatographic (HPLC) determination of plasma oxaprozin concentrations. Time–concentration profiles obtained by each method also are presented.

EXPERIMENTAL

Materials—Anhydrous sodium acetate[1], monobasic and dibasic sodium phosphate[1], absolute ether[1], acetic acid[2], and hydrochloric acid[2] were analytical reagent grade. ACS grade 85% phosphoric acid[3] was used. Glass-distilled acetonitrile[4] was used in the mobile phase. The internal standard was ketoprofen[5].

Macromethod—Aliquots (0.5 ml) of unknown plasma or plasma spiked with standard oxaprozin were placed in 20 × 125-mm screw-capped test tubes to which were added 2.5 ml of distilled water and 1.0 ml of ketoprofen solution in 0.1 *M* acetate buffer (pH 4.8). The concentration of the internal standard ranged from 20 μg/ml for the low range samples and standards (1–10 μg of oxaprozin/ml) to 60 μg/ml for oxaprozin concentrations up to 200 μg/ml, but it was held constant in all cases for each set of samples analyzed. The control plasmas were treated with an identical volume of pH 4.8 buffer without the internal standard.

The samples were adjusted to pH 2 with 1.0 *N* HCl (~ 0.2 ml), and 8 ml of ether was added to each tube. The tubes then were capped, shaken mechanically for 10 min, and centrifuged to 2000 rpm for 5 min. Aliquots (7 ml) of the ether phase were transferred to clean test tubes and evaporated to dryness under reduced pressure at room temperature. The dried extracts were redissolved in 0.5 ml of the mobile phase, and 10-μl aliquots were injected onto the chromatographic column.

Analyses were performed using a high-performance liquid chromatograph[6] equipped with an octadecylsilane column[7]. Separation was achieved by reversed phase using a mobile phase of 62% acetonitrile in 0.05 *M* NaH_2PO_4 (adjusted to pH 3.9 with phosphoric acid) at a flow rate of 1.5 ml/min. The samples were introduced onto the column by means of a syringe-loaded sample injector[8]. At 290 nm, the detection range was 0.02 absorbance unit full scale (aufs) for the lower standards and 0.2–0.5 aufs for those of higher concentration.

A standard curve was generated by plotting the known concentrations of oxaprozin in the extracted standards against the ratios calculated by dividing the oxaprozin peak height (millivolts) by the internal standard peak height (millivolts). Quantitation of the unknowns was achieved by comparing the peak height ratios to this standard curve.

Micromethod—Aliquots (50 μl) of unknown or control plasma were placed in 6 × 50-mm disposable glass tubes. The control plasmas were spiked with 50-μl aliquots of oxaprozin standards (1.0–60 μg/ml) in 0.1 *M* phosphate buffer (pH 7.0). The unknowns were treated with an equal volume of buffer without the standard.

A 50-μl aliquot of a 5-μg/ml solution of ketoprofen in 0.1 *M* phosphate buffer (pH 7) was added to each sample and standard of the low range (0.1–2 μg/ml). Internal standardization of the high range (3–60 μg/ml) samples and standards was achieved with the addition of 50 μl of a 20-μg/ml ketoprofen solution in the same buffer. Two hundred microliters of fresh absolute ether was added to each sample, which then was mixed for 5 sec using a vortex mixer and centrifuged to break up the emulsion. The ether phases were transferred nonquantitatively to fresh tubes, and the extraction was repeated twice. The combined ether extracts were

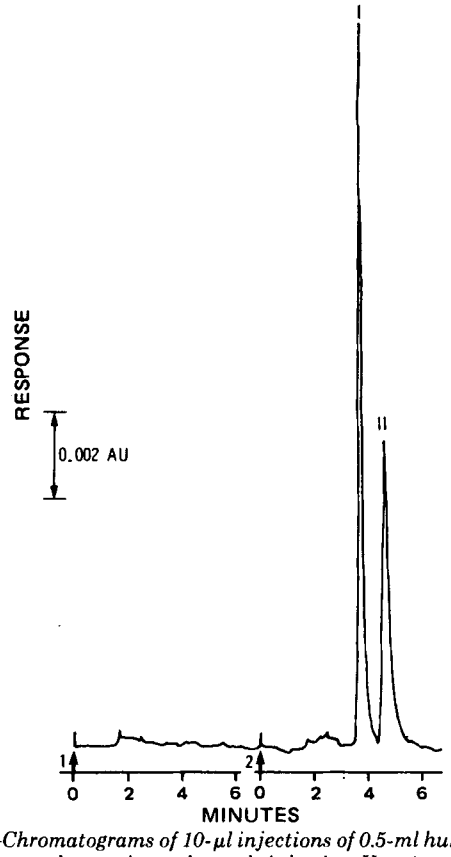

Figure 1—*Chromatograms of 10-μl injections of 0.5-ml human plasma extracts. Arrows denote times of sample injection. Key: 1, control plasma extract; and 2, extract of plasma spiked with ketoprofen (I) (30 μg/ml) and oxaprozin (II) (5 μg/ml).*

[1] Mallinckrodt, St. Louis, Mo.
[2] J. T. Baker Chemical Co., Phillipsburg, N.J.
[3] Fisher Scientific Co., Fair Lawn, N.J.
[4] Burdick & Jackson Laboratories, Muskegon, Mich.
[5] Courtesy of Ives Laboratories, New York, N.Y.
[6] LDC analyst series 7800 with a Spectromonitor III UV monochrometer (or equivalent), a model 308 computing integrator, and a model 3401 strip-chart recorder, Laboratory Data Control, Riviera Beach, Fla.
[7] Chromegabond C_{18}, 10-μm particle size, 30 cm × 4.6 mm i.d., E.S. Industries, Marlton, N.J.
[8] Model 7120, Rheodyne, Berkeley, Calif.

0022-3549/80/0700-0794$01.00/0
© 1980, American Pharmaceutical Association

Table I—Concentrations of Oxaprozin in Human Plasma after a Single 600-mg Oral Dose of Oxaprozin

Hours	Oxaprozin, μg/ml[a]
0	0
1	49.4
2	57.9
4	73.0
6	71.2
9	65.9
12	60.5
24	49.3
48	32.1
96	17.4
144	9.1
168	6.7
240	3.0

[a] Concentrations represent the means for three normal human volunteers.

taken to dryness under a nitrogen stream. The dried extracts were redissolved in 50 μl of the mobile phase, and a 20-μl injection was made.

The HPLC instrument[9] was equipped with a precolumn in addition to the analytical column[7]. The precolumn (5 cm × 2.1 mm i.d.) was filled with dry octadecylsilane[10] by the tap and fill method. The mobile phase was similar to that used in the macromethod, except that the acetonitrile concentration was decreased to 60% to optimize separation. At 280 nm, the detection range was 0.002–0.016 aufs and the peak heights were measured manually. The method of quantitation was the same as for the macromethod.

RESULTS

Macromethod—The chromatograms in Fig. 1 illustrate the absence of interference from control plasma, the peak shape symmetry, and the sensitivity of the detector response. The method achieved good peak separation in <6 min with a lower limit of detectability of 0.5 μg of oxaprozin/ml of plasma. Peak height ratios of the standards over the oxaprozin concentration range of 1–200 μg/ml gave a linear regression line with a correlation coefficient of 0.9993.

The relative accuracy of the method was determined by comparing the HPLC results to the GLC results for a series of human plasma samples taken within 48 hr of an oral 600-mg dose of oxaprozin. The correlation between the two methods of analysis was 0.98. The accuracy of the GLC method was determined previously by comparison with radioactive monitoring of carbon 14 (2). The time–concentration profiles obtained by both HPLC and GLC are presented in Fig. 2. The recovery from plasma was 90.1 ± 3.7%. The coefficient of variation of the HPLC assay was 1.9%. Table I presents the mean drug concentrations in human plasma following a single oral 600-mg dose.

Micromethod—The chromatograms in Fig. 3 represent the analysis of rat plasma extracted by the micromethod. No interference from plasma components was observed, and oxaprozin was separated from its metabolites, including the hydroxylated compounds identified previously[11] (2). The lower limit of detectability was 0.1 μg of oxaprozin/ml of plasma, and the peak height of the standards between 0.1 and 60.0 μg/ml resulted

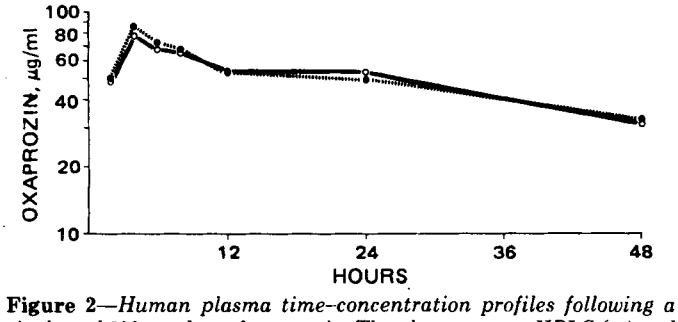

Figure 2—*Human plasma time–concentration profiles following a single oral 600-mg dose of oxaprozin. The plots compare HPLC (●) and GLC (○) results.*

[9] LDC model 2396 dual minipumps with a model 1203 UV-III monitor and a model 3401 strip-chart recorder.

[10] Co:Pell ODS, 37–45-μm particle size, Whatman, Clifton, N.J.

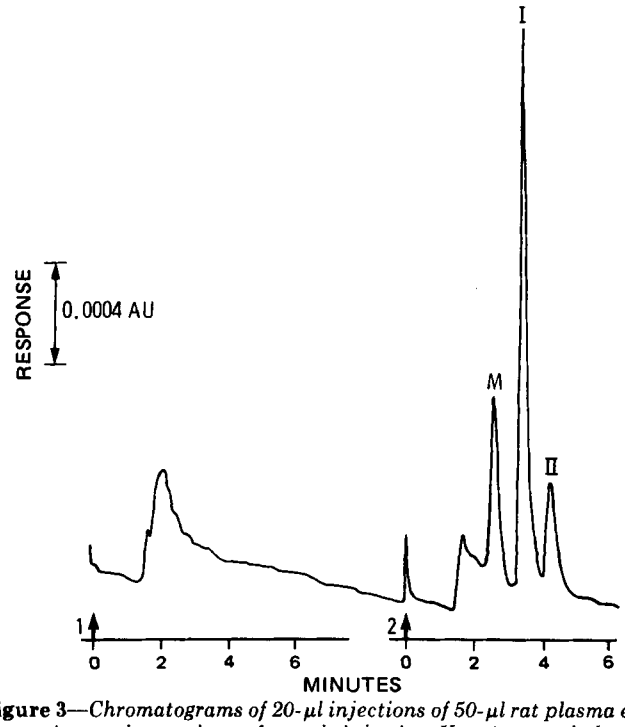

Figure 3—*Chromatograms of 20-μl injections of 50-μl rat plasma extracts. Arrows denote times of sample injection. Key: 1, control plasma extract; and 2, extract of rat plasma obtained 4 hr after a 20-mg/kg oral dose of oxaprozin. The peaks represent 20 μg of ketoprofen/ml (I), 1.9 μg of oxaprozin/ml (II), and a nonquantified amount of oxaprozin metabolites (M).*

in a linear regression correlation coefficient of 0.9994. The coefficient of variation of the micromethod was 3.3%.

A plasma time–concentration profile resulting from an oral dose of 20 mg of oxaprozin/kg to a rat is presented in Fig. 4. The plasma recoveries were similar to those obtained using the macromethod.

DISCUSSION

The HPLC methods outlined here represent several advantages over the GLC method employed previously. Since derivatization is no longer necessary, sample preparation time is shortened and the use of hazardous

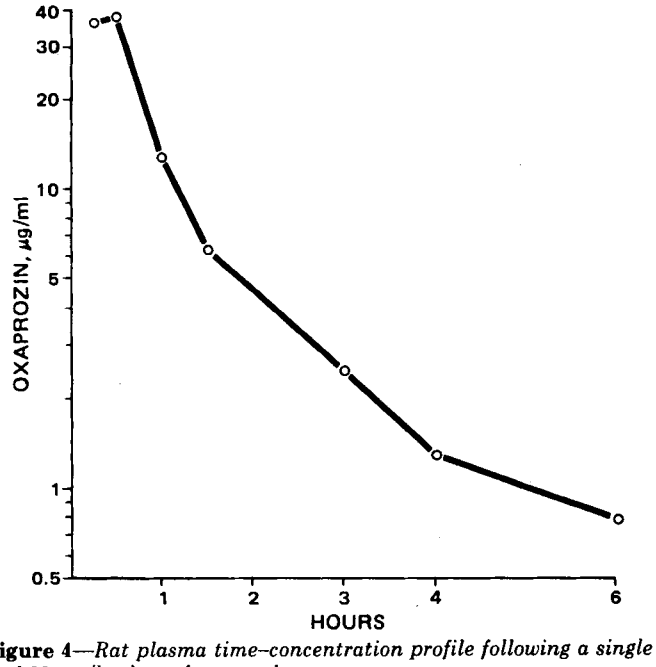

Figure 4—*Rat plasma time–concentration profile following a single oral 20-mg/kg dose of oxaprozin.*

diazomethane is eliminated. The precision of the macromethod is better than that reported for the GLC assay (2), while that of the micromethod is equal to that of the GLC method. The micromethod permits monitoring of drug concentrations in small volumes of plasma, making pharmacokinetic studies in rats and children feasible.

As reported for the GLC method (2), this procedure can be used to determine oxaprozin concentrations in urine by extracting the free drug at pH 7 rather than at pH 2. This modification is necessary in both urine and rat plasma[11] to avoid the partial extraction of oxaprozin glucuronide.

[11] F. W. Janssen and S. K. Kirkman, unpublished data.

Due to the chromatographic separation of oxaprozin from its major metabolites, no other modification in the extraction procedure is necessary.

REFERENCES

(1) K. Brown, J. F. Cavalla, D. Green, and A. B. Wilson, *Nature*, **219**, 164 (1968).

(2) F. W. Janssen, S. K. Kirkman, J. A. Knowles, and H. W. Ruelius, *Drug Metab. Dispos.*, **6**, 465 (1978).

Electronic Study of Receptor Binding of Analgesic Aryl Moiety II: Prodine Analogs

KHALID SABIH A. RAZZAK ˣ and KHAWLA A. HAMID

Received April 12, 1979, from the *College of Pharmacy, University of Baghdad, Baghdad, Iraq.* Accepted for publication February 5, 1980.

Abstract □ Analogs of the prodine analgesics were prepared and tested for analgesic activity. A good correlation seems to exist between the energy level of the highest occupied molecular orbital and biological activity. The energy level of the highest occupied molecular orbital of the aryl moiety of these analogs may permit a charge transfer interaction between the aryl groups of the analgesic molecules and their receptors with the aryl groups acting as charge donors.

Keyphrases □ Prodine analogs—synthesis, testing for analgesic activity, correlation between activity and energy level of highest occupied molecular orbital of aryl moiety □ Analgesic activity—prodine analogs, correlation between potency and energy level of highest occupied molecular orbital of aryl moiety □ Charge transfer interactions—prodine analogs, correlation between analgesic activity and energy level of highest occupied molecular orbital of aryl moiety, complex formation between aryl moiety and receptor

The synthesis of 1-methyl-4-(3-thienyl)-4-propionoxypiperidine (I) and its 2-pyridyl analog (II) was reported previously (1). A similar type of replacement of the benzene ring by heterocyclic rings, such as pyridine, also was reported for propoxyphene, tetralins, and chromanes (2). Compounds I and II were designed to study the receptor binding of the analgesic aryl moiety. The ED_{50} data obtained for I and II at 3.9 and 16.0 mg/kg, respectively, using the mouse–hot plate method and subcutaneous administration pointed to the possible interaction of the aryl group by forces (1) other than van der Waals forces (3, 4) or hydrophobic bonding (5). No further attempt was made to identify these possible forces.

BACKGROUND

Organic compounds containing aromatic rings form charge transfer complexes with other compounds, and they may act as donors or acceptors of the charge (6). Some biochemicals were found to interact in the biological system through the formation of charge transfer complexes (7). Their role as charge donors or acceptors depends on their respective highest occupied molecular orbital or lowest empty molecular orbital energy levels. Correlations between electron densities and the energy levels of the highest occupied molecular orbital or lowest empty molecular orbital and biological activity were described for cholinesterase inhibitors (8, 9), several antimalarials (10), hallucinogens (11), benzothiadiazine antihypertensives (12), and other compounds (13).

Charge transfer complex formation between the aryl moiety of the analgesic molecules and the analgesic receptor is one possibility for explaining variations in analgesic potency. This possibility can be studied by the synthesis of analogs of I and II with aryl groups having different energy levels for their highest occupied molecular orbital or lowest empty molecular orbital. Study of the analgesic activity of these analogs, expressed as their ED_{50} values, together with that of I and II may give more understanding as to how these groups interact with the receptors.

This paper describes the synthesis and analgesic activity of some prodine analogs and correlates the activity with the energy state of the highest occupied molecular orbital or lowest empty molecular orbital of the aryl groups in these analogs.

EXPERIMENTAL[1]

Formation of Aryl Lithium—The aryl halide (0.1 mole) was dissolved in 100 ml of dry ether, placed in a three-necked 500-ml flask, and cooled with a dry ice–acetone bath. An equivalent amount of *n*-butyl lithium[2] (2 moles in 100 ml of hexane) was added dropwise, with stirring, to the aryl halide solution under nitrogen.

Formation of 1-Methyl-4-arylpiperidine-4-ols (IV–VIII)—To the prepared aryl lithium salts was added, with stirring and cooling at the temperature of a dry ice–acetone bath, a solution of 1-methyl-4-piperidone[2] (0.1 mole, 11.3 g) in 100 ml of dry ether over 20 min. The temperature of the reaction mixture then was allowed to rise to 0° and was maintained for 45 min. The reaction mixture then was poured over 100 g of ice–hydrochloric acid (1:1).

The ether layer was separated and washed twice (~50 ml) with dilute hydrochloric acid, and the washings were added to the aqueous acid layer. The mixture was made basic with 10% NaOH and extracted three times (~100 ml) with ether and once with 100 ml of chloroform. The organic washings were mixed and dried over anhydrous sodium sulfate. Removal of the organic solvents under vacuum gave the required alcohols.

Microanalyses were performed on the pure products after recrystallization from the appropriate solvent or on the quaternary salts. The quaternary salts were prepared by treatment of the alcoholic product with methyl iodide or benzyl bromide in methanol and recrystallization from an alcohol–ether mixture.

The IR spectra (chloroform solution) of IV–VIII showed absorption bands in the region of the alcoholic hydroxyl group at 3400–3150 cm^{-1} and at 3100–3000 and 1600–1500 cm^{-1} due to the aryl rings introduced in the piperidine ring.

Esterification of IV–VIII—A solution of IV–VIII (0.02 mole) in 50

[1] All melting points were recorded in an oil bath and are uncorrected. IR spectra were recorded on a Perkin-Elmer model 257 spectrophotometer. All products had IR spectra in agreement with the assigned structures. The aryl halides (Fluka, AG, Bucks, Switzerland) and toluene were distilled before use. Ether was dried over anhydrous sodium sulfate. Microanalyses were performed at Midwest Microlab, Indianapolis, Ind., or by the Department of Medicinal Chemistry, University of Kansas, Lawrence, Kans.

[2] Fluka, AG, Bucks, Switzerland.

0022-3549/80/0700-0796$01.00/0
© 1980, American Pharmaceutical Association

diazomethane is eliminated. The precision of the macromethod is better than that reported for the GLC assay (2), while that of the micromethod is equal to that of the GLC method. The micromethod permits monitoring of drug concentrations in small volumes of plasma, making pharmacokinetic studies in rats and children feasible.

As reported for the GLC method (2), this procedure can be used to determine oxaprozin concentrations in urine by extracting the free drug at pH 7 rather than at pH 2. This modification is necessary in both urine and rat plasma[11] to avoid the partial extraction of oxaprozin glucuronide.

[11] F. W. Janssen and S. K. Kirkman, unpublished data.

Due to the chromatographic separation of oxaprozin from its major metabolites, no other modification in the extraction procedure is necessary.

REFERENCES

(1) K. Brown, J. F. Cavalla, D. Green, and A. B. Wilson, *Nature*, **219**, 164 (1968).

(2) F. W. Janssen, S. K. Kirkman, J. A. Knowles, and H. W. Ruelius, *Drug Metab. Dispos.*, **6**, 465 (1978).

Electronic Study of Receptor Binding of Analgesic Aryl Moiety II: Prodine Analogs

KHALID SABIH A. RAZZAK ˣ and KHAWLA A. HAMID

Received April 12, 1979, from the *College of Pharmacy, University of Baghdad, Baghdad, Iraq.* Accepted for publication February 5, 1980.

Abstract □ Analogs of the prodine analgesics were prepared and tested for analgesic activity. A good correlation seems to exist between the energy level of the highest occupied molecular orbital and biological activity. The energy level of the highest occupied molecular orbital of the aryl moiety of these analogs may permit a charge transfer interaction between the aryl groups of the analgesic molecules and their receptors with the aryl groups acting as charge donors.

Keyphrases □ Prodine analogs—synthesis, testing for analgesic activity, correlation between activity and energy level of highest occupied molecular orbital of aryl moiety □ Analgesic activity—prodine analogs, correlation between potency and energy level of highest occupied molecular orbital of aryl moiety □ Charge transfer interactions—prodine analogs, correlation between analgesic activity and energy level of highest occupied molecular orbital of aryl moiety, complex formation between aryl moiety and receptor

The synthesis of 1-methyl-4-(3-thienyl)-4-propionoxypiperidine (I) and its 2-pyridyl analog (II) was reported previously (1). A similar type of replacement of the benzene ring by heterocyclic rings, such as pyridine, also was reported for propoxyphene, tetralins, and chromanes (2). Compounds I and II were designed to study the receptor binding of the analgesic aryl moiety. The ED_{50} data obtained for I and II at 3.9 and 16.0 mg/kg, respectively, using the mouse–hot plate method and subcutaneous administration pointed to the possible interaction of the aryl group by forces (1) other than van der Waals forces (3, 4) or hydrophobic bonding (5). No further attempt was made to identify these possible forces.

BACKGROUND

Organic compounds containing aromatic rings form charge transfer complexes with other compounds, and they may act as donors or acceptors of the charge (6). Some biochemicals were found to interact in the biological system through the formation of charge transfer complexes (7). Their role as charge donors or acceptors depends on their respective highest occupied molecular orbital or lowest empty molecular orbital energy levels. Correlations between electron densities and the energy levels of the highest occupied molecular orbital or lowest empty molecular orbital and biological activity were described for cholinesterase inhibitors (8, 9), several antimalarials (10), hallucinogens (11), benzothiadiazine antihypertensives (12), and other compounds (13).

Charge transfer complex formation between the aryl moiety of the analgesic molecules and the analgesic receptor is one possibility for explaining variations in analgesic potency. This possibility can be studied by the synthesis of analogs of I and II with aryl groups having different energy levels for their highest occupied molecular orbital or lowest empty molecular orbital. Study of the analgesic activity of these analogs, expressed as their ED_{50} values, together with that of I and II may give more understanding as to how these groups interact with the receptors.

This paper describes the synthesis and analgesic activity of some prodine analogs and correlates the activity with the energy state of the highest occupied molecular orbital or lowest empty molecular orbital of the aryl groups in these analogs.

EXPERIMENTAL[1]

Formation of Aryl Lithium—The aryl halide (0.1 mole) was dissolved in 100 ml of dry ether, placed in a three-necked 500-ml flask, and cooled with a dry ice–acetone bath. An equivalent amount of *n*-butyl lithium[2] (2 moles in 100 ml of hexane) was added dropwise, with stirring, to the aryl halide solution under nitrogen.

Formation of 1-Methyl-4-arylpiperidine-4-ols (IV–VIII)—To the prepared aryl lithium salts was added, with stirring and cooling at the temperature of a dry ice–acetone bath, a solution of 1-methyl-4-piperidone[2] (0.1 mole, 11.3 g) in 100 ml of dry ether over 20 min. The temperature of the reaction mixture then was allowed to rise to 0° and was maintained for 45 min. The reaction mixture then was poured over 100 g of ice–hydrochloric acid (1:1).

The ether layer was separated and washed twice (~50 ml) with dilute hydrochloric acid, and the washings were added to the aqueous acid layer. The mixture was made basic with 10% NaOH and extracted three times (~100 ml) with ether and once with 100 ml of chloroform. The organic washings were mixed and dried over anhydrous sodium sulfate. Removal of the organic solvents under vacuum gave the required alcohols.

Microanalyses were performed on the pure products after recrystallization from the appropriate solvent or on the quaternary salts. The quaternary salts were prepared by treatment of the alcoholic product with methyl iodide or benzyl bromide in methanol and recrystallization from an alcohol–ether mixture.

The IR spectra (chloroform solution) of IV–VIII showed absorption bands in the region of the alcoholic hydroxyl group at 3400–3150 cm^{-1} and at 3100–3000 and 1600–1500 cm^{-1} due to the aryl rings introduced in the piperidine ring.

Esterification of IV–VIII—A solution of IV–VIII (0.02 mole) in 50

[1] All melting points were recorded in an oil bath and are uncorrected. IR spectra were recorded on a Perkin-Elmer model 257 spectrophotometer. All products had IR spectra in agreement with the assigned structures. The aryl halides (Fluka, AG, Bucks, Switzerland) and toluene were distilled before use. Ether was dried over anhydrous sodium sulfate. Microanalyses were performed at Midwest Microlab, Indianapolis, Ind., or by the Department of Medicinal Chemistry, University of Kansas, Lawrence, Kans.

[2] Fluka, AG, Bucks, Switzerland.

0022-3549/80/0700-0796$01.00/0
© 1980, American Pharmaceutical Association

Table I—Data of IV–XIII

Compound	Salt	Formula	Melting Point	Recrystallization Solvent	Yield, %	Analysis, %	Calc.	Found
IV	Methyl iodide	$C_{12}H_{19}N_2O \cdot \frac{1}{2}H_2O$	245–247°	Methanol–ether	86	C	41.98	42.01
						H	5.83	5.62
						N	8.16	8.05
V	—	$C_{16}H_{19}NO$	185–187°	*n*-Hexane[a]	74	C	79.66	79.48
						H	7.88	7.94
VI	Benzyl bromide	$C_{23}H_{26}BrNO$	207–208°	Methanol–ether	88	C	66.99	67.11
						H	6.31	6.36
						N	3.39	3.28
VII	—	$C_{15}H_{18}N_2O$	195–196°	Benzene	85	C	74.37	74.54
						H	7.43	7.34
						N	11.57	11.33
VIII	—	$C_{10}H_{15}NO_2$	138–139°	*n*-Hexane[a]	90	C	66.29	66.53
						H	8.28	8.38
						N	7.73	7.79
IX	Benzyl bromide	$C_{17}H_{20}BrNO$	205–206°	Chloroform–ether	71	C	61.07	61.01
						H	5.98	6.15
						N	4.19	3.92
X	Benzyl bromide	$C_{21}H_{27}BrN_2O_2 \cdot H_2O$	175–176°	Methanol–ether	88	C	57.66	58.02
						H	6.63	6.50
XI	Benzyl bromide	$C_{26}H_{30}BrNO_2 \cdot \frac{1}{2}H_2O$	161–162°	Methanol–ether	77	C	65.40	65.01
						H	6.49	6.59
						N	2.93	3.19
XII	Benzyl bromide	$C_{26}H_{30}BrNO_2 \cdot \frac{1}{4}H_2O$	164–166°	Methanol–ether	82	C	66.03	66.08
						H	6.45	6.42
						N	2.98	3.13
XIII	Benzyl bromide	$C_{25}H_{29}BrN_2O_2 \cdot H_2O$	190–191°	Methanol–ether	72	C	61.60	61.56
						H	6.36	6.35
						N	5.74	5.66

[a] Skellysolve B.

ml of dry toluene was added dropwise, with stirring at room temperature, to a solution of propionyl chloride (0.06 mole, 5.5 g) in 20 ml of dry toluene over 20 min. The reaction mixture then was refluxed for 4 hr and allowed to stand overnight at room temperature. Removal of the solvent under vacuum gave a white solid, which was treated with 5% sodium bicarbonate solution and extracted three times (~50 ml) with ether and once with 50 ml of chloroform.

The combined extracts were dried over anhydrous sodium sulfate. The organic solvents were removed under vacuum, and the residue was treated with excess methyl iodide or benzyl bromide in methanol. The quaternary salts were recrystallized from methanol–ether or chloroform–ether mixtures. The physical constants and microanalyses are shown in Table I.

The IR spectrum of IX (chloroform solution) showed absorption bands at 3020, 2900–2800, 1620, and 1600 cm^{-1}. No absorption band was observed in the carbonyl region. The IR spectra of X–XIII (chloroform solutions) all showed strong absorption bands at 1740–1725 cm^{-1}, indicating an ester carbonyl group.

Biological Testing of X–XIII—Compounds X–XIII were tested for analgesic activity using the mouse–hot plate method and subcutaneous administration. The ED_{50} data are shown in Table II.

RESULTS AND DISCUSSION

Chemistry—Analogs of the prodine analgesics were synthesized according to Scheme I.

The lithium salts of the aromatic or heteroaromatic rings were prepared (14) by treatment of the corresponding bromo derivatives with an equivalent amount of *n*-butyl lithium. Addition of these lithium salts to

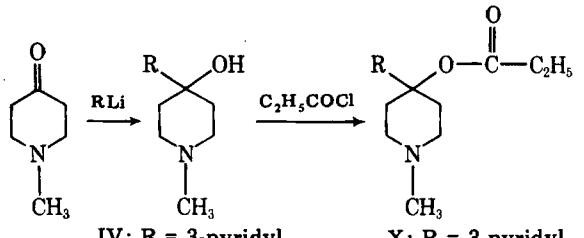

IV: R = 3-pyridyl
V: R = 1-naphthyl
VI: R = 2-naphthyl
VII: R = 3-quinolyl
VIII: R = 2-furyl

X: R = 3-pyridyl
XI: R = 1-naphthyl
XII: R = 2-naphthyl
XIII: R = 3-quinolyl

Scheme I

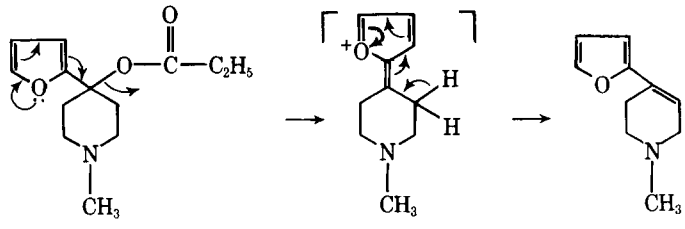

XIV IX

Scheme II

1-methyl-4-piperidone afforded the corresponding alcohols (IV–VIII) in high yields. Treatment of IV–VII with 3 equivalents of propionyl chloride afforded X–XIII. Similar treatment of VIII did not yield the expected ester; instead, olefin IX was the only product obtained from the reaction.

Evidence for the formation of IX was obtained from its IR spectrum, which did not show any absorption band in the carbonyl region and from microanalysis. Furthermore, treatment of 1-methyl-4-(2-thienyl)piperidino-4-ol with propionyl chloride under the same conditions afforded the same type of olefin (15), which was identified by IR and NMR spectroscopy and microanalysis. Changes in the reaction conditions (*i.e.*, ratio of VIII to propionyl chloride, temperature and time of the reaction, and workup of the crude product and solvent) did not change the situation. These results indicate that the heteroatom of the furan ring participates in the elimination of the propionate group after its formation.

If the mechanism of formation of IX was the facile *trans*-diaxial elimination of water from the alcohol during esterification, the same type of olefin would have been produced in all cases reported in this paper. However, the expected esters were obtained in high yields as the only products from the esterification of IV–VII as well as I and II (1). Since the olefin formation was limited to esterification of VIII and its 2-thienyl analog (15), a different mechanism may be involved in this type of elimination. The suggested mechanism involves the electron pair on the oxygen atom of the furan ring assisting in the elimination of the ester group after its formation to give XIV as an intermediate. Loss of a proton from the piperidine ring followed by a shift of the double bonds would produce IX (Scheme II).

Correlation of Pharmacological Data—Compounds IX–XII were tested for analgesic activity using the mouse–hot plate method and subcutaneous administration. The ED_{50} data are summarized in Table II together with those of I and II. The molecular orbital calculations (16) for the highest occupied molecular orbital and lowest empty molecular

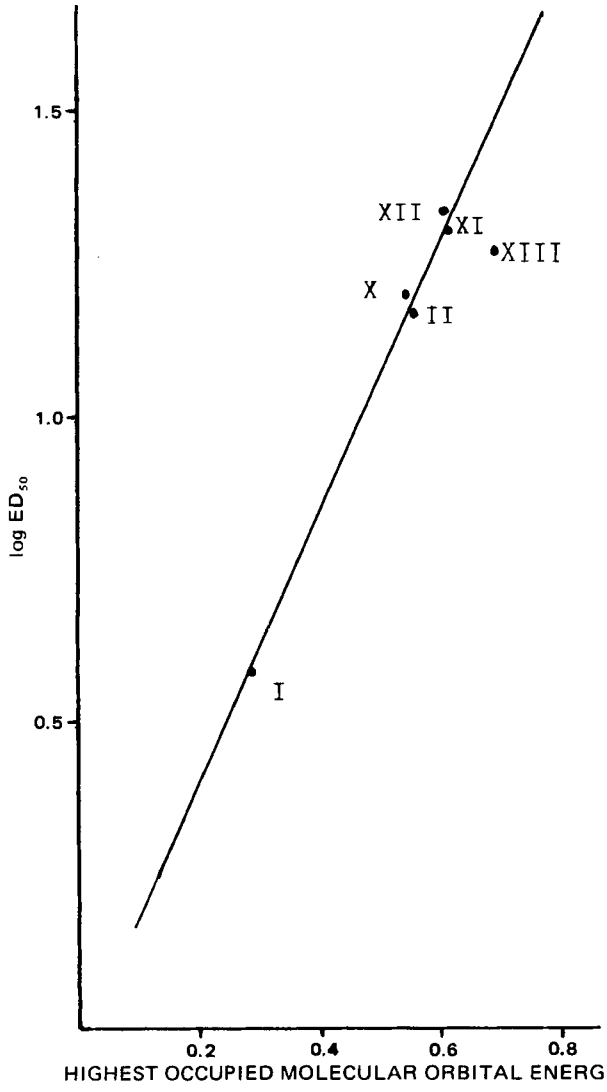

Figure 1—*Plot of log ED_{50} versus highest occupied molecular orbital energy.*

orbital energy levels of aromatic groups present in these molecules also are listed in Table II.

The choice of the aryl groups used in these derivatives was based on the energy level differences of the highest occupied molecular orbital and lowest empty molecular orbital and on the capability of these aryl groups to form charge transfer complexes *in vitro* (17) and *in vivo* (10). The molecular orbital treatment of these molecules was confined to the aromatic planar part, containing the π-electrons. These π-electrons are of primary concern in charge transfer complex formation (18). Other portions of the molecules that are not planar and are not conjugated with the major π-electron system were not included.

The electronic structure indexes considered here are the energy levels in units of the resonance integral (β) of the highest occupied molecular orbital and lowest empty molecular orbital. The energy of the highest occupied molecular orbital is a measure of electron donor ability, and that of the lowest empty molecular orbital is a measure of electron acceptor ability (7). These two energy levels are of primary importance in effecting charge transfer complex formation (7). They also are important in effecting charge transfer complex formation in the biological system (19). The smaller the energy level of the highest occupied molecular orbital, the lower is the energy required to remove a π-electron from the molecule and, thus, the greater are the electron donor properties (19–21). The closer to zero the energy level of the lowest empty molecular orbital, the greater is the electron affinity and, therefore, the greater are the electron acceptor properties (21, 22).

Compound I, the most active in the series, had an ED_{50} of 3.9 mg/kg. The energy levels of the highest occupied molecular orbital and lowest empty molecular orbital of the thienyl group were 0.2928932 and −1.00, respectively (16). These values indicate that the thiophene ring is most likely to form a charge transfer complex in the biological system and acts as a π-electron donor. However, it is the least likely π-electron acceptor because of the high energy level of the lowest empty molecular orbital relative to the other compounds.

Table II—ED_{50} Values and Highest Occupied Molecular Orbital and Lowest Empty Molecular Orbital Energy Data of I, II, and X–XIII

Compound	ED_{50}, mg/kg sc	Energy (π)	
		Highest Occupied Molecular Orbital	Lowest Empty Molecular Orbital
I	3.90	0.2928932	−1.00
II	16.00	0.5602315	−0.5602315
X	16.60	0.5602315	−0.5602315
XI	22.00	0.6180340	−0.6180340
XII	22.50	0.6180340	−0.6180340
XIII	20.00	0.7032833	−0.5270970

Compounds II and X contain a pyridine moiety at position 4 of the piperidine ring. The energy level of the highest occupied molecular orbital of pyridine is 0.5602315 (16), which is lower than that of thiophene. A charge transfer complex of II or X is expected to occur in the biological system in which the pyridine ring acts as a donor but requires a higher energy to transfer the π-electron than that required for the thiophene ring. Thus, a less firm charge transfer complex is expected in this case, which may have been reflected in the ED_{50} values of II and X at 16.0 and 16.6 mg/kg, respectively. The argument presented in comparing the biological activity of I with that of II and X also may hold for naphthalene- and quinoline-containing compounds. The energy levels of the highest occupied molecular orbital of XI–XIII were lower than those for I, II, and X. If a charge transfer complex is expected to occur between the biological system and XI–XIII, they would be weaker than those formed between the thiophene- and pyridine-containing compounds and the biological system. Also, they would require a higher energy for their formation. This difference in the energy requirement may have been the cause of the lower activity of XI–XIII as shown by their higher ED_{50} values.

To test the possibility of a charge transfer complex between the aryl groups of the analgesics and their receptors, the logarithm of the ED_{50} values given in Table II was plotted against the energy values of the corresponding highest occupied molecular orbital. Figure 1 shows a linear relationship between log ED_{50} and the energy of the highest occupied molecular orbital of these compounds. The line is the least-squares line (23) whose equation is $y = 2.2x - 0.04$. This linear relationship may indicate (13) the possibility of a charge transfer complex interaction between these compounds and their receptors, with the aryl groups acting as the charge donors. There was no simple linear relationship when the log ED_{50} values were plotted against the energy values of the lowest empty molecular orbital of these compounds. This finding may exclude the possibility that the aryl groups of these compounds function as electron acceptors.

REFERENCES

(1) K. Sabih and R. A. Wiley, *J. Med. Chem.*, **12**, 922 (1969).

(2) G. DeStevens, A. Halamandaris, P. Strachan, E. Donoghue, L. Dorfman, and C. F. Huchner, *ibid.*, **6**, 357 (1963).

(3) A. H. Beckett and A. F. Casy, *J. Pharm. Pharmacol.*, **6**, 986 (1954).

(4) A. H. Beckett, *Progr. Drug Res.*, **1**, 455 (1959).

(5) P. S. Portoghese, *J. Med. Chem.*, **8**, 609 (1965).

(6) R. Foster, "Organic Charge Transfer Complexes," Academic, New York, N.Y., 1969.

(7) B. Pullman and A. Pullman, "Quantum Biochemistry," Interscience, New York, N.Y., 1963.

(8) W. P. Purcell, *J. Med. Chem.*, **9**, 294 (1966).

(9) W. B. Neely, *Mol. Pharmacol.*, **1**, 137 (1965).

(10) J. A. Singer and W. Purcell, *J. Med. Chem.*, **10**, 754 (1967).

(11) S. H. Snyder and C. R. Meril, *Proc. Natl. Acad. Sci., USA*, **54**, 258 (1965).

(12) A. J. Wohl, *Mol. Pharmacol.*, **6**, 189 (1970).

(13) A. Burger, "Medicinal Chemistry," 3rd ed., Wiley–Interscience, New York, N.Y., 1970, p. 120.

(14) H. Gilman and S. M. Spatz, *J. Org. Chem.*, **16**, 1485 (1951).

(15) K. Sabih, Ph.D. thesis, University of Kansas, Lawrence, Kans., 1968.

(16) C. A. Coulson and A. Streitwieser, "Dictionary of π-Electron

Calculations," W. H. Freeman, San Francisco, Calif., 1965.
(17) R. P. Lang, *J. Am. Chem. Soc.*, **84**, 4438 (1962).
(18) W. O. Foye, "Principles of Medicinal Chemistry," Lea & Febiger, Philadelphia, Pa., 1974, p. 53.
(19) E. M. Kosower, *Progr. Phys. Org. Chem.*, **3**, 81 (1965).
(20) A. Burger, "Medicinal Chemistry," 3rd ed., Wiley-Interscience, New York, N.Y., 1970, p. 157.
(21) B. Pullman, *Biochim. Biophys. Acta*, **88**, 1440 (1964).
(22) P. O. P. Ts'o, I. S. Melvin, and A. C. Olson, *J. Am. Chem. Soc.*, **85**, 1289 (1963).
(23) M. R. Spiegel, "Statistics," McGraw-Hill, New York, N.Y., 1972, p. 217.

ACKNOWLEDGMENTS

The authors thank Dr. Everett L. May for the biological testing of the compounds and the Department of Medicinal Chemistry, University of Kansas, for performing some microanalyses.

Correlation of Hydrophobicity with Protein Binding for Clorobiocin Analogs

C. J. COULSON ˣ **and V. J. SMITH**

Received April 10, 1979, from the *Biochemistry Department, Pharmaceutical Division, May and Baker Ltd., Dagenham, Essex, RM10 7XS, England.* Accepted for publication February 1, 1980.

Abstract □ A new method of equilibrium dialysis was used to measure the binding of analogs of clorobiocin (18631 R.P.) to human serum albumin. Binding constants and numbers of binding sites on human serum albumin were calculated from the binding data and were used to calculate the percentage of compounds free in equilibrium with 4% albumin. Partition coefficients between *n*-octanol and phosphate buffer (0.05 *M*, pH 7.4) also were measured. A positive linear correlation ($r = 0.918$, $s = 0.240$, and $n = 10$) was obtained between log (bound/free compound) and log partition coefficient.

Keyphrases □ Hydrophobicity—clorobiocin analogs, correlation with protein binding □ Protein binding—clorobiocin analogs, correlation with hydrophobicity □ Clorobiocin analogs—correlation of hydrophobicity with protein binding

Clorobiocin (18631 R.P.) (1, 2) has been shown to be tightly bound to human serum albumin (3). In an effort to reduce this binding, various semisynthetic derivatives of the antibiotic were prepared, and the effect of these changes on the binding was monitored.

BACKGROUND

Binding of clorobiocin to human serum albumin was so high (99.97% with 10^{-5} *M* drug and 4% albumin) that the free drug concentration was in the range of 10^{-8}–10^{-9} *M*. To measure this drug level accurately by physicochemical means, radiolabeling of the drug would have been required. As an alternative, a method was developed whereby low concentrations of albumin were used so that the free drug concentration was sufficiently high for detection by UV spectrophotometry. From a plot of bound *versus* free drug, an iterative computer program gave binding constant values and the numbers of primary and secondary binding sites. These plots were used in a program that calculates the percentage of free drug in equilibrium with whole plasma.

The 4-hydroxycoumarin moiety probably contributes to the binding, since this group played a major part in the binding of the warfarin group of anticoagulants to human serum albumin (4). Various reports, listed by Jusko and Gretch (5), indicated that the hydrophobic nature was important for albumin binding. Accordingly, the partition coefficients of several clorobiocin derivatives were measured, and it was found that their hydrophobicity did play a major role in their binding to albumin.

EXPERIMENTAL

Equilibrium Dialysis—The technique was described initially by Coombs and Coulson (6). Two perspex blocks were screwed tightly together with a cellulose membrane[1] in between to form a complete unit with six compartments. Five units were used to hold 14 concentrations of compounds and two blanks (to allow for nonspecific UV absorbance).

For binding measurements, 2 ml of albumin[2] solution (0.25–2 mg/ml) was placed on one side of the membrane. The concentration of albumin appropriate for each compound was selected on the basis of the estimated partition using the Hansch aromatic substituent constants (7). The compounds[3] were dissolved in methanol at a concentration of 10 m*M* and diluted 1 in 50 in phosphate buffer (0.05 *M*, pH 7.4) to give the maximum concentration used. Further dilutions were made in the phosphate buffer. On the other side of the membrane was placed 2 ml of the compound solution (15–200 μM).

A plastic cap was fitted on each compartment to prevent evaporation. The units were shaken in a water bath for 8 hr at 37°, followed by 8 hr without shaking at room temperature. Aliquots from each side of the membrane were taken for the measurement of concentration by UV absorbance at a wavelength where there was no net change in absorbance on binding.

To examine the effect of methanol on the binding, methanolic and aqueous solutions of the sodium salts of clorobiocin and novobiocin were diluted in the buffer and tested; there was no significant difference in binding. The remaining compounds were dissolved initially in methanol since they were insoluble in water at higher concentrations.

Difference Spectra—The binding of each compound to human serum albumin was followed by UV spectroscopy as described previously (3) to find the wavelength for the measurement of the concentration of each compound, *i.e.*, to find the wavelength at which there was no net change in absorbance. Different albumin samples gave different results when binding clorobiocin derivatives according to the amount of dimer present. Therefore, albumin monomer was prepared using Sephadex G-100 as described previously (3).

Calculations—Binding constants and the number of binding sites were obtained from the binding data with an iterative computer program devised in these laboratories. The raw data were fitted to:

$$y = \frac{n_1 k_1 T}{1 + k_1 T} + \frac{n_2 k_2 T}{1 + k_2 T} \qquad \text{(Eq. 1)}$$

where y is the bound drug; T is the free drug; n_1 and n_2 are the numbers of primary and secondary binding sites, respectively; and k_1 and k_2 are the respective binding constants. The inclusion of a third set of binding sites did not improve the fit.

Arbitrary values for n_1, n_2, k_1, and k_2 were entered, and a standard deviation of the curve from the points was calculated. The value of n_1 is increased by 5%, k_1 and k_2 are kept constant, and the best value for n_2 is selected on the basis of a minimal standard deviation. If this standard deviation is lower than the previous one, then n_1 is increased further by

[1] Spectropor 2, M.S.E./Fisons, Crawley, Sussex, England.

[2] Miles.

[3] Clorobiocin was obtained from Dr. Jolles of Rhone Poulenc, novobiocin sodium was obtained from British Drug Houses, and the analogs were obtained from Dr. D. E. Wright, Dr. C. Smith, Dr. R. J. A. Walsh, and Mr. P. J. Warren of May and Baker Ltd. chemical research laboratories.

0022-3549/80/0700-0799$01.00/0
© 1980, American Pharmaceutical Association

Calculations," W. H. Freeman, San Francisco, Calif., 1965.
(17) R. P. Lang, *J. Am. Chem. Soc.*, **84**, 4438 (1962).
(18) W. O. Foye, "Principles of Medicinal Chemistry," Lea & Febiger, Philadelphia, Pa., 1974, p. 53.
(19) E. M. Kosower, *Progr. Phys. Org. Chem.*, **3**, 81 (1965).
(20) A. Burger, "Medicinal Chemistry," 3rd ed., Wiley-Interscience, New York, N.Y., 1970, p. 157.
(21) B. Pullman, *Biochim. Biophys. Acta*, **88**, 1440 (1964).
(22) P. O. P. Ts'o, I. S. Melvin, and A. C. Olson, *J. Am. Chem. Soc.*, **85**, 1289 (1963).
(23) M. R. Spiegel, "Statistics," McGraw-Hill, New York, N.Y., 1972, p. 217.

ACKNOWLEDGMENTS

The authors thank Dr. Everett L. May for the biological testing of the compounds and the Department of Medicinal Chemistry, University of Kansas, for performing some microanalyses.

Correlation of Hydrophobicity with Protein Binding for Clorobiocin Analogs

C. J. COULSON ˣ **and V. J. SMITH**

Received April 10, 1979, from the *Biochemistry Department, Pharmaceutical Division, May and Baker Ltd., Dagenham, Essex, RM10 7XS, England.* Accepted for publication February 1, 1980.

Abstract □ A new method of equilibrium dialysis was used to measure the binding of analogs of clorobiocin (18631 R.P.) to human serum albumin. Binding constants and numbers of binding sites on human serum albumin were calculated from the binding data and were used to calculate the percentage of compounds free in equilibrium with 4% albumin. Partition coefficients between *n*-octanol and phosphate buffer (0.05 *M*, pH 7.4) also were measured. A positive linear correlation ($r = 0.918$, $s = 0.240$, and $n = 10$) was obtained between log (bound/free compound) and log partition coefficient.

Keyphrases □ Hydrophobicity—clorobiocin analogs, correlation with protein binding □ Protein binding—clorobiocin analogs, correlation with hydrophobicity □ Clorobiocin analogs—correlation of hydrophobicity with protein binding

Clorobiocin (18631 R.P.) (1, 2) has been shown to be tightly bound to human serum albumin (3). In an effort to reduce this binding, various semisynthetic derivatives of the antibiotic were prepared, and the effect of these changes on the binding was monitored.

BACKGROUND

Binding of clorobiocin to human serum albumin was so high (99.97% with 10^{-5} *M* drug and 4% albumin) that the free drug concentration was in the range of 10^{-8}–10^{-9} *M*. To measure this drug level accurately by physicochemical means, radiolabeling of the drug would have been required. As an alternative, a method was developed whereby low concentrations of albumin were used so that the free drug concentration was sufficiently high for detection by UV spectrophotometry. From a plot of bound *versus* free drug, an iterative computer program gave binding constant values and the numbers of primary and secondary binding sites. These plots were used in a program that calculates the percentage of free drug in equilibrium with whole plasma.

The 4-hydroxycoumarin moiety probably contributes to the binding, since this group played a major part in the binding of the warfarin group of anticoagulants to human serum albumin (4). Various reports, listed by Jusko and Gretch (5), indicated that the hydrophobic nature was important for albumin binding. Accordingly, the partition coefficients of several clorobiocin derivatives were measured, and it was found that their hydrophobicity did play a major role in their binding to albumin.

EXPERIMENTAL

Equilibrium Dialysis—The technique was described initially by Coombs and Coulson (6). Two perspex blocks were screwed tightly together with a cellulose membrane[1] in between to form a complete unit with six compartments. Five units were used to hold 14 concentrations of compounds and two blanks (to allow for nonspecific UV absorbance).

For binding measurements, 2 ml of albumin[2] solution (0.25–2 mg/ml) was placed on one side of the membrane. The concentration of albumin appropriate for each compound was selected on the basis of the estimated partition using the Hansch aromatic substituent constants (7). The compounds[3] were dissolved in methanol at a concentration of 10 m*M* and diluted 1 in 50 in phosphate buffer (0.05 *M*, pH 7.4) to give the maximum concentration used. Further dilutions were made in the phosphate buffer. On the other side of the membrane was placed 2 ml of the compound solution (15–200 μM).

A plastic cap was fitted on each compartment to prevent evaporation. The units were shaken in a water bath for 8 hr at 37°, followed by 8 hr without shaking at room temperature. Aliquots from each side of the membrane were taken for the measurement of concentration by UV absorbance at a wavelength where there was no net change in absorbance on binding.

To examine the effect of methanol on the binding, methanolic and aqueous solutions of the sodium salts of clorobiocin and novobiocin were diluted in the buffer and tested; there was no significant difference in binding. The remaining compounds were dissolved initially in methanol since they were insoluble in water at higher concentrations.

Difference Spectra—The binding of each compound to human serum albumin was followed by UV spectroscopy as described previously (3) to find the wavelength for the measurement of the concentration of each compound, *i.e.*, to find the wavelength at which there was no net change in absorbance. Different albumin samples gave different results when binding clorobiocin derivatives according to the amount of dimer present. Therefore, albumin monomer was prepared using Sephadex G-100 as described previously (3).

Calculations—Binding constants and the number of binding sites were obtained from the binding data with an iterative computer program devised in these laboratories. The raw data were fitted to:

$$y = \frac{n_1 k_1 T}{1 + k_1 T} + \frac{n_2 k_2 T}{1 + k_2 T} \qquad \text{(Eq. 1)}$$

where y is the bound drug; T is the free drug; n_1 and n_2 are the numbers of primary and secondary binding sites, respectively; and k_1 and k_2 are the respective binding constants. The inclusion of a third set of binding sites did not improve the fit.

Arbitrary values for n_1, n_2, k_1, and k_2 were entered, and a standard deviation of the curve from the points was calculated. The value of n_1 is increased by 5%, k_1 and k_2 are kept constant, and the best value for n_2 is selected on the basis of a minimal standard deviation. If this standard deviation is lower than the previous one, then n_1 is increased further by

[1] Spectropor 2, M.S.E./Fisons, Crawley, Sussex, England.

[2] Miles.

[3] Clorobiocin was obtained from Dr. Jolles of Rhone Poulenc, novobiocin sodium was obtained from British Drug Houses, and the analogs were obtained from Dr. D. E. Wright, Dr. C. Smith, Dr. R. J. A. Walsh, and Mr. P. J. Warren of May and Baker Ltd. chemical research laboratories.

0022-3549/80/0700-0799$01.00/0
© 1980, American Pharmaceutical Association

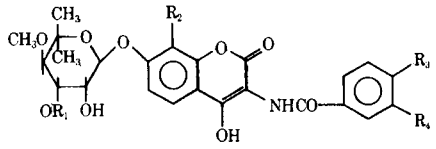

Table I—Binding and Partition Data for Clorobiocin Analogs and Human Serum Albumin

Compound	R_1	R_2	R_3	R_4	Number of Determinations	Average Minimal Standard Deviation of Iterations	Percent of Free[a] Compound	Bound/Free	Partition Coefficient
I	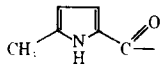	Cl	OCH_3	$CH_2CH{=}C(CH_3)_2$	3	1.21	0.01872	5340	776
II	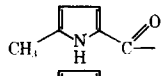	Cl	OH	$CH_2CH_2CH(CH_3)_2$	4	2.25	0.03076	3250	617
Clorobiocin	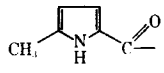	Cl	OH	$CH_2CH{=}C(CH_3)_2$	4	1.33	0.02783	3592	162
Clorobiocin sodium	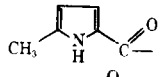	Cl	OH	$CH_2CH{=}C(CH_3)_2$	4	1.90	0.0568	1758	60.3
III	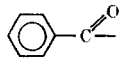	CH_3	OH	$CH_2CH{=}C(CH_3)_2$	2	0.99	0.0841	1188	115.0
IV	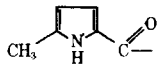	Cl	OCH_2-CH_2OH	$(CH_2)_2CH(CH_3)_2$	3	2.09	0.1079	926	229
V	H	Cl	OH	$CH_2CH{=}C(CH_3)_2$	2	1.49	0.216	462	7.24
VI	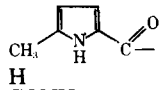	H	OH	$CH_2CH{=}C(CH_3)_2$	5	1.45	0.35	285	14.4
VII	H	CH_3	OH	$CH_2CH{=}(CH_3)_2$	2	0.99	0.64	155	6.03
Novobiocin	$CONH_2$	CH_3	OH	$CH_2CH{=}(CH_2)_2$	2	1.74	0.702	141.5	5.25

[a] Percent of free compound calculated at 40 mg/ml of human serum albumin and 10^{-5} *M* compound.

5%, and the best value for n_2 is obtained. If the second standard deviation is higher, then a 5% reduction in n_1 is made, and the calculation is carried out as before.

The values selected for n_1 continue to fall by 5% until the standard deviation starts to rise, at which point 1% increments are made to n_1 until the lowest standard deviation and corresponding n_2 value are obtained. This value for n_1 is retained while first k_1 and then k_2 are treated in the same way to achieve one complete iteration. Then the process is repeated. At the next stage, n_2 takes the place of n_1, and the process is repeated. A second iteration follows. The process is considered complete when an entire cycle of four iterations (two on n_1 and two on n_2) does not improve the standard deviation by more than 0.1%.

The minimum standard deviation obtained is reported in Table I as the average of two or more runs on each compound. The percentage of free compound at 10 μg/ml in equilibrium with 4% albumin then was calculated (8). This value indicated how much free compound would be present in plasma. The log of bound to free compound was plotted against the log partition coefficient by least-squares regression analysis. All programs were computed on a minicomputer[4].

Partition Coefficients—Partition coefficients between *n*-octanol and phosphate buffer (0.05 *M*, pH 7.4) were measured at five concentrations of the compound between 0.1 and 2.0 m*M*. The UV spectrum of the compound indicated the concentration in both octanol and the buffer. A standard curve was performed in both solvents. This procedure was adopted to detect any glass binding of the compounds, but none was found. The results were averaged (Table I).

Materials—The *n*-octanol was obtained commercially[5], and its absorbance was checked before use to show that it was less than one-tenth of a unit in the range of 270–315 nm[6]. Cellulose membranes were used in the equilibrium dialysis units[7] (Fig. 1).

RESULTS AND DISCUSSION

The partition data and the percentage of free compound in equilibrium with 4% albumin are listed in Table I. The partitions ranged from 1 to 776, and the percentage of free compound ranged from 0.02 to 0.71.

Although at neutral pH the clorobiocin series carried one negative charge due to the 4-hydroxycoumarin residue, the partition coefficients still were noticeably hydrophobic. This result may partially explain the tight binding of the series since, in general, albumin binding is related to hydrophobicity in a positive linear fashion as was shown for numerous series that bind to bovine and human serum albumin (5). These data are in agreement with those of O'Reilly (9), who found that the decrease in lipophilicity produced by the insertion of a hydroxy group into the 6, 7, or 8 position of the 4-hydroxycoumarin nucleus in warfarin reduced binding to human serum albumin of an order of magnitude (albeit at pH 10) when compared with warfarin. Clorobiocin and warfarin probably bind at the same site. In addition, human serum albumin is adapted to carrying anions of fatty acids and tryptophan among others. The methylpyrrole residue present in some derivatives clearly plays a major part in the binding, as is expected from such a hydrophobic structure.

The correlation coefficient for the graph of log bound to free compound against log partition coefficient is 0.918 (s = 0.240, n = 10, F = 43.0, and p = 0.0002), and the relationship is described by log (bound/free compound) = 0.633 log P + 1.839.

Bird and Marshall (10) used the ratio of bound to free compound in analyzing the binding data for 79 penicillin derivatives and human serum on the basis that the ratio was more meaningful and formally analogous to a partition coefficient. In addition, this ratio gave a more complete estimate of the binding, since calculation based on either the binding constant or the number of binding sites failed to indicate the extent of binding. Both parameters were required along with the data from secondary binding sites. The latter contribution was considerable in some cases. Dividing a small figure into a large one clearly will increase the small error in the percentage of free compound. To offset this error, a large number of points was taken to increase the accuracy of each determination.

The binding specificity is supported further by the positive intercept obtained. When the compound is distributed evenly between octanol and buffer (log P = 0), then more compound is bound to the albumin than to the buffer phase. This result implies either that albumin binding is much more hydrophobic than octanol or that some specific binding of these compounds is taking place (the partition then may be seen as an additional factor that modulates this binding). Support for the latter view may be taken from the intercepts obtained by Bird and Marshall (10),

[4] Wang system 2200 B.
[5] Specially pure grade, British Drug Houses.
[6] Spectrophotometric measurements were done on a Pye Unicam SP 800.
[7] Universal Scientific, London, England.

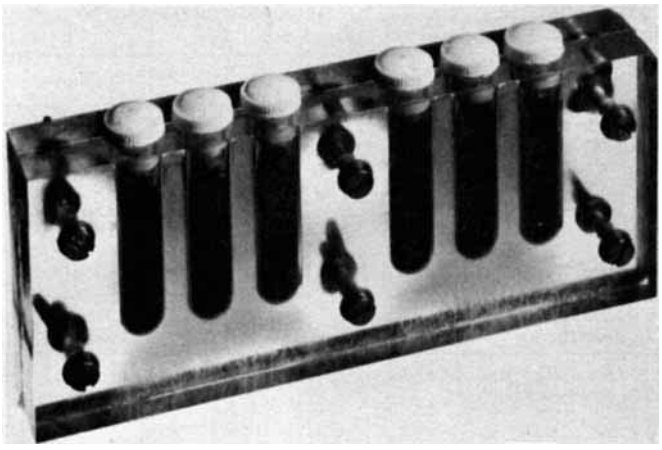

Figure 1—*Equilibrium dialysis units. (Reprinted with permission of the editors of Biochemical Society Transactions).*

Krieglstein *et al.* (11), who investigated the binding of 10 phenothiazines to bovine serum albumin, and Deutsch and Hansch (12), who studied barbiturate binding to the same protein. In each case, log (bound/free) was plotted; negative intercepts of 0.628, 0.578, and 1.22 were obtained, respectively. Penicillins, phenothiazines, and barbiturates apparently do not have as marked a binding site on albumin as do clorobiocins.

The difference in log P of 1.06 between VI and clorobiocin, which differ only by a chlorine atom, is only partially explained by the π value for aromatic chlorine of 0.71 (7), whereas the hydrophobic fragment constant of 0.92 (13) approaches it much more closely. Nevertheless, it seemed important to develop a mathematical relationship based on experimental results rather than on theoretical data for those complex molecules having a great deal of conformational interaction.

Salicylate binding to whole plasma gave a value of −1.32 for log P and 94% drug bound at a concentration of 13.8 μg/ml (6), a result that clearly does not fit the correlation obtained in this work. Other compounds with structures unrelated to either salicylate or clorobiocin also did not fit the correlation, which suggests that they might be binding at a different protein site. Sudlow *et al.* (14) reported that more than one binding site exists on human serum albumin for foreign compounds. The correlation obtained in this study applies to the clorobiocin derivative series. It also may apply to any structure that binds at the same site.

Use of the equilibrium dialysis units has facilitated accurate and reproducible work, which is difficult to carry out by dialysis in a large number of tubing bags. The alternative is to purchase an expensive instrument. The units described here combine the accuracy of the instrument with little more than the cost of the dialysis tubing. Used with the two computer programs, they estimate the binding to plasma albumin of drugs that are tightly bound and are not available in radioactive form. In addition, these units can be used to measure the binding of radioactive drug to whole plasma (6) and, potentially, the binding of any ligand to a macromolecule.

REFERENCES

(1) L. Ninet, F. Benazet, Y. Charpentie, M. Dubost, J. Florent, D. Mancy, J. Preud'homme, T. L. Threlfall, B. Vuillemin, D. E. Wright, A. Abraham, M. Cartier, M. de Chezelles, D. Godard, and J. Theilleux, *C.R. Acad. Sci. Paris (C)*, **275**, 455 (1972).

(2) C. J. Coulson and V. J. Smith, *Enzyme Microb. Technol.*, **1**, 193 (1979).

(3) T. J. Coombs, C. J. Coulson, and V. J. Smith, *Biochem. Pharmacol.*, in press.

(4) R. A. O'Reilly, *Mol. Pharmacol.*, **7**, 209 (1971).

(5) W. J. Jusko and M. Gretch, *Drug Metab. Rev.*, **5**, 43 (1976).

(6) T. J. Coombs and C. J. Coulson, *Biochem. Soc. Trans.*, **6**, 1048 (1978).

(7) C. Hansch, A. Leo, S. H. Unger, K. H. Kim, D. Nikaitani, and E. J. Lien, *J. Med. Chem.*, **16**, 1207 (1973).

(8) R. F. Mais, S. Keresztes-Nagy, J. F. Zaroslinki, and Y. T. Oester, *J. Pharm. Sci.*, **63**, 1423 (1974).

(9) R. A. O'Reilly, *J. Clin. Invest.*, **48**, 193 (1969).

(10) A. E. Bird and A. G. Marshall, *Biochem. Pharmacol.*, **16**, 2275 (1967).

(11) J. Krieglstein, W. Meiler, and J. Staab, *ibid.*, **21**, 985, (1972).

(12) E. W. Deutsch and C. Hansch, *Nature*, **211**, 75, (1966).

(13) G. G. Nys and R. F. Rekker, *Eur. J. Med. Chem.*, **9**, 361 (1974).

(14) G. Sudlow, D. J. Birkett, and D. N. Wade, *Mol. Pharmacol.*, **12** 1052 (1976).

ACKNOWLEDGMENTS

The authors thank Dr. D. E. Wright, Dr. C. Smith, Dr. R. J. A. Walsh, and Mr. P. J. Warren of these chemical research laboratories for helpful discussions. They also thank Mr. B. Basil of the Pharmacology Department for help with the iterative computer program.

Pharmacokinetics of Subcutaneous and Intramuscular Butorphanol in Dogs

M. PFEFFER ˣ, R. D. SMYTH, K. A. PITTMAN, and P. A. NARDELLA

Received September 21, 1979, from *Bristol Laboratories, Syracuse, NY 13201.* Accepted for publication February 8, 1980.

Abstract □ Butorphanol tartrate was administered intramuscularly and subcutaneously to adult male and female dogs at a dose of 0.25 mg/kg. No significant absorption lag time and no significant difference between peak intramuscular and subcutaneous serum concentrations were observed. The mean peak serum concentration was 29 ng/ml at mean times of 28 min after subcutaneous administration and 40 min after intramuscular administration. There were no significant differences in the pharmacokinetics of butorphanol in dogs with either route. The serum half-life was 1.62 hr, and the serum clearance was 3.45 liters/kg/hr. The apparent volume of distribution of butorphanol was 7.96 liters/kg. Although considerable inter- and intraanimal variation in C_{max} and AUC was observed, there was no significant difference in the area under the serum concentration *versus* time curves, and the two administration routes were considered bioequivalent.

Keyphrases □ Butorphanol—pharmacokinetics following subcutaneous and intramuscular administration, dogs □ Pharmacokinetics—butorphanol, subcutaneous and intramuscular administration, dogs □ Analgesics—butorphanol, pharmacokinetics following subcutaneous and intramuscular administration, dogs

Butorphanol tartrate [17-(cyclobutylmethyl)morphinan-3,14-diol tartrate], a new narcotic agonist–antagonist analgesic, is available[1] for use in humans and dogs (1). Previous studies indicated that loss processes account for a decrease in the extent of drug availability from extravascular parenteral injection sites (2). Deposition (3) and degradation (4) of the drug at the injection site can decrease both the rate and extent of absorption. The injection

[1] Stadol, Bristol Laboratories, Syracuse, N.Y.

0022-3549/80/0700-0801$01.00/0

© 1980, American Pharmaceutical Association

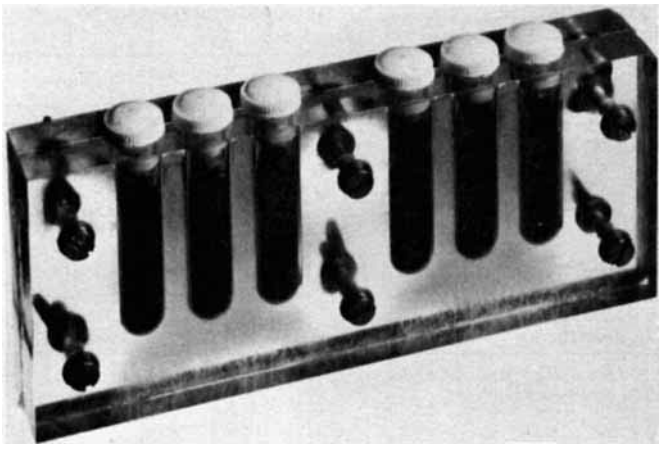

Figure 1—*Equilibrium dialysis units. (Reprinted with permission of the editors of Biochemical Society Transactions).*

Krieglstein *et al.* (11), who investigated the binding of 10 phenothiazines to bovine serum albumin, and Deutsch and Hansch (12), who studied barbiturate binding to the same protein. In each case, log (bound/free) was plotted; negative intercepts of 0.628, 0.578, and 1.22 were obtained, respectively. Penicillins, phenothiazines, and barbiturates apparently do not have as marked a binding site on albumin as do clorobiocins.

The difference in log P of 1.06 between VI and clorobiocin, which differ only by a chlorine atom, is only partially explained by the π value for aromatic chlorine of 0.71 (7), whereas the hydrophobic fragment constant of 0.92 (13) approaches it much more closely. Nevertheless, it seemed important to develop a mathematical relationship based on experimental results rather than on theoretical data for those complex molecules having a great deal of conformational interaction.

Salicylate binding to whole plasma gave a value of −1.32 for log P and 94% drug bound at a concentration of 13.8 μg/ml (6), a result that clearly does not fit the correlation obtained in this work. Other compounds with structures unrelated to either salicylate or clorobiocin also did not fit the correlation, which suggests that they might be binding at a different protein site. Sudlow *et al.* (14) reported that more than one binding site exists on human serum albumin for foreign compounds. The correlation obtained in this study applies to the clorobiocin derivative series. It also may apply to any structure that binds at the same site.

Use of the equilibrium dialysis units has facilitated accurate and reproducible work, which is difficult to carry out by dialysis in a large number of tubing bags. The alternative is to purchase an expensive instrument. The units described here combine the accuracy of the instrument with little more than the cost of the dialysis tubing. Used with the two computer programs, they estimate the binding to plasma albumin of drugs that are tightly bound and are not available in radioactive form. In addition, these units can be used to measure the binding of radioactive drug to whole plasma (6) and, potentially, the binding of any ligand to a macromolecule.

REFERENCES

(1) L. Ninet, F. Benazet, Y. Charpentie, M. Dubost, J. Florent, D. Mancy, J. Preud'homme, T. L. Threlfall, B. Vuillemin, D. E. Wright, A. Abraham, M. Cartier, M. de Chezelles, D. Godard, and J. Theilleux, *C.R. Acad. Sci. Paris (C)*, **275**, 455 (1972).

(2) C. J. Coulson and V. J. Smith, *Enzyme Microb. Technol.*, **1**, 193 (1979).

(3) T. J. Coombs, C. J. Coulson, and V. J. Smith, *Biochem. Pharmacol.*, in press.

(4) R. A. O'Reilly, *Mol. Pharmacol.*, **7**, 209 (1971).

(5) W. J. Jusko and M. Gretch, *Drug Metab. Rev.*, **5**, 43 (1976).

(6) T. J. Coombs and C. J. Coulson, *Biochem. Soc. Trans.*, **6**, 1048 (1978).

(7) C. Hansch, A. Leo, S. H. Unger, K. H. Kim, D. Nikaitani, and E. J. Lien, *J. Med. Chem.*, **16**, 1207 (1973).

(8) R. F. Mais, S. Keresztes-Nagy, J. F. Zaroslinki, and Y. T. Oester, *J. Pharm. Sci.*, **63**, 1423 (1974).

(9) R. A. O'Reilly, *J. Clin. Invest.*, **48**, 193 (1969).

(10) A. E. Bird and A. G. Marshall, *Biochem. Pharmacol.*, **16**, 2275 (1967).

(11) J. Krieglstein, W. Meiler, and J. Staab, *ibid.*, **21**, 985, (1972).

(12) E. W. Deutsch and C. Hansch, *Nature*, **211**, 75, (1966).

(13) G. G. Nys and R. F. Rekker, *Eur. J. Med. Chem.*, **9**, 361 (1974).

(14) G. Sudlow, D. J. Birkett, and D. N. Wade, *Mol. Pharmacol.*, **12** 1052 (1976).

ACKNOWLEDGMENTS

The authors thank Dr. D. E. Wright, Dr. C. Smith, Dr. R. J. A. Walsh, and Mr. P. J. Warren of these chemical research laboratories for helpful discussions. They also thank Mr. B. Basil of the Pharmacology Department for help with the iterative computer program.

Pharmacokinetics of Subcutaneous and Intramuscular Butorphanol in Dogs

M. PFEFFER ˣ, R. D. SMYTH, K. A. PITTMAN, and P. A. NARDELLA

Received September 21, 1979, from *Bristol Laboratories, Syracuse, NY 13201.* Accepted for publication February 8, 1980.

Abstract □ Butorphanol tartrate was administered intramuscularly and subcutaneously to adult male and female dogs at a dose of 0.25 mg/kg. No significant absorption lag time and no significant difference between peak intramuscular and subcutaneous serum concentrations were observed. The mean peak serum concentration was 29 ng/ml at mean times of 28 min after subcutaneous administration and 40 min after intramuscular administration. There were no significant differences in the pharmacokinetics of butorphanol in dogs with either route. The serum half-life was 1.62 hr, and the serum clearance was 3.45 liters/kg/hr. The apparent volume of distribution of butorphanol was 7.96 liters/kg. Although considerable inter- and intraanimal variation in C_{max} and AUC was observed, there was no significant difference in the area under the serum concentration *versus* time curves, and the two administration routes were considered bioequivalent.

Keyphrases □ Butorphanol—pharmacokinetics following subcutaneous and intramuscular administration, dogs □ Pharmacokinetics—butorphanol, subcutaneous and intramuscular administration, dogs □ Analgesics—butorphanol, pharmacokinetics following subcutaneous and intramuscular administration, dogs

Butorphanol tartrate [17-(cyclobutylmethyl)morphinan-3,14-diol tartrate], a new narcotic agonist–antagonist analgesic, is available[1] for use in humans and dogs (1). Previous studies indicated that loss processes account for a decrease in the extent of drug availability from extravascular parenteral injection sites (2). Deposition (3) and degradation (4) of the drug at the injection site can decrease both the rate and extent of absorption. The injection

[1] Stadol, Bristol Laboratories, Syracuse, N.Y.

0022-3549/80/0700-0801$01.00/0

© 1980, American Pharmaceutical Association

site also was demonstrated to be a critical factor in absorption rates due to differences in blood flow (5).

The present study was undertaken to examine and compare the pharmacokinetics and disposition of parenteral butorphanol following intramuscular and subcutaneous administration to dogs and to determine whether any observable differences were attributable to differences in the administration route.

EXPERIMENTAL

Animals—Six healthy adult beagles [three males (10.3 ± 1.8 kg) and three females (11.9 ± 1.9 kg)] were selected. The study was a complete, two-way crossover comparison of intramuscular and subcutaneous butorphanol tartrate at a nominal dose of 0.25 mg/kg (as butorphanol free base equi alent). There was a 2-week recovery period between successive doses.

Treatment—The intramuscular formulation was a solution of 5 mg of butorphanol base (7.29 mg of butorphanol tartrate)/ml of sterile water. The solutions were prepared immediately before administration. The dosing solution was administered into the caudal thigh muscle at a dose of 0.25 mg (0.05 ml)/kg. The subcutaneous formulation contained 1.38 mg of butorphanol base (2.01 mg of butorphanol tartrate)/ml of vehicle. The vehicle formulation was 3.300 g of citric acid USP, 6.400 g of sodium citrate USP, 6.412 g of analytical reagent grade sodium chloride, and water for injection USP to bring the solution to 1 liter. Butorphanol tartrate was stable in this formulation for a minimum of 1 year. Subcutaneous administration was made into the loose skin between the shoulder blades at a dose of 0.25 mg (0.18 ml)/kg.

The dogs had access to food overnight. A 10-ml/kg oral waterload was administered just prior to dosing. A continuous infusion of sterile 0.9% saline solution (25 ml/hr) was maintained for the first 6 hr of the study. The purpose of this waterloading was to eliminate the degree of hydration of individual animals as a variable since the volumes of distribution of solutes can vary with the degree of hydration (6).

Blood samples were collected from a catheterized saphenous vein immediately before the dose (zero time) and at 0.25, 0.50, 0.75, 1, 1.5, 2, 3, 5, and 7 hr after injection. At least 4 ml of serum was prepared from each blood sample and frozen at −20° until it was assayed within 3 weeks of collection. Butorphanol was stable in frozen dog serum for a minimum of 5 weeks.

Serum Butorphanol Assay—All reagents were USP, NF, or ACS grade or better and were used without further purification.

Twenty-five microliters of a 10-ng/μl solution of codeine phosphate, the internal standard, in methanol was added to 3.0 ml of serum. The serum was alkalinized by the addition of 0.1 ml of 5.0 *N* NaOH and shaken[2] for 15 min with 10 ml of chloroform. The mixture was centrifuged[3] for 10 min at 3000 rpm to separate the aqueous and chloroform phases. The chloroform layer was transferred to a clean extraction tube, 4 ml of 0.1 *N* H_2SO_4 was added, and the mixture was shaken for 15 min. The phases then were separated by centrifugation at 3000 rpm for 10 min.

The aqueous acid layer then was transferred to a clean extraction tube and made basic with 0.2 ml of 5 *N* NaOH. Five milliliters of chloroform was added, and the mixture was shaken for 15 min. The chloroform extract was evaporated to dryness under a gentle stream of air[4], the dried residue was dissolved in 95 μl of acetonitrile, and 5 μl of heptafluorobutyric anhydride[5] was added to the acetonitrile solution. After incubation for 10 min at room temperature, the solvent and reagent were evaporated under a gentle stream of air, and the dried residue was reconstituted with 40 μl of acetonitrile.

A 1-μl portion of the final acetonitrile solution was injected[6] into a gas chromatograph[7] equipped with a scandium tritide electron-capture detector operated at 265° with a standing current of 3.2×10^{-8} amp and a nitrogen flow rate of 30 ml/min. The chromatographic column was 3% SE-30 on 100–200-mesh Gas Chrom Q in a 30.5-cm × 4-mm i.d. glass U tube[8]. The retention times of butorphanol and codeine were 6.6 and 3.7 min, respectively.

[2] Roto-Rack model 340, Fisher Scientific Co., Pittsburgh, Pa.
[3] Model UV, International Equipment Co., Needham Heights, Mass.
[4] Evap-O-Rac, Cole Parmer Co., Chicago, Ill.
[5] ICN Pharmaceuticals, Plainview, N.Y.
[6] Microliter syringe, Hamilton, Reno, Nev.
[7] Model 2100, Varian Associates, Palo Alto, Calif.
[8] Applied Science Laboratories, State College, Pa.

Table I—Pharmacokinetic Parameters for Intramuscular and Subcutaneous Butorphanol in Dogs

Parameter	Intramuscular[a]	Subcutaneous[a]	Mean Difference[b]
C_{max}, ng/ml	25.1 ± 6.7	33.3 ± 16.9	8.2 ± 11.7
t_{max}, hr	0.7 ± 0.3	0.5 ± 0.3	−0.2 ± 0.2
AUC, (ng hr)/ml	67.7 ± 16.2	81.7 ± 34.3	14 ± 27.4
$t_{1/2}$, hr	1.53 ± 0.24	1.71 ± 0.40	0.18 ± 0.50
K_a, hr^{-1}	6.12 ± 3.79	7.30 ± 4.73	1.18 ± 2.14
K_{el}, hr^{-1}	0.466 ± 0.092	0.424 ± 0.094	−.042 ± 0.134
C_0, ng/ml	31.5 ± 9.3	34.0 ± 4.7	2.5 ± 10.3
t_0, min	1.3 ± 2.6	−3.8 ± 9.1	5.1 ± 5.4
V, liters/kg	7.51 ± 2.42	8.42 ± 3.08	0.91 ± 1.71
Cl_s, liters/hr/kg	3.41 ± 0.87	3.50 ± 1.32	0.09 ± 1.13

[a] Mean ± *SD*. [b] Mean difference between subcutaneous and intramuscular routes ±95% confidence limit.

A standard curve was prepared by plotting the peak area ratio, the area under the butorphanol peak divided by the area under the codeine peak, *versus* the concentration of butorphanol (as free base equivalent) in spiked serum standards.

Pharmacokinetic and Statistical Analysis—The serum butorphanol *versus* time data for the individual dogs conformed to the linear, open, one-compartment model with first-order drug absorption. The data are described by:

$$C = [K_a C_0/(K_a - K_{el})][\exp(-K_{el}t') - \exp(-K_a t')] \quad \text{(Eq. 1)}$$

where C is the serum concentration; K_a is the first-order absorption rate constant; K_{el} is the first-order elimination rate constant; $C_0 = D/V$, in which D is the dose and V is the volume of distribution; and $t' = t - t_0$, in which t is the time after drug injection and t_0 is the absorption lag time.

The area under the serum concentration *versus* time curve from $t' = 0$ to ∞ (AUC) was found by integrating Eq. 1 between these time limits and simplifying:

$$AUC = C_0/K_{el} \quad \text{(Eq. 2)}$$

The volume of distribution was $V = D/C_0$, and the serum clearance (Cl_s) was $Cl_s = VK_{el} = D/AUC$.

The serum half-life ($t_{1/2}$) was $t_{1/2} = 0.693/K_{el}$. The observed peak serum concentrations, C_{max}, and the time from the dosage to the peak concentration, t_{max}, also were tabulated and analyzed.

The individual serum concentration *versus* time data were optimized and fitted to Eq. 1 by nonlinear regression analysis. The digital computer program AUTOAN, which incorporates Hartley's modification of the Gauss–Newton method, was employed (7, 8).

The values for C_{max}, t_{max}, AUC, $t_{1/2}$, K_a, C_0, Cl_s, and t_0 for the intramuscular and subcutaneous dosing routes were statistically compared using an analysis of variance suitable for a complete, two-way crossover experimental design (9). The K_{el} value was not tested since $t_{1/2}$ was equivalent. The analysis of variance was used to determine whether there were significant differences, at the 5% level, between these parameters on the basis of study periods, interanimal variation, and differences in administration route. The 95% confidence limits for differences in administration routes were calculated using the error term from the analysis of variance and the standard formula (10).

RESULTS

Assay—The linear relationship between butorphanol concentrations and peak area ratios was highly significant ($p < 0.01$) by linear regression analysis. The lower limit of quantitative detectability was equivalent to a serum butorphanol concentration of 0.9 ng/ml. The linear range of the assay was 2–50 ng of butorphanol/ml of serum. The accuracy of the assay with serum standards at a concentration of 15 ng/ml was 97%; there was no significant difference ($p > 0.05$) between the observed and actual concentrations of serum butorphanol as determined by an independent t test.

The reproducibility of the assay was confirmed by replicate analyses of 15 serum samples in the range of 0–37 ng of butorphanol/ml. The mean absolute difference between replicates was 2 ng/ml with a standard deviation of 1.7 ng/ml. There was no significant difference ($p > 0.05$) between the replicate assays as determined by an independent t test.

Serum Butorphanol Concentration—The mean serum concentrations of butorphanol after intramuscular and subcutaneous adminis-

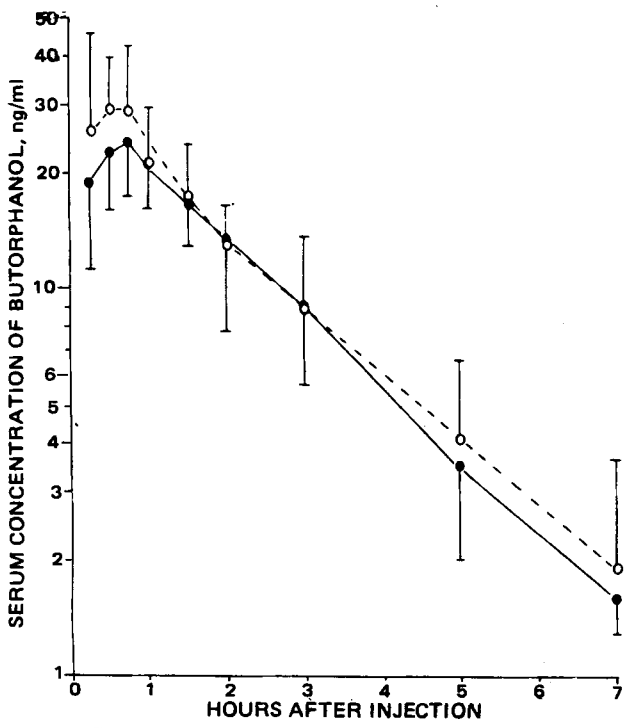

Figure 1—*Serum concentrations of butorphanol in dogs following intramuscular (●) and subcutaneous (○) administration. Mean values from six dogs with standard deviations (vertical bars) are given.*

tration are presented in Fig. 1. The mean pharmacokinetic parameters for intramuscular and subcutaneous administration for male and female dogs are listed in Table I. An analysis of variance indicated that there were no significant differences ($p > 0.05$) between the values of the pharmacokinetic parameters for different administration routes, dosing periods, and animals. There was significant interanimal variability ($p < 0.05$) in the absorption rate constant.

However, inspection of the 95% confidence limits of the mean difference between administration routes indicated considerable variability. This variability was due to both inter- and intraanimal variation. Determination of the bioequivalence of the two routes of administration by comparison of C_{max} and *AUC* within the individual animal demonstrated 85 and 97% relative bioavailability of the intramuscular dose as compared to the subcutaneous dose, respectively, with a coefficient of variation of 35% in both parameters. Although large differences could go undetected in the analysis of variance, the observed differences in the administration route in this study have no clinical, pharmacological, or toxicological significance (1).

DISCUSSION

The extent and time course of drug action can be affected significantly by the route of drug administration (2). There will be an initial lag between injection and the entrance of the drug into the circulation following extravascular parenteral administration. If drug partitioning from subcutaneous tissue and muscle to blood is similar, then the clearance of the drug from the injection site will depend primarily on blood flow. Since butorphanol is a basic (pKa 8.6), moderately lipophilic compound, differences in partitioning between the more lipophilic subcutaneous compartment and the intramuscular compartment could occur. The present studies indicated there were no significant differences in absorption, disposition, or clearance of butorphanol from these extravascular injection sites.

The absorption lag time for butorphanol tartrate in dogs on subcutaneous and intramuscular administration was -1.2 ± 6.9 min, indicating that absorption started immediately. The mean absorption half-times were 5.7 min for subcutaneous administration and 6.8 min for intramuscular administration. There should be a rapid onset of the effect of butorphanol in dogs following parenteral extravascular administration.

The disposition of butorphanol in dogs proceeded independently of the administration route. Although significant inter- and intraanimal variability was observed, the lack of a statistical or biologically significant difference between the *AUC* values indicated that the two routes were bioequivalent. The overall mean serum half-life of butorphanol was 1.62 hr, and the overall mean serum clearance was 3.45 liters/kg/hr. The mean volume of distribution of butorphanol was 7.96 liters/kg. When the apparent volume of distribution exceeds the true body weight in this manner, it usually is interpreted as indicating that the drug is distributed extensively to tissues.

REFERENCES

(1) F. S. Caruso, A. W. Pircio, H. Madissoo, R. D. Smyth, and I. J. Pachter, "Pharmacological and Biochemical Properties of Drug Substances," vol. 2, M. E. Goldberg, Ed., APhA Academy of Pharmaceutical Sciences, Washington, D.C., 1979, p. 19.

(2) L. Z. Benet, *J. Pharmacokinet. Biopharm.*, **6**, 559 (1978).

(3) H. B. Kostenbauder, R. P. Rapp, J. P. Mc Govern, T. S. Foster, D. G. Perrier, H. M. Blacker, W. C. Hulon, and A. W. Kinkel, *Clin. Pharmacol. Ther.*, **18**, 449 (1975).

(4) J. T. Doluisio, J. C. La Piana, and L. W. Dittert, *J. Pharm. Sci.*, **60**, 715 (1971).

(5) E. F. Evans, J. D. Proctor, M. J. Fratkin, J. Velandia, and A. J. Wassermann, *Clin. Pharmacol. Ther.*, **17**, 44 (1975).

(6) M. J. Sweeney, in "Body Fluid Disturbances," W. D. Snively, Jr., Ed., Grune and Stratton, New York, N.Y., 1962, p. 19.

(7) H. O. Hartley, *Technometrics*, **3**, 269 (1961).

(8) A. J. Sedman and J. G. Wagner, "Manual for AUTOAN. A Decision-Making Pharmacokinetic Computer Program," Publication Distribution Service, Ann Arbor, Mich., 1974.

(9) J. E. Grizzle, *Biometrics*, **21**, 467 (1965).

(10) B. Ostle and R. W. Mensing, "Statistics in Research," 3rd ed., Iowa State University Press, Ames, Iowa, 1975, p. 96.

ACKNOWLEDGMENTS

The authors thank Leon Gordon of Bristol Laboratories for advice on the statistical aspects of this report.

Rectal Bioavailability of Lidocaine in Rats: Absence of Significant First-Pass Elimination

A. G. de BOER *x, D. D. BREIMER, J. PRONK, and J. M. GUBBENS-STIBBE

Received April 27, 1979, from the *Department of Pharmacology, Subfaculty of Pharmacy, University of Leiden, Wassenaarseweg 72, Leiden, The Netherlands.* Accepted for publication December 14, 1979. *Present address: Department of Pharmaceutical Technology and Biopharmacy, Subfaculty of Pharmacy, Gorlaeus Laboratories, Wassenaarseweg 76, 2300 RA Leiden, The Netherlands.

Abstract □ Drugs administered rectally generally are considered to enter the systemic circulation without passing first through the liver since the lower hemorrhoidal veins do not drain into the portal system. To test this hypothesis, the systemic availability of the high clearance drug lidocaine was investigated in rats following oral (20 mg) and rectal (20 mg) administration to six rats and intraarterial (5 mg) administration to another six rats. Whole blood concentrations of lidocaine were determined by capillary GLC with nitrogen detection. Systemic availability was evaluated by two methods. For the rectal route, the results were 105.6 ± 43.3 and 83.1 ± 22.3% compared to those for intraarterial administration; for the oral route, these values were 7.7 ± 2.3 and 7.1 ± 2.3%. These results clearly indicate a significant bypass of the liver following rectal administration of lidocaine. Mean elimination half-lives following oral (54 ± 9 min) and rectal (79 ± 36 min) administration were not significantly different; however, rectal elimination half-lives sometimes were slightly prolonged. The mean peak concentration times of 11.5 ± 7.5 (oral) and 15.6 ± 10.6 (rectal) min were not significantly different whereas the mean peak concentrations were significantly different ($p < 0.01$) [0.92 ± 0.49 (oral) and 8.71 ± 3.30 (rectal) μg/ml]. The mean elimination half-life following intraarterial administration (33 ± 3 min) was significantly shorter than both the mean oral and rectal half-lives, and the calculated total blood clearance of lidocaine had an average value of 36 ± 9 ml/min. The results show that it is possible to bypass the liver, at least partially, when giving a high clearance drug rectally to rats. For lidocaine, this bypass is almost complete.

Keyphrases □ Lidocaine—pharmacokinetics following rectal, oral, and intraarterial administration, rats □ Pharmacokinetics—lidocaine following rectal, oral, and intraarterial administration, rats □ First-pass effect—lidocaine following rectal and oral administration, rats □ Bioavailability—lidocaine following rectal, oral, and intraarterial administration, rats

The drug administration route can affect bioavailability markedly. High clearance drugs in particular show substantially decreased bioavailability following oral administration, caused by liver and/or gut wall metabolism. This phenomenon is called the first-pass effect, and it has been demonstrated in several animal species and in humans. Such drugs include lidocaine (1–3), propranolol (4, 5), meperidine (6), salicylamide (7), and nitroglycerin (8, 9).

It has often been speculated that drugs given rectally to humans enter into the general circulation without passing first through the liver (10), but sufficient data are lacking to support this hypothesis. However, the rectal bioavailability of lidocaine (aqueous solution) in humans recently was shown to be about twice as high as the oral bioavailability, indicating a difference in the first-pass effect between the oral and rectal routes (11).

To determine if a similar difference occurs in rats, the systemic availability of lidocaine was studied following oral, rectal, and intraarterial administration. Lidocaine was chosen as the model substrate because it undergoes a substantial first-pass effect on oral and portal administration in humans (1, 2), dogs (3), and monkeys (1) and in rat liver perfusions (12–14).

EXPERIMENTAL

Animals and Sampling Techniques—Male Wistar rats, 200–250 g, were used. Before each experiment, the animals were starved overnight with free access to water. During that period, the animals were kept in a metabolic cage to prevent them from eating their own feces or sawdust.

In the 7-day period between two experiments with one rat, the body weight of the animals generally increased 5–10%.

A cannula[1] (polyvinyl chloride; 50 cm long × 0.5 mm i.d. × 1.0 mm o.d.) filled with heparinized saline[2] (200 IU/ml) was inserted between 9 and 10 am into the right vena jugularis externa ~40 mm from the midpoint of the vena jugularis externa, the vena jugularis anterior, and the acromiodeltoid and cephalic vein under light ether anesthesia. In this way, the end of the cannula was close to the right atrium. To avoid destruction by the animal, the cannula was pulled subcutaneously, emerging on the nape of the neck. The animals then were placed in restraining cages constructed to allow free movement and withdrawal of blood samples without touching the animals.

Each rat received lidocaine orally and rectally with an interval of 1 week. The oral and rectal administrations were given to the same animal. Because no attempt was made to keep the cannula open, the left vena jugularis externa was cannulated after 1 week.

Blood samples were taken at 0, 3, 6, 10, 15, 20, 30, 45, 60, 75, 90, 120, 150, and 180 min following intraarterial and rectal administration and at 3, 6, 10, 15, 20, 30, 45, 60, 75, 90, and 120 min following oral administration. No blood samples were taken during the infusion.

Blood samples, 0.15 ml, were taken with a 1-ml disposable syringe[3] (polypropylene) after discarding the contents of the cannula (±0.10 ml) together with the mixed blood–heparinized saline (total 0.15 ml). After sampling, the cannula was filled with heparinized saline (0.10 ml). The samples were stored in closed heparinized polyethylene containers in a refrigerator at 4° and were assayed the next day.

A check confirmed that no measurable adsorption of lidocaine occurred in the concentration range of 0.1–10.0 μg of lidocaine/ml of blood at the polyvinyl chloride cannula or at the polyethylene containers.

Treatments—Lidocaine was administered intraarterially by introducing a cannula (polyvinyl chloride; 50 cm long × 0.5 mm i.d. × 1.0 mm o.d.) about 1 cm into the left common carotid artery in the caudal direction. To avoid destruction of the cannula by the animal, the cannula was pulled subcutaneously, emerging on the nape of the neck. Lidocaine[4], 5.0 mg in saline solution (0.1 ml), was infused over 2 min by an infusion pump[5] and was followed immediately by a saline infusion (0.2 ml) for 4 min.

Lidocaine was administered orally (20 mg) as a lidocaine[4] solution (0.4 ml) by introduction into the stomach using a stomach tube. It was administered rectally (20 mg) as a lidocaine[4] solution (0.4 ml) through a septum using a syringe with a sharp needle. To prevent expulsion of the solution, the end of the rectum was closed by introduction of the septum. This septum was the tip of the plunger of a 2.5-ml disposable syringe[6] (sterile polypropylene). The septum was kept in place by a ligature with a thread that was introduced subcutaneously around the anus.

Assay of Lidocaine in Plasma—To 0.1 ml of whole blood were added 1.0 ml of distilled water and 50 μl of ethanol containing 0.50 μg of *N*-methylhexobarbital as the internal standard. The mixture was extracted twice with 3 ml of pentane on a whirl mixer for 10 sec. After centrifugation for 3 min at 2500×*g*, the upper organic layers were transferred to a conical

[1] Talas, Ommen, The Netherlands.
[2] Tromboliquine, Organon, Oss, The Netherlands.
[3] BDH, Poole, England.
[4] Lidocaine hydrochloride, Astra, The Netherlands.
[5] Unita I, type 871022, Braun.
[6] H802S, BDH, Poole, England.

0022-3549/80/0700-0804$01.00/0
© 1980, American Pharmaceutical Association

Table I—Elimination Half-Lives and *AUC* Values of Lidocaine[a] following Oral and Rectal Administration (20 mg) to the Same Rat

Rat	Elimination Half-Life, min		*AUC*, μg min/ml[b]		*AUC*, μg min/ml[c]	
	Oral	Rectal	Oral	Rectal	Oral	Rectal
1	45	70	42	551	39	507
2	45	60	58	405	55	363
3	65	65	26	631	23	551
4	55	140	61	706	56	442
5	50	100	48	1056	46	697
6	65	38	34	352	31	351
Mean	54	79	45	617	42	485
SD	9	36	14	253	13	130

[a] Based on whole blood concentrations. [b] Determined according to Method I. [c] Determined according to Method II.

evaporation tube. The solvent was evaporated on a water bath (40°) under a stream of dry nitrogen, and the residue was dissolved in 100 μl of ethanol.

Two microliters of this solution was brought onto the needle of a GLC solid injection system, similar to that used previously for the determination of underivatized nitrazepam in plasma (15). After evaporation of the ethanol, the needle was injected into the injection port of the gas–liquid chromatograph[7] equipped with a dual nitrogen–phosphorus detector[8]. The temperatures were 160° (column), 250° (injection port), and 300° (detector). A 10-m × 0.40-mm i.d. capillary SCOT column[9] was used. The support layer consisted of silanized, fumed silica[10] (particle size of <10 μm) coated with a stationary phase[11].

Linear calibration curves were obtained between 0.10 and 10.0 μg of lidocaine/ml of blood. The sensitivity limit of this method is ~50 ng of lidocaine/ml of blood.

Calculations and Pharmacokinetic Analysis—The postinfusion whole blood concentrations of lidocaine were fitted according to two-compartment kinetics (16). Clearance values were determined by dividing the given dose by the integrated total area under the concentration curves. In the oral and rectal experiments, the elimination rate constant, k_{el}, was obtained by regression analysis of log plasma concentration *versus* time, generally beginning 30 min after dosing. Elimination half-lives, $t_{1/2el}$, subsequently were calculated from:

$$t_{1/2el} = 0.69/k_{el} \qquad \text{(Eq. 1)}$$

The bioavailability, F, of the oral and rectal doses compared to the intraarterial dose was calculated as the ratio of the corresponding areas under the experimental curves (obtained by the trapezoidal rule) corrected for the undetermined area. The area beyond the last sampling point was obtained by two methods (17): (*a*) extrapolating the apparent exponential concentration decay phase of the individual experimental oral and rectal curves to infinite time (Method I); and (*b*) dividing the last experimentally determined concentration by the mean elimination rate constant after intraarterial infusion (Method II).

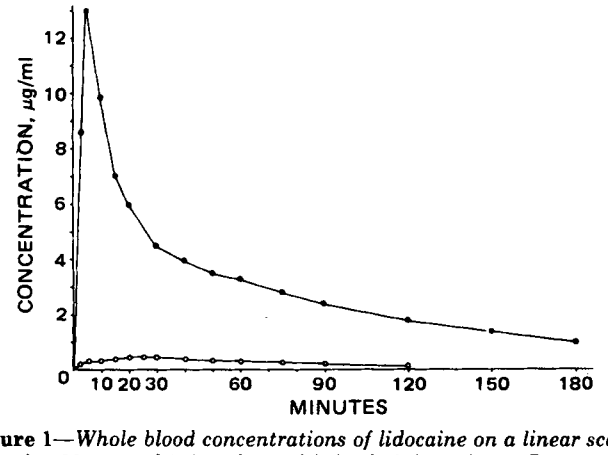

Figure 1—*Whole blood concentrations of lidocaine on a linear scale following 20-mg oral (○) and rectal (●) administration to Rat 1.*

[7] Hewlett-Packard model 5710.
[8] Hewlett-Packard model 18789A.
[9] Duran 50 glass.
[10] Tullanox, Cabot Corp., Boston, Mass.
[11] Carbowax 20M-KOH.

Corrections also were made for differences in the given dose by:

$$F = \frac{D_{ia}AUC_x}{D_xAUC_{ia}} \qquad \text{(Eq. 2)}$$

where D_{ia} and D_x are the intraarterial and the oral or rectal dose, respectively, and AUC_{ia} and AUC_x are the intraarterial and the oral or rectal areas under the curve, respectively. The oral and rectal parameters were determined for each animal and compared to the mean intraarterial value, and statistical differences were tested by a paired t test. When differences between the two groups of animals (intraarterial and rectal or oral) were tested, a nonpaired t test was used.

RESULTS

Figures 1 and 2 show the whole blood lidocaine concentration–time curves for a representative rat following oral and rectal administration. There was a remarkable difference in the concentration peaks. Table I gives the experimentally determined areas under the curve after oral and rectal administration. The AUC_{rect}/AUC_{or} ratios calculated by Methods I and II are given in Table II, indicating that the mean rectal systemic availability was 14.7- (Method I) and 13.0- (Method II) fold higher than the mean oral systemic availability.

A substantial amount of the dose absorbed rectally bypassed the liver and entered directly into the systemic circulation. Although substantial intraindividual differences were noted among the elimination half-lives of lidocaine on oral and rectal administration (Table I), the respective mean values of 54 and 79 min were statistically significantly different (paired t test, $p > 0.10$). Rats 4 and 5 in particular had rectal elimination half-lives that were prolonged compared to the oral administration ones. It is possible that the absorption phase extends partially into the elimination phase.

The peak concentration times, t_{max}, and peak concentrations, C_{max}, were determined with respect to the absorption rate (Table III). The mean t_{max} was 11.5 min orally and 15.6 min rectally ($p > 0.10$). However, the large difference in the mean C_{max} values of 0.92 and 8.71 μg/ml orally and rectally, respectively ($p < 0.01$), reflects the enormously increased *AUC* following rectal administration.

Following intraarterial administration of lidocaine to a second series of rats, the blood concentration–time curves exhibited two distinct phases (Fig. 3) and could be fitted to two-compartment kinetics (16). Table IV shows the data obtained following intraarterial infusion of lidocaine to

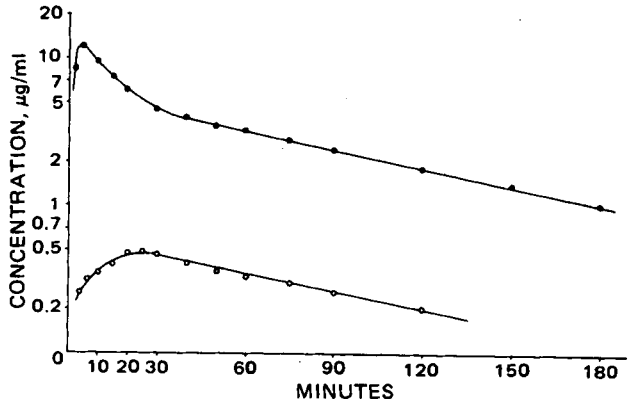

Figure 2—*Whole blood concentrations of lidocaine on a semilog scale following 20-mg oral (○) and rectal (●) administration to Rat 1.*

Table II—*AUC* Ratios (Rectal/Oral) Calculated According to Methods I and II

Rat	AUC_{rect}/AUC_{or} Method I	AUC_{rect}/AUC_{or} Method II	Method I/Method II
1	13.1	13.0	1.00
2	7.0	6.6	1.06
3	24.3	24.0	1.01
4	11.6	7.9	1.47
5	22.0	15.2	1.45
6	10.4	11.3	0.92
Mean	14.7	13.0	1.15
SD	6.9	6.3	0.24

Table III—Peak Concentration Times [a] (t_{max}) and Peak Concentrations [a] (C_{max}) following Oral and Rectal Administration (20 mg) of Lidocaine to the Same Rat

Rat	t_{max}, min Oral	t_{max}, min Rectal	C_{max}, μg/ml Oral	C_{max}, μg/ml Rectal
1	10	30	0.45	6.08
2	5	10	1.75	5.90
3	25	5	0.50	12.34
4	6	21	0.95	5.51
5	15	20	1.16	12.55
6	8	5	0.70	9.87
Mean	11.5	15.6	0.92[b]	8.71[b]
SD	7.5	10.6	0.49	3.30

[a] Based on whole blood concentrations. [b] $p < 0.01$.

Table IV—Pharmacokinetic Parameters of Lidocaine following Intraarterial Infusion Based on Whole Blood Concentrations

Rat	$t_{1/2\beta}$, min[a]	*AUC*, μg min/ml	Clearance, ml/min
A	32	111	45
B	30	119	42
C	35	156	32
D	36	184	27
E	33	194	26
F	31	113	44
Mean	33	146	36
SD	3	37	9

[a] The value $t_{1/2\beta}$ is the half-life of the β-phase.

Table V—Systemic Availability (*F*) of Lidocaine following Oral and Rectal Administration to the Same Rat Calculated According to Methods I and II as the Ratio of the Rectal or Oral Value to the Mean Intraarterial Systemic Availability [a]

Rat	*F*, % Method I Oral	*F*, % Method I Rectal	*F*, % Method II Oral	*F*, % Method II Rectal
1	7.2	94.4	6.7	86.8
2	9.9	69.3	9.4	62.2
3	4.5	108.0	3.9	94.4
4	10.6	120.9	9.6	75.7
5	8.2	180.8	7.9	119.4
6	5.8	60.3	5.3	60.1
Mean	7.7	105.6	7.1	83.1
SD	2.3	43.3	2.3	22.3

[a] Corrections were made for differences in the administered dose.

these rats. The mean elimination half-life was significantly shorter (33 min) than the mean oral and rectal half-lives ($p < 0.001$ and $p < 0.010$, respectively). The total blood clearance of lidocaine calculated by dose/AUC_{ia} had an average value of 36 ml/min (Table IV).

The absolute oral and rectal bioavailability values of lidocaine were calculated for each rat by dividing the corrected individual AUC_{or} or AUC_{rect} by the mean AUC_{ia}. These values varied from 60.3 to 180.8% (Method I) and from 60.1 to 119.4% (Method II), with an average of 105.6 and 83.1%, respectively, for the rectal route, and from 4.5 to 10.6% (Method I) and from 3.9 to 9.6% (Method II), with an average of 7.7 and 7.1%, respectively, for the oral route (Table V).

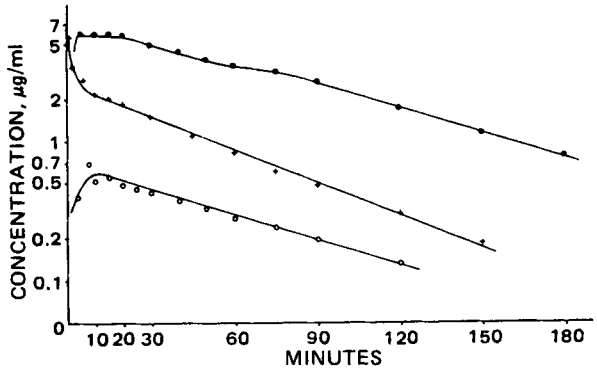

Figure 3—*Mean whole blood concentrations of lidocaine on a semilog scale following oral (○, 20 mg) and rectal (●, 20 mg) administration to Rats 1–6 and intraarterial (+, 5 mg/2 min) administration to Rats A–F.*

DISCUSSION

The experimental results demonstrate that the bioavailability of lidocaine following rectal administration to the rat is far greater than that following oral administration. This result strongly supports the hypothesis that rectal administration can result in a bypass of the liver. For a high clearance drug such as lidocaine, this bypass means increased systemic availability. As derived from the ratio of AUC_{rect} to AUC_{ia} (Table V), the mean bypass of the liver according to Methods I and II was roughly 100 and 80%, respectively, although substantial variations were observed. In addition, Table V shows that calculation of the systemic availability following rectal administration according to Methods I and II results in different mean values, which are due mainly to variations in the data of Rats 4 and 5. This difference also can be observed in Table I, where the oral and rectal *AUC* are calculated according to Methods I and II. The ratio of I to II in Table II shows that only the data of Rats 4 and 5 changed. Both data sets are given since there is no reason to prefer one method to the other (17).

If the liver is not bypassed before a high clearance drug reaches the systemic circulation, the result is extensive drug loss caused by hepatic first-pass metabolism, indicated by the present oral results with lidocaine. In general, differences in the extent of absorption might explain the observed differences in systemic availability. However, lidocaine was administered orally and rectally in an aqueous solution, which probably gives the least chance of pharmaceutical bioavailability problems. The results of this study do not permit definite conclusions about the extent of absorption. To assess the exact amount of lidocaine absorbed following a certain administration route, experiments with radiolabeled drug are indispensable. However, if rectal absorption is not complete whereas oral absorption is, the difference between oral and rectal availability will be even more in favor of the avoidance of first-pass metabolism by the rectal route.

Some pharmacokinetic factors also should be considered. Lennard *et al.* (12) indicated that with low doses of lidocaine, which resulted in initial blood concentrations of ~2 μg/ml, the drug was extracted almost completely by the perfused rat liver (>97%). Similarly, Nyberg *et al.* (13) showed that extraction was ~100% in the perfused rat liver at an initial concentration of 10 μg/ml. Shand *et al.* (14) determined, in the same system, an extraction ratio of 0.95 during constant infusion of lidocaine into the perfusion reservoir at concentrations entering the liver of 5–10 μg/ml. Linear kinetics were observed in all of these cases. One might infer from the shape of the single rectal concentration curve that nonlinear kinetics are involved, but no definite conclusions may be drawn concerning saturation phenomena due to limited data (only Rats 4 and 5 showed this curve shape) (12). Other factors also may be involved; one example is of hemodynamic origin, *i.e.*, a reduced blood flow through the liver results in a lower clearance. In addition, high lidocaine concentrations can cause bradycardia and cardiac depression (18). Finally, it is difficult to distinguish between the experimental situation where the absorption phase extends into the elimination phase and saturation kinetics. In both situations, the experimental curves may look much the same.

The lidocaine clearance value of 36 ml/min (115 ml/min/kg) following intraarterial administration is substantially higher than that reported for liver blood flow (19–23). Following intraarterial administration, ~20% of the cardiac output flows directly through the liver; therefore, with

reference to the venous blood sampling site, this flow will result in a first-pass effect and the actual systemic clearance will be overestimated (24). Even after correcting for this effect by assuming a hepatic extraction of 0.97 (12), the mean systemic clearance of 28.8 ml/min still is greater than the normal liver blood flow. This result could indicate extrahepatic elimination in the rat or an acute hemodynamic effect of lidocaine on its own disposition as a result of an increase in liver blood flow. Such an increase in flow was observed in humans following steady-state intravenous infusion (25).

REFERENCES

(1) N. Benowitz, R. P. Forsyth, K. L. Melmon, and M. Rowland, *Clin. Pharmacol. Ther.*, **16**, 87 (1974).

(2) R. N. Boyes, D. B. Scott, P. J. Jebson, M. J. Godman, and D. G. Julian, *ibid.*, **12**, 105 (1971).

(3) R. N. Boyes, H. J. Adams, and B. R. Duce, *J. Pharmacol. Exp. Ther.*, **174**, 1 (1970).

(4) D. G. Shand and R. E. Rango, *Pharmacology*, **7**, 159 (1972).

(5) D. G. Shand, R. E. Rango, and G. H. Evans, *ibid.*, **8**, 344 (1972).

(6) L. E. Mather and G. T. Tucker, *Clin. Pharmacol. Ther.*, **20**, 535 (1977).

(7) W. H. Barr and S. Riegelman, *J. Pharm. Sci.*, **59**, 164 (1970).

(8) W. R. Taylor, J. S. Forrester, P. Magnusson, T. Takano, K. Chatterjer, and H. J. C. Swan, *Am. J. Cardiol.*, **38**, 469 (1976).

(9) P. S. K. Yap and H. L. Fung, *J. Pharm. Sci.*, **67**, 584 (1978).

(10) T. W. Schwartz, in "American Pharmacy," L. W. Dittert, Ed., Lippincott, Philadelphia, Pa., 1974, p. 280.

(11) A. G. de Boer, D. D. Breimer, H. Mattie, J. Pronk, and J. M. Gubbens-Stibbe, *Clin. Pharmacol. Ther.*, **26**, 701 (1979).

(12) M. S. Lennard, G. T. Tucker, and H. F. Woods, "Abstracts of the 7th International Congress of Pharmacology," Paris, France, 1978, p. 836, no. 2587.

(13) G. Nyberg, B. Karlen, I. Hedlund, R. Grundin, and C. von Bahr, *Acta Pharmacol. Toxicol.*, **40**, 337 (1977).

(14) D. G. Shand, D. M. Kornhauser, and G. R. Wilkinson, *J. Pharmacol. Exp. Ther.*, **195**, 424 (1975).

(15) A. G. de Boer, J. Röst-Kaiser, H. Bracht, and D. D. Breimer, *J. Chromatogr.*, **145**, 105 (1978).

(16) J. C. K. Loo and S. Riegelman, *J. Pharm. Sci.*, **59**, 53 (1970).

(17) J. W. Crow, M. Gibaldi, and G. Levy, *ibid.*, **68**, 958 (1979).

(18) J. G. Sloman, in "Drug Treatment," G. S. Avery, Ed., Adis Press, Sydney, Australia, 1976, chap. 16, p. 450.

(19) E. L. Dobson and H. B. Jones, *Acta Med. Scand. Suppl.*, **273**, 48 (1952).

(20) D. B. Ross, "Perfusion Techniques in Biochemistry: A Laboratory Manual," Clarendon, Oxford, England, 1972.

(21) K. S. Pang and J. R. Gillette, *Drug Metab. Disp.*, **6**, 567 (1978).

(22) M. Tsuchiya, R. A. Ferrone, G. M. Walsh, and E. D. Frohlich, *Am. J. Physiol.*, **235**, H357 (1978).

(23) M. S. Yates, C. R. Hiley, P. J. Roberts, D. J. Back, and F. E. Crawford, *Biochem. Pharmacol.*, **27**, 2617 (1978).

(24) J. R. Gillette and K. S. Pang, *Clin. Pharmacol. Ther.*, **22**, 623 (1977).

(25) G. Tucker, L. Wiklund, A. Berlin-Wahlen, and L. A. Mather, *J. Pharmacokinet. Biopharm.*, **5**, 111 (1977).

Use of Molecular Negentropy to Encode Structure Governing Biological Activity

LEMONT B. KIER

Received October 5, 1979, from the *Department of Pharmaceutical Chemistry, Medical College of Virginia, Virginia Commonwealth University, Richmond, VA 23298.* Accepted for publication February 12, 1980.

Abstract □ A drug molecule is considered to be an information source with an information content available to receptive tissue. In nonspecific interactions, much of the information content has quality as judged by the receptor. Quantitation of the information content using Shannon's equation gives the molecular negentropy. This index is shown to rank molecules according to symmetry and to encode structural characteristics influencing physical properties and biological activity in certain cases.

Keyphrases □ Structure–activity relationships—quantitation of molecular information content by negentropy calculations, correlation between biological activity and molecular structure □ Negentropy—mathematical analysis of correlation between biological activity and molecular structure, molecular information content available to receptor molecule □ Drug–receptor interaction—structure–activity relationships, negentropy of molecules, mathematical analysis of molecular structure and biological potency

A drug molecule may be regarded as a message containing information in the form of electron probability fields distributed in space around a framework of atomic nuclei. Therefore, drug–receptor interaction may be viewed as a presentation of the message, with its information content, to a receiver. Some information in the message may be interpretable by the receiver or receptor, leading to the beginning of events culminating in a biological response.

It follows that the efficacy of a drug depends on the information content and its quality as judged by the receptor. The quality of the information content in the drug molecule depends on the ability of the receptor to interpret the fields and to translate the interactions into a significant change in the receptor and its adjacent structures.

BACKGROUND

Under some circumstances, most if not all of the information content of a drug molecule has quality; that is, a receptor may be capable of interpreting the entire message presented by the drug. These circumstances are commonly referred to as nonspecific actions. In this category are molecules which, by virtue of the mere presence of atoms and bonds, are capable of eliciting a biological response. There usually is a rough correlation between size, expressed as the number of atoms, and the potency. However, various isomers frequently have different potencies. For example, in *in vitro* studies, there often is a decline in activity for the isomer series butanol > isobutanol > *tert*-butanol. Several physicochemical correlates have been presented to explain this trend, but all point to bulk phase phenomena, not to events occurring at the molecular level between the drug and the receptor.

If the information content of a nonspecific-acting molecule is of considerable importance to the potency, then quantitation of this characteristic would be a productive approach in analyzing the structure–activity relationships and the molecular level mechanism.

The information content of a message, whether it is a molecule, a book, or communication network, can be quantitated through information theory (1), particularly by use of the equation developed by Shannon and Weaver (2). This equation has its roots in the probabilities of choice among items classified into sets of equivalent items. A specific example using the propane molecule illustrates the assignment of equivalent atoms

0022-3549/80/0700-0807$01.00/0

© 1980, American Pharmaceutical Association

reference to the venous blood sampling site, this flow will result in a first-pass effect and the actual systemic clearance will be overestimated (24). Even after correcting for this effect by assuming a hepatic extraction of 0.97 (12), the mean systemic clearance of 28.8 ml/min still is greater than the normal liver blood flow. This result could indicate extrahepatic elimination in the rat or an acute hemodynamic effect of lidocaine on its own disposition as a result of an increase in liver blood flow. Such an increase in flow was observed in humans following steady-state intravenous infusion (25).

REFERENCES

(1) N. Benowitz, R. P. Forsyth, K. L. Melmon, and M. Rowland, *Clin. Pharmacol. Ther.*, **16**, 87 (1974).

(2) R. N. Boyes, D. B. Scott, P. J. Jebson, M. J. Godman, and D. G. Julian, *ibid.*, **12**, 105 (1971).

(3) R. N. Boyes, H. J. Adams, and B. R. Duce, *J. Pharmacol. Exp. Ther.*, **174**, 1 (1970).

(4) D. G. Shand and R. E. Rango, *Pharmacology*, **7**, 159 (1972).

(5) D. G. Shand, R. E. Rango, and G. H. Evans, *ibid.*, **8**, 344 (1972).

(6) L. E. Mather and G. T. Tucker, *Clin. Pharmacol. Ther.*, **20**, 535 (1977).

(7) W. H. Barr and S. Riegelman, *J. Pharm. Sci.*, **59**, 164 (1970).

(8) W. R. Taylor, J. S. Forrester, P. Magnusson, T. Takano, K. Chatterjer, and H. J. C. Swan, *Am. J. Cardiol.*, **38**, 469 (1976).

(9) P. S. K. Yap and H. L. Fung, *J. Pharm. Sci.*, **67**, 584 (1978).

(10) T. W. Schwartz, in "American Pharmacy," L. W. Dittert, Ed., Lippincott, Philadelphia, Pa., 1974, p. 280.

(11) A. G. de Boer, D. D. Breimer, H. Mattie, J. Pronk, and J. M. Gubbens-Stibbe, *Clin. Pharmacol. Ther.*, **26**, 701 (1979).

(12) M. S. Lennard, G. T. Tucker, and H. F. Woods, "Abstracts of the 7th International Congress of Pharmacology," Paris, France, 1978, p. 836, no. 2587.

(13) G. Nyberg, B. Karlen, I. Hedlund, R. Grundin, and C. von Bahr, *Acta Pharmacol. Toxicol.*, **40**, 337 (1977).

(14) D. G. Shand, D. M. Kornhauser, and G. R. Wilkinson, *J. Pharmacol. Exp. Ther.*, **195**, 424 (1975).

(15) A. G. de Boer, J. Röst-Kaiser, H. Bracht, and D. D. Breimer, *J. Chromatogr.*, **145**, 105 (1978).

(16) J. C. K. Loo and S. Riegelman, *J. Pharm. Sci.*, **59**, 53 (1970).

(17) J. W. Crow, M. Gibaldi, and G. Levy, *ibid.*, **68**, 958 (1979).

(18) J. G. Sloman, in "Drug Treatment," G. S. Avery, Ed., Adis Press, Sydney, Australia, 1976, chap. 16, p. 450.

(19) E. L. Dobson and H. B. Jones, *Acta Med. Scand. Suppl.*, **273**, 48 (1952).

(20) D. B. Ross, "Perfusion Techniques in Biochemistry: A Laboratory Manual," Clarendon, Oxford, England, 1972.

(21) K. S. Pang and J. R. Gillette, *Drug Metab. Disp.*, **6**, 567 (1978).

(22) M. Tsuchiya, R. A. Ferrone, G. M. Walsh, and E. D. Frohlich, *Am. J. Physiol.*, **235**, H357 (1978).

(23) M. S. Yates, C. R. Hiley, P. J. Roberts, D. J. Back, and F. E. Crawford, *Biochem. Pharmacol.*, **27**, 2617 (1978).

(24) J. R. Gillette and K. S. Pang, *Clin. Pharmacol. Ther.*, **22**, 623 (1977).

(25) G. Tucker, L. Wiklund, A. Berlin-Wahlen, and L. A. Mather, *J. Pharmacokinet. Biopharm.*, **5**, 111 (1977).

Use of Molecular Negentropy to Encode Structure Governing Biological Activity

LEMONT B. KIER

Received October 5, 1979, from the *Department of Pharmaceutical Chemistry, Medical College of Virginia, Virginia Commonwealth University, Richmond, VA 23298.* Accepted for publication February 12, 1980.

Abstract □ A drug molecule is considered to be an information source with an information content available to receptive tissue. In nonspecific interactions, much of the information content has quality as judged by the receptor. Quantitation of the information content using Shannon's equation gives the molecular negentropy. This index is shown to rank molecules according to symmetry and to encode structural characteristics influencing physical properties and biological activity in certain cases.

Keyphrases □ Structure–activity relationships—quantitation of molecular information content by negentropy calculations, correlation between biological activity and molecular structure □ Negentropy—mathematical analysis of correlation between biological activity and molecular structure, molecular information content available to receptor molecule □ Drug–receptor interaction—structure–activity relationships, negentropy of molecules, mathematical analysis of molecular structure and biological potency

A drug molecule may be regarded as a message containing information in the form of electron probability fields distributed in space around a framework of atomic nuclei. Therefore, drug–receptor interaction may be viewed as a presentation of the message, with its information content, to a receiver. Some information in the message may be interpretable by the receiver or receptor, leading to the beginning of events culminating in a biological response.

It follows that the efficacy of a drug depends on the information content and its quality as judged by the receptor. The quality of the information content in the drug molecule depends on the ability of the receptor to interpret the fields and to translate the interactions into a significant change in the receptor and its adjacent structures.

BACKGROUND

Under some circumstances, most if not all of the information content of a drug molecule has quality; that is, a receptor may be capable of interpreting the entire message presented by the drug. These circumstances are commonly referred to as nonspecific actions. In this category are molecules which, by virtue of the mere presence of atoms and bonds, are capable of eliciting a biological response. There usually is a rough correlation between size, expressed as the number of atoms, and the potency. However, various isomers frequently have different potencies. For example, in *in vitro* studies, there often is a decline in activity for the isomer series butanol > isobutanol > *tert*-butanol. Several physicochemical correlates have been presented to explain this trend, but all point to bulk phase phenomena, not to events occurring at the molecular level between the drug and the receptor.

If the information content of a nonspecific-acting molecule is of considerable importance to the potency, then quantitation of this characteristic would be a productive approach in analyzing the structure–activity relationships and the molecular level mechanism.

The information content of a message, whether it is a molecule, a book, or communication network, can be quantitated through information theory (1), particularly by use of the equation developed by Shannon and Weaver (2). This equation has its roots in the probabilities of choice among items classified into sets of equivalent items. A specific example using the propane molecule illustrates the assignment of equivalent atoms

0022-3549/80/0700-0807$01.00/0

© 1980, American Pharmaceutical Association

Table I—Molecular Negentropy and Redundancy of Isomeric Heptanes

Heptane	I	R
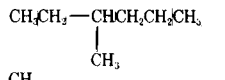	25.219	0.195
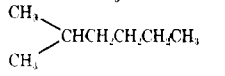	22.811	0.272
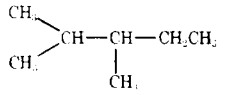	22.584	0.279
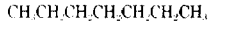	19.426	0.379
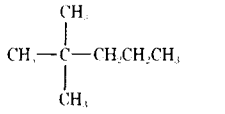	18.665	0.404
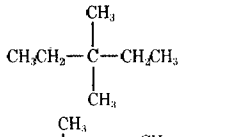	17.768	0.432
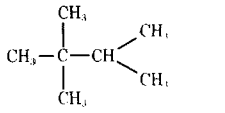	16.029	0.488
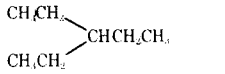	15.200	0.515
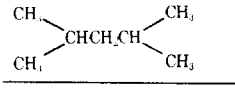	14.155	0.548

into sets and the calculation of the information content. Before proceeding with this illustration, the term molecular negentropy, the negative of information entropy, will be adopted as a measure of the information content of a molecule as suggested previously (1, 3).

THEORETICAL

Calculation of Molecular Negentropy—An approach to the calculation of the negentropy of a molecule can be derived from a consideration of molecular graphs as shown by Rashevsky (4), who pointed out the biological implications of such a parameter. Consider the propane molecule (Fig. 1) as an assemblage of atoms where the six methyl hydrogens are regarded as equivalent. This equivalence is apparent from the performance of symmetry operations on a model and from experimental evidence such as NMR. Each methyl hydrogen possesses the same physical and chemical properties as the other five by virtue of its equivalent topology relative to all of the other atoms.

These six hydrogens comprise a set. Similarly, the two methylene hydrogens are equivalent and comprise a different set with a multiplicity (number in the set) of two. The two methyl carbons comprise a third set with a multiplicity of two. The methylene carbon is in a fourth set with a multiplicity of one. Figure 1 shows the molecule labeled by sets with multiplicities.

The probability of a random selection of a methyl hydrogen is 6/11

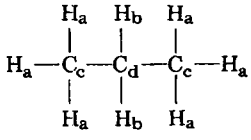

sets	[aaaaaa]	[bb]	[cc]	[d]
multiplicity	6	2	2	1
probabilities of random selection	6/11	2/11	2/11	1/11

Figure 1—*Decomposition of the propane molecule into sets of topologically equivalent atoms, their multiplicities, and probabilities of random selection.*

Table II—Enzyme Inhibitory Potency of Alcohols and Molecular Negentropy

Molecule	I	pC Found	pC Calc.
Methanol	3.24	3.36	3.45
Ethanol	6.55	3.85	3.73
Propanol	10.32	4.28	4.05
Butanol	14.40	4.43	4.39
Pentanol	18.76	5.05	4.76
Hexanol	23.32	5.31	5.15
Heptanol	28.08	5.75	5.55
Octanol	33.00	6.05	5.97
3-Methylbutanol	17.93	4.77	4.69
3-Pentanol	14.31	4.26	4.39
2-Pentanol	18.53	4.40	4.74
2-Methylbutanol	18.53	4.70	4.74
Nonanol	38.07	6.30	6.40
1,2-Dimethyl-propanol	15.89	4.08	4.52
1-Methyl-3-phenyl-propanol	29.91	5.55	5.71
1-Phenylethanol	20.46	4.98	4.91
1-Phenylpropanol	25.09	5.35	5.30

while that for a methylene hydrogen is only 2/11. The complete array of probabilities, P_j, for the four sets is shown in Fig. 1.

The negentropy per atom, i, is computed for propane from Shannon's formula:

$$i = -K \sum_j P_j \log P_j \qquad \text{(Eq. 1)}$$

where K is a constant depending on the logarithmic base and j is the set. For propane, the calculation is:

$$i = -\frac{6}{11}\log\frac{6}{11} - \frac{2}{11}\log\frac{2}{11} - \frac{2}{11}\log\frac{2}{11} - \frac{1}{11}\log\frac{1}{11} \qquad \text{(Eq. 2)}$$

where $i = 0.507$. The molecular negentropy, I for $N = 11$ atoms, is $iN = 5.582$. Note that $\log_{10}$ is used for convenience. Use of $\log_2$ leads to negentropy expressed in bits.

Several properties of negentropy are apparent:

1. The negentropy is maximal when all parts of a structure are unique, resulting in equal probabilities for all parts.

2. The negentropy is zero when all parts of a structure are equivalent.

3. The numerical value of the negentropy decreases with greater multiplicity within each set or for a smaller number of sets. This observation translates into awareness that molecular negentropy ranks molecules according to symmetry. Bonchev *et al.* drew a relationship between negentropy and symmetry only among homologs (5). An example is shown in Table I, in which the nine isomers of heptane are ranked by molecular negentropy. It is apparent that this ranking is the same as that by symmetry and presents the possibility of quantitating the degree of symmetry among molecules. An alternative quantitation would be the use of redundancy, R (1), where $R = 1 - i/\log N$.

Molecular Negentropy as a Structure–Activity Relationship Parameter—If it is hypothesized that in some cases of biological activity the entire information content of a molecule is of quality to the receptor, then the molecular negentropy is a potentially useful parameter of structure. This approach is possible because molecular structure obviously governs the information content (Table I).

Table III—Lipoxygenase Inhibition and Molecular Negentropy

Alcohol	I	pK_I Found	pK_I Calc.
Methanol	3.24	−0.18	−0.10
Ethanol	6.55	0.18	0.26
Isopropanol	7.68	0.37	0.38
Propanol	10.32	0.68	0.67
tert-Butanol	7.62	0.49	0.37
sec-Butanol	14.18	0.86	1.08
Isobutanol	11.77	1.13	0.82
Butanol	14.40	1.15	1.11
Isopentanol	17.93	1.34	1.49
Pentanol	18.76	1.61	1.58
Hexanol	23.33	2.10	2.07
Heptanol	28.08	2.60	2.59

Table IV—Tadpole Narcosis Potency *versus* Molecular Negentropy

Molecule	I	log 1/c		
		Found	Calc.	Calc.[a]
Methanol	3.24	0.24	0.46	0.32
Ethanol	6.55	0.54	0.80	0.66
Propanol	10.32	0.96	1.18	1.05
Butanol	14.40	1.42	1.60	1.48
Octanol	33.00	3.40	3.49	3.41
Isopropanol	7.68	0.89	0.91	0.77
Isobutanol	11.77	1.35	1.33	1.21
tert-Butanol	7.62	0.89	0.91	0.77
Isopentanol	16.13	1.64	1.77	1.66
tert-Pentanol	11.87	1.24	1.35	1.23
Acetone	4.73	0.54	0.61	—
Butanone	11.02	1.04	1.25	—
3-Pentanone	10.99	1.54	1.25	—
2-Pentanone	15.20	1.72	1.68	—
Acetal	14.81	1.98	1.64	—
Ethyl ether	9.36	1.57	1.08	—
Methyl acetate	8.59	1.10	1.01	1.18
Ethyl formate	9.42	1.15	1.09	1.25
Ethyl acetate	12.58	1.52	1.41	1.54
Ethyl propionate	16.85	1.96	1.85	1.93
Propyl acetate	16.85	1.96	1.85	1.93
Ethyl butyrate	21.35	2.37	2.31	2.34
Ethyl isobutyrate	18.72	2.24	2.04	2.10
Butyl acetate	21.35	2.30	2.31	2.34
Isobutyl acetate	18.72	2.24	2.04	2.10
Ethyl valerate	26.05	2.72	2.79	2.76
Amyl acetate	26.05	2.72	2.79	2.76
Butyl valerate	35.93	3.60	3.79	3.66
Methyl carbamate	7.97	0.57	0.94	—
Ethyl carbamate	11.85	1.39	1.34	—
Acetonitrile	3.24	0.44	0.46	—
Acetaldehyde oxime	7.16	0.93	0.86	—

[a] Alcohols calculated from Eq. 6, and esters calculated from Eq. 7.

Sheep Liver Esterase Inhibition—One example of such a relationship is the inhibition of sheep liver esterase by several alcohols (6). In this study, the concentration required to inhibit the enzyme *in vitro* by 25% was deduced from plots of concentration *versus* percent inhibition (Table II). The low activities for 2-butanol and 2-methyl-2-butanol are suspicious. An examination of the original study revealed that these two molecules never achieved 25% inhibition within the concentration range reported. The reported concentration values for these two molecules were extrapolations beyond the concentration range studied. The large uncertainty in those values indicates that they should be deleted in a structure–activity relationship analysis.

The molecular negentropies were computed for each alcohol in Table II. The assignment of atoms into sets and their multiplicities was based on the topological equivalence of the atoms. The equation and statistics are:

$$pC = 0.085(\pm 0.000)\, I + 3.174(\pm 0.16) \qquad \text{(Eq. 3)}$$

$$r = 0.970 \quad s = 0.200 \quad n = 17 \quad F = 239$$

By comparison, a correlation with molecular weight gives $r = 0.940$; a correlation with log P yields $r = 0.931$. The predicted values from Eq. 3 are found in Table II.

Lipoxygenase Inhibition—A second example of alcohol enzyme inhibitors in which molecular negentropy encodes structural features governing potency is found with the enzyme lipoxygenase (7). The data are shown in Table III with *in vitro* potencies predicted from:

$$pK_I = 0.108(\pm 0.000)\, I - 0.450(\pm 0.12) \qquad \text{(Eq. 4)}$$

$$r = 0.986 \quad s = 0.140 \quad n = 12 \quad F = 353$$

A correlation with molecular weight gives $r = 0.974$; a correlation with log P gives $r = 0.984$.

Nonspecific Narcotic Agents—Kier and Hall (8) analyzed several compounds of diverse structure that exhibited narcosis on frog tadpoles (9). The original list of compounds was factorable into two distinct lists based on the relationship between potency (log 1/c) and molecular structure, described by a molecular connectivity index. Two separate nonspecific mechanisms influencing the potency of each list were postulated.

Table V—Vapor Toxicity of Alcohols and Molecular Negentropy

Alcohol	I	pC	
		Found	Calc.
Methanol	3.24	2.80	2.88
Ethanol	6.55	3.00	3.13
Propanol	10.32	3.32	3.43
Isopropanol	7.68	3.26	3.22
Butanol	14.40	3.77	3.74
Pentanol	18.76	4.09	4.08
sec-Butanol	14.18	3.62	3.72
Isopentanol	17.93	4.09	4.01
tert-Pentanol	11.97	3.75	3.55
3-Pentanol	14.31	3.81	3.73
2-Pentanol	18.53	3.90	4.06
2-Methylbutanol	18.53	3.96	4.06
Isobutanol	11.77	3.72	3.54
tert-Butanol	7.62	3.28	3.22

In the present study, 32 molecules (10 alcohols, four ketones, two ethers, 12 esters, two carbamates, one nitrile, and one oxime) were analyzed (Table IV). Dichloropropanol was omitted from the list. The relationship between the negentropy (I) and potency (log 1/c) and the statistics are:

$$\log \frac{1}{c} = 0.102(\pm 0.000)\, I + 0.130(\pm 0.09) \qquad \text{(Eq. 5)}$$

$$r = 0.975 \quad s = 0.187 \quad n = 32 \quad F = 582$$

Analyses of the alcohol and ester subclasses show a definite improvement in the correlations:

$$\log \frac{1}{c}\,(\text{alcohols}) = 0.104(\pm 0.000)\, I - 0.019(\pm 0.077) \qquad \text{(Eq. 6)}$$

$$r = 0.994 \quad s = 0.101 \quad n = 10 \quad F = 654$$

and:

$$\log \frac{1}{c}\,(\text{esters}) = 0.091(\pm 0.000)\, I + 0.396(\pm 0.09) \qquad \text{(Eq. 7)}$$

$$r = 0.994 \quad s = 0.083 \quad n = 12 \quad F = 768$$

Predicted values based on the calculated I values are shown in Table IV for the entire list of compounds (Eq. 5) and for the alcohols (Eq. 6) and esters (Eq. 7).

Toxicity of Alcohols—A number of alcohols have a toxic effect on red spiders when they are exposed to the vapors (10). The potency, expressed as pC, is related to the molecular negentropy by:

$$pC = 0.077(\pm 0.000)\, I + 2.630(\pm 0.14) \qquad \text{(Eq. 8)}$$

$$r = 0.959 \quad s = 0.119 \quad n = 14 \quad F = 136$$

The values calculated from Eq. 8 are shown in Table V.

Heat of Vaporization of Alcohols—A test of the relationship between molecular negentropy and dispersion forces can be made using heats of vaporization available for alcohols found in the described studies. This property is related to molecular negentropy by:

$$\Delta H_{vap} = 0.265(\pm 0.000)\, I + 8.566(\pm 0.29) \qquad \text{(Eq. 9)}$$

$$r = 0.989 \quad s = 0.414 \quad n = 15 \quad F = 563$$

The values calculated from Eq. 9 are shown in Table VI.

DISCUSSION

The significant correlations of molecular negentropy with enzyme inhibitory potencies suggest that this structural index encodes an appreciable description of the structure influencing the activity. Variation in nonspecific activity in these *in vitro* studies may be proposed to result from variation in the receptor interaction rather than the effects on accumulation at, or disturbance of, the receptor environment. This conclusion evolved from a comparison with log P or molecular weight.

In these studies, the receptor may be viewed as responding to the hydroxyl group in a specific way. The response of the receptor to the remainder of the molecule probably is nonspecific; that is, there is no particular need for a specific atom or group to enhance the interaction. The receptor responds to all bonds and atoms in a roughly cumulative way, which is characteristic of dispersion forces among nonpolar moieties.

Table VI—Heat Vaporization of Alcohols and Molecular Negentropy

Alcohol	I	ΔH_{vap}, kcal/mole	
		Found	Calc.
Methanol	3.24	8.94	9.45
Ethanol	6.55	10.18	10.29
Propanol	10.32	11.34	11.25
2-Propanol	7.68	10.90	10.58
Butanol	14.40	12.50	12.29
2-Butanol	14.18	11.89	12.23
2-Methylpropanol	11.77	12.15	11.62
2-Methyl-2-propanol	7.62	11.14	10.56
Pentanol	18.76	13.61	13.40
2-Pentanol	18.53	12.56	13.34
3-Pentanol	14.31	12.36	12.27
2-Methylbutanol	18.53	13.04	13.34
3-Methylbutanol	17.93	13.15	13.19
3-Methyl-2-butanol	15.89	12.27	12.67
Hexanol	23.33	15.00	14.56
Heptanol	28.08	16.20	15.77
Octanol	33.00	17.00	17.03
2-Ethylhexanol	32.77	16.12	16.97
Nonanol	38.07	18.60	18.32
Decanol	43.26	19.82	19.64

Dispersion forces are notable only at close distances, are maximized between similar structural features, and are always attractive (11). Therefore, a molecule with a greater variety of structural features (a molecule with little topological equivalence or symmetry) should be capable of interaction with a greater variety of structural features on a receptor. Stated quantitatively, the greater the information content (negentropy) in a molecule, the greater is its potential for dispersion-type interaction with nonspecific receptive surfaces. Negentropy, which encodes the information content in the molecule, quantitates the variety of structural features and the associated probabilities of interaction with the receptor.

As a test of the relationship between negentropy and dispersion forces, a good correlation can be found between the molecular negentropy of alcohols and the heat of vaporization. This property reflects intermolecular forces in this series due to structural variation, in addition to the common hydroxyl group, for the 15 alcohols in Table VI.

Equations 5–8, which correlate molecular negentropy and the biological activity, show that this index has encoded molecular information of importance to the activity. The operating model of nonspecific interaction admittedly is simplistic. Nevertheless, the probabilities leading to the calculated molecular negentropy values are of great importance to the potencies. The quality of the correlations is good.

In the narcosis study, the greater the variety of information or negentropy, the greater is the potency. The receptive tissue responds to a greater degree to a molecule possessing a greater mix of atoms in differing structural environments. Isomers are ranked correctly by potency with the I value. As an example, the rankings for the observed and calculated potencies for the isomers may be compared (Table IV): propanol > isopropanol, butanol > isobutanol > *tert*-butanol, isopentanol > *tert*-pentanol, 2-pentanone > 3-pentanone, ethyl propionate = propyl acetate, ethyl valerate = isoamyl acetate, and ethyl isobutyrate = isobutyl acetate.

The subclassification into alcohols (Eq. 6) and esters (Eq. 7) (Table IV) considerably improves the correlations. The slopes in Eqs. 6 and 7 are nearly identical and are close to the slope in Eq. 5. It can be concluded that the mechanism is quite similar for alcohols and esters but that there is a uniform difference in potency running through both types of molecules. This difference undoubtedly is due to the roles played by the hydroxyl group and the carbonyl group at receptive tissue, apart from a completely nonspecific definition. Thus, a nonspecific model is useful as a first approximation, and molecular negentropy can encode most of the salient structural characteristics among both types of molecules.

The discussion of the mechanism of action in these studies takes on a probability description. It is evident why, in some studies of nonspecific effects (10, 12, 13), the range of potencies is butanol > isobutanol > *tert*-butanol since the negentropies of these molecules are 14.40, 11.77, and 7.62, respectively. Butanol is composed of 12 different sets of equivalent atoms, isobutanol has eight sets, and *tert*-butanol has five sets. Butanol, with its greater variety of topologically different atoms, can interact with a greater variety of features on a receptor. Its potency would be expected to be higher based on its structure, which governs the probabilities.

A similar situation can be found in observations of the relative affinity contributions of onium groups of muscarinic antagonists (14): $N(CH_3)_3 < N(CH_3)_2(C_2H_5) < N(CH_3)(C_2H_5)_2 > N(C_2H_5)_3$. The calculated negentropies for these moieties parallel the affinity contributions; they are 4.462, 11.962, 14.583, and 13.413, respectively. A similar trend and negentropy relationship can be found in the onium group contribution to affinities among nicotinic agents (15).

It is proposed here that a molecule of biological interest also may be regarded as a message made up of atoms and bonds containing information transmitted to a receptor or receptive tissue. The information content or negentropy is a meaningful parameter in some structure–activity relationship analyses such as in some nonspecific interactions.

It remains to be seen whether molecular negentropy as a structure–activity relationship parameter needs to be confined exclusively to drug molecules postulated to act in a nonspecific manner. Drug molecules that are active at highly structured, specific receptors certainly contain information. The probabilities of atom interaction are altered in a complex way from purely random choice due to marked differences in interaction forces between certain atoms in an agonist molecule and complementary portions of a receptor. Thus, acetylcholine engages its receptor through strong dipolar forces centered on the carbonyl oxygen and the onium group. The statistical picture describing the information content in the previous discussion must be altered to reflect the much greater probability of the onium group and the carbonyl oxygen atom of acetylcholine engaging the receptor. This issue remains for future study.

In conclusion, the calculation of the molecular negentropy of a molecule leads to the quantitation of its relative information content. Molecular negentropy encodes the salient structural characteristics of molecules in some cases where biological activity is nonspecific. It correctly ranks them according to nonspecific biological potency and provides a mechanistic interpretation of action at the molecular level based on probability considerations.

REFERENCES

(1) L. Brillouin, "Science and Information Theory," Academic, New York, N.Y., 1962.

(2) C. E. Shannon and W. Weaver, "The Mathematical Theory of Communication," University of Illinois Press, Urbana, Ill., 1949.

(3) E. Schrodinger, "What is Life?," Cambridge University Press, New York, N.Y., 1945.

(4) N. Rashevsky, *Bull. Math. Biophys.*, **17**, 229 (1955).

(5) D. Bonchev, D. Kamenski, and V. Kamenska, *Bull. Math. Biol.*, **38**, 119 (1976).

(6) D. Glick and C. G. King, *J. Biol. Chem.*, **94**, 497 (1932).

(7) H. Mitsuda, K. Yasumoto, and A. Yamamoto, *Arch. Biochem. Biophys.*, **118**, 664 (1967).

(8) L. B. Kier and L. H. Hall, "Molecular Connectivity in Chemistry and Drug Research," Academic, New York, N.Y., 1976.

(9) E. Overton, "Studies on Narcosis," Fischer, Jena, East Germany, 1901.

(10) P. Read, *Ann. Appl. Biol.*, **19**, 432 (1932).

(11) H. Jahle, W. C. Parke, and A. Salyers, in "Electronic Aspects of Biochemistry," B. Pullman, Ed., Academic, New York, N.Y., 1964.

(12) R. Baechler, *Proc. Am. Wood Pres. Assoc.*, **43**, 94 (1947).

(13) T. T. Herskovitz, B. Gadegbeku, and H. Jaillet, *J. Biol. Chem.*, **245**, 2588 (1970).

(14) R. B. Barlow, K. A. Scott, and R. P. Stephenson, *Br. J. Pharmacol.*, **37**, 555 (1969).

(15) R. B. Barlow, G. M. Thompson, and N. C. Scott, *ibid.*, **37**, 555 (1969).

Acid–Base Equilibria of Tetracycline in Sodium Montmorillonite Suspensions

JEFFREY E. BROWNE *, JOSEPH R. FELDKAMP ‡, JOE L. WHITE ‡, and STANLEY L. HEM *x

Received June 14, 1979, from the **Industrial and Physical Pharmacy Department and the* ‡*Department of Agronomy, Purdue University, West Lafayette, IN 47907.* Accepted for publication February 29, 1980.

Abstract □ Changes in the partial molar free energy of the ionic species of tetracycline as a result of interaction with sodium-saturated montmorillonite were monitored by UV spectroscopic titrations. The stronger interaction between the clay and the protonated (H_3T^+) species relative to the zwitterionic (H_2T^0) species is responsible for the apparent displacement of pK_1 in clay suspensions. The displacement of the first equilibrium favors the H_3T^+ species due to its stabilization by the negative clay surface. Little effect of the clay was observed on pK_2 and pK_3, because the ionic species of tetracycline associated with these equilibria (H_2T^0, HT^-, and T^{2-}) did not interact strongly with the negative clay surface. Therefore, the ionic species distribution of tetracycline in a sodium montmorillonite suspension is significantly different than that expected based on solution equilibria. The degree of equilibrium displacement depended on the accessibility of the negative charge at the clay surface. Fraction bound curves support the hypothesis that the clay surface causes a change in tetracycline equilibria. The H_3T^+ form of tetracycline was highly bound to the sodium montmorillonite, but little adsorption was observed for the H_2T^0 species.

Keyphrases □ Tetracycline—acid-base equilibria in sodium montmorillonite suspensions □ Adsorption—bonding of tetracycline to sodium montmorillonite, acid-base equilibria of tetracycline □ Sodium montmorillonite—effect on acid-base equilibria of tetracycline

The mechanism of adsorption of tetracycline by montmorillonite was studied recently by X-ray diffraction and IR spectroscopy and was found to be highly dependent on the ionic form of tetracycline (1). Feldkamp and White (2) recently examined the effect of clay surfaces on the acid–base equilibria of weak bases in aqueous clay suspensions and showed that protonation was enhanced as a consequence of weak base–clay interactions. Since any changes in the distribution of ionic species present in a system have important consequences, the effect of sodium montmorillonite on the acid–base equilibria of tetracycline was studied.

THEORY

In the thermodynamic analysis given by Feldkamp and White (2), the behavior of the acid–base equilibrium for any weak base, B, was considered in clay suspensions (Scheme I).

$$BH^+ \rightleftarrows B + H^+$$

Scheme I

It was shown that the equilibrium can be displaced due to interactions between constituents participating in the equilibrium (B, BH^+, and H^+) and the clay surface. In particular, protonation in excess of that predicted based on the pK value of the compound and the bulk solution pH of the suspension (pH^b) results from a stronger BH^+–clay interaction than a B–clay interaction. In more concise terms, $\Delta\bar{G}_{BH^+}$ is less than $\Delta\bar{G}_B$, where $\Delta\bar{G}_i$ (i = BH^+, B) is the change in the partial molar Gibbs free energy for constituent i accompanying the addition of clay to the system at constant temperature, pressure, and composition. If $\Delta\bar{G}_{BH^+} = \Delta\bar{G}_B$, indicating that both BH^+ and B interact equally well with the clay, no enhanced protonation effect arises.

The $\Delta\bar{G}_{BH^+}$ and $\Delta\bar{G}_B$ values are related by:

$$\Delta\bar{G}_{BH^+} - \Delta\bar{G}_B = RT \ln \frac{K_{eff}}{K} \qquad \text{(Eq. 1)}$$

where:

$$K = a_{H^+} \frac{a_B}{a_{BH^+}} \qquad \text{(Eq. 2)}$$

and:

$$K_{eff} = a_{H^+} \frac{\bar{C}_B}{\bar{C}_{BH^+}} \qquad \text{(Eq. 3)}$$

The activities are defined by $\bar{G}_i = \bar{G}_i^* + RT \ln a_i$. Because the system is heterogeneous, external electric fields are present (due to the charged clay). As a consequence, $\Delta\bar{G}_i$ may be identified with the electrochemical potential (3), and the activity a_i is regarded as the total activity as described by Low (4). This activity is not to be confused with the activity commonly applied to homogeneous systems (*i.e.*, solutions, for which the activity is defined in terms of the chemical potential and relates to field-free systems). The K_{eff} value is simply an effective or apparent equilibrium constant, and $\bar{C}_i$ (i = B, BH^+, H^+) are average suspension concentrations.

If the ratio of K_{eff} to K is less than one (*i.e.*, $pK_{eff} - pK > 0$), then $\Delta\bar{G}_{BH^+} < \Delta\bar{G}_B$. In addition, when $K_{eff}/K = 1$, then $\Delta\bar{G}_{BH^+} = \Delta\bar{G}_B$. Consequently, K_{eff}/K and $pK_{eff} - pK$ serve as parameters indicating the degree of equilibrium displacement (or enhanced protonation) due to BH^+–clay and B–clay interactions.

The $\Delta\bar{G}_{BH^+}$ and $\Delta\bar{G}_B$ values can be measured individually under certain experimental conditions. If the system is sufficiently dilute with respect to clay and all other solutes, then $\Delta\bar{G}_{BH^+}$ and $\Delta\bar{G}_B$ are given by:

$$\Delta\bar{G}_{BH^+} = RT \ln (1 - f) \left(\frac{K_{eff} + a_{H^+}}{K + a_{H^+}}\right) \qquad \text{(Eq. 4)}$$

$$\Delta\bar{G}_B = RT \ln (1 - f) \left(\frac{K}{K_{eff}}\right) \left(\frac{K_{eff} + a_{H^+}}{K + a_{H^+}}\right) \qquad \text{(Eq. 5)}$$

where f is the fraction of base initially added to the system that is bound to the clay.

This approach may be applied to any acid–base equilibrium of tetracycline (Schemes II–IV) (5), and either K_j (j = 1, 2, 3) or $K_{j,eff}$ can be determined.

$$H_3T^+ \overset{K_1}{\rightleftarrows} H_2T^0 + H^+$$

Scheme II

$$H_2T^0 \overset{K_2}{\rightleftarrows} HT^- + H^+$$

Scheme III

$$HT^- \overset{K_3}{\rightleftarrows} T^{2-} + H^+$$

Scheme IV

Both $K_{j,eff}$ and $\Delta\bar{G}_i$ (i = H_3T^+, H_2T^0, HT^-, T^{2-}) depend on the composition of the system, *i.e.*, pH, ionic strength, temperature, pressure, other solutes, and $\bar{C}_i$. As $\bar{C}_i \to 0$, $K_{j,eff}$ and $\Delta\bar{G}_i$ approach a definite value that reflects an intrinsic interaction of species i with the clay surface, independent of $\bar{C}_i$.

EXPERIMENTAL

Materials—Tetracycline hydrochloride and all other chemicals were official or reagent grade. All water was double distilled. Wyoming bentonite[1] was the source of the montmorillonite used. Characterization by X-ray diffraction[2] and IR spectroscopy[3] showed the Wyoming bentonite

[1] Clay Mineral Repository, Department of Geology, University of Missouri, Columbia, Mo.

[2] Siemens A G Kristalloflex 4 generator and type F diffractometer, Karlsruhe, West Germany.

[3] Model 180, Perkin-Elmer Corp., Norwalk, Conn.

0022-3549/80/0700-0811$01.00/0
© 1980, American Pharmaceutical Association

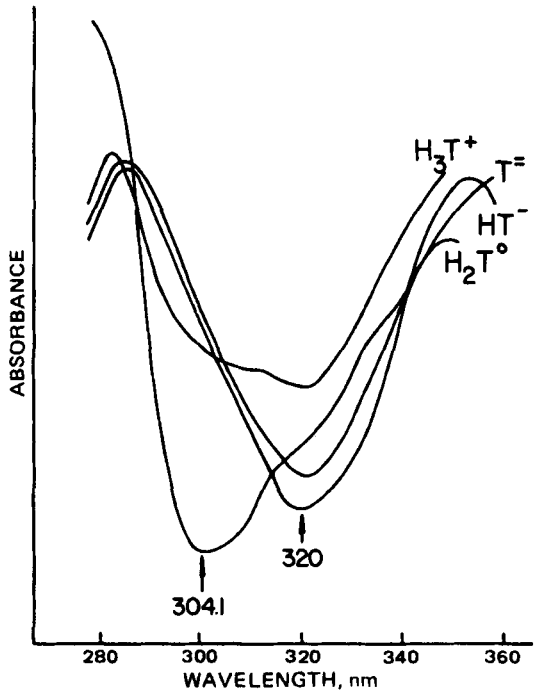

Figure 1—*UV spectra of the four ionic species of tetracycline in aqueous solution (20 mg/liter).*

to be montmorillonite containing a small amount of quartz. The Wyoming bentonite fraction (<2 μm) was washed five times with 1 *M* NaCl and then washed with water until it was salt free, as evidenced by the silver nitrate test to produce the sodium-saturated montmorillonite used. The suspension was passed through a 300-mesh screen to remove any extraneous matter and diluted to obtain a 1% sodium-saturated montmorillonite suspension.

Stock solutions of tetracycline, 200 mg/liter, were prepared fresh before each titration and passed through an ultrafine sintered-glass filter.

Determination of *K* and K_{eff}—UV spectroscopic titrations (6) were performed to determine $\overline{C}_B/\overline{C}_{BH^+}$ as required for Eq. 3. In very dilute solutions (clay free), $\overline{C}_B/\overline{C}_{BH^+} = a_B/a_{BH^+}$ in Eq. 2. The absorbance, A, of a tetracycline solution is related to $\overline{C}_B/\overline{C}_{BH^+}$ by:

$$\frac{\overline{C}_B}{\overline{C}_{BH^+}} = \frac{A - A^+}{A^- - A} \qquad \text{(Eq. 6)}$$

where A^+ is the absorbance when all of the tetracycline is present as BH^+ and A^- is the absorbance when all tetracycline is present as B.

Thus, experimental values for $\overline{C}_{H_2T^0}/\overline{C}_{H_3T^+}$, $\overline{C}_{HT^-}/\overline{C}_{H_2T^0}$, and $\overline{C}_{T^{2-}}/\overline{C}_{HT^-}$ were obtained.

The titrations were performed at a wavelength where A^+ and A^- were significantly different. As shown in Fig. 1, the greatest absorbance difference between H_3T^+ and H_2T^0 occurs at 304.1 nm, while the maximum difference among H_2T^0, HT^-, and T^{2-} occurs at 320 nm. The bandwidth was set at 0.8 nm for all titrations.

Titration curves were constructed by preparing a series of solutions or suspensions at different pH^b values and determining the absorbance at 304.1 nm for the first ionization or 320 nm for the second and third ionizations of tetracycline. Equal volumes of 0.01 *N* HCl and NaOH were pipetted into two 100-ml volumetric flasks, depending on the pH^b desired. Ten milliliters of a 200-mg/liter tetracycline stock solution was added to the sample flask. If sodium chloride was to be added, a level of either 25 mg/liter or 5.844 g/liter was added to both the sample and reference flasks. The sample and reference flasks were diluted to ~95 ml with water. Two milliliters of the 1% sodium-saturated montmorillonite suspension was added to both flasks prior to dilution to 100 ml with water. This procedure minimized the change in pH^b while mixing the tetracycline with the clay. All sample suspensions contained 20 mg of tetracycline and 200 mg of sodium-saturated montmorillonite/liter.

The pH^b of a stirred 50-ml aliquot of the sample suspension was measured[4] after the pH^b had stabilized.

The difference in the absorbance[5] of the sample and reference suspensions, $A_s - A_r$, at the appropriate wavelength was taken as A in Eq. 6. The absorbance at different pH^b values was plotted to construct the titration curves.

[4] Model 801, Orion Research, Cambridge, Mass.

[5] Acta C-II UV-visible spectrophotometer with a light-scattering accessory, Beckman Instruments, Fullerton, Calif.

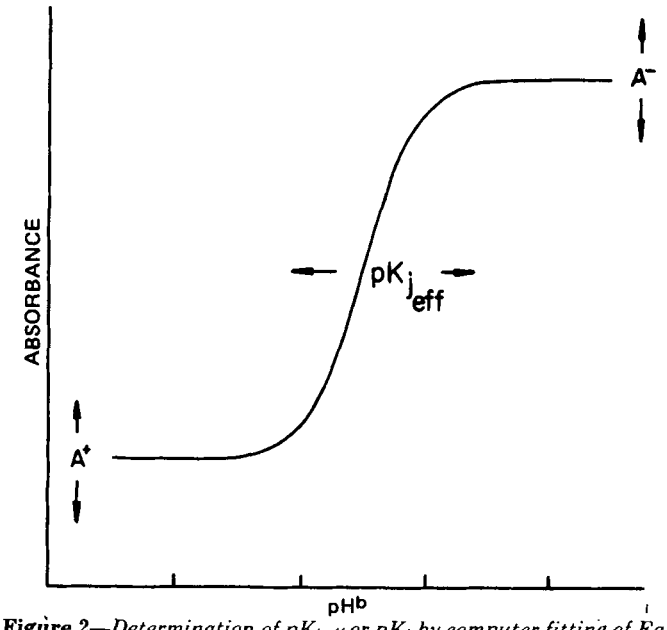

Figure 2—*Determination of $pK_{j,eff}$ or pK_j by computer fitting of Eq. 7 to pH^b versus A.*

The average concentration ratio was computed from the titration curve and used in Eq. 4 to obtain $pK_{j,eff}$. These calculations were restricted to values of $a^b_{H^+}$ such that $0.1K_{j,eff} \leq a^b_{H^+} \leq 10K_{j,eff}$.

In theory, the value of $pK_{j,eff}$ pertains only to the pH^b at which it is measured. However, $pK_{j,eff}$ usually is independent of pH^b over the range of interest, and the plot of pH^b *versus* A has a sigmoidal appearance. Based on this assumption, the Henderson–Hasselbalch equation (rewritten here in the terms of absorbance) describes the pH^b *versus* A graph:

$$A = \frac{A^+ + A^- 10^{(pH^b - pK_{j,eff})}}{1 + 10^{(pH^b - pK_{j,eff})}} \qquad \text{(Eq. 7)}$$

With a computer, the values for A^+, A^-, and $pK_{j,eff}$ were varied until Eq. 7 gave the best fit for the experimental values of pH^b and A (Fig. 2).

Determination of $\Delta\overline{G}_i$—Equations 4 and 5 may be used to calculate $\Delta\overline{G}_i$ following the determination of the fraction bound at a particular pH^b. This determination was accomplished following the pH^b and A measurements described in the preceding section by centrifuging ~30 ml of the remaining sample and reference suspensions and collecting the supernate. Sufficient acid was added to 15 ml of the supernate to ensure that all of the tetracycline was in the protonated form. The absorbance of the sample supernate, A_s, and the reference supernate, A_r, was measured at 304.1 nm.

The fraction bound, f, was calculated from:

$$f = \frac{A_0 - (A_s - A_r)}{A_0} \qquad \text{(Eq. 8)}$$

where A_0 represents the absorbance for a solution containing only the protonated species having a concentration equal to C_0, the initial concentration.

Since $\Delta\overline{G}_i$ is in general a function of pH^b, its value pertains only to the pH^b at which it is calculated. In addition, Eqs. 4 and 5 were developed based on a single equilibrium where only two species are present at any $a^b_{H^+}$ value. These equations cannot be applied to compounds exhibiting multiple acid–base equilibria if significant quantities of a third species are present at the $a^b_{H^+}$ value of interest. Furthermore, $\Delta\overline{G}_i$ values should not be determined at $a^b_{H^+}$ values where very little of species i exists. In general, $\Delta\overline{G}_i$ values are most accurate when measured at pH^b conditions where a substantial amount of species i exists (which can be monitored readily) and where any interference from a second ionization is minimal. These restrictions were followed in all of the $\Delta\overline{G}_i$ determinations.

RESULTS AND DISCUSSION

The first acid–base equilibrium of tetracycline was strongly affected by sodium-saturated montmorillonite as seen in Fig. 3, where titration

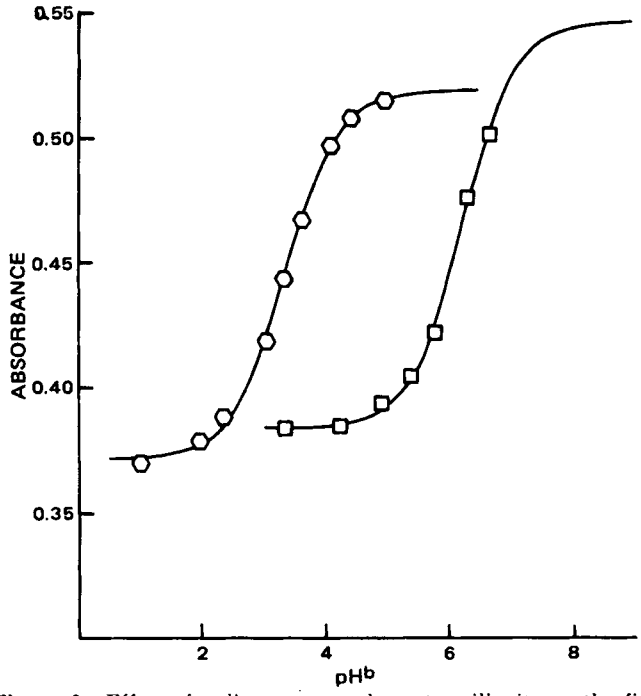

Figure 3—*Effect of sodium-saturated montmorillonite on the first acid–base equilibrium of tetracycline. Key:* ○, *aqueous solution; and* □, *sodium-saturated montmorillonite.*

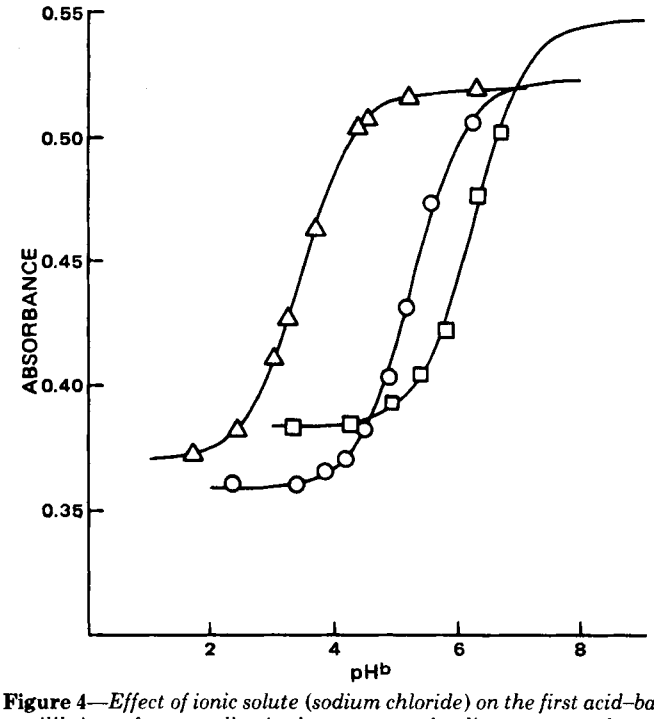

Figure 4—*Effect of ionic solute (sodium chloride) on the first acid–base equilibrium of tetracycline in the presence of sodium-saturated montmorillonite. Key:* □, *no sodium chloride;* ○, *25 mg of sodium chloride/liter; and* △, *5.844 g of sodium chloride/liter.*

curves that best fit the experimental pH^b *versus A* data are plotted. In aqueous solution, pK_1 was 3.34, which agrees well with previously reported values (5, 7). However, in the presence of sodium montmorillonite, $pK_{1,eff}$ was 6.23. The interaction of the protonated species of tetracycline, H_3T^+, with the negative clay surface was responsible for this shift of almost three pH^b units.

As seen in Table I, $\Delta\overline{G}_{H_3T^+}$ was −3.99 kcal/mole, indicating a much greater stabilization of the H_3T^+ species than the H_2T^0 species ($\Delta\overline{G}_{H_2T^0}$ = −0.03 kcal/mole). This stabilization of the H_3T^+ species caused a shift in the acid–base equilibrium in favor of the H_3T^+ species.

The interaction of H_3T^+ with sodium-saturated montmorillonite was affected by other ionic species in the system. As seen in Fig. 4, the shift in the titration curve was reduced in the presence of 25 mg of sodium chloride/liter and approached the solution titration curve when large amounts of sodium chloride (5.844 g/liter) were present.

The value for $pK_{1,eff}$ calculated from Fig. 4 approached pK_1, and $\Delta\overline{G}_{H_3T^+}$ approached zero as large sodium chloride concentrations were added to the tetracycline–sodium-saturated montmorillonite suspension (Table I). The interaction of the H_2T^0 species remained negligible ($\Delta\overline{G}_{H_2T^0}$ = −0.04 kcal/mole) in the presence of sodium chloride.

The titration curve for the second ionization was displaced slightly in the presence of sodium montmorillonite (Fig. 5). As was observed in the first ionization, sodium chloride reduced the displacement of the titration curve.

Calculation of $pK_{2,eff}$, $\Delta\overline{G}_{H_2T^0}$, and $\Delta\overline{G}_{HT^-}$ based on the titration curves in Fig. 5 is tenuous due to the weak interaction of the H_2T^0 and HT^- species with the clay. In addition, the close proximity of pK_2 and pK_3 (7.86 and 9.51, respectively) means that more than two ionic species of tetracycline probably are present in the system in the pH range of interest. However, Eq. 7 was applied to the titration data in Fig. 5, and the resulting increase in $pK_{2,eff}$ was only 0.15 in the presence of the sodium-saturated montmorillonite. This slight increase in $pK_{2,eff}$ may suggest that the zwitterionic form of tetracycline, H_2T^0, interacts slightly with the clay surface. However, this conclusion is made cautiously because of the cited limitations. Furthermore, the values obtained for $\Delta\overline{G}_{H_2T^0}$ and $\Delta\overline{G}_{HT^-}$ were too small to be considered significant.

Virtually no change in the titration curve for the third ionization of tetracycline was observed in the presence of sodium-saturated montmorillonite (Fig. 6), and it was concluded that the clay does not interact significantly with the HT^- and T^{2-} species.

The data in Figs. 3–6 and Table I indicate that the negatively charged sites on montmorillonite are responsible for the strong interaction with the protonated species of tetracycline, H_3T^+. However, this interaction

Table I—Effects of Sodium-Saturated Montmorillonite on Acid–Base Equilibria of Tetracycline

Sample	$pK_{1,eff}$	$pK_{2,eff}$	$\Delta\overline{G}_{H_3T^+}$, kcal/mole	$\Delta\overline{G}_{H_2T^0}$, kcal/mole
Aqueous solution	3.34	7.86	—	—
Sodium-saturated montmorillonite suspension	6.23	8.01	−3.99	−0.03
Sodium-saturated montmorillonite suspension containing 25 mg of sodium chloride/liter	5.25	7.98	−2.72	−0.03
Sodium-saturated montmorillonite suspension containing 5.844 g of sodium chloride/liter	3.45	7.92	−0.27	−0.04

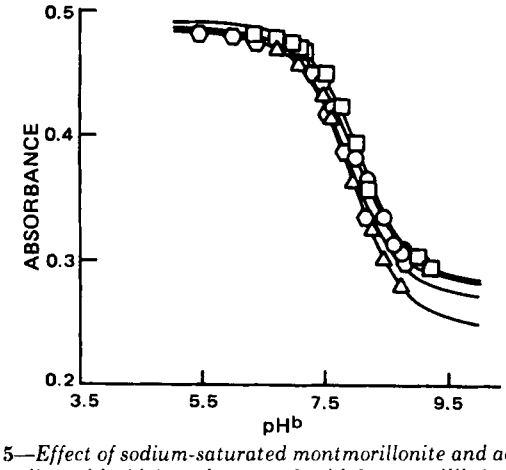

Figure 5—*Effect of sodium-saturated montmorillonite and added ionic solute (sodium chloride) on the second acid–base equilibrium of tetracycline. Key:* ○, *aqueous solution;* □, *sodium-saturated montmorillonite suspension;* ○, *sodium-saturated montmorillonite suspension containing 25 mg of sodium chloride/liter; and* △, *sodium-saturated montmorillonite suspension containing 5.844 g of sodium chloride/liter.*

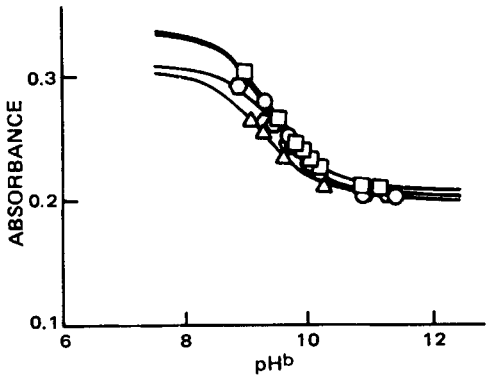

Figure 6—*Effect of sodium-saturated montmorillonite and added ionic solute (sodium chloride) on the third acid–base equilibrium of tetracycline. Key: ○, aqueous solution; □, sodium-saturated montmorillonite suspension; ○, sodium-saturated montmorillonite suspension containing 25 mg of sodium chloride/liter; and △, sodium-saturated montmorillonite suspension containing 5.844 g of sodium chloride/liter.*

is reduced in the presence of other ions such as sodium chloride. It is hypothesized that sodium ions compete with H_3T^+ for the negative sites on the clay surface or, equivalently, that sodium ions screen the negatively charged clay surface, thereby reducing the apparent negative charge of the clay surface. Sodium chloride also may affect the interaction by altering the state of dispersion of the clay so that negative sites are less accessible to the H_3T^+ ions.

Figure 7 shows that $\Delta\overline{G}_{H_3T^+}$ is affected by pH^b and the presence of an additional ionic solute such as sodium chloride. The $\Delta\overline{G}_{H_3T^+}$ value was calculated at each pH^b using Eq. 4 when $(A - A^+)$ and $(A^- - A)$ in Eq. 6 were large enough to determine $pK_{1,eff}$ accurately; if $a^b_{H^+} \gg K_{1,eff}$, $\Delta\overline{G}_{H_3T^+}$ was calculated from:

$$\Delta\overline{G}_{H_3T^+} = RT \ln (1 - f) \frac{a_{H^+}}{K + a_{H^+}} \qquad \text{(Eq. 9)}$$

The change in $\Delta\overline{G}_{H_3T^+}$ seen in the salt-free sodium-saturated montmorillonite suspension and the clay suspension containing a small amount of sodium chloride (25 mg/liter) indicate that increased interaction between H_3T^+ and the clay occurred as the pH^b was increased. At low pH^b values, protons apparently compete with H_3T^+ for the negative clay sites. At pH 4–6, $\Delta\overline{G}_{H_3T^+}$ reached a constant value, indicating an interaction free of competition with H^+. The plateau value of $\Delta\overline{G}_{H_3T^+}$ probably represents an intrinsic interaction of H_3T^+ with the clay since large changes in $\overline{C}_{H_3T^+}$ have little effect on $\Delta\overline{G}_{H_3T^+}$.

The $\Delta\overline{G}_{H_3T^+}$ values seen in Fig. 7 clearly show the reduced interaction of H_3T^+ and the sodium-saturated montmorillonite due to the competitive effect of the added ionic solutes. The effect of pH on $\Delta\overline{G}_{H_3T^+}$ was diminished in the presence of a low level of sodium chloride (25 mg/liter) and could not be observed in a suspension containing 5.844 g of sodium chloride/liter.

The fraction bound curves in Fig. 8 support the conclusions reached based on the titration curves. The fraction of tetracycline bound to the sodium-saturated montmorillonite increased with pH^b until a maximum

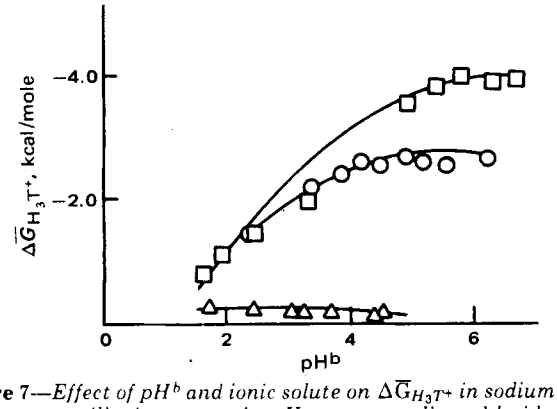

Figure 7—*Effect of pH^b and ionic solute on $\Delta\overline{G}_{H_3T^+}$ in sodium-saturated montmorillonite suspension. Key: □, no sodium chloride; ○, 25 mg of sodium chloride/liter; and △, 5.844 g of sodium chloride/liter.*

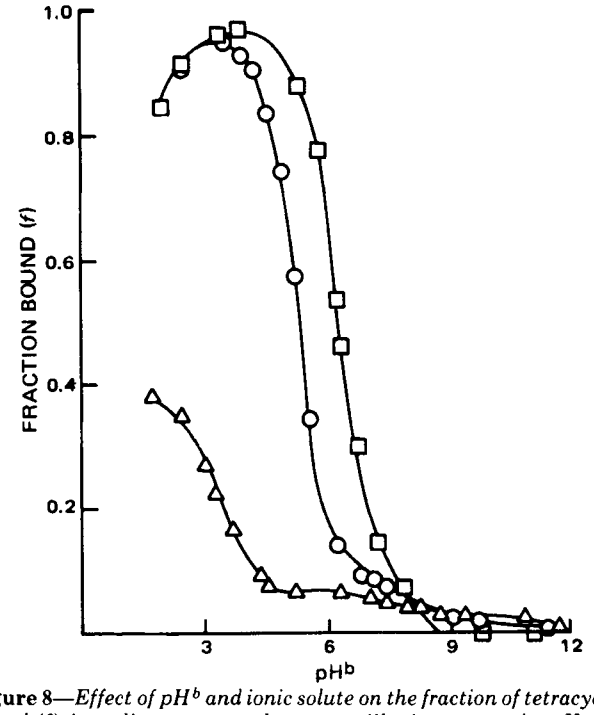

Figure 8—*Effect of pH^b and ionic solute on the fraction of tetracycline bound (f) in sodium-saturated montmorillonite suspension. Key: □, no sodium chloride; ○, 25 mg of sodium chloride/liter; and △, 5.844 g of sodium chloride/liter.*

was observed at pH^b 3.8. This behavior agrees with the reduced interaction of H_3T^+ and clay in the presence of high proton concentrations (Fig. 7). A maximum in the adsorption of tetracycline occurred under pH^b conditions at which the competitive effect of protons was low and the H_3T^+ concentration was still high. This situation occurred at pH 3.8 when no added salt was present. The concentration of H_3T^+ was very high at this pH^b because the $pK_{1,eff}$ under these conditions was 6.23 (Table I).

In the presence of low concentrations of sodium chloride (25 mg/liter), a high fraction of tetracycline was bound by the clay. However, the maximum adsorption occurred at pH^b 3.4, probably reflecting the smaller displacement of $pK_{1,eff}$ in the presence of sodium chloride (Table I).

At high added salt concentrations (5.844 g/liter), only 38% of the tetracycline was adsorbed by the clay (Fig. 8). Under these conditions, H_3T^+ and H^+ cannot compete effectively with sodium ions for negative clay adsorption sites. As a result, $\Delta\overline{G}_{H_3T^+}$ was −0.27 kcal/mole and $pK_{1,eff}$ approached pK_1 (Table I). Thus, a greatly diminished fraction bound curve is seen.

The fraction of tetracycline bound to the sodium-saturated montmorillonite decreased rapidly in all three conditions shown in Fig. 8 because the pH^b conditions allowed the zwitterionic form of tetracycline, H_2T^0, to appear in the system. The $\Delta\overline{G}_{H_2T^0}$ values ranging from −0.03 to −0.04 kcal/mole (Table I) indicate little interaction of this ionic species with the clay.

In the pH^b region above 8.5, the fraction of tetracycline bound to the clay approached zero (Fig. 8) since the pH^b was above $pK_{2,eff}$ (Table I) and only the anionic forms of tetracycline (HT^- and T^{2-}), which cannot interact with the negative clay surface, were present.

Figure 8 shows that a small fraction of tetracycline was bound to the sodium-saturated montmorillonite in the pH region where the anionic forms of tetracycline were present in suspensions containing excess sodium chloride. The added sodium ions are believed to screen the anion–clay repulsive forces by collapsing the electrical double layer associated with the clay and thus allow physical adsorption of the HT^- and T^{2-} species.

The behavior of the fraction bound curves at higher pH^b conditions provides further understanding of the small shift in the titration curve for the second acid–base equilibrium of tetracycline shown in Fig. 5. The interaction of the zwitterionic form of tetracycline with the clay probably is a physical adsorption indicated by the low $\Delta\overline{G}_{H_2T^0}$ value associated with the interaction. This weak interaction led to the displacement of pK_2 from 7.86 to a $pK_{2,eff}$ of 8.02 in the presence of clay. The addition of sodium chloride to the system allows the anionic conjugate base, HT^-, to interact with the clay by collapsing the electrical double layer, and $pK_{2,eff}$ decreased to 7.98 and 7.92 with 25 mg and 5.844 g of sodium chloride/liter,

respectively. This result suggests that H_2T^0 and HT^- interact to approximately the same degree with the clay surface so that $\Delta\bar{G}_{H_2T^0}$ is approximately equal to $\Delta\bar{G}_{HT^-}$, as would be expected if the mechanism of adsorption for each species is physical adsorption.

The distribution of the ionic species of tetracycline in an aqueous solution and in an aqueous sodium-saturated montmorillonite suspension, based on the respective values of pK_1, pK_2, and pK_3 and $pK_{1,eff}$, $pK_{2,eff}$, and $pK_{3,eff}$ found in this study, is shown in Fig. 9. The changes in the acid–base equilibria of tetracycline due to the stabilizing effect of the montmorillonite surface caused the H_3T^+ species to be present over a wider pH range than expected based on acid–base equilibria in solution. In addition, the H_2T^0 form was present over a much smaller pH region when in a clay suspension.

Previous investigators concluded that the zwitterion, H_2T^0, was adsorbed significantly by montmorillonite (1). This conclusion was based on the pK_j (j = 1, 2, 3) values for tetracycline in aqueous solution rather than the $pK_{j,eff}$ (j = 1, 2, 3) values appropriate for clay systems. Feldkamp and White (8) suggested that the ability of a clay to interact with weak bases may increase in concentrated mixtures. Thus, dramatic shifts in species distributions may occur in concentrated suspensions of tetracycline and montmorillonite.

The changes in the distribution of the ionic species of a drug due to interactions with a clay surface may have important consequences in drug therapy. For example, the antimicrobial activity of tetracycline and other antibiotics was reported to be diminished in the presence of clays (9). Tetracycline exhibits its maximum antimicrobial activity between pH 5.5 and 6.0 (10), the region where the zwitterionic form predominates in aqueous solution (Fig. 9). The H_2T^0 species appears to be absorbed preferentially across the GI membranes due to its lipophilic nature (7). In the presence of montmorillonite, the zwitterionic form of tetracycline exists over a dramatically reduced pH region. As a consequence, the most readily absorbable form of tetracycline may be present over a smaller region of the GI tract.

The distribution changes for the ionic forms of a drug also may provide insights into the catalytic effects of a clay on drug degradation. For example, the sequence of steps illustrated in Scheme V is associated with acid-catalyzed hydrolysis of drugs.

$$\text{drug} + H^+ \rightleftarrows \text{drug-}H^+ + H_2O \rightarrow \text{degradation products}$$

Scheme V

The first step of the hydrolysis involves protonation of the drug, followed by nucleophilic attack by water. The degradation rate depends on the concentration of protonated drug. Interaction of the drug with a clay surface may cause a shift in the acid–base equilibrium of the drug that favors the protonated form and thus leads to an accelerated hydrolysis rate in the presence of a clay.

Along with the effect of an increased concentration of reactant (protonated drug), there is the possibility that the activation energy for the hydrolysis reaction might be increased due to the drug–clay interaction. The net effect on the reaction rate will vary for each system, depending on the relative magnitudes of each factor.

Clays have been suggested as a vehicle for controlled-release dosage forms (11). An understanding of the effect of drug–clay interactions on the acid–base equilibria of the drug should provide the information needed to select the proper drug and clay to obtain the desired *in vivo* release pattern.

In summary, the acid–base equilibria of drugs can be affected greatly by interaction with clay surfaces. The thermodynamic quantities, $K_{j,eff}$ and $\Delta\bar{G}_i$, are useful for quantifying and monitoring drug–clay interactions and should be used in the formulation of clay-containing drug products as well as in the evaluation of the effects of the coadministration of drugs and clays.

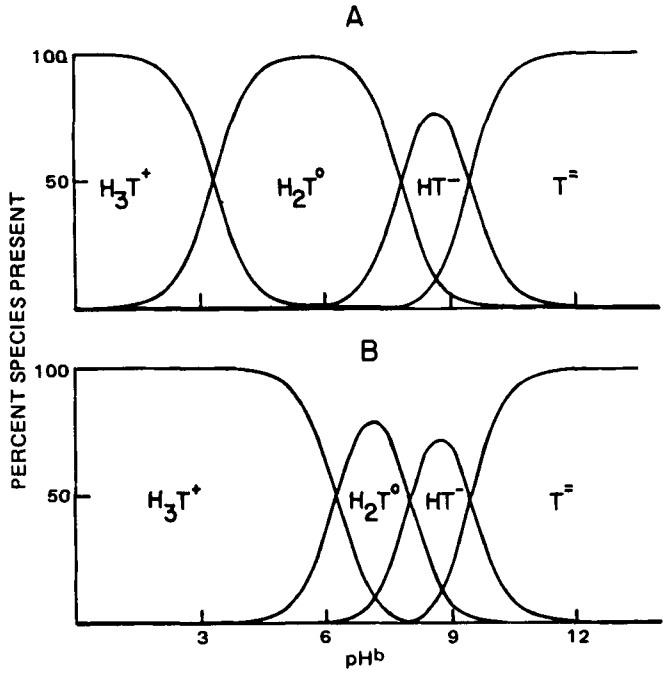

Figure 9—*Distribution of the ionic species of tetracycline. Key: A, aqueous solution; and B, sodium-saturated montmorillonite suspension.*

REFERENCES

(1) L. S. Porubcan, C. J. Serna, J. L. White, and S. L. Hem, *J. Pharm. Sci.*, **67**, 1080 (1978).

(2) J. R. Feldkamp and J. L. White, *J. Colloid Interface Sci.*, **69**, 97 (1979).

(3) E. A. Guggenheim, *J. Phys. Chem.*, **33**, 842 (1929).

(4) P. F. Low, *Soil Sci.*, **71**, 409 (1951).

(5) L. J. Leeson, J. E. Krueger, and R. A. Nash, *Tetrahedron Lett.*, **18**, 1155 (1963).

(6) J. B. Weber, *Spectrochim. Acta*, **23A**, 458 (1967).

(7) J. L. Colaizzi and P. R. Klink, *J. Pharm. Sci.*, **58**, 1184 (1969).

(8) J. R. Feldkamp and J. L. White, in "International Clay Conference 1978," M. M. Mortland and V. C. Farmer, Eds., Elsevier, Amsterdam, The Netherlands, 1979, pp. 187–196.

(9) A. Asher, M. El-Nakeeb, M. Motawi, and N. El-Gindy, *Pharmazie*, **21**, 474 (1973).

(10) C. M. Kunin and M. Finland, *Clin. Pharmacol. Ther.*, **2**, 51 (1961).

(11) J. W. McGinity and J. L. Lach, *J. Pharm. Sci.*, **66**, 63 (1977).

ACKNOWLEDGMENTS

Supported in part by an American Foundation for Pharmaceutical Education Fellowship to J. E. Browne.

This report is Journal Paper 7659, Purdue University Agricultural Experiment Station, West Lafayette, IN 47907.

Characterization and Adsorptive Properties of Pharmaceutical Grade Clays

JEFFREY E. BROWNE *, JOSEPH R. FELDKAMP ‡, JOE L. WHITE ‡, and STANLEY L. HEM *x

Received October 18, 1979, from the *Industrial and Physical Pharmacy Department and the ‡Department of Agronomy, Purdue University, West Lafayette, IN 47907. Accepted for publication January 29, 1980.

Abstract □ The adsorption of tetracycline by clays commonly used in pharmacy can be predicted if the identity and character of the commercial clay sample are established. X-ray diffraction, IR spectroscopy, and chemical analysis were used to identify the clay component and any nonclay diluents present in a series of commercial pharmaceutical grade clays. The major clay components were montmorillonite, hectorite, attapulgite, saponite, and kaolinite. The clay structure, the nature of the exchangeable cation, and the presence of nonclay components are important factors affecting the tetracycline–clay interaction. In general, clay structures with a high surface charge lead to a greater interaction with the protonated form of tetracycline, while interaction with the zwitterionic form of tetracycline occurs in clay structures with minimal surface charge. The presence of multivalent, exchangeable cations on the clay surface diminishes interaction with the protonated form of tetracycline. Nonclay components such as calcite and dolomite increase the interactions of the zwitterionic and anionic forms of tetracycline with the clay.

Keyphrases □ Tetracycline hydrochloride—adsorption onto clay, interaction with pharmaceutical grade clay, adsorptive properties of clay □ Clay—pharmaceutical grade, adsorption of tetracycline, isomorphous substitution □ Adsorption—tetracycline onto pharmaceutical grade clays

The unique properties of clays have led to their use in pharmaceuticals for both therapeutic effects and excipient action. The crystal structure of clay minerals is well understood, and the behavior of clays in pharmaceutical systems is predictable based on structural considerations. Thus, the identity and characterization of a clay are of prime importance to the pharmaceutical scientist.

The purpose of this study was to illustrate the importance of a complete characterization of clays used in pharmaceuticals so that their behavior in formulations and in a patient's drug regimen can be predicted. The influence of clay structure, the nature of the exchangeable cation, and the presence of nonclay components on the interaction of tetracycline with reference or commercial samples of montmorillonite, hectorite, saponite, attapulgite, and kaolinite were studied.

BACKGROUND[1]

The basic structure of clays consists of octahedra of aluminum and magnesium in combination with silica tetrahedra to give layer-like or fibrous structures. Cationic-exchange properties can arise in these structures through isomorphous substitution, *i.e.*, aluminum for silicon, magnesium for aluminum, *etc.* A manifestation of isomorphous substitution is the swelling properties of certain clays with high cation-exchange capacity.

The kaolin group of minerals consists of sheets of silica tetrahedra and alumina octahedra shared in a 1:1 ratio. These minerals have little or no isomorphous substitution and normally are nonswelling in aqueous solutions.

Smectites belong to the 2:1 (ratio of silica tetrahedra to alumina and/or magnesia octahedra) structural group of clays and include montmorillonite, hectorite, and saponite. In these structures, an alumina or magnesia octahedral layer is sandwiched between two silica tetrahedral sheets. Structures are designated as dioctahedral when aluminum occupies the octahedral sites and as trioctahedral when magnesium (or other divalent ions) or lithium occupies the octahedral sites.

Isomorphous substitution occurs in both the tetrahedral and octahedral layers of the 2:1 minerals and gives rise to moderate to high cation-exchange capacities.

Isomorphous substitutions also influence the lattice parameters in clays and appear to be correlated to the swelling properties of smectites. As a consequence of the expanding properties, the smectites also possess very high surface areas.

Montmorillonite represents the aluminum-containing smectite group (dioctahedral). The magnesium end member of the smectite group is designated as saponite (trioctahedral). Substitution of lithium for a portion of the magnesium in trioctahedral compositions results in a clay mineral designated as hectorite (trioctahedral).

Fibrous minerals are represented by sepiolite and attapulgite. These minerals are classified as 2:1-type minerals, but the crystal growth is limited to the c dimension, resulting in ribbons of the 2:1 layer attached at their longitudinal edges. A cross section of the fiber gives a checkerboard arrangement of ribbons and voids with no possibility of expansion.

It appears that fibrous minerals have little or no true cation-exchange capacity. However, because of the very thin nature of the ribbons, the external surface area is moderately high. Fibrous minerals also are very porous due to the channels between the ribbons. However, the dimensions of the pores are such that only small molecules such as water, ammonia, and lower alcohols can be accommodated in them.

EXPERIMENTAL

Materials—Tetracycline hydrochloride and all other chemicals were official or reagent grade. Montmorillonite (Wyoming bentonite), hectorite (Hector, Calif.), attapulgite (Georgia palygorskite), and kaolinite (Hydrite-10) were the reference standards[2]. Samples of pharmaceutical grade clays claimed to represent these minerals were obtained commercially as follows: bentonite USP[3], hectorite[4], saponite[5], attapulgite[6], and kaolin NF[7].

Unless otherwise indicated, all clays were used as received.

The sodium form of the reference clays was prepared by washing a 2% suspension of the clay with 1 *M* NaCl. The washing procedure was repeated five times, and excess salt was removed by repeated washing with water until the addition of silver nitrate to the supernate gave a negative chloride test. Clays exhibiting a cation-exchange capacity that were treated in this manner are termed sodium saturated; clays such as kaolinite and attapulgite, which have little or no cation-exchange capacity, are termed sodium treated if washed with sodium chloride in this manner.

The calcium form of montmorillonite was prepared in an analogous manner using 1 *M* $CaCl_2$ as the exchanging solution.

Preliminary examination of the samples of hectorite and commercial saponite by X-ray diffraction showed significant quantities of calcite and dolomite as nonclay diluents. The removal of these carbonates was attempted by a modification of the pH-stat technique (1). A 2% clay sus-

[1] The information in this section is summarized from R. E. Grim, "Clay Mineralogy," 2nd ed., McGraw-Hill, St. Louis, Mo., 1968.

[2] Clay Mineral Repository, Department of Geology, University of Missouri, Columbia, Mo.

[3] R. F. Revson and Co., New York, N.Y.

[4] Macaloid Lot L-917M22B, NL Industries, Industrial Chemicals Division, Hightstown, N.J.

[5] Veegum, R. T. Vanderbilt Co., Norwalk, Conn.

[6] Pharmasorb, Engelhard Minerals and Chemicals Corp., Menlo Park, N.J.

[7] J. T. Baker Chemical Co., Phillipsburg, N.J.

0022-3549/80/0700-0816$01.00/0
© 1980, American Pharmaceutical Association

pension, 250 ml, was reacted for 24 hr at pH 5.0 in an automatic titration apparatus[8]. The suspension then was washed repeatedly with water until it was salt free as evidenced by the silver nitrate test. The diffractograms of hectorite in Fig. 1 show that the procedure was effective in removing calcite but not dolomite. Clay samples treated in this manner will be referred to as purified.

X-Ray Diffraction—Randomly oriented powder specimens of each clay were prepared using the McCreery method (2), and diffractograms[9] were recorded from 5 to 63° 2θ.

The X-ray step scans were used to determine accurately the 060 peak of commercial saponite. A mixture containing 15% silicon[10] was prepared by trituration and filled into a McCreery mount; X-ray step scans were recorded from 58 to 63° 2θ at a step of 0.02° and a time interval of 90 sec. The 060 spacing of commercial saponite was determined in comparison to the silicon peak at 56.12° 2θ (3).

The Greene-Kelly test (4) is useful in distinguishing between dioctahedral and trioctahedral structures within the smectite group of clays and was utilized in the characterization of the commercial saponite sample. A 1% clay suspension, consisting of the <2-μm fraction, was washed five times with 1 *M* lithium chloride. Excess salt then was removed by washing with double-distilled water until it was salt free by the silver nitrate test. The lithium-saturated clay was air dried on a glass slide and then heated to 200–300° for 12 hr. The sample then was saturated with glycerol using the vaporization method (5); X-ray diffractograms were recorded from 3 to 11° 2θ.

Glycerol solvation was used to investigate the presence of montmorillonite-like impurities in attapulgite, commercial attapulgite, kaolinite, and kaolin NF. Glycerol enters montmorillonite-type minerals and causes a characteristic expansion of the basal spacing to ~17.5 Å (6). Glycerol solvation was achieved by dispersing the clay in a 3% glycerol solution through moderate agitation produced by an ultrasonic probe[11]. The dispersions were air dried on a glass slide, and X-ray diffractograms were recorded from 4 to 8° 2θ.

IR Spectroscopy—Air-dried films of clay were prepared on zinc sulfide windows[12] (7) and used to record the IR spectra[13].

Studies of pleochroism of the IR bands associated with hydroxyl stretching may be used to determine the orientation of hydroxyl bond axes in layer silicates (8) and were used in characterizing commercial saponite and commercial hectorite. An orientation effect is positive evidence for a structure containing trioctahedral character. Self-supporting clay films were prepared by air drying 1% clay suspensions on polyethylene terephthalate films[14]. The clay films were separated from the polyethylene terephthalate film by bending over a sharp corner. IR spectra of the clay films were recorded from 4000 to 3300 cm^{-1} at perpendicular and various incident angles to the IR beam.

Transmission Electron Photomicrographs—Electron microscopic examination[15] of attapulgite was undertaken to confirm the presence of a montmorillonite-type impurity.

Presence of Organic Matter—The peroxide test (9) was used to detect organic matter in the clay samples. Thirty milliliters of 30% H_2O_2 was added to 15 ml of a 1% clay suspension and heated on a steam plate for 15 min. The treated clay was centrifuged along with an untreated reference suspension. The color of the sample sediment was compared to that of the reference sediment. The presence of organic matter was indicated when the color of the sample sediment was significantly lighter than that of the reference sediment.

UV Spectroscopic Titrations—Displacement of the pK_1 of tetracycline in clay suspensions was determined by spectroscopic titration. The $pK_{1,eff}$ and partial molar Gibbs free energy, $\Delta\bar{G}_i$, for H_3T^+ and H_2T° were calculated from the spectroscopic titration curve using the procedure of Feldkamp and White (10).

Titration curves were constructed by preparing a series of tetracycline–clay suspensions at different pH^b (bulk pH) values and determining the absorbance at 304.1 nm. A typical point on the titration curve was obtained by adding equal volumes of 0.01 *N* HCl or NaOH to two 100-ml volumetric flasks, depending on the pH^b desired. Ten milliliters of a

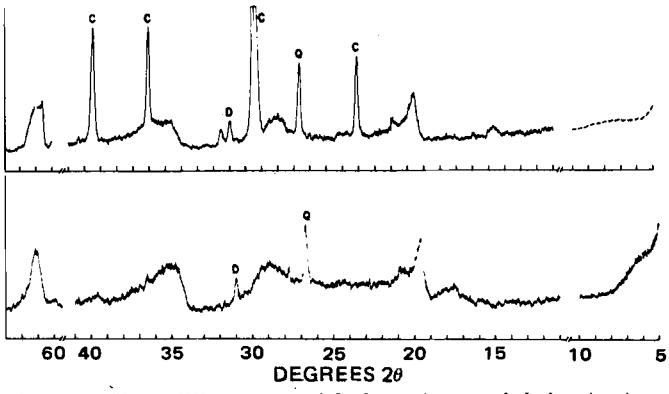

Figure 1—*X-ray diffractogram of the hectorite sample before (top) and after (bottom) carbonate removal using the pH-stat technique at pH 5.0. Key: Q, quartz; C, calcite; and D, dolomite. The solid line represents 100 counts/sec (cps) full scale. The dashed line represents 1000 cps full scale.*

200-mg/liter stock solution of tetracycline hydrochloride was added to the sample flask, and the sample and reference flasks were diluted to near volume with double-distilled water. Two milliliters of a 1% clay suspension was added to both flasks, and the flasks were diluted to 100 ml with distilled water. All sample suspensions contained 20 mg of tetracycline and 200 mg of clay/liter. The pH of the sample suspension was determined[16] after the pH reading stabilized. This value was checked by measuring the pH of the supernate (pH^b) after centrifugation. These pH readings differed by <1%.

This agreement in pH values was expected since the difference in the pH of the suspension and the pH of the supernate (*i.e.*, the suspension effect) increases as the concentration of the suspension increases (11). The clay suspensions studied were dilute enough so that the pH of the suspension accurately represented the system, *i.e.*, $pH_{susp} \simeq pH^b$.

The difference in the absorbance of the sample and the reference suspension ($A_s - A_r$) was measured and plotted *versus* pH^b to construct the titration curves.

Adsorption—The fraction of tetracycline bound by the clay at different pH^b conditions was determined using the samples from the spectroscopic titration experiment. A sample of each suspension was centrifuged, and 15 ml of supernate was collected. Sufficient hydrochloric acid was added to ensure that all of the tetracycline was in the protonated form. The absorbance was measured at 304.1 nm.

The fraction bound, f, was calculated from:

$$f = \frac{A_0 - (A_s - A_r)}{A_0} \qquad \text{(Eq. 1)}$$

where A_0 is the absorbance of a tetracycline solution (20 mg/liter) containing only the protonated form of tetracycline.

RESULTS AND DISCUSSION

Montmorillonite—The X-ray diffractogram of bentonite USP is compared to sodium-saturated montmorillonite in Fig. 2. A comparison of the reflections indicates that montmorillonite was the major clay component in bentonite USP. However, peaks other than those established for montmorillonite appeared in the region between 11 and 41° 2θ in the bentonite USP sample. The intense peak at 26.64° 2θ, corresponding to an interplanar spacing of 3.55 Å, indicates the presence of quartz (12). Other less intense peaks occurring at 11.7, 20.76, and 29.18° 2θ, corresponding to spacings of 7.56, 4.27, and 3.059 Å, are typical of gypsum (12). The peaks at 23.10, 29.42, and 39.40° 2θ, corresponding to spacings of 3.85, 3.035, and 2.285 Å, are associated with calcite (12).

The IR spectra shown in Fig. 3 also indicate that montmorillonite was the major clay constituent in the bentonite USP sample. Characteristic absorption bands for montmorillonite were observed in both samples at 3620, 1200–1000, 915, 878, and 850 cm^{-1} (13–15).

The presence of organic material was confirmed in bentonite USP but not in sodium-saturated montmorillonite using the peroxide test.

The dominant exchangeable cation in the bentonite USP sample was sodium, although 7.1 and 2.7% of the exchange capacity were satisfied by calcium and magnesium ions, respectively (7).

[8] PHM 26 pH meter, TTT II titrator, ABU12 autoburet, TTA3 titration assembly, and SBR2 recorder, Radiometer, Copenhagen, Denmark.

[9] Siemens A G Kristalloflex 4 generator and type F diffractometer, Karlsruhe, West Germany.

[10] Silcon powder, 100 mesh, Alfa Inorganics, Beverly, Mass.

[11] Model W185 sonifier cell disruptor, Heat Systems-Ultrasonic, Plainview, N.Y.

[12] Irtran 2, Eastman Kodak Co., Rochester, N.Y.

[13] Model 180, Perkin-Elmer Corp., Norwalk, Conn.

[14] Mylar.

[15] Hitachi HU-11 100-kv electron microscope, Hitachi Ltd., Tokyo, Japan.

[16] Model 801, Orion Research, Cambridge, Mass.

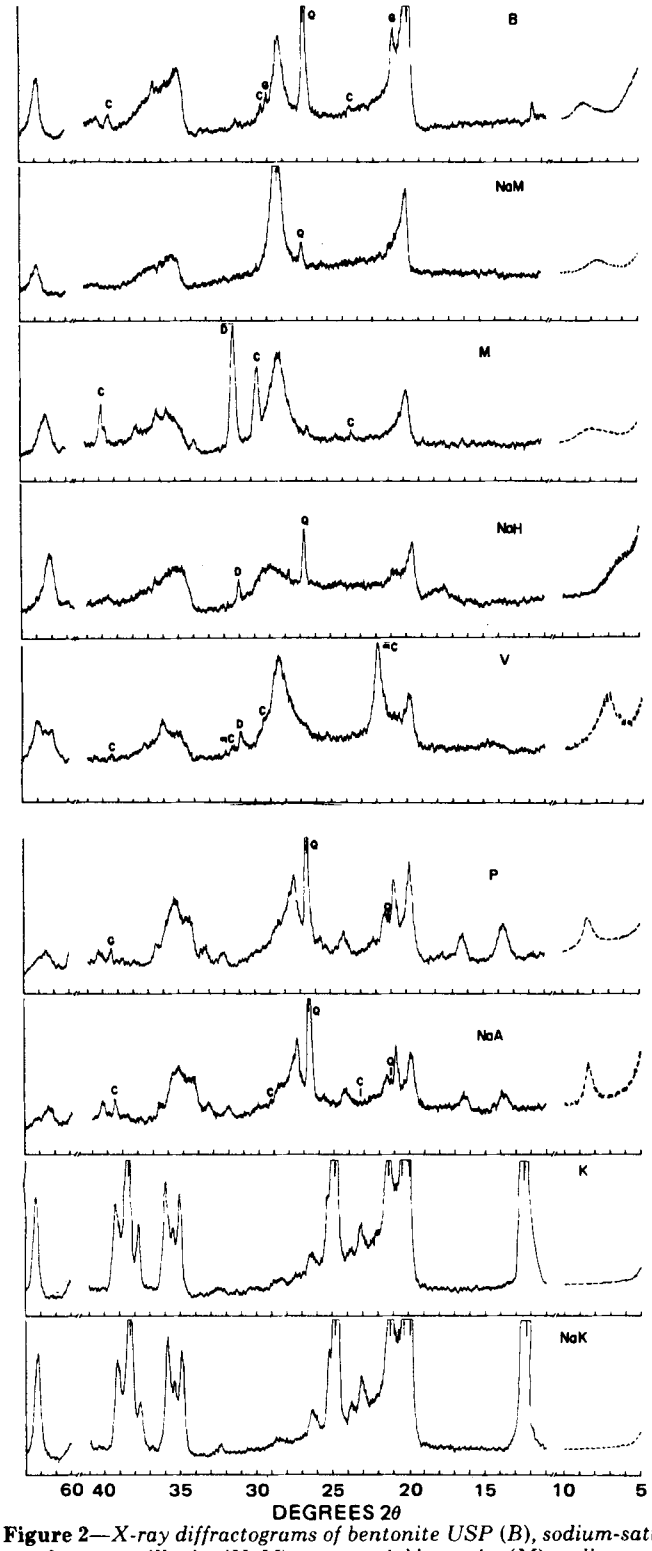

Figure 2—*X-ray diffractograms of bentonite USP (B), sodium-saturated montmorillonite (NaM), commercial hectorite (M), sodium-saturated hectorite (NaH), commercial saponite (V), commercial attapulgite (P), sodium-treated attapulgite (NaA), kaolin NF (K), and sodium-treated kaolinite (NaK). Peaks corresponding to quartz (Q), gypsum (G), dolomite (D), calcite (C), and α-cristobalite (αC) are identified. The solid line represents 100 cps full scale. The dashed line represent 1000 cps full scale.*

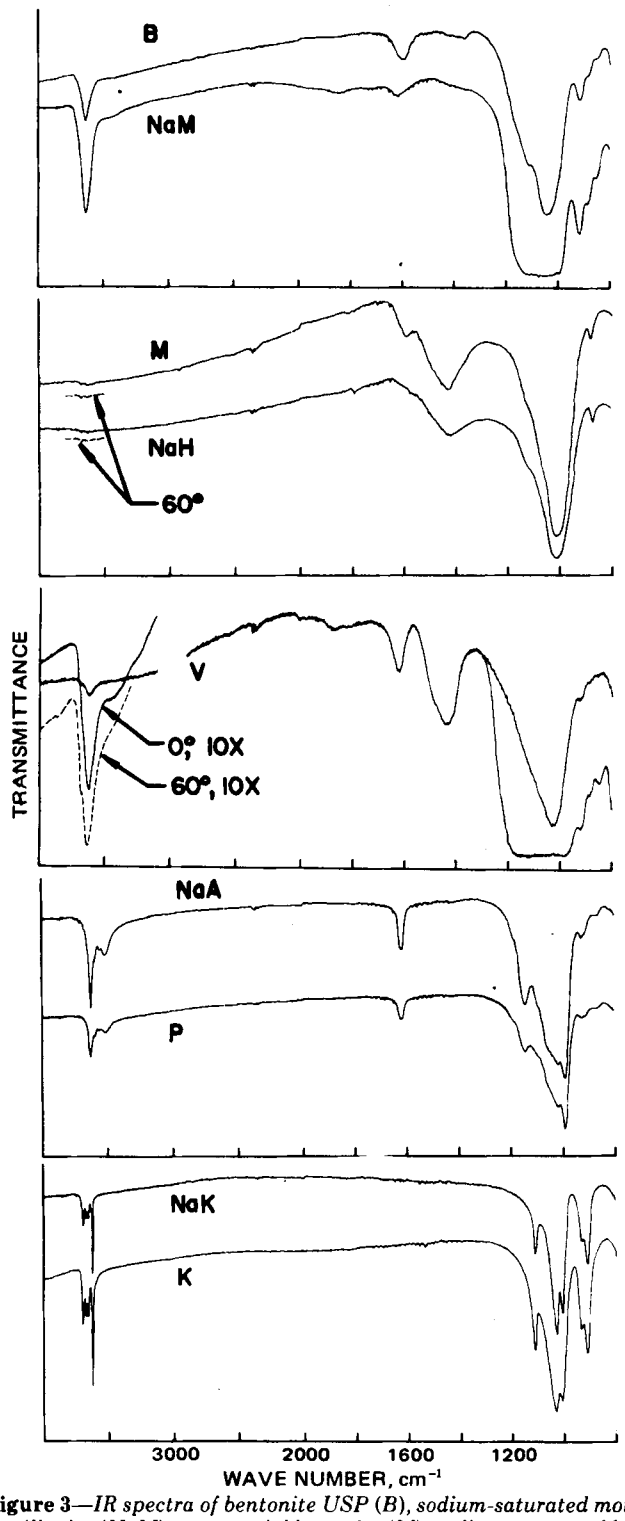

Figure 3—*IR spectra of bentonite USP (B), sodium-saturated montmorillonite (NaM), commercial hectorite (M), sodium-saturated hectorite (NaH), commercial saponite (V), commercial attapulgite (P), sodium-treated attapulgite (NaA), kaolin NF (K), and sodium-treated kaolinite (NaK).*

These findings for the composition of the bentonite USP sample are consistent with previous reports, which indicated that sodium montmorillonite is the major component of bentonite USP (16, 17). However, exchangeable calcium and magnesium ions may constitute 35–65% of the exchange capacity of bentonite USP, and bentonite USP has been found to contain 10–15% quartz as the primary nonclay diluent (18). Other nonclay minerals known to affect the behavior of bentonites include gypsum, calcite, biotite, feldspar, and cristobalite.

The effect of the exchangeable cation on the adsorptive properties of bentonite USP will be illustrated by examining the interaction of bentonite USP, sodium-saturated montmorillonite, and calcium-saturated montmorillonite with tetracycline. As indicated in Table I, interaction with all three forms of montmorillonite caused a shift in the first acid–base equilibrium of tetracycline so that the apparent equilibrium constant

Table I—Effects of Pharmaceutical Grade Clays on the First Acid–Base Equilibrium of Tetracycline

Clay	$pK_{1,eff}$	$\Delta\bar{G}_{H_3T^+}$, kcal/mole	$\Delta\bar{G}_{H_2T^0}$, kcal/mole
Control	3.34	—	—
Bentonite USP	4.15–4.74	−1.13–−1.93	−0.11–−0.16
Sodium-saturated montmorillonite	6.23	−3.99	−0.03
Calcium-saturated montmorillonite	4.39	−1.92	−0.47
Purified, sodium-saturated hectorite	5.99	−3.52	−0.04
Commercial saponite	4.27	−1.26	−0.17
Purified, sodium-saturated commercial saponite	5.23	−2.97	−0.05
Commercial attapulgite	3.51	−0.33	−0.14
Sodium-treated attapulgite	3.46	−0.20	−0.07
Sodium-treated kaolinite	3.02	0.00	−0.16

($pK_{1,eff}$) was significantly different than that observed in solution (pK_1). The magnitude of the shift reflects the degree of perturbation of the equilibrium (10). The greatest shift resulted from interaction with sodium-saturated montmorillonite.

The $pK_{1,eff}$ values of tetracycline in the presence of the sodium and calcium forms of montmorillonite, 6.23 and 4.39, respectively, remained relatively constant over the pH^b range of interest, indicating that $pK_{1,eff}$ was independent of pH^b. However, the $pK_{1,eff}$ values ranged from 4.15 to 4.74, depending on the pH^b of the bentonite USP suspension. This dependency of pK_{eff} on pH^b is attributed to the presence of organic material in the bentonite USP sample since pK_{eff} was found to be dependent on pH^b in suspensions of organic-containing soils (19).

The relative strength of the interaction of the clay with the protonated, H_3T^+, or zwitterionic, H_2T^0, form of tetracycline is expressed by the magnitude of $\Delta\bar{G}_i$ given in Table I, where $\Delta\bar{G}_i$ is the change in the partial molar Gibbs free energy accompanying the addition of clay to the system. Sodium-saturated montmorillonite interacted strongly with H_3T^+ but showed virtually no interaction with H_2T^0. In contrast, calcium-saturated montmorillonite and bentonite USP showed less interaction with H_3T^+, but the $\Delta\bar{G}_{H_2T^0}$ value indicates that a weak interaction occurred with the zwitterionic form.

The fraction of tetracycline bound to the clay (Fig. 4) also indicates that sodium-saturated montmorillonite only interacted with the cationic form because adsorption was observed only under pH^b conditions when H_3T^+ was present.

Tetracycline was bound strongly by calcium-saturated montmorillonite (Fig. 4) under pH conditions favoring the cationic form, as evidenced by the maximum at pH 2.7. However, adsorption also occurred at pH^b conditions favoring the zwitterionic and anionic forms, which caused the secondary maximum at pH 8.

Increased adsorption of tetracycline by calcium-saturated montmorillonite above pH 9.5 is due to complexation of the T^{2-} form of tetracycline with exchangeable calcium ions to form a positively charged calcium–tetracycline complex, which is adsorbed readily by the negative clay surface. The added sodium ions (arising from the sodium hydroxide needed to adjust the pH) cause the displacement of calcium ions from the clay. These calcium ions are available to form higher calcium–tetracycline complexes, which are positively charged and therefore are adsorbed by the clay.

The fraction bound curve for the bentonite USP sample (Fig. 4) showed a maximum adsorption of ~80% of the tetracycline in the system. This degree of adsorption was significantly less than the maximum adsorption of tetracycline by sodium- or calcium-saturated montmorillonite.

The adsorption of tetracycline by bentonite USP had a greater similarity to the fraction bound curve of calcium-saturated montmorillonite than to the fraction bound curve of sodium-saturated montmorillonite. The presence of calcium and magnesium as exchangeable cations in the bentonite USP sample and the calcite impurity was responsible for adsorption of tetracycline at pH conditions where no adsorption would be expected if the montmorillonite were completely sodium saturated.

The lower maximum adsorption of tetracycline by bentonite USP in comparison to sodium-saturated montmorillonite probably was due to the significant nonclay component, which includes quartz, gypsum, calcite, and organic material.

Thus, the nature of the exchangeable cations and the amount of nonclay material have a significant effect on tetracycline adsorption by bentonite USP.

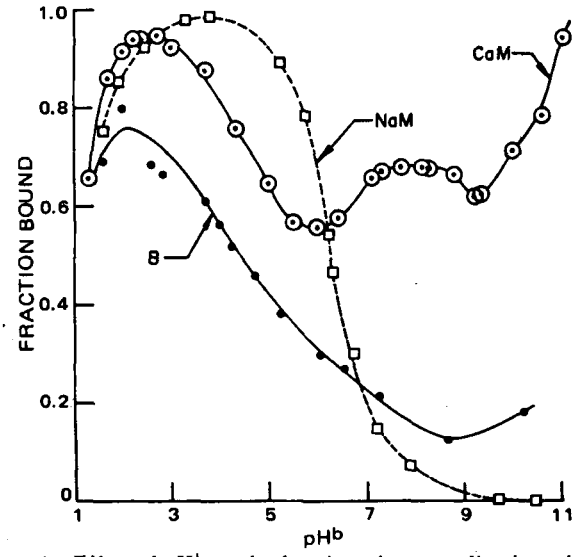

Figure 4—*Effect of pH^b on the fraction of tetracycline bound* (f) *in sodium-saturated montmorillonite (NaM), calcium-saturated montmorillonite (CaM), and bentonite USP (B) suspensions.*

Hectorite—In general, the X-ray reflections for commercial hectorite in Fig. 2 correspond fairly well to those for purified, sodium-saturated hectorite, indicating that hectorite was the major clay mineral contained in the commercial hectorite sample. However, in the region between 60 and 63° 2θ, the 060 reflection of the samples of commercial hectorite and purified, sodium-saturated hectorite had unequal spacings of 1.509 and 1.514 Å, respectively. These differences were expected and probably reflect composition differences due to the amount of lithium substituted for magnesium within the clay structure.

Several nonclay peaks were observed for the sample of commercial hectorite in the region from 11 to 41° 2θ. A very strong, sharp peak was located at 31.12° 2θ, corresponding to a spacing of 2.87 Å, a characteristic spacing for dolomite (11). Additional peaks were found at the established spacings for calcite (3.85, 3.035, and 2.285 Å) and quartz (3.35 Å).

The IR spectra of commercial hectorite and purified, sodium-saturated hectorite (Fig. 3) were essentially identical, thus confirming that hectorite was the major clay contained in the commercial hectorite sample. The absorption shoulder at 1012 cm^{-1} and a weak absorption shoulder at 1120 cm^{-1} typically are observed in hectorite samples. Large quantities of carbonate minerals (calcite and dolomite) were indicated by the 1430- and 877-cm^{-1} bands.

Pleochroism can be used to identify dioctahedral and trioctahedral structures in the smectite group. In trioctahedral minerals, such as hectorite, the transition moment of the hydroxyl group is perpendicular to the plane of the layer, while the hydroxyl groups are tilted out of the plane in dioctahedral minerals (8). Thus, the orientation of an oriented film of a trioctahedral mineral will affect the intensity of the hydroxyl absorbance bands but the IR spectra of dioctahedral minerals are not affected.

Oriented films of commercial hectorite and hectorite, both trioctahedral, are expected to show an orientation effect. When perpendicular to the IR beam, the absorption band at 3680 cm^{-1}, corresponding to the stretching frequency of structural hydroxyl groups in a magnesium-containing trioctahedral mineral, was absent in both spectra (Fig. 3). No increase in intensity was observed at 3680 cm^{-1} when the oriented films were placed at 60° incidence to the IR beam. This finding suggests that the structural hydroxyl groups were replaced by fluorine atoms. These findings agree well with a chemical analysis of hectorite, which indicated the presence of 4.5% fluorine (20).

It was not possible to examine the acid–base equilibria of tetracycline in the presence of commercial hectorite due to severe light scattering. To obtain some indication of the interaction of commercial hectorite with tetracycline, the behavior of tetracycline in the presence of purified, sodium-saturated hectorite was studied. Annoying light-scattering effects did not occur for titrations performed in purified, sodium-saturated hectorite suspensions. Thus, both the presence of carbonate impurities and multivalent ions as exchangeable cations appear to affect significantly the dispersion state of the clay.

As seen in Table I, the displacement of the first acid–base equilibrium of tetracycline in the presence of purified, sodium-saturated hectorite

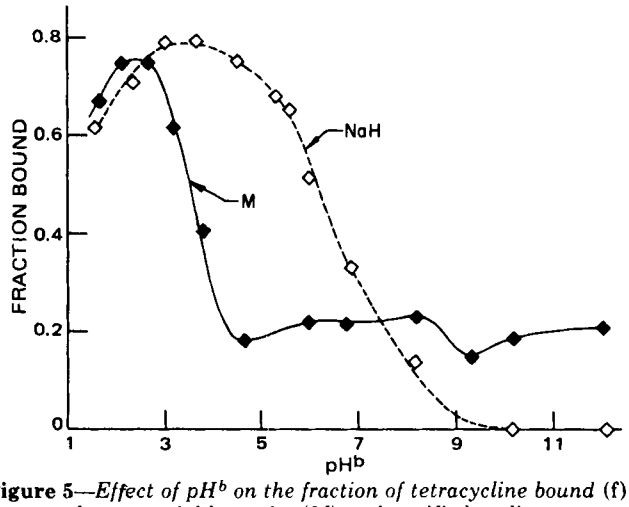

Figure 5—*Effect of pH^b on the fraction of tetracycline bound (f) in untreated commercial hectorite (M) and purified, sodium-saturated hectorite (NaH) suspensions.*

was almost as large as that produced by sodium-saturated montomorillonite. The $pK_{1,eff}$ value of 5.99 remained fairly constant over the pH^b range, indicating that $pK_{1,eff}$ was independent of pH^b. The H_3T^+ species was strongly stabilized by purified, sodium-saturated hectorite, as indicated by the large value of $\Delta\overline{G}_{H_3T^+}$, although virtually no interaction with H_2T^0 was observed.

The fraction bound curve for purified, sodium-saturated hectorite (Fig. 5) showed that adsorption of tetracycline occurred under pH^b conditions where H_3T^+ was present. This adsorption pattern was expected based on the structural similarities between hectorite and montmorillonite. However, a lower maximum was observed in the presence of purified, sodium-saturated hectorite in comparison to sodium-saturated montmorillonite (Fig. 4). It is believed that protons more effectively compete with H_3T^+ for the negative charge sites on the surface of hectorite than on montmorillonite due to differences in the distribution of negative charges arising from the clay structure.

In contrast, the fraction bound curve for commercial hectorite showed a constant adsorption above pH^b 4 in addition to a maximum at pH^b 2.7. The adsorption maximum is believed to represent adsorption of H_3T^+ by the hectorite present in the sample of commercial hectorite, while the constant adsorption above pH^b 4 may be due to complexation of the zwitterionic and anionic species of tetracycline with calcium in the nonclay components. Stern (21) reported that the anionic species of tetracycline is adsorbed onto calcium fluoride surfaces. In a similar manner, it is proposed that tetracycline is adsorbed onto the surfaces of calcite and dolomite present in commercial hectorite.

The adsorptive properties of commercial hectorite cannot be understood based on the structure of hectorite. However, the adsorptive properties of commercial hectorite are predictable when the nonclay components are recognized.

Saponite—The X-ray analysis of commercial saponite (Fig. 2) showed reflections typical of the smectite group of clay minerals. In addition to the smectite reflections, a very sharp, strong peak was noted at 21.40° 2θ, corresponding to an interplanar spacing of 4.15 Å. This peak and a much less intense peak at 31.38° 2θ (2.845 Å) indicated the presence of α-cristobalite (12) in the commercial saponite sample. Other peaks in the region from 11 to 41° 2θ corresponded to dolomite and calcite.

As seen in Fig. 6, the X-ray step scan of the 060 reflection of the commercial saponite sample resulted in spacings at 62.02 and 61.01° 2θ, corresponding to spacings of 1.496 and 1.518 Å. The dioctahedral smectite minerals, such as montmorillonite, have a characteristic 060 spacing of 1.48–1.50 Å, while the trioctahedral smectites, such as saponite and hectorite, are characterized by a spacing of 1.51–1.53 Å for the 060 reflection (22). The 060 reflections suggest that commercial saponite is a mixture of dioctahedral and trioctahedral smectites, with the sample being richer in the dioctahedral component based on the larger peak at 1.496 Å.

The IR spectrum (Fig. 3) of oriented films of the commercial saponite sample produced a number of absorbance bands whose assignments are characteristic of montmorillonite. The absorption band at 3620 cm^{-1} was similar to the hydroxyl-stretching frequency observed in montmorillonite. Characteristic bands for hydroxyl-bending frequencies in montmorillonite at 915, 878, and 850 cm^{-1} also were found in the spectra for commercial saponite. Carbonates are indicated due to the large absorption band at 1430 cm^{-1}.

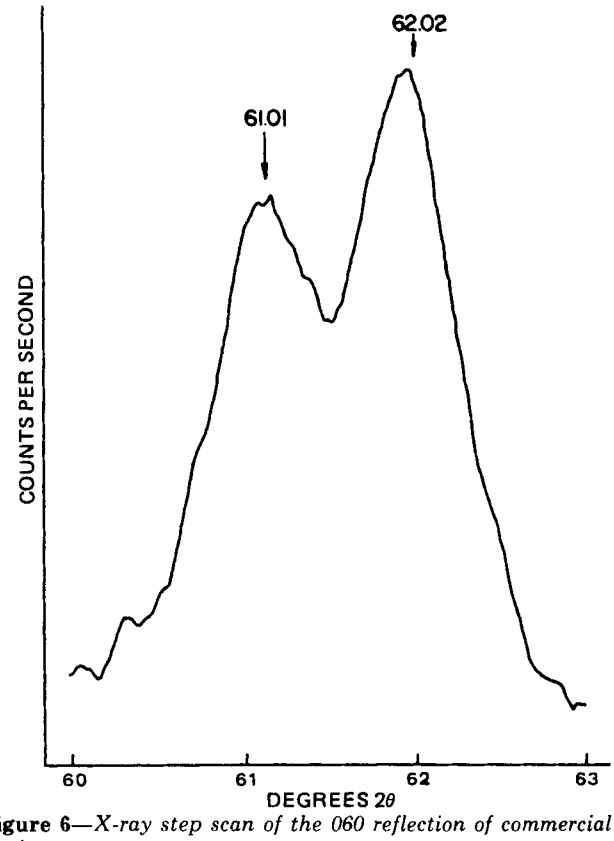

Figure 6—*X-ray step scan of the 060 reflection of commercial saponite.*

An orientation effect was observed in the 10× magnification of the IR spectrum of commercial saponite (Fig. 3) when the sample was placed at 60° incidence to the beam. This prompted further pleochroic studies of commercial saponite, which established the presence of dioctahedral and trioctahedral structures in the clay.

As seen in Fig. 7, the intensity of the band at 3680 cm^{-1} increased with the angle of rotation, confirming the presence of a trioctahedral smectite in commercial saponite. A dioctahedral mineral also was present since no orientation effect was observed for the IR band at 3620 cm^{-1}, which was assigned to the characteristic hydroxyl-stretching frequency of dioctahedral structures. Thus, IR analysis also indicated that the commercial saponite was a mixture of dioctahedral and trioctahedral mineral phases.

Figure 8 shows the results of the Greene-Kelly test on commercial saponite. This test depends on the observation that lithium-saturated smectites (dioctahedral) collapse irreversibly when heated to 200–300°, whereas the collapse of trioctahedral smectites treated similarly is reversible. Upon glycerol solvation of commercial saponite, a collapsed basal (001) spacing of 9.5 Å and an expanded 001 spacing of 18.4 Å were observed, which indicated the presence of dioctahedral and trioctahedral components.

Both X-ray and IR analyses indicated that the commercial saponite sample contained a mixture of dioctahedral and trioctahedral minerals and several nonclay components. The conclusion was supported by a chemical analysis, which reported 13.7% equivalent magnesium oxide in the commercial saponite sample (23). Ross and Hendricks (24) reported the equivalent magnesium oxide content of several montmorillonite samples and found a range of 0.16–8.67% equivalent magnesium oxide. Their analysis of a group of trioctahedral smectites, including saponites and hectorites, yielded an equivalent magnesium oxide content, which ranged from 19.4 to 26.5%.

Because no known smectite mineral contains 13.7% equivalent magnesium oxide and the X-ray and IR studies clearly showed both dioctahedral and trioctahedral character, it is concluded that the sample of commercial saponite was not a one-phase material but a mixture of at least two phases, one similar to montmorillonite and a lesser phase similar to saponite.

The commercial saponite sample caused a shift of the first acid–base

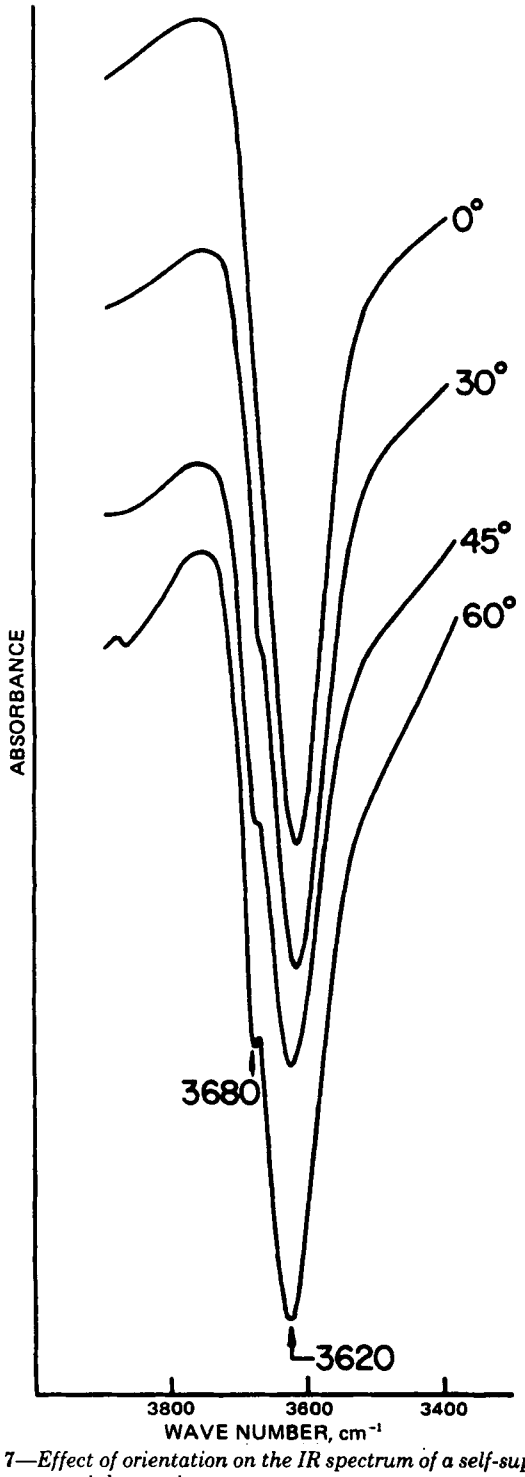

Figure 7—*Effect of orientation on the IR spectrum of a self-supporting film of commercial saponite.*

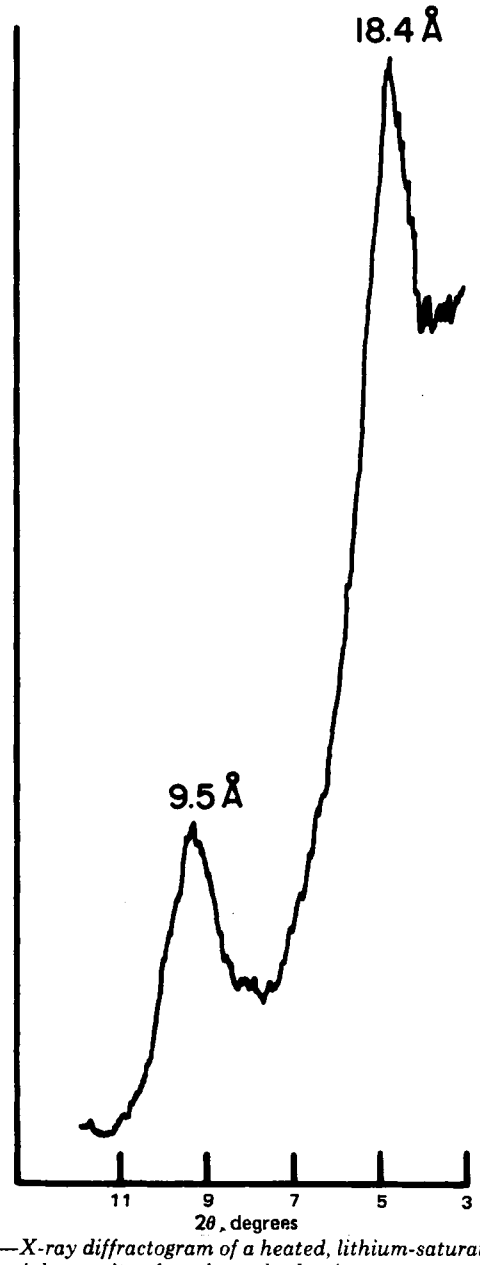

Figure 8—*X-ray diffractogram of a heated, lithium-saturated sample of commercial saponite after glycerol solvation.*

equilibrium of tetracycline to a $pK_{1,eff}$ of 4.27 (Table I). This shift reflects a much stronger interaction with H_3T^+ than H_2T^0, as indicated by the $\Delta\bar{G}_i$ values reported in Table I.

Because both montmorillonite and saponite contain exchangeable cations and the commercial saponite sample contains nonclay diluents, the effect of commercial saponite on the acid–base equilibrium of tetracycline also was studied following purification to remove carbonate impurities and sodium saturation. The displacement in the acid–base equilibrium of tetracycline was much greater in the presence of the purified, sodium-saturated commercial saponite than that observed for commercial saponite (Table I).

The findings are similar to the values observed with sodium-saturated montmorillonite and purified sodium-saturated hectorite, the other smectite minerals studied. Thus, it appears that exchangeable cations other than sodium are present in commercial saponite.

The fraction bound curve for tetracycline in the presence of purified, sodium-saturated commercial saponite (Fig. 9) was very similar to the adsorption profile seen for sodium-saturated montmorillonite (Fig. 4) and purified, sodium-saturated hectorite (Fig. 5). Adsorption only occurred when pH^b conditions permitted H_3T^+ to be present and was close to 100% at the pH^b of maximum adsorption.

The fraction bound curve for tetracycline in a commercial saponite suspension showed a lower maximum fraction bound and also indicated that adsorption occurred at higher pH^b conditions, where the zwitterionic and anionic forms of tetracycline were present. As with bentonite USP and commercial hectorite, the unexpected adsorption profile for commercial saponite is attributed to the effects of the exchangeable cations and the nonclay impurities present in the sample.

Attapulgite—Examination of the X-ray diffractograms in Fig. 2 for commercial attapulgite and sodium-treated attapulgite indicates that attapulgite is the major clay component of commercial attapulgite. Peaks corresponding to quartz and calcite also were seen in the diffractograms. In addition, the presence of a montmorillonite-like component in both commercial attapulgite and sodium-treated attapulgite is suggested since treatment of each sample with glycerol resulted in an expanded spacing

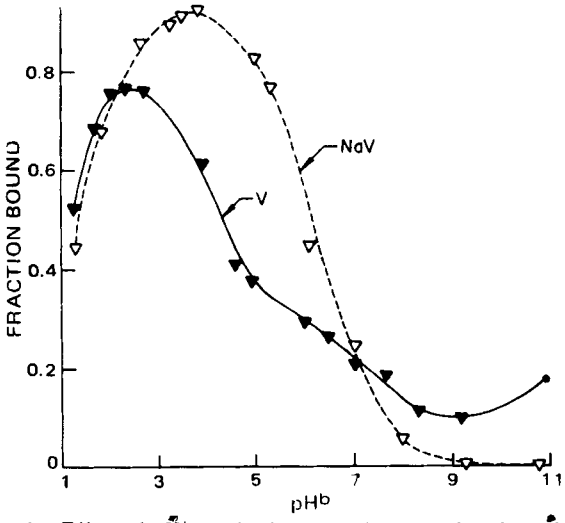

Figure 9—*Effect of pH^b on the fraction of tetracycline bound (f) in untreated commercial saponite (V) and purified, sodium-saturated commercial saponite (NaV) suspensions.*

of 14.5 and 15.2 Å for the 001 reflection of commercial attapulgite and sodium-treated attapulgite, respectively.

Cation-exchange capacity values have been reported for attapulgite. However, some of the higher values reported were attributed to montmorillonite impurities (25).

Transmission electron photomicrographs of sodium-treated attapulgite (Fig. 10) showed elongated, lath-shaped particles characteristic of attapulgite. The irregularly shaped aggregates interwoven among the attapulgite fibers are believed to be the montmorillonite-like impurity and illustrate the difficulty of obtaining pure attapulgite samples.

The IR spectra (Fig. 3) of commercial attapulgite and sodium-treated attapulgite were essentially identical. Both spectra showed the characteristic IR bands for attapulgite at 3625, 3595, 3560, 3505, 1192, 1145, 1090, 1036, 988, and 925 cm^{-1}. Very weak bands were noted at 1425 and 876 cm^{-1}, corresponding to calcite.

A shift of only 0.17 pK unit was observed in the first acid–base equilibrium of tetracycline in the presence of commercial attapulgite (Table I) and was accompanied by a small change in the partial molar Gibbs free energy of the H_3T^+ species. No substantial interaction was expected based on the cation-exchange capacity arising from the clay's structure. The observed interaction is believed to be due largely to interaction of H_3T^+ with the montmorillonite-type impurity in commercial attapulgite.

The effect of pH^b on the fraction of tetracycline bound to the sample of commercial attapulgite also indicates the presence of a montmorillonite-like component. A maximum in the fraction bound curve (Fig. 11) was observed at pH^b conditions favoring the protonated species, H_3T^+. This maximum arose from the cation-exchange capacity due to any isomorphous substitution in attapulgite and the contribution of the montmorillonite. The degree of adsorption decreased from the maximum of 35% as the pH^b increased. Adsorption remained relatively constant at ~15% at pH conditions that favor the zwitterionic and anionic forms of tetracycline.

Although calcium from the calcite impurity may reduce the amount of tetracycline in solution through the formation of calcium–tetracycline complexes, it is more likely that the constant, weak adsorption observed above pH^b 5 was due to physical adsorption. This type of adsorption pattern is expected based on the uncharged structure of attapulgite.

The selective adsorption of the H_3T^+ species indicated by the maximum at pH^b 3 is the adsorption pattern typical of the montmorillonite group of clays and indicates the important effect of the montmorillonite-like impurity on the adsorptive properties of commercial attapulgite.

Sodium-treated attapulgite caused a slightly smaller displacement of the first acid–base equilibrium of tetracycline than did commercial attapulgite and thus resulted in a smaller effect on $pK_{1,eff}$ (Table I). It was less effective in adsorbing tetracycline in comparison to commercial attapulgite (Fig. 11). It is believed that the heat and acid treatments employed to activate commercial attapulgite increase the availability of adsorption sites in attapulgite due to either an increase in the specific surface area of commercial attapulgite or the removal of adsorbed species. Thus, the fraction of tetracycline bound by commercial attapulgite was greater throughout the entire pH range than was observed for sodium-treated attapulgite.

Kaolinite—Identical X-ray diffractograms (Fig. 2) were obtained for sodium-treated kaolinite and kaolin NF and were characteristic of

Figure 10—*Electron photomicrograph of sodium-treated attapulgite showing the elongate lath-shaped particles (A) that are characteristic of attapulgite and the irregularly shaped aggregates (M) believed to be the montmorillonite-like impurity (magnification = 30,000×).*

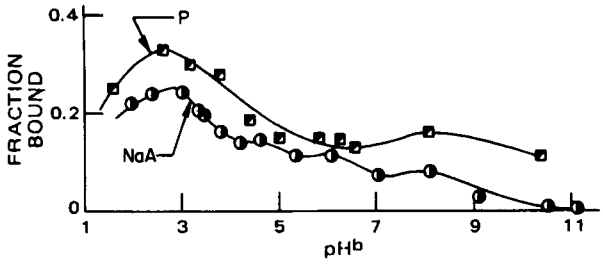

Figure 11—*Effect of pH^b on the fraction of tetracycline bound* (f) *in commercial attapulgite (P) and sodium-treated attapulgite (NaA) suspensions.*

kaolinite, indicating that kaolinite is the major clay present in kaolin NF. Both samples were pure as evidenced by the absence of reflections corresponding to nonclay diluents and the absence of expansion following glycerol treatment.

The IR absorption spectra of sodium-treated kaolinite and kaolin NF showed the characteristic IR bands for kaolinite at 3695, 3670, 3650, 3620, 1108, 1038, 1012, 940, and 915 cm^{-1} (Fig. 3).

Light scattering prevented the study of the acid–base equilibrium of tetracycline in the presence of kaolin NF. However, the first acid–base equilibrium of tetracycline in the presence of sodium-treated kaolinite was examined. As seen in Table I, $pK_{1,eff}$ was decreased slightly in the presence of sodium-treated kaolinite, indicating a displacement in favor of the zwitterionic form of tetracycline. No interaction was found with H_3T^+, but a weak interaction was observed with H_2T^0, as evidenced by the $\Delta\bar{G}_{H_2T^0}$ value of −0.2 kcal/mole.

This behavior is in contrast to the effect of montmorillonite, hectorite, and commercial saponite, where $pK_{1,eff}$ increased due to stabilization of H_3T^+ by the clay. However, kaolinite has little or no cation-exchange capacity and hence no stabilization of H_3T^+ occurs. The shift of $pK_{1,eff}$ in favor of H_2T^0 is consistent with the structure of kaolinite.

Since kaolinite is a nonexpanding mineral, the edge surface comprises a substantial portion (10–20%) of the total surface area. Broken bonds at the edges of the tetrahedral sheet give rise to a small permanent positive charge. A negative charge whose magnitude is related directly to pH results from broken edges of the octahedral sheet (26). Thus, at low pH^b conditions, kaolinite exhibits a small positive charge arising from the tetrahedral sheet; at higher pH^b conditions, the negative charge from the octahedral sheet predominates.

The fraction bound curve for tetracycline in the presence of sodium-treated kaolinite (Fig. 12) showed a very low degree of adsorption. The adsorption profile can be related to the pH-dependent charge arising from broken edges. No adsorption is seen at low pH^b values because the H_3T^+ species is repelled by the positive edge charge. Likewise, at basic pH^b conditions, the anionic forms of tetracycline are repelled by the negative edge charge. A small degree of physical adsorption occurs in the pH^b range where the H_2T^0 species is present.

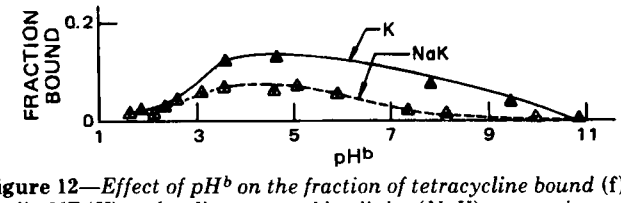

Figure 12—*Effect of pH^b on the fraction of tetracycline bound* (f) *in kaolin NF (K) and sodium-treated kaolinite (NaK) suspensions.*

The fraction bound curve (Fig. 12) for tetracycline in the presence of kaolin NF showed a similar adsorption profile to that of sodium-treated kaolinite. This finding was expected because both X-ray and IR analyses showed that kaolin NF was pure kaolinite.

REFERENCES

(1) N. J. Kerkhof, J. L. White, and S. L. Hem, *J. Pharm. Sci.*, **66**, 1528 (1977).

(2) H. P. Klug and L. E. Alexander, "X-ray Diffraction Procedures for Polycrystalline and Amorphous Materials," Wiley, New York, N.Y., 1954, p. 300.

(3) W. Parrish, *Acta Crystallogr.*, **13**, 838 (1960).

(4) R. Greene-Kelly, *J. Soil Sci.*, **4**, 233 (1953).

(5) G. Brunton, *Am. Mineral.*, **40**, 124 (1955).

(6) D. M. C. MacEwan, *Nature (London)*, **154**, 577 (1944).

(7) L. S. Porubcan, C. J. Serna, J. L. White, and S. L. Hem, *J. Pharm. Sci.*, **67**, 1081 (1978).

(8) J. M. Serrotosa and W. F. Bradley, *J. Phys. Chem.*, **62**, 1164 (1958).

(9) M. L. Jackson, "Soil Chemical Analysis Advanced Course," Department of Soils, University of Wisconsin, Madison, Wis., 1956, p. 35.

(10) J. R. Feldkamp and J. L. White, *J. Colloid Interface Sci.*, **69**, 97 (1979).

(11) H. van Olphen, "An Introduction to Clay Colloid Chemistry," Interscience, New York, N.Y., 1963, pp. 199–202.

(12) "Powder Diffraction File, Inorganic Volume," Joint Committee on Powder Diffraction Standards, Philadelphia, Pa., 1960.

(13) H. W. van der Marel and H. Bentelspacher, "Atlas of Infrared Spectroscopy of Clay Minerals and Their Admixtures," Elsevier, New York, N.Y., 1976.

(14) V. C. Farmer, "The Infrared Spectra of Minerals," Monograph 4, Mineralogical Society, London, England, 1974.

(15) J. L. White, *Soil Sci.*, **112**, 22 (1971).

(16) M. Barr, *J. Am. Pharm. Assoc.*, **NS4**, 4 (1964).

(17) "United States Dispensatory," 27th ed., Lippincott, Philadelphia, Pa., 1973, p. 182.

(18) J. F. Williams, B. C. Elsley, and D. J. Weintritt, *Clays Clay Miner.*, **2**, 141 (1953).

(19) J. R. Feldkamp, Ph.D. thesis, Purdue University, West Lafayette, Ind., 1978.

(20) W. T. Granquist and J. V. Kennedy, *Clays Clay Miner.*, **15**, 103 (1967).

(21) W. S. Stern, Ph.D. thesis, University of Michigan, Ann Arbor, Mich., 1971.

(22) G. Brown, "The X-Ray Identification and Clay Structures of Clay Minerals," 2nd ed., Jarrold and Sons, Norwich, England, 1961, p. 86.

(23) "Veegum: The Versatile Ingredient," Bulletin 15, R. T. Vanderbilt Co., Norwalk, Conn.

(24) C. S. Ross and S. B. Hendricks, U.S. Geological Survey, Paper 205B, 1945, p. 23.

(25) L. W. Zelazny and F. G. Calhoun, in "Minerals in Soil Environments," R. C. Dinauer, Ed., Soil Science Society of America, Madison, Wis., 1977, p. 445.

ACKNOWLEDGMENTS

Supported in part by an American Foundation for Pharmaceutical Education Fellowship to J. E. Browne.

This report is Journal Paper 7953, Purdue University Agricultural Experiment Station, West Lafayette, IN 47907.

Model of Interaction of Ajmaline with Polyvinylpyrrolidone

TOSHIHARU HOSONO *, SEISHI TSUCHIYA, and HIDEO MATSUMARU ˣ

Received August 8, 1979, from the *Tokyo College of Pharmacy, 1432-1 Horinouchi, Hachioji, Tokyo 192-03, Japan.* Accepted for publication February 13, 1980. *Present address: Institute of Research and Development, Yamanouchi Pharmaceutical Co., Ltd., 1-8 Azusawa-1, Itabashi, Tokyo 174, Japan.

Abstract □ The chemical shifts in the Fourier transform ^{13}C-NMR spectrum of ajmaline were assigned from consideration of the acetylation shifts and multiplet splitting in the off-resonance decoupled spectrum. On the basis of the assigned signals, the changes of chemical shifts in ajmaline induced by polyvinylpyrrolidone were investigated, and an interaction model of ajmaline with polyvinylpyrrolidone in chloroform was proposed.

Keyphrases □ Ajmaline—model of interaction with polyvinylpyrrolidone □ Polyvinylpyrrolidone—model of interaction with ajmaline □ ^{13}C-NMR spectroscopy—ajmaline, chemical shifts assigned

Tachibana and Nakamura (1) reported a new method for enhancing the dissolution rates of poorly soluble drugs by using water-soluble polymers such as polyvinylpyrrolidone. The coprecipitate of ajmaline with polyvinylpyrrolidone was prepared (2) in the same manner as the coprecipitate of reserpine (3) and griseofulvin (4), and the enhancement of the dissolution rate of ajmaline from this coprecipitate was ascertained. This effect seemed to be caused largely by some interaction between polyvinylpyrrolidone and ajmaline in chloroform, the solvent in which this coprecipitate was prepared. The interaction sites of polyvinylpyrrolidone and ajmaline in chloroform were investigated. The hydrogen bond formed between the C-21 hydroxyl group in ajmaline and the carbonyl groups in polyvinylpyrrolidone was confirmed (2), and complexation between the aromatic ring in ajmaline and the amide groups in polyvinylpyrrolidone was suggested (5).

This study was conducted to confirm these interactions using Fourier transform ^{13}C-NMR spectroscopy and to propose a model of interaction of polyvinylpyrrolidone with ajmaline in chloroform.

EXPERIMENTAL

The ajmaline, 17,21-diacetylajmaline[1], and polyvinylpyrrolidone[2] (K-15) employed were of the same origin and were purified as described previously (2). ^{13}C-NMR spectra[3] were obtained in deuterochloroform with tetramethylsilane as the internal reference.

RESULTS AND DISCUSSION

To clarify the behavior of the electron density of the carbon atoms in ajmaline caused by the interaction with polyvinylpyrrolidone, the influence of polyvinylpyrrolidone on the ^{13}C-NMR spectrum of ajmaline was investigated. Since there were no previous reports on the ^{13}C-NMR spectrum of ajmaline, the signal assignment was performed initially. The number of signals observed in the complete proton-decoupled ^{13}C-NMR spectrum was equal to the number of carbon atoms constituting ajmaline (Fig. 1). Therefore, no overlap of signals was detected.

From consideration of the chemical shift rules (6) and the multiplet splitting in ^1H-signal frequency off-resonance decoupling experiments, the carbons constituting ajmaline were classified as aromatic carbons (C-8–C-13), carbons adjacent to hydroxyl groups (C-17 and C-21), a quaternary carbon (C-7), methyl carbons (C-18 and C-22), methylene carbons (C-6, C-14, and C-19), and methine carbons (C-2, C-3, C-5, C-15, C-16, and C-20).

The signals of the aromatic carbons in ajmaline were assigned according to previous reports about various compounds containing an indole ring (7, 8) (Table I).

Three signals were observed in the magnetic field of the carbon atoms adjacent to hydroxyl groups, except for the signals derived from deuterochloroform. The signal of δ 88.10 ppm was derived from C-21 because it was adjacent to the nitrogen atom and a hydroxyl group. Generally, the carbon atoms at the α- and β-positions are shifted downfield and upfield, respectively, due to the substituent effects produced by replacement of the hydroxyl group by the acetoxy group (9). Therefore, it seems reasonable that the signal of δ 88.10 ppm was shifted downfield by diacetylation (Table I, $\delta_b - \delta_a$).

On the other hand, the signal of either δ 79.19 or 77.72 ppm corresponded to C-17. The C-17 signal was expected to be shifted significantly downfield by diacetylation because of its α-position to the hydroxyl group. Accordingly, the δ 77.72-ppm signal was determined to be C-17, in spite of the interchangeability of the C-17 assignment with C-2 in the diacetate (δ_b).

The quaternary carbon atom, C-7, was assigned easily from multiplicity.

In the two signals of the methyl carbon atoms (quartet), the δ 34.11-ppm signal was determined to be C-22 because of its adjacency to the nitrogen atom.

For the methylene carbons (C-6, C-14, and C-19), the side-chain carbon (C-19) was attributed to δ 25.39 ppm. Although the assignments of C-6 and C-14 were attempted, the discrimination remained uncertain because one of these signals exhibited the large downfield shift (+1.50 ppm) from diacetylation in spite of the distance from the hydroxyl groups, and this large shift could not be explained by the inductive effect of the acetoxy groups. Further investigation involving an additional steric effect is required to assign these signals.

The signals of the methine carbons (C-2, C-3, and C-5) adjacent to the nitrogen atom were downfield. The signal of C-2 adjacent to the aromatic nitrogen atom in the indole ring was expected to appear considerably downfield (10), and the signal of δ 79.19 ppm was assigned to C-2. The large shift of the δ 77.72-ppm signal by diacetylation also provided convincing evidence that this signal was not derived from C-2.

The signals due to C-15, C-16, and C-20 were expected to be farther upfield than those of C-2, C-3, and C-5. Since C-20 is located at the β-position to C-18 in the aliphatic side chain, this signal seemed to appear significantly upfield. The signal of δ 28.12 ppm was assigned to C-20 and exhibited a reasonable upfield shift by diacetylation (−0.85 ppm). The C-15 and C-16 carbons exist in the ring system, so these signals appear relatively downfield compared with that of C-20. It appears that C-16 is almost as susceptible to influence as C-7 because it is located at the same β-position as C-7 to C-17. The C-15 signal is not influenced by diacetylation due to the long distance between C-15 and either hydroxyl group.

On the basis of these chemical shift rules and acetylation shifts, the possibility that the signals of C-15 or C-16 in ajmaline occur at δ 52.78 or 47.95 ppm is excluded. Consequently, it was concluded that the C-16 signal corresponds to δ 45.22 ppm and that the δ 43.08-ppm signal corresponds to C-15 because the latter was not influenced appreciably by diacetylation. These assignments remained unaltered in spite of the interchangeability of δ 43.65 and 43.01 ppm in the diacetate.

Subsequently, on the basis of these assignments, the change of signals in 0.34 *M* ajmaline by the addition of various concentrations of poly-

[1] Mass spectrum: *m/e* 410 (M^+). *Anal.*—Calc. for $C_{24}H_{30}N_2O_4$: C, 70.37; H, 7.29; N, 6.70. Found: C, 70.16; H, 7.31; N, 6.82.

[2] The mean molecular weight of polyvinylpyrrolidone (K-15) was evaluated to be ~7500 by viscosity measurements at 30°.

[3] JEOL-FX-100 spectrometer operating at 25.0 MHz in the Fourier transform mode.

0022-3549/80/0700-0824$01.00/0
© 1980, American Pharmaceutical Association

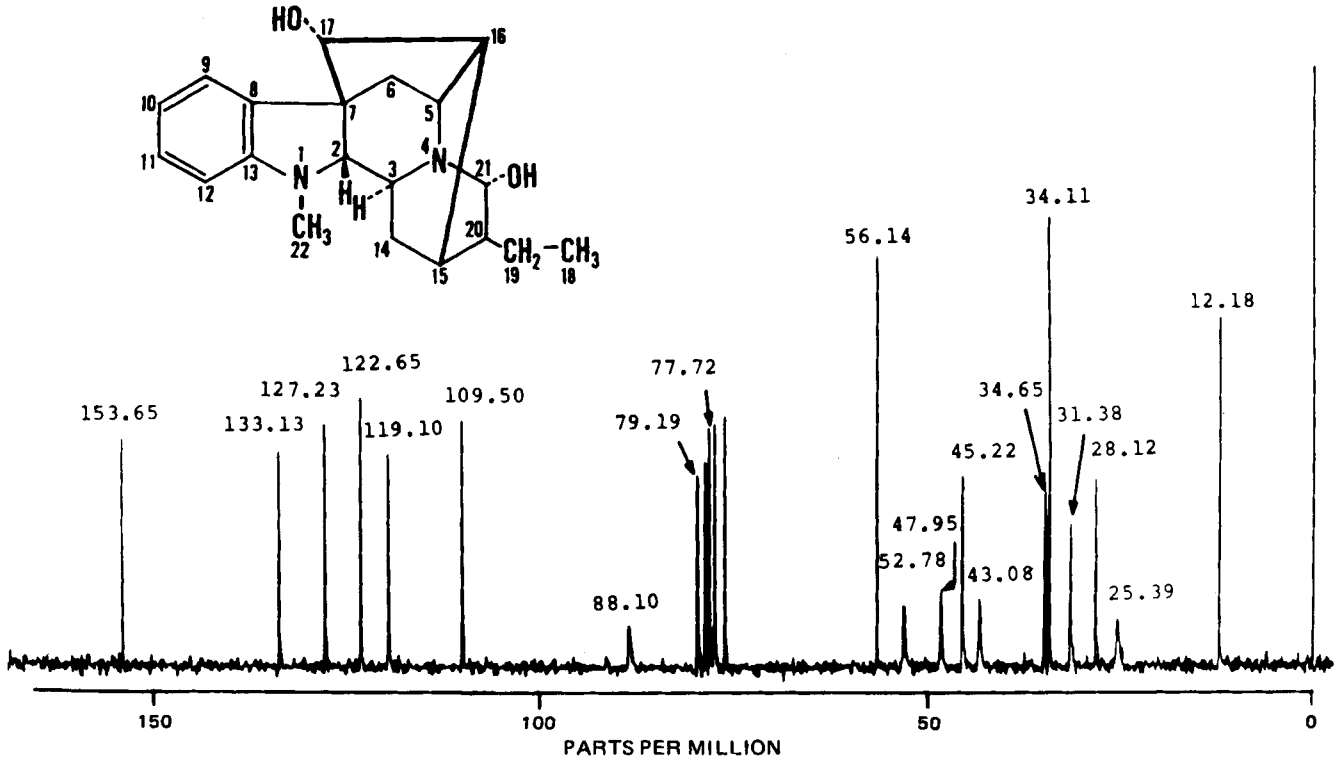

Figure 1—*Structure and complete proton-decoupled ^{13}C-NMR spectrum of ajmaline.*

vinylpyrrolidone was investigated (Fig. 2). Although the chemical shift of the C-17 signal was not distinctly observed by addition of 0.015 and 0.06 *M* polyvinylpyrrolidone due to overlapping with the signals derived from deuterochloroform, the signals of C-21 and C-17 tended to be shielded by an increase in the polyvinylpyrrolidone concentration. However, no significant changes of linewidth in the ajmaline signals induced by polyvinylpyrrolidone could be detected.

By using UV and ^1H-NMR spectra, the hydrogen bond formed between the C-21 hydroxyl group in ajmaline and the carbonyl groups of the pyrrolidone rings in polyvinylpyrrolidone was recognized previously (5). The upfield shifts of C-17 and C-21 were observed by the addition of polyvinylpyrrolidone in the present study. In ^{13}C-NMR spectra, the chemical shift variation is dominated by the electron density (11). The enhancements of electron density in C-21 and C-17 of ajmaline provide sufficient grounds to expect hydrogen bond formation with polyvinylpyrrolidone.

To ascertain this point, the effect of acetone on 2-butanol was examined. The C-2 in 2-butanol was shifted upfield by the addition of 1 drop of acetone (not shown). This upfield shift of C-2 in butanol obviously was attributable to the hydrogen bond formed between 2-butanol and acetone. Accordingly, it is almost certain that the C-17 and C-21 hydroxyl groups in ajmaline formed hydrogen bonds with the carbonyl groups of the pyrrolidone rings in polyvinylpyrrolidone. The fact that the upfield shift of C-21 was smaller than that of C-17 by hydrogen bond formation seemed to result from the smaller influence of C-21 than of C-17 by diacetylation. In addition, from consideration of the changed C-7 signal by diacetylation, the upfield shift of C-7 by the addition of polyvinylpyr-

Table I—Chemical Shift Assignments in ^{13}C-NMR Spectra of Ajmaline and 17,21-Diacetylajmaline [a]

Carbon	Multiplicity	Chemical Shift: Ajmaline (δ_a)	Chemical Shift: Diacetylajmaline (δ_b)	$\delta_b - \delta_a$
13	s	153.65	153.83	+0.18
8	s	133.13	132.09	−1.04
11	d	127.23	127.65	+0.42
10	d	122.65	122.35	−0.30
9	d	119.10	119.24	+0.14
12	d	109.50	109.72	+0.22
21	d	88.10	88.73	+0.63
2	d	79.19	80.03*	+0.84
17	d	77.72	79.22*	+1.50
7	s	56.14	54.37	−1.77
5	d	52.78**	53.56**	+0.78
3	d	47.95**	48.37**	+0.42
16	d	45.22	43.65***	−1.57
15	d	43.08	43.01***	−0.07
6	t	34.65****	36.15****	+1.50
22	q	34.11	34.65	+0.54
14	t	31.38****	31.83****	+0.45
20	d	28.12	27.27	−0.85
19	t	25.39	25.02	−0.37
18	q	12.18	12.17	−0.01
$COCH_3$	s		170.37	
	s		169.11	
$COCH_3$ (X2)	q		21.27	

[a] *, **, ***, and **** may be interchanged in each column. The numbering of the carbons is illustrated in Fig. 1. The designations for signal multiplicity are s = singlet, d = doublet, t = triplet, and q = quartet. Chemical shifts are expressed in parts per million relative to tetramethylsilane.

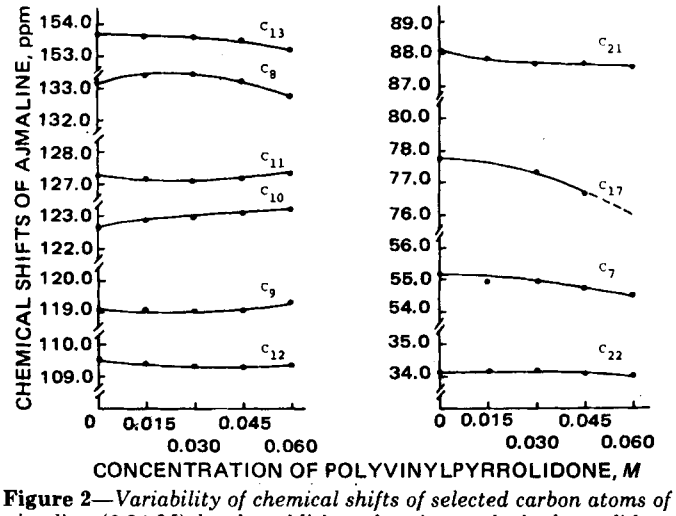

Figure 2—*Variability of chemical shifts of selected carbon atoms of ajmaline (0.34 M) by the addition of various polyvinylpyrrolidone concentrations.*

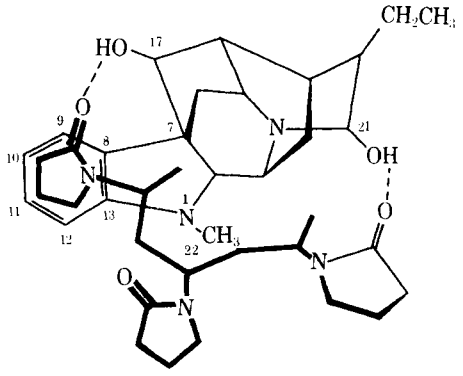

I

rolidone seemed to be influenced by hydrogen bond formation (Table I).

In addition to the influence in the signals of C-7, C-17, and C-21, there was a relatively large influence in the signals of aromatic carbons in ajmaline by polyvinylpyrrolidone; that is, the signals of C-8 and C-13 tended to shift upfield and those of C-9 and C-10 shifted downfield. The electron densities of C-8 and C-13 became higher due to the presence of polyvinylpyrrolidone, and those of C-9 and C-13 became lower.

Considering the relatively small changes of the aromatic carbons by diacetylation, it does not seem that these electron density changes were brought about indirectly through hydrogen bond formation. Furthermore, the upfield shift of C-13 and the downfield shift of C-10 do not seem to support the interaction with the nitrogen atom at position 1 in ajmaline. Accordingly, it is reasonable to consider that a complex was formed between the amide groups of the pyrrolidone ring in polyvinylpyrrolidone and the aromatic ring in ajmaline, as suggested previously (5). It is expected that the electron densities of C-8 and C-13 of the aromatic ring in ajmaline are affected and become higher because of the approach of the positively charged nitrogen atom of the amide group of the pyrrolidone rings of polyvinylpyrrolidone. Considering such mechanisms of complex formation, Laszlo (12) described it as a dipole–induced dipole complex in view of the nomenclature of these complexes.

From these results, an interaction model between polyvinylpyrrolidone and ajmaline is proposed (I). In the coprecipitate, ajmaline apparently was molecularly dispersed in solid polyvinylpyrrolidone through these interactions. As a result, the dissolution rate of ajmaline from the coprecipitate was enhanced markedly.

REFERENCES

(1) T. Tachibana and A. Nakamura, *Kolloid-Z. Z. Polym.*, **203**, 130 (1965).

(2) H. Matsumaru, S. Tsuchiya, and T. Hosono, *Chem. Pharm. Bull.*, **25**, 2504 (1977).

(3) T. R. Bates, *J. Pharm. Pharmacol.*, **21**, 710 (1969).

(4) M. Mayersohn and M. Gibaldi, *J. Pharm. Sci.*, **55**, 1323 (1966).

(5) T. Hosono, S. Tsuchiya, and H. Matsumaru, *Chem. Pharm. Bull.*, **27**, 58 (1979).

(6) J. B. Stothers, "Carbon-13 NMR Spectroscopy," Academic, New York, N.Y., 1972, pp. 55–207.

(7) G. W. Gribble, R. B. Nelson, J. L. Johnson, and G. C. Levy, *J. Org. Chem.*, **40**, 3720 (1975).

(8) E. Wenkert, C. J. Chang, H. P. S. Chawla, D. W. Cochran, E. W. Hagaman, J. C. King, and K. Orito, *J. Am. Chem. Soc.*, **98**, 3645 (1976).

(9) M. Christl, H. J. Reich, and J. D. Roberts, *ibid.*, **93**, 3463 (1971).

(10) P. G. Lukacs, M. De Bellefon, L. Le Men-Oliver, J. Levy, and J. Le Men, *Tetrahedron Lett.*, **1974**, 487.

(11) R. Hagen and J. D. Roberts, *J. Am. Chem. Soc.*, **91**, 4504 (1969).

(12) P. Laszlo, in "Progress in Nuclear Magnetic Resonance Spectroscopy," vol. 3, J. W. Emsley, J. Feeney, and L. H. Sutcliffe, Eds., Pergamon, London, England, 1967, pp. 383–386.

ACKNOWLEDGMENTS

The authors are grateful to Dr. Y. Yamada and Dr. S. Shibuya, Tokyo College of Pharmacy, for helpful discussions and suggestions.

Polarographic Determination of Edetate Disodium in Eyewash and Ophthalmic Decongestant Solutions

MARVIN CARLSON ˣ and LARRY E. HABEGER

Received August 20, 1979, from the *Minneapolis District, Food and Drug Administration, Public Health Service, Department of Health, Education, and Welfare, Minneapolis, MN 55401.* Accepted for publication February 25, 1980.

Abstract □ The quantitative analysis of edetate disodium in nonprescription eyewash and ophthalmic solutions is described. The method involves differential pulse polarography using a dropping mercury electrode. A known concentration of cadmium or zinc is added to a buffer in a polarographic cell. The sample solution is incremented into the cell with a micropipet. The peak current decreases because the resulting chelate is not reducible at the potentials used. The quantity of edetate disodium in the sample then is determined graphically. Some contact lens cleaning and wetting solutions containing polymeric compounds are amenable to assay for edetate disodium if extraction, precipitation, centrifugation, or dilution steps minimize the maximum suppressor effect of the additives. These steps are very effective with cellulose ether compounds but are ineffective with polyvinyl alcohol.

Keyphrases □ Edetate disodium—polarographic determination in eyewash and ophthalmic decongestant solutions □ Polarography, differential pulse—analysis, edetate disodium in eyewash and ophthalmic decongestant solutions □ Ophthalmic preparations—polarographic determination of edetate disodium in eyewash and ophthalmic decongestant solutions

Edetate disodium (I) is added to eyewash and ophthalmic solutions containing bactericides such as benzalkonium chloride, chlorobutanol, and thimerosal to increase their bactericidal properties (1). Compendial methods (2–4) employ classical titrimetric procedures for the quantitative determination of I, but these methods are not suitable for the levels encountered in the drug preparations (0.01–0.25%).

A literature search revealed two methods used to determine I in pharmaceutical preparations. One employed colorimetric detection for ophthalmic solutions (5); the other used atomic absorption for an antibiotic preparation (6).

This paper proposes a sensitive, rapid, and quantitative polarographic method for determining I concentrations by stepwise addition of sample to the cell. The resulting

0022-3549/80/0700-0826$01.00/0

© 1980, American Pharmaceutical Association

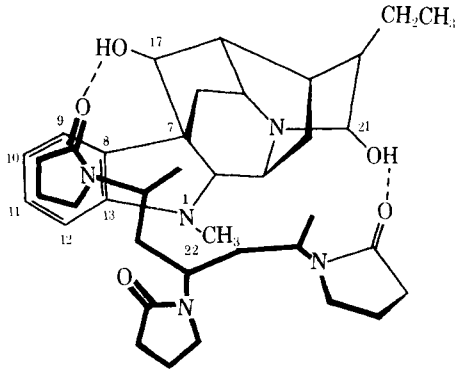

I

rolidone seemed to be influenced by hydrogen bond formation (Table I).

In addition to the influence in the signals of C-7, C-17, and C-21, there was a relatively large influence in the signals of aromatic carbons in ajmaline by polyvinylpyrrolidone; that is, the signals of C-8 and C-13 tended to shift upfield and those of C-9 and C-10 shifted downfield. The electron densities of C-8 and C-13 became higher due to the presence of polyvinylpyrrolidone, and those of C-9 and C-13 became lower.

Considering the relatively small changes of the aromatic carbons by diacetylation, it does not seem that these electron density changes were brought about indirectly through hydrogen bond formation. Furthermore, the upfield shift of C-13 and the downfield shift of C-10 do not seem to support the interaction with the nitrogen atom at position 1 in ajmaline. Accordingly, it is reasonable to consider that a complex was formed between the amide groups of the pyrrolidone ring in polyvinylpyrrolidone and the aromatic ring in ajmaline, as suggested previously (5). It is expected that the electron densities of C-8 and C-13 of the aromatic ring in ajmaline are affected and become higher because of the approach of the positively charged nitrogen atom of the amide group of the pyrrolidone rings of polyvinylpyrrolidone. Considering such mechanisms of complex formation, Laszlo (12) described it as a dipole–induced dipole complex in view of the nomenclature of these complexes.

From these results, an interaction model between polyvinylpyrrolidone and ajmaline is proposed (I). In the coprecipitate, ajmaline apparently was molecularly dispersed in solid polyvinylpyrrolidone through these interactions. As a result, the dissolution rate of ajmaline from the coprecipitate was enhanced markedly.

REFERENCES

(1) T. Tachibana and A. Nakamura, *Kolloid-Z. Z. Polym.*, **203**, 130 (1965).

(2) H. Matsumaru, S. Tsuchiya, and T. Hosono, *Chem. Pharm. Bull.*, **25**, 2504 (1977).

(3) T. R. Bates, *J. Pharm. Pharmacol.*, **21**, 710 (1969).

(4) M. Mayersohn and M. Gibaldi, *J. Pharm. Sci.*, **55**, 1323 (1966).

(5) T. Hosono, S. Tsuchiya, and H. Matsumaru, *Chem. Pharm. Bull.*, **27**, 58 (1979).

(6) J. B. Stothers, "Carbon-13 NMR Spectroscopy," Academic, New York, N.Y., 1972, pp. 55–207.

(7) G. W. Gribble, R. B. Nelson, J. L. Johnson, and G. C. Levy, *J. Org. Chem.*, **40**, 3720 (1975).

(8) E. Wenkert, C. J. Chang, H. P. S. Chawla, D. W. Cochran, E. W. Hagaman, J. C. King, and K. Orito, *J. Am. Chem. Soc.*, **98**, 3645 (1976).

(9) M. Christl, H. J. Reich, and J. D. Roberts, *ibid.*, **93**, 3463 (1971).

(10) P. G. Lukacs, M. De Bellefon, L. Le Men-Oliver, J. Levy, and J. Le Men, *Tetrahedron Lett.*, **1974**, 487.

(11) R. Hagen and J. D. Roberts, *J. Am. Chem. Soc.*, **91**, 4504 (1969).

(12) P. Laszlo, in "Progress in Nuclear Magnetic Resonance Spectroscopy," vol. 3, J. W. Emsley, J. Feeney, and L. H. Sutcliffe, Eds., Pergamon, London, England, 1967, pp. 383–386.

ACKNOWLEDGMENTS

The authors are grateful to Dr. Y. Yamada and Dr. S. Shibuya, Tokyo College of Pharmacy, for helpful discussions and suggestions.

Polarographic Determination of Edetate Disodium in Eyewash and Ophthalmic Decongestant Solutions

MARVIN CARLSON ˣ and LARRY E. HABEGER

Received August 20, 1979, from the *Minneapolis District, Food and Drug Administration, Public Health Service, Department of Health, Education, and Welfare, Minneapolis, MN 55401.* Accepted for publication February 25, 1980.

Abstract □ The quantitative analysis of edetate disodium in nonprescription eyewash and ophthalmic solutions is described. The method involves differential pulse polarography using a dropping mercury electrode. A known concentration of cadmium or zinc is added to a buffer in a polarographic cell. The sample solution is incremented into the cell with a micropipet. The peak current decreases because the resulting chelate is not reducible at the potentials used. The quantity of edetate disodium in the sample then is determined graphically. Some contact lens cleaning and wetting solutions containing polymeric compounds are amenable to assay for edetate disodium if extraction, precipitation, centrifugation, or dilution steps minimize the maximum suppressor effect of the additives. These steps are very effective with cellulose ether compounds but are ineffective with polyvinyl alcohol.

Keyphrases □ Edetate disodium—polarographic determination in eyewash and ophthalmic decongestant solutions □ Polarography, differential pulse—analysis, edetate disodium in eyewash and ophthalmic decongestant solutions □ Ophthalmic preparations—polarographic determination of edetate disodium in eyewash and ophthalmic decongestant solutions

Edetate disodium (I) is added to eyewash and ophthalmic solutions containing bactericides such as benzalkonium chloride, chlorobutanol, and thimerosal to increase their bactericidal properties (1). Compendial methods (2–4) employ classical titrimetric procedures for the quantitative determination of I, but these methods are not suitable for the levels encountered in the drug preparations (0.01–0.25%).

A literature search revealed two methods used to determine I in pharmaceutical preparations. One employed colorimetric detection for ophthalmic solutions (5); the other used atomic absorption for an antibiotic preparation (6).

This paper proposes a sensitive, rapid, and quantitative polarographic method for determining I concentrations by stepwise addition of sample to the cell. The resulting

0022-3549/80/0700-0826$01.00/0

© 1980, American Pharmaceutical Association

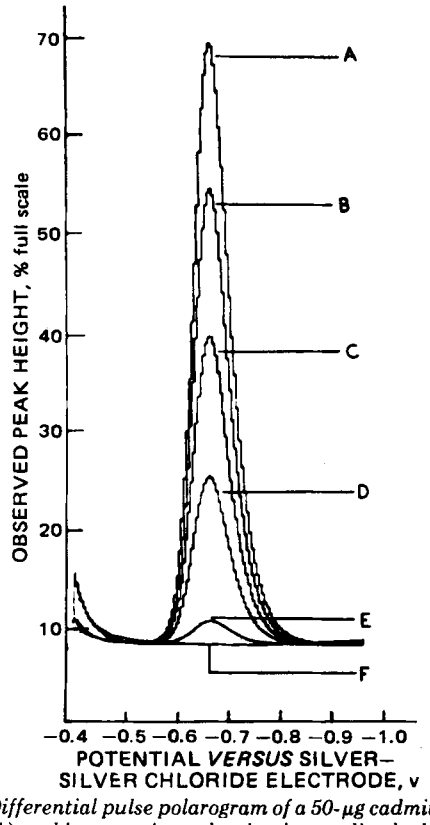

Figure 1—*Differential pulse polarogram of a 50-μg cadmium standard in the cell (A) and its stepwise reduction in amplitude due to the addition of 40-μl increments of a standard 0.1% edetate disodium solution (B–F) (5 μamp full scale).*

chelation causes a corresponding decrease in the peak amplitude of the free metal (cadmium or zinc) originally in the cell.

EXPERIMENTAL

Reagents and Chemicals—Analytical reagent grade chemicals were used.

Solution Preparation—An ammonium–ammonia buffer supporting electrolyte was prepared by diluting 2.0 g of ammonium nitrate and 1.75 ml of concentrated ammonia to 500 ml with water. A maximum suppressor was prepared by dissolving 100 mg of gelatin powder[1] in 100 ml of water. The mixture was warmed to promote dissolution. Gelatin solutions older than 72 hr were not used.

Metal standard solutions (1000 μg/ml) were made by dissolving cadmium wire[2] or zinc shot[2] (99.99%) in 100 ml of 20% HNO_3 and diluting to 1 liter with water. Edetate disodium[3] (99.0–101.0% pure) was assayed (3) and then employed in preparing standard solutions in water and in simulated commercial eye drop and eyewash preparations. Triple-distilled mercury[4] was washed with 10% HNO_3 in a mercury cleaning tower[5] and then pinholed to remove residual wash water.

Instrumentation—Experiments were performed with a commercial polarographic system[6] and an x–y recorder[7]. Adjustable micropipets[8] having volumes of 5–50, 50–250, and 200–1000 μl were used. Nitrogen was passed through a scrubbing tower[9] of vanadous chloride followed by a gas washing tower containing the supporting electrolyte.

[1] BBL, Cockeysville, Md.
[2] Ventron Corp., Beverly, Mass.
[3] Mallinckrodt, St. Louis, Mo.
[4] Bethlehem Apparatus Co., Hellertown, Pa.
[5] Thomas-John, Arthur H. Thomas Co., Philadelphia, Pa.
[6] Princeton Applied Research model 174 polarographic analyzer, model 315 automated electroanalysis controller, and model 303 static mercury drop electrode apparatus.
[7] Houston Instruments model 2000.
[8] Finnpipette, distributed by Markson Science Inc., Del Mar, Calif.
[9] Princeton Applied Research Corp. application note AN-108. The vanadous chloride oxygen scrubbing tower may not be necessary, depending on the nitrogen purity.

Table I—Linearity Data [a] Relating Volume of Sample Added to Adjusted Net Current

0.1% (w/v) edetate disodium added, μl	0	40	80	120	160
Adjusted net current, μamp	3.07	2.35	1.59	0.87	0.12

[a] Linear regression value at x intercept (9) = 166.7 μl, and coefficient of determination (9) = 0.999.

Instrument Parameters—A potential scan from −0.4 to −1.0 v (cadmium) or from −0.8 to −1.5 v (zinc) at a rate of 5 mv/sec was used. The differential pulse mode was employed at a modulation amplitude of 50 mv and a current range of 5 μamp full scale. A dropping mercury electrode with a drop time of 1 sec also was used.

Assay—To the polarographic cell were added 10.0 ml of buffer, 250 μl of gelatin solution, and 50 μl of cadmium or zinc standard solution. Oxygen was removed from the solution by purging with nitrogen for 5 min, and the solution then was scanned to obtain the metal peak. A micropipet was used to add sample to the cell. If the sample solution contained 0.1% I and was complexed with cadmium, 40-μl aliquots were added to the cell. For the sample solutions containing 0.01% I, 400-μl increments were added to the cell. The cell contents were purged for 1 min after each sample addition. Chelation resulted in an ~20% decrease in the observed current for the polarographic peak (Fig. 1). The sample additions were continued until there was no observed metal peak (Fig. 1).

The cadmium–I complex was not readily observed in the potential scan range of 0 to −1.5 v using the differential pulse mode. A broad, low-amplitude wave was observed at ~−1.1 v, which increased in a nonlinear fashion with the addition of I to the cell. Cadmium metal was reduced at −0.67 v.

The zinc–I complex did not exhibit a reduction wave in the potential scan range of 0 to −1.5 v, while zinc metal was reduced at −1.25 v. These potentials were peak maxima *versus* a silver–silver chloride reference electrode. The data of Meites (7) on cadmium and zinc in ammonia–ammonium chloride and I supporting electrolytes agree with the experimental observations.

Calculations—The following formula was used to calculate the adjusted net current after each sample addition:

$$I_A = I_O\left(\frac{V_2}{V_1}\right) \qquad \text{(Eq. 1)}$$

where I_A is the adjusted net current in microamps, I_O is the observed current in microamps, V_1 is the original cell volume in milliliters, and V_2 is the total cell volume in milliliters after each sample addition.

The I_A value is the observed current adjusted to the original cell volume, assuming a linear decrease in response due to dilution.

The sample volume added (microliters) was plotted on the x axis *versus* the adjusted net current on the y axis (Table I).

The x intercept represents the volume of the sample in microliters equivalent to the metal originally present in the cell. The following formula was used to calculate I in the sample:

$$\text{percent sample (w/v)} = V_{std}C_{std}\left(\frac{D}{A}\right)\left(\frac{0.1}{V_{sam}}\right) \qquad \text{(Eq. 2)}$$

where percent sample (w/v) is the percent edetate disodium in the sample calculated on a weight to volume basis, V_{std} is the volume of the metal standard solution in microliters, C_{std} is the concentration of the metal standard solution in micrograms per microliter, D is the molecular weight of edetate disodium, A is the atomic weight of the standard metal (cadmium or zinc), V_{sam} is the end-point volume of the sample solution in microliters, and 0.1 is a factor converting microliters to milliliters, micrograms to grams, and grams per milliliter to percent. The molecular weight of edetate disodium is 372.24, and the atomic weights of cadmium and zinc are 112.40 and 65.37, respectively.

DISCUSSION

The graph of the polarographic peak heights, corrected for dilution, is linear with respect to the sample volume (titrant) added. The most convenient method for calculating sample concentration is to perform a linear regression for the best line fit of the data points (adjusted net current, microamperes *versus* microliters of sample added). A coefficient of determination calculation then is performed to see how well the data fit the linear regression (Table I). Edetate disodium forms 1:1 complexes with many metal ions, but the degree of complex formation is strongly influenced by pH. Since the cadmium and zinc chelates are stable in basic

Table II—Assay Results for Edetate Disodium in Various Solutions Using Cadmium

Type of Product	Amount Declared, %	Amount Found, %	Percent of Declared	Range, %
Standard edetate disodium in water	0.0126	0.0130[a]	103.2	1.6
	0.1040	0.1025[b]	98.6	3.7
	0.5044	0.5033[c]	99.8	4.0
Eye drops[d]	0.1	0.1013[a]	101.3	5.2
Eye drops[e]	0.1	0.1000[a]	100.0	2.5
Eye drops[f]	0.1	0.0994[a]	99.4	3.3
Eye drops[g]	0.1000	0.1028[a]	102.8	3.1
Eyewash[h]	0.10	0.1102[a]	110.2	3.0
Eyewash[g]	0.1000	0.1032[a]	103.2	1.0
Contact lens[i] cleaning solution	0.2	0.1864[a]	93.2[j]	1.1
Contact lens[k] soaking solution	0.01	0.0097[a]	97.0[l]	0.0

[a] Average of two determinations. [b] Average of four determinations. [c] Average of three determinations. [d] Clear Eyes, Abbott Laboratories. [e] Visine, Pfizer. [f] Murine Plus, Abbott Laboratories. [g] Simulated preparation, Minneapolis District, Food and Drug Administration. [h] Lavoptik, Lavoptik Co. [i] Softmate, Barnes-Hind Pharmaceuticals. [j] Ten-milliliter sample extracted with 10 ml of water-washed chloroform and then centrifuged for 20 min at 1500 rpm. [k] Contique, Alcon Laboratories. [l] Five-milliliter sample diluted with 15 ml of water, extracted, centrifuged for 20 min at 1500 rpm, and then allowed to stand until adequately cleared.

or weakly acidic solutions (8), the pH 9.95 buffer used in this assay satisfies a major condition for quantitation in that the uncomplexed metal-ion concentration decreases linearly throughout the titration.

Sample eyewash and eye drop solutions have a pH of ~6–7, so their effect is minimal upon addition to the buffer in the polarographic cell. Some eye drop preparations contain methylcellulose, a viscosity-increasing agent. Since these solutions tend to wet the surface of the plastic micropipet tips, care must be taken to ensure complete removal of the entire sample aliquot from the micropipet tip.

Contact lens cleaning and wetting solutions comprise a large class of samples. These solutions commonly contain I but also may contain polymeric compounds such as methylcellulose and other closely related cellulose ethers, polyvinyl alcohol, and tyloxapol in relatively significant concentrations. From a polarographic analysis viewpoint, these polymers exhibit a strong maximum suppressor effect, resulting in an unusable polarogram.

Table III—Assay Results of Edetate Disodium in Various Solutions Using Zinc

Type of Product	Amount Declared, %	Amount Found, %	Percent of Declared	Range, %
Standard edetate disodium in water	0.0126	0.0134[a]	106.3	0.8
	0.1040	0.1067[b]	102.6	0.7
	0.5044	0.5182[a]	102.7	1.0
Eye drops[c]	0.1	0.1000[a]	100.0	0.6
Eye drops[d]	0.1	0.1039[a]	103.9	2.8
Eye drops[e]	0.1	0.0999[a]	99.9	3.4
Eye drops[f]	0.1000	0.1024[a]	102.4	2.6
Eyewash[g]	0.10	0.1092[a]	109.2	4.5
Eyewash[f]	0.1000	0.1034[a]	103.4	1.3
Contact lens[h] cleaning solution	0.2	0.1808[a]	90.4[i]	4.4
Contact lens[j] soaking solution	0.01	0.0105[a]	105.0[k]	4.0

[a] Average of two determinations. [b] Average of three determinations. [c] Clear Eyes, Abbott Laboratories. [d] Visine, Pfizer. [e] Murine Plus, Abbott Laboratories. [f] Simulated preparation, Minneapolis District, Food and Drug Administration. [g] Lavoptik, Lavoptik Co. [h] Softmate, Barnes-Hind Pharmaceuticals. [i] Ten-milliliter sample extracted with 10 ml of water-washed chloroform and then centrifuged for 20 min at 1500 rpm. [j] Contique, Alcon Laboratories. [k] Five-milliliter sample diluted with 15 ml of water, extracted, centrifuged for 20 min at 1500 rpm, and then allowed to stand until adequately cleared.

The cellulose ether compounds may be precipitated from solution by an extraction procedure using water-washed chloroform. Any remaining suspended material may be removed completely by centrifugation and standing. A preliminary 10-fold sample dilution with water also may reduce cellulose interference, providing the original concentration of I is ≥0.1%. In many instances, this treatment is sufficient for successful sample analysis if polyvinyl alcohol is absent. Polyvinyl alcohol presents several problems: the maximum suppressor effect cannot be diluted out due to the low levels of I present in the samples, extraction of the polymer is compromised due to the freely soluble nature of the alcohol in aqueous solutions, and the alcohol causes undesirable frothing when the polarographic cell contents are purged with nitrogen.

If lens cleaning solutions contain no polyvinyl alcohol, this method can determine the edetate disodium concentration in these samples.

The results in Tables II and III demonstrate the validity of analyzing commercial eyewash, eye drop, and some contact lens cleaning solutions for I. The assay values (Tables II and III) for edetate disodium were generally higher when standard zinc solution was used; however, cadmium exhibited a more reproducible baseline upon addition of certain sample matrixes such as lens cleaning solutions. Based on examination of the tabular data and the experience gained using both cadmium and zinc, cadmium is recommended as the preferred standard.

An important aspect of this assay is the need for accurate dispensing of edetate disodium sample and standard solutions using adjustable micropipets. Since these volumes are <1 ml, the micropipets should be calibrated.

This procedure can be readily used to analyze I in powder and injectable forms as presented in the USP and "Food Chemicals Codex."

Edetate disodium also is widely used in the food industry as a preservative, sequestrant, and stabilizer. It is feasible that I can be extracted from food into a water phase and subjected to further cleanup and that the concentration then can be determined as specified in this method.

REFERENCES

(1) "Handbook of Nonprescription Drugs," 5th ed., American Pharmaceutical Association, Washington, D.C., 1977, pp. 232, 241.

(2) "Official Methods of Analysis of the Association of Official Analytical Chemists," 12th ed., Association of Official Analytical Chemists, Washington, D.C., 1975, p. 663.

(3) "The United States Pharmacopeia," 19th rev., Mack Publishing Co., Easton, Pa., 1975, pp. 164, 165.

(4) "Food Chemicals Codex," 2nd ed., National Academy of Sciences, Washington, D.C., 1972, pp. 258–260.

(5) E. E. Kaminski and D. M. Pacenti, *J. Pharm. Sci.*, **63**, 1133 (1974).

(6) R. J. Hurtubise, *ibid.*, **63**, 1131 (1974).

(7) "Handbook of Analytical Chemistry," 1st ed., L. Meites, Ed., McGraw-Hill, New York, N.Y., 1963, pp. 5-55, 5-58, 5-72, 5-74.

(8) D. Skoog and D. West, "Fundamentals of Analytical Chemistry," Holt, Rinehart, and Winston, New York, N.Y., 1966, pp. 273–275.

(9) "HP-91 Scientific Portable Printing Calculator Owners Handbook," Hewlett-Packard Co., Palo Alto, Calif., 1976, pp. 83–86.

ACKNOWLEDGMENTS

Presented at the Second Voltammetry Users Conference, Chicago, Ill., November 1978, and the Federation of Analytical Chemists and Spectroscopists Society Symposium, Philadelphia, Pa., September 1979.

The authors thank Mr. K. L. Egli, Food and Drug Administration, and Dr. R. W. Ramette, Carleton College, Northfield, Minn., for review of this article.

Size Distribution Characteristics of Mineral Phase in Renal Stones

S. I. ISMAIL and R. TAWASHI ˣ

Received April 16, 1979, from the *Faculté de Pharmacie, Université de Montréal, Montréal, Québec, Canada.* Accepted for publication February 12, 1980.

Abstract □ The size distribution of the mineral phases in three renal stones (whewellite, struvite, and whitlockite) was determined using a particle-counting technique after removal of the organic matrix. The multisized crystallites of the investigated stones revealed close similarity in size distribution characteristics. Whewellite size parameters were in good agreement with the parameters of calcium oxalate monohydrate crystals formed in the kidneys of rats injected with L-4-hydroxyproline. However, these parameters differed significantly from the values calculated from the size distribution of calcium oxalate crystals voided in the urine of recurrent stone formers. The data obtained suggest that critical size distribution characteristics may be instrumental in causing the mineral phase to agglomerate and adopt a close packing in renal stones.

Keyphrases □ Renal stones—size distribution characteristics of mineral phase □ Size distribution—mineral phase of renal stones □ Urinary stones—size distribution characteristics of mineral phase □ Minerals—size distribution characteristics in renal stones

The study of crystal deposits in freshly voided urine and their relation to stone formation has received considerable attention (1–4). The ultrastructure of renal calculi was investigated by various methods to understand stone etiology and growth mechanisms (5–7). However, the size distribution and geometrical characteristics of individual crystals forming the renal calculus were overlooked. The basic question of whether there exists a critical dimension or a critical size range favoring stone construction in humans has not been answered. The quantitative evaluation of these parameters promises a better understanding of the clustering process and the packing stability of the mineral phase in urolithiasis.

The purposes of the present study were to determine the crystal size distribution of calcium oxalate, ammonium magnesium phosphate, and tribasic calcium phosphate in stones using different measuring techniques and to compare the data obtained with data on calcium oxalate crystals formed in the kidneys of rats injected with L-4-hydroxyproline.

EXPERIMENTAL

Three urinary stones[1] characterized as whewellite (calcium oxalate monohydrate), struvite (ammonium magnesium phosphate hexahydrate), and whitlockite (tribasic calcium phosphate) were obtained from recurrent stone formers.

A series of experiments was conducted using different solvents and conditions to remove the organic matrix and to deaggregate the individual crystals from the polycrystalline mass without acting on the mineral phase or changing the crystal morphology. Ten milliliters of an aqueous solvent was added to ~10 mg of the stone and left at room temperature for 7–14 days. The best results were obtained when whewellite, struvite, and whitlockite stones were digested in aqueous 80% ethylenediamine, 30% NaOH, and 12% sodium hypochlorite solutions, respectively. The digested stones were filtered, and the mineral phase residue was washed repeatedly with the respective solvent and subjected to size analysis.

The deaggregated mineral phase of the different stones was analyzed by a particle counter[2] with a 16-channel analyzer and a 100-μm tube. A "clean" electrolyte solution (0.9% NaCl) saturated with the stone material was used as the suspension medium to ensure that no part of the mineral phase dissolved in the electrolyte solution during the size analysis.

RESULTS AND DISCUSSION

Mineral Phase in Renal Stones—Renal stones generally consist of coherent compact mineral phases of very low voidage. The mucoproteinous matrix accounts for 2–2.5% (w/w) (8, 9). The particle-size distribution of the deaggregated mineral phase of the investigated stones is given in Figs. 1 and 2. Particle-size distributions based on the number and volume showed a close similarity among the investigated stones. For example, the number distribution curves (Fig. 1) showed that 50% of the particle population was <5 μm. On the other hand, the volume distribution curves (Fig. 2) indicated that the median sizes (r_{50}) of the investigated stones was 25–30 μm.

The size data in Figs. 1 and 2 were used to estimate the particle population parameters of the mineral phase. The Rosin–Rammler distribution (10), which is given by $G_r = 100[\exp - (r/r_{mean})^{\gamma}]$, was used to describe the multisized particle population, where G_r is the total cumulative volume of the mineral phase oversize in percent, r is the particle size in micrometers, r_{mean} is the statistical mean particle size in micrometers derived graphically (corresponding to the coordinate G_r = 36.8%), and γ is the degree of uniformity of the size distribution, which

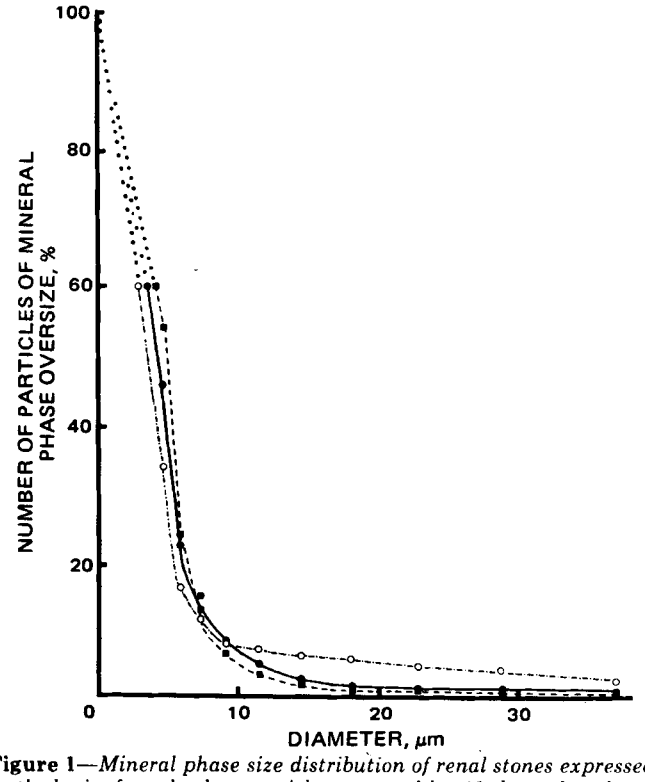

Figure 1—*Mineral phase size distribution of renal stones expressed on the basis of number by a particle counter with a 16-channel analyzer. Key:* ○, *calcium oxalate monohydrate;* ●, *calcium phosphate; and* ■, *ammonium magnesium phosphate.*

[1] Provided by Dr. M. El-Hilali, Department of Urology, University of Sherbrooke, Sherbrooke, Quebec, Canada.

[2] Model TAII, Coulter Electronics, Hialeah, FL 33010.

0022-3549/80/0700-0829$01.00/0
© 1980, American Pharmaceutical Association

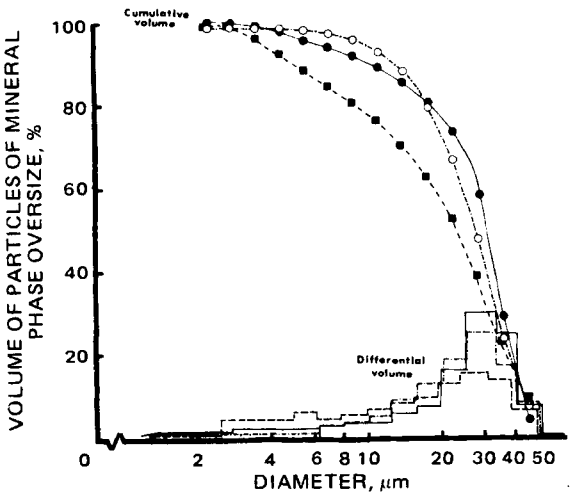

Figure 2—*Mineral phase size distribution of renal stones expressed on the basis of volume by a particle counter with a 16-channel analyzer. Key: ○, calcium oxalate monohydrate; ●, calcium phosphate; and ■, ammonium magnesium phosphate.*

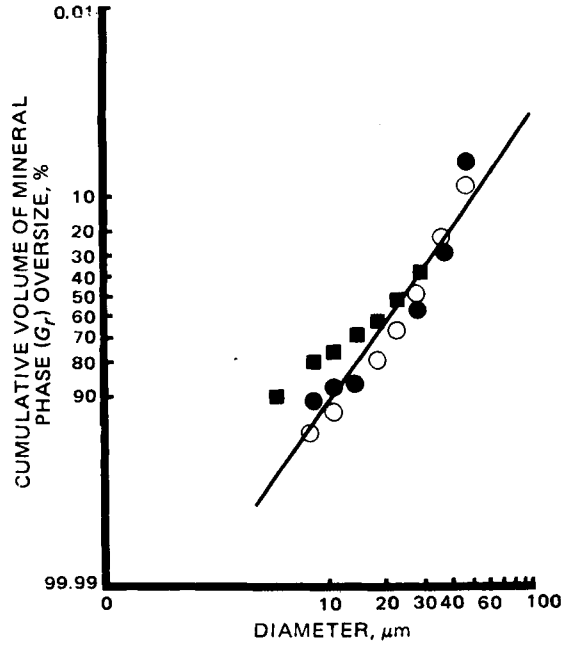

Figure 3—*Scattergraph of the mineral phase size distribution of the investigated renal stones based on the Rosin–Rammler extrapolation. Key: ○, calcium oxalate monohydrate; ●, calcium phosphate; and ■, ammonium magnesium phosphate.*

also is obtained graphically as the slope of the linear relation between log (log $100/G_r$) and log r. The most probable crystal size in the size (10) distribution (r_m) is obtained from $r_m = r_{mean}(\gamma - 1/\gamma)^{1/\gamma}$.

Figure 3 shows a scattergraph and a linear representation of the mineral phase size distribution of the investigated stones. From this plot, the median size (r_{50}) is 25.5 μm, the most probable size in the distribution (r_m) is 26.9 μm, the uniformity factor of the size distribution (γ) is 2.8, and the coefficient of variation (CV) is 63.7%. The coefficient of variation is calculated from $CV\ (\%) = 100[(r_{16} - r_{84})/2r_{50}]$, where r_{16} and r_{84} are the particle sizes when $G_r = 16$ and 84%, respectively.

The examination of the calcium oxalate crystals from the whewellite stone using a scanning electron microscope supported these findings. The mean projected diameter was 28 μm (Fig. 4). This mean projected diameter correlated well with the median size (r_{50}) and the most probable size in the mineral phase size distribution (r_m) obtained by the counter.

***In Vivo* Crystallization of Calcium Oxalate Monohydrate**—The detailed growth history of urinary stones is unknown, and no information is available on the size distribution of the individual crystallites that occur immediately after *in vivo* crystallization. In this study, the size distribution data of calcium oxalate crystallites in renal stones were compared with data for the calcium oxalate crystals produced in rat kidneys after

Table I—Size Characteristics of Calcium Oxalate Monohydrate Crystallized *In Vivo*

Source of Calcium Oxalate Crystals	Median Size (r_{50}), μm	Mean Size (r_{mean}), μm	CV, %	Uniformity Factor (γ)	Most Probable Crystal Size in Size Distribution (r_m), μm
Urinary stone	25.5	31.5	63.7	2.8	26.9
Rat kidneys (experimental urolithiasis)	26.0	31.0	57.7	2.7	26.1
Urine of recurrent stone formers	9.7	14.0	63.8	3.5	8.8

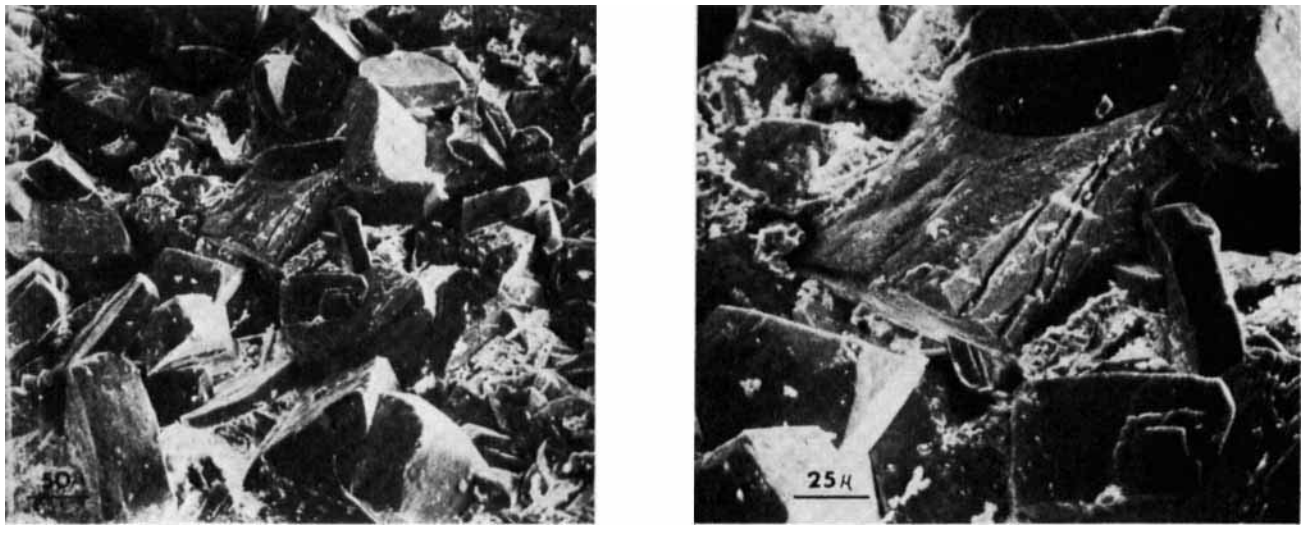

Figure 4—*Scanning electron micrograph of calcium oxalate monohydrate crystals in a calcium oxalate renal stone. The mean projected diameter is 28 μm.*

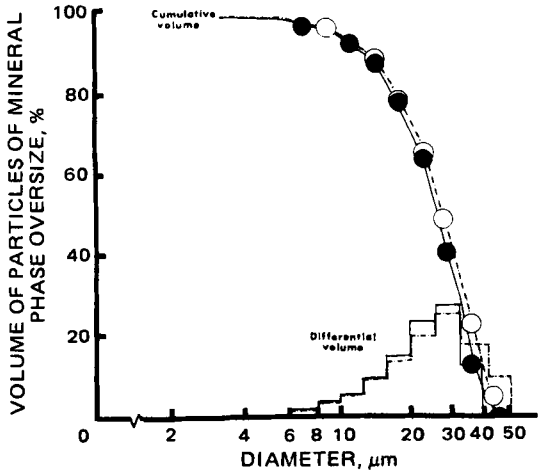

Figure 5—*Size distribution curves of calcium oxalate monohydrate crystals in the renal stone and in experimental urolithiasis. Key:* ○, *calcium oxalate stone; and* ●, *calcium oxalate crystals in rat kidneys.*

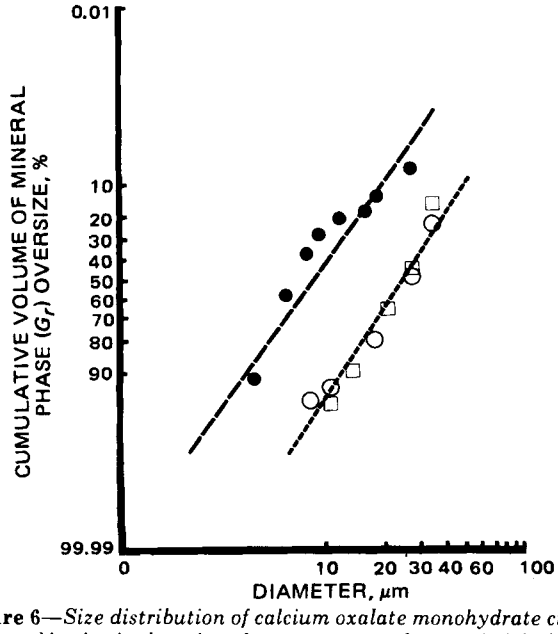

Figure 6—*Size distribution of calcium oxalate monohydrate crystals produced* in vivo *in the urine of recurrent stone formers* (●) *(12), in the urinary stone* (○), *and in rat kidneys (experimental urolithiasis)* (□).

the injection of L-4-hydroxyproline. The experimental details on the formation of calcium oxalate crystals in rat kidneys by injection of L-4-hydroxyproline was described recently (11).

Figure 5 illustrates the size distribution curves of calcium oxalate crystals in the renal stone and calcium oxalate crystals formed in rat kidneys, clearly showing a close similarity in the size distribution of the mineral phase in the rat kidneys and in the human stone. This observation suggests that crystal growth in rat kidneys (experimental urolithiasis) and in the urinary stones may be controlled by similar biological and physicochemical variables.

On the other hand, Robertson and Peacock (12) studied the size distribution of calcium oxalate crystals voided in the urine by recurrent stone formers (those having a history of stones over a period of years). The recurrent stone formers excreted calcium oxalate crystals that gave a bimodal distribution. The examination of the data reported by Robertson and Peacock and data on urinary stones revealed wide variation. To compare the size distribution parameters of calcium oxalate crystals passed in the urine of stone formers with those of calcium oxalate crystals of both renal and rat kidney stones, the Robertson and Peacock data were recalculated and plotted (Fig. 6). The size parameters of calcium oxalate crystals were determined and are given in Table I. The values given in Table I indicate that while the size parameters of the calcium oxalate crystals in both the renal stone and rat kidneys were very close, significant differences existed with calcium oxalate crystals voided in the urine of stone formers. For example, the r_{50} value for crystals in the renal stone was 25.5 μm, and in rat kidneys it was 26.0 μm; for the crystals passed by the recurrent stone formers, it was 9.7 μm.

The uniformity factor (γ), a measure of the uniformity of the distribution, also showed a significant difference between the crystals of the stone and those voided in the urine of stone formers.

Some investigators (9, 13) stated that the coherence of the particles in stones is a function of the surface and shape of the mineral phase particles as well as the presence of the organic matrix. The contribution of the grain size and size distribution characteristics in particle retention and packing still is unclear. More studies are necessary for complete characterization of this problem and for the eventual understanding of stone genesis.

REFERENCES

(1) R. Dyer and B. E. C. Nordin, *Nature*, **215**, 751 (1967).

(2) W. G. Robertson, *Clin. Chim. Acta*, **26**, 105 (1969).

(3) W. G. Robertson, M. Peacock, and B. E. C. Nordin, *Lancet*, **2**, 21 (1969).

(4) F. Catalina and L. Cifuentes Delatte, *Science*, **169**, 183 (1970).

(5) W. Berg, J. D. Schnapp, H. J. Schneider, A. Hesse, and E. Hienzsch, *Eur. Urol.*, **2**, 92 (1976).

(6) M. Gebhardt, *J. Cryst. Growth*, **20**, 6 (1973).

(7) F. Phaneuf-Mimeault and R. Tawashi, *Eur. Urol.*, **3**, 171 (1977).

(8) W. H. Boyce, *Am. J. Med.*, **45**, 673 (1968).

(9) R. S. Malek and W. H. Boyce, *J. Urol.*, **117**, 336 (1977).

(10) J. Nyvlt, "Industrial Crystallisation From Solutions," Butterworths, London, England, 1971, pp. 89–92.

(11) R. Tawashi, M. Cousineau, and M. Sharkawi, *Urol. Res.*, in press.

(12) W. G. Robertson and M. Peacock, *Clin. Sci.*, **43**, 499 (1972).

(13) B. Finlayson, *Kidney Int.*, **13**, 344 (1978).

ACKNOWLEDGMENTS

Presented at the APhA Academy of Pharmaceutical Sciences, Hollywood, Fla. meeting, November 1978.

Supported by the Medical Research Council of Canada.

S. I. Ismail is on a fellowship from the University of Malaysia, Minden, Pulau Pinang, Malaysia.

Solubility and Dissolution Rate Studies of Ergotamine Tartrate

JOHN R. ANDERSON and IAN H. PITMAN ×

Received January 25, 1980, from the *School of Pharmaceutics, Victorian College of Pharmacy, Parkville, Victoria, Australia 3052.* Accepted for publication February 27, 1980.

Abstract □ The solubility of ergotamine tartrate in aqueous solutions of tartaric acid, citric acid, hydrochloric acid, and caffeine and the dissolution rate of ergotamine tartrate in aqueous mixtures containing hydrochloric acid, caffeine, citric acid, or sodium acetate were studied. The Noyes–Whitney model of dissolution is useful for predicting the dissolution rate of ergotamine tartrate in most of the dissolution media. The relative slowness with which ergotamine chloride (a substance with low water solubility) precipitated when ergotamine tartrate was dissolved in 0.1 *M* HCl resulted in the solid dissolving faster in this medium than was predicted using the Noyes–Whitney equation.

Keyphrases □ Ergotamine tartrate—solubility and dissolution rate □ Analgesics—ergotamine tartrate, solubility and dissolution rate □ Solubility—ergotamine tartrate, various dissolution media □ Dissolution rates—ergotamine tartrate, various dissolution media

Relief of migraine headaches by the ergot alkaloid ergotamine depends on its rapid entrance into the systemic circulation during the initial phase of the migraine attack (1). Ergotamine has very low water solubility (2), and its more soluble salts, especially ergotamine tartrate (ergotamine:tartaric acid, 2:1), are used in injections and in solid dosage forms from which rapid drug release is desirable (3).

Although ergotamine tartrate, with a solubility of 1:500 in water (2), is more soluble in water than ergotamine, some confusion exists about the nature of its aqueous solutions. For example, it was stated that ergotamine tartrate is soluble in water but that the addition of tartaric acid often is necessary to maintain a clear solution (4). The present studies concern the solubility of ergotamine in aqueous solutions of tartaric acid, citric acid, hydrochloric acid, and caffeine and the dissolution rate of ergotamine tartrate in several aqueous mixtures. Caffeine was included in some solutions because it is a common ingredient in many dosage forms of ergotamine and it has been postulated that caffeine forms one or more molecular complexes with ergotamine (5).

EXPERIMENTAL

Solubility Studies—Solutions of caffeine, citric acid, and tartaric acid were prepared in the concentration ranges of 0–0.025, 0–0.25, and 0–0.25 *M*, respectively. The pH values of these solutions were adjusted with sulfuric acid, hydrochloric acid, or sodium hydroxide (Table I).

Constant amounts of ergotamine tartrate, in excess of its solubility, were added to screw-capped vials containing a fixed volume of dissolution medium. The vials were sealed and shaken in a water bath at 25.0 ± 0.1°. Preliminary studies were conducted to determine the time required for the solutions to reach equilibrium.

The ergotamine concentration in each equilibrated solution was determined by filtering the contents of the screw-capped vials through a 0.22-μm membrane filter, diluting the filtrate with 1.0% (w/v) tartaric acid solution, and measuring the absorbance of these solutions at 317 nm against an appropriately diluted dissolution medium. Absorbance values were converted to ergotamine concentrations using a Beer's law plot. The Beer's law plot was constructed over the ergotamine concentration range of 0–1.52×10^{-4} *M* and was found to fit $y = 7318x$ ($r = 0.999$), where y is the absorbance and x is the molar concentration of ergotamine.

The amounts of ergotamine tartrate, the volumes of the dissolution media, and the shaking times for each solubility experiment are shown in Table I.

Analysis of Solids—The solid phases remaining in several solubility experiments were collected and dried at 100°. The percentage by weight of ergotamine in the solid phase was determined by dissolving a known amount of the solid and measuring its absorbance at 317 nm. The concentration of ergotamine in the solution was determined from a standard curve, thus allowing the percentage composition of ergotamine in the solid phase to be calculated.

Dissolution Studies—The apparatus used in the dissolution studies was a slight modification of the assembly described in USP XIX. A flow inducer[1] was used to pump the dissolution medium into a flow-through cell mounted in a spectrophotometer[2] and back into the dissolution vessel. The absorbance of ergotamine in the circulating dissolution medium was measured at 317 nm, and a dissolution curve was constructed by plotting ergotamine concentration *versus* time.

The dissolution tests were conducted on 100-mg disks of ergotamine tartrate, manufactured by compression at a force of 5 tons in a hydraulic press. The dissolution medium (1000 ml) was maintained at 25.0 ± 0.1°, and the basket of the dissolution apparatus was rotated at 100 rpm.

The compositions of the dissolution media (Table II) were designed to determine the influence of caffeine and citric acid on the dissolution rate of ergotamine in simulated gastric fluid (0.1 *M* HCl) and at the approximate pH value of the region where the stomach empties its contents into the duodenum (pH 5.0, 0.1 *M* sodium acetate–acetic acid buffer).

RESULTS AND DISCUSSION

Ergotamine Solubility in Aqueous Tartaric Acid Solutions—The phase solubility diagram for ergotamine in aqueous tartaric acid solutions is shown in Fig. 1. The points were calculated from the results of experiments in which water or the tartaric acid solutions were saturated with ergotamine tartrate. The pH values of the various solutions are indicated in Fig. 1. The solution that was prepared by saturating water with ergotamine tartrate [$(EH)_2T$] had a pH value of <5.2, which is the calculated pH value of such a solution [the solution contained 3.2×10^{-3} *M* ergotamine plus ergotamine cation; the pKa value of ergotamine cation is 6.4 (6), and the pKa values for tartaric acid are 2.93 and 4.23 (2)]. This point will be discussed more fully later, but it is believed to arise because the ergotamine tartrate sample was contaminated with tartaric acid or ergotamine acid tartrate (EHTH).

The fact that ergotamine cation has pKa value of 6.4 leads to the conclusion that ergotamine is essentially fully protonated between pH 3 and 1.86, so changes in solubility that accompany changes in tartaric acid concentration cannot be accounted for by changes in the degree of ionization of ergotamine.

The solid phase in the presence of 0.25 *M* added tartaric acid contained 80.3% ergotamine and 19.7% tartaric acid. Since this is a 1:1 molar ratio of ergotamine and tartaric acid, the compound is postulated to be ergotamine acid tartrate. The solid phase in the presence of 0.025 *M* added tartaric acid had an ergotamine to tartaric acid ratio of 1.4:1 and most likely was a mixture of EHTH and ergotamine tartrate [$(EH)_2T$].

These observations and the phase solubility diagram can be accounted for on the basis that the reactions shown in Schemes I–IV occur in saturated aqueous solutions of ergotamine tartrate. In Schemes I–IV, EH^+ is the ergotamine cation; TH_2, TH^-, and T^{2-} are tartaric acid, acid tartrate ion, and tartrate ion, respectively; K_s^1 and K_s^2 are the solubility products of $(EH)_2T$ and EHTH, respectively; and K_a^1 (1.04×10^{-3}) and K_a^2 (4.55×10^{-5}) are the acid dissociation constants of tartaric acid (2).

[1] Watson-Marlow Ltd.
[2] Perkin-Elmer 402 UV–visible spectrophotometer.

0022-3549/80/0700-0832$01.00/0
© 1980, American Pharmaceutical Association

Table I—Composition of the Dissolution Media and Experimental Parameters Used in the Solubility Studies

Medium	Dissolution Medium pH	Composition of Dissolution Medium	Amount of Ergotamine Tartrate, mg	Volume of Dissolution Medium, ml	Shaking Time, hr
1	0.3	0–0.025 *M* caffeine and 0.5 *M* sulfuric acid	100	20	24
2	0.5	0–0.025 *M* caffeine and 0.37 *M* HCl	100	20	24
3	1.0	0–0.025 *M* caffeine and 0.1 *M* HCl	100	20	48
4	1.4	0–0.025 *M* caffeine and 0.037 *M* HCl	100	20	24
5	2.0	0–0.025 *M* caffeine and 0.01 *M* HCl	100	20	48
6	Not controlled	0–0.25 *M* aqueous citric acid solution	250	10	48
7	5.0	0–0.25 *M* aqueous citric acid–sodium hydroxide solution	50	10	48
8	1.0	0–0.25 *M* citric acid and 0.1 *M* HCl	100	20	48
9	1.0	0–0.25 *M* citric acid, 0.025 *M* caffeine, and 0.1 *M* HCl	100	20	48
10	Not controlled	0–0.25 *M* aqueous tartaric acid solution	200	10	48

$$(EH)_2{\cdot}T_{solid} \overset{K_s^1}{\rightleftharpoons} 2\,EH^+ + T^{2-}$$

Scheme I

$$TH_2 \overset{K_a^1}{\rightleftharpoons} TH^- + H^+$$

Scheme II

$$TH^- \overset{K_a^2}{\rightleftharpoons} T^{2-} + H^+$$

Scheme III

$$EH{\cdot}TH_{solid} \overset{K_s^2}{\rightleftharpoons} EH^+ + TH^-$$

Scheme IV

The observation that the solid phase in the presence of 0.025 *M* tartaric acid was a mixture of ergotamine tartrate and ergotamine acid tartrate suggests that the solid phase throughout the ascending portion of the phase solubility diagram, *i.e.*, from 0 to 0.05 *M* added tartaric acid, was a mixture of $(EH)_2T$ and EHTH and that the equilibrium reactions in Schemes I and IV were established. Hence, throughout this region, the relationship:

$$\frac{K_s^1}{K_s^2} = \frac{[EH^+]K_a^2}{[H^+]} \qquad \text{(Eq. 1)}$$

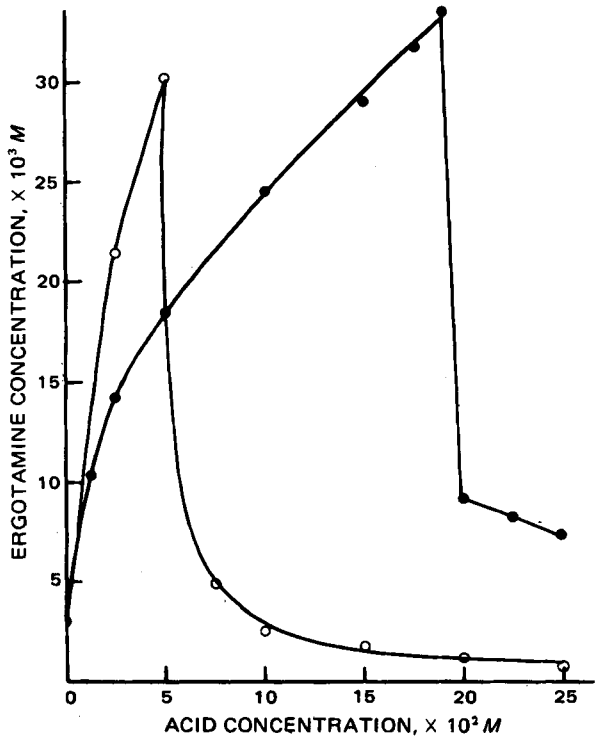

Figure 1—*Effect of the tartaric acid concentration* (○) *and citric acid concentration* (●) *on the solubility of ergotamine tartrate in water. The concentrations of tartaric acid added resulted in various pH values of equilibrated solution: 0* M, *3.0; 0.025* M, *2.33; 0.05* M, *2.15; 0.075* M, *2.10; 0.10* M, *2.04; 0.15* M, *1.98; 0.20* M, *1.92; and 0.25* M, *1.86.*

should apply. Substitution of measured values of $[EH^+]$ and $[H^+]$ in Eq. 1 led to a value of $2.0 \pm 0.1 \times 10^{-4}$ *M* for K_s^1/K_s^2. The solid phase in the presence of 0.25 *M* added tartaric acid was ergotamine acid tartrate. Hence, under these conditions, it is evident that the equilibrium reactions in Schemes II–IV are the only ones operating. Treatment of the data in this region resulted in a value of 2.1×10^{-5} M^2 for K_s^2. Subsequent solution of Eq. 1 gave a value of 4.2×10^{-9} M^3 for K_s^1. Hence, the phase solubility diagram in Fig. 1 may be accounted for by the described postulates and can be quantitated by using values of 4.2×10^{-9} M^3 and 2.1×10^{-5} M^2 for the equilibrium constants K_s^1 and K_s^2 at 25°, respectively.

The presence of EHTH in the EH_2T sample that was obtained commercially could account for the fact that its saturated solution in water had a pH value of 3.0 rather than 5.2 as expected. The analytical results found for this material were: C, 62.11; H, 5.83; N, 10.44; O, 21.52. The formula for $(EH)_2T$ ($C_{70}H_{76}N_{10}O_{16}$) requires: C, 64.01; H, 5.83; N, 10.66; O, 19.49. Therefore, the analytical results are consistent with it containing 50% $(EH)_2T$ and 50% EH·TH (C, 62.36; H, 5.74; N, 10.12; O, 21.77).

If this postulate is correct, then the determinations of ergotamine concentrations made in this study are probably in error by 5% because the Beer's law plots from which concentrations were calculated were constructed on the basis that 1 mole of ergotamine tartrate yielded 2 moles of ergotamine cation. In fact, whereas 1 g of ergotamine tartrate yields 1.52×10^{-3} mole of ergotamine cation, 1 g of a 50:50 mixture of ergotamine tartrate and ergotamine acid tartrate yields 1.45×10^{-3} mole of ergotamine.

Ergotamine Tartrate Solubility in Aqueous Citric Acid Solutions—The phase solubility diagram obtained by saturation of citric acid solutions with ergotamine tartrate is included in Fig. 1. The solid phase in the presence of 0.25 *M* citric acid was a 1:1 mixture of citric acid and ergotamine, presumably the monoergotamine salt of citric acid.

The pH values of solutions in this experiment were not controlled and ranged downward from 3.0. This system was not analyzed further because of its complexity, but it is reasonable to conclude that equilibria similar to those established in the tartaric acid system were in existence as well as others involving the various possible salts of citric acid.

The phase solubility diagram obtained when ergotamine tartrate was added to pH 5.0 citric acid–sodium hydroxide buffers is shown in Fig. 2.

Table II—Dissolution Rates of 100-mg Ergotamine Tartrate Disks in Various Dissolution Media

Composition of Dissolution Medium	pH Value	Gradient of Initial Portion of Dissolution Curve, absorbance units/min × 10^4
0.1 *M* HCl	1.0	35.3 ± 10.5
0.025 *M* caffeine and 0.1 *M* HCl	1.0	288.0 ± 93.1
0.15 *M* citric acid and 0.1 *M* HCl	1.0	83.0 ± 34.1
0.025 *M* caffeine, 0.15 *M* citric acid, and 0.1 *M* HCl	1.0	246.3 ± 99.2
0.1 *M* sodium acetate–acetic acid buffer (acetate buffer)	5.0	37.0 ± 19.1
0.025 *M* caffeine and acetate buffer	5.0	150.3 ± 49.8
0.15 *M* citric acid–sodium hydroxide in acetate buffer	5.0	6.7 ± 1.9
0.025 *M* caffeine and 0.15 *M* citric acid–sodium hydroxide in acetate buffer	5.0	18.3 ± 2.1

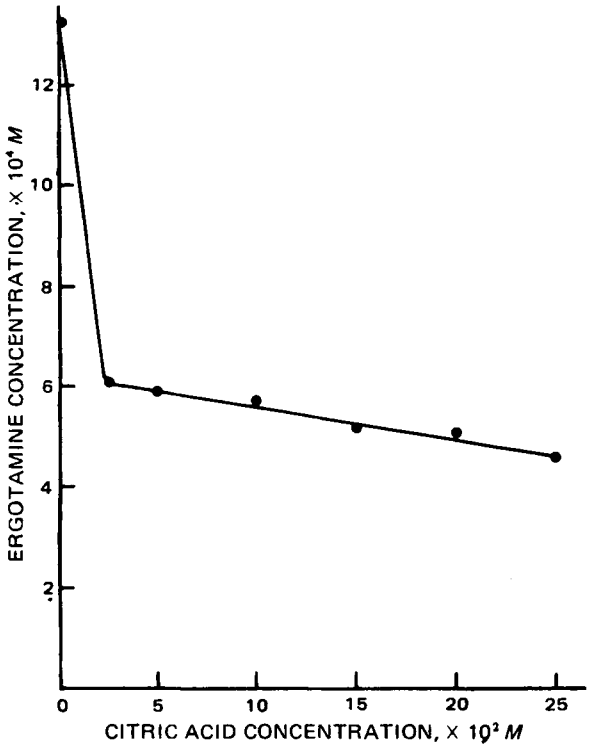

Figure 2—*Solubility of ergotamine tartrate in solutions of citric acid buffered to pH 5.0 with sodium hydroxide.*

In this case, increases in the total citrate concentration caused the ergotamine concentration in solution to decrease. The solid phase in the presence of 0.25 *M* added citric acid contained 72.3% ergotamine. This value is consistent with the solid phase being essentially the monosodium, monoergotamine salt of diionized citric acid, which contains 73.09% ergotamine (EH·HCit·Na). The equilibrium reaction under these conditions is:

$$(EH\cdot HCit\cdot Na)_{solid} \overset{K_2^3}{\rightleftharpoons} EH^+ + Na^+ + HCit^{2-}$$

Scheme V

The decrease in ergotamine concentration in solution that occurred as the sodium citrate concentration was increased resulted from precipitation of EH·HCit·Na by a common-ion effect.

Ergotamine Tartrate Solubility in Aqueous Hydrochloric Acid—The solubilities of ergotamine tartrate in aqueous hydrochloric acid solutions are summarized in Table III. The solid phases were not analyzed[3], but it is postulated that they contained ergotamine chloride. It is known from the pKa value of ergotamine cation (6.4) that the ionic nature of ergotamine does not change appreciably as the pH is lowered from 3.0 (10^{-3} *M* HCl) to ~1.0 (0.1 *M* HCl). Hence, increasing chloride-ion concentrations probably caused precipitation of ergotamine chloride by a common-ion effect. This conclusion is supported by the fact that the product of the concentrations of ergotamine cation [EH^+] and chloride ion in solution was essentially constant (Table III), *i.e.*, it was the solubility product of ergotamine chloride. The slight drift in values could be caused by the change in ionic strength that occurs when the chloride-ion concentration varies by a factor of >100.

The chloride-ion concentrations in the stomach and duodenum are

Table III—Solubility of Ergotamine in Aqueous Hydrochloric Acid

[HCl], *M*	10^4[EH^+], *M*	[Cl^-][a], *M*	K_{SP} = [EH^+][Cl^-], M^2
0.370	0.58	0.362	2.1×10^{-5}
0.100	0.64	0.093	5.9×10^{-6}
0.037	1.77	0.030	5.2×10^{-6}
0.010	7.76	0.003_2	2.5×10^{-6}

[a] Calculated on basis that the solid phase is ergotamine chloride.

[3] A UV spectrum and flame test were consistent with this conclusion.

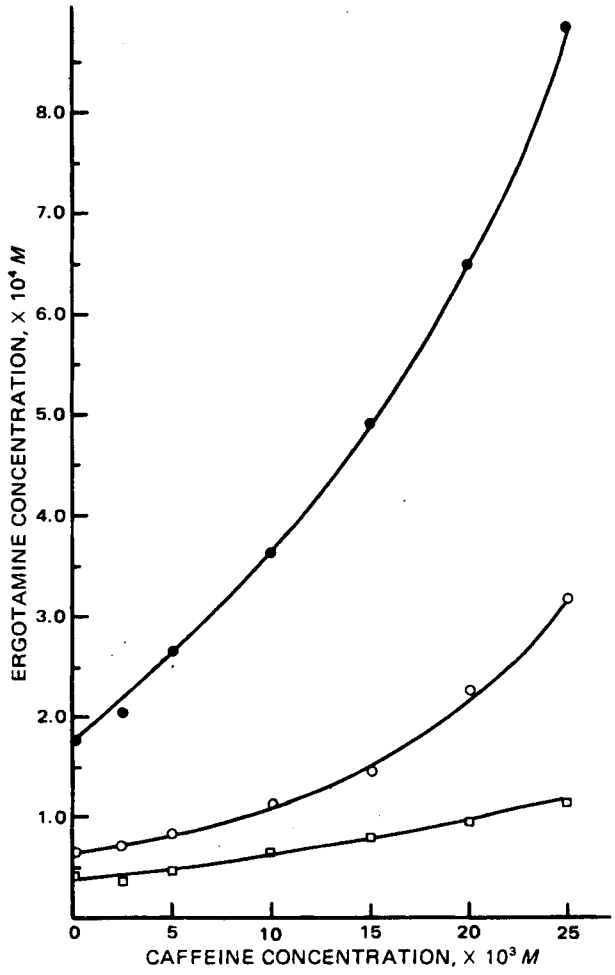

Figure 3—*Effect of caffeine concentration on the solubility of ergotamine in 0.370* M *HCl* (□), *0.100* M *HCl* (○), *and 0.037* M *HCl* (●).

~0.14 *M* (5 mg/ml) and 0.08 *M* (2.6–3.6 mg/ml), respectively (7). Hence, the precipitation of ergotamine chloride in the GI tract may lower the bioavailability of orally administered ergotamine salts.

Zoglio *et al.* (5) determined the solubility of ergotamine tartrate in 0.1 *M* HCl at 30.0° to be ~5.3×10^{-3} *M* ergotamine. This figure is substantially larger than the value of 8.1×10^{-5} *M* calculated in this study under identical conditions. No explanation for this difference can be offered.

Ergotamine Tartrate Solubility in Caffeine Solutions—The phase solubility diagrams that were obtained by saturation of caffeine solutions in aqueous hydrochloric acid with ergotamine tartrate are shown in Figs. 3 and 4. The influence of caffeine on ergotamine tartrate solubility was qualitatively similar to that obtained by Zoglio *et al.* (5) and may be attributed to complex formation between caffeine and ergotamine. The fact that the ergotamine–caffeine phase solubility diagrams are not straight lines suggests that complexes containing more than one caffeine molecule were formed (8).

Dissolution Studies—The dissolution rates of ergotamine from 100-mg ergotamine tartrate disks in various solvents are shown in Table II. The dissolution rates in 0.1 *M* HCl were increased 6.5 times when 0.025 *M* caffeine was included and 2.4 times when 0.15 *M* citric acid was included. The rate was increased seven times in the presence of 0.025 *M* caffeine and 0.15 *M* citric acid. The phase solubility studies indicated that ergotamine tartrate solubility (expressed as ergotamine solubility) in 0.1 *M* HCl was increased six times by 0.025 *M* caffeine and six times by citric acid. Hence, these results were approximately consistent with the Noyes–Whitney model for dissolution (9), which states that the dissolution rate of a solid is proportional to its solubility in dilute solutions.

It is surprising that the dissolution rate of ergotamine in a pH 5.0 acetate buffer was essentially the same as that in 0.1 *M* HCl, whereas its solubility was 20 times greater in the former solvent. A likely explanation is that precipitation of ergotamine chloride, the event that depresses ergotamine solubility in hydrochloric acid solutions, does not occur to an appreciable extent within the diffusion layer. The kinetics of this event apparently are slow with respect to the time taken for a molecule to dif-

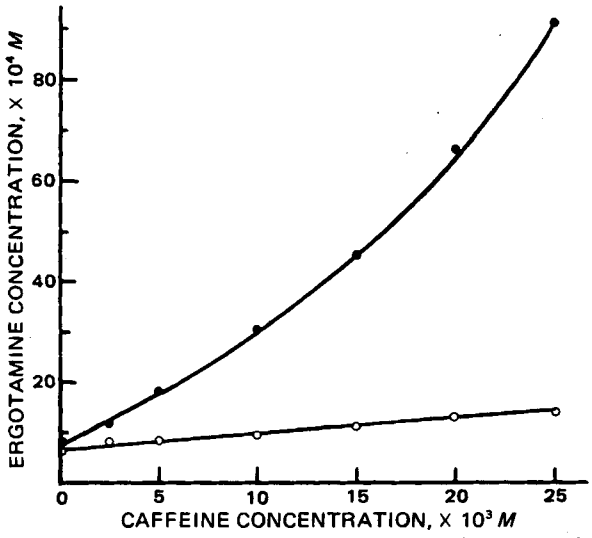

Figure 4—*Solubilizing effect of caffeine on ergotamine tartrate in 0.01 M HCl (●) and 0.50 M sulfuric acid (○).*

fuse from the solid–liquid interface into the bulk of the solution.

The inclusion of 0.025 *M* caffeine in a pH 5 acetate buffer increased the dissolution rate of ergotamine tartrate four times, whereas the inclusion of 0.15 *M* citric acid depressed the rate by a factor of five. The inclusion of 0.15 *M* citric acid in the acetate buffer that contained 0.025 *M* caffeine reduced the rate by a factor of eight.

The rate-enhancing effect of caffeine on ergotamine dissolution at pH 5.0 is consistent with the formation of a soluble molecular complex at this pH as well as at pH 1.0. These studies provided evidence of complex formation at pH 1.0, and Zoglio *et al.* (5) demonstrated complex formation at pH 6.65.

The results in Fig. 2 show that citric acid depressed ergotamine solubility in a pH 5 sodium acetate buffer by a factor of 2.4. Hence, the depressing effect of citric acid on the dissolution rate of ergotamine in a pH 5 buffer is consistent with predictions based on the Noyes–Whitney model.

CONCLUSIONS

1. Chloride ions, a common constituent of the contents of the stomach and duodenum, significantly reduce the concentration of ergotamine in solution by forming ergotamine chloride, a substance with a solubility product of $\sim 5 \times 10^{-6}\ M^2$.

2. The dissolution rate of ergotamine tartrate in water is not depressed appreciably by chloride ions because the precipitation rate of ergotamine chloride apparently is slow compared to the dissolution rate.

3. Protonation of the diionized tartrate anion of ergotamine tartrate by the addition of small amounts of citric acid or tartaric acid increases the solubility of ergotamine. Large amounts of these acids result in the precipitation of 1:1 salts of ergotamine and the acid monoanions. Sodium citrate depresses the solubility of ergotamine.

4. The Noyes–Whitney model for dissolution accounts for the rate-enhancing effect of caffeine and citric acid on ergotamine dissolution at pH 1.0 and the rate-depressing effect of citric acid at pH 5.0.

REFERENCES

(1) J. M. Bradfield, *Curr. Ther.*, **17**, 55 (1976).

(2) "The Merck Index," 9th ed., M. Windholz, Ed., Merck & Co., Rahway, N.J., 1976.

(3) "The Pharmacological Basis of Therapeutics," 5th ed., L. S. Goodman and A. Gilman, Eds., Macmillan, New York, N.Y., 1956, pp. 867–880.

(4) "Martindale: The Extra Pharmacopoeia," 27th ed., N. W. Blacow, Ed., Pharmaceutical Press, London, England, 1977.

(5) M. A. Zoglio, H. V. Maulding, and J. J. Windheuser, *J. Pharm. Sci.*, **58**, 222 (1969).

(6) H. V. Maulding and M. A. Zoglio, *ibid.*, **59**, 700 (1970).

(7) G. J. Martin, "Ion Exchange and Absorption Agents in Medicine," Little, Brown, Boston, Mass., 1955, pp. 10, 11.

(8) T. Higuchi and K. A. Connors, in "Advances in Analytical Chemistry and Instrumentation," vol. 4, C. N. Reilly, Ed., Interscience, New York, N.Y., 1965, pp. 117–212.

(9) A. A. Noyes and W. R. Whitney, *J. Am. Chem. Soc.*, **19**, 930 (1897).

ACKNOWLEDGMENTS

Supported by a grant from the Nicholas Drug Research Consortium.

Wall-Coated Open Tubular Column Coupled with Nitrogen-Selective Detector for Routine GLC Determination of Diazepam, Meprobamate, Phenylbutazone, and Thioridazine in Serum

D. DEBRUYNE ˣ, M. A. MOULIN, R. CAMSONNE, and M.-C. BIGOT

Received March 28, 1979, from the *Laboratory of Pharmacology, Medical School, Laboratory of Functional Explorations B, University Hospital Center of Caen, 14000 Caen, France.* Accepted for publication February 26, 1980.

Abstract □ The selectivity and sensitivity provided by a wall-coated open tubular column coupled with a nitrogen-selective detector allowed rapid, accurate determination of diazepam, meprobamate, phenylbutazone, and thioridazine in serum in the same chromatographic system using 100–200 μl of sample.

Keyphrases □ Diazepam—GLC determination in serum, wall-coated open tubular column coupled with nitrogen-selective detector □ Meprobamate—GLC determination in serum, wall-coated open tubular column coupled with nitrogen-selective detector □ Phenylbutazone—GLC determination in serum, wall-coated open tubular column coupled with nitrogen-selective detector □ Thioridazine—GLC determination in serum, wall-coated open tubular column coupled with nitrogen-selective detector □ GLC—analysis, diazepam, meprobamate, phenylbutazone, and thioridazine in serum, wall-coated open tubular column coupled with nitrogen-selective detector

Various columns and detectors have been used in the GLC determination of diazepam (I) (1–7), meprobamate (II) (8, 9), phenylbutazone (III) (10–14), and thioridazine (IV) (15–17) in serum. Packed columns were used in all of the methods and were coupled to a ^{63}Ni-electron-capture detector (1–5, 7, 14), a flame-ionization detector (6, 8–13,

© 1980, American Pharmaceutical Association

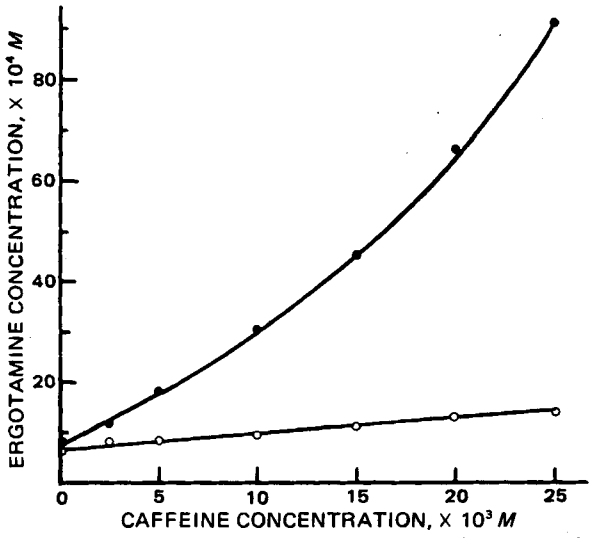

Figure 4—*Solubilizing effect of caffeine on ergotamine tartrate in 0.01 M HCl (●) and 0.50 M sulfuric acid (○).*

fuse from the solid–liquid interface into the bulk of the solution.

The inclusion of 0.025 *M* caffeine in a pH 5 acetate buffer increased the dissolution rate of ergotamine tartrate four times, whereas the inclusion of 0.15 *M* citric acid depressed the rate by a factor of five. The inclusion of 0.15 *M* citric acid in the acetate buffer that contained 0.025 *M* caffeine reduced the rate by a factor of eight.

The rate-enhancing effect of caffeine on ergotamine dissolution at pH 5.0 is consistent with the formation of a soluble molecular complex at this pH as well as at pH 1.0. These studies provided evidence of complex formation at pH 1.0, and Zoglio *et al.* (5) demonstrated complex formation at pH 6.65.

The results in Fig. 2 show that citric acid depressed ergotamine solubility in a pH 5 sodium acetate buffer by a factor of 2.4. Hence, the depressing effect of citric acid on the dissolution rate of ergotamine in a pH 5 buffer is consistent with predictions based on the Noyes–Whitney model.

CONCLUSIONS

1. Chloride ions, a common constituent of the contents of the stomach and duodenum, significantly reduce the concentration of ergotamine in solution by forming ergotamine chloride, a substance with a solubility product of $\sim 5 \times 10^{-6}\ M^2$.

2. The dissolution rate of ergotamine tartrate in water is not depressed appreciably by chloride ions because the precipitation rate of ergotamine chloride apparently is slow compared to the dissolution rate.

3. Protonation of the diionized tartrate anion of ergotamine tartrate by the addition of small amounts of citric acid or tartaric acid increases the solubility of ergotamine. Large amounts of these acids result in the precipitation of 1:1 salts of ergotamine and the acid monoanions. Sodium citrate depresses the solubility of ergotamine.

4. The Noyes–Whitney model for dissolution accounts for the rate-enhancing effect of caffeine and citric acid on ergotamine dissolution at pH 1.0 and the rate-depressing effect of citric acid at pH 5.0.

REFERENCES

(1) J. M. Bradfield, *Curr. Ther.*, **17**, 55 (1976).

(2) "The Merck Index," 9th ed., M. Windholz, Ed., Merck & Co., Rahway, N.J., 1976.

(3) "The Pharmacological Basis of Therapeutics," 5th ed., L. S. Goodman and A. Gilman, Eds., Macmillan, New York, N.Y., 1956, pp. 867–880.

(4) "Martindale: The Extra Pharmacopoeia," 27th ed., N. W. Blacow, Ed., Pharmaceutical Press, London, England, 1977.

(5) M. A. Zoglio, H. V. Maulding, and J. J. Windheuser, *J. Pharm. Sci.*, **58**, 222 (1969).

(6) H. V. Maulding and M. A. Zoglio, *ibid.*, **59**, 700 (1970).

(7) G. J. Martin, "Ion Exchange and Absorption Agents in Medicine," Little, Brown, Boston, Mass., 1955, pp. 10, 11.

(8) T. Higuchi and K. A. Connors, in "Advances in Analytical Chemistry and Instrumentation," vol. 4, C. N. Reilly, Ed., Interscience, New York, N.Y., 1965, pp. 117–212.

(9) A. A. Noyes and W. R. Whitney, *J. Am. Chem. Soc.*, **19**, 930 (1897).

ACKNOWLEDGMENTS

Supported by a grant from the Nicholas Drug Research Consortium.

Wall-Coated Open Tubular Column Coupled with Nitrogen-Selective Detector for Routine GLC Determination of Diazepam, Meprobamate, Phenylbutazone, and Thioridazine in Serum

D. DEBRUYNE ˣ, M. A. MOULIN, R. CAMSONNE, and M.-C. BIGOT

Received March 28, 1979, from the *Laboratory of Pharmacology, Medical School, Laboratory of Functional Explorations B, University Hospital Center of Caen, 14000 Caen, France.* Accepted for publication February 26, 1980.

Abstract □ The selectivity and sensitivity provided by a wall-coated open tubular column coupled with a nitrogen-selective detector allowed rapid, accurate determination of diazepam, meprobamate, phenylbutazone, and thioridazine in serum in the same chromatographic system using 100–200 μl of sample.

Keyphrases □ Diazepam—GLC determination in serum, wall-coated open tubular column coupled with nitrogen-selective detector □ Meprobamate—GLC determination in serum, wall-coated open tubular column coupled with nitrogen-selective detector □ Phenylbutazone—GLC determination in serum, wall-coated open tubular column coupled with nitrogen-selective detector □ Thioridazine—GLC determination in serum, wall-coated open tubular column coupled with nitrogen-selective detector □ GLC—analysis, diazepam, meprobamate, phenylbutazone, and thioridazine in serum, wall-coated open tubular column coupled with nitrogen-selective detector

Various columns and detectors have been used in the GLC determination of diazepam (I) (1–7), meprobamate (II) (8, 9), phenylbutazone (III) (10–14), and thioridazine (IV) (15–17) in serum. Packed columns were used in all of the methods and were coupled to a ^{63}Ni-electron-capture detector (1–5, 7, 14), a flame-ionization detector (6, 8–13,

© 1980, American Pharmaceutical Association

Table I—Extraction Conditions

Serum Sample Extracted, μl	Drug (Solvent)	Concentrations Tested, μg/ml	Amount of Internal Standard (Solvent)	Volume of Acid or Base	Volume of Extraction Solvent	Agitation Time, min	Recovery of Drug, %	Recovery of Internal Standard, %
100	Diazepam (methanol)	0.1, 0.2, 0.5, 1, 1.5, 2	0.125 μg of flunitrazepam (chloroform)	30 μl of 1 *N* NaOH	6.0 ml of ether–chloroform (70:30 v/v)	6	89	69
100	Meprobamate (methanol)	5, 10, 15, 20, 25, 30	0.250 μg of thiopental (water)	200 μl of 0.05 *N* HCl	0.3 ml of chloroform	5	67	62
100	Phenylbutazone (water)	25, 50, 75, 100, 125, 150	5.0 μg of diazepam (methanol)	500 μl of pH 2 phosphate buffer	0.5 ml of chloroform	6	70	77
200	Thioridazine (methanol)	1, 1.5, 2, 2.5, 3, 3.5	1.0 μg of haloperidol (chloroform)	100 μl of 1 *N* NaOH	5.0 ml of hexane–chloroform (70:30 v/v)	12	88	60

Table II—Chromatographic Conditions and Results

Drug	Volume of Sample Injected, μl	Sensitivity and Attenuation	Column Temperature	Linear Carrier Gas Velocity[a], cm/sec	Drug Retention Time	Internal Standard Retention Time	Minimum Detectable Quantity, ng
Diazepam	3–5	1 × 8	235°	46	2 min, 6 sec	3 min, 6 sec	0.5
Meprobamate	10	1 × 2	170°	29	3 min, 28 sec	4 min, 26 sec	5
Phenylbutazone	1–2	1 × 16	245°	36	2 min	2 min, 18 sec	2
Thioridazine	6–8	1 × 2	260°	50	4 min, 36 sec	3 min, 12 sec	6

[a] Nitrogen U.

15, 17), or a ^{90}Sr-ionization detector (16). The columns were packed with Carbowax 20M (1), 3% OV-17 (2–4), 3% OV-225 (5), and 3% SE-30 (6) for I; 3% SE-30 (8) and 3.8% OV-17 (9) for II; 3% OV-210 (10), 3% Apiezon L (11), 3% OV-7 (12), 10% DC 200 (13), and 5% OV-17 (14) for III; and 3% XE-60 (15) and 3% OV-17 (16, 17) for IV.

To overcome the disadvantages of using many materials, one polyvalent chromatographic system, a high-performance wall-coated open tubular column coupled with a nitrogen-specific detector, was used for the determination in serum of these four drugs of various molecular weights and polarities.

The great efficiency (18, 19) and short elution time of the wall-coated open tubular column and the sensitivity and selectivity (20) of the nitrogen detector allow rapid, accurate determination of drugs at therapeutic levels with small samples (100–200 μl) using a simple extraction and no derivatization steps.

EXPERIMENTAL

Standard Solutions—Meprobamate[1] (50 μg/ml), thiopental[2] (5 μg/ml), phenylbutazone[3] (100 μg/ml), diazepam[4] (1, 5, and 100 μg/ml), thioridazine[5] (10 μg/ml), haloperidol[6] (10 μg/ml), and flunitrazepam[4] (5 μg/ml) solutions were prepared by dissolving the pure products in appropriate solvents as indicated in Table I. The solutions were stored at 4°.

Solvents—Chloroform, *n*-hexane, ether[7], and methanol[8] were of high grade purity.

Instrumentation—The gas–liquid chromatograph[9] was equipped with a nitrogen-selective detector[10] and a solid injector[10] and was connected to a recorder[11] with a scale range of 1 mv.

[1] Clin-Comar-Byla, Paris, France.
[2] Abbott, St-Remy sur Avre, France.
[3] Geigy, Rueil-Malmaison, France.
[4] Roche, Neuilly, France.
[5] Sandoz, Rueil-Malmaison, France.
[6] Lebrun, Paris, France.
[7] Merck, Darmstadt, West Germany.
[8] Prolabo, Paris, France.
[9] Model 3000 FC 1 ERPT, Girdel, Suresnes, France.
[10] Girdel, Suresnes, France.
[11] Servotrace PU, Sefram, Paris, France.

Table III—Assay Accuracy

	Serum Concentration, μg/ml		
	Theoretical	Experimental	Percent Difference
Diazepam	0.1	0.095	5
	0.2	0.185	7.5
	0.5	0.515	3
	1	0.985	1.5
	1.5	1.510	0.7
	2	1.995	0.25
Meprobamate	2.5	2.3	8
	5	4.8	4
	10	9.7	3
	15	15.3	2
	20	20.1	0.5
	25	25.5	2
Phenylbutazone	25	24.5	2
	50	50	0
	75	74.5	0.7
	100	99.5	0.5
	125	126.5	1.2
	150	152	1.3
Thioridazine	1	0.98	2
	1.5	1.5	0
	2	1.95	2.5
	2.5	2.37	5.2
	3	2.98	0.7
	3.5	3.54	1.7

The glass capillary column (11.5 m × 0.39 mm) with a phase of SE-30 0.4 μm thick was pretreated and tested by the manufacturer[12]. According to the spot test, it presents an effective number of theoretical plates (n = 16,600) for heptabarbital at 200° for a velocity of 18 cm/sec of the carrier gas (nitrogen U) and a capacity factor of three.

The chromatographic conditions were: injector temperature, 290°; detector temperature, 290°; make-up gas (nitrogen U) flow rate, 40 ml/min; hydrogen flow rate, 24 ml/min; air flow rate, 460 ml/min; and chart speed, 2.5 or 5 mm/min.

The other specific conditions for each compound are summarized in Table II.

Procedure—To 100 or 200 μl of human serum[13] in polytef-lined screw-capped glass test tubes (enveloped in a sheet of aluminum foil to ensure darkness for the thioridazine) were added the drug, the internal standard, acid or base, and the extracting solvent (Table I). The mixture was shaken and centrifuged for 5 min at 15° and 3500 rpm.

[12] Catalog No. 2101-201, LKB, Bromma, Sweden.
[13] Biotrol OOA, Biotrol, Paris, France.

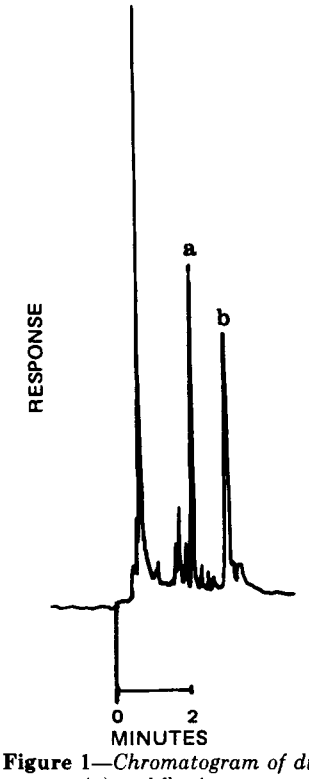

Figure 1—*Chromatogram of diazepam (a) and flunitrazepam as the internal standard (b).*

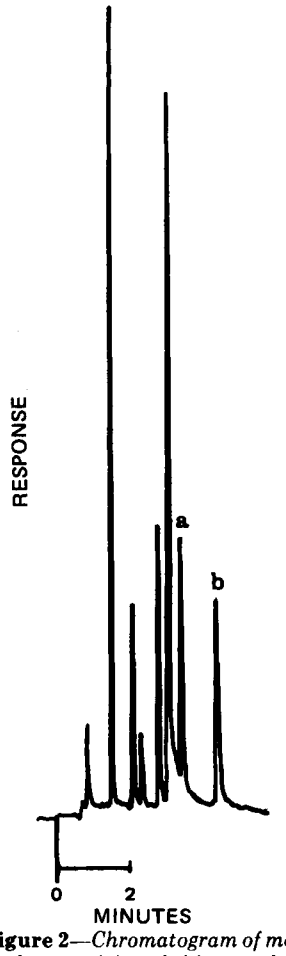

Figure 2—*Chromatogram of meprobamate (a) and thiopental as the internal standard (b).*

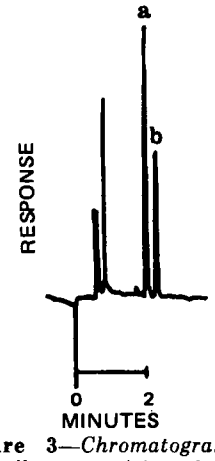

Figure 3—*Chromatogram of phenylbutazone (a) and diazepam as the internal standard (b).*

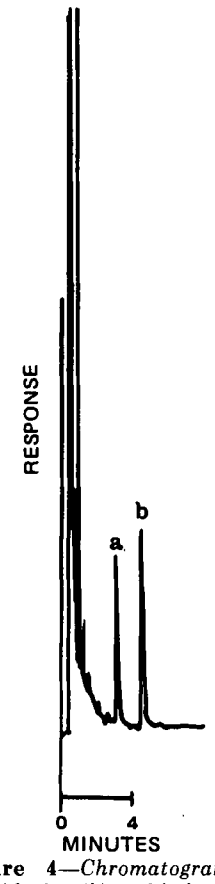

Figure 4—*Chromatogram of thioridazine (b) and haloperidol as the internal standard (a).*

An aliquot (2–10 μl) of the organic phase was injected directly into the chromatograph for II and III. The entire organic phase was evaporated to dryness for I (50° under an air stream) and IV (20° under a nitrogen stream), and the residue was dissolved in 50 μl of chloroform before injection.

RESULTS AND DISCUSSION

Figures 1–4 illustrate the chromatographic responses of the drugs and standards. The chromatographic conditions, retention time, and minimum detectable concentration of each compound are summarized in Table II.

The range of each drug was chosen according to the therapeutic concentrations: 0.7–1.5 (21) or 0.5–2.5 μg/ml (22) for I, 3.4–26.6 (21) or 10 μg/ml (22) for II, 60–150 (21) or 100 μg/ml (22) for III, and 1.1–6.2 (21) or 1–1.5 μg/ml (22) for IV.

The slopes of the regression lines were 1.312, 0.058, 0.015, and 0.527 for I, II, III, and IV, respectively. The correlation coefficient was 0.999 in all cases. The standard deviations ranged from 5 to 3% for 0.5–2 μg of I/ml, from 4 to 3% for 5–30 μg of II/ml, from 4 to 2.5% for 25–150 μg of III/ml, and from 6 to 3% for 1–35 μg of IV/ml over 3 months. Accuracy (Table III) was tested by analyzing spiked samples. Accuracy was improved by avoiding the evaporation step for drugs having sufficiently high therapeutic levels (II and III) and by evaporating the extraction mixture (IV) under nitrogen and in darkness.

For 100-μl serum samples, the minimum detectable concentrations were 0.05, 2, and 5 μg/ml for I, II, and III, respectively. For a 200-μl serum sample of IV, it was 0.3 μg/ml. The twofold determination of the patient serum levels gave the accuracy of the method (Tables III–V). No endogenous interfering substances were found. Exogenous substances such as phenobarbital and lidocaine did not interfere with II; nor did vincamine, quinidine, or clonazepam interfere with I, III, and IV.

The great sensitivity of the wall-coated open tubular column coupled with a nitrogen-specific detector allowed small samples to be used

Table IV—Serum Concentrations of Diazepam in Five Epileptic Patients

Age of Patient, years	Daily Diazepam Dose, mg	Comedication (Daily Dose)	Serum Concentration, μg/ml
8	10	Valproate sodium, 400 mg	0.30 ± 0.02
8	10	Valproate sodium, 800 mg	0.17 ± 0.02
13	8	Phenobarbital, 50 mg; valproate sodium, 600 mg	0.70 ± 0.01
50	15	Phenobarbital, 300 mg	0.42 ± 0.02
56	10	Phenobarbital, 100 mg	0.23 ± 0.01

Table V—Serum Concentrations of Meprobamate in Four Intoxication Cases

Age of Patient, years	Serum Concentration, μg/ml
16	87 ± 2
17	190 ± 5
18	70 ± 1
33	138 ± 2

Table VI—Serum Concentrations of Phenylbutazone in a Nursing Mother after Administration of a 250-mg Suppository Twice Daily for 10 Days

Days of Treatment	Serum Concentration, μg/ml
3	52.0 ± 2.0
6	79.0 ± 2.5
11	66.0 ± 2.0

(100–200 μl), instead of the previous requirements of 1–3 ml for II and III (8, 10–13) and 4–5 ml for IV (15, 17), without increasing the lowest detectable serum concentration. The high resolution of the capillary column (23) reduced the extraction stage to a single step instead of the three steps often suggested to eliminate the interfering substances (12, 13, 15, 17). Furthermore, derivatization steps such as silylation (10) and methylation (12) were unnecessary. The rapid elution time (24) shortened the retention times. These conditions led to shorter extraction and chromatographic stages. Nevertheless, the accuracy and sensitivity were usually improvements over previous assays (3–5, 9, 11, 12, 15, 17).

The determination in serum of four drugs useful in toxicology (25–29) or therapeutic monitoring (30–32) demonstrated the versatility and potential of this chromatographic system and its possible routine use in view of the growing importance of serum level determinations of an increasing number of diverse drugs in clinical practice.

The method was demonstrated by the determination of serum concentrations of diazepam in five epileptic patients (Table IV), of meprobamate in four cases of voluntary overdose (Table V), and of phenylbutazone in a nursing mother given a 250-mg suppository twice daily for 10 days (Table VI).

REFERENCES

(1) J. P. Cano, L. Vignoli, and A. Viala, *Ann. Pharm. Fr.*, **25**, 697 (1967).

(2) J. A. F. De Silva and C. V. Puglisi, *Anal. Chem.*, **42**, 1725 (1970).

(3) H. P. Gelbke, H. J. Schlicht, and G. Schmidt, *Arch. Toxicol.*, **38**, 295 (1977).

(4) M. Linnoila and F. Dorrity, Jr., *Acta Pharmacol. Toxicol.*, **41**, 458 (1977).

(5) E. Rey, J. M. Turquais, and G. Olive, *Clin. Chem.*, **23**, 1338 (1977).

(6) L. B. Foster and C. S. Frings, *ibid.*, **16**, 177 (1970).

(7) F. Marcussi, R. Fonelli, and E. Mussini, *J. Chromatogr.*, **37**, 318 (1968).

(8) L. Martis and R. H. Levy, *J. Pharm. Sci.*, **63**, 834 (1974).

(9) M. P. Rabinowitz, P. Reisberg, and J. I. Bodin, *ibid.*, **61**, 1974 (1972).

(10) R. B. Bruce, W. R. Maynard, and L. K. Dunning, *ibid.*, **63**, 446 (1974).

(11) I. J. McGilveray, K. K. Midha, R. Brien, and L. Wilson, *J. Chromatogr.*, **89**, 17 (1974).

(12) K. K. Midha, I. J. McGilveray, and C. Charette, *J. Pharm. Sci.*, **63**, 1234 (1974).

(13) J. A. Bogan, *J. Pharm. Pharmacol.*, **29**, 125 (1977).

(14) A. Sioufi, F. Caudal, and F. Marfil, *J. Pharm. Sci.*, **67**, 243 (1978).

(15) F. A. J. Vanderheeren, D. J. C. J. Theunis, and M.-T. Rosseel, *J. Chromatogr.*, **120**, 123 (1976).

(16) S. H. Curry and G. P. Mould, *J. Pharm. Pharmacol.*, **21**, 674 (1969).

(17) E. C. Dinovo, L. A. Gottschalk, B. R. Nandi, and P. G. Geddes, *J. Pharm. Sci.*, **65**, 667 (1976).

(18) J. de Graeve and J. Vanroy, *J. Chromatogr.*, **129**, 171 (1976).

(19) F. Berthou, D. Picart, L. Bardou, and H. H. Floch, *ibid.*, **118**, 135 (1976).

(20) J. H. Goudie and D. Burnett, *Clin. Chim. Acta*, **43**, 423 (1973).

(21) R. C. Baselt and R. H. Cravey, *J. Anal. Toxicol.*, **1**, 81 (1977).

(22) C. L. Winek, *Clin. Chem.*, **22**, 832 (1976).

(23) D. Debruyne, H. Kinsun, M. A. Moulin, and M. C. Bigot, *J. Pharm. Sci.*, **68**, 511 (1979).

(24) J. Macloue, M. Rigaud, J. Durand, and X. Chebrou, *Prostaglandins*, **6**, 999 (1976).

(25) R. K. Maddock and H. A. Bloomer, *J. Am. Med. Assoc.*, **201**, 999 (1967).

(26) J. Kanto, R. Sellman, M. Haataja, and P. Hurme, *Int. J. Clin. Pharmacol. Biopharm.*, **16**, 258 (1978).

(27) J. E. Cree, J. Meyer, and D. M. Hailey, *Br. Med. J.*, **4**, 251 (1973).

(28) A. Gaucher, R.-J. Royer, P. Netter, M. J. Royer-Morrot, G. Faure, and J. Pourel, *Sem. Hôp.*, **52**, 1723 (1976).

(29) L. A. Gottschalk, E. Dinovo, R. Biener, and B. R. Nandi, *J. Pharm. Sci.*, **67**, 155 (1978).

(30) M. M. Reidenberg, M. Levy, H. Warner, C. B. Coutinho, M. A. Schwartz, G. Yu, and J. Cheripko, *Clin. Pharmacol. Ther.*, **23**, 371 (1978).

(31) R. J. Royer, M. Meyruey, A. Maillard, C. Monnod, M. J. Morrot, and P. Netter, *Ann. Med. Nancy*, **4**, 1317 (1975).

(32) R. Axelsson and E. Martensson, *Curr. Ther. Res.*, **19**, 242 (1976).

ACKNOWLEDGMENTS

Supported by a grant for 1978–1979 from the Langlois Foundation. The authors thank H. Fusibet for technical collaboration.

Immobilization of Proteins in Microspheres of Biodegradable Polyacryldextran

PETER EDMAN, BO EKMAN, and INGVAR SJÖHOLM ˣ

Received November 13, 1979, from the *Department of Pharmaceutical Biochemistry, Biomedical Center, University of Uppsala, S-751 23 Uppsala, Sweden.* Accepted for publication February 28, 1980.

Abstract □ Macromolecules were immobilized by an emulsion polymerization technique in biodegradable microspheres of polyacryldextran, prepared by copolymerizing bisacrylamide with acryldextran. Such particles can be characterized by D–T–C expressions, where D denotes the concentration of derivatized dextran, T is the total concentration of acrylic compounds in the monomeric solution, and C denotes the fraction of cross-linker. In microparticles based on dextran T40 with a D–T–C of 11–1–75, the yield of immobilized protein was greater than in polyacrylamide particles. The properties of the immobilized proteins, *e.g.*, K_m and V_{max}, were retained. The heat stability of the proteins was improved so that 5–10% of carbonic anhydrase still was active after 30 min at 100°. However, the leakage of proteins from the polyacryldextran particles was greater than from polyacrylamide particles.

Keyphrases □ Microspheres—biodegradable polyacryldextran particles, immobilization of proteins □ Polyacryldextran—microspheres, immobilization of proteins □ Proteins—immobilization in polyacryldextran microspheres

The therapeutic use of proteins *in vivo* usually is hampered by rapid protein inactivation or by immunological reactions when the proteins are immunogenic. For instance, asparaginase is not active for long periods in the treatment of acute leukemias (1). However, the noncovalent immobilization of the proteins in microspheres of

0022-3549/80/0700-0838$01.00/0

© 1980, American Pharmaceutical Association

(100–200 μl), instead of the previous requirements of 1–3 ml for II and III (8, 10–13) and 4–5 ml for IV (15, 17), without increasing the lowest detectable serum concentration. The high resolution of the capillary column (23) reduced the extraction stage to a single step instead of the three steps often suggested to eliminate the interfering substances (12, 13, 15, 17). Furthermore, derivatization steps such as silylation (10) and methylation (12) were unnecessary. The rapid elution time (24) shortened the retention times. These conditions led to shorter extraction and chromatographic stages. Nevertheless, the accuracy and sensitivity were usually improvements over previous assays (3–5, 9, 11, 12, 15, 17).

The determination in serum of four drugs useful in toxicology (25–29) or therapeutic monitoring (30–32) demonstrated the versatility and potential of this chromatographic system and its possible routine use in view of the growing importance of serum level determinations of an increasing number of diverse drugs in clinical practice.

The method was demonstrated by the determination of serum concentrations of diazepam in five epileptic patients (Table IV), of meprobamate in four cases of voluntary overdose (Table V), and of phenylbutazone in a nursing mother given a 250-mg suppository twice daily for 10 days (Table VI).

REFERENCES

(1) J. P. Cano, L. Vignoli, and A. Viala, *Ann. Pharm. Fr.*, **25**, 697 (1967).

(2) J. A. F. De Silva and C. V. Puglisi, *Anal. Chem.*, **42**, 1725 (1970).

(3) H. P. Gelbke, H. J. Schlicht, and G. Schmidt, *Arch. Toxicol.*, **38**, 295 (1977).

(4) M. Linnoila and F. Dorrity, Jr., *Acta Pharmacol. Toxicol.*, **41**, 458 (1977).

(5) E. Rey, J. M. Turquais, and G. Olive, *Clin. Chem.*, **23**, 1338 (1977).

(6) L. B. Foster and C. S. Frings, *ibid.*, **16**, 177 (1970).

(7) F. Marcussi, R. Fonelli, and E. Mussini, *J. Chromatogr.*, **37**, 318 (1968).

(8) L. Martis and R. H. Levy, *J. Pharm. Sci.*, **63**, 834 (1974).

(9) M. P. Rabinowitz, P. Reisberg, and J. I. Bodin, *ibid.*, **61**, 1974 (1972).

(10) R. B. Bruce, W. R. Maynard, and L. K. Dunning, *ibid.*, **63**, 446 (1974).

(11) I. J. McGilveray, K. K. Midha, R. Brien, and L. Wilson, *J. Chromatogr.*, **89**, 17 (1974).

(12) K. K. Midha, I. J. McGilveray, and C. Charette, *J. Pharm. Sci.*, **63**, 1234 (1974).

(13) J. A. Bogan, *J. Pharm. Pharmacol.*, **29**, 125 (1977).

(14) A. Sioufi, F. Caudal, and F. Marfil, *J. Pharm. Sci.*, **67**, 243 (1978).

(15) F. A. J. Vanderheeren, D. J. C. J. Theunis, and M.-T. Rosseel, *J. Chromatogr.*, **120**, 123 (1976).

(16) S. H. Curry and G. P. Mould, *J. Pharm. Pharmacol.*, **21**, 674 (1969).

(17) E. C. Dinovo, L. A. Gottschalk, B. R. Nandi, and P. G. Geddes, *J. Pharm. Sci.*, **65**, 667 (1976).

(18) J. de Graeve and J. Vanroy, *J. Chromatogr.*, **129**, 171 (1976).

(19) F. Berthou, D. Picart, L. Bardou, and H. H. Floch, *ibid.*, **118**, 135 (1976).

(20) J. H. Goudie and D. Burnett, *Clin. Chim. Acta*, **43**, 423 (1973).

(21) R. C. Baselt and R. H. Cravey, *J. Anal. Toxicol.*, **1**, 81 (1977).

(22) C. L. Winek, *Clin. Chem.*, **22**, 832 (1976).

(23) D. Debruyne, H. Kinsun, M. A. Moulin, and M. C. Bigot, *J. Pharm. Sci.*, **68**, 511 (1979).

(24) J. Macloue, M. Rigaud, J. Durand, and X. Chebrou, *Prostaglandins*, **6**, 999 (1976).

(25) R. K. Maddock and H. A. Bloomer, *J. Am. Med. Assoc.*, **201**, 999 (1967).

(26) J. Kanto, R. Sellman, M. Haataja, and P. Hurme, *Int. J. Clin. Pharmacol. Biopharm.*, **16**, 258 (1978).

(27) J. E. Cree, J. Meyer, and D. M. Hailey, *Br. Med. J.*, **4**, 251 (1973).

(28) A. Gaucher, R.-J. Royer, P. Netter, M. J. Royer-Morrot, G. Faure, and J. Pourel, *Sem. Hôp.*, **52**, 1723 (1976).

(29) L. A. Gottschalk, E. Dinovo, R. Biener, and B. R. Nandi, *J. Pharm. Sci.*, **67**, 155 (1978).

(30) M. M. Reidenberg, M. Levy, H. Warner, C. B. Coutinho, M. A. Schwartz, G. Yu, and J. Cheripko, *Clin. Pharmacol. Ther.*, **23**, 371 (1978).

(31) R. J. Royer, M. Meyruey, A. Maillard, C. Monnod, M. J. Morrot, and P. Netter, *Ann. Med. Nancy*, **4**, 1317 (1975).

(32) R. Axelsson and E. Martensson, *Curr. Ther. Res.*, **19**, 242 (1976).

ACKNOWLEDGMENTS

Supported by a grant for 1978–1979 from the Langlois Foundation. The authors thank H. Fusibet for technical collaboration.

Immobilization of Proteins in Microspheres of Biodegradable Polyacryldextran

PETER EDMAN, BO EKMAN, and INGVAR SJÖHOLM ˣ

Received November 13, 1979, from the *Department of Pharmaceutical Biochemistry, Biomedical Center, University of Uppsala, S-751 23 Uppsala, Sweden.* Accepted for publication February 28, 1980.

Abstract □ Macromolecules were immobilized by an emulsion polymerization technique in biodegradable microspheres of polyacryldextran, prepared by copolymerizing bisacrylamide with acryldextran. Such particles can be characterized by D–T–C expressions, where D denotes the concentration of derivatized dextran, T is the total concentration of acrylic compounds in the monomeric solution, and C denotes the fraction of cross-linker. In microparticles based on dextran T40 with a D–T–C of 11–1–75, the yield of immobilized protein was greater than in polyacrylamide particles. The properties of the immobilized proteins, *e.g.*, K_m and V_{max}, were retained. The heat stability of the proteins was improved so that 5–10% of carbonic anhydrase still was active after 30 min at 100°. However, the leakage of proteins from the polyacryldextran particles was greater than from polyacrylamide particles.

Keyphrases □ Microspheres—biodegradable polyacryldextran particles, immobilization of proteins □ Polyacryldextran—microspheres, immobilization of proteins □ Proteins—immobilization in polyacryldextran microspheres

The therapeutic use of proteins *in vivo* usually is hampered by rapid protein inactivation or by immunological reactions when the proteins are immunogenic. For instance, asparaginase is not active for long periods in the treatment of acute leukemias (1). However, the noncovalent immobilization of the proteins in microspheres of

0022-3549/80/0700-0838$01.00/0

© 1980, American Pharmaceutical Association

highly cross-linked polyacrylamide significantly increases stability against denaturation by heat or proteolytic enzymes (2, 3).

BACKGROUND

The proteins are immobilized by two mechanisms: they are partially bound in the polymeric threads and partially entrapped in the polymeric network if they are sufficiently large (2). The leakage is negligible and the biological properties essentially are retained when the particles are small and macroporous (3–5). However, the yield of protein immobilized in the microparticles generally is low (5–10%). After being cleared from the circulation by the reticuloendothelial system, the particles are metabolized slowly, mainly in the liver and spleen (6). The half-life of microspheres injected intravenously or intraperitoneally in the mouse is 10–14 weeks in the liver (6), which in most cases is an inconveniently long half-life.

Preliminary experiments indicated that the yield of proteins in the microspheres can be increased by adding hydrophilic polymers (*e.g.*, dextrans, starch, and polyvinylpyrrolidones) to the monomeric solution during polymerization. In addition if dextran comprises a part of the hydrocarbon chain in the polyacrylamide and forms an intimate part of the microsphere, the polymer should be metabolized more easily. This result can be achieved if the polymeric microspheres are formed from a dextran substituted with acrylic groups and suitable cross-linking agents, *e.g.*, bisacrylamide.

The present paper describes the synthesis of an acryl ether of dextran, the preparation and characteristics of polyacryldextran microparticles, and the properties of the immobilized proteins.

EXPERIMENTAL

Materials—Human serum albumin[1], immunoglobulin G[1], bovine carbonic anhydrase[2] (EC 4.2.1.1), and catalase[3] (EC 1.11.1.6) were used without further purification. Acrylamide[4], *N,N'*-methylenebisacrylamide[4] (I), *p*-nitrophenyl acetate[2], *N,N,N',N'*-tetramethylethylenediamine[2], tris(hydroxymethyl)aminomethane[2], acrylic acid glycidyl ester[3], and other chemicals were analytical grade.

Synthesis of Acrylic Dextrans—Acrylic derivatives of dextran[5] were prepared by reacting acrylic acid glycidyl ester with aqueous alkaline solutions of dextrans of different molecular weights (10,000–2,000,000).

In a typical experiment, dextran (30 g) was dissolved in 250 ml of pH 11, 0.01 *M* carbonate buffer. Acrylic acid glycidyl ester (15 ml) was added, and the two-phase system was stirred magnetically for 5 days at room temperature. The dextran was precipitated with 1000 ml of ethanol and washed with ~300 ml of ethanol. The precipitated dextran was dissolved in 100 ml of distilled water, precipitated again, and washed with ethanol. The procedure was repeated at least four times to free the product from excess glycidyl ester.

Determination of Acrylic Groups—The content of acrylic groups in the dextran derivatives was measured by a method based on the halogenation of the double bonds (7). Aqueous bromine solution was added to the unsaturated acrylic groups, and the subsequent color reduction at 480 nm was measured. The number of acrylic groups was determined from a standard curve obtained with acrylamide as a standard.

Preparation of Microparticles—Microparticles with immobilized proteins were prepared according to a reported method (2, 3). The protein was dissolved in the acrylic monomer solution. In a typical example, the aqueous phase was composed of 3.75 ml of a 2% aqueous solution of I and 6.25 ml of an acryldextran solution (containing 177 mg of derivatized dextran T40/ml with 4.28 mg of acrylic groups/ml).

The water solution was homogenized together with 500 ml of chloroform–toluene (1:4) to produce a water-in-oil emulsion. By addition of catalysts, the water-phase droplets were polymerized to microparticles, which were freed from the organic phase by repeated washings with water and buffer. The microparticles were isolated easily by centrifugation.

^{14}C-Labeled particles were prepared as described by Sjöholm and Edman (6) with [^{14}C]I.

The polyacryldextran gels can be characterized by D–T–C expressions by analogy with the T–C nomenclature suggested by Hjertén (8) for homogeneous polyacrylamide. The first value (D) denotes the concentration of derivatized macromolecules (in this case, dextran) participating in particle formation (grams per 100 ml of solvent). The second value (T) denotes the total concentration of acrylic monomers (grams per 100 ml of solvent). The third value (C) denotes the relative amount of the cross-linker, I, expressed as the percentage (w/w) of the total amount of acrylic monomers. The example given for microparticle preparation yielded particles having a D–T–C of 11–1–75.

Protein Determination—The protein content of the microparticles was determined by amino acid analysis with an automatic amino acid analyzer after hydrolysis in 6 *M* HCl at 105° for 20 hr. The amount of proteins leaking out from the microparticles was determined according to the method of Lowry *et al.* (9). In each case, the protein studied was used as the standard.

Determination of Microparticle Density—The density of the microparticles was determined by density gradient centrifugation using a self-generating gradient medium[6] as reported earlier (2).

Determination of Carbonic Anhydrase Activity—The activity of the carbonic anhydrase was determined using *p*-nitrophenyl acetate as the substrate (10). The enzyme in free form or in microparticles was added to 4.7 ml of 0.05 *M* tris(hydroxymethyl)aminomethane hydrochloride buffer at pH 7.4. The hydrolysis of *p*-nitrophenyl acetate was followed spectrophotometrically at 400 nm at room temperature (22°). From the change of the absorbance, the velocity of the reaction was calculated [$\epsilon = 2.1 \times 10^4$ (10)] and expressed as micromoles hydrolyzed per minute. Correction was made for the spontaneous hydrolysis of the substrate. The microparticles of polyacryldextran did not cause any light scattering at the wavelength used.

Radioactivity—Radioactivity was measured by liquid scintillation counting.

Functional Capacity of Albumin—The functional capacity of albumin was determined as described previously (11). Microparticles with albumin were incubated with [^{14}C]salicylic acid. The amount of albumin binding salicylic acid was calculated from the binding degree and from a standard curve derived by equilibrium dialysis with different albumin concentrations.

Iodination of Human Serum Albumin—Human serum albumin (5 mg) in 0.3 ml of 0.01 *M* phosphate buffer at pH 7.5 was labeled with sodium [^{125}I]iodide[7] (1 mCi) in the presence of lactoperoxidase[2] (EC 1.11.1.7) (40 μg) and hydrogen peroxide (20 μl, 0.005 *M*) according to a literature method (12). The reaction was stopped after 10 min by dilution of the sample with buffer. Separation of ^{125}I-labeled human serum albumin from the reaction mixture was carried out by gel filtration on a column (43 cm^3) of Sephadex G-25[8].

RESULTS

Preparation of Acryldextrans—Acrylic acid glycidyl ester reacts with a hydroxyl group of a glucose residue in the dextran to form a 3-acryloyl 2-hydroxypropyl ether. The molecular weight of the dextrans used (T10, T40, T70, T500, and T2000) ranged from 10,000 to 2,000,000. All dextrans followed a zero-order reaction with the same rate. After 5 days at room temperature (22–24°), one acrylic group was introduced per 20 glucose residues, regardless of the molecular weight of the dextrans.

The best dextran derivative for preparation of the microparticles was T40 (mol. wt. 40,000). Dextrans of higher molecular weight (T70, T500, and T2000) had a solubility too limited for the particle preparation and gave too high a viscosity of the water phase. The lower molecular weight dextran derivative (T10) did not significantly increase the yield of proteins in the particles.

Immobilization of Proteins in Polyacryldextran—The amount of proteins immobilized in polyacrylamide microparticles depends on the size of the protein and the composition of the polymer, which is characterized by the concentration of monomers (T) and the fraction of cross-linking agent (C) in the water phase. The pore radius of the polymer formed is dependent on both T and C. In addition, the radius of the polymeric threads forming the polymeric network is directly proportional to C (2). This relationship generally means that the incorporation of proteins increases with C, but, at the same time, the functional availability of the immobilized proteins is impaired when the pore radius decreases. An increased yield of immobilized proteins also is achieved by increasing

[1] KABI AB, Stockholm, Sweden.
[2] Sigma Chemical Co.
[3] Fluka AG.
[4] Eastman Kodak Co.
[5] Dextrans of different molecular weights (T10, T40, T70, T500, and T2000) were obtained from Pharmacia Fine Chemicals, Uppsala, Sweden.
[6] Percoll, Pharmacia Fine Chemicals, Uppsala, Sweden.
[7] AB Atomenergi, Studsvik, Sweden.
[8] Pharmacia Fine Chemicals, Uppsala, Sweden.

Table I—Amount of Albumin Immobilized in Microparticles of Different Gel Compositions [a]

Particle Composition (D-T-C)	Total Amount of Protein Immobilized, mg	Total Amount of Active Protein in Particles, mg
0-8-35	46.5	17.8
(10)[b]-8-35	59.8	33.2
10-8-35	92.8	56.8
0-4-100	8.0	2.7
4-2-96	22.6	15.0
0-5-80	16.4	3.8
11-1-75	83.5	66.8

[a] The study was carried out with 5 ml of the water phase with 500 mg of ^{125}I-labeled human serum albumin. After the preparation of the particles, their content of protein was measured in a γ-counter. The amount of functionally active protein in the microparticles was determined by estimating the capacity of the albumin to bind [^{14}C]salicylic acid (11). [b] Underivatized dextran.

the concentration of hydrophilic polymers in the water phase, *e.g.*, by adding starch or dextran. Table I summarizes some results from studies on the incorporation of ^{125}I-labeled human serum albumin in different microspheres of highly cross-linked polyacrylamide and polyacryldextran based on dextran T40.

It is evident from Table I that addition of 10% dextran to microparticles with T–C values of 8–35 increased the total yield of protein from 46.5 to 60 mg under the conditions used. The yield was improved further when the dextran was bound covalently in the polymer, as in acryldextran. However, the functional availability measured by the amount of salicylic acid bound was still low. The effect of the acryldextran is illustrated further by the results from other particles. In particles with D–T–C values of 0–4–100 (*i.e.*, those using only I at a concentration of 4%), 8 mg of albumin was incorporated. By adding acryldextran (0.4 g/10 ml) containing 2% acrylic groups, which constitutes only 4% of the total number of monomeric acrylic groups in the water phase, the immobilization of protein was increased significantly. Not even by adding acrylamide (to 20% of the total amount) to D–T–C values of 0–5–80 could the same increase be achieved.

In the subsequent work, polyacryldextran microparticles with D–T–C values of 11–1–75 were used. Dextran T40 containing 2.3% acrylic side chains (w/w) was employed. The amount of I added thus corresponded to 0.075 g/10 ml. The total yield of albumin in such particles was ~83.5 mg, *i.e.*, 16.7% of the total amount present in the water phase, and 80% of this amount was functionally active, *i.e.*, it bound salicylic acid.

Density of Polyacryldextran Microspheres—The density of polyacrylamide microparticles is largely determined by the porosity of the gel (2, 3). Linear polyacrylamide has a density of 1.15 g/ml, which decreases initially when the fraction of the cross-linker increases up to 5–10%. Above this limit, the characteristics of the polymer change to a more macroporous structure, so that the density increases again with C.

Proteins immobilized in the gel decrease the density of the particles (2). As expected, the same phenomenon was seen when dextran was included in the gel. This result most probably was due to two effects: a decreased porosity of the gel and the lower density of dextran compared to that of polyacrylamide. Thus, microparticles with D–T–C values of 11–1–75 have a density of 1.030 g/ml as determined in the colloidal silica density gradient by centrifugation.

Properties of Immobilized Carbonic Anhydrase—The enzymatic properties of carbonic anhydrase in the free state and in polyacryldextran microparticles are compared in Fig. 1*a*. In the two series of experiments, the amounts of enzyme were the same, based on amino acid analysis. From this figure, the Michaelis constant (K_m) for free and immobilized carbonic anhydrase was calculated to be 18 and 22 mM, respectively. The maximal velocity (V_{max}) as calculated from the y axis intercepts was 15% lower with the immobilized enzyme, which means that the enzyme was not utilized efficiently in the microparticles.

Figure 1*b* shows the differences in the enzymatic properties of carbonic anhydrase immobilized in microspheres and after solubilization of the same spheres with dextranase[2] (EC 3.2.1.11) (4 IU/ml of particle suspension incubated for 3 hr at 22°). The Michaelis constant (K_m) was 21 mM for the immobilized enzyme compared to 18 mM for the enzyme released after solubilization of the spheres. This value is the same as that found with the free enzyme. In addition, the dextranase treatment of the microspheres resulted in a 10% increase in V_{max}.

Leakage of Proteins from Polyacryldextran Microspheres—Microparticles (based on dextran T40 with D–T–C values of 11–1–75) were prepared with proteins of various sizes, carbonic anhydrase [mol. wt. 31,000 (13)], human serum albumin [mol. wt. 66,500 (14)], human immunoglobulin G [mol. wt. 150,000 (15)], and catalase [mol. wt. 240,000 (16)]. The microspheres were suspended in pH 7.4 physiological saline so that the protein concentration was 0.2, 4.91, 0.9, and 0.21 mg/ml, respectively. Sodium azide (0.1%) was added as a preservative, and the samples were left at room temperature for 80 days. After centrifugation, the leakage of protein from the spheres was determined in the supernate. Figure 2 summarizes the results. Thus, 65% of carbonic anhydrase was lost from the particles after 80 days, while 33% of human serum albumin, 44% of immunoglobulin G, and 30% of catalase were lost.

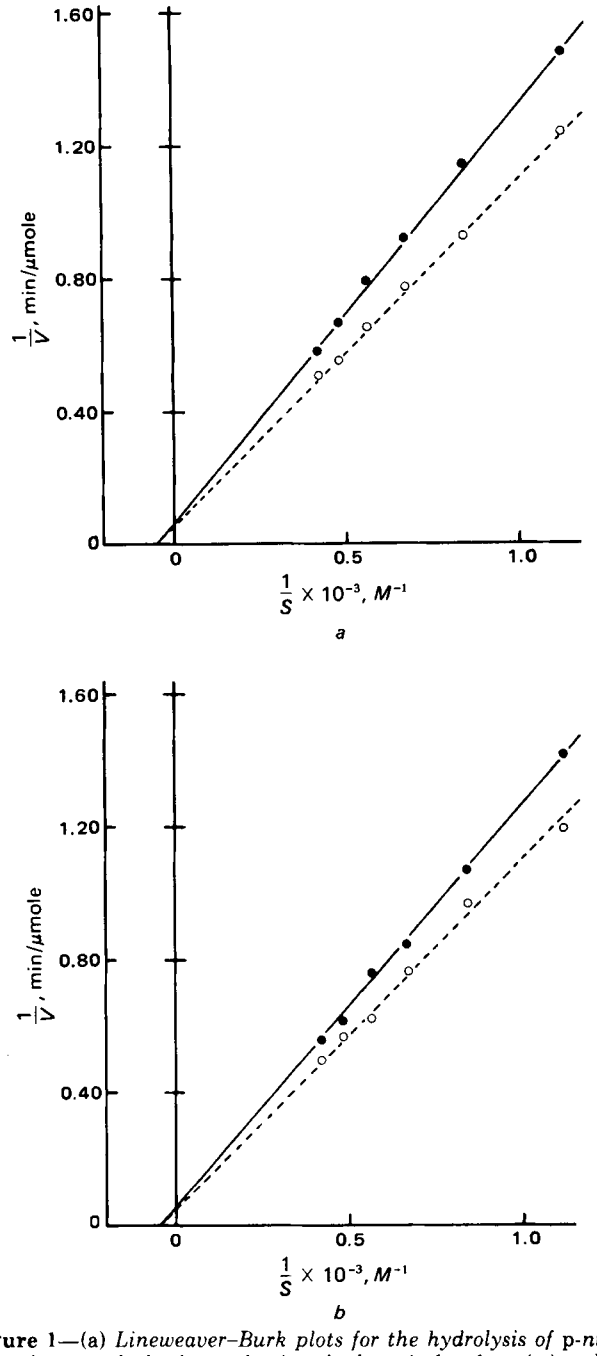

Figure 1—(a) *Lineweaver–Burk plots for the hydrolysis of* p*-nitrophenyl acetate by bovine carbonic anhydrase in free form* (○) *and immobilized* (●) *in microparticles of polyacryldextran.* (b) *Lineweaver–Burk plots obtained with carbonic anhydrase in microparticles before* (●) *and after* (○) *treatment with dextranase.*

Thermostability of Immobilized Carbonic Anhydrase—To investigate the heat stability of immobilized proteins, carbonic anhydrase was incorporated into microspheres of polyacryldextran (based on dextran T40). The spheres were exposed to elevated temperatures for 5 and 30 min. After treatment, the microspheres were cooled in an ice bath for

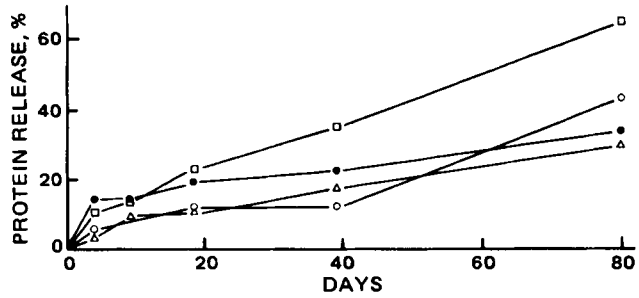

Figure 2—*Leakage of proteins from microspheres during storage at room temperature at pH 7.4. The immobilized proteins were carbonic anhydrase (□), human serum albumin (●), immunoglobulin (○), and catalase (△).*

5 min. After preincubation of the samples at room temperature for 30 min, the remaining activity was measured. Figure 3 shows that the immobilized enzyme was more resistant to heat treatment. All of the free enzyme and 50% of the immobilized enzyme were denatured at 65°. Approximately 5–10% of the enzyme activity was retained even after 30 min at 100°.

Hydrolytic Stability of Polyacryldextran Microspheres—The hydrolytic stability of the polymer, polyacryldextran, was investigated with particles with ^{14}C-labeled I as a cross-linking agent. The labeled microparticles then were incubated at different pH values (2–12) for 2, 4, 8, 12, and 24 hr at 37°. After centrifugation for 15 min at 4°, the supernate was withdrawn and the radioactivity content was measured in the scintillation counter. Figure 4 summarizes the results. The microspheres were not affected significantly at pH 2–9. At pH 11, ~20% of the particles were hydrolyzed in 24 hr. Essentially all of the particles were lost at pH 12 when stored at 37° for 24 hr.

DISCUSSION

The immobilization of proteins in acrylic polymers is influenced strongly by the composition of the polymer, *i.e.*, the total concentration of monomers and the relative fraction of the cross-linker (T and C) in the polymerization mixture. In the present study, the presence of polymers in the mixture, *e.g.*, dextrans or acrylic dextran derivatives, significantly affected the incorporation of protein in the microparticles formed by emulsion polymerization. The yield of protein in the microparticles was increased substantially, even when the total concentration of acrylic monomeric groups in the water phase was decreased substantially. To specify the composition of the polyacryldextran formed, it is suggested that the content of derivatized polymer present is given in grams per 100 ml by adding a D value to the existing nomenclature for characterizing polyacrylamide gels.

The yield of entrapped protein in polyacryldextran may be increased by two mechanisms. First, addition of dextran decreases the gel pore radius. Second, the dextran sterically retains the protein inside the gel during polymerization. The result is increased protein entrapment, implying that the fraction of protein immobilized in the polymeric threads is decreased. This result is evident from the heat stability of incorporated carbonic anhydrase and the leakage of proteins from the microparticles. The fraction of the enzyme that resists treatment at 100° for 30 min is smaller in polyacryldextran (10%) than in polyacrylamide [30% (3)], and the fraction leaking out from polyacryldextran when stored for prolonged periods is substantially larger.

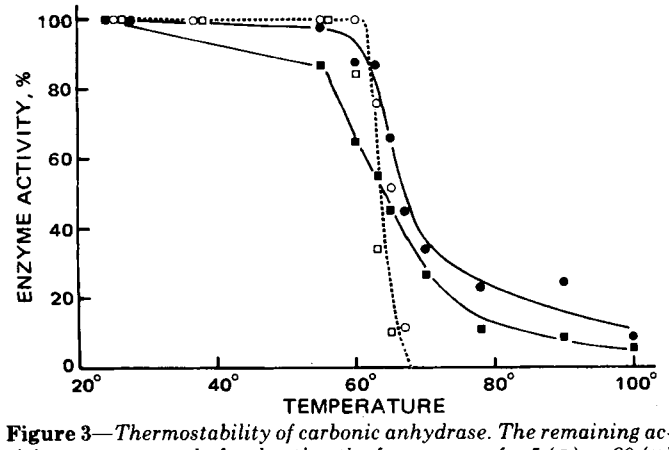

Figure 3—*Thermostability of carbonic anhydrase. The remaining activity was measured after heating the free enzyme for 5 (○) or 30 (□) min and the immobilized enzyme in polyacryldextran for 5 (●) or 30 (■) min.*

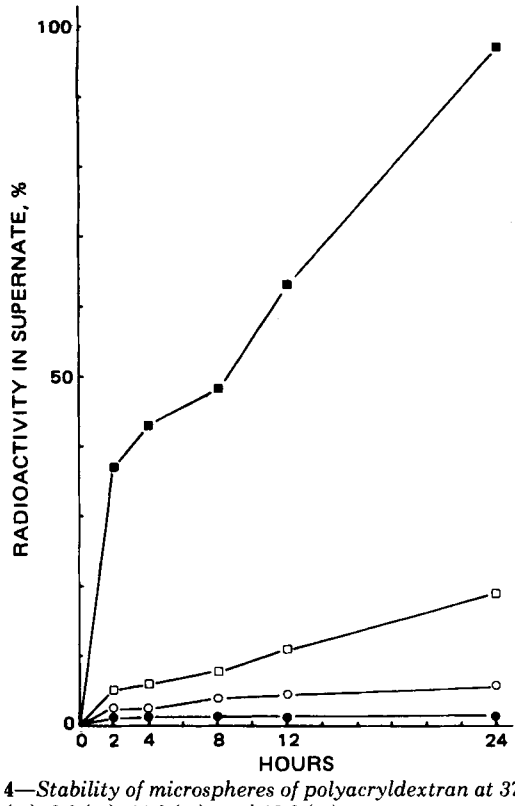

Figure 4—*Stability of microspheres of polyacryldextran at 37° and at pH 2–7 (●), 9.0 (○), 11.0 (□), and 12.0 (■).*

However, in other respects, immobilization in polyacryldextran offers the same advantages as in normal polyacrylamide. For example, the proteins retain their biological properties; K_m and V_{max} of carbonic anhydrase are affected only insignificantly, indicating that the equilibrium between enzyme and substrate is not diffusion dependent, which means that the substrate is not hindered sterically providing the particles are small. Moreover, the incorporation is a mild process as shown by the finding that the small loss in V_{max} and the increase in K_m are recovered almost completely after digestion of the polymer with dextranase.

In addition, other experiments[9] with 11–1–75 particles showed that polyacryldextran was metabolized more rapidly *in vitro* with rat liver homogenates and also was eliminated faster *in vivo* after intraperitoneal injection in mice than in the cases involving polyacrylamide (T–C value of 8–25). These findings were expected since dextran should be degraded easier *in vivo* than hydrocarbon chains, the content of which is comparatively small in polyacryldextran particles with D–T–C values of 11–1–75. The use of dextran thus offers a rich variation in the design of polymeric particles having different biological half-lives. The duration of the enzymatic effects *in vivo* can be controlled adequately without unwanted intracellular accumulation of polymers.

The results presented here were obtained with microparticles of polyacryldextran with D–T–C values of 11–1–75, *i.e.*, those with low T. The total yield of albumin immobilized in the particles was ~15% but could be increased up to ~20% by increasing T, *i.e.*, the concentration of the acrylic monomers in the polymerization mixture. However, the functional availability of the immobilized protein was impaired simultaneously, probably due to the decreased pore radius of the polymer. Furthermore, the leakage of protein from the microspheres was decreased.

In some applications, microparticles with larger amounts of proteins have advantages, even if such particles will be metabolized more slowly. Therefore, for each situation, a compromise must be made between total yield and functional availability and will depend on the desired rate of degradation of the gel, the cost of protein, the acceptable or desired rate of leakage of proteins, and the type of effect aimed at *in vivo*.

[9] P. Edman and I. Sjöholm, manuscript in preparation.

REFERENCES

(1) D. Killander, A. Dohlwitz, L. Engstedt, S. Franzén, G. Gahrton, B. Gullbring, G. Holm, A. Holmberg, S. Höglund, A. Killander, D. Lockner, H. Mellstedt, P. J. Moe, J. Palmblad, P. Reizenstein, K. O. Skårberg, B. Swedberg, A.-M. Udén, B. Wadman, L. Wide, and L. Åhström, *Cancer*, **37**, 220 (1976).

(2) B. Ekman, C. Lofter, and I. Sjöholm, *Biochemistry*, **15**, 5115 (1976).

(3) B. Ekman and I. Sjöholm, *J. Pharm. Sci.*, **67**, 693 (1978).

(4) P. Edman and I. Sjöholm, *J. Pharmacol. Exp. Ther.*, **211**, 663 (1979).

(5) A. Kober, B. Ekman, and I. Sjöholm, *J. Pharm. Sci.*, **67**, 107 (1978).

(6) I. Sjöholm and P. Edman, *J. Pharmacol. Exp. Ther.*, **211**, 656 (1979).

(7) H. Hoppe, J. Koppe, and F. Winkler, *Plaste Kautsch.*, **24**, 105 (1977).

(8) S. Hjertén, *Arch. Biochem. Biophys. Suppl. 1*, 147 (1962).

(9) O. Lowry, N. Rosebrough, L. Farr, and R. Randall, *J. Biol. Chem.*, **193**, 265 (1951).

(10) Y. Pocker and J. Stone, *J. Am. Chem. Soc.*, **87**, 5497 (1965).

(11) I. Sjöholm, B. Ekman, A. Kober, I. Ljungstedt-Påhlman, B. Seiving, and T. Sjödin, *Mol. Pharmacol.*, **16**, 767 (1979).

(12) J. Marchalonis, *Biochem. J.*, **113**, 299 (1969).

(13) S. Lindskog and B. Malmström, *J. Biol. Chem.*, **237**, 1129 (1962).

(14) B. Meloun, L. Morávek, and V. Kostka, *FEBS Lett.*, **58**, 134 (1975).

(15) G. Edelman, B. Cunningham, W. Gall, P. Gottlieb, U. Rutishauser, and M. Waxdal, *Proc. Natl. Acad. Sci. USA*, **63**, 78 (1969).

(16) T. Samejima, W. McCabe, and J. Yang, *Arch. Biochem. Biophys.*, **127**, 354 (1968).

ACKNOWLEDGMENTS

Supported by the Swedish Board for Technical Development and the I. F. Foundation for Pharmaceutical Research.

The authors thank Mr. Per Artursson and Miss Siv Larsson for technical assistance.

Isolation, Identification, and Synthesis of 4-Amino-6,7-dimethoxy-3-quinolinol, the Major Metabolite of Amiquinsin Hydrochloride in Rats and Humans

GEORGE C. WRIGHT *x, RONALD J. HERRETT ‡, JAMES P. HEOTIS ‡, and JAMES L. BUTTERFIELD ‡

Received March 20, 1978, from the **Chemical Research Division and the* ‡*Biological Research Division, Norwich-Eaton Pharmaceuticals, Division of Morton-Norwich Products, Inc., Norwich, NY 13815.* Accepted for publication February 26, 1980.

Abstract □ The metabolism of amiquinsin hydrochloride (4-amino-6,7-dimethoxyquinoline hydrochloride monohydrate, I) was studied in rats and humans. The major metabolite isolated from human urine was identified through synthesis as 4-amino-6,7-dimethoxy-3-quinolinol hydrochloride hydrate (II). Acid hydrolysis of the major metabolite from rat urine also gave II. The structure of the rat metabolite subsequently was tentatively identified as the potassium salt of the 3-*O*-sulfate of II. The pharmacological and toxicological properties of I and II are discussed.

Keyphrases □ Amiquinsin hydrochloride—rat and human metabolites, isolation and identification □ Antihypertensive agents—amiquinsin hydrochloride, rat and human metabolites, isolation and identification □ 4-Amino-6,7-dimethoxy-3-quinolinol—isolation and identification as metabolite of amiquinsin hydrochloride, rats and humans

Wright *et al.* (1) reported that amiquinsin hydrochloride (4-amino-6,7-dimethoxyquinoline hydrochloride monohydrate, I) (Scheme I) demonstrated hypotensive activity. Early biological studies with I included the pharmacological mechanism of action (2) and the absorption, distribution, and elimination of I in dogs (3, 4).

In the present investigation, the metabolism of I was studied in rats and humans. Williams (5) reported that 4-aminoquinoline administered to rabbits was metabolized to 4-amino-3-hydroxyquinoline, which was excreted mainly as an ether sulfate, and that glucuronic acid conjugation was low. Although 4-amino-7-chloroquinoline also was believed to be hydroxylated in rabbits to the 3-hydroxy derivative (5), hydroxylation of this compound in humans was not observed (6).

RESULTS AND DISCUSSION

Isolation and Identification of Metabolites—Metabolite studies with I were done initially in rats. When the rats were dosed orally with [3-^{14}C]I, the major excreted material was parent I; TLC followed by estimation of the activity of the radioactive materials showed the presence of I (61%) and substances at R_f 0.6 (25%), 0.0 (12%), and 0.9 (2%). The materials at R_f 0.0 and 0.9 were not identified.

A preparative method was developed for the isolation of the major rat metabolite at R_f 0.6 that involved separation and purification by gel filtration.

Treatment of the purified R_f 0.6 metabolite with hot methanolic hydrogen chloride gave a hydrolyzed product (hydrochloride of R_f 0.6 metabolite) with physical properties similar to those of the starting R_f 0.6 compound but with significant differences in the NMR spectra and TLC values (Table I). However, a comparison of the physical properties of the hydrolyzed product with those of the synthetic 3-hydroxy derivative II (Table I) clearly demonstrates that the two compounds are identical with respect to their NMR and UV spectra and TLC values. Thus, the hydrochloride of the hydrolyzed R_f 0.6 metabolite was identified as 4-amino-6,7-dimethoxy-3-quinolinol hydrochloride.

The R_f 0.6 metabolite was characterized further through enzymatic hydrolysis with a combination of β-glucuronidase and aryl sulfatase. Isolation of the end-products of enzymatic treatment was attained by extraction and TLC, and each spot then was counted for carbon 14. In the absence of enzymes, or by treatment with β-glucuronidase alone, the structure of the R_f 0.6 metabolite was not altered (Table II). However, treatment with aryl sulfatase and β-glucuronidase together converted the ^{14}C-labeled R_f 0.6 metabolite to [^{14}C]II. Thus, the enzymatic data indicate that the R_f 0.6 metabolite may be the sulfate conjugate of II. The IR spectrum showed a strong S=O stretching band at 8.1 μm, also indicative of a sulfate group in the molecule. The NMR spectra showed that both the R_f 0.6 metabolite and II are substituted in the 3-position. Considering the specificity of the enzymes used, the IR data, and the substitution pattern from the NMR spectra, the R_f 0.6 metabolite probably

0022-3549/80/0700-0842$01.00/0

© 1980, American Pharmaceutical Association

REFERENCES

(1) D. Killander, A. Dohlwitz, L. Engstedt, S. Franzén, G. Gahrton, B. Gullbring, G. Holm, A. Holmberg, S. Höglund, A. Killander, D. Lockner, H. Mellstedt, P. J. Moe, J. Palmblad, P. Reizenstein, K. O. Skårberg, B. Swedberg, A.-M. Udén, B. Wadman, L. Wide, and L. Åhström, *Cancer*, **37**, 220 (1976).

(2) B. Ekman, C. Lofter, and I. Sjöholm, *Biochemistry*, **15**, 5115 (1976).

(3) B. Ekman and I. Sjöholm, *J. Pharm. Sci.*, **67**, 693 (1978).

(4) P. Edman and I. Sjöholm, *J. Pharmacol. Exp. Ther.*, **211**, 663 (1979).

(5) A. Kober, B. Ekman, and I. Sjöholm, *J. Pharm. Sci.*, **67**, 107 (1978).

(6) I. Sjöholm and P. Edman, *J. Pharmacol. Exp. Ther.*, **211**, 656 (1979).

(7) H. Hoppe, J. Koppe, and F. Winkler, *Plaste Kautsch.*, **24**, 105 (1977).

(8) S. Hjertén, *Arch. Biochem. Biophys. Suppl. 1*, 147 (1962).

(9) O. Lowry, N. Rosebrough, L. Farr, and R. Randall, *J. Biol. Chem.*, **193**, 265 (1951).

(10) Y. Pocker and J. Stone, *J. Am. Chem. Soc.*, **87**, 5497 (1965).

(11) I. Sjöholm, B. Ekman, A. Kober, I. Ljungstedt-Påhlman, B. Seiving, and T. Sjödin, *Mol. Pharmacol.*, **16**, 767 (1979).

(12) J. Marchalonis, *Biochem. J.*, **113**, 299 (1969).

(13) S. Lindskog and B. Malmström, *J. Biol. Chem.*, **237**, 1129 (1962).

(14) B. Meloun, L. Morávek, and V. Kostka, *FEBS Lett.*, **58**, 134 (1975).

(15) G. Edelman, B. Cunningham, W. Gall, P. Gottlieb, U. Rutishauser, and M. Waxdal, *Proc. Natl. Acad. Sci. USA*, **63**, 78 (1969).

(16) T. Samejima, W. McCabe, and J. Yang, *Arch. Biochem. Biophys.*, **127**, 354 (1968).

ACKNOWLEDGMENTS

Supported by the Swedish Board for Technical Development and the I. F. Foundation for Pharmaceutical Research.

The authors thank Mr. Per Artursson and Miss Siv Larsson for technical assistance.

Isolation, Identification, and Synthesis of 4-Amino-6,7-dimethoxy-3-quinolinol, the Major Metabolite of Amiquinsin Hydrochloride in Rats and Humans

GEORGE C. WRIGHT *x, RONALD J. HERRETT ‡, JAMES P. HEOTIS ‡, and JAMES L. BUTTERFIELD ‡

Received March 20, 1978, from the **Chemical Research Division and the* ‡*Biological Research Division, Norwich-Eaton Pharmaceuticals, Division of Morton-Norwich Products, Inc., Norwich, NY 13815.* Accepted for publication February 26, 1980.

Abstract □ The metabolism of amiquinsin hydrochloride (4-amino-6,7-dimethoxyquinoline hydrochloride monohydrate, I) was studied in rats and humans. The major metabolite isolated from human urine was identified through synthesis as 4-amino-6,7-dimethoxy-3-quinolinol hydrochloride hydrate (II). Acid hydrolysis of the major metabolite from rat urine also gave II. The structure of the rat metabolite subsequently was tentatively identified as the potassium salt of the 3-*O*-sulfate of II. The pharmacological and toxicological properties of I and II are discussed.

Keyphrases □ Amiquinsin hydrochloride—rat and human metabolites, isolation and identification □ Antihypertensive agents—amiquinsin hydrochloride, rat and human metabolites, isolation and identification □ 4-Amino-6,7-dimethoxy-3-quinolinol—isolation and identification as metabolite of amiquinsin hydrochloride, rats and humans

Wright *et al.* (1) reported that amiquinsin hydrochloride (4-amino-6,7-dimethoxyquinoline hydrochloride monohydrate, I) (Scheme I) demonstrated hypotensive activity. Early biological studies with I included the pharmacological mechanism of action (2) and the absorption, distribution, and elimination of I in dogs (3, 4).

In the present investigation, the metabolism of I was studied in rats and humans. Williams (5) reported that 4-aminoquinoline administered to rabbits was metabolized to 4-amino-3-hydroxyquinoline, which was excreted mainly as an ether sulfate, and that glucuronic acid conjugation was low. Although 4-amino-7-chloroquinoline also was believed to be hydroxylated in rabbits to the 3-hydroxy derivative (5), hydroxylation of this compound in humans was not observed (6).

RESULTS AND DISCUSSION

Isolation and Identification of Metabolites—Metabolite studies with I were done initially in rats. When the rats were dosed orally with [3-^{14}C]I, the major excreted material was parent I; TLC followed by estimation of the activity of the radioactive materials showed the presence of I (61%) and substances at R_f 0.6 (25%), 0.0 (12%), and 0.9 (2%). The materials at R_f 0.0 and 0.9 were not identified.

A preparative method was developed for the isolation of the major rat metabolite at R_f 0.6 that involved separation and purification by gel filtration.

Treatment of the purified R_f 0.6 metabolite with hot methanolic hydrogen chloride gave a hydrolyzed product (hydrochloride of R_f 0.6 metabolite) with physical properties similar to those of the starting R_f 0.6 compound but with significant differences in the NMR spectra and TLC values (Table I). However, a comparison of the physical properties of the hydrolyzed product with those of the synthetic 3-hydroxy derivative II (Table I) clearly demonstrates that the two compounds are identical with respect to their NMR and UV spectra and TLC values. Thus, the hydrochloride of the hydrolyzed R_f 0.6 metabolite was identified as 4-amino-6,7-dimethoxy-3-quinolinol hydrochloride.

The R_f 0.6 metabolite was characterized further through enzymatic hydrolysis with a combination of β-glucuronidase and aryl sulfatase. Isolation of the end-products of enzymatic treatment was attained by extraction and TLC, and each spot then was counted for carbon 14. In the absence of enzymes, or by treatment with β-glucuronidase alone, the structure of the R_f 0.6 metabolite was not altered (Table II). However, treatment with aryl sulfatase and β-glucuronidase together converted the ^{14}C-labeled R_f 0.6 metabolite to [^{14}C]II. Thus, the enzymatic data indicate that the R_f 0.6 metabolite may be the sulfate conjugate of II. The IR spectrum showed a strong S=O stretching band at 8.1 μm, also indicative of a sulfate group in the molecule. The NMR spectra showed that both the R_f 0.6 metabolite and II are substituted in the 3-position. Considering the specificity of the enzymes used, the IR data, and the substitution pattern from the NMR spectra, the R_f 0.6 metabolite probably

0022-3549/80/0700-0842$01.00/0

© 1980, American Pharmaceutical Association

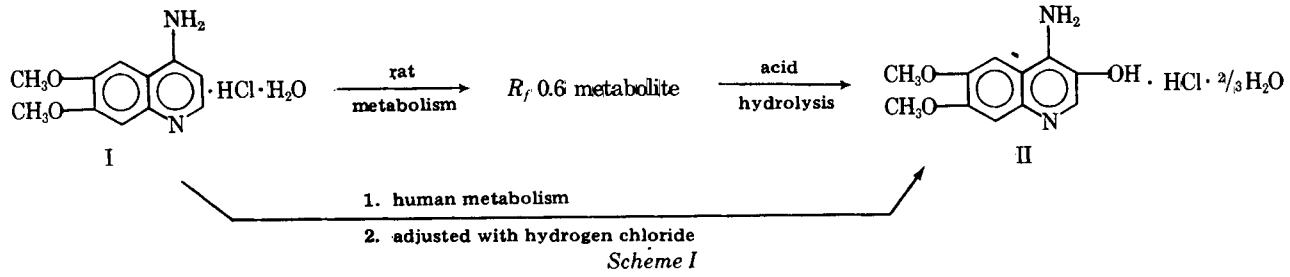

Scheme I

Table I—Physical Data for the R_f 0.6 Metabolite, Hydrochloride of Hydrolyzed R_f 0.6 Metabolite, and Synthetic 3-Hydroxy Derivative

Test	R_f 0.6 Metabolite[a]	Hydrochloride of Hydrolyzed R_f 0.6 Metabolite	Synthetic 3-Hydroxy-Derivative (II)
NMR: proton peaks, δ ppm (integral)	a, 3.92 (6) b, 7.2 (1) or c, 7.5 (1) d, 8.28 (1) e, 6.26 (2)[b] f, — g, 1.92 (2.5)	a, 3.89 (6) b, 7.37 (1) or c, 7.85 (1) d, 8.11 (1) e, 8.03 (2)[b] f, —[c] g, —[c]	a, 3.92 (6) b, 7.29 (1) or c, 7.77 (1) d, 8.07 (1) e, 8.03 (2)[b] f, 10.6 (~1)[b] g, 13.8 (~1)[b]
UV absorption (water)	Maxima: 250 and 321 nm Minimum: 270–275 nm	Maxima: 250 and 316–320 nm Minimum: 275 nm	Maxima: 250 and 316–320 nm Minimum: 275 nm
TLC[d]	0.60	0.25–0.30	0.30–0.35

[a] 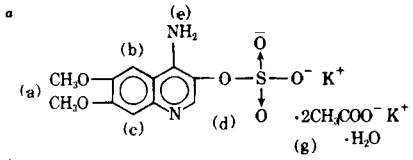

[b] Exchanged with deuterium oxide. [c] These peaks did not appear, probably because of relatively low concentration. [d] Eastman chromatographic sheet type K-301R (silica gel) developed with water-saturated 1-butanol.

is the 3-*O*-sulfate of II. Elemental analysis of the R_f 0.6 metabolite suggested that the isolated form was a hydrated potassium salt, with potassium acetate cocrystallized with the metabolite. No further work on the structural elucidation of the R_f 0.6 metabolite is planned.

Human volunteers were given a single oral dose of I, and the urine was analyzed for metabolites as described under *Experimental*. Although free I was isolated from human urine (the ether–chloroform extract), none of the R_f 0.6 metabolite was present (Table III). However, the R_f values and fluorescence color observed in isopentanol (or 1-butanol) extracts of urine corresponded to values observed for the synthetic 3-hydroxy derivative (II). The structure of the human metabolite was supported further by a comparison of the NMR, fluorescence, and UV absorption spectra of the human metabolite with those of the synthetic compound (Table III). Controls were run on the human urine to rule out the possibility that the R_f 0.6 metabolite initially was present and subsequently was hydrolyzed to II during isolation. Therefore, the human metabolite was identified as 4-amino-6,7-dimethoxy-3-quinolinol hydrochloride hydrate (II).

Pharmacology—Studies were conducted to evaluate the cardiovascular activity of II in anesthetized dogs, the vasodepressor activities of I and II in anesthetized rats, and the LD_{50} values of I and II in mice (see *Experimental*). Significant hypotensive activity in dogs was observed for II. The intensities of the hypotensive responses elicited by comparable intravenous injections of I and II were similar in rats; however, the duration of the hypotensive response in rats was considerably longer for I than for II. The LD_{50} values for I and II administered intravenously to mice were comparable.

Table II—TLC Data on Enzymatic Treatment of R_f 0.6 Metabolite[a]

Compound	Enzyme	R_f
R_f 0.6 metabolite	β-Glucuronidase + aryl sulfatase	0.46
R_f 0.6 metabolite	None	0.96
R_f 0.6 metabolite	β-Glucuronidase	0.93
II	None	0.50

[a] Eastman chromatographic sheet type K-301R2 developed with benzene–95% ethanol (water) (9:1).

Synthesis—The synthesis of II from 6,7-dimethoxy-3-quinolinol (7) (III) was accomplished in a three-step sequence (Scheme II).

In the nitration of IV, it was assumed that the substitution was directed at position 4 to give V; this assumption was based primarily on the published results (8) of the nitration of quinoline 1-oxide, in which 4-nitroquinoline 1-oxide was obtained in 70% yield with only minor amounts of the 5- and 8-nitro isomers. Furthermore, the fact that the properties of synthetic II correspond to those of the metabolite (where the amino substituent must be in position 4) proves that the nitro substituent of V is in position 4.

EXPERIMENTAL[1]

Isolation of Rat Metabolites—A solution of [3-^{14}C]I was administered orally to fasted rats at 10 mg/kg. The excretion of carbon 14 in urine was determined periodically for 24 hr after dosing; of the total [3-^{14}C]I dosage, 81 and 17% were excreted in the urine and feces, respectively. A 50–250-μl aliquot of the urine collected during each period was suspended in thixotropic gel (9) and counted in the liquid scintillation spectrometer.

TLC[2] was used for identification of the ^{14}C-labeled urinary metabolites of [3-^{14}C]I. Several solvent systems were tested initially, but only butanol saturated with water was satisfactory in separating the metabolites of I. The chromatograms were scanned[3] for radioactivity.

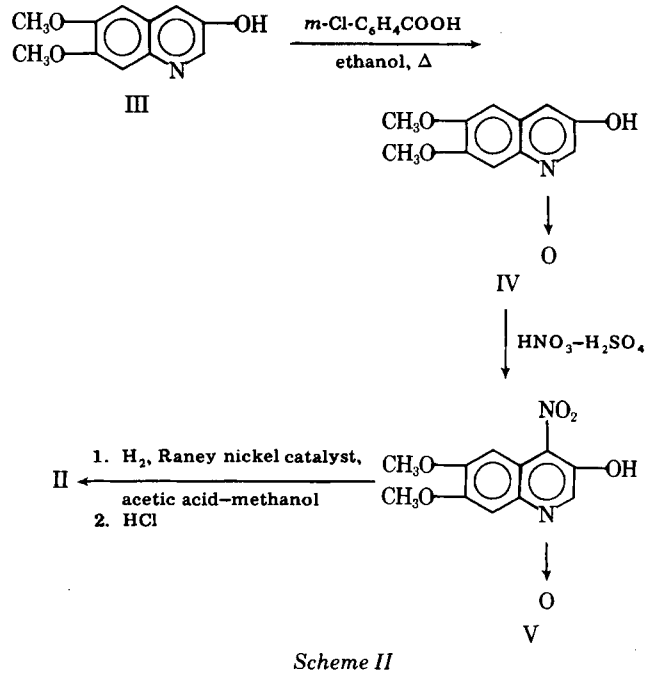

Scheme II

[1] Melting points were determined on a Fisher-Johns hot-stage apparatus and are uncorrected. NMR spectra were determined in dimethylsulfoxide-d_6 with tetramethylsilane as an internal standard on a Varian A60A spectrometer. Fluorescence spectra were obtained on an Aminco-Bowman spectrophotofluorometer.

[2] Eastman Kodak type K301R sheets.

[3] Duo Scan thin-layer scanner.

Table III—Comparison of Physical Data of Human Metabolite of I, R_f 0.6 Metabolite, and II

	I	R_f 0.6 Metabolite	Metabolite from Human Urine	Synthetic 3-Hydroxy Derivative (II)
TLC[a]: R_f (color)				
Water-saturated 1-butanol	0.10 (dark purple)	0.60 (dark blue)	0.10[b] (dark purple) 0.33[c] (bright blue)	0.30 (bright blue)
Chloroform–95% ethanol (water)	0.35 (dark purple)	0.80	0.20[c] (bright blue) 0.35[b] (dark purple)	0.20 (bright blue)
Emission spectra (activation/emission)	260/365 nm	250 nm/—	250/450 nm	250/450 nm
UV absorption	Maximum: 335 nm	Maxima: 250 and 321 nm	Maxima: 250 and 316–320 nm	Maxima: 250 and 316–320 nm
	Minimum: 248–250	Minimum: 270–275 nm	Minimum: 275 nm	Minimum: 275 nm

[a] Commercially prepared silica gel F-254 plates. [b] Found in ether–chloroform or hexanol–heptane (4:1 v/v) extracts. [c] Found in isopentanol or the 1-butanol extracts.

A preparative method was developed for isolation of the major metabolite (R_f 0.6). Forty milliliters of the composite urine sample was placed on a gel filtration column[4] (30 × 4 cm, previously equilibrated with water) and eluted with water (1200–1400 ml). Fractions of ~14 ml were collected with a fraction collector. The absorbance of each fraction was determined at 250 and 320 nm. The R_f 0.6 metabolite fraction was concentrated, placed on a second column[4] (12 × 6 cm), and eluted with water; this procedure resulted in purification of the R_f 0.6 metabolite, as shown by little change in the ratio of the absorbances at 250 and 320 nm, which was 2.9 for the first filtration and 2.8 for the second filtration. The purified R_f 0.6 metabolite was obtained through concentration with an evaporator[5].

The R_f 0.6 metabolite was converted to the hydrochloride of the hydrolyzed R_f 0.6 metabolite by the following procedure. Fifty milligrams of the isolated metabolite was dissolved in 3 ml of absolute methanol, and the resulting solution was purged with hydrogen chloride gas followed by refluxing for 1 hr. Atmospheric moisture was kept from the reaction vessel by a silica gel drying tube. The cooled (tap water) solution was filtered to remove a small amount of insoluble material, and the filtrate was concentrated and filtered with the original precipitate. This procedure yielded 25 mg of dry material. The same procedure was followed with the synthetic 3-hydroxy derivative (II), except that 60 mg of the starting material was used; the yield of the synthetic hydrochloride was 37 mg. Physical data were obtained on these hydrochloride products (Table I).

The enzymatic hydrolysis of the R_f 0.6 metabolite was carried out with β-glucuronidase–aryl sulfatase[6] and β-glucuronidase[7] of bovine origin. The glucuronidase–sulfatase enzyme mix (0.1 ml) was diluted to 5.5 ml with pH 4.5 acetate buffer. This dilution was followed by the addition of a neutral aqueous solution (0.5 ml) containing the ^{14}C-labeled R_f 0.6 metabolite or standard. The 0.5-ml standards were 200 μg of phenolphthalein glucuronide/ml for the β-glucuronidase activity and 200 μg of esterone sulfate/ml for the sulfatase activity. Test tubes containing no enzyme but with all other constituents were included as controls.

All samples were incubated at 37° for 18 hr. At that time, all of the samples of the ^{14}C-labeled R_f 0.6 metabolite and the controls were adjusted to pH 7.5 with 0.1 *N* NaOH and extracted twice with equal volumes of 1-butanol. The butanol extracts were set aside while enzyme activity was checked. This test was done by adding 0.5 ml of 30% trichloroacetic acid to precipitate the enzyme protein, followed by centrifugation and adjustment of the supernate to pH 10.4. Formation of a pink color indicated hydrolysis of the phenolphthalein–glucuronide conjugate to free phenolphthalein. The sulfatase activity was checked by adjusting the solution pH to 7.0 with 0.1 *N* NaOH, followed by extraction of the free estrogen with chloroform. The chloroform extract was reduced in volume *in vacuo*, spotted on thin-layer plates[2], and developed in benzene–95% ethanol (water) (9:1). The free estrone gave a blue spot against a yellow background when the chromatogram was sprayed with 10% phosphomolybdic acid in methanol and heated at 100° for several minutes. TLC[2] of the butanol extracts of samples containing the ^{14}C-labeled R_f 0.6 metabolite were performed with a chloroform–95% ethanol (water) (1:1) solvent system.

Isolation of Human Metabolite—Compound I in gelatin capsules was given to three male adult volunteers as a single oral 50-mg dose, equal to ~0.75 mg/kg. Urine was collected during 0–4 and 8–24 hr. These samples were refrigerated soon after collection and processed for metabolite separation within 1 or 2 weeks.

Solvent extraction of human urine was conducted as follows. The urine was adjusted to pH 10–11.5 with the addition of borate to glycine buffer at pH 10.5, and final adjustment was made with I or 5 *N* NaOH using a pH meter. Extraction with equal volumes of ether–chloroform or hexanol–heptane (4:1) was performed three times, and the extracts were pooled; free amiquinsin was removed in this process. The urines then were adjusted to pH 7–7.5 with 5 *N* HCl and extracted three times with either isopentanol or 1-butanol; free II was removed by this procedure.

Controls were run on the human urine to rule out the possibility that the R_f 0.6 metabolite initially was present and subsequently was hydrolyzed to II during isolation. The R_f 0.6 metabolite was not detected (by TLC) in isopentanol extracts of the human urine but definitely was observed in comparable isopentanol extracts of rat urine.

Additional evidence for the absence of the R_f 0.6 metabolite in human urine was obtained through gel filtration. The urine sample was filtered through a gel filtration column[4] followed by elution with water. The R_f 0.6 metabolite was not in the water eluates, which were examined for UV-absorbing material. However, when previously prepared R_f 0.6 metabolite was added to control human urine and passed through the column[4], it was readily detected by UV absorption at a concentration as low as 1 μg/ml. Thus, the R_f 0.6 metabolite apparently was stable under the conditions of the isolation procedure.

Pharmacology—*Cardiovascular Activity*—Compound II was evaluated for hypotensive activity in three anesthetized (pentobarbital sodium, 35 mg/kg iv) dogs. The compounds were administered intravenously as an aqueous solution, and the blood pressure was recorded from a cannulated femoral artery.

A dose of 1 mg of II/kg iv decreased the arterial blood pressure 48% below the control level within 1 min. After 45 min, the blood pressure returned to within 6% of the control value.

Five milligrams of II/kg given intravenously lowered the arterial blood pressure 68% in <1 min. The pressure gradually rose to a level only 7% below the control by ~120 min postinjection.

Two dogs died after receiving an intravenous 10-mg/kg dose of II.

Vasodepressor Activity—The vasodepressor activities of I and II were evaluated in anesthetized[8], adult male, albino rats[9]. Drug injections were made *via* the femoral vein, and the blood pressure was recorded from a cannulated carotid artery.

A relationship between the dose and the degree of hypotension elicited was not observed; both I and II exhibited a decrease in blood pressure, averaging 30–40% at the doses tested. For II, the time required for the blood pressure to return to 50% of the pretreatment value averaged 2, 3, and 6 min at dose levels of 0.5, 1.0, and 2.0 mg/kg, respectively. However, for I, the 50% return times averaged 8 min at 0.5 mg/kg, 4–55 min at 1.0 mg/kg, and >2 hr at 2.0 mg/kg.

Acute Toxicity—To compare the acute toxicities of I and II, groups of 10 male TFSW mice (19–24 g) were used. For each compound, two doses below and two above the LD_{50} value were administered intravenously. Death within 30 min postinjection was considered as a positive response. The LD_{50} values were calculated by a computerized probit–log dose regression analysis. The observed LD_{50} values for I and II were 67.1 and 66.8 mg/kg, respectively.

[4] Sephadex G-10.
[5] Rinco evaporator.
[6] Calbiochem 34742.
[7] Calbiochem 34743.
[8] Dial-urethan, 0.7 ml/kg ip.
[9] Charles River.

Chemistry—*6,7-Dimethoxy-3-quinolinol 1-Oxide (IV)*—A solution of 6,7-dimethoxy-3-quinolinol (6) (III) (52 g, 0.26 mole) in 95% ethanol (methanol) (786 ml) was treated portionwise with *m*-chlorobenzoic acid (73 g, 0.42 mole) with mechanical stirring. The reaction solution was refluxed for 45 min, stirred for an additional 2 hr, stored in the refrigerator overnight, and filtered to remove a small amount of solid. The filtrate was concentrated to near dryness, and the residue was slurried in ether (500 ml) and stored overnight. The solid product was collected by filtration (50 g), mp 235°. Recrystallization from 95% ethanol (methanol) gave 29.6 g (52% yield) of IV, mp 243–245°.

An analytical sample was prepared by further recrystallization from 95% ethanol (methanol), mp 250–251°; NMR: δ 3.93 (s, 6H, 2 OCH_3), 7.17 (d, 1, aromatic, J = 1.9 Hz), 7.30 (s, 1, aromatic), 7.78 (s, 1, heteroaromatic), 8.18 (d, 1, heteroaromatic, J = 1.6 Hz), and 10.3 (s, 1, OH, exchanged with D_2O).

Anal.—Calc. for $C_{11}H_{11}NO_4$: C, 59.72; H, 5.01; N, 8.33. Found: C, 59.32; H, 4.85; N, 8.29.

6,7-Dimethoxy-4-nitro-3-quinolinol 1-Oxide (V)—To IV (5.0 g, 0.023 mole) was added a cold solution of concentrated nitric acid (7.5 ml) in water (4.0 ml). Concentrated sulfuric acid (15 ml) then was added to the mixture at 10–20° over 15 min with hand stirring. The reaction mixture was allowed to warm (exothermic) to 35° over 6–10 min, warmed to 45° over 3 min, maintained at 45–50° for 30 min, and left at 25° for 1 hr. (Since the heat of reaction was erratic and difficult to control, the sample size was limited to 5 g.) The reaction mixture was added to ice (70 ml), and the resultant yellow, crystalline solid was collected by filtration and washed with cold water (20 ml).

This process was repeated a total of four times, the combined product was treated with hot nitromethane (140 ml), and the insoluble product, assumed to be the sulfate salt of V, was collected by filtration. The cooled filtrate yielded 2.0 g of yellow, crystalline V, mp 232–234°. The nitromethane-insoluble product (5.8 g) was dissolved in 10% Na_2CO_3 (29 ml) with cooling in an ice bath and subsequently acidified with acetic acid (4.0 ml) with cooling. The product (V) was collected by filtration and washed with cold water (4 × 3 ml), cold 2-propanol (2 × 4 ml), and ether to yield 4.4 g, mp 228–232° dec. The total yield was 6.4 g (27%).

An analytical sample was prepared by recrystallization from nitromethane, mp 228–232° dec.; NMR: δ 3.95 and 3.98 [2s, 6, $(OCH_3)_2$], 7.10 and 7.74 (2s, 2, aromatic), and 8.32 (s, 1, heteroaromatic).

Anal.—Calc. for $C_{11}H_{10}N_2O_6$: C, 49.63; H, 3.79; N, 10.52. Found: C, 49.22; H, 3.87; N, 10.93.

4-Amino-6,7-dimethoxy-3-quinolinol Hydrochloride Hydrate (II)—A mixture of V (7.0 g, 0.026 mole), methanol (470 ml), acetic acid (5.8 ml), and Raney nickel catalyst (18 g, wet basis) was subjected to hydrogenation at 48 psig. A pressure drop of 90% (of theory) was observed over 4.0 hr. The reaction mixture was cooled in an ice bath, treated with charcoal, and filtered. The filtrate was treated with a hydrogen chloride–2-propanol solution to pH 3–4, concentrated to 80 ml under reduced pressure, and cooled in an ice bath. The product was collected by filtration and washed with cold methanol, 2-propanol, and ether to give 4.9 g (70% yield), mp 264–267° dec.

An analytical sample was prepared *via* three recrystallizations from methanol, mp 265–267° dec.

Anal.—Calc. for $C_{11}H_{12}N_2O_3 \cdot HCl \cdot 2/3\ H_2O$: C, 49.16; H, 5.37; N, 10.43. Found: C, 49.38; H, 5.74; N, 10.34.

4-Amino-6,7-dimethoxy[3-^{14}C]quinoline Hydrochloride Hydrate ([3-^{14}C]I)—The [3-^{14}C]I was prepared by the same basic procedure as that reported previously (1) for the preparation of I.

Potassium Salt of 3-O-Sulfate of II (VI)—*Anal.*—Calc. for $C_{11}H_{11}KN_2O_6S \cdot 2CH_3COO^-K^+ \cdot H_2O$: C, 32.60; H, 3.47; N, 5.07; S, 5.80. Found: C, 32.87; H, 3.74; N, 4.77; S, 5.52.

REFERENCES

(1) G. C. Wright, E. J. Watson, F. F. Ebetino, G. Lougheed, B. F. Stevenson, A. Winterstein, R. K. Bickerton, R. P. Halliday, and D. T. Pals, *J. Med. Chem.*, **14**, 1060 (1971).

(2) B. S. Jandhyaia, G. J. Gregs, and J. P. Buckley, *Arch. Int. Pharmacodyn. Ther.*, **167**, 217 (1967).

(3) J. D. Conklin and R. D. Hollifield, *Eur. J. Pharmacol.*, **10**, 360 (1970).

(4) J. D. Conklin and R. D. Hollifield, *Life Sci.*, **9**, 577 (1970).

(5) R. T. Williams, "Detoxication Mechanisms," Wiley, New York, N.Y., 1959, p. 651.

(6) E. W. McChesney, W. D. Conway, W. F. Banks, Jr., J. E. Rodgers, and J. M. Shekosky, *J. Pharmacol. Exp. Ther.*, **151**, 482 (1966).

(7) British pat. 942,524 (1963); through *Chem. Abstr.*, **60**, P5469e (1964).

(8) R. C. Elderfield, "Heterocyclic Compounds," Wiley, New York, N.Y., 1952, p. 252. Ochiai, *Imp. Acad. (Tokyo)*, **19**, 307 (1943); through *Chem. Abstr.*, **41**, 5880d (1947).

(9) C. F. Gordon and A. L. Wolfe, *Anal. Chem.*, **32**, 574 (1960).

ACKNOWLEDGMENTS

The authors thank Mr. George Klein for the synthesis of the [3-^{14}C]I, Mr. Charles Williams (deceased) for able assistance, and Dr. Donald Polin for advice in the metabolite identification studies.

Determination of Potential Content of Vitamin D_2 (Ergocalciferol) and Vitamin D_3 (Cholecalciferol) in Gelatin-Coated Beadlets, Oil-Based Mixtures, and Multivitamin Tablet and Capsule Formulations

GUSTAV A. WALKER ˣ, BRUCE E. CARPENTER, and DAVID L. TUESCHER

Received December 17, 1979, from *Control Analytical Research and Development, The Upjohn Company, Kalamazoo, MI 49001.* Accepted for publication February 28, 1980.

Abstract □ A high-performance liquid chromatographic procedure was used to determine routinely the potential vitamin D content in raw materials and multivitamin formulations. The method employs a microparticulate silica column to separate vitamin D from its degradation products as well as other fat-soluble vitamins. Sample preparation is simple, and the chromatographic time is <20 min when progesterone is added to the injection mixture as an internal standard. Replicate analyses of complex multivitamin formulations demonstrate precision with a relative standard deviation of <4%. Spiked placebos typically show 98–100% recovery and a linear chromatographic response. The use of bulk drug as a working reference standard is recommended for the determination of the potential vitamin D concentration in pharmaceutical multivitamin preparations.

Keyphrases □ Vitamin D—high-performance liquid chromatographic determination of potential content of vitamins D_2 and D_3 in gelatin-coated beadlets, oil-based mixtures, and multivitamin tablet and capsule formulations □ Ergocalciferol (vitamin D_2)—high-performance liquid chromatographic determination of potential content in gelatin-coated beadlets, oil-based mixtures, and multivitamin tablet and capsule formulations □ Cholecalciferol (vitamin D_3)—high-performance liquid chromatographic determination of potential content in gelatin-coated beadlets, oil-based mixtures, and multivitamin tablet and capsule formulations □ High-performance liquid chromatography—analysis, potential content of vitamins D_2 and D_3 in gelatin-coated beadlets, oil-based mixtures, and multivitamin tablet and capsule formulations

High-performance liquid chromatography (HPLC) has been established as a rapid, reproducible, and selective method for the separation and analysis of vitamin D in pharmaceutical raw materials. In contrast, current compendial procedures (1) are imprecise and dependent on extensive, time-consuming sample preparation to confer tolerable specificity. For example, the compendial procedure is not suitable for formulations containing vitamin E without the removal of vitamin E from the sample preparation by TLC.

The HPLC methodology allows the separation of the D vitamins from the provitamins, previtamins, and photochemical isomers such as lumisterol, tachysterol, and *trans*-vitamin D. Isocratic separations with adsorption or reversed-phase chromatography have been reported as have gradient elution methods for the determination of vitamin D only or simultaneously with vitamins A and E (2–7).

BACKGROUND

The analysis of vitamin D in bulk drugs as in gelatin-coated beadlets or in oil by HPLC usually is easy and straightforward with minimum sample preparation. However, quantitation of vitamin D in multivitamin products with frequently complex matrixes is difficult without optimum chromatography. The variation in chromatographic cleanliness of excipient components from different suppliers constitutes a special challenge to HPLC methodology. Therefore, few reported HPLC procedures have been equally amenable to all vitamin formulations.

The analysis of vitamin D in pharmaceutical preparations is complicated further by whether this determination should account for the previtamin D content, which is in equilibrium with vitamin D (Scheme I). To allow for conversion of the previtamin into vitamin D, it is necessary to estimate the potential vitamin D content that can be determined through measurement of both the previtamin D (with the appropriate absorptivity correction) and the vitamin D areas. Unfortunately, previtamin D is not always adequately resolved from excipient peaks in the chromatography of products with complex matrixes. Under such chromatographic conditions, it is not quantitated easily.

To account for the previtamin D–vitamin D equilibrium in various products without measuring the previtamin directly, some pharmaceutical manufacturers have recommended a heat equilibration step wherein standards and samples are treated for the same time and at the same temperature (8). Only the vitamin D would have to be measured since the previtamin D should be the same in both the standard and the sample. However, when applied to some multivitamin preparations, this technique is imprecise, and its use frequently results in erroneous estimations of vitamin D content.

The applicability of HPLC methodology is demonstrated in this paper in the determination of vitamin D in bulk drug and in various multivitamin preparations. Sample preparation and chromatographic conditions, modified from previously reported procedures (3, 5, 8), are simple and require minimal changes to accommodate samples with different matrixes. In addition, a practical and reliable approach is recommended for the determination of potential vitamin D content by the use of a bulk drug working standard for samples treated similarly.

EXPERIMENTAL

Reagents and Solvents—Stabilizer-free chloroform[1], *n*-hexane[1], tetrahydrofuran[1], acetic acid[2], and diatomaceous earth[3] were obtained

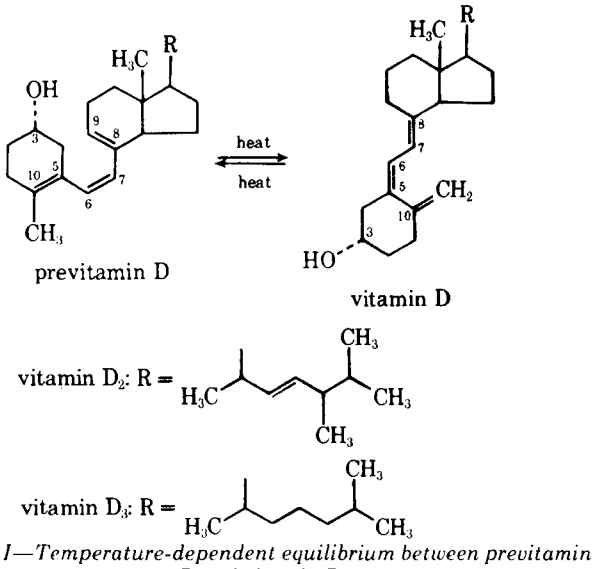

Scheme I—Temperature-dependent equilibrium between previtamin D and vitamin D

[1] Spectroquality grade, Burdick & Jackson Laboratories, Muskegon, Mich.
[2] Analytical grade, Mallinckrodt, St. Louis, Mo.
[3] Florex (Fuller's earth), Floridin Co., Quincy, Fla.

0022-3549/80/0700-0846$01.00/0
© 1980, American Pharmaceutical Association

commercially. Water was deionized. Ergocalciferol USP (vitamin D_2) and cholecalciferol USP (vitamin D_3) were used as reference standards. Progesterone USP served as the internal standard.

Apparatus and Column—The liquid chromatograph[4] was equipped with a fixed-wavelength UV detector[5] (254 nm). A microparticulate silica column[6] (250 × 4.6 mm i.d.) was used. The mobile phase was pumped at a flow rate of 1.5 ml/min and 1200 psi. The column was maintained at room temperature. Chromatograms were traced on a strip-chart recorder[7].

Mobile Phase—A mixture of chloroform–water-saturated *n*-hexane–dry *n*-hexane–tetrahydrofuran–acetic acid (60:15:25:1.5:0.4 v/v) was used. This ratio may be adjusted to achieve satisfactory system suitability.

Internal Standard Solution—The internal standard was prepared by adding ~6 mg of progesterone to 200 ml of mobile phase.

Reference Standard Solution—Approximately 18 mg of vitamin D USP reference standard was weighed accurately, transferred to a 100-ml low actinic volumetric flask, diluted to volume with isooctane, and mixed well. This was reference standard Solution A and could be kept for 1 week if maintained at 0° or below. Exactly 5.0 ml of Solution A was transferred into a 100-ml low actinic volumetric flask and diluted to volume with isooctane. This was reference standard Solution B and was prepared daily.

Prior to chromatography, a 1:1 mixture of Solution B and the mobile phase or the internal standard solution was prepared in a low actinic container and mixed well.

Reference standard Solution B was used to characterize the working standard.

Working Standards—The working standards were vitamin D beadlets USP or cholecalciferol USP in oil.

Approximately 8.0 mg of vitamin D gelatin beadlets was weighed accurately and transferred into a 250-ml centrifuge tube fitted with a 24/40 ground-glass joint. Duplicate weighings of a characterized lot were used. The analysis was continued as described under *Procedure A*.

With a syringe, cholecalciferol in oil equivalent to ~2.6 mg of vitamin D_3 was weighed accurately into a 250-ml low actinic volumetric flask. The flask was filled to volume with hexane, and the contents were mixed well. Duplicate weighings of cholecalciferol were used. The analysis was continued as described under *Procedure B*.

Sample Preparation—*Coated Compressed Tablets*—The weight of 25 tablets was measured accurately, and an average tablet weight was determined. Approximately 12 tablets at a time were ground to a fine powder with a mill[8] and were mixed. A sample equivalent to 20 tablets was weighed accurately and transferred into a 250-ml centrifuge tube fitted with a 24/40 ground-glass joint. The analysis was continued as described under *Procedure A*.

Soft Elastic Capsules—Eighteen capsules were transferred into a suitable container such as a 250-ml centrifuge cup fitted with a 24/40 ground-glass joint. The analysis was continued as described under *Procedure B*.

Oil-Based Mixtures—With a syringe, an accurately weighed sample equivalent to ~260 μg of vitamin D_3 was placed in a 25-ml low actinic volumetric flask. The flask was filled to volume with hexane, and the contents were mixed well. The analysis was continued as described under *Procedure B*.

Procedure A—To each centrifuge cup was added 80 ml of a 3:1 solution of dimethyl sulfoxide and water, which had been cooled to room temperature. The headspace was flushed with nitrogen. The centrifuge cups were stoppered tightly, sonicated for 10 min, and shaken vigorously for 1 hr on a mechanical horizontal shaker. The samples must be protected from heat and prolonged exposure to UV irradiation; contact with oxygen should be minimized.

To each centrifuge cup was added an exact volume of hexane (*e.g.*, 25 ml), and the cups were shaken for 45 min as described previously. The samples were centrifuged at ~1500 rpm for 5 min. For the final preparation of tablet formulations or gelatin-coated beadlets, an aliquot of the hexane layer was transferred into a suitable low actinic container and diluted 1:1 with the internal standard solution. The containers were capped tightly, and the contents were mixed well.

Samples with soft elastic capsules were analyzed for vitamin D as described under *Procedure B*.

Procedure B—Without exposing the samples to UV irradiation, an exact volume of the sample (hexane solution) was pipetted onto the column of diatomaceous earth. Then the column was washed with 100 ml of hexane, and the effluent was discarded. Vitamin D was eluted with the addition of 150 ml of toluene and collected in a suitable low actinic boiling flask containing 3.0 ml of the internal standard solution. The toluene was evaporated using a suitable evaporator and a water bath at 37° under vacuum. The residue was dissolved in 6.0 ml of the mobile phase.

Chromatography—The HPLC column was conditioned with the mobile phase until a relatively stable baseline was obtained. A vitamin D beadlet reference standard and not more than four sample preparations were injected alternately.

A chromatographic run should include at least two beadlet reference standard preparations injected in duplicate. The injection volume usually was 40–50 μl for both reference and sample analysis. Retention times of 8–9 and 14–16 min should be obtained for vitamin D and progesterone, respectively.

Calculations—The amounts of potential vitamin D_2 in micrograms per tablet (or capsule) and vitamin D_3 in micrograms per gram were determined from:

$$\text{amount} = \frac{PR_s}{PR_{std}} \frac{C_{std}}{WT_s} SV \times TW_t \times P_{std} \qquad \text{(Eq. 1}a\text{)}$$

or:

$$\text{amount} = \frac{PR_s}{PR_{std}} \frac{C_{std}}{SN} SV \times P_{std} \qquad \text{(Eq. 1}b\text{)}$$

where PR_s is the peak response ratio of the vitamin D peak to the internal standard peak in the sample preparation, PR_{std} is the peak response ratio of the vitamin D peak to the internal standard peak in the standard preparation, C_{std} is the concentration of the vitamin D reference standard [vitamin D_2 in gelatin beadlets (milligrams of beadlets per milliliter) or cholecalciferol USP in oil solution (milligrams per milliliter)], WT_s is the weight of the sample (grams), SN is the sample number (number of capsules, if applicable), SV is the sample dilution volume [equal to the volume of added hexane in the sample preparation (*e.g.*, 25 ml)], TW_t is the weight of one tablet in grams (factor not applicable when sample number is used), and P_{std} is the assigned potency of the vitamin D beadlet reference standard or cholecalciferol USP in oil in micrograms per milligram.

Calculation of Previtamin D—Previous studies showed that previtamin D and vitamin D form an equilibrium dependent on temperature (9). A solution of reference standard vitamin D_3 dissolved in isooctane and contained under nitrogen in a low actinic flask was heated overnight at 80°. Upon cooling, the solution was injected into the HPLC system, and the amounts of previtamin and vitamin D were determined by peak area. Comparisons were made between the vitamin D concentrations in the freshly prepared solution, which had no detectable traces of previtamin, and the vitamin D concentrations in the heat-treated solution. Since no other degradation products were observed, the amounts of previtamin D formed could be calculated from the decrease in the vitamin D peak. The expected areas of the previtamin (assuming an absorptivity identical to vitamin D) were compared with the areas observed, and the differences were equated with the differences in the respective absorptivities of previtamin D and vitamin D. Results from samples treated as described produced an average value for the absorptivity (254 nm) of the previtamin of 40% of that of vitamin D. This value agrees with the value found by Havingo *et al.* (10).

The concentration of previtamin D_2 was calculated from:

$$\frac{\text{area of previtamin } D_2}{\text{area of vitamin } D_2} \times \frac{\text{vitamin } D_2 \text{ (micrograms per tablet)}}{CF} = \text{micrograms of previtamin } D_2 \text{ per tablet} \qquad \text{(Eq. 2)}$$

and:

$$\frac{\text{previtamin } D_2 \text{ (micrograms per tablet)}}{\text{previtamin } D_2 \text{ (micrograms per tablet)} + \text{vitamin } D_2 \text{ (micrograms per tablet)}} \times 100 = \text{percent of previtamin } D_2 \qquad \text{(Eq. 3)}$$

where CF is the correction factor (0.4).

RESULTS AND DISCUSSION

The chromatographic system used separates vitamin D from its major degradation products. Figure 1 shows the resolved elution profile of the products of partially degraded vitamin D_2. The vitamin D_2 solution was

[4] Model ALC/GPC 244 equipped with a U6K injector, Waters Associates, Milford, Mass.
[5] Model 440, Waters Associates, Milford, Mass.
[6] Si-5A, Brownlee Laboratories, Santa Clara, Calif.
[7] Model B5000 Omniscribe, Houston Instruments, Austin, Tex.
[8] Spex mixer/mill, Metuchen, N.J.

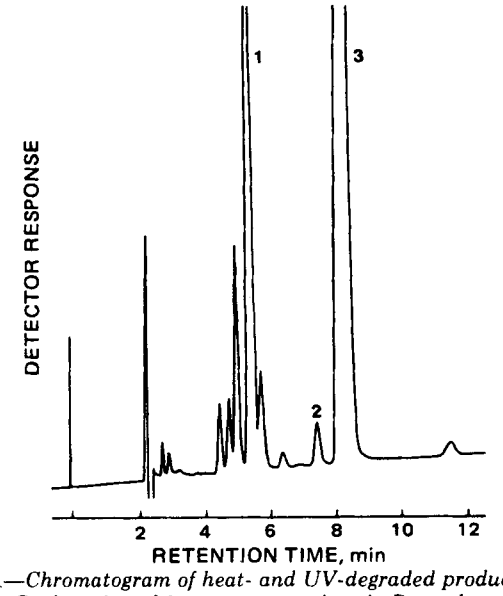

Figure 1—*Chromatogram of heat- and UV-degraded products of vitamin D_2. Peaks 1, 2, and 3 represent previtamin D_2, tachysterol, and vitamin D_2, respectively. The identity of the other peaks was not determined.*

degraded by 2 hr of heat treatment at 90° followed by irradiation for 2 hr at both long and short UV wavelengths. Approximately 6.2 μg of degraded vitamin D_2 was injected. The peaks of interest were associated with previtamin D_2, tachysterol, and vitamin D_2; the respective retention times were 5.4, 7.5, and 8.2 min. Degradation products of vitamin D_3 (not shown) showed a similar elution profile.

Figures 2 and 3 show representative chromatograms of multivitamin preparations. Included are chromatograms of vitamin D_2 in a multivitamin–mineral tablet formulation (Fig. 2) and in a multivitamin capsule formulation (Fig. 3). Chromatograms of placebos showed no interference with the vitamin D peak. Separation of vitamin D from interfering excipient peaks (due largely to degradation of vitamins A and E) and the previtamin D isomer was achieved in each example. Tachysterol was not detected in any preparation, although it was resolved from the vitamin D peak when the degraded D mixture was injected to determine system suitability. Progesterone, which served as an internal standard, was separated completely from vitamin D, its degradation products, and any excipient peaks.

Table I shows an example of a spike recovery study of vitamin D_2 from a multivitamin–mineral placebo formulation. The placebo was spiked with gelatin beadlets from 60 to 120% of theory and carried through the assay. The mean recovery for 10 samples was 99.4% with a relative standard deviation (*RSD*) of 2.2%.

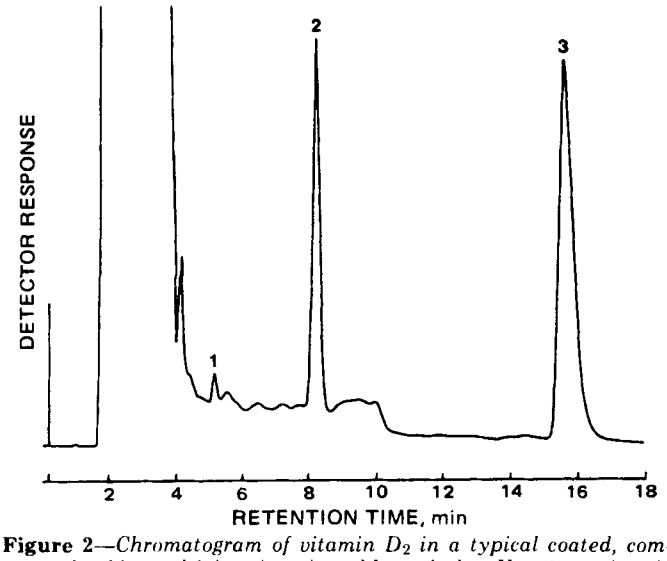

Figure 2—*Chromatogram of vitamin D_2 in a typical coated, compressed, tablet multivitamin–mineral formulation. Key: 1, previtamin D_2; 2, vitamin D_2; and 3, progesterone (internal standard).*

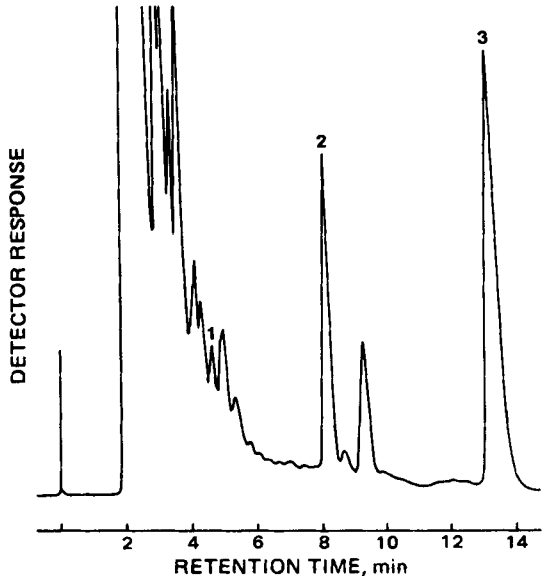

Figure 3—*Chromatogram of vitamin D_2 in a typical capsule multivitamin formulation. Key: 1, previtamin D_2; 2, vitamin D_2; and 3, progesterone (internal standard).*

The data from the recovery studies also provided a comparison of the previtamin D_2 concentration in the bulk drug and in the product formulation. A sample chromatogram (Fig. 2) shows that previtamin D_2 clearly was resolved from excipient peaks. The previtamin D_2 concentration in gelatin beadlets was constant. The mean value for the percentage of previtamin D_2 in seven lots of gelatin beadlets was 11.1% with a relative standard deviation of 3.2%. In comparison, the mean percentage of previtamin D_2 in 14 lots of product formulation was calculated to be 11.0% with a relative standard deviation of 4.2%. Although all product lots were assayed within the expiration date, the age of the samples varied across a range to the limit of expiration.

An alternative to the direct measurement of the previtamin is the use of a well-characterized lot of vitamin D in bulk drug (*i.e.*, gelatin beadlets) as the reference standard. As long as the bulk drug has been maintained at the same temperature as the product formulations and has not been exposed to prolonged UV irradiation, the percentage of previtamin D in the bulk drug is equal to that in the product formulation in accordance with the temperature-dependent equilibrium between these isomers. As indicated previously, the amount of previtamin D_2 in gelatin beadlets and in the formulations in which they had been added was found to be ~11% of the potential vitamin D content when both were stored at room temperature (25°). However, to maintain control of the assay, the potency of the bulk drug was determined periodically *versus* a ergocalciferol USP reference standard.

The use of a well-characterized lot of gelatin beadlets containing vitamin D_2 as a reference standard permits reproducible determinations of the potential vitamin D content in multivitamin formulations. For example, when 12 replicate samples of a multivitamin tablet formulation were assayed over 3 days, the relative standard deviation was 3.5%.

A comparison of assay results obtained by HPLC and the current compendial chemical procedure for the determination of vitamin D_2 in

Table I—Recovery of Vitamin D_2 in Gelatin Beadlets from a Multivitamin–Mineral Placebo Formulation

Day	Percent of Theory	Vitamin D_2 Added, μg	Vitamin D_2 Found, μg	Recovery, %
1	60	140.6	141.3	100.5
1	70	164.2	158.4	96.5
1	80	187.8	185.4	98.7
1	90	211.1	205.2	97.2
1	100	234.8	239.4	102.0
1	120	281.3	273.6	97.3
2	60	140.9	138.7	98.4
2	70	164.8	167.8	101.8
2	90	211.1	216.0	102.3
2	100	234.8	232.4	99.0
Mean				99.4
RSD				2.2

Table II—Potential Vitamin D Content for Several Lots of a Multivitamin–Mineral Formulation [a]

Lot	HPLC Assay Result, μg/tablet	Chemical Assay Result, μg/tablet
A	11.3	11.6
B	11.8	12.5
C	11.1	13.0
D	11.1	11.4
E	12.7	12.8
F	11.4	12.6
G	11.2	11.7
H	11.2	12.4
I	11.2	12.1
J	11.1	11.4
K	11.2	12.1
L	12.0	11.7
M	11.7	12.9
N	12.2	12.2
O	11.6	11.5
Mean	11.5	12.1

[a] Theoretical content was 11.7 μg/tablet.

15 lots of a multivitamin–mineral tablet formulation is shown in Table II. Vitamin D_2 in gelatin-coated beadlets was used as a reference standard for the HPLC analysis. Each assay result was the average of at least two determinations. The relative standard deviations associated with the HPLC and chemical assays were ~4 and 8%, respectively. For the 15 lots of multivitamin formulation, the mean value for the vitamin D content by the HPLC assay was 11.5 μg/tablet (98% of theory); by the chemical assay, it was 12.1 μg/tablet (103% of theory). The chemical assay results were statistically different at the 95% level of confidence from the results obtained by the HPLC assay.

If the photochemical isomers of vitamin D are held to a minimum, the assay values by the chemical procedure should be approximately equal to the sum of the values for previtamin D_2 and vitamin D_2 as determined by HPLC. However, if such isomers are present at a significant concentration, the results of the chemical assay should be significantly higher than those obtained by the HPLC assay because the chemical method is a colorimetric assay that does not distinguish between previtamin D_2, vitamin D_2, or any of the vitamin D_2 photochemical isomers, which, although separated by HPLC, would positively bias vitamin D_2 chemical analysis.

The use of bulk drug as a working reference standard for the determination of the vitamin D content in commercial multivitamin preparations is recommended when it is known that the bulk drug and product formulation have been handled and stored under similar conditions. These conditions preferably are met by storage and sample preparation at room temperature in the absence of UV irradiation. This approach in the quantitation of the potential vitamin D content in product formulations by HPLC is practical and reliable and does not require direct measurement of the previtamin concentration or time-consuming, frequently imprecise, heat equilibration experiments. Sample preparation is quick, with a single extraction step for most formulations. Assay time is <20 min/sample, and the assay can be automated easily. Chromatography is specific and selective. The assay results are reproducible and within 4% of manufacturing theory for the potential vitamin D content.

REFERENCES

(1) "The United States Pharmacopeia," 19th rev., Mack Publishing Co., Easton, Pa., 1975, pp. 633, 634.

(2) R. C. Williams, J. A. Schmit, and R. A. Henry, *J. Chromatogr. Sci.*, **10**, 494 (1972).

(3) D. F. Tomkins and R. J. Techerne, *Anal. Chem.*, **46**, 1602 (1974).

(4) H. Hofsass, A. Grant, N. J. Alicino, and S. B. Greenbaum, *J. Assoc. Off. Anal. Chem.*, **59**, 251 (1976).

(5) K. A. Tartivita, J. P. Saarello, and B. C. Rudy, *J. Pharm. Sci.*, **65**, 1024 (1976).

(6) R. Vanbaelen-Fastre' and M. Vanhaelen, *J. Chromatogr.*, **153**, 219 (1978).

(7) S. A. Barnett and L. W. Frick, *Anal. Chem.*, **51**, 641 (1979).

(8) J. C. Sheridan, "Final Report of the PMA-QC Collaborative Study on Vitamin D using Liquid Chromatography," Jan. 3, 1977.

(9) A. F. Wagner and K. Folkers, "Vitamins and Coenzymes," Interscience, New York, N.Y., 1965, p. 354.

(10) E. Havingo, A. L. Koevoet, and A. Verloop, *Rec. Trav. Chim. Pays-Bas*, **74**, 1230 (1955).

ACKNOWLEDGMENTS

The authors thank Martha Catherman for excellent technical assistance.

Ligand Interaction of Substituted Pyridines with Cytochrome P-450

JERRY L. BORN ˣ and SHERREL EARLY

Received March 12, 1979, from the *College of Pharmacy, University of New Mexico, Albuquerque, NM 87131.* Accepted for publication November 20, 1979.

Abstract □ A series of pyridyl ketones and alkyl pyridines was evaluated as type II ligands for cytochrome P-450. Activity as type II ligands was evaluated in terms of the lipid solubility and the pKa values of the compounds.

Keyphrases □ Ligands—interaction of substituted pyridines and pyridyl ketones with cytochrome P-450, effects of lipid solubility and pKa values on ligand activity □ Pyridines, substituted—ligand interaction with cytochrome P-450, effects of lipid solubility and pKa values on ligand activity □ Ketones, pyridyl—ligand interaction with cytochrome P-450, effects of lipid solubility and pKa values on ligand activity

Cytochrome P-450, the terminal oxidase responsible for many hydroxylation reactions (1, 2), binds to various substrates to produce type II difference spectra (1–6). Compounds that produce type II spectra include alcohols, primary amines, ketones, and pyridines (2).

BACKGROUND

Cytochrome P-450 is an iron-containing porphyrin in which the fifth ligand is a sulfhydryl group and the sixth ligand is a water molecule (7) or an imidazole ring (8). The displacement of the sixth ligand of cytochrome P-450 by pyridine or a pyridine ring of metyrapone[1] (2-methyl-1,2-di-3-pyridyl-1-propanone, I) is thought to result in a pyridine-coordinated cytochrome P-450. The ability of primary amines to produce type II spectra is a function of their ability to bind at a hydrophobic site (5). The base strength of pyridines, as well as an unhindered approach of the pyridine nitrogen to the enzyme, are essential for ligand interaction (9).

Figure 1 shows a proposed (7) binding model for I with cytochrome P-450. The pyridine ring, which is coordinated with the heme site, has a carbonyl attached at position 3; the alkyl-substituted pyridine ring binds at a site removed from the heme portion.

Although this model provides a convenient visualization of the cytochrome P-450 active site, no experimental evidence is available to indicate which pyridine ring of I interacts with the heme site. In addition, the role of secondary binding forces in the interaction of pyridine compounds and cytochrome P-450 has not been investigated.

The difference in the pKa values between the two pyridine rings of I is not likely to be as large as suggested by the pKa values of 5.85 and 3.18 for 3-picoline (II) (10) and 3-pyridyl methyl ketone (III) (11), respectively. Intramolecular steric interactions between the methyl groups of I and the carbonyl-substituted pyridine ring preclude coplanarity of the pyridine ring and the carbonyl group. This situation increases the pKa value of the carbonyl-substituted pyridine ring compared to that of III. Thus, it is not possible to predict which pyridine ring of I coordinates with cytochrome P-450 without considering the role of the carbonyl group in the interaction.

To evaluate further the mode of binding of pyridine compounds to cytochrome P-450, a series of 2-, 3-, and 4-substituted pyridines (Table I) was prepared and evaluated as type II ligands.

EXPERIMENTAL[2]

Pyridyl Ketones—Except for the commercially available pyridyl aldehydes and methyl pyridyl ketones, all pyridyl ketones were prepared by the addition of the appropriate cyanopyridine at 0.05 *M* in 75 ml of benzene to the appropriate alkyl magnesium bromide (ethyl, *n*-propyl, or *n*-butyl) at 0.1 *M* in 150 ml of ether. The reaction mixture was stirred and refluxed for 2 hr, 50 ml of 5% HCl was added slowly, and the mixture was refluxed overnight. The reaction mixture then was made basic with 10% NaOH, cooled, and extracted with ether; the extract then was dried under vacuum. The residue was distilled to give the expected pyridyl ketone. In each case, the physical characteristics of the compounds were as reported previously (12, 13).

4-Alkyl Pyridines—The 4-alkyl pyridines were prepared as described by Wibaut and Hey (14), except for the commercially available methyl- and ethylpyridines. The compounds were purified by repeated recrystallization of their picrates. The free base was obtained by treating the picrates with 10% NaOH and extracting the free base with ether. The ether was dried and removed, and the residue was distilled.

3-Alkyl Pyridines—The 3-alkyl pyridines were prepared by Wolff–Kishner reduction of the 1-(3-pyridyl) ketones. The 1-(3-pyridyl) ketone (0.019 *M*) was dissolved in 25 ml of diethylene glycol, which contained 3.5 g of potassium hydroxide (0.062 *M*) and 4 ml of 85% hydrazine hydrate, and then was refluxed for 4 hr. Distillation directly from the reaction vessel gave a mixture of water and the 3-alkyl pyridine. The 3-alkyl pyridine was separated from the water by extraction with ether, which then was dried and removed. The residue was distilled to give the expected 3-alkyl pyridine. The observed boiling points, literature (15) boiling points, and yields were: *n*-propyl, 76°/40 mm, 182–184°/743 mm, 32%; *n*-butyl, 88°/22 mm, 75–76°/7.5 mm, 41%; and *n*-pentyl, 115–116°/25 mm, 110–112°/20 mm, 37% (15).

Determination of Spectral Binding Constant (K_s)—Phenobarbital sodium (80 mg/kg) was injected intraperitoneally into male Sprague–Dawley rats for 3 consecutive days. The animals then were fasted for 24 hr and sacrificed by decapitation. During the isolation of microsomes, all tissue was maintained at 0–4°. The liver was removed, washed with 0.25 *M* sucrose, and then homogenized in 10 volumes of 0.25 *M* sucrose using a Potter–Elvehjem glass tube and a polytef pestle.

The homogenized material was centrifuged for 15 min at 10,000×*g*,

Table I—Spectral Binding Constants (K_s) and Relative Activities for 3- and 4-Substituted Pyridines

Compound	$K_s \times 10^{-4}$ *M*[a]	*SEM*	Relative Activity
Isonicotinaldehyde (XIX)	10.4	0.731	1.00
Nicotinaldehyde (XVI)	10.4	0.702	1.00
3-Pyridyl methyl ketone (III)	5.17	0.0402	2.01
4-Pyridyl methyl ketone (IV)	5.04	0.405	2.06
β-Picoline (II)	3.53	0.253	2.94
1-(4-Pyridyl)propanone (XX)	2.21	0.130	4.70
1-(3-Pyridyl)propanone (XVII)	2.17	0.032	4.79
1-(3-Pyridyl)butanone (XVIII)	1.74	0.110	5.97
γ-Picoline (XII)	1.66	0.041	6.26
3-Ethylpyridine (IX)	1.61	0.0945	6.45
1-(4-Pyridyl)butanone (XXI)	1.53	0.113	6.79
1-(3-Pyridyl)pentanone (VI)	1.32	0.0120	8.00
4-Ethylpyridine (XIII)	1.11	0.110	9.36
1-(3-Pyridyl)propane (X)	0.934	0.021	11.13
1-(4-Pyridyl)pentanone (V)	0.753	0.0509	13.81
1-(4-Pyridyl)propane (XIV)	0.655	0.456	15.87
1-(3-Pyridyl)butane (XI)	0.483	0.0353	21.53
1-(3-Pyridyl)pentane (VIII)	0.375	0.0182	27.73
1-(4-Pyridyl)butane (XV)	0.375	0.00841	27.73
1-(4-Pyridyl)pentane (VII)	0.256	0.0153	40.62
2-Methyl-1,2-di-3-pyridyl-1-propanone (I)	0.0135	0.000551	800.00

[a] Values are means ± *SEM*, $n = 3$.

[1] Ciba-Geigy.

[2] Difference spectra were obtained using a Beckman M-VI Acta spectrophotometer equipped with a scattered transmission accessory.

0022-3549/80/0700-0850$01.00/0
© 1980, American Pharmaceutical Association

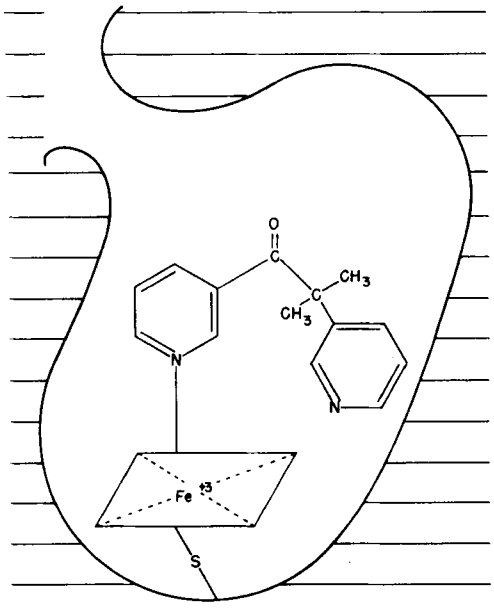

Figure 1—*Proposed interaction (7) of I with the heme portion of cytochrome P-450 via coordination of the carbonyl-substituted pyridine ring of I.*

and the supernate was removed and centrifuged at 100,000×*g* for 1 hr to produce a microsomal pellet. The microsomal pellet was resuspended in 0.15 *M* KCl and recentrifuged at 100,000×*g* for 1 hr. The microsomal pellet obtained by recentrifugation was resuspended in 0.05 *M*, pH 7.4 tromethamine buffer. Then the protein concentration was determined (16) and adjusted to 1 mg/ml with the buffer.

Difference spectra were recorded by placing 3 ml of the protein solution in both the sample and reference cells and then recording the baseline. After the baseline was established, 3-μl portions of the substrate dissolved in tromethamine buffer were added to the sample cell, and successive spectra were recorded. When the solubility of the substrate in the buffer was low, spectroanalyzed methanol was utilized to dissolve the compounds. Addition of as much as 21 μl of methanol to the sample cell did not change the spectra.

Each compound was examined in triplicate at six concentrations. The spectral binding constant, K_s, was determined by substituting the difference between the maximum (427 nm) and minimum (393 nm) absorbances in the spectrum for V in the classical enzyme substrate model (17). The correlation coefficient for the determination of K_s was >0.96 in each case.

Log P values were calculated utilizing the Hansch method (18, 19). Yeh and Higuchi (20) reported π values for methylene substitution on pyridine of 0.61 ± 0.01 and log P values of 3.750 and 3.128 for VII and XV, respectively.

RESULTS AND DISCUSSION

The 2-pyridyl carbonyl compounds investigated failed to produce typical type II spectra. Picolinaldehyde did not produce a recognizable spectrum while 2-pyridyl methyl ketone, 1-(2-pyridyl)propanone, and 1-(2-pyridyl)butanone gave weak type I spectra. 1-(2-Pyridyl)pentanone gave a weak type I spectrum at concentrations up to 2.7×10^{-3} *M*, but a modified type II spectrum was generated when concentrations exceeded 5.6×10^{-3} *M*. The lack of typical type II spectra for the 2-pyridyl carbonyls was not unexpected since their low pKa values, coupled with the steric inhibition of binding by the 2-substituent, would be expected to be unfavorable to type II binding.

On the basis of the pKa values of 3.18 (11) and 3.51 (21) for III and 4-pyridyl methyl ketone (IV), respectively, the 4-pyridyl ketones were expected to be more effective as type II ligands for cytochrome P-450 than the 3-pyridyl ketones. The spectral binding constants, K_s, of these compounds were quite similar, with only 1-(4-pyridyl)pentanone (V) exhibiting an increase in binding as compared to its 3-pyridyl analog (VI) (Table I).

The most basic compounds of this series, the 4-alkyl pyridines (10), also were the most potent type II ligands for cytochrome P-450. The K_s value of 1-(4-pyridyl)pentane (VII) was 1.4 times that of 1-(3-pyridyl)-pentane (VIII) and 2.9 times that of its parent ketone (V).

A plot of log P *versus* log K_s for the 3-alkyl pyridines (II and VIII–XI), the 4-alkyl pyridines (VII and XII–XV), the 3-pyridyl ketones (III, VI, and XVI–XVIII), and the 4-pyridyl ketones (IV, V, and XIX–XXI) produced in each case a straight line with a correlation coefficient of >0.93. This result suggests that lipid solubility of pyridine compounds is important in the ligand interaction.

The role of the carbonyl group in the ligand interaction is observed when alkyl pyridines and pyridyl ketones of similar log P values are compared. The strength of the ligand interaction of pyridyl ketones was surprising in view of their low pKa values. When K_s values for compounds with similar log P values are compared, the pyridyl ketones have equal or greater activity compared to that of the alkyl pyridines. Thus, the K_s values of 1-(3-pyridyl)butanone (XVIII) (log P 1.32) and 1-(4-pyridyl)-butanone (XXI) (log P 1.32) are essentially equal to the K_s value for 4-picoline (XII) (log P 1.26) and greater than that of 3-picoline (II) (log P 1.26). Comparison of the K_s values for V (log P 1.93), 1-(3-pyridyl)pentanone (VI) (log P 1.93), 4-ethylpyridine (XIII) (log P 1.87), and 3-ethylpyridine (IX) (log P 1.87) reveals a similar pattern. The 1-(3-pyridyl)-ketones are more potent ligands for cytochrome P-450 than the 3-alkyl pyridines of similar log P values, suggesting that the introduction of a carbonyl group in the 3-pyridyl series increases the strength of the ligand interaction. This increase in activity occurs in spite of the fact that the pyridyl ketones are less basic than the alkyl pyridines.

In summary, the data indicate that the carbonyl group in simple pyridine compounds is an important determinant in the strength of ligand interactions. The interaction of I with cytochrome P-450 is supported by the data (Fig. 1).

REFERENCES

(1) J. R. Gillette, *Adv. Pharmacol.*, **4**, 219 (1966).

(2) G. J. Mannering, in "Fundamentals of Drug Metabolism and Drug Disposition," B. N. LaDu, H. G. Mandel, and E. L. Way, Eds., Williams & Wilkins, Baltimore, Md., 1979, chap. 12.

(3) J. B. Cshenkman, H. Remer, and R. W. Estabrook, *Mol. Pharmacol.*, **3**, 113 (1967).

(4) Y. Imai and R. Sato, *J. Biochem.*, **62**, 239 (1967).

(5) C. R. E. Jefcoate, J. L. Gaylor, and R. Calabrese, *Biochemistry*, **8**, 3455 (1969).

(6) J. B. Schenkman, *ibid.*, **9**, 2081 (1970).

(7) B. W. Griffin, J. A. Peterson, J. Werringloer, and R. W. Estabrook, *Ann. N.Y. Acad. Sci.*, **244**, 107 (1975).

(8) M. Chevion, J. Peisach, and W. Blumberg, *J. Biol. Chem.*, **252**, 3637 (1977).

(9) J. L. Born and D. Vaughn, *J. Pharm. Sci.*, **66**, 1046 (1977).

(10) N. Ikekana, Y. Sato, and T. Maeda, *Pharm. Bull.*, **2**, 205 (1954).

(11) "Handbook of Tables for Organic Compound Identification," 3rd ed., Z. Rappoport, Ed., Chemical Rubber Co., Cleveland, Ohio, 1967.

(12) C. R. Warner, E. J. Walsh, and R. F. Smith, *J. Chem. Soc.*, **1962**, 1232.

(13) S. Pavlov and V. Arsenijevle, *Glas. Hem. Drus. Beograd*, **32**, 469 (1967).

(14) J. P. Wibaut and J. W. Hey, *Rec. Trav. Chim.*, **72**, 513 (1953).

(15) A. D. Miller and R. Revine, *J. Org. Chem.*, **27**, 168 (1957).

(16) G. H. Lowry, N. J. Rosenbrough, A. L. Farr, and R. J. Randall, *J. Biol. Chem.*, **193**, 265 (1951).

(17) K. C. Leibman, A. G. Hildebrandt, and R. W. Estabrook, *Biochem. Biophys. Res. Commun.*, **36**, 789 (1969).

(18) J. Iwasa, T. Fugita, and C. Hansch, *J. Med. Chem.*, **8**, 150 (1965).

(19) A. Leo, C. Hansch, and D. Gilkins, *Chem. Rev.*, **71**, 525 (1971).

(20) K. C. Yeh and W. I. Higuchi, *J. Pharm. Sci.*, **61**, 1648 (1972).

(21) A. Fisher, W. J. Galloway, and J. Vaughn, *J. Chem. Soc.*, **1964**, 3521.

Saturation Adsorption at Interfaces of Surfactant Solutions

HANS SCHOTT

Received November 19, 1979, from the *School of Pharmacy, Temple University, Philadelphia, PA 19140.* Accepted for publication February 7, 1980.

Abstract □ Plots of the surface or interfacial tension of aqueous surfactant solutions *versus* the logarithm of the bulk concentration of the surfactant frequently become linear at concentrations from 10 to 30% of the critical micelle concentration. According to the Gibbs equation, the surface excess concentration of the surfactant in the linear region is constant; saturation adsorption is said to exist. However, the surface or interfacial tension continues to decrease considerably with increasing bulk concentration of the surfactant throughout the saturation adsorption region until the critical micelle concentration is reached. This decrease is explained as follows. While the surface excess concentration of the surfactant reaches a constant upper limit at the onset of saturation adsorption, the total surfactant concentration in the surface layer, which consists of the surface excess concentration plus the surfactant concentration present in an equivalent volume of bulk solution, continues to increase slightly with increasing bulk concentration throughout the saturation adsorption region. As the bulk concentration approaches the critical micelle concentration, the total surface concentration of the surfactant exceeds its surface excess concentration by small but increasing amounts. Because the surfactant monolayer in the saturation adsorption region is densely packed, slight increases in the total surface concentration produce disproportionately large decreases in the surface or interfacial tension. This explanation is illustrated with experimental data.

Keyphrases □ Surface tension—decrease with increasing bulk concentration of surfactant in saturation adsorption region □ Surfactants—surface tension decrease with increasing bulk concentration of surfactant in saturation adsorption region □ Saturation adsorption region—surface tension decrease with increasing bulk concentration of surfactant

The surface or interfacial tension of aqueous surfactant solutions frequently becomes a linear function of the logarithm of the surfactant concentration when that concentration comes within ~20% of the critical micelle concentration (CMC). According to the Gibbs adsorption equation, the proportionality between the surface or interfacial tension and the logarithm of the bulk concentration of the surfactant indicates that its surface excess concentration has reached a constant value. This fact must be reconciled with the continued decrease of the surface or interfacial tension with increasing surfactant concentration until the critical micelle concentration is reached.

BACKGROUND

Plots of the surface or interfacial tension, γ, of surfactant solutions *versus* the logarithm of the surfactant concentration, c_2, commonly consist of three distinct regions as shown in Fig. 1 for surface tension. Interfacial tensions have lower values, but their curves have similar shapes (1, 2). The curve initially is nearly horizontal but turns gradually steeper as c_2 increases. Eventually, between points B and D, it becomes linear. This segment is followed by another linear segment, DE, that is practically horizontal. The concentration corresponding to point D, where the plot levels off, represents the critical micelle concentration. The surfactant concentration corresponding to point B frequently is reached at concentrations as low as 10–30% of the critical micelle concentration for surfactant adsorption at both air–water and oil–water interfaces (1–3).

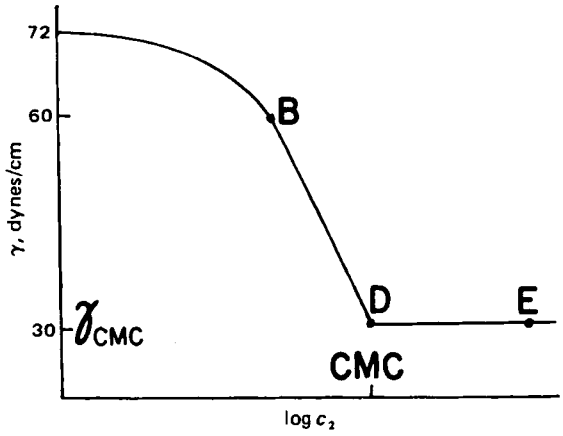

Figure 1—*Schematic plot of surface or interfacial tension* (γ) *versus logarithm of the surfactant concentration* (c_2). *The ordinate scale represents surface tension values.*

The Gibbs equation correlates the surface or interfacial tension of surfactant solutions with their bulk concentration. For nonionic surfactants, or for ionic surfactants in the presence of swamping concentrations of nonsurface-active salts with the same counterion, the equation is (1, 2):

$$\Gamma_2 = -\frac{1}{2.303RT}\frac{d\gamma}{d\log c_2} \qquad \text{(Eq. 1)}$$

where Γ_2 is the surface excess concentration, R is the gas constant (8.314×10^7 ergs/mole/°K), and T is the absolute temperature. The subscript 2 refers to the dissolved surfactant. The solution is assumed to be sufficiently dilute to use surfactant concentration instead of activity.

If a surface layer of area A in square centimeters and thickness τ in centimeters contains $m_2 + n_2$ moles of surfactant while an equal volume of solution $A\tau$ in the bulk contains m_2 moles of surfactant, the surface excess or surface excess concentration of the surfactant is:

$$\Gamma_2 = n_2/A \qquad \text{(Eq. 2)}$$

The surface excess concentration and the total surface concentration of the surfactant, $(m_2 + n_2)/A$, generally are nearly identical because, by definition, surfactants are adsorbed very strongly at interfaces, making $n_2 \gg m_2$.

Along the linear portion BD, the surface excess Γ_2 is constant because the slope $d\gamma/d\log c_2$ is constant. Saturation adsorption has been reached at point B, *i.e.*, the surface excess of the surfactant does not increase further as a result of increases in its bulk concentration beyond point B. However, the surface tension of the solution continues to decrease conspicuously with increasing bulk concentration of the surfactant until point D is reached (1–3). At first glance, these two facts, namely, a constant Γ_2 accompanied by a decreasing γ resulting from an increasing c_2, seem contradictory. In an attempt to reconcile them, it was postulated that as c_2 increases, it becomes easier to bring surfactant molecules to the surface from the progressively more concentrated bulk solution despite attainment of saturation adsorption (1). Surface tension commonly is determined by measuring the resistance to increases in surface area. The continued drop in γ with increasing c_2 along BD was ascribed mainly to the increased activity of the surfactant in the bulk phase rather than at the interface (2).

The purpose of this report is to show that the specific reason for the decrease in surface or interfacial tension of the solution with increasing

0022-3549/80/0700-0852$01.00/0
© 1980, American Pharmaceutical Association

Table I—Comparison of n_2 and m_2 in the Saturation Adsorption Region at Interfaces of Aqueous Surfactant Solutions with Air or Hydrocarbons

Surfactant	Range of Saturation Adsorption, mole/liter		$n_2 \times 10^{10}$, moles	$m_2 \times 10^{13}$, moles[b], at		$\left(\frac{100\,m_2}{n_2}\right)$, %, at		Reference
	$c_{2,L}$[a]	$c_{2,U}$[a]		$c_{2,L}$	$c_{2,U}$	$c_{2,L}$	$c_{2,U}$	
$C_{12}H_{25}O(CH_2CH_2O)_{12}H$[c]	1×10^{-5}	1.4×10^{-4}	2.15	0.02	0.28	0.0009	0.013	4,5
Potassium laurate[d]	0.0016	0.0137	4.24	3.2	27	0.076	0.64	6
Dodecylamine hydrochloride[e]	0.00062	0.0035	5.20	1.2	7	0.024	0.14	6
N-Dodecyl-β-alanine[f]	0.0002	0.001	3.73	0.4	2	0.011	0.054	7
Sodium laurate[g]	0.003	0.017	3.66	6	34	0.16	0.93	3
Sodium lauryl sulfate[h]	0.00015	0.0014	3.16	0.3	2.8	0.009	0.089	3
Sodium nonyl sulfate[h]	0.010	0.043	3.04	20	86	0.66	2.83	3

[a] $c_{2,L}$ is the lower concentration limit of the saturation adsorption range, corresponding to point B; $c_{2,U}$ is the upper limit of the saturation adsorption range, corresponding to point D or the critical micelle concentration. [b] Calculated for a layer with a thickness, τ, of 2×10^{-7} cm and an area, A, of 1 cm^2. [c] Against air. [d] At a constant pH of 10.0 and a constant potassium-ion concentration of 0.1 mole/liter, against air. [e] At a constant pH of 2.0 and a constant chloride-ion concentration of 0.1 mole/liter, against air. [f] At the isoelectric point, against air. [g] At a constant pH of 10.5 and a constant sodium-ion concentration of 0.04 mole/liter, against *n*-heptane. [h] At a constant sodium-ion concentration of 0.1 mole/liter, against petroleum spirit.

bulk concentration of the surfactant in a concentration range where saturation adsorption prevails is that beyond point B, and especially close to point D, $m_2 + n_2$ can no longer be considered equal to n_2. While the surface excess concentration Γ_2 is constant along BD, the total surface concentration $(m_2 + n_2)/A$ continues to increase moderately with increasing c_2 or m_2.

THEORETICAL

Rearrangement of Eq. 1 and integration between the limits γ, c_2 and γ_{CMC},CMC, where γ_{CMC} is the plateau surface tension along DE, yields:

$$\gamma - \gamma_{CMC} = 2.303RT\Gamma_2 \log \text{CMC} - 2.303RT\Gamma_2 \log c_2 \quad \text{(Eq. 3)}$$

The number of moles of surfactant, m_2, contained in $A\tau$ cm^3 of bulk solution is directly proportional to the bulk concentration c_2. If c_2 is expressed in moles per liter:

$$c_2 = 1000m_2/A\tau \quad \text{(Eq. 4)}$$

After substituting and transposing γ_{CMC}, Eq. 3 becomes:

$$\gamma = a - b \log m_2 \quad \text{(Eq. 5)}$$

for the region (BD) of saturation adsorption, where Γ_2 is constant. The constants a and b are equal to $\gamma_{CMC} + 2.303RT\Gamma_2 \log \text{CMC} - 2.303RT\Gamma_2 \log (1000/A\tau)$ and $2.303RT\Gamma_2$, respectively. According to Eq. 5, γ continues to decrease with increasing bulk concentration even after saturation adsorption is reached because c_2 and m_2 increase while Γ_2 and n_2 remain constant.

RESULTS

The values of m_2 at the lower and upper limits of the saturation adsorption range are compared here with the corresponding n_2 values for seven surfactants. Calculations are shown for the nonionic surfactant $C_{12}H_{25}O(CH_2CH_2O)_{12}H$. At 23° (296 °K), $d\gamma/d \log c_2$ in the region of saturation adsorption below the critical micelle concentration was reported as −12.2 dynes/cm (4, 5). Application of the Gibbs equation results in $\Gamma_2 = 2.15 \times 10^{-10}$ mole/cm^2. Hence, $n_2 = A\Gamma_2 = 2.15 \times 10^{-10}$ mole of surfactant for a surface area, A, of 1 cm^2. Saturation adsorption, shown by the linearity of the γ *versus* log c_2 plot, prevailed from the critical micelle concentration of 1.45×10^{-4} mole/liter down to at least $c_2 = 1 \times 10^{-5}$. A surface layer with a thickness, τ, of 20 Å (2×10^{-7} cm) and an area, A, of 1 cm^2 contains $m_2 = c_2A\tau/1000 = 2.0 \times 10^{-15}$ mole of surfactant if the bulk concentration, c_2, is 1×10^{-5} mole/liter but contains 2.8×10^{-14} mole if c_2 is 1.4×10^{-4}. Since $n_2 = 2.15 \times 10^{-10}$ mole, these two m_2 values represent 0.0009 and 0.013% of n_2, respectively. The increase in m_2 from point B to point D amounts to 0.013 − 0.0009 = 0.012% of n_2.

These numerical values and the corresponding data for six additional surfactant systems are listed in Table I. The lower concentration limits of the saturation adsorption range for the three oil–water interfaces probably are smaller than the values shown in the $c_{2,L}$ column since Ref. 3 listed interfacial tension values only at three or four concentrations. The values of m_2 increase by almost an order of magnitude from the lower to the upper concentration limit of the saturation adsorption region, *i.e.*, from point B to point D in Fig. 1. However, most of the m_2 values amount to <1% of n_2. Likewise, the increases in m_2 from the lower to the upper concentration limit of the saturation adsorption region represent <1% of n_2 in most cases. Systems with higher critical micelle concentration values have higher absolute values of m_2 and also higher percentage values of m_2 with respect to n_2 since all seven n_2 values are of the same order of magnitude.

The value of 20 Å for the thickness of the surface region used in the calculations was selected arbitrarily as corresponding approximately to the length of a fully extended surfactant molecule. According to Eq. 4, larger τ values would produce proportionally larger m_2 values for a given bulk concentration, thereby also increasing the percentage of m_2 with respect to the constant n_2 value proportionally.

Despite the fact that the increases in the m_2 values from the lower to the upper concentration limit of the saturation adsorption region constitute only a small fraction of the n_2 values, they are responsible for sizable decreases in surface tension, ranging from 13 dynes/cm for polyoxyethylated dodecanol (4, 5) to 21 and 22 dynes/cm for dodecylamine hydrochloride and potassium laurate (6), respectively, and to 26 dynes/cm for dodecyl alanine (7). The decreases in interfacial tension amount to only 8–13 dynes/cm, but interfacial tensions are lower than surface tensions. Furthermore, the interfacial tension values from Ref. 3 are not available for the entire range of saturation adsorption, so the actual decreases in that range probably are larger.

Evidently, once saturation adsorption is reached, small increases in the total surface concentration of the surfactant produce large decreases in surface or interfacial tension. At that point, the monolayer of surfactant molecules adsorbed at the surface or interface of the aqueous solution is packed so densely that crowding only a few additional surfactant molecules into it substantially reduces the resistance of the surface or interface against expansion in area, *i.e.*, its surface or interfacial tension.

DISCUSSION

The large decrease in surface or interfacial tension that occurs when a small percentage of additional surfactant molecules is crowded into a monolayer in the saturation adsorption region as a result of increases in c_2 and m_2 has an analogy in monomolecular films of insoluble substances spread on water. These insoluble monolayers are characterized by plots of film pressure *versus* area per molecule. Film pressure is the lowering of surface tension caused by the monolayer, *i.e.*, the difference between the surface tension of clean water and of water plus the monolayer. It represents the expanding pressure exerted by the monolayer, which opposes the surface or contracting tension of the clean surface. When a condensed monolayer is compressed beyond the point of close packing, the film pressure–area curve rises steeply. Further small reductions in the area per adsorbed molecule, the equivalent of crowding a few additional molecules into the monolayer, cause large reductions in the surface tension of the system and, hence, large increases in its film pressure (8).

REFERENCES

(1) J. T. G. Overbeek, S. T. Mayr, and R. G. Donnelly, "Colloid and Surface Chemistry, a Self-Study Course," Study Guide, Part 1, Massachusetts Institute of Technology, Cambridge, Mass., 1971, lesson 6.

(2) M. J. Rosen, "Surfactants and Interfacial Phenomena," Wiley, New York, N.Y., 1978, chap. 2.
(3) F. van Voorst Vader, *Trans. Faraday Soc.*, **56**, 1067 (1960).
(4) H. Lange, *Int. Congr. Surface Activity, 3rd*, **1**, 279 (1960).
(5) H. Lange, *Kolloid-Z. Z. Polym.*, **201**, 131 (1965).
(6) C. P. Roe and P. D. Brass, *J. Phys. Chem.*, **76**, 4703 (1954).
(7) T. Okumura, A. Nakamura, K. Tajima, and T. Sasaki, *Bull. Chem. Soc. Jpn.*, **47**, 2986 (1974).
(8) A. W. Adamson, "Physical Chemistry of Surfaces," 3rd ed., Wiley, New York, N.Y., 1976, chap. 3.

ACKNOWLEDGMENTS

The author thanks Dr. E. Astigarrabia and Dr. E. D. Goddard for helpful suggestions and comments.

Simultaneous GLC Analysis of Salicylamide, Phenylpropanolamine Hydrochloride, Caffeine, Chlorpheniramine Maleate, Phenylephrine Hydrochloride, and Pyrilamine Maleate in Capsule Preparations

FABRIZIO DE FABRIZIO

Received November 19, 1979, from *Adcock-Ingram Laboratories, P.O. Box 2368, Johannesburg 2000, South Africa.* Accepted for publication February 2, 1980.

Abstract □ A GLC method is described for the quantitative determination of salicylamide, phenylpropanolamine hydrochloride, caffeine, chlorpheniramine maleate, phenylephrine hydrochloride, and pyrilamine maleate. The sample was dissolved in ethanol, and an aliquot of the solution was brought to dryness and treated with 0.1 ml of 4-(dimethylamino)pyridine in pyridine–acetic anhydride (1:1). The components were isolated and measured by applying 1 μl of the reaction mixture to a chromatograph equipped with a flame-ionization detector and fitted with 8% OV-101 glass columns. The accuracy was good. Dicyclohexylphthalate was used as the internal standard.

Keyphrases □ GLC, flame ionization—simultaneous analysis of salicylamide, phenylpropanolamine, caffeine, chlorpheniramine, phenylephrine, and pyrilamine, capsule preparations □ Salicylamide—GLC analysis, capsule preparations □ Phenylpropanolamine hydrochloride—GLC analysis, capsule preparations □ Caffeine—GLC analysis, capsule preparations □ Chlorpheniramine maleate—GLC analysis, capsule preparations □ Phenylephrine hydrochloride—GLC analysis, capsule preparations □ Pyrilamine maleate—GLC analysis, capsule preparations

GLC procedures have been used extensively for the determination of salicylamide (I), phenylpropanolamine hydrochloride (II), caffeine (III), chlorpheniramine maleate (IV), phenylephrine hydrochloride (V), and pyrilamine maleate (VI) as drug substances and in certain combinations, but no single method has been developed for their simultaneous quantitation. In the preparation used in this study, phenylephrine was the only active ingredient that had to be derivatized before GLC. The other components could have been chromatographed directly using a suitable liquid phase (1, 2).

The determination of phenylephrine as the trifluoroacetate derivative (3) was not applicable to this preparation. The narrow margin allowed for temperature and reaction time was not compatible with those components that gave derivatives with the same reagent. Hista and Laubach (4) showed that a combination of phenylephrine, phenyltoloxamine, chlorpheniramine, and phenylpropanolamine could be chromatographed as trimethylsilyl derivatives using bis(trimethylsilyl)acetamide. However, following the same procedure during a preliminary analysis, the chromatogram exhibited interfering additional peaks, which made the determination of some components difficult.

In this work, the problems encountered were resolved by preparing acetyl derivatives of I, II, and V and using a mixture of 4-(dimethylamino)pyridine, pyridine, and acetic anhydride as the acetylating reagent. Connors and Albert (5) reported that 4-(dimethylamino)pyridine is an excellent catalyst for the formation of acetyl derivatives. It promoted the acetylation of various hydroxyl groups under milder conditions when compared with pyridine alone (6).

EXPERIMENTAL

Apparatus—The gas chromatograph[1] was equipped with a flame-ionization detector and an electronic integrator. The glass-coil columns, 1.8 m × 2 mm, were packed with 8% OV-101 on 80–100-mesh Chromosorb W-HP.

Reagents[2]—4-(Dimethylamino)pyridine (1.2%) in pyridine was prepared weekly. Acetic anhydride also was used.

Solution Preparation—Standard solutions[3] were prepared by weighing accurately ~58, 38, 72, and 49 mg of II, IV, V, and VI, respec-

Table I—Response Factors of I–VI with Respect to the Internal Standard [a]

Compound	Response Factor	*RSD, %*
I	0.890	1.83
II	0.995	1.11
III	0.470	1.41
IV	0.677	1.28
V	0.624	1.64
VI	0.346	2.18

[a] Five solutions were prepared and 15 measurements were made for each compound.

[1] Hewlett-Packard model 5048-A.
[2] All reagents and the internal standard were from Merck, Schuchardt, West Germany.
[3] All standard solutions were prepared from BP raw materials standardized against USP and NF reference standards.

0022-3549/80/0700-0854$01.00/0
© 1980, American Pharmaceutical Association

(2) M. J. Rosen, "Surfactants and Interfacial Phenomena," Wiley, New York, N.Y., 1978, chap. 2.
(3) F. van Voorst Vader, *Trans. Faraday Soc.*, **56**, 1067 (1960).
(4) H. Lange, *Int. Congr. Surface Activity, 3rd*, **1**, 279 (1960).
(5) H. Lange, *Kolloid-Z. Z. Polym.*, **201**, 131 (1965).
(6) C. P. Roe and P. D. Brass, *J. Phys. Chem.*, **76**, 4703 (1954).
(7) T. Okumura, A. Nakamura, K. Tajima, and T. Sasaki, *Bull. Chem. Soc. Jpn.*, **47**, 2986 (1974).
(8) A. W. Adamson, "Physical Chemistry of Surfaces," 3rd ed., Wiley, New York, N.Y., 1976, chap. 3.

ACKNOWLEDGMENTS

The author thanks Dr. E. Astigarrabia and Dr. E. D. Goddard for helpful suggestions and comments.

Simultaneous GLC Analysis of Salicylamide, Phenylpropanolamine Hydrochloride, Caffeine, Chlorpheniramine Maleate, Phenylephrine Hydrochloride, and Pyrilamine Maleate in Capsule Preparations

FABRIZIO DE FABRIZIO

Received November 19, 1979, from *Adcock-Ingram Laboratories, P.O. Box 2368, Johannesburg 2000, South Africa.* Accepted for publication February 2, 1980.

Abstract □ A GLC method is described for the quantitative determination of salicylamide, phenylpropanolamine hydrochloride, caffeine, chlorpheniramine maleate, phenylephrine hydrochloride, and pyrilamine maleate. The sample was dissolved in ethanol, and an aliquot of the solution was brought to dryness and treated with 0.1 ml of 4-(dimethylamino)pyridine in pyridine–acetic anhydride (1:1). The components were isolated and measured by applying 1 μl of the reaction mixture to a chromatograph equipped with a flame-ionization detector and fitted with 8% OV-101 glass columns. The accuracy was good. Dicyclohexylphthalate was used as the internal standard.

Keyphrases □ GLC, flame ionization—simultaneous analysis of salicylamide, phenylpropanolamine, caffeine, chlorpheniramine, phenylephrine, and pyrilamine, capsule preparations □ Salicylamide—GLC analysis, capsule preparations □ Phenylpropanolamine hydrochloride—GLC analysis, capsule preparations □ Caffeine—GLC analysis, capsule preparations □ Chlorpheniramine maleate—GLC analysis, capsule preparations □ Phenylephrine hydrochloride—GLC analysis, capsule preparations □ Pyrilamine maleate—GLC analysis, capsule preparations

GLC procedures have been used extensively for the determination of salicylamide (I), phenylpropanolamine hydrochloride (II), caffeine (III), chlorpheniramine maleate (IV), phenylephrine hydrochloride (V), and pyrilamine maleate (VI) as drug substances and in certain combinations, but no single method has been developed for their simultaneous quantitation. In the preparation used in this study, phenylephrine was the only active ingredient that had to be derivatized before GLC. The other components could have been chromatographed directly using a suitable liquid phase (1, 2).

The determination of phenylephrine as the trifluoroacetate derivative (3) was not applicable to this preparation. The narrow margin allowed for temperature and reaction time was not compatible with those components that gave derivatives with the same reagent. Hista and Laubach (4) showed that a combination of phenylephrine, phenyltoloxamine, chlorpheniramine, and phenylpropanolamine could be chromatographed as trimethylsilyl derivatives using bis(trimethylsilyl)acetamide. However, following the same procedure during a preliminary analysis, the chromatogram exhibited interfering additional peaks, which made the determination of some components difficult.

In this work, the problems encountered were resolved by preparing acetyl derivatives of I, II, and V and using a mixture of 4-(dimethylamino)pyridine, pyridine, and acetic anhydride as the acetylating reagent. Connors and Albert (5) reported that 4-(dimethylamino)pyridine is an excellent catalyst for the formation of acetyl derivatives. It promoted the acetylation of various hydroxyl groups under milder conditions when compared with pyridine alone (6).

EXPERIMENTAL

Apparatus—The gas chromatograph[1] was equipped with a flame-ionization detector and an electronic integrator. The glass-coil columns, 1.8 m × 2 mm, were packed with 8% OV-101 on 80–100-mesh Chromosorb W-HP.

Reagents[2]—4-(Dimethylamino)pyridine (1.2%) in pyridine was prepared weekly. Acetic anhydride also was used.

Solution Preparation—Standard solutions[3] were prepared by weighing accurately ~58, 38, 72, and 49 mg of II, IV, V, and VI, respec-

Table I—Response Factors of I–VI with Respect to the Internal Standard [a]

Compound	Response Factor	*RSD, %*
I	0.890	1.83
II	0.995	1.11
III	0.470	1.41
IV	0.677	1.28
V	0.624	1.64
VI	0.346	2.18

[a] Five solutions were prepared and 15 measurements were made for each compound.

[1] Hewlett-Packard model 5048-A.
[2] All reagents and the internal standard were from Merck, Schuchardt, West Germany.
[3] All standard solutions were prepared from BP raw materials standardized against USP and NF reference standards.

0022-3549/80/0700-0854$01.00/0
© 1980, American Pharmaceutical Association

Table II—Precision and Accuracy of the Standard Solution

Trial	Recovery, % I	II	III	IV	V	VI
1	98.3	99.7	101.0	98.1	98.6	100.3
2	99.5	99.9	101.2	97.3	99.4	98.7
3	98.9	99.7	98.7	98.5	97.2	102.4
4	98.7	99.3	99.9	101.9	101.5	97.9
5	101.9	102.6	98.3	100.0	97.6	99.2
6	102.0	97.6	98.7	97.5	99.2	97.1
7	100.3	99.6	98.7	97.3	101.7	102.0
8	99.7	98.5	99.1	98.5	97.9	97.7
Mean relative error, %	1.11	0.85	0.90	1.03	1.34	1.61
$\bar{X}$	99.9	99.6	99.5	98.6	99.1	99.4
SD	1.33	1.43	1.12	1.54	1.72	1.99
RSD	1.34	1.44	1.13	1.56	1.73	1.99

tively, separately into 25-ml volumetric flasks and dissolving the solid and diluting the solution to 25 ml with ethanol. The internal standard solution was prepared by dissolving ~80 mg of dicyclohexylphthalate in 50 ml of chloroform.

Chromatography—The oven was programmed at 9°/min from 170 to 270° after an initial 3 min; the injection port and detector temperatures were 250 and 290°, respectively. The nitrogen carrier flow rate was 15 ml/min. Hydrogen and air flow rates were adjusted to give maximum response. The attenuation of 13 was reduced to 9 after 10 min.

Standard Preparation—About 240 mg of I and 40 mg of III were weighed accurately into a 50-ml volumetric flask. Standard solutions of II (4 ml), IV (1 ml), V (2 ml), and VI (4 ml) and 5 ml of the internal standard solution were added. The solution was brought to volume with ethanol. A 0.5-ml aliquot was evaporated in a 1-ml glass vial[4] with a gentle nitrogen stream at room temperature.

The residue was allowed to react with 0.1 ml of a 1:1 (v/v) mixture of

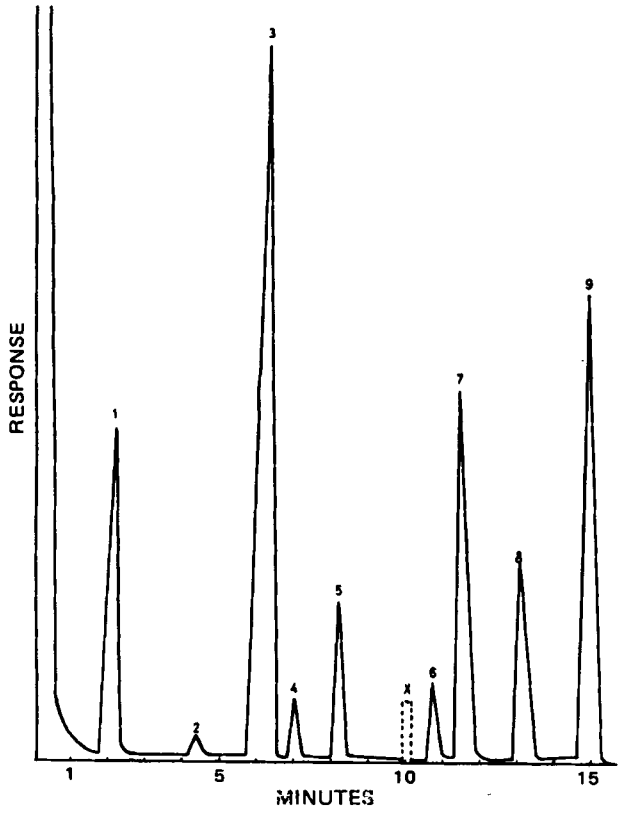

Figure 1—*Representative gas chromatogram. Key: 1 and 2, reagent peaks; 3, salicylamide; 4, phenylpropanolamine; 5, caffeine; 6, chlorpheniramine; 7, phenylephrine; 8, pyrilamine; and 9, internal standard.*

[4] Pierce Chemical Co., Rockford, Ill.

Table III—Precision Study of a Production Lot of Capsules

Parameter	Compound I	II	III	IV	V	VI
Theoretical content, mg/capsule	240	9.25	40	1.5	5.75	7.8
$\bar{X}^a$	241	9.30	40.6	1.56	5.82	7.91
RSD, %	1.41	1.50	1.12	1.34	1.88	1.83

[a] n = 10 determinations.

1.2% 4-(dimethylamino)pyridine solution and acetic anhydride (mixed just before use) for 18 ± 1 min at 40° in a screw-capped vial. One microliter of the reaction mixture was injected.

Sample Preparation—The contents of a representative number of capsules[5] were mixed, and an aliquot of powder corresponding to ~240 mg of I was weighed accurately into a 50-ml volumetric flask. About 30 ml of ethanol was added, and the flask was heated in a water bath at 80° for 15 min. The flask then was shaken mechanically until it was cool. Five milliliters of the internal standard solution was pipetted into the flask, and ethanol was added to the mark. An aliquot of the solution was centrifuged, and 0.5 ml of the clear supernate was treated as described for the standards.

RESULTS AND DISCUSSION

The performance of each component was evaluated by measurement of the response factor, the ratio of the peak area/weight of the substance to the peak area/weight of the internal standard (Table I). The results were obtained by preparing five solutions for each component having the same concentration range as in the commercial preparation. Each solution was analyzed five times.

When the concentration of each component was varied between 80 and 120% of the label claim, the response factor of salicylamide increased by ~3% with the same reproducibility. The pyrilamine maleate response factor decreased by ~5%, and the percent relative standard deviation of solutions of different concentrations was 3.48% compared to 2.18% for one concentration. The remaining components showed similar response factors and reproducibility as for solutions of one concentration.

The acetylation reaction was completed in 5 min for phenylephrine and phenylpropanolamine at room temperature, while salicylamide gave two peaks. Heating the reaction mixture at 40° for 18 min resulted in complete acetylation and a single peak for salicylamide (Fig. 1). The other components, III, IV, and VI, did not undergo nucleophilic catalysis since they did not have active hydrogen atoms. Preliminary injections of the reagent mixture alone after heating at 40° for 18 min showed two peaks at 1.67 and 4.65 min, which did not interfere. Prolonging the heating time beyond 30 min or maintaining the temperature at 90° for 5 min caused a third peak to appear at 13.96 min, which also did not interfere. The reaction mixture of all components was analyzed over a 3-hr period without a significant drifting of the response factor.

The accuracy and precision of the procedure were estimated by analyzing a standard solution containing all six active ingredients plus the internal standard. This solution was determined eight times (Table II). The precision study also was carried out by analyzing capsules of a production batch. The sample was injected 10 times (Table III). The data presented, including the reproducibility, accuracy, and response factor, establish the validity of the method. The procedure is relatively simple and rapid. The six active ingredients were chromatographed and determined in 17 min.

REFERENCES

(1) R. E. Madsen and D. F. Magin, *J. Pharm. Sci.*, **65**, 924 (1976).

(2) K. H. Goebbeler, *Dtsch. Apoth. Ztg.*, **3**, 1291 (1979); through *Anal. Abstr.*, **22**, 4432 (1971).

(3) L. J. Lawrence, P. M. Comi, and E. L. Pratt, *J. Pharm. Sci.*, **62**, 1761 (1973).

(4) C. Hishta, and R. G. Lauback, *ibid.*, **58**, 745 (1969).

(5) K. A. Connors and K. S. Albert, *ibid.*, **62**, 845 (1973).

(6) E. L. Rowe and S. M. Machlovech, *ibid.*, **66**, 273 (1977).

[5] Each capsule contained I (240 mg), II (9.25 mg), III (40 mg), IV (1.5 mg), V (5.75 mg), and VI (7.8 mg).

Structure–Activity Relationships of Benzohydroxamic Acid Inhibitors of Ribonucleotide Reductase

BART van't RIET *x, LEMONT B. KIER *, and HOWARD L. ELFORD ‡

Received July 5, 1979, from the **Department of Pharmaceutical Chemistry and the* ‡*Department of Biochemistry, Medical College of Virginia, Virginia Commonwealth University, Richmond, VA 23298.* Accepted for publication January 31, 1980.

Abstract □ A structure–activity relationship study of 28 substituted benzohydroxamic acids that inhibit ribonucleotide reductase was undertaken to discern the structural features of the molecule contributing to the inhibitory potency of these compounds. An equation containing three molecular connectivity indexes, but not including Hammett σ values, was developed which gives close correlation with observed values for ribonucleotide reductase inhibition. It is postulated that the inhibitory potency involves two parts of the benzohydroxamic acid molecule. One is the hydroxamic portion, which complexes with the metal component of the enzyme, providing a qualitative effect. The other is an interaction involving the benzene ring and its substituents and may provide the quantitative aspect of the observed inhibition values.

Keyphrases □ Hydroxyurea, analogs—substituted aryl hydroxamic acids, inhibition of ribonucleotide reductase, structure–activity relationships, molecular connectivity indexes □ Structure–activity relationships—substituted aryl hydroxamic acids, inhibition of ribonucleotide reductase, molecular connectivity indexes □ Molecular connectivity indexes—substituted aryl hydroxamic acids, inhibition of ribonucleotide reductase, structure–activity relationships □ Antitumor agents—substituted aryl hydroxamic acids, inhibition of ribonucleotide reductase, structure–activity relationships

The reduction of ribonucleotides to deoxyribonucleotides is a rate-limiting step in DNA biosynthesis and, hence, cellular replication. The required enzyme, ribonucleotide reductase, is inhibited by hydroxyurea, which presently is the only clinical antitumor agent with this primary mode of action. Replacement of the amino group of hydroxyurea by various aryl groups gives hydroxamic acids that inhibit ribonucleotide reductase at concentrations lower than those of hydroxyurea (1). The aryl hydroxamic acids also prolong the life of mice with L1210 leukemia (2, 3). Several aryl hydroxamic acids were reported to inhibit DNA synthesis (4, 5).

The possibility of improving on existing chemotherapeutic agents led to an examination of the relationship between the enzyme inhibitory potency and the structures of 28 pyridyl and benzohydroxamic acids, which were tested in this laboratory.

METHODS

Molecular structures can be analyzed in terms of the number of atoms, the kind of atoms, bonding types, and the adjacent environment by the molecular connectivity method (6–10). Molecular connectivity indexes have been computed for each compound in this study (7). In addition, the Hammett σ values for the substituents were summed for each compound and included as an electronic contribution variable. A multivariable search for the best correlation was conducted in a regression analysis.

The synthesis and testing of the *in vitro* inhibitory potency of the aryl hydroxamic acids were reported elsewhere (1, 3). The concentration for the ID_{50} used in this study is expressed as the pC value (Table I). The pC values were determined graphically from at least three concentrations within 1 log unit after determining the inhibition range. In repetitive experiments, the observed pC values agreed within 0.15 pC unit.

RESULTS AND DISCUSSION

A search for the best three-variable equation relating potency (expressed as pC) and structure (encoded with connectivity indexes) was conducted. Hammett σ values were included in the search but did not appear in any equation with a high correlation. The best equation is:

$$pC = 2.36(\pm0.04)^3\chi_p - 3.98(\pm0.53)^0\chi^v + 0.97(\pm0.05)(^1\chi^v)^2 + 9.20(\pm5.50) \quad \text{(Eq. 1)}$$

$$r = 0.943 \quad s = 0.21 \quad n = 28 \quad F = 64$$

Equation 1 explains about 90% of the variation in the data. Because of the experimental variation in pC determinations, the equation is nearly as good as can be expected from the data. Predicted values are found in Table I.

The $^3\chi_p$ index is a weighted count of contiguous three-path fragments, the $^0\chi^v$ index is based on atom deltas, and the $^1\chi^v$ index is a weighted count of bonds. The last two indexes are based on valence deltas. The connectivity index is computed by the general formula $^m\chi_t = \Sigma(\delta_i\delta_j \ldots \delta_n)^{-1/2}$, where m is the order (number of bonds), t is the type (the path in these cases), and the number of deltas in parentheses is equal to the number of bonded atoms in the fragment of order m.

It is apparent that the $^3\chi_p$ index quantifies a structure fragment that plays a favorable role in the pC value. The $^3\chi_p$ index can discriminate among compounds having the same number of substituents in different substitution patterns. Thus, the $^3\chi_p$ index is derived from an additional subgraph wherever two ring substituents are *ortho* to each other. Equation 1 thus describes this structural condition as more favorable for inhibitory potency than the alternative cases.

This situation is illustrated in several examples. Compounds IV, VI, and VIII have *ortho*-, *meta*-, and *para*-hydroxy substitution, respectively, and have the corresponding pC values of 3.82, 3.46, and 3.60. An identical case is found in the comparison of the monoamino derivatives, V, VII, and IX. Again, the *ortho*-substituent is described correctly by the equation as having a larger $^3\chi_p$ term and, hence, a larger pC value. Disubstituted derivatives reinforce this structural analysis (compare XIII–XVIII). Finally, XXVI is correctly described as having the largest pC value by virtue of having four adjacent ring substituents.

The influence of the $^0\chi^v$ and $^1\chi^v$ indexes essentially offsets the information encoded in $^3\chi_p$ (i.e., increasing size increases potency). This result leaves the $^3\chi_p$ index with the exclusive role of encoding the favorable influence of *ortho*-substituents.

The failure to find the Hammett σ term in any high correlation equation indicates that the electronic contribution of the ring substituents is not a prominent factor in the inhibitory potency.

Further evidence for this conclusion can be found in the direct comparison of several compounds. Compounds IV, V, and IX have significantly different Hammett σ values, but their pC values are close. Compounds VI and VII have appreciably different σ values whereas their observed pC values are the same. Thus, regression analysis reveals that electronic effects of the substituents are not prominent but that structural features encoded in the molecular connectivity indexes can account for most of the systematic variation in the pC values in this set of compounds.

These observations indicate that the ring substituents play a role in the inhibitory potency of the hydroxamic acid molecule. This role could take the form of an interaction involving the ring and its substituents or an interaction of the substituents themselves with the active site. Thus, the lack of an electronic contribution to the ring indicates that the general region of the ring must interact with an enzyme binding site. Therefore, it is postulated that two types of interaction occur: (*a*) an underlying constant activity of the hydroxamic acid function with the metal component of the enzyme and (*b*) an additional interaction due to the ring

0022-3549/80/0700-0856$01.00/0
© 1980, American Pharmaceutical Association

Table I—Calculated Inhibitory Potencies of Aryl Hydroxamic Acids

RCNHOH
‖
O

Compound	R	$^3\chi_p$	$^0\chi^v$	$^1\chi^v$	pC Found	pC Calc.
I	Pyridyl-2	3.099	5.112	2.698	3.30	3.23
II	Pyridyl-3	3.099	5.112	2.688	3.10	3.17
III	Unsubstituted phenyl	3.099	5.242	2.838	3.40	3.46
IV	2-Hydroxyphenyl	3.553	5.612	2.979	3.82	3.85
V	2-Aminophenyl	3.553	5.742	3.044	3.92	3.71
VI	3-Hydroxyphenyl	3.426	5.612	2.973	3.46	3.52
VII	3-Aminophenyl	3.426	5.742	3.038	3.46	3.38
VIII	4-Hydroxyphenyl	3.509	5.612	2.972	3.60	3.71
IX	4-Aminophenyl	3.509	5.742	3.038	3.82	3.57
X	4-Methylaminophenyl	3.917	6.665	3.499	3.48	3.79
XI	4-Dimethylaminophenyl	4.208	7.612	3.867	3.30	3.33
XII	4-Methoxyphenyl	3.917	6.573	3.361	3.30	3.24
XIII	2,3-Dihydroxyphenyl	4.145	5.982	3.119	5.10	4.60
XIV	2,4-Dihydroxyphenyl	3.873	5.982	3.113	3.60	3.92
XV	2,5-Dihydroxyphenyl	3.895	5.982	3.113	3.70	3.98
XVI	2,6-Dihydroxyphenyl	3.934	5.982	3.119	4.00	4.11
XVII	3,4-Dihydroxyphenyl	4.087	5.982	3.113	4.52	4.43
XVIII	3,5-Dihydroxyphenyl	3.664	5.982	3.107	3.40	3.40
XIX	2-Hydroxy-3-methylphenyl	4.145	6.535	3.395	3.82	4.15
XX	2-Hydroxy-4-aminophenyl	3.873	6.112	3.178	3.70	3.80
XXI	3,4-Dimethylphenyl	4.087	7.088	3.666	3.52	3.67
XXII	3,4-Diaminophenyl	4.087	6.242	3.243	4.40	4.20
XXIII	3,4-Dimethoxyphenyl	4.678	7.904	3.891	3.60	3.46
XXIV	2,4-Dichlorophenyl	3.873	7.478	3.861	3.35	3.03
XXV	3,4-Dichlorophenyl	4.087	7.478	3.861	3.60	3.54
XXVI	2,3,4-Trihydroxyphenyl	4.732	6.352	3.259	5.46	5.38
XXVII	3,4,5-Trihydroxyphenyl	4.593	6.352	3.253	5.00	5.02
XXVIII	3,4,5-Trimethoxyphenyl	5.391	9.235	4.420	4.00	4.10

and its substituents to give the quantitative differences found in enzyme inhibition values.

REFERENCES

(1) B. van't Riet, G. L. Wampler, and H. L. Elford, *J. Med. Chem.*, **22**, 589 (1979).

(2) H. L. Elford, *Proc. Am. Assoc. Cancer Res.*, **18**, 177 (1977).

(3) H. L. Elford, G. L. Wampler, and B. van't Riet, *Cancer Res.*, **39**, 844 (1979).

(4) G. R. Gale and J. B. Hynes, *J. Med. Chem.*, **11**, 191 (1968).

(5) G. R. Gale, J. B. Hynes, and A. B. Smith, *ibid.*, **13**, 571 (1970).

(6) L. B. Kier, L. H. Hall, W. J. Murray, and M. J. Randic, *J. Pharm. Sci.*, **64**, 1971 (1975).

(7) L. B. Kier and L. H. Hall, "Molecular Connectivity in Chemistry and Drug Research," Academic, New York, N.Y., 1976.

(8) L. B. Kier and R. A. Glennon, *Life Sci.*, **22**, 1589 (1978).

(9) T. DiPaolo, L. B. Kier, and L. H. Hall, *Mol. Pharmacol.*, **13**, 31 (1977).

(10) G. R. Parker, *J. Pharm. Sci.*, **67**, 513 (1978).

ACKNOWLEDGMENTS

Supported by American Cancer Society Grant IN-105C and National Cancer Institute Grant CA 21305.

The authors thank Roberta Elford for editorial assistance.

Sensitive Method for Determination of Ethinyl Estradiol in Presence of Norethindrone

SHINICHIRO HIRAI, ANWAR HUSSAIN ˣ, and SALIM BABHAIR

Received November 14, 1979, from the *College of Pharmacy, University of Kentucky, Lexington, KY 40506.* Accepted for publication February 8, 1980.

Abstract □ A sensitive spectrophotofluorometric procedure for the determination of microamounts of ethinyl estradiol is described. The method is useful for the determination of ethinyl estradiol in the presence of norethindrone and common tablet excipients, especially in dissolution media.

Keyphrases □ Ethinyl estradiol—spectrophotofluorometric analysis in the presence of norethindrone and common tablet excipients □ Spectrophotofluorometry—analysis, ethinyl estradiol in the presence of norethindrone and common tablet excipients □ Dissolution rates—ethinyl estradiol in tablets, spectrophotofluorometric analysis in the presence of norethindrone and common tablet excipients

To study the dissolution rate of ethinyl estradiol and norethindrone from tablets, a sensitive procedure is needed to determine microamounts of these drugs in the presence of each other. The spectrophotometric methods described in the USP (1) for the determination of the two drugs require at least 20 tablets of each and, consequently, cannot be used to determine very small amounts of ethinyl estradiol in the dissolution medium, especially in the pres-

0022-3549/80/0700-0857$01.00/0

© 1980, American Pharmaceutical Association

Table I—Calculated Inhibitory Potencies of Aryl Hydroxamic Acids

RCNHOH
‖
O

Compound	R	$^3\chi_p$	$^0\chi^v$	$^1\chi^v$	pC Found	pC Calc.
I	Pyridyl-2	3.099	5.112	2.698	3.30	3.23
II	Pyridyl-3	3.099	5.112	2.688	3.10	3.17
III	Unsubstituted phenyl	3.099	5.242	2.838	3.40	3.46
IV	2-Hydroxyphenyl	3.553	5.612	2.979	3.82	3.85
V	2-Aminophenyl	3.553	5.742	3.044	3.92	3.71
VI	3-Hydroxyphenyl	3.426	5.612	2.973	3.46	3.52
VII	3-Aminophenyl	3.426	5.742	3.038	3.46	3.38
VIII	4-Hydroxyphenyl	3.509	5.612	2.972	3.60	3.71
IX	4-Aminophenyl	3.509	5.742	3.038	3.82	3.57
X	4-Methylaminophenyl	3.917	6.665	3.499	3.48	3.79
XI	4-Dimethylaminophenyl	4.208	7.612	3.867	3.30	3.33
XII	4-Methoxyphenyl	3.917	6.573	3.361	3.30	3.24
XIII	2,3-Dihydroxyphenyl	4.145	5.982	3.119	5.10	4.60
XIV	2,4-Dihydroxyphenyl	3.873	5.982	3.113	3.60	3.92
XV	2,5-Dihydroxyphenyl	3.895	5.982	3.113	3.70	3.98
XVI	2,6-Dihydroxyphenyl	3.934	5.982	3.119	4.00	4.11
XVII	3,4-Dihydroxyphenyl	4.087	5.982	3.113	4.52	4.43
XVIII	3,5-Dihydroxyphenyl	3.664	5.982	3.107	3.40	3.40
XIX	2-Hydroxy-3-methylphenyl	4.145	6.535	3.395	3.82	4.15
XX	2-Hydroxy-4-aminophenyl	3.873	6.112	3.178	3.70	3.80
XXI	3,4-Dimethylphenyl	4.087	7.088	3.666	3.52	3.67
XXII	3,4-Diaminophenyl	4.087	6.242	3.243	4.40	4.20
XXIII	3,4-Dimethoxyphenyl	4.678	7.904	3.891	3.60	3.46
XXIV	2,4-Dichlorophenyl	3.873	7.478	3.861	3.35	3.03
XXV	3,4-Dichlorophenyl	4.087	7.478	3.861	3.60	3.54
XXVI	2,3,4-Trihydroxyphenyl	4.732	6.352	3.259	5.46	5.38
XXVII	3,4,5-Trihydroxyphenyl	4.593	6.352	3.253	5.00	5.02
XXVIII	3,4,5-Trimethoxyphenyl	5.391	9.235	4.420	4.00	4.10

and its substituents to give the quantitative differences found in enzyme inhibition values.

REFERENCES

(1) B. van't Riet, G. L. Wampler, and H. L. Elford, *J. Med. Chem.*, **22**, 589 (1979).

(2) H. L. Elford, *Proc. Am. Assoc. Cancer Res.*, **18**, 177 (1977).

(3) H. L. Elford, G. L. Wampler, and B. van't Riet, *Cancer Res.*, **39**, 844 (1979).

(4) G. R. Gale and J. B. Hynes, *J. Med. Chem.*, **11**, 191 (1968).

(5) G. R. Gale, J. B. Hynes, and A. B. Smith, *ibid.*, **13**, 571 (1970).

(6) L. B. Kier, L. H. Hall, W. J. Murray, and M. J. Randic, *J. Pharm. Sci.*, **64**, 1971 (1975).

(7) L. B. Kier and L. H. Hall, "Molecular Connectivity in Chemistry and Drug Research," Academic, New York, N.Y., 1976.

(8) L. B. Kier and R. A. Glennon, *Life Sci.*, **22**, 1589 (1978).

(9) T. DiPaolo, L. B. Kier, and L. H. Hall, *Mol. Pharmacol.*, **13**, 31 (1977).

(10) G. R. Parker, *J. Pharm. Sci.*, **67**, 513 (1978).

ACKNOWLEDGMENTS

Supported by American Cancer Society Grant IN-105C and National Cancer Institute Grant CA 21305.

The authors thank Roberta Elford for editorial assistance.

Sensitive Method for Determination of Ethinyl Estradiol in Presence of Norethindrone

SHINICHIRO HIRAI, ANWAR HUSSAIN ˣ, and SALIM BABHAIR

Received November 14, 1979, from the *College of Pharmacy, University of Kentucky, Lexington, KY 40506.* Accepted for publication February 8, 1980.

Abstract □ A sensitive spectrophotofluorometric procedure for the determination of microamounts of ethinyl estradiol is described. The method is useful for the determination of ethinyl estradiol in the presence of norethindrone and common tablet excipients, especially in dissolution media.

Keyphrases □ Ethinyl estradiol—spectrophotofluorometric analysis in the presence of norethindrone and common tablet excipients □ Spectrophotofluorometry—analysis, ethinyl estradiol in the presence of norethindrone and common tablet excipients □ Dissolution rates—ethinyl estradiol in tablets, spectrophotofluorometric analysis in the presence of norethindrone and common tablet excipients

To study the dissolution rate of ethinyl estradiol and norethindrone from tablets, a sensitive procedure is needed to determine microamounts of these drugs in the presence of each other. The spectrophotometric methods described in the USP (1) for the determination of the two drugs require at least 20 tablets of each and, consequently, cannot be used to determine very small amounts of ethinyl estradiol in the dissolution medium, especially in the pres-

0022-3549/80/0700-0857$01.00/0

© 1980, American Pharmaceutical Association

Table I—Composition of Powders Using Common Excipients

Ingredient	Vial 1	Vial 2	Ingredient	Vial 3	Vial 4
Ethinyl estradiol	0[a]	0.035	Ethinyl estradiol	0	0.035
Polyethylene glycol 6000	50	50	Lactose	250	250
Stearic acid	50	50	Cornstarch	74	74
Carbomen[b]	175	175	Microcrystalline cellulose[c]	175	175
Lactose	217	217	Magnesium stearate	1	1
Magnesium stearate	8	8	Total	500	500
Total	500	500			

[a] All values are expressed in milligrams. [b] Carbopol 934. [c] Avicel.

Table II—Effect of Tablet Excipients and Reproducibility of the Fluorometric Method

Vial[a]	Amount Added, μg	Number of Determinations	Mean Amount Found ± *SD*, μg
1	0	4	0.81 ± 0.06
2	35	7	35.5 ± 0.5
3	0	4	0.40 ± 0.08
4	35	7	35.1 ± 0.7

[a] Tablet excipients are shown in Table I.

ence of norethindrone and tablet excipients. It was shown that ethinyl estradiol exhibits fluorescence in the presence of sulfuric acid (2–5).

This report describes a sensitive spectrophotofluorometric procedure for the determination of very small amounts of ethinyl estradiol in dissolution media.

EXPERIMENTAL

Reagents and Equipment—Ethinyl estradiol[1] and norethindrone[1] were used as supplied. All other solvents and reagents were analytical reagent grade. A spectrophotofluorometer[2] was used.

Standard Solution and Sample Preparation—The standard stock solution of ethinyl estradiol was prepared to contain 3.5 μg of ethinyl estradiol/ml in chloroform. To determine if the common excipients used in tablet formulations interfere with the fluorometric analysis of ethinyl estradiol, four powder mixtures (Vials 1–4) were prepared (Table I). To determine the amount of ethinyl estradiol in the dissolution medium, two tablet formulations (Vials 2 and 4) were prepared[3] using 11.9-cm concave punches and die.

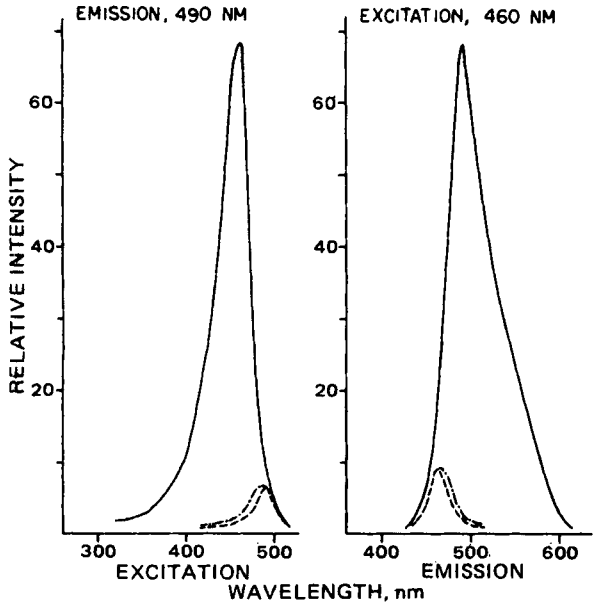

Figure 1—*Excitation and emission spectra of ethinyl estradiol. Key:* —, *ethinyl estradiol (140 ng/ml);* - · -, *norethindrone (2000 ng/ml); and* - - -, *blank.*

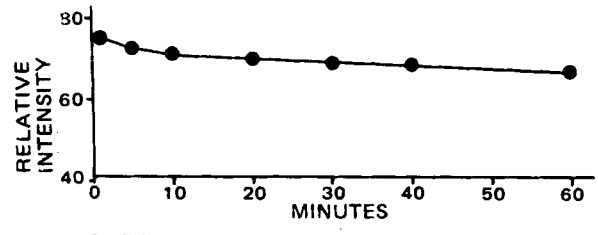

Figure 2—*Stability of fluorescence after the addition of sulfuric acid.*

Calibration Curve—Into screw-capped tubes were placed 0, 0.125, 0.25, 0.5, 1.0, and 2.0 ml of ethinyl estradiol in chloroform stock solution (3.5 μg/ml). The chloroform was removed under a nitrogen stream. The dry residue was redissolved in 0.5 ml of 4% sodium hydroxide–ethanol solution (4 g of sodium hydroxide in 100 ml of 10% ethanol–water). To this solution was added 2 ml of 80% sulfuric acid. The solution was mixed and left standing at room temperature for 30 min. The relative intensities of the fluorescence were measured at excitation and emission wavelengths of 460 and 490 nm, respectively.

Determination of Ethinyl Estradiol in Powder—Exactly 50 mg of each of the four powders (Table I) was suspended in 90 ml of water and extracted with 150 ml of chloroform. The chloroform layer was washed with 60 ml of water and dried over anhydrous sodium sulfate. Then 120 ml of the chloroform layer was evaporated to dryness under vacuum.

The residue was redissolved in 4 ml of ethanol, of which 0.5 ml was placed in a test tube and evaporated to dryness under a nitrogen stream. Ethinyl estradiol then was analyzed as described. The concentration was calculated by comparing the fluorescence of the sample to that of a known concentration treated similarly.

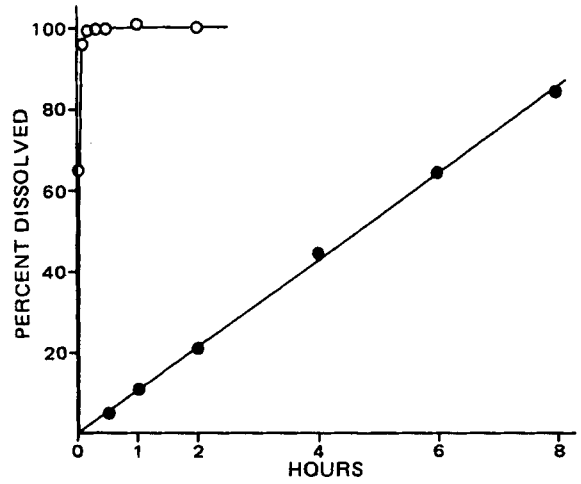

Figure 3—*Dissolution profile of ethinyl estradiol from tablets. Key:* ●, *sustained-release tablet (Vial 2); and* ○, *fast-release tablet (Vial 4).*

[1] Sigma Chemical Co.
[2] Aminco 768G, American Instrument Co., Silver Spring, Md.
[3] Stokes model 511-1 tablet machine, F. J. Stokes Corp., Philadelphia, Pa.

Determination of Ethinyl Estradiol in Dissolution Study—The release rate of ethinyl estradiol was determined at 37° using the USP rotating-basket apparatus in a dissolution medium containing 900 ml of distilled water. The basket was rotated at 100 rpm. At each sampling interval, 6 ml of the medium was withdrawn and extracted with 5 ml of chloroform. Then 4 ml of the chloroform layer was evaporated to dryness under a nitrogen stream. Ethinyl estradiol was analyzed as described.

RESULTS AND DISCUSSION

Figure 1 shows the excitation and emission spectra of ethinyl estradiol. Ethinyl estradiol exhibited strong fluorescence spectra at excitation and emission wavelengths of 460 and 490 nm, respectively. However, norethindrone did not exhibit fluorescence, even at the very high concentration of 2000 ng/ml (Fig. 1).

Figure 2 shows fluorescence stability for 1 hr after sulfuric acid addition. As can be seen in Fig. 2, the fluorescence of ethinyl estradiol was relatively stable; moreover, an excellent linearity between the fluorescence intensity and the ethinyl estradiol concentration over 17.5–280 ng/ml was observed; the minimum detection limit for the drug was ~10 ng/ml using this procedure.

The results of this study also indicate that the reproducibility of the method is excellent and that common tablet excipients do not interfere with the determination of ethinyl estradiol (Table II).

Finally, the method was valuable for the determination of small amounts of the drug in the dissolution study. Figure 3 shows the release rate of ethinyl estradiol from the sustained-release tablet (Vial 2) and the rapid-release tablet (Vial 4).

REFERENCES

(1) "The United States Pharmacopeia," 19th rev., Mack Publishing Co., Easton, Pa., 1975, p. 185.

(2) S. J. Kober, *Biochem. J.*, **32**, 357 (1938).

(3) A. J. Khoury and L. J. Cali, *J. Pharm. Sci.*, **56**, 1485 (1967).

(4) R. J. Templeton, W. A. Arnett, and I. M. Jakovljevic, *ibid.*, **57**, 1168 (1968).

(5) P. Comer and C. Stevenson, *ibid.*, **57**, 147 (1968).

COMMUNICATIONS

Potential Errors in Kinetic Studies of Hydrolysis of Nitrogen Mustards Based on Chloride-Ion Determination

Keyphrases □ Chlorambucil—hydrolysis kinetics, potential errors based on chloride-ion determination □ Hydrolysis—chlorambucil, potential errors in kinetic studies based on chloride-ion determination □ Nitrogen mustards—chlorambucil, hydrolysis, potential errors in kinetic studies based on chloride-ion determination

To the Editor:

Chlorambucil (I), an aromatic nitrogen mustard, has been used clinically in the treatment of chronic lymphocytic leukemia and primary microglobulinemia and in the management of ovarian and testicular carcinomas (1). In aqueous solutions, I and other nitrogen mustards undergo hydrolysis, with the release of chloride ion and the formation of the cyclic ethyleneimmonium ion (1–3). This unstable cyclic intermediate then is attacked by water and other nucleophiles to yield II and other products. The same sequence then is repeated for the hydrolysis of the chloroethyl group in II (Scheme I).

Owen and Stewart recently reported (3) the kinetics of I hydrolysis using the chloride-ion measurement as a parameter for the concentration of intact I remaining. They plotted log $(Cl_\infty - Cl_t)/Cl_\infty$ *versus* time and calculated k_1, the degradation rate of I, from the apparent linear plots. In using chloride-ion measurements to obtain k_1, Owen and Stewart (3) made two important assumptions: (*a*) that the loss of I is always accompanied by the loss of two chloride ions, which is a valid assumption in the case of nitrogen mustards; and (*b*) that both chloride ions must be released simultaneously, *i.e.*, $k_2 \gg k_1$. However, there is no theoretical basis for assuming that $k_2 \gg k_1$.

The mechanism of cyclic ethyleneimmonium-ion formation should be the same for both the k_1 and k_2 steps, and there is no reason to expect that the presence of a hydroxyl function in II would make II much more unstable

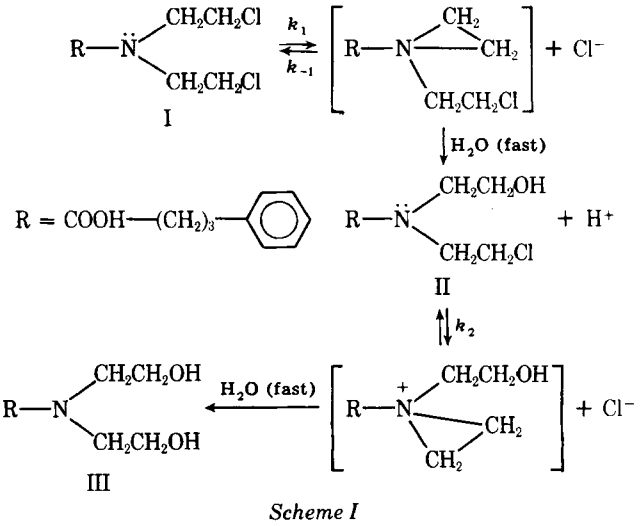

Scheme I

relative to I. From a statistical consideration alone, the k_1 step probably should be faster, because there are two hydrolyzable chloro groups. Furthermore, if k_1 is not the rate-determining step, the plot of log $(Cl_\infty - Cl_t)/Cl_\infty$ *versus* time would be dependent on the relative magnitude of k_2/k_1. This relation can be shown theoretically from the classical kinetic treatment of consecutive reactions (4). Thus, for the reaction shown in Scheme II:

$$I \xrightarrow{k_1} II + Cl^- \xrightarrow{k_2} III + Cl^-$$

Scheme II

it follows that:

$$[I]_t = I_0 e^{-k_1 t} \quad \text{(Eq. 1)}$$

$$[II]_t = \frac{I_0 k_1}{(k_2 - k_1)}(e^{-k_1 t} - e^{-k_2 t}) \quad \text{(Eq. 2)}$$

$$[III]_t = \frac{I_0}{(k_2 - k_1)}[k_2(1 - e^{-k_1 t}) - k_1(1 - e^{-k_2 t})] \quad \text{(Eq. 3)}$$

$$[Cl]_t = [II]_t + 2[III]_t \quad \text{(Eq. 4)}$$

where $[I]_t$, $[II]_t$, $[III]_t$, and $[Cl]_t$ are the concentrations of

0022-3549/80/0700-0859$01.00/0

© 1980, American Pharmaceutical Association

Determination of Ethinyl Estradiol in Dissolution Study—The release rate of ethinyl estradiol was determined at 37° using the USP rotating-basket apparatus in a dissolution medium containing 900 ml of distilled water. The basket was rotated at 100 rpm. At each sampling interval, 6 ml of the medium was withdrawn and extracted with 5 ml of chloroform. Then 4 ml of the chloroform layer was evaporated to dryness under a nitrogen stream. Ethinyl estradiol was analyzed as described.

RESULTS AND DISCUSSION

Figure 1 shows the excitation and emission spectra of ethinyl estradiol. Ethinyl estradiol exhibited strong fluorescence spectra at excitation and emission wavelengths of 460 and 490 nm, respectively. However, norethindrone did not exhibit fluorescence, even at the very high concentration of 2000 ng/ml (Fig. 1).

Figure 2 shows fluorescence stability for 1 hr after sulfuric acid addition. As can be seen in Fig. 2, the fluorescence of ethinyl estradiol was relatively stable; moreover, an excellent linearity between the fluorescence intensity and the ethinyl estradiol concentration over 17.5–280 ng/ml was observed; the minimum detection limit for the drug was ~10 ng/ml using this procedure.

The results of this study also indicate that the reproducibility of the method is excellent and that common tablet excipients do not interfere with the determination of ethinyl estradiol (Table II).

Finally, the method was valuable for the determination of small amounts of the drug in the dissolution study. Figure 3 shows the release rate of ethinyl estradiol from the sustained-release tablet (Vial 2) and the rapid-release tablet (Vial 4).

REFERENCES

(1) "The United States Pharmacopeia," 19th rev., Mack Publishing Co., Easton, Pa., 1975, p. 185.

(2) S. J. Kober, *Biochem. J.*, **32**, 357 (1938).

(3) A. J. Khoury and L. J. Cali, *J. Pharm. Sci.*, **56**, 1485 (1967).

(4) R. J. Templeton, W. A. Arnett, and I. M. Jakovljevic, *ibid.*, **57**, 1168 (1968).

(5) P. Comer and C. Stevenson, *ibid.*, **57**, 147 (1968).

COMMUNICATIONS

Potential Errors in Kinetic Studies of Hydrolysis of Nitrogen Mustards Based on Chloride-Ion Determination

Keyphrases □ Chlorambucil—hydrolysis kinetics, potential errors based on chloride-ion determination □ Hydrolysis—chlorambucil, potential errors in kinetic studies based on chloride-ion determination □ Nitrogen mustards—chlorambucil, hydrolysis, potential errors in kinetic studies based on chloride-ion determination

To the Editor:

Chlorambucil (I), an aromatic nitrogen mustard, has been used clinically in the treatment of chronic lymphocytic leukemia and primary microglobulinemia and in the management of ovarian and testicular carcinomas (1). In aqueous solutions, I and other nitrogen mustards undergo hydrolysis, with the release of chloride ion and the formation of the cyclic ethyleneimmonium ion (1–3). This unstable cyclic intermediate then is attacked by water and other nucleophiles to yield II and other products. The same sequence then is repeated for the hydrolysis of the chloroethyl group in II (Scheme I).

Owen and Stewart recently reported (3) the kinetics of I hydrolysis using the chloride-ion measurement as a parameter for the concentration of intact I remaining. They plotted log $(Cl_\infty - Cl_t)/Cl_\infty$ *versus* time and calculated k_1, the degradation rate of I, from the apparent linear plots. In using chloride-ion measurements to obtain k_1, Owen and Stewart (3) made two important assumptions: (*a*) that the loss of I is always accompanied by the loss of two chloride ions, which is a valid assumption in the case of nitrogen mustards; and (*b*) that both chloride ions must be released simultaneously, *i.e.*, $k_2 \gg k_1$. However, there is no theoretical basis for assuming that $k_2 \gg k_1$.

The mechanism of cyclic ethyleneimmonium-ion formation should be the same for both the k_1 and k_2 steps, and there is no reason to expect that the presence of a hydroxyl function in II would make II much more unstable

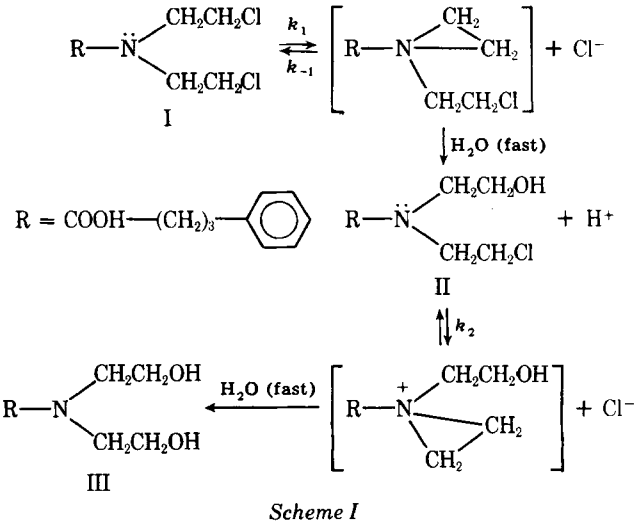

Scheme I

relative to I. From a statistical consideration alone, the k_1 step probably should be faster, because there are two hydrolyzable chloro groups. Furthermore, if k_1 is not the rate-determining step, the plot of log $(Cl_\infty - Cl_t)/Cl_\infty$ *versus* time would be dependent on the relative magnitude of k_2/k_1. This relation can be shown theoretically from the classical kinetic treatment of consecutive reactions (4). Thus, for the reaction shown in Scheme II:

$$I \xrightarrow{k_1} II + Cl^- \xrightarrow{k_2} III + Cl^-$$

Scheme II

it follows that:

$$[I]_t = I_0 e^{-k_1 t} \quad \text{(Eq. 1)}$$

$$[II]_t = \frac{I_0 k_1}{(k_2 - k_1)}(e^{-k_1 t} - e^{-k_2 t}) \quad \text{(Eq. 2)}$$

$$[III]_t = \frac{I_0}{(k_2 - k_1)}[k_2(1 - e^{-k_1 t}) - k_1(1 - e^{-k_2 t})] \quad \text{(Eq. 3)}$$

$$[Cl]_t = [II]_t + 2[III]_t \quad \text{(Eq. 4)}$$

where $[I]_t$, $[II]_t$, $[III]_t$, and $[Cl]_t$ are the concentrations of

0022-3549/80/0700-0859$01.00/0

© 1980, American Pharmaceutical Association

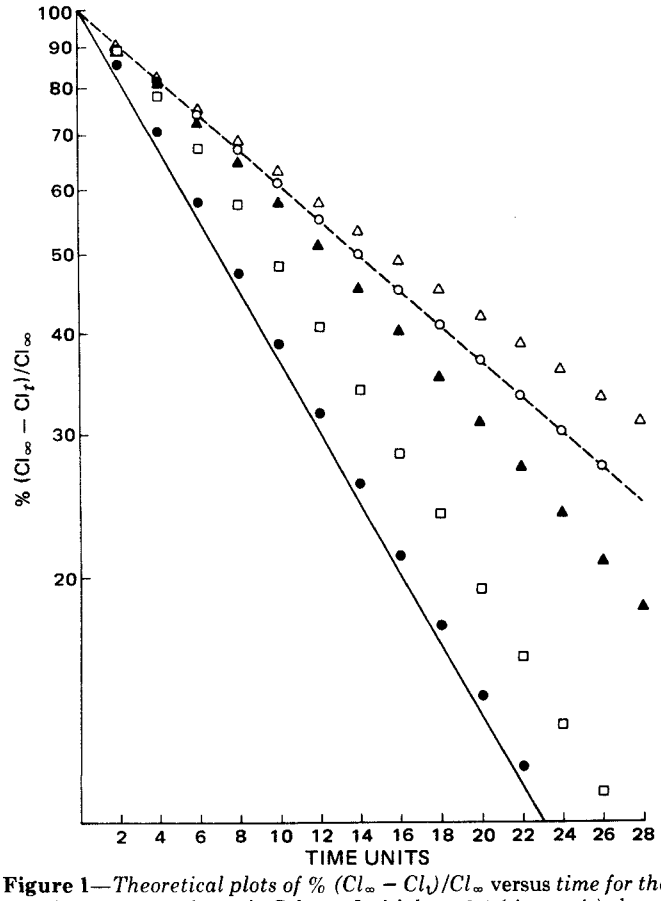

Figure 1—*Theoretical plots of % $(Cl_\infty - Cl_t)/Cl_\infty$* versus *time for the reaction sequence shown in Scheme I with* $k_1 = 0.1$ *(time unit)*$^{-1}$ *and* $I_0 = 1.0$ *and with various values of* k_2/k_1. *Key:* ●, *10.00;* □, *2.00;* ▲, *0.75;* ○, *0.50; and* △, *0.33. The solid line represents the theoretical plot of the percent of I remaining, thus representing the true* k_1 *value; the broken line has a slope equal to* $0.50k_1$.

I, II, III, and chloride ion, respectively, at time t, and I_0 is the initial concentration of I. Since each molecule of I eventually yields two molecules of chloride ion, it follows that the chloride-ion concentration at infinite time is given by:

$$Cl_\infty = 2I_0 \qquad \text{(Eq. 5)}$$

Figure 1 shows theoretical plots obtained by plotting log I or log $(Cl_\infty - Cl_t)/Cl_\infty$ *versus* time for various values of k_2/k_1 (the solid line represents the actual rate of loss of I). As seen in Fig. 1, in addition to the expected linearity of the chloride plot when $k_2 \geq 10k_1$, a perfect linear chloride plot also is obtained when $k_2 = 0.5k_1$[1]. However, the slopes of the two lines are different; only in the case where $k_2 \geq 10k_1$ does the slope yield a value close to k_1. The slope of the straight line plot when $k_2 = 0.5k_1$ is equal to $0.5k_1$.

Therefore, it is apparent that a linear first-order plot of the chloride ion produced does not necessarily establish k_1 as the rate-determining step. In fact, as seen in Table I, an apparent linear relationship of the chloride ion produced can be observed over a wide range of k_2/k_1 values, within experimental errors, particularly if the data are subjected to a computer-assisted linear regression without actually plotting the points. However, the apparent rate constants depend on the value of k_2/k_1 and are smaller than k_1 (Table I). As explained earlier, k_1 probably is not the rate-determining step for the hydrolysis of I, and k_2 probably is of the same magnitude as k_1. Therefore, it is possible that the apparent linear plots of chloride-ion concentrations obtained during I hydrolysis (3) do not yield the true degradation rate of I. To clarify this ambiguity, it is necessary to follow the hydrolysis of I by a method that actually determines the concentration of intact I and to compare the kinetic data obtained with those obtained from chloride titration.

Table I—Correlation of Theoretical Chloride-Ion Plots Shown in Fig. 1 with Similar Calculations for Additional Values of k_2/k_1 Not Shown in Fig. 1

k_2/k_1	Correlation Coefficient[a]	Apparent Rate Constant
20.00	1.0000	0.1000
10.00	0.9999	0.0995
5.00	0.9996	0.0977
2.00	0.9983	0.0880
1.00	0.9986	0.0694
0.75	0.9994	0.0608
0.50	1.0000	0.0500
0.33	0.9991	0.0419
0.25	0.9976	0.0372

[a] Obtained for 15 points, which are two time units apart, up to 28 time units (equal to ~4 half-lives for the k_1 step). The k_1 value was 0.1 (time unit)$^{-1}$ and $I_0 = 1.0$.

A high-pressure liquid chromatographic (HPLC) method was developed to assay intact I in the presence of its major degradation products, II and III. The method involves reversed-phase chromatography[2], in which the hydroxy compounds, II and III, elute earlier than intact I since they are more polar. The details of the HPLC method and the identification of degradation peaks will be reported later.

Solutions of I (0.15 mg/ml) in 0.05 *M* acetate buffer[3] (pH 3.0) and nitric acid solution[3] (pH 2.0) were kept in a 37° water bath. At suitable time intervals, they were assayed for their intact I content by HPLC and for their chloride-ion concentration by an automatic chloride titrator[4]. Figure 2 shows the plot of the I concentration or $(Cl_\infty - Cl_t)/Cl_\infty$[5] *versus* time. The plot of I gave straight lines with half-lives of 25 and 70 min at pH values of 3.0 and 2.0, respectively. However, the points for the chloride-ion plot did not coincide with the HPLC plots (Fig. 2). At pH 3.0, the points appeared to give a straight line with a half-life of 52 min; at pH 2.0, the chloride-ion points showed distinct curvature with an apparent half-life of 165 min (r = 0.993).

Therefore, it is obvious that k_1 is not the rate-determining step in the overall hydrolysis of I. This finding was substantiated further by HPLC analysis of I hydrolysis where the peak due to II was shown to be increasing, through at least one half-life of I, followed by a decrease, as would be expected of a consecutive reaction where the intermediate is not particularly unstable compared to the initial reactants. It also is apparent that the rates calcu-

[1] The straight line nature of the chloride plot, when $k_2 = 0.5k_1$, is mathematically correct, as can be seen by substituting values of $[II]_t$ and $[III]_t$ into Eq. 4 followed by simplification to yield a monoexponential expression, $(Cl_\infty - Cl_t)/Cl_\infty = e^{-0.5k_1t}$.

[2] A Zorbax-C_8 column (DuPont) was used with a running solvent containing 60% methanol, 5% acetonitrile, and 35% acetate buffer (0.15 *M*) (pH 5.0) at a flow rate of 1.6 ml/min. The retention times of I and II were 7.5 and 3.5 min, respectively.

[3] Buffers contained 5% acetone to keep I in solution.

[4] Model 4-4433, American Instrument Co., Silver Spring, Md.

[5] The Cl_∞ and Cl_t values plotted were corrected for the blank, *i.e.*, Cl_0, which is the amount of chloride ion present at time zero.

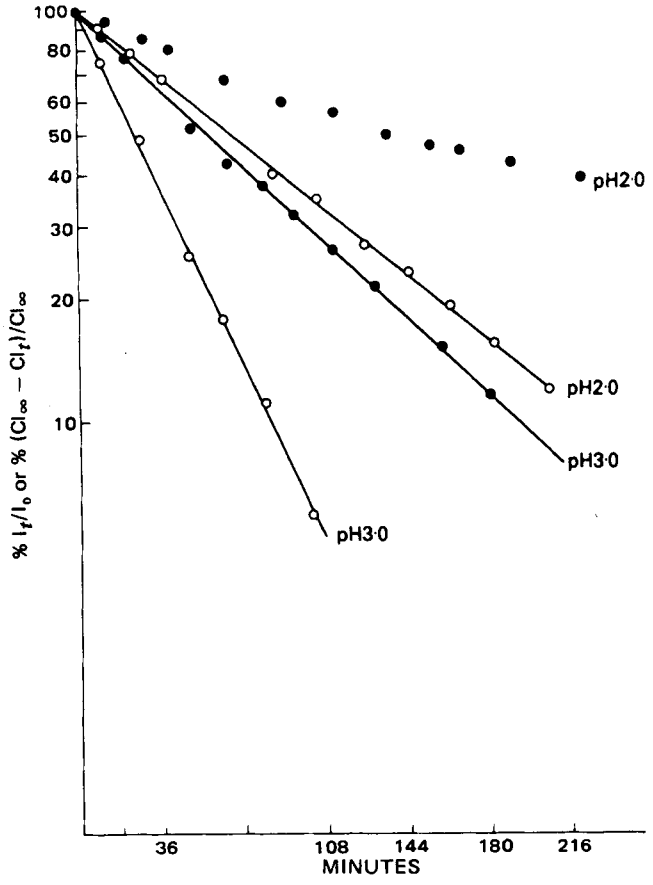

Figure 2—*Plots for the hydrolysis of I. Key:* ○, *data from HPLC runs (% I_t/I_0); and* ●, *data from the chloride-ion determination [% $(Cl_\infty - Cl_t)/Cl_\infty$]; in 0.05* M *acetate buffer (pH 3.0) and in dilute nitric acid (pH 2.0).*

lated from the chloride analyses would considerably overestimate the stability of I, at least in the two buffers tested.

These findings show the inherent potential error in obtaining kinetic parameters of a reactant by following the appearance of a degradation product, particularly when a consecutive reaction is involved as in the hydrolysis of I. The possible error in the rate constants reported for chlorambucil hydrolysis has potential practical implications. Compound I is administered routinely as oral tablets, in which case it is exposed to the pH range of the stomach (1.5–5.0). The relatively short half-lives observed for I hydrolysis at pH 2.0 and 3.0 suggest that a significant amount of I potentially may be degraded before absorption. This observation warrants a more careful study of I hydrolysis using a stability-specific assay. A more detailed kinetic study is in progress using the HPLC method for the analysis of I both to obtain practical stability data under physiological conditions and to elucidate the mechanism of I hydrolysis.

(1) "The Pharmacological Basis of Therapeutics," L. S. Goodman and A. Gilman, Eds., 5th ed., Macmillan, New York, N.Y., 1975, pp. 1254–1265.

(2) W. J. Ross, "Biological Alkylating Agents," Butterworths, London, England, 1962, p. 13.

(3) W. R. Owen and P. J. Stewart, *J. Pharm. Sci.*, **68**, 992 (1979).

(4) K. J. Laidler, "Chemical Kinetics," 2nd ed., McGraw-Hill, New York, N.Y., 1965, p. 322.

Dulal C. Chatterji
Pharmaceutical Development Service
Pharmacy Department
The Clinical Center
National Institutes of Health
Bethesda, MD 20014

Received November 23, 1979.
Accepted for publication March 17, 1980.
The author thanks Dr. Joseph F. Gallelli for helpful criticism of the manuscript and Mr. Russell Yeager for technical assistance.

Potential Errors in Kinetic Studies of Hydrolysis of Nitrogen Mustards Based on Chloride-Ion Determination: A Reply

Keyphrases □ Chlorambucil—hydrolysis kinetics □ Nitrogen mustards—chlorambucil, hydrolysis kinetics □ Hydrolysis—chlorambucil, kinetics

To the Editor:

The hydrolysis of chlorambucil (I) is a complex reaction, involving several reversible and consecutive steps. Chatterji (1) treated the reaction as a consecutive one involving two steps and indicated that k_1 and k_2 may be of the same magnitude. Several comments are appropriate.

The production of chloride from the consecutive model for the hydrolysis of chlorambucil is biexponential, *i.e.*:

$$Cl_t = I_0(1 - e^{-k_1 t}) + \frac{I_0}{k_2 - k_1}[k_2(1 - e^{-k_1 t}) - k_1(1 - e^{-k_2 t})] \quad \text{(Eq. 1)}$$

where Cl_t is the chloride concentration at time t, I_0 is the initial concentration of chlorambucil, and k_1 and k_2 are the rate constants for the two consecutive steps.

Therefore, the theoretical plots of log $(Cl_\infty - Cl_t)/Cl_\infty$ *versus* time will be nonlinear except when $k_2 \gg k_1$ and $k_2 \rightarrow 0.5k_1$. Chatterji (1) suggested that "apparent linear relationships" could be observed over a wide k_2/k_1 range by subjecting data to "computer-assisted linear regression." Apparent linearity was proposed on the basis of the correlation coefficient values. However, this approach is a gross simplification of the model and a misrepresentation of the numerical techniques used in the original work (2).

Table I—Summary of the Analyses of Variance for the Orthogonal Polynomial Analysis of the Theoretical Consecutive Model for Various k_2/k_1 Values

k_2/k_1	Probability[a] of Fitting a Polynomial of Order: Zero	1	2	3	Deviation[b] from Linearity
50	<0.001	<0.001	0.60	0.18	No
30	<0.001	<0.001	0.31	0.17	No
20	<0.001	<0.001	0.08	0.01	Yes?
10	<0.001	<0.001	0.002	<0.001	Yes
5	<0.001	<0.001	<0.001	<0.001	Yes
2	<0.001	<0.001	<0.001	<0.001	Yes
0.75	<0.001	<0.001	<0.001	<0.001	Yes
0.5	<0.001	<0.001	0.78	0.25	No
0.33	<0.001	<0.001	<0.001	0.04	Yes
0.25	<0.001	<0.001	<0.001	0.009	Yes
0.1	<0.001	<0.001	<0.001	<0.001	Yes
0.01	<0.001	<0.001	<0.001	<0.001	Yes

[a] A total of 29 data points was used (up to 28 time units); $k_1 = 0.1$ (time unit)$^{-1}$, $I_0 = 1.0$, and error variance = 0.2×10^{-5}. [b] At $p = 0.05$.

0022-3549/80/0700-0861$01.00/0
© 1980, American Pharmaceutical Association

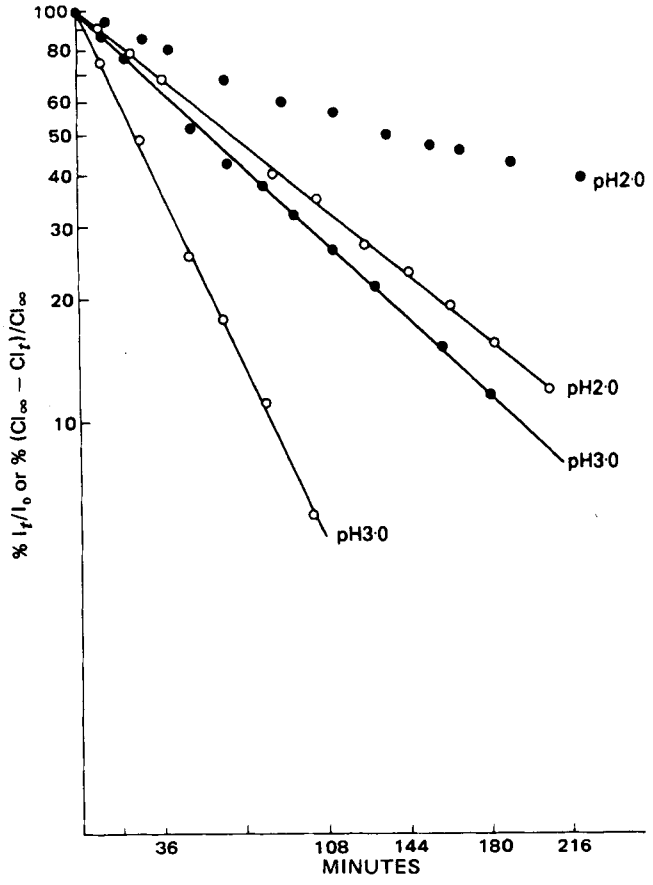

Figure 2—*Plots for the hydrolysis of I. Key:* ○, *data from HPLC runs (% I_t/I_0); and* ●, *data from the chloride-ion determination [% $(Cl_\infty - Cl_t)/Cl_\infty$]; in 0.05* M *acetate buffer (pH 3.0) and in dilute nitric acid (pH 2.0).*

lated from the chloride analyses would considerably overestimate the stability of I, at least in the two buffers tested.

These findings show the inherent potential error in obtaining kinetic parameters of a reactant by following the appearance of a degradation product, particularly when a consecutive reaction is involved as in the hydrolysis of I. The possible error in the rate constants reported for chlorambucil hydrolysis has potential practical implications. Compound I is administered routinely as oral tablets, in which case it is exposed to the pH range of the stomach (1.5–5.0). The relatively short half-lives observed for I hydrolysis at pH 2.0 and 3.0 suggest that a significant amount of I potentially may be degraded before absorption. This observation warrants a more careful study of I hydrolysis using a stability-specific assay. A more detailed kinetic study is in progress using the HPLC method for the analysis of I both to obtain practical stability data under physiological conditions and to elucidate the mechanism of I hydrolysis.

(1) "The Pharmacological Basis of Therapeutics," L. S. Goodman and A. Gilman, Eds., 5th ed., Macmillan, New York, N.Y., 1975, pp. 1254–1265.

(2) W. J. Ross, "Biological Alkylating Agents," Butterworths, London, England, 1962, p. 13.

(3) W. R. Owen and P. J. Stewart, *J. Pharm. Sci.*, **68**, 992 (1979).

(4) K. J. Laidler, "Chemical Kinetics," 2nd ed., McGraw-Hill, New York, N.Y., 1965, p. 322.

Dulal C. Chatterji
Pharmaceutical Development Service
Pharmacy Department
The Clinical Center
National Institutes of Health
Bethesda, MD 20014

Received November 23, 1979.
Accepted for publication March 17, 1980.
The author thanks Dr. Joseph F. Gallelli for helpful criticism of the manuscript and Mr. Russell Yeager for technical assistance.

Potential Errors in Kinetic Studies of Hydrolysis of Nitrogen Mustards Based on Chloride-Ion Determination: A Reply

Keyphrases □ Chlorambucil—hydrolysis kinetics □ Nitrogen mustards—chlorambucil, hydrolysis kinetics □ Hydrolysis—chlorambucil, kinetics

To the Editor:

The hydrolysis of chlorambucil (I) is a complex reaction, involving several reversible and consecutive steps. Chatterji (1) treated the reaction as a consecutive one involving two steps and indicated that k_1 and k_2 may be of the same magnitude. Several comments are appropriate.

The production of chloride from the consecutive model for the hydrolysis of chlorambucil is biexponential, *i.e.*:

$$Cl_t = I_0(1 - e^{-k_1 t}) + \frac{I_0}{k_2 - k_1}[k_2(1 - e^{-k_1 t}) - k_1(1 - e^{-k_2 t})] \quad \text{(Eq. 1)}$$

where Cl_t is the chloride concentration at time t, I_0 is the initial concentration of chlorambucil, and k_1 and k_2 are the rate constants for the two consecutive steps.

Therefore, the theoretical plots of log $(Cl_\infty - Cl_t)/Cl_\infty$ *versus* time will be nonlinear except when $k_2 \gg k_1$ and $k_2 \rightarrow 0.5k_1$. Chatterji (1) suggested that "apparent linear relationships" could be observed over a wide k_2/k_1 range by subjecting data to "computer-assisted linear regression." Apparent linearity was proposed on the basis of the correlation coefficient values. However, this approach is a gross simplification of the model and a misrepresentation of the numerical techniques used in the original work (2).

Table I—Summary of the Analyses of Variance for the Orthogonal Polynomial Analysis of the Theoretical Consecutive Model for Various k_2/k_1 Values

k_2/k_1	Probability[a] of Fitting a Polynomial of Order: Zero	1	2	3	Deviation[b] from Linearity
50	<0.001	<0.001	0.60	0.18	No
30	<0.001	<0.001	0.31	0.17	No
20	<0.001	<0.001	0.08	0.01	Yes?
10	<0.001	<0.001	0.002	<0.001	Yes
5	<0.001	<0.001	<0.001	<0.001	Yes
2	<0.001	<0.001	<0.001	<0.001	Yes
0.75	<0.001	<0.001	<0.001	<0.001	Yes
0.5	<0.001	<0.001	0.78	0.25	No
0.33	<0.001	<0.001	<0.001	0.04	Yes
0.25	<0.001	<0.001	<0.001	0.009	Yes
0.1	<0.001	<0.001	<0.001	<0.001	Yes
0.01	<0.001	<0.001	<0.001	<0.001	Yes

[a] A total of 29 data points was used (up to 28 time units); $k_1 = 0.1$ (time unit)$^{-1}$, $I_0 = 1.0$, and error variance = 0.2×10^{-5}. [b] At $p = 0.05$.

0022-3549/80/0700-0861$01.00/0
© 1980, American Pharmaceutical Association

Table II—Analysis of Variance for the Orthogonal Polynomial Analysis of the Data for Hydrolysis of Chlorambucil at 25.0°

Order of Fit	Regression Sum of Squares	Remainder Sum of Squares	Degrees of Freedom	Remainder Mean Square	Variance Ratio	p
0	0.306E + 01	0.110E + 01	27	0.406E − 01	0.754E + 02	<0.001
1	0.110E + 01	0.538E − 04	26	0.207E − 05	0.529E + 06	<0.001
2	0.101E − 07	0.528E − 04	25	0.215E − 05	0.468E − 02	0.94
3	0.203E − 04	0.335E − 04	24	0.140E − 05	0.145E + 02	0.001
4	0.425E − 06	0.331E − 04	23	0.144E − 05	0.295E + 00	0.60

The use of correlation coefficients to test the goodness of fit of the data to this model is inadequate. A statistical technique capable of testing for curvature of the regression is required. Linear regression with appropriate analysis of variance can be used but requires replicate data that are either extremely difficult or not possible to obtain. Orthogonal polynomial analysis, with the successive fitting of higher order polynomials and subsequent statistical testing to determine whether these higher order polynomials have significantly improved the fit, is the method of choice in these circumstances. The principal orthogonal polynomial algorithms were reviewed (3), and the Gram–Schmidt algorithm (4) was chosen for the original study.

Chatterji's theoretical data were regenerated with a random error variance typical of that obtained in the original study. The log $(Cl_\infty - Cl_t)/Cl_\infty$ *versus* time regressions were subjected to orthogonal polynomial analysis, and a summary of the analyses of variance is provided (Table I). Curvature was detected in all regressions, except in the limiting situations when $k_2 \gg k_1$ and $k_2 = 0.5k_1$. While there may be some doubt as to the linearity of the regression when $k_2/k_1 = 20$, the regression clearly is linear when $k_2/k_1 = 30$ and 50 and when $k_2/k_1 = 0.5$. These results demonstrate clearly the sensitivity of this numerical technique to detect curvature in regressions.

In the original study of chlorambucil hydrolysis (2), typical first-order plots (Fig. 2 in Ref. 2) showed no significant curvature when subjected to orthogonal polynomial analysis (Table II). The literature (5, 6) suggested that the chlorohydrin hydrolyzed much faster than the original dichloroethyl compound, and a rate-determining step involving the hydrolysis of the first chlorine thus was proposed.

Furthermore, Chatterji (1) plotted log $(Cl_\infty - Cl_t)/Cl_\infty$ *versus* time. While this method is satisfactory in the theoretical plots, the Cl_0 term should be added in the chlorambucil hydrolysis, *i.e.*, log $(Cl_\infty - Cl_t)/(Cl_\infty - Cl_0)$ *versus* time. For the true first-order model:

$$Cl_\infty - Cl_t = (Cl_\infty - Cl_0)e^{-kt} \qquad \text{(Eq. 2)}$$

and therefore:

$$\ln (Cl_\infty - Cl_t)/Cl_\infty = -kt + \ln (1 - Cl_0/Cl_\infty) \qquad \text{(Eq. 3)}$$

The absence of a Cl_0 term will force the regression through the zero intercept and cause an error in estimation of the rate constant.

Chatterji (1) also stated that Owen and Stewart assumed that the loss of chlorambucil always is accompanied by the loss of two chloride ions. This hypothesis was clearly tested in the original study by the chloride concentrations at time infinity (2), which demonstrated the loss of two chloride ions.

The present investigator agrees that analytical methods that determine original reactants are preferred over those measuring reaction products, particularly in complex reactions. The original research was initiated over 10 years ago, and methods to measure reactant concentrations, including high-pressure liquid chromatographic (HPLC) methods, were not available. The measurement of chloride ion by specially prepared selective-ion electrodes (3) was the most suitable method to follow the reaction at low concentrations and was amenable to continuous monitoring and automatic data collection. While HPLC methods possess a considerable advantage in the measurement and separation of products and reactants, such methods do have some limitations in fast reactions, *e.g.*, consideration of the extent of decomposition on the column during analysis, difficulties in the calibration of unstable compounds, long-term instability with subsequent changes in retention times, and reduction in the amount of data collected, causing a limitation in the use of numerical techniques.

In addition, the measurement of chloride ion in Chatterji's work may be subject to some error. In a previous study, Chatterji *et al.* (7) pointed out the inaccuracies of the use of the automatic chloride titration in faster reactions due to the production of chloride ion during the titration, the finite time to prepare samples and perform the analysis, and the inaccuracies in pipetting. The use of solid-state chloride-selective electrodes would overcome these difficulties.

Nevertheless, it is difficult to disagree with the results of the current kinetic study, where the k_2 value seems to be about half of the k_1 value. The conclusions in the original study were based on sound numerical techniques that tested for a limiting form of a more complex model ($k_2 \gg k_1$). Consideration was not given to a second limiting form ($k_2 \rightarrow 0.5k_1$) because of the literature indications to the contrary at that time. However, the current work does show that the second limiting form may be a realistic alternative, and further research is warranted.

(1) D. C. Chatterji, *J. Pharm. Sci.*, **69**, 859 (1980).
(2) W. R. Owen and P. J. Stewart, *ibid.*, **68**, 992 (1979).
(3) P. J. Stewart, Ph.D. thesis, University of Queensland, St. Lucia, Australia, 1975.
(4) P. J. Davies, in "Survey of Numerical Analysis," J. Todd, Ed., McGraw-Hill, New York, N.Y., 1962, pp. 347, 363.
(5) W. C. J. Ross, *J. Chem. Soc.*, **1949**, 183.
(6) W. E. Hanby, G. S. Hartley, E. O. Powell, and N. H. Rydon, *ibid.*, **1947**, 520.
(7) D. C. Chatterji, R. F. Green, and J. F. Gallelli, *J. Pharm. Sci.*, **67**, 1527 (1978).

Peter J. Stewart
Department of Pharmacy
University of Queensland
St. Lucia, Australia 4067

Received February 21, 1980.
Accepted for publication April 29, 1980.

Precorneal Retention of Topically Instilled Micronized Particles

Keyphrases □ Micronized particles—precorneal retention, effect of particle size □ Ophthalmic preparations—micronized particles, precorneal retention, effect of particle size

To the Editor:

Aqueous suspensions of micronized drugs are commonly used for topical delivery of low-solubility therapeutic agents to the eye. Previous work was performed to assess the *in vivo* performance of ocular suspensions (1–4), but these studies were primarily drug oriented; they did not quantitate the effects of the physical aspects of the dosage form itself. Parameters specifically important for an ophthalmic suspension include intrinsic solubility, dissolution rate, and particle size.

The particle size of a suspended drug determines the surface area available for dissolution of the drug into the tears and also largely determines the irritation potential of the dosing system. Irritation can cause excessive tearing and accelerated drainage of the instilled dose. To minimize this irritation potential, ophthalmic suspensions generally are prepared using various cost-increasing micronization techniques. This report presents recent preliminary data on the behavior of micronized particles in the precorneal area of the eye and demonstrates the influence of particle size on ocular retention.

Male albino rabbits were used for the particle dynamics studies since most previous ocular work was performed with this species. The animals were preconditioned to sit motionless in specially designed wooden boxes. A normal upright posture was maintained, and local or general anesthetics were not used due to their known effects on tear dynamics (5).

A topical dose of an aqueous suspension containing radiolabeled microspheres[1] was placed carefully into the ocular sac along the lower lid margin using a micropipet. The normal response of the animal is to blink upon instillation, so no further manual mixing or blinking was attempted since it might abnormally force a portion of the dose down the nasolacrimal duct. Immediately after dosing, a γ-probe[2] was positioned to cover the precorneal area without touching the animal; drainage loss and retention of the labeled particles were monitored as a function of time by external scintigraphy[3]. Animals were watched closely by a technician, and all head movements and blinking were recorded carefully. Head movement terminated an individual run due to alteration of the spacial relationship of the precorneal microsphere pool and the monitoring probe.

The results of the studies using 3- and 25-μm particles are shown in Fig. 1. The marked dependence of particle retention on both dosing volume and particle size is readily apparent from these data. Immediately upon instillation of a 3% (w/v) suspension of 3-μm spheres, a washout process swept away a fraction of the dose. Since the duration of this washout phase was dependent on the volume instilled, the percent retention for each dosing volume was different and decreased as the volume was increased. However, since the total number of spheres instilled also varied with the dosing volume, it was not sufficient simply to consider percent retention as a measure of the volume effect as illustrated by the data presented in Table I.

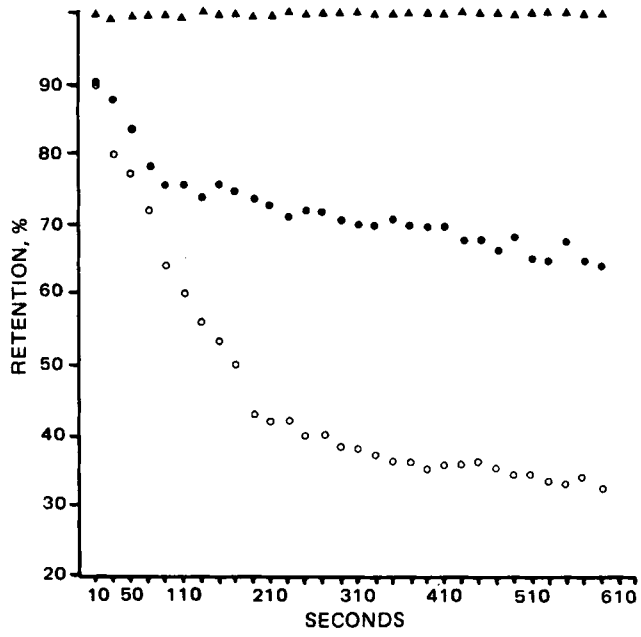

Figure 1—*Precorneal retention of topically instilled micronized particles. Key:* ●, *25-μl dose of 3% (w/v) 3-μm suspension;* ○, *50-μl dose of 3% (w/v) 3-μm suspension; and* ▲, *25- and 50-μl doses of 3% (w/v) 25-μm suspension (both dosing volumes gave virtually identical curves).*

It is clear from this analysis that the twofold increase in percent retention for the 25-μl dose compared with the 50-μl dose exactly offset the twofold sphere number difference between the two dosing volumes. As a result, the total number of spheres retained, as represented by the plateau region in Fig. 1, was the same. It would be tempting to attribute this effect to a maximum surface coverage limit for the conjunctival sac, but this cannot be stated with certainty. Theoretically, if such were the case, a 10-μl dose of the 3-μm suspension should give 100% retention since the total number of spheres instilled would be less than the plateau value for the larger doses. However, the data (Table I) show that the 3-μm spheres still suffered significant washout loss before being deposited within the protective folds of the conjunctiva.

The data for the 25-μm particles (Fig. 1) strikingly contrast with those for the smaller particles. Particle re-

Table I—Ocular Retention of a 3% (w/v) Suspension of 3-μm Particles as a Function of the Dosing Volume

Dose Volume, μl	Milligrams of Spheres	Total Number of Spheres	Percent Retention	Number Retained
50	1.5	8.6×10^7	33	2.8×10^7
25	0.75	4.3×10^7	65	2.8×10^7
10	0.3	1.7×10^7	70	1.2×10^7

[1] Tracer microsphere, Medical Products Division, 3M Co., St. Paul, MN 55101. Radiolabeled microspheres are polystyrene spheres that have been sized under rigid control standards, made radioactive, and annealed to seal radioactivity so that no leaching occurs. The microspheres may be obtained in a range of specific diameters labeled with various isotopes. The microspheres used in the current studies were 3.2 ± 0.6 and 25.7 ± 1.2 μm with a ^{141}Ce label, an isotope with a half-life of 32 days and 145 kev γ-energy. For these initial studies, the spheres were simply suspended in isotonic saline.

[2] Sodium iodide crystal (1.9 × 5.1 cm), TASK 5, Packard Instrument Co., Downers Grove, IL 60515.

[3] Model 9012A multichannel analyzer, Packard Instrument Co., Downers Grove, IL 60515.

0022-3549/80/0700-0863$01.00/0
© 1980, American Pharmaceutical Association

tention was rapid, complete, and independent of the dosing volume up to 50 μl, which is about the limit for a rabbit eye without spillage over the lids. Presumably, the larger diameter and greater particle mass resulted in faster deposition so that the suspending vehicle was drained away independently of the particles. The possibility that the observed retention for the larger particles was due to physical obstruction of the drainage apparatus was checked by subsequent instillation of a radioactive solution of [^{67}Ga]gallium citrate. The mean drainage rate constant obtained for a 25-μl dose of this solution in the presence of the 25-μm spheres was 0.52 min^{-1}, and this value corresponds well with the normal value of 0.545 min^{-1} reported previously for the rabbit (5). Particle size clearly plays a significant role in the rate and extent of particle retention for ophthalmic suspensions.

Studies also were carried out beyond the times indicated by Fig. 1. Only the early postinstillation time intervals are shown to define the washout process clearly. Individual runs lasting several hours were performed, and the presence of particles in the conjunctival sac was demonstrated for at least 12 hr. However, studies are continuing to determine the precise kinetics of the gradual loss of particles that follows the initial washout process, particularly for the 3-μm particles. Preliminary evidence shows that blinking and the associated movement of the tear film play a major role in redistributing small particles within the ocular sac. A blink normally pulls a fresh layer of the precorneal film up from the conjunctival sac and over the corneal surface. Lighter particles are pulled up with the film, and this process leads to gradual loss *via* the drainage apparatus during normal tear turnover.

The data from these studies indicate that a lower limit probably exists for particle-size retention in the eye, in addition to the previously recognized upper limit for irritation. This evidence suggests that caution should be used regarding the extent to which the particle size is reduced for such systems and also may explain the recently documented successes of so-called "economy suspensions," systems characterized by somewhat larger particle sizes than more traditional ophthalmic microsuspensions. Presumably, the smallest particles of the distribution range of a micronized suspension are lost rapidly with the washout of the suspending vehicle and contribute minimally to the ocular drug levels. Thus, the observed *in vivo* performance of an ophthalmic suspension probably is due mainly to the larger particles in the size distribution. Further studies are being conducted to establish more definitively the role of particle size for ocular retention and the influences of suspension concentration and vehicle pH.

(1) A. Kupferman, M. V. Pratt, K. Suckewer, and H. M. Leibowitz, *Arch. Ophthalmol.*, **91**, 373 (1974).

(2) W. V. Cox, A. Kupferman, and H. M. Leibowitz, *ibid.*, **88**, 308 (1972).

(3) K. Green and S. J. Downs, *Invest. Ophthalmol.*, **13**, 316 (1974).

(4) J. W. Sieg and J. R. Robinson, *J. Pharm. Sci.*, **64**, 931 (1975).

(5) S. S. Chrai, T. F. Patton, A. Mehta, and J. R. Robinson, *ibid.*, **62**, 1112 (1973).

James W. Sieg ˣ
John W. Triplett
College of Pharmacy
University of Kentucky
Lexington, KY 40506

Received February 25, 1980.
Accepted for publication April 10, 1980.
The authors thank Brenda N. Hume for technical assistance.

Half-Life of *N*-Acetylprocainamide in Rats

Keyphrases □ Procainamide—metabolism to *N*-acetylprocainamide, half-life of *N*-acetylprocainamide in rats □ *N*-Acetylprocainamide—half-life in rats □ Antiarrhythmic agents—*N*-acetylprocainamide, half-life in rats

To the Editor:

Procainamide is eliminated from the body by renal excretion as unchanged drug and through metabolism to *N*-acetylprocainamide. This metabolite has been shown to have antiarrhythmic activity in animals (1, 2) and humans (3, 4) and is eliminated from the body by urinary excretion. Many patients receiving procainamide chronically have shown plasma levels of *N*-acetylprocainamide in excess of the unmetabolized drug (5).

A most significant therapeutic advantage of *N*-acetylprocainamide is that it does not cause development of lupus erythematosus in patients (6). Additionally, the biological half-life of *N*-acetylprocainamide in humans is more than twice that of procainamide (7, 8), which allows less frequent dosing. We showed previously that *N*-acetylprocainamide decreased the heart rate in rats when the plasma concentration was 16.8 μg/ml, which is quite similar to the therapeutic concentrations in humans (9).

Schneck *et al.* (10) investigated the disposition of procainamide and *N*-acetylprocainamide in rats and found biological half-lives of 55 and 51 min, respectively. These results are in contrast to the data obtained in our laboratory. Therefore, the purpose of this communication is to report our preliminary results showing that the half-life of *N*-acetylprocainamide is two to three times longer than that of procainamide in the same rat and that the disposition of both drugs is qualitatively similar to that in humans.

Eight male Charles River[1] rats, 250–450 g, were selected. A cannula was inserted surgically into the jugular vein of each rat 1 day before the experiment (11). Procainamide hydrochloride (75 mg/kg) and *N*-acetylprocainamide hydrochloride (86 mg/kg) were administered intravenously through the cannula in a randomized crossover design. A 3-day washout period was allowed between administration of the two drugs.

Serial blood samples (0.4 ml) were withdrawn at 0 (just before drug administration), 0.25, 0.5, 0.75, 1, 1.5, 2, 3, 4, 6, and 8 hr following dosing, and the plasma was separated immediately. Urine and feces were collected for 48 hr. The concentrations of procainamide and *N*-acetylprocainamide in plasma and urine were determined by a specific high-pressure liquid chromatographic method (12). Plasma concentrations of the unchanged procainamide and *N*-acetylprocainamide were fitted to one-and two-compartment open models, respectively, using a nonlinear re-

[1] Charles River Breeding Laboratories, Wilmington, Mass.

0022-3549/80/0700-0864$01.00/0
© 1980, American Pharmaceutical Association

tention was rapid, complete, and independent of the dosing volume up to 50 μl, which is about the limit for a rabbit eye without spillage over the lids. Presumably, the larger diameter and greater particle mass resulted in faster deposition so that the suspending vehicle was drained away independently of the particles. The possibility that the observed retention for the larger particles was due to physical obstruction of the drainage apparatus was checked by subsequent instillation of a radioactive solution of [^{67}Ga]gallium citrate. The mean drainage rate constant obtained for a 25-μl dose of this solution in the presence of the 25-μm spheres was 0.52 min^{-1}, and this value corresponds well with the normal value of 0.545 min^{-1} reported previously for the rabbit (5). Particle size clearly plays a significant role in the rate and extent of particle retention for ophthalmic suspensions.

Studies also were carried out beyond the times indicated by Fig. 1. Only the early postinstillation time intervals are shown to define the washout process clearly. Individual runs lasting several hours were performed, and the presence of particles in the conjunctival sac was demonstrated for at least 12 hr. However, studies are continuing to determine the precise kinetics of the gradual loss of particles that follows the initial washout process, particularly for the 3-μm particles. Preliminary evidence shows that blinking and the associated movement of the tear film play a major role in redistributing small particles within the ocular sac. A blink normally pulls a fresh layer of the precorneal film up from the conjunctival sac and over the corneal surface. Lighter particles are pulled up with the film, and this process leads to gradual loss *via* the drainage apparatus during normal tear turnover.

The data from these studies indicate that a lower limit probably exists for particle-size retention in the eye, in addition to the previously recognized upper limit for irritation. This evidence suggests that caution should be used regarding the extent to which the particle size is reduced for such systems and also may explain the recently documented successes of so-called "economy suspensions," systems characterized by somewhat larger particle sizes than more traditional ophthalmic microsuspensions. Presumably, the smallest particles of the distribution range of a micronized suspension are lost rapidly with the washout of the suspending vehicle and contribute minimally to the ocular drug levels. Thus, the observed *in vivo* performance of an ophthalmic suspension probably is due mainly to the larger particles in the size distribution. Further studies are being conducted to establish more definitively the role of particle size for ocular retention and the influences of suspension concentration and vehicle pH.

(1) A. Kupferman, M. V. Pratt, K. Suckewer, and H. M. Leibowitz, *Arch. Ophthalmol.*, **91**, 373 (1974).

(2) W. V. Cox, A. Kupferman, and H. M. Leibowitz, *ibid.*, **88**, 308 (1972).

(3) K. Green and S. J. Downs, *Invest. Ophthalmol.*, **13**, 316 (1974).

(4) J. W. Sieg and J. R. Robinson, *J. Pharm. Sci.*, **64**, 931 (1975).

(5) S. S. Chrai, T. F. Patton, A. Mehta, and J. R. Robinson, *ibid.*, **62**, 1112 (1973).

James W. Sieg ˣ
John W. Triplett
College of Pharmacy
University of Kentucky
Lexington, KY 40506

Received February 25, 1980.
Accepted for publication April 10, 1980.
The authors thank Brenda N. Hume for technical assistance.

Half-Life of *N*-Acetylprocainamide in Rats

Keyphrases □ Procainamide—metabolism to *N*-acetylprocainamide, half-life of *N*-acetylprocainamide in rats □ *N*-Acetylprocainamide—half-life in rats □ Antiarrhythmic agents—*N*-acetylprocainamide, half-life in rats

To the Editor:

Procainamide is eliminated from the body by renal excretion as unchanged drug and through metabolism to *N*-acetylprocainamide. This metabolite has been shown to have antiarrhythmic activity in animals (1, 2) and humans (3, 4) and is eliminated from the body by urinary excretion. Many patients receiving procainamide chronically have shown plasma levels of *N*-acetylprocainamide in excess of the unmetabolized drug (5).

A most significant therapeutic advantage of *N*-acetylprocainamide is that it does not cause development of lupus erythematosus in patients (6). Additionally, the biological half-life of *N*-acetylprocainamide in humans is more than twice that of procainamide (7, 8), which allows less frequent dosing. We showed previously that *N*-acetylprocainamide decreased the heart rate in rats when the plasma concentration was 16.8 μg/ml, which is quite similar to the therapeutic concentrations in humans (9).

Schneck *et al.* (10) investigated the disposition of procainamide and *N*-acetylprocainamide in rats and found biological half-lives of 55 and 51 min, respectively. These results are in contrast to the data obtained in our laboratory. Therefore, the purpose of this communication is to report our preliminary results showing that the half-life of *N*-acetylprocainamide is two to three times longer than that of procainamide in the same rat and that the disposition of both drugs is qualitatively similar to that in humans.

Eight male Charles River[1] rats, 250–450 g, were selected. A cannula was inserted surgically into the jugular vein of each rat 1 day before the experiment (11). Procainamide hydrochloride (75 mg/kg) and *N*-acetylprocainamide hydrochloride (86 mg/kg) were administered intravenously through the cannula in a randomized crossover design. A 3-day washout period was allowed between administration of the two drugs.

Serial blood samples (0.4 ml) were withdrawn at 0 (just before drug administration), 0.25, 0.5, 0.75, 1, 1.5, 2, 3, 4, 6, and 8 hr following dosing, and the plasma was separated immediately. Urine and feces were collected for 48 hr. The concentrations of procainamide and *N*-acetylprocainamide in plasma and urine were determined by a specific high-pressure liquid chromatographic method (12). Plasma concentrations of the unchanged procainamide and *N*-acetylprocainamide were fitted to one-and two-compartment open models, respectively, using a nonlinear re-

[1] Charles River Breeding Laboratories, Wilmington, Mass.

0022-3549/80/0700-0864$01.00/0
© 1980, American Pharmaceutical Association

Table I—Pharmacokinetic Parameters of Procainamide and *N*-Acetylprocainamide

Parameter	Rats				Humans	
	Our Study		Ref. 10			
	Procainamide	*N*-Acetylprocainamide	Procainamide	*N*-Acetylprocainamide	Procainamide[a]	*N*-Acetylprocainamide[b]
Elimination half-life ($t_{1/2}$), hr	0.66	2.13	0.92	0.85	3.5	6.0
Plasma clearance, ml/min/kg	80.7	20.7	64.0	22.0	7.99	3.09
Apparent volume of distribution, liters/kg	4.60	3.82	4.92	1.64	1.91	1.61

[a] From Ref. 7. [b] From Ref. 8.

gression analysis program available in a statistical analysis system package[2].

The biological half-life ranged from 0.54 to 0.83 hr for procainamide and from 1.72 to 2.92 hr for *N*-acetylprocainamide. The ratio of the biological half-life of *N*-acetylprocainamide to that of procainamide in the same rat averaged 3.3. Table I summarizes the values of the pharmacokinetic parameters obtained by Schneck *et al.* (10), those obtained in our study, and values reported for normal subjects.

Determination of the biological half-lives of procainamide and *N*-acetylprocainamide in the same animal, with sufficient time for elimination of the drugs from the body, allowed a more meaningful comparison of the pharmacokinetic parameters of the two drugs. The discrepancy between these results and those reported by Schneck *et al.* (10) may be due to the study design and to the method of determination of pharmacokinetic parameters. Schneck *et al.* sacrificed groups of rats and followed the blood sampling for 4 hr, which appears to be inadequate for *N*-acetylprocainamide. In our study, a distribution phase of ~1 hr was noticed when *N*-acetylprocainamide was administered intravenously. Furthermore, Schneck *et al.* (10) calculated the volume of distribution by dividing the total body clearance by the elimination rate constant, which obviously results in an underestimated value (Table I).

The results of our study were qualitatively similar to those observed in normal human subjects. The ratio of the half-lives, volumes of distribution, and body clearances of procainamide and its metabolite in these two species are similar. These results have important implications in interpretations of metabolism data from acute and chronic toxicity studies.

(1) E. E. Bagwell, T. Walle, D. E. Drayer, M. M. Reidenberg, and J. K. Pruett, *J. Pharmacol. Exp. Ther.*, **197**, 38 (1979).

(2) R. F. Minchin, K. F. Ilett, and J. W. Paterson, *Eur. J. Pharmacol.*, **47**, 51 (1978).

(3) J. J. L. Lertora, A. J. Atkinson, Jr., W. Kushner, M. J. Nevin, W.-K. Lee, C. Jones, and F. R. Schmid, *Clin. Pharmacol. Ther.*, **25**, 273 (1979).

(4) J. Kluger, M. M. Reidenberg, T. Tyberg, V. Lloyd, G. Ellis, J. Hayes, and D. E. Drayer, *Clin. Res.*, **26**, 244A (1978).

(5) M. M. Reidenberg, D. E. Drayer, M. Levy, and J. Warner, *Clin. Pharmacol. Ther.*, **17**, 722 (1975).

(6) R. Lahita, J. Kluger, D. E. Drayer, D. Koffler, and M. M. Reidenberg, *Clin. Res.*, **27**, 235A (1979).

(7) J. Koch-Weser, *Ann. N.Y. Acad. Sci.*, **179**, 370 (1971).

(8) J. M. Strong, J. S. Dutcher, W.-K. Lee, and A. J. Atkinson, Jr., *J. Pharmacokinet. Biopharm.*, **3**, 223 (1975).

(9) A. Yacobi, R. W. Krasula, C.-M. Lai, and B. L. Kamath, *Res. Commun. Chem. Pathol. Pharmacol.*, **24**, 197 (1979).

(10) D. W. Schneck, K. Grove, F. O. Dewitt, R. A. Shiroff, and A. H. Hayes, Jr., *J. Pharmacol. Exp. Ther.*, **204**, 210 (1978).

[2] Statistical Analysis System, SAS Institute, Raleigh, N.C.

(11) P. G. Harms and S. R. Ojeda, *J. Appl. Phys.*, **36**, 391 (1974).

(12) C.-M. Lai, B. L. Kamath, Z. M. Look, and A. Yacobi, *J. Pharm. Sci.*, in press.

Burde L. Kamath ˣ
Avraham Yacobi
Pharmaceutical Development Department
American Critical Care
McGaw Park, IL 60085

Received December 26, 1979.
Accepted for publication April 15, 1980.

Assignment of ^{13}C-NMR Spectra of Strychnine and Brucine

Keyphrases □ Alkaloids—strychnine and brucine, ^{13}C-NMR spectral analyses, chemical shifts assigned □ ^{13}C-NMR spectroscopy—brucine and strychnine, chemical shifts assigned □ Brucine—^{13}C-NMR spectral analysis, chemical shifts assigned □ Strychnine—^{13}C-NMR spectral analysis, chemical shifts assigned

To the Editor:

Singh *et al.* (1) recently reported on the ^{13}C-NMR spectroscopy of the alkaloids strychnine (I) and brucine (II). In this communication, I shall comment on the spectral data and assignments reported by these authors.

Wehrli (2, 3) previously reported on the ^{13}C-NMR spectrum of brucine. The complete assignment of the brucine spectrum (3) was accomplished by using common

Table I—Assignment of ^{13}C-NMR Spectra of Strychnine

Carbon	Ref. 1	Ref. 4	Ref. 5	Ref. 7	Ref. 6	Ref. 8
1	124.2 d	124.25 d	124.12 d	124.99 d	122.3 d	121.9 d
2	122.3 d	122.31 d	122.17 d	122.67 d	124.3 d	123.8 d
3	128.6 d	128.62 d	128.41 d	128.61 d	128.6 d	128.1 d
4	116.3 d	116.24 d	116.12 d	116.52 d	116.2 d	115.8 d
5	142.3 s	142.21 s	142.21 s	142.21 s	142.2 s	141.8 s
6	132.7 s	132.52 s	132.75 s	132.91 s	132.6 s	132.4 s
7	52.0	51.93 s	51.89 s	52.33 s	51.9 s	51.7 s
8	60.2 d	60.06 d	60.08 d	60.42 d	60.1 d	59.9[a] d
10	169.3 s	169.39 s	169.18 s	170.31 s	169.4 s	168.8 s
11	48.2	42.34[a] t	50.28 t	42.46 t	42.3[a] t	42.2 t
12	77.2 d	77.53 d	77.54 d	77.73 d	77.5 d	77.3 d
13	42.9 d	48.17 d	48.18 d	48.44 d	48.2 d	48.0 d
14	42.5 d	31.54 d	31.60 d	31.83 d	31.5 d	31.4 d
15	31.7 t	26.81 t	26.87 t	26.92 t	26.8 t	26.7 t
16	60.2 d	60.06 d	60.08 d	60.42 d	60.1 d	59.8[a] d
17	26.9 t	42.83[a] t	42.43 t	43.05 t	42.8 t	42.6 t
18	52.6	50.23 t	52.67 t	50.49 t	50.2 t	50.1 t
20	50.4	52.65 t	42.87 t	52.76 t	52.7 t	52.4 t
21	140.5 s	140.27 s	140.56 s	140.04 s	140.3 s	140.2 s
22	127.5 d	127.65 d	127.09 d	128.99 d	127.7 d	125.8 d
23	64.6 t	64.55 t	64.57 t	64.84 t	64.6 t	64.3 t

[a] Interchangeable.

0022-3549/80/0700-0865$01.00/0
© 1980, American Pharmaceutical Association

Table I—Pharmacokinetic Parameters of Procainamide and *N*-Acetylprocainamide

Parameter	Rats				Humans	
	Our Study		Ref. 10			
	Procainamide	*N*-Acetylprocainamide	Procainamide	*N*-Acetylprocainamide	Procainamide[a]	*N*-Acetylprocainamide[b]
Elimination half-life ($t_{1/2}$), hr	0.66	2.13	0.92	0.85	3.5	6.0
Plasma clearance, ml/min/kg	80.7	20.7	64.0	22.0	7.99	3.09
Apparent volume of distribution, liters/kg	4.60	3.82	4.92	1.64	1.91	1.61

[a] From Ref. 7. [b] From Ref. 8.

gression analysis program available in a statistical analysis system package[2].

The biological half-life ranged from 0.54 to 0.83 hr for procainamide and from 1.72 to 2.92 hr for *N*-acetylprocainamide. The ratio of the biological half-life of *N*-acetylprocainamide to that of procainamide in the same rat averaged 3.3. Table I summarizes the values of the pharmacokinetic parameters obtained by Schneck *et al.* (10), those obtained in our study, and values reported for normal subjects.

Determination of the biological half-lives of procainamide and *N*-acetylprocainamide in the same animal, with sufficient time for elimination of the drugs from the body, allowed a more meaningful comparison of the pharmacokinetic parameters of the two drugs. The discrepancy between these results and those reported by Schneck *et al.* (10) may be due to the study design and to the method of determination of pharmacokinetic parameters. Schneck *et al.* sacrificed groups of rats and followed the blood sampling for 4 hr, which appears to be inadequate for *N*-acetylprocainamide. In our study, a distribution phase of ~1 hr was noticed when *N*-acetylprocainamide was administered intravenously. Furthermore, Schneck *et al.* (10) calculated the volume of distribution by dividing the total body clearance by the elimination rate constant, which obviously results in an underestimated value (Table I).

The results of our study were qualitatively similar to those observed in normal human subjects. The ratio of the half-lives, volumes of distribution, and body clearances of procainamide and its metabolite in these two species are similar. These results have important implications in interpretations of metabolism data from acute and chronic toxicity studies.

(1) E. E. Bagwell, T. Walle, D. E. Drayer, M. M. Reidenberg, and J. K. Pruett, *J. Pharmacol. Exp. Ther.*, **197**, 38 (1979).

(2) R. F. Minchin, K. F. Ilett, and J. W. Paterson, *Eur. J. Pharmacol.*, **47**, 51 (1978).

(3) J. J. L. Lertora, A. J. Atkinson, Jr., W. Kushner, M. J. Nevin, W.-K. Lee, C. Jones, and F. R. Schmid, *Clin. Pharmacol. Ther.*, **25**, 273 (1979).

(4) J. Kluger, M. M. Reidenberg, T. Tyberg, V. Lloyd, G. Ellis, J. Hayes, and D. E. Drayer, *Clin. Res.*, **26**, 244A (1978).

(5) M. M. Reidenberg, D. E. Drayer, M. Levy, and J. Warner, *Clin. Pharmacol. Ther.*, **17**, 722 (1975).

(6) R. Lahita, J. Kluger, D. E. Drayer, D. Koffler, and M. M. Reidenberg, *Clin. Res.*, **27**, 235A (1979).

(7) J. Koch-Weser, *Ann. N.Y. Acad. Sci.*, **179**, 370 (1971).

(8) J. M. Strong, J. S. Dutcher, W.-K. Lee, and A. J. Atkinson, Jr., *J. Pharmacokinet. Biopharm.*, **3**, 223 (1975).

(9) A. Yacobi, R. W. Krasula, C.-M. Lai, and B. L. Kamath, *Res. Commun. Chem. Pathol. Pharmacol.*, **24**, 197 (1979).

(10) D. W. Schneck, K. Grove, F. O. Dewitt, R. A. Shiroff, and A. H. Hayes, Jr., *J. Pharmacol. Exp. Ther.*, **204**, 210 (1978).

[2] Statistical Analysis System, SAS Institute, Raleigh, N.C.

(11) P. G. Harms and S. R. Ojeda, *J. Appl. Phys.*, **36**, 391 (1974).

(12) C.-M. Lai, B. L. Kamath, Z. M. Look, and A. Yacobi, *J. Pharm. Sci.*, in press.

Burde L. Kamath ˣ
Avraham Yacobi
Pharmaceutical Development Department
American Critical Care
McGaw Park, IL 60085

Received December 26, 1979.
Accepted for publication April 15, 1980.

Assignment of ^{13}C-NMR Spectra of Strychnine and Brucine

Keyphrases □ Alkaloids—strychnine and brucine, ^{13}C-NMR spectral analyses, chemical shifts assigned □ ^{13}C-NMR spectroscopy—brucine and strychnine, chemical shifts assigned □ Brucine—^{13}C-NMR spectral analysis, chemical shifts assigned □ Strychnine—^{13}C-NMR spectral analysis, chemical shifts assigned

To the Editor:

Singh *et al.* (1) recently reported on the ^{13}C-NMR spectroscopy of the alkaloids strychnine (I) and brucine (II). In this communication, I shall comment on the spectral data and assignments reported by these authors.

Wehrli (2, 3) previously reported on the ^{13}C-NMR spectrum of brucine. The complete assignment of the brucine spectrum (3) was accomplished by using common

Table I—Assignment of ^{13}C-NMR Spectra of Strychnine

Carbon	Ref. 1	Ref. 4	Ref. 5	Ref. 7	Ref. 6	Ref. 8
1	124.2 d	124.25 d	124.12 d	124.99 d	122.3 d	121.9 d
2	122.3 d	122.31 d	122.17 d	122.67 d	124.3 d	123.8 d
3	128.6 d	128.62 d	128.41 d	128.61 d	128.6 d	128.1 d
4	116.3 d	116.24 d	116.12 d	116.52 d	116.2 d	115.8 d
5	142.3 s	142.21 s	142.21 s	142.21 s	142.2 s	141.8 s
6	132.7 s	132.52 s	132.75 s	132.91 s	132.6 s	132.4 s
7	52.0	51.93 s	51.89 s	52.33 s	51.9 s	51.7 s
8	60.2 d	60.06 d	60.08 d	60.42 d	60.1 d	59.9[a] d
10	169.3 s	169.39 s	169.18 s	170.31 s	169.4 s	168.8 s
11	48.2	42.34[a] t	50.28 t	42.46 t	42.3[a] t	42.2 t
12	77.2 d	77.53 d	77.54 d	77.73 d	77.5 d	77.3 d
13	42.9 d	48.17 d	48.18 d	48.44 d	48.2 d	48.0 d
14	42.5 d	31.54 d	31.60 d	31.83 d	31.5 d	31.4 d
15	31.7 t	26.81 t	26.87 t	26.92 t	26.8 t	26.7 t
16	60.2 d	60.06 d	60.08 d	60.42 d	60.1 d	59.8[a] d
17	26.9 t	42.83[a] t	42.43 t	43.05 t	42.8 t	42.6 t
18	52.6	50.23 t	52.67 t	50.49 t	50.2 t	50.1 t
20	50.4	52.65 t	42.87 t	52.76 t	52.7 t	52.4 t
21	140.5 s	140.27 s	140.56 s	140.04 s	140.3 s	140.2 s
22	127.5 d	127.65 d	127.09 d	128.99 d	127.7 d	125.8 d
23	64.6 t	64.55 t	64.57 t	64.84 t	64.6 t	64.3 t

[a] Interchangeable.

0022-3549/80/0700-0865$01.00/0
© 1980, American Pharmaceutical Association

Table II—Assignment of ^{13}C-NMR Spectrum of Brucine

Carbon	Ref. 1	Ref. 2	Ref. 3	Ref. 4	Ref. 5	Ref. 6	Ref. 8
1	105.6 d		105.88 d	105.68 d	105.68 d	105.7 d	105.1 d
2	146.2 s	149.13/146.14	149.13/146.14 s	146.24 s	146.11 s	146.2 s	145.6 s
3	149.2 s	146.14/149.13	146.14/149.13 s	149.25 s	149.13 s	149.3 s	148.5 s
4	101.1 d		101.08 d	101.07 d	101.00 d	101.1 d	100.5 d
5	136.0 s	135.97	135.97 s	136.02 s	135.91 s	136.0 s	135.3 s
6	123.6 s	123.46	123.46 s	123.64 s	123.48 s	123.6 s	122.9 s
7	51.8		51.83 s	51.93 s	51.84 s	51.9 s	51.4 s
8	59.9 d		60.22 d	60.30 d	59.84 d	60.3 d	59.8[a] d
10	168.9 s	168.64	168.64 s	168.90 s	168.78 s	168.9 s	168.2 s
11	48.2		42.20 t	42.34 t	50.09 t	42.3 5	41.8 t
12	77.3 d		77.63 d	77.78 d	77.64 d	77.8 d	77.1 d
13	42.4 d		42.15 d	48.29 d	48.18 d	48.3 d	47.7 d
14	42.4 d		31.51 d	31.54 d	31.50 d	31.5 d	31.1 d
15	31.6 t		26.73 t	26.81 t	26.73 t	26.8 t	26.3 t
16	60.3 d		59.82 d	59.94 d	60.28 d	59.9 d	59.3[a] d
17	26.8 t		42.35 t	42.34 t	42.28 t	42.3 t	41.9 t
18	52.6		50.04 t	50.11 t	52.57 t	50.1 t	49.6 t
20	50.2		52.57 t	52.66 t	42.28 t	52.7 t	52.1 t
21	140.6 s	140.29	140.29 s	140.63 s	140.40 s	140.6 s	139.8 s
22	127.1 d		127.14 d	127.16 d	127.14 d	127.2 d	126.7 d
23	64.6 t		64.44 t	64.55 t	64.47 t	64.6 t	64.0 t
	56.4 q		56.45 q	56.42 q	56.43 q	56.4 q	55.7 q
	56.1 q		56.05 q	56.18 q	56.08 q	56.2 q	56.0 q

[a] Interchangeable.

shift rules, off-resonance spectral data, and spin-lattice relaxation time data of the low-field quaternary carbons. Verpoorte and Baerheim Svendsen (4) also reported on the ^{13}C-NMR spectroscopy of strychnine, brucine, and alcuronium, and Srinivasan and Lichter (5) reported on the ^{13}C-NMR spectroscopy of strychnine and brucine.

My extended studies of ^{13}C-NMR spectroscopy of a series of Strychnos alkaloids (6) showed that several assignments made by Srinivasan and Lichter were erroneous. Furthermore, this study (6) made it necessary to reverse my earlier assignment of the signals for C-1 and C-2 in strychnine. Leung and Jones (7) reported their investigation of the ^{13}C-NMR spectroscopy of some Strychnos alkaloids, and their assignment for the spectrum of strychnine was the same (except for C-1 and C-2) as in my second paper (6). Wenkert *et al.* (8) also reported on the ^{13}C-NMR spectroscopy of a series of Strychnos alkaloids. Their assignment of the strychnine spectrum was similar. All spectral data of Refs. 1–8 are summarized in Tables I and II.

If the results reported by Singh *et al.* (1) are compared with those reported by the other investigators, a great deal of discrepancy is observed. The multiplicity for some signals was not reported by Singh *et al.* [C-7 (52.0), C-11 (48.2), C-18 (52.8), and C-20 (50.4) in strychnine]; for other signals [*i.e.*, 42.5 (d), 42.9 (d), and 31.7 (t) in strychnine], the multiplicities were different from those reported in the other studies [42.3 (t), 42.8 (t), and 31.5 (d)] (2–8). In the off-resonance decoupled spectra of strychnine and brucine, not all of the signals show neat first-order splitting patterns. Also, second-order patterns are observed for some signals (9). This finding is readily understood if the PMR spectrum of strychnine is considered, where several methylene groups have the attached *geminal* protons at rather different shifts (10). However, by using different decoupling frequencies in the off-resonance decoupled spectra, the multiplicity of the signals can be established (11). The erroneous interpretation of the multiplicity of some signals necessarily leads to an erroneous assignment of these signals.

Furthermore, the assignment of C-17 by Singh *et al.* (1) is different from the assignments reported by other investigators. However, the assignment of the 42.8-ppm signal to this carbon is confirmed by comparison of the spectra of strychnine and pseudostrychnine (6). In the spectrum of the latter compound, the 26.8-ppm signal is shifted downfield considerably, which makes assignment of this signal to C-15 plausible. These arguments and the data given in Tables I and II indicate that the assignment of the strychnine and brucine spectra according to Singh *et al.* (1) is inaccurate. The assignment of the ^{13}C-NMR spectra of strychnine and brucine as reported by Wehrli (3), Verpoorte *et al.* (6), and Wenkert *et al.* (8) is correct.

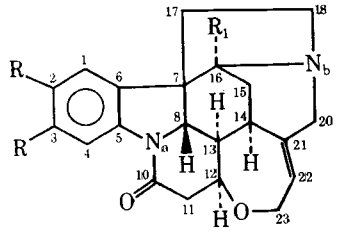

I: R = R_1 = H
II: R = OCH_3, R_1 = H

(1) S. P. Singh, V. I. Stenberg, S. S. Parmar, and S. A. Farnum, *J. Pharm. Sci.*, **68**, 89 (1979).
(2) F. W. Wehrli, *J. Chem. Soc. Chem. Commun.*, **1973**, 379.
(3) F. W. Wehrli, *Adv. Mol. Relaxation Processes*, **6**, 139 (1974).
(4) R. Verpoorte and A. Baerheim Svendsen, *Pharm. Weekbl.*, **111**, 745 (1976).
(5) P. R. Srinivasan and R. L. Lichter, *Org. Magn. Reson.*, **8**, 198 (1976).
(6) R. Verpoorte, P. J. Hylands, and N. G. Bisset, *ibid.*, **9**, 567 (1977).
(7) J. Leung and A. J. Jones, *ibid.*, **9**, 333 (1977).
(8) E. Wenkert, A. H. T. Cheung, H. E. Gottlieb, M. C. Koch, A. Rabaron, and M. M. Plat, *J. Org. Chem.*, **43**, 1099 (1978).
(9) E. W. Hagaman, *Org. Magn. Reson.*, **8**, 389 (1976).
(10) J. C. Carter, G. W. Luther, and T. C. Long, *J. Magn. Reson.*, **15**, 122 (1974).
(11) L. F. Johnson, in "Topics in Carbon-13 NMR Spectroscopy," vol. 3, G. C. Levy, Ed., Wiley–Interscience, New York, N.Y., 1979, p. 7.

R. Verpoorte
Department of Pharmacognosy
Gorlaeus Laboratories
University of Leyden
2300 RA Leyden
The Netherlands

Received November 5, 1979.
Accepted for publication January 29, 1980.

Potential Effect of Early Blood Sampling Schedule on Calculated Pharmacokinetic Parameters of Drugs after Intravenous Administration

Keyphrases □ Pharmacokinetics—effect of blood sampling time on calculated parameters after intravenous administration □ Volume of distribution—effect of blood sampling time on values calculated after intravenous administration □ Blood sampling time—effect on calculated pharmacokinetic parameters after intravenous administration

To the Editor:

The disposition of a drug in the body often can be studied best by intravenous administration (1–5). Differences in experimental methodology are known to affect the results of a pharmacokinetic study. For example, an insufficient sampling period or the lack of a sensitive assay may result in the underestimation of terminal biological half-lives of drugs (4–9). A nonspecific assay can cause overestimation of the plasma area under the curve and underestimation of the total plasma clearance (10). Sampling devices (11) and blood containers (12) might also affect assay results and, hence, the calculated pharmacokinetic parameters. Marked differences in protein binding (possibly also the concentration) of several drugs and bilirubin in serum and heparinized plasma were demonstrated (13). Differences in the curve-fitting technique also might affect the characterization of pharmacokinetic properties (4, 5, 14, 15).

In conventional pharmacokinetic studies, plasma concentration profiles between the beginning of intravenous injection or infusion (*i.e.*, time zero) and the time of the first blood sample collected usually are extrapolated or predicted based on plasma level data obtained at later times. The accuracy of such an extrapolation method has been questioned (16, 17). Marked underestimations of extrapolated plasma concentrations at time zero and probably of extrapolated plasma areas under the curve between time zero and the first sampling time (15 min) after rapid intravenous injection of sulfamethizole to five dogs were found when a constant blood withdrawal device and the conventional multiple blood sampling techniques were employed simultaneously (16). Disposition kinetics of a drug within the first few minutes after intravenous injection are often more complicated than is commonly recognized (17). For example, the true peak plasma concentration might be several times higher than the extrapolated concentration (17). Furthermore, the peak concentration in humans might occur 0.5–2 min after the end of dosing; at time zero, the true plasma concentration at the normal sampling site should always be zero and not the extrapolated zero-time value.

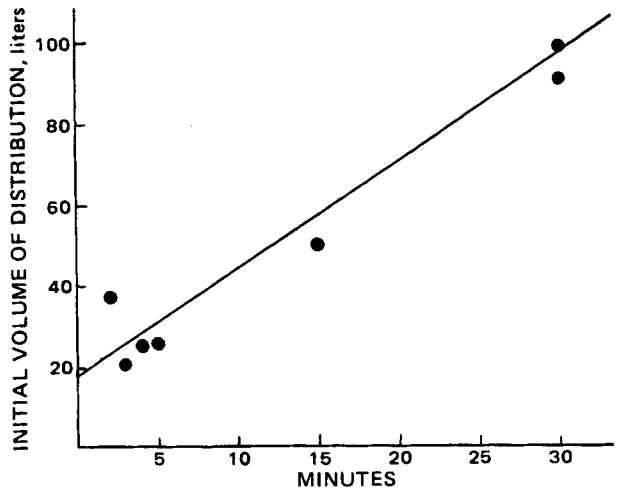

Figure 1—*Correlation between the average initial volume of distribution, V_c, and the time of the first blood sampling after an intravenous dose of digoxin in seven studies on humans with normal renal function; $V_c = 17.4 + 2.53t$ ($r^2 = 0.9452$).*

This review indicates that the early blood sampling schedule used in an intravenous study sometimes might significantly affect the obtained disposition function and, hence, the resultant multicompartmental modeling. In a recent study on quinidine, it was stated that the sampling pattern selected in a study also influences the choice of a model (15). Although it was not elaborated further, this statement is consistent with the contention of the possible early sampling schedule effect.

The literature often shows marked variability in the mean initial volume of distribution or mean volume of the central compartment reported in different intravenous studies on the same drug in similar subjects or patients. Although many factors might account for some of the differences, there often is a general pattern that the mean initial volume of distribution is smaller if the first blood sample is collected earlier in a study. The purpose of this communication is to point out this apparent trend using digoxin, gentamicin, and thiopental as examples.

Mean apparent initial volumes of distribution of digoxin reported or analyzed from six studies (18–23) on healthy adults with normal renal function are used for comparison. Subject characteristics, the duration of intravenous administration, the time of the first blood sampling, and the calculated mean volume value for each study are summarized in Table I. An apparent linear relationship between the mean initial volume of distribution and the time of the first blood sample was found (Fig. 1). The lowest volume, 20 liters, and the highest volume, 99 liters, were obtained from studies with the first blood sample collected at 3 and 30 min, respectively.

Although it is more meaningful to compare the volume of distribution in terms of volume per unit of body weight, this comparison usually is not possible since information on body weight was reported only in one study (21). For that study, the value (24.5 liters) reported in Table I was corrected for a 70-kg body weight. Since these studies involved normal adult subjects with a relatively narrow age range (no age information in Ref. 19), it is unlikely that body weight is a major factor for the marked variation in

0022-3549/80/0700-0867$01.00/0
© 1980, American Pharmaceutical Association

R. Verpoorte
Department of Pharmacognosy
Gorlaeus Laboratories
University of Leyden
2300 RA Leyden
The Netherlands

Received November 5, 1979.
Accepted for publication January 29, 1980.

Potential Effect of Early Blood Sampling Schedule on Calculated Pharmacokinetic Parameters of Drugs after Intravenous Administration

Keyphrases □ Pharmacokinetics—effect of blood sampling time on calculated parameters after intravenous administration □ Volume of distribution—effect of blood sampling time on values calculated after intravenous administration □ Blood sampling time—effect on calculated pharmacokinetic parameters after intravenous administration

To the Editor:

The disposition of a drug in the body often can be studied best by intravenous administration (1–5). Differences in experimental methodology are known to affect the results of a pharmacokinetic study. For example, an insufficient sampling period or the lack of a sensitive assay may result in the underestimation of terminal biological half-lives of drugs (4–9). A nonspecific assay can cause overestimation of the plasma area under the curve and underestimation of the total plasma clearance (10). Sampling devices (11) and blood containers (12) might also affect assay results and, hence, the calculated pharmacokinetic parameters. Marked differences in protein binding (possibly also the concentration) of several drugs and bilirubin in serum and heparinized plasma were demonstrated (13). Differences in the curve-fitting technique also might affect the characterization of pharmacokinetic properties (4, 5, 14, 15).

In conventional pharmacokinetic studies, plasma concentration profiles between the beginning of intravenous injection or infusion (*i.e.*, time zero) and the time of the first blood sample collected usually are extrapolated or predicted based on plasma level data obtained at later times. The accuracy of such an extrapolation method has been questioned (16, 17). Marked underestimations of extrapolated plasma concentrations at time zero and probably of extrapolated plasma areas under the curve between time zero and the first sampling time (15 min) after rapid intravenous injection of sulfamethizole to five dogs were found when a constant blood withdrawal device and the conventional multiple blood sampling techniques were employed simultaneously (16). Disposition kinetics of a drug within the first few minutes after intravenous injection are often more complicated than is commonly recognized (17). For example, the true peak plasma concentration might be several times higher than the extrapolated concentration (17). Furthermore, the peak concentration in humans might occur 0.5–2 min after the end of dosing; at time zero, the true plasma concentration at the normal sampling site should always be zero and not the extrapolated zero-time value.

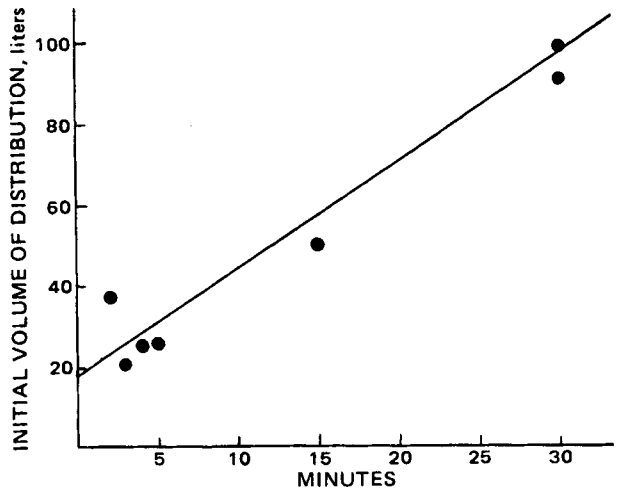

Figure 1—*Correlation between the average initial volume of distribution, V_c, and the time of the first blood sampling after an intravenous dose of digoxin in seven studies on humans with normal renal function; $V_c = 17.4 + 2.53t$ ($r^2 = 0.9452$).*

This review indicates that the early blood sampling schedule used in an intravenous study sometimes might significantly affect the obtained disposition function and, hence, the resultant multicompartmental modeling. In a recent study on quinidine, it was stated that the sampling pattern selected in a study also influences the choice of a model (15). Although it was not elaborated further, this statement is consistent with the contention of the possible early sampling schedule effect.

The literature often shows marked variability in the mean initial volume of distribution or mean volume of the central compartment reported in different intravenous studies on the same drug in similar subjects or patients. Although many factors might account for some of the differences, there often is a general pattern that the mean initial volume of distribution is smaller if the first blood sample is collected earlier in a study. The purpose of this communication is to point out this apparent trend using digoxin, gentamicin, and thiopental as examples.

Mean apparent initial volumes of distribution of digoxin reported or analyzed from six studies (18–23) on healthy adults with normal renal function are used for comparison. Subject characteristics, the duration of intravenous administration, the time of the first blood sampling, and the calculated mean volume value for each study are summarized in Table I. An apparent linear relationship between the mean initial volume of distribution and the time of the first blood sample was found (Fig. 1). The lowest volume, 20 liters, and the highest volume, 99 liters, were obtained from studies with the first blood sample collected at 3 and 30 min, respectively.

Although it is more meaningful to compare the volume of distribution in terms of volume per unit of body weight, this comparison usually is not possible since information on body weight was reported only in one study (21). For that study, the value (24.5 liters) reported in Table I was corrected for a 70-kg body weight. Since these studies involved normal adult subjects with a relatively narrow age range (no age information in Ref. 19), it is unlikely that body weight is a major factor for the marked variation in

0022-3549/80/0700-0867$01.00/0
© 1980, American Pharmaceutical Association

Table I—Subject Characteristics, Duration of Intravenous Digoxin Dosing, Time of First Blood Sampling, and Calculated Initial Volume of Distribution of Digoxin from Six Studies in Normal Adult Subjects and One Study in Neonates and Infants

Study (Ref.)	Number of Subjects	Sex	Age Range, years	Duration of Intravenous Dosing	Time of First Blood Sampling after Dosing, min	Estimated Average V_c[a], liters
1 (18)	4	M	27–35	Bolus	2	37.4[b]
2 (19)	4	—	—	1 min	3	20.0[b]
3 (20)	4	2 M; 2 F	19–40	Bolus	4	25.0[b]
4 (21)	12	M	23–34	60-min infusion	5[c]	24.5[d]
5 (22)	4	3 M; 1 F	22–29	Bolus	15	50.0[b]
6 (23)	6	—	24–26	Bolus	30	99.0[e]
7 (25)	7	—	Neonates and infants	2–3 min	30	91.0[d]

[a] Initial volume of distribution. [b] Estimated by this investigator based on the graphical data from the previous study. [c] Four blood samples also were collected at 0.25, 0.5, 0.75, and 1 hr during infusion. [d] Corrected for 70-kg body weight for comparison. [e] Calculated by Reuning *et al.* (24).

the mean initial volume of distribution. The results (Table I) from a study in neonates and infants (25) also are consistent with the data from the adult studies. The mean initial volume of distribution in these neonates and infants after correction to 70 kg is 91 liters, and the first blood sample in that study (25) was collected at 30 min.

For gentamicin, the mean initial volume of distribution in normal subjects could be estimated as 0.045 liter/kg in one study (26) with the first sample collected 1.0 min after a bolus dose (1.5 mg and 2.0 mg/kg), and as 0.099 liter/kg from another bolus study (27), with the first sample collected at 15 min. In a multiple 1-hr infusion study in patients with normal and moderately impaired renal function, the mean initial volumes of distribution of gentamicin were 0.21 and 0.20 liter/kg, respectively.

The initial volume of distribution of thiopental in one normal subject could be estimated as 6.4 liters from a bolus intravenous study (28) with the first blood sample taken probably at 2.4 min. However, the initial volume of distribution of thiopental in another normal subject in a study conducted in the same laboratory could be estimated as 60.5 liters (29). In the latter study, the first blood sample was collected at ~45 min. In both studies, the data were analyzed based on the two-compartment open model. The plasma thiopental levels at 45 and 120 min in both studies, after correction for the different doses used, were approximately the same.

The results of this study on three drugs indicate that the determination of the apparent initial volume of distribution might be affected by the time at which the first (and probably also the second) blood sample is collected. Although the marked variation in the volume of distribution in these examples might be attributed to the real difference, this factor probably is not major. In general, the most important factor affecting the volume of distribution of the same drug in normal subjects is the body weight. The wide range of the mean initial volume of digoxin from several studies and of thiopental from two (typical) subjects is not accounted for by the presumably relatively much smaller differences in body weight used in each study. Differences in assay accuracy also can be ruled out as a major factor since most assays should be more accurate for plasma samples with higher drug concentrations, which usually were more important in the determination of the initial volume of distribution.

The intersubject variation in the initial volume of distribution from the same study often was much less than the interstudy variation (18, 21, 22, 25), indicating the possible influence of study design on the calculated pharmacokinetic parameter.

The method used in these comparisons of the three drugs is not perfect. A more scientifically designed experiment is being planned to eliminate or minimize most of the other potential contributing factors and to identify the exact mechanisms for the observed phenomena. The results of this preliminary report indicate that one should be prudent in interpreting the markedly different pharmacokinetic parameters, especially the initial volume of distribution, reported in the literature. Some guidelines or standardization of studying and reporting the initial volume of distribution might be useful.

(1) S. Riegelman, J. C. K. Loo, and M. Rowland, *J. Pharm. Sci.*, **57**, 128 (1968).

(2) M. Gibaldi, G. Levy, and H. Weintraub, *Clin. Pharmacol. Ther.*, **12**, 734 (1971).

(3) L. Z. Benet, *J. Pharm. Sci.*, **61**, 536 (1972).

(4) M. Gibaldi and D. Perrier, "Pharmacokinetics," Dekker, New York, N.Y., 1975.

(5) J. G. Wagner, "Fundamentals of Clinical Pharmacokinetics," Drug Intelligence Publications, Hamilton, Ill., 1976.

(6) J. J. Schentag, W. J. Jusko, J. W. Vance, T. J. Cumbo, E. Abrutyn, M. DeLattre, and L. M. Gerbracht, *J. Pharmacokinet. Biopharm.*, **5**, 559 (1977).

(7) L. Z. Benet, *ibid.*, **7**, 1 (1979).

(8) W. L. Chiou, *J. Am. Med. Assoc.*, **337**, 658 (1974).

(9) W. L. Chiou, N. K. Athanikar, and S. M. Huang, *N. Engl. J. Med.*, **300**, 501 (1979).

(10) T. W. Guentert, R. A. Upton, N. H. G. Holford, and S. Riegelman, *J. Pharmacokinet. Biopharm.*, **7**, 303 (1979).

(11) R. H. Cotham and D. Shand, *Clin. Pharmacol. Ther.*, **18**, 535 (1975).

(12) W. L. Chiou and J. H. Hsiao, *J. Pharm. Sci.*, **63**, 1614 (1974).

(13) U. W. Wiegand, J. T. Slattery, K. L. Hintze, and G. Levy, *Life Sci.*, **25**, 471 (1979).

(14) W. G. Kramer, R. P. Lewis, T. C. Cobb, W. F. Forester, J. A. Visconti, L. A. Wanke, H. G. Boxenbaum, and R. H. Reuning, *J. Pharmacokinet. Biopharm.*, **2**, 299 (1974).

(15) T. W. Guentert, N. H. G. Holford, P. E. Coates, R. A. Upton, and S. Riegelman, *ibid.*, **7**, 315 (1979).

(16) C. R. Kowarski, C. Giancatarino, R. Kreamer, D. Brecht, and A. Kowarski, *J. Pharm. Sci.*, **65**, 450 (1976).

(17) W. L. Chiou, *J. Pharmacokinet. Biopharm.*, **7**, 527 (1979).

(18) D. J. Sumner and A. J. Russell, *Br. J. Clin. Pharmacol.*, **3**, 221 (1976).

(19) F. I. Marcus, A. Peterson, A. Salel, J. Scully, and G. G. Kapadia, *J. Pharmacol. Exp. Ther.*, **152**, 372 (1968).

(20) P. M. Blood and W. B. Nelp, *Am. J. Med. Sci.*, **251**, 133 (1966).

(21) B. L. Lloyd, D. J. Greenblatt, M. D. Allen, J. S. Harmatz, and T. W. Smith, *Am. J. Cardiol.*, **42**, 129 (1978).

(22) D. H. Huffman and D. L. Azarnoff, *J. Am. Med. Assoc.*, **222**, 957 (1972).

(23) W. Shapiro, K. Narahara, and K. Taubert, *Circulation*, **42**, 1065 (1970).
(24) R. H. Reuning, R. A. Sams, and R. E. Notari, *J. Clin. Pharmacol.*, **13**, 127 (1973).
(25) G. Wettrell, *Eur. J. Clin. Pharmacol.*, **11**, 329 (1977).
(26) K. L. Lynn, T. J. Neale, P. J. Little, and R. R. Bailey, *N. Z. Med. J.*, **80**, 443 (1974).
(27) A. Mosegaard, P. G. Welling, and P. O. Madsen, *Antimicrob. Agents Chemother.*, **7**, 328 (1975).
(28) B. B. Brodie, L. C. Mark, E. M. Papper, P. A. Lief, E. Bernstein, and E. A. Rovenstine, *J. Pharmacol. Exp. Ther.*, **98**, 85 (1950).
(29) B. B. Brodie, J. J. Burns, L. C. Mark, P. A. Lief, E. Bernstein, and E. M. Papper, *ibid.*, **109**, 26 (1953).

Win L. Chiou
Department of Pharmacy
College of Pharmacy
University of Illinois at the Medical Center
Chicago, IL 60612

Received December 13, 1979.
Accepted for publication April 30, 1980.

Mesophase Formation during Cholesterol Dissolution in Ursodeoxycholate–Lecithin Solutions: New Mechanism for Gallstone Dissolution in Humans

Keyphrases □ Cholesterol—mesophase formation during dissolution in ursodeoxycholate–lecithin solutions, mechanism for gallstone dissolution in humans □ Gallstones—mechanism for dissolution in humans, mesophase formation during cholesterol dissolution in ursodeoxycholate–lecithin solutions

To the Editor:

It is well established that oral administration of chenodeoxycholic acid (I) induces bile desaturation in cholesterol and gradual dissolution of cholesterol gallstones in humans (1). Makino *et al.* (2) reported that ursodeoxycholic acid (II), the 7β-hydroxy epimer of I, also can induce bile desaturation in humans, an observation confirmed by other investigators (3).

The cholesterol saturation of bile (percent saturation) is defined as $(C_{sample}/C_s) \times 100$, where C_s is the concentration in the sample if it is saturated fully with cholesterol, *i.e.*, the solubility at equilibrium. In model systems, C_s is determined almost entirely by the molar proportions of bile acids and lecithin (4–6). The C_s value usually is assumed to be that value determined experimentally for the model system having an identical proportion of bile acids and lecithin, and the actual value for percentage saturation is determined graphically (7) or analytically (8). This approach has been assumed to be correct since C_s determined in bile samples from gallstone patients did not differ significantly from that of the model system (6). Accordingly, there has been rather satisfactory agreement between predicted and measured percent saturation in bile samples obtained from gallstone patients (9). The C_s value was considered to be uninfluenced by biliary bile acid composition since changing the relative proportion of the common bile acids (cholic, deoxycholic, and I) in model systems had little influence on C_s (4, 5).

Igimi *et al.* (10) reported that the ability of II to solubilize cholesterol both in the presence and absence of lecithin was strikingly inferior to that of I and concluded that II might well be less efficacious than I for gallstone dissolution. Carey and coworkers (11) confirmed these observations and also reported (12) that the maximum capacity of model bile systems to solubilize cholesterol was depressed in proportion to the percent of II conjugates in bile salt mixtures. Thus, the micellar zone in the phase diagram simulating bile appears to be reduced by the presence of II. Carey and Ko (12) also proposed that a new C_s value must be used to calculate the percent saturation in gallstone patients receiving II and presented an "urso-correction factor" to facilitate such calculations. Nevertheless, initial clinical studies (3) suggested that gallstone dissolution in patients receiving II did not occur more slowly than in those receiving I. Indeed, several instances of rather rapid dissolution were observed. To rationalize these discrepancies, we undertook a systematic study of cholesterol dissolution with II–lecithin solutions.

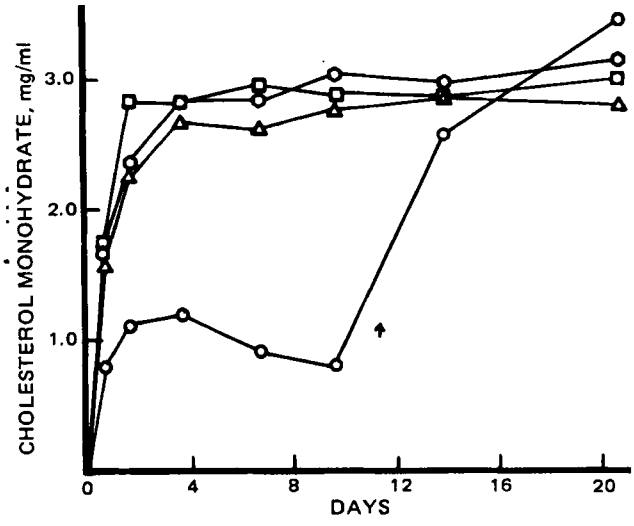

Figure 1—*Apparent solubility profiles of cholesterol monohydrate in 116 mM bile salt, 32 mM lecithin, 0.1 M NaCl, and 0.01 M phosphate buffer media at 37°. Key: ○, glycochenodeoxycholate; □, taurochenodeoxycholate; △, taurocholate; and ○, glycoursodeoxycholate; the arrow indicates the time of occurrence of a nonfilterable cloudiness due to mesophase formation in the glycoursodeoxycholate system.*

In recent dissolution studies[1] under sink conditions using methodology outlined previously (13), we found that over a wide range of bile acid, lecithin, and electrolyte concentrations, the initial dissolution rate of cholesterol monohydrate in II conjugate–lecithin media was two to 70 times lower than in corresponding I media. The dissolution of cholesterol and of gallstones *in vitro* was shown previously (9, 14) to be controlled interfacially, with the interfacial resistance $R = (h/D + 1/P)$ being a function of the dissolution medium composition. The evaluation of R and hence P (the effective permeability coefficient of the interfacial barrier) under sink conditions requires an estimate of C_s, the solute saturation concentration, since $R = AC_s/J$, where A is the area of the dissolving surface and J is the initial dissolution rate (15).

However, in contrast to media containing I and lecithin or I conjugates and lecithin, attempts to measure C_s with

[1] O. I. Corrigan, C. C. Su, W. I. Higuchi, and A. F. Hofmann, manuscript in preparation.

0022-3549/80/0700-0869$01.00/0
© 1980, American Pharmaceutical Association

(23) W. Shapiro, K. Narahara, and K. Taubert, *Circulation*, **42**, 1065 (1970).
(24) R. H. Reuning, R. A. Sams, and R. E. Notari, *J. Clin. Pharmacol.*, **13**, 127 (1973).
(25) G. Wettrell, *Eur. J. Clin. Pharmacol.*, **11**, 329 (1977).
(26) K. L. Lynn, T. J. Neale, P. J. Little, and R. R. Bailey, *N. Z. Med. J.*, **80**, 443 (1974).
(27) A. Mosegaard, P. G. Welling, and P. O. Madsen, *Antimicrob. Agents Chemother.*, **7**, 328 (1975).
(28) B. B. Brodie, L. C. Mark, E. M. Papper, P. A. Lief, E. Bernstein, and E. A. Rovenstine, *J. Pharmacol. Exp. Ther.*, **98**, 85 (1950).
(29) B. B. Brodie, J. J. Burns, L. C. Mark, P. A. Lief, E. Bernstein, and E. M. Papper, *ibid.*, **109**, 26 (1953).

Win L. Chiou
Department of Pharmacy
College of Pharmacy
University of Illinois at the Medical Center
Chicago, IL 60612

Received December 13, 1979.
Accepted for publication April 30, 1980.

Mesophase Formation during Cholesterol Dissolution in Ursodeoxycholate–Lecithin Solutions: New Mechanism for Gallstone Dissolution in Humans

Keyphrases □ Cholesterol—mesophase formation during dissolution in ursodeoxycholate–lecithin solutions, mechanism for gallstone dissolution in humans □ Gallstones—mechanism for dissolution in humans, mesophase formation during cholesterol dissolution in ursodeoxycholate–lecithin solutions

To the Editor:

It is well established that oral administration of chenodeoxycholic acid (I) induces bile desaturation in cholesterol and gradual dissolution of cholesterol gallstones in humans (1). Makino *et al.* (2) reported that ursodeoxycholic acid (II), the 7β-hydroxy epimer of I, also can induce bile desaturation in humans, an observation confirmed by other investigators (3).

The cholesterol saturation of bile (percent saturation) is defined as $(C_{sample}/C_s) \times 100$, where C_s is the concentration in the sample if it is saturated fully with cholesterol, *i.e.*, the solubility at equilibrium. In model systems, C_s is determined almost entirely by the molar proportions of bile acids and lecithin (4–6). The C_s value usually is assumed to be that value determined experimentally for the model system having an identical proportion of bile acids and lecithin, and the actual value for percentage saturation is determined graphically (7) or analytically (8). This approach has been assumed to be correct since C_s determined in bile samples from gallstone patients did not differ significantly from that of the model system (6). Accordingly, there has been rather satisfactory agreement between predicted and measured percent saturation in bile samples obtained from gallstone patients (9). The C_s value was considered to be uninfluenced by biliary bile acid composition since changing the relative proportion of the common bile acids (cholic, deoxycholic, and I) in model systems had little influence on C_s (4, 5).

Igimi *et al.* (10) reported that the ability of II to solubilize cholesterol both in the presence and absence of lecithin was strikingly inferior to that of I and concluded that II might well be less efficacious than I for gallstone dissolution. Carey and coworkers (11) confirmed these observations and also reported (12) that the maximum capacity of model bile systems to solubilize cholesterol was depressed in proportion to the percent of II conjugates in bile salt mixtures. Thus, the micellar zone in the phase diagram simulating bile appears to be reduced by the presence of II. Carey and Ko (12) also proposed that a new C_s value must be used to calculate the percent saturation in gallstone patients receiving II and presented an "urso-correction factor" to facilitate such calculations. Nevertheless, initial clinical studies (3) suggested that gallstone dissolution in patients receiving II did not occur more slowly than in those receiving I. Indeed, several instances of rather rapid dissolution were observed. To rationalize these discrepancies, we undertook a systematic study of cholesterol dissolution with II–lecithin solutions.

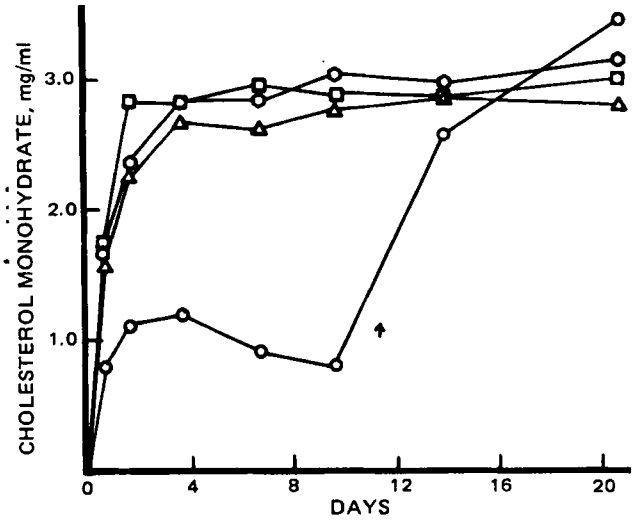

Figure 1—*Apparent solubility profiles of cholesterol monohydrate in 116 mM bile salt, 32 mM lecithin, 0.1 M NaCl, and 0.01 M phosphate buffer media at 37°. Key: ○, glycochenodeoxycholate; □, taurochenodeoxycholate; △, taurocholate; and ○, glycoursodeoxycholate; the arrow indicates the time of occurrence of a nonfilterable cloudiness due to mesophase formation in the glycoursodeoxycholate system.*

In recent dissolution studies[1] under sink conditions using methodology outlined previously (13), we found that over a wide range of bile acid, lecithin, and electrolyte concentrations, the initial dissolution rate of cholesterol monohydrate in II conjugate–lecithin media was two to 70 times lower than in corresponding I media. The dissolution of cholesterol and of gallstones *in vitro* was shown previously (9, 14) to be controlled interfacially, with the interfacial resistance $R = (h/D + 1/P)$ being a function of the dissolution medium composition. The evaluation of R and hence P (the effective permeability coefficient of the interfacial barrier) under sink conditions requires an estimate of C_s, the solute saturation concentration, since $R = AC_s/J$, where A is the area of the dissolving surface and J is the initial dissolution rate (15).

However, in contrast to media containing I and lecithin or I conjugates and lecithin, attempts to measure C_s with

[1] O. I. Corrigan, C. C. Su, W. I. Higuchi, and A. F. Hofmann, manuscript in preparation.

0022-3549/80/0700-0869$01.00/0
© 1980, American Pharmaceutical Association

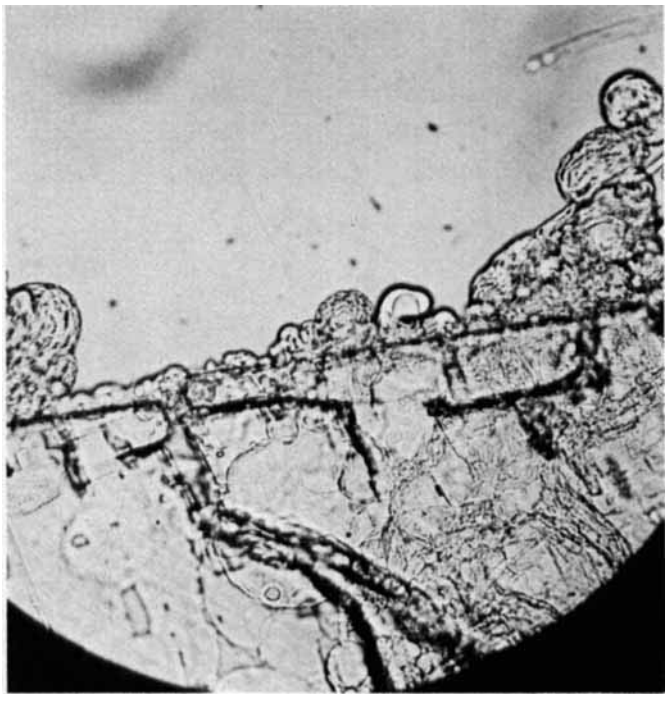

Figure 2—*Mesophase growth on cholesterol monohydrate crystal (original magnification 40×) immersed in a 174 mM ursodeoxycholate–lecithin (48 mM) medium at 37° for 20 hr.*

powder samples of cholesterol monohydrate in media containing II conjugates (glycine or taurine) and lecithin, using conventional methodology, were complicated by the development of turbidity in the supernate, which was not removed by filtration. In addition, the release of cholesterol into the II conjugate–lecithin media continued and even increased beyond the apparent equilibrium solubility (Fig. 1).

Microscopic examination of the cloudy supernate revealed a globular phase of a liquid-crystalline nature, which on analysis, following centrifugation, contained substantial amounts of lecithin (16) and cholesterol. The rate of formation of this mesophase in powder slurries, as judged by the appearance of turbidity and an increase in the apparent solubility, was dependent in the case of glycoursodeoxycholate (III) on the III–lecithin ratio and the total lipid concentration. For example, using a III–lecithin ratio of 3.61 and a III concentration of 116 m*M*, cloudiness did not occur until about the 10th day. However, at a ratio of 3.61 with a III concentration of 174 m*M* or at a ratio of 2.72 with a III concentration of 87 m*M*, the time for mesophase initiation was much shorter (~24 hr). Mesophase formation also was retarded greatly when compressed disks of cholesterol monohydrate were used rather than powder slurries.

These data and other studies[1] suggest that III has a much greater propensity than glycochenodeoxycholate (IV) to promote mesophase formation. To test this possibility, single crystals of cholesterol monohydrate were mounted as described previously (17) in a 1-cm spectroscopic cell and examined during dissolution under static conditions using a horizontally mounted microscope incubated at 37°. During dissolution in a 174 m*M* III–lecithin (48 m*M*) medium, mesophase growth on the cholesterol crystal surface became evident in a few hours. By 24 hr, the crystal surface was coated with mesophase spherulites (~40–150 μm in diameter) (Fig. 2). By contrast, crystals subjected to a IV–lecithin medium of similar composition did not show evidence of mesophase growth; dissolution was more rapid than in III.

In gallstone formation, the problem usually was considered in terms of a solid, crystalline cholesterol monohydrate phase separating from a supersaturated, isotropic micellar phase; for dissolution, the problem was thought to be the slow dissolution of crystalline cholesterol into an unsaturated micellar solution. Although a mesomorphic liquid crystalline phase occasionally has been observed in human bile samples (18, 19) or in animals in which supersaturated bile was induced (20), a mesomorphic phase generally was not considered to be involved in gallstone formation or dissolution since the mesomorphic phase occurred in model systems only at lower ratios of bile acids to lecithin than had been reported for bile samples from gallstone patients (21).

These observations indicate that mesophase formation and dispersion may occur during gallstone dissolution in patients receiving II. Since the mesophase density differs from bile, gallstone dissolution may involve flotation of a mesophase in addition to simple molecular and micellar diffusion and convection.

(1) J. L. Thistle, A. F. Hofmann, B. J. Ott, and D. H. Stephens, *J. Am. Med. Assoc.*, **239,** 1138 (1978).

(2) I. Makino, K. Shinozaki, K. Yoshino, and S. Nakagawa, *Jpn. J. Gastroenterol.*, **72,** 690 (1975).

(3) R. H. Dowling, A. F. Hofmann, and L. Barbara, "Workshop on Ursodeoxycholic Acid," University Park Press, Baltimore, Md., 1979.

(4) M. C. Carey and D. M. Small, *J. Clin. Invest.*, **61,** 998 (1978).

(5) F. G. Hegardt and H. Dam, *Z. Ernaehr.*, **10,** 223 (1971).

(6) R. T. Holzbach, M. E. Marsh, M. Olszewski, and K. Holan, *J. Clin. Invest.*, **52,** 1467 (1973).

(7) A. L. Metzger, S. Heymsfield, and S. M. Grundy, *Gastroenterology*, **62,** 499 (1972).

(8) P. J. Thomas and A. F. Hofmann, *ibid.*, **65,** 698 (1973).

(9) A. M. Molokhia, A. F. Hofmann, W. I. Higuchi, M. Tuchinda, K. Feld, S. Prakongpan, and R. G. Danzinger, *J. Pharm. Sci.*, **66,** 1101 (1977).

(10) H. Igimi, T. Noriyuki, I. Yuichi, and S. Hidehiko, *Life Sci.*, **21,** 1373 (1977).

(11) M. C. Carey, N. A. Mazer, and G. B. Benedek, *Gastroenterology*, **72,** 1036 (1977).

(12) M. C. Carey and G. Ko, in "Biological Effects of Bile Acids," G. Paumgartner, A. Stiehl, and W. Gerok, Eds., MTP Press, Lancaster, England, 1979, pp. 299–308.

(13) K. H. Kwan, W. I. Higuchi, and A. F. Hofmann, *J. Pharm. Sci.*, **67,** 1711 (1978).

(14) W. I. Higuchi, S. Prakongpan, and F. Young, *ibid.*, **62,** 945 (1973).

(15) K. H. Kwan, W. I. Higuchi, A. M. Molokhia, and A. F. Hofmann, *ibid.*, **66,** 1094 (1977).

(16) R. S. Sandhu, *Clin. Chem.*, **22,** 1973 (1976).

(17) S. C. Mehta, P. D. Bernardo, W. I. Higuchi, and A. P. Simonelli, *J. Pharm. Sci.*, **59,** 638 (1970).

(18) M. F. Olszewski, R. T. Holzbach, A. Saupe, and G. H. Brown, *Nature (London)*, **242,** 336 (1973).

(19) K. R. Holan, R. T. Holzbach, R. E. Hermann, A. M. Cooperman, and W. J. Claffey, *Gastroenterology*, **77,** 611 (1979).

(20) R. T. Holzbach, C. Corbusier, M. Marsh, and H. K. Naito, *J. Lab. Clin. Med.*, **87,** 987 (1976).

(21) W. H. Admirand and D. M. Small, *J. Clin. Invest.*, **47,** 1043 (1968).

O. I. Corrigan *
C. C. Su
W. I. Higuchi ˣ
College of Pharmacy
University of Michigan

Ann Arbor, MI 48109
A. F. Hofmann
Division of Gastroenterology
Department of Medicine
University of California
San Diego, CA 92103

Received November 29, 1979.
Accepted for publication February 28, 1980.
Supported by National Institutes of Health Grants AM16694 and AM21506 and grants-in-aid from Canada Packers Ltd., Eli Lilly Co., INTERx Corp., and The Upjohn Co.
The authors thank the Tokyo Tanabe Co., Tokyo, Japan, for a generous sample of ursodeoxycholic acid.
* Present address: School of Pharmacy, Trinity College Dublin, Dublin 4, Ireland.

Coupling of Steroid Hormones to Biodegradable Poly(α-amino acids) I: Norethindrone Coupled to Poly-N^5-(3-hydroxypropyl)-L-glutamine

Keyphrases □ Norethindrone—coupling to poly(α-amino acids), controlled release from coupled compounds □ Contraceptives—norethindrone, coupling to poly(α-amino acids), controlled release from coupled compounds □ Polymers, biodegradable—poly(α-amino acids), coupling to norethindrone, controlled release of norethindrone from coupled compounds

To the Editor:

Sustained release of drugs from polymeric matrixes has received increased interest (1–5). Hormone release from such systems was investigated to obtain devices for long-term contraceptive purposes. A new approach in the release of hormones from polymeric systems is the use of covalently bound polymer–hormone compounds that are biodegradable and do not need removal after implantation. Although a few examples of steroids being bonded covalently to polymers have been reported (6–8), the coupling of steroids to biodegradable polymers was presented only recently (9). We wish to report a new derivatization of 17α-ethynyl-17β-hydroxy steroids, which are appropriate for attachment to biodegradable poly(α-amino acids).

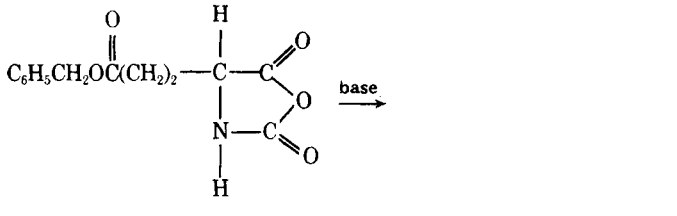

I

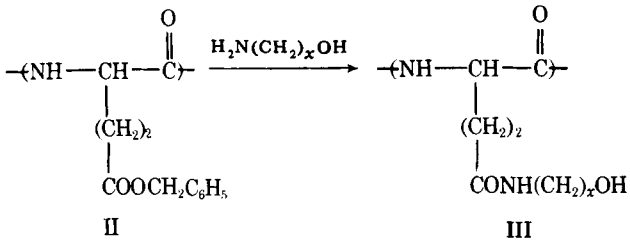

II III

IIIa: $x = 3$

Scheme I

Poly(hydroxyalkyl)-L-glutamines (III) were studied by several investigators (10, 11). These polymers are prepared through the base-catalyzed polymerization of γ-benzyl-L-glutamate N-carboxyanhydride (I), giving the polymeric benzyl-L-glutamate (II), followed by displacement of the benzyl group with the desired hydroxyalkyl amines (12) (Scheme I). The polymers are water soluble but become water insoluble upon substitution with hydrophobic steroids.

The steroid selected for derivatization was norethindrone (IV), an active progestin (Scheme II). Reaction of IV in methylene chloride with a stoichiometric amount of pyridine and an excess of phosgene at room temperature resulted in a 77% yield of norethindrone-17β-chloroformate (V, mp 103–105° dec.). The reaction was monitored by TLC until IV had disappeared completely. The structure of V then was verified; IR (ν, KBr pellet): 1780 (chloroformate) cm^{-1}; ^{1}H-NMR (δ, $CDCl_3$): 5.80 (s, 1H, 4[1]), 2.77 (s, 1H, 21), and 1.00 (s, 3H, 18).

Compound V is unstable and was derivatized to further confirm its structure and to investigate its potential for the coupling with polymer IIIa. Compound V was reacted with

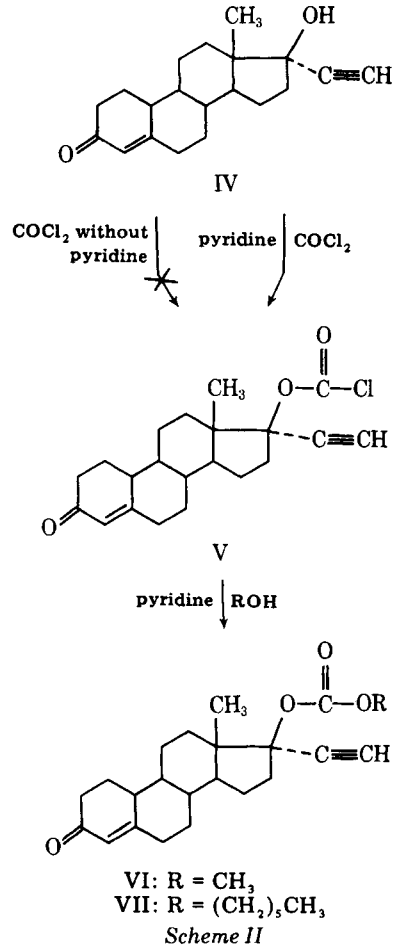

IV V

VI: R = CH_3
VII: R = $(CH_2)_5CH_3$

Scheme II

[1] These numbers correspond to the standard nomenclature for carbon atoms of the steroid skeleton to which the protons are attached. The carbonate carbon is number 22, and the alkyl groups of the carbonate esters are numbered from 23 to 28, where 28 is the terminal carbon of the hexylcarbonate (VII).

0022-3549/80/0700-0871$01.00/0
© 1980, American Pharmaceutical Association

Ann Arbor, MI 48109
A. F. Hofmann
Division of Gastroenterology
Department of Medicine
University of California
San Diego, CA 92103

Received November 29, 1979.
Accepted for publication February 28, 1980.
Supported by National Institutes of Health Grants AM16694 and AM21506 and grants-in-aid from Canada Packers Ltd., Eli Lilly Co., INTERx Corp., and The Upjohn Co.
The authors thank the Tokyo Tanabe Co., Tokyo, Japan, for a generous sample of ursodeoxycholic acid.
* Present address: School of Pharmacy, Trinity College Dublin, Dublin 4, Ireland.

Coupling of Steroid Hormones to Biodegradable Poly(α-amino acids) I: Norethindrone Coupled to Poly-N^5-(3-hydroxypropyl)-L-glutamine

Keyphrases □ Norethindrone—coupling to poly(α-amino acids), controlled release from coupled compounds □ Contraceptives—norethindrone, coupling to poly(α-amino acids), controlled release from coupled compounds □ Polymers, biodegradable—poly(α-amino acids), coupling to norethindrone, controlled release of norethindrone from coupled compounds

To the Editor:

Sustained release of drugs from polymeric matrixes has received increased interest (1–5). Hormone release from such systems was investigated to obtain devices for long-term contraceptive purposes. A new approach in the release of hormones from polymeric systems is the use of covalently bound polymer–hormone compounds that are biodegradable and do not need removal after implantation. Although a few examples of steroids being bonded covalently to polymers have been reported (6–8), the coupling of steroids to biodegradable polymers was presented only recently (9). We wish to report a new derivatization of 17α-ethynyl-17β-hydroxy steroids, which are appropriate for attachment to biodegradable poly(α-amino acids).

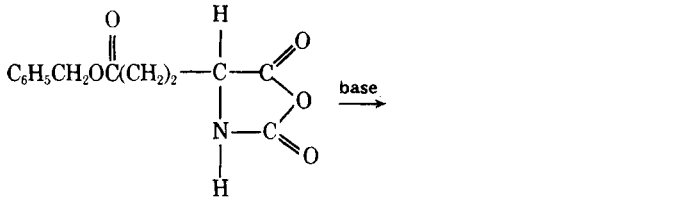

I

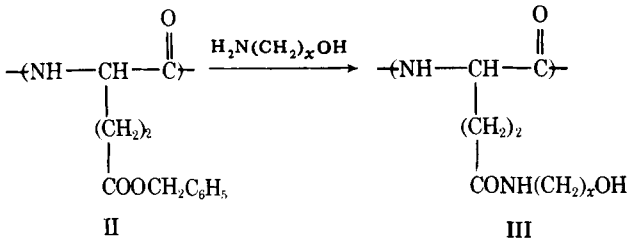

II III

IIIa: $x = 3$

Scheme I

Poly(hydroxyalkyl)-L-glutamines (III) were studied by several investigators (10, 11). These polymers are prepared through the base-catalyzed polymerization of γ-benzyl-L-glutamate N-carboxyanhydride (I), giving the polymeric benzyl-L-glutamate (II), followed by displacement of the benzyl group with the desired hydroxyalkyl amines (12) (Scheme I). The polymers are water soluble but become water insoluble upon substitution with hydrophobic steroids.

The steroid selected for derivatization was norethindrone (IV), an active progestin (Scheme II). Reaction of IV in methylene chloride with a stoichiometric amount of pyridine and an excess of phosgene at room temperature resulted in a 77% yield of norethindrone-17β-chloroformate (V, mp 103–105° dec.). The reaction was monitored by TLC until IV had disappeared completely. The structure of V then was verified; IR (ν, KBr pellet): 1780 (chloroformate) cm^{-1}; ^{1}H-NMR (δ, $CDCl_3$): 5.80 (s, 1H, 4[1]), 2.77 (s, 1H, 21), and 1.00 (s, 3H, 18).

Compound V is unstable and was derivatized to further confirm its structure and to investigate its potential for the coupling with polymer IIIa. Compound V was reacted with

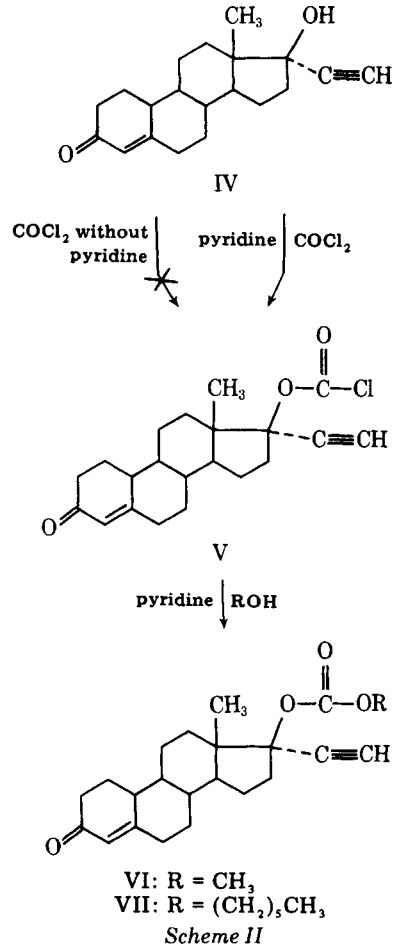

IV V

VI: R = CH_3
VII: R = $(CH_2)_5CH_3$

Scheme II

[1] These numbers correspond to the standard nomenclature for carbon atoms of the steroid skeleton to which the protons are attached. The carbonate carbon is number 22, and the alkyl groups of the carbonate esters are numbered from 23 to 28, where 28 is the terminal carbon of the hexylcarbonate (VII).

0022-3549/80/0700-0871$01.00/0
© 1980, American Pharmaceutical Association

a stoichiometric amount of pyridine and excess methanol or hexanol in dichloromethane to give norethindrone-17β-methylcarbonate (VI, 84% yield, mp 153–154°) or norethindrone-17β-hexylcarbonate (VII, 94% yield, oil).

The spectroscopic data for VI were: IR (ν, KBr pellet): 1750 (carbonate) cm^{-1}; ^{1}H-NMR (δ, $CDCl_3$): 5.80 (s, 1H, 4), 3.77 (s, 3H, 23), 2.63 (s, 1H, 21), and 0.97 (s, 3H, 18); mass spectrum: *m/e* 356 (100%, M^+) and 342 (4.17, $M^+ - CH_3$); satisfactory combustion analysis was obtained. The spectroscopic data for VII were: IR (ν, oil film): 1750 (carbonate) cm^{-1}; ^{1}H-NMR ($CDCl_3$): δ 5.80 (s, 1H, 4), 4.10 (t, 2H, 23), 2.63 (s, 1H, 21), 0.95 (s, 3H, 18), and 0.86 (t, 3H, 28); mass spectrum: *m/e* 426 (3.5%, M^+) and 342 [45, $M^+ - (CH_2)_5CH_3$].

It has been claimed that a base is not necessary for the conversion of primary alcohols into their chloroformates. When tertiary alcohols are converted to their chloroformates, a base is required (13). To check whether a selective reaction with a primary alcohol group in derivatized IV (*e.g.*, the 3-oxime derivative) would be possible, norethindrone (IV) was reacted with phosgene in the absence of pyridine. As anticipated, no chloroformate was formed.

Coupling reactions to poly-N^5-(3-hydroxypropyl)-L-glutamine were monitored using tritiated norethindrone[2]. Compound III*a*[3] was dried for 5 days under high vacuum at room temperature, dissolved in a mixture of anhydrous dimethylformamide and pyridine, and then reacted with the tritiated V, which was synthesized as described. The polymer was isolated from unreacted products by repeated precipitation in ethyl acetate.

The degree of substitution of norethindrone onto the available hydroxyl groups of III*a* was up to 60% as determined by liquid scintillation counting techniques. The following spectroscopic data were obtained: IR (ν, mineral oil): 1760 and 1265 (carbonate) cm^{-1}, 1660 and 1550 (amide) cm^{-1}, and 3300 (hydroxyl) cm^{-1}.

In vivo release studies using norethindrone coupled to poly-N^5-(3-hydroxypropyl)-L-glutamine microparticles, which were implanted subcutaneously in rats, showed a near zero-order release rate for >200 days (14).

[2] Nonspecific tritiated norethindrone, New England Nuclear, Boston, MA 02118.

[3] Obtained from poly(γ-benzyl-L-glutamate), which had a viscosity average molecular weight of 53,000.

(1) T. J. Roseman, *J. Pharm. Sci.*, **61**, 46 (1972).

(2) D. R. Kalkwarf, M. Sikiv, L. Smith, and R. Gordon, *Contraception*, **7**, 474 (1973).

(3) G. Benagiano, M. Ermini, C. C. Chang, K. Sundaram, and F. A. Kind, *Acta Endocrinol.*, **63**, 29 (1970).

(4) S. Yolles, *Acta Pharm. Suec., Suppl. 32*, 13 (1976).

(5) "Controlled Release of Biologically Active Agents," A. C. Tanquari and R. E. Lacey, Eds., Plenum, New York, N.Y., 1974.

(6) H. G. Batz, H. Ringsdorf, and H. Ritter, *Makromol. Chem.*, **175**, 2229 (1974).

(7) C. P. Pinazzi, A. Merril, J. C. Rabadeux, and A. Pleurdeau, *J. Polym. Sci. Symp.*, **52**, 1 (1975).

(8) K. L. Agarwal and M. M. Dhar, *Steroids*, **6**, 105 (1965) and references cited therein.

(9) D. Gregonis, J. Feijen, J. Anderson, and R. V. Petersen, *Polym. Preprints*, **20**, 612 (1979).

(10) N. Lotan, M. Bixon, and A. Berger, *Biopolymers*, **8**, 247 (1969).

(11) M. Miyake, S. Akito, A. Teramoto, T. Norisuye, and H. Fumita, *ibid.*, **13**, 1173 (1974).

(12) N. Lotan, A. Yaron, A. Berger, and M. Sela, *ibid.*, **3**, 625 (1965).

(13) Houben-Weyl, "Methoden der Organischen Chemie," vol. 8, Georg Thieme Verlag, Stuttgart, West Germany, 1952, pp. 101–104.

(14) M. A. Zupon, J. M. Christensen, R. V. Petersen, and S. M. Fang, *Polym. Preprints*, **20**, 604 (1979).

J. Feijen ˣ

Department of Chemical Technology
Twente University of Technology
Enschede, The Netherlands

D. Gregonis
C. Anderson
R. V. Petersen

Department of Pharmaceutics
University of Utah
Salt Lake City, UT 84112

J. Anderson

Department of Macromolecular Sciences
Case Western Reserve University
Cleveland, OH 44106

Received September 14, 1979.

Accepted for publication March 14, 1980.

Supported by National Institute of Child Health and Development Contract NO1-HD-7-2824.

The authors thank Dr. S. W. Kim, Dr. J. R. Cardinal, and Dr. S. M. Fang for stimulating discussions, Mr. H. Lam and Mr. F. Rejali for synthetic support, Mr. J. Silcox, University of Utah Regional Resource Center, for obtaining the NMR spectra, Dr. McCloskey for obtaining mass spectrometry data, and Ms. K. Eggen for typing the manuscript.

REVIEWS

1980 United States Pharmacopeia–National Formulary. The United States Pharmacopeial Convention. 1980. 1505 pp. 21 × 28.5 cm. Price $90.00 postpaid (domestic and foreign), including all annual supplements to USP XX and NF XV; separately, $65.00 for the book and $7.00 for the first supplement. (Available from Mack Publishing Co., 20th and Northampton Streets, Easton, PA 18042; orders also may be placed with state pharmaceutical associations.)

For the first time, the United States Pharmacopeia and the National Formulary are published together in one volume. These compendia set forth legally enforceable standards for drug strength, quality, purity, packaging, and labeling.

USP XX comprises the first portion of this volume. Following a section of introductory material, additions, deletions, and title changes made since USP XIX are listed. Featured next are more than 2300 monographs covering drug substances and dosage forms. The monographs include definitions of identity, packaging and storage information, identification tests, and assays. Category, dose, sizes available, and dispensing information previously included in USP–NF monographs now appears in a separate book, USP Dispensing Information.

The 331-page section of general chapters that follows the monographs includes descriptions of microbiological tests, biological tests and assays, chemical tests and assays, and physical tests and determinations. The general chapters also include discussions of topics such as dosage form stability, controlled drug regulations, and child-resistant containers.

The next section includes descriptions of the reagents, indicators, and solutions that are required in conducting USP and NF tests and assays. The final section of USP XX contains reference tables, among which is a listing of pharmaceutical ingredients by category. A table that gives descriptive and solubility statements for USP and NF substances also is included.

The section of the book corresponding to NF XV also begins with an introductory discussion. Almost 200 monographs for inactive pharmaceutical ingredients are given in NF XV. These monographs also include identity statements along with packaging and storage information, identification tests, and assays.

A 128-page appendix to USP XX follows, which includes excerpts of Federal antibiotic regulations. The book concludes with a combined index to USP XX and NF XV.

The standards set forth by USP and NF are enforced by the U.S. government and by state governments. The USP XX–NF XV standards became official July 1, 1980.

Staff Review

United States Pharmacopeia Dispensing Information. The United States Pharmacopeial Convention. 1980. 20.5 × 28.5 cm. 816 pp. Price $18.75, including updates (quantity discounts available). (Available from Mack Publishing Co., 20th and Northampton Streets, Easton, PA 18042.)

This new companion to the United States Pharmacopeia–National Formulary presents dispensing information for both the practitioner and the patient. Over 300 experts in pharmacy, medicine, dentistry, and nursing participated in the review process, and additional review and input were provided by hundreds of other practitioners and patients.

The first of the three sections of this book contains information oriented toward the health care provider. There are nearly 600 pages of drug monographs arranged in alphabetical order by generic name. Each monograph includes a category statement, precautions to consider, side effects, patient consultation, general dosing information, and dosage forms. There are 364 general monographs providing information on almost 1200 drug substances and products which represent thousands of different brands.

The second section contains patient-oriented information presented in nontechnical language. This material should aid in reinforcing the therapy selected by the prescriber. There are 213 monographs, including 42 class monographs representing 155 drug substances. The information corresponds to that presented in the prescriber-oriented section.

The third section is an index listing drug entities by official names, categories of use, and selected medical information such as pregnancy warnings and breastfeeding warnings. There are cross-references by selected brand names (both U.S. and Canadian) and older nonproprietary names.

Bimonthly updates of this book will provide information on important new drugs as well as changes in information for previously included drugs. Updates are included in the stated price. The first update is provided with the main volume and concentrates on topical and vaginal products.

Staff Review

Fundamentals of Nuclear Pharmacy. By GOPAL B. SAHA. Springer-Verlag New York Inc., 175 Fifth Ave., New York, NY 10010. 1979. 272 pp. 15 × 23 cm. Price $19.90.

This book is meant to be used as a textbook for courses on nuclear pharmacy aimed toward nuclear pharmacists, nuclear medicine technologists, and nuclear medicine residents. It is based on courses taught to such students at the University of Arkansas for Medical Sciences. In the author's own words, "the topics included are comprehensive, ranging from the basic concept of atomic structure to practical clinical uses of radiopharmaceuticals."

Included are 12 chapters on the following topics: The Atom; Radioactive Decay; Production of Radionuclides; Radionuclide Generators; Radiopharmaceuticals; Radiolabeling of Compounds; Characteristics of Specific Radiopharmaceuticals; Quality Control of Radiopharmaceuticals; Radiopharmacy; Radiation Dosimetry, Safety, and Regulations; *In Vitro* Tests; and Radiopharmacology in Nuclear Medicine (which gives a brief description of a variety of nuclear medicine procedures). Each chapter is followed by a series of questions (answers are given in an appendix) designed to test the students' understanding of the material presented.

In general, the chapters are well written, with complex theoretical concepts explained in an easily understandable manner. The depth of the material is appropriate for the indicated audience. Especially well written are those chapters dealing with the more practical aspects of nuclear pharmacy such as the quality control of radiopharmaceuticals, radiopharmacy, safety, *in vitro* tests, and radiopharmacology. In all cases, ample illustrations and examples aid the reader in gaining a practical understanding of the material.

In summary, this is an excellent, reasonably priced textbook for the intended audience and should find widespread acceptance by both students and instructors.

Reviewed by H. Donald Burns
Division of Nuclear Medicine
Johns Hopkins University
Baltimore, MD 21205

Polarography of Molecules of Biological Significance. Edited by W. FRANKLIN SMYTH. Academic, 111 Fifth Ave., New York, NY 10003. 1979. 326 pp. 15 × 23 cm. Price $47.50.

This book covers the polarography of organic molecules that have applications in pharmacy, pharmacology, basic medical sciences, environmental sciences, and agriculture. The authors review the literature published since 1965.

The first part of the book is an introduction to voltammetric analysis and consists of two chapters. The first chapter has a brief outline of the voltammetric methods and their scope and advantages, sampling, initial treatment, separation techniques of the active component, and methods to make an electroactive molecule. Chapter 2 discusses the practical aspects of the voltammetric method, including the choice of solvents, supporting electrolytes, pH, electrodes, cells, and potentiostats. The theoretical aspects of the different voltammetric techniques are discussed to allow optimum selection.

The second part of the book (eight chapters) is the application of polarography to different fields. Three chapters deal with the analysis of pharmaceuticals. The substances discussed include psychotropic, hyp-

REVIEWS

1980 United States Pharmacopeia–National Formulary. The United States Pharmacopeial Convention. 1980. 1505 pp. 21 × 28.5 cm. Price $90.00 postpaid (domestic and foreign), including all annual supplements to USP XX and NF XV; separately, $65.00 for the book and $7.00 for the first supplement. (Available from Mack Publishing Co., 20th and Northampton Streets, Easton, PA 18042; orders also may be placed with state pharmaceutical associations.)

For the first time, the United States Pharmacopeia and the National Formulary are published together in one volume. These compendia set forth legally enforceable standards for drug strength, quality, purity, packaging, and labeling.

USP XX comprises the first portion of this volume. Following a section of introductory material, additions, deletions, and title changes made since USP XIX are listed. Featured next are more than 2300 monographs covering drug substances and dosage forms. The monographs include definitions of identity, packaging and storage information, identification tests, and assays. Category, dose, sizes available, and dispensing information previously included in USP–NF monographs now appears in a separate book, USP Dispensing Information.

The 331-page section of general chapters that follows the monographs includes descriptions of microbiological tests, biological tests and assays, chemical tests and assays, and physical tests and determinations. The general chapters also include discussions of topics such as dosage form stability, controlled drug regulations, and child-resistant containers.

The next section includes descriptions of the reagents, indicators, and solutions that are required in conducting USP and NF tests and assays. The final section of USP XX contains reference tables, among which is a listing of pharmaceutical ingredients by category. A table that gives descriptive and solubility statements for USP and NF substances also is included.

The section of the book corresponding to NF XV also begins with an introductory discussion. Almost 200 monographs for inactive pharmaceutical ingredients are given in NF XV. These monographs also include identity statements along with packaging and storage information, identification tests, and assays.

A 128-page appendix to USP XX follows, which includes excerpts of Federal antibiotic regulations. The book concludes with a combined index to USP XX and NF XV.

The standards set forth by USP and NF are enforced by the U.S. government and by state governments. The USP XX–NF XV standards became official July 1, 1980.

Staff Review

United States Pharmacopeia Dispensing Information. The United States Pharmacopeial Convention. 1980. 20.5 × 28.5 cm. 816 pp. Price $18.75, including updates (quantity discounts available). (Available from Mack Publishing Co., 20th and Northampton Streets, Easton, PA 18042.)

This new companion to the United States Pharmacopeia–National Formulary presents dispensing information for both the practitioner and the patient. Over 300 experts in pharmacy, medicine, dentistry, and nursing participated in the review process, and additional review and input were provided by hundreds of other practitioners and patients.

The first of the three sections of this book contains information oriented toward the health care provider. There are nearly 600 pages of drug monographs arranged in alphabetical order by generic name. Each monograph includes a category statement, precautions to consider, side effects, patient consultation, general dosing information, and dosage forms. There are 364 general monographs providing information on almost 1200 drug substances and products which represent thousands of different brands.

The second section contains patient-oriented information presented in nontechnical language. This material should aid in reinforcing the therapy selected by the prescriber. There are 213 monographs, including 42 class monographs representing 155 drug substances. The information corresponds to that presented in the prescriber-oriented section.

The third section is an index listing drug entities by official names, categories of use, and selected medical information such as pregnancy warnings and breastfeeding warnings. There are cross-references by selected brand names (both U.S. and Canadian) and older nonproprietary names.

Bimonthly updates of this book will provide information on important new drugs as well as changes in information for previously included drugs. Updates are included in the stated price. The first update is provided with the main volume and concentrates on topical and vaginal products.

Staff Review

Fundamentals of Nuclear Pharmacy. By GOPAL B. SAHA. Springer-Verlag New York Inc., 175 Fifth Ave., New York, NY 10010. 1979. 272 pp. 15 × 23 cm. Price $19.90.

This book is meant to be used as a textbook for courses on nuclear pharmacy aimed toward nuclear pharmacists, nuclear medicine technologists, and nuclear medicine residents. It is based on courses taught to such students at the University of Arkansas for Medical Sciences. In the author's own words, "the topics included are comprehensive, ranging from the basic concept of atomic structure to practical clinical uses of radiopharmaceuticals."

Included are 12 chapters on the following topics: The Atom; Radioactive Decay; Production of Radionuclides; Radionuclide Generators; Radiopharmaceuticals; Radiolabeling of Compounds; Characteristics of Specific Radiopharmaceuticals; Quality Control of Radiopharmaceuticals; Radiopharmacy; Radiation Dosimetry, Safety, and Regulations; *In Vitro* Tests; and Radiopharmacology in Nuclear Medicine (which gives a brief description of a variety of nuclear medicine procedures). Each chapter is followed by a series of questions (answers are given in an appendix) designed to test the students' understanding of the material presented.

In general, the chapters are well written, with complex theoretical concepts explained in an easily understandable manner. The depth of the material is appropriate for the indicated audience. Especially well written are those chapters dealing with the more practical aspects of nuclear pharmacy such as the quality control of radiopharmaceuticals, radiopharmacy, safety, *in vitro* tests, and radiopharmacology. In all cases, ample illustrations and examples aid the reader in gaining a practical understanding of the material.

In summary, this is an excellent, reasonably priced textbook for the intended audience and should find widespread acceptance by both students and instructors.

Reviewed by H. Donald Burns
Division of Nuclear Medicine
Johns Hopkins University
Baltimore, MD 21205

Polarography of Molecules of Biological Significance. Edited by W. FRANKLIN SMYTH. Academic, 111 Fifth Ave., New York, NY 10003. 1979. 326 pp. 15 × 23 cm. Price $47.50.

This book covers the polarography of organic molecules that have applications in pharmacy, pharmacology, basic medical sciences, environmental sciences, and agriculture. The authors review the literature published since 1965.

The first part of the book is an introduction to voltammetric analysis and consists of two chapters. The first chapter has a brief outline of the voltammetric methods and their scope and advantages, sampling, initial treatment, separation techniques of the active component, and methods to make an electroactive molecule. Chapter 2 discusses the practical aspects of the voltammetric method, including the choice of solvents, supporting electrolytes, pH, electrodes, cells, and potentiostats. The theoretical aspects of the different voltammetric techniques are discussed to allow optimum selection.

The second part of the book (eight chapters) is the application of polarography to different fields. Three chapters deal with the analysis of pharmaceuticals. The substances discussed include psychotropic, hyp-

REVIEWS

1980 United States Pharmacopeia–National Formulary. The United States Pharmacopeial Convention. 1980. 1505 pp. 21 × 28.5 cm. Price $90.00 postpaid (domestic and foreign), including all annual supplements to USP XX and NF XV; separately, $65.00 for the book and $7.00 for the first supplement. (Available from Mack Publishing Co., 20th and Northampton Streets, Easton, PA 18042; orders also may be placed with state pharmaceutical associations.)

For the first time, the United States Pharmacopeia and the National Formulary are published together in one volume. These compendia set forth legally enforceable standards for drug strength, quality, purity, packaging, and labeling.

USP XX comprises the first portion of this volume. Following a section of introductory material, additions, deletions, and title changes made since USP XIX are listed. Featured next are more than 2300 monographs covering drug substances and dosage forms. The monographs include definitions of identity, packaging and storage information, identification tests, and assays. Category, dose, sizes available, and dispensing information previously included in USP–NF monographs now appears in a separate book, USP Dispensing Information.

The 331-page section of general chapters that follows the monographs includes descriptions of microbiological tests, biological tests and assays, chemical tests and assays, and physical tests and determinations. The general chapters also include discussions of topics such as dosage form stability, controlled drug regulations, and child-resistant containers.

The next section includes descriptions of the reagents, indicators, and solutions that are required in conducting USP and NF tests and assays. The final section of USP XX contains reference tables, among which is a listing of pharmaceutical ingredients by category. A table that gives descriptive and solubility statements for USP and NF substances also is included.

The section of the book corresponding to NF XV also begins with an introductory discussion. Almost 200 monographs for inactive pharmaceutical ingredients are given in NF XV. These monographs also include identity statements along with packaging and storage information, identification tests, and assays.

A 128-page appendix to USP XX follows, which includes excerpts of Federal antibiotic regulations. The book concludes with a combined index to USP XX and NF XV.

The standards set forth by USP and NF are enforced by the U.S. government and by state governments. The USP XX–NF XV standards became official July 1, 1980.

Staff Review

United States Pharmacopeia Dispensing Information. The United States Pharmacopeial Convention. 1980. 20.5 × 28.5 cm. 816 pp. Price $18.75, including updates (quantity discounts available). (Available from Mack Publishing Co., 20th and Northampton Streets, Easton, PA 18042.)

This new companion to the United States Pharmacopeia–National Formulary presents dispensing information for both the practitioner and the patient. Over 300 experts in pharmacy, medicine, dentistry, and nursing participated in the review process, and additional review and input were provided by hundreds of other practitioners and patients.

The first of the three sections of this book contains information oriented toward the health care provider. There are nearly 600 pages of drug monographs arranged in alphabetical order by generic name. Each monograph includes a category statement, precautions to consider, side effects, patient consultation, general dosing information, and dosage forms. There are 364 general monographs providing information on almost 1200 drug substances and products which represent thousands of different brands.

The second section contains patient-oriented information presented in nontechnical language. This material should aid in reinforcing the therapy selected by the prescriber. There are 213 monographs, including 42 class monographs representing 155 drug substances. The information corresponds to that presented in the prescriber-oriented section.

The third section is an index listing drug entities by official names, categories of use, and selected medical information such as pregnancy warnings and breastfeeding warnings. There are cross-references by selected brand names (both U.S. and Canadian) and older nonproprietary names.

Bimonthly updates of this book will provide information on important new drugs as well as changes in information for previously included drugs. Updates are included in the stated price. The first update is provided with the main volume and concentrates on topical and vaginal products.

Staff Review

Fundamentals of Nuclear Pharmacy. By GOPAL B. SAHA. Springer-Verlag New York Inc., 175 Fifth Ave., New York, NY 10010. 1979. 272 pp. 15 × 23 cm. Price $19.90.

This book is meant to be used as a textbook for courses on nuclear pharmacy aimed toward nuclear pharmacists, nuclear medicine technologists, and nuclear medicine residents. It is based on courses taught to such students at the University of Arkansas for Medical Sciences. In the author's own words, "the topics included are comprehensive, ranging from the basic concept of atomic structure to practical clinical uses of radiopharmaceuticals."

Included are 12 chapters on the following topics: The Atom; Radioactive Decay; Production of Radionuclides; Radionuclide Generators; Radiopharmaceuticals; Radiolabeling of Compounds; Characteristics of Specific Radiopharmaceuticals; Quality Control of Radiopharmaceuticals; Radiopharmacy; Radiation Dosimetry, Safety, and Regulations; *In Vitro* Tests; and Radiopharmacology in Nuclear Medicine (which gives a brief description of a variety of nuclear medicine procedures). Each chapter is followed by a series of questions (answers are given in an appendix) designed to test the students' understanding of the material presented.

In general, the chapters are well written, with complex theoretical concepts explained in an easily understandable manner. The depth of the material is appropriate for the indicated audience. Especially well written are those chapters dealing with the more practical aspects of nuclear pharmacy such as the quality control of radiopharmaceuticals, radiopharmacy, safety, *in vitro* tests, and radiopharmacology. In all cases, ample illustrations and examples aid the reader in gaining a practical understanding of the material.

In summary, this is an excellent, reasonably priced textbook for the intended audience and should find widespread acceptance by both students and instructors.

Reviewed by H. Donald Burns
Division of Nuclear Medicine
Johns Hopkins University
Baltimore, MD 21205

Polarography of Molecules of Biological Significance. Edited by W. FRANKLIN SMYTH. Academic, 111 Fifth Ave., New York, NY 10003. 1979. 326 pp. 15 × 23 cm. Price $47.50.

This book covers the polarography of organic molecules that have applications in pharmacy, pharmacology, basic medical sciences, environmental sciences, and agriculture. The authors review the literature published since 1965.

The first part of the book is an introduction to voltammetric analysis and consists of two chapters. The first chapter has a brief outline of the voltammetric methods and their scope and advantages, sampling, initial treatment, separation techniques of the active component, and methods to make an electroactive molecule. Chapter 2 discusses the practical aspects of the voltammetric method, including the choice of solvents, supporting electrolytes, pH, electrodes, cells, and potentiostats. The theoretical aspects of the different voltammetric techniques are discussed to allow optimum selection.

The second part of the book (eight chapters) is the application of polarography to different fields. Three chapters deal with the analysis of pharmaceuticals. The substances discussed include psychotropic, hyp-

REVIEWS

1980 United States Pharmacopeia–National Formulary. The United States Pharmacopeial Convention. 1980. 1505 pp. 21 × 28.5 cm. Price $90.00 postpaid (domestic and foreign), including all annual supplements to USP XX and NF XV; separately, $65.00 for the book and $7.00 for the first supplement. (Available from Mack Publishing Co., 20th and Northampton Streets, Easton, PA 18042; orders also may be placed with state pharmaceutical associations.)

For the first time, the United States Pharmacopeia and the National Formulary are published together in one volume. These compendia set forth legally enforceable standards for drug strength, quality, purity, packaging, and labeling.

USP XX comprises the first portion of this volume. Following a section of introductory material, additions, deletions, and title changes made since USP XIX are listed. Featured next are more than 2300 monographs covering drug substances and dosage forms. The monographs include definitions of identity, packaging and storage information, identification tests, and assays. Category, dose, sizes available, and dispensing information previously included in USP–NF monographs now appears in a separate book, USP Dispensing Information.

The 331-page section of general chapters that follows the monographs includes descriptions of microbiological tests, biological tests and assays, chemical tests and assays, and physical tests and determinations. The general chapters also include discussions of topics such as dosage form stability, controlled drug regulations, and child-resistant containers.

The next section includes descriptions of the reagents, indicators, and solutions that are required in conducting USP and NF tests and assays. The final section of USP XX contains reference tables, among which is a listing of pharmaceutical ingredients by category. A table that gives descriptive and solubility statements for USP and NF substances also is included.

The section of the book corresponding to NF XV also begins with an introductory discussion. Almost 200 monographs for inactive pharmaceutical ingredients are given in NF XV. These monographs also include identity statements along with packaging and storage information, identification tests, and assays.

A 128-page appendix to USP XX follows, which includes excerpts of Federal antibiotic regulations. The book concludes with a combined index to USP XX and NF XV.

The standards set forth by USP and NF are enforced by the U.S. government and by state governments. The USP XX–NF XV standards became official July 1, 1980.

Staff Review

United States Pharmacopeia Dispensing Information. The United States Pharmacopeial Convention. 1980. 20.5 × 28.5 cm. 816 pp. Price $18.75, including updates (quantity discounts available). (Available from Mack Publishing Co., 20th and Northampton Streets, Easton, PA 18042.)

This new companion to the United States Pharmacopeia–National Formulary presents dispensing information for both the practitioner and the patient. Over 300 experts in pharmacy, medicine, dentistry, and nursing participated in the review process, and additional review and input were provided by hundreds of other practitioners and patients.

The first of the three sections of this book contains information oriented toward the health care provider. There are nearly 600 pages of drug monographs arranged in alphabetical order by generic name. Each monograph includes a category statement, precautions to consider, side effects, patient consultation, general dosing information, and dosage forms. There are 364 general monographs providing information on almost 1200 drug substances and products which represent thousands of different brands.

The second section contains patient-oriented information presented in nontechnical language. This material should aid in reinforcing the therapy selected by the prescriber. There are 213 monographs, including 42 class monographs representing 155 drug substances. The information corresponds to that presented in the prescriber-oriented section.

The third section is an index listing drug entities by official names, categories of use, and selected medical information such as pregnancy warnings and breastfeeding warnings. There are cross-references by selected brand names (both U.S. and Canadian) and older nonproprietary names.

Bimonthly updates of this book will provide information on important new drugs as well as changes in information for previously included drugs. Updates are included in the stated price. The first update is provided with the main volume and concentrates on topical and vaginal products.

Staff Review

Fundamentals of Nuclear Pharmacy. By GOPAL B. SAHA. Springer-Verlag New York Inc., 175 Fifth Ave., New York, NY 10010. 1979. 272 pp. 15 × 23 cm. Price $19.90.

This book is meant to be used as a textbook for courses on nuclear pharmacy aimed toward nuclear pharmacists, nuclear medicine technologists, and nuclear medicine residents. It is based on courses taught to such students at the University of Arkansas for Medical Sciences. In the author's own words, "the topics included are comprehensive, ranging from the basic concept of atomic structure to practical clinical uses of radiopharmaceuticals."

Included are 12 chapters on the following topics: The Atom; Radioactive Decay; Production of Radionuclides; Radionuclide Generators; Radiopharmaceuticals; Radiolabeling of Compounds; Characteristics of Specific Radiopharmaceuticals; Quality Control of Radiopharmaceuticals; Radiopharmacy; Radiation Dosimetry, Safety, and Regulations; *In Vitro* Tests; and Radiopharmacology in Nuclear Medicine (which gives a brief description of a variety of nuclear medicine procedures). Each chapter is followed by a series of questions (answers are given in an appendix) designed to test the students' understanding of the material presented.

In general, the chapters are well written, with complex theoretical concepts explained in an easily understandable manner. The depth of the material is appropriate for the indicated audience. Especially well written are those chapters dealing with the more practical aspects of nuclear pharmacy such as the quality control of radiopharmaceuticals, radiopharmacy, safety, *in vitro* tests, and radiopharmacology. In all cases, ample illustrations and examples aid the reader in gaining a practical understanding of the material.

In summary, this is an excellent, reasonably priced textbook for the intended audience and should find widespread acceptance by both students and instructors.

Reviewed by H. Donald Burns
Division of Nuclear Medicine
Johns Hopkins University
Baltimore, MD 21205

Polarography of Molecules of Biological Significance. Edited by W. FRANKLIN SMYTH. Academic, 111 Fifth Ave., New York, NY 10003. 1979. 326 pp. 15 × 23 cm. Price $47.50.

This book covers the polarography of organic molecules that have applications in pharmacy, pharmacology, basic medical sciences, environmental sciences, and agriculture. The authors review the literature published since 1965.

The first part of the book is an introduction to voltammetric analysis and consists of two chapters. The first chapter has a brief outline of the voltammetric methods and their scope and advantages, sampling, initial treatment, separation techniques of the active component, and methods to make an electroactive molecule. Chapter 2 discusses the practical aspects of the voltammetric method, including the choice of solvents, supporting electrolytes, pH, electrodes, cells, and potentiostats. The theoretical aspects of the different voltammetric techniques are discussed to allow optimum selection.

The second part of the book (eight chapters) is the application of polarography to different fields. Three chapters deal with the analysis of pharmaceuticals. The substances discussed include psychotropic, hyp-

notic, and sedative drugs, vitamins, CNS agents, antituberculins, purines, catechols, catecholamines, and antibiotics containing a nitro group. One chapter is concerned with the basic medical sciences, including clinical medicine, chemical carcinogenesis, neurophysiology, virology, immunology, and cells. The polarographic analysis of organic compounds in the aqueous environment is discussed in one chapter. Another chapter discusses the analysis of organic compounds used in agriculture. The last two chapters are concerned with the analysis of organometallic compounds containing mercury, tin, lead, germanium, and arsenic.

This much-needed update discusses developments in the polarographic analysis of organic molecules that have occurred since Peter Zuman wrote "Organic Polarographic Analysis" in 1965. The book is well edited and is easy to read and understand. Each chapter has its own table of contents, and there is a subject index that covers the entire book. Furthermore, each chapter has adequate references that enable the reader to extend beyond the scope of the present book.

There are minor flaws. Chapter 4 should have stated that the $E_{1/2}$ range of $-0.1 \rightarrow -0.4$ v (saturated calomel electrode) is for a nitro group conjugated to an aromatic system. There are other antibiotics containing a nitro group attached to an aliphatic system, such as everninomicins, that can be determined polarographically [Kabasakalian *et al., J. Pharm. Sci.*, **63,** 641 (1974)]. It also is unfortunate that the polarographic analysis of an important compound such as adriamycin (doxorubicin) was omitted [Rao *et al., J. Electrochem. Soc.*, **125,** 534 (1978)]. There is a printing error in the last paragraph on p. 19; ($-1.5 \rightarrow 17$ v) should be 1.7 v.

With the exception of these minor criticisms, the book succeeds admirably in its goal. It is recommended for addition to the library of research workers in the area of pharmaceuticals and allied medicine, analytical chemists, environmental scientists, and agriculture.

Reviewed by Sami Y. Kalliney
Schering Corporation
Bloomfield, NJ 07003

NOTICES

Drug Treatment: Principles and Practice of Clinical Pharmacology and Therapeutics, 2nd Ed. Edited by GRAEME S. AVERY. Adis Press, 515 Madison Ave., New York, NY 10022. 1980. 1382 pp. 17 × 26 cm.

Microbial Drug Resistance, Vol. 2. Edited by SUSUMU MITSUHASHI. University Park Press, 233 E. Redwood St., Baltimore, MD 21202. 1979. 439 pp. 14 × 23 cm. Price $42.50.

Prevention and Detection of Cancer, Part II, Vol. 2: Cancer Detection in Specific Sites. Edited by HERBERT E. NIEBURGS. Dekker, 270 Madison Ave., New York, NY 10016. 1980. 2456 pp. 18 × 25 cm. Price $69.50.

Nutritional Improvement of Food and Feed Proteins. Edited by MENDEL FRIEDMAN. (Advances in Experimental Medicine and Biology, Vol. 105.) Plenum, 227 W. 17th St., New York, NY 10011. 1978. 882 pp. 16 × 25 cm. Price $69.50.

Anatomie Physiologie Pathophysiologie des Menschen: Ein Lehrbuch für Pharmazeuten und Biologen. By GERHARD THEWS, ERNST MUTSCHLER, and PETER VAUPEL. Wissenschaftliche Verlagsgesellschaft, Stuttgart, West Germany. 1980. 792 pp. 16 × 24 cm.

Pharmacology of Ganglionic Transmission. Edited by D. A. KHARKEVICH. (Handbook of Experimental Pharmacology, Vol. 5.) Springer-Verlag New York Inc., 444 Hartz Way, Secaucus, NJ 07094. 1980. 531 pp. 16 × 24 cm. Price $134.75.

Electrophoresis—A Survey of Techniques and Applications. Part A: Techniques. Edited by Z. DEYL. (Journal of Chromatography Library, Vol. 18.) Elsevier/North Holland Inc., 52 Vanderbilt Ave., New York, NY 10017. 1979. 390 pp. 15 × 24 cm. Price $83.00.

Handbook of Water-Soluble Gums and Resins. Edited by ROBERT L. DAVIDSON. McGraw-Hill, 1221 Avenue of the Americas, New York, NY 10020. 1980. 657 pp. 15 × 23 cm. Price $39.50.

The Essential Guide to Prescription Drugs, Revised Edition. By JAMES W. LONG. Harper & Row, 10 E. 53rd St., New York, NY 10022. 1980. 863 pp. 16 × 23 cm. Price $25.00 cloth and $8.95 paper.

Progress in Drug Research, Vol. 23. Edited by ERNST JUCKER. Birkhäuser, Basel, Switzerland. 1979. 320 pp. 16 × 24 cm.

The Neurobiology of Dopamine. Edited by A. S. HORN, J. KORF, and B. H. C. WESTERINK. Academic, 111 Fifth Ave., New York, NY 10003. 1979. 723 pp. 15 × 23 cm. Price $83.00.

Hagers Handbuch der Pharmazeutischen Praxis, 4th Ed., Vol. 6, Part C: T–Z. Edited by P. H. LIST and L. HÖRHAMMER. Springer-Verlag, Heidelberger Platz 3, Postfach D 1000, Berlin 33, West Germany. 1979. 582 pp. 17 × 24 cm. Price $88.00.

Monoamine Oxidase: Structure, Function, and Altered Functions. Edited by THOMAS P. SINGER, R. W. VON KORFF, and DENNIS L. MURPHY. Academic, 111 Fifth Ave., New York, NY 10003. 1979. 557 pp. 15 × 23 cm.

Isoenzyme Analysis. By D. W. MOSS. (Analytical Sciences Monographs No. 6.) The Chemical Society, Burlington House, London W1V OBN, England. 1979. 163 pp. 13 × 22 cm. Price $22.00.

The International Pharmacopoeia, 3rd Ed., Vol. 1: General Methods of Analysis. World Health Organization, 1211 Geneva 27, Switzerland. 1979. 223 pp. 15 × 24 cm. Price Sw. fr. 24.

Clinical Pharmacological Evaluation in Drug Control. (EURO Reports and Studies 13.) World Health Organization, 1211 Geneva 27, Switzerland. 1979. 31 pp. 15 × 21 cm. Price Sw. fr. 5.

The Selection of Essential Drugs. (Technical Report Series 641.) World Health Organization, 1211 Geneva 27, Switzerland. 1979. 44 pp. 14 × 20 cm. Price Sw. fr. 3.

NEW JOURNALS

Biomaterials. Edited by S. D. BRUCK and G. W. HASTINGS. IPC Science and Technology Press, 205 E. 42nd St., New York, NY 10017. 1980. 20 × 30 cm. Price $117.00 (four issues per year).

notic, and sedative drugs, vitamins, CNS agents, antituberculins, purines, catechols, catecholamines, and antibiotics containing a nitro group. One chapter is concerned with the basic medical sciences, including clinical medicine, chemical carcinogenesis, neurophysiology, virology, immunology, and cells. The polarographic analysis of organic compounds in the aqueous environment is discussed in one chapter. Another chapter discusses the analysis of organic compounds used in agriculture. The last two chapters are concerned with the analysis of organometallic compounds containing mercury, tin, lead, germanium, and arsenic.

This much-needed update discusses developments in the polarographic analysis of organic molecules that have occurred since Peter Zuman wrote "Organic Polarographic Analysis" in 1965. The book is well edited and is easy to read and understand. Each chapter has its own table of contents, and there is a subject index that covers the entire book. Furthermore, each chapter has adequate references that enable the reader to extend beyond the scope of the present book.

There are minor flaws. Chapter 4 should have stated that the $E_{1/2}$ range of $-0.1 \rightarrow -0.4$ v (saturated calomel electrode) is for a nitro group conjugated to an aromatic system. There are other antibiotics containing a nitro group attached to an aliphatic system, such as everninomicins, that can be determined polarographically [Kabasakalian *et al., J. Pharm. Sci.*, **63,** 641 (1974)]. It also is unfortunate that the polarographic analysis of an important compound such as adriamycin (doxorubicin) was omitted [Rao *et al., J. Electrochem. Soc.*, **125,** 534 (1978)]. There is a printing error in the last paragraph on p. 19; ($-1.5 \rightarrow 17$ v) should be 1.7 v.

With the exception of these minor criticisms, the book succeeds admirably in its goal. It is recommended for addition to the library of research workers in the area of pharmaceuticals and allied medicine, analytical chemists, environmental scientists, and agriculture.

Reviewed by Sami Y. Kalliney
Schering Corporation
Bloomfield, NJ 07003

NOTICES

Drug Treatment: Principles and Practice of Clinical Pharmacology and Therapeutics, 2nd Ed. Edited by GRAEME S. AVERY. Adis Press, 515 Madison Ave., New York, NY 10022. 1980. 1382 pp. 17 × 26 cm.

Microbial Drug Resistance, Vol. 2. Edited by SUSUMU MITSUHASHI. University Park Press, 233 E. Redwood St., Baltimore, MD 21202. 1979. 439 pp. 14 × 23 cm. Price $42.50.

Prevention and Detection of Cancer, Part II, Vol. 2: Cancer Detection in Specific Sites. Edited by HERBERT E. NIEBURGS. Dekker, 270 Madison Ave., New York, NY 10016. 1980. 2456 pp. 18 × 25 cm. Price $69.50.

Nutritional Improvement of Food and Feed Proteins. Edited by MENDEL FRIEDMAN. (Advances in Experimental Medicine and Biology, Vol. 105.) Plenum, 227 W. 17th St., New York, NY 10011. 1978. 882 pp. 16 × 25 cm. Price $69.50.

Anatomie Physiologie Pathophysiologie des Menschen: Ein Lehrbuch für Pharmazeuten und Biologen. By GERHARD THEWS, ERNST MUTSCHLER, and PETER VAUPEL. Wissenschaftliche Verlagsgesellschaft, Stuttgart, West Germany. 1980. 792 pp. 16 × 24 cm.

Pharmacology of Ganglionic Transmission. Edited by D. A. KHARKEVICH. (Handbook of Experimental Pharmacology, Vol. 5.) Springer-Verlag New York Inc., 444 Hartz Way, Secaucus, NJ 07094. 1980. 531 pp. 16 × 24 cm. Price $134.75.

Electrophoresis—A Survey of Techniques and Applications. Part A: Techniques. Edited by Z. DEYL. (Journal of Chromatography Library, Vol. 18.) Elsevier/North Holland Inc., 52 Vanderbilt Ave., New York, NY 10017. 1979. 390 pp. 15 × 24 cm. Price $83.00.

Handbook of Water-Soluble Gums and Resins. Edited by ROBERT L. DAVIDSON. McGraw-Hill, 1221 Avenue of the Americas, New York, NY 10020. 1980. 657 pp. 15 × 23 cm. Price $39.50.

The Essential Guide to Prescription Drugs, Revised Edition. By JAMES W. LONG. Harper & Row, 10 E. 53rd St., New York, NY 10022. 1980. 863 pp. 16 × 23 cm. Price $25.00 cloth and $8.95 paper.

Progress in Drug Research, Vol. 23. Edited by ERNST JUCKER. Birkhäuser, Basel, Switzerland. 1979. 320 pp. 16 × 24 cm.

The Neurobiology of Dopamine. Edited by A. S. HORN, J. KORF, and B. H. C. WESTERINK. Academic, 111 Fifth Ave., New York, NY 10003. 1979. 723 pp. 15 × 23 cm. Price $83.00.

Hagers Handbuch der Pharmazeutischen Praxis, 4th Ed., Vol. 6, Part C: T–Z. Edited by P. H. LIST and L. HÖRHAMMER. Springer-Verlag, Heidelberger Platz 3, Postfach D 1000, Berlin 33, West Germany. 1979. 582 pp. 17 × 24 cm. Price $88.00.

Monoamine Oxidase: Structure, Function, and Altered Functions. Edited by THOMAS P. SINGER, R. W. VON KORFF, and DENNIS L. MURPHY. Academic, 111 Fifth Ave., New York, NY 10003. 1979. 557 pp. 15 × 23 cm.

Isoenzyme Analysis. By D. W. MOSS. (Analytical Sciences Monographs No. 6.) The Chemical Society, Burlington House, London W1V OBN, England. 1979. 163 pp. 13 × 22 cm. Price $22.00.

The International Pharmacopoeia, 3rd Ed., Vol. 1: General Methods of Analysis. World Health Organization, 1211 Geneva 27, Switzerland. 1979. 223 pp. 15 × 24 cm. Price Sw. fr. 24.

Clinical Pharmacological Evaluation in Drug Control. (EURO Reports and Studies 13.) World Health Organization, 1211 Geneva 27, Switzerland. 1979. 31 pp. 15 × 21 cm. Price Sw. fr. 5.

The Selection of Essential Drugs. (Technical Report Series 641.) World Health Organization, 1211 Geneva 27, Switzerland. 1979. 44 pp. 14 × 20 cm. Price Sw. fr. 3.

NEW JOURNALS

Biomaterials. Edited by S. D. BRUCK and G. W. HASTINGS. IPC Science and Technology Press, 205 E. 42nd St., New York, NY 10017. 1980. 20 × 30 cm. Price $117.00 (four issues per year).

AUGUST 1980
VOLUME 69 NUMBER 8

JOURNAL OF PHARMACEUTICAL SCIENCES

MARY H. FERGUSON
Editor

SHELLY ELLIOTT
Production Editor

MARCIA GARTRELL
Copy Editor

NICOLETTE TRIANTAFELLU
Copy Editor

EDWARD G. FELDMANN
Contributing Editor

SAMUEL W. GOLDSTEIN
Contributing Editor

BELLE R. BECK
Editorial Secretary

DAVID BOHARDT
Director of Publications

L. LUAN CORRIGAN
Assistant Director of Publications

EDITORIAL ADVISORY BOARD

JOHN AUTIAN
NORMAN R. FARNSWORTH
WILLIAM O. FOYE
WILLIAM J. JUSKO
HERBERT A. LIEBERMAN
DAVID E. MANN, JR.
GERALD J. PAPARIELLO
EDWARD G. RIPPIE

The *Journal of Pharmaceutical Sciences* (ISSN 0022-3549) is published monthly by the American Pharmaceutical Association (APhA) at 2215 Constitution Ave., N.W., Washington, DC 20037. Second-class postage paid at Washington, D.C., and at additional mailing office.

All expressions of opinion and statements of supposed fact appearing in articles or editorials carried in this journal are published on the authority of the writer over whose name they appear and are not to be regarded as necessarily expressing the policies or views of APhA.

Offices—Editorial, Advertising, and Subscription: 2215 Constitution Ave., N.W., Washington, DC 20037. All Journal staff may be contacted at this address. Printing: 20th & Northampton Streets, Easton, PA 18042.

Annual Subscriptions—United States and foreign, industrial and government institutions $60, educational institutions $60, individuals *for personal use only* $30; single copies $5. All foreign subscriptions add $5 for postage. Subscription rates are subject to change without notice. Members of APhA may elect to receive the *Journal of Pharmaceutical Sciences* as a part of their annual $80 (foreign $85) APhA membership dues.

Claims—Missing numbers will not be supplied if dues or subscriptions are in arrears for more than 60 days or if claims are received more than 60 days after the date of the issue, or if loss was due to failure to give notice of change of address. APhA cannot accept responsibility for foreign delivery when its records indicate shipment was made.

Change of Address—Members and subscribers should notify at once both the Post Office and APhA of any change of address.

Photocopying—The code at the foot of the first page of an article indicates that APhA has granted permission for copying of the article beyond the limits permitted by Sections 107 and 108 of the U.S. Copyright Law provided that the copier sends the per copy fee stated in the code to the Copyright Clearance Center, Inc., 21 Congress St., Salem, MA 01970. Copies may be made for personal or internal use only and not for general distribution.

Microfilm—Available from University Microfilms International, 300 N. Zeeb Road, Ann Arbor, MI 48106.

© Copyright 1980, American Pharmaceutical Association, 2215 Constitution Ave., N.W., Washington, DC 20037; all rights reserved.

MAINTAINING NAS–NRC CREDIBILITY

This week I had eggs for breakfast—and not just once, but three times, in fact!

As in the case of many Americans who have been diet conscious regarding cholesterol, salt, saturated fats, roughage–fiber, and so on, in recent years I had significantly restricted my intake of cholesterol-rich foods. This regimen was followed in the belief that the risk of coronary disease would be substantially reduced.

But the National Academy of Sciences–National Research Council released a report in late May in which its Food and Nutrition Board said that, in general, there is no reason for a healthy person to reduce his or her intake of cholesterol and fat. Indeed, other than a rather mild caution about daily salt use, the report concluded that there was really no basis for any of the dietary changes of the type noted above.

This conclusion flew in the face of many other reports and recommendations from various other groups that had arrived at an opposite conclusion. For example, just last February the departments of HEW and Agriculture issued dietary guidelines which recommended that healthy Americans should watch how much cholesterol and fat they ate. Most physicians have been influenced by guidelines such as these, and, as such, they have been counseling their patients along these lines for at least the past few years. Consequently, widespread changes have occurred in the dietary practices of a significant portion of the population.

What, then, took place to cause this apparent 180° different conclusion by the NAS–NRC Food and Nutrition Board? They did no new studies; they conducted no new experiments or research; they drew upon no new journal reports or findings. Basically, they just looked at all the same information and data that the other groups had reviewed, but they arrived at quite an opposite conclusion.

Normally, if a single scientist, or even a single group of scientists, disagrees with the mainstream of scientific thought, opinion, or conclusion, little note is taken and little importance is attached. But the NAS–NRC Food and Nutrition Board is not your everyday sort of run-of-the-mill committee.

For example, this same body is responsible for establishing the recommended daily allowances of all vitamins, minerals, and so on that we are constantly reminded of when we see the package labeling for bread, cereals, milk products, and a host of other foods. Beyond their own individual professional credentials, as a group they (FNB members) carry the recognition and reputation of the prestigious NAS–NRC.

But in itself that is no guarantee that biases may not enter the picture. Stories in the public press brought out that the report author, the committee chairman, and a third member who reviewed the report all held paid consultantships with various food producers or food trade organizations. Moreover, several other panel members had connections with the food industry that would appear to render their objectivity suspect in regard to matters with an economic impact on the food industry. Some press reports have highlighted these relationships in an apparent effort to create doubts regarding the scientific objectivity of the FNB's report.

The federal government has made a major effort to eliminate conflict-of-interest considerations from arising within its bodies of advisors as well as staff. But when carried out to its maximum, it becomes difficult to identify highly qualified people because seemingly all the experts have accepted paid industry consultantships or other appointments involving some type of monetary consideration.

We don't know where the truth lies regarding the health hazard of the dietary factors including cholesterol and fat. We suspect that it lies somewhere in between the recent NAS–NRC position and the traditional stand. Perhaps there just aren't sufficient data to make any real decision at this time. But, whatever the case, the NAS–NRC image of prestige and objectivity has now been tarnished in the public eye.

Several years ago, certain elements in the drug industry exerted a major arm-twisting effort to attempt to reverse a position taken by the NAS–NRC Drug Research Board regarding modifying state antisubstitution laws. The drug industry effort came so close to being successful that the NAS–NRC hierarchy undertook a full-scale review of the matter and decided to abolish the Drug Research Board.

NAS–NRC credibility again appears to be at stake as a result of the FNB report. The voice of science in America is too important and too fragile to allow it to suffer the loss of the NAS–NRC as a respected and trusted beacon of scientific truth. Consequently, we hope that officialdom at NAS–NRC will conduct whatever review or investigation is needed to ascertain the objectivity of its FNB's conclusions and recommendations. And, further, we hope that it will institute stringent measures in its committee appointment process to avoid the future potential for any bias to creep into the reports of any of its panels or boards.

In commenting on the problem with the ill-fated Drug Research Board, one of the former DRB members candidly observed that we can hardly find true experts in any field who have no biases; but he suggested that what we must do is identify the experts' biases and then appoint the right mix of people to balance off the respective influences against each other. It would seem that the NAS–NRC would go far in restoring its bruised image if it could successfully follow that sage advice.

Edward G. Feldmann

AUGUST 1980
VOLUME 69 NUMBER 8

JOURNAL OF PHARMACEUTICAL SCIENCES

MARY H. FERGUSON
Editor

SHELLY ELLIOTT
Production Editor

MARCIA GARTRELL
Copy Editor

NICOLETTE TRIANTAFELLU
Copy Editor

EDWARD G. FELDMANN
Contributing Editor

SAMUEL W. GOLDSTEIN
Contributing Editor

BELLE R. BECK
Editorial Secretary

DAVID BOHARDT
Director of Publications

L. LUAN CORRIGAN
Assistant Director of Publications

EDITORIAL ADVISORY BOARD

JOHN AUTIAN
NORMAN R. FARNSWORTH
WILLIAM O. FOYE
WILLIAM J. JUSKO
HERBERT A. LIEBERMAN
DAVID E. MANN, JR.
GERALD J. PAPARIELLO
EDWARD G. RIPPIE

The *Journal of Pharmaceutical Sciences* (ISSN 0022-3549) is published monthly by the American Pharmaceutical Association (APhA) at 2215 Constitution Ave., N.W., Washington, DC 20037. Second-class postage paid at Washington, D.C., and at additional mailing office.

All expressions of opinion and statements of supposed fact appearing in articles or editorials carried in this journal are published on the authority of the writer over whose name they appear and are not to be regarded as necessarily expressing the policies or views of APhA.

Offices—Editorial, Advertising, and Subscription: 2215 Constitution Ave., N.W., Washington, DC 20037. All Journal staff may be contacted at this address. Printing: 20th & Northampton Streets, Easton, PA 18042.

Annual Subscriptions—United States and foreign, industrial and government institutions $60, educational institutions $60, individuals *for personal use only* $30; single copies $5. All foreign subscriptions add $5 for postage. Subscription rates are subject to change without notice. Members of APhA may elect to receive the *Journal of Pharmaceutical Sciences* as a part of their annual $80 (foreign $85) APhA membership dues.

Claims—Missing numbers will not be supplied if dues or subscriptions are in arrears for more than 60 days or if claims are received more than 60 days after the date of the issue, or if loss was due to failure to give notice of change of address. APhA cannot accept responsibility for foreign delivery when its records indicate shipment was made.

Change of Address—Members and subscribers should notify at once both the Post Office and APhA of any change of address.

Photocopying—The code at the foot of the first page of an article indicates that APhA has granted permission for copying of the article beyond the limits permitted by Sections 107 and 108 of the U.S. Copyright Law provided that the copier sends the per copy fee stated in the code to the Copyright Clearance Center, Inc., 21 Congress St., Salem, MA 01970. Copies may be made for personal or internal use only and not for general distribution.

Microfilm—Available from University Microfilms International, 300 N. Zeeb Road, Ann Arbor, MI 48106.

© Copyright 1980, American Pharmaceutical Association, 2215 Constitution Ave., N.W., Washington, DC 20037; all rights reserved.

MAINTAINING NAS–NRC CREDIBILITY

This week I had eggs for breakfast—and not just once, but three times, in fact!

As in the case of many Americans who have been diet conscious regarding cholesterol, salt, saturated fats, roughage–fiber, and so on, in recent years I had significantly restricted my intake of cholesterol-rich foods. This regimen was followed in the belief that the risk of coronary disease would be substantially reduced.

But the National Academy of Sciences–National Research Council released a report in late May in which its Food and Nutrition Board said that, in general, there is no reason for a healthy person to reduce his or her intake of cholesterol and fat. Indeed, other than a rather mild caution about daily salt use, the report concluded that there was really no basis for any of the dietary changes of the type noted above.

This conclusion flew in the face of many other reports and recommendations from various other groups that had arrived at an opposite conclusion. For example, just last February the departments of HEW and Agriculture issued dietary guidelines which recommended that healthy Americans should watch how much cholesterol and fat they ate. Most physicians have been influenced by guidelines such as these, and, as such, they have been counseling their patients along these lines for at least the past few years. Consequently, widespread changes have occurred in the dietary practices of a significant portion of the population.

What, then, took place to cause this apparent 180° different conclusion by the NAS–NRC Food and Nutrition Board? They did no new studies; they conducted no new experiments or research; they drew upon no new journal reports or findings. Basically, they just looked at all the same information and data that the other groups had reviewed, but they arrived at quite an opposite conclusion.

Normally, if a single scientist, or even a single group of scientists, disagrees with the mainstream of scientific thought, opinion, or conclusion, little note is taken and little importance is attached. But the NAS–NRC Food and Nutrition Board is not your everyday sort of run-of-the-mill committee.

For example, this same body is responsible for establishing the recommended daily allowances of all vitamins, minerals, and so on that we are constantly reminded of when we see the package labeling for bread, cereals, milk products, and a host of other foods. Beyond their own individual professional credentials, as a group they (FNB members) carry the recognition and reputation of the prestigious NAS–NRC.

But in itself that is no guarantee that biases may not enter the picture. Stories in the public press brought out that the report author, the committee chairman, and a third member who reviewed the report all held paid consultantships with various food producers or food trade organizations. Moreover, several other panel members had connections with the food industry that would appear to render their objectivity suspect in regard to matters with an economic impact on the food industry. Some press reports have highlighted these relationships in an apparent effort to create doubts regarding the scientific objectivity of the FNB's report.

The federal government has made a major effort to eliminate conflict-of-interest considerations from arising within its bodies of advisors as well as staff. But when carried out to its maximum, it becomes difficult to identify highly qualified people because seemingly all the experts have accepted paid industry consultantships or other appointments involving some type of monetary consideration.

We don't know where the truth lies regarding the health hazard of the dietary factors including cholesterol and fat. We suspect that it lies somewhere in between the recent NAS–NRC position and the traditional stand. Perhaps there just aren't sufficient data to make any real decision at this time. But, whatever the case, the NAS–NRC image of prestige and objectivity has now been tarnished in the public eye.

Several years ago, certain elements in the drug industry exerted a major arm-twisting effort to attempt to reverse a position taken by the NAS–NRC Drug Research Board regarding modifying state antisubstitution laws. The drug industry effort came so close to being successful that the NAS–NRC hierarchy undertook a full-scale review of the matter and decided to abolish the Drug Research Board.

NAS–NRC credibility again appears to be at stake as a result of the FNB report. The voice of science in America is too important and too fragile to allow it to suffer the loss of the NAS–NRC as a respected and trusted beacon of scientific truth. Consequently, we hope that officialdom at NAS–NRC will conduct whatever review or investigation is needed to ascertain the objectivity of its FNB's conclusions and recommendations. And, further, we hope that it will institute stringent measures in its committee appointment process to avoid the future potential for any bias to creep into the reports of any of its panels or boards.

In commenting on the problem with the ill-fated Drug Research Board, one of the former DRB members candidly observed that we can hardly find true experts in any field who have no biases; but he suggested that what we must do is identify the experts' biases and then appoint the right mix of people to balance off the respective influences against each other. It would seem that the NAS–NRC would go far in restoring its bruised image if it could successfully follow that sage advice.

Edward G. Feldmann

Mass Spectra of Dexamethasone and Betamethasone

The work of Attinà[1] in this issue of the Journal questions an earlier report[2] on the distinction between betamethasone and dexamethasone by mass spectrometry. The spectra referred to were obtained, using reference standard materials, on an instrument that was unsophisticated by modern standards. Indeed, the instrument belonged to a local university and was used in a service capacity by the university staff and students. At the time, our laboratories did not possess a mass spectrometer.

On learning of the work of Attinà[1], an attempt was made to repeat the spectra with modern equipment[3]. The spectra obtained were similar but not identical to those reported by Attinà[1].

We can only speculate as to why the spectra obtained in 1969 were so different from each other and from spectra obtained on more modern instruments. There may have been preliminary decomposition because of the minimal control over conditions existing within the instrument, or there may have been a "memory" effect owing to the service nature of the instrument. Nevertheless, based on the spectra received in 1969, the interpretation was reasonable and consistent with analogous work as cited.

We are grateful that this matter has been brought to our attention and thank those involved.

B. A. Lodge
Chemical Standards Division
Drug Research Laboratories
Health Protection Branch
Ottawa, Ontario
Canada, K1A 0L2

P. Toft
Monitoring and Criteria Division
Bureau of Chemical Hazards
Health Protection Branch
Ottawa, Ontario
Canada, K1A 0L2

Received May 2, 1980.

[1] M. Attinà, *J. Pharm. Sci.*, **69**, 991 (1980).
[2] B. A. Lodge and P. Toft, *ibid.*, **59**, 1045 (1970).
[3] Finnigan 4000, Hewlett-Packard 5980 quadrupole.

Commentary on Science

I would like to call attention to some lucid, perspicacious, and appropriate comments on science and then suggest that we all apply the stated criteria to our efforts in the pharmaceutical sciences.

". . .there is a natural history of science— (i.e.) *science, in any given field, goes through a patterned course of growth and development. For example, it seems to me right and natural that in any new field of scientific endeavor the observations are gross, the hypotheses speculative and full of errors, the measurements crude. More important, I hold the opinion that this is just as truly science as the use of the most refined hypotheses and measurements in a more fully developed field of study. The crucial question in either case is not the degree of refinement but the direction of movement. If in either instance the movement is toward more exact measurement, toward more clear-cut and rigorous theory and hypothesis, toward findings which have greater validity and generality, then this is a healthy and growing science. If not, then it is a sterile pseudo science, no matter how exact its methods. Science is a* developing *mode of inquiry, or it is of no particular importance. . . A science (should endeavor) to wrest from the phenomena of experience the inherent order they contain."*[1]

James E. Tingstad
Pharmaceutical Products Division
Abbott Laboratories
North Chicago, IL 60064

Received May 23, 1980.

[1] C. Rogers, in "Psychology: A Study of a Science," vol. III, S. Koch, Ed., McGraw-Hill, New York, N.Y., 1959, p. 189.

Sulfonamide Microcapsules from Gelatin–Acacia Coacervates

The authors of a recent research paper[1] pertaining to sulfamethoxazole microcapsules prepared from gelatin–acacia coacervates cited no studies relating the coacervation pH, the type or concentration of the flocculating (dehydrating) agent, or the exposure duration and concentration of formaldehyde to the properties of powdered products recovered therefrom. The effects of some of these factors as well as the extraction of sulfamerazine from intact microglobules retrieved from gelatin–acacia coacervates were, however, reported previously[2]. It should be apparent from a perusal of these papers[1,2] that there is considerable similarity between the methods used to produce and recover the sulfonamide microcapsules. Therefore, some substantive conclusions from the earlier study[2] would appear to be germane to the results and discussion of the more recent one[1].

David W. Newton
Department of Pharmaceutics
College of Pharmacy
University of Nebraska Medical Center
Omaha, NE 68105

Received June 2, 1980.

[1] H. Takenaka, Y. Kawashima, and S. Y. Lin, *J. Pharm. Sci.*, **69**, 513 (1980).
[2] D. W. Newton, J. N. McMullen, and C. H. Becker, *ibid.*, **66**, 1327 (1977).

Mass Spectra of Dexamethasone and Betamethasone

The work of Attinà[1] in this issue of the Journal questions an earlier report[2] on the distinction between betamethasone and dexamethasone by mass spectrometry. The spectra referred to were obtained, using reference standard materials, on an instrument that was unsophisticated by modern standards. Indeed, the instrument belonged to a local university and was used in a service capacity by the university staff and students. At the time, our laboratories did not possess a mass spectrometer.

On learning of the work of Attinà[1], an attempt was made to repeat the spectra with modern equipment[3]. The spectra obtained were similar but not identical to those reported by Attinà[1].

We can only speculate as to why the spectra obtained in 1969 were so different from each other and from spectra obtained on more modern instruments. There may have been preliminary decomposition because of the minimal control over conditions existing within the instrument, or there may have been a "memory" effect owing to the service nature of the instrument. Nevertheless, based on the spectra received in 1969, the interpretation was reasonable and consistent with analogous work as cited.

We are grateful that this matter has been brought to our attention and thank those involved.

B. A. Lodge
Chemical Standards Division
Drug Research Laboratories
Health Protection Branch
Ottawa, Ontario
Canada, K1A 0L2

P. Toft
Monitoring and Criteria Division
Bureau of Chemical Hazards
Health Protection Branch
Ottawa, Ontario
Canada, K1A 0L2

Received May 2, 1980.

[1] M. Attinà, *J. Pharm. Sci.*, **69**, 991 (1980).
[2] B. A. Lodge and P. Toft, *ibid.*, **59**, 1045 (1970).
[3] Finnigan 4000, Hewlett-Packard 5980 quadrupole.

Commentary on Science

I would like to call attention to some lucid, perspicacious, and appropriate comments on science and then suggest that we all apply the stated criteria to our efforts in the pharmaceutical sciences.

". . .there is a natural history of science— (i.e.) *science, in any given field, goes through a patterned course of growth and development. For example, it seems to me right and natural that in any new field of scientific endeavor the observations are gross, the hypotheses speculative and full of errors, the measurements crude. More important, I hold the opinion that this is just as truly science as the use of the most refined hypotheses and measurements in a more fully developed field of study. The crucial question in either case is not the degree of refinement but the direction of movement. If in either instance the movement is toward more exact measurement, toward more clear-cut and rigorous theory and hypothesis, toward findings which have greater validity and generality, then this is a healthy and growing science. If not, then it is a sterile pseudo science, no matter how exact its methods. Science is a* developing *mode of inquiry, or it is of no particular importance. . . A science (should endeavor) to wrest from the phenomena of experience the inherent order they contain."*[1]

James E. Tingstad
Pharmaceutical Products Division
Abbott Laboratories
North Chicago, IL 60064

Received May 23, 1980.

[1] C. Rogers, in "Psychology: A Study of a Science," vol. III, S. Koch, Ed., McGraw-Hill, New York, N.Y., 1959, p. 189.

Sulfonamide Microcapsules from Gelatin–Acacia Coacervates

The authors of a recent research paper[1] pertaining to sulfamethoxazole microcapsules prepared from gelatin–acacia coacervates cited no studies relating the coacervation pH, the type or concentration of the flocculating (dehydrating) agent, or the exposure duration and concentration of formaldehyde to the properties of powdered products recovered therefrom. The effects of some of these factors as well as the extraction of sulfamerazine from intact microglobules retrieved from gelatin–acacia coacervates were, however, reported previously[2]. It should be apparent from a perusal of these papers[1,2] that there is considerable similarity between the methods used to produce and recover the sulfonamide microcapsules. Therefore, some substantive conclusions from the earlier study[2] would appear to be germane to the results and discussion of the more recent one[1].

David W. Newton
Department of Pharmaceutics
College of Pharmacy
University of Nebraska Medical Center
Omaha, NE 68105

Received June 2, 1980.

[1] H. Takenaka, Y. Kawashima, and S. Y. Lin, *J. Pharm. Sci.*, **69**, 513 (1980).
[2] D. W. Newton, J. N. McMullen, and C. H. Becker, *ibid.*, **66**, 1327 (1977).

Mass Spectra of Dexamethasone and Betamethasone

The work of Attinà[1] in this issue of the Journal questions an earlier report[2] on the distinction between betamethasone and dexamethasone by mass spectrometry. The spectra referred to were obtained, using reference standard materials, on an instrument that was unsophisticated by modern standards. Indeed, the instrument belonged to a local university and was used in a service capacity by the university staff and students. At the time, our laboratories did not possess a mass spectrometer.

On learning of the work of Attinà[1], an attempt was made to repeat the spectra with modern equipment[3]. The spectra obtained were similar but not identical to those reported by Attinà[1].

We can only speculate as to why the spectra obtained in 1969 were so different from each other and from spectra obtained on more modern instruments. There may have been preliminary decomposition because of the minimal control over conditions existing within the instrument, or there may have been a "memory" effect owing to the service nature of the instrument. Nevertheless, based on the spectra received in 1969, the interpretation was reasonable and consistent with analogous work as cited.

We are grateful that this matter has been brought to our attention and thank those involved.

B. A. Lodge
Chemical Standards Division
Drug Research Laboratories
Health Protection Branch
Ottawa, Ontario
Canada, K1A 0L2

P. Toft
Monitoring and Criteria Division
Bureau of Chemical Hazards
Health Protection Branch
Ottawa, Ontario
Canada, K1A 0L2

Received May 2, 1980.

[1] M. Attinà, *J. Pharm. Sci.*, **69**, 991 (1980).
[2] B. A. Lodge and P. Toft, *ibid.*, **59**, 1045 (1970).
[3] Finnigan 4000, Hewlett-Packard 5980 quadrupole.

Commentary on Science

I would like to call attention to some lucid, perspicacious, and appropriate comments on science and then suggest that we all apply the stated criteria to our efforts in the pharmaceutical sciences.

". . .there is a natural history of science— (i.e.) *science, in any given field, goes through a patterned course of growth and development. For example, it seems to me right and natural that in any new field of scientific endeavor the observations are gross, the hypotheses speculative and full of errors, the measurements crude. More important, I hold the opinion that this is just as truly science as the use of the most refined hypotheses and measurements in a more fully developed field of study. The crucial question in either case is not the degree of refinement but the direction of movement. If in either instance the movement is toward more exact measurement, toward more clear-cut and rigorous theory and hypothesis, toward findings which have greater validity and generality, then this is a healthy and growing science. If not, then it is a sterile pseudo science, no matter how exact its methods. Science is a* developing *mode of inquiry, or it is of no particular importance. . . A science (should endeavor) to wrest from the phenomena of experience the inherent order they contain."*[1]

James E. Tingstad
Pharmaceutical Products Division
Abbott Laboratories
North Chicago, IL 60064

Received May 23, 1980.

[1] C. Rogers, in "Psychology: A Study of a Science," vol. III, S. Koch, Ed., McGraw-Hill, New York, N.Y., 1959, p. 189.

Sulfonamide Microcapsules from Gelatin–Acacia Coacervates

The authors of a recent research paper[1] pertaining to sulfamethoxazole microcapsules prepared from gelatin–acacia coacervates cited no studies relating the coacervation pH, the type or concentration of the flocculating (dehydrating) agent, or the exposure duration and concentration of formaldehyde to the properties of powdered products recovered therefrom. The effects of some of these factors as well as the extraction of sulfamerazine from intact microglobules retrieved from gelatin–acacia coacervates were, however, reported previously[2]. It should be apparent from a perusal of these papers[1,2] that there is considerable similarity between the methods used to produce and recover the sulfonamide microcapsules. Therefore, some substantive conclusions from the earlier study[2] would appear to be germane to the results and discussion of the more recent one[1].

David W. Newton
Department of Pharmaceutics
College of Pharmacy
University of Nebraska Medical Center
Omaha, NE 68105

Received June 2, 1980.

[1] H. Takenaka, Y. Kawashima, and S. Y. Lin, *J. Pharm. Sci.*, **69**, 513 (1980).
[2] D. W. Newton, J. N. McMullen, and C. H. Becker, *ibid.*, **66**, 1327 (1977).

JOURNAL OF PHARMACEUTICAL SCIENCES

AUGUST 1980
VOLUME 69 NUMBER 8

RESEARCH ARTICLES

Mechanisms of Anterior Segment Absorption of Pilocarpine following Subconjunctival Injection in Albino Rabbits

JOSEPH M. CONRAD and JOSEPH R. ROBINSON ˣ

Received December 14, 1979, from the *School of Pharmacy, University of Wisconsin, Madison, WI 53706.* Accepted for publication March 13, 1980.

Abstract □ The present study was initiated to provide insight into the mechanisms of drug availability from subconjunctival injection. Pilocarpine nitrate was the probe drug, and the albino rabbit was the experimental animal. Several volumes, from 50 to 500 μl, of drug solution were injected subconjunctivally; drug levels were monitored in the tear, cornea, aqueous humor, and blood as a function of time. The injection site also was examined for residual drug postdosing. Finally, drug was placed in the subconjunctival space either by injection through the conjunctival membrane or through the eyelid. From these experiments, it was concluded that at high injection volumes, *i.e.*, >200 μl, reflux of the drug solution out of the injection site, followed by corneal absorption, is the primary mechanism to explain aqueous humor availability of the drug. At lower injection volumes, multiple mechanisms, including reflux of drug from the injection site and transconjunctival permeation, penetration of the globe of the eye, and systemic absorption followed by return *via* the vascular bed, are necessary to explain drug absorption. High aqueous humor levels of pilocarpine can be achieved from subconjunctival injection as compared to the topical route, provided that large injection volumes, *i.e.*, >200 μl, are employed and correspondingly greater amounts of drug are administered. No true sustaining of drug availability to the aqueous chamber was noted, but local sustaining at the injection site was evident.

Keyphrases □ Pilocarpine—mechanisms of distribution to cornea, tear, aqueous humor, and blood following subconjunctival injection, rabbits □ Absorption, ocular—pilocarpine, mechanisms of distribution following subconjunctival injection, rabbits □ Distribution, ocular—pilocarpine, mechanisms of absorption following subconjunctival injection, rabbits

Subconjunctival administration of ophthalmic drugs represents an important, albeit poorly understood, administration route. Some clinicians select this route because of the expected sustained drug delivery to the eye, whereas others choose it for the expected high drug levels that can be achieved in the anterior segment of the eye as compared to topical dosing. Whether a high level or a sustained effect is achieved appears to depend on the drug, the formulation, and the method of injection.

That drugs do penetrate the eye from subconjunctival injection is certain, although the penetration rate may vary considerably depending on the drug and formulation. However, it is not well understood how the drug moves from the injection site to the aqueous chamber. Until a clear mechanistic picture is established, drug release predictions for different drug entities or formulation changes will be based primarily on experience.

The purpose of the present study was to examine the mechanisms of aqueous chamber absorption from subconjunctival injection for the water-soluble drug pilocarpine.

BACKGROUND

The conjunctiva is the thin membrane covering the front of the eyeball from the lid margin to the corneoscleral junction. The subconjunctival space is the region between the conjunctiva and the eyeball, and subconjunctival injections place the drug in this area either for a local effect or as a repository to provide drug to the aqueous chamber.

Several mechanisms have been proposed to explain the movement of drugs from the subconjunctival site of injection to the anterior segment of the eye, *i.e.*, the aqueous chamber:

1. The drug is absorbed into the conjunctival blood vessels, enters the general circulation, and then enters the anterior segment of the eye.
2. The drug directly penetrates the sclera and underlying layers.
3. The drug refluxes out of the puncture hole produced in the conjunctiva by injection. It then mixes with tears and is absorbed across the cornea.
4. The drug diffuses across the conjunctiva, followed by mixing with tears and eventual corneal absorption.

One early explanation of ocular drug absorption from subconjunctival injection was systemic absorption followed by return to the eye. Without doubt, most of this injected dose is absorbed into the systemic circulation, which represents a considerable loss from the injection site. However, given the large volume of distribution of the vascular bed and the small amount of drug involved, as well as potential metabolism in the blood, it seems unlikely that this route of penetration would be major for most drugs.

The second potential route is direct scleral absorption of drug into the aqueous chamber. While this route is possible, the drug would have to permeate a relatively impermeable scleral coat (1–4) and traverse a rich vascular bed to gain entrance to the aqueous chamber. For most drugs,

0022-3549/80/0800-0875$01.00/0
© 1980, American Pharmaceutical Association

the difficulty of scleral penetration as well as loss to systemic circulation probably would cause little, if any, drug to reach the anterior segment of the eye. In addition, this mechanism would have to be compatible with the very early time of the peak drug level in the aqueous chamber that is commonly observed. Nevertheless, McCartney *et al.* (5), on the basis of autoradiographic techniques, felt that this route was a distinct mechanistic possibility for absorption of hydrocortisone.

Undoubtedly, the most widely accepted route for absorption is the needle puncture and reflux theory. Recent work (6) with small volumes (1 μl) of injected solutions raised doubts about its importance in humans. On the other hand, Wine *et al.* (7) systematically examined the mechanism of absorption of [^{14}C]hydrocortisone and found that the leakage mechanism was the most plausible. Aqueous humor drug levels from normal subconjunctival injections were compared with those achieved from injection through the upper eyelid, which kept the conjunctival membrane intact. The relatively high drug levels from subconjunctival injection compared to those from upper eyelid injection supported the puncture mechanism.

The last possible mechanism is direct permeation of the conjunctiva followed by corneal absorption. The conjunctival permeability coefficient for pilocarpine has been estimated (8) to be in the range of 10^{-3} cm/hr, which is in good agreement with the coefficient of 5×10^{-3} cm/hr found for sodium 22 (2, 9). This sufficiently large permeability coefficient explains the early peak times in the cornea and aqueous humor, provided the concentration of injected drug is very large and little or no drug is lost to the conjunctival blood vessels. Simple diffusion of drugs from subconjunctival injection has been compared with topical dosing (10). Early peaks in the cornea, sclera, and choroid can be attributed to extensive diffusion of drug across the conjunctiva, or leakage, to the tear film or to direct transfer of drug at the corneoscleral junction, presumably through limbal blood vessels.

For any individual drug entity, its physicochemical properties, such as solubility, diffusivity, and partitioning behavior, may give one mechanism precedence over another. In addition, vehicle composition, volume injected, and method of injection also may influence the mechanism. The present study examines some of these variables using pilocarpine as the drug probe.

EXPERIMENTAL

Materials—Tritiated pilocarpine alkaloid with a specific activity of 4.1 Ci/mmole was obtained commercially[1] and purified by vacuum distillation (11) immediately prior to use. All other chemicals were reagent or analytical grade and were used as received.

Male albino rabbits[2], 1.7–2.4 kg, were maintained on a regular diet with no restrictions on the amounts of food and water consumed. Lighting and auditory stimuli were kept constant on a 24-hr basis.

Preparation of Pilocarpine Solutions—Drug solutions were prepared by the addition of the purified labeled material to a 1×10^{-2} *M* (0.2%) pilocarpine solution. The buffer was pH 6.24 isotonic Sorensen buffer. Addition of [^{3}H]pilocarpine had no appreciable effect on the molarity of the final dosing solution. It was determined that 0.25 mCi of the labeled drug/ml of the final dosing solution was sufficient to give good counting efficiency. The dosing solution for injection corresponded to a final concentration of 2.08 μg of pilocarpine alkaloid/μl of solution.

Subconjunctival Injection Administration through Conjunctival Membrane—Rabbits were positioned in restraining boxes to minimize movement and to maintain the normal upright posture. Approximately 10 min prior to dosing, each eye received one drop of 0.5% tetracaine hydrochloride solution[3]. Although topical anesthetics have been shown to cause breakup of the tear film (1–3, 8, 12, 13), this step was necessary to obtain consistent injections.

Following local anesthesia, measured volumes of pilocarpine solution (50, 100, 200, and 500 μl) were injected accurately through the conjunctival membrane in the center of the upper quadrant bulbar conjunctiva, ~3–4 mm back from the corneoscleral junction. A 1-ml tuberculin syringe fitted with a 27-gauge, 1.27-cm needle was employed. Only one eye of each test animal received the dose, with the other eye serving as a control. Alternate eye dosing was used in each animal to eliminate any right to left or left to right eye bias.

Aqueous humor, blood, and corneal samples were obtained at 5, 10, 20, 30, 45, 60, and 120 min postdosing. For the 200-μl injection, samples also were obtained at 180 and 240 min postinjection. At the end of each period, the animal was sacrificed *via* rapid injection of a phenobarbital sodium overdose into the marginal ear vein.

Prior to sampling, the corneal surface was rinsed with isotonic saline and blotted dry with a tissue. Aqueous humor samples were obtained by aspirating the aqueous humor and analyzing the fluid *via* scintillation counting according to reported procedures (14–17). Corneal samples were obtained by excising the cornea immediately after aqueous humor aspiration. The method for obtaining and treating the corneal samples was described previously (14, 17).

Blood samples of 1 ml were obtained by direct cardiac puncture, and then two 100-μl samples were transferred[4] quantitatively to absorbent pads[5] contained in combustion cones[6]. These samples were allowed to dry for 24 hr prior to burning in a tissue oxidizer[7]. The oxidizer automatically deposited the tritiated sample, along with 10 ml of liquid scintillation counting solution[8], into a plastic vial[9]. The vial contents were allowed to cool to room temperature for 6 hr and then were counted and analyzed as described previously (14, 17). At least seven eyes were used for each data point. Mean values and standard errors of the mean were determined from the pooled data at each time point, and the concentration–time profile was fitted to a one-compartment pharmacokinetic model (18, 19).

Subconjunctival Injection Administration through Upper Eyelid—Rabbits were positioned in restraining boxes, and a drop of local anesthetic was instilled into each eye. Accurately measured volumes (50–100 μl) of pilocarpine solution were injected directly through the upper eyelid into the center of the upper quadrant under the bulbar conjunctiva. The injection was made so as to produce a bleb in the same location as the direct subconjunctival injection. Thus, the major difference between this study and the direct subconjunctival injection was that no puncture of the conjunctival membrane occurred.

Tissue sampling and analysis were identical to those described previously. The data treatment and analysis of data also were as described previously.

Tear Film Pilocarpine—*Single-Needle Puncture Hole*—Rabbits were placed in restraining boxes, but no local anesthetic was administered. Pilocarpine solution, 200 μl, was injected subconjunctivally; the tear film was sampled at 0, 0.5, 1, 2, 4, 5, 7, 10, 15, 20, and 30 min postdosing. The tear film samples were obtained by carefully touching a 1-μl capillary pipet[10] to the lacrimal lake at the edge of the lid and aspirating a 1-μl sample. The glass capillary tubes then were treated in a manner similar to that described for the aqueous humor samples. At least 13 eyes were used for each data point, and the data were treated as described previously.

Multiple-Needle Puncture Hole—The study was identical to that described for the single-needle puncture except that multiple punctures were made in the conjunctival membrane. Three protocols were employed: (*a*) nine punctures, followed by dosing of 200 μl of the pilocarpine solution injected during the 10th puncture; (*b*) five punctures, followed by dosing on the sixth puncture, followed by four more punctures into the resulting bleb; and (*c*) injection of 200 μl, followed by nine more punctures into the bleb.

Immediately following the 10th puncture of the conjunctival membrane, 1-μl tear samples were collected over the same period and analyzed in the same way as described for the tear film study.

At the end of the tear sampling period, *i.e.*, 30 min, the animals were sacrificed; the aqueous humor, cornea, and blood samples were obtained. These samples were analyzed as already described.

At least 14 eyes were used for each data point, and the results were treated as described previously.

No Puncture Hole—The dose was injected into the subconjunctival space without puncturing the conjunctival membrane by piercing the upper eyelid and threading the needle to approximately the same spot in the subconjunctival space as from a subconjunctival injection.

Tear samples were collected and analyzed as described previously. At least 11 eyes were used for each data point.

Conjunctival Bleb Analysis—Rabbits were prepared and placed in restraining boxes. Following administration of the topical anesthetic, 200 μl of pilocarpine solution was administered to each eye either by subconjunctival or through-the-eyelid injection. At the end of 60 min, the animals were sacrificed. The upper quadrant conjunctival membrane was

[1] New England Nuclear, Boston, Mass.
[2] Klubertanz Rabbitry, Edgerton, Wis.
[3] Pontocaine, Winthrop Laboratories, New York, N.Y.
[4] Biopette, Schwartz-Mann, Orangeburg, N.Y.
[5] Combusti-Pads, Packard Instrument Co., Downers Grove, Ill.
[6] Combusto-Cone, Packard Instrument Co., Downers Grove, Ill.
[7] Model 2002, Packard Instrument Co., Downers Grove, Ill.
[8] Monophase 40, Packard Instrument Co., Downers Grove, Ill.
[9] The Vial, Research Products International Corp., Elk Grove Village, Ill.
[10] Microcap, Drummond Scientific Co., Bloomfield, N.J.

Table I—Cornea and Aqueous Humor Drug Concentration in the Dosed Eye *versus* Time for 1×10^{-2} *M* Pilocarpine in Various Volumes of pH 6.24 Isotonic Sorensen Buffer Injected Subconjunctivally through the Conjunctival Membrane

Minutes	Micrograms of Pilocarpine per Gram of Cornea (Wet Weight)				Micrograms of Pilocarpine per Milliliter of Aqueous Humor			
	50 μl	100 μl	200 μl	500 μl	50 μl	100 μl	200 μl	500 μl
5	0.304 (0.086)[a] [12][b]	0.200 (0.062)[a] [8][b]	4.203 (0.564)[a] [10][b]	14.802 (1.391)[a] [8][b]	0.047 (0.019)[a] [13][b]	0.089 (0.052)[a] [8][b]	0.386 (0.078)[a] [11][b]	0.704 (0.072)[a] [8][b]
10	0.231 (0.047) [13]	0.314 (0.083) [11]	4.226 (1.043) [11]	14.111 (2.586) [9]	0.127 (0.075) [11]	0.194 (0.063) [13]	0.703 (0.133) [14]	1.747 (0.258) [8]
20	0.059 (0.010) [14]	0.340 (0.069) [12]	6.434 (0.881) [10]	12.013 (0.753) [9]	0.180 (0.102) [11]	0.278 (0.086) [13]	1.442 (0.291) [14]	2.300 (0.140) [8]
30	0.081 (0.017) [8]	0.288 (0.049) [12]	6.482 (1.340) [10]	10.514 (2.278) [9]	0.195 (0.118) [9]	0.329 (0.103) [10]	1.817 (0.314) [13]	3.586 (0.487) [7]
45	0.333 (0.007) [7]	0.254 (0.111) [8]	5.713 (0.984) [12]	9.686 (2.653) [9]	0.136 (0.068) [8]	0.258 (0.110) [10]	1.385 (0.213) [13]	3.156 (0.691) [7]
60	0.030 (0.003) [11]	0.290 (0.052) [8]	1.802 (0.388) [13]	5.635 (2.223) [10]	0.049 (0.006) [8]	0.180 (0.032) [9]	0.505 (0.082) [13]	1.546 (0.498) [11]
90	0.026 (0.005) [7]	0.213 (0.031) [8]	NS[c]	4.798 (0.863) [9]	0.032 (0.012) [11]	0.115 (0.019) [8]	NS	1.370 (0.247) [10]
120	0.033 (0.014) [6]	0.081 (0.023) [8]	0.586 (0.144) [13]	1.894 (0.609) [8]	0.026 (0.008) [9]	0.039 (0.006) [10]	0.199 (0.035) [16]	0.694 (0.222) [8]
180	NS	NS	0.220 (0.051) [12]	NS	NS	NS	0.080 (0.012) [16]	NS
240	NS	NS	0.209 (0.034) [8]	NS	NS	NS	0.063 (0.009) [15]	NS

[a] Numbers in parentheses refer to the standard error of the mean. [b] Numbers in brackets refer to the number of determinations at that point. [c] Not sampled.

Table II—Cornea and Aqueous Humor Drug Concentration in the Contralateral Eye *versus* Time for 1×10^{-2} *M* Pilocarpine in Various Volumes of pH 6.24 Isotonic Sorensen Buffer Injected Subconjunctivally through the Conjunctival Membrane

Minutes	Micrograms of Pilocarpine per Gram of Cornea (Wet Weight)				Micrograms of Pilocarpine per Milliliter of Aqueous Humor			
	50 μl	100 μl	200 μl	500 μl	50 μl	100 μl	200 μl	500 μl
5	0.019 (0.002)[a] [10][b]	0.023 (0.006)[a] [10][b]	0.072 (0.010)[a] [14][b]	0.224 (0.036)[a] [10][b]	0.003 (0.0002)[a] [15][b]	0.004 (0.0002)[a] [10][b]	0.006 (0.001)[a] [14][b]	0.014 (0.002)[a] [11][b]
10	0.018 (0.002) [19]	0.027 (0.002) [12]	0.063 (0.011) [10]	0.406 (0.151) [10]	0.003 (0.0004) [15]	0.007 (0.0003) [14]	0.011 (0.002) [14]	0.037 (0.003) [11]
20	0.018 (0.002) [14]	0.026 (0.001) [14]	0.076 (0.015) [11]	0.408 (0.122) [8]	0.006 (0.0003) [14]	0.012 (0.0004) [15]	0.022 (0.002) [14]	0.053 (0.002) [12]
30	0.013 (0.001) [9]	0.025 (0.002) [13]	0.057 (0.008) [13]	0.205 (0.028) [10]	0.007 (0.001) [8]	0.015 (0.001) [15]	0.027 (0.002) [13]	0.081 (0.003) [11]
45	0.014 (0.001) [9]	0.025 (0.002) [8]	0.214 (0.053) [10]	0.537 (0.119) [9]	0.008 (0.0004) [7]	0.019 (0.002) [10]	0.038 (0.003) [14]	0.107 (0.005) [9]
60	0.015 (0.001) [11]	0.030 (0.002) [10]	0.114 (0.011) [16]	0.186 (0.049) [11]	0.007 (0.0003) [14]	0.020 (0.001) [10]	0.033 (0.001) [16]	0.111 (0.008) [12]
90	0.014 (0.002) [9]	0.027 (0.005) [10]	NS[c]	0.212 (0.031) [8]	0.007 (0.0003) [9]	0.020 (0.001) [10]	NS	0.083 (0.002) [11]
120	0.015 (0.001) [9]	0.025 (0.002) [10]	0.044 (0.008) [7]	0.135 (0.015) [11]	0.007 (0.0004) [10]	0.015 (0.0004) [10]	0.053 (0.004) [16]	0.084 (0.004) [10]
180	NS	NS	0.037 (0.006) [12]	NS	NS	NS	0.032 (0.001) [16]	NS
240	NS	NS	0.028 (0.003) [9]	NS	NS	NS	0.284 (0.001) [16]	NS

[a] Numbers in parentheses refer to the standard error of the mean. [b] Numbers in brackets refer to the number of determinations at that point. [c] Not sampled.

Table III—Circulating Blood Drug Concentration *versus* Time for 1×10^{-2} *M* Pilocarpine in Various Volumes of pH 6.24 Isotonic Sorensen Buffer Injected Subconjunctivally through the Conjunctival Membrane

Minutes	Micrograms of Pilocarpine per Milliliter of Blood			
	50 μl	100 μl	200 μl	500 μl
5	0.035 (0.001)[a] [9][b]	0.069 (0.002)[a] [8][b]	NS[c]	0.214 (0.021)[a] [9][b]
10	0.034 (0.002) [11]	0.058 (0.004) [10]	0.067 (0.009)[a] [9][b]	0.260 (0.029) [12]
20	0.041 (0.002) [12]	0.062 (0.003) [12]	0.108 (0.011) [10]	0.301 (0.014) [12]
30	0.033 (0.001) [11]	0.048 (0.003) [10]	0.048 (0.003) [10]	0.172 (0.014) [9]
45	0.027 (0.002) [12]	0.053 (0.002) [12]	0.132 (0.013) [10]	0.287 (0.020) [12]
60	0.023 (0.001) [10]	0.052 (0.002) [12]	0.101 (0.004) [10]	0.233 (0.015) [9]
90	0.016 (0.001) [10]	0.026 (0.001) [11]	NS	0.132 (0.010) [10]
120	0.014 (0.001) [12]	0.022 (0.001) [10]	0.022 (0.004) [7]	0.097 (0.006) [12]
180	NS	NS	0.007 (0.001) [9]	NS
240	NS	NS	0.007 (0.001) [10]	NS

[a] Numbers in parentheses refer to the standard error of the mean. [b] Numbers in brackets refer to the number of determinations at that point. [c] Not sampled.

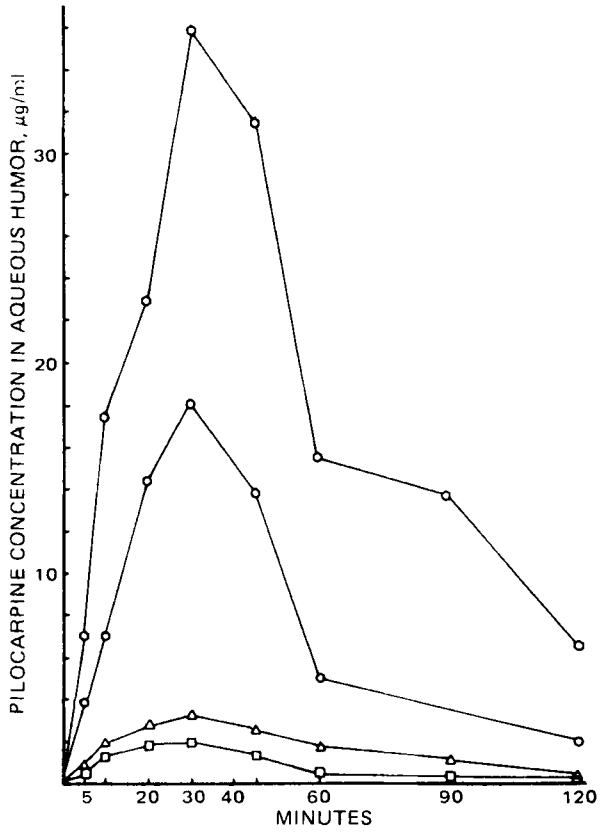

Figure 1—*Aqueous humor drug concentration in the dosed eye* versus *time profiles for 1 × 10^{-2} M pilocarpine in various volumes of pH 6.24 isotonic Sorensen buffer injected subconjunctivally through the conjunctival membrane. Key: □, 50 μl injected; △, 100 μl injected; ○, 200 μl injected; and ○, 500 μl injected. Each point represents a minimum of seven determinations. Error bars were eliminated for clarity.*

dissected and removed, including the bulbar and palpebral portions.

The obtained tissue was placed in a tared combustion cone[6] containing a combustion pad[5] to soak up any fluid and to aid in more even burning of the tissue in the combustion process. The wet weight of each conjunctiva then was determined. Subsequent analytical procedures were identical to those used in the corneal sample analysis.

At least 21 eyes were used for each point in the membrane puncture bleb analysis, and 18 eyes were used per point in the eyelid route bleb analysis. All data were subjected to the same analysis as described previously.

RESULTS

Subconjunctival Injection Delivered through Conjunctival Membrane—Drug concentration *versus* time profiles for each of the four dose volumes were obtained for the aqueous humor, cornea, and blood. Cornea and aqueous humor data were obtained for both the dosed and contralateral eyes.

The data are presented in Tables I–III for the four dose volumes studied. For visual comparison, the aqueous humor data are shown graphically in Fig. 1. An examination of Fig. 1 shows some expected trends. As the dosing volume increased, the amount of drug absorbed into the cornea or aqueous humor increased. The amount of drug absorbed was increased greatly by the increase in dosing volume from 100 to 200 μl. This result also occurred in the contralateral eye, although the drug levels were much smaller and the trend was not as clear.

Subconjunctival Injection Delivered through Upper Eyelid—Drug concentration *versus* time profiles for each of the two dose volumes were obtained for the aqueous humor, cornea, and blood. Cornea and aqueous humor data were obtained for both the dosed and contralateral eyes.

Tables IV–VI contain the pertinent data from this study, and Fig. 2 shows the representative aqueous humor data in graphical form. The drug levels in the cornea and aqueous humor were several orders of magnitude lower than those from the through-the-membrane injection. The levels in the contralateral eyes were about the same as those in the through-the-membrane injection. Finally, the circulating blood level data were comparable from both studies.

Lacrimal Fluid following Subconjunctival Injection—The tear film was monitored for drug as a function of time for three different experimental conditions: one puncture hole in the conjunctiva, multiple-puncture holes in the conjunctiva, and no puncture holes in the conjunctiva (through-the-eyelid injection). The data are shown in Table VII. Drug levels in the through-the-eyelid study were approximately three orders of magnitude less than those in the punctured conjunctival studies. These levels were so low that background radiation levels became important and should be considered when assessing the accuracy of the stated levels.

Data from the punctured conjunctiva are shown graphically in Fig. 3. The profiles were similar at all times except for the first 5 min. Previous reports from this laboratory described the procedures and problems of tear sampling (11, 20–22). Samples were collected for 30 min with emphasis on data obtained during the first 5 min. Therefore, considerable weight is given to the difference shown in Fig. 3 for the first 5 min post-injection.

After 30 min, the experimental animal was sacrificed; samples of the cornea, aqueous humor, and blood were taken (Table VIII). The aqueous humor drug levels for the dosed and contralateral eye in the through-the-eyelid study were not appreciably different. Cornea data from the same study showed the dosed eye levels to be about twice as large as those from the contralateral eye, although both were low relative to the injection study. The small, but measurable, difference in cornea levels is attributed to drug diffusing through the conjunctival membrane to the tear fluid and then absorbed into the cornea.

The aqueous humor and cornea data from the dosed eye in the punctured membrane case were two orders of magnitude greater than those from the through-the-eyelid study. Although the multiple-puncture

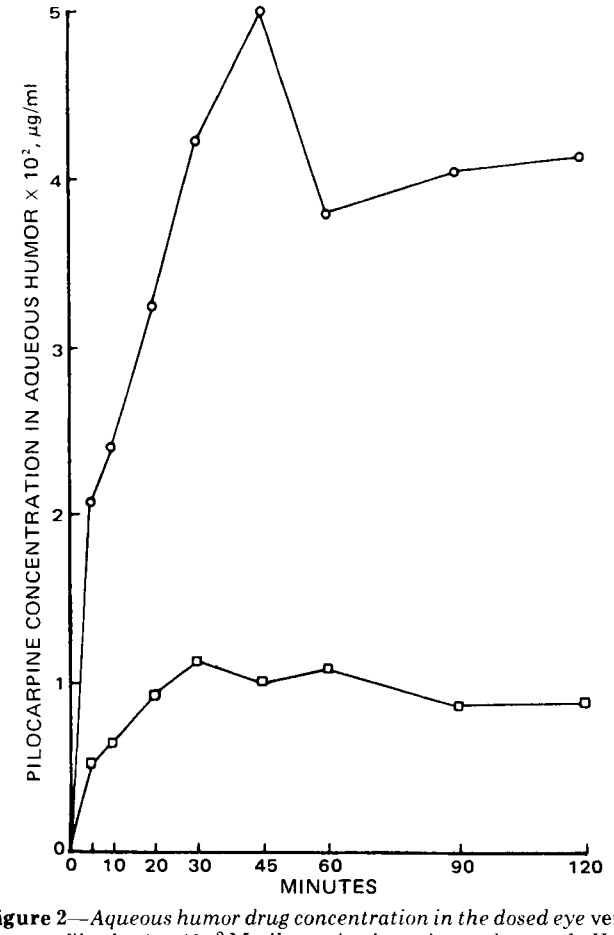

Figure 2—*Aqueous humor drug concentration in the dosed eye* versus *time profiles for 1 × 10^{-2} M pilocarpine in various volumes of pH 6.24 isotonic Sorensen buffer injected subconjunctivally through the upper eyelid. Key: □, 50 μl injected; and ○, 200 μl injected. Each point represents a minimum of seven determinations. Error bars were eliminated for clarity.*

Table IV—Cornea and Aqueous Humor Drug Concentration in the Dosed Eye *versus* Time for 1×10^{-2} *M* Pilocarpine in Various Volumes of pH 6.24 Isotonic Sorensen Buffer Injected Subconjunctivally through the Upper Eyelid

Minutes	Micrograms of Pilocarpine per Gram of Cornea (Wet Weight)		Micrograms of Pilocarpine per Milliliter of Aqueous Humor	
	50 μl	200 μl	50 μl	200 μl
5	0.062 (0.010)[a] [9][b]	0.0676 (0.129)[a] [8][b]	0.005 (0.0004)[a] [9][b]	0.021 (0.003)[a] [8][b]
10	0.064 (0.008) [10]	0.146 (0.22) [10]	0.006 (0.0006) [11]	0.024 (0.001) [10]
20	0.069 (0.009) [11]	0.130 (0.051) [12]	0.009 (0.0004) [12]	0.032 (0.001) [9]
30	0.065 (0.011) [12]	0.119 (0.034) [12]	0.011 (0.0006) [8]	0.042 (0.002) [10]
45	0.070 (0.009) [11]	0.092 (0.010) [9]	0.010 (0.0007) [12]	0.050 (0.003) [12]
60	0.111 (0.009) [7]	0.092 (0.009) [8]	0.011 (0.0007) [11]	0.038 (0.002) [10]
90	0.032 (0.005) [10]	0.104 (0.023) [10]	0.009 (0.0006) [9]	0.040 (0.002) [12]
120	0.039 (0.005) [10]	0.093 (0.13) [10]	0.009 (0.0004) [10]	0.040 (0.001) [7]

[a] Numbers in parentheses refer to the standard error of the mean. [b] Numbers in brackets refer to the number of determinations at that point.

Table V—Cornea and Aqueous Humor Drug Concentration in the Contralateral Eye *versus* Time for 1×10^{-2} *M* Pilocarpine in Various Volumes of pH 6.24 Isotonic Sorensen Buffer Injected Subconjunctivally through the Upper Eyelid

Minutes	Micrograms of Pilocarpine per Gram of Cornea (Wet Weight)		Micrograms of Pilocarpine per Milliliter of Aqueous Humor	
	50 μl	200 μl	50 μl	200 μl
5	0.033 (0.005)[a] [12][b]	0.208 (0.057)[a] [8][b]	0.004 (0.0005)[a] [12][b]	0.012 (0.0007)[a] [12][b]
10	0.053 (0.006) [12]	0.094 (0.020) [10]	.0.005 (0.0004) [12]	0.020 (0.001) [10]
20	0.052 (0.007) [10]	0.062 (0.006) [9]	0.008 (0.0004) [10]	0.032 (0.001) [10]
30	0.059 (0.009) [12]	0.058 (0.007) [12]	0.010 (0.001) [12]	0.036 (0.002) [10]
45	0.057 (0.008) [11]	0.057 (0.008) [10]	0.011 (0.0006) [9]	0.045 (0.002) [10]
60	0.108 (0.008) [8]	0.077 (0.011) [9]	0.011 (0.0007) [12]	0.034 (0.002) [12]
90	0.032 (0.006) [9]	0.081 (0.010) [11]	0.009 (0.001) [12]	0.040 (0.002) [12]
120	0.035 (0.005) [10]	0.088 (0.012) [9]	0.009 (0.0004) [12]	0.043 (0.001) [10]

[a] Numbers in parentheses refer to the standard error of the mean. [b] Numbers in brackets refer to the number of determinations at that point.

Table VI—Circulating Drug Concentration *versus* Time for 1×10^{-2} *M* Pilocarpine in Various Volumes of pH 6.24 Isotonic Sorensen Buffer Injected Subconjunctivally through the Upper Eyelid

Minutes	Micrograms of Pilocarpine per Milliliter of Blood	
	50 μl	200 μl
5	0.051 (0.004)[a] [12][b]	0.158 (0.007)[a] [12][b]
10	0.073 (0.003) [12]	0.172 (0.004) [10]
20	0.057 (0.003) [12]	0.157 (0.007) [10]
30	0.064 (0.004) [12]	0.148 (0.006) [12]
45	0.051 (0.003) [12]	0.112 (0.007) [8]
60	0.044 (0.002) [12]	0.091 (0.003) [10]
90	0.012 (0.002) [10]	0.053 (0.002) [12]
120	0.021 (0.001) [9]	0.061 (0.003) [10]

[a] Numbers in parentheses refer to the standard error of the mean. [b] Numbers in brackets refer to the number of determinations at that point.

aqueous humor and cornea drug levels were slightly higher than the corresponding drug levels from single puncture, they were not statistically different. A partial explanation for this lack of difference is that, upon dissection of the bleb, the area appears as a sponge with numerous aqueous compartments. Multiple punctures do not appear to have a significant effect because it is not like puncturing a balloon but rather like puncturing a sponge.

The drug level in lacrimal fluid at 30 min was as anticipated, with large values in the puncture studies and a low level in the nonpuncture case. The lower lacrimal level in the multiple-puncture case was not statistically different from the single-puncture case. One would expect, *a priori*, lower levels in tears at the 30-min point in the multiple-puncture case if more drug is absorbed into the cornea.

Conjunctival Bleb Injection through Membrane or through Eyelid—The bleb created by subconjunctival injection remains for hours postinjection. It was of interest to determine if the drug also remained for hours or if the bleb merely contained the aqueous injection solution or inflammatory fluid. Thus, at 1 hr postinjection, the bleb was removed surgically and analyzed for drug content. Simple aspiration of the bleb was not possible because of its sponge-like characteristics. The results are shown in Table IX.

After 60 min, there was a considerable amount of pilocarpine in the punctured membrane compared to the through-the-eyelid study. From the wet weights obtained, it is clear that localization of the drug solution in the through-the-eyelid case was much more difficult than in the punctured case. The bleb created by through-the-eyelid injection was distinctly smaller; it was difficult to place it near the bulbar conjunctiva. Undoubtedly, the difference in physical placement and localization of drug solution in the two studies contributed to the difference shown in Table IX. The fact that considerable pilocarpine was left at the site long after appreciable drug levels appeared in the cornea and aqueous humor is significant. This result supports the sustained-release concept of subconjunctival dosing. However, whether the drug is released locally or to the aqueous chamber for long periods depends on the specific drug properties and injection formulation.

DISCUSSION

Each of the four proposed mechanisms for drug movement into the eye interior following subconjunctival injections will be examined, and the

Table VII—Lacrimal Fluid Drug Concentration in the Dosed Eye *versus* Time for 1×10^{-2} *M* Pilocarpine in 200 μl of pH 6.24 Isotonic Sorensen Buffer following Subconjunctival Injection *via* Various Routes of Administration

Minutes	Micrograms of Pilocarpine per Milliliter of Lacrimal Fluid: Single-Puncture Injection through Membrane	Multiple-Puncture Injection through Membrane	Single-Puncture Injection through Eyelid
0.5	270.0 (86.0)[a] [13][b]	416.4 (99.9)[a] [14][b]	0.287 (0.184)[a] [11][b]
1.0	268.2 (93.5) [13]	398.4 (97.6) [14]	0.145 (0.075) [11]
2.0	275.1 (110.4) [13]	350.8 (74.7) [14]	0.082 (0.038) [11]
4.0	238.5 (100.6) [13]	259.3 (52.4) [14]	0.271 (0.143) [11]
5.0	283.5 (93.2) [13]	187.2 (39.7) [14]	0.243 (0.75) [11]
10.0	118.0 (31.7) [13]	95.4 (20.6) [14]	0.161 (0.070) [11]
15.0	75.0 (31.2) [13]	51.1 (11.3) [14]	0.195 (0.079) [11]
20.0	40.1 (12.4) [13]	44.4 (12.6) [14]	0.149 (0.070) [11]
30.0	18.8 (6.4) [13]	11.5 (5.1) [14]	0.437 (0.279) [11]

[a] Numbers in parentheses refer to the standard error of the mean. [b] Numbers in brackets refer to the number of determinations at that point.

results from the present study will be interpreted in light of these proposals. Each mechanism contributes to the overall movement of drug, and it is the magnitude of the contributions that is of concern.

The magnitude and shape of the cornea or aqueous humor pilocarpine–time profile from subconjunctival injection did not differ greatly from those achieved after topical dosing (14, 20, 23), despite the greater amount of drug administered by injection. For example, a 25-μl topical dose of 1×10^{-2} *M* pilocarpine (0.2% solution) produced a maximum level of ~1 μg/ml in ~30 min. A 200-μl injection of the same concentration produced a maximum level of ~1.8 μg/ml in ~30 min, less than a twofold difference despite an eightfold difference in the amount of drug instilled or injected. Moreover, the duration of drug levels was almost identical. Thus, with pilocarpine, no apparent sustaining effect was evident, unless it was at a low level, and only a modest increase in the peak level occurred. It was possible to produce higher aqueous humor levels of drug with the same drug concentration merely by injecting larger volumes.

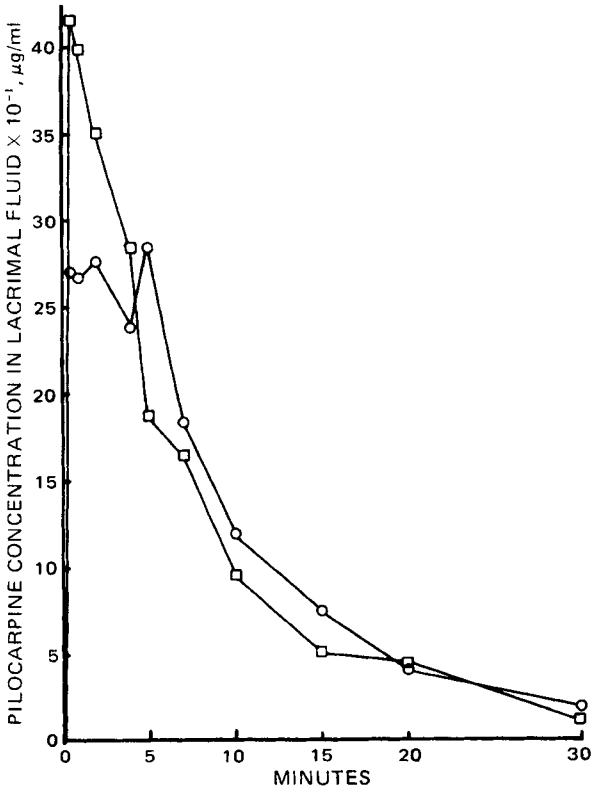

Figure 3—*Lacrimal fluid drug concentration* versus *time profiles for* 1×10^{-2} M *pilocarpine in 200 μl of pH 6.24 isotonic Sorensen buffer following subconjunctival injection* via *various routes in the dosed eye. Key:* ○, *single-puncture injection through the membrane; and* □, *multiple-puncture injection through the membrane. Each point represents a minimum of 13 determinations. Error bars were eliminated for clarity.*

To aid in assessing the experimental changes, the areas under the curve (*AUC*) were measured using a polar planimeter[11] (Table X). In addition, the peak levels and the time to achieve peak levels are important for mechanistic discussion purposes. An assessment of drug bioavailability from this administration route forms the basis for a separate report[12].

The data in Table X are depicted graphically in Figs. 4 and 5 to show the relationship between the dose volume and *AUC* for the cornea and aqueous humor. The insufficient number of points does not fully characterize the lines, but the sigmoidal shape is evident, particularly in the corneal data in Fig. 4. These two graphs may be contrasted with the data for the contralateral eye shown in Fig. 6. A linear relationship was evident over the dose volume range of 50–500 μl. With the contralateral eye, only one mechanism apparently was operative over the dose volume range studied; in the dosed eye, more than one mechanism probably was involved.

Mechanism 1: Drug Passes from Injection Site to Systemic Circulation and Back to Ocular Tissues and Fluids—For this mechanism

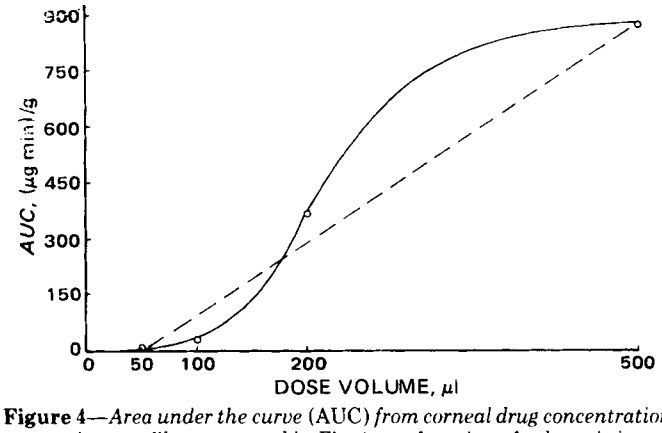

Figure 4—*Area under the curve* (AUC) *from corneal drug concentration* versus *time profiles presented in Fig. 1 as a function of volume injected subconjunctivally through the conjunctival membrane. The dashed line represents the best-fit line through the points, whereas the solid line represents the interpretation of the correct shape of the curve.*

[11] Model 1810-N-10, Dietzgen Corp., Chicago, Ill.
[12] J. Conrad and J. R. Robinson, manuscript in preparation.

Table VIII—Comparison of Fluid or Tissue Drug Concentrations at 30 min following Subconjunctival Dosing with 200 μl of 1×10^{-2} *M* Pilocarpine in pH 6.24 Isotonic Sorensen Buffer *via* Various Routes of Administration

Tissue or Fluid	Single-Puncture Injection through Membrane	Multiple-Puncture Injection through Membrane	Single-Puncture Injection through Eyelid
Aqueous humor[a], dosed eye	1.817 (0.314)[b] [12][c]	2.250 (0.399)[b] [14][c]	0.042 (0.002)[b] [10][c]
Aqueous humor[a], contralateral eye	0.027 (0.002) [13]	0.036 (0.002) [14]	0.036 (0.002) [10]
Cornea, dosed[d] eye	6.482 (1.340) [10]	7.384 (1.285) [13]	0.119 (0.034) [12]
Cornea, contralateral[d] eye	0.057 (0.008) [13]	0.082 (0.006) [13]	0.058 (0.007) [12]
Blood[e]	0.172 (0.014) [10]	0.134 (0.003) [25]	0.148 (0.006) [12]
Lacrimal fluid[f]	18.8 (6.4) [13]	11.5 (5.1) [14]	0.437 (0.279) [11]

[a] Micrograms of pilocarpine per milliliter of aqueous humor. [b] Numbers in parentheses refer to the standard error of the mean. [c] Numbers in brackets refer to the number of determinations at that point. [d] Micrograms of pilocarpine per gram (wet weight) of cornea. [e] Micrograms of pilocarpine per milliliter of blood. [f] Micrograms of pilocarpine per milliliter of lacrimal fluid (tears).

Table IX—Concentration of Drug in Excised Conjunctival Bleb at 60 min following Subconjunctival Dosing with 200 μl of 1×10^{-2} *M* Pilocarpine in pH 6.24 Isotonic Sorensen Buffer *via* Injection through the Conjunctival Membrane or through the Upper Eyelid

	Micrograms of Pilocarpine per Gram of Conjunctiva (Wet Weight)
Through membrane	25.28 (3.11)[a] [21][b,c]
Through eyelid	3.267 (0.966)[a] [18][b,c]

[a] Numbers in parentheses refer to the standard error of the mean. [b] Numbers in brackets refer to the number of determinations at that point. [c] The wet weight of the conjunctival bleb was 240.6 (11.7) μg for the through-the-membrane tissue and 128.2 (7.8) μg for the through-the-eyelid case.

Table X—Comparison of *AUC* Values Obtained after Each Route of Administration for 1×10^{-2} *M* Pilocarpine in pH 6.24 Isotonic Sorensen Buffer Injected Subconjunctivally or Intravenously

Tissue or Fluid	Volume Injected, μl	Through Membrane, Single Puncture, (μg min)/g or ml	Through Upper Eyelid, (μg min)/g or ml
Cornea, dosed[a] eye	50	7.329	7.326
	100	28.363	
	200	367.970	15.136
	500	874.680	
Cornea[a], contralateral eye	50	1.753	4.268
	100	3.140	
	200	11.127	8.498
	500	31.441	
Aqueous humor[a], dosed eye	50	9.742	1.094
	100	20.606	
	200	89.602	4.574
	500	216.598	
Aqueous humor[a], contralateral eye	50	0.759	1.075
	100	1.952	
	200	4.078	4.260
	500	9.701	
Circulating blood[a]	50	2.867	4.603
	100	5.085	
	200	10.279	11.744
	500	24.257	
Lacrimal fluid[b]	200	3265.250	6.699

[a] Measured over first 120 min. [b] Measured over first 30 min. The value was 3137.250 (μg min)/ml in the multiple-puncture through-the-membrane study.

to be important, equivalent, or at least close to equivalent, drug concentration–time profiles should occur in both the dosed and the contralateral eyes. This clearly is not the case, and earlier studies that measured drug in both the dosed and contralateral eye (24, 25) agree with this finding. The time to achieve peak levels in the aqueous humor of the dosed eye was ~30 min, whereas it was ~60 min or longer in the contralateral eye. Moreover, the maximum concentrations achieved in the dosed and contralateral eyes differed by orders of magnitude, as did the *AUC*.

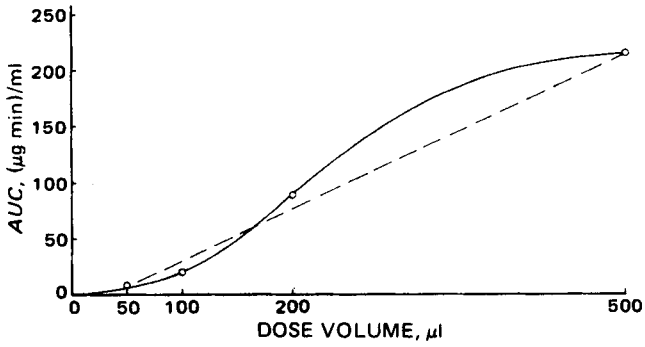

Figure 5—*Area under the curve* (AUC) *from aqueous humor drug concentration* versus *time profiles presented in Fig. 2 as a function of volume injected subconjunctivally through the conjunctival membrane. The dashed line represents the best-fit line through the points, whereas the solid line represents the interpretation of the correct shape of the curve.*

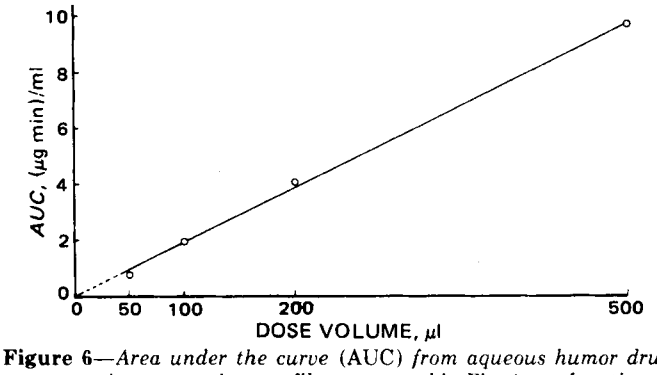

Figure 6—*Area under the curve* (AUC) *from aqueous humor drug concentration* versus *time profiles presented in Fig. 4 as a function of volume injected subconjunctivally through the conjunctival membrane.*

AUC is related directly to the dose volume injected (Fig. 7). Most of the injected drug will be absorbed into the systemic circulation, so a linear relationship is expected.

When the *AUC* for the circulating blood levels at each volume is plotted *versus* the aqueous humor *AUC* for the dosed and contralateral eyes, the relationships shown in Figs. 8 and 9 result. The intercept in the case of the contralateral eye is zero, suggesting that all of the drug in that eye came from drug in the blood. However, for the dosed eye, the intercept is not zero but intercepts on the blood *AUC* axis, suggesting a drug source other than the blood.

Another aspect of the blood level studies related to mechanistic in-

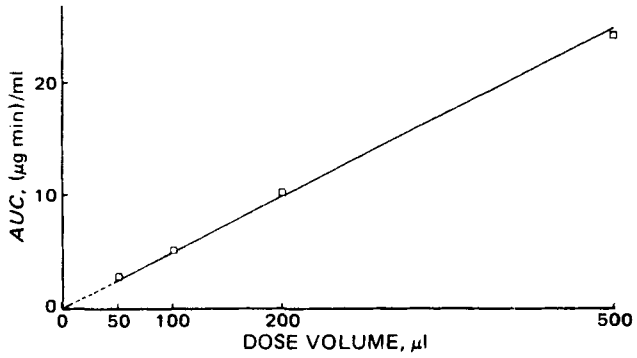

Figure 7—*Area under the curve* (AUC) *from circulating blood drug concentration* versus *time profiles presented in Table III as a function of volume injected subconjunctivally through the conjunctival membrane.*

terpretation is the time–concentration profile resulting from through-the-eyelid injection in contrast to through-the-membrane injection (Table XI). Aside from some minor differences in the peak time, the data are very similar. Moreover, the *AUC*s in these studies are very similar as seen in Table XI.

The present work was conducted in rabbits with an estimated blood volume of about 1 liter. The human eye is similar in size to that of the rabbit, but the circulating blood is 7–8 liters, so the dilution effect is expected to be even more dramatic. It seems reasonable to conclude that a minor amount of drug in the aqueous chamber of the dosed eye comes from the circulating blood.

Mechanism 2: Drug Penetrates Eye from Subconjunctival Injection Site by Simple Diffusion through Tissues Underlying Site—Earlier autoradiographic studies (5) showed that hydrocortisone penetrates the sclera, choroid, and other layers of the globe of the eye. In addition, it is expected that drug moves across limbal vessels to enter the iris and cornea. However, with pilocarpine, this mechanism does not appear to be major for drug gaining access to the anterior segment of the eye.

If movement of drug through the layers of the globe is the principal mechanism, then the method of placement, *i.e.*, puncture or no puncture, should have no effect on the drug levels. Clearly, the through-the-eyelid injection produced drug levels in the cornea and aqueous humor that were orders of magnitude lower (Table XII).

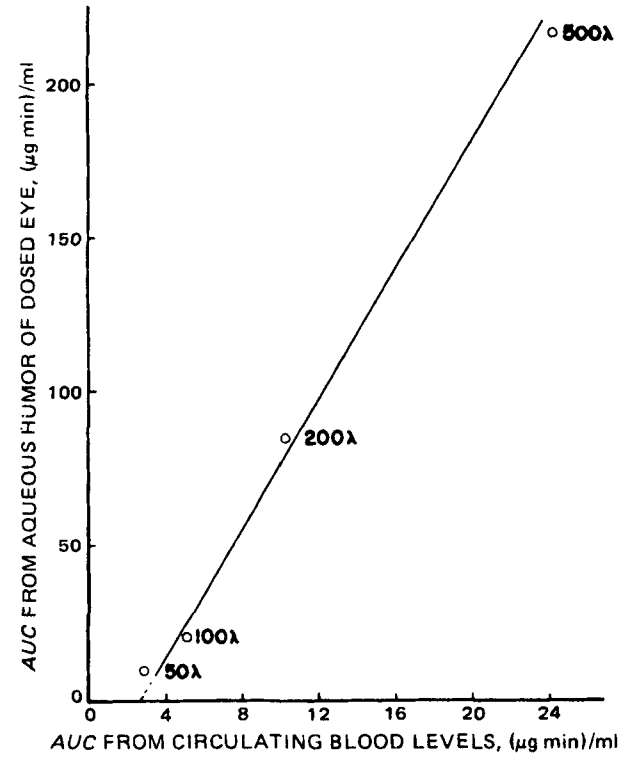

Figure 8—*Comparison of the area under the curve* (AUC) *from aqueous humor drug concentration* versus *time profiles presented in Fig. 2 to the area under the curve* (AUC) *from circulating blood drug concentration* versus *time profiles presented in Fig. 5 at each volume injected subconjunctivally through the conjunctival membrane.*

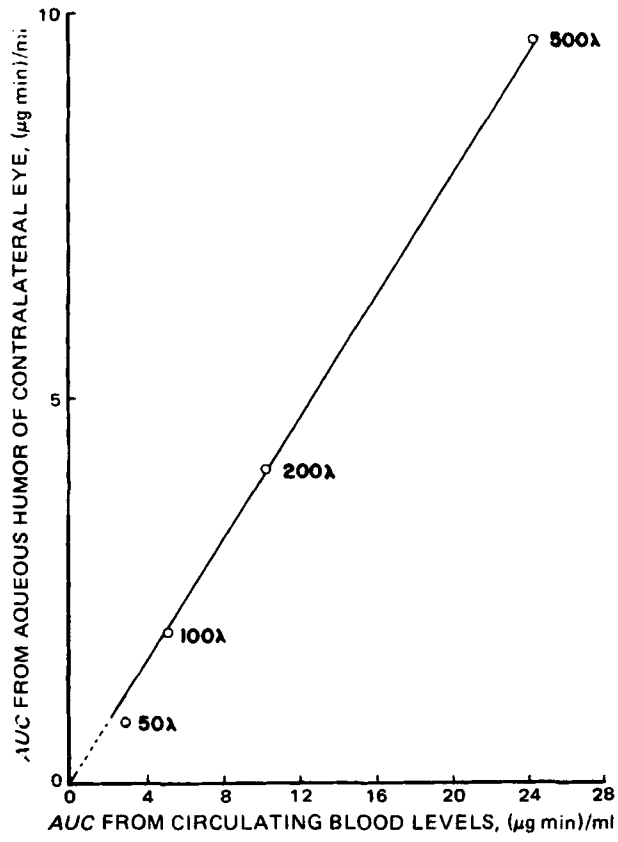

Figure 9—*Comparison of the area under the curve* (AUC) *from aqueous humor drug concentration* versus *time profiles presented in Fig. 4 to the area under the curve* (AUC) *from circulating blood drug concentration* versus *time profiles presented in Fig. 5 at each volume injected subconjunctivally through the conjunctival membrane.*

Additional support for the argument that the majority of drug does not come from penetration of the globe can be seen by comparing the drug level in the cornea with that in the aqueous humor (Fig. 10). The linearity of this plot, particularly at high dose volumes, suggests that almost all of the drug in the aqueous humor is being provided by the cornea. Earlier studies in this laboratory (11, 14, 20, 21, 23, 26) showed that back-diffusion from the aqueous humor to the cornea is not significant, so the high levels in the cornea and the linear relationship with aqueous humor levels suggest that the drug is provided by the cornea and not the globe of the eye.

Thus, for pilocarpine, direct penetration of the globe is not a major factor in getting the drug to the aqueous chamber. For more oil-soluble

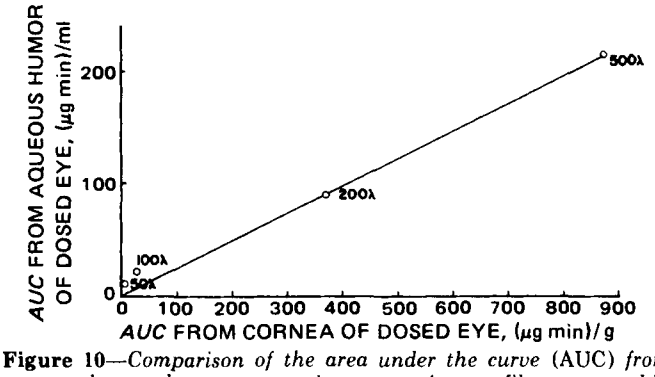

Figure 10—*Comparison of the area under the curve* (AUC) *from aqueous humor drug concentration* versus *time profiles presented in Fig. 1 to the area under the curve* (AUC) *from corneal drug concentration* versus *time profiles presented in Table I at each volume injected subconjunctivally through the conjunctival membrane.*

Table XI—Comparison of Circulating Blood Level Drug Concentration *versus* Time following 50- and 200-μl Subconjunctival Injections of 1×10^{-2} *M* Pilocarpine in pH 6.24 Isotonic Sorensen Buffer [a]

Minutes	50-μl Dose		200-μl Dose	
	Through Membrane, Single Puncture	Through Upper Eyelid	Through Membrane, Single Puncture	Through Upper Eyelid
5	0.035 (0.001)[b] [9][c]	0.051 (0.004)[b] [12][c]	NS[d]	0.158 (0.007)[b] [12][c]
10	0.034 (0.002) [11]	0.073 (0.003) [12]	0.067 (0.009)[b] [9][c]	0.172 (0.004) [10]
20	0.041 (0.002) [12]	0.057 (0.003) [12]	0.108 (0.011) [10]	0.157 (0.007) [10]
30	0.033 (0.001) [11]	0.064 (0.004) [12]	0.172 (0.014) [10]	0.148 (0.006) [12]
45	0.027 (0.002) [12]	0.051 (0.003) [12]	0.132 (0.013) [10]	0.112 (0.005) [8]
60	0.023 (0.001) [10]	0.044 (0.002) [12]	0.101 (0.004) [10]	0.091 (0.003) [10]
90	0.016 (0.001) [10]	0.012 (0.002) [10]	NS[d]	0.053 (0.002) [12]
120	0.014 (0.001) [12]	0.021 (0.001) [9]	0.022 (0.004) [7]	0.061 (0.003) [10]

[a] Values are the micrograms of pilocarpine per milliliter of blood. [b] Numbers in parentheses refer to the standard error of the mean. [c] Numbers in brackets refer to the number of determinations at that point. [d] Not sampled.

drugs, such as some corticosteroids, this route may be important. Additional studies are needed to confirm or reject this possibility.

Mechanism 3: Drug Gains Entrance to Eye by Refluxing out of Injection Site followed by Corneal Absorption—The linearity of the data in Fig. 10 suggests that transcorneal absorption of drug is the primary mechanism for providing pilocarpine to the aqueous humor from a subconjunctival injection. In Fig. 10, the 50- and 100-μl dose volumes fall slightly off the line, suggesting that multiple mechanisms may account for the lower volumes, *i.e.*, Mechanisms 1–3; with larger volumes, a transcorneal mechanism appears predominant. Figures 4 and 5 indicated that multiple mechanisms may have occurred based on the relationship between the *AUC* and dose volume; as the injection volume increases, a back-pressure at the injection site may force leakage out of the puncture hole.

The case for leakage seems evident after comparing aqueous humor drug levels in the dosed eye from through-the-membrane and through-the-eyelid studies. Supportive data come from the lacrimal fluid studies. At the 200-μl injection volume, it is clear from the profiles given in Table VII and in Figs. 3 and 4, as well as from the *AUC* values found in Table XI, that leakage must have occurred in the membrane puncture studies. Injection of drug through the eyelid shows a small quantity of drug in the tear film, presumably from diffusion across the conjunctiva and into the tear film, but the three orders of magnitude difference in tear film concentration shown in Table VII apparently is due to leakage.

It is anticipated that at larger injected volumes, such as 500–1000 μl, the leakage mechanism would remain predominant. On the other hand, smaller volumes are not expected to be as dramatic and, for the 25–100-μl doses, far less drug is expected in the tear film since other mechanisms appear important.

A recent study on the mechanism of the release of fluorescein from subconjunctival injection in the rabbit was reported by Maurice and Ota (6). In this study, small injection volumes (*i.e.*, 1 μl) were employed to avoid a bleb and the drug was administered by membrane puncture and by eyelid puncture. These investigators visually observed the leakage of fluorescein out of the injection site, which is in agreement with the present findings.

Relationship of This Study to Other Drugs and to Humans—The present study was conducted with the water-soluble alkaloid pilocarpine. It is not possible to extrapolate from this single drug entity to other drugs as to their mechanisms of absorption from subconjunctival injection. However, since the principal mechanism for pilocarpine absorption involves leakage, a process independent of drug structure, it is reasonable to assume that a pulse of drug will exit from the injection site and enter the tear film in the early minutes after dosing. Whether this initial dose can establish a high level of drug in the cornea and aqueous humor is dependent primarily on the initial concentration of the drug injected and the injected volume. Presumably, increasing the viscosity of the injected solution or injection of a drug suspension would minimize the reflux process and thus diminish the peak drug level.

It seems unlikely that drugs with a more favorable partition characteristic for absorption will be absorbed so rapidly into the eye, either by direct scleral absorption or absorption across the conjunctiva followed by corneal absorption, so as to overwhelm the contribution from leakage during the early stages following injection. At later times, all drugs probably will show a local sustaining effect since pilocarpine was shown to be present in the bleb a long time after injection. Whether this localized drug can penetrate the globe of the eye over a long time to give a sustaining effect should be a function of its partitioning characteristics. The

Table XII—Comparison of Aqueous Humor Drug Concentration *versus* Time following 50- and 200-μl Subconjunctival Injections of 1×10^{-2} *M* Pilocarpine in pH 6.24 Isotonic Sorensen Buffer [a]

Minutes	50-μl Dose		200-μl Dose	
	Through Membrane, Single-Puncture	Through Upper Eyelid	Through Membrane, Single Puncture	Through Upper Eyelid
5	0.047 (0.019)[b] [13][c]	0.005 (0.0004)[b] [9][c]	0.386 (0.078)[b] [11][c]	0.021 (0.003)[b] [8][c]
10	0.127 (0.075) [11]	0.006 (0.0006) [11]	0.703 (0.133) [12]	0.024 (0.001) [10]
20	0.180 (0.102) [11]	0.009 (0.0004) [12]	1.442 (0.291) [14]	0.032 (0.001) [9]
30	0.195 (0.118) [9]	0.011 (0.0006) [8]	1.817 (0.314) [12]	0.042 (0.002) [10]
45	0.136 (0.068) [8]	0.010 (0.0007) [12]	1.385 (0.213) [13]	0.050 (0.003) [12]
60	0.049 (0.006) [8]	0.011 (0.0007) [11]	0.505 (0.082) [13]	0.038 (0.002) [10]
90	0.032 (0.012) [11]	0.009 (0.0006) [9]	NS[d]	0.040 (0.002) [12]
120	0.026 (0.008) [9]	0.009 (0.0004) [10]	0.199 (0.035) [16]	0.041 (0.001) [7]

[a] Values are the micrograms of pilocarpine per milliliter of aqueous humor. [b] Numbers in parentheses refer to the standard error of the mean. [c] Numbers in brackets refer to the number of determinations at that point. [d] Not sampled.

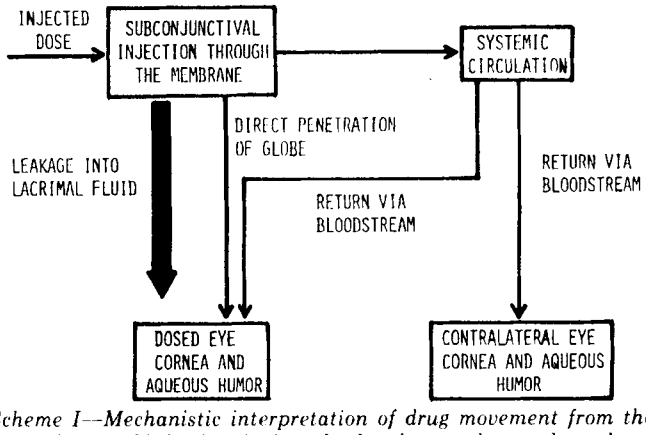

Scheme I—Mechanistic interpretation of drug movement from the subconjunctival injection site into the dosed eye and contralateral eye. At large injection volumes, leakage is the predominant mechanism, illustrated by the thick arrow. At low injection volumes, all mechanisms contribute to the process.

water-soluble drug pilocarpine did not penetrate, but apparently the more oil-soluble hydrocortisone did (5). Additional studies with other drug entities and formulation changes will clarify this picture.

The relationship of the results in rabbits to expected behavior in humans is not as clear. Maurice and Ota (6) injected small volumes of fluorescein subconjunctivally into rabbits and humans. They observed leakage of the dye in the rabbit but not in humans; however, higher levels of fluorescein in the human aqueous humor compared to the rabbit were obtained. Based on these findings, the question of the suitability of the rabbit as a model for subconjunctival injections was raised.

There has been controversy over the behavior of fluorescein in these two species (27), and the differences may be due to the dye itself. Moreover, while the small volume interpretation of these investigators may be accurate, it probably bears little relationship to what occurs at higher volumes. It is probable, based on the work of Maurice and Ota (6), that human and rabbit eyes differ in the importance of one mechanism over another, especially at low volumes. Intuitively, however, since leakage depends on pressure and large volumes are used clinically, it is not unreasonable to assume that humans and rabbits will behave similarly insofar as major mechanisms of drug availability are concerned.

CONCLUSIONS

The study was initiated to provide mechanistic insight into the movement of drug from the site of subconjunctival injection to the aqueous chamber. Several mechanisms apparently are involved in pilocarpine disposition in albino rabbits, depending on the volume of solution injected. At low volumes, it appears that transconjunctival permeation followed by corneal absorption, systemic absorption followed by return *via* the vascular bed, reflux out of the injection site, and, finally, direct penetration of the globe of the eye all contribute to aqueous humor drug levels. However, at larger volumes, leakage from the injection site is the overwhelming mechanism for drug availability (Scheme I).

REFERENCES

(1) K. C. Swan, H. R. Crisman, and P. F. Bailey, *Arch. Ophthalmol.*, **56**, 26 (1956).

(2) R. G. Hardy and C. A. Paterson, *Am. J. Ophthalmol.*, **71**, 1307 (1971).

(3) C. A. Paterson, *Ann. Ophthalmol.*, **5**, 171 (1973).

(4) H. E. Schlegel and K. C. Swan, *Arch. Ophthalmol.*, **52**, 774 (1954).

(5) H. J. McCartney, I. O. Drysdale, A. G. Gornall, and P. K. Basu, *Invest. Ophthalmol.*, **4**, 297 (1965).

(6) D. M. Maurice and Y. Ota, *Jpn. J. Ophthalmol.*, **22**, 95 (1978).

(7) N. A. Wine, A. G. Gornall, and P. K. Basu, *Am. J. Ophthalmol.*, **58**, 362 (1964).

(8) T. F. Patton, Ph.D. thesis, University of Wisconsin, Madison, Wis., 1975.

(9) D. M. Maurice, *Exp. Eye Res.*, **15**, 527 (1973).

(10) R. G. Janes and J. F. Stiles, *Arch. Ophthalmol.*, **62**, 69 (1959).

(11) S. S. Chrai and J. R. Robinson, *Am. J. Ophthalmol.*, **77**, 735 (1974).

(12) M. A. Lemp and J. R. Hamill, *Arch. Ophthalmol.*, **89**, 103 (1973).

(13) F. J. Holly, *Exp. Eye Res.*, **15**, 515 (1973).

(14) J. W. Sieg and J. R. Robinson, *J. Pharm. Sci.*, **65**, 1816 (1976).

(15) J. M. Conrad and J. R. Robinson, *ibid.*, **66**, 219 (1977).

(16) J. M. Conrad, W. A. Reay, R. E. Polcyn, and J. R. Robinson, *J. Parenter. Drug Assoc.*, **32**, 149 (1978).

(17) J. M. Conrad, Ph.D. thesis, University of Wisconsin, Madison, Wis., 1979.

(18) J. G. Wagner, "Pharmacokinetic Notes," J. M. Richards Laboratory, Grosse Pointe Park, Mich., 1969.

(19) J. G. Wagner, "Biopharmaceutics and Relevant Pharmacokinetics," 1st ed., Drug Intelligence Publications, Hamilton, Ill., 1971.

(20) J. W. Sieg and J. R. Robinson, *J. Pharm. Sci.*, **66**, 1222 (1977).

(21) T. F. Patton and J. R. Robinson, *ibid.*, **65**, 1295 (1976).

(22) S. S. Chrai, T. F. Patton, A. Mehta, and J. R. Robinson, *ibid.*, **62**, 1112 (1973).

(23) J. W. Sieg, Ph.D. thesis, University of Wisconsin, Madison, Wis., 1977.

(24) A. Sorsby and J. Ungar, *Br. J. Ophthalmol.*, **31**, 517 (1947).

(25) *Ibid.*, **32**, 864 (1948).

(26) J. W. Sieg and J. R. Robinson, *J. Pharm. Sci.*, **64**, 931 (1975).

(27) K. Shimizu, "Fluorescein Angiography," Igaku Shoin Ltd., Tokyo, Japan, 1974.

ACKNOWLEDGMENTS

Supported in part by Allergan Pharmaceuticals, Irvine, Calif.

Effects of Human Serum Albumin Concentration on Binding of [^{3}H]Amphetamine, [^{3}H]Atropine, [^{3}H]Epinephrine, and [^{14}C]Histamine

JOSEPH JUDIS

Received September 20, 1979, from the *College of Pharmacy, University of Toledo, Toledo, OH 43606.* Accepted for publication February 29, 1980.

Abstract □ The binding of [^{3}H]amphetamine, [^{3}H]atropine, [^{3}H]epinephrine, and [^{14}C]histamine to human serum albumin was examined with a constant ligand concentration and varying albumin concentrations. Two concentrations of each ligand were studied. Scatchard plots of the binding data were linear and had positive slopes; the slopes were greater at the higher ligand concentration. The lowest point was for the highest albumin level and increased in sequence to the lowest albumin concentration. The β (fraction bound) value increased with an increasing amount of albumin in the system. The change in β per change in albumin concentration [$d(\beta)/d$(albumin)] when plotted against albumin concentration yielded curves with negative slopes; the slope was greatest at the lower albumin levels and was much less at the higher albumin levels (equivalent to those encountered in human blood). In agreement with literature data for other systems, the nK value (number of binding sites times the association constant) decreased with increasing albumin concentration. In previous studies of the same ligands and protein, when the albumin concentration was kept constant and the ligand concentration was varied, the Scatchard plots had positive slopes. Positive slopes also were found in this study with constant ligand concentrations and varying albumin levels. These results suggest cooperativity in the binding of these ligands to human serum albumin.

Keyphrases □ Amphetamine—effect of human serum albumin concentration on binding □ Atropine—effect of human serum albumin concentration on binding □ Epinephrine—effect of human serum albumin concentration on binding □ Histamine—effect of human serum albumin concentration on binding □ Binding—effect of human serum albumin concentration on binding of amphetamine, atropine, epinephrine, and histamine

Previous studies on the binding of amphetamine, atropine, epinephrine, and histamine to human serum albumin showed that the Scatchard plots for all four ligands had positive slopes (1). Similar Scatchard plots were observed previously in the binding of codeine, morphine, and methadone to human serum albumin (2). In all of these experiments, the protein concentration was kept constant and the ligand concentration was varied. This approach is typical of most binding studies. In several studies of protein binding in which the ligand concentration was kept constant and the protein concentration was varied, Scatchard plots with positive slopes were reported (3–6).

Bowmer and Lindup (7) commented on the need for data on the effects of protein concentration on binding of ligands for more complete characterization of the protein binding of a ligand. In the usual studies, the protein concentration is kept constant and the ligand concentration is varied. With this concept in mind, the previously described studies of the binding of codeine, morphine, and methadone to human serum albumin were extended to provide data on the effects of varying the human serum albumin concentration. Under these conditions (8), the Scatchard plots had positive slopes, as was reported earlier (1, 2) where the protein concentration was kept constant and the ligand concentration was varied.

The present studies represent an extension of the investigations on the binding of amphetamine, atropine, epinephrine, and histamine to human serum albumin (1). In these additional experiments, the ligand concentration was kept constant and the concentration of human serum albumin was varied.

EXPERIMENTAL

Methods—Protein binding was determined using equilibrium dialysis in multiple-cell blocks, each having a volume of 1 ml on each side of the cellulose membrane, as in previous studies (1, 2). Radioactivity was determined in a liquid scintillation system using techniques described previously (1, 2).

Materials—Tritium-labeled and carbon 14-labeled derivatives of the ligands were obtained from the sources reported previously (1). Crystalline human serum albumin was obtained commercially[1]. The unlabeled forms of the ligands were the highest drug quality available, and all other chemicals were reagent grade.

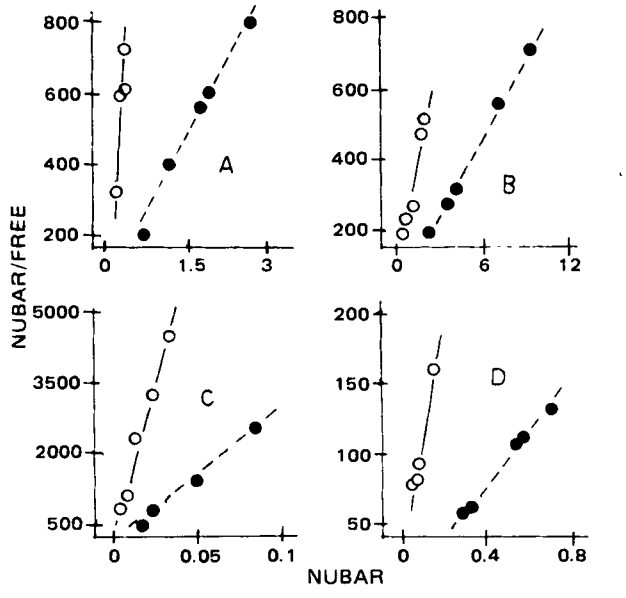

Figure 1—*Scatchard plots of data for binding of [^{3}H]atropine, [^{3}H]amphetamine, [^{3}H]epinephrine, and [^{14}C]histamine to human serum albumin. For each curve, the albumin concentrations are given for each data point starting with the lowest point on the curve. Key: A, [^{3}H]atropine at 4.5×10^{-4} M (○) and 3.43×10^{-3} M (●), with albumin concentrations of 60, 40, 10, and 6 mg/ml for the first ligand concentration and 60, 40, 20, 10, and 6 mg/ml for the second ligand concentration; B, [^{3}H]amphetamine at 3.69×10^{-3} M (○) and 1.48×10^{-2} M (●), with albumin concentrations of 60, 40, 20, 10, and 6 mg/ml for both ligand concentrations; C, [^{3}H]epinephrine at 1.14×10^{-5} M (○) and 4.56×10^{-5} M (●), with albumin concentrations of 60, 40, 20, 10, and 6 mg/ml for the first ligand concentration and 60, 40, 20, and 10 mg/ml for the second ligand concentration; and D, [^{14}C]histamine at 1.15×10^{-3} M (○) and 5.36×10^{-3} M (●), with albumin concentrations of 60, 40, 20, and 10 mg/ml for the first ligand concentration and 60, 40, 20, 10, and 6 mg/ml for the second ligand concentration.*

[1] Nutritional Biochemicals Division, ICN Life Sciences Group.

0022-3549/80/0800-0885$01.00/0
© 1980, American Pharmaceutical Association

Table I—Slopes of Plots of Nubar/Free[a] *versus* Nubar for Binding of [^{3}H]Atropine, [^{3}H]Amphetamine, [^{3}H]Epinephrine, and [^{14}C]Histamine to Human Serum Albumin

Ligand	Total Concentration in System, *M*	Slope	r^b
Atropine	4.5×10^{-4}	1,955.0	0.964
Atropine	3.43×10^{-3}	297.1	0.995
Amphetamine	3.69×10^{-3}	265.4	0.999
Amphetamine	1.48×10^{-2}	69.14	1.000
Epinephrine	1.14×10^{-5}	116,200.0	0.997
Epinephrine	4.56×10^{-5}	28,990.0	1.000
Histamine	1.15×10^{-3}	906.4	0.999
Histamine	5.36×10^{-3}	184.5	1.000

[a] Nubar refers to the molar concentration of ligand bound divided by the molar concentration of human serum albumin in the system. [b] The *r* value refers to the coefficient of correlation of Nubar/free concentration and Nubar.

RESULTS AND DISCUSSION

The human serum albumin concentration was varied from 0.87×10^{-4} to 0.87×10^{-3} *M* (6–60 mg/ml.). Two concentrations of each ligand were used, in the general range of the concentrations used previously (1). The Scatchard plots obtained are shown in Fig. 1. All plots had positive slopes, and the curves were linear (Table I), as can be seen from the coefficients of correlation. In all four cases, a higher slope was obtained with the lower concentration, and higher Nubar (moles of ligand bound per mole of protein in the system) values were seen with the higher concentration.

In the experiments where the protein concentration was kept constant and the ligand concentration was varied, β (fraction bound) values increased with a decrease in ligand concentration (1). In the results obtained in this study, β increased as the albumin concentration increased (Fig. 2). The differences in the plots of β *versus* albumin concentration were not great for the two ligand concentrations. This result is not unexpected when ligand concentrations are not near those required to saturate the protein binding sites. The higher the protein concentration, the more binding sites are available; thus β is expected to increase. For a given ligand, the ratio of the slopes for the two concentrations never exceeded 2.1 (Table II).

Since β varied with albumin concentration for a given ligand, the extent of change of β with a change in albumin concentration was of interest. The rate of change [$d(\beta)/d$(albumin)] was calculated by fitting β values and corresponding albumin concentrations to curves by computer and calculating the first derivative for each albumin concentration for the curve giving the best statistically significant fit (coefficient of correlation of ≥0.95). Plots of these derivatives *versus* albumin concentration are presented in Fig. 3.

The rate of change of β per change in albumin concentration was not constant for all albumin concentrations; it was higher at low albumin concentrations and decreased as the albumin concentration reached that normally found in human blood. Thus, the curves consisted of two major

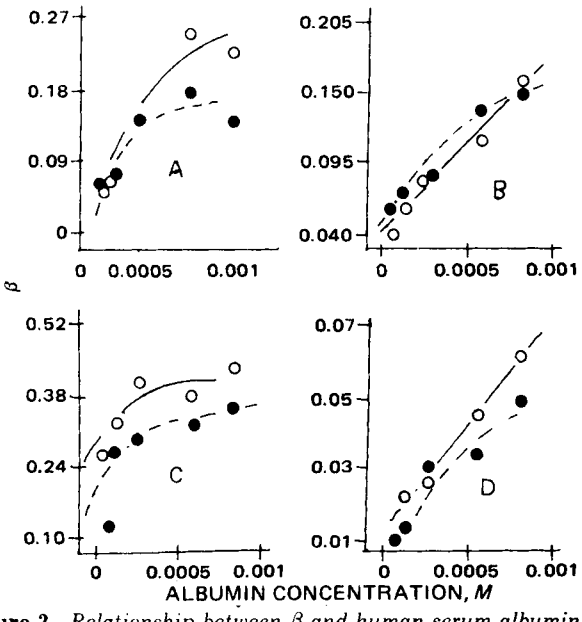

Figure 2—*Relationship between β and human serum albumin concentration for binding of [^{3}H]atropine, [^{3}H]amphetamine, [^{3}H]epinephrine, and [^{14}C]histamine to human serum albumin. Key: A, [^{3}H]atropine at 4.5×10^{-4} M (○) and 3.43×10^{-3} M (●); B, [^{3}H]amphetamine at 3.69×10^{-3} M (○) and 1.48×10^{-2} M (●); C, [^{3}H]epinephrine at 1.14×10^{-5} M (○) and 4.56×10^{-5} M (●); and D, [^{14}C]histamine at 1.15×10^{-3} M (○) and 5.36×10^{-3} M (●).*

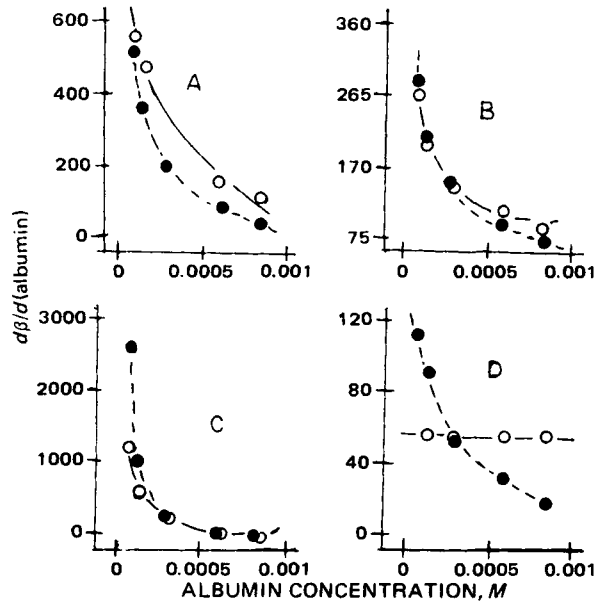

Figure 3—*Change in β per change in human serum albumin concentration* [d(β)/d(*albumin*)] versus *albumin concentration for binding of [^{3}H]atropine, [^{3}H]amphetamine, [^{3}H]epinephrine, and [^{14}C]histamine to human serum albumin. Key: A, [^{3}H]atropine at 4.5×10^{-4} M (○) and 3.43×10^{-3} M (●); B, [^{3}H]amphetamine at 3.69×10^{-3} M (○) and 1.48×10^{-2} M (●); C, [^{3}H]epinephrine at 1.14×10^{-5} M (○) and 4.56×10^{-5} M (●); and D, [^{14}C]histamine at 1.15×10^{-3} M (○) and 5.36×10^{-3} M (●).*

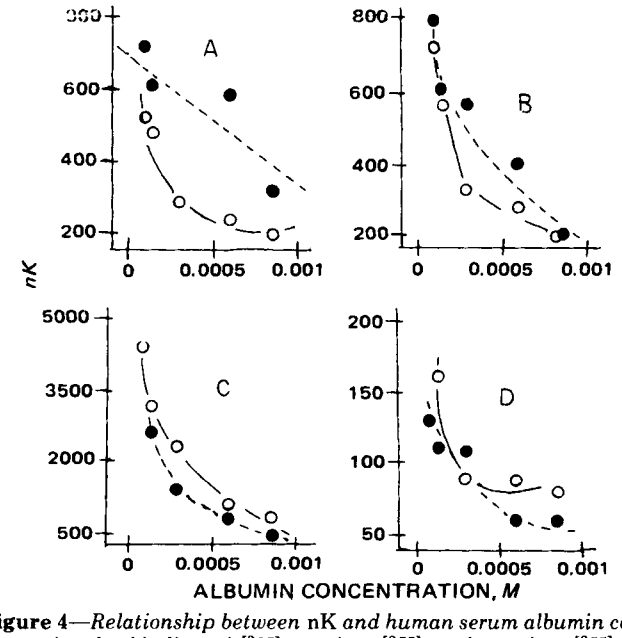

Figure 4—*Relationship between* nK *and human serum albumin concentration for binding of [^{3}H]atropine, [^{3}H]amphetamine, [^{3}H]epinephrine, and [^{14}C]histamine to human serum albumin. Key: A, 3.69×10^{-3} M [^{3}H]amphetamine (○) and 4.5×10^{-4} M [^{3}H]atropine (○); B, 1.48×10^{-2} M [^{3}H]amphetamine (○) and 3.43×10^{-3} M [^{3}H]atropine (●); C, [^{3}H]epinephrine at 1.14×10^{-5} M (○) and 4.56×10^{-5} M (●); and D, [^{14}C]histamine at 1.15×10^{-3} M (○) and 5.36×10^{-3} M (●).*

Table II—Plots of β and nK^a *versus* Human Serum Albumin Concentration (Molar) for Amphetamine, Atropine, Epinephrine, and Histamine

Ligand	Concentration of Ligand, M	β Plot		nK Plot	
		Slope	r^b	Slope	r
Amphetamine	3.69×10^{-3}	142.0	0.995	-3.64×10^5	−0.891
	1.48×10^{-2}	124.7	0.978	-5.58×10^5	−0.870
Atropine	4.5×10^{-4}	241.9	0.906	-3.91×10^5	−0.888
	3.43×10^{-3}	119.0	0.752	-6.44×10^5	−0.964
Epinephrine	1.14×10^{-5}	164.2	0.862	-4.22×10^6	−0.913
	4.56×10^{-5}	98.7	0.922	-2.49×10^6	−0.927
Histamine	1.15×10^{-3}	57.58	0.986	−96,000	−0.748
	5.36×10^{-3}	44.53	0.968	−93,100	−0.946

[a] The n parameter refers to the number of binding sites on the protein molecule, and K is the association constant for the binding system. [b] The r value is the coefficient of correlation for the best fit of the data points to a straight line. The slope given is that calculated for the best-fit straight line.

Table III—Comparison of Slopes of Major Sections of Curves Obtained by Plotting $d(\beta)/d$(Albumin) *versus* Albumin Concentration

Ligand	Concentration of Ligand, M	Slope of Curve Segment[a]		Slope A/Slope B
		A	B	
Amphetamine	3.69×10^{-3}	−1,028,000	−136,100	7.55
	1.48×10^{-2}	−693,000	−114,400	6.06
Atropine	4.5×10^{-4}	−1,780,000	−214,300	8.31
	3.43×10^{-3}	−1,600,000	−249,000	6.43
Epinephrine	1.14×10^{-5}	−4,930,000	−294,000	16.77
	4.56×10^{-5}	−11,960,000	−368,100	32.50
Histamine	1.15×10^{-3}	−253,100	−67,160	3.77
	5.36×10^{-3}	53.54	53.54	1.00[b]

[a] The slope for Segment A was that of the straight line fitted to the three left-hand points of the curve; for Segment B, it was that of the straight line fitted to the three right-hand points. [b] The plot of β *versus* albumin concentration (molar) was a straight line, and $d(\beta)/d$(albumin) was taken as its slope.

segments, one at lower albumin concentrations and the other at higher albumin concentrations. Slopes for the two segments were calculated, and the ratios of the two slopes were computed as a representation of the differences in different albumin concentration ranges (Table III). It appears that β changes the least in the albumin concentration range usually found in human blood. The albumin concentration ranges in which β changes greatly are not encountered clinically.

In several previous studies (7), an increase in protein concentration was accompanied by a decrease in nK[2]. The nK values were calculated using an equation that permits calculation of nK values from β and protein concentrations (9). Plots of nK *versus* albumin concentration are given in Fig. 4. For all four ligands studied, an increase in albumin concentration apparently was accompanied by a decrease in nK. The slopes of these curves are given in Table II; while there were differences in the slopes for the two concentrations of each ligand, these differences were not great (ratios of <2.0), suggesting that the relationship between nK and albumin concentration was essentially independent of ligand concentration for the two ligand concentrations used.

For these four ligands, Scatchard plots with positive slopes were obtained both when the protein concentration was kept constant and the liquid concentration was varied and when the ligand concentration was kept constant and the protein concentration was varied. According to Bowmer and Lindup (7), this result suggests that the positive Scatchard plots may be explained by cooperativity. It also appears that for the compounds examined, the change in β with respect to change in albumin concentration is minor for the albumin concentrations encountered clinically. This finding suggests that β should be similar in normal individuals and those with mild hypoalbuminemia.

[2] The parameter n refers to the number of binding sites or systems on the protein molecule, and the K parameter is the association constant for the protein-ligand system.

REFERENCES

(1) J. Judis, *Can. J. Pharm. Sci.*, **14**, 46 (1979).

(2) J. Judis, *J. Pharm. Sci.*, **66**, 802 (1977).

(3) W. Brunkhorst and E. Hess, *Arch. Biochem. Biophys.*, **111**, 54 (1965).

(4) D. Shen and M. Gibaldi, *J. Pharm. Sci.*, **63**, 1698 (1974).

(5) W. Lindup, *Biochem. Soc. Trans.*, **3**, 635 (1975).

(6) C. Bowmer and W. Lindup, *Biochem. Pharmacol.*, **27**, 937 (1978).

(7) C. Bowmer and W. Lindup, *J. Pharm. Sci.*, **67**, 1193 (1978).

(8) J. Judis, *ibid.*, **69**, 71 (1980).

(9) M. Meyer and D. Guttman, *ibid.*, **57**, 1627 (1968).

ACKNOWLEDGMENTS

The author thanks Mrs. Virginia Matusek for technical assistance.

Structure–Neuromuscular Blocking Activity Relationships of Ketophosphonium Salts

RAYMOND HOUSSIN [x], **JEAN-PIERRE HÉNICHART** *, **MICHEL FOULON** [‡], **and FRANÇOIS BAERT** [‡]

Received October 4, 1979, from the *Institut de Chimie Pharmaceutique, Université de Lille II, rue du Professeur Laguesse, 59045 Lille, France.* Accepted for publication February 26, 1980. *INSERM U16, Place de Verdun, 59045 Lille, France. [‡]Laboratoire de Dynamique des Cristaux Moléculaires, ERA 465, 59650 Villeneuve d'Ascq, France.

Abstract □ Three ketophosphonium salts containing a morpholino group were prepared and evaluated for their neuromuscular blocking effect. Solution and crystal conformations were studied. An attempt was made to explain, in structural terms, different activity levels in connection with the interatomic distances.

Keyphrases □ Ketophosphonium salts—synthesis, relationship between neuromuscular blocking activity and interatomic distances □ Structure–activity relationships—ketophosphonium salts, relationship between neuromuscular blocking activity and interatomic distances □ Neuromuscular blocking activity—ketophosphonium salts, relationship between activity and interatomic distances

The striking relationship between neuromuscular blocking potency and chain length (1–3) or spatial configuration (4–6) in a series of bis-onium salts has been recognized. Replacement of the ammonium moiety by sulfonium, arsonium, or stilbonium has been studied, but the change of one of the two electropositive sites for a phosphonium group has not been well documented (7, 8).

To determine whether it could alter such activity, a triphenylphosphonium salt was introduced on an aliphatic chain with two polar groups. These derivatives exhibit a blocking effect, and the geometric characteristics of the molecules in the crystalline state and in solution were studied to correlate their structure with their biological activity. Their conformations were studied by PMR in solution and by X-ray diffraction in the solid state, enabling evaluation of the distance between the two cations.

EXPERIMENTAL

Methods—Melting points were determined in open glass capillaries and are uncorrected. IR[1] spectra were taken on a double-beam spectrophotometer, utilizing a potassium bromide pellet for solid samples and sodium chloride windows for liquids. PMR[2] spectra were recorded on a 60-MHz instrument. Accurate cell parameters were determined on an automatic diffractometer[3] using Mo K_α radiation. Intensity data also were collected on this instrument.

The structures were solved by direct methods using the Multan program (9). The atoms were normally located by direct and difference Fourier maps, except for some hydrogen atoms. The functional analysis was carried out with the determination of the mean planes and intramolecular distances. Analytical results[4] for the elements were within ±0.4% of theoretical values.

Syntheses—*4-Morpholino-2-butanone (I)*—Concentrated hydrochloric acid (50 ml, 0.5 mole) was added dropwise to a stirred suspension of *s*-trioxane (22.2 g, 0.75 mole) in a cold mixture (5°) of morpholine (43.5 g, 0.5 mole), acetone (200 ml, 2.7 moles), and methanol (30 ml). The mixture was refluxed for 12 hr, cooled, and evaporated to dryness *in vacuo*. A solution of the residue in water (50 ml) was made slightly basic with 10% NaOH and extracted with ether; the combined ethereal solutions were dried over sodium sulfate, evaporated, and distilled under reduced pressure to give 63 g (83% yield) of a colorless liquid, bp 68–74° (0.01 mm).

1-Bromo-4-morpholino-2-butanone Hydrobromide (II)—A solution of bromine (5.1 ml, 0.1 mole) in acetic acid (6 ml) was added dropwise at room temperature to a solution of I (15.7 g, 0.1 mole) in a mixture of hydrobromic acid (20 ml, 0.3 mole) and acetic acid (25 ml). The resulting solution was heated at 40° for 2 hr and then evaporated; crystallization occurred after trituration of the pasty residue with ethanol. Recrystallization from ethanol gave 23.8 g (75% yield) of II, mp 179°.

Anal.—Calc. for $C_8H_{15}Br_2NO_2$: C, 30.31; H, 4.77; N, 4.42. Found: C, 30.39; H, 4.73; N, 4.44.

(2-Oxo-4-morpholino)butyltriphenylphosphonium Bromide Hydrobromide (III)—A mixture of 31.7 g (0.1 mole) of II and 26.2 g (0.1 mole) of triphenylphosphine in 100 ml of anhydrous chloroform was heated to reflux for 12 hr under nitrogen. The solvent was evaporated, and the residue was triturated with an anhydrous ethanol–ether mixture. The resulting solid was recrystallized from ethanol to give 37 g (65% yield) of III, mp 209°.

Anal.—Calc. for $C_{26}H_{30}Br_2NO_2P$: C, 53.91; H, 5.22; N, 2.42. Found: C, 53.61; H, 5.21; N, 2.59.

(2-Oxo-3-chloro)propyltriphenylphosphonium Chloride (IV)—A mixture of 1,3-dichloroacetone (2.5 g, 0.02 mole) and triphenylphosphine (5.2 g, 0.02 mole) in benzene was heated under reflux for 2 hr. The precipitate was collected and crystallized from 95% ethanol to yield 6.9 g (85% yield) of IV·H_2O, mp 173°.

Anal.—Calc. for $C_{21}H_{19}Cl_2OP \cdot H_2O$: C, 61.93; H, 5.20. Found: C, 62.04; H, 5.25.

(2-Oxo-3-morpholino)propyltriphenylphosphonium Chloride Hydrochloride (V)—To a solution of IV (4.1 g, 0.01 mole) and morpholine hydrochloride (1.2 g, 0.01 mole) was added sodium (0.7 g, 0.03 mole) in ethanol. The reaction mixture was refluxed for 3 hr. Sodium chloride was filtered, and ethanolic hydrochloric acid was added to the filtrate. After evaporation of the solvent, the crude product was recrystallized from ethanol to yield 3.5 g (74% yield) of V, mp 165°.

Anal.—Calc. for $C_{25}H_{28}Cl_2NO_2P$: C, 63.03; H, 5.92; N, 2.94. Found: C, 62.92; H, 5.80; N, 2.87.

N-(Chloroacetyl)morpholine (VI) (10)—To a cold solution (−10°) containing 13 g (0.15 mole) of morpholine in a mixture of ethylene dichloride (50 ml) and 20% NaOH (20 ml) was added dropwise 11.3 g (0.1 mole) of chloroacetyl chloride. After stirring at 20° for 1 hr, the reaction mixture was left at 5° overnight. The organic layer was separated, and the aqueous phase was extracted with ethylene dichloride. The organic extracts were washed (10% HCl, 5% $NaHCO_3$, and water), dried (sodium

Table I—Ketophosphonium Salts

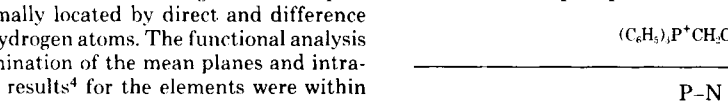

Compound	*n*	X	P–N Distance, Å	Dose, mg/kg ED_{50}[a]	BP[b]	RA[c]	LD_{50}
III[d]	2	Br	6.48	55 ± 1.9	20	55	107 ± 3
V[e]	1	Cl	5.51	84 ± 3.0	50	80	210 ± 5
VII	0	Cl	3.91	25 ± 0.8	40	26	220 ± 3
Gallamine triethiodide				3.5 ± 0.1	4	4	

[a] The ED_{50} values are doses estimated ($p < 0.01$) to decrease the amplitude of the action potential by 50%. [b] The BP values are doses inducing a significant decrease in blood pressure. [c] Doses corresponding to a respiratory arrest. [d] Hydrobromide. [e] Hydrochloride.

[1] Perkin-Elmer 177 spectrometer.
[2] Jeol JNM-MH-60 instrument.
[3] Philips PW 1100.
[4] Perkin-Elmer 240 carbon, hydrogen, and nitrogen analyzer.

0022-3549/80/0800-0888$01.00/0
© 1980, American Pharmaceutical Association

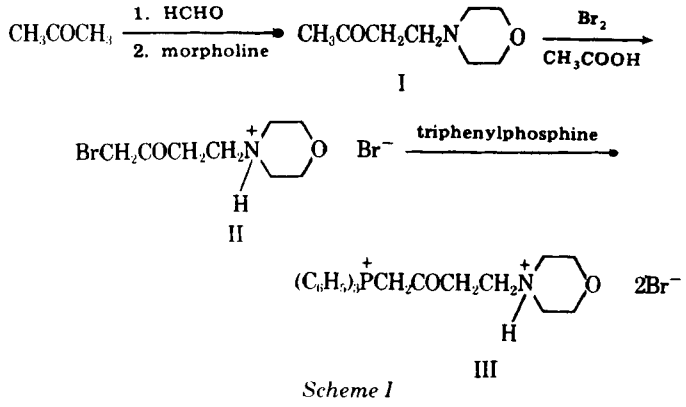

Scheme I

sulfate), and concentrated *in vacuo*. Distillation afforded 12 g (73% yield) of VI, bp 106° (0.01 mm).

(2-Oxo-2-morpholino)ethyltriphenylphosphonium Chloride (VII)—A solution of 16.3 g (0.1 mole) of VI and 26.2 g (0.1 mole) of triphenylphosphine in dry benzene (50 ml) was refluxed for 5 hr under nitrogen. The hot mixture was filtered, and the precipitate was washed with anhydrous ether. Recrystallization from isopropanol yielded 30.6 g (72% yield) of VII, mp 225°; IR (KBr): 1630 (C=O) cm^{-1}; PMR (acetonitrile-d_3): δ 3.47 (m, 4H, CH_2NCH_2), 3.72 (s, 4H, CH_2OCH_2), 5.71 (d, 2H, P^+CH_2, $J_{P,H}$ = 13 Hz), and 7.73 (m, 15H, phenyl).

Anal.—Calc. for $C_{24}H_{25}ClNO_2P$: C, 67.68; H, 5.92; N, 3.29. Found: C, 67.35; H, 6.01; N, 3.34.

(2-Oxo-4-morpholino)butyltriphenylphosphorane (IIIc)—A 10% K_2CO_3 solution (25 ml, 0.017 mole) was added slowly to III (5.8 g, 0.01 mole) dissolved in a minimum of water in a nitrogen atmosphere at 20°. The crude precipitate was filtered after 2 hr and recrystallized from ethyl acetate to afford 3.7 g (88% yield) of IIIc, mp 135°.

Anal.—Calc. for $C_{26}H_{28}NO_2P$: C, 74.81; H, 6.76; N, 3.36. Found: C, 74.70; H, 6.60; N, 3.29.

Pharmacology—*Neuromuscular Blocking Potency*—The gastrocnemius muscle-sciatic nerve preparation was obtained from anesthetized rats (average weight 350 g) by intravenous injection of 0.4 ml of 6% pentobarbital sodium[5]. Contractions were produced by stimulating the nerve within the muscle at a frequency of 1 Hz with rectangular pulses of 1 msec in duration and 30 mv in amplitude and were recorded together with the arterial blood pressure. Animals were placed under artificial respiration.

Tested drugs were compared with gallamine triethiodide[6], with the effects being considered equal when a test concentration produced a 50% inhibition of the action potential (ED_{50}).

LD_{50} Determination—The acute, single-dose toxicity of III, V, and VII in mice following intraperitoneal administration is shown in Table I in terms of the quantitative lethal potency determined by the Miller and Tainter method (11).

RESULTS

Chemistry and Spectral Studies—Schemes I–III illustrate the syntheses of the phosphonium salts. 4-Morpholino-2-butanone (I) was prepared from acetone *via* the Mannich reaction as described previously (12). The corresponding 1-bromo derivative (the hydrobromide salt, II) subsequently was obtained in a good yield from the acetic acid-catalyzed

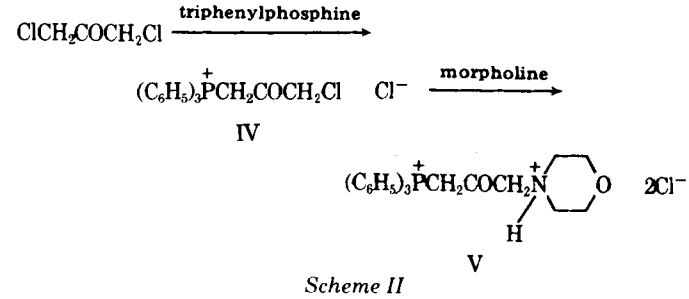

Scheme II

[5] Nembutal, Abbott, Levallois, France.
[6] Flaxedil, Specia, Paris, France.

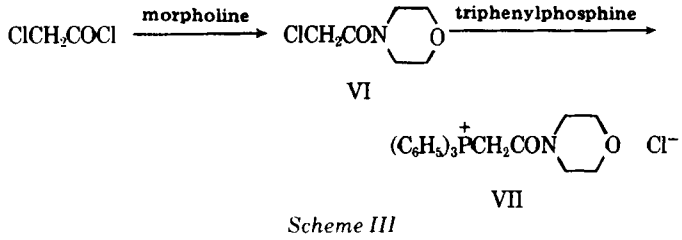

Scheme III

bromination. Direct substitution of II with 1 equivalent of triphenylphosphine in anhydrous chloroform under an inert atmosphere yielded the phosphonium salt (III).

Preparation of (2-oxo-3-morpholino)propyltriphenylphosphonium chloride hydrochloride (V) was achieved by reacting 1,3-dichloroacetone with triphenylphosphine, yielding IV, which then was converted into V with morpholine. Treatment of chloroacetyl chloride with morpholine afforded the amide (VI), and further condensation with triphenylphosphine gave (2-oxo-2-morpholino)ethyltriphenylphosphonium chloride (VII).

The structures of V and VII in the solid state as well as in solution require no special discussion; examination of the X-ray diffraction data and the NMR spectra confirmed the observations revealed by IR spectroscopy, which evidenced their ketonic and amide functions, respectively.

Compound III demands more precise investigation. An X-ray diffraction analysis (Figs. 1 and 2) indicated that the molecule shows an expanded position, probably due to better, stronger packing. Phosphonium and ketone groups are *gauche* with respect to the C_1–C_2 bond, and the C=O does not deviate far from the P–C_1–C_2 plane. The electronic perturbations found here and, in particular, the effect of an α-carbonyl group on the length of the P–C_1 bond confirm previous studies about alkyltriphenylphosphonium salts (13–27). Moreover, the presence of a morpholinyl nitrogen, protonated or not, is apt to bring modifications in the geometry of the PC_1C_2O moiety and to induce a preferential conformation for III in solution. Evidence that III is a mixture of the keto and enol species (Scheme IV) with predominance of the former is given by the presence in the IR spectrum (Table II) of two absorptions at 1720 and 1615 cm^{-1}, the latter being assigned to the C=C stretching of an enolic function. The establishment of the III⇌IIIa equilibrium is confirmed further by the PMR spectral data, which, when obtained in a chloroform medium, included a singlet at a lower field attributable to the hydroxyl hydrogen.

Because the structure of IIIa may give rise to possible *cis–trans* isomers (22), the related phosphorane (IIIc), which presents the same particu-

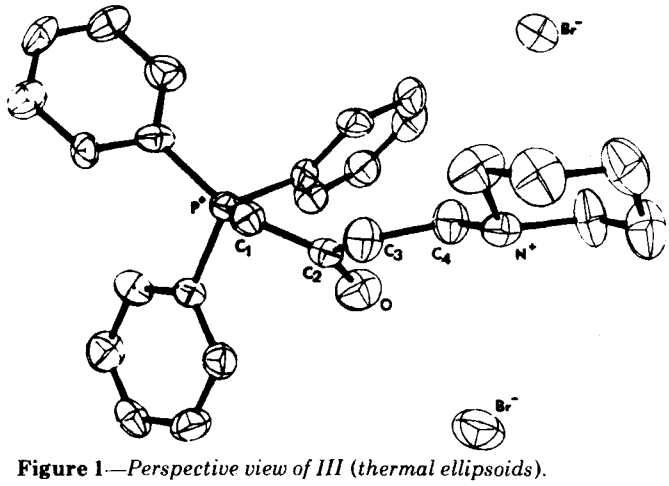

Figure 1—*Perspective view of III (thermal ellipsoids).*

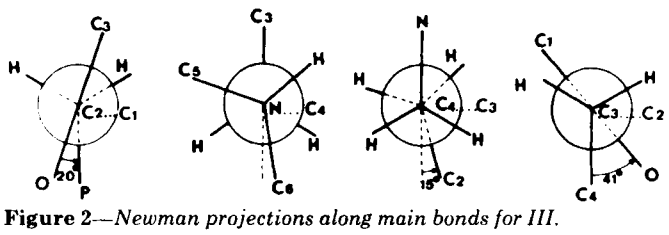

Figure 2—*Newman projections along main bonds for III.*

Table II—PMR and IR Data for III, III*a*, and III*c*

Compound	PMR[a], δ a	b	c	d	e	f	g	Phenyl	IR, cm^{-1}
$(C_6H_5)_3P^+CH_2COCH_2CH_2N$ (O) $2Br^-$	6.10[b] (d, 2)		3.58 (m, 8)		4.03 (m, 4)	10.50 (m, 1)		7.85 (m, 15)	$\nu_{C=O}$ = 1720 (KBr)
$(C_6H_5)_3P^+CH=CCH_2CH_2N$ (O) $2Br^-$	4.25[c] (d, 1)		3.58 (m, 8)		4.03 (m, 4)	10.50 (m, 1)	12.80 (s, 1)	7.85 (m, 15)	$\nu_{C=C}$ = 1615 ($CHCl_3$) ν_{OH} = 3400 ($CHCl_3$)
$(C_6H_5)_3P^+CH-CCH_2CH_2N$ (O)	3.75[d] (d, 1)		2.65[e] (m, 8)		3.70 (m, 4)			7.58 (m, 15)	ν_{C-O} = 1550 (KBr)

[a] PMR spectra were run in deuterochloroform; chemical shifts are expressed in parts per million relative to tetramethylsilane; s = singlet, d = doublet, and m = multiplet. [b] $^2J_{P,H}$ = 12 Hz. [c] $^2J_{P,H}$ = 19.5 Hz. [d] $^2J_{P,H}$ = 26.2 Hz. [e] $^3J_{b,c}$ = 6 Hz.

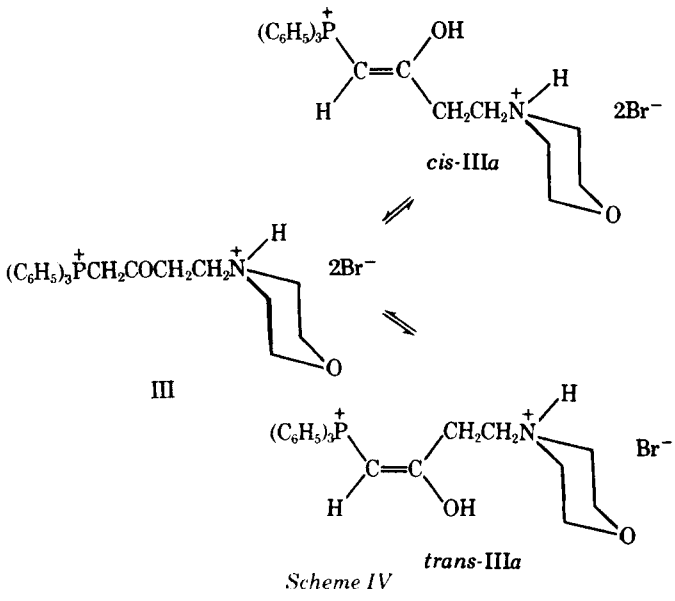

Scheme IV

larity, was studied; its geometry is easier to establish and allows the determination of the respective positions of phosphorus and oxygen in the parent compound (III*a*).

The phosphorane (III*c*) was obtained by addition of a basic reagent in a calculated amount. A first dehydrohalogenation led to the phosphonium bromide (III*b*), whose enolic form is stabilized by hydrogen bonding; its stereochemistry cannot be ascertained from routine experiments. However, further dehydrohalogenation gave the phosphorane (III*c*), and IR data (28–36) revealed the presence of only one rotation isomer (*cis*-III*c*) with the cyclic enolic structure strongly favored by the P^+O^- interaction and by the H···N hydrogen bonding (Scheme V). This latter bonding (37) is confirmed by the dihedral angle ($0 < \alpha < 30°$) determined from $^3J_{b,c}$ = 6 Hz (38–40). Furthermore, the rotation about the C_1–C_2 double bond was observed by NMR at 48° in chloroform, but this phenomenon did not occur up to 150° in dimethyl sulfoxide.

The *cis*-structure of III*c* suggests that its precursor (III*a*) presents the

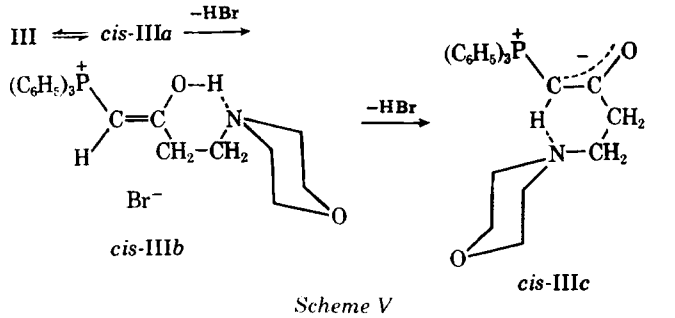

Scheme V

Table III—Crystal Data for III

Formula	$C_{26}H_{30}Br_2NO_2P$
Mol. wt.	579.323
Space group	$P\bar{1}$
a	12.73 (2) Å
b	12.79 (2) Å
c	9.66 (1) Å
α	115°80
β	105°12
γ	66°53
V	1292 $Å^3$
$d_{calc.}$	1.43 g/cm^3
Z	2
Unit cell	Triclinic
R	0.071 (2396 strongest structure factors)
μ	30 cm^{-1}

same configuration in solution and thereby renders the *gauche*-conformation more likely (at the dihedral PC_1C_2O site) for the corresponding ketonic form (III) in solution, as proved by X-ray diffraction (Figs. 1 and 2 and Table III).

Biological Testing—The neuromuscular blocking potencies were tested on the gastrocnemius muscle–sciatic nerve preparation of the anesthetized rat and compared with effects of gallamine triethiodide. The results in Table I are expressed in terms of variations in the amplitude of the action potential. Arterial blood pressure and the frequency of respiration also were recorded. A significant blood pressure decrease was concomitant with the respiratory arrest. Under further artificial respiration, the arterial blood pressure increased to normal values.

DISCUSSION

The levels of neuromuscular blocking activity of the three compounds were not directly related to the P···N distance. The correlation between the curare-like potency and the relative dispositions of the onium groups in bis-onium derivatives has been questioned (41–44). It appears that the activity of some pentamethonium iodides (41) or hexa- and decamethonium bromides (42) may arise from the number of van der Waals contacts between the extreme methyl groups and the receptor sites. In addition, it has been postulated that the ether linkages of the tubocurarines are involved in the interaction with the receptor (43, 45–47).

Similarly, for III, V, and VII, the electronic interaction of the phosphonium cation and the formation of hydrogen bonding between the oxygen atom of the morpholine group and the receptor site can be suggested. Thus, the observed P···O distance for the more potent VII is 6.8 Å, in accordance with the known value found for the cholinergic receptors (48–50).

REFERENCES

(1) W. D. M. Paton and E. J. Zaimis, *Br. J. Pharmacol.*, **6**, 155 (1951).

(2) W. D. M. Paton and E. J. Zaimis, *Pharmacol. Rev.*, **4**, 219 (1952).

(3) F. Bergman, "The Physical Chemistry of Enzymes," Publ. No. 20, Faraday Society, London, England, 1955, p. 126.
(4) E. W. Gill, *Proc. R. Soc., B*, **150**, 381 (1959).
(5) R. Wien, *Arch. Int. Pharmacodyn. Ther.*, **97**, 395 (1954).
(6) F. G. Canepa, *Nature (London)*, **195**, 573 (1962).
(7) H. R. Ing, P. Kordik, and D. P. H. Tudor Williams, *Br. J. Pharmacol.*, **7**, 103 (1952).
(8) K. H. Ginzel, H. Klupp, O. Kraupp, and G. Werner, *Arch. Exp. Pathol. Pharmakol.*, **221**, 336 (1954).
(9) G. Germain, P. Main, and M. M. Woolfson, *Acta Crystallogr.*, **A27**, 368 (1971).
(10) P. C. Hamm and A. J. Speziale, U.S. pat. 2,864,682 (1958); through *Chem. Abstr.*, **54**, 20059h (1960).
(11) L. Miller and M. L. Tainter, *Proc. Soc. Exp. Med.*, **57**, 262 (1944).
(12) N. Grier and S. J. Lederer, French pat. 1,347,339 (1963); through *Chem. Abstr.*, **60**, 10693h (1964).
(13) J. B. Hendrickson, M. L. Maddox, J. J. Sims, and H. D. Kaesz, *Tetrahedron*, **20**, 449 (1964).
(14) D. Seyferth and G. Singh, *J. Am. Chem. Soc.*, **87**, 4156 (1965).
(15) D. J. Martin and C. E. Griffin, *J. Org. Chem.*, **30**, 4034 (1965).
(16) C. E. Griffin and M. Gordon, *J. Am. Chem. Soc.*, **89**, 4427 (1967).
(17) M. J. Gallagher, *Aust. J. Chem.*, **21**, 1197 (1968).
(18) H. J. Bestmann, H. G. Liberda, and J. P. Snyder, *J. Am. Chem. Soc.*, **90**, 2963 (1968).
(19) F. Caesar and W. D. Balzer, *Chem. Ber.*, **102**, 1665 (1969).
(20) H. I. Zeliger, J. P. Snyder, and H. J. Bestmann, *Tetrahedron Lett.*, **1969**, 2199.
(21) G. P. Schiemenz and H. Rast, *ibid.*, **1969**, 2165.
(22) G. A. Gray, *J. Am. Chem. Soc.*, **95**, 7736 (1973).
(23) F. J. Weigert and J. D. Roberts, *Inorg. Chem.*, **12**, 313 (1973).
(24) R. Benassi, M. L. Schenetti, F. Taddei, P. Vivarelli, and P. Dembech, *J. Chem. Soc. Perkin II*, **1974**, 1338.
(25) M. Seno, S. Tsuchiya, H. Kise, and T. Asahara, *Bull. Chem. Soc. Jpn.*, **48**, 2001 (1975).
(26) T. A. Albright, W. J. Freeman, and E. E. Schweizer, *J. Am. Chem. Soc.*, **97**, 940 (1975).
(27) *Ibid.*, **97**, 2942 (1975).
(28) A. J. Speziale and K. W. Ratts, *J. Am. Chem. Soc.*, **85**, 2790 (1963).
(29) *Ibid.*, **87**, 5603 (1965).
(30) F. S. Stephens, *J. Chem. Soc.*, **1965**, 5640. *Ibid.*, **1965**, 5658.
(31) H. J. Bestmann and J. P. Snyder, *J. Am. Chem. Soc.*, **89**, 3936 (1967).
(32) F. J. Randall and A. W. Johnson, *Tetrahedron Lett.*, **1968**, 2841.
(33) A. J. Dale and P. Frøyen, *Acta Chem. Scand. Ser. B*, **24**, 3772 (1970).
(34) I. F. Wilson and J. C. Tebby, *Tetrahedron Lett.*, **1970**, 3769.
(35) H. I. Zeliger, J. P. Snyder, and H. J. Bestmann, *ibid.*, **1970**, 3313.
(36) I. F. Wilson and J. C. Tebby, *J. Chem. Soc. Perkin I*, **1972**, 31.
(37) M. D. Joesten and L. J. Schaad, "Hydrogen Bonding," Dekker, New York, N.Y., 1974, p. 253.
(38) M. Karplus, *J. Chem. Phys.*, **30**, 11 (1959).
(39) M. Karplus, *J. Am. Chem. Soc.*, **85**, 2870 (1963).
(40) R. J. Abraham and K. G. R. Pachler, *Mol. Phys.*, **7**, 165 (1964).
(41) F. G. Canepa, *Acta Crystallogr.*, **16**, 145 (1963).
(42) K. Lonsdale, H. J. Milledge, and L. M. Pant, *ibid.*, **19**, 827 (1965).
(43) I. G. Marshall, J. B. Murray, G. A. Smail, and J. B. Stenlake, *J. Pharm. Pharmacol.*, **19**, 535 (1967).
(44) H. O. J. Collier, *Br. J. Pharmacol.*, **7**, 392 (1952).
(45) J. B. Stenlake, W. D. Williams, N. C. Dhar, and I. G. Marshall, *Eur. J. Med. Chem.*, **9**, 233 (1974).
(46) *Ibid.*, **9**, 239 (1974).
(47) J. B. Stenlake, W. D. Williams, N. C. Dhar, R. D. Waigh, and I. G. Marshall, *Eur. J. Med. Chem.*, **9**, 243 (1974).
(48) P. G. Waser, *Pharmacol. Rev.*, **13**, 365 (1961).
(49) M. Sundaralingham, *Nature (London)*, **217**, 35 (1968).
(50) W. H. Beers and I. Reich, *ibid.*, **228**, 917 (1970).

ACKNOWLEDGMENTS

Supported in part by the Institut National de la Santé et de la Recherche Médicale and in part by the Centre National de la Recherche Scientifique.

The authors thank M. Hurtevent for performing some of the experiments.

General Method for Calculation of Hydrogen-Ion Concentration in Multicomponent Acid–Base Mixtures

D. A. VENTURA and H. Y. ANDO ˣ

Received November 29, 1978, from the *Philadelphia College of Pharmacy and Science, Philadelphia, PA 19104.* Accepted for publication March 6, 1980.

Abstract □ A generalized method for the rapid evaluation of complicated ionic equilibria in terms of the hydrogen-ion concentration was developed. The method was based on the derivation of a single general equation that could be used to evaluate any mixture. A tableau method also was developed which allowed calculation of the numerical solution to the general equation without computer analysis or graphical or intuitive approximations. Examples illustrating the utility of the method are presented. These examples include a mixture of barbital, citric acid, boric acid, monobasic sodium phosphate, and sodium hydroxide. Calculated hydrogen-ion concentrations showed good agreement with experimental values for simple and complex solutions. The major advantages of the method are its simplicity and the obtainment of numerical solutions without initial approximations in the calculations. However, activity corrections are not included in the calculations.

Keyphrases □ Hydrogen-ion concentration—general calculation method for multicomponent acid–base mixtures, calculated results compared with experimental results □ Model, mathematical—calculation of hydrogen-ion concentration in multicomponent acid–base mixtures, comparison with experimental results □ Acid–base mixtures—calculation of hydrogen-ion concentration in multicomponent acid–base mixtures, comparison with experimental results

The calculation of pH values for multicomponent mixtures of weak acids and bases, strong acids and bases, and ampholytes often requires solving a formidable set of simultaneous equations. Although intuitive reasoning may lead to simplifications, it also may lead to erroneous results (1). Although graphical procedures (2) have shown didactic and practical utility, they can become complex and the evaluation may be difficult.

A general method for rapid evaluation of complicated equilibria in terms of the hydrogen-ion concentration is

0022-3549/80/0800-0891$01.00/0
© 1980, American Pharmaceutical Association

(3) F. Bergman, "The Physical Chemistry of Enzymes," Publ. No. 20, Faraday Society, London, England, 1955, p. 126.
(4) E. W. Gill, *Proc. R. Soc., B*, **150**, 381 (1959).
(5) R. Wien, *Arch. Int. Pharmacodyn. Ther.*, **97**, 395 (1954).
(6) F. G. Canepa, *Nature (London)*, **195**, 573 (1962).
(7) H. R. Ing, P. Kordik, and D. P. H. Tudor Williams, *Br. J. Pharmacol.*, **7**, 103 (1952).
(8) K. H. Ginzel, H. Klupp, O. Kraupp, and G. Werner, *Arch. Exp. Pathol. Pharmakol.*, **221**, 336 (1954).
(9) G. Germain, P. Main, and M. M. Woolfson, *Acta Crystallogr.*, **A27**, 368 (1971).
(10) P. C. Hamm and A. J. Speziale, U.S. pat. 2,864,682 (1958); through *Chem. Abstr.*, **54**, 20059h (1960).
(11) L. Miller and M. L. Tainter, *Proc. Soc. Exp. Med.*, **57**, 262 (1944).
(12) N. Grier and S. J. Lederer, French pat. 1,347,339 (1963); through *Chem. Abstr.*, **60**, 10693h (1964).
(13) J. B. Hendrickson, M. L. Maddox, J. J. Sims, and H. D. Kaesz, *Tetrahedron*, **20**, 449 (1964).
(14) D. Seyferth and G. Singh, *J. Am. Chem. Soc.*, **87**, 4156 (1965).
(15) D. J. Martin and C. E. Griffin, *J. Org. Chem.*, **30**, 4034 (1965).
(16) C. E. Griffin and M. Gordon, *J. Am. Chem. Soc.*, **89**, 4427 (1967).
(17) M. J. Gallagher, *Aust. J. Chem.*, **21**, 1197 (1968).
(18) H. J. Bestmann, H. G. Liberda, and J. P. Snyder, *J. Am. Chem. Soc.*, **90**, 2963 (1968).
(19) F. Caesar and W. D. Balzer, *Chem. Ber.*, **102**, 1665 (1969).
(20) H. I. Zeliger, J. P. Snyder, and H. J. Bestmann, *Tetrahedron Lett.*, **1969**, 2199.
(21) G. P. Schiemenz and H. Rast, *ibid.*, **1969**, 2165.
(22) G. A. Gray, *J. Am. Chem. Soc.*, **95**, 7736 (1973).
(23) F. J. Weigert and J. D. Roberts, *Inorg. Chem.*, **12**, 313 (1973).
(24) R. Benassi, M. L. Schenetti, F. Taddei, P. Vivarelli, and P. Dembech, *J. Chem. Soc. Perkin II*, **1974**, 1338.
(25) M. Seno, S. Tsuchiya, H. Kise, and T. Asahara, *Bull. Chem. Soc. Jpn.*, **48**, 2001 (1975).
(26) T. A. Albright, W. J. Freeman, and E. E. Schweizer, *J. Am. Chem. Soc.*, **97**, 940 (1975).
(27) *Ibid.*, **97**, 2942 (1975).
(28) A. J. Speziale and K. W. Ratts, *J. Am. Chem. Soc.*, **85**, 2790 (1963).
(29) *Ibid.*, **87**, 5603 (1965).
(30) F. S. Stephens, *J. Chem. Soc.*, **1965**, 5640. *Ibid.*, **1965**, 5658.
(31) H. J. Bestmann and J. P. Snyder, *J. Am. Chem. Soc.*, **89**, 3936 (1967).
(32) F. J. Randall and A. W. Johnson, *Tetrahedron Lett.*, **1968**, 2841.
(33) A. J. Dale and P. Frøyen, *Acta Chem. Scand. Ser. B*, **24**, 3772 (1970).
(34) I. F. Wilson and J. C. Tebby, *Tetrahedron Lett.*, **1970**, 3769.
(35) H. I. Zeliger, J. P. Snyder, and H. J. Bestmann, *ibid.*, **1970**, 3313.
(36) I. F. Wilson and J. C. Tebby, *J. Chem. Soc. Perkin I*, **1972**, 31.
(37) M. D. Joesten and L. J. Schaad, "Hydrogen Bonding," Dekker, New York, N.Y., 1974, p. 253.
(38) M. Karplus, *J. Chem. Phys.*, **30**, 11 (1959).
(39) M. Karplus, *J. Am. Chem. Soc.*, **85**, 2870 (1963).
(40) R. J. Abraham and K. G. R. Pachler, *Mol. Phys.*, **7**, 165 (1964).
(41) F. G. Canepa, *Acta Crystallogr.*, **16**, 145 (1963).
(42) K. Lonsdale, H. J. Milledge, and L. M. Pant, *ibid.*, **19**, 827 (1965).
(43) I. G. Marshall, J. B. Murray, G. A. Smail, and J. B. Stenlake, *J. Pharm. Pharmacol.*, **19**, 535 (1967).
(44) H. O. J. Collier, *Br. J. Pharmacol.*, **7**, 392 (1952).
(45) J. B. Stenlake, W. D. Williams, N. C. Dhar, and I. G. Marshall, *Eur. J. Med. Chem.*, **9**, 233 (1974).
(46) *Ibid.*, **9**, 239 (1974).
(47) J. B. Stenlake, W. D. Williams, N. C. Dhar, R. D. Waigh, and I. G. Marshall, *Eur. J. Med. Chem.*, **9**, 243 (1974).
(48) P. G. Waser, *Pharmacol. Rev.*, **13**, 365 (1961).
(49) M. Sundaralingham, *Nature (London)*, **217**, 35 (1968).
(50) W. H. Beers and I. Reich, *ibid.*, **228**, 917 (1970).

ACKNOWLEDGMENTS

Supported in part by the Institut National de la Santé et de la Recherche Médicale and in part by the Centre National de la Recherche Scientifique.

The authors thank M. Hurtevent for performing some of the experiments.

General Method for Calculation of Hydrogen-Ion Concentration in Multicomponent Acid–Base Mixtures

D. A. VENTURA and H. Y. ANDO ˣ

Received November 29, 1978, from the *Philadelphia College of Pharmacy and Science, Philadelphia, PA 19104.* Accepted for publication March 6, 1980.

Abstract □ A generalized method for the rapid evaluation of complicated ionic equilibria in terms of the hydrogen-ion concentration was developed. The method was based on the derivation of a single general equation that could be used to evaluate any mixture. A tableau method also was developed which allowed calculation of the numerical solution to the general equation without computer analysis or graphical or intuitive approximations. Examples illustrating the utility of the method are presented. These examples include a mixture of barbital, citric acid, boric acid, monobasic sodium phosphate, and sodium hydroxide. Calculated hydrogen-ion concentrations showed good agreement with experimental values for simple and complex solutions. The major advantages of the method are its simplicity and the obtainment of numerical solutions without initial approximations in the calculations. However, activity corrections are not included in the calculations.

Keyphrases □ Hydrogen-ion concentration—general calculation method for multicomponent acid–base mixtures, calculated results compared with experimental results □ Model, mathematical—calculation of hydrogen-ion concentration in multicomponent acid–base mixtures, comparison with experimental results □ Acid–base mixtures—calculation of hydrogen-ion concentration in multicomponent acid–base mixtures, comparison with experimental results

The calculation of pH values for multicomponent mixtures of weak acids and bases, strong acids and bases, and ampholytes often requires solving a formidable set of simultaneous equations. Although intuitive reasoning may lead to simplifications, it also may lead to erroneous results (1). Although graphical procedures (2) have shown didactic and practical utility, they can become complex and the evaluation may be difficult.

A general method for rapid evaluation of complicated equilibria in terms of the hydrogen-ion concentration is

0022-3549/80/0800-0891$01.00/0
© 1980, American Pharmaceutical Association

described in this paper. A tableau method for the numerical solution also is described. This method eliminates the need for computer analysis.

Activity coefficients were omitted in the following sections to simplify the treatment of the equilibria presented. These corrections may be needed in many pharmaceutical situations.

THEORETICAL

Mixture of Weak Polybasic Acids—Let the mixture contain a concentration TP of a weak polyprotic acid ($H_\alpha P$) with α dissociable hydrogen ions and a concentration TQ of a weak polyprotic acid ($H_\beta Q$) with β dissociable hydrogen ions. The equilibrium expressions for $H_\alpha P$ are:

$$H_\alpha P \overset{KP_1}{\rightleftharpoons} H_{\alpha-1}P^{-1} + H^+$$
Scheme I

$$H_{\alpha-1}P^{-1} \overset{KP_2}{\rightleftharpoons} H_{\alpha-2}P^{-2} + H^+$$
Scheme II

$$\vdots \qquad \vdots$$

$$H_1P^{-(\alpha-1)} \overset{KP_\alpha}{\rightleftharpoons} P^{-\alpha} + H^+$$
Scheme III

and for $H_\beta Q$ are:

$$H_\beta Q \overset{KQ_1}{\rightleftharpoons} H_{\beta-1}Q^{-1} + H^+$$
Scheme IV

$$H_{\beta-1}Q^{-1} \overset{KQ_2}{\rightleftharpoons} H_{\beta-2}Q^{-2} + H^+$$
Scheme V

$$\vdots \qquad \vdots$$

$$H_1Q^{-(\beta-1)} \overset{KQ_\beta}{\rightleftharpoons} Q^{-\beta} + H^+$$
Scheme VI

Let:

$$P_0 = H_\alpha P \qquad \text{(Eq. 1)}$$

$$P_1 = H_{\alpha-1}P^{-1} \qquad \text{(Eq. 2)}$$

$$\vdots \qquad \vdots$$

$$P_\alpha = P^{-\alpha} \qquad \text{(Eq. 3)}$$

and:

$$Q_0 = H_\beta Q \qquad \text{(Eq. 4)}$$

$$Q_1 = H_{\beta-1}Q^{-1} \qquad \text{(Eq. 5)}$$

$$\vdots \qquad \vdots$$

$$Q_\beta = Q^{-\beta} \qquad \text{(Eq. 6)}$$

The individual species for each acid can be expressed as functions of P_0 or Q_0, the respective ionization constants, and the hydrogen-ion concentration. By using Schemes I–VI and Eqs. 1–6, the following equations can be derived:

$$P_0 = P_0 \qquad \text{(Eq. 7)}$$

$$P_1 = KP_1H^{-1}P_0 \qquad \text{(Eq. 8)}$$

$$P_2 = KP_1KP_2H^{-2}P_0 \qquad \text{(Eq. 9)}$$

$$\vdots \qquad \vdots$$

$$P_\alpha = KP_1KP_2 \ldots KP_\alpha H^{-\alpha}P_0 \qquad \text{(Eq. 10)}$$

and:

$$Q_0 = Q_0 \qquad \text{(Eq. 11)}$$

$$Q_1 = KQ_1H^{-1}Q_0 \qquad \text{(Eq. 12)}$$

$$Q_2 = KQ_1KQ_2H^{-2}Q_0 \qquad \text{(Eq. 13)}$$

$$\vdots \qquad \vdots$$

$$Q_\beta = KQ_1KQ_2 \ldots KQ_\beta H^{-\beta}Q_0 \qquad \text{(Eq. 14)}$$

Note that $H^{-1} = 1/H$. Let the charge balance be expressed as:

$$D = \sum_{p=0}^{\alpha} pP_p + \sum_{q=0}^{\beta} qQ_q \qquad \text{(Eq. 15a)}$$

where (1):

$$D = H - OH = H - \frac{K_w}{H} \qquad \text{(Eq. 15b)}$$

Let the mass balance for each acid be expressed as:

$$TP = \sum_{p=0}^{\alpha} P_p \qquad \text{(Eq. 16)}$$

and:

$$TQ = \sum_{q=0}^{\beta} Q_q \qquad \text{(Eq. 17)}$$

Equations 7–10 and Eqs. 11–14, respectively, can be written in general form as:

$$P_p = \prod_{\pi=0}^{p} KP_\pi H^{-p}P_0 \qquad \text{(Eq. 18)}$$

and:

$$Q_q = \prod_{\pi=0}^{q} KQ_\pi H^{-q}Q_0 \qquad \text{(Eq. 19)}$$

where $KP_0 = KQ_0 = 1$.

Substitution of Eq. 18 into Eq. 16 and of Eq. 19 into Eq. 17 yields, respectively:

$$TP = \sum_{p=0}^{\alpha} \prod_{\pi=0}^{p} KP_\pi H^{-p}P_0 \qquad \text{(Eq. 20)}$$

and:

$$TQ = \sum_{q=0}^{\beta} \prod_{\pi=0}^{q} KQ_\pi H^{-q}Q_0 \qquad \text{(Eq. 21)}$$

Rearrangement of Eqs. 20 and 21 yields, respectively:

$$P_0 = \frac{TP}{\sum_{p=0}^{\alpha} \prod_{\pi=0}^{p} KP_\pi H^{-p}} \qquad \text{(Eq. 22)}$$

and:

$$Q_0 = \frac{TQ}{\sum_{q=0}^{\beta} \prod_{\pi=0}^{q} KQ_\pi H^{-q}} \qquad \text{(Eq. 23)}$$

Substitution of Eq. 22 into Eq. 18 and of Eq. 23 into Eq. 19 yields, respectively:

$$P_p = \frac{\prod_{\pi=0}^{p} KP_\pi H^{-p}TP}{\sum_{p=0}^{\alpha} \prod_{\pi=0}^{p} KP_\pi H^{-p}} \qquad \text{(Eq. 24)}$$

and:

$$Q_q = \frac{\prod_{\pi=0}^{q} KQ_\pi H^{-q}TQ}{\sum_{q=0}^{\beta} \prod_{\pi=0}^{q} KP_\pi H^{-q}} \qquad \text{(Eq. 25)}$$

Substitution of Eqs. 24 and 25 into Eq. 15a yields:

$$D = \frac{\sum_{p=0}^{\alpha} p \prod_{\pi=0}^{p} KP_\pi H^{-p}TP}{\sum_{p=0}^{\alpha} \prod_{\pi=0}^{p} KP_\pi H^{-p}} + \frac{\sum_{q=0}^{\beta} q \prod_{\pi=0}^{q} KQ_\pi H^{-q}TQ}{\sum_{q=0}^{\beta} \prod_{\pi=0}^{q} KQ_\pi H^{-q}} \qquad \text{(Eq. 26)}$$

Rearrangement of Eq. 26 followed by multiplication by $H^{(\alpha+\beta)}$ yields:

$$D \sum_{p=0}^{\alpha} \sum_{q=0}^{\beta} \prod_{\pi=0}^{p} KP_\pi \prod_{\pi=0}^{q} KQ_\pi H^{(\alpha+\beta-p-q)} = \sum_{p=0}^{\alpha} \sum_{q=0}^{\beta} \prod_{\pi=0}^{p} KP_\pi \prod_{\pi=0}^{q} KQ_\pi H^{(\alpha+\beta-p-q)}pTP + \sum_{p=0}^{\alpha} \sum_{q=0}^{\beta} \prod_{\pi=0}^{p} KP_\pi \prod_{\pi=0}^{q} KQ_\pi H^{(\alpha+\beta-p-q)}qTQ \qquad \text{(Eq. 27)}$$

Define tensors:

$$H_{pq} = H^{(\alpha+\beta-p-q)} \quad \text{(Eq. 28)}$$

and:

$$K_{pq} = \prod_{\pi=0}^{p} KP_\pi \prod_{\pi=0}^{q} KQ_\pi \quad \text{(Eq. 29)}$$

Substitution of Eqs. 28 and 29 into Eq. 27 yields:

$$D \sum_{p=0}^{\alpha} \sum_{q=0}^{\beta} K_{pq}H_{pq} = \sum_{p=0}^{\alpha} \sum_{q=0}^{\beta} K_{pq}H_{pq}pTP + \sum_{p=0}^{\alpha} \sum_{q=0}^{\beta} K_{pq}H_{pq}qTQ \quad \text{(Eq. 30)}$$

Equation 30 can be simplified by noting that the indexes p and q are repeated in the multiplication of the tensors K_{pq} and H_{pq}. Following the convention proposed by Jeffreys (3), the summation signs will be omitted and the summation will be implied (the indexes are given all possible values of p and q and the terms are added). Equation 30 can be written using this convention as:

$$DK_{pq}H_{pq} = K_{p'q}H_{pq}TP + K_{pq'}H_{pq}TQ \quad \text{(Eq. 31)}$$

where $K_{p'q} = K_{pq}p$ and $K_{pq'} = K_{pq}q$.

The derivation of Eq. 31 can be extended to yield an equation for any number of acids. The resulting equation is:

$$DK_{pq\ldots z}H_{pq\ldots z} = K_{p'q\ldots z}H_{pq\ldots z}TP + K_{pq'\ldots z}H_{pq\ldots z}TQ + K_{pq\ldots z'}H_{pq\ldots z}TZ \quad \text{(Eq. 32)}$$

Mixture of Weak Polyacidic Bases—Let a mixture contain a concentration TR of a weak polyacidic base ($H_\gamma^{+\gamma}R$) with γ ionizations and a concentration TS of a weak polyacidic base ($H_\delta^{+\delta}S$) with δ ionizations. The equilibrium expressions for the bases are:

$$H_\gamma^{+\gamma}R \overset{KR_1}{\rightleftharpoons} H_{\gamma-1}^{+(\gamma-1)}R + H^+$$

Scheme VII

$$H_{\gamma-1}^{+(\gamma-1)}R \overset{KR_2}{\rightleftharpoons} H_{\gamma-2}^{+(\gamma-2)}R + H^+$$

Scheme VIII

$$\vdots \qquad \vdots$$

$$H^+R \overset{KR_\gamma}{\rightleftharpoons} R + H^+$$

Scheme IX

For $H_\delta^{+\delta}S$, they are:

$$H_\delta^{+\delta}S \overset{KS_1}{\rightleftharpoons} H_{\delta-1}^{+(\delta-1)}S + H^+$$

Scheme X

$$H_{\delta-1}^{+(\delta-1)}S \overset{KS_2}{\rightleftharpoons} H_{\delta-2}^{+(\delta-2)}S + H^+$$

Scheme XI

$$\vdots \qquad \vdots$$

$$H^+S \overset{KS_\delta}{\rightleftharpoons} S + H^+$$

Scheme XII

Let:

$$R_0 = H_\gamma^{+\gamma}R \quad \text{(Eq. 33)}$$

$$R_1 = H_{\gamma-1}^{+(\gamma-1)}R \quad \text{(Eq. 34)}$$

$$\vdots \qquad \vdots$$

$$R_\gamma = R \quad \text{(Eq. 35)}$$

and:

$$S_0 = H_\delta^{+\delta}S \quad \text{(Eq. 36)}$$

$$S_1 = H_{\delta-1}^{+(\delta-1)}S \quad \text{(Eq. 37)}$$

$$\vdots \qquad \vdots$$

$$S_\delta = S \quad \text{(Eq. 38)}$$

Let the charge balance be expressed as:

$$D = \sum_{r=0}^{\gamma} (r - NR)R_r + \sum_{s=0}^{\delta} (s - NS)S_s \quad \text{(Eq. 39)}$$

where NR is the number of cationic species possible from the protonation of the neutral base R and NS is the number of cationic species possible from the protonation of the neutral base S.

Let the mass balance equations be expressed as:

$$TR = \sum_{r=0}^{\gamma} R_r \quad \text{(Eq. 40)}$$

and:

$$TS = \sum_{s=0}^{\delta} S_s \quad \text{(Eq. 41)}$$

The individual species for each base can be expressed as a general equation as were the acids in the previous section. The equations for the bases are:

$$R_r = \prod_{\pi=0}^{r} KR_\pi H^{-r}R_0 \quad \text{(Eq. 42)}$$

and:

$$S_s = \prod_{\pi=0}^{s} KS_\pi H^{-s}S_0 \quad \text{(Eq. 43)}$$

A general equation for a system of two polyacidic bases can be derived in a manner analogous to Eq. 31 for the system of two polybasic acids. The equation thus derived is:

$$DK_{rs}H_{rs} = K_{r's}H_{rs}TR + K_{rs'}H_{rs}TS \quad \text{(Eq. 44}a\text{)}$$

where $K_{r's} = K_{rs}(r - NR)$ and $K_{r's} = K_{rs}(s - NS)$.

The derivation of Eq. 44*a* can be extended to a system of any number of bases analogous to the extension of Eq. 31 to Eq. 32. The general equation for any number of polyacidic bases is:

$$DK_{rs\ldots z}H_{rs\ldots z} = K_{r's\ldots z}H_{rs\ldots z}TR + K_{rs'\ldots z}H_{rs\ldots z}TS + \ldots K_{rs\ldots z'}H_{rs\ldots z}TZ \quad \text{(Eq. 44}b\text{)}$$

Mixture of Weak Acids, Weak Bases, Ampholytes, Salts, and Strong Bases—Inspection of Eqs. 31 and 44*a* reveals a mathematical similarity. If an NP term and an NQ term had been defined for the acids, as NR and NS were defined for the bases, then the equations would have been mathematically identical (NP and NQ would have been zero since no cationic species of the acids were formed). Therefore, Eq. 44*a* can be applied to mixtures of acids, mixtures of bases, and mixtures of acids and bases.

Equation 44*a* also is applicable to ampholytes, but caution must be exercised in the determination of the number of cationic species possible.

Salts can be considered as mixtures of acids and bases. Therefore, Eq. 44*a* is applicable to solutions formed from salts. Mathematically, the solution is considered to be formed from a stoichiometric mixture of the acid and base components of the salt.

The addition of a strong acid and/or strong base to any mixture requires modification of the charge balance. Let SB_t denote the total concentration of strong base and SA_t denote the the total concentration of strong acid. If one component of a salt is a strong acid or base, then its concentration must be added to the SA_t or SB_t term, respectively.

Example 1: Ammonium Acetate—This salt is treated as an equimolar mixture of ammonia (TP) and acetic acid (TQ): $TP = TQ$, $NP = 1$, and $NQ = 0$.

Example 2: Sodium Acetate—This salt is treated as an equimolar mixture of acetic acid (TP) and sodium hydroxide (SB_p): $TP = SB_t$, $NP = 0$, and $SB_t = SB_p$.

Example 3: Sodium Carbonate—This salt is treated as a mixture of sodium hydroxide (SB_p) and carbonic acid (TP): $2TP = SB_p$, $NP = 0$, $SB_t = SB_p$.

Example 4: Sodium Carbonate and Sodium Hydroxide—This solution is treated as a mixture of carbonic acid (TP) and sodium hydroxide as in Example 3; however, the additional sodium hydroxide is added to the SB_t term: $2TP = SB_p$, $NP = 0$, and $SB_t = SB_p + SB$.

Therefore, Eq. 44*b* can be extended to mixtures of weak acids, weak bases, ampholytes, salts, strong acids, strong bases, and all of their combinations. The general equation (derived analogously to Eq. 44*b*) is:

$$(SB_t - SA_t + D)K_{pq\ldots z}H_{pq\ldots z} = K_{p'q\ldots z}H_{pq\ldots z}TP + K_{pq'\ldots z}H_{pq\ldots z}TQ + K_{pq\ldots z'}H_{pq\ldots z}TZ \quad \text{(Eq. 44}c\text{)}$$

GENERAL METHOD AND APPLICATION

The substitution of known values into Eq. 44*b* for a particular mixture followed by rearrangement and collection of terms in H results in a

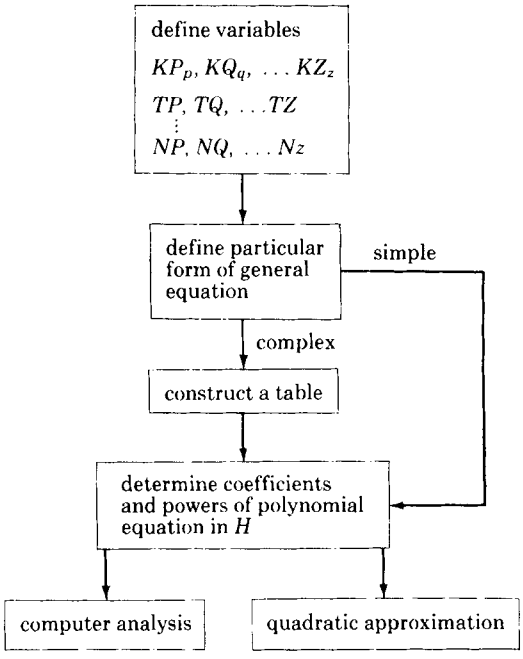

Scheme XIII

polynomial in H. The determination of the coefficients and the order of the polynomial can be facilitated by constructing a table for the systematic enumeration of: (*a*) all possible values of the subscripts of the tensor $K_{pq\ldots z}$, (*b*) the powers of the polynomial in H that correspond to the subscripts, (*c*) the values of the components of $K_{pq\ldots q'}$, and (*d*) the stoichiometric factors for each component.

The table also allows a numerical comparison of the contribution of each term to a particular coefficient. This comparison permits omission of insignificant terms. The advantage of this method increases with the complexity of the mixture.

The final polynomial in H obtained from the table can be solved by numerous numerical computer techniques. However, a quadratic approximation of the polynomial also can be used (1), eliminating the need of a computer.

The general procedure to calculate the hydrogen-ion concentration of a complex system is illustrated in Scheme XIII. A step-by-step approach of the general procedure with specific application to a simple and a complex mixture follows.

Consider the calculation of the hydrogen-ion concentration in a solution of 0.09 M $NaHCO_3$ and 0.01 M Na_2CO_3:

1. The number of actual components is specified. This particular mixture contains two, carbonic acid and sodium hydroxide (refer to previous section).

2. The ionization constants for each component (excluding strong acids and strong bases) are defined. The total number of ionizations for each component also is defined ($\alpha, \beta, \ldots \omega$). The values for this example are: $KP_1 = 4.20E\text{-}07$ for the equilibrium shown in Scheme XIV and $KP_2 = 4.80E\text{-}11$ for the equilibrium shown in Scheme XV, with $\alpha = 2$.

$$H_2CO_3 \overset{KP_1}{\rightleftharpoons} HCO_3^{-1} + H^+$$

Scheme XIV

$$HCO_3^{-1} \overset{KP_2}{\rightleftharpoons} CO_3^{-2} + H^+$$

Scheme XV

3. The number of cationic species formed from each actual component (excluding strong acids and strong bases) is determined. The only component to be considered in this example is carbonic acid, which does not form any cationic species. Therefore, the NP term is equal to zero.

4. The total concentration of each component is determined. The components for this example are carbonic acid and sodium hydroxide. The mass balance for the sodium hydroxide is: $SB_t = 0.09\ M + 2(0.01\ M) = 0.11\ M$ (sodium hydroxide). The mass balance for the carbonic acid is: $TP = 0.09\ M + 0.01\ M = 0.1\ M$ (carbonic acid).

5. By using the general equation (Eq. 44*c*), a particular (general) equation for the mixture is defined. The equation for this example is:

$$(D + SB_t)K_pH_p = PK_{p'}H_p \qquad \text{(Eq. 45)}$$

Table I—Data for Example 1

p	H^n	$p - NP$ ($CP = 1.00E\text{-}01M$)	K_p ($SB_t = 1.10E\text{-}01M$)
0	2	0	1
1	1	1	$4.20E\text{-}07$
2	0	2	$2.00E\text{-}17$

6. The known values (Steps 1–4) are substituted into the equation obtained from Step 5. If the equation is simple, then a direct substitution can be performed after expansion of the equation. Expanding Eq. 45 yields:

$$(D + SB_t)(H^2 + KP_1H + KP_1\,KP_2) = (KP_1H + 2KP_1KP_2)P \qquad \text{(Eq. 46)}$$

Substituting the values from Steps 1–5 and Eq. 15*b* into Eq. 46 yields the final equation for this example:

$$H^4 + (1.1E\text{-}01)H^3 + (4.2E\text{-}09)H^2 - (1.8E\text{-}18)H - 2.01E\text{-}31 = 0 \qquad \text{(Eq. 47)}$$

In more complex situations, rearranging Eq. 45 or whatever general equation results from Step 5 results in a more useful form for substitution of the variables:

$$DK_pH_p + SB_tK_pH_p - PK_{p'}H_p = 0 \qquad \text{(Eq. 48)}$$

A table can be constructed that allows the evaluation of the coefficients of Eq. 48 without expanding the general equation. The table is constructed in the following manner (Table I):

a. A column is constructed that contains each possible combination of $p, q, \ldots z$. The total number of rows (combinations) equals $(\alpha + 1)(\beta + 1)\ldots(\omega + 1)$. In Table I, the three values possible for p in this example are shown in the first column.

b. With the values obtained in the first column, a second column is calculated. This column contains the relative powers of H in the final polynomial. The power is calculated for each row in the second column by using the value of the subscripts $p, q, \ldots z$ in the corresponding row of the first column and solving:

$$(\alpha + \beta + \ldots \omega) - (p + q + \ldots z) = \text{power of } H \qquad \text{(Eq. 49)}$$

c. A column for each component (excluding strong acids and strong bases) is constructed. In Table I, only one column for component CP (carbonic acid) is required for this example. In general, the rows of the component columns are determined from the corresponding entries in the first column and by calculating $p - NP, q - NQ, \ldots, z - NZ$. Since NP is zero, the component column is equivalent to the first column for this example.

d. The last column is constructed by calculating $K_{pq\ldots z}$ from the corresponding values of the subscripts $p, q, \ldots z$ in the first column. The nature of the $K_{pq\ldots z}$ tensor allows each succeeding row after the first to be calculated from a previous row (not necessarily the last row) by multiplication with the next ionization constant corresponding to the new subscript. This column is labeled $K_{pq\ldots z}$ and subtitled with the appropriate concentration of $SB_t - SA_t$. The resultant column for this example is shown in Table I.

7. The next step is to calculate the coefficients and powers of the final polynomial equation. Starting with the highest power of H, the entry is determined under each component for the row corresponding to that power. The value obtained is multiplied by the component concentration (s). This value is subtracted from the $SB_t - SA_t$ concentration. The difference obtained then is multiplied by the corresponding value in the $K_{pq\ldots z}$ column and by the corresponding value of H^n. (In more complex systems, more than one row will be found for a given order. If the values for rows of a given power are equal in magnitude, they are added. If the values are not equal, then the minor contributing row may be ignored.) This procedure is repeated for each decreasing power of H. The values for each power then are added. The values for this example are: power 2 = $(1.10E\text{-}01)(1)H^2$, power 1 = $(1.10E\text{-}01 - 1.00E\text{-}01)(4.20E\text{-}07)H^1$, and power 0 = $(1.10E\text{-}01 - 2.00E\text{-}01)(2.01E\text{-}17)H^0$, so that:

$$\Sigma = (1.10E\text{-}01)H^2 + (4.20E\text{-}09)H^1 - (1.81E\text{-}18)H^0 \qquad \text{(Eq. 50)}$$

The summation obtained in general will equal the total equation (Eq. 48 for this example) minus the term $DK_{pq\ldots z}H_{pq\ldots z}$ (DK_pH_p for this example). This term can be expanded after substituting Eq. 15*b* to yield:

Table II—Data for Example 2

	p	q	r	s	H^n	$p - NP$ TP 2.16E-02	$q - NQ$ TQ 2.16E-02	$r - NR$ TR 2.16E-02	$s - NS$ TS 2.16E-02	K_{pqrs} SB_t 7.07E-02
*[a]	0	0	0	0	8	0	0	0	0	1
	0	0	1	0	7	0	0	0	1	5.80E-10
	0	0	1	0	7	0	0	1	0	3.70E-08
	0	0	1	1	6	0	0	1	1	2.15E-17
*	0	1	0	0	7	0	1	0	0	7.50E-03
	0	1	0	1	6	0	1	0	1	4.35E-12
	0	1	1	0	6	0	1	1	1	2.78E-10
	0	1	1	1	5	0	1	1	1	1.61E-19
	0	2	0	0	6	0	2	0	0	4.65E-10
	0	2	0	1	5	0	2	0	1	2.69E-19
	0	2	1	0	5	0	2	1	0	1.72E-17
	0	2	1	1	4	0	2	1	1	9.98E-27
	0	3	0	0	5	0	3	0	0	2.23E-22
	0	3	0	1	4	0	3	0	1	1.29E-31
	0	3	1	0	4	0	3	1	0	8.25E-30
	0	3	1	1	3	0	3	1	1	4.79E-39
*	1	0	0	0	7	1	0	0	0	8.40E-04
	1	0	0	1	6	1	0	0	1	4.82E-13
	1	0	1	0	6	1	0	1	0	3.11E-11
	1	0	1	1	5	1	0	1	1	1.80E-20
*	1	1	0	0	6	1	1	0	0	6.30E-06
	1	1	0	1	5	1	1	0	1	3.65E-15
	1	1	1	0	5	1	1	1	0	2.33E-13
	1	1	1	1	4	1	1	1	1	1.35E-22
	1	2	0	0	5	1	2	0	0	3.91E-13
	1	2	0	1	4	1	2	0	1	2.27E-22
	1	2	1	0	4	1	2	1	0	1.45E-20
	1	2	1	1	3	1	2	1	1	8.41E-30
	1	3	0	0	4	1	3	0	0	1.89E-25
	1	3	0	1	3	1	3	0	1	1.10E-34
	1	3	1	0	3	1	3	1	0	6.99E-33
	1	3	1	1	2	1	3	1	1	4.05E-42
*	2	0	0	0	6	2	0	0	0	1.50E-08
	2	0	0	1	5	2	0	0	1	8.70E-18
	2	0	1	0	5	2	0	1	0	5.55E-16
	2	0	1	1	4	2	0	1	1	3.22E-25
*	2	1	0	0	5	2	1	0	0	1.13E-10
	2	1	0	1	4	2	1	0	1	6.57E-20
*	2	1	1	0	4	2	1	1	0	4.19E-18
	2	1	1	1	3	2	1	1	1	2.43E-27
*	2	2	0	0	4	2	2	0	0	7.04E-18
	2	2	0	1	3	2	2	0	1	4.09E-27
*	2	2	1	0	3	2	2	1	0	2.61E-25
	2	2	1	1	2	2	2	1	1	1.51E-34
	2	3	0	0	3	2	3	0	0	3.40E-30
	2	3	0	1	2	2	3	0	1	1.98E-39
	2	3	1	0	2	2	3	1	0	1.26E-37
	2	3	1	1	2	2	3	1	1	7.29E-47
	3	0	0	0	5	3	0	0	0	6.00E-14
	3	0	0	1	4	3	0	0	1	3.48E-23
	3	0	1	0	4	3	0	1	0	2.22E-21
	3	0	1	1	3	3	0	1	1	1.29E-29
*	3	1	0	0	4	3	1	0	0	4.52E-16
	3	1	0	1	3	3	1	0	1	2.63E-25
*	3	1	1	0	3	3	1	1	0	1.68E-23
	3	1	1	1	2	3	1	1	1	9.72E-33
*	3	2	0	0	3	3	2	0	0	2.82E-23
*	3	2	0	1	2	3	2	0	1	1.64E-32
*	3	2	1	0	2	3	2	1	0	2.04E-30
*	3	2	1	1	1	3	2	1	1	6.04E-40
	3	3	0	0	2	3	3	0	0	1.36E-35
	3	3	0	1	1	3	3	0	1	7.92E-45
	3	3	1	0	1	3	3	1	0	5.04E-43
*	3	3	1	1	0	3	3	1	1	2.92E-52

[a] The asterisk indicates the row contributing significantly to the total Eq. 55.

$$\left(\frac{H^2 - K_w}{H}\right) K_{pq\ldots z} H_{pq\ldots z} \qquad \text{(Eq. 51)}$$

The $K_{pq\ldots z}H_{pq\ldots z}$ value is computed using the table by recalling the rows used in the determination of the coefficients of the polynomial. Since all three rows were used in this example:

$$K_p H_p = H^2 + (4.20E\text{-}07)H^1 + (2.01E\text{-}17)H^0 \qquad \text{(Eq. 52)}$$

The final equation can be obtained by substituting the values obtained from the summation, the $K_{pq\ldots z}H_{pq\ldots z}$ value, and Eq. 15*b* into the general equation. The result for this example is obtained by substituting Eqs. 50, 52, and 15*b* into Eq. 48 to yield:

$$H^4 + (1.10E\text{-}01)H^3 + (4.20E\text{-}09)H^2 - (1.81E\text{-}18)H^1 - (2.01E\text{-}31)H^0 = 0 \qquad \text{(Eq. 53)}$$

8. The last step is the numerical solution of the final equation. For this example, Eq. 53 can be solved by numerical techniques. However, the quadratic equation obtained from the last three terms of Eq. 53 approximates the total equation. This approximation yields a pH of 9.37, the same as that given by Eq. 53 to this accuracy. Experimentally, a pH of 9.30 was obtained.

The second example is the calculation of the hydrogen-ion concentration of a solution of 0.0216 *M* citric acid (*P*), 0.0216 *M* monobasic sodium phosphate (*Q*), 0.0216 *M* barbital (*R*), 0.0216 *M* boric acid (*S*), and

0.0491 M NaOH, which can be solved as follows:

1. There are five components of this mixture: citric acid, phosphoric acid, barbital, boric acid, and sodium hydroxide.

2. The ionization constants, α, β, γ, and δ, for this example are defined as: $KP_1 = 8.40E\text{-}04$, $KQ_1 = 7.50E\text{-}03$, $KS_1 = 5.80E\text{-}10$, $KP_2 = 1.80E\text{-}05$, $KQ_2 = 6.20E\text{-}08$, $KR_1 = 3.70E\text{-}08$, $KP_3 = 4.00E\text{-}06$, $KQ_3 = 4.80E\text{-}13$, $\alpha = 3$, $\beta = 3$, $\gamma = 1$, and $\delta = 1$.

3. There are no cationic species formed from any of the components. Therefore, $NP = NQ = NR = NS = 0$.

4. The component concentrations are: $TP = TQ = TR = TS = 0.0216$ M and $SB_t = 0.0491$ M (sodium hydroxide) + 0.0216 M (SB_q) = 0.0707 M.

5. The general equation for this particular mixture is then defined from Eq. 44c. Equation 44c for a mixture of four components (TP, TQ, TR, and TS) and SB_t results in:

$$(D + SB_t)K_{pqrs}H_{pqrs} = K_{p'qrs}H_{pqrs}TP + K_{pq'rs}H_{pqrs}TQ + K_{pqr's}H_{pqrs}TR + K_{pqrs'}H_{pqrs}TS \quad \text{(Eq. 54)}$$

6. The tableau method for the calculation of coefficients and powers in the final polynomial is advantageous for this example because of its complexity. Rearranging Eq. 54 and substituting Eq. 15b yield:

$$\left(\frac{H^2 - K_w}{H}\right)K_{pqrs}H_{pqrs} = (SB_tK_{pqrs} - TPK_{p'qrs} - TQK_{pq'rs} - TRK_{pqr's} - TSK_{pqrs'})H_{pqrs} \quad \text{(Eq. 55)}$$

Table II was constructed using the procedure outlined in the previous example. However, in this example, not every row was used in calculating the coefficients. Only 16 rows contributed significantly to the total equation. The values in the K_{pqrs} column for a given power should be compared and the relative values noted. These contributing rows are marked with an asterisk in Table II.

7. The coefficients for each power are determined from Step 6 and summed for all powers of H. This sum equals the right side of Eq. 55. The value of $K_{pqrs}H_{pqrs}$ is calculated by recalling all of the contributing rows used in the determination of the previous summation. The values in the $K_{pqrs}H_{pqrs}$ column corresponding to these rows are added. Substituting the value obtained for the right side of Eq. 55 and the value obtained for $K_{pqrs}H_{pqrs}$ into Eq. 55 and expanding yield the final equation for this system:

$$H^{10} + (7.9E\text{-}02)H^9 + (4.2E\text{-}04)H^8 + (1.7E\text{-}07)H^7 + (6.7E\text{-}13)H^6 - (7.3E\text{-}18)H^5 - (1.72E\text{-}24)H^4 - (6.2E\text{-}32)H^3 - (4.9E\text{-}41)H^2 - (3.6E\text{-}53)H^1 - (2.9E\text{-}66)H^0 = 0 \quad \text{(Eq. 56)}$$

8. This step is performed as in the previous example. The quadratic approximation based on H^7 yields a pH of 5.37, whereas solving the entire Eq. 55 gives a pH of 5.30. The latter pH was the one obtained experimentally.

EXPERIMENTAL

The pH measurements were performed using a digital pH meter[1]. The instrument and test solutions were at 23°. Buffer solutions bracketing the approximate pH of the test solution were used to calibrate the instrument.

RESULTS AND DISCUSSION

The results for two- and five-component mixtures of acids, bases, and ampholytes showed reasonable agreement between experimental and calculated pH values. The general method presented has the advantage that approximations can be made in the final equation rather than in the derivation. This approach allows the approximation to be based on numerical comparison rather than on intuition. Additionally, the method can be used without any approximation if a computer is available (the general nature of the final equation is well suited for computer analysis). In summary, the general equation presented is simple and versatile; it can be used to calculate the hydrogen-ion concentration of simple and complex solutions. However, at high ionic strengths, the lack of activity corrections is expected to limit the accuracy of the method.

REFERENCES

(1) J. E. Ricci, "Hydrogen Ion Concentration," Princeton University Press, Princeton, N.J., 1952, pp. i–v, 121–136.

(2) L. G. Sillen, in "Treatise on Analytical Chemistry," part I, vol. 2, Interscience, New York, N.Y., 1959.

(3) H. Jeffreys, "Cartesian Tensors," Cambridge University Press, London, England, 1963, pp. 2–4.

ACKNOWLEDGMENTS

Presented at the Basic Pharmaceutics Section, APhA Academy of Pharmaceutical Sciences, Montreal meeting, May 1978.

The authors thank Mrs. Margaret Rendler for assistance in manuscript preparation.

D. A. Ventura was the recipient of a Josiah K. Lilly Memorial Fellowship from the American Foundation for Pharmaceutical Education (1977–1979).

[1] Ionalyzer model 807, Orion Research.

Determination of Free Methyldopa in Plasma by High-Pressure Liquid Chromatography and Electrochemical Detection

GREGORY M. KOCHAK and WILLIAM D. MASON ˣ

Received September 21, 1979, from the *Pharmacokinetics Laboratory, Schools of Pharmacy and Medicine, University of Missouri–Kansas City, Kansas City, MO 64108.* Accepted for publication March 7, 1980.

Abstract □ A quantitative method for the analysis of free methyldopa in plasma is described. The method is based on reversed-phase high-pressure liquid chromatography with electrochemical detection utilizing an ion-pairing agent. Separation of methyldopa from plasma is achieved by alumina adsorption. The parameters associated with the adsorption step are described. The lower limit of sensitivity is ~10 ng of methyldopa/ml with a corresponding retention time of 6.9 min.

Keyphrases □ Methyldopa—high-pressure liquid chromatographic analysis using electrochemical detection, separation from plasma by alumina adsorption □ High-pressure liquid chromatography—analysis, methyldopa, plasma □ Adsorption—separation of methyldopa from plasma by alumina adsorption, high-pressure liquid chromatographic analysis

Previous measurements of small quantities of methyldopa (I) and other catechols in biological fluids have been based on separation by alumina adsorption and detection by oxidation to the fluorescent hydroxyindole derivatives. Since most catechol compounds adsorb onto alumina and form the fluorescent derivative, the approach is not specific for any one compound without additional chromatographic procedures. Kwan *et al.* (1) employed no additional chromatography and reported a mean reading for predose plasma equivalent to 280 ± 30 ng of methyldopa/ml. Subtraction of a blank value of this magnitude and variance results in considerable assay variance and severely limits sensitivity.

This paper describes a quantitative method for the determination of methyldopa in plasma that utilizes high-pressure liquid chromatography (HPLC) with electrochemical detection. Electrochemical detection previously was used successfully for detection of catecholamines (2–4). Methyldopa was separated from its metabolites and other endogenous catecholamines with reversed-phase ion-pair HPLC. 3,4-Dihydroxybenzylamine (II) was used as the internal standard.

EXPERIMENTAL

Reagents and Standards—All reagents were reagent grade or better. Water was triple glass distilled. Organic solvents were HPLC grade. The mobile phase was passed through a 0.2-μm filter[1] before introduction into the system. Pure methyldopa[2], 3,4-dihydroxybenzylamine[3], type WN-3 chromatographic alumina[3] (activity grade I), and heptanesulfonic acid[4] (sodium salt) were used. All standard solutions were made in triple glass-distilled water containing 0.005 *M* sodium metabisulfite and acidified to pH 2.6 with phosphoric acid.

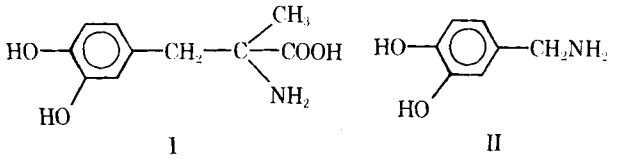

I II

Instrumental Parameters—A chromatographic reciprocating pump[5], a sample injection valve[6], a 5-μm octadecylsilane column[7], a glassy carbon electrochemical detector[8], and a dual-pen recorder[9] comprised the HPLC system.

The mobile phase consisted of 0.07 *M* phosphate buffer adjusted to pH 2.6 with sodium hydroxide, 8% acetonitrile, 0.1 m*M* disodium ethylenediaminetetraacetate, and 5 m*M* heptanesulfonic acid. The anode potential was set at +0.80 v *versus* a silver–silver chloride reference electrode, and amplification was achieved with a polarographic analyzer[10]. With a mobile flow rate of 1.5 ml/min, the retention times for methyldopa (I) and 3,4-dihydroxybenzylamine (II) were 6.9 and 5.2 min, respectively.

Separation from Plasma—One milliliter of plasma was spiked with II. Then 0.1 ml of 0.05 *M* sodium metabisulfite and 0.1 ml of 5% (w/v) disodium ethylenediaminetetraacetate were added to the plasma. The plasma was adjusted to pH 7.0 by the addition of 2 ml of 0.065 *M* tris(hydroxymethyl)aminomethane buffer and then was adjusted further to pH 8.0–8.6 with 1 *M* NaOH after the batchwise addition of 135 ± 1.3 mg of acid-washed alumina (5). The sample was shaken for 15 min, and the supernate was aspirated. The alumina was washed twice with 2 ml of triple-distilled water. The methyldopa was eluted from the alumina by shaking for 15 min with 1 ml of 0.05 *M* phosphoric acid. The acid supernate was transferred immediately to a second tube from which 100 μl subsequently was injected onto the column.

DISCUSSION

Chromatography—Various parameters such as the pH and composition of the mobile phase were evaluated systematically. The ionic strength of the mobile phase greatly affected the electrode response. The effects of various ionic strengths on the bioanalytical electrodes previously were established for phosphate buffer (6) and corresponded to the present results (Fig. 1). Maximal response occurred at 0.07 *M* phosphate buffer. The effect of varying the percent composition of the organic phase in the aqueous mobile phase was described theoretically by Horvath *et al.* (7). Acetonitrile was used as the organic solvent, and the results of varying organic composition *versus* log K' (retardation factor) proved to be linear, verifying the work of Horvath *et al.* (Fig. 2).

The results of the effect of pH on K' are presented in Figs. 3 and 4. Methyldopa has a reported pKa value of 2.2 (8) for the carboxylic acid function at 25°, and K' is related directly to the ionization of the carboxylic acid functional group. The amino group with a pKa of 9.0 at 25° is ionized and is presumed to be paired with heptanesulfonic acid. Increasing the percentage of ionization of the carboxyl group decreased retention up to ~pH 3.20, where elution of methyldopa was at the solvent front. The mobile phase pH must be maintained constant since small pH fluctuations may change the chromatography significantly.

The efficiency of liquid chromatographic columns has been shown to be the greatest for compounds with K' values between 2 and 6 (9). The composition of the mobile phase was adjusted accordingly and resulted in K' values of 2.7 and 3.9 for 3,4-dihydroxybenzylamine and methyldopa, respectively.

[1] Millipore.
[2] Merck Sharp & Dohme Research Laboratories, Rahway, N.J.
[3] Sigma Chemical Co., St. Louis, Mo.
[4] Eastman Chemicals, Rochester, N.Y.
[5] Model 6000A, Waters Associates, Milford, Mass.
[6] Model 7010, Rheodyne Inc., Berkeley, Calif.
[7] Spherisorb, Altex, Berkeley, Calif.
[8] Bioanalytical Systems, West Lafayette, Ind.
[9] Fisher Scientific, St. Louis, Mo.
[10] Model 174A, Princeton Applied Research, Princeton, N.J.

0022-3549/80/0800-0897$01.00/0
© 1980, American Pharmaceutical Association

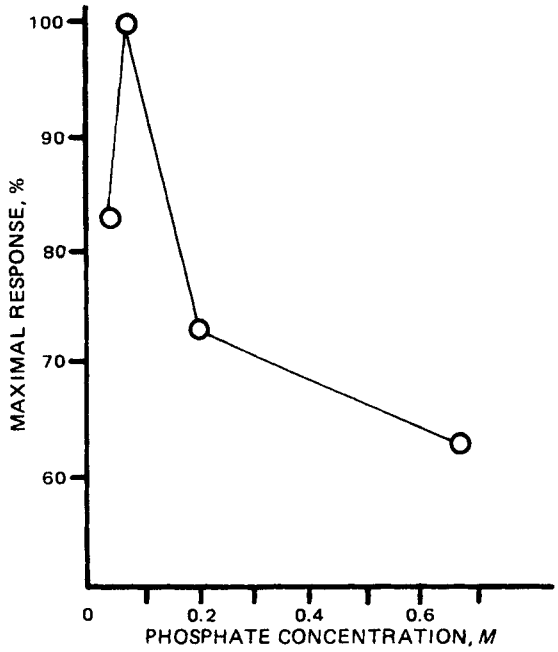

Figure 1—*Effect of ionic strength on the detector response of methyldopa. At a phosphate concentration above 0.07* M, *the current decreased in accordance with the Nernst equation for the diffusion coefficient, in which diffusion is inversely related to the ionic strength. The diminished detector response at low ionic strength is attributed to increased resistance in the electrochemical cell.*

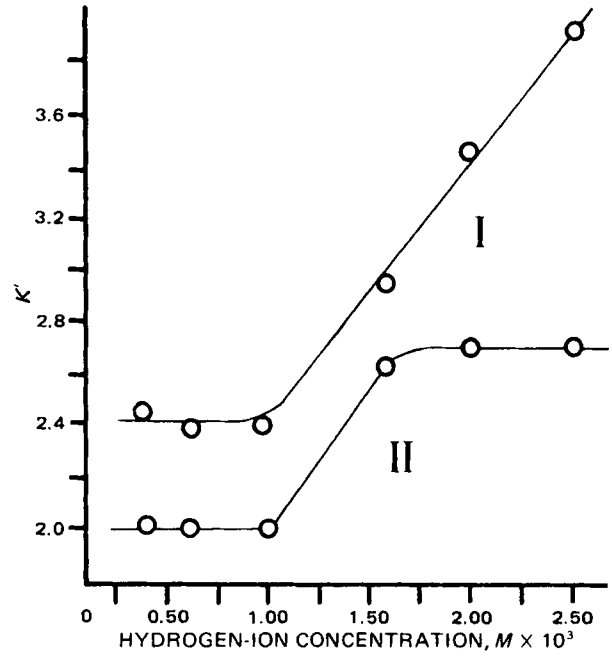

Figure 3—*Effect of hydrogen-ion concentration on the retardation factor. The mobile phase consisted of 0.1* mM *disodium ethylenediaminetetraacetate, 5* mM *heptanesulfonic acid, 0.07* M *phosphate, and 8% acetonitrile; the pH was adjusted by titration with sodium hydroxide before the organic modifier was added. The flow rate was 1.5 ml/min.*

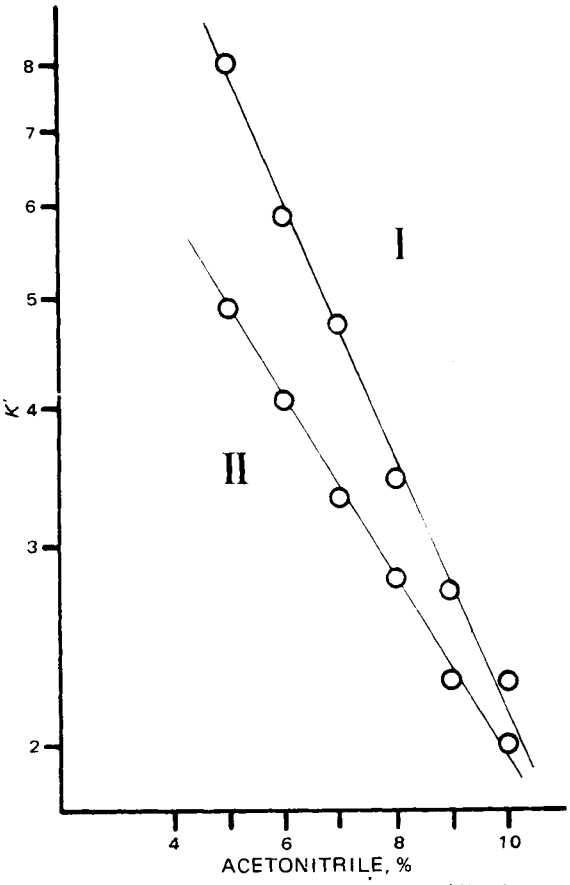

Figure 2—*Retardation factor values at varying mobile phase composition. The mobile phase consisted of 0.1* mM *disodium ethylenediaminetetraacetate, 5* mM *heptanesulfonic acid, and 0.07* M *phosphate buffer at pH 3.0 and a flow rate of 1.5 ml/min. The regression for 3,4-dihydroxybenzylamine was log y = (−0.076 ± 0.004)x + (1.066 ± 0.028), r = 0.995. The regression for methyldopa was log y = (−0.111 ± 0.044)x + (1.41 ± 0.031), r = 0.997.*

Extraction—A modified alumina adsorption method (5) was used to extract 3,4-dihydroxybenzylamine and methyldopa. The adsorption of catecholamines and methyldopa is not linear over a wide range. Both 36 and 135 mg of alumina were tried with various eluents. With 36 mg of alumina, the linear region extended to 150 ng of methyldopa/ml and saturation occurred at 600 ng/ml; 135 mg of alumina/ml produced linearity up to 400 ng/ml with saturation occurring at 750 ng/ml. Using larger

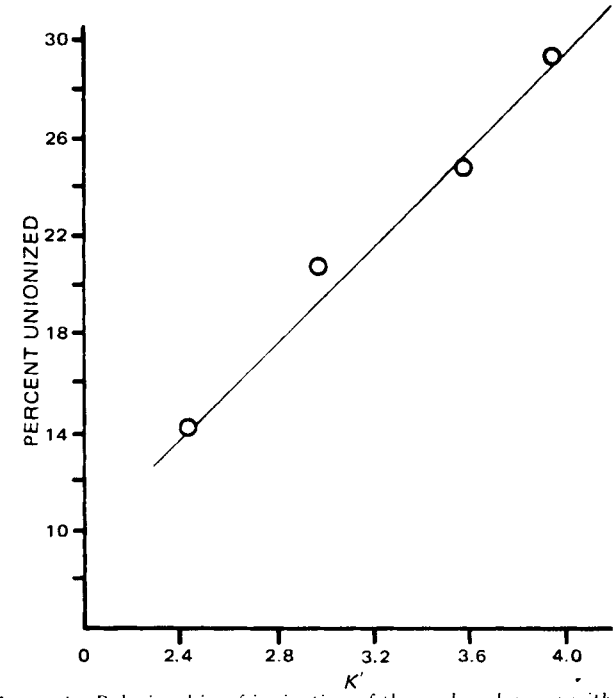

Figure 4—*Relationship of ionization of the carboxyl group with the retardation factor. The percent unionized acid function of methyldopa was calculated using literature pKa values and was not adjusted for the 8% acetonitrile in the mobile phase. The regression was* y = (9.958 ± 0.627)x + (9.490 ± 2.040), r = 0.996.

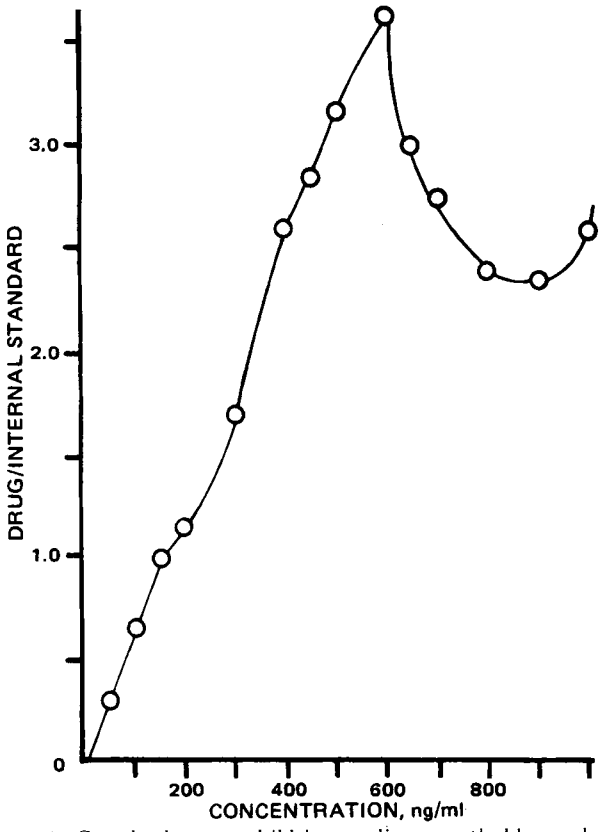

Figure 5—*Standard curve exhibiting nonlinear methyldopa adsorption. Alumina (36 mg) was used to extract methyldopa. Each value is the mean of four determinations.*

amounts of alumina was cumbersome; therefore, 1-ml plasma fractions were utilized when necessary to keep the analysis in the linear range.

The nonlinear nature of alumina adsorption was not mentioned by Kwan *et al.* (1) when measuring up to 7.5 μg of methyldopa/ml. This nonlinearity would account for substantial variation if linearity were assumed. The shape of the standard curves is typical of adsorption of drugs onto solid porous adsorbents (10) (Figs. 5 and 6).

The recovery of known quantities of methyldopa and 3,4-dihydroxybenzylamine from plasma by alumina adsorption varied for differing amounts of alumina as well as for the two drugs. The efficiency of recovery for methyldopa and 3,4-dihydroxybenzylamine was 71 and 72% with coefficients of variation of 3.8 and 3.6%, respectively, when 36 mg of alumina was used in the extraction step. The recovery efficiency changed to 84 and 56% with coefficients of variation of 2.8 and 1.8% for methyldopa and 3,4-dihydroxybenzylamine, respectively, when 135 mg of alumina was used. There were six determinations in both cases.

The linearity of the assay was demonstrated by standard curves over the 0–100- and 0–400-ng/ml ranges in which 36 and 135 mg of alumina adsorbent were used, respectively. The standard curve regressions were: $y = (0.00663 \pm 0.00011)x + (0.00520 \pm 0.00690)$, with $r = 0.999$ for 36 mg of alumina, and $y = (0.00345 \pm 0.00011)x + (0.02800 \pm 0.03100)$, with $r = 0.997$ for 135 mg of alumina, where y is the methyldopa peak height divided by the 3,4-dihydroxybenzylamine peak height and x is the concentration of methyldopa (nanograms per milliliter).

Reproducibility was demonstrated by a day-to-day coefficient of variation based on the change of the standard curve slope of 5.7% ($n = 6$) for 135 mg of alumina. The within-run coefficients of variation (drug/internal standard) were 5.4 and 1.0% ($n = 6$) for 36 and 135 mg of alumina, respectively. The lower limit of this assay with the described instrumentation and procedure (signal to noise ratio of five with no interfering peaks) is ~10 ng/ml of plasma.

Figure 7 is an example of a typical chromatogram. This assay has been applied to over 400 plasma samples and has been reliable. After ~50 assays, the electrode must be removed and the glassy carbon surface must be cleaned by mechanical polishing. Extractions are clean, and the peak resolution is very good. In the development of this assay, consideration also was given for quantitating methylnorepinephrine (III), norepinephrine (IV), and methyldopamine (V). All appeared as resolved peaks with retention times of 4.7, 4.0, and 10.6 min, respectively (Fig. 8).

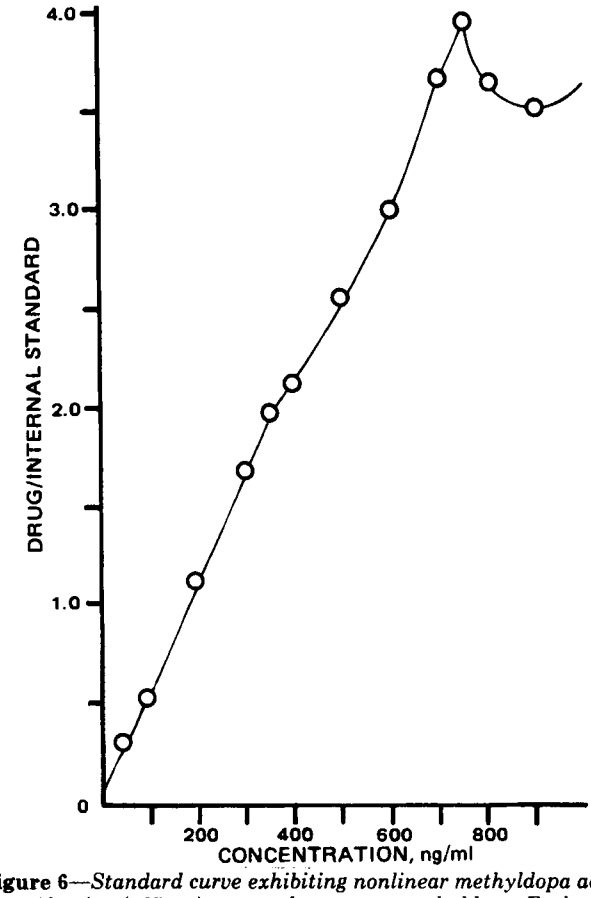

Figure 6—*Standard curve exhibiting nonlinear methyldopa adsorption. Alumina (135 mg) was used to extract methyldopa. Each value is the mean of four determinations. Note that the adsorption isotherms of both 36 and 135 mg of alumina are similar in shape, with the additional alumina shifting the curve in this figure.*

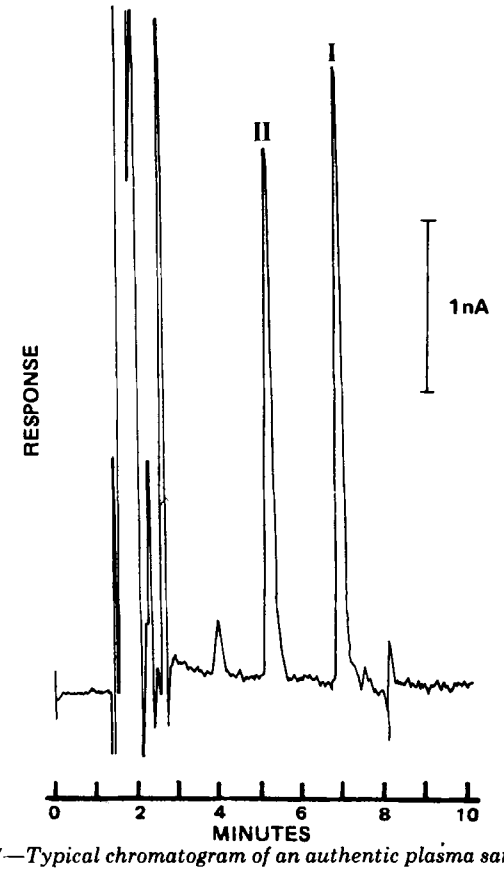

Figure 7—*Typical chromatogram of an authentic plasma sample.*

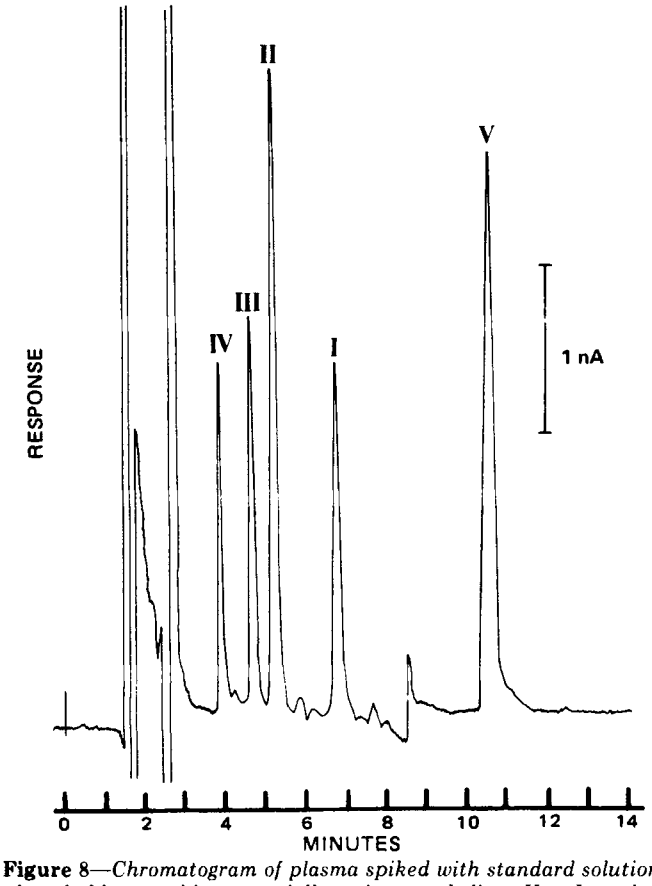

Figure 8—*Chromatogram of plasma spiked with standard solutions of methyldopa and its potentially active metabolites. Key: I, methyldopa; II, 3,4-dihydroxybenzylamine; III, methylnorepinephrine; IV, norepinephrine; and V, methyldopamine.*

Dopamine eluted with methyldopa with a retention time of 6.9 min. However, dopamine does not compromise the assay of methyldopa since normal plasma dopamine concentrations are below the sensitivity of this assay. Blank plasma samples showed no detectable interference. Changing the mobile phase to 9% acetonitrile and pH 2.40 and the ion-pair to 5 m*M* pentanesulfonic acid (sodium salt), with all other parameters remaining constant, allows complete resolution of methyldopa from dopamine. Authentic plasma samples of subjects receiving methyldopa also showed no detectable dopamine in the presence of methyldopa when resolved.

REFERENCES

(1) K. C. Kwan, E. L. Foltz, G. O. Breault, J. E. Baer, and J. A. Totaro, *J. Pharmacol. Exp. Ther.*, **198**, 264 (1976).

(2) R. M. Riggin, R. L. Alcorn, and P. T. Kissinger, *Clin. Chem.*, **22**, 782 (1976).

(3) C. Refshange, P. T. Kissinger, R. Dreiling, L. Blank, R. Freeman, and R. Adams, *Life Sci.*, **14**, 311 (1974).

(4) R. Keller, A. Oke, I. Mefford, and R. Adams, *ibid.*, **19**, 995 (1976).

(5) A. H. Anton and D. F. Sayre, *J. Pharmacol. Exp. Ther.*, **138**, 360 (1962).

(6) T. P. Moyer and N. Jianz, *J. Chromatogr.*, **153**, 365 (1978).

(7) C. Horvath, W. Melander, and I. Molmar, *ibid.*, **125**, 129 (1976).

(8) B. C. Lippold and I. Jaeger, *Arch. Pharm.*, **306**, 106 (Feb. 1973).

(9) E. Johnson and R. Stevenson, "Basic Liquid Chromatography," Varian Associates, Palo Alto, Calif., 1978, pp. 37, 38.

(10) A. Martin, J. Swarbrick, and A. Cammarata, "Physical Pharmacy," 2nd ed., Lea & Febiger, Philadelphia, Pa., 1969, pp. 432–438.

ACKNOWLEDGMENTS

Abstracted in part from a dissertation submitted by G. M. Kochak to the University of Missouri-Kansas City in partial fulfillment of the Doctor of Philosophy degree requirements.

Interactions of Aspirin with Acetaminophen and Caffeine in Rat Stomach: Pharmacokinetics of Absorption and Accumulation in Gastric Mucosa

AD J. M. SEEGERS *x, MARTIN OLLING *, LOWIE P. JAGER ‡, and JACOBUS VAN NOORDWIJK *

Received December 3, 1979, from the **National Institute of Public Health, P.O. Box 1, 3720 BA Bilthoven, The Netherlands*, and the ‡*Department of Pharmacology, Faculty of Pharmacy, State University of Utrecht, Utrecht, The Netherlands.* Accepted for publication February 27, 1980.

Abstract □ To study the pharmacokinetic interactions between aspirin (250 mg/kg) and simultaneously administered oral acetaminophen (125 mg/kg) or caffeine (50 mg/kg) in male adult rats, noninterfering GLC assays for these drugs were developed. Acetaminophen and caffeine both retarded the appearance of salicylate in plasma. During the elimination phase, acetaminophen enhanced plasma salicylate levels whereas caffeine did not. Aspirin reduced the plasma levels of both acetaminophen and caffeine during absorption and elimination. Regardless of whether the drugs had been administered separately or in combination, higher concentrations of salicylate, acetaminophen, and caffeine were found in the glandular part of the stomach compared to the nonglandular part (rumen). In both parts, the absorption of acetaminophen increased in the presence of aspirin. Simultaneous administration of aspirin with caffeine did not influence the absorption of either drug in the glandular and ruminal parts. The inhibitory action of acetaminophen and the potentiating action of caffeine on the erosive activity of aspirin are not due to any effects of these drugs on salicylate accumulation in glandular tissue.

Keyphrases □ Aspirin—administered alone and with acetaminophen or caffeine, absorption, distribution in gastric tissue, blood plasma levels, rats □ Acetaminophen—administered alone and with aspirin, absorption, distribution in gastric tissue, blood plasma levels, rats □ Caffeine—administered alone and with aspirin, absorption, distribution in gastric tissue, blood plasma levels, rats □ Pharmacokinetics—aspirin administered alone and with acetaminophen or caffeine, absorption, distribution in gastric tissue, blood plasma levels, rats

Irritation of the GI mucosa, production of erosions, and GI bleeding are serious side effects of aspirin and other nonsteroidal anti-inflammatory drugs (1, 2). Acidic anti-inflammatory drugs are thought to cause these side effects

0022-3549/80/0800-0900$01.00/0
© 1980, American Pharmaceutical Association

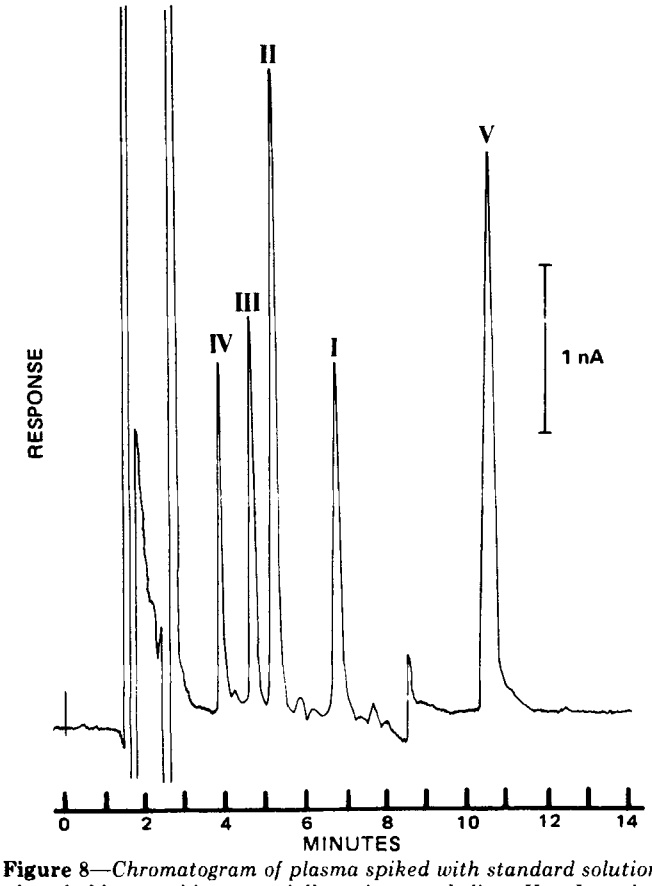

Figure 8—*Chromatogram of plasma spiked with standard solutions of methyldopa and its potentially active metabolites. Key: I, methyldopa; II, 3,4-dihydroxybenzylamine; III, methylnorepinephrine; IV, norepinephrine; and V, methyldopamine.*

Dopamine eluted with methyldopa with a retention time of 6.9 min. However, dopamine does not compromise the assay of methyldopa since normal plasma dopamine concentrations are below the sensitivity of this assay. Blank plasma samples showed no detectable interference. Changing the mobile phase to 9% acetonitrile and pH 2.40 and the ion-pair to 5 m*M* pentanesulfonic acid (sodium salt), with all other parameters remaining constant, allows complete resolution of methyldopa from dopamine. Authentic plasma samples of subjects receiving methyldopa also showed no detectable dopamine in the presence of methyldopa when resolved.

REFERENCES

(1) K. C. Kwan, E. L. Foltz, G. O. Breault, J. E. Baer, and J. A. Totaro, *J. Pharmacol. Exp. Ther.*, **198**, 264 (1976).

(2) R. M. Riggin, R. L. Alcorn, and P. T. Kissinger, *Clin. Chem.*, **22**, 782 (1976).

(3) C. Refshange, P. T. Kissinger, R. Dreiling, L. Blank, R. Freeman, and R. Adams, *Life Sci.*, **14**, 311 (1974).

(4) R. Keller, A. Oke, I. Mefford, and R. Adams, *ibid.*, **19**, 995 (1976).

(5) A. H. Anton and D. F. Sayre, *J. Pharmacol. Exp. Ther.*, **138**, 360 (1962).

(6) T. P. Moyer and N. Jianz, *J. Chromatogr.*, **153**, 365 (1978).

(7) C. Horvath, W. Melander, and I. Molmar, *ibid.*, **125**, 129 (1976).

(8) B. C. Lippold and I. Jaeger, *Arch. Pharm.*, **306**, 106 (Feb. 1973).

(9) E. Johnson and R. Stevenson, "Basic Liquid Chromatography," Varian Associates, Palo Alto, Calif., 1978, pp. 37, 38.

(10) A. Martin, J. Swarbrick, and A. Cammarata, "Physical Pharmacy," 2nd ed., Lea & Febiger, Philadelphia, Pa., 1969, pp. 432–438.

ACKNOWLEDGMENTS

Abstracted in part from a dissertation submitted by G. M. Kochak to the University of Missouri-Kansas City in partial fulfillment of the Doctor of Philosophy degree requirements.

Interactions of Aspirin with Acetaminophen and Caffeine in Rat Stomach: Pharmacokinetics of Absorption and Accumulation in Gastric Mucosa

AD J. M. SEEGERS *x, MARTIN OLLING *, LOWIE P. JAGER ‡, and JACOBUS VAN NOORDWIJK *

Received December 3, 1979, from the **National Institute of Public Health, P.O. Box 1, 3720 BA Bilthoven, The Netherlands*, and the ‡*Department of Pharmacology, Faculty of Pharmacy, State University of Utrecht, Utrecht, The Netherlands.* Accepted for publication February 27, 1980.

Abstract □ To study the pharmacokinetic interactions between aspirin (250 mg/kg) and simultaneously administered oral acetaminophen (125 mg/kg) or caffeine (50 mg/kg) in male adult rats, noninterfering GLC assays for these drugs were developed. Acetaminophen and caffeine both retarded the appearance of salicylate in plasma. During the elimination phase, acetaminophen enhanced plasma salicylate levels whereas caffeine did not. Aspirin reduced the plasma levels of both acetaminophen and caffeine during absorption and elimination. Regardless of whether the drugs had been administered separately or in combination, higher concentrations of salicylate, acetaminophen, and caffeine were found in the glandular part of the stomach compared to the nonglandular part (rumen). In both parts, the absorption of acetaminophen increased in the presence of aspirin. Simultaneous administration of aspirin with caffeine did not influence the absorption of either drug in the glandular and ruminal parts. The inhibitory action of acetaminophen and the potentiating action of caffeine on the erosive activity of aspirin are not due to any effects of these drugs on salicylate accumulation in glandular tissue.

Keyphrases □ Aspirin—administered alone and with acetaminophen or caffeine, absorption, distribution in gastric tissue, blood plasma levels, rats □ Acetaminophen—administered alone and with aspirin, absorption, distribution in gastric tissue, blood plasma levels, rats □ Caffeine—administered alone and with aspirin, absorption, distribution in gastric tissue, blood plasma levels, rats □ Pharmacokinetics—aspirin administered alone and with acetaminophen or caffeine, absorption, distribution in gastric tissue, blood plasma levels, rats

Irritation of the GI mucosa, production of erosions, and GI bleeding are serious side effects of aspirin and other nonsteroidal anti-inflammatory drugs (1, 2). Acidic anti-inflammatory drugs are thought to cause these side effects

0022-3549/80/0800-0900$01.00/0
© 1980, American Pharmaceutical Association

following their rapid absorption to give very high intracellular concentrations, finally resulting in cell death (3–5). However, a causal relationship between the intracellular accumulation of salicylate and the decay of gastric mucosal cells has not been proven. Therefore, the present study was initiated to compare the characteristics of absorption and distribution of aspirin in the rat stomach with those of acetaminophen and caffeine, two drugs that are nonulcerogenic in rats (6).

It also was suggested (5) that the reduced gastric toxicity of slow-release and enteric-coated aspirin formulations (7–9) might be explained by the delayed absorption of aspirin and, thus, a reduction in salicylate trapping in parietal cells. In the rat, acetaminophen reduced the erosive activity of aspirin whereas caffeine potentiated this activity (6, 10). To test this hypothesis, the effects of acetaminophen and caffeine on the absorption of salicylate into the cells of the glandular (containing the parietal cells) and nonglandular parts of the rat stomach were investigated.

EXPERIMENTAL

Reagents and Materials—Aspirin[1], salicylic acid[1], acetaminophen[1], caffeine[1], phenacetin[1], and polysorbate 80[2] were obtained commercially. All other chemicals were analytical reagent grade. Ether[3] was distilled every day. Male Wistar rats of an inbred strain, 180–200 g, were purchased locally[4].

GLC—For aspirin and salicylic acid, a gas chromatograph[5] equipped with a multitemperature programmer, a flame-ionization detector, and an integrator[6] was used. The glass column, 1.00 m × 3 mm i.d., was packed with 3% OV-17[7] on 80–100-mesh Gas Chrom Q[7]. The column oven temperature was programmed for 2 min at 105°, an increase of 4°/min from 105 to 130°, an increase of 30°/min from 130 to 195°, 2 min at 195°, and then cooling down. The injector temperature was 220°, the detector temperature was 220°, the argon carrier gas flow rate was 35 ml/min, the hydrogen flow rate was 40 ml/min, the air flow rate was 400 ml/min, and the amplifier range was at 10. Under these conditions, the retention times of the trimethylsilyl ether derivatives were 3.0 min for *p*-toluic acid (internal standard), 5.0 min for salicylic acid, and 7.5 min for aspirin.

For acetaminophen, a gas chromatograph[8] equipped with a flame-ionization detector and a computing integrator[9] was used. The glass column, 1.80 m × 2 mm i.d., was packed with 3% OV-101[7] on 80–100-mesh Gas Chrom Q. The column oven temperature was 135°, the injector temperature was 200°, the detector temperature was 220°, the nitrogen carrier gas flow rate was 30 ml/min, the hydrogen flow rate was 35 ml/min, and the air flow rate was 350 ml/min. The retention times of the trimethylsilyl ether derivatives were 4.5 min for *p*-bromoacetanilide (internal standard), 7.5 min for acetaminophen, and 6.0 min for phenacetin.

For caffeine, a gas chromatograph[8] equipped with an alkali flame-ionization detector and a computing integrator[9] was used. The glass column, 1.50 × 2 mm i.d., was packed with 3% OV-101 on 80–100-mesh Gas Chrom Q. The column oven temperature was 165°, the injector temperature was 220°, the detector temperature was 220°, the nitrogen carrier gas flow rate was 30 ml/min, the hydrogen flow rate was 35 ml/min, and the air flow rate was 300 ml/min. Under these conditions, the retention times were 5.0 min for phenacetin (internal standard) and 8.0 min for caffeine.

Drug Treatment and Sample Collection—Rats were distributed randomly into groups of eight or 10 animals and were deprived of food, but not water, for 36 hr. They were kept in cages (0.32 × 0.20 × 0.20 m) with a metal grid (8 × 8 mm) to avoid coprophagy. Room temperature was maintained at 21 ± 0.5°. Aspirin, acetaminophen, and caffeine were ground before use (<110 μm). All treatments were administered orally at 5 ml/kg as suspensions in 4% polysorbate 80; control rats received a similar volume of 4% polysorbate 80 solution.

Rats were treated with aspirin (250 mg/kg), acetaminophen (125 mg/kg), caffeine (50 mg/kg), aspirin and acetaminophen (250 and 125 mg/kg), and aspirin and caffeine (250 and 50 mg/kg). Blood samples (1.0 ml) were obtained by decapitation. In the drug elimination studies, dosage groups of 10 rats were decapitated at 0.5, 1.5, 4, 8, and 17 hr after administration. In the drug absorption studies, dosage groups of eight rats were decapitated at 5, 10, 15, 20, and 30 min after administration.

In the absorption experiments, the stomachs were removed immediately after blood sampling, opened along the greater curvature, and rinsed in saline. The glandular part of the gastric tissue was scraped off, and the ruminal part was cut off. Blood was collected in polyethylene snap caps, which contained 1 drop of a solution of 250 IU of heparin[10] and 12 mmoles of sodium fluoride/ml. After centrifugation[11] at 1000×*g*, the plasma was stored at −20°. Tissue samples were weighed wet, stored at −20°, and homogenized[12] in water (1:3 w/v) just before analysis.

Assay of Aspirin and Salicylic Acid—To a 15-ml stoppered conical glass centrifuge tube were added 0.1–0.5 ml of plasma or 1 ml of tissue homogenate, 200–300 mg of sodium chloride, 0.5 ml of buffer solution (17.2 mmoles of potassium sulfate in 100 ml of 0.2 *M* H_2SO_4), and 10 ml of ether. After shaking[13] for 30 min and centrifuging for 10 min at 1000×*g*, as much ether as possible was transferred into a conical tube and evaporated to dryness on a heating block[14] at 30° under a nitrogen stream. To the dry residue was added 0.1 ml of 0.6 m*M* *p*-toluic acid in acetone.

The contents of the tube were transferred with four 0.1-ml portions of acetone to a micro reaction vessel[7]. After evaporation of the acetone, the residue was dissolved in 50 μl of bis(trimethylsilyl)trifluoroacetamide[7], and the vessel was closed with a polytetrafluoroethylene-lined rubber septum[7]. After agitation and heating at 50° for 1 hr, 1 μl was injected into the GLC column and the temperature programming was started.

Assay of Acetaminophen—To a 10-ml glass-stoppered centrifuge tube were added 0.1–1 ml of plasma or 1 ml of tissue homogenate, 2 ml of buffer solution (1 *M* dibasic potassium phosphate saturated with sodium chloride and brought to pH 7.4 with 1 *M* NaOH), and 5 ml of ether containing 24 nmoles of *p*-bromoacetanilide. After shaking for 30 min and centrifuging for 10 min at 1000×*g*, the organic layer was transferred to a conical glass tube and evaporated under a nitrogen stream at room temperature.

The residue was transferred to a micro reaction vessel with two 150-μl portions of acetone; after evaporation of the acetone, the residue was dissolved in 50 μl of bis(trimethylsilyl)trifluoroacetamide and the vessel was closed with a polytetrafluoroethylene-lined rubber septum. After agitation and heating at 50° for 2 hr, 1 μl was injected into the GLC column.

Assay of Caffeine—To a 10-ml glass-stoppered centrifuge tube was added 0.1 ml of a solution of 0.1 m*M* phenacetin in acetone. After evaporation of the acetone, 0.1–0.5 ml of plasma or 1 ml of tissue homogenate and 5 ml of dichloromethane were added. After shaking for 15 min and centrifuging for 5 min at 1000×*g*, the organic layer was dried over sodium sulfate and evaporated to dryness at 40° under a nitrogen stream. The residue was dissolved in 100 μl of methanol, and 1 μl was injected into the GLC column.

Data Analysis—The means and standard errors of the mean (*SEM*) of plasma and tissue concentrations of total salicylate (acetylsalicylate and salicylate), acetaminophen, and caffeine are presented in Figs. 1–4 (the standard error of the mean is presented only when it exceeds the dimensions of the symbol). Rankit tests (11) showed that the assumption that the concentrations within treatment groups were normally distributed was justified.

Differences between the mean concentrations of the treatment groups were tested using the Student *t* test. Because the ratio of two normally distributed variables is not normally distributed, differences in concentration ratios between treatment groups were tested using Wilcoxon's signed rank test. Differences were assumed to be real when tests indicated probability levels of <5%.

[1] O. P. G., Utrecht, The Netherlands.
[2] Brocacef B. V., Maarssen, The Netherlands.
[3] Merck, Darmstadt, West Germany.
[4] Centraal Proefdierenbedrijf T. N. O., Zeist, The Netherlands.
[5] F 22, Perkin-Elmer and Co., GMBH, Uberlingen, West Germany.
[6] Spectra-Physics, Santa Clara, Calif.
[7] Supelco Inc., Bellefonte, Pa.
[8] Model 1440, Varian Aerograph, Walnut Creek, Calif.
[9] CDS 111 C, Varian, Palo Alto, Calif.
[10] Leo, Ballerup, Denmark.
[11] Model GLC-1 centrifuge, Sorvall, Newtown, Conn.
[12] Model S 45 homogenizer, Virtis Co., Gardiner, N.Y.
[13] Griffin flask shaker, Griffin and George Ltd., London, England.
[14] Dri-block DB-3, Techne, Princeton, N.J.

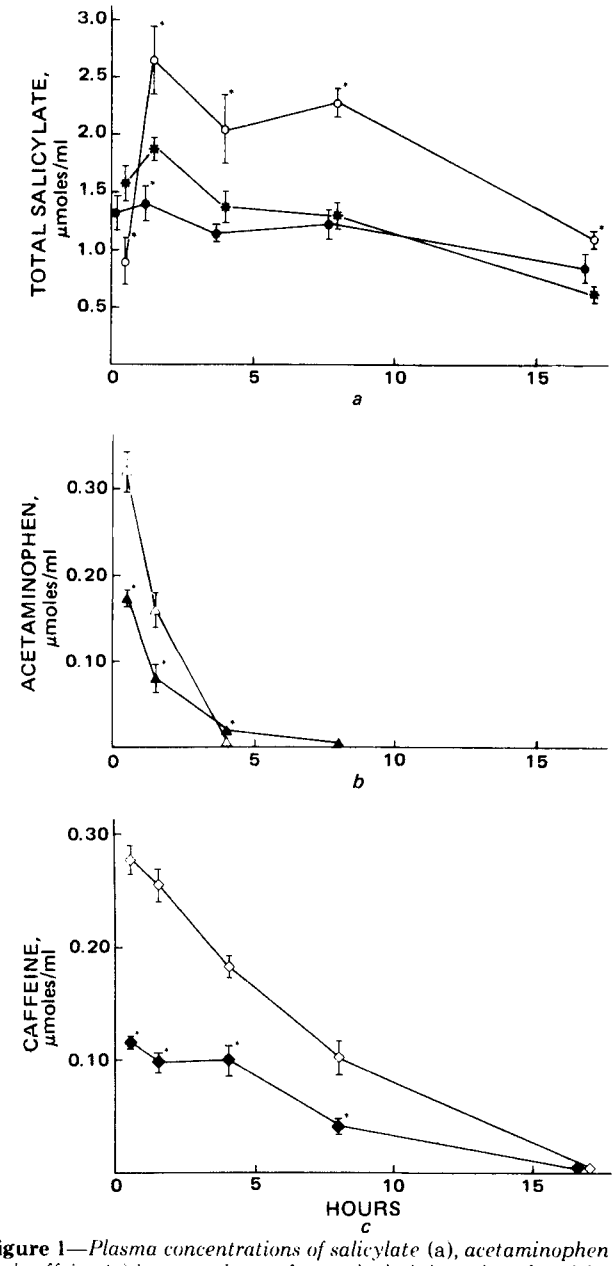

Figure 1—*Plasma concentrations of salicylate* (a), *acetaminophen* (b), *and caffeine* (c) *in starved rats after oral administration of aspirin (250 mg/kg)* (*), *acetaminophen (125 mg/kg)* (△), *caffeine (50 mg/kg)* (◇), *aspirin* (○) *and acetaminophen* (▲) *(250 and 125 mg/kg, respectively), and aspirin* (●) *and caffeine* (♦) *(250 and 50 mg/kg, respectively). Values are means* ± SEM *from 10 rats. An asterisk indicates* $p < 0.05$ *compared to the drugs given alone.*

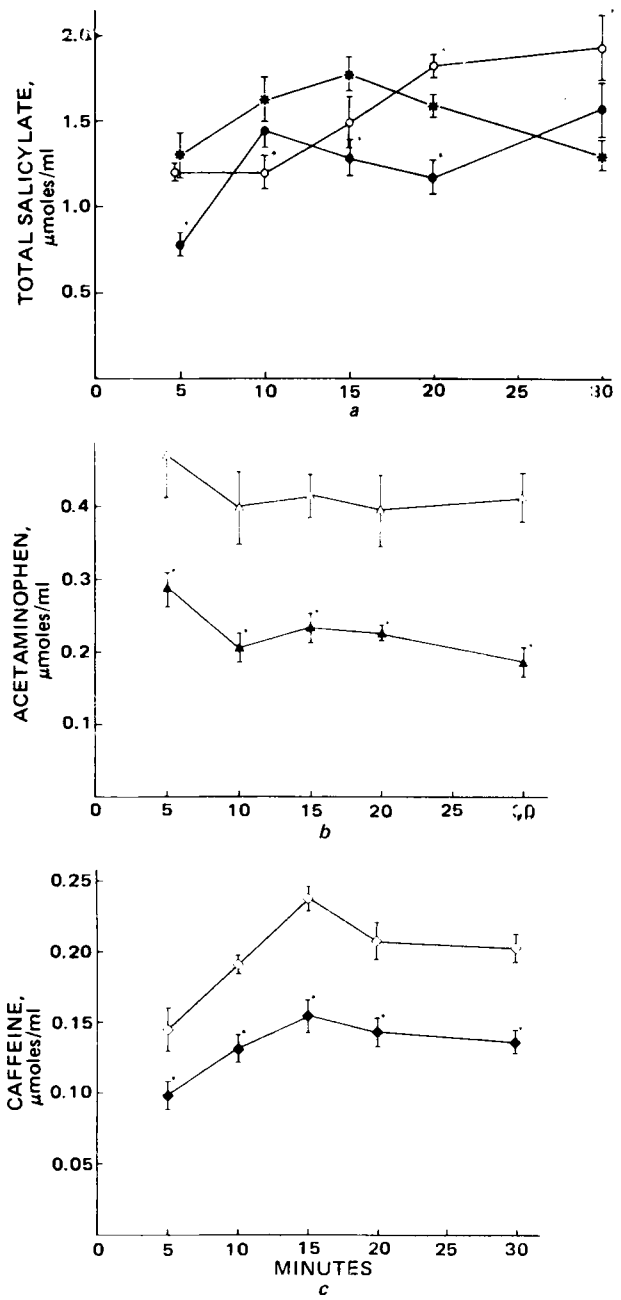

Figure 2—*Plasma concentrations during absorption of salicylate* (a), *acetaminophen* (b), *and caffeine* (c) *in starved rats after oral administration of aspirin (250 mg/kg)* (*), *acetaminophen (125 mg/kg)* (△), *caffeine (50 mg/kg)* (◇), *aspirin* (○) *and acetaminophen* (▲) *(250 and 125 mg/kg, respectively), and aspirin* (●) *and caffeine* (♦) *(250 and 50 mg/kg, respectively). Values are means* ± SEM *from eight rats. An asterisk indicates* $p < 0.05$ *compared to the drugs given alone.*

RESULTS

GLC—Linear relationships were observed between the concentrations of aspirin or salicylic acid (5–100 nmoles/ml) added to normal rat plasma and the peak area ratio measured using *p*-toluic acid as the internal standard ($r = 0.9989$ for aspirin and 0.9976 for salicylic acid). The mean recoveries of added aspirin and salicylic acid from plasma were 98.6 ± 3.5 and 99.9 ± 5.8%, respectively. The recoveries from tissue homogenates were 98.2 ± 3.4 and 99.5 ± 5.0%, respectively ($n = 8$). The detection limit for both compounds was 2 nmoles/ml of plasma; acetaminophen, caffeine, and phenacetin did not interfere with the assay.

In the concentration range of 4–100 nmoles/ml, linear relationships were observed between the concentrations of acetaminophen or phenacetin added to blood plasma and the peak area ratio measured using *p*-bromoacetanilide as the internal standard ($r = 0.9998$ for acetaminophen and 0.9993 for phenacetin). The mean recoveries of acetaminophen and phenacetin from plasma were 70.0 ± 4.0 and 99.0 ± 5.0%, respectively. The recoveries from tissue homogenates were 71.2 ± 4.2 and 99.3 ± 5.3%, respectively ($n = 15$). The detection limit for both compounds was 0.5 nmole/ml of plasma; aspirin, salicylic acid, caffeine, and *p*-aminophenol did not interfere with the assay.

A linear relationship was observed between the concentrations of caffeine (5–50 nmoles/ml) added to blood plasma and the peak area ratio measured using phenacetin as the internal standard ($r = 0.9974$). The recovery of caffeine from plasma samples in the concentration range of 1–175 nmoles/ml was 95.0 ± 4.4% ($n = 17$). The recovery from tissue homogenates in the concentration range of 20–500 nmoles/g was 94.1 ± 5.0% ($n = 8$). The detection limit was 1 nmole/ml of plasma; aspirin, salicylic acid, and acetaminophen did not interfere with the assay.

Plasma Levels during Elimination—The average plasma levels of salicylate, acetaminophen, and caffeine after administration to rats of the individual drugs alone or in combination are shown in Fig. 1.

Administration of aspirin alone or in combination with acetaminophen

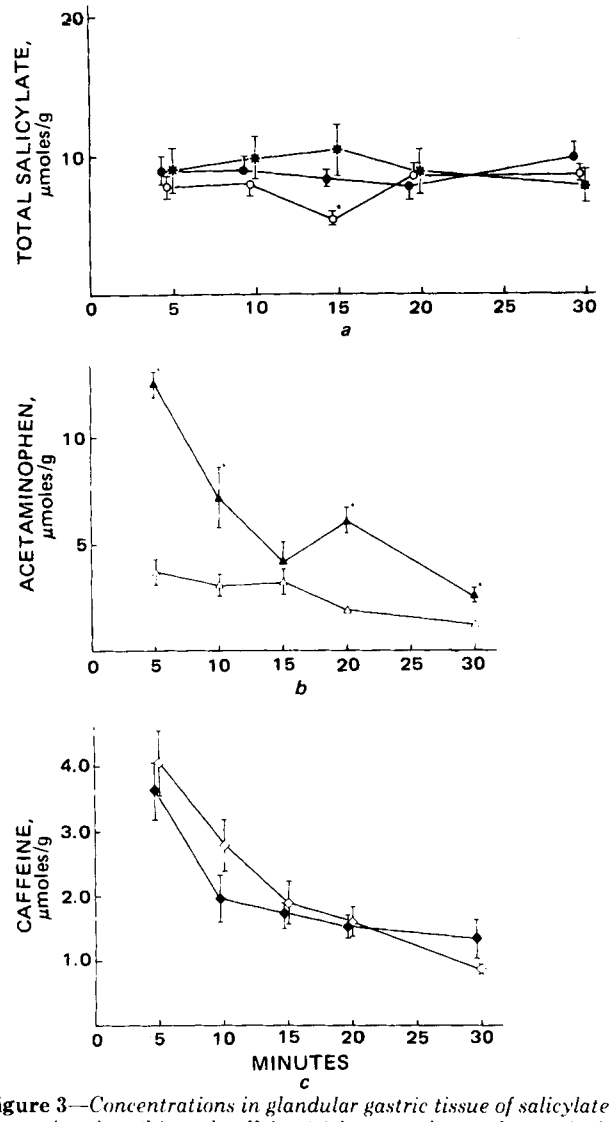

Figure 3—*Concentrations in glandular gastric tissue of salicylate* (a), *acetaminophen* (b), *and caffeine* (c) *in starved rats after oral administration of aspirin (250 mg/kg)* (*), *acetaminophen (125 mg/kg)* (△), *caffeine (50 mg/kg)* (◇), *aspirin* (○) *and acetaminophen* (▲) *(250 and 125 mg/kg, respectively), and aspirin* (●) *and caffeine* (◆) *(250 and 50 mg/kg, respectively). Values are means* ± SEM *from eight rats. An asterisk indicates* $p < 0.05$ *compared to the drugs given alone.*

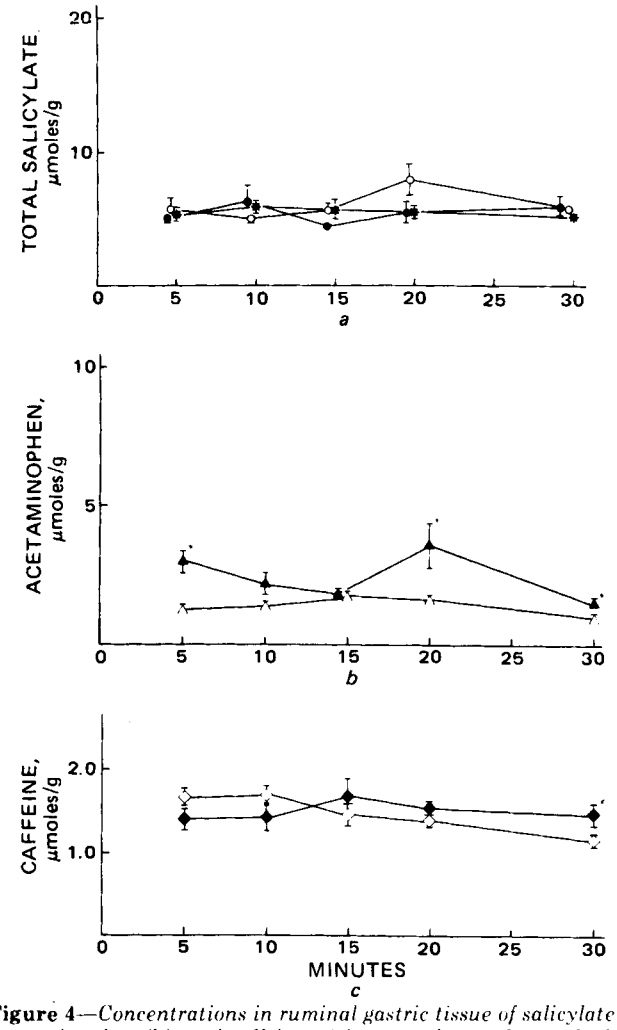

Figure 4—*Concentrations in ruminal gastric tissue of salicylate* (a), *acetaminophen* (b), *and caffeine* (c) *in starved rats after oral administration of aspirin (250 mg/kg)* (*), *acetaminophen (125 mg/kg)* (△), *caffeine (50 mg/kg)* (◇), *aspirin* (○) *and acetaminophen* (▲) *(250 and 125 mg/kg, respectively), and aspirin* (●) *and caffeine* (◆) *(250 and 50 mg/kg, respectively). Values are means* ± SEM *from eight rats. An asterisk indicates* $p < 0.05$ *compared to the drugs given alone.*

or caffeine resulted in maximal plasma salicylate levels within 1.0–1.5 hr. Coadministration of acetaminophen with aspirin significantly reduced the plasma salicylate levels at 0.5 hr, whereas the levels after 1.5 hr were enhanced significantly. Simultaneous administration of caffeine with aspirin significantly reduced plasma salicylate levels at 1.5 hr after administration (Fig. 1*a*).

In the presence of aspirin, the plasma levels of acetaminophen (Fig. 1*b*) and caffeine (Fig. 1*c*) were decreased significantly in comparison to the levels following administration of the individual drugs.

Plasma and Gastric Tissue Concentrations during Absorption—*Plasma Levels*—The average plasma levels of salicylate, acetaminophen, and caffeine during their absorption are shown in Fig. 2 after administration of the individual drugs alone or in combination to rats.

In comparison with aspirin treatment alone, administration of mixtures of aspirin and acetaminophen and aspirin and caffeine resulted in significantly lower plasma salicylate levels during the first few minutes of absorption. However, at $t = 30$ min, the salicylate levels in the presence of caffeine equaled those after aspirin treatment alone; in the presence of acetaminophen, the plasma salicylate levels were enhanced at $t = 20$ and 30 min (Fig. 2*a*). With aspirin, the plasma levels of acetaminophen (Fig. 2*b*) and caffeine (Fig. 2*c*) were reduced significantly during absorption.

Concentrations in Glandular Gastric Tissue—The average concentrations of salicylate, acetaminophen, and caffeine in the glandular tissue of the rat stomach during absorption are presented in Fig. 3 after administration of the individual drugs alone or in combination.

Maximal concentrations of salicylate in the glandular gastric tissue were observed within 5–15 min after administration of aspirin (Fig. 3*a*). Simultaneous administration of acetaminophen with the aspirin tended to retard salicylate absorption, although statistically significant differences between the glandular tissue concentrations could be demonstrated only at $t = 15$ min. Coadministration of caffeine with aspirin did not affect the absorption of salicylate into the glandular tissue.

Acetaminophen (Fig. 3*b*) and caffeine (Fig. 3*c*) were rapidly absorbed into the glandular part of the rat stomach. In the presence of aspirin, the absorption of acetaminophen into the glandular tissue increased significantly whereas the absorption of caffeine was not affected.

During the absorption phase, the ratios of the glandular tissue concentration to the plasma concentration (Table I) remained almost constant for salicylate; for acetaminophen and caffeine, this ratio gradually decreased with time. Coadministration of acetaminophen did not influence the glandular tissue to plasma salicylate concentration ratio; conversely, this ratio for the acetaminophen concentration significantly increased in the presence of aspirin (Table I). Simultaneous administration of caffeine with aspirin tended to increase the concentration ratios for both drugs, although significant differences were observed only at $t = 15$ min for salicylate and at $t = 30$ min for caffeine.

Concentrations in Ruminal Gastric Tissue—The average concentrations of salicylate, acetaminophen, and caffeine in the ruminal tissue of the rat stomach during absorption are presented in Fig. 4 after administration of the individual drugs alone or in combination.

Table I—Mean Concentration Ratios (w/v) of Glandular Gastric Tissue to Blood Plasma following Oral Administration of Drugs and Drug Mixtures to Starved Rats (n = 8)

Treatment	Substance Determined	Time after Administration, min				
		5	10	15	20	30
Aspirin, 250 mg/kg	Salicylate	6.0	6.5	4.9	5.7	6.3
Acetaminophen, 125 mg/kg	Acetaminophen	10.1	8.6	8.1	5.6	3.3
Caffeine, 50 mg/kg	Caffeine	29.0	14.9	8.1	7.9	4.4
Aspirin and acetaminophen, 250 and 125 mg/kg	Salicylate	6.8	7.5	4.2	4.9	4.7
	Acetaminophen	45.5[a]	34.2[a]	18.7[a]	27.4[a]	14.9[a]
Aspirin and caffeine, 250 and 50 mg/kg	Salicylate	12.4	6.8	7.8[b]	6.1	6.5
	Caffeine	40.4	15.6	11.9	10.9	9.6[c]

[a] $p < 0.05$ compared to acetaminophen alone. [b] $p < 0.05$ compared to aspirin alone. [c] $p < 0.05$ compared to caffeine alone.

Table II—Mean Concentration Ratios (w/v) of Ruminal Gastric Tissue to Blood Plasma following Oral Administration of Drugs and Drug Mixtures to Starved Rats (n = 8)

Treatment	Substance Determined	Time after Administration, min				
		5	10	15	20	30
Aspirin, 250 mg/kg	Salicylate	4.6	3.7	3.3	3.5	4.1
Acetaminophen, 125 mg/kg	Acetaminophen	3.0	4.1	4.4	5.3	2.8
Caffeine, 50 mg/kg	Caffeine	12.0	9.0	6.2	6.9	5.9
Aspirin and acetaminophen, 250 and 125 mg/kg	Salicylate	4.9	4.6	4.2	4.5	3.3
	Acetaminophen	11.2[a]	10.5[a]	7.9[a]	15.9[a]	8.9[a]
Aspirin and caffeine, 250 and 50 mg/kg	Salicylate	7.0	4.5	4.2	4.4	4.1
	Caffeine	15.4	11.1	11.6[b]	11.0[b]	11.1[b]

[a] $p < 0.05$ compared to acetaminophen alone. [b] $p < 0.05$ compared to caffeine alone.

Table III—Mean Concentration Ratios (w/w) of Glandular Tissue to Ruminal Tissue of the Stomach following Oral Administration of Drugs and Drug Mixtures to Starved Rats (n = 8)

Treatment	Substance Determined	Time after Administration, min				
		5	10	15	20	30
Aspirin, 250 mg/kg	Salicylate	1.6	1.5	1.6	1.6	1.6
Acetaminophen, 125 mg/kg	Acetaminophen	3.5	2.5	2.2	1.4	1.6
Caffeine, 50 mg/kg	Caffeine	2.4	1.6	1.3	1.1	0.8
Aspirin and acetaminophen, 250 and 125 mg/kg	Salicylate	1.7	1.6	1.0	1.4	1.5
	Acetaminophen	4.9	3.4	2.3	2.1	1.7
Aspirin and caffeine, 250 and 50 mg/kg	Salicylate	1.8	1.9	1.9	1.6	1.8
	Caffeine	2.6	1.4	1.1	1.0	0.9

Aspirin administration, alone as well as in combination with acetaminophen or caffeine, resulted in comparable ruminal salicylate concentrations, which remained constant during the absorption phase (Fig. 4*a*). As in the glandular tissue, the absorption of acetaminophen into the rumen (Fig. 4*b*) was increased significantly in the presence of aspirin whereas the absorption of caffeine (Fig. 4*c*) was not affected.

The ratio of the ruminal tissue concentration to the plasma concentration (Table II) remained almost constant for salicylate and acetaminophen throughout the absorption phase; for caffeine, this ratio gradually decreased with time. The concentration ratios for salicylate were not affected by coadministration of acetaminophen or caffeine; on the other hand, aspirin enhanced the concentration ratios for both acetaminophen and caffeine (Table II).

Glandular Tissue to Ruminal Tissue Concentration Ratios—Table III shows the average glandular tissue to ruminal tissue concentration ratios for salicylate, acetaminophen, and caffeine during their absorption following administration of the individual drugs alone or in combination.

Regardless of whether the drugs were administered separately or in combination, the absorption of all drugs into the glandular tissue was higher than into the rumen. In particular, acetaminophen showed marked accumulation in the glandular tissue. Administration of the drug combinations did not affect the accumulation of the individual drugs in the glandular tissue.

DISCUSSION

Analytical Procedure—The assay used for aspirin and salicylic acid was a modification of earlier methods (12–16). By making derivatives of aspirin and salicylic acid with pure bis(trimethylsilyl)trifluoroacetamide under controlled conditions, more reproducible results were obtained in comparison with methods where the derivatizing agent was diluted with carbon disulfide (12) or acetone (15). With the temperature programming used, an acceptable separation of the desired compounds was obtained from endogenous compounds in plasma and gastric tissue homogenates. Care had to be taken during evaporation of the organic solvent to prevent sublimation (76°) of the aspirin and salicylic acid.

Many stationary phases, such as FFAP (17), OV-1 (18), SP 2250 (19), and OV-17 (20), can be used for the GLC determination of acetaminophen. Because an assay was needed that also could be used in investigations with phenacetin, one assay for both compounds was developed; the use of *p*-bromoacetanilide as an internal standard (21, 22) and an OV-101 column gave the best quantitative results.

Several previous investigations (23–25) involved the determination of caffeine in plasma; none of these reports described a method suitable for tissues. In the present assay, an OV-101 column (24) was used because with an OV-17 column (25) and hexobarbital and phenacetin as internal standards, both compounds gave broad tailing peaks. Extracting caffeine with dichloromethane instead of chloroform (24, 25) rendered the procedure more convenient and less hazardous.

Glandular Accumulation—One theory explaining the gastric toxicity of aspirin assumes an association between its erosive activity and its toxic intracellular actions after absorption (3, 26). Although orally administered aspirin is absorbed mainly from the small intestine (27), considerable amounts also are absorbed *via* the stomach (28). Under the acidic conditions present in the stomach, aspirin (pKa 3.5) is mainly undissociated, which facilitates diffusion of the drug molecules across membranes. In mucosal cells, aspirin is likely to be hydrolyzed to salicylic acid (29), and this compound exists predominantly in an ionized form in the cells (pH ~7.4). Because the back-diffusion of salicylate ions across membranes is very slow, high intracellular concentrations of salicylate rapidly accumulate (30, 31). If sufficiently high concentrations are reached, mitochondrial oxidative phosphorylation is uncoupled, resulting in cessation of synthetic and transport activities in the cell and possibly leading to a reduction in transmucosal resistance (32). However, not all cell types of the gastric mucosa appear to be equally susceptible to damage since erosions induced with aspirin are found only in the glandular part of the rat stomach. Recently, Brune *et al.* (5) showed that the

parietal cells in the glandular mucosa trap salicylate to an excessive extent. It is possible that gastric mucosal damage induced with aspirin starts with the decay of these cells.

In the present study, the salicylate concentrations reached in the glandular tissue during aspirin absorption were higher than those in the rumen (Table III). The concentrations reached in the gastric mucosa depend on the presence of the drug within the stomach lumen since lower levels are obtained in the mucosa after subcutaneous administration of aspirin (33). Acetaminophen (pKa 9.5) and caffeine (pKa 13.2) also accumulated in the glandular tissue after oral administration, to an even larger extent than salicylate (Table III). The fact that acetaminophen and caffeine do not induce gastric erosions (6) might indicate that the intracellular action of these compounds differs from that of salicylate. Thus, accumulation of a drug in glandular tissue *per se* does not account for erosive activity. However, since the erosions are found only in the glandular part of the stomach, in which the highest concentrations of salicylate were reached, an involvement of salicylate accumulation in glandular tissue in the pathogenesis of aspirin-induced erosions cannot be ruled out.

Throughout the absorption period after aspirin treatment, salicylate concentrations in the glandular and ruminal areas of the stomach were not significantly affected by simultaneous administration of either acetaminophen or caffeine (Figs. 3*a* and 4*a*). Only in the group of rats killed after 15 min did salicylate levels in the glandular tissue tend to decrease in the presence of acetaminophen. However, in view of the large number of different observations made at various time points, the possibility that one mean is (significantly) lower by chance is not inconceivable. In any case, the concentrations of salicylate still achieved values of 6–10 μmoles/g in the presence of acetaminophen. Exposure of the gastric mucosa to similar concentrations of salicylate, both *in vitro* (34, 35) and *in vivo* (36, 37), is associated with changes in its electrophysiological properties and permeability characteristics. Furthermore, oral administration of aspirin (50 mg/kg), leading to salicylate concentrations in gastric tissue of 1–2 μmoles/g (33), still causes gastric erosions (6). Hence, it is unlikely that this slight reduction in salicylate accumulation in glandular tissue accounts for the inhibition of the erosive activity of aspirin by acetaminophen.

In the presence of aspirin, the absorption of acetaminophen into the gastric tissues increased (Figs. 3*b* and 4*b*), and this increased absorption might have affected prostaglandin biosynthesis in the gastric wall. According to Vane (38), inhibition of prostaglandin biosynthesis in the gastric mucosa by aspirin-like drugs at least contributes to the formation of gastric erosions. In addition, coadministration of prostaglandins protects the gastric mucosa against irritation by aspirin (39). Therefore, the observation of Robak *et al.* (40) that acetaminophen, in concentrations similar to those measured in blood plasma, stimulates prostaglandin synthetase activity *in vitro* might be important. As a result of its (increased) accumulation, acetaminophen might protect against the erosive activity of aspirin by counteracting the aspirin-induced inhibition of prostaglandin biosynthesis in the glandular part of the stomach.

Blood Plasma Concentrations—The combination of acetaminophen with aspirin retarded the appearance of salicylate in plasma (Fig. 2*a*), and the plasma salicylate levels were enhanced during elimination. A possible explanation for the latter observation might be competition of aspirin with acetaminophen for the glucuronide-forming enzyme system. Such a metabolic interaction between salicylate and acetaminophen could not be demonstrated in humans (41) or rats (42). However, in these studies, considerably lower doses of both drugs were used compared to those used in the present study. In both previous reports (41, 42), the investigators indicated that such an interaction at higher doses may be possible.

The combination of aspirin with acetaminophen appeared to reduce the acetaminophen absorption rate (Fig. 2*b*), an observation that has been reported for the rat (43), guinea pig (44), hamster (45), and mouse (46). Presumably, this retardation is related to the rate of gastric emptying. In this context, Smith and Irving (47) reported that salicylate administered to rats reduced the gastric emptying rate, and it was demonstrated recently that reduction of the gastric emptying rate reduced acetaminophen absorption (48–50). The increment in the acetaminophen concentrations in the glandular and ruminal areas of the stomach corroborates this assumption. After coadministration with aspirin, the elimination rate of acetaminophen from plasma was lower than that of acetaminophen given alone (Fig. 1*b*). This phenomenon might be due to retardation of the acetaminophen absorption and/or to an aspirin-induced decrease in the elimination rate of acetaminophen (43).

Administration of aspirin with caffeine retarded the appearance of both drugs in plasma (Figs. 2*a* and 2*c*). This effect probably is due to a delay in gastric emptying since both caffeine and aspirin relax GI smooth muscles (51, 52). Since simultaneous administration of aspirin and caffeine did not affect the concentrations of either of these drugs in the gastric wall (Figs. 3*a*, 3*c*, 4*a*, and 4*c*), the appearance of salicylate and caffeine in plasma probably depends mainly on absorption from the small intestine and not on absorption from the stomach.

In summary, neither the inhibition by acetaminophen nor the potentiation by caffeine of aspirin-induced erosions in the rat stomach can be attributed to effects of these drugs on salicylate accumulation in glandular mucosa. Furthermore, since simultaneous administration of these drugs to the rat influenced their mutual rates of absorption and elimination, the pharmacological efficacy of the mixtures cannot be predicted simply from the plasma levels of the components.

REFERENCES

(1) L. G. Desbaillets, *Adv. Clin. Pharmacol.*, **6**, 23 (1974).

(2) H. Jick and J. Porter, *Lancet*, **2**, 87 (1978).

(3) B. K. Martin, *Nature*, **198**, 896 (1963).

(4) K. D. Rainsford and K. Brune, *Med. J. Aust.*, **1**, 881 (1976).

(5) K. Brune, A. Schweitzer, and H. Eckert, *Biochem. Pharmacol.*, **26**, 1735 (1977).

(6) A. J. M. Seegers, L. P. Jager, and J. van Noordwijk, *J. Pharm. Pharmacol.*, **30**, 84 (1978).

(7) B. L. J. Treadwell, D. G. Carroll, and E. W. Pomare, *N. Z. Med. J.*, **78**, 435 (1973).

(8) G. D. Champion, R. O. Day, G. G. Graham, and P. D. Paull, *Clin. Rheum. Dis.*, **1**, 245 (1975).

(9) G. B. Howe, G. D. Champion, A. B. Corrigan, J. Hewson, A. Hoshi, R. O. Day, P. D. Paull, and G. G. Graham, *Aust. N. Z. J. Med.*, **7**, 600 (1977).

(10) A. J. M. Seegers, L. P. Jager, and J. van Noordwijk, *J. Pharm. Pharmacol.*, **31**, 840 (1979).

(11) R. A. Fisher and F. Yates, "Statistical Tables for Biological, Agricultural and Medical Research," 4th ed., Oliver and Boyd, Edinburgh, Scotland, 1953, Table XX.

(12) M. Rowland and S. Riegelman, *J. Pharm. Sci.*, **56**, 717 (1967).

(13) B. H. Thomas, G. Solomonraj, and B. B. Coldwell, *J. Pharm. Pharmacol.*, **25**, 201 (1973).

(14) L. J. Walter, D. F. Biggs, and R. T. Coutts, *J. Pharm. Sci.*, **63**, 1754 (1974).

(15) J. P. Tischio, *ibid.*, **65**, 1530 (1976).

(16) M. J. Rance, B. J. Jordan, and J. D. Nichols, *J. Pharm. Pharmacol.*, **27**, 425 (1975).

(17) J. Grove, *J. Chromatogr.*, **59**, 289 (1971).

(18) J. Kalra, O. A. Mamer, B. Gregory, and M. H. Gault, *J. Pharm. Pharmacol.*, **29**, 127 (1977).

(19) M. A. Evans and R. D. Harbison, *J. Pharm. Sci.*, **66**, 1628 (1977).

(20) W. A. Dechtiaruk, G. F. Johnson, and H. M. Solomon, *Clin. Chem.*, **22**, 879 (1976).

(21) L. F. Prescott, *J. Pharm. Pharmacol.*, **23**, 111 (1971).

(22) B. H. Thomas and B. B. Coldwell, *ibid.*, **24**, 243 (1972).

(23) M. Amin and W. Sepp, *J. Chromatogr.*, **118**, 225 (1976).

(24) D. Lavène, M. Guerret, H. Humbert, and J. L. Kiger, *Ann. Pharm. Fr.*, **32**, 505 (1974).

(25) F. L. Grab and J. A. Reinstein, *J. Pharm. Sci.*, **57**, 1703 (1968).

(26) H. W. Davenport, *Gastroenterology*, **46**, 245 (1964).

(27) L. S. Scharker, D. J. Tocco, B. B. Brodie, and C. A. M. Hogben, *J. Pharmacol. Exp. Ther.*, **123**, 81 (1958).

(28) A. R. Cooke and J. N. Hunt, *Am. J. Dig. Dis.*, **15**, 95 (1970).

(29) J. G. Spenney, *Am. J. Physiol.*, **234**, 606 (1978).

(30) E. Morris, A. A. Noujaim, T. S. Miya, and J. E. Christian, *J. Pharm. Sci.*, **56**, 896 (1967).

(31) C. H. Morris, J. E. Christian, T. S. Miya, and W. G. Hansen, *ibid.*, **59**, 325 (1970).

(32) J. G. Spenney and M. Bhown, *Gastroenterology*, **73**, 995 (1977).

(33) H. H. Frey and M. A. El-Sayed, *Arch. Int. Pharmacodyn. Ther.*, **230**, 300 (1977).

(34) A. Garner, *Acta Physiol. Scand.*, **99**, 281 (1977).

(35) J. G. Spenney and M. Bhown, *Gastroenterology*, **73**, 785 (1977).

(36) H. W. Davenport, *ibid.*, **56**, 439 (1969).

(37) K. J. Ivey, S. Morrison, and C. Gray, *J. Appl. Physiol.*, **33**, 81 (1972).

(38) J. R. Vane, *Nature New Biol.*, **231**, 232 (1971).

(39) M. M. Cohen, *Gastroenterology*, **68**, 876 (1975).

(40) J. Robak, A. Wieckowski, and R. Gryglewski, *Biochem. Pharmacol.*, **27**, 393 (1978).
(41) G. Levy and C. G. Regardh, *J. Pharm. Sci.*, **60**, 608 (1971).
(42) G. Ramachander, F. D. Williams, and J. F. Emele, *ibid.*, **62**, 1498 (1973).
(43) B. H. Thomas, W. Zeitz, and B. B. Coldwell, *ibid.*, **63**, 1367 (1974).
(44) L. W. Whitehouse, C. J. Paul, and B. H. Thomas, *ibid.*, **64**, 819 (1975).
(45) L. T. Wong, G. Solomonraj, and B. H. Thomas, *Xenobiotica*, **6**, 575 (1976).
(46) L. W. Whitehouse, C. J. Paul, L. T. Wong, and B. H. Thomas, *J. Pharm. Sci.*, **66**, 1399 (1977).
(47) M. J. H. Smith and J. D. Irving, *Br. J. Radiol.*, **28**, 39 (1955).
(48) R. C. Heading, J. Nimmo, L. F. Prescott, and P. Tothill, *Br. J. Pharmacol.*, **47**, 415 (1973).
(49) J. Nimmo, R. C. Heading, P. Tothill, and L. F. Prescott, *Br. Med. J.*, **1**, 587 (1973).
(50) J. A. Clements, R. C. Heading, W. S. Nimmo, and L. F. Prescott, *Clin. Pharmacol. Ther.*, **24**, 420 (1978).
(51) C. P. Siegers, O. Strubelt, and G. Back, *Eur. J. Pharmacol.*, **20**, 181 (1972).
(52) C. P. Siegers, *Pharmacology (Basel)*, **10**, 19 (1973).

ACKNOWLEDGMENTS

The authors thank P. Besamusca, F. Hagelen, H. Heinen, Y. de Jong, A. van de Kuil, and P. W. M. Zeylmans for excellent technical assistance. They also thank Dr. M. Parnham and Mrs. G. Franchimont for their assistance in manuscript preparation.

This study constitutes part of Joint Project No. 110/79 of the National Institute of Public Health with the Health Inspection for Drugs and the State University of Utrecht.

Rearrangement of Chloramphenicol-3-monosuccinate

D. A. BRENT *x, P. CHANDRASURIN *, A. RAGOUZEOS *, B. S. HURLBERT *, and J. T. BURKE ‡

Received July 19, 1979, from the **Wellcome Research Laboratories, Burroughs Wellcome Co., Research Triangle Park, NC 27709*, and the ‡*School of Pharmacy, University of North Carolina, Chapel Hill, NC 27514.* Accepted for publication March 7, 1980.

Abstract □ The equilibrium mixture of chloramphenicol-3-monosuccinate and its alternate form at neutral pH in aqueous solution was reexamined. The structure of the alternate form was shown by mass spectrometry and NMR spectroscopy to be chloramphenicol-1-monosuccinate and not the cyclic hemi-ortho ester reported previously.

Keyphrases □ Chloramphenicol-3-monosuccinate—identification of alternate form in equilibrium mixture as chloramphenicol-1-monosuccinate □ Antibacterials—chloramphenicol, identification of 1-succinate ester as alternate form in equilibrium mixture with 3-succinate ester □ Prodrugs—chloramphenicol-3-monosuccinate, identification of 1-succinate ester as alternate form in equilibrium mixture with 3-succinate ester

The sodium salt of chloramphenicol-3-monosuccinate[1] (III) is used as a prodrug, generating the broad spectrum antibiotic chloramphenicol by hydrolysis of the succinate ester in the liver (1). Sandmann *et al.* (2) reported that at neutral pH, III exists in equilibrium with a different molecular form, which they identified as a cyclic hemi-ortho ester (II) (Scheme I).

RESULTS AND DISCUSSION

By using a recently developed, sensitive, high-pressure liquid chromatographic (HPLC) assay for III, three products were detected after equilibrating III in aqueous solution at pH 7.5 for 24 hr (3). The first and third peaks (Fig. 1) were identified as chloramphenicol and III, respectively, by comparison with standards and by mass spectrometry of their trimethylsilyl ethers. The mass spectrum of the trimethylsilyl derivative of the first HPLC peak agreed with spectra published for *O*-bis(trimethylsilyl)chloramphenicol (4–6). The mass spectrum of the trimethylsilyl derivative of the third HPLC peak gave ions consistent with IV: *m/e* 551 (2.6%, M − CH_3), 483 (0.6), 377 (2.92), 225 (75.6), 224 (28.9), 173 (25.2), and 73 (100.0).

The second eluted compound exhibited an NMR spectrum identical to that reported by Sandmann *et al.* (2) for II. However, the mass spectrum of the trimethylsilyl derivative of this compound supported the structure of chloramphenicol-1-monosuccinate (I) and not the cyclic hemi-ortho ester (II). The ion having the greatest mass was *m/e* 551 (1.7%,

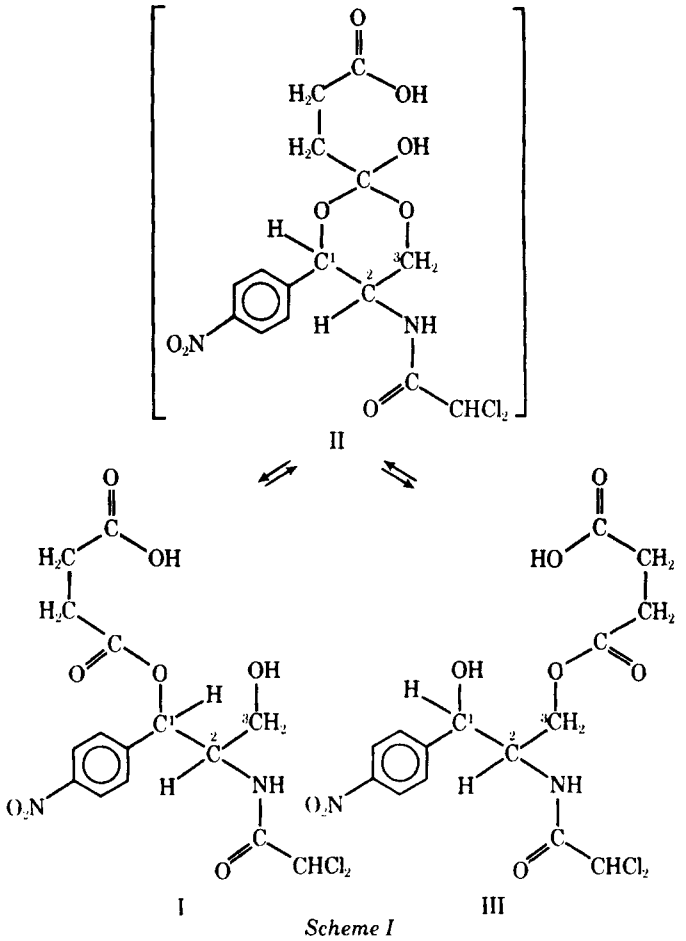

Scheme I

[1] The USAN name chloramphenicol sodium succinate refers to the sodium salt of the 3-monosuccinate ester.

0022-3549/80/0800-0906$01.00/0
© 1980, American Pharmaceutical Association

(40) J. Robak, A. Wieckowski, and R. Gryglewski, *Biochem. Pharmacol.*, **27**, 393 (1978).
(41) G. Levy and C. G. Regardh, *J. Pharm. Sci.*, **60**, 608 (1971).
(42) G. Ramachander, F. D. Williams, and J. F. Emele, *ibid.*, **62**, 1498 (1973).
(43) B. H. Thomas, W. Zeitz, and B. B. Coldwell, *ibid.*, **63**, 1367 (1974).
(44) L. W. Whitehouse, C. J. Paul, and B. H. Thomas, *ibid.*, **64**, 819 (1975).
(45) L. T. Wong, G. Solomonraj, and B. H. Thomas, *Xenobiotica*, **6**, 575 (1976).
(46) L. W. Whitehouse, C. J. Paul, L. T. Wong, and B. H. Thomas, *J. Pharm. Sci.*, **66**, 1399 (1977).
(47) M. J. H. Smith and J. D. Irving, *Br. J. Radiol.*, **28**, 39 (1955).
(48) R. C. Heading, J. Nimmo, L. F. Prescott, and P. Tothill, *Br. J. Pharmacol.*, **47**, 415 (1973).
(49) J. Nimmo, R. C. Heading, P. Tothill, and L. F. Prescott, *Br. Med. J.*, **1**, 587 (1973).
(50) J. A. Clements, R. C. Heading, W. S. Nimmo, and L. F. Prescott, *Clin. Pharmacol. Ther.*, **24**, 420 (1978).
(51) C. P. Siegers, O. Strubelt, and G. Back, *Eur. J. Pharmacol.*, **20**, 181 (1972).
(52) C. P. Siegers, *Pharmacology (Basel)*, **10**, 19 (1973).

ACKNOWLEDGMENTS

The authors thank P. Besamusca, F. Hagelen, H. Heinen, Y. de Jong, A. van de Kuil, and P. W. M. Zeylmans for excellent technical assistance. They also thank Dr. M. Parnham and Mrs. G. Franchimont for their assistance in manuscript preparation.

This study constitutes part of Joint Project No. 110/79 of the National Institute of Public Health with the Health Inspection for Drugs and the State University of Utrecht.

Rearrangement of Chloramphenicol-3-monosuccinate

D. A. BRENT *x, P. CHANDRASURIN *, A. RAGOUZEOS *, B. S. HURLBERT *, and J. T. BURKE ‡

Received July 19, 1979, from the **Wellcome Research Laboratories, Burroughs Wellcome Co., Research Triangle Park, NC 27709*, and the ‡*School of Pharmacy, University of North Carolina, Chapel Hill, NC 27514.* Accepted for publication March 7, 1980.

Abstract □ The equilibrium mixture of chloramphenicol-3-monosuccinate and its alternate form at neutral pH in aqueous solution was reexamined. The structure of the alternate form was shown by mass spectrometry and NMR spectroscopy to be chloramphenicol-1-monosuccinate and not the cyclic hemi-ortho ester reported previously.

Keyphrases □ Chloramphenicol-3-monosuccinate—identification of alternate form in equilibrium mixture as chloramphenicol-1-monosuccinate □ Antibacterials—chloramphenicol, identification of 1-succinate ester as alternate form in equilibrium mixture with 3-succinate ester □ Prodrugs—chloramphenicol-3-monosuccinate, identification of 1-succinate ester as alternate form in equilibrium mixture with 3-succinate ester

The sodium salt of chloramphenicol-3-monosuccinate[1] (III) is used as a prodrug, generating the broad spectrum antibiotic chloramphenicol by hydrolysis of the succinate ester in the liver (1). Sandmann *et al.* (2) reported that at neutral pH, III exists in equilibrium with a different molecular form, which they identified as a cyclic hemi-ortho ester (II) (Scheme I).

RESULTS AND DISCUSSION

By using a recently developed, sensitive, high-pressure liquid chromatographic (HPLC) assay for III, three products were detected after equilibrating III in aqueous solution at pH 7.5 for 24 hr (3). The first and third peaks (Fig. 1) were identified as chloramphenicol and III, respectively, by comparison with standards and by mass spectrometry of their trimethylsilyl ethers. The mass spectrum of the trimethylsilyl derivative of the first HPLC peak agreed with spectra published for *O*-bis(trimethylsilyl)chloramphenicol (4–6). The mass spectrum of the trimethylsilyl derivative of the third HPLC peak gave ions consistent with IV: *m/e* 551 (2.6%, M − CH_3), 483 (0.6), 377 (2.92), 225 (75.6), 224 (28.9), 173 (25.2), and 73 (100.0).

The second eluted compound exhibited an NMR spectrum identical to that reported by Sandmann *et al.* (2) for II. However, the mass spectrum of the trimethylsilyl derivative of this compound supported the structure of chloramphenicol-1-monosuccinate (I) and not the cyclic hemi-ortho ester (II). The ion having the greatest mass was *m/e* 551 (1.7%,

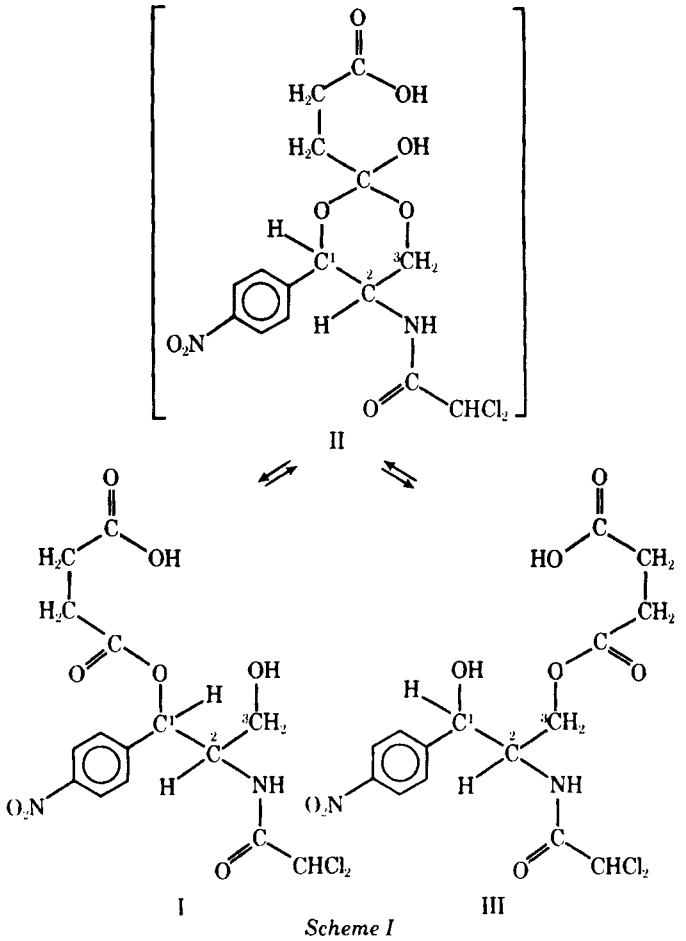

Scheme I

[1] The USAN name chloramphenicol sodium succinate refers to the sodium salt of the 3-monosuccinate ester.

0022-3549/80/0800-0906$01.00/0
© 1980, American Pharmaceutical Association

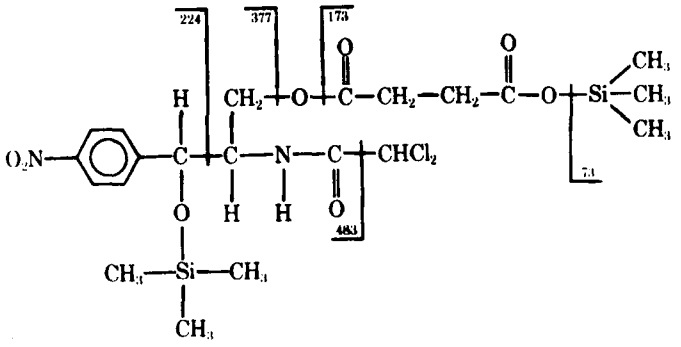

IV (mol. wt. 566)

M − CH_3). The base peak was *m/e* 73. The accurate masses of *m/e* 551 (2.7%), 242 (10.6), and 314 (4.57) were measured by peak matching at 10,000 resolution and 10% valley definition; their accurate masses were 551.0838, 131.0161, and 314.0569, respectively. The corresponding elemental compositions are $C_{20}H_{29}Cl_2N_2O_8Si_2$ (error of 0.1 millimass unit), $C_7H_{14}Cl_2NO_2Si$ (1.0), and $C_{10}H_{22}Cl_2NO_2Si_2$ (0.3). These peaks are consistent with bis- and tris(trimethylsilyl) derivatives of I. The mass spectrum supports the structure of I, but it is unclear whether the derivatizing reagent, which contains a weak base, could cause II to rearrange to I prior to silylation.

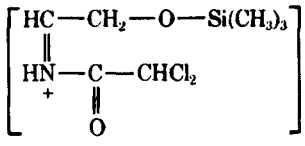

m/e 242

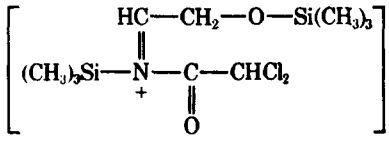

m/e 314

The evidence reported for the alternate form of III, having the structure denoted as II, was reexamined to determine if it really excluded the possibility of this product being I. Sandmann *et al.* (2) reported that chemical evidence indicated that the O→O migration product was incapable of existence in equilibrium under experimental conditions, but they did not describe experiments to prove this point. Within the knowledge of the present investigators, I never has been synthesized. The IR spectrum of III shows three distinct carbonyl absorptions (1690, 1718, and 1745 cm^{-1}), but only two absorptions (1690 and 1745 cm^{-1}) were shown for the alternate form (2). Sandmann *et al.* (2) concluded that this result was due to loss of the ester carbonyl. However, the band at 1718 cm^{-1} is likely the acid carbonyl, which has coalesced with one of the two remaining carbonyl bands or has shifted to 1600 cm^{-1} if it is in the form of a carboxylate anion (7). The optical rotatory dispersion curve for III shows a positive Cotton effect, while the curve for the alternate form shows a negative Cotton effect (2). The optical rotatory dispersion curves for O^1-acetylchloramphenicol-3-monosuccinate and O^1-dichloroacetylchloramphenicol-3-monosuccinate show negative Cotton effects

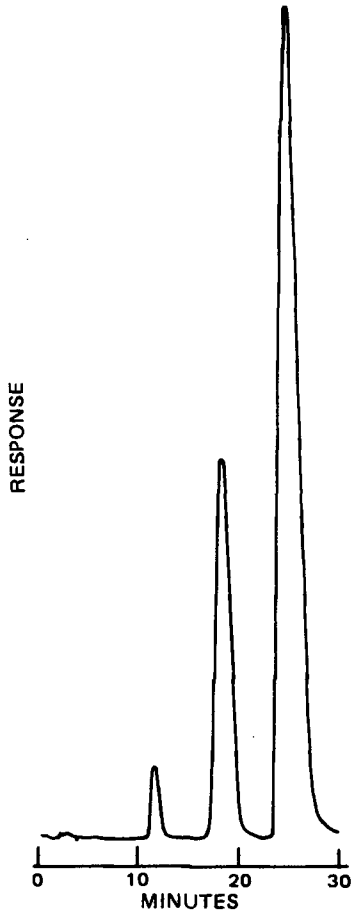

Figure 1—*High-pressure liquid chromatogram of the equilibrium mixture of I. The pH of the mobile phase was 2.5.*

(2). This evidence, used to support Structure II, also supports Structure I.

Sandmann *et al.* (2) reported that attempts to methylate the alternate form of III resulted in complex mixtures. In the present investigation, methylation of the alternate form with diazomethane in ether gave methyl esters of III and I if the reaction was allowed to stand with excess diazomethane. If the diazomethane was added and followed immediately by the addition of acetic acid, only the methyl ester of I resulted. These reactions were followed by HPLC and NMR. The NMR parameters of these products are shown in Table I.

One key factor causing Sandmann *et al.* to assign the alternate form of III as II was the absence of a hydroxylic proton in the NMR spectrum (2). As shown in Table I, this proton is visible in the NMR spectrum of the methyl ester of the alternate form taken in dimethyl sulfoxide-d_6. Furthermore, the downfield shift for H-1 of the alternate form compared with its shift in III is attributed to ester formation at C-1. Whereas ester formation at C-1 should cause such a shift, hemi-ortho esters should shift in the opposite direction, *e.g.*, HCO_2CH_3, δ CH_3 = 3.79; $HOCH_3$, δ CH_3 = 3.47; and $HC(OCH_3)_3$, δ CH_3 = 3.33 (8). None of the NMR data reported previously (2) supports arguments against Structure I as the alternate form of III. In addition, the stability of a hemi-ortho ester (9)

Table I—Proton Chemical Shift Values (Parts per Million) for the Methyl Esters of I and III

Proton	Methyl Ester of I		Methyl Ester of III	
	Chloroform	Dimethyl Sulfoxide-d_6	Chloroform	Dimethyl Sulfoxide-d_6
Phenyl C-3 and C-5 2H	8.18–8.30 m	8.175, 8.27	8.18–8.30 m	8.155–8.24
Phenyl C-2 and C-6 2H	7.54–7.60 m	7.565, 7.65	7.54–7.66 m	7.61–7.695
NH	7.00–7.20 m	8.62 d (J = 9 Hz)	(7.0–7.2)	8.55 d
C-1 H	6.29 d (J = 6.5 Hz)	6.02 d (J = 5 Hz)	5.14 br s	5.05 br s
$CHCl_2$	5.95 s	6.47 s	5.81 s	6.64 s
C-2 H	4.20–4.60 m[a]	4.04–4.42 m	4.2–4.6 m[a]	4.04–4.42 m[a]
OCH_3	3.70 s	3.585	3.72 s	3.61 s
C-3 H	3.50–3.85 m	3.20–3.60	4.2–4.6 m[a]	4.04–4.42 m[a]
C-3 OH	4.2–4.6 m[a]	5.10 t (J = 5 Hz)	—	—
C-1 OH	—	—	?	6.24 d (J = 4.5 Hz)
CH_2CH_2	2.72 s	2.67 m	2.69 s	2.57 s

[a] Two unresolved protons were detected within this shift range.

Table II—^{13}C-NMR Spectra of Chloramphenicol, III, and I [a]

Carbon	Chemical Shift		
	Chloramphenicol	III	I[a,b]
C-1 (CHO)	69.02 (d)	69.51 (d)	72.75 (d)
C-2 (CHN)	56.79 (d)	53.52 (d)	54.94 (d)
C-3 (CH_2O)	60.27 (t)	63.13 (t)	59.67 (t)
Phenyl C-1 (C)	151.18 (s)	150.14 (s)	145.52* (s)
Phenyl C-2 and C-6 (CH)	127.29 (d)	127.42 (d)	127.64 (d)
Phenyl C-3 and 3-5 (CH)	122.84 (d)	122.85 (d)	123.22 (d)
Phenyl C-4 (CNO_2)	146.44 (s)	146.62 (s)	146.98* (s)
Amide C-2 (C=O)	163.38 (s)	163.64 (s)	163.51 (s)
Amide-2 ($CHCl_2$)	66.43 (d)	66.24 (d)	66.37 (d)
Succinyl C-1 (CO_2R)		171.84 (s)	171.18 (s)
Succinyl C-2 (CH_2)		28.60 (t)	28.80+ (t)
Succinyl C-3 (CH_2)		28.60 (t)	28.53+ (t)
Succinyl C-4 (CO_2H)		173.29 (s)	173.21 (s)

[a] Obtained in dimethyl sulfoxide-d_6; values are in parts per million from tetramethylsilane; letters in parentheses refer to peak character in off-resonance decoupled spectrum (s, singlet; d, doublet; and t, triplet). [b] The *, + indicate that these pairs of assignments may be reversed.

under the conditions used to isolate II by Sandmann *et al.* is questionable.

Finally, ^{13}C-NMR (a technique unavailable to Sandmann *et al.* at the time of their investigation) was used to verify the structure of I. The carbon chemical shifts of chloramphenicol and its two succinate derivatives are shown in Table II. The peaks near 163.5 and 66.3 ppm are consistent through the three spectra and are assigned as the carbonyl and methine carbons of the dichloroacetamide moiety, respectively. These shifts are quite consistent with shifts reported by Stothers (10) of 169.7 and 63.8 ppm for dichloroacetic acid and 165.0 and 69.7 ppm for dichloroacetyl chloride.

The assignment of the phenyl carbon shifts for the compounds of this study is based on the shifts of the equivalent carbons of *p*-nitrostyrene (C-1 = 143.6, C-2 and C-6 = 126.0, C-3 and C-5 = 123.1, and C-4 = 146.5 ppm) reported by Dhami and Stothers (11). The upfield shift of C-1 of the phenyl group of I relative to the other two compounds is due to the greater substitution at C-1 of the side chain in I. The assignments of C-1, C-2, and C-3 of the side chain are based on chemical shift and off-resonance decoupling results. The 2-carbon is at the highest field and shows a slight upfield shift on acylation (γ-substitution) at either C-1 or C-3. The 3-carbon is a triplet under off-resonance decoupling conditions. The 1- and 3-carbons show the expected downfield shifts on acylation. The succinyl moiety is assigned on the basis of the succinic acid shifts (CH_2 = 30.0 and CO_2H = 176.4 ppm) reported by Stothers (10). The carboxyl carbons are assigned at a lower field than the ester carbons, as is normally the case.

Most pertinent to the central argument of this paper are the shifts of the succinyl ester carbons at 171.84 and 171.18 ppm. The great similarity of these shifts argues that I is a normal ester, as is III. Furthermore, although reports of chemical shifts for hemi-ortho esters such as II are very rare due to their chemical instability, two such compounds are reported (12) as having shifts of a hemi-orthoacetate carbon at 77.1 ppm. This field shift is surprisingly high and may not be typical, but the ortho ester carbon of ethyl orthoformate absorbs at 112 ppm and those of two orthoacetates absorb at 118.1 and 119.5 ppm (12). It is unreasonable to suppose that the hemi-ortho ester carbon of II absorbs at 171 ppm, which is typical of a normal ester carbonyl carbon.

EXPERIMENTAL

Materials—The equilibrium mixture of III and its alternate form was obtained by dissolving 600 mg of chloramphenicol-3-monosuccinate[2] in 3 ml of water, adjusting the pH to 7.5 with 0.1 *N* NaOH, and allowing the resulting solution to stand at ambient temperature overnight.

Equipment—HPLC was carried out using a reversed-phase column[3] coupled to a UV detector[4] set at 254 nm.

Both the double-focusing mass spectrometer[5] and the NMR spectrometer[6] were coupled to data systems.

Procedures—One hundred microliters of the equilibrium mixture was injected onto the preparative reversed-phase column[5]. The components of the mixture were separated by isocratic elution using 0.01 *M* NaH_2PO_4–40% acetonitrile (final pH adjusted to 2.5 with phosphoric acid) as the mobile phase. A flow rate of 1 ml/min was used for analytical runs, and a rate of 2 ml/min was used for preparative runs. The eluate for each component was extracted with ethyl acetate and dried with magnesium sulfate. The volume of ethyl acetate was reduced by rotary evaporation, and the products were stored at −10° under a nitrogen atmosphere until they were analyzed.

Methylations were carried out by reaction with excess diazomethane[7] in ether. Trimethylsilylation was accomplished by adding 200 μl of *N,O*-bis(trimethylsilyl)acetamide in dimethylformamide[8] (2.5 mg/ml) to a solution of the target compound in acetonitrile.

REFERENCES

(1) F. H. Schmidt and W. Vömel, *Klin. Wochenschr.*, **43**, 535 (1965).

(2) B. Sandmann, D. Szulczewski, J. Windheuser, and T. Higuchi, *J. Pharm. Sci.*, **59**, 427 (1970).

(3) J. T. Burke, W. A. Wargin, and M. R. Blum, *ibid.*, **69**, 909 (1980).

(4) M. Margosis, *ibid.*, **59**, 501 (1970).

(5) G. Janssen and H. Vanderhaeghe, *J. Chromatogr.*, **82**, 297 (1973).

(6) T. Nakagawa, M. Mesada, and T. Uno, *ibid.*, **111**, 355 (1975).

(7) K. Nakanishi, "Infrared Absorption Spectroscopy," Holden Day, San Francisco, Calif., 1962, pp. 43–45.

(8) C. J. Pouchert and J. R. Campbell, Aldrich Library of NMR Spectra, Aldrich Chemical Co., Milwaukee, Wis., 1974.

(9) M. Ahmad, R. G. Bergstrom, M. J. Cashen, Y. Chiang, A. J. Kresge, R. A. McClelland, and M. F. Powell, *J. Am. Chem. Soc.*, **101**, 2669 (1979).

(10) J. B. Stothers, "Carbon-13 NMR Spectroscopy," Academic, New York, N.Y., 1972.

(11) K. S. Dhami and J. B. Stothers, *Can. J. Chem.*, **43**, 510 (1965).

(12) D. A. H. Taylor, *J. Chem. Soc., Perkin Trans. I*, **1974**, 437.

ACKNOWLEDGMENTS

The authors thank Ms. J. Sabatka for assistance with the HPLC.

[2] Obtained from Parke-Davis Co. as chloramphenicol sodium succinate (lot 391769A).

[3] A Bio Rad Bio Sil ODS 10, 25-cm × 4-mm column was used for analytical qualitative analysis. A Waters Associates μBondapak C_{18}, 30-cm × 7.8-mm column was used for preparative work.

[4] Waters Associates model 450 variable-wavelength detector.

[5] Varian MAT 731.

[6] Varian XL-100.

[7] Made by the reaction *p*-tolylsulfonylmethylnitrosamide (Diazaid, Aldrich Chemical Co.) with base.

[8] TRI-SIL/BSA formula D, Pierce Chemical Co.

High-Pressure Liquid Chromatographic Assay for Chloramphenicol, Chloramphenicol-3-monosuccinate, and Chloramphenicol-1-monosuccinate

J. T. BURKE *, W. A. WARGIN *x, and M. R. BLUM ‡

Received July 19, 1979, from the **School of Pharmacy, University of North Carolina, Chapel Hill, NC 27514*, and the ‡*Wellcome Research Laboratories, Burroughs Wellcome Co., Research Triangle Park, NC 27709.* Accepted for publication November 30, 1979.

Abstract □ A high-pressure liquid chromatographic method for the sensitive and rapid determination of chloramphenicol, chloramphenicol-3-monosuccinate, and chloramphenicol-1-monosuccinate is presented. The procedure utilizes a reversed-phase chromatographic column with UV absorption detection. The assay is useful for monitoring patients receiving chloramphenicol, determining the pharmacokinetics of parenteral chloramphenicol sodium succinate, and certifying sterile chloramphenicol sodium succinate.

Keyphrases □ Chloramphenicol—simultaneous high-pressure liquid chromatographic assay with chloramphenicol-3-monosuccinate and chloramphenicol-1-monosuccinate □ High-pressure liquid chromatography—analysis, chloramphenicol, chloramphenicol-3-monosuccinate, and chloramphenicol-1-monosuccinate □ Antibiotics—chloramphenicol, simultaneous high-pressure liquid chromatographic assay with chloramphenicol-3-monosuccinate and chloramphenicol-1-monosuccinate

Chloramphenicol, a broad spectrum antibiotic, is available for parenteral administration as the sodium salt of the 3-monosuccinate ester[1]. This prodrug is biologically inactive and must be converted to chloramphenicol base by hydrolysis of the ester in the liver (1). Glazko *et al.* (2) reported that ~30% of a dose administered to normal adults is excreted unhydrolyzed in the urine. Consequently, impaired renal and/or hepatic function may affect the bioavailability of active chloramphenicol when administered parenterally as the sodium succinate salt.

Chloramphenicol-3-monosuccinate (III) exists in equilibrium with chloramphenicol-1-monosuccinate (I) at pH values near neutrality (3) (Scheme I). A colorimetric assay (4) for the simultaneous measurement of chloramphenicol and chloramphenicol succinate is tedious and lacks specificity. Numerous chromatographic methods have been developed for determining chloramphenicol in biological fluids (5–14), but none included the quantification of chloramphenicol succinate. The current Food and Drug Administration spectrophotometric assay for certifying chloramphenicol sodium succinate for injection (15) does not differentiate among chloramphenicol, III, and I. This paper presents a high-pressure liquid chromatographic (HPLC) method that allows the simultaneous quantification of these compounds.

EXPERIMENTAL

Materials—Reagent grade acetic acid[2], sodium acetate[3], deionized water, and HPLC grade acetonitrile[3] were used to prepare the mobile phase. Pure chloramphenicol[4] and chloramphenicol-3-monosuccinate[5] (III) were dissolved in ethyl acetate[3] to prepare the standard solutions. The internal standard solution was benzocaine[6] in methanol[3] (0.06 mg/ml). Trichloroacetic acid[3] (30%) was used for protein precipitation.

Instrument Conditions—The liquid chromatograph[7] was equipped with a variable-wavelength UV detector. The effluent was monitored at 275 nm with 0.05 aufs. An integrator[8] and a recorder[9] were used to monitor the detector output. A reversed-phase column[10] (25 cm long × 4 mm i.d.) was maintained at 50°. The mobile phase consisted of a 22% solution (v/v) of acetonitrile in 0.05 *M* sodium acetate. The pH of the final solution was adjusted to 5.7 with acetic acid. The flow rate was 1.25 ml/min.

Determination of Equivalence of Molar Absorbance of I and III—A 0.05 *M* phosphate buffer adjusted to pH 7.4 was used to prepare 13 1.0-ml samples of 9.08×10^{-5} *M* III. Immediately after preparation, the samples were incubated at 37° for various periods. The internal standard (50 μl) was added to the sample at the end of the incubation, and a 90-μl portion was injected immediately onto the high-pressure liquid chromatograph.

A standard curve for III and chloramphenicol was prepared in a 0.05 *M* phosphate buffer at pH 4.0. The concentrations of III, I, and chloramphenicol were determined by relating the peak area ratios of the unknowns to the internal standard and comparing them to the standard curves. The standard curve for III was used to quantitate III and I. The apparent first-order forward, k_f, and reverse, k_r, rate constants describing the equilibrium between III and I (Scheme I) were estimated using the NONLIN program (16) with the following equations and unweighted data:

$$A = \frac{A_0 k_r}{k_f + k_r} + \frac{A_0 k_f}{k_f + k_r} e^{-(k_f + k_r)t} \qquad \text{(Eq. 1)}$$

$$B = \frac{A_0 k_f}{k_f + k_r} - \frac{A_0 k_f}{k_f + k_r} e^{-(k_f + k_r)t} \qquad \text{(Eq. 2)}$$

$$K_{eq} = \frac{k_f}{k_r} \qquad \text{(Eq. 3)}$$

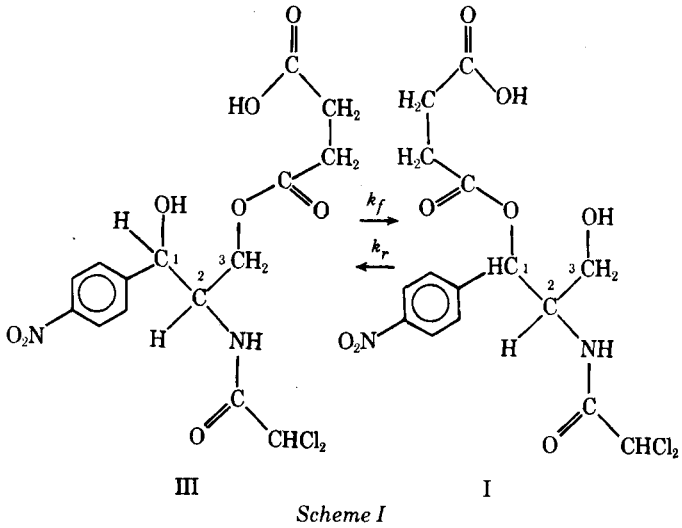

III ⇌ I

Scheme I

[1] The USAN name chloramphenicol sodium succinate refers to the sodium salt of the 3-monosuccinate ester. Chloramphenicol sodium succinate is marketed as Chloromycetin Sodium Succinate by Parke-Davis Co.
[2] J. T. Baker Chemical Co.
[3] Fisher Scientific Co.
[4] Lot 423256, courtesy of Parke-Davis Co.
[5] Lot 441339, courtesy of Parke-Davis Co.
[6] Eastman Kodak Co.
[7] Model 7000, Micromeritics Instrument Corp.
[8] CDS 111, Varian Associates.
[9] Fisher Recordall series 5000, Fisher Scientific Co.
[10] LiChrosorb RP-18, E. Merck.

0022-3549/80/0800-0909$01.00/0
© 1980, American Pharmaceutical Association

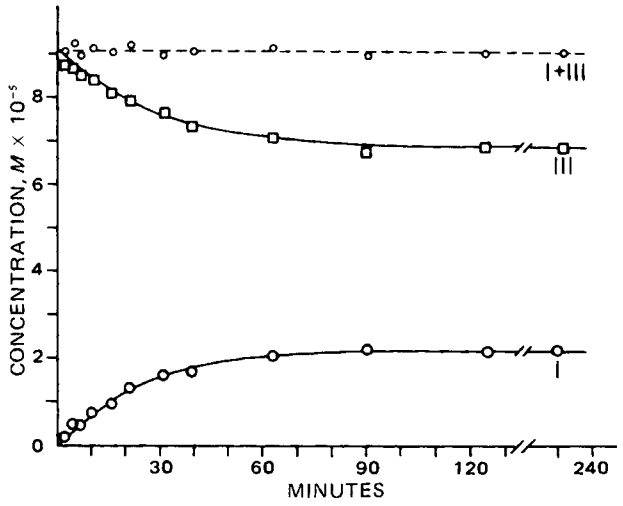

Figure 1—*Rearrangement of III to I in pH 7.4 phosphate buffer at 37°*

where A is the concentration of III, B is the concentration of I, and A_0 is the concentration of III at $t = 0$.

Quantitation of III, I, and Chloramphenicol in Biological Fluids—Blood samples treated with ethylenediaminetetraacetic acid were placed immediately in an ice bath. The plasma was separated and adjusted to pH ~4 by the addition of 20 μl of 4 *N* HCl/ml of plasma. A 250-μl sample was transferred to a 15-ml conical glass tube. The internal standard (25 μl) was added immediately before precipitation with 50 μl of a 30% solution of trichloroacetic acid. The sample was vortexed for 10 sec and then centrifuged for 10 min at 2500 rpm. A portion of the supernate (90 μl) was injected.

Urine samples were centrifuged to remove the sediment and diluted to concentrations of 1:100–1:500. The internal standard (25 μl) was added to 250 μl of the diluted urine sample, and 90 μl then was injected. Plasma standards containing III and chloramphenicol were prepared for each patient using a quantity of his own acidified plasma (pH 4.0). Phosphate buffer (pH 4.0) was used to prepare standards for urine assays.

Stability of III in Plasma—Two portions of fresh human plasma were adjusted to pH 4.0 and 7.4, respectively, and were used to prepare 250-μl samples containing 61.1 μg of III/ml[11]. Sets of plasma samples adjusted to pH 7.4 were incubated at 37, 25, and 0°. The pH 4.0 plasma samples were incubated at 25 and 0°. The concentrations of I, III, and chloramphenicol were determined at 0.5, 1.0, 2.0, 6.0, 12.0, and 24.0 hr.

Effect of Plasma Protein Concentration on Drug Recovery for Assay—Plasma samples from three normal volunteers were each diluted with normal saline to prepare 1:0, 3:1, 1:1, 1:3, and 0:1 dilutions (plasma to normal saline). The pH of each solution was adjusted to 4.0 with 4 *N* HCl and then spiked with 25 μg of chloramphenicol/ml and 19.1 μg of III/ml. Then 100 μl of trichloracetic acid (30%) was added to 0.5-ml samples of each solution. The samples were vortexed for 10 sec and centrifuged for 10 min at 2500 rpm.

A portion of the supernate (250 μl) was transferred to a 15-ml conical glass tube. The internal standard (25 μl) was added to the supernate, the sample was vortexed for 10 sec, and a portion of the supernate (90 μl) was injected. The absolute recoveries of both drugs at the 1:0, 3:1, 1:1, and 1:3 dilutions were determined by relating the peak area ratios of the drugs to the internal standard at these plasma dilutions to the peak area ratios obtained from the 0:1 dilution.

Rearrangement of III to I in Plasma—Citrated human plasma adjusted to pH 7.4 was used to prepare 250-μl samples of 30.5 μg of III/ml. Immediately after preparation, the samples were incubated for various periods at 37°. At the end of the incubation, 50 μl of 30% trichloroacetic acid was added to the sample. The sample then was vortexed for 10 sec and centrifuged for 10 min at 2500 rpm. A portion of the supernate (90 μl) was injected onto the high-pressure liquid chromatograph. The peak area ratio of III to the sum of III and I was determined at the various time intervals. The rate constants for the equilibrium between III and I were estimated by the NONLIN program employing Eq. 1 with unweighted data.

[11] The concentrations of I and III are expressed as chloramphenicol equivalents. The relationship is such that 1.0 mg of the acid form of either ester will yield 0.7635 mg of chloramphenicol upon hydrolysis.

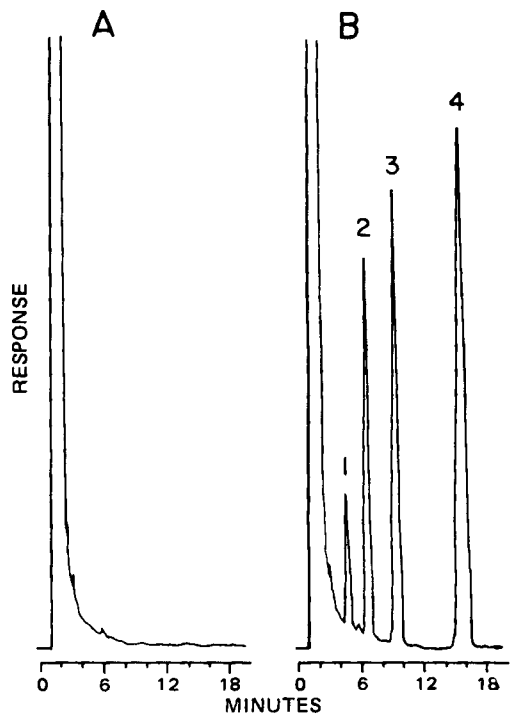

Figure 2—*Sample chromatogram for the assay in plasma. Key: A, blank plasma; B, spiked plasma; 1, I (4.4 μg/ml); 2, III (14.2 μg/ml); 3, chloramphenicol (13.7 μg/ml); and 4, benzocaine internal standard.*

RESULTS AND DISCUSSION

Determination of Equivalence of Molar Absorbance of I and III—The standard curve for the quantification of III also was used to quantitate I. Compound III is commercially available and is stable in crystalline form. Compound I, a pale-yellow oil at room temperature, is difficult to weigh accurately and transfer, rearranges to III under ambient conditions, and can be isolated only by preparative liquid chromatography or other suitable chromatographic methods. Although the technique of utilizing the standard curve for III to quantitate I and III offers numerous advantages, it is valid only if the molar absorptivities for I and III are equivalent for the specified instrument conditions.

The validity of this assumption was tested by measuring the concentrations of III and I as III rearranged to I. If the sum of the concentrations of I and III are constant utilizing a standard curve prepared from III to quantitate both I and III, then the molar absorptivities are equivalent. Figure 1 illustrates the rearrangement of III to I and the resulting equilibrium between the two compounds. The mean sum of the concentrations of I and III was $9.08 \pm 0.10 \times 10^{-5}$ *M* ($\pm SD$, $CV = 1.1\%$) for the 13 determinations. Since this value was constant within very narrow limits and showed no trend as the ratio of the concentration of the two compounds changed, no difference was detected in the molar absorptivities of I and III.

The assumption that the molar absorptivities of I and III are equivalent may not be valid for a different mobile phase or if the effluent is monitored at a different wavelength, although studies demonstrated that the molar absorptivities also were equivalent when the mobile phase pH was adjusted to 4.0 or 7.0. The technique also assumes that neither I nor III forms any other compounds during the sampling interval. The only other compound that could be detected was chloramphenicol, which formed slowly and amounted to only 0.19×10^{-5} *M* at the 230-min sample. This process was considered negligible for the purpose of evaluating the equivalence of the molar absorptivities of III and I.

Quantification in Biological Fluids—A typical chromatogram for the assay in plasma is presented in Fig. 2. Changes in the mobile phase pH had a dramatic effect on the retention times of III and I. Both I and III eluted before chloramphenicol when the mobile phase pH was 5.7 and after chloramphenicol when the mobile phase pH was 4.0. A summary of sample standard curves for chloramphenicol and III in plasma is presented in Table I. Three determinations were performed at each concentration. The intercepts for both standard curves were not significantly different from zero. Linear regression analysis of four-point standard curves for 14 patients demonstrated excellent correlation ($r^2 = 0.991$–1.000 for chloramphenicol and $r^2 = 0.998$–1.000 for III).

Table I—Standard Curves for Chloramphenicol and III

	Chloramphenicol					III				
Concentration, μg/ml	100	40	20	10	1	152.71	76.35	30.54	7.64	0.76
Mean peak area ratio[a]	4.152	1.698	0.874	0.439	0.043	4.816	2.555	1.058	0.265	0.028
CV, %	2.32	1.42	1.02	1.32	0.46	0.26	1.19	0.73	4.15	6.91
Slope[b]			0.0417					0.0320		

[a] Drug to standard. [b] Forced through the origin.

Table II—Stability of III in Plasma Expressed as Percent Converted to Chloramphenicol

Plasma pH	Temperature	Hours 0.5	1.0	2.0	6.0	12.0	24.0
4.0	0°	0	0.1	0.5	0.6	0.9	0.8
4.0	25°	0.4	0.5	1.2	1.4	2.5	4.3
7.4	0°	0.3	0.3	0.5	2.3	4.1	5.3
7.4	25°	0.4	0.7	1.0	2.6	3.5	5.4
7.4	37°	0.8	2.1	1.8	10.8	24.1	27.8

Table III—Stability of III in Plasma Expressed as Percent of I[a]

Plasma pH	Temperature	Hours 0.5	1.0	2.0	6.0	12.0	24.0
4.0	0°	0	0	0	0	0	0
4.0	25°	0	1.7	3.4	4.3	5.0	6.4
7.4	0°	2.8	4.1	5.2	14.8	28.8	32.1
7.4	25°	31.9	32.0	30.8	33.7	33.3	29.8
7.4	37°	30.1	30.8	31.4	30.3	32.1	30.9

[a] (I)/[(I) + (III)].

Potential assay interference was investigated by adding the following drugs to plasma: phenytoin, aspirin, penicillin, ampicillin, cefazolin, cimetidine, oxacillin, theophylline, phenobarbital, isoniazid, gentamicin, ethambutol, probenecid, sulfamethoxazole, and trimethoprim. These compounds did not produce a chromatographic peak or did not have the same retention time as chloramphenicol. Trimethoprim interfered with the quantification of I.

Stability of III in Plasma—Tables II and III illustrate the effects of pH and temperature on the stability of III in plasma. The recovery was 61.3 ± 1.8 μg/ml (±*SD*) for these determinations. The results at physiological conditions confirm findings by previous investigators (1) that chloramphenicol succinate is not rapidly hydrolyzed by plasma esterases to chloramphenicol.

Since rearrangement of III to I proceeded rapidly at pH 7.4 and 25°, it was necessary to acidify plasma to pH 4.0 before preparing a standard curve for III. Optimal conditions to prevent the rearrangement involve placing plasma in an ice bath and acidifying the plasma to pH 4.0. The addition of 20 μl of 4 *N* HCl/ml of plasma is sufficient to lower the pH of plasma to ~4.0.

Both III and I were isolated from the plasma and urine of human subjects. Preparing biological samples to study the rearrangement of III *in vivo* or to study independently the pharmacokinetics of I and III poses certain problems. The best method of plasma preparation involves immediately placing blood samples on ice and separating the plasma in a refrigerated centrifuge. The samples then should be acidified as described previously while the plasma is still cooled to 0°.

Although I and III possess different chemical structures, the usefulness of studying the pharmacokinetics of these compounds independently is mitigated by the fact that the two compounds are in rapid equilibrium. Doses of chloramphenicol succinate contain approximately the same fraction of I that appears in human urine and plasma. An analysis of 13 doses of chloramphenicol succinate[12] prepared in a hospital pharmacy by dilution in 50 ml of 5% dextrose injection revealed that 20.0 ± 1.7% (±*SD*) of the dose existed as I immediately prior to administration. Doses were administered between 1 and 24 hr after preparation.

Effect of Plasma Concentration on Drug Recovery for Assay—The absolute recoveries for chloramphenicol and III were 63.0 ± 2.4 and 49.2 ± 2.3% (±*SD*), respectively, when the samples were prepared with 30% trichloroacetic acid. These relatively low recoveries were the result of drug binding to the denatured protein. The effect of protein concentration on the absolute recovery of chloramphenicol and III is illustrated in Fig. 3.

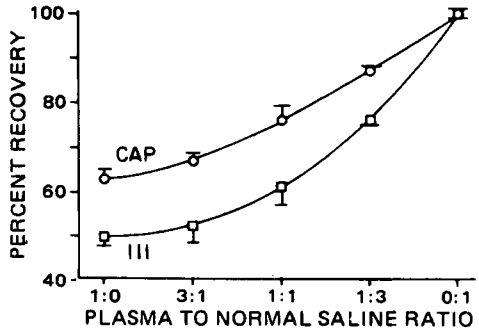

Figure 3—*Effect of protein concentration on drug recovery for assay for various ratios of plasma to normal saline (CAP = chloramphenicol).*

Table IV—Kinetic Parameters for the Rearrangement of III to I

Medium	k_f, min^{-1}	k_r, min^{-1}	$\frac{0.693}{k_f + k_r}$, min	K_{eq}	r^2
Buffer	0.0097	0.0297	17.6	0.327	0.990
Plasma	0.0285	0.0681	7.2	0.418	0.996

Although the absolute recovery for the trichloroacetic acid method is less than optimal, it is adequate for assaying chloramphenicol in the therapeutic range. It offers the advantage of minimal sample preparation time and produces cleaner solutions for injection than does organic solvent extraction. The major disadvantage to the trichloroacetic acid method is that the standard curve should be prepared from the plasma of the individual patient. This approach is preferable because quantitative and qualitative differences in the plasma protein composition might affect the absolute recovery of the compounds assayed.

Kinetics of Rearrangement of III to I—The kinetics of the rearrangement of III to I were studied *in vitro* in a phosphate buffer and plasma at physiological pH and temperature (Table IV). The apparent K_{eq} in the buffer was different from that in plasma (Fig. 4).

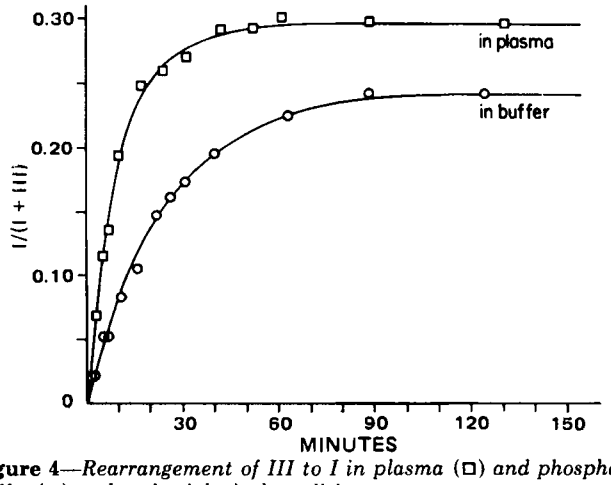

Figure 4—*Rearrangement of III to I in plasma (□) and phosphate buffer (○) under physiological conditions.*

[12] Chloromycetin Sodium Succinate, Parke-Davis Co.

The apparent K_{eq} in plasma may be greater because I is more extensively protein bound. It also may result from the use of trichloroacetic acid as a protein precipitant.

CONCLUSIONS

Chloramphenicol-3-monosuccinate (III) exists in rapid equilibrium with chloramphenicol-1-monosuccinate (I) under physiological conditions and in intravenous solutions prepared for administration. The analytical technique developed permits the quantification of chloramphenicol, I, and III in biological fluids and reconstituted commercial preparations. The methodology may be adapted for certifying chloramphenicol sodium succinate and offers advantages over the current FDA spectrophotometric method, which does not differentiate between these compounds. The analysis of I was simplified by demonstrating that I and III have similar molar absorptivities.

The results of previous investigators who reported that chloramphenicol succinate is not rapidly hydrolyzed by plasma esterases were confirmed. A rapid analytical technique is offered that will allow future studies of the effects of renal and hepatic disease on the pharmacokinetics and bioavailability of chloramphenicol sodium succinate.

REFERENCES

(1) F. H. Schmidt and W. Vomel, *Klin. Wochenschr.*, **43**, 535 (1965).

(2) A. J. Glazko, W. A. Dill, A. W. Kinkel, J. R. Goulet, W. J. Holloway, and R. A. Buchanan, *Clin. Pharmacol. Ther.*, **21**, 104 (1977).

(3) D. A. Brent, P. Chandrasurin, A. Ragouzeos, B. S. Hurlbert, and J. T. Burke, *J. Pharm. Sci.*, **69**, 906 (1980).

(4) A. O'Hara, M. Maruyama, and M. Yamgaki, *Takamine Res. Inst. Annu. Rep.*, **10**, 178 (1958).

(5) J. R. Koup, B. Brodsky, A. Lau, and T. R. Beam, *Antimicrob. Agents Chemother.*, **13**, 439 (1978).

(6) C. J. Least, N. J. Wiegand, G. F. Johnson, and H. M. Soloman, *Clin. Chem.*, **23**, 220 (1977).

(7) R. H. B. Sample, M. R. Glick, M. B. Kleiman, J. W. Smith, and T. O. Oei, *Antimicrob. Agents Chemother.*, **15**, 491 (1979).

(8) I. Nilsson-Ehle, G. Kahlmeter, and P. Nilsson-Ehle, *J. Antimicrob. Chemother.*, **4**, 169 (1978).

(9) J. M. Wal, J. C. Peteran, and G. Bories, *J. Chromatogr.*, **145**, 502 (1978).

(10) R. L. Thies and L. J. Fisher, *Clin. Chem.*, **24**, 778 (1978).

(11) T. Nakagawa, M. Masada, and T. Uno, *J. Chromatogr.*, **111**, 355 (1975).

(12) G. L. Resnick, D. Corbin, and D. H. Sandberg, *Anal. Chem.*, **38**, 582 (1966).

(13) L. K. Pickering, J. L. Hoecker, W. G. Kramer, and J. G. Lieber, *Clin. Chem.*, **25**, 300 (1979).

(14) G. Janssen and H. Vanderhaeghe, *J. Chromatogr.*, **114**, 266 (1975).

(15) *Code of Federal Regulations*, Title 21: Food and Drugs, Section 455: 12a (1977).

(16) C. M. Metzler, G. K. Elfring, and A. J. McEwen, *Biometrics*, **3**, 562 (1974).

ACKNOWLEDGMENTS

Supported in part by Faculty Research Council Grant VF648 from the University of North Carolina at Chapel Hill.

Solubility and Partitioning I: Solubility of Nonelectrolytes in Water

SAMUEL H. YALKOWSKY ˣ **and SHRI C. VALVANI**

Received July 6, 1979, from the *Pharmacy Research Unit, The Upjohn Company, Kalamazoo, MI 49001.* Accepted for publication March 17, 1980.

Abstract □ On the basis of a semiempirical analysis, an equation was obtained that enables the estimation of the aqueous solubility of either liquid or crystalline organic nonelectrolytes:

$$\log S_w \approx -1.00 \log PC - 1.11 \frac{\Delta S_f(MP - 25)}{1364} + 0.54$$

where log PC and ΔS_f are estimated from the chemical structure and MP is either known or experimentally determined. Analysis of this equation provides a means of assessing the role of crystal structure [as reflected by the melting point (MP) and the entropy of fusion (ΔS_f)] and of the activity coefficient [as reflected by the octanol–water partition coefficient (PC)] in controlling the aqueous solubility of a drug. Techniques are also provided for estimating the entropy of fusion of organic compounds.

Keyphrases □ Solubility—nonelectrolytes in water, estimation techniques □ Nonelectrolytes—estimation of solubility in water □ Aqueous solubility—nonelectrolytes, estimation techniques

Aqueous solubility has long been recognized as a key factor in controlling drug efficacy. Before an orally administered drug can become available to its receptor, it first must dissolve in the GI fluid. Both the dissolution rate and the maximum amount of drug that can be dissolved are governed by the solubility of the drug in the medium (1).

The design of orally active drugs must account for the effects of structural modifications on solubility. The lack of sufficient aqueous solubility often causes a drug to appear inactive or less active than some reference compound of a series. Aqueous solubility is a key factor in the design of parenteral and ophthalmic formulations, and it also is important in controlling taste. For these reasons, some appreciation of the relationship between aqueous solubility and chemical structure is needed.

THEORETICAL

In spite of the tremendous importance of aqueous solubility in pharmacy and other applied chemical disciplines, it is a poorly understood phenomenon. There are no generally useful guidelines for estimating the solubility of a substance in water from a consideration of its structure and physical properties. One reason that solubility of crystalline compounds has successfully defied attempts to make it predictable is that it is not a simple equilibrium but rather a combination of equilibria.

This report attempts to provide some guidelines for understanding the factors that govern aqueous solubility and for estimating the aqueous solubility of nonelectrolytes. Subsequent reports will deal with the estimation of the solubility of weak electrolytes.

Factors Influencing Aqueous Solubility—The aqueous solubility of a drug is governed by three major factors: (*a*) the entropy of mixing; (*b*) the difference between the drug–water (DW) adhesive interactions and the sum of the drug–drug (DD) and water–water (WW) cohesive interactions; and (*c*) the additional drug–drug interactions associated with the lattice energy of crystalline drugs, which are designated $\overline{DD}$ and are not applicable to liquids.

The entropy of mixing can be thought of as a force that favors complete

0022-3549/80/0800-0912$01.00/0

© 1980, American Pharmaceutical Association

The apparent K_{eq} in plasma may be greater because I is more extensively protein bound. It also may result from the use of trichloroacetic acid as a protein precipitant.

CONCLUSIONS

Chloramphenicol-3-monosuccinate (III) exists in rapid equilibrium with chloramphenicol-1-monosuccinate (I) under physiological conditions and in intravenous solutions prepared for administration. The analytical technique developed permits the quantification of chloramphenicol, I, and III in biological fluids and reconstituted commercial preparations. The methodology may be adapted for certifying chloramphenicol sodium succinate and offers advantages over the current FDA spectrophotometric method, which does not differentiate between these compounds. The analysis of I was simplified by demonstrating that I and III have similar molar absorptivities.

The results of previous investigators who reported that chloramphenicol succinate is not rapidly hydrolyzed by plasma esterases were confirmed. A rapid analytical technique is offered that will allow future studies of the effects of renal and hepatic disease on the pharmacokinetics and bioavailability of chloramphenicol sodium succinate.

REFERENCES

(1) F. H. Schmidt and W. Vomel, *Klin. Wochenschr.*, **43**, 535 (1965).

(2) A. J. Glazko, W. A. Dill, A. W. Kinkel, J. R. Goulet, W. J. Holloway, and R. A. Buchanan, *Clin. Pharmacol. Ther.*, **21**, 104 (1977).

(3) D. A. Brent, P. Chandrasurin, A. Ragouzeos, B. S. Hurlbert, and J. T. Burke, *J. Pharm. Sci.*, **69**, 906 (1980).

(4) A. O'Hara, M. Maruyama, and M. Yamgaki, *Takamine Res. Inst. Annu. Rep.*, **10**, 178 (1958).

(5) J. R. Koup, B. Brodsky, A. Lau, and T. R. Beam, *Antimicrob. Agents Chemother.*, **13**, 439 (1978).

(6) C. J. Least, N. J. Wiegand, G. F. Johnson, and H. M. Soloman, *Clin. Chem.*, **23**, 220 (1977).

(7) R. H. B. Sample, M. R. Glick, M. B. Kleiman, J. W. Smith, and T. O. Oei, *Antimicrob. Agents Chemother.*, **15**, 491 (1979).

(8) I. Nilsson-Ehle, G. Kahlmeter, and P. Nilsson-Ehle, *J. Antimicrob. Chemother.*, **4**, 169 (1978).

(9) J. M. Wal, J. C. Peteran, and G. Bories, *J. Chromatogr.*, **145**, 502 (1978).

(10) R. L. Thies and L. J. Fisher, *Clin. Chem.*, **24**, 778 (1978).

(11) T. Nakagawa, M. Masada, and T. Uno, *J. Chromatogr.*, **111**, 355 (1975).

(12) G. L. Resnick, D. Corbin, and D. H. Sandberg, *Anal. Chem.*, **38**, 582 (1966).

(13) L. K. Pickering, J. L. Hoecker, W. G. Kramer, and J. G. Lieber, *Clin. Chem.*, **25**, 300 (1979).

(14) G. Janssen and H. Vanderhaeghe, *J. Chromatogr.*, **114**, 266 (1975).

(15) *Code of Federal Regulations*, Title 21: Food and Drugs, Section 455: 12a (1977).

(16) C. M. Metzler, G. K. Elfring, and A. J. McEwen, *Biometrics*, **3**, 562 (1974).

ACKNOWLEDGMENTS

Supported in part by Faculty Research Council Grant VF648 from the University of North Carolina at Chapel Hill.

Solubility and Partitioning I: Solubility of Nonelectrolytes in Water

SAMUEL H. YALKOWSKY ˣ **and SHRI C. VALVANI**

Received July 6, 1979, from the *Pharmacy Research Unit, The Upjohn Company, Kalamazoo, MI 49001.* Accepted for publication March 17, 1980.

Abstract □ On the basis of a semiempirical analysis, an equation was obtained that enables the estimation of the aqueous solubility of either liquid or crystalline organic nonelectrolytes:

$$\log S_w \approx -1.00 \log PC - 1.11 \frac{\Delta S_f(MP - 25)}{1364} + 0.54$$

where log PC and ΔS_f are estimated from the chemical structure and MP is either known or experimentally determined. Analysis of this equation provides a means of assessing the role of crystal structure [as reflected by the melting point (MP) and the entropy of fusion (ΔS_f)] and of the activity coefficient [as reflected by the octanol–water partition coefficient (PC)] in controlling the aqueous solubility of a drug. Techniques are also provided for estimating the entropy of fusion of organic compounds.

Keyphrases □ Solubility—nonelectrolytes in water, estimation techniques □ Nonelectrolytes—estimation of solubility in water □ Aqueous solubility—nonelectrolytes, estimation techniques

Aqueous solubility has long been recognized as a key factor in controlling drug efficacy. Before an orally administered drug can become available to its receptor, it first must dissolve in the GI fluid. Both the dissolution rate and the maximum amount of drug that can be dissolved are governed by the solubility of the drug in the medium (1).

The design of orally active drugs must account for the effects of structural modifications on solubility. The lack of sufficient aqueous solubility often causes a drug to appear inactive or less active than some reference compound of a series. Aqueous solubility is a key factor in the design of parenteral and ophthalmic formulations, and it also is important in controlling taste. For these reasons, some appreciation of the relationship between aqueous solubility and chemical structure is needed.

THEORETICAL

In spite of the tremendous importance of aqueous solubility in pharmacy and other applied chemical disciplines, it is a poorly understood phenomenon. There are no generally useful guidelines for estimating the solubility of a substance in water from a consideration of its structure and physical properties. One reason that solubility of crystalline compounds has successfully defied attempts to make it predictable is that it is not a simple equilibrium but rather a combination of equilibria.

This report attempts to provide some guidelines for understanding the factors that govern aqueous solubility and for estimating the aqueous solubility of nonelectrolytes. Subsequent reports will deal with the estimation of the solubility of weak electrolytes.

Factors Influencing Aqueous Solubility—The aqueous solubility of a drug is governed by three major factors: (*a*) the entropy of mixing; (*b*) the difference between the drug–water (DW) adhesive interactions and the sum of the drug–drug (DD) and water–water (WW) cohesive interactions; and (*c*) the additional drug–drug interactions associated with the lattice energy of crystalline drugs, which are designated $\overline{DD}$ and are not applicable to liquids.

The entropy of mixing can be thought of as a force that favors complete

0022-3549/80/0800-0912$01.00/0

© 1980, American Pharmaceutical Association

miscibility of all components. If $DD + WW - 2DW = 0$ for a liquid solute (*i.e.*, $\overline{DD} = 0$), the solubility is governed only by the entropy of mixing, which is assumed to be ideal. On a mole fraction scale, the ideal solubility of a liquid, X_i^l, is equal to unity and $\log X_i^l = 0$.

In general, the liquid interaction term and the crystal interaction term combine to reduce the aqueous solubility of most drugs by:

$$2.303RT \log X = -(DD + WW - 2DW) - \overline{DD} \qquad \text{(Eq. 1)}$$

If the material is crystalline, the crystalline interactions reduce the solubility by $\overline{DD} = -2.303RT \log X_i^c$, where X_i^c is the ideal solubility of a crystalline compound.

The difference between the adhesive and cohesive forces usually is described (2) by an activity coefficient for the drug in water, γ_w, by:

$$(DD + WW - 2DW) = 2.303RT \log \gamma_w \qquad \text{(Eq. 2)}$$

If the left side is equal to zero, γ_w must equal unity. If $DD + WW - 2DW > 0$, the solubility will be less than ideal. If $DD + WW - 2DW \gg 0$ (as usually is the case for nonelectrolytes in water), there usually will be less than total miscibility and the drug will have a finite solubility in water, X_w. These equations assume that there is no significant mutual miscibility of the drug and water phases. Therefore, *DD* and *WW* refer to the pure phases. A more sophisticated treatment would account for the fact that each phase contains some of the other phase. This treatment would have the effect of increasing *DD* and decreasing *WW*. Mathematically, X_w, X_i, and γ_w are related by:

$$\log X_w = \log X_i - \log \gamma_w \qquad \text{(Eq. 3)}$$

The greater the difference between the adhesive and cohesive forces, the greater is the deviation from ideality and, in general, the lower is the solubility.

If $DD + WW - 2DW = 0$ and the drug is crystalline, $\overline{DD}$ will cause the ideal mole fractional solubility to be less than unity. In most instances, both $DD + WW - 2DW$ and $\overline{DD}$ are greater than zero, so solubility is inhibited by a combination of the liquid interaction term, $\log \gamma_w$, and the crystal interaction term, $\log X_i$. To understand the aqueous solubility of crystalline drugs, it is necessary to consider these terms separately. This report will attempt to provide some insight into the dependence of these terms on chemical structure and, thereby, to present a means for their estimation and thus the estimation of the aqueous solubility of a variety of nonelectrolytes.

Ideal Solubility of Crystals—As already stated, the ideal solubility of a crystalline drug (*i.e.*, its solubility in an ideal solvent) is dependent only on the nature of the crystal. According to Hildebrand and Scott (2), the ideal solubility of a crystalline substance expressed as its mole fraction, X_i^c, is:

$$\log X_i^c = \frac{-\Delta H_f}{2.303R}\left[\frac{T_m - T}{T_m T}\right] + \frac{\Delta C_p}{2.303R}\left[\frac{(T_m - T)}{T} - \log \frac{T_m}{T}\right] \qquad \text{(Eq. 4)}$$

where ΔH_f is the molar heat of fusion of the solid; R is the gas constant; T_m and T are the absolute melting point and temperature of interest, respectively; and ΔC_p is the difference in heat capacity of the crystalline and molten forms of the drug. Since ΔC_p usually is quite small, and since $(T_m - T)/T$ is approximately equal to $\ln(T_m/T)$, the last term in Eq. 4 usually can be ignored without any significant loss in accuracy. Therefore, as a reasonable approximation, X_i^c can be approximated from T_m (°K), T (°K), and ΔH_f by:

$$\log X_i^c \simeq -\frac{\Delta H_f}{2.303RT_m}\frac{(T_m - T)}{T} \qquad \text{(Eq. 5)}$$

Both ΔH_f and T_m depend on the chemical structure of the solute, and both of these parameters tend to increase with increasing molecular weight and increasing polarity. However, these relationships have not proven to be amenable to estimation with any degree of reliability.

Since the free energy of fusion, ΔG, is equal to zero at the melting point, $\Delta H_f/T_m$ can be replaced with ΔS_f, where ΔS_f is the entropy of fusion. At 25 °C, Eq. 5 becomes:

$$\log X_i^c = -\frac{\Delta S_f}{1364}(T_m - 298) \qquad \text{(Eq. 6)}$$

For convenience, the difference in absolute temperatures can be replaced with the difference in centigrade temperatures:

$$\log X_i^c = -\frac{\Delta S_f}{1364}(MP - 25) \qquad \text{(Eq. 7)}$$

where *MP* is the melting point of the drug on the conventional centigrade scale.

The advantage of Eq. 7 over Eq. 5, in addition to its greater simplicity, is that ΔS_f is more understandable and more predictable than ΔH_f (1).

The real aqueous solubility of a crystalline drug, X_w^c, differs from the ideal solubility in the same manner as described for liquids. Thus:

$$\log X_w^c = -\frac{\Delta S_f}{1364}(MP - 25) - \log \gamma_w \qquad \text{(Eq. 8)}$$

From Eq. 8, it is apparent that the estimation of aqueous solubility requires the estimation of two parameters, ΔS_f and $\log \gamma_w$. The remainder of this report deals with the estimation of these parameters for nonelectrolytes and their application to the estimation of aqueous solubility.

EXPERIMENTAL

Entropies of Fusion—All entropies of fusion were calculated from the heats of fusion and melting points. These quantities were either obtained from the literature (3) or were determined experimentally on a differential thermal analyzer with a high-pressure differential scanning calorimeter cell[1]. The literature values were obtained at atmospheric pressure. The experimentally determined values were obtained at 500 psi as described by Martin *et al.* (4) to inhibit sublimation of the more volatile compounds. It was determined that this pressure had little or no effect on the entropy of fusion of nonvolatile compounds; thus, it was assumed that it had no effect on the entropy of fusion of the volatile crystals studied.

Reliable values for the entropy of fusion of three solids could not be determined experimentally. *p*-Aminophenol decomposed before melting, even under 1000 psi of nitrogen. Phthalic acid dehydrated upon melting to form phthalic anhydride. Terephthalic acid sublimed, even under 1000 psi of nitrogen, as evidenced by a coating of the compound around the inside of the calorimeter cell. However, this coating was insoluble in dilute sodium hydroxide and had the texture of a polymer, suggesting that some chemical change (possibly to a linear anhydride) occurred as well. Therefore, the data were excluded from the analysis.

Partition Coefficients—Octanol–water partition coefficients were calculated from the fragment constants, *f*, developed by Nys and Rekker (5) with the following modifications. Secondary and tertiary hydroxyl groups were given *f* values of −1.14 and −0.71, respectively. For the steroids, the experimentally determined values of Tomida *et al.* (6) were used. These values (which were determined under the same conditions as were used to determine the aqueous solubilities) were used because current methods of estimating partition coefficients are unreliable when applied to steroids.

Aqueous Solubilities—The aqueous solubilities of the various classes of compounds were obtained as follows.

The solubilities of halobenzenes were determined spectrophotometrically after equilibration for 24 hr and filtration through sintered glass as described by Yalkowsky *et al.* (7).

Alkyl *p*-aminobenzoate solubilities were determined in the manner described by Yalkowsky *et al.* (8).

The solubilities of polycyclic aromatic compounds were determined as described by MacKay and Shiu (9).

Steroid solubilities were determined as described by Tomida *et al.* (6).

The alcohol solubility data were obtained by averaging data from over 30 sources taken from a compilation[2] of solubility data.

Statistical Analysis of Data—Multiple regression analysis of the data was performed using standard statistical procedures.

RESULTS AND DISCUSSION

Estimation of Entropy of Fusion—In this section, a strictly geometric interpretation of the melting process will be utilized to provide a simple and easily understood means of estimating entropy. Since entropy is a state function, consideration of how the process occurs is not required. Only the initial and final states, *i.e.*, the crystal and the melt, are important. On a molecular level, the most obvious difference between these states is their relative degree of geometric order. The intermolecular distance, the packing arrangement, the orientation, and the conformation of crystalline molecules are held within a much narrower range in the crystal than for the liquid.

[1] DuPont model 910.

[2] S. H. Yalkowsky and S. C. Valvani, unpublished data.

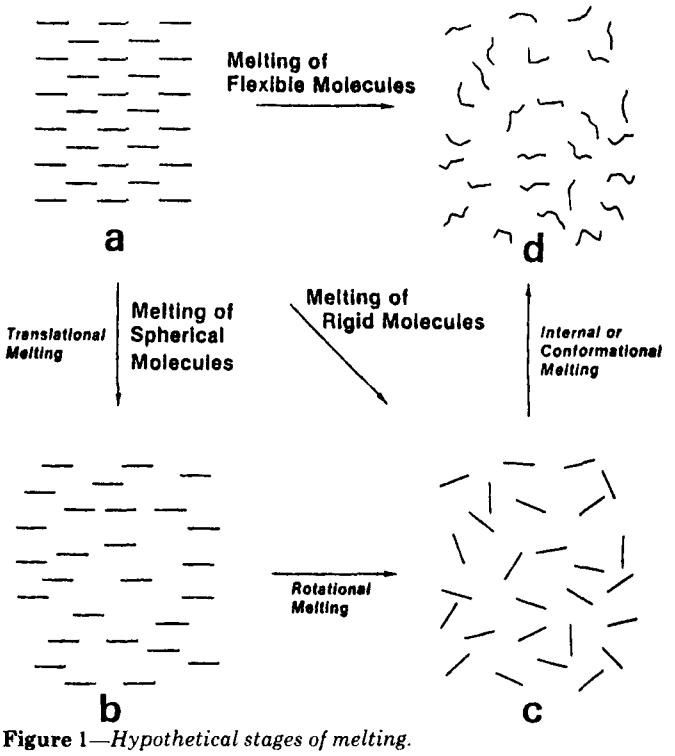

Figure 1—*Hypothetical stages of melting.*

For conceptualization, the melting process can be divided into three subprocesses (4):

1. Translational melting—the change from the ordered arrangement of the molecular centers of gravity in the crystal to the expanded and more randomized arrangement in the liquid.

2. Rotational melting—the change from the ordered arrangement of the major axes of crystalline molecules to the randomly oriented arrangement in the liquid. (This process is not applicable to spherical molecules.)

3. Internal melting—the change from the uniform conformation of flexible molecules of the crystal to the random conformation of such molecules in the liquid. (This process is not applicable to rigid molecules and, thus, to most drugs. However, it does become important for long chain molecules.)

These subprocesses are illustrated in Fig. 1. Since the total entropy is dependent only on the initial and final states, these processes can be treated for convenience as occurring sequentially. For spherical molecules, only translational melting can occur. For rigid nonspherical molecules, both translational and rotational melting exist. All three steps are applicable to the melting of flexible molecules, *i.e.*, those that can undergo conformational changes to an appreciable extent.

The geometrical entropy of a liquid, S_L, is related to the number of ways, W_L, in which its molecules can be arranged that would be consistent with the liquid state by $S_L = R \ln W_L$. Similarly, the geometrical entropy of a crystalline solid, S_c, is related to the number of ways, W_c, of arranging the molecules in the crystal by $S_c = R \ln W_c$. It is assumed that W_c is a subset of W_L; *i.e.*, the crystal arrangement is a special case of the more general, less constrained liquid arrangement.

The molar entropy of fusion, ΔS_f, is equal to the entropy of the liquid minus the entropy of the crystal:

$$\Delta S_f = S_L - S_c = -R \ln \left(\frac{W_c}{W_L}\right) = -R \ln P_f \qquad \text{(Eq. 9)}$$

where P_f is the ratio of the number of ways of achieving the crystal to the number of ways of achieving the liquid. It is equal to the probability (above the melting point) of a collection of 1 mole of liquid molecules spontaneously arranging themselves in such a way as to fulfill the geometrical requirements of the crystal. This quantity will be referred to as the total geometrical probability of fusion and is assumed to be equal to the product of the subprocess probabilities:

$$P_f = P_{trans} P_{rot} P_{int} \qquad \text{(Eq. 10)}$$

Since the entropies of the subprocesses are related to their probability of occurrence by equations analogous to Eq. 9, and since the probabilities are assumed to be multiplicative, the entropies must be additive:

$$\Delta S_f = \Delta S_{trans} + \Delta S_{rot} + \Delta S_{int} \qquad \text{(Eq. 11)}$$

Thus, the total entropy of fusion can be estimated from the probabilities of the component processes of fusion.

Translational Entropy of Fusion—The translational entropy of fusion can be visualized by a two-dimensional analogy. Consider a field of disks or checkers that have been trapped into a nearly closest packed arrangement (Fig. 1*a*) as representing a two-dimensional crystal. When this crystal melts, a slight expansion and a randomization of the positions of the disks occur (Fig. 1*b*). The probability of two-dimensional fusion taking place is equal to the number of arrangements of the disks that are possible within the area allotted for the solid divided by the much greater number of arrangements that are possible within the area allowed for the liquid. This, in turn, is related to the ratio of the areas available within each phase for the disks to occupy, *i.e.*, to the ratio of free areas. In a three-dimensional arrangement of molecules, the ratio of free volumes rather than free areas would be of concern.

As already stated, spherical molecules can gain only translational entropy when they melt. The entropies of fusion for spherical molecules such as the inert gases and for pseudospherical molecules such as methane and carbon tetrachloride usually fall within the range of 3–4 eu. A value of 3.5 eu can be considered as a reasonable approximation for the translational entropy of fusion of all molecules (although nonspherical molecules tend to have a somewhat larger volume change associated with fusion).

Rotational Entropy of Fusion—The rotational entropy of fusion is a component of the total entropy of fusion of all nonspherical molecules. For rigid molecules, it is the only term in addition to the translational entropy that needs to be considered. From the data in Tables I and II, it appears that most rigid aromatic molecules have entropies of fusion between 11 and 16 eu. This constancy of the entropy of fusion has been noted repeatedly in the literature (10–13) but has not been explained.

If it is assumed that the translational contribution to the entropy of fusion is ~3.5 eu, as noted earlier, then the rotational entropy of rigid aromatic molecules must be ~10 ± 3 eu.

An intuitive justification of the nearly constant rotational entropy of fusion is based on the following two assumptions:

1. In the crystal, the molecules (with their centers of mass fixed and accounted for by ΔS_{int}) can wobble or vibrate (~10° in the spherical coordinates ϕ and θ from their most stable position after averaging over all axes).

2. In the liquid, the individual molecules have much greater orientational freedom and can rotate over a much wider range of ϕ and θ.

The probability difference between the two degrees of rotational freedom can be evaluated easily by comparing the areas available to a point on the molecular surface in each phase, provided that the range of ϕ and θ in the two phases is known. If it is assumed for simplicity that a liquid molecule can rotate freely, any reference point will trace out a sphere about the center of gravity of the molecule. If the molecule is restricted orientationally, as it is in the crystal, the reference point will trace out only a spherical segment.

For example, the area of a spherical segment obtained by a ±10° variation in θ and ϕ is 0.00754 times that of a sphere of the same radius. Thus, the probability of n molecules being oriented within the allowed limits for crystallinity is 0.00754^n and the entropy contribution is $-k \ln 0.00754^n$ or ~10 eu. Similarly, the entropy associated with $\theta = \phi = 20°$ is 7 eu. Although the actual values of θ and ϕ probably will depend on the overall geometry of the molecules and their degree of interaction, the relative constancy of ΔS_f for rigid molecules suggests that the variation is not too large or, more likely, that factors inhibiting rotation in the liquid also inhibit rotation in the crystal.

The assumption of free rotation in the liquid is used only for mathematical convenience and probably is physically inappropriate in many cases. However, the entropy estimate is based on the ratio of areas available to the reference point in the two phases. If the liquid rotation is restricted, as it would be in highly elongated or hydrogen-bonded molecules, then the rotation in the solid also is more restricted for the same reasons. The constancy of the entropy of fusion of rigid molecules suggests that, in these cases, the ratio of the rotational freedom in the liquid to the solid is the same.

Pirsch (14, 15) suggested that elongated molecules have higher entropies of fusion; Bondi (10) postulated that, because of their restricted motion in the liquid, hydrogen-bonded molecules have lower entropies of fusion than their hydrocarbon homomorphs. These postulates are not supported by the data available for rigid molecules.

As can be seen in Table I, there is no systematic effect of hydrogen bonding on entropy of fusion. Specifically, the isomeric xylenes and their

Table I—Entropy of Fusion Values for Disubstituted Benzenes

Position	No H-Bonding Groups Substituents		ΔS_f	One H-Bonding Group Substituents		ΔS_f	Two H-Bonding Groups Substituents		ΔS_f
ortho	CH_3	CH_3	13.2	OH	CH_3	12.4	OH	OH	14.4
meta			12.4			9.0			15.2
para			14.2			9.6			14.6
ortho	CH_3	Cl	—	OH	Cl	9.1	OH	NH_2	12.8
meta			—			9.2			11.2
para			12.9			11.1			—
ortho	CH_3	Br	—	OH	Br	9.7	OH	COOH	10.8
meta			—			—			14.7
para			12.0			10.5			12.2
ortho	CH_3	NO_2	—	OH	NO_2	12.5	NH_2	NH_2	12.0
meta			14.6			13.8			11.5
para			13.9			13.0			10.4
ortho	Cl	Cl	12.1	NH_2	CH_3	—	NH_2	COOH	11.8
meta			12.2			—			11.5
para			13.4			13.5			10.8
ortho	Cl	Br	—	NH_2	Cl	—	COOH	COOH	—
meta			12.2			—			18.9
para			13.3			13.8			—
ortho	Cl	NO_2	13.7	NH_2	Br	13.0			
meta			16.1			—			
para			11.7			14.4			
ortho	Br	Br	11.0	NH_2	NO_2	11.2			
meta			12.1			12.0			
para			13.5			14.6			
ortho	Br	NO_2	16.3	COOH	CH_3	14.9			
meta			13.7			9.8			
para			10.0			12.0			
ortho	NO_2	NO_2	13.9	COOH	Cl	14.9			
meta			11.5			13.3			
para			15.1			15.0			
				COOH	Br	13.2			
						11.9			
						15.5			
				COOH	NO_2	15.9			
						11.3			
						17.2			
Average			13.1			12.6			12.7

corresponding dihydroxybenzenes have nearly identical entropies of fusion. The degree of substitution of the benzene ring does not have any systematic effect, as is evidenced by the data for the halobenzenes. Molecular size and shape also appear to have no effect on the entropy of fusion (for compounds larger than benzene).

Surprisingly, there is no systematic difference in entropy with respect to the position of substitution (Table I). The decreased rotational entropy of the more symmetrical compounds evidently is offset by the increased translational entropy that results from their greater packing efficiency. Highly prolate ellipsoids such as diphenyl, anthracene, and naphthacene and highly oblate ellipsoids such as hexamethylbenzene, hexachlorobenzene, and coronene all have entropies of fusion in the range discussed.

Internal Entropy of Fusion—The internal or conformational entropy of fusion results from the fact that molecular configuration is fixed invariably in the crystal but not in the liquid. For example, a molecule of stearic acid is likely to be found only in the *anti*-conformation in a crystal, whereas many bonds are likely to be *gauche* in the liquid.

If twist angles of only 60° (*gauche*), 180° (*anti*), and 300° (*gauche*) are possible and if these three angles are equally probable, then the probability of finding a long chain molecule in the completely outstretched conformation is equal to $(1/3)^{n-3}$, where n is the number of carbon and heteroatoms in the chain and $n - 3$ is the number of twist angles. The entropy associated with this probability is:

$$\Delta S_{int} = -R(n - 3) \ln (1/3) = 2.2(n - 3) \quad \text{(Eq. 12)}$$

For reasons discussed previously (16), the internal entropy of fusion is better approximated by $2.5(n - 5)$. Molecules having less than five units in a flexible chain can be treated as rigid molecules as a first approximation.

Total Entropy of Fusion—On the basis of the preceding discussion, the entropy of fusion is dependent primarily on molecular geometry. For spherical or nearly spherical molecules:

$$\Delta S_f = \Delta S_{trans} = 3.5 \text{ eu} \quad \text{(Eq. 13)}$$

For rigid molecules:

$$\Delta S_f = \Delta S_{trans} + \Delta S_{rot} = 13.5 \text{ eu} \quad \text{(Eq. 14)}$$

For molecules having $n > 5$ nonhydrogen atoms in a flexible chain:

$$\Delta S_f = \Delta S_{trans} + \Delta S_{rot} + \Delta S_{int} = 13.5 + 2.5(n - 5) \text{ eu} \quad \text{(Eq. 15)}$$

Some small nonspherical molecules have very small rotational entropies and thus have entropies of fusion falling between 3.5 and 13 eu. Fortuitously, these compounds, like spherical molecules, melt below room temperature and thus have ideal mole fractional solubilities of unity. In other words, the term involving ΔS_f is equal to zero.

Estimation of Ideal Solubility—The ideal room temperature solubility of the various classes of molecules can be calculated by simply inserting the entropy of fusion approximation into Eq. 7 to give:

$$-\log X_i = 0.01(MP - 25) \quad \text{(Eq. 16)}$$

for rigid nonspherical molecules and:

$$-\log X_i = [0.01 + 0.0018(n - 5)](MP - 25) \quad \text{(Eq. 17)}$$

for partially flexible molecules. The logarithms of the ideal solubilities of a wide variety of compounds calculated from experimentally measured entropies of fusion and from these approximations are listed in Table II. The two values rarely differ by more than 0.3 log unit (*i.e.*, by a factor of two). In fact, the solubility estimates frequently are better than the entropy estimates from which they were generated.

The high accuracy of this approach results in part because compounds that are more spherical or that are highly flexible and thus are likely to have the greatest error in ΔS_f estimation are compounds that tend to have low melting points, so the product $(MP - 25)\ \Delta S_f$ is small and thus does not contribute greatly to the calculation, *i.e.*, $\log X_i$ is near zero.

Statistical analysis of the calculated (from Eq. 7) and approximated (from Eq. 16 or 17) ideal solubilities of the compounds in Table II gives the following:

$$\log X_{calc} = 0.962 \log X_{estim} - 0.020 \quad \text{(Eq. 18)}$$

$$r = 0.96 \quad s = 0.16$$

Since the compounds considered were chosen previously (3) (*i.e.*, there was no subjective selection by the present investigators), this analysis probably can be regarded as an objective test of the relationships dis-

Table II—Calculation of Ideal Solubility of Some Model Compounds [a]

Compound	*MP*	ΔS_f Obs., eu	$n-5$	ΔS_f Estim., eu	log *X* Ideal Calc. (Eq. 7)	log *X* Ideal Estim. (Eq. 16 or 17)	Residual
Cyclohexanol	25.5°	1.41[a]	—	13.5[a]	0.001	0.005	−0.004
Cyanamide	44.0°	1.69	—	13.5	0.024	0.190	−0.166
Succinonitrile	54.5°	2.86	—	13.5	0.062	0.295	−0.233
Trichloroacetic acid	57.5°	4.25	—	13.5	0.101	0.325	−0.224
tert-Butyl alcohol	25.4°	5.44	—	13.5	0.002	0.004	−0.002
Crotonic acid	72.0°	6.32	—	13.5	0.218	0.470	−0.252
Levulinic acid	33.0°	7.20	—	13.5	0.042	0.080	−0.038
Phenol	40.9°	8.60	—	13.5	0.100	0.159	−0.059
cis-Crotonic acid	71.2°	8.73	—	13.5	0.296	0.462	−0.166
α-Chloroacetic acid	61.2°	8.78	—	13.5	0.23-	0.362	−0.129
Menthol	43.5°	9.20	—	13.5	0.125	0.185	−0.060
p-Cresol	34.6°	9.24	—	13.5	0.065	0.096	−0.031
m-Toluic acid	108.8°	9.84	—	13.5	0.605	0.838	−0.233
Phenylacetic acid	76.7°	9.90	—	13.5	0.376	0.517	−0.141
α-Naphthylamine	50.0°	9.90	—	13.5	0.182	0.250	−0.068
β-Chloroacetic acid	56.0°	10.09	—	13.5	0.229	0.310	−0.081
Hydrazobenzene	134.0°	10.36	—	13.5	0.828	1.090	−0.262
Benzoic acid	122.4°	10.47	—	13.5	0.748	0.974	−0.226
p-Bromophenol	63.5°	10.54	—	13.5	0.298	0.385	−0.087
Diphenyl	165.5°	10.69	—	13.5	1.102	1.405	−0.303
DL-Carvoxime	91.0°	10.72	—	13.5	0.519	0.660	−0.141
p-Aminobenzoic acid	188.5°	10.83	—	13.5	1.299	1.635	−0.336
Thiosinamine	77.0°	11.10	—	13.5	0.423	0.520	−0.097
m-Nitrobenzoic acid	141.1°	11.13	—	13.5	0.948	1.161	−0.213
D-Carvoxime	71.5°	11.17	—	13.5	0.381	0.465	−0.084
o-Nitroaniline	71.2°	11.19	—	13.5	0.379	0.462	−0.083
L-Carvoxime	70.0°	11.28	—	13.5	0.372	0.450	−0.078
Urethan	48.7°	11.31	—	13.5	0.197	0.237	−0.040
m-Dinitrobenzene	89.7°	11.45	—	13.5	0.543	0.647	−0.104
β-Naphthol	120.6°	11.46	—	13.5	0.804	0.956	−0.152
Benzoquinone	112.9°	11.48	—	13.5	0.740	0.879	−0.139
m-Aminobenzoic acid	179.5°	11.53	—	13.5	1.306	1.545	−0.239
o-Nitrophenol	45.1°	11.70	—	13.5	0.172	0.201	−0.029
o-Aminobenzoic acid	145.0°	11.80	—	13.5	1.039	1.200	−0.161
p-Bromotoluene	28.0°	11.85	—	13.5	0.026	0.030	−0.004
Allocinnamic acid	68.0°	11.88	—	13.5	0.375	0.430	−0.055
D-Dimethyl tartrate	49.0°	11.89	—	13.5	0.209	0.240	−0.031
m-Nitroaniline	147.0°	12.00	—	13.5	1.074	1.220	−0.146
p-Toluic acid	179.6°	12.00	—	13.5	1.361	1.546	−0.185
Phenanthrene	96.3°	12.07	—	13.5	0.631	0.713	−0.082
2,4,6-Tribromophenol	93.0°	12.09	—	13.5	0.603	0.680	−0.077
m-Diiodobenzene	34.2°	12.39	—	13.5	0.084	0.092	−0.008
Succinic anhydride	119.0°	12.44	—	13.5	0.858	0.940	−0.082
p-Bromoiodobenzene	90.1°	12.59	—	13.5	0.601	0.651	−0.050
Benzil	95.2°	12.65	—	13.5	0.651	0.702	−0.051
Naphthalene	80.2°	12.72	—	13.5	0.515	0.552	−0.037
Thymol	51.5°	12.72	—	13.5	0.247	0.265	−0.018
o-Toluic acid	103.7°	12.79	—	13.5	0.738	0.787	−0.049
p-Dichlorobenzene	53.1°	13.10	—	13.5	0.270	0.281	−0.011
Diphenylamine	53.0°	13.10	—	13.5	0.269	0.280	−0.011
Hydrocinnamic acid	48.0°	13.17	—	13.5	0.222	0.230	−0.008
D-Diiodobenzene	129.0°	13.29	—	13.5	1.014	1.040	−0.026
Resorcinol	110.0°	13.29	—	13.5	0.828	0.850	−0.022
p-Iodotoluene	84.0°	13.32	—	13.5	0.088	0.090	−0.002
Cinnamic acid	133.0°	13.32	—	13.5	1.055	1.080	−0.025
m-Chlorobenzoic acid	154.2°	13.34	—	13.5	1.264	1.292	−0.028
Nitronaphthalene	56.7°	13.36	—	13.5	0.311	0.317	−0.006
Benzophenone	47.9°	13.36	—	13.5	0.224	0.229	−0.005
p-Dibromobenzene	86.0°	13.50	—	13.5	0.604	0.610	−0.006
Benzylaniline	23.4°	13.52	—	13.5	−0.016	−0.016	0.000
Carbazole	243.0°	13.63	—	13.5	2.178	2.180	−0.002
p-Toluidine	43.3°	13.77	—	13.5	0.185	0.183	0.002
Chloral hydrate	47.4°	13.82	—	13.5	0.227	0.224	0.003
Azoxybenzene	36.0°	13.87	—	13.5	0.112	0.110	0.002
o-Dinitrobenzene	116.9°	13.90	—	13.5	0.937	0.919	0.018
p-Chloronitrobenzene	33.5°	13.93	—	13.5	0.597	0.585	0.012
Methyl cinnamate	36.0°	13.93	—	13.5	0.112	0.110	0.002
Hydroxyacetanilide	91.3°	13.94	—	13.5	0.678	0.663	0.015
Anthraquinone	284.8°	13.99	—	13.5	2.665	2.598	0.067
2,4-Dinitrotoluene	70.1°	14.01	—	13.5	0.463	0.451	0.012
Anthracene	216.5°	14.09	—	13.5	1.979	1.915	0.064
Durene	79.3°	14.25	—	13.5	0.567	0.543	0.024
D-Tetrachloroxylene	86.0°	14.28	—	13.5	0.639	0.610	0.029
2,4,6-Trinitrotoluene	80.8°	14.34	—	13.5	0.587	0.558	0.029
Pyrocatechol	105.0°	14.39	—	13.5	0.844	0.800	0.044
Glutaric acid	97.5°	14.54	—	13.5	0.773	0.725	0.048
Quinol	172.3°	14.55	—	13.5	1.572	1.473	0.099
m-Chloronitrobenzene	44.4°	14.58	—	13.5	0.207	0.194	0.013
p-Nitroaniline	114.0°	14.62	—	13.5	0.954	0.890	0.064
p-Tetrachloroxylene	95.0°	14.65	—	13.5	0.752	0.700	0.052

Table II—*Continued*

Compound	*MP*	ΔS_f Obs., eu	$n-5$	ΔS_f Estim., eu	log X Ideal Calc. (Eq. 7)	log X Ideal Estim. (Eq. 16 or 17)	Residual
o-Chlorobenzoic acid	140.2°	14.88	—	13.5	1.257	1.152	0.105
p-Nitrophenol	113.8°	15.00	—	13.5	0.977	0.888	0.089
p-Chlorobenzoic acid	239.7°	15.03	—	13.5	2.367	2.147	0.220
p-Dinitrobenzene	173.5°	15.06	—	13.5	1.640	1.485	0.155
m-Xylene dichloride	34.0°	15.19	—	13.5	0.100	0.090	0.010
α-Naphthol	95.0°	15.26	—	13.5	0.783	0.700	0.083
p-Xylene dichloride	100.0°	15.36	—	13.5	0.845	0.750	0.095
Methyl oxalate	54.4°	15.38	—	13.5	0.332	0.294	0.038
o-Xylene dichloride	55.0°	15.49	—	13.5	0.341	0.300	0.041
Azobenzene	61.7°	15.74	—	13.5	0.424	0.367	0.057
o-Nitrobenzoic acid	148.5°	15.88	—	13.5	1.438	1.235	0.203
m-Xylene dibromide	77.0°	16.18	—	13.5	0.617	0.520	0.097
Dimethylpyrone	132.0°	16.59	—	13.5	1.302	1.070	0.232
p-Nitrobenzoic acid	239.2°	17.23	—	13.5	2.706	2.142	0.564
DL-Dimethyl tartrate	87.0°	17.38	—	13.5	0.790	0.620	0.170
o-Xylene dibromide	95.0°	17.39	—	13.5	0.893	0.700	0.193
Stilbene	124.0°	18.16	—	13.5	1.318	0.990	0.328
Apiol	29.5°	18.95	—	13.5	0.063	0.045	0.018
Undecilic acid	28.3°	19.91	5	26	0.048	0.063	0.015
Capric acid	32.0°	21.95	6	28.5	0.113	0.147	0.034
Methyl fumarate	102.0°	22.26	1	17	1.257	0.963	0.295
Camphene	51.0°	23.26	—	13.5	0.443	0.260	0.183
Cinnamic anhydride	48.0°	24.40	—	13.5	0.411	0.230	0.181
Cetyl alcohol	49.3°	25.43	12	43.5	0.453	0.777	−0.324
Lauric acid	43.2°	27.70	6	28.5	0.370	0.381	−0.011
Palmitic acid	61.8°	30.01	10	38.5	0.810	1.042	−0.232
Tricosane	47.6°	31.13	18	58.5	0.516	0.972	−0.456
Myristic acid	54.0°	33.17	8	33.5	0.705	0.714	−0.007
Nonadecane	32.1°	35.89	14	48.5	0.187	0.253	−0.066
Heneicosane	40.5°	36.37	16	53.5	0.413	0.610	−0.197
Docosane	44.4°	36.86	17	56	0.524	0.799	−0.175
Stearic acid	68.8°	39.57	12	43.5	1.271	1.401	−0.130
Tetracosane	50.9°	40.51	19	61	0.769	1.162	−0.393
Pentacosane	53.7°	42.24	20	63.5	0.889	1.340	−0.451
Heptacosane	59.0°	43.50	21	66	1.085	1.650	−0.565
Octacosane	61.4°	46.21	22	68.5	1.233	1.833	−0.600
Elaidic acid	44.4°	46.35	13	46	0.659	0.656	0.003
Octadecane	28.2°	48.71	13	46	0.114	0.108	0.006
Eicosane	36.8°	53.91	15	51	0.467	0.443	0.024
Tristearin	54.5°	122.67	49	135	2.654	2.928	−0.274

[a] The compounds listed have melting points above 25° for which heat of fusion data are given in Ref. 3. The list therefore is not in any way weighted toward good agreement with theory. All entropy data are in entropy units.

Table III—Calculated Entropies of Fusion and Ideal Solubilities of Alkyl *p*-Aminobenzoates at 37°

Ester	*MP*	ΔS_f Obs. (Ref. 3)	$n-5$	13.5 + 2.5 $(n-5)$	log X_i Calc. (Eq. 6)	log X_i Estim. (Eq. 7)	$\Delta \log X_i$ (Residual)
Methyl	112°	15.1[a]	0	13.5	0.80	0.75	0.05
Ethyl	89°	13.1	0	13.5	0.49	0.53	−0.04
Propyl	74°	14.6	0	13.5	0.37	0.36	0.01
Butyl	56°	17.8	1	16.0	0.24	0.24	0.00
Pentyl	52°	17.8	2	18.5	0.20	0.26	−0.06
Hexyl	61°	25.2	3	21.0	0.43	0.44	−0.01
Heptyl	75°	18.1	4	23.5	0.50	0.76	−0.26
Octyl	71°	28.3	5	26.0	0.68	0.78	−0.10
Nonyl	69°	31.4	6	28.5	0.69	0.78	−0.09
Dodecyl	82°	41.5	9	36.0	1.44	1.39	0.05
Hexadecyl	87°	55.5	13	46.0	1.88	1.99	−0.11

[a] All entropy values are expressed in entropy units.

cussed in this report. If so, Eq. 16 offers a 95% probability of estimating the ideal solubility of a substance to within a factor of two.

The contribution of increasing chain length to the internal entropy of fusion and to the ideal solubility is illustrated specifically for the alkyl *p*-aminobenzoates in Table III.

Experimentally, ideal solubilities can be demonstrated only for solutes in solvents of very similar polarity. The most convenient system for demonstrating the ideal solubility for solids is the aromatic and haloaromatic hydrocarbons in benzene. The observed solubilities of a number of polycyclic aromatics and substituted benzenes in benzene are listed in Table IV along with the ideal solubilities estimated by Eq. 7. The estimated values are in excellent agreement with the experimentally determined values.

Because this treatment is based on many assumptions and approximations, it cannot be expected to provide highly accurate ideal solubility estimates for all compounds. However, it does provide a simple means of obtaining a reasonable estimate of ideal solubility from nothing more than the structure and melting point of the compound in question.

From a pharmaceutical point of view, the value of being able to estimate ideal solubility is not that it enables calculation of the solubility of compounds in ideal solvents but rather that the ideal solubility of a substance is a factor which partially determines its solubility in water and other pharmaceutically important solvents.

Estimation of Aqueous Activity Coefficient—The estimation of the activity coefficient is somewhat more difficult than estimation of the entropy of fusion. The former value is dependent on the nature of two

Table IV—Mole Fraction Solubility of Aromatic Compounds in Benzene

Solute	*MP*	*I*	*X*	log *X* Obs.	log X_i Estim., $0.01(MP - T)$
Diphenyl	68.9°	37.0°	0.5118	−0.29	−0.32
o-Terphenyl	55.5°	28.0°	0.5852	−0.23	−0.28
m-Terphenyl	87.0°	36.8°	0.2827	−0.55	−0.50
p-Terphenyl	213.0°	38.0°	0.0071	−2.15	−1.75
s-Triphenylbenzene	174.9°	25.2°	0.0299	−1.52	−1.50
Naphthalene	80.0°	35.0°	0.3766	−0.42	−0.45
Anthracene	218.0°	35.8°	0.0103	−1.99	−1.82
Phenanthrene	98.4°	32.0°	0.2239	−0.65	−0.62
Pyrene	150.2°	32.4°	0.0734	−1.13	−1.18
Triphenylene	198.1°	39.4°	0.0140	−1.85	−1.59
Chrysene	254.0°	35.6°	0.0021	−2.68	−2.18
Fluorene	113.2°	33.5°	0.1604	−0.79	−0.80
Acenaphthene	94.1°	30.6°	0.1815	−0.74	−0.63
Fluoranthrene	110.2°	44.8°	0.2174	−0.66	−0.65
Hexachlorobenzene	226.0°	29.9°	0.0147	−1.83	−1.96
Hexamethylbenzene	166.0°	29.9°	0.0583	−1.23	−1.36
1,3,5-Trimethyl-2,4,6-trichlorobenzene	205.0	29.9°	0.0190	−1.72	−1.75
1,2,5-Trimethyl-3,4,6-trichlorobenzene	210.0°	29.9°	0.0153	−1.82	−1.94
Tetrachloro-*o*-xylene	228.0°	29.9°	0.0150	−1.82	−1.98
1,2,3,4-Tetramethyl-5,6-dichlorobenzene	193.0°	29.9°	0.0370	−1.43	−1.63
Pentamethylchlorobenzene	154.0°	29.9°	0.0737	−1.13	−1.34
Pentachlorobenzene	86.0°	29.9°	0.242	−0.62	−0.54
4,5-Dichloro-*m*-xylene	76.0°	29.9°	0.305	−0.52	−0.46
Ethylpentachlorobenzene	56.0°	32.4°	0.645	−0.19	−0.24

species, the solute and the solvent (in this case, water), whereas the latter quantity is dependent only on the nature of the solute. Most theoretical treatments of activity coefficients apply to nonpolar solutes in nonpolar solvents [*cf.*, the Scatchard–Hildebrand approach (2)] or to electrolytes in water (*cf.*, Ref. 17).

This report will attempt to develop a practical and easily used semiempirical approach. This approach relates the aqueous activity coefficient to the octanol–water partition coefficient, *PC*, which can in turn be estimated from the chemical structure by established techniques. Some of the more useful schemes used to estimate log *PC* were summarized previously (4).

The aqueous activity coefficient of a drug and its octanol–water partition coefficient are related by:

$$PC_x = \frac{\gamma_w}{\gamma_0} \qquad \text{(Eq. 19)}$$

where γ_0 is the activity coefficient of the drug in octanol. All three terms are expressed in mole fractions. (In its strictest sense, the partition coefficient is the ratio of the activity coefficients of the solute in water-saturated octanol to octanol-saturated water. Since it was shown that the effects of mutual saturation usually are quite small[3], they will be ignored in this report.)

By analogy to the aqueous activity coefficient, the activity coefficient of the drug in octanol can be described by:

$$2.303RT \log \gamma_0 = DD + OO - 2DO \qquad \text{(Eq. 20)}$$

where *OO* represents the octanol cohesive interactions and *DO* is the drug–octanol adhesive interaction term. By combining Eqs. 19 and 20, the following relationship is obtained:

$$2.303RT \log \gamma_w = \log PC_x + DD + OO - 2DO \qquad \text{(Eq. 21)}$$

If the drug has a molar cohesive energy that is similar to that of octanol, the adhesive interactions can be assumed to be equal to the average of the drug and octanol adhesive interactions, so that:

$$DD + OO \cong 2DO \qquad \text{(Eq. 22)}$$

and thus:

$$\log \gamma_w \approx \log PC_x \qquad \text{(Eq. 23)}$$

This treatment is somewhat similar in concept to the Hildebrand and Scott (2) treatment of regular solution theory, with an arithmetic mean being used instead of a geometric mean.

[3] T. J. Roseman and S. H. Yalkowsky, unpublished data.

The fact that most available partition coefficient data are for the octanol–water system is fortuitous. Octanol is a solvent of moderate polarity and is not very different in polarity from most drugs. Octanol has a solubility parameter (δ) of 10.3; for most drugs, this value is $8 \leq \delta \leq 12$. Extremely nonpolar compounds such as hexane have a δ value of >7, and very polar compounds such as ethanol have a δ value of <13. This similarity of polarities is responsible for the near equivalence of *DD* and *OO* and thus for the success of Eqs. 22 and 23. Additional support for the applicability of Eq. 22 is provided by the fact that most organic liquids are miscible in all proportions with octanol[3], indicating that γ_0 is near unity and thus that log γ_0 in Eq. 20 is near zero.

The requirement described by Eq. 22 is important in that it restricts this treatment to nonelectrolytes. If ionized, weak electrolytes can self-interact much more strongly than octanol, the sum of the cohesive forces will be greater than the adhesive forces and the calculated solubility will be erroneous.

Estimation of Aqueous Solubility of Liquids—Equation 23 can be tested on organic liquids that do not self-associate. For these liquids, the activity coefficient can be approximated by the reciprocal of the mole fraction solubility in water, X_w^l:

$$\log \gamma_w \approx -\log X_w^l \qquad \text{(Eq. 24)}$$

By merging the aqueous solubility file of Yalkowsky and Valvani[2] with the octanol–water partition coefficient data of Hansch and Leo (18), over 100 liquids have been found[2] for which apparently reliable solubility and partition coefficient data have been published. The result of regression analysis on these data (which include multiple values for most of the liquids) is:

$$-\log \gamma_w = \log X_w^l = -1.08 \log PC - 1.04 \qquad \text{(Eq. 25)}$$

$$n = 417 \quad r = 0.946 \quad s = 0.356$$

which is in good agreement with Eq. 24.

The slight deviation of the slope from unity is believed to be due to a systematic decrease in *DD* with increasing values of log *PC*, *i.e.*, with decreasing polarity. The intercept of 1.04 is due to the fact that Eq. 23 refers to the mole fractional partition coefficient, which is equal to the conventionally defined partition coefficient minus 0.94 (the logarithm of the ratio of the molarity of pure octanol to that of pure water). This distinction has been discussed more fully (19).

Although verified in this case for liquids, Eq. 25 is not restricted to liquid solutes. It can be expected to hold equally well for crystalline compounds. Therefore, a method has been obtained for estimating log γ_w for all organic nonelectrolytes that do not self-associate.

The reason for the exercise that equated log γ with log *PC* is that the

Table V—Solubility Estimates for Some Polycyclic Hydrocarbons

Name	*MP*	log *PC* Estim.	log *S* Obs.	log *S* Estim.	Residual
Indan	25°	3.57	−3.03	−3.40	0.369
Naphthalene	80°	3.35	−3.61	−3.71	0.108
1-Methylnaphthalene	25°	3.86	−3.70	−3.67	−0.030
2-Methylnaphthalene	35°	3.86	−3.75	−3.77	0.017
1,3-Dimethylnaphthalene	25°	4.38	−4.29	−4.16	−0.129
1,4-Dimethylnaphthalene	25°	4.38	−4.14	−4.16	0.024
1,5-Dimethylnaphthalene	81°	4.38	−4.68	−4.69	0.010
2,3-Dimethylnaphthalene	102°	4.38	−4.72	−4.89	0.171
2,6-Dimethylnaphthalene	108°	4.38	−4.89	−4.94	0.055
1-Ethylnaphthalene	25°	4.39	−4.16	−4.17	0.011
1,4,5-Trimethylnaphthalene	25°	4.90	−4.92	−4.65	−0.271
Diphenyl	71°	4.03	−4.34	−4.27	−0.078
Acenaphthene	96°	4.03	−4.59	−4.50	−0.091
Fluorene	116°	4.47	−4.92	−5.10	0.178
Phenanthrene	101°	4.63	−5.15	−5.11	−0.038
Anthracene	216°	4.63	−6.38	−6.19	−0.183
2-Methylanthracene	209°	5.15	−6.69	−6.62	−0.076
9-Methylanthracene	82°	5.15	−5.87	−5.42	−0.450
9,10-Dimethylanthracene	182°	5.67	−6.57	−6.85	0.284
Pyrene	156°	5.22	−6.18	−6.18	0.007
Fluoranthene	111°	5.22	−5.90	−5.76	−0.138
1,2-Benzofluorene	187°	5.75	−6.68	−6.97	0.290
2,3-Benzofluorene	209°	5.75	−7.27	−7.18	−0.096
Chrysene	255°	5.01	−8.06	−7.76	−0.296
Triphenylene	199°	5.45	−6.73	−6.80	0.077
Naphthacene	357°	5.91	−8.69	−8.72	0.032
1,2-Benzanthracene	160°	5.91	−7.21	−6.87	−0.345
9,10-Dimethyl-1,2-benzanthracene	122°	6.95	−6.63	−7.49	0.863
Perylene	277°	6.50	−8.80	−8.52	−0.282
3,4-Benzopyrene	175°	6.50	−7.82	−7.56	−0.256
3-Methylcholanthrene	178°	7.11	−7.97	−8.17	0.192
Benzo[*ghi*]perylene	277°	7.10	−9.02	−9.09	0.068

Table VI—Solubility Estimates for Halobenzenes

Name	*MP*	log *PC* Estim.	log *S* Obs.	log *S* Estim.	Residual
Hexachlorobenzene	230°	6.53	−7.76	−7.92	0.165
Pentachlorobenzene	86°	5.79	−5.65	−5.82	0.170
1,2,3,4-Tetrachlorobenzene	47°	5.05	−4.70	−4.72	0.017
1,2,3,5-Tetrachlorobenzene	54°	5.05	−4.79	−4.78	−0.006
1,2,4,5-Tetrachlorobenzene	140°	5.05	−5.56	−5.60	0.045
1,2,4,5-Tetrabromobenzene	182°	6.01	−6.98	−6.95	−0.027
1,2,3-Tribromobenzene	87°	4.98	—	−5.03	—
1,2,4-Tribromobenzene	44°	4.98	−4.50	−4.62	0.119
1,3,5-Tribromobenzene	122°	4.98	−5.60	−5.36	−0.236
1,2,3-Trichlorobenzene	53°	4.27	−3.76	−4.00	0.244
1,2,4-Trichlorobenzene	25°	4.27	−3.72	−3.74	0.017
1,3,5-Trichlorobenzene	63°	4.27	−4.44	−4.10	−0.340
1,2,3-Triiodobenzene	116°	5.86	—	−6.18	—
1,2,4-Triiodobenzene	91°	5.85	—	−5.93	—
1,3,5-Triiodobenzene	184°	5.85	—	−6.81	—
1,2-Dibromobenzene	25°	4.07	−3.50	−3.54	0.039
1,3-Dibromobenzene	25°	4.07	−3.38	−3.54	0.159
1,4-Dibromobenzene	87°	4.07	−4.07	−4.13	0.061
1,2-Dichlorobenzene	25°	3.59	−3.20	−3.07	−0.135
1,3-Dichlorobenzene	25°	3.59	−3.09	−3.07	−0.025
1,4-Dichlorobenzene	53°	3.59	−3.21	−3.33	0.123
1,2-Difluorobenzene	25°	2.59	−2.00	−2.08	0.078
1,3-Difluorobenzene	25°	2.58	−2.00	−2.07	0.068
1,4-Difluorobenzene	25°	2.58	−1.97	−2.07	0.098
1,2-Diiodobenzene	27°	4.65	−4.24	−4.13	−0.109
1,3-Diiodobenzene	40°	4.64	−4.57	−4.25	−0.325
1,4-Diiodobenzene	132°	4.64	−5.25	−5.12	−0.127
Bromobenzene	25°	3.07	−2.64	−2.55	−0.088
Chlorobenzene	25°	2.83	−2.35	−2.32	−0.035
Fluorobenzene	25°	2.33	−1.79	−1.82	0.031
Iodobenzene	25°	3.36	−2.95	−2.84	−0.112
Benzene	25°	2.13	−1.64	−1.62	−0.016
2-Bromochlorobenzene	25°	3.83	−3.19	−3.30	0.112
3-Bromochlorobenzene	25°	3.83	−3.21	−3.30	0.092
4-Bromochlorobenzene	68°	3.83	−3.63	−3.71	0.083
2-Bromoiodobenzene	25°	4.36	—	−3.83	—
3-Bromoiodobenzene	25°	4.36	—	−3.83	—
4-Bromoiodobenzene	92°	4.36	−4.56	−4.47	−0.095
2-Chloroiodobenzene	25°	4.12	−3.54	−3.59	0.049
3-Chloroiodobenzene	25°	4.12	−3.55	−3.59	0.039
4-Chloroiodobenzene	57°	4.12	−4.03	−3.89	−0.136

Table VII—Solubility Estimates of Alkyl *p*-Substituted Benzoates

Name	*MP*	log *PC* Estim.	log *S* Obs.	log *S* Estim.	Residual
Methyl *p*-aminobenzoate	112°	1.12	−1.60	−1.49	−0.112
Ethyl *p*-aminobenzoate	89°	1.65	−1.99	−1.78	−0.213
Propyl *p*-aminobenzoate	74°	2.18	−2.33	−2.14	−0.189
Butyl *p*-aminobenzoate	56°	2.70	−2.76	−2.57	−0.194
Pentyl *p*-aminobenzoate	52°	3.23	−3.35	−3.12	−0.231
Hexyl *p*-aminobenzoate	61°	3.76	−3.95	−3.85	−0.100
Heptyl *p*-aminobenzoate	75°	4.29	−4.60	−4.70	0.095
Octyl *p*-aminobenzoate	71°	4.81	−5.40	−5.25	−0.148
Nonyl *p*-aminobenzoate	69°	5.34	−6.00	−5.84	−0.157
Dodecyl *p*-aminobenzoate	82°	6.92	−7.80	−7.90	0.102
Methyl *p*-hydroxybenzoate	131°	1.66	−1.84	−2.18	0.344
Ethyl *p*-hydroxybenzoate	116°	2.19	−2.22	−2.55	0.329
Propyl *p*-hydroxybenzoate	96°	2.71	−2.59	−2.86	0.266
Butyl *p*-hydroxybenzoate	68°	3.24	−2.89	−3.10	0.207

latter value can be estimated by linear free energy (*i.e.*, group contribution) approaches. Due to the efforts of Hansch and coworkers (20, 21) and Nys and Rekker (5), it is possible to estimate, with reasonable accuracy, the value of log *PC* for most organic compounds. The fragment contributions to log *PC* (*f* values) developed by Nys and Rekker for the most common functional groups are summarized in Ref. 5. These *f* values can be used to obtain an approximate log *PC* value for most compounds.

Estimation of Aqueous Solubility of Organic Nonelectrolytes—If the estimations of ΔS_f and γ_w are valid for drugs, they can be inserted into Eq. 8 to give:

$$\log X_w^c \approx -\log PC - \left(\frac{\Delta S_f}{1364}\right)(MP - 25) - 0.94 \qquad \text{(Eq. 26)}$$

which simplifies to:

$$\log X_w \approx -\log PC - 0.01MP - 0.69 \qquad \text{(Eq. 27)}$$

for rigid molecules.

Equations 26 and 27 can be made applicable to liquids simply by replacing the melting point by 25° for compounds that melt below this temperature. This process effectively eliminates the crystal interaction term and causes the equations to revert back to Eq. 25.

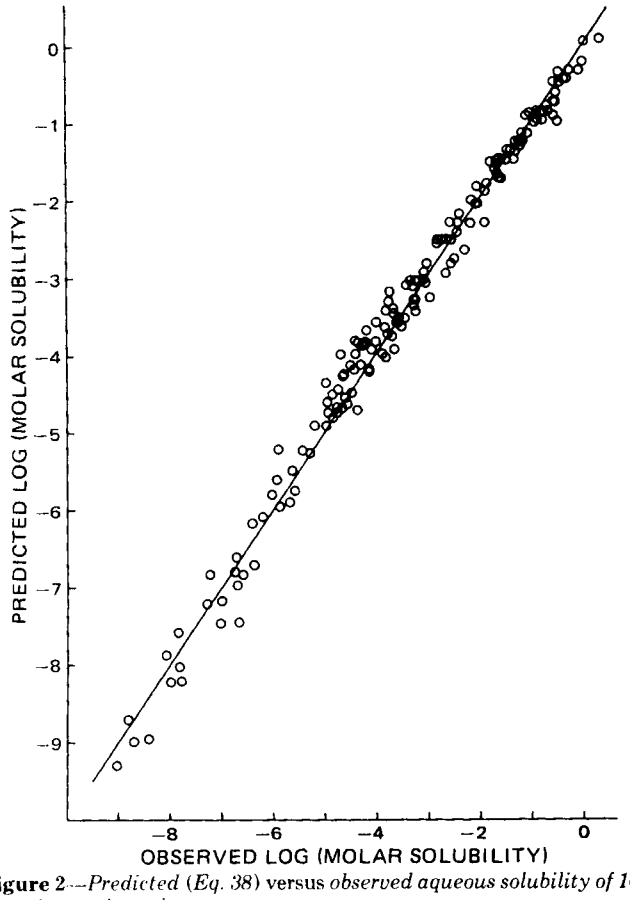

Figure 2—*Predicted (Eq. 38)* versus *observed aqueous solubility of 167 organic nonelectrolytes.*

The aqueous solubility of drugs by convention is reported on a molar rather than a mole fraction scale. For poorly soluble compounds, the molar solubility is simply the mole fraction solubility multiplied by 55.5 (the molarity of water) so that:

$$\log S_m = \log X + 1.74 \qquad \text{(Eq. 28)}$$

where S_m is the solubility in moles per liter. Thus, on a molar scale, Eqs. 26 and 27 become:

$$\log S_m^c \approx -\log PC - \frac{\Delta S_f(MP - 25)}{1364} + 0.80 \qquad \text{(Eq. 29)}$$

in general for nonelectrolytes and:

$$\log S_m^c \approx -\log PC - 0.01MP + 1.05 \qquad \text{(Eq. 30)}$$

for rigid and short chain molecules.

For the more soluble solutes, it is necessary to account for the volume of water displaced by the dissolved solute. The more precise relationship between molar and mole fraction solubilities is:

$$S_w = \frac{1000\rho X_w}{18 + (MW - 18)X_w} \qquad \text{(Eq. 31)}$$

where ρ is the density of the saturated solution and MW is the molecular weight of the solute. Note that as X_w approaches zero and as ρ approaches unity, Eq. 31 approaches Eq. 28. Since S_w is not a truly linear function of X_w, it is not a strictly linear function of MP and log PC, especially at high values of S_w. However, it can be approximated by a linear function with slightly altered coefficients. As long as very soluble solutes are avoided, no serious errors will be encountered as a result of this approximation.

Applications—To test the ability of Eqs. 29 and 30 to estimate the aqueous solubilities of organic nonelectrolytes, several series of compounds will be considered: polycyclic aromatic hydrocarbons; mono- and multihalobenzenes; steroid hormones; normal, branched, and cyclic alcohols; and alkyl *p*-hydroxybenzoates and alkyl *p*-aminobenzoates. These series enable coverage of a wide variety of melting points, partition coefficients, and solubilities. The regression equations of the estimated and observed solubilities for each series and for the combination of all compounds will be given.

Tables V and VI contain the aqueous solubility data for two classes of compounds containing only rigid molecules (the polycyclic aromatic compounds and the halobenzenes). Tables V and VI also contain the estimated partition coefficients and the melting points. In the case of liquids, 25° is used in place of the melting point. For the polycyclic aromatic compounds, the results of regression analysis between the observed and estimated solubilities are:

$$\log S_{obs} = 0.944 \log S_{estim} - 0.785 \qquad \text{(Eq. 32)}$$

$$n = 32 \quad r = 0.989 \quad s = 0.252$$

and for the halobenzenes:

$$\log S_{obs} = 0.980 \log S_{estim} - 0.32 \qquad \text{(Eq. 33)}$$

$$n = 35 \quad r = 0.995 \quad s = 0.136$$

Table VII contains the same type of data for the alkyl *p*-substituted benzoates, a series of both rigid and flexible molecules, all of which are

Table VIII—Solubility Estimates for Aliphatic Alcohols

Name	*MP*	ΔS_f Estim.	log *PC* Estim.	log *S* Obs.	log *S* Estim.	Residual
1-Butanol	25°	13.5	0.84	−0.01	0.05	−0.064
2-Methyl-1-propanol	25°	13.5	0.73	0.06	0.16	−0.101
2-Butanol	25°	13.5	0.73	0.39	0.16	0.232
1-Pentanol	25°	13.5	1.37	−0.61	−0.46	−0.152
2-Methyl-1-butanol	25°	13.5	1.25	−0.48	−0.34	−0.143
3-Methyl-1-butanol	25°	13.5	1.25	−0.51	−0.34	−0.174
2,2-Dimethyl-1-propanol	54°	13.5	1.33	−0.42	−0.69	0.277
2-Pentanol	25°	13.5	1.25	−0.31	−0.31	0.031
3-Pentanol	25°	13.5	1.25	−0.24	−0.34	0.097
3-Methyl-2-butanol	25°	13.5	1.14	−0.21	−0.24	0.022
2-Methyl-2-butanol	25°	13.5	1.33	0.09	−0.42	0.503
1-Hexanol	25°	13.5	1.90	−1.24	−0.96	−0.278
2-Methyl-1-pentanol	25°	13.5	1.78	−1.11	−0.85	−0.267
4-Methyl-1-pentanol	25°	13.5	1.78	−1.14	−0.85	−0.294
2,2-Dimethyl-1-butanol	25°	13.5	1.57	−1.04	−0.65	−0.390
3,3-Dimethyl-1-butanol	25°	13.5	1.57	−0.50	−0.65	0.146
2-Ethyl-1-butanol	25°	13.5	1.78	−1.17	−0.85	−0.325
2-Hexanol	25°	13.5	1.78	−0.88	−0.85	−0.036
3-Hexanol	25°	13.5	1.78	−0.82	−0.85	0.029
3-Methyl-2-pentanol	25°	13.5	1.67	−0.74	−0.74	0.004
4-Methyl-2-pentanol	25°	13.5	1.67	−0.81	−0.74	−0.065
2-Methyl-3-pentanol	25°	13.5	1.67	−0.71	−0.74	0.029
3,3-Dimethyl-2-butanol	25°	13.5	1.74	−0.64	−0.81	0.165
Cyclohexanol	25°	13.5	1.43	−0.45	−0.51	0.058
2-Methyl-2-pentanol	25°	13.5	1.86	−0.51	−0.92	0.414
3-Methyl-3-pentanol	25°	13.5	1.86	−0.39	−0.92	0.529
2,3-Dimethyl-2-butanol	25°	13.5	1.74	−0.41	−0.81	0.403
2,4-Dimethyl-2-pentanol	25°	13.5	2.27	−0.96	−1.32	0.351
1-Heptanol	25°	13.5	2.42	−1.83	−1.46	−0.373
2,2-Dimethyl-1-pentanol	25°	13.5	2.39	−1.52	−1.43	−0.091
2,4-Dimethyl-1-pentanol	25°	13.5	2.19	−1.60	−1.24	−0.360
4,4-Dimethyl-1-pentanol	25°	13.5	2.39	−1.55	−1.43	−0.116
2-Heptanol	25°	13.5	2.31	−1.55	−1.35	−0.193
3-Heptanol	25°	13.5	2.31	−1.44	−1.35	−0.088
4-Heptanol	25°	13.5	2.31	−1.40	−1.35	−0.048
5-Methyl-2-hexanol	25°	13.5	2.19	−1.38	−1.24	−0.145
2-Methyl-3-hexanol	25°	13.5	2.19	−1.32	−1.24	−0.076
2,2-Dimethyl-3-pentanol	25°	13.5	2.27	−1.16	−1.32	0.155
2,4-Dimethyl-3-pentanol	25°	13.5	2.08	−1.23	−1.13	−0.092
2-Methyl-2-hexanol	25°	13.5	2.39	−1.09	−1.43	0.336
3-Methyl-3-hexanol	25°	13.5	2.39	−1.00	−1.43	0.432
2,3-Dimethyl-2-pentanol	25°	13.5	2.27	−0.91	−1.32	0.410
2,3-Dimethyl-3-pentanol	25°	13.5	2.27	−0.86	−1.32	0.451
3-Ethyl-3-pentanol	25°	13.5	2.39	−0.87	−1.43	0.558
2,3,3-Trimethyl-2-butanol	25°	13.5	2.35	−0.72	−1.39	0.670
1-Octanol	25°	13.5	2.95	−2.37	−1.97	−0.404
2-Ethyl-1-hexanol	25°	13.5	2.84	−2.11	−1.86	−0.254
2-Octanol	25°	13.5	2.84	−2.09	−1.86	−0.228
2-Methyl-2-heptanol	25°	13.5	2.91	−1.72	−1.93	0.211
3-Methyl-3-heptanol	25°	13.5	2.91	−1.60	−1.93	0.325
2,2,3-Trimethyl-3-pentanol	25°	13.5	2.88	−1.27	−1.90	0.625
1-Nonanol	25°	13.5	3.48	−3.01	−2.47	−0.533
7-Methyl-1-octanol	25°	13.5	3.36	−2.49	−2.36	−0.137
2,2-Diethyl-1-pentanol	25°	13.5	3.44	−2.42	−2.43	0.015
2-Nonanol	25°	13.5	3.36	−2.74	−2.36	−0.386
3-Nonanol	25°	13.5	3.36	−2.66	−2.36	−0.299
4-Nonanol	25°	13.5	3.36	−2.59	−2.36	−0.227
5-Nonanol	25°	13.5	3.36	−2.49	−2.36	−0.137
2,6-Dimethyl-4-heptanol	25°	13.5	3.13	−2.51	−2.14	−0.370
3,5-Dimethyl-4-heptanol	25°	13.5	3.13	−2.51	−2.14	−0.370
1-Decanol	25°	13.5	4.01	−3.60	−2.98	−0.622
2-Undecanol	25°	13.5	4.42	−2.94	−3.37	0.437
1-Dodecanol	25°	13.5	5.06	−4.80	−3.98	−0.814
1-Tetradecanol	38°	38.5	6.11	−5.84	−5.78	−0.056
1-Pentadecanol	44°	41.0	6.64	−6.35	−6.53	0.180
1-Hexadecanol	49°	43.5	7.17	−7.00	−7.26	0.264
1-Octadecanol	58°	48.5	8.22	−8.40	−8.75	0.350

crystalline. The statistics for this series are:

$$\log S_{obs} = 1.008 \log S_{estim} - 0.270 \qquad \text{(Eq. 34)}$$

$$n = 14 \quad r = 0.990 \quad s = 0.264$$

Table VIII concerns the aliphatic alcohols. The series contains rigid and flexible molecules, most of which are liquids at room temperature. For this series, the observed and estimated solubilities are related by:

$$\log S_{obs} = 0.989 \log S_{estim} - 0.203 \qquad \text{(Eq. 35)}$$

$$n = 67 \quad r = 0.994 \quad s = 0.178$$

Table IX lists the data for some steroid hormones. The data for this group of rigid solids were taken from a study by Tomida *et al.* (6) in which both aqueous solubilities and octanol–water partition coefficients were determined. The experimental data for these cases were used because the group contribution approaches (20, 21) worked poorly for steroids (1). The regression equation for this series is:

$$\log S_{obs} = 0.879 \log S_{estim} - 0.863 \qquad \text{(Eq. 36)}$$

$$n = 19 \quad r = 0.847 \quad s = 0.309$$

In each of the five classes of compounds, there is a definite relationship

Table IX—Solubility Estimates for Some Steroids

Name	*MP*	log *PC* Obs.	log *S* Obs.	log *S* Estim.	Residual
Hydrocortisone	213°	1.55	−2.97	−3.26	0.292
Corticosterone	181°	1.94	−3.24	−3.32	0.084
Deoxycorticosterone	141°	2.90	−3.45	−3.82	0.366
Cortisone	222°	1.42	−3.27	−3.23	−0.043
Hydrocortisone acetate	223°	2.19	−4.34	−3.91	−0.427
Cortisone acetate	236°	2.10	−4.21	−3.95	−0.262
Deoxycorticosterone acetate	157°	3.08	−4.63	−4.11	−0.515
11α-Hydroxyprogesterone	222°	2.36	−3.82	−4.05	0.233
Progesterone	131°	3.87	−4.42	−4.58	0.161
Testosterone	155°	3.29	−4.08	−4.28	0.202
Prednisolone	240°	1.62	−3.18	−3.56	0.381
Prednisolone acetate	238°	2.40	−4.37	−4.23	−0.141
Triamcinolone	270°	1.03	−3.68	−3.31	−0.374
Triamcinolone acetonide	293°	2.31	−4.31	−4.63	0.323
Triamcinolone diacetate	235°	1.92	−4.13	−3.78	−0.349
Dexamethasone	266°	1.83	−3.59	−3.97	0.384
Betamethasone	230°	1.94	−3.77	−3.75	−0.016
Dexamethasone acetate	230°	2.91	−4.90	−4.61	−0.293
Betamethasone-17-valerate	183°	3.49	−4.71	−4.70	−0.006

between the observed and estimated values of log S. In four of the five groups, the coefficient of log S_{estim} is close to 0.96. For the steroids, a lower value is observed. The major variation is observed in the value of the intercept, which varies from −0.863 to −0.203. The reason for the variation (which would be equal to zero if Eqs. 29 and 30 were absolutely correct) is not clear. However, it is clear that the average of Eqs. 32–36:

$$\log S_{obs} \approx \log S_{estim} - 0.5 \qquad \text{(Eq. 37)}$$

can be used as a means of estimating the solubility of nearly any rigid nonelectrolyte regardless of whether it is liquid or solid.

In each of the five classes of compounds, there is a similar relationship between the observed and predicted solubilities. Whether the differences observed are real or are due to systematic errors in calculating log *PC* is not clear.

The complete data set was fitted by multiple linear regression to a function of log *PC* and $\Delta S_f(MP - 25)$. This analysis yielded the following semiempirical equation:

$$\log S_w \sim -1.00 \log PC - 1.11 \frac{\Delta S_f(MP - 25)}{1364} + 0.54 \qquad \text{(Eq. 38)}$$

$$n = 167 \quad r = 0.994 \quad r^2 = 0.988 \quad s = 0.242$$

Equation 38 estimates the solubilities of all but eight of the solutes listed in Tables V–IX to within 0.5 log unit. The agreement between the observed solubilities and the solubilities estimated by Eq. 38 is illustrated in Fig. 2. Although the solubility values span nine orders of magnitude, the error in no case reached a factor of 10.

The pooled data for the rigid molecules gave:

$$\log S_w = -1.05 \log PC - 0.012MP + 0.87 \qquad \text{(Eq. 39)}$$

$$n = 155 \quad r = 0.989 \quad r^2 = 0.979 \quad s = 0.308$$

These equations are believed to be useful because they enable the estimation of aqueous solubility on the basis of a single physical measurement, the melting point. They also enable the chemist to appreciate the likely effect of a structural modification on aqueous solubility.

Although this study was restricted to nonelectrolytes, it appears that Eqs. 38 and 39 can be extended to cover weak electrolytes with only slight modification (22).

REFERENCES

(1) S. H. Yalkowsky and W. Morozowich, in "Drug Design," vol. 9, E. J. Ariens, Ed., Academic, New York, N.Y., 1980, p. 121.

(2) J. H. Hildebrand and R. L. Scott, "Regular Solutions," Prentice Hall, Englewood Cliffs, N.J., 1962.

(3) R. C. Weast, "Handbook of Chemistry and Physics," Chemical Rubber Co., Cleveland, Ohio, 1974.

(4) E. Martin, S. H. Yalkowsky, and J. E. Wells, *J. Pharm. Sci.*, **68**, 565 (1979).

(5) G. G. Nys and R. F. Rekker, *Eur. J. Med. Chem.*, **9**, 361 (1974).

(6) H. Tomida, T. Yotsuyanagi, and K. Ikeda, *Chem. Pharm. Bull.*, **26**, 2832 (1978).

(7) S. H. Yalkowsky, R. J. Orr, and S. C. Valvani, *I&EC Fundam.*, **18**, 351 (1979).

(8) S. H. Yalkowsky, G. L. Flynn, and T. G. Slunick, *J. Pharm. Sci.*, **61**, 852 (1972).

(9) D. MacKay and W. Y. Shiu, *J. Chem. Eng. Data*, **22**, 399 (1977).

(10) A. Bondi, "Physical Properties of Molecular Crystals, Liquids, and Glasses," Wiley, New York, N.Y., 1968.

(11) A. R. Ubbelohde, "Melting and Crystal Structure," Clearendon, Oxford, England, 1965.

(12) P. Walden, *Z. Electrochem.*, **14**, 713 (1908).

(13) S. H. Yalkowsky and S. C. Valvani, *J. Chem. Eng. Data*, **24**, 127 (1979).

(14) J. Pirsch, *Chem. Ber.*, **70**, 12 (1937).

(15) J. Pirsch, *Mikrochim. Acta*, **1–6**, 99 (1956).

(16) S. H. Yalkowsky, *I&EC Fundam.*, **18**, 108 (1979).

(17) H. S. Harned and B. B. Owen, "The Physical Chemistry of Electrolytic Solutions," 3rd ed., Reinhold, New York, N.Y., 1958, p. 667.

(18) C. Hansch and A. Leo, "Pomona College Medicinal Chemistry Project," Pomona, Calif., July 1977.

(19) S. C. Valvani, S. H. Yalkowsky, and T. J. Roseman, "Abstracts," vol. 7, no. 2, APhA Academy of Pharmaceutical Sciences, Washington, D.C., Nov. 1977.

(20) T. Fujita, J. Iwasa, and C. Hansch, *J. Am. Chem. Soc.*, **86**, 5175 (1964).

(21) C. Hansch, A. Leo, and D. Nikaitani, *J. Org. Chem.*, **37**, 3090 (1972).

(22) S. C. Valvani and S. H. Yalkowsky, "Abstracts," vol. 9, no. 2, APhA Academy of Pharmaceutical Sciences, Washington, D.C., Nov. 1979.

ACKNOWLEDGMENTS

The authors thank Dr. Gary L. Bertrand for many helpful comments and criticisms.

Influence of Various Anions on Intestinal Disappearance of Hexamethonium Chloride and Pralidoxime Chloride in Rats

SURYAKANT I. BHUTA *x, EDWIN T. SUGITA, PAUL J. NIEBERGALL ‡, and ROGER L. SCHNAARE

Received May 21, 1979, from the *Department of Pharmacy, Philadelphia College of Pharmacy and Science, Philadelphia, PA 19104.* Accepted for publication March 11, 1980. *Present address: Sandoz Pharmaceuticals, East Hanover, NJ 07936. ‡Present address: Marion Laboratories, Inc., Kansas City, MO 64137.

Abstract □ The intestinal transfer of two poorly absorbed quaternary ammonium drugs, hexamethonium chloride (I) and pralidoxime chloride (II), in the presence of various organic and inorganic anions was investigated in the rat using a modified *in situ* gut technique. The results were in agreement with those of the conventional *in situ* loop and plasma drug level techniques. Of the anions investigated, cholate, desoxycholate, taurocholate, phoscholate, dehydrocholate, and hyodesoxycholate had the greatest effect on increasing the amount and rate of disappearance of I. Similarly, the amount and rate of disappearance of II were enhanced markedly in the presence of phoscholate and trichloroacetate. The effect of cholate and phoscholate was investigated in detail. The membrane permeability and histological studies indicated that these anions may compromise the structural integrity of the membrane tissue, thus enhancing drug transfer.

Keyphrases □ Hexamethonium chloride—influence of various anions on intestinal disappearance in rats □ Pralidoxime chloride—influence of various anions on intestinal disappearance in rats □ Quaternary ammonium drugs—hexamethonium chloride and pralidoxime chloride, influence of various anions on intestinal disappearance in rats □ Absorption—hexamethonium chloride and pralidoxime chloride, influence of various anions on intestinal disappearance in rats

Quaternary ammonium drugs may have limited therapeutic usefulness following oral administration since they are poorly and erratically absorbed. These compounds are ionized completely at all physiological pH values and thus tend to have high aqueous and low lipid solubilities. According to the pH–partition theory of passive absorption, these ionized moieties should be only insignificantly absorbed since they are transported slowly across lipid membranes.

The poor GI absorption of quaternary ammonium drugs can be illustrated by noting the difference in therapeutically effective oral and parenteral doses. For example, much larger doses of the antihypertensive drug hexamethonium and the cholinesterase reactivator pralidoxime chloride must be given by mouth as compared to parenteral administration to achieve a pharmacological response (1–3).

Various attempts have been made to improve the GI absorption of quaternary ammonium drugs. Isolated studies have shown that, in some cases, the amount and rate of absorption of hexamethonium (4), benzomethamine (5), and isopropamide (6) are increased by the addition of anionic substances. For example, Harington (4) showed that the various salts of hexamethonium are absorbed to different extents. These studies imply that the anionic portion of the salt plays a part in the absorption process since the other moiety always was the positively charged quaternary ion.

Although the existence of ion-pair complexes has been speculated, no conclusive evidence has been found. Furthermore, no data are available showing the effect of these anions on *in vivo* membrane permeability. Further work in this area is warranted to elucidate the mechanism of the enhancing action effected by anions.

The purposes of this study were to investigate techniques for increasing GI transfer of two model quaternary ammonium drugs, hexamethonium chloride (I) and pralidoxime chloride (II), and to study the mechanisms involved in this enhancement.

EXPERIMENTAL

Test Animals—Male Sprague–Dawley rats[1], ~140 g, were housed two per cage and had access to food and water until they attained a weight of 180–200 g. Animals were fasted for 24 hr prior to use but had free access to water.

Chemicals—Hexamethonium chloride[2], hexamethonium iodide[2], pralidoxime chloride[3], and pralidoxime iodide[3] were used as purchased. Chemicals used as anions were purchased from various sources.

The concentration of hexamethonium chloride (I) was 2.6×10^{-3} *M*, while that of pralidoxime chloride (II) was 8.7×10^{-3} *M*. The anions were administered as their sodium salts. When a sodium salt was not available, the desired acid was dissolved in deionized, distilled water with an equivalent quantity of sodium hydroxide. All solutions were prepared fresh on the day of the experiment.

Anesthesia—Each rat was anesthetized with urethan[4] (ethyl carbamate), 1 mg/g ip.

Experimental Design—To determine the number of experimental animals required to evaluate each drug–anion combination, preliminary studies were conducted with I and II in four animals on 4 consecutive days. An analysis of variance indicated that there was no statistical difference between the results from the different animals. This finding suggested that each drug–anion combination studied in four animals would give satisfactory results that could differentiate the effects of different anions on drug disappearance. Therefore, each I–anion and II–anion combination to be studied on any particular day was selected randomly.

The results were analyzed statistically using Duncan's new multiple range procedure (7). This procedure groups the ranked means that do not differ statistically ($p = 0.05$) and is suitable for the interpretation of the results since it distinguishes between a single anion and a group of anions that have similar effects on drug absorption.

Methods of Analysis—A slight modification (4% instead of 1.5% washed isopentanol) of the ion-pair technique described by Auerbach (8) and Mitchell and Clark (9) was used for the determination of hexamethonium in aqueous solutions and plasma. The pralidoxime content in biological fluids was analyzed utilizing the method of May *et al.* (10) and Ellin and coworkers (11, 12). The analytical procedure of Roe *et al.* (13) as modified by Schreiner (14) was employed for determining the inulin content in the aqueous solution. In all cases, the standard curves obeyed the Beer–Lambert law.

***In Situ* Gut Technique**—The experimental technique used to study drug transfer kinetics was a modification of a method described previously (15). The earlier technique did not account for intestinal volume changes. To overcome this difficulty, the ilial syringe was replaced with

[1] Huntingdon Farms, West Conshohocken, Pa.
[2] K & K Laboratories, New York, N.Y.
[3] Aldrich Chemical Co., Milwaukee, Wis.
[4] Matheson, Coleman and Bell, East Rutherford, N.J.

0022-3549/80/0800-0923$01.00/0
© 1980, American Pharmaceutical Association

Table I—Intestinal Disappearance of Hexamethonium Chloride (I) in the Presence of Different Anions for the *In Situ* Gut Technique [a]

Anion	Molar Ratio of I to Anion	$k^* \times 10^3$, min^{-1}
Cholate	1:5	8.33 ± 0.13
Desoxycholate	1:5	8.10 ± 0.17
Taurocholate	1:5	6.10 ± 0.40
Phoscholate	1:5	5.35 ± 0.18
Dehydrocholate	1:5	5.14 ± 0.26
Hyodesoxycholate	1:5	4.85 ± 0.11
Bromide	1:4	4.03 ± 0.05
Glycocholate	1:5	3.85 ± 0.12
Phosphate	1:5	3.53 ± 0.09
Iodide	1:5	3.40 ± 0.11
Chloride	1:3	3.05 ± 0.07
Trichloroacetate	1:5	3.00 ± 0.32
Glycotaurocholate	1:4	2.98 ± 0.25
Tartrate	1:5	2.81 ± 0.15
Propionate	1:5	2.76 ± 0.15
Lactate	1:5	2.62 ± 0.11
Acetate	1:5	2.28 ± 0.13
Citrate	1:5	1.95 ± 0.05
Sulfide	1:5	0.99 ± 0.14

[a] Statistical results of Duncan's new multiple range procedure.

a 10.0-ml graduated pipet. At various times, the drug solution from the intestine was emptied gently into the pipet, the volume was measured accurately, a 0.1-ml aliquot was withdrawn for analysis, and the solution was returned to the intestine.

***In Situ* Loop Technique**—This method was an adaptation of the *in situ* gut technique. The experimental procedure and setup were identical up to the point where the drug solution was to be introduced into the washed intestine. At this stage, the syringe was disconnected from the duodenal cannula and replaced with a 5.0-ml pipet containing exactly 5.0 ml of drug solution. This solution was allowed to flow into the intestinal lumen, and the intestine was ligated at the tip of the duodenal cannula. Similarly, the intestine at the ilial cannula was ligated, with care taken to ensure that no drug solution was in the receiving pipet. The pipet and cannulas then were removed.

After 3 hr, the entire section of small intestine was removed and placed in a beaker containing ~50 ml of distilled water. After the intestine was cut into thin rings, the contents in the beaker were stirred vigorously for 30 min. The mixture was filtered, and the solution was diluted to a desired volume. An aliquot of this solution was analyzed for drug content as described previously. The difference between the amount of drug introduced and the amount remaining at the completion of the experiment yielded the drug lost from the intestinal segment.

At the completion of the experiment, a blood sample was obtained *via* heart puncture from the same animal in which the loop technique was studied. The drug concentration in the plasma was determined as described. The blood volume of the rat was estimated from its body weight using the chart published previously for blood volume *versus* the body weight of male rats (16). The product of the plasma drug concentration and the plasma volume yielded a measure of the amount of drug in the plasma of the rat.

Table II—Intestinal Disappearance of Pralidoxime Chloride (II) in the Presence of Different Anions for the *In Situ* Gut Technique [a]

Anion	Molar Ratio of II to Anion	$k^* \times 10^3$, min^{-1}
Phoscholate	1:3	7.37 ± 0.30
Trichloroacetate	1:2	6.56 ± 0.14
Taurocholate	1:2	5.64 ± 0.10
Glycotaurocholate	1:1	5.49 ± 0.21
Hyodesoxycholate	1:2	5.42 ± 0.15
Iodide	1:2	5.25 ± 0.12
Cholate	1:2	5.23 ± 0.27
Dehydrocholate	1:1	5.18 ± 0.51
Glycocholate	1:1	5.19 ± 0.14
Bromide	1:2	4.75 ± 0.71
Chloride	1:2	4.58 ± 0.11
Acetate	1:2	3.73 ± 0.72
Desoxycholate	1:2	3.51 ± 0.13
Tartrate	1:2	3.32 ± 0.12
Propionate	1:2	3.29 ± 0.33
Lactate	1:2	3.24 ± 0.06
Sulfate	1:2	3.16 ± 0.15
Phosphate	1:2	3.07 ± 0.21
Citrate	1:2	2.57 ± 0.38

[a] Statistical results of Duncan's new multiple range procedure.

Membrane Permeability Study—The experimental setup was the same as that used in the *in situ* gut technique. The drug solution was introduced into the intestine; simultaneously, a sterile solution of 20 mg of inulin was injected into the femoral vein. At the end of 3 hr, the volume of the intestinal solution was measured accurately, and an aliquot was taken for inulin analysis.

The amount of inulin determined in the sample aliquot and the volume of the intestinal contents yielded the amount of inulin transferred from the blood to the intestinal lumen.

Histological Study—The *in situ* gut technique was utilized to obtain the intestinal tissue samples. The drug solution was introduced into the intestine; after 3 hr, segments from different intestinal areas were removed, gently flushed out with distilled water, and then fixed for at least 24 hr in a 10% formalin and 1% $CaCl_2$ solution. These sections were fixed permanently for later use.

RESULTS AND DISCUSSION

Intestinal Disappearance—The kinetics of intestinal disappearance of the two quaternary ammonium drugs, hexamethonium chloride (I) and pralidoxime chloride (II), in the presence of various anions were observed for 3 hr. The kinetics between 30 and 180 min followed apparent first-order disappearance and, therefore, could be represented mathematically by:

$$m = m_0 e^{-kt} \qquad \text{(Eq. 1)}$$

where m is the amount of drug in the intestine at any time t, m_0 is the initial amount of drug in the intestine, and k is the disappearance rate constant.

Preliminary studies indicated that the intestinal disappearance rate of the drugs and their combinations with various anions for the initial 30 min did not follow simple first-order kinetics. For this reason, the constant was redefined as an apparent disappearance rate constant and designated as k^*. The behavior during the initial period was studied in detail and will be discussed later. The k^* values for I and II were estimated using linear regression to be $3.05 \pm 0.07 \times 10^{-3}$ and $4.58 \pm 0.11 \times 10^{-3}$ min^{-1}, respectively.

The influence of an excess of chloride ions while utilizing hexamethonium iodide and pralidoxime iodide also was investigated. The disappearance rates of these iodide salts in the presence of an excess of chloride anions were identical to those of the chloride salts of the drugs. Similarly, another study showed that the apparent rates of I and II in the presence of an excess of iodide ions were not different from the rates for the iodide salts of these drugs. The results indicate strongly that the intestinal disappearance kinetics of I and II are affected by the presence of foreign anions and that the drugs behave as the salt of the excess anion present. A possible reason for such behavior is that the quaternary ammonium salts are ionized completely at all physiological pH values to their corresponding cations and anions, and an excess of foreign anion will swamp the anion of the salt.

All anions, except bromide, when used in the molar ratios of drug to anion of 1:2 to 1:5 had the same effect on I and II. With bromide, a progressive increase in the anion concentration caused a corresponding increase in the disappearance rate of I but not of II. The molar ratio of drug to anion was maintained within the range of 1:2 to 1:5; in a few instances, it was necessary to change (±10%) the anion concentration to achieve an isotonic solution to prevent drastic intestinal volume changes. The pH of the solutions during this investigation ranged from 7.5 to 8.3; only the desoxycholate and taurocholate systems gave slightly lower values.

The results for hexamethonium chloride and pralidoxime chloride in the presence of various anions are presented in Tables I and II, respectively. The brackets enclosing the anion or anions in the first column indicate the results of the statistical analysis by Duncan's new multiple range procedure. The effects on the apparent disappearance rate constant of the drug for the anions included in the same bracket do not differ statistically at $p = 0.05$; however, the effects of the anions grouped in different brackets are significantly different at $p = 0.05$.

The simple ion, bromide, increased the disappearance of I but had no effect on the rate constant of II. Iodide increased the value of II and had no significant effect on the value of I. The results of the hexamethonium studies agree with Harington's findings (4); however, the results of the

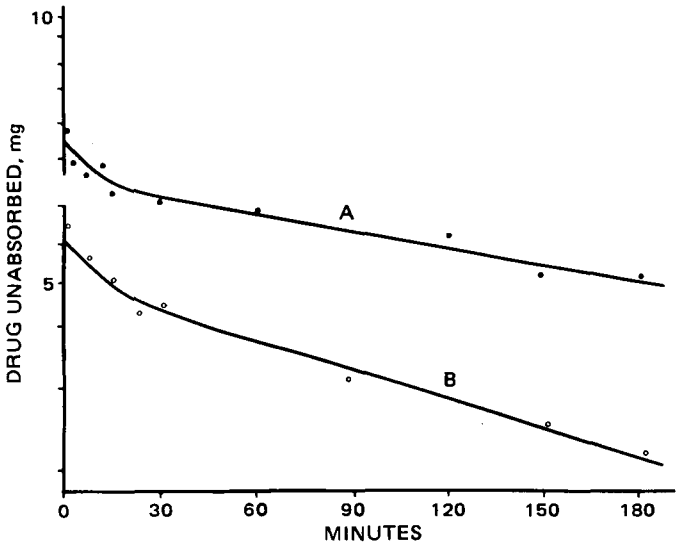

Figure 1—*Intestinal disappearance of hexamethonium chloride (A, ●) and pralidoxime chloride (B, ○) in rats.*

pralidoxime experiments differ from those of Levine and Steinberg (17).

Another anion that had opposing effects on the drug transfer rate was phosphate. It increased the disappearance constant of I while it decreased the value of II appreciably.

Citrate, sulfate, lactate, propionate, tartrate, and acetate had similar effects; they all decreased or had no effect on the disappearance rate constants of I and II. These findings parallel those in the literature, although one investigator (18) reported increased intestinal absorption of the quaternary ammonium compound benzomethamine in the presence of acetate and propionate anions. However, this effect occurred only at high acid concentrations (0.2 *M*) and at relatively low pH values (pH 3–4).

Trichloroacetate had no influence on the results of I while it increased the corresponding value of II. This anion increased the pharmacological response of isopropamide iodide (6).

The most dramatic changes were caused by the bile salt anions. For example, cholate caused an approximately threefold increase in the rate constant for I but only a slight increase for II. Of the bile anions studied, cholate, taurocholate, dehydrocholate, hyodesoxycholate, and glycocholate increased the disappearance rates of I and II. Desoxycholate increased the rate constant of I but was ineffective with II, while glycotaurocholate had an opposite effect.

The most promising of the anions studied was phoscholate. This anion, which is the conjugate base of phoscholic acid (2,2′-phosphinicodilactic acid), significantly increased the disappearance rate constants of both I and II. For example, the rate constant for I in the presence of chloride ions was 3.05×10^{-3} min^{-1}, while its value in the presence of phoscholate was 5.35×10^{-3} min^{-1}. Similarly, the k^* value of II in the presence of chloride ions was 4.58×10^{-3} min^{-1}, which increased to 7.37×10^{-3} min^{-1} when the drug was present with phoscholate.

It was stated previously that the intestinal disappearance of I and II and their combinations with various anions followed a definite pattern; their initial disappearance rate was rapid and was followed by a slower phase. Similar results for other quaternary ammonium drugs (5, 19–21) and other drugs such as phenothiazines (22), haloperidol (22), and steroids (23) also were reported. This pattern may be indicative of the mechanism by which these quaternary ammonium drugs are absorbed through the intestinal barrier.

Figure 1 illustrates the typical kinetic patterns of the intestinal disappearance of I and II. The rate was rapid in the initial period and was followed by a slower phase between 30 and 180 min. An attempt was made to describe mathematically the kinetics of I and II. Of the kinetic models considered, the model shown in Scheme I gave the best fit to the experimental data.

$$A \underset{k_2}{\overset{k_1}{\rightleftharpoons}} B \xrightarrow{k_3} C$$

Scheme I

In Scheme I, A is the drug in the intestinal lumen, k_1 and k_2 are the constants that are part of the equilibrium step, and k_3 is the constant responsible for the disappearance of the drug from the lumen. Assuming that k_1, k_2, and k_3 are first-order rate constants and solving the differential equation for A yield (22, 24, 25):

$$A = A_0 \left[\frac{(k_2 + k_3 - \alpha)e^{-\alpha t} - (k_2 + k_3 - \beta)e^{-\beta t}}{\beta - \alpha}\right] \quad \text{(Eq. 2)}$$

where α and β are given by:

$$\alpha = \tfrac{1}{2}[(k_1 + k_2 + k_3) + \sqrt{(k_1 + k_2 + k_3)^2 - 4k_1k_3}] \quad \text{(Eq. 3)}$$

and:

$$\beta = \tfrac{1}{2}[(k_1 + k_2 + k_3) - \sqrt{(k_1 + k_2 + k_3)^2 - 4k_1k_3}] \quad \text{(Eq. 4)}$$

This derivation gives a mathematical relationship between the defined microconstants k_1, k_2, and k_3 and the disappearance of the drug from the intestine. The β value obtained from the 0–180-min data is identical to the k^* constant determined previously.

The presence of excess chloride did not affect the rate constants of I and II. This finding is in agreement with the results of earlier studies. The presence of cholate and phoscholate increased the disappearance rate constant, k_3, of I and II. They also caused a corresponding increase in the apparent disappearance rate constants of I and II in the *in situ* gut study. For comparison purposes, the k^* values are listed in Tables III and IV in parentheses.

Therefore, it is possible that the quaternary ammonium drugs I and II may be absorbed in the manner described by the proposed mathematical model. Nakamura *et al.* (26–28) investigated the mechanism of intestinal absorption of four highly ionized, poorly lipid-soluble dyes and noted that these compounds must bind to mucus as the first step in absorption. Mucus, which coats the epithelial surface, is secreted by the goblet cells of the small intestine.

Martin *et al.* (29) found that the bile salts sodium deoxycholate, sodium taurodeoxycholate, and sodium glycocholate cause breakdown of the mucus structure. In addition to possibly causing membrane changes, the anions also may elicit their effect in this manner.

The investigation so far indicated that the intestinal disappearance of quaternary ammonium drugs can be influenced by the presence of a suitable anion and also that the *in situ* gut technique can be used to study such enhancement. Since this method determines only the disappearance of drugs from the intestinal lumen, several possibilities could produce misleading results. These possibilities are drug degradation, binding of the drug to the membrane or intestinal contents, intramembrane storage, and mechanical error during sampling. Therefore, before any definite conclusion could be drawn from the study, further investigation of the method was warranted.

To determine the stability of I and II in solution, different drug–anion solutions were prepared and kept at room temperature for 1 week. Almost 100% recovery of each drug from these solutions indicated that the drugs were stable in aqueous solutions containing the different anions. Similar experiments were conducted using the membrane and intestinal contents. Again, almost 100% recovery indicated that the drugs were stable over the experimental period. These results agree with previous reports (4, 17).

Table III—Intestinal Disappearance Rate Constants of Hexamethonium Chloride (I) in the Presence of Different Anions

Anion	Molar Ratio of I to Anion	$k_1 \times 10^2$, min^{-1}	$k_2 \times 10^2$, min^{-1}	$k_3 \times 10^2$, min^{-1}
Chloride	1:3	3.3	11.9	1.1 (0.305)[a]
Cholate	1:5	4.4	12.8	4.1 (0.833)[a]
Phoscholate	1:5	3.0	6.5	1.7 (0.535)[a]

[a] Apparent disappearance rate constant, k^*, in the *in situ* gut technique.

Table IV—Intestinal Disappearance Rate Constants of Pralidoxime Chloride (II) in the Presence of Different Anions

Anion	Molar Ratio of II to Anion	$k_1 \times 10^2$, min^{-1}	$k_2 \times 10^2$, min^{-1}	$k_3 \times 10^2$, min^{-1}
Chloride	1:2	4.2	9.5	1.7 (0.458)[a]
Cholate	1:2	3.1	5.5	1.7 (0.523)[a]
Phoscholate	1:2	1.9	3.6	2.9 (0.730)[a]

[a] Apparent disappearance rate constant, k^*, in the *in situ* gut technique.

Table V—Intestinal Disappearance and Appearance in Plasma of Hexamethonium Chloride (I) and Pralidoxime Chloride (II) in the Presence of Different Anions for the *In Situ* Loop Technique

Anion	I		II	
	Intestinal Loss after 3 hr, mg	Amount in Plasma at 3 hr, mg	Intestinal Loss after 3 hr, mg	Amount in Plasma at 3 hr, mg
Chloride	1.6 ± 0.1	0.46 ± 0.03	3.6 ± 0.1	0.038 ± 0.006
Cholate	2.4 ± 0.2	0.74 ± 0.10	5.4 ± 0.4	0.068 ± 0.007
Phoscholate	2.3 ± 0.1	0.81 ± 0.07	6.3 ± 0.3	0.110 ± 0.004

To determine whether the loss of drug from the intestine was a result of absorption, two experiments were conducted. The first experiment was a study of the effects of selected anions on the intestinal absorption of I and II using a conventional *in situ* loop technique; the second experiment was a study of the amount of drug transferred from the intestine into the blood at the end of 3 hr. Chloride, cholate, and phoscholate were the three anions studied in combination with I and II. The chloride anion was selected because it is the most commonly used anion in the synthesis of quaternary ammonium drugs. Furthermore, the chloride salts of hexamethonium and pralidoxime frequently are used as therapeutically active agents. Cholate was representative of the bile salts, while phoscholate was the most promising anion, and both enhanced the disappearance rates of I and II.

The results for I and II in the presence of cholate and phoscholate as determined by the loop technique are presented in Table V. Both cholate and phoscholate increased the amount of I and II absorbed as compared to the standard, chloride. These findings are in agreement with those of the *in situ* gut technique.

The plasma samples obtained at the completion of the loop experiments indicated the presence of drug, thereby qualitatively substantiating that both I and II were absorbed to some degree. As seen in Table V, both cholate and phoscholate caused increased intestinal loss of I and II (as compared to chloride), and this loss, in turn, increased the quantity of drug in plasma.

The amount of drug lost could be calculated from the *in situ* gut technique data. This value was the difference between the amount of drug known to be present in the intestine at time zero and the amount remaining in the intestine after 180 min. The amount of drug lost was converted to a percentage, and this value then was compared to the results of the *in situ* loop technique. The gut and loop techniques yielded similar values for the percent of drug lost (Table VI). Both cholate and phoscholate enhanced the disappearance of I and II.

During the *in situ* gut technique experiments, if the drug had adhered to or been bound to the intestinal membrane or contents, then the sample aliquot obtained at any time would not have truly represented the actual amount of drug in the lumen. This possibility cannot be fully discounted since no recovery experiments were conducted. However, the results of the two methods were in close agreement. In the *in situ* loop technique, the entire intestine and contents are assayed, so the drug not accounted for must be located in areas other than the intestine. Finally, since no samples are removed until the conclusion of the experiment, mechanical errors such as frequent sampling cannot account for the different kinetic results.

Membrane Permeability—Quaternary ammonium drugs are completely ionized at all physiological pH values, and these drug solutions always contained their corresponding anions. It seemed reasonable that these anions may have affected membrane permeability. This assumption was investigated in a study with a sodium chloride solution as the control. The molar ratios of drug to anion were the same as those of the *in situ* gut technique for all test solutions. Again, the anions selected were chloride, cholate, and phoscholate.

Table VI—Comparison of *In Situ* and Loop Techniques for the Intestinal Disappearance of Hexamethonium Chloride (I) and Pralidoxime Chloride (II) in the Presence of Different Anions

Anion	Drug Lost, %			
	I		II	
	Gut Technique	Loop Technique after 3 hr	Gut Technique	Loop Technique after 3 hr
Chloride	44	46	54	48
Cholate	68	69	67	72
Phoscholate	60	66	79	84

Table VII—Effect of Different Drug–Anion Combinations on Membrane Permeability in the Rat Intestine in the Membrane Permeability Study

Drug–Anion Combination	Molar Ratio of Drug to Anion	Inulin in Intestine after 3 hr, mg × 10^2	Percentage Change[a]
Chloride	—	61 ± 8	Control
I + chloride	1:3	62 ± 5	No change
I + cholate	1:5	84 ± 10	35
I + phoscholate	1:5	90 ± 12	38
I + sulfate	1:5	48 ± 9	−26[b]
II + chloride	1:2	64 ± 8	No change
II + cholate	1:2	86 ± 12	38
II + phoscholate	1:2	83 ± 10	35
II + citrate	1:2	38 ± 5	−39

[a] Percentage change as compared to control. [b] Negative number indicates less than control.

The drug–anion combinations tested for their possible effects on membrane permeability are listed in Table VII. Table VII also shows the percentages of inulin in the intestine after an intravenous dose of 20 mg. The percentages of inulin reported in Table VII are in terms of the control.

The drug–chloride combinations and the chloride alone (control) gave similar results. However, the presence of cholate and phoscholate in the drug solutions increased the amount of inulin in the intestine by ~35%. These results indicate that there were changes in the intestinal membrane permeability when the drug solutions containing cholate and phoscholate were in the intestine for 3 hr.

The control solution containing chloride ion apparently affected the membrane permeability because ~3% of the inulin was found in the intestine when this solution was tested. However, this anion in combination with the drugs gave the same effect as the chloride ion alone. Furthermore, the changes in permeability with phoscholate and cholate in the presence of both drugs were similar. These findings seem to indicate that the anionic components of the solutions were responsible for the permeability changes of the intestinal membrane and not the drug molecules.

Feldman and coworkers (30–34) studied the enhancement of drug absorption by bile salts; in all cases, the increases were attributed to permeability changes. Other investigators (35, 36) demonstrated a similar effect by the bile salts, resulting in better drug absorption. These results suggest that the enhancement of the transfer of I and II caused by cholate and phoscholate is the result of permeability changes in the rat intestine. Also, it is suggested that the anionic components and not the drug molecules are responsible for these effects.

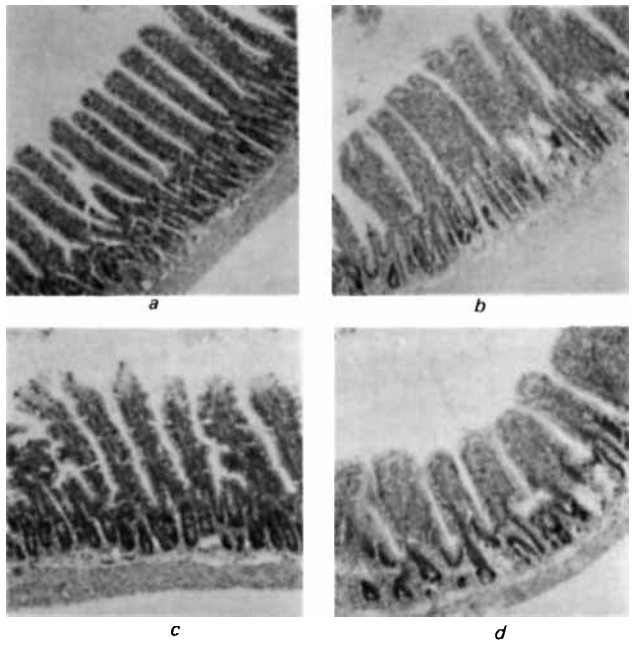

Figure 2—*Examples of intestinal morphological changes. Key:* a, *control;* b, *fusion of villi;* c, *loss of epithelial cells; and* d, *edema of the lamina propria.*

Table VIII—Histological Study of Effect of Drugs and Anions on the Structural Integrity of the Intestinal Membrane [a]

Anion, Drug, or Drug–Anion Combination	Loss of Epithelial Cells	Loss of Goblet Cells	Fusion of Villi	Edema of Lamina Propria	Changes in Mucous Membrane
Control	0	0	0	0	0
I	1	1	2	0	1
II	0	1	1	0	0
Chloride	1	3	1	1	1
Bromide	4	4	3	0	4
Cholate	2	3	2	0	3
Phoscholate	2	2	2	0	2
I + chloride	1	2	1	0	1
I + cholate	2	1	1	0	1
I + phoscholate	1	2	2	0	2
II + chloride	0	3	1	0	2
II + bromide	4	3	3	0	4
II + cholate	2	1	2	0	2
II + phoscholate	3	3	2	0	2

[a] Key: 0 = normal, 1 = slight, 2 = moderate, 3 = severe, and 4 = very severe.

Histological Study—This study was undertaken to investigate the effect of I and II, selected anions, and their combinations on the morphology of the intestine. Since the mucous membrane of the intestine comes in direct contact with the drug, the changes in its structure were of concern. The three layers of importance in absorption are the epithelial lining, lamina propria, and muscularis mucosa. The gross morphological changes in these layers were studied by the following observations:

1. Loss of epithelial cells—These cells form the innermost layer of the intestine, lining the villi of the intestinal mucosa. The epithelium consists of columnar cells and the basement membrane. Since absorption occurs through the columnar cells, any damage or loss of these cells could easily affect the transfer process.

2. Loss of goblet cells—Intermingled with the absorptive cells in the mucous membrane are goblet cells. These cells secrete mucus, which protects the epithelial lining from injury by the materials in the intestine.

3. Fusion of villi—The mucosal surface provides a large surface from which absorption occurs. Since the fusion of the villi means a reduction in the surface area, this fusion possibly could affect the absorption of materials from the intestines.

4. *Edema of lamina propria*—The lamina propria supports the epithelium and connects it to the muscularis mucosa. It carries both the blood and the lymphatic capillaries close to the epithelial surface, and diffusing materials therefore travel only a short distance through the tissue fluid of the lamina propria before gaining entrance into either type of capillary. Damage to the lamina propria could affect the transfer of drugs and their subsequent entrance into the blood.

5. Changes in mucous membrane—These changes did not concern any particular tissue of the mucous membrane but were overall changes in the absorptive surface.

The results of the morphological changes were classified as: 0 = normal, 1 = slight, 2 = moderate, 3 = severe, and 4 = very severe. Examples of these changes are presented in Fig. 2, and the results of this study are shown in Table VIII.

Compound I alone caused only minimal intestinal morphological changes; II caused even milder changes. These results can be correlated with those of the permeability study where the drugs did not affect the permeability of the intestinal membrane.

The responses elicited by the anions were varied. Chloride ions caused considerable loss of goblet cells; however, the overall effect on the mucous membrane was slight. This anion, as well as cholate and phoscholate, earlier was shown to affect membrane permeability. This study demonstrated that these anions had a moderate effect on the morphological structure of the membrane. The most dramatic changes were caused by bromide ions. Bromide was included since it was found previously that increasing the bromide concentration increased the loss of I.

The effects of drugs in combination with anions on the intestinal membrane morphology were similar to the effect of the specific anion alone. This finding supports the view that the drug molecule did not cause any further morphological changes.

None of the drugs or the anions or their combinations caused edema of the lamina propria, while all caused fusion of the villi to varying degrees. Moreover, some goblet cells were lost in all cases. The phoscholate ion and its combination with a drug caused moderate damage to epithelial cells. These findings are in agreement with those of Low-Beer *et al.* (37), who demonstrated a similar morphological change in the presence of foreign materials in the intestine. Cholate ions had a similar effect on the membrane.

The anions that enhanced the absorption of I and II also caused permeability and histological changes in the intestinal membrane. Although these results seem to indicate that the permeability change may have been caused by histological changes, which then led to enhanced drug absorption, they should be viewed cautiously since histological results are not available for the anions that actually decreased drug transfer.

REFERENCES

(1) F. H. Smirk and K. S. Alstad, *Br. Med. J.*, **1**, 1217 (1951).

(2) W. D. M. Paton, *ibid.*, **1**, 773 (1951).

(3) "Physicians' Desk Reference," 33rd ed., Medical Economics Co., Oradell, N.J., 1979.

(4) M. Harington, *Clin. Sci.*, **12**, 185 (1953).

(5) R. R. Levine, *Fed. Proc. Fed. Am. Soc. Exp. Biol.*, **18**, 414 (1959).

(6) G. M. Irwin, H. B. Kostenbauder, L. W. Dittert, R. Staples, A. Mischer, and J. V. Swintosky, *J. Pharm. Sci.*, **58**, 313 (1969).

(7) D. B. Duncan, *Biometrics*, **11**, 1 (1955).

(8) M. E. Auerbach, *Ind. Eng. Chem., Anal. Ed.*, **15**, 492 (1943).

(9) R. Mitchell and B. Clark, *Proc. Soc. Exp. Biol. Med.*, **81**, 105 (1952).

(10) J. R. May, P. Zvirblis, and A. Kondritzer, *J. Pharm. Sci.*, **54**, 1508 (1965).

(11) R. I. Ellin and A. A. Kondritzer, *Anal. Chem.*, **31**, 200 (1959).

(12) W. A. Groff and R. I. Ellin, *Clin. Chem.*, **15**, 72 (1969).

(13) J. H. Roe, J. H. Epstein, and N. P. Goldstein, *J. Biol. Chem.*, **178**, 839 (1949).

(14) G. E. Schreiner, *Proc. Soc. Exp. Biol. Med.*, **74**, 117 (1950).

(15) J. T. Doluisio, N. F. Billups, L. W. Dittert, E. T. Sugita, and J. V. Swintosky, *J. Pharm. Sci.*, **58**, 1196 (1969).

(16) P. O. Alexander and J. M. Rivera-Velez, *Proc. Soc. Exp. Biol. Med.*, **118**, 600 (1965).

(17) R. R. Levine and G. M. Steinberg, *Nature*, **209**, 269 (1966).

(18) R. R. Levine, *J. Pharmacol. Exp. Ther.*, **131**, 328 (1961).

(19) R. M. Levine, M. R. Blair, and B. B. Clark, *ibid.*, **114**, 78 (1955).

(20) R. M. Levine and B. B. Clark, *Arch. Int. Pharmacodyn. Ther.*, **112**, 458 (1957).

(21) R. R. Levine, *Arzneim.-Forsch.*, **16**, 1373 (1966).

(22) J. T. Doluisio, W. G. Crouthamel, G. H. Tan, J. V. Swintosky, and L. W. Dittert, *J. Pharm. Sci.*, **59**, 72 (1970).

(23) A. H. Beckett and M. E. Pickup, *J. Pharm. Pharmacol.*, **27**, 226 (1975).

(24) A. Rescigno and G. Segre, "Drug and Tracer Kinetics," Blaisdell, Waltham, Mass., 1966.

(25) J. S. Roberson, D. C. Tosteson, and J. L. Gamble, Jr., *J. Lab. Clin. Med.*, **49**, 497 (1957).

(26) J. Nakamura, Y. Yoshizaki, M. Yasuhara, T. Kimura, S. Muranishi, and H. Sezaki, *Chem. Pharm. Bull.*, **24**, 683 (1976).

(27) *Ibid.*, **24**, 691 (1976).

(28) J. Nakamura, K. Shima, T. Kimura, S. Muranishi, and H. Sezaki, *Chem. Pharm. Bull.*, **26**, 857 (1978).

(29) G. P. Martin, C. Marriott, and I. W. Kellaway, *J. Pharm. Pharmacol.*, **28**, 76P (1976).

(30) M. Mayersohn, S. Feldman, and M. Gibaldi, *J. Nutr.*, **98**, 288 (1969).

(31) S. Feldman, R. J. Wynn, and M. Gibaldi, *J. Pharm. Sci.*, **57**, 1493

(1968).
(32) S. Feldman, M. Salvino, and M. Gibaldi, *ibid.*, **59**, 705 (1970).
(33) S. Feldman and M. Gibaldi, *Proc. Soc. Exp. Biol. Med.*, **132**, 1031 (1969).
(34) S. Feldman and M. Gibaldo, *J. Pharm. Sci.*, **58**, 425 (1969).
(35) K. Kakemi, H. Sezaki, R. Konishi, T. Kimura, and M. Murakami, *Chem. Pharm. Bull.*, **18**, 275 (1970).
(36) K. Kakemi, H. Sezaki, R. Konishi, T. Kimura, and A. Okita, *ibid.*, **18**, 1034 (1970).
(37) T. S. Low-Beer, R. E. Schneider, and W. O. Dobbins, *Gut*, **11**, 486 (1970).

ACKNOWLEDGMENTS

Abstracted in part from a dissertation submitted by S. I. Bhuta to the Philadelphia College of Pharmacy and Science in partial fulfillment of the Doctor of Philosophy degree requirements.

Separation and Quantitation of Chlortetracycline, 4-Epitetracycline, 4-Epianhydrotetracycline, and Anhydrotetracycline in Tetracycline by High-Performance Liquid Chromatography

NASEEM MUHAMMAD ˣ **and JOY A. BODNAR**

Received September 7, 1979, from *Bristol Laboratories, Division of Bristol-Myers Co., Syracuse, NY 13201.* Accepted for publication March 12, 1980.

Abstract □ The analysis of tetracycline epimers in tetracycline preparations by high-performance liquid chromatography is described. The method uses a microparticulate phenyl column (3.9 mm i.d. × 30 cm) with a step gradient of 12–22% acetonitrile in 0.2 *M* phosphate buffer at pH 2.2. The analysis takes 22 min. The relative standard deviations of the method (2σ, $n = 6$) for the analysis of chlortetracycline, 4-epitetracycline, 4-epianhydrotetracycline, and anhydrotetracycline in tetracycline were ±3.68, ±4.47, ±7.60, and ±2.77%, respectively.

Keyphrases □ Tetracycline—simultaneous high-performance liquid chromatographic analysis of tetracycline epimers in tetracycline preparations □ High-performance liquid chromatography—analysis, tetracycline epimers in tetracycline preparations □ Antibacterials—tetracycline, high-performance liquid chromatographic analysis of tetracycline epimers in tetracycline preparations

Pharmaceutical preparations of tetracycline (I) contain small quantities of related compounds as impurities. The most important compounds are chlortetracycline (II), 4-epitetracycline (quatrimycin, III), 4-epianhydrotetracycline (IV), and anhydrotetracycline (V). Their permitted concentrations are listed in the Federal Register (1) for tetracycline dosage forms marketed in the United States and in the British Pharmacopoeia (2) and European Pharmacopoeia (3) for the European markets. The need for a simple assay prompted this investigation of the conditions under which these compounds could be separated and quantitated by high-performance liquid chromatography (HPLC) without a solvent gradient system.

BACKGROUND

TLC (4, 5), paper chromatography (6), and column chromatography followed by UV spectrophotometry (7, 8) have proved laborious and generally are not sufficiently sensitive or precise. A GLC method (9) requires prior formation of the trimethylsilyl derivative under carefully controlled conditions.

Several HPLC methods have been applied to separate III–V from I using a cation-exchange column with an ethylenediaminetetraacetic acid buffer (10), a C_{18} column (5–7% loading) with phosphate buffer and a linear gradient of 10–60% acetonitrile (11), a C_{18} column (10–18% loading) with a linear gradient of methanol–water–0.2 *M* phosphate buffer at pH 2.5 (30:60:10) and methanol–acetonitrile–water–0.2 *M* phosphate buffer at pH 2.5 (50:30:20:10) (12), and a C_{18} column with water–acetonitrile–perchloric acid in two steps (13).

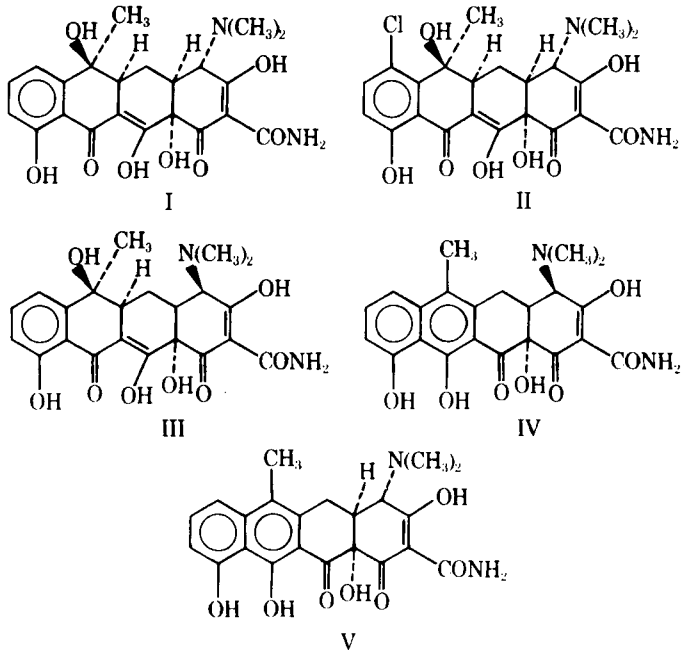

In the present study, a microparticulate phenyl column with a step gradient of 12–22% acetonitrile in 0.2 *M* phosphate buffer at pH 2.2 (using an automatic switching valve) at a flow rate of 2.6 ml/min was used to separate II–V from I in 22 min. The method did not require a solvent gradient system and needed only one pump. It was tested for the analysis of several different tetracycline formulations.

EXPERIMENTAL

Apparatus—The liquid chromatographic apparatus shown in Fig. 1 was used[1].

Reagents and Materials—Ammonium 4-epitetracycline[2], 4-epianhydrotetracycline hydrochloride[2], anhydrotetracycline hydrochloride[2], chlortetracycline hydrochloride[3], acetonitrile[4], phosphoric acid[5], potassium hydroxide[5], and ammonium hydroxide[5] were used.

[1] A Valcor series SV-72 automatic switching valve, a Waters Associates model 6000 A pump, a Valco loop injector, a Waters Associates μBondapak phenyl column, and a Waters Associates model 440 absorbance detector were used.
[2] Bristol reference standards, Bristol Laboratories, Syracuse, N.Y.
[3] USP reference standard.
[4] Burdick & Jackson Laboratories, Muskegon, Mich.
[5] Fisher Scientific Co., Fair Lawn, N.J.

0022-3549/80/0800-0928$01.00/0
© 1980, American Pharmaceutical Association

(1968).
(32) S. Feldman, M. Salvino, and M. Gibaldi, *ibid.*, **59**, 705 (1970).
(33) S. Feldman and M. Gibaldi, *Proc. Soc. Exp. Biol. Med.*, **132**, 1031 (1969).
(34) S. Feldman and M. Gibaldo, *J. Pharm. Sci.*, **58**, 425 (1969).
(35) K. Kakemi, H. Sezaki, R. Konishi, T. Kimura, and M. Murakami, *Chem. Pharm. Bull.*, **18**, 275 (1970).
(36) K. Kakemi, H. Sezaki, R. Konishi, T. Kimura, and A. Okita, *ibid.*, **18**, 1034 (1970).
(37) T. S. Low-Beer, R. E. Schneider, and W. O. Dobbins, *Gut*, **11**, 486 (1970).

ACKNOWLEDGMENTS

Abstracted in part from a dissertation submitted by S. I. Bhuta to the Philadelphia College of Pharmacy and Science in partial fulfillment of the Doctor of Philosophy degree requirements.

Separation and Quantitation of Chlortetracycline, 4-Epitetracycline, 4-Epianhydrotetracycline, and Anhydrotetracycline in Tetracycline by High-Performance Liquid Chromatography

NASEEM MUHAMMAD ˣ **and JOY A. BODNAR**

Received September 7, 1979, from *Bristol Laboratories, Division of Bristol-Myers Co., Syracuse, NY 13201.* Accepted for publication March 12, 1980.

Abstract □ The analysis of tetracycline epimers in tetracycline preparations by high-performance liquid chromatography is described. The method uses a microparticulate phenyl column (3.9 mm i.d. × 30 cm) with a step gradient of 12–22% acetonitrile in 0.2 *M* phosphate buffer at pH 2.2. The analysis takes 22 min. The relative standard deviations of the method (2σ, $n = 6$) for the analysis of chlortetracycline, 4-epitetracycline, 4-epianhydrotetracycline, and anhydrotetracycline in tetracycline were ±3.68, ±4.47, ±7.60, and ±2.77%, respectively.

Keyphrases □ Tetracycline—simultaneous high-performance liquid chromatographic analysis of tetracycline epimers in tetracycline preparations □ High-performance liquid chromatography—analysis, tetracycline epimers in tetracycline preparations □ Antibacterials—tetracycline, high-performance liquid chromatographic analysis of tetracycline epimers in tetracycline preparations

Pharmaceutical preparations of tetracycline (I) contain small quantities of related compounds as impurities. The most important compounds are chlortetracycline (II), 4-epitetracycline (quatrimycin, III), 4-epianhydrotetracycline (IV), and anhydrotetracycline (V). Their permitted concentrations are listed in the Federal Register (1) for tetracycline dosage forms marketed in the United States and in the British Pharmacopoeia (2) and European Pharmacopoeia (3) for the European markets. The need for a simple assay prompted this investigation of the conditions under which these compounds could be separated and quantitated by high-performance liquid chromatography (HPLC) without a solvent gradient system.

BACKGROUND

TLC (4, 5), paper chromatography (6), and column chromatography followed by UV spectrophotometry (7, 8) have proved laborious and generally are not sufficiently sensitive or precise. A GLC method (9) requires prior formation of the trimethylsilyl derivative under carefully controlled conditions.

Several HPLC methods have been applied to separate III–V from I using a cation-exchange column with an ethylenediaminetetraacetic acid buffer (10), a C_{18} column (5–7% loading) with phosphate buffer and a linear gradient of 10–60% acetonitrile (11), a C_{18} column (10–18% loading) with a linear gradient of methanol–water–0.2 *M* phosphate buffer at pH 2.5 (30:60:10) and methanol–acetonitrile–water–0.2 *M* phosphate buffer at pH 2.5 (50:30:20:10) (12), and a C_{18} column with water–acetonitrile–perchloric acid in two steps (13).

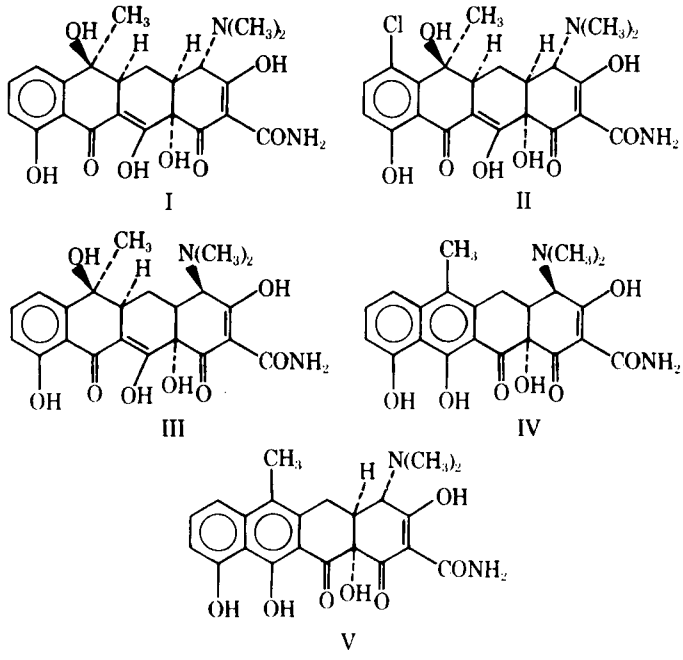

In the present study, a microparticulate phenyl column with a step gradient of 12–22% acetonitrile in 0.2 *M* phosphate buffer at pH 2.2 (using an automatic switching valve) at a flow rate of 2.6 ml/min was used to separate II–V from I in 22 min. The method did not require a solvent gradient system and needed only one pump. It was tested for the analysis of several different tetracycline formulations.

EXPERIMENTAL

Apparatus—The liquid chromatographic apparatus shown in Fig. 1 was used[1].

Reagents and Materials—Ammonium 4-epitetracycline[2], 4-epianhydrotetracycline hydrochloride[2], anhydrotetracycline hydrochloride[2], chlortetracycline hydrochloride[3], acetonitrile[4], phosphoric acid[5], potassium hydroxide[5], and ammonium hydroxide[5] were used.

[1] A Valcor series SV-72 automatic switching valve, a Waters Associates model 6000 A pump, a Valco loop injector, a Waters Associates μBondapak phenyl column, and a Waters Associates model 440 absorbance detector were used.
[2] Bristol reference standards, Bristol Laboratories, Syracuse, N.Y.
[3] USP reference standard.
[4] Burdick & Jackson Laboratories, Muskegon, Mich.
[5] Fisher Scientific Co., Fair Lawn, N.J.

0022-3549/80/0800-0928$01.00/0
© 1980, American Pharmaceutical Association

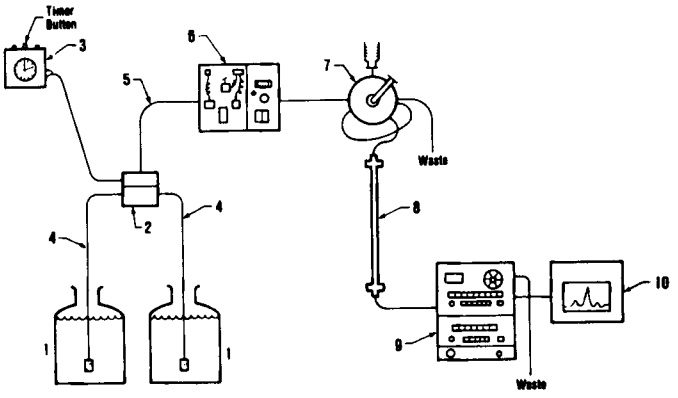

Figure 1—*HPLC step-gradient system for determination of tetracycline epimers. Key: 1, 2-liter reservoirs containing Eluents 1 and 2; 2, automatic switching valve (miniature three-way solenoid); 3, delay timer; 4, polytef tubing (3.2 mm i.d.) used to transfer the eluent from the reservoirs to the switching valve; 5, polytef tubing (16 cm long × 3.2 mm i.d.) used to transfer the eluent from the valve to the pump; 6, pump; 7, 20-μl loop injector operated at 7000 psi; 8, μBondapak phenyl 3.9 mm i.d. × 30-cm column; 9, absorbance detector; and 10, recorder.*

Mobile Phase—Eluent 1 was prepared by adding 240 ml of degassed acetonitrile and 27 ml of phosphoric acid to 1650 ml of degassed, distilled, deionized water. The pH was adjusted to 2.2 with 45% aqueous KOH, and the solution was diluted to 2 liters. The solution was degassed for only 15 sec prior to use.

Eluent 2 was prepared by adding 440 ml of degassed acetonitrile and 27 ml of phosphoric acid to 1500 ml of degassed, distilled, deionized water. The pH was adjusted to 2.2 with 25% aqueous KOH, and the solution was diluted to 2 liters with degassed, distilled, deionized water. The solution was degassed for only 15 sec prior to use.

Standard Solution Preparation—About 20 mg of ammonium 4-epitetracycline, 3 mg of epianhydrotetracycline hydrochloride, 3 mg of anhydrotetracycline hydrochloride, and 10 mg of chlortetracycline hydrochloride reference standards were weighed accurately into a 50-ml volumetric flask, dissolved, and diluted to volume with distilled water. Sonication sometimes was necessary for dissolution.

Sample Preparation—Bulk tetracycline hydrochloride samples were prepared by weighing accurately 500 mg of the sample into a 50-ml volumetric flask. The sample was dissolved and diluted to volume with distilled water.

Tetracycline base samples were prepared by weighing accurately 500 mg of the sample into a 50-ml volumetric flask. The sample was dissolved and diluted to volume with 0.1 *N* aqueous HCl.

Samples of hard, filled capsules containing sodium polymetaphosphate, phenazopyridine hydrochloride, sulfamethizole, and tetracycline phosphate were prepared by weighing accurately 500 mg of capsule blend into a 50-ml volumetric flask. To the flask were added 15 ml of distilled water and 1 ml of concentrated ammonium hydroxide. The flask was shaken until dissolution occurred. The solution was diluted to volume with pH 4.0 phosphate buffer, allowed to stand for 10 min, and filtered.

Sample Analysis—The column was conditioned with Eluent 1. The delay timer (Fig. 1) was set at 10 min. Twenty microliters of the standard solution or sample solution was injected using a loop. The timer was started, and the system was allowed to run. After 10 min, the automatic switching value opened to Eluent 2. The system was allowed to run on Eluent 2 until all peaks eluted (~15 min).

Calculations—The areas of the peaks were measured by the peak height times the half-width method or by a computer. The percentage of each compound was obtained from:

$$\text{factor for II, IV, and V: } F = \frac{\text{peak area of standard}}{\text{mg of standard}} \quad \text{(Eq. 1}a\text{)}$$

or:

$$\text{factor for III: } F = \frac{\text{peak area of standard}}{\text{mg of standard} \times 1.04} \quad \text{(Eq. 1}b\text{)}$$

and the correction factor for tetracycline based on the label claim (K):

$$K = \frac{\text{mg of sample}}{\text{label claim of tetracycline (mg)}} \quad \text{(Eq. 2)}$$

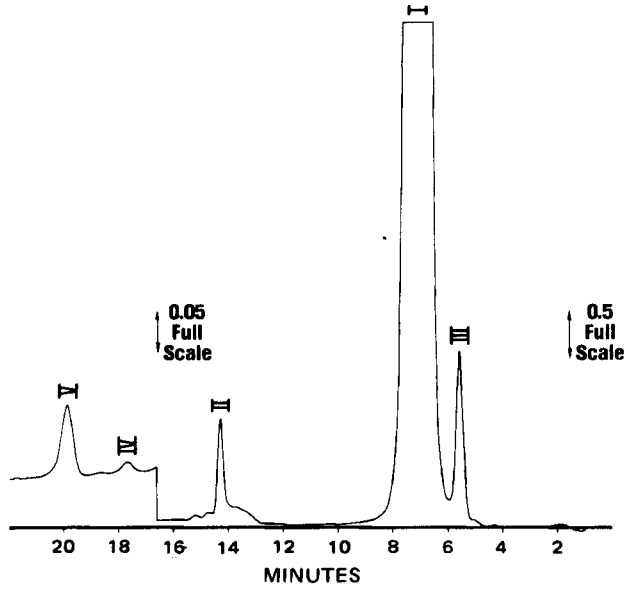

Figure 2—*Representative chromatogram of sample.*

so that:

$$\%\ \text{impurity} = \frac{\text{peak area of individual impurity} \times 100 \times K}{\text{mg of sample} \times F} \quad \text{(Eq. 3)}$$

DISCUSSION

The described HPLC method was developed for use in laboratories without a programmed solvent gradient system. The method requires one pump and an automatic switching valve. The microparticulate phenyl column produced symmetrical peaks without any tailing as compared to the C_{18} (alkyl) column (Figs. 2 and 3).

Standard linearity was checked over the ranges of 0.114–0.306 mg/ml for II, 0.286–0.620 mg/ml for III, 0.0215–0.036 mg/ml for IV, and 0.021–0.084 mg/ml for V. All four compounds responded linearly at the reported concentrations, thus providing more than an adequate range for their analysis as impurities in tetracycline (I).

Chromatographic variability was determined by six identical injections of a solution containing reference standards II–V. Standard variability was determined by a single injection of six different solutions containing reference standards II–V. Sample variability was determined by a single injection of six different preparations of the sample. Procedural variability was determined by a single injection of six individual standards and sample preparations. Standard deviations (s%) and relative standard deviations ($2s$%) for chromatographic variability, standard variability, sample variability, and procedural variability for II–V are shown in Table I.

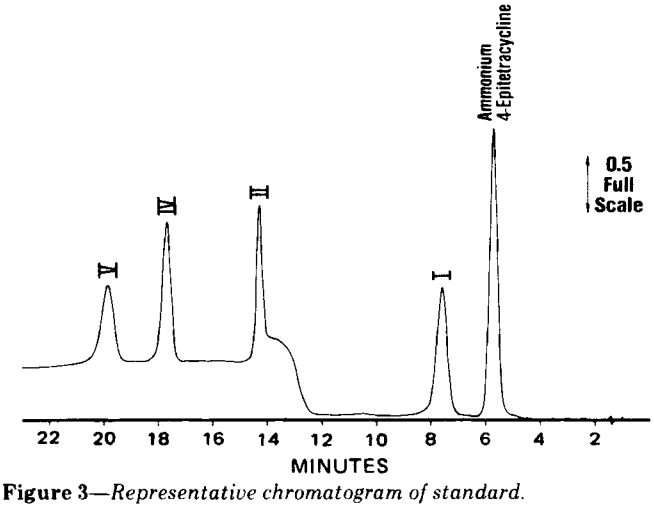

Figure 3—*Representative chromatogram of standard.*

Table I—Standard Deviations and Relative Standard Deviations

	II		III		IV		V	
	s%	$2s$%	s%	$2s$%	s%	$2s$%	s%	$2s$%
Chromatographic variability	0.0075	5.83	0.0663	2.80	0.0083	1.27	0.0183	3.39
Standard variability	0.0040	1.79	0.0081	2.34	0.0051	6.58	0.0016	2.20
Sample variability	0.029	5.44	0.049	4.92	0.0002	8.11	0.0012	4.10
Procedural variability	0.023	3.68	0.044	4.47	0.00017	7.60	0.0008	2.77

Table II—Representative Samples [a]

Sample[b]	II, %	III, %	IV, %	V, %
Capsule 1	1.95	1.13	1.30	3.19
Capsule 2	1.08	1.08	0.05	0.16
Capsule 3	1.98	1.08	0.83	4.01
Capsule 4	2.07	1.05	0.06	0.22
Capsule 5	2.05	1.12	0.02	0.13
Powder 1	1.88	1.09	0.004	0.068
Powder 2	1.99	1.05	0.005	0.054

[a] Percentages are based on the labeled claim of tetracycline. [b] Hard, filled capsules and bulk powders were used.

Accuracy of the assay was determined by spike recoveries of impurities II–V from I. Tetracycline (I) was spiked with impurities at 100% of the target value. The percent recoveries were 96, 102, 104, and 85% for II, III, IV, and V, respectively.

Several tetracycline-containing products were analyzed for impurities (II–V) (Table II).

In summary, the reversed-phase HPLC method described in this paper provides a rapid, sensitive, simple, and quantitative method for the simultaneous determination of impurities (II–V) in tetracycline (I).

REFERENCES

(1) *Fed. Regist.*, **39** (22), Part III, 3935 (1974).

(2) "British Pharmacopoeia, 1973," Her Majesty's Stationery Office, London, England, 1973, p. 468.

(3) "European Pharmacopoeia," Amendments to Vol. II, 39 (1973).

(4) A. A. Fernandoz, V. T. Noceda, and E. S. Carrera, *J. Pharm. Sci.*, **58**, 443 (1969).

(5) P. P. Ascione and G. P. Chrekian, *ibid.*, **59**, 1480 (1970).

(6) E. Addison and R. G. Clark, *J. Pharm. Pharmacol.*, **15**, 268 (1963).

(7) P. P. Ascione, J. B. Zaga, and G. P. Chrekian, *J. Pharm. Sci.*, **61**, 615 (1972).

(8) W. W. Fike and N. W. Brake, *ibid.*, **61**, 615 (1972).

(9) K. Tsujii and J. H. Robertson, *Anal. Chem.*, **45**, 2136 (1973).

(10) R. F. Lindauer, D. M. Cohem, and K. P. Munnelly, *ibid.*, **48**, 1731 (1976).

(11) K. Tsujii and J. H. Robertson, *J. Pharm. Sci.*, **65**, 400 (1976).

(12) K. Tsujii and J. F. Goetz, *J. Antibiot.*, **31**, 302 (1978).

(13) S. L. Ali and T. Strittmatter, *Int. J. Pharm.*, **1**, 185 (1978).

Aminoalkanesulfonic Acids IV: Synthesis of Mitodepressive *N*-Nitrosoaminoalkanesulfonic Acids

Lj. BUTULA ˣ **and Ž. BUKOVEC**

Received September 5, 1978, from the *Faculty of Pharmacy and Biochemistry, University of Zagreb, A. Kovačića 1, Zagreb, Yugoslavia.* Accepted for publication March 12, 1980.

Abstract □ Sodium aminoalkanesulfonates were synthesized from substituted amines and aldehyde sodium bisulfites at 40–60°. Nitrosation yielded the corresponding *N*-nitroso derivatives. Mitodepressive activity on cresse (*Lepidium sativum* L.) was determined, and all compounds examined possessed growth inhibition activity. The *N*-nitroso derivatives were slightly less active but also showed less toxicity than the parent aminoalkanesulfonic acids.

Keyphrases □ Aminoalkanesulfonic acids—synthesis of *N*-nitroso derivatives, evaluation for mitodepressive activity □ Mitodepressive activity—evaluation of aminoalkanesulfonic acids and *N*-nitroso derivatives □ *N*-Nitrosoaminoalkanesulfonic acids—synthesis, evaluation for mitodepressive activity

Aminoalkanesulfonic acids are known to have antiviral (1, 2) and anticancer (3, 4) activities. Some *N*-nitroso compounds, such as *N*-nitrosomethylamine, *N*-nitrosodimethylamine, and *N*-nitrosodiethylamine, showed blastogenic action when applied on Hungarian hamsters (5). Some experiments (6) showed imbalances in DNA and histone synthesis during carcinogenesis induced by nitrosamines. On the other hand, some *N*-nitroso compounds, such as 1,3-bis(2-chloroethyl)-1-nitrosourea (carmustine), are useful in the treatment of certain malignant diseases (7).

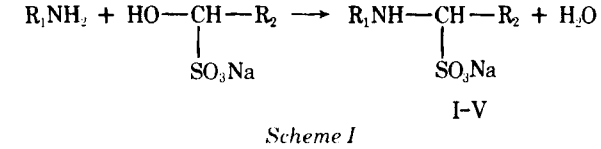

Scheme I

These findings prompted the synthesis of some new derivatives in this series (8–10) to determine their mitodepressive activity.

This report describes the synthesis of some sodium aminoalkanesulfonates (I–V) in which *m*- and *p*-chloroanilines were used with the corresponding aldehyde sodium bisulfites (Scheme I and Table I). In some cases, the desired products were obtained by the addition of sodium metabisulfite to azomethine derivatives (Scheme II).

Nitrosation of I–V and sodium *p*-chloroanilinophenyl-

0022-3549/80/0800-0930$01.00/0

© 1980, American Pharmaceutical Association

Table I—Standard Deviations and Relative Standard Deviations

	II		III		IV		V	
	s%	$2s$%	s%	$2s$%	s%	$2s$%	s%	$2s$%
Chromatographic variability	0.0075	5.83	0.0663	2.80	0.0083	1.27	0.0183	3.39
Standard variability	0.0040	1.79	0.0081	2.34	0.0051	6.58	0.0016	2.20
Sample variability	0.029	5.44	0.049	4.92	0.0002	8.11	0.0012	4.10
Procedural variability	0.023	3.68	0.044	4.47	0.00017	7.60	0.0008	2.77

Table II—Representative Samples [a]

Sample[b]	II, %	III, %	IV, %	V, %
Capsule 1	1.95	1.13	1.30	3.19
Capsule 2	1.08	1.08	0.05	0.16
Capsule 3	1.98	1.08	0.83	4.01
Capsule 4	2.07	1.05	0.06	0.22
Capsule 5	2.05	1.12	0.02	0.13
Powder 1	1.88	1.09	0.004	0.068
Powder 2	1.99	1.05	0.005	0.054

[a] Percentages are based on the labeled claim of tetracycline. [b] Hard, filled capsules and bulk powders were used.

Accuracy of the assay was determined by spike recoveries of impurities II–V from I. Tetracycline (I) was spiked with impurities at 100% of the target value. The percent recoveries were 96, 102, 104, and 85% for II, III, IV, and V, respectively.

Several tetracycline-containing products were analyzed for impurities (II–V) (Table II).

In summary, the reversed-phase HPLC method described in this paper provides a rapid, sensitive, simple, and quantitative method for the simultaneous determination of impurities (II–V) in tetracycline (I).

REFERENCES

(1) *Fed. Regist.*, **39** (22), Part III, 3935 (1974).

(2) "British Pharmacopoeia, 1973," Her Majesty's Stationery Office, London, England, 1973, p. 468.

(3) "European Pharmacopoeia," Amendments to Vol. II, 39 (1973).

(4) A. A. Fernandoz, V. T. Noceda, and E. S. Carrera, *J. Pharm. Sci.*, **58**, 443 (1969).

(5) P. P. Ascione and G. P. Chrekian, *ibid.*, **59**, 1480 (1970).

(6) E. Addison and R. G. Clark, *J. Pharm. Pharmacol.*, **15**, 268 (1963).

(7) P. P. Ascione, J. B. Zaga, and G. P. Chrekian, *J. Pharm. Sci.*, **61**, 615 (1972).

(8) W. W. Fike and N. W. Brake, *ibid.*, **61**, 615 (1972).

(9) K. Tsujii and J. H. Robertson, *Anal. Chem.*, **45**, 2136 (1973).

(10) R. F. Lindauer, D. M. Cohem, and K. P. Munnelly, *ibid.*, **48**, 1731 (1976).

(11) K. Tsujii and J. H. Robertson, *J. Pharm. Sci.*, **65**, 400 (1976).

(12) K. Tsujii and J. F. Goetz, *J. Antibiot.*, **31**, 302 (1978).

(13) S. L. Ali and T. Strittmatter, *Int. J. Pharm.*, **1**, 185 (1978).

Aminoalkanesulfonic Acids IV: Synthesis of Mitodepressive *N*-Nitrosoaminoalkanesulfonic Acids

Lj. BUTULA ˣ **and Ž. BUKOVEC**

Received September 5, 1978, from the *Faculty of Pharmacy and Biochemistry, University of Zagreb, A. Kovačića 1, Zagreb, Yugoslavia.* Accepted for publication March 12, 1980.

Abstract □ Sodium aminoalkanesulfonates were synthesized from substituted amines and aldehyde sodium bisulfites at 40–60°. Nitrosation yielded the corresponding *N*-nitroso derivatives. Mitodepressive activity on cresse (*Lepidium sativum* L.) was determined, and all compounds examined possessed growth inhibition activity. The *N*-nitroso derivatives were slightly less active but also showed less toxicity than the parent aminoalkanesulfonic acids.

Keyphrases □ Aminoalkanesulfonic acids—synthesis of *N*-nitroso derivatives, evaluation for mitodepressive activity □ Mitodepressive activity—evaluation of aminoalkanesulfonic acids and *N*-nitroso derivatives □ *N*-Nitrosoaminoalkanesulfonic acids—synthesis, evaluation for mitodepressive activity

Aminoalkanesulfonic acids are known to have antiviral (1, 2) and anticancer (3, 4) activities. Some *N*-nitroso compounds, such as *N*-nitrosomethylamine, *N*-nitrosodimethylamine, and *N*-nitrosodiethylamine, showed blastogenic action when applied on Hungarian hamsters (5). Some experiments (6) showed imbalances in DNA and histone synthesis during carcinogenesis induced by nitrosamines. On the other hand, some *N*-nitroso compounds, such as 1,3-bis(2-chloroethyl)-1-nitrosourea (carmustine), are useful in the treatment of certain malignant diseases (7).

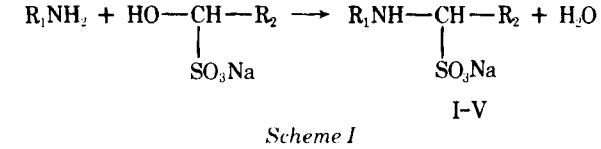

Scheme I

These findings prompted the synthesis of some new derivatives in this series (8–10) to determine their mitodepressive activity.

This report describes the synthesis of some sodium aminoalkanesulfonates (I–V) in which *m*- and *p*-chloroanilines were used with the corresponding aldehyde sodium bisulfites (Scheme I and Table I). In some cases, the desired products were obtained by the addition of sodium metabisulfite to azomethine derivatives (Scheme II).

Nitrosation of I–V and sodium *p*-chloroanilinophenyl-

0022-3549/80/0800-0930$01.00/0

© 1980, American Pharmaceutical Association

Table I—Physical Properties and Reaction Conditions of Sodium Aminoalkanesulfonates

Compound	R_1	R_2	Reaction Conditions (Hours, Temperature, Method)	Yield, %	Melting Point	Recrystallization Solvent	Molecular Formula	Molecular Weight	Analysis, % Calc.	Found	IR ν_{max}, cm^{-1}
I	3-Chloro-phenyl	H	1, 60°, A	75	210–212°	Methanol	$C_7H_7ClNNaO_3S \cdot H_2O$	261.665	N 5.35	5.25	3600, 3320, 1210–1180, 1040
II	3-Chloro-phenyl	CH_3	2, 40°, A	40	123–125°	Ethanol	$C_8H_9ClNNaO_3S \cdot H_2O$	275.691	C 35.00 H 4.05 N 5.12	34.75 4.19 4.77	3535, 3400, 1210–1180, 1020
III	3-Chloro-phenyl	Phenyl	2, 65°, B and C	48	156–158°	Ethanol	$C_{13}H_{11}ClNNaO_3S \cdot H_2O$	355.843	C 43.88 H 4.03 N 4.38	43.90 4.33 4.18	3550, 3350, 1120–1180, 1140
IV	4-Chloro-phenyl	H	1, 60°, A	76	280–284°	Ethanol	$C_7H_7ClNNaO_3S \cdot H_2O$	261.665	N 5.35	5.45	3650, 3300, 1200, 1050
V	4-Chloro-phenyl	CH_3	1, 40–50°, A	45	117–121°	Ethanol	$C_8H_9ClNNaO_3S \cdot H_2O$	275.691	C 35.00 H 4.05 N 5.12	34.91 4.34 5.27	3535, 3400, 1210–1180, 1020
VI[a]	4-Chloro-phenyl	Phenyl	1, 40°, A and C	50, 70	144–147°	Ethanol	$C_{13}H_{11}ClNNaO_3S$	355.843	—	—	3600, 3350, 1215, 1040

[a] Compound VI was synthesized by Neelekantan and Hartung (11).

Table II—Physical Properties and Reaction Conditions of Sodium *N*-Nitrosoaminoalkanesulfonates

Compound	R_1	R_2	Yield, %	Melting Point	Recrystallization Solvent	Molecular Formula	Molecular Weight	Analysis, % Calc.	Found	IR ν_{max}, cm^{-1}
VII	3-Chloro-phenyl	H	50	250–252°	Methanol–water	$C_7H_7ClN_2O_4S$	238.212	N 11.76	11.43	1500–1450, 1210–1180, 1040
VIII	3-Chloro-phenyl	CH_3	83	117–121°	Methanol–ethanol	$C_8H_8ClN_2NaO_4S$	286.687	N 9.77	9.42	1460, 1210–1180, 1040
IX	3-Chloro-phenyl	Phenyl	56	99–103°	Ethanol	$C_{13}H_{20}ClN_2NaO_4S$	348.753	N 8.03	8.17	1470, 1220–1180, 1040
X[a]	4-Chloro-phenyl	H	25	254–255°	Methanol–ethanol	$C_7H_7ClN_2O_4S$	238.213	N 11.76	11.38	1460, 1210, 1040
XI	4-Chloro-phenyl	CH_3	31	119–121°	Ethanol	$C_8H_8ClN_2NaO_4S$	286.687	N 9.77	9.38	1450, 1205–1190, 1040
XII[a]	4-Chloro-phenyl	Phenyl	31.5	250°	Methanol–ethanol	$C_{13}H_{10}ClN_2O_4S$	326.763	C 47.90 H 3.39 N 8.57	48.09 3.51 8.17	3550–3130, 1460, 1210–1180, 1040
XIII	4-Chloro-phenyl	Phenyl	58	119–122°	Ethanol	$C_{13}H_{10}ClNNaO_4S \cdot H_2O$	366.53	C 42.56 H 3.29 N 7.63	42.21 3.35 7.40	1460, 1210–1190, 1040

[a] Isolated in free acid form.

methane sulfonate[1] (VI) yielded the corresponding sodium *N*-nitrosoaminoalkanesulfonates (VII–XIII) (Scheme III and Table II). Compounds X and XII were isolated in the form of free sulfonic acids.

All products were tested for mitodepressive activity on cresse seeds (*Lepidium sativum* L.) by a literature method (12).

DISCUSSION

For the synthesis of the sodium salts of *m*- and *p*-chloroanilinoalkanesulfonic acids (I–VI), Method A was used at lower temperatures and shorter reaction times than those described by Neelekantan and Hartung

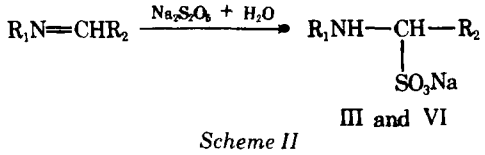

III and VI

Scheme II

[1] Compound VI was synthesized by Neelekantan and Hartung (11).

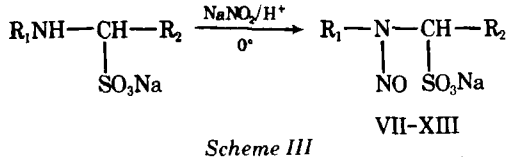

VII–XIII

Scheme III

(11). These conditions produced higher yields of both *m*- and *p*-chloroanilinoalkanesulfonic acids.

The method of Greco *et al.* (13) for nitrosation of α-aminocarboxylic acids was modified by employing a significantly shorter reaction time and a higher reaction pH to avoid extensive decomposition of the products.

In previous work (10), phytobiological experiments were carried out on a group of aminoalkanesulfonates in which 2-aminopyrimidine and 2-aminopyridine were incorporated. Significant inhibitory properties were observed.

The phytobiological experiments (Tables III and IV) showed that inhibitory properties of sodium alkanesulfonates (I–VI) varied between 50 and 80%. The R_1 and R_2 substituents did not influence inhibition greatly. Inhibition properties of *N*-nitroso derivatives (VII–XII) tended to be somewhat lower than those of the parent compounds. On the other hand, aminoalkanesulfonates were more toxic than the corresponding *N*-nitroso derivatives. Cresse seeds recovered their biological properties, such as growth, more readily when treated with *N*-nitroso compounds.

Table III—Inhibitory Properties of Sodium Aminoalkanesulfonates

Compound	R_1	R_2	Inhibition, % 2 mg/ml	1 mg/ml
I	3-Chlorophenyl	H	56	38
II	3-Chlorophenyl	CH_3	78	75
III	3-Chlorophenyl	Phenyl	70	61
IV	4-Chlorophenyl	H	48	38
V	4-Chlorophenyl	CH_3	80	73
VI[a]	4-Chlorophenyl	Phenyl	70	53

[a] Synthesized by Neelekantan and Hartung (11).

Table IV—Inhibitory Properties of Sodium *N*-Nitrosoaminoalkanesulfonates

Compound	R_1	R_2	Inhibition, % 2 mg/ml	1 mg/ml
VII	3-Chlorophenyl	H	41	40
VIII	3-Chlorophenyl	CH_3	60	52
IX	3-Chlorophenyl	Phenyl	52	41
X[a]	4-Chlorophenyl	H	40	30
XI	4-Chlorophenyl	CH_3	46	28
XIII	4-Chlorophenyl	Phenyl	75	67

[a] Isolated in free acid form.

Mitodepressive effects of *N*-nitroso compounds probably result from a combination of the inhibitory effect of the parent sulfonic acids and the growth-stimulating activity of the incorporated *N*-nitroso group in VII–XII. Preliminary experiments with carcinoma Hep-2 cells of the nasopharynx showed that the parent compounds (I–VI) were predominantly cytotoxic while the related *N*-nitroso derivatives (VII–XIII) had mainly cytostatic activity.

EXPERIMENTAL[2]

Preparation of Sodium *m*- and *p*-Chloroanilinoalkanesulfonates—*Method A*—*m*- or *p*-Chloroaniline (6.3 g, 50 mmoles) and formaldehyde, acetaldehyde, or benzaldehyde sodium bisulfite (5.2 mmoles) were mixed in water (10 ml) for 1–2 hr at 40–50°. The reaction mixture was cooled to room temperature, and the crystals that formed were separated and recrystallized.

Method B—Benzaldehyde (5.3 g, 50 mmoles) was stirred with a solution of sodium metabisulfite (5.3 g, 2.8 mmoles) in 30 ml of water at room temperature for 1 hr. *m*- or *p*-Chloroaniline (6.3 g, 50 mmoles) was added to the reaction mixture, and the mixture was stirred and warmed to 60° for 1 hr. After cooling, the resulting crystals were removed by suction, dried in air at room temperature, and recrystallized.

Method C—Benzylidenechloroaniline (2.2 g, 10 mmoles) was warmed in a solution of sodium metabisulfite (2.7 g, 14 mmoles) in 10 ml of water for 1 hr at 40–50°. On cooling, the crystals that formed were isolated and recrystallized.

[2] Melting points were determined using a Buchi (Totoli) melting-point apparatus and are uncorrected. IR spectra were obtained on a Perkin-Elmer 457 grating instrument using potassium bromide wafers. TLC was carried out mainly on silica gel F-254 with butanol–concentrated ammonia (8:2) or benzene–methanol–acetic acid (7:2:1) as the solvent system.

Synthesis of Sodium *N*-Nitrosoaminoalkanesulfonates—A solution of sodium nitrite (7 mmoles) in 1 ml of water was added to a suspension (5 mmoles) of sodium chlorosulfonic acids (I–VI) in 10 ml of water at 0°. Dilute (5%) hydrochloric acid was added with mixing at 0–5° until pH 4 was reached. Stirring was continued for an additional 20 min at room temperature, and the solvent was removed at 30°. Colored crystals were obtained and purified by dissolution in methanol and precipitation in ether at room temperature.

The purity of all products was established chromatographically.

Phytobiological Experiments—Chromatographically pure products were tested for mitodepressive activity on germinating seeds of cresse[3] (*L. sativum* L.) in concentrations of 1 and 2 mg/ml. The values for inhibitory properties are calculated according to:

$$\% I = \frac{L_B - L_X}{L_B} \times 100 \qquad \text{(Eq. 1)}$$

where L_B is the mean value of the length of the cresse radicles formed by germination at 25 ± 1° in water and L_X is the mean value of cresse radicles formed in aqueous solutions of the tested compounds.

The experiments were carried out in the following manner. Twenty to 30 cresse seeds were placed on filter paper in a petri dish and covered with 15 ml of water. After the seeds were incubated for 24 hr at 25 ± 1°, water was decanted and an aqueous solution of the experimental compounds was added. One seed sample left in the water was used as a blank.

After further incubation for 24 hr at the same temperature, test solutions were decanted. The seeds were washed several times with water and fixed with a solution containing 2 g of salicylic acid, 2 g of zinc sulfate, and 15 drops of freshly prepared concentrated sodium phenoxide in 100 ml of distilled water. After fixation, radicles from 20 seeds were measured by using millimetric paper and a lens. A mean value of the measured radicle length was found for each sample, and the inhibitory properties were calculated (Tables III and IV).

REFERENCES

(1) H. McIlwain, *J. Chem. Soc.*, **1941**, 75.

(2) D. M. Greenberg and M. P. Schulman, *Science*, **106**, 271 (1947).

(3) R. L. Thompson, *J. Immunol.*, **55**, 345 (1947).

(4) W. W. Ackerman, *Proc. Soc. Exp. Biol. Med.*, **80**, 362 (1952).

(5) N. H. Vasileva and C. I. Sokova, *Vopr. Onkol.*, **17**, 58 (1971).

(6) M. Gronow, *Eur. J. Cancer*, **2**, 341 (1971).

(7) M. Colvin and J. W. Gowens, *Biochem. Biophys. Res. Commun.*, **60**, 515 (1974).

(8) Lj. Butula and D. Kolbah, *Acta Pharm. Jugosl.*, **16**, 165 (1966).

(9) *Ibid.*, **16**, 173 (1966).

(10) Lj. Butula, *Pharmazie*, **33**, 428 (1978).

(11) L. Neelekantan and W. H. Hartung, *J. Org. Chem.*, **24**, 1943 (1959).

(12) F. Gagiu, A. Cacoveanu, C. Nistor, and C. Daicoviciu, *Chim. Ther.*, **7**, 39 (1972).

(13) C. V. Greco, W. H. Nyberg, and C. C. Cheng, *J. Med. Pharm. Chem.*, **5**, 851 (1962).

[3] Cresse seeds were purchased from Austrosaat-Osterreichische Samenzucht und Handel-saktien-gesellschaft.

4,5-Disubstituted Primaquine Analogs as Potential Antiprotozoan Agents

HANNS BURGHARD and C. DeWITT BLANTON, Jr. ˣ

Received January 7, 1980, from the *Department of Medicinal Chemistry, School of Pharmacy, University of Georgia, Athens, GA 30602.* Accepted for publication March 12, 1980.

Abstract □ 4,5-Dimethylprimaquine and 5-fluoro-4-methylprimaquine were synthesized and evaluated against *Plasmodium berghei* in the mouse. Significant blood schizonticidal activity was observed. The 5-fluoro-4-methylprimaquine analog also was active as a tissue schizonticidal agent when evaluated against *P. cynomolgi* in the rhesus monkey, as an antileishmanial agent when evaluated against *Leishmania donovani* in the hamster, and as a causal prophylactic agent when evaluated against *P. berghei yoelii.*

Keyphrases □ Primaquine analogs—synthesis and evaluation for antiprotozoan activity □ Antiprotozoan agents, potential—primaquine analogs, synthesis and evaluation for activity □ 8-Aminoquinolines, substituted—synthesis and evaluation for antiprotozoan activity

Although generally quite toxic, 8-aminoquinoline derivatives related to primaquine (I*a*) are of interest as potential radical curative and causal prophylactic antimalarial agents (1). Primaquine, the tissue schizonticidal drug of choice, is used mainly with a strong blood schizonticide as a radical cure of relapsing malaria and for chemoprophylaxis or the interruption of transmission (2). A major drawback of primaquine is its relatively low therapeutic index, and modification of the side chain of the molecule exclusively has not resulted in any marked improvement of antimalarial activity combined with reduced toxicity (3, 4).

Substitution of a methyl group onto the 8-amino-6-methoxyquinoline nucleus offers potential for obtaining agents with high antimalarial activity and reduced toxicity relative to the unsubstituted nucleus. For example, 4-methylprimaquine (I*b*) was reported (5, 6) to possess enhanced antimalarial activity and somewhat lower toxicity when evaluated against *Plasmodium cynomolgi* in the rhesus monkey (7, 8) and *P. berghei* in mice (9). Similar trends were reported when 8-aminoquinoline derivatives were screened against *P. gallinaceum* (10). Thus, 8-[(2-diethylaminoethyl)amino]-6-methoxyquinoline (II*a*) had a therapeutic index of 1.8 (10) while the 4-methyl (II*b*) and 5-methyl (II*c*) analogs possessed therapeutic indexes of 20 and 9.1, respectively. Nuclear substitution and modification of the side chain at position 8 led to further improvement in the therapeutic index, as seen with II*d* and II*e*, which had therapeutic indexes of 59 and 33.5 (10). Based on these considerations, a program was initiated to synthesize and evaluate the potential antimalarial activity of 4,5-dimethylprimaquine (I*c*).

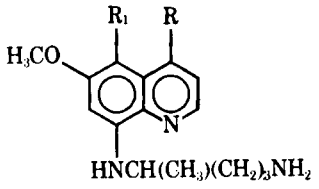

I

I*a*: R = H, R_1 = H
I*b*: R = CH_3, R_1 = H
I*c*: R = R_1 = CH_3
I*d*: R = CH_3, R_1 = F

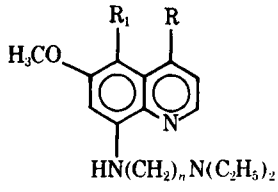

II

II*a*: R = R_1 = H, n = 2
II*b*: R = CH_3, R_1 = H, n = 2
II*c*: R = H, R_1 = CH_3, n = 2
II*d*: R = CH_3, R_1 = H, n = 6
II*e*: R = H, R_1 = CH_3, n = 6

DISCUSSION

Chemistry—The synthesis of the key intermediate (VII) required for the preparation of 4,5-dimethylprimaquine (I*c*) is outlined in Scheme I. 4-Amino-2-fluoro-5-nitroanisole (III) was prepared by the procedure of Elderfield *et al.* (11). Reaction of III with methyl vinyl ketone under modified Skraup conditions (12) gave 4-methyl-5-fluoro-6-methoxy-8-nitroquinoline (IV). Attempts to displace the activated fluorine atom at position 5 with a methyl nucleophile [*e.g.*, methylenetriphenylphosphorane (13)] failed. Similarly, attempts to displace the fluorine atom with a cyanide ion (14) for subsequent reduction (15, 16) to a methyl group failed.

The use of 18-crown-6 ether (17) did not facilitate cyanide-ion displacement of the fluorine atom. However, by reaction of the anion of ethyl malonate and IV in the presence of copper(I) bromide (18) and 18-crown-6 ether, it was possible to displace the fluorine atom with formation of a carbon–carbon bond (V). Acid hydrolysis of the substituted malonate (V) led directly to the desired intermediate (VII). If the hydrolysis step was terminated too soon, the substituted acetic acid derivative (VI) could be isolated. Reduction of 4,5-dimethyl-6-methoxy-8-nitroquinoline (VII) with stannous chloride and alkylation of the amine (VIII) by 4-bromo-1-phthalimidopentane (19) in triethylamine (20, 21) followed by hydrazinolysis gave the desired analog (I*c*).

Since IV then was readily available, 4-methyl-5-fluoroprimaquine (I*d*) also was prepared. Standard reduction of IV and alkylation of the amine (X) followed by hydrazinolysis gave the desired product (I*d*).

Direct synthesis of VII by the Skraup reaction of 2-nitro-4-methoxy-5-methylaniline (XI) (22) and methyl vinyl ketone (Scheme II) was attempted, but the expected intermediate (XII) was the only isolated product; various alterations in experimental conditions or reagents did not change the course of the reaction. (Several of these alterations are summarized in Scheme II, and the uncyclized intermediates XIII and XIV were isolated as in the case of XII.) Steric effects, as well as electronic effects, may prevent direct cyclization to VII. Therefore, Skraup cyclization of III and methyl vinyl ketone, although in low yield, was possible since the fluoro compound (III) presented less of a steric problem than XI.

Antiprotozoan Activity[1]—The blood schizonticidal activity of the potential antimalarials I*c* and I*d* was assessed against *P. berghei* in mice by the method of Osdene *et al.* (9). 4,5-Dimethylprimaquine (I*c*) was active[2] in the Rane test: ΔMST = 7.6 at 160 mg/kg, 9.1 (1C, 2T) at 320 mg/kg, and 0.0 (3C, 2T) and 10.8 (1C, 3T) at 640 mg/kg. 5-Fluoro-4-methylprimaquine (I*d*) showed good activity against *P. berghei* at 10 mg/kg (ΔMST = 6.7). Doses higher than 40 mg/kg produced toxic deaths in all animals (5T). Primaquine diphosphate was active at 80 mg/kg (ΔMST = 9.4) with drug-related toxic deaths at 160 (ΔMST = 10.8, 2T) and 320 (ΔMST = 0.0, 5T) mg/kg.

The tissue schizonticidal potential[1] of I*d* was evaluated in rhesus monkeys by a literature procedure (7, 8). Compound I*d* showed 3/3 cures[3]

[1] Antiprotozoan test results were provided by the Walter Reed Army Institute of Research. Tests for blood schizonticidal and causal prophylactic activity were carried out by the Rane Laboratory, University of Miami, Miami, Fla. Tests for tissue schizonticidal activity were carried out by Dr. L. H. Schmidt, Southern Research Institute, Birmingham, Ala. Tests for antileishmanial activity were carried out by Dr. W. L. Hanson, University of Georgia, Athens, Ga.

[2] The mean survival time (MST) of untreated mice is 6.1 days. A compound is active if ΔMST exceeds 6.1 days. Animals that survive 60 days postinfection are considered cured (C). Deaths on Days 2–5 after drug administration are attributed to drug toxicity (T).

[3] Monkeys that do not relapse in 90 days are considered cured.

0022-3549/80/0800-0933$01.00/0
© 1980, American Pharmaceutical Association

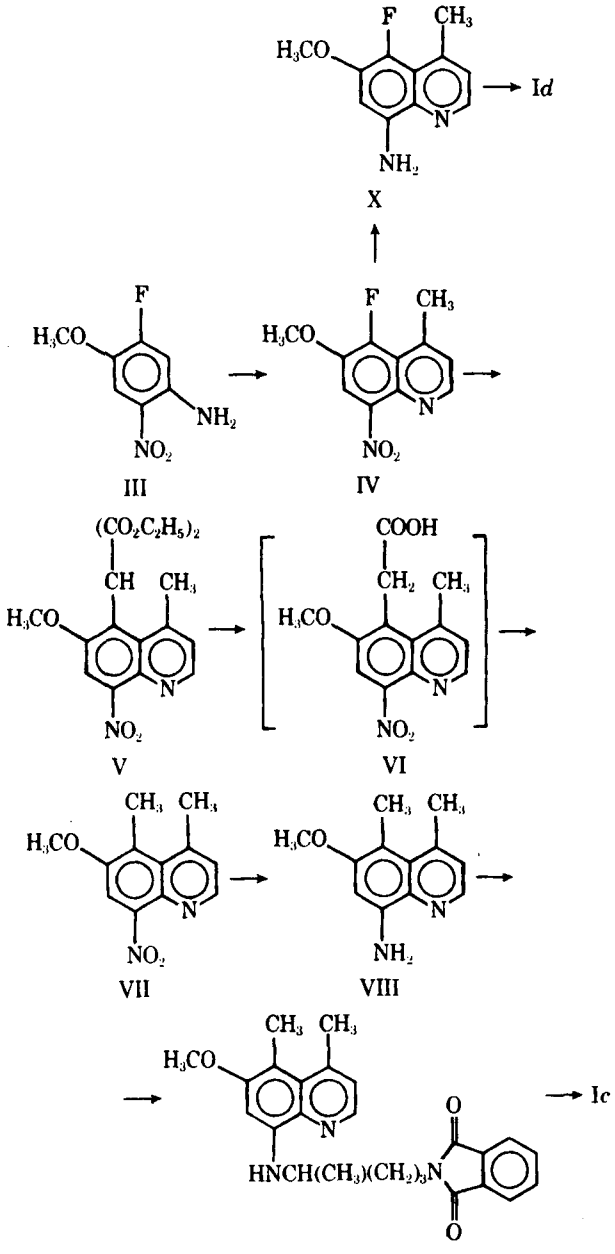

Scheme I

at 0.5 mg/kg. Primaquine diphosphate cured 90% of the monkeys in this test system when administered at a dose of 1.3 mg/kg for 7 days in combination with 5 mg of chloroquine/kg/day.

The antileishmanial activity[1] of Id against *Leishmania donovani* was determined in golden hamsters by the method of Hanson *et al.* (23). The suppressive effects of the test compound were compared to those of the reference compound, *N*-methylglucamine antimoniate[4], and a G index[5] was calculated (4, 23). 5-Fluoro-4-methylprimaquine (Id) showed significant activity in the antileishmanial screen with a G index of 10.98 at 3.25 mg/kg/day. Primaquine possessed a G index of 0.96 at the SD_{90} level, whereas some 8-aminoquinolines with a methyl group at position 4 were reported to have enhanced antileishmanial properties (24); *e.g.*, 8-[(6-diethylaminohexyl)amino]-6-methoxy-4-methylquinoline had a G index of 472 at the SD_{90} level (4).

Compound Id was tested for causal prophylactic activity[1,6] against sporozoite-induced *P. berghei yoelii* in rodents (25, 26). This agent was active at 10 mg/kg when administered subcutaneously (5/5 cures).

[4] Glucantime.

[5] The glucantime index, G, was calculated using G = dose (SD_x) of glucantime/dose (SD_x) of test drug.

[6] Prophylactic activity is evidenced by survival of drug-treated mice for 30 days. Survival of 40% or more of the treated mice indicates activity.

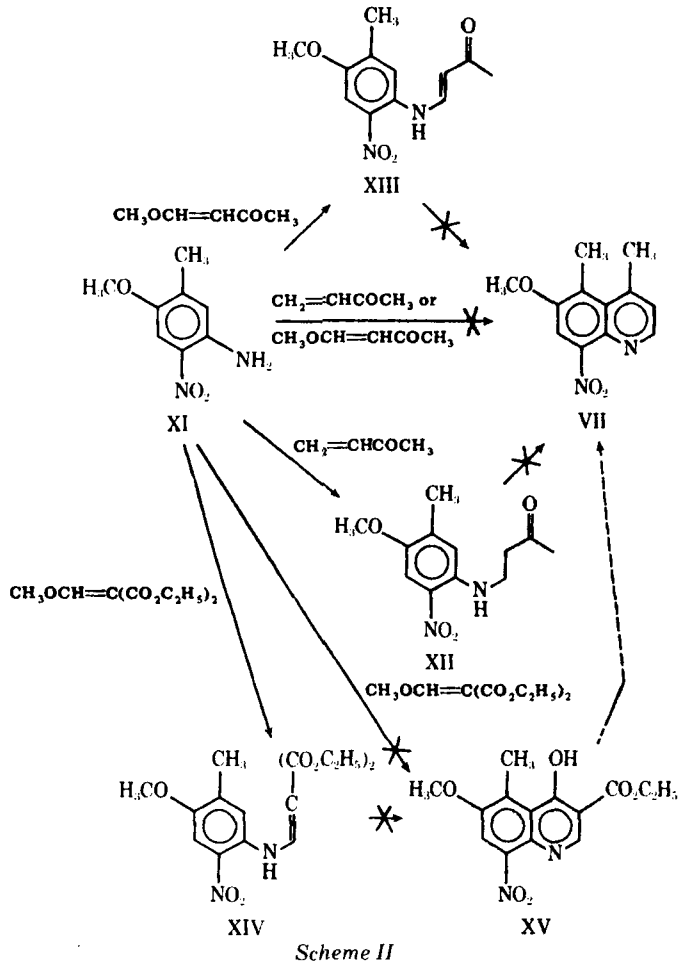

Scheme II

Compound Id given orally was active at 10 and 40 mg/kg (5/5 cures).

Although Ic was not tested for tissue schizonticidal, antileishmanial, or causal prophylactic activity, the data presented confirm that appropriate substituents at the 4- and 5-positions can alter significantly the antiprotozoan activity of 8-aminoquinolines. In the blood schizonticidal test (9), Id was more active at lower doses than primaquine, but it also was more toxic. Compound Ic was not as active as primaquine in this test system, but it was significantly less toxic.

EXPERIMENTAL[7]

4-Methyl-5-fluoro-6-methoxy-8-nitroquinoline (IV)—4-Amino-2-fluoro-5-nitroanisole (III) was prepared by the method of Elderfield *et al.* (11). Compound III (37.23 g, 0.2 mole), 34.96 g of arsenic pentoxide (0.15 mole), and 45 ml of 85% phosphoric acid were mixed to form a viscous slurry. This slurry was stirred vigorously until a homogeneous paste formed. Then 200 ml of 85% phosphoric acid was added gradually while stirring. The suspension was heated to 90°. This mixture was treated with 16.8 g (0.24 mole) of methyl vinyl ketone at such a rate as to maintain the temperature at 90°; the addition required 0.5 hr.

The resulting mixture was kept at 85–95° for 1.5 hr and then was poured into 800 ml of ice-cold water and slowly made basic with 450 ml of concentrated ammonium hydroxide. The dark solid was collected, washed with water, and dried at 50° overnight. The product was dissolved in chloroform (200 ml), but some tar and by-products remained undissolved. A volume of silica gel approximately equal to the volume of crude product was added, and the chloroform mixture was removed *in vacuo*. The brown silica gel complex was transferred onto a short column containing approximately a double volume of fresh silica gel. This column

[7] Melting points were determined on a Thomas-Hoover apparatus (capillary method) and are uncorrected. NMR spectra were determined on a Hitachi Perkin-Elmer R20A high-resolution NMR spectrometer using tetramethylsilane as the internal reference. IR spectra were determined on a Perkin-Elmer 467 grating spectrophotometer using the potassium bromide technique. Elemental analyses were determined by Atlantic Microlab, Atlanta, Ga. Mass spectra were determined on a DuPont 21-490 low-resolution mass spectrometer.

was eluted with chloroform, and the solvent was evaporated *in vacuo* to give a red impure product.

Recrystallization from ethyl acetate gave 11.8 g (25% yield) of product, mp 142°; NMR[8]: δ 2.81 (d, 3H, CH_3 at C-4, J = 7 Hz), 3.90 (s, 3H, CH_3O at C-6), 7.26 (d, H at C-3, J = 5 Hz), 8.67 (d, H at C-2, J = 5 Hz), and 8.95 (*d*, H at C-7, J = 8 Hz). Concentration of the mother liquor gave another 4.3 g (9% yield) for an overall yield of 34%. If the quantity of methyl vinyl ketone is doubled, the yield can be raised to 60–70%.

Anal.—Calc. for $C_{11}H_9FN_2O_3$: C, 55.93; H, 3.84; N, 11.85. Found: C, 55.97; H, 3.88; N, 11.80, 11.82.

Diethyl α-(4-Methyl-6-methoxy-8-nitroquinolyl)malonate (V)—Sodium hydride (0.7 g of 50% dispersion in paraffin oil) was added over 10 min to a stirred mixture of IV (2.95 g, 12.5 mmoles) and copper(I) bromide (0.1 g, 0.7 mmole) in 25 ml of ethyl malonate. The mixture was maintained in an oil bath at 40–45° during the addition of sodium hydride. Ten drops of 18-crown-6 ether were added to the mixture, and the temperature was raised to 80°. Stirring and heating (60–80°) under a nitrogen atmosphere was continued for 6 hr.

The red solution was cooled and diluted with 600 ml of water, and the pH of the aqueous mixture was adjusted to 10 with 10% NaOH. After standing for 48 hr at room temperature, a fluffy yellow solid (5.1 g) was collected by filtration. The material was recrystallized from benzene–petroleum ether (30–60°), mp 162–163° (4.1 g, 87% yield); NMR ($CDCl_3$): δ 1.28 (t, 6H, CH_3 groups of esters), 2.88 (s, 3H, CH_3 at C-4), 3.98 (s, 3H, CH_3O at C-6), 4.25 (q, 4H, CH_2 groups of esters), 5.7 (s, 1H, CH at C-5), 7.28 (broad s, 1H, H at C-3), 7.75 (s, 1H, H at C-7), and 8.65 (broad s, 1H, H at C-2); mol. wt. (mass spectra): calc., 376, and found, 376.

Anal.—Calc. for $C_{18}H_{20}N_2O_7$: C, 57.44; H, 5.36; N, 7.44. Found: C, 57.42; H, 5.38; N, 7.39.

4,5-Dimethyl-6-methoxy-8-nitroquinoline (VII)—Compound V (2.9 g, 7.7 mmoles) was suspended in 50 ml of water and treated with 10 ml of acetic acid and 5 ml of concentrated sulfuric acid. The temperature of the mixture was raised slowly to reflux. The dark mixture was stirred and refluxed for 4 hr (oil bath temperature was maintained between 130 and 150°), cooled, and poured into 250 ml of water containing sufficient 10% NaOH to give a pH of 10. A greenish-gray product separated.

The product was collected by filtration and recrystallized from aqueous dimethylformamide after treatment with charcoal to yield fine yellow needles, mp 177–179° (1.5 g, 83.7% yield); NMR (dimethyl sulfoxide-d_6): δ 2.66 (s, 3H, CH_3 at C-5), 2.85 (s, 3H, CH_3 at C-4), 3.98 (s, 3H, CH_3O at C-6), 7.35 (d, 1H, H at C-3, J = 4.5 Hz), 8.15 (s, 1H, H at C-7), and 8.60 (d, 1H, H at C-2, J = 4.5 Hz).

Anal.—Calc. for $C_{12}H_{12}N_2O_3$: C, 62.06; H, 5.21; N, 12.06. Found: C, 62.12; H, 5.26; N, 12.04.

α-(4-Methyl-6-methoxy-8-nitroquinolyl)acetic Acid (VI)—When the oil bath temperature was not maintained above 130°, hydrolysis and decarboxylation of V was incomplete, and VI was obtained in near quantitative yield, mp 115–117°; NMR (dimethyl sulfoxide-d_6): δ 2.90 (s, 3H, CH_3 at C-4), 4.00 (s, 3H, CH_3O at C-6), 4.30 (s, 2H, CH_2 at C-5), 7.45 (broad s, 1H, H at C-3), 8.3 (s, 1H, H at C-7), and 8.7 (broad s, 1H, H at C-2).

When VI was refluxed with the aqueous acetic acid–sulfuric acid mixture at 130–150° for 4 hr, VII was obtained in a 97.6% yield.

8-Amino-4,5-dimethyl-6-methoxyquinoline (VIII)—A solution of stannous chloride hydrate (31.6 g, 0.14 mole) and 15 ml of concentrated hydrochloric acid was cooled to −5–0°. After the addition of 0.5 g of mossy tin, the mixture was stirred as a precooled solution of VII (8.2 g, 0.035 mole) in 25 ml of concentrated hydrochloric acid was added at a rate such that the temperature remained below 6°. The addition required ~45 min. The brown suspension was stirred for an additional 15 min at 0°, and the ice bath was removed.

After stirring at room temperature for 5 hr, the brown suspension was poured into 200 ml of water. The yellow solid which precipitated became gray when the acidic mixture was made basic with 9 *N* NaOH. The basic solution was covered with 200 ml of ether–ethyl acetate (1:1) and filtered through diatomaceous earth[9] to remove some black insoluble material. The organic layer was separated from the water layer, and the filter cake was washed with ethyl acetate (200 ml) and acetone (200 ml). The aqueous layer was extracted with ethyl acetate (2 × 100 ml). All organic layers were combined and dried (magnesium sulfate).

Removal of the solvents *in vacuo* gave a gold-colored solid. The analytical sample was obtained from aqueous ethanol (4.5 g, 63.6% yield), mp 127–128°; NMR ($CDCl_3$): δ 2.6 (s, 3H, CH_3 at C-4), 2.8 (s, 3H, CH_3 at C-5), 3.80 (s, 3H, CH_3O at C-6), 4.8 (broad s, 2H, NH_2, exchanged by deuterium oxide), 6.7 (s, 1H, H at C-7), 7.05 (d, 1H, H at C-3, J = 4.5 Hz), and 8.39 (d, 1H, H at C-2, J = 4.5 Hz).

Anal.—Calc. for $C_{12}H_{14}N_2O$: C, 71.26; H, 6.98; N, 13.85. Found: C, 70.99; H, 6.98; N, 13.85.

4,5-Dimethyl-6-methoxy -8- [(4-amino-1-methylbutyl)amino]-quinoline (Ic) Maleate—A mixture of VIII (4 g, 0.0198 mole), 4-bromo-1-phthalimidopentane (8.79 g, 0.0297 mole), and triethylamine (3 g, 0.0297 mole) was stirred and heated at 110–135° for 5 hr. Additional 4-bromo-1-phthalimidopentane (2.93 g, 0.0099 mole) and triethylamine (1 g) were added, and heating was continued for 6 hr. The dark reaction mixture was digested in 200 ml of benzene and filtered hot to remove triethylamine hydrobromide. The benzene was removed *in vacuo* to give a dark blood-red oil. This oil was treated with ethanol (150 ml) and 15 ml of 85% hydrazine hydrate.

The mixture was refluxed for 3 hr, cooled to room temperature, and concentrated *in vacuo*. The residue was treated with methylene chloride (200 ml) and filtered to remove phthalhydrazide. The methylene chloride filtrate was dried (magnesium sulfate) and concentrated to an oil. The residual oil was treated with 50 ml of ethanol and 3 g of maleic acid. Addition of ether precipitated a voluminous yellow solid. After recrystallization from ethanol–ether, 1.9 g of the maleate of Ic was obtained (23.8% yield), mp 135–137°.

Anal.—Calc. for $C_{21}H_{29}N_3O_5$: C, 62.51; H, 7.24; N, 10.41. Found: C, 62.49; H, 7.27; N, 10.41.

4-Methyl-5-fluoro-6-methoxy-8-aminoquinoline (X)—Compound IV was reduced by the procedure described for the preparation of VIII. Compound X was obtained in a 91% yield (ethanol) as greenish-white crystals, mp 129°; NMR (dimethyl sulfoxide-d_6): δ 2.64 (d, 3H, CH_3 at C-4, J = 7.0 Hz), 3.9 (s, 3H, CH_3O at C-6), 6.8 (d, H at C-7, J = 8.0 Hz), 7.18 (d, H at C-3, J = 5.0 Hz), and 8.39 (d, H at C-2, J = 5.0 Hz).

Anal.—Calc. for $C_{11}H_{11}FN_2O$: C, 64.06; H, 5.37; N, 13.58. Found: C, 64.22; H, 5.40; N, 13.56.

4-Methyl-5-fluoro-6-methoxy-8-[(4-amino-1-methylbutyl)amino]quinoline (Id) Maleate—The maleate of Id was prepared in a 59% yield (ethanol) by the procedure described for Ic, mp 131°.

Anal.—Calc. for $C_{20}H_{26}FN_3O_5$: C, 58.95; H, 6.43; N, 10.31. Found: C, 58.70; H, 6.48; N, 10.25.

2-Nitro-4-methoxy-5-methyl-*N*-(3-oxobutyl)aniline (XII)—2-Nitro-4-methoxy-5-methylaniline (1.82 g, 0.01 mole), prepared by the procedure of Carmack *et al.* (22), and 40 g of 85% phosphoric acid were heated at 85° while 1.05 g (0.015 mole) of methyl vinyl ketone was added dropwise with vigorous stirring. After 30 min, the addition was completed and the mixture was stirred for an additional 30 min. The brown solution was poured into ice–water and filtered, and the orange product was dried. After recrystallization from ethanol (1.84 g, 73% yield), XII melted at 138°. [This material was identical to that isolated from the Skraup reaction, and no evidence for quinoline (VII) formation was observed.]

Anal.—Calc. for $C_{12}H_{16}N_2O_4$: C, 57.13; H, 6.39; N, 11.10. Found: C, 57.11; H, 6.43; N, 11.12.

4-(2-Nitro-4-methoxy-5-methylanilino)but-3-en-2-one (XIII)—2-Nitro-4-methoxy-5-methylaniline (3.64 0.02 mole) (22) was mixed with 4.0 g (0.04 mole) of 4-methoxybut-3-en-2-one and fused at 150° for 3 hr. The flask was fitted with a condenser to remove methanol. Red crystals were collected when the reaction mixture was cooled and the residue recrystallized from ethanol (71% yield), mp 177°. [This product was identical to that obtained when Skraup reaction conditions were employed, and no evidence of quinoline (VII) formation was obtained.]

Anal.—Calc. for $C_{12}H_{14}N_2O_4$: C, 57.59; H, 5.63; N, 11.19. Found: C, 57.55; H, 5.66; N, 11.22.

Diethyl (3-Methyl-4-methoxy-6-nitroanilino)methylenemalonate (XIV)—2-Nitro-4-methoxy-5-methylaniline (0.91 g, 0.005 mole) (22) and 1.08 g (0.005 mole) of diethyl methoxymethylenemalonic ester were fused (27) and kept at 150° for 45 min. The crude product (XIV) was recrystallized from ethanol (1.61 g, 92% yield, mp 127–128°. [No evidence for quinoline (XV) formation was obtained.]

Anal.—Calc. for $C_{16}H_{20}N_2O_7$: C, 54.54; H, 5.72; N, 7.95. Found: C, 54.41; H, 5.72; N, 7.96.

[8] The solvent was Unisol-D, a blended mixture of deuterated chloroform and deuterated dimethyl sulfoxide, Norell Chemical Co., Landisville, N.J.

[9] Celite.

REFERENCES

(1) P. E. Thompson and L. M. Werbel, "Antimalarial Agents," Academic, New York, N.Y., 1972.

(2) E. A. Steck, "The Chemotherapy of Protozoan Diseases," vol. III, Walter Reed Army Institute of Research Publications, Washington, D.C., 1972.

(3) R. M. Pinder, in "Medicinal Chemistry," 3rd ed., A. Burger, Ed.,

Wiley, New York, N.Y., 1970, p. 507.
(4) J. P. Scovill, D. L. Klayman, T. S. Woods, and T. R. Sweeney, *J. Med. Chem.*, **22**, 1164 (1979).
(5) L. H. Schmidt, R. Fradkin, D. Vaughan, and J. Rasco, *Am. J. Trop. Med. Hyg.*, **26**, 1116 (1977).
(6) M. P. LaMontagne, A. Markovac, and J. R. Menke, *J. Med. Chem.*, **20**, 1122 (1977).
(7) L. H. Schmidt, A. H. Rossan, R. Fradkin, and J. Woods, *Bull. WHO*, **34**, 783 (1966).
(8) "World Health Organization (1972b)," WHO/MAL/72763 (cyclostyled report), World Health Organization, Geneva, Switzerland.
(9) T. S. Osdene, P. B. Russell, and L. Rane, *J. Med. Chem.*, **10**, 431 (1967).
(10) G. R. Coatney, W. C. Cooper, N. B. Eddy, and J. Greenberg, "Survey of Antimalarial Agents," Public Health Monograph No. 9, U.S. Government Printing Office, Washington, D.C., 1953.
(11) R. C. Elderfield, W. J. Gensler, T. A. Williamson, J. M. Griffing, S. M. Kupchan, J. T. Maynard, F. J. Kreysa, and J. B. Wright, *J. Am. Chem. Soc.*, **68**, 1584 (1946).
(12) R. H. F. Manske and M. Kulka, in "Organic Reactions," vol. 7, R. Adams, Ed., Wiley, New York, N.Y., 1953, p. 59.
(13) A. Maercker, in "Organic Reactions," vol. 14, A. C. Cope, Ed., Wiley, New York, N.Y., 1965, p. 270.
(14) L. Friedman and H. Sheckter, *J. Org. Chem.*, **26**, 2522 (1961).
(15) K. Kindler and K. Lührs, *Chem. Ber.*, **99**, 227 (1966).
(16) K. Kindler and K. Lührs, *Ann. Chem.*, **685**, 36 (1965).
(17) F. L. Cook, C. W. Bower, and C. L. Liotta, *J. Org. Chem.*, **39**, 3416 (1974).
(18) A. McKillop and D. P. Rao, *Synthesis*, **1977**, 759.
(19) R. C. Elderfield, H. E. Mertel, R. T. Mitch, I. M. Wempen, and E. Werble, *J. Am. Chem. Soc.*, **77**, 4816 (1955).
(20) E. H. Chen, A. J. Saggiomo, K. Tanabe, B. L. Verma, and E. A. Nodiff, *J. Med. Chem.*, **20**, 1107 (1977).
(21) E. A. Chen, A. J. Saggiomo, and E. A. Nodiff, U.S. pat. 4,167,638 (1979).
(22) M. Carmack, L. W. Kissinger, and I. Von, *J. Am. Chem. Soc.*, **68**, 1551 (1946).
(23) W. C. Hanson, W. L. Chapman, Jr., and K. E. Kinnamon, *Int. J. Parasitol.*, **7**, 443 (1977).
(24) K. E. Kinnamon, E. A. Steck, P. S. Loizeaux, W. L. Hanson, W. L. Chapman, Jr., and V. B. Waits, *Am. J. Trop. Med. Hyg.*, **27**, 751 (1978).
(25) H. Mort and W. Montouri, *ibid.*, **24**, 179 (1975).
(26) K. E. Kinnamon and D. S. Rane, *ibid.*, **28**, 937 (1979).
(27) C. C. Price and R. M. Roberts, *J. Am. Chem. Soc.*, **68**, 1204 (1946).

ACKNOWLEDGMENTS

Supported by the U.S. Army Medical Research and Development Command under Contract DADA-17-71-C1068.

This paper is Contribution 1567 to the Army Research Program on Antiparasitic Drugs.

The authors thank Dr. R. E. Strube, Dr. E. A. Steck, and Dr. T. R. Sweeney of the Walter Reed Army Institute for interest and encouragement.

Aporphines XXVI: GLC and Mass Spectrometric Properties of Trifluoroacetyl Derivatives of *N*-Methyl-, *N*-Propyl-, and Noraporphines

J. F. GREEN *, G. N. JHAM ‡, J. L. NEUMEYER *, and PAUL VOUROS ‡x

Received December 4, 1979, from the **Department of Medicinal Chemistry and the* ‡*Institute of Chemical Analysis, Applications and Forensic Science, Northeastern University, Boston, MA 02115.* Accepted for publication March 12, 1980.

Abstract □ The *O*-trifluoroacetyl and *N,O*-trifluoroacetyl derivatives of a series of aporphine and noraporphine alkaloids were prepared, and their GLC and mass spectrometric characteristics were determined. The positional isomers apocodeine and isoapocodeine were resolved chromatographically as their trifluoroacetyl derivatives, and their mass spectra were distinctly different. Mass spectrometric fragmentation processes apparently unique to *N*-trifluoroacetyl derivatives of noraporphines were observed. Plausible mechanisms for the formation of the major ions in the mass spectra of the various compounds are given.

Keyphrases □ Aporphines—trifluoroacetyl derivatives, GLC and mass spectrometry □ Noraporphines—trifluoroacetyl derivatives, GLC and mass spectrometry □ GLC—trifluoroacetyl derivatives of aporphines and noraporphines

The need for sensitive and quantitative methods for elaborating the metabolism of apomorphine (I*a*) (Scheme I) has increased due to the biological activity of apomorphine and related alkaloids (1–3). Although conjugation was reported as a primary route for the metabolism of I*a* in the rat (4), apocodeine (I*d*) and isoapocodeine (I*e*) formed from *O*-methylation have been reported as possible metabolites in rat liver preparations (5). *N*-Dealkylation also was reported to give an *in vitro* metabolite of several naturally occurring aporphine alkaloids (6). More recent studies in liver microsomal preparations indicated that several aporphine analogs could be converted metabolically to their *O*-demethylated derivatives (*i.e.*, I*d* → I*a* and I*e* → I*a*) (7).

BACKGROUND

N-n-Propylnorapomorphine (I*b*) was reported to be several times more potent than I*a* in several biological systems (3). Monohydroxyaporphines substituted in either the 10- or 11-position were found to be active dopamine agonists, although they were less potent than I*b* (8, 9). It is generally accepted that catechol analogs of apomorphine are more potent dopamine agonists than are the monohydroxy analogs (10). However, the possibility that monohydroxy analogs such as I*j* and I*k* are converted *in vivo* into a catechol-like compound (*e.g.*, I*b*) cannot be excluded (11). Preliminary studies showed no evidence for the microsomal hydroxylation of the monohydroxy aporphines I*j* and I*k* to the corresponding catechol, I*b*, using TLC to distinguish monophenols from catecholic metabolites (7).

To develop more definitive techniques, specifically GLC–mass spectrometric methods for the detection, identification, and quantitation of aporphines, the *O*-trifluoroacetyl derivatives of a series of *N*-methyl- and *N*-propylaporphines were prepared. Since *N*-dealkylation is a common metabolic process, the mass spectra of a series of trifluoroacetyl noraporphine derivatives also were considered. It was hoped that this examination might reveal unique fragmentation processes which could aid in the recognition of noraporphine metabolites or natural products in general.

Paper chromatography, GLC, and TLC were used previously to define

0022-3549/80/0800-0936$01.00/0
© 1980, American Pharmaceutical Association

Wiley, New York, N.Y., 1970, p. 507.
(4) J. P. Scovill, D. L. Klayman, T. S. Woods, and T. R. Sweeney, *J. Med. Chem.*, **22**, 1164 (1979).
(5) L. H. Schmidt, R. Fradkin, D. Vaughan, and J. Rasco, *Am. J. Trop. Med. Hyg.*, **26**, 1116 (1977).
(6) M. P. LaMontagne, A. Markovac, and J. R. Menke, *J. Med. Chem.*, **20**, 1122 (1977).
(7) L. H. Schmidt, A. H. Rossan, R. Fradkin, and J. Woods, *Bull. WHO*, **34**, 783 (1966).
(8) "World Health Organization (1972b)," WHO/MAL/72763 (cyclostyled report), World Health Organization, Geneva, Switzerland.
(9) T. S. Osdene, P. B. Russell, and L. Rane, *J. Med. Chem.*, **10**, 431 (1967).
(10) G. R. Coatney, W. C. Cooper, N. B. Eddy, and J. Greenberg, "Survey of Antimalarial Agents," Public Health Monograph No. 9, U.S. Government Printing Office, Washington, D.C., 1953.
(11) R. C. Elderfield, W. J. Gensler, T. A. Williamson, J. M. Griffing, S. M. Kupchan, J. T. Maynard, F. J. Kreysa, and J. B. Wright, *J. Am. Chem. Soc.*, **68**, 1584 (1946).
(12) R. H. F. Manske and M. Kulka, in "Organic Reactions," vol. 7, R. Adams, Ed., Wiley, New York, N.Y., 1953, p. 59.
(13) A. Maercker, in "Organic Reactions," vol. 14, A. C. Cope, Ed., Wiley, New York, N.Y., 1965, p. 270.
(14) L. Friedman and H. Sheckter, *J. Org. Chem.*, **26**, 2522 (1961).
(15) K. Kindler and K. Lührs, *Chem. Ber.*, **99**, 227 (1966).
(16) K. Kindler and K. Lührs, *Ann. Chem.*, **685**, 36 (1965).
(17) F. L. Cook, C. W. Bower, and C. L. Liotta, *J. Org. Chem.*, **39**, 3416 (1974).
(18) A. McKillop and D. P. Rao, *Synthesis*, **1977**, 759.
(19) R. C. Elderfield, H. E. Mertel, R. T. Mitch, I. M. Wempen, and E. Werble, *J. Am. Chem. Soc.*, **77**, 4816 (1955).
(20) E. H. Chen, A. J. Saggiomo, K. Tanabe, B. L. Verma, and E. A. Nodiff, *J. Med. Chem.*, **20**, 1107 (1977).
(21) E. A. Chen, A. J. Saggiomo, and E. A. Nodiff, U.S. pat. 4,167,638 (1979).
(22) M. Carmack, L. W. Kissinger, and I. Von, *J. Am. Chem. Soc.*, **68**, 1551 (1946).
(23) W. C. Hanson, W. L. Chapman, Jr., and K. E. Kinnamon, *Int. J. Parasitol.*, **7**, 443 (1977).
(24) K. E. Kinnamon, E. A. Steck, P. S. Loizeaux, W. L. Hanson, W. L. Chapman, Jr., and V. B. Waits, *Am. J. Trop. Med. Hyg.*, **27**, 751 (1978).
(25) H. Mort and W. Montouri, *ibid.*, **24**, 179 (1975).
(26) K. E. Kinnamon and D. S. Rane, *ibid.*, **28**, 937 (1979).
(27) C. C. Price and R. M. Roberts, *J. Am. Chem. Soc.*, **68**, 1204 (1946).

ACKNOWLEDGMENTS

Supported by the U.S. Army Medical Research and Development Command under Contract DADA-17-71-C1068.

This paper is Contribution 1567 to the Army Research Program on Antiparasitic Drugs.

The authors thank Dr. R. E. Strube, Dr. E. A. Steck, and Dr. T. R. Sweeney of the Walter Reed Army Institute for interest and encouragement.

Aporphines XXVI: GLC and Mass Spectrometric Properties of Trifluoroacetyl Derivatives of *N*-Methyl-, *N*-Propyl-, and Noraporphines

J. F. GREEN *, G. N. JHAM ‡, J. L. NEUMEYER *, and PAUL VOUROS ‡x

Received December 4, 1979, from the **Department of Medicinal Chemistry and the* ‡*Institute of Chemical Analysis, Applications and Forensic Science, Northeastern University, Boston, MA 02115.* Accepted for publication March 12, 1980.

Abstract □ The *O*-trifluoroacetyl and *N,O*-trifluoroacetyl derivatives of a series of aporphine and noraporphine alkaloids were prepared, and their GLC and mass spectrometric characteristics were determined. The positional isomers apocodeine and isoapocodeine were resolved chromatographically as their trifluoroacetyl derivatives, and their mass spectra were distinctly different. Mass spectrometric fragmentation processes apparently unique to *N*-trifluoroacetyl derivatives of noraporphines were observed. Plausible mechanisms for the formation of the major ions in the mass spectra of the various compounds are given.

Keyphrases □ Aporphines—trifluoroacetyl derivatives, GLC and mass spectrometry □ Noraporphines—trifluoroacetyl derivatives, GLC and mass spectrometry □ GLC—trifluoroacetyl derivatives of aporphines and noraporphines

The need for sensitive and quantitative methods for elaborating the metabolism of apomorphine (I*a*) (Scheme I) has increased due to the biological activity of apomorphine and related alkaloids (1–3). Although conjugation was reported as a primary route for the metabolism of I*a* in the rat (4), apocodeine (I*d*) and isoapocodeine (I*e*) formed from *O*-methylation have been reported as possible metabolites in rat liver preparations (5). *N*-Dealkylation also was reported to give an *in vitro* metabolite of several naturally occurring aporphine alkaloids (6). More recent studies in liver microsomal preparations indicated that several aporphine analogs could be converted metabolically to their *O*-demethylated derivatives (*i.e.*, I*d* → I*a* and I*e* → I*a*) (7).

BACKGROUND

N-n-Propylnorapomorphine (I*b*) was reported to be several times more potent than I*a* in several biological systems (3). Monohydroxyaporphines substituted in either the 10- or 11-position were found to be active dopamine agonists, although they were less potent than I*b* (8, 9). It is generally accepted that catechol analogs of apomorphine are more potent dopamine agonists than are the monohydroxy analogs (10). However, the possibility that monohydroxy analogs such as I*j* and I*k* are converted *in vivo* into a catechol-like compound (*e.g.*, I*b*) cannot be excluded (11). Preliminary studies showed no evidence for the microsomal hydroxylation of the monohydroxy aporphines I*j* and I*k* to the corresponding catechol, I*b*, using TLC to distinguish monophenols from catecholic metabolites (7).

To develop more definitive techniques, specifically GLC–mass spectrometric methods for the detection, identification, and quantitation of aporphines, the *O*-trifluoroacetyl derivatives of a series of *N*-methyl- and *N*-propylaporphines were prepared. Since *N*-dealkylation is a common metabolic process, the mass spectra of a series of trifluoroacetyl noraporphine derivatives also were considered. It was hoped that this examination might reveal unique fragmentation processes which could aid in the recognition of noraporphine metabolites or natural products in general.

Paper chromatography, GLC, and TLC were used previously to define

0022-3549/80/0800-0936$01.00/0
© 1980, American Pharmaceutical Association

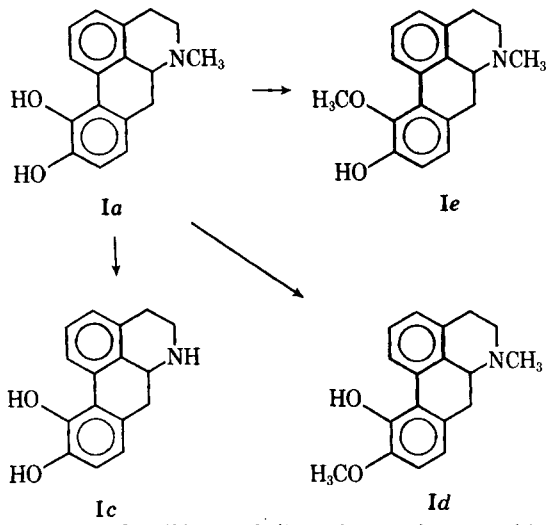

Ia Ie Ic Id

Scheme I—Possible metabolic pathways of apomorphine

the metabolism of such compounds *in vitro* (5, 7) and *in vivo* (12). These techniques *per se* do not necessarily define specificity for such studies. Findings obtained in these laboratories indicated that GLC–mass spectrometry permitted unambiguous analysis of a series of hydroxynoraporphines as their *N*-heptafluorobutyryl-*O*-trimethylsilyl derivatives (13), as well as the trimethylsilyl derivatives for *N*-methyl- and *N*-propylaporphines (14). GLC–mass spectrometry of the trifluoroacetyl derivatives described in this report offers specific advantages over the use of both their trimethylsilyl and heptafluorobutyryl-*O*-trimethylsilyl counterparts.

EXPERIMENTAL

The compounds were available in these laboratories as their hydrochloride or hydroiodide salts. A solution of 1 mg/ml or less of the aporphine and noraporphine in trifluoroacetic anhydride was prepared and heated for 10 min at 60°. The excess reagent was evaporated under a nitrogen stream, and the derivative was dissolved in methylene chloride to yield a 1-mg/ml solution. An aliquot (1–2 μl) was injected into the gas–liquid chromatograph–mass spectrometer system[1] for analysis.

A 183-cm × 2-mm i.d. glass column packed with 1% OV-17 on 100–120-mesh Supelcoport and temperature programmed for 6°/min from 200° was used. The gas chromatograph injection port, detector, and transfer line were maintained at 250, 250, and 200°, respectively. The mass spectrometer ion source was heated to 225°. Mass spectra were recorded in the electron-impact mode (70 ev) at an accelerating voltage of 4.5 kv and a trap current of 50 μamp.

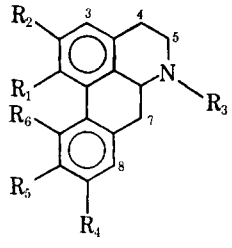

I

Ia: $R_1 = R_2 = R_4 = H, R_3 = CH_3, R_5 = R_6 = OH$
Ib: $R_1 = R_2 = R_4 = H, R_3 = n\text{-}C_3H_7, R_5 = R_6 = OH$
Ic: $R_1 = R_2 = R_3 = R_4 = H, R_5 = R_6 = OH$
Id: $R_1 = R_2 = R_4 = H, R_5 = OCH_3, R_6 = OH, R_3 = CH_3$
Ie: $R_1 = R_2 = R_4 = H, R_5 = OH, R_6 = OCH_3, R_3 = CH_3$
If: $R_1 = R_2 = R_4 = H, R_5 = OCH_3, R_6 = OH, R_3 = n\text{-}C_3H_7$
Ig: $R_1 = R_4 = H, R_2 = R_5 = R_6 = OH, R_3 = CH_3$
Ih: $R_1 = R_4 = H, R_2 = R_6 = OH, R_5 = OCH_3, R_3 = CH_3$
Ii: $R_1 = R_4 = H, R_2 = R_5 = OCH_3, R_6 = OH, R_3 = CH_3$
Ij: $R_1 = R_2 = R_4 = R_6 = H, R_5 = OH, R_3 = C_3H_7$
Ik: $R_1 = R_2 = R_4 = R_5 = H, R_6 = OH, R_3 = C_3H_7$
Il: $R_1 = R_3 = R_4 = H, R_2 = R_5 = OCH_3, R_6 = OH$
Im: $R_1 = R_3 = R_4 = H, R_2 = R_6 = OH, R_5 = OCH_3$
In: $R_1 = R_3 = R_4 = H, R_2 = R_5 = R_6 = OH$
Io: $R_1 = R_5 = OH, R_2 = OCH_3, R_3 = R_4 = R_6 = H$
Ip: $R_1 = OCH_3, R_2 = OH, R_3 = R_4 = R_5 = R_6 = H$
Iq: $R_1 = R_2 = OCH_3, R_3 = R_4 = R_6 = H, R_5 = OH$

[1] Varian Aerograph model 2700 interfaced *via* a 0.15-mm, 25-cm capillary tube to a Nuclide model 12-90-G mass spectrometer.

Table I—GLC Retention Data of Aporphine Derivatives [a]

Compound	Trimethylsilyl Derivatives	Trifluoroacetyl Derivatives
Ia	27.56	23.78
Id	28.50	26.62
Ie	27.79	25.56
IIa	31.60	31.00
2,10,11-Trihydroxy-*N*-methylaporphine	29.12	24.33
2,11-Dihydroxy-10-methoxy-*N*-methylaporphine	30.24	26.83
2,10-Dimethoxy-11-hydroxy-*N*-methylaporphine	30.88	29.33
Ib	28.67	25.04
If	29.52	27.67
Ij	29.08	25.80
Ik	27.07	24.33

[a] Values are in methylene units.

The following compounds were prepared as their *O*-trifluoroacetyl derivatives and studied by GLC–mass spectrometry: apomorphine (Ia), *N*-*n*-propylnorapomorphine (Ib), apocodeine (Id), isoapocodeine (Ie), *N*-*n*-propylnorapocodeine (If), 2,10,11-trihydroxyaporphine (Ig), morphothebaine (Ih), 11-hydroxy-2,10-dimethoxyaporphine (Ii), 10-hydroxy-*N*-*n*-propylnoraporphine (Ij), and 11-hydroxy-*N*-*n*-propylnoraporphine (Ik).

Mass spectrometric data also were acquired on the following noraporphines as their *N*-trifluoroacetyl or *N*,*O*-bis(trifluoroacetyl) derivatives: 11-hydroxy-2,10-dimethoxynoraporphine (Il), 10-methoxy-2,11-dimethoxynoraporphine (Im), and 2,10,11-trihydroxynoraporphine (In). The naturally occurring aporphine alkaloids sparsiflorine (Io), asimilobine (Ip), tuduranine (Iq), bulbocapnine (IIa), nandigerine (IIb), cassyfiline (IIc), xylopine (IId), anolobine (IIe), and actinodaphnine (IIf) also were examined[2].

RESULTS AND DISCUSSION

GLC—N-*Propyl- and* N-*Methylaporphines*—The GLC retention data of the *O*-trifluoroacetyl derivatives of *N*-propyl- and *N*-methylaporphines are given in Table I. For comparison, the methylene unit values for the corresponding trimethylsilyl derivatives reported previously (13) have been included.

In general, the *O*-trifluoroacetyl derivatives of these compounds exhibited good GLC characteristics. The retention data indicate a marked increase in volatility for the *O*-trifluoroacetyl derivatives compared to the corresponding *O*-trimethylsilyl derivatives. For example, this increase in volatility for apomorphine represents a 40° difference in the elution temperature (280 *versus* 240°). This difference not only decreases analysis time but also eliminates the problems of thermal sensitivity associated with these compounds (14).

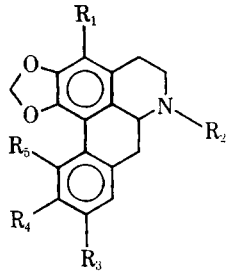

II

IIa: $R_1 = R_3 = H, R_2 = CH_3, R_4 = OCH_3, R_5 = OH$
IIb: $R_1 = R_2 = R_3 = H, R_4 = OH, R_5 = OCH_3$
IIc: $R_1 = R_4 = OCH_3, R_2 = R_5 = H, R_3 = OH$
IId: $R_1 = R_2 = R_4 = R_5 = H, R_3 = OCH_3$
IIe: $R_1 = R_2 = R_4 = R_5 = H, R_3 = OH$
IIf: $R_1 = R_2 = R_4 = H, R_3 = OH, R_5 = OCH_3$

[2] The aporphine alkaloids Io–Iq and IIb–IIf were kindly supplied by Dr. M. Shamma, Pennsylvania State University.

Table II—GLC Retention Data of Noraporphine Derivatives [a]

Compound	Mixed Derivative[b]	Trifluoroacetyl Derivative
Im	30.48	30.60
In	30.00	28.90
Io	28.96	26.30

[a] Values are in methylene units. [b] *N*-Heptafluorobutyryl-*O*-trimethylsilyl derivative.

Of even greater importance is the ability to separate chromatographically, with baseline resolution, the *O*-trifluoroacetyl derivatives of apocodeine (Id) and isoapocodeine (Ie), as substantiated by the retention data in Table I. By contrast, the *O*-trimethylsilyl derivatives of these compounds coelute, a phenomenon that was observed previously (7). Because these two compounds were suggested as possible metabolites of apomorphine, it is essential to identify and to distinguish these products in a biological medium.

Noraporphines—The retention data for the trifluoroacetyl derivatives of noraporphines (Il–In) are given in Table II. These data can be compared to the methylene units of the corresponding mixed derivatives (*O*-trimethylsilyl-*N*-heptafluorobutyryl) reported previously (13). The general improvement in volatility when trifluoroacetyl derivatives are used is apparent. Moreover, temperature variation of the injection port, column, detector, and gas chromatograph–mass spectrometer transfer line over a wide range gave no indication of thermal sensitivity for the trifluoroacetyl derivatives as opposed to their trimethylsilyl counterparts.

Mass Spectrometry—*N-Methyl- and N-Propylaporphines*—The complete mass spectra of the trifluoroacetyl derivatives of apomorphine (Ia), *N*-*n*-propylnorapomorphine (Ib), apocodeine (Id), and isoapocodeine (Ie) are shown in Figs. 1–4, respectively. Partial mass spectra of the compounds in the series are summarized in Tables III and IV.

$M^{+\cdot}$ and $[M-1]^+$ Ions—The mass spectra of the *O*-trifluoroacetyl derivatives of *N*-methyl- and *N*-propylaporphines were noted for the high intensity of the molecular ion peaks or those corresponding to the loss of a hydrogen at $[M-1]^+$. The $[M-1]^+$ ion presumably is formed by the loss of the 6α-hydrogen to yield a quaternary nitrogen (Scheme II). In general, there were few other ions of any significance in the spectra of the

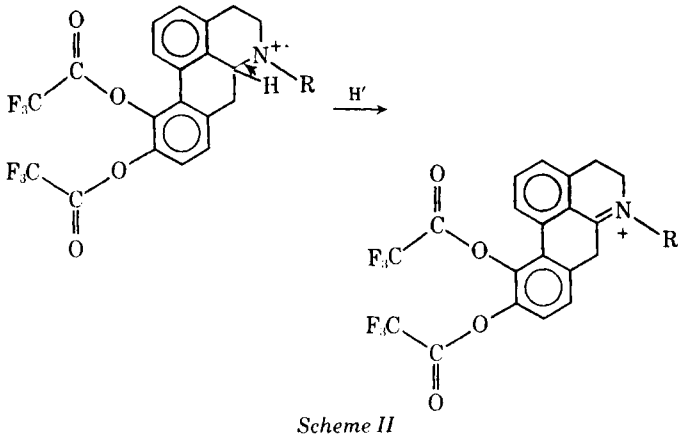

Scheme II

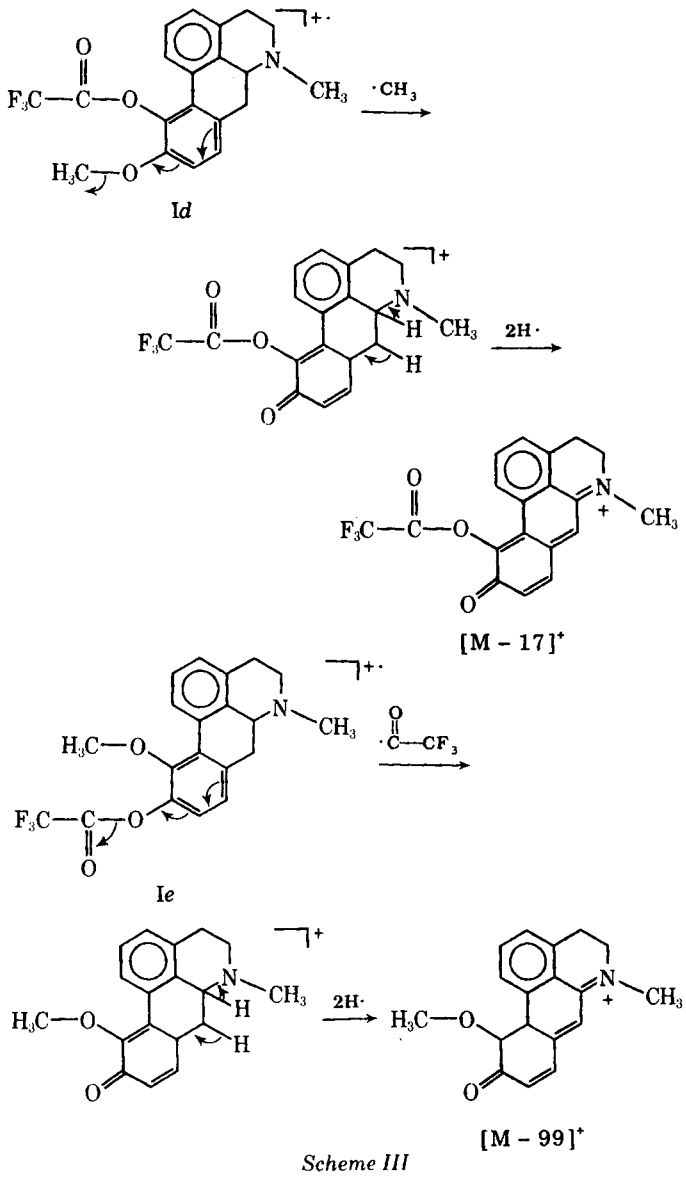

Scheme III

N-methylaporphines. The only peak of any significant intensity in most cases was $[M-97]^+$, arising from the loss of $CF_3C(=O)\cdot$ from $M^{+\cdot}$.

Apocodeine and Isoapocodeine—Two significant differences may be noted (Figs. 3 and 4 and Table III) when the mass spectra of these positional isomers are compared. The spectrum of apocodeine shows a peak at $[M-17]^+$, which was not detected in the spectrum of the trifluoroacetyl derivative of isoapocodeine. In addition, the relative intensities of the peaks at $[M-99]^+$ in the spectra of these two compounds are significantly different, the $[M-99]^+$ ion being much more (10 times)

Table III—Partial Mass Spectra of *N*-Methyl-*O*-trifluoroacetyl Derivatives of Aporphines

Compound	$M^{+\cdot}$	$[M-1]^+$	$[M-15]^+$	$[M-17]^+$	$[M-97]^+$	$[M-99]^+$
Ia	459[a]	458	444	442	362	360
	(100)[b]	(97)	(5)	(—)	(26)	(10)
Id	377	376	362	360	280	278
	(91)	(100)	(26)	(21)	(—)	(5)
Ie	377	376	362	360	280	278
	(76)	(100)	(3)	(—)	(10)	(34)
IIa	421	420	406	404	324	322
	(100)	(56)	(65)	(12)	(—)	(—)
Ig	571	570	556	554	474	472
	(100)	(85)	(6)	(—)	(40)	(6)
2,11-Dihydroxy-10-methyoxyaporphine	489	488	474	472	392	390
	(100)	(86)	(34)	(8)	(9)	(4)
2,10-Dimethoxy-11-hydroxyaporphine	407	406	392	390	310	308
	(87)	(100)	(42)	(30)	(—)	(—)

[a] The *m/e* values. [b] Relative intensity.

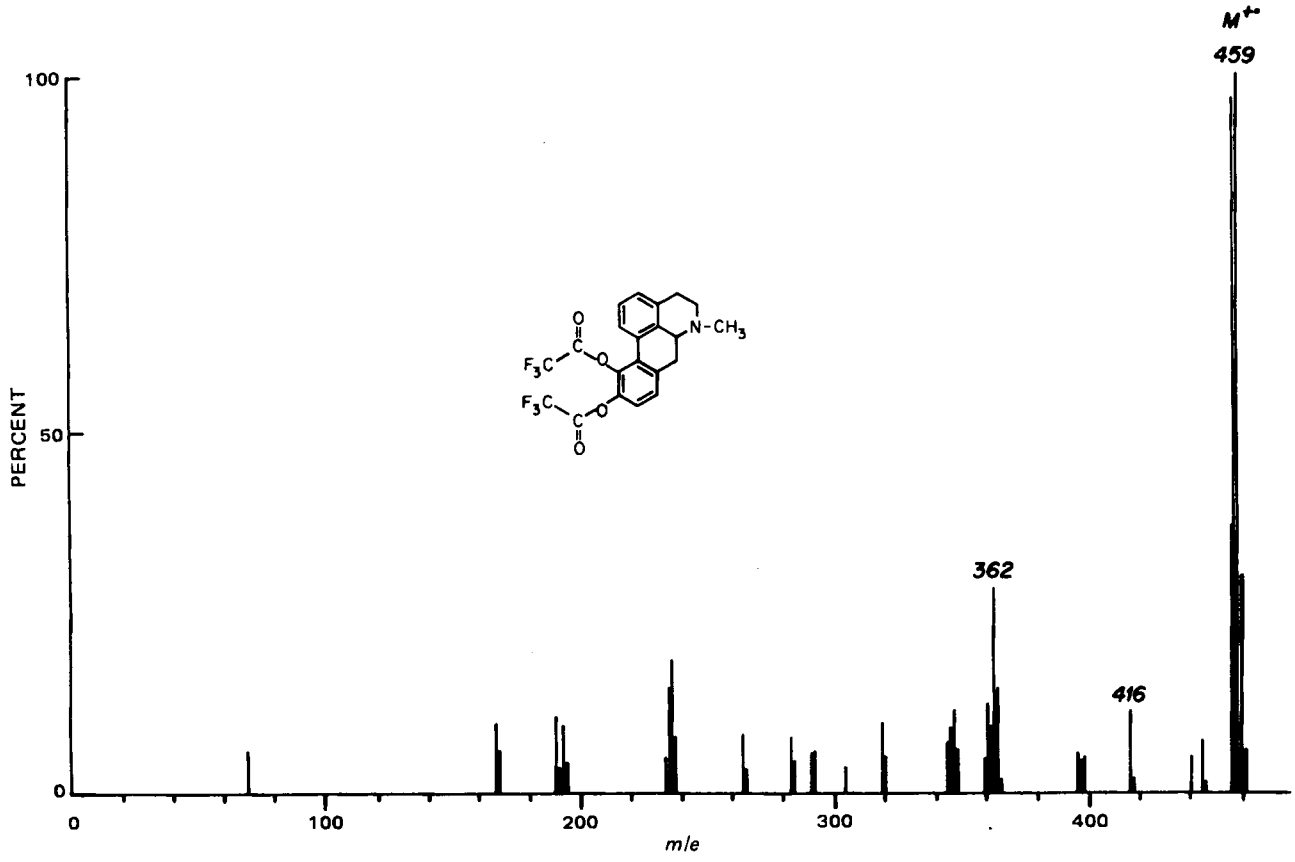

Figure 1—*Mass spectrum of the* O-*bis(trifluoroacetyl) derivative of I*a.

abundant in the spectrum of the isoapocodeine derivative. These differences can be explained by the formation of a quinone-type ion structure (Scheme III). The *O*-trimethylsilyl derivatives of these compounds have virtually identical spectra.

N-n-*Propyl Compounds*—In addition to the $[M - 1]^+$ and $[M - 99]^+$ ions, there are fragmentation pathways specific for compounds containing an *N-n*-propyl substituent. The base peak in the spectra of the *N-n*-propyl compounds studied occurred at $[M - 29]^+$, which results from

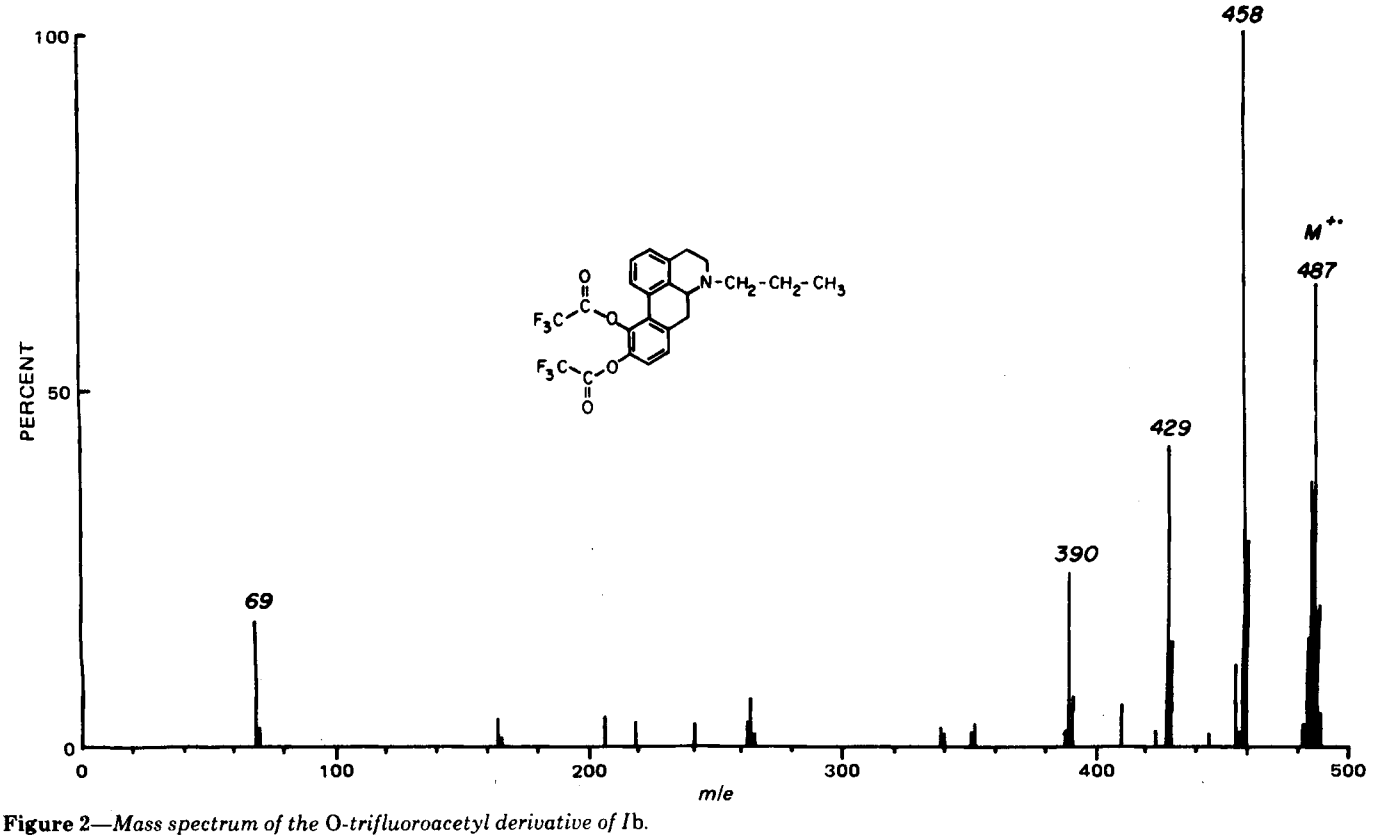

Figure 2—*Mass spectrum of the* O-*trifluoroacetyl derivative of I*b.

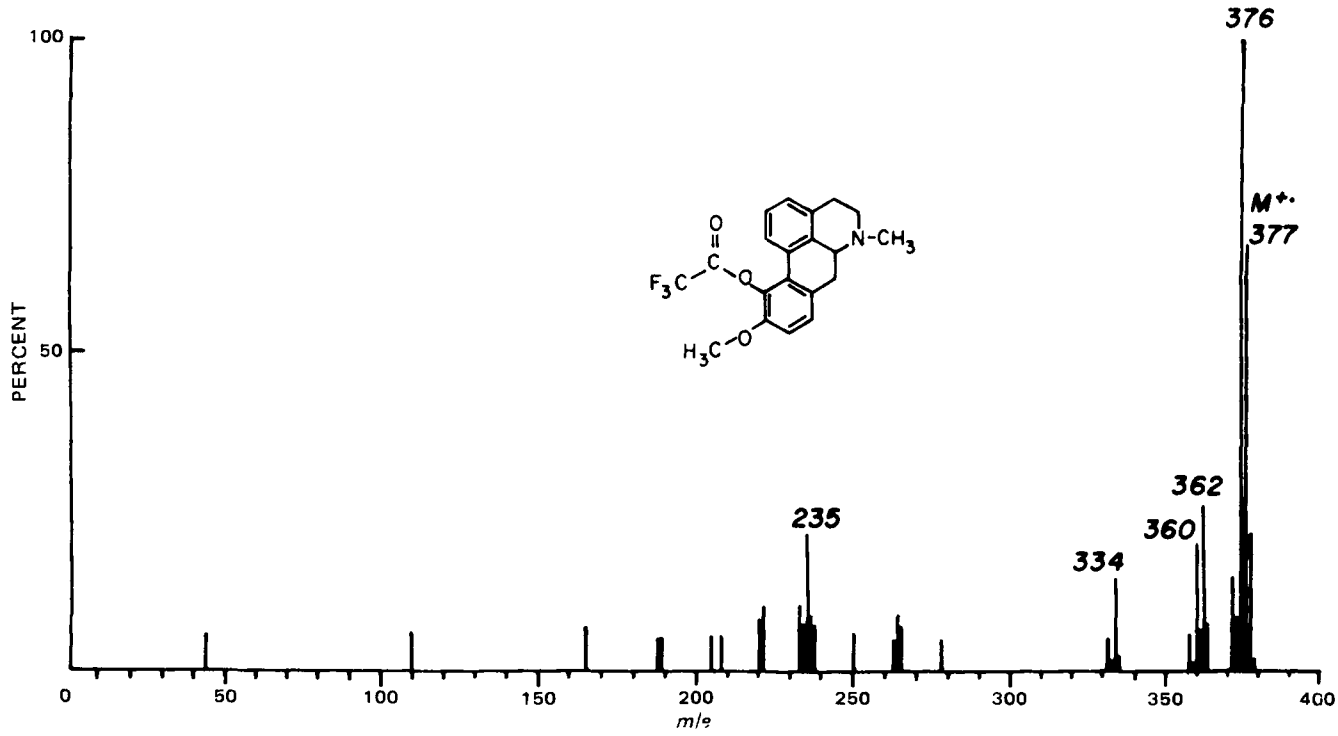

Figure 3—*Mass spectrum of the* O-*trifluoroacetyl derivative of* Id.

cleavage of the carbon–carbon bond beta to the nitrogen. Subsequent fragmentation of this ion gave rise to a peak at $[M - 58]^+$ (Scheme IV).

Noraporphines—The partial mass spectra of the trifluoroacetyl derivatives of the noraporphines (*Il–In*) are listed in Table V. A complete mass spectrum of the *N,O*-bis(trifluoroacetyl) derivative of anolobine (IIe) is shown in Fig. 5. The mass spectrum consists of only a few major ions associated with the fragmentation of the trifluoroacetyl group. This pattern typifies the general spectral characteristics of the trifluoroacetyl derivatives of the noraporphines studied. The ion peaks at $[M - 69]^+$ and $[M - 97]^+$ correspond to the loss of $CF_3\cdot$ and $CF_3C(=O)\cdot$ from $M^{+\cdot}$.

The $[M - 126]^+$ ion is unique to the noraporphine derivatives, and a plausible mechanism for its formation is given in Scheme V. It is suggested that its formation is initiated by a six-membered ring hydrogen transfer (McLafferty rearrangement) from C-7 to the carbonyl oxygen, followed by cleavage of a carbon–carbon bond beta to the heteroatom. The proposed γ-hydrogen transfer is consistent with the general behavior of the structurally related *N*-acetates of biogenic amines (14). Alternatively, the possibility of formation of the $[M - 126]^+$ ion by the loss of a hydrogen from the ion formed by a retro-Diels–Alder fragmentation of $M^{+\cdot}$ cannot *a priori* be ruled out.

In a previous publication, Green *et al.* (15) reported on the GLC–mass spectrometry of mixed *N*-heptafluorobutyryl-*O*-trimethylsilyl derivatives of noraporphines. By comparison, the mass spectra of the trifluoroacetyl derivatives reported here are noted for their overall simplicity. The intensity of the peak at $[M - 126]^+$ is rather striking, and this peak usually dominates the spectra of these derivatives. The analogous peak is of significantly lower relative intensity in the spectra of the *N*-heptafluorobutyryl-*O*-trimethylsilyl derivatives.

In view of the apparent uniqueness of the $[M - 126]^+$ ion, determina-

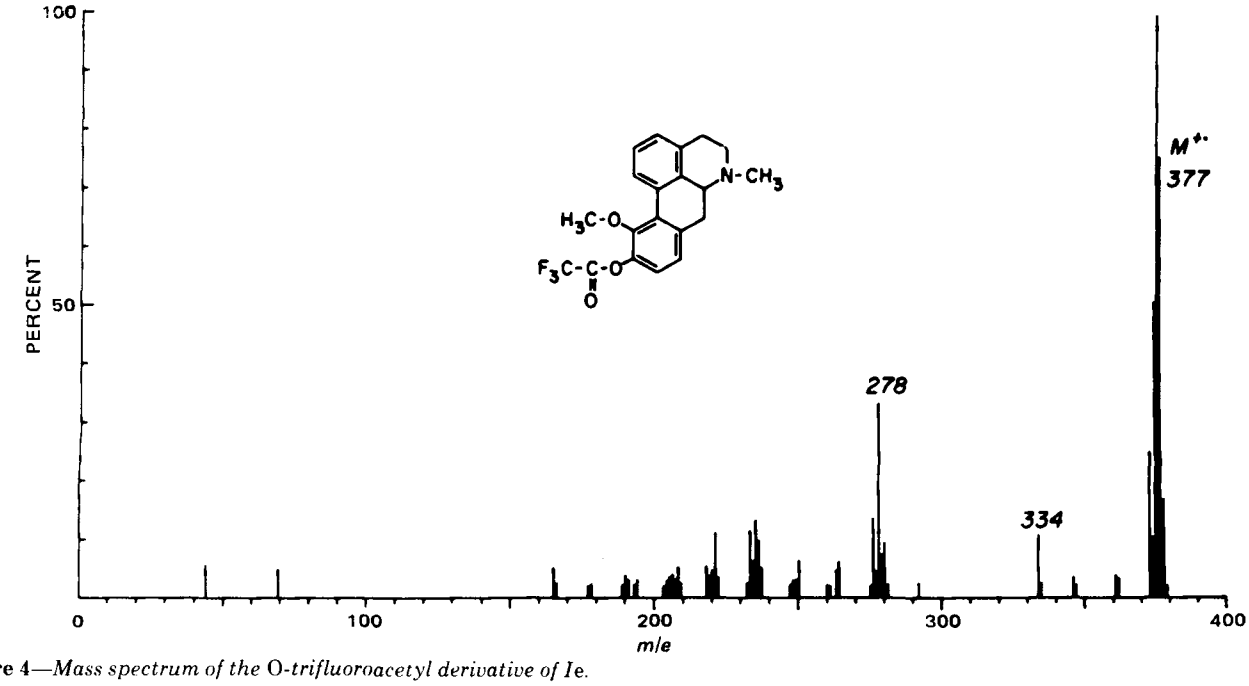

Figure 4—*Mass spectrum of the* O-*trifluoroacetyl derivative of* Ie.

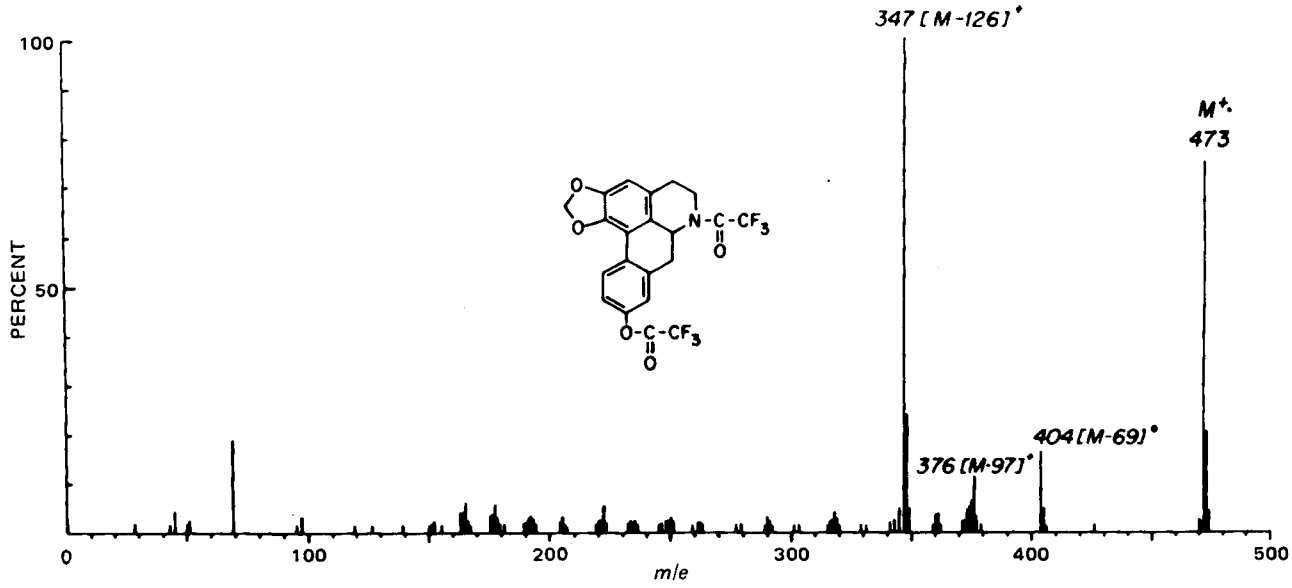

Figure 5—*Mass spectrum of the* N,O-*bis(trifluoroacetyl) derivative of IIe.*

tion of whether this fragmentation could be used diagnostically to recognize the presence of a noraporphine was desired. The type of substitution on the secondary nitrogen of the underivatized aporphine generally is determined on the basis of the retro-Diels–Alder fragmentation. However, in noraporphines, this fragmentation is of reduced intensity (10% relative intensity) compared to that of the *N*-alkyl-substituted alkaloids. Accordingly, the mass spectra of the trifluoroacetyl derivatives of the following naturally occurring noraporphines were studied: sparsiflorine (Io), asimilobine (Ip), tuduranine (Iq), nandigerine (IIb), cassyfiline (IIc), xylopine (IId), anolobine (IIe), and actinodaphnine (IIf).

The partial mass spectra of these derivatives are listed in Table V, and the complete mass spectrum of anolobine is shown in Fig. 5. As with the other noraporphines, the mass spectra again were characterized by few major ions, of which the $[M - 126]^+$ ion was the most prominent. These findings support the earlier supposition that this fragmentation can be used as a diagnostic tool to determine the degree of substitution on the nitrogen of aporphine alkaloids isolated from natural products or as possible metabolites in biological fluids.

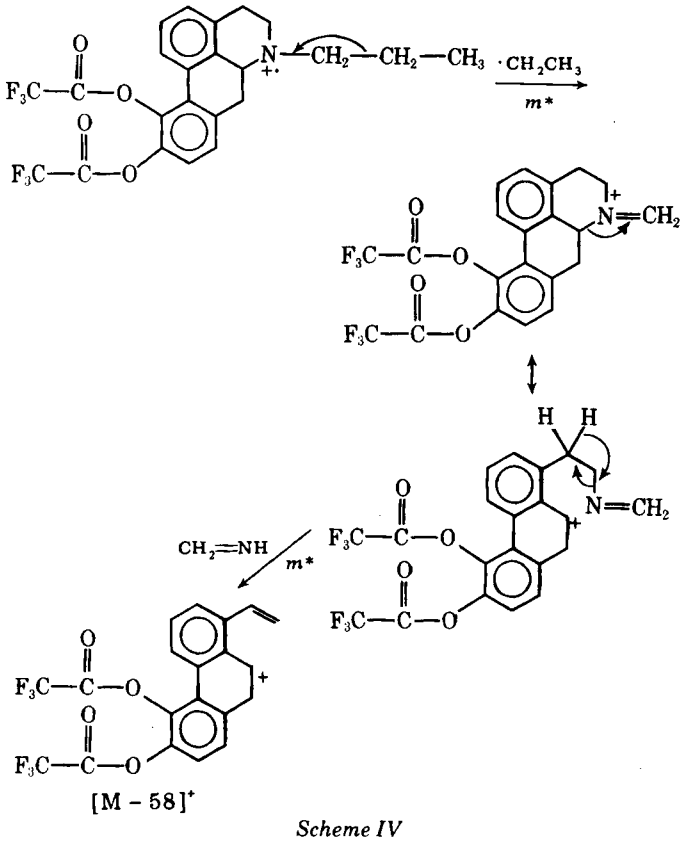

Scheme IV

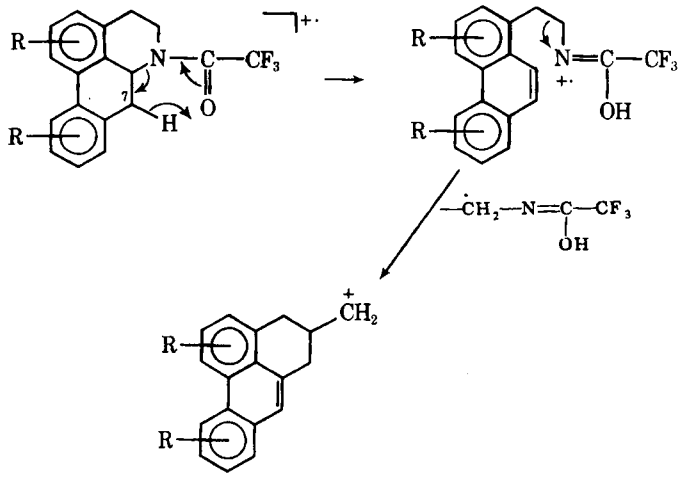

Scheme V

CONCLUSIONS

The trifluoroacetyl derivative formation for aporphine and noraporphine alkaloids represents a reliable technique which has application in the analysis of biological fluids in drug metabolism studies, as well as in the characterization of naturally occurring aporphine alkaloids.

The trifluoroacetyl derivative offers the following advantages over the corresponding trimethylsilyl derivative:

Table IV—Partial Mass Spectra of *N*-*n*-Propyl-*O*-trifluoroacetyl Derivatives of Aporphines

Compound	$M^{+\cdot}$	$[M - 1]^+$	$[M - 29]^+$	$[M - 58]^+$	$[M - 97]^+$
Ib	487[a]	486	458	429	390
	(65)[b]	(38)	(100)	(42)	(24)
If	405	404	376	317	308
	(77)	(45)	(100)	(37)	(4)
Ij	375	374	346	317	278
	(49)	(41)	(100)	(46)	(7)
Ik	375	374	346	317	278
	(62)	(55)	(100)	(48)	(4)

[a] The *m/e* values. [b] Relative intensity.

Table V—Partial Mass Spectra of Trifluoroacetyl Derivatives of Noraporphines

Compound	$M^{+\cdot}$	$[M-69]^+$	$[M-97]^+$	$[M-126]^+$
Il	489[a]	420	392	363
	(100)[b]	(21)	(5)	(46)
Im	571	502	474	445
	(100)	(8)	(36)	(85)
In	653	584	556	527
	(0)	(27)	(17)	(100)
Io	571	502	474	445
	(100)	(11)	(12)	(57)
Ip	459	390	362	333
	(53)	(6)	(4)	(100)
Iq	489	420	392	363
	(71)	(10)	(12)	(100)
IIa	503	436	406	377
	(100)	(6)	(30)	(99)
IIc	533	464	436	407
	(43)	(2)	(8)	(100)
IId	391	322	294	265
	(56)	(7)	(8)	(100)
IIe	473	404	376	347
	(76)	(17)	(11)	(100)
IIf	503	434	406	377
	(49)	(2)	(3)	(100)

[a] The *m/e* values. [b] Relative intensity.

1. The *O*-trifluoroacetyl derivatives have increased volatility.
2. The *O*-trifluoroacetyl derivatives of apocodeine and isoapocodeine can be separated by GLC.
3. The mass spectra of the *O*-trifluoroacetyl derivatives of apocodeine and isoapocodeine show characteristically different fragmentation patterns that can be applied to the characterization of 10- or 11-hydroxylated aporphines.
4. A fragmentation leading to the formation of an ion at a mass value corresponding to $[M-126]^+$ can be used diagnostically to determine the degree of substitution on the nitrogen of aporphine alkaloids.

REFERENCES

(1) G. C. Cotzias, P. S. Papavasiliou, E. S. Papavasiliou, E. S. Tolosa, J. S. Mendez, M. Bell-Midura, and B. Kaufman, *N. Engl. J. Med.*, **294**, 597 (1976).

(2) P. S. Papavasiliou, G. C. Cotzias, V. L. Rosal, and S. T. Miller, *Arch. Neurol.*, **35**, 787 (1978).

(3) M. K. Menon, W. G. Clark, and J. L. Neumeyer, *Eur. J. Pharmacol.*, **52**, 1 (1978).

(4) P. N. Kaul, E. Brochmann-Hanssen, and E. L. Way, *J. Pharm. Sci.*, **50**, 244 (1961). *Ibid.*, **50**, 248 (1961).

(5) K. Missala, S. Lal, and T. L. Sourkes, *Eur. J. Pharmacol.*, **22**, 54 (1973).

(6) R. V. Smith and S. P. Sood, *J. Pharm. Sci.*, **60**, 1654 (1971).

(7) R. V. Smith, P. W. Erhardt, J. L. Neumeyer, and R. J. Borgman, *Biochem. Pharmacol.*, **25**, 2106 (1976).

(8) J. L. Neumeyer, F. E. Granchelli, K. Fuxe, V. Ungerstedt, and H. Corrodi, *J. Med. Chem.*, **17**, 1090 (1974).

(9) J. L. Neumeyer, J. F. Reinhard, W. P. Dafeldecker, J. Guarino, D. S. Kosersky, K. Fuxe, and L. Agnati, *ibid.*, **19**, 25 (1976).

(10) R. I. Schoenfeld, J. L. Neumeyer, W. Dafeldecker, and S. Roffler-Tarlov, *Eur. J. Pharmacol.*, **30**, 63 (1975).

(11) J. L. Neumeyer, N. J. Uretsky, and R. R. Charest, *J. Pharm. Pharmacol.*, **29**, 179 (1977).

(12) R. V. Smith and R. M. Cook, *J. Pharm. Sci.*, **63**, 161 (1974).

(13) J. V. Evans and P. Vouros, *Anal. Biochem.*, **90**, 389 (1978).

(14) R. T. Coutts, G. R. Jones, A. Benderly, and A. L. C. Mak, *J. Chrom. Sci.*, **17**, 350 (1979).

(15) J. F. Green, J. V. Evans, J. L. Neumeyer, and P. Vouros, *Biomed. Mass Spectrom.*, **6**, 282 (1979).

ACKNOWLEDGMENTS

Supported in part by National Institutes of Health Grants USPHS NS 15439-01, GM 22787, and RR07143.

The authors thank Dr. M. Shamma, Pennsylvania State University, for supplying the naturally occurring noraporphine alkaloids.

Decomposition of Aminophylline in Suppository Formulations

JAMES F. BROWER ˣ, ERIC C. JUENGE, DONALD P. PAGE, and MATTHEW L. DOW

Received January 21, 1980, from the *National Center for Drug Analysis, Food and Drug Administration, St. Louis, MO 63101.* Accepted for publication March 13, 1980.

Abstract □ An aminophylline suppository product, when stored at room temperature, was found to be deficient in ethylenediamine content by the USP XIX assay and by a specific method for primary amines. The product also had a melting point that was considerably higher than body temperature. An accelerated decomposition experiment, conducted on normal suppositories of identical original composition, yielded a product refractory at steam bath temperatures and containing no ethylenediamine measurable by the USP assay. The suppositories from both the original sample and the decomposition experiment contained considerable amounts of a white material, which melted at ~150° and which consisted of the diamide products formed by the reaction of ethylenediamine and the fatty acids present in coconut and palm kernel oils. The results, which confirmed the work of Cieszynski, showed that the ethylenediamine constituent of aminophylline can react with suppository base materials to produce insoluble amide decomposition products.

Keyphrases □ Aminophylline—decomposition in suppository formulations □ Suppositories—aminophylline, decomposition in suppository formulations □ Decomposition—aminophylline in suppository formulations

During a study by the Food and Drug Administration which required the analysis of various dosage forms of xanthine derivative drugs, an aminophylline suppository formulation was encountered that unexpectedly failed to melt when heated in a beaker on a steam bath. In fact, the suppositories barely softened, and a composite was prepared for assay only with great difficulty. Analysis by the USP XIX method (1) showed that the suppository contained approximately the labeled amount of theophylline but considerably less than the compendial requirement for ethylenediamine. The suppository sample had been stored at room temperature for a month before analysis, so the original condition of the product was unknown.

An accelerated decomposition experiment was devised to study the phenomenon of hardening and to elucidate the decomposition that apparently had occurred. Ci-

0022-3549/80/0800-0942$01.00/0

© 1980, American Pharmaceutical Association

Table V—Partial Mass Spectra of Trifluoroacetyl Derivatives of Noraporphines

Compound	$M^{+\cdot}$	$[M-69]^+$	$[M-97]^+$	$[M-126]^+$
Il	489[a]	420	392	363
	(100)[b]	(21)	(5)	(46)
Im	571	502	474	445
	(100)	(8)	(36)	(85)
In	653	584	556	527
	(0)	(27)	(17)	(100)
Io	571	502	474	445
	(100)	(11)	(12)	(57)
Ip	459	390	362	333
	(53)	(6)	(4)	(100)
Iq	489	420	392	363
	(71)	(10)	(12)	(100)
IIa	503	436	406	377
	(100)	(6)	(30)	(99)
IIc	533	464	436	407
	(43)	(2)	(8)	(100)
IId	391	322	294	265
	(56)	(7)	(8)	(100)
IIe	473	404	376	347
	(76)	(17)	(11)	(100)
IIf	503	434	406	377
	(49)	(2)	(3)	(100)

[a] The *m/e* values. [b] Relative intensity.

1. The *O*-trifluoroacetyl derivatives have increased volatility.
2. The *O*-trifluoroacetyl derivatives of apocodeine and isoapocodeine can be separated by GLC.
3. The mass spectra of the *O*-trifluoroacetyl derivatives of apocodeine and isoapocodeine show characteristically different fragmentation patterns that can be applied to the characterization of 10- or 11-hydroxylated aporphines.
4. A fragmentation leading to the formation of an ion at a mass value corresponding to $[M-126]^+$ can be used diagnostically to determine the degree of substitution on the nitrogen of aporphine alkaloids.

REFERENCES

(1) G. C. Cotzias, P. S. Papavasiliou, E. S. Papavasiliou, E. S. Tolosa, J. S. Mendez, M. Bell-Midura, and B. Kaufman, *N. Engl. J. Med.*, **294**, 597 (1976).

(2) P. S. Papavasiliou, G. C. Cotzias, V. L. Rosal, and S. T. Miller, *Arch. Neurol.*, **35**, 787 (1978).

(3) M. K. Menon, W. G. Clark, and J. L. Neumeyer, *Eur. J. Pharmacol.*, **52**, 1 (1978).

(4) P. N. Kaul, E. Brochmann-Hanssen, and E. L. Way, *J. Pharm. Sci.*, **50**, 244 (1961). *Ibid.*, **50**, 248 (1961).

(5) K. Missala, S. Lal, and T. L. Sourkes, *Eur. J. Pharmacol.*, **22**, 54 (1973).

(6) R. V. Smith and S. P. Sood, *J. Pharm. Sci.*, **60**, 1654 (1971).

(7) R. V. Smith, P. W. Erhardt, J. L. Neumeyer, and R. J. Borgman, *Biochem. Pharmacol.*, **25**, 2106 (1976).

(8) J. L. Neumeyer, F. E. Granchelli, K. Fuxe, V. Ungerstedt, and H. Corrodi, *J. Med. Chem.*, **17**, 1090 (1974).

(9) J. L. Neumeyer, J. F. Reinhard, W. P. Dafeldecker, J. Guarino, D. S. Kosersky, K. Fuxe, and L. Agnati, *ibid.*, **19**, 25 (1976).

(10) R. I. Schoenfeld, J. L. Neumeyer, W. Dafeldecker, and S. Roffler-Tarlov, *Eur. J. Pharmacol.*, **30**, 63 (1975).

(11) J. L. Neumeyer, N. J. Uretsky, and R. R. Charest, *J. Pharm. Pharmacol.*, **29**, 179 (1977).

(12) R. V. Smith and R. M. Cook, *J. Pharm. Sci.*, **63**, 161 (1974).

(13) J. V. Evans and P. Vouros, *Anal. Biochem.*, **90**, 389 (1978).

(14) R. T. Coutts, G. R. Jones, A. Benderly, and A. L. C. Mak, *J. Chrom. Sci.*, **17**, 350 (1979).

(15) J. F. Green, J. V. Evans, J. L. Neumeyer, and P. Vouros, *Biomed. Mass Spectrom.*, **6**, 282 (1979).

ACKNOWLEDGMENTS

Supported in part by National Institutes of Health Grants USPHS NS 15439-01, GM 22787, and RR07143.

The authors thank Dr. M. Shamma, Pennsylvania State University, for supplying the naturally occurring noraporphine alkaloids.

Decomposition of Aminophylline in Suppository Formulations

JAMES F. BROWER ˣ, ERIC C. JUENGE, DONALD P. PAGE, and MATTHEW L. DOW

Received January 21, 1980, from the *National Center for Drug Analysis, Food and Drug Administration, St. Louis, MO 63101.* Accepted for publication March 13, 1980.

Abstract □ An aminophylline suppository product, when stored at room temperature, was found to be deficient in ethylenediamine content by the USP XIX assay and by a specific method for primary amines. The product also had a melting point that was considerably higher than body temperature. An accelerated decomposition experiment, conducted on normal suppositories of identical original composition, yielded a product refractory at steam bath temperatures and containing no ethylenediamine measurable by the USP assay. The suppositories from both the original sample and the decomposition experiment contained considerable amounts of a white material, which melted at ~150° and which consisted of the diamide products formed by the reaction of ethylenediamine and the fatty acids present in coconut and palm kernel oils. The results, which confirmed the work of Cieszynski, showed that the ethylenediamine constituent of aminophylline can react with suppository base materials to produce insoluble amide decomposition products.

Keyphrases □ Aminophylline—decomposition in suppository formulations □ Suppositories—aminophylline, decomposition in suppository formulations □ Decomposition—aminophylline in suppository formulations

During a study by the Food and Drug Administration which required the analysis of various dosage forms of xanthine derivative drugs, an aminophylline suppository formulation was encountered that unexpectedly failed to melt when heated in a beaker on a steam bath. In fact, the suppositories barely softened, and a composite was prepared for assay only with great difficulty. Analysis by the USP XIX method (1) showed that the suppository contained approximately the labeled amount of theophylline but considerably less than the compendial requirement for ethylenediamine. The suppository sample had been stored at room temperature for a month before analysis, so the original condition of the product was unknown.

An accelerated decomposition experiment was devised to study the phenomenon of hardening and to elucidate the decomposition that apparently had occurred. Ci-

0022-3549/80/0800-0942$01.00/0

© 1980, American Pharmaceutical Association

eszynski (2) had isolated the decomposition products from aged aminophylline suppositories and identified them as the amide reaction products of ethylenediamine with glyceryl esters of the fatty acids in cocoa butter and a suppository base composed of the triglycerides of C_{12}–C_{18} fatty acids[1]. Identification was based on extensive TLC, GLC, and IR spectral analyses of the isolated amides and of products synthesized from authentic materials.

Cieszynski (2) also conducted an accelerated decomposition experiment in which the decomposition reaction described was duplicated. He (2) did not give the melting characteristics of the decomposed suppositories or elemental analyses for the impurities found, but this information may be in one of his earlier papers, which was not available for translation.

The work of Cieszynski allowed this laboratory to concentrate its attention on a small group of possible decomposition compounds. The isolation and identification of the agents responsible for the hardening observed in the aminophylline suppositories are described here.

EXPERIMENTAL

Accelerated Decomposition Study—Fifty 500-mg aminophylline suppositories from another commercial sample of an identical formulation, which originally met all USP XIX requirements, were used. These samples had been stored at room temperature but melted readily on a steam bath and showed only a small loss of ethylenediamine by the USP XIX assay (1). One package of suppositories was stored at 0° during the experiment, and the remaining units were placed in a 40° convection oven. At intervals, four suppository units were removed from the oven. Two were placed in a refrigerator (0°), and the other two were assayed for theophylline (1) and ethylenediamine[2] content.

Isolation of Amide Decomposition Products—The suppository was dispersed in a beaker with 20–30 ml of isooctane[3] to dissolve the fatty base. The undissolved residue was collected on filter paper[4], and the residue was washed with two additional portions of isooctane. The residue on the filter was air dried and washed with two 20-ml portions of hot water to remove the aminophylline and any ethylenediamine or theophylline present. The washed residue was transferred to a beaker, 10 ml of chloroform[3] was added, and the mixture was heated to boiling. Ethanol (95%) was added dropwise until a clear solution was obtained.

The solution was placed in a refrigerator or freezer until crystallization occurred. The precipitate was collected on filter paper and washed with methanol[3]. The material was recrystallized successively from hot methanol and methanol–chloroform (1:1), and the crystals were air dried. Drying was completed in a 105° oven before the melting-point determination or IR scan.

Preparation of Authentic Individual or Mixed Fatty Acid Amides—*Method I (3): Synthesis from Fatty Acids*—Approximately 0.5 g of authentic fatty acid or the fatty acid mixture from saponified base was dissolved in 5 ml of chloroform, 0.2 ml of thionyl chloride was added, and the reaction mixture was cooled. Then 5 ml of chloroform containing 0.5 ml of ethylenediamine[5] (98%) was added slowly, and the mixture was refluxed for an additional 0.5 hr. The mixture was cooled and the precipitated product was collected by filtration. The residue was washed on the filter with methanol and allowed to air dry for ~0.5 hr.

Method II: Preparation from Glyceryl Esters of Fatty Acids—This reaction requires a 2:3 molar ratio of glyceryl ester to ethylenediamine. Approximately 7 g of suppository base was melted in a side-arm test tube and cooled until the onset of crystallization. One milliliter of ethylenediamine was added, and the reactants were mixed thoroughly with a magnetic stirrer. The test tube was fitted with a cold-finger condenser, and the tube was flushed with nitrogen.

The tube was heated in an oil bath, and the reaction mixture was stirred continuously under a nitrogen atmosphere as long as the magnetic bar was operable. The melt gradually became cloudy, and a semisolid appeared as a floating mass. The reaction was allowed to continue until complete solidification occurred. The amide was extracted and the reaction product was recrystallized as described for the isolation of amide decomposition products.

Saponification of Amides—The appropriate amide, 100–500 mg, was placed in a 50-ml round-bottom boiling flask, 10 ml of 20% KOH in propylene glycol was added, and the mixture was refluxed for 3 hr. Then the mixture was cooled, 10 ml of water was added, concentrated hydrochloric acid was added to acidify the solution, and the solution was cooled again. The solution was extracted with methylene chloride in a separator, and the organic phase was evaporated to dryness on a steam bath.

IR Spectra[6]—Sample spectra were prepared neat or as the trifluorovinyl chloride polymer[7] mull of the substance examined.

GLC (4)—The gas chromatograph[8] was equipped with a flame-ionization detector and a 3.05-mm i.d. nickel column[9]. The carrier gas was helium at a flow rate of 28 ml/min. The temperature was 250° for the column, injector, and detector.

Derivatization Procedure (Methylation)—(*m*-Trifluoromethylphenyl)trimethylammonium hydroxide[10], 200 μl, was added to 10 mg of the test substance, and the mixture was allowed to stand for 30 min in a covered vial.

Spectrophotometric Determination of Ethylenediamine in Suppositories[2]—The suppository, or a composite mixture equivalent to one unit, was dispersed in 95% ethanol, and the solution was carried through the automated procedure. The standard may be prepared from a previously analyzed aminophylline drug substance or the USP XIX reference standard. The method is specific for primary aliphatic and secondary cyclic amines.

TLC Identification of Amide Reaction Products—A portion of the reacted mixture was washed with three portions of cold isooctane. The residue was dissolved in boiling chloroform–methanol (1:1) and spotted on 75-mm silica gel plates[11]. Solutions of authentic aminophylline and of the diamide reaction product were spotted adjacent to the sample spots. The chromatogram was developed with chloroform–methanol (9:1) and viewed directly under UV light or by daylight after treatment with iodine vapor. Typical R_f values for aminophylline and the diamide are 0.45 and 0.60, respectively.

The isolation of the high-melting substance from the hardened suppositories was based on consideration of the solubility properties of aminophylline, theophylline, ethylenediamine, and the suppository base[12] used in this product.

The fatty base in the formulation was derived from coconut and palm kernel oils (5), which are rich in the glycerides of lauric and myristic acids, along with smaller amounts of the glycerides of oleic, palmitic, capric, and stearic acids (6). Myristic and palmitic acids were selected as representative of the group, and the pure substances were used for the preparation of authentic amide products by reaction with ethylenediamine after their conversion to acid chlorides.

Authentic suppository base also was used to prepare the amide product by direct reaction with ethylenediamine at 40 and 100°. The higher temperature was used to expedite the reaction and to increase the yield of amide. This experiment was repeated using aminophylline. In all experiments, IR spectrophotometry and TLC were used to monitor the final stages of the amide syntheses.

A portion of the purified high-melting substance isolated from the original, decomposed suppositories and a portion of the synthetic amide mixture prepared from the authentic suppository base were saponified to obtain the free acid mixture from each. These mixtures, another portion of suppository base, and individual lauric, myristic, palmitic, stearic, and oleic acid samples were derivatized and chromatographed by GLC for comparison of acid content.

RESULTS AND DISCUSSION

The results accumulated after storage of the samples at 40° for 3 months showed a progressive diminution of the ethylenediamine content, as measured by both colorimetric amine[2] and USP XIX titration (1)

[1] Witespol.
[2] P. A. McCullen, National Center for Drug Analysis, personal communication.
[3] Glass-distilled isooctane, chloroform, and methanol were used throughout the study.
[4] Whatman No. 1.
[5] Mallinckrodt.
[6] Perkin-Elmer model 337 spectrophotometer.
[7] Fluorolube.
[8] Hewlett-Packard model 5830A.
[9] Packed with 10% Silar-10C on Gas Chrom Q, Applied Science Laboratories, State College, Pa.
[10] Applied Science Laboratories, State College, Pa.
[11] No. 60F-254, E. Merck, Darmstadt, West Germany.
[12] Wecobee M.

Table I—Assay Results on Individual Suppository Units after Incubation at 40°

Elapsed Time, months	Ethylenediamine, % of aminophylline	Aminophylline, % of declared
0 (original analysis)	12.6	100.2[a]
1.0 (start of study)	11.8	100.0
1.5	11.9	102.0
2.0	8.9	95.8
3.5	0	99.2
4.0	0	93.2

[a] Average of six individual suppository assays; results ranged from 97.8 to 106.9%.

methods. The theophylline content showed little or no loss until late in the study (Table I).

The suppositories hardened during the accelerated decomposition experiment, but the increase in their melting point was not readily discernible until the melting point exceeded the steam bath temperature. The accelerated decomposition study had been in progress for 10 weeks by this time, and the ethylenediamine assay results were zero.

A large amount of a white, waxy substance, mp 145–147°, was isolated from the original sample of hardened suppositories. The high melting point of this substance could easily account for the refractory behavior of the suppositories at steam bath temperatures.

The IR spectrum of the trifluorovinyl chloride polymer mull of the dried, extracted material exhibited the following absorption bands: 3290 (NH stretch, amide), 3120 (NH stretch, purine from theophylline), 2930, 2850 (CH_2 symmetrical and unsymmetrical stretch), 1740 (C=O stretch, ester from fatty base), and 1640 (C=O stretch, amide) cm^{-1}. The interpretation was made with the aid of additional IR spectra of the neat suppository base[12], neat ethylenediamine, and the trifluorovinyl chloride polymer mulls of a refrigerated suppository fragment, trimyristin, and the reaction product of myristic acid and ethylenediamine *via* myristoil chloride.

The IR spectrum of the isolated high-melting product is consistent with that of a mixture of an alkyl amide and an alkyl ester (7) and includes all of the principal bands found by Cieszynski (2) in his spectra of amide decomposition products. An alkyl ester band found at 1750 cm^{-1} in the spectrum is believed to be due to unreacted suppository base since the band was absent in the spectrum obtained from the substance recrystallized from hot methanol. A minor NH amide band at 3290 cm^{-1} was found in the spectrum of the refrigerated suppository, which indicates that a small amount of decomposition may have occurred during storage after the original analysis; this observation accounts for the small reduction in the ethylenediamine content of the suppositories between the time of the original analysis and the start of the study.

The recrystallized *N,N'*-(1,2-ethanediyl)bisamides, synthesized from myristic and palmitic acids, had melting points of 150–152° and 147.5–148.0°, respectively, and gave IR spectra that showed the same prominent bands at 3290 and 1640 cm^{-1} that had been obtained from the high-melting substance previously isolated from the suppository.

The purified substance, obtained by direct reaction of myristin and ethylenediamine, melted at 148.5–150° and showed the same prominent IR bands at 3290 and 1640 cm^{-1}.

The spectra of the amide products that had been synthesized directly from aminophylline exhibited strong bands at 3290 and 1640 cm^{-1}, confirming the generation of an amide product by a reaction between aminophylline and the suppository base.

The distribution of fatty acid peaks found by GLC of the substance isolated from the suppositories was the same in kind and rank order as that of the authentic suppository base, confirming the source of the acyl components of the amides (Table II). It was not expected that the ratio percentage of each acid would be the same in both, because the suppository base material is derivatized directly whereas the amide must be saponified and the acids must be extracted before derivatization and GLC.

Table II—Fatty Acid Composition (Percent) of Products Analyzed by GLC

Product	Lauric	Myristic	Palmitic	Stearic	Oleic
Synthetic diamide mixture	45.0	18.2	10.6	26.0	0.2
Suppository base	43.8	17.9	11.1	24.7	2.3
High-melting substance	37.0	18.2	13.4	31.2	0.2

Table III—Elemental Composition of Analyzed Products[a]

Product	C	H	N	Melting Point
Isolated diamide mixture	74.49	12.67	5.84	148.5–149.5°
Synthetic diamide mixture	74.05	12.33	5.73	148.5–150.0°
Calculated for diamide mixture	74.93	12.55	5.79	
Synthetic bispalmitamide	76.21	13.41	5.04	147.5–148.0°
Calculated for *N,N'*-(1,2-ethanediyl)bis-palmitamide	76.06	12.77	5.21	

[a] Based on ratio percent distribution of fatty acids found in suppository base by GLC, expressed as bisamides.

The amide decomposition products isolated from the suppositories are believed to be the 1,2-ethanediamides based on the following experimental evidence. A single stretching band was found at 3290 cm^{-1}. If any primary amide were present, a doublet would have been seen in the region of 3300–3500 cm^{-1} in the IR spectrum. No color reaction was seen with the 2,3-dichloro-1,4-naphthoquinone reagent (8). No monoamide precipitated upon neutralization of the hydrochloric acid extract of the solid material. There was no blue color change when the spot separated by TLC was sprayed with bromcresol green.

Additional confirmation of the presence of diamides was obtained by quantitative elemental microanalyses[13] (Table III).

The results obtained in this study confirm the finding of Cieszynski (2) that the ethylenediamine moiety of aminophylline is capable of reacting with the glyceryl esters of some suppository bases to form insoluble, high-melting amide decomposition products. In a concurrent study conducted in this laboratory, a chemically similar decomposition occurred in rectal theophylline ethanolamine solutions preserved with parabens[14].

The reactions were carried out with authentic materials under conditions likely to exist during the commercial manufacture of suppositories. The reaction between the suppository base and free ethylenediamine at 40° began within 1 hr under an atmosphere of nitrogen, which also showed that prior rancidity was not a necessary condition for the formation of amide products. The reaction of the suppository base with aminophylline at 40° was much slower. Conditions that initiate the reaction, other than heat, have not been determined.

The significance of these results becomes apparent when the manufacturing process for suppositories (3) is examined. Aminophylline is stirred into molten suppository base; the melt is poured into heated molds and slowly cooled to minimize the formation of an unwanted α-state of the base. The maximum batch temperature exceeds 50° for a short time before the addition of drug substance and is kept just above the melting point of the base during pouring. The total elapsed heating time may last up to 1 day, depending on the size of the batch.

The manufacturing process could result in the formation of amide reaction products if temperature and process times are not controlled carefully, especially for the units poured at the end of a large batch run. The same reaction takes place slowly if the finished suppositories are not kept refrigerated, especially under summer temperatures.

A limited number of current commercial products was examined by IR spectrophotometry, which showed the presence of small quantities of amide reaction products. These products were indicated by a weak amide band at 3290 cm^{-1} and a shoulder at 1640 cm^{-1} in most of these spectra. The formulations containing hydrogenated coconut and palm kernel oil mixtures appear to be the most susceptible to decomposition. This observation may be due to the manufacturing process or it may be inherent in the product.

An IR limit test for 1,2-ethanediamides or a melting-point test is recommended for inclusion in the USP monograph for aminophylline suppositories.

REFERENCES

(1) "The United States Pharmacopeia," 19th rev., Mack Publishing Co., Easton, Pa., 1975.

(2) T. Cieszynski, *Acta Pol. Pharm.*, **32**, 371 (1975); through *Chem. Abstr.*, **84**, 79658m (1976).

[13] Galbraith Laboratories, Knoxville, Tenn.

[14] D. F. Gurka, M. A. Kreienbaum, and E. C. Juenge, National Center for Drug Analysis, unpublished results.

(3) R. L. Shriner and R. C. Fuson, "The Systematic Identification of Organic Compounds," 5th ed., Wiley, New York, N.Y., 1964.
(4) D. K. McCreary, W. C. Kossa, S. Ramachandran, and R. R. Kurtz, *J. Chromatogr. Sci.*, **16**, 329 (1978).
(5) "The Wecobee Bases, Cosmetic and Pharmaceutical Applications," PVO International, Boonton, N.J., 1979.
(6) E. W. Eckey, "Vegetable Fats and Oils," Reinhold, New York, N.Y., 1954.
(7) R. M. Silverstein and G. C. Bassler, "Spectrophotometric Identification of Organic Compounds," 2nd ed., Wiley, New York, N.Y., 1967.
(8) A. A. Abou-Ouf, A. M. Taha, and M. B. S. Hom, *J. Pharm. Sci.*, **62**, 1700 (1973).

ACKNOWLEDGMENTS

The analyses of the suppositories in the accelerated decomposition study were performed by M. A. Kreienbaum, P. A. McCullen, and T. W. Moore. W. B. Furman provided assistance and valuable suggestions in the preparation of this paper.

Oxidative Degradation of Hydrocortisone in Presence of Attapulgite

JUAN CORNEJO *, MARIA C. HERMOSIN *, JOE L. WHITE *, GARNET E. PECK ‡, and STANLEY L. HEM ‡x

Received November 1, 1979, from the **Department of Agronomy and the* ‡*Department of Industrial and Physical Pharmacy, Purdue University, West Lafayette, IN 47907.* Accepted for publication March 12, 1980.

Abstract □ Degradation of hydrocortisone in attapulgite suspensions was monitored by high-pressure liquid chromatography and UV spectrophotometry. The rate of oxidative degradation of hydrocortisone was accelerated significantly in the presence of attapulgite. In addition, degradation appeared to be composed of two apparent first-order reactions rather than the single apparent first-order degradation reaction observed for hydrocortisone solutions. However, the same degradation products were obtained in both hydrocortisone solutions and attapulgite suspensions, indicating that interaction with attapulgite did not alter the degradation pathway. Kinetic and adsorption studies suggested that hydrocortisone is adsorbed weakly by attapulgite and undergoes oxidative degradation, which is catalyzed by adsorbed iron oxides or hydroxides as well as by structural ferric iron at the clay surface. Since clay minerals generally contain surface ferric iron, the potential for accelerating the oxidative degradation of drugs should be considered whenever clays and drugs are combined.

Keyphrases □ Attapulgite—effect on hydrocortisone degradation, kinetic and adsorption studies □ Hydrocortisone—oxidative degradation in attapulgite suspensions □ High-pressure liquid chromatography—monitoring of degradation of hydrocortisone in attapulgite suspensions □ Adsorption—hydrocortisone onto attapulgite, oxidative degradation of hydrocortisone

A recent study of the interaction of montmorillonite with digoxin revealed that the clay surface, through its ability to concentrate both digoxin and protons, accelerated the acid-catalyzed hydrolysis of digoxin and suggested that other neutral drugs which are degraded by acid-catalyzed hydrolysis may be affected similarly by interaction with a clay (1). Since oxidation also is a major mechanism of drug degradation, a study was undertaken to determine if interaction with a clay surface could result in accelerated oxidative degradation.

BACKGROUND

Montmorillonite, a member of the smectite group of clays, promotes the oxidation of a number of organic compounds, including the conversion of pyrogallol to quinones of poorly defined structure (2), of dihydroxyquinones to *p*-benzoquinone (3), and of benzidine to a blue monovalent semiquinone (4). In addition, hectorite, a clay belonging to the same structural group as montmorillonite, catalyzes the oxidation of benzidine (5, 6). Surface-adsorbed contaminants or structural ferric iron at the clay surface have been suggested as being responsible for the oxidation of organic materials by these clays.

Attapulgite was chosen for this study because: (*a*) it belongs to the fibrous group of minerals whose effect on oxidative degradation has not been studied extensively, (*b*) the oxidizing action of Fe^{3+} in attapulgite has been demonstrated (7), and (*c*) it is used in pharmaceuticals as a GI adsorbent (8) or excipient. Hydrocortisone was chosen as the model drug because it is known to degrade by oxidation, it may be coadministered orally with a clay-containing pharmaceutical, and it is used in topical dosage forms that also may contain a clay.

Degradation of the C-17 dihydroxyacetone side chain of corticosteroids has been studied extensively (9–13). Transformations and elimination of the side chain occur in both the presence and the absence of oxygen (12). However, autoxidation appears to be the major mechanism of degradation of corticosteroids in pharmaceutical dosage forms (12).

Factors influencing the degradation of prednisolone in aqueous solution were investigated, and trace metals present as contaminants in the buffer reagents were indicated as the cause of accelerated degradation (11).

EXPERIMENTAL

Materials—All chemicals were official or reagent grade. Attapulgite was obtained commercially[1]. X-ray diffraction of the clay sample confirmed that attapulgite was the major mineral but that a small amount of quartz also was present.

The effect of surface ferric iron was studied by treating the attapulgite by the citrate–dithionite procedure (14), which extracts nonstructural iron from the clay surface. The iron extracted was quantified by the *o*-phenanthroline method (15), and the total iron content was determined by the hydrofluoric acid dissolution procedure (16).

Hydrocortisone Assay—A high-pressure liquid chromatographic (HPLC) method, which was recommended for the analysis of hydrocortisone tablets (17), was modified slightly for this study. The liquid chromatograph[2] was equipped with a UV detector operating at 254 nm and a 20-μl injector loop[3]. A commercially packed octadecylsilane[4] column was used with acetonitrile–water (35:65) as the mobile phase. The operating parameters were: flow rate, 1 ml/min; pressure, 1000–1200 psi; temperature, ambient; and UV attenuator, 0.02 aufs. Linear calibration curves were used to quantify hydrocortisone, while the relative concentration of the observed degradation products was characterized by peak heights.

Changes in the A-ring of hydrocortisone were monitored by UV spectrometry at 254 nm.

Self-supporting films were prepared for IR analysis[5] by pipetting appropriate volumes of either the attapulgite or the hydrocortisone–atta-

[1] Pharmabsorb, colloidal, Engelhard Minerals and Chemicals Corp., Menlo Park, N.J.
[2] Model ALC 202, Waters Associates, Framingham, Mass.
[3] Rheodyne, Berkeley, Calif.
[4] Partisil-10 ODS, Whatman Inc., Clifton, N.J.
[5] Model 180, Perkin-Elmer Corp., Norwalk, Conn.

0022-3549/80/0800-0945$01.00/0
© 1980, American Pharmaceutical Association

(3) R. L. Shriner and R. C. Fuson, "The Systematic Identification of Organic Compounds," 5th ed., Wiley, New York, N.Y., 1964.
(4) D. K. McCreary, W. C. Kossa, S. Ramachandran, and R. R. Kurtz, *J. Chromatogr. Sci.*, **16**, 329 (1978).
(5) "The Wecobee Bases, Cosmetic and Pharmaceutical Applications," PVO International, Boonton, N.J., 1979.
(6) E. W. Eckey, "Vegetable Fats and Oils," Reinhold, New York, N.Y., 1954.
(7) R. M. Silverstein and G. C. Bassler, "Spectrophotometric Identification of Organic Compounds," 2nd ed., Wiley, New York, N.Y., 1967.
(8) A. A. Abou-Ouf, A. M. Taha, and M. B. S. Hom, *J. Pharm. Sci.*, **62**, 1700 (1973).

ACKNOWLEDGMENTS

The analyses of the suppositories in the accelerated decomposition study were performed by M. A. Kreienbaum, P. A. McCullen, and T. W. Moore. W. B. Furman provided assistance and valuable suggestions in the preparation of this paper.

Oxidative Degradation of Hydrocortisone in Presence of Attapulgite

JUAN CORNEJO *, MARIA C. HERMOSIN *, JOE L. WHITE *, GARNET E. PECK ‡, and STANLEY L. HEM ‡x

Received November 1, 1979, from the **Department of Agronomy and the* ‡*Department of Industrial and Physical Pharmacy, Purdue University, West Lafayette, IN 47907.* Accepted for publication March 12, 1980.

Abstract □ Degradation of hydrocortisone in attapulgite suspensions was monitored by high-pressure liquid chromatography and UV spectrophotometry. The rate of oxidative degradation of hydrocortisone was accelerated significantly in the presence of attapulgite. In addition, degradation appeared to be composed of two apparent first-order reactions rather than the single apparent first-order degradation reaction observed for hydrocortisone solutions. However, the same degradation products were obtained in both hydrocortisone solutions and attapulgite suspensions, indicating that interaction with attapulgite did not alter the degradation pathway. Kinetic and adsorption studies suggested that hydrocortisone is adsorbed weakly by attapulgite and undergoes oxidative degradation, which is catalyzed by adsorbed iron oxides or hydroxides as well as by structural ferric iron at the clay surface. Since clay minerals generally contain surface ferric iron, the potential for accelerating the oxidative degradation of drugs should be considered whenever clays and drugs are combined.

Keyphrases □ Attapulgite—effect on hydrocortisone degradation, kinetic and adsorption studies □ Hydrocortisone—oxidative degradation in attapulgite suspensions □ High-pressure liquid chromatography—monitoring of degradation of hydrocortisone in attapulgite suspensions □ Adsorption—hydrocortisone onto attapulgite, oxidative degradation of hydrocortisone

A recent study of the interaction of montmorillonite with digoxin revealed that the clay surface, through its ability to concentrate both digoxin and protons, accelerated the acid-catalyzed hydrolysis of digoxin and suggested that other neutral drugs which are degraded by acid-catalyzed hydrolysis may be affected similarly by interaction with a clay (1). Since oxidation also is a major mechanism of drug degradation, a study was undertaken to determine if interaction with a clay surface could result in accelerated oxidative degradation.

BACKGROUND

Montmorillonite, a member of the smectite group of clays, promotes the oxidation of a number of organic compounds, including the conversion of pyrogallol to quinones of poorly defined structure (2), of dihydroxyquinones to *p*-benzoquinone (3), and of benzidine to a blue monovalent semiquinone (4). In addition, hectorite, a clay belonging to the same structural group as montmorillonite, catalyzes the oxidation of benzidine (5, 6). Surface-adsorbed contaminants or structural ferric iron at the clay surface have been suggested as being responsible for the oxidation of organic materials by these clays.

Attapulgite was chosen for this study because: (*a*) it belongs to the fibrous group of minerals whose effect on oxidative degradation has not been studied extensively, (*b*) the oxidizing action of Fe^{3+} in attapulgite has been demonstrated (7), and (*c*) it is used in pharmaceuticals as a GI adsorbent (8) or excipient. Hydrocortisone was chosen as the model drug because it is known to degrade by oxidation, it may be coadministered orally with a clay-containing pharmaceutical, and it is used in topical dosage forms that also may contain a clay.

Degradation of the C-17 dihydroxyacetone side chain of corticosteroids has been studied extensively (9–13). Transformations and elimination of the side chain occur in both the presence and the absence of oxygen (12). However, autoxidation appears to be the major mechanism of degradation of corticosteroids in pharmaceutical dosage forms (12).

Factors influencing the degradation of prednisolone in aqueous solution were investigated, and trace metals present as contaminants in the buffer reagents were indicated as the cause of accelerated degradation (11).

EXPERIMENTAL

Materials—All chemicals were official or reagent grade. Attapulgite was obtained commercially[1]. X-ray diffraction of the clay sample confirmed that attapulgite was the major mineral but that a small amount of quartz also was present.

The effect of surface ferric iron was studied by treating the attapulgite by the citrate–dithionite procedure (14), which extracts nonstructural iron from the clay surface. The iron extracted was quantified by the *o*-phenanthroline method (15), and the total iron content was determined by the hydrofluoric acid dissolution procedure (16).

Hydrocortisone Assay—A high-pressure liquid chromatographic (HPLC) method, which was recommended for the analysis of hydrocortisone tablets (17), was modified slightly for this study. The liquid chromatograph[2] was equipped with a UV detector operating at 254 nm and a 20-μl injector loop[3]. A commercially packed octadecylsilane[4] column was used with acetonitrile–water (35:65) as the mobile phase. The operating parameters were: flow rate, 1 ml/min; pressure, 1000–1200 psi; temperature, ambient; and UV attenuator, 0.02 aufs. Linear calibration curves were used to quantify hydrocortisone, while the relative concentration of the observed degradation products was characterized by peak heights.

Changes in the A-ring of hydrocortisone were monitored by UV spectrometry at 254 nm.

Self-supporting films were prepared for IR analysis[5] by pipetting appropriate volumes of either the attapulgite or the hydrocortisone–atta-

[1] Pharmabsorb, colloidal, Engelhard Minerals and Chemicals Corp., Menlo Park, N.J.
[2] Model ALC 202, Waters Associates, Framingham, Mass.
[3] Rheodyne, Berkeley, Calif.
[4] Partisil-10 ODS, Whatman Inc., Clifton, N.J.
[5] Model 180, Perkin-Elmer Corp., Norwalk, Conn.

0022-3549/80/0800-0945$01.00/0
© 1980, American Pharmaceutical Association

Table I—Stability of Hydrocortisone in Presence of Attapulgite

Temperature	Aqueous Solution at pH 8.4, k_1, hr^{-1}	Attapulgite Suspension[a] at pH 8.4		Dithionite-Citrate-Treated Attapulgite Suspension[a] at pH 8.4	
		k_1, hr^{-1}	k_2, hr^{-1}	k_1, hr^{-1}	k_2, hr^{-1}
23°	—[b]	20.2×10^{-3}	4.4×10^{-3}	8.10×10^{-3}	2.3×10^{-3}
38°	—[b]	25.7×10^{-3}	8.3×10^{-3}	—	—
50°	0.8×10^{-3}	67.0×10^{-3}	14.3×10^{-3}	—	—
69°	1.5×10^{-3}	93.6×10^{-3}	22.2×10^{-3}	—	—

[a] For comparative purposes, the complex degradation pattern of hydrocortisone in attapulgite suspension was treated as consisting of an initial first-order phase characterized by k_1, which was followed by a slower, first-order phase characterized by k_2. [b] No measurable degradation of hydrocortisone occurred in 180 hr.

pulgite suspension onto polyethylene terephthalate[6] and air drying them at room temperature (18).

Hydrocortisone was prepared for IR analysis as a potassium bromide pellet.

Kinetic Studies—The attapulgite concentration was selected as representative of the range of clay usually used in pharmaceuticals; the hydrocortisone concentration was below the solubility limit, 280 μg/ml at 25° (19), to ensure complete solubility during the kinetic studies. Thus, 360 mg of attapulgite was mixed with 30 ml of an aqueous solution of hydrocortisone (200 μg/ml) in a 50-ml stoppered centrifuge tube. The samples were aged in a constant-temperature shaker bath at 23, 38, 50, or 69°. At appropriate intervals, aliquots were centrifuged at 6000 rpm, and the supernate was filtered[7] and analyzed by HPLC.

The pH of each suspension was measured and found to be 8.4 at each sampling interval.

Aqueous solutions of hydrocortisone (200 μg/ml), adjusted to pH 8.4 with sodium hydroxide, were aged with the drug–clay suspensions and served as controls.

The supernate from a suspension of 360 mg of attapulgite in 30 ml of water was filtered and used to prepare a hydrocortisone solution (200 μg/ml). The stability of hydrocortisone in this solution was monitored during aging at 23°.

A hydrocortisone–attapulgite suspension was monitored for 1 week while aging at 23°. After 1 week, the solid phase (attapulgite) was separated by centrifugation and washed three times with distilled water. The washed attapulgite was used to prepare a fresh hydrocortisone–attapulgite suspension whose stability at 23° was monitored as described.

RESULTS AND DISCUSSION

Hydrocortisone exhibited very slow degradation in aqueous solution at pH 8.4, which is consistent with previously reported stability results (20). A hydrocortisone solution at pH 8.4 was monitored every 2 days for 42 days while aging at 69°. During this time, the hydrocortisone concentration decreased from 200 to 33 μg/ml. A plot of log hydrocortisone concentration *versus* time gave a straight line ($r = 0.981$), indicating that degradation of hydrocortisone in solution at pH 8.4 occurs by apparent first-order kinetics (Table I). Earlier reports (9–12) suggested that hydrocortisone degrades by apparent first-order kinetics, although Pitman *et al.* (20) used the tetrazolium assay and observed complex kinetics for the degradation of hydrocortisone in 0.05 *M* NaOH.

Hydrocortisone degraded rapidly in the presence of attapulgite at pH 8.4. For example, the hydrocortisone content of an attapulgite suspension at pH 8.4 decreased from 200 to 100 μg/ml after aging at 23° for ~2 days (Fig. 1). During the same period, the hydrocortisone content of an aqueous solution at pH 8.4 and 23° remained at 200 μg/ml (Table I). The relationship between the hydrocortisone concentration or the logarithm of the hydrocortisone concentration and time was not linear at any temperature studied. To characterize the hydrocortisone degradation rate for comparative purposes, the degradation profile (Fig. 1) was treated as consisting of an initial first-order phase, characterized by k_1 which was followed by a slower, first-order phase characterized by k_2 (Table I).

This approach appears to be justified since both k_1 and k_2 followed the Arrhenius equation and the activation energy for the degradation of hydrocortisone was the same regardless of whether it was calculated from k_1 or k_2 (*i.e.*, 7.13 and 7.16 kcal/mole, respectively).

When the solubility of hydrocortisone was monitored by UV spectrophotometry, no change in absorbance at 254 nm was observed in the control solutions. Similarly, except for a small initial decrease, no change in absorbance at 254 nm was observed when the hydrocortisone–attapulgite suspensions were aged at 23, 38, 50, and 69° (Fig. 1). These results indicate that the degradation of hydrocortisone in the control solutions and the attapulgite suspensions occurred by oxidation of the 17-dihydroxyacetone side chain rather than by photolytic decomposition of the A-ring. The initial decrease in UV absorbance at 254 nm in the presence of attapulgite may be due to a small degree of adsorption of hydrocortisone by the clay.

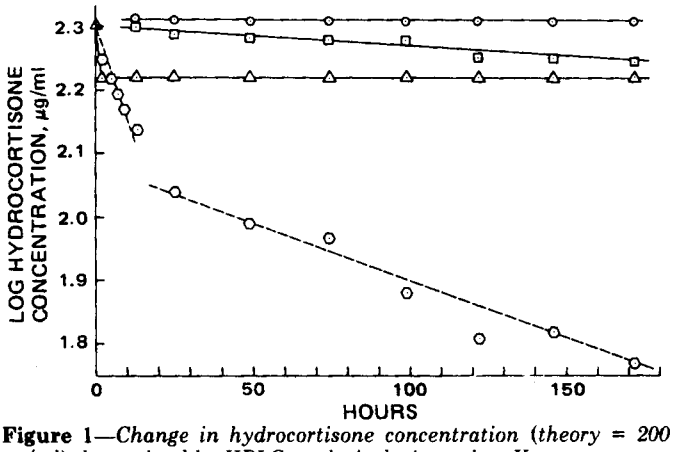

Figure 1—*Change in hydrocortisone concentration (theory = 200 μg/ml) determined by HPLC analysis during aging. Key: □, aqueous solution at pH 8.4 and 50°; ○, solution in supernate from attapulgite suspension at 38°; ○, attapulgite suspension at pH 8.4 and 23°; and △, hydrocortisone concentration of attapulgite suspension at pH 8.4 and 23° determined by UV absorbance at 254 nm.*

The same degradation pathway of hydrocortisone was observed in both the presence and the absence of attapulgite. Other investigators (9, 12) reported two degradation products for prednisolone: a small amount of a neutral keto product and a larger quantity of acidic material. Olson (21) also reported two peaks in addition to hydrocortisone during the HPLC analysis of hydrocortisone in alkaline media.

Figure 2A shows the three peaks observed in the high-pressure liquid chromatograms at 23, 38, and 50°. The peak having a retention time of

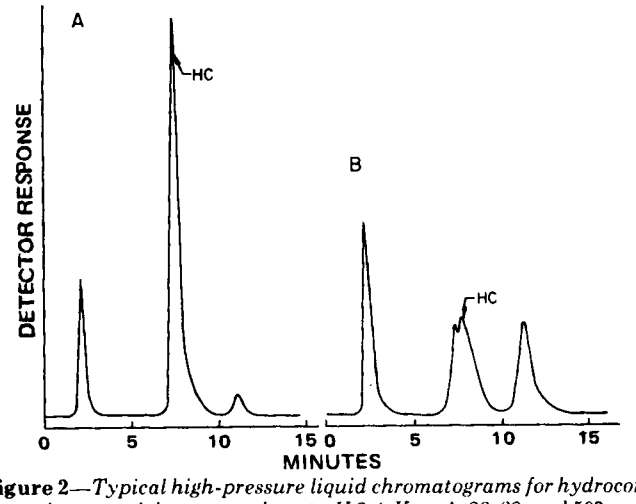

Figure 2—*Typical high-pressure liquid chromatograms for hydrocortisone in attapulgite suspension at pH 8.4. Key: A, 23, 38, and 50°; and B, 69°; HC represents the hydrocortisone peak.*

[6] Mylar.
[7] No. 42, Whatman Inc., Clifton, N.J.

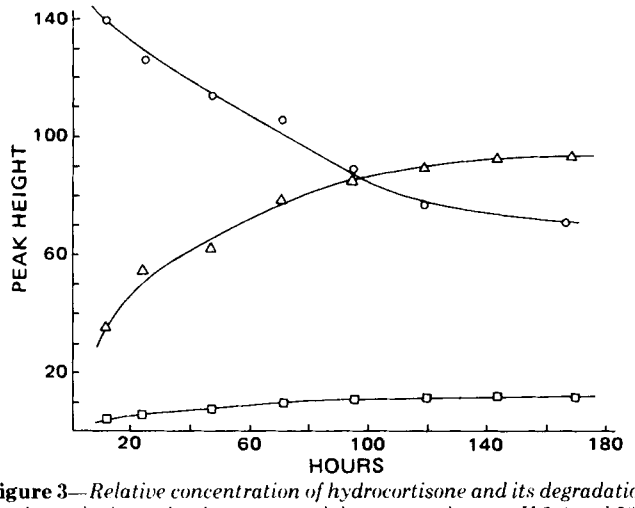

Figure 3—*Relative concentration of hydrocortisone and its degradation products during aging in an attapulgite suspension at pH 8.4 and 23°. Key: ○, hydrocortisone; △, acidic degradation product with retention time of 2.5 min; and □, neutral degradation product with retention time of 11 min.*

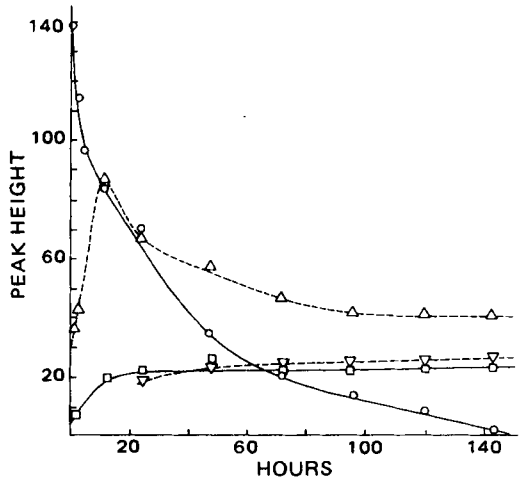

Figure 4—*Relative concentration of hydrocortisone and its degradation products during aging in an attapulgite suspension at pH 8.4 and 69°. Key: ○, hydrocortisone; △, acidic degradation product with retention time of 2.5 min; □, neutral degradation product with retention time of 11 min; and ▽, unknown degradation product with retention time of 7 min.*

8 min corresponded to the hydrocortisone reference standard. No attempt was made to identify the other two peaks. However, the degradation profile seen in Fig. 3 suggests that compounds with retention times of 2.5 and 11 min arise directly from hydrocortisone and that the former compound is the acidic product while the latter compound is the neutral product noted in previous studies. Similar degradation profiles were obtained at 38 and 50°.

A third degradation product having a retention time of 7 min was observed at 69° (Fig. 2B). This compound did not appear until the hydrocortisone was substantially degraded. The third degradation product began to appear after the degradation product with a retention time of 2.5 min (acidic product) reached its maximum concentration (Fig. 4). This type of degradation profile suggests that the third degradation product arises from further decomposition of the acidic product.

The increased degradation rate of hydrocortisone in an attapulgite suspension is not due to any soluble impurity or extractable component of attapulgite since virtually no degradation of hydrocortisone occurred in a solution prepared using the supernate from an attapulgite suspension (Fig. 1). Thus, the accelerated degradation of hydrocortisone in attapulgite suspensions requires contact with the clay surface.

It was hypothesized that oxidation of the C-17 side chain was the mechanism responsible for the accelerated degradation and that the source of the oxidizing action occurring at the surface of attapulgite was ferric iron. Surface ferric iron in attapulgite, as in other clay minerals, may exist either as surface-adsorbed iron oxides or hydroxides or as structural ferric iron, which is located mainly in the octahedral sites of attapulgite. To verify this hypothesis, a portion of attapulgite was treated by the citrate–dithionite method to extract nonstructural ferric iron. The amount of ferric iron extracted was 0.62 mg/g, which represents 2.3% of the total iron (26.6 mg/g) in the sample. Hydrocortisone was much more stable in a suspension of the treated attapulgite, although the degradation was substantially greater than that occurring in aqueous hydrocortisone solutions. The degradation profile did not fit either zero- or first-order kinetics; for comparison, it also was treated as consisting of two first-order phases (Table I). The twofold reduction in the degradation rate of hydrocortisone when surface ferric iron was removed from the attapulgite indicates that nonstructural ferric iron catalyzes the degradation of hydrocortisone. However, structural ferric iron probably also is involved in the catalysis since accelerated degradation occurred in the presence of treated attapulgite.

The IR spectrum of the hydrocortisone–attapulgite suspension did not show any evidence of adsorption of hydrocortisone. However, the small initial decrease in the hydrocortisone content of the supernate of a hydrocortisone–attapulgite suspension (Fig. 1) suggests that hydrocortisone is adsorbed weakly by attapulgite and undergoes oxidative degradation, which is catalyzed by both nonstructural and structural ferric iron at the clay surface.

The catalytic potential of attapulgite appears to be readily regenerated. The degradation rate of hydrocortisone in an attapulgite suspension was determined at 23° (Table I). The attapulgite was recovered and, after washing, was used to prepare a fresh hydrocortisone–attapulgite suspension. The rate profile and k_1 and k_2 values were identical to the results obtained for the original suspension.

It is hypothesized that the two-phase degradation reaction of hydrocortisone observed in the presence of attapulgite may be an indication that two kinds of sites for iron exist in attapulgite. As the oxidizing potential of the more accessible sites is exhausted, the degradation rate decreases.

The rate of diffusion of oxygen to the iron sites may be the rate-limiting factor. In this case, the rapid, initial degradation of hydrocortisone causes the oxidative potential of the iron sites to be exhausted. The regeneration of the sites is limited by the diffusion of oxygen to the sites, and a slower second phase is observed.

A third possible mechanism that may produce the two-phase degradation profile could occur if the hydrocortisone degradation products are adsorbed more strongly by attapulgite than hydrocortisone and preempt the catalytic sites on attapulgite. The two phases also may arise if both an oxidative and a nonoxidative degradation reaction occurs at the C-17 side chain.

Since clay minerals generally contain surface ferric iron, the potential for accelerating the oxidative degradation of drugs should be considered whenever clays and drugs are combined.

REFERENCES

(1) L. S. Porubcan, G. S. Born, J. L. White, and S. L. Hem, *J. Pharm. Sci.*, **68**, 358 (1979).

(2) K. Kumada and H. Kato, *Soil Sci. Plant Nutr.*, **16**, 195 (1970).

(3) T. D. Thompson and W. F. Moll, Jr., *Clays Clay Miner.*, **21**, 337 (1973).

(4) B. K. G. Theng, "The Chemistry of Clay-Organic Reactions," Adam Hilger, London, England, 1974, pp. 263, 264.

(5) D. H. Solomon, B. C. Loft, and A. J. Swift, *Clay Miner.*, **7**, 389 (1968).

(6) M. B. McBride, *Clays Clay Miner.*, **27**, 224 (1979).

(7) J. G. Miller, W. L. Haden, Jr., and T. D. Oulton, in "Proceedings of the Twelfth National Conference on Clays and Clay Minerals," W. F. Bradley, Ed., National Academy of Sciences–National Research Council, Atlanta, Ga., 1963, pp. 381–395.

(8) "Handbook of Nonprescription Drugs," 5th ed., American Pharmaceutical Association, Washington, D.C., 1977, p. 31.

(9) T. Chulski and A. A. Forist, *J. Am. Pharm. Assoc., Sci. Ed.*, **47**, 553 (1958).

(10) E. H. Jensen and D. J. Lamb, *J. Pharm. Sci.*, **53**, 402 (1964).

(11) T. O. Oesterling and D. E. Guttman, *ibid.*, **53**, 1189 (1964).

(12) D. E. Guttman and P. D. Meister, *J. Am. Pharm. Assoc., Sci. Ed.*, **47**, 773 (1958).

(13) E. Caspi, W. Schmid, and T. A. Wittstruk, *Tetrahedron*, **16**, 271 (1961).

(14) M. L. Jackson, "Soil Chemical Analysis—Advanced Course," 2nd ed., University of Wisconsin, Madison, Wis., 1969, p. 44.

(15) *Ibid.*, p. 57.
(16) C. B. Roth, M. L. Jackson, E. G. Lotse, and J. K. Syers, *Isr. J. Chem.*, **6**, 261 (1968).
(17) "Analysis of Pharmaceutical Products," Waters Associates, Milford, Mass., 1976, p. 9.
(18) L. S. Porubcan, C. J. Serna, J. L. White, and S. L. Hem, *J. Pharm. Sci.*, **67**, 1081 (1978).
(19) "The Merck Index," 9th ed., Merck & Co., Inc., Rahway, N.J., 1976, p. 629.
(20) I. H. Pitman, T. Higuchi, M. Alton, and R. Wiley, *J. Pharm. Sci.*, **61**, 918 (1972).
(21) M. C. Olson, *ibid.*, **62**, 2001 (1973).

ACKNOWLEDGMENTS

J. Cornejo gratefully acknowledges the support of the United States–Spanish Joint Committee for Scientific and Technical Cooperation.

This report is Journal Paper 7952, Purdue University Agricultural Experiment Station, West Lafayette, IN 47907.

Quantitative Semiautomated Colorimetric Determination of Thyroid (Iodine) in Thyroid Tablets

E. D. McGARY

Received October 1, 1979, from the *Food and Drug Administration, Department of Health, Education, and Welfare, Kansas City, MO 64106.* Accepted for publication March 21, 1980.

Abstract □ A faster, simpler, more sensitive, and semiautomated method was developed for the analysis of thyroid in individual thyroid tablets and composite samples. The sample is combusted in a Schoniger flask in an oxygen atmosphere, and the liberated iodine is trapped in a dilute sodium hydroxide solution. The solution is acidified with sulfuric acid (1:1), and the iodine is determined colorimetrically using a suitable spectrophotometer equipped with an automated analyzer. The proposed methodology was applied to tablets containing 32.4–324 mg of thyroid. Recoveries ranged from 90.0 to 125.0% of the amount of iodine added as potassium iodide. The proposed method is sensitive to 2.5 ng of iodine/ml.

Keyphrases □ Thyroid—semiautomated colorimetric analysis in individual tablets □ Iodine—semiautomated colorimetric analysis in individual thyroid tablets □ Colorimetry—analysis, thyroid in individual thyroid tablets

This paper describes a simple method for the determination of thyroid in individual thyroid tablets and composite samples. The method is fast and reliable. It permits more samples to be analyzed in an equivalent amount of time than previously reported methodology (1–3) and gives comparable results when applied to individual thyroid tablets and composite samples.

BACKGROUND

The USP XIX procedure for content uniformity (1) employs an empty sample wrapper, which is combusted and used as the blank preparation. When these sample wrappers are used for the oxygen flask combustion in the developed procedure, high and erratic blanks are recorded. Experiments (4) indicated that the high blanks are due to the black dye incorporated in the sample wrappers and can be minimized by washing the sample wrappers several times with distilled water and drying before use. For reliable results, the blank must have <3 ng of iodine/ml for this procedure.

In the procedure developed by Graham (2), iodine is determined spectrophotometrically as the triiodide ion, following the oxygen flask ignition of Moody *et al.* (3), from a sample equivalent to 30 mg of thyroid. The USP assay (1) utilizes essentially the same chemical transformation but requires a sample equivalent to 1 g of thyroid and a final thiosulfate titration. Both procedures give comparable results.

Luchtefeld (5) developed a semiautomated procedure, which was based on the kinetic procedure of Sandell and Kolthoff (6, 7) for the determination of iodine in the Total Diet market basket. By combining the procedures and making selected modifications, a method has been developed that is faster, simpler, more sensitive, and capable of being automated.

EXPERIMENTAL

Apparatus—The automated analyzer[1] system consisted of a water bath maintained at 40°, heating coils [6.1-m (20-ft) inner coil and 12.2-m (40-ft) outer coil of 1.6-mm i.d. glass tubing], tubing S[2] and T[3], a spectrophotometer[4] (gears must be adjusted to permit chart scan with stationary wavelength at 405 nm), and 10-mm flowcells. The schematic diagram in Fig. 1 shows the coils, tubing, and fittings.

The combustion system utilizes sample wrappers[5] (which must be washed prior to use), sample carriers[6], stoppers[7], 1-liter Schoniger oxygen combustion flasks[8], clamps[9], and an oxygen flask igniter[10].

Sample Wrapper Preparation—The sample wrappers were placed in a beaker and covered with distilled water. The beaker was placed in a sonic vibrator for 10–15 min, and the water was discarded. The procedure was repeated five times to decrease the amount of iodides present in the sample wrappers. Then the wrappers were placed on a paper towel and allowed to dry at room temperature.

Reagents—*Ceric Ammonium Nitrate Solution*—Ceric ammonium nitrate, 8.66 g, was dissolved in 100 ml of water in a 2-liter flask, 56.8 ml of sulfuric acid (1:1) was added, and the solution was cooled and diluted to 2 liters with water.

Arsenous Acid Solution—Arsenic trioxide, 15 g, was dissolved in 500 ml of water (made basic with 10 ml of 50% NaOH) by heating on a steam bath. The solution was cooled, 56.8 ml of sulfuric acid (1:1) was added, and the solution was cooled and diluted to 2 liters with water.

Sodium Sulfate Solution—To prepare the sodium sulfate solution, 60 ml of 50% NaOH was transferred to a 2-liter flask with 1 liter of water. Sulfuric acid (1:1), 100 ml, was added cautiously. The solution was cooled and diluted to 2 liters with water.

Sodium Chloride Solution—The sodium chloride solution was a 0.5% aqueous solution.

Standard Preparation—To prepare the standards, 0.1308 g of certified ACS grade potassium iodide[11] was dissolved in water, and the solution was diluted to 1 liter to give a concentration of 0.1 mg of iodine/ml. This solution was diluted with the sodium sulfate solution to give a concentration of 0.1 μg of iodine/ml. Standards containing 2.5, 5.0, 10.0, 15.0, 20.0, and 25 ng of iodine/ml were prepared from the resulting solution and the sodium sulfate solution. These solutions are used for the standard curve and should be prepared fresh daily.

[1] AutoAnalyzer, liquid sampler 1, and proportioning pump 1, Technicon Instruments, Tarrytown, N.Y.
[2] Solvaflex. Technicon Instruments, Tarrytown, N.Y.
[3] Tygon, Plastics and Synthetics Division, Norton Co., Tallmadge, Ohio.
[4] Model DK-2A, Beckman Instruments, Fullerton, Calif.
[5] Block, Catalog No. 6414-F70, Arthur H. Thomas Co., Philadelphia, Pa.
[6] Ogg, Catalog No. 6514-F45, Arthur H. Thomas Co., Philadelphia, Pa.
[7] Thomas-Ogg, Catalog No. 6514-F45, Arthur H. Thomas Co., Philadelphia, Pa.
[8] Catalog No. 4980, Arthur H. Thomas Co., Philadelphia, Pa.
[9] Thomas-Ogg, No. 35, Arthur H. Thomas Co., Philadelphia, Pa.
[10] Thomas-Ogg, model 11, Arthur H. Thomas Co., Philadelphia, Pa.
[11] Fisher Scientific Co., Pittsburgh, Pa.

0022-3549/80/0800-0948$01.00/0
© 1980, American Pharmaceutical Association

(15) *Ibid.*, p. 57.
(16) C. B. Roth, M. L. Jackson, E. G. Lotse, and J. K. Syers, *Isr. J. Chem.*, **6**, 261 (1968).
(17) "Analysis of Pharmaceutical Products," Waters Associates, Milford, Mass., 1976, p. 9.
(18) L. S. Porubcan, C. J. Serna, J. L. White, and S. L. Hem, *J. Pharm. Sci.*, **67**, 1081 (1978).
(19) "The Merck Index," 9th ed., Merck & Co., Inc., Rahway, N.J., 1976, p. 629.
(20) I. H. Pitman, T. Higuchi, M. Alton, and R. Wiley, *J. Pharm. Sci.*, **61**, 918 (1972).
(21) M. C. Olson, *ibid.*, **62**, 2001 (1973).

ACKNOWLEDGMENTS

J. Cornejo gratefully acknowledges the support of the United States–Spanish Joint Committee for Scientific and Technical Cooperation.

This report is Journal Paper 7952, Purdue University Agricultural Experiment Station, West Lafayette, IN 47907.

Quantitative Semiautomated Colorimetric Determination of Thyroid (Iodine) in Thyroid Tablets

E. D. McGARY

Received October 1, 1979, from the *Food and Drug Administration, Department of Health, Education, and Welfare, Kansas City, MO 64106.* Accepted for publication March 21, 1980.

Abstract □ A faster, simpler, more sensitive, and semiautomated method was developed for the analysis of thyroid in individual thyroid tablets and composite samples. The sample is combusted in a Schoniger flask in an oxygen atmosphere, and the liberated iodine is trapped in a dilute sodium hydroxide solution. The solution is acidified with sulfuric acid (1:1), and the iodine is determined colorimetrically using a suitable spectrophotometer equipped with an automated analyzer. The proposed methodology was applied to tablets containing 32.4–324 mg of thyroid. Recoveries ranged from 90.0 to 125.0% of the amount of iodine added as potassium iodide. The proposed method is sensitive to 2.5 ng of iodine/ml.

Keyphrases □ Thyroid—semiautomated colorimetric analysis in individual tablets □ Iodine—semiautomated colorimetric analysis in individual thyroid tablets □ Colorimetry—analysis, thyroid in individual thyroid tablets

This paper describes a simple method for the determination of thyroid in individual thyroid tablets and composite samples. The method is fast and reliable. It permits more samples to be analyzed in an equivalent amount of time than previously reported methodology (1–3) and gives comparable results when applied to individual thyroid tablets and composite samples.

BACKGROUND

The USP XIX procedure for content uniformity (1) employs an empty sample wrapper, which is combusted and used as the blank preparation. When these sample wrappers are used for the oxygen flask combustion in the developed procedure, high and erratic blanks are recorded. Experiments (4) indicated that the high blanks are due to the black dye incorporated in the sample wrappers and can be minimized by washing the sample wrappers several times with distilled water and drying before use. For reliable results, the blank must have <3 ng of iodine/ml for this procedure.

In the procedure developed by Graham (2), iodine is determined spectrophotometrically as the triiodide ion, following the oxygen flask ignition of Moody *et al.* (3), from a sample equivalent to 30 mg of thyroid. The USP assay (1) utilizes essentially the same chemical transformation but requires a sample equivalent to 1 g of thyroid and a final thiosulfate titration. Both procedures give comparable results.

Luchtefeld (5) developed a semiautomated procedure, which was based on the kinetic procedure of Sandell and Kolthoff (6, 7) for the determination of iodine in the Total Diet market basket. By combining the procedures and making selected modifications, a method has been developed that is faster, simpler, more sensitive, and capable of being automated.

EXPERIMENTAL

Apparatus—The automated analyzer[1] system consisted of a water bath maintained at 40°, heating coils [6.1-m (20-ft) inner coil and 12.2-m (40-ft) outer coil of 1.6-mm i.d. glass tubing], tubing S[2] and T[3], a spectrophotometer[4] (gears must be adjusted to permit chart scan with stationary wavelength at 405 nm), and 10-mm flowcells. The schematic diagram in Fig. 1 shows the coils, tubing, and fittings.

The combustion system utilizes sample wrappers[5] (which must be washed prior to use), sample carriers[6], stoppers[7], 1-liter Schoniger oxygen combustion flasks[8], clamps[9], and an oxygen flask igniter[10].

Sample Wrapper Preparation—The sample wrappers were placed in a beaker and covered with distilled water. The beaker was placed in a sonic vibrator for 10–15 min, and the water was discarded. The procedure was repeated five times to decrease the amount of iodides present in the sample wrappers. Then the wrappers were placed on a paper towel and allowed to dry at room temperature.

Reagents—*Ceric Ammonium Nitrate Solution*—Ceric ammonium nitrate, 8.66 g, was dissolved in 100 ml of water in a 2-liter flask, 56.8 ml of sulfuric acid (1:1) was added, and the solution was cooled and diluted to 2 liters with water.

Arsenous Acid Solution—Arsenic trioxide, 15 g, was dissolved in 500 ml of water (made basic with 10 ml of 50% NaOH) by heating on a steam bath. The solution was cooled, 56.8 ml of sulfuric acid (1:1) was added, and the solution was cooled and diluted to 2 liters with water.

Sodium Sulfate Solution—To prepare the sodium sulfate solution, 60 ml of 50% NaOH was transferred to a 2-liter flask with 1 liter of water. Sulfuric acid (1:1), 100 ml, was added cautiously. The solution was cooled and diluted to 2 liters with water.

Sodium Chloride Solution—The sodium chloride solution was a 0.5% aqueous solution.

Standard Preparation—To prepare the standards, 0.1308 g of certified ACS grade potassium iodide[11] was dissolved in water, and the solution was diluted to 1 liter to give a concentration of 0.1 mg of iodine/ml. This solution was diluted with the sodium sulfate solution to give a concentration of 0.1 μg of iodine/ml. Standards containing 2.5, 5.0, 10.0, 15.0, 20.0, and 25 ng of iodine/ml were prepared from the resulting solution and the sodium sulfate solution. These solutions are used for the standard curve and should be prepared fresh daily.

[1] AutoAnalyzer, liquid sampler 1, and proportioning pump 1, Technicon Instruments, Tarrytown, N.Y.
[2] Solvaflex. Technicon Instruments, Tarrytown, N.Y.
[3] Tygon, Plastics and Synthetics Division, Norton Co., Tallmadge, Ohio.
[4] Model DK-2A, Beckman Instruments, Fullerton, Calif.
[5] Block, Catalog No. 6414-F70, Arthur H. Thomas Co., Philadelphia, Pa.
[6] Ogg, Catalog No. 6514-F45, Arthur H. Thomas Co., Philadelphia, Pa.
[7] Thomas-Ogg, Catalog No. 6514-F45, Arthur H. Thomas Co., Philadelphia, Pa.
[8] Catalog No. 4980, Arthur H. Thomas Co., Philadelphia, Pa.
[9] Thomas-Ogg, No. 35, Arthur H. Thomas Co., Philadelphia, Pa.
[10] Thomas-Ogg, model 11, Arthur H. Thomas Co., Philadelphia, Pa.
[11] Fisher Scientific Co., Pittsburgh, Pa.

0022-3549/80/0800-0948$01.00/0
© 1980, American Pharmaceutical Association

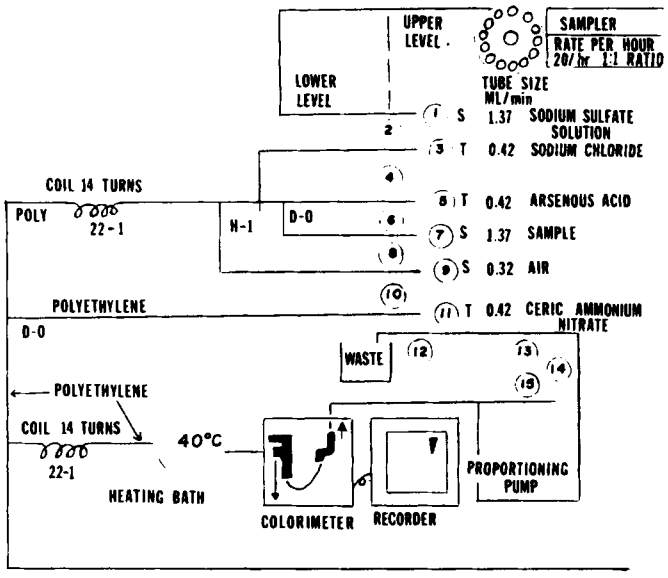

Figure 1—*Flow diagram of semiautomated system for determination of iodine in thyroid tablets.*

Sample Preparation—An amount of tablet or composite sample equivalent to 12–40 mg of thyroid was weighed accurately on a washed sample wrapper. The wrapper was folded, and the sample was transferred to the sample carrier. Thirty milliliters of 0.5 *N* NaOH was placed in a 1-liter Schoniger combustion flask, and the flask was deaerated with a rapid oxygen stream for 4 min with shaking. The mouth of the flask was moistened with water, and the stopper containing the sample was placed immediately in the flask and clamped securely. The joint of the flask around the stopper was moistened with water, and the sample was ignited with the igniter.

After combustion was completed, the flask was shaken vigorously for 1 min and then was allowed to stand for a minimum of 15 min with intermittent shaking. The solution in the flask was transferred quantitatively with water to a 200-ml volumetric flask containing 1 ml of sulfuric acid (1:1), and the solution was diluted to volume with water. Then a 4-ml aliquot was transferred to a 100-ml volumetric flask, and the solution was diluted to volume with the sodium sulfate solution.

Blank Preparation—An empty sample wrapper was subjected to the same procedure as described for sample preparation.

Determinative Step—The automated analyzer pump manifold was set up as shown in Fig. 1. From the water bath, which was maintained at 40 ± 1°, the solution passed through a 10-mm flowcell in a suitable spectrophotometer adjusted to maintain a constant wavelength at ~405 nm and to scan the chart at or near the slowest speed. The reference beam contained an empty 10-mm flowcell.

The instrument was zeroed by placing Tubes 1, 3, 5, and 11 (Fig. 1) in a container of distilled water. The water was pumped through the automated analyzer pump manifold through a 10-mm flowcell in the sample compartment of the spectrophotometer for 30 min. Then the tubes were removed from the water and placed in the following solutions: Tube 1, sodium sulfate solution; Tube 3, sodium chloride solution; Tube 5, arsenous acid solution; and Tube 11, ceric ammonium nitrate solution. The solutions were pumped through the automated analyzer as in zeroing the instrument to establish a baseline (usually from 0.7 to 0.9 absorbance unit). A standard curve (Fig. 2) was obtained by placing the iodine standard solutions in successive cups using a rate of 20/hr. The sample blank and the samples were run in the same manner as the standards.

The iodine content of the samples was determined from the standard curve. Figure 3 shows typical signal peaks used to construct the iodine standard curve.

The percent of iodine per tablet based on the label declaration of thyroid was calculated from:

$$\% \text{ iodine} = \frac{\frac{(S - B)}{1{,}000{,}000} \times DF \times ATW \times 100}{SW \times D} \qquad \text{(Eq. 1)}$$

where S is the nanograms of iodine found in the sample from the standard curve, B is the nanograms of iodine found in the blank from the standard curve, DF is the dilution factor of the sample (5000), ATW is the average tablet weight (grams), 1,000,000 is the factor converting nanograms of iodine to milligrams, SW is the sample weight (grams), and D is the label declaration of thyroid per tablet (milligrams). If the label declaration of thyroid is given in grams per tablet instead of milligrams per tablet, 64.8 mg should be taken as equal to 1 gr.

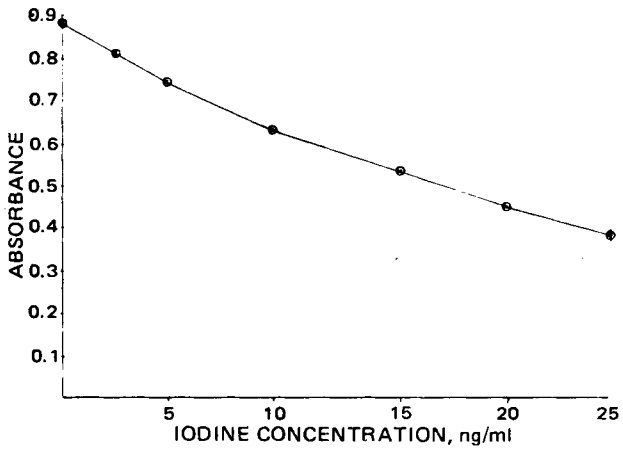

Figure 2—*Standard curve for semiautomated determination of iodine.*

RESULTS

The efficiency of the method was determined by adding known amounts of iodine to the 0.5 *N* NaOH in the combustion flask before the sample combustion and calculating the percent recoveries (Table I).

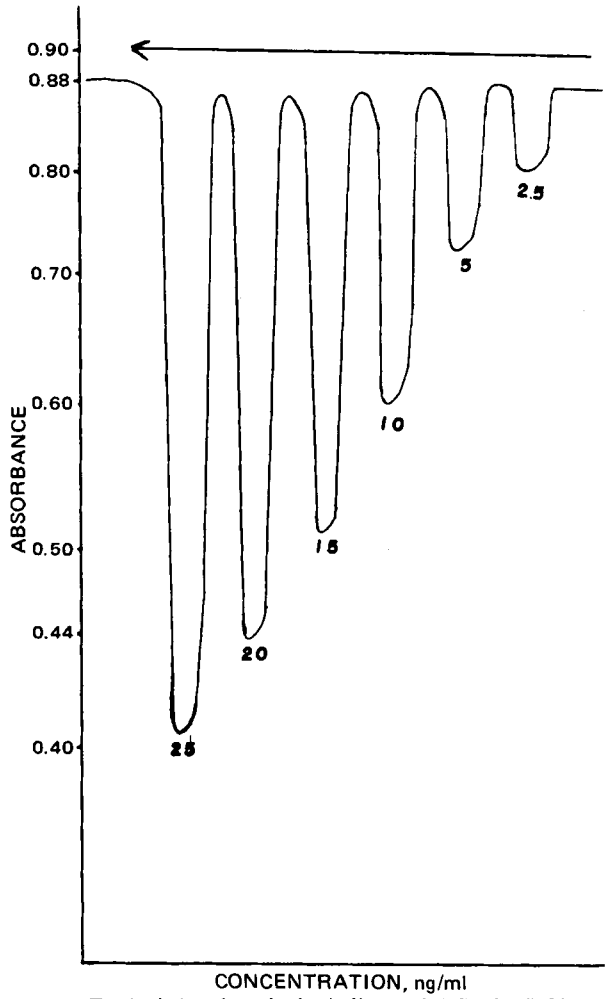

Figure 3—*Typical signal peaks for iodine at 2.5, 5, 10, 15, 20, and 25 ng/ml. Peaks are scanned from right to left.*

Table I—Recovery of Iodine Added to Composite Samples

Sample	Composite	Added, ppm	Found, ppm	Recovery, %
A, 32.4 mg/tablet	1	200	230	115
	2	400	410	102
	3	400	410	102
	4	400	490	122
	5	500	570	114
	6	600	550	92
Average				108
B, 64.8 mg/tablet	1	200	210	105
	2	200	190	95
	3	200	250	125
	4	400	460	115
	5	600	590	98
Average				108
A-1, 64.8 mg/tablet	1	400	360	90
B-1, 120 mg/tablet	1	500	460	92
C-1, 180 mg/tablet	1	222.2	244.5	110
D-1, 240 mg/tablet	1	425.5	468	110
E-1, 300 mg/tablet	1	375	400	107

Four concentrations of uncoated thyroid tablets labeled in milligrams (32.4, 64.8, 130, and 180 mg) and five concentrations of uncoated thyroid tablets labeled in grains (1, 2, 3, 4, and 5 gr) were assayed by the proposed procedure for individual tablets and composite samples. The results were compared to those obtained from the USP assay (1) on the composite samples and are in close agreement (Table II).

DISCUSSION

The primary considerations in developing this semiautomated procedure for content uniformity of individual tablets were its reliability, sensitivity, speed, and simplicity. The proposed procedure addresses all of these concerns.

While this procedure was being developed, much experimentation was required to determine the cause of high blanks. Blanks obtained by using the sample wrappers as received were high, inconsistent, and erratic. In some instances, the absorbance of the blanks indicated that more iodine was present than in the samples; therefore, the quantity of thyroid in the thyroid tablets could not be determined with any accuracy.

Table II—Comparison of Individual Thyroid Tablets and Composite Samples Assayed by the Proposed Procedure and USP (1) Assay for Percent of Labeled Amount of Thyroid

Sample	Composite Sample, %	Individual Tablet Assay[a], %	USP Composite Assay, %
A, 32.4 mg/tablet			
Mean	0.200	0.206	0.216
SD	±0.019[b]	±0.019	±0.005[b]
B, 64.8 mg/tablet			
Mean	0.207	0.214	
SD	±0.008[b]	±0.009	
C, 130 mg/tablet			
Mean	0.213		0.214
SD	±0.007[b]		±0.002[b]
D, 180 mg/tablet			
Mean	0.208		
SD	±0.008[b]		
A-1, 64.8 mg/tablet			
Mean	0.209[c]	0.216	0.200
SD		±0.017	±0.002[d]
B-1, 130 mg/tablet			
Mean	0.200[c]	0.204	0.203
SD		±0.016	±0.002[d]
C-1, 180 mg/tablet			
Mean	0.195[c]	0.198	0.204
SD		±0.012	±0.002[d]
D-1, 240 mg/tablet			
Mean	0.203[c]	0.212	0.204
SD		±0.012	±0.004[d]
E-1, 300 mg/tablet			
Mean	0.214[c]	0.207	0.205
SD		±0.007	±0.005[d]

[a] Assay of 10 individual tablets. [b] $n = 6$. [c] One determination of composite samples A-1, B-1, C-1, D-1, and E-1 was performed using the proposed methodology. [d] $n = 3$.

Table III—Comparison of Analytical Data with and without Solvents Used to Reduce the Amount of Iodine in the Sample Wrappers

Sample	Solvent	Absorbance	Iodine Found, μg
1	Water	0.765	0.1
2	Acetic Acid	0.410	20.8
3	Ethanol	0.382	22.6
4	Methanol	0.351	25.0
5	None		
	Control (1)	0.535	12.4
	(2)	0.515	13.7

A series of four experiments (4) was designed to check experimentally the apparatus as well as the solutions and sample wrappers. The analysis of these results indicated that the high iodine blanks were caused by the black dye incorporated in the paper used to wrap the samples.

The sample wrappers were washed with distilled water, alcohol, methanol, acetic acid, chloroform, acetone, benzene, and heptane in glass beakers of convenient size. The solvents were decanted from the wrappers, and all wrappers were dried first on a steam bath under a current of air and then in a convection oven at 105° (except the wrappers from the water wash, which were allowed to dry at room temperature).

The wrappers from the chloroform, acetone, benzene, and heptane washes were brittle after drying and were discarded. The remaining wrappers (one from each of the water, acetic acid, ethanol, and methanol washes) and two unwashed sample wrappers (controls) were assayed by the proposed procedure, and the amount of iodine remaining in the wrappers was calculated from a standard iodine curve. The results of the analysis (Table III) indicate that the methanol, ethanol, and acetic acid were contaminated with iodine; distilled water was the solvent of choice for decreasing the amount of iodine in the sample wrappers to give negligible iodine blanks.

Several factors influence the determination of iodine in thyroid tablets. One is the increase in absorbance as the temperature is increased. This phenomenon implies that the standards and the sample should be run at the same temperature. This effect also was observed and demonstrated by Moran (8). Another factor is the ionic strengths of the cerium(IV) and arsenic(III) solutions. These solutions should be prepared and maintained as proposed in this procedure if the analysis is to be valid and useful. A previous study (9) supported these views. The final factor is the tubing (S and T); it should be changed when the absorbances of the standard iodine solutions change significantly while the other parameters remain the same.

The reaction rate is not directly proportional to the iodine concentration; therefore, a calibration curve with a slight curvature is obtained (Fig. 2).

In developing this procedure for the analysis of thyroid in thyroid tablets, 0.25 *N* NaOH was used first as the absorbing solution to trap the liberated iodine after the oxygen flask combustion. Low recoveries of iodine were obtained. The next attempt was with 0.5 *N* NaOH, and the recoveries were much improved (Table IV). This contrast in recoveries probably is due to the lower sodium hydroxide concentration not ab-

Table IV—Comparison of Percent Recovery of Iodine Added to Composite Samples Using Two Concentrations of Sodium Hydroxide

Sample	Sodium Hydroxide Concentration, *N*	Composite	Added, ppm	Found, ppm	Recovery, %
A, 32.4 mg/tablet	0.25	1	400	280	70
		2	400	284	71
		3	400	300	75
	0.5	1	400	410	102
		2	400	410	102
		3	400	490	122
B, 64.8 mg/tablet	0.25	1	200	118	59
		2	200	124	62
		3	200	150	75
	0.5	1	200	210	105
		2	200	190	95
		3	200	250	125

sorbing all of the iodine released from the oxygen flask combustion of the tablets.

The combustion apparatus and glassware must be scrupulously cleaned before and after use with distilled water, dilute sodium hydroxide (0.1–0.5 *N*), and again with distilled water to prevent contamination of iodine adsorbed onto these surfaces.

The proposed procedure was not used on coated thyroid tablets, but it should work if a homogeneous sample is obtained.

REFERENCES

(1) "The United States Pharmacopeia," 19th rev., Mack Publishing Co., Easton, Pa., 1975, p. 508.

(2) J. H. Graham, *J. Pharm. Sci.*, **64**, 1393 (1975).

(3) J. E. Moody, J. R. Hohman, and G. B. Kaplin, *ibid.*, **57**, 634 (1968).

(4) E. D. McGary, "FDA Laboratory Information Bulletin," No. 2133, Food and Drug Administration, Washington, D.C., Nov. 1977.

(5) R. G. Luchtefeld, "FDA Laboratory Information Bulletin," No. 1678, Food and Drug Administration, Washington, D.C., Mar. 1974.

(6) E. B. Sandell and I. M. Kolthoff, *J. Am. Chem. Soc.*, **56**, 1426 (1984).

(7) E. B. Sandell and I. M. Kolthoff, *Mikrochim. Acta*, **1**, 9 (1937).

(8) J. J. Moran, *Anal. Chem.*, **24**, 378 (1952).

(9) "Standard Methods of Chemical Analysis," 6th ed., vol. 1, N. H. Furman, Ed., Van Nostrand, Princeton, N.J., 1962, pp. 523, 524.

ACKNOWLEDGMENTS

The author thanks Ronald G. Luchtefeld, Food and Drug Administration, Kansas City, Mo., for constructing the semiautomated iodine system used.

Semiautomated Method for Analysis of Enteric-Coated and Plain Coated Diethylstilbestrol Tablets

RICHARD E. KOLINSKI *x, JAMES W. MYRICK *, and ELAINE A. BUNCH ‡

Received December 13, 1979, from the **National Center for Drug Analysis, Food and Drug Administration, 1114 Market Street, St. Louis, MO 63101*, and the ‡*Food and Drug Administration, Seattle, WA 98174.* Accepted for publication March 19, 1980.

Abstract □ A semiautomated fluorometric method for the analysis of enteric-coated and plain coated diethylstilbestrol tablets is presented. To eliminate interferences from tablet excipients, diethylstilbestrol is extracted into an organic solvent and then into a basic aqueous solution. After UV irradiation, a product of diethylstilbestrol is formed from which a fluorophore is produced chemically. The fluorescence is measured at an excitation wavelength of 335 nm and an emission wavelength of 410 nm. The coefficient of variation measured for the semiautomated procedure was 0.59%. Assay results agreed well with the USP procedure for tablets containing >1 mg of diethylstilbestrol. Tablet dyes and excipients interfered in the USP procedure, which yielded low results for tablets containing <1 mg of diethylstilbestrol. Standard recovery data and assays of tablet composites showed that dyes and other excipients do not interfere with the semiautomated procedure.

Keyphrases □ Diethylstilbestrol—semiautomated fluorometric analysis of enteric-coated and plain coated tablets □ Fluorometry—semiautomated analysis of enteric-coated and plain coated diethylstilbestrol tablets □ Estrogens—diethylstilbestrol, semiautomated fluorometric analysis of enteric-coated and plain coated tablets

Diethylstilbestrol is one of several synthetic estrogens whose use has been the subject of many clinical studies. The estrogenic activity of this stilbenediol derivative was discovered in 1938 (1). In recent years, diethylstilbestrol has been administered for estrogen replacement therapy and treatment of mammary carcinoma and as a contraceptive.

BACKGROUND

The USP (2) content uniformity requirement for diethylstilbestrol tablets increased the analytical workload of many pharmaceutical laboratories. The individual tablet assay described in the monograph is tedious and, because of excipient interference, cannot be used to assay enteric-coated tablets containing <1 mg of diethylstilbestrol. The semiautomated method developed by Hussey *et al.* (3) is similar in principle to the USP XIX procedure (2) but is limited to the analysis of plain tablets and the cores of enteric-coated tablets of dosage levels of >0.25 mg.

The semiautomated method described in this report utilizes a fluorometric determinative step to achieve greater sensitivity for the analysis of low dosage tablets. After UV irradiation of diethylstilbestrol, a fluorophore is produced quantitatively by reducing the irradiation product (4) with an alcoholic hydrochloric acid solution containing 2% pyrocatechol and heating to form a phenanthrenediol. The pyrocatechol increases the fluorescence intensity slightly, which adds to the overall stability of the automated system.

Use of the irradiation product itself as the fluorophore for analysis was investigated by Goodyear and Jenkinson (5). Excipients in enteric coatings were reported to cause some interference, and the fluorescence intensity of the irradiation product without the addition of acid and without heating was not sufficient for quantitation of low dosage tablets in the automated system. However, an intense fluorophore, 3,6-dihydroxy-9,10-diethylphenanthrene, is produced when the UV irradiation product is heated with an alcoholic hydrochloric acid solution containing 2% pyrocatechol. Umberger *et al.* (6) performed a similar reduction by heating the UV irradiation product with acid and bisulfite in alcohol solution to form the phenanthrenediol.

The need to analyze low dosage, enteric-coated diethylstilbestrol tablets from various manufacturers prompted the development of this semiautomated system. The method utilizes the principles and materials of the methods cited, and an extraction step was added to eliminate interferences from tablet excipients.

EXPERIMENTAL

Principles—A solution of diethylstilbestrol in 0.05 *M* alcoholic dibasic potassium phosphate was acidified with 1 *N* HCl and extracted with isooctane–butanol. The drug in the organic phase then was extracted with 1 *N* NaOH. The extract was mixed with phosphoric acid and dibasic potassium phosphate, and the mixture was irradiated with UV light. The irradiation product was reacted with a 2% solution of pyrocatechol in 2 *N* HCl at 70°. The fluorophore thus produced was measured at an excitation wavelength of 335 nm and an emission wavelength of 410 nm.

Apparatus—The automated analyzer[1] system consisted of a sampler, two proportioning pumps, a heating bath at 70°, a fluorometer with a primary[2] and a secondary[3] filter, and a recorder utilizing linear chart paper to record the relative fluorescence intensity. Typical fluorometer

[1] AutoAnalyzer with sampler II, proportioning pump I, and fluorometer II, Technicon Corp., Tarrytown, N.Y.

[2] No. 72786, maximum transmittance at 335 nm, Beckman Instruments, Fullerton, Calif.

[3] No. 5113, 3.8 mm, maximum transmittance at 410 nm, Corning Glass Works, Corning, N.Y.

0022-3549/80/0800-0951$01.00/0

© 1980, American Pharmaceutical Association

sorbing all of the iodine released from the oxygen flask combustion of the tablets.

The combustion apparatus and glassware must be scrupulously cleaned before and after use with distilled water, dilute sodium hydroxide (0.1–0.5 *N*), and again with distilled water to prevent contamination of iodine adsorbed onto these surfaces.

The proposed procedure was not used on coated thyroid tablets, but it should work if a homogeneous sample is obtained.

REFERENCES

(1) "The United States Pharmacopeia," 19th rev., Mack Publishing Co., Easton, Pa., 1975, p. 508.

(2) J. H. Graham, *J. Pharm. Sci.*, **64**, 1393 (1975).

(3) J. E. Moody, J. R. Hohman, and G. B. Kaplin, *ibid.*, **57**, 634 (1968).

(4) E. D. McGary, "FDA Laboratory Information Bulletin," No. 2133, Food and Drug Administration, Washington, D.C., Nov. 1977.

(5) R. G. Luchtefeld, "FDA Laboratory Information Bulletin," No. 1678, Food and Drug Administration, Washington, D.C., Mar. 1974.

(6) E. B. Sandell and I. M. Kolthoff, *J. Am. Chem. Soc.*, **56**, 1426 (1984).

(7) E. B. Sandell and I. M. Kolthoff, *Mikrochim. Acta*, **1**, 9 (1937).

(8) J. J. Moran, *Anal. Chem.*, **24**, 378 (1952).

(9) "Standard Methods of Chemical Analysis," 6th ed., vol. 1, N. H. Furman, Ed., Van Nostrand, Princeton, N.J., 1962, pp. 523, 524.

ACKNOWLEDGMENTS

The author thanks Ronald G. Luchtefeld, Food and Drug Administration, Kansas City, Mo., for constructing the semiautomated iodine system used.

Semiautomated Method for Analysis of Enteric-Coated and Plain Coated Diethylstilbestrol Tablets

RICHARD E. KOLINSKI *x, JAMES W. MYRICK *, and ELAINE A. BUNCH ‡

Received December 13, 1979, from the **National Center for Drug Analysis, Food and Drug Administration, 1114 Market Street, St. Louis, MO 63101*, and the ‡*Food and Drug Administration, Seattle, WA 98174.* Accepted for publication March 19, 1980.

Abstract □ A semiautomated fluorometric method for the analysis of enteric-coated and plain coated diethylstilbestrol tablets is presented. To eliminate interferences from tablet excipients, diethylstilbestrol is extracted into an organic solvent and then into a basic aqueous solution. After UV irradiation, a product of diethylstilbestrol is formed from which a fluorophore is produced chemically. The fluorescence is measured at an excitation wavelength of 335 nm and an emission wavelength of 410 nm. The coefficient of variation measured for the semiautomated procedure was 0.59%. Assay results agreed well with the USP procedure for tablets containing >1 mg of diethylstilbestrol. Tablet dyes and excipients interfered in the USP procedure, which yielded low results for tablets containing <1 mg of diethylstilbestrol. Standard recovery data and assays of tablet composites showed that dyes and other excipients do not interfere with the semiautomated procedure.

Keyphrases □ Diethylstilbestrol—semiautomated fluorometric analysis of enteric-coated and plain coated tablets □ Fluorometry—semiautomated analysis of enteric-coated and plain coated diethylstilbestrol tablets □ Estrogens—diethylstilbestrol, semiautomated fluorometric analysis of enteric-coated and plain coated tablets

Diethylstilbestrol is one of several synthetic estrogens whose use has been the subject of many clinical studies. The estrogenic activity of this stilbenediol derivative was discovered in 1938 (1). In recent years, diethylstilbestrol has been administered for estrogen replacement therapy and treatment of mammary carcinoma and as a contraceptive.

BACKGROUND

The USP (2) content uniformity requirement for diethylstilbestrol tablets increased the analytical workload of many pharmaceutical laboratories. The individual tablet assay described in the monograph is tedious and, because of excipient interference, cannot be used to assay enteric-coated tablets containing <1 mg of diethylstilbestrol. The semiautomated method developed by Hussey *et al.* (3) is similar in principle to the USP XIX procedure (2) but is limited to the analysis of plain tablets and the cores of enteric-coated tablets of dosage levels of >0.25 mg.

The semiautomated method described in this report utilizes a fluorometric determinative step to achieve greater sensitivity for the analysis of low dosage tablets. After UV irradiation of diethylstilbestrol, a fluorophore is produced quantitatively by reducing the irradiation product (4) with an alcoholic hydrochloric acid solution containing 2% pyrocatechol and heating to form a phenanthrenediol. The pyrocatechol increases the fluorescence intensity slightly, which adds to the overall stability of the automated system.

Use of the irradiation product itself as the fluorophore for analysis was investigated by Goodyear and Jenkinson (5). Excipients in enteric coatings were reported to cause some interference, and the fluorescence intensity of the irradiation product without the addition of acid and without heating was not sufficient for quantitation of low dosage tablets in the automated system. However, an intense fluorophore, 3,6-dihydroxy-9,10-diethylphenanthrene, is produced when the UV irradiation product is heated with an alcoholic hydrochloric acid solution containing 2% pyrocatechol. Umberger *et al.* (6) performed a similar reduction by heating the UV irradiation product with acid and bisulfite in alcohol solution to form the phenanthrenediol.

The need to analyze low dosage, enteric-coated diethylstilbestrol tablets from various manufacturers prompted the development of this semiautomated system. The method utilizes the principles and materials of the methods cited, and an extraction step was added to eliminate interferences from tablet excipients.

EXPERIMENTAL

Principles—A solution of diethylstilbestrol in 0.05 *M* alcoholic dibasic potassium phosphate was acidified with 1 *N* HCl and extracted with isooctane–butanol. The drug in the organic phase then was extracted with 1 *N* NaOH. The extract was mixed with phosphoric acid and dibasic potassium phosphate, and the mixture was irradiated with UV light. The irradiation product was reacted with a 2% solution of pyrocatechol in 2 *N* HCl at 70°. The fluorophore thus produced was measured at an excitation wavelength of 335 nm and an emission wavelength of 410 nm.

Apparatus—The automated analyzer[1] system consisted of a sampler, two proportioning pumps, a heating bath at 70°, a fluorometer with a primary[2] and a secondary[3] filter, and a recorder utilizing linear chart paper to record the relative fluorescence intensity. Typical fluorometer

[1] AutoAnalyzer with sampler II, proportioning pump I, and fluorometer II, Technicon Corp., Tarrytown, N.Y.

[2] No. 72786, maximum transmittance at 335 nm, Beckman Instruments, Fullerton, Calif.

[3] No. 5113, 3.8 mm, maximum transmittance at 410 nm, Corning Glass Works, Corning, N.Y.

0022-3549/80/0800-0951$01.00/0

© 1980, American Pharmaceutical Association

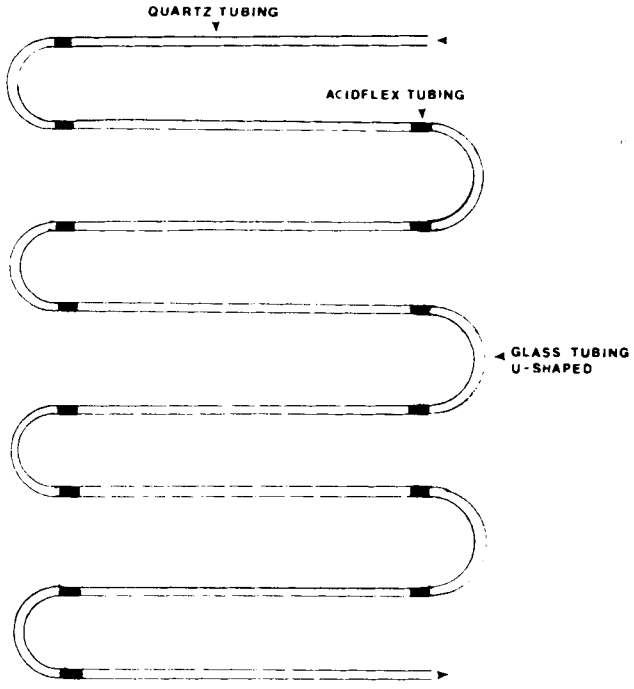

Figure 1—*Section of quartz irradiation coil. The coil consists of 22 37-cm lengths of quartz tubing, 2 mm i.d. × 3 mm o.d., connected by tubing and glass U-tubes. The coil is formed into top and bottom grids, each having 11 lengths of quartz tubing. The grids are shifted out of line to maximize exposure to UV light.*

parameters were: sample aperture, 3; reference aperture, 2; and full-scale recording, 110.

The UV irradiation assembly consisted of clear quartz tubing[4], 2 mm i.d. × 3 mm o.d. and ~9 m long, made into a coil as described by Hussey *et al.* (3) and connected by tubing[5] and glass U-tubes[6] (Fig. 1), and a 15-w germicidal lamp[7] mounted ~10 cm above the quartz coil. Aluminum foil was placed under the coil to provide a reflective background. The entire UV irradiation assembly was covered with aluminum foil for maximum internal reflectance and to prevent leakage of harmful UV radiation.

Reagents—The alcohol used was 95% ethanol.

To prepare 0.05 *M* alcoholic dibasic potassium phosphate, 8.7 g of anhydrous dibasic potassium phosphate was dissolved in 500 ml of water, and the solution was diluted to 1 liter with alcohol.

The 1 *N* HCl was prepared by diluting 83 ml of concentrated hydrochloric acid to 1 liter with water.

For the alcoholic hydrochloric acid, 83 ml of concentrated hydrochloric acid was diluted to 500 ml with water, and the mixture was diluted to 1 liter with alcohol.

The 1 *N* NaOH was prepared by diluting 50 ml of 50% (w/v) NaOH to 1 liter with water.

For the alcoholic phosphoric acid solution, 250 ml of alcohol was added to 60 g of 85% H_3PO_4, and the mixture was diluted to 1 liter with water. The strength of this reagent was adjusted, if necessary, to obtain the correct pH after irradiation.

To prepare the pyrocatechol solution, 20 g of pyrocatechol was dissolved in 500 ml of water, and 178 ml of hydrochloric acid and 250 ml of alcohol were added. The solution was mixed and diluted to 1 liter with water.

The organic solvent was prepared by adding 200 ml of *n*-butanol to 1 liter of isooctane with mixing. *n*-Butanol and distilled-in-glass isooctane that are suitable for spectrophotometry and chromatography were used.

Diethylstilbestrol Standard Solution—Approximately 25 mg of diethylstilbestrol USP reference standard was weighed into a 250-ml volumetric flask. The standard was dissolved and diluted to volume with the alcoholic dibasic potassium phosphate. A 10.0-ml aliquot of the stock standard solution was transferred to a 100-ml volumetric flask and diluted to volume with the alcoholic dibasic potassium phosphate; this solution was stable for at least 10 days. To assay tablets containing <1 mg of diethylstilbestrol, a 10.0-ml aliquot of the stock standard solution was placed in a 100-ml volumetric flask, 40 ml of the alcoholic dibasic potassium phosphate reagent was added, and the mixture was diluted to volume with the alcoholic hydrochloric acid.

Sample Preparation—For tablets containing 1 mg or more of diethylstilbestrol, individual tablets were disintegrated or weighed composites were dispersed in an accurately measured volume of the alcoholic dibasic potassium phosphate reagent to give a concentration of 0.01 mg/ml. Samples were placed in an ultrasonic generator for ~15 min with intermittent swirling to ensure tablet disintegration. Enteric-coated tablets were sonicated until visual examination indicated no trace of intact tablet particles when the sample was swirled. Up to 30 min was required for some products, depending on the enteric-coating formulation. The alcoholic dibasic potassium phosphate reagent was used as the wash solution for the automatic analyzer.

For tablets containing <1 mg of diethylstilbestrol, individual tablets were disintegrated or weighed composites were dispersed in an accurately measured volume of the alcoholic dibasic potassium phosphate reagent to give half of the final volume of the sample solution. The diethylstilbestrol from the tablet material was dissolved by ultrasonic treatment as described. An accurately measured equal volume of the alcoholic hydrochloric acid reagent was added to give a final diethylstilbestrol concentration of 0.01 mg/ml. The solution was allowed to stand until the precipitate had settled. For the automatic analyzer, a wash solution of dibasic potassium phosphate reagent–alcoholic hydrochloric acid reagent (1:1) was used.

Procedure—The automated system was assembled as shown in Fig. 2. The first manifold (Pump A) is the extraction manifold. The second manifold (Pump B) is the irradiation and fluorescence manifold.

The automated system was equilibrated as follows. With the fluorescence manifold pump turned off, the proper reagents were pumped through the extraction manifold. When the B4 fitting on the fluorescence manifold was filled with aqueous and organic layers, the fluorescence manifold pump was turned on and all of the reagents were pumped through the system. Approximately 30 min was allowed for system equilibration. The pH of the phosphate solution was checked after irradiation by collecting, on pH paper, a few drops from the waste line off the C3 resample fitting. A pH of 7–8 was desired.

Portions of the prepared sample and standard solutions were placed in 8.5-ml polystyrene cups on the sampler, which was set to a rate of 20 samples/hr and a sample-to-wash ratio of 2:1. The sampling pattern was three cups of standard, five cups of sample, one cup of standard, five cups of sample, *etc.* Two cups of standard were placed at the end of each run. In the calculations, the first two and the last standard peaks were disregarded.

In the automatic analyzer, the sample was withdrawn, segmented with air, and acidified with 1 *N* HCl. Isooctane–butanol was added and mixed, and the aqueous and organic phases were separated. The organic phase, which contained the drug, was resampled, segmented with air, and mixed with 1 *N* NaOH. The aqueous phase, which then contained the diethylstilbestrol, was separated and mixed with alcoholic dibasic potassium phosphate and phosphoric acid. The solution was irradiated in a quartz coil under a germicidal lamp. The solution was resampled, mixed with 2% pyrocatechol in 2 *N* HCl and alcohol, and heated at 70°. The solution, which then contained a fluorophore of the diethylstilbestrol irradiation product, was cooled and passed through the fluorometer. The fluorescence was measured at an excitation wavelength of 335 nm and an emission wavelength of 410 nm. Typical peaks from the analyzer are shown in Fig. 3.

RESULTS AND DISCUSSION

Four diethylstilbestrol standard solutions having concentrations of 50, 100, 150, and 200 μg/ml were passed through the analyzer. A graph of the fluorescence intensities of these solutions *versus* concentration resulted in a straight line that passed through the origin.

A sampling rate of 25 cups/hr was tested with standard solutions. However, the coefficient of variation for the system increased to 2.00% at 25 cups/hr from 0.60% at 20 cups/hr. Moreover, the percentage of steady state (defined as 100 times the ratio of the sample peak intensity to the steady-state signal intensity) achieved by the peaks decreased from 94.4 to 84.0%.

A composite sample of enteric-coated, 1-mg tablets was prepared from a commercial product. Twenty weighed portions of this composite, each equivalent to a single tablet, were assayed by the semiautomated method. The coefficient of variation obtained was 1.09% (Table I). In addition,

[4] W. A. Sales, Deerfield, Ill.
[5] Acidflex, Technicon Corp., Tarrytown, N.Y.
[6] No. 116-0223, Technicon Corp., Tarrytown, N.Y.
[7] No. E-15763, Crescent Manufacturing Co., Philadelphia, Pa.

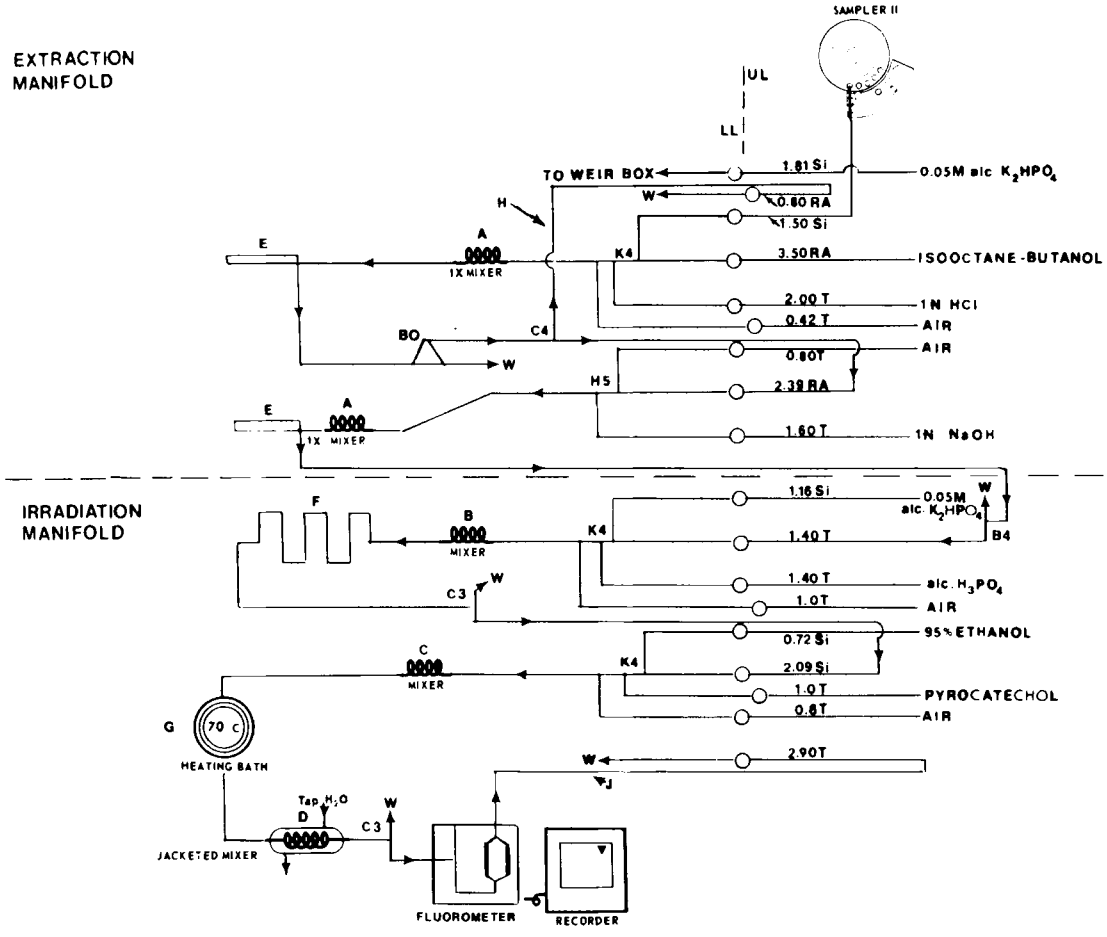

Figure 2—*Flow diagram for the determination of diethylstilbestrol in tablets. Key: A, 1× mixer, 7 turns, 1.0 mm i.d.; B, 1× mixer, five turns, 2 mm i.d.; C, 1× mixer, 14 turns, 2 mm i.d.; D, jacketed mixer, 14 turns, 2.4 mm i.d.; E, delay (settling) coil, 5.5 turns, 2.4 mm i.d.; F, irradiation assembly, consisting of quartz coil (Fig. 1) and 15-w UV lamp; G, heating bath, containing 12-m (40-ft) glass coil, 1.6 mm i.d., set at 70°; H, polyethylene tubing, 0.82 mm (0.034 in.) i.d.; and J, Tygon tubing, 1.59 mm (0.0625 in.) i.d. Transmission tubing is glass, 2 mm i.d. For the pump tubes, RA is red Acidflex, T is Tygon, and Si is silicon; W indicates flow to waste reservoir.*

a single determination on each of 10 days was performed on the same composite to test the day-to-day reproducibility of the system, and the coefficient of variation obtained was 0.59%. The individual standard solutions used in the tests were assayed by comparison to freshly prepared standard solutions. All of the standard solutions were stoppered and stored on a bench top, exposed to room light and to changes in temperature and humidity. These solutions were reexamined after 8 days, and no decomposition was observed.

Table I—Reproducibility Data for 1-mg Diethylstilbestrol Enteric-Coated Tablets Using the Semiautomated Method [a]

	Reproducibility	
	Same Day	Day-to-Day
	102.4	102.0
	101.3	102.2
	100.1	102.3
	101.1	102.2
	104.6	102.3
	102.3	102.4
	100.6	102.2
	100.8	103.2
	99.9	101.0
	100.9	101.3
	101.3	
	101.2	
	102.2	
	99.6	
	100.7	
	101.9	
	100.2	
	101.8	
	101.1	
	101.3	
Mean (20)	101.3	(10) 102.1
SD	1.11	0.60
CV, %	1.09	0.59

[a] Results are reported as percent of label declaration.

Seventy-six cups of a solution prepared from a composite of plain coated tablets were passed through the system. No serious evaporation effects were observed. However, since the samples were dissolved in a 50% alcoholic solution and the sampler was set at 20 cups/hr, the cups were filled and the trays were loaded just before analysis.

Enteric-coated tablets usually are difficult to disintegrate. Normally, an enteric-coated tablet must be crushed or the outer shell must be cracked before the solvent is added; otherwise, tablet disintegration with an ultrasonic generator proceeds slowly and a uniform dispersion of tablet material is not obtained. Use of alcoholic dibasic potassium phosphate as a solvent proved successful for the disintegration of enteric-coated diethylstilbestrol tablets. With the aid of an ultrasonic generator, this solvent disintegrated the tablets into a fine dispersion; the outer shell disintegrated, the tablet core slowly disintegrated, and complete tablet disintegration occurred in a reasonable period. The task of cracking the outer shell of each tablet before solvent addition thus was eliminated.

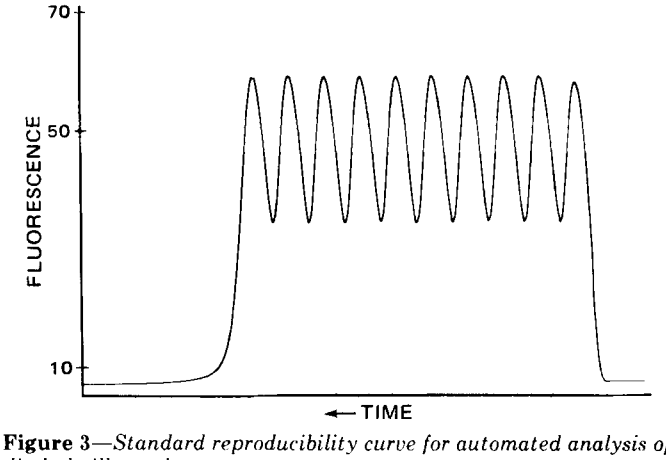

Figure 3—*Standard reproducibility curve for automated analysis of diethylstilbestrol.*

Table II—Comparison of the Semiautomated Method with the USP XIX Method for Assay of Diethylstilbestrol Tablets [a]

Dosage	Semiautomated	USP
Plain coated, 5 mg	96.0	96.5
Plain coated, 5 mg	100.0	99.8
Plain coated, 1 mg (mean)	99.3 (5)	98.6 (2)
CV, %	0.32	
Enteric coated, 5 mg (mean)	100.2 (5)	97.7 (2)
CV, %	0.48	
Enteric coated, 1 mg (mean)	99.2 (5)	98.7 (1)
CV, %	0.54	
Enteric coated, 0.25 mg (mean)	99.0 (5)	95.6 (2)
CV, %	0.68	
Enteric coated, 0.1 mg (mean)	99.8 (5)	86.1 (2)
CV, %	1.24	

[a] Results are reported in percent of label declaration. Numbers of samples analyzed are given in parentheses.

A white precipitate formed in the coils when the enteric-coated tablets from one manufacturer, which contained <1.0 mg of diethylstilbestrol, were assayed. The inner coating of the tablet contained a plasticizer that precipitated when treated with acid on the extraction manifold. The problem was solved by addition of the alcoholic hydrochloric acid reagent to the sample, which previously had been treated with the alcoholic dibasic potassium phosphate reagent, *before* sampling on the automatic analyzer. The precipitate formed and was allowed to settle, and a portion of the supernate then was placed in a cup and sampled.

The extraction manifold was designed to eliminate excipient interference. A mixture of isooctane and butanol was selected as the organic solvent; butanol was added to isooctane to achieve increased polarity for complete extraction of diethylstilbestrol. Dyes present in the outer shells of the enteric-coated tablets remained in the aqueous layer and proceeded to the waste reservoir.

In initial experiments, a coil made from polytetrafluoroethylene[8] tubing was used in the irradiation assembly. However, this tubing was unsuitable; pulsing occurred in the coil because of the presence of air between sample and wash segments. A quartz irradiation coil similar to that described by Hussey *et al.* (3) resulted in a more even flow and more complete irradiation. The extraction step provided a cleaner solution for irradiation and decreased the possibility of interferences in the fluorometric measurement. A 70° temperature in the heating bath for the reaction with pyrocatechol produced the maximal fluorescence.

Results from the semiautomated method compared closely with results from the USP XIX content uniformity method (2) when ground composites of enteric-coated and plain coated 1-mg diethylstilbestrol tablets were analyzed. Ten determinations by the semiautomated method on a ground composite of enteric-coated tablets resulted in a mean of 102.1% of the label declaration and a coefficient of variation of 0.59%. Five determinations on the same composite by the USP method gave a mean of 102.5% of the label declaration and a coefficient of variation of 1.31%. Twenty determinations of a ground composite of plain coated tablets by the semiautomated method resulted in a mean of 95.4% of the label declaration and a coefficient of variation of 0.66%. Five determinations on the same composite by the USP method resulted in a mean of 96.0% of the label declaration and a coefficient of variation of 0.91%.

Composites of enteric-coated and plain coated tablets, obtained from four manufacturers and labeled as containing 0.1–5 mg of diethylstilbestrol, were analyzed by the semiautomated and USP assay methods. Results agreed closely for plain coated and enteric-coated tablets containing 1 mg or more of diethylstilbestrol (Table II) but were low when enteric-coated tablets containing <1 mg of diethylstilbestrol were assayed by the USP method. The large amount of tablet material required for the assay of low dosage, enteric-coated tablets interfered with the USP extraction procedures. Two major problems were encountered: emulsions occurred in the extraction step, and tablet dyes interfered with the color produced by irradiation. These problems were not encountered in the semiautomated method.

A recovery experiment was performed on solutions containing diethylstilbestrol reference standard plus tablet dye and excipients using the semiautomated and manual assay procedures. Two standard solutions, each containing dye to simulate a sample solution of a 0.1-mg diethylstilbestrol tablet, were analyzed by the semiautomated method, and a standard recovery of 100.7% was obtained from each. Two similar standard solutions, containing both dye and excipients, were analyzed by the semiautomated method and gave standard recoveries of 100.8 and 100.6%. The automated analysis of two additional standard solutions of diethylstilbestrol and dye, each equivalent to a sample solution of a 0.25-mg diethylstilbestrol tablet, yielded standard recoveries of 100.1 and 100.3%. A standard solution of diethylstilbestrol, assayed by the USP method, gave a 100.8% standard recovery at a level of 0.1 mg of diethylstilbestrol/tablet. However, a standard solution corresponding to the same diethylstilbestrol level but containing dye and excipients resulted in recovery of only 92.4%. These results indicated that tablet excipients that gave problems in the USP method did not interfere in the semiautomated procedure.

The addition of an extraction and a fluorometric determination to a previously published automated method has made it possible to assay low dosage, enteric-coated tablets without interference from tablet dyes and other excipients. The semiautomated method is reproducible, accurate, and precise and was used to analyze 1500 enteric-coated and 800 plain coated diethylstilbestrol tablets in a survey for content uniformity.

[8] Teflon.

REFERENCES

(1) "Remington's Pharmaceutical Sciences," 15th ed., Mack Publishing Co., Easton, Pa., 1975, p. 917.

(2) "The United States Pharmacopeia," 19th rev., Mack Publishing Co., Easton, Pa., 1975, p. 142.

(3) R. L. Hussey, J. L. Hale, and D. P. Howard, *J. Pharm. Sci.*, **62**, 1171 (1973).

(4) D. Banes, *J. Assoc. Off. Agr. Chem.*, **44**, 323 (1961).

(5) J. M. Goodyear and N. R. Jenkinson, *Anal. Chem.*, **32**, 1203 (1960).

(6) E. J. Umberger, D. Banes, F. Kunze, and S. Colson, *J. Assoc. Off. Agr. Chem.*, **46**, 471 (1963).

Physical Stability of Semisynthetic Suppository Bases

LARRY J. COBEN ˣ **and NICHOLAS G. LORDI** *

Received January 19, 1979, from the *Pharmaceutical Technical Services Department, Parke-Davis Division, Warner-Lambert Company, Morris Plains, NJ 07950.* Accepted for publication March 31, 1980. *College of Pharmacy, Rutgers—The State University, Piscataway, NJ 08854.

Abstract □ Changes in the melting range of several semisynthetic suppository bases were studied over time. X-ray diffraction studies characterized the changes as amorphous to crystalline transitions, with likely polymorphic effects occurring concurrently. Use of a modified Krowczynski apparatus to test pure base and single-ingredient suppositories showed dramatic hardening of the materials over periods as short as 6 weeks. Data were obtained by differential scanning calorimetry on freshly solidified, incrementally aged, and equilibrated samples. These methods may be used as both predictive and ongoing physical stability tests in the evaluation of suppository bases and formulas.

Keyphrases □ Suppositories—physical stability of semisynthetic suppository bases □ Physical stability—semisynthetic suppository bases

Krowczynski (1) noted changes in the deformation time of suppositories during storage using an apparatus of his own design (2). He also noted hardening in polyethylene glycol suppositories (3) but pointed out that plasticizers prevented the phenomenon. Ritschel-Beurlin (4) reported aging in suppository bases by studying the change in "spreading." Torrado-Valeiras (5) studied the stability of suppositories using a hardness tester as well as the Krowczynski device and found that certain excipients could stabilize the "melting point" by a "lubricant action" and stabilization of the metastable form. Mezey *et al.* (6), using a cone flow device, had results similar to those of Torrado-Valeiras. Other studies (7, 8) showed that suppository aging affects the *in vitro* and *in vivo* drug release rates.

Whittam and Rosano (9) studied short-term physical aging in pure monoacid triglycerides using X-ray diffraction analysis, differential thermal analysis, and polarizing microscopy. Lovegren *et al.* (10, 11) utilized differential scanning calorimetry to investigate the polymorphic nature of cocoa butter. Differential scanning calorimetry was employed by Rossell (12) to study cooling phenomena in palm kernel oil products. Correlation to dilatometric means of studying the solids content of fats was shown in a differential scanning calorimetric procedure developed by Miller *et al.* (13).

The aim of this research was to elucidate the aging or hardening phenomena observed in suppositories prepared from semisynthetic suppository bases. The hardening effect, resulting in little or no suppository melting, can cause local irritation, a defecatory reflex, or bowel obstruction. Development of procedures as both predictive and ongoing physical stability tests for both bases and formulated products was undertaken. It was thought that studying the changes through thermal analysis and comparing these results with physical hardening data would allow predictions of shelflife hardening from the initial thermal data. Pure bases and bases with ingredients added were studied.

The combination of the modified Krowczynski procedure, X-ray diffraction analysis, and differential scanning calorimetry gave this study specificity, reproducibility, versatility, and direct application to the dosage form.

EXPERIMENTAL

Materials—Five semisynthetic, commercially available bases were chosen. Table I summarizes their chemical properties and the processes by which they were produced, and Fig. 1 compares their solid fat indexes.

Three excipients were chosen to study the ingredient addition effect. Zinc oxide[1] was selected because of its insolubility, its amorphous nature, and its thickening property in oils. Resorcinol[2] was studied for its crystalline nature and its miscibility with fats. A neutral oil[3], consisting of triglycerides with fatty acid moieties between C-8 and C-12, was used because of its fatty nature and because it was claimed by Mezey *et al.* (6) to inhibit hardening.

Softening Time—The apparatus was a slight modification of Krowczynski's device (2). The original device has a constricted glass tube, with a stoppered bottom, in a glass mantle with an inlet and outlet for thermoregulated water. The suppository sits on the constriction, and a glass rod (29–31 g) is placed on the suppository. When the rod reaches the constriction, the melting time is read. Modifications (Fig. 2) included the use of a constricted U tube to avoid possible back pressure on melting past the constriction, use of a water bath[4] with both refrigeration and heating units (accuracy of ±0.05°), and reduction of the weight of the glass rod from 30 to 14 g.

The first experiment was a screening study of the five bases at 37, 36.5, 36, and 35.5°. Freshly molded suppositories and incrementally aged samples were tested in triplicate. Following Krowczynski's approach, the test was expanded to additional samples if a significant variation was noted. Softening times in excess of 90 min were not continued to the end-point during the screening trials but were noted as such.

Two bases, Bases 1 and 3, were chosen for continuing study because of their stability and instability, respectively, at 37.0°.

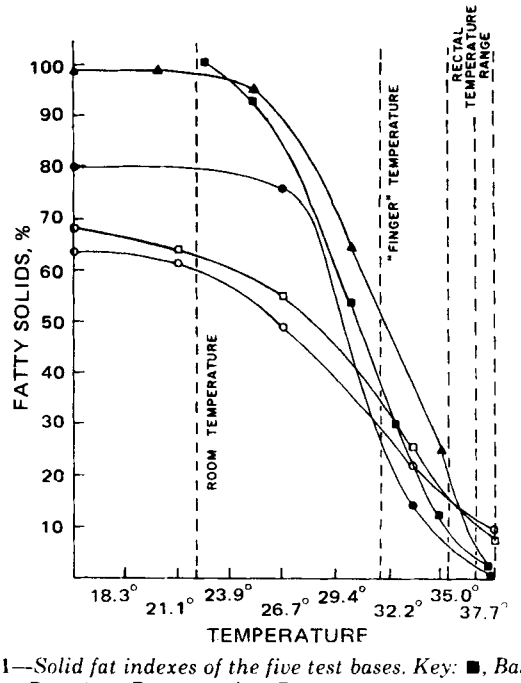

Figure 1—*Solid fat indexes of the five test bases. Key:* ■, *Base 1;* ●, *Base 2;* ▲, *Base 3;* □, *Base 4; and* ○, *Base 5.*

[1] Zinc oxide USP, Westwood Chemical Co., Middletown, N.J.
[2] Resorcinol USP, Koppers, Pittsburgh, Pa.
[3] Miglyol 812, Dynamit Nobel, Witten, West Germany.
[4] Model NK-22, Haake, Saddle Brook, N.J.

0022-3549/80/0800-0955$01.00/0
© 1980, American Pharmaceutical Association

Table I—Chemical Components and Method of Manufacture of Suppository Bases

Base	Fatty Acid Moiety Content, %							Di-esters, %	Mono-esters, %	Process
	C_8	C_{10}	C_{12}	C_{14}	C_{16}	C_{18}	$C_{18.1}$			
1[a]	0.5	2.0	49.0	19.0	14.0	15.0	0.5	9.0	0.5	Reesterified
2[b]	3.0	3.0	55.0	21.0	9.0	9.0	0.0	0.0	0.0	Solvent fractionation
3[c]	2.1	1.9	38.0	13.0	14.8	30.0	0.2	0.0	0.1	Interesterified
4[d]	0.0	0.0	0.2	0.6	17.5	14.4	67.3	0.0	0.0	Solvent fractionation
5[e]	4.0	4.0	48.0	16.0	8.1	17.9	1.4	3.0	0.3	Interesterified

[a] Witepsol H-175, Dynamit Nobel, Witten, West Germany. [b] Satina III, Glidden-Durkee, Rockville Centre, N.Y. [c] Suppocire BCM, Gattefosse, Saint Priest, France. [d] Kaomel, Glidden-Durkee, Rockville Centre, N.Y. [e] Hydrokote 2-7, Capital City Products, Columbus, Ohio.

The second study tested the effect of several parameters on the hardening characteristics of Base 3 since this base was the least stable at 37°. The parameters studied were storage temperature after molding, cooling rate during molding, and ingredient addition. The storage temperatures used were room temperature (22°), refrigeration (4°), and freezer (−5°). For cooling variation, the suppositories were molded using dry ice, refrigeration, and standing at room temperature, varying the molding time (cooling from 50 to 20°) from 5 to 15 to 30 min, respectively. The ingredient addition studies were carried out using 5, 10, and 20% zinc oxide USP, 5% neutral oil, and 0.2, 0.5, 1, and 2% resorcinol USP. Samples were tested at the beginning of the study and after 1-, 2-, 4-, and 6-week periods.

All suppositories were molded in 50-cavity brass molds. All masses were prepared in a 2-liter beaker nested in a 4-liter beaker containing water on a hot plate. Zinc oxide USP was passed through a comminuting machine[5] at high speed with hammers forward before incorporation. Dispersion was accomplished by a laboratory homogenizing mixer[6].

Differential Scanning Calorimetry—A thermal analyzer[7] was used with the differential scanning calorimeter cell attachment. Samples between 7.0 and 10.0 mg were prepared in tightly covered aluminum cups and were tested against an empty, covered cup blank. Sample weight was determined by subtracting the tare weight of the container. The cell containing the blank and sample cups was chilled to −20° using liquid nitrogen. The test runs then were carried out at a heating rate of 2.0°/min over the range of −10–+45°.

Three samples of each base were tested as individual continuous experiments. The experimental design allowed the same samples to be tested at all incremental age periods (initial, 1, 2, 4, and 6 weeks and 6 months or equilibrium).

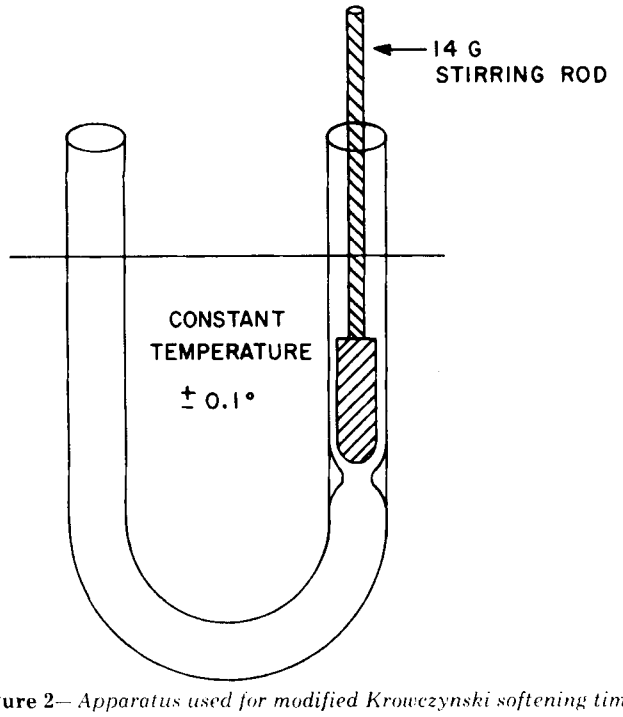

Figure 2— *Apparatus used for modified Krowczynski softening time test.*

[5] Fitzpatrick model M mill with N000 screen.
[6] Arde-Barinco model CJ-3.
[7] Dupont model 900.

After the equilibrium testing of a sample (*e.g.*, 6 months old), the melted sample was held at 45° for 5 min and then cooled back to room temperature using compressed air or nitrogen through the cell over ~20 min. The test then was repeated immediately, with freezing to −20° and running as outlined to establish the initial endotherm. After holding and cooling to room temperature a second time, the sample was stored at the desired temperature for 1, 2, 4, or 6 weeks. Retesting and continued storage were repeated, resolidifying the sample each time, so that full testing of all time periods took 13 weeks. If any test periods were missed, a longer period was measured, and the desired period was repeated that many weeks later.

Bases 1 and 3 then were retested in triplicate at equilibrium, at the initial point, and at 6 weeks, but they were stored at 4, 20, and 30°. Base 3 then was tested with 5% neutral oil (duplicate), 10% zinc oxide USP (duplicate), and 2% resorcinol USP (duplicate as well as single samples with 1, 0.5, and 0.2% resorcinol USP). As before, these samples were tested only at equilibrium, at the initial point, and at 6 weeks.

The recorded endotherms were examined for the position and height of the major peak. This height was measured vertically from the peak tip to a horizontal line drawn between the two equilibrium points at the beginning and end of the run. The height in centimeters was converted to degrees, divided by the sample weight, and recorded as degrees per gram. Heats of fusion, ΔH_f, for the samples were determined by cutting and weighing sample endotherms *versus* a gallium standard.

X-Ray Diffraction—An X-ray diffractometer[8] was used. Samples of each base were prepared by melting the base and molding it in a 0.2-mm thick aluminum frame backed by masking tape. The frame opening created a sample surface measuring 2.0 × 1.0 cm. All five bases were studied initially upon molding and after 1, 2, 4, and 6 weeks. Since this test is nondestructive to the sample, a study could be run in 6 weeks. A second study was done on Bases 1 and 3 stored at 4, 20, and 30° *versus* a polypropylene control since variability was seen in the amplifier from week to week.

RESULTS AND DISCUSSION

Softening Time Testing—Table II summarizes the results of the base screening study performed with the modified Krowczynski apparatus. Observed softening times were noted as a function of temperature for suppositories stored for up to 54 days. Bases 2 and 5 showed no increases in softening time throughout the range of rectal temperature. While Bases 1 (Fig. 3) and 4 showed only slight hardening at 37°, the softening times were increased significantly at lower body temperatures. Base 3 (Fig. 4) showed drastic hardening at all temperatures studied.

Table III summarizes the results of the effects of cooling time, storage temperature, and adjuvant addition on the rise in softening time of Bases 1 and 3 at 37°. Cooling time had no effect on the degree of hardening noted at the test periods, whereas storage temperature had an initial separating effect on the samples but not a lasting one. This finding suggested a discrete, point-to-point process that occurred more slowly as the temperature was lowered as opposed to an ongoing, continuous process. As a control, Base 1 showed little change.

Ingredient addition studies showed the effect on the hardening rate of the three additives: neutral oil, resorcinol USP, and zinc oxide USP. The two oil-soluble materials yielded more dramatic results than the insoluble zinc oxide due to the viscosity-imparting property of this dispersed powder in the melted base. Therefore, the smallest addition of zinc oxide was the most effective in reducing hardening.

Conversely, reducing the concentration of soluble resorcinol reduced its effect on prevention of hardening.

X-Ray Diffraction Studies—In the initial study, all five bases showed similar results both upon molding and after storage.

[8] North American Phillips Co. (Norelco).

Table II—Base Screening Study: Softening Time Stability after Storage at 22°

Age of Base, days	Time to Soften at Test Temperature, min			
	37.0°	36.5°	36.0°	35.5°
Base 1				
1	8.5	10	12	14.5
11	14.5	21	31	60
38	16	22	33	72
53	16	20	28	100
Base 2				
12	6.5	8	10	12
28	7	9	11	12
54	8	9.5	11.5	14
Base 3				
1	14.5	17	21.5	35
9	38	75	>100	>100
18	49	>100	>100	>100
Base 4				
1	8.5	12	18	32
10	11	17	30	44
28	11	21	32	85
43	14	25	35	>100
Base 5				
7	9	11	13.5	30
15	9	11.5	15	22
33	9	11	13.5	30
48	9	11.5	15	22

All bases, upon molding, exhibited a broad peak (~2.2° wide at mid-height) at a 2θ value centering at 20.3–20.6°. A sharper peak (~0.6° wide at half-height) also was seen at a 2θ value of 22.7–23.0°. In the initial samples, the low point between the two peaks was at ~37% of the height of the peak at 20.5°.

After storage, no new major peaks were seen. However, the peak at 20.3° grew sharper and more distinct from the peak at 22.7°, eventually having a smaller width similar to the other peak. The low point between the peaks after 6 weeks approached the baseline (Fig. 5). In Bases 3 and 4, peaks that appeared initially as shoulders on the major peak at 20.5° became more distinct, but in no case did any shift occur to a new position nor did any peak evolve that was not observed initially.

These observations suggest an amorphous to crystalline shift in the materials studied rather than polymorphic changes. Figure 5 shows a typical initial and aged sample scan made on Base 3.

In interpreting these data, it must be kept in mind that all commercial fat products, including semisynthetic suppository bases, are mixtures of many fatty molecules. Thus, these data may not be examined in the same depth as the data for a pure compound or a single crystal. Never-

Table III—Effect of Cooling Time, Storage Temperatures, and Adjuvants on the Softening Time Stability of Bases 1 and 3 at 37°

Base	Excipient	Cooling Time, min	Storage Temperature	Softening Time, min			
				Initial	2 Weeks	4 Weeks	6 Weeks
3[a]	None	15	22°	37	68	103	205
		30	22°	22	70	112	208
		5	22°	24	77	95	200
		15	4°	37	34	90	203
		15	−5°	37	28	27.5	190
	Neutral oil	15	22°	25	34	40	39
	Resorcinol, 0.2%	15	22°	15	35	38	42
	Resorcinol, 0.5%	15	22°	17	33	37	39
	Resorcinol, 1.0%	15	22°	22	31	33	35
	Resorcinol, 2.0%	15	22°	17	26	27	27
	Zinc oxide, 5%	15	22°	35	105	106	102
	Zinc oxide, 10%	15	22°	35	78	95	130
	Zinc oxide, 20%	15	22°	40	80	108	150
1[b]	None	15	22°	7.5	12	20	20
		30	22°	8	10	12	16
		15	4°	8	8	10.5	10

[a] Suppocire BCM. [b] Witepsol H-175.

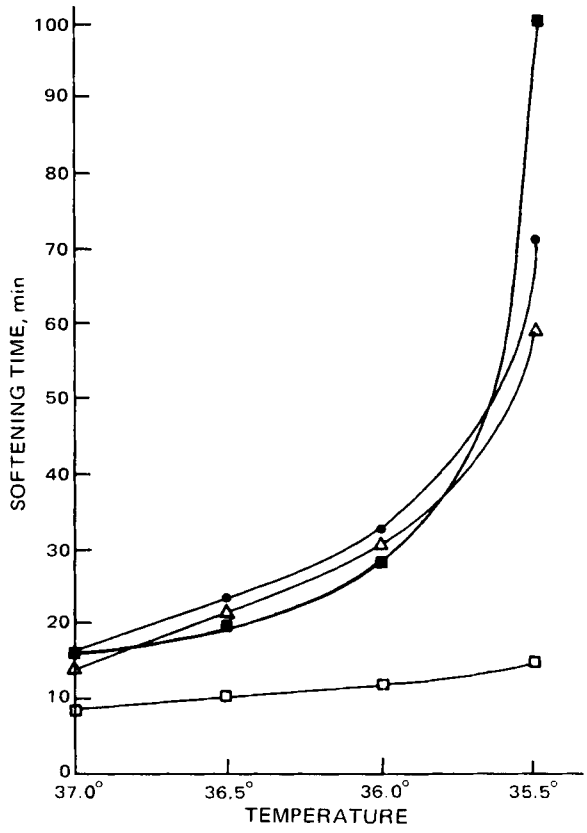

Figure 3—*Softening time stability for Base 1 stored at 22°. Key: □, 1 day; △, 11 days; ●, 38 days; and ■, 53 days.*

theless, the graphs are definitely characteristic. Therefore, while it would be presumptuous to claim that no polymorphism contributes to (or detracts from) the phenomenon under study, it still is obvious from the scans generated that the mechanism responsible for the effect being

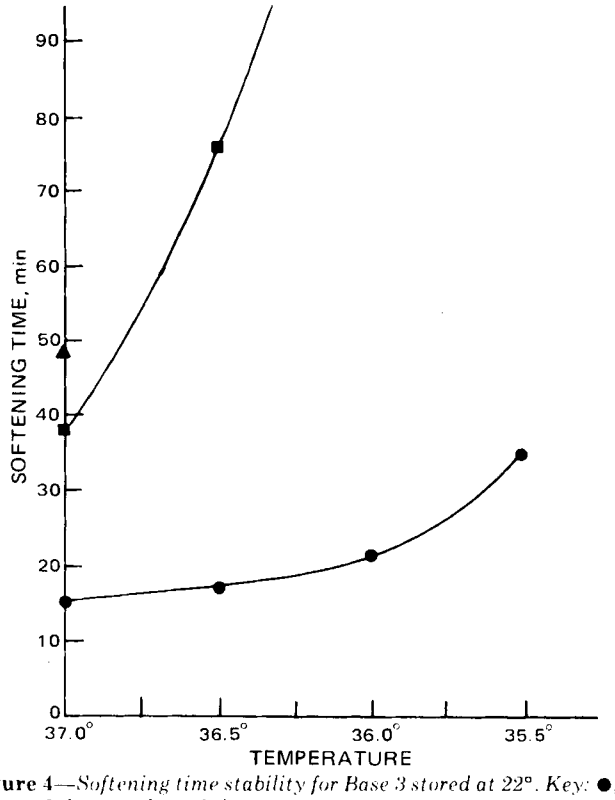

Figure 4—*Softening time stability for Base 3 stored at 22°. Key: ●, 1 day; ■, 9 days; and ▲, 18 days.*

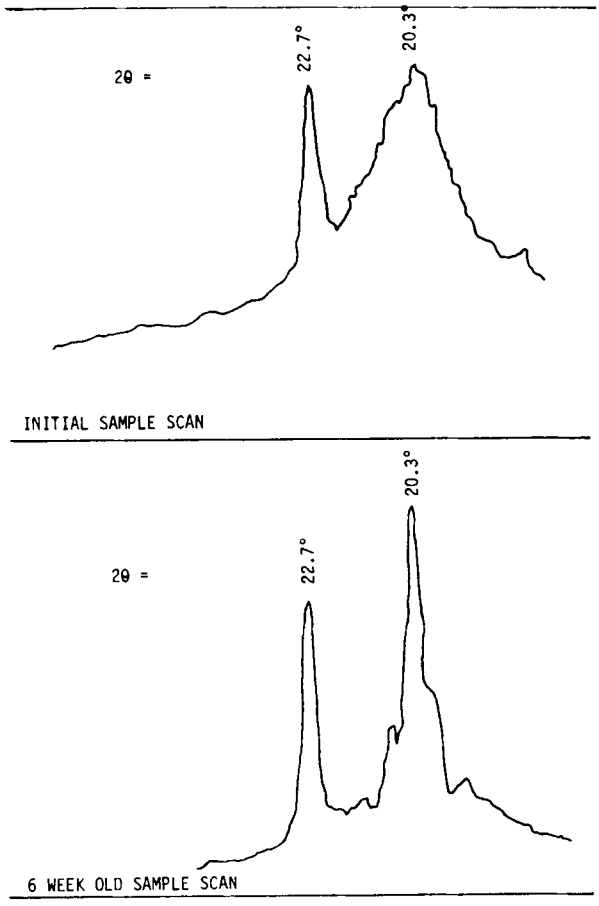

Figure 5—*Comparison of X-ray diffractometer scans for initial and 6-week-old samples of Base 3 stored at 22°.*

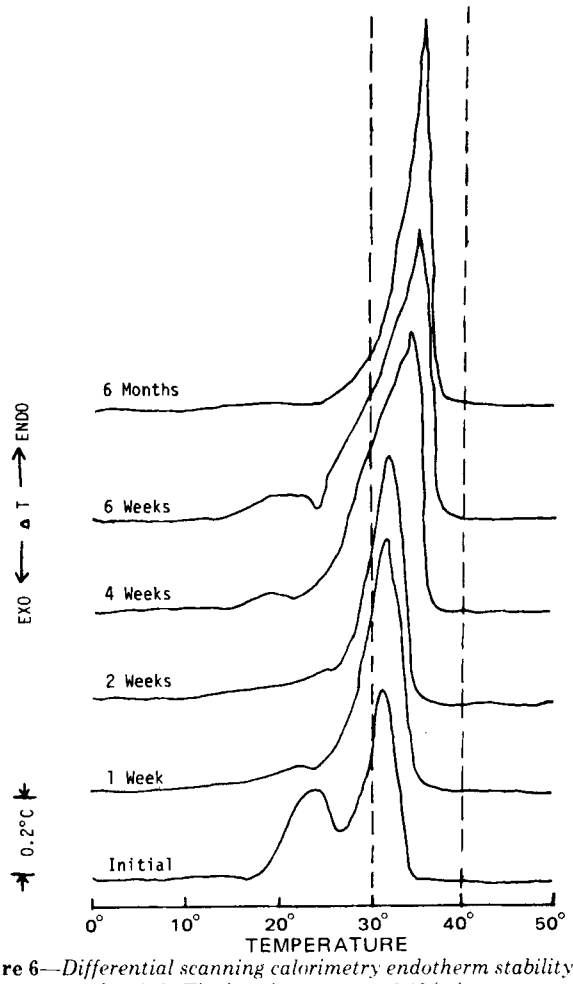

Figure 6—*Differential scanning calorimetry endotherm stability scan of Base 1 stored at 22°. The heating rate was 2.0°/min.*

measured is a crystallization phenomenon. This result reinforces the observation made on comparisons of softening times that a discrete process characterized by a temperature-dependent rate of hardening was taking place.

The hardening rate dependence on temperature was reinforced by the second X-ray study, which showed more rapid peak sharpening at higher storage temperatures in samples aged for 6 weeks at 4, 20, and 30°.

Differential Scanning Calorimetry—Accuracy in melting-range determinations was gained by utilizing a heating rate of 2°/min. The poor heat transfer characteristics of fats (14) prevented the use of faster speeds due to the lag time in the return to a ΔT equilibrium. Speeds of 5°/min and higher totally washed out and shifted the sharp peaks observed at 2°/min. In an experiment where changes in the peak positions of 1° were being sought and metastable transformations were not, this choice was mandatory since slower heating rates yielded sharper endo- or exotherms and located an equilibrium transformation temperature more accurately (10).

Figures 6 and 7 show the general trend observed for Bases 1 and 3 in the initial study conducted with samples stored at room temperature. In all bases, regardless of the initial peak position, a 2.5–3.0° shift upward in the peak positon, a sharpening of the peak, and an increase in peak height were observed over the test period. Tables IV and V summarize the data collected to quantify the measurable parameters of the endotherms in the initial study. Table IV lists the changes in temperature positions of the major peak. Table V lists the ratio of the major peak

Table IV—Base Screening Study: Temperature Position of Major Endotherm Peak [a]

		Storage Time at Room Temperature					
Base	Sample	Initial	1 Week	2 Weeks	4 Weeks	6 Weeks	6 Months
1	A	33.0	34.0	34.5	35.0	34.0	36.0
	B	32.0	34.0	35.0	34.0	34.0	36.0
	C	32.0	32.0	32.0	32.0	32.0	36.5
2	A	31.5	31.5	31.5	32.0	31.0	33.0
	B	31.5	31.5	32.0	31.5	32.0	34.0
	C	31.0	33.5	34.0	34.0	34.0	32.0
3	A	33.0	34.5	36.0	37.5	37.5	37.5
	B	33.5	37.0	37.0	36.5	36.5	37.5
	C	33.0	35.0	37.5	37.0	37.0	37.5
4	A	33.0	33.5	34.0	36.0	34.5	36.0
	B	32.0	33.5	34.0	34.0	34.0	37.0
	C	32.0	34.0	34.0	34.0	34.0	37.0
5	A	33.0	33.0	35.0	35.5	36.0	36.5
	B	32.5	33.0	34.0	35.5	35.5	36.5
	C	32.5	33.5	35.0	35.0	34.0	36.5

[a] Values are in degrees.

Table V—Base Screening Study: Ratio of Height of Major Peak to Sample Weight [a]

		Storage Time at Room Temperature					
Base	Sample	Initial	1 Week	2 Weeks	4 Weeks	6 Weeks	6 Months
1	A	65.6	79.2	70.1	90.9	66.7	109.5
	B	77.5	85.2	59.4	56.8	63.3	148.4
	C	63.6	82.0	79.8	68.5	65.8	88.2
2	A	77.9	75.7	106.6	71.2	112.1	92.9
	B	79.7	80.7	80.2	81.7	72.3	87.2
	C	85.7	48.6	48.1	45.2	48.6	67.2
3	A	51.7	53.3	58.0	73.5	81.1	79.6
	B	47.2	73.7	66.1	66.4	68.1	86.2
	C	42.1	42.1	73.2	71.4	68.1	79.3
4	A	40.6	51.8	63.9	44.3	49.5	50.6
	B	35.3	48.2	47.6	42.9	40.5	58.8
	C	40.5	64.8	67.8	78.7	72.8	65.4
5	A	32.7	40.7	70.9	60.6	54.2	58.6
	B	34.4	33.9	30.4	42.4	38.4	54.8
	C	33.7	35.4	42.2	43.4	47.4	51.4

[a] Values are in degrees per gram.

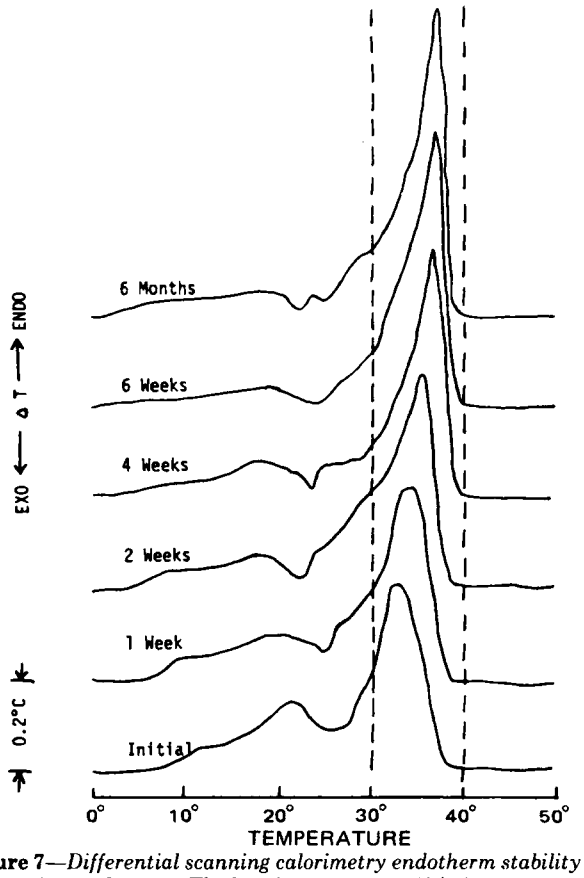

Figure 7—*Differential scanning calorimetry endotherm stability scan of Base 3 stored at 22°. The heating rate was 2.0°/min.*

height to the sample weight and the changes in this parameter over time.

The changes in sample endotherms over the 6-week period correlated perfectly with the observations of Krowczynski softening times and X-ray diffraction patterns. In all cases, a gradual change was seen. As seen in the X-ray diffraction data, changes were observed in all five bases, regardless of the production method or chemical composition.

The differential scanning calorimetry data explain the base to base variation observed in Krowczynski softening times through a correlation to the solid fat index. The solid fat index is determined dilatometrically[9] on samples immediately after solidification and may be considered only as an initial collection of data subject to change upon aging. A correlation between initial differential scanning calorimetry data and the solid fat index was shown by Miller *et al.* (13). Therefore, it is a reasonable assumption that an upward shift in the differential scanning calorimetry endotherm represents a similar upward shift in the solid fat index, *i.e.*, a higher solids content at any measured temperature. A higher solids content at any given temperature would raise the viscosity of the suppository melt at that point and, in turn, increase its softening time in the Krowczynski test.

A correlation between the degree of hardening of the five bases and their solid fat indexes at ~33° was seen (Fig. 1). Base 3, which hardened the most at 37°, had the highest solid fat index at 33° (42%). Bases 1 and 4 were next in hardening and next in decreasing solid fat index values at this temperature (37 and 35%). Base 5 at 33% and Base 2 at 17% hardened the least and were the lowest in the solid fat index at 33°.

While this correlation assumes a total shift of the curves by 4°, this shift is not necessarily the case since the shape of the curve could be changing. Until a method to measure the solid fat index of an aged sample is readily available, the procedure used for this study provides adequate correlation for prediction of hardening effects, rationalized through an upward shift in the solid fat index. In comparison, initial chemical and process information provides only the most general clues as to the melting behavior of the finished base at any age after resolidification. No useful conclusions could be drawn from the heat of fusion data collected or the peak height to sample weight ratios measured.

[9] American Oil Chemists' Society Test Method 113a.

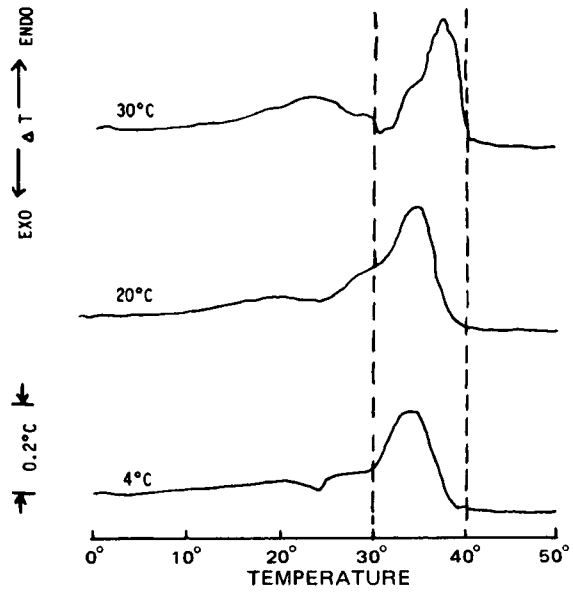

Figure 8—*Effect of storage temperature on differential scanning calorimetry endotherm stability for 6-week-old samples of Base 3. The heating rate was 2.0°/min.*

The effect of the storage temperature on the hardening rate was confirmed by measurements of the endotherms of Bases 1 and 3 stored for 6 weeks at 4, 20, and 30°. The comparative endotherms for Base 3 are shown in Fig. 8. The samples stored at temperatures closer to, but below, their melting ranges reached equilibrium crystallinity more rapidly. This phenomenon is similar to the annealing or tempering process used in metal alloy and glass preparation.

The ingredient addition trial endotherms of Base 3 showed no variation from the endotherms of Base 3 tested without additives either initially or after storage. Thus, it can be concluded that not only is there no significant freezing-point depression but that the mechanism involved in slowing the hardening rate, as evidenced by changes in softening time, is not involved with the phenomenon itself. Since the endotherm still is changing, the amorphous to crystalline shift is still occurring and, likewise, so is the shift in the solid fat index. The explanation lies in the fact that the overall phenomenon being prevented is an increase in the viscosity of the melting suppository since that is what the softening time is measuring. Addition of ingredients provides numerous pockets of discontinuity in the gross crystalline structure of the fatty solids present, lowering the gross viscosity of the semisolid suppository under testing.

This explains the effect seen from different concentrations of resorcinol. As less resorcinol was employed, there was less of a decrease of hardening. With zinc oxide, which is not soluble in the base, diminished hardening was noted at smaller concentrations, but this trend began to reverse when the powders began to add to the viscosity of the melt at higher concentrations.

CONCLUSIONS

The hardening phenomenon has been characterized by multiple test methods to be a finite amorphous to crystalline transition. The rate of this transition is storage temperature dependent but is independent of cooling time during solidification within the bounds of suppository molding rates. This transition is manifested in an upward shift in the solid fat index in the range of body temperatures. This rise in the percent solids in the melt at the temperature under examination results in a rise in viscosity at that temperature, which is perceived as hardening. In other words, there are less meltable solids at body temperature in a suppository that has hardened. Ingredients added to the base do not hinder the transition but may have one of two effects. Base-soluble ingredients disturb the gross crystalline structure of the fatty solids, lowering the achieved viscosity upon melting. Base-insoluble ingredients, in higher concentrations, may raise the viscosity of the melt simply by providing a higher solids content.

Suppository base selection may be simplified in two ways. First, examination of the solid fat index for potential problems upon shifting is an easy investigative early-warning device to narrow the field of choice. Second, differential scanning calorimetric examination of an aged base

sample (as received from a potential supplier) and an instantaneous rerun yield initial *versus* aged data on melting-range shifting after an investment in testing time of <1 hr. Even though the formula ingredients may retard the rate of transition, this test produces a best and worst case melting range to evaluate.

The results of this study in no way reflect on the quality of any base tested or on the ability of any of the manufacturers to supply a range of bases suitable to individual needs.

REFERENCES

(1) L. Krowczynski, *Acta Pol. Pharm.*, **22**(2), 157 (1965).

(2) L. Krowczynski, *Diss. Pharm.*, **11**, 269 (1959).

(3) L. Krowczynski, *Farm. Pol.*, **17**, 506 (1961).

(4) G. Ritschel-Beurlin, *Prap. Pharm.*, **5**, 6 (1969).

(5) J. J. Torrado-Valeiras, *An. Real Acad. Farm.*, **35**(3), 375 (1969).

(6) G. Mezey, G. Regdon, and K. Sztankovanszky, *Pharmazie*, **28**, 465 (1973).

(7) J. Kanto, *Int. J. Clin. Pharmacol.*, **12**, 427 (1975).

(8) C. J. deBlaey and J. Rutten-Kingma, *Pharm. Acta Helv.*, **51**(6), 186 (1976).

(9) J. Whittam and H. Rosano, *J. Am. Oil Chem. Soc.*, **52**(4), 128 (1975).

(10) N. Lovegren, M. Gray, and R. Feuge, *ibid.*, **53**(2), 83 (1976).

(11) *Ibid.*, **53**(3), 108 (1976).

(12) J. B. Rossell, *J. Am. Oil. Chem. Soc.*, **52**, 505 (1975).

(13) W. J. Miller, W. H. Koester, and F. E. Freeberg, *ibid.*, **46**, 341 (1969).

(14) A. E. Bailey, "Melting & Solidification of Fats," Interscience, New York, N.Y., 1950, p. 91.

ACKNOWLEDGMENTS

Presented in part at the Industrial Pharmaceutical Technology Section, APhA Academy of Pharmaceutical Sciences, Phoenix meeting, November 1977.

Abstracted in part from a thesis submitted by L. J. Coben to Rutgers University in partial fulfillment of the Doctor of Philosophy degree requirements.

The authors thank Dr. D. Morrow of the College of Engineering, Rutgers University, for help with the X-ray diffractometer.

Kinetic Study of USP Blue Tetrazolium Assay with Methylprednisolone, Hydrocortisone, and Their Hemisuccinate Esters by High-Pressure Liquid Chromatography

MARILYN DIX SMITH

Received December 7, 1979, from *Abbott Laboratories, North Chicago, IL 60064.* Accepted for publication March 25, 1980. Present address: American Critical Care, McGaw Park, IL 60085.

Abstract □ The reactions of blue tetrazolium (I) with methylprednisolone and hydrocortisone and their hemisuccinate esters at ambient temperature under USP assay conditions in alcohol USP and in absolute alcohol were followed by high-pressure liquid chromatography (HPLC) and spectrophotometry. The disappearance of the ester and the increase and then decrease in the alcohol, as well as the formation of several reaction products with time, were observed by HPLC analysis. The reduction of I was observed spectrophotometrically. A sequential kinetic model was used to describe the overall reaction. The rate constants for the hydrolysis of the hemiester (k_1), the reaction with I (k_2), and the degradation of the parent steroid (k_3) were determined by discrete kinetic experiments using HPLC. The following observations were made: (*a*) k_1 is proportional to $[H_2O]$ and is the rate-limiting step, (*b*) k_2 is about 100 times the value of k_3, and (*c*) k_2 for methylprednisolone is about the same as for hydrocortisone and appears to be independent of the concentration of water. With these rate constants, simulated time–concentration profiles for the reaction of the esters with I favorably compared with experimental data in alcohol USP and absolute alcohol. This study shows that the USP blue tetrazolium assay with these esters has potential for variability and is not stability indicating.

Keyphrases □ Methylprednisolone—and hemisuccinate ester, high-pressure liquid chromatographic and spectrophotometric monitoring of USP assay with blue tetrazolium □ Hydrocortisone—and hemisuccinate ester, high-pressure liquid chromatographic and spectrophotometric monitoring of USP assay with blue tetrazolium □ High-pressure liquid chromatography—kinetic study of USP blue tetrazolium assay with methylprednisolone and hydrocortisone and their hemisuccinate esters

The official USP assay for the corticosteroids, including their esters, is the blue tetrazolium (I) reaction (1). The base-catalyzed reduction of I by the C-17 side chain of corticosteroids is a classical reaction in steroid analysis (2). Meyer and Lindberg (3) established that the α-ketol moiety in corticosteroids is responsible for the reduction of I. However, the reaction mechanism for the C-21 esters of corticosteroids is unknown.

BACKGROUND

Johnson *et al.* (4) reported that color development was unusually slow with hydrocortisone hemisuccinate compared to other steroids. In a study of the reaction of I with cortisone acetate, a C-21 ester, Guttman (5) showed that as the concentration of base catalyst was decreased, the lag time increased and the sigmoid shape of the curve was emphasized. He concluded that hydrolysis of the ester was a prerequisite to a reaction resulting in the generation of formazan. Graham *et al.* (6) also suggested that ester hydrolysis occurs prior to and during formazan development. Their conclusions were derived from graphical kinetic treatment of the spectrophotometric data.

The hydrolysis of the hemiester of corticosteroids in aqueous media has been studied by several investigators. Mauger *et al.* (7) reported that the degradation of its hemisuccinate ester to hydrocortisone was first order. Further degradation to a species devoid of the 17-dihydroxyacetone also was observed. This degradation was followed by separation of the alcohol and ester and subsequent reaction with I. Garrett (8) studied the alkaline hydrolysis of hydrocortisone hemisuccinate by constant pH titration.

High-pressure liquid chromatography (HPLC) has been used recently to study the degradation of hydrocortisone (9). An HPLC method was described (10) that determined simultaneously hydrocortisone (II*a*) and its hemisuccinate ester (III*a*) or methylprednisolone (II*b*) and its hemisuccinate ester (III*b*).

This paper reports a kinetic study of the reaction of I with II and III using this HPLC method. The hydrolysis rates of III to II under compendial blue tetrazolium assay conditions also are reported.

The effect of water in the final reaction mixture of I has been studied. The percentage of water in the official USP method [due to the use of alcohol USP and 10% aqueous tetramethylammonium hydroxide (IV) in the preparation of reagents and samples] is 5.8 (11). Rechnagel and

0022-3549/80/0800-0960$01.00/0

© 1980, American Pharmaceutical Association

sample (as received from a potential supplier) and an instantaneous rerun yield initial *versus* aged data on melting-range shifting after an investment in testing time of <1 hr. Even though the formula ingredients may retard the rate of transition, this test produces a best and worst case melting range to evaluate.

The results of this study in no way reflect on the quality of any base tested or on the ability of any of the manufacturers to supply a range of bases suitable to individual needs.

REFERENCES

(1) L. Krowczynski, *Acta Pol. Pharm.*, **22**(2), 157 (1965).

(2) L. Krowczynski, *Diss. Pharm.*, **11**, 269 (1959).

(3) L. Krowczynski, *Farm. Pol.*, **17**, 506 (1961).

(4) G. Ritschel-Beurlin, *Prap. Pharm.*, **5**, 6 (1969).

(5) J. J. Torrado-Valeiras, *An. Real Acad. Farm.*, **35**(3), 375 (1969).

(6) G. Mezey, G. Regdon, and K. Sztankovanszky, *Pharmazie*, **28**, 465 (1973).

(7) J. Kanto, *Int. J. Clin. Pharmacol.*, **12**, 427 (1975).

(8) C. J. deBlaey and J. Rutten-Kingma, *Pharm. Acta Helv.*, **51**(6), 186 (1976).

(9) J. Whittam and H. Rosano, *J. Am. Oil Chem. Soc.*, **52**(4), 128 (1975).

(10) N. Lovegren, M. Gray, and R. Feuge, *ibid.*, **53**(2), 83 (1976).

(11) *Ibid.*, **53**(3), 108 (1976).

(12) J. B. Rossell, *J. Am. Oil. Chem. Soc.*, **52**, 505 (1975).

(13) W. J. Miller, W. H. Koester, and F. E. Freeberg, *ibid.*, **46**, 341 (1969).

(14) A. E. Bailey, "Melting & Solidification of Fats," Interscience, New York, N.Y., 1950, p. 91.

ACKNOWLEDGMENTS

Presented in part at the Industrial Pharmaceutical Technology Section, APhA Academy of Pharmaceutical Sciences, Phoenix meeting, November 1977.

Abstracted in part from a thesis submitted by L. J. Coben to Rutgers University in partial fulfillment of the Doctor of Philosophy degree requirements.

The authors thank Dr. D. Morrow of the College of Engineering, Rutgers University, for help with the X-ray diffractometer.

Kinetic Study of USP Blue Tetrazolium Assay with Methylprednisolone, Hydrocortisone, and Their Hemisuccinate Esters by High-Pressure Liquid Chromatography

MARILYN DIX SMITH

Received December 7, 1979, from *Abbott Laboratories, North Chicago, IL 60064.* Accepted for publication March 25, 1980. Present address: American Critical Care, McGaw Park, IL 60085.

Abstract □ The reactions of blue tetrazolium (I) with methylprednisolone and hydrocortisone and their hemisuccinate esters at ambient temperature under USP assay conditions in alcohol USP and in absolute alcohol were followed by high-pressure liquid chromatography (HPLC) and spectrophotometry. The disappearance of the ester and the increase and then decrease in the alcohol, as well as the formation of several reaction products with time, were observed by HPLC analysis. The reduction of I was observed spectrophotometrically. A sequential kinetic model was used to describe the overall reaction. The rate constants for the hydrolysis of the hemiester (k_1), the reaction with I (k_2), and the degradation of the parent steroid (k_3) were determined by discrete kinetic experiments using HPLC. The following observations were made: (*a*) k_1 is proportional to $[H_2O]$ and is the rate-limiting step, (*b*) k_2 is about 100 times the value of k_3, and (*c*) k_2 for methylprednisolone is about the same as for hydrocortisone and appears to be independent of the concentration of water. With these rate constants, simulated time–concentration profiles for the reaction of the esters with I favorably compared with experimental data in alcohol USP and absolute alcohol. This study shows that the USP blue tetrazolium assay with these esters has potential for variability and is not stability indicating.

Keyphrases □ Methylprednisolone—and hemisuccinate ester, high-pressure liquid chromatographic and spectrophotometric monitoring of USP assay with blue tetrazolium □ Hydrocortisone—and hemisuccinate ester, high-pressure liquid chromatographic and spectrophotometric monitoring of USP assay with blue tetrazolium □ High-pressure liquid chromatography—kinetic study of USP blue tetrazolium assay with methylprednisolone and hydrocortisone and their hemisuccinate esters

The official USP assay for the corticosteroids, including their esters, is the blue tetrazolium (I) reaction (1). The base-catalyzed reduction of I by the C-17 side chain of corticosteroids is a classical reaction in steroid analysis (2). Meyer and Lindberg (3) established that the α-ketol moiety in corticosteroids is responsible for the reduction of I. However, the reaction mechanism for the C-21 esters of corticosteroids is unknown.

BACKGROUND

Johnson *et al.* (4) reported that color development was unusually slow with hydrocortisone hemisuccinate compared to other steroids. In a study of the reaction of I with cortisone acetate, a C-21 ester, Guttman (5) showed that as the concentration of base catalyst was decreased, the lag time increased and the sigmoid shape of the curve was emphasized. He concluded that hydrolysis of the ester was a prerequisite to a reaction resulting in the generation of formazan. Graham *et al.* (6) also suggested that ester hydrolysis occurs prior to and during formazan development. Their conclusions were derived from graphical kinetic treatment of the spectrophotometric data.

The hydrolysis of the hemiester of corticosteroids in aqueous media has been studied by several investigators. Mauger *et al.* (7) reported that the degradation of its hemisuccinate ester to hydrocortisone was first order. Further degradation to a species devoid of the 17-dihydroxyacetone also was observed. This degradation was followed by separation of the alcohol and ester and subsequent reaction with I. Garrett (8) studied the alkaline hydrolysis of hydrocortisone hemisuccinate by constant pH titration.

High-pressure liquid chromatography (HPLC) has been used recently to study the degradation of hydrocortisone (9). An HPLC method was described (10) that determined simultaneously hydrocortisone (II*a*) and its hemisuccinate ester (III*a*) or methylprednisolone (II*b*) and its hemisuccinate ester (III*b*).

This paper reports a kinetic study of the reaction of I with II and III using this HPLC method. The hydrolysis rates of III to II under compendial blue tetrazolium assay conditions also are reported.

The effect of water in the final reaction mixture of I has been studied. The percentage of water in the official USP method [due to the use of alcohol USP and 10% aqueous tetramethylammonium hydroxide (IV) in the preparation of reagents and samples] is 5.8 (11). Rechnagel and

0022-3549/80/0800-0960$01.00/0

© 1980, American Pharmaceutical Association

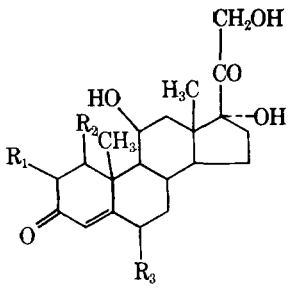

II

IIa: $R_1 = R_2 = R_3 = H$
IIb: $R_1 = R_2$ = missing (unsaturated), $R_3 = CH_3$

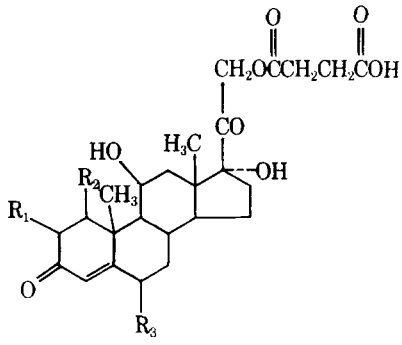

III

IIIa: $R_1 = R_2 = R_3 = H$
IIIb: $R_1 = R_2$ = missing (unsaturated), $R_3 = CH_3$

Litteria (12) found that water inhibits the reaction of I and that the extent of inhibition increases as the concentration of water in the final reaction increases. However, Graham and Kenner (11) showed that the effect of water is essentially negligible if it is present at <6%. This paper reports the effect of the water content of the reaction mixture on the rate constants involved in the reaction of I with II and III.

EXPERIMENTAL

Reagents—Acetonitrile[1], acetic acid[2], anhydrous methanol[3], blue tetrazolium[3] (I), and tetramethylammonium hydroxide[3] (IV) were reagent grade. Alcohol and absolute alcohol were USP grade. Compounds IIa, IIIa, and IIIb were USP reference standards. Compound IIb was an NF reference standard.

Apparatus—A high-pressure liquid chromatograph[4] equipped with a 100-μl injector[5], a fixed-wavelength detector[6] (λ = 254 nm) or a variable-wavelength detector[7], a digital integrator[8], a strip-chart recorder[9], and a scanning spectrophotometer[10] were used.

HPLC Conditions—A microparticulate (5-μm) octadecylsilane column[11] was used. The mobile phase was acetonitrile–water–acetic acid (35:65:2) at a flow rate of 1 ml/min.

Sample Preparation—Fifty milligrams of IIIa or IIIb and 39 mg of IIa and IIb were dissolved separately in 100 ml of alcohol (absolute or USP). Then 12 ml of these solutions was diluted to 500 ml with alcohol (absolute or USP) to a final concentration of ~20 μM for each sample.

Reagent Preparation—Compound I, 500 mg, was dissolved in 100 ml of anhydrous methanol. A 10% solution of IV in water was diluted 1:10 with alcohol USP. A 5% acetic acid solution was prepared by diluting acetic acid 1:20 with water.

[1] Glass distilled, Burdick & Jackson.
[2] Mallinckrodt.
[3] J. T. Baker Chemical Co.
[4] Model 3500, Chromatronix, Spectra-Physics, Santa Clara, Calif.
[5] Valco, Houston, Tex.
[6] Model 8200, Spectra-Physics.
[7] Model 970A (λ 242 nm), Tracor, Austin, Tex.
[8] Autolab Minigrator, Spectra-Physics.
[9] Model 7130A, Hewlett-Packard.
[10] Coleman 570, Perkin-Elmer.
[11] Spherisorb 5-μm ODS, Spectra-Physics.

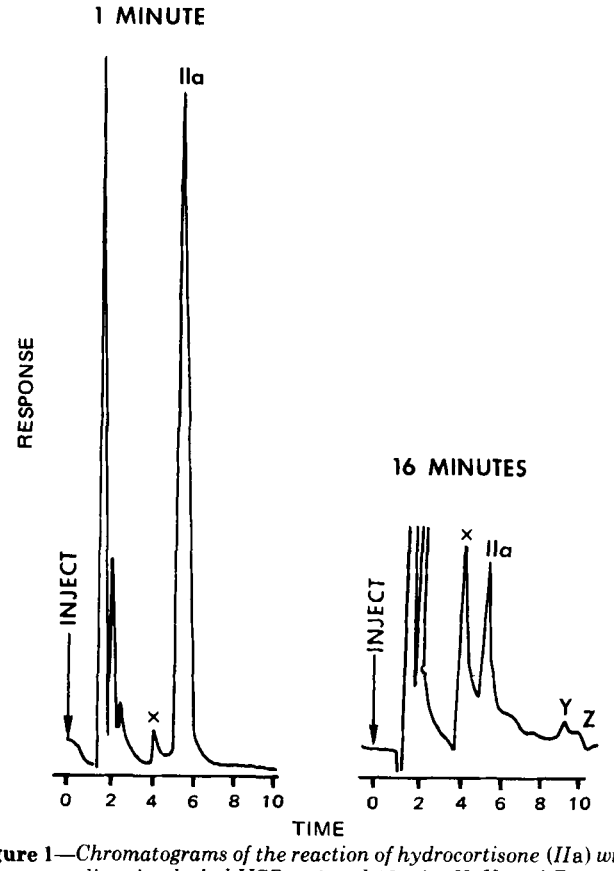

Figure 1—*Chromatograms of the reaction of hydrocortisone (IIa) with blue tetrazolium in alcohol USP at 1 and 16 min; X, Y, and Z are the products of the reaction.*

Kinetic Experiments—*Experiments with I*—Twenty milliliters of the solution of I and 40 ml of diluted IV were added to 200 ml of each sample preparation. The solution was mixed and stored in the dark. At timed intervals, 15 ml of solution was withdrawn and 0.6 ml of acetic acid was added. The absorbance of this solution at 525 nm *versus* a blank preparation was recorded. A portion of the withdrawn solution also was diluted 1:1 with 5% acetic acid and injected onto the HPLC column, and the chromatograms were recorded.

Experiments without I—Twenty milliliters of anhydrous methanol and 40 ml of diluted IV were added to 200 ml of each sample preparation. The solution was mixed. At timed intervals, 15 ml was withdrawn and 0.6 ml of acetic acid was added. This withdrawn solution then was diluted 1:1 with 5% acetic acid and injected onto the HPLC column.

RESULTS AND DISCUSSION

The reactions of I with IIa, IIb, IIIa, and IIIb at ambient temperature under USP assay conditions for III (13) in alcohol USP as well as in absolute alcohol were followed by HPLC and spectrophotometry. The identity and quantitation of each peak were made with respect to standard solutions of IIa, IIb, IIIa, and IIIb.

The percent of water, as determined by the Karl Fischer reaction, was 6.0% in alcohol USP and 0.04% in absolute alcohol. Based on these values, the percent of water in the reaction mixture was calculated to be 6.9% when alcohol USP was used in the sample preparation and 2.3% when absolute alcohol was used.

Chromatograms of these reaction mixtures in alcohol USP at various times are given in Figs. 1–4. Figures 1 and 3 (the reaction of I with IIa and IIb) show a decrease in II with a subsequent increase in peaks X, Y, and Z (possible oxidation products of II) with time. Figures 2 and 4 (the reaction of I with IIIa and IIIb) show a decrease in III with a subsequent increase and then decrease in II and an increase in peaks X and Y with time. These observations suggest that the reaction of the esters of corticosteroids with I is sequential. The intermediate in the reaction sequence is II. Since Gupta (9) showed that IIa is degraded under strongly basic conditions, the decomposition of IIa and IIb under USP assay conditions with alcohol USP and absolute alcohol also was studied.

A kinetic model to describe the overall reaction sequence is given here;

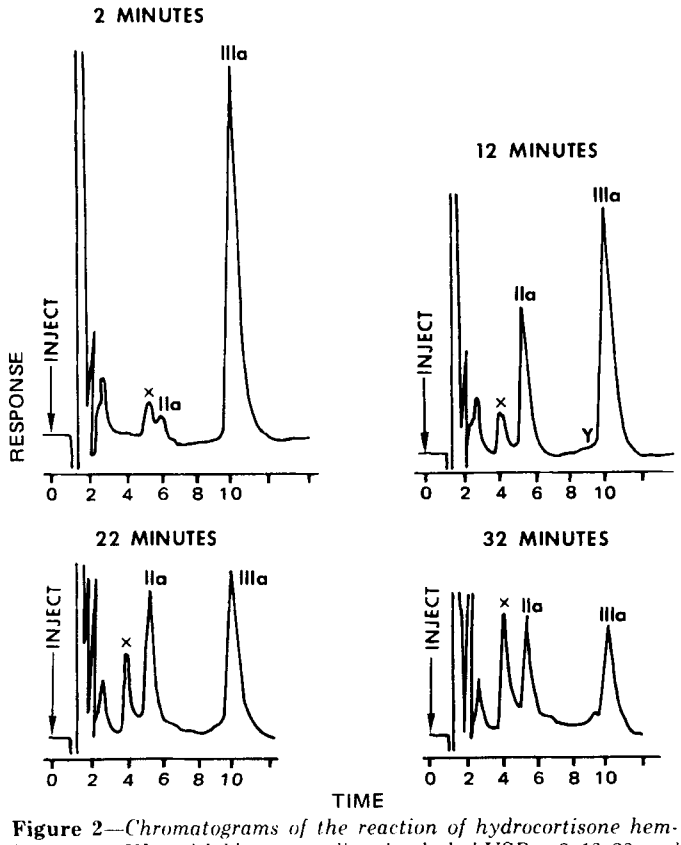

Figure 2—*Chromatograms of the reaction of hydrocortisone hemisuccinate (IIIa) with blue tetrazolium in alcohol USP at 2, 12, 22, and 32 min; X and Z are the reaction products and IIa is hydrocortisone.*

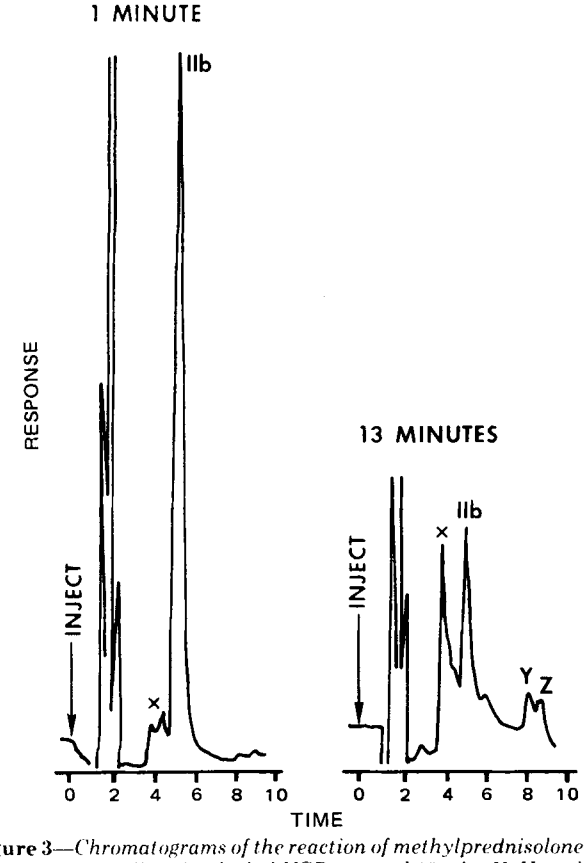

Figure 3—*Chromatograms of the reaction of methylprednisolone (IIb) with blue tetrazolium in alcohol USP at 1 and 13 min; X, Y, and Z are the reaction products.*

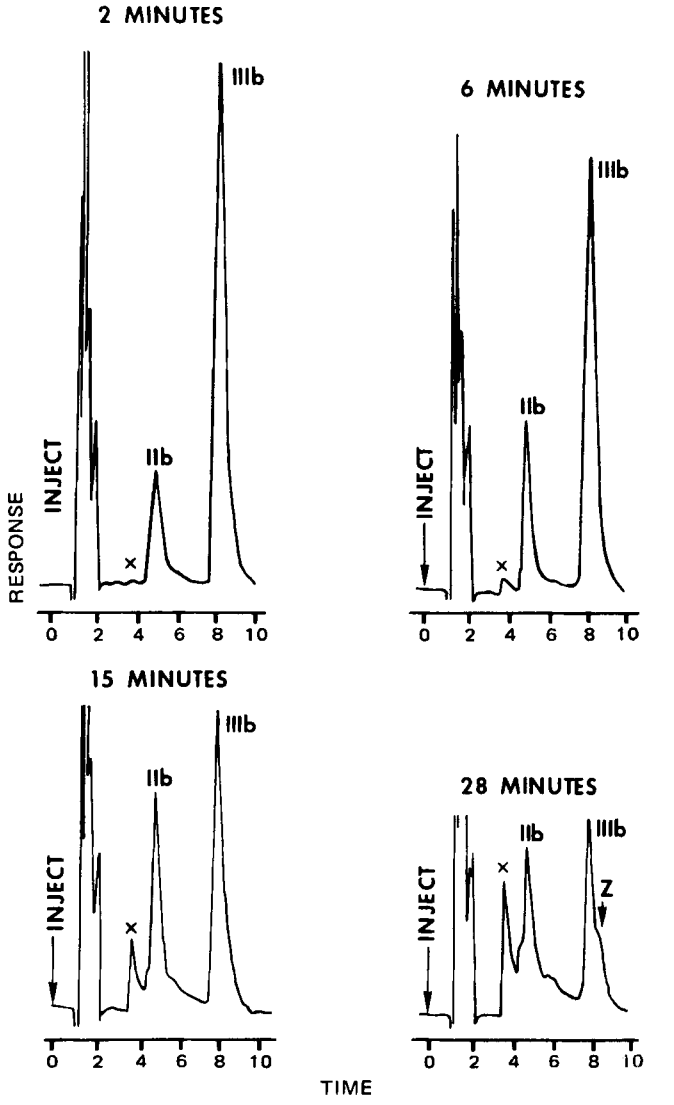

Figure 4—*Chromatograms of the reaction of methylprednisolone hemisuccinate (IIIb) with blue tetrazolium in alcohol USP at 2, 6, 15, and 28 min; X and Z are the reaction products and IIb is methylprednisolone.*

the reformation of I from formazan as postulated by Graham *et al.* (14) is not included. Experimental data of the reaction of II*a* and II*b* with I in 95% alcohol or absolute alcohol suggested that the rate of reformation of I is much slower than the rate of reaction of II with I (Scheme I). Therefore, the loss of formazan (within 100 min of reaction time) would be negligible.

$$\text{III} \xrightarrow[[OH^-]]{k_1} \text{II} \xrightarrow[[I]]{k_2} C + P$$
$$\text{II} \xrightarrow[[OH^-]]{k_3} D$$

Scheme I

P is reduced I; *C* and *D* are decomposition products of II; $[OH^-] = [IV]$, and k_1, k_2, and k_3 are pseudo-first-order rate-constants.

The disappearance of III and the appearance of II and *P* can be described by:

$$\frac{d\text{III}}{dt} = -k_1\text{III} \qquad \text{(Eq. 1)}$$

$$\frac{d\text{II}}{dt} = k_1\text{III} - (k_2 + k_3)\text{II} \qquad \text{(Eq. 2)}$$

$$\frac{dP}{dt} = k_2\text{II} \qquad \text{(Eq. 3)}$$

Table I—Rate Constants of the Blue Tetrazolium–Corticosteroid Reaction

Corticosteroid and Its Ester	Rate Constant, min^{-1}	
	Alcohol USP	Absolute Alcohol
IIa + IIIa		
k_1	0.036	0.014
k_2	0.10	0.10
k_3	0.0015	0.0007
IIb + IIIb		
k_1	0.041	0.018
k_2	0.12	0.13
k_3	0.0021	0.0018

Solutions for these differential equations are:

$$III_t = III_0 e^{-k_1 t} \quad \text{(Eq. 4)}$$

$$II_t = \frac{III_0 k_1}{(k_2 + k_3) - k_1}\left[e^{-k_1 t} - e^{-(k_2+k_3)t}\right] \quad \text{(Eq. 5)}$$

$$P_t = \frac{III_0 k_1 k_2}{k_1 - (k_2 + k_3)}\left[\frac{e^{-k_1 t}}{k_1} - \frac{e^{-(k_2+k_3)t}}{k_2 + k_3}\right] \quad \text{(Eq. 6)}$$

The rate constants k_1, k_2, and k_3 were determined experimentally by following each discrete reaction under USP conditions using either alcohol USP or absolute alcohol as the solvent. The hydrolysis of III, the decomposition of II in IV, and the reaction of II with I were followed independently by HPLC. The results of these kinetic experiments are given in Table I.

These rate constants were used to generate time–concentration profiles for II, III, and *P* to simulate the reaction of III with I under specified solvent conditions. Normalized experimental data obtained by HPLC for the reaction of IIIa and IIIb with I were superimposed on these generated time–concentration profiles (Figs. 5–8). The colorimetric data (*P*) were normalized by dividing each observed absorbance by the absorbance after the reaction was complete (>3 hr). For each ester of II in alcohol USP and absolute alcohol, the predicted concentrations of II, III, and *P* closely agreed with the experimental values. Some estimation of the experimental data (III) occurred since the decomposition products of II (Y and Z) were not totally resolved from III. These observations of the reaction of the hemiester with I corroborate conclusions (5, 6) that hydrolysis of the ester is a prerequisite to the reaction with I.

The following observations can be made about the rate constants for each pseudo-first-order reaction:

1. The rate of decomposition of II in a base (k_3) is ~1% of the rate of reaction with I (k_2) and can be ignored.
2. The rate constants (k_2) under USP assay conditions are about the same for IIa and IIb and are in agreement with the results reported by Graham *et al.* (15) (*i.e.*, k_2 [IIa] = 0.090 and k_2 [IIb] = 0.096).
3. In the ester reaction sequence, ester hydrolysis is the rate-determining step.

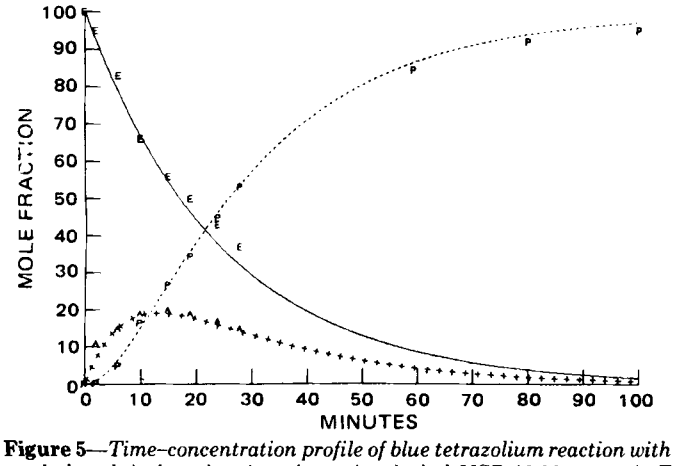

Figure 5—*Time–concentration profile of blue tetrazolium reaction with methylprednisolone hemisuccinate in alcohol USP (6.9% water); E represents the normalized data for methylprednisolone hemisuccinate (IIIb), A represents the normalized data for methylprednisolone (IIb), P represents the normalized data for reduced blue tetrazolium (formazan), and —, +, and . . . are computer-generated curves for E, A, and P, respectively, using rate constants determined independently.*

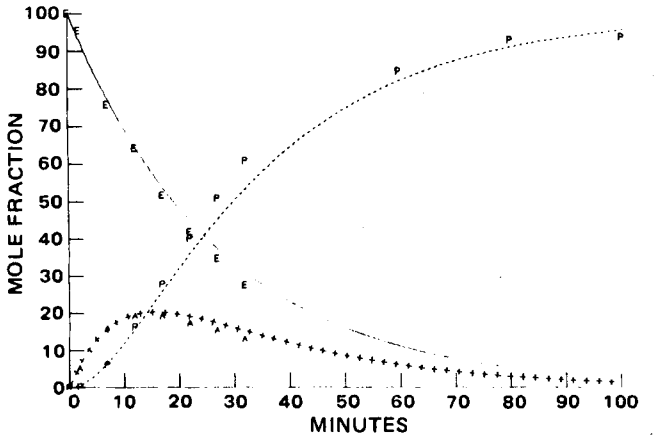

Figure 6—*Time–concentration profile of blue tetrazolium reaction with hydrocortisone hemisuccinate in alcohol USP (6.9% water); E represents the normalized data for hydrocortisone hemisuccinate (IIIa), A represents the normalized data for hydrocortisone (IIa), P represents the normalized data for reduced blue tetrazolium (formazan), and —, +, and . . . are computer-generated curves for E, A, and P, respectively, using rate constants determined independently.*

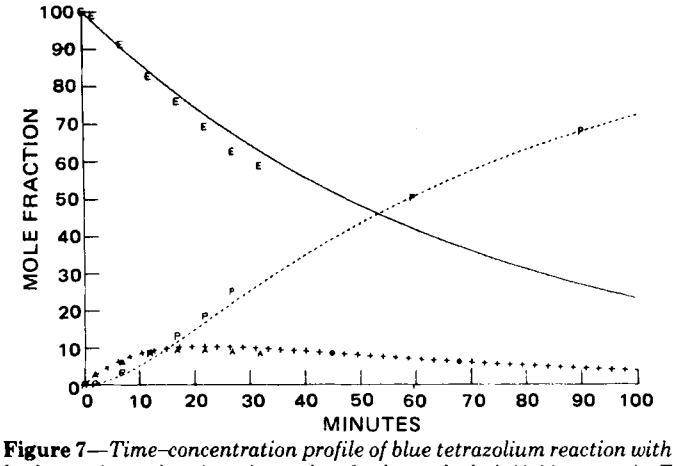

Figure 7—*Time–concentration profile of blue tetrazolium reaction with hydrocortisone hemisuccinate in absolute alcohol (2.3% water); E represents the normalized data for hydrocortisone hemisuccinate (IIIa), A represents the normalized data for hydrocortisone (IIa), P represents the normalized data for reduced blue tetrazolium (formazan), and —, +, and . . . are computer-generated curves for E, A, and P, respectively, using rate constants determined independently.*

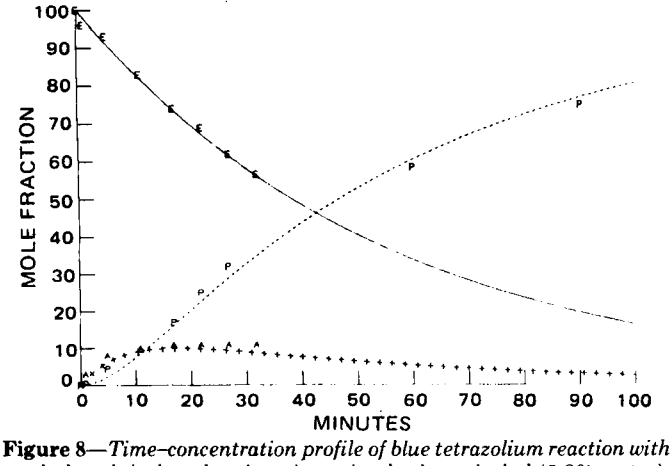

Figure 8—*Time–concentration profile of blue tetrazolium reaction with methylprednisolone hemisuccinate in absolute alcohol (2.3% water); E represents the normalized data for methylprednisolone hemisuccinate (IIIb), A represents the normalized data for methylprednisolone (IIb), P represents the normalized data for reduced blue tetrazolium (formazan), and —, +, and . . . are computer-generated curves for E, A, and P, respectively, using rate constants determined independently.*

4. The water content of the reaction mixture has little effect on the rate of reaction of the corticosteroid (II) with I within the range studied.

5. The hydrolysis rate of the ester (III → II) and subsequently the overall reaction rate appear to be proportional to the water content of the reaction mixture.

These kinetic results imply that the USP blue tetrazolium assay for these corticosteroid hemisuccinate esters has a high variability potential since it is a timed measurement (90 min). These results show that III does not react directly with I and that II must be formed. Therefore, the USP blue tetrazolium assay cannot differentiate between the corticosteroid (II) and its ester (III) and thus is not a stability-indicating assay of III. In fact, if hydrolysis of the ester of these corticosteroids occurred, the results might show an increase in corticosteroid since the reaction rate of the corticosteroid is about three times as fast as the hemiester in alcohol USP.

CONCLUSIONS

1. The reaction of corticosteroid esters (III) with I is sequential. The ester is hydrolyzed first, and the resulting corticosteroid (II) reacts with I. The hydrolysis step is the rate-determining step.

2. The USP blue tetrazolium assay is not stability indicating for the esters of these corticosteroids.

3. As the percent of water in the reaction mixture decreases, the time for complete reaction increases for the USP blue tetrazolium assay of C-21 hemisuccinate esters of corticosteroids.

REFERENCES

(1) "The United States Pharmacopeia," 19th rev., Mack Publishing Co., Easton, Pa., 1975, p. 622.

(2) S. Gorog and G. Szasz, "Analysis of Steroid Hormone Drugs," Elsevier, New York, N.Y., 1978, p. 331.

(3) A. S. Meyer and M. C. Lindberg, *Anal. Chem.*, **27**, 813 (1955).

(4) C. A. Johnson, R. King, and C. Vickers, *Analyst*, **85**, 714 (1960).

(5) D. E. Guttman, *J. Pharm. Sci.*, **55**, 919 (1966).

(6) R. E. Graham, E. R. Biehl, C. T. Kenner, G. H. Luttrell, and D. L. Middleton, *ibid.*, **64**, 226 (1975).

(7) J. W. Mauger, A. N. Paruta, and R. J. Gerraughty, *ibid.*, **58**, 574 (1969).

(8) E. Garrett, *ibid.*, **51**, 445 (1962).

(9) V. D. Gupta, *ibid.*, **67**, 299 (1978).

(10) M. D. Smith and D. Hoffman, *J. Chromatogr.*, **168**, 163 (1979).

(11) R. E. Graham and C. T. Kenner, *J. Pharm. Sci.*, **62**, 103 (1973).

(12) R. O. Rechnagel and M. Litteria, *J. Lab. Clin. Med.*, **45**, 818 (1955).

(13) "The United States Pharmacopeia," 19th rev., Mack Publishing Co., Easton, Pa., 1975, pp. 242, 324.

(14) R. E. Graham, E. R. Biehl, and C. T. Kenner, *J. Pharm. Sci.*, **66**, 965 (1977).

(15) *Ibid.*, **65**, 1048 (1976).

ACKNOWLEDGMENTS

The author thanks Ms. Florence Tucker for technical assistance and Dr. Saul Borodkin and Dr. Philip Carrigan for discussions of the kinetic analysis and help in preparation of this paper.

New Evaluation of Potential Methylmercury Scavengers

LESLIE R. ROBERTS *§x, LARRY K. STEINRAUF *‡, and ROBERT T. BLICKENSTAFF *§

Received November 5, 1979, from the **Department of Biochemistry and the* ‡*Department of Biophysics, Indiana University School of Medicine*, and the §*Veterans Administration Medical Center, Indianapolis, IN 46202.* Accepted for publication March 24, 1980.

Abstract □ A biological assay was developed to evaluate rapidly the relative efficacy of marketed and experimental mercurial scavengers. Rat liver mitochondrial protein (1.0 mg) was titrated against methylmercuric chloride to the inhibitory level of mitochondrial respiration. Respiration induced by adenosine 5′-diphosphate with succinate (plus rotenone) as the substrate was inhibited consistently by 20.7 ± 3.9 nmoles of methylmercury/mg of protein. Adenosine 5′-diphosphate-stimulated respiration (State 3) was restored with dimercaprol, penicillamine, and cysteine but not with serine. The antagonists glutathione, 3-mercaptopropionic acid, 2-mercaptoethanol, dithiothreitol, thioglucose, mercaptosuccinic acid, and thiosalicylic acid were effective. Glutathione was significantly superior to thiosalicylic acid and mercaptosuccinic acid. Sodium sulfide, thioacetamide, and ethylenediaminetetraacetic acid were completely inactive. Substitution of glutamate (plus malate) for succinate (plus rotenone) as the substrate did not alter the responses significantly. The rat liver mitochondrial assay provides preliminary information about the efficacy and toxicity of water-soluble thiols. Investigations utilizing encapsulated water- and lipid-soluble mercaptans are in progress.

Keyphrases □ Mercurial scavengers—thiol-containing compounds, evaluation of efficacy and toxicity using rat liver mitochondrial assay □ Mercaptans—evaluation of efficacy and toxicity as mercurial scavengers using rat liver mitochondrial assay

Agents currently used to alleviate clinical symptoms and to facilitate the rapid removal of methylmercury include chelators such as dimercaprol, penicillamine, and ethylenediaminetetraacetic acid (1–3). Unfortunately, the effectiveness of these antidotes is limited by their toxicity, chemical instability, and relatively short circulation time. Polythiol resins, thioacetylated steroids, mercaptosteroids, and lipid encapsulation of ethylenediaminetetraacetic acid have been proposed to improve on these mercurial scavengers (4–9).

BACKGROUND

Reports on the analysis of subcellular distribution of labeled mercury indicate significant accumulation of mercury by mitochondria (10). Furthermore, dose and time dependence of the mercurial in relation to the extent of damage incurred by isolated mitochondria has been documented (11–13). In addition, the technique for isolation of viable rat liver mitochondria is well known.

Early reports demonstrating reversal of mercurial inhibition by mercaptans dealt with isolated enzymes (14, 15). Thompson and Whittaker (14) showed significant protection of pigeon brain pyruvate oxidase activity against mercuric chloride inhibition by the addition of dimercaprol and glutathione. Barron and Kalnitsky (15) demonstrated 75% reactivation of mercuric chloride-inhibited succinoxidase by the addition of various dithiols. Sone *et al.* (11) recently studied the effects of methylmercuric chloride on mitochondrial respiration and found nearly complete restoration of succinate oxidation with thiol-containing reagents such as 2-mercaptoethanol, glutathione, cysteine, and dithiothreitol. The concentration required for reversal was not given. Less than 10% recovery of nicotinamide-adenine dinucleotide oxidation was restored by these reagents (11).

In summary, direct effects of mercurials on rat liver mitochondria have been demonstrated (10–13). Furthermore, reactivation of mercurial-inhibited enzymes by thiols has been shown (14, 15). In addition, relief of mercurial intoxication in mitochondria by thiols has been shown but has not been quantified (15). This report describes the use of mito-

0022-3549/80/0800-0964$01.00/0
© 1980, American Pharmaceutical Association

4. The water content of the reaction mixture has little effect on the rate of reaction of the corticosteroid (II) with I within the range studied.

5. The hydrolysis rate of the ester (III → II) and subsequently the overall reaction rate appear to be proportional to the water content of the reaction mixture.

These kinetic results imply that the USP blue tetrazolium assay for these corticosteroid hemisuccinate esters has a high variability potential since it is a timed measurement (90 min). These results show that III does not react directly with I and that II must be formed. Therefore, the USP blue tetrazolium assay cannot differentiate between the corticosteroid (II) and its ester (III) and thus is not a stability-indicating assay of III. In fact, if hydrolysis of the ester of these corticosteroids occurred, the results might show an increase in corticosteroid since the reaction rate of the corticosteroid is about three times as fast as the hemiester in alcohol USP.

CONCLUSIONS

1. The reaction of corticosteroid esters (III) with I is sequential. The ester is hydrolyzed first, and the resulting corticosteroid (II) reacts with I. The hydrolysis step is the rate-determining step.

2. The USP blue tetrazolium assay is not stability indicating for the esters of these corticosteroids.

3. As the percent of water in the reaction mixture decreases, the time for complete reaction increases for the USP blue tetrazolium assay of C-21 hemisuccinate esters of corticosteroids.

REFERENCES

(1) "The United States Pharmacopeia," 19th rev., Mack Publishing Co., Easton, Pa., 1975, p. 622.

(2) S. Gorog and G. Szasz, "Analysis of Steroid Hormone Drugs," Elsevier, New York, N.Y., 1978, p. 331.

(3) A. S. Meyer and M. C. Lindberg, *Anal. Chem.*, **27**, 813 (1955).

(4) C. A. Johnson, R. King, and C. Vickers, *Analyst*, **85**, 714 (1960).

(5) D. E. Guttman, *J. Pharm. Sci.*, **55**, 919 (1966).

(6) R. E. Graham, E. R. Biehl, C. T. Kenner, G. H. Luttrell, and D. L. Middleton, *ibid.*, **64**, 226 (1975).

(7) J. W. Mauger, A. N. Paruta, and R. J. Gerraughty, *ibid.*, **58**, 574 (1969).

(8) E. Garrett, *ibid.*, **51**, 445 (1962).

(9) V. D. Gupta, *ibid.*, **67**, 299 (1978).

(10) M. D. Smith and D. Hoffman, *J. Chromatogr.*, **168**, 163 (1979).

(11) R. E. Graham and C. T. Kenner, *J. Pharm. Sci.*, **62**, 103 (1973).

(12) R. O. Rechnagel and M. Litteria, *J. Lab. Clin. Med.*, **45**, 818 (1955).

(13) "The United States Pharmacopeia," 19th rev., Mack Publishing Co., Easton, Pa., 1975, pp. 242, 324.

(14) R. E. Graham, E. R. Biehl, and C. T. Kenner, *J. Pharm. Sci.*, **66**, 965 (1977).

(15) *Ibid.*, **65**, 1048 (1976).

ACKNOWLEDGMENTS

The author thanks Ms. Florence Tucker for technical assistance and Dr. Saul Borodkin and Dr. Philip Carrigan for discussions of the kinetic analysis and help in preparation of this paper.

New Evaluation of Potential Methylmercury Scavengers

LESLIE R. ROBERTS *§x, LARRY K. STEINRAUF *‡, and ROBERT T. BLICKENSTAFF *§

Received November 5, 1979, from the **Department of Biochemistry and the* ‡*Department of Biophysics, Indiana University School of Medicine*, and the §*Veterans Administration Medical Center, Indianapolis, IN 46202.* Accepted for publication March 24, 1980.

Abstract □ A biological assay was developed to evaluate rapidly the relative efficacy of marketed and experimental mercurial scavengers. Rat liver mitochondrial protein (1.0 mg) was titrated against methylmercuric chloride to the inhibitory level of mitochondrial respiration. Respiration induced by adenosine 5′-diphosphate with succinate (plus rotenone) as the substrate was inhibited consistently by 20.7 ± 3.9 nmoles of methylmercury/mg of protein. Adenosine 5′-diphosphate-stimulated respiration (State 3) was restored with dimercaprol, penicillamine, and cysteine but not with serine. The antagonists glutathione, 3-mercaptopropionic acid, 2-mercaptoethanol, dithiothreitol, thioglucose, mercaptosuccinic acid, and thiosalicylic acid were effective. Glutathione was significantly superior to thiosalicylic acid and mercaptosuccinic acid. Sodium sulfide, thioacetamide, and ethylenediaminetetraacetic acid were completely inactive. Substitution of glutamate (plus malate) for succinate (plus rotenone) as the substrate did not alter the responses significantly. The rat liver mitochondrial assay provides preliminary information about the efficacy and toxicity of water-soluble thiols. Investigations utilizing encapsulated water- and lipid-soluble mercaptans are in progress.

Keyphrases □ Mercurial scavengers—thiol-containing compounds, evaluation of efficacy and toxicity using rat liver mitochondrial assay □ Mercaptans—evaluation of efficacy and toxicity as mercurial scavengers using rat liver mitochondrial assay

Agents currently used to alleviate clinical symptoms and to facilitate the rapid removal of methylmercury include chelators such as dimercaprol, penicillamine, and ethylenediaminetetraacetic acid (1–3). Unfortunately, the effectiveness of these antidotes is limited by their toxicity, chemical instability, and relatively short circulation time. Polythiol resins, thioacetylated steroids, mercaptosteroids, and lipid encapsulation of ethylenediaminetetraacetic acid have been proposed to improve on these mercurial scavengers (4–9).

BACKGROUND

Reports on the analysis of subcellular distribution of labeled mercury indicate significant accumulation of mercury by mitochondria (10). Furthermore, dose and time dependence of the mercurial in relation to the extent of damage incurred by isolated mitochondria has been documented (11–13). In addition, the technique for isolation of viable rat liver mitochondria is well known.

Early reports demonstrating reversal of mercurial inhibition by mercaptans dealt with isolated enzymes (14, 15). Thompson and Whittaker (14) showed significant protection of pigeon brain pyruvate oxidase activity against mercuric chloride inhibition by the addition of dimercaprol and glutathione. Barron and Kalnitsky (15) demonstrated 75% reactivation of mercuric chloride-inhibited succinoxidase by the addition of various dithiols. Sone *et al.* (11) recently studied the effects of methylmercuric chloride on mitochondrial respiration and found nearly complete restoration of succinate oxidation with thiol-containing reagents such as 2-mercaptoethanol, glutathione, cysteine, and dithiothreitol. The concentration required for reversal was not given. Less than 10% recovery of nicotinamide-adenine dinucleotide oxidation was restored by these reagents (11).

In summary, direct effects of mercurials on rat liver mitochondria have been demonstrated (10–13). Furthermore, reactivation of mercurial-inhibited enzymes by thiols has been shown (14, 15). In addition, relief of mercurial intoxication in mitochondria by thiols has been shown but has not been quantified (15). This report describes the use of mito-

0022-3549/80/0800-0964$01.00/0
© 1980, American Pharmaceutical Association

chondria in the evaluation of mercaptans as scavengers of methylmercuric chloride.

EXPERIMENTAL[1]

All mercaptans were dissolved in deionized, distilled water just prior to use. These reagents, as well as methylmercury, exhibit chemical instability and volatility. For example, a dilute solution of methylmercuric chloride loses 20% of its capacity to inhibit mitochondrial respiration after standing for 5 hr at room temperature.

Preparation of Mitochondria—Mitochondria were prepared by decapitation of rats (Sprague–Dawley strain) and rapid transfer of the liver to 0.25 *M* sucrose plus 1 m*M* ethylenediaminetetraacetic acid (pH 7.2) at 4°, followed by washing, homogenization, and centrifugation according to the method of Blair (16). The final pellet was resuspended in sucrose–ethylenediaminetetraacetic acid and assayed for total protein by the biuret method (17). The total amount of protein, the volume of material, and the final protein concentration were recorded for each experiment.

Measurement of Redox Reactions—The intactness of isolated mitochondria was determined by incubation of 1.0 mg of mitochondrial protein first with 15 m*M* glutamate plus 0.15 m*M* malate and then with 20 m*M* succinate plus rotenone (500 ng/ml) in a medium containing 250 m*M* sucrose, 5.0 m*M* monobasic sodium phosphate, and 3.0 m*M* $MgCl_2$ (Medium 1). State 3 respiration[2] was initiated by the addition of 1.5 μmoles of adenosine 5′-diphosphate and recorded on an oxygraph[3] equipped with a test platinum electrode and a 2.0-ml partially enclosed reaction vessel maintained at 30° by a circulating water bath. A respiratory control ratio of 5.0 for succinate (plus rotenone) as the substrate was used as a minimum standard. All mitochondria batches were subjected to control runs at the beginning of each experiment.

Inhibition of Mitochondrial Oxidative Metabolism—The minimum level of methylmercury required to inhibit State 3 respiration to the level of State 4 respiration[4] was determined by incubating 1.0 mg of rat liver mitochondrial protein with succinate (20 m*M*) plus rotenone (500 ng/ml) in Medium 1 to which an excess of adenosine 5′-diphosphate (3.0 μmoles) had been added. Approximately 1 min after the initiation of State 3 respiration, methylmercury was pipetted into the reaction vessel. Observations were terminated after several minutes of State 4 respiration or when the rate of State 3 respiration was indistinguishable from State 4 respiration. Titrations were conducted at the beginning of each experiment to evaluate interbatch variation.

The relative efficacy of the water-soluble thiols was examined using succinate plus rotenone as the substrate, adenosine 5′-diphosphate to initiate State 3 respiration, and a constant level of methylmercury in Medium 1. Thiols were titrated to a concentration sufficient to reinstate State 3 respiration. Values reported in Table I represent 50% recovery. These values were calculated by subtracting the State 4 rate from the recovery scavenger rate and dividing by the State 3 rate minus the State 4 rate of respiration, with subsequent matching of the scavenger concentration used to the appropriate percentage recovery. All agents were tested on several preparations of mitochondria.

RESULTS AND DISCUSSION

Inhibition of mitochondrial metabolism as a function of the amount of methylmercury added was reported previously (11, 12). No change in respiration was observed below 0.10 nmole of methylmercury/mg of rat liver mitochondrial protein. Above 11.0 nmoles of methylmercury, >91% inhibition of State 3 minus State 4 respiration was obtained.

Sone *et al.* (11) reported that dimercaprol reverses methylmercury-induced inhibition of rat liver mitochondrial metabolism. To quantify the proposed reversal, a series of experiments was conducted as described. Figure 1 displays actual tracings obtained when appropriate incubations were carried out. Addition of rat liver mitochondria to a reaction medium containing the substrate initiated State 2 respiration[5]. When adenosine 5′-diphosphate was added, State 3 respiration began. Without further additions, State 3 respiration terminated to give State 4 respiration (curve A). If 1.0 μmole of dimercaprol/mg of rat liver mitochondrial protein was mixed with actively respiring mitochondria, no change was observed (curve B). Introduction of a predetermined level of methylmercury slowed the State 3 rate to a pseudo-State 4 rate. Finally, a sufficient quantity of dimercaprol added to the medium immediately relieved mercurial inhibition (curves C–E). With levels of >50 nmoles of dimercaprol/mg of rat liver mitochondrial protein, >60% recovery routinely was obtained.

Table I—Titration of Methylmercury Scavengers [a]

Mercaptan	With Methylmercury: 50% Recovery Concentration, nmoles/mg of rat liver mitochondria	Ratio of Mercaptan to Methylmercury	Without Methylmercury: Control Run Concentration, μmoles/mg of rat liver mitochondria	Effect on State 3 Respiration
Glutathione	14.5[b]	0.54	0.70	None
Thiosalicylic acid	30.4	1.15	2.40	Inhibition
3-Mercaptopropionic acid	41.5	1.76	0.40	None
2-Mercaptoethanol	58.9	2.85	2.40	None
Dithiothreitol	65.1	2.48	4.50	None
Mercaptosuccinic acid	69.2	2.80	2.52	Inhibition
Thioglucose	126[b]	4.81	2.20	None
Sodium sulfide	—	—	1.17	Inhibition
Thioacetamide	—	—	33.2	None

[a] Results are given for the assay of mitochondrial incubations with mercaptans in the presence and absence of methylmercury. Titrations of mercaptans were carried out according to procedures outlined for penicillamine and dimercaprol. Results are reported as 50% recovery levels because of the greater sensitivity in this region of the titration curve to small changes in the concentration of the scavenger. Control runs were conducted in the absence of methylmercury using higher levels of the scavenger than required to produce recovery. Qualitative effects on State 3 respiration are included in the last column. [b] $p < 0.05$ (standard t test); individual 50% recovery concentrations were compared to the mean of all 50% recovery levels.

Since penicillamine has been an alternative therapy for acute mercurial intoxication (18), the efficacy of this compound was compared to dimercaprol with the mitochondrial assay procedure. Cysteine was included as a test reagent because of its close structural similarity to penicillamine and its qualitative scavenger capacity (11, 14). Serine also was selected because it structurally resembles penicillamine but contains a hydroxyl group instead of a sulfhydryl group.

Results of several experiments are shown in Fig. 2. Titration with penicillamine and cysteine produced similar results, although a slightly higher scavenger capacity was demonstrated by penicillamine. The optimal concentration of penicillamine and cysteine required to elicit a given percentage recovery of respiration was significantly higher than the dimercaprol concentration required to produce the same response. Serine has no capacity to reverse mercurial inhibition, thereby substantiating the requirement for sulfhydryl groups on scavenger molecules.

Compounds such as 3-mercaptopropionic acid and glutathione were able to relieve mercuric chloride inhibition of isolated enzyme systems. The scavenger efficacy of these mercaptans, as well as others selected for their variation in carbon chain length, extent of ionization, and location of sulfhydryl groups, was examined (Table I). To verify the requirement of reduced thiols for activity against methylmercury, sodium sulfide and thioacetamide were tested. Because ethylenediaminetetraacetic acid has been used in the treatment of heavy metal poisoning, it was tested also.

Glutathione, a tripeptide containing one sulfhydryl group, exhibited the greatest efficiency in relieving 50% of the mercurial-induced inhibition. Thiosalicylic acid showed 50% recovery with an average of 30.4 nmoles/mg of rat liver mitochondrial protein, making it nearly as effective as glutathione, although it inhibited State 3 respiration during the control run. 3-Mercaptopropionic acid exhibited a slightly superior mercaptan

[1] Methylmercuric chloride was obtained from ICN K and K Laboratories. Sucrose, succinate, rotenone, glutamate, malate, ethylenediaminetetraacetic acid, adenosine 5′-diphosphate, 2-mercaptoethanol, thioglucose, thiosalicylic acid, glutathione, and dithiothreitol were purchased from Sigma Chemical Co. Dimercaprol, penicillamine, and serine were products of Aldrich Chemical Co. Cysteine and mercaptosuccinic acid were supplied by Eastman Organic Chemicals. 3-Mercaptopropionic acid was obtained from Evans Chemetics. Thioacetic acid and thioacetamide were products of Matheson, Coleman and Bell.

[2] Active respiration of mitochondria in the presence of excess added substrate and adenosine 5′-diphosphate.

[3] Gilson model M5P.

[4] Respiration of mitochondria after added adenosine 5′-diphosphate has been phosphorylated but in the presence of exogenous substrate.

[5] Mitochondrial respiration in the presence of added substrate and phosphate.

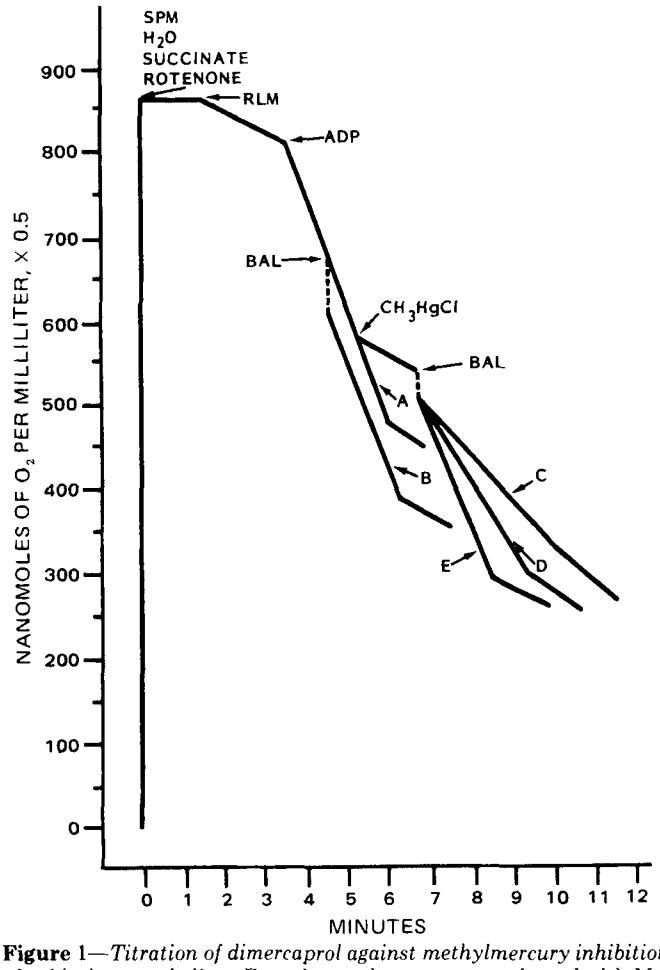

Figure 1—*Titration of dimercaprol against methylmercury inhibition of oxidative metabolism. Experimental runs were conducted with Medium 1 (20 mM succinate, 500 ng of rotenone/ml, 20 mg of mitochondria/ml, and 3.0 μmoles of adenosine 5′-diphosphate). Key: A, control run without methylmercury or dimercaprol; B, scavenger control run of 1.0 μmole of dimercaprol/mg of protein added to mitochondria after the initiation of State 3 respiration; and C–E, inhibitory effect of methylmercury (200 μg/ml) and the level of recovery using 0.05 (C), 0.10 (D), and 10 (E) μmoles of dimercaprol/mg of rat liver mitochondrial protein. Each run required ~10 min. SPM = 250 mM sucrose, 5.0 mM monobasic sodium phosphate, and 3.0 mM $MgCl_2$; RLM = rat liver mitochondria; ADP = adenosine 5′-diphosphate; and BAL = British anti-Lewisite.*

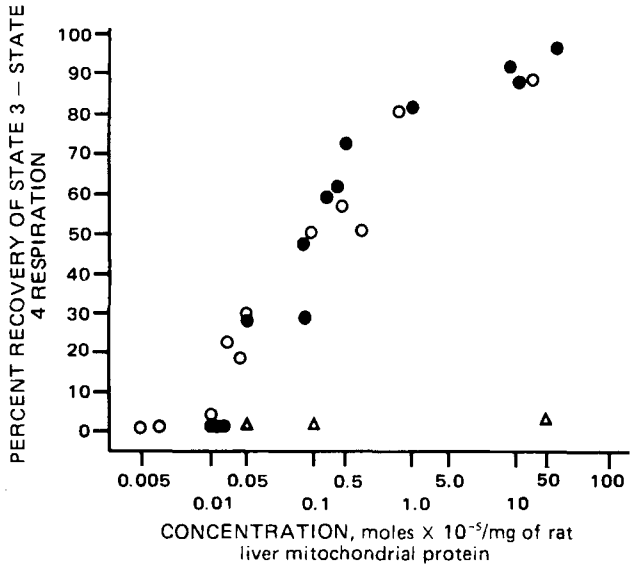

Figure 2—*Titration of penicillamine, cysteine, and serine against methylmercury. Mitochondria (20 mg/ml) were incubated in the presence of Medium 1 (20 mM succinate and 500 ng of rotenone/ml). State 3 respiration was initiated with excess adenosine 5′-diphosphate (3.0 μmoles). Inhibition of State 3 respiration to the level of State 4 respiration was obtained using 200 μg of methylmercury/ml. Aliquots of cysteine (○), penicillamine (●), and serine (△) were added to the reaction vessel, which was observed for reestablishment of State 3 respiration. The calculation of the percent recovery is described under* Experimental.

to methylmercury ratio to those of 2-mercaptoethanol and dithiothreitol, but the concentrations required were not statistically different. Mercaptosuccinic acid relieved 50% of the observed inhibition, although the scavenger capacity was reduced by a progressive increase of State 3 inhibition. Thioglucose was markedly less efficient as a mercurial scavenger. Sodium sulfate and thioacetamide proved to be ineffective scavengers and inhibitory at sufficient levels. Ethylenediaminetetraacetic acid was neither effective as a mercurial scavenger nor toxic at a concentration of 168 nmoles/mg of rat liver mitochondrial protein.

To compare the effect of an alternative substrate on mercurial scavenger efficacy, glutamate plus malate was substituted for succinate plus rotenone and several experiments were conducted as outlined. The test compounds were 3-mercaptopropionic acid, 2-mercaptoethanol, mercaptosuccinic acid, and thioacetamide. In each case, the assay responded as observed when succinate plus rotenone was used as the substrate. Furthermore, levels required for 50% recovery were statistically indistinguishable from those reported here. Thioacetamide was ineffective, as expected.

Dimercaprol proved to be a significantly superior methylmercury scavenger to penicillamine in the assay. The improved efficacy of dimercaprol compared to penicillamine also was observed in whole animal studies (8). Because dimercaprol has a relatively greater lipid solubility than penicillamine and contains an additional thiol group, the differences observed are reasonable. Nevertheless, doubling the number of sulfhydryl groups per molecule does not strictly increase its effectiveness by a factor of two. Thus, the potential of dimercaprol to bind heavy metals perhaps is antagonized by its characteristic tendency to form intermolecular disulfide bridges (18).

In this assay, glutathione was a significantly better mercurial scavenger than are the other mercaptans. Glutathione contains some ionized groups at physiological pH, so ease of transport through the inner mitochondrial membrane is not an applicable explanation. Furthermore, no damage to respiratory components was observed when glutathione was incubated with mitochondria (Table I). The explanation for the enhanced scavenger capacity of glutathione remains undetermined but is under investigation.

With the exception of glutathione and thioglucose, the mercaptans tested were not statistically different, indicating no minimal requirement for structural design beyond the availability of a free sulfhydryl group and water solubility. The inactivity of thioacetamide and sodium sulfide against methylmercury was predictable (14).

The assay is a new approach for preliminary testing of mercurial antidotes. Information is obtained not only about the efficiency of the mercurial scavenger but also about its behavior under control conditions. Although mercaptans such as thiosalicylic acid and mercaptosuccinic acid are effective scavengers, they also inhibit respiration in this system (Table I). The advantages of time and the number of animals involved make this assay attractive for first approximations of scavenger capacity. These studies are being extended to encapsulation of water-soluble mercaptans and lipid-soluble thiols.

REFERENCES

(1) L. Magos, *Br. J. Ind. Med.*, **25**, 152 (1968).

(2) W. T. Longcope, J. A. Leutscher, Jr., E. Calkins, D. Grob, S. W. Bush, and H. Eisenberg, *J. Clin. Invest.*, **25**, 557 (1964).

(3) H. Matsumoto, A. Suzuki, and C. Norita, *Life Sci.*, **6**, 2321 (1967).

(4) T. W. Clarkson, H. Small, and T. Norseth, *Arch. Environ. Health*, **26**, 173 (1973).

(5) L. Magos and T. W. Clarkson, *Chem.-Biol. Interact.*, **14**, 325 (1976).

(6) H. Selye, T. Mels, and S. Szabo, *Int. Urol. Nephrol.*, **2**, 287 (1970).

(7) V. Eybl, J. Sykora, M. Koutenska, J. Koutensky, and F. Mertl, *Arzneim.-Forsch.*, **23**, 867 (1973).

(8) L. K. Steinrauf, B. Cox, E. Foster, and R. T. Blickenstaff, *J. Pharm. Sci.*, **67**, 1739 (1978).
(9) V. E. Rahman, M. W. Rosenthal, and E. A. Cerny, *Science*, **180**, 300 (1973).
(10) T. Norseth and M. Brendeford, *Biochem. Pharmacol.*, **20**, 1101 (1971).
(11) N. Sone, M. K. Larsstuvold, and Y. Kagawa, *J. Biochem.*, **82**, 859 (1977).
(12) J. H. Southard and P. Nitisewojo, *Biochem. Biophys. Res. Commun.*, **52**, 921 (1973).
(13) J. H. Southard, P. Nitisewojo, and D. E. Green, *Fed. Proc. Fed. Am. Soc. Exp. Biol.*, **33**, 2147 (1973).
(14) R. H. S. Thompson and V. P. Whittaker, *Biochem. J.*, **41**, 346 (1947).
(15) E. S. Barron and G. Kalnitsky, *ibid.*, **41**, 351 (1947).
(16) P. V. Blair, *Arch. Biochem. Biophys.*, **181**, 550 (1976).
(17) G. A. Gornall, C. J. Bardawill, and M. M. David, *J. Biol. Chem.*, **177**, 751 (1949).
(18) "The Pharmacological Basis of Therapeutics," 5th ed., L. Goodman and A. Gilman, Eds., Macmillan, New York, N.Y., 1975, pp. 944–958.

ACKNOWLEDGMENTS

Supported by National Science Foundation Grant 74 22992 A_1.

The authors thank Dr. P. V. Blair, Department of Biochemistry, Indiana University School of Medicine, Indianapolis, Ind., for advice and support.

Aspirin—A National Survey IV: *In Vitro* Dissolution of Aspirin Formulations

WILLIAM E. JUHL ˣ and ROSS D. KIRCHHOEFER

Received October 29, 1979, from the *National Center for Drug Analysis, Food and Drug Administration, St. Louis, MO 63101.* Accepted for publication March 26, 1980.

Abstract □ The results of a national survey of the *in vitro* dissolution rates of aspirin tablets are presented. Dissolution profiles by both the proposed USP XX basket method and a paddle method are compared. The methods were used to analyze 59 tablet formulations representing 38 manufacturers. Each tablet was subjected to the dissolution procedure in 500 ml of pH 4.5 buffer solution, and an aliquot was sampled automatically and analyzed by an automated system. In 30 min, 22% of the samples tested using the basket method failed the proposed USP XX dissolution requirement. Seventy-five percent of the samples tested by the paddle method also failed the proposed dissolution requirement.

Keyphrases □ Aspirin—*in vitro* dissolution, comparison of basket and paddle methods □ Analgesics—*in vitro* dissolution of aspirin formulations □ Dissolution—aspirin formulations, *in vitro*, basket and paddle methods compared

A national survey (1) of aspirin tablet products was conducted at the National Center for Drug Analysis during the summer and fall of 1978. The purpose of the survey was to ascertain the quality of these products and the adequacy of the USP monograph (2). The USP presented a dissolution test in the *Pharmaceutical Forum* (3) that specifies use of a basket and requires 80% dissolution in 30 min.

During the survey, selected aspirin samples representing each manufacturer and dosage level were assayed for their dissolution rates *in vitro* using both a basket and a paddle and the dissolution medium (pH 4.5 buffer) and speed of rotation (50 rpm) specified in Ref. 3. The guidelines (4) for the dissolution testing were followed. The dissolution rate for each sample was determined by taking aliquots automatically (5) every 10 min over 60 min and analyzing the dissolution medium for aspirin by an automated procedure. The purpose of this experiment was to compare the dissolution characteristics of the selected marketed samples by the proposed USP XX dissolution test using the proposed basket method and the paddle method. The paddle method also was used because it has been a more discriminating test for differentiating drug products than the basket method in this laboratory.

EXPERIMENTAL

Apparatus—A dissolution apparatus[1] and a 76-liter aquarium tank with a constant-temperature water bath maintained at 37° were used.

For the sampling[2], an automatic analyzer with a sampler[3], three pumps[4], a manifold, and a timer[5] was used together with a cycle timer[6] for the sampling interval timer. Six sampling probes with filters[7] were required.

For the determinative step, an automatic analyzer with a sampler[3], pumps[8], a manifold, and a timer[5] was connected to a spectrophotometer[9] equipped with a quartz flowcell[10]. A 100-mv recorder[11] was connected to the spectrophotometer.

Reagents—ACS grade chloroform was washed with water and filtered through paper on the day of use. The pH 2.2 buffer solution was prepared by diluting 250.0 ml of 0.2 *M* KCl and 39.0 ml of 0.2 *M* HCl to 1 liter with water. The 0.2 *M* KCl was prepared by dissolving 14.911 g of potassium chloride in water and diluting it with water to 1 liter. The 0.2 *M* HCl was prepared by diluting 17.0 ml of concentrated hydrochloric acid to 1 liter with water. The pH 4.5 buffer solution was prepared by adding 2.99 g of sodium acetate to 1.66 ml of acetic acid and diluting to 1 liter with water. The buffer solution used for the dissolution medium was boiled to remove air bubbles.

Standard Preparation (324-mg Tablets)—Approximately 325 mg of USP reference standard aspirin was weighed accurately and dissolved in 5.0 ml of 95% ethanol. This solution was diluted to 1 liter with the pH 4.5 buffer solution. The standard was prepared fresh daily and was used immediately.

Sample Preparation (324-mg Tablets)—One tablet was placed in each dissolution vessel or basket. For 60 min, samples were withdrawn

[1] Model 72RL, Easi-Lift multiple-spindle dissolution drive, Hanson Research Corp., Northridge, CA 91324.
[2] C. E. Wells, T. W. Moore, and W. E. Juhl, unpublished data.
[3] AutoAnalyzer sampler II, 127-A000, Technicon Instruments Corp., Tarrytown, NY 10591.
[4] AutoAnalyzer proportioning pump I, 105-A200-01, Technicon Instruments Corp., Tarrytown, NY 10591.
[5] Flexopulse timer, model HG93A603, Eagle Signal Time Division, Gulf Western Industries, Davenport, IA 52803 (5).
[6] Three-cam, 10-min cycle timer, Westbrook Timer Sales, Westbrook, CT 06498.
[7] Filter tips, 20 μm, Centauer Chemical Co., Stamford, CT 06902.
[8] AutoAnalyzer proportioning pump III, 133-A014-04, Technicon Instruments Corp., Tarrytown, NY 10591.
[9] Model PM2DL, Carl Zeiss, Oberkochen, West Germany.
[10] Ten millimeters, 18 μl (886881) or 80 μl (886878), Beckman Instruments, Fullerton, CA 92634.
[11] Servo/Riter II, PS01W6A, Texas Instruments, Houston, TX 77001.

0022-3549/80/0800-0967$01.00/0
© 1980, American Pharmaceutical Association

(8) L. K. Steinrauf, B. Cox, E. Foster, and R. T. Blickenstaff, *J. Pharm. Sci.*, **67**, 1739 (1978).
(9) V. E. Rahman, M. W. Rosenthal, and E. A. Cerny, *Science*, **180**, 300 (1973).
(10) T. Norseth and M. Brendeford, *Biochem. Pharmacol.*, **20**, 1101 (1971).
(11) N. Sone, M. K. Larsstuvold, and Y. Kagawa, *J. Biochem.*, **82**, 859 (1977).
(12) J. H. Southard and P. Nitisewojo, *Biochem. Biophys. Res. Commun.*, **52**, 921 (1973).
(13) J. H. Southard, P. Nitisewojo, and D. E. Green, *Fed. Proc. Fed. Am. Soc. Exp. Biol.*, **33**, 2147 (1973).
(14) R. H. S. Thompson and V. P. Whittaker, *Biochem. J.*, **41**, 346 (1947).
(15) E. S. Barron and G. Kalnitsky, *ibid.*, **41**, 351 (1947).
(16) P. V. Blair, *Arch. Biochem. Biophys.*, **181**, 550 (1976).
(17) G. A. Gornall, C. J. Bardawill, and M. M. David, *J. Biol. Chem.*, **177**, 751 (1949).
(18) "The Pharmacological Basis of Therapeutics," 5th ed., L. Goodman and A. Gilman, Eds., Macmillan, New York, N.Y., 1975, pp. 944–958.

ACKNOWLEDGMENTS

Supported by National Science Foundation Grant 74 22992 A_1.

The authors thank Dr. P. V. Blair, Department of Biochemistry, Indiana University School of Medicine, Indianapolis, Ind., for advice and support.

Aspirin—A National Survey IV: *In Vitro* Dissolution of Aspirin Formulations

WILLIAM E. JUHL ˣ and ROSS D. KIRCHHOEFER

Received October 29, 1979, from the *National Center for Drug Analysis, Food and Drug Administration, St. Louis, MO 63101.* Accepted for publication March 26, 1980.

Abstract □ The results of a national survey of the *in vitro* dissolution rates of aspirin tablets are presented. Dissolution profiles by both the proposed USP XX basket method and a paddle method are compared. The methods were used to analyze 59 tablet formulations representing 38 manufacturers. Each tablet was subjected to the dissolution procedure in 500 ml of pH 4.5 buffer solution, and an aliquot was sampled automatically and analyzed by an automated system. In 30 min, 22% of the samples tested using the basket method failed the proposed USP XX dissolution requirement. Seventy-five percent of the samples tested by the paddle method also failed the proposed dissolution requirement.

Keyphrases □ Aspirin—*in vitro* dissolution, comparison of basket and paddle methods □ Analgesics—*in vitro* dissolution of aspirin formulations □ Dissolution—aspirin formulations, *in vitro*, basket and paddle methods compared

A national survey (1) of aspirin tablet products was conducted at the National Center for Drug Analysis during the summer and fall of 1978. The purpose of the survey was to ascertain the quality of these products and the adequacy of the USP monograph (2). The USP presented a dissolution test in the *Pharmaceutical Forum* (3) that specifies use of a basket and requires 80% dissolution in 30 min.

During the survey, selected aspirin samples representing each manufacturer and dosage level were assayed for their dissolution rates *in vitro* using both a basket and a paddle and the dissolution medium (pH 4.5 buffer) and speed of rotation (50 rpm) specified in Ref. 3. The guidelines (4) for the dissolution testing were followed. The dissolution rate for each sample was determined by taking aliquots automatically (5) every 10 min over 60 min and analyzing the dissolution medium for aspirin by an automated procedure. The purpose of this experiment was to compare the dissolution characteristics of the selected marketed samples by the proposed USP XX dissolution test using the proposed basket method and the paddle method. The paddle method also was used because it has been a more discriminating test for differentiating drug products than the basket method in this laboratory.

EXPERIMENTAL

Apparatus—A dissolution apparatus[1] and a 76-liter aquarium tank with a constant-temperature water bath maintained at 37° were used.

For the sampling[2], an automatic analyzer with a sampler[3], three pumps[4], a manifold, and a timer[5] was used together with a cycle timer[6] for the sampling interval timer. Six sampling probes with filters[7] were required.

For the determinative step, an automatic analyzer with a sampler[3], pumps[8], a manifold, and a timer[5] was connected to a spectrophotometer[9] equipped with a quartz flowcell[10]. A 100-mv recorder[11] was connected to the spectrophotometer.

Reagents—ACS grade chloroform was washed with water and filtered through paper on the day of use. The pH 2.2 buffer solution was prepared by diluting 250.0 ml of 0.2 *M* KCl and 39.0 ml of 0.2 *M* HCl to 1 liter with water. The 0.2 *M* KCl was prepared by dissolving 14.911 g of potassium chloride in water and diluting it with water to 1 liter. The 0.2 *M* HCl was prepared by diluting 17.0 ml of concentrated hydrochloric acid to 1 liter with water. The pH 4.5 buffer solution was prepared by adding 2.99 g of sodium acetate to 1.66 ml of acetic acid and diluting to 1 liter with water. The buffer solution used for the dissolution medium was boiled to remove air bubbles.

Standard Preparation (324-mg Tablets)—Approximately 325 mg of USP reference standard aspirin was weighed accurately and dissolved in 5.0 ml of 95% ethanol. This solution was diluted to 1 liter with the pH 4.5 buffer solution. The standard was prepared fresh daily and was used immediately.

Sample Preparation (324-mg Tablets)—One tablet was placed in each dissolution vessel or basket. For 60 min, samples were withdrawn

[1] Model 72RL, Easi-Lift multiple-spindle dissolution drive, Hanson Research Corp., Northridge, CA 91324.
[2] C. E. Wells, T. W. Moore, and W. E. Juhl, unpublished data.
[3] AutoAnalyzer sampler II, 127-A000, Technicon Instruments Corp., Tarrytown, NY 10591.
[4] AutoAnalyzer proportioning pump I, 105-A200-01, Technicon Instruments Corp., Tarrytown, NY 10591.
[5] Flexopulse timer, model HG93A603, Eagle Signal Time Division, Gulf Western Industries, Davenport, IA 52803 (5).
[6] Three-cam, 10-min cycle timer, Westbrook Timer Sales, Westbrook, CT 06498.
[7] Filter tips, 20 μm, Centauer Chemical Co., Stamford, CT 06902.
[8] AutoAnalyzer proportioning pump III, 133-A014-04, Technicon Instruments Corp., Tarrytown, NY 10591.
[9] Model PM2DL, Carl Zeiss, Oberkochen, West Germany.
[10] Ten millimeters, 18 μl (886881) or 80 μl (886878), Beckman Instruments, Fullerton, CA 92634.
[11] Servo/Riter II, PS01W6A, Texas Instruments, Houston, TX 77001.

0022-3549/80/0800-0967$01.00/0
© 1980, American Pharmaceutical Association

Table I—National Survey Results[a] (Percent of Label Declaration) for Dissolution of Aspirin Tablets

Manufacturer[b]	Tablet Dosage, mg	Appararus[c]	Dissolution Time, min 10	20	30	40	50	60
A	324	P	38.6 (2.6)	50.2 (3.8)	59.0[d] (4.2)	66.3 (4.5)	72.4 (4.3)	77.7 (4.3)
	324	B	71.2 (3.7)	93.4 (2.4)	97.5 (2.0)	97.4 (1.9)	96.8 (2.1)	96.2 (1.7)
B	421	P	41.3 (10.9)	51.0 (8.0)	58.1[d] (7.3)	62.9 (7.3)	65.9 (7.3)	68.6 (5.8)
	421	B	33.6 (4.0)	56.3 (6.7)	72.3[d] (9.8)	85.4 (12.8)	90.4 (13.2)	92.3 (12.7)
C	324	P	41.6 (3.6)	54.6 (8.1)	61.7[d] (7.9)	66.5 (8.0)	69.6 (7.6)	73.0 (7.2)
	324	B	61.8 (4.2)	94.4 (3.1)	100.3 (1.1)	100.3 (1.4)	99.6 (2.3)	98.6 (1.9)
	81	P	56.6 (4.6)	78.0 (8.1)	88.0 (8.1)	94.4 (7.2)	97.3 (6.8)	98.9 (6.4)
	81	B	55.4 (1.0)	85.2 (1.6)	96.5 (2.0)	100.0 (2.3)	100.8 (2.3)	100.8 (2.2)
	160	P	67.0 (2.4)	80.4 (3.3)	85.0 (3.8)	86.9 (3.7)	88.1 (3.7)	88.9 (3.6)
	160	B	61.8 (2.5)	87.9 (4.0)	98.0 (3.4)	101.2 (3.4)	101.9 (3.6)	102.6 (3.5)
D	486[e]	P	89.7 (6.0)	90.7 (5.2)	92.1 (5.5)	92.0 (5.0)	91.9 (4.9)	92.2 (5.1)
	486[e]	B	62.8 (16.9)	77.2 (14.2)	84.7 (10.3)	88.0 (6.7)	90.2 (3.6)	91.4 (2.3)
	324[e]	P	74.0 (12.2)	77.2 (10.0)	78.0[d] (9.2)	78.9 (8.5)	79.2 (7.7)	79.0 (7.8)
	324[e]	B	85.9 (13.3)	96.3 (4.9)	97.5 (2.6)	97.7 (1.5)	97.6 (1.8)	98.0 (2.0)
F	324[e]	P	98.6 (2.2)	100.3 (1.5)	100.8 (1.9)	100.5 (1.6)	100.7 (1.9)	99.2 (2.4)
	324[e]	B	79.7 (2.4)	87.3 (2.4)	91.4 (2.3)	92.1 (2.1)	92.2 (2.6)	92.9 (1.7)
G	324	P	17.6 (3.1)	27.0 (5.6)	35.4[d] (7.6)	42.3 (6.2)	48.2 (7.2)	54.2 (7.3)
	324	B	11.2 (1.0)	20.2 (2.0)	27.5[d] (3.4)	36.0 (4.8)	44.5 (5.7)	52.4 (6.9)
H	324	P	17.2 (8.7)	34.5 (14.8)	47.0[d] (18.3)	55.4 (19.2)	60.8 (17.8)	65.0 (16.3)
	324	B	37.9 (7.9)	72.9 (7.7)	91.1 (5.2)	96.7 (2.2)	99.4 (1.3)	98.9 (1.4)
	81	P	69.0 (18.7)	90.8 (11.4)	97.1 (7.7)	98.5 (9.1)	100.0 (9.2)	100.3 (8.6)
	81	B	56.2 (7.1)	84.6 (7.5)	93.4 (6.2)	97.6 (6.0)	100.1 (6.1)	102.0 (5.5)
I	81	P	9.1 (2.4)	12.5 (1.2)	16.9[d] (1.5)	20.5 (1.4)	24.2 (2.1)	27.3 (2.5)
	81	B	7.3 (0.4)	12.1 (0.6)	16.6[d] (0.6)	19.8 (0.4)	22.8 (0.5)	25.7 (0.7)
	324	P	16.0 (2.3)	27.4 (4.7)	36.6[d] (6.1)	43.6 (6.6)	49.3 (6.7)	54.2 (6.5)
	324	B	36.5 (14.7)	75.2 (13.9)	93.3 (6.2)	99.1 (1.3)	98.8 (0.7)	98.4 (0.5)
J	324	P	38.1 (3.2)	59.4 (6.3)	72.2[d] (7.8)	80.7 (7.6)	84.8 (6.0)	88.2 (5.4)
	324	B	59.9 (7.3)	81.7 (6.9)	90.4 (6.1)	93.9 (5.7)	95.1 (5.2)	95.0 (4.9)
K	81	P	12.3 (0.9)	24.1 (2.7)	32.4[d] (3.3)	38.7 (2.7)	44.2 (3.1)	47.2 (3.4)
	81	B	37.8 (3.1)	86.1 (6.7)	105.7 (8.5)	107.2 (6.1)	108.0 (6.1)	109.4 (6.6)
	324	P	23.2 (2.3)	34.3 (2.9)	41.4[d] (4.8)	47.3 (5.3)	52.1 (6.5)	55.9 (7.3)
	324	B	62.3 (6.2)	86.5 (5.5)	96.6 (2.6)	99.2 (1.7)	100.1 (1.1)	100.0 (1.5)
L	324[e]	P	93.4 (7.4)	95.0 (6.2)	95.4 (6.4)	95.2 (5.6)	95.1 (6.1)	95.8 (5.5)
	324[e]	B	83.7 (5.9)	90.0 (4.5)	93.0 (4.1)	95.6 (3.3)	96.7 (3.1)	95.4 (3.1)
M	324	P	31.5 (3.5)	46.7 (5.7)	56.5[d] (5.9)	64.4 (5.9)	70.6 (5.5)	75.9 (5.0)
	324	B	55.0 (1.8)	85.7 (3.4)	93.6 (1.5)	95.9 (2.1)	96.6 (2.4)	96.7 (2.2)
N	324	P	21.0 (4.8)	31.7 (7.0)	39.6[d] (7.6)	45.4 (8.0)	49.9 (8.0)	53.8 (7.9)
	324	B	43.5 (4.4)	62.5 (5.5)	73.7[d] (6.5)	80.6 (6.9)	84.8 (6.0)	91.9 (8.5)
O	324	P	24.0 (4.8)	42.3 (7.9)	55.8[d] (9.3)	65.5 (9.3)	72.6 (9.2)	78.2 (8.3)
	324	B	27.5 (6.6)	49.6 (9.2)	64.8[d] (10.2)	76.8 (9.3)	84.8 (8.2)	90.6 (6.6)
P	324	P	22.6 (2.6)	38.1 (5.5)	49.8[d] (6.2)	58.5 (6.4)	65.4 (6.6)	71.3 (5.5)
	324	B	26.6 (4.9)	45.7 (6.2)	59.5[d] (6.1)	69.9 (5.8)	77.9 (4.9)	84.2 (3.5)
Q	324	P	23.6 (2.2)	35.8 (3.8)	45.2[d] (4.9)	52.0 (6.2)	57.4 (7.2)	61.5 (7.6)
	324	B	40.0 (3.7)	69.6 (4.1)	84.1 (4.3)	91.0 (3.4)	94.5 (2.3)	95.9 (1.1)
R	324	P	20.0 (2.1)	29.5 (3.0)	37.1[d] (3.2)	42.5 (3.3)	46.9 (3.1)	50.7 (3.5)
	324	B	52.3 (7.7)	76.6 (10.5)	88.8 (8.5)	95.6 (7.0)	98.4 (5.4)	99.3 (4.2)
S	324	P	38.2 (10.9)	48.2 (11.0)	54.3[d] (10.4)	59.1 (9.9)	63.0 (9.3)	66.7 (9.0)
	324	B	66.0 (7.7)	93.4 (3.9)	97.6 (2.5)	97.1 (2.7)	97.1 (2.2)	96.7 (2.5)
T	81	P	56.4 (8.2)	67.5 (7.2)	75.7[d] (10.1)	79.8 (8.9)	83.0 (8.0)	84.5 (6.7)
	81	B	45.5 (7.8)	64.9 (8.1)	74.6[d] (7.8)	80.4 (6.1)	85.1 (5.5)	87.5 (4.0)
	324[e]	P	87.9 (2.3)	88.7 (2.9)	88.2 (2.8)	88.0 (2.9)	88.0 (2.7)	87.4 (2.5)
	324[e]	B	85.7 (2.3)	93.4 (2.3)	93.9 (2.2)	93.7 (2.0)	93.8 (1.6)	93.3 (1.9)
	81	P	46.9 (8.5)	61.9 (9.0)	70.1[d] (8.5)	74.3 (7.4)	77.3 (7.5)	80.1 (6.3)
	81	B	47.3 (7.8)	63.0 (9.5)	76.2[d] (10.3)	84.0 (9.4)	89.6 (9.1)	90.8 (7.9)
U	324[e]	P	103.7 (5.0)	107.5 (5.7)	105.6 (6.0)	103.6 (4.7)	105.9 (4.6)	107.4 (3.8)
	324[e]	B	90.4 (3.6)	96.4 (4.6)	98.9 (4.3)	99.0 (4.2)	99.9 (4.3)	100.2 (4.4)
	81	P	45.4 (5.6)	67.3 (7.2)	73.5[d] (7.5)	78.0 (7.7)	79.1 (7.1)	79.4 (7.8)
	81	B	50.5 (8.8)	70.9 (10.1)	80.0 (10.0)	84.6 (8.6)	88.1 (7.9)	90.8 (7.7)
V	324[e]	P	74.2 (9.0)	84.8 (7.0)	86.9 (6.8)	87.1 (6.2)	87.6 (5.8)	88.1 (5.1)
	324[e]	B	63.7 (4.8)	98.2 (2.8)	102.4 (1.4)	101.0 (3.0)	100.5 (1.8)	—
	81	P	44.6 (2.0)	68.8 (10.8)	74.2[d] (13.0)	76.9 (13.3)	79.2 (13.6)	80.2 (13.0)
	81	B	77.9 (4.0)	98.8 (3.6)	101.8 (2.8)	101.1 (2.2)	99.7 (2.5)	100.7 (2.7)
W	324	P	8.1 (0.7)	14.0 (2.5)	18.5[d] (3.5)	22.3 (4.3)	25.8 (4.8)	28.5 (5.1)
	324	B	4.1 (1.1)	9.6 (1.5)	14.4[d] (2.0)	19.2 (2.4)	23.1 (3.0)	27.3 (4.0)
X	324	P	16.3 (1.6)	25.9 (2.6)	33.1[d] (2.8)	39.3 (3.2)	44.5 (3.2)	48.9 (3.8)
	324	B	57.9 (4.9)	83.1 (3.1)	93.1 (2.0)	96.0 (2.5)	97.2 (2.1)	97.7 (1.3)
	81	P	60.5 (5.6)	75.2 (5.2)	81.9 (5.6)	85.0 (5.1)	85.9 (4.5)	87.9 (4.8)
	81	B	76.7 (4.1)	94.6 (1.8)	98.9 (2.5)	100.9 (2.1)	100.3 (1.6)	99.1 (1.9)
Y	81	P	37.7 (4.7)	56.7 (4.6)	65.6[d] (5.2)	71.4 (4.8)	73.8 (4.3)	75.1 (4.7)
	81	B	58.2 (6.8)	83.6 (4.0)	92.7 (3.6)	96.7 (1.9)	96.6 (2.5)	96.5 (1.3)
	324	P	19.2 (4.6)	32.1 (4.4)	40.4[d] (4.6)	47.3 (5.0)	52.6 (5.1)	57.0 (5.6)
	324	B	52.3 (12.0)	78.1 (9.8)	91.6 (4.7)	98.0 (1.5)	99.2 (1.5)	97.9 (1.5)
	486	P	48.3 (8.8)	67.7 (6.4)	76.9[d] (5.8)	81.7 (5.4)	84.4 (4.4)	84.9 (4.1)
	486	B	35.0 (3.1)	65.5 (9.4)	80.9 (11.9)	87.1 (9.4)	89.4 (5.4)	91.7 (4.4)

(continued)

Table I—*Continued*

Manufacturer[b]	Tablet Dosage, mg	Apparatus[c]	Dissolution Time, min 10	20	30	40	50	60
	648	P	26.5 (4.9)	44.5 (5.6)	52.8[d] (6.1)	57.5 (7.1)	61.2 (6.9)	63.7 (6.5
	648	B	34.4 (6.2)	65.3 (10.0)	85.3 (9.9)	97.5 (6.7)	103.7 (4.1)	105.4 (1.2)
Z	324	P	25.9 (4.6)	36.8 (5.5)	45.8[d] (5.8)	52.6 (5.8)	58.0 (5.9)	63.1 (5.7)
	324	B	67.5 (1.9)	88.8 (3.9)	93.1 (2.7)	94.5 (2.2)	95.2 (2.4)	95.5 (2.8)
	486	P	10.8 (2.0)	20.8 (5.6)	28.5[d] (8.6)	35.7 (10.1)	41.7 (11.0)	47.7 (12.2)
	486	B	5.7 (0.9)	10.7 (1.4)	15.5[d] (1.8)	20.2 (2.2)	24.5 (2.9)	28.8 (3.5)
AA	300	P	36.9 (2.7)	51.8 (2.8)	60.6[d] (3.1)	66.8 (3.1)	72.4 (2.7)	76.6 (2.1)
	300	B	59.9 (2.7)	87.7 (2.8)	98.9 (2.2)	100.6 (2.4)	100.4 (1.9)	100.3 (2.0)
	81	P	33.6 (3.4)	50.0 (4.3)	61.6[d] (5.6)	70.2 (5.1)	76.8 (5.0)	80.6 (4.8)
	81	B	77.6 (6.3)	98.6 (2.9)	99.5 (1.9)	99.1 (2.1)	98.5 (2.2)	98.1 (2.1)
BB	324	P	40.8 (2.3)	55.1 (3.5)	63.8[d] (3.9)	69.6 (4.1)	73.6 (4.3)	77.8 (4.5)
	324	B	47.3 (1.0)	74.6 (4.3)	91.1 (5.6)	97.0 (3.8)	98.8 (2.1)	99.3 (2.5)
CC	324[e]	P	81.8 (4.5)	84.7 (4.1)	85.3 (3.5)	85.0 (3.5)	84.8 (3.5)	84.3 (3.2)
	324[e]	B	77.7 (3.5)	89.5 (4.2)	92.4 (3.8)	93.7 (4.1)	94.3 (3.7)	96.4 (4.4)
DD	324[e]	P	90.6 (1.7)	89.8 (1.2)	88.4 (1.7)	88.7 (1.9)	90.8 (2.1)	93.2 (2.3)
	324[e]	B	82.6 (4.0)	94.2 (4.1)	94.3 (3.3)	93.1 (2.4)	93.8 (4.4)	95.4 (2.4)
EE	81	P	15.8 (4.1)	45.8 (7.6)	67.1[d] (7.2)	79.3 (7.7)	82.2 (7.7)	84.5 (7.3)
	81	B	56.0 (13.7)	85.0 (9.9)	95.9 (6.3)	99.1 (3.7)	99.3 (5.0)	100.4 (4.7)
	324	P	38.9 (8.4)	46.6 (10.1)	56.5[d] (6.3)	62.6 (6.4)	68.1 (5.6)	72.2 (4.9)
	324	B	62.1 (6.8)	92.0 (2.8)	100.1 (2.8)	101.2 (2.7)	101.3 (1.8)	101.4 (2.4)
FF	324	P	40.3 (2.6)	53.6 (3.3)	63.6[d] (5.0)	71.9 (6.4)	78.1 (6.2)	82.6 (5.5)
	324	B	70.6 (3.9)	97.3 (1.3)	100.4 (1.1)	99.6 (1.1)	99.7 (1.2)	98.7 (1.0)
GG	324[e]	P	29.0 (2.7)	48.9 (1.6)	63.8[d] (2.6)	73.6 (1.8)	77.8 (2.5)	81.3 (2.3)
	324[e]	B	50.5 (4.1)	71.9 (6.8)	83.2 (5.2)	88.7 (6.5)	91.8 (4.5)	92.5 (4.1)
	81	P	12.0 (1.7)	17.5 (2.9)	31.7[d] (5.9)	42.3 (4.1)	53.1 (3.8)	64.3 (4.1)
	81	B	8.1 (1.1)	17.8 (2.0)	33.2[d] (3.7)	54.5 (7.6)	78.4 (4.1)	89.9 (2.3)
	81	P	8.5 (0.6)	17.2 (3.9)	28.5[d] (3.8)	40.0 (6.4)	49.7 (7.0)	54.3 (6.3)
	81	B	6.2 (0.4)	9.9 (0.2)	13.8[d] (0.6)	19.8 (1.2)	30.9 (1.9)	46.4 (4.3)
HH	320	P	13.7 (1.3)	22.4 (2.2)	29.7[d] (4.1)	34.5 (3.1)	39.5 (3.6)	43.9 (3.7)
	320	B	33.1 (6.2)	63.6 (8.0)	80.7 (6.9)	89.7 (6.9)	93.3 (4.2)	95.6 (3.3)
	65	P	45.9 (11.0)	69.6 (11.5)	81.7 (9.3)	88.0 (7.1)	92.6 (6.0)	94.8 (5.1)
	65	B	59.1 (24.7)	79.0 (24.4)	88.1 (21.9)	92.3 (18.8)	93.1 (15.7)	94.2 (13.5)
II	324[e]	P	47.4 (5.2)	58.7 (5.4)	63.5[d] (5.4)	66.3 (4.9)	68.4 (5.0)	70.2 (5.0)
	324[e]	B	41.8 (5.0)	65.2 (4.3)	78.6[d] (5.6)	85.3 (7.2)	89.5 (8.1)	91.1 (8.7)
JJ	324	P	30.5 (2.7)	44.2 (2.8)	55.3[d] (4.9)	65.5 (6.9)	74.3 (8.0)	80.2 (6.9)
	324	B	66.6 (3.8)	92.6 (2.9)	97.2 (1.0)	98.3 (2.8)	97.8 (1.3)	97.8 (1.8)
	81	P	31.5 (2.6)	61.5 (9.1)	70.6[d] (9.6)	73.5 (8.8)	76.3 (8.6)	76.8 (9.1)
	81	B	45.9 (7.6)	74.7 (9.5)	85.6 (8.4)	90.4 (6.5)	92.8 (4.4)	95.5 (3.1)
KK	486[e]	P	81.0 (4.3)	84.9 (4.8)	87.4 (4.4)	88.3 (4.3)	89.0 (4.4)	89.8 (4.6)
	486[e]	B	34.5 (8.5)	77.5 (11.7)	96.6 (3.4)	99.2 (2.8)	99.8 (3.2)	99.0 (2.8)
LL	324[e]	P	47.8 (2.0)	62.2 (2.8)	70.2[d] (3.2)	74.9 (2.8)	78.6 (2.6)	80.9 (2.6)
	324[e]	B	38.3 (3.5)	58.9 (4.1)	70.9[d] (5.3)	78.1 (5.6)	82.4 (5.4)	85.0 (5.6)

[a] Average of six assays. Numbers in parentheses are standard deviations. [b] A = Bell Pharmacal, Greenville, S.C.; B = Block Drug Co., Memphis, Tenn.; C = Bowman Pharmaceuticals, Canton, Ohio; D = Bristol-Myers Co., New York, N.Y.; F = Otis Clapp & Sons, Boston, Mass.; G = Cord Laboratories, Detroit, Mich.; H = Davis Manufacturing Co., Knoxville, Tenn.; I = Dewey Products Co., Grand Rapids, Mich.; J = Ferndale Laboratories, Ferndale, Mich.; K = Freeda Vitamins, New York, N.Y.; L = ICN Pharmaceuticals, Cincinnati, Ohio; M = Lannett Co., Philadelphia, Pa.; N = Eli Lilly & Co., Indianapolis, Ind.; O = Mallard, Detroit, Mich.; P = Manhattan Drug Co., Hillside, N.J.; Q = Marshall Pharmacal Corp., S. Hackensack, N.J.; R = McKesson Laboratories, Fairfield, Conn.; S = Norwich-Eaton Pharmaceuticals, Norwich, N.Y.; T = Oak Park Pharmaceuticals, Fredonia, Wis.; U = Pennex Products Co., Pittsburgh, Pa.; V = L. Perrigo Co., Allegan, Mich.; W = Pill Mill, Grand Rapids, Mich.; X = Plough, Memphis, Tenn.; Y = Rexall Drug Co., St. Louis, Mo.; Z = Richlyn Laboratories, Philadelphia, Pa.; AA = Stein-Mendez Labs, Rio Peidas, Puerto Rico; BB = Stanback Co., Salisbury, N.C.; CC = Standard Pharmacal Co., Chicago, Ill.; DD = Stanley Laboratories, Portland, Ore.; EE = Sterling Drug, New York, N.Y.; FF = E. R. Squibb & Sons, New York, N.Y.; GG = Sun Laboratories, Portland, Ore.; HH = Vale Chemical Co., Allentown, Pa.; II = Walgreen Co., Chicago, Ill.; JJ = West-Ward, Eatontown, N.J.; KK = Whitehall Laboratories, New York, N.Y.; and LL = Zenith Laboratories, Hoboken, N.J. [c] P = paddle, and B = basket. [d] Failed to meet proposed USP XX requirements of 80% dissolution at 30 min. [e] Buffered tablets.

at 10-min intervals using the automated sampling system.

Semiautomated Determination—The automated system was assembled as shown in Fig. 1. The solutions were sampled at a rate of 30 cups per hour with a sample-to-wash ratio of 2:1. A sampling pattern of three standards, six samples, one standard, six samples, *etc.*, was used. Two cups of standard were placed at the end. The first two standards and the last standard were not used in the calculations. A polytetrafluoroethylene strip was inserted into the BO fitting to direct the organic phase downward.

To start the system, ethanol was pumped through the chloroform pump tube for 5 min, and the tube then was pumped dry. The chloroform line was placed in the solution and pumped until the solution reached the spectrophotometer cell. The pH 2.2 buffer line was placed in the solution, and the system was allowed to equilibrate.

The sample stream was diluted with pH 2.2 buffer, and chloroform was added. The chloroform containing the extracted drug was pumped through a flowcell, and the absorbance of the drug was read at 280 nm.

RESULTS AND DISCUSSION

Validation Tests—A series of validation tests was performed on the automated system. A linear response was obtained from four standard solutions containing 0.3–1.3 mg of aspirin/ml (corresponding to 50–200% of the label declaration). The results of an assay of 30 individual cups exhibited a relative standard deviation of 0.9%. A standard solution containing 0.65 mg of aspirin/ml gave reproducible peaks whose height reached ~97.0% of the steady state.

Composite Assays—Portions of tablet composites equivalent to single tablets were analyzed by the paddle method and the proposed USP XX (3) method. The ground tablet composites were prepared from available commercial samples. When four samples were analyzed by the USP and the automated methods, the results obtained were (percentage of label declaration): 97.9, 98.2, 101.0, and 100.9 and 99.3, 98.2, 101.5, and 101.2, respectively. Four individual assays of one composite gave an average of 101.2% of the label declaration with a relative standard deviation of 0.27%.

Effect of Alcohol in Standard—Since aspirin is not very soluble in pH 4.5 buffer solution, the aspirin standard was dissolved in ethanol and then diluted with the buffer solution. To test the effect of the alcohol, solutions containing 1% alcohol and no alcohol were analyzed. There was no difference in absorptivity between the two solutions.

Effect of Boiling pH 4.5 Buffer Solution—Deaerated water usually is recommended for dissolution of tablets. In the proposed method, if the water is deaerated first and the buffer solution then is prepared using this

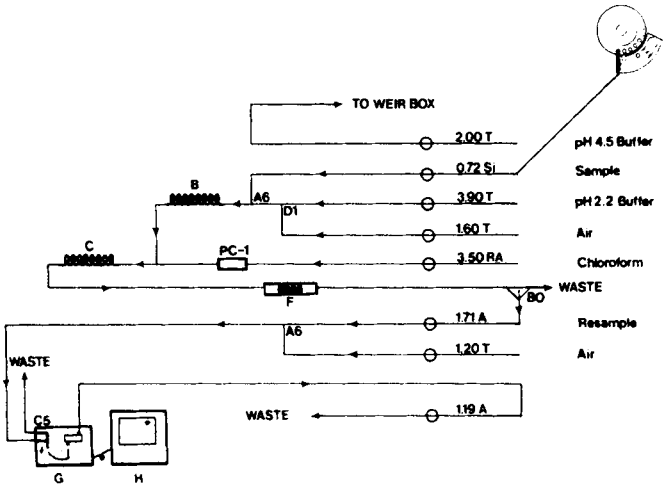

Figure 1—*Flow of automated system for aspirin dissolution. Key: Si, silicon pump tube; T, Tygon tube; A, Acidflex pump tube; RA, red Acidflex pump tube; B, 28-turn × 2.4-mm i.d. mixing coil; C, 28-turn × 2.4-mm i.d. mixing coil with one double end; F, 5.5-turn settling coil; G, UV spectrophotometer; and H, recorder. Pump tube sizes are in milliliters per minute.*

water, air can be introduced into the solution. A test was performed to determine if boiling the pH 4.5 buffer solution affects the pH of the solution. The pH of the freshly prepared solution and the boiled solution was the same.

Survey Results—The automated method was employed to analyze 59 tablet formulations representing 37 manufacturers using both the basket and the paddle techniques (Table I). Of the total samples tested, 22% failed the proposed USP XX dissolution requirement using the basket method and 75% failed using the paddle technique.

Of the 59 formulations tested, 49 were plain aspirin tablets and 10 were buffered tablets. None of the buffered tablets and 26.5% of the plain tablets failed the proposed USP XX requirements by the basket method. Eighty-six percent of the plain tablets and 20% of the buffered tablets failed the proposed USP XX requirements by the paddle method.

During this survey, the basket method gave higher results than the paddle method for ~75% of the samples. For some samples, the basket method results were twice as high as those for the paddle method. Therefore, if the basket method is used as the USP XX requirement, all buffered and most plain tablets would pass the test; but if the paddle method is used, some buffered tablets and most plain tablets would fail the proposed requirement. These results pose the question of which method will predict bioavailability more accurately.

REFERENCES

(1) W. E. Juhl and R. D. Kirchhoefer, *J. Pharm. Sci.*, **69**, 544 (1980).

(2) "The United States Pharmacopeia," 19th rev., Mack Publishing Co., Easton, Pa., 1975.

(3) *Pharmacopeial Forum*, 4, 266 (1978).

(4) D. C. Cox, C. C. Douglas, W. B. Furman, R. D. Kirchhoefer, J. W. Myrick, and C. E. Wells, *Pharm. Technol.*, 2, 40 (1978).

(5) J. W. Myrick and W. B. Furman, Laboratory Information Bulletin 1640, Food and Drug Administration, Rockville, Md., 1974.

ACKNOWLEDGMENTS

The authors thank Margaret Randall, Rudy Kulousek, John Gleason, Daniel Lee, and Anita Klix for technical assistance and Donald P. Page and William B. Furman for editorial assistance.

NOTES

Poloxamer 188 as Vehicle for Injectable Diazepam

ARTHUR V. PRANCAN *[x], BERNARD ECANOW [§], ROBERT J. BERNARDONI [¶], and MAX S. SADOVE [‡]

Received January 8, 1980, from the *Departments of *Pharmacology and [‡]Anesthesiology, Rush-Presbyterian-St. Luke's Medical Center, Chicago, IL 60612.* Accepted for publication February 25, 1980. [§]College of Pharmacy, University of Illinois at the Medical Center, Chicago, IL 60612. [¶]Present address: Department of Family Practice, St. Mary's Hospital, Madison, WI 53715.

Abstract □ The significant occurrence of thrombophlebitis in patients administered diazepam intravenously was described recently. This side effect has been attributed to the crystallization of diazepam and its subsequent precipitation upon contact with blood or intravenous fluids. The current study was designed to reveal whether the solubilizing capability of poloxamer 188 reduces the incidence of thrombotic and inflammatory effects of diazepam in rabbits. The incidence of early (3-hr) ear vein necrosis was 72% in the diazepam-treated ears, while the incidence of necrosis in the ears that received poloxamer 188 as a vehicle for diazepam was 25%. The occurrence of thrombosis and loss of vessel integrity also was higher in diazepam-treated ears than in those treated with diazepam plus poloxamer 188. Solubilization of diazepam with poloxamer 188 may decrease the incidence of the tested side effects.

Keyphrases □ Diazepam—reduction of thrombosis and inflammation using poloxamer 188 as vehicle, rabbits □ Poloxamer 188—use as vehicle for reduction of thrombosis and inflammation induced by injectable diazepam, rabbits □ Sedatives—diazepam, reduction of thrombosis and inflammation using poloxamer 188 as vehicle, rabbits

Diazepam[1] is generally accepted as an intravenous sedative/anesthetic with usefulness in dentistry and medicine (1–6). Its increased use over the past decade has resulted in support for its benefits in various procedures, but the literature also contains references to side effects.

Pain upon injection is a frequent side effect of diazepam use (3, 7–9), and there have been many reports of thrombophlebitis following diazepam injection (1–3, 9). These side effects have been associated with precipitation of di-

[1] Valium Injectable, Hoffmann-La Roche, Nutley, N.J.

0022-3549/80/0800-0970$01.00/0
© 1980, American Pharmaceutical Association

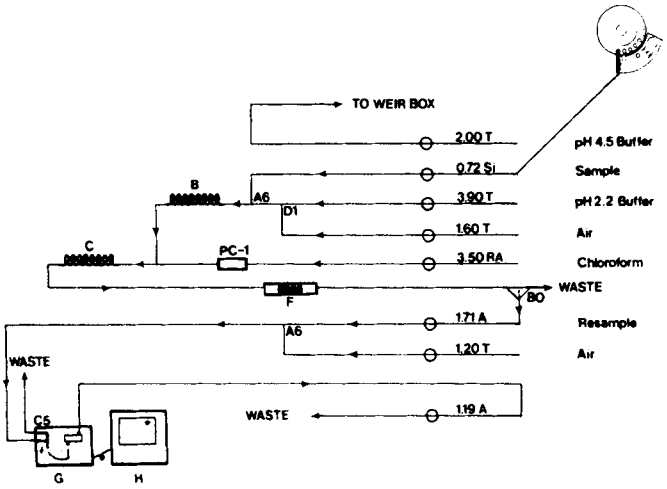

Figure 1—*Flow of automated system for aspirin dissolution. Key: Si, silicon pump tube; T, Tygon tube; A, Acidflex pump tube; RA, red Acidflex pump tube; B, 28-turn × 2.4-mm i.d. mixing coil; C, 28-turn × 2.4-mm i.d. mixing coil with one double end; F, 5.5-turn settling coil; G, UV spectrophotometer; and H, recorder. Pump tube sizes are in milliliters per minute.*

water, air can be introduced into the solution. A test was performed to determine if boiling the pH 4.5 buffer solution affects the pH of the solution. The pH of the freshly prepared solution and the boiled solution was the same.

Survey Results—The automated method was employed to analyze 59 tablet formulations representing 37 manufacturers using both the basket and the paddle techniques (Table I). Of the total samples tested, 22% failed the proposed USP XX dissolution requirement using the basket method and 75% failed using the paddle technique.

Of the 59 formulations tested, 49 were plain aspirin tablets and 10 were buffered tablets. None of the buffered tablets and 26.5% of the plain tablets failed the proposed USP XX requirements by the basket method. Eighty-six percent of the plain tablets and 20% of the buffered tablets failed the proposed USP XX requirements by the paddle method.

During this survey, the basket method gave higher results than the paddle method for ~75% of the samples. For some samples, the basket method results were twice as high as those for the paddle method. Therefore, if the basket method is used as the USP XX requirement, all buffered and most plain tablets would pass the test; but if the paddle method is used, some buffered tablets and most plain tablets would fail the proposed requirement. These results pose the question of which method will predict bioavailability more accurately.

REFERENCES

(1) W. E. Juhl and R. D. Kirchhoefer, *J. Pharm. Sci.*, **69**, 544 (1980).

(2) "The United States Pharmacopeia," 19th rev., Mack Publishing Co., Easton, Pa., 1975.

(3) *Pharmacopeial Forum*, 4, 266 (1978).

(4) D. C. Cox, C. C. Douglas, W. B. Furman, R. D. Kirchhoefer, J. W. Myrick, and C. E. Wells, *Pharm. Technol.*, 2, 40 (1978).

(5) J. W. Myrick and W. B. Furman, Laboratory Information Bulletin 1640, Food and Drug Administration, Rockville, Md., 1974.

ACKNOWLEDGMENTS

The authors thank Margaret Randall, Rudy Kulousek, John Gleason, Daniel Lee, and Anita Klix for technical assistance and Donald P. Page and William B. Furman for editorial assistance.

NOTES

Poloxamer 188 as Vehicle for Injectable Diazepam

ARTHUR V. PRANCAN *[x], BERNARD ECANOW [§], ROBERT J. BERNARDONI [¶], and MAX S. SADOVE [‡]

Received January 8, 1980, from the *Departments of *Pharmacology and [‡]Anesthesiology, Rush-Presbyterian-St. Luke's Medical Center, Chicago, IL 60612.* Accepted for publication February 25, 1980. [§]College of Pharmacy, University of Illinois at the Medical Center, Chicago, IL 60612. [¶]Present address: Department of Family Practice, St. Mary's Hospital, Madison, WI 53715.

Abstract □ The significant occurrence of thrombophlebitis in patients administered diazepam intravenously was described recently. This side effect has been attributed to the crystallization of diazepam and its subsequent precipitation upon contact with blood or intravenous fluids. The current study was designed to reveal whether the solubilizing capability of poloxamer 188 reduces the incidence of thrombotic and inflammatory effects of diazepam in rabbits. The incidence of early (3-hr) ear vein necrosis was 72% in the diazepam-treated ears, while the incidence of necrosis in the ears that received poloxamer 188 as a vehicle for diazepam was 25%. The occurrence of thrombosis and loss of vessel integrity also was higher in diazepam-treated ears than in those treated with diazepam plus poloxamer 188. Solubilization of diazepam with poloxamer 188 may decrease the incidence of the tested side effects.

Keyphrases □ Diazepam—reduction of thrombosis and inflammation using poloxamer 188 as vehicle, rabbits □ Poloxamer 188—use as vehicle for reduction of thrombosis and inflammation induced by injectable diazepam, rabbits □ Sedatives—diazepam, reduction of thrombosis and inflammation using poloxamer 188 as vehicle, rabbits

Diazepam[1] is generally accepted as an intravenous sedative/anesthetic with usefulness in dentistry and medicine (1–6). Its increased use over the past decade has resulted in support for its benefits in various procedures, but the literature also contains references to side effects.

Pain upon injection is a frequent side effect of diazepam use (3, 7–9), and there have been many reports of thrombophlebitis following diazepam injection (1–3, 9). These side effects have been associated with precipitation of di-

[1] Valium Injectable, Hoffmann-La Roche, Nutley, N.J.

0022-3549/80/0800-0970$01.00/0
© 1980, American Pharmaceutical Association

Table I—Effect of Poloxamer 188 on the Incidence of Diazepam-Related Rabbit Ear Vein Alterations [a]

	Thrombosis			Necrosis			Loss of Vascular Integrity		
	I[b]	II	III	I	II	III	I	II	III
Morrhuate sodium[c]	0	0	5	1	4	2	4	0	0
Saline	0	0	0	0	0	0	0	0	0
Diazepam	0	0	3	4	1	1	4	0	1
Diazepam plus poloxamer 188	0	0	1	2	0	0	0	0	0

[a] The values are the number of ears, within each group of eight ears injected, that showed the side effect. [b] Key: I = mild, II = moderate, and III = severe. [c] Known inflammatory agent.

azepam from the injectable solution in the presence of an aqueous medium, including blood (10).

The present study was designed to reveal whether the solubilizing capability of poloxamer 188[2] reduces the incidence of thrombotic and inflammatory effects of diazepam in rabbit ear veins.

EXPERIMENTAL

Sixteen male, adult, albino New Zealand rabbits[3], 2–3 kg, received an injection of a control or test solution in the marginal ear vein. After 180 min, the animals were sacrificed with ether. Vein cross-section samples, beginning 2 cm proximal to the injection site, were taken for pathological evaluation of vasculitis, necrosis, hemorrhage, thrombosis, edema, and vessel integrity. Standard staining and tissue handling techniques were used.

The animals were divided into two test groups. Group A (n = 8) animals received 0.9% saline (0.6 ml/kg) in one ear and morrhuate sodium (10 mg/kg), a known inflammatory agent, in the opposite ear. Group B (n = 8) animals received injectable diazepam[4] diluted (2×) with vehicle (diazepam, 1.5 mg/kg) in one ear and injectable diazepam diluted with water containing 5% poloxamer 188[5] (diazepam, 1.5 mg/kg) in the opposite ear. The diazepam vehicle contained 40% propylene glycol, 10% ethanol, 5% sodium benzoate, and 1.5% benzyl alcohol.

RESULTS AND DISCUSSION

Necrosis was more prevalent in diazepam-treated ear veins than in ear veins treated with diazepam plus poloxamer 188 (Table I). Necrosis also was closely associated with diazepam injection in other studies. Schneider and Mace (11) described an episode of necrosis associated with thrombosis that was related to a diazepam injection in a patient. Knill and Evans (12) injected diazepam into the central artery of rabbit ears and observed consistent necrosis and gangrene.

Antemortem thrombosis was observed in three of eight ear veins biopsied 3 hr after diazepam injection, while one ear vein contained a thrombus following diazepam plus poloxamer 188 (Table I). In ears treated with diazepam, two demonstrated hemorrhage and five showed a loss of vessel integrity. These changes were not seen in the ears treated with diazepam plus poloxamer 188.

Thrombosis after diazepam injection also was a frequent finding in previous studies. Graham *et al.* (13) found that thrombosis developed in the vein used for drug infusion within 48 hr in rats that received at least 0.25 mg of diazepam. Baker (1) reported a 15% incidence of superficial venous thrombosis in 400 patients receiving diazepam anesthesia. Three patient case reports of thrombosis following injection of diazepam also were described (14). Brown (15) observed a 15% incidence of thrombophlebitis or thrombosis following intravenous injection of 35 mg of diazepam and a 30% incidence with 50 mg of diazepam administered intravenously to patients. A 39% incidence of thrombosis was reported in patients 7–10 days after intravenous administration of 10 mg of diazepam (16).

The occurrence of thrombophlebitis probably is related to the insolubility of diazepam in aqueous media. Langdon (17) decreased the incidence of phlebitis from 7 to 2% by using 150–250 ml of saline flush. Jusko *et al.* (10) concluded that the thrombophlebitis associated with diazepam injection probably is due to precipitation of diazepam from solution when injected into a slow intravenous drip or a slow venous stream. Their calculations indicate that only a high flow rate allows the diazepam to stay in solution in an aqueous medium, where it is relatively insoluble.

This flow-related factor may be the reason that some investigators experienced fewer problems with diazepam when it was injected into a large vein (2) and may explain the lower incidence of thrombophlebitis when diazepam was followed by a large volume of saline flush (17). Graham *et al.* (7) reduced the incidence of thrombophlebitis after injection of 10 mg of diazepam in patients from 16 to 3% by diluting the drug in 20 ml of 5% dextrose–Ringer's lactate solution.

Ecanow and coworkers[6] found that a milky precipitate appeared upon introduction of injectable diazepam into whole blood and serum samples *in vitro*. The mixtures were centrifuged, and the precipitate was collected and observed under a light microscope; amorphous and needle-shaped crystalline particles were seen. A similar type of precipitate was obtained by adding the injectable diazepam to distilled water. Reformulation of the injectable diazepam was accomplished by adding poloxamer 188 (5% and more) to the commercial formulation. When the reformulated diazepam was introduced to the *in vitro* serum and whole blood solutions, no precipitation was apparent.

Poloxamer 188[7] [poly(oxypropylene) poly(oxyethylene) condensate], a surface-active agent with low toxicity, is used intravenously in humans. The present data indicate that poloxamer 188-solubilized diazepam causes fewer thrombotic and inflammatory effects in rabbit ear veins than does the injectable form of diazepam. Further studies are indicated to determine if this compound will effectively reduce diazepam side effects in patients.

REFERENCES

(1) A. B. Baker, *Anaesthesia*, **24**, 388 (1969).

(2) T. E. J. Healy, J. S. Robinson, and M. D. Vickers, *Br. Med. J.*, **3**, 10 (1960).

(3) G. M. Wyant and L. J. Studney, *Can. Anesth. Soc. J.*, **17**, 166 (1970).

(4) N. B. Litchfield and P. Gerard, *Aust. Dent. J.*, **16**, 25 (1971).

(5) P. A. Foreman, *Oral Surg.*, **37**, 337 (1974).

(6) K. K. Jain, *Can. J. Neurol. Sci.*, **1**, 141 (1974).

(7) C. W. Graham, R. R. Pagano, and J. T. Conner, *Anaesthesia*, **33**, 188 (1978).

(8) J. Katz, S. C. Finestone, and M. T. Pappas, *Anesth. Analg.*, **46**, 243 (1967).

(9) D. E. Langdon, J. R. Harlan, and R. L. Bailey, *J. Am. Med. Assoc.*, **223**, 184 (1973).

(10) W. J. Jusko, M. Gretch, and R. Gassett, *ibid.*, **225**, 176 (1973).

(11) S. Schneider and J. W. Mace, *Pediatrics*, **53**, 112 (1974).

(12) R. L. Knill and D. Evans, *Can. Anesth. Soc. J.*, **22**, 637 (1975).

(13) C. W. Graham, R. R. Pagano, and R. L. Katz, *Anesth. Analg.*, **56**, 409 (1977).

(14) J. L. Jenkinson and J. I. Tullis, *Edinburgh Dent. Hosp. Gaz.*, **10**, 6 (1970).

(15) S. S. Brown, *Proc. Symp. R. Soc. Med. (London)*, **1967**, 52.

(16) J. E. Hegarty and J. W. Dundee, *Br. Med. J.*, **2**, 1384 (1977).

(17) D. E. Langdon, *J. Am. Med. Assoc.*, **225**, 1389 (1973).

ACKNOWLEDGMENTS

Supported by Hoffmann-La Roche through Dr. John S. Kolina.

The authors thank Dr. James Bryant for evaluating the vein sections.

[2] Pluronic F68, BASF Wyandotte Corp., Wyandotte, Mich.

[3] Thompson Research Foundation, Monee, Ill., and Scientific Small Animal Laboratory and Farm, Arlington Heights, Ill.

[4] Injectable diazepam and placebo for injectable diazepam were generously supplied by Hoffmann-La Roche, Nutley, N.J.

[5] Wyandotte Corp., Wyandotte, Mich.

[6] B. Ecanow and coworkers, College of Pharmacy, University of Illinois at the Medical Center, Chicago, IL 60612, unpublished data.

[7] Poloxelene, Instant Microsphere Kit, Minnesota Mining and Manufacturing Corp., St. Paul, Minn.

Effect of Edetate Disodium on Goldfish Membrane

PETER J. CASCELLA ˣ **and PAUL D. KINDELSPIRE**

Received May 21, 1979, from the *Pharmacy Department, South Dakota State University, Brookings, SD 57007.* Accepted for publication February 13, 1980.

Abstract □ The effect of edetate disodium on the absorption of secobarbital sodium was examined in goldfish. An inverse relationship was observed between the concentration of edetate disodium to which fish were exposed and the time of death induced by secobarbital sodium. This inverse relationship is postulated to be due to an enhanced absorption of the ionized form of secobarbital in goldfish. There appears to be a period of time after exposure of the fish to the chelating agent in which the enhanced permeability of the membrane is absent in most studies. However, once the enhanced permeability effect is obtained, it is present 24 hr after exposure.

Keyphrases □ Edetate disodium—effect on absorption of secobarbital sodium in goldfish □ Secobarbital sodium—absorption in goldfish, effect of edetate disodium □ Permeability—effect of edetate disodium on goldfish membrane

Edetic acid is a sequestering agent capable of forming chelates with alkaline earth and heavy metal ions. Tidball (1) reported a 10-fold increase in the absorption of phenolsulfonphthalein (phenol red) in rats in the presence of edetic acid. Enhanced absorption of heparin and synthetic heparinoids from the GI tract of rats and dogs in the presence of edetic acid was observed (2). Feldman and Gibaldi (3) reported an ~20% increase in the transfer rate of salicylate across the everted rat intestine after exposure to edetic acid but found no apparent change in the transfer rate of salicylamide. They suggested that edetic acid may alter the rate-limiting barrier for water-soluble compounds but not for lipid-soluble compounds.

The purpose of this investigation was to examine the effect of edetate disodium on the permeability of the goldfish membrane. Levy and coworkers (4, 5) utilized goldfish to study the effects of surfactants on the absorption of alcohols and barbiturates. Nightingale *et al.* (6) used goldfish to assess structure–toxicity relationships of some substituted phenothiazines. Feldman *et al.* (7) used goldfish to study various local anesthetic agents and found an apparent relationship between the minimum effective concentration of drug to produce a response in goldfish and the minimum blocking concentration of these agents in isolated nerve or muscle fibers (8).

Therefore, it was of interest to examine the effects of edetate disodium on the goldfish membrane to determine if the permeability effects were similar to those reported previously (1–3) in other biological models.

EXPERIMENTAL

Concentration and Recovery Time Studies—Goldfish (*Carassius auratus*) (1–3 g) were placed in groups of five in tanks containing 2 liters of a solution of edetate disodium[1] at 0.1, 0.2, and 0.4 mg/ml. The solutions were made with glass-distilled[2] water and were adjusted to pH[3] 7.4 using 0.1 *N* NaOH or HCl. The fish were left in the solutions for 24 hr and then were placed for 30 min or 24 hr in recovery tanks containing 2 liters of glass-distilled water. Individual fish then were placed into beakers containing 200 ml of 0.1 m*M* secobarbital sodium[4] in 0.05 *M* phosphate buffer (pH 7.4). Cessation of gill and mouth movements was noted, and the time to death was computed.

Controls were run for each group following the procedure for the edetate disodium-treated fish, except that the chelating agent was omitted from the treatment tank. All investigations were performed at 20 ± 2°.

pH Study—Five fish were placed in tanks containing 2 liters of 0.2 mg/ml edetate disodium in glass-distilled water. The solutions were adjusted to pH 7.4 using 0.1 *N* NaOH or 0.1 *N* HCl. The fish were left in the tanks for 24 hr and then were placed for 30 min or 24 hr in a recovery tank containing 2 liters of glass-distilled water. Individual fish were placed in 200 ml of a 0.1 m*M* secobarbital sodium solution buffered to pH 6.4, 7.4, or 8.4 with 0.05 *M* phosphate buffer. Cessation of gill and mouth movements was noted, and the time to death was computed.

Controls were run in the same manner as described previously. All experiments were performed at 20 ± 2°.

RESULTS AND DISCUSSION

The results of the concentration and recovery time study are summarized in Table I. Comparisons were made within each block using a Student *t* test. There was no significant difference between the treated animals and the controls for the 24-hr treatment, 30-min recovery study, except at the highest concentration of the chelating agent. In the 24-hr treatment, 24-hr recovery study, there was a significant difference between the treated and control fish at all concentrations of edetate disodium. If it is assumed that the amount of secobarbital necessary to produce death is the same for treated and control animals, edetate disodium apparently increases membrane permeability to the barbiturate, as indicated by the shorter times until death for the treated animals.

Although the reason is unknown, there appears to be a time period after exposure in which the enhanced permeability of the membrane is absent, except at the highest concentration (0.4 mg/ml) of the chelating agent. This conclusion is suggested by the fact that there was no significant difference between treated and control animals in the 24-hr treatment, 30-min recovery study for edetate disodium at 0.1 and 0.2 mg/ml, while a significant difference was found for the 24-hr treatment, 24-hr recovery study. The fact that the apparent increased permeability of the membrane, once established, exists 24 hr after exposure suggests that the effect on membrane permeability is relatively long, at least in the system investigated.

It was of interest to determine whether a relationship exists between the concentration of the chelating agent and the increased membrane permeability. Since the condition of the fish employed may have varied, an analysis of variance was performed on the control fish for each concentration of the chelating agent used in the 24-hr treatment, 24-hr recovery study. The results indicated that a significant difference existed between the three control groups ($p < 0.05$). An analysis of the means using the least significant difference method indicated that the control run with the fish treated with 0.2-mg/ml edetate disodium was significantly different ($p < 0.05$) from the controls run with the fish treated with 0.1- and 0.4-mg/ml edetate disodium. A comparison of the means for the fish treated with 0.1- and 0.4-mg/ml edetate disodium using a Student *t* test showed a significant difference ($p < 0.05$) between the two means. Therefore, the higher the concentration of chelating agent to which the fish are exposed, the greater is the apparent increase in permeability.

Studies also were performed in which the fish were treated with 0.2-mg/ml edetate disodium solutions and then exposed to secobarbital sodium solutions buffered to pH 6.4, 7.4, and 8.4 (Table II). There again appeared to be a period of time after exposure of the fish to the chelating agent in which the enhanced permeability of the membrane was absent. This effect was evident in the 24-hr treatment, 30-min recovery study, in which no significant difference was observed between the treated and the control groups. With the 24-hr treatment, 24-hr control, there was

[1] Fisher Scientific Co., Fair Lawn, N.J.
[2] Corning model AG-1B.
[3] Heath model EU-302A.
[4] Robinson Laboratory, San Francisco, Calif.

0022-3549/80/0800-0972$01.00/0
© 1980, American Pharmaceutical Association

Table I—Effect of Concentration of Edetate Disodium and Recovery Time on Time of Death of Goldfish in 0.1 m*M* Secobarbital Sodium [a]

	Concentration of Edetate Disodium					
	0.1 mg/ml		0.2 mg/ml		0.4 mg/ml	
	Mean Time ± *SD*, min	Significance	Mean Time ± *SD*, min	Significance	Mean Time ± *SD*, min	Significance
Treatment[b]	16.56 ± 6.63	NS[c]	20.21 ± 3.74	NS	17.66 ± 2.23	$p < 0.05$
Control[d]	18.93 ± 8.51		23.89 ± 5.80		21.09 ± 4.68	
Treatment[e]	18.88 ± 3.85	$p < 0.05$	23.03 ± 1.79	$p < 0.05$	14.26 ± 3.16	$p < 0.05$
Control[f]	25.07 ± 5.88		32.27 ± 8.07		20.99 ± 2.77	

[a] Results given are for 10 determinations. [b] 24-hr treatment, 30-min recovery. [c] Not significant ($p > 0.05$). [d] 24-hr blank, 30-min recovery. [e] 24-hr treatment, 24-hr recovery. [f] 24-hr blank, 24-hr recovery.

Table II—Effect of pH and Recovery Time on Time of Death of Goldfish Exposed to 0.2-mg/ml Edetate Disodium [a]

	pH 6.4		pH 7.4		pH 8.4	
	Mean Time ± *SD*, min	Significance	Mean Time ± *SD*, min	Significance	Mean Time ± *SD*, min	Significance
Treatment[b]	14.88 ± 0.99	NS[c]	20.21 ± 3.74	NS	52.29 ± 9.70	NS
Control[d]	13.49 ± 2.51		23.89 ± 5.80		62.30 ± 16.93	
Treatment[e]	18.73 ± 5.92	NS	23.03 ± 1.79	$p < 0.05$	58.83 ± 17.31	$p < 0.05$
Control[f]	15.80 ± 3.51		32.27 ± 8.07		97.84 ± 22.19	

[a] Results given are for 10 determinations except for the 24-hr blank, 24-hr recovery study at pH 6.4, for which the results of five determinations are given. [b] 24-hr treatment, 30-min recovery. [c] Not significant ($p > 0.05$). [d] 24-hr blank, 30-min recovery. [e] 24-hr treatment, 24-hr recovery. [f] 24-hr blank, 24-hr recovery.

a significant difference between the treated fish and the controls for secobarbital sodium at pH 7.4 and 8.4. However, there was no difference between the treated fish and the controls for the secobarbital sodium solution buffered at pH 6.4.

Since secobarbital is a weak acid with a pKa of 7.9, it exists ~3, ~24, and ~76% ionized at pH 6.4, 7.4, and 8.4, respectively. Thus, the chelating agent apparently affected the transport of the ionized barbiturate form. However, the increase in the transport rate of the ionized form apparently was not enough to compensate for the decrease in the unionized concentration as the pH of the secobarbital sodium solutions increased. This result was evident from the apparent increase in time necessary to produce death as the pH of the secobarbital sodium solutions increased.

With a model proposed by Levy and Gucinski (9) (see *Appendix*) for the absorption of both the unionized and ionized drug forms in goldfish, a plot of the reciprocal of the response time ($1/t$) as a function of the fraction of drug unionized should be linear with a slope equal to $K_b(K_u - K_i)$ and an intercept equal to K_bK_i:

$$1/t = K_bK_i + K_b(K_u - K_i)f \qquad \text{(Eq. 1)}$$

where K_b is a constant equal to the quotient of the secobarbital concentration to which the fish were exposed divided by the amount of barbiturate in the fish at death and K_i and K_u are the first-order rate constants for the ionized and unionized forms of the drug. Figure 1 is the least-squares regression of the reciprocal of the response time *versus* the fraction of drug unionized for the 24-hr treatment, 24-hr recovery and the 24-hr treatment, 30-min recovery studies. The regression lines are $1/t = 0.0050 + 0.0500f$ ($r = 0.9999$) and $1/t = 0.0029 + 0.0644f$ ($r = 0.9960$), respectively.

Dividing the slope by the intercept yields:

$$\frac{\text{slope}}{\text{intercept}} = \frac{K_b(K_u - K_i)}{K_bK_i} = \frac{K_u}{K_i} - 1 \qquad \text{(Eq. 2)}$$

For the 24-hr treatment, 24-hr recovery study, Eq. 2 yields:

$$11 = K_u/K_i \qquad \text{(Eq. 3)}$$

For the 24-hr treatment, 30-min recovery, it yields:

$$23.3 = K_u/K_i \qquad \text{(Eq. 4)}$$

A rather dramatic change in the magnitude of the unionized to ionized ratio is observed between the two studies. With the assumption that the amount of drug in the fish is the same at the end-point:

$$\frac{\text{intercept 1}}{\text{intercept 2}} = \frac{\frac{C}{\text{amount}}K_i}{\frac{C}{\text{amount}}K_i} = \frac{K_{i1}}{K_{i2}} = 1.7 \qquad \text{(Eq. 5)}$$

Thus, there appears to be an ~70% increase in the rate constant for the ionized drug in the 24-hr treatment, 24-hr recovery study as compared to the 24-hr treatment, 30-min recovery study. Substituting the apparent increase in the rate constant for the absorption of the ionized form into Eq. 2 for the 24-hr treatment, 24-hr recovery study yields $11 = K_u/1.7K_i$ or $18.7 = K_u/K_i$. Although the apparent increase of the ionized rate constant obtained from the intercept values does not explain completely the observed ratio for the 24-hr treatment, 30-min recovery study ($K_u/K_i = 23.3$), it does account for ~80% of the value.

Unfortunately, the controls for both recovery time studies do not appear to fit the model. Although the exact reason for this result is unknown,

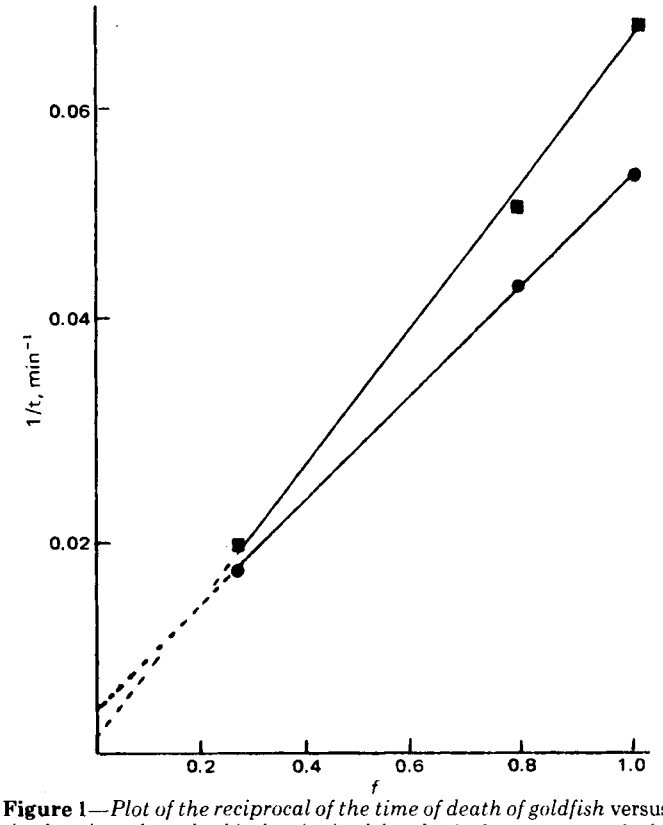

Figure 1—*Plot of the reciprocal of the time of death of goldfish* versus *the fraction of secobarbital unionized for the 24-hr treatment, 24-hr recovery study (●) and the 24-hr treatment, 30-min recovery study (■).*

in the experiment by Levy and Gucinski (9) the fish exposed to secobarbital apparently did fit the model, which led these investigators to conclude that secobarbital was absorbed in both the unionized and ionized forms. For the most part, that experiment was similar to the controls in this experiment.

In summary, there appears to be a period of time after exposure of fish to the chelating agent in which the enhanced permeability of the membrane to the barbiturate is absent. However, once the effect is obtained, it is present 24 hr after exposure. The chelating agent appears to affect the transport of the ionized drug species, but the increase in the transport of the ionized form is not enough to compensate for the reduction of the unionized concentration in the pH study. There also appears to be a direct relationship between the change in permeability and the concentration of chelating agent to which the fish are exposed. Further studies are underway concerning the effects of edetate disodium on the goldfish membrane.

APPENDIX

The model proposed by Levy and Gucinski (9) concerning the absorption of both the unionized and ionized drug forms in the goldfish is:

$$R = K_i C_i + K_u C_u \qquad \text{(Eq. A1)}$$

where R is the absorption rate, K_i and K_u are the first-order rate constants, and C_i and C_u are the concentrations of the ionized and unionized species, respectively. The amount of drug in the fish is equal to the product of the absorption rate and the time the fish is exposed to the bathing solution:

$$\text{amount} = Rt \qquad \text{(Eq. A2)}$$

Substituting Eq. A1 for R in Eq. A2 yields:

$$\text{amount} = (K_i C_i + K_u C_u)t \qquad \text{(Eq. A3)}$$

which is equivalent to:

$$1/t = \frac{K_i C_i + K_u C_u}{\text{amount}} \qquad \text{(Eq. A4)}$$

Since the sum of C_i and C_u represents the total drug concentration, which was constant for these experiments, then:

$$1/t = \frac{C}{\text{amount}}[K_i(1 - f) + K_u f] \qquad \text{(Eq. A5)}$$

where C represents the total concentration of drug and f and $1 - f$ represent the fraction of the drug present in the unionized and ionized forms, respectively. Therefore:

$$1/t = \frac{C}{\text{amount}}(K_i - K_i f + K_u f) \qquad \text{(Eq. A6)}$$

and:

$$1/t = \frac{CK_i}{\text{amount}} + \frac{C(K_u - K_i)f}{\text{amount}} \qquad \text{(Eq. A7)}$$

If it is assumed that the amount of drug necessary to produce death is constant regardless of the pH employed:

$$1/t = K_b K_i + K_b(K_u - K_i)f \qquad \text{(Eq. A8)}$$

where K_b is a constant and equals C/amount. Therefore, a plot of the reciprocal of the response time ($1/t$) as a function of the fraction of drug unionized should be linear with a slope equal to $K_b(K_u - K_i)$ and an intercept equal to $K_b K_i$.

REFERENCES

(1) C. S. Tidball, *Am. J. Physiol.*, **206**, 243 (1964).

(2) E. Windsor and G. E. Cronheim, *Nature*, **190**, 263 (1961).

(3) S. Feldman and M. Gibaldi, *J. Pharm. Sci.*, **58**, 967 (1969).

(4) G. Levy and J. A. Anello, *ibid.*, **57**, 101 (1968).

(5) G. Levy, K. E. Miller, and R. H. Reuning, *ibid.*, **55**, 1498 (1966).

(6) C. H. Nightingale, M. Tse, and E. I. Stupak, *ibid.*, **61**, 1948 (1972).

(7) S. Feldman, M. DeFrancisco, and P. J. Cascella, *ibid.*, **64**, 1713 (1975).

(8) D. Agin, L. Hersh, and D. Holtzman, *Proc. Natl. Acad. Sci. USA*, **53**, 952 (1965).

(9) G. Levy and S. P. Gucinski, *J. Pharmacol. Exp. Ther.*, **146**, 80 (1964).

Stability of Apomorphine in Solutions Containing Ascorbic Acid and Bisulfite and Effects of Antioxidants on Apomorphine-Induced Cage Climbing and Hypothermia in Mice

RICHARD E. WILCOX *, DAVID W. HUMPHREY ‡, WILLIAM H. RIFFEE *, and ROBERT V. SMITH ‡x

Received December 10, 1979, from the **Department of Pharmacology and* ‡*Drug Dynamics Institute, College of Pharmacy, University of Texas at Austin, Austin, TX 78712.* Accepted for publication February 29, 1980.

Abstract □ Ascorbic acid (100 mg/ml) and sodium bisulfite (0.5 and 20 mg/ml) prevented more than 10% oxidation of apomorphine hydrochloride in water maintained at room temperature over 1–3 days. Refrigeration at 5° prevented oxidation of apomorphine hydrochloride in aqueous solutions for 1 week. Neither ascorbic acid nor sodium bisulfite affected murine stereotyped cage climbing or hypothermia induced by apomorphine.

Keyphrases □ Apomorphine—stability in solutions containing ascorbic acid and sodium bisulfite, effects of antioxidants on apomorphine-induced cage climbing and hypothermia in mice □ Antioxidants—ascorbic acid and sodium bisulfite, stability of apomorphine in solutions containing antioxidants, effects of antioxidants on apomorphine-induced cage climbing and hypothermia in mice □ Stability—apomorphine in solutions containing ascorbic acid and sodium bisulfite

Current interest in apomorphine (I) stems from its activity as a dopaminergic agonist and its consequent antiparkinsonian activity (1–3). Its clinical unity has been demonstrated when used alone and in combination with other agents such as levodopa (4). In addition to parkinsonism, recent studies indicated potential new uses for I

0022-3549/80/0800-0974$01.00/0

© 1980, American Pharmaceutical Association

in the experiment by Levy and Gucinski (9) the fish exposed to secobarbital apparently did fit the model, which led these investigators to conclude that secobarbital was absorbed in both the unionized and ionized forms. For the most part, that experiment was similar to the controls in this experiment.

In summary, there appears to be a period of time after exposure of fish to the chelating agent in which the enhanced permeability of the membrane to the barbiturate is absent. However, once the effect is obtained, it is present 24 hr after exposure. The chelating agent appears to affect the transport of the ionized drug species, but the increase in the transport of the ionized form is not enough to compensate for the reduction of the unionized concentration in the pH study. There also appears to be a direct relationship between the change in permeability and the concentration of chelating agent to which the fish are exposed. Further studies are underway concerning the effects of edetate disodium on the goldfish membrane.

APPENDIX

The model proposed by Levy and Gucinski (9) concerning the absorption of both the unionized and ionized drug forms in the goldfish is:

$$R = K_i C_i + K_u C_u \qquad \text{(Eq. A1)}$$

where R is the absorption rate, K_i and K_u are the first-order rate constants, and C_i and C_u are the concentrations of the ionized and unionized species, respectively. The amount of drug in the fish is equal to the product of the absorption rate and the time the fish is exposed to the bathing solution:

$$\text{amount} = Rt \qquad \text{(Eq. A2)}$$

Substituting Eq. A1 for R in Eq. A2 yields:

$$\text{amount} = (K_i C_i + K_u C_u)t \qquad \text{(Eq. A3)}$$

which is equivalent to:

$$1/t = \frac{K_i C_i + K_u C_u}{\text{amount}} \qquad \text{(Eq. A4)}$$

Since the sum of C_i and C_u represents the total drug concentration, which was constant for these experiments, then:

$$1/t = \frac{C}{\text{amount}}[K_i(1 - f) + K_u f] \qquad \text{(Eq. A5)}$$

where C represents the total concentration of drug and f and $1 - f$ represent the fraction of the drug present in the unionized and ionized forms, respectively. Therefore:

$$1/t = \frac{C}{\text{amount}}(K_i - K_i f + K_u f) \qquad \text{(Eq. A6)}$$

and:

$$1/t = \frac{CK_i}{\text{amount}} + \frac{C(K_u - K_i)f}{\text{amount}} \qquad \text{(Eq. A7)}$$

If it is assumed that the amount of drug necessary to produce death is constant regardless of the pH employed:

$$1/t = K_b K_i + K_b(K_u - K_i)f \qquad \text{(Eq. A8)}$$

where K_b is a constant and equals C/amount. Therefore, a plot of the reciprocal of the response time ($1/t$) as a function of the fraction of drug unionized should be linear with a slope equal to $K_b(K_u - K_i)$ and an intercept equal to $K_b K_i$.

REFERENCES

(1) C. S. Tidball, *Am. J. Physiol.*, **206**, 243 (1964).

(2) E. Windsor and G. E. Cronheim, *Nature*, **190**, 263 (1961).

(3) S. Feldman and M. Gibaldi, *J. Pharm. Sci.*, **58**, 967 (1969).

(4) G. Levy and J. A. Anello, *ibid.*, **57**, 101 (1968).

(5) G. Levy, K. E. Miller, and R. H. Reuning, *ibid.*, **55**, 1498 (1966).

(6) C. H. Nightingale, M. Tse, and E. I. Stupak, *ibid.*, **61**, 1948 (1972).

(7) S. Feldman, M. DeFrancisco, and P. J. Cascella, *ibid.*, **64**, 1713 (1975).

(8) D. Agin, L. Hersh, and D. Holtzman, *Proc. Natl. Acad. Sci. USA*, **53**, 952 (1965).

(9) G. Levy and S. P. Gucinski, *J. Pharmacol. Exp. Ther.*, **146**, 80 (1964).

Stability of Apomorphine in Solutions Containing Ascorbic Acid and Bisulfite and Effects of Antioxidants on Apomorphine-Induced Cage Climbing and Hypothermia in Mice

RICHARD E. WILCOX *, DAVID W. HUMPHREY ‡, WILLIAM H. RIFFEE *, and ROBERT V. SMITH ‡x

Received December 10, 1979, from the **Department of Pharmacology and* ‡*Drug Dynamics Institute, College of Pharmacy, University of Texas at Austin, Austin, TX 78712.* Accepted for publication February 29, 1980.

Abstract □ Ascorbic acid (100 mg/ml) and sodium bisulfite (0.5 and 20 mg/ml) prevented more than 10% oxidation of apomorphine hydrochloride in water maintained at room temperature over 1–3 days. Refrigeration at 5° prevented oxidation of apomorphine hydrochloride in aqueous solutions for 1 week. Neither ascorbic acid nor sodium bisulfite affected murine stereotyped cage climbing or hypothermia induced by apomorphine.

Keyphrases □ Apomorphine—stability in solutions containing ascorbic acid and sodium bisulfite, effects of antioxidants on apomorphine-induced cage climbing and hypothermia in mice □ Antioxidants—ascorbic acid and sodium bisulfite, stability of apomorphine in solutions containing antioxidants, effects of antioxidants on apomorphine-induced cage climbing and hypothermia in mice □ Stability—apomorphine in solutions containing ascorbic acid and sodium bisulfite

Current interest in apomorphine (I) stems from its activity as a dopaminergic agonist and its consequent antiparkinsonian activity (1–3). Its clinical unity has been demonstrated when used alone and in combination with other agents such as levodopa (4). In addition to parkinsonism, recent studies indicated potential new uses for I

0022-3549/80/0800-0974$01.00/0

© 1980, American Pharmaceutical Association

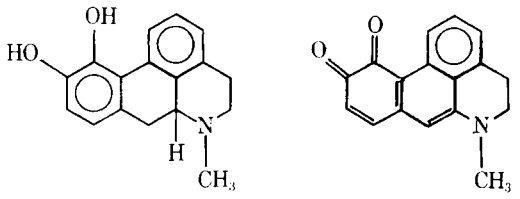

I

II

in treating Huntington's chorea (5), tardive dyskinesia (6, 7), Gilles de la Tourette's syndrome (8), and schizophrenia (9, 10).

BACKGROUND

Recent efforts have focused on extending the pharmacokinetic studies of I in mice. The disposition of I following parenteral administration to mice was reported (11–14). Study of the plasma levels of I in mice following intraperitoneal, intravenous, and oral administrations (15) and preliminary investigations (15, 16) suggested a correlation between circulating levels of I and stereotyped cage climbing (16). Continued work is aimed at extensive comparisons between circulating levels of I and the stereotyped cage climbing and hypothermia induced by I in mice. These studies are being conducted to develop pharmacological models that might be useful in evaluating the efficacy of apomorphine prodrugs, some of which already have been synthesized (17) and evaluated pharmacologically in rats (18).

A problem complicating work with apomorphine is its tendency to undergo air oxidation. Aqueous solutions of I·HCl rapidly become green to blue green due to the accumulation of oxidation products (19). The oxidation process in neutral and acidic media is relatively uncomplicated, leading principally to the orthoquinone, II (20, 21). However, at alkaline pH values, the degradation is considerably more complex and yields four or more products (22, 23).

Burkman (24, 25) studied the oxidation kinetics of I from pH 5.2 to 6.8. The half-lives of I in buffered solutions were 11–166 hr with the more acidic solutions being more stable. An unbuffered 1.2% solution of I·HCl (pH 5.5) was considerably more stable than its buffered counterpart. Various investigators recommended the use of citrate (26), bisulfite (27), ascorbic acid (28), thiourea (29), and edetic acid (26) to stabilize aqueous solutions of apomorphine.

The purpose of this investigation was to reevaluate the use of bisulfite and ascorbate in stabilizing I solutions maintained at room temperature and under refrigerated conditions. The use of a specific high-performance liquid chromatographic (HPLC) assay, developed recently in these laboratories (30), was expected to facilitate this work. Furthermore, studies of the effect of ascorbate and bisulfite on apomorphine-induced stereotyped cage climbing and hypothermia in mice were conducted to determine if the antioxidants interfered in these test systems.

EXPERIMENTAL

Reagents—(*R*)-(−)-Apomorphine hydrochloride hemihydrate[1] [98% pure as determined by UV spectrophotometry (31)], ascorbic acid[2], and sodium bisulfite[2] were used as purchased. Apomorphine orthoquinone (6-methyl-5,6-dihydro-4*H*-dibenzo[*de,g*]quinone-10,11-dione) (II) was prepared according to a literature method (20). The methanol and acetonitrile used in the HPLC studies were distilled in glass[3]. All other solvents and reagents were analytical reagent grade. Water was double distilled in glass.

HPLC Analyses—The apomorphine content of solutions was analyzed using a previously described HPLC method (30). For this application, a UV detector[4] was used at 273 nm with a setting of 1.28 aufs. Under the analytical conditions, authentic II, ascorbic acid, and sodium bisulfite showed no interference in the region of the developed apomorphine peak.

Stability Studies—Samples of I·HCl were prepared at a concentration of 0.2 mg/ml in water, in a 1-mg/ml aqueous ascorbic acid solution, in a 100-mg/ml aqueous ascorbic acid solution, in a 0.52-mg/ml aqueous sodium bisulfite solution, and in a 20-mg/ml aqueous sodium bisulfite solution. Blank and sample solutions were prepared in clear 10-ml glass-stoppered containers and maintained at room temperature (22–25°) under typical laboratory conditions of light exposure. Samples were analyzed in triplicate at time zero and 1, 3, 7, and 8 days following preparation by direct injection of 100-μl portions into the HPLC column. Quantitation was performed by comparison of peak heights to a calibration curve obtained (r = 0.999) from chromatographic development of five freshly prepared solutions of apomorphine (in 1-mg/ml ascorbic acid solution) containing 0.02–0.2 mg of I·HCl/ml.

Refrigerator Stability—This experiment was performed as was the previous study, except that three apomorphine solutions (in water alone, in a 100-mg/ml ascorbic acid solution, and in a 20-mg/ml sodium bisulfite solution) were kept in a laboratory refrigerator (5°) until sampling.

Pharmacological Studies—Experimentally naive CD-1 male mice[5] weighed 20–36 g at the time of testing. Access to food and water was provided *ad libitum*, and the animals were maintained in a 12-hr light–dark cycle (lights on from 6 am to 6 pm); all testing was done between 8 am and 5 pm.

The cage climbing and hypothermia experiments were designed similarly. Each experiment consisted of one between-subject factor, the solution (4.7 mg of I·HCl·1/2H_2O/kg in water, in 100-mg/ml ascorbate, or in 0.52-mg/ml sodium bisulfite), and one within-subject factor, the response (cage climb scores or body temperature changes after one of the three solutions of I).

Cage Climbing Behavior—A modification of the procedure of Protais *et al.* (32) was used. Animals were placed individually into cylindrical cages (12 cm diameter × 14 cm high with walls of vertical bars 2 mm in

Table I—Effects of Antioxidants on the Stability of Apomorphine Hydrochloride Solutions [a]

	Percent I Remaining[b]				
		Ascorbic Acid[d], mg/ml		Sodium Bisulfite[e], mg/ml	
Day	Water[c]	1	100	0.52	20
0	100 (3.3)	100 (0.6)	100 (0.3)	100.2(2.0)	100 (0.7)
1	86.4(3.4)	93.3(3.1)[f]	90.9(2.2)[f]	98.4(0.0)[f]	97.4(0.7)[f]
3	82.3(0.8)	87.3(0.9)[f]	93.6(1.7)[f]	94.3(2.2)[f]	93.0(0.8)[f]
7	76.9(0.5)	71.3(0.6)	—	87.0(1.0)[f]	85.2(0.3)[f]
8	63.6(0.9)	59.1(2.7)	92.0(1.4)[f]	81.5(1.0)[f]	80.3(0.8)[f]

[a] Results are expressed as the percent of drug on Day 0 (for 0.2-mg/ml solutions; see *Experimental*). [b] Mean ± *SD*, n = 3. [c] The initial pH was 5.43. [d] The initial solution pH values were 3.42 (1 mg/ml) and 2.34 (100 mg/ml). [e] The initial solution pH values were 5.61 (0.52 mg/ml) and 4.53 (20 mg/ml). [f] Significantly different than the water sample of that day (Neuman–Keuls tests, p = 0.05); samples were maintained at room temperature (22–25°).

Table II—Stability of Apomorphine Solutions Maintained at 5°

	Percent of I Remaining[a]		
Day	Water[b,c]	Ascorbic Acid[c]	Sodium Bisulfite[c]
0	100 ± 0.5	100 ± 1.3	100 ± 0.5
1	98.4 ± 0.5	99.5 ± 0.0	100.3 ± 0.3
3	97.6 ± 1.7	98.9 ± 0.0	97.6 ± 1.0
7	98.3 ± 1.7	97.0 ± 1.7	94.2 ± 0.8

[a] Results are expressed as the percent of drug on Day 0 (0.2 mg/ml; see *Experimental*). [b] Mean ± *SD*, n = 3. [c] No significant decomposition (analysis of variance, p = 0.05).

Table III—Effects of Antioxidants on Two *In Vivo* Responses to Apomorphine Hydrochloride

Treatment	Hypothermia[b]	Cage Climb Score[c]
I–water[a]	3.7 ± 0.5°	12.7 ± 1.4
I–ascorbic acid	4.0 ± 0.4°	11.8 ± 1.8
I–sodium bisulfite	3.2 ± 0.4°	13.8 ± 1.4

[a] A solution of 4.7 mg of apomorphine hydrochloride hemihydrate was prepared in distilled water or in aqueous solutions of ascorbate (100 mg/ml) or sodium bisulfite (20 mg/ml). [b] Body temperature changes were recorded 60 min after drug administration; analysis of variance showed no significant effects (p = 0.05). [c] Cumulative stereotypic activity for 12 consecutive 5-min periods after drug administration (maximum = 24); analysis of variance showed no significant effects (p = 0.05).

[1] McFarland Smith Ltd., Edinburgh, Scotland.
[2] Sigma Chemical Co., St. Louis, Mo.
[3] Burdick & Jackson Laboratories, Muskegon, Mich.
[4] Model 995, Tracor Instruments, Austin, Tex.
[5] Charles River Laboratories, Wilmington, Mass.

diameter and 1 cm apart) surmounted by fine wire mesh for a 20-min habituation period. Animals then received a pretreatment consisting of isotonic saline (0.1 ml/10 g of body weight ip). One hour later, the behavior of the animals was recorded on videotape as described previously (33) to establish a baseline of activity for each subject. The mice then were injected immediately with I·HCl hemihydrate (4.7 mg/kg) in water, ascorbate, or bisulfite. The behavior of each animal was recorded on videotape for 30 sec every 5 min for 1 hr and later rated "blind" using a rating scale with 0 = four paws on cage floor, 1 = two paws holding the vertical bars of the cage, and 2 = four paws holding the vertical bars of the cage.

Hypothermia—Rectal temperatures were taken immediately prior to administration of I·HCl by insertion of a rectal probe (1.5 cm) connected to a telethermometer[6]. The mice were injected with one of the three I·HCl solutions, and temperatures were taken 60 min later.

RESULTS AND DISCUSSION

As shown in Table I, both antioxidants tested were effective in delaying apomorphine decomposition. The higher levels of each antioxidant were most effective, although neither antioxidant could delay significant degradation for more than 1–3 days when solutions were stored at room temperature. Refrigeration of apomorphine samples at 5° was effective in preventing decomposition for 0–7 days, and the addition of antioxidants was unnecessary under these conditions (Table II).

Table III shows the lack of influence of the antioxidants, ascorbic acid and sodium bisulfite, on apomorphine-induced hypothermia and stereotyping of cage climbing. Neither ascorbate nor sodium bisulfite displayed any significant effects on these *in vivo* responses to I.

In summary, ascorbic acid (100 mg/ml) and sodium bisulfite (0.52 and 20 mg/ml) prevented more than 10% oxidation of apomorphine hydrochloride in water maintained at room temperature for 1–3 days. Refrigeration at 5° prevented oxidation of I·HCl in aqueous solutions for over 1 week. Neither ascorbic acid nor sodium bisulfite affected murine stereotyped cage climbing or hypothermia induced by apomorphine.

REFERENCES

(1) G. C. Cotzias, P. S. Papavasiliou, C. Fehling, B. Kaufman, and I. Mena, *N. Engl. J. Med.*, **282,** 31 (1970).

(2) G. C. Cotzias, P. S. Papavasiliou, E. S. Tolosa, J. S. Mendez, and M. Bell-Midura, *ibid.*, **294,** 567 (1976).

(3) F. Stian, E. Micheler, and O. Benkert, *Pharmacopsychiatry*, **5,** 198 (1972).

(4) G. C. Cotzias, I. Mena, P. S. Papavasiliou, and J. Mendez, in "Advances in Neurology," vol. 5, F. McDowell and A. Barbeau, Eds., Raven, New York, N.Y., 1973, pp. 11–22.

(5) I. Shoulson and T. N. Chase, *Ann. Rev. Med.*, **26,** 419 (1975).

(6) C. D. Marsden, D. Tarsy, and R. J. Baldessarini, in "Psychiatric Aspects of Neurologic Disease," D. F. Benson and D. Blumir, Eds., Grune & Stratton, New York, N.Y., 1975, pp. 219–265.

[6] Model 43, Yellow Springs Instrument Co., Yellow Springs, Ohio.

(7) E. S. Tolosa, *Arch. Neurol.*, **35,** 459 (1978).

(8) R. J. Baldessarini, K. G. Walton, and R. J. Borgman, *Neuropharmacology*, **15,** 471 (1976).

(9) C. A. Tamminga, M. H. Schaffer, R. C. Smith, and J. M. Davis, *Science*, **200,** 567 (1978).

(10) R. C. Smith, C. A. Tamminga, and J. M. Davis, *J. Neurol. Trans.*, **40,** 171 (1977).

(11) P. N. Kaul, E. Brockmann-Hanssen, and E. L. Way, *J. Pharm. Sci.*, **50,** 244 (1961).

(12) *Ibid.*, **50,** 248 (1961).

(13) *Ibid.*, **50,** 840 (1961).

(14) A. M. Burkman, R. E. Notari, and W. K. Van Tyle, *J. Pharm. Pharmacol.*, **26,** 493 (1974).

(15) R. V. Smith, R. E. Wilcox, W. H. Soine, W. H. Riffee, R. J. Baldessarini, and N. S. Kula, *Res. Commun. Chem. Pathol. Pharmacol.*, **24,** 483 (1979).

(16) W. H. Riffee, R. E. Wilcox, and R. V. Smith, *Eur. J. Pharmacol.*, **54,** 273 (1979).

(17) R. J. Borgman, R. J. Baldessarini, and K. G. Walton, *J. Med. Chem.*, **19,** 717 (1976).

(18) R. J. Baldessarini, K. G. Walton, and R. J. Borgman, *Neuropharmacology*, **15,** 471 (1976).

(19) G. Pellagri, *Chem. Ber.*, **10,** 1384 (1877).

(20) H. H. A. Linde and M. S. Ragab, *Helv. Chim. Acta*, **51,** 683 (1968).

(21) K. Rehse, *Arch. Pharm.*, **302,** 487 (1969).

(22) E. R. Atkinson, S. P. Battista, I. E. Ary, D. G. Richardson, L. S. Harris, and W. L. Dewey, *J. Pharm. Sci.*, **65,** 1682 (1976).

(23) P. W. Erhardt, R. V. Smith, T. T. Sayther, and J. E. Keiser, *J. Chromatogr.*, **116,** 218 (1976).

(24) A. M. Burkman, *J. Pharm. Pharmacol.*, **15,** 461 (1963).

(25) A. M. Burkman, *J. Pharm. Sci.*, **54,** 325 (1965).

(26) R. J. Engelhardt, F. M. Schell, and J. L. Lichtin, *J. Am. Pharm. Assoc.*, **NS8,** 198 (1968).

(27) P. Lundgren and L. Landersjo, *Acta Pharm. Suec.*, **7,** 133 (1970).

(28) K. Steiger and M. Bergmann, *Schweiz. Apoth. Z.*, **84,** 812 (1946).

(29) M. Strahar and M. Heliova, *Pharmazie*, **22,** 38 (1967).

(30) D. W. Humphrey, M. E. Goldman, R. E. Wilcox, C. K. Erickson, and R. V. Smith, *Microchem. J.*, in press.

(31) W. H. Soine, P. Salgo, and R. V. Smith, *J. Label Compounds Radiopharm.*, **16,** 597 (1979).

(32) P. Protais, J. Contentin, and J. C. Schwartz, *Psychopharmacology*, **50,** 1 (1976).

(33) R. E. Wilcox, W. H. Riffee, and R. V. Smith, *Pharmacol. Biochem. Behav.*, **10,** 161 (1979).

ACKNOWLEDGMENTS

Supported by Grant NS-12259 from the National Institute of Neurological and Communicative Disorders and Stroke. D. W. Humphrey is grateful for fellowship support from Hoffmann-La Roche Inc.

Serum Protein Binding of Prednisolone in Four Species

MARIO L. ROCCI, Jr., NOREEN F. JOHNSON, and WILLIAM J. JUSKO ˣ

Received August 10, 1979, from the *Clinical Pharmacokinetics Laboratory, Department of Pharmaceutics, School of Pharmacy, State University of New York at Buffalo and the Millard Fillmore Hospital, Buffalo, NY 14209.* Accepted for publication March 6, 1980.

Abstract □ The protein binding of prednisolone in serum from humans, rabbits, dogs, and rats was determined by equilibrium dialysis. Two nonlinear least-squares regression programs were used to characterize transcortin and albumin binding of the steroid. The animal species differed markedly in their ability to bind prednisolone, but the rabbit was most similar to humans in transcortin concentration and affinity constant.

Keyphrases □ Prednisolone—serum protein binding in humans, rabbits, dogs, and rats □ Serum protein binding—prednisolone in humans, rabbits, dogs, and rats □ Binding, serum protein—prednisolone in humans, rabbits, dogs, and rats

The serum protein binding of prednisolone is nonlinear in humans due to saturation of the high affinity binding sites on the α_1-glycoprotein, transcortin (1). As serum concentrations of the steroid increase, the limited capacity of transcortin for binding is exceeded and the fraction of free drug in serum increases. This nonlinear serum protein binding is partially responsible for the dose-dependent disposition of prednisolone observed in humans (2). To examine its pharmacokinetics further, an animal model was sought that would exhibit protein binding characteristics for prednisolone similar to those observed in humans.

EXPERIMENTAL

The serum protein binding of prednisolone was examined in Sprague–Dawley rats, New Zealand White rabbits, a mongrel dog, and a normal man. Serum was spiked with prednisolone in concentrations ranging from 0.024 to 25 μM. The tritiated prednisolone was purified by high-pressure liquid chromatography (HPLC). A 10-μl aliquot (10,000 dpm) of [^{3}H]prednisolone (specific activity of 53 Ci/mmole) was added to 0.8 ml of the serum samples. The samples then were dialyzed against an equal volume of isotonic phosphate buffer (pH 7.4) using plexiglass cells maintained in a water bath at 37°. After dialysis, the counts per minute of the buffer and serum samples were converted to disintegrations per minute using the sample channel ratio technique. The percent of prednisolone bound and the molar concentrations of free (D_F) and bound (D_b) drug then were calculated for each serum sample.

The relationship that governs the protein binding of prednisolone is:

$$D_b = \frac{N_T K_T P_T D_F}{1 + K_T D_F} + \frac{N_A K_A P_A D_F}{1 + K_A D_F} \qquad \text{(Eq. 1)}$$

where N_T and N_A are the number of binding sites on the transcortin and albumin molecules, K_T and K_A are the affinity constants for transcortin and albumin, and P_T and P_A are the molar serum concentrations of transcortin and albumin (3). Albumin binding apparently was nonspecific; *i.e.*, the product of K_A and D_F for the albumin–prednisolone interaction was negligible when compared to unity, permitting simplification of Eq. 1 to yield:

$$D_b = \frac{N_T K_T P_T D_F}{1 + K_T D_F} + N_A K_A P_A D_F \qquad \text{(Eq. 2)}$$

The nonlinear least-squares regression computer program, NONLIN (4), was employed to fit the binding data to Eq. 2. The D_b and D_F variables for each serum sample served as the dependent and independent variables. Least-squares estimates of K_T, $N_T K_T P_T$, and $N_A K_A P_A$ then were computed. The N_T and N_A values were assumed to be equal to one. Albumin concentration (P_A) was measured chemically[1] in all serum samples, making solution of Eq. 2 for all binding parameters possible. The three computer-generated binding parameters (P_T, K_T, and K_A) are apparent values since endogenous corticosteroids present in the serum are likely to compete with prednisolone for protein binding sites.

Least-squares estimates of K_T, $N_T K_T P_T$, and $N_A K_A P_A$ also were obtained by the statistical method of Priore and Rosenthal (5). This method employs the total drug concentration and the fraction bound as the independent and dependent variables. The use of these variables minimizes the effects of experimental error on the magnitude of the generated binding parameters through the use of the most error-free independent variable (total drug concentration). An even distribution of the experimentally determined values around the fitted fraction bound *versus* the total drug concentration binding curve is produced.

[1] Technicon autoanalyzer.

RESULTS AND DISCUSSION

Figure 1 illustrates the protein binding profile for each species as a function of the postdialysis serum prednisolone concentration. All profiles exhibited nonlinearity consistent with saturation in transcortin binding and linear binding to albumin. Dog and rat serum demonstrated the least concentration dependence in the protein binding of prednisolone. The therapeutic range of the serum prednisolone concentration extended up to ~7 μM.

The binding parameters obtained using the modified NONLIN computer program (Method I) and using the MACMOL program of Priore and Rosenthal (Method II) are presented in Table I. The two methods yielded binding parameters in the same general range. There was excellent agreement for all binding parameters in the rabbit and in the K_A values obtained for each species. Differences between the methods existed in the P_T and K_T values obtained in the dog, rats, and human. At low serum prednisolone concentrations, where the protein binding of the steroid exhibits concentration dependence, small errors in the determination of either the fraction bound or the total drug concentration can introduce rather large errors in the calculated values of D_f (total drug concentration × free fraction). Such errors will affect most profoundly the binding parameters obtained using Method I, where D_f is the independent variable. Since this problem is avoided using Method II, it probably generates the closer estimates of the true binding parameters for transcortin.

At high prednisolone concentrations, where albumin is the major binding protein, the values of the prednisolone free fraction are larger and do not vary appreciably in any one species. As a result, the errors incurred in quantitation of the binding systems at high serum concen-

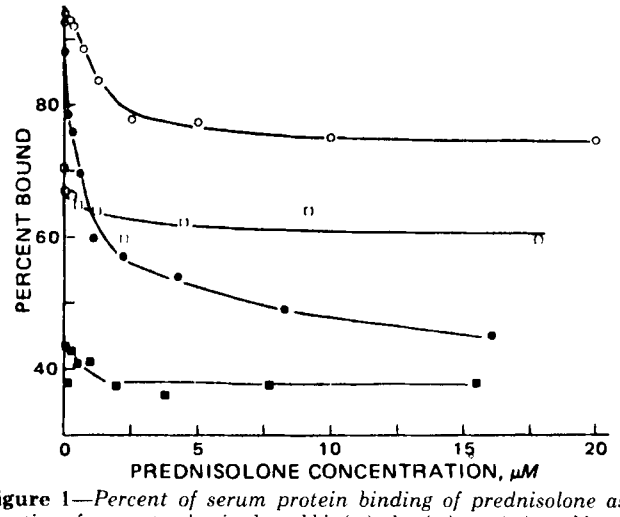

Figure 1—*Percent of serum protein binding of prednisolone as a function of concentration in the rabbit* (○), *dog* (□), *rat* (■), *and human* (●).

0022-3549/80/0800-0977$01.00/0
© 1980, American Pharmaceutical Association

Table I—Serum Protein Binding Parameters for Prednisolone in Four Species Obtained by Methods I and II [a]

Species	Transcortin				Albumin		
	$P_T, M \times 10^7$		$K_T, M^{-1} \times 10^{-7}$		P_A [b], $M \times 10^4$	$K_A, M^{-1} \times 10^{-3}$	
	I	II	I	II		I	II
Rabbit	5.74	6.13	2.33	2.09	4.49	6.22	6.15
Dog	2.21	1.19	0.284	0.569	5.73	2.62	2.69
Rat	0.259	1.01	0.653	0.152	3.96	1.51	1.45
Human	6.19	3.26	0.499	1.63	6.43	1.21	1.400

[a] Method I is from Ref. 4, and Method II is from Ref. 5. [b] Determined by an automatic analyzer.

trations are of less significance, accounting for the good agreement in the K_A values between the two methods.

The binding profile of the rabbit appears most like humans in the degree of nonlinearity in prednisolone binding (Fig. 1). The binding constants in Table I (Method II) confirm this observation. The P_T and K_T values in the rabbit are closest to those values determined in humans, producing similar decreases in binding as the serum prednisolone concentration increases. The binding parameters confirm the presence of high affinity, low capacity transcortin binding and low affinity, high capacity albumin binding in each species.

The transcortin concentrations and affinity constants for all of the species examined are in the general range of values reported by other investigators for cortisol. Westphal (6) obtained P_T and K_T values in the rabbit of 3.6×10^{-7} M and 4×10^7 M^{-1}, which agree well with the present estimates. In contrast, the P_T and K_T values determined by Westphal in the rat were 6.9×10^{-7} M and 1×10^7 M^{-1}. These discrepancies may reflect inherent differences in the interactions of prednisolone and hydrocortisone with transcortin. The use of different strains of the same animal species and physiological factors such as age, sex, and endogenous corticosteroid level might affect the transcortin–steroid interaction and contribute to variability in the binding parameters (7).

In summary, the animal species studied differed markedly in their ability to bind prednisolone. The rabbit was the most similar to humans in transcortin concentration and affinity constant for prednisolone and in the range of free drug fractions at increasing steroid concentrations.

REFERENCES

(1) A. A. Sandberg, W. R. Slaunwhite, Jr., and H. N. Antoniades, *Rec. Progr. Hormone Res.*, **13**, 209 (1957).

(2) J. Q. Rose, A. M. Yurchak, and W. J. Jusko, "Abstracts of the 7th International Congress of Pharmacology, Paris," 1978, p. 400.

(3) H. E. Rosenthal, *Anal. Biochem.*, **20**, 525 (1967).

(4) C. M. Metzler, Technical Report 7292/69/7292/005, The Upjohn Co., Kalamazoo, Mich., Nov. 25, 1969.

(5) R. L. Priore and H. E. Rosenthal, *Anal. Biochem.*, **70**, 231 (1976).

(6) U. Westphal, *Arch. Biochem. Biophys.*, **118**, 556 (1967).

(7) U. Westphal, "Steroid–Protein Interactions," Springer-Verlag, Berlin, Germany, 1971, pp. 225–247.

ACKNOWLEDGMENTS

Supported in part by Grant 24211 from the National Institutes of General Medical Sciences.

The MACMOL computer program (5) was kindly provided by Dr. Roger L. Priore.

Effect of Sodium Bicarbonate on *In Vitro* Conversion of Fibrinogen to Fibrin

DENNIS W. WONG

Received November 8, 1979, from the *Division of Nuclear Medicine, Department of Radiology, Martin Luther King Jr. General Hospital and Charles R. Drew Postgraduate Medical School, Los Angeles, CA 90059.* Accepted for publication March 12, 1980.

Abstract □ The effect of sodium bicarbonate on the conversion of fibrinogen to fibrin clot was investigated using fresh human whole blood and pure human fibrinogen. *In vitro* experimental data demonstrated that sodium bicarbonate interfered with fibrin clot formation during clotting. This study assessed the possibility of synergistic action of sodium bicarbonate with sodium citrate. As expected, sodium citrate potentiated the anticoagulant action of sodium bicarbonate.

Keyphrases □ Sodium bicarbonate—effect on conversion of fibrinogen to fibrin, synergistic action with sodium citrate □ Sodium citrate—effect on fibrin clot formation, synergistic action with sodium bicarbonate □ Fibrin—effect of sodium bicarbonate and sodium citrate on *in vitro* conversion of fibrinogen

In vitro experimental results and clinical patient data demonstrate that sodium and potassium bicarbonate can interfere with the clotting process, as evidenced by prolongation in prothrombin time and thrombin clotting time (1). The anticoagulant effect appears to be caused primarily by the specific anion species and an increase in ionic strength and to a lesser extent by the effect of pH. Thrombin clotting time analyses on citrated whole blood samples containing sodium bicarbonate indicate that the unavailability of calcium ions is not the direct cause of clot inhibition.

Since previous work contained no information dealing directly with the effect of bicarbonate on clotting (2–9), the present study was undertaken to determine the effect of sodium bicarbonate on the conversion of pure human fibrinogen to fibrin clot. The possibility of synergistic action of sodium bicarbonate with sodium citrate on clot inhibition also was investigated.

EXPERIMENTAL

Lyophilized human fibrinogen[1] was reconstituted with water for injection USP to a concentration of 20 mg/ml at pH 6. Prior to the addition of fibrinogen, a predetermined amount of sodium bicarbonate solution[2] (pH 7.8, 7.5%), ranging from 1 to 25 mg in a volume of <0.1 ml, was added to each test tube containing 3.0 ml of 7 mM pH 7.4 Sorensen's phosphate buffer (ionic strength 0.017) and 0.4 ml of a 3.8% sodium citrate solution (pH 9.85, 0.13 M, ionic strength 0.078). The resulting mixture contained one part of citrate solution to nine parts of test sample. The amount of citrate solution used was equivalent to the quantity of anticoagulant present in the blood-collecting test tube. When the required amount of sodium bicarbonate solution to be added to the test samples exceeded 0.1 ml, a weighed amount of reagent grade powder[3] was dissolved in the

[1] Parenogen, Cutter Laboratories, Berkeley, Calif.
[2] Abbott Laboratories, North Chicago, Ill.
[3] American Drug and Chemical Corp., Los Angeles, Calif.

0022-3549/80/0800-0978$01.00/0

© 1980, American Pharmaceutical Association

Table I—Serum Protein Binding Parameters for Prednisolone in Four Species Obtained by Methods I and II [a]

Species	Transcortin				Albumin		
	$P_T, M \times 10^7$		$K_T, M^{-1} \times 10^{-7}$		P_A [b], $M \times 10^4$	$K_A, M^{-1} \times 10^{-3}$	
	I	II	I	II		I	II
Rabbit	5.74	6.13	2.33	2.09	4.49	6.22	6.15
Dog	2.21	1.19	0.284	0.569	5.73	2.62	2.69
Rat	0.259	1.01	0.653	0.152	3.96	1.51	1.45
Human	6.19	3.26	0.499	1.63	6.43	1.21	1.400

[a] Method I is from Ref. 4, and Method II is from Ref. 5. [b] Determined by an automatic analyzer.

trations are of less significance, accounting for the good agreement in the K_A values between the two methods.

The binding profile of the rabbit appears most like humans in the degree of nonlinearity in prednisolone binding (Fig. 1). The binding constants in Table I (Method II) confirm this observation. The P_T and K_T values in the rabbit are closest to those values determined in humans, producing similar decreases in binding as the serum prednisolone concentration increases. The binding parameters confirm the presence of high affinity, low capacity transcortin binding and low affinity, high capacity albumin binding in each species.

The transcortin concentrations and affinity constants for all of the species examined are in the general range of values reported by other investigators for cortisol. Westphal (6) obtained P_T and K_T values in the rabbit of 3.6×10^{-7} M and 4×10^7 M^{-1}, which agree well with the present estimates. In contrast, the P_T and K_T values determined by Westphal in the rat were 6.9×10^{-7} M and 1×10^7 M^{-1}. These discrepancies may reflect inherent differences in the interactions of prednisolone and hydrocortisone with transcortin. The use of different strains of the same animal species and physiological factors such as age, sex, and endogenous corticosteroid level might affect the transcortin–steroid interaction and contribute to variability in the binding parameters (7).

In summary, the animal species studied differed markedly in their ability to bind prednisolone. The rabbit was the most similar to humans in transcortin concentration and affinity constant for prednisolone and in the range of free drug fractions at increasing steroid concentrations.

REFERENCES

(1) A. A. Sandberg, W. R. Slaunwhite, Jr., and H. N. Antoniades, *Rec. Progr. Hormone Res.*, **13**, 209 (1957).

(2) J. Q. Rose, A. M. Yurchak, and W. J. Jusko, "Abstracts of the 7th International Congress of Pharmacology, Paris," 1978, p. 400.

(3) H. E. Rosenthal, *Anal. Biochem.*, **20**, 525 (1967).

(4) C. M. Metzler, Technical Report 7292/69/7292/005, The Upjohn Co., Kalamazoo, Mich., Nov. 25, 1969.

(5) R. L. Priore and H. E. Rosenthal, *Anal. Biochem.*, **70**, 231 (1976).

(6) U. Westphal, *Arch. Biochem. Biophys.*, **118**, 556 (1967).

(7) U. Westphal, "Steroid–Protein Interactions," Springer-Verlag, Berlin, Germany, 1971, pp. 225–247.

ACKNOWLEDGMENTS

Supported in part by Grant 24211 from the National Institutes of General Medical Sciences.

The MACMOL computer program (5) was kindly provided by Dr. Roger L. Priore.

Effect of Sodium Bicarbonate on *In Vitro* Conversion of Fibrinogen to Fibrin

DENNIS W. WONG

Received November 8, 1979, from the *Division of Nuclear Medicine, Department of Radiology, Martin Luther King Jr. General Hospital and Charles R. Drew Postgraduate Medical School, Los Angeles, CA 90059.* Accepted for publication March 12, 1980.

Abstract □ The effect of sodium bicarbonate on the conversion of fibrinogen to fibrin clot was investigated using fresh human whole blood and pure human fibrinogen. *In vitro* experimental data demonstrated that sodium bicarbonate interfered with fibrin clot formation during clotting. This study assessed the possibility of synergistic action of sodium bicarbonate with sodium citrate. As expected, sodium citrate potentiated the anticoagulant action of sodium bicarbonate.

Keyphrases □ Sodium bicarbonate—effect on conversion of fibrinogen to fibrin, synergistic action with sodium citrate □ Sodium citrate—effect on fibrin clot formation, synergistic action with sodium bicarbonate □ Fibrin—effect of sodium bicarbonate and sodium citrate on *in vitro* conversion of fibrinogen

In vitro experimental results and clinical patient data demonstrate that sodium and potassium bicarbonate can interfere with the clotting process, as evidenced by prolongation in prothrombin time and thrombin clotting time (1). The anticoagulant effect appears to be caused primarily by the specific anion species and an increase in ionic strength and to a lesser extent by the effect of pH. Thrombin clotting time analyses on citrated whole blood samples containing sodium bicarbonate indicate that the unavailability of calcium ions is not the direct cause of clot inhibition.

Since previous work contained no information dealing directly with the effect of bicarbonate on clotting (2–9), the present study was undertaken to determine the effect of sodium bicarbonate on the conversion of pure human fibrinogen to fibrin clot. The possibility of synergistic action of sodium bicarbonate with sodium citrate on clot inhibition also was investigated.

EXPERIMENTAL

Lyophilized human fibrinogen[1] was reconstituted with water for injection USP to a concentration of 20 mg/ml at pH 6. Prior to the addition of fibrinogen, a predetermined amount of sodium bicarbonate solution[2] (pH 7.8, 7.5%), ranging from 1 to 25 mg in a volume of <0.1 ml, was added to each test tube containing 3.0 ml of 7 mM pH 7.4 Sorensen's phosphate buffer (ionic strength 0.017) and 0.4 ml of a 3.8% sodium citrate solution (pH 9.85, 0.13 M, ionic strength 0.078). The resulting mixture contained one part of citrate solution to nine parts of test sample. The amount of citrate solution used was equivalent to the quantity of anticoagulant present in the blood-collecting test tube. When the required amount of sodium bicarbonate solution to be added to the test samples exceeded 0.1 ml, a weighed amount of reagent grade powder[3] was dissolved in the

[1] Parenogen, Cutter Laboratories, Berkeley, Calif.
[2] Abbott Laboratories, North Chicago, Ill.
[3] American Drug and Chemical Corp., Los Angeles, Calif.

0022-3549/80/0800-0978$01.00/0

© 1980, American Pharmaceutical Association

Table I—*In Vitro* Anticoagulant Action of Sodium Bicarbonate on Fresh Human Blood Samples

Sample	Sodium Bicarbonate Concentration[a] mEq/kg of Body Weight	mEq/ml of Blood	Total μ	pH	Prothrombin Time, sec	Thrombin Clotting Time, sec
Control	0.00	0.0000	0.154	7.40	11.1	7.5
1	0.81	0.0125	0.167	7.40	11.3	8.1
2	1.62	0.0250	0.179	7.40	11.8	9.0
3	2.43	0.0375	0.192	7.50	12.3	9.5
4	3.24	0.0500	0.204	7.65	13.3	10.5
5	4.05	0.0625	0.217	7.65	14.1	12.1
6	4.86	0.0750	0.229	7.65	15.3	14.0
7	5.67	0.0875	0.242	7.65	17.0	16.5
8	6.48	0.1000	0.254	7.65	19.8	18.0
9	7.29	0.1125	0.267	7.70	22.5	21.0
10	8.10	0.1250	0.279	7.74	26.0	32.0

[a] The amount of sodium bicarbonate added to the samples ranged from 12.5 to 125 mEq/liter of blood, assuming an average adult blood volume of 65 ml/kg of body weight. The plasma ionic strength, μ, was 0.154. All values represent the average of three determinations from three normal healthy volunteers.

sodium citrate–phosphate buffer mixture. Exactly 0.6 ml of fibrinogen solution (12 mg of fibrinogen) was added to each test tube, yielding a final concentration of 3 mg of fibrinogen/ml of sample. (Normal blood fibrinogen concentration ranged from 150 to 350 mg %.) Similar samples but without sodium citrate were prepared to eliminate any synergistic effect of sodium citrate with sodium bicarbonate.

After thorough mixing, the pH of each sample was determined at 37° by a pH meter[4] with a combination glass and ceramic electrode. Coagulation was induced by the addition of 0.1 ml (10 units/ml, pH 6) of topical thrombin[5] in normal saline to 0.2 ml of the test sample previously incubated at 37° for 2–5 min. The thrombin clotting time (expressed in seconds) was recorded mechanically with an automatic clot timer[6]. Control samples were assessed without sodium bicarbonate. The ionic strength of the phosphate-buffered fibrinogen solution in the absence of sodium bicarbonate and sodium citrate was 0.017. With the addition of sodium citrate, the total ionic strength was 0.095.

To determine the effect of sodium bicarbonate on clotting, *in vitro* studies were performed using fresh blood samples collected from healthy volunteers by venipuncture. Prior to addition of the whole blood, a predetermined amount of sodium bicarbonate solution or powder was added to specimen test tubes used for blood collection, each containing 0.3 ml of 3.8%, 0.13 *M* sodium citrate. Exactly 2.7 ml of the fresh whole blood was added immediately to the sample test tube and mixed well. The quantity of sodium bicarbonate added to the blood samples was equivalent to administration of 1–10 mEq/kg to a 70-kg adult, assuming uniform distribution only in the blood.

The blood sample pH was determined prior to plasma separation. Plasma was separated from the whole elements by centrifugation at 2000 rpm (540×*g*) for 30 min. One-stage prothrombin time, by the addition of thromboplastin and calcium ions to 0.2 ml of plasma, was determined according to standard laboratory methods. The same plasma sample was diluted to 1:10 with Owren's pH 7.4 barbital[7] (barbital sodium–sodium chloride) buffer. Thrombin clotting time was determined by adding 0.1 ml (1 unit) of topical thrombin to 0.1 ml of a plasma sample previously incubated at 37°. Both the prothrombin time and the thrombin clotting time were recorded with an automatic clot timer. The plasma ionic strength was assumed to equal that of normal saline (0.9% NaCl), which is 0.154. Control samples were tested without the addition of sodium bicarbonate.

RESULTS

The inhibitory effect of sodium bicarbonate on the conversion of fibrinogen to fibrin clot is illustrated in Fig. 1. At the salt concentration used, the ionic strength of the bicarbonate samples increased from a control value of 0.017 to 0.317 and that of the sodium citrate–sodium bicarbonate samples rose from a control value of 0.095 to 0.395. Thrombin clotting time increased gradually from 6.9 to 8.6 sec as the bicarbonate concentration increased from 0.012 to 0.12 mEq/ml (1–10 mg/ml). The thrombin clotting time of the control sample was 6.4 sec. Increasing the bicarbonate content beyond 0.12 mEq/ml caused a sharp rise in the thrombin clotting time from 10 to 156 sec.

As seen in Fig. 1, sodium citrate potentiated the anticoagulant effect of sodium bicarbonate. While the sodium citrate concentration remained constant at 3.8 mg/ml, the addition of sodium bicarbonate to these samples markedly prolonged the thrombin clotting time.

The pH of the bicarbonate samples gradually rose from 7.2 to 7.8 with the increasing amount of salt added. A similar increase in pH, from 7.2 to 7.7, was observed with sodium citrate–sodium bicarbonate samples. However, results from the pH determination did not demonstrate a linear relationship between the rise in pH and the sharp increase in the thrombin clotting time.

Table I summarizes the *in vitro* prothrombin time and thrombin

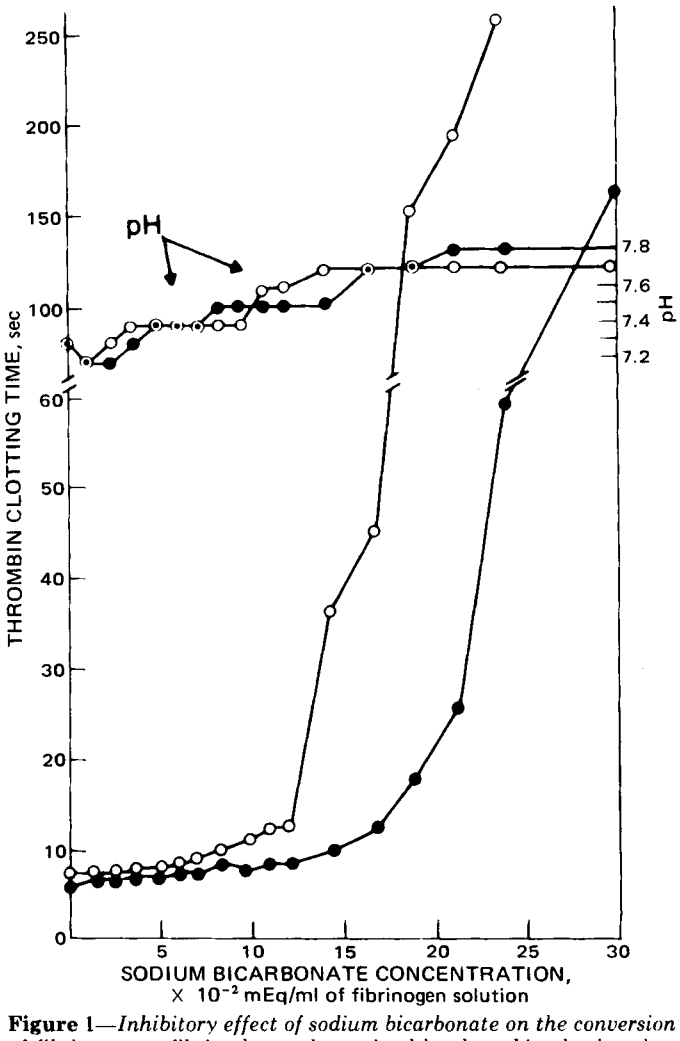

Figure 1—*Inhibitory effect of sodium bicarbonate on the conversion of fibrinogen to fibrin clot as determined by thrombin clotting time assay. Sodium citrate potentiated the anticoagulant action of sodium bicarbonate. Key:* O, *sodium bicarbonate and sodium citrate; and* ●, *sodium bicarbonate alone.*

[4] Instrumentation Laboratory, Lexington, Mass.
[5] Parke-Davis, Detroit, Mich.
[6] Fibrometer, Becton-Dickinson, Rutherford, N.J.
[7] Veronal, Dade Division, American Hospital Supply Corp., Miami, Fla.

clotting time data on fresh blood samples containing various amounts of sodium bicarbonate. The amount of sodium bicarbonate added to the samples ranged from 12.5 to 125 mEq/liter of blood, assuming an average adult blood volume of 65 ml/kg. At added bicarbonate concentrations of 1–2 mEq/kg, significant changes in clotting were observed. Both the prothrombin time and the thrombin clotting time were elevated (Samples 1 and 2, Table I). Increasing the bicarbonate concentration beyond 2 mEq/kg inhibited clotting markedly.

DISCUSSION

Sodium bicarbonate is used widely as a therapeutic agent for acid–base imbalance (10–12). The usual dose of sodium bicarbonate ranges from 1 to 2 mEq/kg and normally is administered intravenously as a 7.5% hypertonic solution or as a 1.5% isotonic solution. Sodium bicarbonate has been regarded as a safe and effective therapeutic agent and is relatively free of serious side effects. With the exception of overdose-induced seizures or tetany secondary to hypocalcemia and hyperalkalosis, no known adverse reactions have been reported (13, 14).

Results from the present investigation demonstrate that sodium bicarbonate inhibits the conversion of fibrinogen to fibrin. Although the mechanism of clot inhibition is unclear, it is well known that some neutral salts retard coagulation and that others accelerate the conversion of fibrinogen to fibrin (2–9). Both cations and anions may bind to the fibrinogen or fibrin molecules during clot formation, and, depending on the individual chemical species, they can either accelerate or inhibit coagulation. The degree of clot inhibition also is affected greatly by the concentration and ionic strength of the salt.

Although data from pH determinations do not correlate well with observed changes in the prothrombin time and the thrombin clotting time, the effect of increasing pH on clotting cannot be ignored. Previous studies revealed that the structure and properties of fibrin clots are modified greatly by variations in pH and ionic strength during coagulation. However, even at constant pH and ionic strength, certain ions and neutral molecules at low concentration greatly affect the structure of the fibrin clot and its formation rate.

REFERENCES

(1) D. W. Wong, F. Mishkin, and T. Tanaka, *J. Am. Med. Assoc.*, in press.

(2) U. Abildgaard, *Scand. J. Clin. Lab. Invest.*, **16**, 521 (1964).

(3) R. Briggs and K. E. W. Denson, in "Human Blood Coagulation, Hemastasis and Thrombosis," Blackwell Scientific Publication, Oxford, England, 1972, pp. 133–135.

(4) J. T. Edsall and W. F. Lever, *J. Biol. Chem.*, **191**, 735 (1951).

(5) C. R. Harmison and E. F. Mammen, in "Blood Clotting Enzymology," W. H. Seegers, Ed., Academic, New York, N.Y., 1967, pp. 48–102, 345–373.

(6) J. E. Lovelock and B. M. Porterfield, *Biochem. J.*, **50**, 415 (1952).

(7) O. D. Ratnoff and A. M. Potts, *J. Clin. Invest.*, **33**, 206 (1954).

(8) K. C. Robbins, *Am. J. Physiol.*, **142**, 581 (1944).

(9) S. Shulman, *Arch. Biochem.*, **30**, 353 (1951).

(10) "The Pharmacological Basis of Therapeutics," 3rd ed., L. Goodman and A. Gilman, Eds., Macmillan, New York, N.Y., 1965, pp. 763–794.

(11) B. W. Grunner, *Med. J. Aust.*, **1**, 275 (1967).

(12) "Harrison's Principles of Internal Medicine," 6th ed., M. M. Winthrobe, G. W. Thorn, R. D. Adams, *et al.*, Eds., McGraw-Hill, New York, N.Y., 1970, pp. 1371–1379.

(13) W. Feldman, D. G. H. Stevens, and P. H. Beaudry, *Can. Med. Assoc. J.*, **94**, 328 (1966).

(14) C. R. Palm, S. C. Ushinski, and P. Frieman, *J. Allergy*, **45**, 104 (1970).

Polydimethylsiloxane Pellets for Sustained Delivery of Morphine in Mice

WILLIAM H. RIFFEE ˣ, RICHARD E. WILCOX, JULIE A. ANDERSON, and JAMES W. McGINITY

Received February 11, 1980, from the *Departments of Pharmacology and Pharmaceutics, Drug Dynamics Institute, College of Pharmacy, University of Texas at Austin, Austin, TX 78712.* Accepted for publication March 13, 1980.

Abstract □ A new dosage form was designed whereby a polymeric silicone elastomer pellet provided sustained delivery of morphine to mice over 11 days. These pellets, which can be made easily and inexpensively with a standard tablet mold, gradually released morphine sulfate into the implanted mice. Maximal morphine-induced physical dependence, measured by jumping during naloxone-induced withdrawal, was observed 3–5 days after implantation. At this time, slightly less than 50% of the morphine sulfate had been released. Drug release continued through Day 11 and was accompanied by a physical dependence of decreased magnitude compared to that observed on Day 3 or 5.

Keyphrases □ Morphine—sustained release from polydimethylsiloxane pellets, mice □ Drug delivery systems—sustained release of morphine from polydimethylsiloxane pellets, mice □ Sustained-release systems—delivery of morphine from polydimethylsiloxane pellets, mice

As a representative of the narcotic analgesic drugs, morphine has been used to induce tolerance and physical dependence in experimental animals (1). Its relatively short half-life in small animals requires frequent injections of morphine to sustain drug levels over an extended period.

BACKGROUND

Attempts have been made to deliver morphine to experimental animals without these injection routines but with the production of maximum tolerance and dependence. For example, Collier *et al.* (2) used an oily sustained-release preparation. Hui and Roberts (3) adsorbed morphine sulfate onto molecular sieves. Goode (4) used an implanted silicone rubber tubing reservoir of morphine solution. Teiger (5) used continuous intraperitoneal infusion. The usefulness of several of these methods is marginal as judged by the lack of utilization by fellow researchers. According to this criterion, employment of implanted tableted pellets that slowly release their morphine content appears to be the most accepted method to date.

The most commonly used morphine implant is the microcrystalline cellulose pellet described by Gibson and Tingstad (6). However, this pellet has several disadvantages as a drug delivery system for morphine. One disadvantage is that drug delivery in the animal ceases after 3 days, with only half of the drug being released from the pellet for absorption; the pellet tends to become encapsulated by membranous tissue, thereby diminishing morphine bioavailability (7, 8). Another disadvantage is that the pellet quickly becomes soft and mushy, so complete removal of the implant from the animal is difficult. This result is due to the fact that the pellet contains ~50% microcrystalline cellulose, a tablet disintegrant. Failure to remove all of the implanted pellet gives erroneously high values

0022-3549/80/0800-0980$01.00/0

© 1980, American Pharmaceutical Association

clotting time data on fresh blood samples containing various amounts of sodium bicarbonate. The amount of sodium bicarbonate added to the samples ranged from 12.5 to 125 mEq/liter of blood, assuming an average adult blood volume of 65 ml/kg. At added bicarbonate concentrations of 1–2 mEq/kg, significant changes in clotting were observed. Both the prothrombin time and the thrombin clotting time were elevated (Samples 1 and 2, Table I). Increasing the bicarbonate concentration beyond 2 mEq/kg inhibited clotting markedly.

DISCUSSION

Sodium bicarbonate is used widely as a therapeutic agent for acid–base imbalance (10–12). The usual dose of sodium bicarbonate ranges from 1 to 2 mEq/kg and normally is administered intravenously as a 7.5% hypertonic solution or as a 1.5% isotonic solution. Sodium bicarbonate has been regarded as a safe and effective therapeutic agent and is relatively free of serious side effects. With the exception of overdose-induced seizures or tetany secondary to hypocalcemia and hyperalkalosis, no known adverse reactions have been reported (13, 14).

Results from the present investigation demonstrate that sodium bicarbonate inhibits the conversion of fibrinogen to fibrin. Although the mechanism of clot inhibition is unclear, it is well known that some neutral salts retard coagulation and that others accelerate the conversion of fibrinogen to fibrin (2–9). Both cations and anions may bind to the fibrinogen or fibrin molecules during clot formation, and, depending on the individual chemical species, they can either accelerate or inhibit coagulation. The degree of clot inhibition also is affected greatly by the concentration and ionic strength of the salt.

Although data from pH determinations do not correlate well with observed changes in the prothrombin time and the thrombin clotting time, the effect of increasing pH on clotting cannot be ignored. Previous studies revealed that the structure and properties of fibrin clots are modified greatly by variations in pH and ionic strength during coagulation. However, even at constant pH and ionic strength, certain ions and neutral molecules at low concentration greatly affect the structure of the fibrin clot and its formation rate.

REFERENCES

(1) D. W. Wong, F. Mishkin, and T. Tanaka, *J. Am. Med. Assoc.*, in press.

(2) U. Abildgaard, *Scand. J. Clin. Lab. Invest.*, **16**, 521 (1964).

(3) R. Briggs and K. E. W. Denson, in "Human Blood Coagulation, Hemastasis and Thrombosis," Blackwell Scientific Publication, Oxford, England, 1972, pp. 133–135.

(4) J. T. Edsall and W. F. Lever, *J. Biol. Chem.*, **191**, 735 (1951).

(5) C. R. Harmison and E. F. Mammen, in "Blood Clotting Enzymology," W. H. Seegers, Ed., Academic, New York, N.Y., 1967, pp. 48–102, 345–373.

(6) J. E. Lovelock and B. M. Porterfield, *Biochem. J.*, **50**, 415 (1952).

(7) O. D. Ratnoff and A. M. Potts, *J. Clin. Invest.*, **33**, 206 (1954).

(8) K. C. Robbins, *Am. J. Physiol.*, **142**, 581 (1944).

(9) S. Shulman, *Arch. Biochem.*, **30**, 353 (1951).

(10) "The Pharmacological Basis of Therapeutics," 3rd ed., L. Goodman and A. Gilman, Eds., Macmillan, New York, N.Y., 1965, pp. 763–794.

(11) B. W. Grunner, *Med. J. Aust.*, **1**, 275 (1967).

(12) "Harrison's Principles of Internal Medicine," 6th ed., M. M. Winthrobe, G. W. Thorn, R. D. Adams, *et al.*, Eds., McGraw-Hill, New York, N.Y., 1970, pp. 1371–1379.

(13) W. Feldman, D. G. H. Stevens, and P. H. Beaudry, *Can. Med. Assoc. J.*, **94**, 328 (1966).

(14) C. R. Palm, S. C. Ushinski, and P. Frieman, *J. Allergy*, **45**, 104 (1970).

Polydimethylsiloxane Pellets for Sustained Delivery of Morphine in Mice

WILLIAM H. RIFFEE ˣ, RICHARD E. WILCOX, JULIE A. ANDERSON, and JAMES W. McGINITY

Received February 11, 1980, from the *Departments of Pharmacology and Pharmaceutics, Drug Dynamics Institute, College of Pharmacy, University of Texas at Austin, Austin, TX 78712.* Accepted for publication March 13, 1980.

Abstract □ A new dosage form was designed whereby a polymeric silicone elastomer pellet provided sustained delivery of morphine to mice over 11 days. These pellets, which can be made easily and inexpensively with a standard tablet mold, gradually released morphine sulfate into the implanted mice. Maximal morphine-induced physical dependence, measured by jumping during naloxone-induced withdrawal, was observed 3–5 days after implantation. At this time, slightly less than 50% of the morphine sulfate had been released. Drug release continued through Day 11 and was accompanied by a physical dependence of decreased magnitude compared to that observed on Day 3 or 5.

Keyphrases □ Morphine—sustained release from polydimethylsiloxane pellets, mice □ Drug delivery systems—sustained release of morphine from polydimethylsiloxane pellets, mice □ Sustained-release systems—delivery of morphine from polydimethylsiloxane pellets, mice

As a representative of the narcotic analgesic drugs, morphine has been used to induce tolerance and physical dependence in experimental animals (1). Its relatively short half-life in small animals requires frequent injections of morphine to sustain drug levels over an extended period.

BACKGROUND

Attempts have been made to deliver morphine to experimental animals without these injection routines but with the production of maximum tolerance and dependence. For example, Collier *et al.* (2) used an oily sustained-release preparation. Hui and Roberts (3) adsorbed morphine sulfate onto molecular sieves. Goode (4) used an implanted silicone rubber tubing reservoir of morphine solution. Teiger (5) used continuous intraperitoneal infusion. The usefulness of several of these methods is marginal as judged by the lack of utilization by fellow researchers. According to this criterion, employment of implanted tableted pellets that slowly release their morphine content appears to be the most accepted method to date.

The most commonly used morphine implant is the microcrystalline cellulose pellet described by Gibson and Tingstad (6). However, this pellet has several disadvantages as a drug delivery system for morphine. One disadvantage is that drug delivery in the animal ceases after 3 days, with only half of the drug being released from the pellet for absorption; the pellet tends to become encapsulated by membranous tissue, thereby diminishing morphine bioavailability (7, 8). Another disadvantage is that the pellet quickly becomes soft and mushy, so complete removal of the implant from the animal is difficult. This result is due to the fact that the pellet contains ~50% microcrystalline cellulose, a tablet disintegrant. Failure to remove all of the implanted pellet gives erroneously high values

0022-3549/80/0800-0980$01.00/0

© 1980, American Pharmaceutical Association

for the percent of morphine absorbed. However, the greatest disadvantage is the need for expensive equipment and pharmaceutical expertise to produce these tableted pellets.

McGinity and Mehta (9) recently reported a method for morphine delivery in rats utilizing a silicone rubber matrix formulated with algin, a water-soluble carrier. This method has been modified for use in mice, and the present study evaluates the ability of this pellet system to render mice physically dependent on morphine.

EXPERIMENTAL

Male experimental CD-1 albino mice[1], 20–35 g, were permitted to acclimate to the animal housing and testing facility (adjacent rooms) for at least 3 days prior to experimentation. Food and water were available *ad libitum*. The animal quarters were maintained on a 12-hr light–dark cycle (lights on at 7 am and off at 7 pm). All testing was done between 8 am and 6 pm.

The drugs and chemicals used were morphine sulfate[2], algin[3], polydimethylsiloxane[4], silicone oil[5], and stannous octate[6].

The pellets were prepared by the addition of silicone oil to the polydimethylsiloxane elastomer in a ratio of 1:1, followed by homogeneous mixing with the powders (morphine sulfate and algin). The method of preparation was described previously (10). When the pellets hardened, edges were trimmed carefully and the pellets were removed from the mold. The cylindrical pellets were 6 mm in diameter and 3 mm in height. Ten percent of the pellets were selected at random and tested for batch uniformity and morphine content. The morphine content in each pellet (both for batch uniformity and for each experimental pellet) was determined spectrophotometrically at 286 nm, and the morphine concentration was calculated using a standard curve.

Light ether anesthesia was used to permit the implantation of two morphine pellets in each mouse (pilot studies indicated two pellets would induce a satisfactory level of physical dependence). The pellets were implanted subcutaneously along the midline of the dorsal neck region posterior to the ears. Placebo pellets (pellets with lactose substituted for morphine) were implanted similarly.

Fifty mice were implanted, and groups of eight were challenged with naloxone at 5 mg/kg on Days 1, 3, 5, 7, 9, and 11 following implantation (each group was used for only one challenge). Each animal was placed in a large, clear glass (4-liter capacity) container and observed for spontaneous jumping off the floor. This behavior was videotaped and subsequently quantified by viewing of the videotapes. Counts for the number of spontaneous jumps were recorded for 5-min intervals up to 30 min after the naloxone challenge. Statistical analysis was done using analysis of variance and *post hoc* tests for differences among means.

RESULTS AND DISCUSSION

Figure 1 shows the concentration of morphine remaining in the pellet over time. Twenty-four hours after implantation, 81% of the morphine remained in the pellet, whereas 56% remained 3 and 5 days after surgery. The concentration of morphine then decreased to 35–40% 7–11 days after implantation.

The spontaneous jumping behavior also is shown in Fig. 1. Approximately 25 spontaneous jumps were shown over a 20-min period following naloxone challenge on Day 1. The peak withdrawal jumping behavior was observed at 3 and 5 days after implantation (207 and 206 jumps, respectively). After Day 5, jumping behavior decreased (Days 7 and 9) to approximately 135 jumps, falling to a level not significantly different from that of placebo-implanted mice on Day 11 (90 jumps).

A morphine-containing silicone rubber implant was reported previously for use in rats (9). This pellet was modified and reformulated for use in mice in the present study. The time course of development of physical dependence agrees well with that obtained by Way *et al.* (11) and Isom *et al.* (12). The former investigators used microcrystalline cellulose pellets, first described by Gibson and Tingstad (6), which contained 75 mg of morphine base; the latter investigators used silicone pellets containing 300 mg of morphine sulfate and mineral oil. The silicone pellet described in the present report contained 32 mg of morphine sulfate and algin, thus providing the implantation of 64 mg of drug/mouse. The major advantage in the use of these sustained-release drug

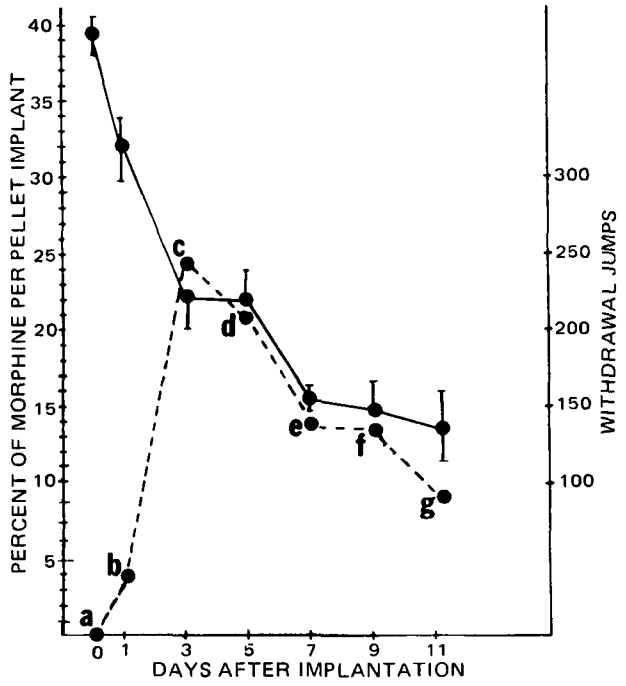

Figure 1—*Percent of morphine remaining in the polydimethylsiloxane pellet (—) (left axis) and the number of jumps observed during withdrawal induced by naloxone (- -) (right axis) plotted against the number of days the pellets were implanted. Symbols a–g represent the mean number of withdrawal jumps per 20 min after naloxone injection. The following symbols were not statistically significantly different from each other ($p < 0.05$): a and b; c and d; d, e, and f; and e, f, and g.*

delivery systems is the rapid induction of physical dependence without time-consuming repetitive injections. However, the microcrystalline cellulose pellets are manufactured *via* tablet presses available to relatively few investigators interested in this area of study.

The silicone pellet containing mineral oil (12) required approximately five times the amount of morphine used in the silicone pellet developed in these laboratories. The former pellet also produced a relatively low level of naloxone-induced jumping (*e.g.*, a peak withdrawal jumping score of 42 over 30 min compared to 247 jumps in 30 min in this study using 4 and 5 mg of naloxone/kg, respectively). The continuous intraperitoneal infusion reported by Teiger (5) allows reliable, controlled, and easily measurable quantities of morphine to be delivered to an experimental animal. However, the extensive surgery, long recovery, and the possible limitation for use in rats or larger animals are distinct disadvantages of this system.

An advantage of the polydimethylsiloxane pellets reported in this study is the use of algin, which causes the pellet to swell in the presence of tissue fluid. As the swelling occurs, the slow release of morphine sulfate within the pellet occurs. The incorporation of algin at the 10% level appears to be optimum for the incorporation and release of morphine sulfate at a concentration of 40% of the pellet weight. The manufacture of these pellets is extremely simple and inexpensive. In addition, only minor surgery and a very brief recovery period are required, thus permitting any investigator the opportunity of developing a sustained-release drug delivery system for morphine with which to study events associated with chronic morphine administration (*e.g.*, tolerance, physical dependence, and morphine-induced alterations of neurotransmitter dynamics).

The quantification of the level of physical dependence on morphine utilizing vertical jumping (as in the present study) *versus* platform jumping was studied by Takemori and Sprague (13). They reported no differences between the two methods. The vertical jumping is a simple method of assessing physical dependence induced by morphine, and the use of videotape greatly enhances the ability to quantitate this behavior accurately.

[1] Charles River, Wilmington, Mass.
[2] Mallinckrodt, St. Louis, Mo.
[3] Kelco Co., Clark, N.J.
[4] Silastic 382 elastomer, Dow Corning Corp., Midland, Mich.
[5] Medical fluid 360, Dow Corning Corp., Midland, Mich.
[6] Catalyst M, Dow Corning Corp., Midland, Mich.

REFERENCES

(1) J. H. Jaffe, in "The Pharmacological Basis of Therapeutics," 5th ed., L. S. Goodman and A. Gilman, Eds., Macmillan, New York, N.Y., 1975, pp. 284–324.

(2) H. O. J. Collier, D. L. Francis, and C. Schneider, *Nature*, **237**, 220

(1973).
(3) K. W. Hui and M. B. Roberts, *J. Pharm. Pharmacol.*, **27**, 569 (1975).
(4) P. E. Goode, *Br. J. Pharmacol.*, **41**, 558 (1971).
(5) D. G. Teiger, *J. Pharmacol. Exp. Ther.*, **190**, 408 (1974).
(6) R. D. Gibson and J. E. Tingstad, *J. Pharm. Sci.*, **59**, 426 (1970).
(7) J. Blasig, A. Reinhald, and K. Zieralgansberger, *Psychopharmacologia*, **33**, 19 (1973).
(8) E. Wei, *ibid.*, **28**, 35 (1973).
(9) J. W. McGinity and C. S. Mehta, *Pharmacol. Biochem. Behav.*, **9**, 705 (1978).
(10) J. W. McGinity, L. A. Hunke, and A. B. Combs, *J. Pharm. Sci.*, **68**, 662 (1979).
(11) E. L. Way, H. H. Loh, and F. H. Shen, *J. Pharmacol. Exp. Ther.*, **167**, 1 (1969).
(12) G. E. Isom, K. D. Meisheri, and M. J. Meldruom, *J. Pharmacol. Methods*, **1**, 121 (1978).
(13) A. E. Takemori and G. L. Sprague, *J. Pharm. Pharmacol.*, **30**, 585 (1978).

Determination of Procainamide and *N*-Acetylprocainamide in Biological Fluids by High-Pressure Liquid Chromatography

CHII-MING LAI, BURDE L. KAMATH, ZEE M. LOOK, and AVRAHAM YACOBI ˣ

Received October 10, 1979, from the *Pharmaceutical Development Department, Research and Medical Affairs, Arnar-Stone Laboratories, Inc., McGaw Park, IL 60085.* Accepted for publication March 12, 1980.

Abstract □ A modification of a high-pressure liquid chromatographic method for the simultaneous determination of procainamide and *N*-acetylprocainamide in plasma is described. The deficiencies in the specificity of the existing method were overcome by replacing the cation-exchange column and the mobile phase. The recovery and reproducibility of both procainamide and *N*-acetylprocainamide from human, dog, and rat plasma and urine spiked with either compound were excellent in the concentration range of 0.05–10 μg/ml for plasma and 0.5–20 μg/ml for urine. The comparison of this method with a specific extraction method for sets of plasma samples from human subjects and rats receiving *N*-acetylprocainamide and procainamide, respectively, showed no statistically significant difference.

Keyphrases □ Procainamide—simultaneous high-pressure liquid chromatographic determination with *N*-acetylprocainamide in biological fluids □ *N*-Acetylprocainamide—simultaneous high-pressure liquid chromatographic determination with procainamide in biological fluids □ High-pressure liquid chromatography—analysis, procainamide and *N*-acetylprocainamide in biological fluids □ Antiarrhythmic agents—procainamide, simultaneous high-pressure liquid chromatographic determination with *N*-acetylprocainamide in biological fluids

High-pressure liquid chromatographic (HPLC) procedures for the determination of procainamide and its major metabolite, *N*-acetylprocainamide, in plasma have been described (1–6). One approach requires selective extraction of the drugs from plasma with an organic solvent, followed by reextraction or evaporation of the organic solvent prior to assay (1–4). The other approach involves deproteinization of plasma with acetonitrile and direct injection of the supernate following centrifugation (5). The former procedure usually is tedious. The latter procedure, while simple and rapid, may exhibit specificity and recovery deficiencies under certain conditions.

Nation *et al.* (7) suggested that the extraction method, although tedious and time consuming, may be a prudent approach for the determination of procainamide and *N*-acetylprocainamide. The present investigators experienced similar difficulties in using the deproteinization method. The purpose of this report is to describe a modified deproteinization method which produced consistent results and eliminated the lack of specificity and recovery. This result was achieved by replacing the cation-exchange column and the mobile phase utilized previously (5, 7).

EXPERIMENTAL

Materials—*N*-Acetylprocainamide hydrochloride[1] (an investigational new drug), procainamide hydrochloride USP[2], dioxane[3], toluene[3], acetonitrile[3], TLC plates[4], heparin USP[5], and a carbonated beverage[6] were obtained from commercial sources. Dioxane, toluene, and acetonitrile were glass distilled and purchased commercially. [^{14}C]Procainamide hydrochloride (specific activity 32 μCi/mg) and [^{14}C]-*N*-acetylprocainamide hydrochloride (specific activity 23.1 μCi/mg) were obtained commercially[7]. The internal standard, *p*-amino-*N*-(2-dipropylaminoethyl)benzamide, was synthesized in these laboratories.

Apparatus and Conditions—The high-pressure liquid chromatograph[8] was equipped with a 30-cm long × 4-mm i.d. alkylphenyl column[9] and a UV detector[10] at 280 nm. The column was eluted with a mobile phase that was a 60:40 mixture of acetonitrile and phosphate buffer (0.01 *M* NaH_2PO_4 and 0.005 *M* Na_2HPO_4, pH 6.6). The final pH of the mobile phase was 7.7. The flow rate was 2.0 ml/min. The solutions containing the drugs and the internal standard were injected into the chromatograph *via* an automatic processor[11].

The TLC plates were developed in an ascending fashion in a saturated chamber containing dioxane–toluene–ammonium hydroxide (80:30:1). The radioactivity on the developed TLC plates was detected by a radiochromatographic scanner[12], and the activity was determined on a liquid scintillation counter[13].

Preparation of Standards—The stock solution of the internal standard was prepared in methanol at a concentration of 2 mg/ml. This solution was diluted with acetonitrile to give a working standard solution of 1.5 μg/ml.

The standard solutions in plasma (human, dog, and rat) were prepared by spiking known amounts of procainamide and *N*-acetylprocainamide from a stock solution containing 1 mg/ml of each drug as the

[1] Napp Chemicals, Lodi, N.J.
[2] Ganes Chemicals, New York, N.Y.
[3] Burdick & Jackson Laboratories, Muskegon, Mich.
[4] Aluminum oxide 60F-254, E. Merck, Rahway, N.J.
[5] Eli Lilly and Co., Indianapolis, Ind.
[6] Coca Cola.
[7] Custom synthesized, New England Nuclear, Boston, Mass.
[8] Model ALC/GPC 204, Waters Associates, Milford, Mass.
[9] μBondapak phenyl column, Waters Associates, Milford, Mass.
[10] Model 440, Waters Associates, Milford, Mass.
[11] Model 710 WISP, Waters Associates, Milford, Mass.
[12] Model 7201, Packard Instrument Co., Downers Grove, Ill.
[13] Model 2425, Packard Instrument Co., Downers Grove, Ill.

0022-3549/80/0800-0982$01.00/0
© 1980, American Pharmaceutical Association

(1973).
(3) K. W. Hui and M. B. Roberts, *J. Pharm. Pharmacol.*, **27**, 569 (1975).
(4) P. E. Goode, *Br. J. Pharmacol.*, **41**, 558 (1971).
(5) D. G. Teiger, *J. Pharmacol. Exp. Ther.*, **190**, 408 (1974).
(6) R. D. Gibson and J. E. Tingstad, *J. Pharm. Sci.*, **59**, 426 (1970).
(7) J. Blasig, A. Reinhald, and K. Zieralgansberger, *Psychopharmacologia*, **33**, 19 (1973).
(8) E. Wei, *ibid.*, **28**, 35 (1973).
(9) J. W. McGinity and C. S. Mehta, *Pharmacol. Biochem. Behav.*, **9**, 705 (1978).
(10) J. W. McGinity, L. A. Hunke, and A. B. Combs, *J. Pharm. Sci.*, **68**, 662 (1979).
(11) E. L. Way, H. H. Loh, and F. H. Shen, *J. Pharmacol. Exp. Ther.*, **167**, 1 (1969).
(12) G. E. Isom, K. D. Meisheri, and M. J. Meldruom, *J. Pharmacol. Methods*, **1**, 121 (1978).
(13) A. E. Takemori and G. L. Sprague, *J. Pharm. Pharmacol.*, **30**, 585 (1978).

Determination of Procainamide and *N*-Acetylprocainamide in Biological Fluids by High-Pressure Liquid Chromatography

CHII-MING LAI, BURDE L. KAMATH, ZEE M. LOOK, and AVRAHAM YACOBI ˣ

Received October 10, 1979, from the *Pharmaceutical Development Department, Research and Medical Affairs, Arnar-Stone Laboratories, Inc., McGaw Park, IL 60085.* Accepted for publication March 12, 1980.

Abstract □ A modification of a high-pressure liquid chromatographic method for the simultaneous determination of procainamide and *N*-acetylprocainamide in plasma is described. The deficiencies in the specificity of the existing method were overcome by replacing the cation-exchange column and the mobile phase. The recovery and reproducibility of both procainamide and *N*-acetylprocainamide from human, dog, and rat plasma and urine spiked with either compound were excellent in the concentration range of 0.05–10 μg/ml for plasma and 0.5–20 μg/ml for urine. The comparison of this method with a specific extraction method for sets of plasma samples from human subjects and rats receiving *N*-acetylprocainamide and procainamide, respectively, showed no statistically significant difference.

Keyphrases □ Procainamide—simultaneous high-pressure liquid chromatographic determination with *N*-acetylprocainamide in biological fluids □ *N*-Acetylprocainamide—simultaneous high-pressure liquid chromatographic determination with procainamide in biological fluids □ High-pressure liquid chromatography—analysis, procainamide and *N*-acetylprocainamide in biological fluids □ Antiarrhythmic agents—procainamide, simultaneous high-pressure liquid chromatographic determination with *N*-acetylprocainamide in biological fluids

High-pressure liquid chromatographic (HPLC) procedures for the determination of procainamide and its major metabolite, *N*-acetylprocainamide, in plasma have been described (1–6). One approach requires selective extraction of the drugs from plasma with an organic solvent, followed by reextraction or evaporation of the organic solvent prior to assay (1–4). The other approach involves deproteinization of plasma with acetonitrile and direct injection of the supernate following centrifugation (5). The former procedure usually is tedious. The latter procedure, while simple and rapid, may exhibit specificity and recovery deficiencies under certain conditions.

Nation *et al.* (7) suggested that the extraction method, although tedious and time consuming, may be a prudent approach for the determination of procainamide and *N*-acetylprocainamide. The present investigators experienced similar difficulties in using the deproteinization method. The purpose of this report is to describe a modified deproteinization method which produced consistent results and eliminated the lack of specificity and recovery. This result was achieved by replacing the cation-exchange column and the mobile phase utilized previously (5, 7).

EXPERIMENTAL

Materials—*N*-Acetylprocainamide hydrochloride[1] (an investigational new drug), procainamide hydrochloride USP[2], dioxane[3], toluene[3], acetonitrile[3], TLC plates[4], heparin USP[5], and a carbonated beverage[6] were obtained from commercial sources. Dioxane, toluene, and acetonitrile were glass distilled and purchased commercially. [^{14}C]Procainamide hydrochloride (specific activity 32 μCi/mg) and [^{14}C]-*N*-acetylprocainamide hydrochloride (specific activity 23.1 μCi/mg) were obtained commercially[7]. The internal standard, *p*-amino-*N*-(2-dipropylaminoethyl)benzamide, was synthesized in these laboratories.

Apparatus and Conditions—The high-pressure liquid chromatograph[8] was equipped with a 30-cm long × 4-mm i.d. alkylphenyl column[9] and a UV detector[10] at 280 nm. The column was eluted with a mobile phase that was a 60:40 mixture of acetonitrile and phosphate buffer (0.01 *M* NaH_2PO_4 and 0.005 *M* Na_2HPO_4, pH 6.6). The final pH of the mobile phase was 7.7. The flow rate was 2.0 ml/min. The solutions containing the drugs and the internal standard were injected into the chromatograph *via* an automatic processor[11].

The TLC plates were developed in an ascending fashion in a saturated chamber containing dioxane–toluene–ammonium hydroxide (80:30:1). The radioactivity on the developed TLC plates was detected by a radiochromatographic scanner[12], and the activity was determined on a liquid scintillation counter[13].

Preparation of Standards—The stock solution of the internal standard was prepared in methanol at a concentration of 2 mg/ml. This solution was diluted with acetonitrile to give a working standard solution of 1.5 μg/ml.

The standard solutions in plasma (human, dog, and rat) were prepared by spiking known amounts of procainamide and *N*-acetylprocainamide from a stock solution containing 1 mg/ml of each drug as the

[1] Napp Chemicals, Lodi, N.J.
[2] Ganes Chemicals, New York, N.Y.
[3] Burdick & Jackson Laboratories, Muskegon, Mich.
[4] Aluminum oxide 60F-254, E. Merck, Rahway, N.J.
[5] Eli Lilly and Co., Indianapolis, Ind.
[6] Coca Cola.
[7] Custom synthesized, New England Nuclear, Boston, Mass.
[8] Model ALC/GPC 204, Waters Associates, Milford, Mass.
[9] μBondapak phenyl column, Waters Associates, Milford, Mass.
[10] Model 440, Waters Associates, Milford, Mass.
[11] Model 710 WISP, Waters Associates, Milford, Mass.
[12] Model 7201, Packard Instrument Co., Downers Grove, Ill.
[13] Model 2425, Packard Instrument Co., Downers Grove, Ill.

0022-3549/80/0800-0982$01.00/0
© 1980, American Pharmaceutical Association

Table I—Recovery and Reproducibility of Procainamide in Plasma and Urine

Concentration, μg/ml	Recovery[a], %				Reproducibility[b]			
	Plasma			Human Urine	Plasma			Human Urine
	Human	Dog	Rat		Human	Dog	Rat	
0.05	96.3 ± 4.98	100.5 ± 3.91	93.6 ± 9.53	—	94.8	96.1	89.8	—
0.1	94.3 ± 5.01	101.9 ± 4.37	96.2 ± 1.91	—	94.7	95.7	98.0	—
0.25	103.5 ± 1.96	94.7 ± 4.32	84.2 ± 3.64	—	98.1	95.4	95.7	—
0.5	99.1 ± 0.960	99.9 ± 0.808	99.0 ± 0.591	94.7 ± 1.01	99.0	99.2	99.4	98.9
0.75	101.0 ± 1.58	98.1 ± 0.693	96.4 ± 0.0	—	98.4	99.3	100.0	—
1.0	96.9 ± 1.15	100.1 ± 0.700	99.3 ± 0.730	102.6 ± 1.27	98.8	99.3	99.3	98.8
2.5	97.6 ± 2.10	98.6 ± 0.650	96.4 ± 0.0	100.9 ± 0.766	97.8	99.3	100.0	99.2
5.0	100.7 ± 2.01	97.9 ± 2.00	94.7 ± 1.23	99.0 ± 1.07	98.0	98.0	98.7	98.9
7.5	99.1 ± 1.40	—[c]	—[c]	99.1 ± 3.39	98.6	98.6	98.5	96.6
10.0	100.0 ± 1.21	100.0 ± 0.231	100.8 ± 0.500	98.3 ± 2.54	98.8	99.8	99.5	97.4
15.0	—	—	—	101.6 ± 2.46	—	—	—	97.6
20.0	—	—	—	102.9 ± 0.877	—	—	—	99.1
Mean	98.8	99.1	95.6	99.9	97.7	98.1	97.9	98.3
SD	3.45	2.99	5.56	3.08	1.60	1.69	3.11	0.972

[a] Mean ± *SD*, $n = 4$. [b] Values equal 100 minus percent coefficient of variation. [c] Contaminated aqueous standards.

Table II—Recovery and Reproducibility of *N*-Acetylprocainamide in Plasma and Urine

Concentration, μg/ml	Recovery[a], %				Reproducibility[b]			
	Plasma			Human Urine	Plasma			Human Urine
	Human	Dog	Rat		Human	Dog	Rat	
0.05	88.9 ± 3.62	95.9 ± 6.99	89.8 ± 0.299	—	95.9	92.7	99.7	—
0.1	93.8 ± 2.88	94.2 ± 3.89	92.9 ± 2.05	—	96.9	95.9	97.8	—
0.25	98.8 ± 2.19	91.2 ± 1.98	81.5 ± 0.750	—	97.8	97.8	99.1	—
0.5	98.3 ± 0.681	93.2 ± 0.751	92.5 ± 0.493	92.2 ± 0.503	99.3	99.2	99.5	99.5
0.75	97.3 ± 1.26	93.7 ± 0.693	92.7 ± 1.10	—	98.7	99.3	98.8	—
1.0	93.4 ± 1.10	93.6 ± 0.800	93.7 ± 0.939	101.7 ± 2.19	98.8	99.4	99.0	97.8
2.5	95.6 ± 1.15	92.9 ± 0.650	91.4 ± 0.450	100.6 ± 1.11	98.8	99.3	99.5	98.9
5.0	96.8 ± 2.08	91.8 ± 1.73	89.4 ± 1.14	97.7 ± 1.45	97.9	98.1	98.7	98.5
7.5	95.8 ± 1.54	—[c]	—[c]	98.6 ± 3.62	98.4	98.1	98.4	96.3
10.0	97.3 ± 1.65	95.5 ± 2.38	95.4 ± 0.245	96.9 ± 2.68	99.8	97.5	99.7	97.2
15.0	—	—	—	101.2 ± 2.46	—	—	—	97.6
20.0	—	—	—	102.0 ± 1.27	—	—	—	98.8
Mean	95.6	93.6	91.0	98.9	98.1	97.7	99.0	98.1
SD	3.33	2.98	3.94	3.65	1.02	2.08	0.616	1.04

[a] Mean ± *SD*, $n = 4$. [b] Values equal 100 minus percent coefficient of variation. [c] Contaminated aqueous standards.

free base in water. The plasma standards were 0.05, 0.1, 0.25, 0.5, 0.75, 1.0, 2.5, 5.0, 7.5, and 10 μg/ml of each drug as the free base.

The standard solutions in human urine were prepared from a stock solution containing 1 mg/ml each of procainamide and *N*-acetylprocainamide as the hydrochloride salts. The concentrations of the standards were 0.5, 1.0, 2.5, 5.0, 7.5, 10, 15, and 20 μg/ml of procainamide hydrochloride and *N*-acetylprocainamide hydrochloride.

Preparation of Samples—To compare the deproteinization method with the extraction method (7), plasma samples were obtained from a clinical study in which a normal subject was given a 500-mg *N*-acetylprocainamide hydrochloride tablet every 6 hr for 54 hr and from a metabolism study in which rats received procainamide hydrochloride (1280 mg/kg/day) mixed in the diet for 6 months. The human plasma samples were collected at 30, 36, 48, 49, 50, 54.5, 55.0, 56, 58, and 60 hr following the first dose.

Procedure—To a 0.1- or 0.5-ml plasma or urine sample containing 0.05–20 μg each of *N*-acetylprocainamide and procainamide/ml was added an equal or double volume, respectively, of acetonitrile containing 1.5 μg of the internal standard [*p*-amino-*N*-(2-dipropylaminoethyl)-benzamide]/ml. The mixture was vortexed for 10 sec and then centrifuged for 5 min at 4500 rpm. The supernatant solution was decanted, and 50 μl was applied for HPLC analysis.

The solvent extraction method consisted of the following sequences. A mixture of 0.1 ml of plasma, 0.5 ml of water, and 0.1 ml of 1 *M* NaOH was vortexed for 1 min with 3 ml of ethyl acetate. After centrifugation, most of the organic layer was transferred to a test tube and vortexed for 1 min with 0.1 ml of 0.5% phosphoric acid. The tube was centrifuged, and the aqueous phase was separated, evaporated to dryness, and reconstituted in water–acetonitrile (1:2). An aliquot of this solution was injected.

The specificity of the HPLC method was examined using [^{14}C]-*N*-acetylprocainamide and [^{14}C]procainamide and TLC. Briefly, plasma samples containing both drugs were deproteinized with two volumes of acetonitrile, vortexed, and centrifuged. Fifty microliters of the supernate was spotted on TLC plates, and the chromatograms then were developed. The developed plates were examined by a radiochromatographic scanner, and the activity corresponding to *N*-acetylprocainamide and procainamide spots was determined by liquid scintillation. Additionally, 20-sec fractions of the HPLC eluate were collected for radioactivity determination to establish the entire high-pressure liquid chromatogram.

RESULTS AND DISCUSSION

The HPLC retention times of *N*-acetylprocainamide, procainamide, and the internal standard were 3.5, 4.4, and 5.6 min, respectively. Tables I and II summarize the recovery and reproducibility of the assay for human, dog, and rat plasma as well as for human urine for a wide range of procainamide and *N*-acetylprocainamide concentrations. The relationships between the peak height ratios and drug concentrations were linear over the entire range studied for both plasma and urine. The assay recovery of procainamide for human, dog, and rat plasma was 98.8, 99.1, and 95.6%, respectively; the recovery of *N*-acetylprocainamide was 95.6, 93.6, and 91.0%, respectively. The recovery of procainamide and *N*-acetylprocainamide for human urine was 99.9 and 98.9%, respectively. Both plasma and urine recoveries were concentration independent throughout the range studied.

The average reproducibility of the assay for each set of samples (n = 32–40) was ~98%. The use of an internal standard with similar physicochemical characteristics to the drugs contributed to the accuracy and high reproducibility. The TLC–HPLC comparison produced essentially the same results with respect to the specificity and recovery of the assay. Additionally, 48-hr incubation of plasma samples containing *N*-acetylprocainamide and procainamide at room temperature showed 93.5 ± 8.31 and 95.6 ± 3.76% (mean ± *SD*, n = 10) of the spiked values, respectively, indicating no significant degradation of either drug. The resolution of the column as tested by radioactivity measurement was consistent at all times, regardless of aging of the alkylphenyl column, and symmetrical peaks were produced with no indication of interfering compounds. Similarly, the radiochromatographic scanning of TLC plates showed no interfering peaks.

Although the lack of specificity of the assay may result from drug metabolites, it often may be due to the presence of endogenous and/or

Table III—Comparison of Direct Deproteinization Method to Extraction Method for the HPLC Determination of Procainamide and *N*-Acetylprocainamide in Plasma

Clinical Study[a]			Metabolic Study of Procainamide in Rats[b]					
Steady-State Plasma Concentrations of *N*-Acetylprocainamide, μg/ml			Procainamide Concentration, μg/ml			*N*-Acetylprocainamide Concentration, μg/ml		
Deproteinization Method (I)	Extraction Method (II)	I/II	Deproteinization Method (I)	Extraction Method (II)	I/II	Deproteinization Method (I)	Extraction Method (II)	I/II
3.27	3.33	0.982	0.720	0.762	0.945	0.672	0.776	0.866
4.10	4.20	0.976	0.833	0.897	0.929	0.610	0.617	0.987
4.08	4.09	0.998	2.23	2.06	1.08	0.904	0.970	0.932
4.39	4.33	1.01	1.67	1.68	0.994	0.877	1.06	0.827
5.65	5.82	0.971	0.698	0.706	0.948	1.09	1.15	0.948
4.32	4.52	0.956	0.281	0.351	0.801	2.27	2.22	1.02
4.49	4.58	0.980	0.338	0.310	1.09	0.397	0.411	0.966
6.95	6.89	1.01	0.737	0.744	0.991	0.820	0.823	0.996
5.54	5.50	1.01	1.34	1.33	1.01	1.17	1.13	1.04
4.34	4.40	0.986	1.02	1.02	1.00	0.726	0.767	0.947
Mean		0.988			0.979			0.953
SD		0.0186			0.082			0.066

[a] A normal subject received 500 mg of *N*-acetylprocainamide hydrochloride every 6 hr for 54 hr. [b] Rats received procainamide hydrochloride mixed in the diet of 1280 mg/kg/day for 6 months.

exogenous compounds. Plasma samples often are heparinized, and traces of heparin can be a source of interference with the drug peaks, particularly in the deproteinization techniques. This problem was observed with at least two HPLC columns differing in their polarity and under various elution systems. Unless a suitable chromatographic system is selected for a given compound, heparin probably will be a source of error in the assay of drugs. In this method, the retention time of heparin was 2.2 min and that of components of coffee or a carbonated beverage was <2 min. Previous investigators (8, 9) noticed that chemicals contained in vacutainer stoppers may interfere with extraction procedures for lidocaine and procainamide for a GLC measurement.

The application of both methods to human and rat plasma samples produced results with no statistically significant differences (paired *t* test) between the method described in this study and the specific extraction method (7) with respect to *N*-acetylprocainamide in humans and procainamide and *N*-acetylprocainamide in rats (Table III). The concentration ratio of the deproteinization method to the extraction method averaged 95.3–97.9%.

The proposed assay offers the same simplicity of the deproteinization procedure published previously (5, 7). However, the use of the alkylphenyl column with an appropriate mobile phase produces more consistent and reliable results. This procedure was tested with numerous samples obtained from subjects or animals given *N*-acetylprocainamide, procainamide, or both without any difficulties or specificity problems.

REFERENCES

(1) R. F. Adams, F. L. Vandermark, and G. Schmidt, *Clin. Acta*, **69**, 515 (1979).

(2) K. Carr, R. L. Woosley, and J. A. Oates, *J. Chromatogr.*, **129**, 363 (1979).

(3) J. S. Dutcher and J. M. Strong, *Clin. Chem.*, **23**, 1318 (1977).

(4) A. G. Butterfield, J. K. Cooper, and K. K. Midha, *J. Pharm. Sci.*, **67**, 839 (1978).

(5) M. A. F. Gadalla, G. W. Peng, and W. L. Chiou, *ibid.*, **67**, 869 (1978).

(6) S. C. Su and W. Y. W. Au, *J. Liquid Chromatogr.*, **1**, 783 (1978).

(7) R. L. Nation, M. G. Lee, S. M. Huang, and W. L. Chiou, *J. Pharm. Sci.*, **68**, 532 (1979).

(8) A. J. Atkinson, Jr., M. Parker, and J. Strong, *Clin. Chem.*, **18**, 643 (1972).

(9) M. M. Reidenberg, D. E. Drayer, M. Levy, and H. Warner, *Clin. Pharmacol. Ther.*, **17**, 722 (1975).

Synthesis and Biological Evaluation of *p*-Bromospiperone as Potential Neuroleptic Drug

C. C. HUANG *x, A. M. FRIEDMAN *‡, R. SO §, M. SIMONOVIC §, and H. Y. MELTZER §

Received February 19, 1980, from the **Chemistry Division, Argonne National Laboratory, Argonne, IL 60439,* and the ‡*Department of Radiology and the* §*Department of Psychiatry, University of Chicago, Chicago, IL 60637.* Accepted for publication March 18, 1980.

Abstract □ *p*-Bromospiperone was prepared from the reaction of spiperone with bromine. It was tested for dopamine receptor binding affinity *in vitro* and its ability to stimulate prolactin secretion *in vivo*. The results indicate no significant change of biological activities due to the bromination of spiperone.

Keyphrases □ Spiperone—*p*-bromo analog, synthesis and biological evaluation as a potential neuroleptic □ Neuroleptics, potential—*p*-bromospiperone, synthesis and biological evaluation □ Prolactin secretion—stimulation by *p*-bromospiperone

Spiperone (I) is one of the most potent neuroleptic drugs in clinical use. This drugs binds extensively to the dopamine receptors in the brains of rats and mice (1, 2). Attempts have been made to study the receptor–drug inter-

0022-3549/80/0800-0984$01.00/0

© 1980, American Pharmaceutical Association

Table III—Comparison of Direct Deproteinization Method to Extraction Method for the HPLC Determination of Procainamide and *N*-Acetylprocainamide in Plasma

Clinical Study[a]			Metabolic Study of Procainamide in Rats[b]					
Steady-State Plasma Concentrations of *N*-Acetylprocainamide, μg/ml			Procainamide Concentration, μg/ml			*N*-Acetylprocainamide Concentration, μg/ml		
Deproteinization Method (I)	Extraction Method (II)	I/II	Deproteinization Method (I)	Extraction Method (II)	I/II	Deproteinization Method (I)	Extraction Method (II)	I/II
3.27	3.33	0.982	0.720	0.762	0.945	0.672	0.776	0.866
4.10	4.20	0.976	0.833	0.897	0.929	0.610	0.617	0.987
4.08	4.09	0.998	2.23	2.06	1.08	0.904	0.970	0.932
4.39	4.33	1.01	1.67	1.68	0.994	0.877	1.06	0.827
5.65	5.82	0.971	0.698	0.706	0.948	1.09	1.15	0.948
4.32	4.52	0.956	0.281	0.351	0.801	2.27	2.22	1.02
4.49	4.58	0.980	0.338	0.310	1.09	0.397	0.411	0.966
6.95	6.89	1.01	0.737	0.744	0.991	0.820	0.823	0.996
5.54	5.50	1.01	1.34	1.33	1.01	1.17	1.13	1.04
4.34	4.40	0.986	1.02	1.02	1.00	0.726	0.767	0.947
Mean		0.988			0.979			0.953
SD		0.0186			0.082			0.066

[a] A normal subject received 500 mg of *N*-acetylprocainamide hydrochloride every 6 hr for 54 hr. [b] Rats received procainamide hydrochloride mixed in the diet of 1280 mg/kg/day for 6 months.

exogenous compounds. Plasma samples often are heparinized, and traces of heparin can be a source of interference with the drug peaks, particularly in the deproteinization techniques. This problem was observed with at least two HPLC columns differing in their polarity and under various elution systems. Unless a suitable chromatographic system is selected for a given compound, heparin probably will be a source of error in the assay of drugs. In this method, the retention time of heparin was 2.2 min and that of components of coffee or a carbonated beverage was <2 min. Previous investigators (8, 9) noticed that chemicals contained in vacutainer stoppers may interfere with extraction procedures for lidocaine and procainamide for a GLC measurement.

The application of both methods to human and rat plasma samples produced results with no statistically significant differences (paired *t* test) between the method described in this study and the specific extraction method (7) with respect to *N*-acetylprocainamide in humans and procainamide and *N*-acetylprocainamide in rats (Table III). The concentration ratio of the deproteinization method to the extraction method averaged 95.3–97.9%.

The proposed assay offers the same simplicity of the deproteinization procedure published previously (5, 7). However, the use of the alkylphenyl column with an appropriate mobile phase produces more consistent and reliable results. This procedure was tested with numerous samples obtained from subjects or animals given *N*-acetylprocainamide, procainamide, or both without any difficulties or specificity problems.

REFERENCES

(1) R. F. Adams, F. L. Vandermark, and G. Schmidt, *Clin. Acta*, **69**, 515 (1979).

(2) K. Carr, R. L. Woosley, and J. A. Oates, *J. Chromatogr.*, **129**, 363 (1979).

(3) J. S. Dutcher and J. M. Strong, *Clin. Chem.*, **23**, 1318 (1977).

(4) A. G. Butterfield, J. K. Cooper, and K. K. Midha, *J. Pharm. Sci.*, **67**, 839 (1978).

(5) M. A. F. Gadalla, G. W. Peng, and W. L. Chiou, *ibid.*, **67**, 869 (1978).

(6) S. C. Su and W. Y. W. Au, *J. Liquid Chromatogr.*, **1**, 783 (1978).

(7) R. L. Nation, M. G. Lee, S. M. Huang, and W. L. Chiou, *J. Pharm. Sci.*, **68**, 532 (1979).

(8) A. J. Atkinson, Jr., M. Parker, and J. Strong, *Clin. Chem.*, **18**, 643 (1972).

(9) M. M. Reidenberg, D. E. Drayer, M. Levy, and H. Warner, *Clin. Pharmacol. Ther.*, **17**, 722 (1975).

Synthesis and Biological Evaluation of *p*-Bromospiperone as Potential Neuroleptic Drug

C. C. HUANG *x, A. M. FRIEDMAN *‡, R. SO §, M. SIMONOVIC §, and H. Y. MELTZER §

Received February 19, 1980, from the **Chemistry Division, Argonne National Laboratory, Argonne, IL 60439,* and the ‡*Department of Radiology and the* §*Department of Psychiatry, University of Chicago, Chicago, IL 60637.* Accepted for publication March 18, 1980.

Abstract □ *p*-Bromospiperone was prepared from the reaction of spiperone with bromine. It was tested for dopamine receptor binding affinity *in vitro* and its ability to stimulate prolactin secretion *in vivo*. The results indicate no significant change of biological activities due to the bromination of spiperone.

Keyphrases □ Spiperone—*p*-bromo analog, synthesis and biological evaluation as a potential neuroleptic □ Neuroleptics, potential—*p*-bromospiperone, synthesis and biological evaluation □ Prolactin secretion—stimulation by *p*-bromospiperone

Spiperone (I) is one of the most potent neuroleptic drugs in clinical use. This drugs binds extensively to the dopamine receptors in the brains of rats and mice (1, 2). Attempts have been made to study the receptor–drug inter-

0022-3549/80/0800-0984$01.00/0

© 1980, American Pharmaceutical Association

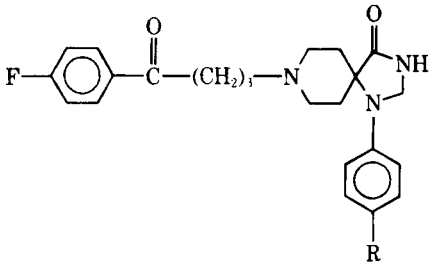

I: R = H
II: R = Br

action by using suitable gamma or positron radionuclides. Since the usual techniques for incorporation of fluorine 18 into an aromatic ring result in compounds of low specific activity, the use of radiobromines (bromine 77, 76, and 75) was investigated. Substitution of bromine for hydrogen at one aromatic ring may represent a minimum structural alteration without much of a change in pharmacological activity. As an essential step in this procedure, the nonradioactive brominated analog of spiperone was prepared to determine the effect of this substitution on its biological utility as a neuroleptic compound.

This report describes the synthesis and biological testing of the brominated spiperone (II).

EXPERIMENTAL[1]

Synthesis—To a solution of spiperone (80 mg, 0.2 mmole) in methylene chloride (5 ml) was added dropwise bromine (35 mg, 0.22 mmole) in carbon tetrachloride (5 ml). The solution was stirred at 0° for 30 min. At the end of the reaction, an equal volume of an aqueous solution of 5% NH_4OH and 1% $Na_2S_2O_3$ was added. The organic phase was separated and dried over anhydrous sodium sulfate. Removal of the solvent gave a white powder. Recrystallization from a mixture of methylene chloride and carbon tetrachloride gave pure II (70 mg, 74%), mp 204–205°.

Anal.—Calc. for $C_{23}H_{25}BrFN_3O_2$: C, 58.23; H, 5.31; Br, 16.85. Found: C, 58.01; H, 5.36; Br, 16.52.

The mass spectrum of the compound showed molecular ions at *m/e* 474 (M) and 476 (M + 2) of equal intensity and other fragmentation peaks at 123, 165, 322, 324, 336, and 338; NMR ($CDCl_3$): δ 1.5–2.2 (m, 4H), 2.3–3.2 (m, 10H), 4.66 (s, 2H), 6.68 (d, 2H *ortho* to N, J = 9 Hz), 6.9–7.5 (m, 4H), 7.97 (q, 2H *ortho* to carbonyl group), and 8.89 (s, 1H); IR (KBr): ν_{max} 814, 839, 1230, 1387, 1507, 1606, and 1717 cm^{-1}; TLC [reversed-phase silica gel[2] with methanol–water (80:20)]: R_f 0.18 for II and 0.23 for I.

Receptor Binding Assay—The ability of bromospiperone to displace [^{3}H]spiperone from its specific binding sites in calf caudate and anterior pituitary homogenates was tested by methods described previously (3). The tissues were homogenized in cold 50 m*M* tris(hydroxymethyl)aminomethane hydrochloride buffer (pH 7.7) and centrifuged twice at 50,000×*g* for 10 min, with rehomogenization of the intermediate pellet in the same buffer. The final pellet was resuspended in a cold incubation medium containing 50 m*M* tris(hydroxymethyl)aminomethane hydrochloride, 10 m*M* pargyline hydrochloride, 0.1% ascorbic acid, 120 m*M* NaCl, 5 m*M* KCl, 2 m*M* $CaCl_2$, and 1 m*M* $MgCl_2$ (pH 7.1) at 25°.

The final concentration of [^{3}H]spiperone was 0.25 n*M* for pituitary and 0.13 n*M* for caudate. Each tube contained ~0.4 mg of protein and was incubated at 37° for 10 (pituitary) or 15 (caudate) min. The assay was terminated by rapid filtration through glass fiber filters[3]. The filters were washed with three 3-ml portions of cold 50 m*M* tris(hydroxymethyl)-aminomethane hydrochloride buffer (pH 7.7), and the radioactivity trapped by the filters was counted with an efficiency of 40–45%. Nonspecific binding was obtained by displacement using 1 μ*M* *d*-butaclamol (3). Specific binding was defined as the difference between the total and the nonspecific binding and ranged from 40 to 50% of the total binding.

Plasma Prolactin Levels—Male Sprague–Dawley rats (175–200 g) were housed six per cage in a temperature- (26°) and humidity- (60%) regulated room with a 12-hr light–dark cycle. The animals had free access to rat chow[4] and water at all times. Rats were decapitated 30 min following the intraperitoneal injection of a test compound or saline. Trunk blood was collected. Serum then was separated and stored at −20° until it was assayed for prolactin by the double-antibody radioimmunoassay as described previously (4).

Table I—IC_{50} Values[a] for Binding of [^{3}H]Spiperone to Calf Anterior Pituitary and Caudate

Drug	IC_{50}, n*M*	
	Caudate	Anterior Pituitary
Spiperone	2.6	2.2
p-Bromospiperone	2.8	3.2

[a] The IC_{50} values are concentrations for 50% reduction in binding of [^{3}H]spiperone.

Table II—Effect of a Low Dose of Spiperone or Its Brominated Derivative on Serum Prolactin in Male Rats

Group	Dose, mg/kg	Prolactin Concentration[a], ng/ml	Comparison	*p*
1 Saline	—	2.0 ± 1.0	—	—
2 Spiperone	0.01	22.0 ± 5.9	1–2	<0.01
3 Bromospiperone	0.01	30.2 ± 8.4	1–3	<0.05
			2–3	NS

[a] Mean serum prolactin level ± *SEM* for a group of five rats. The significance of the difference was assessed using the Student *t* test.

RESULTS AND DISCUSSION

Chemistry—*p*-Bromospiperone (II) was synthesized by direct bromination of spiperone with bromine. Structural identification of II was obtained from various spectral evidence. The mass spectrum of II showed the molecular ions at *m/e* 474 (M) and 476 (M + 2) of approximately equal intensity, characteristic of the presence of a bromine atom. The brominated product was assigned a *para*-position based on the fact that the aniline-type structure favors *ortho*- or *para*-substitution in the electrophilic reaction because of the electron-donating character of nitrogen. In this case, the steric interference would render *ortho*-substitution less favorable. In addition, the NMR spectrum showed a characteristic doublet (δ 6.68) for two protons *ortho* to nitrogen.

The IR spectrum of II did not show much difference from that of I. However, careful examination revealed some information as to the structural identity of the compound. For example, the disappearance of the peak at 755 cm^{-1} is characteristic of monosubstitution due to a C–H bending vibration. This disappearance was accompanied by the appearance of the peak at 814 cm^{-1}, which is indicative of 1,4-disubstitution due to the bromination (5). The peak at 839 cm^{-1}, present in both I and II, probably is due to the CH bending from the other fluorine-substituted aromatic ring.

The similarities in the chemical behavior of spiperone and *p*-bromospiperone can be demonstrated by TLC. TLC on silica gel in several solvent systems (acetone, methanol, methylene chloride, and carbon tetrachloride–methanol) did not separate I and II. However, the separation could be accomplished by reversed-phase TLC[2] with methanol–water (80:20) as the solvent.

Biological Testing—The IC_{50} values determined by the binding assay are shown in Table I. Spiperone and *p*-bromospiperone were essentially equipotent in displacing [^{3}H]spiperone from specific binding sites in both calf caudate and pituitary. This finding indicates that bromination does not interfere with the binding of the spiperone nucleus to dopamine receptors *in vitro*.

Dopamine receptor blockers stimulate prolactin secretion *in vivo* be-

[1] Melting points were determined with an Electrothermal melting-point apparatus and are uncorrected. NMR spectra were obtained with a Varian A-60 spectrometer using tetramethylsilane as the internal standard and deuterochloroform as the solvent. IR spectra were recorded on a Beckman IR 12 spectrophotometer. TLC was performed on silica gel with a fluorescence indicator (Eastman) on plastic sheets or on reversed-phase silica gel with a fluorescence indicator (Whatman KC_{18}); visualization was with either UV light or iodine vapor. The mass spectrum was obtained with a Bendix time-of-flight mass spectrometer. Elemental analyses were performed by Galbraith Laboratory, Knoxville, Tenn. [^{3}H]Spiperone was obtained from New England Nuclear with a specific activity of 25.64 Ci/mmole. Spiperone was a gift of Janssen Pharmaceuticals, Belgium, and Dr. P. Seeman, Toronto, Canada, and *d*-butaclamol was a gift of Ayerst Laboratories.

[2] Whatman KC_{18} silica gel.

[3] Whatman GF/B.

[4] Purina.

cause they interfere with tonic dopaminergic inhibition of prolactin release (6). Previous work showed that spiperone, one of the most potent dopamine receptor antagonists, elevates plasma prolactin levels in rats (3). In the present study, prolactin levels were elevated significantly 30 min after the administration of a low dose of this neuroleptic to male rats (Table II). As shown in Table II, the same low dose of *p*-bromospiperone resulted in a comparable rise in serum prolactin levels. These results indicate that the bromination of the spiperone molecule does not significantly affect its ability to act as a dopamine receptor blocker in pituitary receptors *in vivo*, a finding consistent with results from the *in vitro* binding study. This brominated analog thus has potential as a neuroleptic drug. In addition, the radiobrominated compound may prove to be an extremely useful pharmacological tool for dopamine receptor studies in humans using positron emission tomography.

REFERENCES

(1) P. Laduron and J. Leysen, *Biochem. Pharmacol.*, **26**, 1003 (1977).

(2) V. Höllt and P. Schubert, *Brain Res.*, **151**, 149 (1978).

(3) H. Y. Meltzer, R. So, R. J. Miller, and V. S. Fang, *Life Sci.*, **25**, 573 (1979).

(4) H. Y. Meltzer, S. Daniels, and V. S. Fang, *ibid.*, **17**, 339 (1975).

(5) R. M. Silverstein and G. C. Bassler, "Spectrometric Identification of Organic Compounds," Wiley, New York, N.Y., 1967, p. 73.

(6) R. M. MacLeod and J. E. Lehmeyer, *Endocrinology*, **94**, 1077 (1974).

ACKNOWLEDGMENTS

Supported by the Division of Biological and Environmental Research, U.S. Department of Energy.

The authors thank Dr. J. McDermed, Wellcome Research Laboratories, and Dr. P. Hoffman and Dr. R. Dinerstein, Department of Pharmacological and Physiological Sciences, University of Chicago, for helpful discussions. They also thank Dr. R. Winans, Argonne National Laboratory, for performing the mass spectrometry.

New Compounds: N^1,N^8-Bis(2,3-dihydroxybenzoyl)spermidine and Analogs as Potential Iron-Chelating Drugs

K. K. BHARGAVA, R. W. GRADY ˣ, and A. CERAMI

Received May 3, 1979, from the *Department of Medical Biochemistry, Rockefeller University, New York, NY 10021.* Accepted for publication March 18, 1980.

Abstract □ N^1,N^8-Bis(2,3-dihydroxybenzoyl)spermidine was synthesized and evaluated as an iron-chelating drug. Homologs were prepared and evaluated together with a series of *N,N'*-bis(2,3-dihydroxybenzoyl)-α,ω-diaminoalkanes. Analogous 2-hydroxybenzoyl compounds also were synthesized and evaluated.

Keyphrases □ N^1,N^8-Bis(2,3-dihydroxybenzoyl)spermidine—synthesis and evaluation as iron-chelating drug □ Chelating agents—N^1,N^8-bis(2,3-dihydroxybenzoyl)spermidine and analogs, synthesis and evaluation as iron-sequestering agents

An orally effective, iron-chelating drug is needed to treat patients with Cooley's anemia. Patients suffering from this genetic disease must be transfused every 2–4 weeks. Since the body lacks a physiological means of excreting the iron present in transfused erythrocytes, these patients develop a secondary iron overload, which leads to damage of vital organs and eventually to death. It was suggested that 2,3-dihydroxybenzoic acid might be an orally effective, iron-chelating drug (1). Although subsequent clinical evaluation confirmed this report (2–4), it was not possible to maintain patients in iron balance.

A chelating agent with a greater affinity for iron presumably would be more effective. Several iron-sequestering agents produced by microbes are conjugates of 2,3-dihydroxybenzoic acid (5–9). These compounds all possess affinities for iron that are many orders of magnitude greater than the affinity of the parent compound. One of these compounds, N^1,N^8-bis(2,3-dihydroxybenzoyl)spermidine (8), removes iron from the ferritin of cultured Chang cells and from transferrin, the principal iron-binding protein of serum (10).

The synthesis of N^1,N^8-bis(2,3-dihydroxybenzoyl)-spermidine hydrochloride (XVII) together with a series of simpler analogs is presented in this report. Preliminary evidence suggests that this type of compound may be useful in iron-chelation therapy whereas the corresponding 2-hydroxybenzoyl derivatives are inactive. The *in vitro* and *in vivo* evaluation of these compounds will be presented later.

DISCUSSION

Prior to the synthesis of XVII, a series of simpler analogs, *i.e.*, *N,N'*-bis(2,3-dihydroxybenzoyl)-α,ω-diaminoalkanes, was prepared. Like the spermidine derivative, these compounds would be expected to bind iron strongly, their affinities for iron and perhaps their biological activities being related to the separation of the 2,3-dihydroxybenzoyl moieties. The compounds were obtained readily in a 40–50% yield *via* the reaction of 2,3-dioxosulfinylbenzoyl chloride (11) with the appropriate α,ω-diaminoalkane in tetrahydrofuran (Procedure A). Since the goal of this program was to obtain enough pure material for biological testing, no attempt was made to optimize the yield of this or subsequent reactions.

All compounds were obtained as solids which were purified by recrystallization. The ethane (I) and propane (II) derivatives were somewhat unique in that they were crystallized from aqueous methanol as their hydrates. Compound I was obtained as a monohydrate, with the water of crystallization being lost upon drying under vacuum at 78° for 4 hr. Compound II was obtained from aqueous methanol as the dihydrate. Drying caused the loss of both moles of water, as evidenced by elemental analysis.

The identity of I, II, and V was confirmed *via* independent synthesis. Two moles of 2,3-diacetoxybenzoic acid were condensed with ethylenediamine, 1,3-diaminopropane, or 1,6-diaminohexane *via* activation with *N,N'*-dicyclohexylcarbodiimide (Procedure B). Subsequent hydrolysis of the protecting groups yielded products (40%) identical to those obtained by Procedure A. Compound II also was prepared by fusing methyl 2,3-dihydroxybenzoate and 1,3-diaminopropane at 130° under nitrogen (Procedure C). The latter procedure was used to prepare an analogous series of *N,N'*-bis(2-hydroxybenzoyl)-α,ω-diaminoalkanes (X–XIV).

0022-3549/80/0800-0986$01.00/0

© 1980, American Pharmaceutical Association

cause they interfere with tonic dopaminergic inhibition of prolactin release (6). Previous work showed that spiperone, one of the most potent dopamine receptor antagonists, elevates plasma prolactin levels in rats (3). In the present study, prolactin levels were elevated significantly 30 min after the administration of a low dose of this neuroleptic to male rats (Table II). As shown in Table II, the same low dose of *p*-bromospiperone resulted in a comparable rise in serum prolactin levels. These results indicate that the bromination of the spiperone molecule does not significantly affect its ability to act as a dopamine receptor blocker in pituitary receptors *in vivo*, a finding consistent with results from the *in vitro* binding study. This brominated analog thus has potential as a neuroleptic drug. In addition, the radiobrominated compound may prove to be an extremely useful pharmacological tool for dopamine receptor studies in humans using positron emission tomography.

REFERENCES

(1) P. Laduron and J. Leysen, *Biochem. Pharmacol.*, **26**, 1003 (1977).

(2) V. Höllt and P. Schubert, *Brain Res.*, **151**, 149 (1978).

(3) H. Y. Meltzer, R. So, R. J. Miller, and V. S. Fang, *Life Sci.*, **25**, 573 (1979).

(4) H. Y. Meltzer, S. Daniels, and V. S. Fang, *ibid.*, **17**, 339 (1975).

(5) R. M. Silverstein and G. C. Bassler, "Spectrometric Identification of Organic Compounds," Wiley, New York, N.Y., 1967, p. 73.

(6) R. M. MacLeod and J. E. Lehmeyer, *Endocrinology*, **94**, 1077 (1974).

ACKNOWLEDGMENTS

Supported by the Division of Biological and Environmental Research, U.S. Department of Energy.

The authors thank Dr. J. McDermed, Wellcome Research Laboratories, and Dr. P. Hoffman and Dr. R. Dinerstein, Department of Pharmacological and Physiological Sciences, University of Chicago, for helpful discussions. They also thank Dr. R. Winans, Argonne National Laboratory, for performing the mass spectrometry.

New Compounds: N^1,N^8-Bis(2,3-dihydroxybenzoyl)spermidine and Analogs as Potential Iron-Chelating Drugs

K. K. BHARGAVA, R. W. GRADY ˣ, and A. CERAMI

Received May 3, 1979, from the *Department of Medical Biochemistry, Rockefeller University, New York, NY 10021.* Accepted for publication March 18, 1980.

Abstract □ N^1,N^8-Bis(2,3-dihydroxybenzoyl)spermidine was synthesized and evaluated as an iron-chelating drug. Homologs were prepared and evaluated together with a series of *N,N'*-bis(2,3-dihydroxybenzoyl)-α,ω-diaminoalkanes. Analogous 2-hydroxybenzoyl compounds also were synthesized and evaluated.

Keyphrases □ N^1,N^8-Bis(2,3-dihydroxybenzoyl)spermidine—synthesis and evaluation as iron-chelating drug □ Chelating agents—N^1,N^8-bis(2,3-dihydroxybenzoyl)spermidine and analogs, synthesis and evaluation as iron-sequestering agents

An orally effective, iron-chelating drug is needed to treat patients with Cooley's anemia. Patients suffering from this genetic disease must be transfused every 2–4 weeks. Since the body lacks a physiological means of excreting the iron present in transfused erythrocytes, these patients develop a secondary iron overload, which leads to damage of vital organs and eventually to death. It was suggested that 2,3-dihydroxybenzoic acid might be an orally effective, iron-chelating drug (1). Although subsequent clinical evaluation confirmed this report (2–4), it was not possible to maintain patients in iron balance.

A chelating agent with a greater affinity for iron presumably would be more effective. Several iron-sequestering agents produced by microbes are conjugates of 2,3-dihydroxybenzoic acid (5–9). These compounds all possess affinities for iron that are many orders of magnitude greater than the affinity of the parent compound. One of these compounds, N^1,N^8-bis(2,3-dihydroxybenzoyl)spermidine (8), removes iron from the ferritin of cultured Chang cells and from transferrin, the principal iron-binding protein of serum (10).

The synthesis of N^1,N^8-bis(2,3-dihydroxybenzoyl)-spermidine hydrochloride (XVII) together with a series of simpler analogs is presented in this report. Preliminary evidence suggests that this type of compound may be useful in iron-chelation therapy whereas the corresponding 2-hydroxybenzoyl derivatives are inactive. The *in vitro* and *in vivo* evaluation of these compounds will be presented later.

DISCUSSION

Prior to the synthesis of XVII, a series of simpler analogs, *i.e.*, *N,N'*-bis(2,3-dihydroxybenzoyl)-α,ω-diaminoalkanes, was prepared. Like the spermidine derivative, these compounds would be expected to bind iron strongly, their affinities for iron and perhaps their biological activities being related to the separation of the 2,3-dihydroxybenzoyl moieties. The compounds were obtained readily in a 40–50% yield *via* the reaction of 2,3-dioxosulfinylbenzoyl chloride (11) with the appropriate α,ω-diaminoalkane in tetrahydrofuran (Procedure A). Since the goal of this program was to obtain enough pure material for biological testing, no attempt was made to optimize the yield of this or subsequent reactions.

All compounds were obtained as solids which were purified by recrystallization. The ethane (I) and propane (II) derivatives were somewhat unique in that they were crystallized from aqueous methanol as their hydrates. Compound I was obtained as a monohydrate, with the water of crystallization being lost upon drying under vacuum at 78° for 4 hr. Compound II was obtained from aqueous methanol as the dihydrate. Drying caused the loss of both moles of water, as evidenced by elemental analysis.

The identity of I, II, and V was confirmed *via* independent synthesis. Two moles of 2,3-diacetoxybenzoic acid were condensed with ethylenediamine, 1,3-diaminopropane, or 1,6-diaminohexane *via* activation with *N,N'*-dicyclohexylcarbodiimide (Procedure B). Subsequent hydrolysis of the protecting groups yielded products (40%) identical to those obtained by Procedure A. Compound II also was prepared by fusing methyl 2,3-dihydroxybenzoate and 1,3-diaminopropane at 130° under nitrogen (Procedure C). The latter procedure was used to prepare an analogous series of *N,N'*-bis(2-hydroxybenzoyl)-α,ω-diaminoalkanes (X–XIV).

0022-3549/80/0800-0986$01.00/0

© 1980, American Pharmaceutical Association

Table I—Physical Constants of *N,N'*-Bis(aroyl)-α,ω-diaminoalkanes

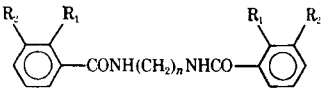

Compound	*n*	R_1	R_2	Method	Yield, %	Melting Point	Recrystallization Solvent	Formula	Analysis, %	Calc.	Found
I	2	OH	OH	A	43	220–221°	Aqueous methanol	$C_{16}H_{16}N_2O_6$	C	57.83	57.63
				B	41				H	4.85	4.86
									N	8.43	8.30
II	3	OH	OH	C	42	168–169°	Aqueous methanol	$C_{17}H_{18}N_2O_6$	C	58.95	59.26
				A	59				H	5.24	5.27
				B	44				N	8.09	8.14
III	4	OH	OH	A	45	210–212°	Aqueous methanol	$C_{18}H_{20}N_2O_6$	C	59.99	59.82
									H	5.59	5.55
									N	7.77	7.70
IV	5	OH	OH	A	40	174–176°	Aqueous methanol	$C_{19}H_{22}N_2O_6$	C	60.95	60.66
									H	5.92	5.95
									N	7.48	7.30
V	6	OH	OH	A	55	184–186°	Aqueous ethanol	$C_{20}H_{24}N_2O_6$	C	61.84	61.69
				B	38				H	6.23	6.24
									N	7.21	7.17
VI	8	OH	OH	A	38	172–174°	Ethyl acetate–petroleum ether	$C_{22}H_{28}N_2O_6$	C	63.45	63.22
									H	6.78	6.70
									N	6.73	6.59
VII	9	OH	OH	A	53	146–147°	Ethyl acetate–petroleum ether	$C_{23}H_{30}N_2O_6$	C	64.16	64.26
									H	7.02	7.04
									N	6.50	6.46
VIII	10	OH	OH	A	51	148–150°	Ethyl acetate–petroleum ether	$C_{24}H_{32}N_2O_6$	C	64.86	64.66
									H	7.20	7.22
									N	6.30	6.26
IX	12	OH	OH	A	54	130–131°	Ethyl acetate–petroleum ether	$C_{26}H_{36}N_2O_6$	C	66.08	66.37
									H	7.68	7.77
									N	5.93	5.94
X	2	OH	H	C	46	187–189°	Ethanol	$C_{16}H_{16}N_2O_4$	C	63.99	64.01
									H	5.37	5.41
									N	9.33	9.34
XI	3	OH	H	C	38	181–182.5°	Ethanol	$C_{17}H_{18}N_2O_4$	C	64.95	65.00
									H	5.77	5.71
									N	8.91	8.79
XII	4	OH	H	C	42	180–181°	Ethanol	$C_{18}H_{20}N_2O_4$	C	65.84	65.91
									H	6.14	6.15
									N	8.53	8.56
XIII	6	OH	H	C	45	141–142.5°	Ethanol	$C_{20}H_{24}N_2O_4$	C	67.39	67.36
									H	6.79	6.73
									N	7.87	7.84
XIV	8	OH	H	C	49	139–140.5°	Ethanol	$C_{22}H_{28}N_2O_4$	C	68.72	68.70
									H	7.34	7.44
									N	7.29	7.32

These compounds chelated iron but failed to induce significant amounts of iron excretion when given intraperitoneally to hypertransfused rats.

Attempts to prepare N^1,N^8-bis(2,3-dihydroxybenzoyl)spermidine *via* Procedure A met with little success. Mixtures were obtained from which the desired compound could not be isolated. The hydrochloride salt (XVII) ultimately was prepared in low yield (14%) *via* treatment of the fusion products of spermidine and methyl 2,3-dihydroxybenzoate with hydrogen chloride (Procedure D). While purification of the free amine proved difficult, the hydrochloride could be purified readily by recrystallization from water. In similar fashion, the corresponding derivatives of diethylenetriamine and 3,3'-diaminodipropylamine were prepared. These hydrochlorides were obtained as the hydrates from which the water was removed upon drying *in vacuo*. N^1,N^5-Bis(2-hydroxybenzoyl)diethylenetriamine (XVIII) also was prepared. This compound was readily obtained as the free amine using Procedure C.

EXPERIMENTAL[1]

Methyl salicylate, 2,3-dihydroxybenzoic acid, *N,N'*-dicyclohexylcarbodiimide, and all of the diamines and triamines were obtained commercially. Methyl 2,3-dihydroxybenzoate was prepared according to the method of Clinton and Laskowski (12), whereas 2,3-diacetoxybenzoic acid was synthesized as described by Simokoriyama (13).

Preparation of Conjugated Derivatives—The general procedures for synthesis of *N,N'*-bis(aroyl)-α,ω-diaminoalkanes and *N,N'*-bis(aroyl)-ω,ω'-diaminodialkylamines are described as follows. The physical constants observed together with the analytical data are summarized in Tables I and II.

Procedure A—A mixture of 15.4 g (0.1 mole) of 2,3-dihydroxybenzoic acid and 35 ml (0.5 mole) of thionyl chloride was heated under reflux for 8 hr. Upon cooling, the residual thionyl chloride was removed under vacuum. To the residue was added ~10 ml of anhydrous benzene, which was evaporated under vacuum. This process was repeated three times.

The solid residue containing 2,3-dioxosulfinylbenzoyl chloride (11) then was dissolved in 200 ml of tetrahydrofuran. To this solution were added 0.04 mole of the diamine and 30 g (0.22 mole) of anhydrous potassium carbonate. The reaction mixture was heated under reflux for 12 hr, cooled, and filtered to remove potassium salts. After evaporation of the solvent, 250 ml of water was added and the mixture was allowed to stand at room temperature for 5–6 hr. After the water was decanted, the residue was recrystallized from aqueous methanol.

Procedure B—A solution of 2.1 g (0.01 mole) of *N,N'*-dicyclohexylcarbodiimide and 4.76 g (0.02 mole) of 2,3-diacetoxybenzoic acid in 200 ml of acetonitrile containing 2 ml of pyridine was stirred at room temperature for 2 hr. The precipitated dicyclohexylurea was removed by filtration, and 0.005 mole of the diamine and 1.75 ml (0.0125 mole) of triethylamine were added. The reaction mixture was allowed to stir overnight at room temperature under nitrogen.

The solvent was evaporated under reduced pressure, and the residue

[1] Melting points were determined with a capillary melting-point apparatus and are uncorrected. TLC was carried out on silica gel with benzene–methanol–acetic acid (45:8:1) as the eluent. Compounds were visualized by spraying first with 0.5% ferric chloride and then with either 1% basic permanganate reagent or 50% H_2SO_4 (charred). For identification, NMR spectra were determined at 60 MHz in acetone-d_6 or dimethyl sulfoxide-d_6 containing a few drops of deuterium oxide. In all cases, the integrals and chemical shifts were in agreement with those expected. The spectra of representative compounds (V, XIII, and XVII) were determined at 220 MHz in dimethyl sulfoxide-d_6 containing deuterium oxide. Values are reported in parts per million (δ) downfield from tetramethylsilane (the internal standard).

Table II—Physical Constants of *N,N'*-Bis(aroyl)-ω,ω'-diaminodialkylamines

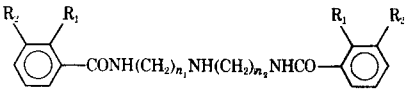

Compound	n_1	n_2	R_1	R_2	Method	Yield, %	Melting Point	Recrystallization Solvent	Formula	Analysis, %	Calc.	Found
XV	2	2	OH	OH	D	18	163–165°	Water	$C_{17}H_{21}N_3O_6$·HCl	C	52.49	52.51
										H	5.34	5.28
										N	10.20	10.12
XVI	3	3	OH	OH	D	16	115–117°	Water	$C_{19}H_{25}N_3O_6$·HCl	C	54.69	54.62
										H	5.95	6.02
										N	9.55	9.31
XVII	3	4	OH	OH	D	14	205–207°	Water	$C_{20}H_{27}N_3O_6$·HCl	C	55.56	55.33
										H	6.17	6.02
										N	9.26	8.98
XVIII	2	2	OH	H	C	37	151.5–153°	Ethanol	$C_{18}H_{21}N_3O_4$	C	62.96	63.02
										H	6.16	6.09
										N	12.24	12.27

was taken up in ethyl acetate. This solution was washed with 10% HCl (two times), 10% $NaHCO_3$, and water. The solvent was evaporated, leaving a residual semisolid, which then was dissolved in methanol (30 ml) to which was added 10 ml of 4 *N* NaOH. This solution was stirred under nitrogen at room temperature for 1 hr, after which it was acidified with 10% HCl. The solvent was evaporated, and the residue was crystallized from aqueous methanol.

Procedure C—To a 50-ml, round-bottom flask were added 21 g (17.9 ml, 0.138 mole) of methyl salicylate and 0.067 mole of the diamine (or triamine). An immediate reaction took place with generation of heat. Precipitation often ensued. The reaction mixture then was heated under nitrogen at 130° for 3 hr. Upon cooling, the residue was recrystallized from 95% ethanol.

Procedure D—To a 100-ml, round-bottom flask were added 0.03 mole of the triamine and 0.06 mole of methyl 2,3-dihydroxybenzoate. This mixture was heated under nitrogen at 130–140° for 3 hr. Upon cooling, the viscous residue was dissolved in 200 ml of methanol. The resulting solution was concentrated to ~50 ml and poured into 200 ml of anhydrous ether.

After stirring at room temperature for 30 min, the precipitate was collected by suction filtration and dissolved in 200 ml of methanol. This solution was saturated with hydrogen chloride, concentrated to ~50 ml, and poured into 200 ml of anhydrous ether. After stirring for 30 min, the ether was decanted and the residue was recrystallized from water.

***N,N'*-Bis(2,3-dihydroxybenzoyl)ethylenediamine (I)**—Compound I was prepared according to Procedure A. The solid obtained was recrystallized twice from aqueous methanol to yield 7.6 g (43%) of I as tiny tan needles, which were pure as evidenced by TLC. Elemental analysis revealed that the material was a monohydrate. Drying *in vacuo* at 78° for 8 hr caused loss of the water of crystallization.

Compound I also was prepared according to Procedure B. The synthesis was carried out as described, except that pyridine was used in place of triethylamine. The semisolid obtained was recrystallized from aqueous methanol to yield 0.72 g (41%) of light-tan needles, mp 220–221°. The melting point was not depressed upon admixture with the sample prepared according to Procedure A. TLC and the NMR spectra showed that the two samples were identical. Elemental analysis of a sample dried at 78° for 8 hr verified it as $C_{16}H_{16}N_2O_6$.

***N,N'*-Bis(2,3-dihydroxybenzoyl)-1,3-diaminopropane (II)**—Compound II was prepared by Procedure C. Upon cooling, the reaction mixture was dissolved in ethanol (50 ml). This solution was poured into 50 ml of water containing a few drops of acetic acid. After stirring at room temperature for 30 min, the solid (6.3 g) was collected by filtration. TLC showed that this solid was nearly pure; it was contaminated with a small amount of methyl 2,3-dihydroxybenzoate together with traces of the mono adduct. Addition of more water to the filtrate gave additional product, but it was very impure.

The solid (6.3 g) was dissolved in 25 ml of ethanol and decolorized with charcoal. Addition of 25 ml of water to the pale-orange solution yielded the desired compound upon cooling. The pink needles (4.8 g, 42%) melted over a wide range, depending on the rate of heating. Elemental analysis revealed that the compound contained 2 moles of water. After drying at 78° for 6 hr, the compound melted at 168–169°. Both moles of water were lost after drying, as evidenced by elemental analysis.

A second sample of II was prepared by Procedure A. The semisolid obtained was recrystallized twice from aqueous methanol to yield 9.0 g (59%) of II. TLC revealed that the material was pure and that it cochromatographed with a sample of the material prepared by Procedure C.

This compound also was synthesized from 2,3-diacetoxybenzoic acid according to Procedure B. The semisolid obtained was recrystallized twice from aqueous methanol to yield 0.85 g (44%) of tiny pink needles. TLC revealed that the material was pure and that it cochromatographed with the product obtained *via* Procedure C. The melting point of a sample dried *in vacuo* at 78° for 4 hr and admixed with a similar sample prepared according to Procedure C was not depressed. Likewise, the NMR spectrum was identical to that of a sample prepared according to Procedure C.

***N,N'*-Bis(2,3-dihydroxybenzoyl)-1,4-diaminobutane (III)**—Compound III was prepared according to Procedure A. The semisolid obtained was crystallized from aqueous ethanol and then was recrystallized from aqueous methanol to yield 5.8 g (45%) of III as an amorphous tan solid, mp 210–212°. The NMR spectrum and elemental analysis were in agreement with those expected.

***N,N'*-Bis(2,3-dihydroxybenzoyl)-1,5-diaminopentane (IV)**—Compound IV was prepared according to Procedure A. The semisolid residue was dissolved in ethyl acetate and then extracted with 10% $NaHCO_3$, water, and saturated sodium chloride. After drying over anhydrous magnesium sulfate, the ethyl acetate was removed *in vacuo*. The residual solid was recrystallized from aqueous methanol to give 5.8 g (40%) of IV as an amorphous tan solid, mp 174–176°.

***N,N'*-Bis(2,3-dihydroxybenzoyl)-1,6-diaminohexane (V)**—Compound V was synthesized *via* Procedure A. The reaction product was recrystallized twice from aqueous ethanol, yielding 8.3 g (55%) of a cream-colored amorphous solid, mp 184–186°; NMR (dimethyl sulfoxide-d_6–deuterium oxide): δ 7.26 [dd, 2H, $^3J(H^6\text{–}H^5) \simeq 8.1$, $^4J(H^6\text{–}H^4) \simeq 1.2$, aromatic C_6-H], 6.93 [dd, 2H, $^3J(H^5\text{–}H^6) \simeq 7.9$, $^4J(H^4\text{–}H^6) \simeq 1.2$, aromatic C_4-H], 6.69 [m, 2H, $^3J(H^5\text{–}H^4) \simeq {}^3J(H^5\text{–}H^6) \simeq 7.9$, $^4J(H^4\text{–}H^6) \simeq 1.2$, aromatic C_5-H], 3.28 (m, 4H, $J \simeq 6.8$, $NHCH_2$), 1.54 (m, 4H, $NHCH_2CH_2$), and 1.34 (m, 4H, $NHCH_2CH_2CH_2$).

Compound V also was synthesized by Procedure B. Pyridine was employed rather than triethylamine. The product obtained was recrystallized twice from aqueous methanol, yielding 0.73 g (38%) of a light-tan solid, mp 184–186°. The mixed melting point of this product with that obtained *via* Procedure A was not depressed. TLC and NMR spectroscopy revealed that the two compounds were identical.

***N,N'*-Bis(2,3-dihydroxybenzoyl)-1,8-diaminooctane (VI)**—Compound VI was prepared according to Procedure A. The reaction product was taken up in ethyl acetate and washed successively with 10% $NaHCO_3$ (twice), water, and saturated sodium chloride. Recrystallization (twice) from ethyl acetate–petroleum ether (60–90°) gave 6.4 g (38%) of tan crystals, mp 172–174°.

***N,N'*-Bis(2,3-dihydroxybenzoyl)-1,9-diaminononane (VII)**—Compound VII was prepared exactly as was VI using Procedure A. The compound was isolated (9.2 g, 53%) as tiny cream-colored needles after recrystallization (twice) from ethyl acetate–petroleum ether (60–90°). The NMR spectrum and elemental analysis were in agreement with the theory.

***N,N'*-Bis(2,3-dihydroxybenzoyl)-1,10-diaminodecane (VIII)**—Compound VIII was prepared exactly as was VI using Procedure A. The product was obtained (9.1 g, 51%) as a tan powder, mp 148–150°. TLC revealed that the material was pure. The elemental analysis and the NMR spectrum were in agreement.

***N,N'*-Bis(2,3-dihydroxybenzoyl)-1,12-diaminododecane (IX)**—Compound IX was prepared as was VI using Procedure A. The product

(10.2 g, 54%) was obtained as a cream-colored powder, mp 130–131°. The NMR spectrum agreed with that expected.

***N,N'*-Bis(2-hydroxybenzoyl)ethylenediamine (X)**—Compound X was prepared according to Procedure C. The reaction mixture was dissolved in methanol, and this solution then was poured into ether. After stirring at room temperature for 1 hr, the solid was collected by filtration. This solid was recrystallized from ethanol to give 8.3 g (46%) of cream-colored crystals, mp 187–189°.

***N,N'*-Bis(2-hydroxybenzoyl)-1,3-diaminopropane (XI)**—Compound XI was prepared according to Procedure C. Upon cooling, the reaction mixture was dissolved in 50 ml of methanol. To this solution was added 50 ml of water containing a few drops of acetic acid. Upon stirring at room temperature, the oily precipitate solidified. The solid (13.5 g) was recrystallized twice from ethanol (100 ml) to yield 7.2 g (38%) of white crystals, which were pure by TLC, mp 181–182.5°.

***N,N'*-Bis(2-hydroxybenzoyl)-1,4-diaminobutane (XII)**—Compound XII was prepared according to Procedure C. The solid reaction mixture was dissolved in methanol, and the product was precipitated *via* the addition of water. The product (15.9 g) was recrystallized from ethanol (75 ml) to yield 8.2 g (42%) of shiny white plates, which were pure by TLC, mp 180–181°.

***N,N'*-Bis(2-hydroxybenzoyl)-1,6-diaminohexane (XIII)**—Compound XIII was prepared according to Procedure C. The waxy solid residue was crystallized from 35 ml of ethanol, yielding 10.9 g of product. TLC showed that this product contained some of the mono adduct. Recrystallization from ethanol gave 9.7 g (45%) of pure product as waxy white plates, mp 141–142.5°; NMR (dimethyl sulfoxide-d_6–deuterium oxide): δ 7.82 [dd, 2H, $^3J(H^6\text{–}H^5) \simeq 8.1$, $^4J(H^6\text{–}H^4) \simeq 1.3$, aromatic C_6-H], 7.41 [m, 2H, $^3J(H^4\text{–}H^3) \simeq {}^3J(H^4\text{–}H^5) \simeq 7.7$, aromatic C_4-H], 6.90 [m, 4H, $^3J(H^3\text{–}H^4) \simeq {}^3J(H^5\text{–}H^4) \simeq {}^3J(H^5\text{–}H^6) \simeq 7.9$, aromatic C_5-H and C_3-H], 3.31 (m, 4H, $J \simeq 6.8$, $NHCH_2$), 1.57 (m, 4H, $NHCH_2CH_2$), and 1.36 (m, 4H, $NHCH_2CH_2CH_2$).

***N,N'*-Bis(2-hydroxybenzoyl)-1,8-diaminooctane (XIV)**—Compound XIV was prepared according to Procedure C. The solid reaction mixture was crystallized from ethanol (50 ml), yielding 12.5 g of product. TLC revealed that this product contained a small amount of the mono adduct. Recrystallization from ethanol gave 11.4 g (49%) of product as waxy white plates, mp 139–140.5°.

***N*^{1},*N*^{5}-Bis(2,3-dihydroxybenzoyl)diethylenetriamine Hydrochloride (XV)**—Compound XV was prepared *via* Procedure D from 5.2 g (0.05 mole) of diethylenetriamine and 16.0 g (0.10 mole) of methyl 2,3-dihydroxybenzoate. The hydrochloride was obtained as a cream-colored powder (3.8 g, 18%), mp 163–165°.

***N*^{1},*N*^{7}-Bis(2,3-dihydroxybenzoyl) -3,3'- diaminodipropylamine Hydrochloride (XVI)**—Compound XVI was prepared according to Procedure D exactly as was XV. The hydrochloride was isolated as a cream-colored powder (2.6 g, 16%). After drying at 78° for 4 hr, the elemental analysis confirmed its formula as $C_{19}H_{25}N_3O_6$·HCl. This material failed to melt sharply; a phase transition occurred at 85–87°, after which it melted with decomposition at 115–117°.

***N*^{1},*N*^{8}-Bis(2,3-dihydroxybenzoyl)spermidine Hydrochloride (XVII)**—Compound XVII was prepared by Procedure D from 5 g (0.034 mole) of spermidine and 11.6 g (0.07 mole) of methyl 2,3-dihydroxybenzoate. The product was obtained as a light-tan powder (2.2 g, 14%), mp 205–207°. TLC revealed that the compound was pure. After drying at 78° for 6 hr, the compound was free from the water of crystallization as evidenced by elemental analysis. The NMR spectrum of the hydrochloride (dimethyl sulfoxide-d_6–deuterium oxide) gave the following values: δ 7.31 [m, 2H, $^3J(H^6\text{–}H^5) \simeq 7.7$, $^4J(H^6\text{–}H^4) < 1.0$, aromatic C_6-H], 6.95 [d, 2H, $^3J(H^4\text{–}H^5) \simeq 7.9$, $^4J(H^4\text{–}H^6) < 1.0$, aromatic C_4-H], 6.70 [m, 2H, $^3J(H^5\text{–}H^4) \simeq {}^3J(H^5\text{–}H^6) \simeq 7.9$, aromatic C_5-H], 3.36 (m, 4H, $CONHCH_2$), 2.93 (m, 4H, CH_2NHCH_2), 1.91 (m, 2H, $NHCH_2CH_2CH_2NH$), and 1.64 (m, 4H, $NHCH_2CH_2CH_2CH_2NH$).

***N*^{1},*N*^{5}-Bis(2-hydroxybenzoyl)diethylenetriamine (XVIII)**—Compound XVIII was prepared according to Procedure C. Upon cooling, the reaction mixture solidified as a glass. This solid was triturated with methanol from which 14.3 g of solid separated. The solid was recrystallized from ethanol to yield 8.4 g (37%) of slightly orange crystals, mp 151.5–153°. The NMR spectrum and elemental analysis were in agreement with those expected.

REFERENCES

(1) J. H. Graziano, R. W. Grady, and A. Cerami, *J. Pharmacol. Exp. Ther.*, **190**, 570 (1974).

(2) C. M. Peterson, J. H. Graziano, R. W. Grady, R. L. Jones, H. V. Vlassara, V. C. Canale, D. R. Miller, and A. Cerami, *Br. J. Haematol.*, **33**, 477 (1976).

(3) C. M. Peterson and R. L. Jones, in "Iron Metabolism and Thalassemia," D. Bergsma, A. Cerami, C. M. Peterson, and J. H. Graziano, Eds., Alan R. Liss, New York, N.Y., 1976, pp. 187–192.

(4) C. M. Peterson, J. H. Graziano, R. W. Grady, R. L. Jones, A. Markenson, V. Levi, V. Canale, G. E. Gray, A. Cerami, and D. R. Miller, *Exp. Hematol.*, **7**, 74 (1979).

(5) T. Ito and J. B. Neilands, *J. Am. Chem. Soc.*, **80**, 4645 (1958).

(6) I. G. O'Brien, G. B. Cox, and F. Gibson, *Biochim. Biophys. Acta*, **177**, 321 (1969).

(7) J. L. Corbin and W. A. Bulen, *Biochemistry*, **8**, 757 (1969).

(8) G. H. Tait, *Biochem. J.*, **146**, 191 (1975).

(9) I. G. O'Brien and F. Gibson, *Biochim. Biophys. Acta*, **215**, 393 (1970).

(10) A. Jacobs, G. P. White, and G. P. Tait, *Biochem. Biophys. Res. Commun.*, **74**, 1626 (1977).

(11) F. W. Weitl and K. N. Raymond, *J. Am. Chem. Soc.*, **101**, 2728 (1979).

(12) R. O. Clinton and S. C. Laskowski, *ibid.*, **70**, 3135 (1948).

(13) V. M. Simokoriyama, *Bull. Chem. Soc. Jpn.*, **16**, 284 (1941).

ACKNOWLEDGMENTS

Supported by National Institutes of Health Grant AM-18894, The National Foundation March of Dimes Grant 1-615, and grants from Cooley's Anemia Volunteers, Cooley's Anemia Foundation, and the American Hellanic Educational Progressive Association.

Indole–Catechol Charge Transfer Complexes I

Keyphrases □ Catechol—charge transfer complex with indoles □ Indoles—charge transfer complex with catechol □ Charge transfer complexes—interaction of catechol and indoles

To the Editor:

The involvement of charge transfer phenomena, based on UV absorption measurements, was hypothesized between catechol-containing substances and the nucleic acid bases in the mechanism of action of biogenic amines as well as in their storage in the adrenal medulla and other nerve endings (1, 2). In continuing efforts to elucidate this effect in nerve conduction, the interaction between (−)-tryptophan and catechol was studied by UV absorption and emission techniques in aqueous solutions.

Figure 1 shows that the mixture containing (−)-tryptophan and catechol is shifted toward longer wavelengths and is accompanied by an increase in absorbance from that representing the sum of the absorbances of the single pure substances, indicating complex formation[1]. The increase in absorbance is attributed to the (−)-tryptophan–catechol complex and is used to calculate the equilibrium constant by applying the Benesi–Hildebrand equation:

$$\frac{[A_0]}{A_\lambda^{AD}} = \frac{1}{\epsilon_\lambda^{AD}} + \frac{1}{K_{abs}\epsilon_\lambda^{AD}[D_0]} \qquad \text{(Eq. 1)}$$

where $[A_0]$ and $[D_0]$ represent the total concentrations of the reactants, A_λ^{AD} and ϵ_λ^{AD} are the absorbance and molar absorptivity at a given wavelength, and K_{abs} is the equilibrium constant. Equation 1 is based on the assumptions that a 1:1 complex is formed and that $[A_0] \ll [D_0]$. A plot of $[A_0]/A_\lambda^{AD}$ *versus* $1/[D_0]$, with $[A_0]$ kept constant, gave a straight line (Fig. 2). The equilibrium constant calculated from the slope and intercept of the plot, when treated by the least-squares method, was 0.178 ± 10% M^{-1} in 10^{-3} M cacodylate buffer at pH 5 and 15° while the molar absorptivity at the wavelength of the measurement (306 nm) was 99.2 ± 2%.

Fluorescence measurements frequently are used to study complex formation (3). To allow meaningful comparison, the system was studied by this method under similar conditions in neutral solutions. When (−)-tryptophan was excited at 275 nm, the maximum emission wavelength observed was 365 nm. The fluorescence of (−)-tryptophan was quenched upon addition of catechol[2] (Fig. 3). The fraction of the fluorescence intensity remaining is a function of the concentrations of both components.

The equilibrium constant obtained from the fluorescence measurements, K_{fluo}, is calculated from:

$$\frac{1-\beta}{\beta} = K_{fluo}\{[D_0] - [A_0](1-\beta)\} \qquad \text{(Eq. 2)}$$

where β represents the relative fluorescence intensity

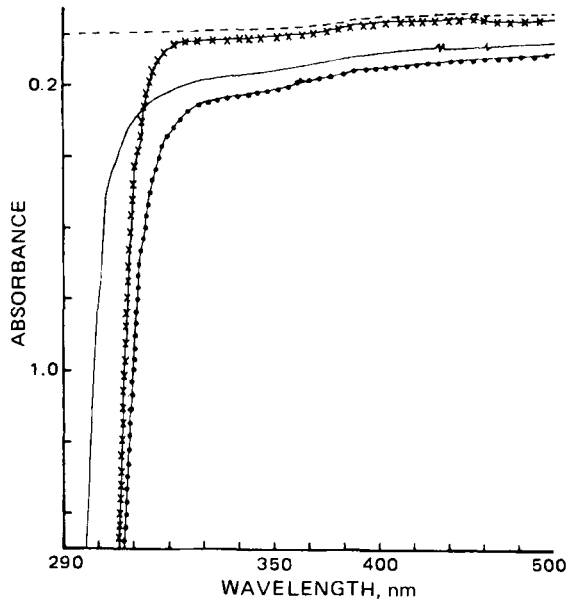

Figure 1—*Absorption spectra of 2 × 10^{-2} M (−)-tryptophan (-×-×), 1 M catechol (—), and 2 × 10^{-2} M (−)-tryptophan with 1 M catechol (-●-●); the broken line (- - -) represents the baseline. All solutions were in 10^{-3} M cacodylate buffer at pH 5. Measurements were made in 0.5-cm path length cells at 15°.*

observed. Equation 2 is based on the assumption that a 1:1 complex is formed; the complex does not fluoresce, and the fluorescence intensity is related linearly to concentration. Nearly equal K_{fluo} values (6.152 × 10^3 ± 17% M^{-1}) were found when fixed concentrations of (−)-tryptophan (10^{-5} and 10^{-4} M) and varying concentrations of catechol (up

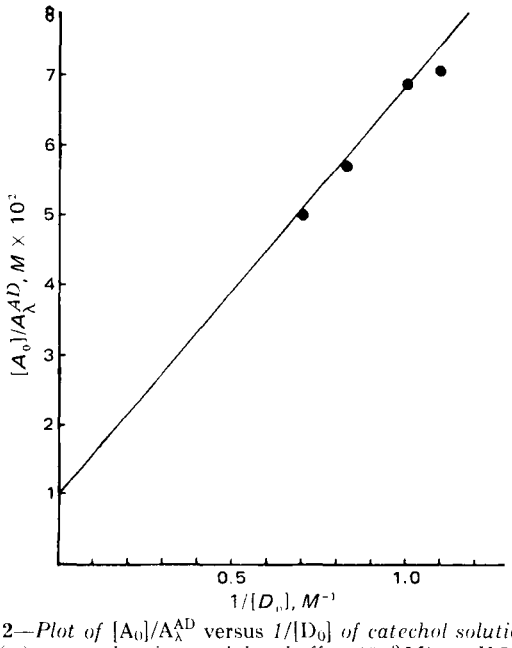

Figure 2—*Plot of $[A_0]/A_\lambda^{AD}$ versus $1/[D_0]$ of catechol solutions containing (−)-tryptophan in cacodylate buffer (10^{-3} M) at pH 5 and 15°. The total concentration of (−)-tryptophan, $[A_0]$, was 2 × 10^{-2} M; the total concentration of catechol, $[D_0]$, was 0.9–1.4 M; A_λ^{AD} represents the absorbance of the complex in a 1-cm path length cell at 306 nm.*

[1] Absorbances were measured with a Perkin-Elmer model 402 UV–visible spectrophotometer.

[2] Fluorescence measurements were made with an Aminco-Bowman model J4-8203G spectrophotofluorometer.

0022-3549/80/0800-0990$01.00/0
© 1980, American Pharmaceutical Association

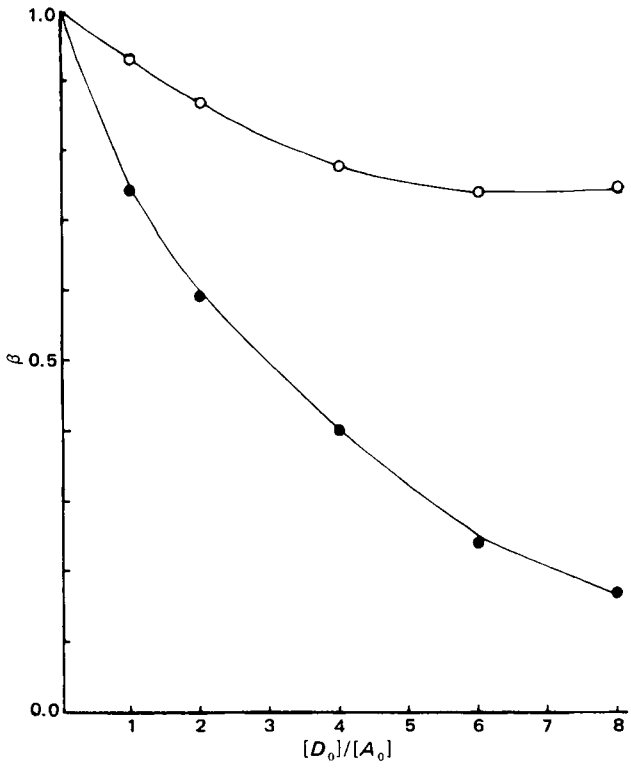

Figure 3—*Change in the relative fluorescence intensity of (−)-tryptophan, β, versus the molar ratio of catechol to (−)-tryptophan, $[D_0]/[A_0]$, at 10^{-5} M (-O-O) and 10^{-4} M (-●-●) (−)-tryptophan in cacodylate buffer (10^{-3} M) at pH 7 and 15°. The excitation wavelength was 275 nm. Fluorescence intensity was measured at 365 nm.*

to eightfold) were used. Furthermore, catechol did not have appreciable fluorescence at the highest concentration used (~5% from the total fluorescence intensity at the wavelength used).

In correlating the equilibrium constants obtained by the methods, a quenching coefficient, γ, is introduced in calculating the true (thermodynamic) equilibrium constant, K_t, from the simple mathematical model proposed:

$$K_{fluo} = \frac{[AD]\gamma_{AD}}{[A]\gamma_A[D]\gamma_D} = \frac{[AD]}{[A][D]}\left(\frac{\gamma_{AD}}{\gamma_A\gamma_D}\right) = K_t K_{quen} \qquad \text{(Eq. 3)}$$

$$K_{quen} = \frac{\gamma_{AD}}{\gamma_A\gamma_D} \qquad \text{(Eq. 4)}$$

where K_{quen} is the quenching constant. When K_{quen} was calculated by assuming $K_t \simeq K_{abs}$, it had a value of 3.4562×10^4.

Fluorescence quenching of tryptophan and some other fluorescing compounds was attributed to charge transfer interactions (4). In those studies, tryptophan was considered as an electron donor. It was suggested that the catechol-containing compounds act as electron donors when forming charge transfer complexes with nucleic acid bases in aqueous acidic solutions (1, 2). It may be reasonably concluded that the results presented in this work can be interpreted on the basis of charge transfer effects. It is difficult to assign the donor or acceptor species of the present molecules since precise theoretical data involving molecular orbital calculations of the highest occupied or lowest empty molecular orbitals are either inconsistent or unavailable and the values usually are expressed in terms of resonance units (uncertain quantities). However, it is assumed tentatively that catechol acts as an electron donor while (−)-tryptophan acts as an electron acceptor.

To explain the differences between the equilibrium constants obtained from the two methods as well as the appearance of the quenching constant, it is proposed that one pair of (−)-tryptophan–catechol out of several thousand pairs of molecules, within the concentration limits used, exists in close proximity in the form of a real complex while the rest remain isolated in solution.

On the other hand, to justify the charge transfer mechanism for the observed quenching, we propose a hypothesis of an electron pump through water. Experimental results indicated an observable quenching at concentrations as low as 10^{-5} *M* each (5.5%). Simple calculations revealed that the distance between molecules at 2×10^{-5} *M* is 436.26 Å; the distance between two molecules of water is 3.1 Å. Therefore, under this proposal, an electron can be pumped through ~140 molecules of water.

It is hoped that the results presented here and the theory advanced may help in understanding many important biological processes such as conduction through nerves and other excitable membranes.

(1) F. A. Al-Obeidi and H. N. Borazan, *J. Pharm. Sci.*, **65**, 892, 982 (1976).

(2) H. M. Taha, F. A. Al-Obeidi, and H. N. Borazan, *ibid.*, **68**, 631 (1979).

(3) R. Foster, "Organic Charge Transfer Complexes," Academic, London, England, 1969, pp. 82–89.

(4) M. A. Slifkin, "Charge Transfer Interactions of Biomolecules," Academic, London, England, 1971, pp. 110–149.

Hanna N. Borazan ˣ
Yousif H. Ajeena
Department of Pharmaceutical Chemistry
College of Pharmacy
University of Baghdad
Baghdad, Republic of Iraq

Received August 21, 1979.
Accepted for publication April 9, 1980.
The authors thank the University of Baghdad for financial support of this work. They also thank Dr. Waleed R. Sulaiman for encouragement.

Mass Spectra of Dexamethasone and Betamethasone

Keyphrases □ Dexamethasone—mass spectral analysis, comparison with mass spectrum of betamethasone □ Betamethasone—mass spectral analysis, comparison with mass spectrum of dexamethasone □ Mass spectrometry—comparison of spectra of betamethasone and dexamethasone

To the Editor:

The application of mass spectrometry to the study of steroids provides a powerful tool for establishing the structure and spatial configuration of these complex molecules (1). In particular, the decomposition of steroidal alcohols under electron impact often is specific, with the position of the hydroxyl group affecting the fragmentation pattern of 17-hydroxysteroids, thus allowing discrimination between epimeric alcohols and their derivatives.

However, the occurrence of unwanted phenomena, *e.g.*,

0022-3549/80/0800-0991$01.00/0
© 1980, American Pharmaceutical Association

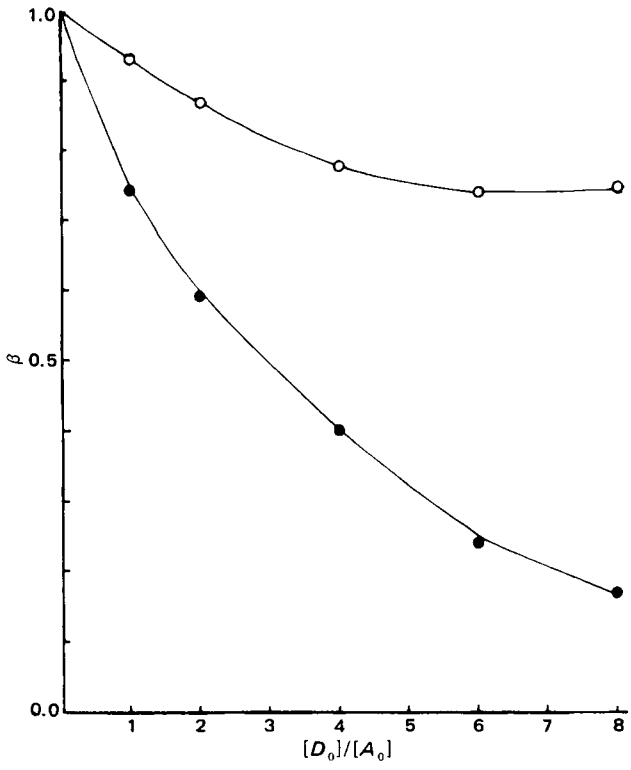

Figure 3—*Change in the relative fluorescence intensity of (−)-tryptophan, β, versus the molar ratio of catechol to (−)-tryptophan, $[D_0]/[A_0]$, at 10^{-5} M (-O-O) and 10^{-4} M (-●-●) (−)-tryptophan in cacodylate buffer (10^{-3} M) at pH 7 and 15°. The excitation wavelength was 275 nm. Fluorescence intensity was measured at 365 nm.*

to eightfold) were used. Furthermore, catechol did not have appreciable fluorescence at the highest concentration used (~5% from the total fluorescence intensity at the wavelength used).

In correlating the equilibrium constants obtained by the methods, a quenching coefficient, γ, is introduced in calculating the true (thermodynamic) equilibrium constant, K_t, from the simple mathematical model proposed:

$$K_{fluo} = \frac{[AD]\gamma_{AD}}{[A]\gamma_A[D]\gamma_D} = \frac{[AD]}{[A][D]}\left(\frac{\gamma_{AD}}{\gamma_A\gamma_D}\right) = K_t K_{quen} \qquad \text{(Eq. 3)}$$

$$K_{quen} = \frac{\gamma_{AD}}{\gamma_A\gamma_D} \qquad \text{(Eq. 4)}$$

where K_{quen} is the quenching constant. When K_{quen} was calculated by assuming $K_t \simeq K_{abs}$, it had a value of 3.4562×10^4.

Fluorescence quenching of tryptophan and some other fluorescing compounds was attributed to charge transfer interactions (4). In those studies, tryptophan was considered as an electron donor. It was suggested that the catechol-containing compounds act as electron donors when forming charge transfer complexes with nucleic acid bases in aqueous acidic solutions (1, 2). It may be reasonably concluded that the results presented in this work can be interpreted on the basis of charge transfer effects. It is difficult to assign the donor or acceptor species of the present molecules since precise theoretical data involving molecular orbital calculations of the highest occupied or lowest empty molecular orbitals are either inconsistent or unavailable and the values usually are expressed in terms of resonance units (uncertain quantities). However, it is assumed tentatively that catechol acts as an electron donor while (−)-tryptophan acts as an electron acceptor.

To explain the differences between the equilibrium constants obtained from the two methods as well as the appearance of the quenching constant, it is proposed that one pair of (−)-tryptophan–catechol out of several thousand pairs of molecules, within the concentration limits used, exists in close proximity in the form of a real complex while the rest remain isolated in solution.

On the other hand, to justify the charge transfer mechanism for the observed quenching, we propose a hypothesis of an electron pump through water. Experimental results indicated an observable quenching at concentrations as low as 10^{-5} *M* each (5.5%). Simple calculations revealed that the distance between molecules at 2×10^{-5} *M* is 436.26 Å; the distance between two molecules of water is 3.1 Å. Therefore, under this proposal, an electron can be pumped through ~140 molecules of water.

It is hoped that the results presented here and the theory advanced may help in understanding many important biological processes such as conduction through nerves and other excitable membranes.

(1) F. A. Al-Obeidi and H. N. Borazan, *J. Pharm. Sci.*, **65**, 892, 982 (1976).

(2) H. M. Taha, F. A. Al-Obeidi, and H. N. Borazan, *ibid.*, **68**, 631 (1979).

(3) R. Foster, "Organic Charge Transfer Complexes," Academic, London, England, 1969, pp. 82–89.

(4) M. A. Slifkin, "Charge Transfer Interactions of Biomolecules," Academic, London, England, 1971, pp. 110–149.

Hanna N. Borazan ˣ
Yousif H. Ajeena
Department of Pharmaceutical Chemistry
College of Pharmacy
University of Baghdad
Baghdad, Republic of Iraq

Received August 21, 1979.
Accepted for publication April 9, 1980.
The authors thank the University of Baghdad for financial support of this work. They also thank Dr. Waleed R. Sulaiman for encouragement.

Mass Spectra of Dexamethasone and Betamethasone

Keyphrases □ Dexamethasone—mass spectral analysis, comparison with mass spectrum of betamethasone □ Betamethasone—mass spectral analysis, comparison with mass spectrum of dexamethasone □ Mass spectrometry—comparison of spectra of betamethasone and dexamethasone

To the Editor:

The application of mass spectrometry to the study of steroids provides a powerful tool for establishing the structure and spatial configuration of these complex molecules (1). In particular, the decomposition of steroidal alcohols under electron impact often is specific, with the position of the hydroxyl group affecting the fragmentation pattern of 17-hydroxysteroids, thus allowing discrimination between epimeric alcohols and their derivatives.

However, the occurrence of unwanted phenomena, *e.g.*,

0022-3549/80/0800-0991$01.00/0
© 1980, American Pharmaceutical Association

Table I—Relative Abundances of the Peaks at *m/e* 315 and 343 in the Mass Spectra of Betamethasone and Dexamethasone

Compound	*m/e*	Relative Abundance[a], %
I	315	3 ± 2[b], 3, ~10
	343	3 ± 2[b], 5, ~12
II	315	40 ± 5[b], 12, ~15
	343	4 ± 2[b], 5, ~76

[a] Refers to the base peak at *m/e* 122. The first value was determined by the present investigator, the second value was taken from Ref. 5, and the third value was obtained from Ref. 2.

thermal decomposition of the sample under the rather drastic conditions prevailing in the ion source, must be given serious consideration with steroids to prevent experimental artifacts.

A case in point is the mass spectral analysis of betamethasone (I) and dexamethasone (II), which are configurational isomers at C-16; their spectra were reported by Lodge and Toft (2, 3). According to these investigators, unequivocal discrimination between the epimers is allowed by the fragment (M − 49) at *m/e* 343, a major peak (actually, the second most abundant ion) in the spectrum of II whose abundance is insignificant in the spectrum of I. Formation of the fragment was traced (2, 3) to the preliminary loss of water from the D-ring followed by cleavage of the 20,21-bond, which should be favored in II according to a mechanism similar to that suggested by Zaretskii *et al.* (4) for the epimers of 17-alkyl-19-nortestosterone.

While these results and their interpretation remain unchallenged in the literature, there are indications (5) of unsuccessful attempts to corroborate the occurrence of a major peak at *m/e* 343 in the mass spectrum of II together with the suggestion that the spectrum may be affected greatly by the thermal decomposition of the sample. In view of the pharmaceutical relevance of the epimeric pair involved, a systematic investigation was undertaken to reconcile the discrepancy and to evaluate the effects of the possible instrumental artifacts.

Authentic samples of I and II from different sources, whose identity and purity had been checked by melting-point determination, IR spectroscopy, and high-pressure liquid chromatography (HPLC), were analyzed on a quadrupole spectrometer[1] and two magnetic sector spectrometers[2]. An effort was made to duplicate as closely as possible the conditions described previously (2, 3), using a direct-insertion probe temperature of 180–200° and an electron energy of 70 ev.

The results confirm that the molecular ion is barely detectable and indicate that the base peak in the spectra of both I and II is the ion at *m/e* 122. However, other significant features of the spectra, including the peaks at *m/e* 315 and 343, differ significantly from previously reported values (Table I).

The discrepancies clearly are too large to be explained by instrumental factors and suggest that thermal decomposition of the sample plays a significant role. This view is supported by the correspondingly large scatter (~22°) of the melting points reported in the literature and their dependence on the heating rate (5).

To gather additional evidence on this point, further experiments were carried out using thermogravimetric analysis and mass spectrometry. A sample of II was heated in a thermoanalyzer[3], both in a self-induced atmosphere and in dry nitrogen, from 25 to 220° at rate of 4°/min and then maintained at 220°. A significant (8.1 ± 0.1%) weight loss occurred above 200°, peaking at ~205°.

In a separate experiment, samples of II were heated at 205° in a glass tube under high vacuum (1.5×10^{-6} torr), and a white sublimate was observed immediately above the heated portion of the tube. The composition of the sublimate could be taken as representative of the composition of the vapors above the heated sample under conditions that closely approach those in the ion source. Accordingly, the mass spectrum of the sublimate was recorded and was significantly different from that of pure II. In particular, the relative abundances of the peaks at *m/e* 315 and 343 were 13 and 7%, respectively, which are very close to the values reported in Ref. 5.

These experiments provide compelling evidence that thermal decomposition plays a significant role in the mass spectrum of II, affecting in particular the relative abundances of the peaks at *m/e* 315 and 343. Consequently, the diagnostic value of the fragment at *m/e* 343 in unequivocally distinguishing between I and II is questionable.

If discrimination between the two epimers has to be achieved by mass spectrometry rather than by more suitable techniques, *e.g.*, HPLC, it appears that the most significant diagnostic peak is the one at *m/e* 315. In fact, not only the present data but also those reported in Ref. 5 show that the fragment at *m/e* 315 is consistently and significantly more abundant in the mass spectrum of II than of I.

Any mechanistic interpretation of the electron-induced fragmentation pattern of complicated molecules, especially in those cases where heat-sensitive substances are involved, should be made cautiously.

(1) Z. V. Zaretskii, "Mass Spectrometry of Steroids," Wiley, New York, N.Y., 1976.

(2) B. A. Lodge and P. Toft, *J. Pharm. Sci.*, **59**, 1045 (1970).

(3) B. A. Lodge and P. Toft, *J. Pharm. Pharmacol.*, **23**, 196 (1970).

(4) V. I. Zaretskii, N. S. Wulfson, V. G. Zaikin, V. N. Leonov, and I. V. Torgov, *Tetrahedron*, **24**, 2339 (1968).

(5) E. M. Cohen, in "Analytical Profiles of Drug Substances," vol. 2, K. Florey, Ed., Academic, New York, N.Y., 1973, p. 190.

Marina Attinà
Institute of Pharmaceutical Chemistry
University of Rome
00100 Rome, Italy

Received July 30, 1979.
Accepted for publication May 6, 1980.
Supported by the Italian National Research Council.
The author thanks Dr. F. Cacace for useful suggestions.

[1] Hewlett-Packard model 5980.
[2] AEI model MS-12 and Varian model MAT 311A.
[3] Model TA1, Mettler Co.

REVIEWS

Index Nominum 1980. 10th ed. The Swiss Pharmaceutical Society. 1979. xiv + 913 pp. 21 x 29.5 cm. (Available from Drug Intelligence Publications, Dept. C78, Hamilton, IL 62341.) (*Introduction in French, German, and English; text in French.*)

Index Nominum 1980 is an alphabetical list of generic and trade names of internationally available drug products containing one active substance. Information is given on International Nonproprietary Names (INN) and other generic names, trade names and manufacturers, chemical names and structures, pharmacopeial monographs on each drug, and main therapeutic uses. The 1980 edition lists approximately 3800 compounds and derivatives, approximately 200 of which are new. More than 26,000 references are given.

As with the previous edition, Index Nominum 1980 is a single volume with a single alphabet; readers never have to look up more than one cross-reference to find the main entry. Among the other convenient features retained in this edition are the listing of monograph titles from pharmacopeias of international importance and the distinction of new substances published for the first time by a point preceding the name or synonym.

Staff Review

Selective Toxicity: The Physico-Chemical Basis of Therapy, 6th ed. By ADRIEN ALBERT. Wiley, One Wiley Drive, Somerset, NJ 08873. 1979. 662 pp. 15 × 23 cm. Price $42.50.

The first edition of this book appeared in 1951, and the sixth edition, published recently, is approximately 10% larger than the fifth edition, which was published in 1973.

The book is divided into two parts. The first part is entitled Topics of General Interest and consists of seven chapters (269 pages). The first chapter briefly discusses the principle of selectivity, and the second chapter outlines various steps in correlating chemical structure with biological activity. This account deals mainly with the concept of receptors followed by a discussion of how minor molecular modifications by methyl or methylene groups may affect biological properties. Chapters 3–5 (129 pages) deal with three general principles of selectivity: differences in the distribution of compounds between "economic and uneconomic cells," a comparison of the biochemistry between the same metabolic routes in different biological systems, and comparisons between the structures of different cells and cellular components. Chapter 6 describes some principles of chemotherapy, including a succinct account of drug resistance. This chapter is prefaced by a short but interesting account of various aspects of the history of chemotherapy. The first section of this book concludes with a chapter on pharmacodynamics (70 pages), in which the theme of selective toxicity of a compound in one organism is amplified.

The second section, Studies, in Depth, of Topics from Part I (285 pages), commences with a chapter on the nature of chemical bonding and absorption followed by a chapter on metabolites and antimetabolites. Chapters 10 and 11 are particularly valuable and emphasize the importance of ionization and chelation of compounds in eliciting biological responses. They are followed by two chapters on the covalent bond and stereochemistry. Chapter 14 discusses surface activity. The next chapter deals with biological activity that is not related to chemical structure. A chapter not appearing in previous editions, entitled The Perfection of a Discovery (approximately 5 pages), emphasizes multiple regression analyses, molecular orbital calculations, and molecular conductivity. Four appendixes follow the second section.

On the positive side, many medicinal chemists, pharmacologists, biochemists, and toxicologists will derive some benefit from portions of this book. A number of recent developments in medicinal chemistry are incorporated into this monograph, including certain aspects of cancer, opioid receptors, and robust metal complexes. The bibliography is excellent, and many recent references are included.

On the negative side, although it is difficult to deal adequately with every facet of selective toxicity, there are areas where the present work is lacking. While the author states that regression analysis and other mathematical models are much used, he gives only a brief account of them. Thus, although he deals with this subject on pages 70–75 and 557–562, this account will be considered by some to be a somewhat cursory treatment. Furthermore, a somewhat truncated summary of information is available on prodrugs. Another criticism is the fragmentation of information throughout the book; although it is understood that the classification of the vast amount of information recorded in this book is a difficult art, the value of dividing the book into two parts is not clear to this reviewer. Why go back in Part II and resurrect a theme that was started in Part I? For example, the subject of receptors is introduced on pages 23–39, mentioned briefly again on pages 250–261, and outlined again in Chapter 13. The same approach is used not only for stereochemistry, which is described initially on pages 39–46 and then becomes the subject of an entire chapter, but also for regression analyses, as noted earlier. Presumably, the author would maintain that it is an unreasonably large jump, and, thus, the book may be regarded as too undergraduate oriented for those who are experienced in the chemical–biological interface.

In summary, this book is valuable reading to those interested in chemicals producing biological responses, but medicinal chemists and others will have to delve into other monographs in many cases to obtain a fuller treatment of the subject.

Reviewed by J. R. Dimmock
College of Pharmacy
University of Saskatchewan
Saskatoon, Saskatchewan, S7N 0W0
Canada

Atlas of the Three-Dimensional Structure of Drugs, Vol. 1. By J. P. TOLLENAERE, H. MOEREELS, and L. A. RAYMAEKERS. Elsevier/North-Holland Inc., 52 Vanderbilt Ave., New York, NY 10017. 1979. 322 pp. 17 × 24.5 cm. Price $36.50.

Medicinal chemists should welcome this volume since it is a successful effort to relate appropriate crystallography to the representation of the molecular architecture of compounds from a variety of pharmacological classes.

Representative compounds from the following categories are included: muscarinic agonists and antagonists; nicotinic agonists and antagonists; phenethylamines, catecholamines, and related compounds; H_1- and H_2-histamine receptor agonists and antagonists; opiate receptor agonists and antagonists; serotonin and related compounds; hallucinogens; local anesthetics; antiarrhythmic agents; Ca^{2+}-antagonists; anticonvulsants and sedative hypnotics; diuretics; nonsteroidal anti-inflammatory agents; and anthelmintic, antifungal, and antiprotozoal agents.

The primary objective was to compare and classify the compounds within each class with respect to geometric and conformational characteristics by using crystallographic data, but it was necessary to visualize molecular structures rather than merely rely on interpretations of numerical data in terms of distances and torsion angles. To determine the optimal orientation of so many molecules, interactive computer techniques were used; an APL (A Programming Language) function PROJ was developed to generate numerous orientations from which the final selection was made. Rotation angles around defined x, y, and z axes, the scale, and viewing distance then were transferred and used in the ORTEP (Oak Ridge Thermal Ellipsoid Program), which draws the picture on a CALCOMP plotter. The ORTEP drawings of the molecular structures then were retouched slightly and thus appear very artistically in the book.

The authors emphasize the idea of pharmacological class relationship by representing molecular structure in space in such a manner that common moieties within each class can be recognized. In many cases, a compromise had to be made between strictly analogous orientation of key moieties and clarity of the representation and the authors' attempt to show the intrinsic beauty of molecular architecture. Due to this compromise, not only medicinal chemists who have expertise in crystallography and three-dimensional structural studies, but also most connoisseurs of fine art and fine science will appreciate the beauty of the struc-

tural representations, with one structure per page covering most of the page.

The introduction includes very helpful, brief explanations regarding the structural data bearing on groups, classes, and subclasses of the compounds. Although these comments are not intended to provide complete explanations, they strengthen the perception of intra- and interclass relationships and differences which are reflected by the pictorial representations.

The authors' intent was for this book "to serve as a bridge between crystallographers and structural chemists and those engaged in drug research." This reviewer concludes that the book does in fact provide such an effective bridge. This book therefore is recommended not only to medicinal chemists but also to graduate and undergraduate students in medicinal chemistry and pharmacology.

Reviewed by Jaime N. Delgado
College of Pharmacy
University of Texas at Austin
Austin, TX 78712

Computer-Assisted Drug Design. Edited by E. C. OLSON and R. E. CHRISTOFFERSEN. (ACS Symposium Series 112.) American Chemical Society, 1155 16th St., N.W., Washington, DC 20036. 1979. 619 pp. 15 × 23 cm. Price $40.00.

This book is a collection of 26 presentations made at a recent American Chemical Society symposium entitled "Computer-Assisted Drug Design." The articles cover a few of the theoretical structure–activity relationship methods in use for drug design. The book is divided into four sections covering the assessment of several techniques, drug receptor modeling, examples of some techniques, and applications. A 15-page index completes the book.

A number of articles stand out and deserve comment. In the first section, a review of a few of the general structure–activity relationship methods is attempted. Unfortunately, it is incomplete in its coverage. An article by Topliss *et al.* is a useful description of chance factors in dealing with structure–activity relationship statistics.

In the second section on drug receptor modeling, Andrews briefly discusses transition state analogs. Articles by *Cole et al.*, Marshall *et al.*, and Humber *et al.* on mapping and modeling are of interest. An article by Loew *et al.* on interaction studies on the opiate receptor is well written and of quality. Rohrer *et al.* describe the use of PROPHET in the same section.

In the third section on examples of techniques, articles by Magee, Bersohn, Weintraub, and Stuper *et al.* present useful descriptions of computer-assisted methods of analysis.

The fourth section on applications in drug design contains a refreshingly thorough and accurate review of theoretical structure–activity relationship contributions over the past 15 years by Grunewald *et al.* Articles by Gund *et al.*, Petit *et al.*, and Hodes reveal computer-based applications of theoretical structure—activity relationships.

A number of problems apparent with this book are common to similar efforts to publish quickly everything presented at a symposium. Because of the requirement for speed, there is little opportunity for screening or review, leading to a wide range of scholarship and quality. Since every presentation is published, the amount of background material that can accompany each article is restricted. As a result, a reader outside of the area is not sufficiently informed. In contrast, an investigator in the field probably would turn to the original journal articles of the authors.

The book should be examined by anyone involved or interested in theoretical structure–activity relationship studies in medicinal chemistry.

Reviewed by Lemont B. Kier
School of Pharmacy
Medical College of Virginia
Virginia Commonwealth University
Richmond, VA 23298

REVIEWS

Index Nominum 1980. 10th ed. The Swiss Pharmaceutical Society. 1979. xiv + 913 pp. 21 x 29.5 cm. (Available from Drug Intelligence Publications, Dept. C78, Hamilton, IL 62341.) (*Introduction in French, German, and English; text in French.*)

Index Nominum 1980 is an alphabetical list of generic and trade names of internationally available drug products containing one active substance. Information is given on International Nonproprietary Names (INN) and other generic names, trade names and manufacturers, chemical names and structures, pharmacopeial monographs on each drug, and main therapeutic uses. The 1980 edition lists approximately 3800 compounds and derivatives, approximately 200 of which are new. More than 26,000 references are given.

As with the previous edition, Index Nominum 1980 is a single volume with a single alphabet; readers never have to look up more than one cross-reference to find the main entry. Among the other convenient features retained in this edition are the listing of monograph titles from pharmacopeias of international importance and the distinction of new substances published for the first time by a point preceding the name or synonym.

Staff Review

Selective Toxicity: The Physico-Chemical Basis of Therapy, 6th ed. By ADRIEN ALBERT. Wiley, One Wiley Drive, Somerset, NJ 08873. 1979. 662 pp. 15 × 23 cm. Price $42.50.

The first edition of this book appeared in 1951, and the sixth edition, published recently, is approximately 10% larger than the fifth edition, which was published in 1973.

The book is divided into two parts. The first part is entitled Topics of General Interest and consists of seven chapters (269 pages). The first chapter briefly discusses the principle of selectivity, and the second chapter outlines various steps in correlating chemical structure with biological activity. This account deals mainly with the concept of receptors followed by a discussion of how minor molecular modifications by methyl or methylene groups may affect biological properties. Chapters 3–5 (129 pages) deal with three general principles of selectivity: differences in the distribution of compounds between "economic and uneconomic cells," a comparison of the biochemistry between the same metabolic routes in different biological systems, and comparisons between the structures of different cells and cellular components. Chapter 6 describes some principles of chemotherapy, including a succinct account of drug resistance. This chapter is prefaced by a short but interesting account of various aspects of the history of chemotherapy. The first section of this book concludes with a chapter on pharmacodynamics (70 pages), in which the theme of selective toxicity of a compound in one organism is amplified.

The second section, Studies, in Depth, of Topics from Part I (285 pages), commences with a chapter on the nature of chemical bonding and absorption followed by a chapter on metabolites and antimetabolites. Chapters 10 and 11 are particularly valuable and emphasize the importance of ionization and chelation of compounds in eliciting biological responses. They are followed by two chapters on the covalent bond and stereochemistry. Chapter 14 discusses surface activity. The next chapter deals with biological activity that is not related to chemical structure. A chapter not appearing in previous editions, entitled The Perfection of a Discovery (approximately 5 pages), emphasizes multiple regression analyses, molecular orbital calculations, and molecular conductivity. Four appendixes follow the second section.

On the positive side, many medicinal chemists, pharmacologists, biochemists, and toxicologists will derive some benefit from portions of this book. A number of recent developments in medicinal chemistry are incorporated into this monograph, including certain aspects of cancer, opioid receptors, and robust metal complexes. The bibliography is excellent, and many recent references are included.

On the negative side, although it is difficult to deal adequately with every facet of selective toxicity, there are areas where the present work is lacking. While the author states that regression analysis and other mathematical models are much used, he gives only a brief account of them. Thus, although he deals with this subject on pages 70–75 and 557–562, this account will be considered by some to be a somewhat cursory treatment. Furthermore, a somewhat truncated summary of information is available on prodrugs. Another criticism is the fragmentation of information throughout the book; although it is understood that the classification of the vast amount of information recorded in this book is a difficult art, the value of dividing the book into two parts is not clear to this reviewer. Why go back in Part II and resurrect a theme that was started in Part I? For example, the subject of receptors is introduced on pages 23–39, mentioned briefly again on pages 250–261, and outlined again in Chapter 13. The same approach is used not only for stereochemistry, which is described initially on pages 39–46 and then becomes the subject of an entire chapter, but also for regression analyses, as noted earlier. Presumably, the author would maintain that it is an unreasonably large jump, and, thus, the book may be regarded as too undergraduate oriented for those who are experienced in the chemical–biological interface.

In summary, this book is valuable reading to those interested in chemicals producing biological responses, but medicinal chemists and others will have to delve into other monographs in many cases to obtain a fuller treatment of the subject.

Reviewed by J. R. Dimmock
College of Pharmacy
University of Saskatchewan
Saskatoon, Saskatchewan, S7N 0W0
Canada

Atlas of the Three-Dimensional Structure of Drugs, Vol. 1. By J. P. TOLLENAERE, H. MOEREELS, and L. A. RAYMAEKERS. Elsevier/North-Holland Inc., 52 Vanderbilt Ave., New York, NY 10017. 1979. 322 pp. 17 × 24.5 cm. Price $36.50.

Medicinal chemists should welcome this volume since it is a successful effort to relate appropriate crystallography to the representation of the molecular architecture of compounds from a variety of pharmacological classes.

Representative compounds from the following categories are included: muscarinic agonists and antagonists; nicotinic agonists and antagonists; phenethylamines, catecholamines, and related compounds; H_1- and H_2-histamine receptor agonists and antagonists; opiate receptor agonists and antagonists; serotonin and related compounds; hallucinogens; local anesthetics; antiarrhythmic agents; Ca^{2+}-antagonists; anticonvulsants and sedative hypnotics; diuretics; nonsteroidal anti-inflammatory agents; and anthelmintic, antifungal, and antiprotozoal agents.

The primary objective was to compare and classify the compounds within each class with respect to geometric and conformational characteristics by using crystallographic data, but it was necessary to visualize molecular structures rather than merely rely on interpretations of numerical data in terms of distances and torsion angles. To determine the optimal orientation of so many molecules, interactive computer techniques were used; an APL (A Programming Language) function PROJ was developed to generate numerous orientations from which the final selection was made. Rotation angles around defined x, y, and z axes, the scale, and viewing distance then were transferred and used in the ORTEP (Oak Ridge Thermal Ellipsoid Program), which draws the picture on a CALCOMP plotter. The ORTEP drawings of the molecular structures then were retouched slightly and thus appear very artistically in the book.

The authors emphasize the idea of pharmacological class relationship by representing molecular structure in space in such a manner that common moieties within each class can be recognized. In many cases, a compromise had to be made between strictly analogous orientation of key moieties and clarity of the representation and the authors' attempt to show the intrinsic beauty of molecular architecture. Due to this compromise, not only medicinal chemists who have expertise in crystallography and three-dimensional structural studies, but also most connoisseurs of fine art and fine science will appreciate the beauty of the struc-

REVIEWS

Index Nominum 1980. 10th ed. The Swiss Pharmaceutical Society. 1979. xiv + 913 pp. 21 x 29.5 cm. (Available from Drug Intelligence Publications, Dept. C78, Hamilton, IL 62341.) (*Introduction in French, German, and English; text in French.*)

Index Nominum 1980 is an alphabetical list of generic and trade names of internationally available drug products containing one active substance. Information is given on International Nonproprietary Names (INN) and other generic names, trade names and manufacturers, chemical names and structures, pharmacopeial monographs on each drug, and main therapeutic uses. The 1980 edition lists approximately 3800 compounds and derivatives, approximately 200 of which are new. More than 26,000 references are given.

As with the previous edition, Index Nominum 1980 is a single volume with a single alphabet; readers never have to look up more than one cross-reference to find the main entry. Among the other convenient features retained in this edition are the listing of monograph titles from pharmacopeias of international importance and the distinction of new substances published for the first time by a point preceding the name or synonym.

Staff Review

Selective Toxicity: The Physico-Chemical Basis of Therapy, 6th ed. By ADRIEN ALBERT. Wiley, One Wiley Drive, Somerset, NJ 08873. 1979. 662 pp. 15 × 23 cm. Price $42.50.

The first edition of this book appeared in 1951, and the sixth edition, published recently, is approximately 10% larger than the fifth edition, which was published in 1973.

The book is divided into two parts. The first part is entitled Topics of General Interest and consists of seven chapters (269 pages). The first chapter briefly discusses the principle of selectivity, and the second chapter outlines various steps in correlating chemical structure with biological activity. This account deals mainly with the concept of receptors followed by a discussion of how minor molecular modifications by methyl or methylene groups may affect biological properties. Chapters 3–5 (129 pages) deal with three general principles of selectivity: differences in the distribution of compounds between "economic and uneconomic cells," a comparison of the biochemistry between the same metabolic routes in different biological systems, and comparisons between the structures of different cells and cellular components. Chapter 6 describes some principles of chemotherapy, including a succinct account of drug resistance. This chapter is prefaced by a short but interesting account of various aspects of the history of chemotherapy. The first section of this book concludes with a chapter on pharmacodynamics (70 pages), in which the theme of selective toxicity of a compound in one organism is amplified.

The second section, Studies, in Depth, of Topics from Part I (285 pages), commences with a chapter on the nature of chemical bonding and absorption followed by a chapter on metabolites and antimetabolites. Chapters 10 and 11 are particularly valuable and emphasize the importance of ionization and chelation of compounds in eliciting biological responses. They are followed by two chapters on the covalent bond and stereochemistry. Chapter 14 discusses surface activity. The next chapter deals with biological activity that is not related to chemical structure. A chapter not appearing in previous editions, entitled The Perfection of a Discovery (approximately 5 pages), emphasizes multiple regression analyses, molecular orbital calculations, and molecular conductivity. Four appendixes follow the second section.

On the positive side, many medicinal chemists, pharmacologists, biochemists, and toxicologists will derive some benefit from portions of this book. A number of recent developments in medicinal chemistry are incorporated into this monograph, including certain aspects of cancer, opioid receptors, and robust metal complexes. The bibliography is excellent, and many recent references are included.

On the negative side, although it is difficult to deal adequately with every facet of selective toxicity, there are areas where the present work is lacking. While the author states that regression analysis and other mathematical models are much used, he gives only a brief account of them. Thus, although he deals with this subject on pages 70–75 and 557–562, this account will be considered by some to be a somewhat cursory treatment. Furthermore, a somewhat truncated summary of information is available on prodrugs. Another criticism is the fragmentation of information throughout the book; although it is understood that the classification of the vast amount of information recorded in this book is a difficult art, the value of dividing the book into two parts is not clear to this reviewer. Why go back in Part II and resurrect a theme that was started in Part I? For example, the subject of receptors is introduced on pages 23–39, mentioned briefly again on pages 250–261, and outlined again in Chapter 13. The same approach is used not only for stereochemistry, which is described initially on pages 39–46 and then becomes the subject of an entire chapter, but also for regression analyses, as noted earlier. Presumably, the author would maintain that it is an unreasonably large jump, and, thus, the book may be regarded as too undergraduate oriented for those who are experienced in the chemical–biological interface.

In summary, this book is valuable reading to those interested in chemicals producing biological responses, but medicinal chemists and others will have to delve into other monographs in many cases to obtain a fuller treatment of the subject.

Reviewed by J. R. Dimmock
College of Pharmacy
University of Saskatchewan
Saskatoon, Saskatchewan, S7N 0W0
Canada

Atlas of the Three-Dimensional Structure of Drugs, Vol. 1. By J. P. TOLLENAERE, H. MOEREELS, and L. A. RAYMAEKERS. Elsevier/North-Holland Inc., 52 Vanderbilt Ave., New York, NY 10017. 1979. 322 pp. 17 × 24.5 cm. Price $36.50.

Medicinal chemists should welcome this volume since it is a successful effort to relate appropriate crystallography to the representation of the molecular architecture of compounds from a variety of pharmacological classes.

Representative compounds from the following categories are included: muscarinic agonists and antagonists; nicotinic agonists and antagonists; phenethylamines, catecholamines, and related compounds; H_1- and H_2-histamine receptor agonists and antagonists; opiate receptor agonists and antagonists; serotonin and related compounds; hallucinogens; local anesthetics; antiarrhythmic agents; Ca^{2+}-antagonists; anticonvulsants and sedative hypnotics; diuretics; nonsteroidal anti-inflammatory agents; and anthelmintic, antifungal, and antiprotozoal agents.

The primary objective was to compare and classify the compounds within each class with respect to geometric and conformational characteristics by using crystallographic data, but it was necessary to visualize molecular structures rather than merely rely on interpretations of numerical data in terms of distances and torsion angles. To determine the optimal orientation of so many molecules, interactive computer techniques were used; an APL (A Programming Language) function PROJ was developed to generate numerous orientations from which the final selection was made. Rotation angles around defined x, y, and z axes, the scale, and viewing distance then were transferred and used in the ORTEP (Oak Ridge Thermal Ellipsoid Program), which draws the picture on a CALCOMP plotter. The ORTEP drawings of the molecular structures then were retouched slightly and thus appear very artistically in the book.

The authors emphasize the idea of pharmacological class relationship by representing molecular structure in space in such a manner that common moieties within each class can be recognized. In many cases, a compromise had to be made between strictly analogous orientation of key moieties and clarity of the representation and the authors' attempt to show the intrinsic beauty of molecular architecture. Due to this compromise, not only medicinal chemists who have expertise in crystallography and three-dimensional structural studies, but also most connoisseurs of fine art and fine science will appreciate the beauty of the struc-

tural representations, with one structure per page covering most of the page.

The introduction includes very helpful, brief explanations regarding the structural data bearing on groups, classes, and subclasses of the compounds. Although these comments are not intended to provide complete explanations, they strengthen the perception of intra- and interclass relationships and differences which are reflected by the pictorial representations.

The authors' intent was for this book "to serve as a bridge between crystallographers and structural chemists and those engaged in drug research." This reviewer concludes that the book does in fact provide such an effective bridge. This book therefore is recommended not only to medicinal chemists but also to graduate and undergraduate students in medicinal chemistry and pharmacology.

Reviewed by Jaime N. Delgado
College of Pharmacy
University of Texas at Austin
Austin, TX 78712

Computer-Assisted Drug Design. Edited by E. C. OLSON and R. E. CHRISTOFFERSEN. (ACS Symposium Series 112.) American Chemical Society, 1155 16th St., N.W., Washington, DC 20036. 1979. 619 pp. 15 × 23 cm. Price $40.00.

This book is a collection of 26 presentations made at a recent American Chemical Society symposium entitled "Computer-Assisted Drug Design." The articles cover a few of the theoretical structure–activity relationship methods in use for drug design. The book is divided into four sections covering the assessment of several techniques, drug receptor modeling, examples of some techniques, and applications. A 15-page index completes the book.

A number of articles stand out and deserve comment. In the first section, a review of a few of the general structure–activity relationship methods is attempted. Unfortunately, it is incomplete in its coverage. An article by Topliss *et al.* is a useful description of chance factors in dealing with structure–activity relationship statistics.

In the second section on drug receptor modeling, Andrews briefly discusses transition state analogs. Articles by *Cole et al.*, Marshall *et al.*, and Humber *et al.* on mapping and modeling are of interest. An article by Loew *et al.* on interaction studies on the opiate receptor is well written and of quality. Rohrer *et al.* describe the use of PROPHET in the same section.

In the third section on examples of techniques, articles by Magee, Bersohn, Weintraub, and Stuper *et al.* present useful descriptions of computer-assisted methods of analysis.

The fourth section on applications in drug design contains a refreshingly thorough and accurate review of theoretical structure–activity relationship contributions over the past 15 years by Grunewald *et al.* Articles by Gund *et al.*, Petit *et al.*, and Hodes reveal computer-based applications of theoretical structure—activity relationships.

A number of problems apparent with this book are common to similar efforts to publish quickly everything presented at a symposium. Because of the requirement for speed, there is little opportunity for screening or review, leading to a wide range of scholarship and quality. Since every presentation is published, the amount of background material that can accompany each article is restricted. As a result, a reader outside of the area is not sufficiently informed. In contrast, an investigator in the field probably would turn to the original journal articles of the authors.

The book should be examined by anyone involved or interested in theoretical structure–activity relationship studies in medicinal chemistry.

Reviewed by Lemont B. Kier
School of Pharmacy
Medical College of Virginia
Virginia Commonwealth University
Richmond, VA 23298

tural representations, with one structure per page covering most of the page.

The introduction includes very helpful, brief explanations regarding the structural data bearing on groups, classes, and subclasses of the compounds. Although these comments are not intended to provide complete explanations, they strengthen the perception of intra- and interclass relationships and differences which are reflected by the pictorial representations.

The authors' intent was for this book "to serve as a bridge between crystallographers and structural chemists and those engaged in drug research." This reviewer concludes that the book does in fact provide such an effective bridge. This book therefore is recommended not only to medicinal chemists but also to graduate and undergraduate students in medicinal chemistry and pharmacology.

Reviewed by Jaime N. Delgado
College of Pharmacy
University of Texas at Austin
Austin, TX 78712

Computer-Assisted Drug Design. Edited by E. C. OLSON and R. E. CHRISTOFFERSEN. (ACS Symposium Series 112.) American Chemical Society, 1155 16th St., N.W., Washington, DC 20036. 1979. 619 pp. 15 × 23 cm. Price $40.00.

This book is a collection of 26 presentations made at a recent American Chemical Society symposium entitled "Computer-Assisted Drug Design." The articles cover a few of the theoretical structure–activity relationship methods in use for drug design. The book is divided into four sections covering the assessment of several techniques, drug receptor modeling, examples of some techniques, and applications. A 15-page index completes the book.

A number of articles stand out and deserve comment. In the first section, a review of a few of the general structure–activity relationship methods is attempted. Unfortunately, it is incomplete in its coverage. An article by Topliss *et al.* is a useful description of chance factors in dealing with structure–activity relationship statistics.

In the second section on drug receptor modeling, Andrews briefly discusses transition state analogs. Articles by *Cole et al.*, Marshall *et al.*, and Humber *et al.* on mapping and modeling are of interest. An article by Loew *et al.* on interaction studies on the opiate receptor is well written and of quality. Rohrer *et al.* describe the use of PROPHET in the same section.

In the third section on examples of techniques, articles by Magee, Bersohn, Weintraub, and Stuper *et al.* present useful descriptions of computer-assisted methods of analysis.

The fourth section on applications in drug design contains a refreshingly thorough and accurate review of theoretical structure–activity relationship contributions over the past 15 years by Grunewald *et al.* Articles by Gund *et al.*, Petit *et al.*, and Hodes reveal computer-based applications of theoretical structure—activity relationships.

A number of problems apparent with this book are common to similar efforts to publish quickly everything presented at a symposium. Because of the requirement for speed, there is little opportunity for screening or review, leading to a wide range of scholarship and quality. Since every presentation is published, the amount of background material that can accompany each article is restricted. As a result, a reader outside of the area is not sufficiently informed. In contrast, an investigator in the field probably would turn to the original journal articles of the authors.

The book should be examined by anyone involved or interested in theoretical structure–activity relationship studies in medicinal chemistry.

Reviewed by Lemont B. Kier
School of Pharmacy
Medical College of Virginia
Virginia Commonwealth University
Richmond, VA 23298

SEPTEMBER 1980
VOLUME 69 NUMBER 9

JOURNAL OF PHARMACEUTICAL SCIENCES

MARY H. FERGUSON
Editor

SHELLY ELLIOTT
Production Editor

MARCIA GARTRELL
Copy Editor

NICOLETTE TRIANTAFELLU
Copy Editor

EDWARD G. FELDMANN
Contributing Editor

SAMUEL W. GOLDSTEIN
Contributing Editor

BELLE R. BECK
Editorial Secretary

DAVID BOHARDT
Director of Publications

L. LUAN CORRIGAN
Assistant Director of Publications

EDITORIAL ADVISORY BOARD

JOHN AUTIAN
HERBERT A. LIEBERMAN
NORMAN R. FARNSWORTH
DAVID E. MANN, JR.
WILLIAM O. FOYE
GERALD J. PAPARIELLO
WILLIAM J. JUSKO
EDWARD G. RIPPIE

The *Journal of Pharmaceutical Sciences* (ISSN 0022-3549) is published monthly by the American Pharmaceutical Association (APhA) at 2215 Constitution Ave., N.W., Washington, DC 20037. Second-class postage paid at Washington, D.C., and at additional mailing office.

All expressions of opinion and statements of supposed fact appearing in articles or editorials carried in this journal are published on the authority of the writer over whose name they appear and are not to be regarded as necessarily expressing the policies or views of APhA.

Offices—Editorial, Advertising, and Subscription: 2215 Constitution Ave., N.W., Washington, DC 20037. All Journal staff may be contacted at this address. Printing: 20th & Northampton Streets, Easton, PA 18042.

Annual Subscriptions—United States and foreign, industrial and government institutions $60, educational institutions $60, individuals *for personal use only* $30; single copies $5. All foreign subscriptions add $5 for postage. Subscription rates are subject to change without notice. Members of APhA may elect to receive the *Journal of Pharmaceutical Sciences* as a part of their annual $80 (foreign $85) APhA membership dues.

Claims—Missing numbers will not be supplied if dues or subscriptions are in arrears for more than 60 days or if claims are received more than 60 days after the date of the issue, or if loss was due to failure to give notice of change of address. APhA cannot accept responsibility for foreign delivery when its records indicate shipment was made.

Change of Address—Members and subscribers should notify at once both the Post Office and APhA of any change of address.

Photocopying—The code at the foot of the first page of an article indicates that APhA has granted permission for copying of the article beyond the limits permitted by Sections 107 and 108 of the U.S. Copyright Law provided that the copier sends the per copy fee stated in the code to the Copyright Clearance Center, Inc., 21 Congress St., Salem, MA 01970. Copies may be made for personal or internal use only and not for general distribution.

Microfilm—Available from University Microfilms International, 300 N. Zeeb Road, Ann Arbor, MI 48106.

© Copyright 1980, American Pharmaceutical Association, 2215 Constitution Ave., N.W., Washington, DC 20037; all rights reserved.

TAKING ANIMALS OUT OF THE LAB

If we were to ask our readers whether they favor "research modernization," undoubtedly the response would be one of overwhelming approval.

If we likewise polled them as to whether or not they favor the elimination of animals in pharmaceutical research, we expect that the response would be equally overwhelming in opposition.

Interestingly enough, however, these two apparently different concepts currently bear a very close relationship. Specifically, legislation is now being seriously and actively considered within the U.S. Congress that bears the title "Research Modernization Act" (H.R. 4805), and which has the specific purpose of working toward significant reduction or complete elimination of the use of animals in research.

In itself, legislation of this general nature is not novel, because many bills affecting the use of animals in research have been introduced on numerous occasions in the past; in fact, there are at least three other bills in the present Congress which also have as their objective the reduction or elimination of the use of animals in biomedical research (H.R. 282, H.R. 4479, and H.R. 6847).

What makes H.R. 4805 relatively novel is the appealing approach embodied in the preamble of the bill which states that a national center is to be established to develop and coordinate "alternative methods of research and testing" which do not involve the use of live animals.

Those of our readers who have occasion to see *Science*, the weekly publication of the American Association for the Advancement of Science, may have noted an article which appeared in the May 9, 1980 issue. The article was entitled "Legislating an End to Animals in the Lab," and it carried the subtitle "A bill backed by animal-rights activists could all but outlaw federally funded research using cats, rats, dogs, rabbits . . . ." This article brought into sharp focus the potential impact of the legislation should it be successfully enacted. Moreover, the article likewise revealed the intense support being given the legislation by antivivisectionists and other animal-rights activists.

On the other hand, from our perception we have seen relatively little discussion of this legislation in the scientific or technical press, nor have we heard much mention of it at scientific or technical meetings. Yet, as brought out in the article in *Science*, "Those in the scientific establishment (who have studied the bill) say the impact of such legislation would be catastrophic, ..."

Certainly, the basic nature of pharmaceutical research is such that any abrupt action to diminish the availability and use of animals for research and testing purposes would have a dramatic impact on both drug research and production—animals being widely used not only as precursors to human clinical testing in drug research but also, in many instances, as test subjects in quality control monitoring of drug products in production.

There is no question but that appropriate care, humane treatment, good housing, and a healthy environment must be accorded all research animals. Any noncompliance calls for stringent measures of regulatory enforcement against the violators. Happily, extensive progress had been made in these areas fully a generation ago, and present conditions of animal treatment in virtually all research centers are at a high level and generally in compliance with current legislation dealing with humane care and housing.

Furthermore, simple economic considerations have provided the scientific community with a strong incentive to devise and adopt *in vitro* methods to replace *in vivo* procedures wherever possible. *In vitro* methods are generally less expensive to conduct; they are more consistent and uniform; and their results are generally considerably more accurate. Hence, even in the absence of animal-rights considerations, there is strong motivation for science to replace animal test procedures with alternative methodology wherever possible.

The primary purpose of this editorial is not to serve as a defense for the use of animals in pharmaceutical research and testing. Our readers are fully cognizant of the importance of the use of animals for such purposes. Indeed, many of our readers are personally engaged in activities which involve their directly working with animals on a regular basis.

What we do wish to achieve by this editorial is the alerting of the pharmaceutical scientific community to the existence of this major legislative threat and the probable severity of the results if this innocent-sounding legislation were to be enacted.

It has only been within the last few months that regulatory measures were finalized to eliminate the use of prisoners in drug research as of June 1, 1981. This development is already having severe impact on human clinical research in the United States. If legislation of the sort now before the Congress were enacted relative to ending the use of animals in the laboratory, the ultimate impact would even dwarf that resulting from the regulatory action eliminating the use of prisoners.

Edward G. Feldmann

SEPTEMBER 1980
VOLUME 69 NUMBER 9

JOURNAL OF PHARMACEUTICAL SCIENCES

MARY H. FERGUSON
Editor

SHELLY ELLIOTT
Production Editor

MARCIA GARTRELL
Copy Editor

NICOLETTE TRIANTAFELLU
Copy Editor

EDWARD G. FELDMANN
Contributing Editor

SAMUEL W. GOLDSTEIN
Contributing Editor

BELLE R. BECK
Editorial Secretary

DAVID BOHARDT
Director of Publications

L. LUAN CORRIGAN
Assistant Director of Publications

EDITORIAL ADVISORY BOARD

JOHN AUTIAN
HERBERT A. LIEBERMAN
NORMAN R. FARNSWORTH
DAVID E. MANN, JR.
WILLIAM O. FOYE
GERALD J. PAPARIELLO
WILLIAM J. JUSKO
EDWARD G. RIPPIE

The *Journal of Pharmaceutical Sciences* (ISSN 0022-3549) is published monthly by the American Pharmaceutical Association (APhA) at 2215 Constitution Ave., N.W., Washington, DC 20037. Second-class postage paid at Washington, D.C., and at additional mailing office.

All expressions of opinion and statements of supposed fact appearing in articles or editorials carried in this journal are published on the authority of the writer over whose name they appear and are not to be regarded as necessarily expressing the policies or views of APhA.

Offices—Editorial, Advertising, and Subscription: 2215 Constitution Ave., N.W., Washington, DC 20037. All Journal staff may be contacted at this address. Printing: 20th & Northampton Streets, Easton, PA 18042.

Annual Subscriptions—United States and foreign, industrial and government institutions $60, educational institutions $60, individuals *for personal use only* $30; single copies $5. All foreign subscriptions add $5 for postage. Subscription rates are subject to change without notice. Members of APhA may elect to receive the *Journal of Pharmaceutical Sciences* as a part of their annual $80 (foreign $85) APhA membership dues.

Claims—Missing numbers will not be supplied if dues or subscriptions are in arrears for more than 60 days or if claims are received more than 60 days after the date of the issue, or if loss was due to failure to give notice of change of address. APhA cannot accept responsibility for foreign delivery when its records indicate shipment was made.

Change of Address—Members and subscribers should notify at once both the Post Office and APhA of any change of address.

Photocopying—The code at the foot of the first page of an article indicates that APhA has granted permission for copying of the article beyond the limits permitted by Sections 107 and 108 of the U.S. Copyright Law provided that the copier sends the per copy fee stated in the code to the Copyright Clearance Center, Inc., 21 Congress St., Salem, MA 01970. Copies may be made for personal or internal use only and not for general distribution.

Microfilm—Available from University Microfilms International, 300 N. Zeeb Road, Ann Arbor, MI 48106.

© Copyright 1980, American Pharmaceutical Association, 2215 Constitution Ave., N.W., Washington, DC 20037; all rights reserved.

TAKING ANIMALS OUT OF THE LAB

If we were to ask our readers whether they favor "research modernization," undoubtedly the response would be one of overwhelming approval.

If we likewise polled them as to whether or not they favor the elimination of animals in pharmaceutical research, we expect that the response would be equally overwhelming in opposition.

Interestingly enough, however, these two apparently different concepts currently bear a very close relationship. Specifically, legislation is now being seriously and actively considered within the U.S. Congress that bears the title "Research Modernization Act" (H.R. 4805), and which has the specific purpose of working toward significant reduction or complete elimination of the use of animals in research.

In itself, legislation of this general nature is not novel, because many bills affecting the use of animals in research have been introduced on numerous occasions in the past; in fact, there are at least three other bills in the present Congress which also have as their objective the reduction or elimination of the use of animals in biomedical research (H.R. 282, H.R. 4479, and H.R. 6847).

What makes H.R. 4805 relatively novel is the appealing approach embodied in the preamble of the bill which states that a national center is to be established to develop and coordinate "alternative methods of research and testing" which do not involve the use of live animals.

Those of our readers who have occasion to see *Science*, the weekly publication of the American Association for the Advancement of Science, may have noted an article which appeared in the May 9, 1980 issue. The article was entitled "Legislating an End to Animals in the Lab," and it carried the subtitle "A bill backed by animal-rights activists could all but outlaw federally funded research using cats, rats, dogs, rabbits . . . ." This article brought into sharp focus the potential impact of the legislation should it be successfully enacted. Moreover, the article likewise revealed the intense support being given the legislation by antivivisectionists and other animal-rights activists.

On the other hand, from our perception we have seen relatively little discussion of this legislation in the scientific or technical press, nor have we heard much mention of it at scientific or technical meetings. Yet, as brought out in the article in *Science*, "Those in the scientific establishment (who have studied the bill) say the impact of such legislation would be catastrophic, ..."

Certainly, the basic nature of pharmaceutical research is such that any abrupt action to diminish the availability and use of animals for research and testing purposes would have a dramatic impact on both drug research and production—animals being widely used not only as precursors to human clinical testing in drug research but also, in many instances, as test subjects in quality control monitoring of drug products in production.

There is no question but that appropriate care, humane treatment, good housing, and a healthy environment must be accorded all research animals. Any noncompliance calls for stringent measures of regulatory enforcement against the violators. Happily, extensive progress had been made in these areas fully a generation ago, and present conditions of animal treatment in virtually all research centers are at a high level and generally in compliance with current legislation dealing with humane care and housing.

Furthermore, simple economic considerations have provided the scientific community with a strong incentive to devise and adopt *in vitro* methods to replace *in vivo* procedures wherever possible. *In vitro* methods are generally less expensive to conduct; they are more consistent and uniform; and their results are generally considerably more accurate. Hence, even in the absence of animal-rights considerations, there is strong motivation for science to replace animal test procedures with alternative methodology wherever possible.

The primary purpose of this editorial is not to serve as a defense for the use of animals in pharmaceutical research and testing. Our readers are fully cognizant of the importance of the use of animals for such purposes. Indeed, many of our readers are personally engaged in activities which involve their directly working with animals on a regular basis.

What we do wish to achieve by this editorial is the alerting of the pharmaceutical scientific community to the existence of this major legislative threat and the probable severity of the results if this innocent-sounding legislation were to be enacted.

It has only been within the last few months that regulatory measures were finalized to eliminate the use of prisoners in drug research as of June 1, 1981. This development is already having severe impact on human clinical research in the United States. If legislation of the sort now before the Congress were enacted relative to ending the use of animals in the laboratory, the ultimate impact would even dwarf that resulting from the regulatory action eliminating the use of prisoners.

Edward G. Feldmann

JOURNAL OF PHARMACEUTICAL SCIENCES

SEPTEMBER 1980
VOLUME 69 NUMBER 9

SOINE MEMORIAL SECTION

The articles in this Section came from the former students, colleagues, and friends of the late Professor T. O. Soine in honor and in memory of his outstanding contributions to the pharmaceutical sciences.

Synthesis, Stereochemical Analysis, and Neuromuscular Blocking Activity of Selected *E,E*- and *Z,Z*-Isomeric *O*-Ethers of 4-Androstene-3,17-dione Dioximes

DAVID B. GARCIA *§, ROBERT G. BROWN ‡, and JAIME N. DELGADO ‡x

Received March 29, 1979, from the **College of Pharmacy, Idaho State University, Pocatello, ID 83209,* and the ‡*College of Pharmacy, University of Texas at Austin, Austin, TX 78712.* Accepted for publication December 28, 1979. §Present address: Alcon Laboratories, Product Services Chemistry, Fort Worth, TX 76134.

Abstract □ A number of selected geometric oxime ethers were synthesized as potential neuromuscular blocking agents. The study consisted of the synthesis, separation, and stereochemical analysis of selected compounds followed by a preliminary pharmacological evaluation for neuromuscular blockade. Synthesis of the compounds began with the double oximination of 4-androstene-3,17-dione followed by TLC, column chromatography, and fractional crystallization as the purification methods. These procedures yielded two of the possible four isomers. Configurational assignments on the isolated pair were based on experiments using IR, UV, and NMR spectroscopy. Isomerically pure diethers were prepared by two methods: (*a*) *O*-alkylation of the stereochemically pure dioximes with the appropriate aminoalkyl halide, and (*b*) *O*-alkylation of the dioxime mixture followed by quaternization and subsequent isolation of configurationally pure salts *via* fractional crystallization. A preliminary pharmacological evaluation was conducted by using mice on a treadmill apparatus. Some structure–activity relationships are discussed.

Keyphrases □ 4-Androstene-3,17-dione dioximes—*E,E*- and *Z,Z*-isomeric *O*-ethers, synthesis, stereochemical analysis, and evaluation for neuromuscular blocking activity □ Neuromuscular blocking agents, potential—*E,E*- and *Z,Z*-isomeric *O*-ethers of 4-androstene-3,17-dione dioximes, synthesis, stereochemical analysis, and pharmacological testing

Recent reports from these laboratories discussed oxime derivatives possessing significant anticholinergic activity (1–4). Furthermore, some of the studies (3, 4) supported the idea that the isomeric character of the oxime function results in potency differences among isomeric pairs that could characterize further the cholinergic receptor. On the basis of these findings, this investigation was initiated to study the neuromuscular blockage and receptor activity of oxime ethers.

The oximino ethers chosen were derived from 4-androstene-3,17-dione dioxime and are bisquaternary ammonium compounds (I). These compounds differ from the more classical neuromuscular blocking agents in that their quaternary nitrogens are bridged by 17 or 19 atoms instead of the usual nine to 11 atoms. This feature places the series in the second peak of potency reported by Barlow and Zoller (5).

DISCUSSION

Synthesis and Resolution—The dioximes of 4-androstene-3,17-dione were prepared in good yield using a reported method (6). This method was applied on the assumption that four geometrical isomers would result (II–V). However, numerous attempts by several methods failed to produce four compounds. TLC, column chromatography, and fractional crystallization proved to be suitable and yielded apparently two isomerically pure compounds (fast and slow[1]). NMR spectroscopy (PMR and ^{13}C-NMR) was utilized to verify their isolation.

[1] Fast and slow designate the relative migration rates of the two compounds on the TLC plates.

0022-3549/80/0900-0995$01.00/0
© 1980, American Pharmaceutical Association

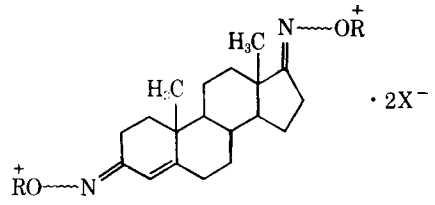

I

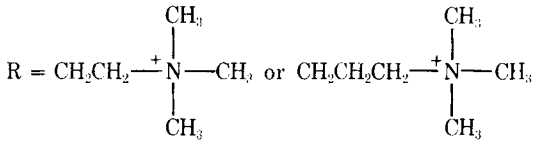

The isolation (and the apparent existence of only two of the possible four isomers) is perplexing since the dioximes that were isolated and stereochemically characterized possess all possible configurations at each oxime site. Furthermore, earlier studies (7–10) involving steroid monooximes showed that the isomeric pairs are separable and distinguishable using available methods. At present, the possibility of specific stereochemical conversion of the *Z,E*- and *E,Z*-isomers to the *E,E*- and *Z,Z*-isomers, respectively, is under consideration. This conversion may be a consequence of the isolation or purification procedures. Indirect evidence for this hypothesis comes from PMR data, which clearly show that the two zones obtained from a dry silica gel column represent configurationally pure compounds. The dioxime mixture is readily distinguishable, with respect to all configurations at both oxime sites, when subjected to PMR analysis.

Two general methods were used in the preparation of isomerically pure oxime ethers. Method A utilized isomerically pure dioximes followed by *O*-alkylation with the appropriate aminoalkyl halide. Method B generated a mixture of ethers from *O*-alkylation of isomerically mixed dioximes. Stereochemically pure material in Method B was obtained by exhaustive quaternization of the free base followed by fractional crystallization.

Stereochemical Analysis—Because of the importance of the stereochemical features of the oxime ethers to the research objectives, several methods were used to identify the configurations at each oxime site. Configurational characterization was restricted mainly to the dioximes and was based on NMR, IR, and UV spectroscopy.

Preliminary NMR Data—There is evidence that, in some cases, proximity of an electronegative atom such as oxygen causes deshielding of protons on adjacent groups (11, 12). Karabotsos *et al.* (13) noted that the α-methylene protons and the imino proton experience greater deshielding as a consequence of the oxime hydroxyl group being in closer proximity; the β-methylene protons are reported to experience a shielding effect under the same conditions (Fragment A). These effects on the α- and β-protons have been verified for this system in carbon tetrachloride,

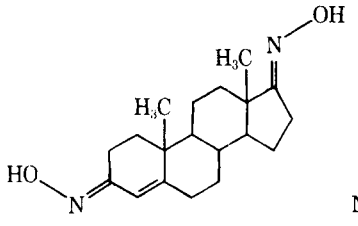

II: *E,E*

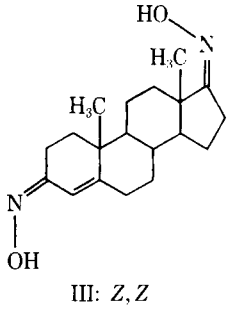

III: *Z,Z*

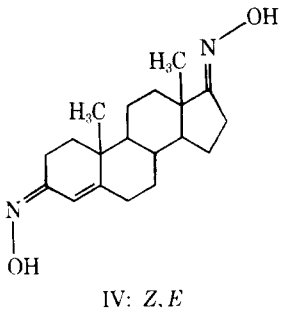

IV: *Z,E*

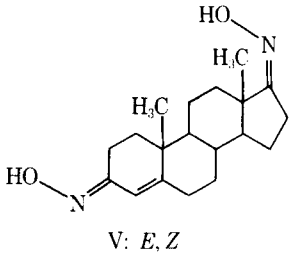

V: *E,Z*

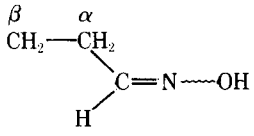

Fragment A

benzene, methylene bromide, and nitrobenzene. The effect on the imino proton appears to be independent of the solvent and the structure. Whereas the imino proton can be used confidently to determine *E*- and *Z*-configurations, assignments based on α- and β-protons are complicated because the structure as well as the solvent reverses the resonance of *E*- and *Z*-hydrogens.

In the present study, preliminary NMR data on the dioximes were generated in dimethyl sulfoxide. A previous study on the oximes of isophorone (compounds resembling the A-ring of the dioximes) supports the suggestion that closer proximity of the oxime hydroxyl group causes deshielding of protons on adjacent groups of the dioximes (11).

For the fast isomer, the chemical shifts were δ 5.63 and 0.94 for the olefinic and 18-methyl protons, respectively. For the slow isomer, the chemical shifts were δ 6.26 and 0.98, respectively.

With the assumption that closer proximity of the oxygen to a group causes deshielding of protons on that group, tentative configurational assignments of *E,E* and *Z,Z* were made for the fast and slow isomers, respectively.

Aromatic Solvent-Induced Shifts—To support the tentative configurational assignments, the two compounds were analyzed *via* the technique of aromatic solvent-induced shifts. Wolkowski *et al.* (14) reported data derived from this technique that allowed identification of the oximes of isophorone.

Using the formula $\Delta\delta = \nu CCl_4 - \nu C_6D_6$, Wolkowski *et al.* (14) obtained $\Delta\delta$ values of −21 and −14 Hz for the olefinic proton of the *Z*-(VII) and *E*-(VI) isomers, respectively. By utilization of the same formula, with the substitution of deuterochloroform for the aliphatic solvent and pyridine (*d*-5) for the aromatic solvent[2], similar calculations were conducted on data derived from the isolated oximes. The fast isomer demonstrated $\Delta\delta$ values of −24 and −3.4 Hz for the olefinic and 18-methyl protons, respectively. The slow isomer showed $\Delta\delta$ values of −32 and −4.4 Hz for the same parameters. Since Wolkowski *et al.* obtained greater negative values for the *Z*-isomer of isophorone oxime, the data indicate that the fast isomer has the *E,E*-configuration and the slow isomer must possess the *Z,Z*-configuration.

NMR Shift Studies—Earlier investigations (15) involving the oximes of isophorone and the shift reagent tris(dipivalomethanato)europium revealed that a greater shift of the olefinic proton is found in the *Z*-isomer. Wolkowski *et al.* (14) extrapolated to an equimolar concentration of the shift reagent and obtained shifts of 27.0 and 22.0 ppm for the *Z*- and *E*-isomers, respectively. However, in the present study, in which the shift reagent tris(1,1,1,1,1,2,2-heptafluoro-7,7-dimethyloctanedione)-europium and the oximes of isophorone were used, the opposite effect was observed (*i.e.*, a greater shift of the olefinic proton in the *E*-isomer). No attempt was made to investigate this apparent anomaly.

Subjecting the dioximes of 4-androstene-3,17-dione to a similar study using the shift reagent tris(1,1,1,1,1,2,2-heptafluoro-7,7-dimethyloctanedione)europium resulted in a greater shift of the olefinic and 18-methyl protons in the fast isomer compared to the shifts in the slow isomer. Since the olefinic proton of the *E*-isomer in isophorone oxime also exhibited greater movement using the same shift reagent, it was concluded that the fast isomer also must possess the *E*-configuration on the A-ring.

The assignments of *E*- and *Z*-configurations at the D-ring to the fast and slow isomers, respectively, unfortunately were not substantiated with a model shift study; consequently, the evidence is not as strong.

IR Data—Several factors have been cited as affecting the stretching

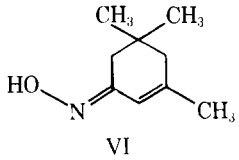

VI

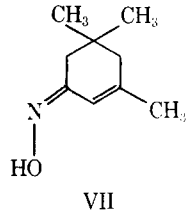

VII

[2] The equation $\Delta\delta = \nu_{aliphatic} - \nu_{aromatic}$ also applies to the substitution of chloroform for carbon tetrachloride and of pyridine for benzene.

frequency of the carbonyl group (16). The position of this particular band in the IR spectrum can be affected by the physical state, electrical and mass effect, conjugation, hydrogen bonding, and ring strain. Since the same factors also are expected to affect the oximino function (C=N) in the same qualitative manner, generalities that apply to a carbonyl system were extrapolated to the oximino systems of the dioximes.

Since ring strain tends to raise the frequency of the C=N group, the higher frequencies in the region of the C=N frequency were assigned to the C=N group of the D-ring. Configurational assignments on the D-ring were made on the basis of data reported by Göndös *et al.* (9). After establishing the configuration of some 17-oximino steroids *via* the Beckman rearrangement reaction, these investigators assigned the higher frequency to the *E*-isomer. Thus, the slow isomer in the present work, which exhibited a frequency of 1681 cm^{-1}, was assigned the *Z*-configuration; the fast isomer, which displayed a frequency of 1704 cm^{-1}, was assigned the *E*-configuration.

By inspection of the oxime function on the A-ring using Dreiding stereomodels, it was noted that more steric hindrance would be realized if the oxime hydroxyl group were in the *Z*-configuration. Since steric hindrance tends to interfere with the coplanarity of the conjugated system, a higher frequency was expected for the isomer with the *Z*-configuration at this site. For the fast isomer, a singlet was recorded at 1634 cm^{-1}; for the slow isomer, a doublet was found at 1642 and 1618 cm^{-1}.

Of significance in these recordings is the fact that the slow isomer did show one elevated frequency (1642 cm^{-1}), but perhaps more informative is the observation that a distinct doublet was detected. This observation possibly could indicate a hybrid situation where perfect overlap between the C=N and C=C groups is not allowed because of the *peri-peri* interactions encounted by the oxime hydroxyl group and the olefinic hydrogen. Thus, on this basis, the slow isomer must be assigned the *Z*-configuration and the fast isomer must have the *E*-configuration.

UV Data—Since oximes show no absorption in the UV spectrum for the C=N group unless it is involved in conjugation (17), the UV analysis was restricted to the oxime function on the A-ring. In this connection, certain α,β-unsaturated carbonyl compounds have been known to possess lower absorptivities when the coplanarity is affected unfavorably (18). Therefore, a lower absorptivity for the *Z*-isomer is expected since, in this isomer, the oxime hydroxyl group would interact significantly with the olefinic hydrogen. Experimentally, the faster isomer demonstrated an absorptivity of 26,898; the slow isomer registered an absorptivity of 22,943. Therefore, the fast isomer was assigned the *E*-configuration and the slow isomer must have the *Z*-configuration at the C-3 oxime site. These assignments are in complete agreement with NMR and IR data.

Conclusion—Based on the evidence, it is concluded that the fast and slow isomers must possess *E,E*- and *Z,Z*-configurations, respectively. These assignments are substantiated by the rule predicting the isomeric ratio (19). The rule predicts that the more nearly equal in bulk the substituent groups attached to the oxime function are, the more nearly equal will be the isomeric ratio.

Oxime Ethers—Studies in these laboratories (3, 4) showed that oximes in general are relatively configurationally stable to the etherification reaction. Thus, in the systems investigated, starting with a configurationally pure oxime will yield a configurationally enriched oxime ether. In the present study, etherification of configurationally enriched dioximes did not produce detectable levels of alternate configurations, as evidenced by PMR spectroscopy. For example, the *Z,Z*- and *E,E*-isomers of the *N,N*-dimethylaminopropyl ethers (free bases) are readily distinguishable by comparison of the chemical shifts for the olefinic protons and the 18-methyl protons. In the *Z,Z*-isomer, the δ values were 5.56 and 1.03, respectively; for the *E,E*-isomer, the same groups had δ values of 6.22 and 1.01.

NMR analysis also was conducted on the quaternary ammonium salts to ensure the configurational purity of the final compounds.

EXPERIMENTAL[3]

Synthesis—4-Androstene-3,17-dione dioximes were prepared according to the method of Crabbé *et al.* (6).

Oxime Ethers—Two general methods were employed for the preparation of isomerically pure oxime ethers. The first method consisted of reacting isomerically pure dioximes (as determined by TLC and NMR spectroscopy) with the appropriate aminoalkyl halide. No problems with configurational conversion were encountered. The second method involved etherification of the mixture of the two dioximes with the appropriate aminoalkyl halide followed by quaternization and fractional crystallization of the mixture produced. Both methods were reliable.

All ethers were prepared by first dissolving the appropriate dioxime in absolute ethanol followed by the addition of the base, potassium *tert*-butoxide. The proper aminoalkyl halide hydrochloride then was added in one portion. All solutions were refluxed and stirred for the prescribed time in a three-necked flask. Subsequent to the reaction interval, the solutions were filtered by suction and evaporated on a rotary evaporator *in vacuo*. This general procedure afforded an oily residue. Variations in reactant quantities and specific procedures, as applicable to the individual ethers, will be given; physical data also are included.

Quaternization of the free bases was effected by dissolving the oily material in absolute ethanol in the presence of excess methyl bromide. The salts were purified by crystallization from a mixture of absolute ethanol and isopropyl ether.

E,E-*4-Androstene-3,17-di*(N,N-*dimethylaminoethyl oximino ether*) *Dimethobromide* (*VIII*)—*E,E*-4-Androstene-3,17-dione dioxime (1.65 g, 0.0052 mole) was dissolved in 90 ml of absolute ethanol. Potassium *tert*-butoxide (2.33 g, 0.021 mole) and 2-dimethylaminoethyl chloride (1.5 g, 0.0104 mole) then were added with constant stirring. After 4.5 hr, the solvent was evaporated, giving an oily residue that was treated with two 25-ml portions of isopropyl ether. Separation of the isopropyl ether layers and evaporation gave a material that subsequently was treated with 20 ml of petroleum ether. The petroleum ether extract was cooled in an acetone–dry ice bath and then removed and allowed to warm to room temperature. Decanting and subsequent evaporation of the warmed petroleum ether extract yielded the first crop of the dioximino ether.

All of the material that was not soluble in the petroleum ether or isopropyl ether was solubilized in ~20 ml of dimethyl sulfoxide and extracted with five 20-ml portions of petroleum ether. Small amounts of water were added between each extraction to reduce the solubility of the ether in the dimethyl sulfoxide. The petroleum ether extracts were combined and treated as before using the acetone–dry ice bath. Evaporation of the petroleum ether yielded a second crop. This procedure yielded a total of 0.7 g of the dioximino ether (29.3% yield); IR: λ_{max} (neat) 1619 (C=N, conjugated), 1667 (C=N, unconjugated), and 1035 (O—C) cm^{-1}; NMR[4]: δ 1.04 (s, 3H, 18-methyl), 2.19 (s, 12H, *N*-methyl protons), ~2.50 (β-methylene protons from both side chains; two almost overlapping A_2X_2 systems), and 5.58 (s, 1H, HC=).

The methobromide salt melted at 221° dec. and was analyzed for carbon, hydrogen, and nitrogen.

Anal.—Calc. for $C_{29}H_{52}Br_2N_4O_2$: C, 53.70; H, 8.08; N, 8.64. Found: C, 53.79; H, 8.13; N, 8.38.

Z,Z-*4-Androstene-3,17-di*(N,N-*dimethylaminoethyl oximino ether*) *Dimethobromide* (*IX*)—A mixture of *Z,Z*- and *E,E*-4-androstene-3,17-dione dioximes (3.0 g, 0.0095 mole) was dissolved in 80 ml of absolute ethanol. While stirring, potassium *tert*-butoxide (4.32 g, 0.039 mole) and 2-dimethylaminoethyl chloride (2.77 g, 0.019 mole) were added. The reaction was allowed to proceed for 8 hr, giving an oily residue upon evaporation of the solvent. The crude product was extracted with several portions of petroleum ether, and the extracts were combined and chilled in an acetone–dry ice bath to precipitate impurities. After the petroleum ether extracts warmed to room temperature, the solvent was decanted and evaporated. This procedure yielded 2.3 g of the ether (40.0% yield).

The oil obtained was dissolved in ~80 ml of absolute ethanol. Excess methyl bromide was added to the alcoholic solution followed by standing for several hours in a stoppered flask. Isopropyl ether was added to the solution of the methobromide salt until cloudiness persisted, and the milky solution was placed on a hot plate until the cloudiness dissipated. Allowing the solution to cool slowly over ~10 hr gave the first crop (0.65 g) of crystals, characterized (*via* NMR) as a mixture of *Z,Z*- and *E,E*-isomers in a 2:1 ratio.

A second crystallization in the same manner afforded a material in which no *E,E*-isomer was detectable. This material was recrystallized four times to ensure the isomeric purity of the product, mp 251° dec.; IR: λ_{max}[3] 1619 (C=N, conjugated), 1646 (C=N, unconjugated), and 1084 (C—O) cm^{-1}; NMR[5]: δ 1.09 (s, 3H, 18-methyl), 3.10 (s, 18H, *N*-methyl protons), and 6.26 (s, 1H, HC=).

[3] Melting points are uncorrected; a Thomas-Hoover Uni-Melt apparatus was used. Elemental analysis were conducted by Schwarzkopf Microanalytical Laboratory, Woodside, N.Y. IR spectra were obtained with a Beckman IR-8 spectrophotometer; spectra of oils were obtained using sodium chloride windows; spectra of salts utilized potassium bromide dispersion pellets. PMR spectra were produced on Varian A-60, Varian 100-MHz, and Jeol C-60hl spectrometers. ^{13}C-NMR spectra were taken on a Bruker WH 90 spectrometer. Optical rotations were obtained with a Perkin-Elmer 141 polarimeter.

[4] Chloroform-*d*; tetramethylsilane was the reference.

[5] Dimethyl sulfoxide-*d* was the solvent; the pentet for dimethyl sulfoxide-*d* at δ 2.5 was used as the reference.

Anal.—Calc. for $C_{29}H_{52}Br_2N_4O_2$: C, 53.70; H, 8.08; N, 8.64. Found: C, 53.63; H, 8.20; N, 8.47.

E,E-*4-Androstene-3,17-di*(N,N-*dimethylaminopropyl oximino ether*) *Dimethobromide* (*X*)—*E,E*-4-Androstene-3,17-dione dioxime (3.0 g, 0.0095 mole) was reacted with potassium *tert*-butoxide (4.3 g, 0.0383 mole) and 3-dimethylaminopropyl chloride (3.0 g, 0.019 mole). A reaction time of ~18 hr was allowed. After filtration and evaporation of the solvent, the resulting material was extracted with 150 ml of petroleum ether. The extract was cooled in an acetone–dry ice bath, allowed to come to room temperature, and decanted; the solvent was evaporated to yield a viscous yellow oil. Further purification was effected by redissolving the material in 40 ml of petroleum ether followed by a second cooling in the acetone–dry ice bath, decantation, and evaporation as already described.

A second crop of the desired material was obtained by dissolving all of the material that was not soluble in the petroleum ether in 17 ml of dimethyl sulfoxide. Several extractions of the dimethyl sulfoxide with petroleum ether afforded additional material, which was purified by employing the acetone–dry ice bath as described. Small amounts of water were added between extractions. The total yield was 2.1 g (35.0% yield); IR: λ_{max} (neat) 1634 (C=N, conjugated), 1730 (C=N, unconjugated), and 1044 (C—O) cm^{-1}; NMR[6]: δ 1.03 (s, 3H, 18-methyl), 2.11 (s, 12H, *N*-methyl), 3.88 (γ-methylene protons from both side chains; two overlapping A_2X_2 systems), and 5.56 (s, 1H, HC=).

Quaternization of the free base followed by crystallization from a mixture of absolute ethanol and isopropyl ether gave a salt that melted at 244° dec.

Anal.—Calc. for $C_{31}H_{56}Br_2N_4O_2$: C, 55.02; H, 8.34; N, 8.29. Found: C, 55.39; H, 8.36; N, 8.28.

Z,Z-*4-Androstene-3,17-di*(N,N-*dimethylaminopropyl oximino ether*) *Dimethobromide* (*XI*)—The *Z,Z*-dioxime of 4-androstene-3,17-dione (2.0 g, 0.0063 mole) was dissolved in 80 ml of absolute ethanol. Potassium *tert*-butoxide (2.85 g, 0.0254 mole) and 3-dimethylaminopropyl chloride (2.0 g, 0.0127 mole) were added, and the mixture was allowed to reflux for 23 hr. The oily residue that resulted after evaporation of the alcohol was extracted several times with petroleum ether. The petroleum ether extracts were combined, and the solvent was evaporated, yielding an oily residue.

The residue was purified further by retreating it with petroleum ether followed by separation of the ether layer and evaporation. This procedure was continued until only petroleum ether-soluble material remained. The procedure yielded 1.4 g of a viscous yellow oil (35% yield), mp 236° dec.; IR: λ_{max} (neat) 1634 (C=N, conjugated), 1734 (C=N, unconjugated), and 1044 (C—O) cm^{-1}; NMR[6]: δ 1.01 (s, 3H, 18-methyl), 2.11 (s, 12H, *N*-methyl protons), 4.08 (γ-methylene protons from both side chains; two overlapping A_2X_2 systems), and 6.22 (s, 1H, HC=).

Crystallization of the methobromide salt from absolute alcohol and isopropyl ether yielded an analytically pure sample.

Anal.—Calc. for $C_{31}H_{56}Br_2N_4O_2$: C, 55.03; H, 8.34; N, 8.28. Found: C, 54.82; H, 8.63; N, 7.98.

Separation Procedures (Dioximes)—*Method I* (*TLC*)—Separation by TLC was accomplished using a cylindrical developing chamber (25 × 5.5 cm) lined with filter paper to enhance saturation. The developing solvent consisted of benzene–ethyl acetate (10:3). Silica gel strips[7] (20 cm) were activated for 30 min at 110° and allowed to cool in a desiccator. After the system reached equilibrium (1 hr), the plates were developed to a distance of 15 cm, resulting in two distinct zones. The fast isomer was at R_f 0.17, and the slow isomer was at R_f 0.11.

Method II (*Dry Column Chromatography*)—With the same solvent system described for TLC and silica gel[8] as the support, column chromatography afforded semipreparative amounts of isomerically pure dioximes.

Method III (*Fractional Crystallization*)—4-Androstene-3,17-dione dioxime (mixture) (10.7 g) was dissolved in 425 ml of hot acetone and filtered. The solution was placed in a 500-ml beaker and covered with aluminum foil. Several small holes were provided near the center of the foil to allow slow and controlled evaporation of the acetone. When the solvent had reached the 350-ml level, the acetone was decanted and the crystals that had formed were washed with 5 ml of fresh acetone.

This first crop amounted to 2.2 g of the fast isomer with traces of the slow isomer. A second crystallization from the same solvent afforded 1.7 g of the fast isomer. The mother liquor was allowed to evaporate further in the manner described until the solvent level reached 250 ml. A second crop was obtained and identified as the slow isomer (0.8 g). Further evaporation yielded crystals that were a mixture of both isomers. This procedure gave two analytically pure samples.

The fast isomer had a melting point of 223° dec.; $[\alpha]_D^{25}$ +231° (methanol, 0.32%); UV: λ_{max} (methanol) 241 (ϵ 26,898) nm; IR[3]: λ_{max} 1634 (C=N, conjugated) and 1704 (C=N, unconjugated) cm^{-1}; NMR[5]: δ 0.780 (s, 3H, 19-methyl), 0.940 (s, 3H, 18-methyl), 5.626 (s, 1H, CH=), 9.930 [s, 1H, HO—N=C (D-ring)], and 10.326 [s, 1H, HO—N=C (A-ring)].

Anal.—Calc. for $C_{19}H_{28}N_2O_2$: C, 72.11; H, 8.92; N, 8.86. Found: C, 72.02; H, 8.89; N, 8.59.

The slow isomer melted at 223–226° dec.; $[\alpha]_D^{25}$ +132° (methanol, 0.23%); UV: λ_{max} (methanol) 243 (ϵ 22,943) nm; IR[3]: λ_{max} 1642 and 1618 (C=N, conjugated) and 1681 (C=N, unconjugated) cm^{-1}; NMR[5]: δ 0.780 (s, 3H, 19-methyl), 0.976 (s, 3H, 18-methyl), 6.259 (s, 1H, CH=), 9.930 [s, 1H, HO—N=C (D-ring)], and 10.026 [s, 1H, HO—N=C (A-ring)].

Anal.—Calc. for $C_{19}H_{28}N_2O_2$: C, 72.11; H, 8.92; N, 8.86. Found: C, 72.29; H, 9.09; N, 8.79.

NMR Shift Studies (Dioximes)—Five milligrams of each dioxime was weighed accurately and dissolved separately in 0.5 ml of deuterochloroform. To each sample was added accurately 0.007 ml of a 10% methanol solution in carbon tetrachloride using a microsyringe[9]. Minimal tetramethylsilane was added to avoid precipitation of the sample. Seven spectra were obtained on each sample, with increasing amounts of tris(1,1,1,1,1,2,2-heptafluoro-7,7-dimethyloctanedione)europium added to effect shifts on the signals[10] of the olefinic proton and C-18 methyl protons.

PHARMACOLOGY

Method—The rolling (rotarod) apparatus was used to evaluate neuromuscular blockade. This device was first described by Dunham and Miya (20), who mentioned the possibility of using such an apparatus to detect muscular relaxation. Subsequent reports (21–24) discussed the use of this method to quantify motor incoordination in laboratory animals under the influence of various drugs. Although this method is not specific for the evaluation of neuromuscular blocking agents, it does provide a reliable and simple screening avenue for such agents.

Female albino mice [Sprague–Dawley SH:ARA (ICR) f], 17–29 g, were used to evaluate the neuromuscular blocking activity of the synthesized compounds. The mice were injected intraperitoneally with solutions of the methyl bromide salts of the compounds in double-distilled water. Approximately 0.1 ml of the solution was used to deliver each dose. Immediately after injection, the mice were placed on a rotating motorized drum (7.150 rpm) and the time was recorded.

To eliminate a prolonged training period for each animal, the drum design included a screen wire walking surface with a diameter of 11.4 cm and partitions (17.8 cm in diameter) isolating each animal. A maximum of 30 min was allowed to record observations. If the animal was unable to remain on the rotating drum for the allotted time, a positive response was recorded; no response was noted if the animal remained the full time. No positive responses were observed with the control group that had been injected previously with double-distilled water.

Because the stock solutions lost significant potency over 24 hr, all stock solutions were used within 8 hr; dilutions from the stock solution were used immediately. All stock solutions were made by weighing at least 30 mg of each compound followed by dissolution with an appropriate volume of double-distilled water. Four doses (10 animals per dose) were used for all compounds tested.

The Litchfield–Wilcoxon method (24) was employed for the statistical evaluation of the data and the fitting of curves.

Results—The pharmacological data provided the following information.

1. The slopes of all curves, including the one for decamethonium, were not significantly different (95% confidence limits).
2. The *Z,Z*-isomers were significantly more potent than the *E,E*-isomers.
3. With respect to potency, the molecular modification from the ethylamino side chains to the propylamino side chains was more significant in *Z,Z*-isomerism (the propylamino homolog was more potent).
4. All of the compounds were considerably more potent than decamethonium.
5. The oxime ethers had a slower onset of action compared to decamethonium.

[6] Carbon tetrachloride; tetramethylsilane was the reference.
[7] Eastman 13181 No. 60-60.
[8] J. T. Baker, 60–200 mesh.

[9] The shift of the proton signal on the hydroxyl group of methanol was used as a relative indication of the concentration of tris(1,1,1,1,1,2,2-heptafluoro-7,7-dimethyloctanedione)europium; *i.e.*, the greater the concentration of the shift reagent, the farther downfield the proton signal would appear.
[10] Varian 100-MHz spectrometer.

Table I—Summary of Pharmacological Data

Compound[a]	ED_{50}, μM/kg	95% Confidence Limit, μM/kg	Average Response Time, min
Decamethonium[b]	1.38	1.21–1.57	5.63
VIII: *E,E*-isomer	10.0×10^{-2}	$8.2–12.2 \times 10^{-2}$	11.5
IX: *Z,Z*-isomer	7.05×10^{-2}	$6.47–7.69 \times 10^{-2}$	9.59
X: *E,E*-isomer	9.80×10^{-2}	$9.30–10.3 \times 10^{-2}$	11.1
XI: *Z,Z*-isomer	5.10×10^{-2}	$4.81–5.41 \times 10^{-2}$	15.7

[a] As the methyl bromide salts. [b] Syncurine, Burroughs Wellcome.

Additionally, from gross observations, it appears that the compounds of this study act primarily *via* a depolarizing type of mechanism. Table I summarizes the pharmacological data.

Discussion—Since the slopes of the dose–effect curves of the synthesized compounds and of decamethonium were not significantly different, the mechanism of action must be mainly depolarizing. This conclusion was supported by gross observation of the similarity in behavioral patterns when the animals were under the influence of decamethonium or the synthesized compounds. Both decamethonium and the test compounds resulted in twitching, some piloerection, pronounced heavy deep breathing, bulging eyes, and apparent convulsions subsequent to injection with an overdose. Death always followed the convulsive episode. The behavioral pattern was readily distinguishable from that produced by the antidepolarizing agent (+)-tubocurarine.

Two observations can be made with respect to possible structure–activity relationships implying drug–receptor interactions. First, in both the ethylamino and propylamino series, the *Z,Z*-isomers were significantly more potent than the *E,E*-isomers. However, the distance between the two quaternary nitrogens in the extended conformation was not significantly altered by the isomerism in question. Given the ethylamino side chain, the intercationic distance was not significantly different between the *Z,Z*- and *E,E*-isomers. Furthermore, conformational analysis using Dreiding molecular models revealed significant conformational bulky differences among the side chains of the two isomeric pairs. In the extended conformation, the side chains in the *Z,Z*-isomers could assume an almost parallel alignment (with themselves); however, *E,E*-isomerism directed the side chains at an angle of ~90°.

Second, the molecular modification from ethylamino to propylamino side chains was more significant in *Z,Z*-isomerism. In this respect, the *Z,Z*-dipropylamino congener was significantly more potent than the *Z,Z*-diethylamino compound; the *E,E*-dipropylamino compound was equipotent with the *E,E*-diethylamino congener.

At least two factors may account for the fact that the synthesized compounds were significantly more potent than decamethonium (one compound was ~27 times more potent). Because of the greater hydrophobic to hydrophilic ratio, the steroidal compounds may interact more favorably with the proposed hydrophobic area within or in close proximity to the receptor. Moreover, the steroidal oxime ethers also have the advantage of interacting with the proposed esterophilic portions of the receptor *via* the polarized oximino function; decamethonium obviously is not able to interact by a similar mechanism.

With respect to the onset of action, these compounds were significantly slower than decamethonium, probably because their greater lipid character leads to poorer transfer in the aqueous medium of the biological system.

REFERENCES

(1) M. M. Kochhar, R. G. Brown, and J. N. Delgado, *J. Pharm. Sci.*, **54,** 393 (1965).

(2) S. K. Gomer, E. I. Isaacson, R. G. Brown, and J. N. Delgado, *ibid.*, **57,** 1586 (1968).

(3) P. L. Huerta, E. I. Isaacson, R. G. Brown, and J. N. Delgado, *ibid.*, **66,** 1120 (1977).

(4) W. G. Haney, R. G. Brown, E. I. Isaacson, and J. N. Delgado, *ibid.*, **66,** 1602 (1977).

(5) R. B. Barlow and A. Zoller, *Br. J. Pharmacol. Chemother.*, **23,** 131 (1964).

(6) P. Crabbé, M. J. Durazo, R. M. Saloma, and P. G. Holton, *Bull. Soc. Chim. Belg.*, **71,** 203 (1962).

(7) "Steroid Reactions," C. Djerassi, Ed., Holden-Day, San Francisco, Calif., 1963, pp. 506–510.

(8) C. W. Shoppe, G. Kruger, and R. N. Mirrington, *J. Chem. Soc. London*, **1962,** 1050.

(9) G. Göndös, B. Matkovics, and O. Kovacs, *Microchem. J.*, **8,** 415 (1966).

(10) B. Matkovics, Z. Tegyey, and G. Göndös, *ibid.*, **11,** 548 (1966).

(11) G. Slomp and W. J. Wechter, *Chem. Ind.*, **Jan. 6,** 41 (1962).

(12) W. D. Phillips, *Ann. N.Y. Acad. Sci.*, **70,** 817 (1958).

(13) G. J. Karabotsos, R. A. Taller, and F. M. Vane, *J. Am. Chem. Soc.*, **85,** 2326 (1963).

(14) Z. W. Wolkowski, N. Thoai, and J. Wiemann, *Tetrahedron Lett.*, **1970,** 93.

(15) Z. W. Wolkowski, *ibid.*, **1971,** 825.

(16) R. M. Silverstein, G. C. Bassler, and T. C. Morrill, "Spectrometric Identification of Organic Compounds," Wiley, New York, N.Y., 1974, p. 96.

(17) *Ibid.*, p. 247.

(18) *Ibid.*, p. 244.

(19) W. E. Bachmann and M. X. Barton, *J. Org. Chem.*, **3,** 300 (1939).

(20) N. W. Dunham and T. S. Miya, *J. Am. Pharm. Assoc., Sci. Ed.*, **46,** 208 (1957).

(21) J. E. Weaver and T. S. Miya, *J. Pharm. Sci.*, **50,** 910 (1961).

(22) W. J. Kinnard, Jr., and C. J. Carr, *J. Pharmacol. Exp. Ther.*, **211,** 354 (1957).

(23) N. Watzman and H. Barry, III, *Psychopharmacologia*, **12,** 414 (1968).

(24) J. T. Litchfield, Jr., and F. Wilcoxon, *J. Pharmacol. Exp. Ther.*, **96,** 99 (1949).

ACKNOWLEDGMENTS

The authors thank Dr. Ben A. Shoulders, Department of Chemistry, University of Texas, for counsel during the evaluation of the spectral data. ^{13}C-NMR spectra were made possible with the aid of a Bruker WH-90 spectrometer purchased with National Science Foundation Grant GP-41570.

Inhibitors of Polyamine Biosynthesis VII: Evaluation of Pyruvate Derivatives as Inhibitors of *S*-Adenosyl-L-methionine Decarboxylase

M. PANKASKIE and M. M. ABDEL-MONEM ˣ

Received April 20, 1979, from the *College of Pharmacy, University of Minnesota, Minneapolis, MN 55455.* Accepted for publication August 6, 1979.

Abstract □ The mechanism of the enzymatic decarboxylation of *S*-adenosyl-L-methionine catalyzed by *S*-adenosyl-L-methionine decarboxylase and its inhibition by methylglyoxal bis(guanylhydrazone) were investigated. The results indicate that the carbonyl group of the pyruvate cofactor does not form an azomethine bond with an amino group of the enzyme protein. The substrate and/or product forms an azomethine bond with the pyruvate cofactor, which can be reduced efficiently with sodium cyanoborohydride. Methylglyoxal bis(guanylhydrazone) appears to interfere with the formation of the enzyme–substrate complex by competing with the substrate for binding with the active enzyme site. The dimethylaminoethylhydrazone, semicarbazone, and guanylhydrazone derivatives of pyruvic acid, ethyl pyruvate, pyruvic acid amide, and pyruvyl glycineamide were synthesized. None of these compounds had significant inhibitory activity on the enzymatic decarboxylation of *S*-adenosyl-L-methionine by *S*-adenosyl-L-methionine decarboxylase from rat liver *in vitro*. These results indicate that the structural requirements for binding of methylglyoxal bis(guanylhydrazone) to the enzyme are strict and that structural modifications of this compound result in a dramatic loss of activity.

Keyphrases □ *S*-Adenosyl-L-methionine decarboxylase—inhibition by pyruvate derivatives □ Enzyme inhibition—effects of pyruvate derivatives on *S*-adenosyl-L-methionine decarboxylase

The polyamines appear to play an essential role in cellular metabolism and cell proliferation (1). Selective inhibitors of polyamine biosynthesis have produced antiproliferative activity in cell culture (2) and *in vivo* (3). Most of the compounds studied have been inhibitors of L-ornithine decarboxylase, the rate-controlling enzyme in the biosynthesis of the polyamines (4). Only a few inhibitors of *S*-adenosyl-L-methionine decarboxylase, the second enzyme in the synthetic pathway of polyamines, have been studied (5, 6). Therefore, studies to develop specific inhibitors of mammalian, putrescine-activated *S*-adenosyl-L-methionine decarboxylase were initiated.

This report presents a tentative scheme for catalysis by *S*-adenosyl-L-methionine decarboxylase and a possible mechanism of its inhibition by methylglyoxal bis(guanylhydrazone) (I*a*). The synthesis of some pyruvate derivatives structurally similar to I*a* and evaluation of them as inhibitors of enzymatic decarboxylation of *S*-adenosyl-L-methionine by the decarboxylase from rat liver also are reported.

BACKGROUND

The identification of covalently bound pyruvate in rat liver *S*-adenosyl-L-methionine decarboxylase was reported recently in two studies (7, 8). The pyruvate group appears to be essential for the catalytic activity of the enzyme and probably is involved in the formation of an azomethine bond with the amino group of the substrate, *S*-adenosyl-L-methionine, to form an intermediate (IV) (Scheme I). Previous studies with pyridoxal phosphate-dependent decarboxylases showed that the pyridoxal phosphate is linked to the ε-amino group of a specific lysyl residue by an azomethine bond and that the enzyme–substrate complex is formed by transaldimination between the enzyme–pyridoxal phosphate complex and the substrate. Unlike pyridoxal-dependent decarboxylases, the carbonyl group of the pyruvate cofactor does not form an azomethine bond with an amino group from the enzyme protein since sodium borohydride reduction of the purified enzyme results in the formation of lactic acid and not an *N*-substituted alanine.

Since studies with model systems indicated that transaldimination proceeds more rapidly than *de novo* Schiff base formation (9), the possibility of *S*-adenosyl-L-methionine decarboxylase activation by putrescine, due to the formation of the ketimine (III) between the pyruvate residue and putrescine, was explored. Transketimination between III and the substrate (II) would result in the more rapid formation of the intermediate (IV). The decarboxylation product (V) of II also may be bound to the enzyme by an azomethine bond.

Imminium compounds such as III–V could be trapped in the presence of free pyruvate residues by selective reduction with cyanoborohydride (10). Thus, the presence of such intermediates in an incubation medium containing *S*-adenosyl-L-methionine decarboxylase and the appropriate ligand could be demonstrated if a loss of enzymatic activity were observed on treatment of the mixture with sodium cyanoborohydride. This approach was used by Satre and Kennedy (11) to demonstrate the formation of a Schiff base between the amino group of phosphatidyl serine and the pyruvate residue of the enzyme as an essential step in the action of phosphatidylserine decarboxylase. Therefore, experiments were carried out to determine the effects on enzyme activity of the addition of sodium cyanoborohydride to *S*-adenosyl-L-methionine decarboxylase preparations containing the activator putrescine and/or the substrate.

EXPERIMENTAL[1]

Melting points were determined in open capillary tubes and are uncorrected. NMR spectra were taken in deuterochloroform or deuterium oxide with tetramethylsilane or sodium 2,2-dimethyl-2-silapentane-5-sulfonate as the internal standard, respectively. Mass spectral analyses were performed at 20–70 ev and chamber temperatures of 25–200°.

Methylglyoxal Disemicarbazone (I*b*)—Methylglyoxal (2.5 g of a 40% aqueous solution) was added to a solution of semicarbazide hydrochloride (1.0 g) and sodium acetate (1.5 g) in water (25 ml). The mixture was heated on a steam bath for 30 min. The precipitate was collected by filtration, washed with warm water, and dried *in vacuo* to give I*b* (2.4 g, 95% yield), mp 252° dec. [lit. (12) mp 254°].

Anal.—Calc. for $C_5H_{10}N_6O_2$: C, 32.25; H, 5.41; N, 45.14. Found: C, 32.47; H, 5.43; N, 45.10.

Methylglyoxal Dithiosemicarbazone (I*c*)—A solution of sodium acetate (2.0 g in 10 ml of water) was added to a solution of methylglyoxal (2.5 g of a 40% aqueous solution) and thiosemicarbazide (1.0 g) in water (25 ml). The mixture was heated on a steam bath for 30 min. A heavy orange precipitate was formed and then collected by filtration. The precipitate was washed with boiling water and dried *in vacuo* overnight to give Ic (2.8 g, 93% yield), mp 250° dec. [lit. (12) mp 253°].

Anal.—Calc. for $C_5H_{10}N_6S_2$: C, 27.51; H, 4.62; N, 38.50. Found: C, 27.77; H, 4.46; N, 38.47.

Pyruvyl Glycineamide Diethyl Ketal (XI)—Ethyl pyruvate diethyl ketal was prepared from ethyl pyruvate and ethyl orthoformate according to the procedure of Wermuth and Marx (13). Ethyl pyruvate diethyl ketal (5.0 g, 26 mmoles) was treated with a 3% aqueous potassium hydroxide solution (50 ml, 30 mmoles) and stirred overnight at room temperature. The aqueous solution was made acidic by the addition of 5% HCl and extracted with ether (2 × 150 ml). The ether extract was concentrated *in vacuo* to give pyruvic acid diethyl ketal (3.5 g, 88% yield); IR (neat):

[1] Instruments used were a Thomas-Hoover melting-point apparatus, a Perkin-Elmer 281 spectrophotometer, Varian A-60D and T-60 NMR spectrophotometers, an AEI MS-30 mass spectrometer, and a Beckman LS-100C liquid scintillation counter. Elemental analyses were performed by M-H-W Laboratories, Phoenix, Ariz.

0022-3549/80/0900-1000$01.00/0
© 1980, American Pharmaceutical Association

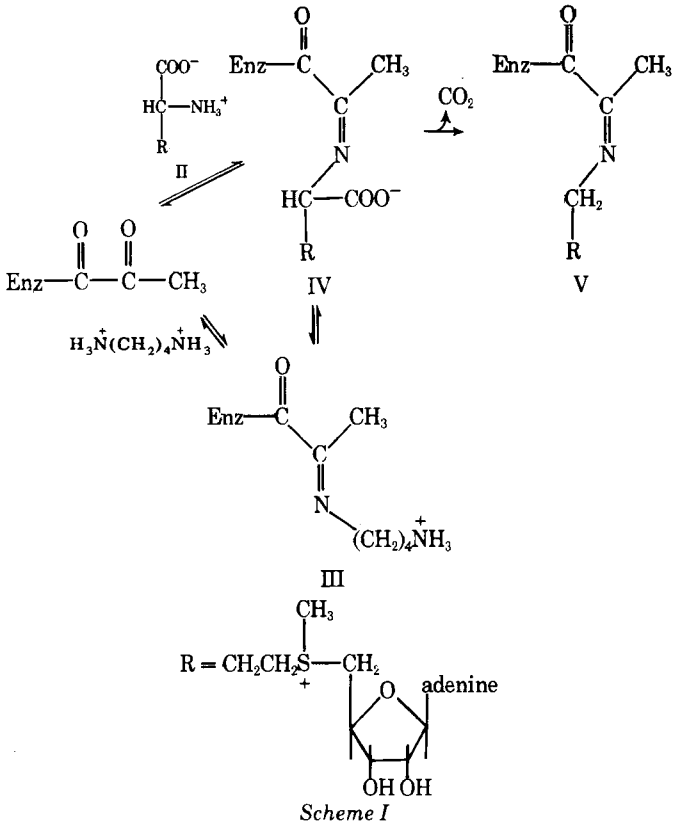

Scheme I

3200 (broad), 2985, 2930, 2895, 1740, 1450, 1370, 1150, 1040, 950, 855, and 740 cm^{-1}; NMR (deuterochloroform): δ 3.6 (m, 4H), 1.6 (s, 3H), and 1.2 (t, 6H) ppm.

A cooled (ice–salt bath) solution of pyruvic acid diethyl ketal (2.0 g, 12 mmoles) in chloroform (100 ml) was treated with triethylamine (1.25 g, 12 mmoles) and ethyl chloroformate (1.35 g, 12 mmoles), and the mixture was stirred for 20 min. The ice–salt bath was removed, and a solution of glycineamide (1.0 g, 15 mmoles) in chloroform (100 ml) was added slowly over 30 min. The reaction mixture was stirred for 4 hr at room temperature, and the chloroform solution was washed with successive portions of 10% $NaHCO_3$ and brine. The chloroform solution was dried over anhydrous sodium sulfate and evaporated to dryness *in vacuo*. The semisolid residue obtained was crystallized from boiling ether to give XI (1.6 g, 60% yield), mp 95–96°; IR (melt): 3320, 2995, 2940, 1670, 1620, 1525, 1450, 1365, 1300, 1200, 1160, 1050, and 950 cm^{-1}; NMR (deuterochloroform): δ 7.6, 6.9, and 6.2 (broad s, 3H, exchangeable with deuterium oxide), 4.0 (d, 2H), 3.5 (q, 4H), 1.5 (s, 3H), and 1.3 (t, 6H) ppm; mass spectrum: *m/e* 219 ($M^+ + 1$), 217 ($M^+ - 1$), 173, 156, 128, 117, 100, 89, 75, 61 (100%), 59, 43, and 30.

Anal.—Calc. for $C_9H_{18}N_2O_4$: C, 49.53; H, 8.31; N, 12.84. Found: C, 49.25; H, 8.49; N, 12.89.

Monoacetyl Hydrazine—Monoacetyl hydrazine was prepared according to the procedure described by Rabini and Vita (14), mp 64–65° [lit. (14) mp 62°]. This compound is hygroscopic and was stored in a vacuum desiccator over anhydrous calcium chloride granules.

***N*-Acetyl-*N*-(dimethylaminoethyl)hydrazine Dihydrochloride (XIV)**—A solution of dimethylaminoacetaldehyde diethyl acetal (XII) (5.0 g, 31 mmoles) in concentrated hydrochloric acid (10 ml) was allowed to stand overnight at 4° and then was concentrated under reduced pressure at 40°. The viscous residue was dissolved in dry methanol (100 ml) and treated with acetylhydrazine (2.5 g, 35 mmoles) and sodium cyanoborohydride (1.3 g, 20 mmoles) under nitrogen. The pH of the reaction mixture was maintained at 2–3 by the addition of methanolic hydrochloric acid, using bromcresol green as an indicator, over 6 hr at room temperature.

After concentration *in vacuo* at room temperature, the residue was dissolved in cold absolute ethanol and filtered. The filtrate was treated with ethanolic hydrochloric acid and stored at 4° overnight. The precipitated solid was filtered and dried *in vacuo* to give XIV (2.8 g, 42% yield), mp 126–128°. An analytical sample was recrystallized from 95% ethanol; IR (KBr): 3400 (broad), 300 (broad), 2040, 1715, 1630, 1460, 1380, 1230, 1000, and 800 cm^{-1}; NMR (deuterium oxide): δ 3.2 (s, 4H), 2.8 (s, 6H), and 2.0 (s, 3H) ppm; mass spectrum: *m/e* 145 ($M^+ - 2HCl$), 87, 71, 59, 58 (100%), 44, and 36.

Anal.—Calc. for $C_6H_{17}Cl_2N_3O$: C, 33.03; H, 7.86; N, 19.26. Found: C, 33.17; H, 8.07; N, 19.20.

Dimethylaminoethylhydrazine Dihydrochloride (XV)—A solution of XIV (2.0 g, 9 mmoles) was dissolved in ethanolic hydrogen chloride solution (20 ml) and warmed gently on a steam bath for 45 min. The mixture was stored at 4° overnight to give a quantitative yield of XV, mp 120–121°. The product was hygroscopic; IR (KBr): 3400 (broad), 3000, 2700, 2050, 1620, 1470, 1150, and 800 cm^{-1}; NMR (deuterium oxide): δ 3.2 (s, 4H) and 2.8 (s, 6H) ppm; mass spectrum: *m/e* 103 ($M^+ - 2HCl$), 58 (100%), 42, and 36.

Anal.—Calc. for $C_4H_{15}Cl_2N_3$: C, 27.28; H, 8.59; N, 23.86. Found: C, 27.47; H, 8.56; N, 23.96.

Dimethylaminoethylhydrazone Derivatives (VI*a*–VI*d*)—The ketone (IX*a*, IX*b*, or IX*c*) or XI (3 mmoles) was added to a solution of XV (0.5 g, 3 mmoles) in ethanol (20 ml) and allowed to stand overnight at room temperature. Ether was added dropwise to the clear solution until turbidity was observed. The mixture was stored at 4°. The precipitated solid was filtered and crystallized to give the desired products (VI*a*–VI*d*) (Table I).

Semicarbazone Derivatives (VII*a*–VII*d*)—One gram of the ketone (IX*a*, IX*b*, or IX*c*) or XI was added to a solution of semicarbazide hydrochloride (1.0 g) and sodium acetate (1.5 g) in water (25 ml). The mixture was heated on a steam bath for 15 min and allowed to stand overnight. The formed solids were filtered, recrystallized from water, and dried *in vacuo* for 12 hr to give the desired products (VII*a*–VII*d*) (Table I).

Guanylhydrazone Derivatives (VIII*a*–VIII*c*)—A suspension of aminoguanidine bicarbonate (50 mmoles) in water (50 ml) was adjusted to pH 5–6 with concentrated hydrochloric acid. Compound IX*a*, IX*b*, or IX*c* was added dropwise to the clear solution of the aminoguanidine, and the reaction mixture was stirred overnight at room temperature. The precipitated solids were filtered, crystallized, and dried overnight *in vacuo* to give the desired products (VIII*a*–VIII*c*) (Table I).

Pyruvyl Glycineamide Guanylhydrazone Hydrochloride (VIII*d*)—Aminoguanidine hydrochloride (0.25 g, 2.5 mmoles) was added to a solution of XI (0.44 g, 2 mmoles) in water (30 ml), and the mixture was heated on a steam bath for 2 hr and stored at 4° overnight. The precipitated crystalline solid was filtered and washed with ice-cold water to give VIII*d* (0.41 g, 87% yield) (Table I).

Pyruvic Acid Guanylhydrazide Guanylhydrazone Dihydrochloride (VIII*e*)—Aminoguanidine hydrochloride (6.6 g, 60 mmoles) was added to a solution of ethyl pyruvate (3.5 g, 30 mmoles) in water (25 ml), and the mixture was heated at 80° overnight. The solution was evaporated to dryness, and the residue after two crystallizations from aqueous ethanol gave VIII*e* (7.3 g, 90% yield), mp 250–251°; IR (KBr): 3200, 2950, 1670, 1590, 1490, 1440, 1420, 1370, 1300, 1150, 1120, 900, and 720 cm^{-1}; NMR (deuterium oxide): δ 1.6 (s, 3H) ppm; mass spectrum: *m/e* 182, 126, 57, 44, 43, 42, 38, and 36 (100%).

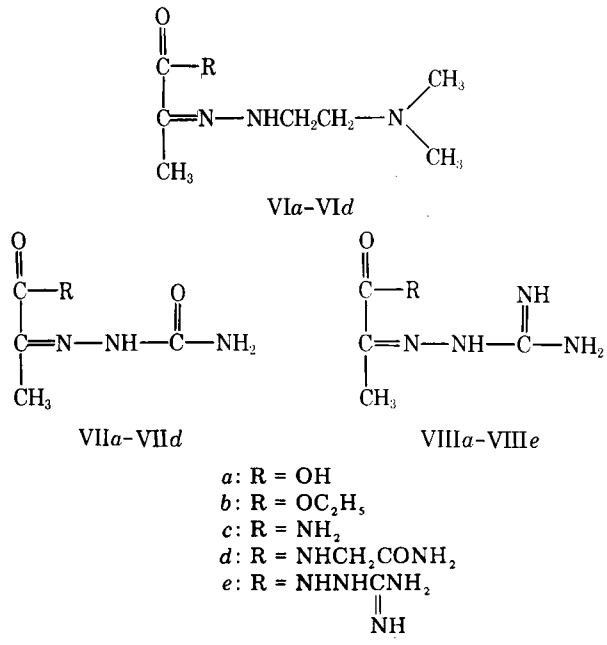

Table I—Analytical Data and Enzyme Inhibitory Activities of Pyruvate Derivatives

Compound	Formula	Yield %	Melting Point	Crystallization Solvent[a]	Inhibition[b], % 20 μM	Inhibition[b], % 10 μM	Analysis, %	Calc.	Found
VI*a*	$C_7H_{15}N_3O_2$·HCl	69	169–170°	A	9	0	C	40.10	40.12
							H	7.69	7.69
							N	20.04	20.20
VI*b*	$C_9H_{19}N_3O_2$·HCl	50	104–105°	B	0	0	C	45.47	45.78
							H	8.48	8.58
							N	17.68	17.86
VI*c*	$C_7H_{16}N_4O$·HCl	78	152–153°	B	2	0	C	40.28	40.64
							H	8.21	8.31
							N	26.85	27.16
VI*d*	$C_9H_{19}N_5O_2$·HCl	70	190–192°	A	3	0	C	40.68	40.40
							H	7.59	7.81
							N	26.36	26.12
VII*a*	$C_4H_7N_3O_3$	95	215–216°	C	0	0	—[c]		
VII*b*	$C_6H_{11}N_3O_3$	93	213–214°	C	8	2	—[c]		
VII*c*	$C_4H_8N_4O_2$	90	241–242°	C	0	0	—[c]		
VII*d*	$C_6H_{11}N_5O_3$	80	240–241°	C	0	0	C	35.81	35.79
							H	5.51	5.43
							N	34.81	34.50
VIII*a*	$C_4H_8N_4O_2$·HCl	87	230–231°	C	2	0	C	26.60	26.93
							H	5.12	5.16
							N	31.03	31.27
VIII*b*	$C_6H_{12}N_4O_2$·HCl	90	150–151°	A	3	0	C	34.54	34.10
							H	6.30	6.16
							N	26.85	26.69
VIII*c*	$C_4H_9N_5O$·HCl	85	255–256°	C	0	0	C	26.75	26.69
							H	5.61	5.65
							N	40.00	39.82
VIII*d*	$C_6H_{12}N_6O_2$·HCl	87	260° dec.	A	0	0	C	28.29	28.61
							H	5.93	5.89
							N	33.01	33.21
VIII*e*	$C_5H_{12}N_8O_2$·HCl	90	250–251°	D	0	0	C	21.99	21.73
							H	5.17	5.00
							N	41.03	40.79

[a] Solvents used were ethanol (A), ethanol–ether (B), water (C), and ethanol–water (D). [b] Inhibition of enzymatic decarboxylation of [1-^{14}C]-*S*-adenosyl-L-methionine by partially purified *S*-adenosyl-L-methionine decarboxylase from rat liver. Compound I*a* produced 100 and 63% inhibition at 10 and 1 μ*M*, respectively. [c] See Ref. 12.

Anal.—Calc. for $C_5H_{12}N_8O$·2HCl: C, 21.99; H, 5.17; N, 41.03. Found: C, 21.73; H, 5.00; N, 40.79.

Enzyme Purification—Rat liver *S*-adenosyl-L-methionine decarboxylase was purified by the method of Pegg (15) with slight modifications. Twelve male Sprague–Dawley[2] rats (250 g) were injected intraperitoneally with methylglyoxal bis(guanylhydrazone)[3] (I*a*, 80 mg/kg) and were sacrificed by cervical dislocation 24 hr later. The livers were removed and homogenized in 200 ml of Buffer A [containing 10 m*M* tris(hydroxymethyl)aminomethane hydrochloride (pH 7.5), 2.5 m*M* putrescine, 1 m*M* dithiothreitol, and 0.1 m*M* ethylenediaminetetraacetic acid disodium] at 4°. All subsequent operations were carried out at 0–5°.

The homogenate was centrifuged at 105,000×*g* for 90 min. The supernate was treated with ammonium sulfate, and the protein fraction precipitating between 35 and 65% saturation was collected by centrifugation. The protein pellet was dissolved in the minimum amount of Buffer A, and the solution was dialyzed overnight against 4 liters of the same buffer.

A glass column (2.5 × 30 cm) was packed with Sepharose[4] linked to I*a* and washed with 200 ml of Buffer A. The dialyzed protein sample was applied to the column at a flow rate of 35–40 ml/hr, and the column was washed with 100 ml of Buffer A followed by 150 ml of Buffer A containing 0.3 *N* NaCl. The protein having *S*-adenosyl-L-methionine decarboxylase activity was eluted off the column with Buffer A containing 0.3 *N* NaCl and 1 m*M* I*a*. The column eluates were collected in 10-ml fractions, and each fraction was assayed for decarboxylase activity using 50 μl in the standard procedure.

Decarboxylase activity usually was found in fractions 4–6, with >80% of the recovered activity in fraction 5 alone. The presence of I*a* in the elution solvent greatly reduced the apparent activity of these fractions. Fractions containing decarboxylase activity were pooled, divided into 5-ml aliquots, and stored at 0–5°. The protein solution was dialyzed against two 1-liter portions of Buffer A, to remove the inhibitor (I*a*), immediately before use as a source of the decarboxylase enzyme. By using this method, an enzyme preparation having a specific activity of ~15 nmoles of carbon dioxide/min/mg of protein routinely was obtained.

Assay of *S*-Adenosyl-L-methionine Decarboxylase Activity—*S*-Adenosyl-L-methionine decarboxylase activity was determined by a modification of a literature method (16). The assay medium contained 0.1 *M* sodium phosphate buffer (pH 7.0), 2.5 m*M* dithiothreitol, 2.5 m*M* putrescine, 0.2 m*M* [1-^{14}C]-*S*-adenosyl-L-methionine (2.0 × 10^5 cpm), and the enzyme fraction[5] in a total volume of 1.0 ml. Reactions were carried out in 16 × 100-mm test tubes sealed with rubber stoppers carrying a polypropylene well[6] containing 0.3 ml of ethanolamine.

After incubation for 30 min at 37°, the reaction was terminated and [^{14}C]carbon dioxide was released by the injection of 0.5 ml of 5 *N* H_2SO_4 through the rubber stopper. The tubes were incubated for an additional 45 min at 25°, and the well and its contents were transferred into a glass scintillation vial containing 10 ml of scintillation cocktail[7]. The samples were stored in the dark overnight and then counted. All counts were corrected for the nonenzymatic production of [^{14}C]carbon dioxide, which was determined by replacing the enzyme fraction in the incubation medium with an equal volume of Buffer A. This method gave the quantitative recovery of the [^{14}C]carbon dioxide released from sodium [^{14}C]-bicarbonate.

Enzyme Inhibition—The test compounds were dissolved in water (I*a* and VI–VIII) or 5% dimethyl sulfoxide in water (I*b* and I*c*) to give 1 m*M* solutions. The incubation medium contained 0.1 *M* sodium phosphate buffer (pH 7.0), 2.5 m*M* dithiothreitol, 2.5 m*M* putrescine, 0.2 m*M* [1-^{14}C]-*S*-adenosyl-L-methionine (2.0 × 10^5 cpm), the inhibitor at concentrations of 50, 20, 10, and 1 μ*M*, and 0.1 ml of the enzyme preparation in a total volume of 1.0 ml. The amount of [^{14}C]carbon dioxide released was measured as described for the assay of *S*-adenosyl-L-methionine decarboxylase activity and corrected for the nonenzymatic release of [^{14}C]carbon dioxide. The presence of dimethyl sulfoxide in solutions of I*b* and I*c* resulted in <5% inhibition of enzymatic activity, and the final

[2] Bio-Lab Corp., St. Paul, Minn.
[3] Aldrich Chemical Co., Milwaukee, Wis.
[4] Prepared according to the procedure described in Ref. 15; Sigma Chemical Co., St. Louis, Mo.
[5] Enzyme fractions were column eluates after recovery of the protein from the Sepharose column or dialyzed protein after preincubation (Tables II and III).
[6] Kontes Glass Co., Vineland, N.J.
[7] Aquasol 2, New England Nuclear, Boston, Mass.

Table II—Effects of pH and Buffer on the Recovery of *S*-Adenosyl-L-methionine Decarboxylase Activity

Buffer	Activity Remaining[a] pH 6.5	pH 7.0	pH 7.5
Tris(hydroxymethyl)aminomethane hydrochloride (10 m*M*)	69	83	58
Phosphate (100 m*M*)	86	100	75

[a] See *Experimental.*

results for these compounds were corrected for inhibition by the solvent.

Effects of pH and Buffer on Recovery of *S*-Adenosyl-L-methionine Decarboxylase Activity—The dialyzed protein fraction containing *S*-adenosyl-L-methionine decarboxylase activity was diluted with Buffer A to a concentration of 0.2 mg of protein/ml. Aliquots (0.1 ml) were diluted to 0.4 ml with one of the buffer solutions listed in Table II and incubated at 37° for 30 min. Aliquots (0.1 ml) were removed and assayed for *S*-adenosyl-L-methionine decarboxylase activity as described for the assay of *S*-adenosyl-L-methionine decarboxylase activity. The activity of the sample incubated in pH 7.0 phosphate buffer was arbitrarily assigned a value of 100, and the activities of the other samples are reported in Table II as a percentage of that activity. Incubation in pH 7.0 phosphate buffer resulted in a 10% loss of activity of the original preparation.

Effects of Different Preincubation Conditions on Recovery of *S*-Adenosyl-L-methionine Decarboxylase Activity—Protein fractions containing *S*-adenosyl-L-methionine decarboxylase activity were dialyzed against a pH 7.5 buffer containing 10 m*M* tris(hydroxymethyl)aminomethane hydrochloride, 1 m*M* dithiothreitol, and 0.1 m*M* ethylenediaminetetraacetic acid disodium. Aliquots of the dialyzed protein were diluted with buffer solution (pH 7.0) containing the additions described in Table III and incubated at 37° for 30 min.

Each sample was dialyzed against Buffer A (two 100-ml portions), and 0.1-ml aliquots of the dialyzed protein were assayed for *S*-adenosyl-L-methionine decarboxylase activity as described for the assay of *S*-adenosyl-L-methionine decarboxylase activity. The activity of the sample preincubated in the buffer with no additions was arbitrarily assigned a value of 100, and the activities of the other samples are reported in Table III as a percentage of that activity.

RESULTS

Incubation of partially purified *S*-adenosyl-L-methionine decarboxylase from rat liver at 37° in a buffer for 30 min resulted in a slight loss of activity. This result is consistent with the previously reported instability of the enzyme at elevated temperatures (16). The nature and pH of the buffer influenced the degree of activity loss (Table II), with optimum stability of the enzyme observed in pH 7.0 phosphate buffer. Addition of sodium cyanoborohydride at 5 and 50 m*M* to the incubation medium [pH 7.0 tris(hydroxymethyl)aminomethane hydrochloride buffer] did not cause additional loss of enzymatic activity (Table III).

Incubation of *S*-adenosyl-L-methionine decarboxylase in pH 7.0 tris(hydroxymethyl)aminomethane hydrochloride buffer containing various concentrations of *S*-adenosyl-L-methionine at 37° for 30 min, followed by dialysis, resulted in a loss of enzymatic activity in the recovered protein. This loss was dependent on the concentration of II in the initial incubation mixture (Table III). Addition of Ia at 1.0 μM to the original incubation mixture resulted in protection of the enzyme from the substrate-induced deactivation.

Addition of sodium cyanoborohydride at 5 and 50 m*M* to a mixture of the decarboxylase and II (0.2 m*M*) in pH 7.0 tris(hydroxymethyl)-aminomethane hydrochloride buffer, followed by incubation at 37° for 30 min, resulted in an essentially complete loss of enzymatic activity in the dialyzed protein. The use of [*S*-C^{3}H$_3$]II (10.13 Ci/mmole) in the experiment resulted in the incorporation of radioactivity in the protein fraction. Extensive dialysis of the protein did not dissociate the radioactivity from the enzyme. The addition of Ia at 0.1 μM significantly lowered the degree of inactivation of *S*-adenosyl-L-methionine by sodium cyanoborohydride treatment in the presence of the substrate and putrescine (Table III).

Addition of sodium cyanoborohydride to a mixture of *S*-adenosyl-L-methionine decarboxylase and putrescine (2.5 m*M*) in pH 7.0 tris(hydroxymethyl)aminomethane hydrochloride buffer and incubation at 37° for 30 min did not result in the loss of enzymatic activity of the dialyzed protein (Table III). The use of [^{3}H]putrescine in the experiment did not lead to the incorporation of radioactivity in the enzyme.

Table III—Effects of Different Preincubation Conditions on the Recovery of *S*-Adenosyl-L-methionine Decarboxylase Activity

Additions to Incubation Medium	Activity Remaining: No Sodium Cyanoborohydride	5 m*M* Sodium Cyanoborohydride	50 m*M* Sodium Cyanoborohydride
None	100[a]	97	96
2.5 m*M* Putrescine	102	101	104
2.5 m*M* Putrescine and 0.2 m*M* *S*-adenosyl-L-methionine	75	4	2
2.5 m*M* Putrescine and 0.1 m*M* *S*-adenosyl-L-methionine	82	ND[b]	ND
2.5 m*M* Putrescine and 0.05 m*M* *S*-adenosyl-L-methionine	90	ND	ND
2.5 m*M* Putrescine, 0.2 m*M* *S*-adenosyl-L-methionine, and 1.0 μM Ia	90	43	34

[a] See *Experimental.* [b] Not determined.

DISCUSSION

The described experiments confirm that the carbonyl group of the pyruvate cofactor does not form an azomethine bond with an amino group from the enzyme since sodium cyanoborohydride reduction of the enzyme did not result in loss of catalytic activity of the protein. It appears that putrescine does not form the intermediate III and that the mechanism of activation of *S*-adenosyl-L-methionine decarboxylase by putrescine does not involve transketimination between III and the substrate as was proposed initially. However, these experiments indicate that intermediates IV and/or V are formed during the decarboxylation of II by the enzyme.

Methylglyoxal bis(guanylhydrazone) (Ia) appears to interfere with the formation of the enzyme–substrate complex as shown by two experiments: (*a*) Ia protected the enzyme from substrate-induced inactivation, and (*b*) the degree of inactivation of the enzyme by sodium cyanoborohydride in the presence of II was much lower when Ia was added to the incubation medium. These findings and the observation that inhibition of *S*-adenosyl-L-methionine decarboxylase by I may have been competitive with respect to II indicate that Ia competes with II for binding at the enzyme active site.

The demonstration that IV and/or V are intermediates in the enzymatic decarboxylation of II prompted the synthesis of some derivatives of pyruvic acid (VI–VIII) and their evaluation as inhibitors of *S*-adenosylmethionine decarboxylase. The structural similarities between VI–VIII and intermediates IV and V suggested that these compounds may form complexes with the enzyme and act as inhibitors of the reaction.

Two other factors suggested that VI–VIII may be inhibitors of *S*-adenosylmethionine decarboxylase. First, Ia, which has structural similarities to intermediates IV and V, inhibits *S*-adenosylmethionine decarboxylase by interfering with the formation of the enzyme–substrate complex. The very high inhibitory activity of Ia (Ia produced 100% inhibition at 10 μM in the presence of 0.2 m*M* substrate) suggested that it may be a transition-state analog rather than an analog of the substrate or product. Second, a number of pyridoxal phosphate analogs, which are structurally similar to the intermediate formed between the cofactor and the substrate, were potent inhibitors of pyridoxal-dependent decarboxylases. However, the intermediates formed between pyridoxal phosphate and substrates are not bound covalently to the enzyme, unlike intermediates IV and V, which would be bound covalently to the enzyme.

Chemistry—The target compounds (VI–VIII) were synthesized using a modification of the procedure of Podrebarac *et al.* (17) by condensing the appropriate pyruvate derivative with the corresponding hydrazine salt in aqueous alcohol (Scheme II). Pyruvyl glycineamide diethyl ketal (XI) was obtained by the condensation of pyruvic acid diethyl ketal with glycineamide using the mixed carbonic–carboxylic anhydride method (18). Condensation of XI with the appropriate hydrazine provided VId, VIId, and VIIId (Scheme III).

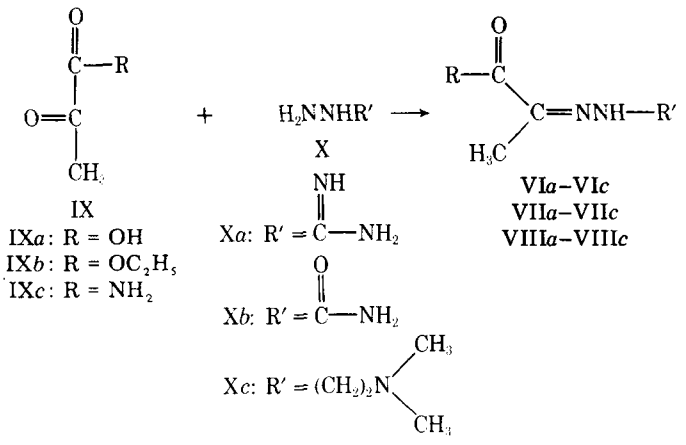

Scheme II

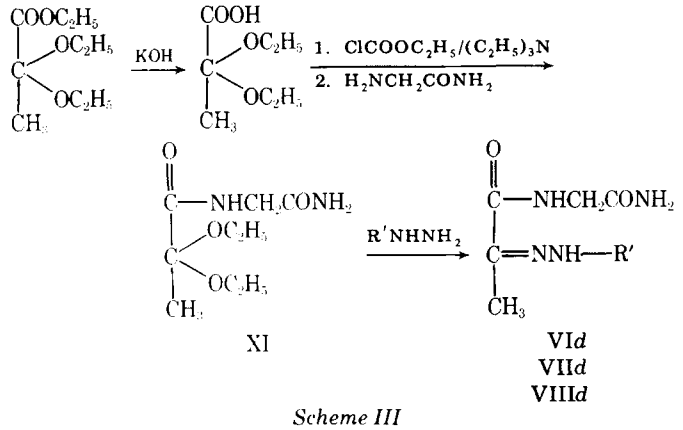

Scheme III

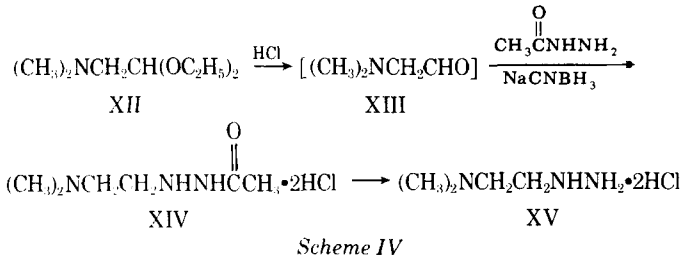

Scheme IV

Acid hydrolysis of dimethylaminoacetaldehyde diethyl ketal (XII) provided the free aldehyde (XIII). Treatment of XIII with acetylhydrazine and sodium cyanoborohydride provided XIV. Acid hydrolysis of XIV provided the dihydrochloride salt, dimethylaminoethylhydrazine dihydrochloride (XV) (Scheme IV). Compounds Ib and Ic were obtained by condensing methylglyoxal pyruvaldehyde with either semicarbazide or thiosemicarbazide in aqueous alcohol using the method of Shriner *et al.* (19) (Scheme V).

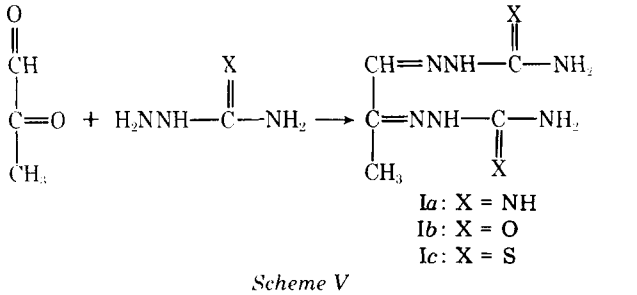

Scheme V

Enzyme Inhibition—The inhibition by the test compounds of the enzymatic decarboxylation of *S*-adenosyl-L-methionine was measured *in vitro*. A partially purified protein from rat liver was used as the source of the *S*-adenosyl-L-methionine decarboxylase, and the decarboxylase activity was measured by determining the amount of [^{14}C]carbon dioxide released from *S*-adenosyl-L-methionine labeled with carbon 14 on the carboxyl group. Under the assay conditions, *S*-adenosyl-L-methionine decarboxylase from rat liver had an apparent K_m value for *S*-adenosyl-L-methionine of 5.14×10^{-5} *M* and a V_{max} value of 8.72 nmoles of carbon dioxide/min/mg of protein.

The addition of Ia at 10 μM caused 100% inhibition of the enzymatic activity. However, the addition of Ib or Ic at 100 μM resulted only in 5 and 3% inhibition of enzymatic activity, respectively. Compounds VI–VIII showed little or no inhibitory activity when added to the reaction mixture in concentrations of 10 and 20 μM (Table I).

These results indicate that the structural requirements for binding of Ia to the enzyme are strict and that structural modifications of this compound result in a dramatic loss of activity. The low inhibitory activities of Ib and Ic underscore the essential role the strongly basic guanidino groups play in the binding of Ia to the enzyme. The lack of significant inhibitory activities for VI–VIII indicates that the inhibitory activity of Ia is not due to its structural similarity to intermediates IV and V in the enzymatic reaction.

REFERENCES

(1) J. Janne, H. Poso, and A. Raina, *Biochim. Biophys. Acta*, **473**, 241 (1978).

(2) P. S. Mamont, M. C. Duchesne, J. Grove, and P. Bey, *Biochem. Biophys. Res. Commun.*, **81**, 58 (1978).

(3) N. J. Parkash, P. J. Schechter, J. Grove, and J. Koch-Weser, *Cancer Res.*, **38**, 3059 (1978).

(4) M. M. Abdel-Monem and E. A. Mikhail, *J. Pharm. Sci.*, **67**, 1174 (1978), and references cited therein.

(5) A. Corti, C. Dave, H. G. Williams-Ashman, E. Mihich, and A. Schenone, *Biochem. J.*, **139**, 351 (1974).

(6) A. E. Pegg, *J. Biol. Chem.*, **253**, 539 (1978).

(7) A. E. Pegg, *FEBS Lett.*, **84**, 33 (1977).

(8) A. A. Demetriou, M. S. Cohen, C. W. Tabor, and H. Tabor, *J. Biol. Chem.*, **253**, 1684 (1978).

(9) E. H. Cordes and W. P. Jencks, *Biochemistry*, **1**, 773 (1962).

(10) R. F. Borch, M. D. Bernstein, and H. D. Durst, *J. Am. Chem. Soc.*, **93**, 2897 (1971).

(11) M. Satre and E. P. Kennedy, *J. Biol. Chem.*, **253**, 479 (1978).

(12) "CRC Handbook of Tables for Organic Compound Identification" 3rd ed., R. C. Weast, Ed., Chemical Rubber Co., Cleveland, Ohio, 1967.

(13) C.-G. Wermuth and H. Marx, *Bull. Soc. Chem. Fr.*, **1964**, 732.

(14) T. Rabini and G. Vita, *J. Org. Chem.*, **30**, 2486 (1965).

(15) A. Pegg, *Biochem. J.*, **141**, 581 (1974).

(16) A. E. Pegg and H. G. Williams-Ashman, *J. Biol. Chem.*, **244**, 682 (1969).

(17) E. G. Podrebarac, W. H. Nyberg, F. A. French, and C. C. Cheng, *J. Med. Chem.*, **6**, 283 (1963).

(18) J. P. Greenstein and M. Winitz, "Chemistry of the Amino Acids," Wiley, New York, N.Y., 1961, p. 978.

(19) R. L. Shriner, R. C. Fuson, and D. Y. Curtin, "The Systemic Identification of Organic Compounds," Wiley, New York, N.Y., 1964.

ACKNOWLEDGMENTS

M. Pankaskie was supported by an American Foundation for Pharmaceutical Education fellowship (1978–1979) and a Mellendy summer fellowship.

N-Acetyl-DL-penicillamine and Acetaminophen Toxicity in Mice

RICHARD T. ZERA and HERBERT T. NAGASAWA ˣ

Received April 23, 1979, from the *Medical Research Laboratories, Veterans Administration Medical Center, and the Department of Medicinal Chemistry, University of Minnesota, Minneapolis, MN 55417.* Accepted for publication January 9, 1980.

Abstract □ *N*-Acetyl-DL-penicillamine (III*b*), a structural analog of *N*-acetyl-L-cysteine (III*a*), did not protect mice from lethal doses of acetaminophen (I), whereas III*a* offered protection. This lack of efficacy of III*b* probably is due to the decreased nucleophilicity of its sulfhydryl group compared to that of III*a*, the probable involvement of cysteine in any conjugate addition to the reactive intermediates of I, and the absence of metabolic conversion of III*b* to inorganic sulfate.

Keyphrases □ *N*-Acetyl-DL-penicillamine—evaluation for protection against acetaminophen toxicity in mice □ Acetaminophen—toxicity, evaluation of protection offered by *N*-acetyl-DL-penicillamine, mice □ Toxicity—acetaminophen, evaluation of protection offered by *N*-acetyl-DL-penicillamine, mice

Acetaminophen (I) is hepatotoxic in large doses (1, 2) and can be toxic even in therapeutic doses in patients with impaired liver function (3). Renal necrosis also has been associated with acetaminophen abuse (1, 2, 4).

THEORY

Animal studies have demonstrated that both the hepatotoxicity (5, 6) and renal toxicity (7) follow cellular glutathione depletion and subsequent covalent binding of a highly reactive metabolic product of I, presumed to be the *p*-quinoneimide (II), to tissue macromolecules (Scheme I).

Numerous sulfhydryl-containing agents, including cysteamine, L-methionine, D-penicillamine, and *N*-acetyl-L-cysteine (III*a*), have been tested and shown to ameliorate acetaminophen toxicity in varying degrees (8–15), ostensibly by covalent intervention with the reactive metabolite, II. Of these compounds, III*a* has become the currently accepted therapy (16, 17). The use of *N*-acetyl-DL-penicillamine (III*b*), a structural analog of III*a*, has not been reported. Compound III*b*, which is effective for the treatment of mercuric chloride poisoning (18, 19), is not catabolized extensively and theoretically could form a pseudomercapturic acid conjugate (IV*b*) by interaction with the quinoneimide (II) *via* its sulfhydryl group. Compound IV*b* then would be expected to be excreted as an analog of the mercapturic acid (IV*a*) (Scheme II).

Accordingly, the effectiveness of III*b* as a protective agent against the hepatotoxicity elicited by I in mice was evaluated and compared to the protection afforded by III*a*.

EXPERIMENTAL

Animals—Randomly bred male Swiss–Webster mice[1], 20–30 g, were

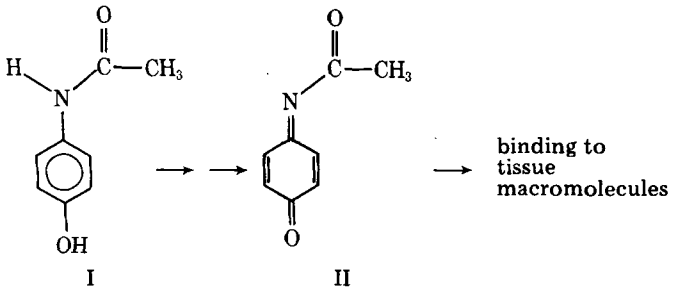

Scheme I

housed individually and fed a standard diet of rat chow and water *ad libitum*.

Chemicals—*N*-Acetyl-DL-penicillamine[2] (III*b*) was recrystallized from hot water. Injection solutions were prepared by dissolving 0.15 g in 15.0 ml of water (10 mg/ml). *N*-Acetyl-L-cysteine (III*a*) was a 20% sterile solution[3]. Solutions for injection were prepared by taking 1.0 ml of the 20% solution and diluting it to 20 ml with 0.9% sterile saline (10 mg/ml). Acetaminophen[4] (I) was recrystallized from hot water. Injection solutions were prepared by dissolving 1.25 g in 50.0 ml of sterile 0.9% saline. The solution was kept at 35–40° for injections.

Treatment Protocol and Histological Criteria—All drugs were administered intraperitoneally. Mice were treated with 750 mg of I/kg and 30 min later were given 400 mg of III*b* or III*a*/kg. Control mice received III*b*, III*a*, or 1.0 ml of sterile 0.9% saline. The mice then were observed for 48 hr with food and water allowed *ad libitum*. Mice that died during this period were examined grossly, and the liver and kidneys were excised, sliced, and fixed in 10% formalin for histological examination.

Survivors were sacrificed by cervical dislocation after the 48-hr period, and the liver and kidneys of all mice were processed as described. Paraffin sections of these tissues were stained with hematoxylin and eosin. Liver injury was graded according to the criteria described by Mitchell *et al.* (20) and quantitated as follows: 0, necrosis absent; 1+, necrosis of <6% of hepatocytes; 2+, necrosis of 6–25% of hepatocytes; 3+, necrosis of 25–50% of hepatocytes; and 4+, necrosis of >50% of hepatocytes.

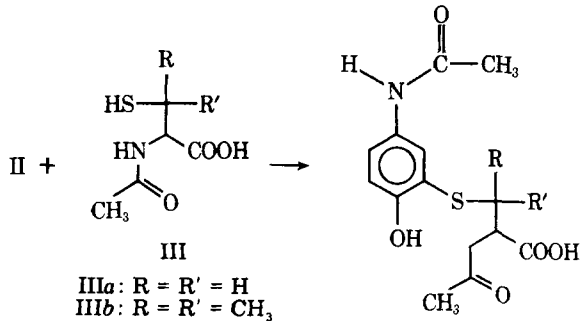

Scheme II

RESULTS

The results of these experiments are summarized in Table I. Mice given 750 mg of I/kg without sulfhydryl treatment did poorly. At 48 hr, 40% had died and 40% had 3–4+ liver necrosis. Mice that were given I and treated with III*b* did not fare much better. At 48 hr, 40% of the animals had died and 50% had 3–4+ necrosis. However, mice given I and III*a* responded well to the latter treatment, as expected. No deaths were noted at 48 hr; no animal had 3–4+ necrosis, and only three of 10 animals had any evidence of liver injury characterized by mild 1+ necrosis. Although the doses of III*b* and III*a* were not exactly equimolar due to differences in their molecular weights, the results clearly indicated that III*b* was ineffective as a protective agent. Some mice in the control groups given III*a* or III*b* alone apparently sustained a low-grade liver injury, an observation noted previously with III*a* (21).

Liver necrosis was of the centrilobular hemorrhagic type in the more severe examples and of the centrilobular type in the less severe cases.

[1] Biolabs, St. Paul, Minn.

[2] Lot 2998, Nutritional Biochemical Corp., Chagrin Falls, Ohio.
[3] Mucomyst (Lot UGH38), Mead-Johnson Co., Evansville, Ind.
[4] Lot A730-2, Aldrich Chemical Co., Milwaukee, Wis.

0022-3549/80/0900-1005$01.00/0
© 1980, American Pharmaceutical Association

Table I—Effect of *N*-Acetyl-DL-penicillamine (III*b*) and *N*-Acetyl-L-cysteine (III*a*) Treatment on the Hepatotoxicity Induced by Acetaminophen (I) in Mice

Treatment	Number of Animals	Deaths (48 hr)	Percent of Animals with Necrosis				
			4+	3+	2+	1+	0
Saline	10	0	0	0	0	0	100
I	10	4	40	0	10	0	50
I + III*b*	10	4	50	0	10	10	30
III*b*	10	0	0	10	0	10	80
I + III*a*	10	0	0	0	0	30	70
III*a*	10	0	0	0	0	20	80

Centrilobular hemorrhagic necrosis was reported previously as a component of acetaminophen overdose in the mouse (21). The histological pattern of centrilobular hemorrhagic necrosis is more typically seen with rapidly progressive congestive heart failure (21). Centrilobular necrosis differs from centrilobular hemorrhagic necrosis only in the absence of extravasated red cells and also was observed after toxic exposure to carbon tetrachloride, chloroform, or naphthalene (22).

DISCUSSION

In a study of the relative nucleophilicities of the sulfhydryl groups in thiol amino acids, Friedman *et al.* (23) observed that the mercaptide ion of III*b* was approximately 50 times less reactive with α,β-unsaturated systems than was III*a*. Since the pK values of the two sulfhydryl groups are similar (9.90 and 9.52, respectively), it was concluded that this differential nucleophilicity was due to steric hindrance in III*b* by the presence of the *gem*-dimethyl groups adjacent to the sulfhydryl group. The failure of III*b* to protect mice against toxic doses of I may reflect this low relative nucleophilicity of its sterically hindered sulfhydryl group.

Chasseaud (24) showed that enzymatic deacetylation of III*a* occurs prior to reaction with electrophiles. This finding suggests that cysteine itself and not III*a* may be involved in any addition reactions with II *in vivo*, a premise supported by the observation that cysteine is approximately 2.5 times more nucleophilic than its acetylated derivative, III*a* (23). Moreover, III*a* is rapidly and nearly quantitatively deacetylated to cysteine in the rat (25). When [^{35}S]acetylcysteine was administered to rats, the major metabolites were cysteine and cystine at 2 hr. At 24 hr, inorganic sulfate was the major product in the urine, with minor amounts of mixed disulfide also present. Thus, III*a* may act as a prodrug form of cysteine and release the latter in the liver as a trapping agent or as a biosynthetic precursor of glutathione.

In contrast, other investigators (26–28) presented indirect evidence for the absence of deacetylation of orally administered III*b* in rats and humans. The present investigators also observed that rat liver homogenates did not deacetylate III*b* under conditions where III*a* was completely deacetylated. In any event, D-penicillamine is not a particularly effective protective agent for I (14). Since the administration of sodium sulfate itself significantly reduced the toxicity of I in mice (29), the efficacy of III*a* treatment in acetaminophen overdoses has been suggested to be due to increased sulfate generation. D-Penicillamine is not catabolized appreciably *in vivo*, and inorganic sulfate has not been demonstrated as a metabolite (30, 31). These observations and the present results with III*b* suggest that the direct formation of conjugates such as IV (as in Scheme II) may not be operative *in vivo*.

Based on metabolic (32) and pharmacokinetic considerations (33), a dual therapeutic regimen designed to (*a*) eliminate much of the excess acetaminophen represented by the overdose *via* conjugation mechanisms on the preformed phenolic hydroxyl group and (*b*) sequester the reactive metabolite(s) generated during the oxidative metabolism of I by administration of a suitable trapping agent appears to be superior to a single-treatment regimen. An obvious choice would be the combination therapy of III*a* with sodium sulfate.

REFERENCES

(1) L. F. Prescott, N. Wright, P. Roscoe, and S. S. Brown, *Lancet*, 1, 519 (1971).

(2) A. T. Proudfoot and N. Wright, *Br. Med. J.*, **3**, 557 (1970).

(3) D. M. Rosenberg, A. A. Meyer, I. H. Manning, and F. A. Neelon, *South. Med. J.*, **70**, 660 (1977).

(4) T. D. Boyer and S. L. Rouff, *J. Am. Med. Soc.*, **218**, 440 (1971).

(5) J. R. Mitchell, D. J. Jallow, W. Z. Potter, J. R. Gillette, and B. B. Brodie, *J. Pharmacol. Exp. Ther.*, **187**, 211 (1973).

(6) D. Labadarios, M. Davis, B. Portman, and R. Williams, *Biochem. Pharmacol.*, **26**, 31 (1977).

(7) R. J. McMurty, W. R. Snodgrass, and J. R. Mitchell, *Toxicol. Appl. Pharmacol.*, **45**, 87 (1978).

(8) P. Crome, G. N. Volans, J. A. Vale, B. Widdop, and R. Goulding, *Lancet*, **2**, 829 (1976).

(9) A. P. Douglas, A. N. Hamlyn, and O. James, *ibid.*, **1**, 111 (1976).

(10) R. C. Peterson and B. H. Rumack, *J. Am. Med. Soc.*, **237**, 2406 (1977).

(11) E. Piperno and D. A. Berssenbruegge, *Lancet*, **2**, 738 (1976).

(12) L. F. Prescott, C. P. Swainson, A. R. W. Forrest, and H. Matthew, *ibid.*, **1**, 588 (1974).

(13) L. F. Prescott, F. R. Sutherland, J. Park, I. J. Smith, and A. J. Proudfoot, *ibid.*, **2**, 109 (1976).

(14) L. F. Prescott, J. Park, and A. T. Proudfoot, *J. Int. Med. Res.*, **4** (Suppl. 4), 112 (1976).

(15) L. F. Prescott, A. Ballantyne, J. Park, P. Adriaenssens, and A. T. Proudfoot, *Lancet*, **2**, 432 (1977).

(16) J. R. Lewis, *J. Am. Med. Soc.*, **240**, 684 (1978).

(17) American Academy of Pediatrics Committee on Drugs, *Pediatrics*, **61**, 108 (1978).

(18) H. V. Aposhian and M. M. Aposhian, *J. Pharmacol. Exp. Ther.*, **126**, 131 (1959).

(19) R. A. P. Kark, D. C. Poskanzer, J. D. Bullock, and G. Boylen, *N. Engl. J. Med.*, **285**, 10 (1971).

(20) J. R. Mitchell, D. J. Jollow, W. Z. Potter, D. C. Davis, J. R. Gillette, and B. B. Brodie, *J. Pharmacol. Exp. Ther.*, **187**, 185 (1973).

(21) E. Piperno, A. H. Mosher, D. A. Berssenbruegge, J. D. Winkler, and R. B. Smith, *Pediatrics*, **62**, 880 (1978).

(22) S. L. Robbins, "The Pathologic Basis of Disease," 4th ed., W. B. Saunders, Philadelphia, Pa., 1974, pp. 999–1001.

(23) M. Friedman, J. F. Cavins, and J. S. Wall, *J. Am. Chem. Soc.*, **87**, 3672 (1965).

(24) L. F. Chasseaud, *Biochem. Pharmacol.*, **23**, 1133 (1974).

(25) A. L. Sheffner, E. M. Medler, K. R. Bailey, D. G. Gallo, A. J. Mueller, and H. R. Sarett, *ibid.*, **15**, 1523 (1966).

(26) J. C. Capps, E. M. Medler, L. W. Jacobs, and A. L. Sheffner, *Am. J. Clin. Nutr.*, **21**, 715 (1968).

(27) A. D. Stephens and R. W. Watts, *Q. J. Med., New Ser. XI*, **355** (1971).

(28) D. A. Gibbs and R. W. Watts, *Clin. Sci. Mol. Med.*, **36**, 87 (1969).

(29) J. T. Slattery and G. Levy, *Res. Commun. Chem. Pathol. Pharmacol.*, **18**, 167 (1977).

(30) F. Planas-Bohne, *Z. Naturforsch.*, **28**, 774 (1973).

(31) F. Planas-Bohne, *Arzneim.-Forsch.*, **22**, 1426 (1972).

(32) J. A. Hinson, L. R. Pohl, and J. R. Gillette, *Life Sci.*, **21**, 2133 (1979).

(33) J. T. Slattery and G. Levy, *Clin. Pharmacol. Ther.*, **25**, 184 (1979).

ACKNOWLEDGMENTS

Supported by a program grant from the Veterans Administration.

Synthesis and Biological Evaluation of 2,3-Diazabicyclo[2.2.1]heptane Derivatives as Prostaglandin Endoperoxide Analogs

SHEUNG-TSAM KAM *, ROBERT N. HANSON ‡, and PHILIP S. PORTOGHESE ×

Received April 11, 1979, from the *Department of Medicinal Chemistry, College of Pharmacy, University of Minnesota, Minneapolis, MN 55455.* Accepted for publication June 26, 1979. *Present address: American Critical Care, McGaw Park, IL 60085. ‡Present address: College of Pharmacy and Allied Health Professions, Northeastern University, Boston, MA 02115.

Abstract □ Three prostaglandin endoperoxide analogs that possess the 2,3-diazabicyclo[2.2.1]heptane skeleton were synthesized and evaluated for activity in human platelets and in the rat fundus. All three compounds were inactive in inhibiting or stimulating platelet aggregation. One compound possessed weak contracting activity on the rat fundus.

Keyphrases □ Platelet aggregation—evaluation of inhibition and stimulation by prostaglandin endoperoxide analogs □ Prostaglandin endoperoxide analogs—synthesis and evaluation for inhibition and stimulation of platelet aggregation

A recent report stated that the prostaglandin endoperoxide analog 9,11-azo-13-oxa-15-hydroxyprostanoic acid (I) is a potent inhibitor of platelet aggregation (1). Some of its congeners also possessed antiaggregatory activity.

Because simple bicyclic systems, such as 2,3-dioxabicyclo[2.2.1]heptane and 2,3-diazabicyclo[2.2.1]hept-2-ene, were reported (2) to inhibit platelet aggregation in the millimolar concentration range, determination of whether less complex congeners of I containing only one side chain exhibit similar activity was of interest. The synthesis and biological evaluation of such compounds (II–IV) are described.

DISCUSSION

The preparation of II was accomplished *via* the olefin synthesis of Zweifel *et al.* (3) using diethyl 2,3-diazabicyclo[2.2.1]hept-5-ene-2,3-dicarboxylate (V) (4) (Scheme I). Two products, the desired *cis*-olefin (VII) (70%) and a ring-opened product, 4-(*N,N'*-dicarboethoxyhydrazino)cyclopentene (VIII) (10%), were obtained. The isolation of VII and VIII can be rationalized by the formation of an intermediate (VI), which can rearrange through two different but competitive pathways. Path a is the dominant alkyl carbanion migration pathway and yields VII; path b leads to rupture of the bicyclic system to give VIII[1]. Treatment of VII with base followed by air oxidation with cupric acetate as a catalyst (6) and acidolysis gave the target compound, II.

The coupling constant of the olefinic protons in II is ~10 Hz, which is within the range of the coupling constant for a *cis*-double bond (7). The *exo*-orientation of the side chain at C-5 is assigned by virtue of the reaction mechanism since hydroboration of bicyclic olefins proceeds by *cis*-addition (8) from the *exo*-face (8) and migration of an alkyl group from the boron atom to an electron-deficient carbon (path a in VI) occurs (9) with the retention of configuration.

Compounds III and IV were synthesized from the *exo*-mesylate (X)

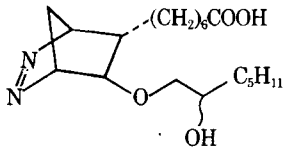

I

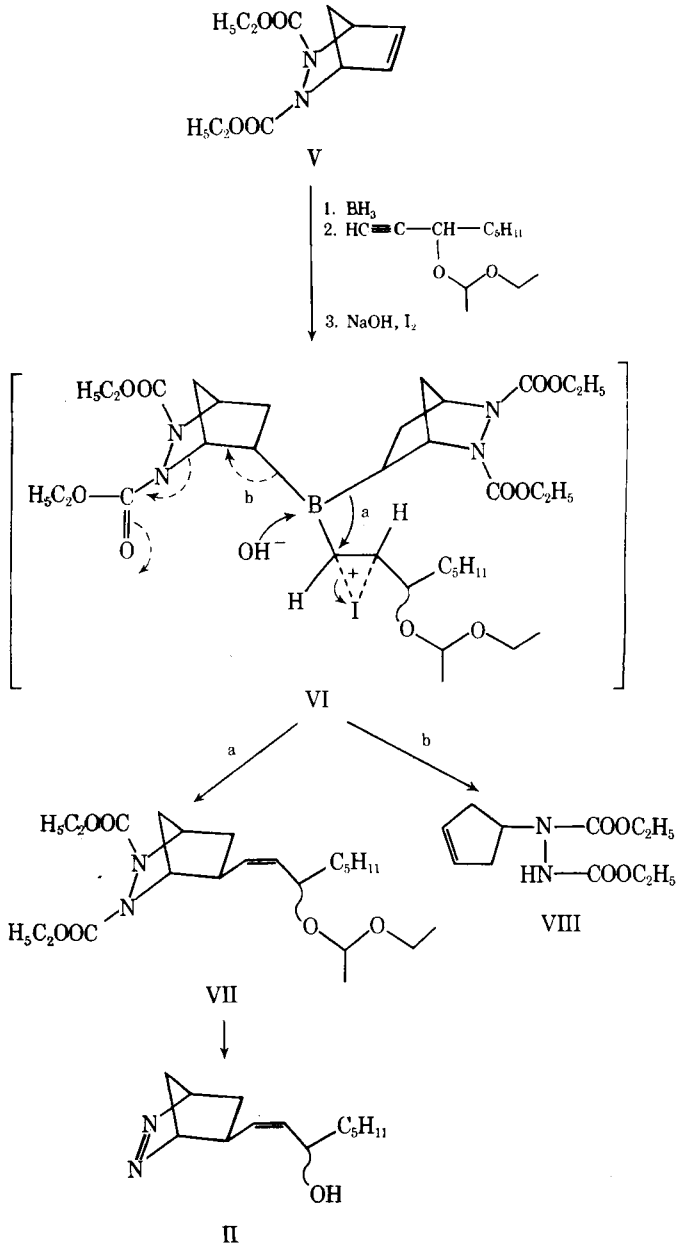

V, VI, VII, VIII, II

Scheme I

(Scheme II) using the aluminum-mediated condensation developed by Nagishi and Baba (10). Compound X, which was prepared from the corresponding alcohol (IX), was reacted with tri-1-octynylalane to yield III (46%) (Scheme II). Deprotection and oxidation of III gave the azo product, IV.

The NMR spectrum of III indicates that the 1-octynyl side chain at C-5 is *exo*. After decoupling of the C-6 *exo*-proton and the C-3' methylene protons of the alkyne side chain, the C-5 methine proton appeared as a broad doublet at δ 2.65. The coupling constant (J = 7 Hz) of this doublet

[1] A similar ring-opened product was reported in the hydroboration–oxidation of dimethyl 2,3-diazabicyclo[2.2.1]hept-5-ene-2,3-dicarboxylate (5).

0022-3549/80/0900-1007$01.00/0
© 1980, American Pharmaceutical Association

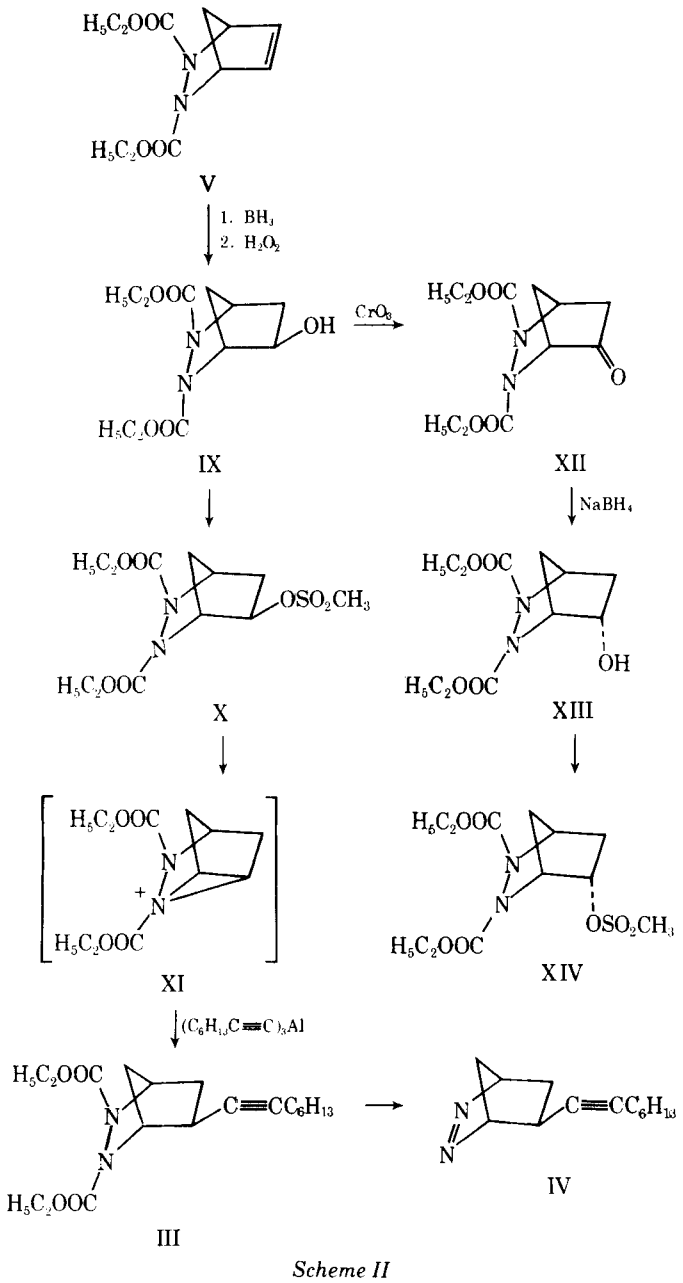

Scheme II

is in the range of *endo-endo* coupling (J = 6–7 Hz) in the norbornane system (11) and is identical to that reported (12) for a related compound.

The *endo*-mesylate isomer (XIV) (Scheme II) did not react with tri-1-octynylalane under identical conditions. This isomer was prepared by a similar procedure (5) and included oxidation of the alcohol (IX) followed by hydride reduction of the resulting ketone (XII) to the *endo*-alcohol (XIII) (Scheme II).

The fact that only the *exo*-mesylate underwent this reaction can be explained by a carbonium-ion mechanism (10) with the assumption that departure of the *exo*-mesylate group is assisted by the electrons of the neighboring carbamate nitrogen. This action would give a symmetrical aziridinium-ion intermediate (XI), which opens on reaction with the alkyne. A similar type of ring opening was reported (12) with a structurally related aziridinium ion to give an *exo*-substituted product. Therefore, the predictable stereochemical consequence of the aziridinium-ion (XI) mechanism is that the newly introduced group at C-5 in III and IV is *exo*. In contrast, the stereochemistry of the *endo*-methanesulfonate group in XIV makes it difficult or impossible to form an aziridinium ion because departure of the *endo*-methanesulfonate function receives no assistance from the neighboring nitrogen.

At 10^{-4} M, none of the compounds (II–IV) induced aggregation of human platelets or inhibited the aggregation induced by 8.2×10^{-4} M arachidonic acid or by 8.5×10^{-7} M of 9,11-methanoepoxy prostaglandin H_2[2] (13). In view of the finding (1) that all analogs of I that possess the carboxyhexyl side chain showed inhibition of the aggregation induced by 9,11-methanoepoxy prostaglandin H_2, the carboxyhexyl side chain might be more important in receptor or enzyme binding relative to the other side chain. The activity of II–IV on the rat fundus also was evaluated. Compound III showed contracting activity at 10^{-4} M but was much less potent ($\sim 3 \times 10^5$-fold) than prostaglandin E_2. The other two compounds were inactive in this test.

EXPERIMENTAL[3]

Diethyl 5-*exo*-[3-[(1-Ethoxy)ethoxy]-*cis*-1-octenyl]-2,3-diazabicyclo[2.2.1]heptane-2,3-dicarboxylate (VII)—To 9.5 ml of diborane–tetrahydrofuran (1.09 M, 10 mmoles) at 0° under nitrogen was added 4.8 g (20 mmoles) of V (4) in tetrahydrofuran (10 ml). After the mixture was stirred at 0° for 6 hr, 1.98 g (10 mmoles) of 3-[(1-ethoxy)-ethoxy]oct-1-yne (14) was added dropwise. Stirring was continued for 1 hr at 0° followed by 1.5 hr at 25°. The mixture then was cooled to 0°, and migration of the diazabicyclic system was induced by addition of sodium hydroxide (6 N, 6 ml) followed by iodine (2.54 g, 10 mmoles) in 15 ml of tetrahydrofuran.

The mixture was maintained at ice temperature for 5 hr and at 25° for an additional 3 hr. Excess iodine in the mixture was destroyed by addition of an aqueous solution of sodium thiosulfate. The organic layer was separated, and the aqueous phase was extracted three times with ether (50 ml). The organic layers were combined and dried (anhydrous magnesium sulfate), and the solvent was removed *in vacuo*. The crude product was chromatographed on silica gel (100 g, 3 × 35 cm) using (*a*) 20% ethyl acetate in petroleum ether (30–60°) (300 ml), (*b*) ethyl acetate in petroleum ether (30–60°) (200 ml), (*c*) ethyl acetate (300 ml), and (*d*) 2% methanol in ethyl acetate (300 ml).

The major product, VII, was eluted with ethyl acetate fractions (3.08 g, 70%). Rechromatography of VII on silica gel (100 g, 3 × 35 cm) using 3% isopropanol in chloroform afforded analytically pure VII; IR (liquid film): 1700 and 1750 (C=O) cm^{-1}; NMR (carbon tetrachloride): δ 0.7–1.57 (m, 25H, C_5H_{11}, 2 $COOCH_2CH_3$, $CHCH_3$, OCH_2CH_3, and 2 methylene protons at C-6), 1.65 (broad s, 3H, 2 bridge protons at C-7 and 1 methine proton at C-5), 3.2–3.7 (m, 2H, OCH_2CH_3), 3.98–4.8 (m, 8H, 2 $COOCH_2CH_3$, bridgehead protons at C-1 and C-4, C=CCH, and O–CH–O), and 5.0–5.65 (m, 2H, olefinic protons); mass spectrum (70 ev): m/e 440 (M^+).

Anal.—Calc. for $C_{23}H_{40}N_2O_6$: C, 62.70; H, 9.15; N, 6.36. Found: C, 62.53; H, 9.28; N, 6.18.

The ring-opened product (VIII) (0.48 g, 10%) was isolated from the 2% methanol in ethyl acetate eluent; IR (liquid film): 3300 (NH) and 1510 (CON) cm^{-1}; NMR (chloroform-d_6): δ 1.13 (t, 6H, 2 $COOCH_2CH_3$), 2.39 (d, 4H, $CH_2C{=}CH_2$), 4.05 (q, 4H, 2 $COOCH_2CH_3$), 4.8 (m, 1H, >CHN), 5.5 (s, 2H, $CH{=}CH$), and 6.8 (s, 1H, NH); mass spectrum (70 ev): m/e 242 (M^+).

Anal.—Calc. for $C_{11}H_{18}N_2O_4$: C, 54.53, H, 7.49; N, 11.57. Found: C, 54.73; H, 7.63; N, 11.32.

5-*exo*-(3-Hydroxy-*cis*-1-octenyl) -2,3- diazabicyclo[2.2.1]hept-2-ene (II)—Compound VII (0.44 g, 1 mmole) was dissolved in ethylene glycol (1 ml) and mixed with a solution of potassium hydroxide (0.336 g, 6 mmoles) in ethylene glycol (6 ml). The mixture was heated at 115° for 4.5 hr followed by the addition of water (50 ml). The aqueous solution was extracted with two 100-ml portions of ether. The volume of the ether was reduced to ~10 ml and mixed with methanol (10 ml) containing a catalytic amount (0.01 g) of cupric acetate. Air was bubbled into the mixture at 0° for 2 hr.

The resulting mixture was partitioned between water (50 ml) and ether (2 × 200 ml). The ether layer was separated and removed *in vacuo* to give an oil, which was chromatographed on silica gel (10 g, 1.3 × 30 cm) with ether to afford 5-*exo*-[3-(1-ethoxy)ethoxy-*cis*-1-octenyl]-2,3-diazabicyclo[2.2.1]hept-2-ene (0.183 g, 65%); IR (liquid film): 1490 (N=N) cm^{-1}; mass spectrum (70 ev): m/e 294 (M^+). Deprotection of the alcohol was achieved by dissolving this product in ethyl acetate–water–tetrahydrofuran (3:1:1) (10 ml) and heating to 45° for 3 hr.

[2] U46619.

[3] Melting points were determined with a Thomas-Hoover melting-point apparatus and are uncorrected. Elemental analyses were performed by M-H-W Laboratories, Phoenix, Ariz. IR spectra were obtained with a Perkin-Elmer model 237B grating spectrophotometer. NMR data (δ) were recorded with Varian models A-60D and T-60 spectrometers. Mass spectral analyses were performed with a Hitachi Perkin-Elmer model RMU-6D spectrometer by the Mass Spectrometry Service Laboratory, School of Chemistry, University of Minnesota.

The solvents were removed *in vacuo* at 25° to leave an oily residue, which was chromatographed on silica gel (10 g, 1.3 × 30 cm) with ether to give II (0.13 g, 59%). This product was a mixture of two racemates; IR (liquid film): 3400 (OH), 1700 (*cis*-C=C), and 1490 (N=N) cm^{-1}; NMR (carbon tetrachloride): δ 1.95–2.2 (broad d, 1H, methine proton at C-5), 3.9–4.5 (m, 1H, C*H*OH), 4.75, 4.9 (2 broad s, 1H, bridgehead proton assigned to the two diastereomers at C-4), 4.95–5.6 (m, 2H, *cis*-C*H*=C*H*, J = 10 Hz), and 5.13 (broad s, 1H, bridgehead proton at C-1); mass spectrum (70 ev): m/e 176 ($M^+ - N_2 - H_2O$); UV: λ_{max} 338 (N=N) nm.

Anal.—Calc. for $C_{13}H_{22}N_2O$: C, 70.22; H, 9.98; N, 12.60. Found: C, 70.07; H, 9.87; N, 12.54.

Diethyl 5-*exo*-Hydroxy-2,3-diazabicyclo[2.2.1]heptane-2,3-dicarboxylate (IX)—Compound IX was obtained from diethyl 2,3-diazabicyclo[2.2.1]hept-5-ene-2,3-dicarboxylate (V) (4) (1 g, 3.7 mmoles) by hydroboration and oxidation *via* a procedure similar to that described by Allred and Smith (5). The oily product was chromatographed on silica gel and eluted with ethyl acetate–ether (3:2) to give 0.7 g (75%) of the *exo*-alcohol (IX) as a colorless oil, R_f 0.31 (silica gel, 10% ethanol in ether); IR (liquid film): 3475 (OH), 1720, and 1750 (C=O) cm^{-1}; NMR (carbon tetrachloride): δ 1.27 (t, 6H, 2 $COOCH_2CH_3$), 1.58 (m, 2H, bridge protons at C-7), 1.78–2.2 (m, 2H, CHOH-CH_2), 4.1 (broad s, 1H, bridgehead proton at C-1), and 4.47 (broad s, 1H, bridgehead proton at C-4); mass spectrum (70 ev): m/e 258 (M^+).

Anal.—Calc. for $C_{11}H_{18}N_2O_5$: C, 51.15; H, 7.02; N, 10.85. Found: C, 50.96; H, 7.24; N, 10.69.

Diethyl 5-*exo*-Methanesulfonyl-2,3-diazabicyclo[2.2.1]heptane-2,3-dicarboxylate (X)—To a solution of IX (3.64 g, 14.1 mmoles) in pyridine–toluene (1:1) (40 ml) was added 1.78 g (15.5 mmoles) of methanesulfonyl chloride in pyridine (20 ml) at 0°. The mixture was allowed to stir at 25° for 12 hr, and the pyridinium hydrochloride salt which precipitated was removed by filtration. The filtrate was concentrated *in vacuo*, and the residue was partitioned between water (50 ml) and methylene chloride (2 × 100 ml). Removal of the methylene chloride afforded an oil, which was chromatographed on silica gel (50 g, 2.3 × 35 cm) using benzene–ether (8:2) to give X.

Compound X was crystallized from carbon tetrachloride–ether to afford a white solid (3.8 g, 80%), R_f 0.52 (silica gel, ether), mp 87.5–88°; NMR (chloroform-d_6): δ 1.26 (2 t, 6H, 2 $COOCH_2CH_3$), 1.5–2.6 (m, 4H, methylene protons at C-6 and bridge protons at C-7), 3.02 (s, 3H, OSO_2CH_3), 4.16 (2 q, 4H, 2 $COOCH_2CH_3$), and 4.45–4.9 (m, 3H, bridgehead protons at C-1 and C-5 and methine proton at C-5); mass spectrum (70 ev): m/e 336 (M^+).

Anal.—Calc. for $C_{12}H_{20}N_2O_7S$: C, 42.85; H, 5.99; N, 8.33. Found: C, 42.58; H, 5.86; N, 8.16.

Diethyl 5-*exo*-(1-Octynyl)-2,3-diazabicyclo[2.2.1]heptane-2,3-dicarboxylate (III)—To a solution of *n*-oct-1-yne (0.9 g, 9.6 mmoles, purified by distillation over anhydrous sodium sulfate) in dry *n*-hexane (15.4 ml) was added, under nitrogen, 3.84 ml of *n*-butyl lithium (2.5 *M*, 9.6 mmoles) in hexane at 0°. The suspension was stirred at 0° for 0.5 hr, and 0.43 g (3.2 mmoles) of aluminium chloride was added. The resulting mixture was stirred at 0° for 0.5 hr, and the solvent was removed *in vacuo* at 25° to give a residue of trioctylalane; this residue was dissolved in 25 ml of dry dichloroethane (dried over phosphorus pentoxide and distilled) under nitrogen.

The trioctylalane solution was cooled to 0°, and a solution of 1.0 g (3 mmoles) of X in 5 ml of dichloroethane was added. After stirring at 25° for 24 hr, the mixture was added to another batch of freshly prepared trioctylalane (9.6 mmoles). Stirring was continued at 25° for another 24 hr, and the mixture then was partitioned between 2% HCl (50 ml) and chloroform (2 × 100 ml). The organic layer was separated, dried (anhydrous sodium sulfate), and filtered, and the solvent was removed *in vacuo* to give an oil; this oil was chromatographed on silica gel (10 g, 1.3 × 30 cm) with ether–pentane (4:1) to afford III (0.43 g, 46%).

Compound III showed a single peak on GLC (3% OV-1, 1.8 m; 200°; nitrogen flow rate, 10 ml/min; retention time, 5 min); NMR (carbon tetrachloride): δ 0.66–1.06 (m, 3H, CH_2CH_3), 1.65 (broad s, 2H, protons at C-7), 1.83 (broad s, 1H, *endo*-proton at C-6), 2.06 (broad s, 3H, 2 C=C-CH_2 and C-6 *exo*-proton), and 2.65 (broad s, 1H, >CH-C≡C-; after decoupling of the δ 2.06 peak, J = 7 Hz); mass spectrum (68 ev, high resolution): calc. M^+ for $C_{19}H_{30}N_2O_4$, m/e 350.2205; found, 350.2212.

Anal.—Calc. for $C_{19}H_{30}N_2O_4$: C, 65.16; H, 8.64; N, 8.00. Found: C, 65.47; H, 8.82; N, 7.97.

5-*exo*-(1-Octynyl)-2,3-diazabicyclo[2.2.1]hept-2-ene (IV)—Compound IV was prepared from III (0.7 g, 2 mmoles) by base hydrolysis and oxidation according to the procedure employed for the preparation of II. The product was extracted with ether after oxidation. The ether was removed *in vacuo*, and the residue was chromatographed on silica gel (10 g, 1.3 × 30 cm) with 10% isopropanol in petroleum ether (30–60°) to give IV (0.37 g, 90%); IR (liquid film): 1590 (N=N) cm^{-1}; NMR (carbon tetrachloride): δ 1.7–2.3 (m, 3H, C*H*-C≡C-CH_2) and 4.9–5.15 (m, 2H, bridgehead protons at C-1 and C-4); mass spectrum (70 ev): m/e 204 (M^+).

Anal.—Calc. for $C_{13}H_{20}N_2$: C, 76.42; H, 9.87; N, 13.72. Found: C, 76.64; H, 9.96; N, 13.75.

Diethyl 2,3-Diazabicyclo[2.2.1]heptane-5-one-2,3-dicarboxylate (XII)—A mixture of chromium trioxide (8.92 g, 88.2 mmoles), 200 ml of methylene chloride (dried over a 3-Å molecule sieve), and 7.0 g (88.2 mmoles) of pyridine (dried over potassium hydroxide pellets) was allowed to stir at 25° for 15 min. A solution containing 3.93 g (14.7 mmoles) of IX in methylene chloride (10 ml) was added to this mixture and stirred for 15 min. The reaction mixture then was filtered, and the methylene chloride was removed *in vacuo*. The residue was dissolved in ether (100 ml) and filtered again to obtain a clear filtrate.

Removal of the ether afforded an oily product (XII) (7.2 g, 82%), which was relatively pure as judged by NMR analysis. This product was used without further purification for the synthesis of XIII because of its instability. A small quantity of pure XII was isolated by using a Florisil column (50 g, 2.3 × 35 cm) with methylene chloride; IR (liquid film): 1775 (C=O) cm^{-1}; NMR (carbon tetrachloride): δ 1.3 (2 t, 6H, 2 $COOCH_2CH_3$), 1.98 (s, 2H, bridge protons at C-7), 2.22 (s, 2H, CH_2C=O), 4.15 (2 q, 4H, 2 $COOCH_2CH_3$), 4.22 (broad s, 1H, bridgehead proton at C-1), and 4.8 (s, 1H, bridgehead proton at C-4); mass spectrum (70 ev): m/e 256 (M^+).

Anal.—Calc. for $C_{11}H_{16}N_2O_5$: C, 52.30; H, 6.29; N, 10.93. Found: C, 52.17; H, 6.50; N, 10.80.

Diethyl 5-*endo*-Hydroxy-2,3-diazabicyclo[2.2.1]heptane-2,3-dicarboxylate (XIII)—To a solution of bicyclic ketone (XII) (4.1 g, 1.6 mmoles) in methanol (46 ml) maintained at −25° were added divided portions of sodium borohydride (0.6 g, 16 mmoles) in methanol–water (80:20) (49 ml). After stirring at −25° for 15 min, the reaction was quenched by addition of dilute hydrochloric acid to pH 7. The methanol was removed *in vacuo*, and the remaining aqueous solution was extracted with methylene chloride (2 × 50 ml). Removal of the methylene chloride *in vacuo* afforded an oily product (XIII), which was purified by column chromatography using silica gel (60 g, 2.3 × 3.5 cm) and eluted first with 250 ml of ether and then with 10% ethanol in ether to obtain the pure alcohol (XIII) (2.26 g, 55%), R_f 0.51 (silica gel, 10% ethanol in ether); IR (liquid film): 3475 (OH) cm^{-1}; NMR (carbon tetrachloride): δ 1.25 (t, 6H, 2 $COOCH_2CH_3$), 1.66 (s, 2H, bridge protons at C-7), 1.5–2.4 (m, 4H, 2 bridge protons at C-6 and 2 bridge protons at C-7), 4.15 (2 q, 4H, 2 $COOCH_2CH_3$), 4.2 (m, 1H, methine proton at C-5 observed after decoupling of the δ 1.25 triplet), 4.28 (s, 1H, bridgehead proton at C-1), and 4.44 (s, 1H, bridgehead proton at C-4); mass spectrum (20 ev): m/e 258 (M^+).

Anal.—Calc. for $C_{11}H_{18}N_2O_5$: C, 51.15; H, 7.02; N, 10.85. Found: C, 51.14; H, 6.99; N, 10.88.

Diethyl 5-*endo*-Methanesulfonyl-2,3-diazabicyclo[2.2.1]heptane-2,3-dicarboxylate (XIV)—Compound XIV was prepared from XIII (0.85 g, 3.3 mmoles) in the manner described for the preparation of X. The crude product was purified on silica gel (10 g, 1.3 × 30 cm) with 20% ethyl acetate in ether to afford an oil. This oil was crystallized from carbon tetrachloride to give pure XIV (10 g, 92%), R_f 0.37 (silica gel, ether), mp 120–120.5°; NMR (chloroform-d_6): δ 3.05 (s, 3H, OSO_2CH_3), 4.48 (broad s, 1H, bridgehead proton at C-1), and 4.92–5.2 (m, 2H, bridgehead proton at C-4 and methine proton at C-5); mass spectrum (70 ev): m/e 336 (M^+).

Anal.—Calc. for $C_{12}H_{20}N_2O_7S$: C, 42.85; H, 5.99; N, 8.33. Found: C, 42.72; H, 6.02; N, 8.28.

Platelet Aggregation Studies—Platelet-rich plasma was prepared according to the method of Gerrard *et al.* (15) and was incubated with II–IV (10^{-4} *M*) at 37.5° for 1.5 min. It then was added to a cell containing a standard quantity of arachidonic acid or 9,11-methanoepoxy prostaglandin H_2. Aggregation (or inhibition of aggregation) was monitored for 5 min on a dual-channel aggregometer[4].

Rat Fundus Studies—A 0.2 × 2.5-cm section of the fundus was cut from the outer curvature of the stomach from male Sprague–Dawley rats and suspended in a tissue bath. The tissue bath was perfused continuously with Krebs solution, and one end of the stomach was tied to an isotonic heart–smooth muscle transducer connected to a recorder[5].

[4] Payton.
[5] Beckman R411 Dynograph.

Compounds II–IV were added to the bath, and muscle contraction was monitored for 1.5 min. Prostaglandin E_2 was used to obtain standard contraction.

REFERENCES

(1) S. T. Kam, P. S. Portoghese, J. M. Gerrard, and E. W. Dunham, *J. Med. Chem.*, **22**, 1402 (1979). S. T. Kam, P. S. Portoghese, E. W. Dunham, and J. M. Gerrard, *Prostaglandins and Medicine*, **3**, 279 (1979).

(2) N. A. Porter, J. H. Roycroft, J. Nixon, D. Gilmore, and D. B. Mengel, *Fed. Proc., Fed. Am. Soc. Exp. Biol.*, **37**, 608 (1978).

(3) G. Zweifel, R. P. Fisher, J. T. Snow, and C. C. Whitney, *J. Am. Chem. Soc.*, **93**, 6309 (1971).

(4) P. G. Gassman and K. T. Mansfield, *Org. Syn.*, **49**, 1 (1969).

(5) E. L. Allred and R. L. Smith, *J. Org. Chem.*, **31**, 3489 (1966).

(6) E. J. Corey, K. C. Nicolaou, Y. Machida, C. L. Malmsten, and B. S. Samuelsson, *Proc. Natl. Acad. Sci., USA*, **72**, 3355 (1975).

(7) L. M. Jackman and S. Sternhell, "Applications of Nuclear Magnetic Resonance Spectroscopy in Organic Chemistry," 2nd ed., Pergamon, Oxford, England, 1969, p. 301.

(8) H. C. Brown and G. Zweifel, *J. Am. Chem. Soc.*, **83**, 2544 (1961).

(9) M. W. Rathke, N. Inoue, K. R. Varma, and H. C. Brown, *ibid.*, **88**, 2870 (1966).

(10) E. Nagishi and S. Baba, *ibid.*, **97**, 7385 (1975).

(11) L. M. Jackman and S. Sternhell, "Applications of Nuclear Magnetic Resonance Spectroscopy in Organic Chemistry," 2nd ed., Pergamon, Oxford, England, 1969, p. 289.

(12) P. S. Portoghese and D. T. Sepp, *Tetrahedron*, **29**, 2253 (1973).

(13) C. Malmsten, *Life Sci.*, **18**, 169 (1976).

(14) G. Stook and M. Isobe, *J. Am. Chem. Soc.*, **97**, 4745 (1975).

(15) J. M. Gerrard, J. D. Peller, T. P. Krich, and J. G. White, *Prostaglandins*, **14**, 39 (1977).

ACKNOWLEDGMENTS

Abstracted in part from a dissertation submitted by S.-T. Kam to the University of Minnesota in partial fulfillment of the Doctor of Philosophy degree requirements.

Supported in part by National Institutes of Health Research Grant HL 16524.

The authors thank Dr. E. W. Dunham, Department of Pharmacology, and Dr. J. M. Gerrard, Department of Pediatrics, University of Minnesota, for assistance in the biological evaluation and Dr. J. E. Pike, The Upjohn Co., for the prostaglandin standards.

Potential Organ- or Tumor-Imaging Agents XIX: Radioiodinated Antiarrhythmic Drugs as Potential Myocardial Imaging Agents

N. KORN, J. K. GIBSON, F. J. KNIFFEN, B. R. LUCCHESI, V. V. RANADE, M. MIMNAUGH, T. YU, and R. E. COUNSELL ˣ

Received April 16, 1979, from the *Department of Pharmacology, Medical School, University of Michigan, Ann Arbor, MI 48109.* Accepted for publication August 22, 1979.

Abstract □ Iodinated and radioiodinated analogs of propranolol and *N,N*-dimethylpropranolol were synthesized wherein an iodophenyl moiety replaced the naphthalene ring of the parent drug. These new compounds were evaluated not only for their β-adrenergic blocking and antiarrhythmic activities but also for their ability to accumulate selectively in myocardial tissue. Like propranolol, the iodinated analogs displayed comparable β-blocking and antiarrhythmic activity, and the order of potency was *ortho-* > *meta-* > *para*-iodophenyl. Quaternization of propranolol and the iodinated analogs eliminated the β-adrenergic blocking activity but retained the antiarrhythmic property of the secondary amine precursors. Among the quaternary salts, the antiarrhythmic potency was *meta-* > *ortho-* > *para*-iodophenyl. Tissue distribution of the radioiodinated derivatives revealed that only the quaternary derivatives were selectively accumulated in myocardial tissue. These results demonstrate that an iodophenyl ring can substitute for the naphthalene ring in propranolol and its quaternary salt without significant alteration of pharmacological properties. The radioiodinated quaternary derivatives may be useful pharmacological tools in experiments aimed at relating antiarrhythmic activity to myocardial uptake.

Keyphrases □ Antiarrhythmic agents—iodinated and radioiodinated analogs of propranolol and *N,N*-dimethylpropranolol, synthesis and evaluation of activity, tissue distribution of radioiodinated analogs, potential as myocardial imaging agents □ Propranolol—iodinated and radioiodinated analogs, synthesis and testing for β-adrenergic blocking and antiarrhythmic activity, tissue distribution of radioiodinated analogs, potential as myocardial imaging agents □ Radionuclide imaging—radioiodinated analogs of propranolol and *N,N*-dimethylpropranolol, tissue distribution, potential as myocardial imaging agents

The synthesis of a compound that selectively concentrates in the myocardium and that also can act as a carrier molecule for a γ-emitting nuclide has been a goal of this laboratory for several years (1–3). The approach has been to select a compound with known or suspected propensity for the target organ and then to modify the structure to allow incorporation of a γ-emitting nuclide while retaining the localizing properties of the parent compound.

BACKGROUND

One possible carrier molecule for myocardial localization is the β-adrenergic blocking agent propranolol (I). Its antiarrhythmic actions were demonstrated in a wide variety of experimentally induced arrhythmias (4, 5) as well as in clinically occurring arrhythmias (6, 7). Tissue distribution studies with [^{14}C]propranolol (8, 9) demonstrated its uptake by the heart, but not to the degree expected in view of the potent action of propranolol in blocking the cardiac effects of catecholamines (8). Instead, other tissues such as the lungs and brain contained higher levels of radioactivity (8, 9).

Previous studies in this laboratory showed that quaternization of propranolol produced a drug (II) that retained the antiarrhythmic activity but eliminated the β-adrenergic blocking property of propranolol (10). Subcutaneous administration of ^{14}C-labeled II to rats revealed a rapid and selective localization of radioactivity in the heart (23 times the blood

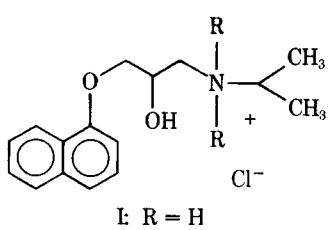

I: R = H
II: R = CH_3

0022-3549/80/0900-1010$01.00/0

© 1980, American Pharmaceutical Association

Compounds II–IV were added to the bath, and muscle contraction was monitored for 1.5 min. Prostaglandin E_2 was used to obtain standard contraction.

REFERENCES

(1) S. T. Kam, P. S. Portoghese, J. M. Gerrard, and E. W. Dunham, *J. Med. Chem.*, **22**, 1402 (1979). S. T. Kam, P. S. Portoghese, E. W. Dunham, and J. M. Gerrard, *Prostaglandins and Medicine*, **3**, 279 (1979).

(2) N. A. Porter, J. H. Roycroft, J. Nixon, D. Gilmore, and D. B. Mengel, *Fed. Proc., Fed. Am. Soc. Exp. Biol.*, **37**, 608 (1978).

(3) G. Zweifel, R. P. Fisher, J. T. Snow, and C. C. Whitney, *J. Am. Chem. Soc.*, **93**, 6309 (1971).

(4) P. G. Gassman and K. T. Mansfield, *Org. Syn.*, **49**, 1 (1969).

(5) E. L. Allred and R. L. Smith, *J. Org. Chem.*, **31**, 3489 (1966).

(6) E. J. Corey, K. C. Nicolaou, Y. Machida, C. L. Malmsten, and B. S. Samuelsson, *Proc. Natl. Acad. Sci., USA*, **72**, 3355 (1975).

(7) L. M. Jackman and S. Sternhell, "Applications of Nuclear Magnetic Resonance Spectroscopy in Organic Chemistry," 2nd ed., Pergamon, Oxford, England, 1969, p. 301.

(8) H. C. Brown and G. Zweifel, *J. Am. Chem. Soc.*, **83**, 2544 (1961).

(9) M. W. Rathke, N. Inoue, K. R. Varma, and H. C. Brown, *ibid.*, **88**, 2870 (1966).

(10) E. Nagishi and S. Baba, *ibid.*, **97**, 7385 (1975).

(11) L. M. Jackman and S. Sternhell, "Applications of Nuclear Magnetic Resonance Spectroscopy in Organic Chemistry," 2nd ed., Pergamon, Oxford, England, 1969, p. 289.

(12) P. S. Portoghese and D. T. Sepp, *Tetrahedron*, **29**, 2253 (1973).

(13) C. Malmsten, *Life Sci.*, **18**, 169 (1976).

(14) G. Stook and M. Isobe, *J. Am. Chem. Soc.*, **97**, 4745 (1975).

(15) J. M. Gerrard, J. D. Peller, T. P. Krich, and J. G. White, *Prostaglandins*, **14**, 39 (1977).

ACKNOWLEDGMENTS

Abstracted in part from a dissertation submitted by S.-T. Kam to the University of Minnesota in partial fulfillment of the Doctor of Philosophy degree requirements.

Supported in part by National Institutes of Health Research Grant HL 16524.

The authors thank Dr. E. W. Dunham, Department of Pharmacology, and Dr. J. M. Gerrard, Department of Pediatrics, University of Minnesota, for assistance in the biological evaluation and Dr. J. E. Pike, The Upjohn Co., for the prostaglandin standards.

Potential Organ- or Tumor-Imaging Agents XIX: Radioiodinated Antiarrhythmic Drugs as Potential Myocardial Imaging Agents

N. KORN, J. K. GIBSON, F. J. KNIFFEN, B. R. LUCCHESI, V. V. RANADE, M. MIMNAUGH, T. YU, and R. E. COUNSELL ˣ

Received April 16, 1979, from the *Department of Pharmacology, Medical School, University of Michigan, Ann Arbor, MI 48109.* Accepted for publication August 22, 1979.

Abstract □ Iodinated and radioiodinated analogs of propranolol and *N,N*-dimethylpropranolol were synthesized wherein an iodophenyl moiety replaced the naphthalene ring of the parent drug. These new compounds were evaluated not only for their β-adrenergic blocking and antiarrhythmic activities but also for their ability to accumulate selectively in myocardial tissue. Like propranolol, the iodinated analogs displayed comparable β-blocking and antiarrhythmic activity, and the order of potency was *ortho-* > *meta-* > *para*-iodophenyl. Quaternization of propranolol and the iodinated analogs eliminated the β-adrenergic blocking activity but retained the antiarrhythmic property of the secondary amine precursors. Among the quaternary salts, the antiarrhythmic potency was *meta-* > *ortho-* > *para*-iodophenyl. Tissue distribution of the radioiodinated derivatives revealed that only the quaternary derivatives were selectively accumulated in myocardial tissue. These results demonstrate that an iodophenyl ring can substitute for the naphthalene ring in propranolol and its quaternary salt without significant alteration of pharmacological properties. The radioiodinated quaternary derivatives may be useful pharmacological tools in experiments aimed at relating antiarrhythmic activity to myocardial uptake.

Keyphrases □ Antiarrhythmic agents—iodinated and radioiodinated analogs of propranolol and *N,N*-dimethylpropranolol, synthesis and evaluation of activity, tissue distribution of radioiodinated analogs, potential as myocardial imaging agents □ Propranolol—iodinated and radioiodinated analogs, synthesis and testing for β-adrenergic blocking and antiarrhythmic activity, tissue distribution of radioiodinated analogs, potential as myocardial imaging agents □ Radionuclide imaging—radioiodinated analogs of propranolol and *N,N*-dimethylpropranolol, tissue distribution, potential as myocardial imaging agents

The synthesis of a compound that selectively concentrates in the myocardium and that also can act as a carrier molecule for a γ-emitting nuclide has been a goal of this laboratory for several years (1–3). The approach has been to select a compound with known or suspected propensity for the target organ and then to modify the structure to allow incorporation of a γ-emitting nuclide while retaining the localizing properties of the parent compound.

BACKGROUND

One possible carrier molecule for myocardial localization is the β-adrenergic blocking agent propranolol (I). Its antiarrhythmic actions were demonstrated in a wide variety of experimentally induced arrhythmias (4, 5) as well as in clinically occurring arrhythmias (6, 7). Tissue distribution studies with [^{14}C]propranolol (8, 9) demonstrated its uptake by the heart, but not to the degree expected in view of the potent action of propranolol in blocking the cardiac effects of catecholamines (8). Instead, other tissues such as the lungs and brain contained higher levels of radioactivity (8, 9).

Previous studies in this laboratory showed that quaternization of propranolol produced a drug (II) that retained the antiarrhythmic activity but eliminated the β-adrenergic blocking property of propranolol (10). Subcutaneous administration of ^{14}C-labeled II to rats revealed a rapid and selective localization of radioactivity in the heart (23 times the blood

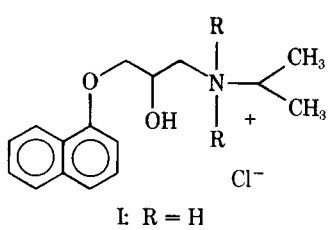

I: R = H
II: R = CH_3

0022-3549/80/0900-1010$01.00/0

© 1980, American Pharmaceutical Association

concentration at 2 hr postinjection) with no marked concentration of radioactivity in the lungs and brain[1]. Similar results were obtained in dogs (11).

Since II and other quaternary antiarrhythmic drugs, such as bretylium, persist in the myocardium long after blood levels have declined, it is believed that the uptake and retention of these drugs by the myocardium account for their antiarrhythmic action (11, 12). In any event, it is clear that plasma levels of these drugs cannot be used to guide individualization of dosage. As a consequence, the purpose of the present study was to synthesize not only a myocardial imaging agent but also an antiarrhythmic drug whose pharmacokinetic properties could be monitored in intact animals by external counting equipment.

Most rectilinear scanners and cameras currently available are used in conjunction with γ-emitting nuclides with an energy of <500 kev. Iodine has two radionuclides, iodine 123 and iodine 131, that fulfill this requirement and that are widely used in nuclear medicine. Accordingly, the present research focused on the synthesis and biological evaluation of iodinated analogs of propranolol and *N,N*-dimethylpropranolol. Since completion of this study, two reports (13, 14) appeared concerning propranolol as a carrier for γ-emitting radionuclides for myocardial imaging.

RESULTS AND DISCUSSION

Chemistry—The synthesis of the iodinated analogs of propranolol (*IV*) and their methylated congeners (V and VI) followed conventional paths as outlined in Scheme I (*a* = *ortho*, *b* = *meta*, and *c* = *para*). For synthesis of the corresponding radioiodinated derivatives, iodine 125 was selected for the initial studies because its longer half-life (60 days) and weak γ-radiation (35 kev) minimized handling and storage problems. In addition, a subsequent switch to iodine 123 or iodine 131 would represent no major change in methodology.

Radioactive iodine was introduced by the isotope-exchange method and involved refluxing an aqueous or ammonium hydroxide solution of IV or V to which the appropriate amount of sodium [^{125}I]iodide had been added. Higher yields of radioisotope incorporation usually were achieved when the exchange reactions were performed in ammonium hydroxide solution. The radioiodinated quaternary salts were obtained by treating the radioiodinated tertiary amine with methyl iodide in methanol at room temperature.

Pharmacology—The results of the pharmacological studies are summarized in Table I.

β-Adrenergic Receptor Blockade—Five of the synthesized compounds were tested for β-adrenergic receptor blocking activity against isoproterenol in isolated rabbit right atrial strips. The iodinated propranolol analogs (IV*a*–IV*c*) all showed β-adrenergic blocking activity. The order of activity was *ortho* > *meta* > *para*. The pA_2 value of 8.7 reported for propranolol by Blinks (15) was comparable to that observed for the *meta*-isomer (IV*b*). Accordingly, the *ortho*-isomer (IV*a*) was somewhat more active than propranolol as a β-adrenergic blocker. *N,N*-Dimethylpropranolol, as well as both of the iodinated analogs tested, lacked significant β-adrenergic receptor blocking activity.

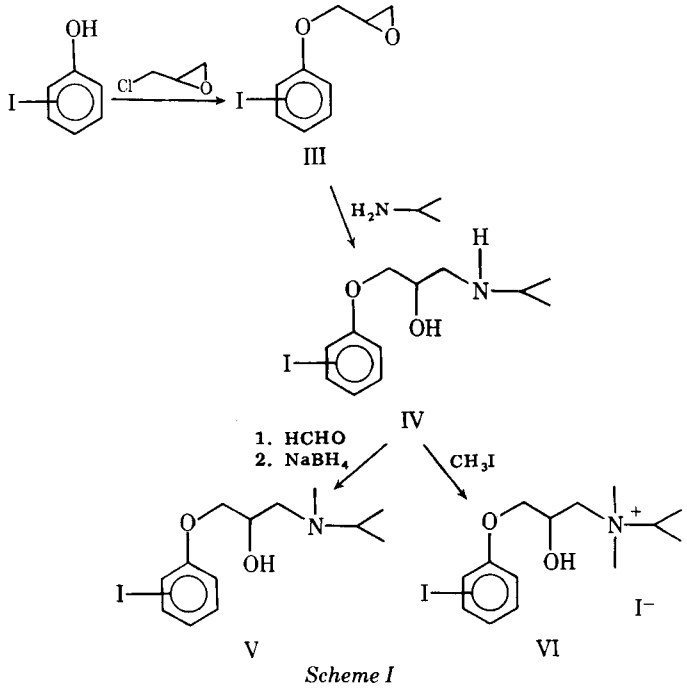

Scheme I

Table I—Pharmacological Activity of Radioiodinated Analogs of Propranolol (I) and *N,N*-Dimethylpropranolol (II)

Compound	β-Adrenergic Receptor Blocking Activity, pA_2	Antiarrhythmic Activity	
		n	Dose, mg/kg
I	8.7[a]		6.1[b]
II	I(4.4)[c]		2–3[c]
IV*a*	10.0	5/5	4.8
IV*b*	8.5	5/5	5.7
IV*c*	6.6	3/3	10.0
VI*a*	I[d]	5/5	7.5
VI*b*	I	5/5	5.0
VI*c*	NT[e]	3/3	9.0

[a] Data from Ref. 15. [b] Data from Ref. 4. [c] Data from Ref. 10. [d] Inactive under conditions described under *Experimental*. [e] Not tested.

Antiarrhythmic Activity—All of the compounds tested were effective in converting the ouabain-induced ventricular tachycardia to normal sinus rhythm. Propranolol analogs IV*a*–IV*c* required doses of 4.8–10.0 mg/kg for conversion compared to 6.1 mg/kg required for propranolol (4). The iodinated analogs of *N,N*-dimethylpropranolol converted the ouabain-induced arrhythmias at doses of 5.0–9.0 mg/kg as compared to 2–3 mg/kg for the parent compound (10). In these preliminary studies, the *meta*-isomer (VI*b*) was the most potent antiarrhythmic agent among the iodinated analogs, followed in turn by the *ortho*-isomer (VI*a*) and the *para*-isomer (VI*c*).

Tissue Distribution—Based on the pharmacological results, the *meta*-iodinated analogs of propranolol and *N,N*-dimethylpropranolol were radioiodinated. The results of tissue distribution studies with these compounds are summarized in Table II. Administration of propranolol analog IV*b* resulted in no selective accumulation of radioactivity in myocardial tissue. On the other hand, there was marked uptake of activity in the lungs and liver. However, administration of the quaternary ammonium salt (VI*b*) resulted in selective concentration of radioactivity in rat myocardial tissue. Adrenal, lung, and thyroid tissues also showed high levels of uptake. The high levels of activity seen in the thyroid were believed to be due to *in vivo* deiodination of the compounds.

These results indicate that replacement of the naphthalene ring system in propranolol and *N,N*-dimethylpropranolol with an iodophenyl moiety does not markedly modify the pharmacological properties of the parent compounds. The iodinated analogs of propranolol all possessed β-adrenergic receptor blocking activity. However, the position of the iodine on the phenyl ring altered the potency of this activity. The β-blocking activities of propranolol and the *meta*-iodinated analog (IV*b*) were about equal and intermediate between the activities noted for the *ortho*-isomer (IV*a*) and the *para*-isomer (IV*c*).

This relationship also was observed for the antiarrhythmic activity of the three propranolol analogs. The doses needed to convert the ouabain-induced arrhythmia were about equal for propranolol (6.1 mg/kg) and the *meta*-iodinated analog, whereas lower and higher doses were required for the *ortho*- and *para*-isomers, respectively. Thus, the antiarrhythmic activity of these compounds paralleled their β-adrenergic receptor blocking activity. Since other drugs without β-adrenergic activity have antiarrhythmic properties, there may be no relationship between these two effects in the propanolol series; the antiarrhythmic action may be due to a direct membrane effect (5).

The absence of any significant localization of radioactivity in the heart following injection of radioiodinated IV*b* also paralleled the absence of marked localization of radioactivity in the myocardium reported after injection of ^{14}C-labeled propranolol (8). Similarly, other radioiodinated analogs of β-adrenergic antagonists have failed to demonstrate appreciable myocardial uptake and retention of radioactivity (13, 14).

Similar to the parent compound, the iodinated analogs of *N,N*-dimethylpropranolol (VI) were devoid of β-adrenergic receptor blocking activity. However, these analogs retained the antiarrhythmic activity of *N,N*-dimethylpropranolol, although larger doses of the analogs were

[1] A. Buswink, M. Johnson, F. Kniffen, and R. E. Counsell, unpublished data.

Table II—Tissue Distribution Profiles of Radioiodinated Analogs of Propranolol and *N,N*-Dimethylpropranolol after Subcutaneous Administration to Rats

Tissue	Percent of Administered Dose per Gram of Tissue[a]			
	IV*b*		VI*b*	
	2 hr	6 hr	2 hr	6 hr
Adrenal	0.362 ± 0.035	0.121 ± 0.016	1.680 ± 0.134	0.996 ± 0.224
Blood	0.140 ± 0.012	0.172 ± 0.009	0.422 ± 0.027	0.261 ± 0.030
Brain	0.318 ± 0.033	0.033 ± 0.010	0.037 ± 0.003	0.013 ± 0.002
Heart	0.166 ± 0.004	0.068 ± 0.012	—	—
Auricle	—	—	2.755 ± 0.320	0.604 ± 0.095
Ventricle	—	—	4.254 ± 0.201	1.013 ± 0.041
Kidney	0.621 ± 0.025	0.390 ± 0.065	0.854 ± 0.069	0.330 ± 0.015
Liver	1.211 ± 0.110	0.345 ± 0.051	0.776 ± 0.093	0.237 ± 0.016
Lung	1.048 ± 0.068	0.195 ± 0.061	1.190 ± 0.121	0.479 ± 0.020
Skeletal muscle	0.111 ± 0.005	0.044 ± 0.004	0.190 ± 0.041	0.114 ± 0.019
Thyroid	—	—	7.762 ± 1.452	9.016 ± 1.595

[a] Values represent the mean ± *SEM*; $n = 3$.

Table III—Experimental Data

Compound	Boiling Point (mm Hg) or Melting Point (Solvent)	Yield, %	Formula	Analysis, %		
					Calc.	Found
III*a*	118–123° (0.2)	44	$C_9H_9IO_2$	C	39.16	39.08
				H	3.28	3.13
III*b*	125° (0.3)	64	$C_9H_9IO_2$	C	39.16	39.00
				H	3.28	3.47
III*c*	120° (0.2)	64	$C_9H_9IO_2$	C	39.16	39.12
				H	3.28	3.12
IV*a*	97–98° (acetone)	60	$C_{12}H_{18}INO_2$	C	43.00	43.02
				H	5.41	5.13
IV*b*	89–90° (acetone)	60	$C_{12}H_{18}INO_2$	C	43.00	42.79
				H	5.41	5.36
IV*c*	112–113° (acetone)	83	$C_{12}H_{18}INO_2$	C	43.00	43.04
				H	5.41	5.44
V*a*	116–117° (methanol–ether)	68	$C_{13}H_{21}ClINO_2$	C	40.48	40.33
				H	5.49	5.51
V*b*	131–132° (methanol–ether)	70	$C_{13}H_{21}ClINO_2$	C	40.48	40.74
				H	5.49	5.60
V*c*	114–116° (methanol–ether)	70	$C_{13}H_{21}ClINO_2$	C	40.48	40.84
				H	5.49	5.72
VI*a*	153–155° (acetone)	82	$C_{14}H_{23}INO_2$	C	34.23	34.15
				H	4.72	4.54
VI*b*	165–166° (acetone)	81	$C_{14}H_{23}INO_2$	C	34.23	34.16
				H	4.72	4.65
VI*c*	215–216° (methanol–acetone)	78	$C_{14}H_{23}INO_2$	C	34.23	34.22
				H	4.72	4.68

required to convert the ventricular tachycardia to normal sinus rhythm. The tissue distribution profile of radioiodinated VI*b* was comparable to that of II. At 2 hr after administration to rats, the heart to lung ratio of VI*b* was 3.6 whereas the ratio for the parent drug was 2.7. Studies are in progress using VI*b* labeled with iodine 131 as a probe for relating the antiarrhythmic activity of these quaternary drugs to their uptake and retention in the myocardium.

EXPERIMENTAL[2]

General procedures are described for the synthesis of III–VI, and experimental data are furnished in Table III.

1-(*o*-Iodophenoxy)-2,3-epoxypropane (III*a*)—Epichlorohydrin (2.7 g, 30 mmoles) was added dropwise at room temperature to a stirred solution of *o*-iodophenol (4.4 g, 20 mmoles) in 5% NaOH (25 ml). The reaction mixture was allowed to stir overnight. The oily layer that resulted was extracted with chloroform. This extract was washed with water and dried over anhydrous sodium sulfate. Removal of the solvent gave an oily residue which, upon distillation *in vacuo*, afforded a colorless oil (2.5 g).

1-(*o*-Iodophenoxy)-3-isopropylamino-2-propanol (IV*a*)—A solution of I*a* (5.4 g, 20 mmoles) and isopropylamine (8 ml) in isopropanol (60 ml) was stirred overnight at room temperature. The solution was evaporated to dryness, redissolved in 10% HCl, and washed with ether. The aqueous layer was made basic with sodium hydroxide and extracted with ether. The extract was washed with water, dried over anhydrous sodium sulfate, and concentrated to yield a solid. Upon recrystallization from acetone, this solid afforded a colorless solid (4.0 g).

1-(*o*-Iodophenoxy)-3-methylisopropylamino-2-propanol (V*a*)—Formaldehyde solution (37%, 0.8 ml) was added with stirring to a solution of II*a* (0.67 g, 2 mmoles) in absolute methanol (10 ml), and the reaction mixture was stirred at room temperature for 2 hr. Sodium borohydride (1.2 g) was added with stirring at ice bath temperature. The mixture was allowed to come to room temperature and then was poured into ice–water (100 ml). The mixture was extracted with ether, and the ether layer was washed with water, dried over anhydrous sodium sulfate, and evaporated to dryness *in vacuo*. The residue was dissolved in methanol–hydrochloric acid and diluted with ether. Filtration resulted in the hydrochloride salt (0.48 g), which was recrystallized from methanol–ether.

***N,N*-Dimethyl-1-(*o*-iodophenoxy)-3-isopropylamino-2-propanol Iodide (VI*a*)**—A mixture of IV*a* (3.35 g, 10 mmoles), sodium carbonate (1.1 g), and methyl iodide (5 ml) in absolute methanol (50 ml) was refluxed with stirring for 1 day. Additional methyl iodide (5 ml) was added, and refluxing was continued for 2 days. The solvent was removed under reduced pressure, and the resulting oily residue was washed with water. The residue was triturated with ethyl acetate and allowed to stand overnight. The resulting solid was filtered, washed with ethyl acetate,

[2] Melting points were taken on a Fisher-Johns melting-point apparatus and are corrected. Elemental analyses were performed by Midwest Microlab, Indianapolis, Ind., or by Spang Microanalytical Laboratory, Ann Arbor, Mich. IR spectra (Perkin-Elmer 337 spectrophotometer, either neat or as potassium bromide pellets) and NMR spectra (Varian A-60 spectrometer, taken in deuterated chloroform or dimethyl sulfoxide) were consistent with the proposed structures. TLC analyses were run on silica gel plates (Eastman Kodak), and spots were detected under UV light. Radiochemical purity of radioiodinated compounds was confirmed by TLC analysis, and they were scanned with an Atomic Associates RCS-363 radiochromatogram scanner. The corresponding authentic nonradioactive compound was cochromatographed with the radioiodinated compounds. Total radioactivities were determined with a Picker nuclear isotope calibrator.

Table IV—Isotope-Exchange Conditions and Results

Parameter	Compound IV*b*	Compound V*b*
Starting material, mg	200	200
Sodium [^{125}I]iodide, mCi	5	6
Solvent (ml)	Water (4.5)	Ammonium hydroxide (2.0)
Temperature	100°	100°
Reaction time	48 hr	5 days
Extract solvent	Chloroform	Ether
Resulting compound, mg	200	160
Total activity, μCi	600	2500
Percent exchange	12.0	41.7

and dried. Recrystallization from acetone or methanol–acetone afforded a colorless solid (3.0 g).

Isotope Exchange—Radioactive iodine was incorporated by heating a solution of the secondary (IV) or tertiary (V) amine in the presence of sodium [^{125}I]iodide. Table IV lists the experimental data. The quaternary derivative (VI) was formed by refluxing a methanolic solution of V in the presence of excess methyl iodide for 2 hr. Radiochemical purity was ascertained by TLC analysis of the compounds on silica gel plates[3] developed in ether–methanol (5:1) for IV and V or chloroform–methanol (3:1) for VI.

Pharmacology—*β-Adrenergic Receptor Blocking Activity*—Chronotropic concentration–effect curves to isoproterenol in spontaneously beating rabbit atrial strips were obtained using the procedure described by Schuster *et al.* (10). Probit analysis (16) was used to compute the median effective dose (ED_{50}) for each concentration–effect curve, and these values then were used to calculate the pA_2 values for the compounds tested according to the method described by Schild (17). The pA_2 value is defined as the negative logarithm of the antagonist concentration that doubles the agonist concentration required to achieve a given effect.

Antiarrhythmic Activity—Arrhythmias were induced in anesthetized male mongrel dogs (9–13 kg) with ouabain according to the procedure described by Schuster *et al.* (10). After establishment of ventricular tachycardia, a saline solution of the test material was administered intravenously until conversion to normal sinus rhythm was attained for at least 30 min with failure of right vagal stimulation to expose automatic ectopic ventricular activity during vagal-induced sinoatrial nodal arrest.

Tissue Distribution—Radioiodinated IV*b* and VI*b* were given by subcutaneous injection to male Sprague–Dawley rats[4], 180–330 g. The doses of radioactivity ranged from 22 to 25 μCi/rat (1.8–8.0 mg/rat) in 0.25 ml of vehicle. The vehicle was saline for VI*b* and 0.1 *N* HCl for IV*b*. At 2 and 6 hr after administration of the compounds, groups of three rats were killed by exsanguination while under ether anesthesia. Adrenal, blood, brain, heart, kidney, liver, lung, muscle, and thyroid samples were removed. Tissue samples were placed in liquid scintillation vials and weighed. Duplicate samples were taken.

The contents of each vial were digested overnight in 0.3–0.5 ml of 2.5 *N* NaOH. The vials were heated at 40–60° for 5–10 min to complete digestion. Four drops of hydrogen peroxide (30% solution) were added to each cooled vial to decolorize the samples. Enough 0.9–1.1 *M* acetic acid to neutralize the base and 10 ml of scintillation cocktail[5] were added to each sample, and the vials were shaken on a vortex mixer. The samples were assayed for radioactivity in a liquid scintillation counter[6] for 5 min or until enough counts had accumulated to reduce the counting error to 1%. Maximum counting error for samples that counted the full 5 min was 7%. Efficiency for iodine 125 was 45%.

Results are expressed as the percentage of the administered dose per gram of tissue and were calculated from:

$$\frac{\text{sample dpm} \times 1000\ \text{mg/g}}{\text{sample weight (mg)} \times 2.22 \times 10^6\ \text{dpm/}\mu\text{Ci} \times \text{dose (}\mu\text{Ci)}} \times 100$$

REFERENCES

(1) R. E. Counsell, T. Yu, V. V. Ranade, and A. Buswink, *J. Med. Chem.*, **16**, 1038 (1973).

(2) R. E. Counsell, T. Yu, V. V. Ranade, A. A. Buswink, E. A. Carr, Jr., and M. Carroll, *J. Nucl. Med.*, **15**, 991 (1974).

(3) R. E. Counsell, V. V. Ranade, W. Kline, B. H. Hong, and A. A. Buswink, *J. Pharm. Sci.*, **65**, 285 (1976).

(4) B. R. Lucchesi, L. S. Whitsitt, and N. L. Brown, *Can. J. Physiol. Pharmacol.*, **44**, 543 (1966).

(5) B. R. Lucchesi, L. S. Whitsitt, and J. L. Stickney, *Ann. N.Y. Acad. Sci.*, **139**, 940 (1967).

(6) D. J. Rowlands, G. Howitt, and P. Markman, *Br. Med. J.*, **1**, 891 (1965).

(7) D. C. Harrison and J. R. Griffin, *Ann. N.Y. Acad. Sci.*, **139**, 997 (1967).

(8) D. Masuoka and E. Hansson, *Acta Pharmacol. Toxicol.*, **25**, 447 (1967).

(9) A. Hayes and R. G. Cooper, *J. Pharmacol. Exp. Ther.*, **176**, 302 (1971).

(10) D. P. Schuster, B. R. Lucchesi, N. L. Nobel, M. N. Mimnaugh, R. E. Counsell, and F. J. Kniffen, *ibid.*, **184**, 213 (1973).

(11) J. K. Gibson, N. J. Korn, R. E. Counsell, and B. R. Lucchesi, *Fed. Proc., Fed. Am. Soc. Exp. Biol.*, **38**, 697 (1979).

(12) D. H. Namm, C. M. Wang, S. El-Sayad, F. C. Copp, and R. A. Maxwell, *J. Pharmacol. Exp. Ther.*, **173**, 344 (1975).

(13) A. Bobik, E. A. Woodcock, C. I. Johnston, and W. J. Funder, *J. Labelled Compd. Radiopharm.*, **12**, 605 (1977).

(14) V. W. Jiang, R. E. Gibson, W. J. Rzeszotarski, W. C. Eckelman, R. C. Reba, F. Vieras, and P. O. Alderson, *J. Nucl. Med.*, **19**, 918 (1978).

(15) J. R. Blinks, *Ann. N.Y. Acad. Sci.*, **135**, 673 (1967).

(16) A. Goldstein, "Biostatistics: An Introductory Text," Macmillan, New York, N.Y., 1964, pp. 153–174.

(17) H. O. Schild, *Br. J. Pharmacol.*, **2**, 189 (1957).

ACKNOWLEDGMENTS

Supported in part by U.S. Public Health Service Grant CA-08349 and National Heart, Lung, and Blood Institute Grant HL-05806-19. J. K. Gibson was supported by a Research Fellowship from the Michigan Heart Association.

The authors thank Mr. Parvis Afiatpour for assistance in the tissue distribution studies.

[3] Eastman Kodak, Rochester, N.Y.
[4] Spartan Research Animals, Haslett, Mich.
[5] Aquasol, New England Nuclear, Boston, Mass.
[6] Beckman LS200.

Potential Organ- or Tumor-Imaging Agents XX: Ovarian Imaging with 19-Radioiodinated Cholesterol

N. KORN, G. NORDBLOM, E. FLOYD, and R. E. COUNSELL ˣ

Received April 16, 1979, from the *Department of Pharmacology, Medical School, University of Michigan, Ann Arbor, MI 48109.* Accepted for publication August 22, 1979.

Abstract □ Cholesterol is stored in the ovaries where it is a precursor in the biosynthesis of the female sex hormones progesterone and estradiol. The purpose of this study was to determine whether a radioiodinated analog of cholesterol, ^{125}I-labeled 19-iodocholesterol, would mimic cholesterol in this capacity and thus offer a means for imaging the ovaries of intact animals. Aside from the thyroid, the adrenal glands and ovaries of the female rat retained the highest levels of radioactivity at 4 days following the intravenous administration of ^{125}I-labeled 19-iodocholesterol. Moreover, the levels of radioactivity were sufficient to obtain clear images of the adrenal glands and ovaries with a small animal scanner. Folch analysis of these tissues revealed that >80% of the radioactivity was associated with the sterol ester fraction.

Keyphrases □ Cholesterol—19-radioiodinated analog, evaluation as ovarian imaging agent □ Radionuclide imaging—19-radioiodinated cholesterol, evaluation as ovarian imaging agent

19-Radioiodinated cholesterol originally was synthesized as an adrenal imaging agent (1). Since that time, this agent and its close relatives have been used in clinical diagnostic procedures for visualization of the adrenal glands and associated tumors (2).

The synthesis of radioiodinated cholesterol as a radiodiagnostic agent was based on the knowledge that the adrenal cortex stores cholesterol for ultimate use in corticosteroid hormone biosynthesis. The ovary is another mammalian organ that is rich in cholesterol and that utilizes this lipid as a precursor for steroid hormone synthesis.

It is generally accepted that the synthesis of steroid hormones in the adrenal gland and ovary is controlled mainly by the trophic hormones adrenocorticotropic hormone and luteinizing hormone, respectively. While many details regarding their modes of action are unclear, they appear to influence the conversion of stored cholesterol ester to free cholesterol and the transformation of the latter compound to pregnenolone (Scheme I) (3).

This similarity between the ovary and the adrenal gland in the storage and utilization of cholesterol suggested that 19-iodocholesterol might accumulate in the ovaries and steroid-secreting ovarian tumors in addition to its predilection for adrenal cortical tissue. Thus, the purpose of this study was to compare the disposition of 19-radioiodinated cholesterol in the adrenal and ovarian tissues of the female rat.

EXPERIMENTAL

Radioiodinated Cholesterol—^{125}I-Labeled 19-iodocholesterol was prepared as described previously (1), yielding 14 mg with an estimated specific activity of 400 μCi/mg. The compound was dissolved in 5.0 ml of benzene and stored at 4° until just prior to use, at which time the material was formulated for injection as follows. An aliquot of the benzene solution was placed in a multidose vial, and the solvent was evaporated. The compound was redissolved in saline containing 1.6% polysorbate 80 and 10% ethanol. Prior to use, one aliquot of the solution was assayed for radioactivity to determine the radioactive concentration, and another aliquot was analyzed by TLC using silica gel G plates[1] developed in benzene–ethyl acetate (9:1).

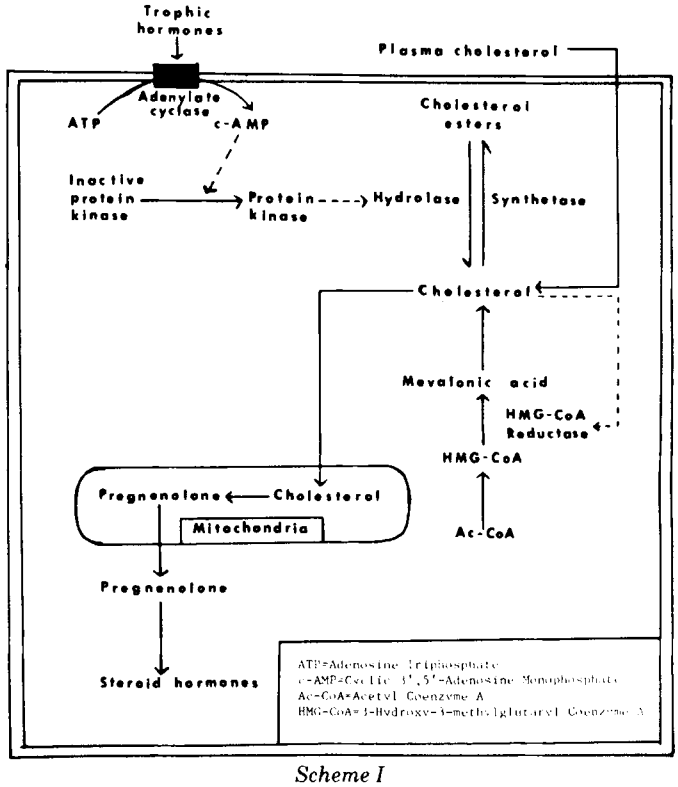

Scheme I

Two solutions were prepared. Solution A, used for tissue distribution studies, was made using 1 ml of the benzene solution. The final volume of this solution was 10 ml (103 μCi/ml). Solution B, used for scanning, was prepared using 2.0 ml of the benzene solution. The final volume of this solution was 5.0 ml (350 μCi/ml). Both solutions showed only one radioactive peak when scanned with a radiochromatogram scanner[2]. The location of this peak was coincident with that of the authentic unlabeled material cochromatographed with the radioiodinated sample.

Tissue Distribution—Ten adult female Sprague–Dawley rats[3], 173–185 g, each received an intravenous injection of 25.8 μCi of ^{125}I-labeled 19-iodocholesterol in 0.25 ml of vehicle (Solution A) *via* the tail vein while under ether anesthesia. Rats were either in estrus or metestrus at the time of injection as determined by vaginal smear. Half of the rats were killed 1 day postadministration and half were killed 4 days postadministration by exsanguination from the heart while under ether anesthesia.

Tissues of the adrenal cortex and medulla, liver, ovary, blood, uterus, and thyroid were removed at sacrifice. Samples of the adrenal cortex, ovary, liver, and blood from each rat were placed on ice for subsequent extraction studies. All tissue samples were placed in tared cellulose acetate capsules and weighed. The capsules then were placed in polystyrene γ-counting tubes and assayed for radioactivity in a well scintillation counter[4] for 10 min or until 100,000 counts had accumulated. Counting efficiency for iodine 125 was 87% in all cases, except when glass culture

[1] Eastman Kodak, Rochester, N.Y.
[2] Berthold model 6000.
[3] Spartan Research Animals, Hasslett, Mich.
[4] Searle 1185 γ-spectrometer.

0022-3549/80/0900-1014$01.00/0
© 1980, American Pharmaceutical Association

Table I—Distribution of Radioactivity following Intravenous Administration of ^{125}I-Labeled 19-Iodocholesterol to Female Rats

Tissue	Percent of Dose per Gram[a] 1 Day Postinjection	4 Days Postinjection
Adrenal cortex	10.195 ± 0.251	9.572 ± 0.349
Adrenal medulla	3.002 ± 0.438	1.990 ± 0.554
Blood	0.252 ± 0.010	0.021 ± 0.002
Liver	0.431 ± 0.026	0.059 ± 0.003
Ovary	5.929 ± 0.343	2.736 ± 0.437
Uterus	0.238 ± 0.010	0.055 ± 0.005
Thyroid	199.096 ± 18.263	152.042 ± 10.606

[a] Values represent the mean ± *SEM* for five rats.

tubes were used to hold samples. In the latter case, the counting efficiency was 77%.

Folch Extraction—Radioactivity was extracted from selected tissues using a variation of the procedure described by Folch *et al.* (4). The samples of the liver, adrenal cortex, and ovary were weighed and placed in a ground-glass homogenizer with sufficient distilled water to bring the combined volume of tissue and water to 0.5 ml (1 g of tissue was assumed to be equal to 1 ml). The samples were homogenized in 2–5 ml of chloroform–methanol (2:1) and filtered through filter paper[5]. The homogenizers then were rinsed twice with 2–4 ml of the solvent, and these rinses were filtered. The combined volume of the homogenizing vehicle plus the rinses for each sample was 10 ml.

Aliquots of blood (0.5 ml) were shaken with 5 ml of chloroform–methanol (2:1) in a conical centrifuge tube. The solvent was filtered, and the tube was rinsed with an additional 5 ml of solvent, which also was filtered and combined with the original filtrate. Similar to the tissue samples, the volume of the combined filtrates for each blood extract was measured and adjusted to 10 ml by addition of chloroform–methanol (2:1).

The filter paper with each precipitate was air dried, placed in a polystyrene γ-tube, and assayed as described to ascertain radioactivity associated with precipitable material. Each filtrate was placed in a 15-ml conical centrifuge tube. Distilled water (2.0 ml) was added, and the tube was shaken. The tubes then were centrifuged at low speed for 10 min to separate the phases. The upper phase of each sample was removed; the lower phase was washed with two 1.0-ml portions of Folch's upper phase solvent (chloroform–methanol–water, 3:48:47), which were combined with the upper phase from each sample. Each upper phase was adjusted to 10 ml by addition of the upper phase solvent, and a 1.0-ml aliquot of each upper phase was placed in a polyethylene microfuge tube, which then was placed in a polystyrene γ-tube and assayed for radioactivity as described.

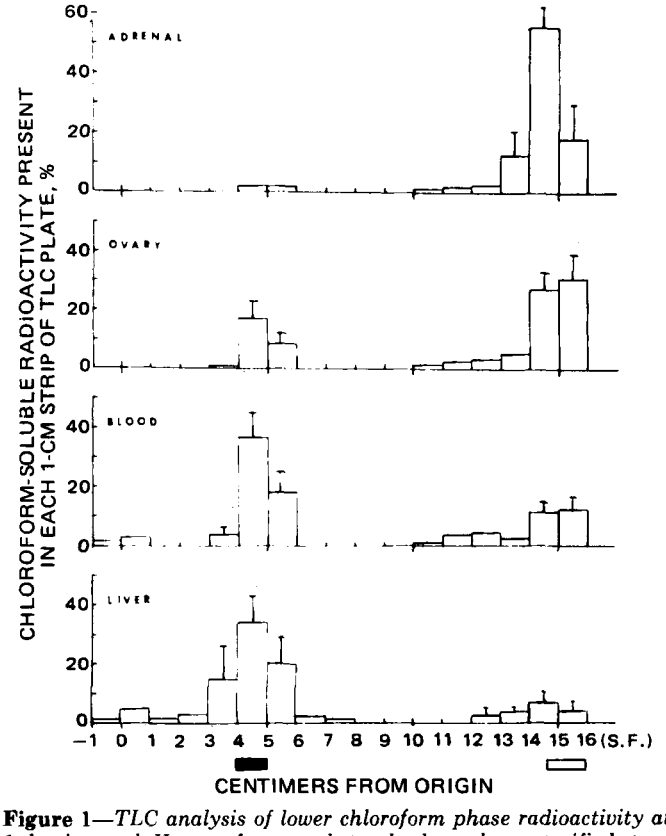

Figure 1—*TLC analysis of lower chloroform phase radioactivity at 1-day interval. Key:* ■, *free sterol standards; and* □, *esterified standards. S.F. = solvent front.*

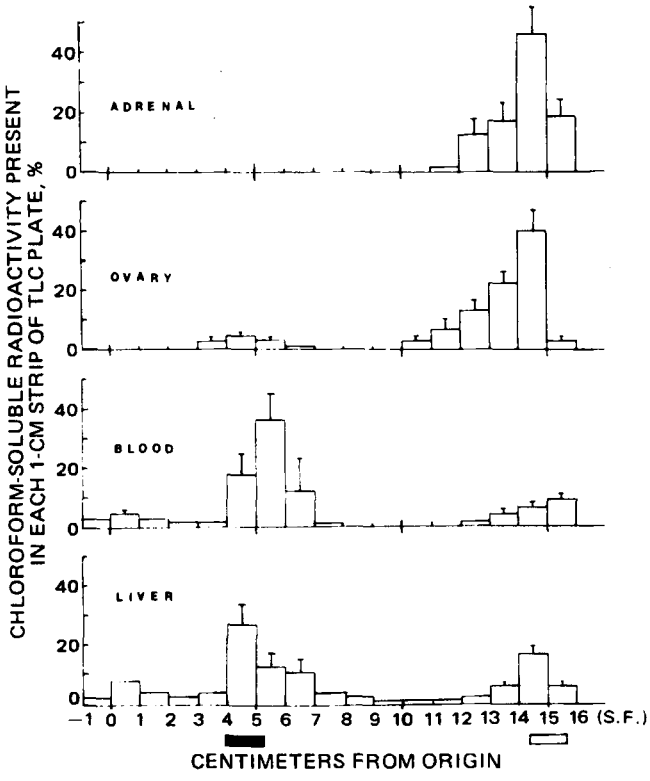

Figure 2—*TLC analysis of lower chloroform phase radioactivity at 4-day interval. Key:* ■, *free sterol standards; and* □, *esterified standards. S.F. = solvent front.*

Each lower phase was evaporated to dryness under nitrogen at 20–30°, and the residues were redissolved in 1.0 ml of benzene. An aliquot (100 μl) of each benzene fraction was placed in a glass culture tube, which then was placed in a polystyrene counting tube and assayed for radioactivity as described. The remainder of the benzene solution for each sample was stored overnight in a capped vial at 4°. The benzene then was evaporated, and the residues were redissolved in ether (10 drops) and spotted on TLC plates[6]. The vials were rinsed with another 10 drops of ether, which also was spotted on the plates. The plates then were developed once in *n*-hexane–ether–acetic acid (90:10:1) to 16 cm, air dried, and redeveloped in the same direction with *n*-hexane–ether–acetic acid (75:25:2). The plates were cut into 1-cm wide strips, starting 1 cm below the origin and continuing to the solvent front. Each strip was placed in a counting tube and assayed for radioactivity as described. Unlabeled 19-iodocholesterol, cholesterol, 19-iodocholesteryl palmitate, cholesteryl oleate, and pregnenolone were cochromatographed with the radioactive samples and visualized with iodine vapor to serve as reference standards.

Scintiscan of Female Rat—Two adult female Sprague–Dawley rats, 212 and 218 g, each received an intravenous injection of 245.4 μCi of ^{125}I-labeled 19-iodocholesterol in 0.7 ml of vehicle (Solution B) *via* the tail vein while under ether anesthesia. At 1 and 4 days postadministration, one rat was anesthetized with pentobarbital sodium by intraperitoneal injection (0.2 ml, 50 mg/ml) and scanned in the prone position using a small animal scanner. Following removal of the left ovary and adrenal gland, the rat was rescanned. The rat then was killed, and samples of the adrenal gland, ovary, and liver were assayed for radioactivity as described previously.

[5] Whatman No. 1.

[6] ITLC, Gelman, Ann Arbor, Mich.

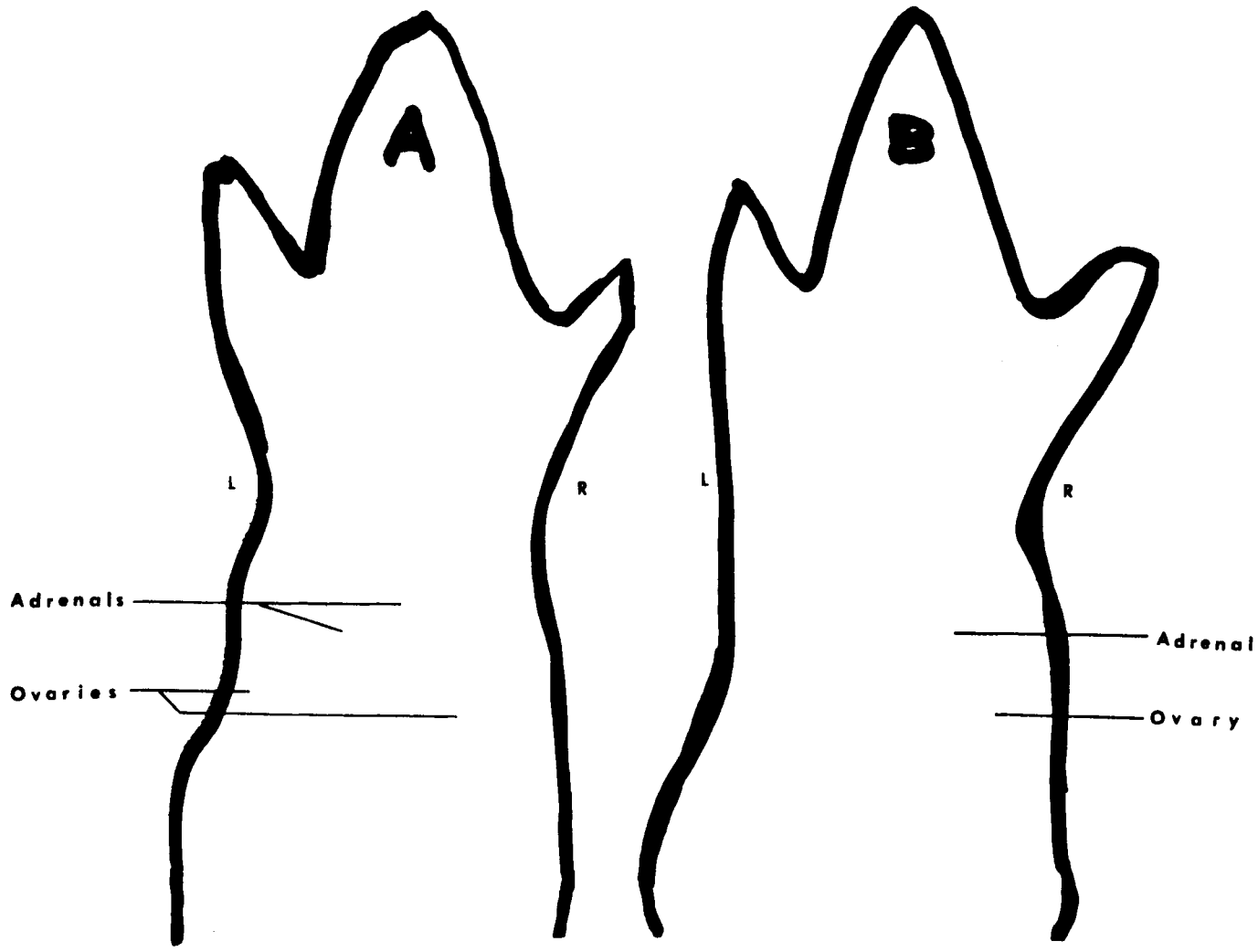

Figure 3—*Scintiscan of female rat 4 days after administration of ^{125}I-labeled 19-iodocholesterol (A) and rescan of the same rat following removal of the left ovary and left adrenal gland (B).*

RESULTS

Tissue Distribution—The distribution of radioactivity following intravenous administration of ^{125}I-labeled 19-iodocholesterol to female rats is summarized in Table I. High levels of radioactivity were noted in the adrenal cortex, ovaries, and thyroid at both times studied. The ovary to blood and ovary to liver ratios were 23 and 14 at 1 day postinjection and 138 and 47 at 4 days postinjection, respectively. The adrenal cortex to blood and adrenal cortex to liver ratios were 41 and 24 at the 1-day interval and 479 and 165 at the 4-day interval, respectively.

Folch Extraction—The results of the Folch extraction studies are summarized in Table II and Figs. 1 and 2. Greater than 90% of the radioactivity in the adrenal cortex was extractable into the lower chloroform phase at both the 1- and 4-day intervals. The remaining activity was found predominantly in the precipitated material, with only trace amounts in the upper aqueous phase. At the 1-day interval, 88% of the lower phase activity comigrated with the esterified standards; this activity increased to 95% by 4 days. While >90% of the radioactivity in the ovary also was extractable into the lower phase, only 58% of this activity comigrated with the esterified standards at the 1-day interval. Activity that comigrated with free sterol standards represented 25% of the lower phase activity. However, by 4 days, 86% of the activity was seen in the ester peak and only 10.4% was seen in the free sterol peak. Again, the remaining radioactivity was associated with the precipitated material.

For blood and liver samples, only 56–78% of the radioactivity was extractable into the lower phase. The remaining activity was found in both the precipitate and the upper phase. TLC analysis of the lower phase radioactivity showed that two distinct peaks were present; one peak corresponded to the free sterol standards, and one corresponded to the esterified sterol standards. However, unlike the adrenal gland and the ovary, most of the radioactivity was located in the free sterol peak.

Scintiscan of Female Rats—Attempts to scan the rat 1 day after administration of ^{125}I-labeled 19-iodocholesterol did not delineate the ovary or adrenal gland. Radioactivity present in the nontarget tissues of the abdominal cavity (*e.g.*, liver) as well as the adrenal glands and ovaries resulted in one large area of abdominal radioactivity. Removal of the left ovary and adrenal gland resulted in no detectable change in the image. Scintiscan of the rat 4 days after administration of ^{125}I-labeled 19-iodocholesterol (Fig. 3) resulted in the visualization of four areas of radioactivity. Removal of the left adrenal gland and ovary resulted in the corresponding disappearance of two radioactive areas when the rat was rescanned. The percent of dose per gram values for this animal were: adrenal, 10.707; ovary, 4.564; and liver, 0.062.

DISCUSSION

Results of tissue distribution and Folch extraction studies in rats showed that radioactivity was selectively accumulated and retained in an esterified form in the ovary as well as in the adrenal cortex following administration of ^{125}I-labeled 19-iodocholesterol. This finding is consistent with the reported similarities between the adrenal gland and ovary with regard to storage and utilization of cholesterol (3).

The retention of high levels of radioactivity in the adrenal gland and ovary several days after administration provides target to nontarget ratios necessary for resolution and visualization of these small organs. Although the level of radioactivity in the liver at 24 hr was considerably lower than that in either the adrenal gland or ovary, it was sufficient to interfere with imaging. However, after 4 days, the nontarget levels of radioactivity dropped significantly so that the target organs could be visualized.

The extremely high levels of radioactivity in the thyroid were noted previously (1) and are thought to be the result of *in vivo* deiodination and subsequent accumulation of free iodide in the thyroid where it becomes protein bound. Evidence for this conclusion lies in the blocking of thyroid

Table II—Percent of Radioactivity [a] Found in Each Phase following Folch Extraction of Tissue Radioactivity at 1 and 4 Days Postadministration of ^{125}I-Labeled 19-Iodocholesterol

Tissue	Day 1			Day 4		
	Precipitate	Upper	Lower	Precipitate	Upper	Lower
Adrenal	5.47 ± 2.36[b]	0.40 ± 0.42[b]	94.14 ± 2.48[b]	9.02 ± 3.54[b]	0.12 ± 0.14[b]	90.87 ± 3.65[b]
Blood	19.50 ± 4.74	13.87 ± 0.96	66.63 ± 5.21	29.00 ± 13.09	14.54 ± 4.98	56.47 ± 14.02
Liver	8.83 ± 2.00[b]	13.60 ± 2.04[b]	77.58 ± 2.29[b]	12.53 ± 1.91	11.18 ± 2.37	76.30 ± 3.87
Ovary	7.89 ± 2.21	0.92 ± 0.53	91.19 ± 1.82	8.81 ± 3.71	0.35 ± 0.10	90.84 ± 3.70

[a] Each value represents the mean ± *SD* for five rats unless noted. [b] Four rats.

uptake of radioactivity by pretreatment with potassium iodide solution (1) and in Folch extraction studies where >98% of the thyroid radioactivity was associated with the precipitated fraction[7].

The TLC systems used gave good separation of the free and esterified sterol. No further identification of radioactive products was attempted. Therefore, the esterified sterol peak could be made up of 19-iodocholesterol esterified with different saturated and unsaturated fatty acids. Similarly, slight alterations in the sterol portion of the molecule also could go undetected. Thus, [^{14}C]cholesterol and ^{125}I-labeled 19-iodocholesterol have the same R_f value in these systems.

Despite these limitations, these studies support the view that 19-iodocholesterol mimics cholesterol with regard to esterification and storage and that this property is a factor in its accumulation and retention for long periods in the adrenal cortex and ovary. In addition to its use in adrenal imaging, 19-radioiodinated cholesterol or related compounds may have clinical utility for the diagnosis of ovarian disorders.

[7] R. E. Counsell, N. Korn, R. Langdon, and J. L. McGauley, unpublished data.

REFERENCES

(1) R. E. Counsell, V. V. Ranade, R. J. Blair, W. H. Beierwaltes, and P. A. Weinhold, *Steroids*, **16**, 317 (1970).

(2) R. E. Counsell and N. Korn, in "Principles of Radiopharmacology," L. G. Columbetti, Ed., CRC, Boca Raton, Fla., 1979, p. 189.

(3) D. Schulster, S. Burstein, and B. A. Cooke, "Molecular Endocrinology of the Steroid Hormones," Wiley, New York, N.Y., 1976, pp. 167, 230.

(4) J. Folch, M. Lees, and G. H. Sloane-Stanley, *J. Biol. Chem.*, **226**, 497 (1957).

ACKNOWLEDGMENTS

Supported in part by U.S. Public Health Service Grant CA-08349. The authors thank Searle Laboratories for the 19-iodocholesterol.

Allyl Derivatives of Zearalenone

M. T. SHIPCHANDLER

Received May 10, 1979, from the *Research & Development Division, International Minerals & Chemical Corporation, Terre Haute, IN 47808.* Accepted for publication June 21, 1979. Present address: Diagnostics Division, Abbott Laboratories, North Chicago, IL 60064.

Abstract □ The Claisen rearrangement of 4-*O*-allylzearalenone led to only one principal product, which was identified as 3-allylzearalenone with the aid of photochemical isomerization and PMR spectroscopy. This general method is useful for distinguishing 3-substituted zearalenone isomers from 5-substituted isomers. Hydrogenation of 3-allylzearalenone gave 3-(1-propyl)zearalanone.

Keyphrases □ Zearalenone—allyl derivatives, synthesis □ Anabolic agents—zearalenone, synthesis of allyl derivatives

Zearalenone (I), a metabolite of *Gibberella zeae*, is produced *via* an industrial fermentation process (1). Several derivatives of I were synthesized to enhance its anabolic activity (2, 3). Zeranol (VI), a tetrahydro derivative, is used commercially as an anabolic agent in feedlot steers. The same fungus also produces four structurally related minor metabolites, one of which was characterized as 3-formylzearalenone (II) (4).

DISCUSSION

Isomeric 3- and 5-substituted zearalenones are not distinguished readily from each other by standard spectroscopic methods. Bolliger and Tamm (4) formylated zearalenone, and extensive PMR spectral scrutiny of the resulting 3- and 5-formylzearalenones and their corresponding dimethyl ethers led to the unequivocal assignment of Structure II to the metabolite (4). In another instance, III, the Kolbe–Schmitt reaction product of zearalenone, was subjected to extensive degradation (5).

This report describes a simple photochemical method coupled with PMR spectroscopy for a facile structural assignment. 4-*O*-Allylzearalenone (IV) was subjected to the Claisen rearrangement at 190–195°, and the principal product, V (mp 116–118°), was isolated in a 48% yield. It was isomerized to 3-allyl-*cis*-zearalenone (VIII) *via* the photochemical method of Peters (6). In the comparative PMR spectra of V and VIII, the upfield shift (13 Hz) of the aromatic proton of C-5 was very distinct, while the shifts of the allyl group protons were practically unchanged (6). Such an upfield shift of the aromatic proton of C-3 is not expected to occur in 5-substituted derivatives. The Claisen product thus was identified as 3-allylzearalenone (V). Low-pressure hydrogenation of VI gave 3-(1-propyl)zearalanone (VII).

EXPERIMENTAL[1]

4-*O*-Allylzearalenone (IV)—Compound I (15.9 g, 0.05 mole), allyl bromide (24.2 g, 0.2 mole), and potassium carbonate (10.0 g, 0.07 mole) were stirred and refluxed in acetone (200 ml) for 8 hr. The filtered inorganic salts were washed well with more solvent. The combined washings and filtrate were evaporated under reduced pressure. The residue was crystallized from 2-propanol to give 10 g of IV, mp 123–125°. In the PMR spectrum, a peak at δ 12.00 indicated the presence of the chelated hydroxyl proton at the 2-position; the absence of a peak at about δ 8.00 of the hydroxyl proton at the 4-position indicated allylation of this site. With two aromatic protons at δ 6.38 and 6.48 (J = 2.5 Hz), the rest of the spectrum was consistent with the assigned structure.

[1] Melting points (uncorrected) were measured with a Thomas-Hoover apparatus. PMR spectra were recorded on a Varian A 60-A instrument in deuterochloroform with tetramethylsilane as the internal standard. Elemental analyses were carried out by Microanalyses Inc.

0022-3549/80/0900-1017$01.00/0

© 1980, American Pharmaceutical Association

Table II—Percent of Radioactivity [a] Found in Each Phase following Folch Extraction of Tissue Radioactivity at 1 and 4 Days Postadministration of ^{125}I-Labeled 19-Iodocholesterol

Tissue	Day 1			Day 4		
	Precipitate	Upper	Lower	Precipitate	Upper	Lower
Adrenal	5.47 ± 2.36[b]	0.40 ± 0.42[b]	94.14 ± 2.48[b]	9.02 ± 3.54[b]	0.12 ± 0.14[b]	90.87 ± 3.65[b]
Blood	19.50 ± 4.74	13.87 ± 0.96	66.63 ± 5.21	29.00 ± 13.09	14.54 ± 4.98	56.47 ± 14.02
Liver	8.83 ± 2.00[b]	13.60 ± 2.04[b]	77.58 ± 2.29[b]	12.53 ± 1.91	11.18 ± 2.37	76.30 ± 3.87
Ovary	7.89 ± 2.21	0.92 ± 0.53	91.19 ± 1.82	8.81 ± 3.71	0.35 ± 0.10	90.84 ± 3.70

[a] Each value represents the mean ± *SD* for five rats unless noted. [b] Four rats.

uptake of radioactivity by pretreatment with potassium iodide solution (1) and in Folch extraction studies where >98% of the thyroid radioactivity was associated with the precipitated fraction[7].

The TLC systems used gave good separation of the free and esterified sterol. No further identification of radioactive products was attempted. Therefore, the esterified sterol peak could be made up of 19-iodocholesterol esterified with different saturated and unsaturated fatty acids. Similarly, slight alterations in the sterol portion of the molecule also could go undetected. Thus, [^{14}C]cholesterol and ^{125}I-labeled 19-iodocholesterol have the same R_f value in these systems.

Despite these limitations, these studies support the view that 19-iodocholesterol mimics cholesterol with regard to esterification and storage and that this property is a factor in its accumulation and retention for long periods in the adrenal cortex and ovary. In addition to its use in adrenal imaging, 19-radioiodinated cholesterol or related compounds may have clinical utility for the diagnosis of ovarian disorders.

[7] R. E. Counsell, N. Korn, R. Langdon, and J. L. McGauley, unpublished data.

REFERENCES

(1) R. E. Counsell, V. V. Ranade, R. J. Blair, W. H. Beierwaltes, and P. A. Weinhold, *Steroids*, **16**, 317 (1970).

(2) R. E. Counsell and N. Korn, in "Principles of Radiopharmacology," L. G. Columbetti, Ed., CRC, Boca Raton, Fla., 1979, p. 189.

(3) D. Schulster, S. Burstein, and B. A. Cooke, "Molecular Endocrinology of the Steroid Hormones," Wiley, New York, N.Y., 1976, pp. 167, 230.

(4) J. Folch, M. Lees, and G. H. Sloane-Stanley, *J. Biol. Chem.*, **226**, 497 (1957).

ACKNOWLEDGMENTS

Supported in part by U.S. Public Health Service Grant CA-08349. The authors thank Searle Laboratories for the 19-iodocholesterol.

Allyl Derivatives of Zearalenone

M. T. SHIPCHANDLER

Received May 10, 1979, from the *Research & Development Division, International Minerals & Chemical Corporation, Terre Haute, IN 47808.* Accepted for publication June 21, 1979. Present address: Diagnostics Division, Abbott Laboratories, North Chicago, IL 60064.

Abstract □ The Claisen rearrangement of 4-*O*-allylzearalenone led to only one principal product, which was identified as 3-allylzearalenone with the aid of photochemical isomerization and PMR spectroscopy. This general method is useful for distinguishing 3-substituted zearalenone isomers from 5-substituted isomers. Hydrogenation of 3-allylzearalenone gave 3-(1-propyl)zearalanone.

Keyphrases □ Zearalenone—allyl derivatives, synthesis □ Anabolic agents—zearalenone, synthesis of allyl derivatives

Zearalenone (I), a metabolite of *Gibberella zeae*, is produced *via* an industrial fermentation process (1). Several derivatives of I were synthesized to enhance its anabolic activity (2, 3). Zeranol (VI), a tetrahydro derivative, is used commercially as an anabolic agent in feedlot steers. The same fungus also produces four structurally related minor metabolites, one of which was characterized as 3-formylzearalenone (II) (4).

DISCUSSION

Isomeric 3- and 5-substituted zearalenones are not distinguished readily from each other by standard spectroscopic methods. Bolliger and Tamm (4) formylated zearalenone, and extensive PMR spectral scrutiny of the resulting 3- and 5-formylzearalenones and their corresponding dimethyl ethers led to the unequivocal assignment of Structure II to the metabolite (4). In another instance, III, the Kolbe–Schmitt reaction product of zearalenone, was subjected to extensive degradation (5).

This report describes a simple photochemical method coupled with PMR spectroscopy for a facile structural assignment. 4-*O*-Allylzearalenone (IV) was subjected to the Claisen rearrangement at 190–195°, and the principal product, V (mp 116–118°), was isolated in a 48% yield. It was isomerized to 3-allyl-*cis*-zearalenone (VIII) *via* the photochemical method of Peters (6). In the comparative PMR spectra of V and VIII, the upfield shift (13 Hz) of the aromatic proton of C-5 was very distinct, while the shifts of the allyl group protons were practically unchanged (6). Such an upfield shift of the aromatic proton of C-3 is not expected to occur in 5-substituted derivatives. The Claisen product thus was identified as 3-allylzearalenone (V). Low-pressure hydrogenation of VI gave 3-(1-propyl)zearalanone (VII).

EXPERIMENTAL[1]

4-*O*-Allylzearalenone (IV)—Compound I (15.9 g, 0.05 mole), allyl bromide (24.2 g, 0.2 mole), and potassium carbonate (10.0 g, 0.07 mole) were stirred and refluxed in acetone (200 ml) for 8 hr. The filtered inorganic salts were washed well with more solvent. The combined washings and filtrate were evaporated under reduced pressure. The residue was crystallized from 2-propanol to give 10 g of IV, mp 123–125°. In the PMR spectrum, a peak at δ 12.00 indicated the presence of the chelated hydroxyl proton at the 2-position; the absence of a peak at about δ 8.00 of the hydroxyl proton at the 4-position indicated allylation of this site. With two aromatic protons at δ 6.38 and 6.48 (J = 2.5 Hz), the rest of the spectrum was consistent with the assigned structure.

[1] Melting points (uncorrected) were measured with a Thomas-Hoover apparatus. PMR spectra were recorded on a Varian A 60-A instrument in deuterochloroform with tetramethylsilane as the internal standard. Elemental analyses were carried out by Microanalyses Inc.

0022-3549/80/0900-1017$01.00/0

© 1980, American Pharmaceutical Association

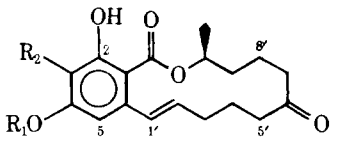

I: $R_1 = R_2 = H$
II: $R_1 = H$, $R_2 = CHO$
III: $R_1 = H$, $R_2 = COOH$
IV: $R_1 = CH_2CH{=}CH_2$, $R_2 = H$
V: $R_1 = H$, $R_2 = CH_2CH{=}CH_2$

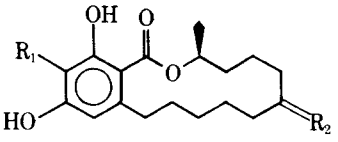

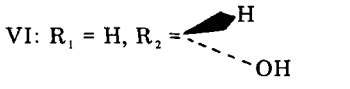

VII: $R_1 = CH_2CH_2CH_3$, $R_2 = {=}O$

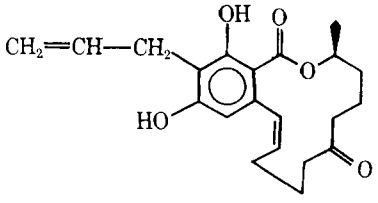

VIII

Anal.—Calc. for $C_{21}H_{26}O_5$: C, 70.37; H, 7.31. Found: C, 70.63; H, 7.13.

3-Allylzearalenone (V)—Compound IV (5.0 g) was placed in an oil bath maintained at 190–195° for 5 hr. TLC examination revealed only one principal product. The melt was chromatographed over a silica gel column[2] (100 g, 28 × 3.3 cm) and eluted with benzene and chloroform mixtures of increasing polarity. The fractions containing the product were evaporated together, and V was crystallized from methanol–water to give 2.5 g of white crystals, mp 116–118°. In the PMR spectrum, only one aromatic proton appeared as a singlet at δ 6.48 and two peaks of phenolic proton resonances appeared at δ 12.00 and 8.64. The C-1′ olefinic proton appeared as a doublet at δ 7.12 (J = 15 Hz).

Anal.—Calc. for $C_{21}H_{26}O_5$: C, 70.37; H, 7.31. Found: C, 70.47; H, 7.33.

3-Allyl-*cis*-zearalenone (VIII)—Compound V (1.3 g) was photoisomerized[3] in methanol (100 ml) for 60 hr according to the method of Peters (6). Evaporation gave a glassy substance (1.2 g), which could not be purified by crystallization. The peak ratio of the C-5 aromatic protons in the PMR spectrum (deuterium oxide was added to remove the interfering resonance of the C-4 phenolic proton) indicated a 90–95% conversion. The singlet resonance of the C-5 aromatic proton appeared at δ 6.26, and the doublet resonance of the C-1′ olefinic proton appeared at δ 6.65 (J = 12 Hz). This observation was consistent with that of Peters (6).

3-(1-Propyl)zearalanone (VII)—Compound V (1.0 g) was hydrogenated under 50 psi in methanol (100 ml) for 3 hr in the presence of palladium-on-carbon (5%, 0.1 g). The catalyst was removed *via* filtration, and the filtrate was evaporated under reduced pressure. The residue was crystallized from methanol–water to yield 1.1 g of white crystals, mp 161–162.5°. There were no resonances of olefinic protons in the PMR spectrum. The singlet resonance of the C-5 aromatic proton appeared at δ 6.27, and the pseudotriplet resonance of the methyl protons (of the propyl group) appeared at δ 1.00 (J = 6 Hz).

Anal.—Calc. for $C_{21}H_{30}O_5$: C, 69.58; H, 8.34. Found: C, 69.70; H, 8.40.

REFERENCES

(1) P. H. Hidy, R. S. Baldwin, R. L. Greasham, C. L. Keith, and J. R. McMullen, in "Advances in Applied Microbiology," vol. 22, D. Perlman, Ed., Academic, New York, N.Y., 1977, p. 59.

(2) W. H. Urry, H. L. Wehrmeister, E. B. Hodge, and P. H. Hidy, *Tetrahedron Lett.*, **1966**, 3109.

(3) M. T. Shipchandler, *Heterocycles*, **3**, 471 (1975).

(4) G. Bolliger and C. Tamm, *Helv. Chim. Acta*, **55**, 3030 (1972).

(5) T. B. Windholz and R. D. Brown, *J. Org. Chem.*, **37**, 1647 (1972).

(6) C. A. Peters, *J. Med. Chem.*, **15**, 867 (1972).

ACKNOWLEDGMENTS

The author thanks Mr. Marvin C. Bachman for continued interest in this research and Mr. R. P. Sidenbender for technical assistance.

[2] Baker No. 3404.

[3] The photoisomerization process does not need to be complete. For example, the shifts at δ 6.48 and 6.26 of the C-5 aromatic protons were distinct in the PMR spectrum of the reaction mixture containing approximately equal amounts of V and VIII.

Carbocyclic Analogs of Arabinosylpurine Nucleosides

HEEJOO LEE and ROBERT VINCE ˣ

Received March 12, 1979, from the *Department of Medicinal Chemistry, College of Pharmacy, University of Minnesota, Minneapolis, MN 55455.* Accepted for publication August 22, 1979.

Abstract □ Carbocyclic analogs of arabinofuranosylguanine (VII) and 2,6-diamino-9-β-arabinofuranosylpurine (VIII) and the corresponding 8-azapurine analogs, 5-amino-7-hydroxy-3-[2α,3β-dihydroxy-4α-(hydroxymethyl)cyclopent-1α-yl]-ν-triazolo[4,5-*d*]pyrimidine (X) and 5,7-diamino-3-[2α,3β-dihydroxy-4α-(hydroxymethyl)cyclopent-1α-yl]-ν-triazolo[4,5-*d*]pyrimidine (XI), were prepared. Carbocyclic nucleoside analogs VII and X exhibited significant cytotoxicity against P-388 mouse leukemia cells in culture. *In vitro* testing against herpes simplex type 1 (strain HF) indicated that only VIII exhibited significant antiviral activity.

Keyphrases □ Arabinosylpurine nucleosides—carbocyclic analogs, synthesis and evaluation for antitumor and antiviral activity □ Antitumor activity—carbocyclic analogs of arabinosylpurine nucleosides, synthesis and testing □ Antiviral activity—carbocyclic analogs of arabinosylpurine nucleosides, synthesis and testing

The significant antiviral and antitumor activities exhibited by the adenosine deaminase-resistant carbocyclic analog of arabinofuranosyladenine (1) prompted the synthesis of a variety of carbocyclic arabinosylpurine nucleosides. Recent studies with other antiviral nucleosides suggested that purine derivatives other than adenine should be explored in cases where an adenine nucleoside exhibits antitumor or antiviral properties (2, 3). In the case cited, the antiviral activity of the guanine analog in a series of 9-(2-hydroxyethoxymethyl)purines was two orders of magnitude greater than that of the corresponding adenine analog. In addition, Elion *et al.* (4) demonstrated high antiviral activity with 2,6-diamino-9-β-arabinofuranosylpurine. However, this analog was deaminated rapidly by adenosine deaminase. These results provide an excellent rationale for the synthesis of the guanosine and 2,6-diaminopurine derivatives of carbocyclic arabinosyl nucleosides.

RESULTS AND DISCUSSION

The synthesis of the carbocyclic purine nucleosides is outlined in Scheme I[1]. Condensation of (±)-4α-amino-2β,3α-dihydroxy-1α-cyclopentanemethanol (I) (1) with 2-amino-4,6-dichloropyrimidine (II) gave the corresponding pyrimidinylamino derivative (III). The 5-(*p*-chlorophenylazo)pyrimidine (IV) was prepared with *p*-chlorobenzenediazonium chloride by the method of Shealy and Clayton (5). Reduction of IV with zinc and acetic acid gave the pyrimidine V, which subsequently was converted to the 9-substituted 2-amino-6-chloropurine (VI) by ring closure with diethoxymethyl acetate and subsequent mild acid hydrolysis. Treatment of VI with 1 *N* HCl under reflux conditions gave carbocyclic arabinosylguanine (VII), while treatment of VI with liquid ammonia gave carbocyclic arabinosyl 2,6-diaminopurine (VIII).

The 8-azapurine analogs were obtained as illustrated in Scheme II. Ring closure of V with sodium nitrite and hydrochloric acid gave an excellent yield of (±)-5-amino-7-chloro-3-[2α,3β-dihydroxy-4α-(hydroxymethyl)cyclopent-1α-yl]-ν-triazolo[4,5-*d*]pyrimidine (IX). Acid hydrolysis of IX gave the 8-aza analog (X) of carbocyclic arabinosylguanine, whereas treatment of IX with liquid ammonia gave the 8-aza analog (XI) of carbocyclic arabinosyl 2,6-diaminopurine.

The ED_{50} cytotoxicity concentrations of VI–XI in P-388 mouse leukemia cell culture are listed in Table I. Carbocyclic arabinosylguanine

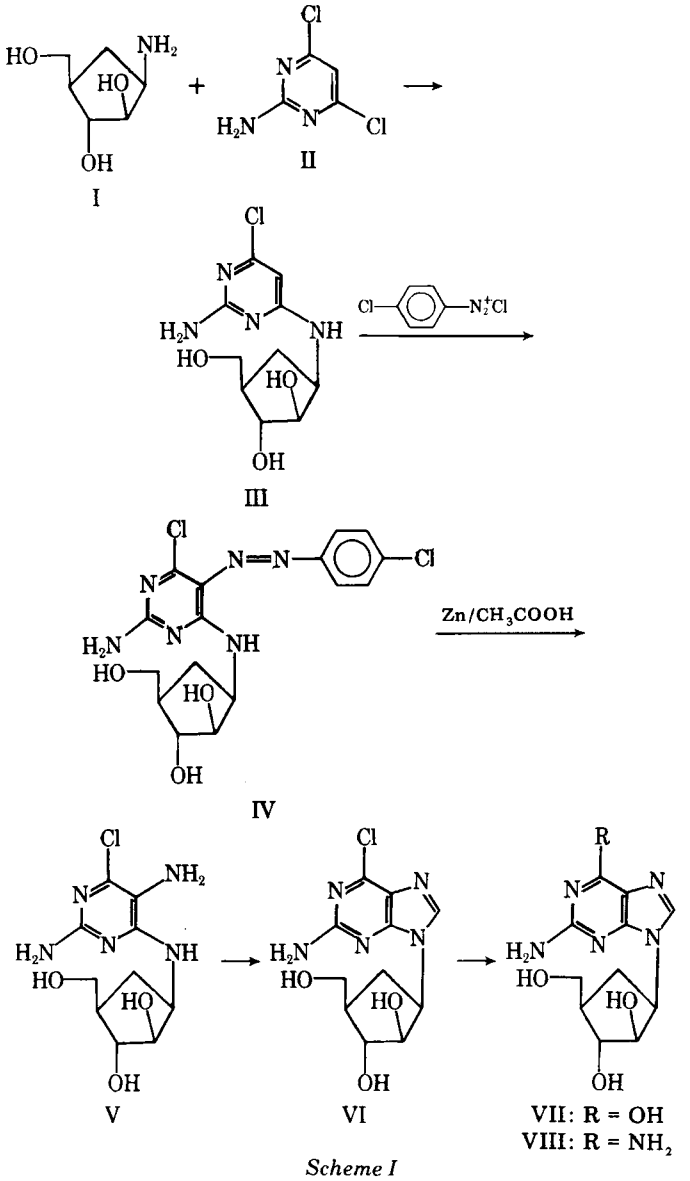

Scheme I

(VII) and 8-aza carbocyclic arabinosylguanine (X) exhibited significant cytotoxicities in this assay. All purine analogs were examined for *in vitro* antiviral activity against herpes simplex virus type 1 (strain HF) by quantitating the inhibition of virus-induced cytopathogenic effects in infected cultures.

The virus was propagated and assayed for infectivity in continuous-

Table I—Inhibitory Concentrations of Carbocyclic Purine Arabinosides for P-388 Leukemia Cells in Culture

Compound	ED_{50}, μM
VI	166.0
VII	4.6
VIII	251.0
IX	33.3
X	6.5
XI	258.0

[1] Structures I–XI depict only one enantiomer of the racemic form that actually was obtained.

0022-3549/80/0900-1019$01.00/0
© 1980, American Pharmaceutical Association

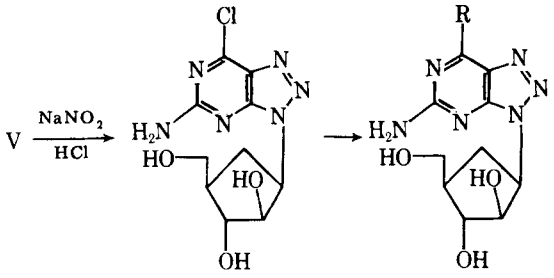

Scheme II

passage, human epidermoid carcinoma of the larynx (H. Ep.-2) cells. Virus ratings were calculated for the activity of each compound using a modification of the method of Ehrlich *et al.* (6) that was described previously (7, 8). Only the carbocyclic arabinosyl 2,6-diaminopurine analog (VIII) exhibited significant antiviral activity with a virus rating of 1.5[2].

EXPERIMENTAL[3]

TLC was performed using 0.25-mm layers of silica gel[4], and column chromatography was performed on silica gel[5]. PMR spectra were taken with a 60-MHz[6] or 100-MHz[7] spectrometer with tetramethylsilane as the internal standard. Melting points were determined in capillaries with a melting-point block[8] and are uncorrected.

(±)-2-Amino-4-*N*-[2α,3β-dihydroxy-4α-(hydroxymethyl)cyclopent-1α-yl]amino-6-chloropyrimidine (III)—A mixture of aminoalcohol I [obtained from hydrolysis of 20 mmoles of (±)-4α-acetamido-2β,3α-diacetoxy-1α-cyclopentanemethyl acetate as described in Ref. 1], 2-amino-4,6-dichloropyrimidine (4.92 g, 30 mmoles), and triethylamine (20 ml) in 1-butanol (100 ml) was refluxed under nitrogen gas for 2 days (9). The solvent was removed under reduced pressure, and the residue was dissolved in water (200 ml). The aqueous solution was washed with methylene chloride (2 × 200 ml) to remove excess 2-amino-4,6-dichloropyrimidine. The aqueous solution was stirred briefly with anion-exchange resin[9] (40 ml), evaporated under reduced pressure, and azeotroped with absolute ethanol to dryness.

The liquid residue was dissolved in methanol–methylene chloride (1:4, 20 ml) and refrigerated. A pale-yellow crystalline product was collected by filtration, and recrystallization from methanol–methylene chloride (1:1) gave III as white granules (4.3 g, 78% from the acetamido acetate), mp 189–190°; UV: λ_{max} ($\epsilon \times 10^{-3}$) 310 (9.0), 274 (11.4), 238 (17.0), and 210 (28.0) in 0.1 *N* HCl, 284 (11.5), 239 (13.0), and 210 (30.0) in water, and 284 (11.3) and 236 (13.3) in 0.1 *N* NaOH; IR (KBr): 3500–3200 (NH and OH), 1640 (NH), and 1585 (C=C and C=N) cm^{-1}; PMR (100 MHz, dimethyl sulfoxide-d_6): δ 1.1–2.2 (m, 3H, CH and CH_2), 3.1–3.8, 4.0–5.1 (m, all other protons with water in the solvent), 5.87 (s, 1H, H at pyrimidine C-5), 6.33 (s, 2H, NH_2), and 6.74 (broad s, 1H, NH).

Anal.—Calc. for $C_{10}H_{15}ClN_4O_3$: C, 43.72; H, 5.50; Cl, 12.91; N, 20.40. Found: C, 43.51; H, 5.41; Cl, 12.94; N, 20.24.

(±)-2-Amino-4-*N*-[2α,3β-dihydroxy-4α-(hydroxymethyl)cyclopent-1α-yl]amino-5-*p*-chlorophenylazo-6-chloropyrimidine (IV)—A cold (0–5°) solution of *p*-chlorobenzenediazonium chloride was prepared by adding a solution of sodium nitrite (0.65 g, 9.5 mmoles) in water (5 ml) to a solution of *p*-chloroaniline (1.15 g, 9 mmoles) dissolved in 12 *N* HCl (5 ml) and water (15 ml) and cooled in an ice–salt bath (5). The cold solution of *p*-chlorobenzenediazonium chloride was added dropwise to a mixture of III (2.15 g, 7.8 mmoles), sodium acetate trihydrate (17 g), acetic acid (40 ml), and water (40 ml) at room temperature. A yellow precipitate formed immediately, but the reaction mixture was stirred at room temperature overnight. The mixture was cooled in an ice bath; the yellow precipitate was filtered, washed with cold water, and dried.

The solid product was crystallized from methanol to yield yellow crystals (2.5 g, 77.6%, mp 243–246°), which were homogeneous by TLC and were used for the next reaction without further purification. An analytical sample of IV was obtained by recrystallization from methanol, mp 256–258°; UV: λ_{max} ($\epsilon \times 10^{-3}$) 372 (27.6), 266, and 228 (24.0) in 0.1 *N* HCl, 386 (29.8), 278 (11.6), and 226 (17.5) in water, and 386 (30.5) and 267 (13.8) in 0.1 *N* NaOH; IR (KBr): 3450–3100 (OH, NH), 1650 (NH), and 1570 (C=C and C=N) cm^{-1}; PMR (100 MHz, dimethyl sulfoxide-d_6): δ 1.15–2.43 (m, 3H, CH_2 and CH in cyclopentane ring), 3.29–3.92 (m, 5H, 3 CH, OH, and HOD), 4.33–4.72 (m, 2H, CH_2), 4.85 and 5.51 (2d, 2H, 2 OH), and 7.37–7.91 (m, 7H, aromatic, NH_2, and NH).

Anal.—Calc. for $C_{16}H_{18}Cl_2N_6O_3$: C, 46.50; H, 4.39; Cl, 17.16; N, 20.34. Found: C, 46.55; H, 4.38; Cl, 17.42; N, 20.23.

(±)-2,5-Diamino-4-*N*-[2α,3β-dihydroxy-4α-(hydroxymethyl)cyclopent-1α-yl]amino-6-chloropyrimidine (V)—A mixture of IV (2.5 g, 6.1 mmoles), zinc dust (200 mesh, 4 g), and acetic acid (2 ml) in ethanol (100 ml) and water (100 ml) was refluxed under nitrogen until the yellow color of IV disappeared (5 hr) (5). Excess zinc was removed by filtration, and the solvent was evaporated under reduced pressure. The brown residue was dissolved in water (150 ml), and the aqueous solution was washed with methylene chloride to remove *p*-chloroaniline. After removal of water under reduced pressure, the residue was dissolved in ethanol–ethyl acetate and the solution was refrigerated overnight.

Filtration and dryness gave a crude brown product[10] (1.545 g, mp 213–215°). Repeated crystallization (three times) from water-ethanol (1:4) gave V as a slightly pink powder, mp 236–238°; UV: λ_{max} ($\epsilon \times 10^{-3}$) 298 (7.9) and 234 (18.9) in 0.1 *N* HCl, 302 (9.3), 242, 226, and 202 (19.1) in water, and 302 (9.0) and 244 in 0.1 *N* NaOH; IR (KBr): 3400–3200 (NH and OH), 1650, 1615, 1575, 1505, and 1470 cm^{-1}; PMR (100 MHz, dimethyl sulfoxide-d_6): δ 0.82–2.17 (m, 3H, CH_2 and CH in cyclopentane ring), 3.1–3.8 and 4.0–4.82 (m, other protons with HOD), 5.40 (broad s, 2H, NH_2), and 5.87 (d, 1H, NH).

Anal.—Calc. for $C_{10}H_{16}ClN_5O_3$: C, 41.45; H, 5.57; Cl, 12.24; N, 24.17. Found: C, 41.64; H, 5.68; Cl, 12.05; N, 24.39.

(±)-2-Amino-6-chloro-9-[2α,3β-dihydroxy-4α-(hydroxymethyl)cyclopent-1α-yl]purine (VI)—Compound V (200 mg, 0.7 mmole) in diethoxymethyl acetate (20 ml) was stirred at room temperature for 1 hr, and the clear solution was heated at 80° for 24 hr with stirring. The solvent was removed under reduced pressure, and the oil residue was dissolved in 0.5 *N* HCl (10 ml) and stirred at room temperature for 30 min. The reaction solution was neutralized with anion-exchange resin[9] (pH 7–8), and the water was evaporated and azeotroped with absolute ethanol. The residue was purified by passing it through a silica gel column with methanol–methylene chloride (3:17) as the eluent.

Evaporation of the solvent of the corresponding fraction left 145 mg (69%) of a pink solid, mp 208–209°, which was homogeneous by TLC. Recrystallization from methanol–methylene chloride gave the analytically pure VI as a pink powder, mp 209–210°; UV: λ_{max} ($\epsilon \times 10^{-3}$) 312 (7.0), 242, and 218 (29.2) in 0.1 *N* HCl, 306 (8.2), 246, and 222 (28.2) in water, and 306 (8.1) and 246 in 0.1 *N* NaOH; IR (KBr): 3490, 3350 (br), 3220, 1658 (NH), 1610, 1565 (C=C and C=N), and 1035 (C–O) cm^{-1}; PMR (100 MHz, dimethyl sulfoxide-d_6): δ 1.65–2.35 (m, 3H, CH_2 and CH in cyclopentane ring), 3.11–4.01, 4.41–5.31 (CH_2O, 2 CHO, CHN, 3 OH, and HOD in dimethyl sulfoxide-d_6), 6.86 (s, 2H, NH_2), and 8.12 (s, 1H, H at purine C-8).

Anal.—Calc. for $C_{11}H_{14}ClN_5O_3$: C, 44.08; H, 4.71; Cl, 11.83; N, 23.37. Found: C, 44.24; H, 4.78; Cl, 11.93; N, 23.50.

(±)-9-[2α,3β-Dihydroxy-4α-(hydroxymethyl)cyclopent-1α-yl]guanine (VII)—A solution of VI (146 mg, 0.49 mmole) in 1 *N* HCl (10 ml) was refluxed for 5 hr, and then the water was evaporated and azeotroped with absolute ethanol. The liquid residue was dissolved in a small amount of water, and the solution was neutralized (pH 6–7) with 6 *N* NaOH. The white precipitate formed immediately, but the solution was refrigerated for 1 hr. The solid product was collected by filtration and washed with cold water to yield 130 mg (94.3%) of a white powder, mp 290–293°.

Recrystallization from water gave VII as a white powder, mp 292–294°; UV: λ_{max} ($\epsilon \times 10^{-3}$) 227 (sh) and 252 (14.1) in 0.1 *N* HCl, 270 (sh) and 251 (13.5) in water, and 267 (12.0) and 254 (sh) in 0.1 *N* NaOH; IR (KBr): 3470, 3320, 3210, 2940–2500 (br), 1735 (C=O), 1630, and 1610 cm^{-1}; PMR (100 MHz, dimethyl sulfoxide-d_6): δ 1.6–2.3 (m, 3H, CH_2 and CH in cyclopentane ring), 3.31 (s, OH and HOD), 3.4–3.9 (m, 4H, CHO, CHN, and

[2] Virus rating (VR) is a weighted measurement of antiviral activity based on the *in vitro* inhibition of virus-induced cytopathogenic effects and the cytotoxicity exhibited by the drug as described in Ref. 6. A VR of >1.0 indicates definite (+) antiviral activity, and a VR of <0.5 indicates no (−) apparent antiviral activity.

[3] Elemental analyses were performed by M-H-W Laboratories, Phoenix, Ariz.

[4] Merck 60 F-254.

[5] Merck 60.

[6] Varian A-60D and T-60.

[7] Varian XL-100.

[8] Mel-Temp apparatus.

[9] Amberlite IRA-400 (OH^-).

[10] The crude brown products usually were contaminated with zinc acetate dihydrate (mp 237°) so that yields were variable.

CH_2O), 4.56–5.20 (m, 4H, 3 OH and CHO), 6.38 (s, 2H, NH_2), and 7.68 (s, 1H, H at purine C-8).

Anal.—Calc. for $C_{11}H_{15}N_5O_4$: C, 46.97; H, 5.38; N, 24.90. Found: C, 46.74; H, 5.42; N, 24.89.

(±)-2-Amino-9-[2α,3β-dihydroxy-4α-(hydroxymethyl)cyclopent-1α-yl]adenine (VIII)—The chloropurine VI (390 mg, 1.3 mmoles) was stirred in excess liquid ammonia in a steel bomb at 75° for 42 hr. The bomb was cooled in a dry ice bath, and the reaction mixture was transferred to a beaker using methanol. The ammonia was allowed to evaporate at room temperature, and evaporation of methanol left a white powder.

Crystallization from water gave VIII as pink crystals (323 mg, 83.3%), mp 266–268°; UV: λ_{max} ($\epsilon \times 10^{-3}$) 290 (11.0), 251 (12.7), and 216 (27.0) in 0.1 *N* HCl, 280 (10.5), 254 (8.7), and 214 (273) in water, and 279 (11.5) and 254 (9.4) in 0.1 *N* NaOH; IR (KBr): 3470, 3410, 3330, 3210, 3130, 2900–2500 (br), 1670, 1630, and 1600 (NH, C=C and C=N) cm^{-1}; PMR (100 MHz, dimethyl sulfoxide-d_6): δ 1.71–2.31 (m, 3H, CH_2 and CH in cyclopentane ring), 3.27–3.91 (m, 8H, CHO, CNH, CH_2O, and H_2O), 4.57–5.33 (m, 4H, 3 OH and CHO), 5.77 (s, 2H, NH_2), 6.63 (s, 2H, NH_2), and 7.71 (s, 1H, H at purine C-8).

Anal.—Calc. for $C_{11}H_{16}N_6O_3 \cdot H_2O$: C, 44.28; H, 6.08; N, 28.18. Found: C, 44.04; H, 6.12; N, 28.56.

(±)-5-Amino-7-chloro-3-[2α,3β-dihydroxy-4α-(hydroxymethyl)-cyclopent-1α-yl]-ν-triazolo[4,5-*d*]pyrimidine (IX)—A solution of V (180 mg, 0.62 mmole) in 1 *N* HCl (1.3 ml) and water (4 ml) was cooled in an ice–salt bath, and sodium nitrite (45 mg, 0.65 mmole) was added with stirring. After 5 min (the solution was frozen), the ice–salt bath was removed and the solution was stirred at room temperature for 1 hr. The reaction solution was neutralized with sodium bicarbonate (109 mg, 1.3 mmoles) and then evaporated to dryness by azeotroping with absolute ethanol. The remainder was passed through a silica gel column with methanol–methylene chloride (1:4) as the eluent and gave a solid product (152 mg, 82%), mp 209–210°.

Recrystallization from methanol gave IX as a white powder, mp 210° dec.; UV: λ_{max} ($\epsilon \times 10^{-3}$) 314 (7.5) and 223 (27.0) in 0.1 *N* HCl, 314 (7.5) and 223 (22.9) in water, and 276 (12.4) in 0.1 *N* NaOH; IR (KBr): 3360, 3320, 3200 (OH and NH), 2960, 2920, 1640 (NH), 1600, 1570, 1510 (C=C and C=N), and 1110 (C—O) cm^{-1}; PMR (100 MHz, dimethyl sulfoxide-d_6): δ 1.80–2.46 (m, 3H, CH and CH_2 in cyclopentane ring), 3.40–4.14 (m, 4H, CHO, CHN, and CH_2O), 4.54–5.14 (m, 4H, CHO and 3 OH), and 7.56 (s, 2H, NH_2).

Anal.—Calc. for $C_{10}H_{13}ClN_6O_3$: C, 39.93; H, 4.35; Cl, 11.79; N, 27.95. Found: C, 39.66; H, 4.31; Cl, 11.79; N, 28.03.

(±)-5-Amino-7-hydroxy-3-[2α,3β-dihydroxy-4α-(hydroxymethyl)cyclopent-1α-yl]-ν-triazolo[4,5-*d*]pyrimidine (X)—A solution of IX (139 mg, 0.46 mmole) in 10 ml of 1 *N* HCl was refluxed for 5 hr, and the solvent was removed under reduced pressure and azeotroped with absolute ethanol. The solid residue was dissolved in a small amount of water, and the aqueous solution was refrigerated. Filtration afforded a fine crystalline product (pale brown, 80 mg, 62%), mp 210–215°.

Recrystallization from water gave X as pale-brown fine crystals, mp 215–217° (shrinking) and 275–277° dec.; UV: λ_{max} ($\epsilon \times 10^{-3}$) 270 (sh) and 252 (15.2) in 0.1 *N* HCl, 270 (sh), 252 (13.5), and 202 (24.0) in water, and 277 (13.0) in 0.1 *N* NaOH; IR (KBr): 3480, 3400, 3360, 3300, 3200 (OH and NH), 2940, 2880, 2800, 2740, 1700 (C=O), 1640, 1590, 1530 (C=C and C=N), and 1035 (C—O) cm^{-1}; PMR (100 MHz, dimethyl sulfoxide-d_6): δ 1.70–2.44 (m, 3H, CH and CH_2 in cyclopentane ring), 3.34 (s, OH and HOD), 3.40–4.10 (m, 4H, CHO, CHN, and CH_2O), 4.46–5.00 (m, 4H, 3 OH and CHO), and 6.80 (s, 2H, NH_2).

Anal.—Calc. for $C_{10}H_{14}N_6O_4$: C, 42.55; H, 5.00; N, 29.78. Found: C, 42.21; H, 5.07; N, 29.52.

(±)-5,7-Diamino-3-[2α,3β-dihydroxy - 4α - (hydroxymethyl)cyclopent-1α-yl]-ν-triazolo[4,5-*d*]pyrimidine (XI)—The chloro compound IX (202 mg, 0.67 mmole) was shaken with excess liquid ammonia in a steel bomb at room temperature for 2 days. Evaporation of ammonia left a solid residue, which was dissolved in hot water (10 ml). Refrigeration of the aqueous solution yielded a solid product (147 mg, 75.6%), mp 245–247°.

Recrystallization from water afforded XI as a white powder, mp 260–262°; UV: λ_{max} ($\epsilon \times 10^{-3}$) 282 (9.2), 252 (13.0), and 211 (32.8) in 0.1 *N* HCl, 283 (11.7), 250 (sh), and 222 (27.2) in water, and 283 (12.6) and 254 (sh) in 0.1 *N* NaOH; IR (KBr): 3500, 3400, 3320, 3140 (OH and NH), 2940, 2880, 1675 (NH), 1610, 1490 (C=C and C=N), and 1050 (C—O) cm^{-1}; PMR (100 MHz, dimethyl sulfoxide-d_6): δ 1.76–2.40 (m, 3H, CH_2 in cyclopentane ring), 3.40–4.12 (m, 4H, CHO, CNH, and CH_2O), 4.50–5.04 (m, 4H, 3 OH and CHO), 6.28 (s, 2H, NH_2), and 7.46 (s, 2H, NH_2).

Anal.—Calc. for $C_{10}H_{15}N_7O_3 \cdot 1/2H_2O$: C, 41.37; H, 5.56; N, 33.78. Found: C, 41.62; H, 5.56; N, 33.63.

REFERENCES

(1) R. Vince and S. Daluge, *J. Med. Chem.*, **20,** 612 (1977).

(2) G. B. Elion, P. A. Furman, J. A. Fyfe, P. deMiranda, L. Beachamp, and H. J. Schaeffer, *Proc. Natl. Acad. Sci., USA,* **74,** 5716 (1977).

(3) H. J. Schaeffer, L. Beachamp, P. deMiranda, G. B. Elion, D. J. Bauer, and P. Collins, *Nature,* **272,** 583 (1978).

(4) G. B. Elion, J. L. Rideout, P. deMiranda, P. Collins, and D. J. Bauer, *Ann. N.Y. Acad. Sci.,* **255,** 468 (1975).

(5) Y. F. Shealy and J. D. Clayton, *J. Pharm. Sci.,* **62,** 1432 (1973).

(6) J. Ehrlich, B. J. Sloan, F. A. Miller, and H. Machamer, *Ann. N.Y. Acad. Sci.,* **130,** 5 (1965).

(7) R. W. Sidwell, G. Arnett, G. J. Dixon, and F. M. Schabel, Jr., *Proc. Soc. Exp. Biol. Med.,* **131,** 1226 (1969).

(8) L. L. Bennett, Jr., W. M. Shannon, P. W. Allan, and G. Arnett, *Ann. N.Y. Acad. Sci.,* **225,** 342 (1975).

(9) S. Daluge and R. Vince, *J. Org. Chem.,* **43,** 2311 (1978).

ACKNOWLEDGMENTS

Supported by Grant CA 13592 from the National Cancer Institute, Department of Health, Education, and Welfare.

The authors thank Dr. W. M. Shannon of the Southern Research Institute for antiviral screening of the compounds.

Latentiated Forms of the Transport-Inhibitory α-Amino Acid Adamantanine

HERBERT T. NAGASAWA ˣ, JAMES A. ELBERLING, and FRANCES N. SHIROTA

Received March 12, 1979, from the *Medical Research Laboratories, Veterans Administration Medical Center, and the Department of Medicinal Chemistry, College of Pharmacy, University of Minnesota, Minneapolis, MN 55417.* Accepted for publication July 10, 1979.

Abstract □ *N*-(γ-L-Glutamyl)adamantanine (Ic) and *N*-hydroxyadamantanine (I*b*) were synthesized as latentiated forms of the transport-inhibitory α-amino acid adamantanine (I*a*), and their biological properties were evaluated. Inhibition of the growth of P-388 tumor cells by I*b* was comparable with that of the antitumor agent *N*-hydroxycycloleucine (II*b*). *In contrast*, Ic was inactive in this system, presumably because it was not a substrate for γ-glutamyltranspeptidase. Nevertheless, the concept proposed here of using the enzyme, γ-glutamyltranspeptidase, to latentiate drugs *in vivo* by synthetic γ-glutamylation of an amino or hydroxyl group on the drug molecule appears to be worthy of further exploration.

Keyphrases □ Adamantanine—synthesis of latentiated forms and biological evaluation □ Antitumor activity—latentiated forms of adamantanine, synthesis and biological evaluation □ Transport inhibitors—latentiated forms of α-amino acid adamantanine, synthesis

The tricyclo aliphatic α-amino acid adamantanine (2-aminoadamantane-2-carboxylic acid, I*a*), a structural analog of the transport-inhibitory and antitumor amino acid cycloleucine (II*a*), is highly effective in inhibiting the transport of L-methionine and L-leucine into Ehrlich ascites carcinoma cells *in vitro* (1). However, the bioavailability of I*a* is compromised severely by its extreme insolubility. Accordingly, methods to convert I*a* systematically to latentiated forms have been sought. The C-terminal and N-terminal glycine and leucine conjugates (dipeptides) of I*a* were inactive, reflecting the inertness of these derivatives to cleavage by leucine aminopeptidase (2).

BACKGROUND

α-Amino acids and certain natural products that are conjugated on the amino group as γ-L-glutamyl derivatives can be considered as latentiated forms of the amino acid or natural product, since the γ-glutamyl group can be cleaved *in vivo* by γ-glutamyltranspeptidase, an enzyme that is abundant in transport-active organs such as the kidneys (3). Synthetic *N*-(γ-glutamyl)-α-amino acids were shown to be substrates for γ-glutamyltranspeptidase to varying degrees (4–6). N^4-(1-Hydroxycyclopropyl)-L-glutamine, a compound found in the edible mushroom species *Coprinus atramentarius*, inhibits aldehyde dehydrogenase *in vivo* but not *in vitro* (7). *N*-(γ-L-Glutamyl)dopamine (8) and *N*-(γ-L-glutamyl)levodopa (9), both prodrugs of dopamine, have demonstrable renal vasodilator activities due to the release of the dopamine moiety *in vivo*.

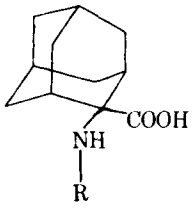

I*a*: R = H
I*b*: R = OH
Ic: R = $COCH_2CH_2CHCOOH$ (NH$_2$)

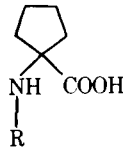

II*a*: R = H
II*b*: R = OH

N-Hydroxylated α-amino acids (α-hydroxyamino acids) also can be considered as precursors of the respective amino acids since the latter compounds can be generated on reduction of the hydroxyamino function *in vivo*. The antitumor agent 1-hydroxyaminocyclopentanecarboxylic acid (*N*-hydroxycycloleucine, II*b*) is active against Ehrlich ascites carcinoma cells *in vivo* (10) and L-1210 leukemia (11); although no precise data are available to suggest the conversion of II*b* to II*a*, rat liver contains an enzyme that can reduce *N*-alkylhydroxyamines to the corresponding *N*-alkylamines (12).

Based on these considerations, several derivatives of I*a*, the γ-glutamyl derivative *N*-(γ-glutamyl)adamantanine (Ic) and the *N*-hydroxylated analog *N*-hydroxyadamantanine (I*b*), were synthesized as latentiated forms. These compounds were evaluated with respect to their ability to be released or converted to I*a* by enzymatic action.

EXPERIMENTAL[1]

Chemistry—*N*-(γ-L-Glutamyl)adamantanine (Ic) was synthesized by coupling *N*-phthaloyl-L-glutamic anhydride (III) with the *N,O*-bis(trimethylsilyl) derivative of adamantanine (IV), both prepared *in situ* (Scheme I). The procedure for the preparation of III was a modification (13) of the method of King and Kidd (14). Hydrazinolysis of the phthaloyl group of α-*N*-phthaloyl-γ-L-glutamyladamantanine (V) afforded Ic in a 74% yield. The fact that Ic was a γ-glutamyl peptide and not the isomeric α-peptide can be assessed by the method of synthesis, a procedure known to yield γ-glutamyl peptides (15), and was verified by chemical-ionization mass spectrometry[2].

N-Hydroxyadamantanine (I*b*) was prepared *via* a three-step procedure (16–18) from adamantan-2-one oxime (VI) (Scheme II). Addition of hydrogen cyanide to VI gave 2-hydroxyamino-2-cyanoadamantane (VII), which was hydrolyzed successively to the carboxamide (VIII) with cold concentrated sulfuric acid and then to the desired I*b* under more vigorous conditions.

Attempts to hydrolyze VII in one step to I*b* at elevated temperatures led to considerable decomposition and reversion (19) to adamantan-2-one. Compound I*b* was stable to acid but rapidly decomposed above pH 8, an alkaline instability typical for α-hydroxyamino acids (17). Compound I*b* also gave a strong color test for hydroxylamine with triphenyltetrazolium chloride (20) and gave a quasimolecular ion (MH^+, base peak) at the expected *m/e* 212 on chemical-ionization mass spectrometry.

α-*N*-*Phthaloyl-γ-L-glutamyladamantanine* (*V*)—To a solution of *N*-phthaloyl-L-glutamic acid (14) (19.25 g, 0.069 mole) in tetrahydrofuran (250 ml) was added dicyclohexylcarbodiimide (14.33 g, 0.070 mole), and the reaction mixture was stirred at room temperature for 2 hr. The mixture then was filtered. The filtrate was added to a solution of the trimethylsilyl derivative (IV), which was prepared *in situ* by heating I*a* (13.56 g, 0.069 mole) and *N,O*-bis(trimethylsilyl)trifluoroacetamide (17.88 g, 0.069 mole) in 300 ml of acetonitrile under reflux for 2 hr. Heating under reflux was continued for 2 hr, and the solvent was evaporated to dryness.

The residue was suspended in 300 ml of water, and the solution was brought to pH 10 with 5% Na_2CO_3 solution. Ether (200 ml) was added

[1] Melting points were determined on a Mettler FP-2 hot-stage apparatus and are corrected. All solvent evaporations were carried out *in vacuo* on a mechanical rotating evaporator using a water aspirator. Microanalyses were performed by Galbraith Laboratories, Knoxville, Tenn. IR spectra were determined on a Beckman IR-10 IR spectrophotometer, and the chemical-ionization mass spectra were provided by Dr. R. Foltz, Battelle Columbus Laboratories, Columbus, Ohio, using an AEI-MS-902 mass spectrometer equipped with an SRIC model CIS-2 combined chemical-ionization–electron-ionization ion source.

[2] R. Foltz, Battelle Columbus Laboratories, Columbus, Ohio, personal communication. The diagnostic value of chemical-ionization mass spectrometry for distinguishing γ-glutamyl dipeptides from the isomeric α-glutamyl dipeptides will be discussed in a separate report.

0022-3549/80/0900-1022$01.00/0
© 1980, American Pharmaceutical Association

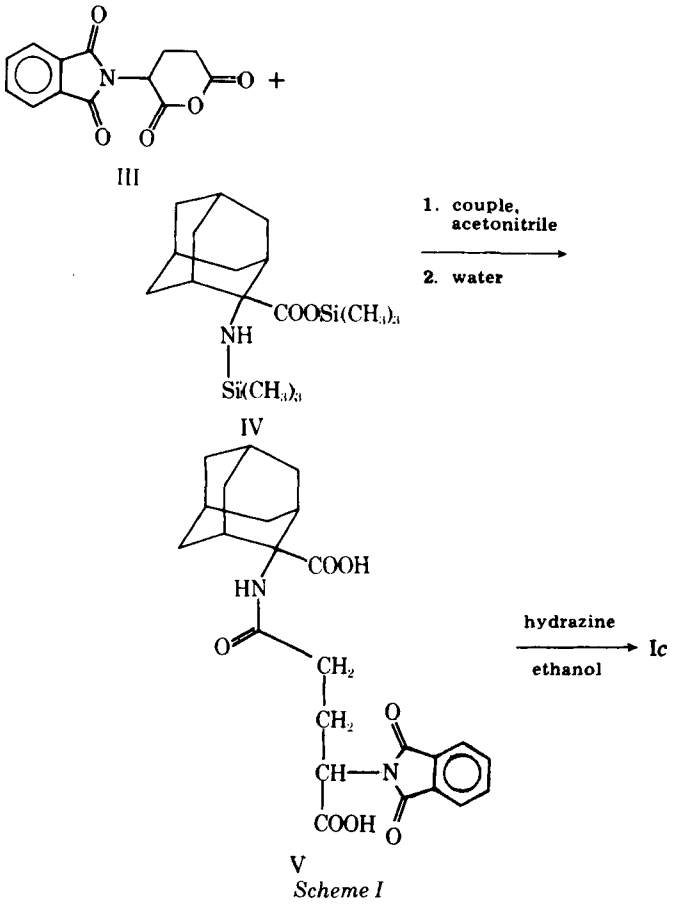

Scheme I

to the cloudy solution, and the three-phase system which contained solids was filtered. The collected solids were dissolved in fresh pH 10 aqueous sodium carbonate, and the solution was extracted with ether. The alkaline aqueous phases were combined, concentrated to remove the ether, and then acidified to pH 3 to precipitate V, which was collected and air dried to yield 23.4 g (74%), mp 135–137°.

Anal.—Calc. for $C_{24}H_{26}N_2O_7 \cdot H_2O$: C, 61.01; H, 5.97; N, 5.93. Found: C, 61.18; H, 5.80; N, 5.94.

N-(γ-*L-Glutamyl*)*adamantanine* (*Ic*)—Compound V (6.00 g, 0.013 mole) was dephthaloylated by heating it with 95% hydrazine (0.440 g, 0.013 mole) in 100 ml of ethanol for 2 hr. After evaporation of the solvent to dryness, the residue was extracted four times with 50 ml of boiling water. The aqueous extracts were combined, heated to boiling, and then filtered to remove residual solids, and the filtrate was evaporated nearly to dryness. The residue was suspended in 50 ml of hot ethanol, and the insoluble solids (1.25 g) were collected by filtration.

Concentration of the filtrate gave a total of 2.70 g of additional solids

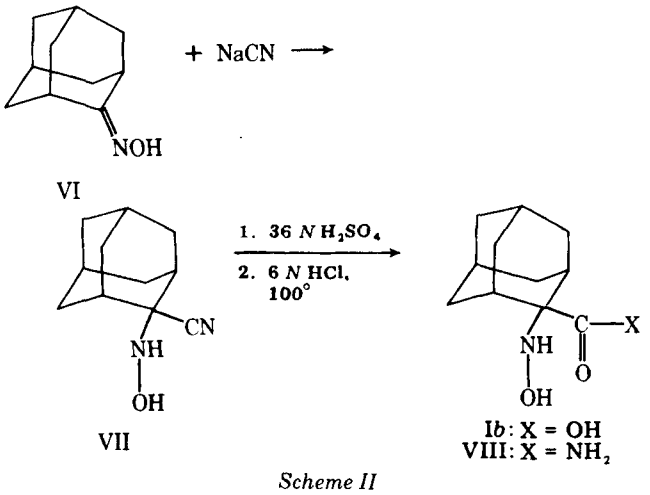

Scheme II

Table I—Formation of γ-Glutamylhydroxamate Catalyzed by γ-Glutamyltranspeptidase

γ-Glutamyl Donor	γ-Glutamylhydroxamate Formed, μmoles/mg of protein/10 min
Ic, 10 m*M*	<0.02
Glutathione, 10 m*M*	4.62
Glutathione + Ic, both at 10 m*M*	4.79

in three successive crops. Since the latter solids were yellow, they were dissolved in 50% ethanol and decolorized with charcoal. The decolorized solution was evaporated to dryness, and the solid residue was recrystallized from ethanol–acetone. This recrystallized product was combined with the 1.25 g of product isolated earlier and once again was recrystallized from ethanol–water to give a powder. This powder was dried under vacuum at 75° to give 2.78 g (63% yield), mp 220–224°; $[\alpha]_D^{26}$ +18.3° (*c*, 1.0 mg in 1.0 *N* HCl, calculated as the monohydrate).

Anal.—Calc. for $C_{16}H_{24}N_2O_5 \cdot H_2O$: C, 56.13; H, 7.65; N, 8.18. Found: C, 56.01; H, 7.45; N, 7.87.

2-Hydroxyamino-2-cyanoadamantane (*VII*)—To a 500-ml glass pressure-reaction bottle were added adamantan-2-one oxime (VI) (21) (25.0 g, 0.15 mole), monobasic potassium phosphate (120 g, 0.88 mole), 100 ml of water, 25 ml of ethanol, and 25.0 g (0.51 mole) of sodium cyanide. The bottle was sealed with a silicone rubber stopper fitted with a dial thermometer and placed in a shaking apparatus. The reaction mixture was heated gradually with shaking to 70° over 30 min, and the temperature was maintained at 70–78° for another 30 min.

The reaction mixture then was cooled, diluted with 2 liters of water, and continuously extracted with chloroform in a liquid–liquid extractor for 4 hr. The chloroform extract was treated with charcoal, and the solvent was evaporated to dryness. The yellow residue was dissolved in methylene chloride, and the solution was treated again with charcoal and filtered. The filtrate was concentrated to ~20 ml and diluted with 40 ml of hexane to give 5.70 g (19.8% yield) of pale-yellow crystals, mp 141–142°; IR (potassium bromide): 3455 (OH), 3270 (NH), and 2210 (CN) cm^{-1}.

Anal.—Calc. for $C_{11}H_{16}N_2O$: C, 68.72; H, 8.39; N, 14.57. Found: C, 68.70; H, 8.39; N, 14.52.

2-Hydroxyaminoadamantane-2-carboxamide (*VIII*)—Compound VII (2.00 g, 0.010 mole) was added slowly to 10 ml of 36 *N* H_2SO_4 with stirring, and the mixture was allowed to stand at room temperature for 90 min. The clear solution then was poured into 100 ml of ice-cold water, and the solution was brought carefully to pH 8 with 6 *N* NaOH. The solids which precipitated were collected, air dried, and then recrystallized from tetrahydrofuran to give 1.65 g (75% yield) of colorless plates, mp 177–178°; IR (potassium bromide): 3430 (OH), 3350, 3320, 3245, 3170 (NH_2, NH), 1635 (C=O, amide I), and 1600 (NH deformation, amide II) cm^{-1}. An analytical sample was recrystallized from tetrahydrofuran and dried for 18 hr under vacuum, mp 177.5–178.5°.

Anal.—Calc. for $C_{11}H_{18}N_2O_2$: C, 62.83; H, 8.63; N, 13.32. Found: C, 62.94; H, 8.49; N, 13.34.

N-*Hydroxyadamantanine* (*Ib*)—Compound VIII (0.300 g, 1.43 mmole) and 6 *N* HCl (3 ml) were added to each of three pressure-reaction tubes. The tubes were sealed and heated for 3 hr at 110°. The cooled reaction mixtures were filtered into a common receiver, and the filtrate was evaporated to dryness *in vacuo*. The residue was dissolved in 20 ml of water and applied to a column of cation-exchange resin[3] (80 g). The column was washed with water until the eluate was chloride free (300 ml) and then eluted with 2 *N* NH_4OH (400 ml).

Evaporation of the eluate *in vacuo* gave 170 mg of crude product. This product was dissolved in 5 ml of ethanol, and the solution was decolorized with charcoal. By concentration to 2 ml, dilution with water (1 ml), and further evaporation of the solvent *in vacuo*, crystals precipitated. The crystals were collected and dried under vacuum at 65° for 18 hr to give 0.060 g (6.6% yield), mp 173.5–174.5°. The chemical-ionization mass spectrum of *Ib* exhibited peaks at *m/e* (relative intensity) 212 (MH^+, 100), 196 (16), 166 (25), and 150 (60).

Anal.—Calc. for $C_{11}H_{17}NO_3$: C, 62.54; H, 8.11; N, 6.63. Found: C, 62.54; H, 8.15; N, 6.56.

***In Vivo* Metabolism Studies**—Solutions of Ic dissolved in dilute aqueous hydrochloric acid (2.5 ml, pH 1) were administered orally at 40 and 400 mg/kg to male rats[4] weighing ~250 g, and 24-hr urine samples were collected in stainless steel metabolism cages. The 24-hr urine sam-

[3] Amberlite IRC-50 (H^+).

[4] Sprague–Dawley strain.

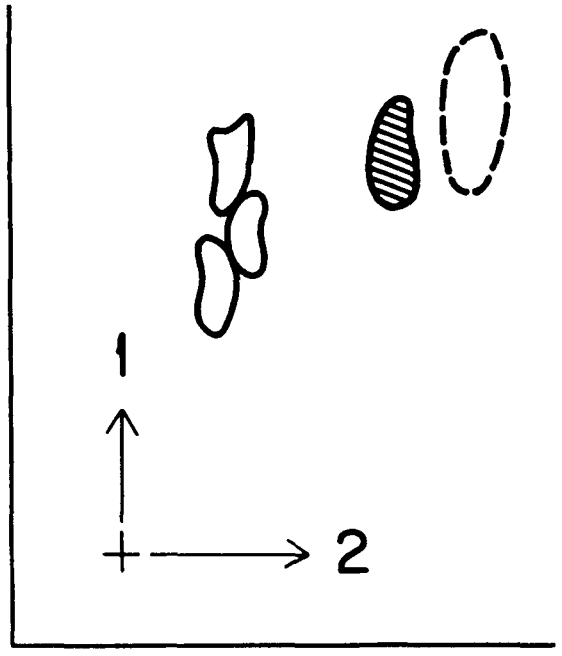

Figure 1—*Composite two-dimensional chromatogram of the urine from a rat given 400 mg of γ-glutamyladamantanine (Ic)/kg and of a control urine sample to which Ic (shaded spot) (1 mg/ml) had been added. Solvent 1 was chloroform–methanol–17% ammonia (2:2:1); Solvent 2 was 1-butanol–acetic acid–water (4:1:1). The point of application is represented by +. The shaded spot was not seen in the urine of the rat treated with Ic, the chromatograms being otherwise similar.*

ples from each rat prior to administration of the peptide served as control urine. The urine samples were spotted on 8 × 8-cm fluorescent silica gel plates and developed two dimensionally, first in chloroform–methanol–17% ammonia (2:2:1) and then in 1-butanol–acetic acid–water (4:1:1). The chromatograms were visualized with 0.3% ethanolic ninhydrin spray reagent. These chromatograms were compared to those of control urine and control urine to which the peptide was added. The results with the high dose are shown in Fig. 1.

***In Vitro* Enzyme and Growth Inhibition**—γ-Glutamyltranspeptidase was isolated from hog kidney cortex (4), and the transfer of the γ-glutamyl group of Ic to hydroxylamine was determined spectrophotometrically (22). Glutathione, the natural substrate for this enzyme, was used as the standard. The results are recorded in Table I.

Growth inhibition of P-388 lymphoid leukemia cells in tissue culture was determined as described previously (21) using varying concentrations of Ib, Ic, and IIb (Table II). Compound Ic in hydroxypropylcellulose also was administered intraperitoneally to host BDF_1 mice bearing 10^5 L-1210 lymphoid leukemia cells at doses of 400 mg/kg once daily for 9 days.

RESULTS AND DISCUSSION

Test doses of *N*-(γ-L-glutamyl)adamantanine (Ic) administered to rats at 40 and 400 mg/kg did not give rise to the excretion of the intact dipeptide (Fig. 1), in contrast to the metabolically inert dipeptides, leucyl- and glycyladamantanine, which were excreted intact in the urine (2). This result suggested that the compound was metabolized *in vivo* or else was poorly (or not at all) absorbed from the GI tract. Although Ic gives a strong ninhydrin chromophore (Fig. 1), the amino acid Ia is not chromogenic with ninhydrin or fluorescamine (23); hence, it was not possible to detect the free amino acid in the urine or plasma.

These results encouraged the evaluation of Ic for substrate activity with a partially purified preparation of γ-glutamyltranspeptidase from hog kidney cortex (22). However, Ic did not transfer its γ-glutamyl moiety to the test acceptor hydroxylamine (Table I). Under the same conditions, glutathione, the natural substrate for this enzyme, readily formed γ-glutamylhydroxamate, indicating that the enzyme preparation was active. Moreover, Ic did not inhibit the latter reaction when present at equimolar concentrations with glutathione.

As can be seen from Table II, Ic did not inhibit the growth of P-388 leukemia cells *in vitro*, nor did Ic increase the survival time of host BDF_1 mice bearing 10^5 L-1210 leukemia cells, even at daily doses of 400 mg/kg for 9 days (data not shown). However, *N*-hydroxyadamantanine (Ib) had activity comparable to *N*-hydroxycycloleucine (IIb) in the P-388 system (Table II), although these compounds were nearly 10 times less active in this system than *N*-hydroxyurea, which was the standard test compound.

Table II—Inhibition of Growth of P-388 Lymphoid Leukemia Cells *In Vitro*

Compound	I_{50} μg/ml	I_{50} m*M*
Ib	168	0.80
Ic	>1000	>3
IIb[a]	50	0.34
N-Hydroxyurea[b]	2.3	0.03

[a] Prepared according to a combination of literature procedures (17, 18), mp 196–198° dec. (corrected) [lit. (26) mp 200–202° dec.]. [b] Schwartz/Mann Division, Becton-Dickinson and Co., Orangeburg, N.Y.

The lack of substrate activity of Ic for γ-glutamyltranspeptidase probably is due to steric hindrance at the peptide bond. Various glycine and leucine dipeptides of adamantanine (both N-terminal and C-terminal) also are resistant to hydrolysis by leucine aminopeptidase (2). Meister (24) showed that γ-glutamyl derivatives of α-alkyl-substituted α-amino acids, *e.g.*, γ-glutamyl-α-aminoisobutyrate, are not good substrates for γ-glutamyltranspeptidase. Since Ia also may be considered as α-alkyl substituted, the present example provided by Ic reinforces this observation.

Although the latentiation of Ia as peptide derivatives has not yet been achieved, perhaps due to the unique structure of this amino acid, the concept of γ-glutamyltranspeptidase-mediated amino acid release should be capable of extension appropriate to the latentiation of biologically active molecules other than amino acids, *e.g.*, drugs. By utilizing this enzyme from the γ-glutamyl cycle (24), selected drugs may be transported *in vivo* as chemically conjugated synthetic γ-glutamyl derivatives with subsequent release at target organ sites. The successful use of this approach to the development of dopamine prodrugs was alluded to previously (8, 9). For the moiety attached to the γ-glutamyl end of the molecule, there is a low order of specificity. For example, whereas the natural substrate is glutathione itself, γ-L- or γ-D-glutamyl-*p*-nitroanilide (4) and *S*-substituted glutathione derivatives (25) are active substrates for the transpeptidase. Furthermore, the amide linkage is not mandatory since γ-esters of L-glutamic acid also serve as substrates (4). Since a large number of pharmacological agents possess free amino or hydroxyl groups, the applications of this concept appear to be unlimited. These possibilities are under study.

REFERENCES

(1) H. T. Nagasawa, J. A. Elberling, and F. N. Shirota, *J. Med. Chem.*, **16**, 823 (1973).

(2) *Ibid.*, **18**, 826 (1975).

(3) M. Orlowski and A. Meister, *Proc. Natl. Acad. Sci. USA*, **67**, 1248 (1970).

(4) M. Orlowski and A. Meister, *J. Biol. Chem.*, **240**, 338 (1965).

(5) O. W. Griffith and A. Meister, *Proc. Natl. Acad. Sci. USA*, **74**, 3330 (1977).

(6) A. M. Karkowsky and M. Orlowski, *J. Biol. Chem.*, **253**, 1574 (1978).

(7) G. M. Hatfield and J. P. Schaumberg, *Lloydia*, **38**, 489 (1975).

(8) J. Kyncl, R. Hollinger, R. Warner, C. W. Ours, F. N. Minard, P. H. Jones, and J. H. Biel, *Kidney Int.*, **10**, 589 (1976).

(9) S. Wilk, H. Mizoguchi, and M. Orlowski, *J. Pharmacol. Exp. Ther.*, **206**, 227 (1978).

(10) J. H. Wilson, J. L. Irwin, J. E. Suggs, and K. Liu, *Cancer Res.*, **19**, 272 (1959).

(11) R. B. Ross, C. I. Noll, W. C. J. Ross, M. W. Nadkarni, B. H. Morrison, and H. W. Bond, *J. Med. Pharm. Chem.*, **3**, 1 (1961).

(12) A. W. Lessin, R. F. Long, and M. W. Parkes, *Biochem. Pharmacol.*, **15**, 481 (1966).

(13) J. A. Elberling, R. T. Zera, S. D. J. Magnan, and H. T. Nagasawa, *Org. Prep. Proc. Int.*, **11**, 67 (1978).

(14) F. King and O. Kidd, *J. Chem. Soc.*, **1949**, 3315.

(15) J. P. Greenstein and M. Winitz, "Chemistry of the Amino Acids," vol. 2, Wiley, New York, N.Y., 1961, p. 1096.

(16) C. C. Porter and L. Hellerman, *J. Am. Chem. Soc.*, **61**, 754 (1939).

(17) E. F. J. Duynstee, J. L. J. P. Henneken, and M. R. A. H. Mevis, *Rec. Trav. Chim. Pays-Bas*, **84**, 1442 (1965).
(18) A. Ahmad, *Bull. Chem. Soc. Jpn.*, **47**, 2583 (1974).
(19) A. W. Coulter, J. B. Lombardini, J. R. Sufrin, and P. Talalay, *Mol. Pharmacol.*, **10**, 319 (1974).
(20) H. T. Nagasawa, J. G. Kohlhoff, P. S. Fraser, and A. A. Mikhail, *J. Med. Chem.*, **15**, 483 (1972).
(21) G. W. Smith and H. D. Williams, *J. Org. Chem.*, **26**, 2211 (1961).
(22) O. Noren, H. Sjöström, and L. Josefson, *Biochim. Biophys. Acta*, **327**, 446 (1973).
(23) S. Udenfriend, S. Stein, P. Böhlen, W. Dairman, W. Leimgruber, and W. Weigele, *Science*, **178**, 871 (1972).
(24) A. Meister, *ibid.*, **180**, 33 (1973).
(25) S. S. Tate and A. Meister, *J. Biol. Chem.*, **249**, 7593 (1974).
(26) L. Neelakantan and W. H. Hartung, *J. Org. Chem.*, **23**, 964 (1958).

ACKNOWLEDGMENTS

Supported by a program grant from the Veterans Administration.
The authors thank J. O. McMahon for the electron-impact spectra, Mrs. O. Hammerston for the IR spectra, and Dr. R. Vince for the P-388 leukemia cells. Dr. Harry B. Wood, Jr., Drug Research and Development Branch, Division of Cancer Treatment, National Cancer Institute, National Institutes of Health, kindly provided the *in vivo* antitumor screening data.

Anti-Inflammatory Activity of Amine Cyanoboranes, Amine Carboxyboranes, and Related Compounds

IRIS H. HALL *x, C. O. STARNES *, A. T. McPHAIL ‡, P. WISIAN-NEILSON ‡, M. K. DAS ‡, F. HARCHELROAD, Jr. ‡, and B. F. SPIELVOGEL ‡

Received April 10, 1979, from the **Division of Medicinal Chemistry, School of Pharmacy, University of North Carolina, Chapel Hill, NC 27514,* and the ‡*Paul M. Gross Chemical Laboratory, Duke University, Durham, NC 27706.* Accepted for publication July 20, 1979.

Abstract □ Amine cyanoboranes and amine carboxyboranes (boron analogs of α-amino acids) were shown to inhibit inflammation. The analogs effectively blocked general inflammation, induced arthritis, and the writhing reflex associated with inflammation pain, while the inflammation associated with pleurisy was marginally inhibited. The boron analogs were shown *in vitro* to inhibit the release of lysosomal enzymes from liver and polymorphonuclear neutrophils. Furthermore, prostaglandin synthesis was blocked by these agents at a low concentration, *i.e.*, 10^{-6} *M*. Liver oxidative phosphorylation processes also were uncoupled by these agents, but the migration of polymorphonuclear neutrophils was unaltered at 10^{-4} *M*. The elevation of cyclic adenosine monophosphate levels in polymorphonuclear neutrophils correlated positively with *in vivo* antiarthritic activity. Initial studies in rodents demonstrated that these boron analogs can be used at safe therapeutic doses.

Keyphrases □ Anti-inflammatory activity—evaluation of amine cyanoboranes, amine carboxyboranes, and related compounds □ Amine cyanoboranes and amine carboxyboranes—evaluation for anti-inflammatory activity

The antineoplastic activity of some α-amino boron analogs was reported previously (1). While studying their metabolic effects on tumor cell metabolism, it was noted that these agents interfered with oxidative phosphorylation processes of mitochondria, inhibited lysosomal enzymatic hydrolytic activities, and elevated cyclic adenosine monophosphate levels. Since commercially available anti-inflammatory agents, *e.g.*, phenylbutazone, salicylates, and indomethacin, have similar effects on cellular metabolism, testing of the boron analogs for anti-inflammatory activity in rodents was undertaken and the data are reported here.

EXPERIMENTAL

Chemistry—Consideration of the isoelectronic formalism between carbon and boron results in the prediction of boron analogs of dipolar α-amino acids, *e.g.*, glycine ammonia carboxyborane, alanine ammonia carboxymethylborane, and betaine triethylamine carboxyborane. Interest in these boron analogs lies mainly in their potential biological activity when compared with the enormous biological activity of the α-amino acids. A highly significant step toward demonstrating the existence of this class of compounds was the synthesis of trimethylamine carboxyborane, the protonated boron analog of betaine (2) (Scheme I).

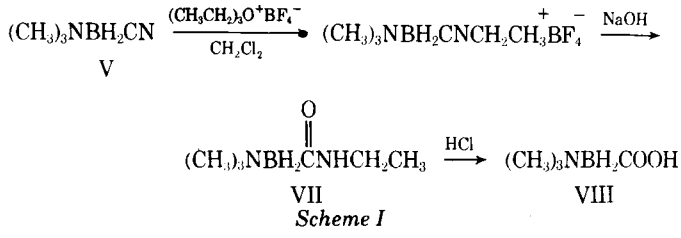

Scheme I

Trimethylamine carboxyborane, a white, crystalline solid whose X-ray crystal structure was determined, is stable in air and water.

Amine Cyanoboranes—One approach to the synthesis of boron analogs of the α-amino acids involves the conversion of an amine cyanoborane to a boroamino acid according to the procedure outlined in Scheme I. To provide adequate quantities of the precursor amine cyanoboranes, a general, convenient, high-yield synthesis (3, 4) of this class of compounds was developed (Scheme II).

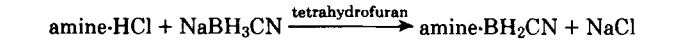

Scheme II

All previous syntheses (5–9) of amine cyanoboranes were limited as to the yield and reaction scale. Several synthetic procedures were developed (5, 6) following initial reports from these laboratories (10, 11) on the preparation of cyanoborane oligomers, *i.e.*, $(BH_2CN)_x$, by the addition of dry hydrogen chloride to a solution containing cyanohydroborate in ether. Thus, addition of amines to solutions of cyanoborane [which also can be prepared (8) by the reaction of cyanohydroborate and halogens] gives the amine cyanoborane. Typical yields have been ~25%, whereas yields up to 90% have been obtained with the amine hydrochloride procedure.

Following Scheme II, amine cyanoboranes were prepared where the amine was trimethylamine (V), dimethylamine (VI), pyridine (XV), 3-dimethylaminopropionitrile (XIX), or *N*-methylmorpholine (XIV). Bis(cyanoboranes) (XI and XX) were prepared (4) from ethylenediamine and tetramethylethylenediamine. However, attempts to prepare the parent ammonia cyanoborane (XVII) by this procedure were not successful. The only other report of the preparation of XVII (7) involved the reaction of trimethylamine iodoborane (IX) with sodium cyanide in liquid ammonia. Attempts to repeat this reaction in these laboratories resulted

0022-3549/80/0900-1025$01.00/0
© 1980, American Pharmaceutical Association

(17) E. F. J. Duynstee, J. L. J. P. Henneken, and M. R. A. H. Mevis, *Rec. Trav. Chim. Pays-Bas*, **84**, 1442 (1965).
(18) A. Ahmad, *Bull. Chem. Soc. Jpn.*, **47**, 2583 (1974).
(19) A. W. Coulter, J. B. Lombardini, J. R. Sufrin, and P. Talalay, *Mol. Pharmacol.*, **10**, 319 (1974).
(20) H. T. Nagasawa, J. G. Kohlhoff, P. S. Fraser, and A. A. Mikhail, *J. Med. Chem.*, **15**, 483 (1972).
(21) G. W. Smith and H. D. Williams, *J. Org. Chem.*, **26**, 2211 (1961).
(22) O. Noren, H. Sjöström, and L. Josefson, *Biochim. Biophys. Acta*, **327**, 446 (1973).
(23) S. Udenfriend, S. Stein, P. Böhlen, W. Dairman, W. Leimgruber, and W. Weigele, *Science*, **178**, 871 (1972).
(24) A. Meister, *ibid.*, **180**, 33 (1973).
(25) S. S. Tate and A. Meister, *J. Biol. Chem.*, **249**, 7593 (1974).
(26) L. Neelakantan and W. H. Hartung, *J. Org. Chem.*, **23**, 964 (1958).

ACKNOWLEDGMENTS

Supported by a program grant from the Veterans Administration.
The authors thank J. O. McMahon for the electron-impact spectra, Mrs. O. Hammerston for the IR spectra, and Dr. R. Vince for the P-388 leukemia cells. Dr. Harry B. Wood, Jr., Drug Research and Development Branch, Division of Cancer Treatment, National Cancer Institute, National Institutes of Health, kindly provided the *in vivo* antitumor screening data.

Anti-Inflammatory Activity of Amine Cyanoboranes, Amine Carboxyboranes, and Related Compounds

IRIS H. HALL *x, C. O. STARNES *, A. T. McPHAIL ‡, P. WISIAN-NEILSON ‡, M. K. DAS ‡, F. HARCHELROAD, Jr. ‡, and B. F. SPIELVOGEL ‡

Received April 10, 1979, from the **Division of Medicinal Chemistry, School of Pharmacy, University of North Carolina, Chapel Hill, NC 27514,* and the ‡*Paul M. Gross Chemical Laboratory, Duke University, Durham, NC 27706.* Accepted for publication July 20, 1979.

Abstract □ Amine cyanoboranes and amine carboxyboranes (boron analogs of α-amino acids) were shown to inhibit inflammation. The analogs effectively blocked general inflammation, induced arthritis, and the writhing reflex associated with inflammation pain, while the inflammation associated with pleurisy was marginally inhibited. The boron analogs were shown *in vitro* to inhibit the release of lysosomal enzymes from liver and polymorphonuclear neutrophils. Furthermore, prostaglandin synthesis was blocked by these agents at a low concentration, *i.e.*, 10^{-6} *M*. Liver oxidative phosphorylation processes also were uncoupled by these agents, but the migration of polymorphonuclear neutrophils was unaltered at 10^{-4} *M*. The elevation of cyclic adenosine monophosphate levels in polymorphonuclear neutrophils correlated positively with *in vivo* antiarthritic activity. Initial studies in rodents demonstrated that these boron analogs can be used at safe therapeutic doses.

Keyphrases □ Anti-inflammatory activity—evaluation of amine cyanoboranes, amine carboxyboranes, and related compounds □ Amine cyanoboranes and amine carboxyboranes—evaluation for anti-inflammatory activity

The antineoplastic activity of some α-amino boron analogs was reported previously (1). While studying their metabolic effects on tumor cell metabolism, it was noted that these agents interfered with oxidative phosphorylation processes of mitochondria, inhibited lysosomal enzymatic hydrolytic activities, and elevated cyclic adenosine monophosphate levels. Since commercially available anti-inflammatory agents, *e.g.*, phenylbutazone, salicylates, and indomethacin, have similar effects on cellular metabolism, testing of the boron analogs for anti-inflammatory activity in rodents was undertaken and the data are reported here.

EXPERIMENTAL

Chemistry—Consideration of the isoelectronic formalism between carbon and boron results in the prediction of boron analogs of dipolar α-amino acids, *e.g.*, glycine ammonia carboxyborane, alanine ammonia carboxymethylborane, and betaine triethylamine carboxyborane. Interest in these boron analogs lies mainly in their potential biological activity when compared with the enormous biological activity of the α-amino acids. A highly significant step toward demonstrating the existence of this class of compounds was the synthesis of trimethylamine carboxyborane, the protonated boron analog of betaine (2) (Scheme I).

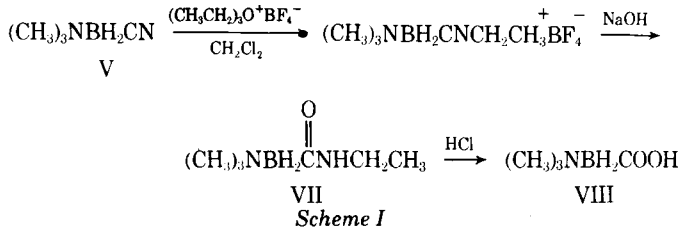

Scheme I

Trimethylamine carboxyborane, a white, crystalline solid whose X-ray crystal structure was determined, is stable in air and water.

Amine Cyanoboranes—One approach to the synthesis of boron analogs of the α-amino acids involves the conversion of an amine cyanoborane to a boroamino acid according to the procedure outlined in Scheme I. To provide adequate quantities of the precursor amine cyanoboranes, a general, convenient, high-yield synthesis (3, 4) of this class of compounds was developed (Scheme II).

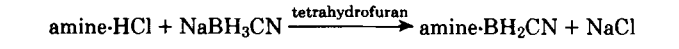

Scheme II

All previous syntheses (5–9) of amine cyanoboranes were limited as to the yield and reaction scale. Several synthetic procedures were developed (5, 6) following initial reports from these laboratories (10, 11) on the preparation of cyanoborane oligomers, *i.e.*, $(BH_2CN)_x$, by the addition of dry hydrogen chloride to a solution containing cyanohydroborate in ether. Thus, addition of amines to solutions of cyanoborane [which also can be prepared (8) by the reaction of cyanohydroborate and halogens] gives the amine cyanoborane. Typical yields have been ~25%, whereas yields up to 90% have been obtained with the amine hydrochloride procedure.

Following Scheme II, amine cyanoboranes were prepared where the amine was trimethylamine (V), dimethylamine (VI), pyridine (XV), 3-dimethylaminopropionitrile (XIX), or *N*-methylmorpholine (XIV). Bis(cyanoboranes) (XI and XX) were prepared (4) from ethylenediamine and tetramethylethylenediamine. However, attempts to prepare the parent ammonia cyanoborane (XVII) by this procedure were not successful. The only other report of the preparation of XVII (7) involved the reaction of trimethylamine iodoborane (IX) with sodium cyanide in liquid ammonia. Attempts to repeat this reaction in these laboratories resulted

0022-3549/80/0900-1025$01.00/0
© 1980, American Pharmaceutical Association

instead in the isolation of the novel complex hexakis(ammonia cyanoborane)sodium iodide (X) (12). The complex, which was characterized by X-ray crystallography, consists of six ammonia cyanoborane (XVII) molecules coordinated octahedrally around the sodium cation. However, pure ammonia cyanoborane could be obtained by dissolution of the complex in water and extraction of the ammonia cyanoborane into ether (13). The compound also was prepared (13) by base displacement (Scheme III).

$$C_6H_5NH_2{\cdot}BH_2CN \xrightarrow{H_3N} \underset{\text{XVII}}{H_3NBH_2CN} + C_6H_5NH_2$$

Scheme III

In both cases, ammonia cyanoborane as prepared in these laboratories differs from that reported previously (7), which was characterized only partially. Ammonia cyanoborane possesses considerable hydrolytic stability, suffering only an 8% loss of hydrogen in concentrated hydrochloric acid after 70 hr at room temperature. In general, the amine cyanoboranes are quite stable to air and moisture.

Amine Carboxyboranes—By using the general synthetic route illustrated in Scheme I, amine carboxyborane compounds where the amine was pyridine (XVI) or *N*-methylmorpholine were prepared (4) from the corresponding amine cyanoborane. Tetramethylethylenediamine bis(carboxyborane) (XII) and its intermediate (XIII) were synthesized (4). Trimethylamine carboxyborane (VIII) derivatives can be prepared readily by the preparation of the ethyl ester. The ethyl ester, a white solid (mp 45–47°), can be prepared in a 34% yield according to Scheme IV.

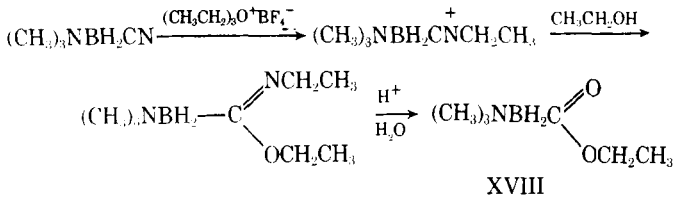

Scheme IV

The ethyl ester was obtained by allowing a solution of 95% ethanol (200 ml), concentrated aqueous hydrochloric acid (8 ml), and the *N*-ethylnitrilium salt [prepared by refluxing for 24 hr a solution of trimethylamine cyanoborane (0.2 mole) and 400 ml of 1 *N* triethyloxonium tetrafluoroborate in methylene chloride (2)] to reflux for 48 hr. After neutralization with a saturated sodium bicarbonate solution and removal of ethanol under reduced pressure, the product was extracted from the aqueous solution with methylene chloride. Drying the organic portion over magnesium sulfate and solvent removal produced a yellow liquid. Purification by recrystallization from ethanol or ether or by sublimation afforded the ester as a white crystalline solid (9.9 g). Satisfactory carbon, hydrogen, nitrogen, and boron analyses were obtained[1]. The PMR signals (deuterochloroform) were those expected for the trimethylamine (δ 2.78 singlet) and ethyl (δ 1.2 triplet and δ 4.10 quartet) functions; strong B–H (2380 cm^{-1}) and C=O (1660 cm^{-1}) stretches were present in the IR spectrum.

The structures of the boron analogs and references for their syntheses are given in Table I.

Pharmacology—*Toxicity Studies*—Acute LD_{50} toxicity studies were carried out in CF_1 male mice (~30 g) using the method of Litchfield and Wilcoxon (14).

Anti-Inflammatory Screen—CF_1 male mice (~30 g) were administered the test drugs at 10 mg/kg ip in 0.05% polysorbate 80–water 3 hr and then 30 min prior to injection of 0.05 ml of 2% carrageenan in 0.9% saline into the plantar surface of the right hindfoot. Saline injected into the left hindfoot served as a baseline. After 3 hr, both feet were excised at the tibiotarsal (ankle) joint according to the modified (15) method of Winter, resulting in a net weight increase of 87 mg in the feet of the control animals.

Antipyretic Screen—Sprague–Dawley rats (~200 g) were administered 2 ml of a 44% solution of baker's yeast subcutaneously (15) 18 hr prior to the injection of drugs at 2.5 or 5 mg/kg ip, resulting in an elevation of 3.46° F. Alternatively, rats were administered 0.25 mg of killed and dried *Mycobacterium butyricum*[2] (16) subcutaneously prior to drug administration. Rectal temperatures were taken immediately before and 2, 4, and 6 hr after drug administration.

Writhing Reflex—CF_1 male mice were administered the test drugs at 20 mg/kg ip 20 min (17) prior to the administration of 0.5 ml of 0.6% acetic acid (18). After 5 min, the number of stretches, characterized by repeated contractures of the abdominal musculature accompanied by hindlimb extension, was counted for the next 10 min. Control mice had 78 stretch reflexes/10 min.

Chronic Adjuvant Arthritic Screen—Male Sprague–Dawley rats (~160 g) were injected at the base of the tail with 0.2 ml of a solution of killed and dried *M. butyricum* and digitonin in mineral oil (19). Test drugs were administered intraperitoneally on Days 3–20 at 2.5 mg/kg/day. Animals were sacrificed on Day 21, and the feet were excised and weighed. Control animals had a net weight gain of 0.830 g.

Antipleurisy Screen—Sprague–Dawley rats were administered the test drugs at 2.5 mg/kg ip 1 hr before injection and 3 hr postinjection of 0.05 ml of a solution of 0.316% Evan's blue and carrageenan into the pleural cavity (20). After 6 hr, the rats were sacrificed and the fluid was collected from the pleural cavity. Control rats produced 2.5 ml of fluid.

Table I—Structures of Boron Analogs

Compound	Formula	Synthetic Reference
I	$(CH_3)_3CNH_2{\cdot}BH_3$[a]	—
II	$O(CH_2CH_2)_2NH{\cdot}BH_3$[a]	—
III	$(CH_3)_3N{\cdot}BH_3$[b]	—
IV	$(CH_3)_2NH{\cdot}BH_3$[b]	—
V	$(CH_3)_3N{\cdot}BH_2CN$	1, 3
VI	$(CH_3)_2NH{\cdot}BH_2CN$	1, 3
VII	$(CH_3)_3N{\cdot}BH_2CONHCH_2CH_3$	1, 2
VIII	$(CH_3)_3N{\cdot}BH_2COOH$	1, 2
IX	$(CH_3)_3N{\cdot}BH_2I$	1, 6
X	$[Na[H_3N{\cdot}BH_2(CH)]_6]I$	1, 12
XI	$[CH_2N(CH_3)_2{\cdot}BH_2CN]_2$	4
XII	$[CH_2N(CH_3)_2{\cdot}BH_2COOH]_2$	4
XIII	$[CH_2N(CH_3)_2{\cdot}BH_2CONHCH_2CH_3]_2$	4
XIV	$O(CH_2CH_2)_2N(CH_3){\cdot}BH_2CN$	3–5
XV	$C_5H_5N{\cdot}BH_2CN$	3–5
XVI	$C_5H_5N{\cdot}BH_2COOH$	4
XVII	$H_3N{\cdot}BH_2CN$	13
XVIII	$(CH_3)_3N{\cdot}BH_2COOCH_2CH_3$	Text
XIX	$NCCH_2CH_2N(CH_3)_2{\cdot}BH_2CN$	4
XX	$(CH_2NH_2{\cdot}BH_2CN)_2$	4

[a] Alfa Products. [b] Aldrich Chemicals.

Table II—*In Vivo* Anti-Inflammatory Activity of Boron Analogs

Compound	LD_{50}, mg/kg	Percent of Control: Anti-Inflammatory Screen, 10 mg/kg × 2	Percent of Control: Writhing Reflex, 20 mg/kg	Percent of Control: Antiarthritic Screen, 2.5 mg/kg/day
I	16	41	—	—
II	475	55	15	33
III	740	65	47	12
IV	200	66	37	61
V	70	42	18	4
VI	39	49	24	25
VII	320	63	29	64
VIII	1800	79	29	53
IX	250	66	37	22
X	100	57	12	0
XI	200	95	76	77
XII	>1000	58	54	19
XIII	>1000	65	55	24
XIV	23	91[a]	78[a]	16
XV	25	83[a]	80	45
XVI	>200	74[a]	53	44
XVII	30	51	50	32
XVIII	>500	87	106	26
XIX	140	74	89	13
XX	>150	87	95	100
Indomethacin[b]	28	22	43	27
Control	—	100	100	100

[a] One-third dose. [b] Tested at 10 mg/kg.

[1] *Anal.*—Calc.: C, 49.70; H, 11.12; B, 7.46; N, 9.66. Found: C, 49.66; H, 11.04; B, 7.56; N, 9.56.

[2] Difco.

Table III—Effects of Boron Analogs on *In Vitro* Lysosomal Enzymatic Activities and Cyclic Adenosine Monophosphate Levels at 5 μMoles

Compound	Percent of Control				
	Liver		Polymorphonuclear Neutrophils		
	Percent of Free Acid Phosphatase Activity (pH 5)	Percent of Free Cathepsin Activity (pH 5)	Percent of Free Acid Phosphatase Activity (pH 5)	Percent of Free Cathepsin Activity (pH 5.0)	Cyclic Adenosine Monophosphate Level
I	77 ± 4	58 ± 5	100 ± 9	100 ± 4	58
II	75 ± 8	107 ± 6	79 ± 5	93 ± 7	107
III	72 ± 6	17 ± 4	57 ± 4	18 ± 3	145
IV	82 ± 3	67 ± 3	82 ± 6	65 ± 5	80
V	69 ± 4	0 ± 2	35 ± 5	4 ± 2	245
VI	73 ± 4	32 ± 5	89 ± 4	22 ± 1	98
VII	78 ± 7	—	100 ± 2	22 ± 5	98
VIII	82 ± 5	56 ± 6	50 ± 3	14 ± 4	99
IX	71 ± 6	14 ± 3	71 ± 5	40 ± 4	133
X	65 ± 3	3 ± 1	34 ± 6	0 ± 3	361
XI	80 ± 6	50 ± 7	84 ± 5	16 ± 5	94
XII	69 ± 5	23 ± 6	84 ± 4	52 ± 4	155
XIII	74 ± 4	—	100 ± 7	70 ± 6	92
XIV	68 ± 7	13 ± 5	50 ± 3	37 ± 5	165
XV	79 ± 3	57 ± 4	57 ± 4	49 ± 7	110
XVI	77 ± 8	58 ± 4	100 ± 5	31 ± 4	100
XVII	75 ± 5	48 ± 6	100 ± 2	26 ± 4	93
XVIII	—	—	—	16 ± 3	—
XIX	66 ± 4	15 ± 3	100 ± 9	17 ± 5	199
XX	77 ± 8	80 ± 7	100 ± 10	57 ± 2	28
Indomethacin	86 ± 4	67 ± 6	100 ± 2	100 ± 1	80
Control	100 ± 7[a]	100 ± 6[b]	100 ± 8[c]	100 ± 6[d]	100[e]

[a] 0.753 mg of inorganic phosphate released/hr/g of wet tissue. [b] 2.69 mg of protein released/hr/g of wet tissue. [c] 0.26 μg of inorganic phosphate released/hr/10^7 cells. [d] 0.225 mg of protein released/hr/10^7 cells. [e] 48 pmoles of cyclic adenosine monophosphate/10^7 cells.

Polymorphonuclear neutrophil migration studies were carried out according to Nelson *et al.* (21). The analogs were tested *in vitro* at 10^{-4} *M*.

Ulcerogenic tests were carried out in Sprague–Dawley rats (~160 g); they were administered II, V, X, XIV, and XIX at 2.5 mg/kg for 3 weeks. After the rats were fasted for 18 hr, the last dose on Day 21 was administered. After 4 hr, the rats were sacrificed and the gastric and duodenum mucosa were examined for bleeding and ulcers (22). In an analogous experiment, animals were bled on Day 21 by the tail vein; the red and white blood cells were counted in a hemocytometer and expressed as the number of cells × 10^6 per cubic centimeter. Hematocrits also were obtained (23).

Biochemistry—*Lysosomal Enzymatic Assays*—Sprague–Dawley rats (~160 g) were sacrificed, the liver was excised, and a 10% homogenate (four times) in 0.25 *M* sucrose and 0.001 *M* ethylenediaminetetraacetic acid (pH 7.2) was prepared.

Polymorphonuclear neutrophils were collected from the peritoneal cavity 4 hr after injection of 35 ml of 0.5% oyster glycogen in isotonic saline (24). The polymorphonuclear neutrophils were centrifuged at 800×*g* for 20 min, washed, and resuspended in minimum essential medium with 10% fetal calf serum (pH 7.4).

Acid phosphatase activity (25) was determined by incubating 0.1 *M* β-glycerol phosphate in 0.1 *M* acetate (pH 5.0) with 5 μmoles of the test drugs in 1% carboxymethylcellulose sodium for 20 min with the liver homogenate and for 60 min with the resuspended polymorphonuclear neutrophils. Lysosome enzymes were released by 0.02% alkylphenoxy polyethoxyethanol 100[3] to obtain the total enzymatic activity. The reaction was stopped with 10% trichloroacetic acid, and the solution was centrifuged. Aliquots of the supernate were assayed for inorganic phosphate content by the method of Chen *et al.* (26). The percentage of free acid phosphatase was calculated.

Cathepsin activity was determined in an analogous manner, except that the substrate was 2% azocasein (27) and 0.1 *M* acetate buffer (pH 5.0). The supernate was assayed for acid-soluble peptide fragments at 366 nm. The percentage of free cathepsin activity was calculated.

Cyclic Adenosine 3′,5′-Monophosphate Levels—Isolated polymorphonuclear neutrophils were incubated with the test drugs at 5 μmoles for 1 hr at 37° in minimum essential medium at pH 7.4. The reaction was stopped with 6% trichloroacetic acid. The cyclic-3′,5′-adenosine monophosphate levels were determined by the radioimmunoassay of Gilman (28) using [^{3}H(G)]cyclic adenosine 3′,5′-monophosphate (39.8 Ci/mmole). Results were calculated in picomoles per 10^7 polymorphonuclear neutrophils.

Prostaglandin Synthetase Activity—The incubation medium of Tomlinson *et al.* (29) was used to determine [^{3}H]prostaglandin formation (prostaglandins E, F_α, and D) from [^{3}H(N)]arachidonic acid (86.2 Ci/mmole) and 10 mg of purified commercial prostaglandin synthetase from beef seminal vesicles[4]. After 1 hr at 37°, the reaction was stopped with 1 *N* HCl and the solution was extracted with ether and evaporated. The residue was taken up in ethyl acetate and spotted on silica gel TLC plates, which were eluted with chloroform–methanol–water–acetic acid (90:8:1:0.8) (30). The plates were dried and developed in iodine vapor; with the use of prostaglandin standards, the appropriate areas were scraped and counted for tritium content. Indomethacin was used as a standard at 10^{-4} *M*. The test drugs were used at 10^{-6} *M*.

Oxidative Phosphorylation Studies—The basal respiration and adenosine diphosphate-stimulated respiration on 10% liver homogenates were measured using succinate or α-ketoglutarate as the substrate (31). The reaction vessel contained sucrose (55 μmoles), potassium chloride (22 μmoles), dibasic potassium phosphate (22 μmoles), test compounds at 5 μmoles in 1% carboxymethylcellulose sodium and sodium succinate (90 μmoles) or α-ketoglutarate (60 μmoles) in a total volume of 1.8 ml. After the basal metabolic (State 4) level was obtained, 0.257 μmole of adenosine diphosphate was added to obtain the adenosine diphosphate-stimulated rate (State 3). The respiration rate was calculated as microliters of oxygen consumed per hour per milligram (wet weight) of liver.

RESULTS

The boron analogs afforded significant anti-inflammatory activity in rodents. Administration of I, V, and VI resulted in at least 50% inhibition of the carrageenan-induced edema in mouse footpads (Table II), while II, X, XII, and XVII resulted in at least 40% inhibition. Administration of II, V, and X caused 80% inhibition of the writhing reflex, which is similar to inflammation pain. Compounds VI–VIII caused 70% inhibition of the reflex. In the induced arthritic screen in rats, 3 weeks of dosing of III, V, X, XIV, and XIX caused >80% inhibition, with X and V causing 100 and 96% inhibition, respectively. Compound V was administered at 1.25–10 mg/kg/day ip. Doses at 1.25 mg/kg/day caused 75% inhibition, doses of 2.5 mg/kg/day caused 96% inhibition, and doses of 5 or 10 mg/kg/day resulted in 100% inhibition. Compounds VI, IX, XIII, and XVIII

[3] Triton X-100.

[4] Miles Research Products.

Table IV—Effects of Boron Analogs on *In Vitro* Prostaglandin Synthesis and Oxidative Phosphorylation Processes

Compound	Percent of Control				
	Prostaglandin Synthesis, × 10^{-6} *M*	Oxidative Phosphorylation (5 μmoles)			
		Succinate		α-Ketoglutarate	
		State 4	State 3	State 4	State 3
I	100 ± 3	118 ± 11	63 ± 8	160 ± 35	63 ± 14
II	100 ± 5	115 ± 15	66 ± 10	97 ± 29	50 ± 11
III	61 ± 3	117 ± 11	56 ± 12	71 ± 8	28 ± 10
IV	100 ± 5	119 ± 9	82 ± 4	67 ± 18	53 ± 16
V	59 ± 6	133 ± 20	51 ± 20	85 ± 21	42 ± 9
VI	63 ± 4	126 ± 19	61 ± 5	128 ± 25	45 ± 12
VII	100 ± 7	114 ± 13	74 ± 9	113 ± 37	45 ± 18
VIII	93 ± 3	122 ± 14	63 ± 4	127 ± 22	70 ± 20
IX	67 ± 5	120 ± 12	63 ± 9	102 ± 16	70 ± 13
X	42 ± 5	110 ± 5	31 ± 10	101 ± 25	37 ± 10
XI	85 ± 4	116 ± 8	122 ± 13	168 ± 38	106 ± 21
XII	60 ± 6	80 ± 11	57 ± 16	122 ± 15	48 ± 30
XIII	100 ± 4	117 ± 8	66 ± 8	162 ± 43	50 ± 24
XIV	38 ± 3	62 ± 10	36 ± 5	140 ± 47	51 ± 16
XV	58 ± 3	124 ± 16	57 ± 16	112 ± 42	52 ± 15
XVI	76 ± 5	110 ± 13	75 ± 15	109 ± 30	63 ± 15
XVII	55 ± 6	112 ± 7	60 ± 11	149 ± 27	40 ± 9
XVIII	—	119 ± 18	61 ± 19	126 ± 51	54 ± 8
XIX	53 ± 7	43 ± 16	24 ± 7	105 ± 33	33 ± 8
XX	81 ± 5	13 ± 5	10 ± 5	50 ± 18	25 ± 8
Indomethacin (10^{-4} *M*)	64 ± 2	—	—	—	—
Control	100[a]	100 ± 6[b]	100 ± 4[c]	100 ± 8[d]	100 ± 9[e]

[a] 6564 dpm of prostaglandin E formed/hr/mg of enzyme. [b] 9.19 μl of oxygen consumed/hr/mg of wet tissue. [c] 13.66 μl of oxygen consumed/hr/mg of wet tissue. [d] 3.38 μl of oxygen consumed/hr/mg of wet tissue. [e] 4.93 μl of oxygen consumed/hr/mg of wet tissue.

afforded >70% inhibition of the induced arthritic state, and II and XVII caused 60% inhibition.

In the antipyretic test, V at 5 or 10 mg/kg caused no inhibition of elevated body temperature. In the antipleurisy screen, inhibition of 33, 35, 49, and 39% was demonstrated for III, V, X, and XIX, respectively. Boron analogs had no effect on the chemotactic migration of polymorphonuclear neutrophils. Dosing for 3 weeks with II, V, X, XIV, and XIX intraperitoneally resulted in no alteration of the red or white blood cell count per cubic millimeter and in no gastric or duodenum mucosa irritations or bleeding.

The percentage of free lysosomal enzymatic activities in the liver and polymorphonuclear neutrophils was inhibited by the presence of boron analogs (Table III). Free acid phosphatase activity in the liver was inhibited 28–35% by III, V, IX, X, XII, XIV, and XIX; in polymorphonuclear neutrophils, inhibition of 43, 65, 50, 66, and 50% was found for III, V, VIII, X, and XIV, respectively. Free proteolytic cathepsin activity of the liver was inhibited at least 75% by III, IX, XII, XIV, and XIX, with 100% inhibition by V and 97% inhibition by X. Inhibition of polymorphonuclear neutrophil cathepsin activity of at least 82% was exhibited by III, VIII, X, XI, XVIII, and XIX, with 96% inhibition by V and 100% inhibition by X.

Cyclic adenosine monophosphate levels in polymorphonuclear neutrophils were elevated after *in vitro* incubation with drugs (Table III). The increases were 45, 145, 33, 261, 55, 65, and 99% for III, V, IX, X, XII, XIV, and XIX, respectively.

At 10^{-6} *M in vitro*, III, V, VI, IX, X, XII, XIV, XV, XVII, and XIX blocked prostaglandin synthesis by >30% (Table IV). Compound X resulted in 58% inhibition, and XIV caused 62% inhibition. The presence of boron analogs at 5 μmoles caused uncoupling of the oxidative phosphorylation processes of liver mitochondria. Several agents (*e.g.*, XX) suppressed basal (State 4) as well as adenosine diphosphate-stimulated respiration (State 3) with both substrates. Uncoupling of the electron transport chain was seen with the substrate succinate, a flavin adenine dinucleotide-linked dehydrogenase, with I–X, XIII, and XV–XVIII. This uncoupling was observed as an increase in State 4 respiration and as a decrease in State 3 respiration. With α-ketoglutarate as the substrate, a nicotinamide diphosphate-linked dehydrogenase, uncoupling was seen with I, VI–VIII, and XII–XVIII. Both States 3 and 4 respiration were inhibited with succinate in the presence of XII, XIV, XIX, and XX and with α-ketoglutarate by III–V and XX. Compounds that demonstrated potent antiarthritic activity also demonstrated potent inhibitory effects on State 3 respiration, *e.g.*, III, V, X, XII, XIV, and XIX with either succinate or α-ketoglutarate. The exception to this observation was XX.

DISCUSSION

Inflammation is a process associated with the release of chemical vasoamines, *e.g.*, histamine, serotonin, slow-reacting substance, and bradykinin, the release of lysosomal hydrolytic enzymes by leukocytes, the synthesis and release of prostaglandins, and the modulation of cyclic nucleotide levels of lymphocytes and leukocytes (32–36). These agents, in turn, cause increased vascular permeability, chemotaxis of polymorphonuclear neutrophils and macrophages, erythema, dermatitis, hypersensitivity, complement fixation, allergy reactions, and edema, and they elicit pain together with increasing the local and body temperature.

The commercially available anti-inflammatory agents are known to interfere with some of these processes, thus retarding the development of inflammation. For example, indomethacin decreases the polymorphonuclear neutrophil motility, uncouples oxidative phosphorylation processes, inhibits prostaglandin synthetase and histidine decarboxylase activities, mucopolysaccharide biosynthesis, and platelet function, stabilizes lysosomal membranes, and thus inhibits hydrolytic enzymatic activity (32). A number of agents are known to inhibit cyclic adenosine monophosphate phosphodiesterase activity (37) and increase cyclic adenosine monophosphate, which supposedly stabilizes the lysosomal membranes, blocks immunoglobulin E-dependent antigen-induced vasoamine release, and inhibits hypersensitivity (38–43).

As seen from the current studies, compounds having potent antiarthritic effects, *e.g.*, III, V, X, XII, XIV, and XIX, also were significant inhibitors of lysosomal-free hydrolytic activity both from the liver and polymorphonuclear neutrophils, indicating membrane stabilization. The inhibition of cathepsin activity was particularly high by the boron analogs. Increased levels of activity of this enzyme have been linked with a number of inflammation states. The boron analogs at the same concentration as indomethacin were more effective in inhibiting polymorphonuclear neutrophil lysosomal rupture.

Prostaglandin synthetase activity also was suppressed by III, V, X, XII, XIV, and XX at 10^{-6} *M*. Indomethacin at 10^{-6} *M* resulted in only 24% inhibition in this system; at 10^{-4} *M*, indomethacin caused 36% inhibition. Analogs V, X, XIV, XV, XVII, and XIX were more potent than indomethacin in inhibiting prostaglandin synthesis by the isolated enzyme system. Oxidative phosphorylation processes were uncoupled at 5 μmoles for the boron compounds, which demonstrated potent *in vivo* antiarthritic activity in rats. The uncoupling and suppression of energy production needed for migration and phagocytosis of polymorphonuclear neutrophils and macrophages were seen with all of the boron analogs; however, the migration of polymorphonuclear neutrophils at 10^{-4} *M* demonstrated no inhibition by boron analogs. Thus, it was more difficult to demonstrate positive correlation of uncoupling of respiration with *in vivo* antiarthritic activity. Nevertheless, excluding XX, those compounds possessing potent antiarthritic activity all suppressed adenosine diphosphate-stimulated respiration (State 3) by 40% or better.

The effects of boron analogs on respiration may be secondary to other metabolic effects. A more positive correlation with *in vivo* antiarthritic

activity is seen with the ability of the drug to elevate intracellular levels of cyclic adenosine monophosphate, which could account for the ability of these agents to block lysosomal enzyme release and prostaglandin synthesis and release. Elevated levels of cyclic adenosine monophosphate have been correlated with the ability to block the release of lysosomal enzymes (25, 41). The exact mechanism by which boron analogs cause elevations in cyclic adenosine monophosphate levels needs further study. Toxicity and side effects did not appear to be problems with boron analogs at the required therapeutic doses.

REFERENCES

(1) I. H. Hall, C. O. Starnes, B. F. Spielvogel, P. Wisian-Neilson, M. K. Das, and L. Wojnowich, *J. Pharm. Sci.*, **68,** 685 (1979).

(2) B. F. Spielvogel, L. Wojnowich, M. K. Das, A. T. McPhail, and K. D. Hargrave, *J. Am. Chem. Soc.*, **98,** 5702 (1976).

(3) P. Wisian-Neilson, M. K. Das, and B. F. Spielvogel, *Inorg. Chem.*, **17,** 2327 (1978).

(4) B. F. Spielvogel, P. Wisian-Neilson, and F. Harchelroad, Jr., *J. Inorg. Nucl. Chem.*, in press.

(5) S. S. Uppal and H. C. Kelly, *Chem. Commun.*, **1970,** 1619.

(6) C. Weidig, S. S. Uppal, and H. C. Kelly, *Inorg. Chem.*, **13,** 1763 (1974).

(7) P. J. Bratt, M. P. Brown, and K. R. Seddon, *J. Chem. Soc. Dalton Trans.*, **1974,** 2161.

(8) D. R. Martin, M. A. Chiusano, M. L. Denniston, D. J. Dye, E. D. Martin, and B. T. Pennington, *J. Inorg. Nucl. Chem.*, **40,** 9 (1978).

(9) O. T. Beachley and B. Washburn, *Inorg. Chem.*, **14,** 120 (1975).

(10) B. F. Spielvogel, J. M. Purser, and C. G. Moreland, *Chem. Eng. News,* **47**(47), 38 (Nov. 10, 1969).

(11) B. F. Spielvogel, R. F. Bratton, and C. G. Moreland, *J. Am. Chem. Soc.*, **94,** 8567 (1972).

(12) K. D. Hargrave, A. T. McPhail, B. F. Spielvogel, and P. Wisian-Neilson, *J. Chem. Soc. Dalton Trans.*, **1977,** 2150.

(13) A. T. McPhail, K. D. Onan, B. F. Spielvogel, and P. Wisian-Neilson, *J. Chem. Res.* (S), **205** (M), 2601 (1978).

(14) J. T. Litchfield and F. Wilcoxon, *J. Pharmacol. Exp. Ther.*, **96,** 99 (1949).

(15) A. P. Roszkowski, W. H. Rooks, A. Tomolonis, and L. M. Miller, *ibid.*, **179,** 114 (1971).

(16) L. O. Randall and H. Baruth, *Arch. Int. Pharmacodyn. Ther.*, **220,** 94 (1976).

(17) L. C. Hendershat and J. Forsaith, *J. Pharmacol. Exp. Ther.*, **125,** 237 (1959).

(18) R. Vingar, J. F. Traux, and J. L. Selph, *Eur. J. Pharmacol.*, **37,** 23 (1976).

(19) B. H. Waksman, C. M. Pearson, and J. T. Sharp, *J. Immunol.*, **85,** 403 (1960).

(20) L. F. Sancilio, *Proc. Soc. Exp. Biol. Med.*, **127,** 597 (1968).

(21) B. D. Nelson, P. G. Quie, and R. L. Simmons, *J. Immunol.*, **115,** 1650 (1975).

(22) D. A. Brodie and B. J. Chase, *J. Gastroenterol.*, **53,** 604 (1967).

(23) S. A. Lang, B. D. Johnson, E. Cohen, A. E. Sloboda, and E. Greenblatt, *J. Med. Chem.*, **19,** 1404 (1976).

(24) R. P. Orange, M. D. Valentine, and K. F. Austen, *J. Exp. Med.*, **127,** 767 (1968).

(25) R. Gianetto and C. de Duve, *Biochem. J.*, **59,** 433 (1955).

(26) P. S. Chen, T. Y. Toribara, and H. Warner, *Anal. Chem.*, **28,** 1756 (1956).

(27) W. D. Schleuning and H. Fritz, *Methods Enzymol.*, **45,** 330 (1976).

(28) A. C. Gilman, *Proc. Natl. Acad. Sci. USA*, **67,** 305 (1970).

(29) R. V. Tomlinson, H. J. Ringold, M. C. Qureshi, and E. Forchielli, *Biochem. Biophys. Res. Commun.*, **46,** 552 (1972).

(30) M. Glatt, H. Kälin, K. Wagner, and K. Boune, *Agents Action*, **7,** 321 (1977).

(31) I. H. Hall and G. L. Carlson, *J. Med. Chem.*, **19,** 1257 (1976).

(32) T. Y. Shen and C. A. Winter, *Adv. Drug Res.*, **12,** 89 (1977).

(33) H. Bourne, L. Lichtenstein, K. Melmom, C. Henncy, C. Weinstein, and G. Shearer, *Science,* **184,** 19 (1974).

(34) M. Kalimer and K. F. Austen, *Biochem. Pharmacol.*, **23,** 763 (1974).

(35) B. Weiss and W. N. Hait, *Annu. Rev. Pharmacol.*, **17,** 441 (1977).

(36) P. Davis and R. J. Bonney, *Annu. Rep. Med. Chem.*, **12,** 152 (1977).

(37) V. Stefanovich, *Res. Commun. Chem. Pathol. Pharmacol.*, **7,** 537 (1974).

(38) S. H. Ferreira and J. R. Vane, *Annu. Rev. Pharmacol.*, **14,** 57 (1974).

(39) H. E. Paulus and M. W. Whitehouse, *ibid.*, **13,** 107 (1973).

(40) W. L. Smith and W. E. M. Lando, *J. Biol. Chem.*, **21,** 6700 (1971).

(41) G. Weissman, P. Dukor, and R. B. Zurier, *Nature New Biol.*, **231,** 131 (1971).

(42) H. R. Bourne, R. I. Lehrer, M. J. Cline, and K. L. Melmom, *J. Clin. Invest.*, **50,** 920 (1971).

(43) L. J. Ignarro, *J. Immunol.*, **112,** 110 (1974).

ACKNOWLEDGMENTS

Supported by Grant VC-785 from the University of North Carolina Research Council to I. H. Hall.

The synthesis of these agents at Duke University was supported in part by a U.S. Army Research Office Grant.

Pattern Recognition of Steroids Using Fragment Molecular Connectivity

DOUGLAS R. HENRY and JOHN H. BLOCK ˣ

Received May 18, 1979, from the *School of Pharmacy, Oregon State University, Corvallis, OR 97331.* Accepted for publication July 6, 1979.

Abstract □ The use of pattern recognition methods to classify a set of steroids into five therapeutic categories was investigated. First-order fragment molecular connectivity values were determined for 10 positions on each molecule using a template-based method of position assignment. Learning set and test set classifications were performed. Although the numbers of compounds misclassified were comparable for all of the methods, the identities of the misclassified compounds varied depending on whether the classification method assumed a local or a global view of the data. The best classification results were comparable to those obtained by linear and quadratic discriminant analyses. For this set of compounds, it was concluded that pattern recognition methods offer no advantages over traditional discriminant analysis methods if classification alone is considered, especially since most discriminant analysis procedures utilize stepwise variable selection, which is not as common in pattern recognition analyses.

Keyphrases □ Steroids—pattern recognition using fragment molecular connectivity □ Fragment molecular connectivity—pattern recognition of steroids □ Pattern recognition methods—classification of steroids in therapeutic categories using fragment molecular connectivity

The use of fragment molecular connectivity values as position descriptors in a template-based discriminant analysis has been demonstrated as a means of classifying structures according to their type of pharmacological activity (1). The use of statistical discriminant analysis in such classification problems is optimal for multivariate, normal random variables (2). For observations that are not distributed normally with respect to the descriptor variables, a discriminant analysis may not be the optimal classification method; certain distribution-free pattern recognition techniques may be more suitable (3). Although pattern recognition methods are not used as commonly in medicinal chemistry as are regression analysis and analysis of variance (4), the application of these techniques is increasing (5–9).

Accordingly, a number of classification-type pattern recognition procedures were applied to a set of steroidal compounds studied previously using linear and quadratic discriminant analysis[1]. These compounds show markedly nonnormal distributions with respect to many of the position variables used to describe them (Table I). It was felt that better classification results and greater insight into the value of molecular connectivity in classification problems possibly could be gained with pattern recognition methods.

Four such methods were selected: Andrews function curves (10), K nearest neighbor analysis (11, 12), multicategory linear learning machine analysis (13), and statistical isolinear multicomponent analysis (SIMCA)[2] (14, 15). The use of the Andrews function for representing multivariate data in statistical research is well documented (16). The remaining methods were used as part of ARTHUR, a pattern recognition program (17, 18).

[1] See D. R. Henry and J. H. Block, *Eur. J. Med. Chem.*, in press.

[2] The term SIMCA also can serve as an acronym for SIMilarity Components Analysis, SImple Modeling by Class Analogy, and other methods.

EXPERIMENTAL

A learning set of 46 steroidal compounds, classified into five therapeutic categories, was used (Table I). A test set of nine steroids also was selected (I–IX) (19). The pharmacological categories of these compounds are estrogens (E or ESTR), progestogens (P or PROG), androgens (A or ANDR), corticosteroids (C or CORT), and cardiac steroids (H or CARD). A template structure (6) was designated, and 10 positions of interest were selected. Each compound in the study was superimposed on the template

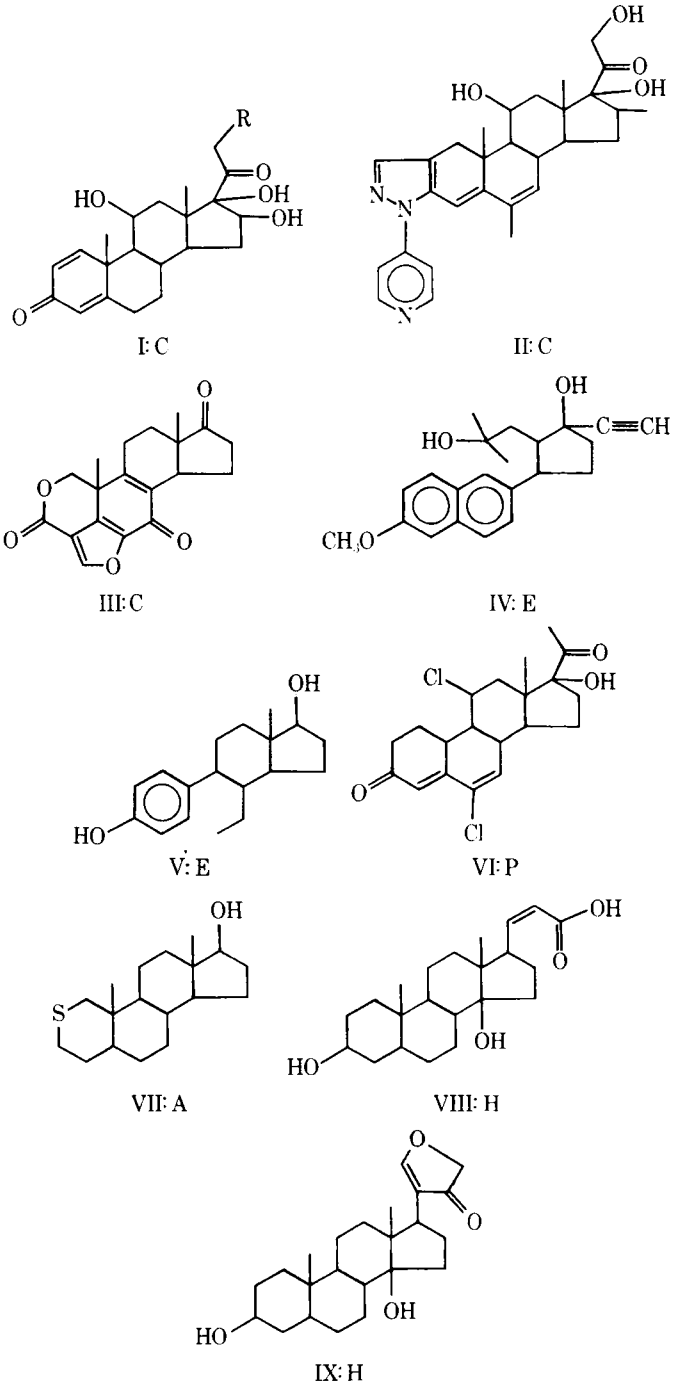

0022-3549/80/0900-1030$01.00/0
© 1980, American Pharmaceutical Association

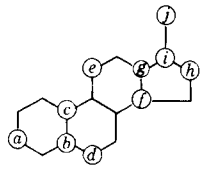

Table I—Raw First-Order Molecular Connectivity Values of Compounds in the Analyses

	Compound[a]	Class[b]	Position									
			a	*b*	*c*	*d*	*e*	*f*	*g*	*h*	*i*	*j*
1	Diethylstilbestrol	E	0.801	0.622	0.827	0.707	1.061	0.827	0.622	0.622	0.801	0.224
2	Dienestrol	E	0.801	0.622	0.827	0.577	0.204	0.827	0.622	0.622	0.801	0.224
3	Methallestril	E	0.781	0.827	0.827	0.622	0.707	1.105	1.115	1.000	0.854	0.781
4	Benzestrol	E	0.801	0.622	0.866	0.707	1.115	0.866	0.622	0.622	0.801	0.224
5	Promethestrol	E	0.742	0.577	0.866	0.707	1.115	0.866	0.622	0.622	0.781	0.408
6	Estradiol	E	0.801	0.892	0.827	0.854	0.908	1.030	1.431	0.908	0.955	0.258
7	Estrone	E	0.801	0.892	0.827	0.854	0.908	1.030	1.392	0.854	0.808	0.204
8	Estriol	E	0.801	0.892	0.827	0.854	0.908	1.030	1.431	0.999	0.880	0.258
9	Equilin	E	0.801	0.892	0.827	0.854	0.908	1.030	1.392	0.854	0.808	0.204
10	Equilinin	E	0.801	0.827	0.789	0.622	0.854	0.986	1392	0.854	0.808	0.204
11	Progesterone	P	0.846	0.892	1.392	0.854	0.908	1.030	1.392	0.854	1.077	0.954
12	17-α-Hydroxyprogesterone	P	0.846	0.892	1.392	0.854	0.908	1.030	1.392	0.854	1.077	0.954
13	Medroxyprogesterone	P	0.846	0.827	1.392	1.274	0.908	1.030	1.392	0.854	1.077	0.954
14	Dihydroprogesterone	P	0.846	0.827	1.392	0.622	0.908	1.030	1.431	0.908	0.986	0.933
15	Ethisterone	P	0.846	0.827	1.392	0.622	0.908	1.030	1.431	0.908	0.986	0.993
16	Norethindrone	P	0.846	0.892	1.392	0.854	0.908	1.030	1.392	0.854	1.077	0.224
17	Norethynodrel	P	0.846	0.931	1.030	0.854	0.908	1.030	1.392	0.854	1.077	0.224
18	Dimethisterone	P	0.846	0.931	1.030	0.854	0.908	1.030	1.246	0.854	1.077	0.224
19	Norgestrel	P	0.846	0.931	1.030	0.854	0.908	1.030	1.246	0.854	1.077	0.224
20	Ethynodiol	P	0.999	0.931	1.030	0.854	0.908	1.030	1.392	0.854	1.077	0.224
21	Testosterone	A	0.846	0.892	1.392	0.854	0.908	1.030	1.430	0.908	0.955	0.258
22	α-Methyltestosterone	A	0.846	0.892	1.392	0.854	0.908	1.030	1.392	0.854	1.327	0.224
23	Oxymetholone	A	0.808	1.105	1.430	0.908	0.908	1.030	1.392	0.854	1.327	0.224
24	Nandrolone	A	0.846	0.931	1.030	0.854	0.908	1.030	1.431	0.908	0.955	0.258
25	Dromostanolone	A	0.846	1.105	1.431	0.908	0.908	1.030	1.431	0.908	0.955	0.258
26	Stanozolol	A	0.827	1.105	1.431	0.908	0.908	1.030	1.392	0.854	1.327	0.224
27	Ethylestrenol	A	0.908	0.931	1.030	0.854	0.908	1.030	1.392	0.854	1.181	0.224
28	Methandrostenolone	A	0.781	0.892	1.327	0.854	0.908	1.030	1.392	0.854	1.327	0.224
29	Oxandrolone	A	0.762	1.105	1.431	0.908	0.908	1.030	1.392	0.854	1.327	0.224
30	Hydrocortisone	C	0.846	0.931	1.030	0.854	1.000	1.030	1.392	0.854	1.077	0.808
31	Prednisone	C	0.781	0.892	1.327	0.854	0.846	1.030	1.392	0.854	1.077	0.808
32	Methylprednisolone	C	0.781	0.827	1.327	1.274	1.000	1.030	1.392	0.854	1.077	0.808
33	Triamcinolone	C	0.781	0.892	1.289	0.854	0.955	1.030	1.392	0.955	1.012	0.808
34	Fluorandrenolone	C	0.781	0.827	1.327	0.567	1.000	1.030	1.392	0.955	1.012	0.808
35	Dexamethasone	C	0.781	0.892	1.288	0.854	0.955	1.030	1.392	1.274	1.012	0.808
36	Paramethasone	C	0.781	0.827	1.327	0.567	1.000	1.075	1.030	1.274	1.051	0.808
37	Flumethasone	C	0.781	0.827	1.288	0.567	0.955	1.030	1.392	1.274	1.012	0.808
38	Fluprednisolone	C	0.781	0.827	1.327	0.567	1.000	1.030	1.392	0.854	1.077	0.808
39	Halcinolone	C	0.846	0.827	1.354	0.854	0.955	1.030	1.392	0.955	1.012	0.808
40	Digitoxigenin	H	1.052	1.105	1.431	0.908	0.908	1.116	1.392	0.908	0.986	0.931
41	Digoxigenin	H	1.052	1.105	1.431	0.908	0.816	1.116	1.193	0.908	0.986	0.931
42	Gitoxigenin	H	1.052	1.105	1.431	0.908	0.908	1.116	1.392	0.999	0.911	0.931
43	Ouabain	H	1.052	1.181	1.181	0.854	0.999	1.116	1.392	0.908	0.986	0.931
44	Strophanthidin	H	1.052	1.181	1.181	0.854	0.908	1.116	1.392	0.908	0.986	0.931
45	Proscillaridin	H	0.927	0.892	1.392	0.854	0.908	1.116	1.392	0.908	0.986	0.781
46	Bufogenin B	H	1.075	1.105	1.431	0.908	0.908	1.116	1.392	0.977	0.911	0.866
	Mean		0.853	0.908	1.196	0.835	0.912	1.029	1.310	0.892	1.016	0.538
	SD		0.090	0.141	0.234	0.162	0.121	0.056	0.227	0.131	0.147	0.324

[a] Structures may be found in Refs. 25 and 26. [b] Key: E = estrogen, P = progestogen, A = androgen, C = corticosteroid, and H = cardiac steroid.

structure, and a value of the descriptor index was assigned to each of the 10 positions on the molecule.

The selected descriptor was first-order molecular connectivity ($^1\chi^v$), which was calculated as the sum of the first-order terms for each bond joining the position of interest (20). This descriptor was selected because this index, when compared to molar refraction and a number of other fragment molecular connectivity indexes, showed lower rates of misclassification when used in linear and quadratic discriminant analyses (1). Using the molecules in the learning set, each position variable was standardized to zero mean and unit variance prior to use. An observation to variable ratio of about 10 was sought. Accordingly, variable selection was performed using both the Fisher and variance weighting methods (18).

The top five variables from a variance-weighted standpoint were, in order of importance, positions *j*, *a*, *i*, *c*, and *b*. These variables were the same as those selected in the stepwise discriminant analysis of the data. Using Fisher weighting, the same variable subset was selected, except that position *f* replaced *b*, which assumed sixth place in significance. Since position *f* had a constant value for three of the groups in the analysis (estrogens, progestogens, and cardiac steroids), the five-variable subset selected by variance weighting was adopted as a basis for performing the pattern recognition analyses.

RESULTS AND DISCUSSION

Andrews Functions—Andrews (21) introduced a trigonometric series expansion with orthonormal coefficients, which is useful for representing multivariate data in two dimensions. This function takes the form:

$$F(x) = x_1\,0.707 + x_2 \sin t + x_3 \cos t + x_4 \sin 2t + x_5 \cos 2t + \cdots \quad \text{(Eq. 1)}$$

where the x values are the values of the respective variables for a given observation. For each observation, a plot of this function over the interval $t = [-\pi,\pi]$ radians gives a curve that is unique to the observation but similar in shape and amplitude to the curves of observations having similar x values (*i.e.*, observations close to each other in multidimensional space). The order of the x variables in Eq. 1 usually is determined based on the contribution of the variable to the between-group differences, with

Table II—Classification by Andrews Function [a]

True Group	Predicted Group ESTR	PROG	ANDR	CORT	CARD	Percent Correct[b]
ESTR	10	0	0	0	0	100.0
PROG	0	7	3	0	0	66.7
ANDR	0	2	5	0	2	55.6
CORT	0	4	0	6	0	60.0
CARD	0	0	1	0	6	85.7
Mean of group	−3.65	0.30	1.22	−0.07	3.33	
SD	0.98	0.67	1.29	0.24	0.90	

[a] For $t = 0.28$ rad, $F(x) = 0.707a + 0.267j + 0.964c + 0.514i + 0.858b$. Variables are ordered according to their contribution to the between-group variation. [b] Learning set results showed 74.5% correct. Compounds misclassified (predicted group) were: 11–13 (ANDR), 21 (PROG), 23 (CARD), 26 (CARD), 27 (PROG), 31 (PROG), 34 (PROG), 37 (PROG), 39 (PROG), and 45 (ANDR). Test set results showed 77.8% correct. Compounds misclassified (predicted group) were II (PROG) and III (ESTR).

the most significant variable being assigned to x_1 and the least significant variable assigned to the last term in the series.

Andrews function plots of prototypes of each therapeutic class are shown in Fig. 1. For this purpose, the group centroids (mean values) of each class were considered to be representative of the class. Other possibilities would be to use median or mode values of the variables for a given group. Each curve in Fig. 1 represents a typical member of its class. There are points along the t axis where between-group separations are large.

Figure 2 shows a plot of the total squared separation, summed over all possible pairs of groups (10 terms). The maximum in overall between-group separation occurs at 0.28 radian. By fixing t at this value, the Andrews function becomes a form of the discriminant function. A histogram of the values of this function for all of the observations is seen in Fig. 3.

Table II shows detailed classification results for the compounds. The results were obtained by determining the distance, in standard deviation units, of the Andrews function value for each observation from the mean value of each group. The observation then was classified into the group for which the absolute value of this distance was the smallest.

A comparison of the results in Table II with the corresponding results of a linear discriminant analysis (Table III) shows that the single Andrews discriminant function performed slightly worse in classifying the learning set (74% correct) compared to a discriminant analysis in which three canonical discriminant functions were used (83% correct). However, for the test set, the Andrews method correctly classified seven out of nine cases while the discriminant analysis was correct in only six cases.

Better classification results might be obtained from the Andrews function by selecting more than one value of t and generating several discriminant functions. Other values of t for which the between-group separation is large are indicated in Fig. 2. As an alternative, a separate value of t and its corresponding function could be selected for each pair of groups, and an observation could be classified based on the number of pairwise comparisons. Neither approach was tried during the present work.

***K* Nearest Neighbor Analysis**—This classification method conceptually is one of the simplest in the pattern recognition literature (22, 23). It differs from most minimum-distance classifiers in that the group centroid is not selected as the prototype of a given class. Instead, an observation is classified into the group to which a majority of its K nearest neighbors in multidimensional space belong. Values of K usually range from one to 10, but classification results suffer whenever the value of K approaches the average class size. In ties, the group showing the smallest aggregate distance is selected.

Table IV shows the results of K nearest neighbor analyses for the learning and test sets of compounds. For the learning set, the results at all levels of K were comparable to the best results obtained by discriminant analysis. For the test set, four compounds were misclassified for all values of K except the first value. This total is one misclassification more than was found with the linear and quadratic discriminant analysis methods.

Table III—Discriminant Analysis Results for Compounds in the Learning Set [a]

Variable	Discriminant Score Coefficients ESTR	PROG	ANDR	CORT	CARD
a	−9.36	2.08	−0.36	−3.36	15.67
b	−1.02	−0.73	1.16	−0.38	1.56
c	−7.09	1.06	2.87	−0.99	6.35
i	−4.24	1.19	2.29	0.50	0.71
j	−1.14	−0.14	−3.16	2.10	2.89
Constant	−13.76	−2.08	−5.60	−3.50	−21.97

[a] Linear classification results were obtained using BMDP7M (27); average results were 82.6% correct. Quadratic classification results were calculated using the University of Wisconsin MULTDIS program (28); average results were 89.1% correct. Test set classification results (both linear and quadratic classification) were 66.7% correct.

Multicategory Linear Learning Machine Analysis—In a manner similar to linear discriminant analysis, a linear learning machine seeks to define a function or boundary that will maximally separate a given group of observations from all other observations (13). However, instead of relying on a fixed statistical criterion (such as maximizing the ratio of between-group variation to within-group variation), a learning machine generates the classification function by iteration and feedback (24). A vector of weighting coefficients is derived for each group. Then, for each observation, a discriminant score is calculated for each group, and the observation is classified into the group for which the discriminant score is highest.

Table V summarizes the results of a multicategory linear learning machine analysis of the steroid data. A total of 201 iterations was performed, although the classification results ceased to improve after 186 cycles through the data. Thirty-nine of the learning set (84.8%) and six of the test set (66.7%) compounds were classified correctly by this method. In each case, the misclassified compounds and the groups into which they were placed were identical to those misclassified in a linear discriminant analysis of the data. This result occurred in spite of the fact that some notable differences existed both in the relative magnitude and in the sign between the weighting vectors derived by the learning machine (Table V) and those calculated in the discriminant analysis (Table III).

All of the misclassified compounds were placed by the learning machine

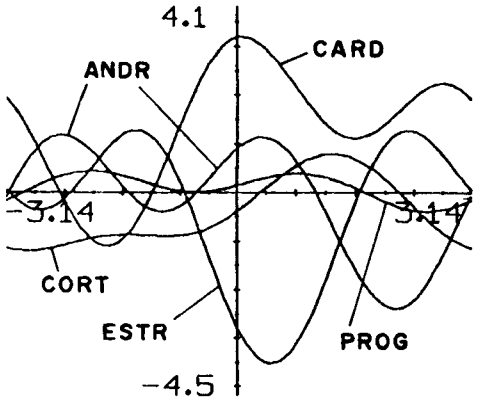

Figure 1—*Andrews function plots of the group centroids of each therapeutic category. The mean values of the position variables* a, j, c, i, *and* b *were used as coefficients in the Andrews function in the order given.*

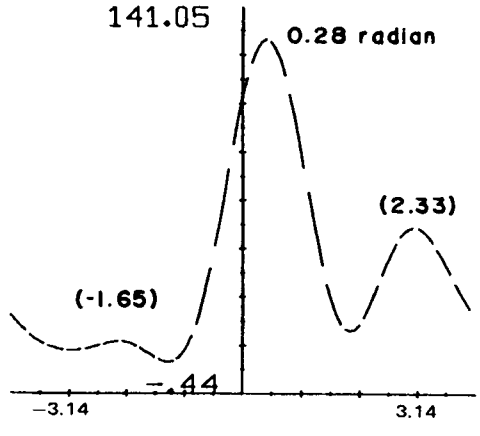

Figure 2—*Plot of the total sum of squares of differences between each possible pair of curves shown in Fig. 1. Values in parentheses are values of* t *(radians) for which local maxima exist; these values of* t *could be used to generate additional discriminant functions.*

Table IV—Results of *K* Nearest Neighbor Analysis [a]

K	Percent Correct	
	Learning Set	Test Set[b]
1	87.0	66.7
3	89.1	55.6
4	89.1	55.6
5	89.1	55.6
6	87.0[c]	55.6[d]

[a] Classification was performed in the space of the standardized position variables *a*, *b*, *c*, *i*, and *j*. [b] Each observation in the test set was classified on the basis of observations in the learning set, omitting other test set compounds. [c] Learning set compounds misclassified (predicted group) were 21 (PROG), 24 (PROG), 25 (PROG), 27 (PROG), 39 (PROG), and 45 (PROG). [d] Test set compounds misclassified (predicted group) were III (ESTR), IV (PROG), VI (CORT), and VII (PROG).

Table V—Multicategory Linear Learning Machine Results: Final Weighting Vectors [a]

Variable	Group				
	ESTR	PROG	ANDR	CORT	CARD
a	0.357	0.646	0.469	−0.442	1.522
b	−1.250	0.747	1.392	−0.992	0.219
c	−0.828	0.373	0.719	−0.498	0.191
i	−0.643	0.194	0.113	0.010	0.209
j	0.527	0.283	−0.102	0.610	0.781
Constant	0.147	0.643	0.601	0.150	0.194

[a] Learning set results were 84.8% correct. Compounds misclassified (predicted group) were 13-15 (CORT), 16 (ANDR), and 19 (ANDR). Test set results were 66.7% correct. Compounds misclassified (predicted group) were IV (CORT), VI (CORT), and VIII (ANDR).

Table VI—Principal Component Models from a SIMCA Study

Group	Component[a]	Variable					Percent Correct in Group[b]
		a	*b*	*c*	*i*	*j*	
ESTR	1	−0.099	−0.150	−0.228	−0.189	−0.110	100.0
	2	−0.091	−0.967	0.052	−0.231	−0.004	
PROG	1	0.023	−0.018	0.025	0.004	−0.006	100.0
	2	0.208	0.177	−0.526	0.112	−0.797	
ANDR	1	−0.039	0.092	0.080	0.174	−0.139	55.6
	2	0.220	−0.235	−0.307	−0.895	0.035	
CORT	1	−0.097	−0.054	0.060	0.026	0.125	80.0
CARD	1	0.299	0.199	0.101	−0.052	0.167	85.7
	2	0.550	0.770	−0.271	−0.027	0.176	
	3	0.429	−0.032	0.841	−0.327	0.045	

[a] Cross-validation was performed to select the optimum number of components for each group, based on a partial *F* test that measures the significance of an added component, given the components already present. [b] Average learning set results were 84.8% correct. Compounds misclassified (predicted group) were 21 (PROG), 24 (PROG), 25 (PROG), 27 (PROG), 30 (PROG), 39 (PROG), and 45 (PROG). Average test set results were 66.7% correct. Compounds misclassified (predicted group) were IV (PROG), VI (CORT), and VII (PROG).

into the progestogen category. Examination of two- and three-dimensional scatter plots and Andrews curves of the progestogens revealed that this class of compounds showed wide within-group variation with respect to the position variables selected. To be classified successfully by a linear learning machine, the compounds must be linearly separable in the space of the descriptor variables, which perhaps is not the case here.

Statistical Isolinear Multicomponent Analysis—A more sophisticated method of pattern recognition than those mentioned previously was developed by Wold (14). The SIMCA method involves generating a separate principal components model for each class of observations. Components are generated iteratively, and the number of components retained for each class may vary. For each group, the model so obtained is solved by least-squares techniques to determine the relationships between the original variables and the derived principal components.

An observation can be classified, and goodness of fit can be determined, by calculating the principal component scores of the observation for each group and then determining the theoretical *x* values the observation should have if it were a member of the given group. The sum of squares of the differences between the calculated *x* values and the observed ones (*i.e.*, the residuals from the regression models) is a measure of how well

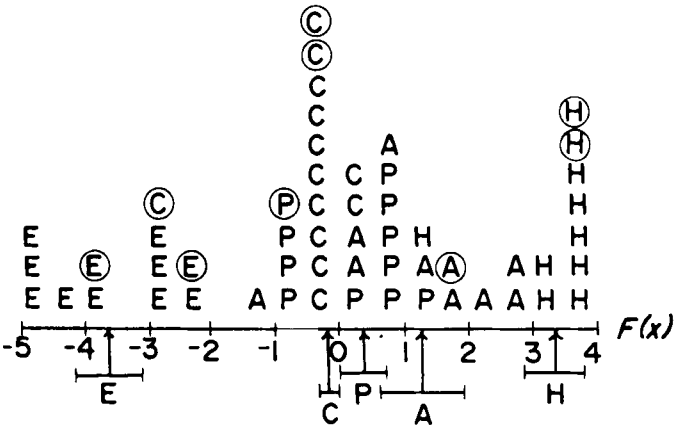

Figure 3—*Histogram of Andrews function values for the compounds in this study. Groups are estrogens (E), progestogens (P), androgens (A), corticosteroids (C), and cardiac steroids (H). Circled entries are test set compounds. Group means (±SD) are shown below the axis.*

the observation fits the model for a particular group. An observation can be placed into the group for which this deviation is smallest or, depending on some preset criteria, it may be placed into a new class instead of into any existing group.

Table VI summarizes the results of a SIMCA study of the data. The number of compounds misclassified by the SIMCA method for both the learning and test sets was the same as for the multiclass separator and the discriminant analysis techniques. However, the identities of the compounds misclassified were different. Those misclassified by the SIMCA method had more in common with the compounds misclassified by the *K* nearest neighbor analysis. This result may reflect a fundamental difference between the multiclass separator and discriminant analysis on the one hand and SIMCA and *K* nearest neighbor analysis on the other. The SIMCA and *K* nearest neighbor methods rely more on local properties of the data set (*i.e.*, the distribution of compounds in the immediate neighborhood of the compound being classified). By contrast, the discriminant function methods rely on a more global view of the data set, considering all groups at once or, in the case of the multiclass separator, comparing a given group with all other groups combined.

CONCLUSIONS

First-order molecular connectivity values contain information that can be used, with varying degrees of success, in the classification of molecular structures into their correct therapeutic categories using pattern recognition techniques. This has been demonstrated using a template-based method of variable assignment. Of course, any method of assigning position variables may be criticized on the basis of its subjectivity. An alternative method, involving whole-molecule molecular connectivity terms, is being studied, and encouraging results have been obtained[3].

For the compounds in this study, pattern recognition methods did not give better classification results than those obtained with the traditional discriminant analysis techniques. The latter methods, due to their statistical nature, have the advantage that stepwise procedures may be employed for variable selection. Such stepwise techniques are not used as commonly in most pattern recognition research.

The classification of observations *per se* is not usually considered a sufficient goal for research of the type reported here. The use of model-building methods of analysis, such as SIMCA, provides a basis for extending such investigations to include both qualitative and quantitative predictions (9). However, it is important that a variety of descriptor variables be studied to determine which variables are most suitable for particular purposes. Molecular connectivity indexes, because of their close relationship to molecular structure, have unique potential for classification problems.

REFERENCES

(1) D. R. Henry and J. H. Block, *J. Med. Chem.*, **22**, 465 (1979).

(2) P. A. Lachenbruch, "Discriminant Analysis," Hafner, New York, N.Y., 1975, p. 40.

[3] See D. R. Henry, Ph.D. thesis, Oregon State University, Corvallis, Ore. (to be published).

(3) L. Kanal, *IEEE Trans. Inform. Theory*, **IT-20**, 697 (1974).
(4) Y. C. Martin, "Quantitative Drug Design-A Critical Introduction," Dekker, New York, N.Y., 1977.
(5) A. J. Stuper and P. C. Jurs, *J. Pharm. Sci.*, **67**, 745 (1978).
(6) A. Cammarata and G. K. Menon, *J. Med. Chem.*, **19**, 739 (1976).
(7) G. K. Menon and A. Cammarata, *J. Pharm. Sci.*, **66**, 304 (1977).
(8) W. J. Dunn, III, and S. Wold, *J. Med. Chem.*, **21**, 1001 (1978).
(9) W. J. Dunn, III, and Y. C. Martin, *ibid.*, **21**, 922 (1978).
(10) D. F. Andrews, in "Discriminant Analysis and Applications," T. Cacoullos, Ed., Academic, New York, N.Y., 1973, pp. 37–47.
(11) E. Fix and J. L. Hodges, U. S. School of Aviation Medicine, Project 21-49-004, Report 4, Randolph Field, Tex., 1951; reprinted in "Machine Recognition of Patterns," A. K. Agrawala, Ed., IEEE Press, New York, N.Y., 1977, pp. 261–279.
(12) T. M. Cover and P. E. Hart, *IEEE Trans. Inform. Theory*, **IT-13**, 21 (1967).
(13) N. J. Nilsson, "Learning Machines," McGraw-Hill, New York, N.Y., 1965.
(14) S. Wold, *Pattern Recognition*, **8**, 127 (1976).
(15) S. Wold and M. Sjöstrom, in "Chemometrics–Theory and Practice," B. R. Kowalski, Ed., ACS Symposium Series No. 52, American Chemical Society, Washington, D.C., 1977, pp. 243–282.
(16) R. Gnanadesikan, "Methods for Statistical Analysis of Multivariate Observations," Wiley, New York, N.Y., 1977, pp. 203–225.
(17) D. L. Duewer, J. R. Koskinen, and B. R. Kowalski, "ARTHUR," available from Alice M. Harper, Department of Chemistry, University of Georgia, Athens, GA 30602.
(18) A. M. Harper, D. L. Duewer, B. R. Kowalski, and J. L. Fasching, in "Chemometrics–Theory and Practice," B. R. Kowalski, Ed., ACS Symposium Series No. 52, American Chemical Society, Washington, D.C., 1977, pp. 14–52.
(19) M. J. Green and B. N. Lutsky, in "Annual Reports in Medicinal Chemistry," vol. 11, F. H. Clarke, Ed., Academic, New York, N.Y., 1976, chap. 16, pp. 149–157.
(20) L. B. Kier and L. H. Hall, *Eur. J. Med. Chem.*, **12**, 307 (1977).
(21) D. F. Andrews, *Biometrics*, **28**, 125 (1972).
(22) P. E. Hart, *IEEE Trans. Inform. Theory*, **IT-14**, 515 (1968).
(23) J. H. Friedman, F. Baskett, and L. J. Shustek, *IEEE Trans. Comput.*, **C-24**, 1000 (1975).
(24) J. T. Tou and P. Gonzales, "Pattern Recognition Principles," Addison-Wesley, Reading, Mass., 1974, pp. 181–186.
(25) D. S. Fullerton, in "Textbook of Organic Medicinal and Pharmaceutical Chemistry," 7th ed., C. O. Wilson, O. Gisvold, and R. F. Doerge, Eds., Lippincott, Philadelphia, Pa., 1977, chap. 20, pp. 731–823.
(26) W. C. Cutting, "Cutting's Handbook of Pharmacology," 5th ed., Appleton-Century Crofts, New York, N.Y., 1972.
(27) "BMDP-Biomedical Computer Programs-1977," W. J. Dixon, Ed., University of California Press, Berkeley, Calif., 1977, pp. 711–733.
(28) R. A. Eisenbeis and R. B. Avery, "Discriminant Analysis and Classification Procedures—Theory and Applications," Heath, New York, N.Y., 1972.

ACKNOWLEDGMENTS

Funds for computer time were supplied by the Oregon State University Computer Center.

Structural Information from Molecular Connectivity $^4\chi_{PC}$ Index

LEMONT B. KIER

Received June 5, 1978, from the *Department of Pharmaceutical Chemistry, Medical College of Virginia, Virginia Commonwealth University, Richmond, VA 23298.* Accepted for publication March 26, 1979.

Abstract □ The molecular connectivity $^4\chi_{PC}$ index was examined for its ability to describe uniquely molecules containing substituted benzene rings. The subgraphs comprising this index were shown to encode information about the number, placement, and type of ring substituents. Several examples illustrate the ability of the index to describe structure-influencing properties.

Keyphrases □ Molecular connectivity—description of molecules containing substituted benzene rings by $^4\chi_{PC}$ index □ Structure–activity relationships—molecules containing substituted benzene rings, interpretation of structure–activity relationship from molecular connectivity $^4\chi_{PC}$ index

Since the development of a new method of molecular structure quantitation called molecular connectivity, it has been utilized in numerous structure–activity relationship studies (1–7). The numerical indexes computed for each molecule are rich in information content; hence, constellations of indexes are of considerable value in describing structural features contributing to the numerical value of a physical property or biological activity. This study explored the information content of one important index, $^4\chi_{PC}$, and revealed how it plays a prominent role in several structure–activity relationship analyses.

THEORY

The molecular connectivity description of molecular structure gives rise to several numerical indexes of the general form $^m\chi_t$, where m is the order of the molecular fragment and t is the type. Indexes may be of the simple connectivity (unweighted adjacency) or valence level. The indexes are weighted counts of fragments within a molecule, conveying information about topological features such as molecular size, branching, cyclization, unsaturation, and heteroatom location and type.

One distinct advantage of a molecular connectivity analysis of structure in a structure–activity relationship study is that the indexes correlating with activity in a regression analysis can be interpreted directly in terms of structural fragments meaningful to the medicinal chemist (8–10). Depending on the study, various indexes will emerge from searches with one or more variables, each conveying various amounts of structural information.

It has become apparent in the studies conducted in these laboratories that certain patterns of index appearance are found in analyses of molecular structure using molecular connectivity. One noteworthy appearance is the $^4\chi_{PC}$ (or the $^4\chi^v_{PC}$) index in studies on the structures of molecules containing substituted benzene rings. This index frequently is important as a second or third variable in regression analyses on molecules in which the benzene rings possess different numbers, positions, and types of substituents.

This recurrence led to the belief that the $^4\chi_{PC}$ index carries a high degree of information content in these structural classes that is common to many drug molecules. The purpose of this report is to analyze and

0022-3549/80/0900-1034$01.00/0
© 1980, American Pharmaceutical Association

(3) L. Kanal, *IEEE Trans. Inform. Theory*, **IT-20**, 697 (1974).
(4) Y. C. Martin, "Quantitative Drug Design-A Critical Introduction," Dekker, New York, N.Y., 1977.
(5) A. J. Stuper and P. C. Jurs, *J. Pharm. Sci.*, **67**, 745 (1978).
(6) A. Cammarata and G. K. Menon, *J. Med. Chem.*, **19**, 739 (1976).
(7) G. K. Menon and A. Cammarata, *J. Pharm. Sci.*, **66**, 304 (1977).
(8) W. J. Dunn, III, and S. Wold, *J. Med. Chem.*, **21**, 1001 (1978).
(9) W. J. Dunn, III, and Y. C. Martin, *ibid.*, **21**, 922 (1978).
(10) D. F. Andrews, in "Discriminant Analysis and Applications," T. Cacoullos, Ed., Academic, New York, N.Y., 1973, pp. 37–47.
(11) E. Fix and J. L. Hodges, U. S. School of Aviation Medicine, Project 21-49-004, Report 4, Randolph Field, Tex., 1951; reprinted in "Machine Recognition of Patterns," A. K. Agrawala, Ed., IEEE Press, New York, N.Y., 1977, pp. 261–279.
(12) T. M. Cover and P. E. Hart, *IEEE Trans. Inform. Theory*, **IT-13**, 21 (1967).
(13) N. J. Nilsson, "Learning Machines," McGraw-Hill, New York, N.Y., 1965.
(14) S. Wold, *Pattern Recognition*, **8**, 127 (1976).
(15) S. Wold and M. Sjöstrom, in "Chemometrics–Theory and Practice," B. R. Kowalski, Ed., ACS Symposium Series No. 52, American Chemical Society, Washington, D.C., 1977, pp. 243–282.
(16) R. Gnanadesikan, "Methods for Statistical Analysis of Multivariate Observations," Wiley, New York, N.Y., 1977, pp. 203–225.
(17) D. L. Duewer, J. R. Koskinen, and B. R. Kowalski, "ARTHUR," available from Alice M. Harper, Department of Chemistry, University of Georgia, Athens, GA 30602.
(18) A. M. Harper, D. L. Duewer, B. R. Kowalski, and J. L. Fasching, in "Chemometrics–Theory and Practice," B. R. Kowalski, Ed., ACS Symposium Series No. 52, American Chemical Society, Washington, D.C., 1977, pp. 14–52.
(19) M. J. Green and B. N. Lutsky, in "Annual Reports in Medicinal Chemistry," vol. 11, F. H. Clarke, Ed., Academic, New York, N.Y., 1976, chap. 16, pp. 149–157.
(20) L. B. Kier and L. H. Hall, *Eur. J. Med. Chem.*, **12**, 307 (1977).
(21) D. F. Andrews, *Biometrics*, **28**, 125 (1972).
(22) P. E. Hart, *IEEE Trans. Inform. Theory*, **IT-14**, 515 (1968).
(23) J. H. Friedman, F. Baskett, and L. J. Shustek, *IEEE Trans. Comput.*, **C-24**, 1000 (1975).
(24) J. T. Tou and P. Gonzales, "Pattern Recognition Principles," Addison-Wesley, Reading, Mass., 1974, pp. 181–186.
(25) D. S. Fullerton, in "Textbook of Organic Medicinal and Pharmaceutical Chemistry," 7th ed., C. O. Wilson, O. Gisvold, and R. F. Doerge, Eds., Lippincott, Philadelphia, Pa., 1977, chap. 20, pp. 731–823.
(26) W. C. Cutting, "Cutting's Handbook of Pharmacology," 5th ed., Appleton-Century Crofts, New York, N.Y., 1972.
(27) "BMDP-Biomedical Computer Programs-1977," W. J. Dixon, Ed., University of California Press, Berkeley, Calif., 1977, pp. 711–733.
(28) R. A. Eisenbeis and R. B. Avery, "Discriminant Analysis and Classification Procedures—Theory and Applications," Heath, New York, N.Y., 1972.

ACKNOWLEDGMENTS

Funds for computer time were supplied by the Oregon State University Computer Center.

Structural Information from Molecular Connectivity $^4\chi_{PC}$ Index

LEMONT B. KIER

Received June 5, 1978, from the *Department of Pharmaceutical Chemistry, Medical College of Virginia, Virginia Commonwealth University, Richmond, VA 23298.* Accepted for publication March 26, 1979.

Abstract □ The molecular connectivity $^4\chi_{PC}$ index was examined for its ability to describe uniquely molecules containing substituted benzene rings. The subgraphs comprising this index were shown to encode information about the number, placement, and type of ring substituents. Several examples illustrate the ability of the index to describe structure-influencing properties.

Keyphrases □ Molecular connectivity—description of molecules containing substituted benzene rings by $^4\chi_{PC}$ index □ Structure–activity relationships—molecules containing substituted benzene rings, interpretation of structure–activity relationship from molecular connectivity $^4\chi_{PC}$ index

Since the development of a new method of molecular structure quantitation called molecular connectivity, it has been utilized in numerous structure–activity relationship studies (1–7). The numerical indexes computed for each molecule are rich in information content; hence, constellations of indexes are of considerable value in describing structural features contributing to the numerical value of a physical property or biological activity. This study explored the information content of one important index, $^4\chi_{PC}$, and revealed how it plays a prominent role in several structure–activity relationship analyses.

THEORY

The molecular connectivity description of molecular structure gives rise to several numerical indexes of the general form $^m\chi_t$, where m is the order of the molecular fragment and t is the type. Indexes may be of the simple connectivity (unweighted adjacency) or valence level. The indexes are weighted counts of fragments within a molecule, conveying information about topological features such as molecular size, branching, cyclization, unsaturation, and heteroatom location and type.

One distinct advantage of a molecular connectivity analysis of structure in a structure–activity relationship study is that the indexes correlating with activity in a regression analysis can be interpreted directly in terms of structural fragments meaningful to the medicinal chemist (8–10). Depending on the study, various indexes will emerge from searches with one or more variables, each conveying various amounts of structural information.

It has become apparent in the studies conducted in these laboratories that certain patterns of index appearance are found in analyses of molecular structure using molecular connectivity. One noteworthy appearance is the $^4\chi_{PC}$ (or the $^4\chi^v_{PC}$) index in studies on the structures of molecules containing substituted benzene rings. This index frequently is important as a second or third variable in regression analyses on molecules in which the benzene rings possess different numbers, positions, and types of substituents.

This recurrence led to the belief that the $^4\chi_{PC}$ index carries a high degree of information content in these structural classes that is common to many drug molecules. The purpose of this report is to analyze and

0022-3549/80/0900-1034$01.00/0
© 1980, American Pharmaceutical Association

Table I—Molecular Connectivity Indexes for Several Substituted Benzenes

Molecule	Number of $^3\chi_C$ Terms	$^3\chi_C$	$^3\chi_C^v$	Number of $^4\chi_{PC}$ Terms	$^4\chi_{PC}$	$^4\chi_{PC}^v$
I 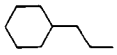	1	0.204	0.118	3	0.433	0.219
II 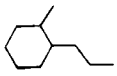	2	0.402	0.102	7	1.020	0.561
III 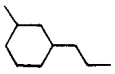	2	0.493	0.285	5	0.777	0.390
IV 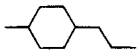	2	0.493	0.285	5	0.841	0.412
V 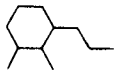	3	0.595	0.371	11	1.638	0.942
VI 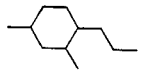	3	0.691	0.413	9	1.360	0.729
VII 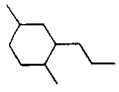	3	0.691	0.413	9	1.369	0.732
VIII 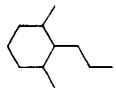	3	0.607	0.377	11	1.500	0.856
IX 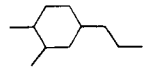	3	0.676	0.407	9	1.514	0.821
X 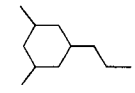	3	0.781	0.451	7	1.047	0.535
XI 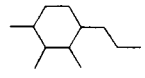	4	0.787	0.496	15	2.245	1.317
XII 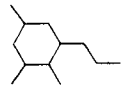	4	0.883	0.538	13	1.919	1.089
XIII 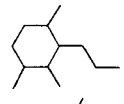	4	0.800	0.502	15	2.127	1.240
XIV 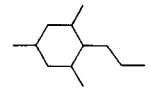	4	0.896	0.544	13	1.772	1.001
XV 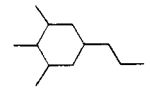	4	0.868	0.531	13	2.053	1.173
XVI 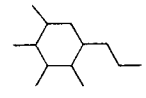	5	0.980	—	19	2.800	1.673
XVII 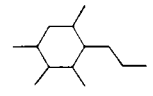	5	0.992	—	19	2.673	1.593
XVIII 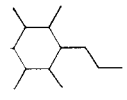	5	0.992	—	19	2.693	1.601
XIX 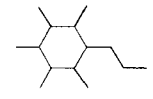	6	1.098	0.713	25	3.448	2.192
XX 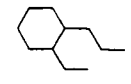	2	0.333	0.204	8	0.992	0.554
XXI 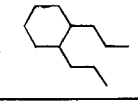	2	0.333	0.204	8	0.943	0.524

(*continued*)

Table I—*Continued*

Molecule	Number of $^3\chi_C$ Terms	$^3\chi_C$	$^3\chi_C^v$	Number of $^4\chi_{PC}$ Terms	$^4\chi_{PC}$	$^4\chi_{PC}^v$
XXII 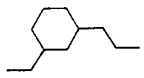	2	0.408	0.236	6	0.873	0.455
XXIII 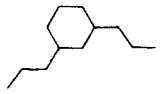	2	0.408	0.236	6	0.813	0.421
XXIV 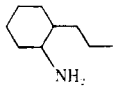	—	—	—	7	1.020	0.404
XXV 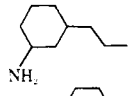	—	—	—	5	0.777	0.314
XXVI 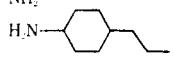	—	—	—	5	0.841	0.331
XXVII 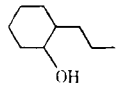	—	—	—	7	1.020	0.356
XXVIII 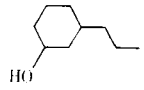	—	—	—	5	0.777	0.291
XXIX 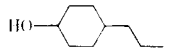	—	—	—	5	0.841	0.305
XXX 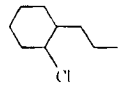	—	—	—	7	1.020	0.633
XXXI 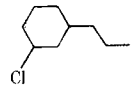	—	—	—	5	0.777	0.425
XXXII 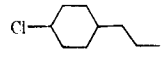	—	—	—	5	0.841	0.449
XXXIII 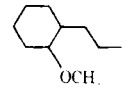	—	—	—	8	0.992	0.400
XXXIV 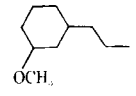	—	—	—	6	0.873	0.352
XXXV 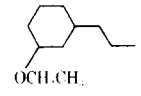	—	—	—	6	0.813	0.332
XXXVI 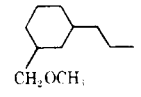	—	—	—	6	0.813	0.385

reveal the information about benzene ring substitution encoded in the $^4\chi_{PC}$ index.

The $^4\chi_{PC}$ index describes the molecular fragment represented as Fragment A.

Fragment A

The index is calculated using the standard algorithm described previously (1, 7, 8). Each atom in the fragment is assigned a δ value based on the number of atoms bonded to it (adjacency) in the original molecule. A valence delta (δ^v) is assigned on the basis of adjacency or, in the case of heteroatoms or unsaturated carbons, use of the prescription $\delta^v = Z^v - h$, where Z^v is the number of valence electrons and h is the number of attached hydrogen atoms. The $^4\chi_{PC}$ (or $^4\chi_{PC}^v$) index then is computed as the sum of the reciprocal square roots of the products of delta values: $^4\chi_{PC} = \Sigma(\delta_i\delta_j\delta_k\delta_l)^{-1/2}$. The $^4\chi_{PC}^v$ index likewise is computed using δ^v values.

The index carries information about the number of benzene ring substituents, the substitution pattern, the length of the substituents up to three bond lengths, and the heteroatom type of substituent. Each category of information will be described, followed by examples of structure–activity relationship studies in which the $^4\chi_{PC}$ index is prominent.

RESULTS AND DISCUSSION

Number of Ring Substituents—The $^4\chi_{PC}$ index appears whenever a branch point in a chain or a ring substituent occurs in a molecular structure. Each ring substituent contributes at least two terms to this index. With substituents longer than one bond length, neglecting hydrogens, the number of terms per substituent is at least three.

Table I presents a number of substituted phenethylamines that were chosen to illustrate the information content of the $^4\chi_{PC}$ index. In the first 19 entries, the number of $^4\chi_{PC}$ terms and the $^4\chi_{PC}$ and $^4\chi_{PC}^v$ values for all possible methyl derivatives are reported. By plotting the number of

Table II—Solubility of Alkyl Benzenes

Molecule	Observed ln S^a	Calculated ln S
Benzene	1.64	1.66
Toluene	2.25	2.24
Ethylbenzene	2.84	2.76
o-Xylene	2.78	2.71
m-Xylene	2.76	2.84
p-Xylene	2.73	2.82
Propylbenzene	3.34	3.34
Isopropylbenzene	3.38	3.26
1,2,4-Trimethylbenzene	3.32	3.31
Butylbenzene	3.94	3.89
sec-Butylbenzene	3.67	3.79
tert-Butylbenzene	3.60	3.69
tert-Amylbenzene	4.15	4.08

[a] Molal solubility in water.

methyl substituents *versus* the $^4\chi_{PC}$ value in Fig. 1, it is obvious that the $^4\chi_{PC}$ values correlate closely with the number of methyl substituents. In other words, the $^4\chi_{PC}$ index carries significant information about the number of single-atom ring substituents (exclusive of hydrogen).

This information content is not unique to the $^4\chi_{PC}$ index. It also is encoded in the $^0\chi$, $^1\chi$, and $^3\chi_C$ indexes. However, the information about the number of substituents encoded in $^4\chi_{PC}$ establishes a base from which the greater utility of this index can be established in molecules containing benzene rings. The $^0\chi$, $^1\chi$, and $^3\chi_C$ indexes fail to perform as well as the $^4\chi_{PC}$ index in encoding additional structural information among substituted benzenes.

Orientation of Ring Substituents—The $^4\chi_{PC}$ index encodes information about the orientation of ring substituents. In general, the greater the adjacency or crowding of single-vertex substituents, the larger is the numerical value of the $^4\chi_{PC}$ index. This effect is illustrated in Fig. 2. In considering the six trisubstituted rings (V–X) in Table I, a plot of the number of adjacent pairs *versus* the $^4\chi_{PC}$ values shows an increase in value with an increased pairing of the substituents. The same effect is illustrated in Fig. 2 with the five tetrasubstituted rings (XI–XV) in Table I. Since there is no quantitative way of describing crowding, it is difficult to illustrate this effect in quantitative terms. In fact, the use of $^4\chi_{PC}$ may be a more meaningful way of quantifying crowding or adjacency of ring substituents.

Other indexes fail to discriminate among substitution isomers in every case. Molecule pairs III, IV; VI, VII; and XVII, XVIII have identical $^3\chi_C$ index values.

An examination of the $^4\chi_{PC}$ terms in these cases makes it apparent why it encodes this information. In Fig. 3, the skeletons of III and IV are shown. The $^3\chi_C$ fragments for each skeleton are identical with respect to the atomic δ values. As a result, the $^3\chi_C$ indexes for III and IV are equivalent.

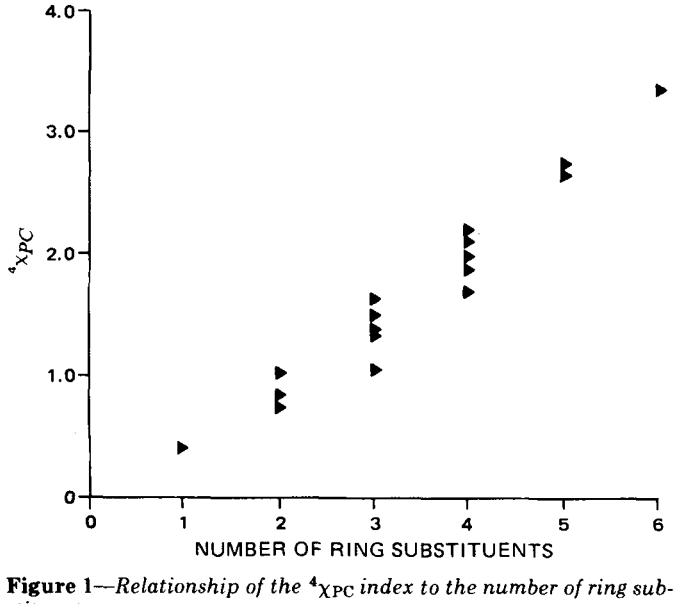

Figure 1—*Relationship of the $^4\chi_{PC}$ index to the number of ring substituents.*

Table III—Cytochrome P-450 Conversion by Substituted Phenols

Substituent	Observed pC^a	Calculated pC
None	1.07	1.02
3-Hydroxy	0.81	1.09
4-Methyl	1.48	1.40
4-Carboxy	1.15	1.30
3-Methyl	1.50	1.44
2-Chloro	1.60	1.36
3-Ethyl	1.82	1.83
4-Bromo	2.04	2.03
2-Iodo	2.09	2.23
2,4-Dichloro	2.11	1.89
2,4,6-Trichloro	2.21	2.33
2,3,4,6-Tetrachloro	2.65	2.59
Pentachloro	2.90	2.92

[a] From Ref. 12.

In contrast, III and IV give rise to differing sets of $^4\chi_{PC}$ fragments because $^4\chi_{PC}$ fragments *b* and *c* of III contain ring atoms that are positions of substitution. Compound IV does not have such fragments. Since a $^4\chi_{PC}$ fragment has a path-three feature, it is able to distinguish *ortho*-, *meta*-, and *para*-substitution patterns. Thus, in Fig. 3, the $^4\chi_{PC}$ index differentiates between the structures, thereby conveying information in numerical form.

Length of Ring Substituents—The effect on the numerical value of $^4\chi_{PC}$ is illustrated by two series of compounds, II, XX, and XXI and III, XXII, and XXIII. With the *ortho*-substitution series (II, XX, and XXI), lengthening the chain by one atom results in a consistent decrease in the $^4\chi_{PC}$ value. With the *meta*-substitution series (III, XXII, and XXIII), there is a decline in the $^4\chi_{PC}$ value beyond one bond length. Substituents with bond lengths of four or more are not distinguishable from those of three-bond length. On the other hand, a branched substituent such as an isopropyl group gives rise to additional $^4\chi_{PC}$ fragments and, hence, an increased numerical value of this index.

An interesting observation can be made about the $^4\chi_{PC}$ indexes and structures discussed in these two series. A ranking of these six compounds based on the extent of interaction between substituent groups is speculated as II, XX, XXI, XXIII, XXII, and III. This ranking closely parallels the decline in the value of their respective $^4\chi_{PC}$ indexes.

Heteroatom-Type Substituent—From Table I, it can be seen for XXIV–XXXVI that the $^4\chi_{PC}$ index is equivalent for all similarly substituted derivatives with the same number of bonds. Thus, XXIV, XXVII, and XXX have identical $^4\chi_{PC}$ indexes. The valence level index $^4\chi^v_{PC}$ must be employed to differentiate between substituents containing atoms of differing δ^v values; XXIV, XXVII, and XXX have different $^4\chi^v_{PC}$ indexes. The larger the δ^v for the heteroatom vertex in these molecules, the smaller is the numerical value of the $^4\chi^v_{PC}$ index.

The $^4\chi^v_{PC}$ index thus can add to the information encoded in the $^4\chi_{PC}$ index the presence of heteroatoms of various kinds in the substituent groups. In addition, the $^4\chi^v_{PC}$ index can distinguish between substituents

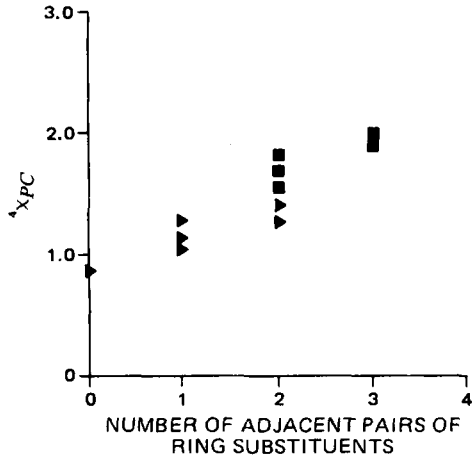

Figure 2—*Relationship of the $^4\chi_{PC}$ index to the number of adjacent pairs of ring substituents, showing the disubstituted (▲) and trisubstituted (●) phenalkylamines in Table I.*

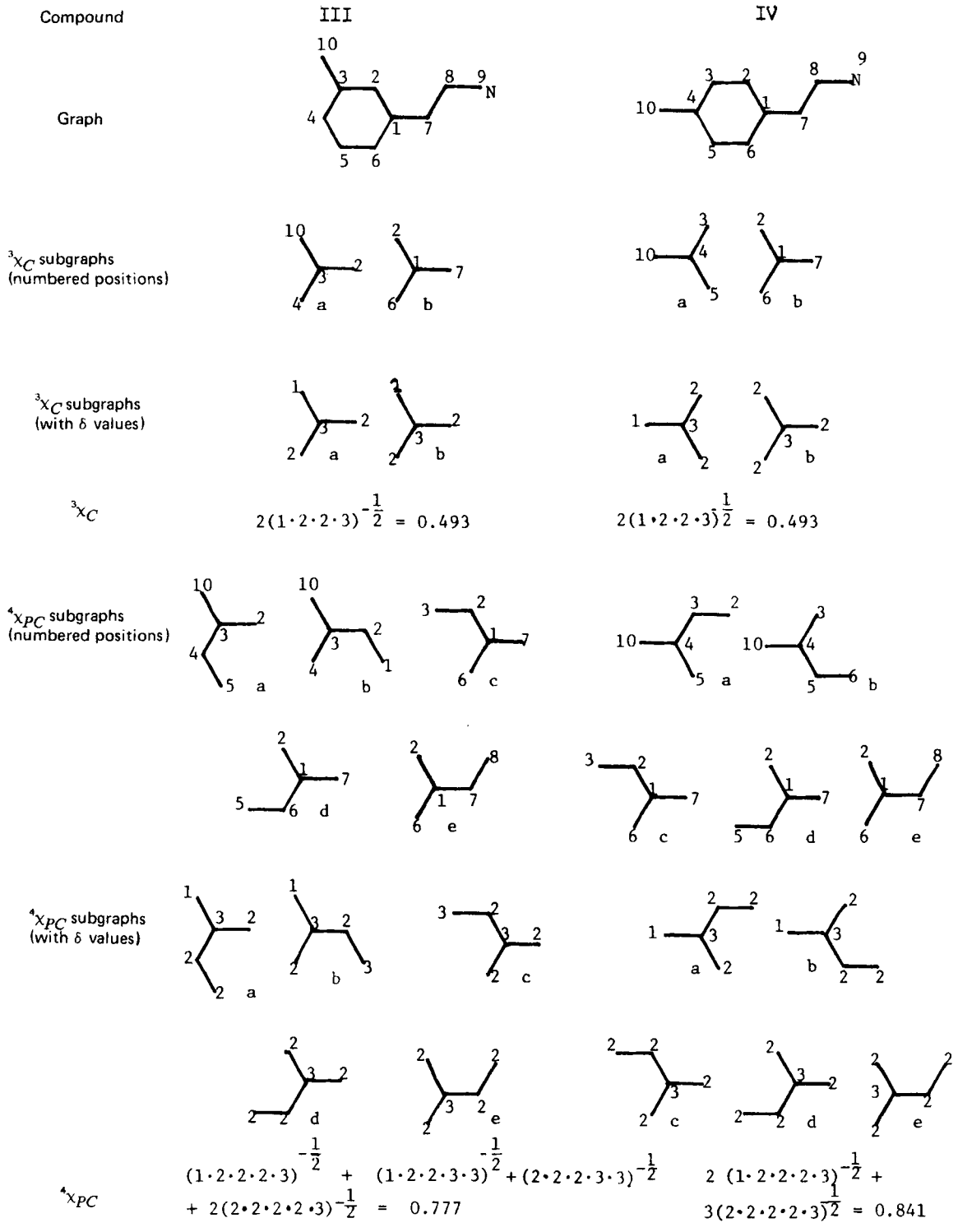

Figure 3—*Comparison of* $^3\chi_C$ *and* $^4\chi_{PC}$ *subgraphs for two molecules.*

containing the same heteroatoms but in different group positions (*e.g.*, XXXV and XXXVI).

Examples of $^4\chi_{PC}$ Indexes in Structure–Activity Relationship Studies—*Propyl Phenyl Ethers*—The first reported use of $^4\chi_{PC}$ in a structure–activity relationship equation was a study on a series of substituted phenyl propyl ethers active against the fungus *Trichophyton mentagrophytes* (1). The same study later was employed in a detailed subgraph analysis (11).

These 28 molecules are related to log 1/*c* by:

$$\log(1/c) = 2.44\,{}^1\chi - 3.29\,{}^3\chi_P + 2.71\,{}^4\chi^v_{PC} - 1.31 \qquad \text{(Eq. 1)}$$

$$r = 0.957 \quad s = 0.149 \quad n = 28 \quad F = 87.4$$

The compounds in the study included mono-, di-, and tri-ring-substituted derivatives including methyl and chloro groups in varying numbers and ring positions.

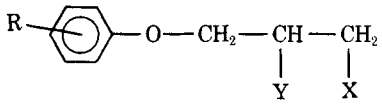

X = H, OH Y = H, OH R = Cl, CH_3

The $^4\chi^v_{PC}$ index conveys the type of information described previously. The greater its magnitude, the greater is the calculated log 1/*c* value.

Table IV—Inhibition of *Aspergillus niger* by Substituted Benzyl Alcohols

Substituent	Observed log $1/c$[a]	Calculated log $1/c$
None	1.51	1.29
4-Chloro	2.07	1.93
2,4-Dichloro	3.07	2.61
3,4-Dichloro	3.07	2.66
2,4,5-Trichloro	3.32	3.34
3,4,5-Trichloro	3.63	3.35
2-Bromo	2.15	2.38
4-Bromo	2.27	2.32
4-Iodo	2.75	2.61
4-Methyl	1.79	1.83
2,4-Dimethyl	2.14	2.41
3,5-Dimethyl, 4-chloro	3.05	3.15
3,5-Dimethyl, 4-iodo	3.42	3.83
2-Nitro	2.49	2.13
4-Nitro	2.00	2.13
4-Cyano	1.67	1.83
2-Hydroxy	1.39	1.62
3-Hydroxy	1.39	1.54
4-Hydroxy	1.39	1.56

[a] From Ref. 13.

Thus, the $^4\chi^v_{PC}$ index indicates that multiple substitution of the ring, particularly in the *ortho*-position and in adjacent ring positions, enhances log $1/c$. Furthermore, the $^4\chi^v_{PC}$ index describes the favorable role of chlorine over methyl as the substituent.

Amphetamines—The $^4\chi^v_{PC}$ index emerged as one of three molecular connectivity indexes in a structure–activity relationship study of 23 ring-substituted amphetamines tested as hallucinogenic agents (8). The ring substituents were methoxy and methylenedioxy with a few alkyl groups and a bromo group.

The regression analysis presented the $^4\chi^v_{PC}$ index in reciprocal form:

$$\log MU = \frac{45.16}{^3\chi_P} + 1.29\,{}^6\chi_P - \frac{4.30}{^4\chi^v_{PC}} - 5.59 \qquad \text{(Eq. 2)}$$

$$r = 0.92 \quad s = 0.25 \quad n = 23 \quad F = 35$$

The $^4\chi^v_{PC}$ index describes the favorable role of substituent orientation, substituent length, and heteroatom presence.

Alkyl Benzenes—Molal solubility data are available for 13 alkylbenzenes (Table II). A two-index equation including the $^4\chi_{PC}$ index gives an excellent correlation with ln S:

$$\ln S = 0.782\,{}^0\chi^v - 0.344\,{}^4\chi_{PC} - 1.051 \qquad \text{(Eq. 3)}$$

$$r = 0.994 \quad s = 0.086 \quad n = 13 \quad F = 394$$

The calculated results in Table II reveal the role played by the $^4\chi_{PC}$ index, in concert with the $^0\chi^v$ index, in describing the various types and orientations of substituents on the benzene ring. The $^4\chi_{PC}$ index predicts the favorable influence of substituent branching on solubility. The influence on this physical property is revealed by the quality of the correlation with ln S.

Phenols—A series of heteroatom-substituted phenols are effective in the cytochrome P-450 conversion (12). These derivatives were subjected to molecular connectivity analysis (Table III). The 50% inhibitory concentration, pC, was found to be related to the two indexes by:

$$pC = 0.628\,{}^0\chi^v - 4.99\,{}^4\chi_{PC} - 1.81 \qquad \text{(Eq. 4)}$$

$$r = 0.971 \quad s = 0.161 \quad n = 13 \quad F = 82$$

The $^4\chi_{PC}$ index describes the number, orientation, and complexity of the substituents to the extent that it accounts for 94% of the variation in the data.

Benzyl Alcohols—A series of benzyl alcohol derivatives modified in the ring are known to inhibit *Aspergillus niger* (13). The molecular connectivity description reveals a correlation with $^1\chi^v$ and $^4\chi_{PC}$ accounting for 88% of the variance in the data:

Table V—Inhibition of *Mycobacterium tuberculosis* by Substituted Phenols

Substituent	Observed pC[a]	Calculated pC
None	0.95	1.02
4-Bromo	1.94	1.92
2-Methyl, 4-bromo	2.35	2.32
2-Ethyl, 4-bromo	2.70	2.70
2-Propyl, 4-bromo	3.18	3.10
2-Butyl, 4-bromo	3.76	3.49
2-Pentyl, 4-bromo	3.99	3.88
2-*sec*-Pentyl, 4-bromo	3.54	3.80
2-Hexyl, 4-bromo	4.26	4.27
2-Cyclohexyl, 4-bromo	3.75	3.88
2-Bromo	1.78	1.83
2-Bromo, 4-*tert*-pentyl	3.39	3.37
2-Bromo, 4-hexyl	4.11	4.20
2-Bromo, 4-propyl, 3,5-dimethyl	3.69	3.61

[a] From Ref. 14.

$$\log 1/c = 0.341\,{}^4\chi_{PC} + 0.979\,{}^1\chi^v - 1.404 \qquad \text{(Eq. 5)}$$

$$r = 0.940 \quad s = 0.268 \quad n = 19 \quad F = 61$$

The results (Table IV) reveal the role of $^4\chi_{PC}$ in describing the number and orientation of ring substituents.

Phenols—A series of alkyl bromophenols was reported as effective in inhibiting *Mycobacterium tuberculosis* (14). A molecular connectivity analysis reveals a high correlation with two variables, including the $^4\chi^v_{PC}$ index:

$$pC = 0.551\,{}^0\chi^v - 0.434\,{}^4\chi^v_{PC} - 1.052 \qquad \text{(Eq. 6)}$$

$$r = 0.992 \quad s = 0.134 \quad n = 14 \quad F = 357$$

The results in Table V show the role of the $^4\chi_{PC}$ index in describing structural information in the relationship.

Conclusion—Because of the structure of the molecular fragment described by $^4\chi_{PC}$, this index is ideally suited to quantifying structural features associated with ring substitution. The fragment may contain up to three consecutive phenyl ring bonds; as a consequence, *ortho-*, *meta-*, and *para*-substitution give rise to different terms, resulting in different $^4\chi_{PC}$ indexes in each case.

The structural information encoded in the $^4\chi_{PC}$ index should make it possible to interpret the structure–activity relationship from molecular connectivity descriptions when this index appears.

REFERENCES

(1) L. B. Kier and L. H. Hall, "Molecular Connectivity in Chemistry and Drug Research," Academic, New York, N.Y., 1976.

(2) L. B. Kier, L. H. Hall, W. J. Murray, and M. Randic, *J. Pharm. Sci.*, **64**, 1971 (1975).

(3) L. B. Kier, W. J. Murray, and L. H. Hall, *J. Med. Chem.*, **18**, 1272 (1975).

(4) T. DiPaolo, L. B. Kier, and L. H. Hall, *Mol. Pharmacol.*, **13**, 31 (1977).

(5) L. B. Kier, T. DiPaolo, and L. H. Hall, *J. Theoret. Biol.*, **67**, 585 (1977).

(6) L. H. Hall and L. B. Kier, *Tetrahedron*, **33**, 1953 (1977).

(7) L. B. Kier and L. H. Hall, *Eur. J. Med. Chem.*, **12**, 307 (1977).

(8) L. B. Kier and L. H. Hall, *J. Med. Chem.*, **20**, 1631 (1977).

(9) L. B. Kier, L. H. Hall, and R. J. Simons, *J. Pharm. Sci.*, **67**, 725 (1978).

(10) L. H. Hall and L. B. Kier, *Eur. J. Med. Chem.*, **13**, 89 (1978).

(11) L. H. Hall and L. B. Kier, *J. Pharm. Sci.*, **67**, 1743 (1978).

(12) Y. Ichikawa and T. Yamano, *Biophys. Acta*, **147**, 518 (1967).

(13) D. V. Carter, P. T. Carlton, A. H. Fenton, J. R. Housey, and B. Lessel, *J. Pharm. Pharmacol., Suppl.*, **10**, 149T (1958).

(14) E. Klarmann, V. Shternov, L. Gates, and P. Cox, *J. Am. Chem. Soc.*, **55**, 4657 (1933).

Synthesis of [8,9-$^2H_2$]Apomorphine and [1,3,8,9-$^2H_4$]Apomorphine for PMR, ^{13}C-NMR, and Mass Spectral Studies

WILLIAM H. SOINE *, JAMES E. HUDSON ‡, BEN A. SHOULDERS ‡, and ROBERT V. SMITH *x

Received March 23, 1979, from the **Drug Dynamics Institute, College of Pharmacy, and the* ‡*Department of Chemistry, University of Texas at Austin, Austin, TX 78712.* Accepted for publication June 6, 1979.

Abstract □ Methods are described for the preparation of [8,9-$^2H_2$]-apomorphine and [1,3,8,9-$^2H_4$]apomorphine based on reaction of apomorphine in trifluoroacetic acid-*d*. The mass spectral properties of these compounds and of the *O,O*-bis(heptafluorobutyrate) ester and the *O,O*-bis(trimethylsilyl) and *O,O*-bis(*tert*-butyldimethylsilyl) ethers of apomorphine, using electron impact and chemical ionization, are reported. [1,3,8,9-$^2H_4$]Apomorphine was used to elaborate the ^{13}C-NMR chemical shifts of the proton-bearing carbons of apomorphine.

Keyphrases □ Apomorphine—synthesis of deuterated analogs for PMR, ^{13}C-NMR, and mass spectral analyses □ Mass spectrometry—analysis, deuterated analogs of apomorphine □ NMR spectroscopy—analysis, deuterated analogs of apomorphine

There is a resurgence of interest in the aporphine alkaloid apomorphine (I) because of its utility in the treatment of Parkinson's disease (1–3), tardive dyskinesia (4), Huntington's chorea (5, 6), and schizophrenia (7). As part of ongoing studies of the mammalian metabolism of I (8–11), methods were desired for the preparation of its specifically deuterated analogs. The latter compounds were envisioned as being potentially useful in mass spectral assays of I and metabolites in biological fluids (12).

Early studies on the deuteration of I gave conflicting evidence on the site and extent of deuteration (13) or provided methodology requiring total synthesis of the aporphine skeleton (14). One report (13) suggested that deuterated analogs of I would not be suitable for use in a mass spectral assay due to proton scrambling during vaporization. Therefore, mass spectral studies were initiated with deuterated I to develop conditions suitable for use in biological assays.

During preliminary analysis, PMR analysis of I in trifluoroacetic acid-*d* showed facile exchange of the 8- and 9-protons with the deuterium ions from the solvent (15). The kinetics for the deuterium exchange of I were studied using PMR spectroscopy, and conditions were developed for the selective preparation of II and III using trifluoroacetic acid-*d*. The ester and silyl ether derivatives of I were used to study the electron-impact and chemical-ionization mass spectral characteristics of II and III for potential use as internal standards in qualitative and quantitative determinations of I. Finally, II was employed to analyze the ^{13}C-NMR spectrum of I.

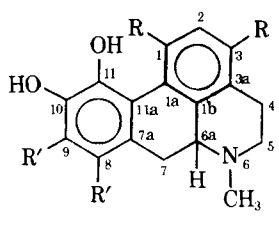

I: R = R′ = H
II: R = R′ = D
III: R = H, R′ = D

RESULTS AND DISCUSSION

The deuteration of apomorphine (I) in trifluoroacetic acid-*d* was studied at various temperatures and in the presence of a transition metal catalyst (5% rhodium on aluminum oxide). Products with increasing deuterium substitution at the aromatic positions were isolated (Table I). PMR spectroscopy was used primarily to determine the sites of substitution, while the extent of incorporation was assessed through mass spectral and PMR analysis. When I was dissolved in trifluoroacetic acid-*d*, there was a collapse of the pair of doublets at δ 6.72 and 6.92 in the PMR spectrum, which is attributable to the exchange of the C-8 and C-9 protons, respectively. Careful analysis of this exchange in excess trifluoroacetic acid-*d* showed that it followed first-order kinetics (Fig. 1) and that C-8 H exchanged significantly faster ($t_{1/2}$ 69.4 min) than C-9 H ($t_{1/2}$ 115 min). This later observation may reflect differences in the resonance stabilization of cationic transition-state intermediates at C-8 and C-9 and correlates with previous work on the bromination of apomorphine dimethyl ether (16).

The protonated amine of apomorphine hydrochloride also underwent exchange in trifluoroacetic acid-*d* as expected. However, it was surprising that the exchange of the amine proton was more than one order of magnitude slower (k = 0.0325 hr^{-1}, r = 0.996, a = 87%, $t_{1/2}$ = 21.3 hr) than the exchange of the aromatic protons at C-8 and C-9.

In contrast to the C-8 and C-9 protons, the exchange of the C-1 and C-3 protons for deuterium in trifluoroacetic acid-*d* was relatively slow at room temperature. With PMR spectroscopy, it appeared that no more than a 15% exchange occurred at C-1 and C-3 in excess trifluoroacetic acid-*d*, even after 216 hr. Elevated temperatures were required to prepare a product significantly enriched in II, and no improvement in incorporation was observed with a rhodium catalyst (Table I). The exchange of the C-1 and C-3 protons for deuterium was observed through loss of the doublets at δ 8.15 and 7.11, respectively. These changes were accompanied by an expected collapse of the triplet observed for C-2 H at δ 7.31 into a singlet integrating for one proton.

The noted assignments parallel those made by Ginos *et al.* (13) for I and II in dimethyl sulfoxide-d_6. These investigators studied the deuteration of apomorphine in 85% D_3PO_4 (in deuterium oxide) and found that II was formed after heating at 95° for several hours or at 140° for 30 min. Convincing PMR evidence was provided for the purity and assign-

Table I—Deuteration of Apomorphine

Deuterated Analog of I	Percent Formation under Various Conditions[a]				
	A	B	C	D	E
d_0	—	—	—	1	—
d_1	10	11	4	6	1
d_2	83	85	19	22	7
d_3	7	2	41	35	32
d_4	—	2	30	29	44
d_5	—	—	6	6	16
Atom percent of deuterium[b]	39	39	63	60	74
Percent of theoretical yield[c]	84	14	42	40	44

[a] Key: A, conditions as indicated under *Experimental* for III; B, same as A only with 50 mg of 5% rhodium on aluminum oxide; C, 5 ml of trifluoroacetic acid-*d* and 0.66 mmole of I·HCl with agitation at 140° for 72 hr; D, identical to C only with 50 mg of 5% rhodium on aluminum oxide; and E, conditions as indicated under *Experimental* for II. [b] Calculations are based on mass spectral analysis and are the atom percent of deuterium of aromatic protons only. [c] Isolated product.

0022-3549/80/0900-1040$01.00/0
© 1980, American Pharmaceutical Association

Table II—Mass Spectral Characteristics of Apomorphine, Its Deuterated Analogs, and Some Potentially Suitable Derivatives for GLC–Mass Spectral Analysis

Compound	Ionization Mode	Scanned	Base Peak	Parent or Pseudoparent Ion (Relative Abundance)	$[M-1]^+/M^+$	Other Important Fragments (Relative Abundance)
I (free base)	EI	36–350	266	267 (64)	1.55	—
I·HCl	EI	50–350	266	267 (72)	1.39	—
II·HCl	EI	70–310	270	271 (75)	1.33	—
III·HCl	EI	70–350	268	269 (70)	1.43	—
I·HCl	CI[a]	70–350	268	268 (100)	—	267 (9)
III·HCl	CI	70–350	270	270 (100)	—	269 (25)
I heptafluorobutyrate[b]	EI	100–730	169	659 (37)	1.03	658 (38)
I trimethylsilyl ether[c]	EI	100–450	410	411 (72)	1.38	322 (79)
II trimethylsilyl ether[c]	EI	100–450	414	415 (90)	1.11	326 (80)
III trimethylsilyl ether[c]	EI	100–450	412	413 (75)	1.33	324 (66)
I trimethylsilyl ether[c]	CI	100–450	412	412 (100)	—	396 (61)
II trimethylsilyl ether[c]	CI	100–450	416	416 (100)	—	400 (46)
III trimethylsilyl ether[c]	CI	100–450	414	414 (100)	—	398 (34)
I *tert*-butyldimethylsilyl ether[d]	EI	100–530	322	495 (4)	0.3	438 (15)

[a] Essentially identical results were obtained when methane or isobutane was used as the ionizing gas. All other chemical-ionization determinations were made with methane. [b] *O,O*-Bis(heptafluorobutyrate) ester. [c] *O,O*-Bis(trimethylsilyl) ether. [d] *O,O*-Bis(*tert*-butyldimethylsilyl) ether.

ment of deuterium atoms in II. However, mass spectral examination of this product proved to be somewhat anomalous; the mass spectrum indicated that ~55% of the aromatic protons had been exchanged for deuterium (d_0, 23; d_1, 0; d_2, 11; d_3, 19; d_4, 41; and d_5, 6), while the PMR spectrum indicated that 80% of the aromatic protons had been exchanged. The relatively high proportion of undeuterated product shown by the mass spectrum was attributed to the exchange between the proton from hydrogen chloride and the deuterium atoms on the aromatic rings (II was analyzed as its hydrochloride salt) during vaporization in the mass spectrometer. The PMR determinations of II and III performed during the present studies were in agreement (within ±4%) with the compositions estimated by mass spectral analysis (Table I).

The exchanges of the C-1 and C-3 protons in trifluoroacetic acid-*d* were facile compared to the exchange of C-2 H. Indeed, no exchange of C-2 H could be detected when I was treated with trifluoroacetic acid-*d* (Table I) or allowed to stand in trifluoroacetic acid-*d* for 9 days at 25°. The ease of exchange of C-1 and C-3 H relative to C-2 H probably results from the influence of the 11-hydroxyl group, which causes resonance stabilization of the developing positive charges at C-1 and C-3. In contrast, a resonance interaction of the 10-oxygen atom across both rings is prevented because of its *meta*-relationship to the A-ring. Furthermore, the 10-hydroxyl group of I may be protonated preferentially in trifluoroacetic acid, which could have important implications for selective *O*-acylations of I in this solvent (17).

Since II and III are proposed for use in biological disposition studies, indication of their stability (with respect to the deuterium–hydrogen exchange) in aqueous media was desired. To determine if the aromatic protons of I at C-8 and C-9 would exchange under mildly acidic conditions, ~60 μmoles of I·HCl was dissolved in 1 ml of 0.02 and 0.3 *M* ascorbic acid (to prevent oxidation of I) prepared in deuterium oxide (pH 2.92 and 2.28, respectively) and stored in screw-capped test tubes at room temperature for 14 days. No incorporation of deuterium was detected after this treatment following GLC–mass spectral analysis of the isolated product as its bis(trimethylsilyl) ether derivative.

The use of II and III as GLC–mass spectral internal standards in metabolic studies requires derivatization to improve volatility and prevent thermal decomposition. Furthermore, the production of suitable (high molecular weight) fragment or parent ions that retain the deuterium label is desired, and these ions should be formed in sufficient amounts (*i.e.*, they should represent a significant proportion of the total ionization current) to permit sensitive detection. Previous work with I (18, 19) indicated that the *O,O*-bis(trimethylsilyl) ether and the *O,O*-bis(heptafluorobutyrate) ester derivatives are readily formed quantitatively and may be applicable to GLC–mass spectral determinations. Compounds converted to *tert*-butyldimethylsilyl ethers frequently form intense ions at high *m/e* values due to loss of a *tert*-butyl radical (M − 57) using electron-impact (EI) conditions, and this derivative was evaluated as well. The electron-impact and chemical-ionization (CI) mass spectral characteristics of I–III and their derivatives are presented in Table II.

A common fragment ion observed in the electron-impact mass spectrum of aporphines is an $[M-1]^+$ species, which is due to loss of the 6a-proton. As indicated in Table II, I and its derivatives, except for apomorphine *O,O*-bis(*tert*-butyldimethylsilyl) ether, give rise to a

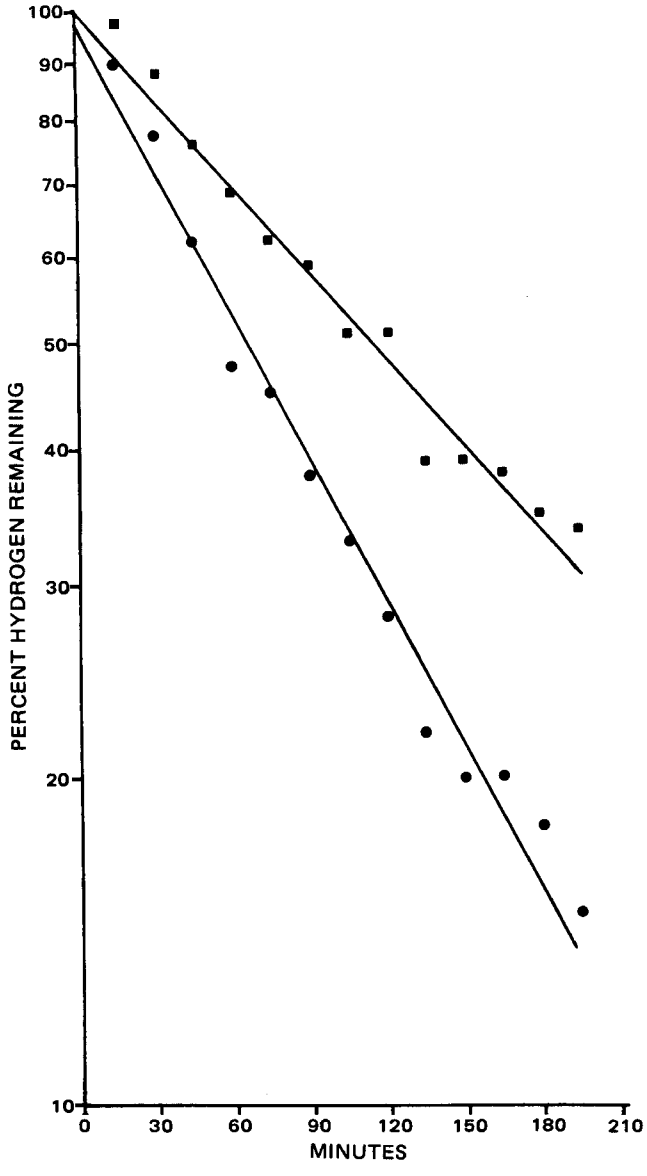

Figure 1—*Kinetics of exchange of C-8 H* (●) (k = *0.60 hr*$^{-1}$, r = *0.992*, a = *97.0%*, $t_{1/2}$ = *69.4 min*) *and C-9 H* (■) (k = *0.36 hr*$^{-1}$, r = *0.989*, a = *101.0%*, $t_{1/2}$ = *114.6 min*) *of apomorphine in trifluoroacetic acid-d at 25°.*

Table III—^{13}C-NMR Spectral Characteristics of Apomorphine in Trifluoroacetic Acid

Carbon	Chemical Shift, δ	Integrated Area[a]
C-1	130.8	2529
C-1a	130.8	—
C-1b	128.9	1265
C-2	129.2	—[b,c]
C-3	129.7	—[c,d]
C-3a	133.5	912
C-4	27.5	860
C-5	55.4	840
C-6a	65.7	1004
C-7	33.4	731
C-7a	127.5	1049
C-8	122.4	—[c,e]
C-9	118.0	940
C-10	143.7	957
C-11	144.8	1031
C-11a	122.1	—[f,g]
N-Methyl	43.5	1183

[a] From broad-band decoupled spectrum. [b] Not sufficiently resolved from C-1b for accurate area measurement. [c] Peak height significantly less than that of quaternary carbons. [d] Not sufficiently resolved from C-2 for accurate area measurement. [e] Not sufficiently resolved from C-11a for accurate area measurement. [f] Not sufficiently resolved from C-8 for accurate area measurement. [g] Peak height significantly greater than aromatic carbons bearing hydrogens.

prominent $[M - 1]^+$ peak. The bis(heptafluorobutyrate) derivative of I under electron-impact conditions gave a moderate parent ion (*m/e* 659) in addition to extensive formation of the imine fragment (*m/e* 658). However, a drawback in using the heptafluorobutyrate derivative is the possibility of exchange of the deuterium atoms at C-8 and C-9 due to small quantities of heptafluorobutyric acid present during derivatization (19).

The electron-impact mass spectrum of the *O,O*-bis(trimethylsilyl) ether of I showed a parent ion that was 75% of the base peak and accounted for 3% of the total ion current. A strong fragment ion was observed at *m/e* 322 for apomorphine as its trimethylsilyl derivative, and corresponding ions at *m/e* 326 and 324 were noted for the same derivative of II and III, respectively. However, in all of these cases, the fragment-ion peaks represented <10% of the total ion currents.

When I was treated with excess *tert*-butyldimethylimidazole, it formed a diether derivative, as evidenced by a parent peak at *m/e* 495. The formation of this derivative was somewhat unexpected since there is significant steric crowding in the resulting derivatized catechol. As anticipated, the parent ion was rather weak in the electron-impact mass spectrum of I as its *tert*-butyldimethylsilyl ether derivative, but there was a fragment ion of moderate intensity at *m/e* 438 ($[M - 57]^+$), which probably arose due to the loss of a *tert*-butyl radical (20). This fragment ion was 15% of the base peak but accounted for only 1% of the total ionization current. A second fragment ion at *m/e* 322 served as the base peak but represented only 6% of the total ionization current. The intensity of these ions may have been enhanced by the use of lower ionization potentials; however, the use of the *tert*-butyldimethylsilyl derivative in GLC–mass spectral work is complicated by its GLC characteristics. Even on a short column (50 cm, 3% methylphenylsiloxane; see *Experimental*), this derivative has long retention times (*e.g.*, 44 min at 210° with a carrier flow rate of 20 ml/min).

Since none of the derivatives had the desired characteristics for quantitative GLC–mass spectral work employing electron-impact conditions, chemical-ionization mass spectrometry was evaluated. The chemical-ionization mode has two advantages over electron-impact spectra. First, it usually is more sensitive than the electron-impact mode. In a typical electron-impact spectrum, the base peak may account for only 20% or less of the total ion current, while many chemical-ionization spectra display base peaks representing as much as 70–80% of the total ion current. Apomorphine proved to be no exception. With the electron-impact mode, the base peak for I was at *m/e* 266 ($[M - 1]^+$) and was 22% of the total ion current; with chemical-ionization mass spectrometry (isobutane), the base peak at *m/e* 268 ($[M + 1]^+$) was 59% of the total ion current.

A second advantage to the chemical-ionization mode is that it often gives a strong pseudoparent ion ($[M + 1]^+$), which may, because of its high molecular weight, be less likely to suffer interference from other components of biological extracts. Apomorphine and its dideuterated analog, III, gave intense pseudoparent ions at *m/e* 268 and 270, respectively, which were the base peaks in both cases. Even when isobutane was used, M^+ and $[M - 1]^+$ ions at *m/e* 266 and 267, respectively, were observed in the chemical-ionization mass spectrum of I. These ions were in approximately the same relative proportion to one another as seen in the electron-impact mass spectrum of I. It has been observed, especially with tertiary amines using methane as the reactant gas, that the amine can undergo electron transfer with one of the reactant ions, giving an M^+ ion (21, 22). This transfer apparently occurs with I. A similar observation was made with glaucine, a related aporphine (23). This observation restricts the use of underivatized I for qualitative work because the noted phenomenon could lead to errors in quantitative determinations.

Of the three derivatives studied, the trimethylsilyl ethers were the most suitable for GLC–mass spectral work. With methane as the GLC carrier gas and the chemical-ionization reactant gas, the chemical-ionization mass spectrum of the trimethylsilyl ethers of I, II, and III showed base peaks at *m/e* 412, 416, and 414, respectively; the ions accounted for 25–32% of the total ion currents for these compounds. However, as was seen with underivatized I, the trimethylsilyl ethers underwent electron transfer with the reactant ions, giving appropriate M^+ and $[M - 1]^+$ ions (*m/e* 411 and 410 for I as its trimethylsilyl derivative) that were quite intense (59 and 29% of the base peak, respectively, for the trimethylsilyl derivative of I). In addition, there appeared to be significant hydrogen abstraction, most likely of the 6a-proton. This phenomenon is observed with tertiary amines in which the hydride loss is enhanced by referring the charge to an adjacent nitrogen atom (22, 24), and it makes the pseudoparent ions of the trimethylsilyl ethers of I–III less desirable for selective-ion monitoring. Fortunately, there are strong and clean fragment ions for the aporphines as their trimethylsilyl derivatives at *m/e* 396 (I), 400 (II), and 398 (III) which account for ~15% of the total ion current in each case. These ion fragments probably occur through the loss of methane from pseudoparent ions, probably from the trimethylsilyl groups. In conclusion, it appears that II and III can function as internal standards for I if chemical-ionization mass spectrometry is used and the noted fragment ions of their trimethylsilyl derivatives are monitored.

The availability of II presented an opportunity to elaborate chemical shifts of the proton-bearing carbons of I. By use of broad-band decoupling, off-resonance white noise decoupling, and selective-proton decoupling, the ^{13}C-NMR data listed in Table III were compiled.

The broad-band decoupling spectrum of I contained only 16 lines; however, the signal at δ 130.8 integrated for two carbons. The off-resonance white noise decoupling spectrum indicated that the signals at δ 144.8, 143.7, 133.5, 130.8, 128.9, 127.5, and 122.1 were nonprotonated carbons. Chemical shifts assigned to aliphatic carbons in I (Table III) were deduced from data reported previously for similar aporphines (25, 26). The ^{13}C-NMR spectrum of II had a single aryl CH signal at δ 129.2.

The use of selective-proton decoupling of the aromatic protons in trifluoroacetic acid presented some problems. Irradiation (0.3 w) at δ H 7.31 to enhance C-2 and δ H 7.11 to enhance C-3 caused enhancement of all of the protonated aromatic carbon signals. In contrast, irradiation at δ H 8.15 to enhance C-1 caused collapse of all of the protonated aromatic carbon signals represented by lines integrating for one carbon; this effect was especially noticeable for the signal at δ 129.7. However, during this experiment, the signal at δ 130.8 (which integrates for two carbons) still integrated for two carbons, indicating that the protonated carbon resonating at δ 130.8 is C-1. By default, the carbon signal at δ 129.7 corresponds to C-3.

Assignment of the carbon signals for C-8–C-11 are based on reported assignments in similar aporphines (25, 26). The carbon assignments for nuciferine and isocorydine suggest that C-11a (*ortho* to phenol) should be the farthest upfield while C-3a should be the farthest downfield of the signals possible for these nuclei. The remaining nonprotonated carbons are provided with proposed assignments (Table III) based on the chemical shifts suggested for analogous carbons in isocorydine (25).

An unusual observation was made with respect to carbon resonance intensities when trifluoroacetic acid was used as the solvent. All of the nonprotonated aromatic carbons possessed intensities greater than or equal to those of the protonated aromatic carbons (during broad-band decoupling); the opposite usually is true because of nuclear Overhauser enhancement. This observation may have general applicability in differentiating nonprotonated from protonated carbons and is under further investigation in these laboratories.

EXPERIMENTAL

Reagents—(*R*)-(−)-Apomorphine hydrochloride hemihydrate was used as purchased[1]. Trifluoroacetic acid-*d* was generated from trifluo-

[1] McFarland Smith Ltd., Edinburgh, Scotland.

roacetic anhydride[2] with deuterium oxide[3] (99.7 atom % D). All other solvents and reagents were analytical reagent grade.

Mass Spectral and GLC–Mass Spectral Studies—Mass spectra were determined in the electron-impact and chemical-ionization modes using an automated GLC–mass spectrometric[4] system consisting of a microprocessor-controlled gas chromatograph coupled (all glass jet separator) to a quadrapole mass spectrometer and data system. Mass spectra of I–III (free base and hydrochloride salts) were obtained by introduction of the sample on a solid probe programmed from 100 to 300° (30°/min). GLC–mass spectral determinations were implemented with a U-shaped glass column (50 cm × 2 mm i.d.) packed with 3% methyl phenyl siloxane on a specially treated silaceous support[5] (100–120 mesh).

Helium (20 ml/min) was the carrier gas in all electron-impact studies; methane was the carrier gas (20 ml/min) in most chemical-ionization work. GLC–mass spectral analyses were carried out with a column temperature of 180–220°. The mass spectrometer was operated with an electron energy of 70 ev, an emission current of 350 μamp, an ion source temperature of 220°, and a scan rate of 30 scans/min from *m/e* 50 or 100 to 700. The final spectrum of each compound was an averaged sum of 10 or more spectra with the average background subtracted.

Trimethylsilyl derivatives were prepared by dissolving ~1 mg of I, II, or III in 100 μl of *N,O*-bis(trimethylsilyl)acetamide and heating at 65° for 30 min. The *tert*-butyldimethylsilyl derivative of I was prepared by reaction of ~1 mg of I·HCl with 200 μl of *tert*-butyldimethylsilylimidazole reagent[6] at 65° for 1 hr. Apomorphine *O,O*-bis(heptafluorobutyrate) was formed by a method reported previously (18).

NMR Studies—PMR and kinetic studies were performed with a 100-MHz[7] instrument, and chemical shifts are reported relative to tetramethylsilane. The rates of deuterium exchange were determined through analyses of integrated areas for C-8 and C-9 H relative to C-2 H in apomorphine hydrochloride. When I·HCl was reacted for 9 days at 25° in trifluoroacetic acid-*d* (containing 2 mg of dithionite/ml to prevent oxidation of I), the integrated area for C-2 H relative to the aliphatic protons remained constant within experimental error.

^{13}C-NMR spectra were obtained with a 90-MHz Fourier transform system[8], and chemical shifts are reported relative to tetramethylsilane. Solutions containing 200 mg of I·HCl/ml of trifluoroacetic acid and 75 mg of II·HCl/ml of trifluoroacetic acid-*d* were analyzed with an external deuterium oxide capillary for locking. For selective-proton decoupling experiments, approximate proton chemical shifts relative to carbon resonances were determined from analysis of acetone-d_6 solutions of I·HCl. The sample for ^{13}C-NMR analysis then was irradiated at the appropriate chemical shift with the source set at 0.3 w.

[1,3,8,9-$^2H_4$]Apomorphine (II)—(*R*)-(−)-Apomorphine hydrochloride hemihydrate (400 mg, 1.2 mmoles) was dissolved in trifluoroacetic acid-*d* (5 ml, 67.3 mmoles) in a silylated 16 × 100-mm polytef-lined screw-capped culture tube and placed in a pipe bomb at 140° for 96 hr. The trifluoroacetic acid-*d* was removed under a nitrogen stream, leaving a pale-brown oil. The oil was treated with a saturated solution of sodium bicarbonate, and the mixture was extracted with ether (4 × 5 ml). The ether was removed under reduced pressure, and the residue was redissolved in dry ether (15 ml). The hydrochloride salt, obtained by bubbling hydrogen chloride through the ether solution, was filtered and dried under vacuum to give 88 mg (44% of theoretical yield) of pale-green powder. Recrystallization from methanol–acetone gave off-white to pale-green crystals.

Purity was >99% as determined by UV spectrophotometry using spectral comparisons and absorbance values at 273 nm from authentic I·HCl [λ_{max} (water) 273 nm, ϵ = 17,300]. The GLC retention time of II as its heptafluorobutyrate derivative was identical to that obtained from similarly derivatized I. The parent peak of II as the free base was at *m/e* 271 ($C_{17}H_{13}D_4NO_2$) with a base peak at *m/e* 270 ($C_{17}H_{12}D_4NO_2$) and a retro-Diels–Alder peak at *m/e* 228 ($C_{15}H_8D_4O_2$). PMR analysis (trifluoroacetic acid-*d*) showed a signal at δ 7.42 (s, C-2 H) and residual signals at δ 8.24 and 7.20 from I-d_3 (Table I).

[8,9-$^2H_2$]Apomorphine (III)—(*R*)-(−)-Apomorphine hydrochloride hemihydrate (200 mg, 0.66 mmole) was dissolved in trifluoroacetic acid-*d* (5 ml, 67.3 mmoles) and kept in the dark at room temperature for 72 hr. The workup was the same as that described for II and gave 140 mg (70% of theoretical yield) of III·HCl as an off-white to pale-green powder. Purity was >99% as determined by UV spectrophotometry, and the GLC retention time of the heptafluorobutyrate derivative of III was identical to that of the corresponding derivative of I. The parent peak of III as the free base was at *m/e* 269 ($C_{17}H_{15}D_2NO_2$), the base peak was at *m/e* 268 ($C_{17}H_{14}D_2NO_2$), and the retro-Diels–Alder peak was at *m/e* 226 ($C_{15}H_{10}D_2O_2$); PMR (trifluoroacetic acid-*d*): δ 8.24 (d, 1H, *J* = 8.0, C-1 H), 7.42 (t, 1H, *J* = 8.0, C-2 H), 7.20 (d, 1H, *J* = 8.0, C-3 H), 6.96 (s, C-9 H, due to the presence of a trace amount of C-8 $^2H_1$), and 6.83 (s, C-8 H, due to the presence of a trace amount of C-9 $^2H_1$) (Table I).

Use of Rhodium Catalyst—Reactions were performed as indicated except that 50 mg of 5% rhodium on aluminum oxide[9] was added and the reaction mixtures were agitated for the times indicated. Workup procedures were identical to those outlined.

REFERENCES

(1) R. S. Schwab, L. V. Amador, and J. Y. Littvin, *Trans. Am. Neurol. Assoc.*, **76,** 521 (1951).

(2) G. C. Cotzias, P. S. Papavasiliou, C. Fehling, B. Kaufman, and I. Mena, *N. Engl. J. Med.*, **282,** 31 (1970).

(3) G. C. Cotzias, P. S. Papavasiliou, E. S. Tolosa, J. S. Mendez, and M. Bell-Midura, *ibid.*, **294,** 567 (1976).

(4) C. D. Marsden, D. Tarsy, and R. J. Baldessarini, in "Psychiatric Aspects of Neurological Disease," D. F. Benson and D. Blumir, Eds., Grune and Stratton, New York, N.Y., 1975, pp. 219–265.

(5) E. S. Tolosa, *J. Am. Med. Assoc.*, **229,** 1579 (1974).

(6) E. S. Tolosa and S. B. Sparber, *Life Sci.*, **15,** 1371 (1974).

(7) C. A. Tamminga, M. H. Schaffer, R. C. Smith, and J. M. Davis, *Science*, **200,** 567 (1978).

(8) J. G. Cannon, R. V. Smith, A. Modiri, S. P. Sood, R. J. Borgman, M. A. Aleem, and J. P. Long, *J. Med. Chem.*, **15,** 273 (1972).

(9) R. V. Smith and A. W. Stocklinski, *Anal. Chem.*, **47,** 1321 (1975).

(10) R. V. Smith, P. W. Erhardt, J. L. Neumeyer, and R. J. Borgman, *Biochem. Pharmacol.*, **25,** 2106 (1976).

(11) W. H. Riffee, R. E. Wilcox, W. H. Soine, and R. V. Smith, *Pharmacologist*, **20,** 184 (1978).

(12) "Mass Spectrometry in Drug Metabolism," A. Frigerio and E. L. Ghisalberti, Eds., Plenum, New York, N.Y., 1977.

(13) J. Z. Ginos, A. LoMonte, G. C. Cotzias, A. K. Bose, and R. J. Brambilla, *J. Am. Chem. Soc.*, **95,** 2991 (1973).

(14) R. Gottlieb and J. L. Neumeyer, *ibid.*, **98,** 7108 (1976).

(15) W. H. Soine, P. Salgo, and R. V. Smith, *J. Labelled Compd. Radiopharm.*, **16,** 597 (1979).

(16) R. V. Smith and A. W. Stocklinski, *Tetrahedron Lett.*, **1973,** 1819.

(17) R. J. Borgman, R. V. Smith, and J. E. Keiser, *Synthesis*, **1975,** 249.

(18) R. V. Smith and A. W. Stocklinski, *Anal. Chem.*, **47,** 1321 (1975).

(19) D. M. Baaske, J. E. Keiser, and R. V. Smith, *J. Chromatogr.*, **140,** 57 (1977).

(20) R. W. Kelly and P. L. Taylor, *Anal. Chem.*, **48,** 465 (1976).

(21) M. S. B. Munson and F. H. Field, *J. Am. Chem. Soc.*, **88,** 2621 (1966).

(22) F. H. Field, in "Advances in Mass Spectrometry," vol. 5, A. Macoll, Ed., MTP International Review of Science, series 1, Butterworths, London, England, 1972, p. 133.

(23) H. M. Fales, H. A. Lloyd, and G. W. A. Milne, *J. Am. Chem. Soc.*, **92,** 1590 (1970).

(24) T. A. Whitney, L. P. Klemann, and H. F. Field, *Anal. Chem.*, **43,** 1048 (1971).

(25) E. Wenkert, B. L. Buckwalter, I. R. Burfitt, M. J. Gassie, H. E. Gottlieb, E. W. Hagaman, F. M. Schell, and P. M. Wovkulich, in "Topics in C-13 N.M.R. Spectroscopy," vol. 2, G. C. Levy, Ed., Wiley–Interscience, New York, N.Y., 1976, p. 105.

(26) M. Shamma, in "The Alkaloids—Specialist Periodical Reports," vol. 7, M. F. Grundon, Ed., The Chemical Society, London, England, 1977, pp. 152–166.

[2] Matheson, Coleman and Bell, Norwood, Ohio.

[3] Merck & Co., Rahway, N.J.

[4] Finnigan 4023 system complete with model 9610 gas chromatograph, model 4000 quadrapole mass spectrometer, and model 2300 INCOS data system, Finnigan Instruments, Sunnyvale, Calif.

[5] OV-17 on Chromosorb WHP, Analabs, North Haven, Conn.

[6] Applied Science Laboratories, State College, Pa.

[7] Model HA-100, Varian Associates, Palo Alto, Calif.

[8] Model WH 90, Bruker Instruments, Billerica, Mass.

[9] Pfaltz & Bauer, Stamford, Conn.

ACKNOWLEDGMENTS

Supported in part by Grant NS-12259 from the National Institute of Neurological and Communicative Disorders and Stroke and Grant GP-41570 from the National Science Foundation.

The authors are grateful to Peter Salgo for technical assistance.

Antitumor Agents XXXVI: Structural Elucidation of Sesquiterpene Lactones Microhelenins-A, B, and C, Microlenin Acetate, and Plenolin from *Helenium microcephalum*

YASUHIRO IMAKURA *, KUO-HSIUNG LEE *x, DONALD SIMS *, RONG-YANG WU *, IRIS H. HALL *, HIROSHI FURUKAWA ‡, MASATAKA ITOIGAWA ‡, and KAZUE YONAHA ‡

Received December 26, 1978, from the **Department of Medicinal Chemistry, School of Pharmacy, University of North Carolina at Chapel Hill, Chapel Hill, NC 27514*, and the ‡*Faculty of Pharmacy, Meijo University, Tempaku, Nagoya, Japan.* Accepted for publication April 6, 1979.

Abstract □ The antitumor sesquiterpene lactones microhelenins-A, B, and C, microlenin acetate, and plenolin were isolated from *Helenium microcephalum*. The structures and stereochemistry of these lactones were determined by physical methods as well as by chemical transformations and correlations. Microlenin acetate appears to be the first novel dimeric sesquiterpene lactone demonstrated to have significant antileukemic activity.

Keyphrases □ Antitumor agents—microhelenins, microlenin acetate, and plenolin, isolation from *Helenium microcephalum*, determination of structure and stereochemistry □ Microhelenins—isolation from *Helenium microcephalum*, determination of structure and stereochemistry □ Sesquiterpene lactones—microhelenins, microlenin acetate, and plenolin, isolation from *Helenium microcephalum*, determination of structure and stereochemistry

Search for an ample supply of helenalin for investigation into the relationship between the structure of sesquiterpene lactones and their cytotoxic antitumor activity led to the use of the plant *Helenium microcephalum*[1] (1). Preexamination of the whole plant extract revealed that the removal of helenalin left a mother liquor, which retained significant inhibitory activity against Walker 256 carcinosarcoma in rats and P-388 lymphocytic leukemia in mice. Further work with the chloroform extract resulted in the isolation[2] and structural determination of the new antitumor agents microhelenins-A (I) (2), B (VI) (3), C (VIII) (3), and D (mexicanin-E, XIV) (3) and microlenin[3] (4, 5), which were described in preliminary reports.

The purpose of this paper is to describe fully the isolation and structural elucidation of microhelenins-A, B, and C, the new dimeric antileukemic agent microlenin acetate[3] (X), and the companion pseudoguaianolide plenolin (VII) (7).

RESULTS AND DISCUSSION

The final chloroform extract of the whole plant of *H. microcephalum* was chromatographed on silica gel using chloroform and chloroform–ethyl acetate (9:1) as the eluents. The initial chloroform eluate afforded a gum of several components. Further silica gel column chromatography and preparative TLC of this mixture led to the isolation of microhelenins-A, B, C, and D. Subsequent elution with chloroform–ethyl acetate (9:1) gave plenolin and microlenin as well as helenalin. Microlenin acetate was isolated from the mother liquor after the removal of helenalin.

Microhelenin-A (I)—Microhelenin-A (I), $C_{15}H_{18}O_4$ (high-resolution mass spectral and elemental analyses), mp 140–141°, $[\alpha]_D^{24}$ +89.0°, showed the partial structure A, with the lactone ring closed at C-7 and C-8 and the methylene group of CH_2OCH attached at C-5 on the basis of IR and NMR (Table I) evidence as reported previously (2).

The circular dichroism and optical rotatory dispersion data of microhelenin-A are listed in Table II together with data for 2,3-dihydrohelenalin (II) (8), whose absolute configuration has been established. Similarities in the sign and magnitude of ketone Cotton effects indicated that I possessed the same *trans*-fused cyclopentanone ring system (C-1α, C-5β-CH_2O) as II. Determination of the *cis*-stereochemistry of the γ-lactone ring in I was based on the generalization that *cis*-fused lactones closed toward C-8, exhibiting a positive lactone Cotton effect, as exemplified by II (9, 10). In addition, Samek's rule (11) ($J_{7,13}$ *trans*-lactone $\geq 3 \geq J_{7,13}$ *cis*-lactone), which generally has been applicable to guaianolides, also indicated that I contains a *cis*-fused lactone since $J_{7,13e}$ = 2.5–3.0 and $J_{7,13f}$ = 2.0–3.0[4]. This evidence led to postulation of possible conformations of the seven-membered ring of I (C and D).

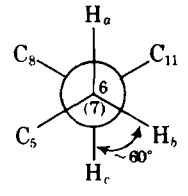

C: boat and half-chair

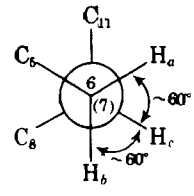

D: chair

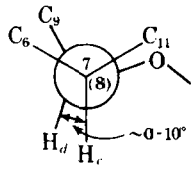

E: boat

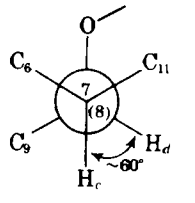

F: half-chair

[1] The constituents of *H. microcephalum* were examined previously and reported to contain helenalin in good yield (1).

[2] Helenalin also was isolated from this chloroform extract.

[3] Microhelenins-A, B, C, and D and microlenin showed significant (T/C ≥ 125%) inhibitory activity against Walker 256 carcinosarcoma in rats at T/C = 148, 138, 159, 144, and 172% at 2.5 mg/kg, respectively. Microlenin and microlenin acetate demonstrated significant (T/C ≥ 120%) inhibitory activity against P-388 lymphocytic leukemia in mice at T/C = 167 and 147% at 12.5 mg/kg, respectively, according to a literature method (6). Plenolin showed T/C = 138% at 25 mg/kg in the P-388 screen.

[4] The coupling constants of $J_{7,13}$ were changed by the conditions of the NMR instrument (XL-100), as shown in the data.

0022-3549/80/0900-1044$01.00/0
© 1980, American Pharmaceutical Association

ACKNOWLEDGMENTS

Supported in part by Grant NS-12259 from the National Institute of Neurological and Communicative Disorders and Stroke and Grant GP-41570 from the National Science Foundation.

The authors are grateful to Peter Salgo for technical assistance.

Antitumor Agents XXXVI: Structural Elucidation of Sesquiterpene Lactones Microhelenins-A, B, and C, Microlenin Acetate, and Plenolin from *Helenium microcephalum*

YASUHIRO IMAKURA *, KUO-HSIUNG LEE *x, DONALD SIMS *, RONG-YANG WU *, IRIS H. HALL *, HIROSHI FURUKAWA ‡, MASATAKA ITOIGAWA ‡, and KAZUE YONAHA ‡

Received December 26, 1978, from the **Department of Medicinal Chemistry, School of Pharmacy, University of North Carolina at Chapel Hill, Chapel Hill, NC 27514*, and the ‡*Faculty of Pharmacy, Meijo University, Tempaku, Nagoya, Japan.* Accepted for publication April 6, 1979.

Abstract □ The antitumor sesquiterpene lactones microhelenins-A, B, and C, microlenin acetate, and plenolin were isolated from *Helenium microcephalum*. The structures and stereochemistry of these lactones were determined by physical methods as well as by chemical transformations and correlations. Microlenin acetate appears to be the first novel dimeric sesquiterpene lactone demonstrated to have significant antileukemic activity.

Keyphrases □ Antitumor agents—microhelenins, microlenin acetate, and plenolin, isolation from *Helenium microcephalum*, determination of structure and stereochemistry □ Microhelenins—isolation from *Helenium microcephalum*, determination of structure and stereochemistry □ Sesquiterpene lactones—microhelenins, microlenin acetate, and plenolin, isolation from *Helenium microcephalum*, determination of structure and stereochemistry

Search for an ample supply of helenalin for investigation into the relationship between the structure of sesquiterpene lactones and their cytotoxic antitumor activity led to the use of the plant *Helenium microcephalum*[1] (1). Preexamination of the whole plant extract revealed that the removal of helenalin left a mother liquor, which retained significant inhibitory activity against Walker 256 carcinosarcoma in rats and P-388 lymphocytic leukemia in mice. Further work with the chloroform extract resulted in the isolation[2] and structural determination of the new antitumor agents microhelenins-A (I) (2), B (VI) (3), C (VIII) (3), and D (mexicanin-E, XIV) (3) and microlenin[3] (4, 5), which were described in preliminary reports.

The purpose of this paper is to describe fully the isolation and structural elucidation of microhelenins-A, B, and C, the new dimeric antileukemic agent microlenin acetate[3] (X), and the companion pseudoguaianolide plenolin (VII) (7).

RESULTS AND DISCUSSION

The final chloroform extract of the whole plant of *H. microcephalum* was chromatographed on silica gel using chloroform and chloroform–ethyl acetate (9:1) as the eluents. The initial chloroform eluate afforded a gum of several components. Further silica gel column chromatography and preparative TLC of this mixture led to the isolation of microhelenins-A, B, C, and D. Subsequent elution with chloroform–ethyl acetate (9:1) gave plenolin and microlenin as well as helenalin. Microlenin acetate was isolated from the mother liquor after the removal of helenalin.

Microhelenin-A (I)—Microhelenin-A (I), $C_{15}H_{18}O_4$ (high-resolution mass spectral and elemental analyses), mp 140–141°, $[\alpha]_D^{24}$ +89.0°, showed the partial structure A, with the lactone ring closed at C-7 and C-8 and the methylene group of CH_2OCH attached at C-5 on the basis of IR and NMR (Table I) evidence as reported previously (2).

The circular dichroism and optical rotatory dispersion data of microhelenin-A are listed in Table II together with data for 2,3-dihydrohelenalin (II) (8), whose absolute configuration has been established. Similarities in the sign and magnitude of ketone Cotton effects indicated that I possessed the same *trans*-fused cyclopentanone ring system (C-1α, C-5β-CH_2O) as II. Determination of the *cis*-stereochemistry of the γ-lactone ring in I was based on the generalization that *cis*-fused lactones closed toward C-8, exhibiting a positive lactone Cotton effect, as exemplified by II (9, 10). In addition, Samek's rule (11) ($J_{7,13}$ *trans*-lactone $\geq 3 \geq J_{7,13}$ *cis*-lactone), which generally has been applicable to guaianolides, also indicated that I contains a *cis*-fused lactone since $J_{7,13e}$ = 2.5–3.0 and $J_{7,13f}$ = 2.0–3.0[4]. This evidence led to postulation of possible conformations of the seven-membered ring of I (C and D).

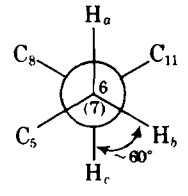

C: boat and half-chair

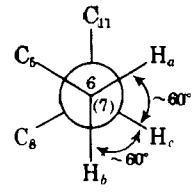

D: chair

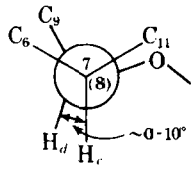

E: boat

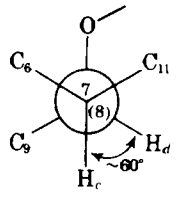

F: half-chair

[1] The constituents of *H. microcephalum* were examined previously and reported to contain helenalin in good yield (1).

[2] Helenalin also was isolated from this chloroform extract.

[3] Microhelenins-A, B, C, and D and microlenin showed significant (T/C ≥ 125%) inhibitory activity against Walker 256 carcinosarcoma in rats at T/C = 148, 138, 159, 144, and 172% at 2.5 mg/kg, respectively. Microlenin and microlenin acetate demonstrated significant (T/C ≥ 120%) inhibitory activity against P-388 lymphocytic leukemia in mice at T/C = 167 and 147% at 12.5 mg/kg, respectively, according to a literature method (6). Plenolin showed T/C = 138% at 25 mg/kg in the P-388 screen.

[4] The coupling constants of $J_{7,13}$ were changed by the conditions of the NMR instrument (XL-100), as shown in the data.

0022-3549/80/0900-1044$01.00/0
© 1980, American Pharmaceutical Association

Table I—Decoupling Experiment Data for IX*b* in PMR Spectrum[a]

Changed Signal Position	Irradiation Position: C-11 CH_3 (δ 1.47)	H-7 (δ 2.74)	H-11 (δ 2.74)	H-8 (δ 4.71)	H-6 (δ 5.38)
C-11 CH_3			d, J = 7.5 ↓ s		
H-7			br dd, J = 6.0 and 10.0 ↓ d, $J_{7,8}$ = 6.0	br dd, J = 6.0 and 10.0 ↓ d, $J_{7,11}$ = 10.0	br dd, J = 6.0 and 10.0 ↓ sharp dd, and J = 6.0 and 10.0
H-11	dq, J = 7.5 and 11.0 ↓ d, $J_{7,11}$ = 10.0	dq, J = 7.5 and 11.0 ↓ d, $J_{11,13}$ = 7.5			
H-8		br t ↓ m			
H-6		br s, $W_{1/2}$ = 2.5 ↓ sharp s			

[a] Values are expressed in parts per million. Multiplicities are indicated by the usual symbols: d, doublet; m, multiplet whose center is given; br s, broad singlet; br t, broad triplet; dd, doublet of doublets; and dq, doublet of quartets. The values are in Hertz. Measurements were recorded with a 100-MHz instrument and were taken in deuterochloroform.

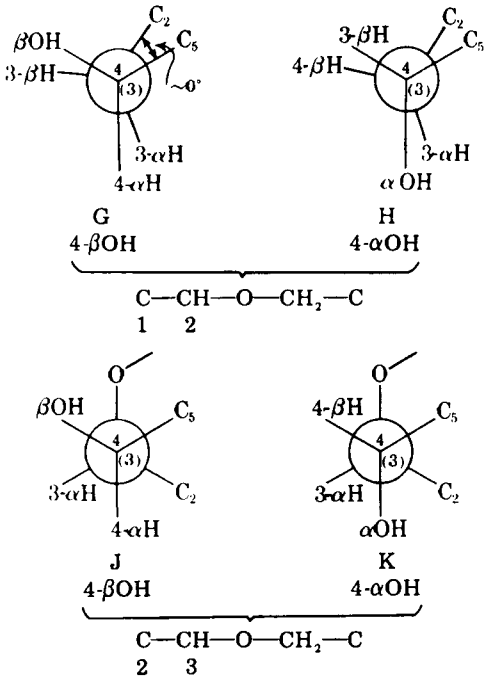

The conformation of the seven-membered ring was determined by a series of INDOR[5] experiments. The magnitude of $J_{6,7}$ determined the relative configuration at C-6 (H_a) and C-7 (H_c); hence, if the configuration of H_c were established as α, then the configurations for H_a and H_b at C-6 would be known accordingly. When the quartet lines of H_a (δ 1.67) were monitored, they gave the INDOR signals arising from H_b at $\delta \sim$ 2.30–2.50 (2). The J values observed between H_a and H_c (J = 13.0 Hz) clearly indicated a diaxial relationship between H_a and H_c, and the value between H_b and H_c (J = 3.0 Hz) indicated a dihedral angle of ~60°, as illustrated in C. Consequently, the conformation of I was assigned the boat or half-chair form.

In addition, the coupling constant ($J_{7,8}$ = 9.0 Hz) between H_c and H_d indicated an eclipsed relationship between H_c and H_d, as illustrated in E, and not a dihedral angle of ~60°, as illustrated in the half-chair form F. Thus, the boat form shown in B was the preferred conformation of the seven-membered ring of I. The linkage position of the remaining methine proton in CH_2OCH was determined as follows. The physical data of I suggested that the methine proton in CH_2OCH could be placed only at C-2 or C-3; in this case, the possible configuration relationships between C-3 and C-4 could be shown as G, H, J, and K (Structure B).

[5] Internal Nuclear Double Resonance.

Treatment of I with sodium borohydride afforded a monohydroxy 11,13-dihydro derivative (III*a*) in which the methylene group of CH_2OCH was linked at C-5 on the basis of spectral evidence (2).

The protons at C-2 and C-4 appeared as a multiplet at δ 4.0. However, the NMR spectrum of III*a* measured in deuterated chloroform–benzene (1:1) showed the presence of H-2 as a multiplet at δ 3.77 and of H-4 as a doublet of doublets of doublets at δ 3.49 (J = 2.0, 4.0, and 10.0 Hz), which indicated that the methine proton of CH_2OCH was placed at C-2, as illustrated in G.

The configuration of the methyl group at C-10 was assigned on the basis of NMR data. If the C-10 methyl group were in the β-axial configuration, the C-2 β-oxygen group would be expected to deshield the C-10 β-methyl group (δ 1.34), as was shown for bipinantin (IV) (12). On the other hand, a C-2 α-hydroxyl group, as found in ivoxathin (V) (13), would be expected to have little or no effect on it (δ 1.11). In addition, a positive Nuclear Overhauser Effect (NOE) between a C-10 β-methyl group and the 5β-axial proton (H_h) should be observed.

The C-10 methyl group of I was observed as a doublet at δ 1.17 and showed no NOE in the NMR spectrum. Therefore, the C-10 methyl group was assigned to an α-configuration and thus gave the complete Structure B for microhelenin-A. The high-resolution mass spectral data of I shown in Scheme I supported this structural assignment.

Microhelenins-B (VI) and C (VIII)—Microhelenin-B (VI), $C_{20}H_{28}O_5$ (high-resolution mass spectrum), mp 111–113°, $[\alpha]_D^{28}$ −84.91°, was recrystallized as colorless needles from chloroform. The IR (tetrachloromethane) and NMR spectra (Table III) showed the presence of an α,β-unsaturated cyclopentenone and an α-methyl-γ-lactone, as found in plenolin (VII) (7) as described previously (3).

The remaining two oxygen atoms of the empirical formula were assigned as part of a five-carbon saturated ester side chain (IR bands at 1741, 1230, and 1190 cm^{-1}), as evidenced by the facile loss of a $C_5H_{10}O_2$ fragment and the appearance of a $C_5H_9O^+$ ion as the base peak in the mass spectrum (Scheme II). The nature of this ester side chain was revealed by the NMR spectrum, which had the same characteristic peaks of a 2-methylbutanoate, as found in tetrahydrobrevilin-A (IX*a*) (14). Based on the physical data, Structure VI was postulated for microhelenin-B. The attachment of the 2-methylbutanoyl side chain at C-6 (δ 5.50, br s, $W_{1/2}$ = 3.0 Hz, H at C-6) and the closing of the lactone ring at C-8 (δ 4.80, br t-like, J = 6.0 Hz, H at C-8) were based on comparable substitution patterns found in other pseudoguaianolides. The high-resolution mass spectral data supported the structural assignment (Scheme II).

Microhelenin-C (VIII), $C_{20}H_{26}O_5$ (high-resolution mass spectrum), $[\alpha]_D^{23}$ −85.0°, was isolated in small quantity as a gum by silica gel column chromatography and preparative TLC. The IR (tetrachloromethane) and NMR spectra (Table III) indicated the presence of an α-methyl-γ-lactone ring, an α,β-unsaturated cyclopentenone of the type found in VI and VII, and a tiglate[6] ester moiety as reported previously (3). In addition,

[6] In general, the βH and βCH_3 protons in methyl tiglate were observed at δ 6.73 and 1.73, respectively, and the protons in methyl tiglate were observed at δ 5.98 and 1.97, respectively (15). The NMR spectrum of VIII indicated the presence of a tiglate ester group, as shown in Table III.

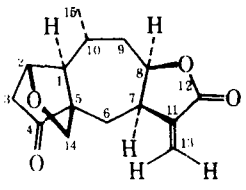

I

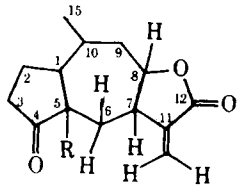

A

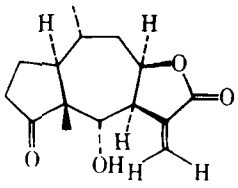

II

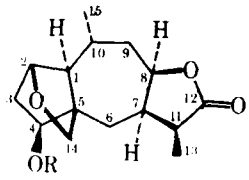

IIIa: R = H
IIIb: R = $COCH_3$

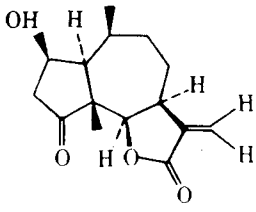

IV

NMR ($CDCl_3$):
δ 1.34 (d, 10-CH_3)

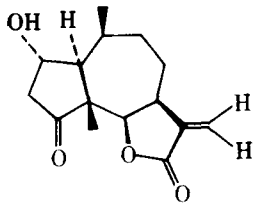

V

NMR ($CDCl_3$):
δ 1.11 (d, 10-CH_3)

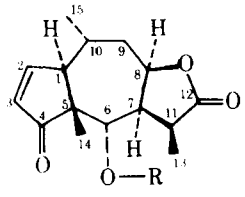

VI: R = $-\overset{1'}{\underset{\underset{O}{\|}}{C}}-\overset{2'}{\underset{\underset{CH_3}{|}}{CH}}-CH_2CH_3$

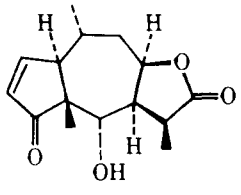

VII

VIII: R = $-\underset{\underset{O}{\|}}{C}-\underset{\underset{CH_3}{|}}{C}=C\overset{H}{\underset{CH_3}{}}$

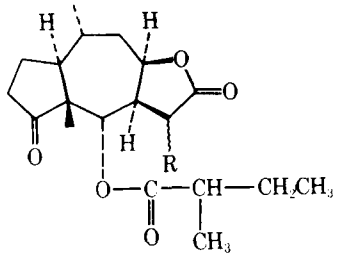

IXa: R = αCH$_3$
IXb: R = βCH$_3$

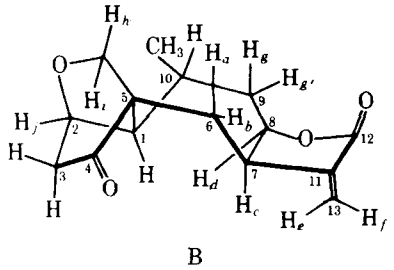

B

the PMR spectrum showed the presence of two methyl signals [δ 1.05 (s, 5-CH_3) and 1.25 (d, J = 6.0 Hz, 10-CH_3)]. In accordance with these deductions, the high-resolution mass spectrum exhibited diagnostically important peaks at m/e 346.1782 ($C_{20}H_{26}O_5$, M^+), 246.1252 ($M^+ - C_5H_8O_2$, base peak), 123.0808 ($C_8H_{11}O^+$), and 83.0494 ($C_5H_7O^+$). Consequently, the structure of microhelenin-C was formulated as VIII, and the stereochemistry was established by direct comparison (TLC and superimposable IR, NMR, and mass spectra) with the synthetic plenolin tiglate prepared from plenolin (VII) and tigloyl chloride in pyridine-benzene.

Catalytic hydrogenation of VI and VIII with 10% palladium-on-carbon in ethanol yielded the same amorphous compound (IX*b*). The IR, PMR, and mass spectra reflected changes resulting from saturation of a cyclopentenone chromophore and a tigloyl side chain. In addition, the PMR spectrum (Table III) was strikingly similar to that of tetrahydrobrevilin-A (IX*a*), which differed only in the stereochemistry of the methyl group at C-11. Thus, the conformations of the seven-membered ring and the configurations of 11-CH_3 could be described as shown in L–N.

The complete assignments of protons for C-6, C-7, C-8, and C-11 of IX*b* were achieved by extensive decoupling experiments (Table I). If the usual assumption is made that the C-7–C-11 bond is equatorial and β as in all sesquiterpene lactones of documented stereochemistry, then the observed large value of $J_{7,11}$ requires that H-11 be *cis* to H-7 and α and the small value of $J_{6,7}$ requires that H-6 be *cis* to H-7 and β. Thus, the lactone ring must be *cis*-fused and the seven-membered ring must be in the chair conformation, as shown in L. In addition, the stereochemistry of tetrahydromicrohelenins-B and C was confirmed to be identical to the

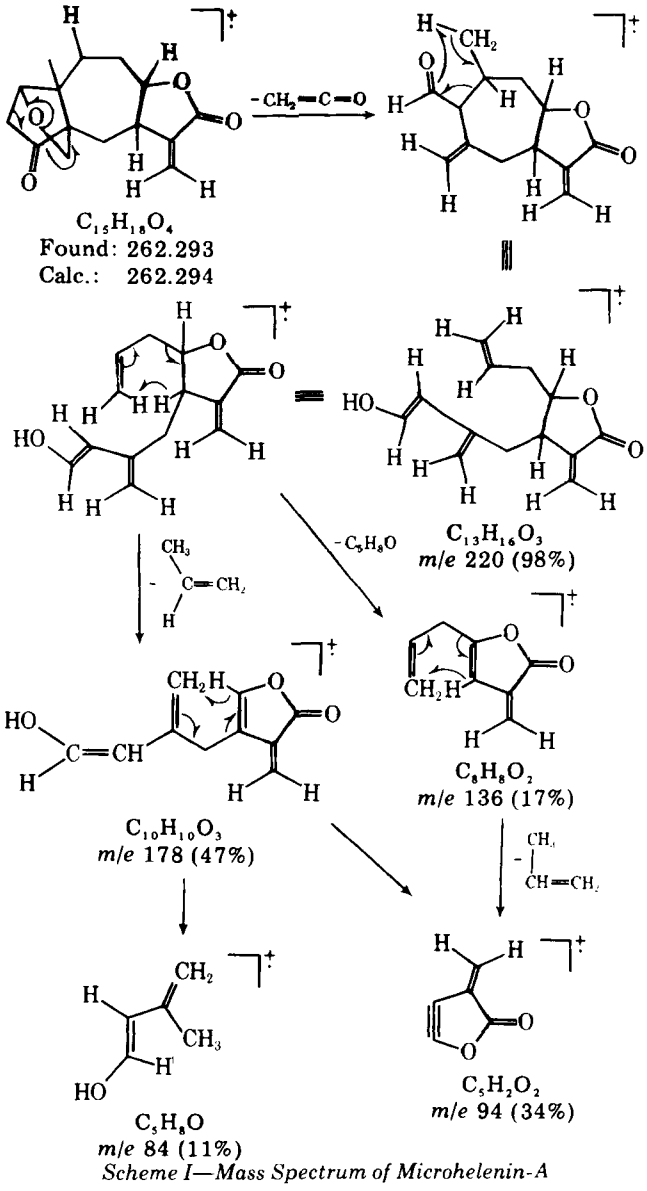

Scheme I—Mass Spectrum of Microhelenin-A

Table II—Optical Rotatory Dispersion and Circular Dichroism Curves of Microhelenin-A (I) and 2,3-Dihydrohelenalin (II)[a]

Compound	Optical Rotatory Dispersion: First Extreme nm	Φ	Second Extreme nm	Φ	Amplitude (a)	Circular Dichroism: Ketone λ_{max}, nm	θ	Lactone λ_{max}, nm	θ
I	313	+5633	277	−4821	+104.5	297	+7598	253	−3144
II	315	+5016	283	−1457	+63.41	300	+5280	262	−3749

[a] Determined on a Cary 60 recording spectrometer in methanol (c, 0.1).

hydrogenation product prepared from plenolin tiglate by direct comparison of TLC results and IR and NMR spectra. Thus, the stereochemistry of tetrahydromicrohelenins-B and C was established as IX*b*. The foregoing evidence led to the establishment of the structures of microhelenins-B and C as VI and VIII, respectively.

Microlenin Acetate (X)—Microlenin acetate (X), $C_{31}H_{36}O_8$, *m/e* 536 (M^+), mp 289–291° dec., was isolated from the mother liquor after the removal of helenalin and recrystallized as colorless needles from chloroform–ether. In the PMR spectrum of X, the presence of one acetyl singlet (δ 1.97), one methyl singlet (δ 0.94), and two methyl doublets [δ 1.18 and 1.23 (d, 3H each, J = 7.0 Hz)] coupled with the characteristic signals corresponding to one cyclopentenone [δ 7.67 (dd, J = 2.0 and 6.0 Hz) and 6.06 (dd, J = 3.0 and 6.0 Hz)] and one α-methylene-γ-lactone moiety [δ 6.28 (d, J = 3.0 Hz) and 5.52 (d, J = 3.0 Hz)] suggested an acetylated dimeric sesquiterpene lactone possessing a cyclopentenone and an α-methylene-γ-lactone for the structure of X. Final identification of X with an acetate of microlenin (XI), prepared by acetylation of XI with acetic anhydride–pyridine, was established by direct comparison (IR, NMR, and mass spectra).

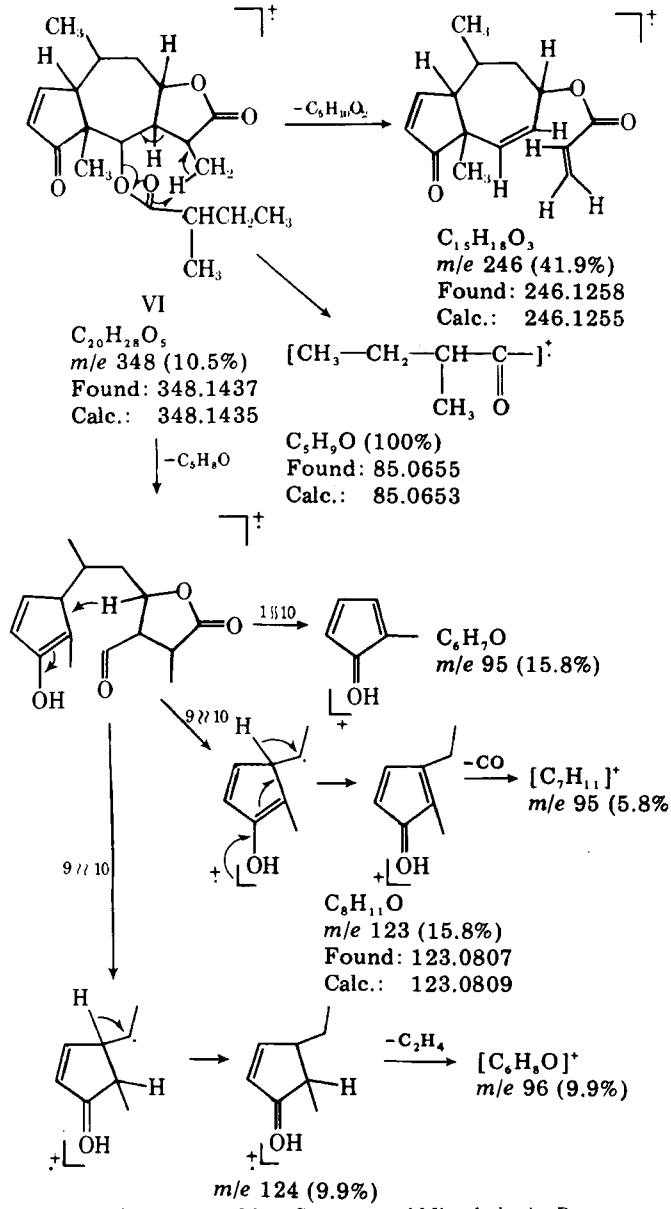

Scheme II—Mass Spectrum of Microhelenin-B

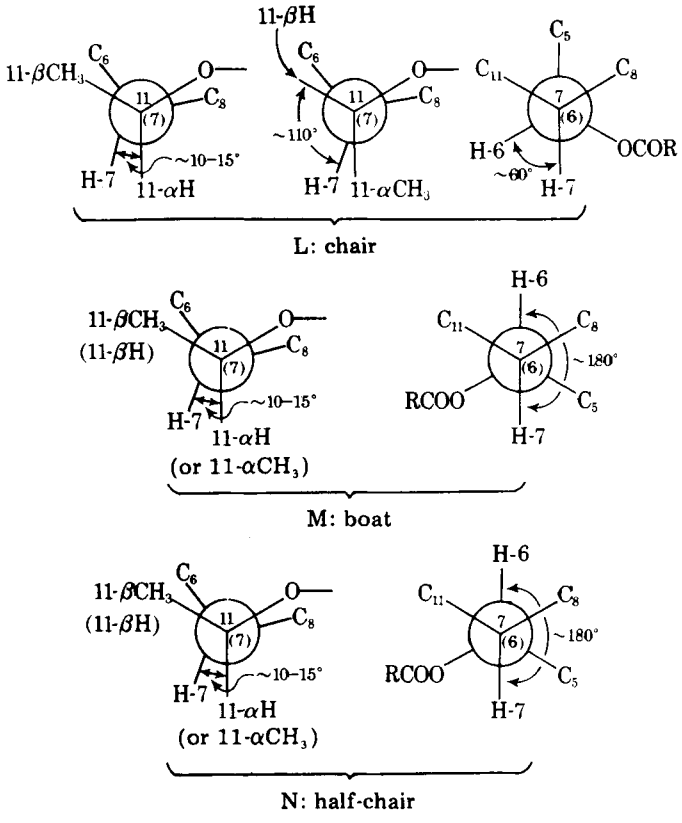

Plenolin (VII)—Plenolin (VII), $C_{15}H_{20}O_4$, *m/e* 264 (M^+), mp 222–224°, was isolated from the chloroform–ethyl acetate (9:1) eluate and recrystallized as colorless needles from chloroform. The IR and NMR

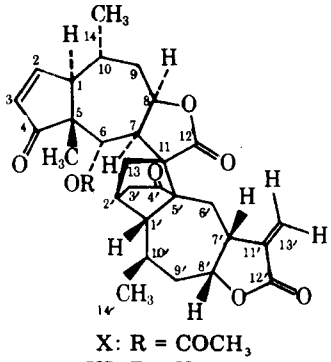

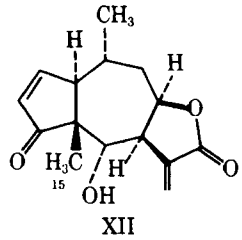

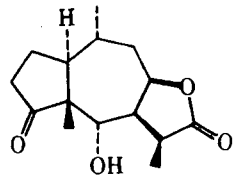

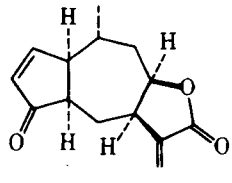

Table III—PMR Spectra of Microhelenins-A (I), B (VI), and C (VIII) and IX*b* [a]

Assignment	I	VI[b]	VIII	IX*b*
H-2	δ 4.53 (m)	δ 7.79 (dd, 2.3 and 6.0)	δ 7.76 (dd, 2.0 and 6.0)	
H-3		δ 6.14 (dd, 3.0 and 6.0)	δ 6.06 (dd, 3.0 and 6.0)	
H-6	δ 1.67 (dd, 13.0 and 15.0, H_a)	δ 5.50 (s-like, $W_{1/2}$ = 3.0)	δ 5.46 (s-like, $W_{1/2}$ = 3.0)	δ 5.38 (br s)
	δ 2.44 (dd, 3.0 and 15.0, H_b)			
H-7	δ 3.12 (m)			δ 2.74 (dd, 6.0 and 10.0)
H-8	δ 4.77 (ddd, 4.0, 9.0, and 11.0)	δ 4.80 (m)	δ 4.78 (m)	δ 4.71 (br t-like, 6.0)
H-11				δ 3.03 (dq, 7.5 and 10.0)
H-13e	δ 5.77 (d, 3.0)			
H-13f	δ 6.34 (d, 3.0)			
H-15	δ 3.64 and 3.85 (*AB*q, 9.0)			
5-CH_3		δ 1.08 (s)	δ 1.05 (s)	δ 0.84
10-CH_3	δ 1.17 (d, 7)	δ 1.28 (d, 6.0)	δ 1.25 (d, 6.0)	δ 1.06 (d, 7.0)
11-CH_3		δ 1.55 (d, 6.0)	δ 1.50 (d, 6.0)	δ 1.47 (d, 7.5)
2′-CH_3		δ 1.08 (d, 7.5)	δ 1.73 (br s)	
3′-CH_3			δ 1.74 (br d, 7.0)	
H-3′			δ 6.64 (m)	
2′-CH_3		δ 1.08 (d, 7.5)	δ 1.73 (br s)	δ 1.06 (d, 7.0)
3′-CH_3		—[c]	δ 1.74 (br d, 7.0)	—[c]
H-3′		—[c]	δ 6.64 (m)	—[c]

[a] Values are in parts per million. Multiplicities are indicated by the usual symbols: d, doublet; m, multiplet whose center is given; and br, slightly broadened singlet. Unmarked signals are singlets. Figures in parentheses are coupling constants in Hertz. Measurements were recorded with a 100-MHz instrument and were taken in deuterochloroform. [b] Measured at 60 MHz (in deuterochloroform). [c] Obscured signal.

spectra of this compound were identical with those of synthetic dihydrohelenalin prepared by catalytic hydrogenation of helenalin. To confirm further the structure of VII, its identity with natural plenolin, isolated from Florida *Helenium autumnale* (15), was established by direct comparison (TLC and superimposable IR, NMR, and mass spectra).

EXPERIMENTAL[7]

Isolation of Microhelenins-A (I), B (VI), C (VIII), and D (XIV), Microlenin Acetate (X), and Plenolin (VII) from *H. microcephalum*.—The *H. microcephalum* (Compositae) used was from a collection made in June 1972 in Burleson County, Tex[8]. The ground, air-dried, whole plant material (7 kg) was extracted exhaustively with chloroform and worked up in the usual manner (16), affording 181 g of a dark-brown gum. The gum (146 g) was chromatographed on silica gel (10 × 70 cm) with chloroform, chloroform–ethyl acetate (9:1), and acetone. Fractions of 250 ml were collected (Fractions a, b, and c) and examined by TLC.

The first chloroform eluate (fractions 7–15 = Fraction a) gave a gummy solid (10 g) upon evaporation of the solvent. The subsequent chloroform eluate (fractions 16–25 = Fraction b) yielded a gum which, upon chromatography on silica gel [200 g, eluted with benzene–chloroform (1:1) and collected at 75 ml/fraction], gave 0.2 g of microhelenin-A upon recrystallization of fractions 13–32 with ether. Recrystallization with ether–tetrachloromethane of the mother liquor after the removal of microhelenin-A afforded 0.2 g of microhelenin-D. The chloroform–ethyl acetate (9:1) eluate (fractions 50 and 51 = Fraction c) yielded helenalin (XII) and plenolin (VII, 80 mg) in addition to a gummy solid (1 g), which was recrystallized from chloroform–ether to give 400 mg of microlenin (XI) as colorless needles. Microlenin acetate (X, 28 mg) was isolated from the mother liquor after the removal of helenalin.

The first chloroform eluate (Fraction a, 10 g) was rechromatographed on silica gel (200 g) with benzene–acetone (25:1) (collected at 20 ml/fraction). Fractions 50–60, after evaporation of the solvent, left a semisolid residue (318 mg). This residue was purified by preparative TLC [benzene–chloroform–acetone (4:4:1), UV detection] to yield a mixture of microhelenins-B and C (205 mg) as indicated by NMR and mass spectra. Further purification of this mixture was achieved by a second preparative TLC procedure [silica gel impregnated with silver nitrate, chloroform–ethyl acetate (3:1), developed twice and detected with UV light] to give 109 mg of microhelenin-B (VI) and 50 mg of microhelenin-C (VIII). Fractions 81–180 gave microhelenin-D (mexicanin-E) (1.8 g) after recrystallization from ether–tetrachloromethane. Fractions 190–250 yielded microhelenin-A (30 mg) upon recrystallization from chloroform.

Microhelenin-A (I)—The analytical data for I were: mp 140–141°, $[\alpha]_D^{24}$ +89.0° (*c*, 1.00 in methanol), C, 68.47; H, 6.88 ($C_{15}H_{18}O_4$ requires C, 68.68; H, 6.92); IR (tetrachloromethane): no hydroxyl group, 1772, 1665 (α-methylene-γ-lactone), and 1758 (cyclopentanone) cm^{-1}; mass spectrum: *m/e* (%) 262.293 (M^+, 100) (calc. 262.294), 220 [M^+ − 42 (CH_2=CO), 98], 178 [M^+ − (42 + CH_3CH=CH_2), 47], 136 [M^+ − (42 + 84), 17], 94 ($C_5H_5O_2^+$, 34), and 84 ($C_5H_8O^+$, 11). The PMR data (100 MHz, deuterochloroform) are shown in Table III.

Microhelenin-B (VI)—The analytical data for VI were: mp 111–113°, $[\alpha]_D^{28}$ −84.91° (*c*, 1.75 in methanol); IR (tetrachloromethane): 1782 (γ-lactone), 1741 (ester), 1726, and 1586 (cyclopentenone) cm^{-1}; mass spectrum: *m/e* (%) 348.1937 (M^+, 6.9) ($C_{20}H_{28}O_5$ requires 348.1935), 246.1258 (M^+ − $C_5H_{10}O_2$, 41.9) ($C_{15}H_{18}O_3$ requires 246.1255), 123.0807 ($C_8H_{11}O^+$, 15.8) ($C_8H_{11}O$ requires 123.0809), and 85.0655 [$CH_3CH_2CH(CH_3)C$=$O)^+$, 100] (C_5H_9O requires 85.0653). The PMR data (60 MHz, deuterochloroform) are shown in Table III.

Microhelenin-C (VIII)—The analytical data for VIII (a gum) were: $[\alpha]_D^{23}$ −85.0° (*c*, 1.30 in methanol); IR (tetrachloromethane): 1782 (α-methyl-γ-lactone), 1725, 1583 (cyclopentenone), 1725, 1651, 1260, and 1182 (tigloyl ester) cm^{-1}; mass spectrum: *m/e* (%) 346.1782 (M^+, 11.8) ($C_{20}H_{26}O_5$ requires 346.1779), 246.1252 (M^+ − $C_5H_8O_2$, 100) ($C_{15}H_{18}O_3$ requires 246.1255), and 83.0494 [$CH_3CH_2CH(CH_3)C$=O^+, 98.1] (C_5H_7O requires 83.0496). The PMR data (60 Hz, deuterochloroform) are shown in Table III.

Sodium Borohydride Reduction of Microhelenin-A (I)—To a solution of I (40 mg) in methanol (2 ml) was added sodium borohydride (20 mg). The total mixture was kept stirring at room temperature for 25 min, treated with acetone (5 ml) and methanol (3 ml), stirred further for 10 min, and worked up in the usual manner. The reaction product was purified by preparative TLC [benzene–methanol (20:2), detection with iodine] to give a monohydroxy dihydro derivative (III*a*) (15 mg), mp 138–140° (chloroform); IR (chloroform): 3590 (OH) and 1762 (γ-lactone) cm^{-1}; mass spectrum: *m/e* (%) 266.1518 (M^+, 9.8) ($C_{15}H_{22}O_4$ requires 266.1518) and 248 (M^+ − H_2O, 4.5); PMR (100 MHz, deuterochloroform): δ 1.07 (d, 3H, *J* = 7.0 Hz, 10-CH_3), 1.18 (d, 3H, *J* = 7.5 Hz, 11-CH_3), 2.84 (dq, 1H, *J* = 7.5 and 10.0 Hz, H-11), 3.50 (dd, 1H, *J* = 2.0 and 8.0 Hz, C-5 CH_2O), 4.18 (d, 1H, *J* = 8.0 Hz, 1H, C-5 CH_2O), 4.0 (m, 2H, H-2 and H-4), and 4.78 (m, 1H, H-8); PMR (100 MHz, deuterated chloroform and benzene, deuterated water treatment): δ 0.81 and 0.99 (d, 3H each, *J* = 7.0 Hz, 10-CH_3 and 11-CH_3), 3.23 (dd, 1H, *J* = 2.0 and 8.0 Hz, C-5 CH_2O), 3.49 (ddd, 1H, *J* = 2.0, 4.0, and 10.0 Hz, H-4), 3.77 (m, 1H, H-2), 3.98 (d, 1H, *J* = 8.0 Hz, C-5 CH_2O), and 4.29 (m, 1H, H-8).

Acetylation of III*a*—Acetylation of III*a* (7 mg) with acetic anhydride (0.5 ml) and pyridine (0.5 ml) at room temperature for 20 hr followed by the usual workup yielded a product (5 mg). This product was purified

[7] Melting points were determined on a Thomas-Hoover melting-point apparatus and are uncorrected. Specific rotations were on a Perkin-Elmer model 141 polarimeter (1 = 1 dm). IR spectra were recorded with a Perkin-Elmer model 257 grating IR spectrometer. The PMR spectrum was determined with either a Jeolco C60 HL or a Varian XL-100 NMR spectrometer (tetramethylsilane as the internal standard). Mass spectra were determined on an AEI MS-902 instrument at 70 ev using a direct-inlet system. Optical rotatory dispersion and circular dichroism spectra were measured on a Cary model 60 spectrometer. Silica gel was used for column chromatography (Mallinckrodt CC-7, 200–325 mesh) and for TLC (Merck silica gel G). Detection of components was made by spraying with 1% cerium sulfate–10% sulfuric acid solution followed by heating. Elemental analyses were performed by Atlantic Microlab, Atlanta, Ga.

[8] Dr. John J. Sperry, Texas A & M University, collected and identified the plant material. A voucher specimen (J. J. Sperry, No. 4020) is available for inspection at the Herbarium, Department of Botany, University of North Carolina at Chapel Hill.

with preparative TLC [chloroform–methanol (40:1), detection with iodine] to give an acetylated derivative (III*b*, 3.5 mg) of III*a*. The analytical data for III*b* were: mp 135–138° (chloroform); mass spectrum: *m/e* (%) 308.1620 (M^+, 100) ($C_{17}H_{24}O_5$ requires 308.1624) and 248 (M^+ – CH_3COOH, 33); PMR (100 MHz, deuterochloroform): δ 2.14 (s, 3H, C-4 $OCOCH_3$), 4.09 (m, 1H, H-2), 4.7, and 5.1 (m, 2H, H-4 and H-8).

Catalytic Hydrogenation of Microhelenin-C (VIII)—A solution of VIII (50 mg) in ethanol (8 ml) was shaken with hydrogen at room temperature (22°) and atmospheric pressure in the presence of 10% palladium-on-charcoal (50 mg). The reaction mixture was filtered after the initial rapid absorption slowed. Removal of ethanol *in vacuo* resulted in a gum (49 mg), which was purified by preparative TLC [benzene–chloroform–acetone (4:4:1), detection with iodine] to give an amorphous compound (IX*b*, 36 mg) from acetone; IR (tetrachloromethane): 1782 (α-methyl-γ-lactone), 1749, and 1740 (sh) (ester and cyclopentanone) cm^{-1}; mass spectrum: *m/e* (%) 350.2091 (M^+, 7.0) ($C_{20}H_{20}O_5$ requires 350.2093), 248 [M^+ – $CH_3CH_2CH(CH_3)COOH$, 58.3], 85 $[CH_3CH_2CH_2C{=}O)^+$, 58.3] and 57 ($CH_3CH_2C^+HCH_3$, 100); PMR (100 MHz, deuterochloroform): δ 0.84 (s, 3H, 5-CH_3), 1.06 (d, 6H, J = 7.0 Hz, 10-CH_3 and 2′-CH_3), 1.47 (d, 3H, J = 7.5 Hz, 11-CH_3), 2.74 (dd, 1H, J = 6.0 and 10.0 Hz, H-7), 3.03 (dq, 1H, J = 7.5 and 10.0 Hz, H-11), 4.71 (br t-like, 1H, J = 6.0 Hz, H-8), and 5.38 (br s, 1H, H-6). The methyl triplet of the side chain was submerged in the methyl and methylene envelope.

Catalytic Hydrogenation of Microhelenin-B (VI)—The hydrogenation of VI was repeated under the described conditions. The product was identical to IX*b* according to TLC (three solvent systems), IR (tetrachloromethane), and PMR spectra (deuterochloroform).

Synthesis of Microhelenin-C (VIII) from Plenolin and Tigloyl Chloride—A solution of plenolin (120 mg) in dry benzene (2 ml) and dry pyridine (1 ml) was treated with tigloyl chloride (0.2 ml). The solution was heated under reflux for 3 hr. Evaporation to dryness under reduced pressure left a solid residue, which was suspended in 5% sodium bicarbonate, extracted with ether, and worked up in the usual manner. The product obtained from the ether extract was purified by silica gel (40 g, eluted with chloroform) column chromatography to give plenolin tiglate (54 mg) as a gum. This gum was identified as VIII by direct comparison with the material isolated previously from this plant; IR (tetrachloromethane): 1781 (α-methyl-γ-lactone), 1725, 1583 (cyclopentenone), 1725, 1651, 1262, and 1182 (tigloyl ester) cm^{-1}; PMR (60 MHz, deuterochloroform): δ 1.05 (s, 3H, 5-CH_3), 1.23 (d, 3H, J = 6.0 Hz, 10-CH_3), 1.51 (d, 3H, J = 6.0 Hz, 11-CH_3), 1.70 (br s, 3H, 2′-CH_3), 1.71 (br d, 3H, J = 6.5 Hz, 3′-CH_3), 4.75 (m, 1H, H-8), 5.47 (s-like, 1H, $W_{1/2}$ = 3.0 Hz, H-6), 6.04 (dd, 1H, J = 3.0 and 6.0 Hz, H-3), 6.65 (m, 1H, H-3′), and 7.70 (dd, 1H, J = 2.0 and 6.0 Hz, H-2).

Catalytic Hydrogenation of Plenolin Tiglate—A solution of the plenolin tiglate (45 mg) in ethanol (8 ml) was hydrogenated with 10% palladium-on-charcoal until hydrogen absorption ceased and then was treated as described. The product was purified by preparative TLC [benzene–chloroform–acetone (4:4:1), detection with iodine] to give an amorphous compound (30 mg) from acetone. The compound was identical with IX*b*, which was obtained previously by hydrogenation of VI and VIII. The IR spectra were superimposable, and the TLC behavior was identical; PMR (60 MHz, deuterochloroform): δ 0.83 (s, 3H, 5-CH_3), 1.05 (d, 3H, J = 6.75 Hz, 10-CH_3), and 1.46 (d, 1H, J = 6.75 Hz, H-10).

Microlenin Acetate (X)—The analytical data for X were: mp 289–291° dec., $[\alpha]_D^{20}$ +47.9° (*c*, 1.90 in methanol); IR (chloroform): no hydroxyl group, 1757 (γ-lactone), 1741, 1662 (α-methylene-γ-lactone), 1715, and 1580 (cyclopentenone) cm^{-1}; NMR (100 MHz, deuterochloroform): δ 0.94 (s, 3H, 5-CH_3), 1.18 and 1.23 (d, 3H each, J = 7.0 Hz, 10-CH_3 and 10′-CH_3), 1.97 (s, 3H, C-6 $OCOCH_3$), 2.48 (d, 1H, J = 8.0 Hz, H-7), 3.29 (m, 1H, H-7′), 4.71 (m, 1H, H-8′), 4.95 (m, 1H, H-8), 5.52 and 6.28 (d, 1H each, J = 3.0 Hz, H-13′), 5.62 (s, 1H, H-6), 6.06 (dd, 1H, J = 3.0 and 6.0 Hz, H-3), and 7.67 (dd, 1H, J = 2.0 and 6.0 Hz, H-2). The IR and NMR spectra of X were identical to those of microlenin acetate prepared from acetylation of microlenin (XI) with acetic anhydride in pyridine (5).

Plenolin (VII)—The analytical data for VII were: mp 222–224°; IR (chloroform): 3450 (hydroxyl), 1752 (γ-lactone), and 1690 (cyclopentenone) cm^{-1}; NMR (100 MHz, deuterochloroform): δ 0.96 (s, 3H, 5-CH_3), 1.21 (d, 3H, J = 7.0 Hz, 10-CH_3), 1.35 (d, 3H, J = 7.0 Hz, 11-CH_3), 4.40 (d, 1H, J = 4.0 Hz, H-6), 4.80 (m, 1H, H-8), 6.05 (dd, 1H, J = 3.0 and 6.0 Hz, H-3), and 7.70 (dd, 1H, J = 2.0 and 6.0 Hz, H-2); mass spectrum: *m/e* 264 (M^+).

Catalytic Hydrogenation of Helenalin (XII)—A solution of XII (60 mg) in ethyl acetate (25 ml) was hydrogenated with hydrogen at room temperature and atmospheric pressure in the presence of 5% palladium-on-carbon (25 mg). After the reaction mixture was filtered and the solvent was removed *in vacuo*, the residue was purified by column chromatography [silica gel, chloroform–ethyl acetate (9:1)] and preparative TLC [chloroform–ethyl acetate (1:1)] to give rise to the dihydro (23 mg, mp 222–224°) and the tetrahydro (XIII, 25 mg, mp 175–176°) derivatives.

The IR and NMR spectra of the dihydro derivative were identical to those of plenolin (VII) (7). The spectral data of the tetrahydro derivative were in accord with the structure of 2,3,11,13-tetrahydrohelenalin (XIII) (8, 17); mass spectrum: *m/e* 266 (M^+); IR (chloroform): 3580 (hydroxyl), 1750 (γ-lactone), and 1720 (cyclopentenone) cm^{-1}; NMR (deuterochloroform): δ 0.80 (s, 3H, 5-CH_3), 1.04 (d, 3H, J = 7.0 Hz, 10-CH_3), 1.36 (d, 3H, J = 7.0 Hz, 11-CH_3), 4.30 (br s, 1H, H-6), 4.75 (t-like, 1H, J = 6.0 Hz, H-8), and 2.95 (m, 2H, H-3).

REFERENCES

(1) R. Adams and W. Herz, *J. Am. Chem. Soc.*, **71**, 2546 (1949).

(2) K. H. Lee, Y. Imakura, and D. Sims, *J. Pharm. Sci.*, **65**, 1410 (1976).

(3) K. H. Lee, Y. Imakura, D. Sims, A. T. McPhail, and K. D. Onan, *Phytochemistry*, **16**, 393 (1977).

(4) K. H. Lee, Y. Imakura, D. Sims, A. T. McPhail, and K. D. Onan, *J. Chem. Soc. Chem. Commun.*, **1976**, 341.

(5) Y. Imakura, K. H. Lee, D. Sims, and I. H. Hall, *J. Pharm. Sci.*, **67**, 1228 (1978).

(6) R. I. Geran, N. H. Greenberg, M. M. MacDonald, A. M. Schumacher, and B. J. Abbott, *Cancer Chemother. Rep. (Part 3)*, **3**, 1 (1972).

(7) K. H. Lee, T. Ibuka, A. T. McPhail, K. D. Onan, T. A. Geissman, and T. G. Waddell, *Tetrahedron Lett.*, **1974**, 1149.

(8) K. H. Lee, H. Furukawa, and E. S. Huang, *J. Med. Chem.*, **15**, 609 (1972).

(9) T. G. Waddell, W. Stöcklin, and T. A. Geissman, *Tetrahedron Lett.*, **1969**, 1313.

(10) W. Stöcklin, T. G. Waddell, and T. A. Geissman, *Tetrahedron*, **26**, 2397 (1970).

(11) Z. Samek, *Tetrahedron Lett.*, **1970**, 671.

(12) E. Rodriguez, H. Yoshioka, and T. J. Mabry, *Phytochemistry*, **10**, 1145 (1971).

(13) A. Samek, M. Holub, V. J. Novikov, J. N. Forostjan, and D. P. Dopa, *Coll. Czech. Chem. Commun.*, **35**, 3818 (1970).

(14) W. Herz, C. M. Gast, and P. S. Subramaniam, *J. Org. Chem.*, **33**, 2780 (1968).

(15) L. M. Jackmann and R. H. Wiley, *J. Chem. Soc.*, **1960**, 2886.

(16) K. H. Lee and T. A. Geissman, *Phytochemistry*, **9**, 403 (1970).

(17) E. P. Clark, *J. Am. Chem. Soc.*, **58**, 1982 (1936).

ACKNOWLEDGMENTS

Presented in part at the APhA Academy of Pharmaceutical Sciences, New Orleans meeting, April 1976.

Supported by National Cancer Institute Grant CA-17625 and American Cancer Society Grant CH-19 to K. H. Lee.

The authors thank Dr. David L. Harris, Department of Chemistry, University of North Carolina at Chapel Hill, for NMR spectra and Dr. David Rosenthal and Mr. Fred Williams, Research Triangle Center for Mass Spectrometry, for the mass spectral data. The XL-100 NMR spectrometer was purchased with grants from the National Science Foundation and the National Institutes of Health to the Chemistry Department, University of North Carolina at Chapel Hill.

Antitumor Agents XXXVIII: Isolation and Structural Elucidation of Novel Germacranolides and Triterpenes from *Elephantopus mollis*

KUO-HSIUNG LEE *x, TOSHIRO IBUKA *, HIROSHI FURUKAWA *, MUTSUO KOZUKA *, RONG-YANG WU *, IRIS H. HALL *, and HUAN-CHANG HUANG ‡

Received April 4, 1979, from the **Department of Medicinal Chemistry, School of Pharmacy, University of North Carolina at Chapel Hill, Chapel Hill, NC 27514,* and the ‡*School of Pharmacy, Kaohsiung Medical College, Kaohsiung, Taiwan, Republic of China.* Accepted for publication July 27, 1979.

Abstract □ The ethanolic extract of *Elephantopus mollis* yielded three novel cytotoxic antitumor germacranolides, molephantin, molephantinin, and phantomolin. The extract also yielded three inactive known triterpenes, β-amyrin acetate, lupeol acetate, and epifriedelanol, as well as stigmasterol. The structure and stereochemistry of the cytotoxic antitumor agents molephantin, molephantinin, and phantomolin were determined on the basis of chemical transformations and spectral evidence. Preliminary *in vivo* tumor assays indicated that molephantinin and phantomolin were potent inhibitors of Ehrlich ascites carcinoma and Walker 256 carcinosarcoma. Molephantinin also showed significant antileukemic activity in the P-388 lymphocytic leukemia screen.

Keyphrases □ *Elephantopus mollis*—isolation and structural determination of molephantin, molephantinin, and phantomolin □ Antineoplastic agents, potential—molephantin, molephantinin, and phantomolin, isolation from *Elephantopus mollis*, structural determination □ Molephantin—isolation from *Elephantopus mollis* and structural determination □ Molephantinin—isolation from *Elephantopus mollis* and structural determination □ Phantomolin—isolation from *Elephantopus mollis* and structural determination

During a continuing search of Formosan plants for agents with potential antitumor activity (1), the alcoholic extract of *Elephantopus mollis*[1] (Compositae) showed significant reproducible inhibitory activity in both *in vitro* (KB cell culture) and *in vivo* (Walker 256 carcinosarcoma) screens[2]. Preliminary reports described the structural determination of three novel cytotoxic antitumor germacranolides, molephantin (I) (4), molephantinin (II) (5), and phantomolin (III) (6). The present report fully describes the isolation and structural elucidation of these novel antitumor sesquiterpene lactones as well as the companion triterpenes β-amyrin acetate (IV), lupeol acetate (V), epifriedelanol (VI), and stigmasterol (VII).

RESULTS AND DISCUSSION

The active alcoholic extract of the whole plant (winter growth) was concentrated and partitioned between water and chloroform. Guided by the assay in KB cells (Scheme I and Table I), the active principles were concentrated in the chloroform extract (Fraction C). Partitioning of this extract between 33% aqueous methanol and hexane concentrated the activity in the aqueous methanolic layer (Fraction D). The aqueous methanolic layer was concentrated and extracted further with chloroform. Chromatography of the active chloroform extract (Fraction G) over silica gel isolated the active principles, molephantin (I), molephantinin (II), and phantomolin (III). Compounds I and III were isolated at 0.025 and 0.023%, respectively, as the major components in this winter collection. In a spring collection of the same plant, I was isolated at ~0.020% as the major cytotoxic principle.

Compound I, mp 212–213°, $C_{19}H_{22}O_6$ (mass spectrum and elemental analysis), contained an α-methylene-γ-lactone, as evidenced by the characteristic NMR signals (Table II) for the methylene protons [δ 6.36 (d, J = 2.5, H_a-13) and 5.83 (d, J = 2.0, H_b-13)] and the IR bands [1773 (γ-lactone) and 1650 (C=C) cm^{-1}]. The UV spectrum of I showed, in addition to the α-methylene-γ-lactone at 210 nm (ε 30,960), a dienone system at 242 nm (ε 18,210, shoulder). The presence of an α,β-unsaturated ester group in I was indicated by IR absorption at 1713 and 1650 (C=C) cm^{-1} and was supported by the base peak at *m/e* 69 [CH_2=$C(CH_3)CO^+$] in the mass spectrum. The NMR spectrum of I suggested a methacrylate pattern for the acid portion of the ester since it showed two multiplets at δ 6.15 and 5.68 (2H, H-19) and one vinyl methyl multiplet at δ 1.96 (H-18)[3], which are typical signals for the methacrylate group (8, 9). Thus, I is an α-methylene-γ-lactone sesqui-

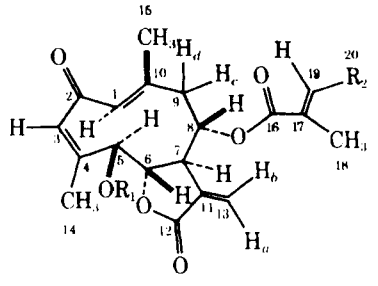

I: R_1 = R_2 = H
Ia: R_1 = $COCH_3$, R_2 = H

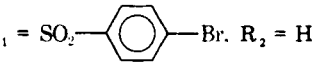

Ie: R_1 = SO_2—(p-Br-C$_6$H$_4$)—, R_2 = H

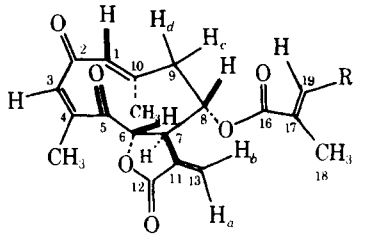

Ib: R = H
IIb: R = CH_3

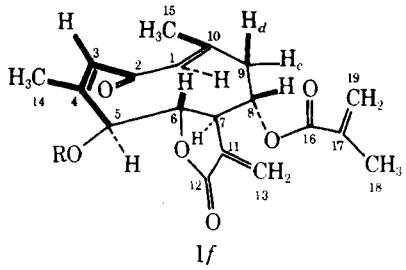

If

[1] *E. mollis* is known as "Péh-Teng-Khiā-U" in Formosan folklore as an herbal remedy for human rheumatism as well as an antipyretic and anti-inflammatory agent (2).

[2] *In vitro* and *in vivo* assays were performed according to literature procedures (3).

[3] The assignment of δ 1.96 to H-18 was confirmed by the double-resonance experiment carried out on molephantin acetate (Ia).

0022-3549/80/0900-1050$01.00/0
© 1980, American Pharmaceutical Association

Table I—*In Vitro* Cytotoxicity and *In Vivo* Antitumor Activity of Fractions and Constituents from *E. mollis*

Fraction Constituent	ED_{50} (KB)[a], μg/ml	*In Vivo* Antitumor Activity ($n = 6$)[b]			
		Ehrlich Ascites Carcinoma, % inhibition (33.3 mg/kg)	Walker 256 Carcinosarcoma, T/C (2.5 mg/kg)	Lewis Lung, T/C (25 mg/kg)	P-388 Lymphocytic Leukemia, T/C (25 mg/kg)
A	5.35	—	—	—	—
B	>20	—	—	—	—
C	<20	—	—	—	—
D	<11.50	—	—	—	—
E	>15	—	—	—	—
F	12.50	—	—	—	—
G	3.60	—	—	—	—
I	1.05	75	149	80	118
II	0.90	88	397	123	146
III	4.03	87	378	123	113
Fluorouracil	—	—	—	—	186
Melphalan	—	96	317	—	168
Cyclophosphamide	—	—	—	140	—
0.05% Polysorbate 80	—	0	100	100	100

[a] KB refers to human carcinoma of the nasopharynx. Cytotoxicity was assayed according to a literature method (3). A compound is active if the average ED_{50} is ≤4 μg/ml for the pure compound. [b] n = number of animals per group. These *in vivo* data were reported previously (7).

terpene lactone that possesses an additional dienone system and a methacrylate ester.

Compound I also possesses a secondary hydroxyl group. It showed an IR absorption band at 3420 cm^{-1} and a M − 18 (water) peak at *m/e* 328.1305[4] in the mass spectrum. The C*H*OH proton (*i.e.*, H-5) was seen as a one-proton singlet at δ 5.46 and was displaced to δ 6.57 in the NMR spectrum of molephantin acetate [I*a*, mp 169°, *m/e* 388.1522 (M^+) for $C_{21}H_{24}O_7$], obtained by acetylation of I with acetic anhydride in pyridine. Since the lactonic proton at C-6 was seen as a doublet (J = 3.5 Hz each) at δ 4.26 in I and 4.35 in I*a*, it indicated that there was almost no coupling between H-5 and H-6 (*i.e.*, the dihedral angle between H-5 and H-6 is ~90°) and that C-4 should be tetrasubstituted, *i.e.*, a vinyl methyl or a carbonyl group was attached at C-4 in I or I*a*.

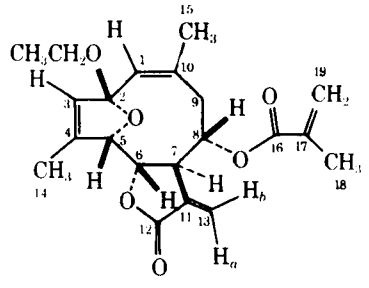

III

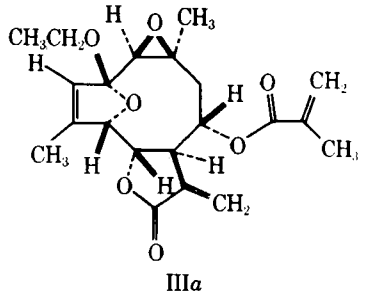

III*a*

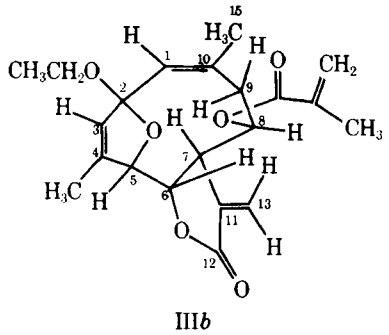

III*b*

The assignment of protons at C-7, C-8, C-9, and C-1, as well as the three vinyl methyl groups at C-17, C-10, and C-4, was made possible by spin-decoupling experiments of I*a*. Thus, irradiation at the frequency of H-7 (multiplet) at δ 3.42 collapsed the two doublets of H_a-13 and H_b-13 at δ 6.35 and 5.79 to two singlets, the doublet of H-6 ($J_{5,6}$ = 0 and $J_{6,7}$ = 3.5 Hz) at δ 4.35 to a singlet, and the doublet of triplets of H-8 ($J_{7,8}$ = 10.5 Hz, $J_{8,d}$ = 4.0 Hz, and $J_{8,c}$ = 0) to a pair of doublets ($J_{8,d}$ = 4.0 Hz and $J_{c,d}$ = 11.0 Hz). Conversely, irradiation of H-8 sharpened the multiplet of H-7 as well as converted the doublet ($J_{c,d}$ = 11.0 Hz) of H_c-9 at 2.58 and the doublet of doublets ($J_{c,d}$ = 11.0 Hz and $J_{8,d}$ = 4.0 Hz) of H_d-9 at 2.79 to a pair of doublets ($J_{c,d}$ = 11.0 Hz), thereby suggesting a tetrasubstitution at C-10.

Since most sesquiterpene lactones, especially the germacranolides, contain methyl groups at C-4 and C-10, the two vinyl methyl groups at δ 1.98 (d, J = 1.5 Hz) and 1.80 (d, J < 1.0 Hz) were assigned to these C-4 and C-10 positions, respectively. Consequently, the last oxygen function was placed at C-2, the last position available, as the dienone carbonyl group. This assignment was confirmed by the fact that H-1 and H-3 appeared as a low-field singlet and multiplet at δ 6.37 and 6.05, respectively. Irradiation of the C-4 methyl group at δ 1.98 collapsed the H-3 multiplet to a singlet. Irradiation of the C-17 methyl group at δ 1.94 changed the two one-proton multiplets of H-19 at δ 6.14 and 5.67 to two doublets (J = 1.8 Hz each), confirming the presence of the methylacrylate ester side chain. The remaining narrowly split three-proton doublet at δ 1.79 then was assigned to the vinyl methyl group at C-10.

The foregoing evidence led to the formulation of Structure I for molephantin, exclusive of the complete stereochemistry. A consideration of the relationship between the J value and the dihedral angle (10) with the aid of a Dreiding model established the stereochemical relationships among protons at C-5, C-6, C-7, C-8, and C-9, as shown in I*f*. These assignments were based on the assumption of a β-oriented H-6, followed by the dihedral angles shown between H-5 and H-6, H-6 and H-7, H-7 and H-8, and H-8 and H-9 deduced from their corresponding J values, *i.e.*, $\phi_{5,6} \simeq 90°$ ($J_{5,6}$ = 0), $\phi_{6,7} \simeq 120°$ ($J_{6,7}$ = 3.5 Hz), $\phi_{7,8} \simeq 140°$ ($J_{7,8}$ = 10.5 Hz), $\phi_{8,d} \simeq 50°$ ($J_{8,d}$ = 4.0 Hz), and $\phi_{8,c} \simeq 90°$ ($J_{8,c}$ = 0).

The establishment of these relationships was possible only when the C-10 methyl group was forced to lie close above the π-electron cloud of the C-3–C-4 double bond. This arrangement was supported by the NMR spectra of I and I*a*, in which the C-10 methyl group (δ 1.79 in I and 1.80 in I*a*) was shifted upfield by 0.23 to 0.18 ppm by the C-3–C-4 double bond compared to the C-4 methyl group (δ 2.02 in I and 1.98 in I*a*). A similar upfield shift of H-6 in I and I*a* (δ 4.26 in I and 4.35 in I*a*) further confirmed that H-6 was located close above the C-1–C-10 double bond. When C_5-OH was oxidized to the corresponding ketone [*i.e.*, dehydromolephantin (I*b*), $C_{19}H_{20}O_6$, mp 132–133°, λ_{max} 211 nm (ε 29,070)] by Jones

[4] The calculated *m/e* value for $C_{19}H_{20}O_5$ was 328.1311, which further confirmed the composition of $C_{19}H_{22}O_6$ for I.

Table II—NMR Spectra of I–III and Derivatives[a]

Compound	H-1	H-3	H-5	H-6	H-7	H-8	H_c-9	H_d-9	H_a-13	H_b-13	H-14	H-15	H-18	H-19	H-20	Miscellaneous
I	6.22 (s)	6.01 (br s)	5.46 (br s)	4.26 (d, 3.5)	3.40 (m)	5.26 (dt, 4.0 and 10.5)	2.56 (d, 11.0)	2.78 (dd, 11.0 and 4.0)	6.36 (d, 2.5)	5.83 (d, 2.0)	2.02 (d, 1.5)	1.79 (s)	1.96 (m)	6.15 (m), 5.68 (m)	—	—
I*a*	6.37 (s)	6.05 (m)	6.57 (s)	4.35 (d, 3.5)	3.42 (m)	5.21 (dt, 4.0 and 10.5)	2.58 (d, 11.0)	2.79 (dd, 11.0 and 4.0)	6.35 (d, 2.5)	5.79 (m)	1.98 (d, 1.5)	1.80 (d, <1.0)	1.94 (m)	6.14 (m), 5.67 (m)	1.83 (m)	2.07 (s, OCO-CH_3)
I*b*[b]	5.98 (m)	5.89 (m)[c]	—	4.73 (d, 5.0)	3.97 (m)	5.23 (dt, 4.0 and 10.5)	2.43 (d, 11.0)	2.73 (dd, 11.0 and 4.0)	6.35 (d, 2.5)	5.89 (d, 2.0)	2.21 (d, 2.0)	1.92 (br s)	2.00 (m)	6.15 (m), 5.67 (m)	—	—
I*c*	2.90 (s)	6.09 (m)	—	4.25 (d, 9.0)	4.08 (m)	5.25 (m)	—	—	6.32 (d, 3.0)	5.78 (d, 3.0)	2.31 (d, 2.0)	1.40 (s)	1.98 (m)	6.22 (m), 5.74 (m)[c]	—	3.90 (m, OH)[d], 3.25 (br s, OH)[d]
I*d*	3.46 (s)	6.09 (m)	—	4.23 (d, 9.0)	3.80 (m)	5.10 (m)[c]	—	—	6.28 (d, 3.0)	5.72 (d, 3.0)	2.31 (d, 2.0)	5.21 (m)	1.99 (m)	6.22 (m), 5.71 (m)[c]	—	3.37 (m, OH)[d]
I*e*	6.35 (m)[c]	6.03 (m)	6.49 (s)	4.30 (d, 3.5)	3.35 (m)	6.27 (dt, 4.0 and 10.5)	—	—	6.37 (d, 2.5)	5.85 (d, 2.0)	1.86 (d, 1.5)	1.80 (s)	1.98 (m)	—	—	7.77 (m, 4H, aromatic)
II	6.21 (s)	6.00 (m)	5.46 (br s)	4.25 (d, 3.5)	3.38 (m)	5.24 (dt, 4.0 and 10.5)	2.54 (d, 11.0)	2.76 (dd, 11.0 and 4.0)	6.35 (d, 2.5)	5.82 (d, 2.0)	2.02 (d, 1.5)	1.80 (s)	1.83 (m)	6.92 (br m)	1.83 (m)	—
II*a*	6.36 (s)	6.04 (m)	6.57 (s)	4.34 (d, 3.5)	3.40 (m)	5.21 (dt, 4.0 and 10.5)	2.56 (d, 11.0)	2.76 (dd, 11.0 and 4.0)	6.34 (d, 2.5)	5.77 (m)	1.98 (d, 1.5)	1.80 (d, <1.0)	1.83 (m)	6.92 (br m)	1.83 (m)	2.07 (s, OCO-CH_3)
II*b*	5.94 (m)[c]	6.04 (m)	—	4.77 (d, 5.0)	3.95 (m)	5.32 (dt, 4.0 and 10.5)	2.39 (d, 11.0)	2.72 (dd, 11.0 and 4.0)	6.41 (d, 2.5)	6.04 (d, 2.0)	2.21 (d, 2.0)	1.91 (br s)	1.87 (m)	6.96 (br m)	1.87 (m)	—
III	5.51 (br s)	5.67 (m)	5.23 (4.0)[c]	4.65 (dd, 4.0 and 6.0)	3.14 (m)	5.24 (m)[c]	—	—	6.33 (d, 3.0)	5.80 (d, 3.0)	1.73 (m)	1.79 (d, 1.5)	1.99 (m)	6.17 (m), 5.72 (m)	3.48 (q, 7.0)	1.20 (t, 7.0, H-21)
III*a*[b]	3.05 (s)	5.82 (m)[c]	5.32 (4.0)[c]	4.52 (dd, 4.0 and 6.0)	3.19 (m)[c]	5.23 (m)[c]	—	—	6.45 (d, 3.0)	5.95 (d, 3.0)	1.80 (d, 1.5)	1.41 (s)	2.04 (d, 1.5)	6.24 (m), 5.82 (m)[c]	3.53 (q, 7.0)	1.25 (t, 7.0, H-21)

[a] Run in deuterochloroform at 100 MHz. Values are in parts per million. Multiplicities are indicated by the usual symbols: s, singlet; d, doublet; t, triplet; q, quartet; m, multiplet whose center is given; and br, slightly broadened singlet. Figures in parentheses are coupling constants in Hertz. [b] Run in deuterochloroform at 60 MHz. [c] Overlapped signals. [d] Signals disappeared upon addition of deuterium oxide.

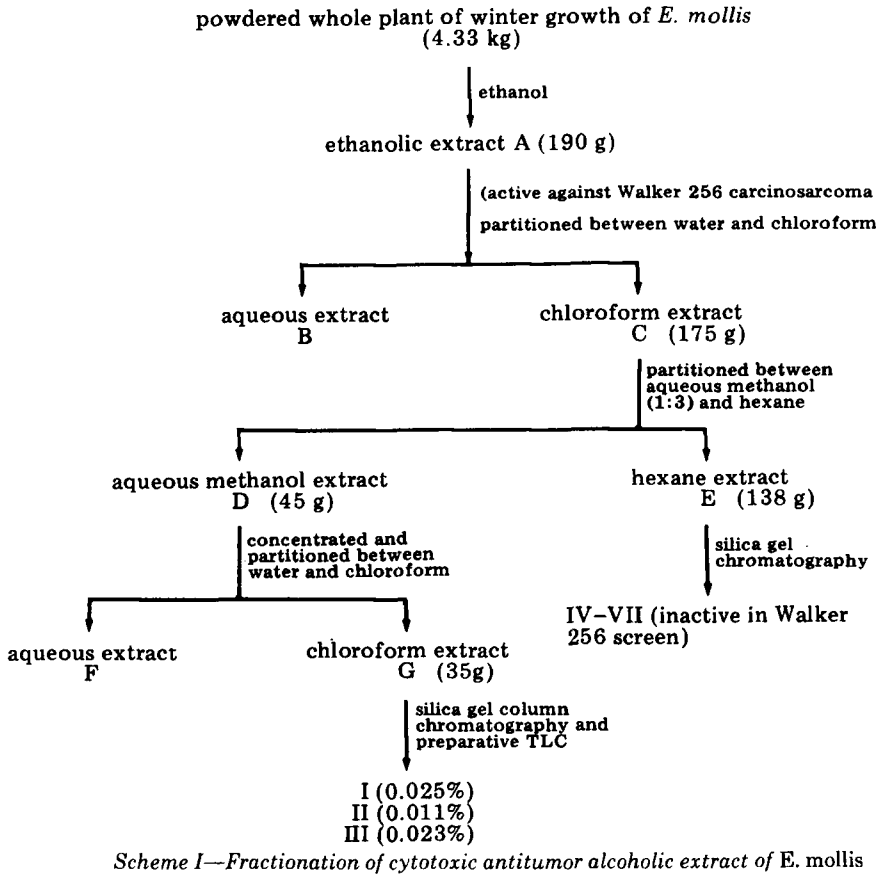

Scheme I—Fractionation of cytotoxic antitumor alcoholic extract of E. mollis

reagent, H-6 (δ 4.73 in I*b*) was shifted downfield by 0.38 to 0.47 ppm compared to the ones found in I and I*a*. This shift, coupled with the significant downfield shift of the C-10 methyl group (δ 1.92) in I*b*, suggested that a conformational change had occurred in I*b*.

An examination of the conformation of the 10-membered ring of I*b* based on the dihedral angles derived from the *J* values of H-6 to H-9 in I*b* (Table II) as illustrated in A–C led to the conclusion that Ig was the preferred conformation of dehydromolephantin, in which the C-10 methyl group was in an α-axial configuration and now was deshielded by the C-3–C-4 double bond. The H-1 (δ 5.98) was in a β-axial position and was shielded by the β-oriented C-5 carbonyl group by 0.24–0.39 ppm compared to those found in I (δ 6.22) and I*a* (δ 6.37). The C-1–C-10 double bond was in proximity to the β-oriented C-5 carbonyl group, and this arrangement gave rise to the intramolecular cyclization products when I*b* was treated with sulfuric acid in acetone. These products, which were formed *via* a mechanism shown in Scheme II, were characterized as two guaianolides, Ic and I*d*.

Compound Ic, $C_{19}H_{22}O_7$, mp 168–170°, showed IR (mineral oil) bands at 1750, 1640 (α-methylene-γ-lactone), and 1715 and 1700 (two α,β-unsaturated carbonyl groups) cm^{-1}. The presence of two hydroxyl groups was revealed by IR bands at 3440 and 3320 cm^{-1}, the disappearance of two signals at δ 3.90 (1H) and 2.90 (s, 1H) in the NMR spectrum on the addition of deuterated water, and by an ion of *m/e* 344.1265[5] (M − 18) in the mass spectrum. The NMR spectrum of Ic disclosed the presence of three methyl groups. The three-proton doublet (J = 2.0 Hz) at δ 2.31 was assigned to the cyclopentenone β-methyl group at C-4. The multiplet at δ 1.98 was attributable to the methacrylate methyl group at C-17 as seen in I, I*a*, and I*b*. The methyl singlet in the higher field at δ 1.40 was assigned to the methyl group attached to the carbon bearing a hydroxyl group at C-10. The lactonic proton at C-6 appeared as a doublet with a larger coupling constant compared to that found in I, I*a*, and I*b* and indicated the presence of a second hydroxyl group at C-5 in a guaianolide structure. Assignment of other protons (Table II) was achieved by extensive decoupling experiments. For example, the multiplets at δ 6.22 and 5.74 were assigned to the protons at C-19 since, upon irradiation of the C-17 methyl group at δ 1.98, both changed to two doublets (J = 1.5 Hz each). Irradiation of the C-4 methyl group at δ 2.31 collapsed the multiplet of H-3 at δ 6.09 to a singlet.

[5] The calculated *m/e* value for $C_{19}H_{20}O_6$ was 344.1260.

Compound I*d*, mp 188–189°, had a composition of $C_{19}H_{20}O_6$ and showed IR (chloroform) bands at 3400, 1770, 1713 (double strength), 1650, and 1625 cm^{-1}. The NMR spectrum of I*d* indicated the absence of the C-10 methyl group as seen in Ic and the presence of one additional terminal methylene group at C-10 at δ 5.21 compared to Ic, suggesting that I*d* was the dehydrated form of Ic. Further assignment of protons (Table II) that supported I*d* as the structure for this product also was achieved by extensive NMR decoupling experiments.

The assignment of a β-hydroxyl and an α-methyl group at C-10 in Ic as well as the β-oriented proton at C-1 and the β-oriented hydroxyl group at C-5 in both Ic and I*d* was based on the mechanism involved in the intramolecular cyclization of I*b* to Ic and I*d*, in which the hydroxyl ion could only make a nucleophilic attack at C-10 of a *trans*-C-1–C-10 double bond from the sterically less hindered β-side since the C-5 carbonyl group was β-oriented. Thus, it gave rise to a β-hydrogen and a β-hydroxyl group at C-1 and C-5, respectively.

This evidence led to the establishment of I*b* for dehydromolephantin, I*a* for molephantin acetate, and I for molephantin. Further unequivocal proof of the structure, stereochemistry, and absolute configuration of I

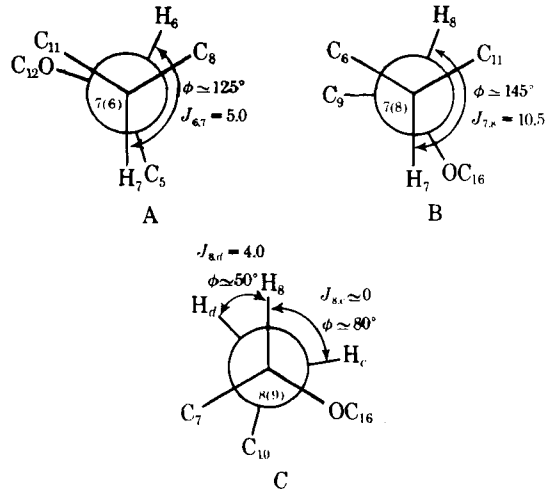

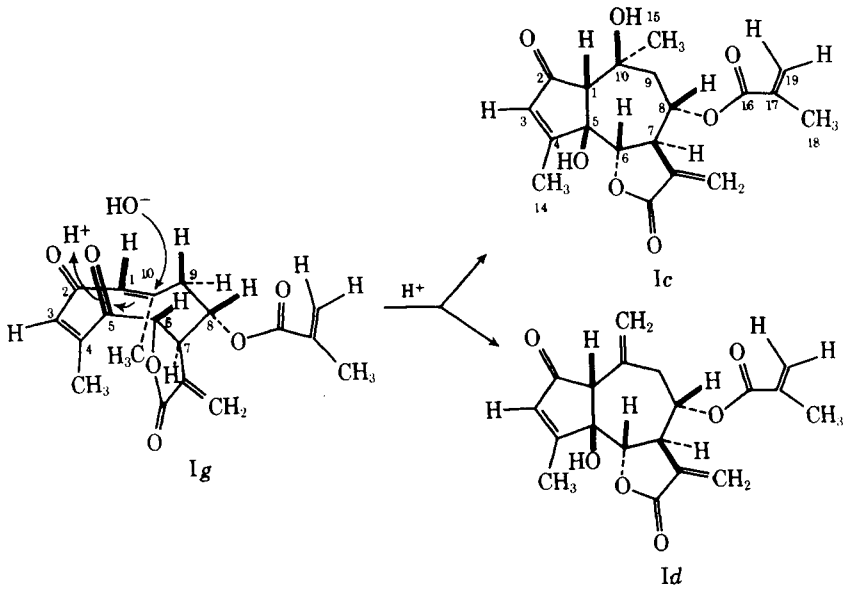

Scheme II

for molephantin was achieved by a single-crystal X-ray analysis of molephantin *p*-bromobenzenesulfonate (Ie, $C_{25}H_{25}BrO_8S$, mp 165–167°) (4).

Molephantinin (II), mp 223–225°, had a composition of $C_{20}H_{24}O_6$ and showed IR, NMR, and mass spectra similar to those of molephantin (I), except for the difference in the acid portion of the ester side chain. The ester moiety in II was identified as a tigloyl group instead of a methacrylate as in I. This assignment was based on the characteristic NMR signals shown in II for the tigloyl group as the broad vinyl multiplets at δ 6.92 (1H, H-19) and the vinyl methyl multiplets at δ 1.83 (6H, H-18 and H-20) (11, 12), as well as a base peak in the mass spectrum at *m/e* 83 due to the cleavage of a tiglic acid ester (13).

Molephantinin yielded an acetate [IIa, mp 131°, $C_{22}H_{26}O_7$ (*m/e* 402.1670, M^+)] upon acetylation with acetic anhydride in pyridine and a dehydro derivative (IIb, mp 136°, $C_{20}H_{22}O_6$) upon oxidation with Jones reagent. The IR, NMR (Table II), and mass spectral data, especially the data obtained from the extensive NMR decoupling experiments[6], of molephantinin, molephantinin acetate, and dehydromolephantinin were in accordance with the assigned structures of II, IIa, and IIb, respectively. The circular dichroism curve of II showed a strong positive Cotton effect at 244 nm, indicating that molephantinin possessed the same stereochemistry and absolute configuration as molephantin. Accordingly, molephantinin acetate and dehydromolephantinin carried exactly the same stereochemistries as those of molephantin acetate (Ia) and dehydromolephantin (Ib), as depicted in IIa and IIb.

Phantomolin (III) was isolated as a colorless oil and had a composition of $C_{21}H_{26}O_6$ on the basis of high-resolution mass spectrometry (M^+ at *m/e* 374.1880). It was an α-methylene-γ-lactone compound [IR (chloroform) bands at 1770 and 1664 cm^{-1}] and contained a methacrylate ester (1719 and 1640 cm^{-1}) side chain. The NMR spectrum (Table II) confirmed these assignments, showing the α-methylene group of the γ-lactone at δ 6.33 (d, J = 3.0 Hz) and 5.80 (d, J = 3.0 Hz) and the methacryl methyl group at C-17 as a multiplet at δ 1.99 and the two protons at C-19 as multiplets at δ 6.17 and 5.72. The assignment of the one-proton signals at δ 5.25 ($J_{5,6}$ = 4.0 Hz) for H-5, 4.65 (dd, $J_{5,6}$ = 4.0 and $J_{6,7}$ = 6.0 Hz) for H-6, 3.14 (m) for H-7, and 5.24 (m) for H-8 was based on decoupling experiments. Thus, irradiation at the frequency of H-7 at δ 3.14 collapsed two doublets for H-13 to two singlets, changed the doublet of doublets at δ 4.65 to a doublet with J = 4.0 Hz, and sharpened the multiplet at δ 5.24 for H-8. Conversely, irradiation at H-6 sharpened the H-7 and H-8 multiplets.

Irradiation at δ 5.25 (H-5) converted H-6 to a doublet with $J_{6,7}$ = 6.0 Hz. The one-proton broad singlet at δ 5.51 was assigned to H-1 since, upon irradiation of the C-10 methyl group (δ 1.79, d, J = 1.5 Hz), it gave rise to a sharp singlet. The remaining low-field one-proton multiplet at δ 5.67 then was assigned to H-3, which coupled with the C-4 methyl group (δ 1.73, m). The characteristic two-proton quartet (J = 7.0 Hz) at δ 3.48 and the three-proton triplet (J = 7.0 Hz) at δ 1.20 were assigned to an *O*-ethyl group[7]. The location of this group at C-2 rather than C-9 was suggested by the fact that no known germacranolide contained oxygenation at C-9. This assignment also was substantiated by a one-proton multiplet at δ 5.24 for H-8, indicating two protons at C-9. Thus, the last oxygen was placed between C-2 and C-5 as an ether linkage, as shown in III.

Consideration of the cooccurrence of phantomolin (III), molephantin (I), and molephantinin (II) suggested the similar *trans*-axial arrangement among protons at C-6, C-7, and C-8. If the configuration of H-6 was β-oriented, as was likely, then H-7 was α and H-8 was β. The coupling constants of $J_{6,7}$ = 6.0 Hz and $J_{5,6}$ = 4.0 Hz were suggestive of the approximate dihedral angles of 38 and 128° for H-6 and H-7 and 51 and 122° for H-5 and H-6. A Dreiding model indicated the feasibility of only one conformation, *i.e.*, with H-5 as β-oriented, CH_3CH_2O as β-oriented and a C-10 vinyl methyl group *cis* to H-1, as shown in IIIb in which the dihedral angles were ~128° for H-6 and H-7 and ~50° for H-5 and H-6.

Further proof of the structure and relative stereochemistry of III was achieved by an X-ray analysis (6) of a *cis*-1,10-epoxide of phantomolin (IIIa), prepared from epoxidation of III with *m*-chloroperbenzoic acid in chloroform.

Fractionation of the inactive hexane extract (Scheme I) led to the isolation of four colorless crystalline substances, IV (mp 239–241°, $C_{32}H_{52}O_2$), V (mp 218°, $C_{32}H_{52}O_2$), VI (mp 285°, $C_{30}H_{50}O$), and VII (mp 170°, $C_{29}H_{48}O_2$), which were identified as triterpenes β-amyrin acetate, lupeol acetate, epifriedelanol, and stigmasterol, respectively (15, 16).

The *in vitro* cytotoxic molephantin, molephantinin, and phantomolin were tested for *in vivo* antitumor activity against four tumor lines (7). As shown in Table I, molephantinin and phantomolin were potent inhibitors of Walker 256 ascites carcinosarcoma in Sprague–Dawley rats at 2.5 mg/kg/day and of Ehrlich ascites tumor in CF_1 male mice at 33.3 mg/kg/day. Molephantinin also showed significant (T/C ≥ 125%) antileukemic activity in the P-388 lymphocytic leukemia screen at T/C = 146% (DBA/2 mice at 25 mg/kg/day). Further studies on the structure–activity relationships and mechanism of action among compounds related to molephantinin and phantomolin are in progress (17).

EXPERIMENTAL[8]

Isolation of Molephantin (I), Molephantinin (II), and Phanto-

[6] Data on NMR decoupling experiments of molephantinin acetate were reported previously (5).

[7] The presence of an ethyl ether is novel and appears to represent the first example in naturally occurring germacranolides and the second instance of the sesquiterpene lactone lactal hymenolide (14).

[8] Unless otherwise specified, melting points were determined on a Thomas-Hoover melting-point apparatus and are uncorrected. Specific rotations were taken on a Perkin-Elmer model 141 polarimeter (1 = 1 dm). IR spectra were recorded with a Perkin-Elmer 257 grating IR spectrometer in chloroform. NMR spectra were determined in deuterochloroform with a Varian XL-100 NMR spectrometer (tetramethylsilane as the internal standard). Mass spectra were determined on an A.E.I. MS-902 instrument at 70 ev using a direct-inlet system. Circular dichroism was measured on a Cary model 60 spectrometer. Silica gel was used for column chromatography (Mallinckrodt CC-7, 200–325 mesh), TLC (Merck silica gel G), and preparative TLC (Merck silica gel GF 254, 2000 μm). Elemental analyses were performed by Atlantic Microlab, Atlanta, Ga.

molin (III) from *E. mollis*—The *E. mollis* (Compositae) used was from a collection made in January 1973 in Chia-Sen, Kaohsiung, Taiwan[9]. The ground, air-dried, whole plant material (4.33 kg) was extracted exhaustively with ethanol. Guided by the bioassay in KB cells (Scheme I and Table I), the final active chloroform extract (35 g, Fraction G) was chromatographed on silica gel[10] (100 mesh, 7 × 32-cm column) with chloroform, chloroform–acetone (1:1), and acetone as the eluting solvents. Fractions of 1 liter each were collected and examined by TLC.

Fractions 1–4 gave traces of residue upon solvent evaporation. Fractions 5–10 yielded 1.44 g of colorless needles, which later proved to be a 1:1 mixture of I and II after a careful NMR analysis, although they showed only a single spot with different solvent systems. Rechromatography of the mother liquor (9 g) after the isolation of the mixture on a silica gel column (3 × 50 cm) in chloroform (1.5 liters) afforded 270 mg of the same mixture as crystalline solids. A final separation of this mixture was achieved by column chromatography on silica gel (4 × 60-cm column) and elution with chloroform to yield 550 mg (0.011%) of pure II from the first 450 ml of the chloroform eluate and 1.26 g (0.025%) of pure I from the second 600 ml of the chloroform eluate. The mother liquors (5 g), after the isolation of pure I and II, were combined and rechromatographed on silica gel (70–230 mesh, 4 × 70-cm column). The chloroform eluates, which showed a new spot different from I and II on TLC, were combined and chromatographed again on silica gel (70–230 mesh, 2.6 × 60-cm column). Evaporation of the solvent resulting from elution with benzene–chloroform (3:2) yielded pure III (1.035 g, 0.023%).

Isolation of I–III from spring growth of the same plant (collected on March 19, 1972 at the same site) using the described procedure gave rise to different yields, *i.e.*, 0.0199% of I, 0.0086% of II, and 0.015% of III.

Molephantin (*I*)—Molephantin was recrystallized from chloroform–ethyl acetate, mp 212–213°; mass spectrum: *m/e* 346 (M^+), 328.1305 (M − 18) ($C_{19}H_{20}O_5$ requires 328.1311), and 69 [base peak, $CH_2{=}C(CH_3)CO^+$]. Table II shows the NMR data.

Anal.—Calc. for $C_{19}H_{22}O_6$: C, 65.88; H, 6.40. Found: C, 66.48; H, 6.67.

Molephantin Acetate (*Ia*)—Molephantin (10 mg) was acetylated with acetic anhydride (0.2 ml) and pyridine (0.2 ml) for 15 hr at room temperature to yield 10 mg of Ia after usual workup and one recrystallization from ether, mp 169°; IR: 1770, 1745, 1720, 1650, and 1620 cm^{-1}; mass spectrum: *m/e* 388.1522 (M^+, $C_{21}H_{24}O_7$ requires 388.1527), 346 [M − 42 ($COCH_3$)], 328 [M − 60 (CH_3COOH)], 319 [M − 69 [$COC(CH_3){=}CH_2$]], 302 [M − 86 [$HOOCC(CH_3){=}CH_2$]], 277 (M − 42 − 69), 260 (M − 42 − 86), 242 (M − 60 − 86), and 69. The NMR data are shown in Table II.

Anal.—Calc. for $C_{21}H_{24}O_7$: C, 64.93; H, 6.23. Found: C, 64.84; H, 6.38.

Dehydromolephantin (*Ib*)—A solution of molephantin (300 mg) in acetone (5 ml) was cooled to 5–10° with stirring and treated with 20 drops of Jones' reagent. After 5 min, methanol (5 ml) was added and the solution was extracted with ether. The ethereal extract was washed with water, dried (anhydrous sodium sulfate), and evaporated *in vacuo* to afford Ib (145 mg) as colorless prisms after one recrystallization from acetone–ether (1:2), mp 132–133°; IR (mineral oil): 1770, 1720, 1705, 1660, and 1640 cm^{-1}; mass spectrum: *m/e* 344.1256 (M^+, $C_{19}H_{20}O_6$ requires 344.1260). The NMR data are shown in Table II.

Treatment of Dehydromolephantin with Sulfuric Acid: Compounds Ic and Id—A mixture of dehydromolephantin (70 mg) in 0.5% sulfuric acid–acetone (5 ml) was stirred for 30 min at room temperature. The mixture was evaporated *in vacuo*, extracted with chloroform, and dried (anhydrous sodium sulfate). The dried chloroform extract was evaporated to furnish a residue showing two spots on TLC. Separation of this residue was achieved by preparative TLC [chloroform–acetone (10:1)] to yield Ic (14 mg) as colorless prisms (from ether) and Id (40 mg) as colorless needles (from ether).

For Ic, the analytical data were: mp 168–170°; IR (chloroform): 3530, 3410, 1772, 1712, 1692, and 1629 cm^{-1}; mass spectrum: *m/e* 362 (M^+) and 344.1265 (M − 18) ($C_{19}H_{20}O_6$ requires 344.1260). The NMR data are given in Table II.

For Id, the analytical data were: mp 188–189°; IR: 3400, 1770, 1713 (double strength), 1650, and 1625 cm^{-1}; mass spectrum: *m/e* 344.1256 (M^+, $C_{19}H_{20}O_6$ requires 344.1260). The NMR data are given in Table II.

Molephantin p-*Bromobenzenesulfonate* (*Ie*)—A solution of molephantin (25 mg) in dry pyridine (0.5 ml) was added with *p*-bromobenzenesulfonyl chloride (35 mg), and the reaction mixture was allowed to stand at 5°. After 12 hr, the mixture was diluted with water and extracted with chloroform, dried, and evaporated to give a product. Recrystallization from isopropanol–ether (1:1) afforded colorless needles, mp 165–167°.

Molephantinin (*II*)—The analytical data for II were: mp 223–225° (ethanol); IR: 3420, 1775, 1713, 1650, and 1615 cm^{-1}; mass spectrum: *m/e* 360 (M^+), 342.1462 (M − 18) ($C_{20}H_{24}O_6$ requires 342.1467), and 83 [base peak, $CH_3CH{=}C(CH_3)C{=}O^+$]. The NMR data are shown in Table II.

Molephantinin Acetate (*IIa*)—Acetylation of molephantinin (10 mg) with acetic anhydride in pyridine in the usual way gave IIa as colorless prisms in quantitative yield, mp 131° (ether); IR: 1775, 1745, 1713, 1655, and 1615 cm^{-1}; mass spectrum: *m/e* 402.1670 (M^+) ($C_{22}H_{26}O_7$ requires 402.1679), 360 [M − 42 ($COCH_3$)], 342 [M − 60 (CH_3COOH)], and 83 [base peak, $CH_3CH{=}C(CH_3)CO^+$]. The NMR data are shown in Table II.

Dehydromolephantinin (*IIb*)—Molephantinin (26 mg) in acetone (2 ml) was oxidized with Jones' reagent (0.3 ml) in the manner described for Ib. The product was purified by preparative TLC [developed with chloroform–acetone (5:1)] and recrystallized from ether to give IIb (24 mg) as colorless pillars, mp 136°; IR: 1776, 1710, 1660, and 1620 cm^{-1}; mass spectrum: *m/e* 400 (M^+). The NMR data are shown in Table II.

Anal.—Calc. for $C_{20}H_{22}O_6$: C, 67.02; Found: C, 67.25: H, 6.23.

Phantomolin (*III*)—Phantomolin was isolated as a colorless oil; IR: 1770, 1725, 1719, 1664, and 1640 cm^{-1}; mass spectrum: *m/e* 374 (M^+). The NMR data are shown in Table II.

Anal.—Calc. for $C_{21}H_{26}O_6$: C, 67.36; H, 7.00. Found: C, 67.40; H, 6.98.

Phantomolin cis-*1,10-Epoxide* (*IIIa*)—A solution of phantomolin (15 mg) in chloroform (1 ml) was treated with a solution of *m*-chloroperbenzoic acid (20 mg) in chloroform (1 ml), and the mixture was allowed to stand at room temperature for 48 hr. The chloroform was evaporated under reduced pressure, and the residue was dissolved in ether. The ether solution was washed with 1% sodium bicarbonate and water, dried, and evaporated *in vacuo* to yield a product. This product, upon preparative TLC separation, yielded IIIa as colorless needles (6 mg) after one recrystallization from ether-hexane (3:1), mp 172°; IR: 1775, 1725, 1672, 1660, and 1643 cm^{-1}; mass spectrum: *m/e* 390 (M^+). The NMR data are shown in Table II.

Anal.—Calc. for $C_{21}H_{26}O_7$: C, 64,60; H, 6.71. Found: C, 64.31; H, 6.68.

Isolation and Characterization of β-Amyrin Acetate (IV), Lupeol Acetate (V), Epifriedelanol (VI), and Stigmasterol (VII)—The nonpolar *n*-hexane extract (~80 g) was chromatographed on a silica gel column[10] (silicic acid, 100 mesh, 10 × 100 cm) with *n*-hexane and then *n*-hexane–chloroform (9:1) as the eluents.

The first eluate from *n*-hexane was evaporated to dryness. Recrystallization of the residue from *n*-hexane afforded 400 mg of IV as colorless needles, mp 239–241°, $[\alpha]_D^{20}$ +74° (*c*, 1.0 in chloroform). The IR spectrum of IV was identical to that of an authentic sample of β-amyrin acetate[11] (15).

Anal.—Calc. for $C_{32}H_{52}O_2$: C, 81.99; H, 11.18. Found: C, 81.99; H, 11.33.

The second eluate from *n*-hexane was evaporated to dryness. Recrystallization of the residue from *n*-hexane–ether (1:1) afforded V (10 mg) as colorless needles, mp 218°, $[\alpha]_D^{20}$ +40.1° (*c*, 1.0 in chloroform). The IR spectrum (in potassium bromide) of V was identical to that of an authentic sample of lupeol acetate[11].

Anal.—Calc. for $C_{32}H_{52}O_2$: C, 81.99; H, 11.18. Found: C, 81.89; H, 11.00.

The first eluate from *n*-hexane–chloroform (9:1) was evaporated to dryness. Recrystallization of the residue from chloroform gave VI (20 mg) as colorless prisms, mp 285°, $[\alpha]_D^{20}$ +21° (*c*, 1.0 in chloroform). The IR spectrum of VI was superimposable with that of an authentic sample of epifriedelanol[11] (16).

Anal.—Calc. for $C_{30}H_{52}O$: C, 84.04; H, 12.33. Found: C, 84.24; H, 12.43.

The second eluate from *n*-hexane–chloroform (9:1) was evaporated to dryness. Recrystallization of the residue from acetone yielded VII (400 mg) as colorless silky needles, mp 170°, $[\alpha]_D^{20}$ −50.0° (*c*, 1.0 in chloroform); mass spectrum: *m/e* 412 (M^+). A mixed melting point of VII with authentic stigmasterol (16) showed no depression, and the IR spectra were identical.

Anal.—Calc. for $C_{29}H_{48}O_2$: C, 84.40; H, 11.72. Found: C, 84.23; H, 11.79.

[9] A voucher specimen is available for inspection at the herbarium of the School of Pharmacy, Kaohsiung Medical College, Kaohsiung, Taiwan.

[10] Mallinckrodt.

[11] Provided by Dr. T. Kikuchi.

REFERENCES

(1) K. H. Lee, Y. Imakura, Y. Sumida, R. Y. Wu, I. H. Hall, and H. C. Huang, *J. Org. Chem.*, **44**, 2180 (1979).

(2) A. T. Hsieh and T. I. Yang, "Nomenclature of Plants in Taiwan," National Taiwan University Press, Taiwan, Republic of China, 1969, p. 924.

(3) R. I. Geran, N. H. Greenberg, M. M. MacDonald, A. M. Schumacher, and B. J. Abbott, *Cancer Chemother. Rep., Part 3*, **3**, 1 (1972).

(4) K. H. Lee, H. Furukawa, M. Kozuka, H. C. Huang, P. A. Luhan, and A. T. McPhail, *J. Chem. Soc. Chem. Commun.*, **1973**, 476.

(5) K. H. Lee, T. Ibuka, H. C. Huang, and D. L. Harris, *J. Pharm. Sci.*, **64**, 1077 (1975).

(6) A. T. McPhail, K. D. Onan, K. H. Lee, T. Ibuka, M. Kozuka, T. Shingu, and H. C. Huang, *Tetrahedron Lett.*, **1974**, 2739.

(7) I. H. Hall, K. H. Lee, C. O. Starnes, S. A. ElGebaly, T. Ibuka, Y. S. Wu, T. Kimura, and M. Haruna, *J. Pharm. Sci.*, **67**, 1235 (1978).

(8) F. A. Bovey, "NMR Data Tables for Organic Compounds," vol. 1, Wiley, New York, N.Y., 1967, p. 136.

(9) S. M. Kupchan, A. Aynehchi, J. M. Cassady, H. K. Schnoes, and A. L. Burlingame, *J. Org. Chem.*, **34**, 3869 (1969).

(10) M. Karplus, *J. Am. Chem. Soc.*, **85**, 2870 (1963).

(11) R. R. Fraser, *Can. J. Chem.*, **38**, 549 (1960).

(12) J. D. Connolly, R. Henderson, R. McCrindle, K. H. Overton, and N. S. Bhacca, *J. Chem. Soc.*, **1965**, 6935.

(13) T. A. Geissman and T. S. Griffin, *Rev. Latinoam. Quim.*, **2**, 81 (1971).

(14) W. Herz, K. Aota, M. Holub, and Z. Samek, *J. Org. Chem.*, **35**, 2611 (1970).

(15) T. Kikuchi, T. Yokoi, M. Niwa, and T. Shingu, *Chem. Pharm. Bull.*, **25**, 2078 (1977).

(16) T. Kikuchi, T. Toyoda, M. Arimoto, M. Takayama, and M. Yamano, *Yakugaku Zasshi*, **89**, 1358 (1969).

(17) K. H. Lee, "Program and Abstracts of the 16th National Medicinal Chemistry Symposium," Medicinal Chemistry Division, A ıerican Chemical Soçiety, Kalamazoo, Mich., 1978, pp. 44–58.

ACKNOWLEDGMENTS

Presented in part at the Medicinal Chemistry Section, APhA Academy of Pharmaceutical Sciences, Chicago meeting, August 1974.

Supported by National Cancer Institute Grant CA-17625 and American Cancer Society Grant CH-19 to K. H. Lee.

The authors thank Dr. Tohru Kikuchi, Research Institute for Wakan-Yaku (Oriental Medicines), University of Toyama, Toyama, Japan, for providing authentic samples of β-amyrin acetate, lupeol acetate, epifriedelanol, and stigmasterol; Dr. D. L. Harris, Department of Chemistry, University of North Carolina at Chapel Hill, for the 100-MHz NMR spectra; and Dr. David Rosenthal and Mr. Fred Williams, Research Triangle Center for Mass Spectrometry, for mass spectral data.

Convenient Synthesis of (*S*)-(+)-Apomorphine from (*R*)-(−)-Apomorphine

PATRICK J. DAVIS *, SELIM SEYHAN *, WILLIAM SOINE ‡§, and ROBERT V. SMITH ‡x

Received May 7, 1979, from the **Division of Pharmaceutical Chemistry and the* ‡*Drug Dynamics Institute, College of Pharmacy, University of Texas at Austin, Austin, TX 78712.* Accepted for publication June 1, 1979. §Present address: Department of Medicinal Chemistry, School of Pharmacy, Virginia Commonwealth University, Richmond, VA 23298.

Abstract □ A method was devised for preparing (*S*)-(+)-apomorphine from (*R*)-(−)-apomorphine. Dehydrogenation of the dimethyl ether of (*R*)-(−)-apomorphine with 10% palladium-on-carbon followed by reduction with sodium cyanoborohydride under acidic conditions resulted in quantitative racemization to give (*R,S*)-apomorphine dimethyl ether, which then was resolved with (−)-tartaric acid. Ether cleavage of (*S*)-(+)-apomorphine dimethyl ether (−)-tartrate with hydriodic acid in acetic anhydride yielded (*S*)-(+)-apomorphine, which was isolated as the hydrochloride salt in 99% enantiomeric excess.

Keyphrases □ Apomorphine—synthesis of (*S*)-(+)-stereoisomer from (*R*)-(−)-stereoisomer □ Dopaminergic agonists—apomorphine, synthesis of (*S*)-(+)-stereoisomer from (*R*)-(−)-stereoisomer □ Stereoisomers—apomorphine, synthesis of (*S*)-(+)-stereoisomer from (*R*)-(−)-stereoisomer

Current interest in apomorphine (I) stems from its activity as a dopaminergic agonist and its consequential antiparkinsonism activity (1–3). Clinical utility has been demonstrated for I alone and in combination with other agents such as levodopa (4). Further studies are aimed at preparing suitable prodrug derivatives to overcome the drawbacks to its use (5). In addition to parkinsonism, recent studies indicated potential new uses for I in ameliorating the symptoms of Huntington's chorea (6), tardive dyskinesia (7), Gilles de la Tourette's syndrome (8), and schizophrenia (9, 10).

BACKGROUND

Most work to date involved the use of (−)-apomorphine (*R*-configuration), synthesized commercially by the acid-catalyzed rearrangement of (−)-morphine (11). Investigations into the pharmacological properties of (*S*)-(+)-apomorphine (II) have been limited to *in vivo* assays including dog emesis, a caudate brain-lesioned mouse preparation (12, 13), and evaluation of the racemate in comparison to (*R*)-(−)-I in these assays as well as on overt behavior in the monkey (13, 14). Previous reports utilized a *de novo* synthesis of (*R,S*)-I *via* Pschorr cyclization followed by resolution of the racemate (12, 15).

Molecular pharmacologists have extended the knowledge of dopaminergic mechanisms by the examination of several receptor assays, culminating in the postulation of several distinct dopamine receptors (16). Along with other criteria, these receptors are distinguished from one another by the differential action of dopaminergic agonists and antagonists, including (*R*)-(−)-I. Thus, apparently difficult to rationalize effects, such as the improvement of schizophrenic symptoms with exceedingly low doses of I, possibly can be understood on the basis of presynaptic dopamine receptors modulating dopaminergic transmission and, consequently, postsynaptic dopaminergic activity (9).

Because of the renewed interest in apomorphine pharmacology and the known differential receptor activity of stereoisomeric pharmacological agents (17), a reexamination of the two antipodes of I was desired. Also, a more direct method was sought for the synthesis of II from the commercially available (*R*)-(−)-antipode rather than the *de novo* synthesis. The synthesis of II reported here is patterned after an earlier procedure for racemization of the related aporphine alkaloid glaucine (18).

EXPERIMENTAL

Reagents—(*R*)-(−)-Apomorphine hydrochloride hemihydrate[1], 10% palladium-on-carbon[2], sodium cyanoborohydride[3], (+)- and (−)-tartaric acid[3], *p*-tolylsulfonylmethylnitrosamide[3], and heptafluorobutyric an-

[1] McFarland Smith Ltd., Edinburg, Scotland.
[2] Alfa-Ventron, Danvers, Mass.
[3] Aldrich Chemical Co., Milwaukee, Wis.

0022-3549/80/0900-1056$01.00/0

© 1980, American Pharmaceutical Association

REFERENCES

(1) K. H. Lee, Y. Imakura, Y. Sumida, R. Y. Wu, I. H. Hall, and H. C. Huang, *J. Org. Chem.*, **44**, 2180 (1979).

(2) A. T. Hsieh and T. I. Yang, "Nomenclature of Plants in Taiwan," National Taiwan University Press, Taiwan, Republic of China, 1969, p. 924.

(3) R. I. Geran, N. H. Greenberg, M. M. MacDonald, A. M. Schumacher, and B. J. Abbott, *Cancer Chemother. Rep., Part 3*, **3**, 1 (1972).

(4) K. H. Lee, H. Furukawa, M. Kozuka, H. C. Huang, P. A. Luhan, and A. T. McPhail, *J. Chem. Soc. Chem. Commun.*, **1973**, 476.

(5) K. H. Lee, T. Ibuka, H. C. Huang, and D. L. Harris, *J. Pharm. Sci.*, **64**, 1077 (1975).

(6) A. T. McPhail, K. D. Onan, K. H. Lee, T. Ibuka, M. Kozuka, T. Shingu, and H. C. Huang, *Tetrahedron Lett.*, **1974**, 2739.

(7) I. H. Hall, K. H. Lee, C. O. Starnes, S. A. ElGebaly, T. Ibuka, Y. S. Wu, T. Kimura, and M. Haruna, *J. Pharm. Sci.*, **67**, 1235 (1978).

(8) F. A. Bovey, "NMR Data Tables for Organic Compounds," vol. 1, Wiley, New York, N.Y., 1967, p. 136.

(9) S. M. Kupchan, A. Aynehchi, J. M. Cassady, H. K. Schnoes, and A. L. Burlingame, *J. Org. Chem.*, **34**, 3869 (1969).

(10) M. Karplus, *J. Am. Chem. Soc.*, **85**, 2870 (1963).

(11) R. R. Fraser, *Can. J. Chem.*, **38**, 549 (1960).

(12) J. D. Connolly, R. Henderson, R. McCrindle, K. H. Overton, and N. S. Bhacca, *J. Chem. Soc.*, **1965**, 6935.

(13) T. A. Geissman and T. S. Griffin, *Rev. Latinoam. Quim.*, **2**, 81 (1971).

(14) W. Herz, K. Aota, M. Holub, and Z. Samek, *J. Org. Chem.*, **35**, 2611 (1970).

(15) T. Kikuchi, T. Yokoi, M. Niwa, and T. Shingu, *Chem. Pharm. Bull.*, **25**, 2078 (1977).

(16) T. Kikuchi, T. Toyoda, M. Arimoto, M. Takayama, and M. Yamano, *Yakugaku Zasshi*, **89**, 1358 (1969).

(17) K. H. Lee, "Program and Abstracts of the 16th National Medicinal Chemistry Symposium," Medicinal Chemistry Division, A ıerican Chemical Soçiety, Kalamazoo, Mich., 1978, pp. 44–58.

ACKNOWLEDGMENTS

Presented in part at the Medicinal Chemistry Section, APhA Academy of Pharmaceutical Sciences, Chicago meeting, August 1974.

Supported by National Cancer Institute Grant CA-17625 and American Cancer Society Grant CH-19 to K. H. Lee.

The authors thank Dr. Tohru Kikuchi, Research Institute for Wakan-Yaku (Oriental Medicines), University of Toyama, Toyama, Japan, for providing authentic samples of β-amyrin acetate, lupeol acetate, epifriedelanol, and stigmasterol; Dr. D. L. Harris, Department of Chemistry, University of North Carolina at Chapel Hill, for the 100-MHz NMR spectra; and Dr. David Rosenthal and Mr. Fred Williams, Research Triangle Center for Mass Spectrometry, for mass spectral data.

Convenient Synthesis of (*S*)-(+)-Apomorphine from (*R*)-(−)-Apomorphine

PATRICK J. DAVIS *, SELIM SEYHAN *, WILLIAM SOINE ‡§, and ROBERT V. SMITH ‡x

Received May 7, 1979, from the **Division of Pharmaceutical Chemistry and the* ‡*Drug Dynamics Institute, College of Pharmacy, University of Texas at Austin, Austin, TX 78712.* Accepted for publication June 1, 1979. §Present address: Department of Medicinal Chemistry, School of Pharmacy, Virginia Commonwealth University, Richmond, VA 23298.

Abstract □ A method was devised for preparing (*S*)-(+)-apomorphine from (*R*)-(−)-apomorphine. Dehydrogenation of the dimethyl ether of (*R*)-(−)-apomorphine with 10% palladium-on-carbon followed by reduction with sodium cyanoborohydride under acidic conditions resulted in quantitative racemization to give (*R,S*)-apomorphine dimethyl ether, which then was resolved with (−)-tartaric acid. Ether cleavage of (*S*)-(+)-apomorphine dimethyl ether (−)-tartrate with hydriodic acid in acetic anhydride yielded (*S*)-(+)-apomorphine, which was isolated as the hydrochloride salt in 99% enantiomeric excess.

Keyphrases □ Apomorphine—synthesis of (*S*)-(+)-stereoisomer from (*R*)-(−)-stereoisomer □ Dopaminergic agonists—apomorphine, synthesis of (*S*)-(+)-stereoisomer from (*R*)-(−)-stereoisomer □ Stereoisomers—apomorphine, synthesis of (*S*)-(+)-stereoisomer from (*R*)-(−)-stereoisomer

Current interest in apomorphine (I) stems from its activity as a dopaminergic agonist and its consequential antiparkinsonism activity (1–3). Clinical utility has been demonstrated for I alone and in combination with other agents such as levodopa (4). Further studies are aimed at preparing suitable prodrug derivatives to overcome the drawbacks to its use (5). In addition to parkinsonism, recent studies indicated potential new uses for I in ameliorating the symptoms of Huntington's chorea (6), tardive dyskinesia (7), Gilles de la Tourette's syndrome (8), and schizophrenia (9, 10).

BACKGROUND

Most work to date involved the use of (−)-apomorphine (*R*-configuration), synthesized commercially by the acid-catalyzed rearrangement of (−)-morphine (11). Investigations into the pharmacological properties of (*S*)-(+)-apomorphine (II) have been limited to *in vivo* assays including dog emesis, a caudate brain-lesioned mouse preparation (12, 13), and evaluation of the racemate in comparison to (*R*)-(−)-I in these assays as well as on overt behavior in the monkey (13, 14). Previous reports utilized a *de novo* synthesis of (*R,S*)-I *via* Pschorr cyclization followed by resolution of the racemate (12, 15).

Molecular pharmacologists have extended the knowledge of dopaminergic mechanisms by the examination of several receptor assays, culminating in the postulation of several distinct dopamine receptors (16). Along with other criteria, these receptors are distinguished from one another by the differential action of dopaminergic agonists and antagonists, including (*R*)-(−)-I. Thus, apparently difficult to rationalize effects, such as the improvement of schizophrenic symptoms with exceedingly low doses of I, possibly can be understood on the basis of presynaptic dopamine receptors modulating dopaminergic transmission and, consequently, postsynaptic dopaminergic activity (9).

Because of the renewed interest in apomorphine pharmacology and the known differential receptor activity of stereoisomeric pharmacological agents (17), a reexamination of the two antipodes of I was desired. Also, a more direct method was sought for the synthesis of II from the commercially available (*R*)-(−)-antipode rather than the *de novo* synthesis. The synthesis of II reported here is patterned after an earlier procedure for racemization of the related aporphine alkaloid glaucine (18).

EXPERIMENTAL

Reagents—(*R*)-(−)-Apomorphine hydrochloride hemihydrate[1], 10% palladium-on-carbon[2], sodium cyanoborohydride[3], (+)- and (−)-tartaric acid[3], *p*-tolylsulfonylmethylnitrosamide[3], and heptafluorobutyric an-

[1] McFarland Smith Ltd., Edinburg, Scotland.
[2] Alfa-Ventron, Danvers, Mass.
[3] Aldrich Chemical Co., Milwaukee, Wis.

0022-3549/80/0900-1056$01.00/0

© 1980, American Pharmaceutical Association

hydride[4] were used without further purification. All other solvents and reagents were analytical reagent grade or better.

Spectral Studies—PMR spectra were obtained on a 60-MHz[5] or a 100-MHz[6] spectrometer, and chemical shifts are reported relative to tetramethylsilane. Optical rotations were analyzed on a spectropolarimeter[7]. Melting points were taken on a digital melting-point analyzer[8] and are corrected. Mass spectra were obtained on a medium-resolution mass spectrometer[9] by direct-probe insertion.

TLC was performed on 0.25-mm silica gel plates[10] that were developed with benzene–methanol (4:1). Plates were visualized under short (254 nm) and long (280 nm) wavelength UV light. GLC of apomorphine was conducted as its *O,O*-heptafluorobutyryl derivative as described previously (19). Apomorphine dimethyl ether also was analyzed using this GLC procedure.

Synthesis of (*R*)-(−)-Apomorphine Dimethyl Ether (III)—(*R*)-(−)-Apomorphine hydrochloride was converted to III by the method of Neumeyer *et al.* (13) using ethereal diazomethane. The free base was crystallized from *n*-hexane[11] to yield pale-yellow needles, mp 75–77° [lit. (20) mp 77.5–79°], $[\alpha]_D^{22}$ −142° (*c*, 1.59 in absolute ethanol) [lit. (21) $[\alpha]_D^{22}$ −148° (*c*, 1.64 in absolute ethanol)]; PMR (100 MHz, $CDCl_3$): δ 2.54 (s, 3H, *N*-CH_3), 2.15–3.30 (m, 7H, aliphatic), 3.71 (s, 3H, C_{11}-OCH_3), 3.88 (s, 3H, C_{10}-OCH_3), 6.84 (m, 2H, H-8 and H-9), 7.07 (m, 1H, H-2), 7.25 (m, 1H, H-3), and 8.25 (dd, 1H, H-1), identical in all respects to the reported spectrum (15); mass spectrum: *m/e* (%) 295 (68) (M^+), 294 (100), 281 (20), 264 (18), and 252 (18).

Synthesis of 6a,7-Dehydroapomorphine Dimethyl Ether (IV)—Compound III (2 g, 6.8 mmoles) was refluxed with 2 g of 10% palladium-on-carbon in 100 ml of acetonitrile under a dry nitrogen atmosphere according to the method of Cava *et al.* (22). TLC analysis indicated complete conversion in 8 hr (R_f of III = 0.50, R_f of IV = 0.85). The catalyst was removed by filtration through sintered glass and was washed repeatedly with acetonitrile. The filtrate was taken to dryness *in vacuo* to give a dark-green oil (1.9 g). This product gave a single spot on TLC and was used without further purification; PMR (60 MHz, $CDCl_3$): δ 3.09 (s, 3H, *N*-CH_3), 3.35 (s, 4H, CH_2CH_2), 3.94 (s, 3H, C_{11}-OCH_3), 4.00 (s, 3H, C_{10}-OCH_3), 6.68 (s, 1H, H-7), 7.0–7.6 (m, 4H, aromatic), and 9.65 (dd, 1H, H-1); mass spectrum: *m/e* (%) 293 (100) (M^+), 278 (80), 263 (12), 250 (25), and 235 (50).

Synthesis of (*S*)-(+)-Apomorphine Dimethyl Ether (V)—Compound IV (1.9 g, 6.5 mmoles) was dissolved in 250 ml of absolute ethanol with heat. The solution and the reaction mixture to follow were purged continuously with dry nitrogen and constant stirring. Sodium cyanoborohydride (2.0 g, 32 mmoles) was added, and the reaction was initiated and maintained at an apparent pH of 5.0 by periodic additions of ethanolic hydrochloric acid. After 18 hr, an additional 2 g of sodium cyanoborohydride was added and the reaction was allowed to continue for 2 hr, at which time TLC analysis indicated a complete conversion to (*R,S*)-apomorphine dimethyl ether. The reaction mixture was taken to dryness *in vacuo*, and the residue was solubilized in 150 ml of water, alkalinized with potassium carbonate, and extracted with ethyl acetate (3 × 200 ml). The organic layer was washed with 50 ml of water, dried with anhydrous sodium sulfate, and taken to dryness *in vacuo* to give a gold oil (1.85 g), $[\alpha]_D^{22}$ −9.2° (*c*, 1.5 in absolute ethanol, indicating 97% racemization). The PMR and mass spectra were identical to those given for III.

The racemate (1.85 g) was dissolved in 10 ml of absolute ethanol and filtered. A filtered solution of 1.2 g (−)-tartaric acid (8.0 mmoles) in 17 ml of absolute ethanol was added, and the cloudy solution was heated to clarification. The white granular crystals that separated (1.15 g) were washed with ethyl acetate and recrystallized repeatedly from absolute ethanol to yield 0.635 g of (*S*)-(+)-apomorphine dimethyl ether (−)-tartrate, $[\alpha]_D^{22}$ +62.1° (*c*, 2.06 in water) [lit. (12) $[\alpha]_D^{22}$ +64.0° (*c*, 1 in water)], mp 189–191° dec. [lit. (12) mp 179–184° dec.]. Authentic (*R*)-(−)-apomorphine dimethyl ether (+)-tartrate prepared from pure (*R*)-(−)-IV (prepared as described) gave $[\alpha]_D^{22}$ −60.0° (*c*, 1 in water) [lit. (12) $[\alpha]_D^{22}$ −59.6° (*c*, 1 in water)], mp 186–187° [lit. (12) mp 177–183°].

***S*-(+)-Apomorphine (II) Hydrochloride**—The free base V was generated from 300 mg of the (−)-tartrate salt prepared by extraction from 10 ml of saturated sodium bicarbonate solution with ethyl acetate (3 × 25 ml). The organic layer was washed once with 10 ml of water, dried *in vacuo*, and dried further by azeotroping twice with 10 ml of benzene. The ether functions were cleaved using hydriodic acid–acetic anhydride according to the method of Neumeyer *et al.* (15) as modified by Saari *et al.* (12). The reaction was monitored by TLC and was complete in 30 min. The reaction was adjusted carefully to pH 7–8 with saturated sodium bicarbonate containing 20 mg of dithionite as an antioxidant and exhaustively extracted with ether. The ethereal extract was dried over anhydrous sodium sulfate and taken to dryness *in vacuo*.

The product was dissolved in ether and filtered, and hydrogen chloride was passed through to yield the hydrochloride salt as a white powder. This powder was collected by filtration and dried *in vacuo* at 65° for 18 hr to give 104 mg (50%) of II·HCl, $[\alpha]_D^{22}$ 47.4° (*c*, 1.13 in 0.02 *N* HCl) [(*R*)-(−)-apomorphine hydrochloride gave $[\alpha]_D^{22}$ −48.7°; lit. (23) $[\alpha]_D^{22}$ −49–−51°], indicating 99% enantiomeric excess. UV comparison to (*R*)-(−)-apomorphine indicated 98.8% purity (λ_{max} 275 nm, ε 17,300), mp 249–260° dec. [lit. (12) mp 258–268° dec.]; mass spectrum: *m/e* (%) 267 (78) (M^+), 266 (100), 250 (22), 224 (34), and 221 (23), identical to the spectrum of (*R*)-(−)-apomorphine hydrochloride. GLC analysis indicated cochromatography with authentic (*R*)-(−)-apomorphine [as the heptafluorobutyryl derivative (19)] and >99% purity.

RESULTS AND DISCUSSION

Interest in racemizing and resolving aporphines continues because naturally occurring aporphines and aporphines generated from natural products [*e.g.*, (−)-apomorphine from (−)-morphine (11)] usually exist as single antipodes. A recent study (24) allowed for the racemization and resolution of the catatonic aporphine (+)-bulbocapnine by a route similar to that described in this study (Scheme I).

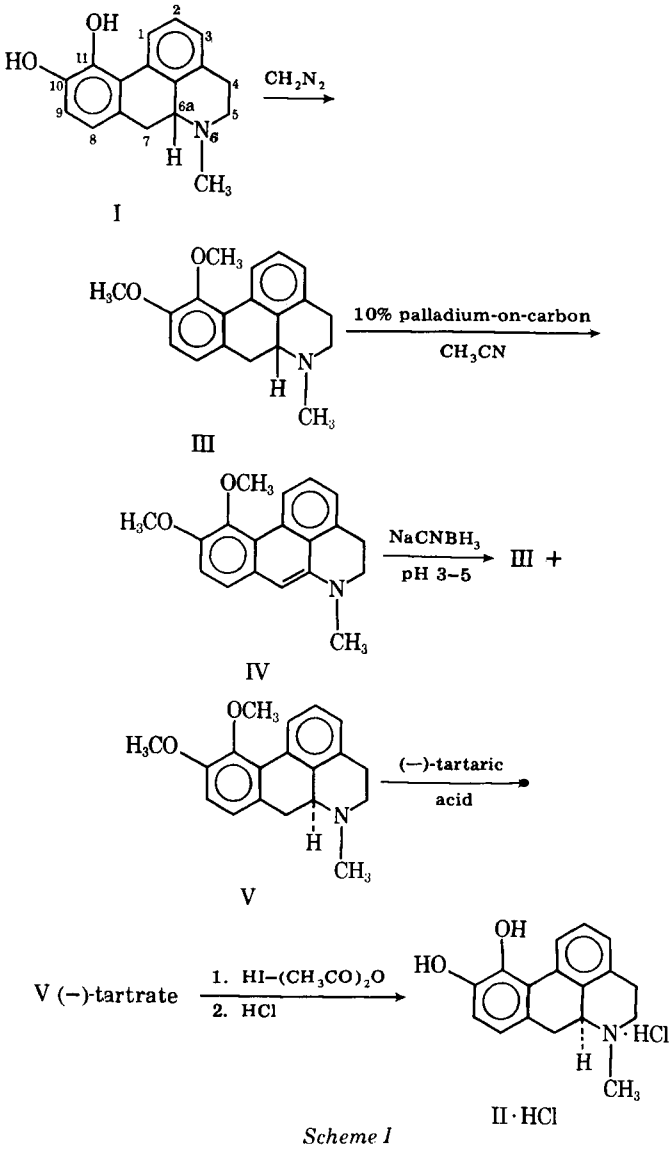

Scheme I

[4] Pierce Chemical Co., Rockford, Ill.
[5] Model R12-A, Perkin-Elmer Corp., Norwalk, Conn.
[6] Model HA-100, Varian Associates, Palo Alto, Calif.
[7] Model 241MC, Perkin-Elmer Corp., Norwalk, Conn.
[8] Model 355, Fisher Scientific Co., Houston, Tex.
[9] Model 21491, Dupont Instrument Products Division, Wilmington, Del.
[10] Polygram silica G/V_{254}, Brinkmann Associates, Westbury, N.Y.
[11] Skelly B.

This reported preparation of (*S*)-(+)-apomorphine represents a facile conversion of the readily available (*R*)-(−)-antipode rather than a *de novo* synthesis of the aporphine skeleton by Pschorr cyclization (12, 15). Due to the instability of the catechol, a protecting group was necessary for subsequent reactions; the dimethyl ether was chosen because of its ease of preparation and subsequent removal (12, 15).

The racemization of III was accomplished in the manner used previously for the preparation of racemic glaucine, which involved oxidation to the dehydroaporphine followed by nonstereospecific reduction (18). While the first step was accomplished earlier by oxidation with iodine and sodium acetate (25) or with mild permanganate oxidation (26), the method described recently (22) of refluxing the aporphine in acetonitrile with 10% palladium-on-carbon proved to be a clean and facile route to IV. The dehydroaporphine corresponding to III exhibited a characteristic PMR spectrum consisting of a relatively deshielded *N*-methyl substituent (δ 3.09 *versus* 2.54 in III) as well as the signal for the H-1 proton (δ 9.65 *versus* 8.25 in III) (26). In addition, the four H-4 and H-5 protons of IV resonated as a broad singlet (δ 3.35) and the H-7 proton resonated as a singlet at δ 6.68. The same characteristics were observed in 6a,7-dehydroglaucine (18) and *O,O*-diacetyl-6a,7-dehydroapomorphine (27).

The dehydroaporphine IV is reduced easily using sodium cyanoborohydride at acidic pH, probably due to an increased development of 6,6a-quaternary imine character under acidic conditions. Other reduction methods such as dissolving metal (28) and catalytic reduction with Adam's catalyst in acetic acid have been used. Some investigators reported a sluggish reaction in the latter case (28). The sodium cyanoborohydride procedure provided a facile and nearly quantitative racemization of IV with inexpensive reagents. The method of Kametani *et al.* (29) also has been used for similar reactions, but this method requires longer reaction times, an apparatus for hydrogenation at atmospheric pressure, and, in most cases, a weight of the expensive Adam's catalyst equal to the weight of the alkaloid.

Resolution of the racemate of apomorphine dimethyl ether was accomplished in a manner similar to that of Saari *et al.* (12). In the present study, however, oiling was encountered repeatedly using ethanol–ethyl acetate as recommended by these investigators (12). Recrystallization from ethanol ultimately was more satisfactory. Repeated recrystallization gave V as the (−)-tartrate salt in 99% enantiomeric excess. The protecting groups were removed by hydriodic acid in acetic anhydride (12, 15). In alternative experiments, TLC and GLC evidence indicated smooth cleavage using boron tribromide in methylene dichloride using a literature method (30) (*i.e.*, when the solvent was not freed of ethanol prior to use).

The (*S*)-(+)-apomorphine hydrochloride isolated through the reactions indicated in Scheme I was in >99% enantiomeric excess and was >98% pure by UV spectroscopy when compared to authentic I. Considerable variability of the optical rotation was observed with high dilutions of the salt (from −74° at *c* 0.16 to −49° at *c* 1.03 or above in 0.02 *N* HCl). Thus, a minimum *c* value of 1.0 was necessary for obtaining accurate optical rotation data. This phenomenon may be attributable to the salt–free base equilibrium, which favors the latter at high dilution. Indeed, when samples were run in 0.2 *N* HCl, lower values were obtained (−63–−47° for the concentration range).

The (*S*)-(+)-compound prepared was submitted for preliminary *in vitro* pharmacological evaluation. In the presynaptic dopaminergic receptor assay of Steinsland and Heible (31), the agent exhibits 1% of the activity of (*R*)-(−)-I, as expected based on its optical purity and its expected inactivity as a dopaminergic agonist (12). However, preliminary results in the receptor assay of Seeman *et al.* (32) show an unexpected affinity similar to that of I. Complete pharmacological evaluation of II will be the subject of a subsequent report from these laboratories.

REFERENCES

(1) G. C. Cotzias, P. S. Papavasiliou, C. Fehling, B. Kaufman, and I. Mena, *N. Engl. J. Med.*, **282,** 31 (1970).

(2) G. C. Cotzias, P. S. Papavasiliou, E. S. Tolosa, J. S. Mendez, and M. Bell-Midura, *ibid.*, **294,** 567 (1976).

(3) F. Stian, E. Micheler, and O. Benkert, *Pharmacopsychiatry*, **5,** 198 (1972).

(4) G. C. Cotzias, I. Mena, P. S. Papavasiliou, and J. Mendez, in "Advances in Neurology," vol. 5, F. McDowell and A. Barbeau, Eds., Raven, New York, N.Y., 1973, pp. 11–22.

(5) R. J. Borgman, R. J. Baldessarini, and K. G. Walton, *J. Med. Chem.*, **19,** 717 (1976).

(6) I. Shoulson and T. N. Chase, *Annu. Rev. Med.*, **26,** 419 (1975).

(7) C. D. Marsden, D. Tarsy, and R. J. Baldessarini, in "Psychiatric Aspects of Neurologic Disease," D. F. Benson and D. Blumir, Eds., Grune & Stratton, New York, N.Y., 1975, pp. 219–265.

(8) R. J. Baldessarini, K. G. Walton, and R. J. Borgman, *Neuropharmacology*, **15,** 471 (1976).

(9) C. A. Tamminga, M. H. Schaffer, R. C. Smith, and J. M. Davis, *Science*, **200,** 567 (1978).

(10) R. C. Smith, C. A. Tamminga, and J. M. Davis, *J. Neural Trans.*, **40,** 171 (1977).

(11) F. C. Colpaert, W. F. M. VanBeven, and J. E. M. F. Leyson, *Int. Rev. Neurobiol.*, **19,** 225 (1976).

(12) W. S. Saari, S. W. King, and V. J. Lotti, *J. Med. Chem.*, **16,** 171 (1973).

(13) J. L. Neumeyer, B. R. Neustadt, K. H. Oh, K. K. Weinhart, C. B. Boyce, F. J. Rosenberg, and D. G. Teiger, *ibid.*, **16,** 223 (1973).

(14) R. I. Schoenfeld, J. L. Neumeyer, W. Dafeldecker, and S. Roffler-Tarlov, *Eur. J. Pharmacol.*, **30,** 63 (1975).

(15) J. Neumeyer, B. Neustadt, and K. Weinhardt, *J. Pharm. Sci.*, **59,** 1850 (1970).

(16) J. W. Kebabian and D. B. Calne, *Nature*, **277,** 93 (1979).

(17) E. J. Simon, *Neurochem. Res.*, **1,** 3 (1976).

(18) P. J. Davis, D. Wiese, and J. P. Rosazza, *J. Chem. Soc., Perkin I*, **1976,** 1.

(19) D. M. Baaske, J. E. Keiser, and R. V. Smith, *J. Chromatogr.*, **140,** 57 (1977).

(20) J. G. Cannon, R. V. Smith, A. Modiri, S. P. Sood, R. J. Borgman, M. A. Aleem, and J. P. Long, *J. Med. Chem.*, **15,** 273 (1972).

(21) L. Knorr and F. Raake, *Chem. Ber.*, **41,** 3050 (1908).

(22) M. P. Cava, D. L. Edie, and J. J. Saa, *J. Org. Chem.*, **40,** 301 (1975).

(23) "Remington's Pharmaceutical Sciences," 14th ed., A. Osol, Ed., Mack Publishing Co., Easton, Pa., 1970, p. 806.

(24) M. Gerecke, R. Borer, and A. Brossi, *Helv. Chim. Acta*, **59,** 2551 (1976).

(25) M. P. Cava, A. Venkateswarbu, M. Srinivasan, and D. L. Edie, *Tetrahedron*, **28,** 4299 (1972).

(26) M. P. Cava, Y. Watanabe, K. Bessho, M. J. Mitchell, A. I. da Rocha, B. Hwang, B. Douglas, and J. A. Weisback, *Tetrahedron Lett.*, **1968,** 2437.

(27) H. A. Linde and M. S. Ragab, *Helv. Chim. Acta*, **51,** 683 (1968).

(28) M. P. Cava, M. J. Mitchell, S. C. Havlicek, A. Lindert, and R. J. Spangler, *J. Org. Chem.*, **35,** 175 (1970).

(29) T. Kametani, M. Ihara, and K. Shima, *J. Chem. Soc. C*, **1968,** 1619.

(30) S. Teitel, J. O'Brien, and A. Brossi, *J. Org. Chem.*, **37,** 1879 (1972).

(31) O. S. Steinsland and J. P. Heible, *Science*, **199,** 443 (1978).

(32) P. Seeman, J. L. Tedesco, T. Lee, M. Chau-Wong, P. Muller, J. Bowles, P. M. Whitaker, C. McManus, M. Tittler, P. Weinreich, W. C. Friend, and G. M. Brown, *Fed. Proc. Fed. Am. Soc. Exp. Biol.*, **37,** 130 (1978).

ACKNOWLEDGMENTS

Supported by Grant NS-12259 from the National Institute of Neurological and Communicative Disorders and Stroke.

Topographical Model of the Renal Vascular Dopamine Receptor

PAUL W. ERHARDT

Received April 27, 1979, from the *Department of Pharmaceutical Research, Arnar-Stone Laboratories, McGaw Park, IL 60085.* Accepted for publication December 6, 1979.

Abstract □ Based on review and examination of recent additions to dopaminergic structure–activity relationships, a topographical model of the renal vascular dopamine receptor is presented. The implications of this model for the design of new dopaminergic drug candidates are discussed briefly.

Keyphrases □ Dopamine—topographical model of renal vascular receptor □ Drug–receptor interactions—topographical model of renal vascular dopamine receptor □ Structure–activity relationships—dopaminergic drugs

Several reports (1–4) suggested that the preferred conformation for dopamine, when it is interacting with its biological receptor sites, resembles the fully extended *trans*-form (I). In this conformation, the catechol ring and amine function are in an antiperiplanar arrangement. Cannon and coworkers (5–7) suggested that a biologically significant conformer has the *m*-hydroxy group rotated toward the amine, as depicted in I. This arrangement has been designated as the α-rotamer, and the antiperiplanar conformation having the *m*-hydroxy group rotated away from the amine function has been designated as the β-rotamer (5). Both a dihedral angle approximating 180° (8, 9) and near coplanarity (5, 7) of the catechol ring and ethylamine system have been implicated as important structural features for dopaminergic activity.

BACKGROUND

The benzazepine derivative II recently was reported to possess significant renal dopaminergic-mediated vasodilator properties[1] (10). In this molecule, the catechol and amine functions can exist only in *gauche* and eclipsed conformations, while the phenyl ring and amine system can assume a nearly antiperiplanar arrangement. Although there are examples of nonoxygenated 2-aminotetralins that show central dopaminergic activity (11, 12), there is no precedent for such systems having renal dopaminergic activity where an intact catechol function appears to be a requisite structural feature for agonist action. Therefore, the pharmacological profile for II seems to contradict the hypothesis that an antiperiplanar arrangement of the key pharmacophoric groups is important in determining dopaminergic activity. Alternatively, as shown in its side view, there is a partially eclipsed conformation for II in which the amine function lies within the plane established by the catechol ring.

Examination of various dopamine agonists reveals that aryl–amine coplanarity or very near coplanarity is a feature common to all of the agents, whereas the dihedral angle varies considerably. Even certain 2-

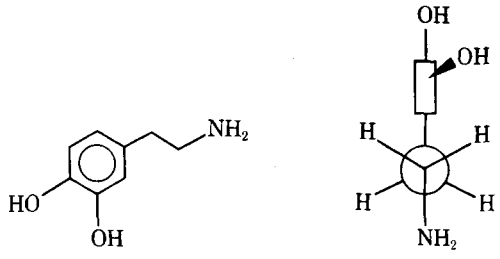

I

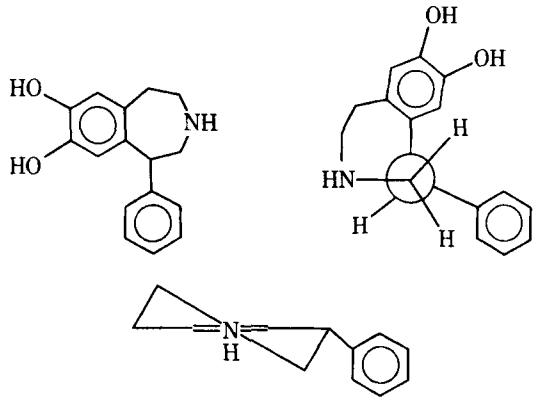

II

indanamine derivatives (III), previously regarded as an enigma (3, 5), possess aryl ring–amine coplanarity when assuming an envelope conformation (13).

In addition to coplanarity, structure–activity relationships indicate that specific nitrogen to hydroxyl group distances are optimal for interaction with certain dopaminergic receptor populations (5, 9, 14). Because of the noted differences in dopamine receptors (15–19), it is important to specify which receptor population is under consideration when addressing this structural parameter. Table I indicates the nitrogen to *p*-hydroxy and nitrogen to *m*-hydroxy distances and the renal dopaminergic activity for several dopamine analogs. In active compounds, the *m*- and *p*-hydroxy groups reside ~7–8 Å away from the amine function. Apomorphine, which has a somewhat shorter nitrogen to *m*-hydroxy group distance, is an exception. However, its pharmacological profile also is somewhat different; apomorphine is best classified as a weak, partial agonist in the renal dopaminergic system (16). Furthermore, its activity may be partially derived from additional binding contributions from its molecular portions outside of its apparent dopaminergic pharmacophore (17).

More interesting is the inactivity observed for isoapomorphine, which satisfies both coplanarity and amine–hydroxy group distance criteria. Two receptor models were proposed to account for this finding. Grol and Rollema (21) suggested that a receptor boundary is present which hampers interaction with molecules bearing bulky groups on the side of the molecule opposite the *m*-hydroxy group. Goldberg *et al.* (16, 17) also attributed isoapomorphine inactivity to a steric parameter and further emphasized an improper orientation of its amine free electron pair for preferred interaction with a stereospecific amine recognition site on the receptor.

Recent experiments in these laboratories provided additional insight into dopaminergic structure–activity relationships. The synthesis (24,

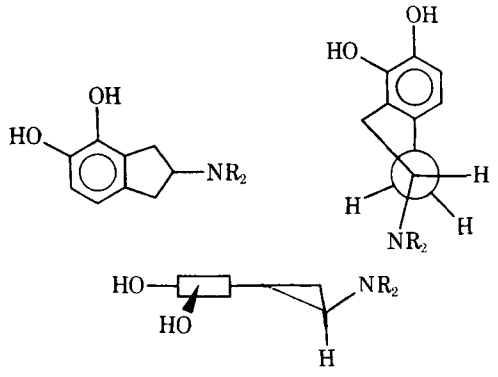

III

[1] Comparison between intravenous injection of II and injection of II directly into the renal artery (10) indicates that II itself is an active drug and not dependent on aromatic hydroxylation or any other metabolic process for its activation.

0022-3549/80/0900-1059$01.00/0
© 1980, American Pharmaceutical Association

Table I—Amine-to-Hydroxy Group Distances [a] for Selected Dopamine Analogs [b]

Compound	Distance, Å		Renal Dopaminergic Activity
	Nitrogen to *p*-Hydroxy	Nitrogen to *m*-Hydroxy[c]	
Apomorphine	7.8	6.5	Partial agonist (16)
Isoapomorphine	7.8	7.3	Inactive (16, 17)
Tetrahydroisoquinolines[d]	6.0	6.4	Inactive (14)
II	7.0	7.0	Active (10)
Dopamine, antiperiplanar, β-rotamer	7.8	7.3	Active[e]
Dopamine, partially eclipsed[f]	7.0	7.0	Active [g]
2-Amino-6,7-dihydroxytetralin[h]	7.8	7.3	Active (14)
2-Amino-5,6-dihydroxytetralin[h]	7.8	6.5	Inactive (14)
IV	7.7	7.4	Inactive (23)

[a] Determinations agree with various literature values within ±0.1 Å (3–5, 20, 21). [b] All compounds can possess aryl ring–amine coplanarity or near coplanarity. [c] Analogous to the *meta*- and *para*-positions of dopamine. [d] 6,7-Dihydroxytetrahydroisoquinoline and *N*-methyl-6,7-dihydroxytetrahydroisoquinoline. Although the preferred conformations for these systems are such that the amine function resides above or below the plane of the aromatic ring (22), coplanarity of these groups is not thermodynamically precluded, especially when considering that drug–receptor associations may produce a net energetically favored situation. [e] The β-rotamer is thought (14) to be optimal for interaction with renal dopaminergic receptors. [f] Conformation superimposed on that depicted for II. [g] By analogy to II. [h] Determined with the nitrogen in a pseudo-equatorial orientation, as is thought to be the active conformer (6, 9).

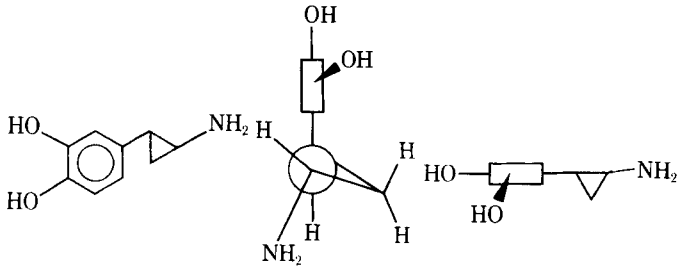

IV

25) and pharmacological activity (23, 25, 26) of *E*- and *Z*-2-(3,4-dihydroxyphenyl)cyclopropylamines, two semirigid analogs of dopamine, were reported. Since the *E*-isomer (IV) is similar to conformer I in terms of aryl–amine coplanarity, its inactivity as a renal dopaminergic agonist or antagonist was surprising. However, the additional steric bulk resulting from incorporation of the methylene unit forming the cyclopropyl system resembles that present in α-methyldopamine, which also is inactive as a renal dopaminergic agonist (27). In α-methyldopamine and in IV, the bond between the β-carbon and the aryl ring is free to rotate such that both the α- and β-rotameric conformers are accessible. Furthermore, this rotation should proceed with minimal thermodynamic constraint; conformational considerations, therefore, seem an unlikely explanation for the inactivity of these compounds.

Alternatively, if one observes IV from the side as shown, it is apparent that the methylene unit protrudes perpendicularly out from the plane established by the aryl ring and amine function. This protrusion results in a molecular thickness of ~2 Å midway between the aromatic ring and the amine moiety. If a steric boundary were localized in a corresponding location above the receptor, then this protrusion would be expected to preclude effective receptor binding. The fact that this boundary must be localized specifically in this region is apparent from the activity observed for compounds such as apomorphine, 2-amino-6,7-dihydroxytetralin, and II, whose somewhat smaller but similar bulk in this region is directed toward the α- and β-carbons. Interestingly, Sheppard and Burghardt (28), employing Newman projections, also referred to a steric parameter localized specifically in the "9 o'clock position" to explain certain structure–activity relationships observed for aryl-substituted analogs derivatized in the 2-position.

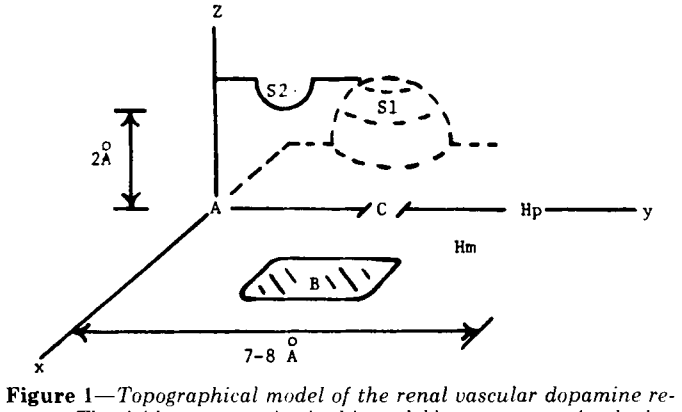

Figure 1—*Topographical model of the renal vascular dopamine receptor. The rigid representation in this model is not meant to imply that a more dynamic relationship, such as mutual molding, is not operative during drug–receptor interaction.*

THEORETICAL

Combining the structural parameters discussed affords a three-dimensional map (29) of the renal dopamine receptor that contains the following topographical features (Fig. 1):

1. A single plane containing amine (A) and catechol (Hm, Hp, and C) recognition sites.
2. A distance between the amine recognition site and *p*- (Hp) and *m*- (Hm) hydroxy group recognition sites of ~7–8 Å.
3. A steric parameter (S1) located to one side of the principal pharmacophoric recognition site. Depending on the α- or β-rotameric relationship, this parameter could limit the bulk on the side opposite to the *m*-hydroxy group of molecules attempting to align with the receptor properly (21). An additional hydrophobic binding region (B) located on the same side as the analogous *m*-hydroxy group also may be present in the plane established by A, C, Hp, and Hm (17).
4. A second steric parameter (S2) located ~2 Å above the plane of the receptor and localized specifically along the analogous α- and β-carbon chain region.

DISCUSSION

Although conceptual in nature, topographical mapping of receptors can be useful in the design of new drug entities. In this regard, the receptor model described here implies that new renal dopaminergic structural candidates should possess overall planarity and a somewhat narrow molecular thickness, especially in the analogous α- and β-carbon region. Concern about an appropriate dihedral angle or even about a classical two-carbon bridge between the amine and aromatic functions is not necessary as long as key nitrogen-to-catechol hydroxyl group distances are maintained. Furthermore, significant steric bulk opposite the position analogous to the dopamine *m*-hydroxy group should be avoided, while incorporation of hydrophobic character on the same side as the analogous *m*-hydroxy group could be beneficial for receptor binding.

REFERENCES

(1) A. S. Horn and S. H. Snyder, *Proc. Natl. Acad. Sci. USA*, **68**, 2325 (1971).

(2) R. F. Rekker, D. J. C. Engel, and G. G. Nys, *J. Pharm. Pharmacol.*, **24**, 589 (1972).

(3) R. M. Pinder, *Adv. Neurol.*, **3**, 295 (1973).

(4) R. Miller, A. Horn, L. Iversen, and R. Pinder, *Nature*, **250**, 238 (1974).

(5) J. G. Cannon, *Adv. Neurol.*, **9**, 177 (1975).

(6) J. G. Cannon, R. V. Smith, M. A. Aleem, and J. P. Long, *J. Med.*

Chem., **18**, 108 (1975).
(7) J. G. Cannon, G. J. Hatheway, J. P. Long, and F. M. Sharabi, *ibid.*, **19**, 987 (1976).
(8) H. L. Komiskey, J. F. Bossart, D. D. Miller, and P. N. Patil, *Proc. Natl. Acad. Sci. USA*, **75**, 2641 (1978).
(9) D. D. Miller, *Fed. Proc. Fed. Am. Soc. Exp. Biol.*, **37**, 2392 (1978).
(10) R. G. Pendleton, L. Samler, C. Kaiser, and P. T. Ridley, *Eur. J. Pharmacol.*, **51**, 19 (1978).
(11) J. D. McDermed, G. M. McKenzie, and A. P. Phillips, *J. Med. Chem.*, **18**, 362 (1975).
(12) J. G. Cannon, T. Lee, H. D. Goldman, B. Costall, and R. J. Naylor, *ibid.*, **20**, 1111 (1977).
(13) B. Fuchs, in "Topics in Stereochemistry," vol. 10, E. Eliel and N. Allinger, Eds., Wiley, New York, N.Y., 1978.
(14) P. H. Volkman, J. D. Kohli, L. I. Goldberg, J. G. Cannon, and T. Lee, *Proc. Natl. Acad. Sci. USA*, **74**, 3602 (1977).
(15) R. G. Pendleton and P. E. Setler, *Gen. Pharmacol.*, **8**, 1 (1977).
(16) L. I. Goldberg, P. H. Volkman, and J. D. Kohli, *Ann. Rev. Pharmacol. Toxicol.*, **18**, 57 (1978).
(17) L. I. Goldberg, J. D. Kohli, A. N. Kotake, and P. H. Volkman, *Fed. Proc. Fed. Am. Soc. Exp. Biol.*, **37**, 2396 (1978).
(18) P. E. Setler, H. M. Sarau, C. L. Zirkle, and H. L. Saunders, *Eur. J. Pharmacol.*, **50**, 419 (1978).
(19) J. W. Kebabian and D. B. Calne, *Nature*, **277**, 93 (1979).
(20) B. Costall, R. J. Naylor, and R. M. Pinder, *J. Pharm. Pharmacol.*, **26**, 753 (1974).
(21) C. J. Grol and H. Rollema, *ibid.*, **29**, 153 (1977).
(22) J. Knabe, *Arch. Pharm.*, **292**, 416 (1959).
(23) R. J. Borgman, P. W. Erhardt, R. J. Gorczynski, and W. G. Anderson, *J. Pharm. Pharmacol.*, **30**, 193 (1978).
(24) P. W. Erhardt, *J. Org. Chem.*, **44**, 883 (1979).
(25) P. W. Erhardt, R. J. Gorczynski, and W. G. Anderson, *J. Med. Chem.*, **22**, 907 (1979).
(26) R. J. Gorczynski, W. G. Anderson, P. W. Erhardt, and D. M. Stout, *J. Pharmacol. Exp. Ther.*, **210**, 252 (1979).
(27) L. I. Goldberg, P. F. Sonneville, and J. L. McNay, *ibid.*, **163**, 188 (1968).
(28) H. Sheppard and C. R. Burghardt, *Mol. Pharmacol.*, **10**, 721 (1974).
(29) P. Pauling and T. J. Petcher, *Chem. Biol. Interact.*, **6**, 351 (1973).

Thalifaurine and Dehydrodiscretine, New Quaternary Protoberberines from *Thalictrum fauriei*

CHUNG-HSIUNG CHEN ˣ, TZER-MING CHEN, and CHRISTINE LEE

Received March 26, 1979, from the *School of Pharmacy, National Taiwan University, Taipei, Taiwan, Republic of China.* Accepted for publication May 4, 1979.

Abstract □ Two new quaternary protoberberines, thalifaurine and dehydrodiscretine, were isolated from the ethanolic extract of *Thalictrum fauriei* Hayata. Based on spectral analysis and correlation with compounds of known structure, thalifaurine was shown to be 3-hydroxy-2-methoxy-10,11-methylenedioxyberbinium chloride and dehydrodiscretine was established as 3-hydroxy-2,10,11-trimethoxyberbinium chloride. The structural assignment was confirmed by synthesis of both compounds. Magnoflorine also was isolated and identified.

Keyphrases □ Thalifaurine—new quaternary protoberberine isolated from *Thalictrum fauriei*, structural determination □ Dehydrodiscretine—new quaternary protoberberine isolated from *Thalictrum fauriei*, structural determination □ Protoberberines, quaternary—thalifaurine and dehydrodiscretine, isolation from *Thalictrum fauriei*, structural determination □ *Thalictrum fauriei*—isolation of thalifaurine and dehydrodiscretine and their structural determination

Thalictrum fauriei Hayata (Ranunculaceae) is a perennial herb that is distributed widely over the mountainous area of Taiwan, especially in wet places (1). In view of an increasing interest in the biological activity of some Thalictrum alkaloids (2), a study was initiated on the alkaloidal constituents of *T. fauriei*.

Previous reports from this laboratory described the isolation and characterization of three known aporphines, (+)-oconovine (Ia) (3), (+)-isocorydine (Ib) (3), and (+)-corydine[1] (Ic), from the tertiary base fraction. Continuing investigation of the quaternary base fraction has provided two new protoberberinium salts, thalifaurine (IIa) and dehydrodiscretine (IIb), in addition to the known aporphine magnoflorine (III). The isolation and structural characterization of these quaternary salts are described in this report.

[1] C.-H. Chen, T.-M. Chen, and C. Lee, unpublished data.

RESULTS AND DISCUSSION

The ethanolic extract of the whole plant material of *T. fauriei* was processed by the usual acid–base treatment and solvent partitioning to separate the quaternary alkaloid fraction from the tertiary base fraction. The quaternary salt was precipitated with Mayer reagent and then was exchanged by an anionic resin into the chloride form. Extensive fractionation of this chloride salt on silica gel columns yielded three crystalline compounds, designated as alkaloids Q-3, Q-4, and Q-6 according to their increasing polarity on TLC plates.

Alkaloid Q-4—Alkaloid Q-4 was isolated as the chloride salt, mp 258–260°, and was optically inactive. The UV spectrum appeared as a complicated pattern with absorption maxima at 241, 263, 291, and 341 nm and shoulders at 310 and 380 nm. This pattern was characteristic of quaternary protoberberine salts, and the shoulder at 310 nm suggested a 2,3,10,11-substituted pseudoprotoberberinium pattern (4). Bathochromic shifts in the presence of bases and the broad IR absorption bands at 3510 and 3326 cm^{-1} indicated the phenolic nature of Q-4. The NMR spectrum of Q-4 revealed one methoxy group at δ 4.02, one methylenedioxy group at δ 6.33, two triplets of two protons each at δ 3.17 and 4.74 (J = 6 Hz), and six aromatic protons at δ 6.87 (s, 1H), 7.51 (s, 2H), 7.64 (s, 1H), 8.59 (s, 1H), and 9.25 (s, 1H) ppm.

Simanek *et al.* (5) made a detailed analysis of the chemical shifts for each aromatic proton on various protoberberinium and pseudoprotoberberinium salts. The data for pseudopalmatinium (IIe) and pseudoepiberberinium (IIf) salts were taken from their report and compared with those of Q-4 (Table I); the data for Q-4 were consistent with the 2,3,10,11-substitution pattern. In the chemical-ionization mass spectrum of Q-4 with isobutane as the reagent gas, the molecular ion M^+ appeared at m/e 322 and base ion c appeared at m/e 320; both were highly abundant, which reflected the unusual stability of the parent ion under the chemical-ionization mode. Ion a at m/e 323 and ion b at m/e 337 represented the result from thermal disproportionation of the parent ion (M^+), a fact proven for berberine derivatives by Habermehl *et al.* (6). Ions d (m/e 177), e (m/e 178), and f (m/e 176) suggested the presence of hydroxy and methoxy groups on ring A. Ion g (m/e 148) served to locate the methylenedioxy group on ring D.

Two structures were compatible with the evidence: 3-hydroxy-2-methoxy-10,11-methylenedioxyberbinium chloride (IIa) and 2-hydroxy-3-methoxy-10,11-methylenedioxyberbinium chloride (IIc).

0022-3549/80/0900-1061$01.00/0
© 1980, American Pharmaceutical Association

Chem., **18**, 108 (1975).
(7) J. G. Cannon, G. J. Hatheway, J. P. Long, and F. M. Sharabi, *ibid.*, **19**, 987 (1976).
(8) H. L. Komiskey, J. F. Bossart, D. D. Miller, and P. N. Patil, *Proc. Natl. Acad. Sci. USA*, **75**, 2641 (1978).
(9) D. D. Miller, *Fed. Proc. Fed. Am. Soc. Exp. Biol.*, **37**, 2392 (1978).
(10) R. G. Pendleton, L. Samler, C. Kaiser, and P. T. Ridley, *Eur. J. Pharmacol.*, **51**, 19 (1978).
(11) J. D. McDermed, G. M. McKenzie, and A. P. Phillips, *J. Med. Chem.*, **18**, 362 (1975).
(12) J. G. Cannon, T. Lee, H. D. Goldman, B. Costall, and R. J. Naylor, *ibid.*, **20**, 1111 (1977).
(13) B. Fuchs, in "Topics in Stereochemistry," vol. 10, E. Eliel and N. Allinger, Eds., Wiley, New York, N.Y., 1978.
(14) P. H. Volkman, J. D. Kohli, L. I. Goldberg, J. G. Cannon, and T. Lee, *Proc. Natl. Acad. Sci. USA*, **74**, 3602 (1977).
(15) R. G. Pendleton and P. E. Setler, *Gen. Pharmacol.*, **8**, 1 (1977).
(16) L. I. Goldberg, P. H. Volkman, and J. D. Kohli, *Ann. Rev. Pharmacol. Toxicol.*, **18**, 57 (1978).
(17) L. I. Goldberg, J. D. Kohli, A. N. Kotake, and P. H. Volkman, *Fed. Proc. Fed. Am. Soc. Exp. Biol.*, **37**, 2396 (1978).
(18) P. E. Setler, H. M. Sarau, C. L. Zirkle, and H. L. Saunders, *Eur. J. Pharmacol.*, **50**, 419 (1978).
(19) J. W. Kebabian and D. B. Calne, *Nature*, **277**, 93 (1979).
(20) B. Costall, R. J. Naylor, and R. M. Pinder, *J. Pharm. Pharmacol.*, **26**, 753 (1974).
(21) C. J. Grol and H. Rollema, *ibid.*, **29**, 153 (1977).
(22) J. Knabe, *Arch. Pharm.*, **292**, 416 (1959).
(23) R. J. Borgman, P. W. Erhardt, R. J. Gorczynski, and W. G. Anderson, *J. Pharm. Pharmacol.*, **30**, 193 (1978).
(24) P. W. Erhardt, *J. Org. Chem.*, **44**, 883 (1979).
(25) P. W. Erhardt, R. J. Gorczynski, and W. G. Anderson, *J. Med. Chem.*, **22**, 907 (1979).
(26) R. J. Gorczynski, W. G. Anderson, P. W. Erhardt, and D. M. Stout, *J. Pharmacol. Exp. Ther.*, **210**, 252 (1979).
(27) L. I. Goldberg, P. F. Sonneville, and J. L. McNay, *ibid.*, **163**, 188 (1968).
(28) H. Sheppard and C. R. Burghardt, *Mol. Pharmacol.*, **10**, 721 (1974).
(29) P. Pauling and T. J. Petcher, *Chem. Biol. Interact.*, **6**, 351 (1973).

Thalifaurine and Dehydrodiscretine, New Quaternary Protoberberines from *Thalictrum fauriei*

CHUNG-HSIUNG CHEN ˣ, TZER-MING CHEN, and CHRISTINE LEE

Received March 26, 1979, from the *School of Pharmacy, National Taiwan University, Taipei, Taiwan, Republic of China.* Accepted for publication May 4, 1979.

Abstract □ Two new quaternary protoberberines, thalifaurine and dehydrodiscretine, were isolated from the ethanolic extract of *Thalictrum fauriei* Hayata. Based on spectral analysis and correlation with compounds of known structure, thalifaurine was shown to be 3-hydroxy-2-methoxy-10,11-methylenedioxyberbinium chloride and dehydrodiscretine was established as 3-hydroxy-2,10,11-trimethoxyberbinium chloride. The structural assignment was confirmed by synthesis of both compounds. Magnoflorine also was isolated and identified.

Keyphrases □ Thalifaurine—new quaternary protoberberine isolated from *Thalictrum fauriei*, structural determination □ Dehydrodiscretine—new quaternary protoberberine isolated from *Thalictrum fauriei*, structural determination □ Protoberberines, quaternary—thalifaurine and dehydrodiscretine, isolation from *Thalictrum fauriei*, structural determination □ *Thalictrum fauriei*—isolation of thalifaurine and dehydrodiscretine and their structural determination

Thalictrum fauriei Hayata (Ranunculaceae) is a perennial herb that is distributed widely over the mountainous area of Taiwan, especially in wet places (1). In view of an increasing interest in the biological activity of some Thalictrum alkaloids (2), a study was initiated on the alkaloidal constituents of *T. fauriei*.

Previous reports from this laboratory described the isolation and characterization of three known aporphines, (+)-oconovine (Ia) (3), (+)-isocorydine (Ib) (3), and (+)-corydine[1] (Ic), from the tertiary base fraction. Continuing investigation of the quaternary base fraction has provided two new protoberberinium salts, thalifaurine (IIa) and dehydrodiscretine (IIb), in addition to the known aporphine magnoflorine (III). The isolation and structural characterization of these quaternary salts are described in this report.

[1] C.-H. Chen, T.-M. Chen, and C. Lee, unpublished data.

RESULTS AND DISCUSSION

The ethanolic extract of the whole plant material of *T. fauriei* was processed by the usual acid–base treatment and solvent partitioning to separate the quaternary alkaloid fraction from the tertiary base fraction. The quaternary salt was precipitated with Mayer reagent and then was exchanged by an anionic resin into the chloride form. Extensive fractionation of this chloride salt on silica gel columns yielded three crystalline compounds, designated as alkaloids Q-3, Q-4, and Q-6 according to their increasing polarity on TLC plates.

Alkaloid Q-4—Alkaloid Q-4 was isolated as the chloride salt, mp 258–260°, and was optically inactive. The UV spectrum appeared as a complicated pattern with absorption maxima at 241, 263, 291, and 341 nm and shoulders at 310 and 380 nm. This pattern was characteristic of quaternary protoberberine salts, and the shoulder at 310 nm suggested a 2,3,10,11-substituted pseudoprotoberberinium pattern (4). Bathochromic shifts in the presence of bases and the broad IR absorption bands at 3510 and 3326 cm^{-1} indicated the phenolic nature of Q-4. The NMR spectrum of Q-4 revealed one methoxy group at δ 4.02, one methylenedioxy group at δ 6.33, two triplets of two protons each at δ 3.17 and 4.74 (J = 6 Hz), and six aromatic protons at δ 6.87 (s, 1H), 7.51 (s, 2H), 7.64 (s, 1H), 8.59 (s, 1H), and 9.25 (s, 1H) ppm.

Simanek *et al.* (5) made a detailed analysis of the chemical shifts for each aromatic proton on various protoberberinium and pseudoprotoberberinium salts. The data for pseudopalmatinium (IIe) and pseudoepiberberinium (IIf) salts were taken from their report and compared with those of Q-4 (Table I); the data for Q-4 were consistent with the 2,3,10,11-substitution pattern. In the chemical-ionization mass spectrum of Q-4 with isobutane as the reagent gas, the molecular ion M^+ appeared at m/e 322 and base ion c appeared at m/e 320; both were highly abundant, which reflected the unusual stability of the parent ion under the chemical-ionization mode. Ion a at m/e 323 and ion b at m/e 337 represented the result from thermal disproportionation of the parent ion (M^+), a fact proven for berberine derivatives by Habermehl *et al.* (6). Ions d (m/e 177), e (m/e 178), and f (m/e 176) suggested the presence of hydroxy and methoxy groups on ring A. Ion g (m/e 148) served to locate the methylenedioxy group on ring D.

Two structures were compatible with the evidence: 3-hydroxy-2-methoxy-10,11-methylenedioxyberbinium chloride (IIa) and 2-hydroxy-3-methoxy-10,11-methylenedioxyberbinium chloride (IIc).

0022-3549/80/0900-1061$01.00/0
© 1980, American Pharmaceutical Association

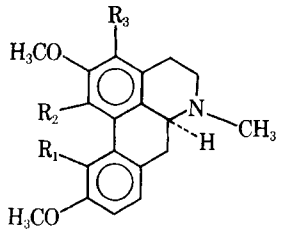

I

Ia: $R_1 = OH$, $R_2 = R_3 = OCH_3$
Ib: $R_1 = OH$, $R_2 = OCH_3$, $R_3 = H$
Ic: $R_1 = OCH_3$, $R_2 = OH$, $R_3 = H$

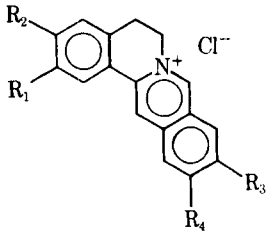

II

IIa: $R_1 = OCH_3$, $R_2 = OH$, $R_3 = R_4 = OCH_2O$
IIb: $R_1 = R_3 = R_4 = OCH_3$, $R_2 = OH$
IIc: $R_1 = OH$, $R_2 = OCH_3$, $R_3 = R_4 = OCH_2O$
IId: $R_1 = OH$, $R_2 = R_3 = R_4 = OCH_3$

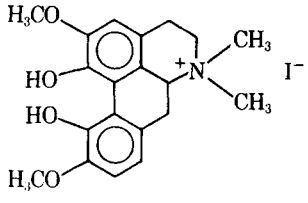

III (as iodide)

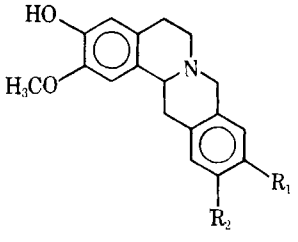

IV

IVa: $R_1 = R_2 = OCH_2O$
IVb: $R_1 = R_2 = OCH_3$

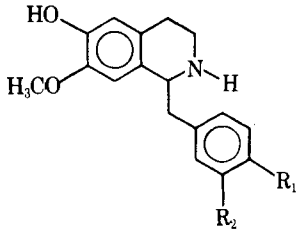

V

Va: $R_1 = R_2 = OCH_2O$
Vb: $R_1 = R_2 = OCH_3$

Structure IIc is dehydropseudocheilanthifoline, a naturally occurring compound isolated from *Isopyrum thalictroides* (7). An authentic sample of IIc was different from Q-4 in all respects. Thus, Structure IIa was assigned tentatively to Q-4.

On reduction with sodium borohydride, Q-4 yielded a tetrahydroprotoberberine, Q-4-H, mp 142–144°. High-resolution mass spectral analysis of the molecular ion at *m/e* 325 agreed with a composition of $C_{19}H_{19}NO_4$. The UV absorption maxima at 230 and 290 nm were consistent with the expected chromophore, and a bathochromic shift on base treatment coupled with the IR bands at 3571 cm^{-1} suggested a phenolic function. The NMR spectrum showed one methoxy group at δ 3.85, one methylenedioxy group at δ 5.86, and four aromatic protons at δ 6.56 (s, 2H), 6.65 (s, 1H), and 6.82 (s, 1H) ppm. The electron-impact mass spectrum revealed the collapse of ring C to give base peak k (*m/e* 148) from ring D and ions i (*m/e* 178) and j (*m/e* 176) from rings A and B.

These data were identical to those of an authentic sample of 3-hydroxy-2-methoxy-10,11-methylenedioxyberbine (IVa), a by-product obtained from Suguna and Pai (8) in their synthesis of tetrahydrogroenlandicine. By a standard procedure, 6-hydroxy-7-methoxy-1-(3′,4′-methylenedioxybenzyl)-1,2,3,4-tetrahydroisoquinoline (Va) was synthesized and condensed with formaldehyde to give IVa, which also was found to be identical to Q-4-H. Further oxidation of IVa with mer-

Table I—Comparison of the NMR Data of Q-4 and Q-3 with Pseudoprotoberberinium Salts IIe and IIf in the Aromatic Region

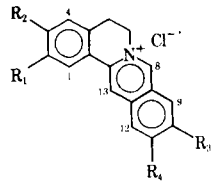

IIa: $R_1 = OCH_3$, $R_2 = OH$, $R_3 = R_4 = OCH_2O$
IIb: $R_1 = R_3 = R_4 = OCH_3$, $R_2 = OH$
IIe: $R_1 = R_2 = R_3 = R_4 = OCH_3$
IIf: $R_1 = R_2 = OCH_3$, $R_3 = R_4 = OCH_2O$

Compound	Proton H-4	H-12	H-1	H-9	H-13	H-8	Solvent
IIe[a]	7.07	7.60	7.63	7.67	8.83	9.50	Dimethyl sulfoxide-d_6
IIf[a]	7.07	7.55	7.62	7.67	8.80	9.47	Dimethyl sulfoxide-d_6
IIa (Q-4)	6.87	7.51	7.51	7.64	8.59	9.25	CD_3OD
IIb (Q-3)	6.53	7.33	7.43	7.43	8.27	9.07	CD_3OD

[a] Values for IIe and IIf were taken from Ref. 5.

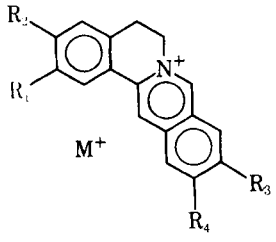

IIa: *m/e* 322 (93.8%)
IIb: *m/e* 338 (0.3%)

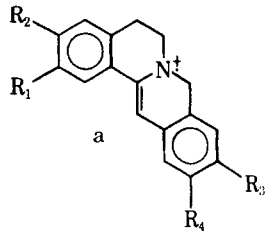

IIa: *m/e* 323 (40.3%)
IIb: *m/e* 339 (0.3%)

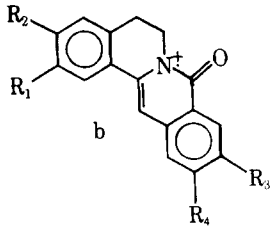

IIa: *m/e* 337 (11.8%)
IIb: *m/e* 353 (2.0%)

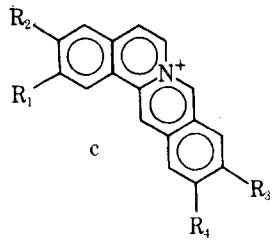

IIa: *m/e* 320 (100%)

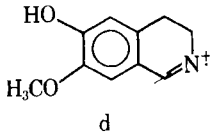

IIa: *m/e* 177 (1.8%)
IIb: *m/e* 177 (1.1%)

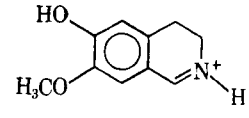

IIa: *m/e* 178 (1.8%)
IIb: *m/e* 178 (1.7%)

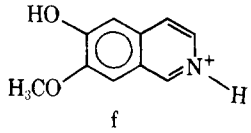

IIa: *m/e* 176 (2.7%)

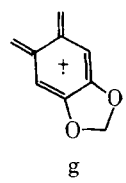

IIa: *m/e* 148 (4.0%)

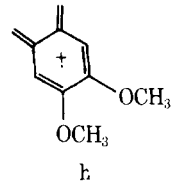

IIb: *m/e* 164 (3.0%)

Chemical-ionization mass spectral fragmentation of Q-4 (IIa) ($R_1 = OCH_3$, $R_2 = OH$, $R_3 = R_4 = OCH_2O$) and Q-3 (IIb) ($R_1 = R_3 = R_4 = OCH_3$, $R_2 = OH$) with isobutane as the reagent gas.

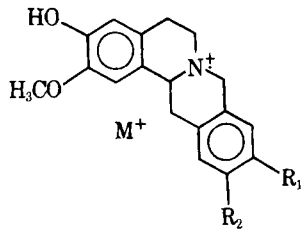

IV*a*: *m/e* 325 (62.5%)
IV*b*: *m/e* 341 (7.8%)

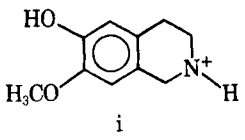

i

IV*a*: *m/e* 178 (1.2%)
IV*b*: *m/e* 178 (2.8%)

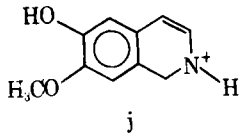

j

IV*a*: *m/e* 176 (29.2%)
IV*b*: *m/e* 176 (12.0%)

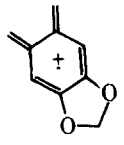

k

IV*a*: *m/e* 148 (100%)

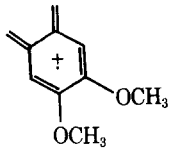

l

IV*b*: *m/e* 164 (100%)

Major fragments from electron-impact mass spectra of Q-4-H (IV*a*) ($R_1 = R_2 = OCH_2O$) and Q-3-H (IV*b*) ($R_1 = R_2 = OCH_3$).

curic acetate provided 3-hydroxy-2-methoxy-10,11-methylenedioxyberbinium chloride (II*a*), which was identical in every respect to Q-4. The structure of Q-4 therefore was firmly established as II*a*, and, since it was a new protoberberine from nature, it was named thalifaurine.

Alkaloid Q-3—Alkaloid Q-3 was isolated in a minute amount as the chloride salt, mp 230–234°, and was optically inactive. The UV spectrum was similar to that of Q-4, showing maximum absorptions at 243, 264.5, 289, 310 (sh), 341, and 379 (sh) nm. A bathochromic shift on base treatment and the IR absorption at 3400 cm^{-1} suggested its phenolic nature. The NMR spectrum showed three methoxy groups at δ 4.07, 4.01, and 3.89 ppm and one triplet of two protons at δ 3.05 ppm (J = 6 Hz), with a similar triplet obscured by the solvent peak. In the aromatic region, six protons were observed at δ 9.07 (s, 1H), 8.27 (s, 1H), 7.43 (s, 2H), 7.33 (s, 1H), and 6.53 (s, 1H) ppm. A comparison in this region with Q-4, II*e*, and II*f* (Table I) suggested that Q-3 is another 2,3,10,11-substituted pseudoprotoberberinium salt.

Examination of its chemical-ionization mass spectrum revealed the molecular ion M^+ (*m/e* 338) and the ions from thermal disproportionation of M^+, a (*m/e* 339) and b (*m/e* 353), all of which supported the skeleton of the parent ion, although they were in significantly lower abundance than similar ions from Q-4. Ions d (*m/e* 177), e (*m/e* 178), and h (*m/e* 164) were in agreement with the presence of three methoxy groups and located the phenolic function on ring A as well.

Two alternative structures were compatible with these data: 3-hydroxy-2,10,11-trimethoxyberbinium chloride (II*b*) and 2-hydroxy-3,10,11-trimethoxyberbinium chloride (II*d*). Structure II*d* is pseudocolumbamine, an alkaloid isolated from *I. thalictroides* (7). An authentic sample of II*d* was entirely different from Q-3, which required the assignment of Structure II*b* to Q-3.

Further evidence came from the reduction of Q-3 with sodium borohydride, giving a tetrahydroprotoberberine, Q-3-H, mp 180–182°. The molecular ion at *m/e* 341 was analyzed for $C_{20}H_{23}NO_4$ by high-resolution mass spectrometry. In agreement with the expected chromophore, the UV spectrum showed maximum absorption at 225 (sh) and 286.5 nm. A bathochromic shift was observed in the presence of base, which corroborated the IR phenolic absorption bands at 3570 and 3440 cm^{-1}. The NMR spectrum revealed three methoxy groups at δ 3.86 (s, 6H), and 3.89 (s, 3H) ppm and four aromatic protons at δ 6.58 (s, 1H), 6.66 (s, 2H), and 6.72 (s, 1H) ppm. The major mode of fragmentation in the electron-impact mass spectrum was the cyclic collapse of ring C, yielding base peak l (*m/e* 164) from ring D and ions i (*m/e* 178) and j (*m/e* 176) from rings A and B.

These spectral data were in good agreement with those of discretine (IV*b*) isolated from *Xylopia discreta* (9). Following literature procedures (10, 11), IV*b* was synthesized by condensing 6-hydroxy-7-methoxy-1-(3′,4′-dimethoxybenzyl)-1,2,3,4-tetrahydroisoquinoline (V*b*) with formaldehyde. This synthetic sample of (±)-discretine (IV*b*) was identical with Q-3-H in all respects. In addition, oxidation of IV*b* with mercuric acetate produced a compound, II*b*, that was identical to Q-3. Therefore, the structure of Q-3 was proven to be 3-hydroxy-2,10,11-trimethoxyberbinium chloride (II*b*). Since it is a dehydro form of discretine, it was named dehydrodiscretine.

Alkaloid Q-6—The major alkaloid in the quaternary base fraction was Q-6, isolated as the iodide salt, mp 250–252°. The spectral properties of this compound were identical to those of an authentic sample of magnoflorine (III) iodide.

EXPERIMENTAL[2]

Plant Material—The whole plant of *T. fauriei* Hayata[3] was collected during spring 1976 from the mountains near Wulai, Taipei County, Taiwan. The whole plant material was dried in an oven at 45° and milled to a fine powder.

Extraction and Initial Fractionation—Powdered plant material (3.29 kg) was extracted with 95% ethanol by percolation at room temperature until a negative test for alkaloids in the extract was shown with Valser reagent. The percolate was concentrated *in vacuo* to give 350 g of a greenish-brown semisolid residue. This residue was triturated with 3% citric acid and filtered. The process was continued until the filtrate showed a negative Valser test.

The combined acidic solution (3.5 liters) was extracted with ethyl acetate (4 liters) to remove the acidic and neutral fractions. The citric acid solution was adjusted to pH 9–10 with concentrated ammonium hydroxide and then extracted successively with ether (2 liters) and chloroform (3 liters), which removed the tertiary base fraction. The aqueous solution was adjusted to pH 4.4 with saturated citric acid solution, and Mayer reagent was added to precipitate the quaternary alkaloids.

After standing overnight in a refrigerator, the precipitate was filtered and washed with ether. The residue (106 g) then was dissolved in methanol–acetone–water (3:1:1), and the insoluble material was filtered off. The filtrate was stirred with an anion-exchange resin[4] for 3 days. After removal of the resin by filtration, the filtrate was evaporated under reduced pressure to give a semisolid residue (27.5 g) of the quaternary alkaloids as the chloride salts. Part of this residue (6.6 g) was chromatographed on a silica gel[5] (313 g) column and eluted with methanol in chloroform, with the methanol concentration increasing stepwise (1, 3, 7.5, 15, 30, 50, and 100%). Each 100 ml of eluate was collected and analyzed by TLC.

Isolation and Identification of Thalifaurine (II*a*, Q-4)—The residue (260 mg) from column fractions 50–52, eluted with 30% methanol in chloroform, was crystallized from methanol and recrystallized from the same solvent, yielding Q-4 as fine yellow needles (50 mg), mp 258–260°, $[\alpha]_D^{25}$ 0° (*c*, 0.2 in methanol); IR (KBr): ν_{max} 3510 (m), 3326 (m, OH), 1640 (m, C=N), 1613 (m), and 933 (w, OCH_2O) cm^{-1}; UV (methanol): λ_{max} (log ϵ) 241 (4.31), 263 (4.28), 291 (4.66), 310 (sh, 4.40), 341 (4.23), and 380 (sh, 3.83) nm; UV (methanol–0.1 *N* NaOH): λ_{max} (log ϵ) 252.5 (4.45), 311 (4.32), and 380 (4.44) nm; NMR (CD_3OD): 3.17, 4.74 (2 t, J = 6 Hz, CH_2CH_2), 4.02 (s, OCH_3), 6.33 (s, OCH_2O), 7.51 (s, 2H, aromatic), and 6.87, 7.64, 8.59, and 9.25 (4 s, 1H each, aromatic); electron-impact mass spectrum: *m/e* (%) 337 ($M^+ + O - H$, 6.2), 336 (8.6), 335 (10.2), 334 (8.5), 323 (19.4), 322 (M^+, 31.4), 321 (71.4), 320 (97.5), 319 (69.9), 318 (91.0), 307 (10.5), 306 (19.3), 305 (10.1), 278 (7.2), 277 (6.4), 261 (6.3), 260 (5.5), 202 (6.0), 177 (1.8), 176 (2.7), 160 (7.0), 159 (7.7), 130 (9.4), 52 (32.4), and 50 (100); chemical-ionization mass spectrum (isobutane as reagent gas):

[2] Melting points were taken with a Thomas-Hoover apparatus and are uncorrected. UV spectra were determined with a Hitachi model 200-20 spectrophotometer. IR spectra were taken with a Perkin-Elmer model 577 spectrophotometer in potassium bromide pellets. NMR spectra were recorded in suitable solvents, with tetramethylsilane as the internal standard, on a Varian A-60A or Bruker HX-90E spectrometer; chemical shifts are reported as δ (parts per million) values.

Optical rotations were measured on a Perkin-Elmer model 241 polarimeter. Mass spectra were obtained using a DuPont 21-491 double-focusing spectrometer *via* a direct-inlet probe, and the chemical-ionization mass spectra employed isobutane as the reactant gas. High-resolution mass spectra were determined on an A.E.I. MS-902 instrument using a direct-inlet system. Elemental analyses were performed by the Laboratory of Microanalysis, Chung-Shan Institute of Science and Technology, Chung-Li, Taiwan.

[3] A specimen of this plant was authenticated by Mr. Muh-Tsuen Kao, Department of Botany, National Taiwan University, and a voucher specimen was deposited in the School of Pharmacy of that University.

[4] IRA-410, chloride form.

[5] E. Merck No. 7734.

m/e (%): 378 (M^+ + 56, 4.0), 376 (2.9), 364 (M^+ + 42, 10.5), 362 (14.9), 337 (M^+ + O − H, 11.8), 336 (16.7), 335 (8.5), 324 (12.7), 323 (40.3), 322 (M^+, 93.8), 321 (90.6), 320 (100), 319 (65.9), 318 (16.3), 178 (1.8), 177 (1.8), 176 (2.7), and 148 (4.0). IR, UV, NMR, and mass spectral comparisons showed that this compound was identical to a synthetic sample of 3-hydroxy-2-methoxy-10,11-methylenedioxyberbinium chloride (II*a*), and a mixed melting-point determination showed no depression.

Reduction of II*a* to Q-4-H (IV*a*)—A solution of Q-4 (61 mg) in methanol (18 ml) was cooled on an ice bath and treated portionwise with sodium borohydride (122 mg). The mixture was stirred at room temperature for 24 hr and then evaporated under reduced pressure to remove methanol. The residue was treated with 6% NH_4OH (30 ml) and extracted with chloroform (4 × 30 ml). The combined chloroform extracts were washed with water (50 ml), dried (anhydrous potassium carbonate), and evaporated to give a syrup.

Crystallization from chloroform–methanol provided Q-4-H (30 mg) as pale-yellow plates, mp 142–144°; IR (KBr): ν_{max} 3571 (m, OH), 2930 (w), 2894 (w), 2853 (w), 2813 (w, *trans*-quinolizidine bands), 1505 (s), 1477 (s), and 930 (m, OCH_2O) cm^{-1}; UV (methanol): λ_{max} (log ϵ) 230 (sh, 4.00) and 290 (3.94) nm; UV (methanol–0.1 *N* NaOH): λ_{max} (log ϵ) 240 (sh, 4.01) and 296 (4.04) nm; NMR (CD_3OD): δ 2.49–3.97 (m, 9H, aliphatic), 3.85 (s, OCH_3), 5.86 (s, OCH_2O), 6.56 (s, 2H, aromatic), and 6.65 and 6.82 (2 s, 1H each, aromatic); electron-impact mass spectrum: *m/e* (%) 326 (13.6), 325 (M^+, 62.5), 324 (24.9), 310 (4.4), 178 (1.2), 177 (5.8), 176 (29.2), 150 (14.7), 149 (27.4), 148 (100), 147 (21.8), and 146 (4.6). The high-resolution mass measurement of *m/e* 325 (M^+) showed a value of 325.1315 for $C_{19}H_{19}NO_4$ (calc. 325.1312). The IR, UV, NMR, and mass spectra and a mixed melting-point determination showed that this compound was identical to an authentic sample of 3-hydroxy-2-methoxy-10,11-methylenedioxyberbine (IV*a*).

Synthesis of IV*a*—A mixture of 6-hydroxy-7-methoxy-1-(3′,4′-methylenedioxybenzyl)-1,2,3,4-tetrahydroisoquinoline (V*a*) (125 mg as the hydrochloride salt) and formaldehyde (4 ml) in acetic acid (4 ml) was refluxed for 3 hr. The reaction mixture was evaporated, and the resulting residue was made alkaline with 10% NH_4OH (30 ml). The aqueous solution was extracted with chloroform (4 × 30 ml), and the combined extracts were washed with water (50 ml), dried (anhydrous sodium sulfate), and evaporated to leave a residue (110 mg). The residue was purified further on a silica gel (7 g) column with the eluent (acetone in benzene) increasing from 1 to 20%.

Each 30-ml eluate was collected and analyzed by TLC. The residue from column fractions 18–61 was crystallized from chloroform–methanol to yield IV*a* (40 mg), mp 145–146°. The spectral properties of this compound were identical in every respect to those of an authentic sample synthesized by another route (8), mixed mp 144–145°. It also was identical to Q-4-H in terms of the IR, UV, NMR, and mass spectra and the mixed melting point (144–145°).

Anal.—Calc. for $C_{19}H_{19}NO_4$: C, 70.14; H, 5.89; N, 4.30. Found: C, 70.02; H, 5.95; N, 4.22.

Synthesis of II*a*—A solution of IV*a* (30 mg) in 25% acetic acid (30 ml) was treated with a saturated solution of mercuric acetate in acetic acid (1.5 ml), and the resulting mixture was refluxed on a water bath for 1 hr. The reaction mixture was evaporated, and the residue was dissolved in anhydrous ethanol (30 ml). A stream of hydrogen sulfide gas was introduced into the solution to precipitate the mercuric ion as the sulfide salt. The precipitate was removed by centrifugation and filtration over a layer of filter aid. The residue was washed with ethanol (3 × 40 ml) and filtered.

The combined ethanolic filtrates were evaporated to leave a residue. This residue was dissolved in warm concentrated hydrochloric acid (10 drops) and set aside to crystallize. The crude crystals were collected and recrystallized from methanol to yield fine yellow needles (15 mg) of II*a*, mp 259–261°. Compound II*a* was identical to Q-4 in terms of their IR, UV, NMR, and mass spectra. The mixed melting point was 258–260°.

Anal.—Calc. for $C_{19}H_{16}ClNO_4 \cdot H_2O$: C, 60.73; H, 4.83; Cl, 9.43; N, 3.73. Found: C, 60.15; H, 4.67; Cl, 9.45; N, 3.84.

Isolation and Identification of Dehydrodiscretine (II*b*, Q-3)—The residue from column fractions 46–49, eluted with 30% methanol in chloroform, was combined (125 mg) and rechromatographed on a small silica gel (15 g) column. Elution was performed by using methanol in chloroform (increasing from 5 to 20%) and collecting each 15-ml fraction. Additional Q-4 (15 mg) was isolated from fractions 34–43. The residue from fractions 46–53 was dissolved in a minimum amount of methanol and set aside in a refrigerator for 3 days.

The fine reddish-brown needles of Q-3 (10 mg) were filtered, mp 230–234°, $[\alpha]_D^{25}$ 0° (*c*, 0.15 in methanol); IR (KBr): ν_{max} 3400 (m, OH), 1633 (m), 1614 (m), 1517 (s), 1500 (s), 1430 (s), 1358 (s), 1290 (s), 1220 (s), 1128 (m), 1008 (m), and 880 (m) cm^{-1}; UV (methanol): λ_{max} (log ϵ) 243 (4.24), 264.5 (4.21), 289 (4.48), 310 (sh, 4.36), 341 (4.19), and 379 (sh, 3.82) nm; UV (methanol–0.1 *N* NaOH): λ_{max} (log ϵ) 254 (4.42), 310 (4.24), and 378 (4.37) nm; NMR (CD_3OD): δ 3.89, 4.01, and 4.07 (3 s, OCH_3 each), 3.05 (t, J = 6 Hz, CH_2), 7.43 (s, 2H, aromatic), and 6.53, 7.33, 8.27, and 9.07 (4 s, 1H each, aromatic); chemical-ionization mass spectrum (isobutane as reagent gas): *m/e* (%) 353 (M^+ + O − H, 2.0), 339 (0.3), 338 (M^+, 0.3), 208 (1.0), 206 (0.7), 178 (1.7), 177 (1.1), 169 (3.0), 167 (7.5), 165 (1.2), 164 (3.0), 163 (1.4), 152 (3.6), 150 (14.5), 149 (14.3), 141 (14.8), 137 (8.3), 128 (5.5), 127 (100), 126 (19.9), 105 (8.2), 103 (3.2), 95 (4.2), 91 (3.2), 85 (5.3), 76 (6.6), 75 (34.6), 74 (87.8), and 73 (5.1). This compound was shown to be 3-hydroxy-2,10,11-trimethoxyberbinium chloride (II*b*) by direct comparison with a synthetic sample.

Reduction of II*b* to Discretine (IV*b*)—A solution of Q-3 (8 mg) in methanol (5 ml) was reduced with sodium borohydride (20 mg) following a procedure similar to that described for the reduction of Q-4. The reduced product was crystallized from methanol as colorless needles (3 mg) and was designated as Q-3-H. Additional Q-3-H was obtained from reduction of the mother liquid of Q-3, which also was admixed with Q-4. The reduced mixture of Q-3-H and Q-4-H was separated on a preparative TLC plate of silica gel[5] (1 mm) and eluted with acetone–benzene (1:3). The zone corresponding to Q-3-H (R_f 0.31) was scraped and extracted with methanol–chloroform (1:9). The extract was evaporated, and the residue was crystallized from methanol to provide 9 mg of Q-3-H.

The combined material of Q-3-H was recrystallized from methanol, mp 180–182°; IR (KBr): ν_{max} 3570 (m), 3440 (m, OH), 2940 (m), 2840 (w), 1615 (m), 1520 (s), 1448 (m), 1350 (m), 1260 (s), 1140 (m), and 1030 (m) cm^{-1}; UV (methanol): λ_{max} (log ϵ) 225 (sh, 4.18) and 286.5 (3.87) nm; UV (methanol–0.1 *N* NaOH): λ_{max} (log ϵ) 245 (4.08), 290.5 (3.96), and 300 (sh, 3.83) nm; NMR ($CDCl_3$): δ 2.50–3.80 (m, 9H, aliphatic), 3.86 (s, 2 OCH_3), 3.89 (s, OCH_3), 6.66 (s, 2H, aromatic), and 6.58 and 6.72 (2s, 1H each, aromatic); electron-impact mass spectrum: *m/e* (%) 342 (1.9), 341 (M^+, 7.8), 340 (3.4), 339 (3.0), 338 (4.3), 283 (5.3), 181 (3.5), 180 (2.4), 178 (2.8), 177 (3.6), 176 (12.0), 166 (11.9), 165 (38.1), 164 (100), 151 (3.0), 150 (4.7), 135 (4.1), and 133 (4.1). The high-resolution mass measurement of *m/e* 341 (M^+) showed a mass for $C_{20}H_{23}NO_4$ of 341.1624 (calc. 341.1626). This compound was identical to a synthetic sample of IV*b* in terms of their IR, UV, NMR, and mass spectra and a mixed melting-point determination.

Synthesis of II*b* from IV*b*—(±)-Discretine was synthesized according to the method of Kametani *et al.* (10, 11) by condensation of 6-hydroxy-7-methoxy-1-(3′,4′-dimethoxybenzyl)-1,2,3,4-tetrahydroisoquinoline (V*b*) with formaldehyde or by debenzylation of *O*-benzyldiscretine. The pure product of IV*b* was crystallized from acetone–ether as white plates, mp 183–184° [lit. (10) mp 182–184°]. Direct comparison of their IR, UV, NMR, and mass spectra showed that this compound was identical to Q-3-H; a mixed melting point of 182–184° was observed.

A solution of IV*b* (300 mg) in acetic acid (12 ml) was added to a warm solution of mercuric acetate (2.1 g) in acetic acid (14 ml). The resulting mixture was refluxed on a water bath for 7 hr. Following a workup similar to that described for the synthesis of II*a*, a yellow residue was obtained. This residue was dissolved in concentrated hydrochloric acid (5 ml). The crude crystal was collected and recrystallized from methanol to yield II*b* as fine reddish-yellow needles (284 mg), mp 232–234°. This compound was identical to Q-3 in terms of their IR, NMR, and UV spectra, and a mixed melting point of 230–233° was obtained.

Anal.—Calc. for $C_{20}H_{20}ClNO_4 \cdot H_2O$: C, 61.30; H, 5.66; Cl, 9.05; N, 3.57. Found: C, 60.95; H, 5.68; Cl, 8.84; N, 3.64.

Isolation and Identification of Magnoflorine (III) Iodide (Q-6)—The crude brown residue (1.76 g) from column fractions 65–118, eluted with 75% methanol in chloroform, was dissolved in methanol. To this solution was added an excess of saturated methanolic potassium iodide solution. The solution was kept at room temperature for 2 days, and the resulting white precipitate was removed by filtration. The precipitate was crystallized twice from methanol to yield Q-6 (85 mg) as white crystals, mp 250–252°. This compound was identified as magnoflorine (III) iodide on the basis of its TLC behavior and IR, UV, circular dichroism, NMR, and mass spectral data, which were identical to those obtained for an authentic sample of magnoflorine iodide. In addition, there was no depression in the mixed melting-point determination with an authentic sample of magnoflorine iodide.

REFERENCES

(1) H.-L. Li, T.-S. Liu, T.-C. Huang, T. Koyama, and C. E. DeVol, "Flora of Taiwan," vol. 2, Epoch Publishing, Taipei, Taiwan, Republic of China, p. 510 (to be published).

(2) P. L. Schiff, Jr., and R. W. Doskotch, *Lloydia*, **33**, 404 (1970).
(3) C.-H. Chen and J. Wu, *Taiwan Yao Hsueh Tsa Chih*, **28**, 121 (1976).
(4) M. Shamma, M. J. Hillman, and C. D. Jones, *Chem. Rev.*, **69**, 779 (1969).
(5) V. Simanek, V. Preininger, and J. Lasovsky, *Coll. Czech. Chem. Commun.*, **41**, 1050 (1976).
(6) G. Habermehl, J. Schunk, and G. Schaden, *Justus Liebigs Ann. Chem.*, **742**, 138 (1970).
(7) C. Moulis, J. Gleye, and E. Stanislas, *Phytochemistry*, **16**, 1283 (1977).
(8) H. Suguna and B. R. Pai, *Coll. Czech. Chem. Commun.*, **41**, 1219 (1976).
(9) J. Schmutz, *Helv. Chim. Acta*, **42**, 335 (1959).
(10) T. Kametani, M. Takeshita, and S. Takano, *J. Chem. Soc. Perkin I*, **1972**, 2834.
(11) T. Kametani, Y. Hirai, F. Satoh, K. Ogasawara, and K. Fukumoto, *Chem. Pharm. Bull.*, **21**, 907 (1973).

ACKNOWLEDGMENTS

Adapted in part from the theses submitted by T.-M. Chen and C. Lee to the National Taiwan University in partial fulfillment of the Master of Science degree requirements.

Supported by the National Science Council of the Republic of China.

The authors thank Dr. Edward H. Fairchild and Dr. Jinn Wu, College of Pharmacy, Ohio State University, for measurement of some PMR and mass spectra and Dr. Kuo-Hsiung Lee, School of Pharmacy, University of North Carolina at Chapel Hill, for measurement of the high-resolution mass spectra. They also thank Dr. B. R. Pai, Department of Chemistry, Presidency University, Madras, India, for an authentic sample of 3-hydroxy-2-methoxy-10,11-methylenedioxyberbine and Dr. C. Moulis, Faculty of Pharmaceutical Sciences, University of Toulouse, France, for authentic samples of pseudocolumbamine and dehydropseudocheilanthifoline. C.-H. Chen also expresses his gratitude to the late Professor Taito O. Soine for his encouragement and interest in this work.

Acetylcarnitine and Cholinergic Receptors

K. W. REED, W. J. MURRAY ˣ, and E. B. ROCHE

Received April 2, 1979, from the *Department of Biomedicinal Chemistry, College of Pharmacy, University of Nebraska Medical Center, Omaha, NE 68105.* Accepted for publication April 28, 1980.

Abstract □ Acetylcarnitine, a naturally occurring compound found in high concentration in heart and skeletal muscle of vertebrates, bears structural resemblance to acetylcholine, and studies have shown that it has slight cholinergic properties. Acetylcarnitine was subjected to conformational analysis by extended Hückel theory (EHT) and complete neglect of differential overlap (CNDO/2) molecular orbital methods. The preferred conformations were examined with respect to their similarity to the Kier and Chothia–Pauling models of cholinergic receptor patterns. The preferred conformations of both isomers did not fit the receptor pattern described by Kier's model, although energy barriers to rotation are low enough to permit accommodation. The Chothia–Pauling model predicts activity for the *S*-isomer only. These studies partially explain the low cholinergic activity found for acetylcarnitine and the higher activity of (*S*)-acetylcarnitine compared to the *R*-isomer.

Keyphrases □ Acetylcarnitine—conformational analysis, comparison to cholinergic receptor patterns □ Cholinergic activity—acetylcarnitine, conformational analysis, comparison to cholinergic receptor patterns □ Structure–activity relationships—acetylcarnitine, conformational analysis, comparison to cholinergic receptor patterns

L-(−)-Carnitine [(*R*)-carnitine, I] is a naturally occurring substance found in high concentrations in plants, microorganisms, and animals. The muscles of vertebrates and invertebrates have especially high levels. Its principal physiological function is to transport free fatty acids into the mitochondria prior to their oxidation *via* the β-oxidation cycle (1).

(*R*)-Acetylcarnitine (II), a derivative of carnitine, also is found in high concentrations in the tissues of vertebrates. Enveloped within the structure of acetylcarnitine is the structure of the parasympathetic neurotransmitter acetylcholine (indicated by the dashed lines in II). The close structural similarity of acetylcarnitine to acetylcholine has

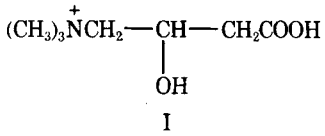

I

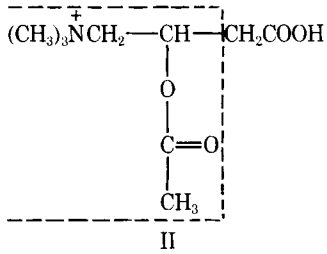

II

prompted investigations into its pharmacological properties as either a cholinomimetic or an anticholinergic compound (2–11).

BACKGROUND

It was reported that high doses of acetylcarnitine exerted a cholinergic effect on the heart which was blocked by atropine (2). Strack and Försterling reported that carnitine had little biological activity (3). However, Dallemagne *et al.* (4) found that carnitine and acetylcarnitine depolarized motor end plates. They reported that (*R,S*)-carnitine was 1/1000 as potent as acetylcholine on frog rectus abdominis muscle and that (*R*)-acetylcarnitine was 10–25% as potent as acetylcholine (4).

In contrast, Blum *et al.* (5) found (*R*)-carnitine to have 1/10,000 and (*S*)-carnitine to have 1/4000 the activity of acetylcholine on rectus abdominis muscle. They also reported that (*R*)- and (*S*)-acetylcarnitine were 1/700 as potent as acetylcholine in lowering arterial blood pressure in dogs (5). They concluded that acetylcarnitine acts at the cholinergic site rather than by blocking acetylcholinesterase. Two other groups found that synthetic (*R,S*)-acetylcarnitine possessed only weak to no nicotinic activity (6, 7).

Hosein and Proulx (8) claimed to have isolated a cholinergic active fraction of brain synaptosomes and identified this fraction as containing the coenzyme A ester derivatives of γ-butyrobetaine, crotonbetaine, carnitine, and acetylcarnitine. Six groups of investigators were unable to verify Hosein's isolation and identification of the active cholinergic substance of the brain, and the substance isolated by Hosein *et al.* apparently was acetylcholine itself (7). Falchetto *et al.* (9) reported that cortical neurons excited by acetylcholine also are excited by carnitine and acetylcarnitine. Carnitine was found to be more potent than acetylcarnitine.

Fritz (10) injected (*R,S*)-acetylcarnitine intracisternally into rat brains and evoked pronounced motor activity, which was not observed with

0022-3549/80/0900-1065$01.00/0
© 1980, American Pharmaceutical Association

(2) P. L. Schiff, Jr., and R. W. Doskotch, *Lloydia*, **33**, 404 (1970).
(3) C.-H. Chen and J. Wu, *Taiwan Yao Hsueh Tsa Chih*, **28**, 121 (1976).
(4) M. Shamma, M. J. Hillman, and C. D. Jones, *Chem. Rev.*, **69**, 779 (1969).
(5) V. Simanek, V. Preininger, and J. Lasovsky, *Coll. Czech. Chem. Commun.*, **41**, 1050 (1976).
(6) G. Habermehl, J. Schunk, and G. Schaden, *Justus Liebigs Ann. Chem.*, **742**, 138 (1970).
(7) C. Moulis, J. Gleye, and E. Stanislas, *Phytochemistry*, **16**, 1283 (1977).
(8) H. Suguna and B. R. Pai, *Coll. Czech. Chem. Commun.*, **41**, 1219 (1976).
(9) J. Schmutz, *Helv. Chim. Acta*, **42**, 335 (1959).
(10) T. Kametani, M. Takeshita, and S. Takano, *J. Chem. Soc. Perkin I*, **1972**, 2834.
(11) T. Kametani, Y. Hirai, F. Satoh, K. Ogasawara, and K. Fukumoto, *Chem. Pharm. Bull.*, **21**, 907 (1973).

ACKNOWLEDGMENTS

Adapted in part from the theses submitted by T.-M. Chen and C. Lee to the National Taiwan University in partial fulfillment of the Master of Science degree requirements.

Supported by the National Science Council of the Republic of China.

The authors thank Dr. Edward H. Fairchild and Dr. Jinn Wu, College of Pharmacy, Ohio State University, for measurement of some PMR and mass spectra and Dr. Kuo-Hsiung Lee, School of Pharmacy, University of North Carolina at Chapel Hill, for measurement of the high-resolution mass spectra. They also thank Dr. B. R. Pai, Department of Chemistry, Presidency University, Madras, India, for an authentic sample of 3-hydroxy-2-methoxy-10,11-methylenedioxyberbine and Dr. C. Moulis, Faculty of Pharmaceutical Sciences, University of Toulouse, France, for authentic samples of pseudocolumbamine and dehydropseudocheilanthifoline. C.-H. Chen also expresses his gratitude to the late Professor Taito O. Soine for his encouragement and interest in this work.

Acetylcarnitine and Cholinergic Receptors

K. W. REED, W. J. MURRAY ˣ, and E. B. ROCHE

Received April 2, 1979, from the *Department of Biomedicinal Chemistry, College of Pharmacy, University of Nebraska Medical Center, Omaha, NE 68105.* Accepted for publication April 28, 1980.

Abstract □ Acetylcarnitine, a naturally occurring compound found in high concentration in heart and skeletal muscle of vertebrates, bears structural resemblance to acetylcholine, and studies have shown that it has slight cholinergic properties. Acetylcarnitine was subjected to conformational analysis by extended Hückel theory (EHT) and complete neglect of differential overlap (CNDO/2) molecular orbital methods. The preferred conformations were examined with respect to their similarity to the Kier and Chothia–Pauling models of cholinergic receptor patterns. The preferred conformations of both isomers did not fit the receptor pattern described by Kier's model, although energy barriers to rotation are low enough to permit accommodation. The Chothia–Pauling model predicts activity for the *S*-isomer only. These studies partially explain the low cholinergic activity found for acetylcarnitine and the higher activity of (*S*)-acetylcarnitine compared to the *R*-isomer.

Keyphrases □ Acetylcarnitine—conformational analysis, comparison to cholinergic receptor patterns □ Cholinergic activity—acetylcarnitine, conformational analysis, comparison to cholinergic receptor patterns □ Structure–activity relationships—acetylcarnitine, conformational analysis, comparison to cholinergic receptor patterns

L-(−)-Carnitine [(*R*)-carnitine, I] is a naturally occurring substance found in high concentrations in plants, microorganisms, and animals. The muscles of vertebrates and invertebrates have especially high levels. Its principal physiological function is to transport free fatty acids into the mitochondria prior to their oxidation *via* the β-oxidation cycle (1).

(*R*)-Acetylcarnitine (II), a derivative of carnitine, also is found in high concentrations in the tissues of vertebrates. Enveloped within the structure of acetylcarnitine is the structure of the parasympathetic neurotransmitter acetylcholine (indicated by the dashed lines in II). The close structural similarity of acetylcarnitine to acetylcholine has

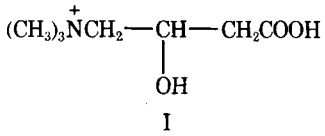

I

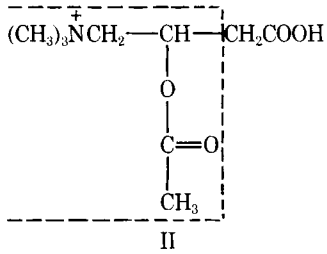

II

prompted investigations into its pharmacological properties as either a cholinomimetic or an anticholinergic compound (2–11).

BACKGROUND

It was reported that high doses of acetylcarnitine exerted a cholinergic effect on the heart which was blocked by atropine (2). Strack and Försterling reported that carnitine had little biological activity (3). However, Dallemagne *et al.* (4) found that carnitine and acetylcarnitine depolarized motor end plates. They reported that (*R,S*)-carnitine was 1/1000 as potent as acetylcholine on frog rectus abdominis muscle and that (*R*)-acetylcarnitine was 10–25% as potent as acetylcholine (4).

In contrast, Blum *et al.* (5) found (*R*)-carnitine to have 1/10,000 and (*S*)-carnitine to have 1/4000 the activity of acetylcholine on rectus abdominis muscle. They also reported that (*R*)- and (*S*)-acetylcarnitine were 1/700 as potent as acetylcholine in lowering arterial blood pressure in dogs (5). They concluded that acetylcarnitine acts at the cholinergic site rather than by blocking acetylcholinesterase. Two other groups found that synthetic (*R,S*)-acetylcarnitine possessed only weak to no nicotinic activity (6, 7).

Hosein and Proulx (8) claimed to have isolated a cholinergic active fraction of brain synaptosomes and identified this fraction as containing the coenzyme A ester derivatives of γ-butyrobetaine, crotonbetaine, carnitine, and acetylcarnitine. Six groups of investigators were unable to verify Hosein's isolation and identification of the active cholinergic substance of the brain, and the substance isolated by Hosein *et al.* apparently was acetylcholine itself (7). Falchetto *et al.* (9) reported that cortical neurons excited by acetylcholine also are excited by carnitine and acetylcarnitine. Carnitine was found to be more potent than acetylcarnitine.

Fritz (10) injected (*R,S*)-acetylcarnitine intracisternally into rat brains and evoked pronounced motor activity, which was not observed with

0022-3549/80/0900-1065$01.00/0
© 1980, American Pharmaceutical Association

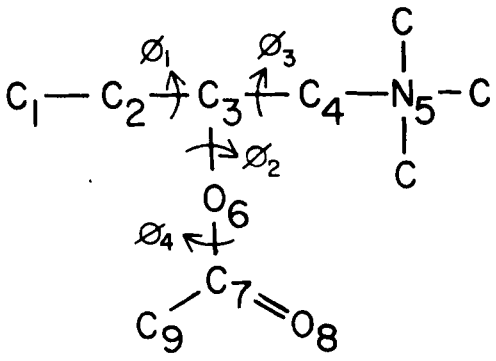

Figure 1—*Torsional angles for acetylcarnitine. Key:* ϕ_1, C_1-C_2-C_3-O_6; ϕ_2, C_2-C_3-O_6-C_7; ϕ_3, C_2-C_3-C_4-N_5; *and* ϕ_4, C_3-O_6-C_7-O_8.

(*R,S*)-carnitine. (*R,S*)-Acetylcarnitine injected intraventricularly caused phonation, pupillary dilatation, and markedly increased motor activity. Walker *et al.* (11) reported carnitine and acetylcarnitine to be less than 1/5000 as active as acetylcholine on excitatory neurons from *Helix aspera*.

Overall, the evidence shows that (*R*)- and (*S*)-acetylcarnitines possess low cholinergic activity. Since atropine is reported to block the cholinergic action of acetylcarnitine, its activity may be primarily at muscarinic receptors (5).

Many models of muscarinic and nicotinic receptors have been proposed based on the activity of potent cholinergic compounds. Therefore, it is of interest to examine the preferred conformations of (*R*)- and (*S*)-acetylcarnitines and to compare their fit to these proposed models. If the models are useful in predicting a pattern for an active cholinergic compound, then low activity compounds should not be expected to fit the pattern.

EXPERIMENTAL

To determine the preferred conformations, two quantum chemical methods were used: the extended Hückel theory (EHT)[1] (12) and complete neglect of differential overlap (CNDO/2)[2] (13). Although EHT usually exaggerates the energy barriers to rotation, it does correctly predict preferred rotational conformers. The CNDO/2 method relies less on empirical parameters than does EHT and uses a self-consistent field technique to estimate electronic interactions (13). Compared to EHT, CNDO/2 gives more realistic estimations of electronic parameters such as electron populations and charge densities and also gives reasonable estimations of energy barriers to rotation. The CNDO/2 method was used to verify the EHT calculations for preferred conformations and allowed the determination of the effect of electrostatic interactions between the quaternary ammonium group and the carboxylate anion.

The conformational problem concerns the steric and electronic effects of the C_1-carboxylate anion and the N_5-quaternary ammonium cation and the effect of the acetyl group in determining the rotational and conformational properties of the carnitine molecule. The numbering scheme and dihedral angles considered are given in Fig. 1. A torsional angle, ϕ (A–B–C–D), between the bonded atoms A–B–C–D represents the angle between planes ABC and BCD.

Viewed from the direction of A, positive rotations of ϕ are clockwise and negative rotations are counterclockwise, with the BCD plane rotating with respect to the ABC plane. The value $\phi = 0°$ corresponds to the *cis*-planar arrangement of bonds AB and CD.

The problem is analogous to that encountered by Kier (14) with cholinergic agents. To simplify calculations for acetylcholine, Kier segmented the molecule into two parts to determine the preferred conformation of each segment, which is dependent only on the nearest neighboring groups. This approach is used in the present study with both acetylcarnitine isomers.

Acetylcarnitine is segmented to include four torsional angles: ϕ_1 (C_1-C_2-C_3-O_6), ϕ_2 (C_2-C_3-O_6-C_7), ϕ_3 (C_2-C_3-C_4-N_5), and ϕ_4 (C_3-O_6-C_7-O_8)

[1] The EHT calculations were carried out with QCPE Program 64.
[2] The CNDO/2 calculations were carried out with QCPE Program 91.

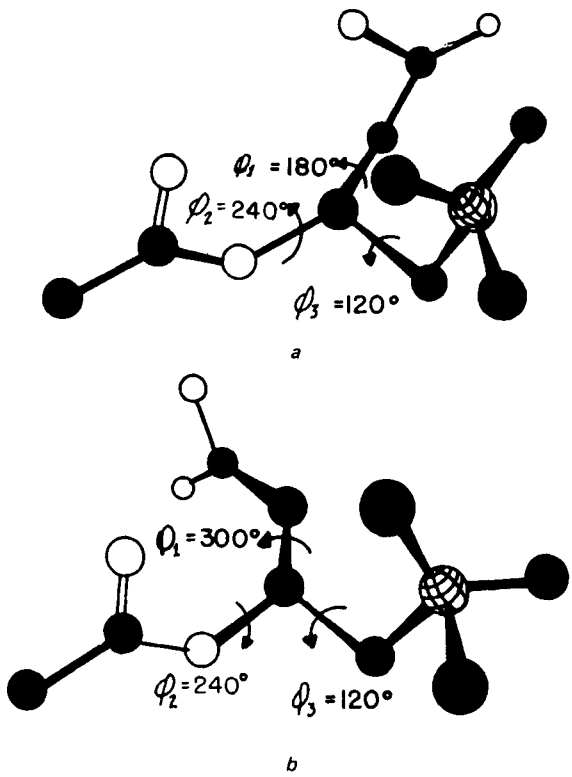

Figure 2—*Preferred conformations for acetylcarnitine. Key: a, folded conformation; and b, extended conformation.*

(Fig. 1). In addition, torsional angles for the preferred orientation of the quaternary ammonium group and carboxylate anion were determined. The optimal conformations of the isolated torsional angles, ϕ_1, ϕ_2, and ϕ_4, were determined first and then were used to find ϕ_3. With the whole molecule, slight variations in each torsional angle were examined to optimize all parameters.

The bond angles and bond lengths were derived from crystallographic data (15, 16). The three-dimensional Cartesian coordinates for each atom in the differing conformations were calculated with PROXYZ, QCPE Program 94, using X-ray data (15, 16).

RESULTS

Kier's (14) partitioning method for determining the lowest energy conformer for each torsional angle as the molecule is constructed was followed. For (*R*)-acetylcarnitine, the torsional angle for the ester group, ϕ_4 (C_3-O_6-C_7-O_8), using III was determined first using 30° increments.

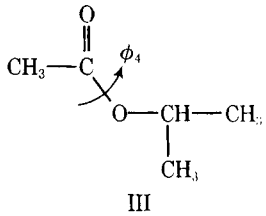

III

The lowest energy conformer was 300°. With this value of ϕ_4, ϕ_2 (C_2-C_3-O_6-C_7) was determined by adding on the carboxylate group to give IV.

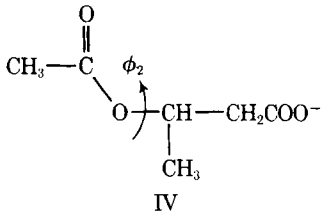

IV

Again, 30° increments in rotation were used and the lowest energy conformer occurred at $\phi_2 = 240°$. With this segment, ϕ_1 (C_1-C_2-C_3-O_6) was

Table I—Comparison of X-Ray and Calculated (EHT) Torsional Angles for (*R*)-Acetylcarnitine

Torsional Angle	Calculated Angle: Folded Conformer	Calculated Angle: Extended Conformer	Angle Observed by X-Ray (16)
ϕ_1 (C_1-C_2-C_3-O_6)	180°	300°	190°
ϕ_2 (C_2-C_3-O_6-C_7)	240°	240°	284.5°
ϕ_3 (C_2-C_3-C_4-N_5)	120°	120°	152.1°
ϕ_4 (C_3-O_6-C_7-O_8)	60°	60°	5.3°

determined to be 300°. Finally, the quaternary ammonium group was added to give V, and the whole molecule, lowest energy conformer was determined by varying ϕ_3 (C_2-C_3-C_4-N_5) in 30° increments.

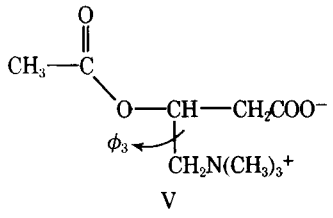

V

This rotamer was determined to be 120° and corresponds to an extended conformation (Fig. 2). Next, whole molecule rotations were done by varying one of the torsional angles and keeping the others constant. Another low energy conformer was found with a variation in ϕ_1; this conformer was determined to be ϕ_1 (C_1-C_2-C_3-O_6) = 180° and corresponds to a folded conformation. The folded conformer has the onium group and carboxylate group in close proximity, whereas the extended conformer corresponds to a molecule having the charged groups separated (Fig. 2). The EHT molecular orbital method was used in these determinations.

The X-ray data of Sass and Werness (16) on acetylcarnitine indicate a folded conformation. The values interpreted from their data are $\phi \approx 190°$, $\phi_2 = 284.5°$, and $\phi_3 = 152°$. Calculations using the CNDO/2 method also show that the preferred conformer of (*R*)-acetylcarnitine is the folded conformer. Table I shows the X-ray and EHT calculated values for the torsional angles of (*R*)-acetylcarnitine.

DISCUSSION

A drug receptor is generally defined as a macromolecule that, when interacting with a small drug molecule, initiates a biological response. Generally, much is known about the small molecules that interact specifically with the receptor, but there usually is only inferential evidence about the nature of the receptor. An analogy can be drawn between the concept of a receptor and the concept of induced fit that occurs in describing enzyme action. Induced fit explains the stereochemistry necessary for a substrate molecule to fit an enzyme, while the receptor concept describes the structural requirements for a drug. However, in enzymes, the substrate becomes altered by the macromolecule. In receptors, the small molecule is thought to cause a conformational change in the large molecule, thereby initiating the response.

As the small molecule approaches certain features on the macromolecule, it may interact if its structural features are complementary to those of the macromolecule, *i.e.*, if the drug is recognized. A drug molecule can be complementary without having agonist activity, in which case it would

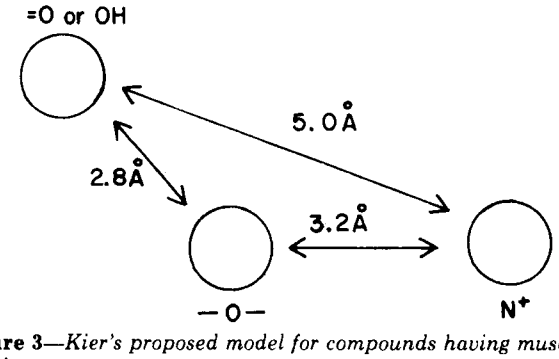

Figure 3—*Kier's proposed model for compounds having muscarinic activity.*

Table II—Comparison of Dihedral Angles of (*R*)-Acetylcarnitine with Chothia–Pauling Model of Acetylcholine

Torsional Angle[a]	Angle for Muscarinic Activity[b] by Chothia–Pauling Model	Angle in (*R*)-Acetylcarnitine[c]
τ_1 (CH_3N-N_5-C_4-C_3)[d]	180°	180°
τ_2 (N_5-C_4-C_3-O_6)	75–137°	240°
τ_3 (C_4-C_3-O_6-C_7)	145–215°	120°
τ_4 (C_3-O_6-C_7-C_9)	180–223°	240°

[a] Atoms numbered according to Fig. 1. [b] All angles are the same dihedral angles reported in Ref. 20 and shown in Fig. 4. [c] Torsional angles transformed from data in Table I. [d] Torsional angle with respect to C_3.

be an antagonist. If the drug is efficacious, specific conformational changes should occur in the macromolecule, leading to a biological action.

For this discussion, the receptor site is described only by the structural requirements necessary for initial recognition of the drug. This definition is limiting and has no applicability to the isolation and determination of the conformational and dynamic properties of the receptor macromolecule. It also does not take into account degrees of biological efficacy. However, the definition is useful in constructing a model of the receptor site topography during the initial approach of the drug. It also allows mapping of areas where primary and secondary interactions must occur for initial complementarity between the drug and its binding site on the macromolecule.

As a result of his EHT calculations for acetylcholine, muscarine, and muscarone, Kier (14) proposed a muscarinic receptor model based on structural similarity among these potent muscarinic compounds. The model defines the distances between three atomic centers as being important to activity: the quaternary nitrogen, the ether oxygen, and a carbonyl or hydroxyl oxygen (Fig. 3). Since three points describe a plane, Kier's model implies that a planar relationship between these groups is required, along with appropriate interatomic distances and electronic properties, for initial recognition by the receptor. As a result of calculations on β-methylacetylcholine, the model was modified (17). The modified distances between atomic centers are (Fig. 3): quaternary nitrogen to ether oxygen, 3.2 ± 0.2 Å; quaternary nitrogen to carbonyl oxygen, 5.0 ± 0.6 Å; and carbonyl oxygen to ether oxygen, 2.8 ± 0.6 Å.

The lowest energy conformer of (*S*)-acetylcarnitine from this study has the following atomic distances between groups: quaternary nitrogen to ether oxygen, 3.59 Å; quaternary nitrogen to carbonyl oxygen, 4.95 Å; quaternary nitrogen to acetyl methyl, 4.64 Å; and carbonyl oxygen to ether oxygen, 2.23 Å. These distances do not match Kier's original cholinergic receptor site model.

In acetylcarnitine, both isomers have a probability of adopting a conformation that enables them to fit Kier's modified receptor model (17).

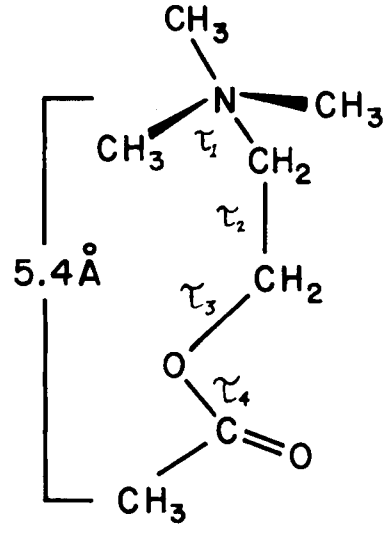

Figure 4—*Chothia–Pauling model for compounds having muscarinic activity. The torsional angles are from Ref. 20. See the text for definitions of these angles.*

To fit, the R-isomer must have the ester methyl group pointing up and the S-isomer must have the methyl group pointing down. These conformations and the receptor model fit are obtained only when ϕ_4 is rotated to 0°. This orientation of the methyl groups may account for the low activity of acetylcarnitine. These conformations are 5 kcal/mole less favorable than the preferred conformation according to EHT calculations. In these conformations, the γ-methylene and carboxylate groups are opposite the ester methyl group for both isomers.

Chothia and coworkers (18–20) also proposed a muscarinic receptor model. Their model was derived from an examination of the X-ray conformations of several cholinergic compounds. It is described in terms of torsional angles (τ) and interatomic distances (Fig. 4). The interatomic distances are: quaternary nitrogen to ether oxygen, 3.3 Å; quaternary nitrogen to carbonyl oxygen, 5.6 Å; and quaternary nitrogen to acetyl methyl, 5.4 Å. It was proposed that for muscarinic activity, the torsional angles shown in Fig. 4 need to have the following values (20): $\tau_1 = 180°$ (with respect to C-3), $\tau_2 = 73–137°$, $\tau_3 = 145–215°$, and $\tau_4 = 180$ or 223°, where the angles are defined, according to the numbering in Fig. 1, as $\tau_1 = CH_3N\text{-}N_5\text{-}C_4\text{-}C_3$, $\tau_2 = N_5\text{-}C_4\text{-}C_3\text{-}O_6$, $\tau_3 = C_4\text{-}C_3\text{-}O_6\text{-}C_7$, and $\tau_4 = C_3\text{-}O_6\text{-}C_7\text{-}C_9$.

The interatomic distances in the lowest energy conformation of (S)-acetylcarnitine from the present study are given for comparison.

For (R)-acetylcarnitine, the torsional angles defined in Ref. 20 are given in Table II. The values of the torsional angles for (R)-acetylcarnitine in Table II were transformed from those in Table I to allow comparison with the data from Ref. 20; however, the same conformation of (R)-acetylcarnitine is described in both Tables I and II.

With (S)-acetylcarnitine, there is very little difference in energy in the conformations for τ_3 between 180 and 300° and for τ_4 between 120 and 240°. (S)-Acetylcarnitine could fit the Chothia–Pauling model for muscarinic activity. However, (R)-acetylcarnitine does not fit because $\tau_2 = 240°$ (Table II and Fig. 4). From EHT, the (R)-acetylcarnitine conformer having $\tau_2 = 137°$ is energetically less favored than the preferred conformation, as shown by the calculated, although exaggerated, value of 300 kcal/mole.

On the basis of this examination, the preferred conformations of (R)- and (S)-acetylcarnitines do not meet the criteria proposed by Kier's model for muscarinic activity. However, the energy barriers to rotation are sufficiently low so that some conformations accommodate the model. However, in these conformations, the methyl group on the acetyl moiety is oriented differently than for acetylcholine. These results may explain the low muscarinic activity found for acetylcarnitine. The Chothia–Pauling model predicts that only the S-isomer will have muscarinic activity.

Some controversy exists concerning whether acetylcarnitine possesses cholinergic activity (2–11). Current evidence suggests that (R)- and (S)-acetylcarnitines possess low cholinergic, muscarinic activity (5, 9). The S-isomer appears to be more potent than the R-isomer, and both isomers are reported to interact at the cholinergic, muscarinic receptor (5). The Chothia–Pauling model correctly predicts activity for the S-isomer but does not predict the interaction of the R-isomer with the receptor. Although the lowest energy conformers of (R)- and (S)-acetylcarnitines do not fit Kier's model, flexibility in the molecule does allow some degree of fit. Kier's model appears to fulfill more satisfactorily the requirements for defining the initial recognition features for interaction. The Chothia–Pauling model appears to be suitable for describing requirements for biological efficacy.

The low order of activity also may be related to the remainder of the carnitine molecule. Acetylcarnitine may be considered as the β-acetic acid derivative of acetylcholine. The steric bulk of this substituent and its highly polar nature may interfere in the interaction and specificity of the conformational perturbation in the receptor.

REFERENCES

(1) I. B. Fritz, *Physiol. Rev.*, **41**, 52 (1961).

(2) P. Weger, *Biochem. Z.*, **287**, 424 (1936).

(3) E. Strack and K. Försterling, *Arch. Exp. Pathol. Pharmakol.*, **185**, 612 (1937).

(4) M. J. Dallemagne, E. Philippot, F. Binon, and E. L. Dumoulin, in "Proceedings of the World Congress of Anesthesiologists," vol. 1, International Anesthesia Research Society, Burgess Publishing, Minneapolis, Minn., 1955, p. 285.

(5) K. Blum, E. Seifter, and J. Seifter, *J. Pharmacol. Exp. Ther.*, **178**, 331 (1971).

(6) E. A. Hosein, S. J. Booth, I. Gasoi, and G. Kato, *ibid.*, **156**, 565 (1967).

(7) V. P. Whittaker and G. H. Dowe, *Int. J. Neuropharmacol.*, **3**, 593 (1964).

(8) E. A. Hosein and P. Proulx, *Arch. Biochem. Biophys.*, **106**, 267 (1964).

(9) S. Falchetto, G. Kato, and L. Provini, *Can. J. Phys. Pharmacol.*, **49**, 1 (1971).

(10) I. B. Fritz, *Adv. Lipid Res.*, **1**, 285 (1963).

(11) R. J. Walker, G. Kato, D. Morris, and G. N. Woodruff, *Comp. Gen. Pharmacol.*, **4**, 65 (1973).

(12) R. Hoffmann, *J. Chem. Phys.*, **39**, 1397 (1963).

(13) J. A. Pople, D. P. Santry, and G. A. Segal, *ibid.*, **43**, S129 (1965). J. A. Pople and G. A. Segal, *ibid.*, **43**, S136 (1965).

(14) L. B. Kier, *Mol. Pharmacol.*, **3**, 487 (1967).

(15) K. Tomita, K. Urabe, Y. B. Kim, and T. Fujiwara, *Bull. Chem. Soc. Jpn.*, **47**, 1988 (1974).

(16) R. L. Sass and P. Werness, *Biochem. Biophys. Res. Commun.*, **55**, 736 (1973).

(17) M. J. Jhon, U. I. Cho, and L. B. Kier, *J. Korean Chem. Soc.*, **16**, 70 (1970).

(18) C. Chothia, *Nature (London)*, **225**, 36 (1970).

(19) C. Chothia and P. Pauling, *ibid.*, **226**, 541 (1970).

(20) R. W. Baker, C. H. Chothia, P. Pauling, and T. J. Petcher, *ibid.*, **230**, 439 (1971).

Scope of Differential UV and Differential Fluorescence Assays for Phenothiazines: Comparison with Official Methods

DONALD F. GURKA *x, RICHARD E. KOLINSKI, JAMES W. MYRICK, and CLYDE E. WELLS

Received September 19, 1979, from the *National Center for Drug Analysis, Food and Drug Administration, St. Louis, MO 63101.* Accepted for publication March 4, 1980. *Present address: Environmental Protection Agency, Environmental Monitoring Systems Laboratory, Las Vegas, NV 89114.

Abstract □ Operational difficulties have been encountered with many of the official phenothiazine assay procedures in this laboratory. Although some difficulties were corrected, the procedures still lack specificity. Accordingly, the general scope of differential UV and differential fluorescence methods was investigated. These specific methods are facile, reproducible, and applicable to both composite and single-tablet assays.

Keyphrases □ Phenothiazines—comparison of differential UV and differential fluorescence methods with official assays □ Differential UV and fluorescence spectrophotometry—analysis, phenothiazines, comparison with official methods

The 10-substituted phenothiazines constitute one of the largest drug classes in the official compendia (1, 2). Nineteen different phenothiazine bases of this type are represented by 74 entries in the USP and NF. A recent drug quality assurance program in this laboratory resulted in the semiautomated analysis of 291 phenothiazine samples, in a wide variety of formulations, from 14 manufacturers.

While checking the results from the automated analyzer by the official assay procedures, considerable difficulty was experienced. Many of the official procedures did not work well and had to be amended. Consequently, the general scope of a differential spectrophotometric assay for phenothiazines was investigated (3). Results from this method were compared with those from the automated method and from modifications of the official procedures.

BACKGROUND

The oxidative degradation of 10-substituted phenothiazines has been studied extensively (see Refs. 4 and 5 for recent reviews). In particular, electrochemical oxidation has been studied in great detail (6–8). It was demonstrated that a 10-substituent raises the oxidation potential and directs oxidation to the sulfur atom. Theoretical considerations supported by electron-spin resonance studies have rationalized this oxidation direction in terms of a steric effect on the phenothiazine electronic system (9, 10). Chemical oxidation in these systems also leads predominantly to sulfur oxidation (11). Among the chemical reagents used have been ozone (12), oxygen (13), sodium nitrite (14), dichromate (15), and hydrogen peroxide (16).

Despite the ease of oxidation of these compounds, specific assay procedures that are stability indicating are not abundant in the literature. Although it is stability indicating, Ryan's palladium complex method (17) has not been widely adopted. A quantitative TLC procedure was described for butaperazine (18), but it is too laborious for routine analysis. GLC (19–21) and high-pressure liquid chromatographic (22, 23) methods are not generally applicable to the entire class of 10-substituted phenothiazines in the presence of their degradation products.

With this background in mind, the following considerations of the official phenothiazine assays indicate the need for their revision. The compendial procedures are of three types: measurement at a single UV wavelength, difference measurements at two UV wavelengths, and measurement of the palladium chloride complex at visible wavelengths. The first method is nonspecific and, at the low wavelengths employed, is susceptible to excipient interference. The difference method apparently involves baseline correction for interfering excipients. Use of the selected correction wavelength (~275 nm) can lead to spurious results since sulfoxide impurities can interfere through their nearby absorption maximum (24). The third method, a variation of Ryan's palladium complexation method, is specific. However, this method has not been widely adopted by the compendia (only one-third of the phenothiazine drugs in this study are officially determined by this method). This lack of acceptance may be a result of poor complex solubility, low complex absorptivity, or unstable complexes. These considerations, as well as a recent report (25) that cited extensive degradation of phenothiazine liquid formulations, emphasize the need for a general, specific assay.

EXPERIMENTAL

Apparatus—A UV-visible double-beam spectrophotometer[1] equipped with 1-cm quartz cells was used for the manual assays. The automated system consisted of a liquid sampler, two proportioning pumps, and two manifolds[2]. This system was equipped with a recorder[3] and interfaced with a minicomputer[4]. Absorbances were measured automatically on a single-beam spectrophotometer[5]. Fluorescence intensities were measured automatically on a ratio fluorometer[6]. Both were determined in a 1-cm flowcell. Manual measurements of fluorescence intensities were taken on the same fluorometer utilizing 1-cm rectangular cells. Tablets were disintegrated in an ultrasonic generator[7] or, if possible, on a mechanical shaker[8].

Materials—Alcohol (95%), acetic acid, hydrochloric acid, *n*-heptane, and *n*-butanol were analytical reagent grade[9] and were used as received. Ammonium hydroxide, sodium nitrite, potassium chloride, sodium hydroxide, and ascorbic acid were ACS grade[10] and were used as received. Hydrogen peroxide (30%) was refrigerated and used as needed. Chromatographic siliceous earth[11] was acid-washed grade and was rewashed with 0.1 *N* HCl on the column.

Standards—All standards were pure drug substances obtained from manufacturers whose products were studied in the quality assurance program. Each drug substance was analyzed *versus* the appropriate USP or NF reference standard by the automated procedure. All substances gave assays in the range of 100 ± 0.4%.

Preparation of Reagents—To prepare 0.1 *N* HCl, concentrated hydrochloric acid (10 ml) was diluted to 1 liter with deionized water.

The peracetic acid oxidizing solution was prepared by pipetting 1.5 ml of 30% H_2O_2 into a 250-ml volumetric flask containing 200 ml of acetic acid. The flask was covered and heated on a steam bath for 1 hr. After

[1] Acta MIV, Beckman Instruments Inc., Fullerton, Calif.
[2] AutoAnalyzer, Technicon Instruments Co., Tarrytown, N.Y.
[3] Servoriter II, Texas Instruments Inc., Houston, Tex.
[4] Series 2116 minicomputer, Hewlett-Packard Inc., Palo Alto, Calif.
[5] PM2DL, Carl Zeiss Inc., New York, N.Y.
[6] Ratio-2 fluorometer, Farrand Optical Co., Valhalla, N.Y.
[7] Model 11, Heat Systems-Ultrasonic Inc., Plainview, N.Y.
[8] Wrist-action shaker, Burrell Co., Pittsburgh, Pa.
[9] Mallinckrodt Chemical Works, St. Louis, Mo.
[10] Fisher Scientific Co., Fair Lawn, N.J.
[11] Celite, Johns-Manville, Denver, Colo.

0022-3549/80/0900-1069$01.00/0
© 1980, American Pharmaceutical Association

Table I—Analysis Parameters for the Modified Official Assay

Drug	Extraction Aliquot Concentration	Assay Concentration, μg/ml
Prochlorperazine maleate or edisylate	3 mg of salt/10 ml	12
Chlorpromazine hydrochloride	2 mg of salt/15 ml	20
Promazine hydrochloride	4 mg of salt/10 ml	40
Trimeprazine tartrate	1.5 mg of salt/10 ml	6

standing overnight at room temperature, the solution was diluted to volume with acetic acid. This solution was discarded after 1 week.

A solution of 0.025% ascorbic acid in 0.1 *N* HCl was prepared by dissolving 250 mg of ascorbic acid in 1 liter of 0.1 *N* HCl.

Three hundred milliliters of 95% alcohol was diluted to 1 liter with pH 2.2 buffer (26) to prepare a solution of alcohol and pH 2.2 buffer.

Equal volumes of *n*-butanol and *n*-heptane were mixed to prepare heptane–butanol (1:1).

The 0.5% $NaNO_2$ oxidizing solution was prepared by dissolving 1 g of sodium nitrite in 200 ml of deionized water.

A solution of 0.1 *N* NaOH was prepared by diluting 5.3 ml of 50% NaOH (w/v) to 1 liter with deionized water.

Modified Official Assay Procedure—Except for the following changes, the official procedures were used as given.

Class I Compounds—Prochlorperazine maleate or edisylate, chlorpromazine hydrochloride, promazine hydrochloride, and trimeprazine tartrate were assayed. To prepare single tablets for assay, the tablet was disrupted ultrasonically in 0.1 *N* HCl. To prepare sample composites, the average tablet weight was determined, and the tablets were ground in a mortar and pestle to pass through a 60-mesh screen. The appropriate weight of tablet powder then was shaken with 0.1 *N* HCl in a volumetric flask (Table I), diluted to volume with 0.1 *N* HCl, and filtered through paper. The first 10 ml of the filtrate was discarded.

An aliquot of the filtrate of the concentration specified in Table I was transferred to a separator. Water (125 ml) and saturated sodium chloride (5 ml) were added, and the solution was made basic with ammonium hydroxide (3 ml). The pH was checked to confirm that the solution was strongly alkaline. The solution then was extracted with four portions of heptane (40, 25, 25, and 25 ml). The combined heptane extracts were extracted with 0.1 *N* HCl (4 × 25 ml), and the combined hydrochloric acid extracts were diluted to the final concentration specified in Table I. The standards were prepared in 0.1 *N* HCl to the same final concentration as that expected for the assay.

Immediately after preparation of the assay and standard solutions, the absorbance was determined as specified in the individual official monograph. With the exception of prochlorperazine maleate and edisylate, all assay and standard operations were carried out in low-actinic glassware. In addition, prochlorperazine maleate and edisylate standards and trimeprazine tartrate standards were carried through the extraction procedure to remove the counterions, which are UV absorbing.

Class II Compounds—Fluphenazine hydrochloride, thiethylperazine maleate, and trifluoperazine hydrochloride were assayed. Sample preparation was the same as that described for the Class I compounds. For thiethylperazine maleate, 20 mg of drug was transferred to a separator. Ten milliliters of 0.1 *N* HCl, 15 ml of water, and 5 ml of saturated sodium chloride were added, after which the procedure in NF XIV was followed. For trifluoperazine hydrochloride tablets, the official NF XIV procedure was used.

For trifluoperazine hydrochloride liquid formulations, an aliquot containing 2 mg of drug dissolved in 10 ml of 0.1 *N* HCl was transferred to a separator. Fifteen milliliters of water, 5 ml of saturated sodium chloride, and 3 ml of stronger ammonia were added. Then the solution was extracted with four portions of heptane (40, 25, 25, and 15 ml). The combined heptane extracts were extracted with 0.1 *N* HCl (4 × 25 ml), and the combined acid extracts were diluted to a final concentration of 10 mg/ml with 0.1 *N* HCl. The absorbance was measured at the wavelength specified in the monograph *versus* a blank of 0.1 *N* HCl. A standard of the same final concentration as expected for the sample was prepared, and its absorbance was read concomitantly. All operations were performed in low-actinic glassware.

For fluphenazine hydrochloride, the official USP procedure was used but the extraction solvent was changed from the specified *n*-hexane to *n*-hexane–*n*-butanol (98:2).

Class III Compounds—Triflupromazine hydrochloride, perphenazine,

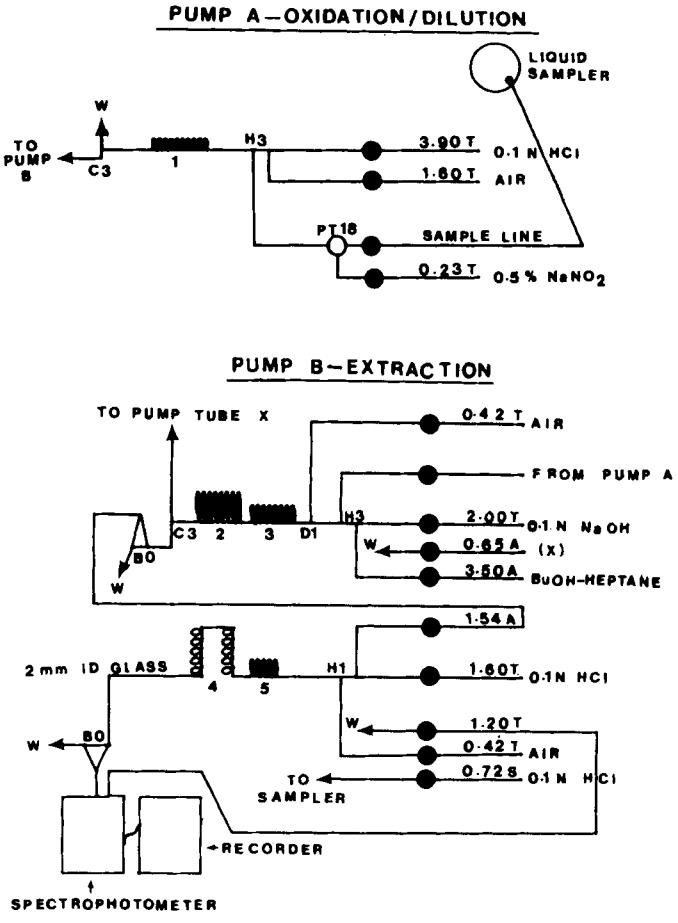

Figure 1—*Diagram of automated analytical system for phenothiazines. Pump tube sizes are listed in milliliters per minute. Key for pump tube materials: T, Tygon; S, silicone; and A, Acidflex. All connectors, mixing coils, and separators are identified with the Technicon designation, but similar units by other suppliers may be used. Key for mixing coils: 1, Technicon 105-0085; 2, eight turns of 2.4-mm (0.095 in.) i.d. Teflon tubing wrapped around a 38.1-mm (1.5-in.) diameter core; 3, Technicon 116-101-2 (beaded coil); 4, Technicon 157-0248; and 5, Technicon 116-0127-05 (1 mm i.d.). All points marked W go to the waste container. All connecting tubing should be as short as possible. The spectrophotometer is equipped with a 1-cm flowcell.*

and carphenazine maleate were assayed. The official procedures were used.

Automated Method—To prepare tablet samples, one tablet was placed in a vial and a sufficient amount of 0.025% ascorbic acid in 0.1 *N* HCl was added to yield the final drug concentration specified in Table II. The capped vial was shaken mechanically until tablet disintegration commenced. Then the vial was transferred to an ultrasonic bath, and the bath was operated until disintegration was complete. The vial was shaken mechanically for 30 min. After the solids settled, the supernate was decanted into a sample cup.

To prepare fluphenazine hydrochloride tablet samples, one tablet was placed in a volumetric flask chosen such that its volume yielded a final concentration of 50 μg/ml. Deionized water was added to equal 5% of the total flask volume. The flask was shaken mechanically until the tablet began to disintegrate. Then the flask was transferred to an ultrasonic bath, and the bath was operated until tablet disintegration was complete. The flask was diluted to volume with 95% alcohol and mixed. After the solids settled, the supernate was decanted into a sample cup.

To prepare the liquid formulation samples, a suitable aliquot was transferred in a "to contain" pipet to a volumetric flask. The pipet and volumetric flask were chosen such that the final assay concentration corresponded to that specified in Table II. The pipet contents were washed into the volumetric flask with 0.025% ascorbic acid in 0.1 *N* HCl, and the solution was diluted to volume with the same solvent. The standard solutions were prepared in this solvent at the same final concentration as that expected for the sample assay.

Table II—Differential UV and Semiautomated Analysis Parameters

Drug	Automated[a] Wavelength, nm	Automated[a] Final Concentration, μg/ml	Differential UV[b] Wavelength, nm	Differential UV[b] Final Concentration, μg/ml
I Carphenazine maleate	251	500	372	208
II Chlorpromazine hydrochloride	241, 298	200	344	40
III Promazine hydrochloride	241, 298	200	342	40
IV Thiethylperazine maleate	276	200	350	83
V Thioridazine hydrochloride	276, 342	200	348	40
VI Triflupromazine hydrochloride	273	400	347	40
VII Trimeprazine tartrate	271	100	342	42
VIII Fluphenazine hydrochloride	256	50	349	4.2
IX Methdilazine hydrochloride	251	160	341	58
X Prochlorperazine maleate	257	100	342	42
XI Trifluoperazine hydrochloride	257	40	349	4.0
XII Perphenazine	255	80	343	33

[a] Drugs I–VII were oxidized and double extracted. Drugs IX–XII were extracted and determined directly. For VIII in tablet strengths of ≥2.5 mg, the extracted drug was determined at a concentration of 50 μg/ml. Tablets containing ≤1 mg were oxidized, double extracted, and determined fluorometrically at a concentration of 10 μg/ml. [b] Drugs VIII and XI were analyzed by differential fluorescence; all others were analyzed by the differential UV method.

The assay (Fig. 1) was carried out by placing the sample and standard solutions in 3-ml polystyrene cups on a liquid sampler set at 24 samples/hr with a sample-to-wash ratio of 4:1. The cups were filled in the following order: three cups of standard, five cups of sample, one cup of standard, five cups of sample, *etc.* Two cups of standard were placed at the end of each run.

For drugs requiring oxidation and dilution, the sample was withdrawn and segmented with air, and 0.1 *N* HCl and 0.5% $NaNO_2$ (if necessary) were added. The solution then was mixed, resampled, and made basic with 0.1 *N* NaOH; heptane–butanol was added. After segmentation with air, the solution was mixed in a beaded coil, and the phases were allowed to coalesce in a phasing coil. Then the phases were separated. The organic phase was segmented with air and mixed with 0.1 *N* HCl. The phases were separated again. The drug was extracted into 0.1 *N* HCl, and the absorbance of the aqueous phase was read at the specified wavelength in a spectrophotometer equipped with a 1-cm flowcell.

For drugs requiring only extraction, the oxidation–dilution manifold was not used. The sample was introduced directly into the extraction manifold at the resample pump tube and made basic with 0.1 *N* NaOH, and heptane–butanol was added. After segmentation with air, the solution was mixed in a beaded coil, and the phases were allowed to coalesce in a phasing coil. The phases were separated. The organic phase was segmented with air and mixed with 0.1 *N* HCl. The phases were separated again. The drug was extracted into 0.1 *N* HCl, and the absorbance of the aqueous phase was read at the specified wavelength in a spectrophotometer equipped with a 1-cm flowcell.

Differential UV Method—The chromatographic columns for single-tablet and composite assays were prepared as follows. For 10-mg and higher strength tablets, a 17 × 250-mm column[12] plugged with glass wool was used. Acid-washed siliceous earth (3 g) was added and tamped down. The column was topped with a glass wool plug. Then 60 ml of 0.1 *N* HCl was passed through the column, and the wash was discarded. The column then was ready for use. For tablets of <10-mg strength, this procedure was modified to use a 13 × 200-mm column[12] packed with 1 g of acid-washed siliceous earth.

Single-tablet assays for promazine hydrochloride, chlorpromazine hydrochloride, triflupromazine hydrochloride, thioridazine hydrochloride, and thiethylperazine maleate were conducted as follows. One tablet was disintegrated in 60 ml of 0.1 *N* HCl in an ultrasonic bath. The tablet suspension was shaken for 1 hr on a mechanical shaker. Composites were prepared by determining the average tablet weight and then grinding the tablets to pass through a 60-mesh screen. A sufficient amount of tablet powder was weighed accurately to contain 10–12.5 mg of phenothiazine salt, to which 60 ml of 0.1 *N* HCl was added. The tablet suspension was shaken mechanically for 1 hr. A standard solution was prepared in 0.1 *N* HCl such that 60 ml contained an accurately known amount (10–12.5 mg) of standard.

Single-tablet, composite, and standard solutions were prepared in the following manner. Sixty milliliters of solution containing 10–12.5 mg of phenothiazine salt was passed through a chromatographic column into a 100-ml volumetric flask. Residual drug was washed through the column with three portions (20, 15, and 15 ml) of 0.1 *N* HCl. The combined eluate was diluted to 100.0 ml with 0.1 *N* HCl. Peracetic acid (5.0 ml) was added to 20.0 ml of the eluate[13], and the solution was mixed and diluted to 50.0 ml with 0.1 *N* HCl.

[12] No. K-420530 or equivalent, Kontes, Evanston, Ill.

Table III—Phenothiazine Sulfoxide Absorptivities[a]

Sulfoxide	Wavelength, nm	Δ Absorptivity[b]	Absorptivity[c]
Prochlorperazine	342	7.95 (3)[d]	9.70
Perphenazine	343	12.0 (5)	14.8
Fluphenazine[e]	349	9.16 (4)	11.0
Chlorpromazine	344	13.8 (8)	18.1
Thioridazine	348	10.9 (8)	13.1
Triflupromazine	347	11.7 (3)	14.0
Carphenazine	372	2.05 (6)	5.44
Thiethylperazine	350	6.87 (2)	8.47
Methdilazine	341	16.2 (1)	18.2
Promazine	342	16.0 (1)	18.8
Trimeprazine	342	14.1 (1)	15.5
Trifluoperazine[e]	349		11.5

[a] Based on grams of phenothiazine salt per liter (1-cm cell). [b] Measured *versus* a blank containing an equal concentration of unoxidized drug. [c] Measured *versus* a solvent blank. [d] Number of determinations. [e] Assayed fluorometrically.

The absorbance of the oxidized composite assay solution was read rapidly *versus* that of a sample blank prepared from 20.0 ml of the assay eluate and 5.0 ml of acetic acid diluted to 50.0 ml with 0.1 *N* HCl. The absorbance of an oxidized standard solution, prepared from 20.0 ml of the standard eluate and 5.0 ml of peracetic acid diluted to 50.0 ml with 0.1 *N* HCl, was measured concomitantly *versus* that of a standard blank prepared from 20.0 ml of the standard eluate and 5.0 ml of acetic acid diluted to 50.0 ml with 0.1 *N* HCl. The absorbance of oxidized single-tablet assay solutions was measured rapidly *versus* that of a solvent blank prepared from 5.0 ml of acetic acid diluted to 50.0 ml with 0.1 *N* HCl. The absorbance of an oxidized standard solution was measured concomitantly *versus* that of a solvent blank. The wavelengths of the assay determination and final assay concentrations are given in Table II. Phenothiazine sulfoxide absorptivities are listed in Table III.

Single-tablet solutions of perphenazine were prepared by disintegrating one tablet in 25 ml of 0.1 *N* HCl in an ultrasonic bath. Composite solutions were prepared by grinding 20 tablets to pass through a 60-mesh screen and adding one tablet weight of composite powder to 25 ml of 0.1 *N* HCl. The single-tablet or composite suspension was shaken mechanically for 1 hr. The suspension was diluted, if necessary, to 80 μg/ml with 0.1 *N* HCl. A perphenazine standard solution of 80 μg/ml in 0.1 *N* HCl was prepared. Then 25 ml of 0.1 *N* HCl containing 2 mg of drug or standard was passed through a chromatographic column into a 50-ml volumetric flask.

Residual drug was washed from the column with three portions (10, 10, and 5 ml) of 0.1 *N* HCl. The combined eluate was diluted to 50.0 ml with 0.1 *N* HCl, and 20.0 ml of the eluate was oxidized with 4.0 ml of peracetic acid. The absorbance of the composite assay solution was measured rapidly at 343 nm *versus* a sample blank prepared from 20.0 ml of the same column eluate and 4.0 ml of acetic acid. The absorbance of an oxidized standard solution was measured concomitantly *versus* that

[13] For thiethylperazine maleate assays, 25.0 ml of the column eluate and 5.0 ml of peracetic acid were used.

Table IV—Percent Recovery of Phenothiazine Salts from Synthetic Formulation Mixtures by the Differential UV–Differential Fluorescence Method

Drug	Percent Recovered[a]	*RSD*, %	Simulated Dosage Strength, mg
Thiethylperazine maleate	99.5	0.93	10
Prochlorperazine maleate	100.2	0.81	5
Chlorpromazine hydrochloride	100.8	0.73	25
Thioridazine hydrochloride	99.0	0.43	10
Perphenazine	100.3	0.42	16
Carphenazine maleate	99.5	0.41	12.5
Promazine hydrochloride	99.8	0.41	25
Trifluprom azine hydrochloride	100.1	0.38	10
Trimeprazine tartrate	100.3	0.21	2.5

[a] Average of eight determinations.

Table V—Precision Study on Composite of 100-mg Chlorpromazine Hydrochloride Tablets

Percent of Label Claim		
Automated[a]	Modified Official	Differential
101.6		
99.7		98.5
98.2	99.2	98.5
99.2	99.8	99.0
100.0	100.3	99.1
99.5	96.1	99.9
99.3	100.1	99.1
99.1	98.7	98.0
99.4	100.3	98.0
Mean (*RSD*, %)		
99.6 (0.92)	99.2 (1.42)	98.8 (0.65)

[a] One sample run on each of 9 days.

of a standard blank prepared from 20.0 ml of the standard eluate and 4.0 ml of acetic acid. The absorbance of the oxidized single-tablet solution and the absorbance of an oxidized standard were measured *versus* a solvent blank prepared from 20.0 ml of 0.1 *N* HCl and 4.0 ml of acetic acid.

Single-tablet solutions of trimeprazine tartrate were prepared by disintegrating one tablet in 25 ml of 0.1 *N* HCl in an ultrasonic bath. Composite solutions were prepared by grinding 20 tablets to pass through a 60-mesh screen and adding one tablet weight of composite powder to 25 ml of 0.1 *N* HCl. The single-tablet or composite suspension was shaken mechanically for 1 hr. A trimeprazine tartrate standard solution of 100 μg/ml in 0.1 *N* HCl was prepared. Then 25 ml of the standard or assay solution containing 2.5 mg of drug was passed through a chromatographic column into a 50-ml volumetric flask. The assay proceeded as directed in the perphenazine assay beginning with the washing of residual drug. The absorbance was read at 342 nm.

Single-tablet solutions of methdilazine hydrochloride were prepared by disintegrating one tablet in 25 ml of 0.1 *N* HCl in an ultrasonic bath. Composite solutions were prepared by grinding 20 tablets to pass through a 60-mesh screen and adding one tablet weight of composite powder to 25 ml of 0.1 *N* HCl. The single-tablet or composite suspension was shaken mechanically for 1 hr. A methdilazine hydrochloride standard solution of 144 μg/ml was prepared in 0.1 *N* HCl. Then 25 ml of the standard or assay solution containing 3.6 mg of methdilazine hydrochloride was passed through a chromatographic column into a 50-ml volumetric flask. The assay proceeded as directed in the perphenazine assay beginning with the washing of residual drug. The absorbance was read at 341 nm.

Single-tablet solutions of prochlorperazine maleate were prepared by disintegrating one tablet in 50 ml of 0.1 *N* HCl in an ultrasonic bath. Composite solutions were prepared by grinding 20 tablets to pass through a 60-mesh screen and adding one tablet weight of composite powder to 50 ml of 0.1 *N* HCl. The single-tablet or composite suspension was shaken mechanically for 1 hr. The suspension was diluted, if necessary, to 100 μg/ml with 0.1 *N* HCl. A prochlorperazine maleate standard solution (100 μg/ml) was prepared in 0.1 *N* HCl. Then 50 ml of the standard or assay solution containing 5 mg of prochlorperazine maleate was passed through a chromatographic column into a 100-ml volumetric flask. The column was washed with three portions (15, 15, and 10 ml) of 0.1 *N* HCl. The combined eluate was diluted to 100.0 ml with 0.1 *N* HCl, and the assay proceeded as directed in the perphenazine assay beginning with the oxidation of the eluate. The absorbance was read at 342 nm.

Single-tablet solutions of carphenazine maleate were prepared by disintegrating one tablet in 25 ml of 0.1 *N* HCl in an ultrasonic bath. Composite solutions were prepared by grinding 20 tablets to pass a 60-mesh screen and adding one tablet weight of the composite powder to 25 ml of 0.1 *N* HCl. The single tablet or composite suspension was shaken mechanically for 1 hr. A carphenazine maleate standard solution (500 μg/ml) was prepared in 0.1 *N* HCl. Then 25 ml of the standard or the assay solution containing 12.5 mg of carphenazine maleate was passed through a chromatographic column into a 50-ml volumetric flask. Residual drug was washed from the column with three portions (15, 15, and 10 ml) of 0.1 *N* HCl. The combined eluate was diluted to 50.0 ml with 0.1 *N* HCl, and the assay proceeded as directed in the perphenazine assay beginning with the oxidation of the eluate. The absorbance was read at 372 nm.

Liquid formulations of chlorpromazine hydrochloride and thioridazine hydrochloride were assayed as follows. An aliquot of liquid containing 100 mg of drug was transferred in a "to contain" pipet to a suitable volumetric flask, and the pipet contents were rinsed into the flask with 0.1 *N* HCl. The solution was diluted quantitatively and stepwise to a final concentration of 50 μg/ml. Standard solutions of thioridazine hydrochloride and chlorpromazine hydrochloride were prepared at a concentration of 50 μg/ml. Then 20.0-ml aliquots of the thioridazine hydrochloride assay solution were pipetted into each of two flasks; 5.0 ml of peracetic acid was pipetted into one flask, and 5.0 ml of acetic acid was pipetted into the other flask. The absorbance of the oxidized thioridazine hydrochloride solution was read at 348 nm *versus* that of the sample blank. The absorbance of the oxidized thioridazine hydrochloride standard solution was measured concomitantly *versus* that of a standard blank. The absorbance of oxidized chlorpromazine hydrochloride assay and standard solutions was measured at 344 nm *versus* that of their appropriate blanks.

To assay liquid formulations of prochlorperazine maleate, an aliquot of liquid containing 10 mg of drug was transferred in a "to contain" pipet to a suitable volumetric flask. The pipet contents were rinsed into the flask with 0.1 *N* HCl, and the solution was diluted quantitatively and stepwise with 0.1 *N* HCl to a final concentration of 50 μg/ml. A standard solution of prochlorperazine maleate was prepared having a final concentration of 50 μg/ml. Then 20.0-ml aliquots of sample and standard solutions were oxidized with 5.0-ml aliquots of peracetic acid. The absorbance of oxidized standard and oxidized sample solutions was measured concomitantly *versus* that of their appropriate blanks at 342 nm.

Differential Fluorometric Method—The fluorescence of oxidized phenothiazines was reported previously (27), but an assay was not developed at that time. Excitation occurs at 365 nm[14]; emission is at 405 nm[15]. A linear relationship between the meter response and the concentration change was demonstrated in the concentration range of interest.

After insertion of the proper excitation and emission filters, the apertures, range, and sensitivity were set to yield a meter deflection of ~90% with an oxidized drug solution. With these instrumental settings, the fluorescence of the freshly oxidized standard, sample, and blank solutions was measured.

To assay 0.25-mg fluphenazine hydrochloride tablets, one tablet was disintegrated in 25 ml of pH 2.2 buffer in an ultrasonic bath. Then 15.0 ml of 95% alcohol[16] was added and shaken mechanically for 1 hr. The solution was diluted to 50.0 ml with pH 2.2 buffer and filtered through paper[17]; the first 10 ml was discarded. Then 25.0-ml aliquots of the filtrate were pipetted into each of two flasks. One aliquot was oxidized with 5.0 ml of peracetic acid, and 5.0 ml of acetic acid was added to the other aliquot. The fluorescence of the sample and blank solutions was determined in 1-cm rectangular cells. The fluorescence of the oxidized standard and standard blank solutions was measured concomitantly.

For tablets containing 1, 2.5, 5, or 10 mg of fluphenazine hydrochloride or trifluoperazine hydrochloride, one tablet was disintegrated in 60 ml of pH 2.2 buffer in an ultrasonic bath. Then 30.0 ml of 95% alcohol was added, and the solution was shaken mechanically for 1 hr. The solution was diluted to 100.0 ml with pH 2.2 buffer and filtered through paper[17]; the first 10 ml was discarded. An aliquot containing 0.5 mg of drug was pipetted into a 100-ml volumetric flask and diluted to volume with alcohol

[14] Filter 5860, Corning Glass Works, Corning, N.Y.

[15] Ditric Optics Inc., Marlboro, Mass. A narrow band filter reduces sample blanks about 75%.

[16] Alcohol hinders the disintegration and must be added after disintegration is complete. The final concentration of alcohol is important since it enhances the fluorescence intensity.

[17] No. 42, Whatman Inc., Clifton, N.J.

Table VI—Comparative Analysis of Commercial Solid Formulations

Drug and Dosage Strength	Assay Type	Percent of Label Claim		
		Differential	Automated	Modified Official
Perphenazine, 2 mg	Tablet	105.5 (10)[a]	—	106.5 (3)
	Composite	106.6 (5)	100.7 (2)	103.7 (4)
Promazine hydrochloride, 10 mg	Tablet	99.2 (20)	102.5 (10)	101.3 (1)
	Composite	100.6 (6)	—	—
Thioridazine hydrochloride				
10 mg	Tablet	98.8 (20)	—	95.8 (3)
	Composite	100.9 (2)	96.5 (10)	96.0 (2)
200 mg	Composite	96.1 (4)	—	100.2 (2)
Triflupromazine hydrochloride				
10 mg	Tablet	105.9 (20)	105.8 (10)	109.2 (2)
	Composite	106.6 (2)	—	—
50 mg	Composite	99.5 (9)	99.7 (2)	100.6 (4)
Prochlorperazine maleate				
5 mg	Tablet	102.1 (10)	96.8 (10)	97.8 (2)
	Composite	101.9 (2)	—	—
75 mg	Composite[b]	98.2 (2)	101.5 (2)	101.3 (1)
Trimeprazine tartrate, 2.5 mg	Tablet	100.8 (10)	99.6 (10)	104.5 (2)
	Composite	101.5 (5)	101.1 (2)	101.3 (4)
Carphenazine maleate				
12.5 mg	Tablet	104.7 (10)	102.0 (10)	109.2 (7)
50 mg	Composite	99.9 (4)	100.4 (2)	100.1 (6)
Methdilazine hydrochloride				
3.6 mg	Tablet	94.9 (10)	—	—
8.0 mg	Composite	96.5 (5)	97.3 (5)	99.9 (5)
Thiethylperazine maleate, 10 mg	Tablet	100.7 (10)	97.9 (10)	101.9 (10)
	Composite	97.8 (5)	98.0 (2)	98.1 (4)
Chlorpromazine hydrochloride, 100 mg	Tablet	102.2 (10)	—	—
	Composite	98.8 (8)	99.6 (9)	—
Trifluoperazine hydrochloride, 1 mg	Tablet	98.2 (7)	98.1 (10)	102.0 (4)
	Composite	102.1 (5)	100.3 (2)	97.9 (4)
Fluphenazine hydrochloride				
5 mg	Tablet	97.7 (10)	95.3 (10)	—
	Composite	100.1 (3)	96.1 (2)	96.1 (3)
1 mg	Tablet	96.8 (10)	96.8 (20)	—
0.25 mg	Tablet	96.7 (20)	92.6 (20	—

[a] Number of determinations. [b] Controlled-release capsule.

in pH 2.2 buffer. Then 25.0-ml aliquots were pipetted into each of two flasks. One aliquot was oxidized with 5.0 ml of peracetic acid, and 5.0 ml of acetic acid was added to the other aliquot. A standard assay and standard solution blank were prepared in the same manner. The fluorescence of each solution was determined concomitantly.

To run composite assays, the average tablet weight was determined. Then 20 tablets were ground to pass through a 60-mesh screen. One tablet weight of powder was used in a manner similar to the single-tablet procedure.

To assay liquid formulations of trifluoperazine hydrochloride, an aliquot of liquid containing 50 mg of drug was transferred in a "to contain" pipet to a suitable volumetric flask. The pipet contents were rinsed into the flask with alcohol in pH 2.2 buffer. The solution was diluted quantitatively and stepwise with this solvent to a final concentration of 5.0 μg/ml. A standard trifluoperazine hydrochloride solution was prepared with this solvent at a concentration of 5.0 μg/ml. Then 25.0-ml aliquots of the sample and standard solutions were oxidized with 5.0-ml portions of peracetic acid. The fluorescence of the sample and standard solutions was read rapidly in 1-cm rectangular cells. Sample and standard blanks were prepared from 25.0 ml of solution and 5.0 ml of acetic acid. The fluorescence of each blank was determined, and the sample and standard fluorescences were corrected.

RESULTS AND DISCUSSION

Validation Tests—A tablet placebo was prepared from the known formulation ingredients. To this placebo was added an aliquot containing an amount of drug corresponding to the label declaration. This synthetic mixture then was subjected to the appropriate differential UV or differential fluorescence composite assay. Recovery results are listed in Table IV.

Modified Official Method—The most serious problem encountered with the official assay methods involved the ether extraction steps (Class I compounds only; thioridazine hydrochloride and trifluoperazine hydrochloride ether extractions did not exhibit this problem). The ether extraction procedures require an aeration step to remove residual ether from the final dilute acid extract. Aeration generated colored solutions, and these solutions exhibited badly distorted UV curves (28). The substitution of nitrogen gas for air did not alleviate the problem. It is well known that hydroperoxides rapidly oxidize phenothiazines to their sulfoxides; thus, ether peroxide impurities were suspected (4). To avoid having to purify ether continuously, heptane was used as the solvent. This choice of solvent solved the problem, but mixtures of heptane and dilute acid are prone to emulsion.

The Class II phenothiazines were extracted incompletely by the official procedures. The simple expedient of using saturated sodium chloride solution solved this problem. In this way, the extraction partition coefficient for thiethylperazine maleate was raised 100-fold. In addition, the fluphenazine assays required the addition of 2% *n*-butanol to the *n*-hexane extraction solvent.

The official procedures worked quite well for the Class III compounds, but carphenazine–palladium complexes are very unstable.

The amendments to the official procedures, although improving their utility, do not make these methods specific.

Semiautomated Method—This procedure was developed initially without an oxidation step, but some dosage levels were too low to permit UV measurement. For most of these drugs, oxidation with 0.5% $NaNO_2$ raised absorbances to convenient working levels, but single tablets containing 0.25 or 1.0 mg of fluphenazine hydrochloride could not be assayed by oxidation followed by UV analysis. These tablet strengths eventually were assayed by oxidation followed by fluorometric determination.

With these modifications, the automated system was applicable to every type of formulation encountered. In most cases, coefficients of variation were as good as or better than those of the modified official method. Table V contains a typical comparative precision study. Since the automated procedure, like the official and modified official methods, employs a UV solvent blank, this method also is nonspecific if impurities are present.

Differential UV and Differential Fluorescence Methods—During the differential UV oxidation studies, it was noted that sulfoxide absorbances declined slowly with time; but it has been demonstrated that for each drug in this study, the ratio of standard and sample absorbances is constant for at least 3 hr after oxidation. In addition, absorbances and fluorescence intensities usually rise and reach a maximum value that is

Table VII—Comparative Analysis of Commercial Liquid Formulations

Drug and Dosage Strength	Percent of Label Claim		
	Differential	Automated	Modified Official
Chlorpromazine hydrochloride concentrate, 100 mg/ml	99.0 (8)[a]	99.6 (2)	101.6 (1)
Trifluoperazine hydrochloride concentrate, 10 mg/ml	97.8 (5)	101.2 (2)	98.8 (2)
Prochlorperazine maleate concentrate, 10 mg/ml	96.1 (2)	97.5 (2)	100.2 (1)
Thioridazine hydrochloride concentrate, 100 mg/ml	97.9 (2)	99.3 (2)	99.7 (1)

[a] Number of determinations.

sufficiently stable for measurement in ~3 min after oxidation. This rise apparently is due to the expulsion of air bubbles formed as a result of mixing acetic acid and dilute hydrochloric acid.

Differential UV assays results were unaffected by 18 commonly used excipients. However, the differential fluorescence method was affected by one excipient, dibasic calcium phosphate. This problem was corrected by changing the fluorescence assay solvent from 0.1 *N* HCl to pH 2.2 buffer containing ~30% alcohol. Comparative assay results for the three methods are summarized in Tables VI and VII.

CONCLUSIONS

Previously published work on the phenothiazine differential oxidation method suggested its general applicability (3). The inclusion of a siliceous earth filtration step and the introduction of a fluorometric procedure for lower formulation strengths make the method facile and accurate. The method was shown to be reproducible to concentrations as low as 1 μg/ml. The procedure was applied to tablets, sustained-release preparations, concentrates, and syrups. Recoveries from known mixtures ranged from 99 to 101%. These results and the specificity of the differential oxidation procedure suggest its superiority to the official assay procedures.

REFERENCES

(1) "The United States Pharmacopeia," 19th rev., Mack Publishing Co., Easton, Pa., 1975.

(2) "The National Formulary," 14th ed., Mack Publishing Co., Easton, Pa., 1975.

(3) A. G. Davidson, *J. Pharm. Pharmacol.*, **28**, 795 (1976).

(4) S. P. Massie, *Chem. Rev.*, **54**, 797 (1954).

(5) C. Bodea and I. Silberg, in "Advances in Heterocyclic Chemistry," vol. 9, A. R. Katritzky, Ed., Academic, New York, N.Y., 1968, p. 321.

(6) J. P. Billon, *Ann. Chim. (Paris)*, **7**, 183 (1962).

(7) T. N. Tozer and L. D. Tuck, *J. Pharm. Sci.*, **54**, 1169 (1965).

(8) P. Kabasakalian and J. McGlotten, *Anal. Chem.*, **31**, 431 (1959).

(9) J. P. Malrieu and B. Pullman, *Theoret. Chim. Acta*, **2**, 293 (1964).

(10) A. Pullman, *J. Chim. Phys.*, **61**, 1666 (1964).

(11) H. Gilman and R. D. Nelson, *J. Am. Chem. Soc.*, **75**, 5422 (1953).

(12) M. Nakanishi and N. Kuriyama, Japanese pat. 15,617 (1961); through *Chem. Abstr.*, **56**, 12908i (1962).

(13) G. P. Brown, J. W. Cole, and T. I. Crowell, *J. Org. Chem.*, **20**, 1772 (1955).

(14) D. Simov Antonov, *Izv. Khim. Inst., Bulgar. Nauk.*, **5**, 51 (1957); through *Chem. Abstr.*, **55**, 1655d (1961).

(15) C. Bodea and M. Raileany, *Ann. Chem.*, **614**, 171 (1958).

(16) L. K. Turner, *J. Forensic Sci.*, **4**, 39 (1963).

(17) J. A. Ryan, *J. Am. Pharm. Assoc., Sci. Ed.*, **48**, 240 (1959).

(18) A. J. Kapadia, M. A. Barber, and A. E. Martin, *J. Pharm. Sci.*, **59**, 1476 (1970).

(19) S. Cooper, J. Albert, R. Dugal, and M. Bertrand, *J. Chromatogr.*, **150**, 263 (1978).

(20) E. C. Dinovo, L. A. Gottschalk, B. R. Nandi, and P. G. Geddes, *J. Pharm. Sci.*, **65**, 667 (1976).

(21) S. H. Curry, *Anal. Chem.*, **40**, 1251 (1968).

(22) R. G. Muusze and J. F. K. Huber, *J. Chromatogr. Sci.*, **12**, 779 (1974).

(23) D. H. Rodgers, *ibid.*, **12**, 743 (1974).

(24) A. DeLeenheer, *J. Assoc. Off. Anal. Chem.*, **56**, 105 (1973).

(25) A. G. Davidson, *J. Pharm. Pharmacol.*, **30**, 410 (1978).

(26) "The United States Pharmacopeia," 19th rev., Mack Publishing Co., Easton, Pa., p. 761.

(27) J. B. Ragland and V. J. Kinross-Wright, *Anal. Chem.*, **36**, 1356 (1964).

(28) R. D. Kirchhoefer and J. W. Myrick, *J. Assoc. Off. Anal. Chem.*, **61**, 1519 (1978).

Pyridones as Potential Antitumor Agents II: 4-Pyridones and Bioisosteres of 3-Acetoxy-2-pyridone

DENG R. HWANG *, GEORGE R. PROCTOR ‡, and JOHN S. DRISCOLL ˣ

Received February 25, 1980, from the *Drug Design and Chemistry Section, Laboratory of Medicinal Chemistry and Biology, Developmental Therapeutics Program, Division of Cancer Treatment, National Cancer Institute, National Institutes of Health, Bethesda, MD 20205.* Accepted for publication March 25, 1980. *Present address: Technicon Inc., Tarrytown, N.Y. ‡Present address: University of Strathclyde, Glasgow, Scotland.

Abstract □ Pyridone structural requirements for activity against murine P-388 leukemia have been extended to isosteric analogs of 3-hydroxy-4-pyridone, a compound previously found to have activity. An amino group can be substituted for the 3-hydroxyl function with retention of activity. A sulfur, but not an amino function, can replace the lactam oxygen in the 2-position. Relocation of the lactam oxygen from the 2- to the 4-position in the pyridine ring also produces active pyridones, including 2-methyl-3-acetoxy-4-pyridone. This compound, which has a T/C value of 179%, is the most active material discovered thus far in the pyridone studies.

Keyphrases □ Pyridones—4-pyridones and bioisosteres of 3-acetoxy-2-pyridone, synthesis and evaluation for antitumor activity □ Antitumor agents, potential—4-pyridones and bioisosteres of 3-acetoxy-2-pyridone, synthesis and evaluation for activity □ Structure–activity relationships—4-pyridones and bioisosteres of 3-acetoxy-2-pyridone, synthesis and evaluation for antitumor activity

It was reported recently that 3-hydroxy- (I) and 3-acetoxy-2-pyridone (II) have reproducible activity against murine P-388 lymphocytic leukemia (1). Eight additional derivatives of 3- and 5-hydroxy-2-pyridone also were active, and a tentative structure–activity relationship was established between antitumor activity and the position of the hydroxyl group relative to the 2-pyridone lactam function. The present investigation extends the study of

0022-3549/80/0900-1074$01.00/0

© 1980, American Pharmaceutical Association

Table VII—Comparative Analysis of Commercial Liquid Formulations

Drug and Dosage Strength	Percent of Label Claim		
	Differential	Automated	Modified Official
Chlorpromazine hydrochloride concentrate, 100 mg/ml	99.0 (8)[a]	99.6 (2)	101.6 (1)
Trifluoperazine hydrochloride concentrate, 10 mg/ml	97.8 (5)	101.2 (2)	98.8 (2)
Prochlorperazine maleate concentrate, 10 mg/ml	96.1 (2)	97.5 (2)	100.2 (1)
Thioridazine hydrochloride concentrate, 100 mg/ml	97.9 (2)	99.3 (2)	99.7 (1)

[a] Number of determinations.

sufficiently stable for measurement in ~3 min after oxidation. This rise apparently is due to the expulsion of air bubbles formed as a result of mixing acetic acid and dilute hydrochloric acid.

Differential UV assays results were unaffected by 18 commonly used excipients. However, the differential fluorescence method was affected by one excipient, dibasic calcium phosphate. This problem was corrected by changing the fluorescence assay solvent from 0.1 *N* HCl to pH 2.2 buffer containing ~30% alcohol. Comparative assay results for the three methods are summarized in Tables VI and VII.

CONCLUSIONS

Previously published work on the phenothiazine differential oxidation method suggested its general applicability (3). The inclusion of a siliceous earth filtration step and the introduction of a fluorometric procedure for lower formulation strengths make the method facile and accurate. The method was shown to be reproducible to concentrations as low as 1 μg/ml. The procedure was applied to tablets, sustained-release preparations, concentrates, and syrups. Recoveries from known mixtures ranged from 99 to 101%. These results and the specificity of the differential oxidation procedure suggest its superiority to the official assay procedures.

REFERENCES

(1) "The United States Pharmacopeia," 19th rev., Mack Publishing Co., Easton, Pa., 1975.

(2) "The National Formulary," 14th ed., Mack Publishing Co., Easton, Pa., 1975.

(3) A. G. Davidson, *J. Pharm. Pharmacol.*, **28**, 795 (1976).

(4) S. P. Massie, *Chem. Rev.*, **54**, 797 (1954).

(5) C. Bodea and I. Silberg, in "Advances in Heterocyclic Chemistry," vol. 9, A. R. Katritzky, Ed., Academic, New York, N.Y., 1968, p. 321.

(6) J. P. Billon, *Ann. Chim. (Paris)*, **7**, 183 (1962).

(7) T. N. Tozer and L. D. Tuck, *J. Pharm. Sci.*, **54**, 1169 (1965).

(8) P. Kabasakalian and J. McGlotten, *Anal. Chem.*, **31**, 431 (1959).

(9) J. P. Malrieu and B. Pullman, *Theoret. Chim. Acta*, **2**, 293 (1964).

(10) A. Pullman, *J. Chim. Phys.*, **61**, 1666 (1964).

(11) H. Gilman and R. D. Nelson, *J. Am. Chem. Soc.*, **75**, 5422 (1953).

(12) M. Nakanishi and N. Kuriyama, Japanese pat. 15,617 (1961); through *Chem. Abstr.*, **56**, 12908i (1962).

(13) G. P. Brown, J. W. Cole, and T. I. Crowell, *J. Org. Chem.*, **20**, 1772 (1955).

(14) D. Simov Antonov, *Izv. Khim. Inst., Bulgar. Nauk.*, **5**, 51 (1957); through *Chem. Abstr.*, **55**, 1655d (1961).

(15) C. Bodea and M. Raileany, *Ann. Chem.*, **614**, 171 (1958).

(16) L. K. Turner, *J. Forensic Sci.*, **4**, 39 (1963).

(17) J. A. Ryan, *J. Am. Pharm. Assoc., Sci. Ed.*, **48**, 240 (1959).

(18) A. J. Kapadia, M. A. Barber, and A. E. Martin, *J. Pharm. Sci.*, **59**, 1476 (1970).

(19) S. Cooper, J. Albert, R. Dugal, and M. Bertrand, *J. Chromatogr.*, **150**, 263 (1978).

(20) E. C. Dinovo, L. A. Gottschalk, B. R. Nandi, and P. G. Geddes, *J. Pharm. Sci.*, **65**, 667 (1976).

(21) S. H. Curry, *Anal. Chem.*, **40**, 1251 (1968).

(22) R. G. Muusze and J. F. K. Huber, *J. Chromatogr. Sci.*, **12**, 779 (1974).

(23) D. H. Rodgers, *ibid.*, **12**, 743 (1974).

(24) A. DeLeenheer, *J. Assoc. Off. Anal. Chem.*, **56**, 105 (1973).

(25) A. G. Davidson, *J. Pharm. Pharmacol.*, **30**, 410 (1978).

(26) "The United States Pharmacopeia," 19th rev., Mack Publishing Co., Easton, Pa., p. 761.

(27) J. B. Ragland and V. J. Kinross-Wright, *Anal. Chem.*, **36**, 1356 (1964).

(28) R. D. Kirchhoefer and J. W. Myrick, *J. Assoc. Off. Anal. Chem.*, **61**, 1519 (1978).

Pyridones as Potential Antitumor Agents II: 4-Pyridones and Bioisosteres of 3-Acetoxy-2-pyridone

DENG R. HWANG *, GEORGE R. PROCTOR ‡, and JOHN S. DRISCOLL ˣ

Received February 25, 1980, from the *Drug Design and Chemistry Section, Laboratory of Medicinal Chemistry and Biology, Developmental Therapeutics Program, Division of Cancer Treatment, National Cancer Institute, National Institutes of Health, Bethesda, MD 20205.* Accepted for publication March 25, 1980. *Present address: Technicon Inc., Tarrytown, N.Y. ‡Present address: University of Strathclyde, Glasgow, Scotland.

Abstract □ Pyridone structural requirements for activity against murine P-388 leukemia have been extended to isosteric analogs of 3-hydroxy-4-pyridone, a compound previously found to have activity. An amino group can be substituted for the 3-hydroxyl function with retention of activity. A sulfur, but not an amino function, can replace the lactam oxygen in the 2-position. Relocation of the lactam oxygen from the 2- to the 4-position in the pyridine ring also produces active pyridones, including 2-methyl-3-acetoxy-4-pyridone. This compound, which has a T/C value of 179%, is the most active material discovered thus far in the pyridone studies.

Keyphrases □ Pyridones—4-pyridones and bioisosteres of 3-acetoxy-2-pyridone, synthesis and evaluation for antitumor activity □ Antitumor agents, potential—4-pyridones and bioisosteres of 3-acetoxy-2-pyridone, synthesis and evaluation for activity □ Structure–activity relationships—4-pyridones and bioisosteres of 3-acetoxy-2-pyridone, synthesis and evaluation for antitumor activity

It was reported recently that 3-hydroxy- (I) and 3-acetoxy-2-pyridone (II) have reproducible activity against murine P-388 lymphocytic leukemia (1). Eight additional derivatives of 3- and 5-hydroxy-2-pyridone also were active, and a tentative structure–activity relationship was established between antitumor activity and the position of the hydroxyl group relative to the 2-pyridone lactam function. The present investigation extends the study of

0022-3549/80/0900-1074$01.00/0

© 1980, American Pharmaceutical Association

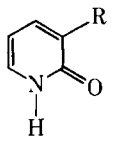

I: R = OH
II: R = $OCOCH_3$
III: R = NO_2
IV: R = NH_2
V: R = $NHCOCH_3$
VI: R = $NHCONHCH_3$

pyridone antitumor activity to 2-pyridones that are bioisosteres of I and to the 4-pyridone system.

RESULTS

An earlier study (1) established that hydroxyl substitution at the 3-position produced optimal P-388 activity in the 2-pyridone series. For this reason, the 2,3-relationship was maintained in the study of the effect of bioisosteric functional groups on 2-pyridone antitumor activity. The objective of the present 2-pyridone study was the determination of the effect on P-388 activity of replacing the oxygen functionality in I and II with nitrogen- and sulfur-containing groups.

3-Amino-2-pyridone (IV) was synthesized by the nitration of 2-pyridone to produce 3-nitro-2-pyridone (III) and subsequent catalytic reduction to produce IV. Compound IV was reacted with acetic anhydride to give V, an analog of II, and with methyl isocyanate to give VI. Both V and VI are nitrogen isosteres of oxygen analogs previously found to be active (1). The importance of the oxygen functionality in the 2-position of I was studied by replacing it with nitrogen- (VII), chlorine- (VIII), and sulfur- (IX) containing groups. 3-Hydroxy-2-thiopyridone (IX) was *O*-acetylated to produce X, a sulfur analog of II, the most active oxygen-containing compound.

Another objective of this investigation was to study the effect of moving the lactam oxygen function in I from the 2-position to the 4-position to produce the other pyridone isomer. The commercially available pyrone plant product, maltol (XI), provided an entry to the desired 4-pyridone series. By a method similar to that of Fisher and Hodge (2), maltol was methylated to give XII, which was reacted with ammonia to produce the 4-pyridone (XIII). Methoxy cleavage with hydrobromic acid produced the target compound, 2-methyl-3-hydroxy-4-pyridone (XIV). The urethan (XV) and acetoxy (XVI) analogs were prepared for the reason mentioned previously.

Compounds III–XVI were evaluated using the standard National Cancer Institute protocol for P-388 lymphocytic leukemia (3). The data for the reproducibly active members of the series, as well as the activities reported (1) for I and II which are shown for comparison, are given in Table I. Duplicate dose–response tests were carried out with each compound. An active test is defined (3) as one that produces a T/C value[1] of ≥125%. Active compounds are defined as those that give active tests in two separate experiments. The compounds among I–XVI that are not shown in Table I were inactive in duplicate experiments.

DISCUSSION

Both 3-hydroxy-2-pyridone (I) and its acetyl derivative (II) have P-388 activity (Table I), with the latter compound being the best among 10 previously reported active analogs (1). Replacement of the 3-hydroxyl group in I with a nitro group (III) resulted in inactivity. However, an amino group in the same position provided a compound (IV) with approximately the same level of activity as its bioisostere, I. Acetylation of IV to produce V, instead of enhancing activity as in the case of II, abolished activity. While the formation of the methylaminocarbonyl derivative of I increased the activity of the resulting urethan (1), the opposite was the case when IV was treated in a similar manner.

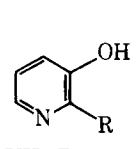

VII: R = NH_2
VIII: R = Cl

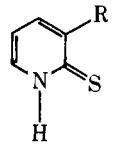

IX: R = OH
X: R = $OCOCH_3$

[1] T/C = (survival time of treated mice/survival time of control mice) × 100%.

Table I—Pyridones Active against P-388 Lymphocytic Leukemia[a]

Compound	Optimum Dose[b], mg/kg/day	T/C[c]	T − C[d]
I	400	138	−2.4
II	600	163	−2.8
IV	200	133	−4.1
IX	200	139	−0.9
XIV	200	153	0.0
XVI	400	179	−3.1

[a] With 10^6 cells implanted intraperitoneally in CDF_1 mice. [b] Dose giving the maximum T/C value on the QD 1–9 treatment schedule. [c] At least one other active test was obtained in a separate, duplicate experiment. [d] Weight difference, in grams, between treated and control mice 5 days after tumor implantation.

The replacement of the lactam oxygen function of I with an amino group to give VII, the position isomer of active IV and the bioisostere of active I, resulted in inactivity. This result may be related to the fact that 2-hydroxypyridines exist mainly in the lactam form while the amino form predominates in 2-aminopyridines (4). A similar replacement with chlorine (VIII), which possesses no tautomeric possibilities, also resulted in inactivity. However, when the same replacement was made with sulfur to produce 3-hydroxy-2-thiopyridone (IX), activity was retained. 2-Mercapto- as well as 2-hydroxypyridines exist as the amide tautomer (pyridone or lactam form) in >99% (4). Acetylation of IX to form X reduced activity (T/C 133, 120, and 110%), contrary to what was observed with I but similar to the finding with IV.

In the isomeric 4-pyridone series, the starting material, maltol (XI), its *O*-methylated derivative (XII), and the 3-methoxy-4-pyridone (XIII) obtained from XII did not possess P-388 activity. However, demethylation of XIII gave 2-methyl-3-hydroxy-4-pyridone (XIV), a compound with an activity level greater than that of I and similar to that of II, the most active compound in the 2-pyridone series. Preparation of a urethan (XV), which had increased activity relative to I in the 2-pyridone series, abolished activity in the 4-pyridone case. However, XVI, the *O*-acetyl derivative of XIV, was the most active compound in either the 2- or 4-pyridone series, producing T/C values of 179 and 176%. Compound XVI also proved active against the less sensitive murine tumor model, L-1210 lymphoid leukemia (T/C 157 and 138), and presently is being evaluated in the National Cancer Institute tumor panel (5).

The mechanism of antitumor activity for the pyridones has not been established. A similarity with the catechol–*ortho*-quinone series involving possible sulfhydryl reactivity was noted (6). Another possible parallel exists between the antitumor activity observed here and the catechol-*O*-methyl transferase inhibitory activity of the 3-hydroxypyridones demonstrated by Borschardt (7). Aminopyridones also were potent inducers of erythroid differentiation in Friend leukemia cells (8).

In summary, it has been found that relative to the 2-pyridone lead compound, I, an amino group can be substituted for the 3-hydroxy group with retention of activity and that a sulfur, but not an amino or a chloro function, can successfully replace the lactam oxygen in the 2-position. Changing the lactam oxygen from the 2- to the 4-position of the pyridine ring produces 3-hydroxy-4-pyridone derivatives with better P-388 leukemia activity than similar 2-pyridones. 2-Methyl-3-acetoxy-4-pyridone (XVI) is the most active compound found thus far in these studies. The 4-pyrone (XI), which differs from the 4-pyridone (XIV) only in the heterocyclic atom, is inactive. The inactivity of the 3-methoxy analog (XIII) is consistent with previous observations that the two vicinal oxygen functions capable of being oxidized further are required for P-388 activity in the pyridones (1) and in a similar, but nonheterocyclic, series of catechol derivatives (6).

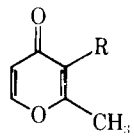

XI: R = OH
XII: R = OCH_3

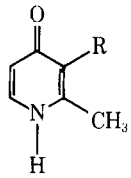

XIII: R = OCH_3
XIV: R = OH
XV: R = $OCONHCH_3$
XVI: R = $OCOCH_3$

EXPERIMENTAL[2]

3-Nitro-2(1*H*)-pyridone (III)—Compound III, mp 224–225° [lit. (9) mp 224–225°], was prepared from 2-pyridone on a 30-g scale by the method of Binz and Maier-Bode (9); NMR: 6.32 (t, 1, CH), 7.78 (m, 1, CH), 8.33 (m, 1, CH), and 12.77 (broad, 1, NH); UV: 361 (3.83) and 248 (3.43); IR: 1675 and 1640.

Anal.—Calc. for $C_5H_4N_2O_3$: C, 42.83; H, 2.88; N, 20.06. Found: C, 42.94; H, 2.89; N, 20.13.

3-Amino-2(1*H*)-pyridone (IV)—3-Nitro-2(1*H*)-pyridone (7.00 g, 0.05 mole) dissolved in 100 ml of methanol was hydrogenated in a Parr shaker (45 psi) in the presence of 10% palladium-on-carbon (400 mg). The catalyst was filtered, and the solution was stirred with activated carbon. The solution was filtered and evaporated to yield 5.47 g (99%) of a pink-white, light-sensitive solid, mp 123–125°; NMR: 4.66 (broad, 2, NH_2), 6.00 (t, 1, CH), and 6.63 (m, 2, CH); UV: 309 (3.94) and 253.5 (3.75); IR: 1650.

Anal.—Calc. for $C_5H_6N_2O$: C, 54.48; H, 5.49; N, 25.52. Found: C, 54.46; H, 5.56; N, 25.18.

3-Acetamido-2(1*H*)-pyridone (V)—A stirred mixture of sodium acetate (7.84 g, 0.08 mole), acetic anhydride (10 ml), and dry IV (8.45 g, 0.077 mole) was refluxed for 2 hr and then stirred for 16 hr at a temperature just high enough to keep the mixture fluid. The excess acetic anhydride was evaporated *in vacuo*, and the resulting solid was extracted first with hot methylene chloride (100 ml) and then with hot ethyl acetate (125 ml). Evaporation of the solvents gave a pink solid, which was dissolved in a limited amount of methanol and stirred with decolorizing carbon. Filtration of the solution and cooling gave 6.70 g (57%) of white crystals, mp 209–211°; NMR: 2.08 (s, 3, CH_3), 6.13 (t, 1, CH), 7.03 (m, 1, CH), 8.17 (m, 1, CH), and 9.12 and 11.82 (broad, 2, NH); UV: 308 (4.00), 256 (3.91), and 247.5 (3.98); IR: 1635 and 1605.

Anal.—Calc. for $C_7H_8N_2O_2$: C, 55.21; H, 5.29; N, 18.48. Found: C, 55.13; H, 5.31; N, 18.28.

3-[[(Methylamino)carbonyl]amino]-2(1*H*)-pyridone (VI)—Methyl isocyanate (3.00 ml, 0.051 mole) was added by syringe to a cold (2°) stirred solution of IV (5.50 g, 0.05 mole) and triethylamine (0.5 ml) in dry dimethylformamide (30 ml). Stirring was continued for 3 hr in the cold and for 50 hr at room temperature. Evaporation of the solvent *in vacuo* gave a brown solid, which was recrystallized from methanol (charcoal) to give 5.76 g (69%) of a white solid, mp >300°; NMR: 2.60 (d, 3, CH_3), 6.10 (t, 1, CH), 6.87 (broad, 2, CH, NH), 7.97 (m, 1, CH), and 8.15 and 11.70 (broad, 2, NH); UV: 305 (4.04) and 251 (4.01); IR: 1640–1605.

Anal.—Calc. for $C_7H_9N_3O_2$: C, 50.24; H, 5.42; N, 25.22. Found: C, 50.13; H, 5.50; N, 25.21.

3-Acetoxy-2(1*H*)-thiopyridone (X)—Acetic anhydride (3.82 ml, 0.0405 mole) was added by syringe to a dry, stirred solution of IX (5.09 g, 0.04 mole) and pyridine (0.0405 mole, 3.3 ml) in acetone (30 ml), which had been freshly distilled from phosphorus pentoxide. The solution was refluxed for 23 hr under nitrogen, during which time the product precipitated from solution. The mixture was stirred at room temperature for an additional 42 hr. The light-yellow product was filtered and then recrystallized from methanol–ethanol to give 5.82 g (86%) of a light-yellow solid, mp 167–171°; NMR: 2.20 (s, 3, CH_3), 6.68 (t, 1, CH), 7.74 (m, 2, CH), and 13.8 (broad, 1, NH); UV: 361.5 (3.89) and 279.5 (4.05); IR: 1765, 1365, and 1310.

Anal.—Calc. for $C_7H_7NO_2S$: C, 49.67; H, 4.17; N, 8.31. Found: C, 49.78; H, 4.40; N, 8.41.

2-Methyl-3-methoxy-4-pyrone (XII)—Compound XII was prepared in a 73% yield on a 20-g scale from XI by the method of Fisher and Hodge (2). The crude product was used immediately for the next reaction without further purification.

2-Methyl-3-methoxy-4(1*H*)-pyridone (XIII)—Crude XII (20.63 g, 0.146 mole) was dissolved in concentrated ammonium hydroxide (600 ml), and the light-yellow solution was refluxed for 12 hr. The reaction mixture was cooled to room temperature, more ammonium hydroxide was added (50 ml), and stirring was continued for 4 hr. Evaporation of the solvent *in vacuo* gave a yellow solid, which was recrystallized from acetone to give 16.39 g (80.5%) of product. Further recrystallization from acetone–ethanol gave analytically pure XIII, mp 155–156° [lit. (2) mp 155–156°]; NMR ($CDCl_3$): 2.33 (s, 3, CH_3), 3.75 (s, 3, OCH_3), 6.40 (d, 1, CH), 7.48 (d, 1, CH), and 9.97 (broad, 1, NH); UV: 264 (4.14); IR: 1620.

Anal.—Calc. for $C_7H_9NO_2$: C, 60.39; H, 6.52; N, 10.10. Found: C, 60.37; H, 6.63; N, 10.05.

2-Methyl-3-hydroxy-4(1*H*)-pyridone (XIV)—A solution of XIII (8.35 g, 0.06 mole) in 48% hydrobromic acid (120 ml) was heated at 140–150° for 4 hr, cooled to room temperature, and concentrated to 30–40 ml. The resulting red crystalline solid was isolated and dissolved in a small amount of water, and the solution was carefully neutralized with sodium carbonate. At pH 6–7, a red-brown solid precipitated. This solid was filtered, dissolved in boiling water, and decolorized with charcoal. A light red-brown product was isolated (5.81 g, 77%), mp 285–288° dec. [lit. (2) mp >250° dec.]; NMR: 2.13 (s, 3, CH_3), 6.03 (m, 2, CH + exchangeable), and 7.3 (m, 2, CH + exchangeable); UV: 276.5 (4.17); IR: 1635.

Anal.—Calc. for $C_6H_7NO_2$: C, 57.57; H, 5.63; N, 11.24. Found: C, 57.30; H, 5.77; N, 11.28.

2-Methyl-3-[[(methylamino)carbonyl]oxy] -4(1*H*)- pyridone (XV)—To a stirred suspension of XIV (2.78 g, 0.02 mole) in dry dimethylformamide (15 ml) and triethylamine (5 drops) under nitrogen was added 1.21 ml (0.02 mole) of methyl isocyanate. During the addition (syringe through a flask septum), the suspended solid changed from red brown to white. After stirring 21 hr at room temperature, the solvent was evaporated, the resulting solid was triturated well with benzene and then ethyl acetate. A pink-white solid (3.61 g, 99%), mp 280–285° dec., was obtained; NMR: 2.08 (s, 3, CH_3), 2.57 (d, 3, NCH_3), 6.07 (d, 1, CH), 7.45 (broad, 2, CH, NH), and 10.2 (broad, 1, NH); UV: 258.5 (4.16); IR: 1730 and 1620.

Anal.—Calc. for $C_8H_{10}N_2O_3$: C, 52.71; H, 5.53; N, 15.43. Found: C, 52.40; H, 5.50; N, 15.13.

2-Methyl-3-acetoxy-4(1*H*)-pyridone (XVI)—A solution of XIV (3.64 g, 0.029 mole) in acetic anhydride (25 ml) was refluxed (130–140°) for 21 hr under a nitrogen atmosphere. Removal of excess acetic anhydride gave a dark oil, which was dissolved in ethyl acetate and cooled at 0°. A dark-brown solid (1.05 g, 22%) resulted, mp 205–208° [lit. (2) mp 205–208°, (10) 204–205°]; NMR: 1.20 (unresolved d, 6, CH_3), 6.12 (broad, 1, CH), and 7.53 (broad, 1, CH); UV: 260 (4.10); IR: 1760 and 1630.

Anal.—Calc. for $C_8H_9NO_3$: C, 57.46; H, 5.42; N, 8.41. Found: C, 56.57; H, 5.47; N, 8.24.

[2] All melting points were recorded on a Thomas-Hoover capillary apparatus and are uncorrected. Elemental analyses were performed by the Microanalytical Services Section, National Institute of Arthritis, Metabolism, and Digestive Diseases, National Institutes of Health, Bethesda, Md. Compounds were identified by NMR, UV, and IR spectroscopy. These spectra were determined in dimethyl sulfoxide-d_6, 95% ethanol, and nujol, respectively, unless otherwise indicated. NMR data are delta values relative to tetramethylsilane, UV values are in nanometers (log ϵ), and IR values are in reciprocal centimeters. Compounds I, II, VII–IX, and XI were purchased from Aldrich Chemical Co.

REFERENCES

(1) D. R. Hwang and J. S. Driscoll, *J. Pharm. Sci.*, **68**, 816 (1979).

(2) B. E. Fisher and J. E. Hodge, *J. Org. Chem.*, **29**, 776 (1964).

(3) R. I. Geran, N. H. Greenberg, M. M. Macdonald, A. M. Schumacher, and B. J. Abbott, *Cancer Chemother. Rep., Part 3*, **3**(2), 1 (1972).

(4) H. Tieckelmann, in "Pyridine and its Derivatives," vol. 14, Suppl. part 3, R. A. Abramovitch, Ed., Interscience, New York, N.Y., 1974, p. 733.

(5) S. A. Schepartz, DHEW Publication (NIH) 76-1200, 1976, pp. 13–25.

(6) J. S. Driscoll, *J. Pharm. Sci.*, **68**, 1519 (1979).

(7) R. T. Borschardt, *J. Med. Chem.*, **16**, 581 (1973).

(8) C. Li, L. S. Rittmann, A. S. Tsiftsoglou, K. K. Bhargava, and A. C. Sartorelli, *J. Med. Chem.*, **21**, 874 (1978).

(9) A. Binz and H. Maier-Bode, *Angew. Chem.*, **49**, 486 (1936).

(10) A. Peratoner and A. Tamburello, *Gazz. Chim. Ital.*, **36**, 33 (1906).

ACKNOWLEDGMENTS

The authors thank Mr. Leo Dudeck and Mr. George Congleton of Hazleton Laboratories for the determination of the antitumor test data under National Cancer Institute Contract N01-CM-57007.

D. R. Hwang was a National Institutes of Health Visiting Postdoctoral Fellow for 1976–1977. G. R. Proctor was a National Cancer Institute Visiting Expert for 1975–1976.

Evaluation of Sustained-Action Chlorpheniramine–Pseudoephedrine Dosage Form in Humans

AVRAHAM YACOBI ×, ROGER G. STOLL, GEORGE C. CHAO, JAMES E. CARTER, DAVID M. BAASKE, BURDE L. KAMATH, ANTON H. AMANN, and CHII-MING LAI

Received November 5, 1979, from the *Department of Pharmaceutical Development, Research and Development, American Critical Care, McGaw Park, IL 60085.* Accepted for publication January 28, 1980.

Abstract □ This investigation compared the bioavailability of chlorpheniramine and pseudoephedrine from a sustained-action capsule and a combination of two reference standard tablets in 24 normal human subjects. The capsule contained 8 mg of chlorpheniramine maleate and 120 mg of pseudoephedrine hydrochloride, and the tablets each contained half of the amount of the chlorpheniramine or pseudoephedrine in the capsule. Because the capsule was a combination product, a new study design had to be developed to accommodate steady-state conditions for both drugs. Each subject received the capsule (every 12 hr) and the combination of the reference tablets (every 6 hr) for 8 days according to a two-way crossover design. Serial blood and urine samples were taken during the entire study. Plasma and urine samples were assayed for chlorpheniramine and pseudoephedrine by sensitive and specific high-pressure liquid chromatographic or GLC methods. There were no significant differences in the plasma concentration profiles of chlorpheniramine and pseudoephedrine at all times, except when the capsule developed peaks or the tablets developed nadirs. The highest mean peak plasma concentrations for the capsule and the tablets were 38.7 and 32.9 ng of chlorpheniramine/ml and 525 and 515 ng of pseudoephedrine/ml, respectively. The mean biological half-lives of chlorpheniramine and pseudoephedrine were 21.6 and 8.0 hr, respectively. The *AUC* and unchanged drug excreted in urine, after a single dose and at steady state, showed that the sustained-action capsule (given every 12 hr) and the reference standard tablets (given every 6 hr) were bioequivalent.

Keyphrases □ Chlorpheniramine—bioavailability in sustained-release dosage form with pseudoephedrine □ Pseudoephedrine—bioavailability in sustained-release dosage form with chlorpheniramine □ Dosage forms, sustained release—bioavailability of chlorpheniramine and pseudoephedrine in combination product □ Bioavailability—chlorpheniramine and pseudoephedrine in sustained-release dosage form

Sustained-action dosage forms often are administered to assure a uniform blood concentration and to provide greater patient convenience and compliance. This dosage form minimizes the occurrence of adverse reactions caused by high plasma concentrations and assures clinical efficacy over the entire regimen. Drugs that are used in sustained-action dosage forms usually possess short half-lives, and their absorption and elimination are affected by physiological factors such as variable urinary pH, enzyme induction or inhibition upon multiple dosing, and variable GI motility.

The physical characteristics of a sustained-release dosage form are such that absorption of the drug is prolonged. The possibility of immediate release of a large amount of drug (dose dumping) is unlikely but requires verification. By considering such factors, a bioavailability study involving multiple doses to achieve steady state will provide a reproducibility test for the *in vivo* performance of a sustained-action dosage form. Pharmacokinetically, such a test will be characterized by more reliable parameters and less variability due to physiological changes.

Ideally, a sustained-action dosage form should release its contents at a constant rate, regardless of changes in the GI pH. Such a dosage form should avoid dose dumping and prevent large fluctuation in plasma concentrations. The objective of this study was to test the bioavailability of chlorpheniramine and pseudoephedrine from a newly developed sustained-action capsule dosage form containing chlorpheniramine and pseudoephedrine by comparison of the plasma concentration *versus* time profile of the drugs following administration of single and multiple doses.

EXPERIMENTAL

In a two-way crossover design study, 24 healthy, nonobese male subjects, 19–41 years old and 62–99 kg (mean 73 kg), were selected randomly. They did not receive any drugs, including enzyme-inducing agents and monoamine oxidase inhibitors, 1 month before and during the study. Eleven subjects were smokers. Alcoholic beverages and those containing caffeine also were withheld during the study.

Each subject received either one sustained-action capsule[1], containing 8 mg of chlorpheniramine maleate and 120 mg of pseudoephedrine hydrochloride, or the combination of one 4-mg chlorpheniramine maleate[2] tablet and one 60-mg pseudoephedrine hydrochloride[3] tablet with 200 ml of water. Either one capsule was given every 12 hr (twice per day) or the combination of the chlorpheniramine and pseudoephedrine tablets was given every 6 hr (four times per day) for 8 days. On Days 1 and 8, only a single capsule or two doses of the combination of the tablets was administered. The subjects were not allowed food overnight, from 10 hr before dosing to 4 hr after administration of the first capsule or first tablet on Days 1 and 8 of the study. A 5-day washout period was allowed between the two treatments.

Heart rate and blood pressure were measured daily during the entire study. Serial blood samples during Day 1 (for 24 hr), Days 2–7 (one sample at the minimum plasma concentration), and Day 8 (for 48 hr) were collected and the plasma was separated. Urine samples were collected during Day 1, at steady state, and for 48 hr after administration of the last capsule and tablet dose. All plasma and urine samples were frozen immediately and were kept frozen until they were assayed.

The plasma chlorpheniramine concentration was determined by a specific high-pressure liquid chromatographic (HPLC) method (1). The recovery and reproducibility of standard samples over the concentration range of 2.5–100 ng/ml were 96.6 and 95.4%, respectively. The plasma pseudoephedrine concentration was determined by GLC with electron-capture detection (2, 3). The recovery and reproducibility of standard samples over the concentration range of 10–700 ng/ml were 99.0 and 93.4%, respectively. Chlorpheniramine and pseudoephedrine concentrations in urine were determined simultaneously by a specific HPLC method (4, 5). The recovery and reproducibility of standard samples were 97.3 and 96.8%, respectively, for chlorpheniramine (0.12–3 μg/ml) and 89.7 and 96.8%, respectively, for pseudoephedrine (3–75 μg/ml). All samples were assayed in duplicate. Samples that showed more than a 15% difference between duplicate assays were reassayed in duplicate, when possible, and the two closest values were taken for final data analysis.

Dissolution testing of the capsule was carried out by a modification of the NF time-release procedure (6). The dissolution fluid consisted of 0.05 *M* potassium phosphate buffer (pH 4.5). There was no variation in the pH during the 7-hr dissolution procedure. The tablet dissolution testing was carried out using the USP XIX rotating-basket procedure. The concentrations of chlorpheniramine and pseudoephedrine in the dissolution fluids were determined by stability-indicating GLC proce-

[1] Isoclor Timesule, American Critical Care, McGaw Park, Ill.
[2] Chlor-Trimeton, Schering Corp., Kenilworth, N.J.
[3] Sudafed, Burroughs Wellcome Co., Research Triangle Park, N.C.

0022-3549/80/0900-1077$01.00/0
© 1980, American Pharmaceutical Association

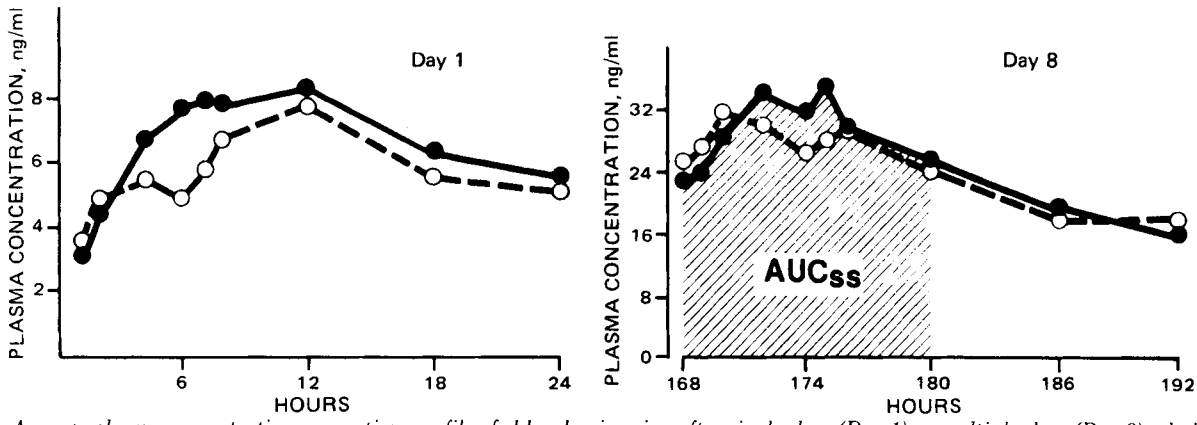

Figure 1—*Average plasma concentration* versus *time profile of chlorpheniramine after single-dose (Day 1) or multiple-dose (Day 8) administration of the sustained-release capsule* (●) *and the reference tablet* (○) *in 24 normal subjects.*

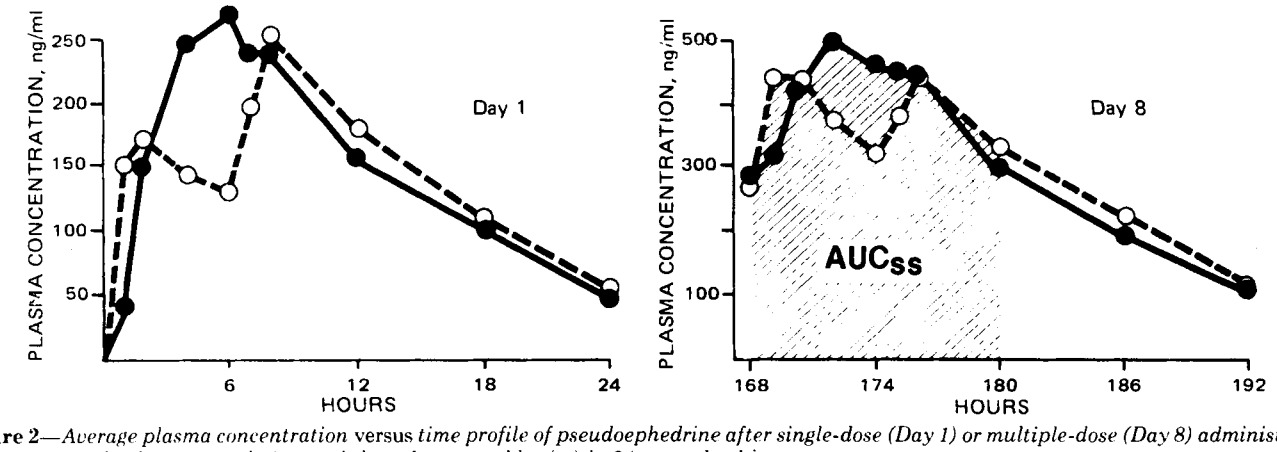

Figure 2—*Average plasma concentration* versus *time profile of pseudoephedrine after single-dose (Day 1) or multiple-dose (Day 8) administration of the sustained-release capsule* (●) *and the reference tablet* (○) *in 24 normal subjects.*

dures (7). This assay also was utilized to verify potency for each dosage form.

The biological half-life, $t_{1/2}$, of each drug in individual subjects was determined from the postabsorption-distribution phase after administration of the last capsule (168 hr). The ratio of the total body clearance, Cl, to the bioavailability factor, F, was determined by dividing the given dose by the area under the plasma concentration *versus* time profile, AUC, at steady state, AUC_{ss} (168–180 hr). The AUC from 0 to 24 hr or at steady state was determined by the trapezoidal method. The ratio of the volume of distribution, V_d, to F was determined from $Cl/\beta F$, where β is the disposition rate constant and is equal to $0.693/t_{1/2}$. The average plasma concentration at steady state, $\overline{C}$, was determined by dividing AUC_{ss} by the dosing interval, *i.e.*, 12 hr. The relative amount of drug absorbed was evaluated by comparing the AUC at steady state and the amount of drug excreted in the urine at steady state.

A nonparametric Wilcoxon's two-sample test (8) with its application to crossover design by Koch (9) was performed to compare formulations for plasma concentrations, urinary excretion and recovery of unchanged drug, and pharmacokinetic parameters of chlorpheniramine and pseudoephedrine following administration of each dosage form. The same test was used for comparison of the blood pressure and heart rate. The period, group, and formulation effects also were tested.

RESULTS

Figures 1 and 2 depict the average plasma concentration *versus* time profiles of chlorpheniramine and pseudoephedrine, respectively. Data after the first and last doses at steady state are shown. The plasma concentrations were significantly higher for the capsule only at 4, 6, and 7 hr after the single dose and at steady state after the last dose.

Table I summarizes the mean peak plasma concentration, peak time of chlorpheniramine and pseudoephedrine, and results of statistical analysis. The mean peak plasma concentrations of chlorpheniramine at steady state were 38.7 ng/ml (range[4] 17.3–75.8 ng/ml) after administration of the capsule and 32.9 ng/ml (range 17.7–79.5 ng/ml) after the tablet. Without the unusual chlorpheniramine data point[4], the mean peak plasma concentration becomes 35.5 ng/ml, which is not significantly different from the mean values obtained for the standard tablet. The mean peak plasma concentration times differed after the single dose ($p < 0.01$) and was the same after multiple dosing for both drugs.

The higher concentrations of chlorpheniramine and pseudoephedrine attained in this study were not associated with an increase in the incidence or the type of adverse side effects.

Figure 3 depicts the mean minimum plasma concentration of chlorpheniramine and pseudoephedrine following multiple-dose administration of the sustained-release capsule and the reference tablets. There was essentially no significant difference between the values obtained for either dosage form. On the average, the steady-state minimum plasma concentration was achieved after 6 days for chlorpheniramine and 2 days for pseudoephedrine. The minimum plasma chlorpheniramine concentration was ~24 ng/ml and remained within a 10% range at Days 6–8; the minimum plasma concentration of pseudoephedrine increased from 260 ng/ml on Day 7 to ~315 ng/ml on Day 8.

Table II summarizes the mean AUC and amounts of unchanged chlorpheniramine and pseudoephedrine excreted in the urine. There was no significant difference between the two treatments. At steady state, the AUC and the urinary values were almost twice as high for chlorpheniramine and were ~27 and 12% higher for pseudoephedrine than those for the respective single doses. Additionally, at steady state, the amounts excreted in the urine for both drugs were higher at 156–168 hr than at 168–180 hr.

Table III lists the average pharmacokinetic parameters for chlorpheniramine and pseudoephedrine. These parameters were essentially identical for the capsule and reference tablets.

The relative amount of drugs absorbed was evaluated by comparing the AUC or the average steady-state plasma concentrations and the

[4] One subject showed an unusually high plasma concentration of 154 ng/ml 7 hr after the last dose; his second highest plasma concentration was 75.8 ng/ml 6 hr after the last dose.

Table I—Mean Peak Plasma Concentration and Peak Time of Chlorpheniramine and Pseudoephedrine and Results of Statistical Analysis

Parameter	Mean ± *SD*		Significance Level by Wilcoxon's Two-Sample Test		
	Capsules	Reference Tablets	Drug	Period	Group
		Chlorpheniramine			
Peak plasma concentration, ng/ml					
0–12 hr	10.6 ± 4.92	8.88 ± 2.47	NS[a]	NS	NS
168–180 hr	38.7[b] ± 27.1	32.9 ± 13.6	NS	NS	NS
Peak time[c], hr					
0–12 hr	7.88 ± 4.83	10.9 ± 4.90	0.01	NS	NS
168–180 hr	5.63 ± 2.90	4.54 ± 2.98	NS	NS	NS
		Pseudoephedrine			
Peak plasma concentration, ng/ml					
0–12 hr	282.7 ± 49.8	264.0 ± 59.6	NS	NS	NS
168–180 hr	525.4 ± 131.3	514.6 ± 98.0	NS	NS	NS
Peak time[c], hr					
0–12	5.83 ± 1.27	7.63 ± 2.55	0.01	NS	NS
168–180 hr	4.67 ± 1.66	4.25 ± 3.15	NS	NS	NS

[a] Not significant. [b] When an unusual plasma concentration of 154 ng/ml in one subject is eliminated, the mean value becomes 35.5 ng/ml, which does not change the statistical results. [c] Relative to administration of the capsule or the first tablet in each interval.

Table II—Mean Area under Plasma Concentration *versus* Time Profile and Unchanged Drug Excreted in Urine

Parameter	Chlorpheniramine[a]		Pseudoephedrine[a]	
	Capsules	Reference Tablets	Capsules	Reference Tablets
AUC, (ng hr)/ml				
Single dose, 0–24 hr	161.3 ± 73.2	140.7 ± 36.1	3620 ± 747	3456 ± 629
Steady state, 168–180 hr	351.8 ± 138.7	333.0 ± 147.1	4986 ± 1248	4647 ± 1123
Urinary excretion[b], mg				
Single dose, 0–24 hr	0.407 ± 0.302	0.424 ± 0.229	96.0 ± 11.3	92.6 ± 14.0
Steady state, 156–168 hr	1.06 ± 0.678	0.967 ± 0.512	109.9 ± 22.3	103.7 ± 30.7
Steady state, 168–180 hr	0.716 ± 0.748	0.667 ± 0.510	101.5 ± 22.7	92.6 ± 16.2
Washout, 168–216 hr	2.07 ± 1.42	1.91 ± 0.996	175.8 ± 31.8	165.1 ± 27.9

[a] Mean ± *SD*; there was no significant difference between treatments. [b] Amount given as chlorpheniramine maleate or pseudoephedrine hydrochloride.

urinary excretion of the drugs at steady state. Table IV summarizes the ratio of these parameters (capsule to reference tablet) with respect to either drug. The capsule showed slightly higher bioavailability than the reference tablet.

The capsule potency was determined to be 101.2 and 104.0% of the labeled quantity of chlorpheniramine and pseudoephedrine, respectively. The chlorpheniramine and pseudoephedrine tablets contained 98.2 and 99.2%, respectively, of the labeled quantity. The dissolution testing indicated that the capsule released 84.5 and 89.0% of chlorpheniramine and pseudoephedrine, respectively, within 7 hr and that the tablets released 99.1 and 101.4% of chlorpheniramine and pseudoephedrine, respectively, within 15 min.

DISCUSSION

Because the sustained-action formulation tested was a combination product of chlorpheniramine and pseudoephedrine, a new study design had to be developed that would assure steady-state conditions for both drugs and use two reference standard tablets for the bioequivalency tests. A standard three-way crossover design would have made the study unduly

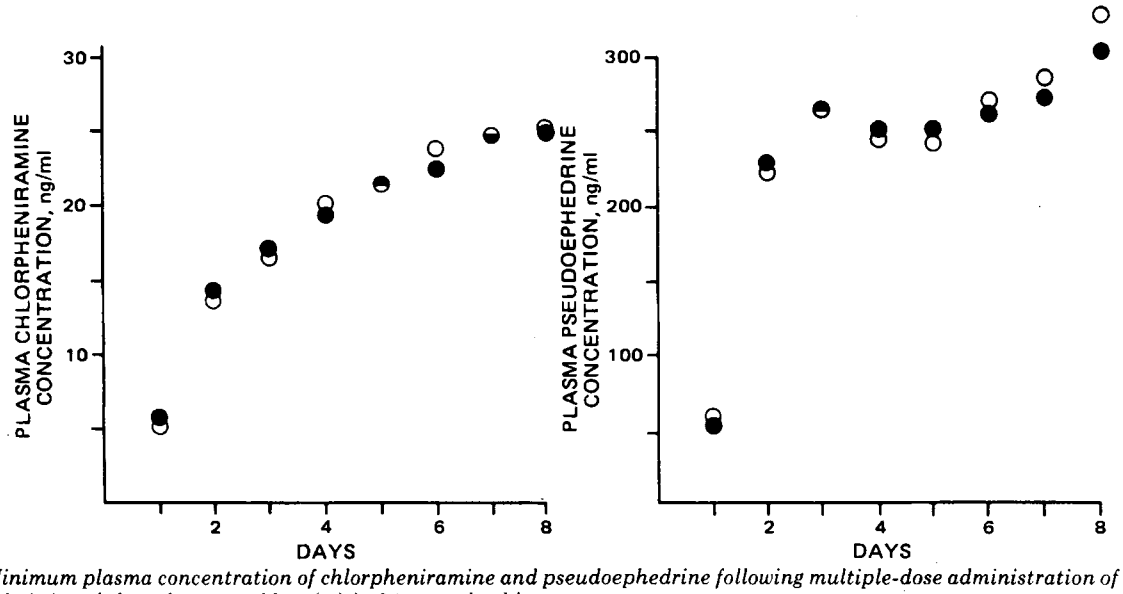

Figure 3—*Minimum plasma concentration of chlorpheniramine and pseudoephedrine following multiple-dose administration of the sustained-release capsule (●) and the reference tablets (○) in 24 normal subjects.*

Table III—Pharmacokinetic Parameters of Chlorpheniramine and Pseudoephedrine

Parameter	Sustained-Release Capsule[a] Mean ± SD	Sustained-Release Capsule[a] Range	Reference Tablets[a] Mean ± SD	Reference Tablets[a] Range
		Chlorpheniramine		
$\bar{C} = AUC_{ss}/12$, ng/ml	29.3 ± 11.6	14.0–63.5	27.8 ± 12.3	16.0–71.0
$t_{1/2}$, hr	22.13 ± 5.92	11.5–35.7	20.96 ± 4.94	13.9–33.0
V_d/F, liters/kg	7.51 ± 2.12	2.12–14.4	7.65 ± 2.06	3.13–11.3
Cl/F, ml/hr/kg	251.5 ± 93.2	111.8–456.8	264.1 ± 84.6	106.2–414.2
		Pseudoephedrine		
$\bar{C} = AUC_{ss}/12$, ng/ml	415.5 ± 104.0	255.0–609.0	387.2 ± 93.7	209.0–582.0
$t_{1/2}$, hr	8.23 ± 1.28	4.65–10.9	7.85 ± 1.63	5.02–10.9
V_d/F, liters/kg	3.40 ± 0.92	1.76–5.11	3.50 ± 1.12	1.46–5.73
Cl/F, ml/hr/kg	289.0 ± 74.6	164.7–434.1	309.8 ± 81.2	188.9–528.6

[a] Mean ± SD, $n = 24$; there was no significant difference between treatments.

cumbersome. The two-way crossover design allowed for simultaneous administration of the two reference standard tablets to one group and the sustained-action formulation to the other and provided the opportunity for a multiple-dose study within a short time period.

The sustained-action capsule showed gradual *in vivo* absorption and produced plasma concentrations virtually identical to those obtained after administration of the reference tablets. Statistical differences were noted when the capsule reached the peak level at approximately the same time as the every 6-hr regimen reached its nadir. There was no indication of dose dumping after capsule administration. This conclusion is substantiated by sustained plasma concentrations during one dosing interval at steady state, similarity of peak plasma concentrations, and similarity of the time of peak plasma concentrations of either dosage form at steady state.

For both dosage forms, the time to achieve the highest peak plasma concentration was examined. Since the tablets were given every 6 hr, it was expected that the peak after the second 6-hr dose (*i.e.*, the second tablet) would be the highest; this expectation was verified statistically. For both drugs and at steady state, every 6-hr administration of the reference tablets should produce virtually the same peak at the same relative time. This response is apparent in the data and also is the reason for having a shorter peak plasma concentration time at steady state than after the single-dose administration (*i.e.*, the first two doses of the every 6-hr regimen) of the reference tablets.

The gradual *in vivo* absorption of the sustained-action capsule was dictated by its *in vitro* dissolution characteristics (Fig. 4). Identical dissolution profiles were observed at pH 1.5, 4.5, and 7.5. Therefore, no changes in the release rate are expected in the GI tract with respect to changes in pH. Other factors such as the presence or absence of enzymes may influence the dissolution rate of the drugs. The pH-independent dissolution of chlorpheniramine and pseudoephedrine in the capsule assures complete release of the drugs and minimizes the chances for dose dumping, which can cause side effects.

The results showed minimum occurrence of side effects during the 8 days of the study, with no effect on the heart rate or blood pressure by either dosage form. The chlorpheniramine and pseudoephedrine doses used in this study are considered safe. In a more rigorous clinical study, Bye *et al.* (10) observed signs of insomnia which lasted for the first 3 days among subjects who received chronic dosing with a 180-mg sustained-action product of pseudoephedrine. In another study, Dickerson *et al.* (11) found that chronic dosing with 120- and 150-mg sustained-action products of pseudoephedrine increased the pulse rate but decreased blood pressure.

Consistent with the half-lives of chlorpheniramine (22 hr) and pseudoephedrine (8 hr), the minimum steady-state plasma concentrations were achieved in 6 and 2 days, respectively. Both chlorpheniramine and pseudoephedrine are weak bases, and their elimination in urine is pH dependent (4, 12, 13). Day-to-day fluctuations in the urine pH will result in a fluctuation in the plasma concentration as well as in the urinary excretion of unchanged drugs. In this study, the minimum steady-state plasma concentration of both drugs, particularly pseudoephedrine, increased during the 168–180-hr interval; the urinary excretion of unchanged drugs in the same interval diminished. This change occurred just after hospitalization of the subjects and standardization of the food, which may have directly affected the urinary pH. In fact, consistent with the decrease in the urinary excretion of the drugs, the average urinary pH values did increase significantly from 5.8 at the 156–168-hr interval to ~6.1 at the 168–180-hr collection interval in both treatments (Table V).

The steady-state approach allowed determination of the pharmacokinetic parameters and bioequivalency of chlorpheniramine and pseudoephedrine between the sustained-action capsule and the reference standard tablets. The single-dose data after 24-hr blood sampling and urinary collection resulted in smaller *AUC* and urinary excretion values of unchanged drugs for both chlorpheniramine (44 and 50%, respectively) and pseudoephedrine (73 and 88%, respectively). This finding warrants a longer washout period for both drugs after a single dose. However, for chlorpheniramine, the sensitivity of the assay also must be considered.

The average plasma concentrations of chlorpheniramine and pseudoephedrine were the same for both dosage forms. In a group of 16 subjects who received a regimen of pseudoephedrine, the estimated minimum steady-state plasma concentration was 447 ng/ml (11), which is consistent with the present finding. The biological half-life of chlorpheniramine was in agreement with values reported in a study that utilized an identical assay (14). The average biological half-life of pseudoephedrine found in the present study (8.0 hr) was higher than values reported previously (5.9 hr) for 16 subjects (11). However, the higher half-life may account for the higher V_d/F value found in this study (3.4 liters/kg) than in the same 16 subjects (2.6 liters/kg). However, these differences also may be due to the study design and methods for estimation of V_d. The reproducibility of the pharmacokinetic parameters is indicative of completeness of absorption of chlorpheniramine and pseudoephedrine from both dosage forms. The reproducibility of the minimum steady-state plasma concentration also suggests that there was no enzyme induction with respect to chlorpheniramine metabolism or

Table IV—Relative Bioavailability of Chlorpheniramine and Pseudoephedrine after the Sustained-Release Capsule

Parameter	Ratio of Parameters[a] of Capsule to Tablets: Chlorpheniramine	Ratio of Parameters[a] of Capsule to Tablets: Pseudoephedrine
Excretion in urine		
0–24 hr	0.96	1.04
156–168[b] hr	1.10	1.06
168–180[b] hr	1.06	1.06
168–216 hr	1.08	1.06
Area under plasma concentration *versus* time profile		
0–24 hr	1.15	1.05
168–180[b] hr	1.06	1.07

[a] Ratio of the mean parameters obtained after administration of the capsule and the combination of the tablets. Ratio of one indicates that two dosage forms are bioequivalent. [b] These parameters are determined at steady state and give the true bioequivalence data.

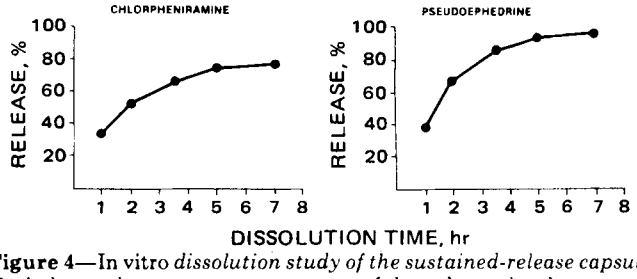

Figure 4—In vitro *dissolution study of the sustained-release capsule. Each data point represents an average of three determinations at each pH. Identical dissolution profiles were obtained at pH 1.5, 4.5, and 7.5.*

Table V—Mean Urine pH at Steady State and Results of Statistical Analysis

Urine Collection Interval, hr	Capsules pH[a]	Capsules p^b	Reference Tablets pH[a]	Reference Tablets p^b
156–168	5.78 ± 0.36		5.84 ± 0.51	
168–174	6.08 ± 0.65	<0.01	6.23 ± 0.68	<0.01
174–180	6.20 ± 0.67	<0.01	6.20 ± 6.16	<0.05
168–180[c]	6.14 ± 0.62	<0.01	6.21 ± 0.55	<0.01

[a] Mean ± *SD*, $n = 24$; there was no statistically significant difference between two treatments. [b] Statistically significant difference from 156–168-hr urine sample pH. [c] Average of 168–174- and 174–180-hr pH values.

changes in urinary excretion of either drug. While the urinary excretion of unchanged chlorpheniramine is a small fraction of the administered dose (4), the urinary excretion of unchanged pseudoephedrine is the major fraction of the administered dose and can be a reliable indicator for bioequivalency tests.

The bioequivalency test for sustained-release dosage forms can be best made at steady state when the amount excreted in urine reflects the amount absorbed. Table II substantiates this premise since the 0–24-hr *AUC* does not accurately reflect the amount of chlorpheniramine absorbed. At steady state, the *AUC* for a single dosing interval was more than twice as large as that found during the 0–24-hr interval following a single dose of the capsule. The slow absorption associated with this sustained-action dosage form makes it difficult to evaluate such systems using a single-dose study design. When the ratio of parameters characterizing the bioavailability of two drugs is one, the dosage forms are considered to be bioequivalent. In this study, the average ratio (capsule to reference tablet) was 1.06. Thus, both the rate of drug absorption as given by the peak plasma concentration and time of peak (Table I) and the extent of absorption (Tables II and IV) showed virtually identical bioavailability for the sustained-action capsule and reference standard tablets.

REFERENCES

(1) N. K. Athanikar, G. W. Pang, R. L. Nation, and W. L. Chiou, *J. Chromatogr.*, **162,** 367 (1979).

(2) L. M. Cummins and M. J. Fourier, *Anal. Lett.*, **2,** 403 (1969).

(3) E. T. Lin, D. C. Brater, and L. Z. Benet, *J. Chromatogr.*, **140,** 275 (1979).

(4) C. M. Lai, R. G. Stoll, Z. M. Look, and A. Yacobi, *J. Pharm. Sci.*, **68,** 1243 (1979).

(5) D. M. Baaske, C. M. Lai, L. Klein, Z. M. Look, and A. Yacobi, *ibid.*, **68,** 1472 (1979).

(6) "The National Formulary," 14th ed., Mack Publishing Co., Easton, Pa., 1975, p. 985.

(7) A. Yacobi, Z. M. Look, and C. M. Lai, *J. Pharm. Sci.*, **67,** 1668 (1978).

(8) M. Hollander and D. Wolfe, "Nonparametric Statistical Methods," Wiley, New York, N.Y., 1973, pp. 68–75, 185.

(9) G. G. Koch, *Biometrics*, **28,** 577 (1972).

(10) C. Bye, H. M. Hill, D. T. D. Hughes, and A. W. Peck, *Eur. J. Clin. Pharmacol.*, **8,** 47 (1975).

(11) J. Dickerson, D. Perrier, M. Mayersohn, and R. Bressler, *ibid.*, **14,** 253 (1978).

(12) G. R. Wilkinson and A. H. Beckett, *J. Pharm. Pharmacol.*, **11,** 256 (1965).

(13) R. G. Kuntzman, I. Tsai, L. Brand, and L. C. Mark, *Clin. Pharmacol. Ther.*, **12,** 62 (1971).

(14) W. L. Chiou, N. K. Athanikar, and S. M. Huang, *N. Engl. J. Med.*, **300,** 501 (1979).

High-Performance Liquid Chromatographic Assay of Codeine in Acetaminophen with Codeine Dosage Forms

C. Y. KO ˣ, F. C. MARZIANI, and C. A. JANICKI

Received March 4, 1980, from the *Pharmacy Research Department, McNeil Laboratories, Fort Washington, PA 19034.* Accepted for publication March 27, 1980.

Abstract □ An accurate, rapid, and specific high-performance liquid chromatographic (HPLC) assay was developed for codeine in acetaminophen with codeine combination products. The internal standard (chlorpheniramine maleate), codeine, acetaminophen, and several other test compounds or impurities were well separated. A complete analysis took <10 min. The relative standard deviations of the retention time, precision, and accuracy were 0.5, 0.4, and 0.5%, respectively. An excellent linear correlation was obtained between the HPLC and GLC methods.

Keyphrases □ Codeine—high-performance liquid chromatographic analysis of capsules, tablets, and elixirs with acetaminophen and codeine, comparison with GLC analysis □ Acetaminophen—high-performance liquid chromatographic analysis of codeine and acetaminophen in capsules, tablets, and elixirs, comparison with GLC analysis □ High-performance liquid chromatography—analysis, codeine and acetaminophen in capsules, tablets, and elixirs, comparison with GLC analysis

Various analytical methods (1–11) have been reported for codeine, a narcotic analgesic and antitussive drug. Sell and Rajzer (1) determined codeine in nonaqueous media using a differentiating potentiometric titration method. Mulé (2) reported UV, TLC, and GLC methods for the determination of narcotic analgesics in humans. GLC methods (3–5) also were used extensively to determine codeine in various media.

Steady progress in high-performance liquid chromatographic (HPLC) analyses of codeine has been reported (6–11). Following reports that the HPLC technique was useful for codeine analysis (6, 7, 11), reversed-phase and ion-pair HPLC techniques were developed (8, 9). Baker *et al.* (10) recently analyzed codeine using a reversed-phase HPLC system equipped with dual-wavelength UV detection. Gupta (12) reported the simultaneous separation of acetaminophen, aspirin, caffeine, codeine phosphate, phenacetin, and salicylamide using a reversed-phase chromatographic method.

The purpose of this study was to develop an HPLC method that could be used routinely to assay codeine in acetaminophen with codeine combination products. This method is fast, simple, specific, precise, and accurate.

EXPERIMENTAL

Reagents and Materials—The *n*-hexane used was distilled in glass. Ammonium hydroxide was ACS grade. Chloroform[1], methanol[1], and sodium hydroxide[1] were analytical reagent grade. The codeine phosphate,

[1] Mallinckrodt, St. Louis, MO 63147.

0022-3549/80/0900-1081$01.00/0

© 1980, American Pharmaceutical Association

Table V—Mean Urine pH at Steady State and Results of Statistical Analysis

Urine Collection Interval, hr	Capsules pH[a]	Capsules p^b	Reference Tablets pH[a]	Reference Tablets p^b
156–168	5.78 ± 0.36		5.84 ± 0.51	
168–174	6.08 ± 0.65	<0.01	6.23 ± 0.68	<0.01
174–180	6.20 ± 0.67	<0.01	6.20 ± 6.16	<0.05
168–180[c]	6.14 ± 0.62	<0.01	6.21 ± 0.55	<0.01

[a] Mean ± *SD*, $n = 24$; there was no statistically significant difference between two treatments. [b] Statistically significant difference from 156–168-hr urine sample pH. [c] Average of 168–174- and 174–180-hr pH values.

changes in urinary excretion of either drug. While the urinary excretion of unchanged chlorpheniramine is a small fraction of the administered dose (4), the urinary excretion of unchanged pseudoephedrine is the major fraction of the administered dose and can be a reliable indicator for bioequivalency tests.

The bioequivalency test for sustained-release dosage forms can be best made at steady state when the amount excreted in urine reflects the amount absorbed. Table II substantiates this premise since the 0–24-hr *AUC* does not accurately reflect the amount of chlorpheniramine absorbed. At steady state, the *AUC* for a single dosing interval was more than twice as large as that found during the 0–24-hr interval following a single dose of the capsule. The slow absorption associated with this sustained-action dosage form makes it difficult to evaluate such systems using a single-dose study design. When the ratio of parameters characterizing the bioavailability of two drugs is one, the dosage forms are considered to be bioequivalent. In this study, the average ratio (capsule to reference tablet) was 1.06. Thus, both the rate of drug absorption as given by the peak plasma concentration and time of peak (Table I) and the extent of absorption (Tables II and IV) showed virtually identical bioavailability for the sustained-action capsule and reference standard tablets.

REFERENCES

(1) N. K. Athanikar, G. W. Pang, R. L. Nation, and W. L. Chiou, *J. Chromatogr.*, **162,** 367 (1979).

(2) L. M. Cummins and M. J. Fourier, *Anal. Lett.*, **2,** 403 (1969).

(3) E. T. Lin, D. C. Brater, and L. Z. Benet, *J. Chromatogr.*, **140,** 275 (1979).

(4) C. M. Lai, R. G. Stoll, Z. M. Look, and A. Yacobi, *J. Pharm. Sci.*, **68,** 1243 (1979).

(5) D. M. Baaske, C. M. Lai, L. Klein, Z. M. Look, and A. Yacobi, *ibid.*, **68,** 1472 (1979).

(6) "The National Formulary," 14th ed., Mack Publishing Co., Easton, Pa., 1975, p. 985.

(7) A. Yacobi, Z. M. Look, and C. M. Lai, *J. Pharm. Sci.*, **67,** 1668 (1978).

(8) M. Hollander and D. Wolfe, "Nonparametric Statistical Methods," Wiley, New York, N.Y., 1973, pp. 68–75, 185.

(9) G. G. Koch, *Biometrics*, **28,** 577 (1972).

(10) C. Bye, H. M. Hill, D. T. D. Hughes, and A. W. Peck, *Eur. J. Clin. Pharmacol.*, **8,** 47 (1975).

(11) J. Dickerson, D. Perrier, M. Mayersohn, and R. Bressler, *ibid.*, **14,** 253 (1978).

(12) G. R. Wilkinson and A. H. Beckett, *J. Pharm. Pharmacol.*, **11,** 256 (1965).

(13) R. G. Kuntzman, I. Tsai, L. Brand, and L. C. Mark, *Clin. Pharmacol. Ther.*, **12,** 62 (1971).

(14) W. L. Chiou, N. K. Athanikar, and S. M. Huang, *N. Engl. J. Med.*, **300,** 501 (1979).

High-Performance Liquid Chromatographic Assay of Codeine in Acetaminophen with Codeine Dosage Forms

C. Y. KO ˣ, F. C. MARZIANI, and C. A. JANICKI

Received March 4, 1980, from the *Pharmacy Research Department, McNeil Laboratories, Fort Washington, PA 19034.* Accepted for publication March 27, 1980.

Abstract □ An accurate, rapid, and specific high-performance liquid chromatographic (HPLC) assay was developed for codeine in acetaminophen with codeine combination products. The internal standard (chlorpheniramine maleate), codeine, acetaminophen, and several other test compounds or impurities were well separated. A complete analysis took <10 min. The relative standard deviations of the retention time, precision, and accuracy were 0.5, 0.4, and 0.5%, respectively. An excellent linear correlation was obtained between the HPLC and GLC methods.

Keyphrases □ Codeine—high-performance liquid chromatographic analysis of capsules, tablets, and elixirs with acetaminophen and codeine, comparison with GLC analysis □ Acetaminophen—high-performance liquid chromatographic analysis of codeine and acetaminophen in capsules, tablets, and elixirs, comparison with GLC analysis □ High-performance liquid chromatography—analysis, codeine and acetaminophen in capsules, tablets, and elixirs, comparison with GLC analysis

Various analytical methods (1–11) have been reported for codeine, a narcotic analgesic and antitussive drug. Sell and Rajzer (1) determined codeine in nonaqueous media using a differentiating potentiometric titration method. Mulé (2) reported UV, TLC, and GLC methods for the determination of narcotic analgesics in humans. GLC methods (3–5) also were used extensively to determine codeine in various media.

Steady progress in high-performance liquid chromatographic (HPLC) analyses of codeine has been reported (6–11). Following reports that the HPLC technique was useful for codeine analysis (6, 7, 11), reversed-phase and ion-pair HPLC techniques were developed (8, 9). Baker *et al.* (10) recently analyzed codeine using a reversed-phase HPLC system equipped with dual-wavelength UV detection. Gupta (12) reported the simultaneous separation of acetaminophen, aspirin, caffeine, codeine phosphate, phenacetin, and salicylamide using a reversed-phase chromatographic method.

The purpose of this study was to develop an HPLC method that could be used routinely to assay codeine in acetaminophen with codeine combination products. This method is fast, simple, specific, precise, and accurate.

EXPERIMENTAL

Reagents and Materials—The *n*-hexane used was distilled in glass. Ammonium hydroxide was ACS grade. Chloroform[1], methanol[1], and sodium hydroxide[1] were analytical reagent grade. The codeine phosphate,

[1] Mallinckrodt, St. Louis, MO 63147.

0022-3549/80/0900-1081$01.00/0

© 1980, American Pharmaceutical Association

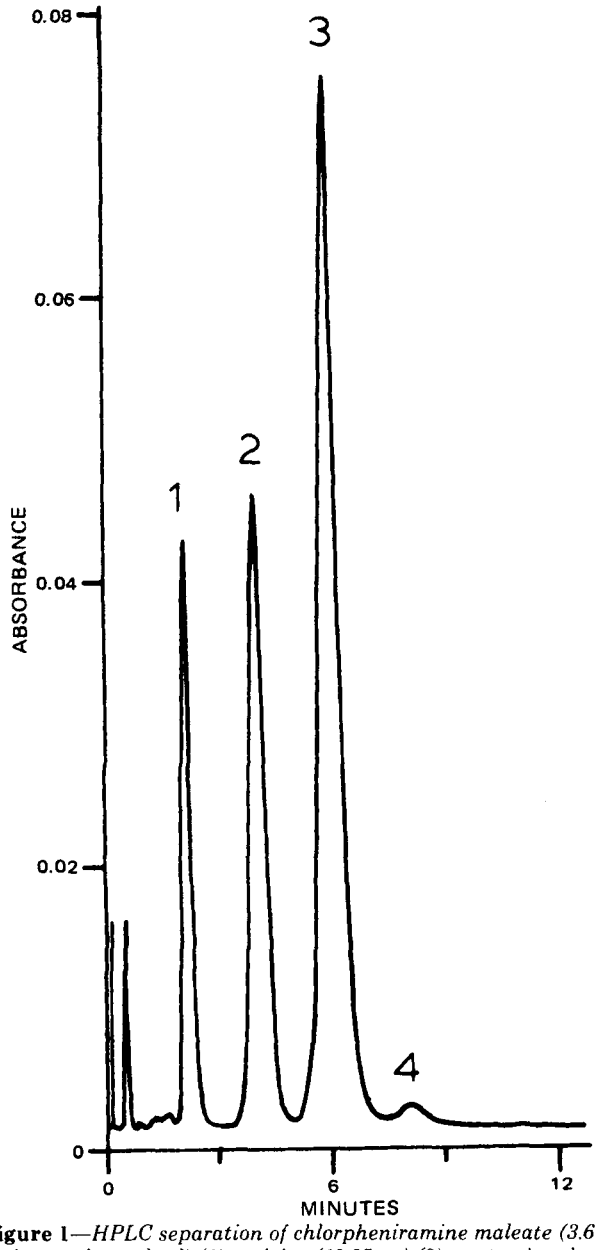

Figure 1—*HPLC separation of chlorpheniramine maleate (3.6 μg as an internal standard) (1), codeine (10.85 μg) (2), acetaminophen (unknown amount) (3), and an unknown compound (4) from an acetaminophen (325 mg) with codeine phosphate (30 mg) tablet sample.*

morphine sulfate, and chlorpheniramine maleate were USP reference standards. Atropine sulfate[2], apomorphine hydrochloride[3], nalorphine hydrochloride[3], naloxone hydrochloride[4], 4-aminophenol[5], acetaminophen[5], and acetaminophen with codeine products[5] were used as received.

Instrumentation—The high-performance liquid chromatograph[6] was equipped with a UV detector (254 nm), a 6000-psi pump, and a loop injector. The output of the UV detector was connected to a recorder and a minicomputer[7]. An automatic sampler[8] also was used.

Silica gel[9], 10 μm, was slurry packed, using a slightly modified packing procedure (13), into a 25-cm × 2.1-mm i.d. stainless steel column. The mobile phase was 23.2% methylene chloride, 4.4% methanol, 72.3% *n*-hexane, and 0.1% ammonium hydroxide. The column flow rate was set at 3.0 ml/min, and the UV detector was set at 0.10 aufs.

Internal Standard Preparation—A 22.5-mg sample of chlorpheniramine maleate was weighed accurately into a 25-ml volumetric flask, chloroform was added, and the flask was shaken until the compound dissolved. The sample was taken to volume with chloroform (0.9 mg/ml).

Codeine Standard Preparation—A 60-mg sample of codeine phosphate (equivalent to 45.20 mg of codeine) was weighed accurately into a 120-ml screw-capped bottle. Exactly 50 ml of chloroform and 40 ml of 0.1 *N* NaOH were added to the sample. It was capped tightly and shaken on a mechanical shaker for 1 hr. After centrifugation, the aqueous layer was aspirated and discarded.

The chloroform layer was filtered through a small pledget of cotton into a clean 60-ml bottle. Fifteen milliliters of the standard solution was pipetted into a 25-ml volumetric flask, 5 ml of the internal standard solution was added, and the solution was diluted to volume with chloroform. Twenty microliters of this solution was injected into the high-performance liquid chromatograph. This volume deposited 3.6 μg of chlorpheniramine maleate and 10.85 μg of codeine on the column.

Sample Preparation—For tablets, 20 tablets were selected randomly, weighed, and triturated to a fine powder. An accurately weighed amount of powder equivalent to 30 mg of codeine phosphate (22.60 mg of codeine) was transferred to a 120-ml screw-capped bottle.

For capsules, 20 capsules were randomly selected and weighed. The average capsule fill was determined. The contents of the capsules were emptied and mixed. An accurately weighed amount of powder equivalent to 30 mg of codeine phosphate (22.60 mg of codeine) was transferred to a 120-ml screw-capped bottle.

For the elixirs, an amount equivalent to 30 mg of codeine phosphate (22.60 mg of codeine) was transferred accurately to a 120-ml screw-capped bottle.

Exactly 25 ml of chloroform and 20 ml of 0.1 *N* NaOH were added to the sample. The bottle was capped tightly, shaken on a mechanical shaker for 1 hr, and centrifuged. The aqueous layer was aspirated and discarded. The chloroform layer (0.904 mg/ml) was filtered through a small pledget of cotton into a clean 60-ml bottle. A 15-ml aliquot of the 0.904-mg/ml chloroform solution was transferred to a 25-ml volumetric flask containing exactly 5 ml of the internal standard solution. It then was diluted to volume with chloroform and shaken. A 20-μl aliquot of this solution was injected into the high-performance liquid chromatograph. Two injections were made for each solution.

Calibration Curve—The relative calibration curve of the internal standard to codeine was prepared as follows. A known concentration of the internal standard was prepared, and different amounts of codeine phosphate were weighed and dissolved with the internal standard solution. The solutions were injected into the high-performance liquid chromatograph, and peak area ratios of codeine to the internal standard *versus* weight ratios of codeine to the internal standard were plotted.

Calculation—The peak area ratio, R, was determined from:

$$R = \frac{\text{area of codeine peak}}{\text{area of internal standard peak}} \qquad \text{(Eq. 1)}$$

The concentration of codeine then was determined from:

$$\text{sample concentration} = \text{codeine standard concentration} \times \frac{R_{\text{sample}}}{R_{\text{standard}}} \qquad \text{(Eq. 2)}$$

The percent of codeine was determined from:

$$\%\ \text{label} = \frac{\text{sample concentration}}{\text{theoretical sample concentration}} \times 100 \qquad \text{(Eq. 3)}$$

Precision Study—Twenty tablets containing acetaminophen with codeine were weighed and triturated to a fine powder. From this powder, seven samples, each containing the equivalent of 30 mg of codeine phosphate (22.60 mg of codeine), were weighed and treated as already described. Duplicate injections were made for each sample.

Accuracy Study—Known weights of codeine phosphate USP and acetaminophen USP were added to four placebo tablets. Samples were prepared as described and then were injected into the high-performance liquid chromatograph.

HPLC and GLC Comparison—The GLC method was similar to the methods described previously (2, 3). The gas–liquid chromatograph[10] was equipped with a flame-ionization detector and a 1.83-m × 2-mm i.d. coiled-glass column packed with 3% OV-17 on Chromosorb W HP (80–100

[2] Sigma Chemical Co., St. Louis, MO 63118.
[3] Merck Chemical Division, Rahway, N.J.
[4] Endo Laboratories, Garden City, N.Y.
[5] McNeil Laboratories, Fort Washington, PA 19034.
[6] Waters Associates, Milford, MA 01757.
[7] Model 3352B laboratory data system, Hewlett-Packard, Avondale, PA 19311.
[8] WISP 710, Waters Associates, Milford, MA 01757.
[9] LiChrosorb Si-60, EM Laboratories, Elmsford, NY 10523.
[10] Model 900, Perkin-Elmer, Norwalk, CT 06856.

Table I—Retention Times and Minimum Detection Limits of Codeine and Related Compounds on a Silica Gel Column

Compound	Retention Time, min	Detection Limit, μg
Naloxone hydrochloride	0.79	0.10
Apomorphine hydrochloride	1.10	0.10
Chlorpheniramine maleate	1.88	—
Nalorphine hydrochloride	3.17	0.10
4-Aminophenol	3.26	0.01
Codeine	3.82	—
Acetaminophen	6.00	—
Morphine sulfate	14.02	0.75

Table II—Reproducibility of Retention Times for Codeine, Chlorpheniramine Maleate, and Acetaminophen

Run	Retention Time, min		
	Codeine	Chlorpheniramine Maleate	Acetaminophen
1	3.79	1.89	5.96
2	3.80	1.87	5.99
3	3.83	1.88	6.03
4	3.83	1.88	6.02
5	3.84	1.88	6.01
Mean ($\bar{x}$)	3.82	1.88	6.00
SD (σ)	0.02	0.01	0.03
RSD[a], %	0.5	0.5	0.5

[a] *RSD* is the relative standard deviation and is derived from 100 ($\sigma/\bar{x}$).

Table III—Precision of HPLC Assay of Codeine in Acetaminophen with Codeine Products

Sample	Percent of Label Found
1	99.8
2	100.2
3	100.1
4	101.2
5	100.1
6	100.2
7	100.2
Mean ($\bar{x}$)	100.3
SD (σ)	0.4
RSD[a], %	0.4

[a] Relative standard deviation derived from 100 ($\sigma/\bar{x}$).

mesh). The column temperature was set at 205°, and the carrier gas was nitrogen. The initial standard was atropine and was prepared by accurately weighing 50 mg of atropine sulfate into a 120-ml screw-capped bottle. Fifty milliliters of chloroform and 25 ml of 0.1 *N* NaOH were added. The bottle then was shaken for 1 hr and centrifuged, and the aqueous layer was aspirated and discarded. The codeine standard and sample preparations were similar to those already described.

Samples of acetaminophen with codeine elixirs, tablets, and capsules were prepared as described. Before addition of the internal standard solution, the sample was split into two parts. One part was assayed by HPLC, and the other part was assayed by GLC.

RESULTS AND DISCUSSION

Figure 1 shows the excellent separation of codeine from acetaminophen and chlorpheniramine maleate in <10 min. This method also separates structurally related compounds from codeine such as naloxone hydrochloride, apomorphine hydrochloride, nalorphine hydrochloride, and morphine sulfate, as well as 4-aminophenol, the hydrolysis product of acetaminophen. The structurally related compounds were chosen to demonstrate the specificity of the method. Their respective retention times and detection limits are listed in Table I. The relative standard deviations of the retention times all were 0.5% (Table II).

Although both codeine and acetaminophen were well separated from each other, the simultaneous quantitation of a very large amount of acetaminophen and a small amount of codeine was chromatographically difficult. Acetaminophen had a much higher ϵ value than codeine at 254 nm. In addition, the simultaneous quantitative extractions of codeine and acetaminophen were unsuccessful. Either codeine or acetaminophen had to be extracted from the various dosage forms. It was decided to extract codeine quantitatively for HPLC analysis.

Table IV—Accuracy of HPLC Assay of Codeine in Acetaminophen with Codeine Products

Sample	Percent of Label	
	Theoretical	Found
1	100.00	101.2
2	100.00	100.0
3	100.00	100.7
4	100.00	100.7
Mean ($\bar{x}$)	100.00	100.7
SD (σ)	—	0.5
RSD[a], %		0.5
95% Confidence limit, %		0.8

[a] Relative standard deviation derived from 100 ($\sigma/\bar{x}$).

Table V—HPLC and GLC Assay Results of Codeine in Acetaminophen with Codeine Products

Sample	Percent of Label Claim		Variation[a]
	HPLC	GLC	
Elixir			
1	98.3	99.1	0.8
2	97.3	98.8	1.5
3	98.6	98.6	0.0
4	87.6	88.7	1.1
5	99.4	97.2	2.2
6	99.4	99.5	0.1
7	97.7	97.6	0.1
Tablet			
1	93.8	95.4	1.6
2	92.7	93.2	0.5
3	89.5	89.5	0.0
4	101.9	105.1	3.2
5	101.6	101.9	0.3
6	102.4	102.6	0.2
7	100.3	103.5	3.2
Capsule			
1	95.7	96.3	0.6
2	93.4	96.9	3.5
3	90.7	94.5	3.8
4	93.7	95.6	1.9
5	94.2	96.9	2.7
6	93.8	96.7	2.9
7	95.4	98.6	3.2
8	92.3	95.2	2.9

[a] The linear correlation coefficient was 0.9999, and the average variation was 1.7%.

The amount of ammonium hydroxide in the mobile phase was critical to the separation. Ammonia was lost slowly from the mobile phase. To keep the retention times constant and to maintain effective separation, fresh solvent should be used daily. Sometimes, it was necessary to adjust slightly the amount of ammonium hydroxide (between 0.1 and 0.2%) to obtain effective separation when a new column was used.

Chlorpheniramine maleate was chosen as the internal standard because its peak was sharp and symmetrical and it was well separated from codeine. Furthermore, chlorpheniramine maleate was stable and did not react with the mobile phase, other sample components, and the column packing. In addition, it is available commercially in high purity. The peak heights of chlorpheniramine maleate and codeine decrease slightly with time due to changing column conditions in the presence of ammonium hydroxide. However, the peak areas and their ratio remain unchanged, which is critical to an accurate assay. The precision of the method showed a relative standard deviation of 0.4% (n = 7) (Table III).

The accuracy of the assay is shown in Table IV. A relative standard deviation of 0.5% (n = 4) was obtained. When the internal standard method was not used, the relative standard deviations of precision and accuracy were >1.0%. For a routine assay with the automatic sampler, the standard codeine with the internal standard was injected as every third sample to ensure reliable results. In addition, the calibration curve obtained for the internal standard to codeine was linear.

The results of the comparison of the HPLC and GLC methods are shown in Table V. Three dosage forms with different amounts of acetaminophen with codeine were used. For 22 samples, the GLC assay results varied on an average of 1.7% from those of the HPLC assay. A linear correlation coefficient of 0.9999 was obtained. The precision of the GLC

assay was ~2%. Besides assaying for composite granulations, the HPLC assay also is applicable to content uniformity analysis.

In conclusion, the HPLC method is simple, precise, fast, specific, and accurate. A complete analysis takes ~10 min. All test compounds and known impurities can be detected. Since the analysis is conducted at ambient temperature, no thermal degradation of codeine is expected.

REFERENCES

(1) E. Sell and D. Rajzer, *Ann. Acad. Med. Gedanensis*, **6**, 127 (1976).

(2) S. J. Mulé, *Anal. Chem.*, **36**, 1907 (1964).

(3) R. Pentz and A. Schuett, *Arch. Toxicol.*, **39**, 225 (1978).

(4) K. D. Parker, C. R. Fontan, and P. L. Kirk, *Anal. Chem.*, **35**, 356 (1963).

(5) "Proceedings of the International Colloquium on Prospective Biology," 3rd ed., G. Siest and D. S. Young, Eds., Basel, Switzerland, 1976, p. 136.

(6) C. Y. Wu, S. Siggia, T. Robinson, and R. D. Waskiewicz, *Anal. Chim. Acta*, **63**, 393 (1973).

(7) R. Verpoorte and A. B. Svendsen, *J. Chromatogr.*, **100**, 227 (1974).

(8) C. Y. Wu and J. J. Wittick, *Anal. Chem.*, **49**, 359 (1977).

(9) C. Olieman, L. Maat, K. Waliszewski, and H. C. Beyerman, *J. Chromatogr.*, **133**, 382 (1977).

(10) J. K. Baker, R. E. Skelton, and C. Y. Ma, *ibid.*, **168**, 417 (1979).

(11) T. H. Beasley, D. W. Smith, H. W. Ziegler, and R. L. Charles, *J. Assoc. Off. Anal. Chem.*, **57**, 85 (1974).

(12) V. D. Gupta, *J. Pharm. Sci.*, **69**, 110 (1980).

(13) R. K. Gilpin, D. J. Camillo, and C. A. Janicki, *J. Chromatogr.*, **121**, 13 (1976).

ACKNOWLEDGMENTS

The authors thank Dr. Joseph S. Ranweiler, Mr. Henry C. Lewis, and Mrs. Elizabeth A. Clemens for carrying out the GLC assays.

High-Performance Liquid Chromatographic Analysis of Nitroglycerin Ointment

LOREN GELBER

Received August 24, 1979, from the *Winchester Engineering and Analytical Center, Food and Drug Administration, Winchester, MA 01890.* Accepted for publication March 22, 1980.

Abstract □ The assay of ointments containing nitroglycerin is described. Sample preparation by direct dissolution in warm dimethyl sulfoxide appeared to be more accurate than extraction. Anisole was used as an internal standard. Chromatographic conditions included a C_{18} microporous silica column and a methanol–water mobile phase (40:60). Detection at 215 nm was superior to detection at 254 nm.

Keyphrases □ Nitroglycerin—ointment, reversed-phase high-performance liquid chromatographic analysis □ Ointments—nitroglycerin, reversed-phase high-performance liquid chromatographic analysis □ High-performance liquid chromatography—analysis, nitroglycerin ointment

The use of topical nitroglycerin for patients with congestive heart failure was reported recently (1). Existing methods for the analysis of nitroglycerin (2–9) lack specificity (7), are too time consuming for convenient uniformity determinations, or require prolonged heating that could lead to decomposition of nitroglycerin, which occurs at 50–60° (10).

Several high-performance liquid chromatographic (HPLC) assays for nitroglycerin dosage forms were reported recently (11, 12). These methods can separate nitroglycerin from its mono- and dinitrate degradation products. Since HPLC has none of the disadvantages of the other methods, its applicability to the analysis of nitroglycerin ointment was studied. A sample preparation method was developed so that the method of Crouthamel and Dorsch (11) could be applied to ointment samples. It was chosen for initial investigation because it uses an octadecylsilane column, which is widely available in HPLC laboratories, and a simple, less expensive, water–methanol mobile phase. The method of Baske *et al.* (12) uses a less retentive phenyl column and a more expensive and complex water–acetonitrile–tetrahydrofuran mobile phase. Contrary to a previous observation (12), no problems of clogging of inlet filters were encountered.

EXPERIMENTAL

Materials—The water used was HPLC grade[1]. The methanol was distilled in glass[2]. Dimethyl sulfoxide (I), butylated hydroxyanisole[3], isooctane, sodium acetate, acetic acid, potassium nitrate, ammonium hydroxide, lanolin, and petrolatum[4] were ACS reagent grade.

A 10% nitroglycerin on lactose triturate[5] was used as a standard and was calibrated by the USP phenoldisulfonic acid method for the assay of nitroglycerin (2). It assayed at 9.62%. The standard solutions were 1 mg/ml in methanol for Method 1, 2 mg/ml in I for Method 2, and 2 mg/ml in the internal standard solution for Method 2a.

Instrumentation—Two liquid chromatographic systems were used. The first system consisted of a dual-head reciprocating piston positive-displacement pump[6], a septumless syringe-loaded loop injector with a 10-μl loop[7], a variable-wavelength detector operated at 254 or 216 nm[8], a 10-mv recorder[9], and a 15-cm × 4-mm column of a slurry of chemically bonded octadecyl reversed-phase material[10] packed in aqueous sodium acetate and methanol according to the manufacturer's directions. The second system contained a dual-head reciprocating piston pump[11], an automatic injector[12], a variable-wavelength detector operated at 215 nm[13], a flat-bed recorder[14], and a 15-cm × 4.6-mm column of chemically

[1] J. T. Baker Chemical Co., Phillipsburg, N.J.
[2] Burdick & Jackson Laboratories, Muskegon, Mich.
[3] Sigma Chemical Co., St. Louis, Mo.
[4] Fisher Scientific Co., Fair Lawn, N.J.
[5] Marion Laboratories, Kansas City, Mo.
[6] Model 100A with preparative scale head, Altex Scientific Inc., Berkeley, Calif.
[7] Model 70-10 with model 70-11 loop filler port, Rheodyne Inc., Berkeley, Calif.
[8] Model 837 spectrophotometer, DuPont Instruments, Wilmington, Del.
[9] Servariter II, Texas Instruments, Houston, Tex.
[10] ODS-Hypersil, Hyperspheres (5 μm), Shandon Southern Products Ltd., Cheshire, England.
[11] Model 6000A, Waters Associates, Milford, Mass.
[12] WI-SP, Waters Associates.
[13] Model LC-75, Perkin-Elmer, Norwalk, Conn.
[14] Model 595, Linear Instruments Corp., Irvine, Calif.

0022-3549/80/0900-1084$01.00/0

© 1980, American Pharmaceutical Association

assay was ~2%. Besides assaying for composite granulations, the HPLC assay also is applicable to content uniformity analysis.

In conclusion, the HPLC method is simple, precise, fast, specific, and accurate. A complete analysis takes ~10 min. All test compounds and known impurities can be detected. Since the analysis is conducted at ambient temperature, no thermal degradation of codeine is expected.

REFERENCES

(1) E. Sell and D. Rajzer, *Ann. Acad. Med. Gedanensis*, **6**, 127 (1976).

(2) S. J. Mulé, *Anal. Chem.*, **36**, 1907 (1964).

(3) R. Pentz and A. Schuett, *Arch. Toxicol.*, **39**, 225 (1978).

(4) K. D. Parker, C. R. Fontan, and P. L. Kirk, *Anal. Chem.*, **35**, 356 (1963).

(5) "Proceedings of the International Colloquium on Prospective Biology," 3rd ed., G. Siest and D. S. Young, Eds., Basel, Switzerland, 1976, p. 136.

(6) C. Y. Wu, S. Siggia, T. Robinson, and R. D. Waskiewicz, *Anal. Chim. Acta*, **63**, 393 (1973).

(7) R. Verpoorte and A. B. Svendsen, *J. Chromatogr.*, **100**, 227 (1974).

(8) C. Y. Wu and J. J. Wittick, *Anal. Chem.*, **49**, 359 (1977).

(9) C. Olieman, L. Maat, K. Waliszewski, and H. C. Beyerman, *J. Chromatogr.*, **133**, 382 (1977).

(10) J. K. Baker, R. E. Skelton, and C. Y. Ma, *ibid.*, **168**, 417 (1979).

(11) T. H. Beasley, D. W. Smith, H. W. Ziegler, and R. L. Charles, *J. Assoc. Off. Anal. Chem.*, **57**, 85 (1974).

(12) V. D. Gupta, *J. Pharm. Sci.*, **69**, 110 (1980).

(13) R. K. Gilpin, D. J. Camillo, and C. A. Janicki, *J. Chromatogr.*, **121**, 13 (1976).

ACKNOWLEDGMENTS

The authors thank Dr. Joseph S. Ranweiler, Mr. Henry C. Lewis, and Mrs. Elizabeth A. Clemens for carrying out the GLC assays.

High-Performance Liquid Chromatographic Analysis of Nitroglycerin Ointment

LOREN GELBER

Received August 24, 1979, from the *Winchester Engineering and Analytical Center, Food and Drug Administration, Winchester, MA 01890.* Accepted for publication March 22, 1980.

Abstract □ The assay of ointments containing nitroglycerin is described. Sample preparation by direct dissolution in warm dimethyl sulfoxide appeared to be more accurate than extraction. Anisole was used as an internal standard. Chromatographic conditions included a C_{18} microporous silica column and a methanol–water mobile phase (40:60). Detection at 215 nm was superior to detection at 254 nm.

Keyphrases □ Nitroglycerin—ointment, reversed-phase high-performance liquid chromatographic analysis □ Ointments—nitroglycerin, reversed-phase high-performance liquid chromatographic analysis □ High-performance liquid chromatography—analysis, nitroglycerin ointment

The use of topical nitroglycerin for patients with congestive heart failure was reported recently (1). Existing methods for the analysis of nitroglycerin (2–9) lack specificity (7), are too time consuming for convenient uniformity determinations, or require prolonged heating that could lead to decomposition of nitroglycerin, which occurs at 50–60° (10).

Several high-performance liquid chromatographic (HPLC) assays for nitroglycerin dosage forms were reported recently (11, 12). These methods can separate nitroglycerin from its mono- and dinitrate degradation products. Since HPLC has none of the disadvantages of the other methods, its applicability to the analysis of nitroglycerin ointment was studied. A sample preparation method was developed so that the method of Crouthamel and Dorsch (11) could be applied to ointment samples. It was chosen for initial investigation because it uses an octadecylsilane column, which is widely available in HPLC laboratories, and a simple, less expensive, water–methanol mobile phase. The method of Baske *et al.* (12) uses a less retentive phenyl column and a more expensive and complex water–acetonitrile–tetrahydrofuran mobile phase. Contrary to a previous observation (12), no problems of clogging of inlet filters were encountered.

EXPERIMENTAL

Materials—The water used was HPLC grade[1]. The methanol was distilled in glass[2]. Dimethyl sulfoxide (I), butylated hydroxyanisole[3], isooctane, sodium acetate, acetic acid, potassium nitrate, ammonium hydroxide, lanolin, and petrolatum[4] were ACS reagent grade.

A 10% nitroglycerin on lactose triturate[5] was used as a standard and was calibrated by the USP phenoldisulfonic acid method for the assay of nitroglycerin (2). It assayed at 9.62%. The standard solutions were 1 mg/ml in methanol for Method 1, 2 mg/ml in I for Method 2, and 2 mg/ml in the internal standard solution for Method 2a.

Instrumentation—Two liquid chromatographic systems were used. The first system consisted of a dual-head reciprocating piston positive-displacement pump[6], a septumless syringe-loaded loop injector with a 10-μl loop[7], a variable-wavelength detector operated at 254 or 216 nm[8], a 10-mv recorder[9], and a 15-cm × 4-mm column of a slurry of chemically bonded octadecyl reversed-phase material[10] packed in aqueous sodium acetate and methanol according to the manufacturer's directions. The second system contained a dual-head reciprocating piston pump[11], an automatic injector[12], a variable-wavelength detector operated at 215 nm[13], a flat-bed recorder[14], and a 15-cm × 4.6-mm column of chemically

[1] J. T. Baker Chemical Co., Phillipsburg, N.J.
[2] Burdick & Jackson Laboratories, Muskegon, Mich.
[3] Sigma Chemical Co., St. Louis, Mo.
[4] Fisher Scientific Co., Fair Lawn, N.J.
[5] Marion Laboratories, Kansas City, Mo.
[6] Model 100A with preparative scale head, Altex Scientific Inc., Berkeley, Calif.
[7] Model 70-10 with model 70-11 loop filler port, Rheodyne Inc., Berkeley, Calif.
[8] Model 837 spectrophotometer, DuPont Instruments, Wilmington, Del.
[9] Servariter II, Texas Instruments, Houston, Tex.
[10] ODS-Hypersil, Hyperspheres (5 μm), Shandon Southern Products Ltd., Cheshire, England.
[11] Model 6000A, Waters Associates, Milford, Mass.
[12] WI-SP, Waters Associates.
[13] Model LC-75, Perkin-Elmer, Norwalk, Conn.
[14] Model 595, Linear Instruments Corp., Irvine, Calif.

0022-3549/80/0900-1084$01.00/0

© 1980, American Pharmaceutical Association

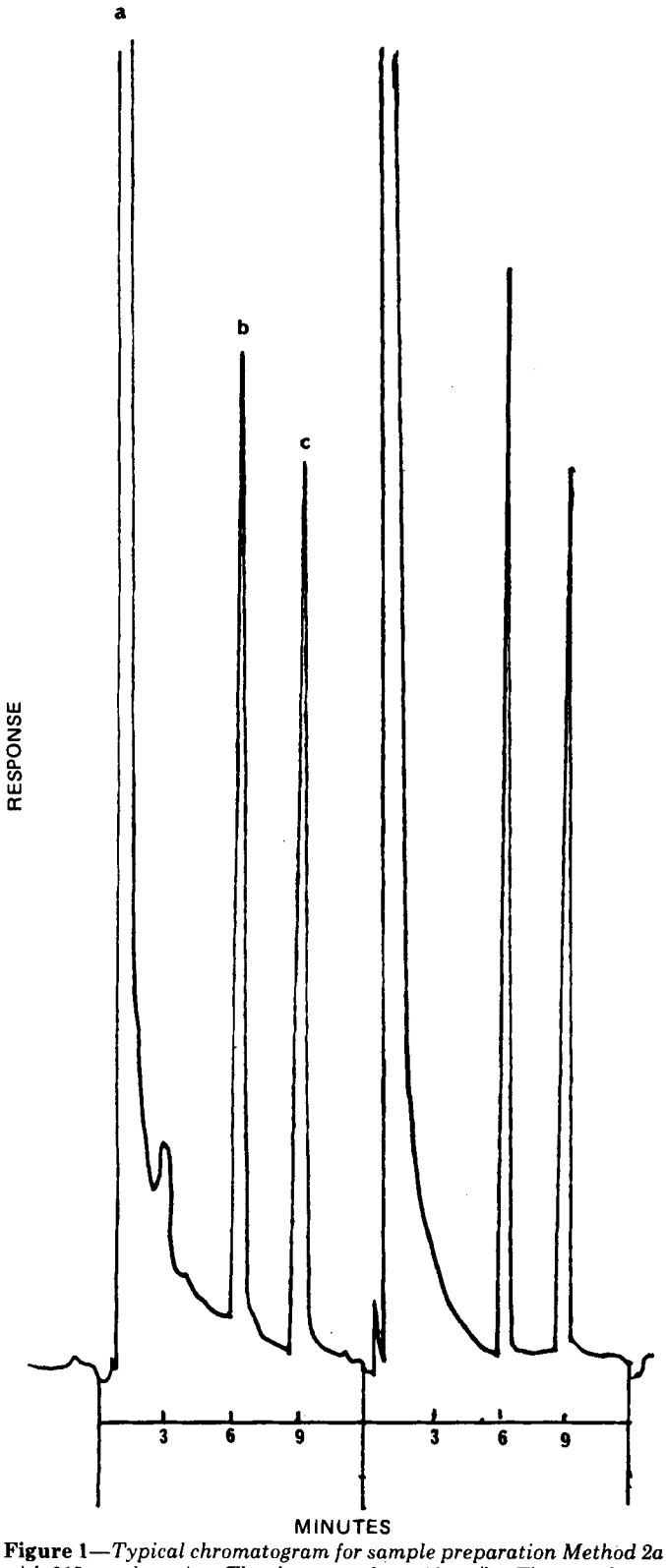

Figure 1—*Typical chromatogram for sample preparation Method 2a with 215-nm detection. The chart speed was 20 cm/hr. The sample was followed by the standard. Key: a, I; b, nitroglycerin; and c, anisole.*

bonded octadecyl reversed-phase material[15] commercially packed and used with a 4-cm × 4.6-mm precolumn dry packed with pellicular octadecyl reversed-phase material[16].

Chromatographic Conditions—The mobile phase was methanol–water (40:60) and was suction filtered through a 0.9-μm filter[17]. This mobile phase was chosen since it was the strongest mobile phase that gave adequate resolution of nitroglycerin from I. Anisole was the internal standard since it was well resolved from the peak of interest and from I or excipient peaks and is very stable and readily available. Diazepam, suggested as an internal standard by Crouthamel and Dorsch (11), was not resolved from nitroglycerin in System 1. The flow rate was 0.8 ml/min with a pressure of 800 psi for System 1 and 2 ml/min with 4400 psi for System 2.

Typical chromatographic parameters for System 1 were $k' = 5.4$ for nitroglycerin and 7.1 for anisole, $N = 2000$ for nitroglycerin and 2500 for anisole, and $R = 3.1$. For System 2, $k' = 8.6$ for nitroglycerin and 12.4 for anisole, $N = 3430$ for nitroglycerin and 5230 for anisole, and $R = 5.95$. The N and R values were evaluated using half-width formulas (13). Tailing (evaluated by dropping a vertical line from the peak maximum, drawing a horizontal line at the 10% peak height, and dividing the distance from the vertical line to the peak back by the distance from the vertical line to the peak front) was 3.4 for nitroglycerin and 3.3 for anisole in System 1 and 1.9 for nitroglycerin and 1.0 for anisole in System 2 (Fig. 1).

Procedure—*Method 1*—About 1 g of ointment (equivalent to 20 mg of nitroglycerin) and 20 ml of isooctane were shaken mechanically for 40 min. After the contents of the flask were transferred to a separator, the flask was washed with water to dissolve the remaining lactose; each water wash was used to extract gently the isooctane. The pooled water was shaken with isooctane. The original flask was washed twice with methanol. Both methanol portions were combined, used to extract the isooctane, and filtered[18]. This procedure was repeated twice, and the extract was taken to 25.0 ml with methanol.

Method 2—About 1 g of ointment was weighed accurately into a beaker, 10.0 ml of I was added, and the solution was heated on a steam bath for 5 min with occasional gentle agitation. After cooling, the coagulated solids were removed with a capillary pipet or left in the beaker when the solution was decanted into a glass-stoppered erlenmeyer flask. An internal standard solution was prepared by combining 0.1 ml of anisole with 10 ml of methanol and diluting 3 ml of the resulting solution to 75 ml with I. An aliquot of 0.50 ml of the internal standard solution was added to 2.0 ml of the sample or standard to produce solutions for injection.

Method 2a—About 1 g of ointment was weighed accurately into a 50-ml glass-stoppered centrifuge tube, 20.0 ml of the internal standard solution (0.0003 ml of anisole/ml in I) was added, and the solution was heated for 5 min on a steam bath with occasional vigorous shaking. The solution then was shaken mechanically for 30 min, which resulted in a ball of coagulated solid floating on top of the liquid, so that the clear liquid could be removed easily with a capillary pipet for injection into the liquid chromatograph.

System 1 was used to evaluate Methods 1 and 2; System 2 was used to evaluate Method 2a.

Table I—Comparison of Sample Preparation Methods with 254-nm Detection [a]

Method	Sample Assay, % label claim	Spike Recovery, % added standard
1	86.4	86.3
	84.7	92.7
2	94.9	100.1
	90.3	105.4

[a] Manufacturer 1.

RESULTS AND DISCUSSION

Table I shows that Method 2, which makes a lipophilic sample suitable for injection into a reversed-phase HPLC system without extraction, is more accurate than Method 1. This fact is indicated most clearly by results of spiked samples, consisting of ~0.5–0.6 g of ointment and 100 mg of standard triturate (10 mg of nitroglycerin), taken through the method. Table II demonstrates that Method 2a gives improved extraction of nitroglycerin from the ointment and more precision due to the presence of the internal standard from the beginning of sample preparation and the increased agitation.

While detection at 254 nm is possible at the concentrations used here, the signal-to-noise ratio is low due to the fact that the UV spectrum of nitroglycerin exhibits a minimum at this wavelength. As shown in Table

[15] Ultrasphere ODS (5 μm), Altex Scientific Inc., Berkeley, Calif.
[16] μBondapak C_{18} Corasil, Waters Associates.
[17] AAWP, Millipore Corp., Bedford, Mass.
[18] Grade 541, Whatman Ltd., England.

Table II—Sample Preparation Method 2a with 215-nm Detection

Manufacturer	Assay, %	Recovery[a], %
1	106.5	100.6
	106.6	102.7
Average	106.6	101.6
2	103.2	101.8
	100.4	101.9
Average	101.8	101.8
3	104.7	97.3
	104.0	100.2
Average	104.4	98.7

[a] Average recovery for all manufacturers = 100.7%.

Table III—Comparison of Detection Wavelengths for Sample Preparation Method 2

	254 nm		216 nm	
Manufacturer	Assay, %	Recovery, %	Assay, %	Recovery, %
1	94.9	100.1	96.8	103.5
	91.0	105.4	92.6	98.8
Average	93.0	102.8	94.7	101.2
3	96.8	104.4	94.4	97.8
	98.1	104.8	93.1	101.0
Average	97.4	104.6	93.8	99.4

Table IV—Authentic Recoveries for Sample Preparation Method 2a with 215-nm Detection

Manufacturer	Recovery of Label Claim[a], %
1	99.2
	98.0
2	101.1
	99.3
3	99.3
	97.9

[a] Average = 99.1%; coefficient of variation = 1.14%.

III, detection at 216 nm gives comparable quantitative results (data were obtained with the same solutions). At 254 nm, peak heights were ~0.01 absorbance unit; at 216 nm, they were ~0.82 absorbance unit. This difference represents approximately an 80-fold enhancement in detection.

Thus, Method 2a and detection at 215 nm were best and were subjected to further validation. The three products tested were all currently marketed, nitroglycerin ointments. Three substances that represented expected excipients, lanolin, butylated hydroxyanisole, and petrolatum, were analyzed individually by this method at levels likely to be used in commercial formulations. Petrolatum gave no peaks, and lanolin gave only a peak before I. Butylated hydroxyanisole gave a peak with a k' value six times that of nitroglycerin and a height 1.4% of that of nitroglycerin (at 254 nm, the butylated hydroxyanisole peak was 4.5% of that of nitroglycerin). This finding indicates that none of the excipients interferes with the method.

By combining individual weighings of the appropriate excipients, authentic mixtures were prepared and assayed (Table IV). The average recovery of 99.1% with a coefficient of variation of 1.14% indicates that the accuracy and reproducibility of the method are acceptable for the analysis of this type of product. With authentic mixtures, the method demonstrated linearity from 0.25 to 1.50 mg/ml, representing 25–150% of the label declaration of 2% nitroglycerin [correlation coefficient >0.9997 (14); levels measured were 0.25, 0.50, 0.75, 1.00, 1.25, and 1.50 mg/ml]. These results indicate that sample preparation Method 2a with detection at 215 nm is appropriate for the analysis of nitroglycerin ointments.

Preliminary testing indicates that the system can be used for the analysis of isosorbide dinitrate, pentaerythritol tetranitrate, and erythritol trinitrate, which are well resolved from one another and from nitroglycerin. With a 50:50 methanol–water mobile phase, k' values of 6.7, 17, and 18.9 were obtained for these three glycosides, respectively; the k' value of nitroglycerin was 9.5. The analysis of these cardiac glycosides in sustained-release preparations will be reported later.

REFERENCES

(1) *The Medical Letter on Drugs and Therapeutics*, **20**, 20 (Oct. 6, 1978).

(2) "The United States Pharmacopeia," 19th rev., Mack Publishing Co., Easton, Pa., 1975, p. 343.

(3) "The United States Pharmacopeia," 14th rev., Mack Publishing Co., Easton, Pa., 1950, p. 416.

(4) "Official Methods of Analysis," 12th ed., Association of Official Analytical Chemists, Washington, D.C., 1975, p. 758.

(5) *Ibid.*, p. 757.

(6) M. T. Rossell, M. G. Bogart, and E. J. Moerma, *J. Chromatogr.*, **53**, 263 (1970).

(7) A. L. Woodsen and L. L. Alber, *J. Assoc. Off. Anal. Chem.*, **52**, 847 (1969).

(8) P. S. K. Yap, E. F. McNiff, and H. Fang, *J. Pharm. Sci.*, **67**, 582 (1978).

(9) J. K. Sturek, T. D. Sokoloski, W. T. Winsley, and P. E. Stach, *Am. J. Hosp. Pharm.*, **67**, 582 (1978).

(10) "The Merck Index," 8th ed., Merck & Co., Rahway, N.J., 1975, p. 859.

(11) W. G. Crouthamel and B. J. Dorsch, *J. Pharm. Sci.*, **68**, 237 (1979).

(12) D. M. Baske, J. E. Carter, and A. H. Amann, *ibid.*, **68**, 481 (1979).

(13) "The National Formulary," 14th ed., Mack Publishing Co., Easton, Pa., 1975, p. 869.

(14) R. G. D. Steel and J. H. Torrie, "Principles and Procedures of Statistics," McGraw-Hill, New York, N.Y., 1960, p. 188.

ACKNOWLEDGMENTS

The author thanks J. Gillingham, B. Williston, and G. Bafus, Marion Laboratories, Kansas City, Mo., for suggesting the modifications of sample preparation Method 2, which resulted in the development of Method 2a.

Pharmacokinetics of Nicotine in Rats after Single-Cigarette Smoke Inhalation

K. S. ROTENBERG *, R. P. MILLER ‡, and J. ADIR §x

Received September 17, 1979, from the *Clinical Pharmacokinetics Laboratory, Department of Pharmaceutics, School of Pharmacy, University of Maryland, Baltimore, MD 21201.* Accepted for publication March 31, 1980. *Present address: Division of Biopharmaceutics, Food and Drug Administration, Rockville, MD 20014. ‡Present address: Department of Pharmacy, School of Pharmacy, West Virginia University, Morgantown, WV 26506. §Present address: Stauffer Chemical Company, Farmington, CT 06032.

Abstract □ The amount of nicotine absorbed following cigarette smoke inhalation was evaluated by comparing the area under the plasma concentration–time curve and urinary recovery with those observed after its intravenous injection to rats. Nicotine was absorbed rapidly, with the maximum plasma concentration occurring immediately after cessation of cigarette smoke exposure. On the average, 68% of the nicotine delivered to the inhalation chamber was absorbed. The absorption and elimination of nicotine, as well as the formation and elimination of its metabolites, followed first-order kinetics, and the derived pharmacokinetic parameters were similar to those observed after the intravenous administration of nicotine.

Keyphrases □ Nicotine—comparison of pharmacokinetic parameters following single-cigarette smoke inhalation and intravenous administration, cotinine as major nicotine metabolite, rats □ Pharmacokinetics—comparison of nicotine pharmacokinetic parameters following single-cigarette smoke inhalation and intravenous administration, cotinine as major metabolite of nicotine, rats □ Cotinine—major metabolite of nicotine, comparison of pharmacokinetic parameters following single-cigarette smoke inhalation and intravenous administration, rats

Reports of the effect of inhalation of tobacco smoke on a wide range of biological systems have increased. The principal concern has been the effect of smoke inhalation on the structure and function of the lungs (1–3), cardiovascular response (4), and teratogenicity (5). These studies have renewed interest in the metabolic fate of nicotine.

Recent studies in these laboratories investigated the pharmacokinetics of nicotine in rats following intravenous injection (6, 7). However, little is known about the rate of absorption of nicotine from cigarette smoke. Most studies on nicotine absorption reported only the blood nicotine concentrations following smoking in humans (8, 9), dogs (10), and cats (11). Armitage *et al.* (8) showed that habitual smokers retained 82–92% and that nonsmokers retained 30–66% of the inhaled nicotine, but they did not assess the absorption rate of nicotine in these subjects. McGovern *et al.* (12), using an isolated perfused rabbit lung preparation, found that nicotine absorption from tobacco smoke was rapid, with peak levels occurring almost immediately after cigarette smoke administration had ceased.

The purpose of this investigation was to characterize the rate and extent of absorption of nicotine in rats after single-cigarette smoke inhalation and to compare its disposition kinetics with those observed after intravenous administration.

EXPERIMENTAL

Chemicals—[*methyl*-^{14}C]Nicotine was obtained commercially[1] and had a specific activity of 61.6 μCi/mg. Radiochemical purity was established by TLC and radioscanning techniques. With acetone–benzene–ammonia–ethanol (40:50:5:5) as the solvent, the compound migrated as a single radioactive spot with an R_f value corresponding to authentic nicotine. Unlabeled nicotine[2] for use as a standard was obtained commercially, and unlabeled cotinine was prepared from nicotine by the method of Bowman and McKennis (13).

Cigarettes—The cigarettes[3] were stored in a desiccator that provided an atmosphere of 65% humidity. They were reported to contain 9.5 mg of nicotine/g of tobacco and to have a smoke condensate pH of 4.9. Analysis in these laboratories using a spectrophotometric assay (14) verified the nicotine content of the cigarettes.

One cigarette was spiked with ^{14}C-labeled nicotine using an infusion pump[4] equipped with a glass tube (17 cm × 8 mm i.d.) to hold the cigarette in place. Another infusion pump[5] was fitted with a 1-ml gas-tight syringe[6] containing the ^{14}C-labeled nicotine solution. The two pumps were set facing each other such that the needle delivering the radiolabeled nicotine solution mounted on one pump penetrated the cigarette mounted on the other pump. This setting allowed the delivery of the spiking solution to the entire length of the cigarette, after which the cigarette was rotated 90° and allowed to dry. This process was repeated until 225 μCi of [*methyl*-^{14}C]nicotine was delivered, yielding a final specific activity of 17.11 μCi/mg. Following spiking, the cigarette was replaced in the desiccator.

Smoke Exposure Apparatus—The intermittent smoke generation–inhalation system[7] (15–17) used was designed to simulate the smoking of a single cigarette. Briefly, a 2-sec negative pressure allowed 35 cm^3 of cigarette smoke to enter an exposure chamber where it was distributed rapidly, forming a 10% smoke aerosol. The rats were placed in restraining cylinders attached to the exposure chamber with only their noses protruding into the chamber. The smoke remained in the chamber for 20 sec, after which air was forced into the chamber to expel the smoke and to maintain an atmosphere of fresh air for 38 sec. This 1-min cycle (puff) was repeated until the cigarette burnt down to a 23-mm butt after a total of 10 puffs were delivered into the exposure chamber.

The exposure unit was modified by attaching a cambridge filter[8] to the exposure chamber. This filter is capable of trapping 99.9% of the total particulate matter, including nicotine, from the smoke forced out of the exposure chamber (18). This modification allowed for an account of the material balance and, hence, calculation of the amount of nicotine delivered to the inhalation chamber and the amount absorbed by rats.

The restraining cylinders also were modified by drilling an orifice at the proximal part to the exposure chamber through which the animal's previously implanted cannula was brought out. Thus, blood samples could be collected during the smoke inhalation period.

Animals—Male Fischer-344 rats[9], 226–263 g, were housed in stainless steel cages and had free access to food[10] and water. At least 48 hr prior to the study, each animal was placed under light ether anesthesia and a chronic cannula was implanted into the abdominal aorta (19). The study was initiated with eight rats, but only four rats completed the study due to a malfunction of the cannula.

Protocol—Rats were placed in the restraining cylinders 30 min prior to lighting the cigarette to condition them to the smoke exposure–inhalation system (20). The cigarette was consumed in 10 min (10 puffs), after which the rats were transferred to plastic metabolism cages for the remainder of the experiment. Blood samples (0.2 ml) were collected into heparinized syringes at 4, 8 (smoking phase), 15, 30, 45, 60, and 90 min and 2, 3, 5, 8, 14, 16.5, 24, and 30 hr (postsmoking phase). The plasma was

[1] ICN, Irving, CA 92664.

[2] Eastman Kodak Co., Rochester, NY 14650.
[3] Code No. 31, provided by Enviro Control, Rockville, MD 20852.
[4] Sage model 341, Orion Research Inc., Cambridge, MA 02139.
[5] Sage model 351, Orion Research Inc., Cambridge, MA 02139.
[6] No. 1001, Hamilton Co., Reno, NV 89510.
[7] Maddox-ORNL, Oak Ridge National Research Laboratory, Oak Ridge, TN 37830.
[8] Phipps and Bird, Richmond, VA 23261.
[9] Microbiological Associates, Walkersville, MD 21793.
[10] Purina Laboratory Chow, Ralston-Purina Co., St. Louis, MO 53188.

0022-3549/80/0900-1087$01.00/0
© 1980, American Pharmaceutical Association

Table I—Nicotine Absorbed following Cigarette Smoke Inhalation by Rats

Rat[a] (weight, kg)	Amount Absorbed Based on *AUC*[b]		Amount Absorbed Based on Urinary Recovery[b]	
	dpm/kg	mg/kg	dpm/kg	mg/kg
1 (0.240)	5.061×10^6	0.04	5.258×10^6	0.04
2 (0.235)	7.752×10^6	0.06	5.234×10^6	0.04
3 (0.226)	7.911×10^6	0.06	8.472×10^6	0.06
4 (0.263)	8.199×10^6	0.06	5.765×10^6	0.04
Mean (0.241)	7.231×10^6 [c]	0.06	6.182×10^6[c]	0.05
SEM (0.008)	0.729×10^6	0.01	0.773×10^6	0.01

[a] Eight rats were placed in the inhalation chamber, but four did not complete the study because of malfunction of the indwelling cannula. [b] No significant differences were observed at the $p = 0.05$ level between the amount calculated from plasma concentrations *versus* time and the urinary recovery data. [c] If it is assumed that the same amount of nicotine also was absorbed by the four rats that did not complete the study, the total amount absorbed represents 69.8 (*AUC* method) and 66.3% (urinary recovery method) of the amount of nicotine delivered to the inhalation chamber, with a mean of 68%.

separated from whole blood by centrifugation and stored at −20° until the time of analysis. Urine was collected in containers immersed in ice for up to 48 hr and frozen until the time of analysis. The separation and quantitation of nicotine and its metabolites were described earlier (6, 7).

Pharmacokinetic Analysis—The concentration–time profiles of nicotine, cotinine, and other metabolites for each rat were plotted on semilogarithmic graph paper, which provided an insight to the operative pharmacokinetic models. These plots also were employed to obtain initial estimates for curve fitting of the data using the SAAM 26 digital computer program (21). Each data point was assigned a statistical weight proportional to the reciprocal of the square of a standard deviation representing 10% of the data point.

The puffing profile of the smoke inhalation machine was incorporated into the pharmacokinetic model used to fit the data both during and after cigarette smoke inhalation. The amount of nicotine absorbed by inhalation (A_{ih}) was computed from (22):

$$A_{ih} = \text{dose}_{iv}(AUC_{ih}/AUC_{iv}) \qquad \text{(Eq. 1)}$$

where dose_{iv} is the dose injected by intravenous administration and AUC_{ih} and AUC_{iv} are the areas under the plasma concentration–time curve ($0 \rightarrow \infty$) following cigarette smoke inhalation and intravenous administration, respectively. The dose and *AUC* from the 0.08-mg/kg iv study reported earlier (7) were used in Eq. 1. An alternative method for calculating A_{ih} is provided by (22):

$$A_{ih} = \text{dose}_{iv}\, Nu_{\infty,ih} f_{iv}/Nu_{\infty,iv} f_{ih} \qquad \text{(Eq. 2)}$$

where Nu_∞ is the amount of nicotine ultimately excreted in urine at time infinity and f_{ih} and f_{iv} represent the fractions of total radioactivity excreted as nicotine following cigarette smoke inhalation and intravenous administration, respectively. The dose and $Nu_{\infty,iv}$ from the 0.08-mg/kg dose reported earlier (7) were used in these calculations.

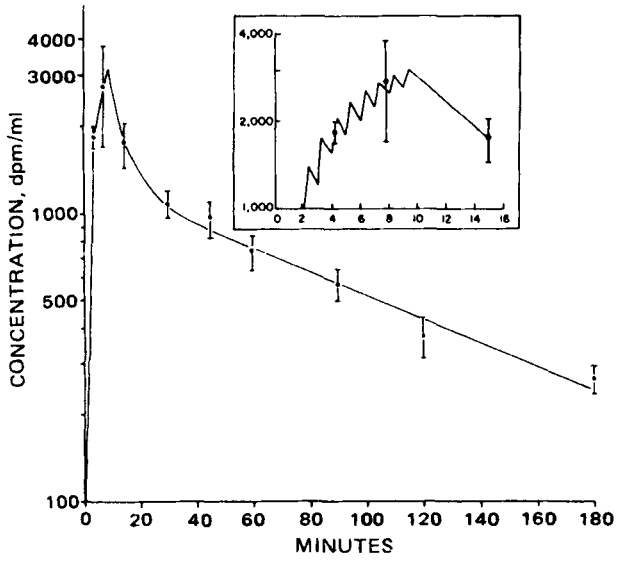

Figure 1—*Semilogarithmic plot of plasma nicotine concentration (mean ± SEM) as a function of time following cigarette smoke absorption of nicotine. Inset shows nicotine absorption during the smoke exposure period.*

The plasma nicotine concentration (C_n) *versus* time data for each rat were fitted to a two-compartment open model with a first-order rate constant of absorption described by (22):

$$C_n = Ae^{-k_a t} + Be^{-\alpha t} + Ce^{-\beta t} \qquad \text{(Eq. 3)}$$

where *A*, *B*, and *C* are constants, k_a is the absorption rate constant, and α and β are hybrid rate constants describing the rapidly and slowly declining phases of the plasma concentration, respectively. The dose absorbed by each rat (calculated using Eqs. 1 and 2) was divided by 10 (each representing one puff) and was included in the data-fitting procedure.

The first-order rate constant of elimination (K_e) and the ratio of the fraction (F) of nicotine converted to cotinine to the volume of distribution of the latter compound (V_d) were obtained by curve fitting of the plasma cotinine concentration–time data to the one-compartment open model with a first-order rate constant of formation (K_f) as reported earlier (6, 7). Also, the pharmacokinetic parameters of the origin activities were estimated as described previously (6, 7).

Renal clearance (*Cl*) was calculated for nicotine and its metabolites employing (22):

$$Cl_{r,i} = Xu_{i,t_1 \rightarrow t_2}/AUC_{i,t_1 \rightarrow t_2} \qquad \text{(Eq. 4)}$$

where i represents nicotine, cotinine, or origin activity, Xu is the amount excreted between t_1 and t_2, and *AUC* is the area under the plasma concentration–time curve over the same time interval.

Statistical Analysis—The t test was used to evaluate differences in the pharmacokinetic parameters of nicotine and its metabolites between the cigarette smoke inhalation and the intravenous administration studies at the $p < 0.05$ and < 0.01 levels (23).

RESULTS AND DISCUSSION

Nicotine—About 4% (2.0×10^7 dpm) of the nicotine present in the mainstream of cigarette smoke (4.9×10^8 dpm) was delivered to the inhalation chamber. This amount represents the sum of the nicotine absorbed by the rats, retained on the filter (4.7×10^6 dpm), and present in the washing of the chamber[11] (1.3×10^6 dpm). The amount of nicotine absorbed calculated from Eqs. 1 and 2 is shown in Table I. Since there were no significant differences between the two methods of computation, the amount of nicotine absorbed can be obtained by either the plasma concentration *versus* time plots or the urinary recovery data. The amount of nicotine absorbed ranged from 0.04 to 0.06 mg/kg[12], representing an average of 68% of the amount of nicotine delivered. This value is similar to that reported by Armitage *et al.* (8), who showed that nonsmokers absorbed between 30 and 60% of the nicotine delivered to their mouths.

The mean plasma nicotine concentration–time profile shown in Fig. 1 indicates that nicotine is absorbed rapidly by inhalation. During the 10 puffs needed to consume the cigarette, the plasma nicotine levels paralleled the intermittent pattern of the smoke exposure machine (shown in the inset of the figure). A maximum of 3000 dpm/ml (79.2 ng/ml) was achieved at the cessation of the cigarette smoke exposure. Following this rapid absorption, which appeared to be described ade-

[11] After delivery of each puff into the airtight exposure chamber, the smoke remained in the chamber for 20 sec. Fresh air then was forced in the chamber, which caused the unabsorbed nicotine (as well as other particulate matter) to be retained on the filter or absorbed onto the inside walls of the chamber, both of which were assayed for radioactivity.

[12] The similarity in the dose and pharmacokinetic parameters obtained in this study and those observed in the 0.08-mg/kg iv study reported earlier (7) warranted the use of the intravenous data in Eqs. 1 and 2.

Table II—Pharmacokinetic Parameters of Nicotine following Cigarette Smoke Inhalation by Rats

Rat	k_a, min^{-1}	α, min^{-1}	β, min^{-1}	$AUC_{0\to\infty}$, (dpm hr)/(ml kg)	Cl_r, ml/hr/kg
1	0.084	—[a]	0.0090	7.64×10^3	402.0
2	0.089	0.0753	0.0105	11.70×10^3	221.0
3	0.404	0.1380	0.0062	11.94×10^3	160.0
4	0.082	0.6470	0.0076	12.37×10^3	119.0
Mean	0.165	0.2870	0.0083	10.91×10^3	226.0
SEM	0.080	0.1810	0.0009	1.10×10^3	62.0

[a] Although the α-phase in this rat was discernible by examination of the log concentration–time plot, it did not include sufficient data points to enable computer estimation of this parameter.

Table III—Pharmacokinetic Parameters of Cotinine following Cigarette Smoke Inhalation of Nicotine by Rats

Rat	t_{max}, hr	K_f, hr^{-1}	K_e, hr^{-1}	$AUC_{0\to\infty}$[a], (dpm hr)/(ml kg)	Cl_r, ml/hr/kg	$\frac{AUC_{cot}}{AUC_{nic}}$	F/V_d, kg/liter[b] From *AUC*	F/V_d, kg/liter[b] From Urinary Excretion
1	1.50	1.544	0.118	56.35×10^3	14.71	7.88	0.303	0.292
2	1.50	1.205	0.103	104.58×10^3	11.32	8.80	0.314	0.466
3	2.00	1.351	0.077	104.86×10^3	17.48	10.64	0.229	0.214
4	2.00	1.366	0.096	94.10×10^3	8.90	7.51	0.273	0.389
Mean	1.75	1.366	0.099	89.97×10^3	13.10	8.71	0.280	0.340
SEM	0.14	0.069	0.009	11.48×10^3	1.88	0.70	0.019	0.055

[a] Obtained by extrapolation of the plasma cotinine concentration data to infinity. [b] There were no significant differences between the F/V_d values calculated from the *AUC* and those from the urinary excretion data.

quately by first-order kinetics, plasma nicotine concentrations declined biexponentially in a fashion similar to that of intravenous administration.

The pharmacokinetic parameters derived from these data are reported in Table II. The mean half-life of absorption ($t_{1/2,k_a}$) was 6.6 min; the mean half-life values of the rapidly and slowly declined phases ($t_{1/2,\alpha}$ and $t_{1/2,\beta}$) were 5.1 and 86.5 min, respectively. There were no significant differences in α and β between the present cigarette smoke inhalation study and the intravenous studies reported previously (6, 7).

Armitage *et al.* (8) estimated that the half-life of nicotine following cigarette smoke inhalation in humans, assuming a one-compartment open model, ranged from 24 to 84 min, with a mean of 40 min. Unfortunately, these investigators carried out their experiment for only 1 hr; nicotine distribution may not have been completed at this time and their reported half-lives may have been underestimated. The results in Table II also indicate that the renal clearance of nicotine following cigarette smoke inhalation ranged from 119 to 402 (mean 226) ml/hr/kg. This renal clearance accounted for ~9% of the total plasma clearance of nicotine observed at the same dose following intravenous administration (7).

Cotinine—Figure 2 shows the plasma concentration–time profile of this major metabolite of nicotine (mean ± *SEM*). The formation of cotinine is rapid. Approximately 20% of the maximum cotinine concentration was achieved within the first 3 min of cigarette smoke inhalation. The pharmacokinetic parameters of cotinine are reported in Table III. The time to reach the maximum plasma concentration (t_{max}) ranged from 1.5 to 2.0 hr. When statistical analysis was performed on t_{max}, there were no significant differences between intravenous administration and cigarette smoke inhalation of nicotine.

The mean half-life of formation of cotinine was 30.6 min and that of its elimination ranged from 5.9 to 9.0 hr. There were no significant differences among the means between cigarette smoke inhalation and intravenous administration with respect to the rate constants of formation and elimination (Table III). The renal clearance of cotinine ranged from 8.9 to 17.48 ml/hr/kg. This range is ~6% of the renal clearance of nicotine, indicating that cotinine is cleared by the kidney at a much slower rate than nicotine. There were no significant differences between the means of renal clearance following cigarette smoke inhalation and intravenous administration of nicotine (Table III).

To determine if changes occurred in the formation of cotinine from nicotine following cigarette smoke inhalation compared to the intravenous study, the ratio AUC_{cot}/AUC_{nic} was examined. The ratio ranged from 7.5 to 10.6 (Table III) and appeared to be slightly lower ($p < 0.01$) than that observed after the intravenous administration of nicotine at a comparable dosage (7). It is not clear whether this difference is biologically significant or is indicative of a first-pass metabolism of nicotine in the lungs. McGovern *et al.* (12) found no significant first-pass effect of nicotine in the isolated rabbit lung preparation.

Changes in the fraction of nicotine converted to cotinine (F), as well as in the apparent volume of distribution of cotinine, also were evaluated by examining the F/V_d ratio. This ratio (Table III) ranged from 0.21 to 0.47 kg/liter. There were no significant differences in the F/V_d ratios between those calculated from the plasma and urine data. However, these ratios were somewhat lower ($p < 0.05$) than those observed following the intravenous administration of similar doses of nicotine (7). This observation implies an increase in the volume of distribution or a decrease in the fraction of the dose converted to cotinine.

Table IV—Pharmacokinetic Parameters of Origin Activity following Cigarette Smoke Inhalation by Rats

Rat	t_{max}, hr	$t_{1/2}$, hr	$AUC_{0\to\infty}$, (dpm hr)/(ml kg)	Cl_r, ml/hr/kg	$\frac{AUC_{orig\ act}}{AUC_{nic}}$
1	1.50	24.75	65.38×10^3	117.29	9.14
2	0.75	28.88	112.66×10^3	75.96	9.48
3	0.50	24.79	68.96×10^3	160.04	7.00
4	0.75	26.67	157.53×10^3	38.14	12.58
Mean	0.88	26.27	101.13×10^3	97.86	9.55
SEM	0.22	0.98	21.65×10^3	26.28	1.15

Other Metabolites—Some of the nicotine metabolites remained at the origin of the thin-layer plate, and their possible compositions were discussed previously (6, 7). It is evident from the time course of these metabolites (Fig. 3) that ~25% of their maximum concentration (c_{max}) was formed within the first 3 min following the inhalation of cigarette smoke. Table IV reports the pharmacokinetic parameters derived from these data. There were no significant differences in t_{max} between intravenous administration and cigarette smoke inhalation. This observation suggests that the rate constants of formation and elimination have not

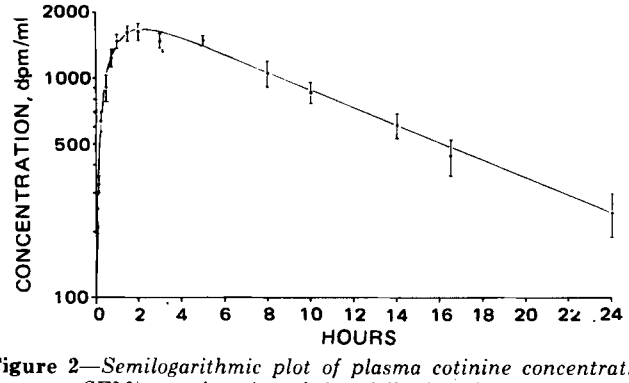

Figure 2—*Semilogarithmic plot of plasma cotinine concentration (mean ± SEM) as a function of time following cigarette smoke absorption of nicotine.*

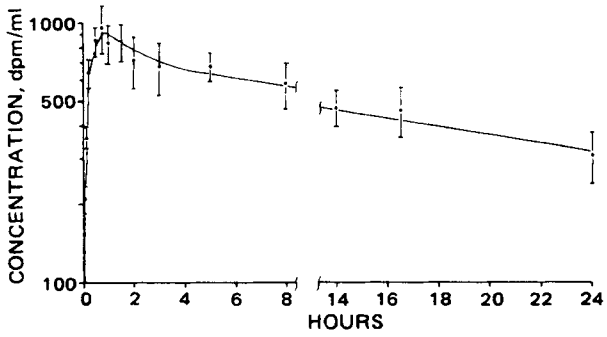

Figure 3—*Semilogarithmic plot of plasma origin activity concentration (mean ± SEM) as a function of time following cigarette smoke absorption of nicotine.*

changed between cigarette smoke inhalation and intravenous administration. Although the origin activity is composed of more than one metabolite, an overall half-life of elimination was determined for comparative purposes. The overall half-life of elimination mean (±*SEM*) was 26.27 (±0.98) hr. There were no significant differences in this parameter between the intravenous administration of nicotine (7) and the present study.

The amount of origin activity formed following cigarette smoke inhalation was compared to that observed after intravenous nicotine administration (7) by assessing the ratio of $AUC_{\text{orig act}}$ to AUC_{nic} in each study. The ratios (range of 7.0–12.6 with an overall mean of 9.5) were not significantly different from those obtained in the intravenous study (7). Therefore, the formation of the origin activity appears to be independent of the route of administration of nicotine. The renal clearance of the origin activity also appears to be independent of the route of administration, since there were no significant differences in this parameter between cigarette smoke inhalation and intravenous administration studies (7).

Urinary Excretion of Nicotine and Metabolites—The 48-hr excretion of nicotine and its metabolites following cigarette smoke inhalation is shown in Table V. There were no significant differences among the mean recoveries of radiolabeled substances in the urine between intravenous administration and cigarette smoke inhalation. The average recovery was ~66% of the amount absorbed. Approximately 16 and 13% of the total radioactivity excreted in urine consisted of nicotine and cotinine, respectively, while 33% was composed of the origin activity. No significant differences were found when these values were compared to the intravenous results. Consistent with the plasma concentration data, the ratios of cotinine or the origin activity to that of nicotine excreted in the urine in the present study also were not significantly different from those found in the intravenous study (7).

CONCLUSION

This study indicates that the absorption of nicotine present in the mainstream of cigarette smoke is rapid and does not seem to undergo first-pass metabolism through the lungs. In addition, the pharmacokinetics of nicotine and its metabolites were essentially similar to those observed previously following the intravenous injection of a single dose of nicotine (6, 7). The effect of multiple-cigarette smoke inhalation on the pharmacokinetics of these compounds is being investigated.

Table V—Urinary Excretion of Nicotine and Its Metabolites in Rats 48 hr after Cigarette Smoke Inhalation

Rat	Percent of Absorbed Dose Excreted in Urine as Total Radioactivity	Percent of Total Radioactivity Excreted in Urine as		
		Nicotine	Cotinine	Origin Activity
1	78.5	23.4	13.1	37.0
2	51.0	18.0	14.0	37.3
3	80.9	9.3	9.2	17.9
4	53.1	11.5	15.0	40.6
Mean	65.9	15.6	12.8	33.2
SEM	8.0	3.2	1.3	5.2

REFERENCES

(1) R. Binns and G. C. Clark, *Ann. Occup. Hyg.*, **15**, 237 (1972).

(2) D. M. Aviado and T. Watanabe, *Toxicol. Appl. Pharmacol.*, **30**, 185 (1974).

(3) H. Ito, T. Watanabe, S. R. Shore, and D. M. Aviado, *ibid.*, **35**, 403 (1976).

(4) C. Agué, *Psychopharmacologia*, **30**, 135 (1973).

(5) G. Reckzeh, W. Dontenwill, and F. Leuschner, *Toxicology*, **4**, 289 (1975).

(6) J. Adir, R. P. Miller, and K. S. Rotenberg, *Res. Commun. Chem. Pathol. Pharmacol.*, **13**, 173 (1976).

(7) R. P. Miller, K. S. Rotenberg, and J. Adir, *Drug Metab. Disp.*, **5**, 436 (1977).

(8) A. K. Armitage, C. T. Dollery, C. F. George, T. H. Houseman, P. J. Lewis, and D. M. Turner, *Br. Med. J.*, **4**, 313 (1975).

(9) H. Schievelbein, R. Eberhardt, and K. Loschenkohl, *Agents Actions*, **3/4**, 254 (1973).

(10) P. F. Isaac and M. J. Rand, *Eur. J. Pharmacol.*, **8**, 269 (1969).

(11) A. K. Armitage, T. H. Houseman, and D. M. Turner, *Q. J. Exp. Physiol.*, **59**, 55 (1974).

(12) J. P. McGovern, W. C. Lubawy, and H. B. Kostenbauder, *J. Pharmacol. Exp. Ther.*, **199**, 198 (1976).

(13) E. R. Bowman and H. McKennis, *Biochem. Prep.*, **10**, 36 (1963).

(14) M. A. El-Sayad and Y. A. Mohamed, *Planta Med.*, **27**, 140 (1975).

(15) M. R. Guerin, "Tobacco Smoke Analysis Program Progress Report, ORNL Report No. 4735," Oak Ridge National Laboratory, Oak Ridge, Tenn., 1971.

(16) M. R. Guerin and P. Nettesheim, "Tobacco Smoke Research Program Progress Report, ORNL Report No. 4879," Oak Ridge National Laboratory, Oak Ridge, Tenn., 1973.

(17) J. Kendrick, J. B. Rubin, D. A. Creasia, W. L. Maddox, M. R. Guerin, and P. Nettesheim, *Arch. Environ. Health*, **May/June**, 131 (1976).

(18) W. B. Wartman, E. G. Cogbill, and E. S. Harlow, *Anal. Chem.*, **31**, 1705 (1959).

(19) J. R. Weeks and J. A. Jones, *Proc. Soc. Exp. Biol. Med.*, **104**, 646 (1960).

(20) J. Kendrick, P. Nettesheim, M. Guerin, J. Caton, W. Dalbey, R. Griesemer, I. Rubin, and W. Maddox, *Toxicol. Appl. Pharmacol.*, **37**, 557 (1976).

(21) M. Berman and M. F. Weiss, "Simulation Analysis and Modeling Manual," U.S. Department of Health, Education, and Welfare, Public Health Service, National Institutes of Health, 1974.

(22) M. Gibaldi and D. Perrier, "Pharmacokinetics," Dekker, New York, N.Y., 1972, pp. 80–155.

(23) R. G. D. Steele and J. H. Torrie, "Principles and Procedures of Statistics," McGraw-Hill, New York, N.Y., 1960, p. 43.

ACKNOWLEDGMENTS

Abstracted in part from a dissertation submitted by K. S. Rotenberg to the University of Maryland in partial fulfillment of the Doctor of Philosophy degree requirements.

Supported in part by National Cancer Institute Contract N01-CP-43312.

Degradation of Chlorambucil in Aqueous Solution

HANS EHRSSON ˣ, STAFFAN EKSBORG, INGER WALLIN, and STEN-OVE NILSSON

Received April 9, 1979, from *Karolinska Pharmacy, Fack, S-104 01 Stockholm 60, Sweden.* Accepted for publication March 31, 1980.

Abstract □ The stability of chlorambucil and its degradation product 4-[*p*-(2-chloroethyl-2-hydroxyethylamino)phenyl]butyric acid (I) was studied using reversed-phase high-pressure liquid chromatography. The degradation rate of chlorambucil was unaffected by pH between pH 5 and 10 but decreased at lower pH. The degradation rates of chlorambucil and I differed only slightly (pH > 6). The proteolytic properties of the compounds were studied using spectrophotometric and partition techniques.

Keyphrases □ Chlorambucil—degradation in aqueous solution, influence of pH and temperature □ Degradation—chlorambucil and metabolites, in aqueous solution, effect of pH and temperature □ Antineoplastic agents—chlorambucil, degradation in aqueous solution, influence of pH and temperature

Nitrogen mustards are important drugs in the treatment of neoplastic diseases. A detailed and accurate knowledge of their chemical properties is important for an understanding of their behavior *in vivo*.

BACKGROUND

The nitrogen mustards are believed to react *via* an intermediate aziridinium ion (1) according to Scheme I. The aliphatic nitrogen mustards given an accumulation of the aziridinium ion, B, during the initial phase of degradation since Step I is faster than Step II (2). The aromatic nitrogen mustards differ in this respect from the aliphatic compounds (3). However, chlorambucil was proposed to follow a reaction profile similar to that of the aliphatic nitrogen mustards based on results obtained using a spectrophotometric procedure involving the reaction of the alkylating agents with 4-(*p*-nitrobenzyl)pyridine (4). However, this technique is not selective since both the parent compound and the degradation product, C (Scheme I), are derivatized and codetermined (5).

The influence of pH on the degradation rate of chlorambucil was studied previously (6), and a continuous increase in the stability of chlorambucil from pH 7 to 4.5 was observed. However, this study was performed at such a high concentration that the results might have been affected by aggregation phenomena (*cf.*, 7).

The present investigation considered the stability of chlorambucil and its degradation product 4-[*p*-(2-chloroethyl-2-hydroxyethylamino)-phenyl]butyric acid between pH 1.5 and 10 using a selective and sensitive high-pressure liquid chromatographic (HPLC) technique. The sensitivity of the technique made study of low concentrations possible, where chlorambucil is present only as the monomer.

EXPERIMENTAL

All experiments were carried out at 25.00 ± 0.05° and at the same ionic strength (0.1) unless otherwise stated.

Preparation of 4-[*p*-(2-Chloroethyl-2-hydroxyethylamino)-phenyl]butyric Acid (I)—Chlorambucil (10 mg in methanol, 0.5 ml) was mixed with 100 ml of distilled water. The solution was kept at 25° for 2 hr (final pH of 4) and extracted with ethyl acetate (100 ml). The extract was evaporated to 0.2 ml under a nitrogen atmosphere and separated by TLC[1]. The silica gel zone containing I was scraped from the plate, packed into a Pasteur pipet, and eluted with methanol (5 ml). The yield was 15% as determined spectrophotometrically. The mass spectrum was consistent with the expected structure. Prominent peaks were located at *m/e* (relative intensity, %) 250 (17), 249 (62), 191 (19), 177 (17), 176 (100), 132 (19), 131 (35), 118 (55), 117 (14), and 91 (18).

[1] Silica gel 60, F_{254}, 2 mm, Merck, Darmstadt, West Germany. The eluting solvent was toluene–methanol–heptane–isopropylacetone (8:6:3:4). The spots were 4-[*p*-[di(2-hydroxyethyl)amino]phenyl]butyric acid (R_f 0.4), I (R_f 0.6), and chlorambucil (R_f 0.7).

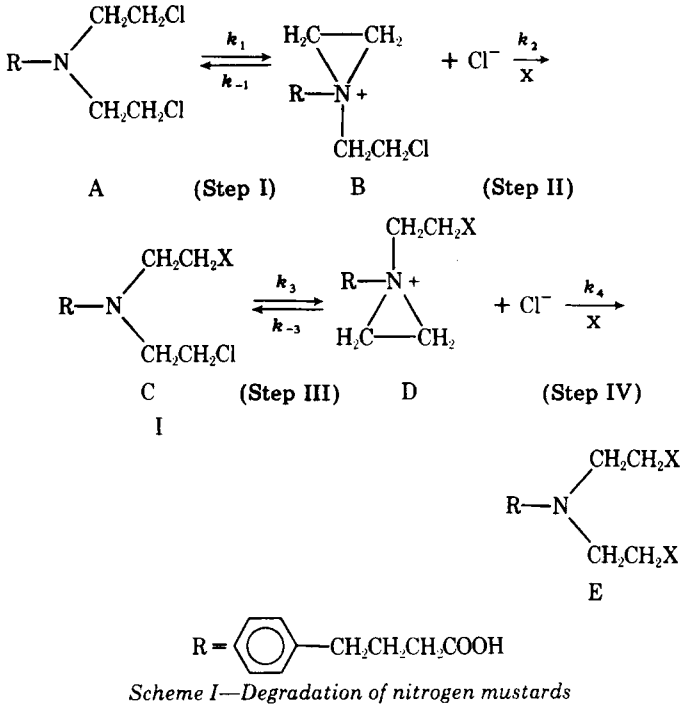

Scheme I—Degradation of nitrogen mustards

Spectrophotometric Determination of Acid Dissociation Constants—A stock solution of chlorambucil or I in ethanol (3.4×10^{-3} *M*) was diluted (1:40) with 1 *M* HCl, phosphate buffer, or citrate buffer. The absorbance was determined at 257 nm[2]. The slit width of the spectrophotometer was kept constant within each experimental series. The absorbance of at least three dilutions was measured at each pH value[3].

Determination of Acid Dissociation Constants by Partition Studies—Partition experiments were performed in centrifuge tubes using equal volumes (10 ml) of hexane and buffer and mechanical shaking for 30 (pH < 3.5) or 15 (pH > 3.5) min. Chlorambucil was dissolved initially in the organic phase to a concentration of 1.2×10^{-4} *M*.

The concentration of chlorambucil was determined spectrophotometrically (257 nm) in both phases. The organic phase was measured directly. Chlorambucil in the aqueous phase was measured by extraction into methylene chloride, buffering to pH 3.4, and mechanical shaking for 30 min.

Degradation Studies—Chlorambucil or I in methanol (0.1 ml) was mixed with the appropriate buffer (10 ml) to give a final alkylating agent concentration of 3×10^{-5} *M*, unless otherwise stated.

The solutions were analyzed by reversed-phase HPLC[4].

RESULTS AND DISCUSSION

Proteolytic Properties—The general proteolysis of an amino acid is summarized in Scheme II. The compound may occur in four forms: ammonium ($^+HR_2NMCOOH$), carboxylate (R_2NMCOO^-), uncharged ($R_2NMCOOH$), and zwitterion ($^+HR_2NMCOO^-$). The microscopic constants k'_1, k'_2, k'_{12}, and k'_{21} were defined previously (8).

[2] Zeiss PMQ III spectrophotometer.

[3] Orion Research model 701 digital pH meter equipped with an Ingold combined electrode type 401.

[4] The detector (Altex model 153) measured at 253.7 nm. The cell volume was 8 μl, and the path length was 10 mm. The pump was model LDC 711. A stainless steel 150-mm long × 4-mm i.d. column and a Rheodyne (model 70-10) injection valve with a 300-μl sample loop were used. The chromatographic support, LiChrosorb RP-18 (Merck, Darmstadt, West Germany), had a mean particle diameter of 5 μm. Methanol–water containing 0.01 *M* phosphoric acid was used as the mobile phase.

0022-3549/80/0900-1091$01.00/0
© 1980, American Pharmaceutical Association

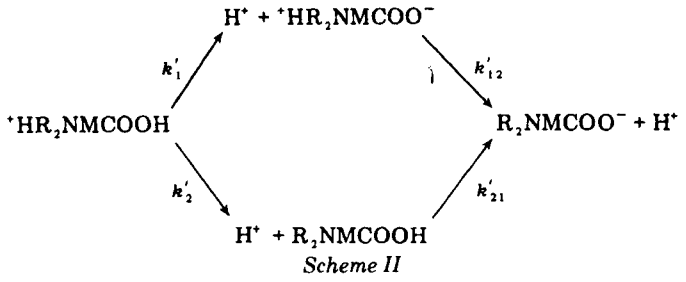

Scheme II

Spectrophotometric Determination of Acid Dissociation Constants—The absorption spectrum of chlorambucil and 4-[*p*-(2-chloroethyl-2-hydroxyethylamino)phenyl]butyric acid (1) were strongly pH dependent due to proteolysis of the amino group. Spectrophotometric determination of the microscopic constants with graphic evaluation according to a literature method (8) is illustrated in Fig. 1. The fraction of species with an unprotonized amino group, α_{R_2N}, was calculated from:

$$\alpha_{R_2N} = \frac{[R_2NMCOOH + R_2NMCOO^-]}{C_M} = \frac{A - A_A}{A_B - A_A} \quad \text{(Eq. 1)}$$

where C_M is the total concentration and A, A_A, and A_B are the absorbances at 257 nm in buffer, 1 *M* HCl, and buffer at pH 8.5, respectively. From the spectral data, it was concluded that $C_M = [^+HR_2NMCOOH]$ in 1 *M* HCl and that $C_M = [R_2NMCOO^-]$ in buffer at pH 8.5. Furthermore, M_{R_2N} was defined by:

$$M_{R_2N} = \frac{a_h([R_2NMCOOH] + [R_2NMCOO^-])}{[^+HR_2NMCOOH] + [^+HR_2NMCOO^-]} \quad \text{(Eq. 2)}$$

From Fig. 1 and Ref. 8, it was concluded that the pk'_2 value of chlorambucil is 2.49 ± 0.02. A similar evaluation for I gave a pk'_2 value of 3.63 ± 0.04. It was not possible to evaluate the pk'_{12} values from the graphs with sufficient precision, but the most likely pk'_{12} for chlorambucil was >4.2; for I, it was >6. An evaluation of pk'_1 for the two compounds also was not possible. However, since pM_{R_2N} was almost constant when α_{R_2N} was within the range of 0.1–0.6, it was concluded that zwitterion formation was negligible, *i.e.*, $pk'_1 \gg pk'_2$ (*cf.*, 9).

Determination of Acid Dissociation Constants for Chlorambucil by Partition Studies—Chlorambucil probably partitions from an aqueous phase into an organic phase in the uncharged form. The distribution ratio, D, then is given by:

$$D = \frac{[R_2NMCOOH]_{org}}{[R_2NMCOOH] + [R_2NMCOO^-] + [^+HR_2NMCOOH] + [^+HR_2NMCOO^-]} \quad \text{(Eq. 3)}$$

which can be rewritten as:

$$D = \frac{k_d}{1 + k'_{21}/a_h + a_h/k'_2 + k'_{21}/k'_{12}} \quad \text{(Eq. 4)}$$

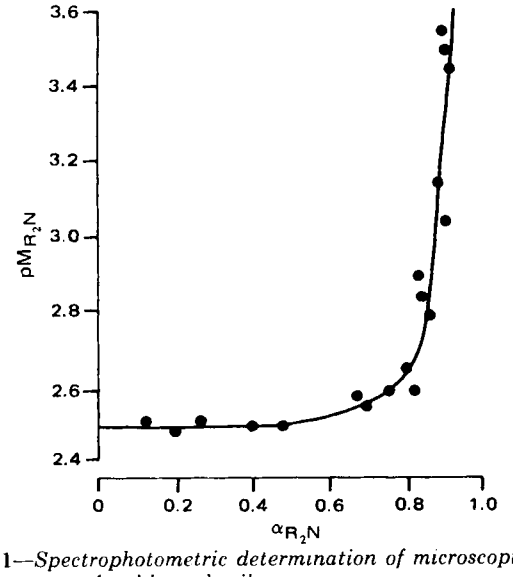

Figure 1—*Spectrophotometric determination of microscopic dissociation constants for chlorambucil.*

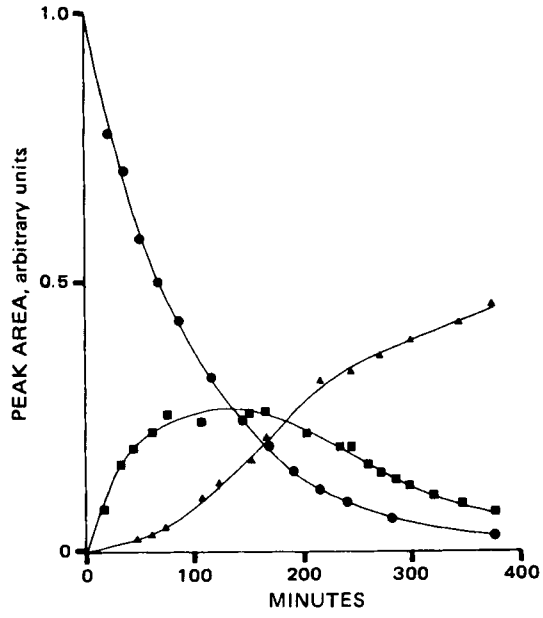

Figure 2—*Time course for chlorambucil and degradation products in aqueous solution. Key:* ●, *chlorambucil (A, Scheme I);* ■, *I (C, Scheme I); and* ▲, *4-[p-[di(2-hydroxyethyl)amino)phenyl]butyric acid (E, Scheme I). The molar absorbance and yield from the chromatographic column were considerably lower for E compared to A and C.*

where k_d, the partition coefficient, is defined by:

$$k_d = \frac{[R_2NMCOOH]_{org}}{[R_2NMCOOH]} \quad \text{(Eq. 5)}$$

Since zwitterion formation was negligible as revealed by spectrophotometric determination of acid dissociation constants, $k'_{21}/k'_{12} \ll 1$. At low pH, *i.e.*, $k'_{21}/a_h \ll 1$, Eq. 4 can be reduced to:

$$\frac{1}{D} = \frac{1}{k_d} + \frac{a_h}{k'_2 k_d} \quad \text{(Eq. 6)}$$

A plot of $1/D$ *versus* a_h for pH 1.2–2.4 gave a straight line with a small positive intercept. However, evaluation of the partition coefficient, k_d, was not possible from the intercept. The value for $-\log(k_d \times k'_2)$ was calculated from the slope as 1.04 ± 0.02; by substituting k_2 with the value determined spectrophotometrically, log k_d was evaluated as 1.45 ± 0.04.

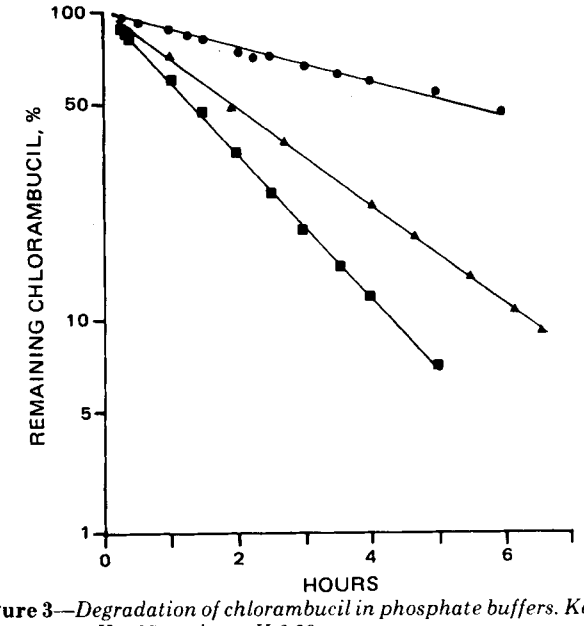

Figure 3—*Degradation of chlorambucil in phosphate buffers. Key:* ●, *pH 1.92;* ▲, *pH 2.95; and* ■, *pH 6.99.*

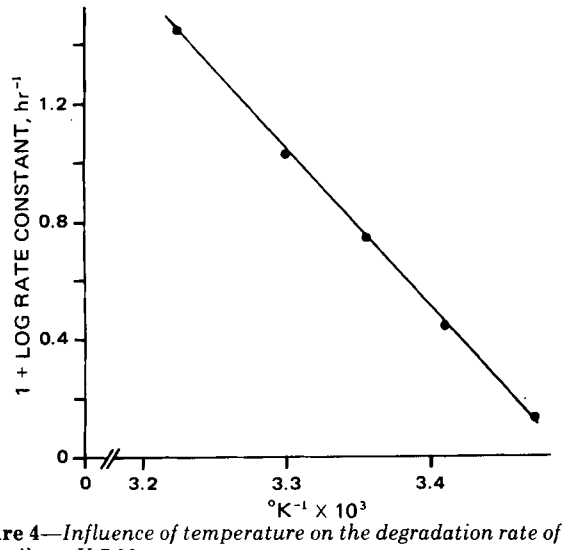

Figure 4—*Influence of temperature on the degradation rate of chlorambucil at pH 7.00.*

At high pH, *i.e.*, $a_h/k_2' \ll 1$, Eq. 4 can be rewritten as:

$$\frac{1}{D} = \frac{1}{k_d} + \frac{k_{21}'}{a_h k_d} \qquad \text{(Eq. 7)}$$

A plot of $1/D$ *versus* $1/a_h$ for pH 4.8–5.9 gave a straight line, indicating the validity of Eq. 7. From the slope and the previously evaluated value of k_d, the pk_{21}' value of 4.46 ± 0.04 was determined.

Degradation of Chlorambucil—The degradation of chlorambucil in pure aqueous solution was studied by reversed-phase HPLC. The time course of peak areas for chlorambucil and its degradation products, C and E (X = OH, Scheme I), is given in Fig. 2. The concentration of C was ~30% of the initial chlorambucil concentration after 2 hr (assuming the same molar absorbance of A and C).

The rate of loss of the alkylating activity [established by the 4-(*p*-nitrobenzyl)pyridine method] was slower initially, as reported previously by Williamson and Witten (3), who concluded that significant amounts of the aziridinium ion (B, Scheme I) accumulated during the initial degradation of chlorambucil. However, this conclusion might be incorrect since a similar rate profile is observed for a codetermination of chlorambucil and C.

A pseudo-first-order plot of the degradation of chlorambucil in phosphate buffers is shown in Fig. 3. Linear relationships were observed throughout the reaction. No change in degradation rates was observed compared to reactions in pure aqueous solutions, indicating no buffer catalysis at the pH values used. The same rate constant for chlorambucil degradation was obtained within the concentration range of 3×10^{-6}–3×10^{-5} *M*, establishing that no aggregation phenomena occurred.

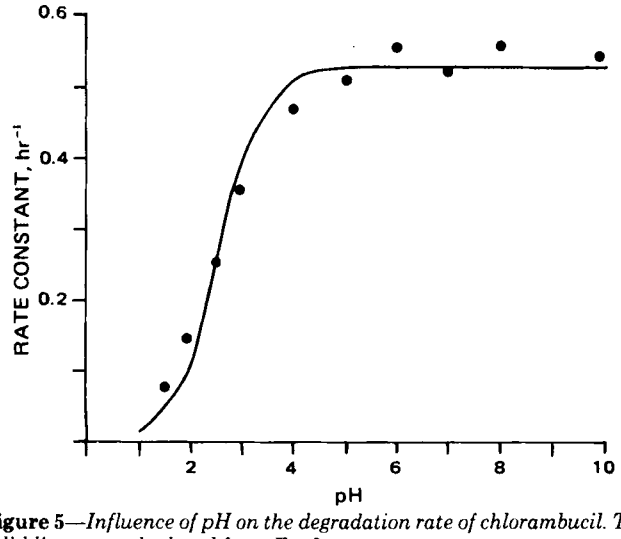

Figure 5—*Influence of pH on the degradation rate of chlorambucil. The solid line was calculated from Eq. 8.*

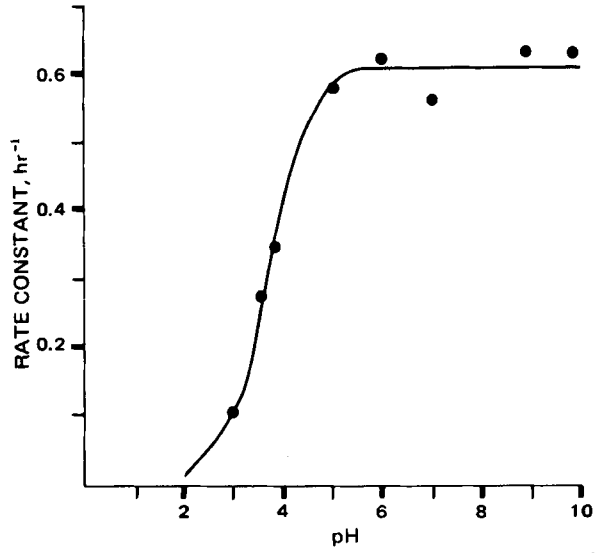

Figure 6—*Influence of pH on the degradation rate of I. The solid line was calculated from Eq. 8.*

Table I—Pseudo-First-Order Rate Constants for Degradation of Chlorambucil and I

Compound	pk_2'	k_1^*, hr^{-1} [a]
Chlorambucil	2.49 ± 0.02	0.54 ± 0.02 (n = 12)
I	3.63 ± 0.04	0.61 ± 0.04 (n = 6)

[a] Determined at pH 6–10.

Influence of Temperature—The relationship between the logarithm of the first-order rate constant and the reciprocal of temperature is given in Fig. 4. The activation energy was 102 kJ/mole, in general agreement with the data given by Linford (10).

Influence of pH on Degradation Rate of Chlorambucil and I—The degradation rate of chlorambucil was unaffected by pH in the range of pH 5–10 but decreased below pH 5 (Fig. 5). The solid line is calculated using (2):

$$k_1^* = \frac{k_2' k_1}{k_2' + a_h} \qquad \text{(Eq. 8)}$$

where k_1^* is the observed pseudo-first-order rate constant, k_1 is the pseudo-first-order rate constant for the alkylating compound with an unprotonized nitrogen atom, and k_2' is the apparent acid dissociation constant for the amino group.

The good agreement between the calculated and experimental values suggests that the nitrogen mustard group is stable when present in the protonized form and that the degree of protonization of the carboxylic group (pk_{21} 4.46) does not affect its stability. These results contradict those of Linford (6) who observed a continuous increase in the stability of chlorambucil in the pH range of 7–4.5. This finding probably was due to the high concentrations used, where the degradation rate was affected by aggregation phenomena (7).

The degradation rates of I and chlorambucil differed only slightly (Table I). These results are in contrast to those found for *N*-ethyl-*N*-(2-chloroethyl)aniline, which has a degradation rate considerably higher than does *N*,*N*-di(2-chloroethyl)aniline (11).

The influence of pH on the degradation rate of I is given in Fig. 6. The rate profile was similar to that of chlorambucil but the rate declined at higher pH, reflecting the higher base strength of the amino group.

REFERENCES

(1) M. H. Benn, P. Kazmaier, and C. Watanatada, *Chem. Commun.*, **1970**, 1685.

(2) B. Cohen, E. R. van Artsdalen, and J. Harris, *J. Am. Chem. Soc.*, **70**, 281 (1948).

(3) C. E. Williamson and B. Witten, *Cancer Res.*, **27**, 33 (1967).

(4) J. Epstein, R. W. Rosenthal, and R. J. Ess, *Anal. Chem.*, **27**, 1435 (1955).

(5) M. K. Balazs, C. A. Anderson, R. H. Iwamoto, and P. Lim, *J. Pharm. Sci.*, **59**, 563 (1970).

(6) J. H. Linford, *Biochem. Pharmacol.*, **12**, 317 (1963).
(7) D. Blakeslee, M. Chen, and J. C. Kennedy, *Br. J. Cancer*, **31**, 689 (1975).
(8) J. T. Edsall, R. B. Martin, and B. R. Hollingworth, *Proc. Natl. Acad. Sci. USA*, **44**, 505 (1958).
(9) S. Eksborg, *J. Pharm. Sci.*, **67**, 782 (1978).
(10) J. H. Linford, *Biochem. Pharmacol.*, **8**, 343 (1961).
(11) W. C. J. Ross, *J. Chem. Soc.*, **1949**, 183.

ACKNOWLEDGMENTS

The authors thank Dr. Ragnar Ryhage and Yvonne Mårde for the mass spectrometric analysis.

GLC Determination of Aprindine in Human Plasma Using a Nitrogen–Phosphorus Flame-Ionization Detector

J. F. NASH ˣ and R. H. CARMICHAEL

Received November 30, 1979, from *Lilly Research Laboratories, Indianapolis, IN 46206.* Accepted for publication April 1, 1980.

Abstract □ A procedure for the determination of aprindine in human plasma was developed. After the addition of *N,N*-diethyl-*N'*-(1,2,3,4-tetrahydro-2-naphthyl)-*N'*-phenyl-1,3-propanediamine as an internal standard, the plasma was buffered to pH 8.0, and the drug and the internal standard were extracted into ethyl acetate–hexane (9:1 v/v). The compounds then were extracted from the organic phase into 0.02 *N* HCl. The acidic solution was made basic with 0.2 *M* tribasic sodium phosphate, and aprindine and the internal standard were extracted into a small volume of hexane. The compounds were analyzed by GLC using a nitrogen–phosphorus flame-ionization detector. The drug concentration and instrument response were linear for 0.10–1.00 μg of aprindine/ml, the slope was 1.1416 (0.0141), the *y* intercept was 0.0096 ± 0.0082, and the correlation coefficient was 0.99960 ± 0.00002. The sensitivity of the method was 0.02 μg of aprindine/ml. The within-day coefficient of variation was 9.50, 3.10, 3.14, and 2.21% for 0.05, 0.20, 0.40, and 0.80 μg of aprindine/ml, respectively. The between-day coefficient of variation was 17.4, 3.40, 2.07, and 1.54% at the same concentrations. Total precision values of 19.9, 4.60, 4.26, and 2.69% were obtained. The overall relative error of the method was +1.33, +2.00, −0.07, and +0.25% at these concentrations.

Keyphrases □ Aprindine—GLC analysis in human plasma using nitrogen–phosphorus flame-ionization detection □ GLC—analysis, aprindine, nitrogen–phosphorus flame-ionization detection, human plasma □ Antiarrhythmic agents—aprindine, GLC analysis using nitrogen–phosphorus flame-ionization detection, human plasma

Aprindine[1] (*N,N*-diethyl-*N'*-2-indanyl-*N'*-phenyl-1,3-propanediamine), an oral, long-acting, antidysrhythmic agent, has been used in Europe since the early 1970's. A sensitive (0.1 μg/ml), specific, and precise (coefficient of variation 5%) GLC method was developed (1) and then modified (2) that satisfactorily monitors plasma aprindine levels in patients. Lagerström and Persson (3) reported a sensitive (0.5 μg/ml) high-performance liquid chromatographic assay for monitoring plasma aprindine levels. These methods appear to be suitable for monitoring plasma aprindine levels of ≥0.5 μg/ml. However, for pharmacokinetic and bioavailability studies following unit doses of 10, 25, or 50 mg of aprindine, a more sensitive method was necessary.

This report describes a GLC method using a dual nitrogen–phosphorus flame-ionization detector that optimizes the sensitivity and specificity of the measurement of aprindine and still retains the precision of the assay.

[1] Christiaens Pharmaceutical Co., Brussels, Belgium.

EXPERIMENTAL

Chemicals and Reagents—Ethyl acetate[2], hexane[2], and methanol[2] were distilled in glass; all other chemicals and reagents were analytical reagent grade. Aprindine hydrochloride[3], *N,N*-diethyl-*N'*-(1,2,3,4-tetrahydro-2-naphthyl)-*N'*-phenyl-1,3-propanediamine hydrochloride[4], and [*N-phenyl*-1-^{14}C]aprindine hydrochloride[5] with a specific activity of 29.4 μCi/mg were synthesized.

The aprindine standard solution (10 μg/ml) was prepared by weighing accurately 1.12 mg of aprindine hydrochloride into a 100-ml volumetric flask and diluting the solution to volume with distilled water.

The *N,N*-diethyl-*N'*-(1,2,3,4-tetrahydro-2-naphthyl)-*N'*-phenyl-1,3-propanediamine solution (the internal standard) (5 μg/ml) was prepared by weighing accurately 1.11 mg of the hydrochloride salt of the internal standard into a 200-ml volumetric flask and diluting the solution to volume with distilled water.

GLC System—Table I summarizes the GLC equipment, materials, and conditions for the identification and analysis of aprindine in plasma. Disposable 15-ml centrifuge tubes with plastic-lined screw caps[6] were used throughout the extraction.

Procedure—A plasma calibration curve was prepared by pipetting 1.0 ml of fresh, human, drug-free plasma into each of five disposable 15-ml centrifuge tubes and adding 250 μl of the internal standard solution to give a concentration of 1.25 μg/ml. The first tube served as the blank. Ten microliters of the aprindine standard solution was added to the second tube, 25 μl was added to the third tube, 50 μl was added to the fourth tube, and 100 μl was added to the fifth tube. These plasma standards contained aprindine concentrations of 0.00, 0.10, 0.25, 0.50, and 1.00 μg/ml, respectively.

Borate buffer USP, 0.5 ml, was mixed thoroughly with the plasma standards. Then 10 ml of ethyl acetate–hexane (9:1 v/v) was shaken with each tube of plasma standard for 2 min, and the phases were separated by centrifugation. Approximately 8 ml of the supernate was pipetted into a clean 15-ml centrifuge tube, with care taken not to remove any of the aqueous phase. The compounds were extracted into 5 ml of 0.02 *N* HCl, the contents of the tube were centrifuged, and the organic layer was discarded. The aqueous solution was made basic by mixing with 1.5 ml of 0.2 *M* tribasic sodium phosphate, the drug and the internal standard were extracted into 0.3 ml of hexane, and the phases were separated again by centrifugation. Two microliters of the hexane solution was injected onto the chromatographic column.

When assaying plasma samples, a 1.0-ml sample was placed into a 15-ml disposable centrifuge tube and 250 μl of the internal standard solution was added. After 0.5 ml of borate buffer was added, the plasma samples were handled as were the calibration curve samples.

A least-squares line was prepared by analysis of the calibration curve of the peak height ratio of aprindine to the internal standard *versus*

[2] Burdick & Jackson, Muskegon, Mich.
[3] Fibocil, Eli Lilly and Co., Indianapolis, Ind.
[4] Eli Lilly and Co., Indianapolis, Ind.
[5] New England Nuclear, Boston, Mass.
[6] Corning Glass Works, Corning, N.Y.

0022-3549/80/0900-1094$01.00/0
© 1980, American Pharmaceutical Association

(6) J. H. Linford, *Biochem. Pharmacol.*, **12**, 317 (1963).
(7) D. Blakeslee, M. Chen, and J. C. Kennedy, *Br. J. Cancer*, **31**, 689 (1975).
(8) J. T. Edsall, R. B. Martin, and B. R. Hollingworth, *Proc. Natl. Acad. Sci. USA*, **44**, 505 (1958).
(9) S. Eksborg, *J. Pharm. Sci.*, **67**, 782 (1978).
(10) J. H. Linford, *Biochem. Pharmacol.*, **8**, 343 (1961).
(11) W. C. J. Ross, *J. Chem. Soc.*, **1949**, 183.

ACKNOWLEDGMENTS

The authors thank Dr. Ragnar Ryhage and Yvonne Mårde for the mass spectrometric analysis.

GLC Determination of Aprindine in Human Plasma Using a Nitrogen–Phosphorus Flame-Ionization Detector

J. F. NASH ˣ and R. H. CARMICHAEL

Received November 30, 1979, from *Lilly Research Laboratories, Indianapolis, IN 46206.* Accepted for publication April 1, 1980.

Abstract □ A procedure for the determination of aprindine in human plasma was developed. After the addition of *N,N*-diethyl-*N'*-(1,2,3,4-tetrahydro-2-naphthyl)-*N'*-phenyl-1,3-propanediamine as an internal standard, the plasma was buffered to pH 8.0, and the drug and the internal standard were extracted into ethyl acetate–hexane (9:1 v/v). The compounds then were extracted from the organic phase into 0.02 *N* HCl. The acidic solution was made basic with 0.2 *M* tribasic sodium phosphate, and aprindine and the internal standard were extracted into a small volume of hexane. The compounds were analyzed by GLC using a nitrogen–phosphorus flame-ionization detector. The drug concentration and instrument response were linear for 0.10–1.00 μg of aprindine/ml, the slope was 1.1416 (0.0141), the *y* intercept was 0.0096 ± 0.0082, and the correlation coefficient was 0.99960 ± 0.00002. The sensitivity of the method was 0.02 μg of aprindine/ml. The within-day coefficient of variation was 9.50, 3.10, 3.14, and 2.21% for 0.05, 0.20, 0.40, and 0.80 μg of aprindine/ml, respectively. The between-day coefficient of variation was 17.4, 3.40, 2.07, and 1.54% at the same concentrations. Total precision values of 19.9, 4.60, 4.26, and 2.69% were obtained. The overall relative error of the method was +1.33, +2.00, −0.07, and +0.25% at these concentrations.

Keyphrases □ Aprindine—GLC analysis in human plasma using nitrogen–phosphorus flame-ionization detection □ GLC—analysis, aprindine, nitrogen–phosphorus flame-ionization detection, human plasma □ Antiarrhythmic agents—aprindine, GLC analysis using nitrogen–phosphorus flame-ionization detection, human plasma

Aprindine[1] (*N,N*-diethyl-*N'*-2-indanyl-*N'*-phenyl-1,3-propanediamine), an oral, long-acting, antidysrhythmic agent, has been used in Europe since the early 1970's. A sensitive (0.1 μg/ml), specific, and precise (coefficient of variation 5%) GLC method was developed (1) and then modified (2) that satisfactorily monitors plasma aprindine levels in patients. Lagerström and Persson (3) reported a sensitive (0.5 μg/ml) high-performance liquid chromatographic assay for monitoring plasma aprindine levels. These methods appear to be suitable for monitoring plasma aprindine levels of ≥0.5 μg/ml. However, for pharmacokinetic and bioavailability studies following unit doses of 10, 25, or 50 mg of aprindine, a more sensitive method was necessary.

This report describes a GLC method using a dual nitrogen–phosphorus flame-ionization detector that optimizes the sensitivity and specificity of the measurement of aprindine and still retains the precision of the assay.

[1] Christiaens Pharmaceutical Co., Brussels, Belgium.

EXPERIMENTAL

Chemicals and Reagents—Ethyl acetate[2], hexane[2], and methanol[2] were distilled in glass; all other chemicals and reagents were analytical reagent grade. Aprindine hydrochloride[3], *N,N*-diethyl-*N'*-(1,2,3,4-tetrahydro-2-naphthyl)-*N'*-phenyl-1,3-propanediamine hydrochloride[4], and [*N-phenyl*-1-^{14}C]aprindine hydrochloride[5] with a specific activity of 29.4 μCi/mg were synthesized.

The aprindine standard solution (10 μg/ml) was prepared by weighing accurately 1.12 mg of aprindine hydrochloride into a 100-ml volumetric flask and diluting the solution to volume with distilled water.

The *N,N*-diethyl-*N'*-(1,2,3,4-tetrahydro-2-naphthyl)-*N'*-phenyl-1,3-propanediamine solution (the internal standard) (5 μg/ml) was prepared by weighing accurately 1.11 mg of the hydrochloride salt of the internal standard into a 200-ml volumetric flask and diluting the solution to volume with distilled water.

GLC System—Table I summarizes the GLC equipment, materials, and conditions for the identification and analysis of aprindine in plasma. Disposable 15-ml centrifuge tubes with plastic-lined screw caps[6] were used throughout the extraction.

Procedure—A plasma calibration curve was prepared by pipetting 1.0 ml of fresh, human, drug-free plasma into each of five disposable 15-ml centrifuge tubes and adding 250 μl of the internal standard solution to give a concentration of 1.25 μg/ml. The first tube served as the blank. Ten microliters of the aprindine standard solution was added to the second tube, 25 μl was added to the third tube, 50 μl was added to the fourth tube, and 100 μl was added to the fifth tube. These plasma standards contained aprindine concentrations of 0.00, 0.10, 0.25, 0.50, and 1.00 μg/ml, respectively.

Borate buffer USP, 0.5 ml, was mixed thoroughly with the plasma standards. Then 10 ml of ethyl acetate–hexane (9:1 v/v) was shaken with each tube of plasma standard for 2 min, and the phases were separated by centrifugation. Approximately 8 ml of the supernate was pipetted into a clean 15-ml centrifuge tube, with care taken not to remove any of the aqueous phase. The compounds were extracted into 5 ml of 0.02 *N* HCl, the contents of the tube were centrifuged, and the organic layer was discarded. The aqueous solution was made basic by mixing with 1.5 ml of 0.2 *M* tribasic sodium phosphate, the drug and the internal standard were extracted into 0.3 ml of hexane, and the phases were separated again by centrifugation. Two microliters of the hexane solution was injected onto the chromatographic column.

When assaying plasma samples, a 1.0-ml sample was placed into a 15-ml disposable centrifuge tube and 250 μl of the internal standard solution was added. After 0.5 ml of borate buffer was added, the plasma samples were handled as were the calibration curve samples.

A least-squares line was prepared by analysis of the calibration curve of the peak height ratio of aprindine to the internal standard *versus*

[2] Burdick & Jackson, Muskegon, Mich.
[3] Fibocil, Eli Lilly and Co., Indianapolis, Ind.
[4] Eli Lilly and Co., Indianapolis, Ind.
[5] New England Nuclear, Boston, Mass.
[6] Corning Glass Works, Corning, N.Y.

0022-3549/80/0900-1094$01.00/0
© 1980, American Pharmaceutical Association

Table I—Conditions for the GLC Identification and Analysis of Aprindine and the Internal Standard [a] in Plasma Extracts

Instrument	Gas Chromatograph[b]	Gas Chromatograph–Mass Spectrograph[c]
Detector	Nitrogen–phosphorus flame-ionization detector[b]	Mass spectrograph[c]
Recorder	Model 7127A, 1 mv[b]	Model 6000[c]
Packing	3.8% W-98[d]	2% OV-7[d]
Support	Chromosorb G-HP[d] (80–100 mesh)	Chromosorb W-HP[d] (80–100 mesh)
Column length, cm	91.4	91.4
Column inner diameter, mm	3	2
Gases and flow rates, ml/min		
Carrier	Helium, 60	Source pressure
Flame	Hydrogen, 60	800–1000 μm
Support	Oxygen, 240	Methane, 18
Oven temperature	255°	240°
Injection port temperature	250°	270°
Detector temperature	250°	180°
Attenuation	1×10^{-9}	—
Chart speed, cm/min	0.635	—
Ionization energy, ev	—	110

[a] *N,N*-Diethyl-*N'*-(1,2,3,4-tetrahydro-2-naphthyl)-*N'*-phenyl-1,3-propanediamine. [b] HP 5700A, Hewlett-Packard Co., Avondale, Pa. [c] Model 3200, Finnigan Corp., Sunnyvale, Calif. [d] Ohio Valley Specialty Chemical Co., Marietta, Ohio.

concentration. The concentration of aprindine in the plasma samples was determined from their peak height ratios and the least-squares line.

RESULTS AND DISCUSSION

With [*N-phenyl*-1-^{14}C]aprindine hydrochloride, it was found that ~80% of the aprindine in spiked plasma samples was recovered following the described procedure (Table II).

During the development of the method, aprindine adsorbed irreversibly to the glass surface during the evaporation of hexane in the final concentration step. Silylation of the dry-down tubes and/or addition of 20 μl of dimethylformamide to the hexane only partially prevented the binding. Therefore, only a small volume of hexane was used as the collection solvent for the compounds. When the final hexane layer was not concentrated, the binding of aprindine to glass was prevented and the

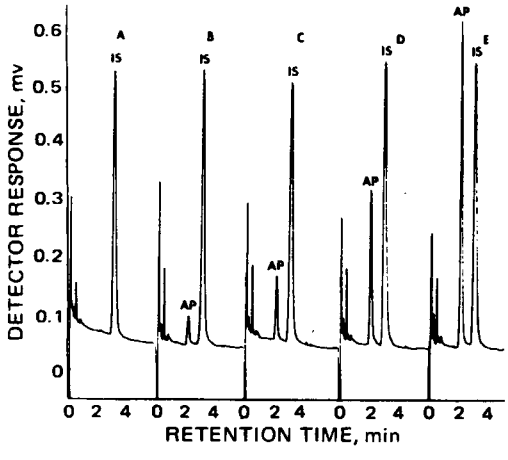

Figure 1—*Gas–liquid chromatograms (nitrogen–phosphorus detector) of a plasma blank with the internal standard (A) and plasma standards with aprindine at 0.10 (B), 0.25 (C), 0.50 (D), and 1.00 (E) μg/ml. Key: AP, aprindine; and IS, internal standard. The temperature was 255°. The 91.4-cm column was packed with 3.8% W-98 on Chromosorb G (HP). The attenuation was 64. Two microliters was injected.*

Table II—Analytical Recovery of [*N-phenyl*-1-^{14}C]Aprindine Added to Plasma

Concentration Added[a], μg/ml	Recovery[b], %	*CV*, %
0.5	82.6	7.0
2.0	80.0	3.3

[a] As [*N-phenyl*-1-^{14}C]aprindine hydrochloride; five replicates. [b] Found in hexane phase after analyzing samples by the reported procedure, correcting for volume transferred, and comparing to the same unextracted concentration of [*N-phenyl*-1-^{14}C]aprindine in hexane.

Table III—Standard Curves for Aprindine in Plasma [a]

Aprindine[b] Added to Plasma, μg/ml	Peak Height Ratio, Aprindine to Internal Standard	Aprindine[c] Found in Plasma, μg/ml
0.10	0.1197 (0.0086)	0.113 (0.0003)
0.25	0.2628 (0.0086)	0.238 (0.0013)
0.50	0.5536 (0.0124)	0.493 (0.0132)
1.00	1.1376 (0.0167)	1.005 (0.0036)

[a] Linear regression equation: $y = 1.1416\ (0.0141)x - 0.0096\ (0.0082)$; $r = 0.99960$ (0.00002). [b] As aprindine hydrochloride. [c] Mean (±*SD*) of three replicate curves assayed on 3 different days by the same analyst.

reproducibility of the method was improved greatly while suitable sensitivity was maintained.

Table III shows that the data from three typical plasma calibration curves were linear over at least a 10-fold concentration range with an intercept of near zero. The small standard deviations of the data used to prepare the least-squares lines and the correlation coefficients indicate the reproducibility of the method.

Figure 1 shows typical chromatograms of blank human plasma and a plasma calibration curve obtained by using the nitrogen–phosphorus flame-ionization detector. Chromatograms of blank human plasma and a plasma calibration curve obtained using a flame-ionization detector are given in Fig. 2. Comparison of the nitrogen–phosphorus chromatograms to the flame-ionization chromatograms shows that the former detector was 16 times more sensitive under the conditions stated for the detection of aprindine (calculated by noting four times the peak height of aprindine standards at four times the instrument attenuation). It was necessary to acid wash glassware and to optimize the nitrogen–phosphorus detector daily, as reported by Pierce *et al.* (4), to maintain good reproducibility and sensitivity.

The major metabolite of aprindine, desethylaprindine (1), eluted at ~60 sec, which separated it from the aprindine (150 sec) and the internal standard (190 sec). When humans were given therapeutic doses of aprindine hydrochloride, desethylaprindine was never seen in their plasma; however, the metabolite was seen and quantitated in dog plasma after the dogs were dosed with the drug[7]. Standard vacuum containers[8], used to collect blood samples, produced no interference in the determination of aprindine by this method.

Gas–liquid chromatograms–mass spectrograms (methane as positive ion for chemical ionization) of plasma extracts were similar to solid-probe

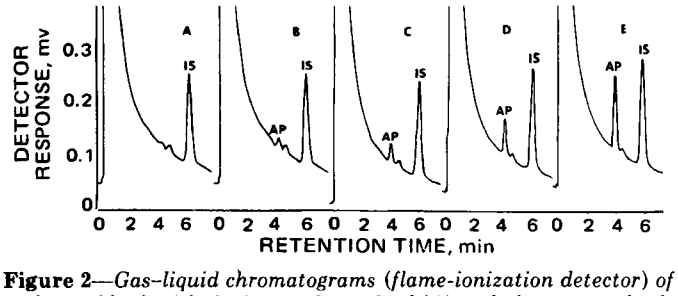

Figure 2—*Gas–liquid chromatograms (flame-ionization detector) of a plasma blank with the internal standard (A) and plasma standards with aprindine at 0.10 (B), 0.25 (C), 0.50 (D), and 1.00 (E) μg/ml. Key: AP, aprindine; and IS, internal standard. The temperature was 240°. The 91.4-cm column was packed with 3.8% W-98 on Chromosorb C (HP). The attenuation was 16. Two microliters was injected.*

[7] J. F. Nash and R. H. Carmichael, Eli Lilly and Co., Indianapolis, Ind., unpublished data.

[8] Vacutainer, Becton-Dickinson Co., Rutherford, N.J.

Table IV—Precision and Accuracy in Assay of Added Aprindine to Human Plasma

	In Vitro Pools, μg/ml			
	0.050	0.200	0.400	0.800
Number of replicates	5	5	5	5
Mean, μg/ml	0.048	0.200	0.390	0.796
CV, %	9.32	3.54	4.80	2.45
Number of replicates	5	5	5	5
Mean, μg/ml	0.046	0.202	0.400	0.796
CV, %	11.91	2.21	1.77	1.43
Number of replicates	5	5	5	5
Mean, μg/ml	0.058	0.210	0.408	0.814
CV, %	7.71	3.37	2.05	2.55
Overall precision				
Between-day *CV*, %	17.4	3.40	2.07	1.54
Within-day *CV*, %	9.50	3.10	3.14	2.21
Total *CV*, %	19.9	4.60	4.26	2.69
Overall accuracy				
Mean, μg/ml	0.051	0.204	0.399	0.802
Total relative error, %	+1.33	+2.00	−0.07	+0.25

spectrograms of aprindine. The protonated $[M + H]^+$ ion at *m/e* 323 and fragmentation ions at *m/e* 113, 117, and 207 confirmed the presence and integrity of aprindine in the plasma of subjects administered the drug.

The accuracy and precision of the method were determined by preparing four plasma pools of known aprindine concentrations. The same analyst assayed five replicates from each pool on each of 3 days (Table IV). Good reproducibility was indicated by the within-day coefficients of variation of 9.50, 3.10, 3.14, and 2.21% for 0.05, 0.20, 0.40, and 0.80 μg of aprindine/ml, respectively, as well as by the between-day variations of 17.4, 3.40, 2.07, and 1.54% at the same concentrations. The total coefficients of variation were 19.9, 4.60, 4.26, and 2.69%, respectively. The overall relative errors at 0.05, 0.20, 0.40, and 0.80 μg of aprindine/ml were +1.33, +2.00, −0.07, and +0.25%, respectively.

Because of the specificity, sensitivity, precision, and accuracy of the reported method for the determination of aprindine in plasma, bioavailability and pharmacokinetic studies of aprindine can be undertaken at therapeutic doses. These studies will be reported later.

REFERENCES

(1) L. Dodion, J. M. Desuray, M. DeBlecker, and A. Georges, *Thérapie*, **29**, 221 (1974).

(2) J. P. Van Durme, M. G. Bogaert, and M.-T. Rosseel, *Eur. J. Clin. Pharmacol.*, **7**, 343 (1974).

(3) P. O. Lagerström and B.-A. Persson, *J. Chromatogr.*, **149**, 331 (1978).

(4) W. O. Pierce, T. C. Lamoreaux, F. M. Urry, L. Kopjak, and B. S. Finkle, *J. Anal. Toxicol.*, **2**, 26 (1978).

ACKNOWLEDGMENTS

The authors thank Dr. R. L. Wolen for the GLC–mass spectrometric analyses, Mr. W. E. Legan for help in development of the method and analyses of the plasma samples, and Mrs. K. Z. Farid for helpful suggestions in method development.

NOTES

Measurement of Pilocarpine and Its Degradation Products by High-Performance Liquid Chromatography

JAMES J. O'DONNELL ˣ, ROBERT SANDMAN, and MICHAEL V. DRAKE

Received January 22, 1980, from the *Department of Ophthalmology, University of California Medical Center, San Francisco, CA 94143.* Accepted for publication March 21, 1980.

Abstract □ An assay method for pilocarpine using reversed-phase high-performance liquid chromatography is presented. This method also measures isopilocarpine, the stereoisomer of pilocarpine, and the degradation products pilocarpic acid and isopilocarpic acid. Maximum sensitivity was obtained with optical absorbance at 216 nm.

Keyphrases □ Pilocarpine—reversed-phase high-performance liquid chromatographic analysis □ High-performance liquid chromatography—analysis, *pilocarpine*, isopilocarpine, pilocarpic acid, and isopilocarpic acid □ Ophthalmic drugs—pilocarpine, high-performance liquid chromatographic analysis

Pilocarpine (I) is a natural alkaloid used for the parasympathomimetic treatment of glaucoma. Isopilocarpine (II), the therapeutically inactive stereoisomer of pilocarpine, is present in nature and in commercial preparations of pilocarpine (1, 2). The degradation products,

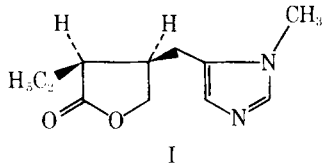

I

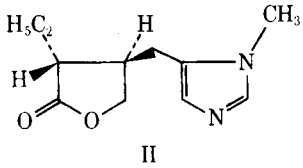

II

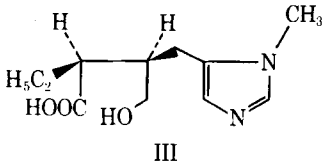

III

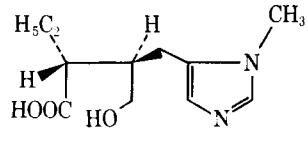

IV

pilocarpic acid (III) and isopilocarpic acid (IV), also are found in commercial products (3). This report presents an efficient and sensitive assay for I–IV using reversed-phase high-performance liquid chromatography (HPLC). This method is a modification of a procedure described recently (4).

EXPERIMENTAL

Pilocarpine hydrochloride USP[1] and isopilocarpine hydrochloride[2] were obtained commercially. Pilocarpic acid and isopilocarpic acid were prepared by hydrolysis of pilocarpine and isopilocarpine in 0.1 *N* NaOH. Isocratic reversed-phase chromatography was accomplished by pumping[3]

[1] Mallinckrodt, St. Louis, Mo.
[2] Aldrich, Milwaukee, Wis.
[3] Model 310 high-performance liquid chromatograph, Altex Scientific Inc., Berkeley, Calif.

0022-3549/80/0900-1096$01.00/0

© 1980, American Pharmaceutical Association

Table IV—Precision and Accuracy in Assay of Added Aprindine to Human Plasma

	In Vitro Pools, μg/ml			
	0.050	0.200	0.400	0.800
Number of replicates	5	5	5	5
Mean, μg/ml	0.048	0.200	0.390	0.796
CV, %	9.32	3.54	4.80	2.45
Number of replicates	5	5	5	5
Mean, μg/ml	0.046	0.202	0.400	0.796
CV, %	11.91	2.21	1.77	1.43
Number of replicates	5	5	5	5
Mean, μg/ml	0.058	0.210	0.408	0.814
CV, %	7.71	3.37	2.05	2.55
Overall precision				
Between-day *CV*, %	17.4	3.40	2.07	1.54
Within-day *CV*, %	9.50	3.10	3.14	2.21
Total *CV*, %	19.9	4.60	4.26	2.69
Overall accuracy				
Mean, μg/ml	0.051	0.204	0.399	0.802
Total relative error, %	+1.33	+2.00	−0.07	+0.25

spectrograms of aprindine. The protonated $[M + H]^+$ ion at *m/e* 323 and fragmentation ions at *m/e* 113, 117, and 207 confirmed the presence and integrity of aprindine in the plasma of subjects administered the drug.

The accuracy and precision of the method were determined by preparing four plasma pools of known aprindine concentrations. The same analyst assayed five replicates from each pool on each of 3 days (Table IV). Good reproducibility was indicated by the within-day coefficients of variation of 9.50, 3.10, 3.14, and 2.21% for 0.05, 0.20, 0.40, and 0.80 μg of aprindine/ml, respectively, as well as by the between-day variations of 17.4, 3.40, 2.07, and 1.54% at the same concentrations. The total coefficients of variation were 19.9, 4.60, 4.26, and 2.69%, respectively. The overall relative errors at 0.05, 0.20, 0.40, and 0.80 μg of aprindine/ml were +1.33, +2.00, −0.07, and +0.25%, respectively.

Because of the specificity, sensitivity, precision, and accuracy of the reported method for the determination of aprindine in plasma, bioavailability and pharmacokinetic studies of aprindine can be undertaken at therapeutic doses. These studies will be reported later.

REFERENCES

(1) L. Dodion, J. M. Desuray, M. DeBlecker, and A. Georges, *Thérapie*, **29**, 221 (1974).

(2) J. P. Van Durme, M. G. Bogaert, and M.-T. Rosseel, *Eur. J. Clin. Pharmacol.*, **7**, 343 (1974).

(3) P. O. Lagerström and B.-A. Persson, *J. Chromatogr.*, **149**, 331 (1978).

(4) W. O. Pierce, T. C. Lamoreaux, F. M. Urry, L. Kopjak, and B. S. Finkle, *J. Anal. Toxicol.*, **2**, 26 (1978).

ACKNOWLEDGMENTS

The authors thank Dr. R. L. Wolen for the GLC–mass spectrometric analyses, Mr. W. E. Legan for help in development of the method and analyses of the plasma samples, and Mrs. K. Z. Farid for helpful suggestions in method development.

NOTES

Measurement of Pilocarpine and Its Degradation Products by High-Performance Liquid Chromatography

JAMES J. O'DONNELL ˣ, ROBERT SANDMAN, and MICHAEL V. DRAKE

Received January 22, 1980, from the *Department of Ophthalmology, University of California Medical Center, San Francisco, CA 94143.* Accepted for publication March 21, 1980.

Abstract □ An assay method for pilocarpine using reversed-phase high-performance liquid chromatography is presented. This method also measures isopilocarpine, the stereoisomer of pilocarpine, and the degradation products pilocarpic acid and isopilocarpic acid. Maximum sensitivity was obtained with optical absorbance at 216 nm.

Keyphrases □ Pilocarpine—reversed-phase high-performance liquid chromatographic analysis □ High-performance liquid chromatography—analysis, *pilocarpine*, isopilocarpine, pilocarpic acid, and isopilocarpic acid □ Ophthalmic drugs—pilocarpine, high-performance liquid chromatographic analysis

Pilocarpine (I) is a natural alkaloid used for the parasympathomimetic treatment of glaucoma. Isopilocarpine (II), the therapeutically inactive stereoisomer of pilocarpine, is present in nature and in commercial preparations of pilocarpine (1, 2). The degradation products,

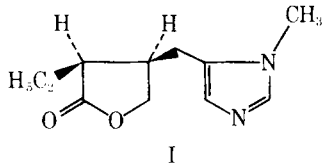

I

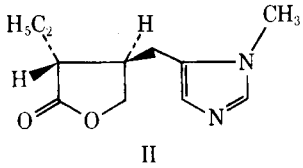

II

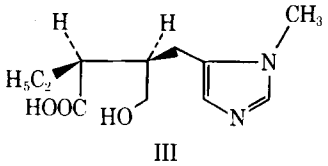

III

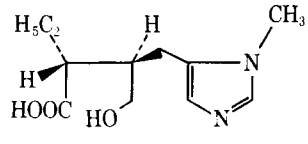

IV

pilocarpic acid (III) and isopilocarpic acid (IV), also are found in commercial products (3). This report presents an efficient and sensitive assay for I–IV using reversed-phase high-performance liquid chromatography (HPLC). This method is a modification of a procedure described recently (4).

EXPERIMENTAL

Pilocarpine hydrochloride USP[1] and isopilocarpine hydrochloride[2] were obtained commercially. Pilocarpic acid and isopilocarpic acid were prepared by hydrolysis of pilocarpine and isopilocarpine in 0.1 *N* NaOH. Isocratic reversed-phase chromatography was accomplished by pumping[3]

[1] Mallinckrodt, St. Louis, Mo.
[2] Aldrich, Milwaukee, Wis.
[3] Model 310 high-performance liquid chromatograph, Altex Scientific Inc., Berkeley, Calif.

0022-3549/80/0900-1096$01.00/0

© 1980, American Pharmaceutical Association

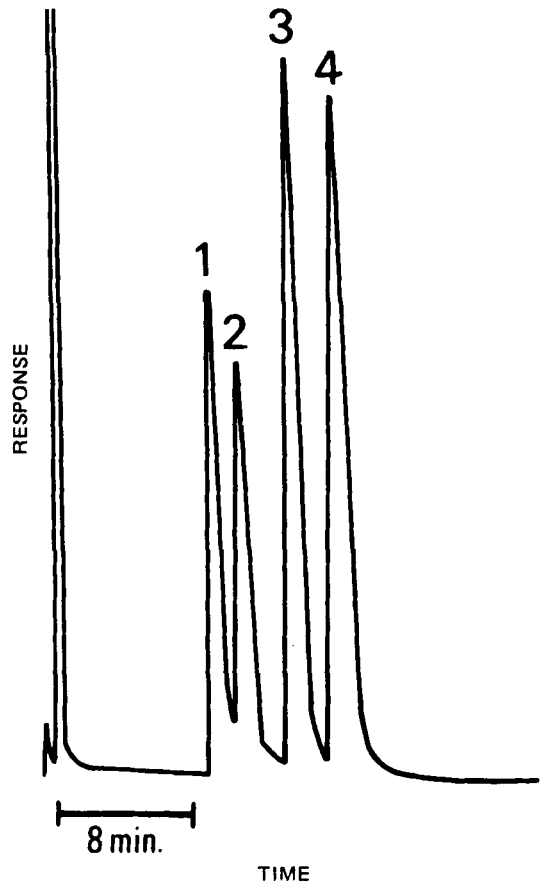

Figure 1—*HPLC separation of isopilocarpine (1), pilocarpine (2), pilocarpic acid (3), and isopilocarpic acid (4).*

97% H_2O–3% CH_3OH containing 5% KH_2PO_4 (pH 2.5) through a C_{18} column[4] at 1.5 ml/min at ambient temperature. The compounds were detected[5] by their optical absorbance at 216 nm.

RESULTS AND DISCUSSION

The chromatographic separation of pilocarpine, isopilocarpine, pilocarpic acid, and isopilocarpic acid is shown in Fig. 1. The maximum sensitivity obtainable in this system with a peak height signal of twice the short-term baseline noise is 300 ng. Detection of isopilocarpine in pilocarpine dosage forms is a problem in pilocarpine analysis. Since the isopilocarpine and pilocarpine peaks overlap, the lower limit of detection of isopilocarpine in the presence of pilocarpine by this method is one part of isopilocarpine in 100 parts of pilocarpine.

Despite long ophthalmic use, sensitive measurement of pilocarpine and its metabolites has been possible only recently. The USP method uses extraction and an insensitive colorimetric determination (5). Polarographic (6), GLC (7, 8), and NMR (3) assays have been reported. HPLC offers the convenience of speed, selectivity, sensitivity, mild and nondestructive conditions, and direct measurement. Ion-exchange HPLC (1, 2, 9) has the disadvantages of variable retention time, poor resolution, and destructive alkaline pH. The method used here was adapted from a reported reversed-phase HPLC method that used refractive index detection (4). Optical absorbance detection at 216 nm was used for increased ease and sensitivity. External standards can be used for pilocarpine analysis.

Sensitive measurement of pilocarpine and its metabolites will allow studies of the purity of dosage forms and investigation of the pharmacokinetics of pilocarpine.

[4] Lichrosorb RP C_{18} (10 μm) in 4.6 × 250-mm column, Altex Scientific Inc., Berkeley, Calif.

[5] Model 785 variable-wavelength detector, Micromeritics Instrument Corp., Norcross, Ga.

REFERENCES

(1) T. Urbanyi, A. Piedmont, E. Willis, and G. Manning, *J. Pharm. Sci.*, **65**, 257 (1976).

(2) J. D. Weber, *J. Assoc. Off. Anal. Chem.*, **59**, 1409 (1976).

(3) G. A. Neville, F. B. Hasan, and I. C. P. Smith, *J. Pharm. Sci.*, **66**, 638 (1977).

(4) A. Noordam, K. Waliszewski, C. Olieman, L. Maat, and H. C. Beyerman, *J. Chromatogr.*, **153**, 271 (1978).

(5) "The United States Pharmacopeia," 19th rev., Mack Publishing Co., Easton, Pa., 1975, pp. 384–386.

(6) H. K. Muller, O. Hockwin, and O. Kleifeld, *Graefes Arch. Ophthalmol.*, **162**, 107 (1960).

(7) W. F. Bayne, L. C. Chu, and F. T. Tao, *J. Pharm. Sci.*, **65**, 1724 (1976).

(8) S. W. Dziedzic, S. E. Gitlow, and D. L. Krohn, *ibid.*, **65**, 1262 (1976).

(9) F. I. DeGraw, J. S. Engstrom, and E. Willis, *ibid.*, **64**, 1700 (1975).

ACKNOWLEDGMENTS

Supported in part by National Eye Institute Grants EY-01786 and EY-02706 and by a Basil O'Connor starter research grant from the National Foundation–March of Dimes to J. J. O'Donnell.

Synthesis of 1-Aryl-3-formyl-3-methyltriazenes, Potential Metabolites of 1-Aryl-3,3-dimethyltriazenes

LUCIA LASSIANI *, **CARLO NISI** *x, **FABIO SIGON** *, **GIANNI SAVA** ‡, **and TULLIO GIRALDI** ‡

Received January 9, 1980, from the *Istituto di Chimica Farmaceutica and the ‡Istituto di Farmacologia, Università di Trieste, 34127, Trieste, Italy. Accepted for publication March 20, 1980.

Abstract □ Some *para*-substituted 1-aryl-3,3-dimethyltriazenes were oxidized with *tert*-butyl hydroperoxide in the presence of vanadium pentoxide as a catalyst. Under these conditions, the corresponding 1-aryl-3-formyl-3-methyltriazenes, 1-aryl-3-*tert*-butylperoxymethyl-3-methyltriazenes, and *p*-nitrobenzenes were obtained. The 1-aryl-3-formyl-3-methyltriazenes might play a role in the metabolic oxidation of the 1-aryl-3,3-dimethyltriazenes, which are active as mutagenic, carcinogenic, and antitumor agents.

Keyphrases □ 1-Aryl-3-formyl-3-methyltriazenes—synthesis as potential metabolites of 1-aryl-3,3-dimethyltriazenes □ Antitumor agents—1-aryl-3,3-dimethyltriazenes, synthesis of 1-aryl-3-formyl-3-methyltriazenes as potential metabolites □ Metabolites, potential—1-aryl-3-formyl-3-methyltriazenes, synthesis as oxidation products of 1-aryl-3,3-dimethyltriazenes

Dimethyltriazenes have been reported to cause mutagenic (1), carcinogenic (2), and antineoplastic (3) effects, and their mechanism of action has been investigated. Their local carcinogenic effects have been attributed to aryldiazonium cations generated by hydrolysis (4), whereas their antitumor and systemic carcinogenic effects have been attributed to the methylation of cellular components by monomethyltriazenes (5) produced by microsomal oxidative *N*-demethylation (4, 6).

BACKGROUND

However, it is possible that some biological effects observed for dimethyltriazenes are due to other metabolites formed by oxidation of the nitrogen atoms or methyl groups in the triazene moiety. The *N*-hydroxymethyltriazenes suggested as intermediates in the microsomal *N*-demethylation of dimethyltriazenes (6) recently were synthesized (7) and isolated as metabolites (8). Therefore, it seemed interesting to attempt the chemical oxidation of dimethylaryltriazenes because of the potential of the resulting compounds as possible metabolites or as antitumor agents themselves.

The possibility of performing the oxidation without the destructive reactions reported using Udenfried's system (9) was investigated. Of the several attempts using hydrogen peroxide, oxygen, *m*-chloroperoxybenzoic acid, and *tert*-butyl hydroperoxide in the presence of molybdenum dioxyacetylacetonate (10) or vanadium pentoxide, only the latter combination of oxidizing agent and catalyst was successful and gave satisfactory yields. In this way, the *N*-formyl derivatives (I*a*–I*d*), peroxides (II*a*–II*d*), and *p*-nitrobenzenes resulting from the oxidative breakdown of the triazene function were obtained.

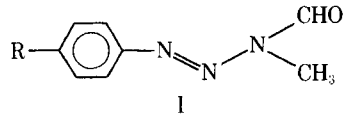

I

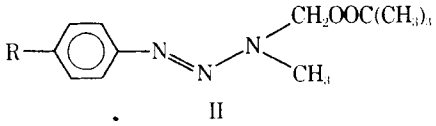

II

I*a* and II*a*: R = NO_2
I*b* and II*b*: R = Cl
I*c* and II*c*: R = Br
I*d* and II*d*: R = I

The reported structures were assigned on the basis of elemental analyses as well as NMR, IR, and mass spectral data. For I*a*–I*d*, the presence of a formyl group and a single methyl group was indicated by a singlet at δ ~9.30 for one proton and a singlet at δ ~5.40 for three protons, respectively. Furthermore, a strong band at ~1700 cm^{-1}, attributable to C=O stretching, was observed in the IR spectra. For II*a*–II*d*, the NMR spectra showed the presence of a singlet for nine protons at δ ~1.25, a singlet for three protons at δ ~3.30, and a singlet for two protons at δ ~5.50. Further investigation is in progress to evaluate the antitumor effect of these formyltriazenes and their possible role in the metabolism of dimethyltriazenes.

EXPERIMENTAL[1]

General Procedure—A 3,3-dimethyl-1-aryltriazene (5 mmoles) and vanadium pentoxide (50 mg) were suspended in 25 ml of benzene, and 6 ml of 80% *tert*-butyl hydroperoxide (47 mmoles) was added dropwise with stirring. The temperature was raised to 45°, and stirring was maintained for 26–30 hr, or for 50 hr for I*d* and II*d*, to ensure complete disappearance of the starting triazene. The starting material was detected by TLC on silica gel plates developed with 5% hexane in benzene (v/v) or 30% ethyl acetate in hexane for II*b*. The reaction mixture was filtered, and the filtrate was evaporated under reduced pressure.

Compounds I*a* and II*a*—The residue dissolved in 2 ml of acetone was chromatographed on silica gel. The elution with 1% acetone in benzene (v/v) afforded three fractions detected by TLC. The first fraction, which contained only 1,4-dinitrobenzene, was discarded. The second fraction, after evaporation of the solvent under reduced pressure, gave 30 mg of II*a*. The third fraction, which contained a mixture of I*a* and II*a*, was chromatographed again, after evaporation, on silica gel with ethyl acetate in hexane (1:2 v/v) as the eluent.

The first fraction yielded 350 mg of 1-(4-nitrophenyl)-3-*tert*-butylperoxymethyl-3-methyltriazene (II*a*), mp 86°, after crystallization from hexane; UV: 345 nm; NMR: δ 1.24 (s, 9H), 3.32 (s, 3H), 5.48 (s, 2H), and 7.45–8.35 (m, 4H); mass spectrum: *m/e* 282 (M).

Anal.—Calc. for $C_{12}H_{18}N_4O_4$: C, 51.05; H, 6.42; N, 19.84. Found: C, 51.08; H, 6.40; N, 19.81.

The second fraction, after evaporation, yielded 200 mg of 1-(4-nitrophenyl)-3-formyl-3-methyltriazene (I*a*) after crystallization from methanol, mp 117–119°; UV: 215 and 302 nm; IR: 1700–1720 (C=O) cm^{-1}; NMR: δ 3.44 (s, 3H), 7.73–8.44 (m, 4H), and 9.35 (s, 1H); mass spectrum: *m/e* 208 (M).

Anal.—Calc. for $C_8H_8N_4O_3$: C, 46.15; H, 3.87; N, 26.91. Found: C, 46.03; H, 3.85; N, 26.95.

Compounds I*b* and II*b*—To obtain I*b*, the residue was dissolved in 2 ml of benzene and chromatographed on silica gel. Elution with 5% hexane in benzene (v/v) afforded three fractions detected by TLC. The first fraction, which contained *p*-chloronitrobenzene, was discarded. The second fraction contained II*b*, and the third fraction, after evaporation under reduced pressure, gave 150 mg of 1-(4-chlorophenyl)-3-formyl-3-methyltriazene (I*b*) as a crystalline residue, mp 89°, after crystallization twice from methanol; UV: 223 and 283 nm; IR: 1733 (C=O) cm^{-1}; NMR: δ 3.36 (s, 3H), 7.28–7.72 (m, 4H), and 9.26 (s, 1H).

Anal.—Calc. for $C_8H_8ClN_3O$: C, 48.62; H, 4.08; N, 21.26. Found: C, 48.65; H, 4.11; N, 21.28.

[1] Melting points were determined in open glass capillaries using a Büchi apparatus and are uncorrected. IR spectra were obtained as potassium bromide disks with a Perkin-Elmer model 225 spectrometer. UV spectra of methanol solutions were determined on a Hitachi Perkin-Elmer model 124 spectrometer. NMR spectra were recorded on a Perkin-Elmer R12B spectrometer, in deuterochloroform, with tetramethylsilane as the internal standard. Mass spectra were recorded on a Hitachi Perkin-Elmer RMU-6L spectrometer. Silica gel (Merck) of 230–240 mesh activated 5 hr at 200° and HF (254 + 366) were used for column chromatography and TLC, respectively.

0022-3549/80/0900-1098$01.00/0
© 1980, American Pharmaceutical Association

To obtain IIb, the residue dissolved in 2 ml of benzene was chromatographed on silica gel. The elution with hexane–ether (7:1 v/v) afforded a first fraction containing a mixture of *p*-chloronitrobenzene and IIb. The second fraction was evaporated under reduced pressure. The residue, after crystallization from hexane chilled in a dry ice–acetone bath to avoid losses, gave 150 mg of 1-(4-chlorophenyl)-3-*tert*-butylperoxymethyl-3-methyltriazene (IIb), mp 44.5°; UV (ethanol): 218, 222, and 282 nm; NMR: δ 1.23 (s, 9H), 3.30 (s, 3H), 5.52 (s, 2H), and 7.35–7.43 (m, 4H).

Anal.—Calc. for $C_{12}H_{18}ClN_3O_2$: C, 53.04; H, 6.68; N, 15.46. Found: C, 53.03; H, 6.64; N, 15.50.

Compounds Ic and IIc—The residue dissolved in 2 ml of benzene was chromatographed on silica gel. Three fractions resulted from elution with 5% hexane in benzene (v/v). The first fraction was *p*-bromonitrobenzene. The second fraction, after evaporation of the solvent under reduced pressure, gave 200 mg of 1-(4-bromophenyl)-3-*tert*-butylperoxymethyl-3-methyltriazene (IIc), mp 54°; UV: 218, 222, and 281 nm.

Anal.—Calc. for $C_{12}H_{18}BrN_3O_2$: C, 45.58; H, 5.74; N, 13.29. Found: C, 45.80; H, 5.84; N, 13.10.

The third fraction gave 200 mg of 1-(4-bromophenyl)-3-formyl-3-methyltriazene (Ic), mp 102–104°, after crystallization from methanol and from hexane; UV: 224 and 284 nm; IR: 1733 (C=O) cm^{-1}; NMR: δ 3.37 (s, 3H), 7.55 (m, 4H), and 9.24 (s, 1H).

Anal.—Calc. for $C_8H_8BrN_3O$: C, 39.69; H, 3.33; N, 17.36. Found: C, 39.63; H, 3.30; N, 17.30.

Compounds Id and IId—The residue was suspended in 2 ml of methanol and filtered. The filtrate was chromatographed on silica gel, and elution with 5% hexane in benzene gave three fractions. The first fraction, which contained *p*-iodonitrobenzene, was discarded. The second fraction, after evaporation of the solvent, gave 250 mg of 1-(4-iodophenyl)-3-*tert*-butylperoxymethyl-3-methyltriazene (IId), mp 56°; UV: 224 and 284 nm.

Anal.—Calc. for $C_{12}H_{18}IN_3O_2$: C, 39.68; H, 4.99; N, 11.57. Found: C, 39.80; H, 4.93; N, 11.30.

The third fraction gave 50 mg of 1-(4-iodophenyl)-3-formyl-3-methyltriazene (Id), mp 123–124°, after crystallization from methanol; UV: 230 and 293 nm; IR: 1700 (C=O) cm^{-1}; NMR: δ 3.38 (s, 3H), 7.25–7.95 (m, 4H), and 9.30 (s, 1H).

Anal.—Calc. for $C_8H_8IN_3O$: C, 33.24; H, 2.79; N, 14.54. Found: C, 33.23; H, 2.69; N, 14.45.

REFERENCES

(1) C. Malaveille, G. F. Kolar, and H. Bartsch, *Mutation Res.*, **36**, 1 (1976).

(2) R. Preussmann, S. Ivankovic, C. Landschutz, J. Gimmy, E. Flohr, and U. Griesbach, *Z. Krebforsch.*, **81**, 285 (1974).

(3) T. A. Connors, P. M. Goddard, K. Merai, W. C. J. Ross, and D. E. V. Wilman, *Biochem. Pharmacol.*, **25**, 241 (1976).

(4) G. F. Kolar and R. Preussmann, *Z. Naturforsch.*, **26**, 950 (1971).

(5) P. Kleihues, G. F. Kolar, and G. F. Margison, *Cancer Res.*, **36**, 2189 (1976).

(6) G. F. Kolar, "Advances in Antimicrobial and Antineoplastic Chemotherapy," Proceedings of the 7th International Congress of Chemotherapy, Prague, 1971, vol. II, Urban and Schwarzenberg, Munich, West Germany, 1972, p. 121.

(7) A. Gescher, J. A. Hickman, R. J. Simmonds, M. F. G. Stevens, and K. Vaughan, *Tetrahedron Lett.*, **50**, 5041 (1978).

(8) G. F. Kolar and R. Carubelli, *Cancer Lett.*, **7**, 209 (1979).

(9) V. Zvěřina, J. Diviš, J. Marhold, and M. Matrka, *Collect. Czech. Chem. Commun.*, **36**, 1598 (1971).

(10) W. C. Cornelius, K. Terada, and B. E. Bryant, *Inorg. Synth.*, **6**, 147 (1960).

ACKNOWLEDGMENTS

The authors thank Dr. A. Bigotto, Istituto di Chimica Fisica, Università di Trieste, for advice in the examination of IR spectra and Mr. Paolo D'Errico for elemental analyses and technical assistance.

Stability of Solid Drugs: Degradation of Ergocalciferol (Vitamin D_2) and Cholecalciferol (Vitamin D_3) at High Humidities and Elevated Temperatures

L. T. GRADY and K. D. THAKKER ˣ

Received November 1, 1979, from the *United States Pharmacopeia, Rockville, MD 20852.* Accepted for publication March 17, 1980.

Abstract □ Ergocalciferol and cholecalciferol powders were studied at 25 and 40° and at different humidities. Ergocalciferol decomposed rapidly at 25 and 40° when stored in dry air. Decomposition of ergocalciferol led to the formation of products of higher polarity. Cholecalciferol was not as labile under dry conditions, but decomposed rapidly at high temperature.

Keyphrases □ Vitamin D—ergocalciferol (vitamin D_2) and cholecalciferol (vitamin D_3), effects of temperature and humidity on decomposition □ Stability—ergocalciferol (vitamin D_2) and cholecalciferol (vitamin D_3), effects of humidity and temperature □ Ergocalciferol—stability, effects of temperature and humidity □ Cholecalciferol—stability, effects of temperature and humidity

Ergocalciferol and cholecalciferol are fat-soluble vitamins essential for their antirachitic activity. The adverse effects of light, air, and temperature on solutions of these 9,10-secosterols are well documented (1–4).

Previous studies on the solid-state decomposition of ergocalciferol (initially a white, crystalline powder) showed the formation of a yellow powder having a lowered melting point (5). These observations also were made in this laboratory. GLC analysis of ergocalciferol and cholecalciferol resulted in the decomposition of the parent product, with the formation of two peaks (6). These two peaks were identified as pyro- and isopyro vitamin D[1], formed as a result of thermal cyclization of vitamin D (6). The decomposition of ergocalciferol in powder preparations was reported to depend directly on the surface acidity of the excipients and their ability to adsorb moisture (7).

These studies on the decomposition of vitamin D are valuable but do not predict its stability under normal storage conditions. A labile reference material such as vitamin D must be stored at optimum conditions. Therefore, to determine these conditions, the effects of temperature and humidity on the stability of ergocalciferol and cholecalciferol in the absence of light were investigated.

[1] Vitamin D refers to vitamins D_2 and D_3.

0022-3549/80/0900-1099$01.00/0

© 1980, American Pharmaceutical Association

To obtain IIb, the residue dissolved in 2 ml of benzene was chromatographed on silica gel. The elution with hexane–ether (7:1 v/v) afforded a first fraction containing a mixture of *p*-chloronitrobenzene and IIb. The second fraction was evaporated under reduced pressure. The residue, after crystallization from hexane chilled in a dry ice–acetone bath to avoid losses, gave 150 mg of 1-(4-chlorophenyl)-3-*tert*-butylperoxymethyl-3-methyltriazene (IIb), mp 44.5°; UV (ethanol): 218, 222, and 282 nm; NMR: δ 1.23 (s, 9H), 3.30 (s, 3H), 5.52 (s, 2H), and 7.35–7.43 (m, 4H).

Anal.—Calc. for $C_{12}H_{18}ClN_3O_2$: C, 53.04; H, 6.68; N, 15.46. Found: C, 53.03; H, 6.64; N, 15.50.

Compounds Ic and IIc—The residue dissolved in 2 ml of benzene was chromatographed on silica gel. Three fractions resulted from elution with 5% hexane in benzene (v/v). The first fraction was *p*-bromonitrobenzene. The second fraction, after evaporation of the solvent under reduced pressure, gave 200 mg of 1-(4-bromophenyl)-3-*tert*-butylperoxymethyl-3-methyltriazene (IIc), mp 54°; UV: 218, 222, and 281 nm.

Anal.—Calc. for $C_{12}H_{18}BrN_3O_2$: C, 45.58; H, 5.74; N, 13.29. Found: C, 45.80; H, 5.84; N, 13.10.

The third fraction gave 200 mg of 1-(4-bromophenyl)-3-formyl-3-methyltriazene (Ic), mp 102–104°, after crystallization from methanol and from hexane; UV: 224 and 284 nm; IR: 1733 (C=O) cm^{-1}; NMR: δ 3.37 (s, 3H), 7.55 (m, 4H), and 9.24 (s, 1H).

Anal.—Calc. for $C_8H_8BrN_3O$: C, 39.69; H, 3.33; N, 17.36. Found: C, 39.63; H, 3.30; N, 17.30.

Compounds Id and IId—The residue was suspended in 2 ml of methanol and filtered. The filtrate was chromatographed on silica gel, and elution with 5% hexane in benzene gave three fractions. The first fraction, which contained *p*-iodonitrobenzene, was discarded. The second fraction, after evaporation of the solvent, gave 250 mg of 1-(4-iodophenyl)-3-*tert*-butylperoxymethyl-3-methyltriazene (IId), mp 56°; UV: 224 and 284 nm.

Anal.—Calc. for $C_{12}H_{18}IN_3O_2$: C, 39.68; H, 4.99; N, 11.57. Found: C, 39.80; H, 4.93; N, 11.30.

The third fraction gave 50 mg of 1-(4-iodophenyl)-3-formyl-3-methyltriazene (Id), mp 123–124°, after crystallization from methanol; UV: 230 and 293 nm; IR: 1700 (C=O) cm^{-1}; NMR: δ 3.38 (s, 3H), 7.25–7.95 (m, 4H), and 9.30 (s, 1H).

Anal.—Calc. for $C_8H_8IN_3O$: C, 33.24; H, 2.79; N, 14.54. Found: C, 33.23; H, 2.69; N, 14.45.

REFERENCES

(1) C. Malaveille, G. F. Kolar, and H. Bartsch, *Mutation Res.*, **36**, 1 (1976).

(2) R. Preussmann, S. Ivankovic, C. Landschutz, J. Gimmy, E. Flohr, and U. Griesbach, *Z. Krebforsch.*, **81**, 285 (1974).

(3) T. A. Connors, P. M. Goddard, K. Merai, W. C. J. Ross, and D. E. V. Wilman, *Biochem. Pharmacol.*, **25**, 241 (1976).

(4) G. F. Kolar and R. Preussmann, *Z. Naturforsch.*, **26**, 950 (1971).

(5) P. Kleihues, G. F. Kolar, and G. F. Margison, *Cancer Res.*, **36**, 2189 (1976).

(6) G. F. Kolar, "Advances in Antimicrobial and Antineoplastic Chemotherapy," Proceedings of the 7th International Congress of Chemotherapy, Prague, 1971, vol. II, Urban and Schwarzenberg, Munich, West Germany, 1972, p. 121.

(7) A. Gescher, J. A. Hickman, R. J. Simmonds, M. F. G. Stevens, and K. Vaughan, *Tetrahedron Lett.*, **50**, 5041 (1978).

(8) G. F. Kolar and R. Carubelli, *Cancer Lett.*, **7**, 209 (1979).

(9) V. Zvěřina, J. Diviš, J. Marhold, and M. Matrka, *Collect. Czech. Chem. Commun.*, **36**, 1598 (1971).

(10) W. C. Cornelius, K. Terada, and B. E. Bryant, *Inorg. Synth.*, **6**, 147 (1960).

ACKNOWLEDGMENTS

The authors thank Dr. A. Bigotto, Istituto di Chimica Fisica, Università di Trieste, for advice in the examination of IR spectra and Mr. Paolo D'Errico for elemental analyses and technical assistance.

Stability of Solid Drugs: Degradation of Ergocalciferol (Vitamin D_2) and Cholecalciferol (Vitamin D_3) at High Humidities and Elevated Temperatures

L. T. GRADY and K. D. THAKKER ˣ

Received November 1, 1979, from the *United States Pharmacopeia, Rockville, MD 20852.* Accepted for publication March 17, 1980.

Abstract □ Ergocalciferol and cholecalciferol powders were studied at 25 and 40° and at different humidities. Ergocalciferol decomposed rapidly at 25 and 40° when stored in dry air. Decomposition of ergocalciferol led to the formation of products of higher polarity. Cholecalciferol was not as labile under dry conditions, but decomposed rapidly at high temperature.

Keyphrases □ Vitamin D—ergocalciferol (vitamin D_2) and cholecalciferol (vitamin D_3), effects of temperature and humidity on decomposition □ Stability—ergocalciferol (vitamin D_2) and cholecalciferol (vitamin D_3), effects of humidity and temperature □ Ergocalciferol—stability, effects of temperature and humidity □ Cholecalciferol—stability, effects of temperature and humidity

Ergocalciferol and cholecalciferol are fat-soluble vitamins essential for their antirachitic activity. The adverse effects of light, air, and temperature on solutions of these 9,10-secosterols are well documented (1–4).

Previous studies on the solid-state decomposition of ergocalciferol (initially a white, crystalline powder) showed the formation of a yellow powder having a lowered melting point (5). These observations also were made in this laboratory. GLC analysis of ergocalciferol and cholecalciferol resulted in the decomposition of the parent product, with the formation of two peaks (6). These two peaks were identified as pyro- and isopyro vitamin D[1], formed as a result of thermal cyclization of vitamin D (6). The decomposition of ergocalciferol in powder preparations was reported to depend directly on the surface acidity of the excipients and their ability to adsorb moisture (7).

These studies on the decomposition of vitamin D are valuable but do not predict its stability under normal storage conditions. A labile reference material such as vitamin D must be stored at optimum conditions. Therefore, to determine these conditions, the effects of temperature and humidity on the stability of ergocalciferol and cholecalciferol in the absence of light were investigated.

[1] Vitamin D refers to vitamins D_2 and D_3.

0022-3549/80/0900-1099$01.00/0

© 1980, American Pharmaceutical Association

Table I—Degradation of Ergocalciferol and Cholecalciferol at 25°

Days	Ergocalciferol Remaining[a,b], %			Cholecalciferol Remaining[a,b], %		
	In a Desiccator	85% RH	Anaerobic	In a Desiccator	85% RH	Anaerobic
1	101, 106	101, 101	100			99
7	99, 97	99, 100		99, 96	99, 96	
15	88, 89, 88, 87	97, 96	100, 98	100, 100	99, 100	101, 103
25	71, 72	100, 100	98	100, 101, 100	91, 90	99, 100
56	3, 5, 4, 2	79, 77	101, 100	99, 99	86, 89	101, 103

[a] Samples always were stored in the dark. [b] Individual values are individual assays of separate weighings, and each is based on an average of at least two injections. When more than two values appear in a single block, they were obtained at 6-month intervals as a check of reproducibility.

Table II—Degradation of Ergocalciferol and Cholecalciferol at 40°

Days	Ergocalciferol Remaining[a,b], %		Cholecalciferol Remaining, %	
	85% RH	45% RH	85% RH	45% RH
0.66	100, 97, 98	99, 99	80, 79	85, 82
1	99, 99, 98	96, 97, 97	65, 63	75, 79
3	91, 94	91, 91	49, 47	69, 68
7	89, 86, 85	20, 19	20, 15, 16	62, 69
10	78, 78, 78, 79	—[c]	7, 10, 9	
14	51, 52			
21	35, 33, 31	—[c]	3, 3	4, 3

[a,b] Same as in Table I. [c] Not detectable.

EXPERIMENTAL

Reagents—Ergocalciferol and cholecalciferol USP[2] were used as received. Hexane[3] and 1-pentanol[4] were high-pressure liquid chromatographic (HPLC) grade.

Controlled-Temperature and Humidity Microenvironments—Commercial constant-humidity ovens[5] were used to achieve 40° with 85% relative humidity (RH) and 40° with 45% RH. For all of the other controlled-temperature–humidity microenvironments, saturated salt solution systems (8) were used to achieve constant humidity in a thermostatically regulated room (25 ± 1°).

A glove box[6] was used to achieve dry, anaerobic conditions as follows. It first was allowed to equilibrate to very low humidity by placing flat dishes of silica gel in it for 2 days. The dry air then was evacuated, and dry nitrogen was flushed throughout the glove box; this evacuation–flushing cycle was repeated twice. While the glove box was used, dry nitrogen was bled into it continuously at a low rate to ensure an anaerobic environment above the samples.

Sample Assay—The assay to determine the percentage of vitamin D remaining in the preweighed samples after storage at specified time intervals was based on the method described by deVries *et al.* (9). The gradient elution high-pressure liquid chromatograph[7] was equipped with a variable-wavelength UV detector[8], a recorder[9], and an integrator[10]. A commercial liquid chromatographic column[11] packed with microporous silica was the stationary phase. A mixture of 1-pentanol and dry hexane (9) was the mobile phase. The concentration of 1-pentanol in hexane was varied (0.05–0.1% v/v) when necessary to meet the system suitability test.

System Suitability Test—A mixture of cholecalciferol and its known isomers, *e.g.*, precholecalciferol lumisterol, isotachysterol, tachysterol, and 7-dehydrocholesterol, was available from samples left from a previous collaborative study (9). This mixture was injected onto the HPLC column. The resolution, R, between cholecalciferol and tachysterol and the resolution between precholecalciferol and *trans*-cholecalciferol were determined by:

$$R = 2D/B + C \qquad \text{(Eq. 1)}$$

where D is the distance between the peak maxima and B and C are the peak widths of the two peaks.

The system conditions were adjusted to obtain $R > 1.0$ for cholecalciferol–tachysterol peaks and $R > 0.8$ for precholecalciferol–*trans*-cholecalciferol peaks. Under these conditions, separation of all isomers listed was possible; their elution order remained fixed so that the peaks could be identified by comparison with reported chromatograms (9).

Procedure—About 1–2 mg of ergocalciferol or cholecalciferol was weighed on an electronic balance[12] as quickly as possible and transferred to a disposable, aluminum weighing boat. Weighings were done in subdued light only. The samples were introduced immediately into the various controlled-temperature–humidity microenvironments. At the designated time intervals, the samples were removed from the microenvironments, dissolved promptly in the mobile phase, and transferred to a 10-ml volumetric flask. The sample dish was washed successively with small volumes of the mobile phase to ensure quantitative transfer. After the volume was adjusted to 10 ml, ~10 μl was injected onto the chromatographic column with a loop injector[13].

Standard Solution—About 1–2 mg of ergocalciferol USP or cholecalciferol USP, accurately weighed, was transferred to a 10-ml volumetric flask and dissolved in the mobile phase. After the volume was adjusted to 10.0 ml, 10 μl of the resulting solution was injected into the HPLC column[11] with a loop injector[13]. The standard solution was prepared fresh daily and was injected at least three times for each assay.

Calculations—The integrator counts for the peak due to ergocalciferol or cholecalciferol (duplicate injections) were compared with the area counts obtained for the peak due to ergocalciferol USP or cholecalciferol USP in the standard solution, and the percentage of ergocalciferol or cholecalciferol remaining in the samples was calculated with a correction applied for the weights of the powders.

Other Tests—Reversed-phase HPLC separation of ergocalciferol and its decomposition products also was performed. The same liquid chromatograph[7] was used as in the assay of decomposed samples. The stationary phase consisted of octadecylsilane chemically bonded to microporous silica[14], and the mobile phase was methanol–acetonitrile (50:50 v/v).

TLC also was used to separate ergocalciferol and the decomposition products. The following four systems were used on silica gel[3] plates: 1, cyclohexane–ether (1:1 v/v); 2, chloroform; 3, chloroform–ether–methanol (4:4:2 v/v/v); and 4, toluene–hexane–ether (2:2:1 v/v/v). All solvents were chromatographic grade[4].

RESULTS

Table I shows the stability of ergocalciferol and cholecalciferol at room temperature for 56 days. In general, ergocalciferol was more labile at room temperature in the presence of a desiccant. After 21 days, samples stored in dry air (in a desiccator) had only ~66% remaining; those stored under very moist air (85% RH) or anaerobic (dry) conditions (dry nitrogen box) had >95% remaining. On the other hand, cholecalciferol was more stable

[2] Provided by Philips-Duphar, Weesp, The Netherlands.
[3] E. Merck, Darmstadt, West Germany.
[4] Fisher Scientific Co., Fair Lawn, N.J.
[5] Blue-M Electric Co., Blue Island, Ill.
[6] Lab-Con-Co., Kansas City, Mo.
[7] Varian Associates, Palo Alto, Calif.
[8] Gilson Medical Electronics, Middleton, Wis.
[9] Linear Instruments, Irvine, Calif.
[10] Spectra-Physics, Santa Clara, Calif.
[11] Zorbaxsil, Dupont Instruments, Wilmington, Del.
[12] Mettler Instruments Corp., Princeton, N.J.
[13] Valco Instruments, Houston, Tex.
[14] Micropak MCH-10, Varian Associates, Palo Alto, Calif.

Table III—Degradation of Ergocalciferol and Cholecalciferol on Different Container Surfaces

Container	Isomer Remaining after 7 Days at 40° and 45% RH, %	
	Ergocalciferol	Cholecalciferol
Aluminum weighing boats	16, 17	69, 62
Glass weighing dishes	19, 20	69, 69
Polystyrene weighing boats (disposable)	38, 35	66, 72
High-density polyethylene bottles	26, 30	73, 73
Polypropylene bottles (multiple-unit containers)	45	76

at room temperature. After 21 days, cholecalciferol samples stored under all three conditions had >99% remaining, indicating no degradation.

After 15 days, ergocalciferol samples that were stored in a desiccator acquired a yellow tinge, which deepened as time progressed. On thin-layer chromatograms, separation of ergocalciferol and the decomposition products was obtained in System 1, but the new spot due to the decomposition product remained at the origin. There were no extra peaks on the chromatograms of ergocalciferol (obtained during adsorption chromatography), although the samples turned distinctly yellow. However, separation of ergocalciferol and the degradation products was obtained on reversed-phase liquid chromatograms. The decomposition products from a yellowed sample of ergocalciferol eluted with the solvent front (Fig. 1).

Table II shows the stability of ergocalciferol and cholecalciferol at 40°. Both compounds were less stable at elevated temperatures. After 7 days, samples of ergocalciferol stored at 40° and 85% RH had 87% remaining; those stored at 40° and 45% RH had only 20% remaining. Both samples had turned yellow. Cholecalciferol showed the reverse trend. After 7 days, samples stored at 40° and 85% RH had 15% of the cholecalciferol remaining; those stored at 40° and 45% RH had about 65% of the cholecalciferol remaining.

Table III shows the stability of ergocalciferol and cholecalciferol (at 40° and 45% RH for 7 days) on different types of containers (surfaces) used as sample dishes. Both ergocalciferol and cholecalciferol were more stable when stored on plastic containers than when stored on glass or aluminum weighing dishes. In all cases, cholecalciferol was more stable than ergocalciferol.

DISCUSSION

Solutions of ergocalciferol and cholecalciferol undergo thermal, photochemical, and oxidative reactions that lead to a host of degradation products (1–4). Scheme I shows the known pathways of decomposition for these compounds.

Powder preparations of ergocalciferol were reported to undergo isomerization, which resulted in the formation of 5,6-*trans*-vitamin D_2 (7). Neither this isomer nor any known ergocalciferol isomer (Scheme I) was present in any decomposed sample. Since Scheme I lists reactions involving the sterol nucleus, which require considerable freedom of molecular motion, the absence of these isomers in decomposed ergocalciferol samples indicates that such freedom of molecular motion is not available to molecules of ergocalciferol for solid-state decomposition.

The effect of moisture on reactions of ergocalciferol is apparent. Moisture adsorbed on the surface of the molecules seems to inhibit the decomposition of ergocalciferol. Such inhibition by moisture adsorbed by the excipients was reported for some powder preparations of ergocalciferol (7). Furthermore, the decomposition is faster in the presence of air since oxygen is required. In short, it can be inferred that the solid-state decomposition reactions of ergocalciferol in the absence of light is of a dry, oxidative type.

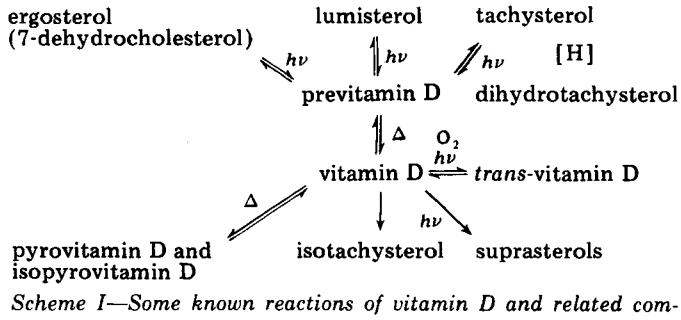

Scheme I—Some known reactions of vitamin D and related compounds

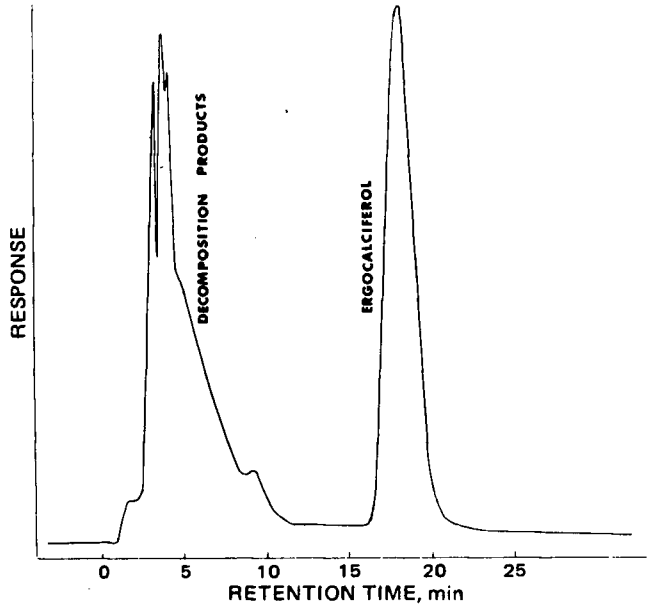

Figure 1—*Chromatogram of a partially decomposed, yellowed sample of ergocalciferol on Micropak MCH-10. The mobile phase was methanol–acetonitrile (50:50 v/v).*

The decomposition reactions of cholecalciferol apparently differ from these of ergocalciferol (Tables I–III). Cholecalciferol was more stable than ergocalciferol under all but one condition. The sharp decomposition of ergocalciferol in a dry aerobic atmosphere was not seen with cholecalciferol. Decomposition of cholecalciferol was a little faster at the more humid of the two conditions at 40°. This finding was the exact opposite of the behavior seen for ergocalciferol.

Since the only structural difference between the two molecules is in the side chain, the solid-state decomposition reactions of both compounds must involve the side chain only. This observation also is consistent with the observation that no known isomers involving reactions of the sterol nucleus are found. If the sterol nucleus were to take part in the solid-state decomposition of ergocalciferol and cholecalciferol, such differences as were obtained on decomposition of these two compounds (Table II) would not have been obtained. A double bond in the side chain of ergocalciferol must make it a substrate for attack by oxygen. Since the solid-state reactions must occur with little freedom of movement, the decomposition reactions of ergocalciferol (involving the double bond of the side chain and oxygen) may occur *via* a free radical pathway. Free radical reactions can be accomplished in the solid state and may be effected more readily by the presence of molecules with high dipole moment. Cholecalciferol is stable at room temperature but is quite labile at 40°; thus, the decomposition reaction of cholecalciferol seems to have a low activation energy.

The nature of the decomposition products of ergocalciferol or cholecalciferol is not known, and their chromatographic behavior is puzzling. Normal-phase liquid chromatography and TLC revealed that the decomposition products bound strongly to the silica supports. Reversed-phase liquid chromatography of the same decomposition products revealed that they had a highly polar nature as seen by their fairly high solubility in methanol. These observations cannot be clarified further until more information is gathered to allow proposal of a mechanism for decomposition reactions of ergocalciferol and cholecalciferol.

REFERENCES

(1) T. Kanzawa and S. Kotaku, *J. Pharm. Soc. Jpn.*, **73**, 1357 (1953).

(2) K. S. Keuning, *Pharm. Weekbl.*, **100**, 889 (1965).

(3) L. Velluz, G. Amiard, and A. Petit, *Bull. Soc. Chim. Fr.*, **1949**, 501.

(4) K. H. Hanewald, M. P. Rappoldt, and J. R. Ruborgh, *Recueil*, **80**,

1003 (1961).
(5) S. R. Byrn, *J. Pharm. Sci.*, **65**, 16 (1976).
(6) P. P. Nair and S. deLeon, *Arch. Biochem. Biophys.*, **128**, 663 (1968).
(7) T. Takahashi and R. Yamamoto, *Yakagaku Zasshi*, **89**, 909 (1969).
(8) "Handbook of Chemistry and Physics," 53rd ed., Chemical Rubber Co., Cleveland, Ohio, 1972–1973, p. E-40.
(9) E. J. deVries, J. Zeeman, R. J. E. Esser, B. Borsje, and F. J. Mulder, *J. Assoc. Off. Anal. Chem.*, **62**, 129 (1979).

Synthesis and Antidepressant Activity of 5-(4-Dimethylaminobenzyl)imidazolidine-2,4-dione

F. L. WESSELS ˣ, T. J. SCHWAN, and S. F. PONG

Received November 21, 1979, from the *Scientific Affairs Department, Norwich-Eaton Pharmaceuticals, Division of Morton-Norwich Products, Inc., Norwich, NY 13815.* Accepted for publication March 24, 1980.

Abstract □ 5-(4-Dimethylaminobenzyl)imidazolidine-2,4-dione was prepared by catalytic hydrogenation of the corresponding benzylidene compound. Antidepressant testing in mice indicated that its ED_{50} values for antagonism of tetrabenazine-induced ptosis and potentiation of levodopa-induced behavioral changes were 42 and 17 mg/kg po, respectively. *In vitro* neurochemical studies demonstrated that this compound did not inhibit the uptake of selected biogenic amines into crude synaptosomes of mouse whole brain, and it did not have significant monoamine oxidase inhibitory activity *in vivo* and *in vitro*. Thus, this compound possesses potential antidepressant activity with a mechanism different from that of the tricyclic antidepressants and monoamine oxidase inhibitors.

Keyphrases □ 5-(4-Dimethylaminobenzyl)imidazolidine-2,4-dione—synthesis and testing for antidepressant activity □ Antidepressant activity—5-(4-dimethylaminobenzyl)imidazolidine-2,4-dione, *in vitro* and *in vivo* testing

The tricyclic antidepressant drugs are the most useful drugs for the treatment of depression. However, these drugs are not effective in all patients and are not without compromising side effects (1, 2). Monoamine oxidase inhibitors also are effective antidepressants; however, because of their propensity to cause hypertensive crisis, they now have limited use in the treatment of depression (3).

As part of a program directed at the discovery and development of novel agents affecting the central nervous system (CNS), 5-(4-dimethylaminobenzyl)imidazolidine-2,4-dione (I) was synthesized as a chemical intermediate and unexpectedly demonstrated antidepressant activity in selected experimental models (4). This paper presents the synthesis and results of pharmacological testing of this compound.

EXPERIMENTAL[1]

Synthesis of 5-(4-Dimethylaminobenzyl)imidazolidine-2,4-dione (I)—A mixture of 69.3 g (0.30 mole) of 5-(4-dimethylaminobenzylidene)imidazolidine-2,4-dione (IV) (5), 600 ml of 1 *N* KOH, and 15 g of wet No. 28 Raney nickel catalyst was shaken with hydrogen at 3–4 atm for 28 hr until the theoretical quantity was consumed. The catalyst was washed with two 100-ml portions of 1 *N* KOH, and the filtrate and combined washings were acidified with acetic acid to give the crude product (60 g). Recrystallization from methanol gave 35 g (50%) of I, mp 180–186°; IR: 3.10, 3.21 (NH), 5.66, 5.90 (C=O), and 6.20 (C=C) μm; NMR (dimethyl sulfoxide-d_6): δ 2.75–2.85 [m, 8, $(CH_3)_2N$ and aryl CH_2], 4.20 (t, 1, CH_2CHNH), 6.60, 7.01 (d, 4, J = 9 Hz, aromatic CH), 7.78 (broad exchangeable s, 1, imidazolidine 1-NH), and 11.0 (broad exchangeable m, 1, imidazolidine 3-NH).

Anal.—Calc. for $C_{12}H_{15}N_3O_2$: C, 61.78; H, 6.48; N, 18.02. Found: C, 61.79; H, 6.45; N, 18.02.

Tetrabenazine Antagonism—The method used was similar to that described by Barnett *et al.* (6). Groups of five unfasted male mice (TAC:SW/N fBr), 20–27 g, were pretreated with the test compound at 50 mg/kg po as a 0.5% suspension in 0.5% methylcellulose 4000 cps[2] or methylcellulose alone. Thirty minutes later, each animal received tetrabenazine methanesulfonate[3] (36 mg/kg ip in saline) or saline at a volume of 10 ml/kg. After an additional 30 min, the degree of palpebral narrowing was estimated as a measure of ptosis and compared to the methylcellulose and tetrabenazine control groups. The degree of ptosis was evaluated using a rating scale of 0–4, with a score of 4 representing a normal palpebral opening and scores of 3, 2, 1, and 0 representing slight, moderate, marked, and complete active closure of the palpebral opening, respectively. The percent prevention of ptosis was calculated as described by Barnett *et al.* (6).

Compound I at a dose of 50 mg/kg antagonized the effect of tetrabenazine by 50% or greater and, therefore, was evaluated further for dose-response effect as an ED_{50} value. The method described by Litchfield and Wilcoxon (7) was used for determining the ED_{50} value.

Levodopa Potentiation—The levodopa potentiation model is a reflection of increased dopaminergic activity, and the method used was that described by Everett (8). Groups of unfasted male mice [TAC:(SW)fBr] were administered pargyline[4] at a dose of 40 mg/kg po (0.4% in 0.5% methylcellulose) 4 hr prior to the administration of graded doses of test drugs or methylcellulose only. One hour after administration of the test drugs, levodopa (100 mg/kg ip, 1% in saline) was administered to all mice.

Observations of the levodopa-induced response were recorded 25 min after administration on a scale similar to that described by Everett (8). The degree of potentiation was scored as: 0 = no unusual irritability; 1 = increased alertness and responsiveness to touch; 2 = aggressive response to touch (hyperreactive); and 3 = markedly aggressive response to touch, spontaneous fighting with salivation and piloerection, or near prostrate. The percent of levodopa potentiation was calculated as described by Everett (8). The ED_{50} values were obtained using the method described by Litchfield and Wilcoxon (7).

Tryptamine Potentiation—Tedeschi *et al.* (9) hypothesized that tryptamine increases brain serotonin levels but that convulsions do not occur because the destruction of serotonin by monoamine oxidase keeps pace with its formation. The interruption of the metabolism of serotonin (*i.e.*, by monoamine oxidase inhibitors) and tryptamine will cause convulsions. The method used was similar to that described by Tedeschi *et al.* (9). Groups of 10 unfasted male mice [TAC:(SW)fBr] were administered the test compounds suspended in 0.5% methylcellulose at a dose 10 times their levodopa potentiation ED_{50} values. Four hours later, tryptamine[5] was administered at 50 mg/kg iv. The compounds were considered to potentiate tryptamine if >50% of the animals in the treated group convulsed.

[1] Melting points were determined on a Mel-Temp apparatus and are corrected. The IR spectrum was determined as a mineral oil mull using a Perkin-Elmer 137B spectrophotometer. The NMR spectrum was obtained on a Varian A-60 instrument and was compared with tetramethylsilane as the internal standard.

[2] Methocel, Dow Chemical Co.
[3] Hoffmann-La Roche.
[4] Abbott Laboratories.
[5] Aldrich Chemical Co.

0022-3549/80/0900-1102$01.00/0
© 1980, American Pharmaceutical Association

1003 (1961).
(5) S. R. Byrn, *J. Pharm. Sci.*, **65**, 16 (1976).
(6) P. P. Nair and S. deLeon, *Arch. Biochem. Biophys.*, **128**, 663 (1968).
(7) T. Takahashi and R. Yamamoto, *Yakagaku Zasshi*, **89**, 909 (1969).
(8) "Handbook of Chemistry and Physics," 53rd ed., Chemical Rubber Co., Cleveland, Ohio, 1972–1973, p. E-40.
(9) E. J. deVries, J. Zeeman, R. J. E. Esser, B. Borsje, and F. J. Mulder, *J. Assoc. Off. Anal. Chem.*, **62**, 129 (1979).

Synthesis and Antidepressant Activity of 5-(4-Dimethylaminobenzyl)imidazolidine-2,4-dione

F. L. WESSELS ˣ, T. J. SCHWAN, and S. F. PONG

Received November 21, 1979, from the *Scientific Affairs Department, Norwich-Eaton Pharmaceuticals, Division of Morton-Norwich Products, Inc., Norwich, NY 13815.* Accepted for publication March 24, 1980.

Abstract □ 5-(4-Dimethylaminobenzyl)imidazolidine-2,4-dione was prepared by catalytic hydrogenation of the corresponding benzylidene compound. Antidepressant testing in mice indicated that its ED_{50} values for antagonism of tetrabenazine-induced ptosis and potentiation of levodopa-induced behavioral changes were 42 and 17 mg/kg po, respectively. *In vitro* neurochemical studies demonstrated that this compound did not inhibit the uptake of selected biogenic amines into crude synaptosomes of mouse whole brain, and it did not have significant monoamine oxidase inhibitory activity *in vivo* and *in vitro*. Thus, this compound possesses potential antidepressant activity with a mechanism different from that of the tricyclic antidepressants and monoamine oxidase inhibitors.

Keyphrases □ 5-(4-Dimethylaminobenzyl)imidazolidine-2,4-dione—synthesis and testing for antidepressant activity □ Antidepressant activity—5-(4-dimethylaminobenzyl)imidazolidine-2,4-dione, *in vitro* and *in vivo* testing

The tricyclic antidepressant drugs are the most useful drugs for the treatment of depression. However, these drugs are not effective in all patients and are not without compromising side effects (1, 2). Monoamine oxidase inhibitors also are effective antidepressants; however, because of their propensity to cause hypertensive crisis, they now have limited use in the treatment of depression (3).

As part of a program directed at the discovery and development of novel agents affecting the central nervous system (CNS), 5-(4-dimethylaminobenzyl)imidazolidine-2,4-dione (I) was synthesized as a chemical intermediate and unexpectedly demonstrated antidepressant activity in selected experimental models (4). This paper presents the synthesis and results of pharmacological testing of this compound.

EXPERIMENTAL[1]

Synthesis of 5-(4-Dimethylaminobenzyl)imidazolidine-2,4-dione (I)—A mixture of 69.3 g (0.30 mole) of 5-(4-dimethylaminobenzylidene)imidazolidine-2,4-dione (IV) (5), 600 ml of 1 *N* KOH, and 15 g of wet No. 28 Raney nickel catalyst was shaken with hydrogen at 3–4 atm for 28 hr until the theoretical quantity was consumed. The catalyst was washed with two 100-ml portions of 1 *N* KOH, and the filtrate and combined washings were acidified with acetic acid to give the crude product (60 g). Recrystallization from methanol gave 35 g (50%) of I, mp 180–186°; IR: 3.10, 3.21 (NH), 5.66, 5.90 (C=O), and 6.20 (C=C) μm; NMR (dimethyl sulfoxide-d_6): δ 2.75–2.85 [m, 8, $(CH_3)_2N$ and aryl CH_2], 4.20 (t, 1, CH_2CHNH), 6.60, 7.01 (d, 4, J = 9 Hz, aromatic CH), 7.78 (broad exchangeable s, 1, imidazolidine 1-NH), and 11.0 (broad exchangeable m, 1, imidazolidine 3-NH).

Anal.—Calc. for $C_{12}H_{15}N_3O_2$: C, 61.78; H, 6.48; N, 18.02. Found: C, 61.79; H, 6.45; N, 18.02.

Tetrabenazine Antagonism—The method used was similar to that described by Barnett *et al.* (6). Groups of five unfasted male mice (TAC:SW/N fBr), 20–27 g, were pretreated with the test compound at 50 mg/kg po as a 0.5% suspension in 0.5% methylcellulose 4000 cps[2] or methylcellulose alone. Thirty minutes later, each animal received tetrabenazine methanesulfonate[3] (36 mg/kg ip in saline) or saline at a volume of 10 ml/kg. After an additional 30 min, the degree of palpebral narrowing was estimated as a measure of ptosis and compared to the methylcellulose and tetrabenazine control groups. The degree of ptosis was evaluated using a rating scale of 0–4, with a score of 4 representing a normal palpebral opening and scores of 3, 2, 1, and 0 representing slight, moderate, marked, and complete active closure of the palpebral opening, respectively. The percent prevention of ptosis was calculated as described by Barnett *et al.* (6).

Compound I at a dose of 50 mg/kg antagonized the effect of tetrabenazine by 50% or greater and, therefore, was evaluated further for dose-response effect as an ED_{50} value. The method described by Litchfield and Wilcoxon (7) was used for determining the ED_{50} value.

Levodopa Potentiation—The levodopa potentiation model is a reflection of increased dopaminergic activity, and the method used was that described by Everett (8). Groups of unfasted male mice [TAC:(SW)fBr] were administered pargyline[4] at a dose of 40 mg/kg po (0.4% in 0.5% methylcellulose) 4 hr prior to the administration of graded doses of test drugs or methylcellulose only. One hour after administration of the test drugs, levodopa (100 mg/kg ip, 1% in saline) was administered to all mice.

Observations of the levodopa-induced response were recorded 25 min after administration on a scale similar to that described by Everett (8). The degree of potentiation was scored as: 0 = no unusual irritability; 1 = increased alertness and responsiveness to touch; 2 = aggressive response to touch (hyperreactive); and 3 = markedly aggressive response to touch, spontaneous fighting with salivation and piloerection, or near prostrate. The percent of levodopa potentiation was calculated as described by Everett (8). The ED_{50} values were obtained using the method described by Litchfield and Wilcoxon (7).

Tryptamine Potentiation—Tedeschi *et al.* (9) hypothesized that tryptamine increases brain serotonin levels but that convulsions do not occur because the destruction of serotonin by monoamine oxidase keeps pace with its formation. The interruption of the metabolism of serotonin (*i.e.*, by monoamine oxidase inhibitors) and tryptamine will cause convulsions. The method used was similar to that described by Tedeschi *et al.* (9). Groups of 10 unfasted male mice [TAC:(SW)fBr] were administered the test compounds suspended in 0.5% methylcellulose at a dose 10 times their levodopa potentiation ED_{50} values. Four hours later, tryptamine[5] was administered at 50 mg/kg iv. The compounds were considered to potentiate tryptamine if >50% of the animals in the treated group convulsed.

[1] Melting points were determined on a Mel-Temp apparatus and are corrected. The IR spectrum was determined as a mineral oil mull using a Perkin-Elmer 137B spectrophotometer. The NMR spectrum was obtained on a Varian A-60 instrument and was compared with tetramethylsilane as the internal standard.

[2] Methocel, Dow Chemical Co.
[3] Hoffmann-La Roche.
[4] Abbott Laboratories.
[5] Aldrich Chemical Co.

0022-3549/80/0900-1102$01.00/0
© 1980, American Pharmaceutical Association

Table I—Effect of I and Selected Compounds in Various Tests for Potential Antidepressant Activity

Compound	Anti-tetrabenazine[a] ED_{50}, mg/kg po	Levodopa[b] Potentiation ED_{50}, mg/kg po	Potentiation of Tryptamine[c]	Biogenic Amine[d] Uptake Inhibition *In Vitro* IC_{50}, μM			Inhibition[e] of Liver Monoamine Oxidase *In Vitro* IC_{50}, μM
				Norepinephrine	5-Hydroxy-tryptamine	Dopamine	
I	42 (14–126)	17 (8–38)	No	>100	>100	>100	44 ± 4.0
Desipramine	0.25 (0.03–0.58)	1.1 (0.5–2.3)	No	6.6 ± 1.3	0.6 ± 0.06	8.6 ± 1.3	75 ± 13.0
Imipramine	1.3 (0.8–2.1)	5.0 (2.3–11)	No	15 ± 3	0.11 ± 0.02	12 ± 1.0	23 ± 5.0
Pargyline	25 (3–81)	5.1 (2.2–12)	Yes[f]	Inactive	—	—	0.14 ± 0.01
Benzotropine	—	—	—	0.35 ± 0.11	11 ± 2.0	0.17 ± 0.02	—

[a] Dose of the compound that inhibited tetrabenazine-induced ptosis in 50% of the mice. The 95% confidence limits are indicated in the parentheses. [b] Dose of the compound that potentiated the response of levodopa in 50% of the mice. The 95% confidence limits are indicated in the parentheses. [c] Dose of the compound that potentiated the response of tryptamine in mice. Tested at a dose 10 times or greater than the levodopa ED_{50}. [d] Concentration of the compound that caused 50% inhibition of the uptake in mice crude synaptosomes of norepinephrine, 5-hydroxytryptamine, and dopamine (mean ± *SE*). [e] Concentration of the compound that inhibited monoamine oxidase by 50% (mean ± *SE*). [f] Dose of pargyline was 100 mg/kg, approximately four times the antitetrabenazine ED_{50} value.

Inhibition of Biogenic Transmitter Uptake into Crude Synaptosomes of Mouse Brain *In Vitro*—A modification of the technique described by Kuhar (10) was used. The procedure included isolation of crude synaptosomes of mouse whole brain by differential centrifugation, incubation of synaptosomes with the test compound and a tracer amount of tritiated neurotransmitter[6] (norepinephrine, 5-hydroxytryptamine, and dopamine), separation of the free neurotransmitter by vacuum filtration, and radioactivity measurement of the bound neurotransmitter remaining on the cellulose membrane[7] filter by means of liquid scintillation spectrophotometry. The micromolar concentrations of test compound producing 50% inhibition of neurotransmitter uptake (IC_{50}) were estimated from log dose–response curves based on at least three concentrations with at least three determinations at each concentration.

***In Vitro* Monoamine Oxidase Inhibition in Mouse Liver—**The method used was essentially that described by Wurtman and Axelrod (11) with [side chain-2-^{14}C]tryptamine as the substrate. The micromolar concentrations of test compound producing 50% inhibition of monoamine oxidase (IC_{50}) were estimated from log dose–response curves on three concentrations with three determinations at each concentration.

RESULTS AND DISCUSSION

Condensation of imidazolidine-2,4-dione (II) with the aldehyde (III) gave rise to a benzylidene compound (IV) (5) which, upon catalytic hydrogenation in the presence of Raney nickel, afforded 5-(4-dimethylaminobenzyl)imidazolidine-2,4-dione (I) (Scheme I).

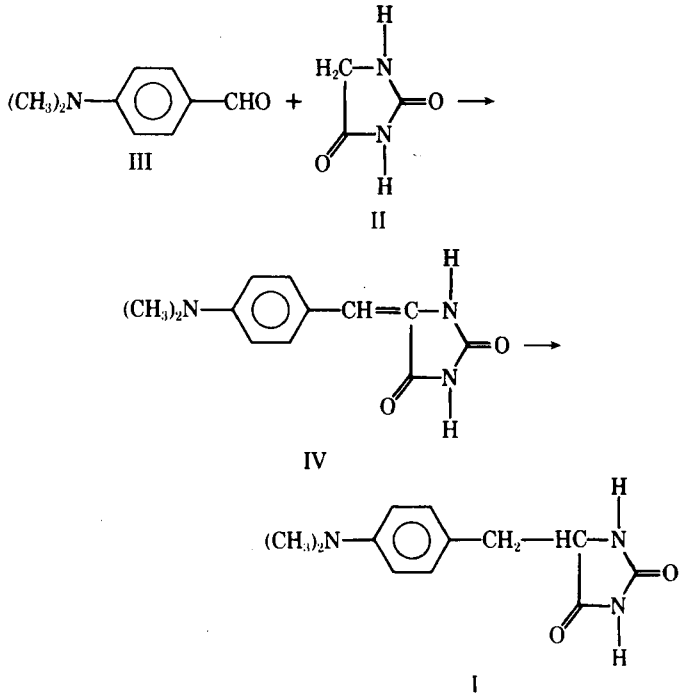

Scheme I

In preliminary testing at a dose of 50 mg/kg po, I inhibited tetrabenazine-induced ptosis by >90%. Therefore, a dose–response effect (7) was established and an antitetrabenazine ED_{50} value of 42 mg/kg was estimated (Table I).

This antidepressant activity of I was evaluated further using the levodopa potentiation test, which provides a measure of antidepressant activity more clearly related to CNS events (8) than to responses involving peripheral biogenic amines, such as the eyelid (ptosis) response to tetrabenazine. The usefulness of the levodopa potentiation model rests on its being a behavioral response and a reflection of the CNS effects of increased dopaminergic activity (8). However, this test is particularly sensitive to monoamine oxidase inhibitors because of the requirement for monoamine oxidase inhibitor pretreatment. In this test, I potentiated the levodopa response, and the estimated oral ED_{50} value was 17 mg/kg. Two tricyclic antidepressants, desipramine and imipramine, as well as a monoamine oxidase inhibitor, pargyline, also were effective with oral ED_{50} values of 1.1, 5.0, and 5.1 mg/kg, respectively.

Since the levodopa test is highly susceptible to monoamine oxidase inhibition, and since I was found to be an active potentiator of levodopa, I was evaluated for potentiation of tryptamine-induced convulsions. When administered intravenously, tryptamine causes an increase in brain 5-hydroxytryptamine levels (9). However, convulsions do not occur because the rate of destruction of 5-hydroxytryptamine by monoamine oxidase is directly related to the formation of 5-hydroxytryptamine. But in the presence of a monoamine oxidase inhibitor, with the metabolism of 5-hydroxytryptamine interrupted, tryptamine causes convulsions. This action is presumptive evidence of monoamine oxidase inhibitory activity (9). In this test, I at a dose of 174 mg/kg po (greater than 10 times the levodopa potentiating ED_{50}), as well as the tricyclic antidepressants, did not potentiate the tryptamine response, indicating that the potentiation of levodopa action was not a function of monoamine oxidase inhibition. On the other hand, pargyline at a dose of 100 mg/kg po did potentiate the tryptamine response, indicating the involvement of monoamine oxidase inhibition.

Compound I then was evaluated for effects on the uptake of selected biogenic amines *in vitro* (10). At a concentration of 100 μM, I did not prevent the uptake of norepinephrine, 5-hydroxytryptamine, and dopamine into crude synaptosomes prepared from the whole mouse brain, whereas the reference drugs all were effective. Desipramine inhibited norepinephrine uptake with an IC_{50} value of 6.6 μM, imipramine inhibited 5-hydroxytryptamine uptake with an IC_{50} value of 0.11 μM, and benzotropine inhibited dopamine uptake with an IC_{50} value of 0.17 μM.

In vitro monoamine oxidase of mouse liver (11) was inhibited by I with an IC_{50} value of 44 μM. However, I was more than 100 times less active than pargyline (IC_{50} 0.14 μM) under the same conditions.

Table I summarizes the results of the pharmacological evaluation presented in this paper.

[6] New England Nuclear Corp.
[7] Millipore type HA, 0.45 μm.

REFERENCES

(1) "International Drug Therapy Newsletter," F. J. Ayd, Jr., Ed., vol. 10, No. 6, Ayd Medical Communications, Baltimore, Md., June 1975.

(2) L. Jacobsson, K. Glitterstam, and U. Palm, *Acta Psychiat. Scand., Suppl.*, **255**, 47 (1974).

(3) N. H. Neff and H.-Y. T. Yang, *Life Sci.*, **14**, 2061 (1974).
(4) T. J. Schwan, U.S. pat. 3,932,449 (Jan. 13, 1976); through *Chem. Abstr.*, **84**, 135659b (1976).
(5) L. Y. Ladna and A. L. Boiko, *Farm. Zh. (Kiev)*, **21**, 10 (1966); through *Chem. Abstr.*, **65**, 13686d (1966).
(6) A. Barnett, R. I. Taber, and D. D. Greenhouse, *Int. J. Neuropharmacol.*, **8**, 353 (1960).
(7) J. T. Litchfield and F. Wilcoxon, *J. Pharmacol. Exp. Ther.*, **96**, 99 (1949).
(8) G. M. Everett, "Proceedings of the 1st International Symposium on Antidepressant Drugs," Milan, Italy, 1966.
(9) D. H. Tedeschi, R. E. Tedeschi, and E. J. Fellows, *J. Pharmacol. Exp. Ther.*, **126**, 223 (1959).
(10) M. M. Kuhar, *Life Sci.*, **13**, 1623 (1973).
(11) R. J. Wurtman and J. Axelrod, *Biochem. Pharmacol.*, **12**, 1439 (1963).

ACKNOWLEDGMENTS

The authors thank Mr. Warren Smith for the microanalyses, Ms. Patricia Curtis for the NMR spectrum, Mr. Richard Burns and Mr. Walton Dauchy for the *in vivo* pharmacological studies, and Ms. Christine Tinkham for the *in vitro* studies. They also thank Ms. K. Thompson for typing the manuscript. Tetrabenazine methanesulfonate, desipramine, imipramine, and benzotropine were generous gifts from Hoffmann–La Roche, U.S.V. Pharmaceutical Corp., Geigy Pharmaceuticals, and Merck Sharp & Dohme Research Laboratories, respectively.

Evaluation of 2-Azabicyclo[2.2.2]octane Analogs of 4-Anilidopiperidine Analgesics

RONALD F. BORNE ˣ, SAY-JONG LAW, JOHN C. KAPEGHIAN, and LAWRENCE W. MASTEN

Received January 14, 1980, from the *Departments of Medicinal Chemistry and Pharmacology, School of Pharmacy, University of Mississippi, University, MS 38677.* Accepted for publication March 28, 1980.

Abstract □ Eight analogs of the fentanyl-type analgesics, in which the piperidine ring is restricted into a boat conformation, were evaluated for analgesic activity. All analogs were less active than fentanyl, but interesting conformational and structural relationships were observed. Results of the study are discussed.

Keyphrases □ Analgesic activity—evaluation of 2-azabicyclo[2.2.2]-octane analogs of 4-anilidopiperidines, mice □ 4-Anilidopiperidines—2-azabicyclo[2.2.2]octane analogs, evaluation for analgesic activity, mice □ Structure–activity relationships—evaluation of 2-azabicyclo[2.2.2]-octane analogs of 4-anilidopiperidines for analgesic activity, mice

Studies designed to clarify the structural and conformational factors influencing the interactions of centrally acting analgesic agents with analgesic receptors have received considerable attention (1), and the recent discovery of the natural opiates has intensified this interest (2). Structural modification of methadone and methadone derivatives led to the development of a new series of agents, the acyclic basic anilides (3), which are represented by diampromide (I). Subsequent development (4) of the 4-anilidopiperidines, represented by fentanyl (II), led to a potent new class of analgesics. Differences in the modes of receptor binding of the various classes have been suggested.

BACKGROUND

The acyclic basic anilides have been proposed to differ from the methadone-type analgesics (5), and the 4-anilidopiperidines apparently differ from the acyclic basic anilides and the 4-phenylpiperidines, although they more closely resemble the former group (6). Differences in the modes of receptor binding between the acyclic basic anilides and the 4-anilidopiperidines have been proposed on the basis of structure–activity relationships and may be due to differences in receptor conformations (6). Based on spectroscopic evidence (7), a conformation of I has been suggested in which, among other features, the protonated basic center lies in close proximity to the anilido nitrogen. The preferred conformation of II has been suggested (6) as that in which the anilido function assumes the equatorial position of the chair form of the piperidine ring. Such a conformation would place the protonated basic center at a greater distance from the anilido nitrogen in II than in I. Additionally, this conformation of II would differ from the preferred conformation of the 4-phenylpiperidines, which has been suggested to be a skew boat conformation (8). However, the possibility that boat-type conformations of II may contribute to receptor interactions has not been tested directly. Analogs of fentanyl in which the flexibility of the piperidine ring has been restricted through incorporation of the tropane nucleus, designed to simulate frozen chair conformations of fentanyl, were reported recently (9). The 3-β-(propanilido) isomers were more potent than the 3-α-(propanilido) isomers and were nearly as potent as fentanyl itself.

The 2-azabicyclo[2.2.2]octane ring system was employed previously to restrict acetylcholine (10) and procaine (11) in *trans-* and *gauche-*conformations. More recently, this ring system was employed to restrict the piperidine ring of prodine-type analgesics in boat conformations (12). This report concerns the pharmacological evaluation of boat conformers of fentanyl-type analgesics. Casy *et al.* (6) reported the effects of substituents on the ring nitrogen atom of 4-anilidopiperidines and noted that analgesic activity increases significantly in the order $CH_3 < CH_2C_6H_5 < CH_2CH_2C_6H_5$. The analogs prepared in this study would permit the evaluation of this effect as well as the effect of positional isomerism in the boat conformers III–X. The synthesis and stereochemical analyses of these analogs were reported previously (13).

EXPERIMENTAL

The analgesic potency of the fentanyl analogs was determined by a modification of the D'Amour–Smith tail-flick method (14) using male albino ICR mice[1], 25–30 g, and an analgesiometer. All mice had their tails blackened with a black magic marker at least 15 min prior to testing to ensure a short, uniform tail-flick response time. The challenge to thermal stimulus occurred 30 min postinjection with the vehicle alone or the respective drugs. A control group of 10 mice was used to establish the baseline response time.

The criterion for analgesia (antinociception) was defined as a tail-flick response time greater than or equal to the mean response time of the

[1] Harlan Industries, Cumberland, Ind.

0022-3549/80/0900-1104$01.00/0
© 1980, American Pharmaceutical Association

(3) N. H. Neff and H.-Y. T. Yang, *Life Sci.*, **14**, 2061 (1974).
(4) T. J. Schwan, U.S. pat. 3,932,449 (Jan. 13, 1976); through *Chem. Abstr.*, **84**, 135659b (1976).
(5) L. Y. Ladna and A. L. Boiko, *Farm. Zh. (Kiev)*, **21**, 10 (1966); through *Chem. Abstr.*, **65**, 13686d (1966).
(6) A. Barnett, R. I. Taber, and D. D. Greenhouse, *Int. J. Neuropharmacol.*, **8**, 353 (1960).
(7) J. T. Litchfield and F. Wilcoxon, *J. Pharmacol. Exp. Ther.*, **96**, 99 (1949).
(8) G. M. Everett, "Proceedings of the 1st International Symposium on Antidepressant Drugs," Milan, Italy, 1966.
(9) D. H. Tedeschi, R. E. Tedeschi, and E. J. Fellows, *J. Pharmacol. Exp. Ther.*, **126**, 223 (1959).
(10) M. M. Kuhar, *Life Sci.*, **13**, 1623 (1973).
(11) R. J. Wurtman and J. Axelrod, *Biochem. Pharmacol.*, **12**, 1439 (1963).

ACKNOWLEDGMENTS

The authors thank Mr. Warren Smith for the microanalyses, Ms. Patricia Curtis for the NMR spectrum, Mr. Richard Burns and Mr. Walton Dauchy for the *in vivo* pharmacological studies, and Ms. Christine Tinkham for the *in vitro* studies. They also thank Ms. K. Thompson for typing the manuscript. Tetrabenazine methanesulfonate, desipramine, imipramine, and benzotropine were generous gifts from Hoffmann–La Roche, U.S.V. Pharmaceutical Corp., Geigy Pharmaceuticals, and Merck Sharp & Dohme Research Laboratories, respectively.

Evaluation of 2-Azabicyclo[2.2.2]octane Analogs of 4-Anilidopiperidine Analgesics

RONALD F. BORNE ˣ, SAY-JONG LAW, JOHN C. KAPEGHIAN, and LAWRENCE W. MASTEN

Received January 14, 1980, from the *Departments of Medicinal Chemistry and Pharmacology, School of Pharmacy, University of Mississippi, University, MS 38677.* Accepted for publication March 28, 1980.

Abstract □ Eight analogs of the fentanyl-type analgesics, in which the piperidine ring is restricted into a boat conformation, were evaluated for analgesic activity. All analogs were less active than fentanyl, but interesting conformational and structural relationships were observed. Results of the study are discussed.

Keyphrases □ Analgesic activity—evaluation of 2-azabicyclo[2.2.2]-octane analogs of 4-anilidopiperidines, mice □ 4-Anilidopiperidines—2-azabicyclo[2.2.2]octane analogs, evaluation for analgesic activity, mice □ Structure–activity relationships—evaluation of 2-azabicyclo[2.2.2]-octane analogs of 4-anilidopiperidines for analgesic activity, mice

Studies designed to clarify the structural and conformational factors influencing the interactions of centrally acting analgesic agents with analgesic receptors have received considerable attention (1), and the recent discovery of the natural opiates has intensified this interest (2). Structural modification of methadone and methadone derivatives led to the development of a new series of agents, the acyclic basic anilides (3), which are represented by diampromide (I). Subsequent development (4) of the 4-anilidopiperidines, represented by fentanyl (II), led to a potent new class of analgesics. Differences in the modes of receptor binding of the various classes have been suggested.

BACKGROUND

The acyclic basic anilides have been proposed to differ from the methadone-type analgesics (5), and the 4-anilidopiperidines apparently differ from the acyclic basic anilides and the 4-phenylpiperidines, although they more closely resemble the former group (6). Differences in the modes of receptor binding between the acyclic basic anilides and the 4-anilidopiperidines have been proposed on the basis of structure–activity relationships and may be due to differences in receptor conformations (6). Based on spectroscopic evidence (7), a conformation of I has been suggested in which, among other features, the protonated basic center lies in close proximity to the anilido nitrogen. The preferred conformation of II has been suggested (6) as that in which the anilido function assumes the equatorial position of the chair form of the piperidine ring. Such a conformation would place the protonated basic center at a greater distance from the anilido nitrogen in II than in I. Additionally, this conformation of II would differ from the preferred conformation of the 4-phenylpiperidines, which has been suggested to be a skew boat conformation (8). However, the possibility that boat-type conformations of II may contribute to receptor interactions has not been tested directly. Analogs of fentanyl in which the flexibility of the piperidine ring has been restricted through incorporation of the tropane nucleus, designed to simulate frozen chair conformations of fentanyl, were reported recently (9). The 3-β-(propanilido) isomers were more potent than the 3-α-(propanilido) isomers and were nearly as potent as fentanyl itself.

The 2-azabicyclo[2.2.2]octane ring system was employed previously to restrict acetylcholine (10) and procaine (11) in *trans-* and *gauche-*conformations. More recently, this ring system was employed to restrict the piperidine ring of prodine-type analgesics in boat conformations (12). This report concerns the pharmacological evaluation of boat conformers of fentanyl-type analgesics. Casy *et al.* (6) reported the effects of substituents on the ring nitrogen atom of 4-anilidopiperidines and noted that analgesic activity increases significantly in the order $CH_3 < CH_2C_6H_5 < CH_2CH_2C_6H_5$. The analogs prepared in this study would permit the evaluation of this effect as well as the effect of positional isomerism in the boat conformers III–X. The synthesis and stereochemical analyses of these analogs were reported previously (13).

EXPERIMENTAL

The analgesic potency of the fentanyl analogs was determined by a modification of the D'Amour–Smith tail-flick method (14) using male albino ICR mice[1], 25–30 g, and an analgesiometer. All mice had their tails blackened with a black magic marker at least 15 min prior to testing to ensure a short, uniform tail-flick response time. The challenge to thermal stimulus occurred 30 min postinjection with the vehicle alone or the respective drugs. A control group of 10 mice was used to establish the baseline response time.

The criterion for analgesia (antinociception) was defined as a tail-flick response time greater than or equal to the mean response time of the

[1] Harlan Industries, Cumberland, Ind.

0022-3549/80/0900-1104$01.00/0
© 1980, American Pharmaceutical Association

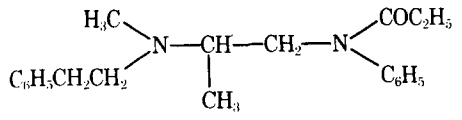

I

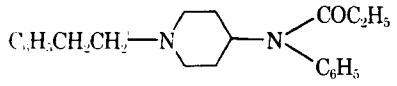

II

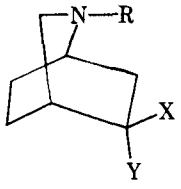

III: R = CH_3, X = $N(C_6H_5)COC_2H_5$, Y = H
IV: R = CH_3, X = H, Y = $N(C_6H_5)COC_2H_5$
V: R = $CH_2CH_2C_6H_5$, X = $N(C_6H_5)COC_2H_5$, Y = H
VI: R = $CH_2CH_2C_6H_5$, X = H, Y = $N(C_6H_5)COC_2H_5$

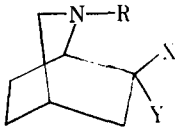

VII: R = CH_3, X = $N(C_6H_5)COC_2H_5$, Y = H
VIII: R = CH_3, X = H, Y = $N(C_6H_5)COC_2H_5$
IX: R = $CH_2CH_2C_6H_5$, X = $N(C_6H_5)COC_2H_5$, Y = H
X: R = $CH_2CH_2C_6H_5$, X = H, Y = $N(C_6H_5)COC_2H_5$

control group plus two standard deviations of their mean. Groups of eight mice were used for each dose of drug. Morphine sulfate alone and together with fentanyl citrate served as the positive controls. All AD_{50} values and their 95% confidence limits were determined by the method of Litchfield and Wilcoxon (15).

All injections were made intraperitoneally with saline as the vehicle. The drug preparation was injected at 0.01 ml/g. The *N*-methyl analogs (III, IV, VII, and VIII) were administered as the hydrochloride salts, while the *N*-phenethyl analogs (V, VI, IX, and X) were administered as suspensions of free bases in 4% polysorbate–saline because of the difficulty in producing homogeneous solutions at neutral pH in pure saline. Compounds that produced no analgesia at 100 mg/kg were tested further for possible antagonism to the narcotics. For the antagonism study, at least four mice per group were pretreated with 5.0 mg of morphine sulfate/kg or 500 μg of fentanyl citrate/kg 5–10 min before injection of the test compound and subsequent analgesic testing 30 min postinjection.

RESULTS AND DISCUSSION

The results of the analgesic evaluation and antagonism study are summarized in Tables I and II, respectively. Both *N*-methyl-5-propanilido analogs (III and IV) were analgesically inactive at 100 mg/kg. With the *exo*-isomer (III), central nervous system effects were observed clearly. Mice treated at that dose showed decreased motor activity, labored respiration, and tremor. No blockade of the morphine analgesic effect was demonstrated for III and IV, although most of the animals treated with morphine and III (100 mg/kg) failed to produce the Straub tail effect.

Both *N*-methyl-6-propanilido analogs (VII and VIII) showed analgesic activity with AD_{50} values of 60.0 and 71.5 mg/kg, respectively. However, in both cases, no Straub tail effect was produced along with the analgesic effect. Both of these agents also were highly toxic, with LD_{50} values of 62.5 and 91.0 mg/kg, respectively. The animals evidenced severe dyspnea and convulsions at higher doses. In the *exo*-isomer (VII), overlap occurred between the confidence intervals for the AD_{50} and LD_{50}. This overlap was possible since analgesic testing of the survivors at a given dose contributed data to the AD_{50} determination.

Unlike the *N*-methyl derivatives, water-soluble hydrochloride salts of the *N*-phenethyl analogs could not be prepared, suggesting large differences in hydrophobic properties in the two series. Of the four isomeric *N*-phenethyl analogs (V, VI, IX, and X), only X showed activity (AD_{50} value of 43.0 mg/kg). Compound X also had a relatively wider safety margin (therapeutic index > 3) as compared to the two active *N*-methyl-6-propanilido analogs (VII and VIII). Toxicity was observed only when the dosage was raised to 150 mg/kg, resulting in extreme excitation, convulsions, and lethality in two of eight mice. The three analgesically inactive *N*-phenethyl analogs (V, VI, and IX) produced only mild dyspnea and convulsions, and no deaths occurred in all dosage groups tested. These analogs also were unable to antagonize the analgesic activity of fentanyl.

Prior to the utilization of 4% polysorbate 60–saline as a suspending vehicle for the four *N*-phenethyl analogs, suspensions of V, VI, IX, and X in 3% acacia–saline were used for administration *via* the intracerebroventricular route. The intracerebroventricular injections were made after careful removal of the skin from the top of the skull with a razor. Injections were made at a point of 1 mm posterior to the bregma and 1 mm laterally to the right of the midline of the skull (16). Five microliters then was injected (for a 25-g mouse) slowly ~1 mm into the right lateral ventricle.

Analgesia was determined at 20 and 60 min postinjection. While the AD_{50} values of morphine sulfate and fentanyl citrate were 0.21 mg/kg and 14 μg/kg by this administration route, the experiment did not lead to an AD_{50} determination of the analogs due to the limitations of concentration. Table III summarizes the results of this analgesic study. Each dosage shown was the highest attainable for that particular compound in a single intracerebroventricular injection.

Table II—Results of Antagonism Study for 2-Azabicyclo[2.2.2]-octane Analogs of Fentanyl-Type Analgesics

Agonist	Antagonist	Dose of Antagonist, mg/kg	Analgesic Response	Lethality
Morphine[a]	III·HCl	100	6/6	2/8
Morphine	IV·HCl	100	8/8	0/8
Fentanyl[b]	V	100	4/4	0/4
Fentanyl	VI	50	2/2	2/4
Fentanyl	IX	25	4/4	0/4
X[c]	Naloxone	4.0	0/4	0/4

[a] Dose of morphine sulfate = 5.0 mg/kg. [b] Dose of fentanyl citrate = 500 μg/kg. [c] Dose of X = 75 mg/kg.

Table I—Analgesic Activity of the 2-Azabicyclo[2.2.2]octane Analogs of Fentanyl-Type Analgesics and the Positive Controls with 95% Confidence Limits

Compound	AD_{50}	LD_{50}	AD_{50} of Positive Control
III·HCl	Inactive at 100 mg/kg	—[a]	M[b] = 1.32 mg/kg (0.84–2.07)
IV·HCl	Inactive at 100 mg/kg	—[a]	M = 1.32 mg/kg (0.84–2.07)
VII·HCl	60.0 mg/kg (44.1–81.4)	62.5 mg/kg (55.5–70.3)	M = 1.32 mg/kg (0.84–2.07)
VIII·HCl	71.5 mg/kg (61.1–83.7)	91.0 mg/kg (84.9–97.5)	M = 3.0 mg/kg (2.3–4.0)
V	Inactive at 100 mg/kg	—[a]	M = 5.0 mg/kg (1.55–16.0)
VI	Inactive at 100 mg/kg	—[a]	M = 5.0 mg/kg (1.55–16.0) F[c] = 68.5 μg/kg (52.3–89.7)
IX	Inactive at 100 mg/kg	—[a]	M = 5.0 mg/kg (1.55–16.0) F = 68.5 μg/kg (52.3–89.7)
X	43.0 mg/kg (31.2–59.3)	—[d]	M = 5.0 mg/kg (1.55–16.0) F = 68.5 μg/kg (52.3–89.7)

[a] No deaths occurred at 100 mg/kg. [b] M = morphine sulfate. [c] F = fentanyl citrate. [d] Death occurred in two of eight mice at a dose of 150 mg/kg.

Table III—Analgesic Response to the Isomeric *N*-Phenethyl 2-Azabicyclo[2.2.2]octane Analogs of Fentanyl-Type Analgesics in Mice *via* Intracerebroventricular Route with 3% Acacia–Saline as the Vehicle [a]

Compound	Dose, mg/kg	Analgesic Response	
		20 min	60 min
V	3.0	0/4	0/4
VI	5.0	1/4	0/4
IX	20.0	0/4	0/4
X	5.0	1/4	2/4

[a] Morphine sulfate AD_{50} = 0.21 mg/kg; fentanyl citrate AD_{50} = 14.0 μg/kg.

Several conclusions can be drawn from these studies.

1. Since the most potent analog (as the free base) of the eight isomeric compounds prepared had a potency ratio of <1/600 (on the basis of the AD_{50} values determined) when compared to fentanyl citrate, the boat conformations do not appear to contribute to receptor interactions of the fentanyl-type analgesics; this finding suggests the importance of chair conformations in this class of analgesics. A recent report (9) on tropane analogs of fentanyl supports this conclusion.

2. The argument that boat conformations do not contribute to analgesic activity can be applied more readily for V and VI, the two *N*-phenethyl analogs of the 4-substituted piperidine-type analgesics. Analogous structures such as the 2,5-dimethyl derivatives of fentanyl were examined by Riley *et al.* (17) for analgesic activity. Although the exact configurations of the two ring methyl groups were not elucidated, ring methylation at C-2 and C-5 of fentanyl does not seem to destroy the analgesic effect since this compound was still 5% as active as fentanyl. Since V and VI can be regarded as analogs having the C-2 and C-5 methyl groups linked together, with the resultant restriction of the piperidine ring into a boat conformation, the liability of boat conformations was even more obvious.

3. The lack of analgesic activity of III and IV, the two *N*-methyl analogs of the 4-substituted piperidine-type analgesics, is consistent with the report (6) that, unlike the prodine-type analgesics, fentanyl-type analgesics possessing *N*-methyl substituents display weak analgesic activity at best.

4. Since three of the four *N*-methyl and *N*-phenethyl analogs that correspond to 3-substituted piperidine-type analgesics displayed moderate activity and since the *N*-phenethyl analog X was only slightly more active than the corresponding *N*-methyl analogs, positional isomerism apparently accounts for a fundamental alteration in the mode of binding of the molecules at the analgesic receptor.

5. The similar order of analgesic activity observed for the four *N*-phenethyl analogs (V, VI, IX, and X) when the intracerebroventricular route was employed suggests that the differences in apparent analgesic activity truly reflect differences in intrinsic activity and not large differences in disposition. To support this argument, attempts were made to determine the pKa values and partition coefficients of these four analogs. Due to their highly hydrophobic nature and thus their limited solubility, the pKa values that were obtained by following the method of Mathison and Tidwell (18) were questionable, and these determinations were discontinued. A similar fate was encountered in the partition coefficient study. The solubility (in pH 7.4 buffer saturated with octanol) of VI was lower than 2×10^{-6} *M* (or 0.0008 mg/ml). This value was determined by measuring, in duplicate, the UV absorbance (λ_{max} 252.5) prior to and after filtration. The absorbance of the mixture (previously stirred overnight at room temperature) before filtration was invariably far more intense than that after filtration, suggesting that the octanol-saturated buffer was still saturated with VI at that concentration.

6. The abolition of the analgesic effect of X by naloxone and the observation of the Straub tail effect at all doses of X producing analgesia implied the mediation of analgesia through binding to the opiate receptor.

REFERENCES

(1) A. H. Soloway, in "Principles of Medicinal Chemistry," W. O. Foye, Ed., Lea & Febiger, Philadelphia, Pa., 1974, chap. 12.

(2) R. J. Kobylecki and B. A. Morgan, *Ann. Rep. Med. Chem.*, **14**, 31 (1979).

(3) W. R. Wright, H. J. Brabender, and R. A. Hardy, *J. Am. Chem. Soc.*, **81**, 1518 (1959).

(4) P. A. J. Janssen, *Br. J. Anaesth.*, **34**, 260 (1962).

(5) P. S. Portoghese and D. L. Larson, *J. Pharm. Sci.*, **53**, 302 (1964). P. S. Portoghese and T. N. Riley, *ibid.*, **54**, 1831 (1965).

(6) A. F. Casy, M. M. A. Hassan, A. B. Simmonds, and D. Staniforth, *J. Pharm. Pharmacol.*, **21**, 434 (1969).

(7) A. F. Casy and M. M. A. Hassan, *ibid.*, **19**, 114 (1967).

(8) A. F. Casy, *J. Med. Chem.*, **11**, 188 (1968).

(9) T. N. Riley and J. R. Bagley, *ibid.*, **22**, 1167 (1979).

(10) R. F. Borne, C. R. Clark, and I. W. Waters, *J. Pharm. Sci.*, **63**, 1559 (1974).

(11) R. F. Borne, C. R. Clark, and J. M. Holbrook, *J. Med. Chem.*, **16**, 853 (1973).

(12) C. R. Clark, J. M. Holbrook, and R. F. Borne, *ibid.*, **19**, 852 (1976).

(13) S. J. Law, D. H. Lewis, and R. F. Borne, *J. Heterocycl. Chem.*, **15**, 273 (1978).

(14) F. E. D'Amour and D. L. Smith, *J. Pharmacol. Exp. Ther.*, **72**, 74 (1941).

(15) J. T. Litchfield and F. Wilcoxon, *ibid.*, **96**, 99 (1949).

(16) T. J. Haley and W. G. McCormick, *Br. J. Pharmacol.*, **12**, 12 (1957).

(17) T. N. Riley, D. B. Hale, and M. C. Wilson, *J. Pharm. Sci.*, **62**, 983 (1973).

(18) I. W. Mathison and R. R. Tidwell, *J. Med. Chem.*, **18**, 1227 (1975).

ACKNOWLEDGMENTS

Supported in part by Grant 1 R01 NS09188 from the National Institute of Neurological Diseases and Stroke and in part by the Research Institute of Pharmaceutical Sciences, School of Pharmacy, University of Mississippi.

What is Odoratin?

Keyphrases □ Odoratin—recommended assignment of name only to isolate from *Cedrela odorata* □ Undecanortriterpenoids—odoratin, recommended assignment of name only to isolate from *Cedrela odorata* □ *Cedrela odorata*—recommended assignment of odoratin as name for isolate from *Cedrela odorata* only

To the Editor:

In 1966, Chan *et al.* (1, 2) assigned the name odoratin (I) to a novel undecanortriterpenoid isolated from the West Indian cedar *Cedrela odorata* L. (Meliaceae). To our knowledge, this was the first time that the name odoratin was assigned to any plant principle.

Two years later, Ortega *et al.* (3) isolated a novel pseudoguaianolide (II) from the Mexican Compositae *Hymenoxys odorata* DC. and also assigned it the trivial name odoratin.

In 1973, Bose *et al.* (4, 5) reported the isolation of a novel chalcone from *Eupatorium odoratum* L. (Compositae), which was shown to be 6′-hydroxy-4,2′,3′,4′-tetramethoxychalcone (III), and confused the literature further by naming it odoratin.

Finally, Galina and Gottlieb (6) and Hayashi and Thomson (7) simultaneously reported the isolation of a novel isoflavone from *Pterodon apparicioi* Pedersoli (Leguminosae) and *Dipteryx odorata* Willd. (Leguminosae), respectively. This compound also was assigned (7) the name odoratin (IV) and subsequently was synthesized (8).

In spite of the repetitive assignments of the trivial name odoratin to four classes of natural products over an 8-year period, odoratin recently has been used again to designate the chalcone (III) isolated from *Eupatorium odoratum* (9) and the pseudoguaianolide (II) isolated from *Baileya pauciradiata* Harv. and Gray (Compositae) (10).

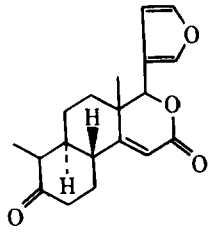

I

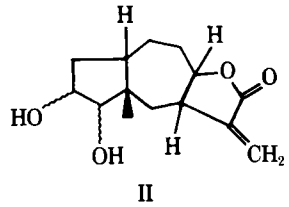

II

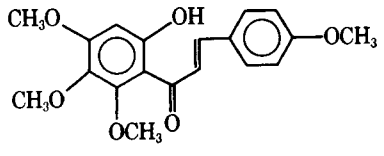

III

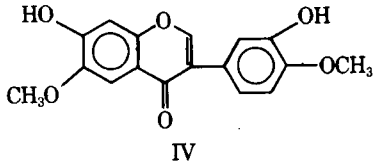

IV

Because of the confusion created by this failure to check the literature prior to the assignment of a trivial name, we suggest that the name odoratin be retained for the first isolate, the undecanortriterpenoid represented by I. Structures II–IV should be referred to by the systematic names 3,4,8β-trihydroxyambros-11(13)-en-12-oic acid γ-lactone (II), 6′-hydroxy-4,2′,3′,4′-tetramethoxychalcone (III), and 7,3′-dihydroxy-6,4′-dimethoxyisoflavone (IV).

(1) W. R. Chan, D. R. Taylor, and R. T. Aplin, *Chem. Commun.*, **1966**, 576.

(2) W. R. Chan, D. R. Taylor, and R. T. Aplin, *Tetrahedron*, **28**, 431 (1972).

(3) A. Ortega, A. Romo de Vivar, and J. Romo, *Can. J. Chem.*, **46**, 1539 (1968).

(4) P. K. Bose, P. Chakrabarti, S. Chakravarti, S. P. Dutta, and A. K. Barua, *Phytochemistry*, **12**, 667 (1973).

(5) P. K. Bose, P. Chakrabarti, S. Chakravarti, S. P. Dutta, and A. K. Barua, *Trans. Bose. Res. Inst. (Calcutta)*, **37**, 25 (1974).

(6) E. Galina and O. R. Gottlieb, *Phytochemistry*, **13**, 2593 (1974).

(7) T. Hayashi and R. H. Thomson, *ibid.*, **13**, 1943 (1974).

(8) S. N. Seshagiri, R. K. Gupta, and M. Krishnamurti, *Indian J. Chem.*, **14B** 1011 (1976).

(9) E. O. Arene, G. R. Pettit, and R. H. Ode, *Lloydia*, **41**, 68 (1978).

(10) J. J. Hoffman, S. D. Joland, S. J. Torrance, D. J. Luzbetak, R. M. Wiedhopf, and J. R. Cole, *J. Pharm. Sci.*, **67**, 1633 (1978).

N. R. Farnsworth ˣ
G. A. Cordell
C. J. Kaas
Department of Pharmacognosy and Pharmacology
College of Pharmacy
University of Illinois at the Medical Center
Chicago, IL 60612

Received April 25, 1980.
Accepted for publication June 4, 1980.

Monitoring *In Vivo* Disintegration Time of Tablets by External Scintigraphy

Keyphrases □ Disintegration—monitoring of *in vivo* tablet disintegration time by external scintigraphy □ Scintigraphy, external—monitoring of *in vivo* tablet disintegration time □ Tablets—disintegration *in vivo*, monitoring by external scintigraphy

To the Editor:

Several investigators developed techniques for the determination of *in vivo* disintegration times of pharmaceutical solid formulations. One technique had the tablet attached at the end of a string. The tablet was administered orally; at predetermined time intervals, the tablet was pulled back, and the degree of disintegration was observed (1). In another case, the tablet was recovered by inducing vomiting (1). Other techniques involved direct visualization of the tablet in the stomach by means of a gastroscope or a fiberscope (1, 2) or by using roentgenography or fluoroscopy with or without a radiopaque material

0022-3549/80/0900-1107$01.00/0
© 1980, American Pharmaceutical Association

What is Odoratin?

Keyphrases □ Odoratin—recommended assignment of name only to isolate from *Cedrela odorata* □ Undecanortriterpenoids—odoratin, recommended assignment of name only to isolate from *Cedrela odorata* □ *Cedrela odorata*—recommended assignment of odoratin as name for isolate from *Cedrela odorata* only

To the Editor:

In 1966, Chan *et al.* (1, 2) assigned the name odoratin (I) to a novel undecanortriterpenoid isolated from the West Indian cedar *Cedrela odorata* L. (Meliaceae). To our knowledge, this was the first time that the name odoratin was assigned to any plant principle.

Two years later, Ortega *et al.* (3) isolated a novel pseudoguaianolide (II) from the Mexican Compositae *Hymenoxys odorata* DC. and also assigned it the trivial name odoratin.

In 1973, Bose *et al.* (4, 5) reported the isolation of a novel chalcone from *Eupatorium odoratum* L. (Compositae), which was shown to be 6′-hydroxy-4,2′,3′,4′-tetramethoxychalcone (III), and confused the literature further by naming it odoratin.

Finally, Galina and Gottlieb (6) and Hayashi and Thomson (7) simultaneously reported the isolation of a novel isoflavone from *Pterodon apparicioi* Pedersoli (Leguminosae) and *Dipteryx odorata* Willd. (Leguminosae), respectively. This compound also was assigned (7) the name odoratin (IV) and subsequently was synthesized (8).

In spite of the repetitive assignments of the trivial name odoratin to four classes of natural products over an 8-year period, odoratin recently has been used again to designate the chalcone (III) isolated from *Eupatorium odoratum* (9) and the pseudoguaianolide (II) isolated from *Baileya pauciradiata* Harv. and Gray (Compositae) (10).

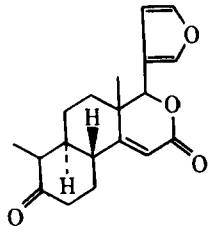

I

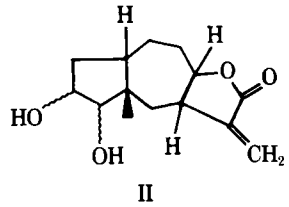

II

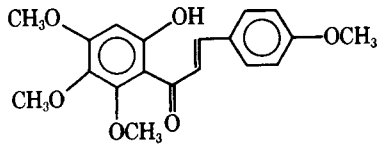

III

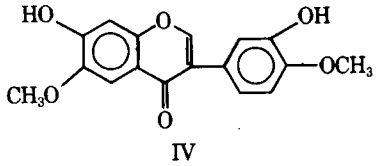

IV

Because of the confusion created by this failure to check the literature prior to the assignment of a trivial name, we suggest that the name odoratin be retained for the first isolate, the undecanortriterpenoid represented by I. Structures II–IV should be referred to by the systematic names 3,4,8β-trihydroxyambros-11(13)-en-12-oic acid γ-lactone (II), 6′-hydroxy-4,2′,3′,4′-tetramethoxychalcone (III), and 7,3′-dihydroxy-6,4′-dimethoxyisoflavone (IV).

(1) W. R. Chan, D. R. Taylor, and R. T. Aplin, *Chem. Commun.*, **1966**, 576.

(2) W. R. Chan, D. R. Taylor, and R. T. Aplin, *Tetrahedron*, **28**, 431 (1972).

(3) A. Ortega, A. Romo de Vivar, and J. Romo, *Can. J. Chem.*, **46**, 1539 (1968).

(4) P. K. Bose, P. Chakrabarti, S. Chakravarti, S. P. Dutta, and A. K. Barua, *Phytochemistry*, **12**, 667 (1973).

(5) P. K. Bose, P. Chakrabarti, S. Chakravarti, S. P. Dutta, and A. K. Barua, *Trans. Bose. Res. Inst. (Calcutta)*, **37**, 25 (1974).

(6) E. Galina and O. R. Gottlieb, *Phytochemistry*, **13**, 2593 (1974).

(7) T. Hayashi and R. H. Thomson, *ibid.*, **13**, 1943 (1974).

(8) S. N. Seshagiri, R. K. Gupta, and M. Krishnamurti, *Indian J. Chem.*, **14B** 1011 (1976).

(9) E. O. Arene, G. R. Pettit, and R. H. Ode, *Lloydia*, **41**, 68 (1978).

(10) J. J. Hoffman, S. D. Joland, S. J. Torrance, D. J. Luzbetak, R. M. Wiedhopf, and J. R. Cole, *J. Pharm. Sci.*, **67**, 1633 (1978).

N. R. Farnsworth ˣ
G. A. Cordell
C. J. Kaas
Department of Pharmacognosy and Pharmacology
College of Pharmacy
University of Illinois at the Medical Center
Chicago, IL 60612

Received April 25, 1980.
Accepted for publication June 4, 1980.

Monitoring *In Vivo* Disintegration Time of Tablets by External Scintigraphy

Keyphrases □ Disintegration—monitoring of *in vivo* tablet disintegration time by external scintigraphy □ Scintigraphy, external—monitoring of *in vivo* tablet disintegration time □ Tablets—disintegration *in vivo*, monitoring by external scintigraphy

To the Editor:

Several investigators developed techniques for the determination of *in vivo* disintegration times of pharmaceutical solid formulations. One technique had the tablet attached at the end of a string. The tablet was administered orally; at predetermined time intervals, the tablet was pulled back, and the degree of disintegration was observed (1). In another case, the tablet was recovered by inducing vomiting (1). Other techniques involved direct visualization of the tablet in the stomach by means of a gastroscope or a fiberscope (1, 2) or by using roentgenography or fluoroscopy with or without a radiopaque material

0022-3549/80/0900-1107$01.00/0
© 1980, American Pharmaceutical Association

in the tablet formulation (1, 3–7). Casey *et al.* (8) used technetium 99m to label capsules and a γ-camera to monitor the *in vivo* disintegration of the formulation. Alpsten *et al.* (9) labeled capsules with chromium 51 and monitored the *in vivo* disintegration with a shielded scintillation crystal probe.

The major disadvantages of these techniques were that they were invasive, causing discomfort to the animal model or to the human subject; they did not allow continuous observation of the solid formulation in the stomach; they exposed the subject to high doses of X-ray radiation; and they always tampered considerably with the physical integrity of the tablet or capsule formulation.

This communication presents a noninvasive method for monitoring the *in vivo* disintegration time of tablets. This method involves external scintigraphy for monitoring the *in vivo* disintegration times of tablets (10), combined with a new method for labeling the tablet with a short-lived radionuclide. This labeling process interferes to a lesser degree with the physical integrity of the formulation.

In a typical experiment, the tablet[1] was labeled with iodine 131 by exposing it to vapors of iodine 131 (5 mCi) in carbon tetrachloride[2] for 5 hr in a glass chamber. The $^{131}I_2$ was adsorbed onto the tablet surface, and some diffused into the tablet. The extent of the penetration of the $^{131}I_2$ into the tablet was examined by autoradiography. Slices ~2 mm thick were taken from different labeled tablets at different distances from the center of the tablet using a microtome[3]. Due to friability of the tablet, it was impossible to obtain thinner slices or more than one slice per tablet. Each slice was placed on medical X-ray film[4] for ~1 hr. The *in vitro* disintegration time of the labeled tablets was found to be within the range of the nonlabeled tablets.

The labeled tablet (~100,000 cpm) was administered orally to an anesthetized[5] animal with a pill gun. The animal was placed in a supine position on a table, and the abdomen then was positioned under the collimated detector of a multicrystal scintillation camera[6]. Data were accumulated for up to 30 min. During that period, scintiphotographs of the abdominal area were taken (Figs. 1A–1D). In a second animal, data were accumulated for 50 min (Figs. 1E–1H). Figure 1A shows the scintigraphic image of the tablet outside of the stomach of the dog, while Figs. 1B–1D show the tablet inside the dog at various times. The onset of the tablet disintegration is shown in Fig. 1D, while a better picture of the disintegration is given in Figs. 1E–1H, taken from another dog.

This method for measuring the disintegration time of tablets *in vivo* has good potential in the assessment of tablet formulations for the following reasons. The labeling of the tablet is achieved by exposing the tablet to vapors of $^{131}I_2$ in carbon tetrachloride. Iodine 131 is adsorbed onto the tablet surface and, to a lesser extent, is diffused into the tablet. This labeling process interferes the least, compared to other techniques, with the physical integrity of the formulation. The technique is based on external scintigraphy and does not require sacrifice of the experimental animal. If the scintillation camera is coupled with a video recording device for replay capability and a computer for image processing, then it is possible to follow the disintegration process minute by minute and to determine accurately the onset and end of the disintegration process within the animal's stomach.

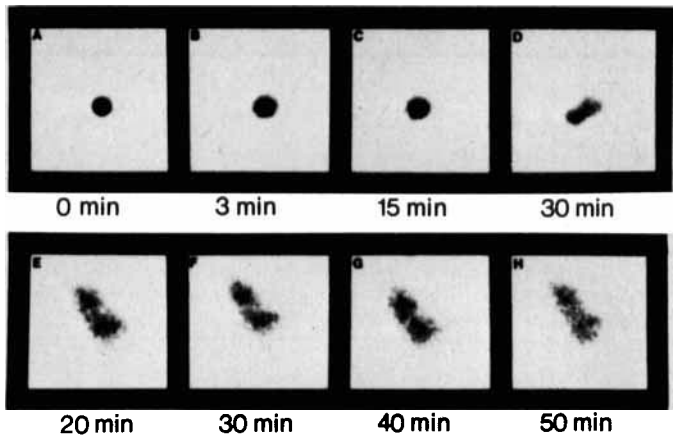

Figure 1—*Sequence scintiphotographs of a tablet ingested by a dog. Key: A–D, Dog 1, and E–H, Dog 2.*

Further research is in progress to assess the effect of the labeling process on the physical integrity of the formulation and the effectiveness of this process with respect to the penetrability and uniformity of diffusion of the label into various types of tablets.

(1) W. H. Steinberg, G. H. Frey, J. N. Masci, and H. H. Hutchins, *J. Pharm. Sci.*, **54**, 747 (1965).

(2) A. Weiss, E. R. Pitman, and E. C. Graham, *Am. J. Med.*, **31**, 266 (1961).

(3) L. Lachman, W. Burrett, R. K. Rinehart, and H. Sheppard, *Curr. Ther. Res.*, **6**, 49 (1964).

(4) E. Lozinski and G. R. Diver, *J. Am. Pharm. Assoc., Sci. Ed.*, **22**, 143 (1933).

(5) F. S. Buckey and C. W. Bliven, *ibid.*, **25**, 119 (1936).

(6) J.G. Wagner, W. Veldkamp, and S. Long, *ibid.*, **47**, 681 (1958).

(7) G. Levy, *J. Pharm. Sci.*, **52**, 1039 (1963).

(8) D. L. Casey, R. M. Beihn, G. A. Digenis, and M. B. Shambhu, *ibid.*, **65**, 1412 (1976).

(9) M. Alpsten, C. Bogentoft, G. Ekenved, and L. Sölvell, *J. Pharm. Pharmacol.*, **31**, 480 (1979).

(10) M. C. Theodorakis, M. D. Devous, Sr., and D. R. Simpson, "Abstracts," vol. 10, no. 1, APhA Academy of Pharmaceutical Sciences, Washington, D.C., 1980, p. 79.

Michael C. Theodorakis ˣ
Michael D. Devous, Sr.
David R. Simpson
Division of Nuclear Medicine and Radiopharmacology and Department of Bioengineering
Colleges of Veterinary Medicine and Engineering
University of Illinois at Urbana–Champaign
Urbana, IL 61801

Received September 17, 1979.
Accepted for publication June 12, 1980.
Supported by Grant CA 09067 awarded by the National Cancer Institute, Department of Health, Education, and Welfare, and by the University of Illinois Research Board.

[1] Vitamin C (250 mg/tablet), S. S. Kresge Co., Troy, Mich.
[2] ICN, Chemical and Radioisotope Division, Irvine, Calif.
[3] A-20 microtome, Scientific Instruments Division, American Optical Inc., Buffalo, N.Y.
[4] RP/R-14, Eastman Kodak Co., Rochester, N.Y.
[5] Rompun (xylazine), 1.1 mg/kg, Bagvet, Division of Cutter Laboratories, Shawnee, Kans.
[6] Nuclear of Chicago, Pho/Gamma HP, Searle Diagnostics, Des Plaines, Ill.

REVIEWS

Pharmaceutical Handbook, 19th ed. Edited by AINLEY WADE. The Pharmaceutical Press, 1 Lambeth High St., London SE1 7JN, England. 1980. 783 pp. 18 × 20 cm. Price $35.00. (Available from Rittenhouse Book Distributors, 251 S. 24th St., Philadelphia, PA 19103.)

Developed as a companion to *Martindale: The Extra Pharmacopoeia*, the *Pharmaceutical Handbook* contains a wealth of information of use to students, practicing pharmacists, and practitioners of allied professions. The 19th edition is the most recent volume in a series that originated in 1906.

The *Handbook* has been thoroughly revised and updated since its previous edition in 1970. The 117-page section on the preparation and supply of medicines has been rewritten. A new checklist of potential incompatibilities of additives to intravenous preparations has been included, and the table of drug interactions has been extended.

The other major sections of the book cover diverse topics such as computers and their applications in pharmacy, sterilization methods and tests, disinfectants and antiseptics, physiological values for body fluids, drug absorption, poisoning, microbiology, immunology, nomenclature of organic compounds, and weights and measures.

The 24-page section of miscellaneous data includes geometrical formulas, mathematical notations, signs, and symbols, calculus equations, the Russian and Greek alphabets, a table for the determination of body surface area from height and weight, and a periodic table. A glossary of proprietary names and equivalent approved names lists trade names for single-entity preparations available in the United Kingdom along with their approved names.

A 136-page glossary gives concise definitions of medical and pharmaceutical terms along with definitions of radiological terms, terms used in foreign prescriptions, and units and measures. The book concludes with a 38-page index.

The *Handbook* is a convenient reference source that contains valuable information which otherwise could be found only by consulting many other sources.

Staff Review

Substituent Constants for Correlation Analysis in Chemistry and Biology. By CORWIN HANSCH and ALBERT LEO. Wiley, 605 Third Ave., New York, NY 10016. 1979. 339 pp. 21 × 28 cm. Price $24.95.

This book is organized into two sections: a descriptive section that lightly covers the fundamentals of chemical structure–physical parameter theory and estimation (65 pages) and a set of tables, in the form of computer printouts, that contain fragment constants and partition coefficients which were extracted from the literature. The tables are provided as separate appendixes. The first appendix contains about 100 pages and is entitled Electronic, Steric, and Hydrophobic (π) Constants. The second appendix contains about 160 pages and is entitled Partition Coefficients. The last appendix contains four pages and is entitled Hydrophobic Fragment Constants.

The expressed purpose of this book (the authors refer to it as a monograph) is "to provide a comprehensive listing of parameters of proven value for the correlation of structure with chemical or biologic reactivity." The tables provided seem to represent the most complete source of information yet organized for such use, and the book therefore admirably accomplishes its stated goal. The tables are not the easiest to decipher, given their computerized structure, but they nevertheless are a rich source of well-referenced information on the influences of structure on physical and chemical events. Partitioning data listed are for diverse solvent systems.

The opening, narrative section of the book has very brief discussions of electronic, steric, and hydrophobic parameters; molar refractivity and parachor; and cluster analysis. These discussions are provided at the advanced undergraduate level. They provide a minimal preparation for the use of the extensive tabulations that follow. To an extent, this aspect of the book is disappointing since the discussions are largely phenomenological and fail to deal with physicochemical events, such as hydrophobicity, in terms of present understanding of their fundamental molecular origins.

While limitations and/or uncertainties in parameter estimations are presented fairly, severe mechanistic shortcomings of quantitative structure–activity relationship approaches are skirted completely. The idea of the prospective use of quantitative structure–activity relationships is sold; the fact that applications have been largely retrospective goes unmentioned.

On balance, the book contains much useful information in tables and material in short chapters which should be part of the coursework of medicinal chemistry and pharmaceutics programs. It makes a valuable library addition but should be considered for personal collections only by those emphasizing quantitative structure–activity relationships in their teaching or research.

Reviewed by Gordon L. Flynn
College of Pharmacy
University of Michigan
Ann Arbor, MI 48104

Toxic Plants. Edited by A. DOUGLAS KINGHORN. Columbia University Press, 562 W. 113th St., New York, NY 10025. 1979. 195 pp. 15 × 23.5 cm. Price $20.00.

This book is the result of a symposium on toxic plants held at the University of Miami in 1977 as part of the annual Society for Economic Botany meeting. It features contributions by eight major authors on various aspects of plant poisoning. It is an up-to-date treatment providing chemical, biochemical, and toxicological information on a wide range of poisonous plants.

The problem of poisonous plants is described in general in the first chapter. Problems related to phytotoxicology are discussed such as plants with known toxic constituents that are not always poisonous, the uneven quality of the existing literature, the need for accurate identification to access information, the question of labeling poisonous ornamental plants, and the difficulty of improving the present body of information.

The remaining chapters cover and update several specific and important areas of interest in poison plants such as toxic mushrooms (amatoxins, phallotoxins, phallolysin, antamanide, ibotenic acid, muscimol, psilocybin, muscarine, gyromitrin, and coprine); toxins and teratogens of the Solanaceae and Liliaceae (nonalkaloidal toxins, tropane alkaloids, pyridine/piperidine alkaloids, and steroidal alkaloids); pokeweed and other lymphocyte mitogens (lectins, mitogens, Abrus lectin, abrin, and Hura and Robinia lectins); a literature review and clinical management of household ornamental plants potentially toxic to humans; cocarcinogenic irritant Euphorbiaceae (phorbol esters, ingenol esters, daphnane esters, and diterpene esters); the poisonous Anacardiaceae (botany, phenolic compounds, and immunological studies); and contact hypersensitivity and photodermatitis evoked by Compositae (sesquiterpene lactones and acetylenic compounds).

Overall, the chapters provide recent data, data of significance to human poisonings, and much insight into the complexity of poisoning by natural products. Chemical structures are provided for many classical poisons as well as for some recently characterized molecules. Finally, clinical management is provided where available on a number of poisonous plants.

This book will be of interest to numerous specialists such as botanists, chemists, pharmacognosists, and horticulturalists as well as those in the medical and health professions. The topics discussed are a welcome addition to the relatively sparse literature in the field.

Reviewed by Ara Der Marderosian
Philadelphia College of Pharmacy and Science
Philadelphia, PA 19104

REVIEWS

Pharmaceutical Handbook, 19th ed. Edited by AINLEY WADE. The Pharmaceutical Press, 1 Lambeth High St., London SE1 7JN, England. 1980. 783 pp. 18 × 20 cm. Price $35.00. (Available from Rittenhouse Book Distributors, 251 S. 24th St., Philadelphia, PA 19103.)

Developed as a companion to *Martindale: The Extra Pharmacopoeia*, the *Pharmaceutical Handbook* contains a wealth of information of use to students, practicing pharmacists, and practitioners of allied professions. The 19th edition is the most recent volume in a series that originated in 1906.

The *Handbook* has been thoroughly revised and updated since its previous edition in 1970. The 117-page section on the preparation and supply of medicines has been rewritten. A new checklist of potential incompatibilities of additives to intravenous preparations has been included, and the table of drug interactions has been extended.

The other major sections of the book cover diverse topics such as computers and their applications in pharmacy, sterilization methods and tests, disinfectants and antiseptics, physiological values for body fluids, drug absorption, poisoning, microbiology, immunology, nomenclature of organic compounds, and weights and measures.

The 24-page section of miscellaneous data includes geometrical formulas, mathematical notations, signs, and symbols, calculus equations, the Russian and Greek alphabets, a table for the determination of body surface area from height and weight, and a periodic table. A glossary of proprietary names and equivalent approved names lists trade names for single-entity preparations available in the United Kingdom along with their approved names.

A 136-page glossary gives concise definitions of medical and pharmaceutical terms along with definitions of radiological terms, terms used in foreign prescriptions, and units and measures. The book concludes with a 38-page index.

The *Handbook* is a convenient reference source that contains valuable information which otherwise could be found only by consulting many other sources.

Staff Review

Substituent Constants for Correlation Analysis in Chemistry and Biology. By CORWIN HANSCH and ALBERT LEO. Wiley, 605 Third Ave., New York, NY 10016. 1979. 339 pp. 21 × 28 cm. Price $24.95.

This book is organized into two sections: a descriptive section that lightly covers the fundamentals of chemical structure–physical parameter theory and estimation (65 pages) and a set of tables, in the form of computer printouts, that contain fragment constants and partition coefficients which were extracted from the literature. The tables are provided as separate appendixes. The first appendix contains about 100 pages and is entitled Electronic, Steric, and Hydrophobic (π) Constants. The second appendix contains about 160 pages and is entitled Partition Coefficients. The last appendix contains four pages and is entitled Hydrophobic Fragment Constants.

The expressed purpose of this book (the authors refer to it as a monograph) is "to provide a comprehensive listing of parameters of proven value for the correlation of structure with chemical or biologic reactivity." The tables provided seem to represent the most complete source of information yet organized for such use, and the book therefore admirably accomplishes its stated goal. The tables are not the easiest to decipher, given their computerized structure, but they nevertheless are a rich source of well-referenced information on the influences of structure on physical and chemical events. Partitioning data listed are for diverse solvent systems.

The opening, narrative section of the book has very brief discussions of electronic, steric, and hydrophobic parameters; molar refractivity and parachor; and cluster analysis. These discussions are provided at the advanced undergraduate level. They provide a minimal preparation for the use of the extensive tabulations that follow. To an extent, this aspect of the book is disappointing since the discussions are largely phenomenological and fail to deal with physicochemical events, such as hydrophobicity, in terms of present understanding of their fundamental molecular origins.

While limitations and/or uncertainties in parameter estimations are presented fairly, severe mechanistic shortcomings of quantitative structure–activity relationship approaches are skirted completely. The idea of the prospective use of quantitative structure–activity relationships is sold; the fact that applications have been largely retrospective goes unmentioned.

On balance, the book contains much useful information in tables and material in short chapters which should be part of the coursework of medicinal chemistry and pharmaceutics programs. It makes a valuable library addition but should be considered for personal collections only by those emphasizing quantitative structure–activity relationships in their teaching or research.

Reviewed by Gordon L. Flynn
College of Pharmacy
University of Michigan
Ann Arbor, MI 48104

Toxic Plants. Edited by A. DOUGLAS KINGHORN. Columbia University Press, 562 W. 113th St., New York, NY 10025. 1979. 195 pp. 15 × 23.5 cm. Price $20.00.

This book is the result of a symposium on toxic plants held at the University of Miami in 1977 as part of the annual Society for Economic Botany meeting. It features contributions by eight major authors on various aspects of plant poisoning. It is an up-to-date treatment providing chemical, biochemical, and toxicological information on a wide range of poisonous plants.

The problem of poisonous plants is described in general in the first chapter. Problems related to phytotoxicology are discussed such as plants with known toxic constituents that are not always poisonous, the uneven quality of the existing literature, the need for accurate identification to access information, the question of labeling poisonous ornamental plants, and the difficulty of improving the present body of information.

The remaining chapters cover and update several specific and important areas of interest in poison plants such as toxic mushrooms (amatoxins, phallotoxins, phallolysin, antamanide, ibotenic acid, muscimol, psilocybin, muscarine, gyromitrin, and coprine); toxins and teratogens of the Solanaceae and Liliaceae (nonalkaloidal toxins, tropane alkaloids, pyridine/piperidine alkaloids, and steroidal alkaloids); pokeweed and other lymphocyte mitogens (lectins, mitogens, Abrus lectin, abrin, and Hura and Robinia lectins); a literature review and clinical management of household ornamental plants potentially toxic to humans; cocarcinogenic irritant Euphorbiaceae (phorbol esters, ingenol esters, daphnane esters, and diterpene esters); the poisonous Anacardiaceae (botany, phenolic compounds, and immunological studies); and contact hypersensitivity and photodermatitis evoked by Compositae (sesquiterpene lactones and acetylenic compounds).

Overall, the chapters provide recent data, data of significance to human poisonings, and much insight into the complexity of poisoning by natural products. Chemical structures are provided for many classical poisons as well as for some recently characterized molecules. Finally, clinical management is provided where available on a number of poisonous plants.

This book will be of interest to numerous specialists such as botanists, chemists, pharmacognosists, and horticulturalists as well as those in the medical and health professions. The topics discussed are a welcome addition to the relatively sparse literature in the field.

Reviewed by Ara Der Marderosian
Philadelphia College of Pharmacy and Science
Philadelphia, PA 19104

REVIEWS

Pharmaceutical Handbook, 19th ed. Edited by AINLEY WADE. The Pharmaceutical Press, 1 Lambeth High St., London SE1 7JN, England. 1980. 783 pp. 18 × 20 cm. Price $35.00. (Available from Rittenhouse Book Distributors, 251 S. 24th St., Philadelphia, PA 19103.)

Developed as a companion to *Martindale: The Extra Pharmacopoeia*, the *Pharmaceutical Handbook* contains a wealth of information of use to students, practicing pharmacists, and practitioners of allied professions. The 19th edition is the most recent volume in a series that originated in 1906.

The *Handbook* has been thoroughly revised and updated since its previous edition in 1970. The 117-page section on the preparation and supply of medicines has been rewritten. A new checklist of potential incompatibilities of additives to intravenous preparations has been included, and the table of drug interactions has been extended.

The other major sections of the book cover diverse topics such as computers and their applications in pharmacy, sterilization methods and tests, disinfectants and antiseptics, physiological values for body fluids, drug absorption, poisoning, microbiology, immunology, nomenclature of organic compounds, and weights and measures.

The 24-page section of miscellaneous data includes geometrical formulas, mathematical notations, signs, and symbols, calculus equations, the Russian and Greek alphabets, a table for the determination of body surface area from height and weight, and a periodic table. A glossary of proprietary names and equivalent approved names lists trade names for single-entity preparations available in the United Kingdom along with their approved names.

A 136-page glossary gives concise definitions of medical and pharmaceutical terms along with definitions of radiological terms, terms used in foreign prescriptions, and units and measures. The book concludes with a 38-page index.

The *Handbook* is a convenient reference source that contains valuable information which otherwise could be found only by consulting many other sources.

Staff Review

Substituent Constants for Correlation Analysis in Chemistry and Biology. By CORWIN HANSCH and ALBERT LEO. Wiley, 605 Third Ave., New York, NY 10016. 1979. 339 pp. 21 × 28 cm. Price $24.95.

This book is organized into two sections: a descriptive section that lightly covers the fundamentals of chemical structure–physical parameter theory and estimation (65 pages) and a set of tables, in the form of computer printouts, that contain fragment constants and partition coefficients which were extracted from the literature. The tables are provided as separate appendixes. The first appendix contains about 100 pages and is entitled Electronic, Steric, and Hydrophobic (π) Constants. The second appendix contains about 160 pages and is entitled Partition Coefficients. The last appendix contains four pages and is entitled Hydrophobic Fragment Constants.

The expressed purpose of this book (the authors refer to it as a monograph) is "to provide a comprehensive listing of parameters of proven value for the correlation of structure with chemical or biologic reactivity." The tables provided seem to represent the most complete source of information yet organized for such use, and the book therefore admirably accomplishes its stated goal. The tables are not the easiest to decipher, given their computerized structure, but they nevertheless are a rich source of well-referenced information on the influences of structure on physical and chemical events. Partitioning data listed are for diverse solvent systems.

The opening, narrative section of the book has very brief discussions of electronic, steric, and hydrophobic parameters; molar refractivity and parachor; and cluster analysis. These discussions are provided at the advanced undergraduate level. They provide a minimal preparation for the use of the extensive tabulations that follow. To an extent, this aspect of the book is disappointing since the discussions are largely phenomenological and fail to deal with physicochemical events, such as hydrophobicity, in terms of present understanding of their fundamental molecular origins.

While limitations and/or uncertainties in parameter estimations are presented fairly, severe mechanistic shortcomings of quantitative structure–activity relationship approaches are skirted completely. The idea of the prospective use of quantitative structure–activity relationships is sold; the fact that applications have been largely retrospective goes unmentioned.

On balance, the book contains much useful information in tables and material in short chapters which should be part of the coursework of medicinal chemistry and pharmaceutics programs. It makes a valuable library addition but should be considered for personal collections only by those emphasizing quantitative structure–activity relationships in their teaching or research.

Reviewed by Gordon L. Flynn
College of Pharmacy
University of Michigan
Ann Arbor, MI 48104

Toxic Plants. Edited by A. DOUGLAS KINGHORN. Columbia University Press, 562 W. 113th St., New York, NY 10025. 1979. 195 pp. 15 × 23.5 cm. Price $20.00.

This book is the result of a symposium on toxic plants held at the University of Miami in 1977 as part of the annual Society for Economic Botany meeting. It features contributions by eight major authors on various aspects of plant poisoning. It is an up-to-date treatment providing chemical, biochemical, and toxicological information on a wide range of poisonous plants.

The problem of poisonous plants is described in general in the first chapter. Problems related to phytotoxicology are discussed such as plants with known toxic constituents that are not always poisonous, the uneven quality of the existing literature, the need for accurate identification to access information, the question of labeling poisonous ornamental plants, and the difficulty of improving the present body of information.

The remaining chapters cover and update several specific and important areas of interest in poison plants such as toxic mushrooms (amatoxins, phallotoxins, phallolysin, antamanide, ibotenic acid, muscimol, psilocybin, muscarine, gyromitrin, and coprine); toxins and teratogens of the Solanaceae and Liliaceae (nonalkaloidal toxins, tropane alkaloids, pyridine/piperidine alkaloids, and steroidal alkaloids); pokeweed and other lymphocyte mitogens (lectins, mitogens, Abrus lectin, abrin, and Hura and Robinia lectins); a literature review and clinical management of household ornamental plants potentially toxic to humans; cocarcinogenic irritant Euphorbiaceae (phorbol esters, ingenol esters, daphnane esters, and diterpene esters); the poisonous Anacardiaceae (botany, phenolic compounds, and immunological studies); and contact hypersensitivity and photodermatitis evoked by Compositae (sesquiterpene lactones and acetylenic compounds).

Overall, the chapters provide recent data, data of significance to human poisonings, and much insight into the complexity of poisoning by natural products. Chemical structures are provided for many classical poisons as well as for some recently characterized molecules. Finally, clinical management is provided where available on a number of poisonous plants.

This book will be of interest to numerous specialists such as botanists, chemists, pharmacognosists, and horticulturalists as well as those in the medical and health professions. The topics discussed are a welcome addition to the relatively sparse literature in the field.

Reviewed by Ara Der Marderosian
Philadelphia College of Pharmacy and Science
Philadelphia, PA 19104

NOTICES

Microbiology—1980. Edited by DAVID SCHLESSINGER. American Society for Microbiology, 1913 I St., N. W., Washington, DC 20006. 1980. 400 pp. 17 × 26 cm. Price $22.00.

Vitamin E: A Comprehensive Treatise. Edited by LAWRENCE J. MACHLIN. (Basic and Clinical Nutrition, Vol. 1.) Dekker, 270 Madison Ave., New York, NY 10016. 1980. 660 pp. 15 × 23 cm. Price $79.50.

Antifungal Chemotherapy. Edited by D. C. E. SPELLER. Wiley, 605 Third Ave., New York, NY 10016. 1980. 446 pp. 15 × 23 cm. Price $80.00.

Topics in Antibiotic Chemistry, Vol. 4: The Chemistry and Antimicrobial Activity of New Synthetic β-Lactam Antibiotics. By P. G. SAMMES. Wiley, 605 Third Ave., New York, NY 10016. 1980. 273 pp. 15 × 23 cm. Price $75.00.

Advances in Sex Hormone Research, Vol. 4. Edited by J. A. THOMAS and R. L. SINGHAL. Urban & Schwarzenberg, 7 E. Redwood St., Baltimore, MD 21202. 1980. 364 pp. 15 × 23 cm. Price $32.50.

Vaccine Preparation Techniques. Edited by J. I. DUFFY. Noyes Data Corp., Mill Rd. at Grand Ave., Park Ridge, NJ 07656. 1980. 403 pp. 16 × 23 cm. Price $48.00.

Invertebrate Neuropharmacology. By LUCY D. LEAKE and ROBERT J. WALKER. Wiley, 605 Third Ave., New York, NY 10016. 1980. 358 pp. 15 × 23 cm. Price $59.95.

Current Chemotherapy and Infectious Disease, Vols. 1 and 2. Edited by JOHN D. NELSON and CARLO GRASSI. American Society for Microbiology, 1913 I St., N. W., Washington, DC 20006. 1980. 774 and 1023 pp. 17 × 26 cm. Price $75.00 per two-volume set.

Advances in Steroid Biochemistry and Pharmacology, Vol. 7. Edited by M. H. BRIGGS and A. CORBIN. Academic, 111 Fifth Ave., New York, NY 10003. 1980. 125 pp. 15 × 23 cm. Price $23.00.

An Introduction to the Chemistry and Biochemistry of Pyrimidines, Purines and Pteridines. By DEREK T. HURST. Wiley, 605 Third Ave., New York, NY 10016. 1980. 266 pp. 15 × 23 cm. Price $39.00.

The Laser Doppler Techniques. By L. E. DRAIN. Wiley, 605 Third Ave., New York, NY 10016. 1980. 241 pp. 15 × 23 cm. Price $39.95.

Semisynthetic Proteins. By R. E. OFFORD. Wiley, 605 Third Ave., New York, NY 10016. 1980. 235 pp. 15 × 23 cm. Price $46.75.

Fragrances and Flavors: Recent Developments. Edited by S. TORREY. Noyes Data Corp., Mill Rd. at Grand Ave., Park Ridge, NJ 07656. 1980. 233 pp. 15 × 23 cm. Price $45.00.

Photochemistry, Vol. 10. D. BRYCE-SMITH, Senior Reporter. (A Specialist Periodical Report.) The Chemical Society. 1979. 717 pp. 12 × 22 cm. Price $103.00. (Available from Special Issues Sales, American Chemical Society, 1155 16th St., N. W., Washington, DC 20036.)

Carbohydrate Chemistry, Vol. 11. D. S. BRIMACOMBE, Senior Reporter. (A Specialist Periodical Report.) The Chemical Society. 1980. 546 pp. 13 × 22 cm. Price $95.00. (Available from Special Issues Sales, American Chemical Society, 1155 16th St., N. W., Washington, DC 20036.)

Aliphatic and Related Natural Product Chemistry, Vol. 1. (A Specialist Periodical Report.) The Chemical Society. 1979. 308 pp. 13 × 22 cm. Price $55.00. (Available from the American Chemical Society, 1155 16th St., N. W., Washington, DC 20036.)

Drug Disposition in Humans: The Basis of Clinical Pharmacology. By WILLIAM A. CREASEY. Oxford University Press, 200 Madison Ave., New York, NY 10016. 1979. 237 pp. 15 × 23 cm. Price $9.95.

Progress in Drug Metabolism, Vol. 3. Edited by J. W. BRIDGES and L. F. CHASSEAUD. Wiley, 605 Third Ave., New York, NY 10016. 1979. 372 pp. 15 × 23 cm. Price $48.50.

Noncatecholic Phenylethylamines, Part 2: Phenylethanolamine, Tyramines, and Octopamine. Edited by ARON D. MOSNAIM and MARION E. WOLF. (Modern Pharmacology–Toxicology Series, Vol. 12.) Dekker, 270 Madison Ave., New York, NY 10016. 1980. 365 pp. 15 × 23 cm. Price $55.00.

Drugs and the Elderly: Perspectives in Geriatric Clinical Pharmacology. Edited by J. CROOKS and I. H. STEVENSON. University Park Press, 233 E. Redwood St., Baltimore, MD 21202. 1979. 304 pp. 15 × 23 cm. Price $49.50.

Analysis of Drugs and Metabolites by Gas Chromatography–Mass Spectrometry, Vol. 6: Cardiovascular, Antihypertensive, Hypoglycemic, and Thyroid-Related Agents. By BENJAMIN J. GUDZINOWICZ and MICHAEL J. GUDZINOWICZ. Dekker, 270 Madison Ave., New York, NY 10016. 1979. 446 pp. 15 × 23 cm. Price $47.50.

Lecture Notes on Pharmaceutics. By LUCY S. C. WAN. Medical Book Center, 204 Textile Center, Singapore 7, Singapore. 1979. 256 pp. 14 × 20 cm.

Principal Drugs: An Alphabetical Guide, 6th ed. By S. J. HOPKINS. Faber and Faber. 1980. 164 pp. 10 × 16 cm. Price $4.50 (soft cover). (Available from Merrimack Book Service, 99 Main St., Salem, NH 03079.)

Thermoregulatory Mechanisms and Their Therapeutic Implications. Edited by B. COX, P. LOMAX, A. S. MILTON, and E. SCHÖNBAUM. S. Karger AG, Arnold-Böcklin-Strasse 25, CH-4101 Basel, Switzerland. 1980. 303 pp. 17 × 24 cm.

IARC Monographs on the Evaluation of the Carcinogenic Risk of Chemicals to Humans, Supplement 1: Chemical and Industrial Processes Associated with Cancer in Humans. International Agency for Research on Cancer. 1979. 71 pp. 17 × 24 cm. Price Sw. fr. 10. (Available from the World Health Organization, 1211 Geneva 27, Switzerland.)

IARC Monographs on the Evaluation of the Carcinogenic Risk of Chemicals to Humans: Some Halogenated Hydrocarbons, Vol. 20. International Agency for Research on Cancer. 1979. 609 pp. 17 × 24 cm. Price Sw. fr. 60. (Available from the World Health Organization, 1211 Geneva 27, Switzerland.)

Handbook of Biological Psychiatry, Part II: Brain Mechanisms and Abnormal Behavior—Psychophysiology. Edited by HERMAN M. van PRAAG, MALCOLM H. LADER, OLE J. RAFAELSEN, and EDWARD J. SACHAR. Dekker, 270 Madison Ave., New York, NY 10016. 1980. 491 pp. 15 × 23 cm.

Increasing the Impact of Social Innovations Funded by Grantmaking Organizations. Edited by JACK LINDQUIST. W. K. Kellogg Foundation, 400 North Ave., Battle Creek, MI 49016. 1980. 324 pp. 14 × 23 cm.

Problems of Drug Dependence, 1979. Edited by LOUIS S. HARRIS. (NIDA Research Monograph 27.) National Institute on Drug Abuse, 5600 Fishers Lane, Rockville, MD 20857. 1979. 482 pp. 15 × 23 cm. (Available from the Superintendent of Documents, U.S. Government Printing Office, Washington, DC 20402.)

Bibliography of Doctoral Theses in Pharmaceutical Sciences, Indian Universities, 1951–1979. Edited by A. P. HARDAS. Swastik Printing Press, Huns Talkies Road, Belgaum-590002, India. 1979. 28 pp. 10 × 12 cm. Price $1.00.

Chemicals Which Cause Birth Defects—Teratogens: A Brief Guide. By VERA KOLB MEYERS and CAL Y. MEYERS. 1980. 37 pp. 14 × 21 cm. Price $3.00. (Available from Vera Kolb Myers, School of Medicine, Southern Illinois University, Carbondale, IL 62901.)

NEW JOURNALS

Asian Journal of Pharmaceutical Sciences. Edited by LUCY S. C. WAN. Medical Book Center, Crawford P. O. Box 666, Singapore 7, Singapore. 1979. 16 × 21.5 cm. Price $18.00 per volume.

Medicinal and Aromatic Plants Abstracts. Publications & Information Directorate, Council of Scientific & Industrial Research, Hillside Rd., New Delhi-110012, India. 15 × 24 cm. Price $17.00 per volume (six issues), $3.00 per single copy.

NOVEMBER 1980
VOLUME 69 NUMBER 11

JOURNAL OF PHARMACEUTICAL SCIENCES

MARY H. FERGUSON
Editor

SHELLY ELLIOTT
Production Editor

NICOLETTE TRIANTAFELLU
Copy Editor

EDWARD G. FELDMANN
Contributing Editor

SAMUEL W. GOLDSTEIN
Contributing Editor

BELLE R. BECK
Editorial Secretary

DAVID BOHARDT
Director of Publications

L. LUAN CORRIGAN
Assistant Director of Publications

EDITORIAL ADVISORY BOARD

JOHN AUTIAN
NORMAN R. FARNSWORTH
WILLIAM O. FOYE
WILLIAM J. JUSKO
HERBERT A. LIEBERMAN
DAVID E. MANN, JR.
GERALD J. PAPARIELLO
EDWARD G. RIPPIE

The *Journal of Pharmaceutical Sciences* (ISSN 0022-3549) is published monthly by the American Pharmaceutical Association (APhA) at 2215 Constitution Ave., N.W., Washington, DC 20037. Second-class postage paid at Washington, D.C., and at additional mailing office.

All expressions of opinion and statements of supposed fact appearing in articles or editorials carried in this journal are published on the authority of the writer over whose name they appear and are not to be regarded as necessarily expressing the policies or views of APhA.

Offices—Editorial, Advertising, and Subscription: 2215 Constitution Ave., N.W., Washington, DC 20037. All Journal staff may be contacted at this address. Printing: 20th & Northampton Streets, Easton, PA 18042.

Annual Subscriptions—United States and foreign, industrial and government institutions $60, educational institutions $60, individuals *for personal use only* $30; single copies $5. All foreign subscriptions add $5 for postage. Subscription rates are subject to change without notice. Members of APhA may elect to receive the *Journal of Pharmaceutical Sciences* as a part of their annual $80 (foreign $85) APhA membership dues.

Claims—Missing numbers will not be supplied if dues or subscriptions are in arrears for more than 60 days or if claims are received more than 60 days after the date of the issue, or if loss was due to failure to give notice of change of address. APhA cannot accept responsibility for foreign delivery when its records indicate shipment was made.

Change of Address—Members and subscribers should notify at once both the Post Office and APhA of any change of address.

Photocopying—The code at the foot of the first page of an article indicates that APhA has granted permission for copying of the article beyond the limits permitted by Sections 107 and 108 of the U.S. Copyright Law provided that the copier sends the per copy fee stated in the code to the Copyright Clearance Center, Inc., 21 Congress St., Salem, MA 01970. Copies may be made for personal or internal use only and not for general distribution.

Microfilm—Available from University Microfilms International, 300 N. Zeeb Road, Ann Arbor, MI 48106.

© Copyright 1980, American Pharmaceutical Association, 2215 Constitution Ave., N.W., Washington, DC 20037; all rights reserved.

SCIENTIFIC INFORMATION IN FORMULATING PUBLIC POLICY

In the August issue of this journal, we published an editorial relating to the publicity and controversy surrounding the issuance of a report, entitled "Toward Healthful Diets," by the Food and Nutrition Board of the National Academy of Sciences–National Research Council. Although our editorial touched on the significant recommendations concerning human diet, health, and nutrition contained in the report, we directed our principal focus at the alleged bias and conflict-of-interest charges which were widely discussed in the public press.

We also expressed our sorrow at the damage this brouhaha was having on the public image of the prestigious sponsoring organization. In fact, the editorial was entitled "Maintaining NAS–NRC Credibility," because of our emphasis on this aspect and our gratuitous suggestions as to how the NAS–NRC might reorient its committee appointment process to minimize future reoccurrences.

The NAS President, Philip Handler, responded to our comments and we are pleased to publish his letter in the *Open Forum* section of this month's journal. His letter serves to bring out several points that were not included in our editorial—either (*a*) because of our inadvertent oversight, or (*b*) because those points were personally unknown to us. In the first category, Dr. Handler correctly points out that even those scientists who have disagreed with the report recommendations "*have not found the Board's work or its assessment unsound or unscientific.*" In the second category, Dr. Handler explains that the problem of apparent bias "*cropped up through news reports that stopped short of the full truth*" by pointing out that some members were identified with one side of the issue but neglecting to point out that other members were equally identified with the other side of the issue. Hence, Dr. Handler tells us, the Board did, in fact, have the balanced "mix of people" that we urged in the conclusion of our editorial.

Referring to the technical dispute concerning the FNB report, President Handler poignantly states in his letter, "*The scientific disagreement has turned not on the evidence but on what advice to offer the public at large under these shaky circumstances.*"

Whether, as scientists, we like it or not, and whether or not we feel that is how decision-making should operate, this last observation of Dr. Handler's reflects more and more how the system of public policy is functioning in today's world.

Indeed, in early October a symposium—and by sheer coincidence also sponsored by the NAS–NRC—was held on the subject of "The Role of Scientific Information in Decision-Making." The announcement publicizing the conference explained that 10 years ago words like benzene, DES, 2,4,5-T, and chlorofluorocarbons were found only in chemistry textbooks. But today they are seen in front-page stories in newspapers across the country. All of these terms became familiar for the same reason—the government has restricted the use of these substances based on scientific evidence of adverse effects.

The symposium further brought out that the pertinent scientific information is only a single dimension in a total process that involves many considerations including legal, economic, environmental, political, statistical, and various other factors.

We feel that it is important for all of us to recognize that such is the total process by which public policy decision-making is performed today. Indeed, this is how the process currently operates under the best of circumstances; often there is no scientific input at all and the decision may simply turn on one or two of these other factors, such as the political considerations.

At any rate, the day is now gone when public policy decisions are determined solely by scientific data and technical findings. Moreover, leaving our bias for science aside for the moment, this writer is inclined to conclude that this latter development is a good thing. For all its virtues, science provides too narrow a perspective, and the best decisions are going to be those that embody all considerations—including, but not limited to, the scientific aspects.

—EGF

NOVEMBER 1980
VOLUME 69 NUMBER 11

JOURNAL OF PHARMACEUTICAL SCIENCES

MARY H. FERGUSON
Editor

SHELLY ELLIOTT
Production Editor

NICOLETTE TRIANTAFELLU
Copy Editor

EDWARD G. FELDMANN
Contributing Editor

SAMUEL W. GOLDSTEIN
Contributing Editor

BELLE R. BECK
Editorial Secretary

DAVID BOHARDT
Director of Publications

L. LUAN CORRIGAN
Assistant Director of Publications

EDITORIAL ADVISORY BOARD

JOHN AUTIAN
NORMAN R. FARNSWORTH
WILLIAM O. FOYE
WILLIAM J. JUSKO
HERBERT A. LIEBERMAN
DAVID E. MANN, JR.
GERALD J. PAPARIELLO
EDWARD G. RIPPIE

The *Journal of Pharmaceutical Sciences* (ISSN 0022-3549) is published monthly by the American Pharmaceutical Association (APhA) at 2215 Constitution Ave., N.W., Washington, DC 20037. Second-class postage paid at Washington, D.C., and at additional mailing office.

All expressions of opinion and statements of supposed fact appearing in articles or editorials carried in this journal are published on the authority of the writer over whose name they appear and are not to be regarded as necessarily expressing the policies or views of APhA.

Offices—Editorial, Advertising, and Subscription: 2215 Constitution Ave., N.W., Washington, DC 20037. All Journal staff may be contacted at this address. Printing: 20th & Northampton Streets, Easton, PA 18042.

Annual Subscriptions—United States and foreign, industrial and government institutions $60, educational institutions $60, individuals *for personal use only* $30; single copies $5. All foreign subscriptions add $5 for postage. Subscription rates are subject to change without notice. Members of APhA may elect to receive the *Journal of Pharmaceutical Sciences* as a part of their annual $80 (foreign $85) APhA membership dues.

Claims—Missing numbers will not be supplied if dues or subscriptions are in arrears for more than 60 days or if claims are received more than 60 days after the date of the issue, or if loss was due to failure to give notice of change of address. APhA cannot accept responsibility for foreign delivery when its records indicate shipment was made.

Change of Address—Members and subscribers should notify at once both the Post Office and APhA of any change of address.

Photocopying—The code at the foot of the first page of an article indicates that APhA has granted permission for copying of the article beyond the limits permitted by Sections 107 and 108 of the U.S. Copyright Law provided that the copier sends the per copy fee stated in the code to the Copyright Clearance Center, Inc., 21 Congress St., Salem, MA 01970. Copies may be made for personal or internal use only and not for general distribution.

Microfilm—Available from University Microfilms International, 300 N. Zeeb Road, Ann Arbor, MI 48106.

© Copyright 1980, American Pharmaceutical Association, 2215 Constitution Ave., N.W., Washington, DC 20037; all rights reserved.

SCIENTIFIC INFORMATION IN FORMULATING PUBLIC POLICY

In the August issue of this journal, we published an editorial relating to the publicity and controversy surrounding the issuance of a report, entitled "Toward Healthful Diets," by the Food and Nutrition Board of the National Academy of Sciences–National Research Council. Although our editorial touched on the significant recommendations concerning human diet, health, and nutrition contained in the report, we directed our principal focus at the alleged bias and conflict-of-interest charges which were widely discussed in the public press.

We also expressed our sorrow at the damage this brouhaha was having on the public image of the prestigious sponsoring organization. In fact, the editorial was entitled "Maintaining NAS–NRC Credibility," because of our emphasis on this aspect and our gratuitous suggestions as to how the NAS–NRC might reorient its committee appointment process to minimize future reoccurrences.

The NAS President, Philip Handler, responded to our comments and we are pleased to publish his letter in the *Open Forum* section of this month's journal. His letter serves to bring out several points that were not included in our editorial—either (*a*) because of our inadvertent oversight, or (*b*) because those points were personally unknown to us. In the first category, Dr. Handler correctly points out that even those scientists who have disagreed with the report recommendations "*have not found the Board's work or its assessment unsound or unscientific.*" In the second category, Dr. Handler explains that the problem of apparent bias "*cropped up through news reports that stopped short of the full truth*" by pointing out that some members were identified with one side of the issue but neglecting to point out that other members were equally identified with the other side of the issue. Hence, Dr. Handler tells us, the Board did, in fact, have the balanced "mix of people" that we urged in the conclusion of our editorial.

Referring to the technical dispute concerning the FNB report, President Handler poignantly states in his letter, "*The scientific disagreement has turned not on the evidence but on what advice to offer the public at large under these shaky circumstances.*"

Whether, as scientists, we like it or not, and whether or not we feel that is how decision-making should operate, this last observation of Dr. Handler's reflects more and more how the system of public policy is functioning in today's world.

Indeed, in early October a symposium—and by sheer coincidence also sponsored by the NAS–NRC—was held on the subject of "The Role of Scientific Information in Decision-Making." The announcement publicizing the conference explained that 10 years ago words like benzene, DES, 2,4,5-T, and chlorofluorocarbons were found only in chemistry textbooks. But today they are seen in front-page stories in newspapers across the country. All of these terms became familiar for the same reason—the government has restricted the use of these substances based on scientific evidence of adverse effects.

The symposium further brought out that the pertinent scientific information is only a single dimension in a total process that involves many considerations including legal, economic, environmental, political, statistical, and various other factors.

We feel that it is important for all of us to recognize that such is the total process by which public policy decision-making is performed today. Indeed, this is how the process currently operates under the best of circumstances; often there is no scientific input at all and the decision may simply turn on one or two of these other factors, such as the political considerations.

At any rate, the day is now gone when public policy decisions are determined solely by scientific data and technical findings. Moreover, leaving our bias for science aside for the moment, this writer is inclined to conclude that this latter development is a good thing. For all its virtues, science provides too narrow a perspective, and the best decisions are going to be those that embody all considerations—including, but not limited to, the scientific aspects.

—EGF

Maintaining NAS–NRC Credibility: A Reply

The editorial in your August issue, "Maintaining NAS–NRC Credibility," leaves the mistaken impression that the National Academy of Sciences–National Research Council has no system for protecting against the introduction of bias in its studies. You then go on to endorse a system that would identify experts' biases and then balance those when a committee is appointed by finding "the right mix of people." That is precisely the system that the NAS–NRC has been using for many years.

Our system is designed to protect against both the reality and the appearance of bias, but it failed to eliminate the appearance of bias within the Food and Nutrition Board recently because of a previously unrecognized gap in our procedures. I remain convinced that appearances, and only appearances, have been offended in this instance. Even fellow scientists who have disagreed with the Board's recommendations in "Toward Healthful Diets" have not found the Board's work or its assessment unsound or unscientific; all agree that the available evidence is inconclusive. The scientific disagreement has turned not on the evidence but on what advice to offer the public at large under these shaky circumstances.

The real issue is: How did the apparent bias gain such importance in the public eye when it had such limited importance in reality? The problem cropped up through news reports that stopped short of the full truth by pointing out that some members of the Food and Nutrition Board had connections with organizations that produce foods high in cholesterol. Almost universally ignored was the fact that some of this group (even some of the *same* individuals who consult for "procholesterol" companies) had connections with firms that deliberately produce foods *low* in cholesterol and saturated fats. The members of the Board are experts in nutrition and health, and their advice is sought on that basis by government, by industry, and by independent organizations such as ours. Their credibility and, consequently, that of the report and of the Academy itself became an issue only when the news media failed to provide a balanced perspective or the whole truth.

With hindsight, it might have been prudent to ask some members at the Food and Nutrition Board to step aside so as to ensure that the report proper and not its authors would be the center of attention and debate. But the professional credentials of those Board members are impressive and impeccable—and in the end, that must be what counts.

Philip Handler, President
National Academy of Sciences
Washington, DC 20418

Received September 26, 1980.

FD&C COLORS
(Crompton & Knowles)

for all three
1 Primary Dyes
2 Aluminum Lakes
3 Aluminum Lake Dispersions
PLUS
- sales/market research, counseling
- importing, exporting, warehousing

AUSTIN CHEMICAL COMPANY, INC.
205 West Touhy Avenue • Park Ridge, IL 60068
(312) 823-9020 TELEX 254-121

If your library shelves are getting a little crowded

It's time to consider *J. Pharm. Sci.* backfiles, now available on 35-mm. positive microfilm from:

University Microfilms, Inc.
300 N. Zeeb Road
Ann Arbor, Michigan 48106

Complete backfile, Vols. 1–54 (1912–1965) $658.80

Volumes 55 through last complete year $21.20/reel

(one volume/reel)

a Subsidiary of Xerox Corporation

JOURNAL OF PHARMACEUTICAL SCIENCES

NOVEMBER 1980
VOLUME 69 NUMBER 11

RESEARCH ARTICLES

Metabolism of Carprofen, a Nonsteroidal Anti-Inflammatory Agent, in Rats, Dogs, and Humans

F. RUBIO ˣ, S. SEAWALL, R. POCELINKO *, B. DeBARBIERI, W. BENZ, L. BERGER, L. MORGAN, J. PAO, T. H. WILLIAMS, and B. KOECHLIN

Received January 3, 1980, from the *Roche Research Center, Hoffmann-La Roche Inc., Nutley, NJ 07110.* Accepted for publication May 29, 1980. *Present address: Department of Clinical Pharmacology, American Cyanamid Company, Pearl River, NY 10905.

Abstract □ The metabolic disposition of ^{14}C-labeled carprofen [(±)-6-chloro-α-methylcarbazole-2-acetic acid] was investigated in rats, dogs, and humans. Carprofen is eliminated predominantly by biotransformation in these three species. In dogs and rats, the direct conjugation of carprofen to form an ester glucuronide and oxidation to the C-7 and the C-8 phenols followed by their conjugation represent the major metabolic pathways. Small amounts of the α-hydroxy derivative also are formed by these species and are excreted free in the urine. In dogs, biliary secretion predominates, and 70% of an intravenous dose of carprofen is excreted in the feces while 8–15% of the dose is excreted in the urine. In rats, fecal excretion due to biliary secretion varies from 60 to 75%, and urinary excretion accounts for 20–30% of an intravenous dose. In humans, direct conjugation of carprofen represents the only significant pathway of metabolism. Between 65 and 70% of the orally administered carprofen was found to be excreted as the ester glucuronide in the urine, and most of the remaining dose was estimated to be secreted as this metabolite in the bile. Due to enterohepatic circulation, only a fraction of the biliary metabolite was recovered in the feces in humans. Less than 5% of the dose was excreted in human urine as free, intact carprofen. In dogs and humans, plasma levels of carprofen and of total radioactivity exhibit a multiphasic decline. In the three human subjects studied, the terminal component declined with a 13–26-hr half-life; the terminal half-life was ~40 hr in dogs.

Keyphrases □ Carprofen—metabolism in rats, dogs, and humans □ Metabolism—carprofen in rats, dogs, and humans □ Anti-inflammatory agents—carprofen, metabolism in rats, dogs, and humans

Carprofen [(±)-6-chloro-α-methylcarbazole-2-acetic acid], a nonsteroidal drug, exhibits anti-inflammatory activity in several screening tests in rats (1, 2).

Fluorometric (3, 4) measurements of blood carprofen levels in human volunteers (5) and in dogs[1] receiving single doses of the drug showed a biexponential decline composed of a fast initial component and a very slow terminal component. Comparison of blood levels measured after single and multiple doses indicated predictable drug accumulation (6). As in dogs and rats, a small volume of distribution was consistent with the high drug concentration in the central plasma compartment that was observed in these subjects.

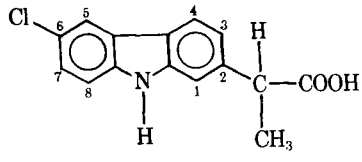

carprofen

The objectives of the present study were to establish and to compare the biotransformation of carprofen in dogs, rats, and human volunteers using ^{14}C-labeled drug and to determine further the disposition of the drug in these three species. A preliminary report on these investigations was published previously (7).

EXPERIMENTAL

Dose—[^{14}C]Carprofen, labeled in the α-position ($C_{15}H_{12}ClNO_2$, mol. wt. 273.2), was synthesized[2] with specific activities of 14.2 and 51.98 mCi/mmole. The radiopurity was at least 95%, and it was checked periodically by TLC. To minimize radiodecomposition during storage, the compound was dissolved in 10% ethanol in benzene. For the metabolic experiments, the specific activity was reduced to $1.0–6.0 \times 10^6$ dpm/mg for the dog and rat studies and to 0.5×10^6 dpm/mg for the human studies.

For the oral and intravenous dosing of dogs and rats, solutions were prepared containing 2.5 mg of [^{14}C]carprofen (0.0092 mEq)/ml in a mixture of five parts of propylene glycol, one part of 0.1 *N* NaOH (0.1 mEq), and four parts of distilled water.

[1] D. Maynard and S. A. Kaplan, Hoffmann-La Roche, Nutley, NJ 07110, reports on file.

[2] Syntheses were performed by Dr. Liebman and Dr. Muccino of the Roche Radiosynthesis Laboratory.

0022-3549/80/1100-1245$01.00/0
© 1980, American Pharmaceutical Association

Table I—TLC of Carprofen and Metabolites (R_f Values [a])

Solvent System	Carprofen	Carprofen Ester	I	I Ester	III	III Ester	IV	IV Ester
1 Chloroform–ethanol–formic acid (90:10:5)	0.48	0.69	0.27	0.55	0.36	0.53	0.36	0.51
2 Chloroform–ethanol–acetic acid (90:10:1)	0.38		0.0		0.28	0.53	0.22	
3 Chloroform–methanol–acetic acid (70:30:5)	0.79				0.76		0.76	
4 Chloroform–methanol–concentrated ammonia (70:30:1)	0.13		0.09 (trail)		0.13		0.13	
5 Chloroform–ethanol–formic acid (85:15:10)	0.65		0.44					
6 Chloroform–methanol–acetic acid (85:15:5)	0.60				0.51		0.51	

[a] These R_f values represent averages of several TLC runs and are reproducible within 10%. The metabolite esters all are methyl esters.

For oral administration to human subjects, radioactive carprofen was incorporated into tablets that were identical with the formulation used clinically. Each tablet contained 50 mg of [^{14}C]carprofen with a specific activity of 0.5 μCi/mg.

Animal Experiments—Two male beagle dogs, 12.8 and 10.1 kg, received a single intravenous dose of 1 mg of [^{14}C]carprofen/kg (Experiments D-I and D-V). Subsequently, the same dogs received a 1-mg/kg oral dose of this drug (D-II and D-VI). Two other dogs (D-III and D-XI) received single intravenous 10-mg/kg doses as a solution of 25 mg (0.092 mEq)/ml.

Blood specimens (5–10 ml, heparinized) were drawn by heart puncture or from the jugular vein at the indicated intervals. Aliquots of whole blood were taken for determination of the total carbon 14 content and for the hematocrit. The remaining blood was centrifuged. The radioactivity in the plasma was quantitated and fractionated, and the carbon 14 levels in the erythrocytes were calculated.

The dogs were kept in metabolism cages; urine (under toluene) and feces were collected for 96 hr at 24-hr intervals. Feces were homogenized in five volumes of 70% aqueous ethanol, and the radioactivity of these homogenates was determined using 10-fold dilutions.

In two additional male dogs weighing 10.5 (Experiment D-IV) and 7.6 (Experiment D-X) kg, the bile ducts were cannulated. The dogs were anesthetized by intravenous injection of 25–30 mg of pentobarbital sodium/kg. Anesthesia was maintained by additional 2.5-mg/kg pentobarbital sodium injections given about every 2 hr after the initial administration, as required. After intravenous injection of single 1-mg/kg doses of [^{14}C]carprofen, bile was collected for 5 hr at 0.5-hr intervals. Blood specimens were collected periodically from the cannulated femoral vein during the experiment.

After 5 hr, the dogs were sacrificed. The major tissues were excised, rinsed with ice-cold saline, and frozen. Aliquots (2–5 g) were homogenized with 10–20 volumes of ice-cold, aqueous, 0.2 *M* acetate buffer (pH 5) in a high-speed homogenizer.

Male 180–200-g Sprague–Dawley rats[3] were injected intravenously (tail vein) with 5 mg of [^{14}C]carprofen/kg in the described solution. Groups of three rats were sacrificed by decapitation after 10 min, 1 hr, and 4 hr, and plasma and the major tissues were collected. The tissues were homogenized as described, individually or as pools.

The bile ducts in two rats (320 g) were cannulated under light ether anesthesia, 5-mg/kg doses of [^{14}C]carprofen were administered intravenously, and bile was collected at 2-hr intervals for 6–7 hr, with the rats being in a conscious state and confined in restraining cages. Other animals were kept anesthetized with pentobarbital sodium (40 mg/kg), and their temperature was maintained at 37° during bile cannulation. In some experiments, Charles River CD rats of different ages and weights were used.

Urinary and fecal excretion (0–96 hr) of a 5-mg/kg iv dose of [^{14}C]-carprofen was determined in another group of three male rats.

Clinical Study[4]—Three male volunteers, 59–87 kg and 43–58 years old, were administered single 50-mg tablets of [^{14}C]carprofen orally with 240 ml of water. They fasted from 8 hr before until 4 hr after drug ingestion.

Blood specimens (10–15 ml, oxalated) were drawn before dosing and at 0.25, 0.5, 1, 2, 4, 6, 8, 12, and 24 hr and daily at 24-hr intervals after dosing for a minimum of 8 days or until no more radioactivity was detectable.

Urine was collected for intervals of 0–2, 2–4, 4–6, 6–9, 9–12, and 12–24 hr and as 24-hr pooled daily specimens thereafter until no more radioactivity was detected (for ~8–10 days). The creatinine content of each specimen was measured to provide an indication of completeness of urine collection. Feces were collected as 24-hr portions.

Quantification of Radioactivity—The isotope disintegration rates of all specimens were determined by liquid scintillation spectrometry[5] using the external standard channels ratio technique. Counting mixtures were prepared as follows. One milliliter of an aqueous tissue homogenate was mixed with 1.5 ml of distilled water and 10 ml of scintillation fluid[6] to produce a stable gelatinous suspension. Silica gel zones scraped from thin-layer chromatograms were suspended similarly in a mixture of 2.5 ml of water and 10 ml of scintillation fluid. Plasma aliquots of 0.1–1 ml were diluted to 2.5 ml with water and mixed with 10 ml of scintillation fluid. Aqueous solutions, diluted urine not exceeding 2 ml, and solvent extracts were mixed directly with the scintillation fluid.

Isotope disintegration rates in whole blood aliquots of 0.1–0.5 ml were determined following combustion[7].

Extraction and Fractionation of Drug Components from Urine, Bile, and Plasma—Intact carprofen and its unconjugated metabolites were extracted quantitatively (>95%) with 10 ml of ether from 0.5–1.0 ml of plasma diluted to 2 ml with 1.0 *M* acetate buffer (pH 5). The drug was extracted with two equal volumes of ether from urine titrated to pH 5. The extracted aqueous phase was titrated to pH 1 and was reextracted with ethyl acetate or with butanol at pH 5, using two extractions with equal solvent volumes. Diluted bile fractions, combined with 1 ml of 1.0 *M* acetate buffer (pH 5), were extracted twice with two volumes of ether to remove the free drug. The conjugates remaining in the aqueous phase were fractionated by cleaving first the ester glucuronide of carprofen at pH 11 (titration with 6 *N* NaOH) for 2 hr at room temperature and then the ethereal glucuronides by readjusting the pH to 5, adding 0.1 ml of glusulase enzyme[8], and incubating for 2 hr at 37°. Each treatment was followed by ether extraction of the freed metabolites at pH 5. The extracts were evaporated under nitrogen at 40–50°. The residues were taken up in 250 μl of ethanol immediately before aliquots were taken for measurement of the isotope disintegration rate and for TLC.

Suitable aliquots of these concentrated extracts were subjected to TLC on precoated silica gel 60 F254 plates[9] using the solvent systems listed in Table I. For preparative isolation (quantities up to 1 mg), each extract concentrate was streaked as a band across the plate; after development, the silica gel bands corresponding to the purified components were scraped off, suspended in a buffer, and extracted with a solvent.

The presence of intact [^{14}C]carprofen and other radioactive metabolites in plasma or tissue homogenates was determined by one-dimensional TLC of pH 5 ether extracts with System 1 and subsequent scanning[10]. These components were quantitated by two-dimensional TLC with System 2 and then System 4, scraping, and measurement of the isotope disintegration rates of the silica gel areas bearing the detected components.

Carprofen β-glucuronide ester in human plasma and urine was extracted (following removal of the free drug by ether extraction at pH 5) with ethyl acetate at pH 1. After cleavage of this ester at alkaline pH as

[3] Carworth Farm, N.Y.

[4] Special Treatment Unit, Newark Beth Israel Medical Center, Newark, N.J. (Dr. Robert Pocelinko, Scientific Director). The protocol of this study and the informed consent procedure were approved by the Institutional Review Committee, Newark Beth Israel Medical Center, Newark, N.J., on June 12, 1975. Use of radioactively labeled material in this human isotope study was approved as Amendment 14 of the Medical By-Product Material License 29-11847, assigned to Dr. Edward D. Fram, Newark Beth Israel Medical Center, by the U.S. Nuclear Regulatory Commission on March 13, 1975. It was approved by the Division of Oncology and Radiopharmaceutical Products of the Food and Drug Administration on February 5, 1976, as an addendum to IND 10,049 (carprofen) of Hoffmann-La Roche.

[5] Model 3380, Packard Instruments, Downers Grove, Ill.

[6] Aquasol, New England Nuclear Corp., Boston, Mass.

[7] Oxymat, Intertechnique Corp.

[8] Endo Laboratories, Garden City, N.Y.

[9] Brinkmann Instruments, Westbury, N.Y.

[10] Model 7201 scanner with a model 835 recording rate meter, Packard Instruments.

Table II—Excretion of Total Radioactivity in Urine and Feces of [^{14}C]Carprofen-Treated Dogs (Expressed as Cumulative Percent of Dose)

	Experiment					
	D-I	D-V	D-XI	D-III	D-II	D-VI
Dose, mg/kg	1.0	1.0	10.0	10.0	1.0	1.0
Route	Intravenous	Intravenous	Intravenous	Intravenous	Oral	Oral
Urinary excretion (at end of period)						
24 hr	10.29	8.02	5.52	9.41	17.34	8.07
48 hr	14.99	9.32	6.77	10.63	18.92	8.60
72 hr	15.20	9.50	—[a]	—[a]	19.07	8.72
96 hr	15.28	9.61	—[a]	—[a]	—[a]	—[a]
120 hr	15.31	—[a]	—[a]	—[a]	—[a]	—[a]
Fecal excretion (at end of period)						
24 hr	2.54	0.0	59.71	—[a]	32.0	45.01
48 hr	61.37	61.84	70.6	—[a]	66.7	65.71
72 hr	67.41	67.34	—[a]	—[a]	67.68	67.25
96 hr	67.97	68.26	—[a]	—[a]	—[a]	—[a]
Total excretion	83.28	77.87	77.37	—	86.75	75.97

[a] These specimens were not collected and analyzed.

Table III—Tissue Distribution of Total Radioactivity 5 hr after an Intravenous Dose of 1 mg of [^{14}C]Carprofen/kg in Two Bile Duct-Cannulated Dogs (D-IV and D-X)

Sample	Carbon 14 Found[a]		Percent of Dose		Tissue Concentration/ Plasma Concentration	
	D-IV	D-X	D-IV	D-X	D-IV	D-X
Plasma[b]	5.85	5.45	29.3[b]	27.1[b]	1.00	1.00
Liver	2.24	1.95	6.1	6.3	0.38	0.36
Kidneys	1.24	1.16	0.79	0.94	0.21	0.21
Brain	0.09	0.08	0.07	0.06	0.016	0.015
Lungs	1.40	1.09	1.23	0.81	0.24	0.20
Spleen	0.25	n.m.[c]	0.15	n.m.	0.04	n.m.
Heart	1.24	0.7	0.79	0.51	0.21	0.13
Muscle[d]	0.22	0.25	8.7[d]	9.9[d]	0.037	0.045
Testes	0.33	0.12	0.05	0.02	0.056	0.021
Fat[e]	0.50	0.46	2.5[e]	2.3[e]	0.093	0.085
Small intestine tissue	0.96	0.82	1.19	2.47	0.16	0.15
Large intestine tissue	0.61	0.51	0.65	0.34	0.10	0.094
Stomach and contents	0.46	0.49	0.43	0.40	0.08	0.09
Small intestine contents	—	—	0.54	0.69	—	—
Large intestine contents	—	—	0.06	0.08	—	—
Bile	—	—	23.5	26.9	—	—
Total	—	—	76.6	78.8	—	—

[a] In microgram equivalents per gram. [b] Assuming that plasma is 5% of the total body weight. [c] n.m. = nonmeasurable. [d] Assuming that muscle tissue is 40% of the total body weight. [e] Assuming that fat tissue is 5% of the total body weight.

described, glucuronic acid was identified by TLC on cellulose-precoated plates with the solvent system *n*-butanol–acetic acid–water (2:1:1) followed by naphthoresorcinol spray. Glucuronic acid was quantitated by the naphthoresorcinol assay (8, 9) following cleavage of the conjugate by mammalian liver β-glucuronidase[11].

Representative portions of all human urine specimens collected during the first 24 hr from each subject were pooled. One 2-ml aliquot of these pools and of each subsequent 24-hr urine portion (up to 120 hr) were extracted directly with ether at pH 5. A second aliquot was cleaved with sodium hydroxide as described, and the deconjugated carprofen was extracted with ether at pH 5. Both extracts were subjected to one- and two-dimensional TLC, and carprofen was quantitated as described.

To check specifically for the presence of Metabolites I and III in human urine, 10-ml portions of 0–72-hr urine pools (1% of each fraction) were extracted after both alkaline and glusulase cleavage, and the two extracts were subjected to one- and two-dimensional TLC in the presence of

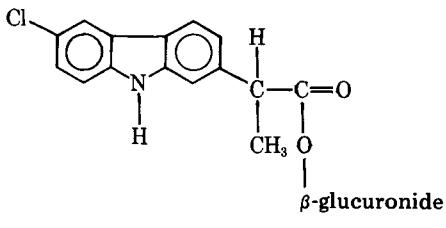

carprofen ester glucuronide

[11] Calbiochem, La Jolla, Calif.

nonlabeled standards of these metabolites. Since the recoveries of urinary carprofen varied from 85 to 95%, the values reported are uncorrected.

Analysis of Feces—Ten milliliters of a fecal homogenate in 70% ethanol was diluted with 10 ml of 1 *M* phosphate buffer (pH 7), and the dilution (35% ethanol) was extracted twice with 20 ml of ether followed by a backwash with 10 ml of water. The residue of the combined ether extracts was redissolved in 5 ml of ethanol–aqueous 0.1 *N* HCl (4:1). This solution was equilibrated twice with 10 ml of hexane. The hexane extracts were washed consecutively with a second 5-ml portion of the same ethanol–hydrochloric acid mixture and then were discarded. Both ethanol–hydrochloric acid solutions were diluted with 5 ml of 0.1 *N* HCl and extracted twice with 10 ml of a 3:2 mixture of ether and hexane. These extracts, containing 60–70% of the original radioactivity of a typical fecal homogenate, were combined, concentrated, and analyzed by one- and two-dimensional TLC essentially as described for the solvent extracts of urines.

Metabolite Characterization—UV spectra of solutions of ~5 μg/ml in 0.1 *N* HCl and in 0.1 *N* NaOH in 20% aqueous ethanol were measured using a microcell (0.5 ml) assembly in a spectrophotometer[12].

The fluorescence spectra of the individual metabolites of carprofen, dissolved in ethanol–1% acetic acid, were determined in a spectrofluorometer[13].

High-resolution and low-resolution mass spectra[14] were obtained. The ionizing energy was 70 ev, and the interface temperature was 270°. The

[12] DU, Beckman Instruments.

[13] Farrand.

[14] High-resolution mass spectra were obtained with a CEC 21-110 and low-resolution mass spectra were obtained with a Hitachi RMU-6L coupled to a Perkin-Elmer 990 gas chromatograph.

Table IV—UV and Fluorescent Spectra of Carprofen and Its Metabolites

Compound	Fluorescence (1% Acetic Acid in Ethanol)		UV Absorption			
			0.1 *N* HCl–20% Ethanol		0.1 *N* NaOH–20% Ethanol	
	$\lambda_{act}/\lambda_{emit}$, nm	TM[a]/μg/ml	A_{max}[b], nm	E[b], × 10^4	A_{max}[b], nm	E[b], × 10^4
I	295/375	123	240	5.10	240	5.21
			300	2.10	300	2.13
III	340/395	52 → 180[c]	245	5.35	255	5.02
			295	1.47	300	1.1
IV	310/360	422	240	5.05	245	4.37
			310	1.66	340	1.75
Carprofen	295/375	102	240	4.26	240	4.37
			300	1.67	300	1.75

[a] TM = fluorescence intensity reading. [b] E = molar absorptivity; A_{max} = wavelength of absorbance peak. [c] The first TM value represents the reading taken immediately after placing the sample into the light path of the fluorometer; the second TM value represents the final constant reading taken after leaving the sample in the light path for 5–10 min.

metabolite structures given in the text are based on integer masses combined with other information. GLC was performed on 3% OV-17 on 80–100-mesh Gas Chrom Q (183-cm × 4-mm i.d. column) at 250° or with temperature programming (4°/min to 300°) using a flame-ionization detector. The carrier gas was helium at 30 ml/min.

[^{14}C]Carprofen and its metabolites were esterified with diazomethane freshly prepared from *N,N*-nitrosomethylurea in ether in the presence of 40% KOH and distilled directly into the methanolic drug solution. Trimethylsilyl derivatives were prepared by reacting the compound under strictly anhydrous conditions with *N,O*-bis(trimethylsilyl)acetamide in silylation grade pyridine[15] for 30 min at room temperature. Methyl esters and trimethylsilyl methyl esters of carprofen and of some of its metabolites were separated and characterized by GLC[16] on a 122-cm column of 3% OV-17 on Gas Chrom Q (60–80 mesh) at a column temperature of 250° and a port temperature of 285°. The flame-ionization detector was operated at 300° at a hydrogen flow rate of 2.5 ml/min. The nitrogen carrier gas flow rate was 3.0 ml/min.

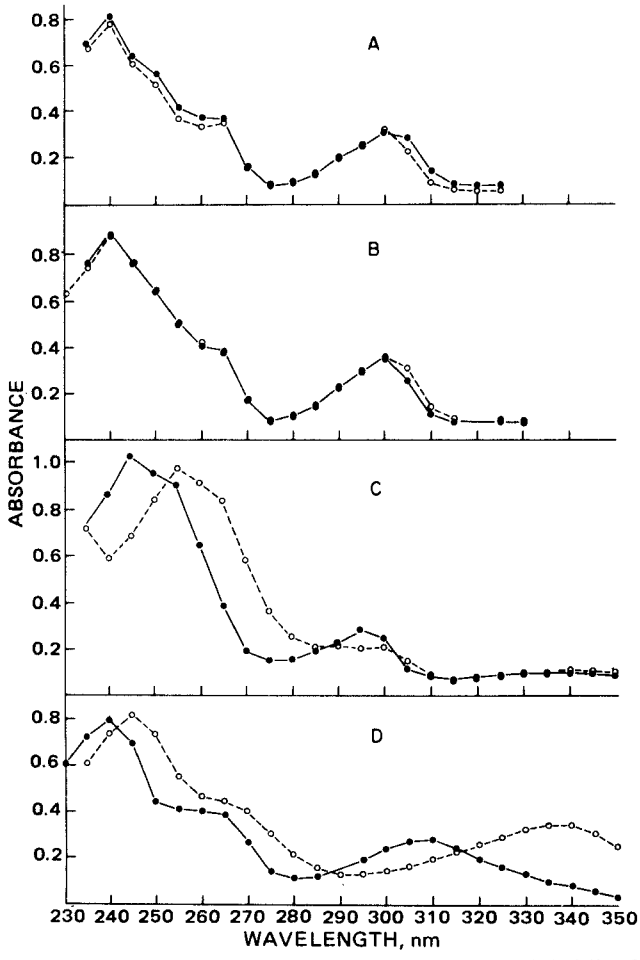

Figure 1—*Relative UV absorption spectra of carprofen (A), I (B), III (C), and IV (D) in acidic (●) and basic (○) media.*

[15] SIL BSA reagent, Pierce Chemical Co., Rockford, Ill.

RESULTS

Dog Experiments—*Excretion*—The cumulative excretion of total radioactivity by the dogs after intravenous and oral administration of 1 or 10 mg of labeled carprofen/kg accounted for 67–71% of the dose in the feces and for 7–19% in the urine (Table II). Twenty-four and 27% of the dose were excreted in the bile of two anesthetized bile duct-cannulated dogs within the first 5 hr after the intravenous administration of 1 mg of labeled carprofen/kg (Table III). Most of the radioactive fraction excreted in the feces by the intact dog after the intravenous dose (Table II) represented bile-secreted material since <1% of the dose was present in the intestinal contents in the bile duct-cannulated dogs within 5 hr after the dose of carprofen (Table III).

Identification of Urinary Metabolites of [^{14}C]*Carprofen*—The urinary metabolite patterns after a 1-mg/kg dose and after a 10-mg/kg dose were very similar. Dog urine excreted the 1st day after a 10-mg/kg iv dose of [^{14}C]carprofen (containing 9.41% of the dose) was fractionated. Direct extraction of the urine at pH 5 with ether removed 51% of the total urinary radioactivity. Subsequent extraction with butanol at pH 5 or with ethyl acetate at pH 1–2 removed an additional 28%. TLC of the ether extract in System 1 separated two quantitatively equal components of R_f 0.29 and 0.18, respectively. Intact carprofen (R_f 0.48) was absent.

UV-absorbing impurities were separated by preparative TLC with System 2, whereby the radioactive components remained at the origin. They were extracted together from the plate and separated from one another and from a remaining UV impurity by preparative TLC with System 5. Final purification, adequate for physical–chemical characterization, was achieved by extraction of each component from ether into 0.2 *N* NaOH, acidification of the alkaline extract, and reextraction into ether. Of these two radioactive excretion products, only the R_f 0.29 product represented a genuine metabolite of carprofen (Metabolite I); the R_f 0.18 component (Compound II) was an artifact[17].

Metabolite I—The UV spectrum of Metabolite I was independent of pH, and the maxima and respective molar absorptivities were similar to those of intact carprofen (Table IV and Fig. 1A). The two fluorescence spectra also were indistinguishable. These characteristics pointed to an intact, unsubstituted carbazole moiety.

The methyl ester of Metabolite I differed by TLC (Table I) from the free acid; on GLC, it appeared as a homogeneous peak with an R_t value of 8.2 min, distinct from that of carprofen methyl ester (R_t 5.5 min).

The mass spectrum of Metabolite I (the free acid) indicated a molecular ion at *m/e* 289 ($C_{15}H_{12}ClNO_3$), representing addition of one oxygen to carprofen, and a fragment at *m/e* 271 ($C_{15}H_{10}ClNO_2$), arising from the

[16] Model 402, Hewlett-Packard.

[17] Compound II proved to be derived from a labeled contaminant of the [^{14}C]-carprofen dose, which was not detected on TLC. Since the addition of carrier carprofen to prepare the doses did not reduce the specific activity of this contaminant to that of [^{14}C]carprofen, the specific activity of isolated Compound II, identified as α-hydroxy-α-desmethylcarprofen (by NMR, GLC–mass spectrometry, and synthesis), was several times that of the administered [^{14}C]carprofen. The fact that the same contaminant also is present, although to a lesser extent (0.5%), in unlabeled carprofen preparations is evidenced by the excretion of the same α-hydroxy-α-desmethylcarprofen derivative by dogs dosed with unlabeled drug.

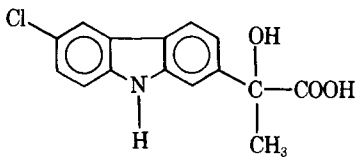

Metabolite I

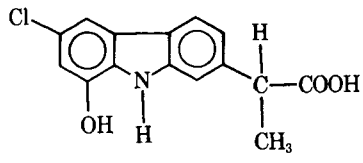

Metabolite III

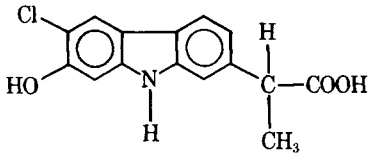

Metabolite IV

loss of water. GLC–mass spectrometry of the methyl ester revealed a molecular ion of *m/e* 303 ($C_{16}H_{14}ClNO_3$), indicative of the addition of one oxygen atom to the carprofen ester ($C_{16}H_{14}ClNO_2$). The fragmentation pattern suggested an unsubstituted carbazole ring structure, consistent with the UV spectral evidence.

The GLC–mass spectral pattern, TLC properties, and NMR spectra of Metabolite I and the authentic α-hydroxy derivative of carprofen, whose structure had been unambiguously established as that of a tertiary α-hydroxy compound by its synthesis from the α-keto acid by the Grignard reaction, were identical.

Metabolites III and IV—The polar urinary radioactivity extracted from dog urine with *n*-butanol at pH 5 did not migrate on TLC with System 1. However, it was converted to a compound with a higher R_f value when exposed to either alkaline or acidic conditions and, partly, after incubation with glusulase at pH 5. The converted (high R_f) fraction was extractable with ether at pH 1 and 5. It was prepared for further characterization (from dog urine preextracted with ether at pH 5 to remove Metabolite I and Compound II) in 83% yield by slow, repeated equilibration of the acidified urine (0.4 *N* HCl) with ether.

UV-absorbing contaminants were removed by equilibrating the ether solution with 0.2 *M* phosphate buffer (pH 7) and by extracting the metabolites into 0.2 *N* NaOH and returning them to ether at pH 5 with a recovery of 85%. Preparative TLC with System 2 achieved complete resolution of Metabolites III (R_f 0.27–0.32) and IV (R_f 0.21–0.25), representing 16 and 2.4% of the urinary radioactivity, respectively. Metabolite III discolored when it was left on a TLC plate and was unstable in alkaline solution. With adequate precautions, preparative TLC produced both metabolites in sufficiently pure form for physical–chemical identification.

Metabolite III exhibited a major absorption maximum in acidic solution at 245 nm which was shifted to 255 nm at alkaline pH (Table IV and Fig. 1C). This bathochromic shift indicated a phenolic structure. Spectrofluorometric analysis revealed maxima at 290 and 340 nm, both with emission maxima at 395 nm. The fluorescence intensity increased during the exposure of the solution to the 290-nm light source to a value that remained stable.

Methylation resulted in a major reaction product, which was purified by preparative TLC (R_f 0.56 in System 1). Its high-resolution mass spectrum revealed a molecular ion of *m/e* 303.0688 ($C_{16}H_{14}ClNO_3$), compatible with a methyl ester of a monohydroxy derivative of carprofen. Substitution in the carbazole ring was supported by the fragment of *m/e* 217.0308 ($C_{12}H_8ClNO$), which retains the added oxygen and arises from loss of the $C_4H_6O_2$ side chain, consistent with the phenolic structure evidenced by the pH-dependent UV spectrum of this metabolite.

To determine the position of this phenolic function, Metabolite III methyl ester was dissolved in 0.35 ml of deuterochloroform, and its PMR spectrum was determined. A single scan revealed a methyl ester band at δ 3.68 and a CH_3CH doublet (J = 6.5 Hz) at 1.59, indicating that the side chain was intact. A time-averaged spectrum of 229 scans of the δ 5–10 region revealed the following parameters: δ 6.81 (d, 1H, J *meta* = 2 Hz,

Table V—Excretion of Carprofen and Metabolites by Humans, Dogs, and Rats

Species	Number of Animals or Subjects	Dose, mg/kg	Administration Route	Excretion Route (Collection Period)	Percent of Dose[a]								Total Percent of Dose per Fraction
					Carprofen		Free I	III		IV	Polar Component	Total Recovered	
					Free	β-Glucuronide		Free	β-Glucuronide	β-Glucuronide			
Human, male	3	0.74 ± 0.15	Oral	Urine (0–120 hr)	2.84 ± 0.47	63.1 ± 10.8	0.3	—[b]	0.4	—	—	66.6	67.7
				Feces[c] (0–120 hr)	7.3	—	0.95	0.7	—	—	8.0	17.0	23.7
Dog, male	2	1.0	Intravenous	Urine (0–24 hr)	—	—	2.28 ± 0.3	—	1.30 ± 0.35	0.20 ± 0.05	2.40 ± 0.7	6.2	10.3
	1	1.0	Intravenous	Feces (24–48 hr)	7.8	—	—	7.2[d]	—	—	33.0	48.0	59.0
	2	1.0	Intravenous	Bile (0–5 hr)	2.25 ± 0.52	12.6 ± 2.2	0.73 ± 0.04	0.25[d] ± 0.05	2.58 ± 0.17	0.34 ± 0.04	2.88 ± 0.18	21.6	24.0 ± 1.1
	1	1.0	Oral	Urine (0–24 hr)	—	—	3.67	—	2.70	0.39	4.35	11.1	17.3
Rat, male	3 pooled	5.0	Intravenous	Urine (0–72 hr)	0.79	—	1.55	5.23[d]	—	—	7.46	15.0	19.2
				Feces (0–40 hr)	7.19	—	—	22.9[d]	—	—	15.9	46.0	57.2
	1	5.0	Intravenous	Bile (0–7 hr)	—	34.1	—	—	3.1	5.0	3.5	45.7	53.7

[a] The mean ± range is given for two values, and the mean ± *SD* is given for three values. [b] The dash indicates that the amounts found were <0.1% of the dose. [c] Quantitative distribution of carbon 14 component in human feces represents an estimate in one subject. [d] In these specimens, the TLC system did not differentiate between free III and free IV.

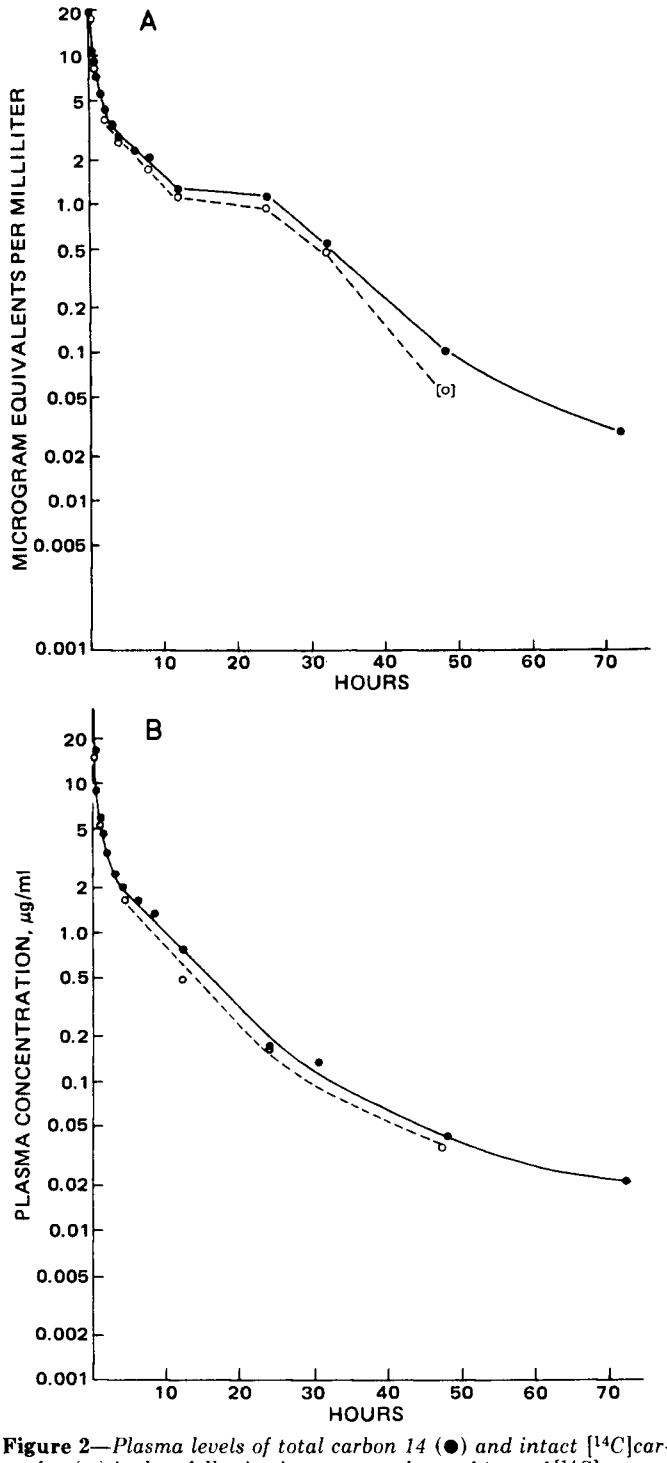

Figure 2—*Plasma levels of total carbon 14 (●) and intact [^{14}C]carprofen (○) in dogs following intravenous doses of 1 mg of [^{14}C]carprofen/kg. Key: A, Experiment D-I; and B, Experiment D-V.*

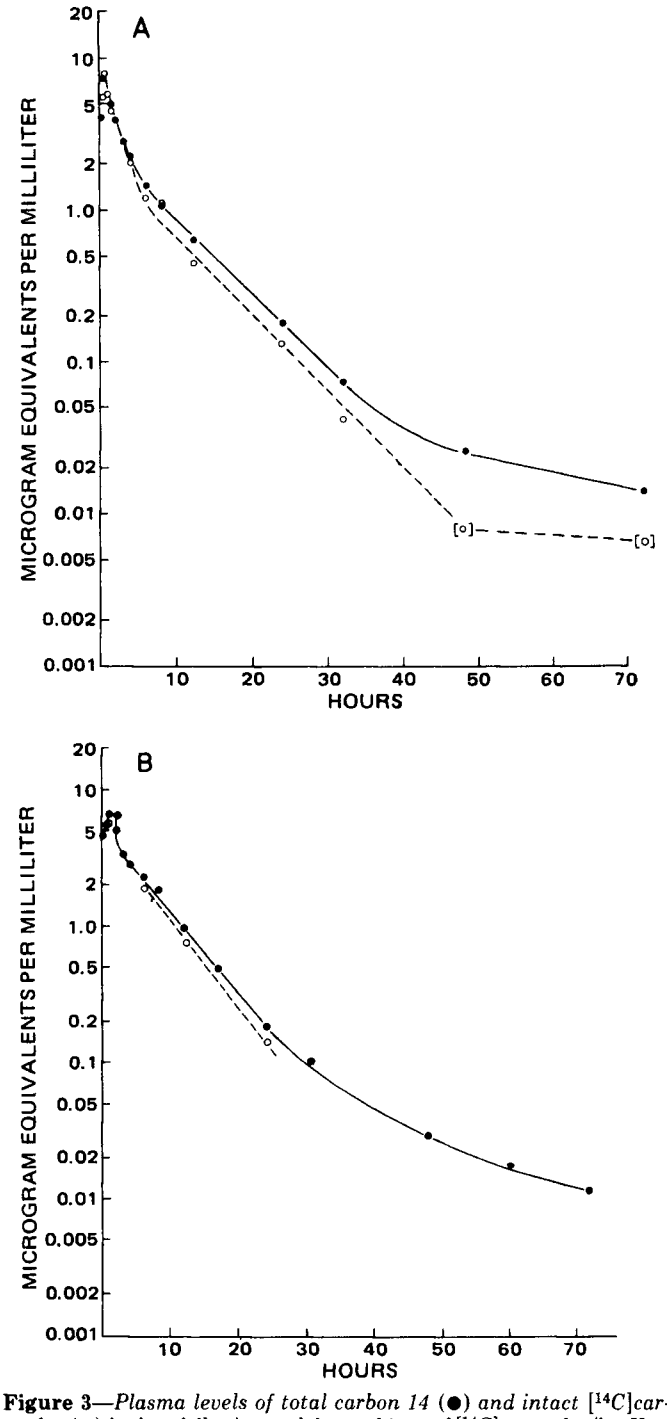

Figure 3—*Plasma levels of total carbon 14 (●) and intact [^{14}C]carprofen (○) in dogs following oral doses of 1 mg of [^{14}C]carprofen/kg. Key: A, Experiment D-II; and B, Experiment D-VI. Brackets indicate an estimated value.*

H-7), 7.17 (broad d, 1H, *J ortho* = 8 Hz, H-3), 7.38 (broad s, 1H, H-1), 7.59 (broad s, 1H, H-5), 7.90 (d, *J ortho* = 8 Hz, H-4), and 8.17 (broad, NH). The chemical shifts of the aromatic protons (H-1, H-3, and H-4) correspond (within ±0.02 ppm) with those of the parent ester and clearly showed that the alkyl-substituted ring was not hydroxylated. However, the bands at δ 6.81 and 7.59 were at δ 7.33 and 7.99 in the parent and indicated large significant upfield shifts of 0.52 (*ortho*) and 0.40 (*para*) ppm, respectively, which were attributed to the new hydroxyl group at C-8. This conclusion was confirmed by a resolved *meta*-splitting ($J_{5,7}$ = 2 Hz) observed in the H-7 signal. Thus, hydroxylation occurred definitely at C-8, and Metabolite III was characterized conclusively as 6-chloro-8-hydroxy-α-methylcarbazole-2-acetic acid.

The UV and fluorescence spectra of Metabolite IV differed from those of Metabolite III (Table IV and Fig. 1D). The UV spectrum of Metabolite IV exhibited a bathochromic shift from maxima at 240 and 310 nm to maxima at 245 and 340 nm. The fluorescence spectrum showed activation/emission maxima at 310/360 nm with a high intensity that was stable when exposed to light.

The high-resolution mass spectrum of the purified methyl ester of Metabolite IV indicated a molecular ion of *m/e* 303.0681 ($C_{16}H_{14}ClNO_3$), isomeric with that of Metabolite III methyl ester. The fragment of *m/e* 217.0206 ($C_{12}H_8ClNO$), arising from loss of the side chain ($C_4H_6O_2$), demonstrated oxygen addition in the carbazole moiety. These data support a structure for Metabolite IV of a phenolic monohydroxy derivative distinct from Metabolite III.

The position of the phenolic hydroxy function of Metabolite IV was elucidated by the NMR spectrum of its dimethyl derivative. Thus, the

Table VI—Excretion Patterns of [^{14}C]Carprofen and of Metabolites in Rats

Number of Rats	Strain (Sex)	Age, weeks	Weight, g	Dose mg/kg	Dose mg/Rat	Percent of Dose Excreted: Urine (0–72 hr)	Feces (0–72 hr)	Bile ^{14}C (0–4 hr)	Biliary Metabolites: Carprofen Glucuronide	III	IV	Polar Carbon 14
2	Carworth[a] Farm (M)	8	326	5.0	1.63	19.2	57.2	38.2[b]	24.3 ± 0.4	2.22 ± 0.38	3.55 ± 0.11	2.52 ± 0.11
3	Charles River (M)	10	410 ± 10	5.0	2.05 ± 0.05	—	—	34.8 ± 1.1	13.9 ± 0.44	11.0 ± 1.8	3.58 ± 0.21	2.96 ± 0.66
6	Charles River (F)	8–10	265 ± 14	5.0	1.33 ± 0.07	—	—	38.6 ± 6.7	12.6 ± 1.7	12.31 ± 3.1	4.75 ± 0.73	5.60 ± 2.1
3	Charles[c] River (M)	10	337 ± 32	3.0	1.04 ± 0.10	20.4 ± 2.0	74.6 ± 2.5	44.7 ± 6.3	15.4 ± 1.4	14.8 ± 3.8	5.9 ± 0.97	5.0 ± 2.0
3	Charles[c] River (M)	88	728 ± 90	3.0	2.27 ± 0.23	30.8 ± 6.7	58.3 ± 7.3	22.9 ± 3.8	11.0 ± 1.2	5.08 ± 1.8	3.23 ± 1.7	1.93 ± 0.74

[a] In these two experiments, rats used to measure excretion in urine and feces were different from those used to collect bile following bile duct cannulation. [b] Incomplete collection. [c] In these experiments, the same rats were used, first for the urinary and fecal excretion experiment and then, after 1 week, for the biliary secretion experiments.

Table VII—Tissue Distribution of Total Carbon 14 and [^{14}C]Carprofen in Rats at Different Times following Intravenous Administration of 5 mg of [^{14}C]Carprofen/kg

Tissue	10 Min: Carbon 14 Found[a]	Carbon 14 Ratio[b]	% of Carbon 14 Dose	μg of Carprofen/g	1 Hr: Carbon 14 Found[a]	Carbon 14 Ratio[b]	% of Carbon 14 Dose	μg of Carprofen/g	4 Hr: Carbon 14 Found[a]	Carbon 14 Ratio[b]	% of Carbon 14 Dose	μg of Carprofen/g
Plasma[c]	34.0	1.0	32.9[d]	29.6	20.2	1.00	19.5[d]	16.1	8.62	1.00	8.32[d]	5.9
Liver[c]	15.5	0.46	11.9	14.6	10.4	0.57	7.63	7.39	5.73	0.66	4.73	2.43
Kidneys[c]	21.7	0.64	3.3	20.5	16.3	0.81	2.45	13.5	7.44	0.86	1.09	5.19
Muscle[c]	1.9	0.056	—	1.81	1.65	0.082	—	1.33	0.64	0.07	—	0.45
Carcass[e]	2.36	0.069	32.9	2.18	2.28	0.110	32.4	1.64	0.87	0.10	12.3	0.55
Heart[f]	3.37	0.10	0.18	—	3.34	0.167	0.18	—	1.50	0.17	0.81	—
Brain[f]	0.66	0.019	0.11	—	0.44	0.022	0.07	—	0.19	0.02	0.03	—
Spleen[f]	2.18	0.063	0.09	—	1.74	0.086	0.08	—	1.04	0.04	0.04	—
Testes[f]	0.61	0.018	0.14	—	1.61	0.080	0.36	—	1.06	0.26	0.26	—
Fat[f]	0.77	0.022	—	—	1.31	0.065	—	—	0.82	0.14	—	—
Lungs[f]	3.57	0.11	0.63	—	9.25	0.46	0.64	—	2.86	0.33	0.23	—
GI tract[g] tissues	—	—	1.47	—	—	—	4.34	—	—	—	2.9	—
Small intestine[h]	—	—	3.26	—	—	—	20.5	—	—	—	19.0	—
Large intestine[h]	—	—	n.m.[i]	—	—	—	1.3	—	—	—	33.7	—
Total	—	—	86.88	—	—	—	89.45	—	—	—	83.41	—

[a] In microgram equivalents per gram. [b] Ratio of concentration in tissue to concentration in plasma. [c] Average of three individual values. [d] Total plasma carbon 14 estimated assuming plasma volume = 5% of body weight. [e] Value from one carcass at each time. [f] Value from three pooled tissues. [g] Stomach and intestinal tissue free of contents. [h] Value from three pooled contents. [i] n.m. = nonmeasurable.

methoxy methyl ester of Metabolite IV dissolved in dimethyl sulfoxide-d_6 provided a methyl ester band at δ 3.59 and a CH_3CH doublet (J = 7 Hz) at 1.45, indicating that the side chain was intact. The rest of the spectrum was assigned as follows: δ 3.91 (q, 1H, J = 7 Hz, CH_3CH), 3.93 (s, 3H, CH_3O ether), 7.04 (dd, 1H, J *meta* = 1.5 and J *ortho* = 8 Hz, H-3), 7.13 (s, 1H, H-8), 7.34 (d, 1H, J *meta* = 1.5 Hz, H-1), 7.96 (d, 1H, J *ortho* = 8 Hz, H-4), 8.13 (s, 1H, H-5), and 11.19 (s, 1H, NH). The chemical shifts and multiplicities of the bands assigned to H-1, H-3, and H-4 indicated definitely that the alkyl-substituted ring was not hydroxylated. The singlet character of the bands at δ 7.13 and 8.13 showed that oxygenation had occurred at C-7. Therefore, Metabolite IV is the 7-hydroxy derivative of carprofen.

The amounts of Metabolites I, III, and IV excreted in the 0–24-hr dog urines are included in Table V.

Metabolites in Bile and Feces of Dogs—The distribution of the biliary metabolites in two dogs (D-IV and D-X) is shown in Table V. A small portion of the biliary carbon 14 was present as pH 5 ether-extractable metabolites, predominantly as intact [^{14}C]carprofen. The other components appeared to be identical to the metabolites seen in urine according to TLC evidence (Systems 1 and 2). About 50% of the biliary carbon 14 consisted of the ester glucuronide of [^{14}C]carprofen, while 12% represented conjugates of Metabolites III and IV (in a ratio of 8:1) that were cleaved by glusulase.

About half of the fecal radioactivity was ether extractable at pH 5. This extract contained similar parts of carprofen and the phenolic fraction (mixture of Metabolites III and IV).

Plasma Levels and Tissue Distribution—The levels of total radioactivity and of intact [^{14}C]carprofen measured in the plasma of two dogs (D-I and D-V) following 1-mg/kg iv doses of [^{14}C]carprofen are presented in Fig. 2. In the first 48 hr, most of the radioactivity in the plasma represented intact drug. A minor ether-extractable metabolite with an R_f value (0.27–0.29) in System 1 corresponding to that of Metabolite I was detected in the 3–12-hr plasma samples of these intravenously dosed dogs. No radioactivity was found in the erythrocytes.

The plasma levels of carprofen showed a triexponential decline that was most distinct in Experiment D-V (Fig. 2B). In this study, the half-lives of the three phases were 0.5, 6, and 40 hr. In Experiment D-I (Fig. 2A), the plasma levels, after an initial decline, plateaued between 12 and 24 hr and then declined again.

Following oral administration of the same dose as a solution to the same two dogs (D-II and D-VI), plasma levels peaked at 0.5–1 hr, indicating that absorption of the drug was rapid (Fig. 3). Absorption, as estimated from comparison of the intravenous and oral areas under the total plasma carbon 14 level curves, was 106% in D-VI. In D-II, the lower value of 50% appeared to be related to a secondary drug uptake, reflected in the plateau of the intravenous curve.

Evaluation of the plasma levels obtained after a 10-times higher intravenous dose of 10 mg/kg (D-III and D-XI) indicated that in the 1–10-mg/kg dose range, the plasma levels were proportional to dose whereas the disposition rates were independent of the dose.

The distribution of total carbon 14 into the major tissues of two bile duct-cannulated dogs (D-IV and D-X) 5 hr after intravenous doses of 1 mg of [^{14}C]carprofen/kg is shown in Table III. Very low concentrations of carbon 14 in all of these tissues relative to plasma were evident. Of the radioactivity in the liver and in the kidneys, close to 70% represented intact carprofen. Both tissues contained trace levels of Metabolite I.

Rat Experiments—*Excretion*—After intravenous administration of [^{14}C]carprofen, the radioactivity was excreted predominantly in the

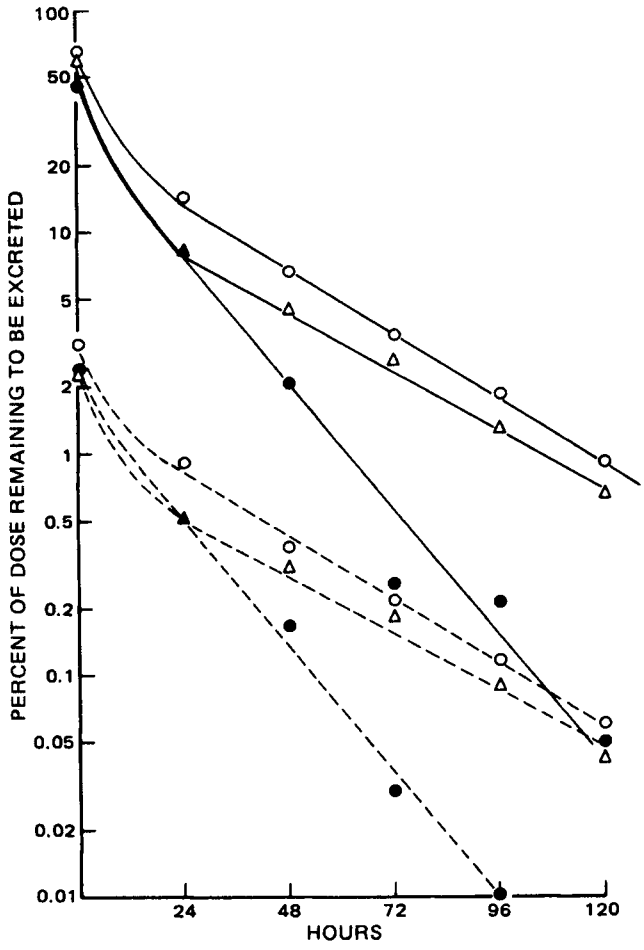

Figure 4—*Urinary excretion in three human subjects, following oral doses of 50 mg of* [^{14}C]*carprofen, of free intact carprofen* (- - -) *and of carprofen ester glucuronide* (—) *by Subject 1* (○), *Subject 2* (△), *and Subject 3* (●).

feces. Experiments in bile duct-cannulated animals showed this finding to result almost exclusively from biliary secretion of labeled carprofen metabolites.

The distribution of the radioactivity between feces (bile) and urine varied depending on the age and size of the rats (Table VI). In 337-g Charles River rats, 75% of a 3-mg/kg dose was excreted in the feces within 72 hr (45% in the bile in 4 hr) and 20% was excreted in the urine, with both forms of excretion being rapid and almost complete within 24 hr. In the larger and older Charles River rats (>700 g), only 58% of the same dose was excreted in the feces within 72 hr (23% in the bile in 4 hr) and 31%

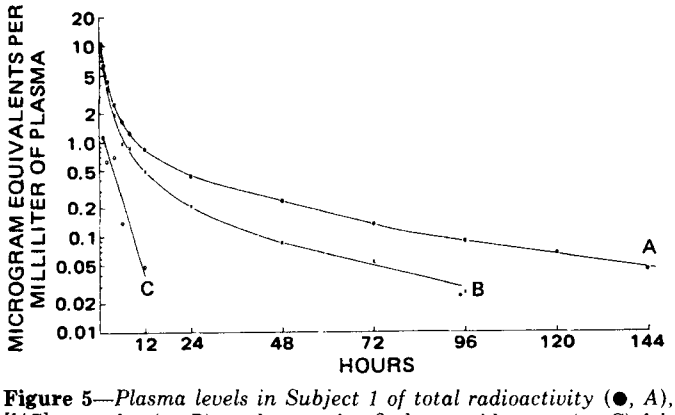

Figure 5—*Plasma levels in Subject 1 of total radioactivity* (●, *A*), [^{14}C]*carprofen* (×, *B*), *and carprofen β-glucuronide ester* (○, *C*) *following a 50-mg oral dose of* [^{14}C]*carprofen. Data expressed as log of microgram equivalents per milliliter of plasma are plotted* versus *time in hours.*

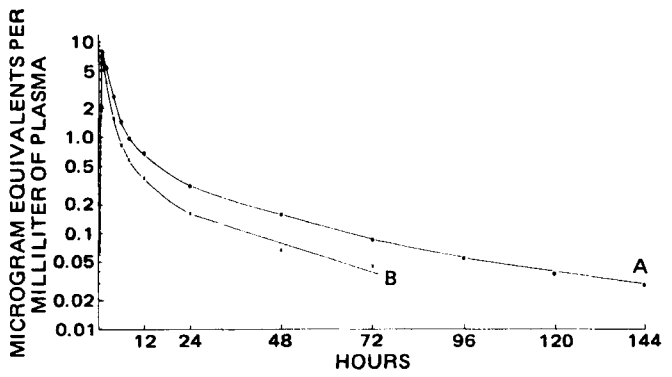

Figure 6—*Plasma levels in Subject 2 of total radioactivity* (●, *A*) *and of* [^{14}C]*carprofen* (×, *B*) *following a 50-mg oral dose of* [^{14}C]*carprofen. Data expressed as log of microgram equivalents per milliliter of plasma are plotted* versus *time in hours.*

was excreted in the urine, both at a slower rate of excretion. The biliary metabolite fraction contained exclusively conjugates, including the carprofen ester glucuronide and the ethereal glucuronides of the phenolic Metabolites III and IV, identified by cochromatography (in three systems) with the metabolites isolated from dog bile and urine. The quantitative distribution of the secreted metabolites appeared to vary depending on the strain and age (size) of the rats. Relatively less hydroxylated metabolites were secreted in the bile of the old (large) rats than in the bile of the young (small) rats. A somewhat larger fraction was secreted as the carprofen ester glucuronide by male rats of the Carworth Farm Sprague–Dawley (CF-D) strain than by the Charles River CD strain. No sex differences were evident.

Analysis of the intestinal and fecal carbon 14 fractions of the rats indicated a progressive deconjugation of the biliary metabolites and a decrease of the ratio of carprofen to the phenolic metabolites (III and IV) as the radioactivity moved from bile (ratio of 4.2) to the large intestine (ratio of 0.8) and feces (ratio of 0.31). This finding suggests a selective reabsorption of enterically deconjugated carprofen.

TLC of an extract obtained with ethyl acetate at pH 1 from a 0–24-hr rat urine specimen (containg 16.3% of a 5-mg/kg [^{14}C]carprofen dose) distinguished labeled components, which, from their R_f values in System 1, appeared to include intact carprofen, Metabolites III and/or IV, Metabolite I, and a polar component that remained at the origin (Table V).

Tissue Distribution—The tissue distribution of total carbon 14 and of [^{14}C]carprofen and the tissue to plasma carbon 14 ratios in rats at 10 min and 1 and 4 hr after intravenous administration of 5 mg of [^{14}C]-carprofen/kg are presented in Table VII. At each time, the carbon 14 levels were highest in the plasma. Intact carprofen prevailed in the plasma and tissues at all times. The residual radioactivity consisted mostly of ether-unextractable polar material.

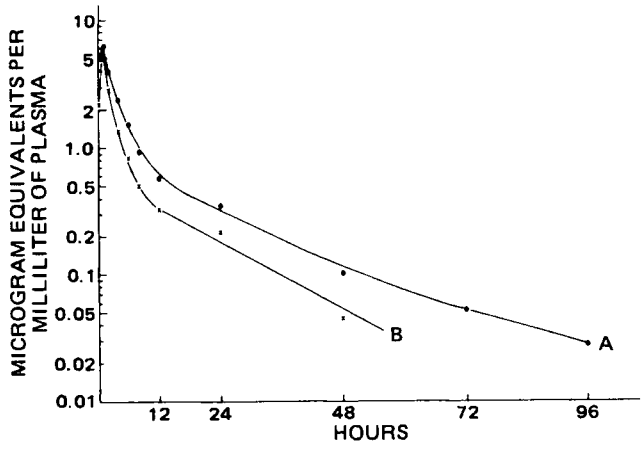

Figure 7—*Plasma levels in Subject 3 of total radioactivity* (●, *A*) *and of* [^{14}C]*carprofen* (×, *B*) *following a 50-mg oral dose of* [^{14}C]*carprofen. Data expressed as log of microgram equivalents per milliliter of plasma are plotted* versus *time in hours.*

Human Studies—*Excretion*—After oral administration of 50 mg of [^{14}C]carprofen, the main portion of the dose was excreted in the urine (75% of the dose in Subjects 1 and 2 and 55% in Subject 3). The ester glucuronide of carprofen represented >90% of the urinary carbon 14, and intact carprofen represented 3–5%. Only trace amounts of free Metabolite I and of conjugated Metabolite III could be detected (Table V). A semilog plot of intact carprofen and of its ester glucuronide, expressed as the percentages remaining to be excreted, *versus* time (Fig. 4) produced parallel curves for each component, reflecting biexponential excretion. The fast excretion rate was characterized by half-lives of 2.4–3.6 hr, whereas the terminal phase exhibited apparent half-lives of 24–25 hr in Subjects 1 and 2 and of 13 hr in Subject 3. These half-lives are in close agreement with the plasma half-lives for carprofen.

The fecal excretion of radioactivity represented 17–20% of the dose and extended from Day 2 to Day 10 in Subjects 1 and 2. In Subject 3, 33% of the radioactivity was excreted in the feces at a considerably faster rate than in the other two subjects.

The fraction extracted from the ethanolic homogenates of the human feces by the described procedures contained 60–70% of the fecal radioactivity. Of this fraction, 25–30% (~7% of the administered dose) was separated and identified as intact carprofen by TLC and by high-resolution mass spectrometry. The TLC pattern of the fecal extracts suggested the presence of small quantities of Metabolite I and two additional components not detected in dogs and rats. UV and mass spectral analysis of the two additional components yielded spectra similar to those of carprofen, suggesting that these metabolites may represent lipid-soluble addition products rather than true metabolites of carprofen.

Plasma Levels—Intact drug was the dominant radioactive component in human plasma during the first 12 hr. A polar component increased with time to more than half of the total radioactivity in plasma. One of these polar metabolites, identified in Subject 1 as the β-glucuronide ester of carprofen, declined rapidly with a half-life close to 2 hr.

The elimination rate in plasma of both carprofen and total radioactivity decreased with time (Figs. 5–7). A biphasic fall off of the plasma levels of carprofen occurred in all three subjects. The initial plasma carprofen levels declined with a half-life of 1.8–2.2 hr to reach values corresponding to ~5% of the peak levels within 12 hr. During the terminal phase, the levels declined with half-lives of 25–27 hr in Subjects 1 and 2 and ~13 hr in Subject 3. No drug-related radioactivity was detectable in the red cells throughout the experiment[18].

DISCUSSION

The disposition of [^{14}C]carprofen is similar in rats, dogs, and humans. It has many characteristics in common with the disposition of other acidic nonsteroidal anti-inflammatory compounds (10–16). Like most members of this class of drugs, carprofen is strongly bound to plasma proteins (17), and this binding is associated with a high ratio of the concentration of carprofen in plasma relative to its concentration in tissues. Intact carprofen accounts for most of the radioactivity in plasma and in the major tissues of rats and dogs. Drug elimination from plasma is characterized in dogs and humans by a bi- or multiphasic decline.

The main metabolites, primarily conjugates, do not accumulate and are rapidly eliminated, except for a small polar metabolite fraction that persists in human plasma.

Carprofen is eliminated from rats, dogs, and humans primarily by biotransformation. Probably <5% of the dose is cleared directly as the free, intact drug. The carprofen found in the feces probably arose from deconjugation of the ester glucuronide, which predominated in the bile (Table V).

The ester glucuronide of the intact drug represents the major metabolite in rats, dogs, and humans. The rapid formation and the characteristic rate and mode of elimination of this metabolite determine the pharmacokinetics of the drug. In rats and dogs but to a very minor extent in humans, oxidation in positions 7 and 8 of the carbazole moiety to phenolic derivatives (probably *via* a common arene oxide precursor) and their conjugation to form ethereal glucuronides represent alternate pathways. A small percentage of the dose also is metabolized by side chain oxidation to the α-hydroxy derivative, which is excreted free in the urine by dogs and rats. In rats and dogs, the ester glucuronide of carprofen and the ethereal glucuronides of the two phenolic metabolites are eliminated predominantly by biliary secretion.

Human subjects, in contrast to rats and dogs, excrete most of an oral carprofen dose as urinary ester glucuronide. However, the relatively small fecal ^{14}C-labeled component apparently represents only a fraction of a substantially larger biliary component because of enterohepatic circulation. A comparison of the initial 90% decline of the drug in plasma with the 50–60% of the dose excreted in the urine during the same 12-hr period suggests that the remaining 30–40% of the dose had been eliminated with the bile. This estimate of extensive biliary excretion of metabolites in humans was supported by analysis of biliary aspirates from an intubated human volunteer[19].

Extensive enterohepatic circulation in humans was suggested by the protracted fecal excretion of radioactivity in two of the three subjects discussed in the present report. Furthermore, the slow terminal decline of plasma levels and of the urinary excretion rates in these two subjects may be related to a continuous reabsorption of the biliary fraction. The extent of this reabsorption determines the fraction of the primary biliary portion that is excreted in the feces and the fraction that ultimately is excreted in the urine. In the third subject, the enterohepatic process may be concluded to have been less pronounced, resulting in a higher and more rapid fecal excretion and in a shorter apparent half-life of the radioactivity in plasma.

REFERENCES

(1) L. O. Randall and H. Baruth, *Arch. Int. Pharmacodyn. Ther.*, **220**, 94 (1976).

(2) M. Maeda, Y. Tanaka, T. Suzuki, and K. Nakamura, *Folia Pharmacol. Jpn.*, **73**, 757 (1977).

(3) J. A. F. de Silva, N. Strojny, and M. A. Brooks, *Anal. Chim. Acta*, **73**, 283 (1974).

(4) C. V. Puglisi, J. C. Meyer, and J. A. F. de Silva, *J. Chromatogr.*, **136**, 391 (1977).

(5) J. E. Ray, J. O. Bostram, and D. N. Wade, *Clin. Exp. Pharmacol. Physiol.*, **5**, 271 (1978).

(6) J. H. Gustafson, A. A. Holazo, H. Boxenbaum, M. L. Jack, R. E. Weinfeld, W. Glover, R. A. Dickey, L. Weissman, and S. A. Kaplan, "Abstracts," vol. 8, no. 2, APhA Academy of Pharmaceutical Sciences, Washington, D.C., 1978, p. 93.

(7) F. Rubio, S. Seawall, B. Koechlin, and R. Pocelinko, *Fed. Proc. Fed. Am. Soc. Exp. Biol.*, **37**, 605 (1978).

(8) W. H. Fishman and S. Green, *J. Biol. Chem.*, **215**, 527 (1955).

(9) C. A. Marsh, in "Glucuronic Acid, Free and Combined", G. J. Dutton, Ed., Academic, New York, N.Y., 1966, p. 3.

(10) H. B. Hucker, A. G. Zacchei, S. V. Cox, D. A. Brodie, and N. H. Cantwell, *J. Pharmacol. Exp. Ther.*, **153**, 237 (1966).

(11) A. Rubin, P. Warrick, R. L. Wolen, S. M. Chernish, A. S. Ridolfo, and C. M. Gruber, Jr., *ibid.*, **183**, 449 (1972).

(12) J. Pottier, D. Berlin, and J. R. Raynau, *J. Pharm. Sci.*, **66**, 1030 (1977).

(13) R. F. N. Mills, S. S. Adams, E. F. Cliffe, W. Dickson, and J. S. Nicholson, *Xenobiotica*, **3**, 589 (1973).

(14) M. L. Selley, J. Glass, E. J. Triggs, and J. Thomas, *Clin. Pharmacol. Ther.*, **17**, 599 (1975).

(15) V. Tamassia, G. Corvi, E. Moro, G. P. Tosolini, and L. M. Fucella, *Eur. J. Clin. Pharmacol.*, **10**, 257 (1973).

(16) L. M. Fucella, G. C. Goldaniga, E. Moro, V. Tamassia, and G. Valzelli, *ibid.*, **6**, 256 (1973).

(17) G. Sullow, D. J. Birket, and D. N. Wade, *Mol. Pharmacol.*, **12**, 1052 (1976).

ACKNOWLEDGMENTS

The authors thank Mrs. K. Catala and Mrs. K. Heusser for assistance in the preparation of this report.

[18] Because of the nonuptake of the drug by the red cells, plasma levels would be higher by a factor of $(1 - \text{hematocrit})^{-1}$ than the blood levels determined for the same specimen.

[19] Bile samples from collaborative study of Dr. C. Dujovne, Kansas City Medical Center, and Dr. J. Gustafson, Roche Department of Pharmacokinetics and Biopharmaceutics.

Negligible Excretion of Unchanged Ketoprofen, Naproxen, and Probenecid in Urine

R. A. UPTON ˣ, J. N. BUSKIN, R. L. WILLIAMS, N. H. G. HOLFORD, and S. RIEGELMAN

Received March 20, 1980, from the *Drug Studies Unit, University of California, San Francisco, CA 94143.* Accepted for publication May 5, 1980.

Abstract □ On the average, 0.6% of a dose of ketoprofen or naproxen or 1.2% of a dose of probenecid was found in the urine of normal male volunteers assayed immediately after its collection. Between ~60 and 85% of the dose of these drugs can be excreted in the urine as conjugates, which rapidly hydrolyze at body temperature, at room temperature, and even during frozen storage, thereby regenerating the parent drug. Since urine collections involved sample retention in the bladder at 37° for collection intervals as long as 2–3 hr, the given percentages excreted unchanged probably are overestimates. It is possible that no unchanged ketoprofen, naproxen, or probenecid is excreted in urine. This study contrasts with previous reports of up to 50% of a dose of ketoprofen and 15–17% of doses of naproxen and probenecid being excreted in urine as the parent compound. Those reports probably reflect primarily the duration of frozen sample storage between collection and assay along with the urine collection schedules employed, the speed of the clinical procedures, and the analytical procedures used. Attention should be given to potential conjugate hydrolysis whenever the pharmacokinetics of carboxylic acids are studied.

Keyphrases □ Ketoprofen—urinary excretion of unchanged drug □ Naproxen—urinary excretion of unchanged drug □ Probenecid—urinary excretion of unchanged drug

Previous reports suggested that up to 50% of a dose of ketoprofen (1–4), 15% of a dose of naproxen (5–7), and 17% of a dose of probenecid (8–10) are excreted in urine as the unchanged drug. It also has been claimed that the percentage of each of these drugs excreted unchanged is variable among individuals or within individuals (2, 5, 10) and that the percentage excreted unchanged might be depressed with concurrent administration of other drugs (6). In contrast, this report presents evidence that, even in normal individuals, the renal excretion of ketoprofen, naproxen, and probenecid is negligible. Data reported previously probably reflected the collection, storage, and handling of urine samples instead of the urinary excretion of these compounds.

EXPERIMENTAL

The data were derived from several studies in which ketoprofen, naproxen, or probenecid was given orally to adult male volunteers judged to be normal after a physical examination, an extensive blood screen, and urinalysis. Participants received other drugs only where specifically stated.

Urine was analyzed within 30 min of serial collections from 0 to 1, 1 to 2, 2 to 3, 3 to 4, and 4 to 6 hr after the 13th dose of a regimen of 50 mg of ketoprofen[1] given every 6 hr or after the 13th dose of a regimen of 500 mg of probenecid[2] given every 6 hr. Urine was analyzed within 30 min of collection from 0 to 1, 1 to 2, 2 to 3, 3 to 6, 6 to 8, 8 to 10, and 10 to 12 hr after the seventh dose of a regimen of 500 mg of naproxen[3] given every 12 hr.

Ketoprofen, naproxen, probenecid, and their conjugates were analyzed by a sensitive high-pressure liquid chromatographic (HPLC) assay described previously (11). Conjugates were analyzed as the parent drug after simple alkaline hydrolysis (11).

[1] Orudis capsules, Ives Laboratories, New York, N.Y.
[2] Benemid tablets, Merck Sharp and Dohme, West Point, Pa.
[3] Naprosyn tablets, Syntex Laboratories, Palo Alto, Calif.

Table I—Urinary Excretion of Ketoprofen, Naproxen, and Probenecid in an Interdose Interval at Steady-State Plasma Concentrations with Urine Assayed Immediately after Collection

Dose and Interval	Volunteer	Percent of Dose Unchanged	Percent of Dose as Conjugates
Ketoprofen, 50 mg, 6 hr	1	0.5	67.9
	2	0.5	70.7
	3	0.7	82.9
	4	0.8	77.7
	5	0.5	69.1
Mean ± *SD*		0.6 ± 0.1	73.7 ± 6.4
Naproxen, 500 mg, 12 hr	6	0.4	64.4
	7	0.9	61.7
	8	0.4	42.5
	9	0.7	58.6
Mean ± *SD*		0.6 ± 0.2	56.8 ± 9.8
Probenecid, 500 mg, 6 hr (with ketoprofen regimen)	10	1.3	57.0
	11	1.4	33.4
	12	1.0	40.2
Mean ± *SD*		1.2 ± 0.2	43.5 ± 12.1

RESULTS

Table I shows the percentage of a dose of ketoprofen, naproxen, or probenecid appearing unchanged or as alkali-hydrolyzable conjugates in urine at steady-state plasma concentrations. On the average, only 0.6% of the ketoprofen dose, 0.6% of the naproxen dose, and 1.2% of the probenecid dose appeared in urine as the unchanged drug, but 74, 57, and 44% of these drugs were excreted as conjugates, respectively. None of the five people taking ketoprofen alone and none of the four subjects taking naproxen alone excreted >0.9% of unchanged drug in the urine.

The three individuals taking probenecid were simultaneously following the described ketoprofen regimen. None excreted >1.4% of the dose of probenecid (mean, 1.2%) or >0.2% of the ketoprofen dose as the unchanged drugs.

In an additional three individuals taking the ketoprofen regimen with aspirin[4] (975 mg every 6 hr), the maximum urinary excretion of unchanged ketoprofen observed was 0.9% of the dose (0.8 ± 0.1%), but 59.7 ± 3.6% was excreted as conjugates. When three of the four individuals taking naproxen undertook a further naproxen regimen together with 300 mg of cimetidine[5] given every 6 hr, the maximum urinary excretion of naproxen was 0.7% (0.5 ± 0.2%), and 65.6 ± 8.3% was excreted as conjugates. The data on the urinary excretion of ketoprofen, naproxen, and probenecid were derived from 14 volunteers.

Some samples were stored at −15° for assay at various dates after collection (Table II). Over a period of <2 months, the ketoprofen and naproxen content of these samples increased up to threefold at the apparent expense of the alkali-hydrolyzable conjugates, presumably as a result of conjugate hydrolysis, even in the frozen state. Furthermore, since a different sample of the same urine collection was stored for each repetition of the assay, the progressive accumulation in content of the unchanged drug (Table II) was specifically an effect of storage rather than of repeated freezing and thawing, which also appear to have an effect. When samples were frozen and then thawed after 12 hr, a period during which (by reference to Table II) one might expect a negligible increase in unchanged drug specifically due to storage, the content of unchanged ketoprofen increased by 14.2 ± 5.9% (n = 4), and the content of naproxen increased by 17.1 ± 14.6% (n = 3).

[4] Unbuffered 325-mg tablets, Eli Lilly & Co., Indianapolis, Ind.
[5] Tagamet tablets, Smith Kline and French Laboratories, Philadelphia, Pa.

0022-3549/80/1100-1254$01.00/0
© 1980, American Pharmaceutical Association

Table II—Urine Sample Content after Storage at −15°

Sample Designation	Day of Assay	Concentration of Unchanged Drug, μg/ml	Concentration of Unchanged Drug plus Conjugates, μg/ml[a]	Increase in Unchanged Drug	
				μg/ml/day	μg/day/μg of conjugates
Ketoprofen 1	0	0.196	19.0		
	26	0.357	17.6	0.00619	0.000330
Ketoprofen 2	0	0.0728	3.39		
	28	0.0922			
	54	0.211			
	106	0.228	3.40	0.00160	0.000482
	$r = 0.904$, $\alpha(1) < 0.05$				
Ketoprofen 3	0	1.66	165.0		
	28	3.23		0.0561	0.000343
Ketoprofen 4	0	0.0281	1.26		
	28	0.0436			
	54	0.0864			
	106	0.362	1.26	0.00325	0.00263
	$r = 0.935$, $\alpha(1) < 0.05$				
Mean ± *SD*				0.0168 ± 0.0263	0.00094 ± 0.00112
Naproxen 1	0	22.0	679		
	8	26.3			
	22	30.9	676		
	60	46.7	728	0.405	0.000616
	$r = 0.999$, $\alpha(1) < 0.001$				
Naproxen 2	0	3.28	607		
	8	4.71	565		
	50	10.4	587	0.140	0.000232
	$r = 0.999$, $\alpha(1) < 0.025$				
Naproxen 3	0	2.32	321		
	1	3.09	289		
	43	7.67	315	0.117	0.000367
	$r = 0.994$, $\alpha(1) < 0.05$				
Mean ± *SD*				0.221 ± 0.160	0.000406 ± 0.000195

[a] Micrograms per milliliter of unchanged drug after alkaline hydrolysis (11).

Because all samples other than those assayed on Day 0 were stored frozen, their assay was subject to the effects not only of storage but also of freezing and thawing. As a result, elucidation of the kinetics of conjugate hydrolysis might be complex, requiring more detailed data than are presented here. However, regardless of whether the hydrolysis rates observed are interpreted as zero or first order, they are sufficient to account for the levels of unchanged drug that have been reported in the literature. A zero-order rate of production of 17 ng/ml/day (the average zero-order rate from Table II) leads to a 5% apparent excretion of unchanged ketoprofen in an individual who had taken a 50-mg dose and produced 1.5 liters of urine to be assayed 3 months later. A first-order daily rate of production of 0.9 ng of ketoprofen/μg of conjugates (Table II) would lead to an apparent 6% excretion of unchanged ketoprofen when the urine of an individual excreting 74% (Table I) of the dose as conjugates is assayed after frozen storage for 3 months. Similar calculations show that an apparent excretion of naproxen of ~4% could arise by delaying the assay of urine samples by 3 months. These calculations indicate that after 8 months of frozen storage, 13% of the dose as unchanged ketoprofen might be expected.

Figure 1 shows the apparent urinary excretion of unchanged ketoprofen by 12 volunteers (each taking three single 50-mg doses) whose 24-hr urine was stored at −15° for 20–100 days between collection and assay. A linear correlation between the apparent ketoprofen excretion by each volunteer[6] and the time of storage of the urine is significant ($r = 0.6$, $p < 0.0005$, $n = 32$). As predicted, after 3 months of storage, ~4–5% of the dose appeared to be in the urine as unchanged ketoprofen. In another study, 12 additional volunteers (each taking three single 50-mg doses), whose urine was frozen shortly after collection and thawed for the first time after 8 months, appeared to excrete 9.6 ± 2.0% ($n = 36$) of the dose unchanged.

Greater rates of hydrolysis were observed at room temperature (Table III). Samples doubled in their content of unchanged ketoprofen or naproxen within 4–5 hr. (The pH of eight urine samples taken from three volunteers at various times within 24 hr after dosage ranged between 5.4 and 6.7 immediately after collection.) Therefore, analytical units not alerted to the potential facile hydrolysis of ketoprofen or naproxen conjugates during extended processing of urine in the clinic or during sample workup might report even higher percentages of the drug excreted unchanged than the figures discussed here.

Furthermore, hydrolysis rates even higher than those at room temperature were observed at 37° (Table IV). Therefore, the extent of excretion of unchanged ketoprofen, naproxen, and probenecid shown in Table I, while less than that reported previously, probably is still an overestimate since urine collections at 2–3-hr intervals involve sample retention in the bladder at 37° for sufficient time for significant conjugate hydrolysis. It is possible that no unchanged drug is excreted into urine.

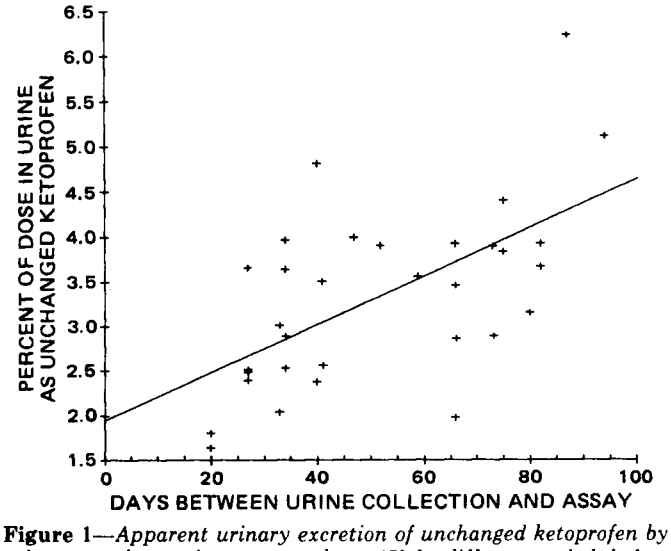

Figure 1—*Apparent urinary excretion of unchanged ketoprofen by volunteers whose urine was stored at −15° for different periods before assay.*

[6] Data on the third dose of four of the individuals are incomplete.

Table III—Urine Sample Content after Storage at Room Temperature

Sample Designation	Time of Assay, hr	Concentration of Unchanged Drug, μg/ml	Concentration of Conjugated Drug, μg/ml[a]	Increase in Unchanged Drug	
				μg/ml/hr	μg/hr/μg of conjugates
Ketoprofen 1	0	0.179	27.9		
	3.5	0.351			
	11	0.726			
	23	1.27			
	28	1.41		0.0448	0.00161
	$r = 0.998$, $\alpha(1) < 0.0005$				
Ketoprofen 2	0	0.148	32.3		
	3.5	0.337			
	11	0.625			
	23	1.23			
	28	1.37		0.0444	0.00137
	$r = 0.998$, $\alpha(1) < 0.0005$				
Mean ± *SD*				0.0446 ± 0.0003	0.00149 ± 0.00017
Naproxen 1	0	22.0	657		
	1	25.2			
	2	28.9		3.49	0.00531
	$r = 0.999$, $\alpha(1) < 0.025$				
Naproxen 2	0	3.28	604		
	5	6.93			
	11	10.1		0.616	0.00102
	$r = 0.996$, $\alpha(1) < 0.05$				
Naproxen 3	0	1.21	208		
	1	1.43			
	10	3.99			
	23	6.98		0.253	0.00121
	$r = 0.999$, $\alpha(1) < 0.025$				
Mean ± *SD*				1.45 ± 1.77	0.00251 ± 0.00242
Probenecid 1	0	13.9	203		
	3.5	19.2			
	11	20.6			
	23	33.3			
	28	36.0		0.787	0.00376
	$r = 0.985$, $\alpha(1) < 0.0025$				
Probenecid 2	0	42.8	332		
	3.5	45.6			
	11	52.1			
	23	69.3			
	28	77.1		1.23	0.00359
	$r = 0.994$, $\alpha(1) < 0.0005$				
Probenecid 3	0	4.14	138		
	3.5	4.60			
	11	5.70			
	23	7.61			
	28	7.73		0.128	0.000903
	$r = 0.993$, $\alpha(1) < 0.0005$				
Mean ± *SD*				0.715 ± 0.555	0.00275 ± 0.00160

[a] As the equivalent concentration of unchanged drug.

For ketoprofen and naproxen, at least three conjugates apparently are excreted in urine. If urine is assayed by the previously reported HPLC method (11) with the hydrolysis step omitted and acidic extraction conditions used as for plasma analysis, peaks are seen at 1.8 (largest), 2.0, and 2.9 (smallest) times the retention time for ketoprofen or at 2.5 (largest), 3.1 (smallest), and 4.1 times the retention time for naproxen. After extracts of urine from subjects taking either ketoprofen or naproxen were chromatographed, fractions of the eluent, each containing one of the three peaks, were collected. An aliquot of each eluent fraction was rechromatographed to ensure that fractions were not cross-contaminated with other conjugates or with the parent drug. The remaining part of each fraction underwent alkaline hydrolysis and then reextraction.

Further chromatography revealed a ketoprofen or a naproxen peak alone. For the first and second conjugate peaks of ketoprofen and the first and third conjugate peaks of naproxen, the conjugate gave rise to the parent compound on an equal peak area basis (to within 20%). For the other peaks (the smallest) from either compound, this finding was less certain due to the less straightforward concentration and extraction procedures that were necessary. Equivalence of peak areas confirms that conjugation does not involve the major chromophoric moiety but rather the carboxylic function and, hence, the ease of subsequent conjugate hydrolysis.

DISCUSSION

A negligible fraction of the dose of ketoprofen, naproxen, or probenecid is excreted in the urine as the unchanged drug, but a large fraction (up to 85%) appears as conjugates. Glucuronides of ketoprofen (12) and naproxen (8) were reported previously. Evidence in this study suggests that there are at least three conjugates of ketoprofen and three of naproxen. These conjugates are rapidly hydrolyzed to the parent compound by mild alkaline conditions (11). Hydrolysis of one or more conjugates of each drug appears to occur even in urine stored frozen, the most commonly employed mode of storage. Furthermore, freezing and thawing appear to promote hydrolysis, and even more rapid hydrolysis occurs at room temperature or at 37°.

Earlier reports of significant urinary excretion of unchanged ketoprofen, naproxen, and probenecid probably reflect not only the time of frozen storage between collection and assay but also the urine collection schedules employed, the speed of the clinical procedures, and the analytical procedures used, particularly the conditions and speed of the sample workup. The previously reported variability in ketoprofen, naproxen, and probenecid urinary excretion (2, 5, 10) probably is related to variability in these conditions, especially the time between collection and assay. Differences between different experimental groups might have

Table IV—Urine Sample Content after Storage at 37°

Sample Designation	Time of Assay, hr	Concentration of Unchanged Drug, μg/ml	Concentration of Conjugated Drug, μg/ml[a]	Increase in Unchanged Drug μg/ml/hr	Increase in Unchanged Drug μg/hr/μg of conjugates
Ketoprofen	0	0.196	18.8		
	0.25	0.235			
	0.5	0.276			
	0.75	0.335			
	1.0	0.375			
	2.0	0.502		0.155	0.00825
	$r = 0.994$, $\alpha(1) < 0.0005$				
Naproxen	0	22.0	657		
	0.25	23.6			
	0.5	26.2			
	0.75	27.6			
	1.0	30.2			
	2.0	40.3		0.24	0.0141
	$r = 0.997$, $\alpha(1) < 0.0005$				
Probenecid 1	0	20.6	203		
	12	51.7		2.59	0.0128
Probenecid 2	0	52.1	332		
	12	167		9.58	0.0288
Probenecid 3	0	5.7	138		
	12	12.9		0.600	0.00435
Mean ± *SD*				4.26 ± 4.7	0.0153 ± 0.0124

[a] As the equivalent concentration of unchanged drug.

a similar source, particularly where clinical and analytical schedules were not both randomized.

Since virtually no naproxen appears to be excreted unchanged in urine, reports of a decrease in naproxen excretion with concomitant doses of other drugs such as probenecid (6) must be questioned. The apparent decrease in unchanged naproxen excretion probably is a direct consequence of reduced naproxen conjugate excretion, which results in a diminished rate of postexcretion conjugate hydrolysis. The previously reported increase in renal clearance of probenecid with metabolic alkalosis (6, 9, 13) induced by intravenous sodium bicarbonate may largely result from improved conditions for conjugate hydrolysis in the alkaline urine in the bladder.

The ease of hydrolysis of the conjugates described probably is attributable to their being carboxylic acid esters. The greater apparent excretion of unchanged drug found for probenecid possibly is related to its being a benzoic acid, a stronger acid than the alkanoic acids, and it therefore forms a conjugate more susceptible to hydrolysis in urine between the times of excretion and assay. Data describing urinary excretion of other carboxylic acids, including many nonsteroidal anti-inflammatory drugs, should be interpreted with caution unless adequate attention was given to potential conjugate hydrolysis both *in vivo* and *in vitro*. The best safeguard at present is immediate assay after short urine collection intervals. If this procedure is not possible, immediate frozen storage for short periods might yield insignificant hydrolysis. It is conceivable, but by no means can it be assumed, that temperatures of $<-15°$ might permit negligible hydrolysis.

The virtual absence of unchanged compound in the urine may arise because alternative forms of elimination are extremely rapid. However, the total plasma clearances of ketoprofen and naproxen are only 5 and 0.7 liters/hr, respectively (5, 13). Even if these clearances are considered to be totally metabolic, extraction ratios of only 0.06 and 0.01 are apparent, respectively (assuming 1:1 partitioning of these drugs between plasma and the red blood cells). Ketoprofen, naproxen, and probenecid all are highly lipophilic compounds, a characteristic discusssed in a previous report (11), where it was noted that they can be extracted into ether and can be retained on lipophilic chromatographic columns even when they are almost completely ionized in water. Such compounds are potentially highly susceptible to renal tubular reabsorption (10). Perhaps reabsorption from the glomerular filtrate is so efficient that virtually no ketoprofen, naproxen, or probenecid is excreted into urine as such.

Since plasma rather than urine concentrations are more central to most pharmacokinetic interpretations, a similar ease of hydrolysis in plasma samples might lead to even more misleading descriptions of the general pharmacokinetic behavior of these drugs. However, in analyzing ketoprofen or naproxen in plasma immediately upon collection of blood samples, the ratio of the total concentration (parent drug and its conjugates) to that of unchanged ketoprofen or naproxen, respectively, was only 1.42 ± 0.14 (11 samples from one subject at various times up to 24 hr postdosing) or 1.10 ± 0.05 (39 samples from three subjects). If immediate assay did in fact reflect the relative proportions of compounds in the bloodstream, then even complete hydrolysis upon storage would affect the apparent ketoprofen or naproxen plasma levels only slightly, at least by comparison with the potential change in urine concentrations. After ~2 months of storage at −15° there appeared to be little change in the ketoprofen samples (total drug to parent drug ratio of 1.37 ± 0.08), but repeating the analysis for ketoprofen in five samples between 3 and 6 months after collection (involving further freezing and thawing) revealed that the content of unchanged ketoprofen had increased by 10–25%. Repeated analysis for naproxen only 2 months after collection showed that the conjugates had almost disappeared, with a commensurate increase (~10%) in the content of unchanged drug.

REFERENCES

(1) E. Castegnaro, F. Iannotta, and C. Pollini, *Farmaco*, **29**, 520 (1974).

(2) O. R. W. Lewellen and R. Templeton, *Scand. J. Rheumatol., Suppl.*, **14**, 53 (1976).

(3) F. Delbarre, J. C. Roucayrol, B. Amor, J. Ingrand, G. Bourat, J. Fournel, and J. Courjaret, *ibid.*, **14**, 45 (1976).

(4) T. M. Jefferies, W. O. A. Thomas, and R. T. Parfitt, *J. Chromatogr.*, **162**, 122 (1979).

(5) R. Runkel, M. D. Chaplin, H. Sevelius, E. Ortega, and E. Segre, *Clin. Pharmacol. Ther.*, **20**, 269 (1976).

(6) R. Runkel, E. Mroszczak, M. Chaplin, H. Sevelius, and E. Segre, *ibid.*, **24**, 706 (1978).

(7) V. H. Held, *J. Clin. Chem. Clin. Biochem.*, **16**, 579 (1978).

(8) D. Schachter, *J. Clin. Invest.*, **36**, 297 (1957).

(9) J. M. Perel, P. G. Dayton, T. F. Yu, and A. B. Gutman, *Eur. J. Clin. Pharmacol.*, **3**, 106 (1971).

(10) S. Melethil and W. D. Conway, *J. Pharm. Sci.*, **65**, 861 (1976).

(11) R. A. Upton, J. N. Buskin, T. W. Guentert, R. L. Williams, and S. Riegelman, *J. Chromatogr.*, **190**, 119 (1980).

(12) P. Populaire, B. Terlain, S. Pascal, B. Decouvelaere, A. Renard, and J.-P. Thomas, *Ann. Pharm. Fr.*, **31**, 735 (1973).

(13) R. A. Upton, R. L. Williams, T. W. Guentert, J. N. Buskin, and S. Riegelman, *Eur. J. Clin. Pharmacol.*, in press.

ACKNOWLEDGMENTS

Ms. A. F. Fast managed the clinical sections of this study.

Simultaneous High-Performance Liquid Chromatographic Determination of Suxibuzone and Its Metabolites in Plasma and Urine

TERUYOSHI MARUNAKA ˣ, TOSHIAKI SHIBATA, YOSHINORI MINAMI, YUKIHIKO UMENO, and TAKASHI SHINDO

Received March 5, 1980, from the *Research Laboratory, Taiho Pharmaceutical Co., Ltd., Kawauchi-cho, Tokushima, 771-01, Japan.* Accepted for publication May 2, 1980.

Abstract □ A high-performance liquid chromatographic method is described for the simultaneous determination of the anti-inflammatory agent suxibuzone and its metabolites, 4-hydroxymethylphenylbutazone, phenylbutazone, oxyphenbutazone, and γ-hydroxyphenylbutazone, in plasma and urine. Acidified plasma or urine is extracted with benzene–cyclohexane (1:1). The organic extract is reduced to dryness, and the resulting residue is redissolved in methanol. Aliquots of this solution are chromatographed on a reversed-phase column using a mobile phase of methanol–0.5 *M* KH_2PO_4 (linear gradient from 0 to 100% methanol at 8%/min with a flow rate of 2.0 ml/min) on a high-performance liquid chromatograph equipped with a UV absorbance detector (254 nm). Detection is limited to 0.10 μg/ml for suxibuzone and 4-hydroxymethylphenylbutazone and to 0.05 μg/ml for the other metabolites.

Keyphrases □ Suxibuzone—simultaneous high-performance liquid chromatographic determination with metabolites in plasma and urine □ Metabolites—suxibuzone, simultaneous high-performance liquid chromatographic determination with parent drug in plasma and urine □ High-performance liquid chromatography—analysis, suxibuzone and metabolites in plasma and urine

Suxibuzone [4-butyl-4-(hydroxymethyl)-1,2-diphenyl-3,5-pyrazolidinedione hydrogen succinate] is a new derivative of phenylbutazone that was developed as an anti-inflammatory agent. It was reported that suxibuzone was equipotent to phenylbutazone in pharmacological activity and that its toxicity was one-third to one-fifth of that of phenylbutazone in experiments with animals, indicating greater safety (1–3).

Suxibuzone is metabolized in the body mainly to phenylbutazone through 4-hydroxymethylphenylbutazone as an intermediate, with the phenylbutazone then proceeding to oxyphenbutazone and γ-hydroxyphenylbutazone (Scheme I) (4).

BACKGROUND

An assay for suxibuzone and its metabolites in plasma and urine was reported (4) in which suxibuzone and its metabolites are determined by GLC as their trimethylsilyl derivatives.

For the assay of phenylbutazone and its metabolites in plasma and urine after phenylbutazone administration, several UV (5–13), GLC (14–19), and high-performance liquid chromatographic (HPLC) (20, 21) methods have been reported. The UV method reported by Burns *et al.* (5) has many sensitivity and specificity problems. With the GLC methods, phenylbutazone and oxyphenbutazone were determined as their methyl derivatives by Midha *et al.* (16), phenylbutazone and the heptafluorobutyryl derivative of oxyphenbutazone were determined by Bruce *et al.* (17), and Tanimura *et al.* (18) assayed phenylbutazone and the trimethylsilyl derivatives of oxyphenbutazone and γ-hydroxyphenylbutazone.

An HPLC method using an adsorption chromatographic column (SIL-X) was used to determine phenylbutazone and oxyphenbutazone (20, 21).

In the present study, an HPLC method using a reversed-phase column for determination of suxibuzone and its metabolites, 4-hydroxymethylphenylbutazone, phenylbutazone, oxyphenbutazone, and γ-hydroxyphenylbutazone, in plasma and urine after administration of suxibuzone was examined; an accurate and sensitive assay for their measurements was established.

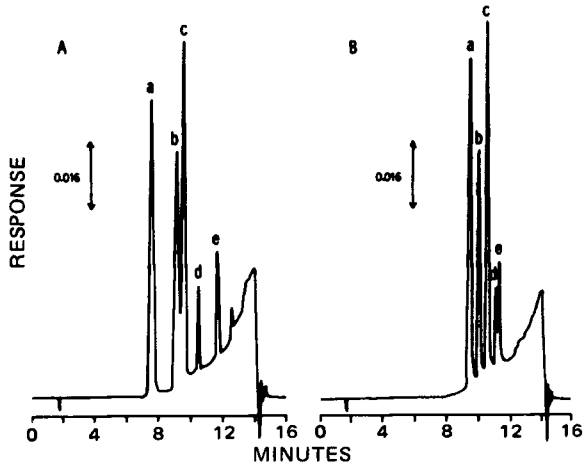

Figure 1—*High-performance liquid chromatograms of authentic samples using a mobile phase of methanol–water (A) and methanol–0.05 M KH_2PO_4 (B) with a linear gradient (0–100% methanol at 8%/min with a flow rate of 2.0 ml/min). Key: a, γ-hydroxyphenylbutazone; b, oxyphenbutazone; c, phenylbutazone; d, suxibuzone; and e, 4-hydroxymethylphenylbutazone.*

EXPERIMENTAL

Materials—Suxibuzone[1], phenylbutazone[1], oxyphenbutazone[1], and γ-hydroxyphenylbutazone[1] were used as received. 4-Hydroxymethylphenylbutazone[2] was synthesized and purified. Benzene, cyclohexane, and methanol were liquid chromatographic grade[3], and the other chemicals used were analytical grade[3].

HPLC Conditions—The high-performance liquid chromatograph[4] was equipped with a high-pressure injection port[5], gradient elution equipment[6], and a fixed-wavelength (254-nm) UV absorbance detector[7].

A reversed-phase chromatographic column[8] (30 cm × 3.9 mm i.d.) was used for the separation and was maintained at room temperature. The mobile phase was a linear gradient of methanol and 0.05 *M* KH_2PO_4 (0 to 100% methanol at 8%/min) at a flow rate of 2.0 ml/min. The mobile phase was degassed by applying a vacuum (~100 mm) to the solvent reservoir for ~2 min before use.

A computer system[9] was employed for quantitative calculation.

GLC Conditions—The gas chromatograph[10] was equipped with a

[1] Laboratory, Esteve, S. A., Barcelona, Spain.
[2] Research Laboratory, Taiho Pharmaceutical Co., Tokushima, Japan.
[3] Wako Pure Chemicals Co., Osaka, Japan.
[4] Model LC-2, Shimadzu, Kyoto, Japan.
[5] Model SIL-1A, Shimadzu.
[6] Model GRE-2, Shimadzu.
[7] Model UVD-2, Shimadzu.
[8] μBondapak C_{18}, Waters Associates, Milford, Mass.
[9] Chromatopac 1A, Shimadzu.
[10] Model GC-4CM, Shimadzu.

0022-3549/80/1100-1258$01.00/0
© 1980, American Pharmaceutical Association

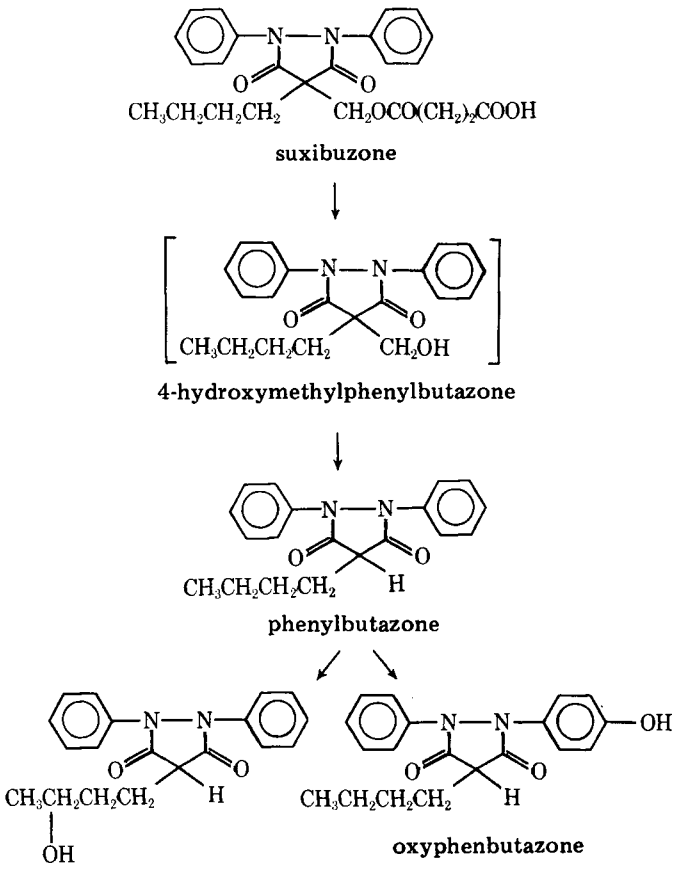

Scheme I—Main metabolic pathways of suxibuzone.

flame-ionization detector. The GLC conditions were described previously (4).

Mass Spectrometric Conditions—A mass spectrometer[11] with an electron-impact ion source was used for identification of suxibuzone and its metabolites. The mass spectrometric analysis was carried out under the following conditions: ionization energy, 75 ev; ionization current, 200 μamp; and acceleration voltage, 10 kv.

Analytical Procedure—Samples of 1.0 ml of plasma or 2.0 ml of urine

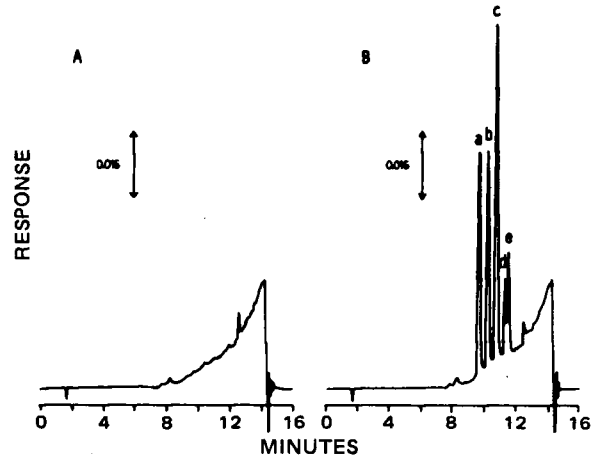

Figure 2—*High-performance liquid chromatograms of beagle dog control plasma (A) and beagle dog plasma extracts following addition of authentic samples at 5.0 μg/ml for each compound (B). Key: a, γ-hydroxyphenylbutazone; b, oxyphenbutazone; c, phenylbutazone; d, suxibuzone; and e, 4-hydroxymethylphenylbutazone.*

[11] Model JMS-01SG02, JEOL, Tokyo, Japan.

Table I—Recoveries on Extraction of Suxibuzone and Its Metabolites from Plasma and Urine of a Beagle Dog

Compound	Added, μg/ml	Recovery[a], %
Suxibuzone	50	99.4
	25	99.6
	5	99.5
Mean ± *SD*		99.5 ± 1.1
4-Hydroxymethylphenylbutazone	50	98.2
	25	97.8
	5	97.9
Mean ± *SD*		97.9 ± 1.4
Phenylbutazone	50	96.5
	25	96.4
	5	97.3
Mean ± *SD*		96.7 ± 1.7
Oxyphenbutazone	50	92.9
	25	92.5
	5	94.0
Mean ± *SD*		93.1 ± 3.7
γ-Hydroxyphenylbutazone	50	92.1
	25	93.4
	5	91.8
Mean ± *SD*		92.4 ± 4.2

[a] Each value is the mean of three HPLC determinations.

were diluted with distilled water, adjusted to pH 2.0 with 5 *N* HCl, and extracted with benzene–cyclohexane (1:1 v/v) (20 ml for plasma and 30 ml for urine) for 20 min. The organic layer containing suxibuzone and its metabolites was separated by centrifugation at 2000×*g*. This extraction was repeated once. The combined organic layer was evaporated to a suitable volume under nitrogen at 30°, transferred to a test tube (10-ml capacity), and dried under nitrogen. The residue was dissolved in 100 μl of methanol, and 2–10 μl of this solution was injected into the liquid chromatograph with a 10-μl syringe[12].

Calibration curves for the determination of suxibuzone, 4-hydroxymethylphenylbutazone, phenylbutazone, oxyphenbutazone, and γ-hydroxyphenylbutazone by HPLC were prepared by plotting the peak area against the concentration of each compound. All of these calibration curves were linear.

The procedure for GLC determination was the same as that reported previously (4).

RESULTS AND DISCUSSION

An efficient solvent system (4), benzene–cyclohexane (1:1 v/v) acidified

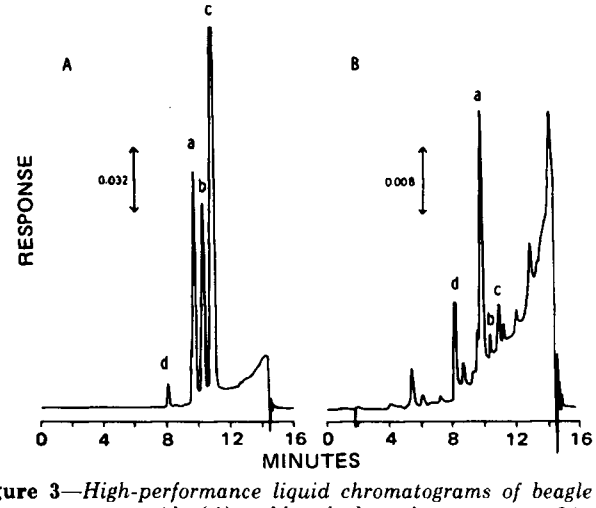

Figure 3—*High-performance liquid chromatograms of beagle dog plasma extracts at 4 hr (A) and beagle dog urine extracts at 24–48 hr (B) following a single oral dose of 142 mg of suxibuzone/kg. Key: a, γ-hydroxyphenylbutazone; b, oxyphenbutazone; c, phenylbutazone; and d, unknown metabolite.*

[12] Model 10A-RN-GP, Scientific Glass Engineering Ltd., North Melbourne, Australia.

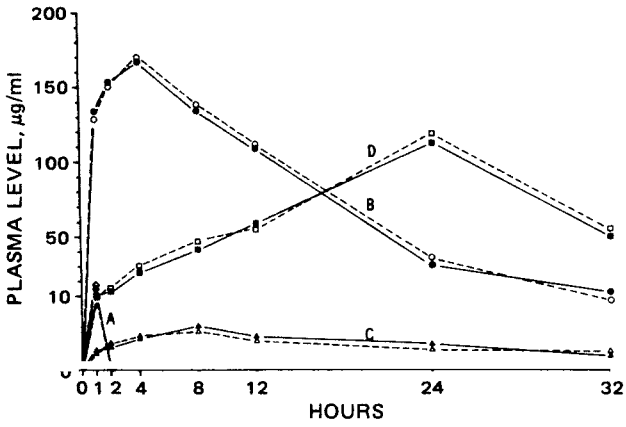

Figure 4—*Comparison of plasma levels of suxibuzone and its metabolites determined by HPLC (closed symbols) and GLC (open symbols) methods following a single oral dose of 142 mg of suxibuzone/kg to a beagle dog. Key: A (◆ and ◇), suxibuzone; B (● and ○), phenylbutazone; C (▲ and △), oxyphenbutazone; and D (■ and □), γ-hydroxyphenylbutazone.*

with hydrochloric acid, was used for the extraction of suxibuzone and its metabolites from plasma and urine. Chloroform, methylene chloride, and ethylene dichloride could not be used as the solvent because of the decomposition, such as oxidation, of the extract during the extraction and evaporation.

A reversed-phase column[8] was used for the HPLC separation. Chromatographic separation of suxibuzone, 4-hydroxymethylphenylbutazone, phenylbutazone, oxyphenbutazone, and γ-hydroxyphenylbutazone was first examined using authentic samples. When a linear gradient system with methanol–0.01 *M* sodium acetate buffer (pH 4.0) was used as the mobile phase, suxibuzone and 4-hydroxymethylphenylbutazone were not separated, even when the initial methanol concentration was varied. As shown in Fig. 1, a linear gradient system with methanol–water or methanol–0.05 *M* KH_2PO_4 (0–100% methanol at 8%/min) gave good separation of suxibuzone and the four metabolites. Each compound gave only one chromatographic peak under this condition. Furthermore, no interfering peaks of biological extracts from the plasma and urine of a beagle dog were observed in either of these mobile phases.

On the basis of these results and the knowledge that phenylbutazone, oxyphenbutazone, and γ-hydroxyphenylbutazone are major metabolites of suxibuzone (4), the linear gradient system with methanol–0.05 *M* KH_2PO_4 as the mobile phase, which had given the best separation of these compounds, was employed for subsequent experiments.

Methanol was used as a solvent for redissolving the residue obtained by the evaporation to dryness of the benzene–cyclohexane extract from plasma and urine since suxibuzone and its metabolites all are readily soluble in this solvent. The dissolution was made immediately before the chromatographic assay. No decomposition of suxibuzone and its metabolites in methanol was observed. Similar assay results also were obtained when water was used as a solvent for the sample residue.

The chromatogram of suxibuzone, 4-hydroxymethylphenylbutazone, phenylbutazone, oxyphenbutazone, and γ-hydroxyphenylbutazone extracted from beagle dog plasma following addition of 5.0 μg/ml of each compound and the chromatogram of a control plasma extract are shown in Fig. 2. The chromatogram of the beagle dog urine extract was similar to that of the plasma extract. The retention times of suxibuzone, 4-hydroxymethylphenylbutazone, phenylbutazone, oxyphenbutazone, and γ-hydroxyphenylbutazone were 11.0, 11.2, 10.5, 10.0, and 9.4 min, respectively, and the time required for the assay was 15 min. Each fraction eluted from the HPLC column was collected separately, and the substances were confirmed by mass spectrometric analysis; suxibuzone: *m/e* 438 [M^+], 308, 264, and 183; 4-hydroxymethylphenylbutazone: *m/e* 338 [M^+], 308, 264, and 183; phenylbutazone: *m/e* 308 [M^+], 252, and 183; oxyphenbutazone: *m/e* 324 [M^+], 268, and 199; and γ-hydroxyphenylbutazone: *m/e* 324 [M^+], 309, 280, 266, and 183.

Table II—Comparison of Urine Levels of Suxibuzone and Its Metabolites Determined by HPLC and GLC Methods following a Single Oral Dose of 142 mg of Suxibuzone/kg to a Beagle Dog

Compound	Mole Percent of Dose					
	0–12 hr		12–24 hr		24–48 hr	
	HPLC	GLC	HPLC	GLC	HPLC	GLC
Suxibuzone	ND[a]	ND	ND	ND	ND	ND
4-Hydroxymethylphenylbutazone	ND	ND	ND	ND	ND	ND
Phenylbutazone	0.04	0.05	0.98	1.04	1.23	1.27
Oxyphenbutazone	ND	ND	0.11	0.09	0.31	0.33
γ-Hydroxyphenylbutazone	0.85	0.82	1.96	1.93	19.11	18.99

[a] Not detectable.

The detection limits under these HPLC conditions were 0.1 μg/ml for suxibuzone and 4-hydroxymethylphenylbutazone and 0.05 μg/ml for the other suxibuzone metabolites. The present method had an accuracy of ±2.3–3.1% and very good reproducibility.

Known amounts (5, 25, and 50 μg/ml) of suxibuzone and the four metabolites were added to the plasma and urine (1.0 ml) of beagle dogs, and the recovery of each compound was determined. The results are given in Table I.

One metabolite, *p*,γ-dihydroxyphenylbutazone (4), showed an extraction recovery of <20–30% using benzene–cyclohexane; therefore, this metabolite could not be assayed quantitatively by the present method. A GLC method (4) showed the same result. Although chloroform and ethylene dichloride were able to extract this metabolite efficiently, these solvents were unsuitable because of its decomposition. The retention time for *p*,γ-dihydroxyphenylbutazone under the present HPLC conditions was 10.2 min, and this metabolite had no effect on the separation of suxibuzone and the other metabolites.

A 142-mg/kg (0.32-mmole) dose of suxibuzone was administered orally to the beagle dog, and the concentration of suxibuzone and its metabolites in the plasma and urine was determined using the present method. The chromatogram of the plasma extract at 4 hr and that of the urine extract at 24–48 hr after administration are shown in Figs. 3A and 3B, respectively. With the beagle dog, 4-hydroxymethylphenylbutazone was not detected, as was reported previously (4). The concentrations of suxibuzone and its metabolites in plasma and urine determined by the HPLC method were compared with those reported previously for a GLC determination (4) (Fig. 4 and Table II). The overall difference between the value obtained by the two methods was 4.6%.

The present assay then was applied to the plasma and urine of other animals and humans to which suxibuzone and its metabolites were added. The results obtained for the chromatographic separation, recovery, and sensitivity were in good agreement with those obtained with beagle dog plasma and urine.

The present method is simple and rapid and has high accuracy and sensitivity. It should be useful for basic and clinical pharmacological investigations on suxibuzone.

REFERENCES

(1) A. Kanda, J. Yamamoto, H. Murakami, K. Tashima, and H. Fujimura, *Oyo Yakuri*, **19**, 133 (1980).

(2) H. Fujimura, K. Tsurumi, I. Morikawa, and T. Suzuki, *ibid.*, **14**, 379 (1977).

(3) R. Yoshida, A. Maruden, H. Sudo, O. Yamakita, M. Inubishi, K. Morita, T. Sakamoto, and M. Enomoto, *ibid.*, **19**, 1 (1980).

(4) T. Shindo, Y. Yasuda, K. Tahira, N. Mitani, A. Kanda, and A. Akazawa, *Yakugaku Zasshi*, **99**, 1186 (1979).

(5) J. J. Burns, R. K. Rose, T. Chenkin, A. Goldman, A. Schulert, and B. B. Brodie, *J. Pharmacol. Exp. Ther.*, **109**, 346 (1953).

(6) B. Hermann, *Med. Exp.*, **1**, 170 (1960).

(7) M. W. Fuchs, *Rheumatology*, **16**, 489 (1964).

(8) J. E. Wallace, *J. Pharm. Sci.*, **57**, 2053 (1968).

(9) H. M. Stevens, *Clin. Chem.*, **16**, 437 (1970).

(10) G. R. Van Petten, H. Ferg, R. J. Withey, and H. F. Letten, *J. Clin. Pharmacol.*, **11**, 117 (1971).

(11) E. Jähnchen and G. Levy, *Clin. Chem.*, **18**, 984 (1972).

(12) G. Lukas, C. B. Borman, and S. B. Zak, *J. Pharm. Sci.*, **65**, 86 (1976).

(13) R. Pulver, *Schweiz. Med. Wochenschr.*, **80**, 308 (1957).

(14) R. Perego, E. Martinelli, and P. C. Vanoni, *J. Chromatogr.*, **54**, 280 (1971).

(15) I. J. McGilveray, K. K. Midha, R. Brien, and L. Wilson, *ibid.*, **89**, 17 (1974).

(16) K. K. Midha, I. J. McGilveray, and C. Charette, *J. Pharm. Sci.*, **63**, 1234 (1974).

(17) R. B. Bruce, W. R. Maynard, and L. K. Dunning, *ibid.*, **63**, 446 (1974).

(18) Y. Tanimura, Y. Saitoh, F. Nakagawa, and T. Suzuki, *Chem.*

Pharm. Bull., **23**, 651 (1975).
(19) A. Sioufi, F. Caudal, and F. Marfil, *J. Pharm. Sci.*, **67**, 243 (1978).
(20) N. J. Pound, I. J. McGilveray, and R. Sears, *J. Chromatogr.*, **89**, 23 (1974).
(21) N. J. Pound and R. W. Sears, *J. Pharm. Sci.*, **64**, 284 (1975).

Kinetics of Hydrolysis of Methenamine

J. G. STROM, Jr., and H. WON JUN ˣ

Received March 19, 1979, from the *Department of Pharmaceutics, School of Pharmacy, University of Georgia, Athens, GA 30602.* Accepted for publication April 25, 1980.

Abstract □ The kinetics of degradation of methenamine were studied in citrate–phosphate buffers between pH 2.0 and 7.4 at 37.5°. GLC was used to monitor the rate of hydrolysis. The conversion of methenamine to formaldehyde was found to be pH dependent in the buffers of constant ionic strength, with the reaction half-life decreasing from 13.8 hr at pH 5.8 to 1.6 hr at pH 2.0. The kinetics of degradation also were measured at 47, 57, and 67°, and the reaction obeyed the Arrhenius relationship. At pH 2.0, the activation energy was calculated to be 23.5 kcal/mole; at pH 5.1, it was 12.0 kcal/mole.

Keyphrases □ Methenamine—hydrolysis kinetics in citrate–phosphate buffers □ Hydrolysis kinetics—methenamine in citrate–phosphate buffers □ Kinetics—hydrolysis of methenamine in citrate–phosphate buffers

Methenamine (hexamethylenetetramine) is a urinary antibacterial useful in the long-term therapy of chronic urinary tract infections. The antibacterial activity of methenamine is derived from formaldehyde produced upon hydrolysis of methenamine in the bladder. The amount of hydrolysis is a function of the acidity of the urine (1).

BACKGROUND

Methenamine was introduced for the treatment of urinary infections in 1894 (2). Although this drug has been used for over 80 years and its pharmacological activity depends on the extent and rate of hydrolysis of the parent compounds in acidic media (3), there are few reported studies on the *in vitro* hydrolysis of methenamine. In 1935, Philippi and Löbering (4) studied the hydrolysis of methenamine in buffer solutions. Their assay method was based on the formation of a silver nitrate–methenamine complex. According to Slowick and Kelley (5), this procedure produces inaccurate and undependable results, so the findings of Philippi and Löbering (4) probably are in error.

A paper published by Tada (6) summarized work done from 1951 to 1958 (7–10) in Japan and listed the rates of decomposition of methenamine in hydrochloric acid at pH ≤1.6. Decomposition also was measured in acetic acid–sodium acetate buffer solutions in the pH range of ~4–6. Tada's (6) assay involved the titration of excess acid not consumed in the degradation reaction. Titration procedures normally are tedious and time consuming.

Investigations into the pharmacology of methenamine have been difficult because all of the methods are based on the measurement of formaldehyde liberated from methenamine. Early studies used methods that were relatively insensitive. Many of the analytical procedures are not applicable in the presence of intact methenamine (11). Most studies on urinary formaldehyde concentrations used the colorimetric method of Tanenbaum and Bricker (12). The acidity of the reagents used in this method recently was found to convert 20–30% of the residual methenamine to formaldehyde (13).

Useful scientific data for methenamine compounds generally are not available. The pharmacokinetics and mechanisms of action of this drug have not been well elucidated. Because of the use of other urinary tract antibacterials like nitrofurantoin and the sulfonamides, few recent studies on methenamine have been reported.

This report presents a study of the hydrolysis of methenamine between pH 2.0 and 7.4 in aqueous buffers. The rate of hydrolysis of methenamine was followed by measuring the change in the concentration of intact methenamine determined by the specific and accurate GLC procedure of Strom and Jun (14).

EXPERIMENTAL

Apparatus—The gas chromatograph[1] was equipped with a dual flame-ionization detector. A 1.8-m × 6-mm i.d. glass column was packed with 3% OV-17 on 80–100-mesh Chromosorb W-HP. The operating temperatures were 245° for the injection port, 190° (isothermal) for the column oven, and 250° for the detector. Nitrogen at a flow rate of 45 ml/min was the carrier gas. The flow rates of hydrogen and compressed air were adjusted to optimum sensitivity. The electrometer range was 10^{-10} amp/mv.

Calibration Curve—Methenamine[2] was recrystallized from absolute ethanol. Methylparaben[3] (methyl *p*-hydroxybenzoate), the internal standard, was used as received. Aliquots of 0.5, 1.5, 2.5, 5.0, 7.5, and 10 ml of methenamine solution (2 mg/ml in water containing 2 mg of methylparaben/ml) were added to individual 10-ml volumetric flasks and diluted to volume with water (containing 2 mg of methylparaben/ml). Each solution (1 μl) was injected into the chromatograph. The calibration curve was obtained by plotting the known concentration of methenamine *versus* the corresponding peak height ratio (methenamine/methylparaben).

Buffer Solutions—All buffer solutions were prepared in deionized, distilled water and were adjusted to an ionic strength of 0.5 with potassium chloride. Buffer solutions in the pH range of 2.0–7.4 were prepared by combining various amounts of 0.1 *M* citric acid and 0.2 *M* dibasic sodium phosphate stock solutions (15).

Stability Studies—*Effect of pH*—Amounts of methenamine equal to 0.75 mg/ml were weighed and placed in volumetric flasks. At time zero, the methenamine was dissolved in buffer solutions of pH 2.0, 2.4, 3.4, 4.6, 5.1, 5.5, 5.8, or 7.4 previously equilibrated at 37.5°. After dilution with the respective buffers, 10.0-ml samples were removed and placed in 16 × 125-mm culture tubes with polytef-lined screw caps. These tubes were placed into a constant-temperature water bath.

At suitable time intervals, one culture tube was removed and cooled to room temperature by quenching in an ice bath. One milliliter of the internal standard solution (22 mg of methylparaben/ml in methanol) was added, and the sample was subjected immediately to the GLC analysis. The pH was measured at the beginning and end of each run, and no significant change was found.

Effect of Temperature—Methenamine at 0.75 mg/ml also was studied kinetically at 47, 57, and 67° in pH 2.0, 5.1, and 7.4 buffers.

RESULTS AND DISCUSSION

Figure 1 shows a typical gas chromatogram obtained for an aqueous solution of methenamine (t_R = 0.8 min) and methylparaben, the internal standard (t_R = 1.7 min). Both methenamine and the internal standard gave sharp, well-resolved peaks (resolution, R_s = 5.4) with no tailing. A

[1] Varian Aerograph model 1830, Varian Instruments Division, Palo Alto, CA 94304.
[2] Riker Laboratories, Northridge, CA 91324.
[3] Fisher Scientific Co., Fair Lawn, NJ 07410.

0022-3549/80/1100-1261$01.00/0
© 1980, American Pharmaceutical Association

Pharm. Bull., **23**, 651 (1975).
(19) A. Sioufi, F. Caudal, and F. Marfil, *J. Pharm. Sci.*, **67**, 243 (1978).
(20) N. J. Pound, I. J. McGilveray, and R. Sears, *J. Chromatogr.*, **89**, 23 (1974).
(21) N. J. Pound and R. W. Sears, *J. Pharm. Sci.*, **64**, 284 (1975).

Kinetics of Hydrolysis of Methenamine

J. G. STROM, Jr., and H. WON JUN ˣ

Received March 19, 1979, from the *Department of Pharmaceutics, School of Pharmacy, University of Georgia, Athens, GA 30602.* Accepted for publication April 25, 1980.

Abstract □ The kinetics of degradation of methenamine were studied in citrate–phosphate buffers between pH 2.0 and 7.4 at 37.5°. GLC was used to monitor the rate of hydrolysis. The conversion of methenamine to formaldehyde was found to be pH dependent in the buffers of constant ionic strength, with the reaction half-life decreasing from 13.8 hr at pH 5.8 to 1.6 hr at pH 2.0. The kinetics of degradation also were measured at 47, 57, and 67°, and the reaction obeyed the Arrhenius relationship. At pH 2.0, the activation energy was calculated to be 23.5 kcal/mole; at pH 5.1, it was 12.0 kcal/mole.

Keyphrases □ Methenamine—hydrolysis kinetics in citrate–phosphate buffers □ Hydrolysis kinetics—methenamine in citrate–phosphate buffers □ Kinetics—hydrolysis of methenamine in citrate–phosphate buffers

Methenamine (hexamethylenetetramine) is a urinary antibacterial useful in the long-term therapy of chronic urinary tract infections. The antibacterial activity of methenamine is derived from formaldehyde produced upon hydrolysis of methenamine in the bladder. The amount of hydrolysis is a function of the acidity of the urine (1).

BACKGROUND

Methenamine was introduced for the treatment of urinary infections in 1894 (2). Although this drug has been used for over 80 years and its pharmacological activity depends on the extent and rate of hydrolysis of the parent compounds in acidic media (3), there are few reported studies on the *in vitro* hydrolysis of methenamine. In 1935, Philippi and Löbering (4) studied the hydrolysis of methenamine in buffer solutions. Their assay method was based on the formation of a silver nitrate–methenamine complex. According to Slowick and Kelley (5), this procedure produces inaccurate and undependable results, so the findings of Philippi and Löbering (4) probably are in error.

A paper published by Tada (6) summarized work done from 1951 to 1958 (7–10) in Japan and listed the rates of decomposition of methenamine in hydrochloric acid at pH ≤1.6. Decomposition also was measured in acetic acid–sodium acetate buffer solutions in the pH range of ~4–6. Tada's (6) assay involved the titration of excess acid not consumed in the degradation reaction. Titration procedures normally are tedious and time consuming.

Investigations into the pharmacology of methenamine have been difficult because all of the methods are based on the measurement of formaldehyde liberated from methenamine. Early studies used methods that were relatively insensitive. Many of the analytical procedures are not applicable in the presence of intact methenamine (11). Most studies on urinary formaldehyde concentrations used the colorimetric method of Tanenbaum and Bricker (12). The acidity of the reagents used in this method recently was found to convert 20–30% of the residual methenamine to formaldehyde (13).

Useful scientific data for methenamine compounds generally are not available. The pharmacokinetics and mechanisms of action of this drug have not been well elucidated. Because of the use of other urinary tract antibacterials like nitrofurantoin and the sulfonamides, few recent studies on methenamine have been reported.

This report presents a study of the hydrolysis of methenamine between pH 2.0 and 7.4 in aqueous buffers. The rate of hydrolysis of methenamine was followed by measuring the change in the concentration of intact methenamine determined by the specific and accurate GLC procedure of Strom and Jun (14).

EXPERIMENTAL

Apparatus—The gas chromatograph[1] was equipped with a dual flame-ionization detector. A 1.8-m × 6-mm i.d. glass column was packed with 3% OV-17 on 80–100-mesh Chromosorb W-HP. The operating temperatures were 245° for the injection port, 190° (isothermal) for the column oven, and 250° for the detector. Nitrogen at a flow rate of 45 ml/min was the carrier gas. The flow rates of hydrogen and compressed air were adjusted to optimum sensitivity. The electrometer range was 10^{-10} amp/mv.

Calibration Curve—Methenamine[2] was recrystallized from absolute ethanol. Methylparaben[3] (methyl *p*-hydroxybenzoate), the internal standard, was used as received. Aliquots of 0.5, 1.5, 2.5, 5.0, 7.5, and 10 ml of methenamine solution (2 mg/ml in water containing 2 mg of methylparaben/ml) were added to individual 10-ml volumetric flasks and diluted to volume with water (containing 2 mg of methylparaben/ml). Each solution (1 μl) was injected into the chromatograph. The calibration curve was obtained by plotting the known concentration of methenamine *versus* the corresponding peak height ratio (methenamine/methylparaben).

Buffer Solutions—All buffer solutions were prepared in deionized, distilled water and were adjusted to an ionic strength of 0.5 with potassium chloride. Buffer solutions in the pH range of 2.0–7.4 were prepared by combining various amounts of 0.1 *M* citric acid and 0.2 *M* dibasic sodium phosphate stock solutions (15).

Stability Studies—*Effect of pH*—Amounts of methenamine equal to 0.75 mg/ml were weighed and placed in volumetric flasks. At time zero, the methenamine was dissolved in buffer solutions of pH 2.0, 2.4, 3.4, 4.6, 5.1, 5.5, 5.8, or 7.4 previously equilibrated at 37.5°. After dilution with the respective buffers, 10.0-ml samples were removed and placed in 16 × 125-mm culture tubes with polytef-lined screw caps. These tubes were placed into a constant-temperature water bath.

At suitable time intervals, one culture tube was removed and cooled to room temperature by quenching in an ice bath. One milliliter of the internal standard solution (22 mg of methylparaben/ml in methanol) was added, and the sample was subjected immediately to the GLC analysis. The pH was measured at the beginning and end of each run, and no significant change was found.

Effect of Temperature—Methenamine at 0.75 mg/ml also was studied kinetically at 47, 57, and 67° in pH 2.0, 5.1, and 7.4 buffers.

RESULTS AND DISCUSSION

Figure 1 shows a typical gas chromatogram obtained for an aqueous solution of methenamine (t_R = 0.8 min) and methylparaben, the internal standard (t_R = 1.7 min). Both methenamine and the internal standard gave sharp, well-resolved peaks (resolution, R_s = 5.4) with no tailing. A

[1] Varian Aerograph model 1830, Varian Instruments Division, Palo Alto, CA 94304.
[2] Riker Laboratories, Northridge, CA 91324.
[3] Fisher Scientific Co., Fair Lawn, NJ 07410.

0022-3549/80/1100-1261$01.00/0
© 1980, American Pharmaceutical Association

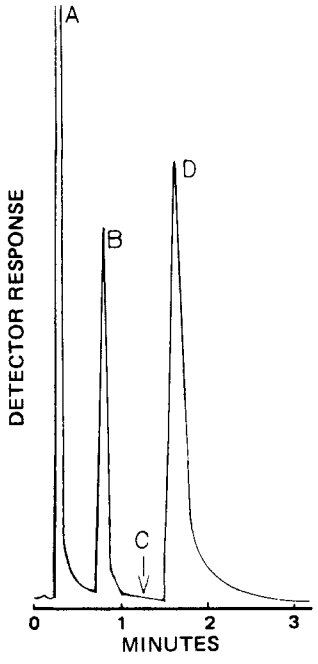

Figure 1—*Gas chromatogram of methenamine and the internal standard in water on a 3% OV-17 column. Key: A, solvent; B, methenamine; C, recurrent unidentified peak; and D, methylparaben.*

peak that appeared repeatedly in all kinetic runs had a retention time of 1.25 min (point C in Fig. 1). This peak, possibly the hydrolysis product formaldehyde or, more probably, a polymer of formaldehyde, would be well resolved from both methenamine (R_s = 4.4) and from the internal standard (R_s = 2.2). A plot of the ratio of the peak height of methenamine to the height of the internal standard *versus* the concentration of methenamine produced a linear relationship between 0.10 and 2.00 mg/ml. The calibration curve had a slope of 0.89 ml/mg, an intercept of 3.24×10^{-2}, and a correlation coefficient of 0.9997.

The kinetics of hydrolysis of methenamine were followed at various pH values by monitoring the decrease of the ratio of the peak height for the peak at the methenamine retention time to the peak height of the internal standard as a function of time. A plot of the hydrolysis data obtained at various pH values is shown in Fig. 2.

The logarithms of the difference of the final peak height ratio, H_∞ (the peak height ratio at the end of 10 half-lives), and the peak height ratio at any time, H_t, *versus* time produced linear plots. The apparent first-order rate constants were calculated from the slopes of the linear regression lines fitted to:

$$\ln(H_t - H_\infty) = \ln(H_0 - H_\infty) - kt \qquad \text{(Eq. 1)}$$

where H_0 is the peak height ratio at time zero and k is the apparent first-order rate constant. At all of the pH values studied, H_∞ was essentially zero after storage for several days at the selected temperature, indicating that the reaction went to completion. The rate constants derived from the data are presented in Table I.

A concentration of 0.75 mg/ml was chosen as the initial concentration because this value is the expected physiological concentration following a normal dose in humans (16). Six hours would be the maximum time a solution of methenamine would remain in the bladder. No decomposition (*i.e.*, no change in the peak height ratio) was observed in the pH 7.4 buffer over a 6-hr period.

Table I—Apparent First-Order Rate Constants for Hydrolysis of Methenamine in Buffer at 37.5°

pH	k, $hr^{-1} \times 10^2$	$t_{1/2}$, hr	r^a
2.0	43.3	1.60	0.9978
2.4	32.7	2.12	0.9848
3.4	22.4	3.09	0.9920
4.6	18.6	3.73	0.9993
5.1	8.36	8.29	0.9882
5.5	6.35	10.9	0.9856
5.8	5.01	13.8	0.9935
7.4	—[b]	—	

[a] Correlation coefficient for the linear regression line. [b] No observable degradation over the time interval studied.

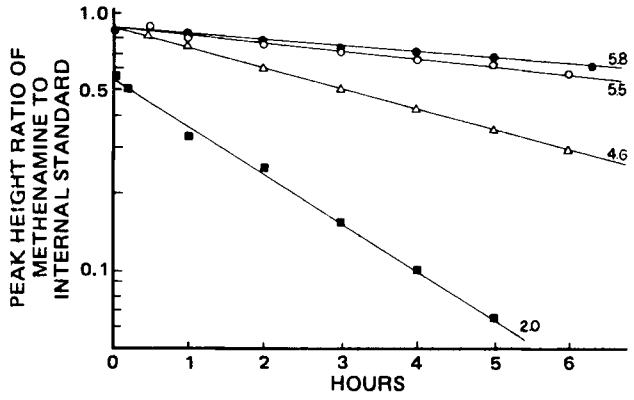

Figure 2—*Semilogarithmic plots of the ratio of the height of the GLC peak for methenamine to the peak for the internal standard* versus *time at specified pH values. Each point is an average of two kinetic runs. Key: ●, pH 5.8; ○, pH 5.5; △, pH 4.6; and ■, pH 2.0.*

The effect of temperature on the hydrolysis rate was investigated at pH 2.0, 5.1, and 7.4 at several temperatures. Table II lists the apparent first-order rate constants calculated at each temperature for each pH value. There was no observable change in the peak height ratio in pH 7.4 buffer at any temperature over a 6-hr period. Arrhenius plots of the logarithms of the observed rate constants *versus* $1/T$ produced straight lines (Fig. 3). The activation energy for the reaction then was calculated from the slopes of the lines fitted to the data (Table II).

The studies of Tada (6) showed that:

$$k_{obs} = (k_w + k_h[H^+])f^+ \qquad \text{(Eq. 2)}$$

where k_{obs} is the observed rate constant; k_w and k_h are the rate constants for the water solvolysis reaction and the hydrogen-ion-catalyzed reaction, respectively; and f^+ is the fraction of methenamine present in the protonated form. Tada (6) calculated k_w and k_h values at 30° of 6.05×10^{-6} sec^{-1} and 6.33×10^{-4} liter/mole/sec, respectively. Tada (6) also determined the dissociation constant of protonated methenamine to be 7.0×10^{-6}, from which values of f^+ as a function of pH can be calculated. This relationship is shown graphically in Fig. 4. The value from Table I for hydrolysis at pH 2.0 and 37.5° was set equal to the value from Tada (6) at pH 2.0 and 30°, and the remaining values from Table I were scaled

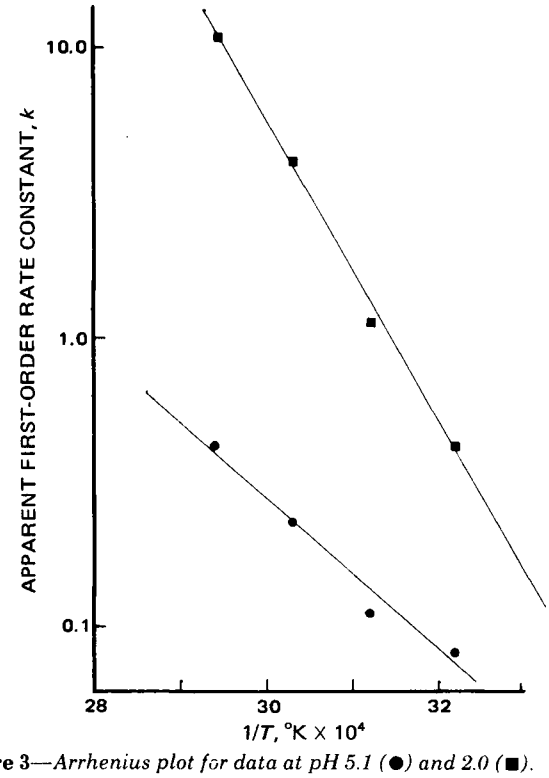

Figure 3—*Arrhenius plot for data at pH 5.1 (●) and 2.0 (■).*

Table II—Apparent First-Order Rate Constants and Thermodynamic Parameters for the Hydrolysis of Methenamine at Various Temperatures

pH	k, $hr^{-1} \times 10$				E_a, kcal/mole	ln A^a	r^b
	37.5°	47°	57°	67°			
2.0	4.33	11.5	41.9	111.0	23.5	37.2	0.9985
5.1	0.836	1.11	2.33	4.27	12.0	16.8	09853

[a] A is the frequency factor. [b] The correlation coefficient for the linear regression line obtained by fitting the data to the Arrhenius relationship.

accordingly and plotted in Fig. 4. The scaled values from this study agreed very well with the values predicted by Tada (6).

The Arrhenius activation energy (E_a) of 23.5 kcal/mole at pH 2.0 and an ionic strength of 0.5 compared favorably with Tada's (6) value of 23.3 kcal/mole in highly acidic media at an ionic strength of 3.08. This E_a value can be largely associated with the hydrogen-ion-catalyzed reaction. The E_a value of 12.0 kcal/mole calculated at pH 5.1 would be almost entirely a function of the rate constant of the water reaction, k_w.

The conversion of methenamine to formaldehyde in biological fluids, particularly urine, is of clinical importance since formaldehyde is the pharmacologically active product and is effective against urinary bacteria only above a concentration of ~20 μg/ml (17). Methenamine solution remains in the bladder for only a certain time (~6 hr), and it is necessary to know the amount of conversion that occurs over that period. It also would be useful for successful therapy to know the effect of the urinary pH on the rate of that conversion. Several recent reports discussed hydrolysis of methenamine in urine (18–20). Possible errors from the assay method used in these studies were minimized in part by use of the Jackson and Stamey method (13), a modification of the Tanenbaum and Bricker (12) procedure, or by use of the Chen and Chafetz method (21). A possibly better method would be use of the Jackson and Stamey procedure to quantitate the free formaldehyde concentration simultaneously with the GLC procedure for intact methenamine.

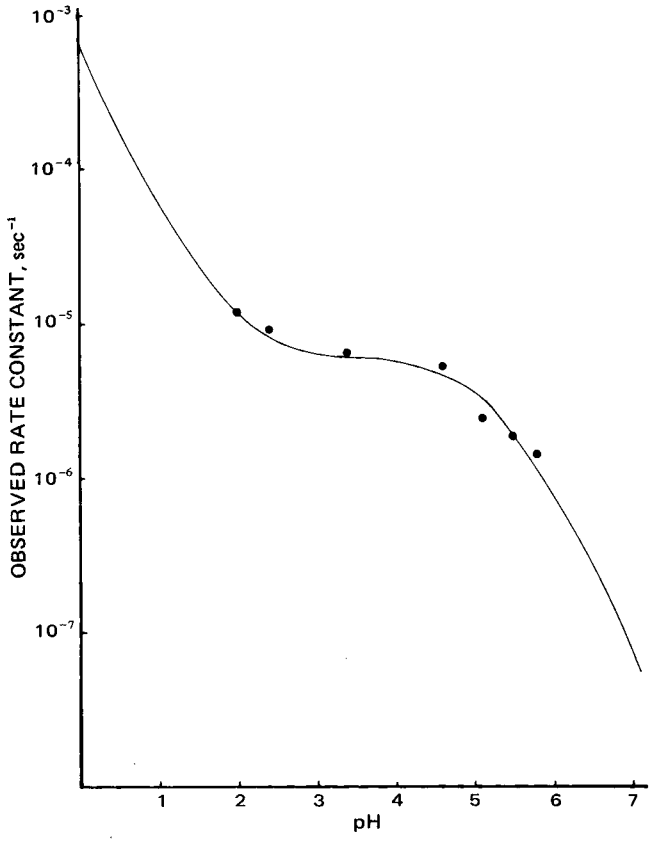

Figure 4—*The pH–rate profile of methenamine degradation. The solid line is the predicted relationship from the work of Tada (6). The points are the data from Table I scaled to 30°.*

According to the data of the present study, methenamine should circulate in the blood as the intact drug and be rapidly converted to formaldehyde when it reaches the acidic urine. If the drug were converted at a similar rate in the urine as in the buffers of this study, sufficient formaldehyde would be produced within 2 hr at pH ≤5.8. However, it may not be possible to make quantitative predictions of the *in vivo* behavior of methenamine from the data of this study because of possible kinetic salt effects. Tada's (6) work demonstrated a linear increase in the observed rate constant with an increase in the ionic strength up to a value of 3 or 4. This effect was shown for about 15 mono- and divalent salts, such as sodium chloride, sodium iodide, potassium chloride, potassium iodide, lithium chloride, calcium chloride, and ammonium chloride.

The reported study demonstrated that the GLC procedure can be used to observe and quantitate the degradation kinetics of methenamine *in vitro* in a buffer system.

REFERENCES

(1) P. J. Hanzlik and A. B. Collins, *Arch. Intern. Med.*, **12**, 578 (1913).

(2) A. Nicolaier, *Dtsch. Med. Wochenschr.*, **21**, 541 (1895).

(3) R. S. A. Heathcote, *Br. J. Urol.*, **7**, 9 (1935).

(4) E. Philippi and J. Löbering, *Biochem. Z.*, **277**, 365 (1935).

(5) E. F. Slowick and R. S. Kelley, *J. Am. Pharm. Assoc., Sci. Ed.*, **31**, 15 (1942).

(6) H. Tada, *J. Am. Chem. Soc.*, **82**, 255 (1960).

(7) S. Kambara and H. Tada, *J. Chem. Soc. Jpn.*, **55**, 360 (1952).

(8) H. Tada, *ibid.*, **56**, 445 (1953).

(9) *Ibid.*, **57**, 37 (1954).

(10) *Ibid.*, **58**, 10 (1955).

(11) J. A. Stamey, "Urinary Infections," Williams & Wilkins, Baltimore, Md., 1972, p. 266.

(12) M. Tanenbaum and C. E. Bricker, *Anal. Chem.*, **23**, 354 (1951).

(13) J. Jackson and T. A. Stamey, *Invest. Urol.*, **9**, 124 (1971).

(14) J. G. Strom, Jr., and H. W. Jun, *J. Pharm. Sci.*, **66**, 589 (1977).

(15) "Scientific Tables," 7th ed., K. Diem and C. Lentner, Eds., Ciba-Geigy, Basel, Switzerland, 1970, pp. 280–282.

(16) V. Knight, J. W. Draper, E. A. Brady, and C. A. Attmore, *Antibiot. Chemother.*, **2**, 615 (1962).

(17) H. Miller and E. Phillips, *Invest. Urol.*, **8**, 21 (1970).

(18) D. M. Musher and D. P. Griffith, *Antimicrob. Agents Chemother.*, **6**, 708 (1974).

(19) D. M. Musher, D. P. Griffith, and Y. Richie, *Invest. Urol.*, **13**, 380 (1976).

(20) J. M. T. Hamilton-Miller and W. Brumfitt, *ibid.*, **14**, 287 (1977).

(21) T. Chen and L. Chafetz, *ibid.*, **10**, 212 (1972).

ACKNOWLEDGMENTS

The authors thank the reviewer for constructive comments and suggestions.

Quantitation of Carbenicillin Disodium, Cefazolin Sodium, Cephalothin Sodium, Nafcillin Sodium, and Ticarcillin Disodium by High-Pressure Liquid Chromatography

V. DAS GUPTA [x] **and KENNETH R. STEWART** [*]

Received February 22, 1980, from the *College of Pharmacy, University of Houston, Houston, TX 77004.* Accepted for publication May 2, 1980. *Ben Taub General Hospital Pharmacy, Houston, TX 77030.

Abstract □ High-pressure liquid chromatographic (HPLC) methods for the quantitation of carbenicillin, cefazolin, cephalothin, nafcillin, and ticarcillin were developed. The stability of 2% solutions of the antibiotics in normal saline and in 5% dextrose in water were studied at 24 and 5°. The assays were conducted using a previously reported colorimetric method, and some assays also were performed using HPLC. For discolored solutions of cephalothin, the colorimetric method was not stability indicating. The percent relative standard deviations by HPLC based on six injections were 1.69, 0.94, 1.30, 1.59, and 1.6 for carbenicillin, cefazolin, cephalothin, nafcillin, and ticarcillin, respectively. Both carbenicillin and ticarcillin apparently may be mixtures of two isomers at equilibrium with each other. The shelflives recommended by the manufacturers at 5° may be too conservative.

Keyphrases □ Carbenicillin disodium—high-pressure liquid chromatographic analysis □ Cefazolin sodium—high-pressure liquid chromatographic analysis □ Cephalothin sodium—high-pressure liquid chromatographic analysis □ Nafcillin sodium—high-pressure liquid chromatographic analysis □ Ticarcillin disodium—high-pressure liquid chromatographic analysis □ Antibiotics—carbenicillin disodium, cefazolin sodium, cephalothin sodium, nafcillin sodium, and ticarcillin disodium, high-pressure liquid chromatographic analysis

The preparation of intravenous admixtures is a common service provided by hospital pharmacies in the United States. Most pharmacists are concerned about the stability of the solutions after mixing. Some of these solutions contain antibiotics such as carbenicillin disodium, cefazolin sodium, cephalothin sodium, nafcillin sodium, and ticarcillin disodium in normal saline or in 5% dextrose in water. The stability studies must be conducted using a stability-indicating assay.

Pharmaceutical manufacturers have begun to report limited information on the stability of antibiotics in intravenous admixtures. For example, the following information has been reported in the package inserts. Intravenous solutions of carbenicillin disodium (1), cefazolin sodium (2), cephalothin sodium (3), and ticarcillin disodium (4) are stable for 1 day at room temperature and for 3, 4, 4, and 3 days, respectively, when stored in a refrigerator. The intravenous solution of nafcillin sodium has been reported to be stable for 3 days at room temperature and for 7 days when stored in a refrigerator (5).

BACKGROUND

Brief studies on the stability of frozen and refrigerated solutions of cefazolin sodium (6, 7) and cephalothin sodium (8, 9) have been reported. These reports did not describe the methodology in detail, especially the analytical techniques. One study (9) recommended expiration dates of 2 days at 5° and of 6–24 hr at 25° for a 1% solution of cephalothin sodium in normal saline or in 5% dextrose in water. Other reports (6–8) recommended an expiration date of 4 days for both cefazolin sodium and cephalothin sodium when stored in a refrigerator. Longer expiration dates were recommended for frozen solutions.

Zia and Zargarbashi (10) reported the kinetics of carbenicillin sodium in aqueous solution at 35°. The degradation products of cephalothin and cefazolin in alkaline and neutral aqueous solutions at 35° were reported also (11).

Several analytical techniques have been used for the stability studies. A fluorometric method for cephalothin and cefazolin was reported (12). Zia and Zargarbashi (10) preferred the iodometric method, and Yamana and Tsuji (11) used anion-exchange chromatography for cephalothin and high-pressure liquid chromatography (HPLC) for cefazolin. One method for the quantitation of cefazolin was based on a reaction with hydroxylamine hydrochloride (13). This method was modified (14) and applied to other penicillins including carbenicillin and cephalothin.

The high experimental errors inherent in microbiological assays were reported (15), and the factors affecting the iodometric assay technique and its limitations were described (16, 17).

The purposes of this investigation were to develop accurate and reproducible stability-indicating assays for the quantitation of carbenicillin disodium (I), cefazolin sodium (II), cephalothin sodium (III), nafcillin

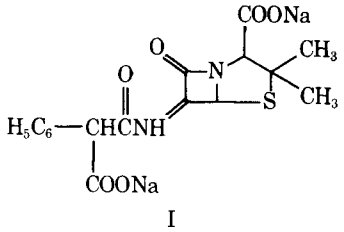

I

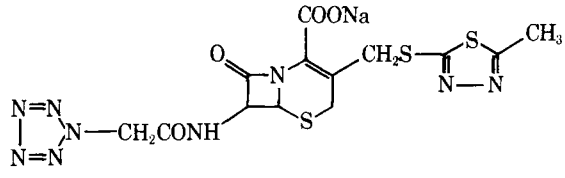

II

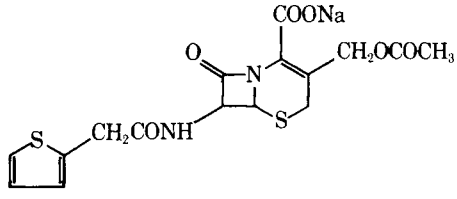

III

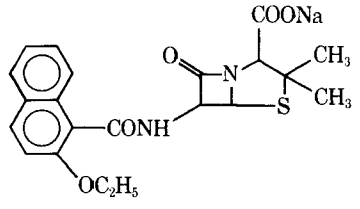

IV

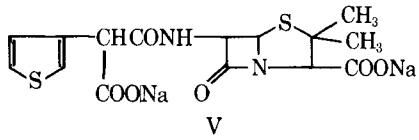

V

0022-3549/80/1100-1264$01.00/0
© 1980, American Pharmaceutical Association

Table I—Chromatographic Conditions

Antibiotic	Mobile Phase	Flow Rate, ml/min	Detector Setting, nm	Sensitivity Setting	Chart Speed, cm/hr	Concentration[a] of Standard Solution, μg/ml
Carbenicillin	0.01 *M* NH_4OOCCH_3 in water	1.6	245	0.04	30.5	600
Cefazolin	0.01 *M* NH_4OOCCH_3 in 30% methanol in water	1.3	254	0.1	30.5	60
Cephalothin	0.01 *M* NH_4OOCCH_3 in 30% methanol in water	2.2	254	0.04	30.5	50
Nafcillin	0.01 *M* NH_4OOCCH_3 in 50% methanol in water	2.0	280	0.04	30.5	80
Ticarcillin	0.01 *M* NH_4OOCCH_3 in water	1.6	245	0.1	30.5	600

[a] The concentrations reported are in terms of total sterile powder. The temperature was ambient.

Table II—Colorimetric Assay Results for Solutions (2 g/100 ml) Stored at Room Temperature (24 ± 1°)

		Percent of Potency Retained (Based on Label Claim) after						
Antibiotic	Solvent	1 day	4 days	5 days	5 days (HPLC)[a]	7 days	13 days (HPLC)[a]	15 days
Carbenicillin	NS[b]	96.8	89.7	86.5	87.4	—[c]	—[c]	60.1
Cefazolin	NS	98.0	95.4	93.9	93.0	90.9	—[c]	86.4
Cephalothin	NS	96.1	79.2[d]	78.0	62.2	—[c]	33.4	—[c]
Nafcillin	D5W[e]	97.9	93.6	91.6	92.0	89.5	—[c]	—[c,f]
Ticarcillin	NS	96.4	88.8	85.1	85.5	—[c]	—[c]	60.1

		Percent of Potency Retained (Based on Label Claim) after										
Antibiotic	Solvent	1 day	3 days	5 days	5 days (HPLC)[a]	6 days	6 days (HPLC)[a]	7 days	9 days	9 days (HPLC)[a]	11 days	11 days (HPLC)[a]
Carbenicillin	D5W	99.1	79.6	—[c]	—[c]	67.5	68.6	61.7	—[c]	—[c]	31.4	—[c]
Cefazolin	D5W	99.1	76.6	94.0	93.2	—[c]	—[c]	—[c]	89.4	88.5	86.1	—[c]
Cephalothin	D5W	95.8	88.4[d]	78.6	56.1	—[c]	—[c]	—[c]	72.1	50.5	60.6	40.9
Nafcillin	NS	100	94.3	—[c]	—[c]	87.5	86.5	85.1	—[c]	—[c]	—[c,f]	—[c]
Ticarcillin	D5W	99.2	81.4	—[c]	—[c]	45.0	43.5	43.3	—[c]	—[c]	14.3	—[c]

[a] By the HPLC method. [b] Normal saline. [c] Not assayed on this day. [d] Solution had discolored to light yellow. The intensity of the color increased with further storage. [e] Five percent dextrose in water. [f] There was precipitation in the bag (light yellow).

sodium (IV), and ticarcillin disodium (V) using HPLC and to study the stability of some intravenous admixtures containing these antibiotics. All of the antibiotics studied have a β-lactam ring.

EXPERIMENTAL

Chemicals and Reagents—All chemicals and reagents were USP, NF, or ACS quality and were used without further purification. The sterile powders of carbenicillin disodium[1], cefazolin sodium[2], cephalothin sodium[2], nafcillin sodium[3], and ticarcillin disodium[4] were used as received. The powder of III contained sodium bicarbonate and the powder of IV contained sodium citrate as a buffering agent. The presence of buffering agents did not interfere in these investigations.

Apparatus—The high-pressure liquid chromatograph[5] was equipped with a multiple-wavelength detector[6], a recorder[7], and an integrator[8].

Column—A semipolar[9] column (30 cm long × 4 mm i.d.) was used.

Chromatographic Conditions—The chromatographic conditions are reported in Table I.

Preparation of Solutions—The standard solutions in water were prepared fresh. Their concentrations are reported in Table I. Solutions of other concentrations were prepared fresh as needed using a simple solution method.

Preparation of Antibiotic Solutions (Similar to Intravenous Admixtures)—Solutions of I–V (2.00%)[10] were prepared in either sterile normal saline[11] or in sterile 5% dextrose in water[11]. The final solutions were not sterile. All solutions were divided into two parts and transferred to the original containers[12]. One set of the solutions was stored at room temperature (24 ± 1°), and the other set was stored in a refrigerator (5 ± 1°). The solutions were assayed at appropriate intervals.

Assay Procedures—*Colorimetric Procedure*—The colorimetric procedure was reported previously (14). The method has been claimed to be stability indicating. The results are reported in Tables II and III.

HPLC Procedures—At appropriate intervals, solutions of antibiotics also were assayed using HPLC methods developed in this laboratory. Before analysis, all solutions were diluted with water to the appropriate concentrations (identical to the standard solutions; see Table I). A 20.0-μl aliquot of the assay solution was injected into the chromatograph using the described conditions (Table I). For comparison, an identical volume of the appropriate standard solution was injected after the assay solution eluted.

Calculations—Since preliminary investigations indicated that the peak areas (also peak heights) were related directly to the concentration (ranges tested were: I, 8–16 μg; II, 0.8–1.6 μg; III, 0.5–1.2 μg; IV, 1.3–2.0 μg; and V, 8–16 μg), the results were calculated using:

$$\text{percent of label claim} = \frac{(Ph)_a}{(Ph)_s} \times 100 \qquad \text{(Eq. 1)}$$

where $(Ph)_a$ is the peak height of the assay solution and $(Ph)_s$ is the peak height of the standard solution of identical concentration. For I and V, heights of the taller peaks (peak 1) were compared. The results are presented in Tables II and III and Figs. 1–3. The pH values are presented in Table IV.

RESULTS AND DISCUSSION

Carbenicillin—The results (Table II) indicate that the manufacturer-recommended expiration date of 1 day at room temperature is reasonable. At room temperature, a 2.00% solution of carbenicillin appears to have greater stability in normal saline (60.1% potency after 15

[1] Roerig, a Division of Pfizer, New York, NY 10017.
[2] Eli Lilly and Co., Indianapolis, IN 46206.
[3] Wyeth Laboratories, Philadelphia, PA 19101.
[4] Beecham Laboratories, Bristol, TN 37620.
[5] Model ALC 202 equipped with a U6K universal injector, Waters Associates, Milford, Mass.
[6] Spectroflow monitor SF770, Schoeffel Instrument Corp., Westwood, N.J.
[7] Omniscribe 5313-12, Houston Instruments, Austin, Tex.
[8] Autolab minigrator, Spectra-Physics, Santa Clara, Calif.
[9] Waters Associates μBondapak phenyl (Catalog No. 27198).
[10] The concentrations are in terms of total sterile powder.
[11] Travenol Laboratories, Deerfield, IL 60015.
[12] The original plastic Viaflex PL 146 bags from which either normal saline or 5% dextrose in water was withdrawn for making the solutions.

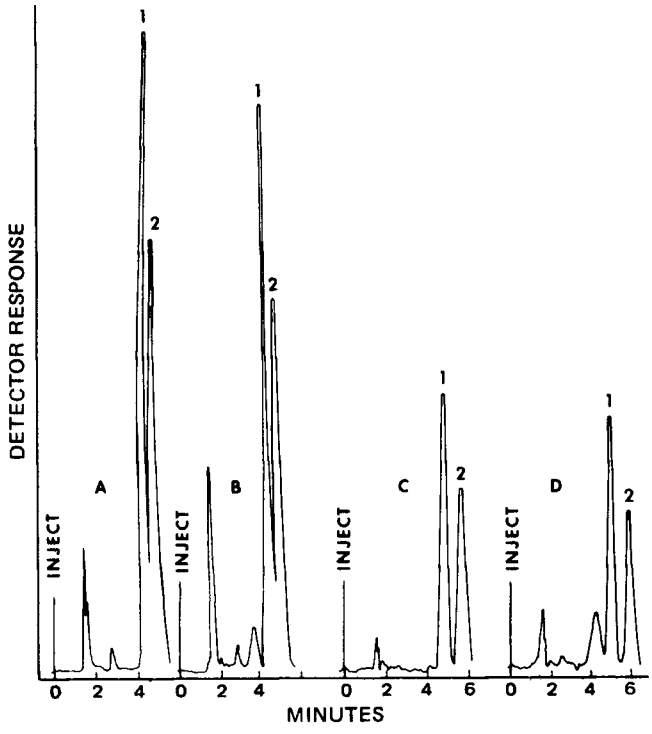

Figure 1—*Sample chromatograms. Peaks 1 and 2 in chromatograms A and B are from ticarcillin (V); in chromatograms C and D, they are from carbenicillin (I). Key: A and C, standard solutions of V and I, respectively; and B and D, 5-day-old solutions of V and I, respectively, in normal saline (storage at 24°). The chromatographic conditions are given in Table I.*

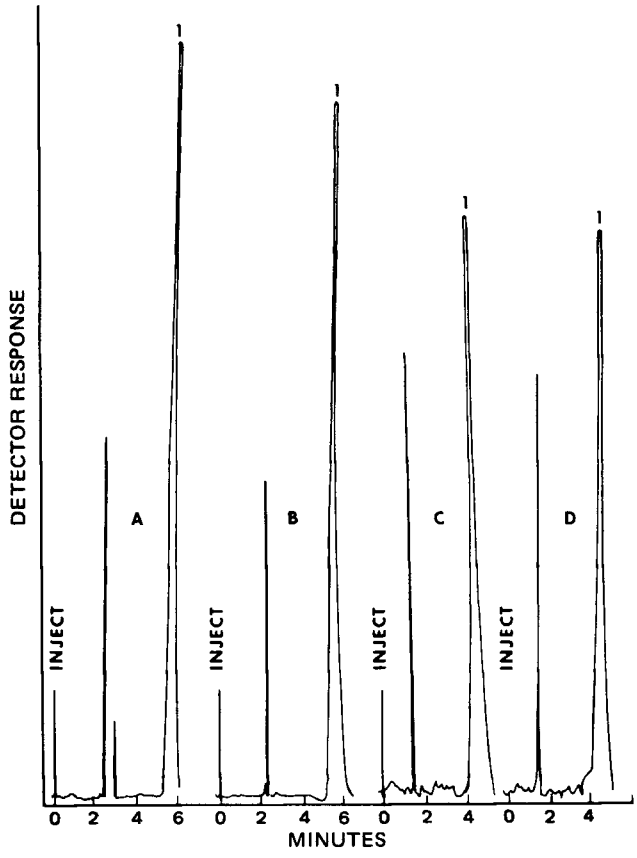

Figure 2—*Sample chromatograms. Peak 1 in chromatograms A and B is from cefazolin (II); in chromatograms C and D, it is from nafcillin (IV). Key: A and C, standard solutions of II and IV, respectively; B, 5-day-old solution of II in normal saline (storage at 24°); and D, 15-day-old solution of IV in normal saline (storage at 5°). The chromatographic conditions are given in Table I.*

days of storage) *versus* 31.4% (after only 11 days of storage) in 5% dextrose in water. After 7 days, the potency retained in dextrose solution was about the same as that after 15 days in normal saline.

Both solutions were stable (based on 90% potency) for 15 days at 5°. Therefore, the manufacturer-recommended expiration date of 3 days (1) is too conservative.

The colorimetric assay reported previously (14) appears to be stability indicating. The results by the literature method and by the HPLC method were almost the same (Table II), considering experimental errors. Nevertheless, the HPLC method gave more information than the assay results alone. For example, it appears that carbenicillin is a mixture of two isomers (peaks 1 and 2 in Fig. 1C), and the percent decomposition in both isomers was the same. The isomers apparently are at equilibrium with each other, which is normal.

For the HPLC method, the percent relative standard deviation based on six injections was 1.69.

Cefazolin—The results (Table II) indicate that the cefazolin solutions, both in normal saline and in dextrose, were stable for at least 5 days (based on 90% potency) at room temperature and for 15 days at 5°. Therefore, the recommended (2) expiration dates of 1 and 4 days at room temperature and at refrigerator temperature, respectively, are very conservative.

Of the five antibiotics studied, cefazolin appears to have the greatest stability (Tables II and III). This result may have been due to the fact that the pH values of cefazolin solutions increased during storage (Table IV), while the pH values of all of the other solutions decreased (Table IV).

Table III—Colorimetric Assay Results for Solutions (2 g/100 ml) Stored at 4 ± 1°

Antibiotic	Solvent	Percent of Potency Retained (Based on Label Claim) after 4 days	7 days	15 days
Carbenicillin	NS[a]	98.4	97.5	94.0
Cefazolin	NS	99.5	94.7	94.7
Cephalothin	NS	96.5	96.3	95.0
Nafcillin	D5W[b]	97.4	96.0	91.8
Ticarcillin	NS	97.9	94.6	91.0

Antibiotic	Solvent	Percent of Potency Retained (Based on Label Claim) after 3 days	4 days	7 days	8 days	9 days	9 days (HPLC)[c]	15 days	15 days (HPLC)[c]	24 days
Carbenicillin	D5W	100.0	—[d]	99.6	—[d]	99.2	99.7	90.9	—[d]	—[d]
Cefazolin	D5W	—[d]	99.7	—[d]	97.1	96.5	95.2	95.0	—[d]	95.1
Cephalothin	D5W	—[d]	100.0	—[d]	96.4	96.8	96.5	95.0	93.5	—[d]
Nafcillin	NS	99.8	—[d]	98.3	—[d]	—[d]	94.9	95.5	95.4	94.1
Ticarcillin	D5W	99.3	—[d]	98.4	—[d]	—[d]	96.6	97.6	93.3	—[d]

[a] Normal saline. [b] Five percent dextrose in water. [c] By the HPLC method. [d] Not assayed on this day.

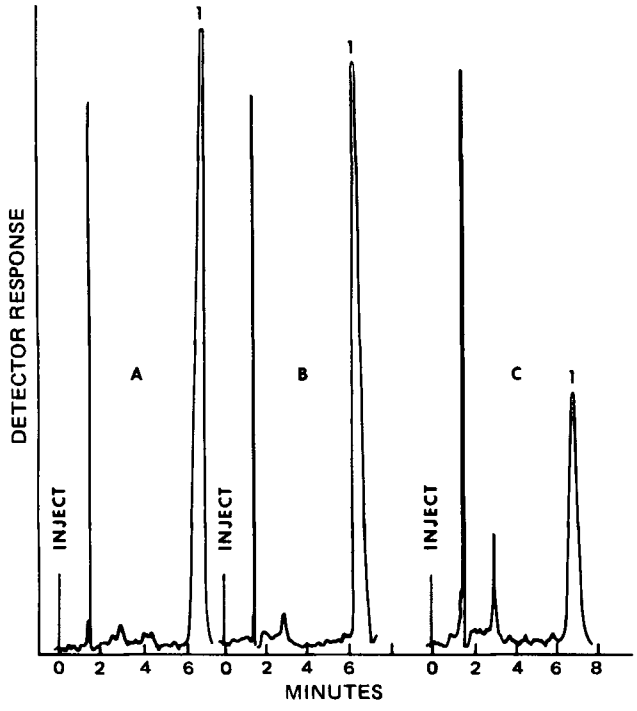

Figure 3—*Sample chromatograms. Peak 1 is from cephalothin (III). Key: A, standard solution; B, 15-day-old solution of III in 5% dextrose in water (storage at 5°); and C, 11-day-old solution of III in 5% dextrose in water (storage at 24°). The chromatographic conditions are given in Table I.*

The results using the HPLC method (Table II) were similar to those obtained using the literature method (14). Since these solutions did not decompose much, there was no significant difference between the chromatogram of a standard solution (Fig. 2A) and a chromatogram from a 5-day-old solution in normal saline when stored at room temperature (Fig. 2B).

For the HPLC method, the percent relative standard deviation based on six injections was 0.94.

Cephalothin—The results at room temperature (Table II) indicate that the manufacturer-recommended (3) expiration date of 1 day is reasonable. However, if stored in a refrigerator, the solutions were stable for at least 15 days (Table II), compared to the manufacturer-recommended (3) shelflife of 4 days. Moreover, the solutions that were stored in a refrigerator remained colorless during the investigation. However, at room temperature, the solutions started discoloring to a light-yellow color within 48–72 hr. The intensity of this color increased on further storage.

Once the solutions became discolored, the colorimetric analysis gave misleading results (Table II). For example, after 5 days of storage at 24°, cephalothin in normal saline and in dextrose solutions indicated a potency of ~78% (Table II). When assayed using the HPLC method (Fig. 3), the potencies were 62.2 and 56.1% for solutions in normal saline and dextrose, respectively (Table II). After 11 days, the solution with dextrose indicated 60.6% potency by the colorimetric method compared to 40.9% by the HPLC method. Therefore, the literature method (14) probably is unreliable for stability studies of III once the solutions become discolored.

For the HPLC method, the percent relative standard deviation based on six injections was 1.3.

Nafcillin—The results at room temperature (Table II) indicate that the expiration date of 3 days recommended by the manufacturer (5) is reasonable. However, when stored in a refrigerator, the solutions were stable for at least 15 days (Table III). The manufacturer recommends (5) an expiration date of 7 days.

The results with the HPLC method were similar (Table II) to those with the colorimetric method (14). For the HPLC method, the percent relative standard deviation based on six injections was 1.59.

Ticarcillin—The results at room temperature (Table II) indicate that the manufacturer-recommended shelflife (4) of 1 day is reasonable. However, when stored in a refrigerator, the solutions were stable for at least 15 days (Table III). Therefore, the recommended shelflife of 3 days is too conservative.

Table IV—Change in pH of the Antibiotic Solutions (2 g/100 ml) with Various Storage Times and Temperatures

Antibiotic	Solvent	pH Value (±0.1) after Initial	1 day at 24°	7 days at 24°	7 days at 5°
Carbenicillin	NS[a]	6.5	6.0	5.6	6.4
Cefazolin	NS	4.4	5.8	6.4	5.2
Cephalothin	NS	7.5	6.4	4.6[b]	7.3
Nafcillin	D5W[c]	6.6	6.4	5.6	6.4
Ticarcillin	NS	6.1	5.8	5.6	5.9

Antibiotic	Solvent	pH Value (±0.1) after Initial	1 day at 24°	15 days at 24°	15 days at 5°
Carbenicillin	D5W	6.5	5.9	5.1	5.9
Cefazolin	D5W	4.6	5.6	6.2	5.6
Cephalothin	D5W	7.6	6.3	4.6[b]	6.9
Nafcillin	NS	6.6	6.4	4.6[d]	6.1
Ticarcillin	D5W	6.2	5.7	5.1	5.6

[a] Normal saline. [b] Solution had discolored to yellow. [c] Five percent dextrose in water. [d] Precipitation occurred (light yellow).

The colorimetric analysis appears to be stability indicating, but the HPLC method gave some new information. Ticarcillin appears to be a mixture of two isomers (Figs. 1A and 1B). These isomers are at equilibrium, as explained for carbenicillin, since the percent decomposition in both isomers was similar.

For the HPLC method, the percent relative standard deviation based on six injections was 1.6.

The data could not be treated mathematically since the pH values of the solutions were not constant (Table IV). The degradation products of cefazolin and cephalothin were reported previously (11). General information about the degradation of carbenicillin (10) and other penicillins (18) is available in the literature.

REFERENCES

(1) Geopen, Insert 60-1856-00-4, Roerig, a Division of Pfizer, New York, NY 10017, rev. Feb. 1978.

(2) Kefzol, Insert PA 7341 AMP, Eli Lilly and Co., Indianapolis, IN 46206, rev. Sept. 19, 1978.

(3) Keflin, Insert PA 7420 AMP, Eli Lilly and Co., Indianapolis, IN 46206, rev. Sept. 1, 1978.

(4) Ticar, Insert 7182/C, Beecham Laboratories, Bristol, TN 37620, rev. Feb. 1978.

(5) Unipen, Insert CI 2622-1, Wyeth Laboratories, Philadelphia, PA 19101, rev. Nov. 15, 1977.

(6) S. M. Carone, M. Bornstein, D. L. Coleman, P. N. Thomas, and J. C. Boylan, *Am. J. Hosp. Pharm.*, **33**, 639 (1976).

(7) M. Bornstein, P. N. Thomas, D. L. Coleman, and J. C. Boylan, *ibid.*, **31**, 296 (1974).

(8) J. C. Boylan, J. L. Simmons, and C. L. Winely, *ibid.*, **29**, 687 (1972).

(9) J. M. Mann, D. L. Coleman, and J. C. Boylan, *ibid.*, **28**, 760 (1971).

(10) H. Zia and R. Zargarbashi, *Can. J. Pharm. Sci.*, **9**, 112 (1974).

(11) T. Yamana and A. Tsuji, *J. Pharm. Sci.*, **65**, 1563 (1976).

(12) A. B. C. Yu, C. H. Nightingale, and D. R. Flanagan, *ibid.*, **66**, 213 (1977).

(13) W. W. Holl, M. O'Brien, J. Filan, T. R. Mazeika, A. Post, D. Pitkin, and P. Actor, *ibid.*, **64**, 1232 (1975).

(14) J. W. Munson, D. Papadimitriou, and P. P. DeLuca, *ibid.*, **68**, 1333 (1979).

(15) M. Mundell, H. Fischbach, and T. Eble, *J. Am. Pharm. Assoc., Sci. Ed.*, **35**, 373 (1946).

(16) P. J. Weiss, *Antibiot. Chemother.*, **9**, 660 (1959).

(17) B. Ortenblad, *Acta Chem. Scand.*, **4**, 518 (1950).

(18) K. A. Connors, G. L. Amidon, and L. Kennon, "Chemical Stability of Pharmaceuticals—A Handbook for Pharmacists," Wiley, New York, N.Y., 1979.

High-Pressure Liquid Chromatographic Determination of Salicylsalicylic Acid, Aspirin, and Salicylic Acid in Human Plasma and Urine

L. I. HARRISON ˣ, M. L. FUNK, and R. E. OBER

Received March 10, 1980, from the *Drug Metabolism Department, Riker Laboratories, Inc., Subsidiary of 3M, 3M Center, St. Paul, MN 55144.* Accepted for publication May 2, 1980.

Abstract □ A high-pressure liquid chromatographic method was developed for the separation and quantitation of salicylsalicylic acid (I), aspirin (II), and salicylic acid (III) in human plasma and urine. The method for plasma involves the selective extraction of I–III and an internal standard, α-phenylcinnamic acid, into methylene chloride from acidified plasma, followed by evaporation of the organic phase and dissolution of the residue in methanol. A 25-μl aliquot is analyzed on a reversed-phase column with UV detection. Urine is treated similarly with hexane as the extracting solvent. If 300 nm is used as the monitoring wavelength, the assays of I and III are linear over the concentration range of 1–150 μg/ml in both plasma and urine. If 280 nm is used as the monitoring wavelength, II can be quantitated along with I and III; however, detector sensitivities of I and III are two to three times greater at 300 nm. The accuracy and precision of the methods for I–III are adequate for clinical pharmacokinetic studies. Following therapeutic doses of I in humans, the method was applied successfully to the determination of I and III in plasma and urine.

Keyphrases □ Aspirin—high-pressure liquid chromatographic analysis with salicylsalicylic acid and salicylic acid in human plasma and urine □ Salicylsalicylic acid—high-pressure liquid chromatographic analysis with aspirin and salicylic acid in human plasma and urine □ Salicylic acid—high-pressure liquid chromatographic analysis with salicylsalicylic acid and aspirin in human plasma and urine □ High-pressure liquid chromatography—analysis, salicylsalicylic acid, aspirin, and salicylic acid in human plasma and urine

Salicylsalicylic acid (I) was developed as a salicylate alternative for aspirin (II) and sodium salicylate. Although I was available as early as 1920, its usefulness in salicylate therapy has been explored only recently (1). Double-blind clinical trials have shown that I causes significantly less GI bleeding and gastric erosions at anti-inflammatory doses than does II (2–6). The therapeutic response of arthritic patients to I appears to be equivalent to that of II (6–11). Thus, I appears to be an important salicylate derivative and offers efficacy with diminished GI distress.

Compound I is hydrolyzed in the body to give salicylic acid (III). Metabolic studies of I measured only levels of III following single and multiple doses of I (5, 11–16). Studies of plasma and urine levels of I used the difference between levels of III before and after hydrolysis as an estimate of the concentrations of I (11, 16). A high-pressure liquid chromatographic (HPLC) assay was described recently for monitoring I as an impurity in aspirin tablets (17). The present report describes a specific and sensitive HPLC assay for the quantitation of I–III in biological samples.

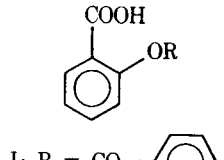

I: R = CO— (OH)

II: R = $COCH_3$

III: R = H

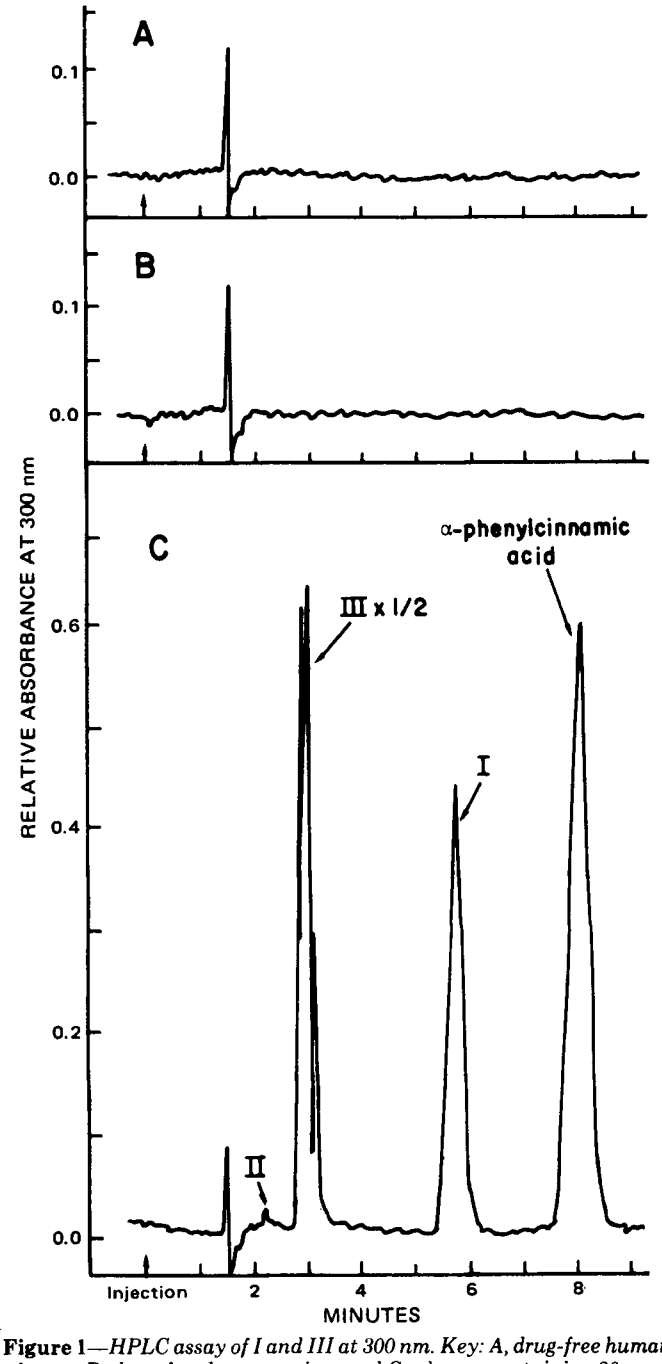

Figure 1—*HPLC assay of I and III at 300 nm. Key: A, drug-free human plasma; B, drug-free human urine; and C, plasma containing 20 μg of I–III and α-phenylcinnamic acid/ml.*

0022-3549/80/1100-1268$01.00/0
© 1980, American Pharmaceutical Association

Table I—Accuracy and Precision of the HPLC Analysis of Salicylsalicylic Acid and Salicylic Acid in Human Plasma at 300 nm

Drug Added to Plasma, μg/ml	Salicylsalicylic Acid		Salicylic Acid	
	Detected, μg/ml	Difference, μg/ml	Detected, μg/ml	Difference, μg/ml
5.0	5.2	0.2	6.2	1.2
	5.1	0.1	6.2	1.2
	5.0	0.0	6.0	1.0
	5.5	0.5	6.1	1.1
	5.3	0.3	6.0	1.0
	5.2 ± 0.2[a]	0.2 *ME*[b]	6.1 ± 0.1[a]	1.1 *ME*
	4% *CV*[c]	4% *RE*[d]	2% *CV*	18% *RE*
20.0	20.7	0.7	20.7	0.7
	20.0	0.0	21.4	1.4
	20.8	0.8	21.2	1.2
	20.8	0.8	20.3	0.3
	20.9	0.9	20.1	0.1
	20.6 ± 0.4[a]	0.6 *ME*	20.7 ± 0.6[a]	0.7 *ME*
	2% *CV*	3% *RE*	3% *CV*	3% *RE*
50.0	48.1	−1.9	47.7	−2.3
	50.8	0.8	47.8	−2.2
	49.3	−0.7	52.4	2.4
	49.0	−1.0	48.9	−1.1
	52.0	2.0	51.2	1.2
	49.8 ± 1.6[a]	−0.2 *ME*	49.6 ± 2.1[a]	−0.4 *ME*
	3% *CV*	−0.4% *RE*	4% *CV*	−0.8% *RE*

[a] Mean ± *SD*. [b] *ME* = mean error. [c] *CV* = coefficient of variation × 100. [d] *RE* = relative error.

Table II—Accuracy and Precision of the HPLC Analysis of Salicylsalicylic Acid and Salicylic Acid in Human Urine at 300 nm

Drug Added to Urine, μg/ml	Salicylsalicylic Acid		Salicylic Acid	
	Detected, μg/ml	Difference, μg/ml	Detected, μg/ml	Difference, μg/ml
5.0	5.1	0.1	5.5	0.5
	5.9	0.9	5.8	0.8
	5.6	0.6	6.0	1.0
	4.9	−0.1	5.4	0.4
	5.4 ± 0.46[a]	0.4 *ME*[b]	5.7 ± 0.28[a]	0.7 *ME*
	8.5% *CV*[c]	7% *RE*[d]	4.9% *CV*	12% *RE*
10.0	9.8	−0.2	8.6	−1.4
	9.6	−0.4	9.7	−0.3
	9.2	−0.8	9.3	−0.7
	9.7	−0.3	9.3	−0.7
	9.6 ± 0.26[a]	−0.4 *ME*	9.2 ± 0.46[a]	−0.8 *ME*
	2.7% *CV*	−4% *RE*	5.0% *CV*	−9% *RE*

[a-d] See Table I.

EXPERIMENTAL

Materials—All solvents were glass distilled and suitable for liquid chromatographic analyses[1], and all reagents were analytical grade. Analytically pure standards of I[2]–III and α-phenylcinnamic acid[3] were used. Aqueous solutions were prepared in distilled water. Drug-free plasma and urine were obtained from normal human volunteers.

A high-pressure liquid chromatograph[4] equipped with a septumless injector[5] and a variable-wavelength UV detector[6] were used. The detector was operated at either 0.02 or 0.04 aufs. The mobile phase of methanol–1% acetic acid (60:40 v/v) was pumped at 2.0 ml/min (2800 psi) through a stainless steel column (30 cm × 4 mm i.d.) packed with a high-efficiency, reversed-phase packing[7].

Methods—α-Phenylcinnamic acid served as the internal standard. To a 0.5-ml aliquot of plasma were added 0.9 ml of 0.27 *N* HCl, 10 μg of α-phenylcinnamic acid (100 μl of a 0.1-mg/ml solution in methanol), and 10 ml of methylene chloride. The tubes were shaken for 15 min on a mechanical shaker at 125 cycles/min and centrifuged for 5 min at 750×*g*.

[1] Burdick & Jackson Laboratories, Muskegon, Mich.
[2] Riker Laboratories, Northridge, Calif.
[3] Aldrich Chemical Co., Milwaukee, Wis.
[4] Model 6000, Waters Associates, Milford, Mass.
[5] Model U6K, Waters Associates, Milford, Mass.
[6] Model SF 770, Schoeffel Instrument Corp., Waterford, N.J.
[7] μBondapak C_{18}, Waters Associates, Milford, Mass.

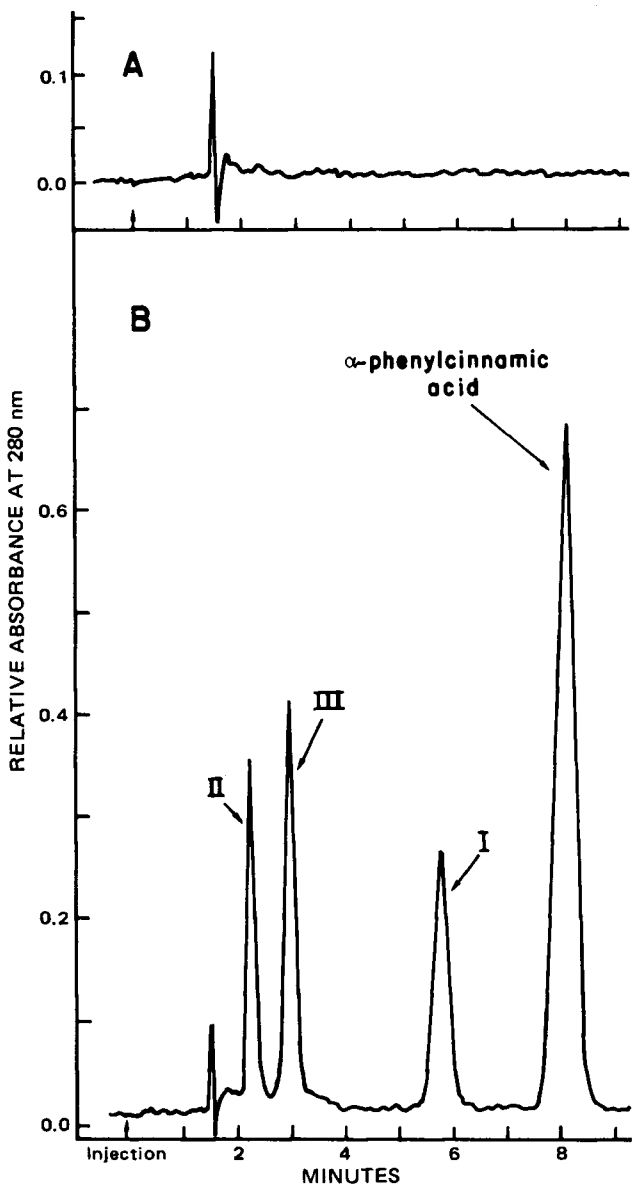

Figure 2—*HPLC assay of I–III at 280 nm. Key: A, drug-free human plasma; and B, plasma containing 20 μg of I–III and α-phenylcinnamic acid/ml.*

The methylene chloride phase was separated and evaporated to dryness[8]. The residue was dissolved in 0.5 ml of methanol, and 25 μl was injected into the chromatograph.

A similar procedure was used for the urine extraction, except that 2-ml urine aliquots were extracted with 10 ml of hexane. A solvent less polar than methylene chloride was required for the urine extractions to eliminate interfering substances.

Plasma and urine standards were prepared by adding I and III (and in some cases II) dissolved in 100 μl of methanol to aliquots of drug-free human plasma and urine. UV absorbance was measured at 300 nm. Peak height ratios were used to determine concentrations.

RESULTS AND DISCUSSION

Reversed-phase HPLC was an effective method to quantitate I and III simultaneously in human plasma and urine. Figure 1 shows a representative chromatogram. Baseline separation between I, III, and α-phenylcinnamic acid (the internal standard) was achieved. No interference by endogenous materials from either drug-free human plasma or urine was seen (Fig. 1). Under the experimental conditions, the elution

[8] Evapo-Mix, Buchler Instruments, Fort Lee, N.J.

Table III—Accuracy and Precision of the HPLC Analysis of Salicylsalicylic Acid, Aspirin, and Salicylic Acid in Human Plasma at 280 nm

Drug Added to Plasma, μg/ml	Salicylsalicylic Acid		Aspirin		Salicylic Acid	
	Detected, μg/ml	Difference, μg/ml	Detected, μg/ml	Difference, μg/ml	Detected, μg/ml	Difference, μg/ml
5.0	5.9	0.9	5.1	0.1	5.6	0.4
	5.6	0.6	5.2	0.2	6.1	1.1
	5.8	0.8	5.2	0.2	5.9	0.9
	6.3	1.3	5.2	0.2	6.1	1.1
	5.9	0.9	4.4	−0.6	6.4	1.4
	5.9 ± 0.3[a]	0.9 *ME*[b]	5.0 ± 0.3[a]	0.02 *ME*	6.0 ± 0.3[a]	1.0 *ME*
	4% *CV*[c]	15% *RE*[d]	6% *CV*	0.4% *RE*	5% *CV*	17% *RE*
20.0	20.2	0.2	20.3	0.3	20.2	0.2
	19.9	−0.1	19.8	−0.2	21.2	1.2
	20.8	0.8	20.6	0.6	20.6	0.6
	20.9	0.9	20.4	0.4	20.6	0.6
	20.5	0.5	20.1	0.1	19.7	−0.3
	20.5 ± 0.4[a]	0.5 *ME*	20.2 ± 0.3[a]	0.2 *ME*	20.5 ± 0.6[a]	0.5 *ME*
	2% *CV*	2% *RE*	1% *CV*	1% *RE*	3% *CV*	2% *RE*
50.0	48.1	−1.9	49.6	0.4	48.4	−1.6
	50.5	0.5	49.4	0.6	48.1	−1.9
	49.3	−0.7	50.0	0.0	52.0	2.0
	49.3	−0.7	49.7	−0.7	49.2	−0.8
	52.0	2.0	50.7	0.7	51.1	1.1
	49.8 ± 1.5[a]	−0.2 *ME*	49.9 ± 0.5[a]	−0.2 *ME*	49.8 ± 1.7[a]	−0.2 *ME*
	3% *CV*	−0.4% *RE*	1% *CV*	0.4% *RE*	3% *CV*	−0.4% *RE*

[a–d] See Table I.

volumes for I, III, and the internal standard were 11.5 (5.8 min), 6.0 (3.0 min), and 16 (8.0 min) ml, respectively.

The assay of I and III was linear over the concentration range of 1–150 μg/ml in both plasma and urine. The minimum detectable level of I and III was 1 μg/ml. However, this sensitivity could be increased by adding <500 μl of methanol at the final extraction step. The accuracy and precision of the method were tested at three concentrations of I and III in plasma. Both compounds were present in all plasma samples; five samples of each concentration were assayed on the same day (Table I).

The coefficient of variation was ≤4% for all three levels of I and III. Thus, good precision was demonstrated. The accuracy of the method is indicated by the mean error between the detected and theoretical values. The mean error was small in most cases, except for III at 5 μg/ml. Similar accuracy and precision were seen with urine samples (Table II).

Compound II was quantitated along with I and III by changing the wavelength to 280 nm (Fig. 2). Compound II had weak UV absorbance at 300 nm (Fig. 1) and could not be quantitated at that wavelength. The elution volume for II was 4.5 ml (2.3 min). Since the elution volumes for I, III, and the internal standard were unchanged, the analysis time remained at 9 min/sample. The assay at 280 nm for II (and also for I and III) was linear over the concentration range of 2–100 μg/ml. The accuracy and precision of the method at 280 nm were tested at three concentrations of I–III in plasma and were similar to those observed at 300 nm (Table III).

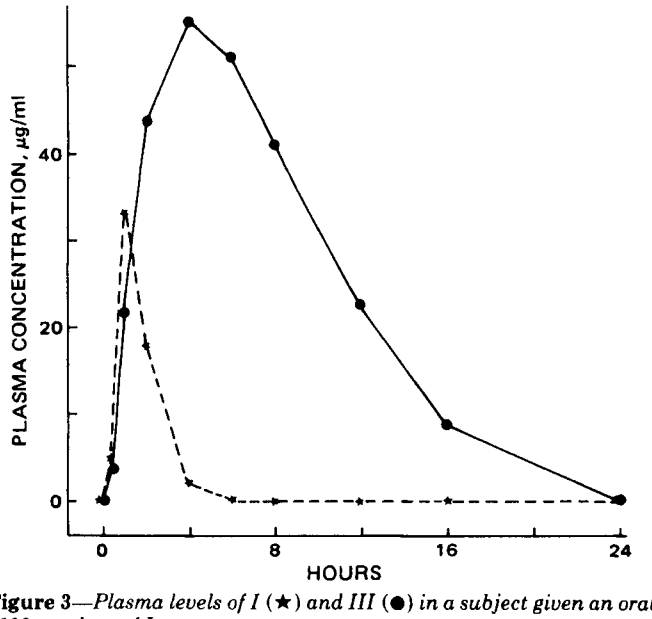

Figure 3—*Plasma levels of I (★) and III (●) in a subject given an oral 1000-mg dose of I.*

For maximum sensitivity, I and III should be quantitated at 300 nm and II should be quantitated at 280 nm. As shown in Fig. 2, the 280-nm wavelength can be used to quantitate I–III simultaneously in plasma, although the absorbances of I and III at 280 nm under the present experimental conditions were only 65 and 35%, respectively, of the absorbances at 300 nm.

The HPLC method was used in the analysis of plasma and urine samples from a 10-subject absorption study of I. The healthy male volunteers were given a single, oral, 1000-mg dose of I as two tablets[9]. Heparinized blood samples were taken immediately before dosing and at 0.5, 1, 2, 4, 6, 8, 12, 16, and 24 hr postdosing. The plasma levels of I and III were determined by the HPLC method at 300 nm and are plotted for a representative subject in Fig. 3. A peak plasma level for I of 33.4 μg/ml was reached in this subject at 1 hr postdosing, and the decrease in plasma levels followed a monoexponential decline with an estimated plasma half-life for I of 0.8 hr. The *in vivo* hydrolysis of I to III resulted in a peak plasma level of III of 55.2 μg/ml at 4 hr; the plasma half-life of III was 3.5 hr. The 24-hr urinary excretions of I and III in this subject were 10.0 and 29.8 mg, respectively.

During this absorption study, analytical results showed that the assay yielded only minimal day-to-day and operator-to-operator variations. Eleven plasma standard curves were run for each compound over a 2-month period. The coefficient of correlation of each plasma standard curve was 0.997 or better for I; it was 0.994 or better, with one exception (0.989), for III. Zero was contained within the standard error of the intercept. Linear regression of a line forced through the origin for the mean standard curve gave slopes of 0.035 ± 0.0031 (mean ± *SD*) for I and 0.084 ± 0.0062 for III. Comparable agreement was obtained for four urine standard curves.

Several multiple-dose studies at anti-inflammatory doses have shown that the assay is more than adequate to determine plasma concentrations of I in humans. However, simultaneous quantitation of III may require sample dilution to keep the level of III below 150 μg/ml. The HPLC assay requires 9 min/sample. Approximately 30 samples can be extracted and analyzed daily.

REFERENCES[10]

(1) W. W. Downie and V. Wright, *Practitioner*, **219**, 465 (1977).

[9] Disalcid, Riker Laboratories, Northridge, Calif.

[10] *Note added in proof:* Another HPLC assay for the quantitation of I and III in plasma was published recently (18).

(2) J. R. Leonards, *J. Lab. Clin. Med.*, **74**, 911 (1969).
(3) D. Edmar, *Acta Radiol.*, **11**, 57 (1971).
(4) S. Thune, *Nord. Med.*, **79**, 352 (1968).
(5) A. Cohen, *J. Clin. Pharmacol.*, **19**, 242 (1979).
(6) S. P. Liyanage and P. K. Tambar, *Curr. Med. Res. Opinion*, **5**, 450 (1978).
(7) L. J. Denson and W. R. Thompson, *J. Med. Soc. N.J.*, **85**, 314 (1960).
(8) L. Paris and H. Newfield, *Clin. Med.*, **70**, 2029 (1963).
(9) R. G. Regalado, *Curr. Med. Res. Opinion*, **5**, 454 (1978).
(10) O. N. Re, *J. Int. Med. Res.*, **7**, 90 (1979).
(11) P. Nordqvist, presented at the Congress of the Swedish Medical Society, Stockholm, Sweden, Nov. 26, 1964.
(12) P. Nordqvist, J. G. L. Harthon, and R. Karlsson, *Nord. Med.*, **74**, 1074 (1965).
(13) A. Cohen, *Curr. Ther. Res.*, **23**, 772 (1978).
(14) I. W. French and C. A. Mildon, *Clin. Ther.*, **1**, 353 (1978).
(15) I. Santillan, *Curr. Ther. Res.*, **23**, 345 (1978).
(16) P. J. Hanzlik and N. E. Presho, *J. Pharmacol. Exp. Ther.*, **26**, 61 (1926).
(17) J. C. Reepmeyer and R. D. Kirchhoefer, *J. Pharm. Sci.*, **68**, 1167 (1979).
(18) M. M. Lubran, S. N. Steen, and R. L. Smith, *Ann. Clin. Lab. Sci.*, **9**, 501 (1979).

Preparation, Characterization, and Stability of New Prostaglandin E_2 Gel for Local Administration

A. S. HARRIS *x, A. KIRSTEIN-PEDERSEN ‡, P. STENBERG §, U. ULMSTEN ¶, and L. WINGERUP ¶

Received March 18, 1980 from **Perstorp AB, Box 5000, S-28400 Perstorp, Sweden*, the ‡*Department of Pharmacology, University of Aarhus, DK-8000 Aarhus C, Denmark*, and the §*Hospital Pharmacy and* ¶*Departments of Obstetrics and Gynecology, Malmö General Hospital, S-214-01 Malmö, Sweden.* Accepted for publication May 2, 1980.

Abstract □ A new gel delivery system for the local application of prostaglandin E_2 consists of drug incorporated in the matrix of a cross-linked starch polymer. The properties of the starch powder provide a stabilizing milieu for the labile prostaglandin E_2 and, by addition of saline, a ready-to-use gel for immediate local administration. The gel offers advantages over existing preparations in terms of chemical and microbiological stability, homogeneity, and dosage safety. This report outlines the pharmaceutical aspects involved in the development of the delivery system.

Keyphrases □ Prostaglandin E_2—preparation, characterization, and stability of gel delivery system □ Drug delivery systems—prostaglandin E_2 gel, preparation, characterization, and stability

The discovery, isolation, and characterization of the various prostaglandins have created substantial interest in their physiological role and therapeutic applications (1). Their use in human reproduction (2) clearly demonstrates their clinical value. However, the broad spectrum of pharmacological responses and the general instability of the prostaglandins have made it difficult to achieve specific therapeutic aims without significant side effects.

BACKGROUND

In the E series, for example, the cervical ripening effect of prostaglandin E_2 first was observed in early studies using intravenous infusion prior to therapeutic abortion or induction of labor in patients at term (3). The large dose required to achieve these effects was associated with frequent systemic side effects such as vomiting and diarrhea (4). The most recent phase in such use of prostaglandin E_2 has been a low dose local (intracervical or vaginal) administration in a viscous gel or a lipid-based pessary (5, 6).

The prostaglandin E_2 regimen is simple and highly acceptable to patients, causing no significant side effects and improving the prospects of labor. There is now extensive evidence of the efficacy and safety of this method (7–9). The obstacle to wider utilization lies in the inherent lability of prostaglandin E_2 compared to the less effective prostaglandin $F_{2\alpha}$ (10). Existing formulations in simple gels and pessaries do not provide sufficient long-term stability and involve problems concerning homogeneity, sterility, and dosage safety (11, 12).

The absence of a suitable delivery vehicle and a standardized preparation of the gel has discouraged commercial production and hindered clinical usage of the prostaglandin E_2 technique. This report presents a new prostaglandin E_2 gel delivery system and affords a definite solution to the problems afflicting the practical handling of the drug for local administration. This system consists of drug distributed in the matrix of a cross-linked starch derivative. The properties of the starch powder provide a stabilizing milieu for the labile prostaglandin E_2 and, by addition of saline, a ready-to-use gel for immediate local administration.

The safety and efficacy of the starch gel prepared with prostaglandin E_2 in cervical ripening were established in clinical trials (13), and this paper outlines the pharmaceutical aspects involved in the development of such a delivery system.

EXPERIMENTAL

Materials—Prostaglandin E_2[1](I) was used in the crystalline form. [1-^{14}C]Prostaglandin E_2[2] (specific activity 2.07 GBq/mmole) was supplied as a solution in ethanol–water (7:3). The cross-linked starch polymer[3] was supplied as a dry powder (particle size 50–100 μm). All reagents were analytical grade.

Gel Formulations—The prostaglandin E_2 gel powder was prepared under aseptic conditions. A freshly prepared, sterile-filtered solution of I (50 mg) in 80% (v/v) aqueous ethanol (25 ml) was added to 50 g of the heat-sterilized (160° for 1 hr) cross-linked starch powder. During the subsequent manual mixing for 10 min, the starch material swelled to twice its original volume. After lyophilization and homogenization, the prostaglandin E_2 gel powder was dispensed in 0.5-g portions (0.5 mg of I/dose) in sterile, disposable, 10-ml syringes.

The radiolabeled prostaglandin E_2 gel powder was prepared in a similar manner with the addition of 92.5 KBq of [1-^{14}C]prostaglandin E_2 to the solution of I. For practical reasons, this batch was prepared at one-half the scale (*i.e.*, 50 doses) and under nonaseptic conditions.

The ready-to-use-gel for clinical administration was prepared by adding 2.2 ml of sterile saline *via* a hypodermic needle to the prostaglandin E_2 gel powder in the syringe. A uniform gel consistency was obtained without agitation within 30 sec.

The prostaglandin E_2 gel fortified with X-ray contrast medium was prepared by adding 1 ml of saline and 2 ml of contrast medium (6.75 g of metrizamide[4] dissolved in 7.8 ml of 0.6 m*M* sodium bicarbonate) to

[1] The Upjohn Co.
[2] The Radiochemical Centre.
[3] Perstorp AB.
[4] Amipaque, Nyegaard & Co., Oslo, Norway.

0022-3549/80/1100-1271$01.00/0
© 1980, American Pharmaceutical Association

(2) J. R. Leonards, *J. Lab. Clin. Med.*, **74**, 911 (1969).
(3) D. Edmar, *Acta Radiol.*, **11**, 57 (1971).
(4) S. Thune, *Nord. Med.*, **79**, 352 (1968).
(5) A. Cohen, *J. Clin. Pharmacol.*, **19**, 242 (1979).
(6) S. P. Liyanage and P. K. Tambar, *Curr. Med. Res. Opinion*, **5**, 450 (1978).
(7) L. J. Denson and W. R. Thompson, *J. Med. Soc. N.J.*, **85**, 314 (1960).
(8) L. Paris and H. Newfield, *Clin. Med.*, **70**, 2029 (1963).
(9) R. G. Regalado, *Curr. Med. Res. Opinion*, **5**, 454 (1978).
(10) O. N. Re, *J. Int. Med. Res.*, **7**, 90 (1979).
(11) P. Nordqvist, presented at the Congress of the Swedish Medical Society, Stockholm, Sweden, Nov. 26, 1964.
(12) P. Nordqvist, J. G. L. Harthon, and R. Karlsson, *Nord. Med.*, **74**, 1074 (1965).
(13) A. Cohen, *Curr. Ther. Res.*, **23**, 772 (1978).
(14) I. W. French and C. A. Mildon, *Clin. Ther.*, **1**, 353 (1978).
(15) I. Santillan, *Curr. Ther. Res.*, **23**, 345 (1978).
(16) P. J. Hanzlik and N. E. Presho, *J. Pharmacol. Exp. Ther.*, **26**, 61 (1926).
(17) J. C. Reepmeyer and R. D. Kirchhoefer, *J. Pharm. Sci.*, **68**, 1167 (1979).
(18) M. M. Lubran, S. N. Steen, and R. L. Smith, *Ann. Clin. Lab. Sci.*, **9**, 501 (1979).

Preparation, Characterization, and Stability of New Prostaglandin E_2 Gel for Local Administration

A. S. HARRIS *x, A. KIRSTEIN-PEDERSEN ‡, P. STENBERG §, U. ULMSTEN ¶, and L. WINGERUP ¶

Received March 18, 1980 from **Perstorp AB, Box 5000, S-28400 Perstorp, Sweden*, the ‡*Department of Pharmacology, University of Aarhus, DK-8000 Aarhus C, Denmark*, and the §*Hospital Pharmacy and* ¶*Departments of Obstetrics and Gynecology, Malmö General Hospital, S-214-01 Malmö, Sweden.* Accepted for publication May 2, 1980.

Abstract □ A new gel delivery system for the local application of prostaglandin E_2 consists of drug incorporated in the matrix of a cross-linked starch polymer. The properties of the starch powder provide a stabilizing milieu for the labile prostaglandin E_2 and, by addition of saline, a ready-to-use gel for immediate local administration. The gel offers advantages over existing preparations in terms of chemical and microbiological stability, homogeneity, and dosage safety. This report outlines the pharmaceutical aspects involved in the development of the delivery system.

Keyphrases □ Prostaglandin E_2—preparation, characterization, and stability of gel delivery system □ Drug delivery systems—prostaglandin E_2 gel, preparation, characterization, and stability

The discovery, isolation, and characterization of the various prostaglandins have created substantial interest in their physiological role and therapeutic applications (1). Their use in human reproduction (2) clearly demonstrates their clinical value. However, the broad spectrum of pharmacological responses and the general instability of the prostaglandins have made it difficult to achieve specific therapeutic aims without significant side effects.

BACKGROUND

In the E series, for example, the cervical ripening effect of prostaglandin E_2 first was observed in early studies using intravenous infusion prior to therapeutic abortion or induction of labor in patients at term (3). The large dose required to achieve these effects was associated with frequent systemic side effects such as vomiting and diarrhea (4). The most recent phase in such use of prostaglandin E_2 has been a low dose local (intracervical or vaginal) administration in a viscous gel or a lipid-based pessary (5, 6).

The prostaglandin E_2 regimen is simple and highly acceptable to patients, causing no significant side effects and improving the prospects of labor. There is now extensive evidence of the efficacy and safety of this method (7–9). The obstacle to wider utilization lies in the inherent lability of prostaglandin E_2 compared to the less effective prostaglandin $F_{2\alpha}$ (10). Existing formulations in simple gels and pessaries do not provide sufficient long-term stability and involve problems concerning homogeneity, sterility, and dosage safety (11, 12).

The absence of a suitable delivery vehicle and a standardized preparation of the gel has discouraged commercial production and hindered clinical usage of the prostaglandin E_2 technique. This report presents a new prostaglandin E_2 gel delivery system and affords a definite solution to the problems afflicting the practical handling of the drug for local administration. This system consists of drug distributed in the matrix of a cross-linked starch derivative. The properties of the starch powder provide a stabilizing milieu for the labile prostaglandin E_2 and, by addition of saline, a ready-to-use gel for immediate local administration.

The safety and efficacy of the starch gel prepared with prostaglandin E_2 in cervical ripening were established in clinical trials (13), and this paper outlines the pharmaceutical aspects involved in the development of such a delivery system.

EXPERIMENTAL

Materials—Prostaglandin E_2[1](I) was used in the crystalline form. [1-^{14}C]Prostaglandin E_2[2] (specific activity 2.07 GBq/mmole) was supplied as a solution in ethanol–water (7:3). The cross-linked starch polymer[3] was supplied as a dry powder (particle size 50–100 μm). All reagents were analytical grade.

Gel Formulations—The prostaglandin E_2 gel powder was prepared under aseptic conditions. A freshly prepared, sterile-filtered solution of I (50 mg) in 80% (v/v) aqueous ethanol (25 ml) was added to 50 g of the heat-sterilized (160° for 1 hr) cross-linked starch powder. During the subsequent manual mixing for 10 min, the starch material swelled to twice its original volume. After lyophilization and homogenization, the prostaglandin E_2 gel powder was dispensed in 0.5-g portions (0.5 mg of I/dose) in sterile, disposable, 10-ml syringes.

The radiolabeled prostaglandin E_2 gel powder was prepared in a similar manner with the addition of 92.5 KBq of [1-^{14}C]prostaglandin E_2 to the solution of I. For practical reasons, this batch was prepared at one-half the scale (*i.e.*, 50 doses) and under nonaseptic conditions.

The ready-to-use-gel for clinical administration was prepared by adding 2.2 ml of sterile saline *via* a hypodermic needle to the prostaglandin E_2 gel powder in the syringe. A uniform gel consistency was obtained without agitation within 30 sec.

The prostaglandin E_2 gel fortified with X-ray contrast medium was prepared by adding 1 ml of saline and 2 ml of contrast medium (6.75 g of metrizamide[4] dissolved in 7.8 ml of 0.6 m*M* sodium bicarbonate) to

[1] The Upjohn Co.
[2] The Radiochemical Centre.
[3] Perstorp AB.
[4] Amipaque, Nyegaard & Co., Oslo, Norway.

0022-3549/80/1100-1271$01.00/0
© 1980, American Pharmaceutical Association

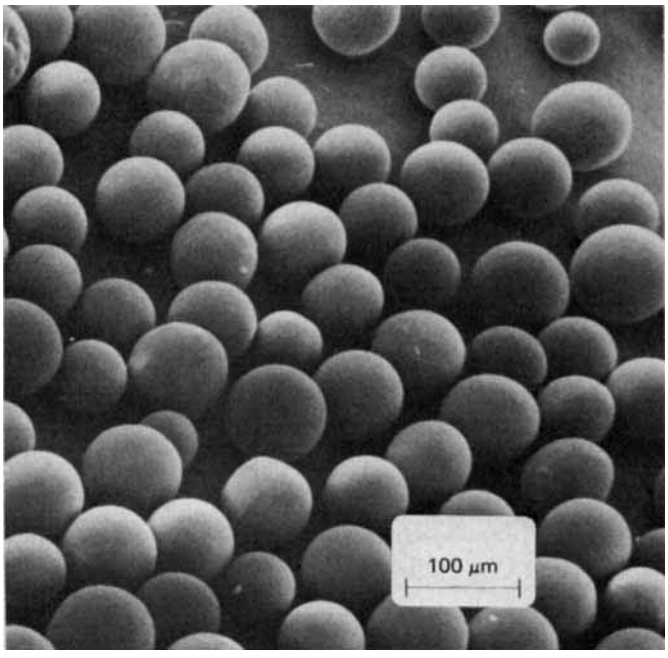

Figure 1—*Scanning electron micrograph of the dry starch microspheres prepared with I (×150).*

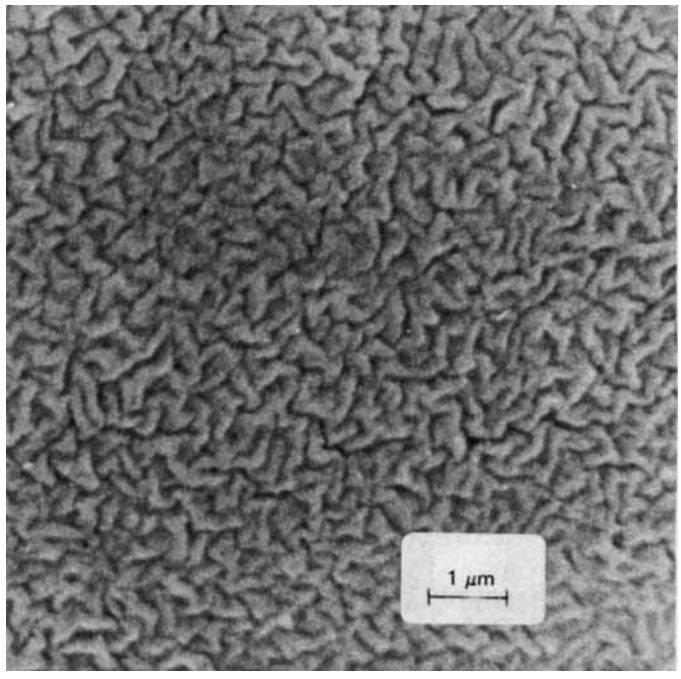

Figure 2—*Scanning electron micrograph of the sphere surface structure (×10,000).*

the prostaglandin E_2 gel powder. The gel was administered to a 28-year-old II-gravida at a gestational age of 30 weeks with an intrauterine dead fetus.

Characterization of Prostaglandin E_2 Gel Powder—The water content in the powder was determined by Karl Fischer titration. Particle-size fractionation was performed using a mechanical oscillating sieve[5]. The pH measurements were made using a standard pH meter[6]. The absorption capacity was determined using the method described by Granath and Flodin (14). Micrographs were taken using a scanning electron microscope[7]. Sterility tests on five batches were performed according to the European Pharmacopoeia.

Homogeneity Studies—Twenty samples of 100.0 mg of the radiolabeled I gel powder were selected randomly according to the table of random numbers[8]. After addition of 10 ml of gel scintillation fluid[9] to each sample, the radioactivity was measured using a liquid scintillation spectrometer[10]. The absence of quenching due to the starch powder was verified by measuring the radioactivity in successively increasing amounts (10–300 mg) of the I gel powder from the same samples.

The distribution of I in the swollen, ready-to-use gel was determined in a similar manner by measuring the radioactivity of ~300.0-mg portions of the gel when expelled in a standard manner from the syringe.

Stability Studies—Compound I was tested for stability in the dry powder and in the swollen, ready-to-use viscous gel. Stability was monitored at 4 and 23° in the dry powder for 12 months and at 4, 20, and 37° in the freshly prepared, ready-to-use viscous gel for 24 hr.

Assay and Analytical Procedure—Compound I was determined by extraction from the gel, separation from the degradation products by TLC, and spectrophotometric assay[11] after conversion to prostaglandin B_2 by alkali treatment.

Aqueous ethanol (80% v/v) was prepared, and 2.00 ml was added to 500.0 mg of the dry I gel; after vortexing for 2 min, 50 μl of the supernate was applied to a silica gel thin-layer plate[12] together with standards of 80% (v/v) aqueous ethanol solutions of known concentrations of I. The plate was developed in a solvent system of chloroform–methanol–acetic acid–water (90:9:1:0.65). This system separates I from its major degradation products, prostaglandin A_2 and the ethyl esters (15).

The zone of I was visualized by spraying the standards at the edge of the plate with 10% phosphomolybdic acid in ethanol. The areas corresponding to I were removed from the plate, and I was eluted with methanol (3 × 2.00 ml). The sample was treated with potassium hydroxide to give a final concentration of 1 *M* and then was heated at 50° for 1 hr. The absorbance at 277 nm was read against a blank (containing a corresponding amount of silica gel treated similarly) and compared with the standards.

RESULTS AND DISCUSSION

The described formulation procedure results in an off-white, free-flowing powder consisting of microspheres of 50–100 μm in diameter (Fig. 1). Each microsphere is a highly hydrophilic, three-dimensional network of a cross-linked starch derivative. Scanning electron micrographs show a regular matrix surface structure (Fig. 2). The hydrophilic nature of the starch microspheres is illustrated by the absorption capacity in polar liquids. For example, upon addition of saline, the I gel powder swells to assume a gel consistency, with absorption up to eight times the original weight of the dry powder. Upon addition of 80% aqueous ethanol, the starch powder swells to about twice its own volume as the microspheres enlarge in size. The solution is absorbed by the microspheres and incorporated as intraparticulate liquid. The solution of I thus is distributed

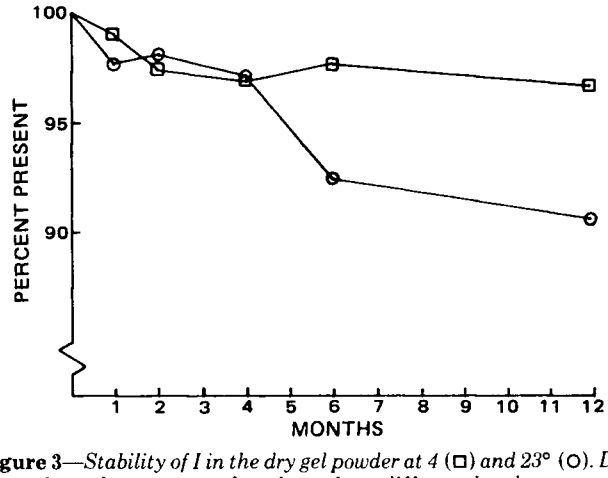

Figure 3—*Stability of I in the dry gel powder at 4 (□) and 23° (○). Data plotted are the average values from three different batches.*

[5] Retsch plane model 330.
[6] Radiometer model 26, Copenhagen, Denmark.
[7] ISM-4S Jeol Ltd., Tokyo, Japan.
[8] See "Geigy Scientific Tables," Ciba-Geigy Ltd., Basel, Switzerland.
[9] Lumac Systems AG, Basel, Switzerland.
[10] Tri-Carb, Packard No. 3320.
[11] Cary model 110 spectrophotometer.
[12] Merck No. 5721 TLC plates.

Table I—Stability of Prostaglandin E_2 (I) in the Freshly Prepared Ready-to-Use I Gel [a]

Incubation, hr	Recovered I, %		
	+4°	+20°	+37°
4	99.1 ± 7.0	99.3 ± 6.9	91.8 ± 5.6
24	94.7 ± 5.4	88.5 ± 4.8	78.0 ± 1.5

[a] Each value is the mean ± *SD* of four samples from the same batch.

throughout the gel bed. During the subsequent lyophilization, the solvent is removed and the starch microspheres are restored to their original size, thereby facilitating the even distribution of I throughout the starch gel powder.

The water content of the I gel powder is ~2–4% and, when protected from moisture, does not significantly alter during storage in plastic syringes.

The results of studies to determine the intrabatch distribution of I in the dry radiolabeled I gel powder prepared at the 50-dose scale showed a relative standard deviation of 2.1% (mean ± *SD*, 24,053 ± 507 dpm/100 mg of dry powder). This value reveals good homogeneity and suggests that the I gel powder can be manufactured commercially with a satisfactory intrabatch variation. The homogeneous nature of the swollen I gel is illustrated by the distribution of radioactivity throughout the gel bed, having a relative standard deviation of 15% (mean count ± *SD*, 11,836 ± 1800 dpm/300 mg). This finding suggests that, in clinical routine, I is distributed satisfactorily in the gel when administered, for example, into the cervical canal.

The solid-state stability of I in the gel delivery system is shown in Fig. 3. The stability profile presents a promising trend and shows little difference between storage temperatures of 4 and 23° for up to 1 year. This finding may be of significance when considering storage conditions for preparations to be used clinically. The stability pattern of the bulk drug presents an increasing degradation rate beginning at 6 months at room temperature (16) and has a 6-month shelflife. In sharp contrast, I in the gel delivery system was quite stable at room temperature for at least 1 year. The starch gel powder functions not only as a delivery vehicle for I but also as a stabilizer for this labile substance. The mechanism controlling the long-term stability of I probably is related to the inherent hydrophilic nature of the starch powder. The degradation rate of the bulk I powder seems to increase and indeed be catalyzed by the presence of the degradation products.

It is likely that I is distributed throughout the starch gel powder and is diluted to such an extent that the degradation products formed have no catalytic effect on the stability profile of I. Moreover, the individual microspheres probably present a very large surface area onto which I adheres to increase the dilution effect. Furthermore, the three-dimensional network probably provides a means of distributing I throughout the whole matrix of the starch microspheres, thereby stabilizing the drug by enclosure. Work is in progress to determine the precise mechanism involved in stabilizing I.

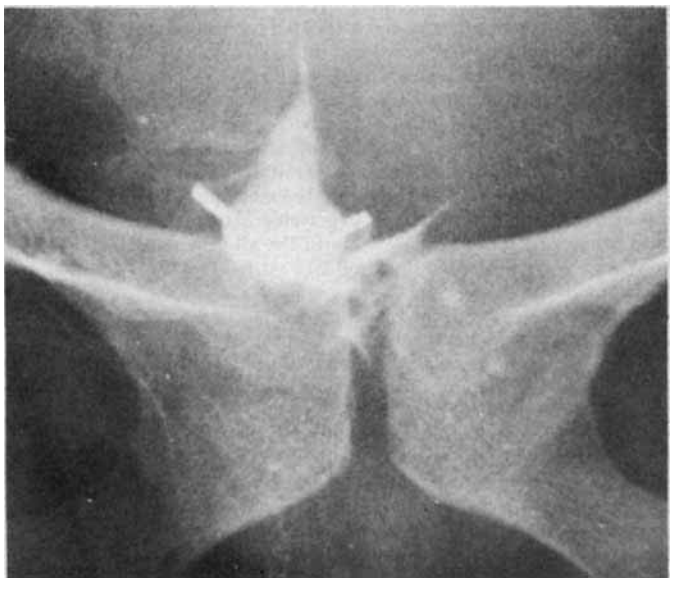

Figure 4—*X-ray picture illustrating the intracervically located gel. Clips were applied at the level of the external os.*

The stability of I in the freshly prepared gel after addition of saline is shown in Table I. Even at elevated temperatures, I is stable in the gel preparation for at least 4 hr, after which the degradation pattern follows the trend seen for the drug in other solvent systems (17). In clinical practice, once the gel is constituted by addition of saline, no further preparative steps are necessary, and the preparation is ready for use. Therefore, the stability of the drug in the swollen gel at room temperature is satisfactory for a sufficient period prior to administration.

The results of sterility testing of five batches showed no microbiological contamination throughout the testing period of 1 year. Thus, the more standardized method of preparation of the I gel powder, compared with more involved methods of I gel preparation, and the dry form of the final product contribute to lowering the risk of microbiological contamination during preparation and subsequent storage.

After the addition of 2.2 ml of saline, the viscous I gel has a final pH of 6.9; therefore, from this point of view, the preparation presents no risk for tissue irritation in the cervix canal when used clinically. Figure 4 shows an *in vivo* X-ray photograph of the viscous I gel located in the cervical canal of a 28-year-old II-gravida. The X-ray, taken 10 min after intracervical administration, shows that the gel clearly adheres to the surface of the cervical canal walls and illustrates the unique property of the gel in facilitating strict intracervical delivery of I.

The new prostaglandin E_2 gel delivery system offers the following advantages over existing gel preparations: (*a*) the final dosage form is a sterile, homogeneous, and clinically ready-to-use preparation for local administration; (*b*) the shelflife of the preparation is at least 12 months at room temperature; and (*c*) the delivery system has a gel consistency, so strict intracervical administration is possible.

REFERENCES

(1) A. Robert, in "Advances in Prostaglandin and Thromboxane Research," vol. 2, B. Samuelsson and R. Paoletti, Eds., Raven, New York, N.Y., 1976, p. 507.

(2) "Prostaglandins and Reproduction," S. M. M. Karim, Ed., MTP Press, St. Leonard's-on-sea, Great Britain, 1975.

(3) M. P. Embrey, *J. Obstet. Gynaecol. Br. Commonw.*, **76**, 783 (1969).

(4) A. H. Ross and W. L. Whitehouse, *Br. Med. J.*, **1**, 642 (1974).

(5) L. Wingerup, K.-E. Andersson, and U. Ulmsten, *Acta Obstet. Gynaecol. Scand.*, **57**, 403 (1978).

(6) A. A. Calder, M. P. Embrey, and T. Tait, *Br. J. Obstet. Gynaecol.*, **84**, 264 (1977).

(7) U. Ulmsten and L. Wingerup, *Acta Obstet. Gynaecol. Scand. Suppl. 84* (1979).

(8) U. Ulmsten, K.-E. Andersson, and L. Wingerup, *Obstet. Gynaecol.*, **54**, 581 (1979).

(9) I. Z. MacKenzie and M. P. Embrey, *Br. Med. J.*, **2**, 1381 (1977).

(10) I. Z. MacKenzie and M. P. Embrey, *Br. J. Obstet. Gynaecol.*, **86**, 167 (1979).

(11) M. P. Embrey, *Br. Med. J.*, **2**, 793 (1979).

(12) T. J. Roseman, B. Sims, and R. G. Stehele, *Am. J. Hosp. Pharm.*, **30**, 236 (1973).

(13) U. Ulmsten, A. Kirstein-Pedersen, P. Stenberg, and L. Wingerup, *Acta Obstet. Gynaecol. Scand. Suppl.*, **84**, 19 (1979).

(14) K. Granath and P. Flodin, *Macromol. Chem.*, **48**, 160 (1961).

(15) K. Greén and B. Samuelsson, *J. Lipid Res.*, **5**, 117 (1961).

(16) S. H. Yalkowsky and T. J. Roseman, *J. Pharm. Sci.*, **68**, 114 (1979).

(17) K. C. Srivastava and J. Clausen, *Lipids*, **8**, 592 (1973).

ACKNOWLEDGMENTS

The authors thank Ms. Lotte Påby, University of Aarhus, for technical assistance and Mr. Lennart Johansson, University of Lund, Sweden, for preparing electron micrographs.

Effects of Short-Term Dietary Exposure to Polychlorinated Biphenyls on Pharmacokinetics of Intravenous Pentobarbital in Rats

V. J. STELLA ˣ and C. K. CHU *

Received October 29, 1979, from the *Department of Pharmaceutical Chemistry, University of Kansas, Lawrence, KS 66045.* Accepted for publication May 9, 1980. *Present address: Department of Pharmaceutics, School of Pharmacy, State University of New York at Buffalo, Amherst, NY 14260.

Abstract □ The intravenous pharmacokinetics of pentobarbital (30 mg/kg as pentobarbital sodium) in rats were studied at 0, 1, 2, 3, and 10 days after pretreatment with 0, 1, 5, 25, and 125 ppm of polychlorinated biphenyls in food. The polychlorinated biphenyls then were removed from the food, and the residual effects of the exposure on pentobarbital pharmacokinetics were studied at 15, 25, 45, and 70 days after initiation of the polychlorinated biphenyl exposure. The pharmacokinetics of pentobarbital were approximated to a one-compartment model. After pretreatment at 1 and 5 ppm for up to 10 days, all pentobarbital pharmacokinetic parameters obtained were comparable to control values. Pretreatment at 125 ppm significantly reduced the biological half-life and raised the total body elimination rate constant, total body clearance, and intrinsic clearance of pentobarbital after a 1-day exposure; all parameters apparently reached a new steady-state value by Days 5–10. Enhanced pentobarbital elimination at 25 ppm was observed after a 3-day exposure, but, again, the elimination parameters appeared to have reached a steady state after 5–10 days of pretreatment. Upon removal of the polychlorinated biphenyls, the various pharmacokinetic parameters showed a lag phase *prior* to a gradual return to control values. The study shows that intrinsic clearances rather than total body clearances or half-lives are more appropriate in assessing enzymatic induction in agents undergoing facile liver metabolic clearance that borders on blood flow rate dependency.

Keyphrases □ Polychlorinated biphenyls—effect of short-term dietary exposure on pharmacokinetics of intravenous pentobarbital, rats □ Pentobarbital—effect of short-term dietary exposure to polychlorinated biphenyls on pharmacokinetics following intravenous administration, rats □ Pharmacokinetics—pentobarbital, effect of short-term dietary exposure to polychlorinated biphenyls following intravenous administration, rats

The objective of this study was to observe the effects of short-term exposure to a class of environmental contaminants and hepatic enzyme inducers, polychlorinated biphenyls, on the pharmacokinetics of pentobarbital in rats. Pentobarbital, whose pharmacokinetics in rats (1) and humans (2) have been documented, is eliminated primarily *via* side-chain hydroxylation by liver microsomal enzymes (3–8). These enzyme systems are induced by exposure to polychlorinated biphenyls (9–14). Therefore, pentobarbital pharmacokinetics can be used as a probe for measuring the inducing effects of polychlorinated biphenyls on the liver microsomal enzymes in rats.

Drug pharmacokinetics can be altered by factors such as diet, age, sex, genetics, disease states, and environmental factors. Exposure to environmental contaminants such as polychlorinated biphenyls, which accumulate in human tissues (11, 15–21) and induce human hepatic enzymes (22–26), could drastically reduce the disposition half-life of drugs. Therefore, a thorough understanding of drug pharmacokinetics as affected by polychlorinated biphenyls and other environmental contaminants is useful in predicting their possible effects on drug therapy.

In a previous study (14), the effects of long-term (0–140-day) dietary exposure to a polychlorinated biphenyl mixture (0–25 ppm) on the pharmacokinetics of intravenously administered pentobarbital in rats were quantitated. The present study examined the effects of short-term dietary exposure to polychlorinated biphenyls (0–125 ppm for 0–10 days) on the elimination kinetics of intravenously administered pentobarbital in rats. The polychlorinated biphenyls were removed from the food at the end of 10 days, and the residual effects of the exposure were followed for 70 days. This procedure allowed a time profile to be established for the inducing effects of the polychlorinated biphenyls. Some qualitative observations concerning the time profile for the alteration of pentobarbital pharmacokinetics by polychlorinated biphenyl exposure are presented. The significance of the effects of accidental human exposure to polychlorinated biphenyls also is discussed.

EXPERIMENTAL

Animals—Male Sprague–Dawley rats[1], 201–225 g, were housed in stainless steel cages in groups of four. All animals were fed standard laboratory rat food[2] for 1 week before the prepared polychlorinated biphenyl[3]-containing diet was introduced. Tap water was available *ad libitum*. Groups of animals then were put on the prepared diet for 0, 1, 2, 3, 5, 10, 15, 25, 45, or 70 days. The rats were exposed (for a maximum of 10 days) to the polychlorinated biphenyl-containing powdered rat food prepared as described previously (13, 14). For animals on the 15-, 25-, 45-, and 70-day diet schedules, the polychlorinated biphenyl-containing powdered rat food was removed after 10 days and replaced with polychlorinated biphenyl-free powdered rat food.

The polychlorinated biphenyl diet was initiated in the afternoon, and all blood sampling studies were carried out in the mornings of the specified days. For example, rats on a 1-day diet were given the polychlorinated biphenyl-containing food in the afternoon of Day 0, and the pharmacokinetics of intravenously administered pentobarbital were studied on the following morning (*i.e.*, the morning of Day 1). Similarly, rats on a 15-day diet were exposed to polychlorinated biphenyl-containing food from the afternoon of Day 0 until the afternoon of Day 10, when powdered polychlorinated biphenyl-free rat food replaced the contaminated food.

For each time period, the rats were divided into groups of eight and were fed powdered laboratory rat food containing 0, 5, 25, or 125 ppm of polychlorinated biphenyls. An additional group of eight animals fed 1 ppm of polychlorinated biphenyl-containing food was included in the 10- and 70-day studies.

Five rats from each group were studied at the end of each time period. Pentobarbital sodium[4], 30 mg/kg (equivalent to 27.7 mg of pentobarbital/kg), was administered to each rat intravenously *via* the dorsal vein of the penis (27). The blood sampling procedure was similar to that described previously (14). Blood samples were collected in microcapillary tubes pretreated with 10% sodium ethylenediaminetetraacetate at 5, 7, 10, 15, 20, 30, 45, 60, and 90 min postdosing. Rats were sacrificed after

[1] ARS/Sprague–Dawley, Madison, Wis.
[2] Wayne Lab-Blox, Allied Mills, Chicago, Ill.
[3] Aroclor 1254 containing 54% (w/w) chlorine, lot KA601, Monsanto Chemical Co., St. Louis, Mo.
[4] Nembutal Sodium, lot 53-967-AF, Abbott Laboratories, North Chicago, Ill.

0022-3549/80/1100-1274$01.00/0
© 1980, American Pharmaceutical Association

Table I—Biological Half-Lives[a] of Pentobarbital in Rats Pretreated at Four Levels of Polychlorinated Biphenyls Compared to the Controls over Periods of up to 10 Days

Pretreatment Time, days	Control	1-ppm Pretreatment	5-ppm Pretreatment	25-ppm Pretreatment	125-ppm Pretreatment
0	50.9 ± 2.1	—	—	—	—
1	52.6 ± 6.9	—	57.9 ± 9.7 (NS)	53.1 ± 4.4 (NS)	38.6 ± 3.1 ($p < 0.02$)[b]
2	52.7 ± 10.7	—	51.2 ± 4.6 (NS)	43.3 ± 5.4 (NS)	29.6 ± 3.0 ($p < 0.01$)[b]
3	51.6 ± 3.5	—	51.5 ± 4.5 (NS)	37.9 ± 4.6 ($p < 0.01$)[b]	28.9 ± 4.8 ($p < 0.01$)[b]
5	51.1 ± 12.0	—	51.0 ± 4.5 (NS)	34.9 ± 6.9 ($p < 0.01$)[b]	23.5 ± 1.4 ($p < 0.01$)[b]
10	54.8 ± 9.9	59.2 ± 16.2 (NS)	52.2 ± 8.0 (NS)	35.5 ± 4.3 ($p < 0.05$)[b]	23.2 ± 1.8 ($p < 0.01$)[b]

[a] All values are means ± *SD* in minutes ($n = 5$). [b] Results are significantly different from the same-day control group at the level indicated.

Table II—Total Body Clearances[a] of Pentobarbital in Rats Pretreated at Four Levels of Polychlorinated Biphenyls Compared to the Controls over Periods of up to 10 Days

Pretreatment Time, days	Control	1-ppm Pretreatment	5-ppm Pretreatment	25-ppm Pretreatment	125-ppm Pretreatment
0	20.5 ± 3.3	—	—	—	—
1	19.9 ± 2.6	—	17.1 ± 3.2 (NS)	17.9 ± 1.8 (NS)	26.9 ± 5.9 ($p < 0.05$)[b]
2	17.1 ± 2.5	—	18.2 ± 3.4 (NS)	22.5 ± 3.3 (NS)	34.2 ± 6.0 ($p < 0.01$)[b]
3	19.9 ± 1.4	—	17.6 ± 3.4 (NS)	22.6 ± 2.4 (NS)	33.2 ± 6.7 ($p < 0.01$)[b]
5	18.7 ± 3.9	—	17.8 ± 3.0 (NS)	28.2 ± 3.8 ($p < 0.01$)[b]	42.5 ± 5.2 ($p < 0.01$)[b]
10	19.0 ± 1.3	17.2 ± 5.5 (NS)	18.5 ± 4.8 (NS)	24.4 ± 2.9 (NS)	46.8 ± 3.4 ($p < 0.01$)[b]

[a] All values are means ± *SD* in milliliters per minute per kilogram of body weight ($n = 5$). [b] Results are significantly different from the same-day control group at the level indicated.

each pretreatment period. The livers were removed, patted dry, and weighed.

Pentobarbital Assay—The plasma pentobarbital concentration was assayed as described previously (14) but with the following modifications. To each 100 μl of plasma sample were added 25 μl of the internal standard (0.099 mg of secobarbital/ml in methanol) and 50 μl of 4 *M* monobasic sodium phosphate. The mixture was extracted with 1.0 ml of water-saturated ether on a vortex mixer for 1 min. After centrifugation, the ether extract was removed to a glass-stoppered 5-ml conical centrifuge tube.

Just before injection in the gas chromatograph, 25 μl of alkaline aqueous 0.02 *M* trimethylanilinium hydroxide was added to the sample, which then was agitated and centrifuged. The trimethylanilinium hydroxide solution was prepared by the method of Stella (28). The ether layer was removed by aspiration, and 1–2 μl of the aqueous lower layer was injected in a gas chromatograph. Chromatographic conditions and column packings were as described previously (14). A standard curve of the peak height ratios of pentobarbital sodium to secobarbital *versus* plasma concentrations of pentobarbital (2–80 μg/ml) was prepared and used to determine pentobarbital in unknown samples.

Pharmacokinetic Data Analysis—In an earlier study (14), a fast distribution phase was observed in the disposition kinetics of pentobarbital in the rat. The distribution kinetics, apart from being rapid, were not affected significantly by the polychlorinated biphenyl pretreatments (14). Based on these observations, the data in this study were treated as a one-compartment model by linear least-squares fitting of the postdistribution data points on a semilog plot. The B and β values obtained from the intercept and slope of the log concentration–time curve were used to calculate the volume of distribution (extrapolated), V_d(ext), and the total body clearance, Cl_{TB} (14). The total body clearance of any compound that is eliminated solely *via* liver metabolism is given by:

$$Cl_{TB} = QE \qquad \text{(Eq. 1)}$$

where Q is the liver blood flow rate and E is the liver extraction constant (29). The extraction constant is not an independent variable but varies with Q, the fraction of unbound drug in the blood (f), and the intrinsic clearance of the drug (Cl_{int}) (29, 30). If the measured intrinsic clearance ($Cl_{int}f$) is represented by Cl_{INT}, then for a drug metabolized exclusively by the liver, the total body clearance, which approximates the hepatic clearance, can be expressed by:

$$Cl_{TB} = Q\frac{Cl_{INT}}{Q + Cl_{INT}} \qquad \text{(Eq. 2)}$$

The intrinsic clearance, defined as the clearance of a drug when there are no flow limitations (29), is a measure of the available metabolic activity of the liver and the properties of the enzyme system associated with hepatic removal. The Cl_{INT} values were calculated from Eq. 2 using blood flow rates calculated from the individual liver to body weight ratios for the particular animal and a blood flow rate of ~2 ml/min/g of liver (30).

The mean values and standard deviations for all parameters for each pretreatment were calculated and compared statistically to the same parameter for the same-day control group. Multiple means within a day were analyzed by a randomized analysis of variance. When the analysis indicated that a significant difference existed, the means of each group were compared by a two-tailed Dunnett multiple mean test (31). This test is for multiple mean comparisons to a control.

RESULTS AND DISCUSSION

Tables I and II summarize the half-lives ($t_{1/2}$) and total body clearances (Cl_{TB}) of intravenously administered pentobarbital in rats pretreated with different polychlorinated biphenyl doses over various time periods compared to the controls. The elimination rate of pentobarbital was increased significantly in rats pretreated for 1 day at 125 ppm of polychlorinated biphenyl in the food. On Day 1, $t_{1/2}$ was reduced significantly to 39 ± 3 min compared to the control group, which showed a $t_{1/2}$ of 53 ± 7 min; the $t_{1/2}$ appeared to reach a constant value of 23 ± 1 min by Days 5–10. The Cl_{TB} values also increased from 21 ml/min/kg of body weight on Day 1 and seemed to approach a constant clearance of 43–47 ml/min/kg of body weight in <1 week. No significant changes in the elimination kinetics of pentobarbital were observed for rats pretreated at the 1- and 5-ppm levels relative to control rats.

Enhanced pentobarbital elimination for rats pretreated with 25 ppm of polychlorinated biphenyls in food was observed after 2–3 days of pretreatment. The elimination parameters again began to plateau after ~5–10 days of pretreatment, as was the case with the 125-ppm polychlorinated biphenyl-pretreated rats. The $t_{1/2}$ was lowered significantly to 38 ± 5 min relative to the control value of 52 ± 4 min after 3 days of pretreatment and remained rather constant at 35 ± 4 min after ~5–10 days. The Cl_{TB} value was similarly significantly increased to 28 ml/min/kg of body weight after 5 days on a polychlorinated biphenyl-contaminated diet and appeared to begin leveling off at a clearance of 24–28 ml/min/kg of body weight after ~5–10 days of the diet.

Upon removal of the polychlorinated biphenyls from the diet after 10 days (Tables III and IV), the enhanced pentobarbital elimination as measured by $t_{1/2}$ and Cl_{TB} started to decline toward the control values after apparent time lags of ~10 and ~20 days for the 25- and 125-ppm polychlorinated biphenyl-pretreated animals, respectively. The lag time for the loss of residual effects appeared to be dose dependent. Induced enzyme activity as shown by enhanced pentobarbital elimination due to exposure to 25 ppm of polychlorinated biphenyls receded within 60 days following removal of polychlorinated biphenyls from the diet. Rats pretreated at the 125-ppm level still demonstrated an elevated, but not statistically significant, enhancement of pentobarbital elimination at 70 days, *i.e.*, 60 days after removal of the polychlorinated biphenyls from the food.

The Cl_{TB} values (Tables II and IV) for the control group decreased slightly but insignificantly over the 70 days of the study; in the 5-ppm

Table III—Biological Half-Lives [a] of Pentobarbital in Rats Pretreated at Four Levels of Polychlorinated Biphenyls Compared to the Controls over the Periods Studied

Pretreatment Time, days	Control	1-ppm Pretreatment	5-ppm Pretreatment	25-ppm Pretreatment	125-ppm Pretreatment
10	54.8 ± 9.9	59.2 ± 16.2 (NS)	52.2 ± 8.0 (NS)	35.5 ± 4.3 ($p < 0.01$)[b]	23.2 ± 1.8 ($p < 0.05$)[b]
15[c]	55.1 ± 7.0	—	50.8 ± 4.1 (NS)	36.0 ± 5.2 ($p < 0.01$)[b]	22.3 ± 1.6 ($p < 0.01$)[b]
25[c]	54.3 ± 8.1	—	50.2 ± 8.7 (NS)	41.8 ± 7.6 ($p < 0.05$)[b]	22.5 ± 1.5 ($p < 0.01$)
45[c]	52.3 ± 8.8	—	50.5 ± 6.5 (NS)	48.2 ± 8.3 (NS)	24.0 ± 3.1 ($p < 0.01$)[b]
70[c]	56.7 ± 7.0	54.7 ± 8.3 (NS)	66.2 ± 10.3 (NS)	53.8 ± 20.6 (NS)	45.9 ± 5.7 (NS)

[a] All values are means ± *SD* in minutes ($n = 5$). [b] Results are significantly different from the same-day control group at the level indicated. [c] Animals were treated with polychlorinated biphenyls at the levels indicated for 10 days, at which time the polychlorinated biphenyl-contaminated food was replaced with polychlorinated biphenyl-free food.

Table IV—Total Body Clearances [a] of Pentobarbital in Rats Pretreated at Four Levels of Polychlorinated Biphenyls Compared to the Controls over the Periods Studied

Pretreatment Time, days	Control	1-ppm Pretreatment	5-ppm Pretreatment	25-ppm Pretreatment	125-ppm Pretreatment
10	19.0 ± 1.3	17.2 ± 5.5 (NS)	18.5 ± 4.8 (NS)	24.4 ± 2.9 (NS)	46.8 ± 3.4 ($p < 0.01$)[b]
15[c]	17.1 ± 3.9	—	16.8 ± 1.2 (NS)	26.3 ± 7.4 ($p < 0.01$)[b]	43.7 ± 3.0 ($p < 0.01$)[b]
25[c]	18.8 ± 3.5	—	18.6 ± 3.6 (NS)	25.4 ± 5.0 ($p < 0.05$)[b]	38.9 ± 1.6 ($p < 0.01$)[b]
45[c]	16.1 ± 2.1	—	16.3 ± 0.8 (NS)	22.8 ± 11.0 (NS)	33.2 ± 6.2 ($p < 0.01$)[b]
70[c]	16.0 ± 1.6	17.9 ± 2.5 (NS)	18.1 ± 3.2 (NS)	18.4 ± 6.0 (NS)	23.4 ± 5.3 (NS)

[a] All values are means ± *SD* in milliliters per minute per kilogram of body weight ($n = 5$). [b] Results are significantly different from the same-day control group at the level indicated. [c] Animals were treated with polychlorinated biphenyls at the levels indicated for 10 days, at which time the polychlorinated biphenyl-contaminated food was replaced with polychlorinated biphenyl-free food.

treated animals, the Cl_{TB} remained at a level similar to the control animals prior to exposure. This finding may suggest some minimal induction by the polychlorinated biphenyls at 5 ppm. However, as suggested by the Dunnett test, no statistically significant differences were seen between the controls and the 5-ppm treated animals at any time.

Figure 1 shows the induction time profiles for β. The dotted lines represent the range (mean ± *SD*) for the β values of the control animals

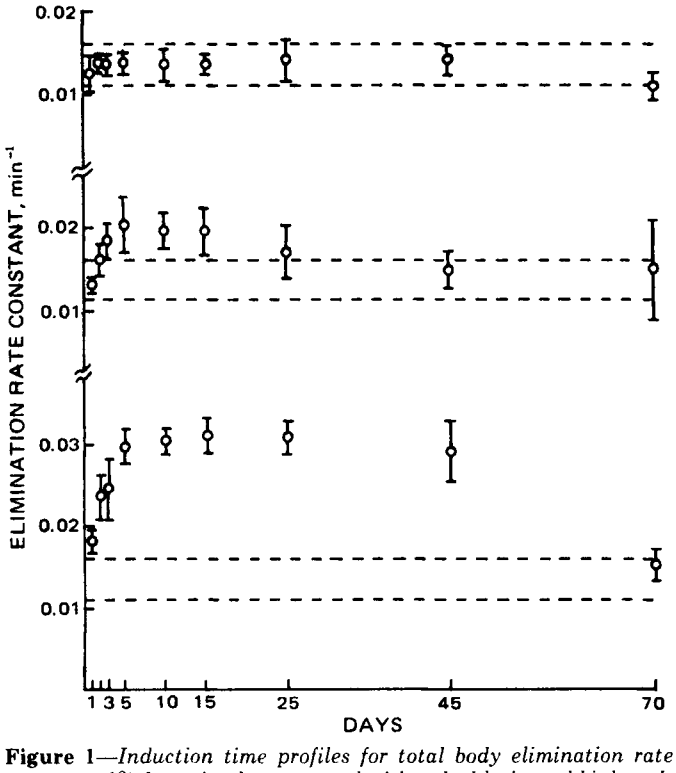

Figure 1—*Induction time profiles for total body elimination rate constants (β) for animals pretreated with polychlorinated biphenyls at 5 ppm (top profile), 25 ppm (middle profile), and 125 ppm (bottom profile) over 70 days. The polychlorinated biphenyl diet was provided up to 10 days, after which time it was replaced with polychlorinated biphenyl-free food. Dotted lines represent the range of the mean control value obtained by averaging the control values at the 10 times studied* (i.e., *mean* ± SD).

averaged over all of the time periods studied. There were no significant effects of polychlorinated biphenyl exposure as measured by β in rats pretreated at the 5-ppm level. Figure 1 also shows that the enhanced elimination of pentobarbital in rats at 25 ppm of polychlorinated biphenyls was observed only after a lag time of ~1–3 days. This pattern resembles the 5-ppm polychlorinated biphenyl-pretreated rats in the earlier study (14), which did not show any effects of polychlorinated biphenyl induction until exposure for >35 days. The increased elimination rate of pentobarbital in rats pretreated with 125 ppm of polychlorinated biphenyls was statistically significant, even after 1 day. The enhanced elimination resulted from exposure to the higher polychlorinated biphenyl doses.

After removal of the polychlorinated biphenyl-contaminated diet on Day 10, induced enzyme activity as measured by β appeared to recede completely by Day 70 in the 25-ppm polychlorinated biphenyl-pretreated rats. Despite the still elevated, but not statistically significant, elimination for pentobarbital in rats pretreated with 125 ppm of polychlorinated biphenyls at Day 70, an apparent decrease in the induced enzyme activity as measured by the same parameters was noticeable.

Body Weights and Liver Weights—No significant trend of body weight increase was observed in rats pretreated at the different levels of polychlorinated biphenyls compared to the control rats. However, the mean liver weight to body weight ratios were higher in rats pretreated at 125 ppm of polychlorinated biphenyls (Table V) throughout induction and remained elevated until ~35 days after the removal of polychlorinated biphenyls (*i.e.*, at Day 45). The liver weights and the liver weight to body weight ratios in the 25-ppm pretreated rats were not significantly different from the control group. Dose-dependent liver weight increases were reported for mice pretreated with polybrominated biphenyls at 100- and 200-ppm dietary levels (32).

It has been shown that exposure to up to 1000 ppm of polychlorinated biphenyls for periods of up to months results in modest proliferation of the smooth endoplasmic reticulum and lipid vacuolation of liver cells but causes no cellular injury in the liver (33–36). Thus, this small increase in the liver weight and the liver weight to body weight ratio probably is an adaptive response, as suggested by Bruckner *et al.* (13) rather than a hepatotoxic effect. Other investigators also suggested that such changes in hepatic morphology upon exposure to polychlorinated biphenyls represent an adaptive response to eliminate foreign compounds by increasing their rate of metabolism (37). The observed enhanced rate of elimination of pentobarbital in polychlorinated biphenyl-pretreated rats probably reflects the increased activities of certain metabolic enzymes due to the exposure.

Intrinsic Clearances—Both the biological half-life and total body clearance values are limited in use as an index of intrinsic hepatic metabolism (38). The former is a complex parameter and depends on the distribution characteristics as well as the elimination of the substance under investigation. The latter can approximate hepatic clearance only

Table V—Percent of Liver Weight to Body Weight [a] for Rats Pretreated at Four Levels of Polychlorinated Biphenyls Compared to the Controls over the 10 Periods Studied

Pretreatment Time, days	Control	1-ppm Pretreatment	5-ppm Pretreatment	25-ppm Pretreatment	125-ppm Pretreatment
0	4.3 ± 0.4	—	—	—	—
1	4.0 ± 0.3	—	3.7 ± 0.3	4.0 ± 0.2	4.5 ± 0.2
2	3.4 ± 0.2	—	3.8 ± 0.2	4.2 ± 0.3	4.7 ± 0.3
3	4.3 ± 0.3	—	4.4 ± 0.4	4.2 ± 0.4	4.5 ± 0.2
5	4.6 ± 0.3	—	4.4 ± 0.2	4.6 ± 0.1	5.3 ± 0.4
10	4.3 ± 0.3	3.9 ± 0.2	3.8 ± 0.3	4.2 ± 0.3	5.6 ± 0.5
15[b]	3.8 ± 0.3	—	3.7 ± 0.3	4.1 ± 0.1	5.1 ± 0.1
25[b]	3.6 ± 0.2	—	3.9 ± 0.2	4.0 ± 0.1	4.7 ± 0.3
45[b]	3.7 ± 0.4	—	3.6 ± 0.2	3.6 ± 0.2	3.9 ± 0.6
70[b]	3.7 ± 0.1	3.4 ± 0.2	3.5 ± 0.1	3.8 ± 0.2	4.0 ± 0.5

[a] All values are means ± *SD* as (liver weight/body weight) × 100 (n = 5). [b] Animals were treated with polychlorinated biphenyls at the levels indicated for 10 days, at which time the polychlorinated biphenyl-contaminated food was replaced with polychlorinated biphenyl-free food.

if the drug is eliminated and metabolized exclusively by the liver. Even for pentobarbital, whose route of elimination is primarily hepatic, an estimation of the total body clearance still may not suffice as the index for intrinsic metabolic activity. As seen by examining Eq. 2, total body clearance is governed not only by the intrinsic clearance but also by the liver blood flow rate. Only when this rate is very much larger than the intrinsic clearance does the total body clearance directly reflect the intrinsic metabolic activity of the liver or the intrinsic clearance. On the other hand, when the intrinsic clearance is very large compared to the blood flow rate through the liver, the total body clearance becomes limited by the flow rate and is no longer proportional to the intrinsic clearance. To quantitate the apparent metabolic activity of the liver enzymes using pharmacokinetic parameters, estimation of the intrinsic clearance is more appropriate.

By using a literature value of 2 ml/min/g of liver for the liver blood flow rate and the measured experimental total body clearances, intrinsic clearances were estimated; the induction time profiles are presented in Fig. 2. The absence of induction of the hepatic metabolic enzymes due to 5-ppm polychlorinated biphenyl exposure as measured by the intrinsic clearances is readily seen in Fig. 2. Again, a statistically significant induction at the 25-ppm pretreatment level is seen after a 3-day lag time and an immediate (<1 day) and more pronounced induction is seen at the 125-ppm polychlorinated biphenyl pretreatment level. The absolute values of Cl_{INT} are dependent on the value used for the liver blood flow rate. Recently developed pharmacokinetic techniques (30, 39, 40) and more traditional measurements (41–44) suggested that the value of ~2 ml/min/g of liver is a reasonable estimate of the liver blood flow rate in rats. Determination of the intrinsic clearances for pentobarbital in rats using the oral and intravenous pharmacokinetic techniques (30, 39, 40) will be presented later.

If $t_{1/2}$, β, or Cl_{TB} is used as a measure of polychlorinated biphenyl induction of pentobarbital elimination, it can be seen from Fig. 1 and Tables I–IV that the percent change in the parameters relative to controls reaches a steady-state level ~5–10 days after an apparent initial lag phase. This also was seen in an earlier chronic exposure study (14). A possible explanation might be that the liver, in response to an inducer, increases the synthesis of microsomal enzymes in an amount proportional to the dose of the inducer. Since the pentobarbital total body clearance, even in the absence of induction, is a reasonably high percentage of the liver blood flow, the percentage increase in the inducing effect of the polychlorinated biphenyls is not reflected totally in the total body clearance.

For example, the steady-state total body clearance after the 10-day exposure at 125 ppm amounted to ~46 ml/min/kg. When this parameter is used as a measure of induction and compared with the control value (19 ml/min/kg), a 142% increase is indicated. If the intrinsic clearances are used instead, the results indicate an increase of 229% (80.8 ml/min/kg in treated animals *versus* 24.5 ml/min/kg in the controls). Thus, the total body clearances do not always reflect the large increases in intrinsic

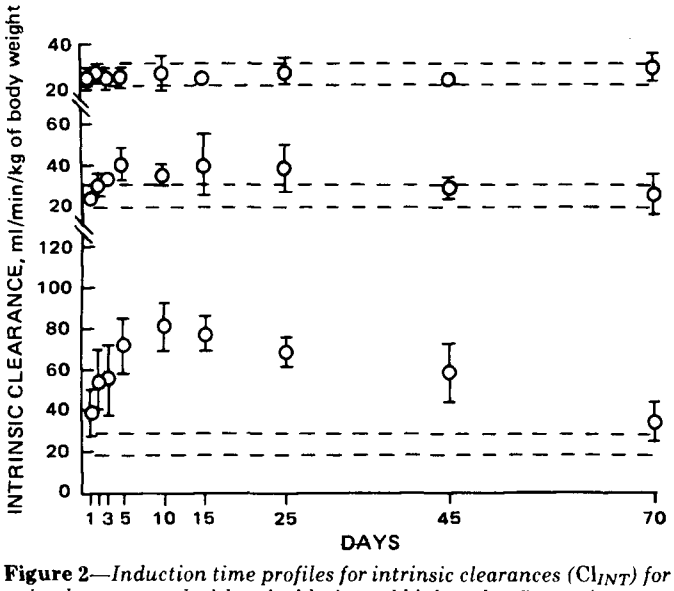

Figure 2—*Induction time profiles for intrinsic clearances* (Cl_{INT}) *for animals pretreated with polychlorinated biphenyl at 5 ppm (top profile), 25 ppm (middle profile), and 125 ppm (bottom profile) in food over 70 days. The polychlorinated biphenyl diet was provided up to 10 days, after which time it was replaced by a polychlorinated biphenyl-free diet. Dotted lines represent the range of the mean control value obtained by averaging the control values at the 10 times studied* (i.e., *mean* ± SD).

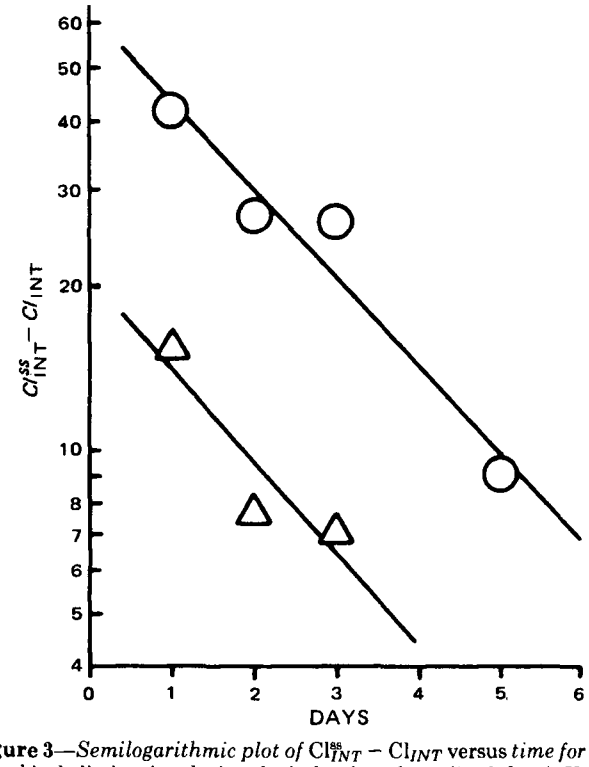

Figure 3—*Semilogarithmic plot of* $Cl_{INT}^{ss} - Cl_{INT}$ versus *time for pentobarbital elimination during the induction phase (0–10 days). Key:* △, *data for the 25-ppm pretreatment, and* ○, *data for the 125-ppm pretreatment.*

clearances, which are more realistic indexes of the degree of induction. This is especially true if the probe molecule under control conditions undergoes a facile liver metabolic clearance that borders on liver blood flow rate dependency.

The lack of significant short-term effects of the 1- and 5-ppm pretreatments on pentobarbital pharmacokinetics suggests that a critical mass of inducer is needed to initiate liver microsomal enzyme stimulation. At the 25-ppm level, an increase in the pentobarbital intrinsic clearance was seen only on Day 5 of exposure, whereas a significant increase in the intrinsic clearance was seen on the 1st day of exposure at the 125-ppm level. These results are consistent with the need for a critical mass of inducer to accumulate before induction is initiated.

Levy and coworkers (45–51) recently published several reports dealing with the time profiles of drug induction. An attempt was made to fit the induction time profile seen in the present work by estimating an average steady-state intrinsic clearance, Cl^{ss}_{INT} (38.4 ml/min/kg for 25 ppm and 80.8 ml/min/kg for 125 ppm), and plotting log ($Cl^{ss}_{INT} - Cl_{INT}$) *versus* time for the induction phase. Good first-order plots were obtained (Fig. 3), giving apparent induction half-lives of ~2 days for both the 25- and 125-ppm data. Similarly, postinduction data were treated by plotting log ($Cl_{INT} - Cl^{0}_{INT}$) *versus* time, where Cl^{0}_{INT} is the mean value of the intrinsic clearance for the control animals. Although half-lives for the loss of residual induction effects of ~11 days were obtained for both the 25- and 125-ppm data, care must be taken in interpreting these values because of the limited number of points available in the postinduction phase.

Based on the observations in this study, the following tentative conclusions can be made about polychlorinated biphenyl induction of pentobarbital elimination.

1. Induction by the polychlorinated biphenyls shows an apparent lag time that appears to be dose dependent.
2. The kinetics of induction, once initiated, appear to be first order, and the induction half-life seems to be dose independent.
3. The extent of induction is polychlorinated biphenyl dose dependent, but there is an apparent minimum exposure below which significant induction is not seen.
4. After removal of the polychlorinated biphenyls, there appears to be a lag time before the various induced pharmacokinetic parameters begin to return to control values (Figs. 1–3).
5. An apparent half-life for the loss of residual induction effects seems to be dose independent.

Although these conclusions must be tempered because of the limited number of data points and doses studied, it is interesting to speculate on their significance. If relationships such as those implied here can be substantiated, they may allow prediction of the time course of induction by various levels and times of exposure of enzyme-inducing agents such as polychlorinated biphenyls and of the effect of this induction on the pharmacokinetics of drugs such as pentobarbital. A better understanding of this phenomenon will allow more quantitative prediction of the therapeutic consequences of accidental acute or chronic exposure to agents such as polychlorinated biphenyls and other environmental enzyme inducers.

REFERENCES

(1) Y. L. Lin, S. Awazu, M. Hanano, and H. Nogami, *Pharm. Chem. Bull.*, **21**, 2749 (1973).

(2) R. B. Smith, L. W. Dittert, W. O. Griffen, Jr., and J. T. Doluisio, *J. Pharmacokinet. Biopharm.*, **1**, 5 (1973).

(3) J. R. Cooper and B. B. Brodie, *J. Pharmacol. Exp. Ther.*, **120**, 75 (1957).

(4) E. W. Maynert, *ibid.*, **150**, 118 (1965).

(5) T. C. Gould and F. E. Shideman, *ibid.*, **104**, 427 (1952).

(6) M. T. Bush, T. C. Butler, and H. L. Dickinson, *ibid.*, **108**, 104 (1953).

(7) B. B. Brodie, L. C. Mard, E. M. Papper, P. A. Lief, E. Berstein, and E. A. Rovenstine, *ibid.*, **98**, 85 (1950).

(8) E. O. Titus and H. Weiss, *J. Biol. Chem.*, **214**, 807 (1955).

(9) J. Marniemi, M. Nokkala, H. Vainio, and K. J. W. Hartiala, *Chem. Biol. Interact.*, **18**, 247 (1974).

(10) J. V. Bruckner, K. L. Khanna, and H. H. Cornish, *Toxicol. Appl. Pharmacol.*, **28**, 189 (1974).

(11) K. Akiyama, G. Ohi, K. Fujitani, H. Yagyu, M. Ogino, and T. Kawana, *Bull. Environ. Contam. Toxicol.*, **14**, 588 (1975).

(12) J. V. Bruckner, K. L. Khanna, and H. H. Cornish, *Toxicol. Appl. Pharmacol.*, **24**, 434 (1973).

(13) J. V. Bruckner, W.-D. Jiang, J. W. Brown, L. Puchta, C. K. Chu, and V. J. Stella, *J. Pharmacol. Exp. Ther.*, **202**, 22 (1977).

(14) C. K. Chu, V. J. Stella, J. V. Bruckner, and W.-D. Jiang, *J. Pharm. Sci.*, **66**, 238 (1977).

(15) M. Karatsune, T. Yoshimura, J. Matsuzaka, and A. Yamaguchi, *Environ. Health Persp.*, **1**, 119 (1972).

(16) H. A. Price and R. L. Welch, *ibid.*, **1**, 73 (1972).

(17) A. R. Yobs, *ibid.*, **1**, 79 (1972).

(18) K. Higuchi, "PCBs Poisoning and Pollution," Academic, New York, N.Y., 1976.

(19) R. W. Miller, *U.S. Public Health Rep.*, **59**, 1085 (1944).

(20) H. B. Matthews and M. W. Anderson, *Drug Metab. Disp.*, **3**, 371 (1975).

(21) F. J. Biros, A. C. Walker, and A. Medbery, *Bull. Environ. Contam. Toxicol.*, **5**, 317 (1970).

(22) R. W. Riseborough, P. Riche, D. B. Peakall, S. B. Herman, and M. N. Kirven, *Nature (London)*, **220**, 1098 (1968).

(23) A. P. Alvares and A. Kappas, *Clin. Pharmacol. Ther.*, **22**, 809 (1977).

(24) J. G. Babish and G. S. Stoewsand, *J. Toxicol. Environ. Health*, **3**, 673 (1977).

(25) J. A. Goldstein, P. Hickman, V. W. Burse, and H. Bergman, *Toxicol. Appl. Pharmacol.*, **32**, 461 (1975).

(26) G. J. Johnstone, D. J. Ecobichon, and O. Hutzinger, *ibid.*, **28**, 66 (1974).

(27) M. Virolainen, *Transplantation*, **5**, 1530 (1967).

(28) V. J. Stella, *J. Pharm. Sci.*, **66**, 1510 (1977).

(29) M. Rowland, L. Z. Benet, and G. G. Graham, *J. Pharmacokinet. Biopharm.*, **1**, 123 (1973).

(30) K. S. Pang and J. R. Gillette, *Drug Metab. Disp.*, **6**, 567 (1978).

(31) B. J. Winer, "Statistical Principles in Experimental Design," McGraw-Hill, New York, N.Y., 1962, pp. 89–91.

(32) S. S. Steiner and C. E. Mueller, *Circ. Res.*, **14**, 99 (1961).

(33) L. Kasza, M. A. Weinberger, C. Carter, D. E. Hinton, B. F. Trump, and E. A. Brouwer, *J. Toxicol. Environ. Health*, **1**, 689 (1976).

(34) D. L. Grant, C. A. Moodie, and W. E. J. Phillips, *Environ. Physiol. Biochem.*, **4**, 214 (1974).

(35) A. Schmoldt, E. Altenahr, W. Grote, H. G. Dammann, B. Sidau, and H. F. Benthe, *Arch. Toxicol.*, **37**, 203 (1977).

(36) J. V. Bruckner, K. L. Khanna, and H. H. Cornish, *Food Cosmet. Toxicol.*, **12**, 323 (1974).

(37) R. Schulte-Hermann, *CRC Crit. Rev. Toxicol.*, **3**, 97 (1974).

(38) D. Perrier and M. Gibaldi, *J. Pharmacol. Exp. Ther.*, **191**, 17 (1974).

(39) D. G. Shand, D. M. Kornhauser, and G. R. Wilkinson, *ibid.*, **195**, 424 (1975).

(40) D. M. Kornhauser, A. J. J. Wood, R. E. Vestal, G. R. Wilkinson, R. A. Branch, and D. G. Shand, *Clin. Pharmacol. Ther.*, **23**, 165 (1978).

(41) A. S. Neis, G. R. Wilkinson, B. D. Rush, J. T. Strother, and D. G. McDevitt, *Biochem. Pharmacol.*, **25**, 99 (1976).

(42) G. C. Rice, D. P. Lieberman, R. T. Mathie, C. J. Ryan, A. M. Harper, and L. H. Blumgart, *Br. J. Exp. Pathol.*, **58**, 243 (1977).

(43) D. Dhumeaux and P. Berthelot, *Biol. Gastroenterol.*, **6**, 161 (1973).

(44) E. E. Ohnhans and J. T. Locker, *Eur. J. Pharmacol.*, **31**, 161 (1975).

(45) R. H. Levy, A. A. Lai, and M. S. Dumain, *J. Pharm. Sci.*, **68**, 398 (1979).

(46) W. H. Pitlick, R. H. Levy, A. S. Troupin, and J. R. Green, *ibid.*, **65**, 462 (1976).

(47) R. H. Levy, W. H. Pitlick, A. S. Troupin, and J. R. Green, in "The Effect of Disease States on Drug Pharmacokinetics," L. Z. Benet, Ed., American Pharmaceutical Association, Washington, D.C., 1976, pp. 87–95.

(48) W. H. Pitlick and R. H. Levy, *J. Pharm. Sci.*, **66**, 647 (1977).

(49) A. A. Lai, R. H. Levy, and R. E. Cutler, *Clin. Pharmacol. Ther.*, **34**, 316 (1978).

(50) A. A. Lai and R. H. Levy, *J. Pharm. Sci.*, **68**, 416 (1979).

(51) R. H. Levy and M. S. Dumain, *ibid.*, **68**, 934 (1979).

ACKNOWLEDGMENTS

Supported by National Institutes of Health Grant GM 22357.

The authors thank Dr. J. V. Bruckner for the Aroclor 1254, M. Riedy and J. Dishinger for technical assistance, and Dr. G. Schlager, Dr. Y. Yamaoka, and Dr. K. Yamaoka for help with the statistics.

Effect of Short-Term Exposure to Polychlorinated Biphenyls on First-Pass Metabolism of Pentobarbital in Rats

V. J. STELLA [x] and C. K. CHU *

Received October 29, 1979, from the *Department of Pharmaceutical Chemistry, University of Kansas, Lawrence, KS 66045.* Accepted for publication May 9, 1980. *Present address: Department of Pharmaceutics, School of Pharmacy, State University of New York at Buffalo, Amherst, NY 14260.

Abstract □ The enhancement of the first-pass metabolism of orally administered pentobarbital in rats was examined after a 10-day exposure to food contaminated with polychlorinated biphenyls at 25 and 125 ppm. The degree of the first-pass effect and the influence of the polychlorinated biphenyl exposure were quantitated by comparing the areas under the plasma concentration–time curves after oral and intravenous dosing in control and treated animals. By using the clearance model and assuming that pentobarbital was eliminated totally by liver metabolism, the experimentally determined oral availability was predicted adequately from both the oral and intravenous data. The enhanced first-pass effect was principally in the intrinsic clearance term, although liver blood flow rates also appeared to be enhanced in animals treated with polychlorinated biphenyls at 125 ppm.

Keyphrases □ Polychlorinated biphenyls—effect of short-term exposure on first-pass metabolism of pentobarbital, rats □ Pentobarbital—effect of short-term exposure to polychlorinated biphenyls on first-pass metabolism, rats □ First-pass metabolism—pentobarbital, effect of short-term exposure to polychlorinated biphenyls, rats

Induction of liver microsomal enzymes by polychlorinated biphenyls, a class of environmental contaminants, has been reported in both humans and rats (1–11). Enhanced metabolism of drugs that are eliminated *via* these enzymes can have clinical implications because the hepatic clearance of drugs, such as pentobarbital (12–14), that are metabolized mainly by liver enzymes can be altered by exposure to these enzyme inducers. Such exposure may require therapeutic dosage adjustments of affected drugs to maintain comparable clinical effectiveness to the preexposure period.

In this study, the enhancement of the first-pass metabolism of pentobarbital in rats was examined after a 10-day exposure to a polychlorinated biphenyl-contaminated diet. It was determined previously (15) that the extent of enzyme induction due to polychlorinated biphenyl exposure is dose dependent and that a 10-day exposure results in an apparent steady-state level of enzyme induction. Therefore, the purpose of this study was to investigate the dose dependency and predictability of enhanced first-pass metabolism and bioavailability parameters for pentobarbital as a result of hepatic enzyme induction by polychlorinated biphenyls.

EXPERIMENTAL

Male Sprague–Dawley rats[1], 201–225 g, were housed in stainless steel cages in groups of four. All animals were fed standard laboratory rat food[2] for 1 week, and tap water was available *ad libitum*. After this preconditioning period, the rats were divided randomly into groups and fed powdered laboratory rat food containing 0, 25, or 125 ppm of polychlorinated biphenyls[3]. Food preparation was the same as described previously (16).

Four rats from each group were studied at the end of 10 days. The same dose of pentobarbital sodium[4], 30 mg/kg (equivalent to 27.7 mg of pentobarbital/kg), was administered orally to one group of rats and intravenously to another group of rats receiving the same polychlorinated biphenyl pretreatment. The oral dose was introduced *via* gastric intubation, and the intravenous dose was administered *via* the dorsal vein of the penis (17).

Blood samples were collected in microcapillary tubes pretreated with a 10% sodium ethylenediaminetetraacetate solution following the oral dose at 15, 30, 45, 60, 75, 90, 120, 150, and 180 min and similarly following the intravenous dose at time intervals as described previously (15). Because of anticipated faster pentobarbital elimination in the animals pretreated with 125 ppm of polychlorinated biphenyls, the last two time points were replaced for this group by additional samples at 5 and 10 min.

After centrifugation, the plasma samples were kept frozen until analysis. Plasma pentobarbital concentrations were assayed as described previously (15). All animals were sacrificed at the end of the blood sampling study. The liver was removed from each animal, patted dry, and weighed.

Experimental systemic availability of pentobarbital was evaluated in rats on the 10-day diet from the ratios of the area under the plasma level–time curves of the oral dosing compared to that from the intravenous dosing schedule:

$$\text{systemic availability} = (AUC_{\text{oral}})_0^\infty/(AUC_{\text{iv}})_0^\infty \qquad \text{(Eq. 1)}$$

where AUC represents the area under the plasma level–time curve. The AUC values were estimated by the trapezoidal method with extrapolation to infinite time from the last data point using standard procedures (18). The total body and intrinsic clearances (Cl_{TB} and Cl_{INT}, respectively) for these animals were evaluated using (19–24):

$$Cl_{TB} = \text{dose}/(AUC_{\text{iv}})_0^\infty \qquad \text{(Eq. 2)}$$

$$Cl_{\text{INT}} = \text{dose}/(AUC_{\text{oral}})_0^\infty \qquad \text{(Eq. 3)}$$

where Cl_{TB} and Cl_{INT} are related by:

$$Cl_{TB} = \frac{QCl_{\text{INT}}}{Q + Cl_{\text{INT}}} \qquad \text{(Eq. 4)}$$

where Q is the liver blood flow rate. The assumption of these equations is that extrahepatic elimination is negligible (19, 20, 23).

The mean values and standard deviations for all parameters for each treatment were calculated and compared statistically to the same parameter for the control. Multiple means were analyzed by a one-way randomized analysis of variance. When analysis indicated that a significant difference existed, the means of each group were compared by a two-tailed Dunnett multiple mean test (25). This test is for multiple mean comparisons to a control.

RESULTS AND DISCUSSION

The plasma level–time curves of pentobarbital sodium administered orally and intravenously at the same dosage (30 mg/kg) to animals on the polychlorinated biphenyl-free control diet are shown in Fig. 1. The bioavailability of pentobarbital in the orally dosed group of animals was

[1] ARS/Sprague–Dawley, Madison, Wis.
[2] Wayne Lab-Blox, Allied Mills, Chicago, Ill.
[3] Aroclor 1254, lot KA601, Monsanto Chemical Co., St. Louis, Mo.
[4] Nembutal Sodium, lot 53-967-AF, Abbott Laboratories, North Chicago, Ill.

0022-3549/80/1100-1279$01.00/0
© 1980, American Pharmaceutical Association

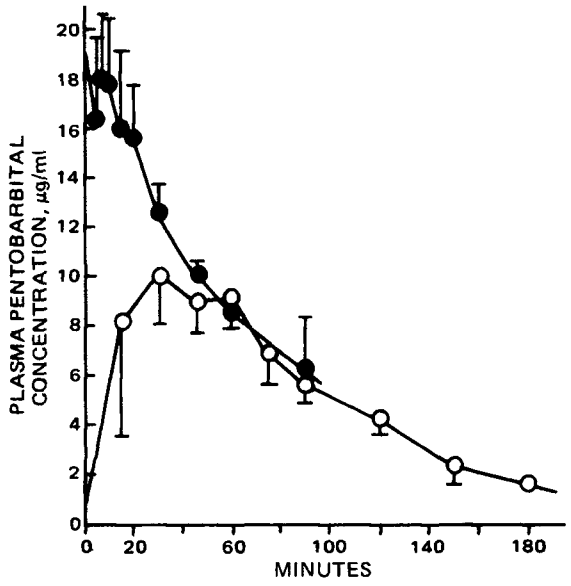

Figure 1—*Time course of plasma pentobarbital concentration* (±SD) *in rats pretreated for 10 days with polychlorinated biphenyl-free control diet. Key:* ●, *obtained after intravenous administration of 30 mg of pentobarbital sodium/kg; and* ○, *obtained after oral administration of 30 mg of pentobarbital sodium/kg.*

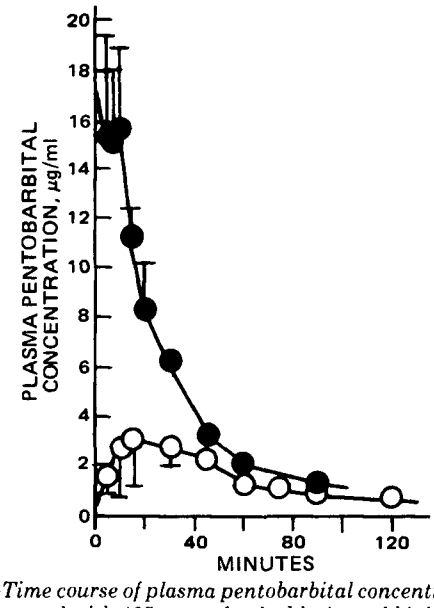

Figure 3—*Time course of plasma pentobarbital concentration* (±SD) *in rats pretreated with 125 ppm of polychlorinated biphenyls in food for 10 days. Key:* ●, *obtained after intravenous administration of 30 mg of pentobarbital sodium/kg; and* ○, *obtained after oral administration of 30 mg of pentobarbital sodium/kg.*

incomplete. Since pentobarbital is well absorbed from the GI tract (26–28) and eliminated almost exclusively (>95%) *via* liver metabolism in the rat (14), the observed reduction in oral bioavailability may be attributed to the first-pass metabolism by the liver, *i.e.*, the first-pass effect.

The disposition profiles of orally and intravenously administered pentobarbital in rats pretreated with 25 or 125 ppm of polychlorinated biphenyls in food for 10 days are given in Figs. 2 and 3. A more pronounced first-pass effect in rats exposed to 25 ppm of polychlorinated biphenyls in food can be discerned from the reduced ratio of the areas under the plasma level–time curves (AUC_{oral}/AUC_{iv}). Rats pretreated with 125 ppm of polychlorinated biphenyls showed an even greater reduction in the *AUC* ratio. This finding indicated an even lower apparent bioavailability of the intact pentobarbital. By comparing AUC_{oral} to AUC_{iv} within a pretreatment group, the effect of clearance in reducing AUC_{iv} when compared to control animals is taken into account.

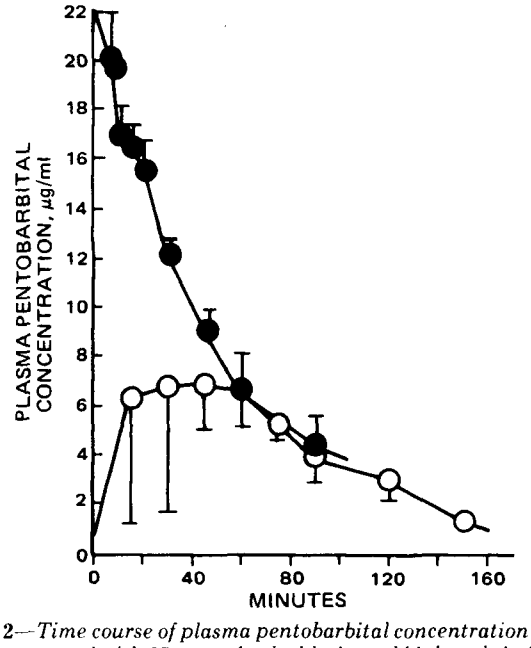

Figure 2—*Time course of plasma pentobarbital concentration* (±SD) *in rats pretreated with 25 ppm of polychlorinated biphenyls in food for 10 days. Key:* ●, *obtained after intravenous administration of 30 mg of pentobarbital sodium/kg; and* ○, *obtained after oral administration of 30 mg of pentobarbital sodium/kg.*

Table I summarizes the pharmacokinetic parameters for intravenously and orally administered pentobarbital in rats pretreated at two levels of polychlorinated biphenyls for 10 days compared to control rats. Pentobarbital was ~76% bioavailable in rats on the control diet. Upon exposure to polychlorinated biphenyls, increases in the degree of the first-pass effect were observed for both the 25- and 125-ppm pretreatments.

The relationship between the systemic availability after oral dosing and the total body clearance for exclusively liver-metabolized drugs was discussed by various investigators (18–24) and is defined by Eqs. 1–4. By rearrangement of Eqs. 1–4, an expression predicting the systemic availability can be obtained using Cl_{TB} values from the intravenous data:

$$\text{systemic availability} = 1 - Cl_{TB}/Q \qquad \text{(Eq. 5)}$$

Table I compares the predicted oral bioavailability for pentobarbital (calculated by Eq. 5 using the Cl_{TB} values from the intravenous data and the blood flow rates, which were calculated from the liver weights and the literature blood flow of 2 ml/min/g of liver) with the experimentally determined oral pentobarbital bioavailabilities for the variously treated animals. The predicted systemic bioavailability of pentobarbital was calculated from the individual Cl_{TB} and calculated Q values for individual animals and not from the mean Cl_{TB} and mean liver blood flow rates. Excellent agreement between the predicted and experimental bioavailability is seen. This result again illustrates the usefulness of intravenous data in assessing apparent systemic availabilities when the drug of interest is eliminated only by liver metabolism (18–24).

Rearrangement of Eqs. 1–4 yields a third expression for computing bioavailability from the liver blood flow rate and intrinsic clearance estimated from oral data:

$$\text{systemic availability} = Q/(Q + Cl_{INT}) \qquad \text{(Eq. 6)}$$

The percent systemic availability values calculated from Eq. 6 were 76.7 ± 2.1, 71.6 ± 3.1 (NS), and 47.8 ± 5.2 ($p < 0.01$) for the control and the 25- and 125-ppm polychlorinated biphenyl-pretreated rats, respectively. Again, these values were calculated from individual animal Q and Cl_{INT} values. These numbers showed excellent agreement with those estimated from the experimental *AUC* ratios.

The total body and intrinsic clearances in Table I were obtained from the dose and the areas under the intravenous and oral plasma level–time curves, respectively, using Eqs. 2 and 3. The induction effects due to polychlorinated biphenyl exposure at the 25- and 125-ppm levels as demonstrated by the Cl_{TB} values increased only by 31 and 193% relative to the controls, respectively. However, the Cl_{INT} values indicate ~47 and

Table I—Pharmacokinetic Parameters [a] for Intravenously and Orally Administered Pentobarbital in Rats Pretreated at Two Levels of Polychlorinated Biphenyls for 10 Days Compared to the Control Animals

Parameter	Control	25-ppm Pretreatment	125-ppm Pretreatment
Cl_{TB} [b], ml/min/kg of body weight	19.3 ± 3.8	25.3 ± 4.0 (NS)	56.5 ± 6.4 ($p < 0.01$) [c]
Cl_{INT} [d], ml/min/kg of body weight	24.4 ± 1.0	35.8 ± 6.7 (NS)	107.3 ± 20.8 ($p < 0.01$) [c]
Liver weight/body weight, %	4.2 ± 0.3	4.3 ± 0.3 (NS)	5.2 ± 0.6 ($p < 0.01$) [c]
Liver blood flow rate [e], ml/min/kg of body weight	82.7 ± 6.2	86.5 ± 6.0 (NS)	106.0 ± 12.2 ($p < 0.01$) [c]
Systemic availability calculated from AUC_{oral}/AUC_{iv} ratios, %	76.0 ± 8.7	71.2 ± 24.2 (NS)	53.9 ± 9.5 ($p < 0.05$) [c]
Systemic availability calculated from Eq. 5, %	77.6 ± 5.0	69.8 ± 2.9 (NS)	49.5 ± 8.3 ($p < 0.01$) [c]

[a] All values are means ± SD ($n = 4$). [b] Calculated from dose/AUC_{iv}. [c] Results are significantly different from the control group of animals at the level indicated. [d] Calculated from dose/AUC_{oral}. [e] Calculated from the literature value of 2.0 ml/min/g of liver.

340% increases over the control values at the 25- and 125-ppm pretreatment levels, respectively. Therefore, the degree of enzyme induction due to exposure to polychlorinated biphenyls is underestimated if only Cl_{TB} values are considered. This point was adequately discussed previously (15).

The relationship of liver blood flow to systemic availability and the clearance terms in Eqs. 5 and 6 provides a means of estimating liver blood flow rates from the experimentally determined bioavailability data. Rearrangement of Eqs. 5 and 6 and Eqs. 1–3 give:

$$Q = \frac{D}{(AUC_{iv})_0^\infty - (AUC_{oral})_0^\infty} \qquad \text{(Eq. 7)}$$

The blood flow rates calculated from Eq. 7 for the present data are given in Table II.

The estimated values compare favorably with the blood flow rates calculated using the literature value of 2 ml/min/g of liver (29). The agreement between the experimental and predicted liver blood flow for the control, 25-, and 125-ppm data supports the possibility of increased liver blood flow with enlarged livers without an increase in the flow per gram of liver.

The hepatic clearance of pentobarbital, the primary route of elimination in rats, can be approximated by the Cl_{TB} value (19, 20, 23). By converting clearances from milliliters per minute per kilogram of body weight to milliliters per minute per gram of liver in individual rats, the relationship between the hepatic clearance (equivalent to the total body clearance in this case) and the intrinsic clearance can be depicted as shown in Fig. 4. The lines represent the relationship between these parameters drawn by substituting a literature blood flow rate of 1.2 ml/min/g of liver (30) and 2 and 3 ml/min/g of liver (29) for Q in Eq. 4. Close agreement between the data points and the prediction using 2 ml/min/g of liver (29) for Q is readily seen and again supports the possibility of increased liver blood flow in polychlorinated biphenyl-treated rats with enlarged livers without an increase in the flow per gram of liver.

The clearance model suggests that substances that are highly extracted by the liver and, therefore, have a high intrinsic clearance relative to the blood flow display a higher sensitivity to blood flow changes. For instance, *d*-propranolol has a high intrinsic clearance (219 ml/min). The enhanced clearance subsequent to phenobarbital treatment is mainly (57%) due to the increase in the hepatic blood flow rate (31). On the other hand, antipyrine has a lower intrinsic clearance (54 ml/min); upon phenobarbital induction, only ~15% of the enhanced clearance results from increased blood flow. At the high level of polychlorinated biphenyl pretreatment, the intrinsic clearance of pentobarbital is increased due to the increased activity of the metabolic enzymes. A higher sensitivity to blood flow changes, reflected by the slightly higher blood flow, therefore is expected to contribute to the enhanced clearance with the 125-ppm pretreatment relative to the 25-ppm pretreatment.

In conclusion, this study showed that hepatic enzyme induction precipitated by environmental factors can significantly affect the bioavailability of drugs that are eliminated largely *via* facile hepatic metabolism. The reduction in the apparent oral bioavailability of pentobarbital in rats increased with the level of polychlorinated biphenyl exposure. As anticipated, the reduction in the apparent bioavailability or the increase in the first-pass effect was more pronounced at the 125-ppm pretreatment level than at the 25-ppm pretreatment level. Although inter- and intraspecies differences do prevail with such dose–effect relationships and extrapolation of the current findings to human subjects may not be valid, the potential clinical implications should not be overlooked. Accidental

Table II—Calculated Liver Blood Flow Rates in Rats Pretreated with Two Doses of Polychlorinated Biphenyls in Food for 10 Days Compared to Control Animals

Liver Blood Flow Rate	Control	25-ppm Pretreatment	125-ppm Pretreatment
Calculated from literature value of 2 ml/min/g of liver	82.7 ± 6.2	86.5 ± 6.0 (NS)	106.0 ± 12.2 ($p < 0.01$)
Calculated from Eq. 7	77.4 [a]	85.8 [a]	121.5 [a]
	1.84 [b]	1.99 [b]	2.33 [b]

[a] Milliliters per minute per kilogram of body weight. [b] Milliliters per minute per gram of liver.

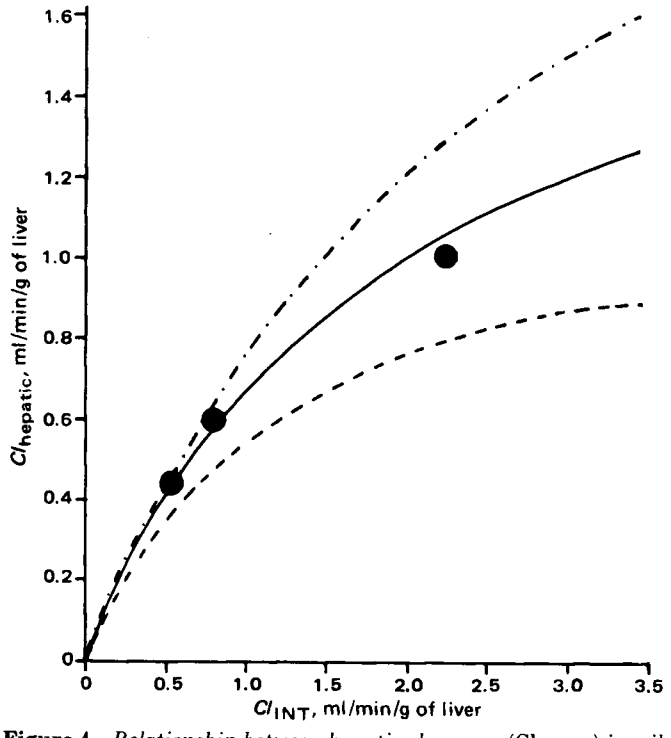

Figure 4—*Relationship between hepatic clearance* ($Cl_{hepatic}$) *in milliliters per minute per gram of liver and intrinsic liver clearance* (Cl_{INT}) *in milliliters per minute per gram of liver. The points are experimentally determined values from oral and intravenous studies, and the lines are for liver blood flow values of 1.2 (– –), 2 (——), and 3 (· – · – ·) ml/min/g of liver.*

exposure of humans to enzyme inducers such as polychlorinated biphenyls may lower the oral bioavailability of facile liver-metabolized drugs and require dosage adjustments.

The apparent agreement of the bioavailability estimation from intravenous or oral data with that determined experimentally from *AUC* values tends to support the validity of the clearance model in assessing systemic availability due to the first-pass effect for drugs exclusively metabolized by the liver. Estimation of the liver blood flow for the control and polychlorinated biphenyl-treated animals showed excellent agreement with literature values. This finding suggests that the blood flow rate on a liver weight basis does not change with induction but that the total hepatic blood flow may be affected by enzyme inducers.

REFERENCES

(1) J. Marniemi, M. Nokkala, H. Vainio, and K. J. W. Hartiala, *Chem. Biol. Interact.*, **18**, 247 (1974).

(2) J. V. Bruckner, K. L. Khanna, and H. H. Cornish, *Toxicol. Appl. Pharmacol.*, **28**, 189 (1974).

(3) K. Akiyama, G. Ohi, K. Fujitani, H. Yagyu, M. Ogino, and T. Kawana, *Bull. Environ. Contam. Toxicol.*, **14**, 588 (1975).

(4) J. V. Bruckner, K. L. Khanna, and H. H. Cornish, *Toxicol. Appl. Pharmacol.*, **24**, 434 (1973).

(5) R. W. Riseborough, P. Riche, D. B. Peakall, S. B. Herman, and M. N. Kirven, *Nature (London)*, **220**, 1098 (1968).

(6) A. P. Alvares and A. Kappas, *Clin. Pharmacol. Ther.*, **22**, 809 (1977).

(7) J. G. Babish and G. S. Stoewsand, *J. Toxicol. Environ. Health*, **3**, 673 (1977).

(8) J. A. Goldstein, P. Hickman, V. W. Burse, and H. Bergman, *Toxicol. Appl. Pharmacol.*, **32**, 461 (1975).

(9) G. J. Stone, D. J. Ecobichon, and O. Hutzinger, *ibid.*, **28**, 66 (1974).

(10) L. S. Birnbaum and M. B. Baird, *Exp. Gerontol.*, **13**, 469 (1978).

(11) J. R. Allen and L. J. Abrahamson, *Arch. Environ. Contam. Toxicol.*, **8**, 191 (1979).

(12) B. B. Brodie, J. J. Burns, L. C. Mard, and P. A. Lief, *J. Pharmacol. Exp. Ther.*, **109**, 26 (1953).

(13) A. H. Conney and J. J. Burns, *Science*, **178**, 576 (1972).

(14) F. W. Ossenberg, M. Peignoux, D. Bourdiau, and J. P. Benhamou, *J. Pharmacol. Exp. Ther.*, **194**, 111 (1975).

(15) V. J. Stella and C. K. Chu, *J. Pharm. Sci.*, **69**, 1274 (1980).

(16) C. K. Chu, V. J. Stella, J. V. Bruckner, and W. D. Jiang, *ibid.*, **66**, 238 (1977).

(17) M. Virolainen, *Transplantation*, **5**, 1530 (1967).

(18) M. Gibaldi and D. Perrier, "Pharmacokinetics," Dekker, New York, N.Y., 1975, p. 293.

(19) D. Perrier and M. Gibaldi, *J. Pharmacol. Exp. Ther.*, **191**, 17 (1974).

(20) D. M. Kornhauser, A. J. J. Wood, R. E. Vestal, G. R. Wilkinson, R. A. Branch, and D. G. Shand, *Clin. Pharmacol. Ther.*, **23**, 165 (1978).

(21) M. Gibaldi, R. N. Boyes, and S. Feldman, *J. Pharm. Sci.*, **60**, 1338 (1971).

(22) W. A. Colburn and M. Gibaldi, *Drug. Metab. Disp.*, **6**, 193 (1978).

(23) M. Rowland, *J. Pharm. Sci.*, **61**, 70 (1972).

(24) M. Rowland, L. Z. Benet, and G. G. Graham, *J. Pharmacokinet. Biopharm.*, **1**, 123 (1973).

(25) B. J. Winer, "Statistical Principles in Experimental Design," McGraw-Hill, New York, N.Y., 1962, pp. 89–91.

(26) A. Hume, M. Bush, J. Renick, and B. H. Douglas, *Arch. Int. Pharmacodyn. Ther.*, **171**, 122 (1968).

(27) K. Kakemi, T. Arita, R. Hori, and R. Konishi, *Chem. Pharm. Bull.*, **15**, 1883 (1967).

(28) *Ibid.*, **15**, 1705 (1967).

(29) K. S. Pang and J. R. Gillette, *Drug Metab. Disp.*, **6**, 567 (1978).

(30) J. Grayson and D. Mendel, "Physiology of the Sphlanchnic Circulation," Williams & Wilkins, Baltimore, Md., 1965, p. 74.

(31) R. Schulte-Hermann, *CRC Crit. Rev. Toxicol.*, **3**, 97 (1974).

ACKNOWLEDGMENTS

Supported by National Institutes of Health Grant GM 22357.

The authors thank Dr. J. V. Bruckner for the Aroclor 1254 and Dr. G. Schlager, Dr. Y. Yamaoka, and Dr. K. Yamaoka for help with the statistics.

Effects of Antibiotics on Platelet Functions in Human Plasma *In Vitro* and Dog Plasma *In Vivo*

M. I. GENUA *, J. GIRALDEZ *, E. ROCHA *x, and A. MONGE ‡

Received November 20, 1979, from the **Clínica Universitaria and the* ‡*Facultad de Farmacia, Universidad de Navarra, Pamplona, Spain.* Accepted for publication May 1, 1980.

Abstract □ The effects of 31 antibiotics on platelet aggregation in human plasma in the presence of adenosine 5′-diphosphate were studied. The marked activity of tetracycline hydrochloride led to a study of its effects on various platelet functions *in vivo* in dogs.

Keyphrases □ Antibiotics—effects on platelet functions □ Platelet aggregation—effect of antibiotics

Many compounds, including some antibiotics (1–6), interfere with platelet activity under certain conditions. The present investigation was concerned with whether antibiotics in current clinical use affect platelet aggregation, either *in vitro* in human plasma or *in vivo* in dog plasma. When such an effect was found, the mechanism was studied; the investigation was broadened to include other platelet functions such as platelet adhesiveness, platelet factor 3 liberation, platelet mobility in an electric field, and the aggregation of platelets filtered in Sepharose gel.

EXPERIMENTAL

The *in vitro* experiments were carried out with plasma from apparently healthy subjects. The aggregation results correspond to the mean values of at least three trials.

The *in vivo* experiments were carried out on five dogs with similar physical characteristics. The results correspond to the mean values of three trials.

Plasma Samples—Human plasma samples were obtained by forearm venipuncture. The blood was collected in silanized tubes containing 3.8% sodium citrate (1:9) to obtain both platelet-rich plasma and platelet-poor plasma for the aggregation studies.

Dog plasma samples were obtained in a similar manner from mongrel dogs weighing 16–20 kg.

Platelet-rich plasma was obtained by sedimentation or centrifugation of samples at 800 rpm for 10 min for human plasma and for 8 min for dog

0022-3549/80/1100-1282$01.00/0

© 1980, American Pharmaceutical Association

exposure of humans to enzyme inducers such as polychlorinated biphenyls may lower the oral bioavailability of facile liver-metabolized drugs and require dosage adjustments.

The apparent agreement of the bioavailability estimation from intravenous or oral data with that determined experimentally from *AUC* values tends to support the validity of the clearance model in assessing systemic availability due to the first-pass effect for drugs exclusively metabolized by the liver. Estimation of the liver blood flow for the control and polychlorinated biphenyl-treated animals showed excellent agreement with literature values. This finding suggests that the blood flow rate on a liver weight basis does not change with induction but that the total hepatic blood flow may be affected by enzyme inducers.

REFERENCES

(1) J. Marniemi, M. Nokkala, H. Vainio, and K. J. W. Hartiala, *Chem. Biol. Interact.*, **18**, 247 (1974).

(2) J. V. Bruckner, K. L. Khanna, and H. H. Cornish, *Toxicol. Appl. Pharmacol.*, **28**, 189 (1974).

(3) K. Akiyama, G. Ohi, K. Fujitani, H. Yagyu, M. Ogino, and T. Kawana, *Bull. Environ. Contam. Toxicol.*, **14**, 588 (1975).

(4) J. V. Bruckner, K. L. Khanna, and H. H. Cornish, *Toxicol. Appl. Pharmacol.*, **24**, 434 (1973).

(5) R. W. Riseborough, P. Riche, D. B. Peakall, S. B. Herman, and M. N. Kirven, *Nature (London)*, **220**, 1098 (1968).

(6) A. P. Alvares and A. Kappas, *Clin. Pharmacol. Ther.*, **22**, 809 (1977).

(7) J. G. Babish and G. S. Stoewsand, *J. Toxicol. Environ. Health*, **3**, 673 (1977).

(8) J. A. Goldstein, P. Hickman, V. W. Burse, and H. Bergman, *Toxicol. Appl. Pharmacol.*, **32**, 461 (1975).

(9) G. J. Stone, D. J. Ecobichon, and O. Hutzinger, *ibid.*, **28**, 66 (1974).

(10) L. S. Birnbaum and M. B. Baird, *Exp. Gerontol.*, **13**, 469 (1978).

(11) J. R. Allen and L. J. Abrahamson, *Arch. Environ. Contam. Toxicol.*, **8**, 191 (1979).

(12) B. B. Brodie, J. J. Burns, L. C. Mard, and P. A. Lief, *J. Pharmacol. Exp. Ther.*, **109**, 26 (1953).

(13) A. H. Conney and J. J. Burns, *Science*, **178**, 576 (1972).

(14) F. W. Ossenberg, M. Peignoux, D. Bourdiau, and J. P. Benhamou, *J. Pharmacol. Exp. Ther.*, **194**, 111 (1975).

(15) V. J. Stella and C. K. Chu, *J. Pharm. Sci.*, **69**, 1274 (1980).

(16) C. K. Chu, V. J. Stella, J. V. Bruckner, and W. D. Jiang, *ibid.*, **66**, 238 (1977).

(17) M. Virolainen, *Transplantation*, **5**, 1530 (1967).

(18) M. Gibaldi and D. Perrier, "Pharmacokinetics," Dekker, New York, N.Y., 1975, p. 293.

(19) D. Perrier and M. Gibaldi, *J. Pharmacol. Exp. Ther.*, **191**, 17 (1974).

(20) D. M. Kornhauser, A. J. J. Wood, R. E. Vestal, G. R. Wilkinson, R. A. Branch, and D. G. Shand, *Clin. Pharmacol. Ther.*, **23**, 165 (1978).

(21) M. Gibaldi, R. N. Boyes, and S. Feldman, *J. Pharm. Sci.*, **60**, 1338 (1971).

(22) W. A. Colburn and M. Gibaldi, *Drug. Metab. Disp.*, **6**, 193 (1978).

(23) M. Rowland, *J. Pharm. Sci.*, **61**, 70 (1972).

(24) M. Rowland, L. Z. Benet, and G. G. Graham, *J. Pharmacokinet. Biopharm.*, **1**, 123 (1973).

(25) B. J. Winer, "Statistical Principles in Experimental Design," McGraw-Hill, New York, N.Y., 1962, pp. 89–91.

(26) A. Hume, M. Bush, J. Renick, and B. H. Douglas, *Arch. Int. Pharmacodyn. Ther.*, **171**, 122 (1968).

(27) K. Kakemi, T. Arita, R. Hori, and R. Konishi, *Chem. Pharm. Bull.*, **15**, 1883 (1967).

(28) *Ibid.*, **15**, 1705 (1967).

(29) K. S. Pang and J. R. Gillette, *Drug Metab. Disp.*, **6**, 567 (1978).

(30) J. Grayson and D. Mendel, "Physiology of the Sphlanchnic Circulation," Williams & Wilkins, Baltimore, Md., 1965, p. 74.

(31) R. Schulte-Hermann, *CRC Crit. Rev. Toxicol.*, **3**, 97 (1974).

ACKNOWLEDGMENTS

Supported by National Institutes of Health Grant GM 22357.

The authors thank Dr. J. V. Bruckner for the Aroclor 1254 and Dr. G. Schlager, Dr. Y. Yamaoka, and Dr. K. Yamaoka for help with the statistics.

Effects of Antibiotics on Platelet Functions in Human Plasma *In Vitro* and Dog Plasma *In Vivo*

M. I. GENUA *, J. GIRALDEZ *, E. ROCHA *x, and A. MONGE ‡

Received November 20, 1979, from the **Clínica Universitaria and the* ‡*Facultad de Farmacia, Universidad de Navarra, Pamplona, Spain.* Accepted for publication May 1, 1980.

Abstract □ The effects of 31 antibiotics on platelet aggregation in human plasma in the presence of adenosine 5′-diphosphate were studied. The marked activity of tetracycline hydrochloride led to a study of its effects on various platelet functions *in vivo* in dogs.

Keyphrases □ Antibiotics—effects on platelet functions □ Platelet aggregation—effect of antibiotics

Many compounds, including some antibiotics (1–6), interfere with platelet activity under certain conditions. The present investigation was concerned with whether antibiotics in current clinical use affect platelet aggregation, either *in vitro* in human plasma or *in vivo* in dog plasma. When such an effect was found, the mechanism was studied; the investigation was broadened to include other platelet functions such as platelet adhesiveness, platelet factor 3 liberation, platelet mobility in an electric field, and the aggregation of platelets filtered in Sepharose gel.

EXPERIMENTAL

The *in vitro* experiments were carried out with plasma from apparently healthy subjects. The aggregation results correspond to the mean values of at least three trials.

The *in vivo* experiments were carried out on five dogs with similar physical characteristics. The results correspond to the mean values of three trials.

Plasma Samples—Human plasma samples were obtained by forearm venipuncture. The blood was collected in silanized tubes containing 3.8% sodium citrate (1:9) to obtain both platelet-rich plasma and platelet-poor plasma for the aggregation studies.

Dog plasma samples were obtained in a similar manner from mongrel dogs weighing 16–20 kg.

Platelet-rich plasma was obtained by sedimentation or centrifugation of samples at 800 rpm for 10 min for human plasma and for 8 min for dog

0022-3549/80/1100-1282$01.00/0

© 1980, American Pharmaceutical Association

Table I—Percent Inhibition of Human Platelet Aggregation Induced by Adenosine 5′-Diphosphate *In Vitro*[a]

Compound	*a*, mg/ml	*A*	*b*, mg/ml	*B*
Penicillin G sodium	12	70	0.12	10
Penicillin G potassium	8	95	0.08	10
Penicillin G benzathine	30	100	0.3	10
Cloxacillin sodium	14.28	80	0.14	0
Ampicillin sodium	25	100	0.25	0
Metampicillin sodium	16.6	100	0.16	0
Carbenicillin disodium	28.5	90	0.28	0
Cephalothin sodium	25	100	0.25	0
Cephaloridine	33.3	70	0.33	25
Cefazolin	25	85	0.25	10
Cephapirin sodium	10	75	0.1	10
Cephacetrile	40	90	0.4	0
Cephradine	50	100	0.5	10
Cefamandole	10	100	0.1	0
Cefoxitin	100	95	1	15
Streptomycin sulfate	25	55	0.25	0
Kanamycin sulfate	25	100	0.25	0
Gentamicin sulfate	4	100	0.04	0
Amikacin sulfate	25	100	0.25	10
Dibekacin sulfate	1.25	100	0.01	0
Colistin sulfate	1.13	0	0.01	0
Lincomycin hydrocloride	30	100	0.3	15
Rifamycin sodium	7.57	100	0.07	20
Spectinomycin	62.5	100	0.62	0
Tetracycline hydrochloride	12.5	100	0.12	30
Oxytetracycline	5	100	0.05	10
Erythromycin	5	100	0.05	0
Chloramphenicol	10	100	0.1	0
Fosfomycin	25	100	0.25	0
Vancomycin	5	100	0.05	10
Amphotericin B	0.5	100	0.005	20

[a] The *a* value is 10% of the concentration of the drug in its dosage form, *A* is the percent inhibition of adenosine 5′-diphosphate-induced platelet aggregation by the antibiotic at concentration *a*, *b* is the maximum concentration that the drug reaches in human plasma through the administration of a therapeutic dose, and *B* is the percent inhibition of adenosine 5′-diphosphate-induced platelet aggregation by the antibiotic at concentration *b*.

plasma, with platelet-poor plasma added to give a concentration of 250,000 platelets/mm^3.

Platelet-poor plasma was obtained by centrifugation of human and dog samples at 4000 rpm for 30 min.

Antibiotics—The 31 antibiotics used were penicillin G sodium, penicillin G potassium, penicillin G benzathine, cloxacillin sodium, ampicillin sodium, metampicillin sodium, carbenicillin disodium, cephalothin sodium, cephaloridine, cefazolin, cephapirin sodium, cephacetrile, cephradine, cefamandole, cefoxitin, streptomycin sulfate, kanamycin sulfate, gentamicin sulfate, amikacin sulfate, dibekacin sulfate, colistin sulfate, lincomycin hydrochloride, rifamycin sodium, spectinomycin, tetracycline hydrochloride, oxytetracycline, erythromycin, chloramphenicol, fosfomycin, vancomycin, and amphotericin B[1].

Aggregating Agents—Adenosine 5′-diphosphate was used at a concentration of 2×10^{-5} *M* in pH 7.4 phosphate buffer for the *in vitro* tests and at 10^{-4} *M* in pH 7.4 phosphate buffer for the *in vivo* tests. Epinephrine at a concentration of 10^{-4} *M* in phosphate buffer was used. An initial collagen solution was prepared by the addition of 5 ml of 0.1 *N* acetic acid (pH 3.5) to 10 mg of collagen, followed by dilution with pH 7.4 phosphate buffer to give a final concentration of 0.2 mg of collagen/ml. The solution then was incubated at 37° for at least 30 min until opalescence was observed.

Platelet Aggregation—Platelet aggregation was measured by the absorbance method of Born and Cross (7) using a platelet aggregation meter[2,3].

In the *in vitro* tests[2], 0.1 ml of the test sample was added to a polyethylene cell containing 0.8 ml of platelet-rich plasma. The cell was incubated for 90 sec at 37°. At this point, 0.1 ml of a solution of adenosine 5′-diphosphate, epinephrine, or collagen in buffer was added.

[1] The trade names are Unicilina, Cidan-cilina, Bencetacil Simple, Orbenin, Cilleral, Actuapen, Pyopen, Keflin, Kefloridine, Cefamecin, Brisfirina, Celospor, Velocef, Mandokef, Mefoxitin, Neodual Estrepto, Kanahidro, Genticina, Biclin, Klobamicina, Colimicina, Lincocin, Rifocina, Kempi, Tetralen, Terramicina, Pantomicina, Chloromycetin, Fosfocina, Diatracin, and Fungizona, respectively.

[2] Evans EE1 169.

[3] Dual-channel Aggro-Meter.

Table II—Percent Inhibition of Human Platelet Aggregation Induced by Adenosine 5′-Diphosphate, Epinephrine, and Collagen *In Vitro*

Antibiotic	Adenosine 5′-Diphosphate	Epinephrine	Collagen
Cephaloridine	25	0	15
Rifamycin sulfate	20	5	15
Tetracycline hydrochloride	30	10	55
Amphotericin B	20	0	30

In the *in vivo* tests[3], 0.05 ml of the aggregating agent was added to 0.4 ml of platelet-rich dog plasma treated with tetracycline, using a procedure similar to that used for the *in vitro* tests.

Platelet Factor 3—The liberation of platelet factor 3 was studied by the Hardisty–Hutton method (8).

Platelet Electrophoretic Mobility—Alteration in the charge of the platelet cell membrane was studied by the determination of platelet mobility in an electric field using a cytopherometer[4]. Platelet-rich dog plasma (0.5 ml) was diluted with 9.5 ml of isotonic saline. The time required for platelets to travel a specified distance at the current strength used was determined.

Platelet Adhesiveness—Platelet adhesiveness was determined by the method of Salzman (9).

Platelet Filtration—Silanized K 15/30 columns, 30 cm × 1.5 cm i.d.[5], were used. Nylon filters with 40-μm diameter pores were placed in the bottom of the columns. The 2B Sepharose gel[5] was dissolved 1:4 in normal saline, kept at 4° for 24 hr, and cleared of bubbles before use.

The columns were filled with the gel to a height of ~16 cm. Then 6 ml of normal saline was added to cover the gel until the columns were used. From 4 to 6 ml of platelet-rich plasma was used for each filtration, which was carried out at a rate of 6–9 drops/min. The eluate was collected in 2-ml fractions in polyethylene tubes in ethylenediaminetetraacetic acid (0.077 *M*) and subsequently was centrifuged for 20 min at 3000 rpm.

The sedimented platelets were diluted with phosphate buffer to a final concentration of 400,000 platelets/mm^3. The aggregation of normal filtered platelets in plasma from dogs treated with tetracycline and of platelets from untreated dogs was studied, and the results were compared.

Statistical Analysis—The statistical analysis was performed using a *t* test.

RESULTS AND DISCUSSION

Most of the antibiotics studied inhibited the aggregation of platelets induced by 2×10^{-5} *M* adenosine 5′-diphosphate (Table I) at 10% of the concentration of the dosage form. At the maximum drug concentration in human plasma after the administration of a therapeutic dose, four drugs (cephaloridine, rifamycin sodium, tetracycline hydrochloride, and amphotericin B) inhibited adenosine 5′-diphosphate-induced aggregation by more than 20% and only one compound (tetracycline hydrochloride) clearly maintained its inhibitory effect *in vitro* in the presence of epinephrine (10%) and collagen (55%) (Table II).

The study of the various aggregating agents in dog blood led to the

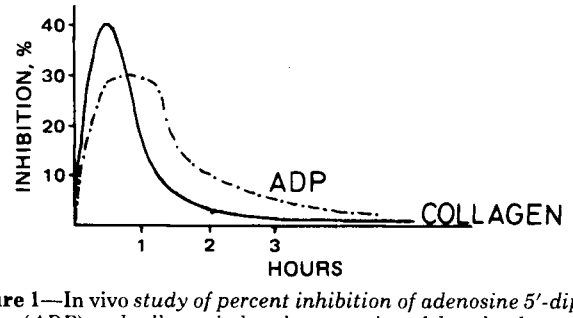

Figure 1—In vivo *study of percent inhibition of adenosine 5′-diphosphate- (ADP) and collagen-induced aggregation of dog platelets treated with tetracycline hydrochloride according to the time elapsed since its administration.*

[4] Zeiss 477500.

[5] Pharmacia, Uppsala, Sweden.

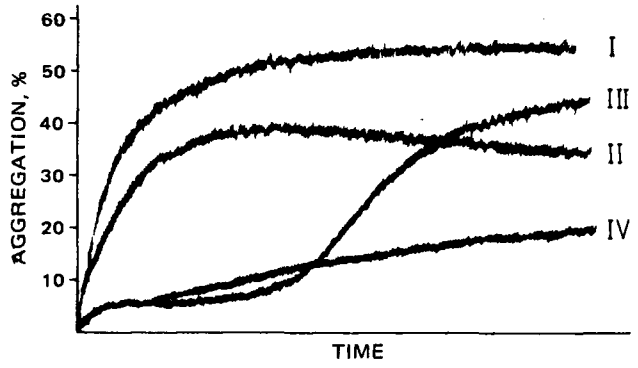

Figure 2—*Aggregation induced by adenosine 5′-diphosphate in filtered dog platelets (I) and in filtered dog platelets previously treated with tetracycline hydrochloride (II) and aggregation induced by collagen in filtered dog platelets (III) and in filtered dog platelets previously treated with tetracycline hydrochloride (IV).*

conclusion that solutions of 10^{-4} *M* adenosine 5′-diphosphate gave identical results to solutions of 2×10^{-5} *M* adenosine 5′-diphosphate in human plasma. The 0.2-mg/ml collagen solutions used in human plasma gave similar results in dog plasma, although the latency period for aggregation with platelet-rich dog plasma was approximately twice that obtained with platelet-rich human plasma. No significant aggregation in platelet-rich dog plasma was obtained with epinephrine, so this aggregating agent was not used for *in vivo* tests in dogs.

Platelet aggregation *in vivo* was studied at 0, 30, 60, and 90 min and 2, 24, 48, and 72 hr after intramuscular administration of tetracycline hydrochloride. As shown in Fig. 1, tetracycline hydrochloride inhibited 40% of collagen-induced platelet aggregation in blood extracted 30 min after the intramuscular administration of 5 mg of antibiotic/kg and 30% of adenosine 5′-diphosphate-induced platelet aggregation in blood extracted 30 and 45 min after a similar dose of the antibiotic. Platelet factor 3 values in dog plasma were similar to those found in human plasma. In dogs treated with tetracycline hydrochloride, factor 3 release was decreased significantly ($p < 0.0001$), with a mean value of 32.5 sec, compared to liberation in untreated dogs, where the mean value was 26 sec.

Electrophoretic mobility was identical for platelets from treated and untreated dogs, indicating unaltered platelet membrane potentials. The results were $x/N = 12.65 \pm 0.05$ and $x_1/N = 13.15 \pm 0.05$, where x is the time required for dog platelets to travel 64 μm (32 μm to the left and 32 μm to the right by varying the polarity), x_1 is the time required for tetracycline-treated dog platelets to travel the same distance, and N is the number of determinations (in this case, 20).

To determine whether the alteration in platelet aggregation produced by tetracycline was due to the platelets themselves or to the surrounding plasma, the platelets were filtered. The activity of normal filtered platelets with tetracycline-treated dog plasma and of tetracycline-treated platelets with untreated dog plasma in the presence of adenosine 5′-diphosphate and collagen was studied; the aggregation of untreated filtered platelets was greater than that of tetracycline-treated platelets (30% inhibition in the presence of adenosine 5′-diphosphate and 85% in the presence of collagen) (Fig. 2).

In conclusion, high concentrations of antibiotics usually completely inhibit the *in vitro* aggregation of platelets induced by adenosine 5′-diphosphate. At concentrations equivalent to plasma levels after administration of a therapeutic dose, only cephaloridine, rifamycin sodium, tetracycline hydrochloride, and amphotericin B partially inhibit adenosine 5′-diphosphate-induced aggregation and only tetracycline hydrochloride maintains this activity in the presence of other aggregating agents. In addition, tetracycline hydrochloride exerts an inhibitory effect *in vivo* on platelet aggregation in dog blood, affecting the platelets themselves and not the surrounding plasma, as shown by the results obtained with platelets filtered in Sepharose columns. It appears to alter the liberation of platelet factor 3.

REFERENCES

(1) J. P. Cazenave, M. A. Guccione, M. A. Packham, and J. F. Mustard, *Br. J. Haematol.*, **35**, 135 (1977).

(2) K. Andrassy, E. Ritz, B. Hasper, M. Scherz, E. Walter, H. Storch, and W. Vomel, *Lancet*, **1**, 1039 (1976).

(3) L. Houbouyan, J. F. Stolz, and A. Goguel, *Acta Haematol.*, **53**, 300 (1975).

(4) J. P. Cazenave, M. A. Packham, M. A. Guccione, and J. F. Mustard, *Proc. Soc. Exp. Biol. Med.*, **142**, 159 (1973).

(5) J. F. Mustard and M. A. Packham, *Chem. Pharmacol.*, **22**, 3151 (1973).

(6) H. Johnson and P. M. Niklassom, *Thromb. Res.*, **11**, 237 (1977).

(7) G. V. R. Born and M. J. Cross, *J. Physiol.*, **168**, 178 (1963).

(8) R. M. Hardisty and R. A. Hutton, *Br. J. Haematol.*, **11**, 258 (1965).

(9) E. W. Salzman, *J. Lab. Clin. Med.*, **62**, 724 (1963).

ACKNOWLEDGMENTS

Supported by a grant from the Comisión Asesora de Investigación Cientifica y Técnica, Spain.

Binding of Toxic Metabolites of Isoniazid by Aconiazide

HANS R. HELD * and SILVIO LANDI *‡x

Received October 17, 1979, from **Connaught Laboratories Limited, Willowdale, Ontario, Canada*, and the ‡*Faculty of Medicine, University of Toronto, Toronto, Ontario, Canada.* Accepted for publication May 12, 1980.

Abstract □ Isoniazid, the hydrazide of isonicotinic acid, is widely used in the treatment and prophylaxis of tuberculosis. The toxicity and carcinogenicity of isoniazid have been attributed to the action of its metabolites, hydrazine and acetylhydrazine. Aconiazide, the isonicotinylhydrazone of 2-formylphenoxyacetic acid, has been used in the treatment and prophylaxis of tuberculosis. Aconiazide is hydrolyzed in the body to isoniazid and 2-formylphenoxyacetic acid. 2-Formylphenoxyacetic acid has been shown to bind hydrazine and acetylhydrazine. This binding could explain the lower toxicity of aconiazide and also could provide a reason for postulating its lack of carcinogenicity.

Keyphrases □ Isoniazid—binding of toxic metabolites by aconiazide □ Aconiazide—binding of toxic metabolites of isoniazid, potential as antitubercular agent □ Antitubercular agents, potential—aconiazide, binding of toxic metabolites of isoniazid

Isoniazid (isonicotinic acid hydrazide) was introduced in 1952 as a drug for the treatment of tuberculosis and it soon became recognized as the most effective drug for the treatment and prevention of tuberculosis. It later became apparent that prolonged treatment with isoniazid may affect the peripheral and central nervous systems, and

0022-3549/80/1100-1284$01.00/0
© 1980, American Pharmaceutical Association

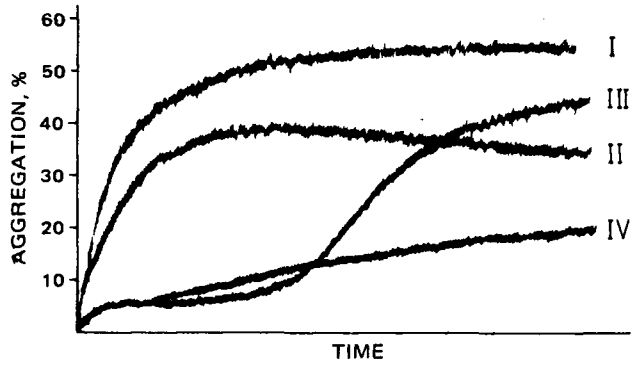

Figure 2—*Aggregation induced by adenosine 5′-diphosphate in filtered dog platelets (I) and in filtered dog platelets previously treated with tetracycline hydrochloride (II) and aggregation induced by collagen in filtered dog platelets (III) and in filtered dog platelets previously treated with tetracycline hydrochloride (IV).*

conclusion that solutions of 10^{-4} *M* adenosine 5′-diphosphate gave identical results to solutions of 2×10^{-5} *M* adenosine 5′-diphosphate in human plasma. The 0.2-mg/ml collagen solutions used in human plasma gave similar results in dog plasma, although the latency period for aggregation with platelet-rich dog plasma was approximately twice that obtained with platelet-rich human plasma. No significant aggregation in platelet-rich dog plasma was obtained with epinephrine, so this aggregating agent was not used for *in vivo* tests in dogs.

Platelet aggregation *in vivo* was studied at 0, 30, 60, and 90 min and 2, 24, 48, and 72 hr after intramuscular administration of tetracycline hydrochloride. As shown in Fig. 1, tetracycline hydrochloride inhibited 40% of collagen-induced platelet aggregation in blood extracted 30 min after the intramuscular administration of 5 mg of antibiotic/kg and 30% of adenosine 5′-diphosphate-induced platelet aggregation in blood extracted 30 and 45 min after a similar dose of the antibiotic. Platelet factor 3 values in dog plasma were similar to those found in human plasma. In dogs treated with tetracycline hydrochloride, factor 3 release was decreased significantly ($p < 0.0001$), with a mean value of 32.5 sec, compared to liberation in untreated dogs, where the mean value was 26 sec.

Electrophoretic mobility was identical for platelets from treated and untreated dogs, indicating unaltered platelet membrane potentials. The results were $x/N = 12.65 \pm 0.05$ and $x_1/N = 13.15 \pm 0.05$, where x is the time required for dog platelets to travel 64 μm (32 μm to the left and 32 μm to the right by varying the polarity), x_1 is the time required for tetracycline-treated dog platelets to travel the same distance, and N is the number of determinations (in this case, 20).

To determine whether the alteration in platelet aggregation produced by tetracycline was due to the platelets themselves or to the surrounding plasma, the platelets were filtered. The activity of normal filtered platelets with tetracycline-treated dog plasma and of tetracycline-treated platelets with untreated dog plasma in the presence of adenosine 5′-diphosphate and collagen was studied; the aggregation of untreated filtered platelets was greater than that of tetracycline-treated platelets (30% inhibition in the presence of adenosine 5′-diphosphate and 85% in the presence of collagen) (Fig. 2).

In conclusion, high concentrations of antibiotics usually completely inhibit the *in vitro* aggregation of platelets induced by adenosine 5′-diphosphate. At concentrations equivalent to plasma levels after administration of a therapeutic dose, only cephaloridine, rifamycin sodium, tetracycline hydrochloride, and amphotericin B partially inhibit adenosine 5′-diphosphate-induced aggregation and only tetracycline hydrochloride maintains this activity in the presence of other aggregating agents. In addition, tetracycline hydrochloride exerts an inhibitory effect *in vivo* on platelet aggregation in dog blood, affecting the platelets themselves and not the surrounding plasma, as shown by the results obtained with platelets filtered in Sepharose columns. It appears to alter the liberation of platelet factor 3.

REFERENCES

(1) J. P. Cazenave, M. A. Guccione, M. A. Packham, and J. F. Mustard, *Br. J. Haematol.*, **35**, 135 (1977).

(2) K. Andrassy, E. Ritz, B. Hasper, M. Scherz, E. Walter, H. Storch, and W. Vomel, *Lancet*, **1**, 1039 (1976).

(3) L. Houbouyan, J. F. Stolz, and A. Goguel, *Acta Haematol.*, **53**, 300 (1975).

(4) J. P. Cazenave, M. A. Packham, M. A. Guccione, and J. F. Mustard, *Proc. Soc. Exp. Biol. Med.*, **142**, 159 (1973).

(5) J. F. Mustard and M. A. Packham, *Chem. Pharmacol.*, **22**, 3151 (1973).

(6) H. Johnson and P. M. Niklassom, *Thromb. Res.*, **11**, 237 (1977).

(7) G. V. R. Born and M. J. Cross, *J. Physiol.*, **168**, 178 (1963).

(8) R. M. Hardisty and R. A. Hutton, *Br. J. Haematol.*, **11**, 258 (1965).

(9) E. W. Salzman, *J. Lab. Clin. Med.*, **62**, 724 (1963).

ACKNOWLEDGMENTS

Supported by a grant from the Comisión Asesora de Investigación Cientifica y Técnica, Spain.

Binding of Toxic Metabolites of Isoniazid by Aconiazide

HANS R. HELD * and SILVIO LANDI *‡x

Received October 17, 1979, from **Connaught Laboratories Limited, Willowdale, Ontario, Canada*, and the ‡*Faculty of Medicine, University of Toronto, Toronto, Ontario, Canada.* Accepted for publication May 12, 1980.

Abstract □ Isoniazid, the hydrazide of isonicotinic acid, is widely used in the treatment and prophylaxis of tuberculosis. The toxicity and carcinogenicity of isoniazid have been attributed to the action of its metabolites, hydrazine and acetylhydrazine. Aconiazide, the isonicotinylhydrazone of 2-formylphenoxyacetic acid, has been used in the treatment and prophylaxis of tuberculosis. Aconiazide is hydrolyzed in the body to isoniazid and 2-formylphenoxyacetic acid. 2-Formylphenoxyacetic acid has been shown to bind hydrazine and acetylhydrazine. This binding could explain the lower toxicity of aconiazide and also could provide a reason for postulating its lack of carcinogenicity.

Keyphrases □ Isoniazid—binding of toxic metabolites by aconiazide □ Aconiazide—binding of toxic metabolites of isoniazid, potential as antitubercular agent □ Antitubercular agents, potential—aconiazide, binding of toxic metabolites of isoniazid

Isoniazid (isonicotinic acid hydrazide) was introduced in 1952 as a drug for the treatment of tuberculosis and it soon became recognized as the most effective drug for the treatment and prevention of tuberculosis. It later became apparent that prolonged treatment with isoniazid may affect the peripheral and central nervous systems, and

0022-3549/80/1100-1284$01.00/0
© 1980, American Pharmaceutical Association

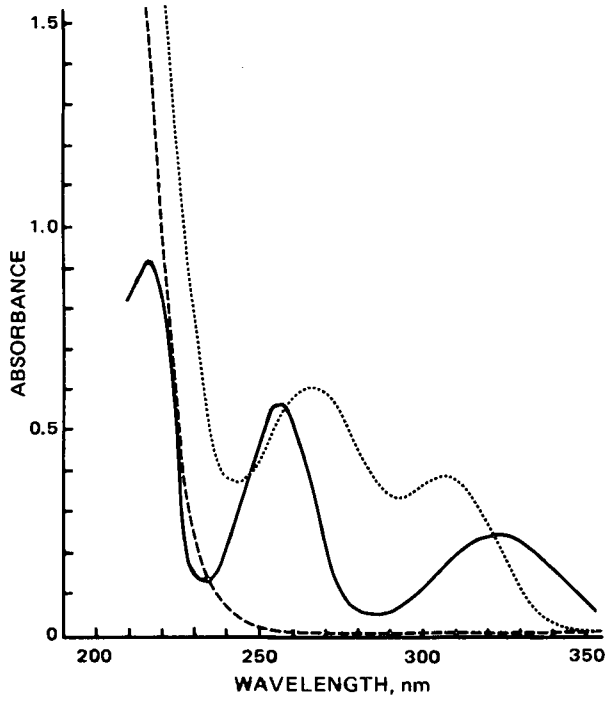

Figure 1—*UV spectra of 2-formylphenoxyacetic acid (0.05 mM) (—), hydrazine (25 mM) (– –), and a mixture of 2-formylphenoxyacetic acid (0.05 mM) and hydrazine (25 mM) (• • •). The spectra were taken within 2 min after the solutions were prepared in 0.1% $NaHCO_3$.*

numerous reports indicated that isoniazid could induce hepatitis (1, 2). Furthermore, it has been well established that isoniazid is carcinogenic in animals (3).

Isoniazid (I) is metabolized to isonicotinyl acetylhydrazine (II), which is metabolized further to isonicotinic acid (III), acetylhydrazine (IV), and hydrazine (V). Free IV and V undergo enzymatic conversion to hepatotoxic (4) and carcinogenic products (3). Therefore, there is obviously a need for antituberculous drugs with the same efficacy as I but with no carcinogenicity and reduced toxicity.

In a search for such drugs, many derivatives of I have been prepared. One compound, aconiazide (the isonicotinylhydrazone of 2-formylphenoxyacetic acid, VI) (5–12),

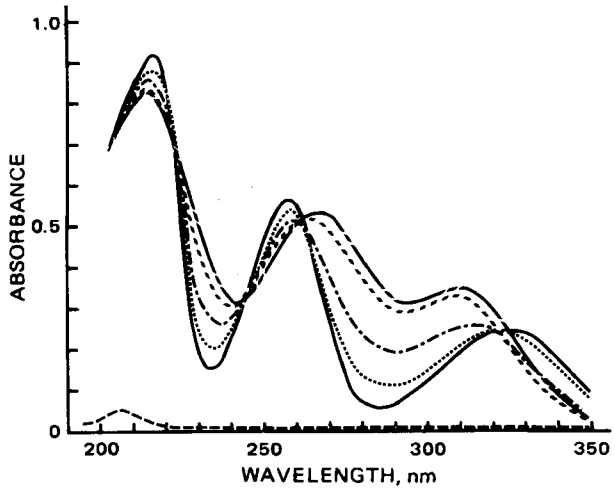

Figure 2—*UV spectra of 2-formylphenoxyacetic acid (0.05 mM) (—), hydrazine (0.05 mM) (– –), and a mixture of the two compounds taken after 30 min (• • •), 4 hr (• – •), 24 hr (– – –), and 3 days (— – —) after its preparation. All solutions were prepared in 0.1% $NaHCO_3$.*

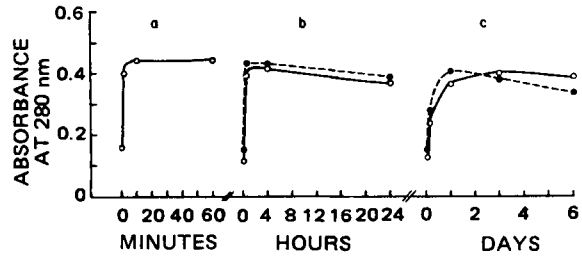

Figure 3—*Reaction of 2-formylphenoxyacetic acid (0.05 mM) with different concentrations of hydrazine in 0.1% $NaHCO_3$ at 23 (—) and 37° (– –). Key: a, 5 mM; b, 0.5 mM; and c, 0.05 mM.*

formed from I and 2-formylphenoxyacetic acid (VII), showed antituberculous activity in animals (6) and humans (8) equivalent to that of I and had a much lower toxicity (5, 7, 8). Aconiazide[1] was used in humans in Canada as a substitute for I (8). The manufacturing of this antituberculous drug was discontinued for economic reasons, although it is still listed in the Compendium of Pharmaceuticals and Specialties (9). However, economic considerations alone should not prevent the use of an antituberculous drug that may have no carcinogenic activity and reduced side effects as compared with I. Therefore, studies were undertaken to determine if the carcinogenic metabolites (IV and V) of I could be bound and hence inactivated by VII, which is a component of VI.

EXPERIMENTAL

Reagents—Isoniazid[2] (I) (mol. wt. 137.14), aconiazide[3] (VI) (mol. wt.

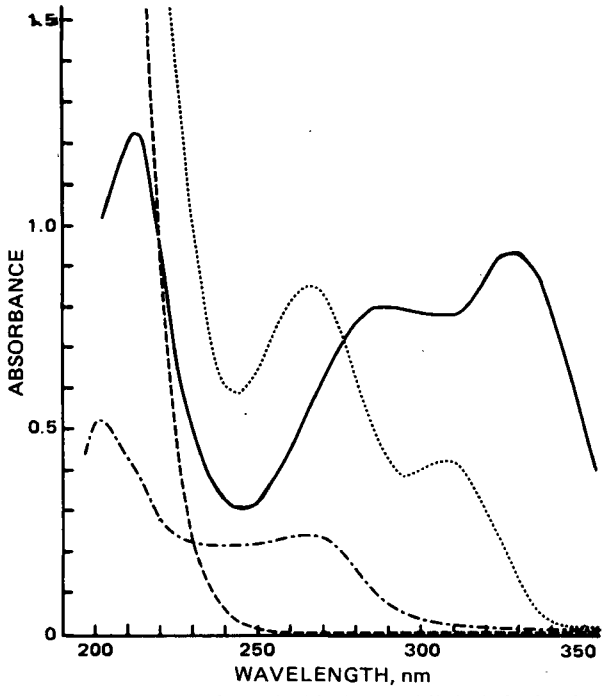

Figure 4—*UV spectra of aconiazide (0.05 mM) (—), hydrazine (25 mM) (– –), and a mixture of aconiazide (0.05 mM) and hydrazine (25 mM) (• • •). The spectrum of isoniazid (0.05 mM) (• – •), which is a component of aconiazide, also is shown. The spectra were taken within 2 min after the solutions were prepared in 0.1% $NaHCO_3$.*

[1] Also known as Compound 377 (6, 7) and later as phenoxalid or aconiazide (9, 10) by the World Health Organization.
[2] Farbenfabriken Bayer A.G., Leverkusen, West Germany.
[3] Connaught Laboratories Ltd., Toronto, Ontario, Canada.

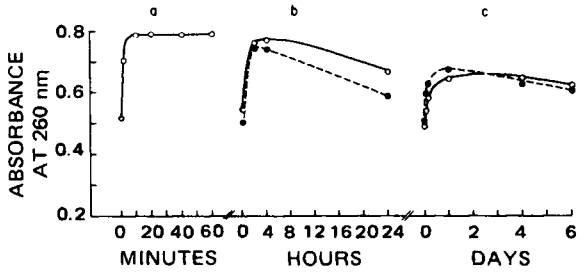

Figure 5—*Reaction of aconiazide (0.05 mM) with different concentrations of hydrazine in 0.1% $NaHCO_3$ at 23 (—) and 37° (- -). Key: a, 5 mM; b, 0.5 mM; and c, 0.05 mM.*

299.28), 2-formylphenoxyacetic acid[4] (VII) (mol. wt. 180.16), acetylhydrazine[5] (IV) (mol. wt. 74.08), and hydrazine[6] (V) (95%) were obtained commercially.

Buffer Solutions—A 0.1% $NaHCO_3$ solution was used to dissolve the reagents and record their UV spectra (Figs. 1–8). The pH of a freshly prepared sodium bicarbonate solution was ~8.4; a 1.25% phosphate buffer of pH 7.2 also was used. It was prepared by dissolving 27.4 g of monobasic potassium phosphate and 72.6 g of dibasic sodium phosphate in 8 liters of water.

UV Spectrophotometry—Due to the sensitivity and characteristics of their UV absorption spectra, the progression of the binding of hydrazine (V) or acetylhydrazine (IV) by 2-formylphenoxyacetic acid (VII) or its isonicotinylhydrazone (VI) can be followed easily. A UV spectrophotometer[7] was used to obtain the spectra.

The progression of the reaction between IV or V and VII in solution was studied by recording the absorbance at 280 nm at various intervals. The progression of the reaction between IV or V and VI in solution was studied at various intervals by recording the absorbance at 260 nm.

RESULTS

Reaction of 2-Formylphenoxyacetic Acid (VII) with Hydrazine (V)—Figure 1 shows the UV spectra of VII and of V at 0.05 and 25 m*M*, respectively. The UV spectrum of a solution containing both substances also is shown. From this spectrum, it appears that a compound, most likely a hydrazone of VII, formed within 2 min after mixing VII and V at final concentrations of 0.05 and 25 m*M*, respectively.

Figure 2 shows the UV spectrum of a solution containing VII and V, both at concentrations of 0.05 m*M*, taken at various time intervals. At this concentration of V (0.05 m*M*), the same new compound was formed but at a much slower rate than when a higher concentration of V (25 m*M*) was used (Fig. 1).

The speed at which VII (0.05 m*M*) reacts with V at different concentrations can be seen more clearly if the absorbance at 280 nm is plotted *versus* time. In fact, Fig. 3 shows that at 23°, the reaction was complete in ~20 min, 2 hr, and 3 days for V at concentrations of 5, 0.5, and 0.05 m*M*, respectively. At 37°, the reaction was approximately two to three times faster than at room temperature and was complete in ~1 hr and 1 day for V at concentrations of 0.5 and 0.05 m*M*, respectively.

Reaction of Aconiazide (VI) with Hydrazine (V)—Figure 4 shows the UV absorption spectra of a solution of VI at 0.05 m*M*[8] (15 μg/ml) and of VI in an excess of V (25 m*M*). Figure 4 also shows that a new compound formed from VI and V within 2 min after these two substances were mixed. Since this new compound has its UV maxima at exactly the same wavelengths as the compound formed from VII and V (Fig. 1), it indicated that the 2-formylphenoxyacetic acid component of VI had reacted with V. Furthermore, Fig. 5 shows that the reaction between VI and V slowed down in exactly the same way as was observed for VII and V when lower concentrations were used.

Reaction of 2-Formylphenoxyacetic Acid (VII) with Acetylhydrazine (IV)—Figure 6 shows the UV absorption spectra of solutions of VII and of IV at 0.05 and 25 m*M*, respectively. Figure 6 also shows the UV spectrum of a solution containing both substances. From this spectrum, it appears that a compound, most likely an acetylhydrazone of VII,

[4] Aldrich Chemical Co., Milwaukee, Wis.
[5] Acethydrazide, Aldrich Chemical Co., Milwaukee, Wis.
[6] Distillation Products Industries, Eastman Organic Chemicals Department, Division of Eastman Kodak Co., Rochester, N.Y.
[7] Pye Unicam SP1800 with linear recorder model AR25.
[8] This concentration can be expected in the serum of patients treated with VI.

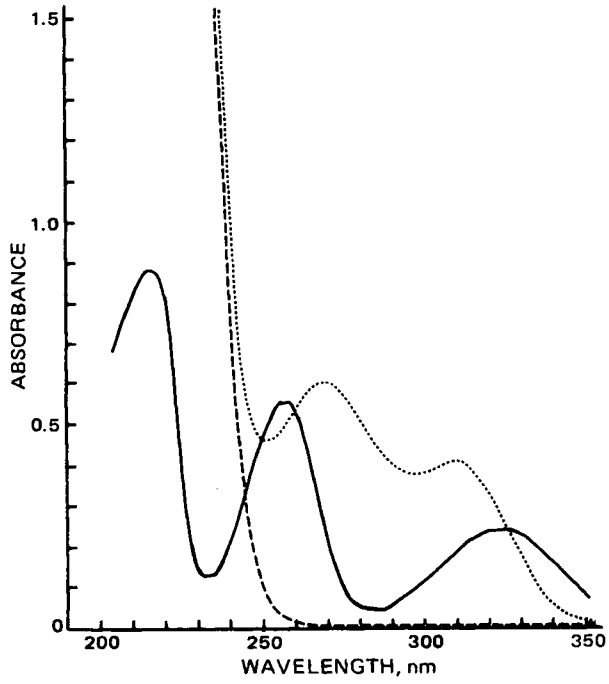

Figure 6—*UV spectra of 2-formylphenoxyacetic acid (0.05 mM) (—), acetylhydrazine (25 mM) (- -), and a mixture of 2-formylphenoxyacetic acid (0.05 mM) and acetylhydrazine (25 mM) (· · ·). The spectrum of the mixture was taken 4 hr after preparation. All solutions were prepared in 0.1% $NaHCO_3$.*

formed within 4 hr after mixing of VII and IV at final concentrations of 0.05 and 25 m*M*, respectively.

Figure 7 shows the speed at which VII reacted with IV at three concentrations (25, 0.5, and 0.1 m*M*). By comparing this reaction with the reaction of VII with V (Figs. 1–3), it is obvious from Figs. 6 and 7 that IV reacted with VII at a much slower rate than V.

Reaction of Aconiazide (VI) with Acetylhydrazine (IV)—Figure 8 shows the UV absorption spectra of VI and of IV at 0.05 and 25 m*M*, respectively. Figure 8 also shows the UV spectrum of a solution containing both substances. From this spectrum, it appears that a new compound formed within 4 hr after mixing VI and IV at final concentrations of 0.05 and 25 m*M*, respectively. Since this new compound has its UV maxima at exactly the same wavelengths as the compound formed from VII and IV (Fig. 6), it can be surmised that the 2-formylphenoxyacetic acid component of VI had reacted with IV.

Reaction of 2-Formylphenoxyacetic Acid (VII) with Hydrazine (V) and Acetylhydrazine (IV) at pH 7.2—The reactions between VII and V or IV were carried out in freshly prepared 0.1% $NaHCO_3$ at a pH of ~8.4. Therefore, it was of interest to find out if the same reactions also would occur at the physiological pH of 7.2 in a phosphate-buffered solution. At this pH, the reactions were not different from those obtained in 0.1% $NaHCO_3$, except that they proceeded at a significantly faster rate.

DISCUSSION

Aconiazide (VI) is formed from I and VII, and VII is a derivative of

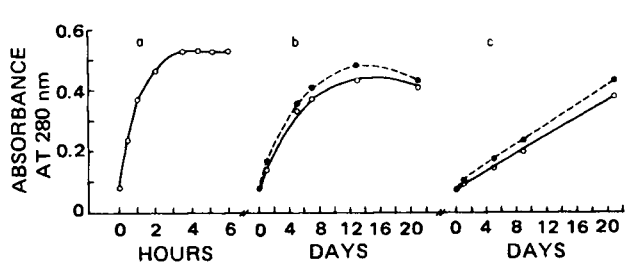

Figure 7—*Reaction of 2-formylphenoxyacetic acid (0.05 mM) with different concentrations of acetylhydrazine in 0.1% $NaHCO_3$ at 23 (—) and 37° (- -). Key: a, 25 mM; b, 0.5 mM; and c, 0.1 mM.*

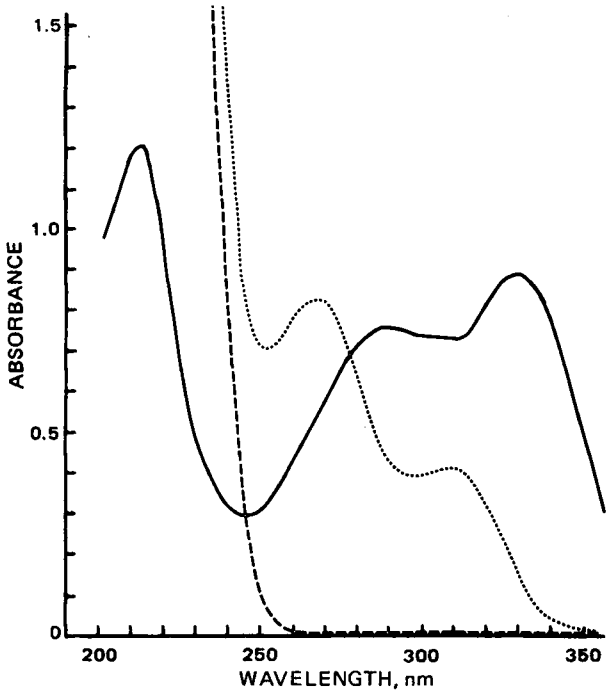

Figure 8—*UV spectra of aconiazide (0.05 mM) (—), acetylhydrazine (25 mM) (– –), and a mixture of aconiazide (0.05 mM) and acetylhydrazine (25 mM) (· · ·). The spectra of the solutions were taken 4 hr after preparation in 0.1% $NaHCO_3$.*

salicylaldehyde. It is well known that aldehydes react with hydrazines. Therefore, the reaction between VII and V or IV, as evidenced by the spectra in Figs. 1–3 and Figs. 4 and 5, respectively, could result in the formation of the hydrazone or acetylhydrazone of VII. Regardless of whether VII or VI was used in the presence of V or IV, the same new compounds were formed, although their levels of absorbance in the 265- and 305-nm regions were different (Figs. 1 and 4 and Figs. 6 and 8). This difference in the level of absorbance is due to the fact that I, which also has an absorption maximum around 265 nm (Fig. 4), is liberated from VI.

The reaction product between VII and V, namely, the sodium salt of the hydrazone of VII, could easily be obtained in crystalline form by mixing a fairly strong solution of the sodium salt of VII with an excess of V and evacuating the mixture to dryness. The preparation so obtained showed a UV absorption spectrum identical to the spectra shown in Figs. 1 and 2.

The fact that V and IV react with VI to form new compounds indicates that VII has a greater affinity for V and IV than for isoniazid (I). One interesting feature of VI is that for each liberated amount of I, the equivalent amount of VII is liberated simultaneously, making it available to bind an equivalent amount of the toxic metabolites released from I, namely, V and IV. This binding could account for the lower toxicity of VI compared to I (7, 8).

It also was shown conclusively that lung tumors can be induced in mice fed isoniazid (I) over 6–12 months and that the tumors are caused by the metabolites of I, namely, acetylhydrazine (IV) and hydrazine (V) (1, 13–15). The demonstration by UV spectrophotometry that a dissociation product of aconiazide (VI) (namely, 2-formylphenoxyacetic acid, VII) binds the carcinogenic metabolites of I strongly suggests that VI may not be carcinogenic. Hence, a comparative study between VI and I in animals is warranted to ascertain whether VI is carcinogenic.

Should these studies show that aconiazide (VI) is noncarcinogenic, and since clinical studies (8), although limited, have shown that VI is as effective as and less toxic than isoniazid (I) in patients with tuberculosis, there should be no reason why VI could not be used as a substitute for I.

REFERENCES

(1) D. E. Kopanoff, D. E. Snider, and G. J. Caras, *Am. Rev. Resp. Dis.*, **117**, 991 (1978).

(2) J. D. Moss, J. E. Lewis, and C. M. Knauer, *ibid.*, **106**, 849 (1972).

(3) "U.S. Registry of Toxic Effects of Chemical Substances," 1976, p. 635.

(4) J. R. Mitchell, presented at the International Conference on Lung Disease, Montreal, Canada, May 1975.

(5) A. Zubrys and C. O. Siebenmann, *Can. J. Chem.*, **33**, 11 (1955).

(6) C. O. Siebenmann and A. Zubrys, *Antibiot. Ann.*, **1954–1955**, 442.

(7) C. O. Siebenmann and C. Barbara, in "Trans. 22nd Res. Conf. on Pulmonary Diseases," Cincinnati, Ohio, Feb. 1963.

(8) Canadian Food and Drug Directorate, "New Drug Submission for Phenoxalid, Vol. II, Clinical Trials," July 20, 1961.

(9) "Compendium of Pharmaceuticals and Specialties (CPS)," 14th ed., Canadian Pharmaceutical Association, Toronto, Ontario, Canada, 1979, p G1.

(10) "Canadian Food and Drug Regulations," Supply & Services Canada, Ottawa, Ontario, Canada, Dec. 1, 1977, p. 148A.

(11) C. O. Siebenmann and A. Zubrys, Canadian pat. 590,941 (Jan. 19, 1960).

(12) C. O. Siebenmann and A. Zubrys, U.S. pat. 2,844,588 (July 22, 1958).

(13) K. Mori, A. Yasuno, and K. Matsumoto, *Gann*, **51**, 83 (1960).

(14) C. Biancifiori and R. Ribacchi, *Nature*, **194**, 488 (1962).

(15) L. Severi and C. Biancifiori, *J. Natl. Cancer Inst.*, **41**, 331 (1968).

Identification of Canine Urinary Metabolites of the Antiprotozoal Agent 3a,4,5,6,7,7a-Hexahydro-3-(1-methyl-5-nitro-1*H*-imidazol-2-yl)-1,2-benzisoxazole

W. J. A. VANDENHEUVEL ˣ, DAVID ONOFREY, J. S. ZWEIG, JOSEPH PILE, NAOMI KIRKMAN-BEY, and B. H. ARISON

Received November 14, 1979, from *Merck Sharp & Dohme Research Laboratories, Rahway, NJ 07065.* Accepted for publication May 12, 1980.

Abstract □ Metabolite fractions from the urine of a dog dosed with 3a,4,5,6,7,7a-hexahydro-3-(1-methyl-5-nitro-1*H*-imidazol-2-yl)-1,2-benzisoxazole (MK-0436) were obtained by the use of high-performance liquid chromatography. These fractions were of suitable purity for structural elucidation. Data obtained by mass spectrometry and NMR spectroscopy allowed the identification of seven major metabolites of this drug. Biotransformation in each case involved hydroxylation (mono or di) of the hexahydrobenzisoxazole ring.

Keyphrases □ 3a,4,5,6,7,7a-Hexahydro-3-(1-methyl-5-nitro-1*H*-imidazol-2-yl)-1,2-benzisoxazole—identification of urinary metabolites, dogs □ Metabolites—of 3a,4,5,6,7,7a-hexahydro-3-(1-methyl-5-nitro-1*H*-imidazol-2-yl)-1,2-benzisoxazole, identification, dog urine □ Antiprotozoal agents—3a,4,5,6,7,7a-hexahydro-3-(1-methyl-5-nitro-1*H*-imidazol-2-yl)-1,2-benzisoxazole, identification of urinary metabolites by NMR spectroscopy, mass spectrometry, and capillary column GLC–mass spectrometry

3a,4,5,6,7,7a-Hexahydro-3-(1-methyl-5-nitro-1*H*-imidazol-2-yl)-1,2-benzisoxazole (MK-0436, I) is an antiprotozoal agent (1) active against *Trypanosoma cruzi* (2) (Fig. 1). This nitroimidazole displayed antibacterial activity during mutagenicity testing[1] using the host-mediated mouse test and the Ames test with S9 liver microsomes (3) but not when the simple Ames spot test (4) was employed (5). These observations led to the presumption that metabolites of I might be antibacterial.

Several metabolite-containing fractions from the urine of a dog given I were found to possess antibacterial activity, and several canine metabolites (both unconjugated and the aglycones from conjugated metabolites) were partially characterized as mono- and dihydroxy species with substitution at positions 4, 5, 6, and/or 7 of the hexahydrobenzisoxazole ring (5). Further characterization of the metabolite mixture and unequivocal identification of several major metabolites of this drug are presented here.

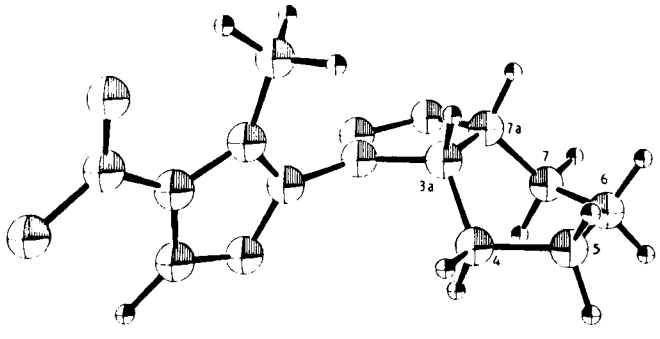

Figure 1—*Computer-generated ORTEP plot of I.*

[1] H. Skeggs, Merck Sharp & Dohme Research Laboratories, West Point, PA 19486, personal communication.

EXPERIMENTAL

Two methanol solutions containing canine urinary metabolites of I (those originally present in the urine as unconjugated metabolites and the aglycones of those originally present as conjugates) were obtained as described previously (5). The two solutions were stored at 4°, and aliquots were taken for isolation and chromatographic purification of the metabolites.

Aliquots of the aglycone metabolite fraction (dissolved in methylene chloride) were subjected to high-performance liquid chromatography (HPLC) using a C_8 reversed-phase preparative column[2] with a step gradient (4.4 ml/min) of methanol–water (1:4) for 40 min, methanol–water (1:2) for 40 min, and methanol for 20 min. Fourteen fractions were collected in each of seven chromatographic runs. The initial column system conditions were regenerated following each run by passage of methanol–water (1:4) through the column for 15 min.

Five fractions (II–VI) yielded sufficient quantities of metabolites to pursue structural elucidation. Aliquots of the metabolite fraction from unhydrolyzed urine also were subjected to HPLC for metabolite isolation using a semipreparative C_{18} reversed-phase column[3]. The quantities of metabolites obtained were, except in one case, too small for successful characterization. Because the amount of bioactivity in the aglycone fraction was approximately twice that found in the nonconjugate fraction, efforts were concentrated on the former. Analytical HPLC was carried out on a C_{18} reversed-phase column[4] with methanol–water (1:4) at a flow rate of 1.5 ml/min. UV detection at 330 nm was used in all HPLC work.

GLC[5] and GLC–mass spectrometric[6] analyses were carried out on trimethylsilylated [bis(trimethylsilyl)trifluoroacetamide[7]–pyridine (3:1) for 3 hr at room temperature] metabolites using 10- or 15-m × 0.3-mm SE-30 glass capillary columns at 240° with helium as the carrier gas. The mass spectrometer[6] was operated with a 70-ev ionizing potential and a 0.8-mamp emission current. Direct-probe mass spectrometry[8] was carried out with a 70-ev ionizing potential, a 60-μamp trap current, and a 3.5-kv accelerating voltage. NMR spectra[9] were obtained from samples dissolved in deuterochloroform.

RESULTS AND DISCUSSION

HPLC (Fig. 2) and GLC (Fig. 3) (trimethylsilyl derivatives) analyses of the aglycone fraction resulting from enzyme hydrolysis of the urinary conjugates demonstrated that it was a multicomponent mixture. Although GLC–mass spectrometry indicated that most of the eluted components (trimethylsilyl derivatives) were drug related [earlier work showed the presence of at least six metabolites of I (5)], it was not possible to discern exact structures on the basis of the mass spectrometric data alone. NMR spectroscopic examination was needed to establish the metabolite structures unequivocally; but to utilize this technique, it was necessary to isolate and purify the metabolites. HPLC appeared to be the method of choice.

Preparative HPLC, followed in some cases by further purification on an analytical HPLC column, gave five metabolite fractions (II–VI in Fig.

[2] Lion Industries.
[3] E. S. Industries.
[4] Waters Associates.
[5] Hewlett-Packard model 5730A instrument with an SGE inlet splitter and a nitrogen-selective detector.
[6] Finnigan model 3200 instrument with a splitless injector.
[7] Supelco.
[8] LKB model 9000 instrument.
[9] Varian SC-300-MHz instrument equipped with a Fourier transform accessory.

0022-3549/80/1100-1288$01.00/0
© 1980, American Pharmaceutical Association

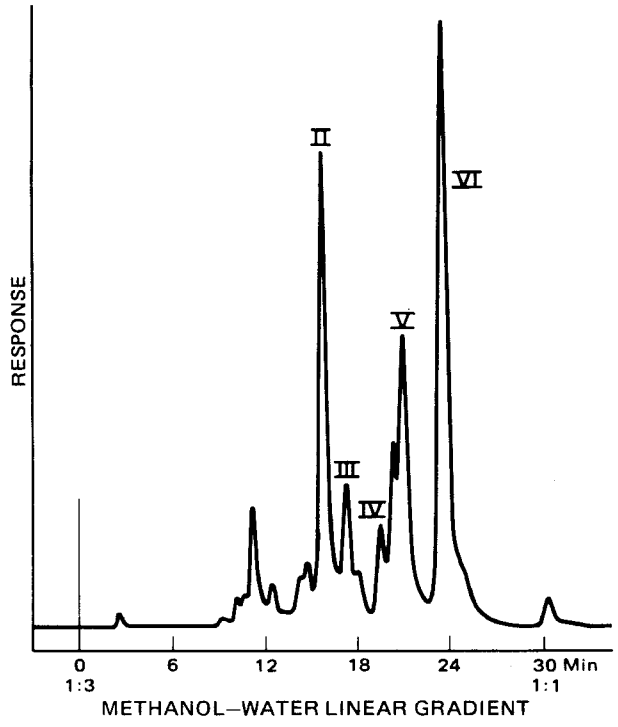

Figure 2—*High-performance liquid chromatogram (C_{18} reversed-phase column) of aglycone fraction (arising from enzyme hydrolysis of canine urinary conjugates).*

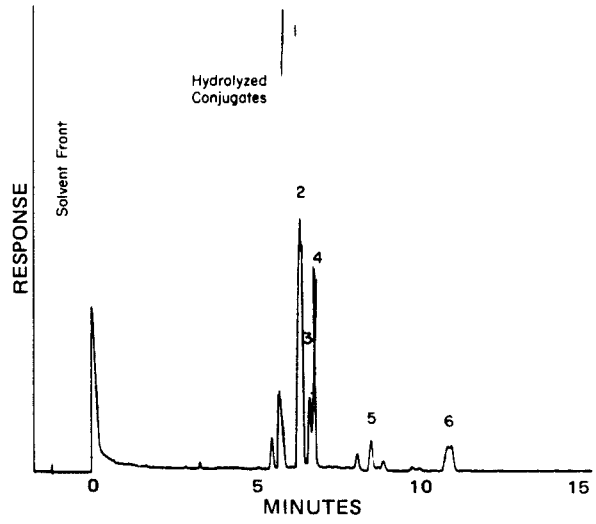

Figure 3—*Gas–liquid chromatogram produced from analysis of the trimethylsilylated aglycone fraction (arising from enzyme hydrolysis of canine urinary conjugates).*

2) of quality and quantity suitable for NMR examination. These fractions were examined first by direct-probe mass spectrometry. The resulting data (major, pertinent ions) are summarized in Table I. Capillary column GLC–mass spectrometric analysis of these samples (following trimethylsilylation) also showed that each sample contained mono- and/or dihydroxylated analogs of the parent drug [molecular ions for the derivatives of *m/e* 426 (dihydroxy metabolites) or *m/e* 338 (monohydroxy metabolites)].

The NMR spectrum (Fig. 4) of I must be understood before structural assignments for the metabolites of this drug can be made. Since previous work demonstrated that the metabolic transformations occurred on carbons 4–7 (5), knowledge of the signal characteristics for the protons on the cyclohexane (hexahydrobenzisoxazole) ring was crucial. The parent drug exhibited proton absorption at δ 8.07 (imidazole H, not shown in Fig. 4), 4.43 (H_{7a}), 4.33 (NCH_3), 3.53 (H_{3a}), 2.29 (H_{7eq}), 2.14 (H_{4eq}), 1.82 (H_{7ax}), 1.67 (H_{6eq} and H_{5eq}), 1.53 (H_{6ax}), and 1.25 (H_{4ax} and H_{5ax}). The assignments, derived from inspection and double-irradiation experiments, provided the basis for the NMR characterization of the metabolites (Table II). The observed coupling constants in the sequence C_7H_2–$C_{7a}H$–$C_{3a}H$–C_4H_2 are consistent with a *cis*-ring fusion and a twist chair configuration for the six-membered ring. Spectrometric and chromatographic details for each isolated metabolite fraction will be given.

Metabolite Fraction II—GLC of the trimethylsilyl derivative of this fraction showed one main component (~80%) and two minor components (~10% each). GLC–mass spectrometry of the major component indicated a molecular ion of *m/e* 426, showing it to be a dihydroxylated metabolite of I. This also was true for the minor components. Direct-probe mass spectrometry of underivatized II gave spectra (Table I) with intense ions of *m/e* 282 (molecular ion of dihydroxy metabolites), and there was no evidence of monohydroxy metabolites (molecular ions of *m/e* 266). HPLC also indicated one major component and two minor components in the sample. The NMR spectrum of II showed two resonances that were not seen in the parent drug in the δ 3.5–4.0 region, indicating incorporation of two hydroxyl groups. Double-irradiation experiments established that the two carbinol methines were vicinal and that one was vicinal to H_{3a}. These findings allowed identification of the major metabolite as a 4,5-dihydroxy analog of I. Since $J_{4,5}$ and $J_{5,6ax}$ are large (>8 Hz), an axial–axial stereochemical relationship is indicated; thus, II must be the 4,5-di(equatorial)hydroxy derivative.

Metabolite Fraction III—Analytical HPLC of this fraction showed one major component and two minor components. However, capillary column GLC indicated the presence of only one minor component (~10%) and one major component (~90%). GLC–mass spectrometry of the trimethylsilylated sample showed that the more abundant component possessed a molecular ion of *m/e* 338, demonstrating that it is a monohydroxy analog of I. The minor component exhibited a molecular ion of *m/e* 426; thus, it is the bis(trimethylsilyl) derivative of a dihydroxy metabolite. The direct-probe mass spectrometric data for III (Table I) also demonstrate that this metabolite fraction is predominantly a

Table I—Major Ions Found in the Mass Spectra of I and Metabolites II–VIII

		Ion and Relative Intensity									
Compound	Substitution	*m/e* 282	*m/e* 266	*m/e* 265	*m/e* 250	*m/e* 249	*m/e* 247	*m/e* 237	*m/e* 233	*m/e* 195[a]	*m/e* 153[b]
I	—	—	—	—	M, 100	—	—	—	M-17, 42	36	70
II	4,5-Di-(eq)OH	M, 10	—	M − 17, 7	—	—	M − 35, 6	—	—	100	10
III	6-(ax)OH	(1)[c]	M, 9	—	—	M − 17, 9	—	—	—	100	76
IV	5-(eq)OH	(5)[c]	M, 37	—	—	M − 17, 27	—	M − 29, 32	—	100	66
V	7-(ax)OH	—	M, 19	—	—	M − 17, 13	M − 19, 19	M − 29, 6	—	72	100
VI	7-(eq)OH	—	M, 31	—	—	M − 17, 42	M − 19, 66	—	—	50	100
VII	6-(eq)OH	(6)[c]	M, 74	—	—	M − 17, 54	M − 19, 15	—	—	100	83
VIII	5-(eq), 7a-di-OH	M, 24	—	M − 17, 48	—	—	—	—	—	100	62

[a] 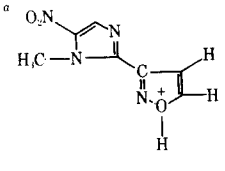

[b] 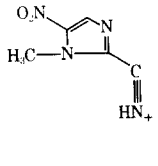

[c] M of minor dihydroxy metabolite component.

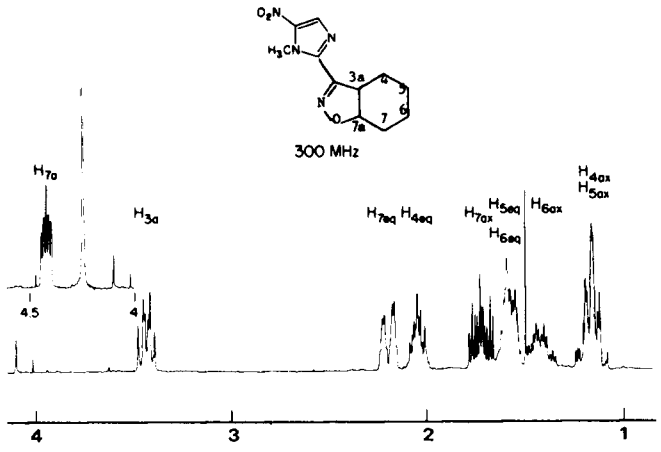

Figure 4—*NMR spectrum of I.*

monohydroxy metabolite contaminated with some dihydroxylated drug.

Metabolite III is assigned as the 6-(axial)hydroxyl derivative of I based on the absence of the characteristic 12.5-Hz coupling constant in the H_{7ax} resonance (Fig. 5). This large splitting is characteristic of an axial–axial relationship and has been identified as J_{H7ax}, J_{H6ax} in the parent drug. As expected, the multiplicities of the H_{3a} and H_{7a} signals are essentially unchanged from those of I, indicating that no substitution has occurred on the neighboring C-7 and C-4 atoms.

Metabolite Fraction IV—As with Fraction III, the direct-probe mass spectrometric data from Fraction IV (Table I) showed that the latter is composed mainly of monohydroxy metabolites plus a lesser amount of dihydroxy metabolites. Capillary column GLC of the trimethylsilyl derivative of IV showed a major component and three minor components, with the minor components each having an area of ~10% of that of the major peak. GLC–mass spectrometry of the major component gave a molecular ion of *m/e* 338, consistent with a monohydroxylated derivative of I. The multicomponent nature of the metabolite fraction (with one major component) also was indicated by analytical HPLC.

The major component of Fraction IV was characterized by NMR spectroscopy as having a single equatorial hydroxyl group at C-5. This conclusion was reached following elimination of other structural possibilities. The C-4 and C-7 sites were eliminated as possible positions of hydroxylation since the H_{3a} and H_{7a} signals retained the same multiplicity as in the parent drug. This required that the neighboring C-4 and C-7 positions be unsubstituted. The two C-6 possibilities were ruled out by Metabolites III and V, in which substitution at C-6 was firmly established by the reduced multiplicity of the recognizable axial H_7 signal. Finally, the linewidth of the carbinol CH group after deuterium oxide exchange ($W_{1/2}$ 20–24 Hz) necessitated at least one large vicinal constant, which is compelling evidence for an axial configuration.

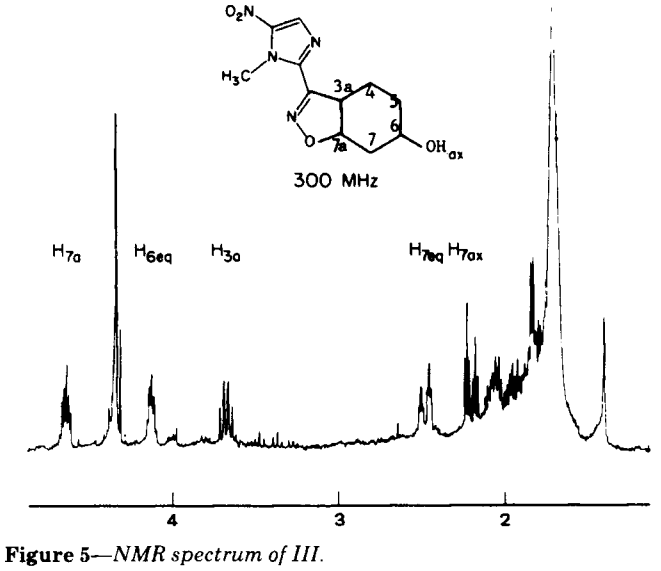

Figure 5—*NMR spectrum of III.*

Table II—NMR Data for I, Related Compounds, and Metabolites

Compound	3a	4 eq	4 ax	5 eq	5 ax	6 eq	6 ax	7 eq	7 ax	7a	NHC_3	HC=	OH
I	3.53 (10.0, 7.5, and 7.5)	2.14	~1.25	~1.67	~1.25	~1.67	~1.53	2.29	1.82 (15.0, 12.5, 4.5, and 4.5)	4.43 (7.5, 4.0, and 4.0)	4.33	8.07	—
Synthetic[a] 4-(eq)OH	3.22 t (8.3)	—	3.59 (11.5, 8.3, and 5.0)	~1.5[b]	1.28	2.10	~1.77	2.33	~1.77[b]	4.66	4.36	8.08	6.03
Synthetic[a] 6-(eq)OH, 7-(ax)OH	3.81 (8.8 and 6.8)	2.34	~1.65	~1.65	1.82	—	4.01	4.14	—	4.70 (8.6 and 4.3)	4.31	8.08	2.08 (3.7) C-6 3.53 (2.7) C-7
Synthetic[a] 5-(ax)OH, 6-(eq)OH	3.75 (11.0 and 7.7)	2.51 (14.5, 6.7, and 4.7)	~1.45	4.05	—	—	3.97	2.42 (14.5, 5.5, and 2.5)	2.20 (14.8, 10.7, and 5.0)	4.68	4.32	8.08	1.93 (6.0) C-6
II [4,5-di-(eq)OH]	3.33	—	3.45	—	3.59	~1.97	~1.65	2.43	~1.98	4.66	4.35	8.07	— —
III [6-(ax)OH]	3.64 q (8.0)	~1.93	~1.83	~1.7	~1.7	4.10 qn (~4.2)	—	2.38 (15.5 and 3.3)	2.10 (15.5, 4.0, and 4.0)	4.66	4.33	8.08	— —
IV [5-(eq)OH]	3.66	—	—	—	3.75	—	—	—	—	4.54	—	—	— —
V [7-(ax)OH]	3.76 q (8.0)	—	—	—	—	—	—	3.95	—	4.65 (8.0 and 3.7)	4.32	8.06	— —
VI [7-(eq)OH]	3.85 q (8.0)			2.0–2.8				—	4.06	4.47 (8.8 and 5.2)	4.29	8.07	— —
VII[c] [6-(eq)OH]	3.51	2.30	~1.32	—	—	—	—	2.63	1.78	4.71	—	—	— —
VIII [5-(eq)OH 7a-OH]	3.74 (12.0 and 7.5)	1.90[b]	1.70[b]	4.16	—	2.55[b]	1.30[b]	2.24	2.35	—	4.32	8.08	2.84

[a] Model compounds prepared by Dr. H. Mrozik, Synthetic Organic Department, Merck Sharp & Dohme Research Laboratories. [b] Tentative assignments. [c] Same as the minor component of metabolite Fraction V.

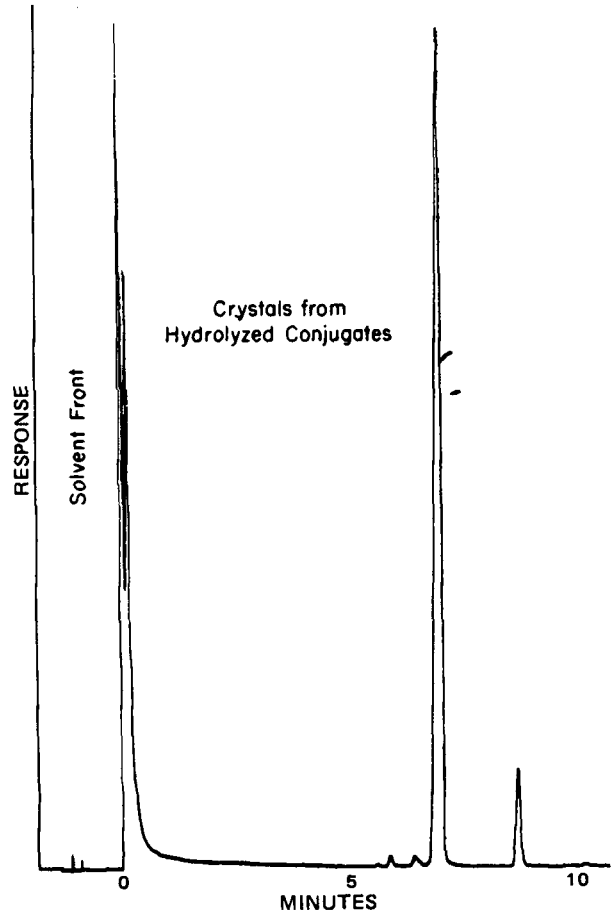

Figure 6—*Gas–liquid chromatogram produced by analysis of the trimethylsilylated metabolite Fraction VII.*

Metabolite Fractions V and VI—HPLC suggested that Fraction V contained one major and one minor component. GLC of the trimethylsilyl derivative showed three peaks with a relative area ratio of approximately 2:4:3. GLC–mass spectrometry of the three peaks gave molecular ions for each of *m/e* 338, as required for monohydroxylated metabolites; however, the fragmentation patterns in each case were somewhat different, suggesting isomeric species. Direct-probe mass spectrometry (Table I) of this metabolite fraction indicated the presence of monohydroxy metabolites only.

Analytical HPLC of Fraction VI and GLC of the trimethylsilyl product indicated a single component of >90% purity. GLC–mass spectrometry indicated a molecular ion at *m/e* 338, required for a monohydroxy compound. The direct-probe mass spectra from Fraction VI also showed that only monohydroxy (and no dihydroxy) metabolites were present (Table I).

The NMR spectra of Fractions V (major component) and VI showed an H_{7a} signal with reduced multiplicity, indicating substitution on a neighboring carbon atom. Since both spectra contained a normal H_{3a} resonance, it follows that the site of hydroxylation is C-7 and that the two metabolites are related as stereoisomers. Stereochemical assignments are not clearcut since the coupling constants between H_{7a} and the two C-7 protons are essentially the same in the parent molecule and differ by only 1 Hz in these two metabolites. However, there is reason for associating the larger J value with an axial H_7 [*i.e.*, a 7-(equatorial)hydroxyl group] since this would correspond to the findings for Metabolite III in which the assignments are unequivocal.

Inspection of the NMR features of the minor component in metabolite Fraction V eliminated C-4 and C-7 as possible sites for the hydroxylation since both the H_{3a} and H_{7a} signals retained a full complement of lines. Irradiation of the equatorial H_7 signal at δ 2.63 reduced the multiplicity of the axial H_7 to a doubled doublet (J = 11.5 and 4.5 Hz). Since the 4.5-Hz coupling constant represents $J_{7,7a}$ and J = 11.5 Hz arises from an axial–axial relationship, it follows that the axial H_7 has suffered a loss of spin interaction with its equatorial neighbor at C-6. Therefore, the minor component in Fraction V was assigned the C-6 equatorial hydroxy structure.

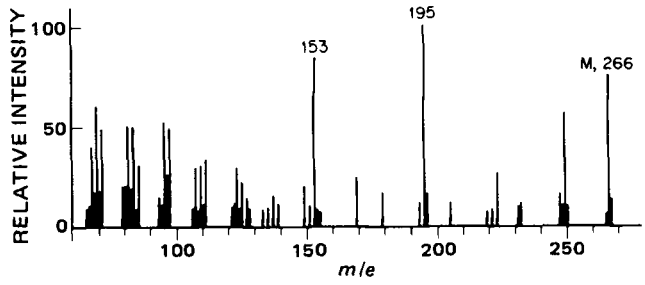

Figure 7—*Mass spectrum from metabolite Fraction VII.*

Metabolite Fraction VII—A small quantity (0.1 mg) of material crystallized in the bottom of the centrifuge tube (stored at 4°) containing the methanol solution of the aglycone metabolite fraction. GLC analysis of the crystals (Fraction VII) following their trimethylsilylation gave the chromatogram shown in Fig. 6. The major and minor components exhibited molecular ions of *m/e* 338 and 426, respectively, characterizing them as mono- and dihydroxy derivatives of I. The major component exhibited the same retention time as the shoulder (peak 3) on the leading edge of peak 4 in Fig. 3. Direct-probe mass spectrometry of underivatized VII gave the spectrum presented in Fig. 7. The molecular ion of *m/e* 266 confirmed that the spectrum arose from a monohydroxylated derivative of I, and the intense fragment ions of *m/e* 153 and 195 demonstrate that the hydroxyl group is substituted on C-4–C-7 of the hexahydrobenzisoxazole ring (5).

NMR examination of VII also indicated the presence of two components in the approximate ratio of 9:1. Signals for the major component matched those for the minor component of Fraction V. This finding indicates that the hydroxyl group in the major component is at C-6 and is in the equatorial configuration. The NMR data for the minor component in Fraction VII indicated it to be a dihydroxy metabolite of I, but no positional or conformational assignments could be made, except that substitution is on C-4–C-7 of the hexahydrobenzisoxazole ring.

Metabolite Fraction VIII—Both HPLC and GLC (following trimethylsilylation) of this nonconjugated metabolite fraction from unhydrolyzed dog urine indicated the presence of a major drug-related component (which appeared to be a dihydroxy metabolite) plus at least two related minor components. The dihydroxy nature of this metabolite also was suggested by direct-probe mass spectrometric data (Table I). Although only limited NMR data were obtained for Fraction VIII, analysis of the spectral features allowed a tentative structural assignment to the major component as 5-(axial),7a-dihydroxy-substituted drug. Key observations that led to this conclusion were: (*a*) the absence of a resonance in the δ 4.5–4.7 region diagnostic for H_{7a}; (*b*) a reduced multiplicity of the H_{3a} and both H_7 signals, indicative of hydroxylation on a neighboring carbon; and (*c*) the appearance of a new, weakly coupled, single proton peak at δ 4.18.

Observations *a* and *b*, taken together, constitute compelling evidence for hydroxylation at C_{7a}. The multiplicities of the H_{3a} and both H_7 signals require that C-4 and C-6 are unsubstituted, thus leaving C-5 as the site for the second hydroxyl group. The new carbinol CH group appears essentially as a broadened singlet with a width at half height of 9.5–10.0 Hz. This indicates that its couplings with the four neighboring protons at C-4 and C-6 all are small, strongly implying an equatorial configuration. Based on this tentative structural assignment, this is the first metabolite of I in which hydroxylation of the drug has occurred at a site other than C-4–C-7, but it is still on the hexahydrobenzisoxazole or cyclohexane ring portion of the drug.

When it was found that hydroxy metabolites of I are bioactive (5), several hydroxy analogs of the drug were synthesized[10]. Although NMR spectroscopy (and mass spectrometry) showed that these analogs were not identical to the metabolites, their NMR spectral data are presented in Table II for comparison.

This and other studies (5–8) have demonstrated that hydroxylation is a common metabolic route for cyclohexanes. Both mono- and dihydroxy metabolites are observed, and the latter probably arise from sequential hydroxylation steps. Thus, Elliott *et al.* (6) showed that cyclohexanol, a urinary metabolite of cyclohexane in the rabbit, is metabolized further to yield *trans*-cyclohexane-1,2-diol.

[10] H. Mrozik, P. Eskola, P. Kulsa, B. H. Arison, W. J. A. VandenHeuvel, J. A. Conroy, and B. M. Miller, Merck Sharp & Dohme Research Laboratories, Rahway, NJ 07065, unpublished data.

Agosin *et al.* (9) reported that the epimastigotes of *T. cruzi* possess an active drug-detoxifying (hydroxylating) system associated with the microsomal fraction, with properties like those of a monooxygenase system linked to cytochrome P-450. These authors speculated that the ability of *T. cruzi* to hydroxylate drugs to inactive metabolites may partially explain why no chemotherapeutic agents that cure Chagas' disease have been found; however, I, for which hydroxylation is a major route of metabolism in dogs (and mice) (5), is active against *T. cruzi* in mice (2, 5). Furthermore, since a synthetic dihydroxy derivative of this compound (the 6,7-*cis*-diol) exhibits severalfold greater activity than the parent drug (5), the possibility is raised that the enzyme system suggested (9) to detoxify other chemotherapeutic agents actually may enhance the bioactivity of I. Thus, the proposal of Agosin *et al.* (9) is of limited validity.

REFERENCES

(1) P. Kulsa and C. S. Rooney, U.S. pat. 3,711,495 (Jan. 16, 1973).

(2) C. M. Malanga, J. Conroy, and A. C. Cuckler, *J. Parasitol.*, in press.

(3) B. N. Ames, J. McCann, and E. Yamasaki, *Mut. Res.*, **31**, 347 (1975).

(4) B. N. Ames, W. E. Durston, E. Yamasaki, and F. D. Lee, *Proc. Natl. Acad. Sci., USA*, **70**, 2281 (1973).

(5) W. J. A. VandenHeuvel, B. H. Arison, T. W. Miller, P. Kulsa, P. Eskola, H. Mrozik, A. K. Miller, H. Skeggs, S. B. Zimmerman, and B. M. Miller, *J. Pharm. Sci.*, **68**, 1156 (1979).

(6) T. H. Elliott, D. V. Parke, and R. T. Williams, *Biochem. J.*, **72**, 13 (1958).

(7) A. G. Renwick and R. T. Williams, *ibid.*, **129**, 857 (1972).

(8) B. Testa and P. Jenner, *J. Pharm. Pharmacol.*, **28**, 731 (1976).

(9) M. Agosin, C. Naquira, J. Paulin, and J. Capdevila, *Science*, **194**, 195 (1976).

ACKNOWLEDGMENTS

The authors thank Dr. Graham Smith for generation of the ORTEP plot, Mr. T. W. Miller for the methanol solutions of urinary metabolites, and Dr. J. E. Baer, Dr. B. M. Miller, Dr. F. J. Wolf, and Mrs. Helen Skeggs for their continuing interest in this work.

Ms. Naomi Kirkman-Bey, Mr. David Onofrey, and Mr. Joseph Pile were participants in the Merck Sharp & Dohme Research Laboratories Summer Student Program.

Antimicrobial Activity of *N*-Chloramine Compounds

H. H. KOHL ˣ, W. B. WHEATLEY, S. D. WORLEY, and N. BODOR *

Received October 12, 1979, from the *Department of Chemistry, Auburn University, Auburn, AL 36830.* Accepted for publication May 9, 1980. *Present address: Department of Medicinal Chemistry, University of Florida, Gainesville, FL 32610.

Abstract □ Cellular mechanisms of action of two representative *N*-chloramines were studied. Both compounds, 3-chloro-4,4-dimethyl-2-oxazolidinone (I) and *N*-chlorosuccinimide (III), inhibited bacterial growth and exerted profound inhibition of bacterial DNA, RNA, and protein synthesis at a concentration of 10^{-5} *M*. Enzymes containing sulfhydryl groups generally were significantly inhibited by these chloramines at 10^{-4} *M*. Dihydrofolate reductase, which contains no sulfhydryl groups, also was inhibited but at much higher chloramine concentrations (10^{-2} *M*); ribonuclease, which also contains no sulfhydryl groups, was unaffected. All of these inhibitory effects of the chloramines could be prevented if sulfhydryl-containing reagents (mercaptoethanol or dithiothreitol) were added before or together with the chloramine. Once inhibition was produced by the chloramine, it was not reversible by later addition of the sulfhydryl reagents. These results suggest that these chloramines act at sulfhydryl sites as well as at other sites in both cells and purified enzymes.

Keyphrases □ *N*-Chloramines—antimicrobial activity, inhibition of bacterial DNA, RNA, and protein synthesis □ Antimicrobial activity—*N*-chloramine-induced inhibition of bacterial DNA, RNA, and protein synthesis □ Enzyme inhibition—*N*-chloramine-induced inhibition of sulfhydryl-containing enzymes in bacteria

Recent studies of the chemical (1–5) and antimicrobial (6–8) properties of *N*-chloramine compounds suggested that many of these compounds may be potentially useful antibacterial agents. Preliminary results indicated that these *N*-chloramines are effective antibacterial agents. It was hypothesized that the bactericidal actions of *N*-chloramines are derived from the direct transfer of positive chlorine ions from the *N*-chloramines to an appropriate cellular receptor (5).

The present study was an attempt to elucidate the cellular processes affected by these agents which might account for their observed antimicrobial properties. In seeking the mechanisms of action of such agents, the determination of the primary targets in terms of overall cellular function is vitally important. This paper reports the effects of two representative *N*-chloramines on overall DNA, RNA, and protein synthesis in bacteria. A more specific action in terms of direct inhibition of cellular enzymes also is discussed.

EXPERIMENTAL

Bacterial Cultures—Bacteria [*Escherichia coli* (ATCC 25922) and *Staphylococcus epidermidis* (ATCC 12228)] were grown and harvested as described previously (9). The bacterial cells then were resuspended in fresh nutrient medium[1] at a density of 3×10^8 colony-forming units/ml. Bacterial purity and the absence of contamination were established routinely by the Gram stain and by colony characteristics on blood agar plates.

DNA, RNA, and Protein Synthesis—All stock solutions of 3-chloro-4,4-dimethyl-2-oxazolidinone (I), 4,4-dimethyl-2-oxazolidinone (II), and *N*-chlorosuccinimide (III) were prepared in 0.1 *M* phosphate buffer (pH 7). The stock solutions were diluted with distilled, deionized water.

The bacterial suspensions were added to test tubes containing the respective agents diluted in water. All determinations were made in duplicate or triplicate along with controls containing an identical volume of bacteria without the agents. The bacteria then were incubated at 37° for 1 hr with various concentrations of the *N*-chloramines. Then 1–2 μCi of the following radioisotopes[2] were added: [*methyl*-^{3}H]thymidine, 90

[1] Bacto nutrient broth 003-03, Difco Laboratories.

[2] New England Nuclear Corp., Boston, Mass.

0022-3549/80/1100-1292$01.00/0

© 1980, American Pharmaceutical Association

Agosin *et al.* (9) reported that the epimastigotes of *T. cruzi* possess an active drug-detoxifying (hydroxylating) system associated with the microsomal fraction, with properties like those of a monooxygenase system linked to cytochrome P-450. These authors speculated that the ability of *T. cruzi* to hydroxylate drugs to inactive metabolites may partially explain why no chemotherapeutic agents that cure Chagas' disease have been found; however, I, for which hydroxylation is a major route of metabolism in dogs (and mice) (5), is active against *T. cruzi* in mice (2, 5). Furthermore, since a synthetic dihydroxy derivative of this compound (the 6,7-*cis*-diol) exhibits severalfold greater activity than the parent drug (5), the possibility is raised that the enzyme system suggested (9) to detoxify other chemotherapeutic agents actually may enhance the bioactivity of I. Thus, the proposal of Agosin *et al.* (9) is of limited validity.

REFERENCES

(1) P. Kulsa and C. S. Rooney, U.S. pat. 3,711,495 (Jan. 16, 1973).

(2) C. M. Malanga, J. Conroy, and A. C. Cuckler, *J. Parasitol.*, in press.

(3) B. N. Ames, J. McCann, and E. Yamasaki, *Mut. Res.*, **31**, 347 (1975).

(4) B. N. Ames, W. E. Durston, E. Yamasaki, and F. D. Lee, *Proc. Natl. Acad. Sci., USA*, **70**, 2281 (1973).

(5) W. J. A. VandenHeuvel, B. H. Arison, T. W. Miller, P. Kulsa, P. Eskola, H. Mrozik, A. K. Miller, H. Skeggs, S. B. Zimmerman, and B. M. Miller, *J. Pharm. Sci.*, **68**, 1156 (1979).

(6) T. H. Elliott, D. V. Parke, and R. T. Williams, *Biochem. J.*, **72**, 13 (1958).

(7) A. G. Renwick and R. T. Williams, *ibid.*, **129**, 857 (1972).

(8) B. Testa and P. Jenner, *J. Pharm. Pharmacol.*, **28**, 731 (1976).

(9) M. Agosin, C. Naquira, J. Paulin, and J. Capdevila, *Science*, **194**, 195 (1976).

ACKNOWLEDGMENTS

The authors thank Dr. Graham Smith for generation of the ORTEP plot, Mr. T. W. Miller for the methanol solutions of urinary metabolites, and Dr. J. E. Baer, Dr. B. M. Miller, Dr. F. J. Wolf, and Mrs. Helen Skeggs for their continuing interest in this work.

Ms. Naomi Kirkman-Bey, Mr. David Onofrey, and Mr. Joseph Pile were participants in the Merck Sharp & Dohme Research Laboratories Summer Student Program.

Antimicrobial Activity of *N*-Chloramine Compounds

H. H. KOHL ˣ, W. B. WHEATLEY, S. D. WORLEY, and N. BODOR *

Received October 12, 1979, from the *Department of Chemistry, Auburn University, Auburn, AL 36830.* Accepted for publication May 9, 1980. *Present address: Department of Medicinal Chemistry, University of Florida, Gainesville, FL 32610.

Abstract □ Cellular mechanisms of action of two representative *N*-chloramines were studied. Both compounds, 3-chloro-4,4-dimethyl-2-oxazolidinone (I) and *N*-chlorosuccinimide (III), inhibited bacterial growth and exerted profound inhibition of bacterial DNA, RNA, and protein synthesis at a concentration of 10^{-5} *M*. Enzymes containing sulfhydryl groups generally were significantly inhibited by these chloramines at 10^{-4} *M*. Dihydrofolate reductase, which contains no sulfhydryl groups, also was inhibited but at much higher chloramine concentrations (10^{-2} *M*); ribonuclease, which also contains no sulfhydryl groups, was unaffected. All of these inhibitory effects of the chloramines could be prevented if sulfhydryl-containing reagents (mercaptoethanol or dithiothreitol) were added before or together with the chloramine. Once inhibition was produced by the chloramine, it was not reversible by later addition of the sulfhydryl reagents. These results suggest that these chloramines act at sulfhydryl sites as well as at other sites in both cells and purified enzymes.

Keyphrases □ *N*-Chloramines—antimicrobial activity, inhibition of bacterial DNA, RNA, and protein synthesis □ Antimicrobial activity—*N*-chloramine-induced inhibition of bacterial DNA, RNA, and protein synthesis □ Enzyme inhibition—*N*-chloramine-induced inhibition of sulfhydryl-containing enzymes in bacteria

Recent studies of the chemical (1–5) and antimicrobial (6–8) properties of *N*-chloramine compounds suggested that many of these compounds may be potentially useful antibacterial agents. Preliminary results indicated that these *N*-chloramines are effective antibacterial agents. It was hypothesized that the bactericidal actions of *N*-chloramines are derived from the direct transfer of positive chlorine ions from the *N*-chloramines to an appropriate cellular receptor (5).

The present study was an attempt to elucidate the cellular processes affected by these agents which might account for their observed antimicrobial properties. In seeking the mechanisms of action of such agents, the determination of the primary targets in terms of overall cellular function is vitally important. This paper reports the effects of two representative *N*-chloramines on overall DNA, RNA, and protein synthesis in bacteria. A more specific action in terms of direct inhibition of cellular enzymes also is discussed.

EXPERIMENTAL

Bacterial Cultures—Bacteria [*Escherichia coli* (ATCC 25922) and *Staphylococcus epidermidis* (ATCC 12228)] were grown and harvested as described previously (9). The bacterial cells then were resuspended in fresh nutrient medium[1] at a density of 3×10^8 colony-forming units/ml. Bacterial purity and the absence of contamination were established routinely by the Gram stain and by colony characteristics on blood agar plates.

DNA, RNA, and Protein Synthesis—All stock solutions of 3-chloro-4,4-dimethyl-2-oxazolidinone (I), 4,4-dimethyl-2-oxazolidinone (II), and *N*-chlorosuccinimide (III) were prepared in 0.1 *M* phosphate buffer (pH 7). The stock solutions were diluted with distilled, deionized water.

The bacterial suspensions were added to test tubes containing the respective agents diluted in water. All determinations were made in duplicate or triplicate along with controls containing an identical volume of bacteria without the agents. The bacteria then were incubated at 37° for 1 hr with various concentrations of the *N*-chloramines. Then 1–2 μCi of the following radioisotopes[2] were added: [*methyl*-^{3}H]thymidine, 90

[1] Bacto nutrient broth 003-03, Difco Laboratories.

[2] New England Nuclear Corp., Boston, Mass.

0022-3549/80/1100-1292$01.00/0

© 1980, American Pharmaceutical Association

Table I—Incorporation of ^{3}H-Labeled Precursors into DNA, RNA, and Protein of *E. coli* [a]

Reaction Time at 37°, hr	Thymidine (DNA)	Uridine (RNA)	Leucine (Protein)
1	9,120	6,100	3,410
2	20,500	12,900	7,500
3	31,221	18,928	11,500
3, acid blank	295	190	300
3. ice blank	210	220	310

[a] The values are in counts per minute, which represent the average of triplicate determinations; each value was within 10% of the average shown.

Ci/mmole; [5,6-^{3}H]uridine, 42 Ci/mmole; and [4,5-^{3}H]-L-leucine, 40 Ci/mmole. Incorporation was allowed to proceed for 2 hr at 37°. Five milliliters of ice-cold trichloroacetic acid (10% w/v) containing nonradioactive thymidine, uridine, and leucine (10^{-4} *M*) was added. This addition terminated the incorporation reactions and precipitated DNA, RNA, and protein. The added nonradioactive thymidine, uridine, or leucine helped to displace adsorbed but unincorporated radioactivity and contributed to the low blank values seen in Table I.

Samples were refrigerated for 30 min, and the precipitated material was suspended mechanically using a vortex mixer. This material then was filtered through glass fiber filters[3]. Each filter was washed with 70 ml of 1.3 *N* HCl followed by 40 ml of absolute ethanol. The filters were dried under a heat lamp and placed into liquid scintillation vials. A solubilizing agent[4] (0.5 ml) was added to the vials and left overnight to digest the radioactive film on the filter surface. Scintillation fluid[5] (15 ml) was added, and the vials were mixed gently. Complete solubilization was assured by removing the filters and noting the residual radioactivity remaining on the filter. At least 95% of the radioactivity associated with the filters usually was solubilized by this process.

Radioactivity was counted in the solution phase using a liquid scintillation spectrometer[6]; the counting efficiency was established by the channels ratio method and was verified periodically through the use of a tritiated toluene standard. Toluene-soluble tritium was counted at an efficiency of 45%. Counting of the toluene-insoluble material contained on the filter could be done at 7% efficiency. Further details concerning these procedures may be obtained from the literature (9–12).

Thymidine is a specific precursor of DNA, while uridine and leucine are incorporated into RNA and protein, respectively. The specific nature of these processes was confirmed in this study by both chemical and enzymatic techniques as outlined previously (10, 13, 14).

The effect of the chloramines on the uptake of [^{3}H]thymidine into the acid-soluble pool of *E. coli* was studied. The concentrations of radioactive precursors found in the acid-soluble pool reflect the level of precursor transport into the bacterial cell (15). Acid-soluble radioactive thymidine was measured as follows. Bacteria were incubated at 37° for 60 min in contact with the chloramine (5×10^{-5} *M*) and radioactive thymidine or with thymidine alone (controls). Tubes containing bacteria then were centrifuged and washed three times with ice-cold bacterial nutrient broth containing 0.1 *M* thymidine. Tubes were drained thoroughly, and 5 ml of ice-cold 0.2 *N* perchloric acid was added to the precipitated bacterial pellets. After 15 min, the perchloric acid solutions were collected, and the tubes were rinsed with an additional 2 ml of 0.2 *N* perchloric acid. Radioactivity in the combined 0.2 *N* perchloric acid solutions was determined by liquid scintillation counting.

The effects of I–III on the activities of several enzymes were studied. The following enzymes were obtained commercially[7] and used without further purification: malate dehydrogenase (EC 1.1.37), fumarase (EC 4.2.1.2), and pancreatic ribonuclease (EC 3.1.4.22). Dihydrofolate reductase (EC 1.5.1.3) was purified from a methotrexate-resistant strain of *Lactobacillus casei* (15). Lactate dehydrogenase (EC 1.1.1.27) and creatine phosphokinase (EC 2.7.3.2) were studied using a reconstituted lyophilized bovine enzyme control serum[8].

Enzyme Assays—Chloramines were added to buffered enzyme solutions and allowed to incubate at room temperature for 30 min before being assayed. The specific assays employed the following literature methods: malic dehydrogenase (16), lactic dehydrogenase (17), creatine phosphokinase (18, 19), pancreatic ribonuclease (20), dihydrofolate reductase (21), and fumarase (22).

[3] GF/C, Scientific Products.
[4] Protosol, New England Nuclear.
[5] Omnifluor (4 g/liter of toluene), New England Nuclear.
[6] Serle Delta 300.
[7] Sigma Chemical Co.
[8] Worthington Biochemical Corp., Freehold, N.J.

Table II—Inhibitory Actions of I and II on *E. coli* DNA, RNA, and Protein Synthesis

Concentration, *M*	Inhibition, % DNA	RNA	Protein
4×10^{-6} [a]	0	0	0
8×10^{-6} [a]	14	0	0
1.6×10^{-5} [a]	29	0	0
3.3×10^{-5} [a]	80	5	0
6.6×10^{-5} [a]	89	62	31
1.33×10^{-4} [a]	98	89	88
2.67×10^{-4} [a]	100	98	98
2.67×10^{-3} [a]	100	100	100
2.67×10^{-3} [b]	0	0	0

[a] I. [b] II (unchlorinated precursor).

Table III—Inhibitory Actions of I and II on *S. epidermidis* DNA, RNA, and Protein Synthesis

Concentration, *M*	Inhibition, % DNA	RNA	Protein
4×10^{-6} [a]	0	0	0
8×10^{-6} [a]	16	0	0
1.6×10^{-5} [a]	20	0	0
3.3×10^{-5} [a]	29	8	0
6.6×10^{-5} [a]	32	16	0
1.33×10^{-4} [a]	36	29	22
2.67×10^{-4} [a]	95	63	86
2.67×10^{-3} [a]	100	73	96
2.67×10^{-3} [b]	0	0	0

[a] I. [b] II (unchlorinated precursor).

RESULTS

The data shown in Table I demonstrate increasing tritium incorporation into the DNA, RNA, and protein of *E. coli* for up to 3 hr at 37° in all three processes. The low counts observed by the addition of acid at zero time or by placing the tube in an ice bath to quench the reactions indicate that the washing procedure used is effective in removing adsorbed but unincorporated radioactivity. Variation of the bacterial stock solution from 0.3 to 0.9 ml also showed proportionally increased incorporation of the radioactive precursor when studied for 1 hr of incubation. Similar results were seen using *S. epidermidis*.

The percent inhibitions of DNA, RNA, and protein synthesis by the *N*-chloramines shown in Tables II–V represent the mean of two experiments, each of which was carried out in triplicate. The individual values of these triplicate determinations were within 10% of the mean values indicated. Table II shows progressively increasing inhibitory effects with increasing concentration of 3-chloro-4,4-dimethyl-2-oxazolidinone (I) for all three cellular processes studied using *E. coli*. Similar conclusions are apparent from the data of Table III with *S. epidermidis*.

Tables IV and V show the effects of the chloramine molecule *N*-chlorosuccinimide (III) on the same two bacterial species shown in Tables II and III. The effects of III were similar to those seen using I, namely, progressively increasing inhibition for all three cellular biochemical processes with increasing chloramine concentration. The effects of 4,4-dimethyl-2-oxazolidinone (II), the unchlorinated precursor molecule of I, also were studied, and it was completely inert (Tables II and III). The

Table IV—Inhibitory Actions of III on *S. epidermidis* DNA, RNA, and Protein Synthesis

III Concentration, *M*	Inhibition, % DNA	RNA	Protein
4×10^{-6}	0	0	0
8×10^{-6}	0	0	0
1.6×10^{-5}	0	13	0
3.3×10^{-5}	19	14	4
6.6×10^{-5}	22	17	12
1.33×10^{-4}	37	35	29
2.67×10^{-4}	47	40	30
2.67×10^{-3}	100	80	96

Table V—Inhibitory Actions of III on *E. coli* DNA, RNA, and Protein Synthesis

III Concentration, *M*	Inhibition, %		
	DNA	RNA	Protein
4×10^{-6}	0	0	0
8×10^{-6}	0	0	0
1.6×10^{-5}	4	0	0
3.3×10^{-5}	10	5	8
6.6×10^{-5}	15	12	10
1.33×10^{-4}	32	16	16
2.67×10^{-4}	60	45	40
2.67×10^{-3}	100	100	95

Table VI—Effect of Addition of a Sulfhydryl-Containing Compound on the Chloramine Inhibition of Bacterial DNA Synthesis

Agent (2.67×10^{-3} *M*)	Dithiothreitol Concentration, *M*	Inhibition of DNA Using *E. coli*, %
I	0	100
I[a]	5.4×10^{-3} [a]	0
I[b]	2.67×10^{-3} [b]	26
I[b]	5.4×10^{-3} [b]	0
I[c]	5.4×10^{-3} [c]	0
None	5.4×10^{-3}	0
II	0	0
III	0	100
III[a]	2.67×10^{-3} [a]	36
III[b]	2.67×10^{-3} [b]	4
III[b]	5.4×10^{-3} [b]	0

[a] Mixed together and added to bacteria as a mixture. [b] Dithiothreitol added to bacteria first, followed by chloramine. [c] Compound I added to the bacteria containing tritiated thymidine and incubated at 37° for 1 hr followed by the addition of dithiothreitol. Fresh bacteria were added, and the incorporation of tritiated thymidine was measured 2 hr later.

unchlorinated precursor molecule (II) was studied under exactly the same conditions as the chloramines (I and III).

Table VI shows that addition of dithiothreitol can protect against the inhibition of DNA synthesis in bacteria. This result was seen when I was combined with dithiothreitol and then added to bacteria or, alternatively, when the bacteria were supplemented with dithiothreitol before the addition of I. Similar protective actions of dithiothreitol using III also have been demonstrated. Again, II had no inhibitory action. Addition of dithiothreitol or mercaptoethanol also could protect against the inhibition of RNA and protein synthesis.

The inhibitory actions of I are not due to chemical alteration of the tritiated thymidine, uridine, or leucine by the chloramine in which these precursors are rendered inert. This conclusion was reached since the chloramines, when added to bacteria with tritiated thymidine and incubated for 60 min at 37°, showed no significant inhibition of incorporation after fresh bacteria were added and incorporation was allowed to proceed for 2 additional hr (Table VI). Residual chloramine was inactivated by adding dithiothreitol immediately before the addition of fresh bacteria. Experiments using tritiated thymidine, uridine, and leucine with I or III gave similar results under identical experimental conditions. However, partial inactivation of the tritiated precursors at far higher chloramine concentrations (1×10^{-2} *M*) was observed.

The data obtained indicate that while the bacterial synthesis of DNA was significantly inhibited based on a *t* test for paired samples ($p < 0.001$), the chloramine did not produce statistically significant inhibition of the uptake or transport of tritiated thymidine into the bacterial cells. Bacteria were incubated together with 5×10^{-5} *M* I and [^{3}H]thymidine for 1 hr at 37°. The amount of tritiated precursor found in the bacterial acid-soluble pool is a direct reflection of the extent of thymidine transport into the bacterial cell (15). Similar results also were obtained using tritiated uridine and leucine.

These chloramines were effective inhibitors of sulfhydryl-containing enzymes (Table VII). Three general groups of enzymes were compared: (*a*) enzymes containing sulfhydryl groups at their active sites [malic dehydrogenase (23), lactic dehydrogenase (24), and creatine phosphokinase (25)]; (*b*) enzymes containing no sulfhydryl groups at their active sites but having sulfhydryl groups at other sites [fumarase (26)]; and (*c*) enzymes containing no sulfhydryl groups at any site [ribonuclease (27) and dihydrofolate reductase (21)].

The enzymes in the first group are inhibited easily (Table VII). The sulfhydryl group does not have to be present at the active site for inhibition to occur since fumarase also is quite sensitive. Some enzymes containing no sulfhydryl groups (dihydrofolate reductase) also can be inhibited but only at much higher chloramine concentrations ($\geq 10^{-2}$ *M*). However, ribonuclease was not inhibited, even at 10^{-2} *M*. All of the chloramine-induced enzymatic inhibitions could be prevented if the chloramines were mixed first with twice the concentration of the sulfhydryl-containing reagent dithiothreitol. The limiting amount of dithiothreitol that was capable of preventing chloramine-induced enzymatic inhibition was not explored. Reactivation of the inhibited enzymes by later addition of sulfhydryl agents after first reacting the enzyme with chloramine was not achieved. The unchlorinated precursor (II) was not effective in inhibiting any of the sulfhydryl-containing enzymes (Table VII).

The effects of increasing I concentrations on the overall growth of *E. coli* also were studied but are not presented in tabular form. Inhibition of bacterial growth was studied by incubating inoculated cultures of *E. coli* at 37° and monitoring the effect on turbidity (absorbance increase) at 450 nm against time at 10-hr intervals. The bacterial growth data represent the mean of triplicate determinations. Varying concentrations of I were added to the bacterial suspensions, and bacterial growth was followed for 4 days. The chloramine appeared to act as a bacteriostatic agent, at concentrations ranging from 5×10^{-5} to 4×10^{-4} *M*, in that bacterial growth was delayed. At concentrations of 5×10^{-4} *M* and higher, no bacterial growth was evident. When the organisms exposed to these higher doses were subcultured, no growth was apparent. These results suggest death of the organisms and show that I exerts bactericidal actions at higher concentrations.

Chemical Verification—Bacterial incorporation was allowed to proceed for 3 hr using radioactive thymidine, uridine, or leucine in different tubes. Cold 0.2 *N* perchloric acid was added, and the precipitates were washed twice with 0.2 *N* perchloric acid. The supernates were discarded, and the precipitates were dissolved and incubated in 0.3 *N* KOH for 1 hr at 37°. The material was reprecipitated with 0.7 *N* perchloric acid,

Table VII—Percent Inhibition of Enzyme Activity by Agent

Agent Concentration, *M*	Inhibition, %					
	Malic Dehydrogenase	Lactic Dehydrogenase	Creatine Phosphokinase	Fumarase	Ribonuclease	Dihydrofolate Reductase
1.33×10^{-5} [a]	0	0	0	50	0	—
2.67×10^{-5} [a]	0	0	0	—	0	—
5.34×10^{-5} [a]	16	10	0	—	0	—
1.07×10^{-4} [a]	20	15	5	100	0	—
2.14×10^{-4} [a]	48	30	15	—	0	—
4.28×10^{-4} [a]	54	40	30	100	0	—
8.56×10^{-4} [a]	62	50	53	100	0	—
1.28×10^{-2} [a]	100	100	85	100	0	—
1.72×10^{-2} [a]	100	100	100	100	0	50
1.72×10^{-2} [a] Added to dithiothreitol						
3.4×10^{-2} [a] (SH)	0	0	0	0	0	0
1.72×10^{-2} [b]	0	0	0	0	0	0

[a] I. [b] II (unchlorinated precursor).

collected on filters, and counted as described previously. The potassium hydroxide treatment resulted in >90% breakdown of the radioactive polymer produced with radioactive uridine.

The polymers produced with radioactive thymidine or leucine were not significantly affected by the alkaline treatment. RNA is known to be degraded by alkali, whereas DNA and protein are not affected (10, 13, 14). Heat treatment (70°) of the radioactive polymers with 0.5 *N* perchloric acid for 30 min resulted in the breakdown of the polymer produced using thymidine, while the polymer produced with leucine was unaffected. DNA is known to be degraded under these conditions of heating in the presence of acid (10, 13, 14).

Enzymatic Verification—The filters containing the radioactive polymers were immersed in solutions of deoxyribonuclease[7], ribonuclease[7], and a mixture of proteolytic enzymes[7] for 1 hr at 37°. The polymer produced using thymidine was degraded by deoxyribonuclease but was not affected by ribonuclease or the proteolytic enzymes. The polymer produced using uridine was degraded only by ribonuclease, and the polymer resulting from leucine incorporation was degraded only by proteolytic enzymes. These reactions strongly support the specific nature of these incorporation processes. (Further details may be obtained from Ref. 10.)

DISCUSSION

The data presented here and previous data (1–5) indicate that chloramines exert both bacteriostatic and bactericidal actions. The extent of the antimicrobial actions depends on the ratio of the bacterial concentration to that of chloramine and the length of exposure. These parameters also control the extent of enzyme inhibition. Both the antibacterial effects and the enzymatic inhibitory actions appear to be due to the powerful oxidative action of the chlorine component of the chloramine molecules. Support for this view is contributed by the facts that the unchlorinated precursor molecule is inactive and that the inhibitory effects of I and III can be abolished completely by first mixing the chloramine with the sulfhydryl compounds dithiothreitol or mercaptoethanol.

Thus, the present study indicates that one cellular mechanism for these antibacterial actions might be that these chloramines effectively attack the sulfhydryl groups, which can lead to enzymatic inactivation or denaturation. A natural consequence of such actions would be interference with major cellular processes (not shown previously) such as DNA, RNA, and protein synthesis, which depend on the subtle interaction of many sulfhydryl-containing enzymes. All three processes appear to be inhibited, and the antimicrobial actions apparently are not due to the selective inhibition of any one specific cellular function that is vastly more sensitive than the others. The data in Tables II and III suggest that DNA synthesis is slightly more sensitive to the action of I than is RNA or protein synthesis. The basis of action of these chloramine agents appears to be similar to that proposed for the bactericidal actions of chlorine (28).

The data in Tables II–V suggest that these chloramines inhibit bacterial synthesis of DNA, RNA, and protein. These results have several possible causes:

1. Chemical alteration of the radioactive precursors by the chloramine, resulting in the decreased incorporation into DNA, RNA, or protein. However, the data presented in Table VI show that this is not true. When bacteria, radioactive precursors, and chloramine were first incubated, no inhibition of incorporation was found after inactivating the chloramine by adding dithiothreitol and then adding fresh, viable bacteria. If the chloramines had reacted with the radioactive precursors and rendered them inert, normal incorporation would not have been demonstrated after inactivating the residual chloramine and adding fresh viable bacteria.

2. Chloramine inhibition of the transport of the radioactive precursor into the bacterial cell. However, the data discussed previously do not support inhibition of precursor transport but rather synthesis inhibition.

The data in Table VII demonstrate that enzymes containing sulfhydryl sites are inhibited by I at 10^{-4} *M*. Other enzymes without sulfhydryl sites (dihydrofolate reductase) may be inhibited at far higher concentrations (10^{-2} *M*) of chloramine, while another enzyme (ribonuclease) appears to be completely resistant. Attempts were made to protect the sulfhydryl groups of malate dehydrogenase and fumarase by reacting these enzymes with agents that reversibly combine with sulfhydryl groups (29). Both enzymes were incubated with 5,5-dithiobis(2-nitrobenzoic acid) and with *p*-hydroxymercuribenzoate. Chloramine was added later, and the incubation was continued. Dithiothreitol then was added to remove the protective agents and to inactivate any residual chloramine. No protective effects were evident against the actions of chloramine by these reversible sulfhydryl agents. It generally can be concluded that the sulfhydryl groups are attacked by these chloramine agents but that other sites also are attacked since non-sulfhydryl-containing enzymes are inhibited and since the chloramines still are capable of causing enzyme inhibition, even when the sulfhydryl groups are protected. The chloramine-induced inhibitions were not reversed simply by adding sulfhydryl reagents to bacteria or to purified enzymes after first incubating with chloramine.

While some enzymes containing sulfhydryl groups are inhibited by chloramines, this fact may not mean that all sulfhydryl-containing enzymes are inhibited, although they could be. Reversal of antibacterial activity by dithiothreitol also does not prove that a compound reacts by a sulfhydryl inhibition.

REFERENCES

(1) J. J. Kaminski, S. D. Worley, and N. Bodor, *Org. Mass Spectrom.*, **12,** 145 (1977).

(2) S. H. Gerson, S. D. Worley, N. Bodor, J. J. Kaminski, and T. W. Flechtner, *J. Electron. Spectrosc., Relat. Phenom.*, **13,** 421 (1978).

(3) S. D. Worley, S. H. Gerson, N. Bodor, J. J. Kaminski, and T. W. Flechtner, *J. Chem. Phys.*, **68,** 1313 (1978).

(4) J. J. Kaminski and N. Bodor, *Tetrahedron*, **32,** 1097 (1976).

(5) J. J. Kaminiski, N. Bodor, and T. Higuchi, *J. Pharm. Sci.*, **65,** 553 (1976).

(6) N. Bodor, J. J. Kaminski, S. D. Worley, R. J. Colton, T. H. Lee, and J. W. Rabalais, *ibid.*, **63,** 1387 (1974).

(7) J. J. Kaminski, M. M. Huycke, S. H. Selk, N. Bodor, and T. Higuchi, *ibid.*, **65,** 1737 (1976).

(8) M. Kosugi, J. J. Kaminski, S. H. Selk, I. H. Pitman, N. Bodor, and T. Higuchi, *ibid.*, **65,** 1743 (1976).

(9) H. H. Kohl, S. Haghighi, and C. A. McAuliffe, *Chem.-Biol. Interact.*, **29,** 327 (1980).

(10) D. Kennell, "Methods in Enzymology," vol. 12, part A, Academic, New York, N.Y., 1967, p. 686.

(11) H. H. Kohl, M. E. Friedman, P. Melius, E. C. Mora, and C. A. McAuliffe, *Chem.-Biol. Interact.*, **24,** 209 (1979).

(12) H. H. Kohl and O. Z. Sellinger, *J. Neurochem.*, **19,** 699 (1972).

(13) H. N. Munro, *Methods Biochem. Anal.*, **14,** 158 (1966).

(14) W. C. Hutchinson and H. N. Munro, *Analyst*, **86,** 768 (1961).

(15) H. Harder and B. Rosenberg, *Int. J. Cancer*, **6,** 207 (1970).

(16) M. E. Friedman, B. Musgrove, K. Lee, and J. E. Teggins, *Biochim. Biophys. Acta*, **250,** 286 (1971).

(17) W. E. C. Wacker, D. P. Ulmer, and B. L. Valler, *N. Engl. J. Med.*, **255,** 499 (1956).

(18) J. T. Oliver, *Biochem. J.*, **61,** 116 (1955).

(19) S. B. Rosalki, *J. Lab. Clin. Med.*, **69,** 696 (1967).

(20) M. Kunitz, *J. Biol. Chem.*, **164,** 563 (1964).

(21) L. E. Gundersen, R. B. Dunlap, N. G. Harding, J. H. Freisheim, F. M. Huennekens, and F. Otting, *Biochemistry* **11,** 1018 (1972).

(22) E. Racker, *Biochim. Biophys. Acta*, **4,** 20 (1950).

(23) P. D. Boyer, "The Enzymes," vol. 11, 3rd ed., Academic, New York, N.Y., 1975, p. 369.

(24) *Ibid.*, p. 191.

(25) *Ibid.*, vol. 8, 1973, p. 384.

(26) *Ibid.*, vol. 5, 1971, p. 539.

(27) *Ibid.*, vol. 4, 1971, p. 647.

(28) W. E. Knox, P. K. Stumpf, D. E. Green, and V. H. Auerbach, *J. Bacteriol.*, **55,** 451 (1948).

(29) J. L. Aull, A. C. Rice, and L. A. Tebbetts, *Biochemistry*, **16,** 672 (1977).

ACKNOWLEDGMENTS

H. H. Kohl was supported by Auburn University Grant-In-Aid 78-162.

High-Pressure Liquid Chromatographic Determination of Ftorafur [1-(Tetrahydro-2-furanyl)-5-fluorouracil] and GLC–Mass Spectrometric Determination of 5-Fluorouracil and Uracil in Biological Materials after Oral Administration of Uracil plus Ftorafur

TERUYOSHI MARUNAKA *x, YUKIHIKO UMENO *, KOZO YOSHIDA *, MASAHIRO NAGAMACHI *, YOSHINORI MINAMI *, and SETSURO FUJII ‡

Received November 14, 1979, from the **Research Laboratory, Taiho Pharmaceutical Co., Ltd., Tokushima, 771-01, Japan,* and the ‡*Division of Regulation of Macromolecular Function, Institute for Protein Research, Osaka University, Osaka, Japan.* Accepted for publication May 19, 1980.

Abstract □ Oral adminstration of uracil plus ftorafur [1-(tetrahydro-2-furanyl)-5-fluorouracil] has a greater antitumor effect than that of ftorafur alone. A high-pressure liquid chromatographic method was developed for the determination of ftorafur in plasma and visceral tissues with a sensitivity of 0.025 μg/ml or g of wet weight. A combination of GLC–mass fragmentography and GLC–mass spectrometry with total-ion monitoring was developed for the specific, simultaneous determination of 5-fluorouracil, an active metabolite, and uracil as their trimethylsilylated derivatives. The detection limits for 5-fluorouracil and uracil in the first method were 0.001 μg/ml for plasma and 0.001–0.005 μg/ml for visceral tissues, and those in the second method were 0.2 μg/ml or g of wet weight. The precision and sensitivity of the assay appear to be satisfactory for determination of the levels of these compounds in plasma and visceral tissues.

Keyphrases □ Ftorafur—high-pressure liquid chromatographic analysis in biological materials □ 5-Fluorouracil—GLC–mass spectrometric analysis in biological materials □ Uracil—GLC–mass spectrometric analysis in biological materials □ High-pressure liquid chromatography—analysis, ftorafur in biological materials □ GLC–mass spectrometry—analysis, 5-fluorouracil and uracil in biological materials □ Antineoplastic agents—uracil plus ftorafur, high-pressure liquid chromatographic and GLC–mass spectrometric analysis in biological materials

5-Fluorouracil and its derivatives have been widely used in cancer chemotherapy. Ftorafur [1-(tetrahydro-2-furanyl)-5-fluorouracil], a masked form of 5-fluorouracil, is an effective antitumor agent. It can be given orally and has lower toxicity than 5-fluorouracil (1–3).

Fujii and coworkers (4–8) recently reported that oral administration of uracil plus ftorafur (4:1 mole/mole) was more effective than that of ftorafur or 5-fluorouracil alone and resulted in a higher level of 5-fluorouracil, an active substance, in tumor tissues than did administration of an equimolar amount of ftorafur or 5-fluorouracil.

For elucidation of the mechanism of action of uracil, it seemed important to establish a quantitative method for the determination of the concentrations of uracil, ftorafur, and 5-fluorouracil in the blood and visceral tissues after uracil plus ftorafur treatment. A method already was reported for the determination of ftorafur and 5-fluorouracil in plasma and visceral tissues after administration of ftorafur in studies on a new antitumor agent, 1,3-bis(tetrahydro-2-furanyl)-5-fluorouracil (9–11); ftorafur was determined by TLC scanning densitometry or high-pressure liquid chromatography (HPLC), and 5-fluorouracil was determined by a microbiological assay using a sensitive bacterial strain or GLC–mass fragmentography with selected-ion monitoring.

Several other methods also have been reported: separate microbiological assays of ftorafur and 5-fluorouracil in plasma and visceral tissues (12, 13), simultaneous HPLC analysis of ftorafur and 5-fluorouracil in plasma and urine using a reversed-phase column (14, 15), and assay of ftorafur by GLC and of 5-fluorouracil by GLC–mass fragmentography in plasma and urine (16, 17).

The present paper describes a precise and sensitive method for the assay of ftorafur, 5-fluorouracil, and uracil in plasma and visceral tissues. Ftorafur is separated from the other compounds by solvent extraction and analyzed by HPLC using an adsorption chromatographic system. 5-Fluorouracil and uracil are silylated and then analyzed by GLC–mass fragmentography. Uracil also is determined simultaneously by GLC–mass spectrometry with total-ion monitoring.

EXPERIMENTAL

Materials—Ftorafur was synthesized and purified (18). 5-Fluorouracil[1], uracil[1], [1,3-$^{15}N_2$]-5-fluorouracil[2] (95% enrichment), and [1,3-$^{15}N_2$]uracil[3] (95% enrichment) were used as received. *N,O*-Bis(trimethylsilyl)trifluoroacetamide[4] and pyridine[4] were derivatizing agents for silylation. Chloroform, methanol, ethanol, and ethyl acetate were liquid chromatographic reagent grade[5]. The other chemicals[5] were analytical reagent grade. Ethylene dichloride[5] was dehydrated and distilled before use.

The samples of blood and visceral tissues were from male AH-130 tumor-bearing rats (160–180 g, 6–7 weeks old).

HPLC Conditions—The liquid chromatograph[6] was equipped with a high-pressure injection valve[7] and a UV detector[8] operating at 254 nm. An adsorption chromatographic column[9] (25 cm × 6.2 mm i.d.) was used for separation with a mobile phase of ethylene dichloride–ethanol (24:1 v/v) at a flow rate of 1.7 ml/min. The column was maintained at room temperature. A gradientor[10] was used for controlling the mobile phase concentration. For quantitative calculations, a computer system[11] was employed.

GLC–Mass Fragmentographic and GLC–Mass Spectrometric Conditions—A mass spectrometer[12] with an electron-impact ion source connected to a gas chromatograph[13] was used.

The coiled glass column (1.0 m × 2.0 mm i.d.) of the gas chromatograph was packed with 3% OV-17 on Chromosorb W AW[14] (80–100 mesh) and

[1] Sigma Chemical Co., St. Louis, Mo.
[2] PCR Inc., Gainesville, Fla.
[3] Merck Sharp and Dohme Canada Ltd., Quebec, Canada.
[4] Pierce Chemical Co., Rockford, Ill.
[5] Wako Pure Chemical Co., Osaka, Japan.
[6] Model LC-2, Shimadzu, Kyoto, Japan.
[7] Model SIL-1A, Shimadzu, Kyoto, Japan.
[8] Model UVD-2, Shimadzu, Kyoto, Japan.
[9] Zorbax SIL (Du Pont), purchased from Shimadzu, Kyoto, Japan.
[10] Model GRE-2, Shimadzu, Kyoto, Japan.
[11] Model 1A Chromatopac, Shimadzu, Kyoto, Japan.
[12] Model JMS-D 300, JEOL, Tokyo, Japan.
[13] Model JGC-20KP, JEOL, Tokyo, Japan.
[14] Gaschro Kogyo Co., Tokyo, Japan.

0022-3549/80/1100-1296$01.00/0
© 1980, American Pharmaceutical Association

was conditioned at 280° for 24 hr. The injector, column, and ion source temperatures were 210, 150, and 230°, respectively. After 5-fluorouracil, uracil, and their internal standard had been detected, the temperature of the column was raised to 280° for 3 min to burn out the remaining materials and then was returned to the operational temperature before the next analysis. The carrier gas was helium, and the flow rate was 30 ml/min.

For mass fragmentography, the mass spectrometer was set at the following conditions: ionization energy, 70 ev; ionization current, 300 μamp; accelerating voltage, 3.0 kv; and ion multiplier voltage, 1.4 kv. The peaks of the molecular ions of the trimethylsilyl derivatives of 5-fluorouracil, uracil, and the respective internal standards ([1,3-$^{15}N_2$]-5-fluorouracil and [1,3-$^{15}N_2$]uracil), *m/e* 274, 256, 276, and 258, respectively, were selected for mass fragmentographic analysis. When necessary, uracil was simultaneously analyzed by GLC–mass spectrometry.

Analytical Procedure—Blood samples were collected in heparinized containers and centrifuged to separate the plasma. Visceral tissues were collected by the freeze-clamping technique and rapidly bled or perfused with cold physiological saline to remove blood. The plasma and visceral tissues then were frozen until analysis.

The plasma (0.5 ml) was diluted to 2.0 ml with distilled water containing 0.1 μg of [1,3-$^{15}N_2$]-5-fluorouracil and 0.5 μg of [1,3-$^{15}N_2$]uracil as internal standards. A sample of 0.5–1.0 g of visceral tissue was homogenized in an ice bath with physiological saline containing 0.1 μg of [1,3-$^{15}N_2$]-5-fluorouracil and 5.0 μg of [1,3-$^{15}N_2$]uracil and then centrifuged at 2000×*g* for 20 min; 1.0 ml of the resulting supernate was diluted to 2.0 ml with distilled water. The samples of plasma and visceral tissue homogenates were adjusted to pH 4.0 with 5 *N* HCl and shaken vigorously with 20 ml of chloroform at room temperature for 10 min.

This extraction was repeated again, and the combined chloroform extracts containing ftorafur were evaporated to dryness at <25°, transferred to a 10-ml test tube by washing with chloroform, and dried under nitrogen. The residue was dissolved in 100 μl of ethylene dichloride, and 20 μl of this solution was injected into the liquid chromatograph.

The aqueous layer containing 5-fluorouracil and uracil separated from the chloroform layer was neutralized with sodium hydroxide solution, adjusted to pH 6.0 with 0.2 ml of 0.5 *M* NaH_2PO_4, and centrifuged at 2000×*g* for 15 min to remove protein. The supernate was extracted with 40 ml of ethyl acetate by vigorous shaking for 20 min. The ethyl acetate layer was evaporated at 40°, transferred to a 1.0-ml reaction vial by washing with methanol, and dried under nitrogen at 40°. The residue was dried thoroughly over phosphorus pentoxide under reduced pressure and subjected to silylation at 70° for 20 min by addition of a freshly prepared solution of 100 μl of pyridine containing 20% *N,O*-bis(trimethylsilyl)-trifluoroacetamide. Then 1–3 μl of the solution was injected into the gas chromatograph–mass spectrometer.

Calibration Curves—Calibration curves were prepared by adding known amounts of ftorafur (20.0, 10.0, 5.0, 1.0, 0.5, 0.1, and 0.05 μg/ml), 5-fluorouracil (1.0, 0.5, 0.25, 0.10, 0.05, 0.01, and 0.005 μg/ml), and uracil (50.0, 25.0, 10.0, 5.0, 2.5, 1.0, 0.5, 0.25, 0.10, 0.05, 0.01, and 0.005 μg/ml) to plasma (1.0 ml) and organ homogenates (1.0 ml from 1.0 g of wet weight) and then analyzing by the same extraction procedure.

The calibration curve for the determination of ftorafur by HPLC was prepared by plotting the peak area against the concentration of ftorafur. Calibration curves for 5-fluorouracil and uracil analyzed by GLC–mass fragmentography and GLC–mass spectrometry were obtained by plotting the ratio of the peak heights of the respective trimethylsilyl derivatives to those of the trimethylsilyl derivatives of the internal standards, [1,3-$^{15}N_2$]-5-fluorouracil and [1,3-$^{15}N_2$]uracil, using GLC–mass fragmentography against the concentrations of these compounds. All of the calibration curves gave good results.

RESULTS AND DISCUSSION

The investigation of the simultaneous determination of ftorafur, 5-fluorouracil, and uracil by HPLC using a reversed-phase column and by GLC based on silylation or on-column methylation with a flame-ionization detector showed that a suitable HPLC retention time of each compound could not be obtained and that ftorafur and 5-fluorouracil were difficult to separate by GLC after silylation, while 5-fluorouracil and uracil were not separated by on-column methylation. Thus, reversed-phase HPLC and GLC were not suitable for the simultaneous assay of ftorafur, 5-fluorouracil, and uracil.

Two independent assay procedures were investigated next on the basis of the physicochemical properties of these compounds. Ftorafur could be recovered from aqueous solution with an organic solvent, and 5-fluorouracil and uracil remained in the aqueous layer. Therefore, extraction

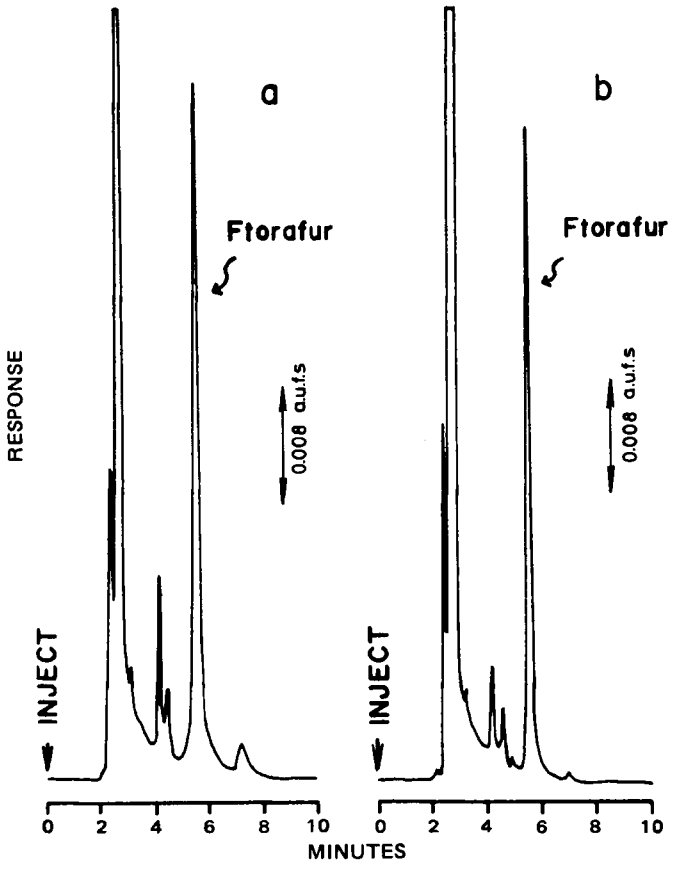

Figure 1—*High-pressure liquid chromatograms showing the separation of ftorafur extracted from plasma* (a) *and tumor tissue* (b) *of AH-130 tumor-bearing rats after addition at 5.0 μg/ml or g of wet weight. The conditions were: column, Zorbax SIL (25 cm × 6.2 mm i.d.); mobile phase, ethylene dichloride–ethanol (24:1 v/v); and flow rate, 1.7 ml/min (room temperature).*

with chloroform from an aqueous solution acidified with hydrochloric acid was employed for quantitative separation of ftorafur from 5-fluorouracil and uracil. Ftorafur then was determined by HPLC using an adsorption column, and 5-fluorouracil and uracil were analyzed by GLC–mass fragmentography and GLC–mass spectrometry.

A Zorbax SIL column was used for the separation of ftorafur extracted from chloroform. Ftorafur was well separated from biological constituents when a mixture of a nonpolar solvent (*e.g.*, chloroform, methylene chloride, ethylene dichloride, or *n*-hexane) containing 1–5% alcohol (*e.g.*,

Table I—Recoveries of Ftorafur, 5-Fluorouracil, and Uracil from Plasma and Visceral Tissues of AH-130 Tumor-Bearing Rats

Tissue	Recovery[a], %		
	Ftorafur	5-Fluorouracil	Uracil
Saline	100.7 ± 1.5	91.4 ± 3.2	84.1 ± 3.1
Plasma	100.3 ± 1.2	86.1 ± 3.7	81.5 ± 3.8
Heart	99.9 ± 1.4	72.0 ± 4.1	66.8 ± 4.3
Intestine	100.1 ± 1.2	76.8 ± 3.5	69.3 ± 3.2
Kidney	99.8 ± 1.6	67.5 ± 4.8	65.0 ± 3.7
Liver	99.6 ± 1.8	63.5 ± 5.1	62.4 ± 4.1
Lung	100.5 ± 1.3	71.0 ± 3.5	64.7 ± 4.9
Muscle	101.1 ± 1.3	79.0 ± 3.4	73.3 ± 3.3
Spleen	100.0 ± 1.8	71.0 ± 4.1	64.9 ± 4.2
Stomach	100.1 ± 1.4	77.0 ± 3.3	69.8 ± 3.2
Testis	99.9 ± 1.1	72.0 ± 3.5	63.2 ± 4.4
Thymus	99.7 ± 1.3	64.5 ± 4.3	61.4 ± 4.6
Tumor	100.4 ± 1.5	81.0 ± 3.3	76.3 ± 3.3

[a] Each value is the mean of five determinations for the particular amount added. Amounts added were: ftorafur, 20.0, 5.0, 0.5, 0.1, and 0.05 μg/ml or g of wet weight; 5-fluorouracil, 0.5, 0.1, 0.05, 0.01, and 0.005 μg/ml or g of wet weight; and uracil, 50.0, 25.0, 10.0, and 2.5 μg/g of wet weight and 0.5, 0.1, 0.05, 0.01, and 0.005 μg/ml for saline, plasma, and visceral tissues.

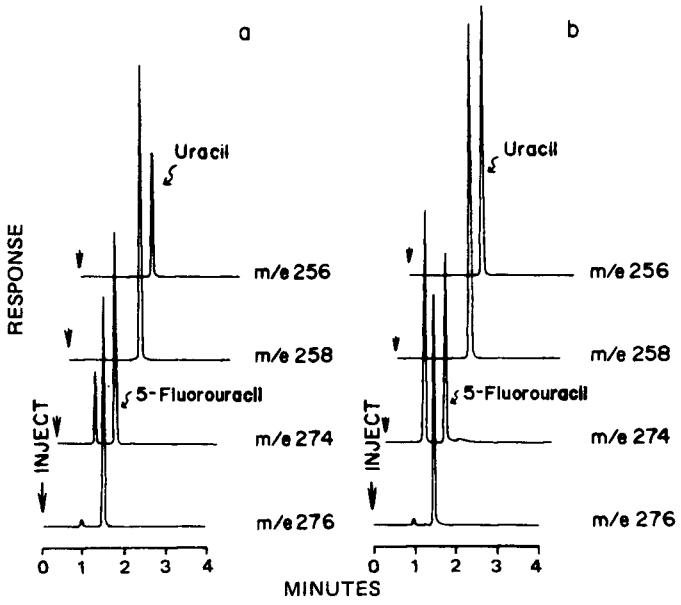

Figure 2—*Mass fragmentograms showing the separation of 5-fluorouracil, uracil, and the respective internal standards extracted from plasma* (a) *and tumor tissue* (b) *of AH-130 tumor-bearing rats. Results are for the trimethylsilylated derivatives.*

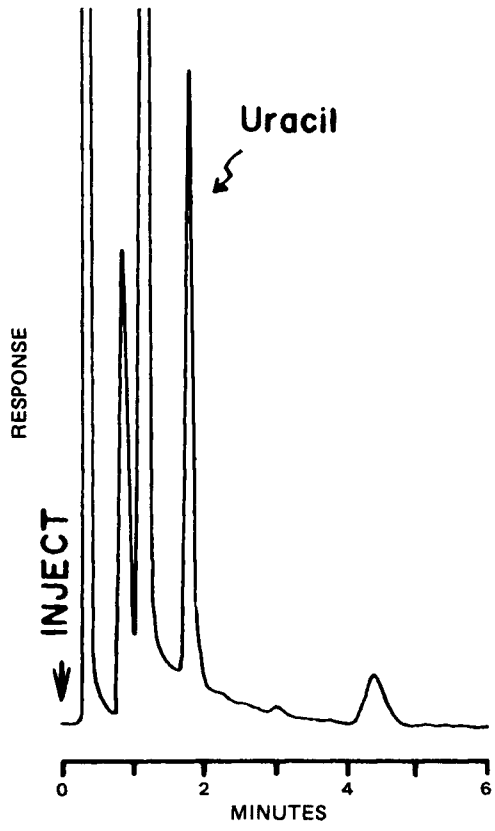

Figure 3—*Chromatogram by GLC–mass spectrometry showing the separation of uracil extracted from tumor tissue of AH-130 tumor-bearing rats. Results are for the trimethylsilyl derivatives.*

methanol, ethanol, or isopropanol) was the mobile phase. Of the solvent systems tested, ethylene dichloride–ethanol (24:1) was chosen as the mobile phase because it gave suitable chromatographic separation and analysis time.

The supernate of each organ homogenate must be extracted with chloroform; otherwise, the large amounts of lipid-soluble materials extracted with chloroform disturb the HPLC analysis.

Known amounts of ftorafur were added to plasma and homogenates of various organs of AH-130 tumor-bearing rats. The HPLC separation of ftorafur extracted from plasma and tumor tissue is shown in Fig. 1. The retention time of ftorafur was 6.3 min. As shown in Table I, the recoveries of ftorafur from plasma and each organ were quantitative, and the detection limit for ftorafur using this HPLC method was 0.025 μg/ml or g of wet weight for plasma and visceral tissues. The reproducibility was ±1.5–2.1%.

5-Fluorouracil and uracil have similar physicochemical properties. Thus, the addition of 0.5 *M* NaH_2PO_4 to the aqueous layer containing 5-fluorouracil and uracil and subsequent extraction with ethyl acetate as described previously (10, 11) resulted in good, constant recoveries.

The silylation procedure with *N,O*-bis(trimethylsilyl)trifluoroacetamide was sensitive, giving excellent GLC–mass fragmentographic and GLC–mass spectrometric separations of 5-fluorouracil and uracil extracted with ethyl acetate.

The internal standards, [1,3-$^{15}N_2$]-5-fluorouracil and [1,3-$^{15}N_2$]uracil, which are labeled with the stable isotope of nitrogen, were used for the simultaneous determination of 5-fluorouracil and uracil by the multiple-ion detection technique. The mass fragment ions detected for GLC–mass fragmentography were the molecular ion peaks (M^+) in the mass spectra of the trimethylsilyl derivatives of 5-fluorouracil and uracil since their base peaks ($M - CH_3$) were not separated clearly in some samples.

The best ion multiplier voltage of the mass spectrometer was 1.4 kv for the simultaneous determination of 5-fluorouracil and uracil by GLC–mass fragmentography. At this voltage, these compounds could be measured at concentrations of 0.001–2.5 μg/100 μl of silylating solvent. Under this condition, the concentrations of 5-fluorouracil could be analyzed in most samples, but the concentrations of uracil exceeded the upper detection limit. In particular, an extremely large difference was observed between the concentrations of 5-fluorouracil and uracil in tumor tissue having a large pool of uracil and those in the plasma collected soon after coadministration of uracil and ftorafur. In such samples, the two compounds could not be measured simultaneously at the ion multiplier voltage of 1.4 kv since the concentration of uracil was saturated. This problem could be overcome by two analytical runs at different values of the ion multiplier voltage: 5-fluorouracil was measured at an ion multiplier voltage of 1.4 kv, and uracil was measured at 1.2 kv. However, in this study, simultaneous detection by GLC–mass fragmentography and GLC–mass spectrometry was used, and conditions were developed for the simultaneous measurement of 5-fluorouracil and uracil in all kinds of samples.

Known amounts of 5-fluorouracil and uracil were added to plasma and homogenates of various organs of AH-130 tumor-bearing rats, and the samples were analyzed. The GLC–mass fragmentographic separation

Table II—Changes in the Concentration of Uracil Pooled in the Plasma, Liver, and Tumor of AH-130 Tumor-Bearing Rats by Incubation with Shaking at Various Temperatures

Incubation Conditions	Concentration of Uracil Detected[a]		
	Plasma, μg/ml	Tumor, μg/g	Liver, μg/g
Control	0.283 ± 0.067	32.793 ± 1.783	15.803 ± 0.998
−20 – −30°, 24 hr	0.282 ± 0.031	32.864 ± 1.345	15.834 ± 0.878
5°, 2 hr	0.283 ± 0.024	32.866 ± 1.567	15.821 ± 0.985
5°, 24 hr	0.283 ± 0.064	35.416 ± 1.857	16.751 ± 1.007
Room temperature, 12 hr	0.281 ± 0.058	57.654 ± 4.171	26.783 ± 3.110
Room temperature, 24 hr	0.276 ± 0.074	124.900 ± 7.895	56.406 ± 5.157
37°, 24 hr	0.255 ± 0.088	339.576 ± 23.694	140.078 ± 14.953

[a] Average of three determinations.

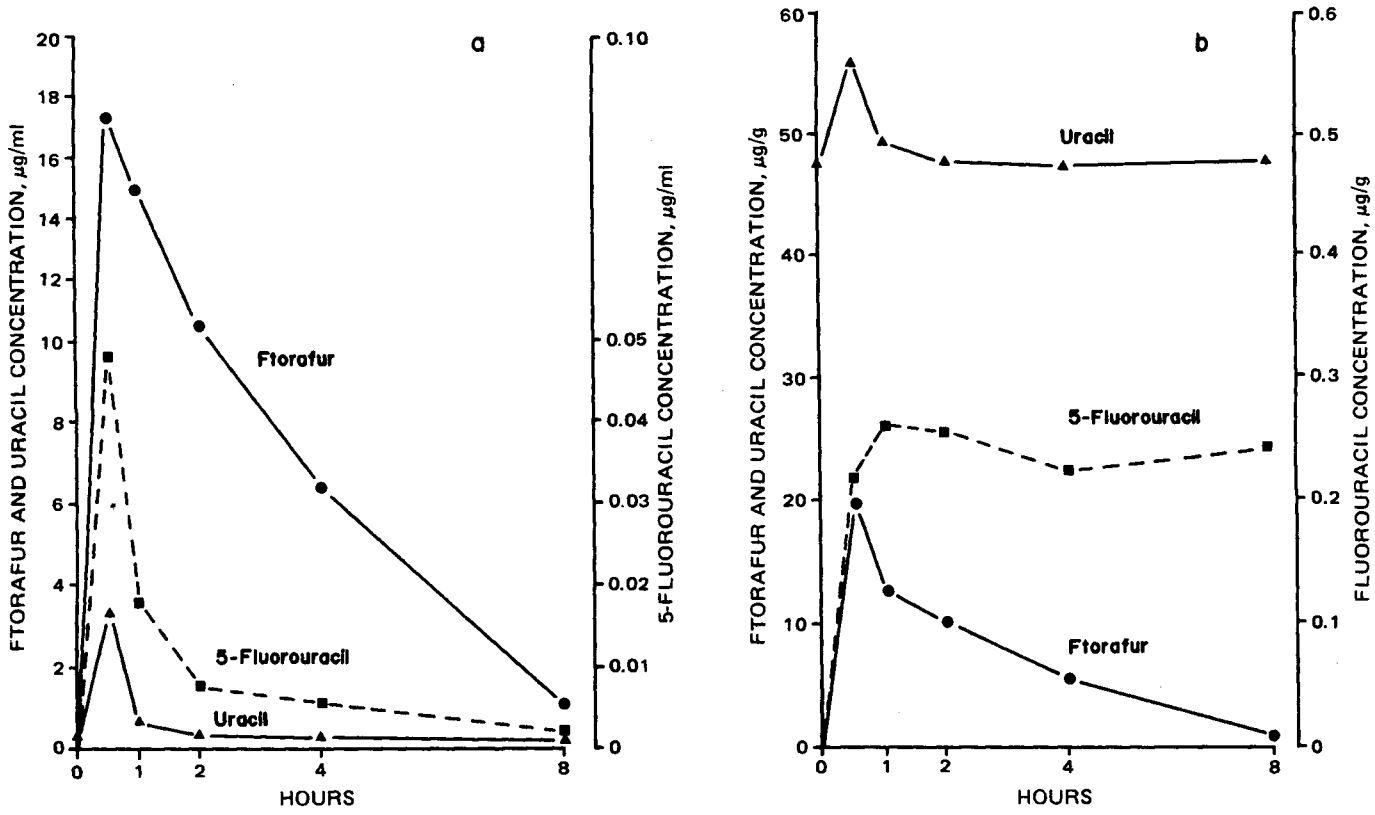

Figure 4—*Plasma levels* (a) *and tumor levels* (b) *of ftorafur, 5-fluorouracil, and uracil after a single oral dose of uracil (33.6 mg) plus ftorafur (5.0 mg) (4:1 mole/mole) to AH-130 tumor-bearing rats.*

of the trimethylsilyl derivatives of 5-fluorouracil, uracil, and their internal standard extracted from plasma and tumor tissue is shown in Fig. 2. The GLC–mass spectrometric separation of uracil extracted from tumor tissue is shown in Fig. 3. The retention times of 5-fluorouracil and uracil as their trimethylsilyl derivatives were 1.5 and 1.8 min, respectively. The recoveries from plasma were 86.1 ± 3.7% for 5-fluorouracil and 81.5 ± 3.8% for uracil, and those from visceral tissues were ~75% for 5-fluorouracil and ~70% for uracil. Since uracil forms pools naturally in all biological materials, the recovery of uracil was determined in a separate experiment by GLC–mass fragmentography and GLC–mass spectrometry utilizing [1,3-$^{15}N_2$]uracil and 5-chlorouracil (ion peak detected was *m/e* 275, M − CH_3) as internal standards.

The detection limits for 5-fluorouracil and uracil for GLC–mass fragmentography were 0.001 μg/ml for plasma and 0.001–0.005 μg/g of wet weight for visceral tissues; the detection limit for GLC–mass spectrometry was 0.2 μg/ml or g of wet weight. The reproducibility of this method was ±2.2–3.4%.

As reported previously (10, 11), the decomposition of ftorafur and 5-fluorouracil nucleosides or nucleotides had no significant effect on the assay of 5-fluorouracil. To examine the effect of decomposition of uracil nucleosides or nucleotides, authentic samples of these compounds were dissolved in physiological saline, plasma, and tissue homogenates of the liver and tumor and then analyzed for their uracil concentration. The results showed no significant differences between the values of the control and test samples and that decomposition of uracil nucleosides and nucleotides had no appreciable influence on the measurement of uracil with the present method.

The results obtained with the present method showed that the pools of uracil in various tissues were fairly high, as reported by Fujimoto *et al.* (19). Thus, the following experiments were conducted. First, changes in the uracil concentration were examined by incubation of plasma and tissue homogenates of the liver and tumor with shaking at various temperatures before measurement. As shown in Table II, the uracil concentration did not differ significantly from control values after incubation at various temperatures for plasma and at 5 or −20–−30° (frozen) for the liver and tumor. However, the uracil concentration increased with incubation at room temperature or 37° for the liver and tumor. This change in the uracil concentration probably is due mainly to the enzymatic decomposition of nucleosides and nucleotides.

Next, plasma and tissue homogenates of the tumor and liver were acidified with hydrochloric acid and extracted with chloroform, and the supernate of the aqueous layer was incubated with shaking at 37° for 24 hr. No significant difference between the concentration of uracil in the control and test samples was observed. Thus, as well as causing deproteinization, extraction with chloroform in hydrochloric acid inactivated enzymes that hydrolyzed the glycoside bonds of nucleosides and nucleotides.

On the basis of these observations, it was concluded that the present method, in which tissues were homogenized in an ice bath at a temperature below 5° and the supernate was acidified with hydrochloric acid and extracted with chloroform, did not involve any procedure that affects the determination of 5-fluorouracil and uracil.

The present method also can be applied to plasma and visceral tissues of other animals. The results obtained for the chromatographic separation, recoveries, and sensitivities were in good agreement with those obtained with AH-130 tumor-bearing rats. It is not ethically possible to obtain all kinds of human tissues; however, results with plasma and tumor tissue from humans gave similar results to those obtained with animals, indicating the applicability of the present method to human tissues.

Uracil plus ftorafur (4:1 mole/mole) was given orally to AH-130 tumor-bearing rats, and the time course of changes in the concentrations of ftorafur, 5-fluorouracil, and uracil in plasma and tumor tissue was measured by the present method (Fig. 4). Since the concentration of uracil represents the sum of the original amount and that resulting from uracil plus ftorafur treatment, individual differences in the original pools of uracil, especially in organs, sometimes were so large that they masked the time course of change in exogenous uracil after administration of uracil plus ftorafur. However, it should be possible to measure the time course using a labeled compound.

Because ftorafur and 5-fluorouracil are metabolized together with uracil, the present method for the simultaneous determination of ftorafur, 5-fluorouracil, and uracil in plasma and visceral tissues should be useful. Furthermore, this method will be helpful for basic and clinical pharmacological studies on uracil plus ftorafur and ftorafur alone.

REFERENCES

(1) C. Konda, H. Niitani, N. Sakauchi, A. Suzuki, Y. Sakai, T. Sakano, M. Shimoyama, T. Kitahara, S. Kumaoka, and K. Kimura, *Jpn. J. Cancer*

Clin., **19**, 495 (1973).
(2) Y. Takemasa, M. Suehara, Y. Koyama, and K. Kimura, *Cancer Chemother. (Tokyo)*, **1**, 259 (1974).
(3) T. Saito, A. Wakui, M. Yokoyama, H. Takahashi, K. Takahashi, H. Tshigaki, K. Watanabe, and S. Tada, *J. Jpn. Soc. Cancer Ther.*, **9**, 395 (1974).
(4) S. Fujii, K. Ikenaka, M. Fukushima, and T. Shirasaka, *Gann*, **69**, 763 (1978).
(5) S. Fujii, S. Kitano, K. Ikenaka, and T. Shirasaka, *Cancer Chemother. (Tokyo)*, **6**, 377 (1979).
(6) *Ibid.*, **70**, 209 (1979).
(7) T. Taguchi, Y. Nakano, K. Jikuya, S. Fujii, K. Ikenaka, and M. Fukushima, *Cancer Chemother. (Tokyo)*, **5**, 1161 (1978).
(8) T. Taguchi, Y. Nakano, S. Fujii, and T. Shirasaka, *ibid.*, **5**, 1167 (1978).
(9) Y. Kawaguchi, Y. Nakamura, T. Sato, S. Takeda, T. Marunaka, and S. Fujii, *Yakugaku Zasshi*, **98**, 525 (1978).
(10) T. Marunaka and Y. Umeno, *J. Chromatogr.*, **157**, 321 (1978).
(11) T. Marunaka, Y. Umeno, and Y. Minami, *ibid.*, **188**, 270 (1980).
(12) H. Fujita, *Cancer Chemother. (Tokyo)*, **1**, 497 (1974).
(13) Y. Yasuda, T. Togo, N. Unemi, S. Watanabe, K. Harima, and T. Suzue, *Nippon Kagaku Ryohogakukai Zasshi*, **21**, 1171 (1973).
(14) L. A. Benvenuto, K. Lu, and T. L. Loo, *J. Chromatogr.*, **134**, 219 (1977).
(15) A. T. Wu, J. L. Au, and W. Sadee, *Cancer Res.*, **38**, 210 (1978).
(16) A. T. Wu, H. J. Schwandt, C. Finn, and W. Sadee, *Res. Commun. Chem. Pathol. Pharmacol.*, **14**, 89 (1976).
(17) J. P. Horwitz, *Proc. Am. Assoc. Cancer Res.*, **18**, 20 (1977).
(18) M. Yasumoto, I. Yamawaki, T. Marunaka, and S. Hashimoto, *J. Med. Chem.*, **21**, 738 (1978).
(19) S. Fujimoto, T. Akao, B. Itoh, I. Koshizuka, K. Koyano, Y. Kistukawa, M. Takahashi, T. Minami, H. Ishigami, Y. Nomura, and K. Itoh, *Cancer Res.*, **36**, 33 (1976).

Use of Stable Isotopes in the Study of Pharmacokinetics of Drugs by Mass Fragmentography II: Detailed Examination of Pharmacokinetics of a Single Oral Dose of Phenytoin in Humans

SHIGEO BABA ˣ, TSUYOSHI GOROMARU, KAZUSHIGE YAMAZAKI, and YASUJI KASUYA

Received May 14, 1979, from the *Tokyo College of Pharmacy, 1432-1 Horinouchi, Hachioji, Tokyo 192-03, Japan.* Accepted for publication May 16, 1980.

Abstract □ To study the pharmacokinetics of phenytoin in detail, a mass fragmentographic method was applied for the precise, sensitive, and specific analysis of phenytoin, 5-(4-hydroxyphenyl)-5-phenylhydantoin, and 5-(4-hydroxyphenyl)-5-phenylhydantoin glucuronide in plasma and urine after administration of a single oral dose of phenytoin to two healthy volunteers. Salivary phenytoin concentrations also were measured. Phenytoin and 5-(4-hydroxyphenyl)-5-phenylhydantoin were analyzed after the addition of deuterium-labeled internal standards and conversion to volatile methyl derivatives for mass fragmentographic analysis. The lower limit of detection was ~10 ng/ml. The simultaneous pharmacokinetic analysis of the plasma levels and urinary excretion data of phenytoin and its major metabolite, 5-(4-hydroxyphenyl)-5-phenylhydantoin, yielded detailed information about the pharmacokinetics of phenytoin.

Keyphrases □ Mass fragmentography—application to pharmacokinetic study of single oral phenytoin dose using stable isotope labeling, humans □ Phenytoin—pharmacokinetics, application of mass fragmentography after single oral dose using stable isotope labeling, humans □ Pharmacokinetics—phenytoin, application of mass fragmentography after single oral dose using stable isotope labeling, humans

GLC–mass spectrometry coupled with selected-ion monitoring is used increasingly in drug research because of its high sensitivity and specificity. In this technique, stable isotope-labeled carriers serve as ideal internal standards to correct for losses of the compound under study in the initial isolation procedures. The usefulness of mass fragmentography in conjunction with stable isotope labeling has been of recent interest in the measurement of trace amounts of substances in biological materials (1–3). This method was used in these laboratories for the metabolic study of drugs in animals and humans (4–6). The mass fragmentographic technique also has been applied for the sensitive, specific, and reliable determination of plasma testosterone levels in humans (7).

Pharmacokinetic studies represent one field in which the sensitivity and specificity of the mass fragmentographic technique offer an advantage. Sullivan and coworkers (8, 9) successfully used stable isotope-labeled drugs together with mass fragmentography to study steady-state pharmacokinetics. An investigation of the elimination kinetics of drugs was carried out in these laboratories by measuring the nanogram levels of a drug and its major metabolites in human urine using this technique (10).

The present paper describes the use of deuterium-labeled phenytoin (I) and its major metabolite, 5-(4-hydroxyphenyl)-5-phenylhydantoin (II), along with mass fragmentography to follow saliva, plasma, and urinary concentrations of I and II for a reasonable period after a single oral administration of I to humans. A detailed analysis and interpretation of the pharmacokinetic data of I from two healthy volunteers also are presented.

EXPERIMENTAL

Synthesis of Deuterated Internal Standards—*Pentadeuterophenytoin (I-*d_5*)*—Deuterobenzophenone (benzophenone-d_5) was prepared by refluxing a mixture of 9.50 g of hexadeuterobenzene[1] (99.5 atom % D) and 2.44 g of benzoyl chloride[2] for 5 hr with 2.70 g of anhydrous aluminum chloride. The I-d_5 then was synthesized from the benzophenone-d_5 according to the method described by Baty and Robinson (11).

[1] Merck.
[2] Wako Pure Chemical Industries.

0022-3549/80/1100-1300$01.00/0
© 1980, American Pharmaceutical Association

Clin., **19**, 495 (1973).
(2) Y. Takemasa, M. Suehara, Y. Koyama, and K. Kimura, *Cancer Chemother. (Tokyo)*, **1**, 259 (1974).
(3) T. Saito, A. Wakui, M. Yokoyama, H. Takahashi, K. Takahashi, H. Tshigaki, K. Watanabe, and S. Tada, *J. Jpn. Soc. Cancer Ther.*, **9**, 395 (1974).
(4) S. Fujii, K. Ikenaka, M. Fukushima, and T. Shirasaka, *Gann*, **69**, 763 (1978).
(5) S. Fujii, S. Kitano, K. Ikenaka, and T. Shirasaka, *Cancer Chemother. (Tokyo)*, **6**, 377 (1979).
(6) *Ibid.*, **70**, 209 (1979).
(7) T. Taguchi, Y. Nakano, K. Jikuya, S. Fujii, K. Ikenaka, and M. Fukushima, *Cancer Chemother. (Tokyo)*, **5**, 1161 (1978).
(8) T. Taguchi, Y. Nakano, S. Fujii, and T. Shirasaka, *ibid.*, **5**, 1167 (1978).
(9) Y. Kawaguchi, Y. Nakamura, T. Sato, S. Takeda, T. Marunaka, and S. Fujii, *Yakugaku Zasshi*, **98**, 525 (1978).
(10) T. Marunaka and Y. Umeno, *J. Chromatogr.*, **157**, 321 (1978).
(11) T. Marunaka, Y. Umeno, and Y. Minami, *ibid.*, **188**, 270 (1980).
(12) H. Fujita, *Cancer Chemother. (Tokyo)*, **1**, 497 (1974).
(13) Y. Yasuda, T. Togo, N. Unemi, S. Watanabe, K. Harima, and T. Suzue, *Nippon Kagaku Ryohogakukai Zasshi*, **21**, 1171 (1973).
(14) L. A. Benvenuto, K. Lu, and T. L. Loo, *J. Chromatogr.*, **134**, 219 (1977).
(15) A. T. Wu, J. L. Au, and W. Sadee, *Cancer Res.*, **38**, 210 (1978).
(16) A. T. Wu, H. J. Schwandt, C. Finn, and W. Sadee, *Res. Commun. Chem. Pathol. Pharmacol.*, **14**, 89 (1976).
(17) J. P. Horwitz, *Proc. Am. Assoc. Cancer Res.*, **18**, 20 (1977).
(18) M. Yasumoto, I. Yamawaki, T. Marunaka, and S. Hashimoto, *J. Med. Chem.*, **21**, 738 (1978).
(19) S. Fujimoto, T. Akao, B. Itoh, I. Koshizuka, K. Koyano, Y. Kistukawa, M. Takahashi, T. Minami, H. Ishigami, Y. Nomura, and K. Itoh, *Cancer Res.*, **36**, 33 (1976).

Use of Stable Isotopes in the Study of Pharmacokinetics of Drugs by Mass Fragmentography II: Detailed Examination of Pharmacokinetics of a Single Oral Dose of Phenytoin in Humans

SHIGEO BABA ˣ, TSUYOSHI GOROMARU, KAZUSHIGE YAMAZAKI, and YASUJI KASUYA

Received May 14, 1979, from the *Tokyo College of Pharmacy, 1432-1 Horinouchi, Hachioji, Tokyo 192-03, Japan.* Accepted for publication May 16, 1980.

Abstract □ To study the pharmacokinetics of phenytoin in detail, a mass fragmentographic method was applied for the precise, sensitive, and specific analysis of phenytoin, 5-(4-hydroxyphenyl)-5-phenylhydantoin, and 5-(4-hydroxyphenyl)-5-phenylhydantoin glucuronide in plasma and urine after administration of a single oral dose of phenytoin to two healthy volunteers. Salivary phenytoin concentrations also were measured. Phenytoin and 5-(4-hydroxyphenyl)-5-phenylhydantoin were analyzed after the addition of deuterium-labeled internal standards and conversion to volatile methyl derivatives for mass fragmentographic analysis. The lower limit of detection was ~10 ng/ml. The simultaneous pharmacokinetic analysis of the plasma levels and urinary excretion data of phenytoin and its major metabolite, 5-(4-hydroxyphenyl)-5-phenylhydantoin, yielded detailed information about the pharmacokinetics of phenytoin.

Keyphrases □ Mass fragmentography—application to pharmacokinetic study of single oral phenytoin dose using stable isotope labeling, humans □ Phenytoin—pharmacokinetics, application of mass fragmentography after single oral dose using stable isotope labeling, humans □ Pharmacokinetics—phenytoin, application of mass fragmentography after single oral dose using stable isotope labeling, humans

GLC–mass spectrometry coupled with selected-ion monitoring is used increasingly in drug research because of its high sensitivity and specificity. In this technique, stable isotope-labeled carriers serve as ideal internal standards to correct for losses of the compound under study in the initial isolation procedures. The usefulness of mass fragmentography in conjunction with stable isotope labeling has been of recent interest in the measurement of trace amounts of substances in biological materials (1–3). This method was used in these laboratories for the metabolic study of drugs in animals and humans (4–6). The mass fragmentographic technique also has been applied for the sensitive, specific, and reliable determination of plasma testosterone levels in humans (7).

Pharmacokinetic studies represent one field in which the sensitivity and specificity of the mass fragmentographic technique offer an advantage. Sullivan and coworkers (8, 9) successfully used stable isotope-labeled drugs together with mass fragmentography to study steady-state pharmacokinetics. An investigation of the elimination kinetics of drugs was carried out in these laboratories by measuring the nanogram levels of a drug and its major metabolites in human urine using this technique (10).

The present paper describes the use of deuterium-labeled phenytoin (I) and its major metabolite, 5-(4-hydroxyphenyl)-5-phenylhydantoin (II), along with mass fragmentography to follow saliva, plasma, and urinary concentrations of I and II for a reasonable period after a single oral administration of I to humans. A detailed analysis and interpretation of the pharmacokinetic data of I from two healthy volunteers also are presented.

EXPERIMENTAL

Synthesis of Deuterated Internal Standards—*Pentadeuterophenytoin (I-*d_5*)*—Deuterobenzophenone (benzophenone-d_5) was prepared by refluxing a mixture of 9.50 g of hexadeuterobenzene[1] (99.5 atom % D) and 2.44 g of benzoyl chloride[2] for 5 hr with 2.70 g of anhydrous aluminum chloride. The I-d_5 then was synthesized from the benzophenone-d_5 according to the method described by Baty and Robinson (11).

[1] Merck.
[2] Wako Pure Chemical Industries.

0022-3549/80/1100-1300$01.00/0
© 1980, American Pharmaceutical Association

The overall yield was 5.1% based on benzene-d_6, mp 301°, 99.3 atom % D.

5-(4-Hydroxyphenyl)-5-pentadeuterophenylhydantoin (II-d_5)—Condensation of 3.07 g of anisoyl chloride with 9.50 g of hexadeuterobenzene[1] (99.5 atom % D) by refluxing for 5 hr with stirring in the presence of anhydrous aluminum chloride produced 2.68 g of 4-methoxybenzophenone-d_5, mp 151°. This compound (2.63 g) then was refluxed at 120° in 50 ml of nitrobenzene for 4 hr with 6.00 g of aluminum chloride to convert it to the phenol. The reaction mixture was poured into ice-cold water and extracted with dichloroethane. Filtration of the dichloroethane layer, extraction with 5% NaOH, acidification with 5% HCl, and reextraction into dichloroethane followed by drying over sodium sulfate and evaporation under reduced pressure gave 1.01 g of 4-hydroxybenzophenone-d_5, mp 140°.

Compound II-d_5 was obtained when 1.00 g of 4-hydroxybenzophenone-d_5 was subjected to reaction with 13.00 g of acetamide, 2.50 g of ammonium carbonate, and 0.40 g of potassium cyanide in a 50-ml sealed tube at 100° for 48 hr (12). After cooling, the reaction mixture was transferred into water, and the product was extracted with ether under alkaline conditions. Evaporation of the ether and recrystallization from aqueous ethanol gave 0.60 g of II-d_5, mp 320° dec., 98.7 atom % D. The overall yield of this reaction was 2% based on benzene-d_5.

Mass Fragmentography—Mass fragmentographic measurements were made with a gas chromatograph–mass spectrometer[3] equipped with a multiple-ion detector. The electron energy was set at 20 ev, and the trap current was set at 60 μamp. The multiple-ion detector was focused on the ions of the methyl derivatives at *m/e* values of 266 (I) and 271 (I-d_5) for the determination of I and at 296 (II) and 301 (II-d_5) for the determination of II to measure the peak height ratio.

GLC was performed on a glass column (2 m × 3 mm i.d.) packed with 1.5% SE-30 on Chromosorb W (80–100 mesh). The column temperature was 250° for I and 290° for II. The temperature of the flash heater was 280° for I and 300° for II, and the separator was at 280° for I and at 300° for II. The temperature of the ion source was 310°. The helium carrier gas flow rate was ~20 ml/min.

Sample Preparation for Mass Fragmentography—*Phenytoin (I)*—A 0.5–1.0-ml plasma sample was diluted with three volumes of water in a 30-ml centrifuge tube, and 1.0 ml of the internal standard (1.0 μg of I-d_5) was added. After 1.0 ml of 0.5 *N* HCl was added, the plasma sample was extracted with 2 × 5 ml of chloroform. The chloroform phase was collected and dried over anhydrous sodium sulfate. After evaporation of the solvent, the residue of the chloroform extract was dissolved in 0.1 ml of methanol, and 0.2 ml of diazomethane in ether was added. The sample then was allowed to stand for 15 hr at 4°, and the organic solvents were evaporated.

The residue was dissolved in a small amount (0.1–0.2 ml) of acetone and subjected to TLC on Kieselgel 60 F_{254} plates[4] (5 cm × 20 cm × 0.25 mm thick). The plate was developed with benzene–acetone–acetic acid (50:25:1 v/v/v), and the UV-positive zone corresponding to standard 3-methyl-I (monomethyl-I) with R_f 0.77 was scraped off. The methyl derivatives of I and I-d_5 were eluted with 10 ml of acetone, and the solvent was evaporated. The residue was dissolved in 0.1 ml of methanol, and 1 μl of the sample was subjected to GLC–mass spectrometry. The observed peak height ratio of *m/e* 266 to *m/e* 271 was determined in triplicate. Saliva (0.7–1.0 ml) and urine (1.0–10.0 ml) samples were not diluted with water and were processed as for plasma I samples.

5-(4-Hydroxyphenyl)-5-phenylhydantoin (II)—To a 0.5–1.0-ml plasma sample were added three volumes of water and 1.0 ml of the internal standard (1.0 μg of II-d_5). The subsequent procedures were the same as the isolation procedures described for plasma I levels, except that the UV-positive zone corresponding to standard *O*-methyl-3-methyl-II (dimethyl-II) with R_f 0.72 was scraped off. For the mass fragmentographic analysis, 1 μl of the sample was introduced into the gas chromatograph–mass spectrometer. The observed peak height ratio of *m/e* 296 to *m/e* 301 was determined in triplicate. Urine (1.0–10.0 ml) samples were not diluted with water and were processed as for plasma II samples.

5-(4-Hydroxyphenyl)-5-phenylhydantoin Glucuronide (III)—A 0.5–1.0-ml plasma sample was diluted with three volumes of water, and 1.0 ml of the internal standard (1.0 μg of II-d_5) was added in a 30-ml centrifuge tube. The plasma sample was treated with 1.0 ml of 10 *N* HCl for 1 hr on a boiling water bath (90–95°) and neutralized with 3 ml of sodium hydroxide solution. The subsequent procedures were the same as the isolation procedures described for plasma II samples. Urine (1.0 ml) samples were not diluted with water and were processed as described for plasma III samples.

Preparation of Calibration Curve—To each of six standards containing 0.05, 0.1, 0.5, 1.0, 5.0, and 10.0 μg of I or II in 0.1 ml of methanol was added 10 μg of I-d_5 or II-d_5 in 0.1 ml of methanol. After evaporation of the solvent to dryness, the residue was dissolved in 0.1 ml of methanol. To each sample was added 0.2 ml of freshly prepared diazomethane in ether. After standing for 15 hr at 4°, the excess diazomethane and the organic solvents were evaporated to dryness under reduced pressure, and the residue was dissolved in 0.1 ml of methanol. A 1-μl volume of the methanol solution was analyzed by GLC–mass spectrometry. The mass fragmentographic analysis was performed using the methyl derivatives by measuring the molecular ions at *m/e* 266 for monomethyl-I, *m/e* 271 for monomethyl-I-d_5, *m/e* 296 for dimethyl-II, and *m/e* 301 for dimethyl-II-d_5. The peak height ratios of I to I-d_5 and of II to II-d_5 were measured.

Determination of Accuracy—*Phenytoin (I)*—Compound I in amounts of 0.05, 0.5, 2.5, 5.0, and 10.0 μg in 1.0 ml of methanol was mixed with 10 μg of I-d_5 dissolved in 1.0 ml of methanol, and the solution was concentrated to ~20 μl. To the concentrated solution were added 0.5-ml aliquots of pooled plasma, and the sample was allowed to stand for 30 min at room temperature. The sample then was processed as described for the sample preparation for mass fragmentography.

5-(4-Hydroxyphenyl)-5-phenylhydantoin (II)—Compound II in amounts of 0.05, 0.5, 1.0, and 5.0 μg in 1.0 ml of methanol was mixed with 1.0 μg of II-d_5 dissolved in 1.0 ml of methanol, and the solution was concentrated to ~20 μl. To the concentrated solution were added 1.0-ml aliquots of pooled plasma, and the sample was allowed to stand for 30 min at room temperature. One set of plasma samples was treated with 1.0 ml of 10 *N* HCl for 1 hr on a boiling water bath and neutralized with 3 ml of sodium hydroxide solution. The other set was not treated with hydrochloric acid. The samples then were processed as described for the sample preparation for mass fragmentography.

Urine samples (1.0-ml aliquots of human urine) also were used for the accuracy determination. The procedures were essentially the same as those described for the plasma samples.

Drug Administration—Two healthy adult male volunteers, 25 (KY) and 36 (YK) years old, weighed 60 and 65 kg, respectively. They had not taken any drugs during the preceding two months. A single oral dose of I as its sodium salt, prepared by dissolving 250 mg of I and 37.5 mg of sodium hydroxide in 100 ml of water, was given in the morning after an overnight fast. The drug solution container was rinsed with 100 ml of water, and the rinsings also were swallowed. Each subject received 400 ml of water 1 hr before dosing and 100 ml of water at hourly intervals for 4 hr after dosing. The subjects urinated completely just prior to drug intake. No food was permitted for 4 hr after drug administration.

Sample Collection—Ten milliliters of heparinized blood samples was taken just prior to dosing and at 1, 2, 3, 4, 5, 6, 7, 8, 10, 12, 24, 48, 72, 96, and 120 hr after dosing. Plasma was separated and kept in a frozen state until analysis. Saliva samples (5 ml) were collected at the time of blood sampling. The saliva pH was measured, and the samples were kept frozen until analysis. Complete collections of urine were made at 0–2, 2–4, 4–6, 6–8, 8–12, 12–36, 36–60, 60–84, 84–108, and 108–132 hr after dosing. The urine volumes and pH were measured, and the samples were kept frozen until analysis. Compound I in saliva and I–III in plasma and urine samples were analyzed in duplicate by mass fragmentography. The initial extraction and isolation procedures were described under *Sample Preparation for Mass Fragmentography*.

RESULTS

Prerequisites for Mass Fragmentographic Analysis—*Preparation of Methyl Derivatives*—In the mass spectra of I and II, relatively abundant molecular ions (*m/e* 252 for I: Σ% 14.3; *m/e* 268 for II: Σ% 33.9)

Table I—Accuracy of Mass Fragmentographic Analysis of I in Plasma

Amount Added, μg	Amount Measured, μg[a]	Relative Error, %
0.0503	0.0502 ± 0.0002	−0.3
0.5026	0.5178 ± 0.0007	+3.0
2.5125	2.4916 ± 0.0062	−0.8
5.0250	4.8802 ± 0.0135	−2.9
10.0500	10.0584 ± 0.0113	−0.1

[a] Mean ± *SD* of triplicate measurements.

[3] Shimadzu LKB 9000.
[4] Merck, Darmstadt, West Germany.

Table II—Accuracy of Mass Fragmentographic Analysis of II in Plasma and Urine [a]

Amount Added, μg	Blood: Amount Measured, μg [b]	Blood: Relative Error, %	Urine: Amount Measured, μg [b]	Urine: Relative Error, %
0.0506	0.0526 ± 0.0002	+4.0	0.0530 ± 0.0005	+4.7
	(0.0482 ± 0.0003)	(−4.7)	(0.0528 ± 0.0001)	(+4.3)
0.1012	0.1053 ± 0.0039	+4.1	0.1043 ± 0.0034	+3.1
	(0.0994 ± 0.0004)	(−1.8)	(0.0974 ± 0.0043)	(−3.8)
0.5060	0.5187 ± 0.0029	+2.5	0.4911 ± 0.0020	−2.9
	(0.5236 ± 0.0013)	(+3.5)	(0.5103 ± 0.0008)	(+0.8)
1.0120	1.0039 ± 0.0045	−0.8	1.0286 ± 0.0013	+1.6
	(1.0322 ± 0.0128)	(+2.5)	(1.0152 ± 0.0035)	(+0.3)
5.0600	5.0499 ± 0.0216	−0.2	5.0523 ± 0.0096	−0.2
	(5.1858 ± 0.0132)	(+2.5)	(5.0687 ± 0.0042)	(+0.2)

[a] Figures in parentheses indicate accuracy determinations with hydrochloric acid treatment. [b] Mean ± *SD* of triplicate measurements.

Table III—Plasma Concentrations of I–III after Single Oral 250-mg Dose of I

Hours	Plasma Concentration, μg/ml [a]: Subject YK I	Subject YK II	Subject YK III	Subject KY I	Subject KY II	Subject KY III
1	3.9216	0.0318	0.7236	2.1200	0.0484	0.5095
2	4.0674	0.0411	0.9753	4.1870	0.0943	0.9753
3	3.9552	0.0477	1.1718	4.7260	0.0993	1.3961
4	4.3498	0.0545	1.3872	5.0336	0.1173	1.5844
5	4.0390	0.0548	1.4065	4.7968	0.1077	1.5462
6	4.0226	0.0594	1.5175	5.2586	0.1145	1.7553
7	3.7546	0.0577	1.6076	4.8334	0.1121	1.7408
8	3.5358	0.0585	1.6248	4.8854	0.1146	1.8967
10	3.8494	0.0602	1.5952	4.4282	0.1200	2.1725
12	3.3232	0.0454	1.5404	3.7540	0.1075	1.9620
24	2.0792	0.0387	1.1915	2.1618	0.0859	1.6122
48	0.4654	0.0121	0.3598	0.6211	0.0344	0.7483
72	0.0772	0	0.0720	0.1294	0.0145	0.2385
96	0.0178	0	0.0114	0.0232	0	0.0359
120	0	0	0	0	0	0

[a] Mean of triplicate measurements.

were observed. However, without derivative formation, both I and II did not possess good GLC properties. On the other hand, the methyl derivatives were suitable for GLC analysis, and molecular ions of monomethyl-I (*m/e* 266) and dimethyl-II (*m/e* 296) were prominent in the mass spectra. The abundance of the molecular ions was Σ% 19.7 for monomethyl-I and Σ% 26.5 for dimethyl-II, providing good potential for use in mass fragmentography.

Selective-ion recordings of I and II showed that no contaminating by-products with retention times close to those of the methyl derivatives of I and II were seen in the mass fragmentograms. After the initial extraction and purification procedures, there was no interference for both I and II in the molecular ion peaks from other materials in the saliva, plasma, or urine extract at these masses.

Sensitivity—The sensitivity of the procedure described here was judged based on the signal to noise ratio. The lower limit of detection of the mass spectrometer was 100 pg for I and II.

Calibration Curve—Compounds I-d_5 and II-d_5 were used as internal standards. Known mixtures of I and I-d_5 and of II and II-d_5 were prepared so that the sample size (1 μl) injected into the gas chromatograph–mass spectrometer covered the I or II range of 0.5–100 ng with a fixed amount (100 ng) of I-d_5 or II-d_5. Each mixture then was analyzed as the methyl derivative, using the *m/e* settings for the molecular ions at 266 (I), 271 (I-d_5), 296 (II), and 301 (II-d_5). In constructing calibration curves, corrections were made for the contributions of the molecular ion to the *m/e* values 5 mass units higher (I → I-d_5 and II → II-d_5) and 5 mass units lower (I-d_5 → I and II-d_5 → II). There was a good correlation between the mixed molar ratio and the observed peak height ratio. Least-squares analysis of the observed ratio gave a regression line with a slope of 1.000.

Table IV—Saliva to Plasma Ratio of I

Hours	Subject YK	Subject KY
4	0.070	0.088
5	0.075	0.091
6	0.070	0.081
7	0.072	—
8	0.065	0.075
10	0.067	0.075
12	—	0.080
24	0.055	0.076
48	0.085	0.069
72	0.130	—
96	0.220	0.073

Accuracy—The accuracy of measurements was determined for I and II added to aliquots of pooled plasma or urine. The plasma or urine samples contained 10 (I-d_5) or 1.0 (II-d_5) μg of the internal standard and different amounts of I (0.05–10.0 μg) or II (0.05–5.0 μg). The amount of I or II then was measured by the present method. The amounts of I and II added were in good agreement with the amounts of I and II measured (Tables I and II). The relative error was <3% for I and <5% for II. In the subsequent experiment, hydrochloric acid was used for the hydrolysis of III. Treatment of plasma or urine samples with hydrochloric acid did not affect the measurement of II in these samples (Table II).

Pharmacokinetics of Phenytoin—A single oral dose of 250 mg of I as its sodium salt dissolved in water was administered to two male volunteers, 25 (KY) and 36 (YK) years old. Time courses of I–III concentrations in plasma, saliva, and urine then were followed by the present method.

Plasma Concentration—Plasma was analyzed for I–III at various times for 120 hr after the administration of I (Table III). In Subject YK, there was a relatively rapid rise in the plasma I concentration to 3.9 μg/ml at 1 hr, giving a peak level of 4.3 μg/ml at 4 hr. In Subject KY, the plasma I concentration became 5.0 μg/ml at 4 hr, and this plasma level was maintained until 10 hr after the administration of I. Semilogarithmic plots of the plasma concentrations *versus* time indicated that, after absorption, a distribution phase was not visible and that the terminal decline phase was monoexponential at time points later than 48 hr for Subjects YK and KY.

Plasma III concentrations were the highest (1.6 μg/ml) at 8 hr in Subject YK, and the plasma decline of III thereafter was parallel to that of I. In Subject KY, a higher peak plasma III concentration of 2.2 μg/ml was obtained at 10 hr, and the plasma III levels exceeded the plasma I levels at 48 hr and later.

There was an excellent parallelism in the time course of the plasma

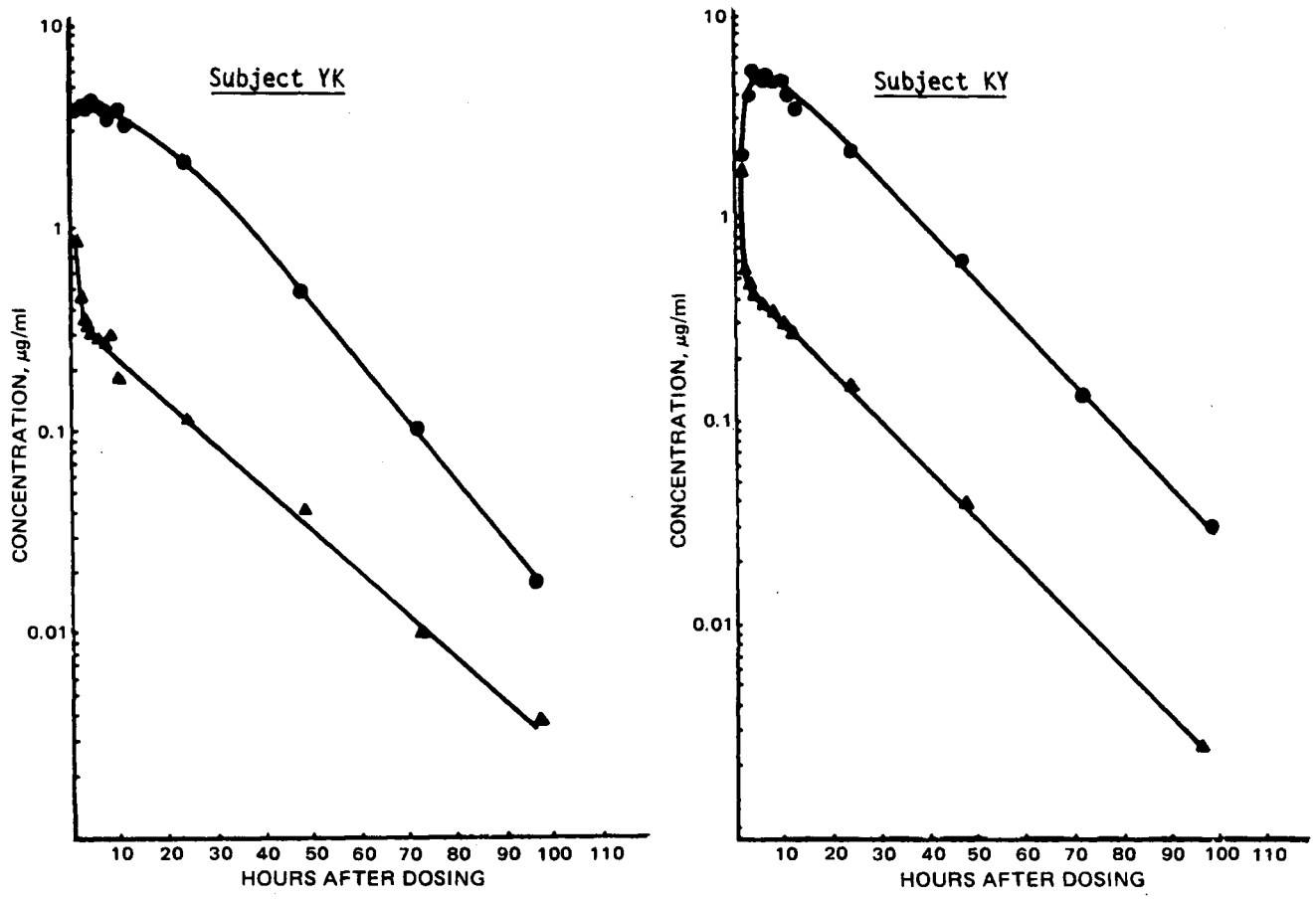

Figure 1—*Semilogarithmic plot of plasma* (●) *and saliva* (▲) *concentrations of I* versus *time after a single oral 250-mg dose of I.*

concentrations of II to that of III in both subjects. However, the levels of II were much lower in Subject YK than in Subject KY. At each time point, the plasma level of II was about 0.033 of the plasma level of III in Subject YK; in Subject KY, the level of II was ~0.1 of the level of III.

Saliva Concentration—Saliva samples were obtained at each time point of blood sampling. The results of measurements of saliva I concentrations are shown in Fig. 1, together with the time course of plasma I concentrations for comparison. Both subjects showed a rapid drop in saliva concentrations of I during the first 3 hr after administration of I; thereafter, the log concentration–time curves could be computed as straight lines. There was a close similarity in the decline of the slope of the saliva elimination curve to that of the plasma elimination curve for I. The slopes of the saliva and plasma elimination curves coincided with each other, especially in Subject KY, with the saliva to plasma ratios after 3 hr being consistent (Table IV). In Subject YK, there was only a slight fluctuation in the saliva to plasma ratio at each time point between 4 and 48 hr, while the ratio became higher at 72 and 92 hr.

Urinary Excretion—Urine samples were collected at appropriate time periods until 132 hr after the administration of I. The urinary pH and flow rate at each urine collection period are presented in Table V. These urine samples were analyzed for I–III, and the urinary excretion data are summarized in Tables VI–VIII. During the first 12 hr, fluctuations in the elimination rate were largely reflected in the excretion rate plots of I–III. After this period, plots of urinary excretion rates against the midpoints of urine collection periods were not scattered so much.

Subject YK excreted a much higher percentage of administered I as III (81%) than did Subject KY (56%) up to 132 hr. The excretion of unconjugated II and unmetabolized I was very small in both subjects, with the percentage being ~1% of the administered I dose. The concentration of conjugated II in plasma and urine was calculated by subtracting the unconjugated II from the total II measured after acid hydrolysis. However, a minor metabolite of I, 5-(3,4-dihydroxy-1,5-cyclohexadien-1-yl)-5-phenylhydantoin, is partially converted to II (13, 14). Therefore, in the present assay, the total plasma or urine II includes these minor pathways.

The sigma-minus plots shown in Fig. 2 apparently were much less sensitive to fluctuations in the elimination rate of I. Figure 2 shows that the slopes of the terminal monoexponential phase in the plots of the log amount remaining to be excreted against time for I–III were parallel to each other in both subjects. This finding indicates that the slopes of the terminal straight lines for the metabolites (II and III) reflect the elimination rate constant for the substrate (I). The half-lives of I calculated

Table V—Urinary pH and Flow Rate in Subjects KY and YK

Urine Collection Time, hr	Urine Collection Period, hr	pH		Urine Volume, ml		Flow Rate, ml/min	
		Subject KY	Subject YK	Subject KY	Subject YK	Subject KY	Subject YK
2	2	5.0	5.4	694	760	5.8	6.3
4	2	5.2	5.6	366	235	3.1	2.0
6	2	6.4	5.6	189	160	1.6	1.3
8	2	5.6	5.6	267	229	2.2	1.9
12	4	6.8	6.6	795	336	3.3	1.4
36	24	5.8	6.2	1130	2175	0.8	1.5
60	24	5.4	5.8	1850	2000	1.3	1.4
84	24	6.2	6.6	2750	2255	1.9	1.6
108	24	6.0	6.4	1800	1675	1.3	1.2
132	24	6.2	6.4	2290	2160	1.6	1.5

Table VI—Urinary Excretion Data for I in Subjects YK and KY

t, hr	Δt, hr	Midpoint t, hr	Subject YK ΔX, μg	Subject YK $\Delta X/\Delta t$, μg/hr	Subject YK ΣX, μg	Subject YK $X^\infty - X$, μg	Subject KY ΔX, μg	Subject KY $\Delta X/\Delta t$, μg/hr	Subject KY ΣX, μg	Subject KY $X^\infty - X$, μg
2	2	1	344.97	172.49	344.97	1865.60	342.08	171.04	342.08	1711.79
4	2	3	221.51	110.76	566.48	1644.09	415.87	207.94	757.95	1295.92
6	2	5	130.88	65.44	697.36	1513.21	181.63	90.82	939.58	1114.29
8	2	7	155.07	92.54	882.43	1328.14	264.50	132.25	10,204.08	849.79
12	4	10	232.71	58.18	1115.14	1095.43	327.56	81.89	1,531.64	522.23
36	24	24	888.36	37.02	2003.50	207.07	329.42	13.73	1,861.06	192.81
60	24	48	170.92	7.12	2174.42	36.15	152.37	6.35	2,013.43	40.44
84	24	72	30.62	1.28	2205.04	5.53	30.00	1.25	2,043.43	10.44
108	24	96	4.17	0.17	2209.21	1.36	10.44	0.44	2,053.87	—
132	24	120	1.36	0.06	2210.57	—	—	—	—	—

Table VII—Urinary Excretion Data for II in Subjects YK and KY

t, hr	Δt, hr	Midpoint t, hr	Subject YK ΔX, μg	Subject YK $\Delta X/\Delta t$, μg/hr	Subject YK ΣX, μg	Subject YK $X^\infty - X$, μg	Subject KY ΔX, μg	Subject KY $\Delta X/\Delta t$, μg/hr	Subject KY ΣX, μg	Subject KY $X^\infty - X$, μg
2	2	1	59.98	29.99	59.98	2379.06	84.10	42.05	84.10	3202.81
4	2	3	107.83	53.92	167.81	2271.23	184.54	92.27	268.64	3018.27
6	2	5	112.84	56.42	280.65	2158.39	152.66	76.33	421.30	2865.61
8	2	7	162.01	81.01	442.66	1996.38	176.09	88.05	597.39	2689.52
12	4	10	295.49	73.87	738.15	1700.89	162.09	40.52	759.48	2527.43
36	24	24	1145.01	47.71	1883.16	555.88	1689.58	70.40	2449.06	837.85
60	24	48	456.84	19.04	2340.00	99.04	662.60	27.61	3111.66	175.25
84	24	72	76.26	3.18	2416.26	22.78	136.62	5.69	3248.28	38.63
108	24	96	19.93	0.83	2436.19	2.85	38.63	1.61	3286.91	—
132	24	120	2.85	0.12	2439.04	—	—	—	—	—

Table VIII—Urinary Excretion Data for III in Subjects YK and KY

t, hr	Δt, hr	Midpoint t, hr	Subject YK ΔX, mg	Subject YK $\Delta X/\Delta t$, mg/hr	Subject YK ΣX, mg	Subject YK $X^\infty - X$, mg	Subject KY ΔX, mg	Subject KY $\Delta X/\Delta t$, mg/hr	Subject KY ΣX, mg	Subject KY $X^\infty - X$, mg
2	2	1	5.723	2.862	5.723	209.700	2.494	1.247	2.494	145.300
4	2	3	10.840	5.420	16.563	198.860	7.698	3.849	10.192	137.602
6	2	5	10.914	5.457	27.477	187.946	8.378	4.189	18.570	129.224
8	2	7	14.555	7.278	42.032	173.391	11.377	5.689	29.947	117.847
12	4	10	26.711	6.678	68.743	146.680	10.741	2.685	40.688	107.106
36	24	24	106.058	4.419	174.801	40.622	70.696	2.946	111.384	36.410
60	24	48	32.642	1.360	207.443	7.980	26.954	1.123	138.338	9.456
84	24	72	6.422	0.268	213.865	1.558	7.375	0.307	145.713	2.081
108	24	96	1.174	0.049	215.039	0.384	1.476	0.062	147.189	0.605
132	24	120	0.384	0.016	215.423	—	0.605	0.025	147.749	—

from these slopes were 9.4 hr for Subject YK and 11.5 hr for Subject KY.

Pharmacokinetic Parameters—Linear regression of $(t_{n+1} - t_n)/(\ln C_n - \ln C_{n+1})$ on $(C_nC_{n+1})^{1/2}$ was used to differentiate between first-order and Michaelis–Menten elimination kinetics (15), where C_n and C_{n+1} are the plasma concentrations at time points t_n and t_{n+1}, respectively. The regression line of the plasma data (Table III) beginning at 12 hr after administration of I gave an apparent straight line whose slope was not equal to zero. Therefore, preliminary estimates of the maximum rate of the process (V_m) and the Michaelis–Menten constant (K_m) were obtained from the y-axis intercept and the slope of the line (16). Since it already was reported that I follows a two-compartment open model after intravenous administration (17), the observed set of plasma data in the present study was fitted to a two-compartment open model with Michaelis–Menten elimination kinetics (Scheme I).

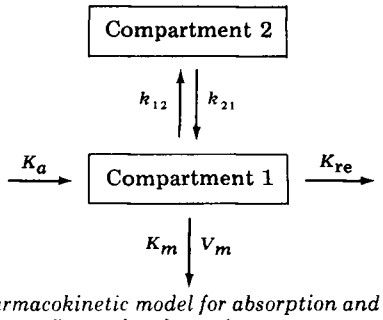

Scheme I—Pharmacokinetic model for absorption and elimination of I. Key: K_a, *apparent first-order absorption rate constant;* k_{12}, *apparent first-order distribution rate constant from Compartment 1 to Compartment 2;* k_{21}, *apparent first-order distribution rate constant from Compartment 2 to Compartment 1;* K_{re}, *apparent first-order rate constant for renal excretion of I;* V_m, *maximum rate of metabolism of I; and* K_m, *Michaelis–Menten constant.*

The differential equations for the model shown in Scheme I are:

$$\frac{dC_1}{dt} = K_aC_0e^{-K_at} - \left(k_{12} + \frac{V_m}{K_m + C_1}\right)C_1 + k_{21}C_2 - K_{re}C_1 \quad \text{(Eq. 1)}$$

$$\frac{dC_2}{dt} = k_{12}C_1 - k_{21}C_2 \quad \text{(Eq. 2)}$$

where C_0 is the fraction absorbed (F) times the administered dose (D) divided by the volume of distribution (V_d), C_1 is the drug concentration in Compartment 1, C_2 is the drug concentration in Compartment 2, t is time, K_a is the first-order absorption rate constant, k_{12} is the first-order distribution rate constant from Compartment 1 to Compartment 2, k_{21} is the first-order distribution rate constant from Compartment 2 to Compartment 1, and K_{re} is the first-order rate constant for renal excretion of I.

Equations 1 and 2 were numerically integrated by a computer[5] using

[5] CMB model 2001-32 personal computer.

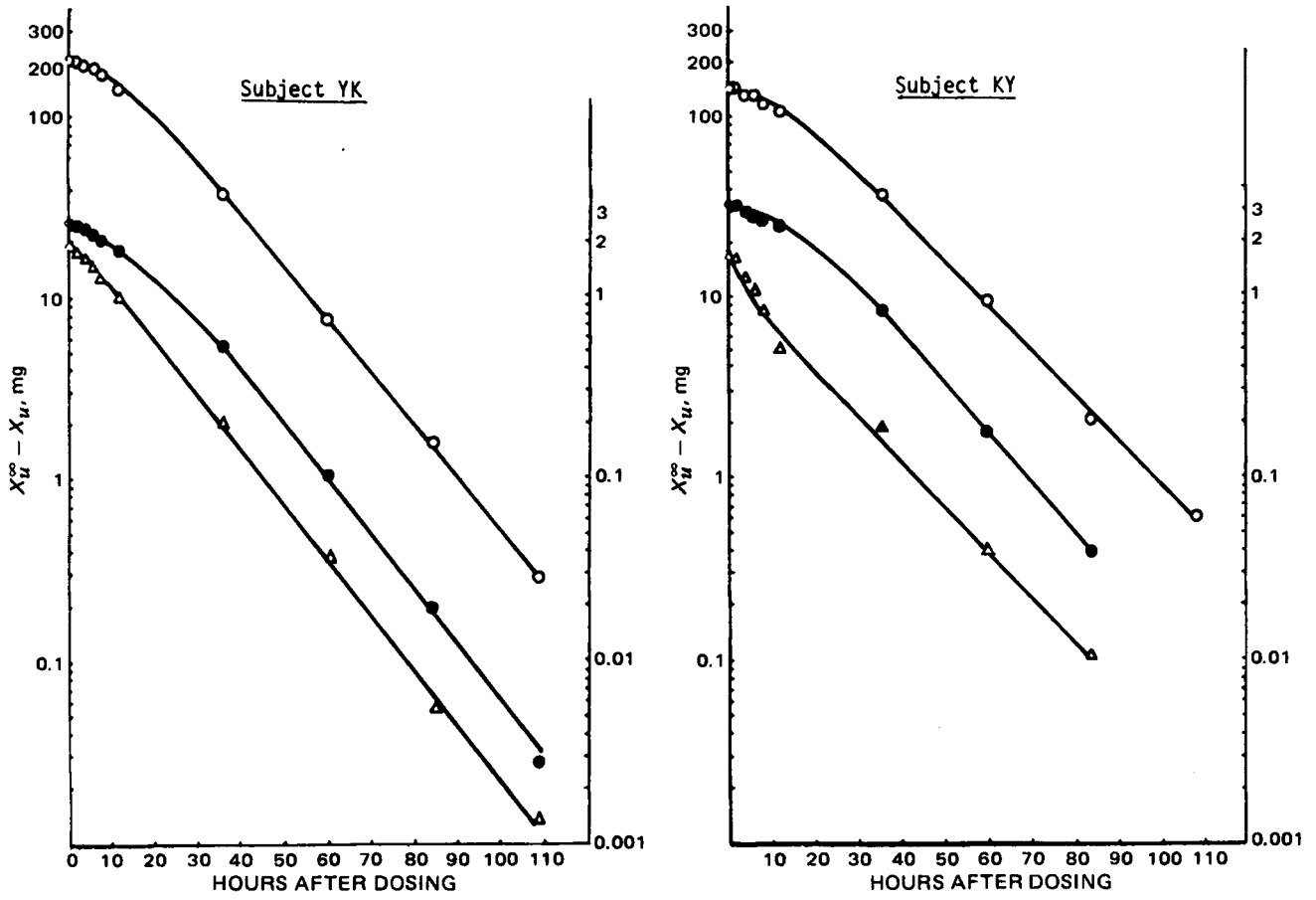

Figure 2—*Semilogarithmic plot of amounts of I–III remaining to be excreted* ($X_u^\infty - X_u$) versus *time for the determination of the elimination rate constant from urinary excretion data. Key:* △, *I (right axis);* ●, *II (right axis); and* ○, *III (left axis).*

the Runge–Kutta method, and the values for the pharmacokinetic parameters (K_a, V_m, K_m, k_{12}, k_{21}, and V_d) were obtained by a least-squares estimation using the steepest descent method. The estimate of the elimination half-life ($t_{1/2}$) was obtained from $t_{1/2} = 0.693/(V_m/K_m)$, without consideration of the minor contribution of K_{re}. The total plasma clearance (Cl_{pl}) was expressed as the amount absorbed divided by the area under the plasma concentration curve, assuming 100% absorption (18). The area under the plasma concentration–time curve (AUC) from t = 0–120 (infinity) was measured by the trapezoidal rule.

Renal clearance (Cl_{re}) for I and II was obtained from the slope of the straight line resulting from a plot of the average excretion rate ($\Delta X_u/\Delta t$) *versus* the plasma concentration at the midpoint of the urine collection period (19). The rate constant for renal excretion of I (K_{re}) was determined by employing $K_{re} = Cl_{re}/V_d$. These pharmacokinetic parameters are listed in Table IX. There were no large differences in V_m, K_m, $t_{1/2}$, Cl_{pl}, and V_d between the two subjects. On the other hand, the values for K_a, K_{re}, AUC, and Cl_{re} were considerably different, except that only a small difference was observed for the AUC value for I.

Table IX—Pharmacokinetic Parameters Derived after Single Oral 250-mg Dose of I

Subject	K_a, hr^{-1}	V_m, μg/ml/hr	K_m, μg/ml	$t_{1/2}$, hr	k_{12}, hr^{-1}
YK	0.80	0.87	12.3	9.8	0.09
KY	0.52	0.81	11.7	10.0	0.06

Subject	k_{21}, hr^{-1}	K_{re}, hr^{-1}	Cl_{pl}, liters/hr	V_d, liters/kg
YK	0.57	0.00041	2.18	0.64
KY	0.78	0.00020	1.91	0.60

	AUC, (μg hr)/ml			Cl_{re}, ml/hr		
Subject	I	II	III	I	II	III
YK	114.80	1.84	57.05	17.2	1359.3	3737.0
KY	131.00	4.55	83.80	7.1	811.5	1684.7

DISCUSSION

The usefulness of a mass fragmentographic technique in conjunction with stable isotope labeling in the pharmacokinetic study of I was a major interest in the present study. Various analytical techniques such as GLC, radioimmunoassay, enzyme immunoassay, liquid chromatography, and spectrophotometry are used frequently for monitoring plasma levels of I during chronic therapy, and comparisons of these analytical methods have been reported (20, 21). The pharmacokinetics of I have been examined by GLC (22–24), colorimetry (25, 26), radioimmunoassay (17), and a radioisotope tracer technique (27, 28). However, the sensitivity or specificity of these methods often does not provide reliable and precise determination of I in biological samples. In addition, no detailed information is available regarding the simultaneous pharmacokinetic analysis of plasma levels and urinary excretion data of I together with its major metabolite II. The present single-dose study in two healthy male volunteers was designed to give information about the precise and detailed pharmacokinetics of I determined from both blood level curves and urinary excretion data for I and II.

The metabolic fate of I has been studied extensively (29–31). Butler (32) showed that I is *para*-hydroxylated in the liver to yield II. This metabolite is conjugated with glucuronic acid, is present in plasma largely as the conjugate, and is excreted in the urine. The colorimetric method described by Dill *et al.* (33) and GLC measurement using derivatization with either trimethylsilyl groups (34) or flash methylation (35) are not sensitive enough to detect unconjugated II in plasma.

A mass fragmentographic method using deuterium-labeled internal standards was described recently (11, 36) for the sensitive quantitative determination of I and II in human plasma. The lower limit of detection was ~0.01 μg/ml for I and II using an extractive alkylation technique (36). Rane *et al.* (37) studied the fate of transplacentally transferred I in newborn infants by a mass fragmentographic method. The molecular ions

Table X—Ratio of II to I in Plasma

t, hr	Subject YK	Subject KY
4	0.013	0.023
12	0.014	0.029
24	0.019	0.040
48	0.026	0.055

were used for the detection of the monomethyl derivatives of I and the internal standard (I-d_{10}). The analytical procedure permitted precise determinations of I in plasma in concentrations down to 0.01 μg/ml. The high sensitivity generally can be obtained by introducing appropriate volatile derivatives for mass fragmentographic analysis.

The mass fragmentographic method described here was satisfactory for the sensitive and specific measurement of I in saliva, plasma, and urine and I and II in plasma and urine. Compound I and its internal standard (I-d_5) were analyzed as the monomethyl derivatives, and II and its internal standard (II-d_5) were converted to the dimethyl derivatives by simple derivatization with diazomethane. The lower limit of detection in this study was ~0.01 μg/ml for both I and II, which was comparable to that reported previously (11, 36, 37).

In the present study, I was administered as the sodium salt dissolved in water, and relatively high saliva I concentrations were observed during the first 3 hr after drug administration (Fig. 1). This result must have been due to residual I in the mouth, although care was taken to avoid this influence by administration of 100 ml of water immediately after drug intake. After this period, the saliva I concentration declined in parallel with the plasma I concentration. Several recent studies (38–40) demonstrated a significant linear correlation between salivary concentrations of I and the plasma total and plasma free concentrations. The data in Table III substantiate the close relationship between the whole salivary and the plasma free I concentrations.

Pharmacokinetic studies in humans usually have been performed with drugs that are present unchanged in the blood or are excreted unchanged in the urine. However, it sometimes is important to carry out simultaneous analysis of blood levels and urinary excretion of both the unchanged drug and its metabolites to determine correct pharmacokinetic parameters, especially when interindividual variations in the pharmacokinetics of a drug are to be investigated. The analysis and interpretation of pharmacokinetic data presented here give some insight into interindividual differences in the metabolic disposition of I.

The shape and peak concentrations of the plasma concentration curves for unchanged I did not differ considerably between Subjects YK and KY. Furthermore, the slopes of the sigma-minus plots for unchanged I (Fig. 2) were very similar in the two subjects. Although there was an approximately twofold difference in the rate constant for renal excretion of I (K_{re}) between Subjects YK and KY, this difference contributed little to the difference in the overall elimination of I since extensive metabolism of I was the predominant route of its elimination. Consequently, it may be stated from these findings that the pharmacokinetic behavior of I in Subjects YK and KY was practically the same.

However, the precise analysis of plasma concentration–time data for I–III revealed that the kinetics of urinary excretion characterized by renal clearance values (Cl_{re}) not only for I but also for II and III differed considerably between the two subjects (Table IX), although both subjects gave normal creatinine clearances of 95.2 (YK) and 105.2 (KY) ml/min. This difference was reflected by the difference in *AUC*. Bochner *et al.* (22) suggested that I is actively secreted in the renal tubules, a process that may differ between subjects. Such a mechanism may explain the difference in renal clearance observed in this study.

It is well known that the clearance of I decreases as the dose of I is increased (41–43). Therefore, it is not unreasonable to assume that the ratio of II to I in plasma could serve as an indicator to predict when one will show these dose-dependent kinetics, regardless of the mechanisms involved. Along this line, Hoppel *et al.* (44) used a mass fragmentographic method to determine II and III in the plasma of patients treated with I. However, no apparent relationship was found in the ratio of the plasma concentrations of I and II at similar doses. Comparison of the ratio of II to I in plasma in the present single-dose study revealed that the ratio tended to increase with the time after administration of I and that the ratio was about two times higher in Subject KY than in Subject YK at each time point (Table X). When the ratio of II to I was compared by calculating the ratio of the *AUC* values for II and I, there also was an approximately twofold difference between the two subjects (KY = 0.035 and YK = 0.016). This in part explains the interindividual differences in the ratios between I and unconjugated II in plasma at a constant dose reported by Hoppel *et al.* (44).

In summary, the mass fragmentographic method described in this study adequately meets the criterion of reliability for the precise, sensitive, and specific determination of I and its main metabolite (II) in biological samples. The pharmacokinetics of I were examined in detail based on the analysis of blood level and urinary excretion data from a single oral dose study in two healthy volunteers.

REFERENCES

(1) "Proceedings of the Second International Conference on Stable Isotopes," E. R. Klein and P. D. Klein, Eds., Argonne National Laboratory, Argonne, Ill., Oct. 1975.

(2) E. R. Klein and P. D. Klein, *Biomed. Mass Spectrom.*, **5**, 91 (1978).

(3) I. Björkhem, R. Blomstrand, O. Lantto, L. Svensson, and G. Öhman, *Clin. Chem.*, **22**, 1789 (1976).

(4) K. Kawai and S. Baba, *Chem. Pharm. Bull.*, **24**, 2728 (1976).

(5) S. Morishita, S. Baba, and Y. Nagase, *J. Pharm. Sci.*, **67**, 757 (1978).

(6) S. Baba, S. Kato, S. Morishita, and H. Sone, *J. Med. Chem.*, **21**, 525 (1978).

(7) S. Baba, Y. Shinohara, and Y. Kasuya, *J. Chromatogr.*, **162**, 529 (1979).

(8) H. R. Sullivan, F. J. Marshall, and R. E. McMahon, *Biomed. Mass Spectrom.*, **2**, 197 (1975).

(9) H. R. Sullivan, D. G. Wood, and R. E. McMahon, *ibid.*, **3**, 212 (1976).

(10) S. Baba, S. Morishita, and Y. Kasuya, *J. Pharmacobio- Dyn.*, **1**, 222 (1978).

(11) J. D. Baty and P. R. Robinson, *Biomed. Mass Spectrom.*, **4**, 36 (1977).

(12) H. R. Henz and A. F. Isbell, *J. Am. Chem. Soc.*, **76**, 4152 (1954).

(13) T. Chang, A. Savory, and A. J. Glazko, *Biochem. Biophys. Res. Commun.*, **38**, 444 (1970).

(14) W. A. Dill, J. Baukema, T. Chang, and A. J. Glazko, *Proc. Soc. Exp. Biol. Med.*, **137**, 674 (1971).

(15) J. G. Wagner, "Fundamentals of Clinical Pharmacokinetics," Drug Intelligence Publications, Hamilton, Ill., 1975, pp. 256–258.

(16) A. J. Sedman and J. G. Wagner, *J. Pharmacokinet. Biopharm.*, **2**, 161 (1974).

(17) R. Gugler, C. V. Manion, and D. L. Azarnoff, *Clin. Pharmacol. Ther.*, **19**, 135 (1976).

(18) R. Gugler, W. Fröschner, M. Eichelbaum, and G. Hildenbrand, *J. Neurol.*, **216**, 155 (1977).

(19) M. Gibaldi and D. Perrier, "Pharmacokinetics" (Drugs and Pharmaceutical Sciences, vol. 1, J. Swarbrick, Ed.), Dekker, New York, N.Y., 1975, pp. 11–14.

(20) P. E. Stanley and M. R. Peikert, *Epilepsia*, **19**, 265 (1978).

(21) A. Castro, J. Ibanez, J. L. DiCesare, R. F. Adams, and H. Malkus, *Clin. Chem.*, **24**, 710 (1978).

(22) F. Bochner, W. D. Hooper, J. M. Sutherland, M. J. Eadie, and J. H. Tyrer, *Clin. Pharmacol. Ther.*, **14**, 791 (1973).

(23) L. Lund, G. Alvan, A. Berlin, and B. Alexanderson, *Eur. J. Clin. Pharmacol.*, **7**, 81 (1974).

(24) L. K. Garrettson and W. J. Jusko, *Clin. Pharmacol. Ther.*, **17**, 481 (1975).

(25) A. J. Glazko, T. Chang, J. Baukema, W. A. Dill, J. R. Goulet, and R. A. Bauchanan, *ibid.*, **10**, 498 (1969).

(26) K. Arnold and N. Gerber, *ibid.*, **11**, 121 (1970).

(27) T. Suzuki, Y. Saitoh, and K. Nishihara, *Chem. Pharm. Bull.*, **18**, 405 (1970).

(28) E. Perucca, K. Makki, and A. Richens, *Clin. Pharmacol. Ther.*, **24**, 46 (1978).

(29) A. J. Glazko, *Epilepsia*, **16**, 367 (1975).

(30) R. M. Thompson, J. Beghim, W. K. Fife, and N. Gerber, *Drug Metab. Dispos.*, **4**, 349 (1976).

(31) K. K. Midha, K. W. Hindmarsh, I. J. McGilveray, and J. K. Cooper, *J. Pharm. Sci.*, **66**, 1596 (1977).

(32) T. C. Butler, *J. Pharmacol. Exp. Ther.*, **119**, 1 (1957).

(33) W. A. Dill, J. Baukema, T. Chang, and A. J. Glazko, *Proc. Soc. Exp. Biol. Med.*, **137**, 674 (1971).

(34) T. Chang and A. J. Glazko, *J. Lab. Clin. Med.*, **75**, 145 (1970).

(35) A. Estas and P. A. Dumont, *J. Chromatogr.*, **82**, 307 (1973).

(36) C. Hoppel, M. Garle, and M. Elander, *ibid.*, **116**, 53 (1976).
(37) A. Rane, M. Garle, O. Borgå, and F. Sjöqvist, *Clin. Pharmacol. Ther.*, **15**, 39 (1974).
(38) J. C. Mucklow, M. R. Bending, G. C. Kahn, and C. T. Dollery, *ibid.*, **24**, 563 (1978).
(39) S. N. Anavekar, R. H. Saunders, W. M. Wardell, I. Shoulson, F. G. Emmings, C. E. Cook, and A. J. Gringeri, *ibid.*, **24**, 629 (1978).
(40) M. Danhof and D. D. Breimer, *Clin. Pharmacokinet.*, **3**, 39 (1978).
(41) F. Bochner, W. D. Hooper, J. H. Tyrer, and M. J. Eadie, *J. Neurol. Neurosurg. Psychiat.*, **35**, 873 (1972).
(42) N. Gerber and J. G. Wagner, *Res. Commun. Chem. Pathol. Pharmacol.*, **3**, 455 (1972).
(43) A. Richens, *Epilepsia*, **16**, 627 (1975).
(44) C. Hoppel, M. Garle, A. Rane, and F. Sjöqvist, *Clin. Pharmacol. Ther.*, **21**, 294 (1977).

Correlation of *In Vivo* Bioavailability of Erythromycin Stearate Tablets with *In Vitro* Tests

S. STAVCHANSKY *x, J. T. DOLUISIO *, A. MARTIN *, C. MARTIN *, B. CABANA ‡, S. DIGHE *‡, and A. LOPER *

Received February 8, 1980, from the **Drug Dynamics Institute, College of Pharmacy, University of Texas at Austin, Austin, TX 78712,* and the ‡*Division of Biopharmaceutics, Food and Drug Administration, Rockville, MD 20852.* Accepted for publication May 21, 1980.

Abstract □ Correlations between the bioavailability parameters for erythromycin stearate tablets from five manufacturers and *in vitro* tests of these tablets were examined using forward (stepwise), multiple linear regression analysis. Bioavailability parameters were determined in clinical studies employing a balanced, incompete block design. *In vitro* tests used disintegration, dissolution, and dissolution/dialysis as the independent variables in regression equations. Significant correlations were found between linear combinations of these parameters and the time to peak and the peak serum levels. The inclusion of an *in vitro* disintegration test to describe peak serum levels of erythromycin is noteworthy since it has been suggested that disintegration tests are of less value than dissolution tests in predicting tablet performance *in vivo*. The multiple regression techniques employed in the present investigation may be useful for selection of appropriate physicochemical tests for continued monitoring of the bioavailability of erythromycin stearate tablets.

Keyphrases □ Erythromycin stearate—correlation of bioavailability of tablets with *in vitro* tests □ Antibiotics—erythromycin stearate, correlation of bioavailability of tablets with *in vitro* tests □ Multiple regression analysis—correlation of bioavailability of erythromycin stearate tablets with *in vitro* tests

Erythromycin stearate is erratically absorbed from the GI tract (1) and is subject to degradation by acids (2). Food and the volume of fluid taken with erythromycin stearate tablets affect the serum erythromycin levels in humans (3). The bioavailability variations, coupled with the numerous erythromycin stearate products marketed, create a potential bioequivalence problem. The difficulties encountered with clinical studies in terms of cost and human safety provide an impetus for prediction of product bioavailability from *in vitro* tests.

BACKGROUND

Bivariate correlations of *in vivo* with *in vitro* results have been reported for a variety of drugs. Dissolution rates of three brands of prednisone tablets indicated the clinical efficacy of the tablets (4). Chloramphenicol bioavailability was correlated with *in vitro* dissolution tests by Ogata *et al.* (5). Aguiar *et al.* (6) reported correlations of both the deaggregation and dissolution rates of four commercial lots of chloramphenicol capsules with human plasma levels.

An *in vitro* dissolution rate test that quantitatively predicted the GI absorption of aspirin from three different dosage forms was developed by Levy *et al.* (7). A linear correlation between salicylate excretion following oral administration of two aspirin tablets and the rate of tablet dissolution also was shown (8). In addition, a linear correlation was found between *in vivo* aspirin absorption and the *in vitro* dissolution rate using a rotating-flask apparatus (9). Similar linear correlations also were demonstrated for salicylamide tablets and suspensions (10).

Bergan *et al.* (11) compared the *in vitro* dissolution rates of two tetracycline and seven oxytetracycline products with their absorption characteristics in healthy human volunteers. Correlations were significant for some of these tetracycline products but not for others. Smolen and Weigand (12) developed a flow-through dissolution apparatus which could be optimized through feedback control to simulate *in vivo* drug release properties. They found that systematic adjustment of dissolution conditions resulted in improved *in vitro* to *in vivo* correlations.

These studies, with the exception of the chloramphenicol deaggregation studies, used *in vitro* dissolution results to predict drug absorption *in vivo*. However, bioavailability is a complex parameter which is influenced by the physicochemical properties of the drug, the dosage form, and the physiological conditions of the system. Thus, dissolution testing should be complemented by other *in vitro* tests to increase the prediction ability of *in vivo* drug absorption from *in vitro* results. Data on dissolution, dialysis, disintegration, and other physical tests are presented, and the usefulness of multiple linear regression analysis in the correlation between *in vivo* bioavailability and *in vitro* parameters for five commercially available erythromycin stearate tablets is demonstrated.

EXPERIMENTAL

***In Vitro* Studies**—*In vitro* tests were performed on selected lots of 250-mg film-coated erythromycin stearate tablets from five manufacturers. All tablets were from the same lots as those used in the clinical studies (13). Tablet hardness was measured with a motorized pendulum tablet hardness tester[1]. When the tablet was harder than 16 kg, a spring-type hand-held tester was used[2]. Weight variation was determined by weighing 10 tablets from each lot.

Four disintegration methods were investigated using the USP XIX apparatus at 37 ± 2°. In Method 1, tablets were run for 30 min in a 0.2% aqueous NaCl solution adjusted to pH 3 with dilute hydrochloric acid. These tablets then were placed in a pH 7.35 phosphate buffer solution containing 6.8 g of monobasic potassium phosphate and 190 ml of 0.2 *N* NaOH adjusted to 1000 ml with water. Method 2 involved placing the tablets in USP XIX simulated gastric fluid test solution (pH 1.22) for 30 min and then removing the tablets and placing them in USP XIX simulated intestinal fluid test solution (pH 7.55) for the time required to bring about disintegration. Method 3 was the same as Method 2, except that no enzymes were used in the simulated gastric and intestinal fluids. Method 4 also was the same as Method 2, except that the time in the gastric fluid was increased to 1 hr.

Dissolution studies on the five erythromycin stearate lots were per-

[1] Heberlein, Dr. K. Scheuniger and Co., Zurich, Switzerland.
[2] F. J. Stokes Machine Co., Philadelphia, Pa.

0022-3549/80/1100-1307$01.00/0
© 1980, American Pharmaceutical Association

Heterogeneous Model of Drug Release from Polymeric Matrix

S. K. CHANDRASEKARAN ˣ **and R. HILLMAN**

Received December 10, 1979, from *Alza Research, Palo Alto, CA 94304.* Accepted for publication May 22, 1980.

Abstract □ The kinetics of drug release from a polymeric matrix originally proposed by Higuchi were extended for the case of high drug loading (relative to the solubility of the drug in the polymer). The model of a granular matrix in which an effective porosity and tortuosity are assumed to modify the normal Higuchi kinetics is reviewed. A new model, which allows the prediction of the kinetics of drug release from properties of the polymer and drug, is based on the assumption that the permeability of the dispersed matrix is a function of drug loading.

Keyphrases □ Release rates—heterogeneous model of drug release from polymeric matrix □ Kinetics—heterogeneous model of drug release from polymeric matrix □ Diffusion—heterogeneous model of drug release from polymeric matrix

The kinetics of release of a solute dispersed in a polymeric matrix are of general interest in the controlled delivery of drugs (1). When the total loading of the solute (dissolved plus dispersed), C_0, is higher than its solubility in the matrix, C_s, the kinetics of release have been described by Higuchi (2). In this model, when the matrix is placed in an infinite sink, it is assumed that solid drug dissolves and diffuses from the surface layer of the matrix; when this layer becomes exhausted of drug, the next layer begins to be depleted.

BACKGROUND

In a planar system, the release of solute per unit time, dM_t/dt, is described by:

$$\frac{dM_t}{dt} = A\left[\frac{D(2C_0 - C_s)C_s}{t}\right]^{1/2} \quad \text{(Eq. 1)}$$

where A is the area of the slab, D is the diffusivity of the drug in the matrix, C_0 is the drug loading, and C_s is the solubility of the drug in the matrix at time t.

When the drug loading becomes much greater than the solubility and a granular matrix (with the possibility of interparticle contact) is formed, Eq. 1 usually is modified to give (2–4):

$$\frac{dM_t}{dt} = A\left[\frac{\frac{\epsilon}{\tau}D(2C_0 - \epsilon C_s)C_s}{t}\right]^{1/2} \quad \text{(Eq. 2)}$$

which becomes:

$$\frac{dM_t}{dt} = A\left(\frac{2\epsilon DC_0C_s}{\tau}\right)^{1/2} t^{-1/2} \quad \text{(Eq. 3)}$$

in the case where $C_0 \gg \epsilon C_s$. Thus, Eq. 1 is modified by an effective porosity, ϵ, which can be related to the volume fraction of drug in the matrix, and an effective tortuosity, τ, which describes the tortuous diffusion path a solute molecule must follow. In addition, the D value is taken as the diffusivity of the solute in the receptor solution. In other words, it is assumed that the solute is released by leaching through channels that are formed in the continuous matrix.

When Eq. 3 is rewritten as:

$$Q = Kt^{-1/2} \quad \text{(Eq. 4)}$$

with:

$$Q = \left(\frac{1}{A}\right)\frac{dM_t}{dt} \quad \text{(Eq. 5)}$$

and:

$$K = \left(\frac{2\epsilon DC_0C_s}{\tau}\right)^{1/2} \quad \text{(Eq. 6)}$$

it can be seen that this model predicts that the release rate constant changes in proportion to the square root of the initial drug loading, C_0. The ratio ϵ/τ then expresses the fractional area available for release.

There are several conceptual and practical drawbacks to the model. One would expect that by introducing flux enhancers or increasing the amount of drug in the matrix, the structure of the matrix, and, hence, the diffusivity of the drug in the matrix should be changed. In this model, the diffusivity is assumed to be independent of the drug concentration. Practically, it is difficult to measure the tortuosity and porosity of a polymer matrix. It is far more desirable to relate drug release to the molecular weight of the drug, the loading of drug in the matrix, and the diffusivity of the drug in pure polymer, all easily obtainable properties.

Davis (5) proposed an equation relating the diffusivity of several drugs in polyacrylamide and povidone gels based on the concentration and molecular weight of the drug in the polymer matrix and the diffusivity of the drug in the receptor solvent. The diffusion coefficient of the drug in the polymer, D_p, is related to the diffusion coefficient of the drug in pure solvent, D_0, by:

$$\log D_p = \log D_0 - k_sP \quad \text{(Eq. 7)}$$

where P is the volume percent of polymer and k_s is defined by:

$$k_s = -\frac{d \log D_p}{dP} \quad \text{(Eq. 8)}$$

and can be shown empirically to be a function of the molecular weight of the solute, M:

$$k_s = k_1 + k_2M \quad \text{(Eq. 9)}$$

Combining Eqs. 7 and 9 gives:

$$D_p = D_0 \exp[-(k_1 + k_2M)P] \quad \text{(Eq. 10)}$$

where k_1 and k_2 are empirical constants.

Davis pointed out that the logarithmic relationship between the diffusivity and the polymer concentration could be anticipated from previous work (6) on porosity in polymer networks. Thus, the exponential term in Eq. 10 could be redefined as porosity, which is defined by the space available for collision-free diffusion. The fundamental drawback in Davis' work is that it is based on an empirical correlation where four constants must be determined experimentally.

An attempt was made in this study to develop a heterogeneous model of drug diffusion from a dispersed polymer matrix for which fewer experimental measurements related directly to fundamental physicochemical properties are required.

THEORY

The polymer matrix is visualized as a heterogeneous system consisting of a continuous (polymer) phase with a discontinuous drug phase as

Table I—Release Rate Constant (K') for Salicylic Acid at Various Drug Concentrations (C_0) in a Polyethylene Glycol–Ethylcellulose Film

Drug, mg/ml	Release Rate Constant, mg/36 cm²/min$^{1/2}$	
	Calculated	Measured (3)
55	0.3	0.25
100	0.6	0.65
200	1.45	1.4
300	2.63	2.7
350	3.36	3.65

0022-3549/80/1100-1311$01.00/0
© 1980, American Pharmaceutical Association

Table II—Release Rate Constant (K') for Salicylic Acid at Various Drug Concentrations (C_0) in an Ethylcellulose Film

Drug, mg/ml	Release Rate Constant, mg/36 cm²/min$^{1/2}$	
	Calculated	Measured (3)
55	0.1	0.1
100	0.2	0.2
200	0.47	0.4
300	0.86	0.6

Table III—Release Rate Constant (K') for Tripelennamine at Various Drug Concentrations (C_0) in a Polyethylene Glycol–Ethylcellulose Film

Drug, mg/ml	Release Rate Constant, mg/36 cm²/min$^{1/2}$	
	Calculated	Measured (3)
55	0.1	0.1
100	0.2	0.3
200	0.47	0.7
300	0.86	1.2
400	1.45	1.99
450	1.8	2.45

particles dispersed uniformly throughout the matrix. Initially, the particles will be assumed to be a uniform array of spheres in the matrix. This assumption allows use of Maxwell's work on the conductivity of a dilute suspension of homogeneous nonpolarizable spheres (7). These assumptions are made to reduce the many particle problem to the case of one particle in a homogeneous field. This work also has been extended to the thermal conductivity of heterogeneous mixtures (8).

From Fick's law, the permeability of a dispersed polymer matrix can be expressed by:

$$P = \frac{D_p V_p \left(\frac{dc}{dx}\right)_p + D_d V_d \left(\frac{dc}{dx}\right)_d}{V_p \left(\frac{dc}{dx}\right)_p + V_d \left(\frac{dc}{dx}\right)_d} \qquad \text{(Eq. 11)}$$

or:

$$P = \frac{D_p V_p F_p + D_d V_d F_d}{V_p F_p + V_d F_d} \qquad \text{(Eq. 12)}$$

where:

$$F_d = \left(\frac{dc}{dx}\right)_d \qquad \text{(Eq. 13)}$$

$$F_p = \left(\frac{dc}{dx}\right)_p \qquad \text{(Eq. 14)}$$

Equation 11 expresses the permeability (P) as a function of the volume fraction of polymer (V_p) and drug (V_d), the diffusivity of the drug through the pure polymer phase (D_p) and the dispersed polymer phase (D_d), and the overall concentration gradient (F_p and F_d) in the two phases.

From Maxwell's work, the average gradient ratio for spheres can be expressed as:

$$F_d = \left[1 + \left(k\frac{D_p}{D_d} - 1\right)V_d\right]^{-1} \qquad \text{(Eq. 15)}$$

assuming $F_p = 1$. Substituting Eq. 15 into Eq. 12 and rearranging terms yield:

$$\frac{P}{P_p} - 1 = 3V_d\left[\frac{(kD_d/D_p) + 2}{(kD_d/D_p) - 1} - V_d\right]^{-1} \qquad \text{(Eq. 16)}$$

where P is the net normalized permeability of the dispersed matrix, P_p is the normalized permeability of the polymer matrix, V_d is the volume fraction of dispersed particles, and k is the partition coefficient.

With the assumption that $kD_d/D_p \gg 1$, Eq. 16 reduces to:

$$\frac{P}{P_p} = \frac{1 + 2V_d}{1 - V_d} \qquad \text{(Eq. 17)}$$

The volume fraction of the dispersed particles can be related to the total loading of particles by:

$$V_d = \frac{C_0}{\rho} \qquad \text{(Eq. 18)}$$

Table IV—Release Rate Constant (K') for Tripelennamine at Various Drug Concentrations (C_0) in an Ethylcellulose Film

Drug, mg/ml	Release Rate Constant, mg/36 cm²/min$^{1/2}$	
	Calculated	Measured (3)
55	0	0
100	0	0
200	0.2	0.2
300	0.37	0.4
400	0.59	0.5
450	0.74	0.7

Table V—Release Rate Constant (K') for Caffeine at Various Drug Contents in an Ethylcellulose Film

Drug, % w/w	Release Rate Constant, mg/7.95 cm²/sec$^{1/2}$ × 10³	
	Calculated	Measured (9)
2	5.0	4.9
5	7.5	7.6
10	11.5	20.4
15	15.5	31.0

Table VI—Release Rate Constant (K') for Salicylic Acid at Various Drug Contents in an Ethylcellulose Film

Drug, % w/w	Release Rate Constant, mg/7.95 cm²/sec$^{1/2}$ × 10³	
	Calculated	Measured (9)
5	6.9	6.3
10	10.3	7.6
15	14.0	16.8

where ρ is the density of the dispersed phase.

Equation 17 now becomes:

$$\frac{DC}{D_p C_p} = \frac{\rho + 2C_0}{\rho - C_0} \qquad \text{(Eq. 19)}$$

where D_pC_p is the normalized permeation rate in the pure polymer (*i.e.*, very low solute loadings) and DC is the normalized rate in the dispersed matrix at a particle loading of C_0.

The basic Higuchi model now may be modified for the release of drug from a dispersed polymer matrix to account for the change in diffusivity. Again, the basic Higuchi model can be written as:

$$\frac{1}{A}\frac{dM_t}{dt} = \left(\frac{2DC_0C_s}{t}\right)^{1/2} \qquad \text{(Eq. 20)}$$

Accounting for the effect of the addition of a dispersed phase by substituting Eq. 19 into Eq. 20 yields:

$$\frac{1}{A}\frac{dM_t}{dt} = \left[2D_pC_pC_0\left(\frac{\rho + 2C_0}{\rho - C_0}\right)\right]^{1/2} t^{-1/2} \qquad \text{(Eq. 21)}$$

The release rate constant, K', for a porous matrix becomes:

$$K' = \left[2D_pC_pC_0\left(\frac{\rho + 2C_0}{\rho - C_0}\right)\right]^{1/2} \qquad \text{(Eq. 22)}$$

and:

$$\frac{1}{A}\frac{dM_t}{dt} = K't^{-1/2} \qquad \text{(Eq. 23)}$$

Thus, the release rate of drug from a porous matrix can be calculated from the density of the dispersed phase, the drug loading, and the permeability of the drug in the pure polymer.

RESULTS AND DISCUSSION

There are few data in the literature on the incorporation of a drug or a solute at high loadings into polymeric films or matrixes. Samuelov *et al.* (3) recently published data on the release rate characteristics of salicylic acid and tripelennamine from polyethylene glycol–ethylcellulose films as a function of solute loading, and an attempt was made to utilize their data to test the validity of the proposed model. The release rate constant, K', was computed using Eq. 22, and the results of these computations as a function of solute loading are presented in Tables I–IV.

The release rate constants measured by Samuelov *et al.* (3) also are shown.

The release rate constants for salicylic acid in polyethylene glycol–ethylcellulose and pure ethylcellulose films are shown in Tables I and II. The density of the salicylic acid was taken as 1.443 g/cm^3, and the normalized permeation rate, D_pC_p, of salicylic acid in the polymer was calculated from the lowest solute loading (55 mg/ml) and used in all subsequent computations. The agreement between the release rate constants determined experimentally and those calculated from the model is good.

Similarly, the release rate constants for tripelennamine in polyethylene glycol–ethylcellulose and pure ethylcellulose films are presented in Tables III and IV. The normalized permeation rate of tripelennamine in the polymer was calculated from the lowest solute loading (55 mg/ml), and the density of the dispersed solute was taken as 1.35 g/cm^3. The agreement between theory and experiment again is good.

Friedman *et al.* (9) prepared timed-release dosage forms using ethylcellulose as the polymeric matrix and salicylic acid and caffeine as model drugs. They determined drug release rates for different initial drug concentrations, and their experimental results are presented in Tables V and VI. The values of the release rate constant, K', computed using Eq. 22 also are shown. The diffusivity in the polymer of caffeine and salicylic acid was 2.26×10^{-11} and 1.96×10^{-11} cm^2/sec, respectively. The agreement between the release rate constants determined experimentally and those calculated from the model is good.

There is a good correlation between the model predictions and the measured release rate constants for the drugs. The deviation at very high drug loadings (>30%) can be attributed to interparticle contact. The interparticle contact leads to the formation of channels in the membrane through which the drug can be leached. Therefore, a model of a porous network must be applied. However, up to this limit, the release of drug can be predicted simply from a knowledge of drug loading, drug density, and the permeation rate of the drug in the pure polymers (very low loadings). Comparison of Tables I and II or Tables III and IV shows that plasticized films (with polyethylene glycol) have significantly higher release rate constants than do pure ethylcellulose films. Thus, the diffusivity and solubility of the drug are altered by the addition of plasticizers. The theory could be suitably modified to predict the release rate based on flux enhancer content and will be the subject of a subsequent communication.

Clearly, many properties of the polymer matrix can influence the permeation of drug including the geometry of the dispersed phase (shape, size, and size distribution), the composition of the dispersed phase, and interactions between the phases. However, the simplified model proposed here apparently gives a good correlation to experimental evidence.

REFERENCES

(1) R. W. Baker and H. K. Lonsdale, "Controlled Release of Biologically Active Agents," A. C. Tanquary and K. E. Lacy, Eds., Plenum, New York, N.Y., 1974, p. 21.

(2) T. Higuchi, *J. Pharm. Sci.*, **50**, 874 (1961).

(3) Y. Samuelov, M. Donbrow, and M. Friedman, *ibid.*, **68**, 325 (1979).

(4) H. Fessi, J. P. Marty, F. Puiseux, and J. T. Carstensen, *Int. J. Pharm.*, **1**, 265 (1978).

(5) B. K. Davis, *Proc. Natl. Acad. Sci. USA*, **71**, 3120 (1974).

(6) A. G. Ogsten, *Trans. Faraday Soc.*, **54**, 1754 (1958).

(7) C. Maxwell, "Treatise of Electricity and Magnetism," vol. 1, Oxford University Press, London, England, 1882, p. 365.

(8) R. L. Hamilton and O. K. Crosser, *I & EC Fundam.*, **1**, 189 (1962).

(9) M. Friedman, M. Donbrow, and Y. Samuelov, *J. Pharm. Pharmacol.*, **31**, 396 (1979).

Synthesis and Evaluation of Substituted Quinazolone Derivatives for Antibacterial, Antifungal, and Antiacetylcholinesterase Activities

ANIL K. SEN GUPTA ˣ and HEMANT K. MISRA

Received March 19, 1980, from the *Department of Chemistry, University of Lucknow, Lucknow-226007, India.* Accepted for publication May 19, 1980.

Abstract □ The synthesis of new 6-bromo- and 6,8-dibromo-2-[*N*-(2′-alkyl-1′,3′,4′-thiadiazol-5′-yl)carbamoylmethylthio]-3-aryl/cyclohexyl-4-(3*H*)-quinazolones is described. The synthesized derivatives were screened for antibacterial, antifungal, and antiacetylcholinesterase activities *in vitro*. Most of the compounds exhibited significant biological activity. The relation between their biological activity and chemical structure was studied.

Keyphrases □ Quinazolones—substituted derivatives, synthesis and evaluation for antibacterial, antifungal, and antiacetylcholinesterase activities □ Antibacterial activity—evaluation of substituted quinazolone derivatives □ Antifungal activity—evaluation of substituted quinazolone derivatives □ Antiacetylcholinesterase activity—evaluation of substituted quinazolone derivatives

Various quinazolone derivatives were investigated recently for biological and pharmacological activities such as antibacterial (1–4), antifungal (5, 6), antitubercular (7), antiamoebic (8), antiviral (9), anti-inflammatory (10), anticonvulsant (11, 12), hypotensive (13), and sedative (14, 15) activities. Parmar and coworkers (16, 17) reported the antiacetylcholinesterase activity of quinazolone derivatives.

Since the 1,3,4-thiadiazole nucleus already is well known for its biological activity (18–20), it was decided to combine different 5-chloroacetylamino-2-alkyl-1,3,4-thiadiazole

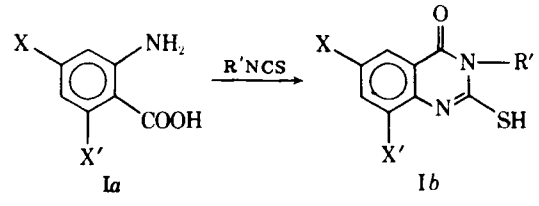

Ia Ib

X = Br, X′ = H
X = X′ = Br

Scheme I

0022-3549/80/1100-1313$01.00/0

© 1980, American Pharmaceutical Association

The release rate constants measured by Samuelov *et al.* (3) also are shown.

The release rate constants for salicylic acid in polyethylene glycol–ethylcellulose and pure ethylcellulose films are shown in Tables I and II. The density of the salicylic acid was taken as 1.443 g/cm^3, and the normalized permeation rate, D_pC_p, of salicylic acid in the polymer was calculated from the lowest solute loading (55 mg/ml) and used in all subsequent computations. The agreement between the release rate constants determined experimentally and those calculated from the model is good.

Similarly, the release rate constants for tripelennamine in polyethylene glycol–ethylcellulose and pure ethylcellulose films are presented in Tables III and IV. The normalized permeation rate of tripelennamine in the polymer was calculated from the lowest solute loading (55 mg/ml), and the density of the dispersed solute was taken as 1.35 g/cm^3. The agreement between theory and experiment again is good.

Friedman *et al.* (9) prepared timed-release dosage forms using ethylcellulose as the polymeric matrix and salicylic acid and caffeine as model drugs. They determined drug release rates for different initial drug concentrations, and their experimental results are presented in Tables V and VI. The values of the release rate constant, K', computed using Eq. 22 also are shown. The diffusivity in the polymer of caffeine and salicylic acid was 2.26×10^{-11} and 1.96×10^{-11} cm^2/sec, respectively. The agreement between the release rate constants determined experimentally and those calculated from the model is good.

There is a good correlation between the model predictions and the measured release rate constants for the drugs. The deviation at very high drug loadings (>30%) can be attributed to interparticle contact. The interparticle contact leads to the formation of channels in the membrane through which the drug can be leached. Therefore, a model of a porous network must be applied. However, up to this limit, the release of drug can be predicted simply from a knowledge of drug loading, drug density, and the permeation rate of the drug in the pure polymers (very low loadings). Comparison of Tables I and II or Tables III and IV shows that plasticized films (with polyethylene glycol) have significantly higher release rate constants than do pure ethylcellulose films. Thus, the diffusivity and solubility of the drug are altered by the addition of plasticizers. The theory could be suitably modified to predict the release rate based on flux enhancer content and will be the subject of a subsequent communication.

Clearly, many properties of the polymer matrix can influence the permeation of drug including the geometry of the dispersed phase (shape, size, and size distribution), the composition of the dispersed phase, and interactions between the phases. However, the simplified model proposed here apparently gives a good correlation to experimental evidence.

REFERENCES

(1) R. W. Baker and H. K. Lonsdale, "Controlled Release of Biologically Active Agents," A. C. Tanquary and K. E. Lacy, Eds., Plenum, New York, N.Y., 1974, p. 21.

(2) T. Higuchi, *J. Pharm. Sci.*, **50**, 874 (1961).

(3) Y. Samuelov, M. Donbrow, and M. Friedman, *ibid.*, **68**, 325 (1979).

(4) H. Fessi, J. P. Marty, F. Puiseux, and J. T. Carstensen, *Int. J. Pharm.*, **1**, 265 (1978).

(5) B. K. Davis, *Proc. Natl. Acad. Sci. USA*, **71**, 3120 (1974).

(6) A. G. Ogsten, *Trans. Faraday Soc.*, **54**, 1754 (1958).

(7) C. Maxwell, "Treatise of Electricity and Magnetism," vol. 1, Oxford University Press, London, England, 1882, p. 365.

(8) R. L. Hamilton and O. K. Crosser, *I & EC Fundam.*, **1**, 189 (1962).

(9) M. Friedman, M. Donbrow, and Y. Samuelov, *J. Pharm. Pharmacol.*, **31**, 396 (1979).

Synthesis and Evaluation of Substituted Quinazolone Derivatives for Antibacterial, Antifungal, and Antiacetylcholinesterase Activities

ANIL K. SEN GUPTA ˣ and HEMANT K. MISRA

Received March 19, 1980, from the *Department of Chemistry, University of Lucknow, Lucknow-226007, India.* Accepted for publication May 19, 1980.

Abstract □ The synthesis of new 6-bromo- and 6,8-dibromo-2-[*N*-(2′-alkyl-1′,3′,4′-thiadiazol-5′-yl)carbamoylmethylthio]-3-aryl/cyclohexyl-4-(3*H*)-quinazolones is described. The synthesized derivatives were screened for antibacterial, antifungal, and antiacetylcholinesterase activities *in vitro*. Most of the compounds exhibited significant biological activity. The relation between their biological activity and chemical structure was studied.

Keyphrases □ Quinazolones—substituted derivatives, synthesis and evaluation for antibacterial, antifungal, and antiacetylcholinesterase activities □ Antibacterial activity—evaluation of substituted quinazolone derivatives □ Antifungal activity—evaluation of substituted quinazolone derivatives □ Antiacetylcholinesterase activity—evaluation of substituted quinazolone derivatives

Various quinazolone derivatives were investigated recently for biological and pharmacological activities such as antibacterial (1–4), antifungal (5, 6), antitubercular (7), antiamoebic (8), antiviral (9), anti-inflammatory (10), anticonvulsant (11, 12), hypotensive (13), and sedative (14, 15) activities. Parmar and coworkers (16, 17) reported the antiacetylcholinesterase activity of quinazolone derivatives.

Since the 1,3,4-thiadiazole nucleus already is well known for its biological activity (18–20), it was decided to combine different 5-chloroacetylamino-2-alkyl-1,3,4-thiadiazole

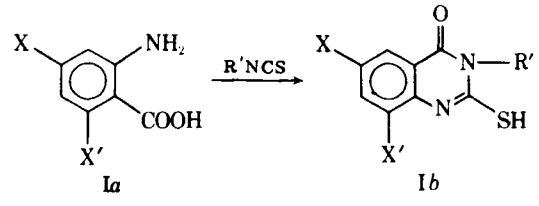

Ia Ib

X = Br, X′ = H
X = X′ = Br

Scheme I

0022-3549/80/1100-1313$01.00/0

© 1980, American Pharmaceutical Association

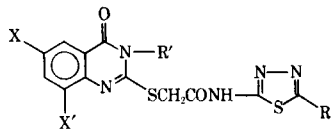

Table I—Physical Constants of Substituted Quinazolone Derivatives

Compound	X	X′	R′	R	Melting Point	Yield, %	Molecular Formula	Nitrogen Analysis, % Calc.	Found
II	Br	H	Benzyl	CH_3	206°	79	$C_{20}H_{16}BrN_5O_2S_2$	13.94	13.71
III	Br	H	Benzyl	C_2H_5	218°	76	$C_{21}H_{18}BrN_5O_2S_2$	13.56	13.37
IV	Br	H	Benzyl	C_3H_7	250°	67	$C_{22}H_{20}BrN_5O_2S_2$	13.20	13.10
V	Br	H	2-Ethylphenyl	CH_3	274°	63	$C_{21}H_{18}BrN_5O_2S_2$	13.56	13.40
VI	Br	H	2-Ethylphenyl	C_2H_5	190°	59	$C_{22}H_{20}BrN_5O_2S_2$	13.20	13.18
VII	Br	H	2-Ethylphenyl	C_3H_7	171°	60	$C_{23}H_{22}BrN_5O_2S_2$	12.86	12.75
VIII	Br	H	Cyclohexyl	CH_3	259°	71	$C_{19}H_{20}BrN_5O_2S_2$	14.17	14.13
IX	Br	H	Cyclohexyl	C_2H_5	258°	67	$C_{20}H_{22}BrN_5O_2S_2$	13.77	13.70
X	Br	H	Cyclohexyl	C_3H_7	228°	69	$C_{21}H_{24}BrN_5O_2S_2$	13.41	13.40
XI	Br	H	4-Methoxyphenyl	CH_3	318°	59	$C_{20}H_{16}BrN_5O_3S_2$	13.51	13.71
XII	Br	H	4-Methoxyphenyl	C_2H_5	324°	57	$C_{21}H_{18}BrN_5O_3S_2$	13.13	13.50
XIII	Br	H	4-Methoxyphenyl	C_3H_7	310°	53	$C_{22}H_{20}BrN_5O_3S_2$	12.82	12.80
XIV	Br	Br	Benzyl	CH_3	220°	76	$C_{20}H_{15}Br_2N_5O_2S_2$	12.05	12.00
XV	Br	Br	Benzyl	C_2H_5	225°	79	$C_{21}H_{17}Br_2N_5O_2S_2$	11.76	11.43
XVI	Br	Br	Benzyl	C_3H_7	218°	71	$C_{22}H_{19}Br_2N_5O_2S_2$	11.49	11.57
XVII	Br	Br	2-Ethylphenyl	CH_3	237°	76	$C_{21}H_{17}Br_2N_5O_2S_2$	11.76	11.75
XVIII	Br	Br	2-Ethylphenyl	C_2H_5	239°	67	$C_{22}H_{19}Br_2N_5O_2S_2$	11.49	11.40
XIX	Br	Br	2-Ethylphenyl	C_3H_7	240°	61	$C_{23}H_{21}Br_2N_5O_2S_2$	11.23	11.20
XX	Br	Br	Cyclohexyl	CH_3	230°	59	$C_{19}H_{19}Br_2N_5O_2S_2$	11.20	11.37
XXI	Br	Br	Cyclohexyl	C_2H_5	240°	55	$C_{20}H_{21}Br_2N_5O_2S_2$	11.92	11.99
XXII	Br	Br	Cyclohexyl	C_3H_7	238°	50	$C_{21}H_{23}Br_2N_5O_2S_2$	11.48	11.50
XXIII	Br	Br	4-Methoxyphenyl	CH_3	232°	61	$C_{20}H_{15}Br_2N_5O_3S_2$	11.72	11.80
XIV	Br	Br	4-Methoxyphenyl	C_2H_5	235°	67	$C_{21}H_{17}Br_2N_5O_3S_2$	11.45	11.21
XV	Br	Br	4-Methoxyphenyl	C_3H_7	231°	59	$C_{22}H_{19}Br_2N_5O_3S_2$	11.20	11.03

Table II—Antiacetylcholinesterase Activity of Substituted Quinazoline Derivatives[a]

Compound	Inhibition at 6.6×10^{-5} M, %	I_{50}[b], $M \times 10^{-5}$
II	5.89	56.0
III	21.06	15.6
IV	25.0	13.2
VIII	15.79	20.8
IX	15.79	20.8
XII	26.32	12.5
XIII	15.79	20.8
XV	21.06	15.6
XVII	26.32	12.5
XVIII	36.843	8.95
XIX	15.80	20.8
XXII	21.06	15.6
XXIV	31.58	10.4
XXV	26.32	12.5

[a] The I_{50} value for neostigmine, a potent acetylcholinesterase inhibitor, used as a standard under similar conditions was 1.96×10^{-7} M. [b] The I_{50} values indicate the molar concentration at which there was 50% inhibition.

Table III—Antibacterial Activity of Substituted Quinazolones

Compound	Average Size of Zone of Inhibition, mm *Staph. aureus*	*B. pumilus*	*B. subtilis*	*Sar. lutea*	*Sal. typhi* H091	*M. tuberculosis*
II	15	7	8	9	11	13
III	9	8	9	13	15	10
IV	—[a]	—[a]	7	10	7	8
V	—[a]	7	—[a]	7	8	—[a]
VI	7	—[a]	8	8	8	—[a]
VII	7	8	—[a]	9	—[a]	7
VIII	7	10	9	7	—[a]	—[a]
IX	—[a]	9	13	12	9	11
X	7	8	13	10	—[a]	7
XI	13	19	17	15	13	18
XII	11	10	9	7	—[a]	13
XIII	10	7	13	9	8	10
XIV	9	13	9	15	17	13
XV	13	15	19	18	9	7
XVI	15	20	17	13	17	14
XVII	7	8	—[a]	7	—[a]	9
XVIII	—[a]	9	15	9	8	—[a]
XIX	10	11	7	8	10	9
XX	7	10	14	7	9	13
XXI	7	9	13	10	12	7
XXII	—[a]	—[a]	7	8	10	—[a]
XXIII	19	15	19	13	17	19
XXIV	15	20	21	17	10	13
XXV	17	10	13	7	13	15
Chloramphenicol[b]	18	17	16	19	17	17
Tetracycline[b]	20	15	16	21	18	15

[a] —, compound inactive. [b] Used as a control in the antibacterial screening.

derivatives with the quinazolone nucleus and to study the biological activities of the quinazolone derivatives in continuation of previous work (21–23).

The present report describes the synthesis, characterization, and *in vitro* antibacterial, antifungal, and antiacetylcholinesterase activities of these quinazolone derivatives (II) (Schemes I–III).

EXPERIMENTAL[1]

Chemistry—Several 6-bromo- and 6,8-dibromo-2-mercapto-3-aryl/cyclohexyl-4-(3*H*)-quinazolones (Ib) were synthesized by condensation of 5-bromo- and 3,5-dibromo-2-aminobenzoic acids (Ia) with different substituted aryl isothiocyanates in ethanol. With the method of Gagiu and Mavrodin (24), different 5-chloroacetylamino-2-alkyl-1,3,4-thiadiazole derivatives (Id) were obtained in good yield by refluxing 2-alkyl-5-amino-1,3,4-thiadiazoles (Ic) in dry benzene with chloroacetyl chloride. The intermediate 2-alkyl-5-amino-1,3,4-thiadiazoles were prepared by a literature method (25). When the 2-mercapto-3-aryl/cyclohexyl-4-

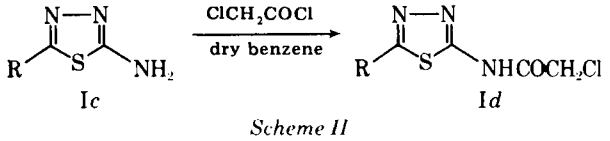

Ic Id

Scheme II

[1] All compounds were analyzed for their nitrogen content. Melting points were taken in open capillary tubes with a partial immersion thermometer and are corrected. IR spectra were obtained with a Perkin-Elmer model 137 Infracord spectrophotometer, equipped with sodium chloride optics, in potassium bromide films in the 700–3500-cm^{-1} range.

Table IV—Antifungal Activity of Substituted Quinazolones [a]

Compound	Concentrations	Average Inhibition after 1 Week, %					
		A. niger	*M. canis*	*A. fumigatus*	*F. moniliforme*	*P. nonatum*	*R. stolonifer*
II	1:1000	41.6	56.7	51.7	38.5	49.3	58.3
	1:10,000	33.3	51.3	47.3	35.3	42.3	47.3
	1:100,000	20.0	42.3	40.0	32.7	39.7	35.2
III	1:1000	58.5	51.4	56.7	67.3	43.7	35.5
	1:10,000	47.3	42.3	45.3	56.4	45.6	28.0
	1:100,000	32.3	37.4	40.1	40.7	47.6	25.3
IV	1:1000	51.3	54.7	47.3	43.7	25.3	27.3
	1:10,000	45.3	50.3	45.3	38.7	19.3	21.3
	1:100,000	47.9	45.5	40.1	25.3	15.4	20.3
V	1:1000	45.5	37.5	55.5	45.6	41.4	35.5
	1:10,000	41.3	33.4	45.6	41.6	40.0	32.3
	1:100,000	37.5	30.0	40.0	37.3	38.0	27.3
VI	1:1000	76.3	67.3	67.3	56.7	87.3	67.9
	1:10,000	45.3	56.4	47.4	53.3	79.5	63.7
	1:100,000	35.7	41.4	40.0	51.2	70.3	60.4
VII	1:1000	81.3	74.4	67.4	45.5	42.7	47.3
	1:10,000	73.7	70.5	60.4	40.1	40.1	45.2
	1:100,000	54.3	61.5	57.5	37.5	37.5	40.3
VIII	1:1000	37.5	25.3	35.5	45.5	36.5	50.0
	1:10,000	30.1	21.5	31.5	40.1	31.3	45.7
	1:100,000	29.1	17.3	27.9	37.5	27.9	41.3
IX	1:1000	47.3	37.3	27.3	25.3	35.6	29.3
	1:10,000	43.2	29.5	25.3	20.4	31.7	25.4
	1:100,000	39.3	25.3	20.9	17.4	28.5	21.4
X	1:1000	37.3	28.3	57.3	47.3	41.5	21.5
	1:10,000	31.4	21.5	45.3	42.1	37.5	20.1
	1:100,000	27.3	17.5	37.4	39.5	30.8	18.3
XI	1:1000	87.3	93.4	81.1	82.1	71.4	47.3
	1:10,000	71.5	87.1	73.3	73.8	67.3	42.1
	1:100,000	69.0	75.6	67.5	56.7	59.7	37.5
XII	1:1000	56.3	67.3	51.5	40.0	51.5	59.0
	1:10,000	47.3	51.8	45.3	37.3	47.5	51.1
	1:100,000	31.5	47.5	41.0	29.0	41.0	49.1
XIII	1:1000	45.0	57.3	43.0	42.0	49.0	47.0
	1:10,000	41.0	51.5	40.0	40.0	41.0	40.0
	1:100,000	40.0	45.7	35.0	33.3	35.5	38.8
XIV	1:1000	97.3	87.3	75.5	85.5	95.5	89.0
	1:10,000	95.4	82.1	71.5	80.0	90.0	85.0
	1:100,000	90.5	76.1	67.9	78.8	85.0	80.0
XV	1:1000	85.6	81.1	70.1	67.3	73.4	70.0
	1:10,000	81.7	80.0	67.1	61.1	70.9	65.5
	1:100,000	75.5	71.0	57.1	56.1	65.9	61.6
XVI	1:1000	51.5	67.3	59.0	61.6	73.1	41.5
	1:10,000	47.7	62.3	57.4	51.1	68.5	39.1
	1:100,000	41.1	51.4	51.5	45.7	56.3	34.5
XVII	1:1000	67.5	56.1	57.1	67.1	49.5	47.1
	1:10,000	63.2	51.1	41.1	61.5	40.0	41.0
	1:100,000	57.1	45.5	34.5	49.0	35.6	37.0
XVIII	1:1000	57.1	45.1	49.0	67.3	61.0	57.5
	1:10,000	40.1	42.1	45.5	61.0	57.3	53.4
	1:100,000	35.3	39.5	40.0	57.3	51.4	50.0
XIX	1:1000	41.5	40.0	41.0	29.0	47.3	40.0
	1:10,000	37.5	35.5	29.0	27.0	41.5	37.9
	1:100,000	30.5	31.6	27.3	21.0	40.1	34.5
XX	1:1000	87.3	76.6	65.5	42.2	67.7	51.0
	1:10,000	81.5	74.0	60.0	41.0	61.1	45.0
	1:100,000	78.1	70.0	57.7	39.1	55.0	42.0
XXI	1:1000	81.1	73.3	69.0	57.0	61.1	63.3
	1:10,000	78.3	71.0	62.0	51.0	59.9	61.0
	1:100,000	70.1	65.0	60.0	45.8	55.5	57.7
XXII	1:1000	67.7	68.0	53.5	41.1	47.7	63.1
	1:10,000	61.1	40.0	40.0	34.4	41.1	57.3
	1:100,000	53.4	37.0	37.3	30.0	35.7	41.1
XXIII	1:1000	89.0	93.7	87.0	81.1	97.0	90.0
	1:10,000	81.0	90.0	81.0	78.1	91.0	85.5
	1:100,000	76.6	85.0	78.0	75.5	87.7	80.0
XXIV	1:1000	78.3	67.3	71.8	84.1	78.1	58.0
	1:10,000	75.1	65.0	65.1	80.0	70.1	51.0
	1:100,000	70.0	60.6	61.1	70.0	59.0	45.5
XXV	1:1000	67.5	57.1	45.0	61.6	45.4	37.3
	1:10,000	61.0	51.0	40.0	59.0	41.4	30.1
	1:100,000	57.7	47.0	37.7	51.5	37.4	28.7

[a] Griseofulvin, a potent fungicide, was used as a control.

(3*H*)-quinazolones were refluxed in alcoholic sodium hydroxide with different 5-chloroacetylamino-2-alkyl-1,3,4-thiadiazoles, 24 new 6-bromo- and 6,8-dibromo-2-[*N*-(2′-alkyl-1′,3′,4′-thiadiazol-5′-yl)carbamoylmethylthio]-3-aryl/cyclohexyl-4-(3*H*)-quinazolones (II) with varying alkyl groups in the thiadiazole nucleus and different aryl functions in the quinazolone nucleus were obtained (Table I).

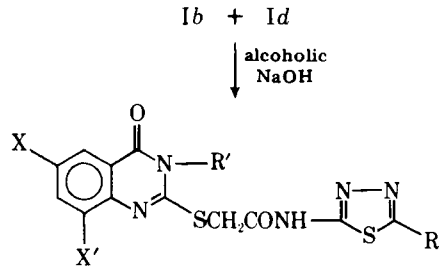

II

Scheme III

Synthesis—*6-Bromo- and 6,8-Dibromo-2-mercapto-3-aryl/cyclohexyl-4-(3H)-quinazolones (Ib)*—These compounds were prepared by the method described by Bhargava and Lakhan (26).

To a solution of 5-bromo-2-aminobenzoic acid (0.01 mole) in absolute ethanol (50 ml) was added 1.41 g (0.01 mole) of cyclohexylisothiocyanate. The resulting solution was heated under reflux on a steam bath for 5 hr, at which time a crystalline solid mass was obtained. The solid mass was separated by filtration, washed with cold ethanol, and recrystallized from ethanol.

Various other quinazolones (Ib) were prepared in a similar manner.

6-Bromo- and 6,8-Dibromo-2-[N-(2'-alkyl-1',3',4'-thiadiazol-5'-yl)carbamoylmethylthio] -3- aryl/cyclohexyl -4- (3H)-quinazolones (II)—To a solution of sodium hydroxide (0.4 g, 0.1 mole) in 30 ml of 80% ethanol was added 3.47 g (0.01 mole) of 6-bromo-2-mercapto-3-benzyl-4-(3*H*)-quinazolone, and the mixture was stirred until a clear solution was obtained. 5-Chloroacetylamino-2-methyl-1,3,4-thiadiazole (1.92 g, 0.01 mole) was added, and the solution was heated under reflux for 5 hr. After cooling, the reaction mixture was poured into 200 ml of ice-cold water; the solid mass was filtered, washed with cold water, and crystallized from ethanol.

Other quinazolone derivatives (II) were prepared in a similar manner and are listed in Table I.

All of the synthesized quinazolone derivatives (II) (Table I) were characterized by their sharp melting points and elemental analyses. The IR spectra of the final compounds (II) showed the characteristic absorption bands of C=N (~1600 cm^{-1}), CH_2CON (~1680 cm^{-1}), CONH (~1660 cm^{-1}), and C=O (1700 cm^{-1}). Absence of the SH vibration at 2550 cm^{-1} provided further support for their molecular structure. These absorption bands correspond to the characteristic quinazolone bands (27).

Biological Screening—All compounds reported in Table I were assayed *in vitro* for antibacterial activity against six bacteria: *Staphylococcus aureus*[2] (NCTC 7447), *Bacillus pumilus*[2] (NCTC 8241), *Bacillus subtilis*[2] (NCTC 8236), *Sarcina lutea*[2] (ATCC 9341), *Salmonella typhi*[3] H091 (NCTC 3111), and *Mycobacterium tuberculosis*[3] ($H_{37}Rv$). Their antifungal activity was screened against several fungi: *Aspergillus niger*[4] (ATCC 12845), *Microsporum canis*[3] (VM 200-USPHS), *Aspergillus fumigatus*[3] (68LI), *Fusarium moniliforme*[4] (ATCC 10052), *Penicillium nonatum*[4] (ATCC 9179), and *Rhizopus stolonifer*[4] (ATCC 10404).

Of the 24 quinazolone derivatives (Table I), 14 also were tested for their antiacetylcholinesterase activity (Table II).

Determination of Antibacterial Activity—The *in vitro* antibacterial activity was determined by an agar plate diffusion method (28). The agar medium was inoculated with 1 ml of a 24-hr-old culture of the test organism. Filter paper disks (5 mm in diameter) saturated with the test compounds (10 mg/ml in ethanol) were placed on nutrient agar after the ethanol was dried. After incubation for 36 hr, the zones of inhibition around the disks were measured.

All experiments were performed in duplicate, and the results are recorded in Table III.

Determination of Antifungal Activity—The agar plate diffusion technique (29) was employed for the determination of the antifungal activity of the synthesized compounds. Three concentrations (1:1000, 1:10,000, and 1:100,000) were used. One milliliter of each compound was poured into separate petri dishes. Approximately 20–25 ml of molten Czapek-Dox agar medium was added to each petri dish.

All experiments were performed in triplicate. The average percentage inhibition given by the various compounds after 1 week is given in Table IV.

Determination of Antiacetylcholinesterase Activity—Male rats, ~150–200 g, were decapitated, and the brains were removed quickly, weighed, and homogenized in a glass homogenizer[5] using a polytef pestle. A 1% (w/v) homogenate in phosphate saline was used without further purification as the enzyme source.

The enzyme activity was assayed essentially according to the method proposed by Diggle and Gage (30), which is a modification of Hestrin's (31) method. The 2.7-ml assay system contained 0.5 ml of phosphate saline, 1.0 ml of acetylcholine bromide solution, 0.2 ml of inhibitor solution in propylene glycol, and 1.0 ml of the enzyme source. The enzyme was kept with the inhibitor at 37° for 5 min. The reaction was started with the addition of acetylcholine (only in experimental tubes).

The tubes were kept at 37° for 15 min, after which the reaction was stopped by the addition of 2.0 ml of alkaline hydroxylamine hydrochloride. Thereafter, 1.0 ml of acetylcholine solution was added to the control tubes. Then 1.0 ml of diluted hydrochloric acid was added to all of the tubes, followed by the addition of 1.5 ml of ferric chloride solution and water to bring the volume to 7.5 ml in each tube. The absorbance was recorded in a spectrophotometer[6] at 540 nm. The inhibition obtained was recorded in Table II along with the I_{50} values of the quinazolone derivatives, which indicate the concentration required to produce 50% enzyme inhibition.

RESULTS AND DISCUSSION

The results shown in Table III indicate that all of the compounds exhibited antibacterial activity against at least one type of bacteria. In comparison to the 6-bromo quinazolone derivatives (II–XIII), 6,8-dibromo quinazolone derivatives (XIV–XXV) were more effective antibacterial compounds. When the benzyl or 4-methoxyphenyl group was substituted at the 3-position in the quinazolone nucleus, the activity increased (II–IV, XI–XVI, and XXIII–XXV). 2-Ethylphenyl-substituted quinazolone derivatives (V–VII and XVII–XIX) exhibited comparatively poor antibacterial activity. All compounds exhibited increased antibacterial activity against *S. lutea* (ATCC 9341). Compounds XI, XVI, and XXIII exhibited good antibacterial activity.

From the toxicity data given in Table IV, it is evident that all of the compounds possess variable antifungal activity against the fungi tested. The 6,8-dibromo quinazolone derivatives were more effective antifungal agents than the 6-bromo quinazolone derivatives. Substitution of the benzyl group at the 3-position of the quinazolone nucleus led to II–IV and XIV–XVI, which were more effective antifungal compounds. Furthermore, the electron-donating group 2-ethylphenyl decreased the fungitoxicity of the test compounds while the electron-withdrawing group 4-methoxyphenyl increased the fungitoxicity. Cyclohexyl substitution at the 3-position of the quinazolone nucleus rendered VIII–X and XX–XXII less fungitoxic against the fungi tested.Compounds XI and XXIII were better antifungal agents.

The results of the antiacetylcholinesterase test *in vitro* against 14 synthesized quinazolone derivatives are recorded in Table II. The screening data indicate that all of these derivatives exhibited marginal activity. Compounds XVIII and XXIV were more active, while II was inactive. Furthermore, 6,8-dibromo-substituted quinazolone derivatives were more potent in comparison to 6-bromo-substituted derivatives. Compounds III, XV, and XXII exhibited equal I_{50} values, as did XII, XVII, and XXV and also VIII, IX, and XIII.

REFERENCES

(1) P. N. Bhargava and M. R. Chaurasia, *J. Indian Chem. Soc.*, **53**, 46 (1976).

(2) S. K. V. Seshavataram and N. V. Subba Rao, *Proc. Indian Acad. Sci., Sec. A*, **85**, 81 (1977).

(3) R. S. Verma, *J. Indian Chem. Soc.*, **52**, 344 (1975).

(4) J. Klosa, German pat. 1,200,307 (1965); through *Chem. Abstr.*, **63**, 18113e (1965).

(5) P. C. Joshi and P. C. Joshi, *J. Indian Chem. Soc.*, **55**, 465 (1978).

(6) N. Home and H. Reinshagen, German pat. 2,619,110 (1976); through *Chem. Abstr.*, **88**, 72696e (1977).

(7) M. K. Jain and K. S. Narang, *J. Indian Chem. Soc.*, **30**, 711

[2] Obtained from Public Analyst Department, U.P. Government, Lucknow, India.

[3] Obtained from Central Drug Research Institute, Lucknow, India.

[4] Obtained from Cane Sugar Research Institute, Lucknow, India.

[5] Potter Elvehjem type A.

[6] Spectrochem.

(1953).
(8) A. B. Sen and S. K. Gupta, *ibid.*, **39**, 369 (1962).
(9) B. M. Gupta, S. K. Khan, and U. Agarwal, *J. Sci. Ind. Res.*, **21**, 189 (1962).
(10) M. Seth and N. M. Khanna, *Indian J. Chem.*, **14**, 536 (1976).
(11) M. L. Gujral, K. N. Sareen, and R. P. Kohli, *Indian J. Med. Res.*, **45**, 207 (1957).
(12) K. C. Joshi, V. K. Singh, D. S. Mehta, R. C. Sharma, and L. Gupta, *J. Pharm. Sci.*, **64**, 1428 (1975).
(13) H. C. Scarborough, U.S. pat. 3,073,826 (1963).
(14) B. Camillo and A. David, *J. Pharm. Pharmacol.*, **12**, 501 (1960).
(15) G. B. Jackman, V. Petrov, and O. Stephensen, *ibid.*, **12**, 529 (1960).
(16) S. S. Parmar, L. D. Joshi, K. Kishore, and R. Kumar, *Biochem. Pharmacol.*, **15**, 723 (1966).
(17) J. P. Barthwal, S. K. Tandon, V. K. Agarwal, K. S. Dixit, and S. S. Parmar, *J. Pharm. Sci.*, **62**, 613 (1973).
(18) H. Kawada, E. Yoshinaga, I. Chiyomaru, and H. Ito, Japanese pat. 7,748,178 (1977); through *Chem. Abstr.*, **88**, 132018p (1978).
(19) L. Nuesslein, E. A. Pieroch, and K. Roeder, U.S. pat. 4,061,645 (1977); through *Chem. Abstr.*, **88**, 62397k (1978).
(20) K. John (Velsicol Chemical Corp.), U.S. pat. 4,052,193 (1977); through *Chem. Abstr.*, **88**, 22929d (1978).
(21) A. K. Sen Gupta and H. K. Misra, *Indian J. Chem.* **17**, 185 (1979).
(22) *Ibid.*, **18**, 381 (1979).
(23) A. K. Sen Gupta and H. K. Misra, *Agr. Biol. Chem., Jpn.*, **44**, 1009 (1980).
(24) F. Gagiu and Al. Mavrodin, *Bull. Soc. Chim. Fr.*, **3**, 1010 (1967).
(25) Japanese pat. 20,944 (1966); through *Chem. Abstr.*, **66**, 46430f (1967).
(26) P. N. Bhargava and R. Lakhan, *Curr. Sci.*, **36**, 575 (1967).
(27) H. Culbertoson, J. C. Decius, and B. E. Christensen, *J. Am. Chem. Soc.*, **74**, 4834 (1952).
(28) R. S. Varma, S. A. Imam, and W. L. Nobles, *J. Pharm. Sci.*, **62**, 140 (1973).
(29) J. G. Horshfall, *Bot. Rev.*, **5**, 357 (1945).
(30) W. M. Diggle and J. G. Gage, *Biochem. J.*, **49**, 491 (1951).
(31) S. Hestrin, *J. Biol. Chem.*, **180**, 249 (1949).

ACKNOWLEDGMENTS

The authors thank Dr. T. N. Srivastava, Department of Chemistry, Lucknow University, Lucknow, India, for providing the facilities. They also thank Dr. Nitya Nand, Central Drug Research Institute, Lucknow, India, for allowing microanalysis and screening of the compounds and Dr. M. C. Joshi, Public Analyst Department, Lucknow, India, and Mr. F. A. Khan, Biochemistry Department, Lucknow University, Lucknow India, for their help during the antibacterial and antiacetylcholinesterase screening. H. K. Misra thanks the Council of Scientific and Industrial Research, New Delhi, India, for the award of a senior research fellowship.

Comparison of Polyethylene Glycol and Polyoxyethylene Stearate as Excipients for Solid Dispersion Systems of Griseofulvin and Tolbutamide I: Phase Equilibria

RABINDER KAUR *, D. J. W. GRANT *x, and T. EAVES ‡§

Received March 4, 1980, from the **Department of Pharmacy, University of Nottingham, University Park, Nottingham NG7 2RD, England,* and the ‡*Hoechst Pharmaceuticals Research Laboratories, Walton Manor, Milton Keynes, Buckinghamshire MK7 7AJ, England.* Accepted for publication May 27, 1980. §Present address: Merrell International, Slough, Berkshire SL1 1YY, England.

Abstract □ Phase equilibrium diagrams were constructed based on hot-stage microscopy and differential scanning calorimetry of solid dispersions of griseofulvin or tolbutamide in polyethylene glycol 2000 or polyoxyethylene 40 stearate. The solid dispersions were prepared by physical mixing, fusion, and coprecipitation from ethanol. The phase diagrams were largely independent of the method of preparation of the dispersion systems. The diagrams were of the monotectic type for polyethylene glycol 2000 with each drug and for griseofulvin with each excipient, with the monotectic species being the pure drug. Polyoxyethylene 40 stearate with tolbutamide gave eutectic systems in which liquid polyoxyethylene 40 stearate dissolved up to 20% of the tolbutamide. The phase diagrams showed greater solubility of tolbutamide in liquid polyoxyethylene 40 stearate than in polyethylene glycol 2000 but showed a similar solubility of griseofulvin in each excipient. Solid solution formation was not detected.

Keyphrases □ Excipients—polyethylene glycol and polyoxyethylene stearate, comparison as excipients for solid dispersion systems of griseofulvin and tolbutamide, phase equilibria □ Polyethylene glycol—comparison with polyoxyethylene stearate as excipient for solid dispersion systems of griseofulvin and tolbutamide, phase equilibria □ Polyoxyethylene stearate—comparison with polyethylene glycol as excipient for solid dispersion systems of griseofulvin and tolbutamide, phase equilibria

The use of a eutectic mixture containing a water-soluble compound to increase the dissolution rate and bioavailability of a sparingly soluble drug first was demonstrated by Sekiguchi and Obi (1). As the water-soluble matrix dissolves, the insoluble drug is exposed to the dissolution medium in a very fine state of subdivision. This type of formulation, a solid dispersion system, has been investigated extensively and has been extended to include solid solutions of drug in water-soluble excipients (2). Solid solutions should offer greater increases in the dissolution rate and bioavailability than eutectic mixtures, because the drug is dispersed as single molecules in solid solutions but as solid microscopic particles in the latter case.

BACKGROUND

Solid dispersions of griseofulvin in polyethylene glycols of high molecular weight (3, 4) have excited much interest. The dissolution rate and bioavailability of griseofulvin from such solid dispersions clearly are greater than those of the micronized or microcrystalline drug (5). These phenomena previously were attributed to the formation of solid solutions, but Chiou (6) recently showed that griseofulvin has negligible or very limited solid solubility in polyethylene glycol dispersion systems. The marked enhancement of the dissolution and absorption rates of griseo-

0022-3549/80/1100-1317$01.00/0
© 1980, American Pharmaceutical Association

(1953).
(8) A. B. Sen and S. K. Gupta, *ibid.*, **39**, 369 (1962).
(9) B. M. Gupta, S. K. Khan, and U. Agarwal, *J. Sci. Ind. Res.*, **21**, 189 (1962).
(10) M. Seth and N. M. Khanna, *Indian J. Chem.*, **14**, 536 (1976).
(11) M. L. Gujral, K. N. Sareen, and R. P. Kohli, *Indian J. Med. Res.*, **45**, 207 (1957).
(12) K. C. Joshi, V. K. Singh, D. S. Mehta, R. C. Sharma, and L. Gupta, *J. Pharm. Sci.*, **64**, 1428 (1975).
(13) H. C. Scarborough, U.S. pat. 3,073,826 (1963).
(14) B. Camillo and A. David, *J. Pharm. Pharmacol.*, **12**, 501 (1960).
(15) G. B. Jackman, V. Petrov, and O. Stephensen, *ibid.*, **12**, 529 (1960).
(16) S. S. Parmar, L. D. Joshi, K. Kishore, and R. Kumar, *Biochem. Pharmacol.*, **15**, 723 (1966).
(17) J. P. Barthwal, S. K. Tandon, V. K. Agarwal, K. S. Dixit, and S. S. Parmar, *J. Pharm. Sci.*, **62**, 613 (1973).
(18) H. Kawada, E. Yoshinaga, I. Chiyomaru, and H. Ito, Japanese pat. 7,748,178 (1977); through *Chem. Abstr.*, **88**, 132018p (1978).
(19) L. Nuesslein, E. A. Pieroch, and K. Roeder, U.S. pat. 4,061,645 (1977); through *Chem. Abstr.*, **88**, 62397k (1978).
(20) K. John (Velsicol Chemical Corp.), U.S. pat. 4,052,193 (1977); through *Chem. Abstr.*, **88**, 22929d (1978).
(21) A. K. Sen Gupta and H. K. Misra, *Indian J. Chem.* **17**, 185 (1979).
(22) *Ibid.*, **18**, 381 (1979).
(23) A. K. Sen Gupta and H. K. Misra, *Agr. Biol. Chem., Jpn.*, **44**, 1009 (1980).
(24) F. Gagiu and Al. Mavrodin, *Bull. Soc. Chim. Fr.*, **3**, 1010 (1967).
(25) Japanese pat. 20,944 (1966); through *Chem. Abstr.*, **66**, 46430f (1967).
(26) P. N. Bhargava and R. Lakhan, *Curr. Sci.*, **36**, 575 (1967).
(27) H. Culbertoson, J. C. Decius, and B. E. Christensen, *J. Am. Chem. Soc.*, **74**, 4834 (1952).
(28) R. S. Varma, S. A. Imam, and W. L. Nobles, *J. Pharm. Sci.*, **62**, 140 (1973).
(29) J. G. Horshfall, *Bot. Rev.*, **5**, 357 (1945).
(30) W. M. Diggle and J. G. Gage, *Biochem. J.*, **49**, 491 (1951).
(31) S. Hestrin, *J. Biol. Chem.*, **180**, 249 (1949).

ACKNOWLEDGMENTS

The authors thank Dr. T. N. Srivastava, Department of Chemistry, Lucknow University, Lucknow, India, for providing the facilities. They also thank Dr. Nitya Nand, Central Drug Research Institute, Lucknow, India, for allowing microanalysis and screening of the compounds and Dr. M. C. Joshi, Public Analyst Department, Lucknow, India, and Mr. F. A. Khan, Biochemistry Department, Lucknow University, Lucknow India, for their help during the antibacterial and antiacetylcholinesterase screening. H. K. Misra thanks the Council of Scientific and Industrial Research, New Delhi, India, for the award of a senior research fellowship.

Comparison of Polyethylene Glycol and Polyoxyethylene Stearate as Excipients for Solid Dispersion Systems of Griseofulvin and Tolbutamide I: Phase Equilibria

RABINDER KAUR *, D. J. W. GRANT *x, and T. EAVES ‡§

Received March 4, 1980, from the **Department of Pharmacy, University of Nottingham, University Park, Nottingham NG7 2RD, England,* and the ‡*Hoechst Pharmaceuticals Research Laboratories, Walton Manor, Milton Keynes, Buckinghamshire MK7 7AJ, England.* Accepted for publication May 27, 1980. §Present address: Merrell International, Slough, Berkshire SL1 1YY, England.

Abstract □ Phase equilibrium diagrams were constructed based on hot-stage microscopy and differential scanning calorimetry of solid dispersions of griseofulvin or tolbutamide in polyethylene glycol 2000 or polyoxyethylene 40 stearate. The solid dispersions were prepared by physical mixing, fusion, and coprecipitation from ethanol. The phase diagrams were largely independent of the method of preparation of the dispersion systems. The diagrams were of the monotectic type for polyethylene glycol 2000 with each drug and for griseofulvin with each excipient, with the monotectic species being the pure drug. Polyoxyethylene 40 stearate with tolbutamide gave eutectic systems in which liquid polyoxyethylene 40 stearate dissolved up to 20% of the tolbutamide. The phase diagrams showed greater solubility of tolbutamide in liquid polyoxyethylene 40 stearate than in polyethylene glycol 2000 but showed a similar solubility of griseofulvin in each excipient. Solid solution formation was not detected.

Keyphrases □ Excipients—polyethylene glycol and polyoxyethylene stearate, comparison as excipients for solid dispersion systems of griseofulvin and tolbutamide, phase equilibria □ Polyethylene glycol—comparison with polyoxyethylene stearate as excipient for solid dispersion systems of griseofulvin and tolbutamide, phase equilibria □ Polyoxyethylene stearate—comparison with polyethylene glycol as excipient for solid dispersion systems of griseofulvin and tolbutamide, phase equilibria

The use of a eutectic mixture containing a water-soluble compound to increase the dissolution rate and bioavailability of a sparingly soluble drug first was demonstrated by Sekiguchi and Obi (1). As the water-soluble matrix dissolves, the insoluble drug is exposed to the dissolution medium in a very fine state of subdivision. This type of formulation, a solid dispersion system, has been investigated extensively and has been extended to include solid solutions of drug in water-soluble excipients (2). Solid solutions should offer greater increases in the dissolution rate and bioavailability than eutectic mixtures, because the drug is dispersed as single molecules in solid solutions but as solid microscopic particles in the latter case.

BACKGROUND

Solid dispersions of griseofulvin in polyethylene glycols of high molecular weight (3, 4) have excited much interest. The dissolution rate and bioavailability of griseofulvin from such solid dispersions clearly are greater than those of the micronized or microcrystalline drug (5). These phenomena previously were attributed to the formation of solid solutions, but Chiou (6) recently showed that griseofulvin has negligible or very limited solid solubility in polyethylene glycol dispersion systems. The marked enhancement of the dissolution and absorption rates of griseo-

0022-3549/80/1100-1317$01.00/0
© 1980, American Pharmaceutical Association

Table I—Effect of Pretreatment on the Melting Ranges

Compound	Ground Materials	Recrystallized from Ethanol	After Fusion and Cooling
I	53–58°	53–58°	54–58°
II	46–50°	46–50°	37–45°
Griseofulvin	220–222°	220–222°	220–224°
Tolbutamide	127–133°	127–133°	125–131°

fulvin dispersed in polyethylene glycol seems to be primarily a result of the reduced size of the griseofulvin crystals; however, other factors, such as increased wettability, reduction or absence of aggregation and agglomeration, and solubilization of the drug by the carrier at the diffusion layer of particles also may contribute (6).

The formation of solid dispersions of tolbutamide in polyethylene glycol polymers also increases the dissolution rate of this drug (7), and this increase has been attributed to the formation of a solid solution, the dispersion of the drug in a fine state of subdivision, or improved wetting of the drug particles. Polyethylene glycol is a hydrophilic polymer with no hydrophobic or lipophilic moiety and, therefore, is not surface active. Esterification with a long-chain *n*-acyl residue (such as stearate, to form, for example, polyoxyethylene stearate) produces a water-soluble, surface-active macromolecule, which might offer certain advantages as an excipient in solid dispersion systems of drugs, such as griseofulvin or tolbutamide, that are poorly soluble in water. The nonpolar hydrophobic moiety, *e.g.*, $C_{17}H_{35}$, might promote solid solution formation, with consequent advantages for drug release, as well as surface activity, a potent factor in enhancing rates of dissolution and absorption. The possibility of solid solution formation is considered in the present report, and the consequences of surface activity are discussed elsewhere (8).

Polyoxyethylene 40 stearate has been evaluated by the joint Food and Agriculture Organization and World Health Organization Expert Committee on Food Additives (9) and is claimed to be acceptable for daily intake of up to 25 mg/kg. Further biological data, including biochemical aspects, toxicological studies, and observations in humans, also have confirmed the relative nontoxicity of polyoxyethylene 40 stearate (10–15).

Polyoxyethylene 40 stearate is a mixture of monoacid stearates of polyoxyethylene polymers consisting of 40 oxyethylene units on the average, and its mean molecular weight is similar to that of polyethylene glycol 2000. It is a solid that melts at 45–52° and is miscible with water in all proportions. Its hydrophile–lipophile balance value is 16.9, and it stabilizes oil-in-water emulsions.

Using thermal methods of analysis, the physicochemical interactions between two model drugs and polyoxyethylene 40 stearate (average molecular weight of 2044) were compared with those between the drugs and polyethylene glycol 2000. The model drugs, griseofulvin and tolbutamide, were chosen based on their low solubility in water and biological fluids.

Dispersion systems containing each drug and each excipient were prepared (*a*) by grinding the drug and excipient together, (*b*) by fusing the drug and excipient together and then grinding the mass, and (*c*) by coprecipitating the drug and excipient from the same solvent (ethanol) followed by grinding. Mixtures covering the entire range of composition, including the single components, were subjected to differential thermal analysis and hot-stage microscopy, from room temperature to temperatures above those of complete melting. The solid–liquid phase diagrams were plotted and compared.

The next report in this series (8) compares the influence of polyoxyethylene 40 stearate (II) with that of polyethylene glycol 2000 (I) on the dissolution rate of the two drugs from certain dispersion systems and assesses the factors responsible for the differences. A preliminary report of the work was published previously (16).

EXPERIMENTAL

Materials—The following materials and drugs were of food or pharmaceutical grade and were used as supplied: polyoxyethylene 40 stearate[1] (II), polyethylene glycol 2000[2] (I), griseofulvin[2], and tolbutamide[2]. Ethanol (95%) was spectroscopic grade. The pH 7 buffer was phosphate buffer BP (17). The pH 1 buffer was 0.1 *M* HCl. All water was double distilled from an all-glass still.

[1] Myrj 52, Atlas Chemicals Ltd., Carshalton, Surrey, England.
[2] Hoechst UK Ltd., Milton Keynes, Bucks, England.

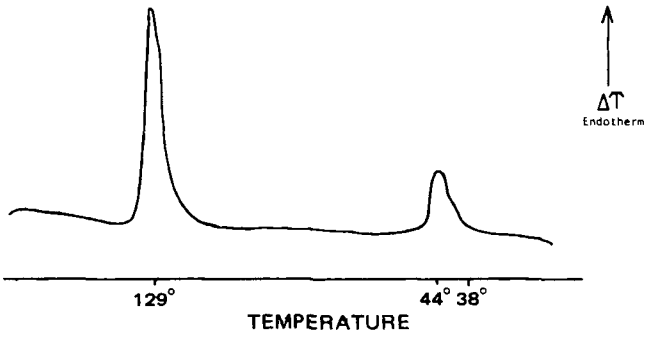

Figure 1—*Differential thermal analysis curve of a coprecipitated dispersion of tolbutamide (90% w/w) and II (10% w/w).*

Preparation of Dispersion Systems—*Physical Mixtures*—The physical mixtures were prepared by thoroughly grinding together weighed quantities of the drug and excipient for 5 min using a glass pestle and mortar. Homogeneity of the mixtures was tested by subjecting the samples to thermal microscopy and to differential thermal analysis.

Fused Mixtures—The fused mixtures were prepared by heating 1–2 g of the corresponding ground physical mixture in a wide test tube to a few degrees above the melting point of the excipient, *i.e.*, <65°, with rotation of the tube for 30 sec. The sample was allowed to cool in a desiccator at 4°. The resulting solid then was scraped out of the tube and ground using a glass pestle and mortar.

Coprecipitated Mixtures—Coprecipitated mixtures were prepared by dissolving weighed quantities of the drug and excipient in ethanol, mixing thoroughly, and allowing the solvent to evaporate slowly in a rotary film evaporator[3] at ~40° under vacuum. The resulting semisolid mass was dried under vacuum[4] at 20° in the presence of phosphorus pentoxide. The dry solid was ground using a glass pestle and mortar.

Differential Thermal Analysis—Five milligrams of sample was heated at 5°/min in a thermal analyzer[5] coupled to a two-channel potentiometric recorder[6]. Alumina was used as the reference material, and static air was the gas phase. The instrument was calibrated using benzoic acid[7] (thermochemical grade).

The onset of each peak was characterized by the temperature at the point of intersection of the line of the steepest slope and the baseline. The completion of each peak was characterized by the temperature at the summit. These two temperatures were used to define the melting ranges from differential thermal analysis.

Hot-Stage Microscopy—About 1 mg of sample was placed between a microscope slide and a cover slide and heated at 1–5°/min under a hot-stage microscope[8] fitted with polarizers. The onset of melting was characterized by the first appearance of liquid, and the completion of melting was considered as the final disappearance of solid. These two temperatures were used to define the melting ranges from hot-stage microscopy.

Preparation of Dispersion Systems for Differential Thermal Analysis and Hot-Stage Microscopy—The excipients under study are waxy at room temperature and crystalline and brittle at the temperature of solid carbon dioxide. Therefore, differential thermal analysis and hot-stage microscopy of the excipients were compared after grinding at each temperature followed by standing for 30 min in a desiccator. Since no significant difference in melting was found, grinding subsequently was carried out at room temperature.

Using differential thermal analysis and hot-stage microscopy, the phase equilibria of physical, fused, and coprecipitated mixtures of each drug (tolbutamide and griseofulvin) with each excipient (I and II) were studied.

RESULTS

Melting Behavior of Original Materials—Compounds I and II, griseofulvin, and tolbutamide, when subjected to differential thermal analysis, each gave a single peak corresponding to fusion. Furthermore,

[3] Buchi, Switzerland.
[4] Vacuum drier, Gallenkamp, London, England.
[5] Stanton Redcroft model 671, London, England.
[6] Servoscribe 2S, Smiths Industries Ltd., Cricklewood, London, England.
[7] BDH Chemicals Ltd., Poole, Dorset, England.
[8] Kofler type, C. Reichert Optische Werke, Austria.

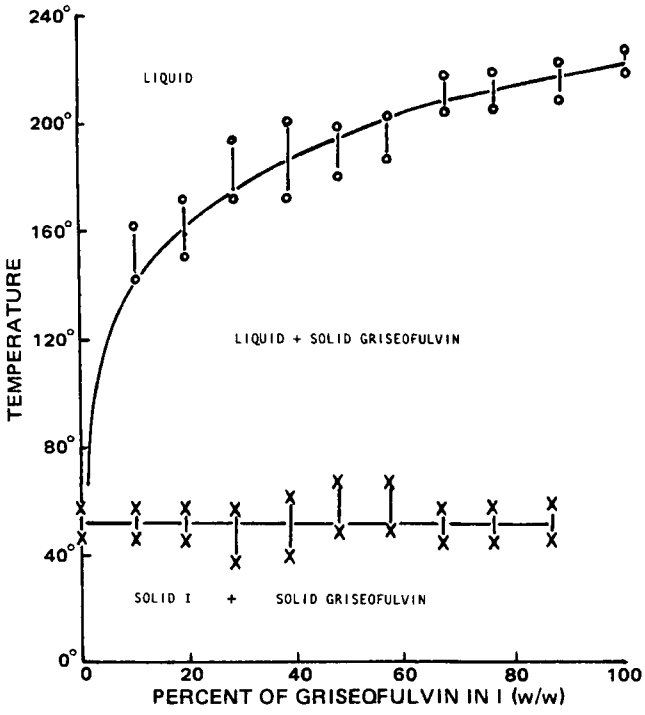

Figure 2—*Phase diagram of coprecipitated mixtures of griseofulvin and I determined using differential thermal analysis and hot-stage microscopy.*

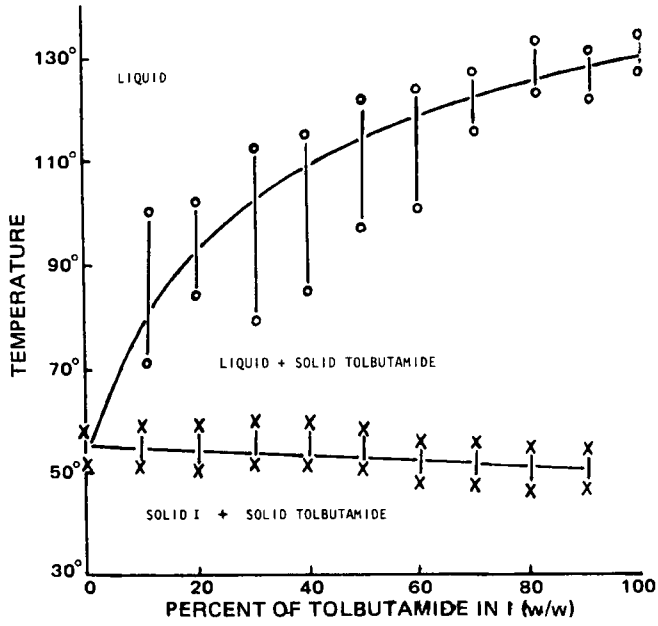

Figure 4—*Phase diagram of coprecipitated mixtures of tolbutamide and I determined using differential thermal analysis and hot-stage microscopy.*

when heated slowly under hot-stage microscopy, each substance melted over the same temperature range as that defined by the beginning and summit of the corresponding peak in differential thermal analysis. The two techniques afforded the melting ranges shown in Table I. Reductions in the melting point were observed only with tolbutamide and II after fusion and cooling.

Melting Behavior of Drug–Excipient Mixtures—Whether prepared by physical mixing, fusion–cooling, or coprecipitation, dispersion systems of each drug (griseofulvin or tolbutamide) in each excipient (I or II), exhibited two transitions in differential thermal analysis (Fig. 1). These transitions corresponded to fusion of the excipient and drug, respectively, as observed under hot-stage microscopy over the temperature range studied. The lower temperature transition always corresponded to fusion of I or II, and the higher temperature transition always corresponded to fusion of griseofulvin or tolbutamide. This behavior and the corresponding binary phase diagram were qualitatively independent and quantitatively almost independent of the method used to prepare a given drug–excipient mixture. Typical phase equilibrium diagrams are shown in Figs. 2–5.

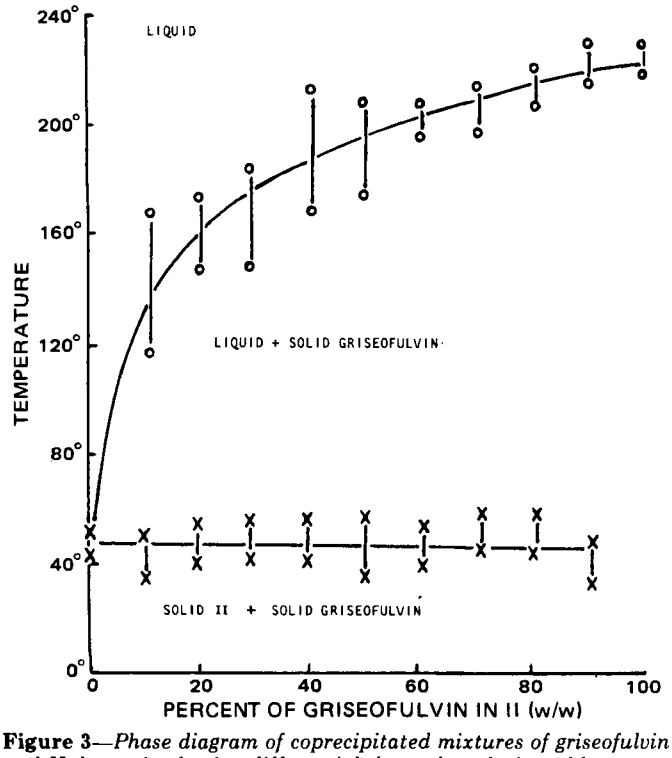

Figure 3—*Phase diagram of coprecipitated mixtures of griseofulvin and II determined using differential thermal analysis and hot-stage microscopy.*

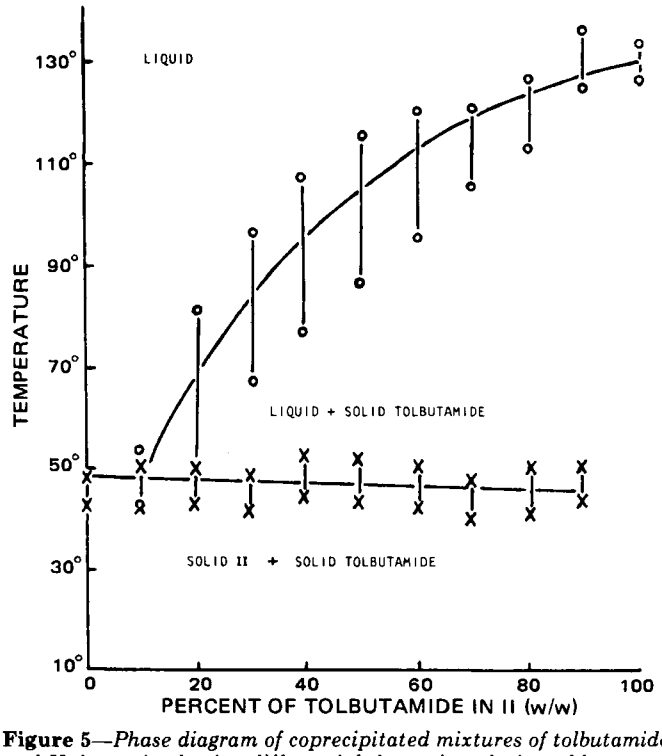

Figure 5—*Phase diagram of coprecipitated mixtures of tolbutamide and II determined using differential thermal analysis and hot-stage microscopy.*

Table II—Classification of Phase Equilibrium Diagrams

Drug	Excipient I			Excipient II		
	Physical Mixing	Fusion	Coprecipitation	Physical Mixing	Fusion	Coprecipitation
Griseofulvin	A	A	A	A	A	A
Tolbutamide	A	A	A	B	B	B

Hot-stage microscopy of the mixtures of all compositions showed a constant melting point of I at 48–58° and of II at 42–52°, corresponding to the endothermic peaks in differential thermal analysis (the solidus or melting point). Hot-stage microscopy showed that, in general, increasing amounts of drug dissolved in the liquid excipient as the temperature increased so that the drug crystals disappeared completely at a temperature (the liquidus or freezing point) between the melting point of the excipient and the melting point of the pure drug. The freezing point was quoted as that temperature above which no more crystals were visible between crossed polarizers. If this transition was not sharp, the sample was allowed to cool gradually and the freezing point was recorded as that temperature at which drug crystals just became visible. Crystals of griseofulvin and tolbutamide have distinctive crystalline habits, which are clearly recognizable compared with the amorphous appearance of the excipients. As the drug crystals dissolved in the liquid excipient on heating, their corners and edges were eroded first, as is normally encountered (18).

When the proportion of each drug in each solid dispersion system was increased, hot-stage microscopy and differential thermal analysis showed, in general, that the solidus temperature (freezing point of the drug) increased. This solidus transition appeared as a second endothermic peak in differential thermal analysis, but the instrument, unlike hot-stage microscopy, was unable to detect this transition for a drug content of <~50% (w/w). Thus, in general, the two techniques were confirmatory or complementary, and no evidence of polymorphism was apparent from either method.

Each of the 12 phase diagrams (2 drugs × 2 excipients × 3 methods of mixing) fell into one of two groups, arbitrarily designated as Types A and B (Table II). Type A was a monotectic system and occurred with all six griseofulvin systems and with the three tolbutamide–I systems. It was characterized by the absence of complete dissolution of the drug in the molten excipient at the melting point of the excipient. Examples of a Type A phase equilibrium diagram are shown in Figs. 2–4. There was very limited solubility of solid griseofulvin in just molten I (Fig. 2) or just molten II (Fig. 3).

Type B diagrams were shown by the three tolbutamide–II systems and were characterized by features common to both eutectic and monotectic behavior. Figure 5 gives an example for the coprecipitated tolbutamide–II system. The liquid II at its melting point (~50°) was capable of dissolving ~10% (w/w) tolbutamide. This contrasts sharply with the immeasurably low solubility of the drug in liquid I at its melting point (Fig. 4).

For any one of the four drug–excipient pairs, the methods of preparing the dispersion systems gave almost identical diagrams with the following exceptions:

1. Physical and fused mixtures of tolbutamide and II gave approximately twice the solubility of tolbutamide in just molten II, as did the coprecipitated mixtures; *i.e.*, concentrations of ~20% were obtained.

2. Physical mixtures of griseofulvin and I showed a more steeply rising liquidus curve than did the fused or coprecipitated systems.

Liquid mixtures containing 1% (w/w) griseofulvin or tolbutamide in I or II froze to a solid, which microscopic examination showed to consist of drug crystals dispersed in the excipient. Therefore, the extent of solid solubility of each drug in each excipient was judged to be negligible (<1% w/w).

DISCUSSION

The only form of tolbutamide encountered under the conditions of the present work was the commercial form which melted at 127° (19), namely, Modification A (20) or I (21, 22). This polymorph is the most stable at room temperature (21, 22). In view of the reported polymorphism of tolbutamide (19–22), it may seem surprising that no polymorphic transitions were observed in the present work; this finding is illustrated by the differential thermal analysis plot shown in Fig. 1. The most likely explanation is that either polymeric polar excipient (polyethylene glycol 2000 or polyoxyethylene 40 stearate) stabilizes the original commercial modification (I or A) relative to the other modifications produced under different conditions (19–22). In an analogous manner, the presence of the polar polymer povidone, for example, slows down the rate of transformation of the polymorphic form (II) of sulfameter to form III in aqueous suspension (23).

All of the phase diagrams involving I or griseofulvin, either separately or together, were of the monotectic type (Figs. 2–4). This type of system has not been reported previously in pharmacy but is well known to metallurgists, *e.g.*, the silicon–tin system (24).

A monotectic phase diagram has the form of a eutectic diagram in which one arm is missing and in which the lower melting component replaces the eutectic composition. The rising liquidus curve on the left of each monotectic diagram corresponds to the solubility curve of the drug in the liquid excipient.

Comparison of the phase diagrams (Figs. 2–5) shows that the differences between I and II as excipients for solid dispersion systems are much less marked for griseofulvin than for tolbutamide dispersions. The position and shape of the rising curve at the left of each phase diagram show a greater solubility of tolbutamide in liquid II than in I (Figs. 4 and 5) but a similar solubility of griseofulvin in each (Figs. 2 and 3).

The phase diagrams for the tolbutamide–II dispersions prepared in three ways can be considered to be eutectic systems in which the liquidus (freezing-point curve of tolbutamide) and the solidus (melting-point curve of II) have become superimposed. The first molten II (at ~40°) is capable of dissolving completely up to 10 or 20% (w/w) tolbutamide, depending on the preparation method.

However, the phase diagrams of the dispersion systems are changed little by the preparation method and appear to be dominated by the solvent properties of liquid I or II for each drug. The presence of a small amount of I or II with each drug causes little depression of the melting point of the drug, and, conversely, the presence of a small amount of griseofulvin or tolbutamide hardly affects the melting point of the excipient. This behavior contrasts sharply with the dispersion systems using small molecules as excipients, *e.g.*, urea (25, 26), succinic acid (27), and citric acid (28). These systems are eutectic with or without the formation of solid solutions. All of the dispersion systems of griseofulvin or tolbutamide with I or II showed negligible formation of solid solutions (<1% w/w), in contrast to the small molecule systems. This absence of solid solutions in polyethylene glycol–griseofulvin systems also was reported on the basis of X-ray diffraction evidence (6).

Finally, the phase diagrams obtained for fused–cooled and coprecipitated mixtures of each drug with each excipient were similar to those of physical mixtures of the two components, and there was no evidence of the formation of solid complexes between the two components. This absence of chemical interactions between the drug–excipient pairs on fusion, which was reported earlier for polyethylene glycol with griseofulvin (3) and tolbutamide (29), indicates that I or II can only influence the dissolution rate of the drugs by altering their surface properties such as the surface area or the nature of the drug–water interface. These factors were considered in a separate report (8).

REFERENCES

(1) K. Sekiguchi and N. Obi, *Chem. Pharm. Bull.*, **9**, 866 (1961).

(2) A. H. Goldberg, M. Gibaldi, J. L. Kanig, and M. Mayersohn, *J. Pharm. Sci.*, **55**, 581 (1966).

(3) W. L. Chiou and S. Riegelman, *ibid.*, **58**, 1505 (1969).

(4) W. L. Chiou and L. D. Smith, *ibid.*, **60**, 125 (1971).

(5) W. L. Chiou and S. Riegelman, *ibid.*, **60**, 1281 (1971).

(6) W. L. Chiou, *ibid.*, **66**, 989 (1977).

(7) N. N. Salib, S. A. El-Gamal, and A. A. Ismail, *Pharm. Ind.*, **38**, 918 (1976).

(8) R. Kaur, D. J. W. Grant, and T. Eaves, *J. Pharm. Sci.*, **69**, 1321 (1980).

(9) "Toxicological Evaluation of Some Food Additives with a Review of General Principles and of Specifications," 17th report, FAO/WHO Expert Committee on Food Additives, FAO Nutrition Meetings Report Series 53, WHO Technical Report Series 539, Rome, Italy, 1974, p. 36.

(10) P. J. Culver, C. S. Wilcox, C. M. Jones, and R. S. Rose, Jr., *J. Pharmacol. Exp. Ther.*, **103**, 377 (1951).

(11) B. L. Oser and M. Oser, *Int. J. Nutr.*, **60**, 367, 489 (1956).

(12) *Ibid.*, **61**, 149, 235 (1957).

(13) O. G. Fitzhugh, A. R. Bourke, A. A. Nelson, and J. P. Crawley, *Toxicol. Appl. Pharmacol.*, **1**, 315 (1959).

(14) J. F. Treon, *Am. Perfum. Cosmet.*, **77**, 35 (1962).

(15) "Guide to the Physiological Suitability of Atlas Surfactants," ICI Americas, Wilmington, Del., 1977, pp. 8–11.

(16) R. Kaur, D. J. W. Grant, and T. Eaves, *J. Pharm. Pharmacol.*, **31S**, 48P (1978).
(17) "British Pharmacopoeia," Her Majesty's Stationery Office, London, England, 1973, p. A-128.
(18) R. J. Withey and A. J. Bowker, *J. Pharm. Pharmacol.*, **24**, 345 (1972).
(19) M. Kuhnert-Brandstätter, "Thermomicroscopy in the Analysis of Pharmaceuticals," Pergamon, Oxford, England, 1971, p. 128.
(20) D. L. Simmons, R. J. Ranz, N. D. Gyanchandani, and P. Picotte, *Can. J. Pharm. Sci.*, **7**, 121 (1972).
(21) A. Burger, *Sci. Pharm.*, **43**, 161 (1975).
(22) A. Burger and R. Ramberger, *Mikrochim. Acta*, **II**, 273 (1979).
(23) A. Ebian, M. Moustafa, S. Khalil, and M. Motawi, *J. Pharm. Pharmacol.*, **25**, 13 (1973).
(24) S. T. Bowden, "The Phase Rule and Phase Reactions: Theoretical and Practical," Macmillan, London, England, 1938, p. 153.
(25) K. Sekiguchi, N. Obi, and Y. Ueda, *Chem. Pharm. Bull.*, **12**, 134 (1964).
(26) A. H. Goldberg, M. Gibaldi, and J. L. Kanig, *J. Pharm. Sci.*, **55**, 482, 487 (1966).
(27) W. L. Chiou and S. Niazi, *ibid.*, **62**, 498 (1973).
(28) M. P. Summers and R. P. Enever, *ibid.*, **66**, 825 (1977).
(29) S. A. Said, H. M. El-Fatatry, and A. Sh. Geneidi, *Aust. J. Pharm. Sci.*, **NS3**, 42 (1974).

Comparison of Polyethylene Glycol and Polyoxyethylene Stearate as Excipients for Solid Dispersion Systems of Griseofulvin and Tolbutamide II: Dissolution and Solubility Studies

RABINDER KAUR *, D. J. W. GRANT *x, and T. EAVES ‡§

Received March 4, 1980, from the **Department of Pharmacy, University of Nottingham, University Park, Nottingham NG7 2RD, England,* and the ‡*Hoechst Pharmaceuticals Research Laboratories, Walton Manor, Milton Keynes, Buckinghamshire MK7 7AJ, England.* Accepted for publication May 27, 1980. §Present address: Merrell International, Slough, Berkshire SL1 1YY, England.

Abstract □ The effects of joining a long-chain ester group with the polyethylene glycol molecule were studied in solid dispersion systems by comparing the dissolution and solution properties of such systems prepared from polyethylene glycol 2000 with those prepared from the nontoxic, water-soluble, solid excipient polyoxyethylene 40 stearate. Solid dispersion systems of griseofulvin and tolbutamide were prepared by physical mixing, fusion, or coprecipitation from ethanol. The compacted dispersion systems dissolved by progressive erosion, releasing floccules of microcrystals. The released microcrystals of tolbutamide (3–10 μm) were smaller than the original drug particles (~20 μm), but those of griseofulvin were of similar size to the original particles. In general, the rate and extent of release of each drug were greater from polyoxyethylene 40 stearate than from polyethylene glycol 2000 dispersions. The aqueous solubility and dissolution rate of nondisintegrating disks of each pure drug increased only slightly in the presence of polyethylene glycol 2000 but increased considerably with increasing concentration of polyoxyethylene 40 stearate due to micellar solubilization. Thus, polyoxyethylene 40 stearate generally is superior to polyethylene glycol 2000 in promoting the dispersion of the drugs in solids, disintegration of the compacted solids, and solubilization of the drugs during dissolution.

Keyphrases □ Excipients—polyethylene glycol and polyoxyethylene stearate, comparison as excipients for solid dispersion systems of griseofulvin and tolbutamide, dissolution and solubility studies □ Polyethylene glycol—comparison with polyoxyethylene stearate as excipient for solid dispersion systems of griseofulvin and tolbutamide, dissolution and solubility studies □ Polyoxyethylene stearate—comparison with polyethylene glycol as excipient for solid dispersion systems of griseofulvin and tolbutamide, dissolution and solubility studies

Solid dispersion systems may provide a means of increasing the dissolution rate and improving the bioavailability of drugs that are poorly soluble in water (1, 2). Polyethylene glycol has proven to be a valuable water-soluble matrix material for dispersion systems. In particular, the dissolution rate and bioavailability of griseofulvin from polyethylene glycol dispersions are greater than those of the micronized or microcrystalline drug (2). Chiou (3) recently showed that griseofulvin has negligible or very limited solid solubility in polyethylene glycol dispersion systems, a fact supported by phase equilibrium diagrams (4). Chiou (3) suggested that the marked enhancement of the dissolution and absorption rates of griseofulvin dispersed in polyethylene glycol primarily is a result of the reduced size of the griseofulvin crystals. However, other factors, such as increased wettability, solubilization of the drug by the carrier at the diffusion layer, and the reduction or absence of aggregation and agglomeration, also may contribute.

The formation of solid dispersions of tolbutamide in polyethylene glycol polymers also increased the dissolution rate of this drug, an effect that has been attributed to the formation of a solid solution, the dispersion of the drug in a fine state of subdivision, or improved wetting of the drug particles (5). However, in previous studies in these laboratories (4), solid solution formation was not found.

BACKGROUND

Esterification of polyethylene glycol (I) with a long-chain *n*-acyl residue such as stearate to form polyoxyethylene stearate, for example, produces a nontoxic (6), surface-active macromolecule, which may be a better excipient in dispersion systems than the non-surface-active material, I. This hypothesis is being tested by comparing the properties of dispersion systems of the poorly water-soluble drugs griseofulvin and tolbutamide in polyoxyethylene 40 stearate (II) with those in I. A previous report (4) showed no evidence of solid solution formation, even with II (<1% drug). Tolbutamide was more soluble in II than in I at the same temperature, but griseofulvin showed similar solubility in each liquid excipient. Griseofulvin with either II or I and tolbutamide with I gave monotectic systems, which may be considered as eutectic systems where the eutectic composition is pure griseofulvin or pure tolbutamide. Tolbutamide with

0022-3549/80/1100-1321$01.00/0
© 1980, American Pharmaceutical Association

(16) R. Kaur, D. J. W. Grant, and T. Eaves, *J. Pharm. Pharmacol.*, **31S**, 48P (1978).
(17) "British Pharmacopoeia," Her Majesty's Stationery Office, London, England, 1973, p. A-128.
(18) R. J. Withey and A. J. Bowker, *J. Pharm. Pharmacol.*, **24**, 345 (1972).
(19) M. Kuhnert-Brandstätter, "Thermomicroscopy in the Analysis of Pharmaceuticals," Pergamon, Oxford, England, 1971, p. 128.
(20) D. L. Simmons, R. J. Ranz, N. D. Gyanchandani, and P. Picotte, *Can. J. Pharm. Sci.*, **7**, 121 (1972).
(21) A. Burger, *Sci. Pharm.*, **43**, 161 (1975).
(22) A. Burger and R. Ramberger, *Mikrochim. Acta*, **II**, 273 (1979).
(23) A. Ebian, M. Moustafa, S. Khalil, and M. Motawi, *J. Pharm. Pharmacol.*, **25**, 13 (1973).
(24) S. T. Bowden, "The Phase Rule and Phase Reactions: Theoretical and Practical," Macmillan, London, England, 1938, p. 153.
(25) K. Sekiguchi, N. Obi, and Y. Ueda, *Chem. Pharm. Bull.*, **12**, 134 (1964).
(26) A. H. Goldberg, M. Gibaldi, and J. L. Kanig, *J. Pharm. Sci.*, **55**, 482, 487 (1966).
(27) W. L. Chiou and S. Niazi, *ibid.*, **62**, 498 (1973).
(28) M. P. Summers and R. P. Enever, *ibid.*, **66**, 825 (1977).
(29) S. A. Said, H. M. El-Fatatry, and A. Sh. Geneidi, *Aust. J. Pharm. Sci.*, **NS3**, 42 (1974).

Comparison of Polyethylene Glycol and Polyoxyethylene Stearate as Excipients for Solid Dispersion Systems of Griseofulvin and Tolbutamide II: Dissolution and Solubility Studies

RABINDER KAUR *, D. J. W. GRANT *x, and T. EAVES ‡§

Received March 4, 1980, from the **Department of Pharmacy, University of Nottingham, University Park, Nottingham NG7 2RD, England,* and the ‡*Hoechst Pharmaceuticals Research Laboratories, Walton Manor, Milton Keynes, Buckinghamshire MK7 7AJ, England.* Accepted for publication May 27, 1980. §Present address: Merrell International, Slough, Berkshire SL1 1YY, England.

Abstract □ The effects of joining a long-chain ester group with the polyethylene glycol molecule were studied in solid dispersion systems by comparing the dissolution and solution properties of such systems prepared from polyethylene glycol 2000 with those prepared from the nontoxic, water-soluble, solid excipient polyoxyethylene 40 stearate. Solid dispersion systems of griseofulvin and tolbutamide were prepared by physical mixing, fusion, or coprecipitation from ethanol. The compacted dispersion systems dissolved by progressive erosion, releasing floccules of microcrystals. The released microcrystals of tolbutamide (3–10 μm) were smaller than the original drug particles (~20 μm), but those of griseofulvin were of similar size to the original particles. In general, the rate and extent of release of each drug were greater from polyoxyethylene 40 stearate than from polyethylene glycol 2000 dispersions. The aqueous solubility and dissolution rate of nondisintegrating disks of each pure drug increased only slightly in the presence of polyethylene glycol 2000 but increased considerably with increasing concentration of polyoxyethylene 40 stearate due to micellar solubilization. Thus, polyoxyethylene 40 stearate generally is superior to polyethylene glycol 2000 in promoting the dispersion of the drugs in solids, disintegration of the compacted solids, and solubilization of the drugs during dissolution.

Keyphrases □ Excipients—polyethylene glycol and polyoxyethylene stearate, comparison as excipients for solid dispersion systems of griseofulvin and tolbutamide, dissolution and solubility studies □ Polyethylene glycol—comparison with polyoxyethylene stearate as excipient for solid dispersion systems of griseofulvin and tolbutamide, dissolution and solubility studies □ Polyoxyethylene stearate—comparison with polyethylene glycol as excipient for solid dispersion systems of griseofulvin and tolbutamide, dissolution and solubility studies

Solid dispersion systems may provide a means of increasing the dissolution rate and improving the bioavailability of drugs that are poorly soluble in water (1, 2). Polyethylene glycol has proven to be a valuable water-soluble matrix material for dispersion systems. In particular, the dissolution rate and bioavailability of griseofulvin from polyethylene glycol dispersions are greater than those of the micronized or microcrystalline drug (2). Chiou (3) recently showed that griseofulvin has negligible or very limited solid solubility in polyethylene glycol dispersion systems, a fact supported by phase equilibrium diagrams (4). Chiou (3) suggested that the marked enhancement of the dissolution and absorption rates of griseofulvin dispersed in polyethylene glycol primarily is a result of the reduced size of the griseofulvin crystals. However, other factors, such as increased wettability, solubilization of the drug by the carrier at the diffusion layer, and the reduction or absence of aggregation and agglomeration, also may contribute.

The formation of solid dispersions of tolbutamide in polyethylene glycol polymers also increased the dissolution rate of this drug, an effect that has been attributed to the formation of a solid solution, the dispersion of the drug in a fine state of subdivision, or improved wetting of the drug particles (5). However, in previous studies in these laboratories (4), solid solution formation was not found.

BACKGROUND

Esterification of polyethylene glycol (I) with a long-chain *n*-acyl residue such as stearate to form polyoxyethylene stearate, for example, produces a nontoxic (6), surface-active macromolecule, which may be a better excipient in dispersion systems than the non-surface-active material, I. This hypothesis is being tested by comparing the properties of dispersion systems of the poorly water-soluble drugs griseofulvin and tolbutamide in polyoxyethylene 40 stearate (II) with those in I. A previous report (4) showed no evidence of solid solution formation, even with II (<1% drug). Tolbutamide was more soluble in II than in I at the same temperature, but griseofulvin showed similar solubility in each liquid excipient. Griseofulvin with either II or I and tolbutamide with I gave monotectic systems, which may be considered as eutectic systems where the eutectic composition is pure griseofulvin or pure tolbutamide. Tolbutamide with

0022-3549/80/1100-1321$01.00/0
© 1980, American Pharmaceutical Association

II gave a eutectic system for which II completely dissolved up to 20% of the tolbutamide.

Compound II is a surface-active agent with a critical micelle concentration in water of 0.014% (w/v); I is not surface active. Surface activity has long been recognized as a potent factor in enhancing dissolution and absorption rates. For example, the addition of a surfactant, *e.g.*, cetomacrogol or lysolecithin, to the dissolution medium increases the dissolution rate of sparingly soluble drugs, such as griseofulvin (7, 8), by micellar solubilization and improved wettability. Furthermore, the addition of aqueous surfactants during recrystallization increases the *in vitro* dissolution of drugs that are poorly soluble in water (9). Since the amount of surfactant released is insufficient to increase significantly the solubility of the drug in the bulk solution, the presence of the surfactant within and outside the crystals might increase the solubility of the drug in the diffusion layer during dissolution.

The objective of the present study was to probe the advantages, if any, of II over I as an excipient for solid dispersion systems of drugs that are poorly soluble in water. The drugs studied were griseofulvin and tolbutamide. *In vitro* release rates of the drug and the contributing processes are compared, and attempts are made to ascertain which factors are involved. A preliminary account of this work was published previously (10).

EXPERIMENTAL

Materials—The following materials and drugs were of food or pharmaceutical grade and were used as supplied: polyoxyethylene 40 stearate[1] (II), polyethylene glycol 2000[2] (I), griseofulvin[2], and tolbutamide[2]. Ethanol (95%) was spectroscopic grade. The pH 7 buffer was phosphate buffer BP (11). The pH 1 buffer was 0.1 *M* HCl. All water was double distilled from an all-glass still.

Preparation of Dispersion Systems—Physical mixtures, fused mixtures, and coprecipitated mixtures of griseofulvin or tolbutamide with I or II were prepared as described previously (4).

Preparation of Solid Compacts—Nondisintegrating disks contained 250 g of powdered griseofulvin or tolbutamide. For griseofulvin, it was necessary to grind up the first disks prepared and to recompress the powder, because the initial compression produced flaky or fragile disks. Disintegrating disks contained 1 g of the dispersion system consisting of the drug and the excipient. The disks (13 mm in diameter) were prepared by compression of powdered materials under vacuum for 5 min in a die[3] assembly for preparing potassium bromide disks for IR spectrophotometry. The load was 10 tons for nondisintegrating disks and 1 ton for disintegrating disks, corresponding to compaction pressures of 739 and 73.9 MN/m^2, respectively. To prevent the dispersion systems from sticking to the platen and anvil in the die, small pieces of greaseproof paper, used for interleaving membrane filters, were placed between each metal surface and the dispersion system.

Dissolution Rate Determination—A modified beaker–stirrer method was employed (12). The Pyrex glass beaker had an internal diameter of 13.8 cm, a height of 20.2 cm, and a capacity of 3 liters. The compact was secured to the center of the base of the beaker with a thin film of silicon paste, and 2 liters of dissolution medium was added. The stirrer motor[4], rotating at 300 rpm, drove a stirrer blade (0.5 × 2.4 cm), which was centrally placed 5 cm above the base of the beaker. Samples (4 ml) were withdrawn by a syringe fitted with a membrane filter[5] (pore diameter 0.45 μm) and were analyzed by UV spectrophotometry[6] at 296 nm for griseofulvin and 228 nm for tolbutamide. The volumes withdrawn were not replaced. For this system, the absorbance values of I and II at the concentrations released were negligible at the λ_{max} values for griseofulvin and tolbutamide. The dissolution profiles were repeated and good agreement was found. Each point reported is the mean of at least two determinations.

Solubility Measurements—The solubility of each drug in aqueous solution at 37° was determined by shaking an excess of powdered drug with the solvent, sampling the solution by means of a calibrated plastic syringe fitted with a membrane filter[5] (pore diameter 0.45 μm), diluting the sample quantitatively, and determining the absorbance by UV spectrophotometry[6] at the λ_{max} values. Two equilibration procedures were compared. In the first procedure, equilibration was achieved by shaking the solutions in a water bath at 37° for 3 and 5 days. Identical results after each period indicated that equilibrium had been attained. In the second procedure, the solid drug was shaken with the solvent in a water bath at 45° for 4 hr and then at 37° for 24 hr. Both methods of equilibration gave identical results. Based on this finding, the second method was adopted, because it was quicker and less liable to permit decomposition of the dissolved drug or the dissolved excipient.

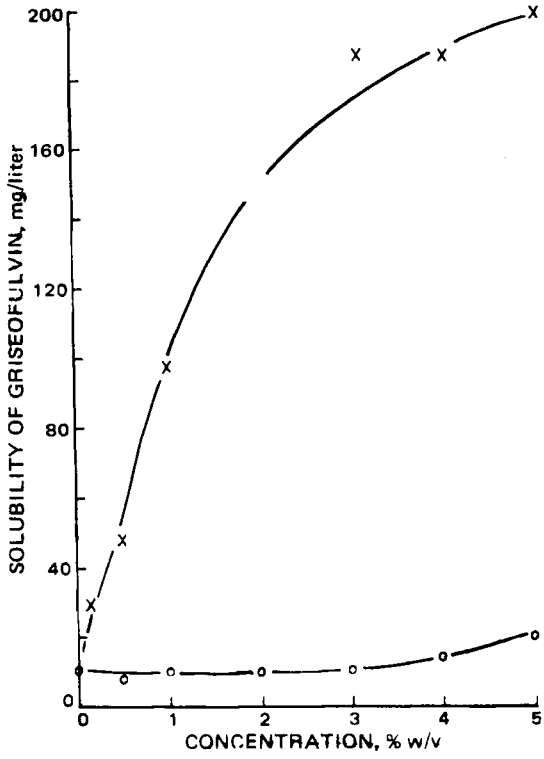

Figure 1—*Solubility of griseofulvin in aqueous solutions of II (×) or I (○) at 37°.*

Surface Tension Measurements—The Du Noüy tensiometer[7] (13) was used, and triplicate readings were taken.

Viscosity Measurements—Viscosity measurements were taken on aqueous solutions of I and II using a cone and plate rheometer[8].

Particle-Size Analysis—The particle-size analysis was carried out using an electronic particle counter[9] with 0.9% (w/v) aqueous NaCl[10], previously saturated with the drug, as the electrolyte.

Optical Microscopy—The drug particles released from dispersion systems were suspended in water saturated with the drug in question. A drop of the suspension on a microscope slide was examined and photographed using a light microscope with a camera attachment.

RESULTS

Effects of Excipients on Aqueous Solubility of Drugs and on Surface Tension and Viscosity of Water—Compounds I and II were reported by the manufacturers to be miscible with water in all proportions. This claim was confirmed for the samples purchased.

Figures 1 and 2 show that the presence of dissolved I or II increased the solubility of griseofulvin or tolbutamide in water. However, a given concentration of II brought about a much greater increase in the solubility of each drug than did the same concentration of I. For example, griseofulvin and tolbutamide were more soluble in 0.5% (w/v) II than in the same concentration of I by factors of about four and two, respectively; at the 5% (w/v) level, the factors were even greater (about 12 and five).

The presence of I or II lowered the surface tension of water (Fig. 3), and the effect was much greater for II. The sharp discontinuity in the curve for II occurs at the critical micelle concentration (CMC) (0.014% w/v). The absence of a discontinuity for I agrees with the fact that it is not a surface-active material and is unlikely to form micelles.

[1] Myrj 52, Atlas Chemicals Ltd., Carshalton, Surrey, England.
[2] Hoechst UK Ltd., Milton Keynes, Bucks, England.
[3] Specac, England.
[4] Fisons Ltd., Loughborough, England.
[5] Millipore (UK) Ltd., London, England.
[6] Cecil, Cambridge, England, or Beckman model 25, Glenrothes, Scotland
[7] Cambridge Instrument Co., Cambridge, England.
[8] Deer rheometer, Integrated Petronics Systems Ltd., London, England.
[9] Model TA/1, Coulter Electronics, Harpenden, England.
[10] Travenol, Thetford, Cambridgeshire, England.

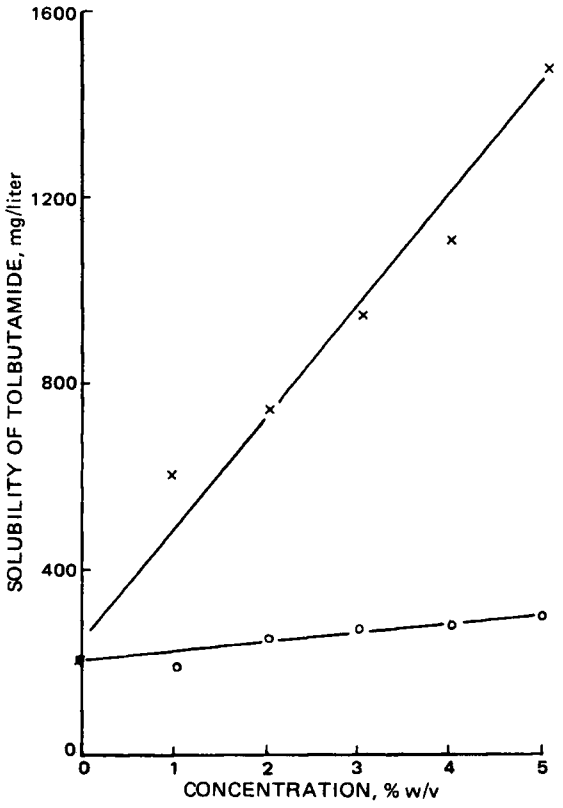

Figure 2—*Solubility of tolbutamide in aqueous solutions of II (×) or I (○) at 37°.*

From the negative gradients of the lines in Fig. 3, the surface excesses of the excipients were calculated by means of the Gibbs absorption isotherm and were found to be 0.178 and 1.09 moles/m^2 for I and II, respectively. From these values, the apparent area per molecule of excipient at the air–water interface was calculated to be 9.32 nm^2 for I and 1.53 nm^2 for II.

The viscosity of water (69 cps at 37°) was increased by the presence of II or I. At 37°, the viscosities were: 1% II, 70 cps; 10% (w/v) II, 103 cps; 1% I, 78 cps; and 10% (w/v) I, 98 cps. The viscosity was an approximately linear function of concentration within the 1–10% (w/v) range.

Dissolution Profiles of Nondisintegrating Disks of Pure Griseofulvin and Tolbutamide—The rate and extent of dissolution of nondisintegrating disks of griseofulvin (Fig. 4) and tolbutamide (Fig. 5) in water were reduced by increasing concentrations of I in the dissolution medium but were increased by increasing concentrations of II.

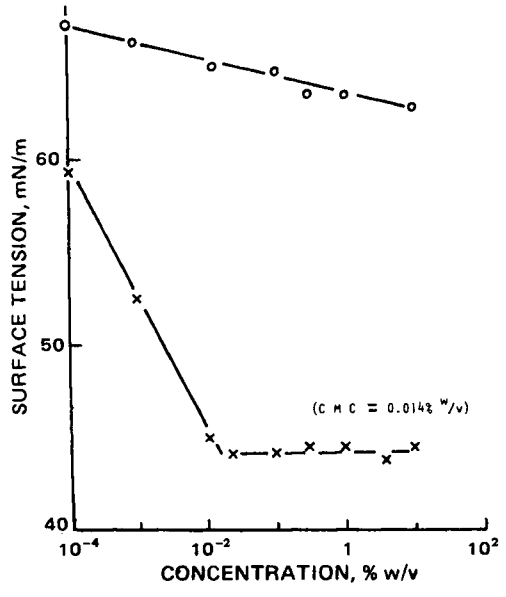

Figure 3—*Effect of concentration (log scale) of I (○) and II (×) on the surface tension of water at 37°.*

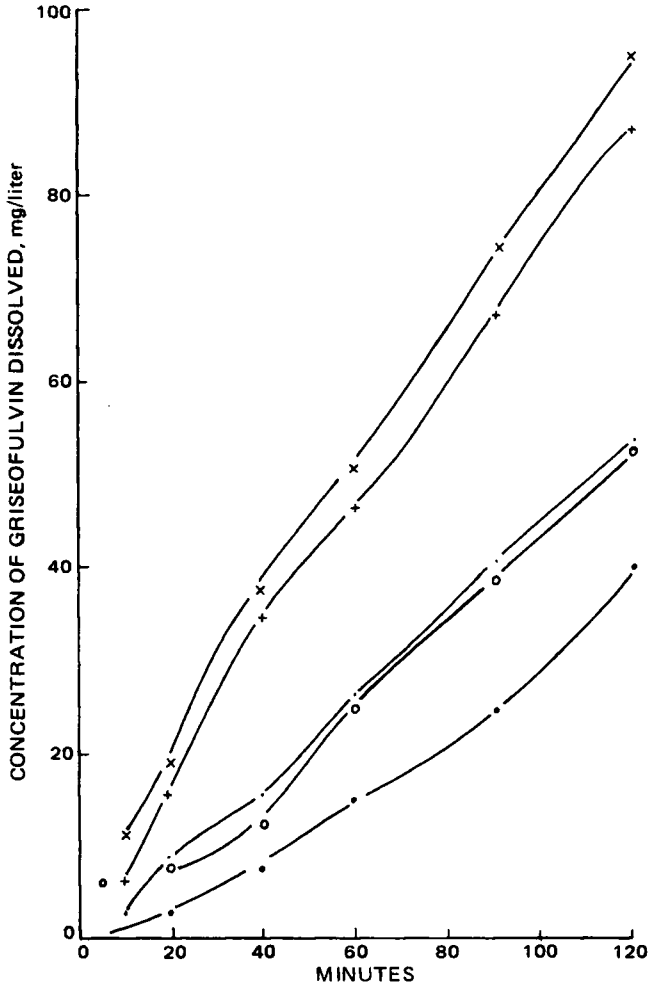

Figure 4—*Dissolution profile of nondisintegrating disks of griseofulvin in water (·), aqueous I at 0.1% (w/v) (○) and 1.0% (w/v) (●), and aqueous II at 0.1% (w/v) (+) and 1.0% (w/v) (×).*

Dissolution Profiles of Fused Dispersion Systems—Since just molten II dissolved up to 20% (w/w) tolbutamide (4), fused mixtures containing 10% (w/w) tolbutamide were selected for the preparation of compacts for dissolution in water and in pH 1 and 7 buffers. The negligible solubility of griseofulvin in just molten II (4) suggested that less of this drug would be more comparable with the tolbutamide preparations, so the fused griseofulvin mixtures chosen contained 2% (w/w) griseofulvin.

The compacted preparations disintegrated gradually by progressive erosion of the exposed surface, and the compacts of both drugs had disintegrated completely within 30 min. The concentration of drug released plateaued (Table I) after 60–120 min at values close to those corresponding to 100% release (10 mg/liter for griseofulvin and 50 mg/liter for tolbutamide). Microscopic examination of the solutions showed the absence of drug particles. The amount of drug in the 1-g compacts (100 mg of tolbutamide or 20 mg of griseofulvin) was insufficient to saturate the dissolution medium (2 liters).

Table I shows that the initial dissolution rate of griseofulvin (2% w/w) from fused dispersions in II was similar to that from fused dispersions in I, but the initial dissolution rate of tolbutamide (10% w/w) was ~45% greater from fused dispersions in II than from those in I. Thus, the dissolution of tolbutamide from fused dispersions was favored by II.

When 1 g of a fused mixture of griseofulvin or tolbutamide with I or II was added to 100 ml of water, a cloudy or frothy suspension was rapidly produced. On standing for a few hours, it gave a clear supernate and a fine powder at the bottom of the flask. By microscopic examination, it could be seen that, as a eutectic mixture was exposed to water, the excipient dissolved in water and a microcrystalline dispersion of the drug in water was obtained. After standing, some microcrystals grew to large macrocrystals at the expense of the smaller crystals. However, if 1 g was exposed

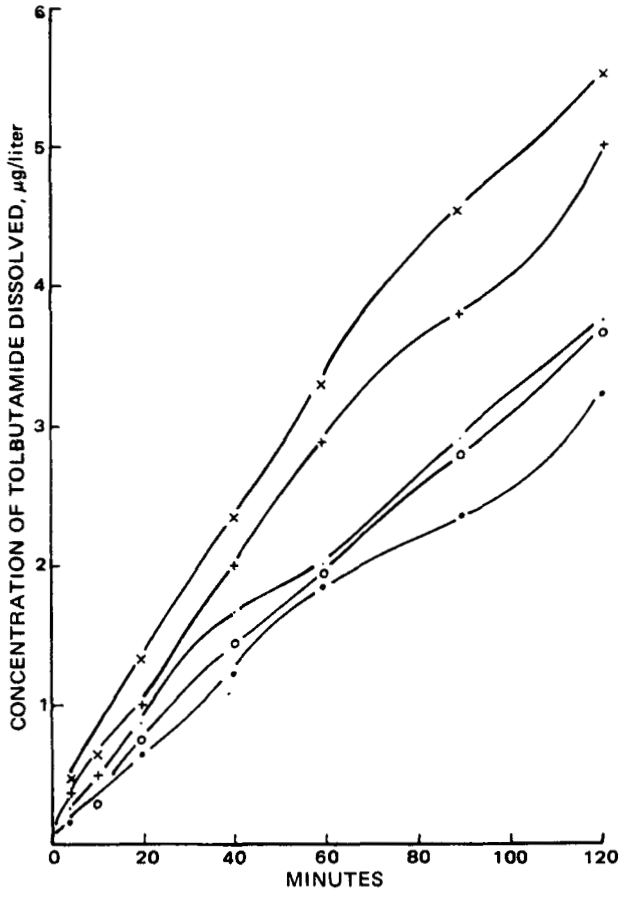

Figure 5—*Dissolution profile of nondisintegrating disks of tolbutamide in water (·), aqueous I at 0.1% (w/v) (○) and 0.5% (w/v) (●), and aqueous II at 0.1% (w/v) (+) and 0.5% (w/v) (×).*

to 1 liter or more of water, then no microcrystals or crystals were observed, because there was sufficient solvent to dissolve all of the drug from the eutectic mixture.

Dissolution Profiles of Coprecipitated Dispersion Systems—The composition of coprecipitated mixtures chosen for the dissolution rate analysis was 60% (w/w) griseofulvin or tolbutamide. Thus, 1 g contained 600 mg of either drug. This composition was a compromise between the need for an appreciable dilution of the solid drug and the need for an acceptable tablet or capsule weight in an eventual pharmaceutical preparation.

Microscopic examination of the coprecipitated mixtures showed agglomerates of micro- and macrocrystals of drug interspersed with the excipient.

In contact with the aqueous dissolution medium, the compacts disintegrated by progressive erosion of the exposed surface. Small floccules of drug crystals were obtained, not a uniform microcrystalline dispersion of the drug. The compacted preparation of each drug disintegrated completely, leaving no drug particles.

For a given dissolution medium, the amount of each drug released at any given time from a II coprecipitate was greater than that from the corresponding I coprecipitate (Figs. 6 and 7). The concentration of griseofulvin released in neutral dissolution medium reached a plateau after 60 min from II coprecipitates (Fig. 6). The plateau effect was not observed with the tolbutamide coprecipitates; this drug continued to be released after 120 min (Fig. 7). The amount of drug incorporated into the 1-g compacts (600 mg of tolbutamide or griseofulvin) was in excess of the amount required to saturate 2 liters of water (the volume of the dissolu-

Table I—Initial Dissolution Rate and Final Mean Concentration Attained between 60 and 120 min after Introducing Fused Dispersions (1 g) Containing Griseofulvin or Tolbutamide in Polyethylene Glycol 2000 (I) or Polyoxyethylene 40 Stearate (II) into Aqueous Solution (2 Liters)

Fused Dispersion System	Initial Dissolution Rate, mg/liter/min			Final Mean Concentration, mg/liter		
	pH 1	Water	pH 7	pH 1	Water	pH 7
2% (w/w) Griseofulvin + I	0.62	—	0.52	10.2	—	10.1
2% (w/w) Griseofulvin + II	0.53	0.57	0.54	8.1	8.8	8.9
10% (w/w) Tolbutamide + I	2.66	—	2.83	60.4	—	49.6
10% (w/w) Tolbutamide + II	3.96	3.99	4.02	55.7	52.0	51.5

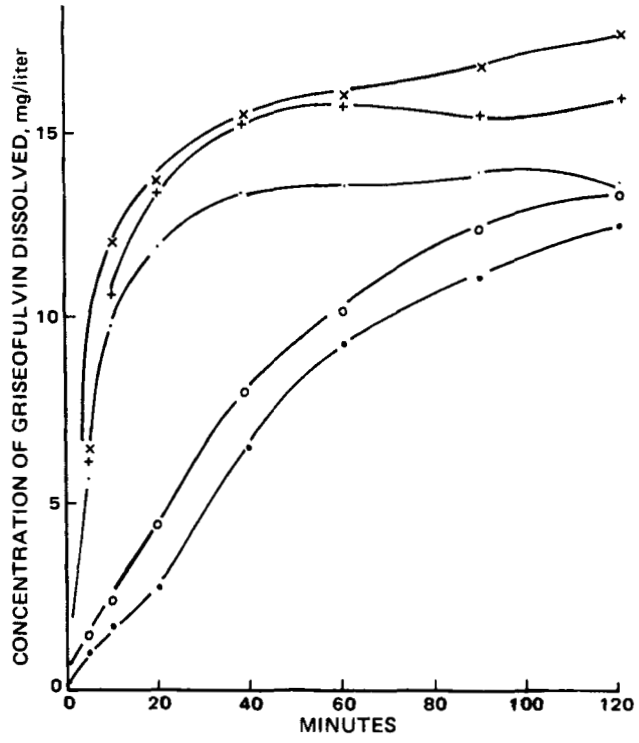

Figure 6—*Dissolution profiles of coprecipitated dispersions of griseofulvin (60% w/w) with I in pH 1 buffer (○) and pH 7 buffer (●) and of griseofulvin (60% w/w) with II in water (·), pH 1 buffer (×), and pH 7 buffer (+).*

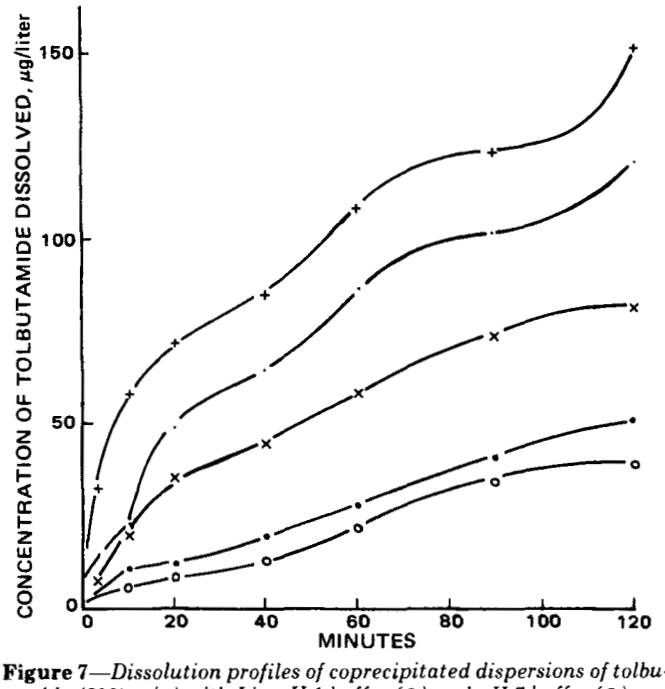

Figure 7—*Dissolution profiles of coprecipitated dispersions of tolbutamide (60% w/w) with I in pH 1 buffer (○) and pH 7 buffer (●) and of tolbutamide (60% w/w) with II in water (·), pH 1 buffer (×), and pH 7 buffer (+).*

Table II—Initial Dissolution Rate and Final Mean Concentration Attained between 60 and 120 min after Introducing Coprecipitated Dispersions (1 g) Containing Griseofulvin in Polyoxyethylene 40 Stearate (II) into Aqueous Solution (2 Liters)

Coprecipitated Dispersion	Initial Dissolution Rate, mg/liter/min		Final Mean Concentration, mg/liter	
	pH 1	pH 7	pH 1	pH 7
12.5% (w/w) Griseofulvin in II	0.507	0.322	18.2	14.9
60% (w/w) Griseofulvin in II	1.22	0.980	16.9	12.9

tion medium). Therefore, the II that was dissolved from the compact was solubilizing each drug.

To test the effect of the griseofulvin concentration, 1-g compacts of a coprecipitate containing 12.5% (w/w) of this drug in II were studied (Table II). The amount of drug (125 mg) corresponds to a dosage level currently administered to patients. The 12.5% (w/w) griseofulvin coprecipitates disintegrated completely within 20 min, and microcrystals of griseofulvin were found at the bottom of the beaker after 180 min of dissolution. The concentration of drug released between 60 and 120 min from coprecipitates containing 12.5% (w/w) griseofulvin was much the same (~15 mg/liter) as from those containing 60% (w/w) of the drug. However, the initial dissolution rate from the 12.5% coprecipitates was about one-third of that from the 60% coprecipitates. Thus, a fivefold reduction in the concentration of the drug in II coprecipitates reduced the initial dissolution rate only threefold.

Changes in Particle-Size Distribution of Drugs before Formulation and during Disintegration—Fused dispersion systems containing 2% (w/w) griseofulvin or 10% (w/w) tolbutamide in II disintegrated rapidly, releasing drug particles whose size distribution was analyzed within 25–30 min of exposure of the dispersion systems to water. Different cooling rates of the fused mixtures during preparation of the dispersion systems prior to compression might be expected to affect the particle-size distribution of the drugs. Comparison of the size distribution of griseofulvin particles released from the dispersion systems with that of the micronized drug originally supplied showed only relatively small differences, which bore no obvious relationship to the cooling rate. Thus, fused-cooled and coprecipitated dispersions released griseofulvin particles that were similar in appearance to those of the original (micronized) griseofulvin. These particles were difficult to discern under the microscope.

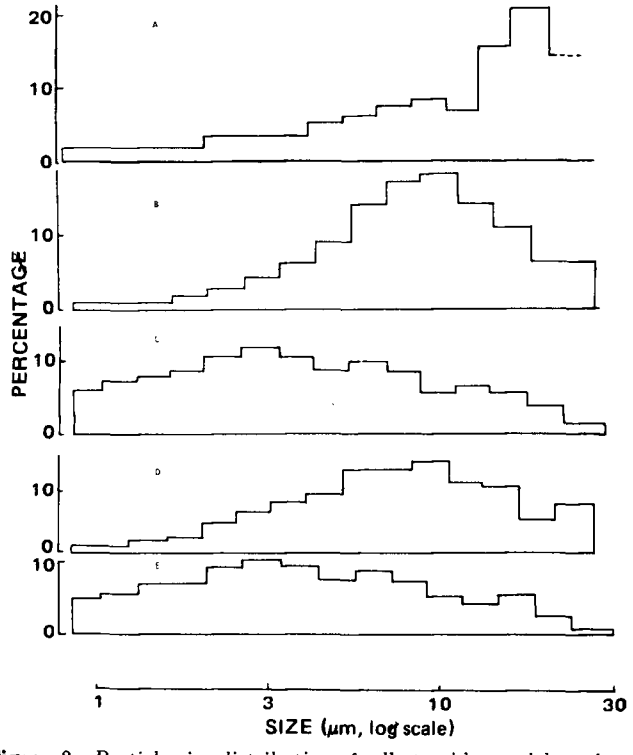

Figure 8—*Particle-size distribution of tolbutamide particles released (into electrolyte saturated with tolbutamide) from the original powder (A) and from fused mixtures of tolbutamide (10%) in II cooled slowly in a paraffin bath (B), cooled by natural cooling to 20° (C), cooled by refrigeration at 4° (D), and cooled rapidly in solid carbon dioxide to −78° (E).*

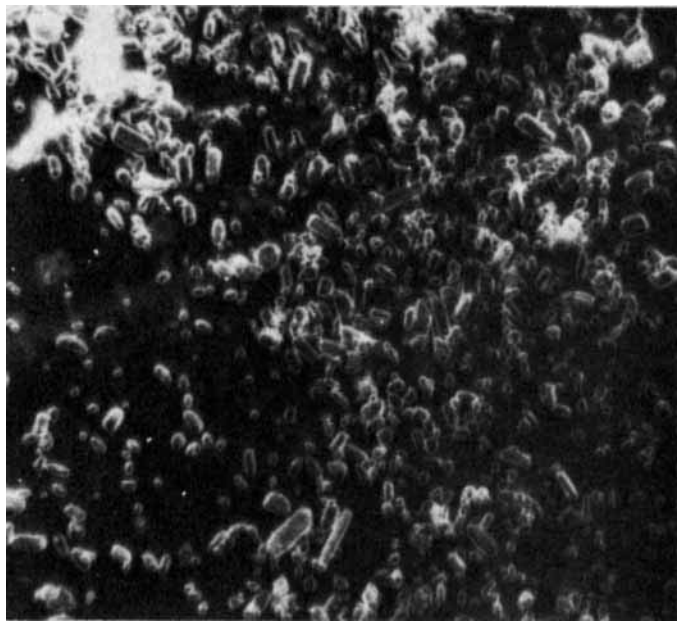

Figure 9—*Micrograph of tolbutamide particles released from a coprecipitated dispersion of tolbutamide (10% w/w) and II into aqueous sodium chloride solution (0.9% w/w) previously saturated with tolbutamide (×100).*

Although dispersion in II did not reduce significantly the particle size of micronized griseofulvin, it did reduce the particle size of commercial tolbutamide. Figures 8 and 9 show that the tolbutamide powder supplied consisted of particles with a mean diameter of ~20 μm or more, and the distribution suggests that some particles with a mean diameter of >30 μm were present, beyond the upper range of the particle counter. Figure 8 shows that the tolbutamide particles released from the fused and cooled dispersion systems in II were considerably smaller, with the mean particle diameters being 3–10 μm. There were relatively small differences between

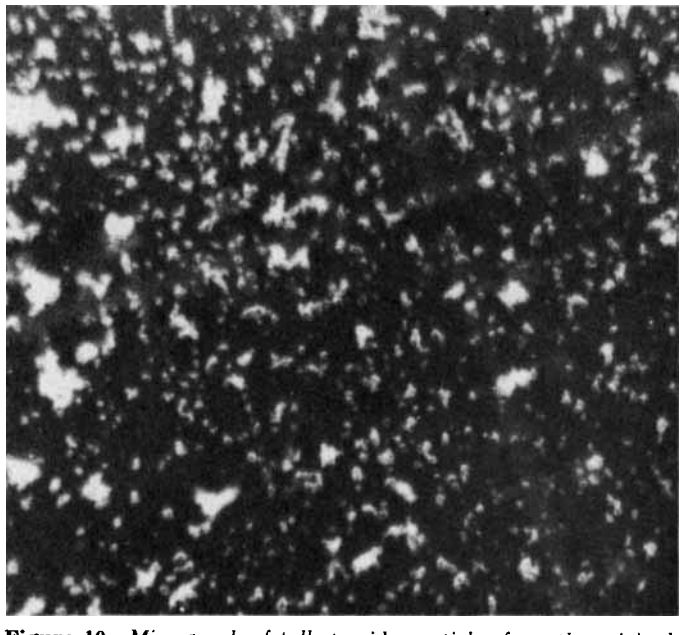

Figure 10—*Micrograph of tolbutamide particles from the original commercial sample of the drug from which the dispersion systems were prepared. The particles were suspended in aqueous sodium chloride solution (0.9% w/w) previously saturated with tolbutamide (×100).*

the size distribution elicited by different cooling rates, but no obvious relationships were apparent. The microscopic appearance of the small tolbutamide particles released from the fused–cooled dispersion systems in II was indistinguishable from that of tolbutamide released from coprecipitated dispersions in II (Fig. 10). The original tolbutamide particles clearly were much larger (Fig. 9).

DISCUSSION

The presence of I in water exerts little solubilizing action on griseofulvin (Fig. 1) or tolbutamide (Fig. 2). This finding agrees with a previous report (3) on the influence of longer polyoxyethylene molecules (polyethylene glycol 6000) on the solubility of griseofulvin. On the other hand, the presence of II in water considerably increases the solubility of both griseofulvin (Fig. 1) and tolbutamide (Fig. 2) by a process of micellar solubilization (Fig. 3) at II concentrations greater than 0.014% (w/v) (the critical micelle concentration). This finding agrees with the reported influence (14) of various nonionic surface-active agents, including some related polyoxyethylene derivatives, on the solubility of griseofulvin.

The presence of II in the aqueous dissolution medium also increases the dissolution rate of solid compressed disks of both drugs (Figs. 4 and 5). The experiments show that micellar solubilization, by increasing the drug solubility at the solid–liquid interface, plays a major role in increasing the dissolution rate of the drugs from solid dispersions of II. However, the presence of 0.1–1.0% (w/v) I in the aqueous dissolution medium actually reduces the dissolution rate of solid compressed disks of griseofulvin or tolbutamide (Figs. 4 and 5). This effect may result from the marked increase in viscosity of the aqueous dissolution medium, which is brought about by the presence of I. Since the diffusivity of small molecules frequently is inversely proportional to the solution viscosity, the effect of I suggests that dissolution of both griseofulvin and tolbutamide is diffusion controlled. The increase in viscosity then would reduce the diffusion rate of the drug in the diffusion layer and thereby reduce the dissolution rate. Evidently, the marked increase in viscosity (a 12% increase is produced by 1% I) more than compensates for the small increase in the solubility of each drug (increase of ~5% produced by 1% I).

Although the viscosity of water is increased by both II and I, the effect is greater for I at low concentrations since the viscosity of water is virtually unaffected by the presence of up to 1% II. Thus, solubilization and viscosity phenomena both favor II over I in promoting dissolution of the drugs, whereas viscosity increases actually disfavor solutions of I compared with pure solvent or buffer solutions (Figs. 4 and 5). This discussion readily explains the greater release rate of griseofulvin and tolbutamide from coprecipitates with II than from coprecipitates with I as the excipient (Figs. 6 and 7). The excipients dissolve rapidly due to their high solubility in water, and this dissolution creates the conditions in solution that influence the dissolution rate.

The difference between I and II as excipients for fused dispersion systems was less marked for griseofulvin than for tolbutamide. This result is apparent in the dissolution behavior of fused drug–excipient mixtures (Table I) and in the phase diagrams of the dispersion systems (4). The mean particle size of griseofulvin was changed little by incorporation into fused II dispersions and subsequent release by dissolution, but that of tolbutamide (Fig. 8) was reduced greatly. These differences may be accounted for by the low solubility of griseofulvin in each molten excipient and by the much greater solubility of tolbutamide in molten II than in molten I (4). On rapid cooling of a solution, the deposited solute, in this case solid tolbutamide, usually has a reduced particle size, because the rate of crystal nucleation is increased relative to the rate of crystal growth (15). When the dispersion systems are prepared by coprecipitation from ethanol, the differences in the dissolution rate between I and II as excipients are as large for griseofulvin as for tolbutamide (Figs. 6 and 7). In these cases, the particles of solid drug are deposited from solution in ethanol, and this process is largely independent of the precise nature of the excipient. Other factors, particularly solubility in and the viscosity of the dissolution medium, then can exert an overwhelming influence.

The release rate of tolbutamide from dispersion systems in polyethylene glycol 4000 or 6000 was found to be greater from coprecipitated dispersions than from fused dispersions (7). The state of subdivision, *i.e.*, the total surface area of the drug, seems the most likely explanation for differences arising from the method of preparation of the dispersion systems.

Polymorphic changes did not occur in the preparation of the dispersion systems (4) and, therefore, cannot be used to explain any of the phenomena reported here.

The surface activity of II may be advantageous in promoting the bioavailability of griseofulvin. For instance, II may be capable of acting like bile salts, which can solubilize and increase the dissolution rate of griseofulvin and other drugs (16–18). In this connection, polyoxyethylene 40 stearate, like the triglycerides, possesses a fatty acid residue, although the ability of triglycerides to increase the bioavailability of griseofulvin is claimed to be due solely to enhanced dissolution and not to enhanced absorption of the dissolved drug (19).

REFERENCES

(1) K. Sekiguchi and N. Obi, *Chem. Pharm. Bull.*, **9**, 866 (1961).

(2) W. L. Chiou and S. Riegelman, *J. Pharm. Sci.*, **60**, 1281 (1971).

(3) W. L. Chiou, *ibid.*, **66**, 989 (1977).

(4) R. Kaur, D. J. W. Grant, and T. Eaves, *ibid.*, **69**, 1317 (1980).

(5) N. N. Salib, S. A. El-Gamal, and A. A. Ismail, *Pharm. Ind.*, **38**, 918 (1976).

(6) "Toxicological Evaluation of Some Food Additives with a Review of General Principles and of Specifications," 17th report, FAO/WHO Expert Committee on Food Additives, FAO Nutrition Meetings Report Series 53, WHO Technical Report Series 539, Rome, Italy, 1974, p. 36.

(7) P. H. Elworthy and F. J. Lipscomb, *J. Pharm. Pharmacol.*, **20**, 817 (1968).

(8) T. R. Bates, S. L. Lin, and M. Gibaldi, *J. Pharm. Sci.*, **56**, 1492 (1967).

(9) W. L. Chiou, S.-J. Chen, and N. Athanikar, *ibid.*, **65**, 1702 (1976).

(10) R. Kaur, D. J. W. Grant, and T. Eaves, *J. Pharm. Pharmacol.*, **31S**, 48P (1979).

(11) "British Pharmacopoeia 1973," Her Majesty's Stationery Office, London, England, 1973, p. A-128.

(12) G. Levy and B. A. Hayes, *N. Engl. J. Med.*, **262**, 1053 (1960).

(13) W. D. Harkins and J. F. Jordan, *J. Am. Chem. Soc.*, **52**, 1751 (1930).

(14) A. A. Kassem and N. M. Mursi, *Bull. Fac. Pharm. Cairo Univ.*, **9**, 11 (1970).

(15) J. W. Mullin, "Crystallisation," Butterworth, London, England, 1972.

(16) T. R. Bates, M. Gibaldi, and J. L. Kanig, *J. Pharm. Sci.*, **55**, 191, 901 (1966).

(17) T. R. Bates, M. Gibaldi, and J. L. Kanig, *Nature*, **220**, 1331 (1966).

(18) S. A. Said, H. M. El-Fatatry, and A. Sh. Geneidi, *Aust. J. Pharm. Sci.*, **NS3**, 42 (1974).

(19) J. A. Grisafe and W. L. Hayton, *J. Pharm. Sci.*, **67**, 895 (1978).

Propoxyphene and Norpropoxyphene: Influence of Type of Controlled-Release Formulation on Intra- and Intersubject Variations

HELLE BECHGAARD *x **and S. BAGGESEN** ‡

Received December 17, 1979, from the *Controlled Release Division and the ‡Quality Assurance Department, A/S Alfred Benzon, 29 Halmtorvet, DK-1700 Copenhagen V, Denmark. Accepted for publication May 22, 1980.

Abstract □ Two types of controlled-release formulations of propoxyphene hydrochloride, one with a buffer system in the pellet core, were studied with regard to intra- and intersubject variations of C_{max} and T_{max} of propoxyphene as well as propoxyphene plus norpropoxyphene in 35 volunteers after administration of a single 150-mg dose. Statistically significant differences between the formulations in intrasubject variance were revealed, and the availability rate of the buffered product showed significantly better reproducibility, presumably due to the established low sensitivity of its release rate to the *in vitro* environment, *i.e.*, pH.

Keyphrases □ Propoxyphene—influence of type of controlled-release formulation on drug release, pH dependency □ Dosage forms, controlled release—propoxyphene, influence of type of formulation on drug release, pH dependency □ Release rates—propoxyphene, influence of type of controlled-release formulation, pH dependency

The analgesic α-*d*-propoxyphene currently is available in two types of multiple-unit controlled-release formulations. One formulation is supported with a buffer system in the pellet core (1) to secure a pH-independent drug release. The other formulation does not have such a system. *In vitro* studies have shown a pronounced difference in the sensitivity of these two formulations to the nature of the dissolution medium, particularly its pH (Fig. 1).

The present study concerns the significance *in vivo*, in terms of intra- and intersubject variations, of these formulation-related differences in *in vitro* drug release with respect to selected pharmacokinetic parameters.

EXPERIMENTAL

Subjects—Thirty-five volunteers [15 females and 20 males, 18–60 years old (median 24 years old) and 47.4–83.5 kg (median 65 kg)] served as test subjects. Prior to the study, the subjects were found to be healthy by clinical examination and various laboratory tests, including serum creatinine, serum bilirubin, liver enzymes, and hemoglobin. Twenty-four subjects were nonsmokers, and 11 were smokers. Four females were taking oral contraceptives. Informed consent was obtained from all of the subjects.

Blood Sampling—Venous heparinized blood samples (~20 ml) were drawn before (0 hr) and 2, 3, 4, 6, 8, and 12 hr after drug administration. Immediately after sampling, the plasma was separated by centrifugation and frozen at −20° until it was assayed. No deterioration was found with storage.

Assay of Plasma Samples—The plasma concentrations of propoxyphene and norpropoxyphene were measured by a mass fragmentographic method (2). The lower detection limit of the method was 4 ng/ml for propoxyphene and 3 ng/ml for norpropoxyphene. The coefficient of variation was <6%.

Propoxyphene Products—Seven batches of Formulation A[1] and two batches of Formulation B[2] were used. Formulation A (without a buffer system) consisted of a sugar core coated with the drug and a lacquer. Formulation B consisted of the drug and a buffer system in a homogeneous core coated with a lacquer (1). The release rate patterns of both formulations (containing 150 mg of α-*d*-propoxyphene hydrochloride) were designed to yield a controlled, sustained release (Table I). Both formulations were supplied in identical red, hard gelatin capsules.

Dosage Schedule—Except for the contraceptive pill, no drugs were allowed for 7 days before the study. During the study, alcoholic beverages and smoking were not permitted.

Subjects fasted overnight before each treatment and were not permitted to eat until 2 hr after dosing, at which time a standardized breakfast with 300 ml of fluid was given. During the remaining observation period, the ambulatory subjects had free access to fluid and food intake and in this respect imitated the clinical situation. Single 150-mg doses of controlled-release propoxyphene hydrochloride were administered at 9 am with 300 ml of tap water.

Experimental Designs—The study involving Formulation A was performed as an unbalanced, incomplete block design with at least 7 days between dosage days. Each subject received one to three different batches. The study involving Formulation B was performed as a nonrandomized crossover trial with at least 7 days between the two dosage days.

Calculations and Statistical Analyses—The peak plasma concentration (C_{max}) and the time to the peak concentration (T_{max}) of propoxyphene and propoxyphene plus its major metabolite, norpropoxyphene, were used as dependent variables in the statistical analyses.

The intra- and intersubject variations, expressed as the variances in the variance components model (Eq. 1), were estimated using the standard computer program GLIM (3). To estimate intersubject variance corrected for interbatch variation and the standard errors of these parameters, the method described by Searle (4) was applied to the data obtained for Formulation A. The estimation was straightforward in the balanced design for the study involving Formulation B.

A comparison between formulations was made by standard variance ratio F tests for intrasubject variance and by an approximate variance ratio test (5) for intersubject variance. For each formulation, the variation of each dependent pharmacokinetic characteristic (y_{ij}) is expressed by:

$$y_{ij} = \mu + \pi_i + \beta_j + \epsilon_{ij} \qquad \text{(Eq. 1)}$$

for subject i receiving a dose from batch j, where π_i, β_j, and ϵ_{ij} are the values of the independent, normally distributed, random variables with

Table I—Dissolution Test (pH 1.2 USP Buffer excluding Enzymes) of Controlled-Release Propoxyphene of Different Batches of Formulations A [a] and B [b] (n = 4)

Batch	Mean (±*SD*) Amount of Propoxyphene Released, mg: Within 1 hr	Within 2 hr	Within 6 hr
83602[a]	47 (3.0)	79 (2.7)	140 (6.3)
83606[a]	56 (4.2)	89 (4.9)	142 (4.2)
83612[a]	49 (1.5)	89 (5.0)	153 (7.5)
84150[a]	49 (3.6)	86 (1.6)	155 (6.3)
84154[a]	52 (3.5)	87 (5.7)	132 (9.9)
84403[a]	60 (5.2)	91 (5.2)	136 (3.6)
83610[a]	50 (5.0)	77 (3.9)	134 (3.5)
Average	51.9	85.4	141.7
(Pooled estimate)	(3.5)	(4.4)	(6.3)
87055[b]	57 (3.2)	91 (1.7)	132 (1.2)
87056[b]	60 (2.0)	91 (1.7)	132 (1.2)
Average	58.5	91.0	132.0
(Pooled estimate)	(2.7)	(1.7)	(1.2)

[a] Diffucap. [b] Repro-Dose.

[1] Diffucap controlled-release propoxyphene (Batches 83602, 83606, 83612, 84150, 84154, 84403, and 83610), Eurand, Milan, Italy.

[2] Repro-Dose controlled-release propoxyphene (Batches 87055 and 87056), A/S Alfred Benzon, Copenhagen, Denmark.

0022-3549/80/1100-1327$01.00/0
© 1980, American Pharmaceutical Association

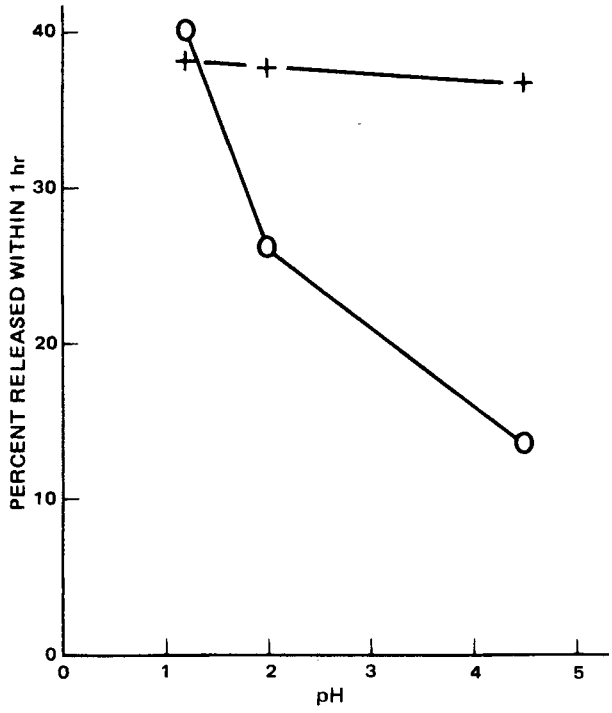

Figure 1—*The pH dependency of drug release from Formulation A (Batch 84403) (○) and from Formulation B (Batch 87055) (+).*

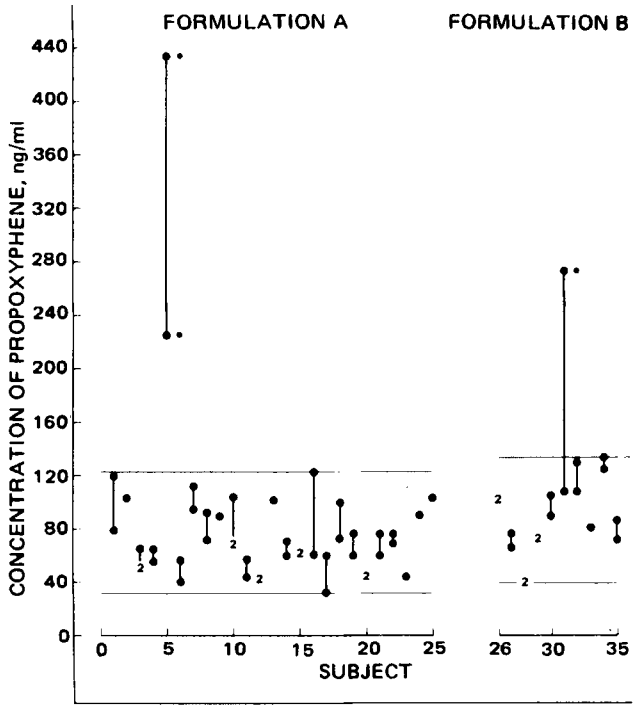

Figure 2—*Individual peak concentrations of propoxyphene after administration of 150 mg of propoxyphene hydrochloride from a batch of Formulation A or B. The symbol 2 indicates equal C_{max} values obtained with different batches; * represents an outlier.*

zero means and variances and are the intersubject, interbatch, and intrasubject variance components, respectively.

The intrasubject variance results from differences in the response from the same subject at different times, but it also is due to subject–batch interactions, to intrabatch variation, and to errors of measurement. The different kinds of variation cannot be separated further on the basis of the existing data.

The fit of the model was assessed with a normal probability plot of residuals in the case where C_{max} was the dependent variable.

Since T_{max} is a discrete variable and thus is in disagreement with the normality assumption of the model, it is irrelevant to test the fit of the model in this case. For the same reason, the variance ratio F test used for comparison of the intersubject variance must be considered as an approximate test with T_{max}.

Dissolution Procedure—The cumulative release of propoxyphene was determined at 1, 2, and 6 hr by means of the NF XIV rotating-bottle procedure (6), which was modified to maintain a constant pH during the dissolution test and to include only one measurement per dosage unit. The rotation speed was 30 ± 1 rpm, and the dissolution medium was 25 ml of sulfate buffer at pH 1.2 or 2.0 or citrate buffer at pH 4.5, thermostated at 37 ± 0.1°. The amount of propoxyphene released was determined by measuring the absorbance at 257 nm (Table I).

RESULTS

Batch Testing *In Vitro*—The release rate pattern of each batch was analyzed (Table I) and found to be in compliance with the specifications for the products, *i.e.*, at least 90% of the capsules released an amount of propoxyphene within 60 ± 15 mg at 1 hr, 93 ± 20 mg at 2 hr, and 132 ± 20 mg at 6 hr. The release data were normally distributed. Both products released 100% of the propoxyphene within 10 hr.

The observed intrabatch standard deviation for Formulation B was statistically significantly lower at 2 ($p < 0.05$) and 6 ($p < 0.001$) hr than the standard deviation for Formulation A (Table I).

pH Dependency *In Vitro*—The amount of propoxyphene released after 1 hr was tested at pH 1.2, 2.0, and 4.5 (Fig. 1). The sensitivity to the pH of the dissolution medium was pronounced for Formulation A, ranging from 40 to 10% of drug released at pH 1.2 and 4.5, respectively. In contrast, virtually no pH-dependent change in released propoxyphene was observed with Formulation B.

Outliers—Three subjects (A5, A17, and B31) were outliers with respect to specific values of C_{max} and T_{max} since the normality assumption of the variance components model (Eq. 1) for these values was not met (Table II). In the statistical tests involving these parameters, as well as for consideration of the ranges (Figs. 1–4), outliers were excluded. No clinical reasons or connection to the smoking or taking of contraceptive pills by the subjects could be applied to the outliers.

Plasma Propoxyphene—The peak concentration of propoxyphene displayed a considerable within-subject variation, with the widest range being 61–123 ng/ml after administration of Formulation A compared to a variation of 107–130 ng/ml after administration of Formulation B (Fig. 2). Total variation, including intra- and intersubject variations, ranged from 32 to 123 ng/ml after administration of Formulation A and from 40 to 134 ng/ml after administration of Formulation B (Fig. 2).

Table II—Comparison of Formulations A [a] and B [b] with Respect to Residual Variance (Intrasubject Variance)

		Formulation A		Formulation B			
	Parameter	Residual Variance, ng^2/ml^2	*DF*	Residual Variance, ng^2/ml^2	*DF* [c]	Variance Ratio, A/B	Outliers: Formulation, Subject, Value
Propoxyphene	C_{max}	226.0	14	76.9	7	2.9 NS [d]	A, 5, 433 A, 5, 224 B, 31, 274
	T_{max}	2.9	14	0.4	8	6.8 ($p < 0.01$)	A, 17, 12 [e]
Propoxyphene plus norpropoxyphene	C_{max}	1242.1	14	185.7	7	6.7 ($p < 0.01$)	A, 5, 588
	T_{max}	4.5	14	0.4	8	11.9 ($p < 0.001$)	B, 31, 432

[a] Diffucap. [b] Repro-Dose. [c] Subject 33 was excluded due to a missing blood sample 4 hr after ingestion of Batch 87056. [d] Not significant. [e] Or later.

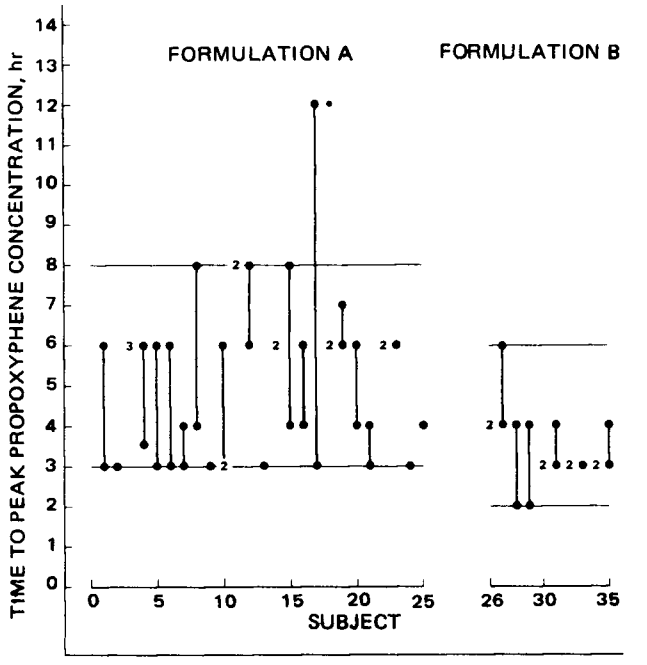

Figure 3—*Individual time to peak concentrations of propoxyphene after administration of 150 mg of propoxyphene hydrochloride from a batch of Formulation A or B. The symbol 2 indicates equal T_{max} values obtained with different batches; * represents an outlier.*

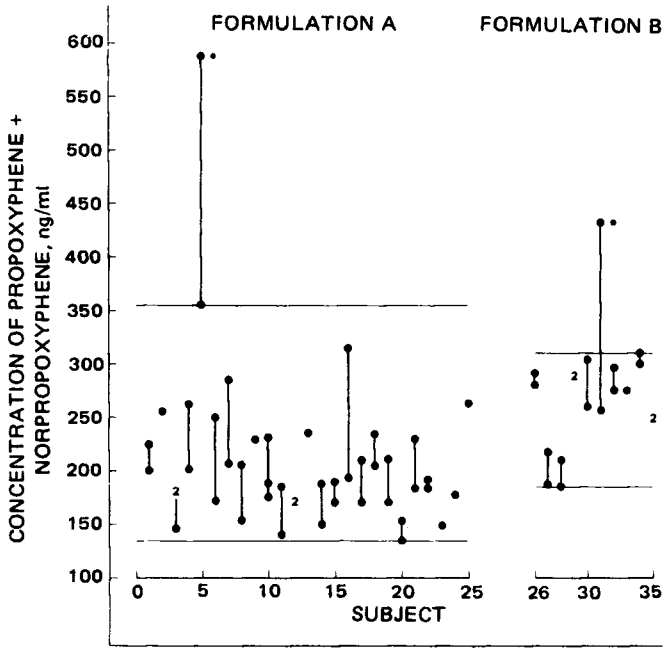

Figure 4—*Individual peak concentrations of propoxyphene plus norpropoxyphene after administration of 150 mg of propoxyphene hydrochloride from a batch of Formulation A or B. The symbol 2 indicates equal C_{max} values obtained with different batches; * represents an outlier.*

The maximum range of T_{max} within a subject was 4 hr or more after ingestion of Formulation A and only 2 hr after ingestion of Formulation B (Fig. 3).

In total, the time to the peak concentration ranged from 3 to 8 hr and from 2 to 6 hr after ingestion of Formulations A and B, respectively (Fig. 3).

Comparison of the two types of controlled-release products with respect to intrasubject variation showed a statistically significantly ($p < 0.01$) lower variance of T_{max}, with a variance 6.8 times greater after administration of Formulation A than after Formulation B (Table II). With respect to C_{max}, the difference in the intrasubject variation between the two formulations was less pronounced; the variance ratio between Formulations A and B was 2.9 but was not statistically significant (Table II). The difference between the two formulations with respect to intersubject variations in C_{max} and T_{max} also was not statistically significant.

Propoxyphene plus Norpropoxyphene—As with propoxyphene, the amount of propoxyphene and its major metabolite, norpropoxyphene, displayed a pronounced intrasubject variation in C_{max}, reaching a maximum of 193–313 ng/ml and of 259–305 ng/ml after administration of Formulations A and B, respectively (Fig. 4). Overall, the peak concentrations ranged from 134 to 355 ng/ml after ingestion of Formulation A and from 184 to 311 ng/ml after administration of Formulation B (Fig. 4).

The maximum range of T_{max} within a subject was >8 hr after administration of Formulation A and only 2 hr after administration of Formulation B (Fig. 5). The total ranges of T_{max} were from 3 to 12 hr or more and from 3 to 6 hr after ingestion of Formulations A and B, respectively (Fig. 5).

Compared to Formulation B, the intrasubject variances of C_{max} and T_{max} were statistically significantly ($p < 0.01$) larger after administration of Formulation A by factors of 6.7 and 11.9, respectively (Table II).

As in the case of propoxyphene alone, no statistically significant difference in the intersubject variance components for C_{max} and T_{max} of propoxyphene plus norpropoxyphene was found.

DISCUSSION

No statistically significant difference was found in either the intra- or intersubject variation of C_{max} of propoxyphene after administration of the two formulations, although the intrasubject variance ratio between Formulations A and B was 2.9 (Table II).

The total range, including the intra- and intersubject variations, of C_{max} of propoxyphene showed a threefold variation (Fig. 2), which was a narrower range compared to the one observed after ingestion of plain propoxyphene products, where C_{max} values showed five- to 10-fold ranges (2, 7–9). Hence, the C_{max} value of propoxyphene for the two controlled-release formulations seems to be subject to a significantly smaller intersubject variation compared to plain products, contrary to what usually is assumed (10). This finding indicates that with controlled-release products, an optimal effect might be obtained by a standard dose regimen with a minimized risk of toxic peak concentrations of propoxyphene. Because single-dose studies are not always applicable to multiple-dose conditions, *i.e.*, the clinical situation, this assumption has to be confirmed.

Among the physiological factors that may influence the bioavailability of a drug from an oral, controlled-release dosage form are the gastric

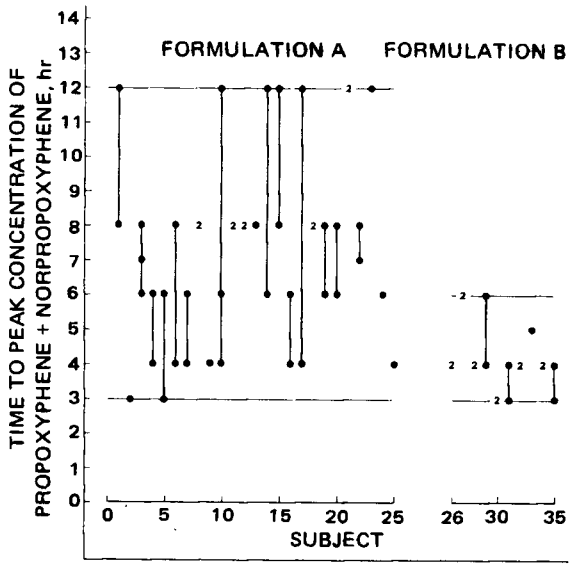

Figure 5—*Individual time to peak concentrations of propoxyphene plus norpropoxyphene after administration of 150 mg of propoxyphene hydrochloride from a batch of Formulation A or B. The symbol 2 indicates equal T_{max} values obtained with different batches; * represents an outlier.*

emptying time, intestinal motility, surface area, specific absorption site, blood flow, and first-pass metabolism (11, 12). The influence of the gastric emptying time and intestinal motility on intra- and intersubject variations in the rate and extent of availability largely can be avoided by the use of multiple-unit, controlled-release dosage forms (11, 13). These dosage forms are comprised of subunits, *e.g.*, pellets or microencapsulated crystals, that are dispersed and distributed throughout the GI tract when the capsule or tablet disintegrates (14).

In the present single-dose study dealing with intra- and intersubject variations in the rate of availability, both formulations were multiple-unit dosage forms, but they showed a highly significant difference in release properties with respect to pH dependency (Fig. 1). When a multiple-unit dosage form is under consideration, the importance of pH dependency is expected to be closely related to the pharmacokinetic characteristics of the drug (*i.e.*, saturable or with an absorption rate-dependent first-pass metabolism) since the influence of gastric emptying on intra- and intersubject variations can be eliminated. However, corroboration of such suggestions is not obtained easily from the literature.

The intrasubject variance of C_{max} of propoxyphene plus norpropoxyphene was significantly lower ($p < 0.01$), by factor of 6.7, after administration of Formulation B (Table II). The rate of appearance of norpropoxyphene in the circulation is a function both of the absorption rate of propoxyphene and of its *N*-demethylation. Because the highest intrasubject variance was observed after ingestion of the formulation whose drug release was most sensitive to the pH of the environment, *i.e.*, Formulation A (Fig. 1), the possibility of an absorption rate-dependent first-pass metabolism cannot be excluded.

With respect to T_{max} of both propoxyphene and propoxyphene plus norpropoxyphene, a significantly ($p < 0.01$) lower intrasubject variance, by factors of 6.7 and 11.9, respectively, was observed after ingestion of Formulation B (Table II). Expressed in terms of intrasubject ranges, identical ranges, *i.e.*, 2 hr for both parameters, were observed after administration of Formulation B. In contrast, the ranges observed for Formulation A were larger and not the same; the ranges were 4 and 8 hr or more, respectively (Figs. 3 and 5). The greater reproducibility of the rate of availability after administration of Formulation B can be ascribed directly to its lower sensitivity to the surrounding pH with respect to drug release. Thus, the significance of the type of controlled-release formulation with regard to minimizing the intrasubject variance in C_{max} and T_{max} has been demonstrated.

Clinically, increased predictability of the time of onset of action presumably is the primary advantage of the improved reproducibility of the plasma concentration pattern with Formulation B compared to Formulation A.

REFERENCES

(1) A. M. Pedersen, U.S. pats. 3,917,813 and 3,954,959 (1975).

(2) A. Melander, A. Berlin-Wahlén, N. O. Bodin, K. Danielson, B. Gustafsson, S. Lindgren, and D. Westerlund, *Acta Med. Scand.*, **202,** 119 (1977).

(3) R. J. Baker and J. A. Nelder, "Manual of the GLIM System," Numerical Algorithms Group, Oxford, England, 1978.

(4) S. R. Searle, "Linear Models," Wiley, New York, N.Y., 1971, p. 421.

(5) B. L. Welch, *J. Am. Statist. Assoc.*, **51,** 132 (1956).

(6) "The National Formulary," 14th ed., Mack Publishing Co., Easton, Pa., 1975, p. 985.

(7) G. W. A. Slywka, A. P. Melikian, P. L. Whyatt, and M. C. Meyer, *J. Clin. Pharmacol.*, **15,** 598 (1975).

(8) R. L. Wolen, C. M. Gruber, Jr., G. F. Kiplinger, and N. E. Scholz, *Toxicol. Appl. Pharmacol.*, **19,** 480 (1971).

(9) B. E. Rodda, N. E. Scholz, C. M. Gruber, Jr., and R. L. Wolen, *ibid.*, **19,** 480 (1971).

(10) B. E. Cabana and C. S. Kumkumian, paper presented at 13th Annual International Industry Pharmacy Conference, Austin, Tex., 1974.

(11) L. Z. Benet, in "Drug Design," vol. IV, E. J. Ariëns, Ed., Academic, New York, N.Y., 1973, p. 1.

(12) C. R. Garcia, A. Siqueiros, and L. Z. Benet, *Pharm. Acta Helv.*, **53,** 99 (1978).

(13) H. Bechgaard and G. Hegermann Nielsen, *Drug Dev. Ind. Pharm.*, **4,** 53 (1978).

(14) H. Bechgaard and K. Ladefoged, *J. Pharm. Pharmacol.*, **30,** 690 (1978).

ACKNOWLEDGMENTS

The authors thank N. E. Larsen, Division of Clinical Pharmacology, Glostrup Hospital, Denmark, for assaying the plasma samples, Dr. N. Shephard, Medical Science Research, United Kingdom, for being the medical evaluator of the project, and Mrs. Liselotte Hansen for carrying out the dissolution tests. They also thank K. Schmidt, Spadille ApS, for performing the statistical evaluation.

Reversible Ring-Opening Reactions of Nimetazepam and Nitrazepam in Acidic Media at Body Temperature

NOBUO INOTSUME and MASAHIRO NAKANO *x

Received January 4, 1980, from the *Faculty of Pharmaceutical Sciences, Hokkaido University, Sapporo 060, Japan.* Accepted for publication May 23, 1980. *Present address: Department of Pharmacy, Kumamoto University Hospital, Honjo 1-chome, Kumamoto 860, Japan.

Abstract □ Hydrolytic reactions of nimetazepam and nitrazepam in acidic solutions at body temperature were studied spectrophotometrically. The open-ring compounds produced by hydrolysis were in equilibrium with the corresponding closed-ring compounds (protonated nimetazepam and nitrazepam). Forward-reaction rate constants of both drugs were greater than the rate constant of diazepam. In nimetazepam, the forward-reaction rate constant was smaller than the reverse-reaction rate constant; in nitrazepam, the reverse-reaction rate constant was much smaller than the forward-reaction rate constant, and possible amide bond cleavage was indicated. The activation energies of the forward and reverse reactions of nimetazepam and the forward reaction of nitrazepam were calculated from Arrhenius-type plots, whereas no clear temperature dependency was observed in the reverse-reaction rate constant of nitrazepam. The effect of pH on these reactions also was examined. In addition, the pKa values of nimetazepam and nitrazepam were calculated to be 2.53 and 2.77, respectively.

Keyphrases □ 1,4-Benzodiazepines—nimetazepam and nitrazepam, kinetics and mechanisms of reversible hydrolysis □ Nimetazepam—kinetics and mechanisms of reversible hydrolysis, pKa determination □ Nitrazepam—kinetics and mechanisms of reversible hydrolysis, pKa determination □ Hydrolysis—nimetazepam and nitrazepam, kinetics and mechanisms, reversible reaction

The hydrolytic cleavage of benzodiazepines has been considered to take place only at elevated temperatures (1–4). On the other hand, pyrazolodiazepinones have been shown to be hydrolyzed easily at ambient temperatures (5). During permeation studies of benzodiazepines at 30°, chemical changes of some benzodiazepines were noted in the receptor solution, which was kept acidic (6). This observation prompted a kinetic investigation of the hydrolytic reaction in acidic media at 37°, and the results indicated that diazepam undergoes reversible ring-opening reactions at its azomethine bond, even at 37° (7).

Since reactions of drugs in acidic media may cause errors in the measurement of dissolution rates in acidic dissolution media and also may influence absorption from the GI tract following oral administration of acid-labile drugs, it is worthwhile to examine the relationship between the chemical structures of benzodiazepines and the rate and extent of hydrolytic reactions. The present report compares the rate constants of nimetazepam (*N*-methylnitrazepam) and nitrazepam with the rate constant of diazepam (7) and relates the different rate constants to structural differences.

EXPERIMENTAL

Materials—Nimetazepam[1], nitrazepam[2], 2-glycylamino-5-nitrobenzophenone hydrochloride[2], and 2-amino-5-nitrobenzophenone[1] were used as received, and their identity and purity were verified by their NMR spectra. Chloroform and ethanol were distilled prior to use. Other chemicals were reagent grade[3] and were used without further purification.

[1] Pharmaceutical Division, Sumitomo Chemical Co., Osaka, Japan.
[2] Nippon Roche K.K., Tokyo, Japan.
[3] Wako Pure Chemical Industries, Osaka, Japan.

Kinetic Studies—The kinetic studies of the hydrolysis of nimetazepam and nitrazepam were carried out spectrophotometrically. Detailed procedures were given previously (7). For experiments at pH 2.2, 2.8, 3.3, and 7.4, 0.1 *M* citric acid–0.2 *M* Na_2HPO_4 or 0.1 *M* phosphate buffers were used.

By employing the molar absorptivity of nimetazepam, nitrazepam, the chloroform-unextractable species from nimetazepam, and 2-glycylamino-5-nitrobenzophenone, the concentration of each species was computed from the observed absorbance in the UV spectra. The forward- and reverse-reaction rate constants (k_f and k_r) for the reversible first-order reactions were obtained from (8):

$$\log \frac{P_t - P_\infty}{P_0 - P_\infty} = -\frac{k_f + k_r}{2.303} t \qquad \text{(Eq. 1)}$$

$$K_{eq} = \frac{k_f}{k_r} = \frac{P_0 - P_\infty}{P_\infty} \qquad \text{(Eq. 2)}$$

where P_0, P_t, and P_∞ are the concentrations or fractions of unreacted nimetazepam or nitrazepam at time zero, t, and infinity, respectively, and K_{eq} is an equilibrium constant.

Separate determinations of protonated nimetazepam and the chloroform-unextractable species in the kinetic studies in the constant-temperature bath and partition kinetic experiments were carried out as reported previously (7).

Determination of pKa of Nimetazepam and Nitrazepam—Stock solutions of nimetazepam and nitrazepam in ethanol were diluted with 0.1 *N* HCl, pH 7.4 phosphate buffer, and 1 *M* sodium acetate–1 *N* HCl of at least seven pH values around pH 2.5 and 2.7, respectively. The absorbance of the diluted solutions was measured quickly at 280 nm to minimize errors due to changes in the chemical species by hydrolysis. The pKa values were calculated according to the standard spectrophotometric method (9).

RESULTS

Nature of Reaction and Properties of Reaction Products of Nimetazepam—The spectral change of nimetazepam in 0.1 *N* HCl at 37° is shown in Fig. 1. Following chloroform extraction of the acidic solution of nimetazepam that had equilibrated for >210 min, the spectrum of the aqueous layer was quite different from that of the equilibrated solution (before extraction). This observation indicates the presence in the equilibrated solution of at least two species that differed markedly in their partition coefficients.

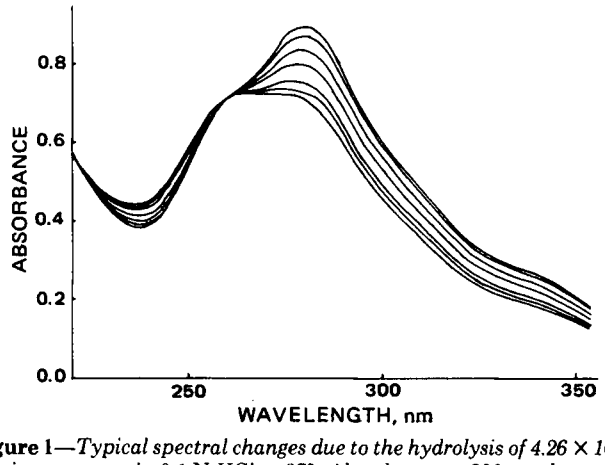

Figure 1—*Typical spectral changes due to the hydrolysis of 4.26 × 10^{-5} M nimetazepam in 0.1 N HCl at 37°. Absorbance at 280 nm decreased with time [measured at 0, 5, 15, 30, 60, 90, and 210 (∞) min].*

0022-3549/80/1100-1331$01.00/0
© 1980, American Pharmaceutical Association

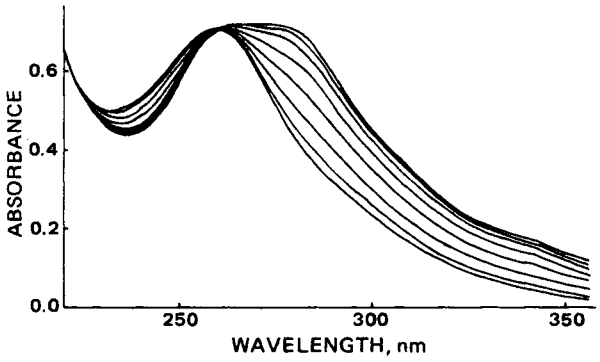

Figure 2—*Typical spectral changes due to the ring-closure reaction of the chloroform-unextractable species at 4.19 × 10^{-5} M formed from nimetazepam in 0.1 N HCl saturated with chloroform at 37°. Absorbance at 280 nm increased with time [measured at 0, 5, 15, 30, 50, 80, 120, and 240 (∞) min].*

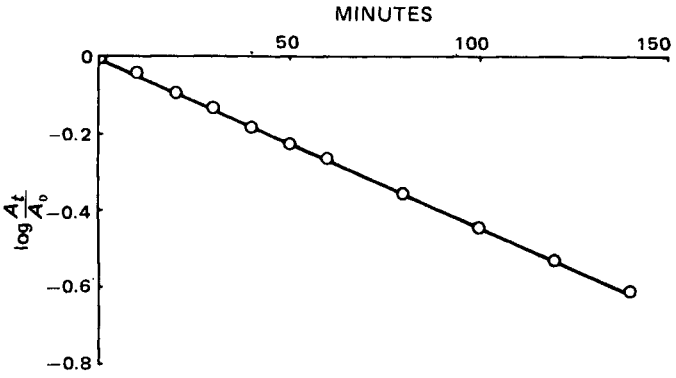

Figure 4—*Changes in absorbance (A) with time of the chloroform-unextractable species in the aqueous layer (0.1 N HCl) in the partition kinetics experiment using chloroform at 37°. Nimetazepam solution (1.36 × 10^{-4} M) was incubated in 0.1 N HCl at 37° for 5.5 hr prior to the partition experiment.*

Since nimetazepam was extracted quantitatively into chloroform immediately after acidification of the aqueous nimetazepam solution, protonated nimetazepam was shown to be chloroform unextractable. The species that remained in the aqueous solution after chloroform extraction was essentially unextractable with chloroform since a second extraction did not significantly affect the spectrum of the aqueous layer.

The reversible nature of the reaction was demonstrated by the formation of protonated nimetazepam from the chloroform-unextractable species. A spectrum of this species with a λ_{max} value of 259.5 nm, which was taken immediately following extraction (Fig. 2, 0 min), changed with time to give a spectrum (Fig. 2, 240 min) that was quite similar to that of the equilibrium mixture starting from protonated nimetazepam (Fig. 1, 210 min). The spectrum in the equilibrium state changed quickly to that of nimetazepam when the pH value of the medium was raised to pH 7.4 by the addition of 2.5 and 0.0025 *N* NaOH and pH 7.4 phosphate buffer. In addition, a spectrum of the species extracted with chloroform from the equilibrated mixture starting from the chloroform-unextractable species was identical to that of nimetazepam extracted with chloroform from an acidic solution of nimetazepam immediately after dilution of the stock nimetazepam solution. Figure 3 depicts the changes in the concentration of both species obtained by separate determinations of each species. An approach to and eventual attainment of the equilibrium are apparent.

Results of the partition kinetics experiments are shown in Fig. 4. An essentially first-order decrease in the amount of the chloroform-unextractable species indicates that nimetazepam is removed from the system as soon as it is formed and that the reaction can go to completion. This process may be used to synthesize nimetazepam from the chloroform-unextractable species in aqueous solutions. Since all of the chloroform-unextractable species was converted to nimetazepam, the reaction is quantitatively reversible.

Nature of Reaction and Properties of Reaction Products of Nitrazepam—The spectral change of nitrazepam in 0.1 *N* HCl at 37° (Fig. 5) differed from the changes of nimetazepam and diazepam. Although the isosbestic points of nitrazepam in Fig. 5 were observed initially at 251 and 363 nm (not shown), they gradually moved to 252 and 346 nm after incubation for 11 hr, and the spectral change continued for >29 hr. Appearance of a new λ_{max} at 358 nm when the test solution was incubated for 18 days at 37° indicates formation of a benzophenone derivative, 2-amino-5-nitrobenzophenone, which was produced by hydrolysis of both the azomethine and amide bonds of nitrazepam. Authentic 2-amino-5-nitrobenzophenone has a λ_{max} at 362 nm.

A spectrum obtained from an equilibrated solution of authentic 2-glycylamino-5-nitrobenzophenone, an opened form of nitrazepam, with an original λ_{max} of 263.5 nm was quite similar to that of the test solution incubated for 11 hr (protonated nitrazepam) (Fig. 5, 11 hr). In addition, a spectrum of the equilibrated nitrazepam in 0.1 *N* HCl rapidly changed to that of nitrazepam by the addition of 2.5 and 0.0025 *N* NaOH and pH 7.4 phosphate buffer. This result indicates the reversibility of the reaction of nitrazepam in the acidic solution.

Although a quinazoline derivative with a λ_{max} at ~295 nm in 0.1 *N* HCl was reported to be produced by incubation of nitrazepam in 0.1 *N* HCl at 90° for 28 hr (2), no increase in absorbance at 295 nm was noted in the spectrum of nitrazepam (Fig. 5). Furthermore, Fig. 5 has an isosbestic point at 251 nm. This observation indicates that this reaction is essentially one step. Therefore, ring contraction upon closure to quinazoline may be negligible under mild conditions.

Structural Assignment of Chloroform-Unextractable Species—Similar to the case of diazepam, although definite identification of the chloroform-unextractable species from nimetazepam is yet to be achieved, the observations discussed earlier ruled out 2-methylamino-5-nitrobenzophenone, which is not expected to be cyclized, as the

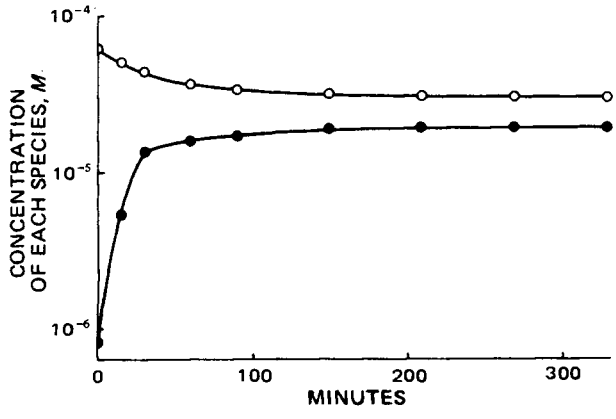

Figure 3—*Separately determined concentrations of protonated nimetazepam (○) and the chloroform-unextractable species (●) for the hydrolysis of 8.29 × 10^{-5} M nimetazepam in 0.1 N HCl at 37°.*

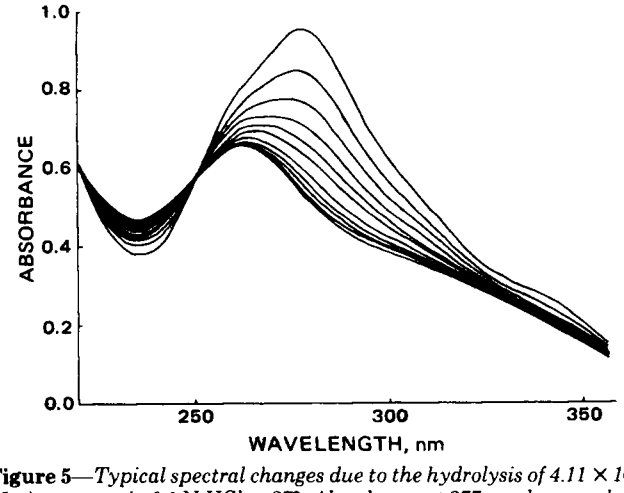

Figure 5—*Typical spectral changes due to the hydrolysis of 4.11 × 10^{-5} M nitrazepam in 0.1 N HCl at 37°. Absorbance at 277 nm decreased with time (measured at 0, 0.67, 1.5, 2.5, 3.5, 5, 7, 9, 13, 18, and 27 hr).*

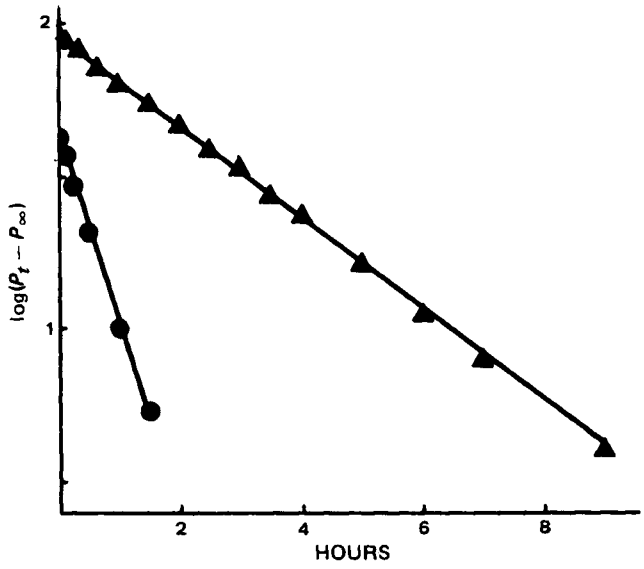

Figure 6—*Plots according to Eq. 1 for 4.26 × 10^{-5} M nimetazepam (●) and 4.11 × 10^{-5} M nitrazepam (▲) in 0.1 N HCl at 37°.*

chloroform-unextractable species. Since assignment of an open-ring compound at the azomethine bond as the structure of the chloroform-unextractable species did not contradict any spectrophotometric and partition characteristics of the species, 2-glycyl(methyl)amino-5-nitrobenzophenone was tentatively assigned to the chloroform-unextractable species.

In nitrazepam, the same reaction as for diazepam and nimetazepam is likely to take place initially, but an additional hydrolysis of the amide bond to produce 2-amino-5-nitrobenzophenone seems to occur, as judged from spectral changes.

As with diazepam, the chloroform-unextractable species could not be isolated as such from aqueous solutions because of the reversible nature of the reaction in 0.1 *N* HCl and because they are rapidly cyclized to form nimetazepam and nitrazepam at pH values above their pKa values. Thus, any attempt to extract the ionized form of the chloroform-unextractable species into organic solvents after neutralization failed.

Quantitative Aspects—The linear relations were obtained in plots according to Eq. 1 (Fig. 6). The reversible first-order reactions with respect to nimetazepam and nitrazepam are indicated. Reaction rate constants calculated for nimetazepam according to Eqs. 1 and 2 are recorded in Table I. Although the general magnitude of the rate constants reasonably agreed, they differed somewhat from each other depending on the experimental method employed. In any case, both the forward- and the reverse-reaction rate constants of nimetazepam were greater than those of diazepam (7), and the rate constant of ring closure was greater than that of the ring-opening reaction. The former observation was attributed to a greater effect of the nitro group than the chloro group on the reactivity. The latter observation indicates a greater concentration of the closed-ring compound (protonated nimetazepam) than the open-ring compound in the equilibrium state at 37°.

Effect of Temperature—The rate constants at 25, 50, and 61° for nimetazepam and at 25 and 50° for nitrazepam were calculated from spectral changes similar to those at 37°. Arrhenius-type rate constant *versus* temperature plots for nimetazepam (Fig. 7) indicate that the reverse-reaction rate constants of nimetazepam were greater than the forward-reaction rate constants below 50° and that the former constant was smaller than the latter constant at temperatures above 50°. This result indicates a greater concentration of the open-ring compound than the closed-ring compound (protonated nimetazepam) at equilibrium at temperatures above 50°.

In nitrazepam, the rate constants of the reverse reaction at 25, 37, and 50° were much smaller than those of the forward reaction and were within the range of experimental error; therefore, no clear dependency of the reverse-reaction rate constants on temperature was noted. The activation energies (mean ± *SE*) calculated were 16.1 ± 0.3 and 11.7 ± 0.8 kcal/mole for the forward and reverse reactions of nimetazepam, respectively. These values were smaller than corresponding values in diazepam (7). The activation energy (mean ± *SE*) for the forward reaction of nitrazepam was 17.2 ± 2.1 kcal/mole.

Effect of pH—Preliminary studies indicated that spectral changes

Table I—Rate Constants of Ring-Opening and Ring-Closure Reactions Estimated by Four Procedures

Estimation Procedure	Rate Constant at 37°, hr^{-1}	
	Ring Opening	Ring Closure
Spectral change starting from protonated nimetazepam (Fig. 1)	0.61	0.82
Spectral change starting from chloroform-unextractable species (Fig. 2)	0.53	0.91
Assay of nimetazepam extracted into chloroform layer (Fig. 3)	0.45	0.74
Decrease in absorbance in aqueous layer during partition kinetics experiments (Fig. 4)	—	0.61

similar to those shown in Figs. 1 and 5 took place in the buffers at pH 2.2 and 3.3 for nimetazepam and at pH 2.8 for nitrazepam. However, the changes in absorbance were smaller than those in 0.1 *N* HCl, indicating that the reactions proceeded to a lesser extent. At pH values higher than the pKa values of nimetazepam and nitrazepam, little change in the absorbance with time was observed. As already indicated, open-ring compounds, once formed in the acidic solutions, reverted back to nimetazepam and nitrazepam when the pH values of the media were increased.

pKa Values of Nimetazepam and Nitrazepam—The calculated pKa values were 2.53 for nimetazepam and 2.77 for nitrazepam. The latter value is smaller than the reported pKa value (3.2) of nitrazepam (10).

DISCUSSION

At body temperature, the reversible reactions involving hydrolysis of 4,5-azomethine bonds of nimetazepam and nitrazepam are expected to take place. The result that the forward-reaction rate constant of nimetazepam is greater than that of diazepam may be explained by the lower electron density of the A-ring of nimetazepam (nitrobenzene group) caused by the higher electron-withdrawing tendency of the nitro group in nimetazepam relative to that of the chlorine in diazepam. The same mechanism may be applicable to the acidic hydrolysis of *m*-nitrobenzoate, which was hydrolyzed faster than *m*-chlorobenzoate to the same degree (11).

The result that the forward-reaction rate constant of nimetazepam is greater than that of nitrazepam may be explained by the higher electron density of the A-ring of nitrazepam caused by the delocalization of the lone electron on the amide nitrogen. In nimetazepam, the lone electron

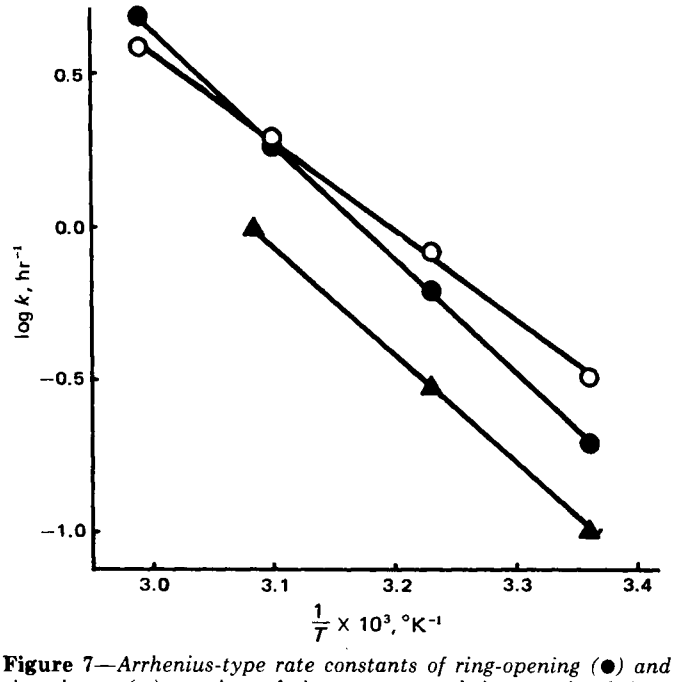

Figure 7—*Arrhenius-type rate constants of ring-opening (●) and ring-closure (○) reactions of nimetazepam and ring-opening (▲) reaction of nitrazepam in 0.1 N HCl.*

on the amide nitrogen is fixed by the methyl group. This difference is not unique in nimetazepam and nitrazepam because the same trend was observed with diazepam and desmethyldiazepam. Diazepam in acidic solution reached equilibrium after incubation for 11 hr (7), whereas desmethyldiazepam in acidic solution did not reach equilibrium, even after incubation for 210 hr[4].

Since further hydrolysis of the amide bond of the chloroform-unextractable species from nitrazepam to 2-amino-5-nitrobenzophenone is expected to be irreversible, such a hydrolysis in the stomach may reduce the amount of the chloroform-unextractable species that reverts back to the original drug and then is absorbed from the intestine. However, since the irreversible hydrolysis of the amide bond of nitrazepam proceeds only at a slow rate, it is not expected to affect the bioavailability of orally administered nitrazepam. The rate constant of formation of 2-amino-5-nitrobenzophenone was not determined in the present study. However, the magnitude of this rate relative to that of the reverse-reaction rate, the dissolution rate of the drug in the stomach, the forward-reaction rate constant, and the stomach-emptying rate is expected to affect the bioavailability of nitrazepam.

Based on the experimental data obtained in the present *in vitro* study, it may be postulated that after administration of dosage forms of nimetazepam and nitrazepam, some nimetazepam and nitrazepam dissolved in the stomach is hydrolyzed to the open-ring compounds because of the acidic pH of the stomach contents. When the open-ring compounds empty from the stomach to the intestine, they are expected to revert back to the parent drugs upon increase in the pH value of the media. Therefore, there can be little loss in drug bioavailability.

[4] N. Inotsume and M. Nakano, unpublished data.

REFERENCES

(1) J. T. Carstensen, K. S. E. Su, P. Maddrell, J. B. Johnson, and H. N. Newmark, *Bull. Parent. Drug Assoc.*, **25**, 193 (1973).

(2) W. Mayer, S. Erbe, and R. Voigt, *Pharmazie*, **27**, 32 (1972).

(3) H. V. Maulding, J. P. Nazareno, J. E. Pearson, and A. F. Michaelis, *J. Pharm. Sci.*, **64**, 278 (1975).

(4) W. W. Han, G. J. Yakatan, and D. D. Maness, *ibid.*, **66**, 795 (1977).

(5) W. H. Hong, C. Johnston, and D. Szulczewski, *ibid.*, **66**, 1703 (1977).

(6) M. Nakano, N. Kohri, Y. Arakawa, and T. Arita, *Chem. Pharm. Bull.*, **27**, 573 (1979).

(7) M. Nakano, N. Inotsume, N. Kohri, and T. Arita, *Int. J. Pharm.*, **3**, 195 (1979).

(8) J. H. Espenson, "Investigation of Rates and Mechanisms of Reactions," 3rd ed., Wiley, New York, N.Y., 1974, pp. 558, 559.

(9) A. Albert and E. Serjeant, "Ionization Constants of Acids and Bases," 2nd ed., Chapman and Hall, London, England, 1971, pp. 44–64.

(10) J. Barrett, W. F. Smyth, and I. E. Davidson, *J. Pharm. Pharmacol.*, **25**, 387 (1973).

(11) E. W. Timm and C. N. Hinshelwood, *J. Chem. Soc.*, **1958**, 862.

ACKNOWLEDGMENTS

The authors thank Sumitomo Chemical Co. and Nippon Roche K.K. for generous gifts of materials.

Structure–Activity Relationships of Pyrrole Amidine Antiviral Antibiotics III: Preparation of Distamycin and Congocidine Derivatives Based on 2,5-Disubstituted Pyrroles

MEIR BIALER *§x, BORIS YAGEN *, RAPHAEL MECHOULAM *, and YECHIEL BECKER ‡

Received March 17, 1980, from the **Department of Natural Products, Pharmacy School, and the* ‡*Department of Molecular Virology, Medical School, Hebrew University, Jerusalem, Israel.* Accepted for publication May 22, 1980. §Present address: Pharmacy Department, Pharmacy School, Hebrew University, Jerusalem, Israel.

Abstract □ Isomers of distamycin A and tripyrrole congocidine containing 2,5-disubstituted pyrroles were synthesized along with distamycin and congocidine homologs containing a single pyrrole ring. Selected compounds were evaluated for their cytotoxicity and antiviral activity. All of the tripyrrole derivatives tested in this series were nontoxic but were less active than distamycin A. The monopyrrole derivative, *N*-methyl-5-nitropyrrole-2-carboxamido-β-propionamidine hydrochloride, was nontoxic and was almost as active antivirally as distamycin A.

Keyphrases □ Antibiotics—distamycin A and congocidine derivatives based on 2,5-disubstituted pyrroles, synthesis and evaluation for cytotoxicity and antiviral activity, structure–activity relationships □ Structure–activity relationships—distamycin A and congocidine derivatives based on 2,5-disubstituted pyrroles, antiviral activity □ Distamycin—derivatives based on 2,5-disubstituted pyrroles, synthesis and evaluation for cytotoxicity and antiviral activity, structure–activity relationships □ Congocidine—derivatives based on 2,5-disubstituted pyrroles, synthesis and evaluation for cytotoxicity and antiviral activity, structure–activity relationships

Distamycin A (I), a basic oligopeptide antibiotic isolated from the fermentation medium of *Streptomyces distallicus* (1), has interesting antibacterial (2) and antiviral activities. As an antiviral drug, distamycin A inhibits the multiplication of DNA viruses and certain retroviruses (3–7). The mechanism of its antiviral activity is believed to be related to its ability to bind to single- and double-stranded DNA molecules, with a particularly high affinity for adenine–thymine-rich DNA sequences. Subsequent formation of a DNA–distamycin A complex destroys the DNA molecule, which serves as a template for the enzyme DNA polymerase (3–7). Distamycin A has been used clinically in cases of herpes virus infections (8).

Distamycin A belongs to a group of compounds known as pyrrole amidine antiviral antibiotics. Another member of this group is congocidine (netropsin, II) (6, 7). This

0022-3549/80/1100-1334$01.00/0

© 1980, American Pharmaceutical Association

on the amide nitrogen is fixed by the methyl group. This difference is not unique in nimetazepam and nitrazepam because the same trend was observed with diazepam and desmethyldiazepam. Diazepam in acidic solution reached equilibrium after incubation for 11 hr (7), whereas desmethyldiazepam in acidic solution did not reach equilibrium, even after incubation for 210 hr[4].

Since further hydrolysis of the amide bond of the chloroform-unextractable species from nitrazepam to 2-amino-5-nitrobenzophenone is expected to be irreversible, such a hydrolysis in the stomach may reduce the amount of the chloroform-unextractable species that reverts back to the original drug and then is absorbed from the intestine. However, since the irreversible hydrolysis of the amide bond of nitrazepam proceeds only at a slow rate, it is not expected to affect the bioavailability of orally administered nitrazepam. The rate constant of formation of 2-amino-5-nitrobenzophenone was not determined in the present study. However, the magnitude of this rate relative to that of the reverse-reaction rate, the dissolution rate of the drug in the stomach, the forward-reaction rate constant, and the stomach-emptying rate is expected to affect the bioavailability of nitrazepam.

Based on the experimental data obtained in the present *in vitro* study, it may be postulated that after administration of dosage forms of nimetazepam and nitrazepam, some nimetazepam and nitrazepam dissolved in the stomach is hydrolyzed to the open-ring compounds because of the acidic pH of the stomach contents. When the open-ring compounds empty from the stomach to the intestine, they are expected to revert back to the parent drugs upon increase in the pH value of the media. Therefore, there can be little loss in drug bioavailability.

[4] N. Inotsume and M. Nakano, unpublished data.

REFERENCES

(1) J. T. Carstensen, K. S. E. Su, P. Maddrell, J. B. Johnson, and H. N. Newmark, *Bull. Parent. Drug Assoc.*, **25**, 193 (1973).

(2) W. Mayer, S. Erbe, and R. Voigt, *Pharmazie*, **27**, 32 (1972).

(3) H. V. Maulding, J. P. Nazareno, J. E. Pearson, and A. F. Michaelis, *J. Pharm. Sci.*, **64**, 278 (1975).

(4) W. W. Han, G. J. Yakatan, and D. D. Maness, *ibid.*, **66**, 795 (1977).

(5) W. H. Hong, C. Johnston, and D. Szulczewski, *ibid.*, **66**, 1703 (1977).

(6) M. Nakano, N. Kohri, Y. Arakawa, and T. Arita, *Chem. Pharm. Bull.*, **27**, 573 (1979).

(7) M. Nakano, N. Inotsume, N. Kohri, and T. Arita, *Int. J. Pharm.*, **3**, 195 (1979).

(8) J. H. Espenson, "Investigation of Rates and Mechanisms of Reactions," 3rd ed., Wiley, New York, N.Y., 1974, pp. 558, 559.

(9) A. Albert and E. Serjeant, "Ionization Constants of Acids and Bases," 2nd ed., Chapman and Hall, London, England, 1971, pp. 44–64.

(10) J. Barrett, W. F. Smyth, and I. E. Davidson, *J. Pharm. Pharmacol.*, **25**, 387 (1973).

(11) E. W. Timm and C. N. Hinshelwood, *J. Chem. Soc.*, **1958**, 862.

ACKNOWLEDGMENTS

The authors thank Sumitomo Chemical Co. and Nippon Roche K.K. for generous gifts of materials.

Structure–Activity Relationships of Pyrrole Amidine Antiviral Antibiotics III: Preparation of Distamycin and Congocidine Derivatives Based on 2,5-Disubstituted Pyrroles

MEIR BIALER *§x, BORIS YAGEN *, RAPHAEL MECHOULAM *, and YECHIEL BECKER ‡

Received March 17, 1980, from the **Department of Natural Products, Pharmacy School, and the* ‡*Department of Molecular Virology, Medical School, Hebrew University, Jerusalem, Israel.* Accepted for publication May 22, 1980. §Present address: Pharmacy Department, Pharmacy School, Hebrew University, Jerusalem, Israel.

Abstract □ Isomers of distamycin A and tripyrrole congocidine containing 2,5-disubstituted pyrroles were synthesized along with distamycin and congocidine homologs containing a single pyrrole ring. Selected compounds were evaluated for their cytotoxicity and antiviral activity. All of the tripyrrole derivatives tested in this series were nontoxic but were less active than distamycin A. The monopyrrole derivative, *N*-methyl-5-nitropyrrole-2-carboxamido-β-propionamidine hydrochloride, was nontoxic and was almost as active antivirally as distamycin A.

Keyphrases □ Antibiotics—distamycin A and congocidine derivatives based on 2,5-disubstituted pyrroles, synthesis and evaluation for cytotoxicity and antiviral activity, structure–activity relationships □ Structure–activity relationships—distamycin A and congocidine derivatives based on 2,5-disubstituted pyrroles, antiviral activity □ Distamycin—derivatives based on 2,5-disubstituted pyrroles, synthesis and evaluation for cytotoxicity and antiviral activity, structure–activity relationships □ Congocidine—derivatives based on 2,5-disubstituted pyrroles, synthesis and evaluation for cytotoxicity and antiviral activity, structure–activity relationships

Distamycin A (I), a basic oligopeptide antibiotic isolated from the fermentation medium of *Streptomyces distallicus* (1), has interesting antibacterial (2) and antiviral activities. As an antiviral drug, distamycin A inhibits the multiplication of DNA viruses and certain retroviruses (3–7). The mechanism of its antiviral activity is believed to be related to its ability to bind to single- and double-stranded DNA molecules, with a particularly high affinity for adenine–thymine-rich DNA sequences. Subsequent formation of a DNA–distamycin A complex destroys the DNA molecule, which serves as a template for the enzyme DNA polymerase (3–7). Distamycin A has been used clinically in cases of herpes virus infections (8).

Distamycin A belongs to a group of compounds known as pyrrole amidine antiviral antibiotics. Another member of this group is congocidine (netropsin, II) (6, 7). This

0022-3549/80/1100-1334$01.00/0

© 1980, American Pharmaceutical Association

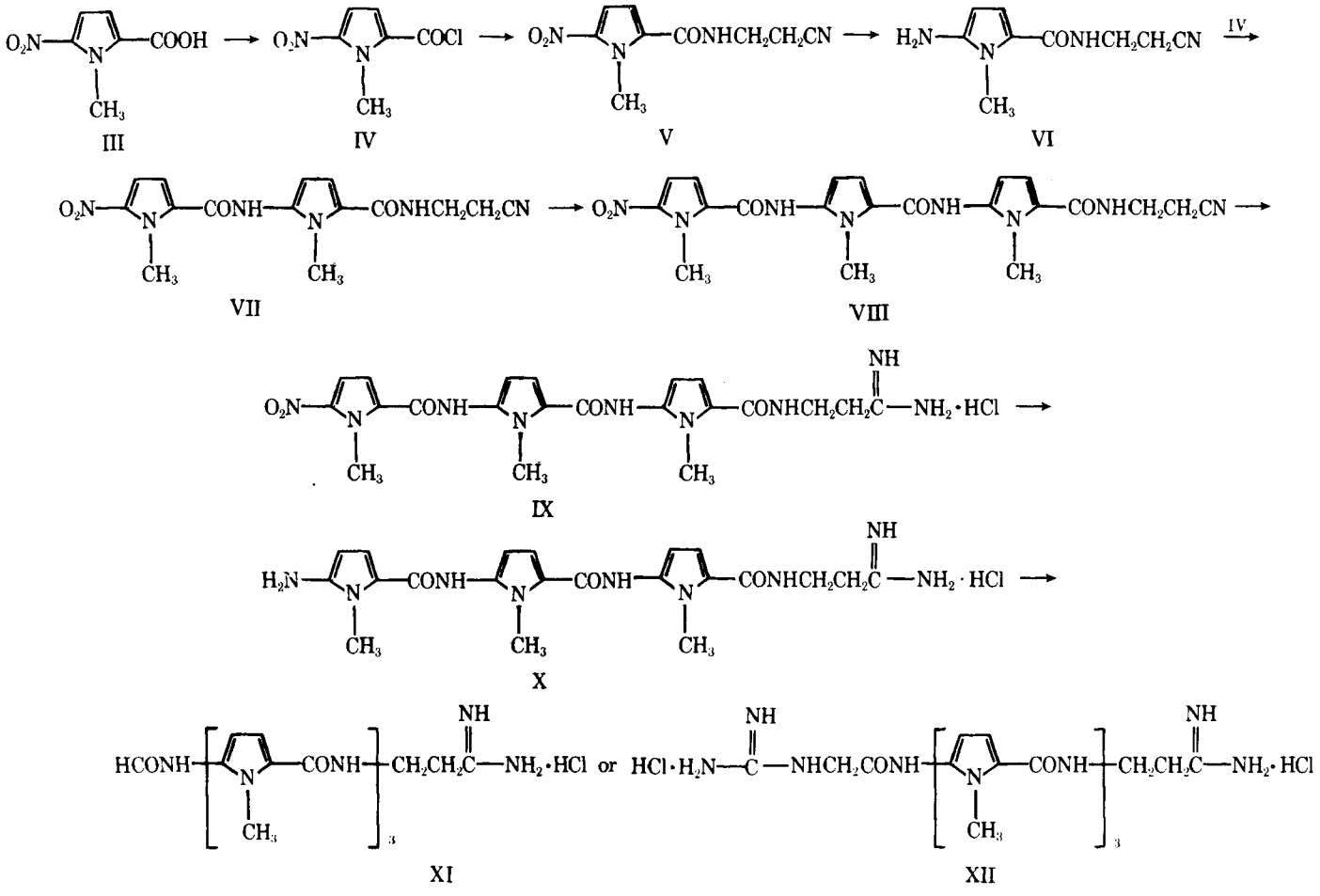

Scheme I

compound has biological activities similar to those of distamycin A.

DISCUSSION

Little information is available on the structural requirements for the antiviral activity of distamycin A (9–17) and congocidine (18, 19). Due to the lack of clinically useful antiviral drugs, a thorough investigation into the structure–activity relationships of the known antiviral compounds is of importance. In continuation of previous research on the structure–activity relationships of pyrrole amidine antiviral antibiotics (13, 16), the present study concerned the synthesis of novel distamycin and congocidine analogs and evaluation of their antiviral activity.

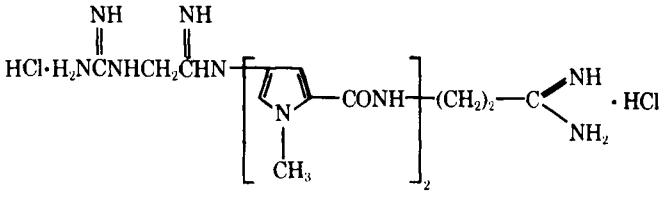

II·2HCl

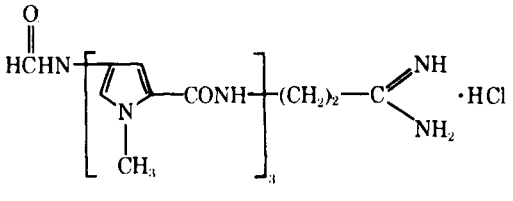

I·HCl

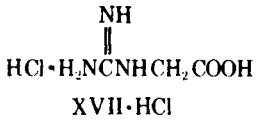

XVII·HCl

In all of the previous work (9–20), the peptide bonds were between positions 2 and 4 of the pyrrole ring. Thus, it was decided to determine if the location of the peptide in the pyrrole ring was critical for the antiviral activity of this series. Accordingly, isomers and homologs of distamycin A (I) and congocidine (II) in which the peptide bonds were moved to positions 2 and 5 of the pyrrole ring were synthesized.

Chemistry—The synthetic route is outlined in Scheme I and is similar to the first total synthesis of distamycin A (21). The starting material was *N*-methyl-5-nitropyrrole-2-carboxylic acid (III) (22). Compound III was prepared and purified similarly to its 4-nitro isomer. The acid (III) was converted to its acyl chloride (IV), which was condensed with β-aminopropionitrile to give the nitro nitrile (V). Compound V was reduced catalytically to the amine (VI) which, without further purification, was condensed with *N*-methyl-5-nitropyrrole-2-carboxyl chloride (IV) to give the dipeptide (VII).

The reduction–condensation process was repeated, leading to the intermediate nitro nitrile (VIII). Compound VIII was converted to the nitroamidine compound (IX) by the standard reaction with hydrochloric acid followed by ammonia (23). Compound IX served as a precursor for the synthesis of the distamycin and the tripyrrole congocidine isomers. Reduction of IX yielded the amino amidine compound (X), which, due to its sensitivity and instability, was condensed directly with formic acid in the presence of dicyclohexylcarbodiimide (24) to give the distamycin isomer (XI) or with glycocyamine hydrochloride (XVII) (25) to give the congocidine analog (XII). The total yield in this synthesis was lower than the yield obtained in the synthesis of analogs containing peptide bonds between positions 2 and 4 (21, 22). This result can be explained by the instability and minor chemical reactivity of α-amino pyrrole derivatives during condensation (26). Chemical reactions not requiring condensation of an α-amino pyrrole, such as in the preparation of V and IX, showed

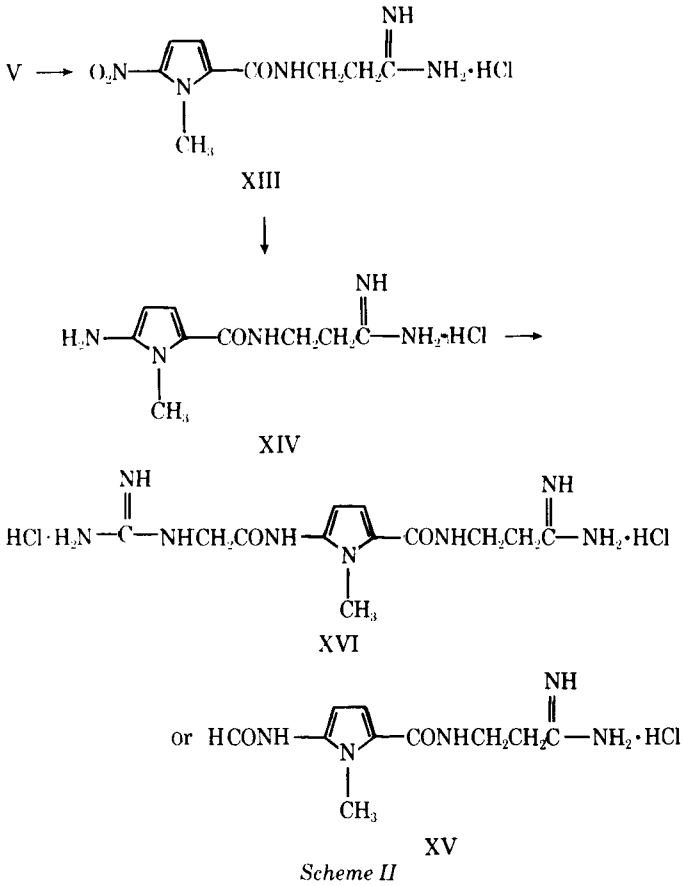

Scheme II

similar yields as the analogs with peptide bonds between positions 2 and 4 (21, 22).

In comparing the UV data of IX and XI to those of analogous compounds in the distamycin series, a bathochromic shift of 30 nm was noted. In the NMR spectra of IV, V, VII, and VIII, the pyrrolic *N*-methyl group that was closest to the aliphatic side chain appeared at 4.1–4.2 ppm, and the aromatic hydrogens showed an *AB* system with J = 4 Hz.

Compound V served as a starting material for the preparation of 2,5-disubstituted monopyrrole derivatives of distamycin and congocidine (Scheme II). It was converted to the nitroamidine (XIII) by the standard reaction with hydrochloric acid followed by ammonia (23). Compound XIII was reduced catalytically to give the amino compound (XIV), which, without isolation, was condensed with formic acetic anhydride (21) or glycocyamine hydrochloride in the presence of dicyclohexylcarbodiimide to give XV or XVI, respectively. The IR, NMR, and mass spectra of the monopyrrole compounds (V, XIII, XV, and XVI) were similar to those of tripyrroles.

Virology—Selected compounds of this series were tested for their cytotoxicity and ability to inhibit Herpes simplex Type 1 viral replication in cultured cells. The details of these techniques were given previously (17).

EXPERIMENTAL

Unless otherwise stated, the following procedures were followed. UV measurements were made for solutions in ethanol or dimethylformamide[1]. IR[2] spectra were taken in potassium bromide pellets. PMR[3] data were determined in dimethyl sulfoxide-d_6 as the solvent with sodium 3′-(trimethylsilyl)tetradeuteropropionate as the external standard. TLC was performed on 0.3-mm silica gel plates, which were developed with Ehrlich's reagent [2% *N,N*-(dimethylamino)benzaldehyde in 6 *N* HCl] or by irradiation at 254 nm. Mass spectra[4] were obtained by direct inlet at 80 ev; in several cases, the technique of field desorption was used.

***N*-Methyl-5-nitropyrrole-2-carboxylic Acid (III)**—*N*-Methyl-5-nitropyrrole-2-carboxylic acid methyl ester (22) (5 g, 27.1 mmoles) was dissolved in ethanol (50 ml), and a solution of sodium hydroxide (1.9 g in 125 ml of water) was added. The reaction mixture was stirred overnight at room temperature, and the ethanol was evaporated. The solution was cooled and acidified with 6 *N* HCl.

The precipitate formed was filtered off and crystallized from ethanol–water to give III, 4 g (87%), mp[5] 198°; NMR: δ 4.22 (s, 3H, *N*-CH_3), 6.82, and 7.08 (d, 2H, J = 4 Hz, aromatic H); UV (ethanol): λ_{max} 225 (ϵ 11,000) and 392 (15,500) nm; IR: ν_{max} 3100, 2600–2900, 1680, 1450, 1350, 1290, and 1250 cm^{-1}; mass spectrum: m/e 170 (M^+, 100%), 152 (17), 122 (65), and 109 (48).

Anal.—Calc. for $C_6H_4N_2O_4$: C, 42.4, H, 3.53; N, 16.5. Found: C, 42.5; H, 3.37; N, 16.1.

***N*-Methyl-5-nitropyrrole-2-carboxamido-β-propionitrile (V)**—Compound III (3 g, 18.2 mmoles) was dissolved in thionyl chloride and boiled under reflux for 1 hr. The remaining thionyl chloride was evaporated. The residue (IV) was dissolved in benzene (30 ml) and added gradually to a solution of β-aminopropionitrile[6] (1.23 g, 176 mmoles) and sodium bicarbonate (2.1 g) in water (25 ml). The reaction mixture was stirred at room temperature and filtered.

The precipitate formed was crystallized from methanol–water to give V, 3.3 g (84%), mp 117–119°; NMR: δ 2.79 (t, 2H, J = 4.8 Hz, *C*-CH_2), 3.52 (t, 2H, J = 4.8 Hz, *N*-CH_2), 4.12 (s, 3H, *N*-CH_3), 6.78, and 7.02 (d, 2H, J = 3.6 Hz, aromatic H); UV (ethanol): λ_{max} 271 (ϵ 10,700) and 345 (14,200) nm; IR: ν_{max} 3270, 3110, 2960, 2250, 1640, 1530, 1460, 1490, 1160, and 1070 cm^{-1}; mass spectrum: m/e 222 (M^+, 32%), 205 (5), 192 (32), 182 (5), 174 (6), and 153 (100).

Anal.—Calc. for $C_9H_{10}N_4O_3$: C, 48.65; H, 4.54; N, 25.22. Found: C, 48.58; H, 4.69; N, 24.78.

***N*-Methyl-5-(*N*-methyl-5-nitropyrrole -2 -carboxamido)pyrrole-2-carboxamido-β-propionitrile (VII)**—Compound V (4 g, 18 mmoles) was dissolved in dimethylformamide (30 ml) and reduced at atmospheric pressure with 10% palladium-on-charcoal (1.2 g) to give VI. Water (90 ml) was added, and the catalyst was filtered off. Sodium bicarbonate (2.25 g) was introduced into the filtrate, followed by a solution of IV (3.06 g, 18 mmoles) in benzene (15 ml). The mixture was stirred overnight. The precipitate formed was filtered off and washed with 5% $NaHCO_3$ and water.

The residue was crystallized from ethanol to give VII, 1.1 g (18%), mp 241–245°; NMR: δ 2.74 (t, 2H, J = 5 Hz, *C*-CH_2), 3.44 (t, 2H, J = 5 Hz, *N*-CH_2), 4.12 (s, 6H, *N*-CH_3), 6.02 (d, 1H, J = 3 Hz), 6.76 (d, 1H, J = 3 Hz), 6.98 (d, 1H, J = 4.8 Hz), 7.2 (d, 1H, J = 4.8 Hz, aromatic H), 8.16 (t, 1H, aliphatic amide H), and 10.2 (s, 1H, aromatic amide H); UV (ethanol): λ_{max} 271 (ϵ 17,000) and 345 (14,200) nm; IR: ν_{max} 3320, 3230, 1670, 1640, 1540, 1460, 1370, 1350, 1290, and 1240 cm^{-1}; mass spectrum: m/e 344 (M^+, 100%), 328 (3.5), 312 (14), and 275 (8).

Anal.—Calc. for $C_{15}H_{16}N_6O_4 \cdot H_2O$: C, 49.72; H, 4.97; N, 23.20. Found: C, 50.11; H, 5.01; N, 23.30.

***N*-Methyl-5-[*N*-methyl-5-(*N*-methyl-5-nitropyrrole-2-carboxamido)pyrrole-2-carboxamido]pyrrole -2 -carboxamido-β -propionitrile (VIII)**—Compound VII (1 g, 3.2 mmoles) was dissolved in dimethylformamide (10 ml). The reduction procedure followed was that described for obtaining VII from V. Sodium bicarbonate (330 mg) was introduced into the filtrate, followed by a solution of IV (620 mg, 36 mmoles) in benzene (8 ml). The mixture was stirred overnight. The precipitate formed was filtered off and washed with 5% $NaHCO_3$ and water.

The precipitate obtained was crystallized from methanol to give VIII, 700 mg (47%), mp 270°; NMR: δ 2.80 (t, 2H, J = 5 Hz, *C*-CH_2), 3.41 (t, 2H, J = 5 Hz, *N*-CH_2), 3.80, 3.81, 4.28 (s, 9H, *N*-CH_3), 6.02 (d, 1H, J = 4 Hz), 6.12 (d, 1H, J = 4 Hz), 6.83 (d, 1H, J = 4 Hz), 7.1 (d, 1H, J = 2 Hz), 7.16 (d, 1H, J = 2 Hz), 7.32 (d, 1H, J = 4 Hz, aromatic H), 8.25, 9.7, and 10.3 (amide H); UV (dimethylformamide): λ_{max} 298 (ϵ 15,200) and 348 (12,900) nm; IR: ν_{max} 3250, 3060, 2960, 2250, 1640, 1540, 1470, 1360, 1230, and 1040 cm^{-1}; mass spectrum: m/e 466 (M^+, 10%), 370 (2), 369 (2), 344 (24), 340 (38), 314 (10), 299 (24), and 275 (100).

Anal.—Calc. for $C_{21}H_{22}N_8O_5 \cdot H_2O$: C, 52.66; H, 4.96; N, 23.14. Found: C, 52.76; H, 5.18; N, 23.11.

***N*-Methyl-5-[*N*-methyl-5-(*N*-methyl-5-nitropyrrole-2-carboxamido)pyrrole-2-carboxamido]pyrrole -2 -carboxamido-β -propionamidine Hydrochloride (IX)**—Compound VIII (700 mg, 1.5 mmoles) was dissolved in absolute ethanol (20 ml). The solution was cooled to 0° and stirred, and dry hydrochloric acid was bubbled through it for 1 hr.

[1] Unican S. P. 1800.
[2] Perkin-Elmer model 577.
[3] Bruker (60 Hz).
[4] Varian CH-5.
[5] Fisher Jones melting-point apparatus.
[6] K and K Co.

Table I—Toxicity and Plaque Inhibition by Distamycin and Congocidine Derivatives

Compound	Maximal Nontoxic Concentration, μg/ml[a]	Inhibition of Virus Progeny[b], %
I	25	99.7
IX	>200[c]	98.45
XI	>200	96.3
XIII	>200	99.12
XVI	>200	76.4

[a] Toxic effect is regarded as cell death within 2 days of incubation of cultured cells with the drug at 37°. The maximal nontoxic concentration is defined as the nontoxic drug concentration whose twofold increase causes toxicity. [b] The titer of virus progeny produced in untreated infected cells and in cells treated with each distamycin derivative was determined by plaque assay on BSC-1 cells. The virus progeny yielded by infected cells was taken as 100%, and the yield of virus from infected treated cells was related to the yield from untreated infected cells. All compounds were tested at a concentration of 200 μg/ml except for I, which was tested at 25 μg/ml. [c] The designation >200 indicates that the drug was nontoxic at 400 μg/ml.

The solution was kept at 0° for an additional 12 hr, the ethanol was evaporated, and the dry residue was washed with ether. Then the residue was dissolved in absolute ethanol (15 ml). The solution was cooled to 0° and stirred, and dry ammonia was bubbled through it for 1 hr.

After the bubbling was stopped, the solution was stirred at room temperature for 12 hr. The ethanol was evaporated, and the residue was crystallized from methanol to give IX, 520 mg (67%), mp 192–198°; NMR: δ 2.89 (d, 2H, *C*-CH_2), 3.6 (d, 2H, *N*-CH_2), 3.78, 3.81, 4.29 (s, 9H, *N*-CH_3), 6.02 (d, 1H, J = 4 Hz), 6.18 (d, 1H, J = 4 Hz), 6.94 (d, 1H, J = 3.84 Hz), 7.21, 7.36 (d, 2H, J = 4 Hz, aromatic H), 8.26, 9.66 (amide H), and 8.74 (amidine H); UV (ethanol): λ_{max} 261 (ε 8800) and 295 (10,000) nm; IR: ν_{max} 3100–3300, 1640, 1540, 1450, 1300, and 1260 cm^{-1}; mass spectrum (field desorption): m/e 466 (M − NH_3), 412, 344, 248, and 218.

***N*-Methyl-5-[*N*-methyl-5-(*N*-methyl-5-(formylamido)pyrrole-2-carboxamido)pyrrole -2-carboxamido]pyrrole-2-carboxamido-β-propionamidine Hydrochloride (XI)**—Compound IX (400 mg, 0.77 mmole) was dissolved in dimethylformamide (7 ml) and reduced at atmospheric pressure with 10% palladium-on-charcoal (120 mg). The mixture was filtered. The intermediate amine (X) presumably obtained was not purified due to instability. Formic acid (53 mg, 1.15 mmoles) in dimethylformamide (10 ml) was gradually added under nitrogen to a solution of X and kept at 0° for 1 hr.

The reaction mixture was stirred at room temperature overnight and filtered, and the filtrate was evaporated. The residue was crystallized from ethanol–ethyl acetate to give XI, 20 mg (5%), mp 182–190°; UV (ethanol): λ_{max} 324 (ε 24,400) nm; IR: ν_{max} 3000–3440, 2440, 2860, 1680, 1640, 1520, 1450, 1370, 1330, 1250, and 1100 cm^{-1}; mass spectrum: m/e 421 (1%), 382 (2), 340 (40), 314 (10), 220 (12), and 218 (100).

***N*-Methyl-5-[*N*-methyl-5-(*N*-methyl-5-(guanidinoacetamido)-pyrrole-2-carboxamido)pyrrole -2- carboxamido]pyrrole-2-carboxamido-β-propionamidine Dihydrochloride (XII)**—Compound XII was obtained from IX as described for XI. The only difference was that the intermediate amine (X) was condensed with glycocyamine hydrochloride[7] (XVII) (1.18 mg, 0.77 mmole), 2 mg (2%); UV (ethanol): λ_{max} 237 (ε 17,100) and 298 (11,200) nm; IR: ν_{max} 2980–3440, 1680, 1640, 1490, 1280, and 1230 cm^{-1}; mass spectrum: m/e 344 (9%), 340 (7), 314 (5), 289 (8), 220 (100), and 218 (26).

***N*-Methyl-5-nitropyrrole -2 -carboxamido -β- propionamidine Hydrochloride (XIII)**—Compound XIII was obtained from the nitrile (V) (2 g, 9 mmoles). The reaction procedure followed was the same as that described for obtaining IX from VIII, 1.5 g (73%), mp 189°; UV (ethanol): λ_{max} 240 (ε 8100) and 344 (9800) nm; IR: ν_{max} 3340, 3240, 3080, 1670, 1540, 1470, 1290, 1250, 1200, and 1150 cm^{-1}; NMR: δ 2.81 (t, 2H, J = 6 Hz, *C*-CH_2), 3.79 (t, 2H, J = 6 Hz, *N*-CH_2), 4.24 (s, 3H, *N*-CH_3), 6.94, 7.27 (d, 2H, J = 4 Hz, aromatic H), and 8.94 (amidine H); mass spectrum: m/e 222 (M − NH_3, 80%), 209 (100), 192 (75), and 153 (65).

Anal.—Calc. for $C_9H_{13}N_5O_3$·HCl: C, 39.20; H, 5.12; Cl, 12.9; N, 25.6. Found: C, 39.31; H, 5.42; Cl, 12.63; N, 25.53.

***N*-Methyl-5-formylamidopyrrole-2-carboxamido -β- propionamidine Hydrochloride (XV)**—The nitropyrrole derivative (XIII) (1.5 g, 5.4 mmoles) was dissolved in 80% methanol (30 ml) and reduced at atmospheric pressure with 10% palladium-on-charcoal (0.4 g). The mixture was filtered and evaporated. The intermediate amine (XIV) presumably obtained was not purified due to its instability. Formic acetic anhydride (21), freshly prepared, was gradually added to the cooled residue. The reaction mixture was stirred at room temperature for 1 hr and then was poured into ether (50 ml).

A white precipitate formed and was washed with ether. The crude precipitate was purified by chromatography on a silica gel column (90 g); the eluent was chloroform–ethanol–water (100:50:4). Compound XV (230 mg, 16%) was obtained; UV (ethanol): λ_{max} 280 (ε 20,900) nm; IR: ν_{max} 3000–3500, 1760, 1620, 1500, 1380, 1330, 1270, and 1150 cm^{-1}; NMR: δ 2.81 (t, 2H, *C*-CH_2), 3.79 (t, 2H, *N*-CH_2), 3.91 (s, 3H, *N*-CH_3), 6.16, 6.94 (d, 2H, J = 5 Hz, aromatic H), 8.14 (amide H), 8.84, 9.30 (amidine H), and 10.34 (formyl H).

***N*-Methyl-5-(guanidinoacetamido)pyrrole -2- carboxamido -β-propionamidine Dihydrochloride (XVI)**—Compound XVI was obtained from XIII following the procedure described for the preparation of XII from IX (2% yield), mp 190–195°; UV (ethanol): λ_{max} 235 (ε 21,100) nm; IR: ν_{max} 3370, 3180, 2940, 2780, 2700, 1650, 1500, 1280, and 1120 cm^{-1}; NMR: δ 3.39 (t, 2H, *N*-CH_2), 3.74 (s, 3H, *N*-CH_3), 6.7, and 7.8 (d, 2H, aromatic H); mass spectrum: m/e 232 (53%), 219 (30), 193 (8), 181 (100), and 169 (65).

Virology—The details for the virological experiment were given previously (17).

RESULTS

The four compounds tested were nontoxic at 400 μg/ml (Table I). The most marked inhibition was shown by XIII. Isomer XI showed lower inhibition than its precursor (IX) and most of the other tripyrrole derivatives of distamycin and congocidine (17, 20).

The tripyrrole compounds tested showed less antiviral activity than distamycin A and the tripyrrole derivatives of congocidine (17, 20). Apparently, the peptide bond at positions 2 and 4 of the pyrrole rings is critical for the antiviral activity in the distamycin or congocidine series. The greatest antiviral activity in the 2,5-disubstituted pyrrole series was demonstrated by XIII, which was less toxic and had almost the same antiviral activity as distamycin A. Compound XIII is more antivirally active than similar monopyrrole homologs of distamycin A or congocidine (13, 20).

REFERENCES

(1) F. Arcamone, S. Penco, P. G. Orezzi, V. Nicollela, and A. Pirelli, *Nature*, **203**, 1064 (1964).

(2) H. Thrum, I. Haupt, G. Bradler, C. Zimmer, and K. E. Reinert, *Int. Congr. Chemother.*, **1**, A-11-9 (1971).

(3) P. Chandra, *Fortschr. Chem. Forsch.*, **52**, 99 (1974).

(4) Y. Becker, *Isr. J. Med. Sci.*, **11**, 1135 (1975).

(5) Y. Becker, "Antiviral Drugs: Mode of Action and Chemotherapy of Viral Infections of Man," Karger, Basel, Switzerland, 1976.

(6) C. Zimmer, *Progr. Nucl. Acid. Res. Mol. Biol.*, **15**, 285 (1975).

(7) F. E. Hahn, in "Antibiotics," vol. 3, J. W. Concoran and F. E. Hahn, Eds., Springer-Verlag, New York, N.Y., 1975, p. 79.

(8) D. Bassetti, *Minerva Med.*, **64**, 2077 (1973).

(9) P. Chandra, A. Gotz, A. Wacker, M. A. Verini, A. M. Casazza, A. Fioretti, F. Arcamone, and M. Ghione, *FEBS Lett.*, **19**, 327 (1972).

(10) P. Chandra, A. Gotz, A. Wacker, F. Zunino, A. Di Marco, M. A. Verini, A. M. Casazza, A. Fioretti, F. Arcamone, and M. Ghione, *Hoppe-Seylers Z. Physiol. Chem.*, **353**, 393 (1972).

(11) P. Chandra, S. Hausmann, and H. Metz, *Pharmacol. Res. Commun.*, **6**, 311 (1974).

(12) R. Arcamone, S. Penco, and F. Delle Moache, *Gazz. Chim. Ital.*, **99**, 620 (1969).

(13) F. Arcamone, V. Nicolella, S. Penco, and S. Redaelli, *ibid.*, **99**, 632 (1969).

(14) F. Arcamone, *Med. Chem. Spec. Contrib. Int. Symp.*, **34d, 1972**, 29 (1973).

(15) P. Chandra, A. Gotz, A. Wacker, M. A. Verini, A. M. Casazza, A. Fioretti, F. Arcamone, and M. Ghione, *FEBS Lett.*, **16**, 249 (1971).

(16) E. G. Werner, J. Obernmier, A. Maidhof, and R. K. Zahn, *Chem. Biol. Interact.*, **8**, 183 (1974).

(17) M. Bialer, B. Yagen, R. Mechoulam, and Y. Becker, *J. Med. Chem.*, **22**, 1296 (1979).

(18) D. H. Jones and K. R. H. Wooldridge, *J. Chem. Soc. C*, **1968**, 550.

(19) C. Zimmer, G. Luck, H. Thrum, and C. Pitra, *Eur. J. Biochem.*, **26**, 81 (1972).

(20) M. Bialer, B. Yagen, R. Mechoulam, and Y. Becker, *J. Med. Chem.*, in press.

(21) S. Penco, S. Redaelli, and F. Arcamone, *Gazz. Chim. Ital.*, **97**,

[7] Fluka, Switzerland.

1110 (1967).
(22) M. Bialer, B. Yagen, and R. Mechoulam, *Tetrahedron*, **34**, 2389 (1978).
(23) B. L. Shriner and F. W. Newmann, *Chem. Rev.*, **35**, 351 (1944).
(24) J. O. Thomas, *Tetrahedron Lett.*, **1967**, 335.
(25) M. Julia and N. Preau Joseph, *Bull. Soc. Chim. Fr.*, **1967**, 4348.
(26) K. Schofield, "Hetero-Aromatic Nitrogen Compounds, Pyrroles and Pyridines," Butterworths, London, England, 1967, p. 97.

ACKNOWLEDGMENTS

The chemical research was partially supported by the Israeli National Council on Research and Development. The virological studies were supported in part by a grant from Dr. H. Hermann, Hermal Chemie, Hamburg, West Germany.

The authors thank Jehudit Hamburger, Jael Asher, Eynat Tavor, and Yaffa Cohen for technical assistance and Mr. D. Linder for mass spectra.

NOTES

Pharmacological Disposition of Negatively Charged Phospholipid Vesicles in Rats

YIN J. KAO and TI LI LOO ×

Received January 21, 1980, from the *Department of Developmental Therapeutics, University of Texas System Cancer Center M. D. Anderson Hospital and Tumor Institute, Houston, TX 77030.* Accepted for publication May 9, 1980.

Abstract □ The pharmacological disposition of four negatively charged phospholipid vesicles with radioactive cholesteryl oleate as a tracer was investigated in rats. The acidic phospholipids included phosphatidylserine, phosphatidylglycerol, phosphatidylinositol, and diphosphatidylglycerol (cardiolipin). The blood half-life of phosphatidylserine vesicles was the shortest (<2 min), while that of phosphatidylinositol was the longest (90 min). Cardiolipin and phosphatidylglycerol vesicles had intermediate blood half-lives (7 and 18 min, respectively). The distribution of these vesicles in six major organs (liver, spleen, heart, kidneys, lungs, and brain) varied greatly. Contrary to the long-held belief, it was possible to prepare negatively charged phospholipid vesicles with long blood half-lives. Furthermore, tissue disposition of these negatively charged vesicles could be manipulated partially by judicious selection of their components.

Keyphrases □ Phospholipid vesicles, negatively charged—tissue distribution in rats □ Drug delivery systems—negatively charged phospholipid vesicles, tissue distribution in rats

Phospholipid vesicles, or liposomes when in combination with several similar preparations, are small (20–50 nm in diameter), single-bilayered, aqueous dispersions of phospholipids (1). The solutes entrapped in the closed interior aqueous compartment of phospholipid vesicles are protected from reacting with exterior chemicals. This property makes phospholipid vesicles an ideal pharmaceutical system for the *in vivo* delivery of biologically active material to target cells (2–5).

BACKGROUND

The interaction between cells and phospholipid vesicles consists of two known mechanisms (6), endocytosis and membrane fusion. Cells can take up phospholipid vesicles *via* endocytosis, producing intracellular vesicles that subsequently are degraded through fusion with lysosomes. Alternatively, phospholipid vesicles can fuse directly with the cell membrane, and the contents become incorporated into the cytoplasm. In terms of therapeutic efficacy, membrane fusion offers certain pharmacological advantages. For example, in enzyme replacement therapy in the treatment of storage disease, vesicle-entrapped enzymes retain their activity if they do not encounter the catalytic proteases in lysosomes (4).

Negatively charged phospholipids are involved in cell membrane fusion (7, 8). Vesicles prepared with negatively charged phospholipids have been used successfully to deliver biologically active chemicals to cells in culture (9). However, difficulties frequently are encountered in the *in vivo* application of negatively charged phospholipid vesicles. In plasma (or any calcium-containing medium), negatively charged liposomes sometimes aggregate to form larger particles, which are removed rapidly from circulation by the reticuloendothelial system (10). In addition, various blood proteins interact with phospholipid vesicles, and phospholipid molecules from blood lipoproteins are apt to exchange with those of the phospholipid vesicles (11, 12). These complicated interactions are expected to influence the pharmacological fate of circulating phospholipid vesicles.

These considerations prompted an investigation of the pharmacokinetics of four negatively charged phospholipid vesicles in rats, particularly since negatively charged liposomes with long blood half-lives may have enhanced bioavailability to the target tissue.

EXPERIMENTAL

Chemicals—Phosphatidylserine[1] (bovine brain), phosphatidylglycerol[1], phosphatidylinositol[1], cardiolipin[1], cholesterol[2] (chromatographically pure), cholesteryl [1-^{14}C]oleate[3] (20 mCi/mmole), and ethylenediaminetetraacetic acid disodium salt[4] were used as received. All solvents were glass distilled[5].

Liposome Preparation—Well-characterized single-bilayer vesicles were prepared by the simple method of Batzri and Korn (13). A solution of 3.75 mg of the phospholipid, 1 mg of cholesterol, and 0.05 μmole of cholesteryl [1-^{14}C]oleate (1 μCi) in 0.5 ml of chloroform was dried first under a nitrogen stream at room temperature and then in a vacuum desiccator for 2 hr at 10^{-5} torr. This procedure was essential to obtain a consistent liposome preparation.

The lipid mixtures were dissolved in 100 μl of ethanol at 37°. The ethanolic lipid solution was added as a fine stream with a 100-μl gastight

[1] Sigma Chemical Co., St. Louis, Mo.
[2] Applied Science Laboratories, State College, Pa.
[3] New England Nuclear, Boston, Mass.
[4] Matheson, Coleman and Bell, Norwood, Ohio.
[5] Burdick & Jackson Laboratories, Muskegon, Mich.

0022-3549/80/1100-1338$01.00/0
© 1980, American Pharmaceutical Association

1110 (1967).
(22) M. Bialer, B. Yagen, and R. Mechoulam, *Tetrahedron*, **34**, 2389 (1978).
(23) B. L. Shriner and F. W. Newmann, *Chem. Rev.*, **35**, 351 (1944).
(24) J. O. Thomas, *Tetrahedron Lett.*, **1967**, 335.
(25) M. Julia and N. Preau Joseph, *Bull. Soc. Chim. Fr.*, **1967**, 4348.
(26) K. Schofield, "Hetero-Aromatic Nitrogen Compounds, Pyrroles and Pyridines," Butterworths, London, England, 1967, p. 97.

ACKNOWLEDGMENTS

The chemical research was partially supported by the Israeli National Council on Research and Development. The virological studies were supported in part by a grant from Dr. H. Hermann, Hermal Chemie, Hamburg, West Germany.

The authors thank Jehudit Hamburger, Jael Asher, Eynat Tavor, and Yaffa Cohen for technical assistance and Mr. D. Linder for mass spectra.

NOTES

Pharmacological Disposition of Negatively Charged Phospholipid Vesicles in Rats

YIN J. KAO and TI LI LOO ×

Received January 21, 1980, from the *Department of Developmental Therapeutics, University of Texas System Cancer Center M. D. Anderson Hospital and Tumor Institute, Houston, TX 77030.* Accepted for publication May 9, 1980.

Abstract □ The pharmacological disposition of four negatively charged phospholipid vesicles with radioactive cholesteryl oleate as a tracer was investigated in rats. The acidic phospholipids included phosphatidylserine, phosphatidylglycerol, phosphatidylinositol, and diphosphatidylglycerol (cardiolipin). The blood half-life of phosphatidylserine vesicles was the shortest (<2 min), while that of phosphatidylinositol was the longest (90 min). Cardiolipin and phosphatidylglycerol vesicles had intermediate blood half-lives (7 and 18 min, respectively). The distribution of these vesicles in six major organs (liver, spleen, heart, kidneys, lungs, and brain) varied greatly. Contrary to the long-held belief, it was possible to prepare negatively charged phospholipid vesicles with long blood half-lives. Furthermore, tissue disposition of these negatively charged vesicles could be manipulated partially by judicious selection of their components.

Keyphrases □ Phospholipid vesicles, negatively charged—tissue distribution in rats □ Drug delivery systems—negatively charged phospholipid vesicles, tissue distribution in rats

Phospholipid vesicles, or liposomes when in combination with several similar preparations, are small (20–50 nm in diameter), single-bilayered, aqueous dispersions of phospholipids (1). The solutes entrapped in the closed interior aqueous compartment of phospholipid vesicles are protected from reacting with exterior chemicals. This property makes phospholipid vesicles an ideal pharmaceutical system for the *in vivo* delivery of biologically active material to target cells (2–5).

BACKGROUND

The interaction between cells and phospholipid vesicles consists of two known mechanisms (6), endocytosis and membrane fusion. Cells can take up phospholipid vesicles *via* endocytosis, producing intracellular vesicles that subsequently are degraded through fusion with lysosomes. Alternatively, phospholipid vesicles can fuse directly with the cell membrane, and the contents become incorporated into the cytoplasm. In terms of therapeutic efficacy, membrane fusion offers certain pharmacological advantages. For example, in enzyme replacement therapy in the treatment of storage disease, vesicle-entrapped enzymes retain their activity if they do not encounter the catalytic proteases in lysosomes (4).

Negatively charged phospholipids are involved in cell membrane fusion (7, 8). Vesicles prepared with negatively charged phospholipids have been used successfully to deliver biologically active chemicals to cells in culture (9). However, difficulties frequently are encountered in the *in vivo* application of negatively charged phospholipid vesicles. In plasma (or any calcium-containing medium), negatively charged liposomes sometimes aggregate to form larger particles, which are removed rapidly from circulation by the reticuloendothelial system (10). In addition, various blood proteins interact with phospholipid vesicles, and phospholipid molecules from blood lipoproteins are apt to exchange with those of the phospholipid vesicles (11, 12). These complicated interactions are expected to influence the pharmacological fate of circulating phospholipid vesicles.

These considerations prompted an investigation of the pharmacokinetics of four negatively charged phospholipid vesicles in rats, particularly since negatively charged liposomes with long blood half-lives may have enhanced bioavailability to the target tissue.

EXPERIMENTAL

Chemicals—Phosphatidylserine[1] (bovine brain), phosphatidylglycerol[1], phosphatidylinositol[1], cardiolipin[1], cholesterol[2] (chromatographically pure), cholesteryl [1-^{14}C]oleate[3] (20 mCi/mmole), and ethylenediaminetetraacetic acid disodium salt[4] were used as received. All solvents were glass distilled[5].

Liposome Preparation—Well-characterized single-bilayer vesicles were prepared by the simple method of Batzri and Korn (13). A solution of 3.75 mg of the phospholipid, 1 mg of cholesterol, and 0.05 μmole of cholesteryl [1-^{14}C]oleate (1 μCi) in 0.5 ml of chloroform was dried first under a nitrogen stream at room temperature and then in a vacuum desiccator for 2 hr at 10^{-5} torr. This procedure was essential to obtain a consistent liposome preparation.

The lipid mixtures were dissolved in 100 μl of ethanol at 37°. The ethanolic lipid solution was added as a fine stream with a 100-μl gastight

[1] Sigma Chemical Co., St. Louis, Mo.
[2] Applied Science Laboratories, State College, Pa.
[3] New England Nuclear, Boston, Mass.
[4] Matheson, Coleman and Bell, Norwood, Ohio.
[5] Burdick & Jackson Laboratories, Muskegon, Mich.

0022-3549/80/1100-1338$01.00/0
© 1980, American Pharmaceutical Association

Table I—Normalized Tissue Distribution of Negatively Charged Phospholipid Liposomes in Rats 90 min after Intravenous Administration [a]

Organ	Phosphatidylserine	Cardiolipin	Phosphatidylglycerol	Phosphatidylinositol
Heart	1.01 ± 0.07	1.14 ± 0.16	1.39 ± 0.10	2.09 ± 0.11[b]
Lungs	1.49 ± 0.17	2.26 ± 0.68	1.79 ± 0.35	4.81 ± 0.54[b]
Liver	94.42 ± 0.16	92.27 ± 0.41	94.51 ± 0.76	87.40 ± 0.85[b]
Spleen	1.74 ± 0.08	3.43 ± 0.39[b]	0.89 ± 0.09[b]	2.96 ± 0.56[b]
Kidneys	1.11 ± 0.06	0.74 ± 0.09	1.15 ± 0.24	1.99 ± 0.23
Brain	0.24 ± 0.05	0.15 ± 0.02	0.27 ± 0.04	0.53 ± 0.05[b]
Percent of dose recovered	45	70	40	20

[a] Each value is the mean ± *SE* of six determinations (two groups of three rats). [b] $p < 0.05$ compared with corresponding phosphatidylserine values.

microsyringe[6] to 2 ml of isotonic saline containing 10 m*M* ethylenediaminetetraacetic acid (pH 7.4) while being vortexed at 37°. Vesicles thus prepared were transparent and remained so for at least 10 hr at room temperature. However, in these experiments, liposomes always were prepared fresh on the day of use.

Pharmacokinetic Studies—Male Sprague–Dawley rats, 200–300 g, were used. Laboratory rat chow and water were provided freely. While the rat was under pentobarbital anesthesia, a 0.5-ml vesicle preparation was administered intravenously *via* the lateral tail vein. Blood samples of 100 μl were collected by clipping the tail at various intervals and then were combusted in a sample oxidizer[7]. The radioactive carbon dioxide was absorbed in 6 ml of a high-capacity carbon dioxide-absorbing solution[8], and this solution was diluted with an equal volume of xylene-based counting fluid[9]. The radioactivity of the samples was determined with a scintillation spectrometer[10]. Quenching was determined and corrected automatically with an external standard; the counting efficiency for carbon 14 was 95%.

After 90 min, the rat was killed by decapitation. The blood was drained, and the internal organs were removed, rinsed with deionized water, blotted with tissue paper, and weighed. Tissue samples were processed in the same manner as the blood except that 11 ml each of the carbon dioxide-absorbing solution and the counting fluid was used. In the phosphatidylserine study, three rats were killed at 20 min because of the short plasma half-life of the vesicles. The tissue disposition patterns were similar to those from rats killed at 90 min.

RESULTS AND DISCUSSION

The disappearance of the four negatively charged liposomes from the blood after a single intravenous administration is depicted in Fig. 1. Phosphatidylserine liposomes were eliminated quickly from the circulation; 4 min after liposome administration, the blood radioactivity decreased almost 10-fold, with the half-life estimated to be 1.2 min by nonlinear regression analysis. In contrast, phosphatidylinositol liposomes persisted much longer (half-life of 90 min); phosphatidylglycerol and cardiolipin liposomes showed half-lives of 18 and 7 min, respectively.

Table I summarizes the normalized percent distribution of radioactivity in six major organs 90 min after intravenous administration of the four liposomes. These results must be considered in light of the fraction of the administered dose recovered in these organs: 45% of phosphatidylserine, 70% of cardiolipin, 40% of phosphatidylglycerol, and 20% of phosphatidylinositol. Clearly, in all of the studies, the liver took up almost all of the radioactivity. However, although it was still high, the hepatic radioactivity of phosphatidylinositol was the lowest (87.4%) of the four liposomes. Since the recovery of the administered phosphatidylinositol also was the lowest (20%), the smallest amount of this liposome persisted in the liver 90 min after its administration.

As a major component of the reticuloendothelial system, the liver undoubtedly plays a critical role in the elimination of liposomes from the blood. Compared with the other three liposomes, phosphatidylinositol liposomes were taken up to the least extent by the liver. Consequently, their elimination from the blood is expected to be much slower than the elimination of the other liposomes. This finding is consistent with the observation that phosphatidylinositol showed the longest half-life in the blood *in vivo*.

The comparative distribution of liposomal radioactivity in the six organs is shown in Fig. 2, with the hepatic radioactivities normalized to 100%. Of the total administered radioactivity recovered, more phosphatidylinositol liposomes than any other liposomes were found in all organs except the spleen. This finding is attributed to the more protracted exposure of the organs to phosphatidylinositol liposomes due to the relatively long blood half-life of these liposomes.

The optimal application of liposomes to drug delivery depends on the mechanism of liposomal internalization. For encapsulated, biologically active chemicals that are resistant to liposomal enzyme catalysis, endocytosis may not be detrimental. However, for other drugs, particularly enzymes for replacement therapy, endocytosis may lead to their degradation by lysosomes. In contrast, fusion of the plasma membrane with liposomes can result in the release of encapsulated materials directly into the cytoplasm. Accordingly, membrane fusion would be preferred for liposomal delivery of drugs.

Negatively charged phospholipids are believed to be essential in the fusion process (8, 14). Tissue membranes that actively participate in fusion are high in negatively charged phospholipids, particularly in neural tissues in which exocytosis contributes significantly in neurotransmission (15). Liposomes recently were used as a model biomembrane system (16–18). The fusion of liposomes under defined conditions provides information on the nature of this process. Generally, the chemical properties of the phospholipid and the cation are critical to fusion. Of the

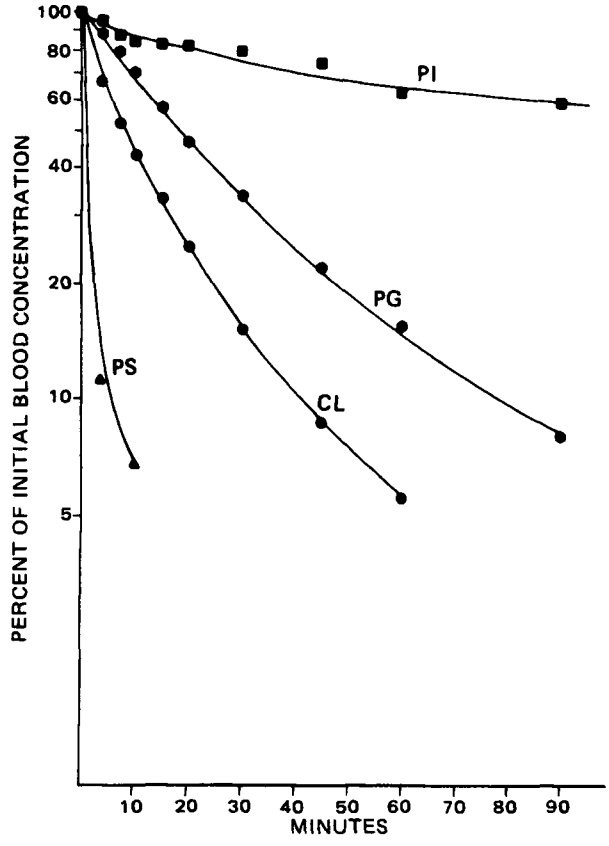

Figure 1—*Plasma disappearance of negatively charged phospholipid vesicles. Key: PS, phosphatidylserine; PG, phosphatidylglycerol; PI, phosphatidylinositol; and CL, cardiolipin. Each point represents the average value from six animals.*

[6] Hamilton.
[7] Model B306, Packard Instrument Co., Downers Grove, Ill.
[8] Carbo-sorb, Packard Instrument Co., Downers Grove, Ill.
[9] Permafluor V, Packard Instrument Co., Downers Grove, Ill.
[10] Tri-carb model 2650, Packard Instrument Co., Downers Grove, Ill.

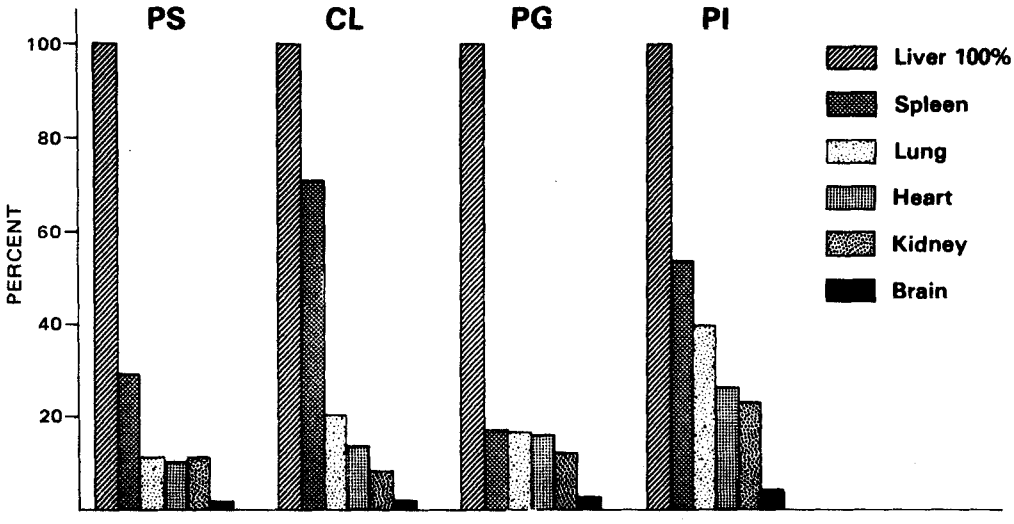

Figure 2—*Relative organ distribution of vesicle-associated radioactivities in the rat. Key: PS, phosphatidylserine; CL, cardiolipin; PG, phosphatidylglycerol; and PI, phosphatidylinositol. The liver-specific uptake was normalized to 100%. For each phospholipid, the data represent the average values from six rats (two experiments with three animals each).*

negatively charged phospholipids, phosphatidylserine fuses at the lowest cation concentration. Furthermore, among divalent cations, calcium is the most effective in inducing fusion. The free calcium concentration in plasma is ~1 m*M*. At this calcium concentration, phosphatidylserine vesicles alone, but not other negatively charged phospholipid vesicles, precipitate and cause disorganization of the membrane and leakage of the contents. This finding is consistent with the observation that the phosphatidylserine liposome blood half-life is <2 min, indicating that phosphatidylserine vesicles are not useful for drug delivery.

The various components in plasma may interact with liposomes. Some phospholipids exchange with blood lipoproteins and vesicles, and various apolipoproteins may bind to liposomes. These interactions must be quantified before a serious application of negatively charged liposomes to drug delivery can be attempted. The interactions between blood components and phosphatidylglycerol and cardiolipin liposomes probably account for their relatively short blood half-life. Although the pharmacological experiments were not designed to identify these interactions, the results suggested their existence.

Phosphatidylinositol liposomes were comparatively stable in the bloodstream since their half-life *in vivo* was the longest. Dapergolas *et al.* (19) showed that insulin encapsulated with phosphatidylinositol liposomes had hypoglycemic activity in rats when given orally. It is inferred that phosphatidylinositol liposomes can maintain their integrity in an extreme chemical environment. Because inositol, a carbohydrate, is highly hydrated in aqueous media, the bonded water molecules surrounding a phosphatidylinositol liposome may contribute to its low reactivity and thus sustain its long blood half-life.

In conclusion, based on pharmacokinetic observations of four negatively charged phospholipid vesicles in the rat, phosphatidylinositol vesicles clearly deserve further studies; they have a very long circulation half-life and a relative high uptake by organs in which the reticuloendothelial system plays a minor role.

REFERENCES

(1) C. Huang, *Biochemistry*, **8**, 344 (1969).

(2) G. Gregoriadis, *FEBS Lett.*, **36**, 292 (1973).

(3) A. D. Bangham, *Prog. Biophys. Mol. Biol.*, **18**, 29 (1968).

(4) G. Sessa and G. Weissman, *J. Biol. Chem.*, **245**, 3295 (1970).

(5) V. E. Rahman and B. J. Wright, *J. Cell Biol.*, **59**, 276 (1973).

(6) S. Batzri and E. D. Korn, *ibid.*, **66**, 621 (1975).

(7) D. Papahadjopoulos, W. J. Vail, K. Jacobson, and G. Poste, *Biochim. Biophys. Acta*, **394**, 483 (1975).

(8) M. Lao and J. H. Prestegard, *ibid.*, **550**, 157 (1979).

(9) G. Poste and D. Papahadjopoulos, *Proc. Natl. Acad. Sci. USA*, **73**, 1603 (1976).

(10) R. L. Juliano and D. Stamp, *Biochem. Biophys. Res. Commun.*, **63**, 651 (1975).

(11) D. Hoekstra and G. Scherphof, *Biochim. Biophys. Acta*, **551**, 109 (1979).

(12) L. C. Smith, H. J. Pownall, and A. M. Gotto, Jr., *Ann. Rev. Biochem.*, **47**, 751 (1978).

(13) S. Batzri and E. D. Korn, *Biochim. Biophys. Acta*, **298**, 1015 (1973).

(14) T. D. Ingolia and D. E. Koshland, Jr., *J. Biol. Chem.*, **253**, 3821 (1978).

(15) G. S. Getz, W. Bartley, D. Lurie, and B. M. Notton, *Biochim. Biophys. Acta*, **152**, 325 (1968).

(16) D. Papahadjopoulos, W. J. Vail, W. A. Pangborn, and G. Poste, *ibid.*, **448**, 265 (1976).

(17) D. Papahadjopoulos, W. J. Vail, C. Newton, S. Nir, K. Jacobson, G. Poste, and R. Lazo, *ibid.*, **465**, 579 (1977).

(18) D. P. Via, Y. J. Kao, and L. C. Smith, *Biophys. J.*, **25**, 262 (1979).

(19) G. Dapergolas, E. D. Neerunjun, and G. Gregoriadis, *FEBS Lett.*, **63**, 235 (1978).

ACKNOWLEDGMENTS

Supported by National Cancer Institute Contract N01-CM-87185 and Grant CA-11520.

High-Pressure Liquid Chromatographic Determination of Lidocaine and Its Active Deethylated Metabolites

JÉRÉMY HILL *, **ANDRÉ ROUSSIN** ‡, **JACQUES LELORIER** *‡x, and **GILLES CAILLE** *

Received January 22, 1980, from the *Department of Pharmacology, Faculty of Medicine, University of Montreal, Montreal, Quebec, Canada, and the ‡Department of Medicine, Hôtel-Dieu Hospital, Montreal, Quebec, Canada. Accepted for publication May 2, 1980.

Abstract □ A simple, specific, high-pressure liquid chromatographic method for lidocaine and its active dealkylated metabolites, monoethylglycinexylidide (I) and glycinexylidide (II), is described. Recoveries were 94% for lidocaine, 98% for I, 77% for II, and 99% for the internal standard, ethylmethylglycinexylidide (III). The sensitivity of the assay is 0.04 μg/ml. Coefficients of variation for day-to-day replicate analyses of lidocaine and the metabolites were <7%.

Keyphrases □ Lidocaine—high-pressure liquid chromatographic analysis, human plasma □ High-pressure liquid chromatography—analysis, lidocaine and active dealkylated metabolites, human plasma □ Antiarrhythmics—lidocaine, high-pressure liquid chromatographic analysis, human plasma

Lidocaine, a widely used antiarrhythmic drug, undergoes extensive metabolism in the liver. Two of its principal metabolites, monoethylglycinexylidide (I) and glycinexylidide (II), often are found in significant concentrations in plasma and both possess pharmacological and toxicological properties (1–4). The pharmacokinetic parameters of lidocaine are affected by disease states (5–7) as well as by the duration of the infusion (6, 8, 9). The elimination of I was shown to be reduced in heart failure (6, 10), and that of II was reduced in both renal (11) and heart (6) failure.

The wide interpatient variability of plasma lidocaine, I, and II levels (5, 10, 12), the narrow margin between therapeutic and toxic plasma lidocaine levels, and the possible contribution of I and II to the therapeutic and toxic effects of lidocaine warrant routine monitoring of plasma lidocaine, I, and II levels in patients receiving lidocaine infusions.

A simple, rapid, accurate, and specific analytical method for quantitating lidocaine, I, and II in plasma by high-pressure liquid chromatography (HPLC) is presented.

EXPERIMENTAL

Materials—The amounts and concentrations of lidocaine[1], I[1], II[1], and ethylmethylglycinexylidide[1] (III) are expressed as the free base. Hydrochloric acid[2] was ultrex grade. Phosphoric acid[3], monobasic potassium phosphate[3], and methylene chloride[3] were reagent grade. Acetonitrile[3] was HPLC grade.

Apparatus—The analyses were performed on a liquid chromatograph equipped with a variable-wavelength UV detector[4]. Separation was carried out on an RP-8 10-μm column[5]. The instrumental conditions included a mobile phase of 18% acetonitrile in 0.1 *M* phosphate buffer adjusted to pH 3.2 at a flow rate of 2 ml/min, and the detector was set at 195 nm.

Procedure—To 2 ml of plasma contained in a culture tube were added 0.1 ml of 0.5 *N* NaOH and 50 μl of the internal standard (III, 5 μg/100 μl). The solution was vortexed for 30 sec. Following the addition of 2.5 ml of methylene chloride, the mixture was shaken for 10 min on a reciprocating shaker and then centrifuged at 3500 rpm. The aqueous phase was discarded; the organic phase was dried over anhydrous sodium sulfate and transferred to a second culture tube, to which was added 0.5 ml of 0.01 *N* HCl. The mixture was shaken for 60 min on a reciprocating shaker and centrifuged, and 150 μl of the aqueous phase was injected into the chromatograph.

Standard samples were prepared by spiking human plasma with increasing concentrations of lidocaine (0.1, 0.4, 0.8, 2, 3, 4, and 5 μg/ml) and the metabolites (0.04, 0.16, 0.32, 0.8, 1.2, 1.6, and 2 μg/ml). Calibration curves, which were identical whether prepared in plasma or in water, were constructed by plotting the ratios of the peak heights of lidocaine, I, and II to the peak height of the internal standard against the concentrations of lidocaine, I, and II.

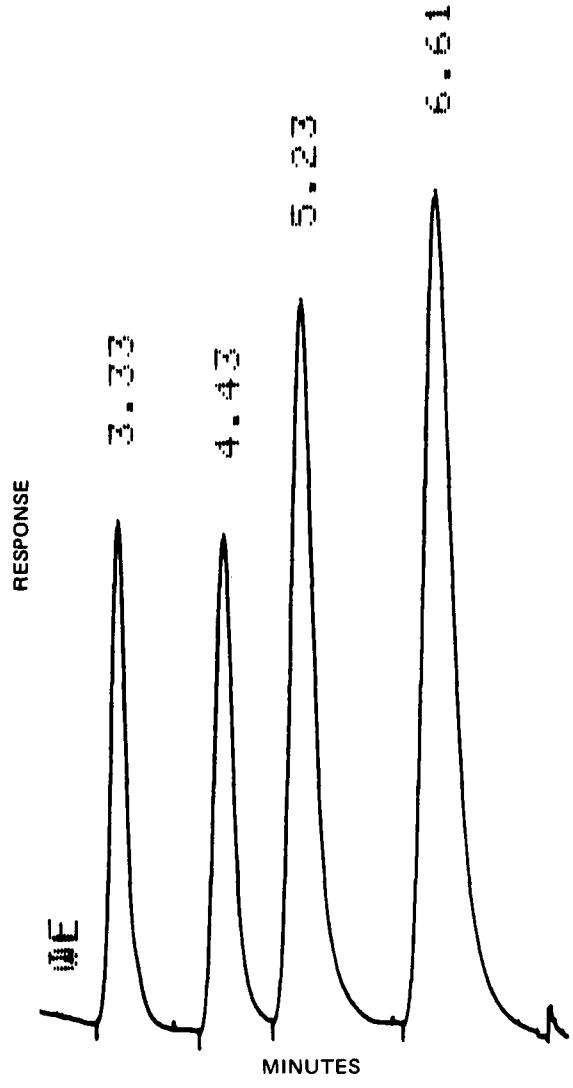

Figure 1—*Typical chromatogram. The retention times were 3.33 min for I (0.53 μg/ml), 4.43 min for II (0.60 μg/ml), 5.23 min for III, and 6.61 min for lidocaine (2.35 μg/ml).*

[1] Astra Pharmaceuticals.
[2] J. T. Baker Chemical Co.
[3] Fisher Scientific Co.
[4] Hewlett-Packard series 1084.
[5] Hewlett-Packard Co.

0022-3549/80/1100-1341$01.00/0
© 1980, American Pharmaceutical Association

Table I—Day-to-Day Reproducibility

Compound	Plasma Concentration, μg/ml	n	CV, %
Lidocaine	2.0	22	4.8
	0.8	11	3.0
I	0.8	22	2.2
	0.32	11	4.1
II	0.8	21	3.5
	0.32	10	6.8

Analytical recovery of lidocaine and I–III was determined by comparing the peak areas obtained by direct injection of standard aqueous solutions with those obtained from the injection of the same standard solutions after running them through the extraction procedure. Three samples were run at each of the seven different concentrations.

Blood samples were obtained from 75 patients receiving lidocaine for therapeutic or prophylactic indications and were analyzed by both the presently described method and by a GLC method (13).

RESULTS AND DISCUSSION

The standard curves were linear throughout the ranges studied (r^2 = 0.998, 0.999, and 0.998 for lidocaine, I, and II, respectively). The average ($\pm SD$) analytical recoveries were 94.3 ± 3.4% for lidocaine, 98.4 ± 4.1% for I, 77.2 ± 2.7% for II, and 99.7 ± 2.1% for III. The retention times were 3.33, 4.43, 5.23, and 7.01 min for II, I, III, and lidocaine, respectively. The day-to-day reproducibility of replicate analyses of standard plasma samples containing different concentrations of lidocaine, I, and II is presented in Table I. A typical chromatogram is shown in Fig. 1.

Concomitantly administered drugs included digoxin, propranolol, procainamide, nitroglycerin, carbamazepine, diazepam, flurazepam, isosorbide dinitrate, chlorpropamide, dipyridamole, allopurinol, methyldopa, furosemide, spironolactone, sulfinpyrazone, hydrochlorothiazide, hydralazine, morphine, aspirin, and oxazepam. None interfered with the assay. The sensitivity of the assay is 0.04 μg/ml, and a concentration as low as 0.01 μg/ml can be detected in the plasma.

The least-squares regression analysis of the data for the GLC method (X) *versus* the presently described method (Y) gave the following results: Y intercept, 0.08; slope, 0.99; r^2, 0.99; and S_Y, 0.57. These results suggest that the HPLC method is relatively free of significant systematic errors (14).

Plasma levels of II in one patient whose myocardial infarction was complicated by severe heart failure rose progressively, attaining 3.2 μg/ml on the 5th day of continuous lidocaine therapy. The corresponding lidocaine and I levels were 2.4 and 0.5 μg/ml, respectively. The infusion rate was 20 μg/kg/min, and there were no signs of lidocaine toxicity. The relatively low lidocaine concentration in this patient was surprising since previous work in this (9) and other (6) laboratories indicated that both heart failure and prolonged infusions should produce plasma lidocaine concentrations of 4 μg/ml at an infusion rate of 20 μg/kg/min.

The highest level of I (1.5 μg/ml) recorded was in another myocardial infarction patient with heart failure after 19 hr of continuous lidocaine infusion (35 μg/kg/min). In this patient, the plasma lidocaine concentration was 5.2 μg/ml and the concentration of II was 0.70 μg/ml. Immediately after the sample was taken, the infusion was ceased, and samples were taken hourly (Fig. 2). The lidocaine concentration fell exponentially to 0.16 μg/ml after 12 hr ($t_{1/2}$, 141 min), and the concentration of I also appeared to decline exponentially, reaching 0.23 μg/ml after 12 hr. The concentration of II was still 0.59 μg/ml 12 hr later. The half-lives cannot be determined for the metabolites from the slopes of their plasma disappearance curves since they are both synthesized from lidocaine and eliminated during the sampling period. This patient recently had suffered a stroke, rendering evaluation of possible neurological toxic effects difficult.

The elevated levels of metabolites in heart failure were reported by other investigators. Prescott *et al.* (6) reported progressively rising I and II levels in patients in whom the myocardial infarction was complicated by heart failure. Halkin *et al.* (10) found higher I levels in patients with heart failure but did not measure II levels. Narang *et al.* (15) described one patient with mild congestive heart failure whose I level was 183% of that of lidocaine (lidocaine, 1.38 μg/ml; I, 2.53 μg/ml), thus contributing more than unchanged lidocaine to the antiarrhythmic effect.

Few conclusions can be drawn concerning the relative contributions of I and II to the pharmacological and toxic effects of lidocaine therapy because their concentrations have been measured in only a limited number of patients. The availability of this method, as well as other HPLC and GLC methods (15–19) that simultaneously measure lidocaine, I, and II, should result in further studies of lidocaine and its active metabolites.

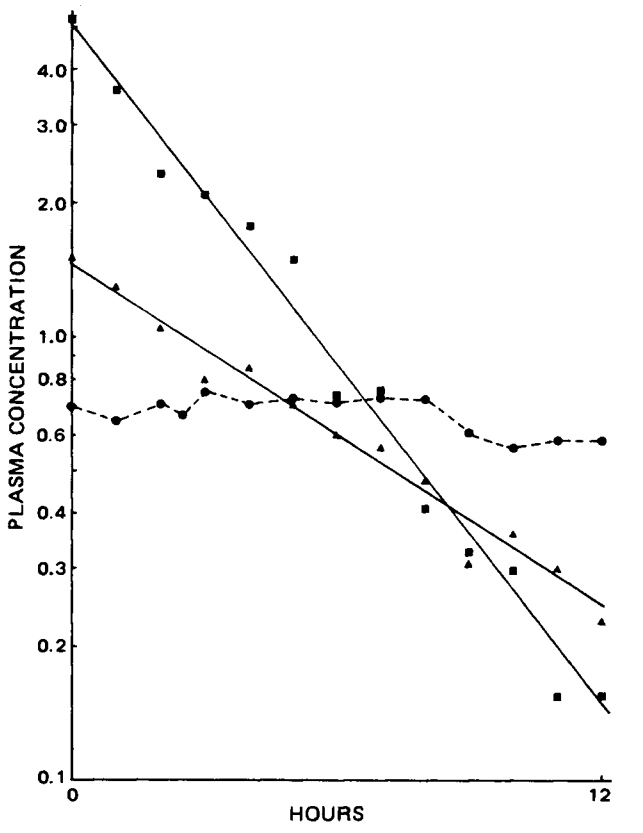

Figure 2—*Plasma concentrations of lidocaine (■), II (▲), and I (●) over the 12-hr period immediately following cessation of the lidocaine infusion.*

REFERENCES

(1) J. Blumer, J. M. Strong, and A. J. Atkinson, Jr., *J. Pharmacol. Exp. Ther.*, **186**, 31 (1973).

(2) R. G. Burney and C. A. Difazio, *Am. Heart J.*, **88**, 765 (1974).

(3) E. R. Smith and B. R. Duce, *J. Pharmacol. Exp. Ther.*, **179**, 580 (1971).

(4) J. M. Strong, D. E. Mayfield, A. J. Atkinson, Jr., B. E. Harris, F. Raymond, and L. T. Webster, Jr., *Clin. Pharmacol. Ther.*, **17**, 184 (1975).

(5) R. L. Nation and E. J. Triggs, *Br. J. Clin. Pharmacol.*, **4**, 439 (1977).

(6) L. F. Prescott, K. K. Adjepon-Yamoah, and R. B. Talbot, *Br. Med. J.*, **1**, 939 (1976).

(7) P. D. Thompson, K. L. Melmon, J. A. Richardson, K. Cohn, W. Steinbrunn, R. Cudihee, and M. Rowland, *Ann. Intern. Med.*, **78**, 499 (1973).

(8) J. LeLorier, R. Moisan, J. Gagné, and G. Caillé, *J. Pharmacol. Exp. Ther.*, **203**, 507 (1977).

(9) J. LeLorier, D. Grenon, Y. Latour, G. Caillé, G. Dumont, A. Brosseau, and A. Solignac, *Ann. Intern. Med.*, **87**, 700 (1977).

(10) H. Halkin, P. Meffin, K. L. Melmon, and M. Rowland, *Clin. Pharmacol. Ther.*, **17**, 669 (1975).

(11) K. A. Collinsworth, J. M. Strong, A. J. Atkinson, Jr., R. A. Winkle, F. Perlroth, and D. C. Harrison, *ibid.*, **18**, 59 (1975).

(12) J. M. Strong, M. Parker, and A. J. Atkinson, Jr., *ibid.*, **14**, 67 (1973).

(13) G. Caillé, J. LeLorier, Y. Latour, and J. G. Besner, *J. Pharm. Sci.*, **66**, 1383 (1977).

(14) J. O. Westgaid and M. R. Hunt, *Clin. Chem.*, **19**, 49 (1973).

(15) P. K. Narang, W. G. Crouthamel, N. H. Carliner, and M. L. Fisher, *Clin. Pharmacol. Ther.*, **24**, 654 (1978).

(16) R. L. Nation, G. W. Peng, and W. L. Chiou, *J. Chromatogr.*, **162**, 466 (1979).
(17) M. J. Rosseel and M. G. Bogaert, *ibid.*, **154**, 99 (1978).
(18) J. L. Wisnicki, W. P. Tong, and D. B. Ludlum, *Clin. Chim. Acta*, **93**, 279 (1979).
(19) K. K. Adjepon-Yamoah and L. F. Prescott, *J. Pharm. Pharmacol.*, **26**, 889 (1974).

ACKNOWLEDGMENTS

The authors thank Claudette Lamoureux and Doris Roy for technical assistance.

Synthesis and Structure–Activity Relationship of a Pyrimido[4,5-*d*]pyrimidine Derivative with Antidepressant Activity

J. L. BERNIER *x, J. P. HENICHART *, V. WARIN ‡, and F. BAERT ‡

Received April 10, 1979, from **INSERM U16, Place de Verdun, 59045 Lille Cedex, France*, and the ‡*Laboratoire de Dynamique des cristaux moléculaires associé au CNRS (ERA 465), Bât. P.5, Université des Sciences et Techniques de Lille, 59650 Villeneuve d'Ascq, France.* Accepted for publication May 2, 1980.

Abstract □ The synthesis and antidepressant properties of a new pyrimido[4,5-*d*]pyrimidine are described. Spectral data determined in solution and in the solid state allowed establishment of the relationship between the activity and the conformation of the molecule. The spatial structure seems to be in accordance with a possible binding at the presynaptic α-receptor sites.

Keyphrases □ Pyrimido[4,5-*d*]pyrimidines—synthesis and evaluation for antidepressant activity, binding at presynaptic α-receptor sites, structure–activity relationships □ Structure–activity relationships—pyrimido[4,5-*d*]pyrimidines, synthesis and evaluation for antidepressant activity, binding at presynaptic α-receptor sites □ Antidepressant activity—pyrimido[4,5-*d*]pyrimidines, synthesis and evaluation for antidepressant activity, binding at presynaptic α-receptor sites, structure–activity relationships

The basic assumptions in the analysis of a structure–activity relationship are that the drug and the receptor exhibit mutual complementarity and that the study of drug conformation yields information relevant to the geometry of the binding sites of the receptors. As a continuation of studies on 1,3-dimethyl-2,4-dioxo-6-substituted octahydropyrimido[4,5-*d*]pyrimidines (1), the particular behavior of the 6-benzyl derivative (I) was evaluated. This compound appears to possess significant antidepressant activity. Antidepressant drugs containing the pyrimido[4,5-*d*]pyrimidine ring system have not been described. In addition, the apparent importance of the benzyl moiety[1] in inducing such properties prompted the establishment of relationships between three-dimensional molecular structure and pharmacological response.

The mechanism of action of antidepressant drugs has been studied recently (2). It is generally accepted that the therapeutic effect of antidepressant agents may be a consequence of an increased availability of norepinephrine at postsynaptic sites. A 3-week administration of tricyclic antidepressant drugs gradually decreased the sensitivity of the presynaptic α-receptor (3), which would explain the delay in the onset of the clinical effect. On the other hand,

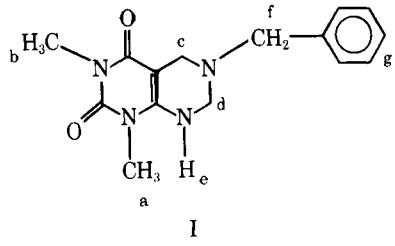

I

the feedback inhibition of brain norepinephrine neurons by tricyclic antidepressants was due to an α-receptor mediation (4). This finding would explain the increase of the availability of norepinephrine at postsynaptic receptor sites after an antidepressant treatment. A correlation may be postulated between antidepressant activity and the action of the drug at the α-adrenergic receptors.

EXPERIMENTAL[2]

1,3-Dimethyl-2,4-dioxo-6-benzyl-1,2,3,4,5,6,7,8-octahydropyrimido[4,5-*d*]pyrimidine (I)—To an ethanolic solution of 9 g (0.06 mole) of 1,3-dimethyl-6-aminouracil were added successively 8.5 g (0.08 mole) of benzylamine and 12 ml of 35% aqueous formaldehyde (0.12 mole) solution. The mixture was stirred and heated under reflux for 2 hr and then concentrated *in vacuo* to dryness. The residual solid was washed with acetone and recrystallized from ethanol to give 14 g (81%) of white crystals. Further recrystallization from ethanol gave an analytical sample, mp 160°; IR(KBr pellets): 1630 and 1690 (C=O), 3150 (NH), and 2750 and 2810 (CH_2) cm^{-1}; PMR (dimethyl sulfoxide-d_6): δ 3.23 (s, 3H, CH_3a), 3.36 (s, 3H, CH_3b), 3.75 (s, 2H, CH_2c), 4.15 (d, 2H, CH_2d), 7.48 (t, 1H, J_{d-e} = 3 Hz, NHe), 3.56 (s, 2H, CH_2f), and 7.56 (s, 5H, phenyl g) ppm.

Anal.—Calc. for $C_{15}H_{18}N_4O_2$: C, 62.92; H, 6.34; N, 19.56. Found: C, 62.88; H, 6.33; N, 19.56.

Pharmacological Assays—Compound I was subjected to the classical tests for psychopharmacological effects. The central nervous system (CNS) activity was evaluated first as described by Irwin (5). Graded doses were given to groups of five mice, and the animals were observed con-

[1] Other pyrimido[4,5-*d*]pyrimidines with a 6-alkyl or aryl group were devoid of such activity (1).

[2] Melting points were determined with a Büchi capillary melting-point apparatus and are uncorrected. PMR spectra were obtained with a Jeol-MH 60 spectrometer using tetramethylsilane as the internal standard. IR spectra were recorded on a Perkin-Elmer 177 spectrometer. Crystallographic data were collected on a Philips PW 1100 diffractometer with graphite monochromated *M* kα radiation at room temperature. Elemental analyses were performed with a Perkin-Elmer CHN 240 instrument.

0022-3549/80/1100-1343$01.00/0
© 1980, American Pharmaceutical Association

(16) R. L. Nation, G. W. Peng, and W. L. Chiou, *J. Chromatogr.*, **162**, 466 (1979).
(17) M. J. Rosseel and M. G. Bogaert, *ibid.*, **154**, 99 (1978).
(18) J. L. Wisnicki, W. P. Tong, and D. B. Ludlum, *Clin. Chim. Acta*, **93**, 279 (1979).
(19) K. K. Adjepon-Yamoah and L. F. Prescott, *J. Pharm. Pharmacol.*, **26**, 889 (1974).

ACKNOWLEDGMENTS

The authors thank Claudette Lamoureux and Doris Roy for technical assistance.

Synthesis and Structure–Activity Relationship of a Pyrimido[4,5-*d*]pyrimidine Derivative with Antidepressant Activity

J. L. BERNIER *x, J. P. HENICHART *, V. WARIN ‡, and F. BAERT ‡

Received April 10, 1979, from **INSERM U16, Place de Verdun, 59045 Lille Cedex, France*, and the ‡*Laboratoire de Dynamique des cristaux moléculaires associé au CNRS (ERA 465), Bât. P.5, Université des Sciences et Techniques de Lille, 59650 Villeneuve d'Ascq, France.* Accepted for publication May 2, 1980.

Abstract □ The synthesis and antidepressant properties of a new pyrimido[4,5-*d*]pyrimidine are described. Spectral data determined in solution and in the solid state allowed establishment of the relationship between the activity and the conformation of the molecule. The spatial structure seems to be in accordance with a possible binding at the presynaptic α-receptor sites.

Keyphrases □ Pyrimido[4,5-*d*]pyrimidines—synthesis and evaluation for antidepressant activity, binding at presynaptic α-receptor sites, structure–activity relationships □ Structure–activity relationships—pyrimido[4,5-*d*]pyrimidines, synthesis and evaluation for antidepressant activity, binding at presynaptic α-receptor sites □ Antidepressant activity—pyrimido[4,5-*d*]pyrimidines, synthesis and evaluation for antidepressant activity, binding at presynaptic α-receptor sites, structure–activity relationships

The basic assumptions in the analysis of a structure–activity relationship are that the drug and the receptor exhibit mutual complementarity and that the study of drug conformation yields information relevant to the geometry of the binding sites of the receptors. As a continuation of studies on 1,3-dimethyl-2,4-dioxo-6-substituted octahydropyrimido[4,5-*d*]pyrimidines (1), the particular behavior of the 6-benzyl derivative (I) was evaluated. This compound appears to possess significant antidepressant activity. Antidepressant drugs containing the pyrimido[4,5-*d*]pyrimidine ring system have not been described. In addition, the apparent importance of the benzyl moiety[1] in inducing such properties prompted the establishment of relationships between three-dimensional molecular structure and pharmacological response.

The mechanism of action of antidepressant drugs has been studied recently (2). It is generally accepted that the therapeutic effect of antidepressant agents may be a consequence of an increased availability of norepinephrine at postsynaptic sites. A 3-week administration of tricyclic antidepressant drugs gradually decreased the sensitivity of the presynaptic α-receptor (3), which would explain the delay in the onset of the clinical effect. On the other hand,

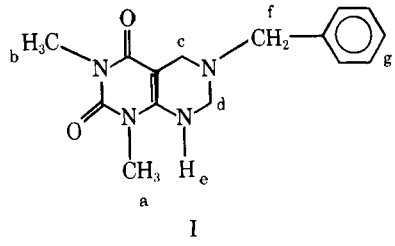

I

the feedback inhibition of brain norepinephrine neurons by tricyclic antidepressants was due to an α-receptor mediation (4). This finding would explain the increase of the availability of norepinephrine at postsynaptic receptor sites after an antidepressant treatment. A correlation may be postulated between antidepressant activity and the action of the drug at the α-adrenergic receptors.

EXPERIMENTAL[2]

1,3-Dimethyl-2,4-dioxo-6-benzyl-1,2,3,4,5,6,7,8-octahydropyrimido[4,5-*d*]pyrimidine (I)—To an ethanolic solution of 9 g (0.06 mole) of 1,3-dimethyl-6-aminouracil were added successively 8.5 g (0.08 mole) of benzylamine and 12 ml of 35% aqueous formaldehyde (0.12 mole) solution. The mixture was stirred and heated under reflux for 2 hr and then concentrated *in vacuo* to dryness. The residual solid was washed with acetone and recrystallized from ethanol to give 14 g (81%) of white crystals. Further recrystallization from ethanol gave an analytical sample, mp 160°; IR(KBr pellets): 1630 and 1690 (C=O), 3150 (NH), and 2750 and 2810 (CH_2) cm^{-1}; PMR (dimethyl sulfoxide-d_6): δ 3.23 (s, 3H, CH_3a), 3.36 (s, 3H, CH_3b), 3.75 (s, 2H, CH_2c), 4.15 (d, 2H, CH_2d), 7.48 (t, 1H, J_{d-e} = 3 Hz, NHe), 3.56 (s, 2H, CH_2f), and 7.56 (s, 5H, phenyl g) ppm.

Anal.—Calc. for $C_{15}H_{18}N_4O_2$: C, 62.92; H, 6.34; N, 19.56. Found: C, 62.88; H, 6.33; N, 19.56.

Pharmacological Assays—Compound I was subjected to the classical tests for psychopharmacological effects. The central nervous system (CNS) activity was evaluated first as described by Irwin (5). Graded doses were given to groups of five mice, and the animals were observed con-

[1] Other pyrimido[4,5-*d*]pyrimidines with a 6-alkyl or aryl group were devoid of such activity (1).

[2] Melting points were determined with a Büchi capillary melting-point apparatus and are uncorrected. PMR spectra were obtained with a Jeol-MH 60 spectrometer using tetramethylsilane as the internal standard. IR spectra were recorded on a Perkin-Elmer 177 spectrometer. Crystallographic data were collected on a Philips PW 1100 diffractometer with graphite monochromated *M* kα radiation at room temperature. Elemental analyses were performed with a Perkin-Elmer CHN 240 instrument.

0022-3549/80/1100-1343$01.00/0
© 1980, American Pharmaceutical Association

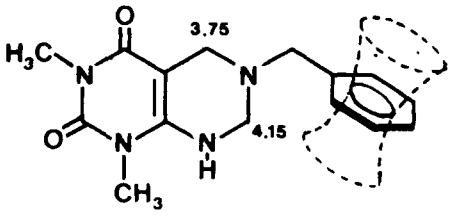

I

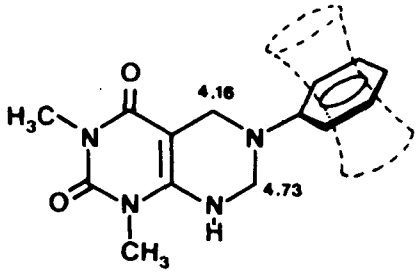

II

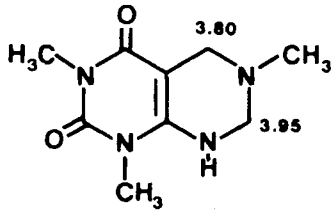

III

Figure 1—*Computer drawn perspective view of I.*

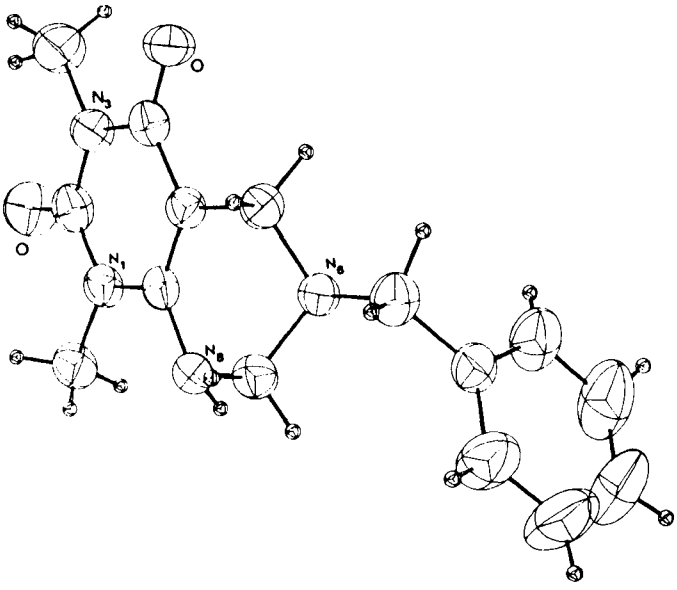

Figure 2—*Comparison between the chemical shifts of the* c *proton (and* d *proton) for different 8-substituted pyrimidopyrimidines.*

tinuously over 6 hr. Lethality and delayed effects were noted 24 hr after drug administration.

Tests for Neurological Deficit—*Activity Chambers (6)*—Sedative activity was measured in groups of 10 mice housed singly in photobeam cages. The number of beam interruptions occurring during the 60-min periods immediately prior to and after dosing was recorded.

Traction Test (7)—The percentage of mice unable to climb onto a wire and balance themselves within 5 sec after being suspended by the forepaws was determined 60 min after administration of the test compound.

Forced Motor Activity (8)—This activity was evaluated by the use of a rod revolving at 14 rpm. The number of mice remaining on the rod for >1 min was used as the measure.

Anticonvulsant Activity—*Convulsions from Pentylenetetrazol (9)*—Pentylenetetrazol was administered in a convulsifying dose (125 mg/kg ip) to groups of 10 mice pretreated for 1 hr with the test compound. Animals that did not have any tonic–clonic attack for 30 min after the pentylenetetrazol were considered to be protected.

Convulsions from Electroshock (10)—The effect of the compound on the maximal electroshock seizure was investigated in mice after intraperitoneal administration. The stimulation was carried out by means of corneal electrodes at 30 mamp for 0.2 sec. The percentage of mice protected from the tonic phase of the seizure was recorded.

Antipsychotic Activity (11)—The ability to reverse a conflict of motivation between exploration and punishment was assessed. The floor of the cage was divided into four plates. When a mouse went from one plate to another, it was subjected to an electrical shock.

Prevention of Prochlorperazine-Induced Catalepsy (12)—This measurement was used as an index of antidepressant activity. Groups of five rats were pretreated with prochlorperazine (10 mg/kg sc); 5.5 hr later, they were treated with the test compound having anticataleptic activity. The test compound was given again 0.5, 1.5, and 2.5 hr thereafter.

***d*-Amphetamine-Induced Lethality (13)**—*d*-Amphetamine-induced lethality was used to evaluate antipsychotic activity. Mice were medicated orally with test drugs 0.5 hr before intraperitoneal injection of *d*-amphetamine (20 mg of the free base/kg). Deaths were recorded during the following 4 hr.

RESULTS

The Irwin test (5) showed that I was not toxic up to 300 mg/kg po. No peculiar symptomatology was observed. Compound I had no effect on the motor activity for mice at a dose of 100 mg/kg (6). At the same dose,

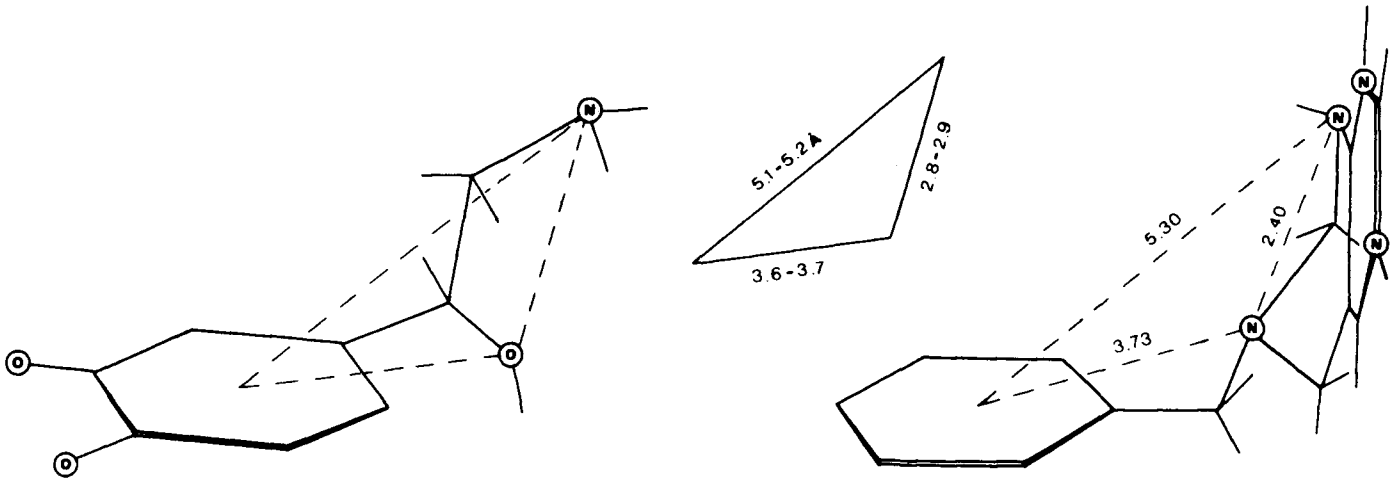

Figure 3—*Proposed binding mode at α-adrenergic receptor sites for norepinephrine and I.*

traction (7) and equilibration (8) reflexes were not changed, and pentylenetetrazol- or electroshock-induced convulsive effects (9, 10) were not antagonized. No anxiolytic activity was observed until 30 mg/kg was administered (11). No central anticholinergic action was noted at 100 mg/kg by the classical antipilocarpine test in rats (14).

Prochlorperazine-induced catalepsy (13) was inhibited at the ED_{50} value of 30 mg/kg ($p \leq 0.05$, Student t test). The amphetaminic group toxicity effect was potentiated at 50 mg/kg (13). Thus, the results reported here suggest that I may be a significant and selective antidepressant compound.

Structural Determinations—The crystal data were: space group P2/C; a = 7.109(3), b = 12.766(3), and c = 16.110(4) Å; β = 97.52(5); V = 1395.2 Å^3; Z = 4; D_c = 1.33; and R = 0.052.

The distances between the center of the phenyl ring and N-6 and N-8 atoms are 3.73 and 5.30 Å, respectively (Fig. 1). The interatomic distance[3] between N-6 and N-8 is 2.40 Å.

PMR Spectrographic Results—The shifts (expressed in δ parts per million using deuterated dimethyl sulfoxide as the solvent) (Fig. 2) corresponding to the methylene protons (c and d) of I were designed unambiguously and compared to shifts reported previously for other compounds (II and III) (1).

The chemical shifts of protons c and d unequivocally indicate that the anisotropic cone of the phenyl ring is closed to proton d (deshielding effect) and that, in solution, I exhibits a privileged conformation in accordance with that observed in the solid state.

DISCUSSION

A number of binding sites at the receptor are known to be important for α-adrenergic activity: the catechol moiety, the β-hydroxyl group, and the ammonium function (Fig. 3). The extended Hückel theory (16) and the perturbative configuration interaction using localized orbitals (17, 18) calculations have permitted postulation of the distance between the center of the aryl ring and the oxygen atom (3.6–3.7 Å), the center of the ring and the nitrogen atom (5.1–5.2 Å), and the nitrogen–oxygen distance (2.8–2.9 Å) as the main characteristics of the molecule binding the α-adrenergic receptor sites.

The spatial configuration of I fits this proposed model.

It can be concluded that I displays structural features making it suitable for binding the presynaptic receptor sites. Nevertheless, I cannot activate them; the bulky group attached to the nitrogen atom accounts for this inhibition. As such, when it partially occupies the site, it hinders the feedback inhibition of norepinephrine, increasing its release in the synaptic cleft. This effect could account for its pharmacological properties and provides information on the activity of certain antidepressant drugs.

[3] Full details concerning the crystallographic data (interatomic distances, angles, and coordinates) are available (15).

REFERENCES

(1) J. L. Bernier, A. Lefebvre, C. Lespagnol, J. Navarro, A. Pério, and E. Vallée, *Eur. J. Med. Chem.*, **12**, 239 (1977).

(2) F. Sulser, J. Vetulani, and P. L. Mobley, *Biochem. Pharmacol.*, **27**, 257 (1978).

(3) F. T. Crews and C. B. Smith, *Science*, **202**, 322 (1978).

(4) T. H. Svensson and T. Usdin, *ibid.*, **202**, 1091 (1978).

(5) S. Irwin, *Psychopharmacologia*, **13**, 222 (1968).

(6) J. R. Boissier and P. Simon, *Arch. Int. Pharmacodyn. Ther.*, **158**, 212 (1965).

(7) J. R. Boissier and P. Simon, *Thérapie*, **15**, 1170 (1960).

(8) H. Van Riezen and L. Boersma, *Eur. J. Pharmacol.*, **6**, 353 (1969).

(9) G. Chen, *Proc. Soc. Exp. Biol. Med.*, **87**, 334 (1954).

(10) R. E. Tedeschi, D. H. Tedeschi, A. Mucha, L. Cook, P. A. Mattis, and E. J. Fellows, *J. Pharmacol. Exp. Ther.*, **125**, 28 (1959).

(11) C. Aron-Samuel, Thèse, Fac. Médecine, Paris, France, 1970.

(12) J. R. Boissier and P. Simon, *Thérapie*, **18**, 1257 (1963).

(13) D. N. Johnson and W. H. Furderburk, *Fed. Proc. Fed. Am. Soc. Exp. Biol.*, **33**, 285 (1974).

(14) P. A. J. Janssen and C. J. E. Niemegeers, *Psychopharmacologia*, **11**, 231 (1967).

(15) V. Warin, F. Baert, M. Lobry, J. L. Bernier, and J. P. Hénichart, *Acta Crystallogr. Sect. B*, **35**, 2165 (1979).

(16) L. B. Kier, *J. Pharmacol. Exp. Ther.*, **164**, 75 (1968).

(17) B. Pullman, J. L. Coubeils, P. Courrière, and J. P. Gervois, *J. Med. Chem.*, **15**, 17 (1972).

(18) J. L. Coubeils, P. Courrière, and B. Pullman, *J. Med. Chem.*, **15**, 453 (1972).

ACKNOWLEDGMENTS

The authors thank A. Pério, Clin-Midy Laboratory, Montpellier, France, for the pharmacological assays.

Effect of Sodium Oleate on Salicylic Acid Binding to Human Serum Albumin

PETER A. SCHWARTZ, DOUGLAS S. GREENE, and C. T. RHODES ˣ

Received January 3, 1980, from the *Department of Pharmacy, College of Pharmacy, University of Rhode Island, Kingston, RI 02881.* Accepted for publication May 19, 1980.

Abstract □ The pharmacological activity of salicylates is related to the nonprotein-bound fraction of drug in the plasma. Free fatty acids have been shown to displace bound drug and to increase the serum levels of salicylates. Continuous ultrafiltration was used to measure unbound salicylic acid at 37°. A nonlinear analysis of the ultrafiltration data using whole number values for the number of binding sites indicates that sodium oleate displaces the salicylic acid competitively at both binding sites. Increased concentrations of fatty acids due to disease or the infusion of fatty acid emulsions perhaps may produce toxic levels of salicylic acid.

Keyphrases □ Sodium oleate—effect on binding of salicylic acid to human serum albumin □ Salicylic acid—binding to human serum albumin, effect of sodium oleate □ Protein binding—effect of sodium oleate on binding of salicylic acid to human serum albumin

Since the pharmacological activity of many drugs is related to the non-protein-bound fraction of the drug in plasma (1–3), any decrease in the fraction of protein-bound drug may be expected to result in an increased pharmacological effect. Free fatty acids bind rapidly to albumin at more than one site (4–6), have a higher affinity for albumin than do most drugs (7, 8), and increase the concentration of unbound drug *in vivo* by displacement of

0022-3549/80/1100-1345$01.00/0

© 1980, American Pharmaceutical Association

traction (7) and equilibration (8) reflexes were not changed, and pentylenetetrazol- or electroshock-induced convulsive effects (9, 10) were not antagonized. No anxiolytic activity was observed until 30 mg/kg was administered (11). No central anticholinergic action was noted at 100 mg/kg by the classical antipilocarpine test in rats (14).

Prochlorperazine-induced catalepsy (13) was inhibited at the ED_{50} value of 30 mg/kg ($p \leq 0.05$, Student t test). The amphetaminic group toxicity effect was potentiated at 50 mg/kg (13). Thus, the results reported here suggest that I may be a significant and selective antidepressant compound.

Structural Determinations—The crystal data were: space group P2/C; a = 7.109(3), b = 12.766(3), and c = 16.110(4) Å; β = 97.52(5); V = 1395.2 Å^3; Z = 4; D_c = 1.33; and R = 0.052.

The distances between the center of the phenyl ring and N-6 and N-8 atoms are 3.73 and 5.30 Å, respectively (Fig. 1). The interatomic distance[3] between N-6 and N-8 is 2.40 Å.

PMR Spectrographic Results—The shifts (expressed in δ parts per million using deuterated dimethyl sulfoxide as the solvent) (Fig. 2) corresponding to the methylene protons (c and d) of I were designed unambiguously and compared to shifts reported previously for other compounds (II and III) (1).

The chemical shifts of protons c and d unequivocally indicate that the anisotropic cone of the phenyl ring is closed to proton d (deshielding effect) and that, in solution, I exhibits a privileged conformation in accordance with that observed in the solid state.

DISCUSSION

A number of binding sites at the receptor are known to be important for α-adrenergic activity: the catechol moiety, the β-hydroxyl group, and the ammonium function (Fig. 3). The extended Hückel theory (16) and the perturbative configuration interaction using localized orbitals (17, 18) calculations have permitted postulation of the distance between the center of the aryl ring and the oxygen atom (3.6–3.7 Å), the center of the ring and the nitrogen atom (5.1–5.2 Å), and the nitrogen–oxygen distance (2.8–2.9 Å) as the main characteristics of the molecule binding the α-adrenergic receptor sites.

The spatial configuration of I fits this proposed model.

It can be concluded that I displays structural features making it suitable for binding the presynaptic receptor sites. Nevertheless, I cannot activate them; the bulky group attached to the nitrogen atom accounts for this inhibition. As such, when it partially occupies the site, it hinders the feedback inhibition of norepinephrine, increasing its release in the synaptic cleft. This effect could account for its pharmacological properties and provides information on the activity of certain antidepressant drugs.

[3] Full details concerning the crystallographic data (interatomic distances, angles, and coordinates) are available (15).

REFERENCES

(1) J. L. Bernier, A. Lefebvre, C. Lespagnol, J. Navarro, A. Pério, and E. Vallée, *Eur. J. Med. Chem.*, **12**, 239 (1977).

(2) F. Sulser, J. Vetulani, and P. L. Mobley, *Biochem. Pharmacol.*, **27**, 257 (1978).

(3) F. T. Crews and C. B. Smith, *Science*, **202**, 322 (1978).

(4) T. H. Svensson and T. Usdin, *ibid.*, **202**, 1091 (1978).

(5) S. Irwin, *Psychopharmacologia*, **13**, 222 (1968).

(6) J. R. Boissier and P. Simon, *Arch. Int. Pharmacodyn. Ther.*, **158**, 212 (1965).

(7) J. R. Boissier and P. Simon, *Thérapie*, **15**, 1170 (1960).

(8) H. Van Riezen and L. Boersma, *Eur. J. Pharmacol.*, **6**, 353 (1969).

(9) G. Chen, *Proc. Soc. Exp. Biol. Med.*, **87**, 334 (1954).

(10) R. E. Tedeschi, D. H. Tedeschi, A. Mucha, L. Cook, P. A. Mattis, and E. J. Fellows, *J. Pharmacol. Exp. Ther.*, **125**, 28 (1959).

(11) C. Aron-Samuel, Thèse, Fac. Médecine, Paris, France, 1970.

(12) J. R. Boissier and P. Simon, *Thérapie*, **18**, 1257 (1963).

(13) D. N. Johnson and W. H. Furderburk, *Fed. Proc. Fed. Am. Soc. Exp. Biol.*, **33**, 285 (1974).

(14) P. A. J. Janssen and C. J. E. Niemegeers, *Psychopharmacologia*, **11**, 231 (1967).

(15) V. Warin, F. Baert, M. Lobry, J. L. Bernier, and J. P. Hénichart, *Acta Crystallogr. Sect. B*, **35**, 2165 (1979).

(16) L. B. Kier, *J. Pharmacol. Exp. Ther.*, **164**, 75 (1968).

(17) B. Pullman, J. L. Coubeils, P. Courrière, and J. P. Gervois, *J. Med. Chem.*, **15**, 17 (1972).

(18) J. L. Coubeils, P. Courrière, and B. Pullman, *J. Med. Chem.*, **15**, 453 (1972).

ACKNOWLEDGMENTS

The authors thank A. Pério, Clin-Midy Laboratory, Montpellier, France, for the pharmacological assays.

Effect of Sodium Oleate on Salicylic Acid Binding to Human Serum Albumin

PETER A. SCHWARTZ, DOUGLAS S. GREENE, and C. T. RHODES ˣ

Received January 3, 1980, from the *Department of Pharmacy, College of Pharmacy, University of Rhode Island, Kingston, RI 02881.* Accepted for publication May 19, 1980.

Abstract □ The pharmacological activity of salicylates is related to the nonprotein-bound fraction of drug in the plasma. Free fatty acids have been shown to displace bound drug and to increase the serum levels of salicylates. Continuous ultrafiltration was used to measure unbound salicylic acid at 37°. A nonlinear analysis of the ultrafiltration data using whole number values for the number of binding sites indicates that sodium oleate displaces the salicylic acid competitively at both binding sites. Increased concentrations of fatty acids due to disease or the infusion of fatty acid emulsions perhaps may produce toxic levels of salicylic acid.

Keyphrases □ Sodium oleate—effect on binding of salicylic acid to human serum albumin □ Salicylic acid—binding to human serum albumin, effect of sodium oleate □ Protein binding—effect of sodium oleate on binding of salicylic acid to human serum albumin

Since the pharmacological activity of many drugs is related to the non-protein-bound fraction of the drug in plasma (1–3), any decrease in the fraction of protein-bound drug may be expected to result in an increased pharmacological effect. Free fatty acids bind rapidly to albumin at more than one site (4–6), have a higher affinity for albumin than do most drugs (7, 8), and increase the concentration of unbound drug *in vivo* by displacement of

0022-3549/80/1100-1345$01.00/0

© 1980, American Pharmaceutical Association

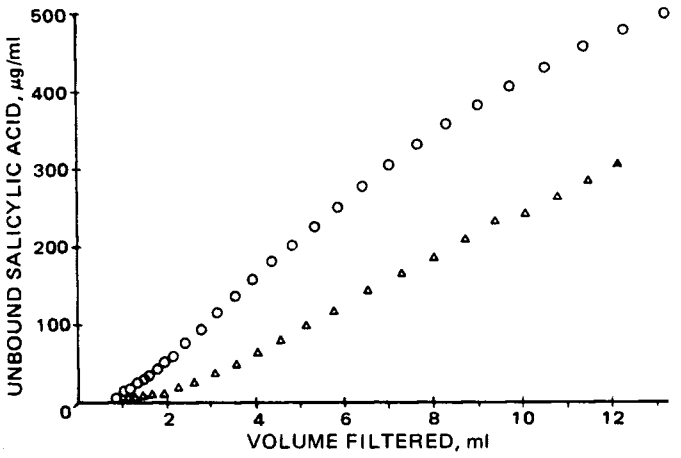

Figure 1—*Relationship between unbound salicylic acid and ultrafiltration volume for salicylic acid alone (△) and salicylic acid with 2.0 mEq of sodium oleate (○).*

bound drug (9, 10). Since salicylates can be relatively highly protein bound at certain concentrations (11–14), drug displacement due to elevated free fatty acid concentrations may have significant clinical implications (15).

Palmitic, oleic, and linoleic acids are the major free fatty acids present in serum (16, 17). Elevated concentrations of free fatty acids, *i.e.*, above the normal range of 0.3–0.8 mEq/liter, have been reported in renal disease (18), diabetes (19), hyperthyroidism (20), stress and exercise (21–23), myocardial infarction (24), and infection (25). Because free fatty acid increases are common in clinical practice and may result in significant drug displacement, the changes in salicylic acid binding in the presence of varying free fatty acid concentrations were investigated *in vitro* using human serum albumin at 37°.

EXPERIMENTAL

Human serum albumin[1] was prepared in pH 7.4 phosphate buffer at a physiological concentration of 4 g/100 ml. Salicylic acid[2] solutions were prepared in pH 7.4 phosphate buffer at concentrations between 700 and 800 μg/ml. Sodium oleate[3] was added to the human serum albumin to yield concentrations of 0.5, 1.0, 1.5, and 2.0 mEq/liter.

The bound fraction of drug was determined using continuous ultrafiltration (26). The salicylic acid solution was placed in the reservoir above the 25-mm ultrafiltration cell, equipped with a membrane having a 10,000 Dalton molecular weight cutoff[4]. The cell then was filled with either human serum albumin or a human serum albumin–sodium oleate mixture. The contents of the cell and reservoir were kept at 37° in a water bath.

The ultrafiltrate was collected under nitrogen (<20 psi) in tared, glass-stoppered test tubes at a flow rate of ~10 ml/hr. After an initial collection of 1 ml (to allow for the void volume), samples were collected and the collected filtrate volumes were determined by reweighing the tubes and converting weights to volumes, assuming a solution density of one (filtrate volumes varied between 0.1 and 0.7 ml).

Salicylate concentrations were determined spectrophotometrically at the absorption maximum of 295 nm from suitably diluted filtrate samples. A regression line of absorbance as a function of salicylate concentration was linear up to 40 μg/ml ($r = 0.999$, $n = 8$). A control study performed without protein showed no evidence of drug binding by the membrane or other parts of the cell.

The method of Greene and Nightingale (27) was used to calculate the number of binding sites and the affinity constants for each site. The raw data, *i.e.*, the filtrate concentration, C_f, as a nonlinear function of the volume filtered, V, were fitted using a computer[5] and the NONLIN program (28):

$$\frac{dC_f}{dV} = \frac{(C_r - C_f)/V_c}{1 + \frac{n_1K_1P}{(1 + K_1C_f)^2} + \frac{n_2K_2P}{(1 + K_2C_f)^2}} \quad \text{(Eq. 1)}$$

where C_r, V_c, and P are the reservoir concentration, ultrafiltration cell volume, and moles of protein, respectively.

All calculations were corrected by subtraction of the void volume from the total volume filtered (26). The void volume, V', was calculated using the NONLIN program to fit the following equation iteratively (27):

$$C_f = C_r - C_re^{\left(\frac{-V+V'}{V_c}\right)} \quad \text{(Eq. 2)}$$

Initial estimates of binding constants were obtained from the computer program MAP (28), which calculates the map of the sum of squares surface. All fits were obtained for a two-site model either with four parameters, *i.e.*, n_1, K_1, n_2, and K_2, or with two parameters, *i.e.*, K_1 and K_2, with whole numbers assigned to n_1 and n_2.

RESULTS AND DISCUSSION

The salicylic acid concentration in the ultrafiltrate is a nonlinear function of the volume filtered (Fig. 1). From these data, a Scatchard plot (Fig. 2) can be constructed using a mass balance analysis of the cell (29). Examination of the intercept on the r axis in Fig. 2 for salicylic acid alone and in the presence of 2.0 mEq of sodium oleate/liter suggests at least four salicylate binding sites on human serum albumin distributed between

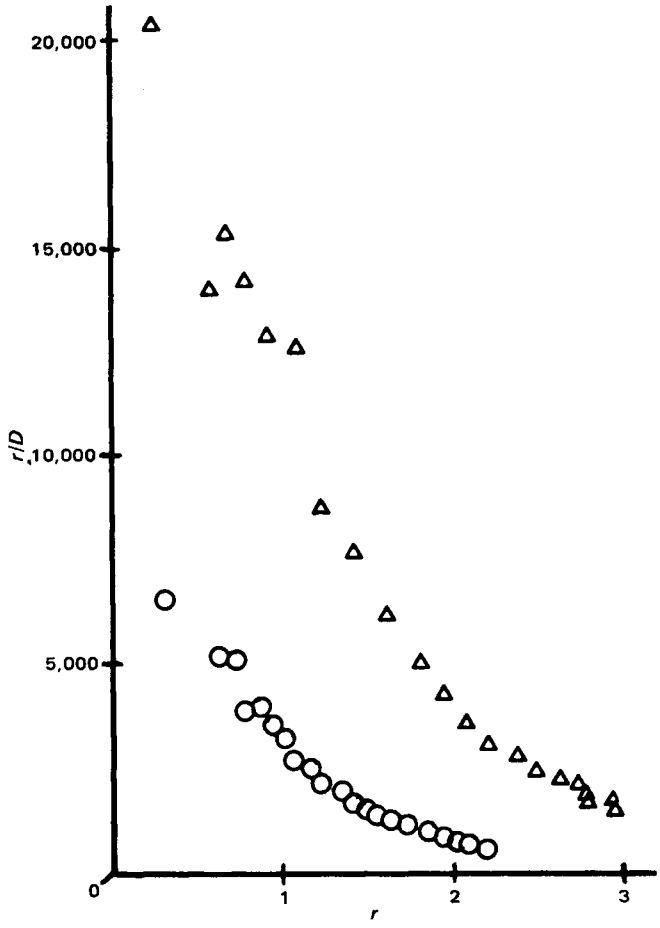

Figure 2—*Scatchard plot of salicylic acid binding. Key: △, salicylic acid alone; and ○, salicylic acid with 2.0 mEq of sodium oleate; r is the moles of salicylic acid bound per mole of human serum albumin and D equals moles of unbound salicylic acid.*

[1] Fraction V powder, Calbiochem.
[2] A-277, Fisher.
[3] Pfaltz and Bauer.
[4] Millipore, PTSC.
[5] Itel AS-5 model 3.

Table I—Scatchard Parameters for Salicylic Acid Binding to 4% Human Serum Albumin at 37°

Model	n_1	K_1, liters/mole	n_2	K_2, liters/mole
Unconstrained	1.33 (0.22)[a]	18,750 (10,600)	2.48 (0.21)	840 (310)
Constrained	2	7440 (2460)	2	430 (48)

[a] The standard deviation is given in parentheses.

two classes of sites. The data are quite clear for the systems that did not contain sodium oleate but are not unequivocal for the systems containing sodium oleate.

Table I lists the Scatchard parameters of a two-class binding model that were obtained by fitting the filtrate data as a function of volume to Eq. 1 using the NONLIN program. The estimates for these parameters are in reasonable agreement with those of other investigations at 37° (30, 31).

The NONLIN program can be modified to constrain the number of binding sites to whole numbers (32). The most likely combination of whole numbers of a two-class binding model, *i.e.*, n_1 and n_2, appears to be one of the following constrained systems: 1, 3; 1, 4; 1, 5; 2, 2; 2, 3; and 2, 4. The best-fit constrained model for the two binding sites (n_1 and n_2) using the criteria of smaller sums of squares was 2, 2. This result differs from a similar analysis of a Scatchard plot of salicylic acid binding to 0.3% human serum albumin at 25°, in which 1, 4 was reported for n_1 and n_2, respectively (32). The 2, 2 model also appeared to describe adequately the salicylic acid binding in the presence of 0.5–2.0 mEq of sodium oleate/liter.

Figure 3 demonstrates that the apparent dissociation constants for both classes of binding sites decreased apparently linearly with increasing oleate concentration. Decreased affinity for binding without a change in the number of binding sites also was shown for diazepam in the presence of oleic acid (10).

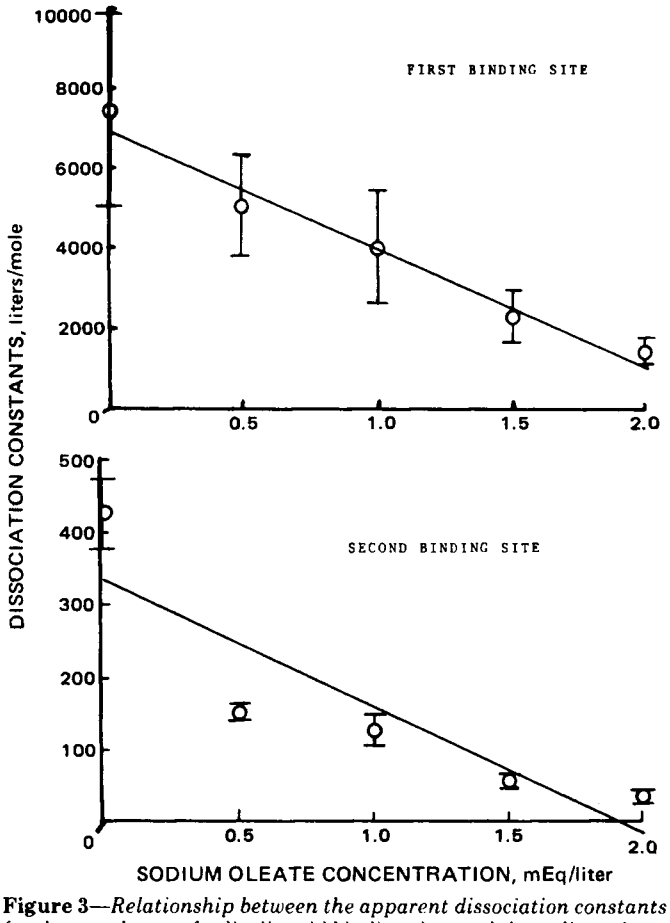

Figure 3—*Relationship between the apparent dissociation constants for the two classes of salicylic acid binding sites and the sodium oleate concentration.*

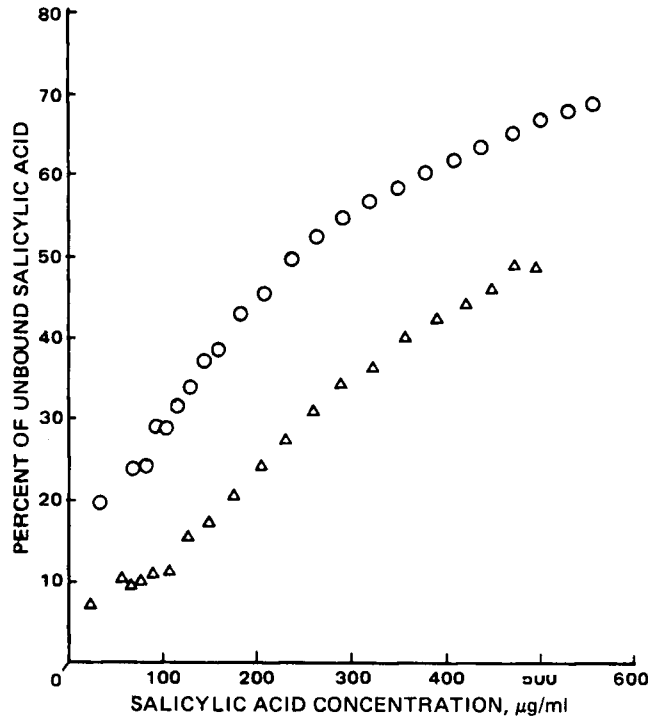

Figure 4—*Relationship between the percent of unbound salicylic acid and the total drug concentration. Key: △, salicylic acid alone; and ○, salicylic acid with 2.0 mEq of sodium oleate.*

Oleic acid appears to alter the binding affinity for salicylic acid to human serum albumin without affecting the number of binding sites. Similar competitive effects of free fatty acids on the binding of salicylic acid and other drugs have been attributed to allosteric conformational changes of protein molecules (32).

The unbound percent of salicylic acid as a function of total drug concentration calculated from the mass balance of cell contents is shown in Fig. 4. A twofold increase in the percent unbound salicylic acid, *i.e.*, from ~20 to 40%, occurred at oleic acid levels of 2.0 mEq/liter, as compared to normal free fatty acid levels of ~0.5 mEq/liter.

This investigation was purely *in vitro* in nature, and there always is an uncertainty in any attempt to extrapolate *in vitro* data to *in vivo* clinical situations. However, it is known that the toxic effects of salicylic acid are related to its unbound concentration, the dose-related volume of distribution, and the clinical status of the patient, *e.g.*, acidosis (15). Since salicylic acid binding can be reduced considerably by elevation of the free fatty acid level, any substantial increase in free fatty acids due to disease or the use of fatty acid emulsion infusions may perhaps be potentially clinically relevant. Since salicylic acid has a quite high therapeutic ratio, the effect may not be hazardous; however, it would be desirable to study the effects of the free fatty acid concentration on several strongly bound drugs with low therapeutic indexes.

REFERENCES

(1) B. B. Brodie, *Proc. R. Soc. Med.*, **58**, 946 (1965).

(2) R. R. Levine, "Pharmacology—Drug Actions and Reactions," Little, Brown, Boston, Mass., 1973, p. 103.

(3) J. R. Gillette, *Ann. N.Y. Acad. Sci.*, **226**, 6 (1973).

(4) D. S. Goodman, *J. Am. Chem. Soc.*, **80**, 3892 (1958).

(5) G. Wilding, R. C. Feldhoff, and E. S. Vessell, *Biochem. Pharmacol.*, **26**, 1143 (1977).

(6) H. H. Ott, J. B. Hayes, G. Ott, and R. S. Gordon, *Fluid*, **13**, 301 (1966).

(7) R. Gugler, D. W. Shoeman, and D. L. Azarnoff, *Pharmacology*, **12**, 160 (1974).

(8) A. A. Spector, *J. Lipid Res.*, **16**, 165 (1975).

(9) D. Rudman, T. J. Bixler, and A. E. DelRio, *J. Pharmacol. Exp. Ther.*, **176**, 261 (1971).

(10) T. Sjokin, *Biochem. Pharmacol.*, **26**, 2157 (1977).

(11) W. D. Wosilait, *Eur. J. Clin. Pharmacol.*, **9**, 285 (1976).

(12) R. C. Baselt and C. B. Stewart, *Res. Commun. Chem. Pathol.*

Pharmacol., **15**, 351 (1976).
(13) J. F. Zaroslinski, S. Keresztes-Nagy, R. F. Mais, and Y. T. Oester, *Biochem. Pharmacol.*, **23**, 1767 (1974).
(14) R. F. Mais, S. Keresztes-Nagy, J. F. Zaroslinski, and Y. T. Oester, *J. Pharm Sci.*, **63**, 1423 (1974).
(15) A. K. Done, *Pediatrics*, **54**, 670 (1974).
(16) K. Diem and C. Lentner, Eds., "Scientific Tables," 7th ed., Ciba-Geigy, Basel, Switzerland, 1970, pp. 600–602.
(17) A. Saifer and L. Goldman, *J. Lipid Res.*, **2**, 268 (1961).
(18) M. S. Losowsky and D. H. Kenward, *J. Lab. Clin. Med.*, **71**, 736 (1968).
(19) J. A. Moorehouse, J. Steinberg, and N. J. Rosen, *J. Clin. Endocrinol. Metab.*, **23**, 1080 (1963).
(20) C. E. Rich, E. L. Bierman, and I. L. Schwartz, *J. Clin. Invest.*, **38**, 275 (1959).
(21) R. J. Havel, A. Naimark, and C. F. Borchgrevink, *ibid.*, **42**, 1054 (1963).
(22) K. Rodahl, H. I. Miller, and B. Issekutz, *J. Appl. Physiol.*, **19**, 489 (1964).
(23) P. Paul and W. L. Holmes, *Lipids*, **8**, 142 (1973).
(24) V. A. Kurien and M. F. Oliver, *Lancet*, **2**, 122 (1966).
(25) J. I. Gallin, D. Kay, and W. M. O'Leary, *N. Engl. J. Med.*, **281**, 1081 (1969).
(26) W. F. Blatt, S. M. Robinson, and J. J. Bixler, *Anal. Biochem.*, **26**, 151 (1968).
(27) D. S. Greene and C. H. Nightingale, *Acad. Pharm. Sci. Abstr.*, **6**, 117 (1976).
(28) C. M. Metzler, G. L. Elfring, and A. J. McEwen, *Biometrics*, **30**, 562 (1974).
(29) D. S. Campion and R. Olsen, *J. Pharm. Sci.*, **63**, 249 (1974).
(30) V. P. Shah, S. M. Wallace, and S. Riegelman, *ibid.*, **63**, 1364 (1974).
(31) O. Borga, I. Odar-Cederlof, V. A. Ringberger, and A. Norlin, *Clin. Pharm. Ther.*, **20**, 464 (1976).
(32) J. E. Fletcher and A. A. Spector, *Mol. Pharmacol.*, **13**, 387 (1977).

Novel Potential Anticancer Agents Derived from Benzimidazole

EL-SEBAII A. IBRAHIM, A.-MOHSEN M. E. OMAR ˣ, and M. A. KHALIL

Received March 4, 1980, from the *Pharmaceutical Chemistry Department, Faculty of Pharmacy, University of Alexandria, Alexandria, Egypt.* Accepted for publication May 20, 1980.

Abstract □ Two novel series of benzimidazole derivatives bearing structural modifications of certain drugs were prepared for evaluation for potential anticancer activity. The first series was a group of alkylating agents, and the second series was a variety of 4-substituted-1-thioacetyl-3-thiosemicarbazides. The tests of some representative products for antileukemic activity against P-388 lymphocytic leukemia indicated no significant effects.

Keyphrases □ Antineoplastic agents, potential—benzimidazole sulfonic esters and nitrogen mustards, synthesis and evaluation for antileukemic activity □ Benzimidazole derivatives—sulfonic esters and nitrogen mustards, synthesis and evaluation for anticancer activity

Among the benzimidazole alkylating agents whose syntheses have been described (1–5), only 2-[bis(2-chloroethyl)aminoethyl]benzimidazole (benzimidazole mustard NSC 23891, I) has shown pronounced anticancer activity (6, 7). Interest in the effect of structural modification on the anticancer activity of such compounds prompted the synthesis of benzimidazole sulfonic esters (IV–IX) and nitrogen mustards (X and XI) (Scheme I), in which the thioethyl chain replaced the methylenic group in I. In addition, 4-substituted-1-(2-mercaptoacetylbenzimidazole)-3-thiosemicarbazides (XIV–XX) (Scheme II) were prepared to compare their anticancer properties with those reported for some heterocyclic α-formylthiosemicarbazone derivatives (8–11).

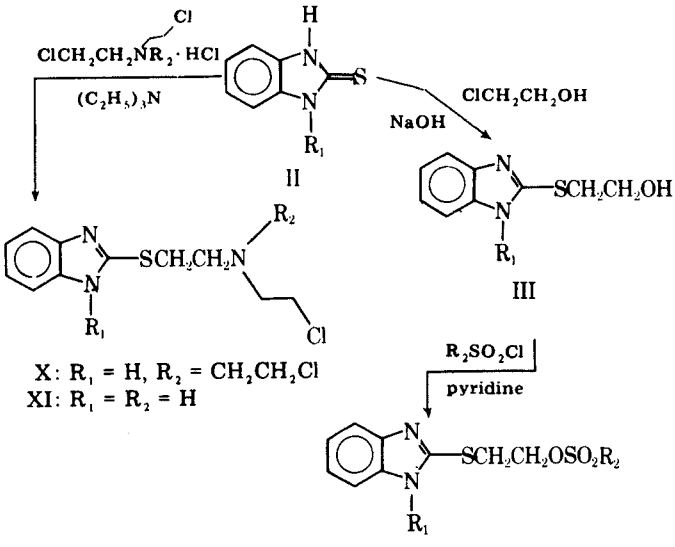

Scheme I

RESULTS AND DISCUSSION

Chemistry—The sulfonic esters (IV–IX) were prepared starting with *S*-alkylation of benzimidazole-2-thione or the 1-substituted derivatives (II) with ethylene chlorohydrin in the presence of potassium hydroxide, followed by treatment of the resulting alcohols (III) with methanesulfonyl chloride or *p*-toluenesulfonyl chloride and pyridine (12) (Scheme I). When the 1-position in the alcohols (III) was vacant, the reactions proceeded with the production of the disulfonated products (VIII and IX) (Table I). The bi- and monofunctional nitrogen mustards (X and XI) were synthesized by reacting benzimidazole-2-thione with a mixture of tris(2-chloroethyl)amine hydrochloride or bis(2-chloroethyl)amine hydrochloride and triethylamine in absolute ethanol.

Treatment of benzimidazole-2-thione (II) with ethyl bromoacetate gave

0022-3549/80/1100-1348$01.00/0
© 1980, American Pharmaceutical Association

Pharmacol., **15**, 351 (1976).
(13) J. F. Zaroslinski, S. Keresztes-Nagy, R. F. Mais, and Y. T. Oester, *Biochem. Pharmacol.*, **23**, 1767 (1974).
(14) R. F. Mais, S. Keresztes-Nagy, J. F. Zaroslinski, and Y. T. Oester, *J. Pharm Sci.*, **63**, 1423 (1974).
(15) A. K. Done, *Pediatrics*, **54**, 670 (1974).
(16) K. Diem and C. Lentner, Eds., "Scientific Tables," 7th ed., Ciba-Geigy, Basel, Switzerland, 1970, pp. 600–602.
(17) A. Saifer and L. Goldman, *J. Lipid Res.*, **2**, 268 (1961).
(18) M. S. Losowsky and D. H. Kenward, *J. Lab. Clin. Med.*, **71**, 736 (1968).
(19) J. A. Moorehouse, J. Steinberg, and N. J. Rosen, *J. Clin. Endocrinol. Metab.*, **23**, 1080 (1963).
(20) C. E. Rich, E. L. Bierman, and I. L. Schwartz, *J. Clin. Invest.*, **38**, 275 (1959).
(21) R. J. Havel, A. Naimark, and C. F. Borchgrevink, *ibid.*, **42**, 1054 (1963).
(22) K. Rodahl, H. I. Miller, and B. Issekutz, *J. Appl. Physiol.*, **19**, 489 (1964).
(23) P. Paul and W. L. Holmes, *Lipids*, **8**, 142 (1973).
(24) V. A. Kurien and M. F. Oliver, *Lancet*, **2**, 122 (1966).
(25) J. I. Gallin, D. Kay, and W. M. O'Leary, *N. Engl. J. Med.*, **281**, 1081 (1969).
(26) W. F. Blatt, S. M. Robinson, and J. J. Bixler, *Anal. Biochem.*, **26**, 151 (1968).
(27) D. S. Greene and C. H. Nightingale, *Acad. Pharm. Sci. Abstr.*, **6**, 117 (1976).
(28) C. M. Metzler, G. L. Elfring, and A. J. McEwen, *Biometrics*, **30**, 562 (1974).
(29) D. S. Campion and R. Olsen, *J. Pharm. Sci.*, **63**, 249 (1974).
(30) V. P. Shah, S. M. Wallace, and S. Riegelman, *ibid.*, **63**, 1364 (1974).
(31) O. Borga, I. Odar-Cederlof, V. A. Ringberger, and A. Norlin, *Clin. Pharm. Ther.*, **20**, 464 (1976).
(32) J. E. Fletcher and A. A. Spector, *Mol. Pharmacol.*, **13**, 387 (1977).

Novel Potential Anticancer Agents Derived from Benzimidazole

EL-SEBAII A. IBRAHIM, A.-MOHSEN M. E. OMAR ˣ, and M. A. KHALIL

Received March 4, 1980, from the *Pharmaceutical Chemistry Department, Faculty of Pharmacy, University of Alexandria, Alexandria, Egypt.* Accepted for publication May 20, 1980.

Abstract □ Two novel series of benzimidazole derivatives bearing structural modifications of certain drugs were prepared for evaluation for potential anticancer activity. The first series was a group of alkylating agents, and the second series was a variety of 4-substituted-1-thioacetyl-3-thiosemicarbazides. The tests of some representative products for antileukemic activity against P-388 lymphocytic leukemia indicated no significant effects.

Keyphrases □ Antineoplastic agents, potential—benzimidazole sulfonic esters and nitrogen mustards, synthesis and evaluation for antileukemic activity □ Benzimidazole derivatives—sulfonic esters and nitrogen mustards, synthesis and evaluation for anticancer activity

Among the benzimidazole alkylating agents whose syntheses have been described (1–5), only 2-[bis(2-chloroethyl)aminoethyl]benzimidazole (benzimidazole mustard NSC 23891, I) has shown pronounced anticancer activity (6, 7). Interest in the effect of structural modification on the anticancer activity of such compounds prompted the synthesis of benzimidazole sulfonic esters (IV–IX) and nitrogen mustards (X and XI) (Scheme I), in which the thioethyl chain replaced the methylenic group in I. In addition, 4-substituted-1-(2-mercaptoacetylbenzimidazole)-3-thiosemicarbazides (XIV–XX) (Scheme II) were prepared to compare their anticancer properties with those reported for some heterocyclic α-formylthiosemicarbazone derivatives (8–11).

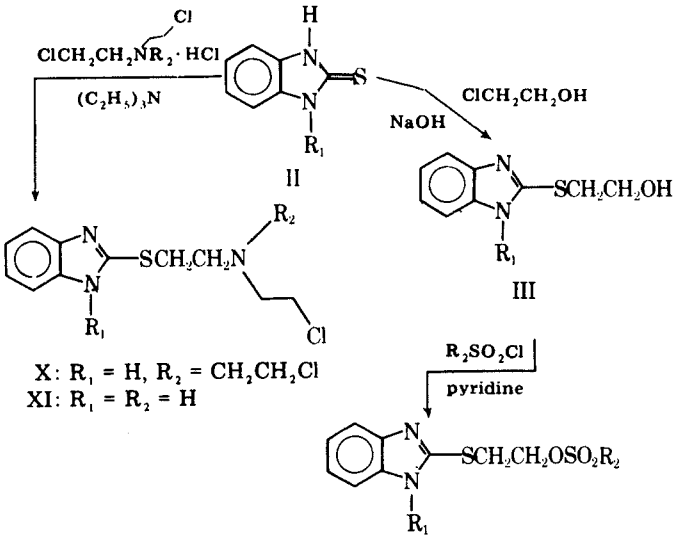

Scheme I

RESULTS AND DISCUSSION

Chemistry—The sulfonic esters (IV–IX) were prepared starting with *S*-alkylation of benzimidazole-2-thione or the 1-substituted derivatives (II) with ethylene chlorohydrin in the presence of potassium hydroxide, followed by treatment of the resulting alcohols (III) with methanesulfonyl chloride or *p*-toluenesulfonyl chloride and pyridine (12) (Scheme I). When the 1-position in the alcohols (III) was vacant, the reactions proceeded with the production of the disulfonated products (VIII and IX) (Table I). The bi- and monofunctional nitrogen mustards (X and XI) were synthesized by reacting benzimidazole-2-thione with a mixture of tris(2-chloroethyl)amine hydrochloride or bis(2-chloroethyl)amine hydrochloride and triethylamine in absolute ethanol.

Treatment of benzimidazole-2-thione (II) with ethyl bromoacetate gave

0022-3549/80/1100-1348$01.00/0
© 1980, American Pharmaceutical Association

Table I—1-Substituted-2-(alkyl or arylsulfonoxyethyl)thiobenzimidazoles

Compound	Melting Point	Yield, %	Molecular Formula	Analysis, % Calc.	Found
IV	73–75°	82	$C_{11}H_{14}N_2O_3S_2$	C 46.01	45.90
				H 4.90	4.80
				N 9.70	10.10
				S 22.30	22.70
V	87°	85	$C_{17}H_{18}N_2O_3S_2$	C 56.30	56.10
				H 5.00	5.00
				N 7.70	7.20
				S 17.69	17.80
VI	87–88°	78	$C_{17}H_{18}N_2O_3S_2$	C 56.30	56.50
				H 5.00	4.90
				N 7.70	7.70
				S 17.69	17.20
VII	100–101°	81	$C_{23}H_{22}N_2O_3S_2$	C 62.90	62.73
				H 5.00	5.14
				N 6.39	6.30
				S 14.60	14.70
VIII	197–199°	85	$C_{11}H_{14}N_2O_5S_3$	C 37.70	38.00
				H 4.02	4.10
				N 8.00	8.30
				S 27.42	27.30
IX	127–128°	90	$C_{23}H_{22}N_2O_5S_3$	C 54.90	54.50
				H 4.40	4.40
				N 5.57	5.90
				S 19.10	19.20

the corresponding *S*-alkyl ester (XII) (13), which, on reaction with hydrazine hydrate in ice, yielded benzimidazole-2-mercaptoacetohydrazide (XIII) (13). Heating this acid hydrazide with the equivalent amount of alkyl-, aryl-, or aralkylisothiocyanates in refluxing ethanol (14) produced the required 4-substituted-1-(2-mercaptoacetylbenzimidazole)-3-thiosemicarbazides (XIV–XX) (Scheme II and Table II). The new products were identified by microanalysis and IR spectra and, for some representative compounds, by PMR and mass spectra.

Anticancer Screening—Compounds IV–VIII, X, XI, XIV–XVI, and XX were evaluated against P-388 lymphocytic leukemia in mice[1]. The activities were measured as the ratio of the mean survival time of the test animals to that of the control animals expressed as a percentage (% T/C). All compounds tested were inactive since their % T/C values were <125.

The inactivity of the synthesized alkylating agents was assumed to be due to the presence of sulfur in the thioethyl chain separating the alkylating function from the benzimidazole ring. This assumption is supported by the fact that no loss in carcinostatic activity or therapeutic index was observed when the methyl group in methylbis(2-chloroethyl)amine (HN_2 NSC 762) was replaced by a longer or more complex substituent (7). On the other hand, the lack of anticancer activity of the thiosemicarbazides (XIV–XX) was attributed to their inability to form the tridentate ligands (15) with the iron required by ribonucleoside diphosphate reductase; as a result, they cannot block DNA synthesis.

EXPERIMENTAL[2]

2-(2-Hydroxyethyl)thiobenzimidazole and Corresponding 1-Methyl- and 1-Benzyl Derivatives (III)—Ethylene chlorohydrin (7 g, 0.1 mole) was added dropwise to an ice-cold solution of benzimidazole-2-thione (II) (0.1 mole) in 12% KOH (40 ml). The mixture was stirred for 3 hr and set aside overnight at room temperature. The separated products were crystallized from ethanol or aqueous ethanol, identified by their IR spectra, and used for the preparation of the sulfonic esters; IR (mineral oil): 3175 (associated OH and NH), 1620 (C=N), 1510 (δ NH), 1265 (OH, out of plane bending), and 1065 (C–O) cm^{-1}.

1-Substituted-2-(alkyl or arylsulfonoxyethyl)thiobenzimidazoles (IV–IX)—Methanesulfonyl chloride or *p*-toluenesulfonyl chloride (0.3 mole) was added to a well-stirred and cooled (ice–salt bath) solution of the 2-(2-hydroxyethyl)thiobenzimidazoles (III) in dry pyridine (10 ml). Stirring was continued for 3 hr, and the mixture was left in the refrigerator overnight. Sufficient ice-cold water was added with vigorous stirring. The separated products were filtered, washed well with water, and crystallized from a benzene–light petroleum mixture. The yields and physical constants of the products are given in Table I; IR (KBr): 1355 and 1170 (asymmetric and symmetric SO_2) cm^{-1}; PMR for V (deuterochloroform): δ 2.29 (s, 3H, aromatic CH_3), 3.89 (s, 3H, *N*-CH_3), 4.38–4.62 (m, distorted, 2H, *S*-CH_2), 4.80–5.25 (m, distorted, 2H, CH_2OSO_2), and 6.89–7.81 (m, 8H, aromatic H) ppm.

2-[2-[Bis(2-chloroethyl)amino]ethyl]thiobenzimidazole Hydrochloride (X)—A mixture of benzimidazole-2-thione (0.45 g, 0.003 mole), tris(2-chloroethyl)amine hydrochloride (0.72 g, 0.003 mole), and triethylamine (0.3 g) in absolute ethanol (20 ml) was heated under reflux for 6 hr. The separated product was filtered and crystallized from absolute ethanol as white crystals, 0.55 g (72%), mp 223–225°; TLC: R_f 0.53

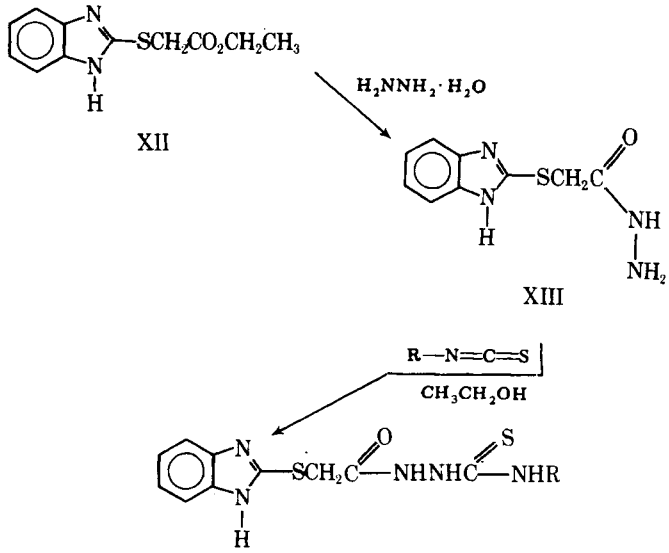

XIV: R = *n*-C_4H_9
XV: R = C_6H_5
XVI: R = 2-$CH_3C_6H_4$
XVII: R = 3-$CH_3C_6H_4$
XVIII: R = 4-$CH_3C_6H_4$
XIX: R = 2-$CH_3OC_6H_4$
XX: R = $C_6H_5CH_2$

Scheme II

[1] Assays were performed in accordance with the protocol of the Drug Evaluation Branch, National Cancer Institute, Bethesda, MD 20014. The compounds, dissolved or suspended in saline with Tween 80, were given as intraperitoneal injections 24 hr after tumor implantation in BDF_1 male and female mice. With a multiple-dose assay, the antileukemic activity of the products was evaluated on Day 30 after tumor implantation.

[2] All melting points are uncorrected. IR spectra were measured on a Beckman 4210 IR spectrophotometer. PMR and mass spectra were measured at Janssen Pharmaceutica Laboratories, Belgium.

Table II—4-Substituted-1-(2-mercaptoacetylbenzimidazole)-3-thiosemicarbazides

Compound	Melting Point	Yield, %	Molecular Formula	Analysis, %	Calc.	Found
XIV	172–174°	83	$C_{14}H_{19}N_5OS_2$	C	49.85	50.10
				H	5.60	5.70
				N	20.77	21.00
				S	18.99	18.60
XV	186–188°	85	$C_{16}H_{15}N_5OS_2$	C	53.60	53.70
				H	4.20	4.37
				N	19.56	19.00
				S	17.80	17.60
XVI	176–178°	85	$C_{17}H_{17}N_5OS_2$	C	54.98	54.89
				H	4.58	4.09
				N	18.80	18.50
				S	17.20	17.00
XVII	173–174°	86	$C_{17}H_{17}N_5OS_2$	C	54.98	54.89
				H	4.58	4.82
				N	18.80	19.20
				S	17.20	17.30
XVIII	168–169°	88	$C_{17}H_{17}N_5OS_2$	C	54.98	55.06
				H	4.58	4.67
				N	18.80	19.10
				S	17.20	17.60
XIX	130–132°	86	$C_{17}H_{17}N_5O_2S_2$	C	52.71	52.34
				H	4.39	4.73
				N	18.00	17.50
				S	16.49	16.60
XX	181–182°	93	$C_{17}H_{17}N_5OS_2$	C	54.98	55.27
				H	4.58	4.67
				N	18.80	18.70
				S	17.20	17.00

(chloroform–benzene–ethanol 2.5:3:0.5); IR (KBr): 2600 (broad, N^+H) cm^{-1}.

Anal.—Calc. for $C_{13}H_{18}Cl_3N_3S$: C, 44.10; H, 5.05; Cl, 30.04; N, 11.84; S, 9.02. Found: C, 44.00; H, 5.10; Cl, 29.60; N, 12.00; S, 8.60.

The PMR spectrum of the free base in deuterochloroform showed: δ 2.99 and 3.09 [2t, overlapping, 6H, J = 5 Hz, $CH_2N(CH_2)CH_2$], 3.42 and 3.53 [2t, overlapping, 6H, J = 5 Hz, SCH_2 and $(CH_2Cl)_2$], 7.11–7.32 (m, 2H, aromatic H), and 7.4–7.61 (m, 2H, aromatic H of benzimidazole) ppm; mass spectrum: *m/e* (relative abundance, %) (M^+ absent) 281 and 283 (2), 264 (3), 232 (26), 176 (44), 161 (14), 150 (100), 118 (16), 91 (8), 65 (11), 36 (16), and 28 (26).

2-[2-[(2-Chloroethyl)amino]ethyl]thiobenzimidazole (XI)—Compound XI was prepared as described for X except that bis(2-chloroethyl)amine hydrochloride was used instead of tris(2-chloroethyl)amine hydrochloride; TLC: R_f 0.61.

Anal.—Calc. for $C_{11}H_{14}ClN_3S$: C, 51.60; H, 5.50; Cl, 13.80; N, 16.40; S, 12.52. Found: C, 51.50; H, 5.50; Cl, 13.40; N, 16.00; S, 12.70.

1-(2-Mercaptoacetylbenzimidazole)-4-alkyl-, aryl-, and aralkyl-3-thiosemicarbazides (XIV–XX)—A solution of equimolar amounts of an alkyl-, aryl-, or aralkylisothiocyanate and benzimidazole-2-mercaptoacetohydrazide (XIII) (13) in ethanol was left overnight at room temperature to deposit the products. They were filtered and crystallized from ethanol or aqueous ethanol. The yields and physical constants of the products are summarized in Table II; IR (mineral oil): 3270–3140 (NH), 1670 (C=O, amide I band), 1350 (amide II band and, in part, N+C=S amide band), 1250 (amide III band), and 1565–1530, 1345–1325, 1075–1050, and 870–830 (N+C=S I, II, III, and IV amide bands, respectively) cm^{-1} (14).

REFERENCES

(1) R. C. Elderfield, I. S. Covey, J. B. Geiduschek, W. L. Meyer, A. B. Ross, and J. H. Ross, *J. Org. Chem.*, **23**, 1749 (1958).

(2) O. F. Ginzburg, B. A. Porai-Koshits, M. I. Krylova, and S. M. Lotareichok, *Zh. Obshchei. Khim.*, **27**, 411 (1957); through *Chem. Abstr.*, **51**, 15500d (1957).

(3) W. S. Gump and E. J. Nikawitz, *J. Org. Chem.*, **24**, 712 (1959).

(4) K. C. Tsou, D. J. Rabiger, and D. Sobel, *J. Med. Chem.*, **12**, 818 (1969).

(5) W. A. Skinner, M. G. M. Schelstraete, and B. R. Baker, *J. Org. Chem.*, **24**, 1827 (1959).

(6) E. Hirschberg, A. Gellhorn, and W. S. Gump, *Cancer Res.*, **17**, 904 (1957).

(7) M. Ochoa, Jr., and E. Hirschberg, "Experimental Chemotherapy," vol. V, Academic, New York, N.Y., 1967, p. 19.

(8) K. C. Agrawal, S. Clayman, and A. C. Sartorelli, *J. Pharm. Sci.*, **65**, 297 (1976), and references cited therein.

(9) W. E. Antholine, J. N. Knight, and D. H. Petering, *J. Med. Chem.*, **19**, 339 (1976).

(10) J. A. Crim and G. Petering, *Cancer Res.*, **27**, 1268 (1967).

(11) I. Antonini, F. Claudi, P. Franchetti, M. Grifantini, and S. Martelli, *J. Med. Chem.*, **20**, 447 (1977).

(12) I. M. Roushdi, A.-M. M. E. Omar, M. S. Ragab, and M. Awad, *ibid.*, **19**, 1333 (1976).

(13) S. Kakimoto and I. Sekikawa, *Nippon Kagaku Zasshi*, **77**, 480 (1956); through *Chem. Abstr.*, **52**, 4084d (1958).

(14) A.-M. M. E. Omar, F. A. Ashour, A. B. Makar, and M. R. I. Soliman, *Pharmazie*, **34**, 110 (1979).

(15) F. A. Frensh and E. J. Blaur, *Cancer Res.*, **25**, 1454 (1965).

ACKNOWLEDGMENTS

The authors thank the members of Drug Research and Development, Division of Cancer Research, National Cancer Institute, Bethesda, MD 20014, for screening the compounds. They also thank the members of the Microanalytical Unit, Faculty of Science, Cairo University, Cairo, Egypt, for the microanalytical data.

Electron-Capture GLC Determination of Clobazam and Desmethylclobazam in Plasma

DAVID J. GREENBLATT

Received November 13, 1979, from the *Division of Clinical Pharmacology, Tufts-New England Medical Center, Boston, MA 02111.* Accepted for publication May 6, 1980.

Abstract □ Electron-capture GLC was utilized for simultaneous quantitation of clobazam, a 1,5-benzodiazepine derivative, and its active metabolite, desmethylclobazam, in human plasma and serum. After addition of diazepam as the internal standard, samples were extracted into benzene–isopentanol. The organic extracts were evaporated to dryness, reconstituted, and subjected to chromatographic analysis without derivatization or cleanup. All three compounds were resolved completely and had favorable chromatographic properties using an OV-101 liquid phase. The limits of detection are 3–5 ng/ml for clobazam and 5–10 ng/ml for desmethylclobazam. Relative standard deviations for identical samples do not exceed 6%. The application of the method to a clinical pharmacokinetic study is demonstrated.

Keyphrases □ Clobazam—electron-capture GLC analysis with desmethylclobazam, human plasma □ Desmethylclobazam—electron-capture GLC analysis with clobazam, human plasma □ GLC, electron capture—analyses, clobazam and desmethylclobazam, human plasma

Clobazam (I) is a 1,5-benzodiazepine derivative utilized as a sedative and antianxiety agent (1–3). The major metabolic pathway of clobazam in humans appears to involve hepatic *N*-demethylation, yielding desmethylclobazam (II) (4). This metabolite also has pharmacological activity (5). The present report describes a rapid and sensitive method for simultaneous quantitation of clobazam and desmethylclobazam in plasma following therapeutic doses of the parent compound.

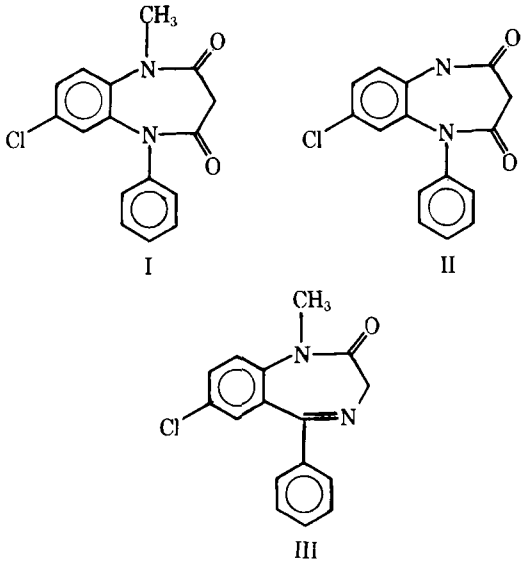

EXPERIMENTAL

Apparatus and Chromatographic Conditions—The analytical instrument was a gas chromatograph[1] equipped with a 15-mCi ^{63}Ni-electron-capture detector and an electronic integrator. The column was coiled glass (122 cm long × 4 mm i.d.) packed with 10% OV-101 on 80–100-mesh Chromosorb WHP[2]. The carrier gas was argon–methane[3] (95:5) at a flow rate of 25 ml/min. The operating temperatures were: injection port, 310°; column, 265°; and detector, 320°. At the beginning of each workday, the column was primed by injection of 2–3 μl of a solution of azolectin[4] (1 mg/ml) in benzene.

Preparation of Stock Solutions—Clobazam[5] and desmethylclobazam[5] (10 mg) each were dissolved in 2–3 ml of absolute ethanol and diluted to 100 ml with benzene. The stock solution, containing 100 μg/ml, were stored in amber bottles at −4°. Freezing of the stock solutions is recommended because desmethylclobazam may deteriorate when stored unfrozen. Diazepam[6] (III) served as the internal standard in all analyses, and the stock solution of diazepam was prepared similarly.

Working standards, containing 1.0 μg of each compound/ml, were prepared daily by appropriate dilution with benzene or toluene.

Preparation of Samples—A constant amount (100 μl) of a 1-μg/ml working solution of the internal standard was added to round-bottom 13-ml glass culture tubes equipped with polytef-lined screw-top caps. The solutions were evaporated to dryness at 40–50° under mildly reduced pressure in a vacuum oven. Calibration standards were prepared by addition of known amounts of clobazam and desmethylclobazam, ranging from 25 to 300 ng, to some of these tubes. The solvents again were evaporated to dryness.

One milliliter of drug-free control plasma was added to each calibration tube, and 0.5–1 ml of unknown plasma was added to each tube that contained only the internal standard. The calibration standards were extracted and analyzed daily together with each set of unknowns. Samples found to contain clobazam or desmethylclobazam concentrations exceeding the limits of the standard curve were reextracted using a smaller aliquot of plasma.

Extraction—To each tube was added 3–5 ml of benzene (containing 1.5% isopentanol to minimize adherence to glassware). The tubes were agitated for 30 sec on a vortex-type mixer and then centrifuged at room temperature for 10 min at 400×*g*. An aliquot of the organic layer was transferred to another tube and evaporated to dryness at 40° under mildly reduced pressure. The residue was redissolved in 100–200 μl of toluene (containing 15% isopentanol), of which 1–6 μl was injected into the chromatograph.

Clinical Pharmacokinetic Study—A healthy 30-year-old male volunteer participated after giving informed consent. After an overnight fast, a single 20-mg dose of clobazam (two 10-mg tablets) was administered with 150 ml of water. Venous blood samples were drawn into heparinized tubes at multiple time points over the next 168 hr. Plasma was separated and frozen until it was assayed. Plasma concentrations of clobazam and desmethylclobazam were determined as described.

The apparent elimination half-life of clobazam during the terminal (β) phase of the plasma concentration curve was determined by least-squares regression analysis.

RESULTS

Evaluation of Method—Under the described chromatographic conditions, the approximate retention times were: diazepam, 5.5 min; clobazam, 7.4 min; and desmethylclobazam, 8.8 min (Fig. 1).

The relation between the plasma concentration of clobazam or desmethylclobazam and the peak area ratio[7] of each compound to the internal standard was linear through plasma concentrations of at least 300 ng/ml (Table I). The relative standard deviations (*RSD*) for replicate

[1] Hewlett-Packard model 5830A.
[2] Supelco Inc., Bellefonte, Pa.
[3] Matheson Gas Products, Gloucester, Mass.
[4] Associated Concentrates, Woodside, N.Y.
[5] Supplied by Dr. S. K. Puri, Hoechst-Roussel Pharmaceuticals, Somerville, N.J.
[6] Supplied by Dr. W. E. Scott, Hoffmann-La Roche Inc., Nutley, N.J.
[7] Peak height ratio can be used.

0022-3549/80/1100-1351$01.00/0
© 1980, American Pharmaceutical Association

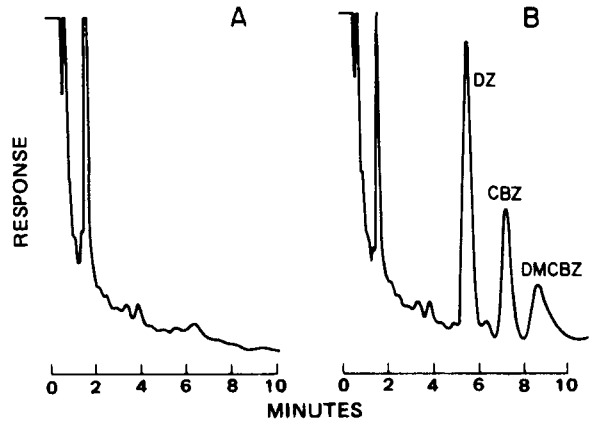

Figure 1—*Chromatogram of a drug-free control plasma extract (A) and chromatogram of the same plasma sample to which was added: diazepam (DZ), 100 ng/ml; clobazam (CBZ), 50 ng/ml; and desmethylclobazam (DMCBZ), 50 ng/ml (B). The chromatographic conditions are given in the text.*

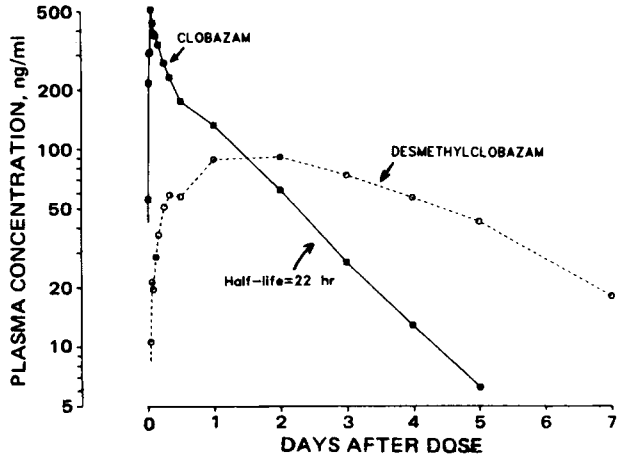

Figure 2—*Plasma concentrations of clobazam and desmethylclobazam over 168 hr after a single 20-mg oral dose of clobazam administered to a healthy male volunteer.*

samples (n = 10) containing 25 ng of clobazam and desmethylclobazam/ml were 1.8 and 5.4%, respectively. At 50 ng/ml, the *RSD* values were 2.5 and 2.9%. The approximate detection limits were 3–5 ng/ml of original sample for clobazam and 5–10 ng/ml of original sample for desmethylclobazam; below these limits, the *RSD* values exceeded 10%. Residue analysis indicated that recovery of clobazam, desmethylclobazam, and diazepam was >95% complete and independent of concentration.

Plasma samples from patients receiving clobazam are stable at room temperature for at least 24 hr. Freezing is recommended for prolonged storage. Plasma extracts also are stable at room temperature and can be stored frozen after reconstitution. Samples are not sensitive to ambient light or to temperatures of <40°.

Pharmacokinetic Study—A peak plasma clobazam concentration of 510 ng/ml was reached at 1.5 hr after dosage (Fig. 2). The elimination half-life during the terminal (β) phase of the curve was 22 hr. Disappearance of clobazam was mirrored by formation of its metabolic product. The highest desmethylclobazam concentration was 91 ng/ml, which was reached 48 hr after clobazam dosage.

DISCUSSION

The sensitivity and specificity of the electron-capture detector have facilitated development of quantitative assays for a number of benzodiazepines in human blood and plasma following therapeutic doses (6–10). The present report describes the application of this approach to the simultaneous quantitation of clobazam and its major pharmacologically active metabolite, desmethylclobazam. Preliminary studies in this laboratory suggested that phenyl methyl silicone liquid phases (such as OV-17) could be used for this purpose. However, chromatographic peaks for the desmethyl metabolite were asymmetric, thereby complicating reliable quantitation. Utilization of a less polar silicone phase (OV-101) substantially improves the chromatographic properties of desmethylclobazam but still allows complete resolution of clobazam and its metabolite from the internal standard and from endogenous plasma contaminants, provided a relatively high phase load (10%) is used.

The clinical pharmacokinetic study illustrates that the method is suitable for pharmacokinetic studies of clobazam and its metabolite following single therapeutic doses. Absorption of clobazam following oral dosage in the fasting state was rapid, with the peak plasma concentration attained 1.5 hr after administration. Clobazam elimination proceeded with a half-life of 22 hr and was mirrored by the formation of desmethylclobazam, which, in turn, was eliminated more slowly than the parent drug. Since both compounds have pharmacological activity, plasma concentrations of both compounds must be measured simultaneously and considered to elucidate the clinical implications of the kinetic properties of clobazam.

Table I—Representative Calibration Data

Concentration, ng/ml	Area Ratio	
	Clobazam	Desmethylclobazam
25	0.17	0.18
50	0.33	0.35
75	0.54	0.56
100	0.70	0.74
150	1.07	1.14
200	1.44	1.56
300	2.12	2.35
Correlation coefficient	0.999	0.999
Slope (±*SE*)	0.00714 (±0.000066)	0.00795 (±0.0000607)
Intercept (±*SE*)	−0.009 (±0.01)	−0.039 (±0.01)
Slope through origin (±*SE*)	0.00710 (±0.000036)	0.00774 (±0.000066)

REFERENCES

(1) D. Koeppen, *Br. J. Clin. Pharmacol.*, **7**, 139S (1979).

(2) J. Mendels, S. Secunda, A. Schless, K. Sandler, and J. Singer, *J. Clin. Pharmacol.*, **18**, 353 (1978).

(3) D. R. Doongaji, A. Sheth, J. S. Apte, P. D. Lakdawala, C. B. Khare, and S. S. Thatte, *ibid.*, **18**, 358 (1978).

(4) M. Volz, O. Christ, H.-M. Kellner, H. Kuch, H.-W. Fehlhaber, D. Gantz, P. Hajdu, and F. Cavagna, *Br. J. Clin. Pharmacol.*, **7**, 41S (1979).

(5) S. Fielding and I. Hoffmann, *ibid.*, **7**, 7S (1979).

(6) J. A. F. deSilva, I. Bekersky, C. V. Puglisi, M. A. Brooks, and R. E. Weinfeld, *Anal. Chem.*, **48**, 10 (1976).

(7) D. M. Hailey, *J. Chromatogr.*, **98**, 527 (1974).

(8) J. M. Clifford and W. F. Smyth, *Analyst*, **99**, 241 (1974).

(9) D. J. Greenblatt, *Clin. Chem.*, **24**, 1838 (1978).

(10) D. J. Greenblatt, K. Franke, and R. I. Shader, *J. Chromatogr.*, **146**, 311 (1978).

ACKNOWLEDGMENTS

Supported in part by Grant MH-12279 from the U.S. Public Health Service, by Grant 77-611 from the Foundations' Fund for Research in Psychiatry, and by a grant-in-aid from Hoechst-Roussel Pharmaceuticals, Somerville, N.J.

The author thanks Ann Locniskar, Marcia Divoll Allen, Ann Werner, Dr. Richard I. Shader, Dr. Surendra K. Puri, and Dr. Dean S. MacLaughlin for assistance. Dr. MacLaughlin was supported by Grant GM-23430 from the U.S. Public Health Service to the Boston Collaborative Drug Surveillance Program.

Use of Nitrogen-Specific Detector for GLC Determination of Caramiphen in Whole Blood

P. LEVANDOSKI ˣ **and T. FLANAGAN**

Received March 10, 1980, from *Smith Kline and French Laboratories, Philadelphia, PA 19101.* Accepted for publication May 27, 1980.

Abstract □ A sensitive GLC determination of caramiphen in whole blood was developed using a nitrogen-specific detector. The method permits the determination of levels of caramiphen as low as 2.5 ng/ml of blood and provides sufficient sensitivity and reproducibility for clinical use.

Keyphrases □ Caramiphen—analysis in whole blood by GLC with nitrogen-specific detector □ GLC—analysis, caramiphen, nitrogen-specific detector □ Antitussives—caramiphen, GLC analysis in whole blood with nitrogen-specific detector

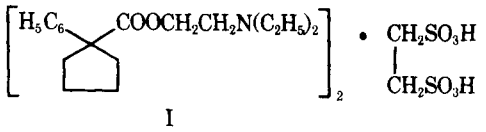

I

Caramiphen ethanedisulfonate[1] (β-diethylaminoethyl 1-phenylcyclopentane-1-carboxylate ethanedisulfonate, I) is an antitussive used as an active ingredient in cough/cold preparations.

A sensitive determination of caramiphen in blood was developed to support clinical studies. The use of a nitrogen-specific detector was proven to be specific and sensitive for other nitrogen-containing compounds in this laboratory and in reported methods for imipramine and desipramine (1), pemoline (2), and bucainide (3).

EXPERIMENTAL

Reagents—Hexane[2] was nanograde, and methanol[3] and sodium hydroxide[4] were reagent grade. Diphenylpyraline hydrochloride[5] was used as the internal standard.

All glassware was washed with chromic acid, silanized with 5% dichlorodimethylsilane[6] in toluene, and rinsed with toluene and then methanol.

Instrumentation—The gas chromatograph[7] was equipped with a nitrogen–phosphorus flame-ionization detector and a 1-mv recorder. The chromatograph was fitted with a 183-cm × 4-mm i.d. coiled glass column packed with 3% OV-17 on 80–100-mesh Chromosorb WHP[6]. The column was conditioned overnight at 310° with a helium flow and several 25-μl injections of a silylating agent[8]. Normal operating temperatures were 270, 300, and 300° for the oven, injection port, and manifold, respectively. The recorder speed was 20 mm/min. Helium was used as the carrier gas at a flow rate of 60 ml/min. The air gauge was set at 3.5 kg/cm². The detector was run in the nitrogen mode at a setting of 710.

Preparation of Standards—Standard stock solutions of 10 mg/100 ml (as the free base) of caramiphen and the internal standard were pre-

Table I—Reproducibility of Caramiphen Standards

Blood Concentration, ng/ml	*n*	Mean Peak Height Ratio ± *SE*	*SE*, %
2.5	2	0.05 ± 0.004	6.7
5	4	0.12 ± 0.012	10.0
10	5	0.28 ± 0.010	3.6
15	4	0.43 ± 0.021	4.9
20	5	0.59 ± 0.011	1.9
30	5	0.93 ± 0.008	0.9
40	4	1.21 ± 0.051	4.2

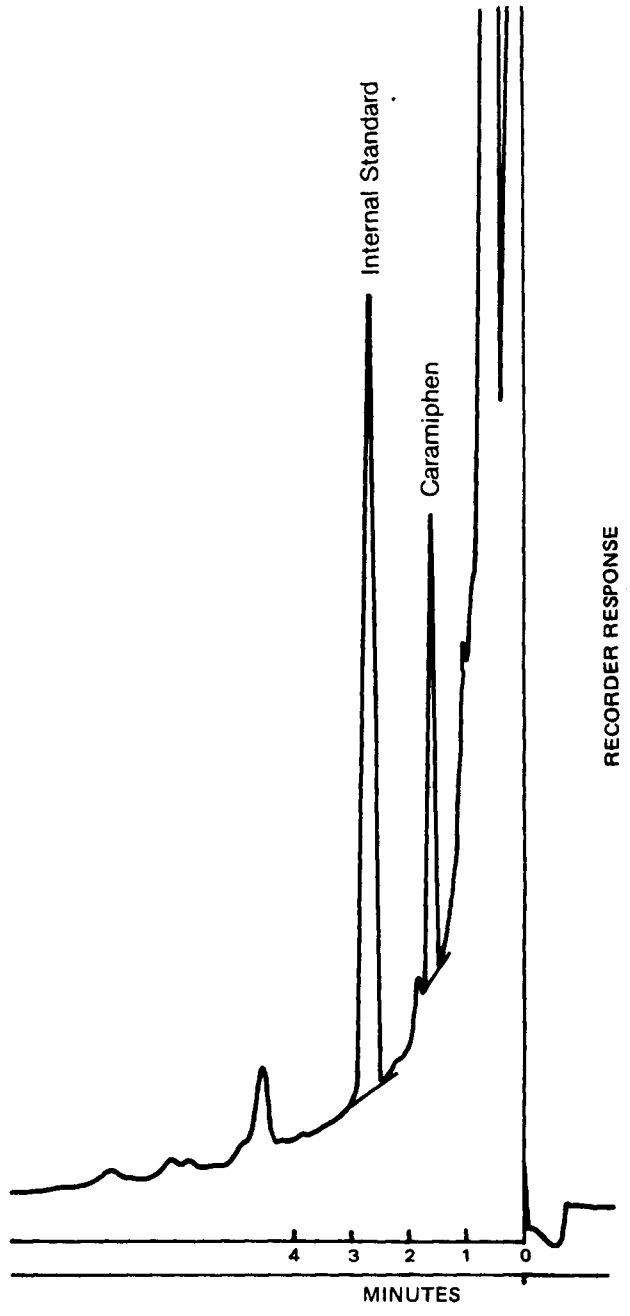

Figure 1—*Chromatogram of a control blood sample that was spiked with the caramiphen reference standard and the internal standard. The peak at 1.6 min represents 20 ng of caramiphen/ml whereas the internal standard (total of 250 ng) has a retention time of 2.7 min.*

[1] Synthesized at SmithKline Corp.
[2] Mallinckrodt.
[3] J. T. Baker Chemical Co.
[4] Fisher Scientific Co.
[5] Napco Chemical Co.
[6] Supelco Inc.
[7] Perkin-Elmer model 3920.
[8] Rejuv-8, Supelco Inc.

0022-3549/80/1100-1353$01.00/0
© 1980, American Pharmaceutical Association

Table II—Blood Levels of Caramiphen in 11 Subjects Receiving 20 mg of Caramiphen Edisylate at 0, 4, and 8 hr Daily for 4 Consecutive Days

Subject	Concentration of Caramiphen, ng/ml											
	0 hr	1 hr	2 hr	4 hr	5 hr	6 hr	8 hr	9 hr	10 hr	13 hr	18 hr	24 hr
1	7.0	43.5	43.5	20.0	74.5	65.0	20.3	21.3	46.0	31.0	13.5	7.5
2	2.5	4.0	11.5	4.5	9.3	17.5	5.0	9.5	12.8	5.8	2.5	3.3
3	3.3	27.8	18.0	9.5	16.0	45.5	17.0	21.0	40.0	14.0	5.3	2.5
4	<1	3.4	31.4	14.6	24.8	21.5	7.9	7.0	21.5	6.3	2.8	1.2
5	9.6	46.6	32.7	15.5	64.5	48.5	21.0	25.0	53.0	22.5	11.6	7.0
6	2.7	16.4	10.6	4.0	5.7	27.8	6.8	4.0	4.0	6.3	7.0	2.0
7	3.5	25.0	23.0	9.0	27.0	34.0	14.0	10.0	29.0	10.0	4.0	3.0
8	5.3	6.0	57.3	29.0	28.5	78.0	30.5	41.5	59.5	36.0	15.5	6.0
9	3.0	15.5	26.0	11.0	28.0	19.0	9.8	10.0	24.5	13.5	6.8	4.0
10	3.0	21.8	27.0	16.5	47.0	34.5	13.0	63.8	34.8	11.5	7.5	4.0
11	2.5	11.5	11.0	3.5	3.3	23.0	10.5	25.0	18.0	5.0	2.8	2.0
Average	3.9	20.1	26.5	12.5	29.9	37.7	14.2	21.6	31.2	14.7	7.2	3.9

pared in methanol. A working internal standard solution (0.5 μg/ml) was prepared by diluting 1 ml of the stock solution to 200 ml with distilled water. A working standard caramiphen solution (100 ng/0.1 ml) was prepared by diluting 1 ml of the stock solution to 100 ml with distilled water.

Extraction Procedure—Aliquots of 0, 12.5, 25, 50, 75, 100, 150, 200, 300, and 400 μl of the working standard solution of I were added to 5 ml of blank whole blood in 12-ml silanized test tubes. A 0.5-ml aliquot of the working internal standard solution was added to each tube. These samples were used to generate a standard curve. A 0.5-ml aliquot of the internal standard solution was added to all unknown samples (5-ml aliquots).

The pH was adjusted to 9.0 with 5% NaOH. A 1-ml aliquot of hexane was added, and the tubes were stoppered and shaken slowly (65 shakes/min) on an automatic shaker[9] for 30 min and centrifuged[10] for 10 min. The hexane layer was transferred to a second 12-ml silanized test tube, and the blood was extracted with another 1-ml aliquot of hexane with shaking for 30 min and centrifugation for 10 min. The second hexane extract was added to the first extract, and the combined solution was evaporated to dryness under a nitrogen stream. The residue was dissolved in 25 μl of methanol. Aliquots (2 μl) were injected into the gas chromatograph.

Calculations—A calibration curve was constructed by plotting the peak height ratio of caramiphen to the internal standard against the blood concentration of caramiphen on linear coordinate paper. Unknown values were read from the calibration curve.

RESULTS AND DISCUSSION

Figure 1 is a typical chromatogram of a spiked blood sample used for the standard curve. The peak at 1.6 min represents 20 ng of caramiphen/ml, and the peak at 2.7 min represents the internal standard (total of 250 ng added).

Spiked standards over the range of 2.5–40 ng/ml were analyzed. Table I shows the standard deviation and standard error obtained.

The assay sensitivity was <2.5 ng/ml of blood. Calibration curves were linear over the range of 2.5–80 ng of caramiphen/ml of blood.

Caramiphen is stable in frozen whole blood specimens for at least 1 week. Its stability was not studied beyond this period.

After overnight fasting, 11 subjects received 20 mg of caramiphen edisylate (plain drug in capsule) at 0, 4, and 8 hr daily for 4 consecutive days. On the 4th day, blood was drawn in heparinized syringes at 0, 1, 2, 4, 5, 6, 8, 9, 10, 13, 18, and 24 hr. The levels of caramiphen found are shown in Table II.

All 11 blood samples were screened before drug administration, and no interference peaks appeared in the area of caramiphen or its internal standard. These control bloods were spiked with the caramiphen standards and the internal standard. Based on these studies, the method was judged as specific for the determination of caramiphen in blood from controlled clinical studies when the subjects were free from other medication.

The sensitivity, reproducibility, and specificity make this method desirable for bioavailability and pharmacokinetic studies.

[9] Arthur H. Thomas Co.
[10] International, Arthur H. Thomas Co.

REFERENCES

(1) D. N. Bailey and P. I. Jatlow, *Clin. Chem.*, **22**, 1697 (1976).
(2) D. J. Hoffman, *J. Pharm. Sci.*, **68**, 445 (1979).
(3) H. H. C. Li, W. P. Feeney, and M. M. Johnston, *ibid.*, **68**, 569 (1979).

ACKNOWLEDGMENTS

The authors thank Dr. R. Stote and the staff of the Clinical Research Group of the Presbyterian University of Pennsylvania Medical Center for conducting the bioavailability study.

Comparative Plasma Salicylate and Urine Salicylurate Levels following Administration of Aspirin, Magnesium Salicylate, and Choline Magnesium Trisalicylate

WILLIAM D. MASON

Received April 25, 1980, from the *Pharmacokinetics Laboratory, Schools of Pharmacy and Medicine, University of Missouri-Kansas City, Kansas City, MO 64108.* Accepted for publication May 23, 1980.

Abstract □ Eighteen healthy volunteers were administered single doses of commercially available solid dosage forms of aspirin, magnesium salicylate (I), and choline magnesium trisalicylate (II), equivalent to ~500 mg of salicylic acid, in a randomized, complete crossover design. Plasma salicylate and urine salicylurate levels were measured by high-pressure liquid chromatography at frequent intervals following dosing; the resultant profiles, areas under the curve (*AUC*), and percentages of dose excreted as salicylurate were statistically analyzed by an analysis of variance. The plasma salicylate levels following the two dosage forms containing I and II were virtually identical when corrected for small differences in the dose. The plasma salicylic acid level following aspirin was ~10% lower during the 1.5–3.0-hr interval due to a portion of unhydrolyzed aspirin, but the dose-corrected *AUC* for the products tested did not differ significantly ($p < 0.05$). During the 24 hr following dosing, 66.5 ± 12.1, 68.4 ± 7.1, and 60.9 ± 14.1% of the salicylic acid were excreted as urine salicylurate for aspirin, I, and II, respectively, with no significant difference ($p < 0.05$). Based on this study, there are no significant differences in the rate and extent of absorption of salicylate following the three dosage forms tested, and the elimination kinetics of salicylic acid are not altered by these dosage forms.

Keyphrases □ Salicylate—comparison of plasma levels following administration of aspirin, magnesium salicylate, and choline magnesium trisalicylate □ Aspirin—plasma salicylate levels following administration of solid dosage form, comparison with magnesium salicylate and choline magnesium trisalicylate □ Magnesium salicylate—plasma salicylate levels following administration of solid dosage form, comparison with aspirin and choline magnesium trisalicylate □ Choline magnesium trisalicylate—plasma salicylate levels following administration of solid dosage form, comparison with aspirin and magnesium salicylate

Relatively high doses of salicylate, primarily as aspirin, frequently are indicated for prolonged periods in the treatment of rheumatoid arthritis. This intensive salicylate therapy commonly is associated with GI disturbances and acute blood loss (1). Recent reports (2–4) suggested that choline magnesium trisalicylate (II) can effectively deliver salicylate without the gastric irritation associated with aspirin. Magnesium salicylate (I) also was reported[1] to be less irritating to the gastric mucosa than aspirin.

If the two salts of salicylic acid are to be used as alternatives to aspirin, it is important to know the rate and extent of their absorption compared to aspirin. Furthermore, because the kinetics of metabolism and excretion of salicylate are complex and serum concentration dependent, the potential influence of the dosage form on elimination also should be evaluated. In the present study, plasma salicylate and urine salicylurate profiles following equivalent single doses of aspirin, I, and II were measured.

EXPERIMENT

Drug Products—Three commercially available products were chosen to provide aspirin[2], magnesium salicylate[3], and choline magnesium salicylate[4]. The salicylate content of each was determined and is reported with the results.

Clinical Protocol—Eighteen male volunteers underwent a comprehensive examination including urine analysis and hematological and blood chemistry determinations to ensure that they were in good health. Volunteers ranged in age from 18 to 24 years and in weight from 62 to 85 kg, and all were within ±20% of ideal body weight. No volunteer had a history of chronic drug use, and none had taken any medications, including salicylate, during the 14 days preceding the study. The three drugs were administered as single doses, equal to ~500 mg of salicylic acid, following a randomized, complete crossover design with a minimum of 3 days between doses.

Following an 8-hr fast, drugs were administered with 240 ml of water; no additional food or water was allowed until a standard meal was given following the 4-hr blood sample. Blood samples were taken *via* an indwelling catheter from a forearm vein, with heparin used to maintain the patency of the catheter. Vacutainer tubes[5] were chilled and samples were handled as described previously (5) to ensure stability. Blood (7 ml) was collected prior to dosing and at 15, 30, 45, and 60 min and 1.5, 2, 3, 4, 8, 12, and 16 hr after dosing. All urine voided was collected 6 hr prior to dosing and for the 0–12- and 12–24-hr intervals following dosing.

Plasma salicylate and urine salicylurate levels were determined by the previously described (5) high-pressure liquid chromatographic method with two modifications. Since the unhydrolyzed aspirin was not to be measured, the retention times of salicylic acid and urine salicylurate were decreased by increasing the amount of acetonitrile in the mobile phase to 22.5%. Only fluorescence detection was employed, with metaanisic acid as the internal standard. A comprehensive evaluation of the method proved its sensitivity, specificity, and reproducibility to be equal or better than published values (5). Samples were stored at −30° prior to analysis.

RESULTS AND DISCUSSION

Table I presents the mean plasma salicylic acid and urine salicylurate levels with the computed parameters and statistical analysis. Estimates of the area under the curves (*AUC*) up to the 16-hr sample [AUC_{0-16} in (micrograms times hours) per milliliter] were computed by the trapezoidal method, and the half-lives were calculated by linear regression of the natural logarithm of the plasma concentration *versus* time for the 4-, 8-, 12-, and 16-hr samples. The *AUC* to infinity [$AUC_{-\infty}$ in (micrograms times hours) per milliliter] was computed as $AUC_{0-16} + 1.44t_{1/2}C_{p16}$, while the maximum plasma concentration, $C_{p\max}$, and the time of $C_{p\max}$, $t_{\max}$, were read directly from the data for each volunteer. The urine salicylurate level is reported as the total milligrams excreted during the 0–12-, 12–24-, and 0–24-hr periods and as the percentage of the dose of salicylate excreted as salicylurate in 24 hr.

As expected, the analysis of variance showed no significant difference in the plasma salicylate level between I and II at any time, while the plasma salicylate level following aspirin was slightly lower during the 1.5–3.0-hr interval. This small difference in the plasma salicylate level probably was due to a portion of the aspirin being unhydrolyzed during the early part of the sampling period. Over the 16 hr, the hydrolysis of aspirin produced more salicylate, with the dose-corrected AUC_{∞},

[1] D. Earnest, Arizona Medical Center, University of Arizona, Tucson, Ariz., personal communication.

[2] Bayer Aspirin, Glenbrook Laboratories, Division of Sterling Drug, New York, N.Y.

[3] Magan, Adria-Warren Teed Pharmaceuticals, Columbus, Ohio.

[4] Trilisate, Purdue Frederick Co., Norwalk, Conn.

[5] Becton-Dickinson 278-069, 7.0 ml containing 14 mg of potassium oxalate and 17.5 mg of sodium fluoride.

0022-3549/80/1100-1355$01.00/0
© 1980, American Pharmaceutical Association

Table I—Mean Plasma Salicylic Acid and Urine Salicyluric Acid Levels following Three Sources of Salicylate

Parameter	Plasma Concentration, μg/ml [Mean[a] ± *SD* (*n* = 18)]		
	Aspirin (494 mg of Salicylic Acid)	Magnesium Salicylate (481 mg of Salicylic Acid)	Choline Magnesium Trisalicylate (500 mg of Salicylic Acid)
0 hr	<0.05 *a*	<0.05 *a*	<0.05 *a*
0.25 hr	10.7 ± 8.94 *a*	11.2 ± 8.71 *a*	7.27 ± 4.81 *a*
0.50 hr	22.7 ± 10.5 *a*	24.5 ± 11.0 *a*	19.0 ± 8.17 *a*
0.75 hr	28.0 ± 9.49 *a*	31.2 ± 12.2 *a*	28.4 ± 10.42 *a*
1.0 hr	30.9 ± 8.98 *a*	33.6 ± 11.5 *a*	35.4 ± 10.42 *a*
1.5 hr	32.9 ± 7.41 *a*	36.5 ± 6.10 *a,b*	37.5 ± 7.97 *b*
2.0 hr	33.1 ± 5.74 *a*	35.0 ± 5.06 *b*	36.5 ± 5.71 *b*
2.5 hr	31.9 ± 5.39 *a*	33.0 ± 4.65 *a,b*	34.4 ± 5.41 *b*
3.0 hr	30.5 ± 5.28 *a*	30.8 ± 4.53 *a*	32.0 ± 5.36 *b*
4.0 hr	26.4 ± 5.35 *a*	25.5 ± 4.88 *a*	27.4 ± 4.65 *a*
8.0 hr	11.0 ± 3.92 *a*	10.5 ± 2.82 *a*	11.1 ± 3.18 *a*
12.0 hr	3.27 ± 2.09 *a*	2.86 ± 1.14 *a*	3.20 ± 1.39 *a*
16.0 hr	0.908 ± 0.786 *a*	0.695 ± 0.322 *a*	0.783 ± 0.388 *a*
AUC_{16}, (μg hr)/ml	224 ± 49.6 *a*	223 ± 40.5 *a*	232 ± 42.1 *a*
$t_{½}$, hr	2.02 ± 0.399 *a*	2.01 ± 0.196 *a*	2.05 ± 0.198 *a*
AUC_{∞}, (μg hr)/ml	226 ± 52.5 *a*	225 ± 41.4 *a*	235 ± 43.2 *a*
$C_{p_{max}}$, μg/ml	35.9 ± 5.87 *a*	39.1 ± 6.21 *b*	41.4 ± 6.75 *b*
t_{max}, hr	1.64 ± 0.698 *a*	1.44 ± 0.670 *a*	1.54 ± 0.583 *a*
$AUC_{\infty}/D \times 10^3$, hr/ml	0.46 ± 0.11 *a*	0.47 ± 0.09 *a*	0.47 ± 0.09 *a*
$C_{p_{max}}/D \times 10^3$, ml^{-1}	0.07 ± 0.01 *a*	0.08 ± 0.01 *b*	0.08 ± 0.01 *b*
SU_{0-12^b}, mg	407 ± 90.5 *a*	393 ± 69.3 *a*	369 ± 77.7 *a*
SU_{12-24}, mg	57.4 ± 33.2 *a*	69.9 ± 68.3 *a*	65.7 ± 48.1 *a*
SU_{0-24}, mg	464 ± 84.7 *a*	465 ± 48.5 *a*	430 ± 99.3 *a*
Percent salicylic acid as salicylurate	66.5 ± 12.1 *a*	68.4 ± 7.1 *a*	60.9 ± 14.1 *a*

[a] A common letter indicates no significant difference ($p < 0.05$) by an analysis of variance and the least-significant difference method (8). [b] Salicylurate excreted.

AUC_{∞}/D, being equivalent to the products containing salicylate salts. Furthermore, the absorption rate as indicated by the time to reach the maximum plasma concentration did not differ significantly among the three products tested.

The percentage of salicylate excreted as salicylurate agreed closely with previous observations (6, 7) and did not differ significantly ($p < 0.05$) among the three treatments. Moreover, the apparent elimination half-life of 2.0 hr was identical for the three treatments and was as expected for a single 500-mg dose. Although chronic administration should produce a longer half-life (6, 7), this result will not be dependent on the dosage form as long as the rate and extent of absorption do not differ substantially.

Based on the present study, the absorption and elimination kinetics and the resultant plasma concentration of salicylate following administration of the commercially available solid dosage forms of I and II are virtually identical. Furthermore, administration of commonly employed aspirin tablets provides a plasma salicylate level that is only slightly lower (10%) at the peak time due to some unhydrolyzed aspirin being present. Over a 16-hr period, and probably on chronic dosing, there would be no significant differences in the plasma salicylate level.

The possible therapeutic implications of these observations depend on the importance of unhydrolyzed aspirin in the body and the possible effects the different forms of salicylate may have on the GI mucosa over time. However, based solely on the plasma salicylate concentration produced, there is no reason to differentiate among the three sources of salicylate evaluated in the present study.

REFERENCES

(1) B. M. Rothschild, *Clin. Pharmacol. Ther.*, **26**, 145 (1979).

(2) A. Cohen and H. E. Carber, *Curr. Ther. Res.*, **23**, 187 (1978).

(3) A. Cohen, *ibid.*, **23**, 772 (1978).

(4) S. Cassell, D. Furst, S. Dromgoole, and H. Paulus, *Arthritis Rheum.*, **22**, 384 (1979).

(5) E. N. Amick and W. D. Mason, *Anal. Lett.*, **12**, 629 (1979).

(6) T. Tsuchiya and G. Levy, *J. Pharm. Sci.*, **61**, 800 (1972).

(7) G. Levy, *ibid.*, **54**, 959 (1965).

(8) J. C. R. Li, "Statistical Inference," vol. 1, Edwards Brothers, Ann Arbor, Mich., 1964, p. 265.

New Compounds: Synthesis of *para*-Substituted Nortropanyl Benzoates

J. L. WALLACE *, M. R. KIDD *x, S. E. CAUTHEN *, and J. D. WOODYARD ‡

Received January 28, 1980, from the **Department of Chemistry, Northeast Louisiana University, Monroe, LA 71201,* and the ‡*Department of Chemistry and Killgore Research Center, West Texas State University, Canyon, TX 79016.* Accepted for publication May 7, 1980.

Abstract □ The syntheses of the *p*-methyl-, *p*-*tert*-butyl-, *p*-chloro-, *p*-cyano-, *p*-amino-, and unsubstituted benzoate esters of nortropine are reported. These compounds were characterized by their NMR, IR, and mass spectra and analytical data.

Keyphrases □ Nortropanyl benzoate—*para*-substituted derivatives, synthesis, NMR, IR, and mass spectral characterization □ Tropanyl esters—demethylation to yield nortropanyl esters for comparison of kinetic data

To investigate the role of the tropanyl *N*-methyl group in the substrate specificity of rabbit serum atropin esterase, a series of nortropanyl benzoate esters was required. Specifically, the kinetic data will be compared to those obtained with the tropanyl benzoates (1). These compounds also will be useful in a continuing study of the anticholinergic properties of tropanyl benzoate (*endo*-8-azabicyclo[3.2.1]octan-3-yl benzoate) and its *para*-substituted methyl, methoxy, *tert*-butyl, chloro, cyano, and amino derivatives.

The most direct approach for producing the nortropanyl esters is demethylation of the corresponding tropanyl esters. Of the methods available for removal of *N*-methyl

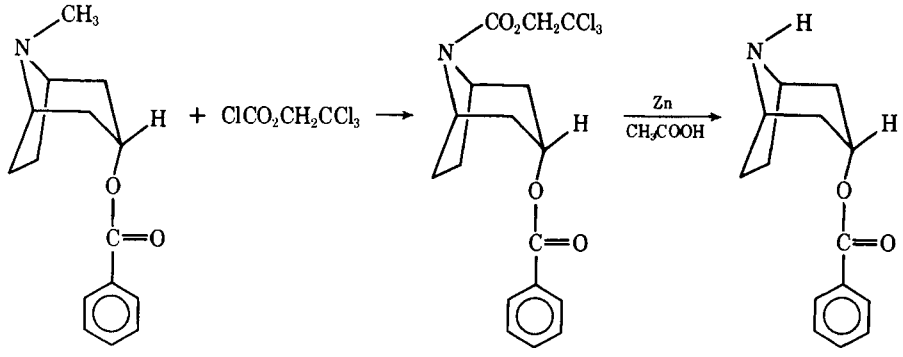

Scheme I

Table I—Physical Data of *para*-Substituted Nortropanyl Benzoates

Substituent	Melting Point	Melting Point of Hydrochloride	Yield, %	Formula	Analysis, % Calc.	Found
H	92–93°	314–315° dec. 214–216° (4) 241–244°[a]	27	$C_{14}H_{17}NO_2$	C 72.70 H 7.41 N 6.06 O 13.83	72.53 7.44 6.06 13.58
CH_3	83–84°	343–345° dec.	47	$C_{15}H_{19}NO_2$	C 73.43 H 7.81 N 5.71 O 13.05	73.23 7.78 5.65 12.86
OCH_3	61–63°	302–303° dec.	46	$C_{15}H_{19}NO_3$	C 68.93 H 7.33 N 5.36 O 18.37	69.79 7.46 5.31 18.22
tert-Butyl	117–118°	258–265° dec.	36	$C_{18}H_{25}NO_2$	C 75.23 H 8.77 N 4.78 O 11.13	75.09 8.94 4.87 11.23
Cl	117–118°	317–318° dec.	17	$C_{14}H_{16}ClNO_2$	C 63.28 H 6.07 Cl 13.34 N 5.27 O 12.04	63.17 6.23 13.27 5.27 11.87
CN	144–145°	293–294° dec.	22	$C_{15}H_{16}N_2O_2$	C 70.29 H 6.29 N 10.93 O 12.48	70.40 6.37 10.87 12.30
NH_2	153–155°	250–252° dec.	30	$C_{14}H_{18}N_2O_2$	C 68.27 H 7.37 N 11.37 O 12.99	68.20 7.38 11.19 12.69

[a] As the picrate.

0022-3549/80/1100-1357$01.00/0
© 1980, American Pharmaceutical Association

Table II—Spectral Data of *para*-Substituted Nortropanyl Benzoates

Substituent	Molecular Ion, *m/e* (% of base peak)	IR Spectrum (Potassium Bromide), cm^{-1}	^{1}H-NMR Spectrum (Deuterochloroform), δ					
			Aromatic	H-3	H-1, H-5	H-8[a]	H-2, H-4, H-6, H-7	R
H	231 (0.7)	3400 b, 3160, 2960, 1710, 1455, 1325, 1280, 1260, 1220, 1180, 1125, 1075, 1030, 860, 710	7.27–8.10	5.28	3.52	—	1.80, 1.87, 1.95, 2.00, 2.05, 2.10, 2.15, 2.23 (sh)	—
CH_3	245 (3.6)	3400 b, 3240, 2950, 1710, 1605, 1360, 1280, 1260, 1180, 1110, 1085, 1000, 855, 760, 690	7.15–7.70	5.30	3.54	1.75	1.85, 1.87 (sh), 2.00, 2.05, 2.07, 2.17, 2.23	2.43
OCH_3	261 (1.4)	3400 b, 2940, 1695, 1600, 1570, 1500, 1420, 1280, 1260, 1170, 1115, 1100, 1035, 845, 770	6.79–8.05	5.27	3.52	—	1.70, 1.80, 1.83, 1.93 (sh), 2.00, 2.03, 2.10, 2.15, 2.23	3.82
tert-Butyl	287 (0.7)	3420 b, 3300, 2960, 1705, 1610, 1465, 1410, 1280, 1260, 1190, 1125, 970, 855, 775, 710	7.42–8.07	5.32	3.57	1.80	1.95, 2.02, 2.07, 2.15, 2.17, 2.27	1.37
Cl	265 (4.3)	3400 b, 3240, 2940, 1710, 1590, 1485, 1400, 1360, 1275, 1260, 1170, 1120, 1000, 855, 760	7.20–8.00	5.27	3.53	1.63	1.77, 1.85, 1.95, 2.02, 2.05, 2.18, 2.27	—
CN	256 (2.9)	3400 b, 3235, 2940, 2245, 1710, 1410, 1315, 1285, 1265, 1120, 1090, 1005, 855, 775, 700	6.67–8.27	5.35	3.58	1.73	1.80 (sh), 1.90, 1.98 (sh), 2.08, 2.12 (sh), 2.20, 2.27, 2.32	—
NH_2	246 (0.4)	3440, 3375, 3290, 2940, 1680, 1600, 1515, 1310, 1280, 1260, 1165, 1110, 1000, 850, 770	6.65–7.96	5.26	3.54	—	1.76, 1.80, 1.84, 1.95, 1.98, 2.03, 2.09, 2.15, 2.23	4.13

[a] These assignments were determined upon addition of deuterium oxide.

groups, the use of 2,2,2-trichloroethyl chloroformate followed by reductive cleavage by zinc in acetic acid (Scheme I) appeared to be the best procedure since it preserves the ester linkage and avoids the benzoylation of a secondary amine alcohol. This method was reported by Woodward (2) and later used (3) to obtain nortropanyl acetate. The nortropanyl esters reported here were characterized by their NMR, IR, and mass spectra and analytical data.

EXPERIMENTAL[1]

The tropanyl benzoate was dissolved in 30 ml of benzene; if a cloudy solution was obtained, the benzene–water azeotrope was distilled until the solution was clear. Potassium carbonate and distilled 2,2,2-trichloroethyl chloroformate were added, and the mixture was refluxed for 4 days. A second portion of the chloroformate, equal to the first portion, was added after 2 days. The mixture was filtered, and the solvent was removed from the filtrate.

The clear residue was dissolved in a minimum amount of acetic acid. Zinc dust was added slowly over 2 hr, with sufficient cooling to maintain room temperature, until bubbling was no longer evident. The acetic acid was removed by evaporation, and 100 ml of water was added. The slurry was made basic with sodium hydroxide, which produced a copious white precipitate. This mixture was extracted with ethyl acetate. The extract was dried over magnesium sulfate, and the solvent was removed. The resulting free base was purified by recrystallization of its hydrochloride salt in ethanol. Analytical samples were sublimed (Table I).

[1] Mass spectra were obtained on a DuPont Dimaspec 321 gas chromatograph–mass spectrometer with a DuPont 320 data system using solid-probe introduction and ionization at 70 ev. NMR spectra were determined in deuterochloroform with a Varian Associates EM-390 NMR spectrometer using tetramethylsilane as the internal standard. IR spectra were recorded on a Beckman Acculab 6 spectrometer. Melting points were obtained using an Electrothermal apparatus and are corrected. Elemental analyses were performed by Galbraith Laboratories, Knoxville, Tenn. The 2,2,2-trichloroethyl chloroformate was obtained from Aldrich Chemical Co.

RESULTS AND DISCUSSION

All of the esters furnished the expected NMR spectra. They were comparable to those of the previously reported tropanyl benzoates except that the bridgehead protons appeared ~0.4 ppm downfield. The mass spectra base peak for all of the compounds was *m/e* 110, corresponding to the nortropanyl ion. In all spectra, there were peaks at *m/e* 68, 80, and 126. The substituted benzoyl and phenyl fragments were detected in all cases except for the *p-tert*-butyl compound. The molecular ion peaks were observed and were of low relative intensity compared to the tropanyl benzoates (1). A summary of these data appears in Table II.

REFERENCES

(1) J. L. Wallace, M. R. Kidd, S. E. Cauthen, and J. D. Woodyard, *J. Heterocycl. Chem.*, **15**, 317 (1978).

(2) R. B. Woodward, *Science*, **153**, 487 (1966).

(3) T. A. Montzka, J. D. Matiskella, and R. A. Partyka, *Tetrahedron Lett.*, **1974**, 1325.

(4) G. Fodor and K. Nádor, *J. Chem. Soc.*, **1953**, 721.

ACKNOWLEDGMENTS

The authors thank Dr. M. G. Reinecke, Texas Christian University, for helpful suggestions and the School of Pharmacy, Northeast Louisiana University, for the mass spectra. The authors also acknowledge the financial support of the Public Health Service (Grant GM 20977) and the Robert A. Welch Foundation (Grant AE-361).

Acetylation of Sulfisoxazole by Isolated Perfused Rat Kidney

Keyphrases □ Sulfisoxazole—renal metabolism to N^4-acetyl metabolite using the isolated perfused rat kidney □ Metabolism, renal—sulfisoxazole, acetylation by the isolated perfused rat kidney

To the Editor:

Although the kidneys contain many metabolizing enzymes of the liver (1), renal drug metabolism has received limited attention, due partially to the relegation of the kidneys to organs of excretion. The isolated perfused kidney is a useful technique for studies of the renal disposition of drugs. In many cases, experiments with the isolated perfused kidney give results that are consistent with data obtained from *in vivo* studies and more clearly define the role of the kidneys in the overall disposition of a drug. In our laboratory, the isolated perfused kidney has been used in renal clearance studies of several compounds (2, 3) as well as in studies of renal metabolism and interconversion of salicylic and salicyluric acids (4).

Since sulfisoxazole (I) is eliminated largely by renal excretion, it can be influenced by protein binding, urinary pH, and the urine flow rate (5, 6). Studies in our laboratory on the renal clearance of sulfisoxazole by the isolated perfused kidney indicated that rat kidneys metabolize this drug to its N^4-acetyl metabolite (II).

Male Sprague–Dawley rats, 350–375 g, were used in the isolated perfused kidney experiments. The surgical technique and experimental details were reported previously (2–4). Sulfisoxazole (6.5 mg) was administered to attain an initial concentration of ~100 μg/ml, and perfusion was continued for 90 min. The experimental time was divided into nine 10-min urine collection periods. Urine samples were assayed for sulfisoxazole and N^4-acetylsulfisoxazole by a modified high-performance liquid chromatographic assay (7).

The mean urinary excretion rates for N^4-acetylsulfisoxazole and sulfisoxazole from five perfusion experiments are presented in Table I. Although the amounts of N^4-acetylsulfisoxazole excreted in the urine were low, they accounted for 5–7% of the total drug excreted as sulfisoxazole plus N^4-acetylsulfisoxazole during the 90-min experiment. Previous *in vivo* experiments on elimination of sulfisoxazole in the rat indicated that, of the total drug excreted in the urine, 12% is excreted as the N-acetyl metabolite (8). The present results thus indicate that half of the excreted N-acetyl metabolite is due to renal metabolism and that, in the rat, the kidneys contribute significantly to the metabolic disposition of sulfisoxazole.

Table I—Urinary Excretion Rates of N^4-Acetylsulfisoxazole (II) Formed by the Perfused Rat Kidney following Administration of 6.5 mg of Sulfisoxazole (I)

Minutes	Urinary Excretion Rate, μg/10 min	
	II	I
10	0.87 ± 0.25[a]	11.12 ± 4.24[a]
20	1.16 ± 0.62	18.78 ± 10.02
30	1.08 ± 0.57	18.40 ± 5.72
40	1.74 ± 0.55	27.98 ± 12.82
50	1.58 ± 0.48	31.13 ± 18.28
60	1.45 ± 0.47	34.70 ± 18.21
70	1.58 ± 0.38	28.30 ± 8.42
80	1.53 ± 0.19	27.30 ± 6.09
90	1.43 ± 0.27	28.38 ± 7.08
Total	12.06	226.02

[a] Mean ± *SD*, $n = 5$.

(1) P. D. Boyer, H. Landy, and K. Myrback, "The Enzymes," vol. 4, 2nd ed., Academic, New York, N.Y., 1960.
(2) I. Bekersky, W. J. Poynor, and W. A. Colburn, *Drug Metab. Disp.*, **8**, 64 (1980).
(3) I. Bekersky, L. Fishman, S. A. Kaplan, and W. A. Colburn, *J. Pharmacol. Exp. Ther.*, **212**, 309 (1980).
(4) I. Bekersky, W. A. Colburn, L. Fishman, and S. A. Kaplan, *Drug Metab. Disp.*, **8**, 319 (1980).
(5) M. Cohen and R. Pocelinko, *J. Pharmacol. Exp. Ther.*, **185**, 703 (1973).
(6) A. Yacobi and G. Levy, *J. Pharm. Sci.*, **68**, 742 (1979).
(7) D. Jung and S. Øie, *Clin. Chem.*, **26**, 51 (1980).
(8) D. C. Bloedow and W. L. Hayton, *J. Pharm. Sci.*, **65**, 334 (1976).

Ihor Bekersky
Wayne A. Colburn ˣ
Department of Pharmacokinetics and Biopharmaceutics
Hoffmann-La Roche Inc.
Nutley, NJ 07110

Received June 6, 1980.
Accepted for publication August 26, 1980.

Anti-Inflammatory Activity of Cannabichromene Homologs

Keyphrases □ Anti-inflammatory activity—evaluation of cannabichromene homologs □ Cannabichromene homologs—evaluation for anti-inflammatory activity

To the Editor:

As part of our continuing study of the cannabinoids, we recently reported that cannabichromene has anti-inflammatory activity. The two tests used to show this activity were the carrageenan-induced rat paw edema test and the red cell stabilization assay (1). To determine the effect of changing the length and position of the side chain of cannabichromene on its anti-inflammatory activity, four homologs were prepared and tested.

Cannabichromene-C_5 (I), cannabichromene-C_1 (II), and cannabichromene-C_0 (III) were prepared following the procedure outlined previously (2), starting from olivetol, orcinol, and resorcinol, respectively. The yield of I was

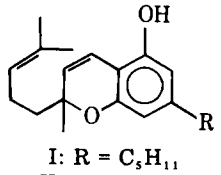

I: R = C_5H_{11}
II: R = CH_3
III: R = H

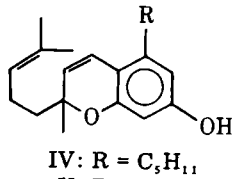

IV: R = C_5H_{11}
V: R = H

0022-3549/80/1100-1359$01.00/0
© 1980, American Pharmaceutical Association

Acetylation of Sulfisoxazole by Isolated Perfused Rat Kidney

Keyphrases □ Sulfisoxazole—renal metabolism to N^4-acetyl metabolite using the isolated perfused rat kidney □ Metabolism, renal—sulfisoxazole, acetylation by the isolated perfused rat kidney

To the Editor:

Although the kidneys contain many metabolizing enzymes of the liver (1), renal drug metabolism has received limited attention, due partially to the relegation of the kidneys to organs of excretion. The isolated perfused kidney is a useful technique for studies of the renal disposition of drugs. In many cases, experiments with the isolated perfused kidney give results that are consistent with data obtained from *in vivo* studies and more clearly define the role of the kidneys in the overall disposition of a drug. In our laboratory, the isolated perfused kidney has been used in renal clearance studies of several compounds (2, 3) as well as in studies of renal metabolism and interconversion of salicylic and salicyluric acids (4).

Since sulfisoxazole (I) is eliminated largely by renal excretion, it can be influenced by protein binding, urinary pH, and the urine flow rate (5, 6). Studies in our laboratory on the renal clearance of sulfisoxazole by the isolated perfused kidney indicated that rat kidneys metabolize this drug to its N^4-acetyl metabolite (II).

Male Sprague–Dawley rats, 350–375 g, were used in the isolated perfused kidney experiments. The surgical technique and experimental details were reported previously (2–4). Sulfisoxazole (6.5 mg) was administered to attain an initial concentration of ~100 μg/ml, and perfusion was continued for 90 min. The experimental time was divided into nine 10-min urine collection periods. Urine samples were assayed for sulfisoxazole and N^4-acetylsulfisoxazole by a modified high-performance liquid chromatographic assay (7).

The mean urinary excretion rates for N^4-acetylsulfisoxazole and sulfisoxazole from five perfusion experiments are presented in Table I. Although the amounts of N^4-acetylsulfisoxazole excreted in the urine were low, they accounted for 5–7% of the total drug excreted as sulfisoxazole plus N^4-acetylsulfisoxazole during the 90-min experiment. Previous *in vivo* experiments on elimination of sulfisoxazole in the rat indicated that, of the total drug excreted in the urine, 12% is excreted as the N-acetyl metabolite (8). The present results thus indicate that half of the excreted N-acetyl metabolite is due to renal metabolism and that, in the rat, the kidneys contribute significantly to the metabolic disposition of sulfisoxazole.

Table I—Urinary Excretion Rates of N^4-Acetylsulfisoxazole (II) Formed by the Perfused Rat Kidney following Administration of 6.5 mg of Sulfisoxazole (I)

Minutes	Urinary Excretion Rate, μg/10 min	
	II	I
10	0.87 ± 0.25[a]	11.12 ± 4.24[a]
20	1.16 ± 0.62	18.78 ± 10.02
30	1.08 ± 0.57	18.40 ± 5.72
40	1.74 ± 0.55	27.98 ± 12.82
50	1.58 ± 0.48	31.13 ± 18.28
60	1.45 ± 0.47	34.70 ± 18.21
70	1.58 ± 0.38	28.30 ± 8.42
80	1.53 ± 0.19	27.30 ± 6.09
90	1.43 ± 0.27	28.38 ± 7.08
Total	12.06	226.02

[a] Mean ± *SD*, $n = 5$.

(1) P. D. Boyer, H. Landy, and K. Myrback, "The Enzymes," vol. 4, 2nd ed., Academic, New York, N.Y., 1960.
(2) I. Bekersky, W. J. Poynor, and W. A. Colburn, *Drug Metab. Disp.*, **8**, 64 (1980).
(3) I. Bekersky, L. Fishman, S. A. Kaplan, and W. A. Colburn, *J. Pharmacol. Exp. Ther.*, **212**, 309 (1980).
(4) I. Bekersky, W. A. Colburn, L. Fishman, and S. A. Kaplan, *Drug Metab. Disp.*, **8**, 319 (1980).
(5) M. Cohen and R. Pocelinko, *J. Pharmacol. Exp. Ther.*, **185**, 703 (1973).
(6) A. Yacobi and G. Levy, *J. Pharm. Sci.*, **68**, 742 (1979).
(7) D. Jung and S. Øie, *Clin. Chem.*, **26**, 51 (1980).
(8) D. C. Bloedow and W. L. Hayton, *J. Pharm. Sci.*, **65**, 334 (1976).

Ihor Bekersky
Wayne A. Colburn ˣ
Department of Pharmacokinetics and Biopharmaceutics
Hoffmann-La Roche Inc.
Nutley, NJ 07110

Received June 6, 1980.
Accepted for publication August 26, 1980.

Anti-Inflammatory Activity of Cannabichromene Homologs

Keyphrases □ Anti-inflammatory activity—evaluation of cannabichromene homologs □ Cannabichromene homologs—evaluation for anti-inflammatory activity

To the Editor:

As part of our continuing study of the cannabinoids, we recently reported that cannabichromene has anti-inflammatory activity. The two tests used to show this activity were the carrageenan-induced rat paw edema test and the red cell stabilization assay (1). To determine the effect of changing the length and position of the side chain of cannabichromene on its anti-inflammatory activity, four homologs were prepared and tested.

Cannabichromene-C_5 (I), cannabichromene-C_1 (II), and cannabichromene-C_0 (III) were prepared following the procedure outlined previously (2), starting from olivetol, orcinol, and resorcinol, respectively. The yield of I was

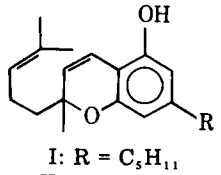

I: R = C_5H_{11}
II: R = CH_3
III: R = H

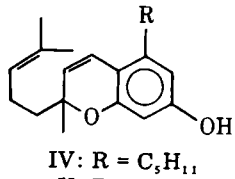

IV: R = C_5H_{11}
V: R = H

0022-3549/80/1100-1359$01.00/0
© 1980, American Pharmaceutical Association

Table I—Effectiveness of Cannabichromene and Its C_1 Homolog in Inhibiting Carrageenan-Induced Rat Paw Edema [a]

Compound	Dose, mg/kg	Inhibition, %	Mean Difference[b]	SEM	n	p[c]
Vehicle control	—	—	0.340	0.560	24	—
I	120	70	0.102	0.049	8	0.01
	240	86	0.048	0.020	8	0.001
	480	100	0.002	0.058	8	0.001
II	60	53	0.160	0.037	8	0.01
	120	63	0.126	0.031	8	0.001
	240	92	0.027	0.038	7	0.001
Phenylbutazone	60	52	0.163	0.023	8	0.01
	120	76	0.082	0.046	8	0.01

[a] Rats received intraperitoneal injections of test compounds 30 min prior to injection of carrageenan, and postinjection measurements were taken after 3 hr. [b] Preinjection volume − postinjection volume. [c] Each test group was compared to the vehicle control group using the Student t test.

~60% (molar conversion) and that of III was 48.3%, while the yield of II was only 10.8%. Although only trace amounts of the *iso*-compounds were formed from the C_5 and C_1 homologs, almost equal quantities of II and isocannabichromene-C_0 (V) were formed under the same conditions. Thus, the same reaction was used to prepare II and V. Similar yields of II and V were formed when the same reaction was carried out in pyridine. However, isocannabichromene-C_5 (IV) was prepared by refluxing olivetol with citral in pyridine at 110° for 7 hr following literature procedures (3, 4). Purification was carried out in all cases by column chromatography on silica gel with benzene–chloroform (1:1) as the solvent system.

Because cannabinoids often have been misidentified, all natural and synthetic cannabinoids were subjected to GLC and GLC–mass spectrometric analysis using electron voltage–mass fragment intensity graphs for positive identification. Trimethylsilyl derivatives were used when needed. All analyses were conducted in accordance with published protocols (5, 6).

Compounds I–V were tested using the red cell stabilization assay, and I and II also were tested using the rat paw edema assay. All testing was conducted using previously described methods (1). All of the test compounds and phenylbutazone (used as a positive control) were tested in the red cell stabilization assay at a final concentration of 1×10^{-4} *M*. Compounds I and II and phenylbutazone were tested in the rat paw edema assay at the intraperitoneal doses indicated in Table I. The intraperitoneal route was chosen because our previous work showed that cannabichromene is more effective by the intraperitoneal route than by the conventional oral route. Positive and negative controls were tested to ensure that the effects observed were true anti-inflammatory effects rather than the result of counterirritation.

Table II—Effectiveness of Cannabichromene Homologs on the Red Cell Stabilization Assay (n = 3) [a]

Compound	Inhibition, %	Mean[b]	SEM
Vehicle control	—	13.43	0.13
I	94	0.76	0.05
II	86	1.86	0.13
Phenylbutazone	66	4.59	0.11
Vehicle control	—	17.21	0.52
I	79	3.66	0.52
IV	75	4.27	0.25
III	69	5.34	0.75
V	43	9.86	0.53
Phenylbutazone	54	7.86	0.70

[a] All compounds were tested at a final concentration of 1×10^{-4} *M*. [b] Mean of three replicates of blood taken from the same dog. Compounds I and II were tested using blood from one dog, and I and III–V were tested using blood from a second dog. Vehicle positive controls from both tests are given.

Cannabichromene and its derivatives stabilized red cell membranes, as indicated by the inhibition of heat-induced hemolysis (Table II). They inhibited hemolysis more effectively than did phenylbutazone at equimolar concentrations, except for V. Both I and II inhibited carrageenan-induced rat paw edema at all doses tested. The percent inhibition produced by I and II was roughly equivalent to the inhibition produced by phenylbutazone when all were tested at 120 mg/kg. Phenylbutazone was not tested at 240 and 480 mg/kg since it is lethal at those doses.

The length and position of the side chain on the cannabichromene moiety appear to have little or no effect on its potency, with the possible exception of V. This indication is of interest since Hollister (7) found that the psychological effects of another *Cannabis* compound, (−)-*trans*-Δ^9-tetrahydrocannabinol, were diminished as the length of the side chain was reduced. For example, the C-3 side-chain homolog of (−)-*trans*-Δ^9-tetrahydrocannabinol was only ~25% as active as (−)-*trans*-Δ^9-tetrahydrocannabinol itself.

Further experiments on the anti-inflammatory effects of cannabichromene are in progress, and the results will be reported.

(1) P. W. Wirth, E. S. Watson, M. A. ElSohly, C. E. Turner, and J. C. Murphy, *Life Sci.*, **26**, 1991 (1980).

(2) M. A. ElSohly, E. G. Boren, and C. E. Turner, *J. Heterocycl. Chem.*, **15**, 699 (1978).

(3) L. Crombie and R. Ponsford, *Chem. Commun.*, **1968**, 894.

(4) L. Crombie and R. Ponsford, *J. Chem. Soc.*, **1971**, 796.

(5) C. E. Turner, K. W. Hadley, J. H. Holley, S. Billets, and M. L. Mole, Jr., *J. Pharm. Sci.*, **64**, 810 (1975).

(6) S. Billets, F. El-Feraly, P. S. Fetterman, and C. E. Turner, *Org. Mass. Spectrom.*, **11**, 741 (1976).

(7) L. E. Hollister, *Pharmacology*, **11**, 3 (1974).

Philip W. Wirth [x]
E. Sue Watson
Mahmoud A. ElSohly
Roger Seidel
James C. Murphy
Carlton E. Turner
Research Institute of Pharmaceutical Sciences
School of Pharmacy
University of Mississippi
University, MS 38677

Received May 27, 1980.
Accepted for publication August 27, 1980.
Supported by the Research Institute of Pharmaceutical Sciences.

REVIEWS

Principles of Pharmaceutical Accounting. By FRANCIS A. MARINO, EDWARD J. ZABLOSKI, and COLMAN M. HERMAN. Lea & Febiger, 600 Washington Square, Philadelphia, PA 19106. 1980. xi + 241 pp. 18 × 26 cm. Price $19.50.

Undergraduate pharmacy students and practicing pharmacists are the intended audience for this book on accounting principles. The major advantage of this book is that it was designed specifically for this audience. It ignores the concepts relevant primarily to multinational manufacturing conglomerates which are found in standard accounting texts, while including topics such as reconciliation of bank statements and determining prescription dispensing costs.

Most of the book is devoted to financial accounting (bookkeeping or the accumulation and summarization of financial data) rather than managerial accounting (the use of financial data to make management decisions). This reviewer recognizes that it is difficult for students to learn to use data properly without some background in how the data were generated.

While tables and figures are abundant, the amount of actual textual material is sparse. Terms tend not to be defined. It is assumed that the reader knows what gross profit is or will figure it out from its use. Examples tend to be used in place of definitions ("Cash includes . . . ." "Inventory consists of items such as . . . ."). It is 150 pages after "cash" is introduced that the reader learns that a certificate of deposit is an investment, not cash. The reader never is told that a bottle of aspirin for resale to a patient is inventory, while if the aspirin is consumed in the pharmacy by employees with a headache, it is a supplies expense.

Conspicuously absent in the book is any mention of UCAS (Uniform Cost Accounting System for Pharmacy). Also lacking is any guidance on what the pharmacy owner should look for in selecting an accountant or what services can be provided by an accountant.

The review questions and exercises at the end of each chapter are helpful aids in reinforcing the concepts presented.

It is not a compliment to say that this book is long overdue. It reflects a concept of the pharmacist keeping his or her own books and being his or her own accountant rather than managing a practice in which annual sales may be in excess of a half-million dollars.

As the only text of its kind in print, individual faculty members should review this book for possible use by students. Managers of community pharmacy practice are more likely to find that, although it is considerably more expensive, UCAS will more effectively satisfy their needs.

Reviewed by Maven J. Myers
Philadelphia College of Pharmacy and Science
Philadelphia, PA 19104

Activated Charcoal: Antidotal and Other Medical Uses. By DAVID O. COONEY. (Drugs and the Pharmaceutical Sciences, Vol. 9.) Dekker, 270 Madison Ave., New York, NY 10016. 1980. 160 pp. 15 × 23 cm. Price $23.50.

This book provides a much needed review of the literature concerning the use of activated charcoal for the treatment of acute drug overdose or poison ingestion. The first chapter emphasizes the advantages of orally administered activated charcoal for the treatment of acute poison ingestion relative to other common emergency measures, such as induced emesis and gastric lavage. Chapter 2 points out the historical highlights of charcoal, indicating that the use of medicinal charcoal was recorded in an Egyptian papyrus in 1500 B.C., that a great variety of starting materials were used in its manufacture, and that the process of activation (which greatly increases the adsorbent capacity of charcoal) was not introduced until 1900.

Chapter 3 describes the manufacture, physicochemical properties, and adsorptive process of activated charcoal. Such knowledge is important for understanding the differences among various charcoal preparations and why a certain charcoal may be more effective than other charcoals for adsorption of a specific chemical. Chapter 4 is devoted to a discussion of the five classical papers of A. H. Anderson, which were published between 1946 and 1948. These publications are important because they summarized many earlier studies on activated charcoal and reported the definitive studies of Anderson, which served as the basis for subsequent work by many investigators.

Chapter 5 discusses the antidotal aspects of activated charcoal, with commentaries on characteristics to be considered in the selection of the most suitable charcoal preparation for oral antidotal uses (*e.g.*, acid-washed charcoal, pore-size distribution predominantly in the 20-Å range, high internal surface areas, and a fine powder as opposed to granules or tablets), dosages, effects of delayed administration, stability of the charcoal–drug complex in the GI tract, storage stability of activated charcoal suspension, safety of activated charcoal, fallacies and dangers of the so-called universal antidote, and the development of palatable formulations of activated charcoal suspension.

Chapter 6 reviews the results of *in vitro* and *in vivo* studies of the binding and antidotal potentials of activated charcoal. A great amount of previously published data is included. Chapter 7 describes investigations of other possible medical or diagnostic applications of activated charcoal. Most of these works were published in the 1930s and are mainly of historical interest, *e.g.*, intravenous injection of activated charcoal for treatment of systemic infections. However, use of activated charcoal to bind bacterial toxins in certain GI infections appears rational, and the use of activated charcoal for hemoperfusion appears to be effective.

A few errors were obvious to the reviewer. On page 40, it is stated that the adsorption isotherm for strychnine nitrate (based on *in vitro* studies in human gastric contents) is presented in Fig. 4.8, but this figure is concerned with diethylbarbituric acid. On page 41, a statement is made in reference to Fig. 4.8 that a change in pH from 8.4 to 5.0 decreases charcoal adsorption of diethylbarbituric acid, whereas the reverse is shown in the figures. Also, the data presented in Fig. 4.3 and Table 5.7 are credited to the wrong authors. However, these errors do not detract from the usefulness of the book.

Probably very few references have escaped citation in this small volume. This book is a convenient source of information concerning the antidotal application of activated charcoal for management of drug overdose or poison ingestion and should be a useful reference for health professionals involved in the treatment of poisoning cases, poison control information centers, and people engaged in research.

Reviewed by Lincoln Chin
Department of Pharmacology and Toxicology
College of Pharmacy
University of Arizona
Tucson, AZ 85721

Prescription Drugs in Short Supply. By MICHAEL A. SCHWARTZ. (Drugs and the Pharmaceutical Sciences, Vol. 8.) Dekker, 270 Madison Ave., New York, NY 10016. 1980. 130 pp. 15 × 23 cm. Price $17.50.

This interesting book documents, by case histories, the shortage of some vital drugs that occurred between 1973 and 1976. Among the major sources of documented information are Senatorial hearings, reports to the Drug Enforcement Administration, various symposia, and the *Federal Register*.

Shortages of five substances are discussed in detail: opium, quinidine, heparin, two injectable penicillins, and some large- and small-volume parenterals. Although no deaths are known to have resulted from the shortages, it is highly likely that there were cases in which optimum patient care was not possible because substitute drugs had to be used.

The shortages were caused by a number of factors which were different in most instances for each substance. The demand for codeine increased significantly, which contributed to the shortage of opium. This increased demand was attributed to: (*a*) increases in population, (*b*) aging of the population, (*c*) an increase in third-party payments for medication, and

REVIEWS

Principles of Pharmaceutical Accounting. By FRANCIS A. MARINO, EDWARD J. ZABLOSKI, and COLMAN M. HERMAN. Lea & Febiger, 600 Washington Square, Philadelphia, PA 19106. 1980. xi + 241 pp. 18 × 26 cm. Price $19.50.

Undergraduate pharmacy students and practicing pharmacists are the intended audience for this book on accounting principles. The major advantage of this book is that it was designed specifically for this audience. It ignores the concepts relevant primarily to multinational manufacturing conglomerates which are found in standard accounting texts, while including topics such as reconciliation of bank statements and determining prescription dispensing costs.

Most of the book is devoted to financial accounting (bookkeeping or the accumulation and summarization of financial data) rather than managerial accounting (the use of financial data to make management decisions). This reviewer recognizes that it is difficult for students to learn to use data properly without some background in how the data were generated.

While tables and figures are abundant, the amount of actual textual material is sparse. Terms tend not to be defined. It is assumed that the reader knows what gross profit is or will figure it out from its use. Examples tend to be used in place of definitions ("Cash includes . . . ." "Inventory consists of items such as . . . ."). It is 150 pages after "cash" is introduced that the reader learns that a certificate of deposit is an investment, not cash. The reader never is told that a bottle of aspirin for resale to a patient is inventory, while if the aspirin is consumed in the pharmacy by employees with a headache, it is a supplies expense.

Conspicuously absent in the book is any mention of UCAS (Uniform Cost Accounting System for Pharmacy). Also lacking is any guidance on what the pharmacy owner should look for in selecting an accountant or what services can be provided by an accountant.

The review questions and exercises at the end of each chapter are helpful aids in reinforcing the concepts presented.

It is not a compliment to say that this book is long overdue. It reflects a concept of the pharmacist keeping his or her own books and being his or her own accountant rather than managing a practice in which annual sales may be in excess of a half-million dollars.

As the only text of its kind in print, individual faculty members should review this book for possible use by students. Managers of community pharmacy practice are more likely to find that, although it is considerably more expensive, UCAS will more effectively satisfy their needs.

Reviewed by Maven J. Myers
Philadelphia College of Pharmacy and Science
Philadelphia, PA 19104

Activated Charcoal: Antidotal and Other Medical Uses. By DAVID O. COONEY. (Drugs and the Pharmaceutical Sciences, Vol. 9.) Dekker, 270 Madison Ave., New York, NY 10016. 1980. 160 pp. 15 × 23 cm. Price $23.50.

This book provides a much needed review of the literature concerning the use of activated charcoal for the treatment of acute drug overdose or poison ingestion. The first chapter emphasizes the advantages of orally administered activated charcoal for the treatment of acute poison ingestion relative to other common emergency measures, such as induced emesis and gastric lavage. Chapter 2 points out the historical highlights of charcoal, indicating that the use of medicinal charcoal was recorded in an Egyptian papyrus in 1500 B.C., that a great variety of starting materials were used in its manufacture, and that the process of activation (which greatly increases the adsorbent capacity of charcoal) was not introduced until 1900.

Chapter 3 describes the manufacture, physicochemical properties, and adsorptive process of activated charcoal. Such knowledge is important for understanding the differences among various charcoal preparations and why a certain charcoal may be more effective than other charcoals for adsorption of a specific chemical. Chapter 4 is devoted to a discussion of the five classical papers of A. H. Anderson, which were published between 1946 and 1948. These publications are important because they summarized many earlier studies on activated charcoal and reported the definitive studies of Anderson, which served as the basis for subsequent work by many investigators.

Chapter 5 discusses the antidotal aspects of activated charcoal, with commentaries on characteristics to be considered in the selection of the most suitable charcoal preparation for oral antidotal uses (*e.g.*, acid-washed charcoal, pore-size distribution predominantly in the 20-Å range, high internal surface areas, and a fine powder as opposed to granules or tablets), dosages, effects of delayed administration, stability of the charcoal–drug complex in the GI tract, storage stability of activated charcoal suspension, safety of activated charcoal, fallacies and dangers of the so-called universal antidote, and the development of palatable formulations of activated charcoal suspension.

Chapter 6 reviews the results of *in vitro* and *in vivo* studies of the binding and antidotal potentials of activated charcoal. A great amount of previously published data is included. Chapter 7 describes investigations of other possible medical or diagnostic applications of activated charcoal. Most of these works were published in the 1930s and are mainly of historical interest, *e.g.*, intravenous injection of activated charcoal for treatment of systemic infections. However, use of activated charcoal to bind bacterial toxins in certain GI infections appears rational, and the use of activated charcoal for hemoperfusion appears to be effective.

A few errors were obvious to the reviewer. On page 40, it is stated that the adsorption isotherm for strychnine nitrate (based on *in vitro* studies in human gastric contents) is presented in Fig. 4.8, but this figure is concerned with diethylbarbituric acid. On page 41, a statement is made in reference to Fig. 4.8 that a change in pH from 8.4 to 5.0 decreases charcoal adsorption of diethylbarbituric acid, whereas the reverse is shown in the figures. Also, the data presented in Fig. 4.3 and Table 5.7 are credited to the wrong authors. However, these errors do not detract from the usefulness of the book.

Probably very few references have escaped citation in this small volume. This book is a convenient source of information concerning the antidotal application of activated charcoal for management of drug overdose or poison ingestion and should be a useful reference for health professionals involved in the treatment of poisoning cases, poison control information centers, and people engaged in research.

Reviewed by Lincoln Chin
Department of Pharmacology and Toxicology
College of Pharmacy
University of Arizona
Tucson, AZ 85721

Prescription Drugs in Short Supply. By MICHAEL A. SCHWARTZ. (Drugs and the Pharmaceutical Sciences, Vol. 8.) Dekker, 270 Madison Ave., New York, NY 10016. 1980. 130 pp. 15 × 23 cm. Price $17.50.

This interesting book documents, by case histories, the shortage of some vital drugs that occurred between 1973 and 1976. Among the major sources of documented information are Senatorial hearings, reports to the Drug Enforcement Administration, various symposia, and the *Federal Register*.

Shortages of five substances are discussed in detail: opium, quinidine, heparin, two injectable penicillins, and some large- and small-volume parenterals. Although no deaths are known to have resulted from the shortages, it is highly likely that there were cases in which optimum patient care was not possible because substitute drugs had to be used.

The shortages were caused by a number of factors which were different in most instances for each substance. The demand for codeine increased significantly, which contributed to the shortage of opium. This increased demand was attributed to: (*a*) increases in population, (*b*) aging of the population, (*c*) an increase in third-party payments for medication, and

REVIEWS

Principles of Pharmaceutical Accounting. By FRANCIS A. MARINO, EDWARD J. ZABLOSKI, and COLMAN M. HERMAN. Lea & Febiger, 600 Washington Square, Philadelphia, PA 19106. 1980. xi + 241 pp. 18 × 26 cm. Price $19.50.

Undergraduate pharmacy students and practicing pharmacists are the intended audience for this book on accounting principles. The major advantage of this book is that it was designed specifically for this audience. It ignores the concepts relevant primarily to multinational manufacturing conglomerates which are found in standard accounting texts, while including topics such as reconciliation of bank statements and determining prescription dispensing costs.

Most of the book is devoted to financial accounting (bookkeeping or the accumulation and summarization of financial data) rather than managerial accounting (the use of financial data to make management decisions). This reviewer recognizes that it is difficult for students to learn to use data properly without some background in how the data were generated.

While tables and figures are abundant, the amount of actual textual material is sparse. Terms tend not to be defined. It is assumed that the reader knows what gross profit is or will figure it out from its use. Examples tend to be used in place of definitions ("Cash includes . . . ." "Inventory consists of items such as . . . ."). It is 150 pages after "cash" is introduced that the reader learns that a certificate of deposit is an investment, not cash. The reader never is told that a bottle of aspirin for resale to a patient is inventory, while if the aspirin is consumed in the pharmacy by employees with a headache, it is a supplies expense.

Conspicuously absent in the book is any mention of UCAS (Uniform Cost Accounting System for Pharmacy). Also lacking is any guidance on what the pharmacy owner should look for in selecting an accountant or what services can be provided by an accountant.

The review questions and exercises at the end of each chapter are helpful aids in reinforcing the concepts presented.

It is not a compliment to say that this book is long overdue. It reflects a concept of the pharmacist keeping his or her own books and being his or her own accountant rather than managing a practice in which annual sales may be in excess of a half-million dollars.

As the only text of its kind in print, individual faculty members should review this book for possible use by students. Managers of community pharmacy practice are more likely to find that, although it is considerably more expensive, UCAS will more effectively satisfy their needs.

Reviewed by Maven J. Myers
Philadelphia College of Pharmacy and Science
Philadelphia, PA 19104

Activated Charcoal: Antidotal and Other Medical Uses. By DAVID O. COONEY. (Drugs and the Pharmaceutical Sciences, Vol. 9.) Dekker, 270 Madison Ave., New York, NY 10016. 1980. 160 pp. 15 × 23 cm. Price $23.50.

This book provides a much needed review of the literature concerning the use of activated charcoal for the treatment of acute drug overdose or poison ingestion. The first chapter emphasizes the advantages of orally administered activated charcoal for the treatment of acute poison ingestion relative to other common emergency measures, such as induced emesis and gastric lavage. Chapter 2 points out the historical highlights of charcoal, indicating that the use of medicinal charcoal was recorded in an Egyptian papyrus in 1500 B.C., that a great variety of starting materials were used in its manufacture, and that the process of activation (which greatly increases the adsorbent capacity of charcoal) was not introduced until 1900.

Chapter 3 describes the manufacture, physicochemical properties, and adsorptive process of activated charcoal. Such knowledge is important for understanding the differences among various charcoal preparations and why a certain charcoal may be more effective than other charcoals for adsorption of a specific chemical. Chapter 4 is devoted to a discussion of the five classical papers of A. H. Anderson, which were published between 1946 and 1948. These publications are important because they summarized many earlier studies on activated charcoal and reported the definitive studies of Anderson, which served as the basis for subsequent work by many investigators.

Chapter 5 discusses the antidotal aspects of activated charcoal, with commentaries on characteristics to be considered in the selection of the most suitable charcoal preparation for oral antidotal uses (*e.g.*, acid-washed charcoal, pore-size distribution predominantly in the 20-Å range, high internal surface areas, and a fine powder as opposed to granules or tablets), dosages, effects of delayed administration, stability of the charcoal–drug complex in the GI tract, storage stability of activated charcoal suspension, safety of activated charcoal, fallacies and dangers of the so-called universal antidote, and the development of palatable formulations of activated charcoal suspension.

Chapter 6 reviews the results of *in vitro* and *in vivo* studies of the binding and antidotal potentials of activated charcoal. A great amount of previously published data is included. Chapter 7 describes investigations of other possible medical or diagnostic applications of activated charcoal. Most of these works were published in the 1930s and are mainly of historical interest, *e.g.*, intravenous injection of activated charcoal for treatment of systemic infections. However, use of activated charcoal to bind bacterial toxins in certain GI infections appears rational, and the use of activated charcoal for hemoperfusion appears to be effective.

A few errors were obvious to the reviewer. On page 40, it is stated that the adsorption isotherm for strychnine nitrate (based on *in vitro* studies in human gastric contents) is presented in Fig. 4.8, but this figure is concerned with diethylbarbituric acid. On page 41, a statement is made in reference to Fig. 4.8 that a change in pH from 8.4 to 5.0 decreases charcoal adsorption of diethylbarbituric acid, whereas the reverse is shown in the figures. Also, the data presented in Fig. 4.3 and Table 5.7 are credited to the wrong authors. However, these errors do not detract from the usefulness of the book.

Probably very few references have escaped citation in this small volume. This book is a convenient source of information concerning the antidotal application of activated charcoal for management of drug overdose or poison ingestion and should be a useful reference for health professionals involved in the treatment of poisoning cases, poison control information centers, and people engaged in research.

Reviewed by Lincoln Chin
Department of Pharmacology and Toxicology
College of Pharmacy
University of Arizona
Tucson, AZ 85721

Prescription Drugs in Short Supply. By MICHAEL A. SCHWARTZ. (Drugs and the Pharmaceutical Sciences, Vol. 8.) Dekker, 270 Madison Ave., New York, NY 10016. 1980. 130 pp. 15 × 23 cm. Price $17.50.

This interesting book documents, by case histories, the shortage of some vital drugs that occurred between 1973 and 1976. Among the major sources of documented information are Senatorial hearings, reports to the Drug Enforcement Administration, various symposia, and the *Federal Register*.

Shortages of five substances are discussed in detail: opium, quinidine, heparin, two injectable penicillins, and some large- and small-volume parenterals. Although no deaths are known to have resulted from the shortages, it is highly likely that there were cases in which optimum patient care was not possible because substitute drugs had to be used.

The shortages were caused by a number of factors which were different in most instances for each substance. The demand for codeine increased significantly, which contributed to the shortage of opium. This increased demand was attributed to: (*a*) increases in population, (*b*) aging of the population, (*c*) an increase in third-party payments for medication, and

(*d*) increased prescribing of codeine. Other factors contributing to the opium shortage were the ban on opium growing in Turkey and reduced production in India due to unfavorable weather conditions.

A Dutch cartel succeeded in gaining control of a significant portion of the world's supply of quinidine, which resulted in alleged shortages of this drug and subsequent price increases.

The heparin shortage resulted from increased demand and also from a short supply of the major raw material, the intestinal mucosa of the hog. This shortage occurred when the number of hogs being slaughtered was reduced.

The penicillin shortage was attributed to an 11-month shutdown of a major manufacturer's facilities for making the product.

The author points out that there is a lack of information concerning drug shortages and that no agency has the authority and responsibility to gather and apply such information. Such an agency, along with a national advisory group with representatives from the pharmaceutical industry, the health professions, and government, is recommended by the author as a means to prevent shortages of essential drugs.

This book is interesting reading for anyone associated with the health professions or the pharmaceutical industry. Most of us are unaware that shortages of vital drugs have occurred and can occur in the future.

Reviewed by Clyde W. Whitworth
School of Pharmacy
University of Georgia
Athens, GA 30602

Nuclear Medicine: Review Syllabus. Edited by PETER T. KIRCHNER. Society of Nuclear Medicine, 475 Park Ave. S., New York, NY 10016. 1980. 619 pp. 15 × 23 cm. Price $30.00.

This book is a product of over 50 contributors. It is an update of the major scientific and clinical advances that have occurred in nuclear medicine since the early 1970s. This volume is not presented as a textbook of nuclear medicine nor as an exposition of basic knowledge. In the preface, the senior editor states his hope that this book "will achieve its goal of assisting physicians in their efforts to maintain or reach clinical competence in the specialty of nuclear medicine."

The book offers an overview of 12 major areas in nuclear medicine. Chapters are included on radiopharmacology, instrumentation, radiation effects and radiation protection, cardiovascular, the central nervous system, endocrinology, gastroenterology, the genitourinary system, hematology–oncology, pulmonary, radioassay, and the skeletal system. The majority of the material is presented in a descriptive manner, with illustrations and tables kept to a minimum. With few exceptions, the text is well written, clear, and easy to follow. Difficulty may be encountered in attempting to locate a reference in a bibliography that was cited within the text.

The text contains a great amount of pertinent information beneficial to nuclear medicine physicians. This book is an excellent source of information for nuclear pharmacy practitioners and educators as well. Although not useful as an entry level textbook, it is of value as a library reference source in institutions with active research and educational programs in nuclear medicine or nuclear pharmacy.

Reviewed by Stanley M. Shaw
Department of Bionucleonics
School of Pharmacy and Pharmacal Sciences
Purdue University
West Lafayette, IN 47907

Catalog of Teratogenic Agents, 3rd Ed. Edited by THOMAS H. SHEPARD. Johns Hopkins University Press, Baltimore, MD 21218. 1980. 410 pp. 16 × 23.5 cm.

This reference text is essentially an alphabetized listing of known and suspected teratogenic agents that are believed to be involved in the development of congenital anomalies in experimental animals and humans. It is an updated version of previous editions, and the reader is made aware that yearly revisions probably will be forthcoming. Easy and quick revision is made possible by the fact that the material has been collected in the usual way and then transferred to computer cards and finally to tape for storage. New material can be inserted at the proper places without totally revising the previously written material. Both positive and negative results and full bibliographic references are included in the discussion of each agent. In addition, there are adequate subject and author indexes.

The stated purpose of the book is to help link the available information on experimental teratogenic agents with malformations occurring in humans. It is clearly pointed out in the introductory material that this task is not easy and that it often is impossible for a variety of reasons.

The most outstanding contribution to the literature provided by this book is the tables of comparative time periods of embryonic and fetal development in humans and experimental animals. One can determine easily what organ or tissue is developing at any time in gestation and consequently predict which tissues may be affected should a suspected teratogen be present at that particular time.

Many obviously important references have been left out, a deficiency that the author admits may be the case. To remedy this problem, the author states that anyone wishing to add material or provide corrections for future editions should do so on the address form provided in the last pages of the text. Unfortunately, this form is not present.

Because this catalog contains information concerning congenital defects due to pharmaceuticals, chemicals, environmental pollutants, food additives, household products, and viruses, it is recommended as a reference souce for anyone who has to answer questions concerning the teratogenic nature of the many agents included in these categories. Along with teratologists, obstetricians, pediatricians, geneticists, pharmacologists, and general practitioners would be particularly interested in this book.

Reviewed by Ronald F. Gautieri
Department of Pharmacology
School of Pharmacy
Temple University
Philadelphia, PA 19140

British Pharmacopoeia 1980. Her Majesty's Stationery Office, Atlantic House, Holborn Viaduct, London EC1P 1BN, England. 1980. 1196 pp. 22 × 31.5 cm. Price £60.

The *1980 British Pharmacopoeia* provides standards for the quality of substances and preparations used in medicine and pharmacy which will become effective in the United Kingdom on December 1, 1980. The 1980 BP incorporates, in edited form, all of the relevant monographs and methods currently contained in the *European Pharmacopoeia*. It also presents, in updated form, a large number of monographs formerly contained in the *British Pharmaceutical Codex*.

The increase in the range of entries covered in the BP resulted in its expansion to two volumes. Volume I contains monographs of medicinal and pharmaceutical substances, including simple organic salts, complex synthetic chemicals, vegetable drugs, antibiotics, and hormones and vitamins. The standards are accompanied by information on their action, use, dose, solubility, storage, and labeling. Style changes in this edition include indication of the stereochemical configuration in structural formulas, where possible. SI units have been introduced where practicable, and an approximate equivalent in the more familiar cgs system is given in parentheses.

Volume II includes an extensive formulary section. It also features discussions of blood products, immunological products, radiopharmaceutical preparations, and surgical materials. The 24 appendixes in Volume II describe procedures and requirements that are necessary for interpretation of the standards. Among the subjects featured in the appendixes are reagents, spectroscopic and chromatographic analyses, determinations of physical properties, limit tests, disintegration tests for dosage forms, and biological and biochemical assays and tests for antibiotics, immunological products, hormones, blood and related products, and enzymes. Tests for sterility, microbial contamination, and efficacy of preservatives also are included. A 48-page index is provided at the end of Volume II.

The significant expansion of the *British Pharmacopoeia* since its previous (1973) edition enhances its value as a reference source.

Staff Review

(*d*) increased prescribing of codeine. Other factors contributing to the opium shortage were the ban on opium growing in Turkey and reduced production in India due to unfavorable weather conditions.

A Dutch cartel succeeded in gaining control of a significant portion of the world's supply of quinidine, which resulted in alleged shortages of this drug and subsequent price increases.

The heparin shortage resulted from increased demand and also from a short supply of the major raw material, the intestinal mucosa of the hog. This shortage occurred when the number of hogs being slaughtered was reduced.

The penicillin shortage was attributed to an 11-month shutdown of a major manufacturer's facilities for making the product.

The author points out that there is a lack of information concerning drug shortages and that no agency has the authority and responsibility to gather and apply such information. Such an agency, along with a national advisory group with representatives from the pharmaceutical industry, the health professions, and government, is recommended by the author as a means to prevent shortages of essential drugs.

This book is interesting reading for anyone associated with the health professions or the pharmaceutical industry. Most of us are unaware that shortages of vital drugs have occurred and can occur in the future.

Reviewed by Clyde W. Whitworth
School of Pharmacy
University of Georgia
Athens, GA 30602

Nuclear Medicine: Review Syllabus. Edited by PETER T. KIRCHNER. Society of Nuclear Medicine, 475 Park Ave. S., New York, NY 10016. 1980. 619 pp. 15 × 23 cm. Price $30.00.

This book is a product of over 50 contributors. It is an update of the major scientific and clinical advances that have occurred in nuclear medicine since the early 1970s. This volume is not presented as a textbook of nuclear medicine nor as an exposition of basic knowledge. In the preface, the senior editor states his hope that this book "will achieve its goal of assisting physicians in their efforts to maintain or reach clinical competence in the specialty of nuclear medicine."

The book offers an overview of 12 major areas in nuclear medicine. Chapters are included on radiopharmacology, instrumentation, radiation effects and radiation protection, cardiovascular, the central nervous system, endocrinology, gastroenterology, the genitourinary system, hematology–oncology, pulmonary, radioassay, and the skeletal system. The majority of the material is presented in a descriptive manner, with illustrations and tables kept to a minimum. With few exceptions, the text is well written, clear, and easy to follow. Difficulty may be encountered in attempting to locate a reference in a bibliography that was cited within the text.

The text contains a great amount of pertinent information beneficial to nuclear medicine physicians. This book is an excellent source of information for nuclear pharmacy practitioners and educators as well. Although not useful as an entry level textbook, it is of value as a library reference source in institutions with active research and educational programs in nuclear medicine or nuclear pharmacy.

Reviewed by Stanley M. Shaw
Department of Bionucleonics
School of Pharmacy and Pharmacal Sciences
Purdue University
West Lafayette, IN 47907

Catalog of Teratogenic Agents, 3rd Ed. Edited by THOMAS H. SHEPARD. Johns Hopkins University Press, Baltimore, MD 21218. 1980. 410 pp. 16 × 23.5 cm.

This reference text is essentially an alphabetized listing of known and suspected teratogenic agents that are believed to be involved in the development of congenital anomalies in experimental animals and humans. It is an updated version of previous editions, and the reader is made aware that yearly revisions probably will be forthcoming. Easy and quick revision is made possible by the fact that the material has been collected in the usual way and then transferred to computer cards and finally to tape for storage. New material can be inserted at the proper places without totally revising the previously written material. Both positive and negative results and full bibliographic references are included in the discussion of each agent. In addition, there are adequate subject and author indexes.

The stated purpose of the book is to help link the available information on experimental teratogenic agents with malformations occurring in humans. It is clearly pointed out in the introductory material that this task is not easy and that it often is impossible for a variety of reasons.

The most outstanding contribution to the literature provided by this book is the tables of comparative time periods of embryonic and fetal development in humans and experimental animals. One can determine easily what organ or tissue is developing at any time in gestation and consequently predict which tissues may be affected should a suspected teratogen be present at that particular time.

Many obviously important references have been left out, a deficiency that the author admits may be the case. To remedy this problem, the author states that anyone wishing to add material or provide corrections for future editions should do so on the address form provided in the last pages of the text. Unfortunately, this form is not present.

Because this catalog contains information concerning congenital defects due to pharmaceuticals, chemicals, environmental pollutants, food additives, household products, and viruses, it is recommended as a reference souce for anyone who has to answer questions concerning the teratogenic nature of the many agents included in these categories. Along with teratologists, obstetricians, pediatricians, geneticists, pharmacologists, and general practitioners would be particularly interested in this book.

Reviewed by Ronald F. Gautieri
Department of Pharmacology
School of Pharmacy
Temple University
Philadelphia, PA 19140

British Pharmacopoeia 1980. Her Majesty's Stationery Office, Atlantic House, Holborn Viaduct, London EC1P 1BN, England. 1980. 1196 pp. 22 × 31.5 cm. Price £60.

The *1980 British Pharmacopoeia* provides standards for the quality of substances and preparations used in medicine and pharmacy which will become effective in the United Kingdom on December 1, 1980. The 1980 BP incorporates, in edited form, all of the relevant monographs and methods currently contained in the *European Pharmacopoeia*. It also presents, in updated form, a large number of monographs formerly contained in the *British Pharmaceutical Codex*.

The increase in the range of entries covered in the BP resulted in its expansion to two volumes. Volume I contains monographs of medicinal and pharmaceutical substances, including simple organic salts, complex synthetic chemicals, vegetable drugs, antibiotics, and hormones and vitamins. The standards are accompanied by information on their action, use, dose, solubility, storage, and labeling. Style changes in this edition include indication of the stereochemical configuration in structural formulas, where possible. SI units have been introduced where practicable, and an approximate equivalent in the more familiar cgs system is given in parentheses.

Volume II includes an extensive formulary section. It also features discussions of blood products, immunological products, radiopharmaceutical preparations, and surgical materials. The 24 appendixes in Volume II describe procedures and requirements that are necessary for interpretation of the standards. Among the subjects featured in the appendixes are reagents, spectroscopic and chromatographic analyses, determinations of physical properties, limit tests, disintegration tests for dosage forms, and biological and biochemical assays and tests for antibiotics, immunological products, hormones, blood and related products, and enzymes. Tests for sterility, microbial contamination, and efficacy of preservatives also are included. A 48-page index is provided at the end of Volume II.

The significant expansion of the *British Pharmacopoeia* since its previous (1973) edition enhances its value as a reference source.

Staff Review

(*d*) increased prescribing of codeine. Other factors contributing to the opium shortage were the ban on opium growing in Turkey and reduced production in India due to unfavorable weather conditions.

A Dutch cartel succeeded in gaining control of a significant portion of the world's supply of quinidine, which resulted in alleged shortages of this drug and subsequent price increases.

The heparin shortage resulted from increased demand and also from a short supply of the major raw material, the intestinal mucosa of the hog. This shortage occurred when the number of hogs being slaughtered was reduced.

The penicillin shortage was attributed to an 11-month shutdown of a major manufacturer's facilities for making the product.

The author points out that there is a lack of information concerning drug shortages and that no agency has the authority and responsibility to gather and apply such information. Such an agency, along with a national advisory group with representatives from the pharmaceutical industry, the health professions, and government, is recommended by the author as a means to prevent shortages of essential drugs.

This book is interesting reading for anyone associated with the health professions or the pharmaceutical industry. Most of us are unaware that shortages of vital drugs have occurred and can occur in the future.

Reviewed by Clyde W. Whitworth
School of Pharmacy
University of Georgia
Athens, GA 30602

Nuclear Medicine: Review Syllabus. Edited by PETER T. KIRCHNER. Society of Nuclear Medicine, 475 Park Ave. S., New York, NY 10016. 1980. 619 pp. 15 × 23 cm. Price $30.00.

This book is a product of over 50 contributors. It is an update of the major scientific and clinical advances that have occurred in nuclear medicine since the early 1970s. This volume is not presented as a textbook of nuclear medicine nor as an exposition of basic knowledge. In the preface, the senior editor states his hope that this book "will achieve its goal of assisting physicians in their efforts to maintain or reach clinical competence in the specialty of nuclear medicine."

The book offers an overview of 12 major areas in nuclear medicine. Chapters are included on radiopharmacology, instrumentation, radiation effects and radiation protection, cardiovascular, the central nervous system, endocrinology, gastroenterology, the genitourinary system, hematology–oncology, pulmonary, radioassay, and the skeletal system. The majority of the material is presented in a descriptive manner, with illustrations and tables kept to a minimum. With few exceptions, the text is well written, clear, and easy to follow. Difficulty may be encountered in attempting to locate a reference in a bibliography that was cited within the text.

The text contains a great amount of pertinent information beneficial to nuclear medicine physicians. This book is an excellent source of information for nuclear pharmacy practitioners and educators as well. Although not useful as an entry level textbook, it is of value as a library reference source in institutions with active research and educational programs in nuclear medicine or nuclear pharmacy.

Reviewed by Stanley M. Shaw
Department of Bionucleonics
School of Pharmacy and Pharmacal Sciences
Purdue University
West Lafayette, IN 47907

Catalog of Teratogenic Agents, 3rd Ed. Edited by THOMAS H. SHEPARD. Johns Hopkins University Press, Baltimore, MD 21218. 1980. 410 pp. 16 × 23.5 cm.

This reference text is essentially an alphabetized listing of known and suspected teratogenic agents that are believed to be involved in the development of congenital anomalies in experimental animals and humans. It is an updated version of previous editions, and the reader is made aware that yearly revisions probably will be forthcoming. Easy and quick revision is made possible by the fact that the material has been collected in the usual way and then transferred to computer cards and finally to tape for storage. New material can be inserted at the proper places without totally revising the previously written material. Both positive and negative results and full bibliographic references are included in the discussion of each agent. In addition, there are adequate subject and author indexes.

The stated purpose of the book is to help link the available information on experimental teratogenic agents with malformations occurring in humans. It is clearly pointed out in the introductory material that this task is not easy and that it often is impossible for a variety of reasons.

The most outstanding contribution to the literature provided by this book is the tables of comparative time periods of embryonic and fetal development in humans and experimental animals. One can determine easily what organ or tissue is developing at any time in gestation and consequently predict which tissues may be affected should a suspected teratogen be present at that particular time.

Many obviously important references have been left out, a deficiency that the author admits may be the case. To remedy this problem, the author states that anyone wishing to add material or provide corrections for future editions should do so on the address form provided in the last pages of the text. Unfortunately, this form is not present.

Because this catalog contains information concerning congenital defects due to pharmaceuticals, chemicals, environmental pollutants, food additives, household products, and viruses, it is recommended as a reference souce for anyone who has to answer questions concerning the teratogenic nature of the many agents included in these categories. Along with teratologists, obstetricians, pediatricians, geneticists, pharmacologists, and general practitioners would be particularly interested in this book.

Reviewed by Ronald F. Gautieri
Department of Pharmacology
School of Pharmacy
Temple University
Philadelphia, PA 19140

British Pharmacopoeia 1980. Her Majesty's Stationery Office, Atlantic House, Holborn Viaduct, London EC1P 1BN, England. 1980. 1196 pp. 22 × 31.5 cm. Price £60.

The *1980 British Pharmacopoeia* provides standards for the quality of substances and preparations used in medicine and pharmacy which will become effective in the United Kingdom on December 1, 1980. The 1980 BP incorporates, in edited form, all of the relevant monographs and methods currently contained in the *European Pharmacopoeia*. It also presents, in updated form, a large number of monographs formerly contained in the *British Pharmaceutical Codex*.

The increase in the range of entries covered in the BP resulted in its expansion to two volumes. Volume I contains monographs of medicinal and pharmaceutical substances, including simple organic salts, complex synthetic chemicals, vegetable drugs, antibiotics, and hormones and vitamins. The standards are accompanied by information on their action, use, dose, solubility, storage, and labeling. Style changes in this edition include indication of the stereochemical configuration in structural formulas, where possible. SI units have been introduced where practicable, and an approximate equivalent in the more familiar cgs system is given in parentheses.

Volume II includes an extensive formulary section. It also features discussions of blood products, immunological products, radiopharmaceutical preparations, and surgical materials. The 24 appendixes in Volume II describe procedures and requirements that are necessary for interpretation of the standards. Among the subjects featured in the appendixes are reagents, spectroscopic and chromatographic analyses, determinations of physical properties, limit tests, disintegration tests for dosage forms, and biological and biochemical assays and tests for antibiotics, immunological products, hormones, blood and related products, and enzymes. Tests for sterility, microbial contamination, and efficacy of preservatives also are included. A 48-page index is provided at the end of Volume II.

The significant expansion of the *British Pharmacopoeia* since its previous (1973) edition enhances its value as a reference source.

Staff Review

(*d*) increased prescribing of codeine. Other factors contributing to the opium shortage were the ban on opium growing in Turkey and reduced production in India due to unfavorable weather conditions.

A Dutch cartel succeeded in gaining control of a significant portion of the world's supply of quinidine, which resulted in alleged shortages of this drug and subsequent price increases.

The heparin shortage resulted from increased demand and also from a short supply of the major raw material, the intestinal mucosa of the hog. This shortage occurred when the number of hogs being slaughtered was reduced.

The penicillin shortage was attributed to an 11-month shutdown of a major manufacturer's facilities for making the product.

The author points out that there is a lack of information concerning drug shortages and that no agency has the authority and responsibility to gather and apply such information. Such an agency, along with a national advisory group with representatives from the pharmaceutical industry, the health professions, and government, is recommended by the author as a means to prevent shortages of essential drugs.

This book is interesting reading for anyone associated with the health professions or the pharmaceutical industry. Most of us are unaware that shortages of vital drugs have occurred and can occur in the future.

Reviewed by Clyde W. Whitworth
School of Pharmacy
University of Georgia
Athens, GA 30602

Nuclear Medicine: Review Syllabus. Edited by PETER T. KIRCHNER. Society of Nuclear Medicine, 475 Park Ave. S., New York, NY 10016. 1980. 619 pp. 15 × 23 cm. Price $30.00.

This book is a product of over 50 contributors. It is an update of the major scientific and clinical advances that have occurred in nuclear medicine since the early 1970s. This volume is not presented as a textbook of nuclear medicine nor as an exposition of basic knowledge. In the preface, the senior editor states his hope that this book "will achieve its goal of assisting physicians in their efforts to maintain or reach clinical competence in the specialty of nuclear medicine."

The book offers an overview of 12 major areas in nuclear medicine. Chapters are included on radiopharmacology, instrumentation, radiation effects and radiation protection, cardiovascular, the central nervous system, endocrinology, gastroenterology, the genitourinary system, hematology–oncology, pulmonary, radioassay, and the skeletal system. The majority of the material is presented in a descriptive manner, with illustrations and tables kept to a minimum. With few exceptions, the text is well written, clear, and easy to follow. Difficulty may be encountered in attempting to locate a reference in a bibliography that was cited within the text.

The text contains a great amount of pertinent information beneficial to nuclear medicine physicians. This book is an excellent source of information for nuclear pharmacy practitioners and educators as well. Although not useful as an entry level textbook, it is of value as a library reference source in institutions with active research and educational programs in nuclear medicine or nuclear pharmacy.

Reviewed by Stanley M. Shaw
Department of Bionucleonics
School of Pharmacy and Pharmacal Sciences
Purdue University
West Lafayette, IN 47907

Catalog of Teratogenic Agents, 3rd Ed. Edited by THOMAS H. SHEPARD. Johns Hopkins University Press, Baltimore, MD 21218. 1980. 410 pp. 16 × 23.5 cm.

This reference text is essentially an alphabetized listing of known and suspected teratogenic agents that are believed to be involved in the development of congenital anomalies in experimental animals and humans. It is an updated version of previous editions, and the reader is made aware that yearly revisions probably will be forthcoming. Easy and quick revision is made possible by the fact that the material has been collected in the usual way and then transferred to computer cards and finally to tape for storage. New material can be inserted at the proper places without totally revising the previously written material. Both positive and negative results and full bibliographic references are included in the discussion of each agent. In addition, there are adequate subject and author indexes.

The stated purpose of the book is to help link the available information on experimental teratogenic agents with malformations occurring in humans. It is clearly pointed out in the introductory material that this task is not easy and that it often is impossible for a variety of reasons.

The most outstanding contribution to the literature provided by this book is the tables of comparative time periods of embryonic and fetal development in humans and experimental animals. One can determine easily what organ or tissue is developing at any time in gestation and consequently predict which tissues may be affected should a suspected teratogen be present at that particular time.

Many obviously important references have been left out, a deficiency that the author admits may be the case. To remedy this problem, the author states that anyone wishing to add material or provide corrections for future editions should do so on the address form provided in the last pages of the text. Unfortunately, this form is not present.

Because this catalog contains information concerning congenital defects due to pharmaceuticals, chemicals, environmental pollutants, food additives, household products, and viruses, it is recommended as a reference souce for anyone who has to answer questions concerning the teratogenic nature of the many agents included in these categories. Along with teratologists, obstetricians, pediatricians, geneticists, pharmacologists, and general practitioners would be particularly interested in this book.

Reviewed by Ronald F. Gautieri
Department of Pharmacology
School of Pharmacy
Temple University
Philadelphia, PA 19140

British Pharmacopoeia 1980. Her Majesty's Stationery Office, Atlantic House, Holborn Viaduct, London EC1P 1BN, England. 1980. 1196 pp. 22 × 31.5 cm. Price £60.

The *1980 British Pharmacopoeia* provides standards for the quality of substances and preparations used in medicine and pharmacy which will become effective in the United Kingdom on December 1, 1980. The 1980 BP incorporates, in edited form, all of the relevant monographs and methods currently contained in the *European Pharmacopoeia*. It also presents, in updated form, a large number of monographs formerly contained in the *British Pharmaceutical Codex*.

The increase in the range of entries covered in the BP resulted in its expansion to two volumes. Volume I contains monographs of medicinal and pharmaceutical substances, including simple organic salts, complex synthetic chemicals, vegetable drugs, antibiotics, and hormones and vitamins. The standards are accompanied by information on their action, use, dose, solubility, storage, and labeling. Style changes in this edition include indication of the stereochemical configuration in structural formulas, where possible. SI units have been introduced where practicable, and an approximate equivalent in the more familiar cgs system is given in parentheses.

Volume II includes an extensive formulary section. It also features discussions of blood products, immunological products, radiopharmaceutical preparations, and surgical materials. The 24 appendixes in Volume II describe procedures and requirements that are necessary for interpretation of the standards. Among the subjects featured in the appendixes are reagents, spectroscopic and chromatographic analyses, determinations of physical properties, limit tests, disintegration tests for dosage forms, and biological and biochemical assays and tests for antibiotics, immunological products, hormones, blood and related products, and enzymes. Tests for sterility, microbial contamination, and efficacy of preservatives also are included. A 48-page index is provided at the end of Volume II.

The significant expansion of the *British Pharmacopoeia* since its previous (1973) edition enhances its value as a reference source.

Staff Review

DECEMBER 1980
VOLUME 69 NUMBER 12

JOURNAL OF PHARMACEUTICAL SCIENCES

MARY H. FERGUSON
Editor

SHELLY ELLIOTT
Production Editor

NICOLETTE TRIANTAFELLU
Copy Editor

EDWARD G. FELDMANN
Contributing Editor

SAMUEL W. GOLDSTEIN
Contributing Editor

BELLE R. BECK
Editorial Secretary

DAVID BOHARDT
Director of Publications

L. LUAN CORRIGAN
Assistant Director of Publications

EDITORIAL ADVISORY BOARD

JOHN AUTIAN
NORMAN R. FARNSWORTH
WILLIAM O. FOYE
WILLIAM J. JUSKO
HERBERT A. LIEBERMAN
DAVID E. MANN, JR.
GERALD J. PAPARIELLO
EDWARD G. RIPPIE

The *Journal of Pharmaceutical Sciences* (ISSN 0022-3549) is published monthly by the American Pharmaceutical Association (APhA) at 2215 Constitution Ave., N.W., Washington, DC 20037. Second-class postage paid at Washington, D.C., and at additional mailing office.

All expressions of opinion and statements of supposed fact appearing in articles or editorials carried in this journal are published on the authority of the writer over whose name they appear and are not to be regarded as necessarily expressing the policies or views of APhA.

Offices—Editorial, Advertising, and Subscription: 2215 Constitution Ave., N.W., Washington, DC 20037. All Journal staff may be contacted at this address. Printing: 20th & Northampton Streets, Easton, PA 18042.

Annual Subscriptions—United States and foreign, industrial and government institutions $60, educational institutions $60, individuals *for personal use only* $30; single copies $5. All foreign subscriptions add $5 for postage. Subscription rates are subject to change without notice. Members of APhA may elect to receive the *Journal of Pharmaceutical Sciences* as a part of their annual $80 (foreign $85) APhA membership dues.

Claims—Missing numbers will not be supplied if dues or subscriptions are in arrears for more than 60 days or if claims are received more than 60 days after the date of the issue, or if loss was due to failure to give notice of change of address. APhA cannot accept responsibility for foreign delivery when its records indicate shipment was made.

Change of Address—Members and subscribers should notify at once both the Post Office and APhA of any change of address.

Photocopying—The code at the foot of the first page of an article indicates that APhA has granted permission for copying of the article beyond the limits permitted by Sections 107 and 108 of the U.S. Copyright Law provided that the copier sends the per copy fee stated in the code to the Copyright Clearance Center, Inc., 21 Congress St., Salem, MA 01970. Copies may be made for personal or internal use only and not for general distribution.

Microfilm—Available from University Microfilms International, 300 N. Zeeb Road, Ann Arbor, MI 48106.

© Copyright 1980, American Pharmaceutical Association, 2215 Constitution Ave., N.W., Washington, DC 20037; all rights reserved.

ETHICAL CONSIDERATIONS IN RESEARCH PUBLICATION

Periodically, news reports in the public press and the broadcast media inform us about a new scandal rocking either Congress or some governmental agency. The scandal might be anything from taking bribes, to exerting improper influence, to improper moral behavior, to any other of a host of misdeeds.

Only relatively rarely, however, do we hear about comparable situations in the world of science and research.

In part, this may be because the people involved are more honorable or have a greater sense of ethics. It may also be because they are simply less likely to face the pressures and temptations that persons who are in positions of greater public prominence routinely encounter.

But we suspect that there is also another explanation. In short, most people in research, in science, and in the health professions are inclined to treat such matters with reserve, discretion, and perhaps even a sense of incredulity. It is almost as if they refuse to believe that such misdeeds occur or that their colleagues and associates could be guilty of the purported practices. For example, the general reluctance of physicians to testify against fellow physicians in malpractice cases is widely recognized within the legal profession.

The psychology underlying this behavior can be explained in a number of ways. But whatever the reason for it, there is no question but that it exists.

These observations are prompted by a detailed exposé of an alleged scientific fraud that was reported this past October in a two-part story appearing in *Science* magazine. Many of the central figures named read like a Who's Who of American medical science. The principal institutions involved are the revered Yale University School of Medicine, the Columbia College of Physicians and Surgeons, and the National Institutes of Health.

The articles in *Science* are entitled, respectively, "Imbroglio at Yale (I): Emergence of a Fraud" and "Imbroglio at Yale (II): A Top Job Lost." We shall not attempt to summarize the story because it is exceedingly complex and a brief summary might treat one or another of the parties unfairly. As a consequence, we recommend to our readers that they read the entire report as it is fully laid out in *Science*. The specific wrong-doing includes plagiarism, destruction of data, falsification of data, and efforts to conceal or down-play the problem. For the principal scientist involved, the episode became an "intellectual Watergate."

In reviewing the scenario, the account in *Science* reveals that initially the incident appeared of minor significance: *"The so-called plagiarism consisted of a few unimportant phrases containing, in total, some 60 words."* After first reviewing the case, the dean at Yale was inclined to dismiss it. However, over the next year, matters gradually snowballed and eventually led to the retraction of 11 papers published in prominent scientific journals, the forced resignation of the chairman of the department of medicine at Columbia, and a host of other sordid consequences.

With this background, we would particularly like to highlight a couple of key conclusions in the *Science* articles:

- *"The Yale part of the story is a case study in how a busy senior investigator lost touch with the laboratory of a junior associate. It raises serious questions about the career pressures that lead to coauthorship and about the health of team research in general."*
- *"The subtle effects of the Yale imbroglio might never be measured, but they will be there nonetheless. Senior researchers, for instance, may hesitate a bit in the future before signing a paper not carefully checked out."*
- *"The fabric of the reward system of coauthorship was torn. To the extent that there are [other researchers of similar bent] at large in the labs, doctoring data, the incident stands as a threat and a warning."*

All of this may appear to be very remote to the *Journal of Pharmaceutical Sciences* and its readers, authors, reviewers, and editors. At most, we might consider the Yale–Columbia incident to be of only casual and incidental interest.

Regrettably, however, over the past decade we have experienced several comparable and analogous situations. Fortunately, in most of these cases, the unethical behavior was uncovered before publication of the pertinent manuscripts; as a result, appropriate corrective action was taken to prevent soiling the published literature. In several other instances, the particular problem only came to light following the paper's publication and the opportunity thereby afforded an affected party to read the paper, to recognize the existence of a problem, and to bring that problem to the attention of the editors and other pertinent parties.

Because these instances of apparent fraud or unethical behavior are not widely publicized like those mentioned in the opening paragraph above, few of our readers, authors, or reviewers are ever aware of them. Nevertheless, they do result in a serious embarrassment and a permanent taint on the reputations of the scientist or scientists involved. Consequently, when it comes to research publication, we wish to counsel the utmost care and caution on the part of all those who would author or coauthor papers, as well as on the part of those who have the responsibility to review or otherwise pass judgment on such manuscripts for possible publication.

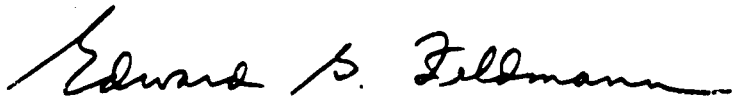

DECEMBER 1980
VOLUME 69 NUMBER 12

JOURNAL OF PHARMACEUTICAL SCIENCES

MARY H. FERGUSON
Editor

SHELLY ELLIOTT
Production Editor

NICOLETTE TRIANTAFELLU
Copy Editor

EDWARD G. FELDMANN
Contributing Editor

SAMUEL W. GOLDSTEIN
Contributing Editor

BELLE R. BECK
Editorial Secretary

DAVID BOHARDT
Director of Publications

L. LUAN CORRIGAN
Assistant Director of Publications

EDITORIAL ADVISORY BOARD

JOHN AUTIAN
NORMAN R. FARNSWORTH
WILLIAM O. FOYE
WILLIAM J. JUSKO
HERBERT A. LIEBERMAN
DAVID E. MANN, JR.
GERALD J. PAPARIELLO
EDWARD G. RIPPIE

The *Journal of Pharmaceutical Sciences* (ISSN 0022-3549) is published monthly by the American Pharmaceutical Association (APhA) at 2215 Constitution Ave., N.W., Washington, DC 20037. Second-class postage paid at Washington, D.C., and at additional mailing office.

All expressions of opinion and statements of supposed fact appearing in articles or editorials carried in this journal are published on the authority of the writer over whose name they appear and are not to be regarded as necessarily expressing the policies or views of APhA.

Offices—Editorial, Advertising, and Subscription: 2215 Constitution Ave., N.W., Washington, DC 20037. All Journal staff may be contacted at this address. Printing: 20th & Northampton Streets, Easton, PA 18042.

Annual Subscriptions—United States and foreign, industrial and government institutions $60, educational institutions $60, individuals *for personal use only* $30; single copies $5. All foreign subscriptions add $5 for postage. Subscription rates are subject to change without notice. Members of APhA may elect to receive the *Journal of Pharmaceutical Sciences* as a part of their annual $80 (foreign $85) APhA membership dues.

Claims—Missing numbers will not be supplied if dues or subscriptions are in arrears for more than 60 days or if claims are received more than 60 days after the date of the issue, or if loss was due to failure to give notice of change of address. APhA cannot accept responsibility for foreign delivery when its records indicate shipment was made.

Change of Address—Members and subscribers should notify at once both the Post Office and APhA of any change of address.

Photocopying—The code at the foot of the first page of an article indicates that APhA has granted permission for copying of the article beyond the limits permitted by Sections 107 and 108 of the U.S. Copyright Law provided that the copier sends the per copy fee stated in the code to the Copyright Clearance Center, Inc., 21 Congress St., Salem, MA 01970. Copies may be made for personal or internal use only and not for general distribution.

Microfilm—Available from University Microfilms International, 300 N. Zeeb Road, Ann Arbor, MI 48106.

© Copyright 1980, American Pharmaceutical Association, 2215 Constitution Ave., N.W., Washington, DC 20037; all rights reserved.

ETHICAL CONSIDERATIONS IN RESEARCH PUBLICATION

Periodically, news reports in the public press and the broadcast media inform us about a new scandal rocking either Congress or some governmental agency. The scandal might be anything from taking bribes, to exerting improper influence, to improper moral behavior, to any other of a host of misdeeds.

Only relatively rarely, however, do we hear about comparable situations in the world of science and research.

In part, this may be because the people involved are more honorable or have a greater sense of ethics. It may also be because they are simply less likely to face the pressures and temptations that persons who are in positions of greater public prominence routinely encounter.

But we suspect that there is also another explanation. In short, most people in research, in science, and in the health professions are inclined to treat such matters with reserve, discretion, and perhaps even a sense of incredulity. It is almost as if they refuse to believe that such misdeeds occur or that their colleagues and associates could be guilty of the purported practices. For example, the general reluctance of physicians to testify against fellow physicians in malpractice cases is widely recognized within the legal profession.

The psychology underlying this behavior can be explained in a number of ways. But whatever the reason for it, there is no question but that it exists.

These observations are prompted by a detailed exposé of an alleged scientific fraud that was reported this past October in a two-part story appearing in *Science* magazine. Many of the central figures named read like a Who's Who of American medical science. The principal institutions involved are the revered Yale University School of Medicine, the Columbia College of Physicians and Surgeons, and the National Institutes of Health.

The articles in *Science* are entitled, respectively, "Imbroglio at Yale (I): Emergence of a Fraud" and "Imbroglio at Yale (II): A Top Job Lost." We shall not attempt to summarize the story because it is exceedingly complex and a brief summary might treat one or another of the parties unfairly. As a consequence, we recommend to our readers that they read the entire report as it is fully laid out in *Science*. The specific wrong-doing includes plagiarism, destruction of data, falsification of data, and efforts to conceal or down-play the problem. For the principal scientist involved, the episode became an "intellectual Watergate."

In reviewing the scenario, the account in *Science* reveals that initially the incident appeared of minor significance: *"The so-called plagiarism consisted of a few unimportant phrases containing, in total, some 60 words."* After first reviewing the case, the dean at Yale was inclined to dismiss it. However, over the next year, matters gradually snowballed and eventually led to the retraction of 11 papers published in prominent scientific journals, the forced resignation of the chairman of the department of medicine at Columbia, and a host of other sordid consequences.

With this background, we would particularly like to highlight a couple of key conclusions in the *Science* articles:

- *"The Yale part of the story is a case study in how a busy senior investigator lost touch with the laboratory of a junior associate. It raises serious questions about the career pressures that lead to coauthorship and about the health of team research in general."*
- *"The subtle effects of the Yale imbroglio might never be measured, but they will be there nonetheless. Senior researchers, for instance, may hesitate a bit in the future before signing a paper not carefully checked out."*
- *"The fabric of the reward system of coauthorship was torn. To the extent that there are [other researchers of similar bent] at large in the labs, doctoring data, the incident stands as a threat and a warning."*

All of this may appear to be very remote to the *Journal of Pharmaceutical Sciences* and its readers, authors, reviewers, and editors. At most, we might consider the Yale–Columbia incident to be of only casual and incidental interest.

Regrettably, however, over the past decade we have experienced several comparable and analogous situations. Fortunately, in most of these cases, the unethical behavior was uncovered before publication of the pertinent manuscripts; as a result, appropriate corrective action was taken to prevent soiling the published literature. In several other instances, the particular problem only came to light following the paper's publication and the opportunity thereby afforded an affected party to read the paper, to recognize the existence of a problem, and to bring that problem to the attention of the editors and other pertinent parties.

Because these instances of apparent fraud or unethical behavior are not widely publicized like those mentioned in the opening paragraph above, few of our readers, authors, or reviewers are ever aware of them. Nevertheless, they do result in a serious embarrassment and a permanent taint on the reputations of the scientist or scientists involved. Consequently, when it comes to research publication, we wish to counsel the utmost care and caution on the part of all those who would author or coauthor papers, as well as on the part of those who have the responsibility to review or otherwise pass judgment on such manuscripts for possible publication.

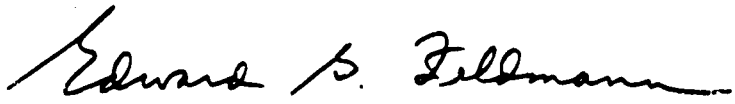

JOURNAL OF PHARMACEUTICAL SCIENCES

DECEMBER 1980
VOLUME 69 NUMBER 12

RESEARCH ARTICLES

Improving Intestinal Absorption of Water-Insoluble Compounds: A Membrane Metabolism Strategy

G. L. AMIDON ˣ, G. D. LEESMAN, and R. L. ELLIOTT

Received February 27, 1980, from the *School of Pharmacy, University of Wisconsin, Madison, WI 53706.* Accepted for publication June 11, 1980.

Abstract □ A strategy for improving the intestinal absorption of water-insoluble drugs was developed and tested. The strategy is based on making a soluble derivative of an insoluble compound which, in turn, is a substrate for enzymes in the surface coat of the brush border region of the microvillous membrane. Consequently, just prior to reaching the membrane, the physical properties of the diffusing species are changed from polar to nonpolar. The experimental test used two drug–drug derivative pairs, estrone–lysine estrone ester and *p*-nitroaniline–lysine *p*-nitroanilide. Wall permeabilities were determined using an external perfusion technique in the rat intestine and a laminar flow convective diffusion model for transport in the lumen. Analysis of the permeability results indicates that the derivatives have higher wall permeabilities than the parent compounds and that the microvillous surface coat may be a significant contributor to the intestinal wall resistance. Comparison of the absorption rates for estrone and the lysine estrone ester indicates that the absorption rate of the derivative could be up to five orders of magnitude greater than that for the parent compound.

Keyphrases □ Permeability—intestinal absorption of water-insoluble drugs, improved membrane permeability through synthesis of soluble derivative as prodrug □ Absorption, intestinal—water-insoluble drugs, improved membrane permeability through synthesis of soluble derivative as prodrug □ Models—intestinal absorption of water-insoluble drugs, improved membrane permeability through synthesis of soluble derivative as prodrug

Water-insoluble compounds frequently are absorbed slowly due to slow dissolution of the solid and/or a very low solution concentration, leading to a small diffusive driving force. Two approaches often are used in these cases to improve absorption: formulation and soluble derivative formation (1). The formulation approach uses physical methods such as micronization or dispersion in a soluble carrier to increase the dissolution rate of the drug product and, hence, the absorption rate. The soluble derivative (prodrug) approach attaches a solubilizing progroup (*e.g.*, phosphate or succinate) to the drug, taking advantage of the usually high solubility and dissolution rate of the derivative salt. Examples of the successful application of both approaches are available (1).

BACKGROUND

Each approach has its limitations. With the formulation approach, the maximal diffusive driving force still is limited by the low aqueous solubility of the drug. While it may be possible to maintain a supersaturated solution for a finite period of time, the supersaturation often is only a factor of two or less, which is not sufficient to ensure complete absorption for very insoluble compounds. The solubilizing progroup approach is limited by the fact that while the aqueous solubility may be increased by several orders of magnitude, the increase in solubility is coupled to a decrease in the membrane–water partition coefficient (2–4) and, consequently, results in a reduction in the membrane permeability. While the transport basis for this trade-off will be discussed in more detail, the significant point is that increased aqueous solubility usually is obtained at the expense of reduced membrane permeability. If, for oral dosage forms, the conversion back to the nonpolar drug occurs rapidly, chemically or biochemically, in the gut lumen, then the reduced membrane permeability of the drug derivative is of no consequence. However, as with the formulation approach, the diffusive transport of the drug again is limited by its low solubility.

This report discusses an approach that may avoid this compromise. The essential strategy is to make derivatives of insoluble compounds that are substrates for enzymes in the brush border region of the mucosal cells. In the next section, the biochemical background is reviewed briefly and the prodrug strategy is developed. Next, the transport processes involved are analyzed. The approach is tested experimentally using two drug–drug derivative pairs in an externally perfused rat intestine preparation. The results then are discussed in light of the transport models and the potential of this approach for improving oral absorption.

Protein Digestion and Absorption—Understanding of the digestion and absorption of proteins has increased over the past 20 years, as demonstrated by numerous reviews and symposium volumes (5–14). Prior to reaching the intestine, ingested protein is acted on by gastric and pancreatic enzymes. This process is intraluminal and reduces the protein to a mixture of free amino acids (<30%) and oligopeptides having two to six residues. This mixture is presented to the intestinal mucous membrane where an active, sodium-dependent carrier transports the free amino acids into the cell. Final hydrolysis of the remaining oligopeptides occurs along the mucous membrane and is complete so that, for practical purposes, only amino acids enter the portal circulation.

For many years, it was assumed that all of the protein was reduced to free amino acids prior to transport across the intestinal wall. Then, in a pioneering series of reports published between 1959 and 1962, Newey and Smyth (15–17) demonstrated that intraluminal hydrolysis accounted

0022-3549/80/1200-1363$01.00/0
© 1980, American Pharmaceutical Association

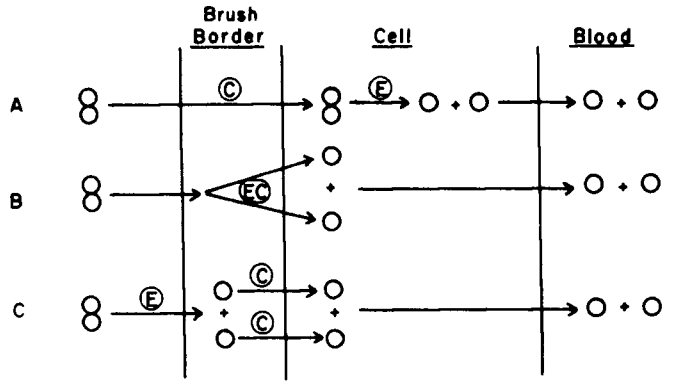

Figure 1—*Peptide absorption mechanisms. Key: A, peptide transport and cellular hydrolysis; B, coupled transport and hydrolysis; C, interfacial hydrolysis and transport;* Ⓒ, *carrier;* Ⓔ, *enzyme; and* ⒺⒸ, *enzyme–carrier system.*

for only a minor portion of the total protein hydrolyzed. In addition, they showed that small amounts of dipeptides could be absorbed into the enterocytes intact, a finding also reported by Prockop *et al.* (18). Matthews and coworkers (19, 20) made the important observation that dipeptides could be absorbed more rapidly than amino acids. This finding established that dipeptides could be transported by a mechanism independent of that used by amino acids. This result was supported by reports that patients with defective intestinal amino acid absorption, as in Hartnup's disease or cystinuria, are able to absorb dipeptides without difficulty (20, 21). Several schemes were proposed to account for the final stages of hydrolysis and absorption of oligopeptides (22–26), and these schemes include one or both of the following mechanisms (Fig. 1):

1. Hydrolysis of the small peptides by enzymes in the brush border region to amino acids. The amino acids then are transported into the cell by a unique carrier system.

2. The small peptides are reduced to (mostly) dipeptides and tripeptides by enzymes on the external surface of the cell, followed by uptake of the di- and tripeptides into the cell where the final hydrolysis takes place.

Membrane Metabolism Strategy—While the nature and specificity of the brush border region enzymes still are the subject of intensive research, the extensive enzymatic activity in the region is well established (6, 7, 11, 23). The significance of this fact, from the point of view of a prodrug strategy, is based on the solubility–partition coefficient trade-off. Increasing the membrane permeability by increasing the membrane–water partition coefficient usually results in reduced solubility, leading to an optimum partition coefficient. That is, the aqueous (luminal) phase and the nonpolar membrane phase have conflicting physical property requirements.

The basis for the prodrug solubilization strategy is as follows. If a (soluble) derivative of an insoluble (high membrane–water partition coefficient) compound can be made that is a substrate for the brush border enzymes located at the interface between the polar and nonpolar phases, then conversion back to the high partition coefficient (low aqueous solubility) compound would occur immediately adjacent to the nonpolar (membrane) sink. This, in turn, would preclude or minimize precipitation of the insoluble drug. In other words, the prodrug strategy involves the use of interfacial enzymes to convert a drug (derivative) that has desirable properties in the one phase (high solubility) to one having desirable properties in the other phase (high partition coefficient). A scheme for this approach is presented in Fig. 2.

THEORETICAL

Membrane Permeability—The transport of a solute through a composite planar membrane will be considered first. The rate of mass transport per unit area, J, is given by (using the film model) (2, 3):

$$J = P_{\text{eff}}\,\Delta C \qquad \text{(Eq. 1)}$$

$$P_{\text{eff}} = \frac{P_a P_m}{P_a + P_m} \qquad \text{(Eq. 2)}$$

$$P_a = D/\delta_a \qquad \text{(Eq. 3)}$$

$$P_m = PCD/\delta_m \qquad \text{(Eq. 4)}$$

where ΔC is the concentration difference between the two sides of the composite barrier, P_{eff} is the effective permeability coefficient, P_a is the aqueous permeability, P_m is the membrane permeability, δ_a and δ_m are the respective film thicknesses, and PC is the membrane–water partition coefficient. Equation 2 can be rewritten as:

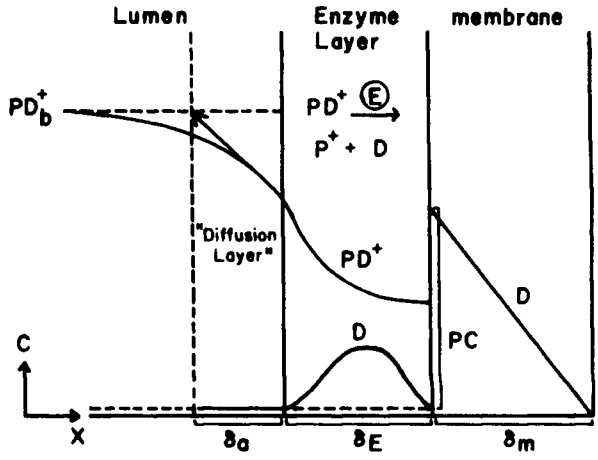

Figure 2—*Reaction diffusion model for absorption of soluble derivatives of insoluble compounds. Drug* (D) *may or may not build up in the enzyme layer. Key:* PD^+, *charged prodrug;* Ⓔ, *enzyme;* δ_a, *diffusion layer thickness;* δ_E, *enzyme layer thickness;* δ_m, *membrane thickness; and* PC, *membrane–enzyme layer partition coefficient.*

$$P_{\text{eff}} = \frac{D}{\delta_a + (\delta_m/PC)} \qquad \text{(Eq. 5)}$$

Under sink conditions, Eq. 1 becomes:

$$J = P_{\text{eff}} C_b \qquad \text{(Eq. 6)}$$

From Eq. 5, it is clear that as PC increases, P_{eff} increases and, hence, the absorption rate increases (Eq. 6). In the limit $PC \to \infty$, $P_{\text{eff}} = D/\delta_a$. However, as PC increases, a significant physical constraint must be considered: as PC increases, the aqueous solubility decreases and, as a result, C_b in Eq. 6 eventually must be replaced by C_s, the aqueous solubility:

$$J = P_{\text{eff}} C_s \qquad \text{(Eq. 7)}$$

Equation 7 represents the flux from suspensions. In this situation, increasing PC increases P_{eff} but decreases C_s to a greater extent. This trade-off leads to the existence of an optimum PC value (2, 3). Equations 5–7 are significant to a prodrug strategy since one can increase C_s but, in most cases, not without a corresponding decrease in P_{eff}[1]. However, given the preceding discussion of the interfacial (brush border) enzymatic activity, a prodrug strategy based on interfacial reconversion may be particularly effective. The transport basis for this approach is as follows. The model (Fig. 2) requires three layers with an enzymatic reaction occurring in the middle layer. The composite barrier is assumed to be planar[2], and the enzymatic reaction is assumed to be first order.

The solution for the three-layer model with a first-order reaction in the enzyme layer (rate constant = k) is:

$$J = P_R C_{A_0} \qquad \text{(Eq. 8)}$$

where P_R is a complex function of δ_w, δ_E, δ_m, K, k, and D (Fig. 2). However, a much simpler expression is obtained if it is assumed that the membrane layer is a sink for the drug and the membrane is impermeable to the (soluble) drug derivative (27). For this two-layer model, P_R from Eq. 8 becomes:

$$P_R = \frac{P_a P_E}{P_a + P_E} \qquad \text{(Eq. 9)}$$

with:

$$P_E = \alpha D \tanh(\alpha \delta_E) \qquad \text{(Eq. 10)}$$

$$\alpha^2 = k/D \qquad \text{(Eq. 11)}$$

[1] See Ref. 4 for examples where this is not the case.

[2] The error involved with this assumption for a cylinder having a radius of 0.2 cm is only 2–3% (27).

where k is the first-order reaction rate in the enzyme layer and P_a is D/δ_a. Note that:

$$\lim_{k\to 0} P_R = 0 \quad \text{and} \quad \lim_{k\to\infty} P_R = P_a$$

The most significant point regarding Eqs. 8–11 is that C_{A_0} is the concentration of the soluble drug derivative and that the membrane–aqueous solution partition coefficient does not enter into the equation. If the enzymatic reaction is fast (large k), the flux of the soluble drug derivative can be orders of magnitude greater than that of the insoluble drug.

Convective Diffusion Model—The experimental test system used a perfused rat intestine. Consequently, a model accounting for both convection and diffusion in a tube is required. The most appropriate model with the present experimental procedure is a laminar flow model (28). The solution to the convective diffusion problem for steady flow in a cylindrical tube with a permeable wall gives (27):

$$C_m/C_0 = \Sigma M_n \exp(-\beta_n^2 Gz) \qquad \text{(Eq. 12)}$$

where:

C_m = outlet (cup-mixing) concentration
C_0 = inlet concentration
$Gz = \pi DL/2Q$
D = aqueous diffusivity of the solute
L = length of the perfused intestine
Q = flow rate

and the M_n and β_n values are functions of the dimensionless (membrane) wall permeability, P_w^*, defined as:

$$P_w^* = \frac{P_w R}{D} \qquad \text{(Eq. 13)}$$

where R is the radius of the intestine.

The P_w value is defined by the boundary condition at the tube wall:

$$-D\left.\frac{\partial C}{\partial r}\right|_{r=R} = P_w C_w \qquad \text{(Eq. 14)}$$

where $C_w = C(R,z)$ is the wall concentration. The results in this study were analyzed using the laminar flow model, although other models could be applied to the data (28). It is important to note that P_w (or P_w^*) does not contain any contribution from the luminal diffusion of the drug. That is, there is no diffusion layer in the model; the luminal diffusion of the drug is accounted for by solution of the appropriate transport equation (27). For passively absorbed compounds, P_w^* is equal to P_m^* in Eq. 4; for the reactive compounds, P_w^* is equal to P_k^* of Eq. 10. Consequently, in interpreting the results, P_w^* must be interpreted appropriately.

The preceding analysis can be related to a pharmacokinetic analysis through a mass balance on the tube. This approach gives:

$$dm/dt = C_0(1 - C_m/C_0)Q \qquad \text{(Eq. 15)}$$

where dm/dt is the mass transported across the absorbing surface per unit time and can be computed directly from the perfusion results. A pharmacokinetic analysis would give $dm/dt = k_{abs}VC_0$, where V is the volume of the intestinal segment. Hence:

$$k_{abs} = (1 - C_m/C_0)Q/V \qquad \text{(Eq. 16)}$$

where C_m/C_0 is a function of the wall permeability (Eq. 12) and Q/V is the residence time of the fluid in the perfused segment. Equation 16 indicates that k_{abs} increases as Q/V increases. That is, the fluid stays in the intestinal segment longer and increases as C_m/C_0 decreases, *i.e.*, as P_w^* or Gz increases.

EXPERIMENTAL

Materials—The drug–prodrug pairs used were p-nitroaniline[3]–L-lysine p-nitroanilide[3] and [^{3}H]estrone[4]–[^{3}H]estrone-3′-L-lysine ester (I). [^{14}C]Polyethylene glycol[4] was used as a volume marker. [^{3}H]Estrone-3′-L-lysine ester was synthesized from [^{3}H]estrone and L-lysine. The synthesis and physicochemical properties of I will be the subject of a subsequent report (29).

Perfusion Experiments—Male Holtzman rats (300–350 g), fasted 12–18 hr, were anesthetized intramuscularly (gluteal muscle) with a 50% urethan solution (150 mg/100 g). A midline longitudinal incision was made in the abdomen, and a glass cannula was placed 2 and 10 cm distal to the ligament of Treitz. A pump[5] was used for perfusion at flow rates of 0.05–1.2 ml/min. Glass tubing was used throughout. [^{14}C]Polyethylene glycol was used as the volume marker. Volume changes rarely exceeded 3%.

An isotonic Sorensen phosphate buffer (pH 6.72) was used. The intestine was perfused first with buffer for 30 min and then for 30–60 min (until steady state) with drug solution. At the conclusion of the experiment, the animal was sacrificed. The intestine was excised and the length of the intestine from cannula to cannula was measured. The radius was calculated from the volume of the excised segment.

Assay—p-Nitroaniline and L-lysine p-nitroanilide were assayed spectrometrically at 375 and 315 nm, respectively. [^{3}H]Estrone, [^{3}H]lysine estrone ester, and [^{14}C]polyethylene glycol were assayed by liquid scintillation. In experiments with lysine p-nitroanilide, the effluent solution was analyzed for both lysine p-nitroanilide and p-nitroaniline. Measurable amounts of p-nitroaniline were not detected in any experiments with lysine p-nitroanilide.

Table I—Coefficients and Exponents for Eq. 19

n	${}^0M_n$	${}^0\beta_n$
1	0.81905	2.7044
2	0.09753	6.6790
3	0.03250	10.6734
4	0.01544	14.6712
5	0.00879	18.6699

RESULTS AND DISCUSSION

The experimental design was such that luminal reconversion (either biochemical or chemical) of the drug derivatives would not be significant, and none was observed. The conditions also maximized the possible attainment of laminar flow in the lumen (28). The results were analyzed using the method of Elliott *et al.*[6], interpreting the wall permeability appropriately (Eq. 4 or 10). The approximate wall permeability, ${}^0P_w^*$, was calculated from:

$$\frac{1}{{}^0P_w^*} = \frac{1}{P_{eff}^*} - \frac{1}{{}^0P_{aq}^*} \qquad \text{(Eq. 17)}$$

where:

$${}^0P_{aq}^* = \frac{\ln(C_m/C_0)\exp}{-4Gz} \qquad \text{(Eq. 18)}$$

and:

$${}^0P_{aq}^* = -\left[\sum_{n=1}^{5} {}^0M_n \exp(-{}^0\beta_n^2 Gz)\right] \Big/ 4Gz \qquad \text{(Eq. 19)}$$

The coefficient and exponents in Eq. 19 are given in Table I. This approach is equivalent to the diffusion layer approach but with the diffusion layer thickness calculated *a priori* (27). The exact expression for the diffusion layer thickness is:

$$\delta/R = \frac{1}{p_{aq}^*} = \frac{-4Gz}{\Sigma M_n \exp(-\beta_n^2 Gz)} - \frac{1}{P_w^*} \qquad \text{(Eq. 20)}$$

using the M_n and β_n values that are appropriate to the wall permeability, P_w^*. While P_w^* is unknown, analysis of the model shows that δ/R is only slightly dependent on P_w^*; hence, Eq. 19, which is appropriate for sink conditions [$P_w^* = \infty$ or $C(R,z) = 0$], provides a good estimate. A small correction then can be applied to the estimated ${}^0P_w^*$ from Eq. 17 to obtain P_w^* (27).

Wall Permeabilities—The experimental results and the calculated

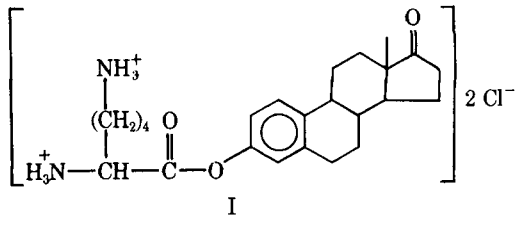

I

[3] U.S. Biochemical Corp., Cleveland, Ohio.
[4] New England Nuclear, Boston, Mass.
[5] Harvard.
[6] R. L. Elliott, G. L. Amidon, and E. N. Lightfoot, *J. Theor. Biol.*, in press.

Table II—Results for Estrone Experiments

C_m/C_0	Gz	P^*_{eff}	${}^0P^*_{aq}$	${}^0P^*_m$ [a]
0.909	0.00891	2.67	4.64	6.31
0.847	0.0178	2.33	3.71	6.27
0.739	0.045	1.68	2.81	4.17
0.784	0.036	1.68	2.99	3.87
0.92	0.0094	2.21	4.56	4.31
0.889	0.0086	3.42	4.70	12.5
0.908	0.0089	2.71	4.64	6.50
0.903	0.0092	2.77	4.59	6.98
0.864	0.012	3.04	4.21	10.9
0.882	0.01	3.13	4.47	10.5
0.921	0.0074	2.78	4.94	6.34
0.751	0.035	2.04	3.02	6.33
0.659	0.086	1.21	2.39	2.45
0.762	0.033	2.05	3.07	6.24
0.683	0.082	1.16	2.41	2.23
0.814	0.021	2.44	3.52	8.04
0.762	0.041	1.65	2.88	3.89

[a] Average ${}^0P^*_m = 6.3$, $s = 2.9$, and $SEM = 0.7$.

permeabilities are given in Tables II–V. Table VI presents a summary of the results, including the correction factors that are required to obtain an estimate of the (laminar flow) wall permeability. In analyzing the data in Tables II–V, the negative membrane permeabilities were omitted. In these cases, P^*_{eff} is greater than the calculated ${}^0P^*_{aq}$, predominantly with the reactive enzyme substrates having high P^*_w values. The possible reasons for this result are as follows. With the laminar flow model at any given Gz value, C_m/C_0 approaches a finite limit as $P^*_w \to \infty$. Since $P^*_{aq} \doteq 3$ as P^*_w increases above this value, the method loses sensitivity to P^*_w; that is, small changes in the experimentally determined C_m/C_0 values give rise to widely different P^*_w values. Experimental variation and error then can give rise to C_m/C_0 values that actually are lower than the values that the model can predict. In addition, the flow in the intestine in any given experiment may depart from laminar flow. Such mixing decreases C_m/C_0 below that expected by the model for very permeable compounds.

Since the variables of the flow rate and the length of the perfused intestine both are incorporated into the dimensionless variable Gz and since P^*_w should be independent of Gz[7] (27), regression analysis on ${}^0P^*_w$ *versus* Gz was performed. The results for estrone are shown in Fig. 3, and the regression equation is:

$${}^0P^*_w = 8.57 - 80.5Gz \qquad \text{(Eq. 21)}$$

$$n = 17 \quad s = 2.14 \quad r = 0.69$$

While there is considerable scatter and the variance does not appear to be constant, an increase in ${}^0P^*_w$ with decreasing Gz (increasing flow rate) is suggested by the data. A possible explanation might be that increasing the flow rate increases the diameter of the intestine. Since the Graetz number is independent of the radius[8] ($Gz = \pi DL/2Q$), the result is likely to be due to a change in the wall characteristics with the flow rate. For example, the surface coat on the microvillous membrane may become thinner as the radius increases, and, hence, the resistance would be lower.

Parent Compound Permeabilities—The wall permeabilities, P^*_w, for *p*-nitroaniline and estrone are interpreted following Eq. 4 as:

$$P^*_w = P^*_m = \frac{P_m R}{D} = PCR/\delta_m \qquad \text{(Eq. 22)}$$

Thus, a direct proportionality of P^*_w with the partition coefficient is expected. The octanol–water partition coefficients are ~25 and 600, respectively (30, 31). Hence, the wall permeabilities (P^*_w) of 6 and 3 are in the correct order, *i.e.*, estrone > *p*-nitroaniline. Since the aqueous resistance has been accounted for, the fact that the wall permeability ratio of estrone $[P^*_w(E_1)]$ to *p*-nitroaniline $[P^*_w(\text{pNA})]$ is 2 while the partition coefficient ratio is 25, combined with the model:

$$\frac{P^*_w(E_1)}{P^*_w(\text{pNA})} = \frac{P_w(E_1)}{P_w(\text{pNA})} = \frac{PC(E_1)}{PC(\text{pNA})} \qquad \text{(Eq. 23)}$$

clearly suggests that the model for the wall permeability must be improved. Some factors to be considered include: (*a*) the octanol–water partition coefficient does not reflect the physiological situation, (*b*) the aqueous phase and the membrane phase diffusivities differ greatly, and (*c*) the wall resistance term is composed of more than just a term for the nonpolar phase. The first factor undoubtedly is true, but it certainly is not the only (or perhaps major) reason. The effect of differing membrane diffusivities is analyzed as follows. The convective mass transport model used for analysis of the data was solved subject to the first-order boundary condition:

$$-\left.\frac{\partial C}{\partial r}\right|_{r=R} = \frac{P_w R}{D} C_w = P^*_w C_w \qquad \text{(Eq. 24)}$$

[7] The analysis is based on ${}^0P^*_w$ rather than P^*_w since the variation of the correction factor with Gz is small.

[8] The Gz value does not depend on R because the R dependence of the residence time cancels the R dependence of the radial penetration time when the flow rate is held constant.

Table III—Results of Lysine Estrone Experiments [a]

C_m/C_0	Gz	P^*_{eff}	${}^0P^*_{aq}$	${}^0P^*_m$ [b]
0.781	0.0062	9.96	5.25	−11.1
0.84	0.0057	7.64	5.41	−18.5
0.958	0.005	2.14	5.66	3.45
0.883	0.0061	5.09	5.28	144.0
0.955	0.0054	2.13	5.51	3.47
0.924	0.0061	3.23	5.28	3.36
0.661	0.0062	16.6	5.25	−7.67
0.914	0.0059	3.81	5.34	13.2

[a] Negative values were not included in the statistics (see text). Average ${}^0P^*_m = 34$, $s = 62$, and $SEM = 28$.

Table IV—Results for *p*-Nitroaniline Experiments [a]

C_m/C_0	Gz	P^*_{eff}	${}^0P^*_{aq}$	${}^0P^*_m$ [b]
0.892	0.0137	2.08	4.03	4.31
0.768	0.0055	11.9	5.47	−10.0
0.888	0.016	1.85	3.83	3.59
0.696	0.0064	14.1	5.19	−8.21
0.885	0.016	1.90	3.83	3.79
0.91	0.016	1.47	3.83	2.39
0.916	0.0137	1.60	4.03	2.65
0.912	0.017	1.35	3.76	2.11
0.892	0.0137	2.08	4.03	4.31
0.888	0.016	1.85	3.83	3.59

[a] Negative values were not included in the statistics (see text). [b] Average ${}^0P^*_m = 3.3$, $s = 0.9$, and $SEM = 0.3$.

Table V—Results for Lysine *p*-Nitroanilide Experiments [a]

C_m/C_0	Gz	P^*_{eff}	${}^0P^*_{aq}$	${}^0P^*_m$
0.772	0.0185	3.49	3.66	75.6
0.746	0.0145	5.05	3.96	−18.3
0.767	0.012	5.52	4.21	−17.7
0.878	0.017	1.91	3.76	3.88
0.775	0.012	5.31	4.21	−20.3
0.806	0.012	4.49	4.21	−67.5
0.856	0.013	2.99	4.10	11.0
0.807	0.014	3.82	4.00	86.0
0.635	0.01	11.3	4.47	−7.38
0.881	0.01	3.16	4.47	10.8
0.915	0.01	2.22	4.47	4.41
0.576	0.016	8.61	3.83	−6.92
0.858	0.011	3.48	4.33	17.6
0.852	0.011	3.64	4.33	22.7
0.915	0.0096	2.31	4.53	4.72
0.791	0.0096	6.10	4.53	−17.6

[a] Negative values are not included in the statistics (see text). [b] Average ${}^0P^*_m = 26$, $s = 32$, and $SEM = 11$.

Table VI—Wall Permeability Values for Compounds Studied

Compound	${}^0P^*_w$ [a]	γ [b]	P^*_w [c]
Estrone	6.3	0.92	6
Estrone-3′-L-lysine ester	34	0.87	30
p-Nitroanilide	3.3	0.93	3
L-Lysine *p*-nitroanilide	26	0.87	23

[a] Approximate (dimensionless) wall permeability (Eq. 17). [b] Correction factor (27). [c] Estimated wall permeability, $P^*_w = \gamma {}^0P^*_w$, for laminar flow model (Eqs. 12 and 13).

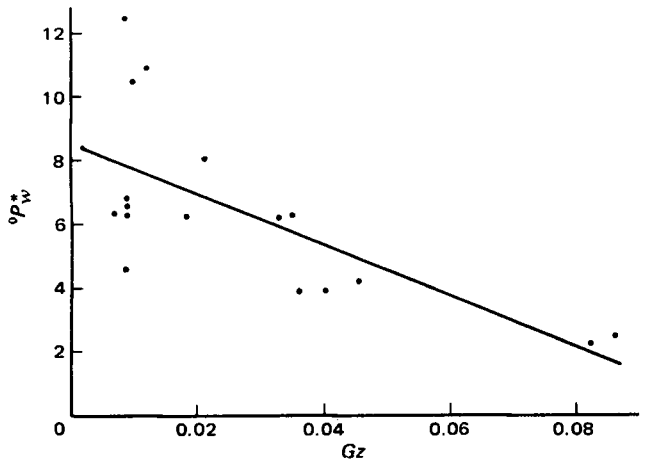

Figure 3—*Plot of the wall permeability,* $^0P^*_w$, *for estrone as a function of the Graetz number* (Gz).

or:

$$-D\left.\frac{\partial C}{\partial r}\right|_{r=R} = P_w C_w = J_w \qquad \text{(Eq. 25)}$$

where J_w is the flux at the wall, P_w is the permeability of the wall, and D is the aqueous diffusivity. A membrane model for the wall would give:

$$J_w = \frac{PCD_m C_w}{\delta_m} \qquad \text{(Eq. 26)}$$

where D_m and δ_m are the membrane parameters. Hence:

$$P_w = \frac{PCD_m}{\delta_m} \qquad \text{(Eq. 27)}$$

and:

$$P^*_w = \frac{PCD_m R}{D\delta_m} \qquad \text{(Eq. 28)}$$

Thus, the ratio of wall permeabilities is:

$$\frac{P^*_w(E_1)}{P^*_w(\text{pNA})} = \frac{PC(E_1)}{PC(\text{pNA})} = \frac{D_m(E_1)}{D_m(\text{pNA})} \qquad \text{(Eq. 29)}$$

assuming equal aqueous diffusivities for estrone and *p*-nitroaniline but not equal membrane permeabilities. Thus, the small ratio of dimensionless wall permeabilities may be due in part to a significantly lower D_m for estrone.

The third factor, an additional wall resistance term, is suggested by the presence of a surface coat on the microvillous membrane (32). If this glycoprotein layer is the major contributor to the membrane resistance, then the simple membrane model again would give Eq. 4, but, in this case, the partitioning would be into a more polar environment and the diffusivities of estrone and *p*-nitroaniline could be substantially different in the glycoprotein layer. Hence, both factors may reduce the permeability ratio.

Reactive Solute Permeabilities—For the reactive solutes, lysine estrone and lysine *p*-nitroanilide, the wall permeability may be interpreted following Eq. 10. Two limits are of interest: high reactivity, where $\alpha\delta_E > 1$ ($\tanh \alpha\delta_E \doteq 1$), for which:

$$P_w = \alpha D \qquad \text{(Eq. 30)}$$

or:

$$P^*_w = \alpha R \qquad \text{(Eq. 31)}$$

and low reactivity, where $\alpha\delta_E \ll 1$ ($\tanh \alpha\delta_E \doteq \alpha\delta_E$), for which:

$$P_w = \alpha^2 D\delta_E \qquad \text{(Eq. 32)}$$

or:

$$P^*_w = \alpha^2\delta^R_E \qquad \text{(Eq. 33)}$$

The lysine estrone–lysine *p*-nitroanilide permeability ratio $[P^*_w(\text{LE}_1)/P^*_w(\text{LpNA})]$ becomes:

$$\frac{P^*_w(\text{LE}_1)}{P^*_w(\text{LpNA})} = \frac{k_{\text{LE}_1}}{k_{\text{LpNA}}} \qquad \alpha\delta_E > 1 \qquad \text{(Eq. 34)}$$

and:

$$\frac{P^*_w(\text{LE}_1)}{P^*_w(\text{LpNA})} = \left(\frac{k_{\text{LE}_1}}{k_{\text{LpNA}}}\right)^2 \qquad \alpha\delta_E \ll 1 \qquad \text{(Eq. 35)}$$

While the membrane enzymes involved in the hydrolysis reactions are not well characterized, kinetic results for trypsin have shown amides to be much poorer substrates than the corresponding esters (33). Consequently, the similar permeability values for LE_1 and LpNA are not likely to be explained in this manner.

As with the passively absorbed compounds, it may be that the surface coat on the microvillous membrane serves as an additional resistance. In this case, the enzymes at the interface (and perhaps to some extent in the surface coat) would provide the effective sink rather than the partitioning into the membrane. Although the scatter in the data is considerably larger for the reactive substrates, the results clearly indicate that the effective wall permeability of the reactive substrates is higher than the corresponding passively absorbed compounds by a factor of five to 10. Based on the suggested interpretation, the reason could be that the effective thickness of the surface coat is smaller for the reactive substrates.

While the interpretation of the permeability values clearly requires more experimental work, the most important point to be obtained from these results is that the derivatives have permeabilities at least as great as those of the parent compounds. Consequently, they are absorbed very efficiently, even though the compounds have smaller diffusivities and much higher polarity (lower partition coefficients) due to the protonated α- and ϵ-amino groups. Thus, an equal or greater effective permeability has been achieved along with much higher aqueous solubility. Since absorption of the intact derivatives is unlikely, hydrolysis at the membrane interface apparently is very effective.

The results also imply that the interfacial reaction is as fast or faster than aqueous diffusion or diffusion through the surface coat since the results approach (and exceed) the value that would be obtained if sink conditions ($P^*_w = \infty$) prevail. Furthermore, lysine *p*-nitroanilide is relatively stable in solution and yet is absorbed very efficiently. This finding suggests that the hydrolysis of amides is at least as fast as luminal diffusion. Consequently, amide derivatives of amines, which otherwise are too stable for chemical reconversion to be effective, may be effective using this strategy.

Absorption Rate—To illustrate further the potential of this approach, the results of the estrone and lysine estrone experiments are graphed in Fig. 4 following Eq. 15 in the form:

$$\log dm/dt = \log[(1 - C_m/C_0)Q] + \log C_0 \qquad \text{(Eq. 36)}$$

A single line is drawn through the estrone and lysine estrone data since their effective permeabilities are nearly the same. That is, at the same flow rate, the fraction absorbed $(1 - C_m/C_0)$ is the same, provided that C_0 is below the saturation concentration. When saturation is reached, $C_0 = C_s$ and the amount absorbed per unit time levels off at a constant value.

On the other hand, for lysine estrone, the mass transfer per unit time increases until the solubility of 0.3 *M* is reached (29). The result is that the amount of lysine estrone absorbed per unit time could be about five orders of magnitude greater than that for estrone (note that Fig. 4 is a log–log plot).

Clearly, many questions remain to be investigated, both with respect

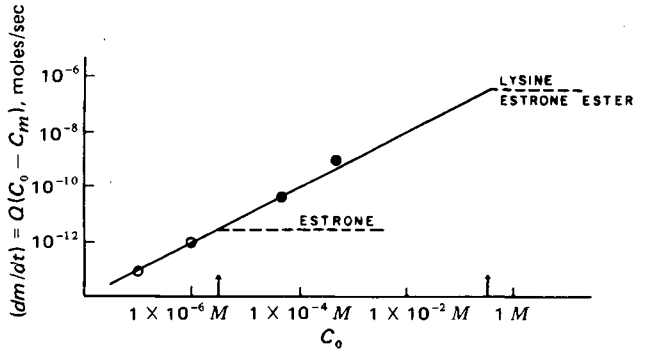

Figure 4—*Amount of drug absorbed per unit time* (dm/dt) *as a function of the initial perfusing concentration* (C_0) *for estrone and lysine estrone. Key:* ○, *estrone;* ●, *lysine estrone;* ↑, *solubilities; and* – –, *theoretical limits.*

to the absorption mechanism and to the actual effectiveness of the strategy in normal physiological situations. However, the results obtained to date strongly suggest that the biochemical strategy offers a new approach with great potential for improving drug product efficacy.

CONCLUSION

A biochemical strategy for improving the absorption of water-insoluble drugs has been tested and shown to have potential for increasing the absorption rates of insoluble compounds by several orders of magnitude. The strategy is based on the use of the enzymes in the interfacial brush border region of the mucosal cells to effect a conversion of the soluble derivative back to the insoluble, high partition coefficient parent compound. Since the aqueous luminal fluid and nonpolar membrane phases have conflicting physical property requirements, the interfacial reaction is, in effect, being used to change the physical properties of a compound from one having desirable aqueous (luminal) properties to one having desirable membrane permeation properties.

Results on two drug–drug derivative pairs, estrone–lysine estrone and *p*-nitroaniline–lysine *p*-nitroanilide, show that the effective intestinal membrane permeability of the derivatives is actually five to 10 times greater than that of the parent compounds. Since the derivatives are significantly more polar than the parent compound, the results indicate that the effective permeability associated with the interfacial enzymatic reaction is not a determining resistance. Thus, the usual physical property compromise necessary to obtain efficient drug absorption by other strategies is avoided. Analysis of the permeability data for both the parent compounds and derivatives suggests that the surface coat on the microvillous membrane may be an important resistance in the absorption process. The apparent residual dependence of the wall permeability on Gz also may be due to a thinning of this coat as *Gz* decreases. In addition, the higher wall permeabilities of the derivatives compared to the parent compounds may be due in part to hydrolysis partially occurring in this layer, reducing its effective thickness.

Analysis of the data in terms of the absorption rate (mass transport per unit time) indicates that an improvement of several orders of magnitude is possible. For lysine estrone–estrone, a two to three order of magnitude increase has been demonstrated, with a four or five order of magnitude increase possible. Given the high solubility, dissolution rate, and permeability of lysine estrone, the biochemical strategy appears to be capable of significantly improving the absorption of water-insoluble drugs.

REFERENCES

(1) "Solubilization," S. H. Yalkowsky, Ed., Dekker, New York, N.Y., 1980.

(2) G. L. Flynn and S. H. Yalkowsky, *J. Pharm. Sci.*, **61**, 838 (1972).

(3) S. H. Yalkowsky and G. L. Flynn, *ibid.*, **62**, 210 (1973).

(4) G. L. Amidon, in "Solubilization," S. H. Yalkowsky, Ed., Dekker, New York, N.Y., 1980.

(5) W. S. Saari, M. B. Freedman, R. D. Hartman, S. W. King, A. W. Raab, W. C. Randall, E. L. Englehardt, and R. Hirschmann, *J. Med. Chem.*, **21**, 746 (1978).

(6) "Peptide Transport and Hydrolysis," Ciba Foundation Symposium 50, Elsevier, Amsterdam, The Netherlands, 1977.

(7) "Peptide Transport in Bacteria and Mammalian Gut," Ciba Foundation Symposium 4, Elsevier, Amsterdam, The Netherlands, 1972.

(8) M. D. Hellier and C. D. Holdsworth, in "Intestinal Absorption in Man," I. McColl and G. E. Sladen, Eds., Academic, New York, N.Y., 1975, pp. 143–186.

(9) M. H. Sleisenger and Y. S. Kim, *N. Engl. J. Med.*, **300**, 659 (1979).

(10) D. M. Matthews, *Gastroenterology*, **73**, 1267 (1977).

(11) D. M. Matthews, *Physiol. Rev.*, **55**, 537 (1975).

(12) D. M. Matthews and S. A. Adibi, *Gastroenterology*, **71**, 151 (1976).

(13) D. M. Matthews, in "Peptide Transport in Protein Nutrition," D. M. Matthews and J. W. Payne, Eds., North-Holland, Amsterdam, The Netherlands, 1975, pp. 61–146.

(14) G. M. Gray and H. L. Cooper, *Gastroenterology*, **61**, 535 (1971).

(15) H. Newey and D. H. Smyth, *J. Physiol.*, **145**, 48 (1959).

(16) *Ibid.*, **152**, 367 (1960).

(17) *Ibid.*, **164**, 527 (1962).

(18) D. J. Prockop, H. R. Keiser, and A. Smoerdsma, *Lancet*, **2**, 527 (1962).

(19) I. L. Craft, D. Geddes, C. W. Hyde, I. J. Wise, and D. M. Matthews, *Gut*, **9**, 425 (1968).

(20) D. M. Matthews, I. L. Craft, D. M. Geddes, I. J. Wise, and C. W. Hyde, *Clin. Sci.*, **35**, 415 (1968).

(21) A. M. Asatoor, B. Cheng, K. D. G. Edwards, A. F. Lant, D. M. Matthews, M. D. Milne, F. Navab, and A. J. Richards, *Gut*, **11**, 380 (1970).

(22) A. M. Ugolev, in "Peptide Transport in Bacteria and Mammalian Gut," Ciba Foundation Symposium 4, Elsevier, Amsterdam, The Netherlands, 1972, pp. 123–127.

(23) A. M. Ugolev, in "Biomembranes," vol. 4A, D. M. Smyth, Ed., Plenum, New York, N.Y., 1974, pp. 285–362.

(24) A. M. Ugolev, in "Peptide Transport and Hydrolysis," Ciba Foundation Symposium 50, Elsevier, Amsterdam, The Netherlands, 1977, pp. 221–238.

(25) D. M. Matthews, *Physiol. Rev.*, **55**, 595 (1975).

(26) A. N. Radhakrishnan, in "Peptide Transport and Hydrolysis," Ciba Foundation Symposium 50, Elsevier, Amsterdam, The Netherlands, 1977, p. 50.

(27) R. L. Elliott, Ph.D. thesis, University of Wisconsin, Madison, Wis., 1979.

(28) G. L. Amidon, J. Kou, R. L. Elliott, and E. N. Lightfoot, *J. Pharm. Sci.*, **69**, 1369 (1980).

(29) G. D. Leesman, Ph.D. thesis, University of Wisconsin, Madison, Wis., 1980.

(30) N. F. H. Ho, J. Y. Park, W. Morozowich, and W. I. Higuchi, in "Design of Biopharmaceutical Properties through Prodrugs and Analogs," E. B. Roche, Ed., APhA Academy of Pharmaceutical Sciences, Washington, D.C., 1977, p. 155.

(31) A. Leo, C. Hansch, and D. Elkins, *Chem. Rev.*, **71**, 525 (1971).

(32) J. S. Trier, in "Alimentary Canal," vol. 3, "Handbook of Physiology," American Physiological Society, Washington, D.C., 1968, p. 1138.

(33) B. Keil, in "The Enzymes," vol. 3, P. D. Boyer, Ed., Academic, New York, N.Y., 1971, p. 266.

ACKNOWLEDGMENTS

Supported by The Upjohn Co., Biomedical Research Support Grant SO 7RR05456-17, and GM 27680.

The authors thank Ms. Shannon Sullivan and Mr. James Kou for assistance with portions of this work.

Analysis of Models for Determining Intestinal Wall Permeabilities

G. L. AMIDON *x, J. KOU *, R. L. ELLIOTT *, and E. N. LIGHTFOOT ‡

Received February 27, 1980, from the *School of Pharmacy and the ‡Department of Chemical Engineering, University of Wisconsin, Madison, WI 53706. Accepted for publication June 11, 1980.

Abstract □ In determining intestinal wall permeabilities, several mass transport models may be applied to analyze the results from external perfusion experiments. The appropriateness of any given model depends on the applicability of the model assumptions to the experimental system. This report compares several mass transport models with respect to their assumptions and applicability to a particular experimental design. The models are shown to differ in their assumptions regarding convection and diffusion in the perfusing fluid. However, since the wall permeability is an unknown parameter in each model and is estimated from the data, all of the models fit the mass transfer results reasonably well, despite fundamentally different assumptions. However, the determined permeabilities differ. Residence time distribution analysis of the experimental system is more sensitive to the model assumptions. It is shown that, in a particular experimental system, laminar flow in a cylindrical tube is the most appropriate model. The model also has the advantage of implicitly accounting for the convection–diffusion problem in the perfusing fluid. Hence, the diffusion layer thickness is not estimated from the data. With the hydrodynamics defined, the relative permeabilities resulting from the application of the several models to the data can be interpreted. The wall permeability determined in the suggested manner provides an estimate of the limiting assistance under perfect mixing conditions.

Keyphrases □ Permeability—mass transport models of intestinal wall permeability □ Models, hydrodynamic—mass transport models of intestinal wall permeability □ Diffusion—mass transport models of intestinal wall permeability

In determining the permeability of the intestinal wall by external perfusion techniques, several models have been proposed (1–5). In each model, assumptions must be made regarding the convection and diffusion conditions in the experimental system. These assumptions, in turn, affect the interpretation of the resulting permeabilities. In addition, the appropriateness of the assumptions in the models to the actual experimental situation must be determined. Often, good agreement between the predicted (theoretical) result and the experimental result is used to support the validity of the model. However, in many cases, several models may be equally satisfactory, particularly when significant variation occurs from experiment to experiment. In this situation, independent experiments that are more sensitive to the assumptions in the models are needed to substantiate their validity.

This report shows that several reasonable models for mass transfer in external perfusion experiments can account for the data reasonably well because the actual wall permeability is unknown. That is, if the permeability is treated as a parameter and is estimated from the data, all of the models can describe the data relatively well.

However, the resulting permeabilities differ, and their interpretation rests on the validity of the assumptions. Consequently, residence time distribution analysis is used to obtain more direct insight into the convection and diffusion assumptions of the mass transfer models. Since the laminar flow model discussed previously (5) has the advantage of providing a direct measure of the wall permeability, the experimental system used was one that maximizes the possible attainment of these conditions.

EXPERIMENTAL

[^{14}C]Polyethylene glycol[1] was used for the residence time studies. Assays were conducted by liquid scintillation. For the residence time perfusion experiments, male Holtzman rats (250–350 kg) were fasted for 12–18 hr and anesthetized with an intramuscular (gluteal muscle) dose of 150 mg/100 g with a 50% urethan solution. A midline abdominal incision was made, and the intestine was cannulated 2 and 10 cm distal to the ligament of Treitz. The entrance tubing was connected to a three-way stopcock such that the test solution would flow straight through the stopcock. The buffer solution, isotonic Sorensen's buffer at pH 7.3, was perfused through the remaining stopcock arm for 20–30 min.

The experiment was initiated by turning the stopcock to the test solution (polyethylene glycol–Sorensen's buffer) at time zero. Samples were collected at 15-sec intervals for ~2 min ($2\bar{t}$) and then at 30-sec intervals for up to ~6 min ($6\bar{t}$). From the collected samples, 0.1 ml was transferred by micropipet to the counting vial. For the step change in concentration, the test solution was perfused throughout the experiment. For the (finite) pulse change, the stopcock was switched from the buffer to the test solution and back to the buffer over about a 2-sec interval. The flow rate was 0.5 ml/min for all experiments.

At the conclusion of the experiment, the animal was sacrificed and the cannulated intestine was excised. The length and volume of the excised intestine were measured to estimate the residence time in the perfused segment. The mass transfer studies used [^{3}H]estrone[1] and followed a procedure described previously (6).

RESULTS AND DISCUSSION

Mass Transfer Models—Four models will be described that differ in their convection and diffusion assumptions (Fig. 1). These models include the laminar flow, plug flow, and complete radial mixing (diffusion layer) models for convective mass transport in a tube and the perfect mixing tank model. It is convenient to begin with the solute transport equation in cylindrical coordinates (5, 7):

$$v_z \frac{\partial C}{\partial z} = D \frac{1}{r} \frac{\partial}{\partial r}\left(r \frac{\partial C}{\partial r}\right) \qquad \text{(Eq. 1)}$$

where:

v_z = axial velocity distribution
D = solute diffusivity in the solvent
C = concentration of A in B
z = axial coordinate
r = radial coordinate

Introduction of the dimensionless variables:

$z^* = z/L$
$r^* = r/R$
$v_z^* = v_z/V_m$
$Gz = DL/V_mR^2 = \pi DL/2Q$
R = radius of the tube
L = length of the tube
V_m = maximum velocity
Q = perfusion flow rate

gives:

[1] New England Nuclear, Boston, Mass.

0022-3549/80/1200-1369$01.00/0
© 1980, American Pharmaceutical Association

Table I—Summary of Various Models

Model	Equation	Variables	Comments
Laminar flow	$C_m/C_0 = \Sigma M_n \exp(-\beta_n^2 Gz)$	P_w^* and Gz	M_n and β_n are functions of P_w^* (Ref. 5)
Plug flow	$C_m/C_0 = \Sigma M'_n \exp(-\beta_n'^2 Gz)$	$P_w'^*$ and Gz	M'_n and β'_n are functions of $P_w'^*$ (Ref. 8)
Complete radial mixing	$C_m/C_0 = \exp(-4P_{eff}^* Gz)$	P_{eff}^* and Gz	$P_{eff}^* = \frac{P_a^* P_w^*}{P_a^* + P_w^*}$
Mixing tank	$C_m/C_0 = (1 + 4P_{eff}'^* Gz)^{-1}$	$P_{eff}'^*$ and Gz	$P_{eff}'^* = \frac{P_a'^* P_w^*}{P_a'^* + P_w^*}$

$$v_z^* \frac{\partial C}{\partial z^*} = Gz \left(\frac{1}{r^*} \frac{\partial}{\partial r^*} r^* \frac{\partial C}{\partial r^*} \right) \quad \text{(Eq. 2)}$$

This relationship is subject to the first-order boundary condition at the wall:

$$\left. \frac{\partial C}{\partial r^*} \right|_{r^*=1} = -P_w^* C_w \quad \text{(Eq. 3)}$$

where $P_w^* = P_w R/D$ = the dimensionless wall permeability.

The main assumptions in arriving at Eqs. 1 and 2 are: (*a*) the diffusivity and density are constant; (*b*) the solution is dilute so that the solvent convection is unperturbed by the solute; (*c*) the system is at steady state ($\partial C/\partial t = 0$); (*d*) the solvent flows only in the axial (z) direction; (*e*) the tube radius, R, is independent of Gz; and (*f*) axial diffusion is small compared to axial convection (7). The boundary condition (Eq. 3) is true for many models having a tube wall but does not describe a carrier transport or Michaelis–Menten process at the wall, except at low solute concentrations. Rewriting Eqs. 2 and 3[2] gives:

$$v_z^* \frac{\partial C}{\partial z} = Gz \left(\frac{1}{r} \frac{\partial}{\partial r} r \frac{\partial C}{\partial r} \right) \quad \text{(Eq. 4)}$$

$$\left. \frac{\partial C}{\partial r} \right|_{r=1} = -P_w^* C_w \quad \text{(Eq. 5)}$$

It is clear that the solution is $C = C(r, z, Gz, P_w^*)$. That is, Gz and P_w^* are the two fundamental independent (dimensionless) variables. Since the measured exit concentration is generally a velocity-averaged concentration (cup-mixing concentration), averaging over r gives:

$$C_m(Gz, P_w^*) = \frac{\int_0^{2\pi} \int_0^1 v_z C r \, dr \, d\theta}{\int_0^{2\pi} \int_0^1 v_z r \, dr \, d\theta} \quad \text{(Eq. 6)}$$

where z (dimensionless) is set equal to 1 (*i.e.*, the concentration is measured at the end of the tube). For the several models discussed here, the given solution refers to the cup-mixing concentration, and Gz and P_w^* are the only fundamental independent variables. However, the P_w^* value will have different interpretations within the context of the different models.

Laminar Flow Model—In the laminar flow model, the velocity profile is taken to be that for a Newtonian fluid in a tube:

$$v_z^* = v_z/V_m = 1 - r^2 \quad \text{(Eq. 7)}$$

where $V_m = 2\langle v \rangle$ and $\langle v \rangle$ is the average flow velocity; *i.e.*, $Q = \langle v \rangle \pi R^2$. With this velocity profile, Eq. 4 is separable and with the boundary condition in Eq. 5 has the solution (5):

$$C_m/C_0 = \sum_n M_n \exp(-\beta_n^2 Gz) \quad \text{(Eq. 8)}$$

where C_m is the exit cup-mixing concentration at length L and C_0 is the inlet concentration (constant). The laminar flow model will be discussed in detail in a report[3] that also contains tabulated values of the M_n and β_n values as a function of P_w^*.

Plug Flow Model—In the plug flow model, the velocity profile is considered to be independent of both r and z. That is, $v_z = Q/\pi R^2$ and is constant; hence, $V_z = V_m$ and $V_z^* = 1$. The solution to Eqs. 4 and 5 is (8):

$$C_m/C_0 = \Sigma M'_n \exp(-\beta_n'^2 Gz) \quad \text{(Eq. 9)}$$

where $M'_n = -4P_w'^*/(\beta_n'^4 + \beta_n'^2 P_w'^{*2})$ and the β'_n values are the roots of the equation:

$$\beta' J_1(\beta') - P_w'^* J_0(\beta) = 0 \quad \text{(Eq. 10)}$$

with J_1 and J_0 being zero-order bessel functions of the first and second kinds. The roots of Eq. 10 are tabulated in Refs. 8 and 9.

With this model, the assumption that V_z is constant is one of perfect slip at the wall. That is, V_z is constant throughout the fluid while the velocity of the wall is zero. However, there is radial diffusion as well as a corresponding concentration gradient toward the wall. The $P_w'^*$ value is the true wall permeability if the actual hydrodynamics are of this type. For a given wall permeability, the plug flow model predicts greater absorption of the solute compared to the laminar flow model due to greater convection near the wall.

Complete Radial Mixing Model—For this model, the velocity profile is assumed to be constant as with the plug flow model. In addition, the concentration is assumed to be constant radially but not axially. That is, there is complete radial, but not axial, mixing to give uniform radial velocity and concentration profiles. With these assumptions, Eq. 4 and

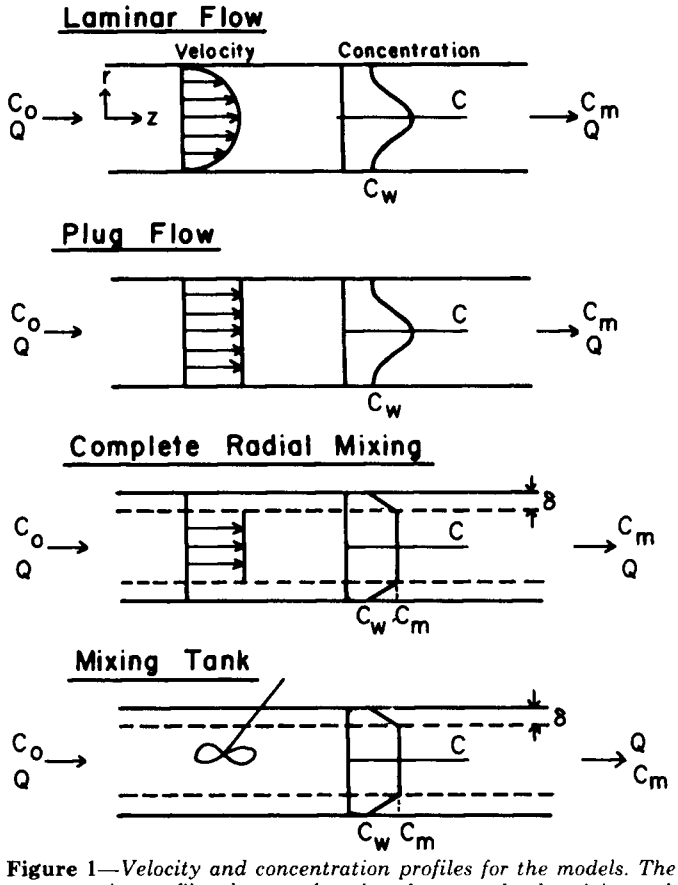

Figure 1—*Velocity and concentration profiles for the models. The concentration profiles also are a function of z except for the mixing tank model.*

[2] Hereafter, all equations will be in dimensionless form but the asterisk will be deleted from the r and z symbols except where the context clearly indicated otherwise.

[3] See R. L. Elliott, G. L. Amidon, and E. N. Lightfoot, *J. Theor. Biol.*, in press.

the boundary condition (Eq. 5) have the solution (5):

$$C_m/C_0 = \exp(-4P^*_{eff}Gz) \quad \text{(Eq. 11)}$$

where P^*_{eff} replaces P^*_w. Since no aqueous resistance is included directly in the model, the wall resistance usually is augmented with a film or diffusion layer resistance. That is, complete radial mixing occurs up to a thin region or film adjacent to the membrane. The aqueous (luminal) resistance is confined, within this model, entirely to this region in series with the membrane. Hence, the wall permeability includes an aqueous or luminal resistance term and can be written as:

$$P^*_{eff} = \frac{P^*_w P^*_a}{P^*_w + P^*_a} \quad \text{(Eq. 12)}$$

where P^*_w is the true wall permeability and P^*_a is the effective aqueous permeability (1–3, 5).

The aqueous permeability often is written as:

$$P_a = D/\delta \quad \text{(Eq. 13)}$$

or:

$$P^*_a = R/\delta \quad \text{(Eq. 14)}$$

where δ is the film thickness and represents an additional parameter that needs to be determined from the data to obtain P^*_w. Since the assumed hydrodynamic conditions probably are not realistic at the low Reynolds numbers for typical experiments, P^*_a or δ/R is an empirical parameter.

The complete radial mixing model also can be derived from a differential mass balance approach (1) and often is referred to as the diffusion layer model. A comparison of the laminar flow and complete radial mixing models will be reported later[3].

Mixing Tank Model—This model takes the next step and assumes that both radial and axial mixing are complete. The aqueous resistance again is thought to be confined to a region (film) next to the membrane where only molecular diffusion occurs, whereas the rest of the contents are well mixed (perfect mixer). This model is described most easily by a mass balance on the system:

$$(\text{mass/time})_{inlet} - (\text{mass/time})_{outlet} = (\text{mass/time})_{absorbed} \quad \text{(Eq. 15a)}$$

or:

$$QC_0 - QC_m = (2\pi RL)(P'_{eff})C_m \quad \text{(Eq. 15b)}$$

where $2\pi RL$ is the area of the mass transfer surface (cylinder) of length L and radius R, P'_{eff} is the permeability or mass transfer coefficient of the surface, and C_m is the concentration in the tube (which is constant and equal to the outlet concentration by the perfect mixing assumption). From Eq. 15b is obtained:

$$\frac{C_0 - C_m}{C_m} = P'_{eff}\frac{2\pi RL}{Q} \quad \text{(Eq. 16)}$$

or:

$$C_0/C_m = 1 + 4P'^*_{eff}Gz \quad \text{(Eq. 17)}$$

As with the complete radial mixing model, P'^*_{eff} contains the additional parameter $P'^*_a = R/\delta'$ that must be estimated from the data. The P'^*_a and P'^*_{eff} values for the mixing tank model differ from those for the complete radial mixing model by nature of the different hydrodynamic assumptions. While this model probably is not appropriate to most perfusion experiments, it will be useful to compare its ability to correlate mass transfer data with the other models.

Model Comparison and Summary—Table I summarizes the models with respect to the predicted mass transfer. If the true wall permeability, P^*_w, were known, then each model could be tested against the data to determine its ability to reproduce the data. Since this is not the case, the appropriate P^*_w or P^*_{eff} value must be determined from the data. A test of the model then is to determine its ability to correlate the data, given a value for the permeability (estimated from the data). That is, the equations in Table I correlate the observed C_m/C_0 as a function of the Gz value, with the permeability being used as a variable parameter.

Mass Transfer Results—Figure 2 presents the results using the simple mixing tank model (Eq. 17). The best-fit line (with zero intercept) is:

$$(C_0/C_m) - 1 = 6.97Gz \quad \text{(Eq. 18)}$$

with $n = 17$, $s = 0.064$, and $p < 0.0005$. The standard error of the slope is 0.43. The P'^*_{eff} calculated from Eq. 17 is 1.7. Given the simplicity of the model, it accounts for the data reasonably well. However, from the graph, it is clear that systematic deviations occur from the best-fit line. If the two data points at the highest Gz value were removed from the data set, the model would do quite well.

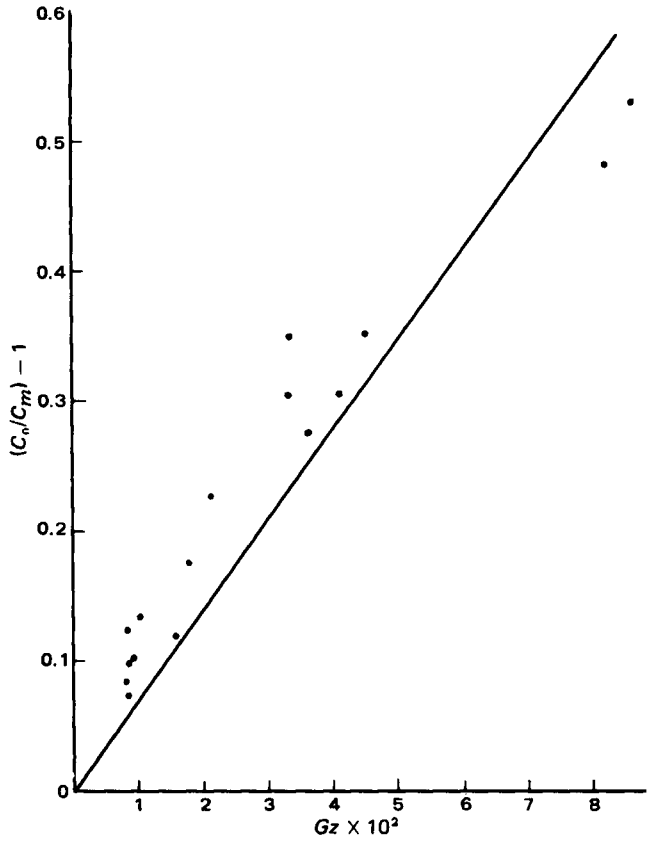

Figure 2—*Graph of* $(C_0/C_m) - 1$ versus Gz *following the mixing tank model* (—) *and the experimental data* (●) *for estrone.*

Figure 3 presents the data as well as the best-fit lines for all four models. The permeabilities were estimated *via* linear regression following Eqs. 11 and 17 and by nonlinear regression following Eqs. 8 and 9 for the respective models. The resulting permeabilities are given in Table II. From Fig. 3, it is clear that it is not possible to choose from among the models on the basis of the mass transfer data if the permeability itself is estimated from the data. The permeabilities differ for the various models. Interpretation of the respective permeabilities requires knowledge as to which model most closely reflects the actual experimental situation.

Residence Time Distribution Analysis—To interpret the mass transfer results and the associated permeabilities, it is necessary to establish the actual hydrodynamics. Since, as noted, the mass transfer data are not sensitive to the model if the wall permeability is known, an independent method that is more sensitive to the hydrodynamics is required. In any given situation, the hydrodynamics implied (assumed) by one or another of the mass transfer models may be the most appropriate. The experimental design used for this study maximized the possible attainment of laminar flow.

Residence time distribution analysis provides one method for determining flow characteristics (10–12). A step or pulse change in the inlet concentration of a completely inert tracer is made, and the resulting appearance of the tracer in the outlet stream is monitored. The appear-

Table II—Permeability Values Estimated from the Data for the Various Models

Model	Permeability[a]
Mixing tank	1.7 (±0.9)
Complete radial mixing	2.0 (±0.3)
Plug flow	3.1 (±0.5)
Laminar flow	5.7 (±1.3)

[a] Dimensionless permeability. Values in parentheses represent the approximate 95% confidence intervals.

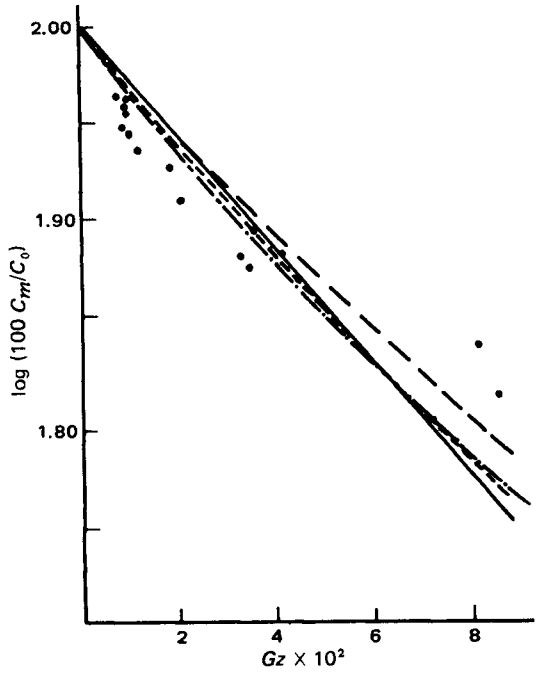

Figure 3—*Graph of log(100*C_m/C_0*) versus Gz for the several models and the experimental data (●) for estrone. Key: – –, mixing tank model; —, complete radial mixing model; - - -, plug flow model; and · – ·, laminar flow model.*

ance of tracer in the outlet stream is a function of the flow (hydrodynamic) conditions since these conditions, in turn, determine the length of time a given fluid element entering the inlet stays in the apparatus. In dealing with potentially very simple hydrodynamics, three simple models are appropriate: mixing tank, plug flow, and laminar tube flow. The step change in concentration, $C = 0$ at $t < 0$ and $C = C_0$ at $t > t_0$, at the inlet gives the F curve, while a finite pulse change (12) gives the E curve. The F curve is defined as:

$$F = \langle C \rangle / C_0 \qquad \text{(Eq. 19)}$$

where $\langle C \rangle$ is the exit cup-mixing concentration and C_0 is the inlet concentration.

The E curve is defined by:

$$E = dF/dt \qquad \text{(Eq. 20)}$$

For a pulse change in concentration at the inlet with a total mass, M, of tracer injected:

$$M = \int_0^\infty \langle C \rangle \, dt \qquad \text{(Eq. 21)}$$

and the E curve is obtained from:

$$E = \frac{\langle C \rangle}{M} \qquad \text{(Eq. 22)}$$

The (experimental) mean residence time, $\bar{t}$, in the apparatus is obtained from:

$$\bar{t} = \int_0^\infty \bar{t} E \, dt \qquad \text{(Eq. 23)}$$

for the pulse change and from:

$$\bar{t} = \int_0^\infty (1 - F) \, dt \qquad \text{(Eq. 24)}$$

for the step change. The corresponding F and E functions for the plug flow model are:

$$F = 0 \qquad t < \bar{t} \qquad \text{(Eq. 25a)}$$

$$F = 1 \qquad t > \bar{t} \qquad \text{(Eq. 25b)}$$

$$E = 0 \qquad t \neq \bar{t} \qquad \text{(Eq. 25c)}$$

$$E = \text{input function} \qquad t = \bar{t} \qquad \text{(Eq. 25d)}$$

For the perfect mixer model, they are:

$$F = 1 - e^{-t/\bar{t}} \qquad \text{(Eq. 26a)}$$

$$E = \frac{1}{\bar{t}} e^{-t/\bar{t}} \qquad \text{(Eq. 26b)}$$

For the laminar flow model, they are:

$$F = 1 - \left(\frac{\bar{t}}{2t}\right)^2 \qquad t > \bar{t}/2 \qquad \text{(Eq. 27a)}$$

$$E = \frac{\bar{t}^2}{2} \frac{1}{t^3} \qquad t > \bar{t}/2 \qquad \text{(Eq. 27b)}$$

The theoretical E and F curves for these models using $\theta = t/\bar{t}$ as dimensionless time are shown in Fig. 4. These models contain only one parameter, $\bar{t}$.

More complex, two- (or more) parameter models, *e.g.*, tanks in series or a dispersion model, could be fitted to the data. However, given the simplicity of the flow situation, this is unnecessary.

The experimental results from the intestinal perfusion studies also are shown in Fig. 4. Since the plug flow model clearly is inappropriate, it will not be analyzed further.

Table III presents the mean residence times estimated by the following three methods: (*a*) the volume measurement of the intestine at $\bar{t} = V/Q$,

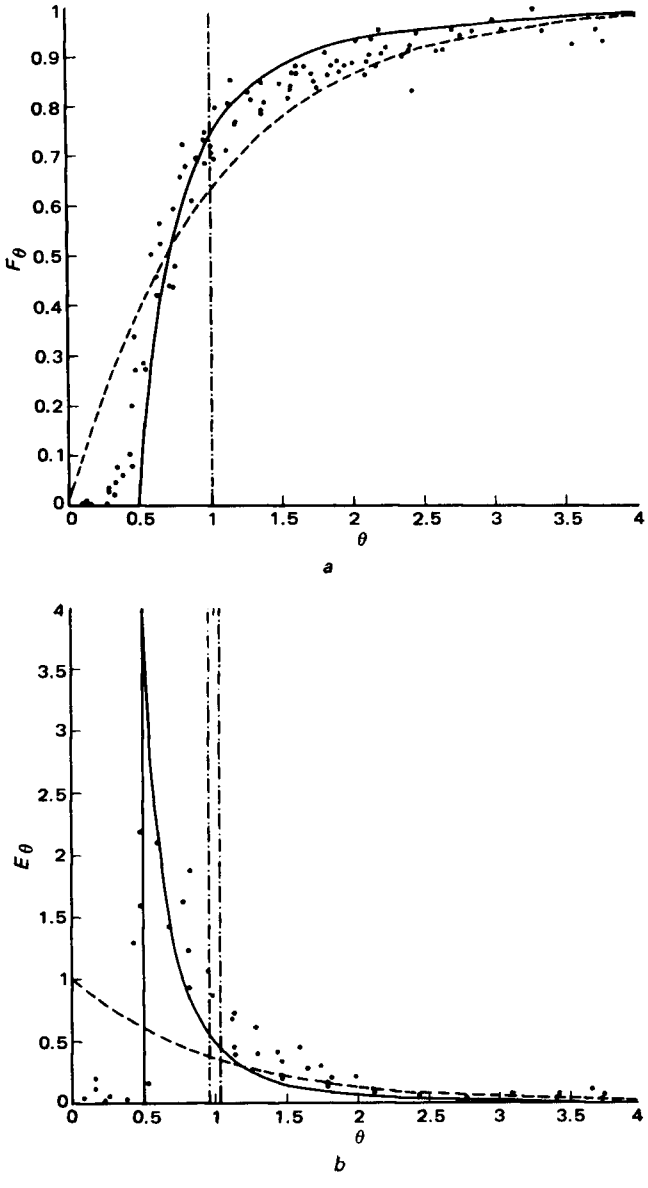

Figure 4—*Curves for perfusion experiments,* F versus θ = t/$\bar{t}$ (a) *and* E versus θ (b). *Key: - - -, mixing tank model; —, laminar flow model; - · -, plug flow model; and ●, experimental results.*

Table III—Estimated Mean Residence Times

Experiment[a]	$\bar{t}\left(\frac{V}{Q}\right)$	$\bar{t}$ (Area)	Mixing Tank $\bar{t}$ (regression)[b]	Laminar Flow $\bar{t}$ (regression)[b]
1	65	60.6	63.9 (13)	60.8 (5)
2	65	51.5	52.4 (8)	57.8 (5)
3	65	52.6	53.0 (11)	56.8 (4)
4	97	70.1	67.5 (13)	76.1 (9)
5	97	86.2	82.7 (23)	79.4 (5)
6	97	82.3	74.8 (11)	77.2 (13)
7	78	65.5	55.8 (11)	55.7 (5)
8	78	71.5	68.7 (16)	65.0 (2)
9	78	81.2	75.8 (14)	76.2 (10)
10	43	46.0	73.6 (75)	37.4 (2)
11	43	46.2	70.6 (63)	34.6 (3)
12	85	86.6	230.3 (300)	89.9 (8)
13	85	99.2	237.0 (310)	74.9 (1)

[a] Experiments 1–9 represent step changes in inlet concentration, and Experiments 10–13 represent pulse changes in concentration. [b] Numbers in parentheses represent approximate 95% confidence intervals.

(*b*) integration following Eq. 23 or 24, and (*c*) nonlinear regression fitting of the mixing tank and laminar flow models to the data using the mean residence time, $\bar{t}$, as the only parameter.

The results in Fig. 4 and Table II clearly suggest that the laminar flow model is the most appropriate of the three simple models. However, the data suggest that some mixing or dispersion is occurring in the system since the tracer appears at the outlet somewhat faster than laminar flow would predict.

Interpretation of Mass Transfer Data—Given the results of the residence time studies, the permeabilities are interpreted most appropriately on the basis of laminar flow hydrodynamics. The estrone permeability value of 6, determined under the assumption of laminar flow, represents an estimate of the true wall permeability. The luminal diffusive component, P^*_{aq}, is not included in the wall permeability. In fact, if the flow is laminar, P^*_{aq} can be calculated from the model (5).

Assuming that the laminar flow permeability measures the wall permeability, the permeabilities resulting from application of the other models can be interpreted. The plug flow value of 3 is lower than the laminar flow result since a larger membrane resistance is needed to compensate for the lower estimate of the aqueous resistance. That is, the larger amount of convection near the wall in the plug flow model leads to a larger P^*_{aq} than actually is the case. Consequently, the membrane permeability must be lower to account for the observed result.

The permeability value for the complete radial mixing model of 2 is lower than the plug flow (and laminar flow) model since this model assumes radial mixing, which leads to still lower estimated luminal (aqueous) resistance values and a higher estimated membrane resistance (lower permeability value). However, the usual interpretation of the complete radial mixing model recognizes that the permeability value includes an aqueous (film) resistance.

The mixing tank model takes the final step in assuming both radial and axial mixing. The permeability value for this model is the lowest of all of the models. Again, this result is due to the low luminal resistance implied by the model. As with the complete radial mixing model, a film resistance usually is included in the wall permeability to account for the presence of an aqueous resistance.

If, as suggested, the complete radial mixing permeability includes a film (diffusion layer) aqueous resistance, the permeability value should be that obtained from the laminar flow model augmented by a P^*_{aq} value following Eq. 12. However, P^*_{aq} is a function of both P^*_w and Gz and, hence, must be calculated at every flow rate (Gz value) using the known P^*_w value. However, an estimate of P^*_{aq} can be made that is not greatly in error by using the ${}^0P^*_{aq}$ value for sink conditions at the wall and an average Gz value (5). This approach gives ${}^0P^*_{aq} = 3.7$. The predicted permeability for the complete radial mixing model thus is 2.2, which is in good agreement with the estimated value of 2.0. A more detailed discussion of the basis for this calculation was given previously (5, 6).

This discussion illustrates one major advantage of the laminar flow approach. The diffusion layer thickness is not a parameter in the model, and the wall permeability can be calculated directly. In the complete radial mixing model, the P^*_{aq} (equal to R/δ) value enters the model to account for the unknown hydrodynamics and, hence, must be estimated from the data as well. The residence time distribution analysis indicates that laminar flow can be established to a reasonable approximation in external perfusion experiments. Consequently, there is no need to introduce a new parameter.

With respect to the normal physiological situation, the hydrodynamics clearly are much more complex. However, the wall permeability is of intrinsic interest since it represents the limiting (controlling) resistance under perfect mixing conditions. Consequently, the wall permeability can be used to quantitate the absorption characteristics of drugs as well as for an experimental approach to the study of the nature of the wall resistance.

CONCLUSION

Four mass transport models that can be applied to intestinal perfusion studies were developed and compared. The models differ with respect to the assumptions regarding convection and diffusion in the perfusing fluid. If the wall permeability is estimated from the experimental results, all of the models work reasonably well. The wall permeabilities fall in the order mixing tank < complete radial mixing (diffusion layer) < plug flow < laminar flow.

Residence time distribution analysis was employed as a more sensitive measure of the validity of the underlying model assumptions. In the experimental system employed, laminar flow in a circular duct is the most appropriate model. This model provides the most direct measure of the intrinsic wall (membrane) permeability. The permeabilities for the various models are in the expected order for the test system, with the wall permeability decreasing in direct proportion to the extent to which the models overestimate the aqueous permeability.

It is concluded that laminar flow in an externally perfused intestine is attainable experimentally and provides the most direct measure of the intrinsic wall permeability. The wall permeability, in turn, represents the limiting permeability under perfect mixing conditions.

REFERENCES

(1) N. F. H. Ho and W. I. Higuchi, *J. Pharm. Sci.*, **63**, 686 (1974).

(2) J. M. Dietschy and H. Westergaard, in "Intestinal Absorption and Malabsorption," T. Z. Csaky, Ed., Raven, New York, N.Y., 1975, p. 197.

(3) D. Winne, *Arch. Pharmacol.*, **304**, 175 (1978).

(4) *Ibid.*, **307**, 265 (1979).

(5) R. L. Elliott, Ph.D. thesis, University of Wisconsin, Madison, Wis., 1979.

(6) G. L. Amidon, G. D. Leesman, and R. L. Elliott, *J. Pharm. Sci.*, **69**, 1363 (1980).

(7) R. B. Bird, W. E. Stewart, and E. N. Lightfoot, "Transport Phenomena," Wiley, New York, N.Y., 1960, p. 559.

(8) H. S. Carslaw and J. C. Jaeger, "Conduction of Heat in Solids," 2nd ed., Oxford University Press, Oxford, England, 1959, p. 195.

(9) M. Abramowitz and I. A. Stegun, "Handbook of Mathematical Functions," Dover, New York, N.Y., 1972, p. 414.

(10) O. Levenspiel, "Chemical Reaction Engineering," 2nd ed., Wiley, New York, N.Y., 1972, p. 253.

(11) C. G. Hill, "An Introduction to Chemical Engineering Kinetics and Reactor Design," Wiley, New York, N.Y., 1977, p. 388.

(12) C. Y. Wen and L. T. Fan, "Models for Flow Systems and Chemical Reactors," Dekker, New York, N.Y., 1975.

ACKNOWLEDGMENTS

Supported by the University of Wisconsin Graduate School, The Upjohn Company, Biomedical Research Support Grant SO 7RR05456-17, and GM 27680.

Dosage Form Design for Improvement of Bioavailability of Levodopa III: Influence of Dose on Pharmacokinetic Behavior of Levodopa in Dogs and Parkinsonian Patients

KUNIHIRO SASAHARA ˣ, TAKASHI NITANAI, TAEKO HABARA, TADASHI MORIOKA, and EIICHI NAKAJIMA

Received September 7, 1979, from the *Product Development Laboratories, Sankyo Company, Ltd., 1-2-58, Hiromachi, Shinagawa, Tokyo, Japan.* Accepted for publication February 21, 1980.

Abstract □ The relationship between the dose of levodopa and its pharmacokinetic behavior following intravenous and oral administration was investigated in dogs and parkinsonian patients. Six beagle dogs received single doses of 2.4, 4.8, and 9.6 mg of levodopa/kg iv and single doses of 4.8, 9.6, and 19.2 mg of levodopa/kg po in a crossover fashion on separate occasions. Three parkinsonian patients received single oral doses of ~3.8, 7.7, and 15.4 mg of levodopa/kg in a crossover test. Plasma samples were analyzed for intact levodopa and total dopamine. The relationship between the area under the plasma concentration–time curve (*AUC*) of levodopa and the intravenous dose to dogs was linear. However, in both dogs and patients, the relationship after oral dosing was nonlinear, with the relative *AUC* increasing with increasing dose. Therefore, the pharmacokinetic behavior of levodopa after oral administration to dogs and patients was dose dependent.

Keyphrases □ Levodopa—pharmacokinetics, effect of dose, dogs and parkinsonian patients □ Pharmacokinetics—levodopa, effect of dose, dogs and parkinsonian patients □ Bioavailability—levodopa, effect of dose, dogs and parkinsonian patients

It was shown previously (1, 2) that the bioavailability of intact levodopa after oral administration was ~35% in both dogs and parkinsonian patients but that the total amount absorbed, including levodopa metabolites, was 80–90% of the administered dose, probably due to extensive metabolism of levodopa during absorption (2). On the other hand, Cotzias *et al.* (3) succeeded in treating parkinsonian patients with high doses of levodopa, and other investigators reported the effectiveness of high doses and the ineffectiveness of low doses in levodopa therapy (4–7).

The first-pass metabolism and clinical facts described indicate the need for an investigation of the absolute bioavailability of levodopa at different doses after intravenous and oral administration in beagle dogs and in patients.

EXPERIMENTAL

Intravenous Dose Studies of Levodopa in Dogs—Six healthy male beagle dogs, 10.3–13.3 kg, were fasted for ~16 hr and divided into three groups of two dogs each. Levodopa injection solution[1] was injected intravenously, over 30 sec, at 2.4 mg/kg to the first group, at 4.8 mg/kg to the second group, and at 9.6 mg/kg to the third group. Crossover experiments were carried out at 1-week intervals.

Blood samples were withdrawn with a heparinized syringe from the contralateral brachial vein. Sampling times were 0, 2, 5, 15, and 30 min and 1, 1.5, 2, 3, 4, and 6 hr postdosing. Urine was collected before the dose and over 48 hr after intravenous administration. The blood and urine specimens were processed as described previously (1, 2).

Oral Dose Studies of Levodopa in Dogs—The same six beagle dogs that were used in the intravenous dose studies were fasted for ~16 hr and divided into three groups of two dogs each. Levodopa in capsule form[2] was administered forcefully orally at 4.8 mg/kg to the first group, at 9.6 mg/kg to the second group, and at 19.2 mg/kg to the third group with 10 ml of warm water. Emesis was prevented by keeping the mouth closed by hand. Crossover experiments were carried out at 1-week intervals.

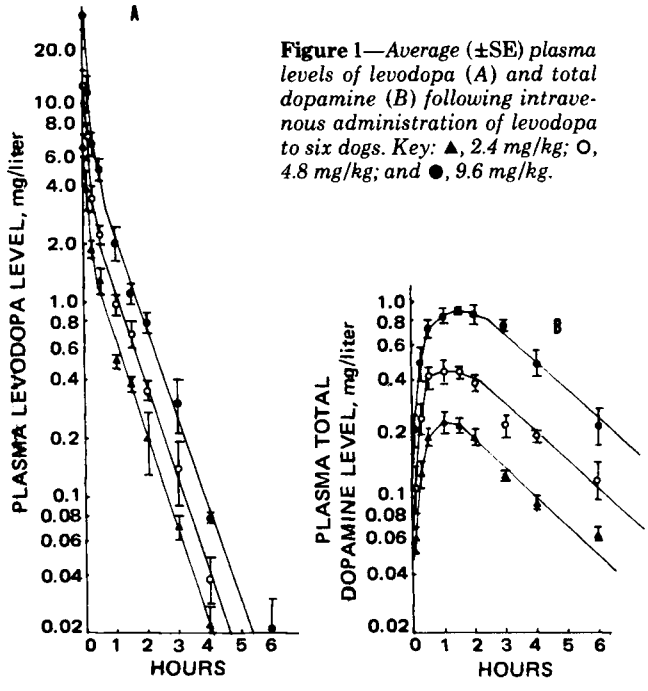

Figure 1—*Average (±SE) plasma levels of levodopa (A) and total dopamine (B) following intravenous administration of levodopa to six dogs. Key: ▲, 2.4 mg/kg; ○, 4.8 mg/kg; and ●, 9.6 mg/kg.*

Blood samples were withdrawn with a heparinized syringe before and at 0.5, 1, 2, 3, 4, and 6 hr after oral administration. Urine also was collected before the dose and over 48 hr. The blood and urine samples were processed as described previously (1, 2).

Oral Dose Studies of Levodopa in Parkinsonian Patients—Three parkinsonian patients, 26–63 years old, participated in this study. Three days prior to the experiments, all levodopa preparations and other drugs administered for the treatment of Parkinson's disease were withdrawn. Levodopa capsules[3] were administered orally at ~3.8 mg/kg together with a cup of water at ~9 am to the first subject, at ~7.7 mg/kg to the second subject, and at ~15.4 mg/kg to the third subject in the same manner. Crossover experiments were carried out at 1-week intervals.

On the day of the experiment, the patients ate breakfast at ~7:00 am, lunch at about noon, and dinner at ~5:30 pm. Blood was withdrawn with a heparinized syringe before dosing and at 0.5, 1, 2, 3, 4, and 6 hr after oral administration. The blood sample processing was carried out as described previously (1, 2). During the 3 days between the experiments of the crossover test, to prevent the appearance of parkinsonian syndrome, 500-mg doses of levodopa capsules were administered three times per day ~30 min after each meal instead of withdrawing the drug.

Assay of Levodopa and Its Metabolites in Plasma and Urine—Levodopa and its metabolites in plasma and urine were assayed according to the method reported previously (1).

[1] Dopaston injection, Sankyo Co., Ltd., Tokyo, Japan.

[2] Levodopa in capsule form was prepared in the same prescription preparation as Dopaston capsules, Sankyo Co., Ltd., Tokyo, Japan.

[3] Dopaston capsules, Sankyo Co., Ltd., Tokyo, Japan.

0022-3549/80/1200-1374$01.00/0
© 1980, American Pharmaceutical Association

Table I—Average (±*SE*) Pharmacokinetic Parameters of Levodopa and *AUC* of Levodopa and Total Dopamine following Administration of 2.4, 4.8, and 9.6 mg of Levodopa/kg to Six Dogs

Parameter	Dose, mg/kg		
	2.4	4.8	9.6
α, hr^{-1}	13.7 ± 2.8	13.6 ± 3.5	14.4 ± 3.0
β, hr^{-1}	1.16 ± 0.10	1.08 ± 0.12	1.04 ± 0.11
$0.693/\beta$, hr	0.62 ± 0.04	0.65 ± 0.05	0.67 ± 0.06
k_{12}, hr^{-1}	6.7 ± 0.61	7.1 ± 0.58	6.8 ± 0.57
k_{21}, hr^{-1}	3.5 ± 0.31	3.4 ± 0.39	3.7 ± 0.31
k_{10}, hr^{-1}	4.5 ± 0.41	4.4 ± 0.34	4.7 ± 0.38
V_1, liter/kg	0.25 ± 0.025	0.23 ± 0.021	0.27 ± 0.024
AUC of levodopa, (mg hr)/liter/kg	0.198 ± 0.015	0.359 ± 0.031	0.751 ± 0.069
Clearance of levodopa, liters/kg/hr	1.14 ± 0.11	1.18 ± 0.13	1.10 ± 0.12
AUC of total dopamine, (mg hr)/liter/kg	0.106 ± 0.009	0.215 ± 0.017	0.418 ± 0.035
Ratio of *AUC* for total dopamine to levodopa	0.52 ± 0.04	0.58 ± 0.04	0.56 ± 0.05

Pharmacokinetic Analysis—The plasma levodopa concentration curves following intravenous administration to dogs were analyzed using the program of Hanano *et al.* (8). The plasma levodopa concentration curves following oral administration to dogs and patients were analyzed using the BMDP-3R nonlinear regression program (9) with a one-compartment open model.

RESULTS

Intravenous Dose Studies of Levodopa in Dogs—The average plasma levels of levodopa and total dopamine[4] following intravenous administration of 2.4-, 4.8-, and 9.6-mg/kg doses of levodopa to six dogs are shown in Fig. 1. Plasma levels of levodopa and total dopamine increased proportionally with the dose of levodopa administered. The linear relationship between the dose and the *AUC* of levodopa is shown in Fig. 2. Pharmacokinetic parameters of the disposition of intravenously administered levodopa were estimated for each dog by fitting the data to the two-compartment open model, assuming linear kinetics. The resultant parameter estimates are summarized in Table I. The *AUC* values of levodopa and total dopamine corrected for body weight also are shown in Table I, as is the ratio of the *AUC* values of total dopamine to levodopa. This ratio, as well as the parameter estimates, is essentially constant and independent of the dose of levodopa administered.

The average urinary excretion of levodopa and its metabolites over 48 hr after intravenous administration of 2.4, 4.8, and 9.6 mg of levodopa/kg to six dogs is shown in Fig. 3. These results show that the total amount excreted in the urine following intravenous administration of 2.4, 4.8, and 9.6 mg of levodopa/kg was similar, indicating 60–65% of the administered dose. The patterns of urinary levodopa and its metabolites were essentially constant, independent of the levodopa dose among the doses administered.

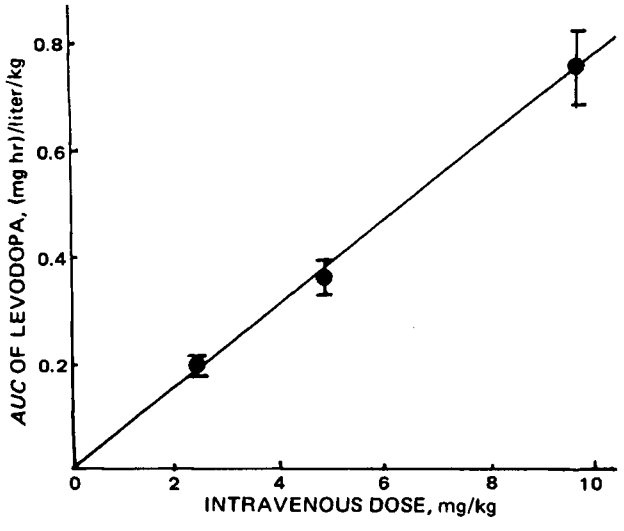

Figure 2—*Relationship between the intravenous dose and the observed* AUC *of levodopa corrected for body weight in dogs (average ± SE).*

[4] Total dopamine = conjugated dopamine + unconjugated dopamine.

Oral Administration of Levodopa in Dogs—The average plasma levels of levodopa and total dopamine following oral administration of 4.8, 9.6, and 19.2 mg of levodopa/kg to six dogs are shown in Fig. 4. As the levodopa dose administered increased, plasma levels of levodopa appeared to be disproportionally high. However, total dopamine, one of its metabolites, revealed an inverse situation; as the dose increased, the relative plasma levels of total dopamine were progressively lower. The average dose-normalized peak concentrations for levodopa were 0.11 ± 0.01, 0.14 ± 0.02, and 0.18 ± 0.01 kg/liter. While the differences do not appear to be statistically significant in most cases, they reflect a trend. The relationship between the levodopa dose administered and the ob-

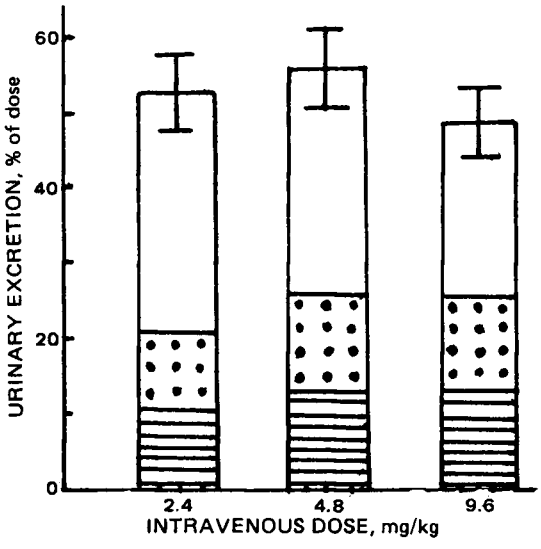

Figure 3—*Average urinary excretion of levodopa and its metabolites following intravenous administration of 2.4, 4.8, and 9.6 mg of levodopa/kg to six dogs. Key:* ▩, *total levodopa;* ■, *total dopamine;* ▨, *total 3,4-dihydroxyphenylacetic acid; and* □, *total homovanillic acid.*

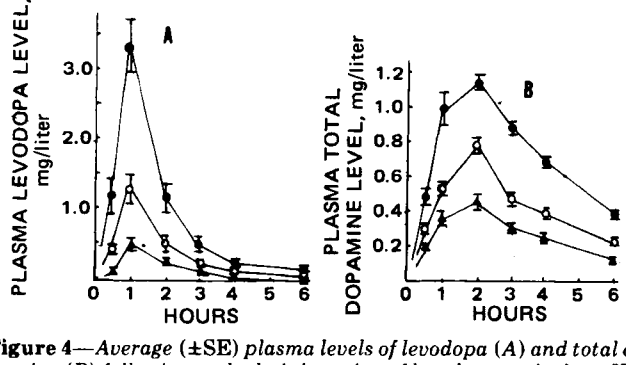

Figure 4—*Average* (±SE) *plasma levels of levodopa (A) and total dopamine (B) following oral administration of levodopa to six dogs. Key:* ▲, *4.8 mg/kg;* ○, *9.6 mg/kg; and* ●, *19.2 mg/kg.*

Table II—Average (±*SE*) Pharmacokinetic Parameters of Levodopa and *AUC* of Levodopa and Total Dopamine following Oral Administration of 4.8, 9.6, and 19.2 mg of Levodopa/kg to Six Dogs

Dose, mg/kg	Pharmacokinetic Parameters: k_{el}[a], hr^{-1}	Pharmacokinetic Parameters: $t_{1/2}$, hr	*AUC* of Levodopa Corrected for Weight, (mg hr)/liter/kg	*AUC* of Total Dopamine Corrected for Weight, (mg hr)/liter/kg	Ratio of *AUC* for Total Dopamine to Levodopa
4.8	0.97 ± 0.09	0.70 ± 0.07	0.080 ± 0.010	0.158 ± 0.013	1.79 ± 0.18
9.6	0.88 ± 0.11	0.74 ± 0.08	0.208 ± 0.024	0.299 ± 0.029	1.47 ± 0.14
19.2	0.96 ± 0.10	0.71 ± 0.07	0.478 ± 0.051	0.548 ± 0.051	1.09 ± 0.11

[a] Elimination rate constant of levodopa obtained by fitting the data to the one-compartment open model.

Table III—Average Urinary Excretion of Levodopa and Its Metabolites as Percentage of Administered Dose following Oral Administration of 4.8, 9.6, and 19.2 mg of Levodopa/kg to Six Dogs

Dose, mg/kg	Percent Dose Excreted in 0–48-hr Urine (Average ± *SE*): Total Levodopa[a]	Total Dopamine	Total 3,4-Dihydroxyphenylacetic Acid[b]	Total Homovanillic Acid[c]	Total[d]
4.8	0.45 ± 0.04 [e]	10.2 ± 1.0	10.1 ± 1.1	31.5 ± 3.1	52.5 ± 4.9
9.6	0.54 ± 0.05 [e]	12.8 ± 1.1	12.3 ± 1.2	29.5 ± 3.0	55.1 ± 5.1
19.2	0.64 ± 0.06 [e] [f]	12.5 ± 1.2	12.9 ± 1.4	24.5 ± 2.1	50.6 ± 4.5

[a] Total levodopa = unconjugated levodopa + conjugated levodopa. [b] Total 3,4-dihydroxyphenylacetic acid = unconjugated 3,4-dihydroxyphenylacetic acid + conjugated 3,4-dihydroxyphenylacetic acid. [c] Total homovanillic acid = unconjugated homovanillic acid + conjugated homovanillic acid. [d] Sum of total levodopa, total dopamine, total 3,4-dihydroxyphenylacetic acid, and total homovanillic acid. [e] Not significant ($p > 0.05$). [f] Significant ($p < 0.05$).

served *AUC* of levodopa is shown in Fig. 5. As the dose increased, the *AUC* increased disproportionately.

Elimination rate constants of levodopa after oral administration to dogs were calculated for each dog by fitting the data to the one-compartment open model. These values are summarized in Table II, along with the *AUC* of levodopa and total dopamine corrected for body weight and the ratio of the *AUC* of total dopamine to that of levodopa. The estimated elimination half-lives were essentially constant, independent of the levodopa dose, but the ratio of the *AUC* decreased with an incease in the dose. On the other hand, the average urinary excretion of levodopa and its metabolites over 48 hr after oral administration of 4.8, 9.6, and 19.2 mg of levodopa/kg to six dogs is shown in Table III. The total amount excreted in the urine following oral administration of the three different doses was similar, but the total levodopa excreted in the urine appeared to increase as the dose increased; only the differences between the 4.8- and 19.2-mg/kg doses were statistically significant ($p < 0.05$).

The absolute bioavailability and the total amount absorbed from the GI tract, including levodopa and its metabolites, following oral administration of 4.8, 9.6, and 19.2 mg of levodopa/kg to six dogs were calculated, based on the assumed linear kinetics, using the respective *AUC* or urinary excretion from intravenous doses of 4.8 and 9.6 mg/kg and also using the dose-corrected *AUC* or urinary excretion from an intravenous 19.2-mg/kg dose (Table IV). The absolute bioavailability of oral levodopa in dogs was dose dependent, while the total amount absorbed was essentially constant, independent of the dose administered.

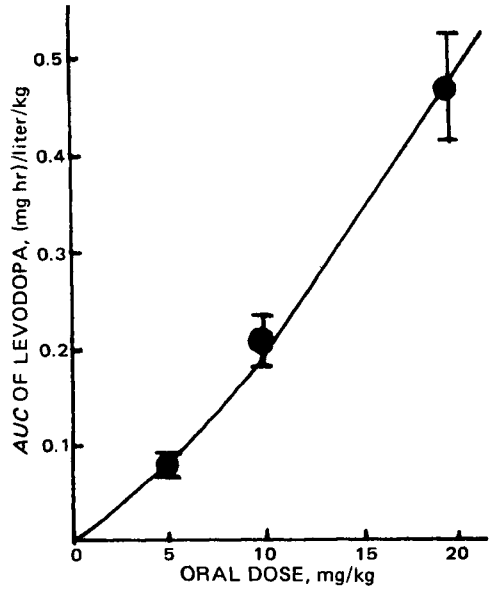

Figure 5—*Relationship between the oral dose and the observed* AUC *of levodopa corrected for body weight in dogs (average ± SE).*

Oral Dose Studies of Levodopa in Parkinsonian Patients—The average plasma levels of levodopa and total dopamine following oral administration of 3.8, 7.7, and 15.4 mg of levodopa/kg to three patients are shown in Fig. 6. The relationship between the dose administered and the plasma levels of levodopa and total dopamine was not directly proportional to the dose. As the dose increased, the relative plasma levels of levodopa were progressively higher but the relative plasma levels of total dopamine were progressively lower: *i.e.*, the dose-normalized plasma levels of levodopa increased with the dose while that of total dopamine decreased with the dose. The relationship between the levodopa dose and the *AUC* of levodopa is shown in Fig. 7. As found with the dogs, the *AUC* value of levodopa showed a nonlinear relationship as the dose increased.

The elimination rate constant of levodopa after oral administration to patients was calculated for each patient by fitting the data to a one-compartment open model. In addition, the ratio of the *AUC* of total dopamine to that of levodopa was calculated (Table V). The *AUC* values of levodopa and total dopamine corrected for body weight also are shown. The *AUC* of levodopa was constant and independent of the levodopa dose, but the *AUC* of total dopamine decreased with an increase in the dose.

The absolute bioavailability of doses of ~3.8, 7.7, and 15.4 mg of levodopa/kg after oral administration to three patients was evaluated on the assumptions that levodopa in the body obeys linear kinetics and that it is appropriate to compare the two different population groups, using the dose-corrected *AUC* from the intravenous dose reported previously (2). This result is listed in Table VI. The absolute bioavailability of oral levodopa in three different doses in patients was dose dependent in the same way as in dogs.

DISCUSSION

To evaluate the influence of the dose of levodopa on the pharmacoki-

Table IV—Absolute Bioavailability and Total Amount Absorbed, Including Metabolites, after Oral Administration to Six Dogs

Dose, mg/kg	Absolute Bioavailability, %	Total Amount Absorbed, %
4.8	22.1 ± 2.2[a]	81.7 ± 8.2[a]
9.6	27.7 ± 2.6[a]	93.1 ± 9.4[a]
19.2	31.9 ± 3.2[b]	78.1 ± 7.5[b]

[a] Based on the assumed linear kinetics using the respective *AUC* or urinary excretion from intravenous dosing (average ± *SE*). [b] Based on the assumed linear kinetics using the dose-corrected *AUC* or urinary excretion from intravenous dosing (average ± *SE*).

Table V—Average (±*SE*) Pharmacokinetic Parameters of Levodopa and *AUC* of Levodopa and Total Dopamine following Oral Administration of Doses of ~3.8, 7.7, and 15.4 mg of Levodopa/kg to Three Patients

Dose, mg/kg	Pharmacokinetic Parameters		*AUC* of Levodopa Corrected for Body Weight, (mg hr)/liter/kg	*AUC* of Total Dopamine Corrected for Body Weight, (mg hr)/liter/kg	Ratio of *AUC* for Total Dopamine to Levodopa
	k_{el}[a], hr^{-1}	$t_{1/2}$, hr			
3.8	0.88 ± 0.09	0.79 ± 0.08	0.008 ± 0.001	0.040 ± 0.003	4.81 ± 0.11
7.7	0.91 ± 0.06	0.77 ± 0.05	0.026 ± 0.003	0.061 ± 0.006	2.62 ± 0.28
15.4	0.90 ± 0.08	0.77 ± 0.07	0.069 ± 0.007	0.105 ± 0.040	1.62 ± 0.61

[a] Elimination rate constant of levodopa obtained by fitting the data to the one-compartment open model.

Table VI—Absolute Bioavailability of Doses of ~3.8, 7.7, and 15.4 mg of Levodopa/kg after Oral Administration to Three Patients

Dose, mg/kg	Absolute Bioavailability[a], % (Average ± *SE*)
3.8	15.2 ± 1.3
7.7	23.4 ± 1.9
15.4	31.2 ± 3.9

[a] Based on the assumed linear kinetics using the dose-corrected *AUC* from the intravenous dose.

netic behavior and bioavailability of the drug, plasma levodopa and total dopamine, one of its main metabolites, and urinary excretion following intravenous and oral administration to dogs and parkinsonian patients were determined. These results indicated that the pharmacokinetic behavior of levodopa and its total urinary excretion, including its metabolites, following intravenous administration to dogs was essentially constant within the dose range tested. Although the total urinary excretion was constant within the dose range after oral administration to dogs, the bioavailability of oral levodopa was dose dependent in both dogs and patients, and the urinary total dopamine also appeared to be dose dependent in dogs.

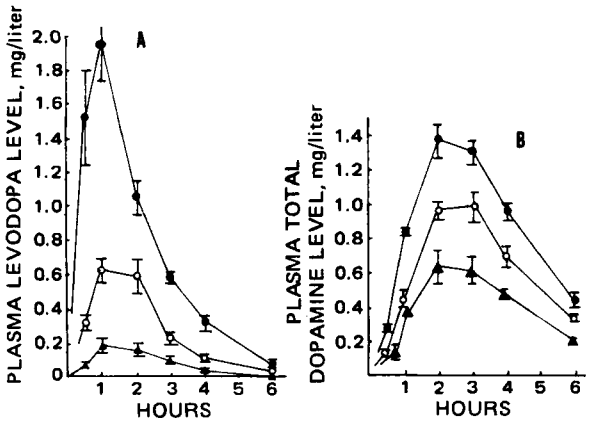

Figure 6—*Average* (±SE) *plasma levels of levodopa* (*A*) *and total dopamine* (*B*) *following oral administration of levodopa to three patients. Key:* ▲, *3.8 mg/kg;* O, *7.7 mg/kg; and* ●, *15.4 mg/kg.*

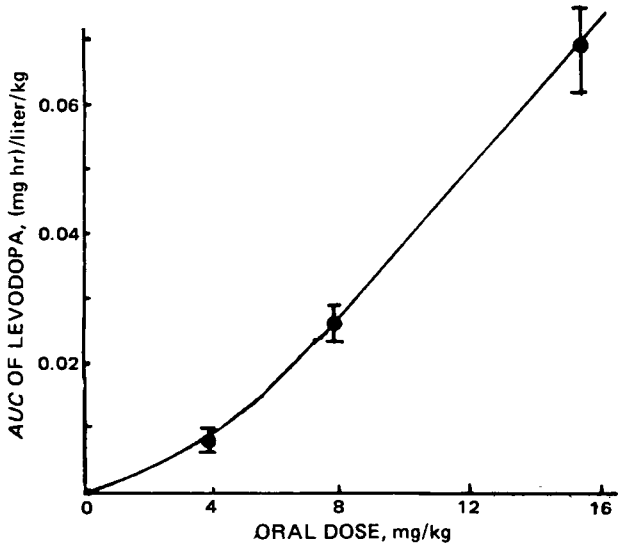

Figure 7—*Relationship between oral doses and observed* AUC *of levodopa in patients* (*average* ± SE).

The absolute bioavailability of oral levodopa must be calculated based on the assumption that levodopa in the body obeys linear kinetics. To test this assumption, an experiment is needed in which radiolabeled levodopa is given intravenously and unlabeled levodopa is given orally to the same subject at the same time. However, this assumption might be true since the clearance of levodopa in the plasma following intravenous administration proved to be constant, independent of the dose, and the elimination rate constant of levodopa in the plasma after oral administration was unchanged within the dose range tested, with nearly the same value found after intravenous administration. Furthermore, the change in total levodopa excreted in the urine after oral administration was proportional to the increase in the fraction of oral levodopa absorbed.

Bioavailability of the drug following oral administration is controlled by at least two factors: the rate and extent of uptake of levodopa in the gut and first-pass metabolism as a function of the dose. If active transport is the main process controlling the bioavailability of levodopa, then the total amount excreted in the urine can be expected to decrease as the dose increases. The observed results are contrary to this expectation. Therefore, if the active transport of levodopa in the GI tract occurs within the dose range tested, it does not play a significant role in affecting bioavailability. The elimination rate constant of levodopa in the plasma was observed to be constant, independent of the oral levodopa dose. This finding suggests the absence of saturation in the systemic elimination as the levodopa dose increased. In addition, the ratio of the *AUC* of total dopamine to that of levodopa after oral administration was small as the dose increased. This ratio reflects the extent of presystemic metabolism when compared to the ratio after intravenous administration (2).

These data support the contention that the dose-dependent bioavailability of levodopa is due to saturable first-pass metabolism during absorption. As the oral dose of levodopa is increased, the fraction of the dose metabolized to dopamine is reduced, and a larger fraction of the oral dose reaches the systemic circulation as intact, pharmacologically active drug. This phenomenon seems to be the most important factor in new dosage form design for improvement of the bioavailability of levodopa.

These results are interesting when they are related to the clinical use of levodopa. Hornykiewicz's assertion (10) that Parkinson's disease could be improved by offsetting the cerebral dopamine deficiency in parkinsonian patients with the administration of levodopa was not achieved at low doses of the drug. However, the high-dose therapy administered in 1967 by Cotzias *et al.* (11) led to the first successful treatment of Parkinson's disease and several subsequent studies (6, 12–14) supported their findings. The results in this report help explain these results.

REFERENCES

(1) K. Sasahara, T. Nitanai, T. Habara, A. Ninomiya, T. Morioka, and E. Nakajima, *Ann. Rep. Sankyo Res. Lab.*, **30**, 65 (1978).

(2) K. Sasahara, T. Nitanai, T. Habara, T. Morioka, and E. Nakajima, *J. Pharm. Sci.*, **69**, 261 (1980).

(3) G. C. Cotzias, M. H. Van Woert, and L. M. Schiffer, *N. Engl. J. Med.*, **276**, 374 (1967).

(4) M. D. Yahr, R. C. Duvoisin, M. J. Shear, R. E. Barrett, and M. M. Hoehn, *Arch. Neurol.*, **21**, 343 (1969).

(5) A. Barbeau, *Can. Med. Assoc. J.*, **101**, 791 (1969).

(6) H. L. Klawans and J. S. Garvin, *Dis. Nerv. Syst.*, **30**, 737 (1969).

(7) F. McDowell, J. E. Lee, T. Swift, R. D. Sweet, J. S. Ogsbury, and J. J. Kessler, *Ann. Intern. Med.*, **72**, 29 (1970).

(8) M. Hanano, S. Awazu, K. Bun, T. Fuwa, R. Iga, and K. Nogami, presented at the 2nd Symposium of Metabolism, Effect and Toxicity of Drug, Kyoto, Japan, Nov. 1972.
(9) W. J. Dixon and M. B. Brown, "BMDP Biomedical Computer Program," University of California Press, Berkeley, Calif., 1977.
(10) O. Hornykiewicz, *Dtsch. Med. Wochenschr.*, **87**, 1807 (1962).
(11) G. C. Cotzias, M. H. Van Woert, and L. M. Schiffer, *N. Engl. J. Med.*, **276**, 374 (1967).
(12) M. D. Yahr, R. C. Duvoisin, M. J. Shear, R. E. Barrett, and M. M. Hoehn, *Arch. Neurol.*, **21**, 343 (1969).
(13) A. Barbeau, *Can. Med. Assoc. J.*, **101**, 791 (1969).
(14) F. Mcdowell, J. E. Lee, T. Swift, R. D. Sweet, J. S. Ogsbury, and J. J. Kessler, *Ann. Intern. Med.*, **72**, 29 (1976).

ACKNOWLEDGMENTS

Presented in part at the Pharmaceutics Section, 97th Meeting of the Pharmaceutical Society of Japan, Tokyo, Japan, April 1977.

The authors thank Dr. A. Noguchi for help in designing the protocol and supervising drug administration and blood and urine sampling in patients, Mr. S. Yamane for technical assistance in the bioavailability studies in patients, Dr. T. Higuchi for valuable discussions, Dr. H. Negoro, Dr. S. Akagi, and Dr. T. Miki for promotion of the research project, Dr. S. Riegelman for constructive comments on the manuscript, and Ms. Ellen Buoncristiani for typing the manuscript.

Simultaneous Determination of Cephalexin and Lysine in Their Salt Using High-Performance Liquid Chromatography of Derivatives

J. L. FABREGAS ˣ and J. E. BENEYTO

Received November 2, 1979, from the *Analytical Department, Laboratorios Almirall, C/Cardoner, 68-74, Barcelona 24, Spain.* Accepted for publication February 29, 1980.

Abstract □ A sensitive and useful high-performance liquid chromatographic method using derivatization was developed for the simultaneous determination of intact cephalexin and lysine in their salt. This method is rapid and reliable, and its inherent specificity makes it an improvement over the common wet chemical methods for stability studies.

Keyphrases □ Cephalexin—simultaneous high-performance liquid chromatographic determination with lysine in their salt using derivatization □ Lysine—simultaneous high-performance liquid chromatographic determination with cephalexin in their salt using derivatization □ High-performance liquid chromatography—analysis, cephalexin and lysine in their salt, derivatization

The sodium salt of cephalexin is absorbed poorly after intramuscular injection (1, 2). Similar observations were made with a related compound, cephradine (3). Investigations with other soluble salts of cephalexin showed that some basic amino acids increased the absorption and bioavailability of cephalexin (4). The extensive use of the lysine salt of cephalexin necessitated the development of methods for the simultaneous determination of both components in this salt. Alkalimetric determination of carboxylic groups and nonaqueous titration of α-amino groups cannot be used because these two groups are present in both components. For the same reason, the Folin reaction with sodium β-naphthoquinone-4-sulfonate or hypobromite and α-naphthol (5) and the Saxena method (6) for microtitration of amino acid mixtures are unsatisfactory, and the selective titration of the ϵ-amino group of lysine in aqueous media with sulfuric acid is insufficiently accurate.

A recent report described the intramolecular aminolysis of some cephalosporins, caused by the nucleophilic attack of an α-amino group in the C-7 side chain in the β-lactam nucleus, which yields piperazine-2,5-dione derivatives (7). Estimation of the rate of disappearance of free amino groups was carried out by the 2,4,6-trinitrobenzenesulfonic acid (I) assay of Satake *et al.* (8) in a modified form. Applications of this technique to cephalexin lysinate was not possible due to interference by lysine.

A high-performance liquid chromatographic (HPLC) procedure for the analysis of lysine and cephalexin trinitrophenyl derivatives (II and III, respectively) is presented here. It is a rapid, sensitive, and specific method for the simultaneous determination of these two substances.

EXPERIMENTAL

Apparatus—Absorption spectra were obtained with a double-beam spectrophotometer[1] with a 1.0-cm cell. HPLC assays were performed with a liquid chromatograph[2] equipped with a variable-wavelength detector[3] and a 1-μl loop injection valve[4]. A stainless steel column (25 × 0.46 cm) loaded with alkylamine[5] (13 μm) was used.

Reagents—Cephalexin monohydrate[6], lysine hydrochloride[7], the lysine salt of cephalexin[8], and trinitrobenzenesulfonic acid[9] were used. The buffer solutions of pH values up to 7.6 were McIlvaine's buffers (9), the pH 7.6 buffer was prepared according to the method of Bundgaard (7), and the buffer solutions of higher pH were those of Clark and Lubs (10). All other reagents were analytical reagent grade.

General HPLC Procedure—An aqueous solution containing the lysine salt of cephalexin (2.0 ml) (5×10^{-4}–2×10^{-3} *M*) was mixed in a 100-ml volumetric flask with buffer solution (pH 10, 2.0 ml) and I (0.4% in water, 5.0 ml). The mixture was shaken and kept in the dark for 1 hr. Acetate buffer (pH 4.8, 20.0 ml) and aqueous 0.1% *o*-nitrophenol (2.0 ml as the internal standard) were added, and the solution was brought to volume with water.

A sample of this solution (1 μl) was injected into the liquid chromatograph and developed using an eluent system of 1% citric acid in a methanol–water mixture (5:40 v/v) with an isocratic flow rate of 0.75

[1] Perkin-Elmer 323.
[2] Perkin Elmer 601.
[3] Perkin-Elmer LC-55.
[4] Chrompack.
[5] Amino Sil-X-I.
[6] Lilly.
[7] Merck.
[8] Laboratorios Almirall.
[9] Aldrich.

0022-3549/80/1200-1378$01.00/0
© 1980, American Pharmaceutical Association

(8) M. Hanano, S. Awazu, K. Bun, T. Fuwa, R. Iga, and K. Nogami, presented at the 2nd Symposium of Metabolism, Effect and Toxicity of Drug, Kyoto, Japan, Nov. 1972.
(9) W. J. Dixon and M. B. Brown, "BMDP Biomedical Computer Program," University of California Press, Berkeley, Calif., 1977.
(10) O. Hornykiewicz, *Dtsch. Med. Wochenschr.*, **87**, 1807 (1962).
(11) G. C. Cotzias, M. H. Van Woert, and L. M. Schiffer, *N. Engl. J. Med.*, **276**, 374 (1967).
(12) M. D. Yahr, R. C. Duvoisin, M. J. Shear, R. E. Barrett, and M. M. Hoehn, *Arch. Neurol.*, **21**, 343 (1969).
(13) A. Barbeau, *Can. Med. Assoc. J.*, **101**, 791 (1969).
(14) F. Mcdowell, J. E. Lee, T. Swift, R. D. Sweet, J. S. Ogsbury, and J. J. Kessler, *Ann. Intern. Med.*, **72**, 29 (1976).

ACKNOWLEDGMENTS

Presented in part at the Pharmaceutics Section, 97th Meeting of the Pharmaceutical Society of Japan, Tokyo, Japan, April 1977.

The authors thank Dr. A. Noguchi for help in designing the protocol and supervising drug administration and blood and urine sampling in patients, Mr. S. Yamane for technical assistance in the bioavailability studies in patients, Dr. T. Higuchi for valuable discussions, Dr. H. Negoro, Dr. S. Akagi, and Dr. T. Miki for promotion of the research project, Dr. S. Riegelman for constructive comments on the manuscript, and Ms. Ellen Buoncristiani for typing the manuscript.

Simultaneous Determination of Cephalexin and Lysine in Their Salt Using High-Performance Liquid Chromatography of Derivatives

J. L. FABREGAS ˣ and J. E. BENEYTO

Received November 2, 1979, from the *Analytical Department, Laboratorios Almirall, C/Cardoner, 68-74, Barcelona 24, Spain.* Accepted for publication February 29, 1980.

Abstract □ A sensitive and useful high-performance liquid chromatographic method using derivatization was developed for the simultaneous determination of intact cephalexin and lysine in their salt. This method is rapid and reliable, and its inherent specificity makes it an improvement over the common wet chemical methods for stability studies.

Keyphrases □ Cephalexin—simultaneous high-performance liquid chromatographic determination with lysine in their salt using derivatization □ Lysine—simultaneous high-performance liquid chromatographic determination with cephalexin in their salt using derivatization □ High-performance liquid chromatography—analysis, cephalexin and lysine in their salt, derivatization

The sodium salt of cephalexin is absorbed poorly after intramuscular injection (1, 2). Similar observations were made with a related compound, cephradine (3). Investigations with other soluble salts of cephalexin showed that some basic amino acids increased the absorption and bioavailability of cephalexin (4). The extensive use of the lysine salt of cephalexin necessitated the development of methods for the simultaneous determination of both components in this salt. Alkalimetric determination of carboxylic groups and nonaqueous titration of α-amino groups cannot be used because these two groups are present in both components. For the same reason, the Folin reaction with sodium β-naphthoquinone-4-sulfonate or hypobromite and α-naphthol (5) and the Saxena method (6) for microtitration of amino acid mixtures are unsatisfactory, and the selective titration of the ϵ-amino group of lysine in aqueous media with sulfuric acid is insufficiently accurate.

A recent report described the intramolecular aminolysis of some cephalosporins, caused by the nucleophilic attack of an α-amino group in the C-7 side chain in the β-lactam nucleus, which yields piperazine-2,5-dione derivatives (7). Estimation of the rate of disappearance of free amino groups was carried out by the 2,4,6-trinitrobenzenesulfonic acid (I) assay of Satake *et al.* (8) in a modified form. Applications of this technique to cephalexin lysinate was not possible due to interference by lysine.

A high-performance liquid chromatographic (HPLC) procedure for the analysis of lysine and cephalexin trinitrophenyl derivatives (II and III, respectively) is presented here. It is a rapid, sensitive, and specific method for the simultaneous determination of these two substances.

EXPERIMENTAL

Apparatus—Absorption spectra were obtained with a double-beam spectrophotometer[1] with a 1.0-cm cell. HPLC assays were performed with a liquid chromatograph[2] equipped with a variable-wavelength detector[3] and a 1-μl loop injection valve[4]. A stainless steel column (25 × 0.46 cm) loaded with alkylamine[5] (13 μm) was used.

Reagents—Cephalexin monohydrate[6], lysine hydrochloride[7], the lysine salt of cephalexin[8], and trinitrobenzenesulfonic acid[9] were used. The buffer solutions of pH values up to 7.6 were McIlvaine's buffers (9), the pH 7.6 buffer was prepared according to the method of Bundgaard (7), and the buffer solutions of higher pH were those of Clark and Lubs (10). All other reagents were analytical reagent grade.

General HPLC Procedure—An aqueous solution containing the lysine salt of cephalexin (2.0 ml) (5×10^{-4}–2×10^{-3} *M*) was mixed in a 100-ml volumetric flask with buffer solution (pH 10, 2.0 ml) and I (0.4% in water, 5.0 ml). The mixture was shaken and kept in the dark for 1 hr. Acetate buffer (pH 4.8, 20.0 ml) and aqueous 0.1% *o*-nitrophenol (2.0 ml as the internal standard) were added, and the solution was brought to volume with water.

A sample of this solution (1 μl) was injected into the liquid chromatograph and developed using an eluent system of 1% citric acid in a methanol–water mixture (5:40 v/v) with an isocratic flow rate of 0.75

[1] Perkin-Elmer 323.
[2] Perkin Elmer 601.
[3] Perkin-Elmer LC-55.
[4] Chrompack.
[5] Amino Sil-X-I.
[6] Lilly.
[7] Merck.
[8] Laboratorios Almirall.
[9] Aldrich.

0022-3549/80/1200-1378$01.00/0
© 1980, American Pharmaceutical Association

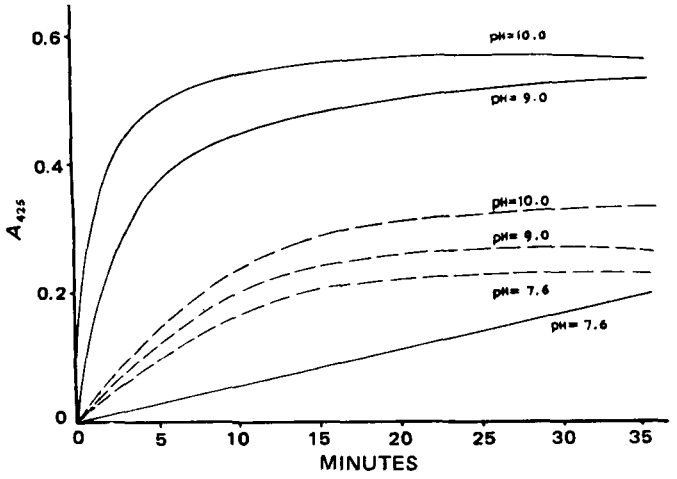

Figure 1—*Time effect on reaction of cephalexin* (- -) *and lysine* (—) *at different pH values.*

ml/min and detection at 425 nm. Good chromatographic performance was achieved only when the column temperature was 50°.

Any significant degradation products were detected by TLC after the initial reaction at pH 10.

Procedure in Basic Degradation Study—Solutions ($\sim 10^{-3}$ *M*) of cephalexin and lysine in 0.5 *N* NaOH were prepared. The assay was carried out on samples taken after standing for 20 and 60 min, respectively, at room temperature. The pH was adjusted to pH 4.8 with 2 *N* HCl, and HPLC of II and III was carried out as described.

Procedure in Acid Degradation Study—Solutions of cephalexin and lysine ($\sim 10^{-3}$ *M*) in 1 *N* HCl were maintained at 60° for 1 hr. These solutions were brought to pH 4.8 with 1 *N* NaOH, and HPLC of II and III was carried out as described.

RESULTS AND DISCUSSION

The simple spectrophotometric method of Bundgaard (7) could not be used for the simultaneous analysis of lysine and cephalexin because both derivatives show identical absorption maxima (425 nm). The velocity constants of the reaction of I with the primary amino compounds is known to be related exponentially to the pH of the reaction medium (11). Consequently, a study was made to find conditions for the direct spectrophotometric assay of cephalexin and lysine in mixtures of these two components. Cephalexin and lysine do not react with I at an appreciable rate below pH 6. Both II and III are stable over long periods and, at other pH values, the reaction obeys pseudo-first-order kinetics, except the reaction of lysine and I at pH 7.6, which is linear with time (Fig. 1).

The different reaction rates of the α- and ϵ-amino groups of lysine with

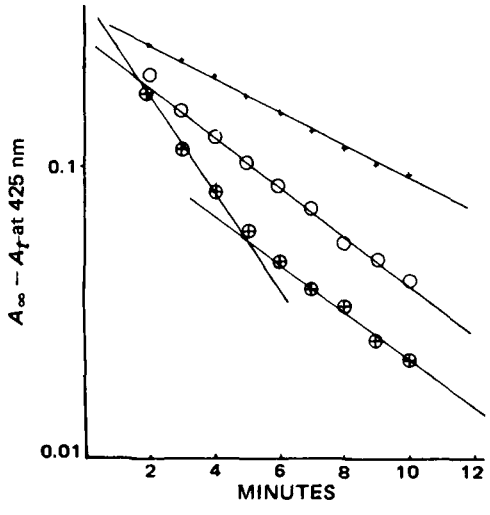

Figure 2—*Reaction kinetics of I at pH 10.0. Key:* ×, *cephalexin;* ○, *salt; and* ⊕, *lysine.*

Table I—Absolute Retention Times (Minutes) on Amino Sil-X-I Using Different Eluents

Compound	Eluent[a] A	B	C	D
I	3.3	>60	7.6	7.6
II	6.7	4.2	3.8	3.9
III	>60	>60	7.3	11.6
o-Nitrophenol	—	—	—	5.5

[a] Eluent A is methanol, Eluent B is 1% acetic acid in methanol–water (5:40 v/v), Eluent C is methanol–0.01 *M* sulfuric acid (5:40 v/v), and Eluent D is 1% citric acid in methanol–water (5:40 v/v).

Table II—Parameters of Calibration Curves

Equation[a]	Compound	a_0, mg/ml	Correlation Coefficient	*n*
$c(\text{mg/ml}) = a_0 + a_1 \frac{h}{h_s}$	II	0.0477	0.9909	8
	III	0.7501	0.9873	8
$c(\text{mg/ml}) = a_0 + a_1 h(\text{mm})$	II	0.0177	0.9916	15
	III	0.0833	0.9977	15

[a] h and h_s are the heights of the sample and internal standard chromatographic peaks, respectively.

I are apparent from a change in the slope of the rate curve (Fig. 2). The slope of the absorbance–time curve for lysine at pH 7.6 is proportional to the concentration of lysine and is linear over the concentration range of 0.5–1.3 × 10^{-3} *M*. By measuring the change of absorbance with time at pH 7.6, it is possible to measure the concentration of both cephalexin and lysine, but there are only small changes in the slope of the line with large changes in the lysine concentration, leading to low sensitivity.

For these reasons, the liquid chromatography of derivatives of I was selected since these derivatives are stable (12), they behave well on alkylamine columns (13), and lysine does not absorb appreciably in the visible or UV regions.

Quantitative formation of II and III occurred most rapidly when the reaction medium was at pH 10 (Fig. 1). However, Amino Sil-X-I columns are not stable at this pH, and the pH of the medium after formation of these derivatives was reduced to pH 4.8. The cephalexin derivative is stable for up to 20 hr at this pH and the lysine derivative is stable for 2 hr, after which it slowly decomposes. The retention times of II and III using different eluents are shown in Table I.

Lysine and especially cephalexin (14) are degraded in both alkaline and acidic solutions. Many of the degradation products contain primary amino groups and are a potential source of interference in the specific analysis of lysine and cephalexin, particularly in pharmaceutical products undergoing stability studies.

Pure solutions of lysine and cephalexin were degraded under acidic and alkaline conditions for different times, and the chromatograms of II and III were studied. Under alkaline conditions, the original peaks of unchanged lysine and cephalexin derivatives (retention times of 3.9 and 11.6 min, respectively) disappeared, and well-defined peaks of degradation products appeared (at 8.8 min from II and at 1.8, 2.4, and 9.4 min from III). However, none of these peaks interfered with the main peaks

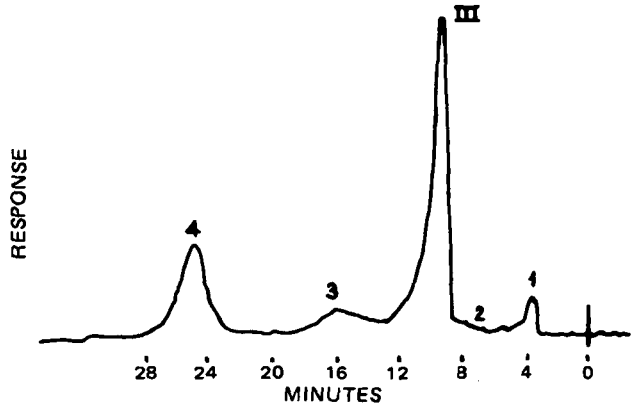

Figure 3—*Chromatogram of III and acid-degraded cephalexin derivative mixture.*

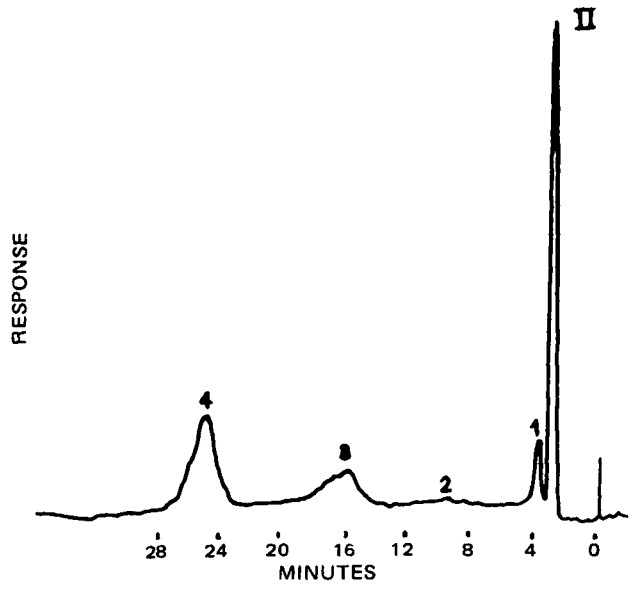

Figure 4—*Chromatogram of II and acid-degraded cephalexin derivative mixture.*

used in the assay of lysine and cephalexin. Cephalexin solutions stored under acidic conditions at 60° yielded four secondary peaks (retention times of 4.1, 11.0, 15.2, and 27.2 min), which could interfere with the chromatographic assay. Trinitrophenyl derivatives were prepared from mixtures containing 50% of acid-hydrolyzed cephalexin solutions and 50% of a pure cephalexin or pure lysine solution (Figs. 3 and 4), respectively. It is apparent that the peak of II was not affected by the acid decomposition products of cephalexin and that the peak of III was affected only minimally. The chromatogram of II after acid hydrolysis (1 hr) showed only two small additional peaks at 16.4 and 26.0 min.

The calibration factors used for the quantitative analysis of cephalexin and lysine are given in Table II. The low values of the intercept at the origin (a_0), when operating with the loop-injection technique but without the internal standard, allow use of this technique. Table II shows that similar calibration parameters were obtained by both techniques (with and without an internal standard), corresponding to the listed straight-line equations. The average response factors for II and III were 110.94 and 36.92 mm/mg with standard deviations of 0.76 and 1.05, respectively, for a set of 45 chromatograms. Sensitivity was three times higher for lysine than for cephalexin, but the sensitivity of the instrument allows lower detection limits of 0.1 and 0.3 μg/ml for lysine and cephalexin, respectively.

The high reproducibility and sensitivity of the HPLC method described here recommend it as a suitable procedure for the simultaneous analysis of cephalexin and lysine in mixtures of these two products for quality control and stability studies of pharmaceutical formulations containing cephalexin lysinate.

REFERENCES

(1) P. E. Gower, C. H. Dash, and C. H. O'Callaghan, *J. Pharm. Pharmacol.*, **25**, 376 (1973).

(2) P. Nicholas, B. R. Meyers, and S. Z. Hirschman, *J. Clin. Pharmacol.*, **13**, 325 (1973).

(3) T. W. Mischler, A. A. Sugerman, D. A. Villard, L. J. Braunick, and E. S. Neiss, *ibid.*, **14**, 604 (1974).

(4) S. Barrios, J. H. Sorensen, and R. G. W. Spickett, *J. Pharm. Pharmacol.*, **27**, 711 (1975).

(5) J. W. Keyser, *Biochem. J.*, **43**, 488 (1948).

(6) O. C. Saxena, *Microchem. J.*, **18**, 652 (1973).

(7) H. Bundgaard, *Arch. Pharm. Chem. Sci.*, **4**, 25 (1976).

(8) K. Satake, T. Okuyama, M. Ohashi, and T. Shinoda, *J. Biochem. (Tokyo)*, **47**, 654 (1960).

(9) P. J. Elving, J. M. Markowitz, and I. Rosenthal, *Anal. Chem.*, **28**, 1179 (1956).

(10) A. B. Clark and H. A. Lubs, *J. Biol. Chem.*, **25**, 479 (1916).

(11) A. R. Goldfarb, *Biochemistry*, **5**, 2570 (1966).

(12) A. Eklund, *Anal. Biochem.*, **70**, 434 (1976).

(13) R. E. Majors, *J. Chromatogr. Sci.*, **15**, 334 (1977).

(14) D. W. Huches, A. Vilim, and W. L. Wilson, *Can. J. Pharm. Sci.*, **11**, 97 (1976).

ACKNOWLEDGMENTS

The authors thank Dr. R. G. W. Spickett for helpful discussions and Miss M. P. Fernández for technical assistance.

Determination of Dextromethorphan Hydrobromide by High-Performance Liquid Chromatography Using Ion-Pair Formation

E. J. KUBIAK and J. W. MUNSON ˣ

Received February 25, 1980, from *Quality Control, The Upjohn Company, Kalamazoo, MI 49001.* Accepted for publication April 9, 1980.

Abstract □ The chromatographic retention behavior of dextromethorphan hydrobromide on an octadecylsilane column was investigated as a function of the pairing ion and the mobile phase composition. Dramatic increases in the capacity factor were observed with pairing ions containing more than eight carbons and with decreasing organic modifier (acetonitrile) concentration. Several pharmaceutically important amines exhibited similar behavior with respect to acetonitrile concentration. An analytical method was developed for dextromethorphan hydrobromide bulk drug and syrups and was applied to commercial preparations.

Keyphrases □ Dextromethorphan hydrobromide—high-performance liquid chromatographic analysis using ion-pair formation □ High-performance liquid chromatography—analysis, dextromethorphan hydrobromide, ion-pair formation □ Antitussives—dextromethorphan hydrobromide, high-performance liquid chromatographic analysis using ion-pair formation

Dextromethorphan hydrobromide [(+)-3-methoxy-17-methyl-9α,13α,14α-morphinan hydrobromide, I] is a centrally active antitussive which, unlike codeine, is devoid of analgesic properties and exhibits little or no depression of the central nervous system. Because of its lack of addiction potential, it is widely used in nonprescription

0022-3549/80/1200-1380$01.00/0
© 1980, American Pharmaceutical Association

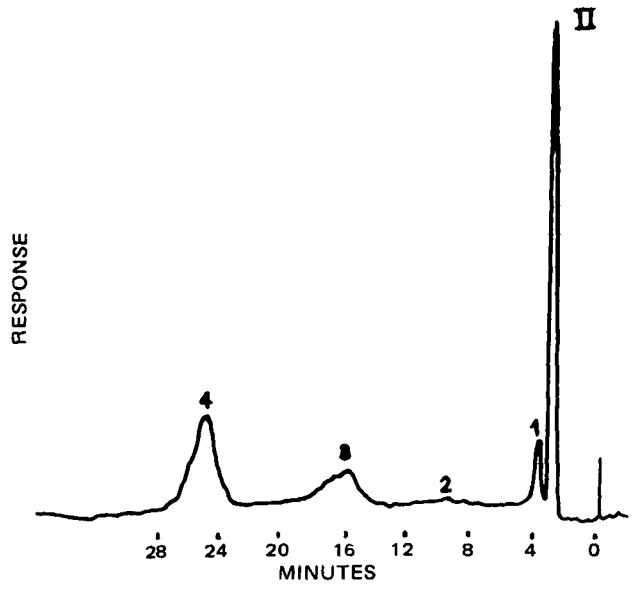

Figure 4—*Chromatogram of II and acid-degraded cephalexin derivative mixture.*

used in the assay of lysine and cephalexin. Cephalexin solutions stored under acidic conditions at 60° yielded four secondary peaks (retention times of 4.1, 11.0, 15.2, and 27.2 min), which could interfere with the chromatographic assay. Trinitrophenyl derivatives were prepared from mixtures containing 50% of acid-hydrolyzed cephalexin solutions and 50% of a pure cephalexin or pure lysine solution (Figs. 3 and 4), respectively. It is apparent that the peak of II was not affected by the acid decomposition products of cephalexin and that the peak of III was affected only minimally. The chromatogram of II after acid hydrolysis (1 hr) showed only two small additional peaks at 16.4 and 26.0 min.

The calibration factors used for the quantitative analysis of cephalexin and lysine are given in Table II. The low values of the intercept at the origin (a_0), when operating with the loop-injection technique but without the internal standard, allow use of this technique. Table II shows that similar calibration parameters were obtained by both techniques (with and without an internal standard), corresponding to the listed straight-line equations. The average response factors for II and III were 110.94 and 36.92 mm/mg with standard deviations of 0.76 and 1.05, respectively, for a set of 45 chromatograms. Sensitivity was three times higher for lysine than for cephalexin, but the sensitivity of the instrument allows lower detection limits of 0.1 and 0.3 μg/ml for lysine and cephalexin, respectively.

The high reproducibility and sensitivity of the HPLC method described here recommend it as a suitable procedure for the simultaneous analysis of cephalexin and lysine in mixtures of these two products for quality control and stability studies of pharmaceutical formulations containing cephalexin lysinate.

REFERENCES

(1) P. E. Gower, C. H. Dash, and C. H. O'Callaghan, *J. Pharm. Pharmacol.*, **25**, 376 (1973).

(2) P. Nicholas, B. R. Meyers, and S. Z. Hirschman, *J. Clin. Pharmacol.*, **13**, 325 (1973).

(3) T. W. Mischler, A. A. Sugerman, D. A. Villard, L. J. Braunick, and E. S. Neiss, *ibid.*, **14**, 604 (1974).

(4) S. Barrios, J. H. Sorensen, and R. G. W. Spickett, *J. Pharm. Pharmacol.*, **27**, 711 (1975).

(5) J. W. Keyser, *Biochem. J.*, **43**, 488 (1948).

(6) O. C. Saxena, *Microchem. J.*, **18**, 652 (1973).

(7) H. Bundgaard, *Arch. Pharm. Chem. Sci.*, **4**, 25 (1976).

(8) K. Satake, T. Okuyama, M. Ohashi, and T. Shinoda, *J. Biochem. (Tokyo)*, **47**, 654 (1960).

(9) P. J. Elving, J. M. Markowitz, and I. Rosenthal, *Anal. Chem.*, **28**, 1179 (1956).

(10) A. B. Clark and H. A. Lubs, *J. Biol. Chem.*, **25**, 479 (1916).

(11) A. R. Goldfarb, *Biochemistry*, **5**, 2570 (1966).

(12) A. Eklund, *Anal. Biochem.*, **70**, 434 (1976).

(13) R. E. Majors, *J. Chromatogr. Sci.*, **15**, 334 (1977).

(14) D. W. Huches, A. Vilim, and W. L. Wilson, *Can. J. Pharm. Sci.*, **11**, 97 (1976).

ACKNOWLEDGMENTS

The authors thank Dr. R. G. W. Spickett for helpful discussions and Miss M. P. Fernández for technical assistance.

Determination of Dextromethorphan Hydrobromide by High-Performance Liquid Chromatography Using Ion-Pair Formation

E. J. KUBIAK and J. W. MUNSON ˣ

Received February 25, 1980, from *Quality Control, The Upjohn Company, Kalamazoo, MI 49001.* Accepted for publication April 9, 1980.

Abstract □ The chromatographic retention behavior of dextromethorphan hydrobromide on an octadecylsilane column was investigated as a function of the pairing ion and the mobile phase composition. Dramatic increases in the capacity factor were observed with pairing ions containing more than eight carbons and with decreasing organic modifier (acetonitrile) concentration. Several pharmaceutically important amines exhibited similar behavior with respect to acetonitrile concentration. An analytical method was developed for dextromethorphan hydrobromide bulk drug and syrups and was applied to commercial preparations.

Keyphrases □ Dextromethorphan hydrobromide—high-performance liquid chromatographic analysis using ion-pair formation □ High-performance liquid chromatography—analysis, dextromethorphan hydrobromide, ion-pair formation □ Antitussives—dextromethorphan hydrobromide, high-performance liquid chromatographic analysis using ion-pair formation

Dextromethorphan hydrobromide [(+)-3-methoxy-17-methyl-9α,13α,14α-morphinan hydrobromide, I] is a centrally active antitussive which, unlike codeine, is devoid of analgesic properties and exhibits little or no depression of the central nervous system. Because of its lack of addiction potential, it is widely used in nonprescription

0022-3549/80/1200-1380$01.00/0
© 1980, American Pharmaceutical Association

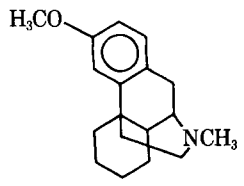

I

cough–cold preparations. The bulk drug and a syrup are described in USP XX (1). This drug is present in over 50 nonprescription antitussive preparations (2).

For USP XX, bulk I is analyzed by titration with acetous perchloric acid (1). The official method for the syrup employs extraction into hexane from a basic aqueous phase, back-extraction into dilute hydrochloric acid, and spectrophotometric quantitation. An automated system was developed which employs formation of an ion-pair with bromcresol green at pH 5.3, extraction of the ion-pair into chloroform, and measurement at 420 nm (3). This method has been used for the analysis of I in mixtures with guaifenesin and phenylpropanolamine in cough syrups. GLC after isolation by extraction into chloroform also has been employed (4). Reversed-phase high-pressure liquid chromatography (HPLC) has been used to measure I in syrups containing I and chlorpheniramine maleate (5). Ion-pair HPLC recently was employed to measure I in syrups along with pseudoephedrine hydrochloride and brompheniramine maleate (6). This report discussed a method that used a microparticulate octadecylsilane column with an acetonitrile–water mobile phase containing the sodium salt of octanesulfonic acid as the pairing ion.

A comprehensive study was made recently on the effects of the carbon chain length of the anionic ion-pairing reagents on the retention behavior of codeine, morphine, and

Table I—Comparison of Capacity Factors [a] for Several Amines Using Different Acetonitrile–Water Mixtures as the Mobile Phase

Amine	k'_A	k'_B	k'_B/k'_A
Dextromethorphan	4.60	97.9	21.3
Codeine	1.11	8.22	7.4
Methoxyphenamine	1.79	19.00	10.6
Tetracaine	3.16	45.60	14.4
Diazepam	2.02	14.22	7.0
Ephedrine	1.32	11.22	8.5
Cocaine	2.21	24.67	11.2
Naloxone	1.11	8.00	7.2
Morphine	0.89	5.56	6.2
Scopolamine	1.21	9.56	7.9
Lidocaine	1.84	18.33	10.0
Hydralazine	1.00	12.22	12.2
Meperidine	2.37	38.30	16.2
Methadone	5.63	>150	—
Methylphenidate	2.16	31.12	14.4
Quinine	4.26	>150	—

[a] k'_A is the capacity factor obtained in the 55:45 (v/v) acetonitrile–water mobile phase; k'_B is the capacity factor obtained in the 37:63 (v/v) acetonitrile–water mobile phase.

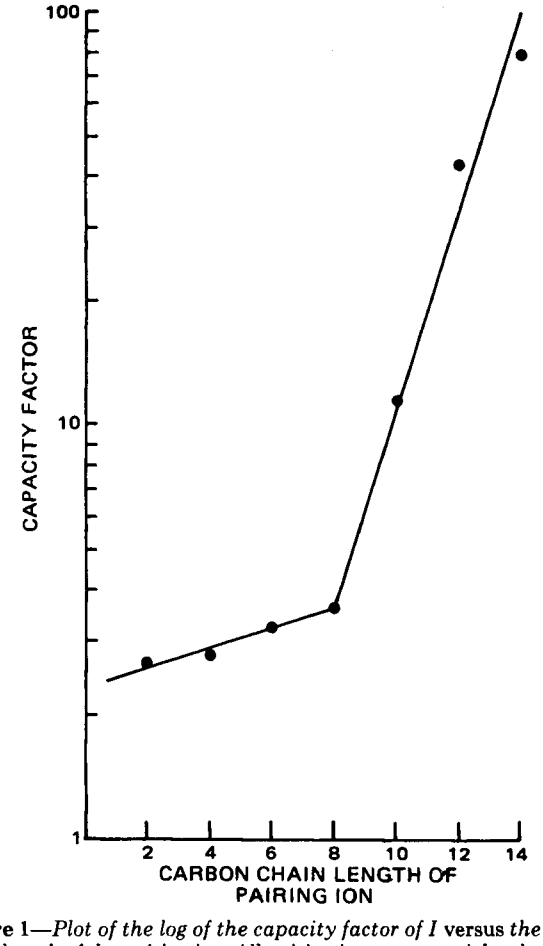

Figure 1—*Plot of the log of the capacity factor of I* versus *the carbon chain length of the pairing ion. All pairing ions were straight-chain alkyl sulfates or sulfonates. The mobile phase was the same as reported previously (7).*

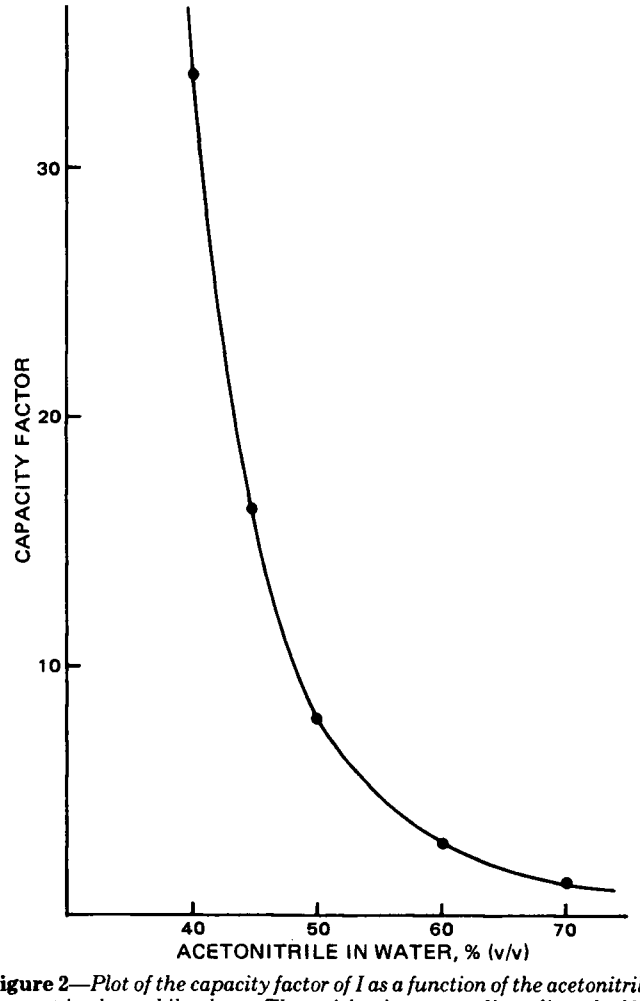

Figure 2—*Plot of the capacity factor of I as a function of the acetonitrile content in the mobile phase. The pairing ion was sodium dioctylsulfosuccinate.*

Table II—Analysis of Dextromethorphan Hydrobromide Syrup [a]

Recovery Data, mg/5 ml of placebo syrup		
Added, mg	Found, mg	Recovery, %
2.02	2.03	100.6
4.08	4.08	100.0
6.11	6.13	100.3
8.01	8.07	100.7
10.02	10.04	100.2
12.10	12.13	100.2
14.17	14.28	100.7
Average		100.4

Precision Data		
	Day 1, mg/5 ml	Day 2, mg/5 ml
	10.11	10.10
	10.14	10.06
	10.12	10.06
	10.13	10.08
	10.08	10.09
	10.10	10.14
Average	10.12	10.09
RSD, %	0.3	0.3

[a] The placebo syrup contained 100 mg of guaifenesin/5 ml and 4.75% alcohol.

ethylmorphine (7). In that study, dioctyl sodium sulfosuccinate was an effective ion-pairing reagent for the analysis of codeine in syrups. Utilizing the conditions developed for codeine as a starting point, a systematic study was undertaken to test the applicability of the method for dextromethorphan in syrups. This paper reports the results of this study and describes a reversed-phase ion-pair HPLC method for I in syrups and as the bulk drug. The chromatographic behavior of several pharmaceutically important amines also was examined using the conditions employed for the analysis of I.

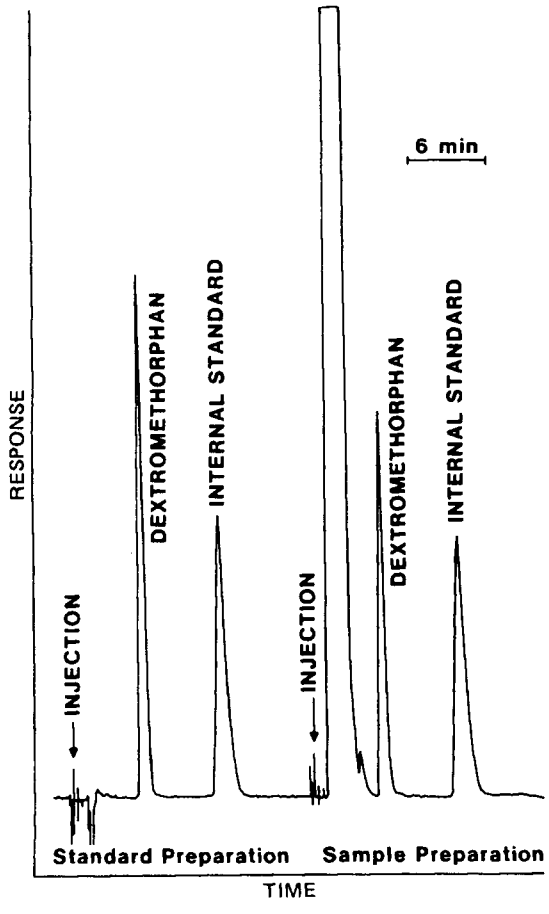

Figure 3—*Typical chromatographic tracings of a standard preparation and a sample preparation. The internal standard was testosterone propionate. The mobile phase was 55% (v/v) acetonitrile in water and contained 0.01 M ammonium nitrate and 0.005 M sodium dioctylsulfosuccinate. The pH of the mobile phase was adjusted to 3.3 with acetic acid. The flow rate was 2.0 ml/min.*

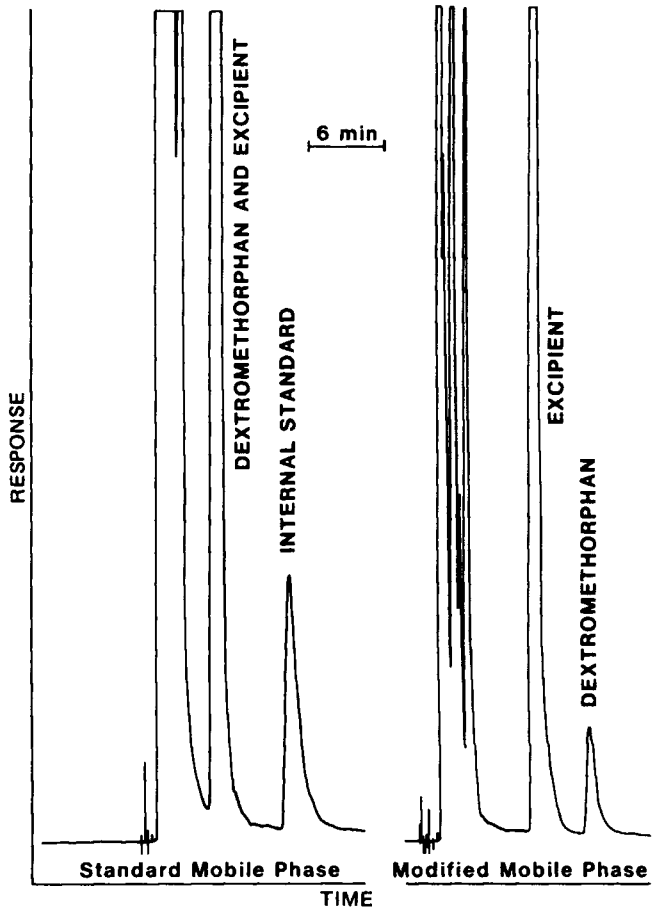

Figure 4—*Chromatographic tracings of a sample syrup preparation containing a large excipient interference. The standard mobile phase was the same as described in Fig. 3. The modified mobile phase was the same, except that the acetonitrile content was lowered from 55 to 45%. The flow rate was 2.0 ml/min.*

EXPERIMENTAL

Materials—Ethanesulfonic acid[1], sodium butanesulfonate[1], sodium hexanesulfonate[1], sodium octanesulfonate[1], sodium decylsulfate[1], sodium dodecylsulfate[1], sodium tetradecylsulfate[1], and sodium dioctylsulfosuccinate[2] were used as received. Dextromethorphan hydrobromide, codeine phosphate, methoxyphenamine hydrochloride, tetracaine hydrochloride, diazepam, ephedrine sulfate, cocaine hydrochloride, naloxone hydrochloride, morphine sulfate, scopolamine hydrobromide, lidocaine hydrochloride, hydralazine hydrochloride, meperidine hydrochloride, methadone hydrochloride, methylphenidate hydrochloride, and quinine sulfate were USP or NF quality.

The internal standard, testosterone propionate, was used as received[3]. Distilled-in-glass acetonitrile[4] and deionized water were used for all mobile phase preparations. All other chemicals were reagent grade. Samples of syrups containing dextromethorphan hydrobromide were obtained from a local wholesale drug distributor.

Apparatus—A modular high-performance liquid chromatograph

[1] Eastman Kodak Co., Rochester, NY 14650.
[2] Aldrich Chemical Co., Milwaukee, WI 53233.
[3] Steraloids, Wilton, N.H.
[4] Burdick & Jackson Laboratories, Muskegon, MI 49442.

Table III—Analyses of Dextromethorphan Hydrobromide Syrups

Syrup	Theory, mg/5 ml	Actual[a], mg/5 ml
A[b]	15.0	15.0 and 14.8
B[b]	15.0	15.0 and 14.9
C[c]	10.0	10.3 and 10.4
D[d]	15.0	15.1 and 15.4
E[e]	10.0	9.7 and 10.2
F[f]	3.5	3.3 and 3.1

[a] Two individual assays. [b] Contained 100 mg of guaifenesin/5 ml and 1.4% alcohol. [c] Contained 100 mg of guaifenesin and 12.5 mg of phenylpropanolamine hydrochloride/5 ml and 4.75% alcohol. [d] Contained 100 mg of guaifenesin/5 ml and 5% alcohol. [e] Contained 50 mg of guaifenesin and 12.5 mg of phenylpropanolamine hydrochloride/5 ml and 10% alcohol. [f] Contained 25 mg of guaifenesin/5 ml and 200 mg of sodium citrate/5 ml and 5% alcohol.

consisting of a reciprocating piston pump equipped with a pulse dampener[5], an automated loop injector[6], a UV detector[7] (254 nm), and a recorder[8] was used for all measurements. For quantitative measurements, data were collected and processed by a digital computer[9].

Mobile Phase—All mobile phases contained 0.005 *M* pairing ion and 0.01 *M* ammonium nitrate in acetonitrile–water. After mixing, the mobile phases were adjusted to pH 3.3 with acetic acid and filtered through a 5-μm filter. A mobile phase containing acetonitrile and water in a 55:45 ratio (v/v) was used for the final analysis of I.

Columns—A microparticulate octadecylsilane column[10] (10-μm particles, 30 cm × 4 mm) was obtained from commercial sources. When not in use, the column was flushed with acetonitrile–water (80:20 v/v) and stored in the same solvent. Flow rates of 2–3 ml/min gave adequate resolution with reasonable analysis times.

Quantitation of Dextromethorphan Hydrobromide in Syrup—Exactly 5.0 ml of the syrup was transferred quantitatively to a 125-ml erlenmeyer flask containing 40.0 ml of the internal standard solution (15 mg of testosterone propionate in 1 liter of the mobile phase) and mixed well. In some cases, 20.0 ml of the internal standard solution was used. When a clear solution did not form upon mixing, 5 ml of water was added to the mixture. Aliquots (25 μl) of the samples were chromatographed at a detector setting of 0.032 aufs. Concentrations were determined by comparison of peak height ratios from sample preparations to those from a standard preparation.

Bulk drug samples were prepared by adding accurately weighed samples (~10 mg) to 40.0 ml of the internal standard solution to produce the sample preparation.

RESULTS AND DISCUSSION

Dextromethorphan hydrobromide exhibited retention behavior similar to that of codeine under the conditions described previously (7). Figure 1 shows a plot of the log of the capacity factor for I as a function of the carbon chain length of the pairing ion. A dramatic increase in the capacity factor was observed with pairing ions containing more than eight carbons. When sodium dioctylsulfosuccinate (II) was used, a capacity factor of about 100 was obtained. This finding clearly represents a retention time far greater than that required for a reasonable retention time. Since I lacks the 4,5-ether linkage and the 6-hydroxyl group of codeine, the ion-pair resulting from I and II would be predicted to be considerably less polar than that resulting from codeine and II. Consequently, a reduction in the polarity of the mobile phase should reduce the capacity factor for I.

This idea was tested by measuring capacity factors of I as a function of the acetonitrile content in the mobile phase while keeping the pairing ion (II) and the pH constant. The results of this study are shown in Fig. 2. Below 60% (v/v) acetonitrile, the concentration of the organic modifier had a dramatic effect on the capacity factor. As a compromise between a short analysis time and resolution of I from syrup excipients, 55% acetonitrile was chosen for the analytical development. To test the generality of the observed relationship of the capacity factor and the acetonitrile concentration, several amines were studied using acetonitrile and water in ratios of 55:45 (v/v) and 37:63 (v/v) (II as the pairing ion). The results

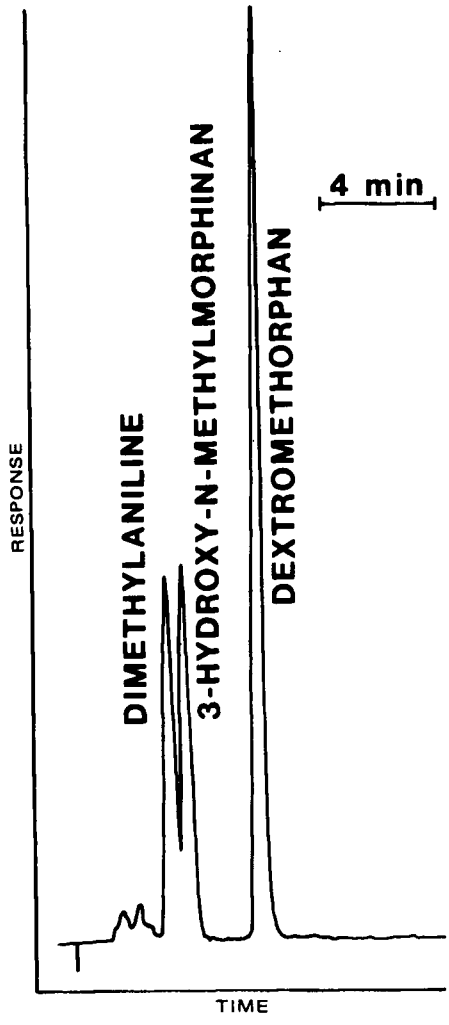

Figure 5—*Chromatographic tracing of a synthetic mixture of dimethylaniline, 3-hydroxy-N-methylmorphinan, and dextromethorphan. See Fig. 3 for the mobile phase composition and flow rate.*

are shown in Table I. With the exception of methadone and quinine, a seven- to 22-fold increase in the capacity factor was observed in going to the 37:63 acetonitrile–water mobile phase [this mobile phase has been used for the analysis of codeine (7)].

Typical chromatographic tracings for standard and sample prepara-

Table IV—Analysis of Bulk Dextromethorphan Hydrobromide

Recovery Data		
Added, mg	Found, mg	Recovery, %
8.08	8.09	100.2
9.10	9.15	100.6
9.85	9.71	98.6
10.77	10.73	99.7
11.86	11.85	99.2
Average		99.7
Precision Data		
Added, mg	Found, mg	Recovery, %
10.05	10.09	100.4
10.08	10.15	100.7
10.05	10.01	99.6
10.04	10.10	100.6
9.99	10.00	100.0
10.28	10.31	100.3
9.91	10.02	101.1
10.09	10.17	100.8
Average		100.4
RSD, %		0.5

[5] Model 110, Altex Corp., Berkeley, CA 94710.
[6] Upjohn LC Autosampler.
[7] UV III, Laboratory Data Control, Riviera Beach, Fla.
[8] Model XKR, Sargent Welch Co., Skokie, IL 60067.
[9] PDP 11, Digital Equipment Co., Maynard, MA 01754.
[10] μBondapak C_{18}, Waters Associates, Milford, MA 01757.

tions are shown in Fig. 3. Total analysis time was ~15 min. Spiked samples of a placebo syrup were analyzed by this method, giving quantitative recovery from 2.0 to 14.0 mg/5 ml (Table II). Replicate analyses of a single lot of syrup (n = 6) on 2 days gave precision (expressed as the relative standard deviation) of 0.3% (Table II).

Other commercially available syrups containing I were obtained and analyzed by this method. The results are summarized in Table III. Excellent agreement with the labeled contents was obtained. One syrup tested showed a rather large excipient peak that was not resolved from the I peak. To solve this problem, the percentage of acetonitrile in the mobile phase was reduced to 45% (v/v). Under these conditions, the excipient peak was resolved completely from the I peak (Fig. 4) but the internal standard peak did not elute in a reasonable time. Using peak height measurements, a value of 9.4 mg/5 ml (label claim was 10.0 mg/5 ml) was obtained for this syrup. This approach demonstrates that the acetonitrile content, as well as the carbon chain length of the pairing ion, can be manipulated to produce resolution of the I peak from interfering components in the mixture.

The method also was applied to the analysis of bulk drug samples. In this case, consideration must be given to the resolution of I and potential impurities arising from the synthetic process. Compound I is synthesized by the methylation of (+)-3-hydroxy-17-methyl-9α,13α,14α-morphinan (III) with phenyltrimethylammonium bromide. The by-product of the reaction is dimethylaniline. Compendial assays for I include tests for dimethylaniline and phenolic compounds (*e.g.*, III). Since dimethylaniline and III both are amines, trace amounts would be expected to be carried over in any acid–base extraction of I used for purification. A chromatographic tracing of a mixture of I, III, and dimethylaniline is shown in Fig. 5. The two potential impurities are well resolved from I. The results of the analyses of bulk I are shown in Table IV. Quantitative recovery and excellent precision are observed.

REFERENCES

(1) "The United States Pharmacopeia," 20th rev., United States Pharmacopeial Convention, Rockville, Md., 1980.

(2) J. F. Cormier and B. G. Bryant, in "Handbook of Nonprescription Drugs," 5th ed., American Pharmaceutical Association, Washington, D.C., 1977.

(3) O. W. A. Weber and J. E. Heveran, *J. Pharm. Sci.*, **62**, 1174 (1973).

(4) J. F. Fabregas and A. Margalet, *ibid.*, **64**, 1005 (1975).

(5) A. Menyharth, F. P. Mahn, and J. E. Heveran, *ibid.*, **63**, 430 (1974).

(6) M. K. Chao, I. J. Holcomb, and S. A. Fusari, *ibid.*, **68**, 1463 (1979).

(7) E. J. Kubiak and J. W. Munson, *ibid.*, **69**, 152 (1980).

ACKNOWLEDGMENTS

Methylphenidate was a gift from Ciba-Geigy, and naloxone hydrochloride was a gift from Dr. Robert E. Willette, National Institute on Drug Abuse, National Institute of Mental Health.

High-Performance Liquid Chromatographic Assay for Benzocaine and *p*-Aminobenzoic Acid Including Preliminary Stability Data

P. K. NARANG, G. BIRD, and W. G. CROUTHAMEL *x

Received February 19, 1980, from the *Department of Pharmacy, School of Pharmacy, University of Maryland, Baltimore, MD 21201.* Accepted for publication May 29, 1980.

*Present address: Department of Pharmacokinetics and Biopharmaceutics, Hoffmann–La Roche Inc., Nutley, NJ 07110.

Abstract □ A high-performance liquid chromatographic assay was developed that separates and quantitates benzocaine and its primary degradation product, *p*-aminobenzoic acid. This method is rapid, sensitive, and specific. Preliminary stability data obtained with this method demonstrate its utility for this purpose.

Keyphrases □ Benzocaine—high-performance liquid chromatographic analysis with *p*-aminobenzoic acid, effects of pH, temperature, and phosphate ion on benzocaine stability □ *p*-Aminobenzoic acid—degradation product of benzocaine, high-performance liquid chromatographic analysis with benzocaine □ High-performance liquid chromatography—analysis, benzocaine and *p*-aminobenzoic acid, stability studies of benzocaine □ Degradation—benzocaine, effect of pH, temperature, and phosphate ion

In spite of the long history of benzocaine as a therapeutic agent, little information has appeared regarding its stability. It has been reported to be relatively unstable under certain conditions, and attempts have been made to decrease its degradation through the use of complexing agents (1) and surfactants (2). Benzocaine also may be unstable in the presence of pharmaceutical excipients such as citric acid, glucose, and cherry flavoring (3). This lack of information is due in part to the absence of a rapid, specific, stability-indicating assay for benzocaine in the presence of its degradation products.

Over the years, benzocaine has been assayed quantitatively by titration (4), diazotization (5), colorimetry (6), potentiometry (7), and crystal formation (8), all of which take advantage of the basic and aromatic character imparted by the aryl amino group. Some initial benzocaine stability work was undertaken by Higuchi and Lachman (1) using a partition spectroscopic method of analysis. GLC was used later for the analysis of benzocaine (9–11). However, recent data (12, 13) showed interference by *p*-hydroxybenzoates in the UV, GLC, and column chromatographic methods for benzocaine, thereby raising questions about the specificity of these commonly employed methods.

A recently developed high-performance liquid chromatographic (HPLC) assay was reported which measures intact benzocaine (14), but the report did not mention the separation or identification of the primary degradation product of benzocaine, *p*-aminobenzoic acid. This paper describes a rapid, precise, and sensitive method for the simultaneous analysis of benzocaine and *p*-aminobenzoic

0022-3549/80/1200-1384$01.00/0

© 1980, American Pharmaceutical Association

tions are shown in Fig. 3. Total analysis time was ~15 min. Spiked samples of a placebo syrup were analyzed by this method, giving quantitative recovery from 2.0 to 14.0 mg/5 ml (Table II). Replicate analyses of a single lot of syrup (n = 6) on 2 days gave precision (expressed as the relative standard deviation) of 0.3% (Table II).

Other commercially available syrups containing I were obtained and analyzed by this method. The results are summarized in Table III. Excellent agreement with the labeled contents was obtained. One syrup tested showed a rather large excipient peak that was not resolved from the I peak. To solve this problem, the percentage of acetonitrile in the mobile phase was reduced to 45% (v/v). Under these conditions, the excipient peak was resolved completely from the I peak (Fig. 4) but the internal standard peak did not elute in a reasonable time. Using peak height measurements, a value of 9.4 mg/5 ml (label claim was 10.0 mg/5 ml) was obtained for this syrup. This approach demonstrates that the acetonitrile content, as well as the carbon chain length of the pairing ion, can be manipulated to produce resolution of the I peak from interfering components in the mixture.

The method also was applied to the analysis of bulk drug samples. In this case, consideration must be given to the resolution of I and potential impurities arising from the synthetic process. Compound I is synthesized by the methylation of (+)-3-hydroxy-17-methyl-9α,13α,14α-morphinan (III) with phenyltrimethylammonium bromide. The by-product of the reaction is dimethylaniline. Compendial assays for I include tests for dimethylaniline and phenolic compounds (*e.g.*, III). Since dimethylaniline and III both are amines, trace amounts would be expected to be carried over in any acid–base extraction of I used for purification. A chromatographic tracing of a mixture of I, III, and dimethylaniline is shown in Fig. 5. The two potential impurities are well resolved from I. The results of the analyses of bulk I are shown in Table IV. Quantitative recovery and excellent precision are observed.

REFERENCES

(1) "The United States Pharmacopeia," 20th rev., United States Pharmacopeial Convention, Rockville, Md., 1980.

(2) J. F. Cormier and B. G. Bryant, in "Handbook of Nonprescription Drugs," 5th ed., American Pharmaceutical Association, Washington, D.C., 1977.

(3) O. W. A. Weber and J. E. Heveran, *J. Pharm. Sci.*, **62**, 1174 (1973).

(4) J. F. Fabregas and A. Margalet, *ibid.*, **64**, 1005 (1975).

(5) A. Menyharth, F. P. Mahn, and J. E. Heveran, *ibid.*, **63**, 430 (1974).

(6) M. K. Chao, I. J. Holcomb, and S. A. Fusari, *ibid.*, **68**, 1463 (1979).

(7) E. J. Kubiak and J. W. Munson, *ibid.*, **69**, 152 (1980).

ACKNOWLEDGMENTS

Methylphenidate was a gift from Ciba-Geigy, and naloxone hydrochloride was a gift from Dr. Robert E. Willette, National Institute on Drug Abuse, National Institute of Mental Health.

High-Performance Liquid Chromatographic Assay for Benzocaine and *p*-Aminobenzoic Acid Including Preliminary Stability Data

P. K. NARANG, G. BIRD, and W. G. CROUTHAMEL *x

Received February 19, 1980, from the *Department of Pharmacy, School of Pharmacy, University of Maryland, Baltimore, MD 21201.* Accepted for publication May 29, 1980.

*Present address: Department of Pharmacokinetics and Biopharmaceutics, Hoffmann–La Roche Inc., Nutley, NJ 07110.

Abstract □ A high-performance liquid chromatographic assay was developed that separates and quantitates benzocaine and its primary degradation product, *p*-aminobenzoic acid. This method is rapid, sensitive, and specific. Preliminary stability data obtained with this method demonstrate its utility for this purpose.

Keyphrases □ Benzocaine—high-performance liquid chromatographic analysis with *p*-aminobenzoic acid, effects of pH, temperature, and phosphate ion on benzocaine stability □ *p*-Aminobenzoic acid—degradation product of benzocaine, high-performance liquid chromatographic analysis with benzocaine □ High-performance liquid chromatography—analysis, benzocaine and *p*-aminobenzoic acid, stability studies of benzocaine □ Degradation—benzocaine, effect of pH, temperature, and phosphate ion

In spite of the long history of benzocaine as a therapeutic agent, little information has appeared regarding its stability. It has been reported to be relatively unstable under certain conditions, and attempts have been made to decrease its degradation through the use of complexing agents (1) and surfactants (2). Benzocaine also may be unstable in the presence of pharmaceutical excipients such as citric acid, glucose, and cherry flavoring (3). This lack of information is due in part to the absence of a rapid, specific, stability-indicating assay for benzocaine in the presence of its degradation products.

Over the years, benzocaine has been assayed quantitatively by titration (4), diazotization (5), colorimetry (6), potentiometry (7), and crystal formation (8), all of which take advantage of the basic and aromatic character imparted by the aryl amino group. Some initial benzocaine stability work was undertaken by Higuchi and Lachman (1) using a partition spectroscopic method of analysis. GLC was used later for the analysis of benzocaine (9–11). However, recent data (12, 13) showed interference by *p*-hydroxybenzoates in the UV, GLC, and column chromatographic methods for benzocaine, thereby raising questions about the specificity of these commonly employed methods.

A recently developed high-performance liquid chromatographic (HPLC) assay was reported which measures intact benzocaine (14), but the report did not mention the separation or identification of the primary degradation product of benzocaine, *p*-aminobenzoic acid. This paper describes a rapid, precise, and sensitive method for the simultaneous analysis of benzocaine and *p*-aminobenzoic

0022-3549/80/1200-1384$01.00/0

© 1980, American Pharmaceutical Association

Table I—Degradation of Benzocaine in Aqueous Solutions at Room Temperature [a]

Minutes	Benzocaine Remaining[b], %			*p*-Aminobenzoic Acid Formed[c], %		
	pH 2	pH 7	pH 11	pH 2	pH 7	pH 11
0	100.0	100.0	100.0	—	—	—
5	100.1	100.4	97.5	—	—	2.20
10	100.3	—	90.7	—	—	9.00
15	99.2	100.4	88.3	—	—	11.82
30	98.0	100.8	83.6	2.40	—	16.21
45	96.5	99.2	77.7	3.70	—	22.10
60	95.5	99.5	73.1	6.20	—	27.92
120	92.4	98.8	52.0	9.51	—	49.25
180	87.6	99.2	40.6	13.60	—	62.32
240	85.1	98.3	28.9	16.32	1.25	69.05
300	78.5	98.0	20.0	24.0	2.20	79.93

[a] 25 ± 1°. [b] Average of two determinations. [c] Percent of amount formed from complete hydrolysis of benzocaine.

acid and reports preliminary stability data using this assay method.

EXPERIMENTAL

Apparatus—A high-performance liquid chromatograph equipped with a multiwavelength detector[1] was employed in conjunction with a microparticulate C_{18} column[2] for separation.

Reagents—All chemicals and reagents were analytical grade unless otherwise indicated. Benzocaine[3], *p*-aminobenzoic acid[4], monobasic potassium phosphate[5], and glass-distilled methanol[6] were used as received. Glass-distilled water was used throughout the study.

Analytical Procedure—All standard solutions of benzocaine and *p*-aminobenzoic acid were prepared in water. The concentrations of benzocaine and *p*-aminobenzoic acid were determined directly from their respective peak heights by comparison to a standard curve. The mobile phase was methanol–acetic acid–water (33:4:63). At ambient temperature and a solvent flow rate of 2 ml/min, the retention times for *p*-aminobenzoic acid and benzocaine were 2 min 28 sec and 7 min 10 sec, respectively.

The sensitivity of *p*-aminobenzoic acid and benzocaine at an injection volume of 10 μl was 0.3 and 0.7 μg/ml, respectively, which was equivalent to 3 and 7 ng injected on column. The assay sensitivity can be increased by increasing the injection volume or decreasing the dilution. Similarly, the assay sensitivity can be increased about fourfold by using 294 nm rather than the more conventional 254 nm as the detector wavelength, although this capability may not be available in all laboratories. Injections of benzocaine and *p*-aminobenzoic acid solutions prepared in nonbuffered and buffered solutions of pH 2, 7, and 11 are chromatographically similar. The solutions to be chromatographed are primarily aqueous, and there is little risk of evaporation at room temperature. Adequate reproducibility can be obtained without the use of an internal standard.

Stability Studies—*Effect of pH and Phosphate Ion*—A methanolic stock solution of benzocaine (5 mg/ml) was diluted to ~40 μg/ml with water and adjusted to pH 2, 7, or 11 with 0.1 *N* NaOH or 0.1 *N* HCl. These solutions were placed in glass vessels at room temperature (25 ± 2°). Each experiment was conducted in duplicate. Aliquots (10 μl) were withdrawn periodically and assayed for benzocaine and *p*-aminobenzoic acid.

In a similar experiment, phosphate (adjusted to 0.1 *M*) was used in place of sodium hydroxide or hydrochloric acid to adjust the solution pH. Only phosphate-ion-containing salts and their corresponding acids were used in preparing these solutions, as calculated by the Henderson–Hasselbach equation (15).

Effect of Temperature—Benzocaine solutions prepared in phosphate buffer (pH 7.0) were placed in sealed glass containers at 40, 60, and 70 ± 1.0°. Aliquots (10 μl) were assayed periodically for benzocaine and *p*-aminobenzoic acid over a 24-hr period.

Treatment of Data—Semilogarithmic plots of the benzocaine concentration as a function of time were constructed to evaluate the order and rate of benzocaine degradation. All plots were consistent with first-order kinetics, *i.e.*, plots of log benzocaine concentration *versus* time were linear. An Arrhenius plot (15) was constructed from the data obtained for the experiment on the effect of temperature. The line of best fit was determined by linear regression.

RESULTS

A typical chromatogram for benzocaine and *p*-aminobenzoic acid is shown in Fig. 1. Retention times varied slightly from day to day, but no interfering peaks were encountered. Standard curves for both benzocaine and *p*-aminobenzoic acid were linear over the concentration range of 0–100 mg/liter, using peak height or peak area as a function of concen-

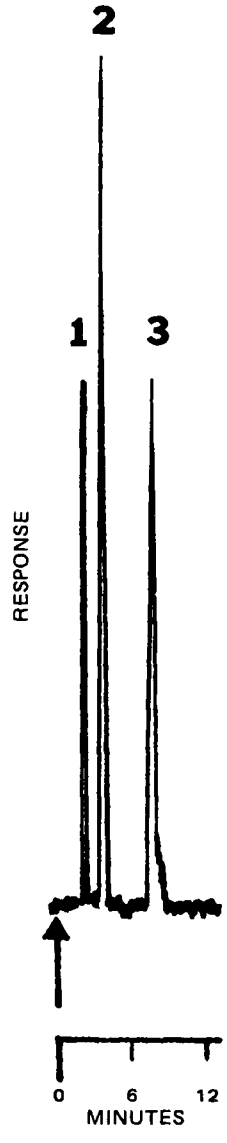

Figure 1—*Representative chromatogram for benzocaine and p-aminobenzoic acid. Key: 1, solvent peak; 2, p-aminobenzoic acid; and 3, benzocaine. The arrow indicates the time when the injection was made.*

[1] Model 1202 with model 711 solvent delivery system, Laboratory Data Control, Riviera Beach, Fla.
[2] Catalog No. 27324, Waters Associates, Milford, Mass.
[3] Amend Drugs and Chemical Co., Irvington, N.J.
[4] Ruger Chemical Co., Irvington, N.Y.
[5] Fisher Scientific Co., Fair Lawn, N.J.
[6] Burdick & Jackson Laboratories, Muskegon, Mich.

Table II—Degradation of Benzocaine in 0.1 *M* Phosphate Buffer Solutions at Room Temperature [a]

Minutes	Benzocaine Remaining[b], %			*p*-Aminobenzoic Acid Formed[c], %		
	pH 2	pH 7	pH 11	pH 2	pH 7	pH 11
0	100.0	100.0	100.0	—	—	—
5	99.4	99.76	99.7	—	—	—
10	99.1	99.97	99.5	—	—	—
15	99.5	99.5	98.7	—	—	—
30	98.3	99.8	97.8	—	—	0.84
45	99.1	99.8	96.6	—	—	1.50
60	98.8	100.0	94.6	—	—	2.02
120	96.9	99.0	93.3	0.82	—	3.20
180	95.7	99.0	88.2	1.10	0.42	6.20
240	93.8	98.2	85.5	2.50	0.96	9.60
300	92.3	98.2	83.6	6.53	0.80	11.35

[a] 25 ± 1°. [b] Average of two determinations. [c] Percent of total amount available for formation.

Table III—Apparent First-Order Rate Constants for Benzocaine Degradation at 25°

pH	Rate Constant, hr^{-1}	
	Nonbuffered Solution	Buffered Solution
2	0.0446	0.00604
7	0.0050	0.00385
11	0.314	0.03920

tration. The correlation coefficient for the standard curves over the concentration range used in this study, 0–100 mg/liter, was ≥0.99 (n = 8) in all cases. Standard solutions assayed repetitively over 15 weeks showed a coefficient of variation of 2% for benzocaine and 1.5% for *p*-aminobenzoic acid. No significant differences were observed (p = 0.05) between the mean peak height obtained from repeated injections (n = 10) on 2 days. The coefficient of variation in the slope obtained from eight standard curves over a 2-month period for benzocaine and *p*-aminobenzoic acid was <3%. The pH of the injected solutions did not affect the retention times.

Table I shows the percent of benzocaine remaining and the percent of *p*-aminobenzoic acid formed (based on the total amount available for formation) at three pH values. Benzocaine degradation was most rapid at pH 11, intermediate at pH 2, and slowest at pH 7. Good agreement was found between the amount of benzocaine lost and the amount of *p*-aminobenzoic acid formed, suggesting that *p*-aminobenzoic acid is the only major degradation product of benzocaine under these conditions. This conclusion is supported by the fact that no other peaks are seen in the chromatograms of degraded benzocaine solutions. A plot of log benzocaine concentration as a function of time for various pH values is shown in Fig. 2. The apparent first-order half-lives determined from these data were 2.2 hr at pH 11, 15.5 hr at pH 2, and 139 hr at pH 7.

Table II shows the disappearance of benzocaine and the appearance of *p*-aminobenzoic acid in solutions containing 0.1 *M* phosphate buffer. As was observed in water, benzocaine degradation was most rapid at pH 11 and slowest at pH 7; good agreement existed between benzocaine loss

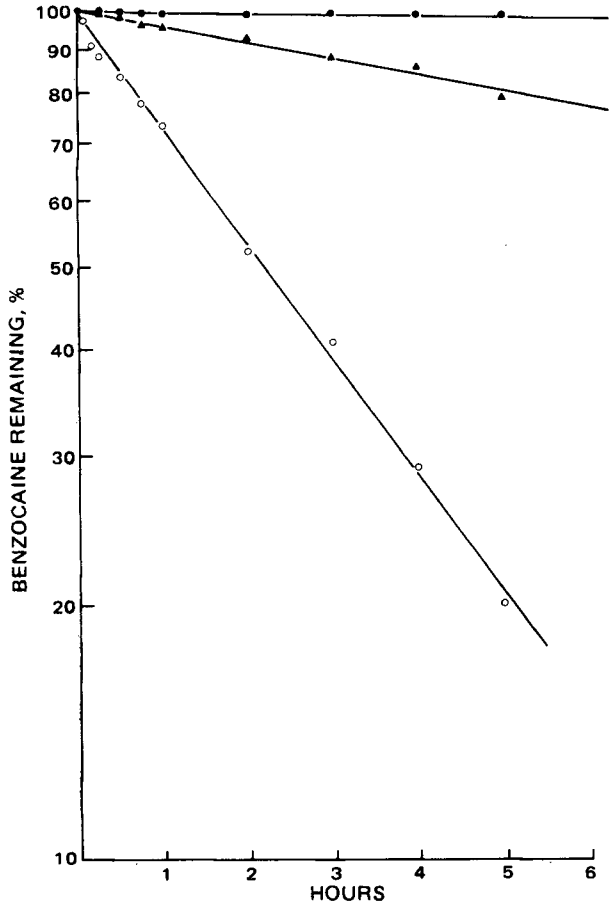

Figure 2—*Benzocaine degradation in aqueous solutions of three pH values at 25°. Key: ●, pH 7, ▲, pH 2; and ○, pH 11.*

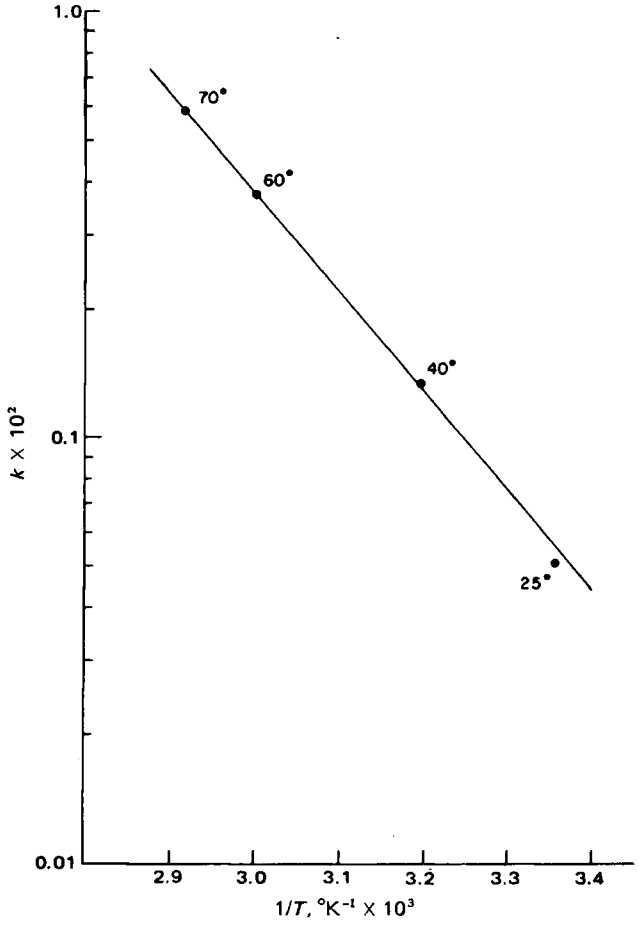

Figure 3—*Arrhenius plot of benzocaine stability in 0.1* M *phosphate buffer (pH 7).*

Table IV—Observed and Predicted Values for Benzocaine Stability at pH 7 in 0.1 *M* Phosphate Buffer [a]

Temperature (t), °C	$1/T$, °K^{-1} × 10^3	k, hr^{-1}	log k	Time for 10% Degradation, hr	Time for 50% Degradation, hr
40	3.195	0.0136	−1.866	7.75	50.96
60	3.003	0.0376	−1.425	2.80	18.44
70	2.915	0.0586	−1.232	1.80	11.82
25	3.356	0.0051	−3.295	20.78	136.70
25		0.0057[b]	−2.444[b]	18.49[b]	121.60[b]

[a] Frequency factor (A) = 2.35 × 10^7 hr^{-1}. Activation energy (E_a) = 5.217 kcal/mole. [b] From Arrhenius plot, based on data at 40, 60, and 70°C.

and *p*-aminobenzoic acid appearance. However, at all three pH values, the degradation rate was slower in phosphate buffer than in water. Half-lives for the loss of benzocaine in the presence of 0.1 *M* phosphate were 17.7 hr at pH 11, 115 hr at pH 2, and 180 hr at pH 7. Thus, benzocaine was approximately 1.3 (pH 7), 7.3 (pH 2), and 8.0 (pH 11) times more stable in phosphate buffer than in nonbuffered solutions of equivalent pH (Table III). The reason for the protective effect of phosphate ion is unknown. However, increasing the phosphate buffer concentration from 0.1 to 0.5 *M* while maintaining a constant ionic strength with sodium chloride did not alter the degradation rate at room temperature and pH 7.

Benzocaine stability was studied at 25, 40, 60, and 70°C in 0.1 *M* phosphate buffer at pH 7.0. An Arrhenius plot (15) constructed by plotting the apparent first-order rate constants obtained as a function of the inverse of temperature (°K) is shown in Fig. 3. Extrapolation of the elevated temperature data to room temperature (25°C) results in a predicted first-order rate constant of 0.0057 hr^{-1}, which compares favorably with the rate constant of 0.0051 hr^{-1} observed at room temperature (Table IV).

DISCUSSION

Various analytical methods were employed in previous stability studies of benzocaine. These methods suffer from several deficiencies, including the inability to quantitate or separate the primary degradation product of benzocaine and the lack of a chromatographic step to separate benzocaine from other potentially interfering materials. The potential interference of *p*-aminobenzoic acid in the methods used in some previous stability studies (1, 11) has been discussed (13). The official assay (16) employs a diazotization titration and hence may not be specific for benzocaine alone. The assay described here is rapid and precise and allows simultaneous quantitation of benzocaine and its primary degradation product, *p*-aminobenzoic acid. This capability allows for the continuous monitoring of mass balance during stability studies and precludes nonspecific losses such as loss into packaging materials.

The new assay has been used to study several stability characteristics of benzocaine, including the effects of pH, temperature, and phosphate ion. Benzocaine degradation is both acid and base catalyzed but is much slower in the presence of phosphate ion. First-order kinetics are observed in all cases. Studies at elevated temperatures indicate that benzocaine obeys the Arrhenius equation. Degradation rates at room temperature agree with those predicted from elevated temperature studies.

Essentially all of the benzocaine lost due to degradation can be accounted for by the appearance of *p*-aminobenzoic acid; hence, *p*-aminobenzoic acid appears to be the only significant degradation product under the study conditions used.

The sensitivity of this assay is ~0.7 μg/ml for benzocaine and ~0.3 μg/ml for *p*-aminobenzoic acid. The sensitivity can be enhanced fourfold if a multiple-wavelength detector is used at 294 nm or if the injection volume is increased.

The method described here suffers from no known interference and is applicable for the content uniformity and quality control of products containing benzocaine. This rapid assay is good for the evaluation of raw materials and employs basic equipment found in most analytical laboratories.

REFERENCES

(1) T. Higuchi and L. Lachman, *J. Am. Pharm. Assoc., Sci. Ed.*, **44**, 521 (1955).

(2) S. Riegelman, *ibid.*, **49**, 339 (1960).

(3) P. Kabasakalian, G. Cannon, and G. Pinchuk, *J. Pharm. Sci.*, **58**, 45 (1969).

(4) C. Burson and C. W. Sodern, *Pharm. Arch.*, **14**, 17 (1943).

(5) P. Jannke, *ibid.*, **16**, 25 (1945).

(6) E. G. Feldmann, *J. Am. Pharm. Assoc., Sci. Ed.*, **48**, 197 (1959).

(7) P. C. Mardunas and J. A. Riddick, *Anal. Chem.*, **23**, 337 (1951).

(8) J. R. Clark and S. M. Wang, *ibid.*, **26**, 1230 (1954).

(9) J. L. Lach and J. S. Sawardeker, *J. Pharm. Sci.*, **54**, 424 (1965).

(10) S. J. Donato, *ibid.*, **54**, 917 (1965).

(11) M. Wilcox, *ibid.*, **56**, 642 (1967).

(12) M. Batchelder, H. I. Tarlin, and G. Williamson, *ibid.*, **61**, 252 (1972).

(13) F. F. Cantwell, *Anal. Chem.*, **48**, 1854 (1976).

(14) V. D. Gupta and S. Sachanandini, *J. Pharm. Sci.*, **66**, 897 (1977).

(15) A. N. Martin, J. Swarbrick, and A. Cammarata, "Physical Pharmacy," 2nd ed., Lea & Febiger, Philadelphia, Pa., 1969.

(16) "The National Formulary," 14th ed., Mack Publishing Co., Easton, Pa., 1975, p. 69.

ACKNOWLEDGMENTS

The authors thank Mr. Benjamin Kowaski for technical assistance during the initial portion of the project.

Preparation of Enteric-Coated Microcapsules for Tableting by Spray-Drying Technique and *In Vitro* Simulation of Drug Release from the Tablet in GI Tract

H. TAKENAKA, Y. KAWASHIMA ˣ, and SHAN-YANG LIN

Received March 27, 1980, from the *Gifu College of Pharmacy, Mitahora, Gifu 502, Japan.* Accepted for publication May 29, 1980.

Abstract □ Improved methods were developed for the preparation of enteric-coated microcapsules for tableting by a spray-drying technique, and the drug release behavior from the tableted microcapsules was investigated using a disintegration apparatus and a new *in vitro* method of simulating the GI tract. As a model system, ammonium solutions of sulfamethoxazole and cellulose acetate phthalate were spray dried using a centrifugal wheel atomizer at 140°. Additives such as colloidal silica, montmorillonite clay, and talc were included in the formulations for spray drying. The influence of the additives on the particle diameter, density, packing properties, and compressibility of the product and on the release characteristics of the resultant tablet *in vitro* were investigated. The additives in the formulations greatly improved the flow properties of the spray-dried products, which could be tableted easily. Products from the nonadditive formulations could not be tableted due to their poor flowability. The hardness and disintegration rate of the tablet increased with increasing concentration of additives in the formulations. X-ray analysis and IR spectroscopy confirmed that the crystals of sulfamethoxazole in the spray-dried microcapsules with cellulose acetate phthalate were converted from Form I to Form II. *In vitro* release characteristics of the tablets were studied using a disintegrator (JP) in buffer solutions (pH 1.2 and 7.5) and distilled water. Enteric action of the spray-dried products was proved by comparison with the original nontreated powders. The additives in the tablet increased the release rate at the initial stage in all dissolution media used. A new *in vitro* release simulator was devised consisting of a flow-type dissolution container in which the pH of the medium was changed continuously from 1.2 to 7.0 to simulate the pH change of tablets exposed to the GI tract.

Keyphrases □ Microcapsules—preparation of enteric-coated microcapsules for tableting by a spray-drying technique, drug release from tableted microcapsules □ Tablets—preparation of enteric-coated microcapsules for tableting, drug release from tableted microcapsules □ Dissolution—tableted enteric-coated microcapsules

Spray-drying techniques have been used widely for drying heat-sensitive foods, pharmaceuticals, and other substances because of the rapid evaporation of the solvent from the droplets. Interest has been renewed in this technique for the preparation of agglomerates or microcapsules of pharmaceuticals. Speiser *et al.* (1) prepared microcapsules of barbituric acid employing a spray polycondensation method. Kawashima and Takenaka (2) produced sustained-action antacid tablets by compressing spray-dried microcapsules of magnesium carbonate. The successful results from these studies encouraged further development of this technique for preparation of a new dosage form.

One objective of the present study was to prepare enteric-coated microcapsules of sulfamethoxazole efficiently by a spray-drying technique instead of by a phase separation method (3). Proper formulation and spray-drying conditions were sought for producing microcapsules with enteric action that meet the requirement for tableting. Another objective was to devise a new *in vitro* simulator for the GI tract to evaluate the enteric action of the tablet prepared by compressing the spray-dried products.

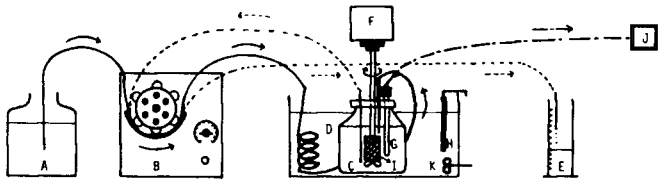

Figure 1—*Apparatus for a new* in vitro *release simulator. Key: A, alkaline solution supplier; B, roller pump (1.27 ml/min); C, modified dissolution apparatus; D, water bath (37°); E, receiving reservoir; F, motor (94 rpm); G, pH electrode; H, heater; I, USP basket modified by attaching four-blade propeller; J, pH meter; K, stirrer; and — and ---, polyethylene tube plugged with cotton at initial points.*

EXPERIMENTAL

Spray-Drying Technique—Sulfamethoxazole[1] was used as received as a model pharmaceutical for microencapsulation or agglomeration. Sulfamethoxazole and cellulose acetate phthalate[2] (50 g each) were dissolved in 1 liter of 5% NH_4OH. To this solution were added 0, 30, and 50 g of colloidal silica[3], montmorillonite clay[4], and talc[5]. Formulations without cellulose acetate phthalate also were prepared as a reference for testing the enteric action.

The slurries or solutions were atomized into a drying chamber by a centrifugal wheel atomizer at 40,000 rpm. The drying chamber was maintained at 140 ± 10°. The dried products were collected by a cyclone collector.

Measurement of Physicochemical Properties—The particle size of the spray-dried products was measured by a photographic counting method using a particle-size analyzer[6]. Packing properties and particle density were measured by a tapping powder method and with a helium–air comparison pycnometer[7], respectively. The surface topography of the spray-dried particles coated with gold was investigated with a scanning electron microscope[8]. To analyze the crystalline form of sulfamethoxazole in the spray-dried products, X-ray diffraction patterns[9] and IR spectra[10] were obtained.

Dissolution Test of Tablets Prepared from Spray-Dried Products—Spray-dried products with additives and the mixtures with microcrystalline cellulose[11] (1:1) were tableted using a single-punch tablet machine. The dimensions and weights of 10 tablets were measured. The hardness of the tablets was measured by a moving platen-type hardness tester[12]. Tablet hardness is presented as average values.

The dissolution test of a tablet was undertaken using the JP IX disintegration apparatus and the specified disintegration test solutions (pH 1.2 and 7.5) and distilled water at 37°. Tests also were conducted with a new *in vitro* release simulator (Fig. 1) with a flow-type dissolution container in which the pH of the medium was changed continuously to simulate the pH change on the surface of the tablets exposed in the GI tract.

[1] Shionogi Pharmaceutical Co., Japan.
[2] Kishida Chemical Co., Japan.
[3] Japan Aerosil K.K., Japan.
[4] Veegum-K, R. T. Vanderbilt Co.
[5] Matsumura Sangyo Co., Japan.
[6] Karl Zeiss TGZ-3.
[7] Model 1302, Micromeritics Instrument Co.
[8] Nihon Denshi JMS-S1.
[9] Nihon Denshi JDX.
[10] Nihon Denshi DS-403G.
[11] Asahi Kasei Kogyo K.K., Japan.
[12] Kyowa Seiko K.K., Japan.

0022-3549/80/1200-1388$01.00/0
© 1980, American Pharmaceutical Association

Table I—Micromeritic Properties of Powdered and Tableted Spray-Dried Products [a]

Property	Montmorillonite Clay		Colloidal Silica		Talc		No Additive
			With Cellulose Acetate Phthalate				
Weight of additive, g	30	50	30	50	30	50	—
D_{av}, μm	8.8	12.8	12.8	15.9	13.4	9.9	22.2
S_w, cm^2/g	4947	3386	3190	2498	2986	4126	2159
ρ, g/cm^3	1.38	1.39	1.50	1.50	1.50	1.50	1.25
a	0.29	0.32	0.14	0.06	0.36	0.31	0.37
b	0.05	0.08	0.07	0.12	0.05	0.05	0.07
ϵ	0.12	0.05	0.07	0.07	0.19	0.16	—
H, kg	3.7	24.2	2.2	12.4	1.1	2.3	—
			Without Cellulose Acetate Phthalate				
Weight of additive, g	30		30	50	30	50	
D_{av}, μm	8.1		7.1	3.6	3.5	8.8	
S_w, cm^2/g	4619		5093	9898	10,988	3940	
ρ, g/cm^3	1.61		1.66	1.68	1.55	1.72	
a	0.31		0.13	0.16	0.39	0.45	
b	0.06		0.13	0.07	0.07	0.09	
ϵ	0.21		0.63	0.45	0.31	0.32	
H, kg	8.7		45	—	2.27	3.77	

[a] Key: D_{av}, geometric mean diameter; S_w, specific area measured by air permeability method; ρ, porosity of tablet; and H, hardness of tablet.

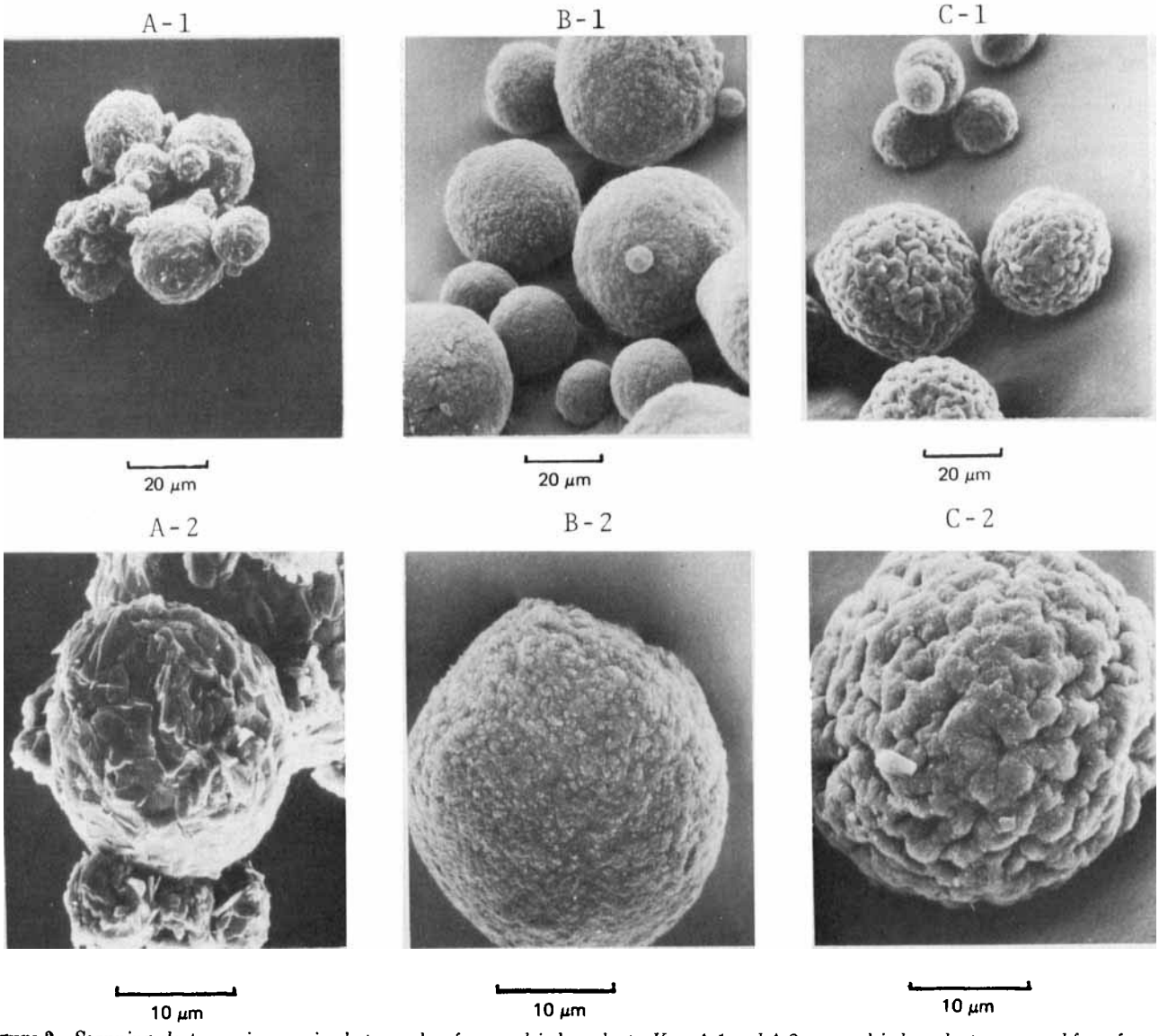

Figure 2—*Scanning electron microscopic photographs of spray-dried products. Key: A-1 and A-2, spray-dried products prepared from formulations containing cellulose acetate phthalate (50 g); B-1 and B-2, spray-dried products prepared from formulations containing cellulose acetate phthalate (50 g) and colloidal silica (50 g); and C-1 and C-2, spray-dried products prepared from formulations containing colloidal silica (50 g).*

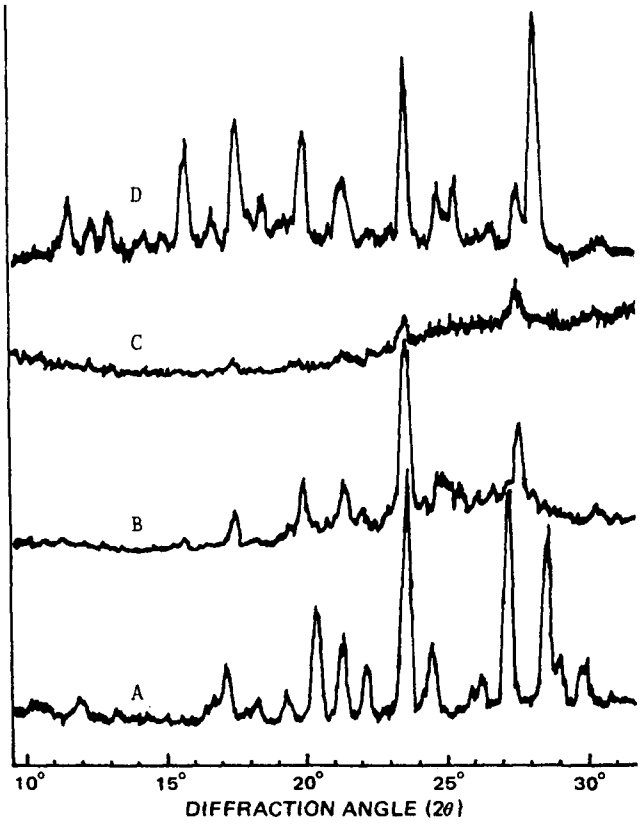

Figure 3—*X-ray diffraction patterns of original and spray-dried sulfamethoxazole. Key: A, Form I, original sulfamethoxazole; B, Form II, sulfamethoxazole recrystallized in water at dry ice–acetone temperature; C, spray-dried products prepared from formulations containing cellulose acetate phthalate (50 g) and colloidal silica (50 g); and D, spray-dried products prepared from formulations containing talc (50 g).*

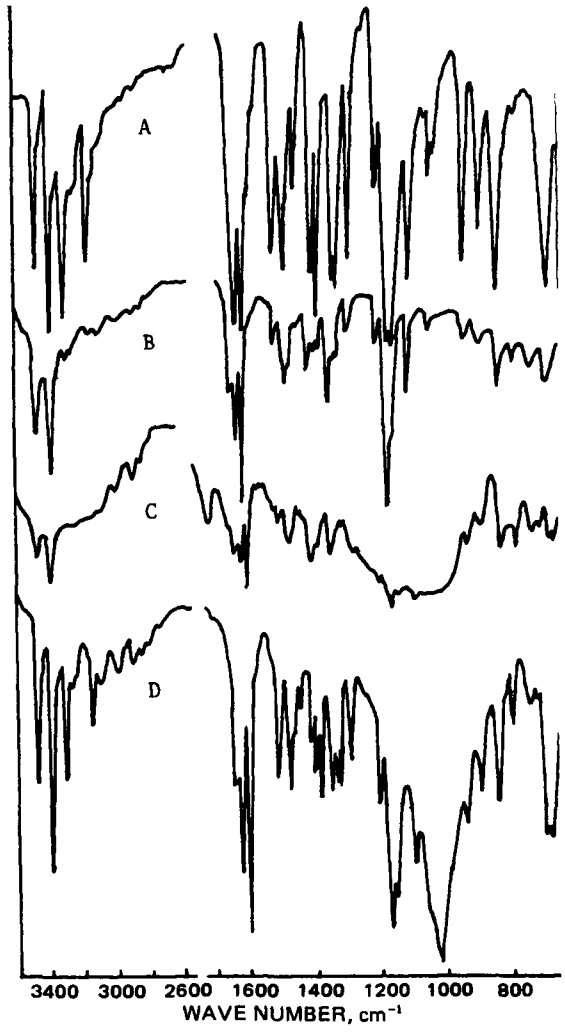

Figure 4—*IR spectra of original and spray-dried sulfamethoxazole. Key: A, Form I, original sulfamethoxazole; B, Form II, sulfamethoxazole recrystallized in water at dry ice–acetone temperature; C, spray-dried products prepared from formulations containing cellulose acetate phthalate (50 g) and colloidal silica (50 g); and D, spray-dried products prepared from formulations containing talc (50 g).*

The test was carried out by placing a tablet in the basket specified in the USP dissolution apparatus, which was modified by attaching a four-blade propeller. This basket was set 1.0 ± 0.2 cm from the bottom of the container and was rotated at 94 rpm. The pH 1.2 medium (300 ml) was introduced into the dissolution apparatus, followed by the addition of the alkaline medium (pH 7.5) at a rate of 1.27 ml/min. Simultaneously, the agitated dissolution medium was removed at the same rate to a reservoir using a rotating-type pump[13]. With this technique, the volume of medium in the container was held to 300 ml and the pH of the medium was changed continuously from 1.2 to 7.0. This pH change corresponds to that of the GI tract. The pH change in the dissolution medium was monitored by a pH meter placed in the dissolution medium.

Aliquots of 2 ml of the dissolution medium in the apparatus and the reservoir were sampled at prescribed intervals through a pipet plugged with cotton and were filtered through a Millipore filter (0.3 μm). Aliquots of distilled water (same volume and temperature) were added immediately to the dissolution apparatus to keep the volume of the dissolution medium in the container constant during the test. The concentration of dissolved sulfamethoxazole in the medium was determined spectrophotometrically at a suitable UV region using a double-beam spectrophotometer[14].

RESULTS AND DISCUSSION

Physicochemical Properties of Spray-Dried Products—The size distribution of the spray-dried particles was described in log-normal form. The geometric mean diameter ranged from 3.6 to 22.0 μm. The formulations including cellulose acetate phthalate and the additives yielded smaller products than the formulations without the additives. The products prepared from the formulations with the additives alone became smaller compared to the others (Table I).

Scanning electron microscopic photographs of the spray-dried products are shown in Fig. 2. The surfaces of the products prepared from the nonadditive formulations were covered with flake-like crusts (Fig. 2A). When the additives were added to the formulations, no flakes appeared, and the surface had an orange peel texture (Fig. 2B). Figure 2C shows an

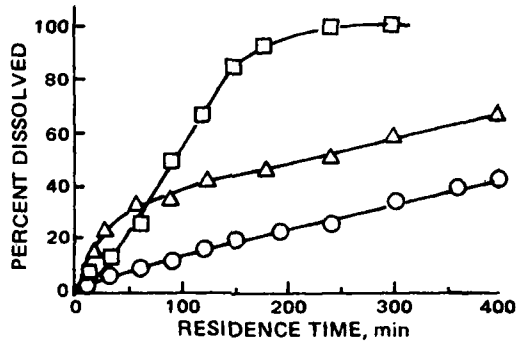

Figure 5—*Release patterns of tablets without microcrystalline cellulose in various media. Key: ○, distilled water; △, pH 1.2; and □, pH 7.5. The additive was 30 g of colloidal silica.*

[13] Furue Science Co., Japan.
[14] Hitachi model 556.

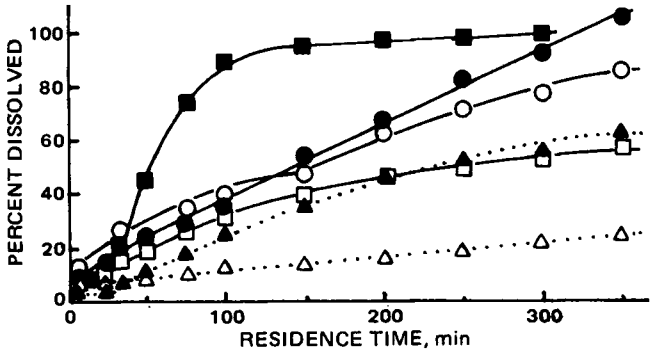

Figure 6—*Drug release patterns of tablets without cellulose acetate phthalate and microcrystalline cellulose and with varying amounts of colloidal silica in various dissolution media. Key: ●, 30 g, pH 1.2 medium; ○, 50 g, pH 1.2 medium; ■, 30 g, pH 7.5 medium; □, 50 g, pH 7.5 medium; ▲, 30 g, distilled water; and △, 50 g, distilled water.*

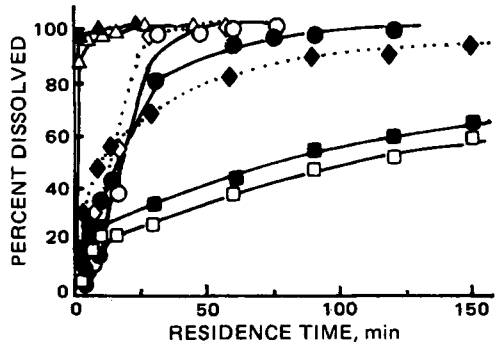

Figure 8—*Drug release patterns of tablets containing microcrystalline cellulose with varying amounts of colloidal silica in various dissolution media. Key: □, 0 g, pH 1.2 medium; ■, 30 g, pH 1.2 medium; ○, 0 g, pH 7.5 medium; ●, 30 g, pH 7.5 medium; ◇, 0 g, distilled water; and ♦, 30 g, distilled water. The original powder also was dissolved in pH 1.2 (△) and 7.5 (▲) media.*

image of the product with the additives alone, which seems to be an agglomerate composed of lobes. Many sulfamethoxazole crystals apparently are adsorbed onto the surface.

The characteristic bulkiness of the spray-dried product from the formulations with cellulose acetate phthalate alone (Fig. 2A) suggests that their particle density and packing property differ from those of the other formulations. It was assumed that these products might be lighter than those with the additives. This assumption was proved by the particle density data given in Table I. The products including the additives alone had a higher particle density. The packing process of the spray-dried products in a tapped graduated cylinder was represented by (4):

$$n/c = 1/ab + n/a \quad \text{(Eq. 1)}$$

$$c = (V_0 - V_n)/V_n \quad \text{(Eq. 2)}$$

where b is a constant, n is the number of taps, V_0 is the volume of powder in a measuring cylinder at the loosest packing, and V_n is the volume after the nth tapping. The parameter a in Eq. 1 for the products without additives was found to be larger than that of the particles with montmorillonite clay and colloidal silica. This finding indicates that the particles with the additives might be packed more easily since a corresponds to the proportion of consolidation at the closest packing attained.

Tablets could not be made directly by compressing the products without the additives due to their poor flowabilities. The products including the additives were tableted easily. Compressibility of the spray-dried products including the additives was improved with increasing amounts of the additives, as indicated by their greater hardness and smaller porosity. This trend clearly appeared with the tablets containing colloidal silica and montmorillonite clay (Table I).

The crystalline forms of the spray-dried products were investigated by X-ray diffraction analysis and IR spectroscopy. The IR spectra and X-ray diffraction patterns of the untreated original sulfamethoxazole used in the present study identified the crystals as Form I, as defined previously (5). The peaks in the X-ray diffraction patterns of the spray-dried products were less intense than those of the original crystals (Fig. 3). This finding indicated that some sulfamethoxazole crystals were converted to a disordered form due to rapid crystallization.

In the patterns of the products with cellulose acetate phthalate, regardless of whether the additives were included, fairly characteristic peaks of Form II appeared. Form II was prepared as a reference by recrystallization in water at dry ice–acetone temperature (Fig. 3). The X-ray diffraction patterns of the products with colloidal silica and montmorillonite clay proved that they were Form I. The patterns of the products with talc exhibited peaks of both Forms I and II, indicating that they were a mixture.

The polymorphic forms of the spray-dried products also were confirmed by their IR spectra (Fig. 4). The spray-dried products with cellulose acetate phthalate exhibited the characteristic bands of Form II at 3080, 2990, and 1640 cm^{-1}, which did not appear in the spectrum of Form I. Differences in the spectra from Form I also were found at 1395, 1330, 1150, and 750 cm^{-1}. When cellulose acetate phthalate was excluded from the formulations, the spectra of the spray-dried products changed to those of Form I. Spectra of the products with talc exhibited the intense bands at 3300 and 3150 cm^{-1} and several characteristic bands of Form II. This result suggests that the products with talc contain Forms I and II.

It has been suggested that polymorphism in sulfonamides may be

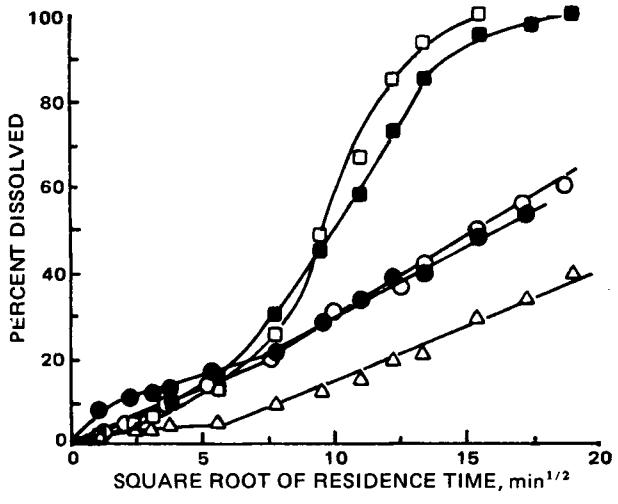

Figure 7—*Percentage of drug release as a function of the square root of the residence time with and without cellulose acetate phthalate, without microcrystalline cellulose, and with varying amounts of colloidal silica in various dissolution media. Key for formulations with cellulose acetate phthalate: ●, 50 g, pH 1.2 medium; □, 30 g, pH 7.5 medium; ■, 50 g, pH 7.5 medium; and △, 30 g, distilled water; ○ represents a formulation without cellulose-acetate phthalate and containing 50 g of colloidal silica in a pH 7.5 medium.*

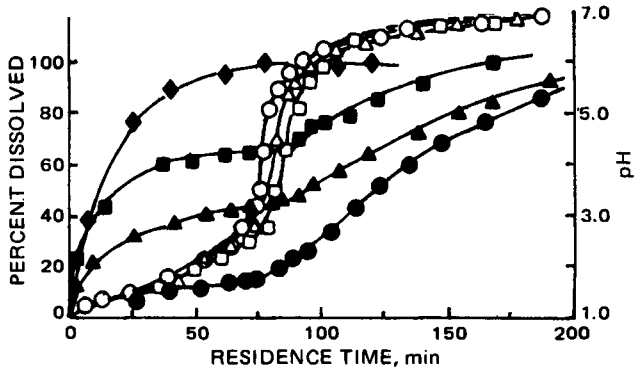

Figure 9—*Drug release (closed symbols) and pH change (open symbols) patterns in a flow-type simulator for formulations containing varying amounts of colloidal silica. Key for formulations containing cellulose acetate phthalate: ●, ○, 0 g; ▲, △, 30 g; and ■, □, 50 g. The formulation without cellulose acetate phthalate and containing 50 g of colloidal silica is represented by ♦.*

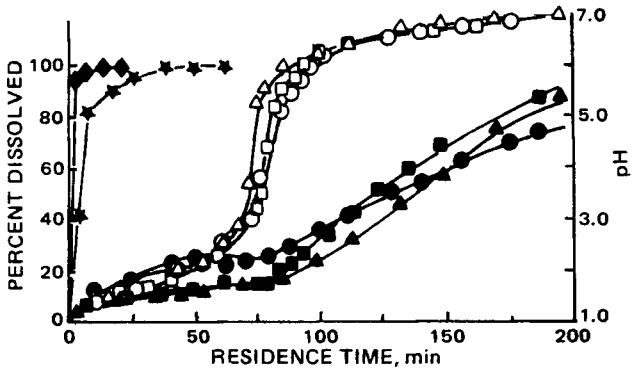

Figure 10—*Drug release (closed symbols) and pH change (open symbols) patterns in a flow-type simulator for formulations containing varying amounts of additives. Key for formulations with cellulose acetate phthalate: ●, ○, 50 g of talc; ▲, △, 50 g of montmorillonite clay; and ■, □, no additive. Key for formulations without cellulose acetate phthalate: ★, ☆, 30 g of talc; and ♦, ◇, 30 g of montmorillonite clay.*

brought about due to the intermolecular hydrogen bonding (6, 7). Hydrogen bonding in the alkaline solutions used might be attained mainly by the interaction between the hydrogen of the *p*-amino group and the oxygen of the S–O group in the sulfamethoxazole molecule. Furthermore, cellulose acetate phthalate molecules might influence the way in which the sulfamethoxazole molecules associate in the solution. This effect was confirmed by the fact that the products from the simple formulations without cellulose acetate phthalate or the additives exhibited Form I but not Form II. Such a polymorphism might make the drug metastable, but it could improve solubility.

Dissolution Behavior of Tablets in Disintegration Apparatus—Dissolution patterns of the tablets of the spray-dried products with colloidal silica and cellulose acetate phthalate in the disintegration test solutions (pH 1.2 and 7.5) and distilled water were determined using a disintegration apparatus (Fig. 5). The dissolution curves in the alkaline solution were distinguished by their much faster release rate from those in the other media used due to the enteric-coating action of the cellulose acetate phthalate contained in the tablet. Although the initial release rate in the acidic solution was faster than in distilled water, the slope of the release curve became almost identical at the later stage. In the alkaline solution, the tablets were gradually disintegrated to fine particles and a few small pieces; in the acidic media, disintegration did not occur, and only the size of the tablet slowly decreased during the dissolution process.

The dissolution behavior of the tablets prepared from the formulations with colloidal silica but without cellulose acetate phthalate is shown in Fig. 6. There was less variation in the rate in the three dissolution media used. The colloidal silica may have acted as a disintegrating agent due to its wettability, which might have resulted in an increased release rate. However, when the concentration of colloidal silica in the tablet was increased, the release rate was decreased significantly, which might have been due to a matrix-like structure of the tablet binding strongly with colloidal silica.

These differences in the release behavior of the tablets were explained by plotting the data on a semisquare root graph (Fig. 7). In the acidic solution and distilled water, all release patterns of the tablets, regardless of the formulation, became fairly straight lines after enhanced dissolution periods. This finding indicates that the release process at the later stage obeys the Higuchi model (8) represented by:

$$Q = [D(2A - C_s)C_s t]^{1/2} \quad \text{(Eq. 3)}$$

where Q is the amount dissolved per unit area of exposure at time t, A is the total amount of drug present in the matrix per unit volume, C_s is the solubility of the drug in the external phase of the matrix, and D is the diffusion constant. When $C_s \ll A$, Eq. 3 can be transformed to a more convenient form to exhibit the release patterns described in Fig. 7 (9):

$$C_r = 100[S_v(2DC_s t/A)^{1/2}] \quad \text{(Eq. 4)}$$

where C_r is the percent of the drug dissolved and S_v is the specific surface area. In alkaline solution, the release patterns of the tablets with and without cellulose acetate phthalate exhibited sigmoid curves and straight lines, respectively.

When microcrystalline celluloses were mixed into the spray-dried products in a 1:1 ratio, tablets could be made even if the products without the additives were used. However, the hardness of the tablet was insufficient for practical use compared with the tablets containing the additives. The dissolution rate of the tablets containing microcrystalline cellulose became faster than that of the tablets without it in all dissolution media due to their rapid disintegration. The distinct discrepancies of the release patterns depended on the type of dissolution medium used (Fig. 8). The prolonged release in the acidic medium was clearly evident when compared to the mixtures of microcrystalline cellulose and original sulfamethoxazole. Thus, the effectiveness of the enteric coating of the spray-dried products containing cellulose acetate phthalate is proved in Figs. 7 and 8.

In the alkaline medium and in distilled water, the dissolution rate was delayed when the additives were included in the formulations. In the acidic solution, the release rate of the tablet with the additives was faster than for those without them. This result might have been due to the fact that the additives included in the discrete microcapsules could promote penetration of the solvent.

Dissolution Behavior of Tablet Containing Various Additives in a Flow-Type Simulator—Gastric contents do not become alkaline merely as a result of passing through the pylorus. The upper small intestine is more likely to be slightly acidic. Thus, to simulate *in vivo* action, it may be desirable to conduct the enteric test in a dissolution medium whose pH is changed continuously from 1.2 to 7.0 rather than in a medium fixed at pH 7.0 or above. Release patterns of tablets prepared from the mixtures of microcrystalline cellulose and the spray-dried products containing various additives exposed to a medium whose pH changed continuously from 1.2 to 7.0 are shown in Figs. 9 and 10. The pH change of the medium with residence time followed a sigmoid curve which varied slightly from batch to batch, although the patterns were almost identical.

The release rate of the tablets with cellulose acetate phthalate was relatively fast at the initial stage, followed by a stage with a decreased rate. After the residence time of 70–90 min at pH 3.5–5.5, the release rate increased rapidly again, which caused an inflection on the release curve. It is reasonable to assume that this point corresponds to the starting point of the enteric action. By increasing the concentration of colloidal silica, the release rate at the initial stage (pH values of <3.5–4.0) increased due to enhancement of the solvent penetrating action by colloidal silica (Fig. 9).

The release patterns of the tablets without cellulose acetate phthalate were characterized by a smooth convex curve without an inflection point. With talc and montmorillonite clay, similar enteric action of the tablets containing cellulose acetate phthalate was observed; however, some solvent penetration appeared at the lower concentrations of these additives. At the later stage (pH > 5.0), the release rate was more delayed compared to that of the additive-free tablets. This result might have been due to the fact that the drug was adsorbed firmly in the pores of the additives, forming a matrix-like structure.

From these results, it is concluded that the enteric-coating behavior of the tablets was more clearly demonstrated by using the flow-type simulator and a medium whose pH changed continuously than by studying dissolution and disintegration at constant pH values. By this technique, it also was possible to detect the pH above which the enteric action was overcome.

REFERENCES

(1) P. Speiser, H. P. Merkle, and L. Schibler, Ger. Offen. 2,233,428 (1973).

(2) Y. Kawashima and H. Takenaka, *J. Pharm. Sci.*, **63**, 1546 (1974).

(3) H. P. Merkle and P. Speiser, *ibid.*, **62**, 1445 (1973).

(4) K. Kawakita, *Zairyo*, **13**, 421 (1964).

(5) S. S. Yang and J. K. Guillory, *J. Pharm. Sci.*, **61**, 26 (1972).

(6) S. S. Yang, *Diss. Abstr.*, **30**, 585 B (1969).

(7) R. J. Mesley and E. E. Houghton, *J. Pharm. Pharmacol.*, **19**, 295 (1967).

(8) T. Higuchi, *J. Pharm. Sci.*, **52**, 1145 (1963).

(9) H. Takenaka, Y. Kawashima, and S. Y. Lin, *Chem. Pharm. Bull.*, **27**, 3054 (1979).

ACKNOWLEDGMENTS

The authors thank Prof. A. Otsuka, Meijyo University, Nagoya, Japan, for use of the X-ray diffractometer.

Potential of Organic Cation-Saturated Montmorillonite as Treatment for Poisoning by Weak Bases

JEFFREY E. BROWNE *, JOSEPH R. FELDKAMP ‡, JOE L. WHITE ‡, and STANLEY L. HEM *x

Received March 13, 1980, from the *Industrial and Physical Pharmacy Department and the ‡Department of Agronomy, Purdue University, West Lafayette, IN 47907. Accepted for publication May 21, 1980.

Abstract □ The preferential adsorption of the protonated form of weak bases by montmorillonite causes an increase in the pK_{eff} of atrazine. The effect on the acid–base equilibrium of atrazine is related to the exchangeable cation on the surface of montmorillonite. The greatest effect was produced by the presence of 3-hydroxypropylammonium-saturated montmorillonite, which caused the pK_{eff} of atrazine to increase 5.3 units to 6.9. This shift in pK_{eff} causes the protonated form of atrazine to be the predominate species in the pH range encountered in the GI tract and should result in a high degree of adsorption of atrazine. Fraction-bound studies confirmed this hypothesis by demonstrating virtually complete adsorption of atrazine by 3-hydroxypropylammonium-saturated montmorillonite up to pH 6. The fraction-bound studies also verified that protonated atrazine is adsorbed more completely by 3-hydroxypropylammonium-saturated montmorillonite than by bentonite USP or sodium-saturated montmorillonite. It is believed that saturation of the clay surface by an organic cation alters the surface environment of the clay, which results in enhanced adsorption of the protonated form of atrazine. The potential utility of montmorillonite saturated with an organic cation as an adsorbent for the emergency treatment of poisoning by weak bases is suggested.

Keyphrases □ Montmorillonite—saturation with organic cations for potential treatment of poisoning by weak bases □ Adsorbents—montmorillonite saturated with organic cations, potential treatment of poisoning by weak bases □ Poisoning—weak bases, potential treatment with organic cation-saturated montmorillonite

A major limitation in the use of clays as adsorbents in the treatment of poisoning is that their strongest adsorption mechanism is chemisorption of cations due to the negative charge of clays arising from isomorphous substitution (1). Clays such as montmorillonite have a high adsorptive capacity for cations but do not interact strongly with neutral molecules (2). Thus, weak bases, which constitute a large chemical class of potential poisons, are well adsorbed by montmorillonite if the pK is high so that the protonated form of the weak base is present in the pH range encountered in the GI tract. However, montmorillonite is a less effective adsorbent if the pK of the weak base is low since these weak bases then exist as neutral molecules in the GI tract.

It was observed recently that the first acid–base equilibrium of tetracycline was displaced in the presence of montmorillonite while the second and third acid–base equilibria were not altered (3). The presence of montmorillonite thus caused the protonated form of tetracycline to be present in a montmorillonite suspension over a wider pH range than occurs in an aqueous solution. As a result, adsorption of tetracycline by montmorillonite occurred over a wider pH range than was expected based on solution pK values. The nature of the exchangeable cation influenced the magnitude of the shift in the first acid–base equilibrium of tetracycline (4). For example, sodium-saturated montmorillonite caused a greater shift than did calcium-saturated montmorillonite.

It was hypothesized that montmorillonite that was specially treated to replace the naturally occurring inorganic cations with an organic exchangeable cation might have a desirable effect on the acid–base equilibrium of weak bases. 3-Hydroxypropylammonium hydrochloride was chosen as the organic cation because it is a cation in the pH range of interest and is relatively small.

Atrazine (2-chloro-4-ethylamino-6-isopropylamine-*s*-triazine) was chosen as a model weak base because it was expected to be neutral in the pH range of the GI tract due to its pK of 1.64 (5).

EXPERIMENTAL

Materials—Atrazine[1] and bentonite USP[2] were obtained commercially. Montmorillonite (Wyoming bentonite) was a reference standard[3]. The presence of organic matter in the bentonite USP sample was established by the peroxide method (6). Thirty milliliters of 30% H_2O_2 was added to 15 ml of a 1% clay suspension and heated in a steam bath for 15 min. The treated clay was centrifuged along with an untreated reference suspension. The presence of organic matter was indicated when the color of the sample sediment was significantly lighter than the reference sediment.

Metal-ion analysis by atomic absorption spectrometry[4] was used to identify the exchangeable cations in the bentonite USP, and X-ray diffraction[5] was used to identify the nonclay components.

Sodium-saturated montmorillonite was prepared by washing a 2% montmorillonite suspension with 1 *M* NaCl. The washing procedure was repeated five times, and excess salt was removed by repeated washing with water until the addition of silver nitrate to the supernate gave a negative chloride test.

Calcium-saturated montmorillonite was prepared in the same manner using 1 *M* $CaCl_2$ as the exchanging solution.

3-Hydroxypropylammonium-saturated montmorillonite was prepared similarly using a 1 *M* 3-hydroxypropylammonium hydrochloride solution as the exchanging solution.

To confirm that 3-hydroxypropylammonium was the exchangeable cation after the washing procedure, the following comparison was made. Since ammonium washing is commonly used to remove calcium from montmorillonite (7), the amount of calcium exchanged by washing calcium-saturated montmorillonite with 1 *M* ammonium acetate was compared to the amount of calcium replaced by washing an identical aliquot of calcium-saturated montmorillonite with 1 *M* 3-hydroxypropylammonium chloride. Two aliquots of a 2% calcium-saturated montmorillonite suspension were washed five times with either 1 *M* ammonium acetate or 1 *M* 3-hydroxypropylammonium chloride. Following centrifugation, the calcium content of the pooled supernate from all five washings was determined by atomic absorption spectrometry[4]. Complete exchange of calcium by 3-hydroxypropylammonium chloride was indicated by the recovery from three individually tested clay samples of 72.9 ± 2.5 mEq of Ca^{2+}/100 g following ammonium acetate washing and 69.8

[1] Ciba-Geigy Corp., Ardsley, N.Y.
[2] R. F. Revson and Co., New York, N.Y.
[3] Clay Mineral Repository, Department of Geology, University of Missouri, Colorado, Mo.
[4] Techtron 6, Varian Associates, Palo Alto, Calif.
[5] Siemens AG Kristalloflex 4 generator, type F diffractometer, Karlsruhe, West Germany.

0022-3549/80/1200-1393$01.00/0
© 1980, American Pharmaceutical Association

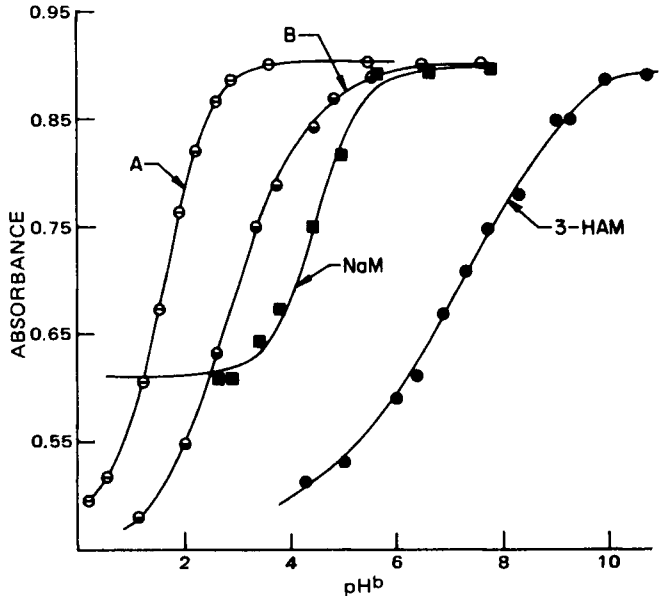

Figure 1—*Acid–base titration of atrazine in clay suspensions. Key: ⊖, aqueous solution; ⊖, bentonite USP; ■, sodium-saturated montmorillonite; and ●, 3-hydroxypropylammonium-saturated montmorillonite.*

± 3.1 mEq of Ca^{2+}/100 g following 3-hydroxypropylammonium chloride treatment.

UV Spectroscopic Titrations—Displacement of the pK of atrazine in clay suspensions was determined by spectroscopic titration. The pK_{eff} and the partial molar Gibbs free energy change upon addition of the clay, $\Delta\overline{G}_i$, for atrazine and atrazine–H^+ were calculated from the spectroscopic titration curve using the procedure of Feldkamp and White (8).

The UV spectra of the protonated and neutral forms of atrazine show the greatest difference in absorbance at 223 nm. Thus, titration curves were constructed by preparing a series of atrazine–clay suspensions containing 5 mg of atrazine and 200 mg of clay/liter at different pH^b (bulk pH) conditions and determining the absorbance at 223 nm.

Titration of atrazine in aqueous solution was done using the same procedure except that the clay was omitted.

Adsorption Studies—The fraction of atrazine bound by the clay at different pH^b conditions was determined using the samples from the spectroscopic titration experiment. A sample of each suspension was centrifuged, and 15 ml of supernate was collected. Sufficient hydrochloric acid was added to ensure that all of the atrazine was in the protonated form (pH^b = 0.5). The absorbance was measured at 223 nm.

The fraction of atrazine bound, f, was calculated from:

$$f = \frac{A_0 - (A_s - A_r)}{A_0} \qquad \text{(Eq. 1)}$$

where A_0 is the absorbance of an atrazine solution (5 mg/liter) containing only the protonated form of atrazine, A_s is the absorbance of the sample supernate, and A_r is the absorbance of the reference supernate.

RESULTS AND DISCUSSION

The effect of bentonite USP, sodium-saturated montmorillonite, and 3-hydroxypropylammonium-saturated montmorillonite on the acid–base equilibrium of atrazine is shown in Fig. 1. In aqueous solution, the pK of atrazine was found to be 1.64, which agrees with previously reported values (5).

In general, pK_{eff} and $\Delta\overline{G}_i$ depend on the composition of the system, *i.e.*, pH, ionic strength, temperature, pressure, other solutes, and concentration. Therefore, the reported values for pK_{eff} and $\Delta\overline{G}_i$ represent average values over the pH range of interest.

The presence of bentonite USP caused the titration curve of atrazine to shift to higher pH values, indicating that the protonated form of atrazine interacts with the clay to a greater extent than does the neutral form of atrazine. This interaction caused a shift in the apparent dissociation constant, pK_{eff}, of atrazine. The magnitude of the interaction of each species of atrazine with the clay can be characterized by $\Delta\overline{G}_i$ (8).

As seen in Table I, the apparent dissociation constant of atrazine increased from 1.64 to 2.80 in the presence of bentonite USP. The change in the partial molar Gibbs free energy of the protonated form of atrazine was −1.46 kcal/mole, indicating that this species of atrazine interacted with the clay. In contrast, virtually no interaction occurred between the neutral atrazine molecule and the clay since $\Delta\overline{G}_B$ was approximately zero.

Table I—Effect of Bentonite USP, Sodium-Saturated Montmorillonite, and 3-Hydroxypropylammonium-Saturated Montmorillonite on the Acid–Base Equilibrium of Atrazine

Sample	pK_{eff}	$\Delta\overline{G}_{BH^+}$, kcal/mole	$\Delta\overline{G}_B$, kcal/mole
Aqueous solution	1.64	—	—
Bentonite USP suspension	2.80	−1.46	~0
Sodium-saturated montmorillonite suspension	4.40	−3.61	~0
3-Hydroxypropylammonium-saturated montmorillonite	6.90	−7.21	~0

The acid–base equilibrium of atrazine was affected more strongly by sodium-saturated montmorillonite. The value of pK_{eff} increased by almost 3 units, reflecting the increased interaction of the protonated form of atrazine with the sodium-saturated montmorillonite (Table I).

Although bentonite USP is predominantly a sodium-saturated montmorillonite (9, 10), the effect of bentonite USP on the acid–base equilibrium of atrazine was not as great as that produced by sodium-saturated montmorillonite. The sample of bentonite USP contained sodium as the major exchangeable cation, although 7.1 and 2.7% of the exchange capacity was satisfied by calcium and magnesium ions, respectively. In addition, X-ray diffraction showed the presence of quartz, gypsum, and calcite, while the peroxide test indicated the presence of organic material.

Thus, the smaller effect of bentonite USP on the acid–base equilibrium of atrazine may be due to the screening effect of the divalent exchangeable

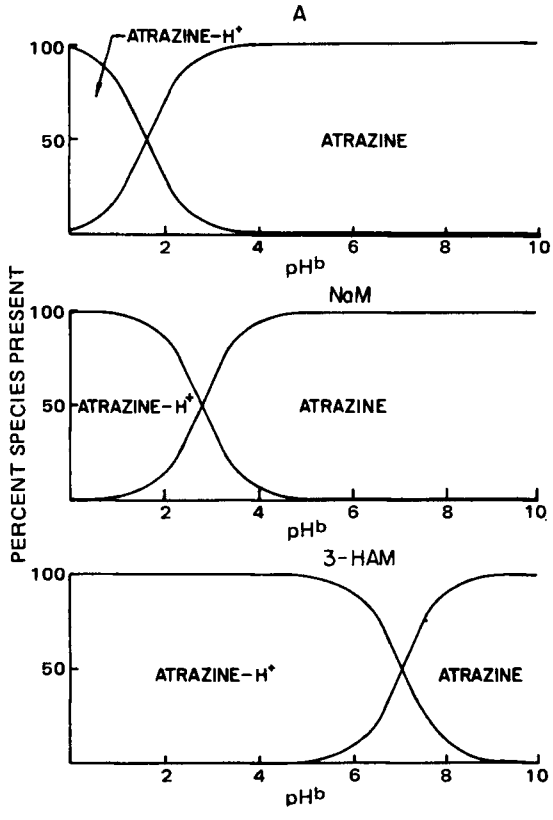

Figure 2—*Distribution of ionic species of atrazine in clay suspensions based on pK_{eff}. Key: A, aqueous solution; NaM, bentonite USP suspension; and 3-HAM, 3-hydroxypropylammonium-saturated montmorillonite.*

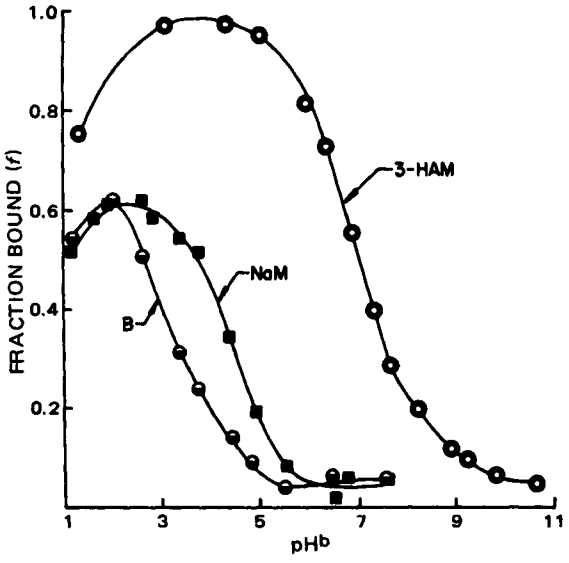

Figure 3—*Effect of pH^b on the fraction of atrazine bound, f, in clay suspensions. Key: ⊖, bentonite USP; ■, sodium-saturated montmorillonite; and ○, 3-hydroxypropylammonium-saturated montmorillonite.*

cations. It also is possible that the organic material in bentonite USP reduces the protonated atrazine–clay interaction. Similar findings were reported by Feldkamp (11), who observed a reduced ability of charged sites to interact with the protonated form of bases in soils containing organic matter.

The presence of 3-hydroxypropylammonium-saturated montmorillonite produced the greatest effect on the acid–base equilibrium of atrazine. The pK_{eff} of atrazine in a 3-hydroxypropylammonium-saturated montmorillonite suspension was 6.9, an increase of more than 5 units in comparison to the pK of atrazine. This shift was caused by the strong interaction of the protonated form of atrazine with the 3-hydroxylpropylammonium-saturated montmorillonite, as evidenced by the magnitude of $\Delta\bar{G}_{BH^+}$ and the virtual absence of any interaction of atrazine with the specially treated clay (Table I).

The interaction of atrazine with the clay surfaces caused a substantial shift in pK_{eff}, which resulted in an altered distribution of the protonated and neutral forms of atrazine. Figure 2 demonstrates the dramatic shift in the pH region in which the protonated form of atrazine predominated due to the presence of 3-hydroxypropylammonium-saturated montmorillonite.

The changes in the acid–base equilibrium of atrazine in the presence of bentonite USP, sodium-saturated montmorillonite, or 3-hydroxypropylammonium-saturated montmorillonite resulted in dramatic changes in the adsorption profile of atrazine (Fig. 3). Bentonite USP and sodium-saturated montmorillonite both adsorbed ~60% of the atrazine, although the maximum adsorption occurred at a higher pH^b (2.6) for sodium-saturated montmorillonite than for bentonite USP (2.0). The fraction of atrazine bound by 3-hydroxypropylammonium-saturated montmorillonite approached 100% at pH^b values up to 5.

The pH^b of maximum adsorption of atrazine reflects the pK_{eff} of atrazine in the presence of each clay. At low pH^b conditions, both protons and protonated atrazine cations compete for the negatively charged sites on the clay surface. The pH^b of maximum adsorption occurs when the interaction of protonated atrazine with the clay surface predominates. At pH^b conditions favoring the formulation of the neutral atrazine species based on pK_{eff}, the fraction bound curves decreased. Virtually no adsorption occurred at higher pH^b conditions, where the unionized atrazine would predominate. This observation confirms that $\Delta\bar{G}_B$ is virtually zero as reported in Table I.

The fraction-bound study also suggests that saturation of montmorillonite with an organic cation such as 3-hydroxypropylammonium increases the interaction between the protonated form of atrazine and the clay. It is believed that the 3-hydroxypropylammonium cation induced a highly diffuse, electrical double layer at the surface of montmorillonite. Thus, 3-hydroxypropylammonium was less effective than sodium in countering the negative surface charge of montmorillonite.

A number of factors may be responsible for this effect. The distribution of the electrostatic charge on the organic cation might render it less effective than sodium in satisfying the surface charge. Geometric considerations also may prevent effective balancing of the surface charge by the organic cation.

It is not surprising that the protonated form of atrazine was able to replace the exchangeable cations in montmorillonite since large organic cations are adsorbed by van der Waals forces in addition to electrostatic forces (1). Hendricks (12) reported that large organic cations adsorbed by montmorillonite were nearly impossible to replace by smaller cations.

In addition to the formation of a highly diffuse, electrical double layer, the strong interaction of atrazine with 3-hydroxypropylammonium-saturated montmorillonite may be enhanced by a surface environment that is highly compatible with protonated atrazine. This is possible if the exchangeable organic cation induces a structured environment at the clay surface in which the polarity of the surface phase is similar to the polarity of protonated atrazine. As a consequence, protonated atrazine will exhibit a greater preference for the clay phase than for the solution phase.

Surface modification of montmorillonite through organic cation saturation may have an important therapeutic application in the treatment of poisoning. For weak bases with low pK values, the uncharged base should exist throughout the small intestine where systemic absorption is most likely. Conventional clay adsorbents such as bentonite USP do not strongly interact with neutral molecules and, therefore, are not effective in treating poisoning by weak bases. However, when montmorillonite is saturated with an organic cation such as 3-hydroxypropylammonium, the fraction of weak base bound and the pH^b range over which adsorption takes place should be greatly increased. Evaluation of the toxicity of small organic cations that may serve as exchangeable cations in montmorillonite may lead to the development of organic cation-saturated montmorillonite, which may prove valuable in the treatment of poisoning by weak bases.

REFERENCES

(1) J. L. White, *ACS Symp. Ser.*, **29**, 208 (1976).

(2) L. S. Porubcan, G. S. Born, J. L. White, and S. L. Hem, *J. Pharm. Sci.*, **68**, 358 (1979).

(3) J. E. Browne, J. R. Feldkamp, J. L. White, and S. L. Hem, *ibid.*, **69**, 811 (1980).

(4) *Ibid.*, **69**, 816 (1980).

(5) J. B. Weber, *Spectrochim. Acta*, **23A**, 458 (1967).

(6) M. L. Jackson, "Soil Chemical Analysis Advanced Course," Department of Soils, University of Wisconsin, Madison, Wis., 1956, p. 35.

(7) M. L. Jackson, "Soil Chemistry Analysis," Prentice-Hall, Englewood Cliffs, N.J., 1958, p. 461.

(8) J. R. Feldkamp and J. L. White, *J. Colloid Interface Sci.*, **69**, 97 (1979).

(9) M. Barr, *J. Am. Pharm. Assoc.*, **NS4**, 4 (1964).

(10) "United States Dispensatory," 27th ed., Lippincott, Philadelphia, Pa., 1973, p. 182.

(11) J. R. Feldkamp, Ph.D. thesis, Purdue University, West Lafayette, Ind., 1978.

(12) S. B. Hendricks, *J. Phys. Chem.*, **45**, 65 (1941).

ACKNOWLEDGMENTS

Supported in part by an American Foundation for Pharmaceutical Education Fellowship to J. E. Browne.

This report is Journal Paper 8074, Purdue University Agricultural Experiment Station, West Lafayette, IN 47907.

Comparison of Two High-Pressure Liquid Chromatographic Assays for Carboprost, a Synthetic Prostaglandin

LEO W. BROWN and BRUCE E. CARPENTER ˣ

Received January 17, 1980, from *Control Research and Development, The Upjohn Company, Kalamazoo, MI 49002.* Accepted for publication June 25, 1980.

Abstract □ A high-pressure liquid chromatographic assay for carboprost tromethamine as the bulk drug and in a sterile solution formulation is described. The procedure involves derivatization of the prostaglandin to form the UV-absorbing naphthacyl ester, which then is chromatographed on a silica gel column using methylene chloride–1,3-butanediol–water (496:4:0.25) as the mobile phase. This procedure is compared with a nonderivatization procedure with refractive index detection. Both procedures separate the 15*R*-epimer of carboprost from carboprost, but only the derivatization procedure separates the 5-*trans*-isomer of carboprost. Possible reasons for the better separation using the derivatization procedure are discussed. Both procedures gave a coefficient of variation of ~1% for carboprost. The derivatization procedure gave a coefficient of variation of ~7% for the 15*R*-epimer and 5-*trans*-isomer when present at 2% of the carboprost level.

Keyphrases □ Carboprost—comparison of high-pressure liquid chromatographic assays with and without derivatization □ High-pressure liquid chromatography—analysis, carboprost, comparison of procedures with and without derivatization □ Prostaglandins—carboprost, high-pressure liquid chromatographic analysis, comparison of procedures with and without derivatization

Several reviews of prostaglandins have been published. Oesterling *et al.* (1) reviewed the nomenclature, chemistry, stability, analytical methods, metabolism, and biology of many prostaglandins. Analytical methods have been developed for the assay of prostaglandins in biological matrixes using GLC, radioimmunoassay, and GLC–mass spectrometry. Liquid chromatography has been used to separate prostaglandins of similar structures (2–4).

The high-pressure liquid chromatographic (HPLC) assays presented here were developed for carboprost [(15*S*)-15-methyldinoprost, I] and its possible impurities or degradation products in bulk drug and pharmaceutical formulations. A similar prostaglandin, dinoprost (II), was used as the internal standard in the nonderivatization procedure.

Carboprost and dinoprost are present initially as their tromethamine salts. The free acids are formed during extraction.

EXPERIMENTAL

Nonderivatization Assay—*HPLC Conditions*—A high-pressure liquid chromatograph[1] was used with a differential refractometer detector[2]. Two 3.9-mm × 30-cm microparticulate silica gel columns[3] were used in series. The flow rate of the mobile phase was maintained at 1 ml/min, and a 25-μl injection volume was used with a loop injector[4]. The chart speed was 0.64 cm/min, and attenuation of the refractive index detector was set at 9.6×10^{-5} unit full scale. The mobile phase was acetonitrile–methanol–acetic acid (96:3:1).

Internal Standard Solution—An aqueous solution containing ~3.4 mg of dinoprost tromethamine/ml was prepared.

Bulk Drug Carboprost Tromethamine Reference Preparation—To a separator were added ~3.3 mg of carboprost tromethamine reference standard, accurately weighed, 1.0 ml of the internal standard solution, and 0.5 g of boric acid. The mixture was swirled to dissolve the boric acid partially, and the carboprost free acid and the internal standard were extracted from the aqueous layer using two 5-ml portions of chloroform. The chloroform extracts were combined and evaporated to dryness with a nitrogen stream.

Carboprost Tromethamine Sterile Solution Reference Preparation—Ten milliliters of 0.9% benzyl alcohol[5] in water was added to a separator, followed by the same additions as used for the reference preparation of bulk drug carboprost tromethamine.

Bulk Drug Sample Preparation—The same procedure as that for the reference preparation was used, substituting the bulk drug sample for the carboprost tromethamine reference.

Carboprost Tromethamine Sterile Solution Sample Preparation—Ten milliliters of sterile solution (0.25 mg carboprost equivalents/ml) was added to a separator, followed by 0.5 g of boric acid and 1.0 ml of the internal standard solution. Carboprost and the internal standard were extracted from the aqueous layer using two 5-ml portions of chloroform. The extracts were combined and evaporated to dryness with a nitrogen stream.

Procedure—To the residues of both the reference and the sample was added 0.5 ml of the mobile phase. The vials were swirled to dissolve the residue and chromatographed using the described HPLC conditions.

Derivatization Assay—*HPLC Conditions*—A high-pressure liquid chromatograph[1] was used with a UV detector[6] at 254 nm. A single 3.9-mm × 30-cm microparticulate silica gel column[3] was used. The flow rate was maintained at ~1.8 ml/min, and a 10-μl injection volume was used with a loop injector[4]. The recorder chart speed was 0.64 cm/min, and attenuation on the UV detector was set at 0.08 aufs. The mobile phase was methylene chloride–1,3-butanediol–water (496:3.5:0.25).

Internal Standard Solution—A mobile phase solution containing ~3 or 7 mg of guaifenesin/ml was prepared for the assay of carboprost sterile solution (0.25 mg/ml) or the bulk drug, respectively.

Derivatization Reagents—An acetonitrile solution containing 20 mg of α-bromo-2-acetonaphthone[7] or 10 μl of diisopropylethylamine[8]/ml was used.

Bulk Drug Reference Preparation—Approximately 5.0 mg of carboprost tromethamine reference was weighed accurately and transferred to a stoppered 35-ml centrifuge tube.

Sterile Solution Reference Preparation—A solution containing ~0.332 mg of carboprost tromethamine reference/ml in water and 9 mg of benzyl alcohol[5]/ml was accurately prepared.

Bulk Drug Sample Preparation—Approximately 5 mg of the carboprost tromethamine sample was weighed accurately and transferred to a 35-ml centrifuge tube.

Sterile Solution Sample Preparation—The solution (0.25 mg of carboprost equivalent/ml) was used without dilution.

Procedure—For bulk drug, 20.0 ml of methylene chloride and 2.0 ml of citrate buffer (0.5 *M*, pH 4.0) were added to the sample and reference tubes. After the tubes were shaken for 10 min and centrifuged, the top aqueous layer was discarded. A 4.0-ml aliquot of the methylene chloride layer was transferred to a small vial and evaporated to dryness. Eighty microliters of the α-bromo-2-acetonaphthone solution was added, followed by 60 μl of the diisopropylethylamine solution. The vials were swirled to dissolve the residue and allowed to stand for 1 hr or heated at 30–35° for 15 min. Then the solutions were evaporated to dryness, and 2.0 ml of the internal standard was added. After mixing, the solutions

[1] DuPont model 830.
[2] Waters model R-401.
[3] Waters Micro-Porasil.
[4] Valco.
[5] The benzyl alcohol was added to provide similar extraction conditions for the reference and samples.
[6] Component of DuPont model 830 liquid chromatograph.
[7] Aldrich Chemical Co. The derivation effectiveness of this reagent varied from lot to lot. A satisfactory reagent was obtained by hot filtration through activated charcoal using carbon tetrachloride, followed by recrystallization.
[8] Aldrich Chemical Co.

0022-3549/80/1200-1396$01.00/0
© 1980, American Pharmaceutical Association

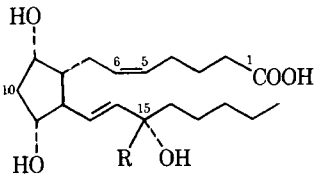

I: R = CH_3
II: R = H

were chromatographed within 24 hr of derivatization using the described HPLC conditions. The standard and sample preparations were protected from light, because light was shown to cause degradation of the naphthacyl ester of carboprost.

For the sterile solution, 2.0 ml of the sample solution and 2.0 ml of the reference solution were added to separate stoppered 35-ml centrifuge tubes. To each tube were added 20.0 ml of methylene chloride and 1.0 ml of citrate buffer. The tubes were shaken for 10 min and centrifuged. The top aqueous layer was discarded, and an 8.0-ml aliquot of the methylene chloride layer was transferred to a small vial and evaporated using a nitrogen stream (complete evaporation was not obtained due to the presence of benzyl alcohol extracted from the aqueous solution). Forty microliters of α-bromo-2-acetonaphthone solution was added, followed by 30 μl of diisopropylethylamine solution. After swirling to mix and dissolve the residue, the solution was allowed to stand for 1 hr or heated at 30–35° for 15 min. The acetonitrile then was evaporated, and 1.0 ml of the internal standard solution was added. After mixing, the solutions were chromatographed within 24 hr of derivatization using the described HPLC conditions. Standard and sample preparations were protected from light, because light was shown to cause degradation of the naphthacyl ester of carboprost.

Table I—Comparison of Extent of Reaction Completeness for Carboprost Tromethamine and Carboprost Free Acid after 1 hr

Sample Weight, mg	Peak Height Ratio	Ratio/ Weight
	Carboprost Tromethamine	
0.2720	0.6961	2.559
0.2720	0.8815	3.241
0.2720	0.7379	2.713
Mean		2.838
CV, %		12.6
	Carboprost Free Acid	
0.1991	0.9455	4.749
0.2079	0.9926	4.774
0.2297	1.0826	4.713
Mean		4.745
CV, %		0.6

Table II—Reaction of Carboprost with α-Bromo-2′-acetonaphthone Solution Containing Diisopropylethylamine at Several Time Intervals

Minutes	Sample Weight, mg	Peak Height Ratio	Ratio/ Weight
25	0.2614	1.1989	4.586
40	0.2614	1.2787	4.892
60	0.2614	1.2945	4.952
81	0.2614	1.2988	4.969
105	0.2614	1.3039	4.988
150	0.2614	1.3132	5.024

Table III—Precision in the Assay of Carboprost Bulk Drug

Sample Weight, mg	Peak Height Ratio	Ratio/ Weight
	Derivatization Procedure	
2.585	1.601	0.619
2.834	1.766	0.623
2.613	1.648	0.631
2.522	1.567	0.621
2.523	1.596	0.633
Average		0.625
CV, %		0.9
	Nonderivatization Procedure	
3.467	1.567	0.452
3.464	1.571	0.454
3.181	1.452	0.457
3.533	1.592	0.451
3.460	1.588	0.459
3.166	1.453	0.459
Average		0.455
CV, %		0.8

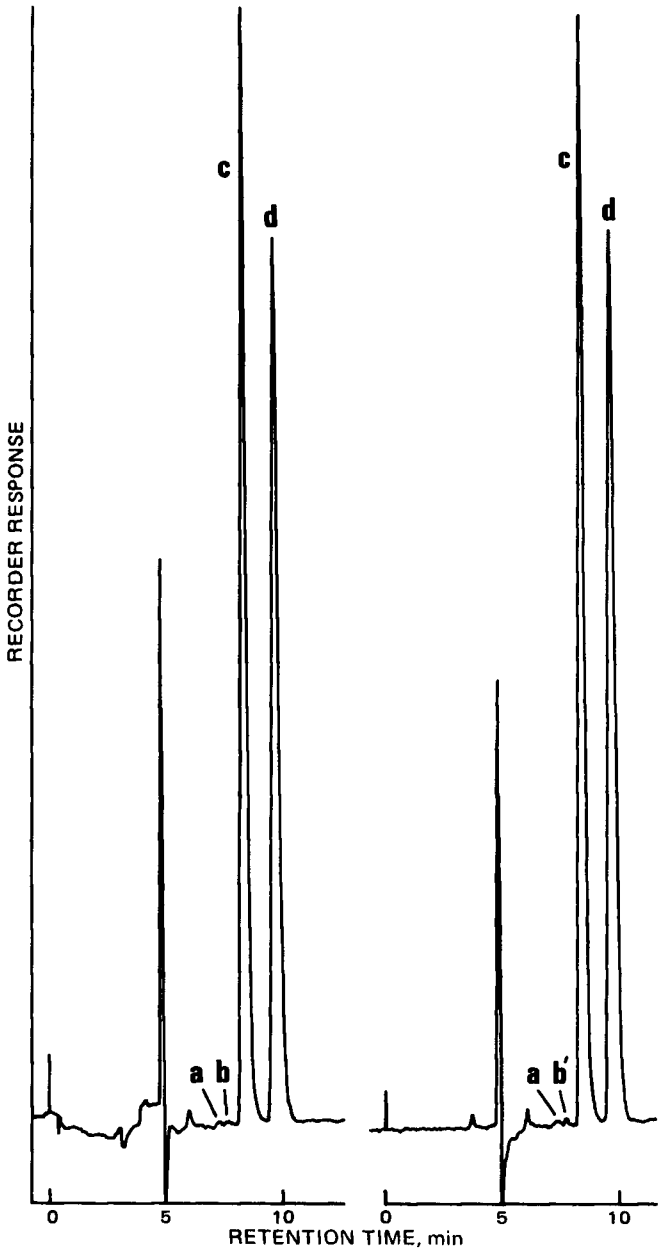

Figure 1—*Chromatograms of the 15R-epimer of dinoprost (a), the 15R-epimer of carboprost at 0.5% (b), the 15R-epimer of carboprost at 1.0% (b′), carboprost (c), and dinoprost (internal standard) (d) using the nonderivatization HPLC procedure with refractive index detection.*

Calculations—For the bulk drug:

$$\% \text{ purity of carboprost tromethamine} = \frac{R_s}{R_{ref}} \times \frac{W_{ref}}{W_s} \times P \quad \text{(Eq. 1)}$$

where R_s is the peak height ratio of the carboprost peak to the internal standard peak in the sample preparation; R_{ref} is the peak height ratio of the carboprost peak to the internal standard peak in the reference preparation; W_{ref} is the weight, in milligrams, of carboprost tromethamine

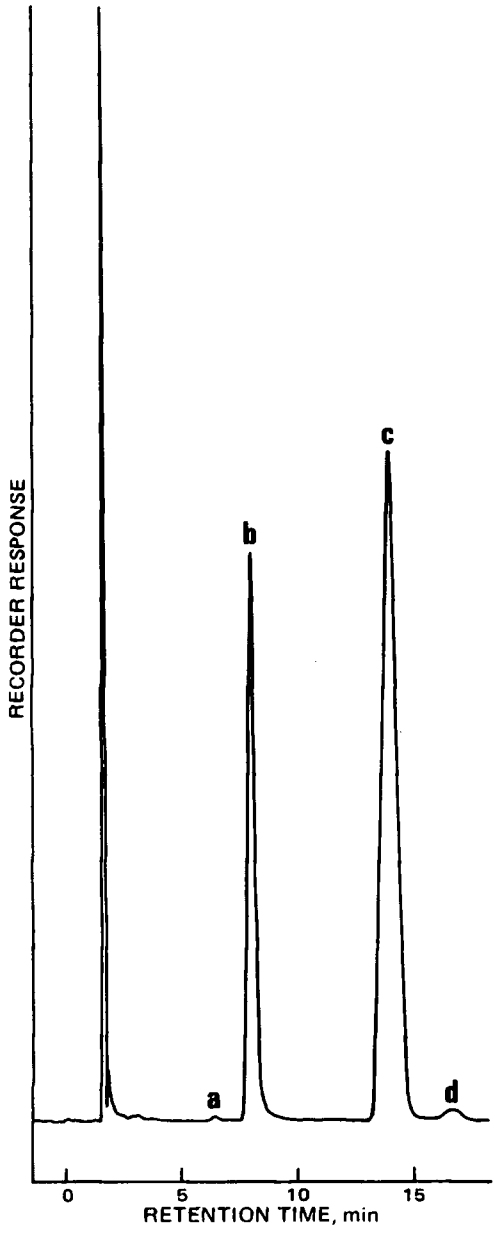

Figure 2—*Chromatogram of guaifenesin impurity (a), guaifenesin (internal standard) (b), 2-naphthacyl carboprost (c), and the 2-naphthacyl 5-*trans*-isomer of carboprost (d) using the derivatization procedure with UV detection.*

amine reference standard; W_s is the weight, in milligrams, of sample; and P is the purity of the carboprost tromethamine reference expressed in percent.

For the sterile solution:

$$\text{mg of carboprost/ml of sterile solution} = \frac{R_s}{R_{\text{ref}}} \times \frac{W_{\text{ref}}}{V_s} \times F_c \times P \qquad \text{(Eq. 2)}$$

where R_s is the peak height ratio of the carboprost peak to the internal standard peak in the sample preparation; R_{ref} is the peak height ratio of the carboprost peak to the internal standard peak in the reference preparation; W_{ref} is the weight, in milligrams, of carboprost tromethamine reference standard used in the procedure; V_s is the volume, in milliliters, of sample; F_c is the factor to convert carboprost tromethamine (mol. wt. 489.65) to carboprost (mol. wt. 368.50) = 0.7526; and P is the purity of the carboprost tromethamine reference expressed as a decimal.

For the impurities:

$$\% \text{ impurity} = \frac{A_a \text{ or } A_c}{A_a + A_b + A_c} \times 100 \qquad \text{(Eq. 3)}$$

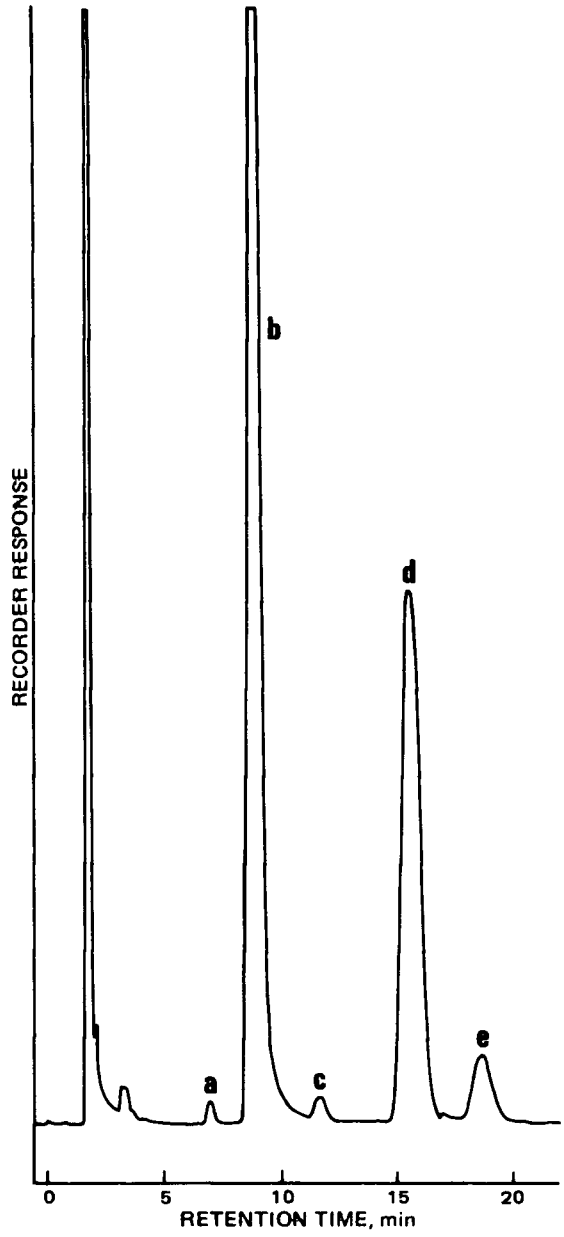

Figure 3—*Chromatogram of a guaifenesin impurity (a), guaifenesin (internal standard) (b), 2-naphthacyl 15*R*-epimer of carboprost at 0.5% (c), 2-naphthacyl carboprost at an attenuation four times that of the other peaks (d), and 2-naphthacyl 5-*trans*-isomer of carboprost at 2.3% (e) using the derivatization procedure with UV detection.*

or:

$$\% \text{ impurity} = \frac{F_aH_a \text{ or } F_cH_c}{F_aH_a + H_b + F_cH_c} \times 100 \qquad \text{(Eq. 4)}$$

where A_a is the area of the 15*R*-epimer peak, A_b is the area of the carboprost peak, A_c is the area of the 5-*trans*-isomer peak, F_a is the factor to normalize the 15*R*-epimer peak height (0.78), F_c is the factor to normalize the 5-*trans*-isomer peak height (1.12), H_a is the peak height of the 15*R*-epimer peak, H_b is the height of the carboprost peak, and H_c is the height of the 5-*trans*-isomer peak.

RESULTS AND DISCUSSION

Both assay procedures (derivatization and nonderivatization) involve extraction of the prostaglandin as the free acid from an acidified aqueous solvent into an organic solvent. This extraction is tailored for the assay of dilute sterile solutions of the prostaglandin in which a concentration step is necessary when using the nonderivatization procedure. Furthermore, the derivatization reaction proceeds much more rapidly with the

Table IV—Assay Results by the Derivatization Procedure of Replicate Samples of the 15*R*-Epimer and 5-*trans*-Isomer in Carboprost Bulk Drug at Concentration Levels of 1.7 and 2.3%

	15*R*-Epimer Content, %	5-*trans*-Isomer Content, %
	1.6	2.4
	1.9	2.5
	1.6	2.6
	1.7	2.4
	1.5	2.3
	1.6	2.0
	1.7	2.4
	1.7	2.4
Average	1.7	2.4
CV, %	7.1	7.4

free acid than with the tromethamine salt (Table I). After 1 hr, the tromethamine salt samples exhibit a low mean ratio and a high variation between samples, while the free acid samples exhibit a high mean ratio and little variation between samples. The derivatization reaction for the free acid is essentially complete after 1 hr (Table II).

Recovery studies showed that the extraction procedure produced nearly complete recovery (~96%) of the prostaglandin. To eliminate possible bias, the reference is carried through the complete procedure along with the sample to be assayed. Replicate samples assayed by either method gave a relative standard deviation of <1% (Table III).

Chromatograms of carboprost (nonderivatization procedure) are shown in Fig. 1; authentic samples of the 15*R*-epimer of carboprost had been added at concentrations of ~0.5 and 1.0% of the carboprost concentration. The epimer peak is baseline separated from the carboprost peak, making the assay satisfactory for stability studies (carboprost degrades to the 15*R*-epimer under acidic conditions). The small peak on the front side of the 15*R*-epimer is the 15*R*-epimer of dinoprost, which was used as the internal standard.

To obtain greater sensitivity for the assay of the 15*R*-epimer in carboprost samples, the derivatization procedure was developed. Formation of the 2-naphthacyl ester has been used for fatty acids (5) and is similar to *p*-nitrophenacyl derivatization of prostaglandins (4). The 2-naphthacyl ester of carboprost was found to exhibit greater absorptivity than the *p*-nitrophenacyl ester at 254 nm with the UV detector. A chromatogram of 2-naphthacyl carboprost using guaifenesin as the internal standard is shown in Fig. 2.

In comparing the nonderivatization and derivatization methods, it is evident that derivatization produced better chromatography. The 15*R*-epimer is better separated, and another impurity, the 5-*trans*-isomer of carboprost, is baseline separated from carboprost. Although the nonderivatization procedure is less time consuming because of the absence of a derivatization step, it is not satisfactory if the 5-*trans*-isomer is present in the carboprost sample. Although several mobile phases were tried, the 5-*trans*-isomer could not be separated from carboprost using the nonderivatization procedure, even with two silica columns in series. With the derivatization procedure, greater separation than is shown in Fig. 2 can be achieved by decreasing the relative concentration of 1,3-butanediol in the mobile phase. This is a definite advantage of the derivatization procedure.

Increased liquid chromatographic separation of the 15-position epimers of carboprost is observed with the derivatization procedure, probably because of the reduced polarity of the carboxyl group by naphthacyl ester formation. The presence of the highly polar carboxyl group masks subtle polarity differences due to the position of the hydroxyl groups in the isomers. Thus, the blocking of the carboxyl group maximizes the effect of the hydroxyl groups, and the polarity differences between the 15-position epimers become more significant.

Figure 3 shows a chromatogram (derivatization procedure) of carboprost with the 15*R*-epimer added. In the absence of reference samples to quantitate the impurities by peak height percent, the 15*R*-epimer and 5-*trans*-isomer peak heights must be multiplied by response factors of 0.78 and 1.12, respectively. The response factors were required to normalize peak height differences due to retention times. These factors were determined using authentic samples. Since the UV chromophore in each compound is the naphthacyl ester, carboprost and the two impurities should have the same absorptivity. By measuring peak area instead of peak height, response factors were not needed. Results by peak area percent showed good agreement with carboprost samples spiked with impurities at known concentrations. Assay results of replicate samples of the 15*R*-epimer at a concentration of 1.7% and of the 5-*trans*-isomer at a concentration of 2.3% in carboprost bulk drug are shown in Table IV. A coefficient of variation of ~7% was obtained for both impurities by peak area percent at 2% of the carboprost concentration.

Light caused degradation of the naphthacyl ester of carboprost. When derivatized samples were placed near a light source, a noticeable increase in the peak corresponding to the 5-*trans*-isomer was observed. No significant change was observed in derivatized samples protected from light for 24 hr. The peak height ratios of carboprost to the internal standard and of the 5-*trans*-isomer to carboprost showed no significant changes. The degradation in light may be due to the chromophore. Acetophenone and several similar compounds have been shown to act as photosensitizers for *cis–trans*-isomerization (6).

REFERENCES

(1) T. O. Oesterling, W. Morozowich, and T. J. Roseman, *J. Pharm. Sci.*, **61**, 1861 (1972).

(2) R. K. Lustgarten, *ibid.*, **65**, 1533 (1976).

(3) N. H. Andersen and E. M. K. Leovey, *Prostaglandins*, **6**, 361 (1974).

(4) W. Morozowich and S. L. Douglas, *ibid.*, **10**, 19 (1975).

(5) M. J. Cooper and M. W. Anders, *Anal. Chem.*, **46**, 1849 (1974).

(6) C. Moussebois and J. Dale, *J. Chem. Soc. C*, **1966**, 260.

Comparative Pharmacokinetics of Quinidine and Its *O*-Desmethyl Metabolite in Rabbits

CLARENCE T. UEDA [x] **and JEANNETTA G. NICKOLS**

Received March 4, 1980, from the *Department of Pharmaceutics, College of Pharmacy, and the Cardiovascular Center, University of Nebraska Medical Center, Omaha, NE 68105.* Accepted for publication June 9, 1980.

Abstract □ The pharmacokinetics of quinidine and the *O*-desmethyl metabolite 6′-hydroxycinchonine were studied in rabbits. After intravenous bolus injections of equimolar doses, the blood concentration–time curves of each agent declined biexponentially, which was characteristic of a two-compartment open model. A significant difference between quinidine and 6′-hydroxycinchonine was observed for the following parameters: $t_{1/2\alpha}$, β, $t_{1/2\beta}$, k_{12}, Vd_β, and the intercompartmental distribution ratio, k_{12}/k_{21}. The results showed that the distribution of the metabolite was slower than quinidine and suggested that it *also* was less extensive. The Vd_β value for 6′-hydroxycinchonine was approximately one-half of the value observed for quinidine, and its k_{12}/k_{21} ratio was about one-fourth of the quinidine value. The terminal half-lives for quinidine and the metabolite were 132.4 ± 27.1 and 65.4 ± 34.4 min, respectively. Total body clearance was similar for both compounds. The findings of this study could be explained by the greater polarity or greater water solubility of 6′-hydroxycinchonine. The limited data in humans coupled with the results of this investigation suggest that, although it is intrinsically active, the *O*-demethylated metabolite probably contributes little to the antiarrhythmic effects seen after quinidine administration in humans.

Keyphrases □ Quinidine—and its *O*-desmethyl metabolite, comparison of pharmacokinetics in rabbits □ Pharmacokinetics—comparison of quinidine and its *O*-desmethyl metabolite, rabbits □ Antiarrhythmic agents—quinidine and its *O*-desmethyl metabolite, pharmacokinetics, rabbits

6′-Hydroxycinchonine (*O*-desmethylquinidine, V) is a newly reported metabolite of quinidine (I) (1, 2). Nwangwu *et al.* (3, 4) reported that the antiarrhythmic potency of V was equivalent to that of I when tested against aconitine-induced arrhythmias in mice. They also suggested that V was less toxic than I. Drayer *et al.* (1, 2) showed that V possessed ~60% of the antiarrhythmic activity exhibited by quinidine using a chloroform- and hypoxia-induced ventricular fibrillation animal model.

Quinidine metabolites such as 2′-oxoquinidinone (IV), 3-hydroxyquinidine (III), and V are believed to contribute to the antiarrhythmic effects seen after the administration of I in humans[1] (5), but they have not been tested directly for such activity.

The purpose of this study was to investigate the comparative pharmacokinetics of I and V in rabbits. This information could provide important insight into the behavior of this metabolite relative to quinidine in humans.

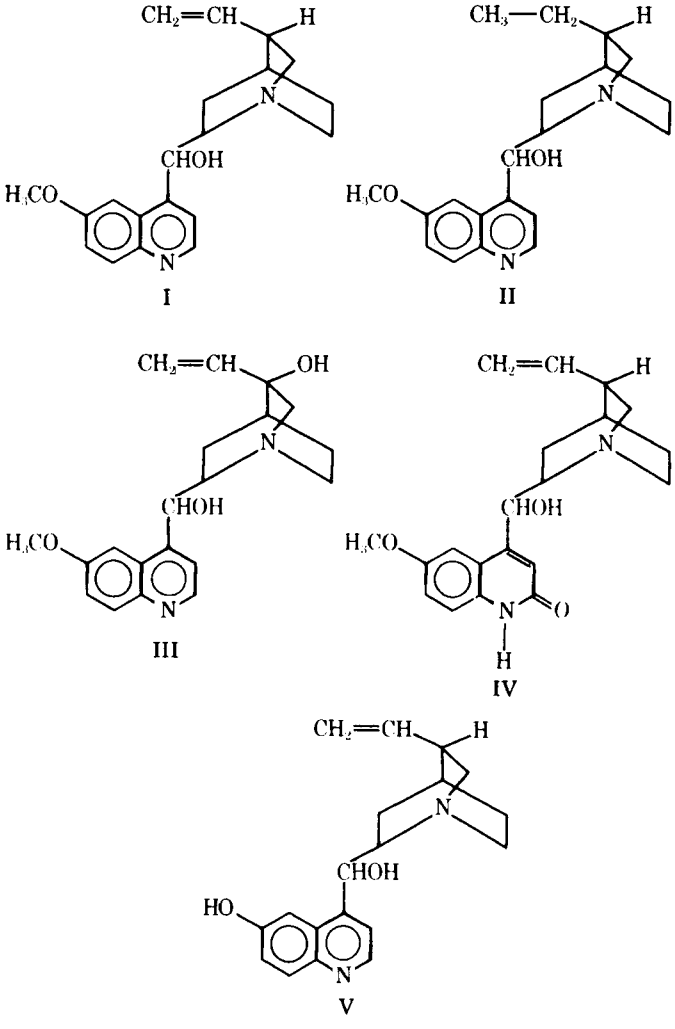

EXPERIMENTAL

Materials—Restrained, male New Zealand White rabbits[2], 4–5 kg, were used.

Quinidine base, free of the dihydro analog (II), was obtained as described previously (6) and was used to prepare a parenteral solution of quinidine sulfate containing 20 mg (0.062 mmole) of quinidine base/ml of solution. An injectable solution containing 19.14 mg (0.062 mmole) of V[3]/ml was prepared fresh from the dihydrochloride salt just before individual experiments. Chromatographic analysis of V revealed 8% of a substance that was presumed to be its dihydro derivative since this material also was prepared from commercial quinidine sulfate powder[4]. Because it did not interfere with the assay for V, no attempt was made to remove this minor impurity.

Methods—To give the intravenous bolus injections and to withdraw blood samples for drug and metabolite analysis, a 25-gauge vein infusion set with a winged adapter[5] was placed in a marginal ear vein and secured to the external ear with adhesive tape. After a control blood specimen was obtained, 1 ml of drug solution was given as an intravenous bolus dose. Complete administration of each dose was achieved by flushing the contents of the infusion set with ~0.8 ml of heparinized normal saline (5 units/ml). Blood specimens of 0.5 ml for the analysis of I and V were collected in heparinized tubes[6] at 5, 10, 15, 30, 45, and 60 min and thereafter at 0.5-hr intervals for up to 3–4 hr after the dose. The blood samples were stored at −20° until they were assayed.

Blood concentrations of V were determined by the following high-

[1] B. S. Dzindzio, W. M. Vosik, and C. T. Ueda, unpublished data.
[2] Earl B. Daubert, Breeding and Laboratory Rabbits, Omaha, Neb.
[3] Prepared by Dr. Laverne D. Small.
[4] Sigma Chemical Co., St. Louis, Mo.
[5] Miniset 2C0075, Travenol Laboratories, Deerfield, Ill.
[6] Becton-Dickinson, Rutherford, N.J.

0022-3549/80/1200-1400$01.00/0
© 1980, American Pharmaceutical Association

performance liquid chromatographic procedure. After the previously frozen samples were thawed, 0.5 ml of whole blood was diluted in a 15-ml culture tube with 0.5 ml of distilled water and 0.5 ml of 0.2 *M* phosphate buffer (pH 7.4), containing 40 ng of dihydroquinidine (II) as the internal standard. Following the addition of 100 μl of 95% ethanol to this mixture, the sample was vortexed[7] and extracted with 4 ml of benzene by shaking for 2 hr on a reciprocating shaker[8] at room temperature.

The benzene extract was separated by centrifugation, and the upper organic layer was carefully removed by pipet and transferred to a 5-ml conical tube. The benzene extract, to which was added 100 μl of absolute alcohol, then was evaporated to dryness at room temperature under a nitrogen stream. The residue was reconstituted with 25 μl of the mobile phase, and an aliquot was injected into a preconditioned liquid chromatograph.

The concentrations of V in the unknown samples were determined from standard calibration curves prepared with the experimental specimens. In the concentration range of 0.5–10 μg/ml for V, the peak height ratio of V to the internal standard was linearly related to the metabolite concentration. The best-fitting equations for the standard curves were obtained by linear regression analysis.

The liquid chromatograph[9] was equipped with a loop injector[10], a μBondapak C_{18} reversed-phase column[11] (30 cm × 3.9 mm i.d.), and a fluorescence detector[12]. The mobile phase, which was filtered and degassed before use, consisted of 15% (v/v) acetonitrile[13] in a 2.5% (v/v) solution of acetic acid and was pumped at a flow rate of 2 ml/min (about 1800 psi). The column eluate was monitored with an excitation wavelength of 315 nm and a KV 418 emission cutoff filter. The detector sensitivity setting was 0.5–1.0 μamp full scale with a time constant set at 4 sec and a chart speed[14] of 0.5 cm/min.

As shown in Fig. 1, with the chromatographic conditions used, V and the internal standard (II) were readily separable with elution times of ~2 and 4 min, respectively. The minor impurity, presumed to be the dihydro analog of V, eluted about midway between the metabolite and internal standard peaks. Peak c in Fig. 1 was an unknown benzene-extractable substance in rabbit blood.

Blood quinidine concentrations were determined with the TLC–fluorometric procedure described previously (7).

After the quinidine and V bolus doses, the blood concentration–time curves for both agents declined biexponentially (Fig. 2). Therefore, the data were fitted using the least-squares computer program NONLIN (8) and a digital computer to:

$$C_b = Ae^{-\alpha t} + Be^{-\beta t} \qquad \text{(Eq. 1)}$$

where C_b is the concentration of alkaloid in the blood at time t, A and B are ordinate intercept constants, and α and β are first-order disposition rate constants. Each value was weighted by the reciprocal of the concentration squared. Initial parameter estimates were obtained with the CSTRIP computer program (9).

Equation 1 describes the two-compartment open model shown in Scheme I. This model was used to characterize the disposition of I and V in rabbits. The pharmacokinetic parameters were derived as reported previously (10, 11). The Student t test was used to evaluate the significance of the observed difference.

RESULTS AND DISCUSSION

As shown in Fig. 2 for a representative animal, the blood concentration–time curves for I and V declined biexponentially after intravenous injection of equimolar doses of the two agents. The pharmacokinetic constants derived for each compound are presented in Table I. Three rabbits were given both I and V. The remaining animals received only one agent.

A significant difference between quinidine and the *O*-demethylated metabolite was observed for the following parameters: $t_{1/2\alpha}$, β, $t_{1/2\beta}$, k_{12} (the first-order rate constant for movement of the drug from the central to the peripheral compartment), $V_d\beta$ (the apparent volume of distribution), and k_{12}/k_{21} (the intercompartmental distribution ratio). No difference was observed in the remaining parameters between the two

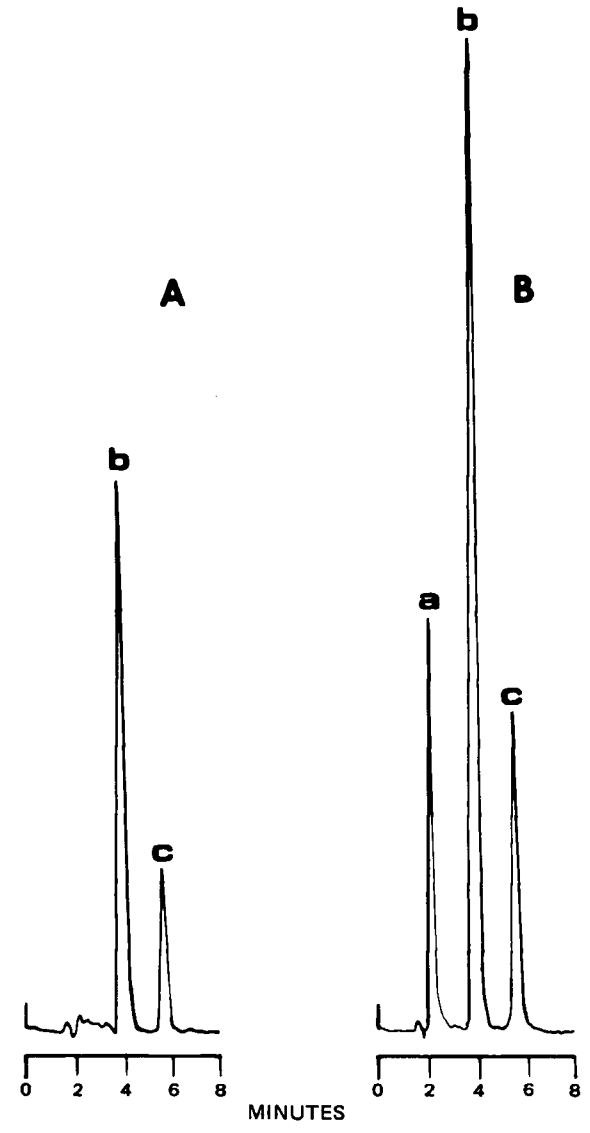

Figure 1—*Liquid chromatograms of blank blood (A) containing the internal standard (II) (b) and a blood sample (B) containing V (a) and II (b). Peak c is an unknown element extracted from rabbit blood.*

compounds; I and V exhibited similar total body clearance rates.

Compared to quinidine, the α or distribution half-life for the metabolite was longer (2.9 *versus* 1.7 min), indicating that it distributed more slowly in the body. The smaller k_{12} value for V (0.134 *versus* 0.226 min^{-1}) agreed with this finding. Furthermore, the distribution of V did not appear to be as extensive as I. The apparent volume of distribution of V of 1.56 ± 0.92 liters/kg was about one-half of the distribution volume for I, which was 3.26 ± 1.11 liters/kg. However, the central compartment volumes for both compounds were of similar size. Thus, the volume of the peripheral or tissue compartment was smaller for the metabolite.

The observed k_{12}/k_{21} ratio, an intercompartmental distribution coefficient, was substantially smaller for the *O*-demethylated metabolite compared to quinidine (4.65 *versus* 17.08). Since the blood flow between the two compartments probably was the same for both agents, the dif-

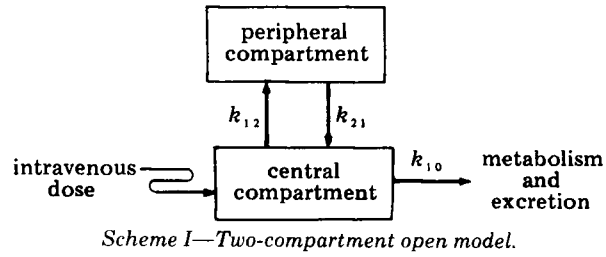

Scheme I—Two-compartment open model.

[7] Vortex-Genie, Scientific Industries, Springfield, Mass.
[8] Eberbach Corp., Ann Arbor, Mich.
[9] Series 2, model 2/2, Perkin-Elmer, Norwalk, Conn.
[10] Model 7105, Rheodyne, Berkeley, Calif.
[11] Waters Associates, Milford, Mass.
[12] Model FS-970, Schoeffel Instrument Corp., Westwood, N.J.
[13] Burdick & Jackson Laboratories, Muskegon, Mich.
[14] Model 23, Perkin-Elmer, Norwalk, Conn.

Table I—Mean Disposition Constants for 6'-Hydroxycinchonine (V) and Quinidine (I) after Intravenous Bolus Injections in Rabbits (±*SD*)

Parameter	V[a]	I[b]	*t* Value	Significance Level
α, min^{-1}	0.290 ± 0.141	0.445 ± 0.143	2.02	$p < 0.10$
$t_{1/2\alpha}$, min	2.86 ± 1.29	1.72 ± 0.62	2.21	$p < 0.05$
β, min^{-1}	0.013 ± 0.006	0.006 ± 0.002	3.17	$p < 0.01$
$t_{1/2\beta}$, min	65.35 ± 34.39	132.44 ± 27.11	4.09	$p < 0.005$
k_{12}, min^{-1}	0.134 ± 0.048	0.226 ± 0.089	2.28	$p < 0.05$
k_{21}, min^{-1}	0.037 ± 0.024	0.019 ± 0.015	1.73	NS[c]
k_{10}, min^{-1}	0.133 ± 0.131	0.207 ± 0.136	1.03	NS
V_c, liters/kg	0.22 ± 0.15	0.20 ± 0.27	0.14	NS
Cl, ml/min/kg	16.84 ± 5.08	16.80 ± 4.51	0.02	NS
$V_d\beta$, liters/kg	1.56 ± 0.92	3.26 ± 1.11	3.04	$p < 0.02$
k_{12}/k_{21}	4.65 ± 3.10	17.08 ± 9.44	3.08	$p < 0.01$
$V_c \times k_{10}$, ml/min/kg	15.5 ± 4.2	17.0 ± 4.8	0.59	NS

[a] $n = 6$. [b] $n = 8$. [c] Not significant.

ferences in the k_{12}/k_{21} ratio between I and V as well as the observed differences in $t_{1/2\alpha}$, k_{12}, and $V_d\beta$ most likely were the results of the greater lipid solubility of I.

The terminal half-life values of 65.4 ± 34.4 and 132.4 ± 27.1 min for V and I, respectively, showed that the metabolite was eliminated more rapidly than the parent drug. This observation is in agreement with the greater polarity or greater water solubility of the *O*-demethylated molecule and indicates that the metabolite would accumulate to a lesser extent than I on repeated dosing of the parent drug (12).

On the basis of its greater polarity, it was anticipated that V would be cleared at a faster rate than I. Therefore, the similarity in total body clearance for V and I was unexpected. Nevertheless, this finding is explained by the following reason. It is widely recognized that metabolism alters the physicochemical properties (*e.g.*, lipid solubility) of a drug molecule, which then leads to changes in its disposition characteristics. For drugs that are converted to more polar metabolites, these biotransformation products would be expected to have smaller volumes of distribution because their ability to cross lipid membranes by diffusion would be diminished. Furthermore, it is reasonable to expect that they would be eliminated more rapidly (*i.e.*, larger β) since they are more water soluble. From the relationship for total body clearance, $Cl = V_d\beta$, it can be seen that a decrease in V_d and an increase in β tend to offset each other and, thus, minimize the anticipated changes in Cl from situations where V_d or β changes alone.

When metabolism involves the conversion to less polar metabolites, a similar situation would be in effect wherein the volumes of distribution and first-order elimination rate constants of the metabolites would increase and decrease, respectively. This situation was observed recently (13) for diethyldithiocarbamate (a metabolite of disulfiram) and its metabolite, methyl diethyldithiocarbamate in dogs. Diethyldithiocarbamate, with a V_d value of 0.16 liter/kg and a β value of 0.205 min^{-1}, is readily soluble in water. Methyl diethyldithiocarbamate (V_d = 2.53 liters/kg and β = 0.014 min^{-1}) is virtually insoluble in water (highly lipid soluble). The observed total body clearances for the respective drug species were 33.1 and 31.9 ml/min/kg.

In this study, the clearance of V and I from the central compartment ($k_{10} \times V_c$) also was similar (16 *versus* 17 ml/min/kg).

In humans, quinidine is eliminated essentially by metabolism (14, 15). The fate of V is not known. Drayer *et al.* (2) detected conjugated and unconjugated V in the urine of four patients receiving quinidine and estimated that both forms accounted for ~1–2% of the quinidine dose. Preliminary findings in this laboratory also suggest that the *O*-demethylation pathway is a minor route for quinidine elimination in humans. These observations, coupled with the results of this study on the disposition and accumulation characteristics of V in rabbits, suggest that, although the *O*-demethylated metabolite possesses intrinsic antiarrhythmic activity (1–4), it probably contributes little to the antiarrhythmic effects seen after the administration of quinidine in humans.

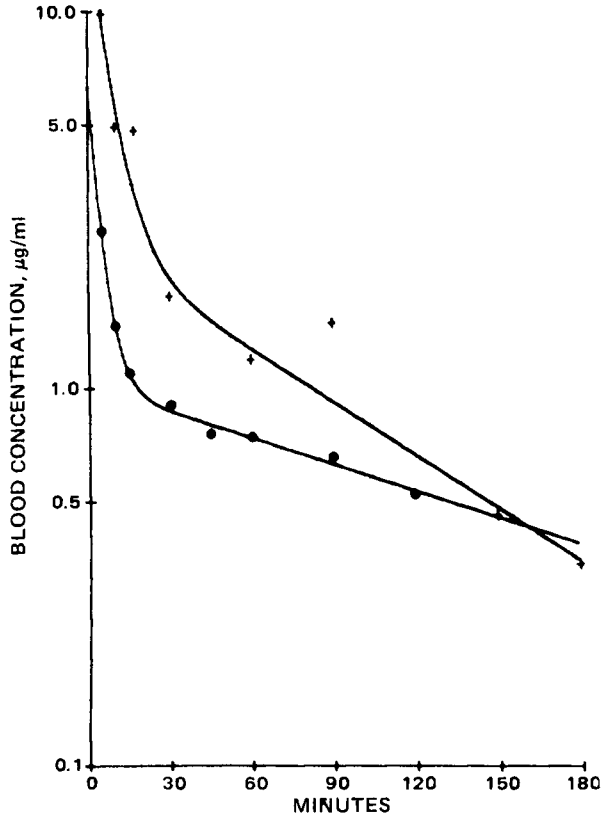

Figure 2—*Computer-simulated curves and experimental data points following intravenous bolus injections of 20 mg of I (●) and 19 mg of V (+) in a single rabbit.*

REFERENCES

(1) D. E. Drayer, C. E. Cook, and M. M. Reidenberg, *Clin. Res.*, **24**, 623A (1976).

(2) D. E. Drayer, D. T. Lowenthal, K. M. Restivo, A. Schwartz, C. E. Cook, and M. M. Reidenberg, *Clin. Pharmacol. Ther.*, **24**, 31 (1978).

(3) P. U. Nwangwu, T. L. Holcslaw, L. D. Small, and S. J. Stohs, *Pharmacologist*, **19**, 152 (1977).

(4) P. U. Nwangwu, T. L. Holcslaw, H. Rosenberg, L. D. Small, and S. J. Stohs, *J. Pharm. Pharmacol.*, **31**, 488 (1979).

(5) N. H. G. Holford, P. E. Coates, T. W. Guentert, S. Riegelman, and L. B. Sheiner, *Pharmacologist*, **21**, 200 (1979).

(6) H. Thron and W. Dirscherl, *Justus Liebigs Ann. Chem.*, **515**, 252 (1935).

(7) C. T. Ueda, B. J. Williamson, and B. S. Dzindzio, *Clin. Pharmacol. Ther.*, **20**, 260 (1976).

(8) C. M. Metzler, G. L. Elfring, and A. J. McEwen, *Biometrics*, **30**, 562 (1974).

(9) A. J. Sedman and J. G. Wagner, *J. Pharm. Sci.*, **65**, 1006 (1976).

(10) S. Riegelman, J. C. K. Loo, and M. Rowland, *ibid.*, **57**, 117 (1968).

(11) *Ibid.*, **57**, 128 (1968).

(12) M. Gibaldi and D. Perrier, "Pharmacokinetics," Dekker, New York, N.Y., 1975, pp. 97–128.

(13) J. Cobby, M. Mayersohn, and S. Selliah, *J. Pharmacokinet. Biopharm.*, **6**, 369 (1978).
(14) C. T. Ueda, D. S. Hirschfeld, M. M. Scheinman, M. Rowland, B. J. Williamson, and B. S. Dzindzio, *Clin. Pharmacol. Ther.*, **19**, 30 (1976).
(15) K. A. Conrad, B. L. Molk, and C. A. Chidsey, *Circulation*, **55**, 1 (1977).

ACKNOWLEDGMENTS

Supported by a grant in aid from the Nebraska affiliate of the American Heart Association.

The authors thank Dr. Laverne D. Small for the 6′-hydroxycinchonine used in this study and Mrs. Donna Earnshaw for typing this manuscript.

Interaction of Povidone with Aromatic Compounds I: Evaluation of Complex Formation by Factorial Analysis

J. A. PLAIZIER-VERCAMMEN ˣ **and R. E. De NÈVE**

Received January 28, 1980, from the *Faculteit Geneeskunde en Farmacie, Vrije Universiteit Brussel, Laarbeeklaan 103, B-1090, Brussel, Belgium.* Accepted for publication June 2, 1980.

Abstract □ In a study of complex formation between macromolecules and small ligands such as drugs, it appeared that the association constants must be calculated with more care (*i.e.*, after a thorough investigation of the influencing parameters such as buffer composition, ionic strength, and temperature) to allow meaningful interpretations of the phenomena. For this purpose, factorial analysis seems to be the method of choice; it offers the advantage of evaluating the influence of several variables and their interactions at the same time with a minimum of experiments. The method was applied to the association of povidone with two ligands, salicylic acid and benzoic acid. Parameters such as buffer composition and ionic strength, which affect binding, could be distinguished. Especially at pH 7.00, a great positive influence of buffer ions (phosphate buffer) and a relative positive interaction between temperature and ionic strength were noted. Knowledge of the influences of these parameters allowed comparison of the effects of the functional groups attached to the ligand molecules, as well as their degree of dissociation, on adsorption to permit more meaningful interpretation of thermodynamic constants.

Keyphrases □ Salicylic acid—binding to povidone, effects of temperature, buffer composition, and ionic strength □ Benzoic acid—binding to povidone, effects of temperature, buffer composition, and ionic strength □ Povidone—complex formation with salicylic acid and benzoic acid, effects of temperature, buffer composition, and ionic strength □ Complexation—povidone with salicylic acid and benzoic acid, effects of temperature, buffer composition, and ionic strength

The binding of various drugs with macromolecules in aqueous solution has been reviewed (1–3). Vallner (3) showed the discrepancies among the results obtained by several investigators and cited the need for the calculation of the association constants in a more meaningful manner. These discrepancies often are due to the uncontrolled influence of variables such as buffer composition, pH, ionic strength, and temperature. There have been few reports concerning the influence of buffer ions on the binding onto macromolecules (4, 5). The parameters usually are studied in the classical manner, *i.e.*, by successively changing one parameter at a time. However, as demonstrated previously (6), an accurate interpretation of the individual effects of the variables or their interactions is not possible with that approach.

Factorial analysis offers the possibility of evaluating the influence of individual variables and their interactions at the same time with a minimum of experiments. This method seems to be a first step for a thorough study of complex formation. Once the influence of these parameters is known, comparison of the effects of the functional groups attached to the ligands and their degree of dissociation on adsorption is possible, and the association constants can be interpreted more meaningfully. The application of factorial analysis to the binding of two simple ligands, benzoic acid and salicylic acid, onto povidone demonstrates the advantages and possibilities of this method in the study of complex formation.

EXPERIMENTAL

Reagents—Povidone[1] with a molecular weight of 700,000 was used as the macromolecule and was oven dried at 50° until a constant weight was reached. Salicylic acid[2] (p.a.) and benzoic acid[3] (p.a.) were used without further purification.

Buffer solutions were used at pH 7.00 (phosphate buffer) and at pH values equal to the pKa value of the two cosolutes (McIllvaine buffers) plus and minus 0.80; the solutions were brought to a determined ionic strength with sodium chloride. To control the influence of buffer ions, two kinds of buffer solutions were used; the normal buffers are denoted by 1 and those with half of the normal capacity are indicated as 0.5. The pH of the solutions at 25 and 50° was controlled with a potentiometric pH measurement[4] and adjusted if necessary.

Methods—The solutions containing the ligand and povidone were prepared in the respective buffers and allowed to stand overnight to attain equilibrium. Ultrafiltration[5] was performed, using a membrane of regenerated cellulose with a claimed cutoff value of ~10,000 mol. wt. units. Compressed nitrogen (4 kg/cm^2) was used, and the filtration was performed under continuous stirring of the sample solution to avoid accumulation of the macromolecule at the membrane–solution interface (7).

The concentration of unbound ligand in the filtrate was assayed spectrophotometrically. Corrections were made for membrane adsorption effects, and the concentration of bound ligand was calculated. The spectrophotometric measurements were performed with a double-beam spectrophotometer[6] at 296 nm for salicylic acid and at 224 nm for benzoic acid.

Calculations—Complex formation can be studied as a function of either macromolecule concentration or ligand concentration. In the first method, the relative tendencies of several ligands to form complexes are expressed as the ratio of the total ligand concentration, T, to the con-

[1] Polyvinylpyrrolidone (Kollidon K90), BASF, Brussels, Belgium.
[2] Merck.
[3] U.C.B.
[4] Radiometer, Copenhagen, Denmark.
[5] Amicon model 52.
[6] Perkin-Elmer model 124.

0022-3549/80/1200-1403$01.00/0
© 1980, American Pharmaceutical Association

(13) J. Cobby, M. Mayersohn, and S. Selliah, *J. Pharmacokinet. Biopharm.*, **6**, 369 (1978).
(14) C. T. Ueda, D. S. Hirschfeld, M. M. Scheinman, M. Rowland, B. J. Williamson, and B. S. Dzindzio, *Clin. Pharmacol. Ther.*, **19**, 30 (1976).
(15) K. A. Conrad, B. L. Molk, and C. A. Chidsey, *Circulation*, **55**, 1 (1977).

ACKNOWLEDGMENTS

Supported by a grant in aid from the Nebraska affiliate of the American Heart Association.

The authors thank Dr. Laverne D. Small for the 6′-hydroxycinchonine used in this study and Mrs. Donna Earnshaw for typing this manuscript.

Interaction of Povidone with Aromatic Compounds I: Evaluation of Complex Formation by Factorial Analysis

J. A. PLAIZIER-VERCAMMEN ˣ **and R. E. De NÈVE**

Received January 28, 1980, from the *Faculteit Geneeskunde en Farmacie, Vrije Universiteit Brussel, Laarbeeklaan 103, B-1090, Brussel, Belgium.* Accepted for publication June 2, 1980.

Abstract □ In a study of complex formation between macromolecules and small ligands such as drugs, it appeared that the association constants must be calculated with more care (*i.e.*, after a thorough investigation of the influencing parameters such as buffer composition, ionic strength, and temperature) to allow meaningful interpretations of the phenomena. For this purpose, factorial analysis seems to be the method of choice; it offers the advantage of evaluating the influence of several variables and their interactions at the same time with a minimum of experiments. The method was applied to the association of povidone with two ligands, salicylic acid and benzoic acid. Parameters such as buffer composition and ionic strength, which affect binding, could be distinguished. Especially at pH 7.00, a great positive influence of buffer ions (phosphate buffer) and a relative positive interaction between temperature and ionic strength were noted. Knowledge of the influences of these parameters allowed comparison of the effects of the functional groups attached to the ligand molecules, as well as their degree of dissociation, on adsorption to permit more meaningful interpretation of thermodynamic constants.

Keyphrases □ Salicylic acid—binding to povidone, effects of temperature, buffer composition, and ionic strength □ Benzoic acid—binding to povidone, effects of temperature, buffer composition, and ionic strength □ Povidone—complex formation with salicylic acid and benzoic acid, effects of temperature, buffer composition, and ionic strength □ Complexation—povidone with salicylic acid and benzoic acid, effects of temperature, buffer composition, and ionic strength

The binding of various drugs with macromolecules in aqueous solution has been reviewed (1–3). Vallner (3) showed the discrepancies among the results obtained by several investigators and cited the need for the calculation of the association constants in a more meaningful manner. These discrepancies often are due to the uncontrolled influence of variables such as buffer composition, pH, ionic strength, and temperature. There have been few reports concerning the influence of buffer ions on the binding onto macromolecules (4, 5). The parameters usually are studied in the classical manner, *i.e.*, by successively changing one parameter at a time. However, as demonstrated previously (6), an accurate interpretation of the individual effects of the variables or their interactions is not possible with that approach.

Factorial analysis offers the possibility of evaluating the influence of individual variables and their interactions at the same time with a minimum of experiments. This method seems to be a first step for a thorough study of complex formation. Once the influence of these parameters is known, comparison of the effects of the functional groups attached to the ligands and their degree of dissociation on adsorption is possible, and the association constants can be interpreted more meaningfully. The application of factorial analysis to the binding of two simple ligands, benzoic acid and salicylic acid, onto povidone demonstrates the advantages and possibilities of this method in the study of complex formation.

EXPERIMENTAL

Reagents—Povidone[1] with a molecular weight of 700,000 was used as the macromolecule and was oven dried at 50° until a constant weight was reached. Salicylic acid[2] (p.a.) and benzoic acid[3] (p.a.) were used without further purification.

Buffer solutions were used at pH 7.00 (phosphate buffer) and at pH values equal to the pKa value of the two cosolutes (McIllvaine buffers) plus and minus 0.80; the solutions were brought to a determined ionic strength with sodium chloride. To control the influence of buffer ions, two kinds of buffer solutions were used; the normal buffers are denoted by 1 and those with half of the normal capacity are indicated as 0.5. The pH of the solutions at 25 and 50° was controlled with a potentiometric pH measurement[4] and adjusted if necessary.

Methods—The solutions containing the ligand and povidone were prepared in the respective buffers and allowed to stand overnight to attain equilibrium. Ultrafiltration[5] was performed, using a membrane of regenerated cellulose with a claimed cutoff value of ~10,000 mol. wt. units. Compressed nitrogen (4 kg/cm^2) was used, and the filtration was performed under continuous stirring of the sample solution to avoid accumulation of the macromolecule at the membrane–solution interface (7).

The concentration of unbound ligand in the filtrate was assayed spectrophotometrically. Corrections were made for membrane adsorption effects, and the concentration of bound ligand was calculated. The spectrophotometric measurements were performed with a double-beam spectrophotometer[6] at 296 nm for salicylic acid and at 224 nm for benzoic acid.

Calculations—Complex formation can be studied as a function of either macromolecule concentration or ligand concentration. In the first method, the relative tendencies of several ligands to form complexes are expressed as the ratio of the total ligand concentration, T, to the con-

[1] Polyvinylpyrrolidone (Kollidon K90), BASF, Brussels, Belgium.
[2] Merck.
[3] U.C.B.
[4] Radiometer, Copenhagen, Denmark.
[5] Amicon model 52.
[6] Perkin-Elmer model 124.

0022-3549/80/1200-1403$01.00/0
© 1980, American Pharmaceutical Association

Table I—Binding of Salicylic Acid (1.00×10^{-2} *M*) to Povidone (6.00%) at pH 2.20

Ionic Strength	Buffer	Temperature	Percentage of Ligand Bound		Difference
		Influence of Temperature[a]	25°	50°	
Low	Low	—	56.9	54.0	−2.9
Low	High	—	57.1	55.0	−2.1
High	Low	—	62.9	62.2	−0.7
High	High	—	62.8	62.4	−0.4
		Influence of Ionic Strength[b]	μ = 0.15	μ = 1.00	
—	Low	Low	56.9	62.9	+6.0
—	Low	High	54.0	62.2	+8.2
—	High	Low	57.1	62.8	+5.7
—	High	High	55.0	62.4	+7.4
		Influence of Buffer Ions[c]	0.5 Buffer	1 Buffer	
Low	—	Low	56.9	57.1	+0.2
Low	—	High	54.0	55.0	+1.0
High	—	Low	62.9	62.8	−0.1
High	—	High	62.2	62.4	+0.2

[a] Factor A = temperature; low level = 25° and high level = 50°. [b] Factor B = ionic strength (μ); low level = 0.15 and high level = 1.00. [c] Factor C = buffer ions; low level = 0.5 and high level = 1.

centration of the free form, *F*, as a function of the percentage of povidone (8–10):

$$Q = \frac{T}{F} = \frac{r}{F}[\text{PVP}] + 1 \qquad \text{(Eq. 1)}$$

where *r* is the number of moles of ligand bound per mole of macromolecule and [PVP] is the molar concentration of povidone in the solution. If *r*/*F* is constant (*i.e.*, if the same type of binding is taking place with increasing povidone concentration), a linear relationship is obtained (11) between *T*/*F* and [PVP].

The second method permits the calculation of equilibrium constants and the maximum number of binding sites on the macromolecule. The basic theory of the calculation of ligand–macromolecule equilibria was described previously (12–15). If no interaction phenomena take place, then reversible binding can be described by:

$$r = \frac{nkF}{1 + kF} \qquad \text{(Eq. 2)}$$

where *n* represents the total number of sites available and *k* is the intrinsic binding constant. The relationship between the intrinsic binding constant, *k*, and the constants for the individual equilibrium reactions, k_i, is given by (16):

$$k_i = \left[\frac{n - (i-1)}{i}\right]k \qquad \text{(Eq. 3)}$$

where *n* is the total number of available sites and *i* is the number of possible combinations of *n* binding sites taken exactly *i* at a time.

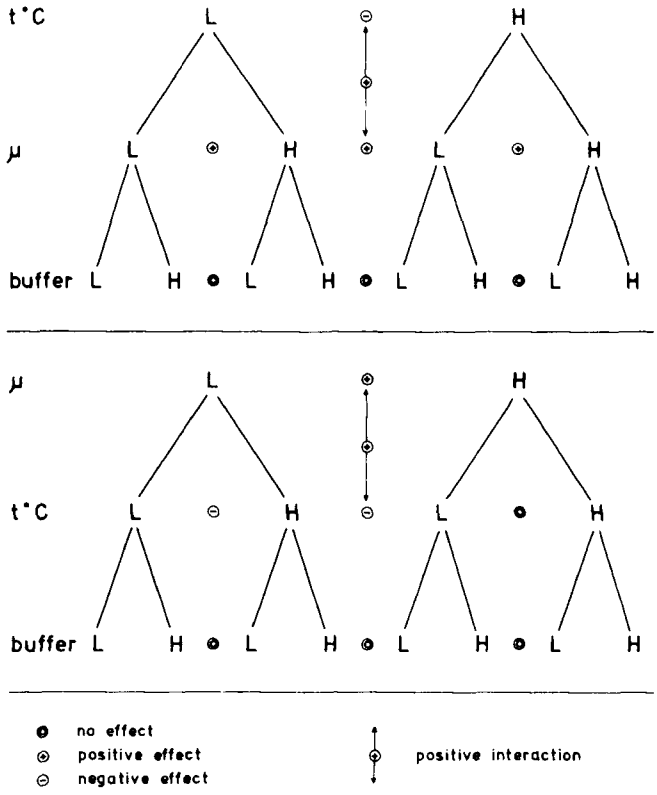

Figure 1—*Influence of parameters on the complexing of salicylic acid (1.00×10^{-2} M) with povidone (6.00%) at pH 2.20.*

The hyperbolic graph of *r versus F* (Eq. 2) can be converted into linear form. The approach of Klotz *et al.* (12) usually is used:

$$\frac{1}{r} = \frac{1}{n} + \frac{1}{nkF} \qquad \text{(Eq. 4)}$$

The Scatchard equation (15) is:

$$\frac{r}{F} = kn - kr \qquad \text{(Eq. 5)}$$

Consequently, graphical representations of $1/r$ *versus* $1/F$ or r/F *versus* *r* are used to obtain *n* (the number of binding sites) and *k* (the intrinsic binding constant). Curvature of such plots usually indicates the existence of more than one class of sites (17).

Factorial Analysis—The overall objective of factorial analysis is to obtain a general picture of how the results are affected by changing the parameters or factors. The theory and practice of factorial analysis were given by Philippe (6) and Chatfield (18). In complex formation, the principal parameters or factors to be considered are ionic strength, buffer

Table II—Experimental Conditions of the Treatment Combinations with the Resulting Percentage of Ligand Bound and the Analysis of Variance of Binding of Salicylic Acid (1.00×10^{-2} *M*) to Povidone (6.00%) at pH 2.20

Column 1: Source of Variation	Column 2: Percentage of Ligand Bound Exp. 1	Exp. 2	Column 3: Sum	Column 4	Column 5	Column 6	Column 7: Degrees of Freedom	Column 8: Sum of Squares (Column 6)^2 / 2 × 8	Column 9: Variance	Column 10: *F*	Column 11: Significant Level $F_8^{1\ 5\%\ 5.32}_{1\%\ 11.26}$
1	57.0	56.8	113.8	221.8	471.9	946.4					
A[a]	53.7	54.3	108.0	250.1	474.5	−12.2	1	9.303	9.303	33.83	Temperature: $-0.001 < p$
B[b]	63.2	62.6	125.8	224.2	−7.3	54.4	1	184.960	184.960	672.58	Ionic strength: $+0.001 < p$
AB	62.5	61.8	124.3	250.3	−4.9	7.4	1	3.423	3.423	12.45	Temperature and ionic strength: $+0.01 < p < 0.001$
C[c]	56.9	57.2	114.1	−5.8	28.3	2.6	1	0.423	0.423	1.54	Buffer ions: 0
AC	55.7	54.4	110.1	−1.5	26.1	2.4	1	0.360	0.360	1.31	
BC	62.6	63.0	125.6	−4.0	4.3	−2.2	1	0.303	0.303	1.10	
ABC	62.9	61.8	124.7	−0.9	3.1	−1.2	1	0.090	0.090	0.33	
Experimental error							8		4.40/2 × 8		

[a,b,c] See Table I footnotes for explanation.

Table III—Analysis of Variance at the Different Levels of Binding of Salicylic Acid (1.00×10^{-2} *M*) to Povidone (6.00%) at pH 2.20

Factor	Degrees of Freedom	Sum of Squares	Variance	*F*	Significant Level $F^{1\ 5\%\ 7.71}_{4\ 1\%\ 21.20}$
			Low Temperature (25°)		
1					
B	1	69.031	69.031	849.62	Ionic strength: $+0.001 < p$
C	1	0.001	0.001	0.02	Buffer ions: 0
BC	1	0.031	0.031	0.39	
Experimental error	4		0.65/2 × 4		
			High Temperature (50°)		
A					
AB	1	119.351	119.351	254.62	Ionic strength: $+0.001 < p$
AC	1	0.781	0.781	1.67	Buffer ions: 0
ABC	1	0.361	0.361	0.77	
Experimental error	4		3.75/2 × 4		
			Low Ionic Strength ($\mu = 0.15$)		
1					
A	1	12.005	12.005	44.06	Temperature: $-0.001 < p$
C	1	0.720	0.720	2.64	Buffer ions: 0
AC	1	0.405	0.405	1.49	
Experimental error	4		2.18/2 × 4		
			High Ionic Strength ($\mu = 1.00$)		
B					
AB	1	0.720	0.720	2.60	Temperature: 0
BC	1	0.005	0.005	0.02	Buffer ions: 0
ABC	1	0.045	0.045	0.16	
Experimental error	4		2.22/2 × 4		

ions, and temperature. In the present experiment, all of these factors were investigated at two levels. For simplicity, a letter was written when the corresponding factor was in the high level and not written when it was in the low level. When all of the factors were in the low level, a number one was written. Generally, with n factors at two levels, 2^n treatment combinations were possible. To obtain an estimation of the experimental error, each factor was determined in duplicate. The sum of the duplicates was analyzed using the Yates method (19), which is a systematic method for estimating the individual effects and performing the analysis of variance.

RESULTS AND DISCUSSION

To determine the influence of the dissociation of the ligand molecules on their binding to povidone, each ligand was investigated at two pH values: at pH = pKa − 0.80 and at pKa + 0.80. At these pH values, the drugs are 86.3% in the undissociated and dissociated state, respectively. Salicylic acid also was investigated at pH 7.00, where the drug is fully dissociated.

Salicylic Acid (pKa 3.0)—Salicylic acid was investigated at pH 2.20 and 3.80. Table I summarizes the factors and their respective levels at pH 2.20. To demonstrate the difficulties in interpreting the results, they are represented in Table I by changing one parameter from the low to the high level, with the other variables being either at a low or high level. For instance, by observing the ionic strength at the low and the high levels, the positive influence of this variable can be seen since the results change from ~56 to 62% of the ligand bound. However, the results obtained by changing the temperature from 25 to 50° are not so easy to interpret. The influence seems to be negative and is greater at low than at high ionic strength, probably due to an interaction of the temperature and the ionic strength. An accurate interpretation is impossible.

With factorial analysis, the parameter effects and interaction phenomena can be interpreted easily and accurately. In Table II, the results given in Table I are analyzed according to Yates (19). In the first column, all of the treatment combinations are listed in a systematic way; the results are determined in duplicate for each factor and are expressed as the percentage of ligand bound (column 2); their sum is listed in column 3.

According to Yates, with three factors, three columns have to be calculated (columns 4–6). Each column is generated from the preceding column in the same way. The first 2^{n-1} values in a column are the sums of successive pairs of numbers in the preceding column. The next 2^{n-1} values are the differences of the successive pairs. In this way, the final column gives the total effect corresponding to the particular treatment combinations. With these estimates, an analysis of variance is performed. This analysis consists of splitting a total sum of squares into sums of squares for the factors considered. The total effect of each factor is squared (column 8) and divided by the number of observations ($2^3 \times 2$), with each factor possessing one degree of freedom. The estimate of the residual variation, *i.e.*, the variance of the experimental error, is calculated by the sum of squares of the variations between the duplicates, divided by 2×8.

With an F test, the significance of the observed effects is tested (column 10). Table II shows that the ionic strength has an overall positive influence; however, increasing the temperature reduces the adsorption, and buffer ions have no influence at all. Moreover, a relative positive interaction is noted between ionic strength and temperature (factor AB).

By splitting up the results at low and high temperatures, more infor-

Table IV—Experimental Conditions of the Treatment Combinations with the Resulting Percentage of Ligand Bound and the Analysis of Variance of the Binding of Salicylic Acid (1.00×10^{-2} *M*) to Povidone (6.00%) at pH 2.20

Source of Variation	Percentage of Ligand Bound		Degrees of Freedom	Sum of Squares	Variance	*F*	Significant Level $F^{1\ 5\%\ 5.32}_{8\ 1\%\ 11.26}$
	Exp. 1	Exp. 2					
1	57.0	56.8					
A[a]	53.7	54.3	1	38.131	38.131	217.11	Temperature: $-0.001 < p$
B[b]	56.8	57.5	1	0.051	0.051	0.29	Ionic strength: 0
AB	53.2	54.2	1	0.076	0.076	0.43	
C[c]	56.9	57.2	1	0.001	0.001	0.00	Buffer ions: 0
AC	53.7	54.4	1	0.031	0.031	0.17	
BC	56.7	57.0	1	0.031	0.031	0.17	
ABC	53.6	54.1	1	0.076	0.076	0.43	
Experimental error			8		2.81/2 × 8		

[a] Factor A = temperature; low level = 25° and high level = 50°. [b] Factor B = ionic strength (μ); low level = 0.15 and high level = 0.40. [c] Factor C = buffer ions; low level = 0.5 and high level = 1.

Table V—Experimental Conditions of the Treatment Combinations with the Resulting Percentage of Ligand Bound and the Analysis of Variance of the Binding of Salicylic Acid (1.00×10^{-2} *M*) to Povidone (6.00%) at pH 3.80

Source of Variation	Percentage of Ligand Bound Exp. 1	Exp. 2	Degrees of Freedom	Sum of Squares	Variance	*F*	Significant Level $F^{1}_{8}{}^{5\%}_{1\%}{}^{5.32}_{11.26}$
1	52.4	53.1					
A[a]	46.6	45.5	1	147.623	147.623	524.88	Temperature: $0.001 < p$
B[b]	52.0	52.4	1	0.063	0.063	0.22	Ionic strength: 0
AB	45.9	46.8	1	1.103	1.103	3.92	
C[c]	52.2	53.1	1	0.000	0.000	0.00	Buffer ions: 0
AC	45.8	46.5	1	0.160	0.160	0.57	
BC	51.8	52.0	1	0.000	0.000	0.00	
ABC	46.3	47.0	1	0.040	0.040	0.14	
Experimental error			8		4.50/2 × 8		

[a,b,c] See Table I footnotes for explanation.

Table VI—Experimental Conditions of the Treatment Combinations with the Resulting Percentage of Ligand Bound and the Analysis of Variance of the Binding of Salicylic Acid (1.00×10^{-2} *M*) to Povidone (5.00%) at pH 7.00

Source of Variation	Percentage of Ligand Bound Exp. 1	Exp. 2	Degrees of Freedom	Sum of Squares	Variance	*F*	Significant Level $F^{1}_{8}{}^{5\%}_{1\%}{}^{5.32}_{11.26}$
1	49.0	50.2					
A[a]	42.8	41.6	1	268.141	268.141	1059.32	Temperature: $-0.001 < p$
B[b]	49.3	50.0	1	0.001	0.001	0.00	Ionic strength: 0
AB	42.0	42.5	1	0.006	0.006	0.02	
C[c]	56.6	56.4	1	102.516	102.516	405.00	Buffer ions: $+0.001 < p$
AC	47.6	47.6	1	2.481	2.481	9.80	Temperature and ionic strength: $-0.05 < p < 0.01$
BC	56.4	56.7	1	0.006	0.006	0.02	
ABC	47.8	47.5	1	0.006	0.006	0.02	
Experimental error			8		4.05/2 × 8		

[a] Factor A = temperature; low level = 25 and high level = 50°. [b] Factor B = ionic strength (μ); low level = 0.25 and high level = 0.50. [c] Factor C = buffer ions; low level = 0.5 and high level = 1.

Table VII—Experimental Conditions of the Treatment Combinations with the Resulting Percentage of Ligand Bound and the Analysis of Variance of the Binding of Benzoic Acid (1.00×10^{-2} *M*) to Povidone (6.00%) at pH 3.40

Source of Variation	Percentage of Ligand Bound Exp. 1	Exp. 2	Degrees of Freedom	Sum of Squares	Variance	*F*	Significant Level $F^{1}_{8}{}^{5\%}_{1\%}{}^{5.32}_{11.26}$
1	39.0	39.2					
A[a]	41.0	40.9	1	14.251	14.251	281.49	Temperature: $+0.001 < p$
B[b]	39.4	38.9	1	0.016	0.016	0.31	Ionic strength: 0
AB	41.2	40.9	1	0.001	0.001	0.01	
C[c]	39.1	39.0	1	0.001	0.001	0.01	Buffer ions: 0
AC	41.3	40.7	1	0.001	0.001	0.01	
BC	39.1	39.2	1	0.001	0.001	0.01	
ABC	41.1	40.9	1	0.006	0.006	0.11	
Experimental error			8		0.81/2 × 8		

[a,b,c] See Table VI footnotes for explanation.

Table VIII—Experimental Conditions of the Treatment Combinations with the Resulting Percentage of Ligand Bound and the Analysis of Variance of the Binding of Benzoic Acid (1.00×10^{-2} *M*) to Povidone (6.00%) at pH 5.00

Source of Variation	Percentage of Ligand Bound Exp. 1	Exp. 2	Degrees of Freedom	Sum of Squares	Variance	*F*	Significant Level $F^{1}_{8}{}^{5\%}_{1\%}{}^{5.32}_{11.26}$
1	16.7	16.8					
A[a]	14.3	14.8	1	17.640	17.640	109.40	Temperature: $-0.001 < p$
B[b]	16.9	16.6	1	0.040	0.040	0.25	Ionic strength: 0
AB	14.4	14.6	1	0.090	0.090	0.56	
C[c]	17.0	16.3	1	0.023	0.023	0.14	Buffer ions: 0
AC	15.2	14.7	1	0.063	0.063	0.39	
BC	17.2	16.3	1	0.023	0.023	0.14	
ABC	14.1	14.9	1	0.063	0.063	0.39	
Experimental error			8		2.58/2 × 8		

[a,b,c] See Table VI footnotes for explanation.

mation about the influence of the ionic strength can be obtained; by considering the results at low and high ionic strengths, the influence of temperature can be analyzed more specifically. The results obtained by splitting at the different levels together with their analysis of variance are given in Table III. Considering the results at the different levels (Table III), the overall positive influence of ionic strength is maintained for the two temperatures, while the negative influence of temperature is observed at low ionic strength.

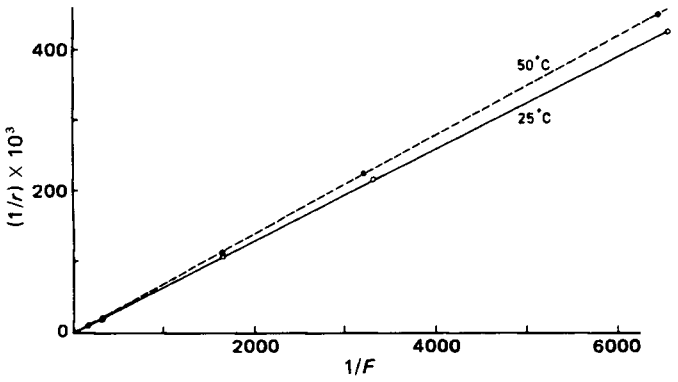

Figure 2—*Influence of temperature on the complexing of salicylic acid with povidone at pH 2.20. The salicylic acid concentration was 5.00 × 10^{-4}–1.00 × 10^{-2} M, the povidone concentration was 6.00% (8.57 × 10^{-5} M), the ionic strength was 0.15, and the buffer ions were 1.*

In Fig. 1, the influence of the different variables investigated before and after splitting the results at the different levels is represented. This figure also offers a good idea of how much information can be obtained from factorial analysis. In the middle of the graph, the overall effects are indicated; on the side, the results after splitting the results are represented.

By lowering the high level of the ionic strength from 1.0 to 0.40 and maintaining the other factors at their original levels, the percentage of ligand bound is determined by ultrafiltration, and a factorial analysis is carried out again. From these results (Table IV), it is noted that ionic strength no longer has an effect on the binding at these levels whereas temperature and buffer ions behave as indicated in Table I.

For salicylic acid at pH 3.80, where the drug is mainly dissociated, the same factors as are given in Table I were investigated. The levels used and the corresponding results are summarized in Table V. In contrast with the phenomena observed at pH 2.20, ionic strength no longer influenced the binding of salicylic acid to povidone while increasing the temperature also diminished the adsorption. The observations remained after splitting the results at the different levels of ionic strength and temperature.

The adsorption of salicylic acid in the dissociated state onto povidone was investigated at pH 7.00 using a phosphate buffer. Factorial analysis was carried out with three factors at two levels (Table VI). Increasing the temperature and the ionic strength had a negative and no influence, respectively, on the binding of salicylic acid. At pH 7.00, in contrast to pH 2.20 and 3.80, the buffer ions enhanced complex formation (from 49.6 to 56.9% of the ligand was bound). At the two lower pH values, the buffer ions were mainly monovalent phosphate and citrate ions. At pH 7.00, the phosphate ions were present as dibasic phosphate ions at 38%, indicating the great influence of these ions on complex formation. However, dibasic phosphate ions do not always enhance complex formation. Thus, no influence was found for the binding of methyl orange to povidone at pH 7.00 (20). On the other hand, dibasic phosphate ions increased binding for chlorpromazine with carboxymethylcellulose sodium (21), as well as citrate ions, by complex formation of local anesthetics and polyvinyl alcohol (22).

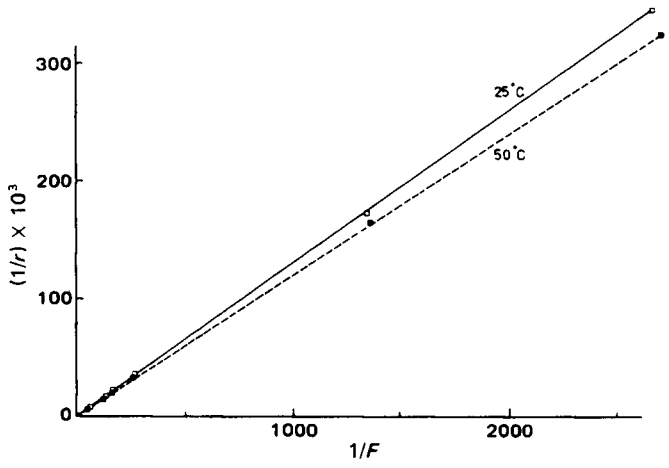

Figure 4—*Influence of temperature on the complexing of benzoic acid with povidone at pH 3.40. The benzoic acid concentration was 1.00 × 10^{-4}–1.00 × 10^{-2} M, the povidone concentration was 6.00% (8.57 × 10^{-5} M), the ionic strength was 0.25, and the buffer ions were 1.*

It is concluded that binding depends not only on the kind of buffer ions present but also on the structure of the macromolecule and the ligand. A second important conclusion is evident; without knowledge of the influence of buffer ions, the binding tendency of the undissociated and dissociated forms of salicylic acid cannot be compared.

Benzoic Acid (pKa 4.2)—For benzoic acid, the same factors and levels were investigated as for salicylic acid. However, the buffers used were McIllvaine buffers at pH 3.40 and 5.00. The ionic strength was maintained at 0.25 and 0.50. At pH 3.40 and 5.00, the ionic strength and buffer ions had no influence on the binding of benzoic acid to povidone (Tables VII and VIII). At pH 3.40, where benzoic acid is mainly undissociated, the adsorption was enhanced by increasing the temperature; at pH 5.00, the binding was diminished.

Isotherms and Thermodynamic Calculations—Isotherms were obtained at 25 and 50°; they are represented graphically using the Klotz isotherm (Eq. 4) in Figs. 2 and 3 for salicylic acid and in Figs. 4 and 5 for benzoic acid.

For the two derivatives, a linear relationship was observed, with the two lines nearly going through the origin. From Eq. 2, it is seen that this finding implies that $kF \ll 1$; from Eq. 4, it is shown that $1/n$ equals zero or n is infinite, indicating a nearly infinitely large number of adsorption sites. The fraction of the ligand bound to the macromolecule does not vary significantly with the ligand concentration, and the binding process ap-

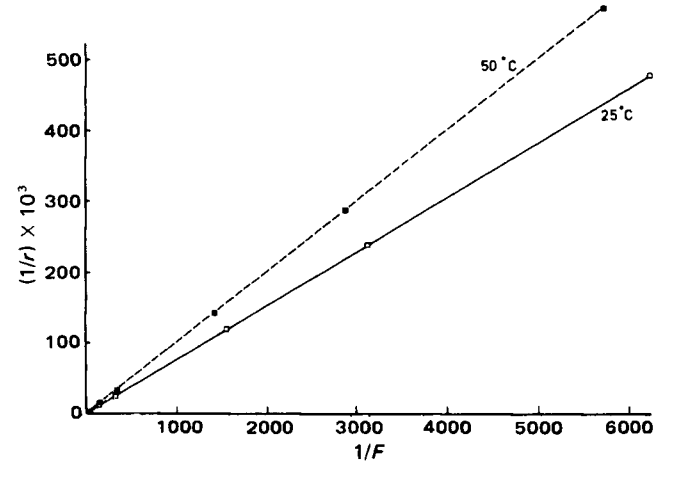

Figure 3—*Influence of temperature on the complexing of salicylic acid with povidone at pH 3.80. The salicylic acid concentration was 5.00 × 10^{-4}–1.00 × 10^{-2} M, the povidone concentration was 6.00% (8.57 × 10^{-5} M), the ionic strength was 0.15, and the buffer ions were 1.*

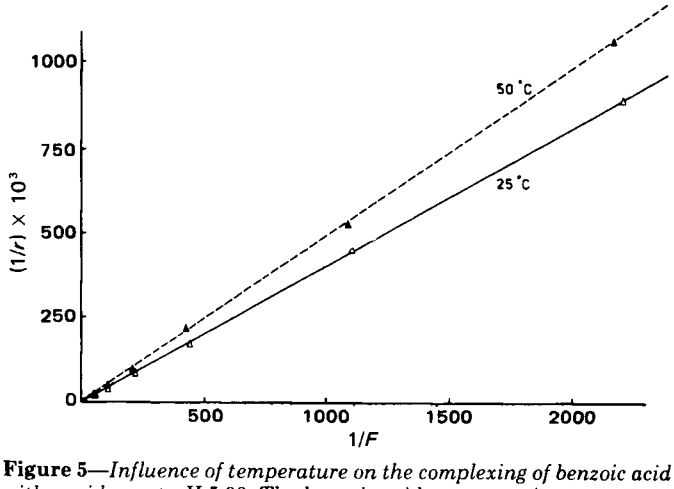

Figure 5—*Influence of temperature on the complexing of benzoic acid with povidone at pH 5.00. The benzoic acid concentration was 1.00 × 10^{-4}–1.00 × 10^{-2} M, the povidone concentration was 6.00% (8.57 × 10^{-5} M), the ionic strength was 0.25, and the buffer ions were 1.*

Table IX—Thermodynamic Data for the Binding of Salicylic Acid and Benzoic Acid to Povidone

Cosolute	pH	nk ($\times 10^{-3}$) at 298 °K, liters/mole	nk ($\times 10^{-3}$) at 323 °K, liters/mole	$\Delta F°$ (323 °K), kcal/mole	$\Delta H°$, kcal/mole	$\Delta S°$, kcal/mole degree
Salicylic acid	2.20	16.2	15.4	−6.2	−0.4	+18.0
	3.80	13.1	9.3	−5.9	−2.1	+11.8
Benzoic acid	3.40	7.8	8.5	−5.8	+0.7	+20.1
	5.00	2.5	2.0	−4.9	−1.5	+10.4

pears to be unsaturable. The same finding was made by Higuchi and Kuramoto (23) in a study of complex formation between benzoic acid and povidone[7] in aqueous solution. Values for nk are deduced from the slopes. According to Scholtan (20), the value of n can be determined only with much uncertainty, so it has little physical meaning. In this case, it is better to use the value of $nk = k_1$, which is a measure for the strength of the binding, while n is indicative of the binding capacity.

The thermodynamic functions calculated from k_1 do not necessarily refer to a single site on the macromolecule. However, the values are useful in considering the nature of the binding, in comparing the binding of different ligands with the same macromolecule, and in analyzing the effects of parameters such as pH and ionic strength (14). The standard free energy, $\Delta F°$, for complex formation is calculated from:

$$\Delta F° = -RT \ln nk \qquad \text{(Eq. 6)}$$

With the assumption that there is no significant temperature dependence of the enthalpy change within the temperature range used, the standard enthalpy change, $\Delta H°$, for the association of 1 mole of ligand with 1 mole of macromolecule is given by:

$$\ln \frac{nk_{25\,°C}}{nk_{50\,°C}} = -\frac{\Delta H°}{R}\left(\frac{1}{298} - \frac{1}{323}\right) \qquad \text{(Eq. 7)}$$

and the entropy change, $\Delta S°$, is obtained by substituting $\Delta H°$ and $\Delta F°$ in the Gibbs–Helmholtz equation:

$$\left(\frac{\delta \Delta F°}{\delta T}\right)_p = -\Delta S° = \frac{\Delta F° - \Delta H°}{T} \qquad \text{(Eq. 8)}$$

Thermodynamic data for the association reactions are reported in Table IX. The negative sign for $\Delta F°$ means that the binding process occurs spontaneously. The high positive entropy and small negative enthalpy values are characteristic for hydrophobic binding (24–26). The positive entropies are associated with many reactions involving the binding of ligands to macromolecules as well as proteins (27–30) and to macromolecules such as polymethacrylic acid (31), polyvinyl alcohol (32), methylcellulose (33), hydroxyethyl cellulose (33), and povidone (34–36). With the knowledge that the buffer composition and ionic strength have no influence on the adsorbing tendency of the two derivatives studied, the thermodynamic constants calculated from the isotherms are due entirely to the binding of the ligand to the macromolecule. Thus, comparison of the thermodynamic constants and the effect of the substituted groups as well as the effect of their degree of dissociation on the binding tendency is possible now.

For salicylic acid (Table IX), the binding strength was lowered by increasing temperature, both for the undissociated and dissociated forms; at the two temperatures, binding was highest for the undissociated form. The same findings can be noted for benzoic acid, except for the undissociated form, where the binding strength was highest at 323 °K. Substitution of a hydroxyl function in the *ortho*-position of the carboxyl function increased the binding strength at 298 °K by a factor of 2.1 for the undissociated form and by a factor of 5.3 for the dissociated form; at 323 °K, it increased by factors of 1.8 and 4.6, respectively. The observations indicate that hydrogen binding also may play an important role in the binding. The application of factorial analysis is under investigation in the study of complex formation between povidone and a series of benzene and pyridine derivatives.

REFERENCES

(1) M. C. Meyer and D. E. Guttman, *J. Pharm. Sci.*, **57**, 895 (1968).

(2) S. Keipert, J. Becker, H. H. Schultze, and R. Voigt, *Pharmazie*, **28**, 145 (1973).

(3) J. J. Vallner, *J. Pharm. Sci.*, **66**, 447 (1977).

(4) F. Karush, *J. Am. Chem. Soc.*, **72**, 2705 (1950).

(5) E. Ullmann and G. Bauer, *Arch. Pharm.*, **306**, 81 (1973).

(6) J. Philippe, "Les Méthodes Statistiques en Pharmacie et en Chimie," Masson, Paris, France, 1967.

(7) C. F. Chignell, *Crit. Rev. Toxicol.*, **1**, 413 (1972).

(8) C. K. Bahal and H. B. Kostenbauder, *J. Pharm. Sci.*, **53**, 1027 (1964).

(9) S. M. Blaug and P. S. Ebersman, *ibid.*, **53**, 35 (1964).

(10) N. K. Patel and N. E. Foss, *ibid.*, **53**, 94 (1964).

(11) G. Jürgensen Eide and P. Speiser, *Acta Pharm. Suec.*, **4**, 185 (1967).

(12) I. M. Klotz, F. M. Walker, and R. B. Pivan, *J. Am. Chem. Soc.*, **68**, 1486 (1946).

(13) J. T. Edsall and J. Wyman, "Biophysical Chemistry," vol. 1, Academic, New York, N.Y., 1960.

(14) R. M. Rosenberg and I. M. Klotz, in "A Laboratory Manual of Analytical Methods of Protein Chemistry," vol. 2, P. Alexander and R. J. Block, Eds., Pergamon, New York, N.Y., 1960, p. 131.

(15) G. Scatchard, *Ann. N.Y. Acad. Sci.*, **51**, 660 (1949).

(16) H. Neurath and K. Bailey, "The Proteins," vol. I, part B, Academic, New York, N.Y., 1953.

(17) I. M. Klotz, *Biochemistry*, **10**, 3065 (1971).

(18) C. Chatfield, "Statistics for Technology," Chapman and Hall, London, England, 1975, p. 271.

(19) F. Yates, "Design and Analysis of Factorial Experiments," Imperial Bureau of Soil Sciences, 1937 (cited in Ref. 6).

(20) W. Scholtan, *Makromol. Chem.*, **11**, 131 (1953).

(21) S. Keipert, J. Becker, and R. Voigt, *Pharmazie*, **32**, 280 (1977).

(22) S. Keipert and R. Voigt, *ibid.*, **30**, 589 (1975).

(23) T. Higuchi and R. Kuramoto, *J. Am. Pharm. Assoc., Sci. Ed.*, **43**, 398 (1954).

(24) P. Alexander and R. J. Block, "Analytical Methods of Protein Chemistry," vol. 2, Pergamon, London, England, 1960.

(25) G. Glasstone and D. Lewis, "Elements of Physical Chemistry," 2nd ed., Macmillan, London, England, 1963.

(26) C. B. Anfinsen, M. L. Anson, K. Bailey, and J. T. Edsall, "Advances in Protein Chemistry," vol. XIV, Academic, London, England, 1959.

(27) A. Ray, J. A. Reynolds, H. Polet, and J. Steinhardt, *Biochemistry*, **5**, 2606 (1966).

(28) W. Scholtan, *Arzneim.-Forsch.*, **14**, 348 (1964).

(29) *Ibid.*, **14**, 469 (1964).

(30) M. J. Cho, A. G. Mitchell, and M. Pernarowski, *J. Pharm. Sci.*, **60**, 196 (1971).

(31) B. C. Lippold and B. H. Lippold, *Pharmazie*, **29**, 534 (1974).

(32) R. Voigt, J. Becker, and S. Keipert, *ibid.*, **32**, 284 (1977).

(33) S. Keipert, J. Becker, and R. Voigt, *ibid.*, **32**, 228 (1977).

(34) R. Voigt, H. H. Schultze, and S. Keipert, *ibid.*, **31**, 863 (1976).

(35) S. Keipert, I. Korner, and R. Voigt, *ibid.*, **3**, 790 (1976).

(36) E. Ullmann, K. Thoma, and P. Mohrschulz, *Arch. Pharm.*, **302**, 756 (1969).

ACKNOWLEDGMENTS

Presented at the F.I.P. Congress, Brighton, England, September 1979.

Abstracted in part from a thesis submitted by J. A. Plaizier-Vercammen to the Vrije Universiteit Brussel in partial fulfillment of the Doctor of Philosophy degree requirements.

[7] Kollidon K-30.

Suppression of Endogenous Hydrocortisone with Dexamethasone

THOMAS J. GOEHL *x, GLORIA M. SUNDARESAN *, JOHN P. HUNT *, VADLAMANI K. PRASAD *, ROGER D. TOOTHAKER ‡, and PETER G. WELLING ‡

Received March 17, 1980, from the *Biopharmaceutics Laboratory Branch, Division of Biopharmaceutics, Food and Drug Administration, Washington, DC 20204, and the ‡School of Pharmacy, University of Wisconsin, Madison, WI 53706. Accepted for publication June 12, 1980.

Abstract □ A newly developed high-pressure liquid chromatographic method was used to study the optimum dosage regimen needed to suppress endogenous hydrocortisone. Nine volunteers were randomly placed in three groups. Each group received 1 mg of dexamethasone at 11 pm (Treatment A), 2 mg of dexamethasone at 11 pm (Treatment B), or 1 mg at 11 pm and an additional 1 mg at 6 am the following day (Treatment C). Analysis of multiple blood samples obtained the day before and the day after drug administration showed suppression in all three groups. Although the duration and extent of this suppression varied, adequate suppression to permit bioavailability studies was observed for Treatments B and C.

Keyphrases □ Hydrocortisone—suppression of endogenous hydrocortisone with dexamethasone □ Dexamethasone—suppression of endogenous hydrocortisone

The principal natural glucocorticoid in humans is hydrocortisone (1). Although numerous synthetic glucocorticoids have been prepared, hydrocortisone remains an important agent in modern adrenocorticosteroid therapy, and many generic formulations have appeared on the market. However, the bioequivalence of these products has not been established. To conduct bioequivalence studies, assay methodology must be available with the required sensitivity, specificity, accuracy, and precision. A number of apparently adequate high-pressure liquid chromatographic (HPLC) methods have been reported recently (2–9).

BACKGROUND

Hydrocortisone production follows a circadian rhythm, so suppression of hydrocortisone production is necessary to simplify the interpretation of bioavailability data. Therefore, in addition to an appropriate analytical procedure, a method that will adequately suppress the endogenous hydrocortisone levels is needed. Without this suppression, it is not possible to quantitate the bioavailability of the administered hydrocortisone dosage forms. One way to achieve this suppression is to administer dexamethasone. This procedure was used in studies on prednisone (10, 11) and prednisolone (12, 13). In these cases, dexamethasone administration was necessary since endogenous steroids cross react with the antiserums used in these radioimmunoassays.

Dexamethasone is thought to act by blocking the release of endogenous ACTH (14). However, no extended detailed quantitative study has been performed to determine the amount of dexamethasone required to suppress endogenous steroids. The duration of such suppression also is not clearly established.

In one study (15), hydrocortisone levels were determined at 2 and 4 hr after administration of 1 mg of dexamethasone. During this period, hydrocortisone levels dropped to 14% of their basal values. In another study (16), the degree of suppression of endogenous hydrocortisone was related to the time of day the dexamethasone was administered. In a third study (17), 8 mg of dexamethasone was given for 2 days. The mean plasma hydrocortisone level for the subjects was 6.8 ng/ml; the blood sampling time was not given.

The present paper explores the extent and duration of dexamethasone suppression of circulating endogenous hydrocortisone using a newly developed, highly sensitive and specific HPLC assay.

EXPERIMENTAL

The nine normal male volunteers (22–45 years old) involved in this study had normal vital signs and selected laboratory parameters. The subjects, 63–80 kg, were randomly assigned to three groups of three each (Table I). Group A received 1 mg of dexamethasone, Group B received 2 mg of dexamethasone, and Group C received 2 mg of dexamethasone in two 1-mg divided doses administered 7 hr apart. Dexamethasone was given as an oral elixir[1] (0.5 mg/5 ml) in all cases.

Table I—Subject Data

Identification	Group	Height, cm	Weight, kg	Age, years
1	A	185	73	28
2	A	180	80	22
3	A	170	63	25
4	B	168	74	37
5	B	170	77	31
6	B	178	66	28
7	C	185	75	39
8	C	180	75	22
9	C	178	64	45

Basal values for plasma hydrocortisone levels were determined from heparinized blood samples (8 ml each) obtained at 8 am, 10 am, 12 noon, 2 pm, 4 pm, 6 pm, and 8 pm on Day 1 of the study. Prior to receiving the evening dexamethasone dose, the subjects were required to fast after 8 pm and to maintain that fast until noon the following day. At 11 pm on the same evening, dexamethasone (Groups A and C, 1 mg; and Group B, 2 mg) was administered to all volunteers followed by 180 ml of water. The following morning (Day 2), subjects in Group C received an additional 1 mg of dexamethasone followed by 180 ml of water at 6 am. Heparinized blood samples then were taken from all volunteers beginning at 8 am and continuing at 10 am, 12 noon, 2 pm, 4 pm, 6 pm, and 8 pm. All samples were collected, and the plasma was separated and frozen until it was assayed for hydrocortisone.

All plasma samples were assayed using a previously reported HPLC method (9) with minor modifications. An internal standard (4-pregnene-17α, 20α,21-triol-3,11-dione) was added to the plasma, which then was extracted with methylene dichloride–ether (60:40). After separation and evaporation of the organic phase, derivatization was carried out with dansylhydrazine. Upon completion of the reaction, the excess dansylhydrazine was reacted with pyruvic acid and a second extraction was performed.

The samples were placed in a water bath at room temperature and were evaporated just to dryness under a gentle nitrogen stream. The residue was immediately taken up in 200 μl of the HPLC mobile phase. Five microliters of this solution was injected[2] later onto a well-conditioned microparticulate silica column[3]. Elution[4] was carried out with an ethylene dichloride–butanol–water (93:6.6:0.4) mobile phase (1.5 ml/min). Conditioning of the column was achieved by pumping the mobile phase through the column for 1–2 days. The effluent was monitored with a fluorescence detector[5] [excitation, 240 nm; emission, 470 nm (cutoff filter)]. A linear calibration curve was found for hydrocortisone concentrations from 3 to 1000 ng/ml.

A special glassware cleaning procedure was adopted to eliminate extraneous chromatographic peaks that sometimes were observed. The procedure consisted of rinsing the glassware with distilled water (no soap was used), placing it into a commercial oven[6], which then was carried through a self-cleaning cycle, and rinsing all of the items with distilled water and methanol.

The hydrocortisone levels present in the clinical plasma samples were

[1] Decadron, lot A3240, Merck Sharp and Dohme.
[2] Model U6K sample injection valve, Waters Associates, Milford, Mass.
[3] Prepacked Hibar II column with LiChrosorb SI-60 5-μm silica, Applied Science Laboratories, State College, Pa.
[4] Model M6000A pump, Waters Associates, Milford, Mass.
[5] Model FS970, Schoeffel Instruments, Westwood, N.J.
[6] Kenmore model 423 self-cleaning oven, Sears, Roebuck and Co., Chicago, Ill.

0022-3549/80/1200-1409$01.00/0
© 1980, American Pharmaceutical Association

Table II—Basal Plasma Hydrocortisone Levels on Day 1 of Study

	Hydrocortisone Concentration, ng/ml								
	Group A			Group B			Group C		
Time	Subject 1	Subject 2	Subject 3	Subject 4	Subject 5	Subject 6	Subject 7	Subject 8	Subject 9
8 am	116	182	150	114	162	212	208	138	78
10 am	148	218	102	126	120	182	210	164	98
Noon	56	108	108	100	94	130	92	92	86
2 pm	76	164	128	76	144	138	74	122	86
4 pm	94	120	90	62	60	100	78	88	42
6 pm	102	148	148	28	94	96	88	126	58
8 pm	44	102	24	14	46	68	42	104	28

Table III—Plasma Hydrocortisone Levels on Day 2 after Dexamethasone Administration

	Hydrocortisone Concentration, ng/ml								
	Group A			Group B			Group C		
Time	Subject 1	Subject 2	Subject 3	Subject 4	Subject 5	Subject 6	Subject 7	Subject 8	Subject 9
8 am	7	8	12	10	10	7	16	8	16
10 am	12	7	4	7	9	7	9	6	8
Noon	24	8	18	6	9	10	7	8	11
2 pm	10	8	12	10	11	10	11	10	14
4 pm	13	7	9	11	8	8	7	7	12
6 pm	40	82	36	10	7	9	8	9	7
8 pm	14	44	14	8	36	9	8	19	9

determined from standard curves prepared by plotting the peak height ratios of the dansylhydrazones of hydrocortisone and the internal standard *versus* the concentrations of the known standards. To correct the standard curve for endogenous levels of hydrocortisone present in the control plasma, the peak height ratio of the control plasma was subtracted from all data points used in the standard curve.

RESULTS AND DISCUSSION

To establish the regimen for dexamethasone administration that would sufficiently suppress endogenous hydrocortisone production, three dexamethasone regimens were evaluated. The basal plasma levels of hydrocortisone in all nine subjects on Day 1 are recorded in Table II. There was a general trend, but not a smooth progression, of decreasing plasma levels from morning to evening. This trend agrees with the observation that plasma hydrocortisone levels follow a circadian rhythm.

The plasma levels of hydrocortisone on Day 2 are given in Table III. Substantial suppression was seen in all subjects. The plasma levels in subjects on Treatment C did not exceed 16 ng/ml from 8 am to 6 pm. Volunteers receiving Treatment B had plasma levels below 11 ng/ml throughout the same period. The plasma levels achieved with both Treatments B and C were quite stable. Suppression of endogenous hydrocortisone was not as complete in the subjects receiving Treatment A and showed greater variations. All three volunteers in Group A had plasma levels of at least 36 ng/ml by 6 pm on Day 2.

Since stress is known to affect the plasma levels of endogenous hydrocortisone (18), concern existed about the possibility of endogenous hydrocortisone levels fluctuating after suppression had been achieved with dexamethasone administration. In this study, the plasma level fluctuations seen during the control period were virtually absent in the postadministration period. This finding is important since any significant variations in the suppressed plasma hydrocortisone levels would seriously hinder the interpretation of bioavailability data of hydrocortisone dosage forms.

A profile analysis (19) using an F test for the average treatment effects, time effects, treatment with time effects, and subject effects was performed on the basal and suppressed plasma hydrocortisone levels. The data were analyzed by comparing Treatment A with Treatments B and C as well as Treatment B with Treatment C. The statistical analysis of basal plasma levels indicated that there were no significant differences due to what were evaluated as treatment effects ($p = 0.52$ and 0.90) and no significant differences due to treatment with time effects ($p = 0.29$ and 0.56). However, there were significant differences due to time ($p = 0.0001$) and intersubject variability ($p = 0.0001$), which could be expected. For the suppressed plasma hydrocortisone levels, the analysis indicated Treatment A was significantly different from Treatments B and C ($p = 0.007$). Treatments B and C were not significantly different ($p = 0.97$). A test of the treatment with time effects likewise indicated that Treatment A was significantly different from Treatments B and C ($p = 0.0001$) but that Treatments B and C were not ($p = 0.98$).

As shown in the preceding analysis, the extent and duration of the suppression of endogenous plasma hydrocortisone were similar with Treatments B and C. Therefore, selection of either regimen for subsequent bioavailability studies would be reasonable. However, since Treatment C requires an evening and a morning dose, Treatment B is more convenient. In addition, the possibility cannot be ruled out that an early morning dose of dexamethasone may affect the kinetics of orally administered hydrocortisone.

A study is underway to investigate the kinetics of hydrocortisone following a single oral dose; Treatment B administration of dexamethasone is being used.

REFERENCES

(1) "Remington's Pharmaceutical Sciences," 15th ed., A. Osol and J. E. Hoover, Eds., Mack Publishing Co., Easton, Pa., 1975, p. 893.

(2) J. Van Den Berg, C. R. Mol, R. S. Deelder, and J. H. H. Thijssen, *Clin. Chim. Acta*, **78**, 165 (1977).

(3) D. Gorg, J. Ayres, and J. Wagner, *Res. Commun. Chem. Pathol. Pharmacol.*, **18**, 137 (1977).

(4) D. Ishii, K. Hibi, K. Asai, M. Nagaya, K. Mochizuki, and K. Mochida, *J. Chromatogr.*, **156**, 173 (1978).

(5) N. R. Scott and P. F. Dixon, *ibid.*, **164**, 29 (1979).

(6) T. Kawasaki, M. Maeda, and A. Tsuji, *ibid.*, **163**, 143 (1979).

(7) J. Q. Rose and W. J. Juski, *ibid.*, **162**, 273 (1979).

(8) F. J. Frey, B. M. Frey, and L. Z. Benet, *Clin. Chem.*, **25**, 1944 (1979).

(9) T. J. Goehl, G. M. Sundaresan, and V. K. Prasad, *J. Pharm. Sci.*, **68**, 1374 (1979).

(10) T. J. Sullivan, M. R. Hallmark, E. Sakmar, D. J. Weidler, R. H. Earhart, and J. G. Wagner, *J. Pharmacokinet. Biopharm.*, **4**, 157 (1976).

(11) T. J. Sullivan, E. Sakmar, K. S. Albert, D. C. Blair, and J. G. Wagner, *J. Pharm. Sci.*, **64**, 1723 (1975).

(12) R. Leclercq and G. Copinschi, *J. Pharmacokinet. Biopharm.*, **2**, 175 (1974).

(13) T. J. Sullivan, R. G. Stoll, E. Sakmar, D. C. Blair, and J. G. Wagner, *ibid.*, **2**, 29 (1974).

(14) J. Kolanowski, M. A. Pizarro, and J. Crabbe, *J. Clin. Endocrinol. Metab.*, **41**, 453 (1975).

(15) S. Nishida, S. Matsumura, M. Horino, H. Oyama, and A. Tenku, *ibid.*, **45**, 585 (1977).

(16) T. Nichols, C. A. Nugent, and F. H. Tyler, *ibid.*, **25**, 343 (1965).

(17) H. H. Newsome, Jr., A. S. Clements, and E. H. Borum, *ibid.*, **34**, 473 (1972).

(18) M. M. Tacker, C. S. Leach, C. A. Owen, and J. A. Rummel, *J. Endocrinol.*, **76**, 165 (1978).

(19) B. J. Winer, "Statistical Principles in Experimental Design," 2nd ed., McGraw-Hill, New York, N.Y., 1971, p. 515.

Nasal Absorption of Propranolol from Different Dosage Forms by Rats and Dogs

ANWAR HUSSAIN ˣ, SHINICHIRO HIRAI, and RIMA BAWARSHI

Received October 22, 1979, from the *College of Pharmacy, University of Kentucky, Lexington, KY 40506.* Accepted for publication June 9, 1980.

Abstract □ The blood levels of propranolol in rats and dogs were compared after the administration of nasal, intravenous, and oral solutions. The results indicate that the blood drug levels after nasal and intravenous administration were identical, but the oral administration resulted in considerably lower blood levels. Sustained-release formulations of the drug also were administered nasally and resulted in low initial but prolonged blood levels. The bioavailability of the sustained-release formulation was identical to that of the intravenous administration.

Keyphrases □ Propranolol—nasal absorption from different dosage forms, rats and dogs □ Bioavailability—propranolol, comparison of sustained-release nasal formulation with intravenous administration, rats and dogs □ Absorption, nasal—propranolol from different dosage forms, rats and dogs

The oral administration of propranolol in human subjects resulted in considerable variation in plasma drug levels. Peak plasma levels in five subjects given 80-mg oral doses varied sevenfold, while 10-mg doses given intravenously to the same subjects varied only twofold (1). Furthermore, the bioavailability of an 80-mg oral dose in several subjects varied from 16 to 60% of that of a 10-mg iv dose. The variations in blood levels as well as the low bioavailability from oral doses have been attributed to extensive drug metabolism during absorption and first passage through the liver (1–3). A previous report (4) indicated that the blood levels of propranolol after intravenous and nasal administration of 1-mg doses in rats were identical but that oral administration of the same dose resulted in considerably lower blood levels.

This report presents the results on the nasal absorption of propranolol in rats and dogs after its administration in a solution and a sustained-release formulation.

Table I—Composition of Sustained-Release Dosage Forms of Propranolol Used in Rat Studies

Ingredient	Formulation		
	SR-A	SR-B	SR-C
Propranolol hydrochloride, mg	1	—	—
Propranolol (base), mg	—	0.88[a]	—
Propranolol stearate, mg	—	—	1.84[a]
Methylcellulose, mg	3	3	3
Saline, ml	0.1	0.1	0.1

[a] One milligram as propranolol hydrochloride.

Table II—Composition of Dosage Forms of Propranolol Used in Dog Studies

Ingredient	Intravenous	Oral	Nasal		
			Solution	SR-D	SR-E
Propranolol hydrochloride, mg	20	20	20	—	—
Propranolol stearate, mg	—	—	—	36.8[a]	36.8[a]
Methylcellulose, mg	—	—	—	—	15
Saline, ml	1	50	0.2	0.5	0.5

[a] Twenty milligrams as propranolol hydrochloride.

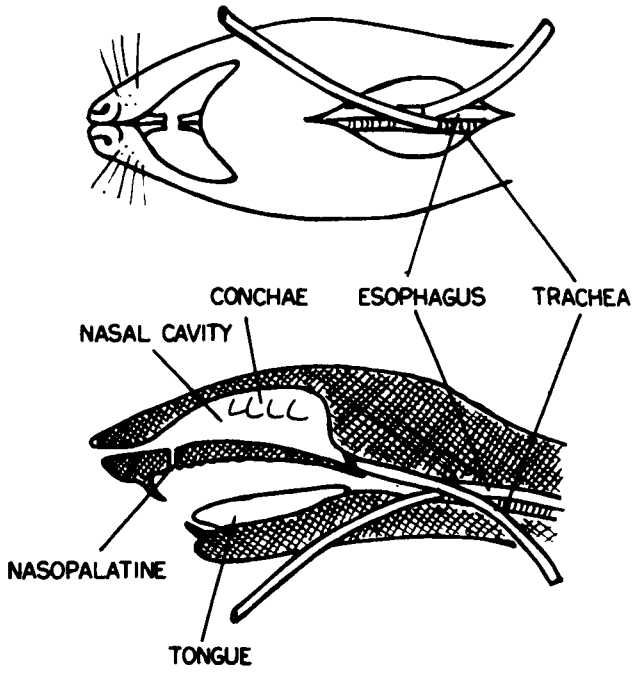

Figure 1—*Diagram of the surgical procedure of nasal absorption in the rat.*

EXPERIMENTAL

Materials—Propranolol hydrochloride USP[1], propranolol free base, and propranolol stearate were used. Propranolol free base and propranolol stearate were prepared from propranolol hydrochloride.

Composition of Formulations—The formulations used in the rat and dog studies are listed in Tables I and II, respectively.

***In Vitro* Dissolution**—The dissolution study was carried out using the USP rotating-basket method; 0.2 g of Formulation SR-A, SR-B, or SR-C was placed in the basket, which was lined from the inside with filter paper. (The filter paper was used as a barrier for the diffusion of methylcellulose.) The dissolution medium consisted of 500 ml of pH 7.4 isotonic buffer at 37°. The basket was rotated at 100 rpm. A 0.5-ml volume of the medium was withdrawn periodically, added to 0.2 ml of 0.1 *N* HCl, and assayed later.

Animal Studies—*Rats*—Male Sprague–Dawley rats, ~270 g, were anesthetized with pentobarbital (50 mg/kg). The surgical operation carried out on the rats was that described by Hirai *et al.*[2] (Fig. 1). An incision was made in the neck, and the trachea was cannulated with a polyethylene tube[3]. Another tube was inserted from the esophagus to the posterior part of the nasal cavity. The nasopalatine was closed with an adhesive agent[4] to prevent drainage of the drug from the nasal cavity to the mouth. The sustained-release preparation (equivalent to 1 mg of propranolol hydrochloride) was administered to the nasal cavity through the tube by means of a syringe. Blood (0.1–0.2 ml) was sampled from the femoral aorta periodically and analyzed later.

Dogs—Three beagle dogs, ~10 kg, were used in this crossover study.

[1] Ayerst Laboratories, New York, N.Y.

[2] S. Hirai, T. Yashiki, and T. Matsuzawa, presented at the 98th annual meeting of the Pharmaceutical Society of Japan, Okayama, Japan, April 1978.

[3] PE 260, Intramedic, Clay Adams, New York, N.Y.

[4] Super Glue, Woodhill Permetex, Cleveland, Ohio.

0022-3549/80/1200-1411$01.00/0
© 1980, American Pharmaceutical Association

Table III—Peak Blood Level (C_{max}), Time to Peak (T_{max}), and Area under Curve (AUC) after Nasal Administration of Sustained-Release Dosage Forms of Propranolol in Rats

Route	C_{max}, ng/ml[a]	T_{max}, min	$AUC_{0-\infty}$, (ng hr)/ml[a]	$\frac{AUC_{oral,nasal}}{AUC_{iv}}$
Intravenous	—	—	1033.8 ± 30.8	—
Oral	96.9 ± 18.6	50.0	196.9 ± 25.8	0.190
Nasal				
Solution	1161.4 ± 29.0	6.3	1033.0 ± 48.7	0.999
SR-A	949.0 ± 46.5	10.0	968.4 ± 15.4	0.936
SR-B	912.3 ± 88.3	13.3	1031.1 ± 42.1	0.997
SR-C	341.5 ± 35.5	71.2	1044.1 ± 30.5	1.009

[a] Mean ± SE (n = 3 or 4).

Table IV—Peak Plasma Level (C_{max}), Time to Peak (T_{max}), and Area under Curve (AUC) after Intravenous, Oral, and Nasal Administration of Propranolol in Dogs

Route	C_{max}, ng/ml[a]	T_{max}, min	$AUC_{0-\infty}$, (ng hr)/ml[a]	$\frac{AUC_{oral,nasal}}{AUC_{iv}}$
Intravenous	—	—	1892.1 ± 102.1	—
Oral	42.5 ± 7.2	50	130.1 ± 8.2	0.068
Nasal				
Solution	1539.2 ± 70.9	5	1942.1 ± 64.2	1.026
SR-D	236.6 ± 24.3	80	1902.3 ± 66.4	1.005
SR-E[b]	64.3 ± 5.6	180	—	—

[a] Mean ± SE (n = 3). [b] Not enough points to calculate $AUC_{0-\infty}$.

For the intravenous administration, the dogs were anesthetized with the intravenous injection of 30 mg of pentobarbital sodium/kg. The administered solution (20 mg of propranolol hydrochloride) was injected through the cubital vein. For the oral administration, the dogs were not anesthetized and the drug was administered by a stomach tube. For the nasal administration, the dogs were anesthetized and both the solution and the sustained-release preparation were administered to the nasal cavity through the nostrils with a micropipet and a syringe, respectively. Blood was sampled periodically from the cubital vein. After centrifugation, 0.5 ml of plasma was separated and analyzed later.

Analytical Method—Blood and plasma levels of propranolol were assayed spectrophotofluorometrically by a minor modification of the method of Shand *et al.* (1). Distilled water (0.5 ml) was added to 0.1–0.5 ml of blood or plasma. The mixture then was made alkaline with 0.5 ml of 1 *N* NaOH and extracted into 10 ml of heptane. After shaking and centrifugation, 8 ml of the heptane layer was extracted into 1.5 ml of 0.1 *N* HCl; the fluorescence of the acid layer was determined by a spectrophotofluorometer[5] (maximum excitation at 295 nm and maximum emission at 360 nm). The minimum detectable concentration was 3 ng/ml; pentobarbital did not interfere with the assay. Corrections were made for the blank.

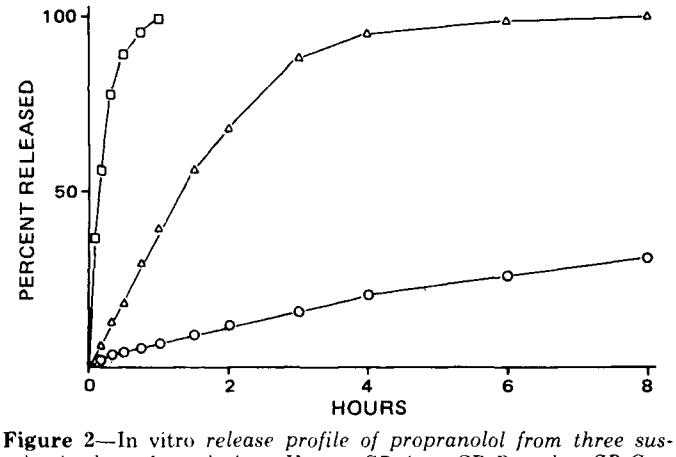

Figure 2—In vitro *release profile of propranolol from three sustained-release formulations. Key:* □, *SR-A;* △, *SR-B; and* ○, *SR-C.*

[5] Aminco-Bowman model 768 G, American Instrument Co., Silver Spring, Md.

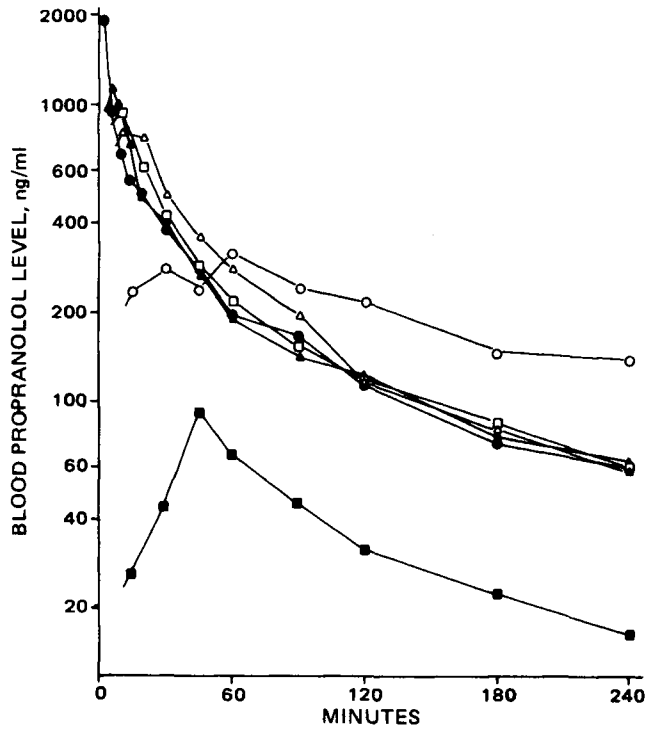

Figure 3—*Mean blood levels of propranolol in rats* (n = *3 or 4*). *Key:* □, *nasal SR-A;* △, *nasal SR-B;* ○, *nasal SR-C;* ▲, *nasal solution;* ●, *intravenous; and* ■, *oral.*

The samples of the *in vitro* dissolution study also were analyzed spectrophotofluorometrically.

RESULTS

Figure 2 shows the *in vitro* release profile of propranolol from three sustained-release formulations (SR-A, SR-B, and SR-C) administered nasally to rats.

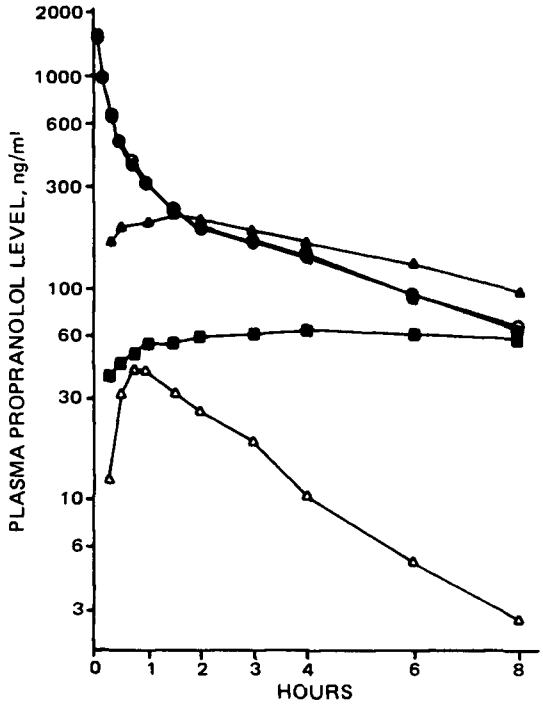

Figure 4—*Mean blood levels of propranolol in dogs* (n = *3*). *Key:* ○, *intravenous;* △, *oral;* ●, *nasal solution;* ▲, *nasal SR-D; and* ■, *nasal SR-E.*

Figure 3 shows the mean blood propranolol levels in rats after the nasal administration of the sustained-release formulations as compared to those obtained previously (4) after intravenous, oral, and nasal administration of an isotonic solution of the drug.

The pharmacokinetic parameters calculated for the different formulations and for the different administration routes are shown in Table III.

Figure 4 shows the mean plasma level in dogs after the nasal administration of the solution and two sustained-release formulations as well as the intravenous and oral solutions. Table IV shows the pharmacokinetic parameters in dogs calculated for the different formulations and for the different administration routes.

DISCUSSION

The oral administration of propranolol to human subjects resulted in low and variable plasma drug levels compared to intravenous administration (1). Similar results were obtained in rats and dogs after the oral administration of propranolol solution (Figs. 3 and 4). However, the data in Figs. 3 and 4 clearly show that the nasal administration of the drug solution in both rats and dogs resulted in plasma drug levels similar to those of an intravenous administration. The data in Figs. 3 and 4 show that the sustained-release formulations resulted in lower initial blood levels of the drug. However, the drug level in the blood was maintained longer. Furthermore, the blood drug profile from the sustained-release formulations administered to rats correlated with the *in vitro* (Fig. 2) release of the drug from these formulations.

The pharmacokinetic parameters for the different formulations and different administration routes obtained for both rats and dogs are shown in Tables III and IV, respectively. The maximum blood levels of the drug observed after administration of the sustained-release formulations were much lower than those observed after administration of the nasal solutions. However, the bioavailability calculated from the area under the blood level curves was identical.

The results of this study strongly suggest that the nasal administration of propranolol is superior to the oral route and as effective as the intravenous route. A study is underway on the bioavailability of propranolol from nasal dosage forms in humans.

REFERENCES

(1) D. G. Shand, E. M. Nuckolls, and J. A. Oates, *Clin. Pharmacol. Ther.*, **11**, 112 (1970).

(2) T. Suzuki, Y. Saitoh, S. Isozaki, and R. Ishida, *Chem. Pharm. Bull.*, **20**, 2731 (1972).

(3) T. Walle, T. C. Fagan, E. C. Conradi, U. K. Walle, and T. E. Gaffney, *Clin. Pharmacol. Ther.*, **26**, 167 (1979).

(4) A. A. Hussain, S. Hirai, and R. Bawarshi, *J. Pharm. Sci.*, **68**, 1196 (1979).

Pharmacokinetics of Phenylbutazone in Healthy Subjects after Oral Administration of Single and Multiple Doses

A. SIOUFI *x, D. COLUSSI *, F. CAUDAL *, J. P. SCHOELLER ‡, and P. MASSIAS §

Received December 10, 1979, from the **Biopharmaceutical Research Center and the* ‡*Medical Department, Ciba-Geigy, Rueil-Malmaison, France,* and the §*Department of Rheumatic Diseases, Antoine Béclère Hospital, Clamart, France.* Accepted for publication June 23, 1980.

Abstract □ Plasma concentration profiles were studied after single oral doses of phenylbutazone of 100, 300, and 600 mg in cachets to six healthy volunteers. The pharmacokinetics of phenylbutazone can be described by a two-compartment open model. The drug is absorbed rapidly and distributed partially into an extravascular compartment; about one-third remains in the plasma. The mean elimination half-life was 77 hr (54–99 hr), and there was a linear relationship between the dose and the area under the plasma concentration curve. In a multiple-dose study, six healthy volunteers received 150 mg of phenylbutazone in cachets twice daily every 11–13 hr for 17 days. A steady state was reached after ~200 hr of chronic treatment. The resultant steady-state plasma concentrations were about four times higher than the peak concentration produced by a single 150-mg dose. The half-lives corresponding to the apparent elimination rate constant for the first and last administrations did not differ in each subject. The theoretical minimum concentrations are higher than the pseudosteady state reached during chronic treatment.

Keyphrases □ Phenylbutazone—pharmacokinetics after single and multiple oral doses □ Pharmacokinetics—phenylbutazone, single and multiple oral doses □ Anti-inflammatory agents—phenylbutazone, pharmacokinetics after single and multiple oral doses

Phenylbutazone has been used as an anti-inflammatory agent for about 25 years. After oral administration, it is completely and rapidly (1) absorbed and almost completely metabolized (1–3). Its half-life in plasma ranges from 1 to 3 days (1, 2, 4–6) and shows large interindividual differences. Phenylbutazone is highly protein bound (~99%) (1). The drug is eliminated mainly in the urine (60–70%) (1, 2).

The single-dose kinetics of phenylbutazone have been studied (1, 7, 8), and two-compartment model was proposed for it (8). There is an almost linear relationship between the dose and the area under the plasma concentration curve (*AUC*) (9).

No precise information is available on multiple-dose kinetics. The steady-state plasma levels of phenylbutazone were measured by several investigators (1, 10–14) and were predicted by Orme *et al.* (12) from knowledge of the half-lives of antipyrine in individual subjects but not from the single-dose kinetics of phenylbutazone. The discrepancy between predicted and measured steady-state plasma levels of phenylbutazone has been discussed, and it was suggested that an increase in the volume of distribution occurs after multiple dosing (14).

Recent advances in analytical methodology (15) have made possible the investigation of the pharmacokinetics of phenylbutazone in humans in greater detail. This report describes the plasma concentration profiles obtained after the oral administration of phenylbutazone in single doses of 100, 300, and 600 mg and after repeated administration of 150 mg twice daily for 17 days.

0022-3549/80/1200-1413$01.00/0
© 1980, American Pharmaceutical Association

Figure 3 shows the mean blood propranolol levels in rats after the nasal administration of the sustained-release formulations as compared to those obtained previously (4) after intravenous, oral, and nasal administration of an isotonic solution of the drug.

The pharmacokinetic parameters calculated for the different formulations and for the different administration routes are shown in Table III.

Figure 4 shows the mean plasma level in dogs after the nasal administration of the solution and two sustained-release formulations as well as the intravenous and oral solutions. Table IV shows the pharmacokinetic parameters in dogs calculated for the different formulations and for the different administration routes.

DISCUSSION

The oral administration of propranolol to human subjects resulted in low and variable plasma drug levels compared to intravenous administration (1). Similar results were obtained in rats and dogs after the oral administration of propranolol solution (Figs. 3 and 4). However, the data in Figs. 3 and 4 clearly show that the nasal administration of the drug solution in both rats and dogs resulted in plasma drug levels similar to those of an intravenous administration. The data in Figs. 3 and 4 show that the sustained-release formulations resulted in lower initial blood levels of the drug. However, the drug level in the blood was maintained longer. Furthermore, the blood drug profile from the sustained-release formulations administered to rats correlated with the *in vitro* (Fig. 2) release of the drug from these formulations.

The pharmacokinetic parameters for the different formulations and different administration routes obtained for both rats and dogs are shown in Tables III and IV, respectively. The maximum blood levels of the drug observed after administration of the sustained-release formulations were much lower than those observed after administration of the nasal solutions. However, the bioavailability calculated from the area under the blood level curves was identical.

The results of this study strongly suggest that the nasal administration of propranolol is superior to the oral route and as effective as the intravenous route. A study is underway on the bioavailability of propranolol from nasal dosage forms in humans.

REFERENCES

(1) D. G. Shand, E. M. Nuckolls, and J. A. Oates, *Clin. Pharmacol. Ther.*, **11**, 112 (1970).

(2) T. Suzuki, Y. Saitoh, S. Isozaki, and R. Ishida, *Chem. Pharm. Bull.*, **20**, 2731 (1972).

(3) T. Walle, T. C. Fagan, E. C. Conradi, U. K. Walle, and T. E. Gaffney, *Clin. Pharmacol. Ther.*, **26**, 167 (1979).

(4) A. A. Hussain, S. Hirai, and R. Bawarshi, *J. Pharm. Sci.*, **68**, 1196 (1979).

Pharmacokinetics of Phenylbutazone in Healthy Subjects after Oral Administration of Single and Multiple Doses

A. SIOUFI *x, D. COLUSSI *, F. CAUDAL *, J. P. SCHOELLER ‡, and P. MASSIAS §

Received December 10, 1979, from the **Biopharmaceutical Research Center and the* ‡*Medical Department, Ciba-Geigy, Rueil-Malmaison, France,* and the §*Department of Rheumatic Diseases, Antoine Béclère Hospital, Clamart, France.* Accepted for publication June 23, 1980.

Abstract □ Plasma concentration profiles were studied after single oral doses of phenylbutazone of 100, 300, and 600 mg in cachets to six healthy volunteers. The pharmacokinetics of phenylbutazone can be described by a two-compartment open model. The drug is absorbed rapidly and distributed partially into an extravascular compartment; about one-third remains in the plasma. The mean elimination half-life was 77 hr (54–99 hr), and there was a linear relationship between the dose and the area under the plasma concentration curve. In a multiple-dose study, six healthy volunteers received 150 mg of phenylbutazone in cachets twice daily every 11–13 hr for 17 days. A steady state was reached after ~200 hr of chronic treatment. The resultant steady-state plasma concentrations were about four times higher than the peak concentration produced by a single 150-mg dose. The half-lives corresponding to the apparent elimination rate constant for the first and last administrations did not differ in each subject. The theoretical minimum concentrations are higher than the pseudosteady state reached during chronic treatment.

Keyphrases □ Phenylbutazone—pharmacokinetics after single and multiple oral doses □ Pharmacokinetics—phenylbutazone, single and multiple oral doses □ Anti-inflammatory agents—phenylbutazone, pharmacokinetics after single and multiple oral doses

Phenylbutazone has been used as an anti-inflammatory agent for about 25 years. After oral administration, it is completely and rapidly (1) absorbed and almost completely metabolized (1–3). Its half-life in plasma ranges from 1 to 3 days (1, 2, 4–6) and shows large interindividual differences. Phenylbutazone is highly protein bound (~99%) (1). The drug is eliminated mainly in the urine (60–70%) (1, 2).

The single-dose kinetics of phenylbutazone have been studied (1, 7, 8), and two-compartment model was proposed for it (8). There is an almost linear relationship between the dose and the area under the plasma concentration curve (*AUC*) (9).

No precise information is available on multiple-dose kinetics. The steady-state plasma levels of phenylbutazone were measured by several investigators (1, 10–14) and were predicted by Orme *et al.* (12) from knowledge of the half-lives of antipyrine in individual subjects but not from the single-dose kinetics of phenylbutazone. The discrepancy between predicted and measured steady-state plasma levels of phenylbutazone has been discussed, and it was suggested that an increase in the volume of distribution occurs after multiple dosing (14).

Recent advances in analytical methodology (15) have made possible the investigation of the pharmacokinetics of phenylbutazone in humans in greater detail. This report describes the plasma concentration profiles obtained after the oral administration of phenylbutazone in single doses of 100, 300, and 600 mg and after repeated administration of 150 mg twice daily for 17 days.

0022-3549/80/1200-1413$01.00/0
© 1980, American Pharmaceutical Association

EXPERIMENTAL

Subjects—Six healthy volunteers were instructed to take no drugs of any kind for at least 1 week prior to the study and no drugs other than phenylbutazone during the experiment.

Five males and one female, 23–29 years and 58–95 kg, participated in the single-dose study. Subjects 2, 3, and 5 took part in the later multiple-dose study together with three additional volunteers. The subjects in this group of four males and two females were 22–29 years old and 59–80 kg.

Procedure—Phenylbutazone was given as the pure active ingredient in cachets without any excipient.

Single-Dose Study—Each subject received 100, 300, and 600 mg at 4-week intervals according to the crossover design. The doses were given to the fasting subjects with 100 ml of water at ~8 am, 2 hr before a light standardized breakfast. A standard lunch was given 4 hr later.

Blood samples (5 ml) were collected in heparinized tubes before and 0.5, 1, 2, 3, 4, 6, 8, 24, 48, 72, 96, and 168 hr after drug administration. The 48-hr sample was omitted after the 600-mg single dose, but additional samples were collected after 240 and 336 hr. Plasma was separated by centrifugation and kept at −20° until analysis.

Multiple-Dose Study—Each subject received one 150-mg dose on the 1st and 22nd days and 150 mg twice daily from the 5th day until the 21st day. The interval after the first dose was allowed so that the total plasma concentration curve of the first dose could be plotted over 96 hr. Morning doses were taken at ~9 am during breakfast. Evening doses were taken during the meal at ~8 pm.

Blood samples were collected in heparinized tubes at various times after the first and last administrations and just before each morning dose during chronic treatment. Plasma was obtained by centrifugation and kept at −20° until the time of analysis.

Drug Assay—Phenylbutazone was assayed in plasma samples from the single-dose study by a GLC method using a flame-ionization detector that measured concentrations as low as 250 ng/ml of plasma. All samples were assayed in duplicate.

In the meantime, a new GLC method (15) was developed using an electron-capture detector capable of determining concentrations down to 10 ng/ml of plasma with the same extraction procedure as used in the flame-ionization technique. Plasma samples from the multiple-dose study were analyzed for phenylbutazone by the electron-capture GLC method. All samples were assayed in duplicate.

Both methods yielded similar results for the same set of samples. Two spiked plasma solutions were prepared (250 and 2500 ng of phenylbutazone/ml of plasma) and analyzed six times by the flame-ionization method and six times by the electron-capture method for each concentration. The results were 250.8 ± 3.6 (*CV*%, n = 6) and 2473.3 ± 4.3 with flame-ionization detection and 249.8 ± 5.0 and 2483.0 ± 5.3 with electron-capture detection.

Moreover, the three unconjugated metabolites of phenylbutazone in plasma (15) were tested by the flame-ionization and electron-capture methods. None of these metabolites interfered with phenylbutazone chromatography.

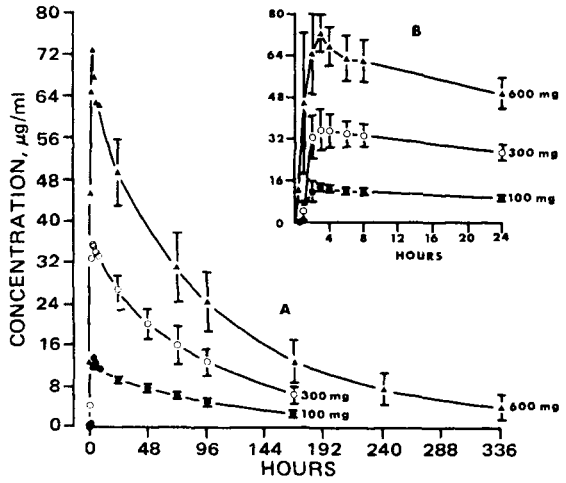

Figure 1—*Mean plasma phenylbutazone concentrations* (±SD) *in six healthy volunteers for doses of 100* (●), *300* (○), *and 600* (▲) *mg. Curve A shows concentrations up to 168 hr for 100 and 300 mg and up to 336 hr for 600 mg. Curve B shows concentrations up to 24 hr.*

Table I—Individual Pharmacokinetic Parameters of Phenylbutazone from Single-Dose Study [a]

Dose, mg	Subject	C_{max}, μg/ml	T_{max}, hr	$T_{1/2}$, hr	AUC_∞, (μg hr)/ml
100	1	12.48	1.81	99.0	1188
	2	17.05	2.88	74.5	1496
	3	14.25	3.22	73.7	1080
	4	12.63	7.03	83.5	1596
	5	13.80	2.90	66.0	1167
	6	15.32	1.81	63.6	1108
	Mean	14.25		76.7	1272
	SD	1.73		13.0	217
	Median		2.89		
300	1	35.05	3.29	86.6	3470
	2	42.96	5.09	54.1	3050
	3	30.77	5.86	74.5	3461
	4	46.33	1.85	78.7	4046
	5	35.43	3.23	82.5	3362
	6	39.97	2.86	70.7	3083
	Mean	38.41		74.5	3412
	SD	5.73		11.5	360
	Median		3.26		
600	1	51.18	6.38	92.4	6615
	2	81.44	3.57	70.0	6349
	3	81.34	2.35	82.5	7430
	4	83.30	2.96	94.8	9734
	5	88.11	1.73	62.4	5629
	6	65.87	0.99	70.0	4441
	Mean	75.20		78.7	6700
	SD	13.94		13.2	1795
	Median		2.65		

[a] C_{max}, T_{max}, and k_E values were calculated from the multiexponential equation giving the best fit to the experimental results. The $T_{1/2}$ values were derived from k_E, and the AUC values were extrapolated to time infinity according to the $T_{1/2}$ values.

Mathematical Methods—The calculations, curve fitting, and statistical analysis were carried out with the aid of a computer[1] equipped with a plotter[2].

RESULTS

Single-Dose Study—*Plasma Concentration–Time Curves*—The curves were obtained by using a multiexponential computer program that selects the equation giving the best fit to the experimental results. The individual curves, as well as the average curves (Fig. 1), exhibited a two-phase decline of the plasma concentration as a function of time. This finding indicates a distribution phase that is sufficiently slow, as compared to the absorption phase, to be visible after absorption is almost completed.

The pharmacokinetics of phenylbutazone, therefore, can be described by a two-compartment open model. With the assumption that all transfer processes, including absorption, are first order, such a model corresponds to a three-term exponential equation. In fact, 16 of the 18 individual curves fitted such an equation.

The equations of the average curves are as follows. For the 100-mg dose:

$$C = -88.00e^{-1.651t} + 12.22e^{-0.5606t} + 10.74e^{-0.0093t} \quad \text{(Eq. 1)}$$

For the 300-mg dose:

$$C = -180.00e^{-1.802t} + 4.87e^{-0.0920t} + 30.78e^{-0.0101t} \quad \text{(Eq. 2)}$$

For the 600-mg dose:

$$C = -152.38e^{-0.994t} + 5.94e^{-0.4005t} + 55.67e^{-0.0092t} \quad \text{(Eq. 3)}$$

The individual equations permitted the calculation of the pharmacokinetic parameters shown in Table I.

Absorption—Phenylbutazone was absorbed rapidly, with the maximum concentration being reached ~3 hr after administration. Nevertheless, the individual values of T_{max} were scattered, and there was a variable delay in some subjects before absorption started (lag time).

In six of 18 cases, the rate of absorption appeared to be slow initially and then increased gradually. This finding indicates that drug absorption was fast enough to have little, if any, effect on the other two phases, *i.e.*, distribution and elimination.

[1] Wang 720 C.
[2] IBM.

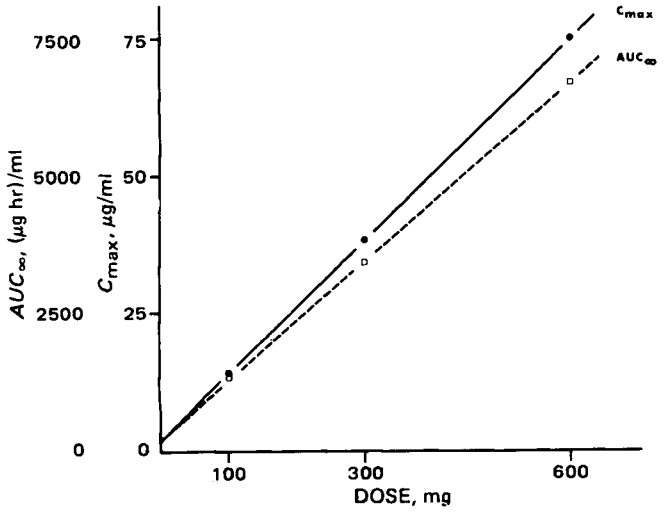

Figure 2—*Relationship between dose and* C_{max} (●) *and between dose and* AUC_∞ (□) *for phenylbutazone in a single-dose study.*

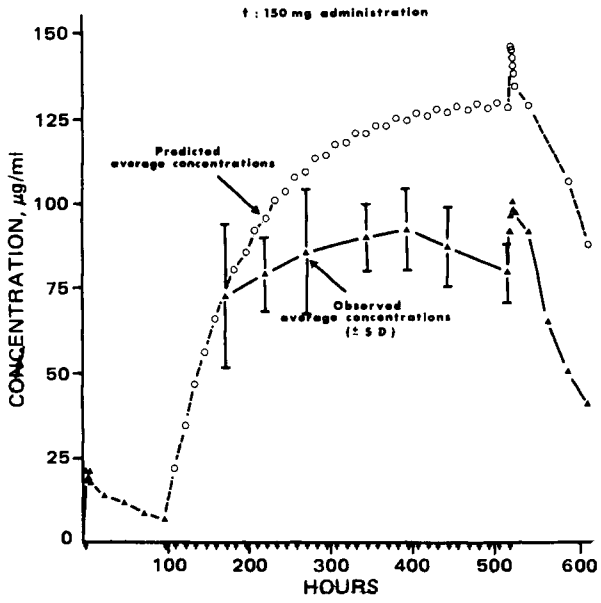

Figure 3—*Predicted* (○) *and observed* (▲) *average plasma concentrations of phenylbutazone during chronic treatment.*

Distribution—The apparent volume of distribution can be estimated from the area under the plasma concentration curve (AUC) and the elimination rate constant (k_E):

$$V_{area} = \frac{F \text{ dose}}{k_E AUC} \qquad \text{(Eq. 4)}$$

where F is the fraction of the dose absorbed.

The average value of the apparent volume of distribution (V_{area}) for all doses was 10.2 liters, assuming that $F = 1$. The volume of plasma (calculated on the basis of 41 ml/kg of body weight) was 2.9 liters. Since F is ≤ 1, ~30% of the administered phenylbutazone remained in the plasma.

Elimination—The overall elimination rate constant, k_E (Table I), clearly was independent of the dose. The mean elimination half-life for all doses was 77 hr, but the individual values varied from 54 to 99 hr. The intrasubject variation was less but was not negligible.

Dose Dependency of Pharmacokinetic Parameters—As shown in Fig. 2, there was a satisfactory linear relationship between the dose and C_{max} and between the dose and AUC_∞ (AUC extrapolated to infinity).

Multiple-Dose Study—Phenylbutazone elimination half-lives ($T_{1/2}$) estimated from the slope of the terminal linear segment of log–linear plots of the plasma concentration were similar at the beginning and end of the chronic treatment. Mean values (±SD) were 65.5 (±8.9) and 66.8 (±12.0) hr, respectively. The areas under the concentration profiles following administration of the first dose were measured by the trapezoidal rule and extrapolated to time infinity using the $T_{1/2}$ values. Their mean value (±SD) was 1697 (±231) (μg hr)/ml, which was in good agreement with the value calculated from the single-dose study [1706 (μg hr)/ml].

The AUC values after single doses were larger than those for a dose interval after multiple dosing; the mean values for the six subjects were 1697 (μg hr)/ml for AUC_0^∞ after a single dose and 1140 (μg hr)/ml for AUC_{504}^{516} after multiple doses. (Plasma levels after 516 hr were estimated roughly by interpolation from the 512- and 528-hr values.) The ratio of these two mean AUC values is similar to the ratio of the measured (~90 μg/ml) to the predicted (~130 μg/ml) steady-state plasma levels (~0.7).

As chronic treatment proceeded, the plasma phenylbutazone concentration measured just before the morning dose increased progressively up to values about four times higher than the peak concentration following the administration of the first dose of the treatment (mean value ± SD, 24.7 ± 6.2 μg/ml). Theoretical phenylbutazone concentrations just before the morning dose were obtained by the superposition technique and were distinctly higher than the corresponding experimental values (Fig. 3).

DISCUSSION

The pharmacokinetics of single doses of phenylbutazone can be described by a two-compartment open model. The drug was absorbed rapidly after oral administration in a single dose. It was distributed partially to an extravascular compartment, but at least one-third of the absorbed drug remained in the plasma. This finding is in agreement with the data reported by Burns *et al.* (1). The mean elimination half-life of phenylbutazone was ~77 hr, with individual values varying from 54 to 99 hr, which are within the reported range (1, 2, 4–6). There was a satisfactory linear relationship between the dose and the AUC. This finding is in agreement with the results reported by Lukas *et al.* (9); the fourfold increase of the dose did not cause a qualitative change in the elimination kinetics of phenylbutazone.

Single doses showed a linear relationship of AUC, C_{max}, and dose up to 600 mg, whereas upon multiple dosing, the plasma levels were lower than would be expected from a linear superposition of single-dose kinetics.

The differences found between single-dose predictions and actual steady-state concentrations cannot be correlated to the fact that two analytical procedures were used for the two phases of the study. Both methods yielded similar results for the same samples, and there was no interference between phenylbutazone and its three metabolites in the two methods.

In the multiple-dose study, the half-lives corresponding to the apparent elimination rate constant in each subject did not differ greatly for the first and last administrations. The theoretical minimum concentrations were much higher than the pseudosteady-state concentrations reached during chronic treatment in healthy volunteers.

The same effects were noticed by Edström (8) in patients with ankylosing spondylitis and by Orme and coworkers (12, 13) in patients with rheumatoid arthritis.

Burns *et al.* (1) showed that, after multiple dosing, increases in the dosage of phenylbutazone did not produce a proportional increase in plasma levels, which tended to reach a limiting concentration. Moreover, when phenylbutazone was administered intravenously to a subject whose plasma level was at this limiting concentration, the drug disappeared rapidly from the plasma until the level declined to the limiting value; after this level was reached, the concentration decreased at a much slower rate. Burns *et al.* (1) assumed that this phenomenon was due to a greatly increased rate of metabolism at higher dosages. The present results are not in agreement with this assumption; the half-life is at least as long at the end of chronic treatment as at the beginning.

On the condition that absorption is complete after multiple dosing, the present data show an increase in drug clearance from the plasma, since the steady-state levels are lower than predicted. However, since the elimination half-life is unchanged, the volume of distribution probably is increased. This is reasonable since phenylbutazone has a low extraction ratio and is highly protein bound. An increase in the free fraction at high concentrations (12, 13) would explain the increase in the clearance and the volume of distribution with no change in the half-life.

REFERENCES

(1) J. J. Burns, R. K. Rose, T. Chenkin, A. Goldman, A. Schulert, and B. B. Brodie, *J. Pharmacol. Exp. Ther.*, **109**, 346 (1953).

(2) W. Dieterle, J. W. Faigle, F. Früh, W. Theobald, K. O. Alt, and W. J. Richter, *Arzneim.-Forsch.*, **26**, 572 (1976).
(3) J. J. Burns, R. K. Rose, S. Goodwin, J. Reichenthal, E. C. Horning, and B. B. Brodie, *J. Pharmacol. Exp. Ther.*, **113**, 481 (1955).
(4) J. J. Burns, T. F. Yü, P. G. Dayton, A. B. Gutman, and B. B. Brodie, *Ann. N.Y. Acad. Sci.*, **86**, 253 (1960).
(5) A. B. Gutman, R. G. Dayton, T. F. Yü, L. Berger, W. Chen, L. E. Sicam, and J. J. Burns, *Am. J. Med.*, **29**, 1017 (1960).
(6) B. Herrmann, *Med. Exp.*, **1**, 170 (1960).
(7) G. R. Petten, H. Feng, R. J. Withey, and H. F. Lettau, *J. Clin. Pharmacol.*, **11**, 177 (1971).
(8) B. Edström, *Proc. Int. Symp. Stockholm*, A. Lindgren and Söner A. B., Mölndal, 1973, p. 84.
(9) G. Lukas, M. B. Maggio-Cavaliere, C. B. Borman, and J. D. Arnold, *J. Clin. Pharmacol.*, **14**, 397 (1974).
(10) D. S. Davies and S. S. Thorgeirsson, *Ann. N.Y. Acad. Sci.*, **79**, 411 (1971).
(11) D. S. Davies and S. S. Thorgeirsson, *Acta Pharmacol., Suppl. 3*, **29**, 181 (1971).
(12) M. Orme, P. J. L. Holt, G. R. V. Hughes, C. J. Bulpitt, G. H. Draffan, S. S. Thorgeirsson, F. Williams, and D. S. Davies, *Br. J. Clin. Pharmacol.*, **3**, 185 (1976).
(13) M. Orme, *J. Intern. Med. Res., Suppl. 2*, **5**, 40 (1977).
(14) D. S. Davies, *ibid.*, **5**, 15 (1977).
(15) A. Sioufi, F. Caudal, and F. Marfil, *J. Pharm. Sci.*, **67**, 243 (1978).

Bioavailability and Pharmacokinetics of a New, Slow-Release Potassium Chloride Capsule

J. ARNOLD *x, J. T. JACOB ‡, and B. RILEY ‡

Received November 20, 1979, from **Quincy Research Center, Kansas City, MO 64127*, and ‡*Berlex Laboratories Inc., Cedar Knolls, NJ 07927.* Accepted for publication June 26, 1980.

Abstract □ The bioavailability of a new, slow-release potassium chloride product consisting of coated beads in a hard gelatin capsule was compared with the bioavailability of two marketed products, an elixir and a slow-release tablet, by determining the urinary excretion of potassium. Twelve healthy male volunteers were dosed with a total of 80 mEq of potassium, in a single dose for the capsule and tablet and in three 26.6-mEq doses at 6-hr intervals for the elixir. Mean recoveries in 24-hr urine potassium levels from all three dosage forms after subtracting normal urine potassium excretion levels were 50.8% from the capsule, 53.9% from the elixir, and 63.1% from the tablet. Maximum excretion rates were reached at 2.0 hr for the elixir, 6.8 hr for the capsule, and 4.0 hr for the tablet. Fewer side effects were reported with the capsule than with the elixir and tablet.

Keyphrases □ Potassium chloride—bioavailability and pharmacokinetics of slow-release capsule □ Bioavailability—potassium chloride in slow-release capsule □ Pharmacokinetics—potassium chloride in slow-release capsule

Potassium chloride is indicated for the treatment of hypokalemic alkalosis associated with various cardiovascular disorders. Aqueous solutions of potassium chloride are effective potassium supplements when taken as prescribed; however, because of an unpleasant taste due to the chloride ion, patient compliance during long-term therapy has been a problem. More palatable forms of potassium salts, such as the gluconate or mixtures of bicarbonate, citrate, and acetate, are available, but the chloride ion has been shown to be a prerequisite for effective treatment (1).

BACKGROUND

A new, slow-release potassium chloride preparation containing 600 mg (8 mEq) of potassium chloride[1] in the form of small, nearly spherical beads enclosed in a hard gelatin capsule was developed to avoid or minimize a high localized concentration of potassium within the GI tract. The potassium chloride crystals are specially coated to permit a uniform, controlled *in vivo* release over 8–10 hr. Extensive toxicity testing in animals was carried out to compare the new capsule preparation with a marketed wax-matrix tablet[2]. The results indicated a marked difference in the ulcerogenic potential of the tablet and capsule dosage forms (2). Based on the animal toxicity data, it was concluded that the new capsule dosage form is not likely to cause local irritation of the GI mucosa.

Certain pharmacokinetic characteristics of potassium make accurate determination of bioavailability difficult. Up to 98% of the physiological potassium in humans is distributed within the intracellular space. The major elimination pathway of potassium is *via* urinary excretion; the secondary elimination pathway is *via* the feces and perspiration. Bioavailability estimates derived from serum potassium levels are inaccurate because of the homeostatic mechanisms that maintain serum potassium levels within a relatively narrow range (3).

Attempts to determine the bioavailability of potassium preparations by measuring urinary potassium levels have been reported (4–6). To achieve any success, the bioavailability study must be conducted where there can be careful control of the diet, fluid intake, physical activity, and urine collection. Fixed menus with a known potassium content should be given throughout the study. Strenuous exercises that might cause

Table I—Cumulative Potassium Recovery from 12 Subjects after 24 hr

Subject	Mean[a] Control Potassium Level, mEq	Net Increase in Urine Potassium in 24 hr, mEq		
		Elixir	Capsule	Tablet
1	51.0 ± 7.3	46.6	22.0	49.1
2	47.9 ± 6.1	48.4	38.3	55.4
3	52.9 ± 8.2	43.3	40.1	53.8
4	61.7 ± 5.6	51.0	37.2	61.6
5	66.7 ± 6.3	42.1	31.0	65.1
6	52.9 ± 4.1	52.5	39.0	52.1
7	45.8 ± 10.1	56.0	42.4	45.3
8	41.6 ± 12.0	50.6	61.0	41.6
9	64.2 ± 1.3	12.3	38.7	42.9
10	48.8 ± 3.2	37.3	32.9	42.6
11	52.2 ± 12.8	37.6	62.5	44.8
12	54.1 ± 5.9	39.2	42.2	51.9
Mean ± *SD*	53.3 ± 7.5	43.1 ± 11.4	40.6 ± 11.4	50.5 ± 7.6

[a] Average of 3 control days (Days 0, 4, and 8).

[1] Berlex Laboratories Inc., Cedar Knolls, N.J.

[2] Slow-K, Ciba Pharmaceutical Co., Summit, N.J.

0022-3549/80/1200-1416$01.00/0
© 1980, American Pharmaceutical Association

(2) W. Dieterle, J. W. Faigle, F. Früh, W. Theobald, K. O. Alt, and W. J. Richter, *Arzneim.-Forsch.*, **26**, 572 (1976).
(3) J. J. Burns, R. K. Rose, S. Goodwin, J. Reichenthal, E. C. Horning, and B. B. Brodie, *J. Pharmacol. Exp. Ther.*, **113**, 481 (1955).
(4) J. J. Burns, T. F. Yü, P. G. Dayton, A. B. Gutman, and B. B. Brodie, *Ann. N.Y. Acad. Sci.*, **86**, 253 (1960).
(5) A. B. Gutman, R. G. Dayton, T. F. Yü, L. Berger, W. Chen, L. E. Sicam, and J. J. Burns, *Am. J. Med.*, **29**, 1017 (1960).
(6) B. Herrmann, *Med. Exp.*, **1**, 170 (1960).
(7) G. R. Petten, H. Feng, R. J. Withey, and H. F. Lettau, *J. Clin. Pharmacol.*, **11**, 177 (1971).
(8) B. Edström, *Proc. Int. Symp. Stockholm*, A. Lindgren and Söner A. B., Mölndal, 1973, p. 84.
(9) G. Lukas, M. B. Maggio-Cavaliere, C. B. Borman, and J. D. Arnold, *J. Clin. Pharmacol.*, **14**, 397 (1974).
(10) D. S. Davies and S. S. Thorgeirsson, *Ann. N.Y. Acad. Sci.*, **79**, 411 (1971).
(11) D. S. Davies and S. S. Thorgeirsson, *Acta Pharmacol., Suppl. 3*, **29**, 181 (1971).
(12) M. Orme, P. J. L. Holt, G. R. V. Hughes, C. J. Bulpitt, G. H. Draffan, S. S. Thorgeirsson, F. Williams, and D. S. Davies, *Br. J. Clin. Pharmacol.*, **3**, 185 (1976).
(13) M. Orme, *J. Intern. Med. Res., Suppl. 2*, **5**, 40 (1977).
(14) D. S. Davies, *ibid.*, **5**, 15 (1977).
(15) A. Sioufi, F. Caudal, and F. Marfil, *J. Pharm. Sci.*, **67**, 243 (1978).

Bioavailability and Pharmacokinetics of a New, Slow-Release Potassium Chloride Capsule

J. ARNOLD *x, J. T. JACOB ‡, and B. RILEY ‡

Received November 20, 1979, from **Quincy Research Center, Kansas City, MO 64127*, and ‡*Berlex Laboratories Inc., Cedar Knolls, NJ 07927.* Accepted for publication June 26, 1980.

Abstract □ The bioavailability of a new, slow-release potassium chloride product consisting of coated beads in a hard gelatin capsule was compared with the bioavailability of two marketed products, an elixir and a slow-release tablet, by determining the urinary excretion of potassium. Twelve healthy male volunteers were dosed with a total of 80 mEq of potassium, in a single dose for the capsule and tablet and in three 26.6-mEq doses at 6-hr intervals for the elixir. Mean recoveries in 24-hr urine potassium levels from all three dosage forms after subtracting normal urine potassium excretion levels were 50.8% from the capsule, 53.9% from the elixir, and 63.1% from the tablet. Maximum excretion rates were reached at 2.0 hr for the elixir, 6.8 hr for the capsule, and 4.0 hr for the tablet. Fewer side effects were reported with the capsule than with the elixir and tablet.

Keyphrases □ Potassium chloride—bioavailability and pharmacokinetics of slow-release capsule □ Bioavailability—potassium chloride in slow-release capsule □ Pharmacokinetics—potassium chloride in slow-release capsule

Potassium chloride is indicated for the treatment of hypokalemic alkalosis associated with various cardiovascular disorders. Aqueous solutions of potassium chloride are effective potassium supplements when taken as prescribed; however, because of an unpleasant taste due to the chloride ion, patient compliance during long-term therapy has been a problem. More palatable forms of potassium salts, such as the gluconate or mixtures of bicarbonate, citrate, and acetate, are available, but the chloride ion has been shown to be a prerequisite for effective treatment (1).

BACKGROUND

A new, slow-release potassium chloride preparation containing 600 mg (8 mEq) of potassium chloride[1] in the form of small, nearly spherical beads enclosed in a hard gelatin capsule was developed to avoid or minimize a high localized concentration of potassium within the GI tract. The potassium chloride crystals are specially coated to permit a uniform, controlled *in vivo* release over 8–10 hr. Extensive toxicity testing in animals was carried out to compare the new capsule preparation with a marketed wax-matrix tablet[2]. The results indicated a marked difference in the ulcerogenic potential of the tablet and capsule dosage forms (2). Based on the animal toxicity data, it was concluded that the new capsule dosage form is not likely to cause local irritation of the GI mucosa.

Certain pharmacokinetic characteristics of potassium make accurate determination of bioavailability difficult. Up to 98% of the physiological potassium in humans is distributed within the intracellular space. The major elimination pathway of potassium is *via* urinary excretion; the secondary elimination pathway is *via* the feces and perspiration. Bioavailability estimates derived from serum potassium levels are inaccurate because of the homeostatic mechanisms that maintain serum potassium levels within a relatively narrow range (3).

Attempts to determine the bioavailability of potassium preparations by measuring urinary potassium levels have been reported (4–6). To achieve any success, the bioavailability study must be conducted where there can be careful control of the diet, fluid intake, physical activity, and urine collection. Fixed menus with a known potassium content should be given throughout the study. Strenuous exercises that might cause

Table I—Cumulative Potassium Recovery from 12 Subjects after 24 hr

Subject	Mean[a] Control Potassium Level, mEq	Net Increase in Urine Potassium in 24 hr, mEq		
		Elixir	Capsule	Tablet
1	51.0 ± 7.3	46.6	22.0	49.1
2	47.9 ± 6.1	48.4	38.3	55.4
3	52.9 ± 8.2	43.3	40.1	53.8
4	61.7 ± 5.6	51.0	37.2	61.6
5	66.7 ± 6.3	42.1	31.0	65.1
6	52.9 ± 4.1	52.5	39.0	52.1
7	45.8 ± 10.1	56.0	42.4	45.3
8	41.6 ± 12.0	50.6	61.0	41.6
9	64.2 ± 1.3	12.3	38.7	42.9
10	48.8 ± 3.2	37.3	32.9	42.6
11	52.2 ± 12.8	37.6	62.5	44.8
12	54.1 ± 5.9	39.2	42.2	51.9
Mean ± *SD*	53.3 ± 7.5	43.1 ± 11.4	40.6 ± 11.4	50.5 ± 7.6

[a] Average of 3 control days (Days 0, 4, and 8).

[1] Berlex Laboratories Inc., Cedar Knolls, N.J.

[2] Slow-K, Ciba Pharmaceutical Co., Summit, N.J.

0022-3549/80/1200-1416$01.00/0
© 1980, American Pharmaceutical Association

Table II—Cumulative Potassium Excretion (Milliequivalents) per Time Period for Each of 12 Subjects [a]

Interval, hr	Subject 1	2	3	4	5	6	7	8	9	10	11	12	Mean ± *SD*
Elixir													
0–6	9.7	17.8	11.2	7.9	12.1	11.3	9.2	21.0	2.9	14.6	2.3	13.2	11.1 ± 5.4
6–12	16.7	10.3	14.2	9.1	16.0	17.5	12.0	11.2	7.8	10.7	19.8	6.3	12.6 ± 4.2
12–24	20.1	20.3	17.9	34.0	13.9	23.7	34.8	18.4	1.6	12.0	15.5	19.7	19.3 ± 9.0
Total	46.5	48.4	43.3	51.0	42.0	52.5	56.0	50.6	12.3	37.3	37.6	39.2	43.0 ± 11.4
Capsule													
0–6	8.2	25.5	16.0	6.3	9.1	12.4	0.2	28.5	13.0	11.5	19.3	12.2	13.6 ± 7.9
6–12	7.5	9.7	11.1	19.8	12.9	21.6	32.2	32.5	17.7	11.3	26.6	16.3	18.3 ± 8.2
12–24	3.9	3.1	13.0	11.1	9.0	5.3	10.8	0.0	8.0	10.1	16.0	13.7	8.7 ± 4.8
Total	19.6	38.3	40.1	37.2	31.0	39.3	43.2	61.0	38.7	32.9	61.9	42.2	40.6 ± 11.4
Tablet													
0–6	25.0	37.2	33.8	41.3	29.5	28.9	30.5	24.9	19.4	21.3	29.3	39.8	30.1 ± 7.0
6–12	13.8	7.8	13.2	11.9	18.9	16.1	12.5	16.7	11.8	11.9	15.5	8.4	13.2 ± 3.3
12–24	10.3	10.4	6.8	8.4	16.7	7.1	2.3	0.0	11.7	9.4	0.0	3.7	7.2 ± 5.0
Total	49.1	55.4	53.8	61.6	65.1	52.1	45.3	41.6	42.9	42.6	44.8	51.9	50.5 ± 7.6

[a] After correcting for control values for each urine collection period.

excessive perspiration, and thus loss of electrolytes, should be avoided.

The following three-way crossover study was designed to determine the bioavailability and pharmacokinetics of potassium chloride sustained-release capsules by urinary potassium excretion in volunteers maintained in a cloistered environment.

EXPERIMENTAL

Twelve healthy male volunteers, 19–55 years (mean 31 years) and weighing within ±10% of the ideal weight for their height and frame (7), participated in the study. Informed consent was obtained. The subjects were examined and found to have no hepatic, renal, or cardiovascular disease or history of GI disorders due to peptic or duodenal ulcer. Routine laboratory determinations, 12-lead ECGs, and physical examinations were conducted before admission to the study center[3].

The subjects remained in the study center under the supervision of the medical and nursing staff throughout the 15-day study. To avoid salt and water loss through perspiration, the subjects stayed indoors in air-conditioned rooms from 9:00 am to 4:30 pm every day and did not engage in strenuous exercise.

The first 3 days after admission (Days −3, −2, and −1) were diet-adaptation days. Day 0 was the control day for the treatment on Day 1. After two rest days (Days 2 and 3), a second control day (Day 4) was observed and then was followed by the second treatment on Day 5. Days 6 and 7 were rest days, followed by the third control day (Day 8) and the final treatment on Day 9. On Day 12, 3 days after the final treatment, the subjects were released from the center.

The three potassium chloride products, capsules[4], elixir[5], and tablets[6], were administered in a randomly assigned fashion in an open-label, three-way crossover treatment. The total dose of elixir, equivalent to 80 mEq of potassium, was divided into three 26.6-mEq doses administered at 6-hr intervals. The capsules and tablets were administered as single doses, each consisting of 80 mEq of potassium (10 capsules and 10 tablets, respectively). On the three treatment days (Days 1, 5, and 9), each subject received one of the three treatments after an 8-hr fast.

All urine voided on Days −3–+11 was collected. On the control days (Days 0, 4, and 8) and treatment days (Days 1, 5, and 9), urine was collected hourly for 16 hr beginning at 6:00 am. On the other days, urine was collected every 4 hr for 16 hr. A 16–24-hr collection was made on the control days as well as on the treatment days. The volume of each collection was recorded, and a sample was analyzed for its potassium and creatinine concentration. Urine potassium was determined by flame photometry (8). The assay sensitivity was ±0.1 mEq/liter. Creatinine was determined by the alkaline picrate method (9). Stool guaiac tests were performed on all feces to determine any loss of blood.

The subjects were required to drink 5200 ml of fluid each day. They received a uniform diet containing an average of 100 mEq of potassium, 340 mEq of sodium, and 4920 cal/day. No additional food or snacks were permitted. Meals were served at 7:00 am, 12:30 pm, 5:00 pm, and 10:00 pm. Drugs were administered, and the effects of the treatments were monitored by the attending staff physician.

All subjects received the constant attention of the nursing staff and were encouraged to report any untoward effect, however trivial it might appear to them. During morning, afternoon, and evening rounds, drug effects and general health problems were discussed with every subject.

[3] Quincy Research Center, Kansas City, Mo.
[4] Potassium Chloride SR Capsules (lot L-7717), Berlex Laboratories Inc.
[5] Kay Ciel Elixir (lot w60920), Berlex Laboratories Inc., Cedar Knolls, N.J.
[6] Slow-K (lot 1670), Ciba Pharmaceutical Co., Summit, N.J.

RESULTS AND DISCUSSION

Changes in the urine potassium levels for each collection were determined by first averaging the urine potassium levels for the three predosing control days for each subject and then subtracting these values from the corresponding urine potassium levels of the treatment day. Each subject's cumulative urine levels for 24 hr on the control days and treatment days are listed in Table I. The mean control value for 12 subjects was 59.0 mEq. The mean increase in the 24-hr potassium level was 43.1 mEq for the elixir, 40.6 mEq for the capsule, and 50.5 mEq for the tablet. These values correspond to 53.9% recovery from the 80-mEq dose administered for the elixir, 50.8% for the potassium chloride sustained-release capsule, and 63.1% for the tablet.

The 24-hr urine collection data were divided into three fractions to determine the potassium elimination patterns of the capsule and tablet in comparison to the elixir. The results (Table II) indicate that the elixir, which was administered every 6 hr, showed eliminations of 11.1 mEq in 0–6 hr, 12.6 mEq from 6 to 12 hr, and 19.3 mEq from 12 to 24 hr. The corresponding figures for the capsule were 13.6, 18.3, and 8.7 mEq, respectively, indicating slow and sustained release of potassium. In contrast, the tablet showed eliminations of 30.1 mEq in 0–6 hr, 13.2 mEq from 6 to 12 hr, and 7.2 mEq from 12 to 24 hr. Sixty percent of the total potassium eliminated from the tablet was eliminated in the first 6 hr, compared to 33.5% for the capsule.

The mean maximum excretion rate and the time for the maximum excretion rate were calculated for each dosage form. The excretion rate maximum was 6.1 mEq/hr (average of three doses) for the elixir, 8.1 mEq/hr for the capsule, and 10.1 mEq/hr for the tablet (Table III). The mean time for the maximum excretion rate was 2.0 hr for the elixir (average of three doses), 6.8 hr for the capsule, and 4.0 hr for the tablet. The capsule showed a slow excretion rate, characteristic for a sustained-release

Table III—Potassium Excretion Kinetics

	Elixir First Dose	Elixir Second Dose	Elixir Third Dose	Capsule	Tablet
Mean maximum excretion rate ± *SD*, mEq/hr	6.2 ± 2.9	5.1 ± 1.9	6.9 ± 3.1	8.1 ± 4.0	10.1 ± 3.0
Mean time of maximum excretion rate ± *SD*, hr	1.8 ± 1.1	1.9 ± 1.1	2.3 ± 0.8	6.8 ± 3.0	4.0 ± 2.5

[a] Excretion rate (mEq/hr) = [urine potassium (mEq) − mean control urine potassium (mEq) for urine collection period]/urine collection period (hr).

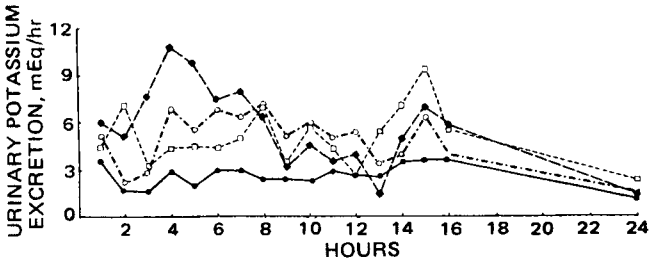

Figure 1—*Mean urinary potassium excretion rate before and after administration of 80-mEq oral doses of potassium chloride as slow-release capsules, elixir, and tablets in 12 subjects. Data for dosage forms were corrected for the mean potassium excretion during each collection period on the control days. Key: – • – O • –, capsules; - - □ - -, elixir; – – ■ – –, tablets; and —●—, control (mean of 3 control days).*

product, and reached a maximum much later than the immediately available elixir dosage form. The tablet also showed delayed release; however, the time for the maximum excretion rate was considerably shorter than for the capsule. The excretion rate curve of each product is shown in Fig. 1. Urine creatinine values for all subjects were within the normal range. Stool guaiac tests were negative for all subjects.

A Friedman two-way analysis of variance nonparametric, K-sample, related-measures test was significant at the 0.05 level, and differences in potassium excretion between the various formulations for each time interval were analyzed further using Wilcoxon's matched-pairs signed-ranks procedure (one tailed) (Table IV). For the mean 24-hr cumulative potassium recovery, both the elixir and the capsule were significantly lower than the tablet but were not significantly different from each other. This also was true for the early period of potassium excretion (0–6 hr), where the mean potassium level from the tablet was almost triple that of the other two formulations. During the 6–12-hr period, both the elixir and tablet means were significantly lower than the capsule mean; in the 12–24-hr period, both the capsule and the tablet gave significantly lower values than the elixir.

There also were significant differences between the mean potassium excretion between the time intervals for each formulation. For tablets, the greatest excretion occurred during the first 6 hr, and each succeeding interval featured significantly less excretion than its predecessor. For capsules and the elixir, the 12–24-hr period was significantly different from the two earlier periods.

Because of the complexity of potassium distribution and elimination kinetics in humans, the comparatively low recoveries seen in this study are not surprising. In another well-controlled crossover study with strict management of the diet, exercise, and fluid intake, only 27.4% of the potassium was recovered from the tablet[2] compared to 59.7% from a 10% solution of potassium chloride (4).

In a study of subjects receiving an effervescent tablet form of potassium chloride, only 46.4% of the potassium was recovered from the urine (5). Higher recoveries of potassium from urine have been reported (10, 11). However, these results are questionable because the controls seemed to be inadequate.

Despite the fact that 10 potassium chloride sustained-release capsules were administered as a single dose, there were no serious adverse reactions in any of the 12 subjects. Subject 1 complained of diarrhea from 2 to 10 hr after receiving the dose. A similar dose of the tablets elicited complaints of stomach pains starting 20 min after the dose and lasting for ~1 hr in Subjects 1, 3, and 9. Abdominal cramps and nausea lasting ~1 hr were reported by Subject 7 who received the tablets. The elixir produced nausea in Subject 10 30 min after the second dose of 26.6 mEq, and Subject 1 vomited 45 min after the second dose. Thus, of the seven complaints, four were related to the tablet, two to the elixir, and one to the capsule.

Table IV—Differences in Cumulative Potassium Excretion for Three Formulations

Formulation	Interval			
	0–6 hr	6–12 hr	12–24 hr	0–24 hr
Elixir – capsule	NS[a]	0.05	0.05	NS
Elixir – tablet	0.05	NS	0.05	0.05
Capsule – tablet	0.05	0.05	NS	0.05

[a] Not significant.

CONCLUSION

The results of this study show that the new potassium chloride slow-release capsule dosage form is equal in bioavailability to a 10% solution of potassium chloride. When tested in a three-way crossover study in 12 normal, healthy male volunteers, the rate of elimination, and thereby the rate of absorption, of potassium chloride sustained-release capsules were slower and more uniform than for the tablets or the elixir. The two slow-release products produced prolonged potassium levels after administration of a single dose. The potassium chloride sustained-release capsule was well tolerated, even though the subjects were given an unusually high single dose of 10 capsules, equivalent to 80 mEq of potassium.

REFERENCES

(1) J. P. Kassirer, P. M. Berkman, D. R. Lawrenz, and W. B. Schwartz, *Am. J. Med.*, **38**, 172 (1965).

(2) F. C. Goble, W. G. Lillis, J. Baldridge, J. T. Jacob, and D. R. Casorso, *Curr. Ther. Res.*, **27**, 40 (1980).

(3) A. Müller, M. Thoma, and H. Renker, *Schweiz. Med. Wochensch.*, **106**, 27 (1976).

(4) D. Ben-Ishay and K. Engelman, *Clin. Pharmacol. Ther.*, **40**, 250 (1973).

(5) D. L. Levine, *C.M.A. J.*, **108**, 1482 (1973).

(6) A. Cordano, J. J. Vitale, B. J. Gunther, H. Velez, and T. Franco, *Curr. Ther. Res.*, **20**, 156 (1976).

(7) "Metropolitan Life Insurance Tables," Statistical Bull. 40, Metropolitan Life Insurance Co., New York, N.Y., 1959.

(8) J. Bauer, G. Toro, and P. Ackerman, "Bray's Clinical Laboratory Methods," C. V. Mosby, St. Louis, Mo., 1962, pp. 68, 69.

(9) W. White and S. Frankel, "Chemistry for Medical Technology," 2nd ed., C. V. Mosby, St. Louis, Mo., 1965, pp. 124, 125.

(10) C. Graffner and J. Sjogren, *Acta Pharm. Suec.*, **8**, 13 (1971).

(11) U. Otto and G. Rooth, *ibid.*, **10**, 337 (1973).

ACKNOWLEDGMENTS

The authors thank J. Baldridge for contributions in the preparation of the protocol and J. Meinders, A. Berger, and the Quincy Research Center staff for conducting the study.

Radioimmunoassay for Terfenadine in Human Plasma

C. E. COOK *x, DAVID L. WILLIAMS *, MARY MYERS *, C. RAY TALLENT *, G. A. LEESON ‡, R. A. OKERHOLM ‡, and G. J. WRIGHT ‡§

Received February 25, 1980, from the *Research Triangle Institute, Research Triangle Park, NC 27709, and the ‡Merrell Research Center, Cincinnati, OH 45215. Accepted for publication June 24, 1980. §Present address: A. H. Robins Company, Richmond, VA 23220.

Abstract □ A radioimmunoassay procedure was developed for the antihistamine terfenadine {α-[4-(1,1-dimethylethyl)phenyl]-4-(hydroxydiphenylmethyl)-1-piperidinebutanol}. The keto analog of terfenadine was converted to its *O*-carboxymethyloxime derivative, which was conjugated to bovine thyroglobulin by a mixed anhydride technique. Rabbits were immunized with the resulting conjugate, and antiserums capable of binding radiolabeled terfenadine were obtained. Tritium-labeled terfenadine was prepared by a combination of exchange and reduction with platinum oxide in the presence of tritium gas, and the procedure yielded a specific activity of 48 Ci/mmole. Plasma containing terfenadine was diluted with sodium carbonate solution and extracted with hexane, and the hexane extracts were evaporated and analyzed. The between-assay coefficient of variation on control samples ranged from 8% at 10 ng/ml to 14% at 1 ng/ml. The lower practical sensitivity limit was at least as low as 0.25 ng/ml (25 pg measured). Two metabolites of terfenadine cross-reacted 16–30% with the antiserum used. However, extraction eliminated essentially all of these compounds. Analysis of plasma samples from human subjects given terfenadine showed marked intersubject variability and low plasma levels.

Keyphrases □ Radioimmunoassay—terfenadine, human plasma □ Terfenadine—radioimmunoassay, human plasma □ Antihistaminics—terfenadine, radioimmunoassay, human plasma

A new antihistamine, terfenadine (I*a*), is under clinical study[1]. Metabolism studies in animals[2] indicated that plasma levels of the parent drug could be expected to be in the low nanogram per milliliter range. Therefore, for bioavailability studies, a sensitive analytical procedure was needed. Radioimmunoassay was chosen because of its sensitivity, specificity, and simplicity.

This report describes the synthesis of an immunogen containing a haptenic moiety corresponding to terfenadine, the production of antiserum in rabbits, the synthesis of tritium-labeled terfenadine as a radioligand for competitive binding studies, and the development of a radioimmunoassay procedure for terfenadine which was applied to human studies.

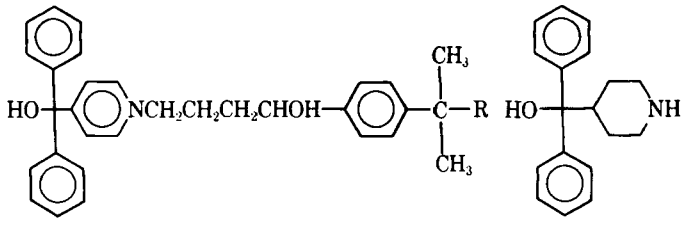

I*a*: R = CH_3
I*b*: R = CH_2OH
I*c*: R = COOH

I*d*

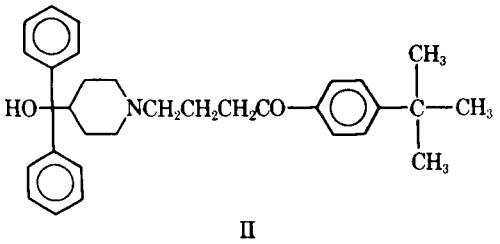

II

[1] Merrell Research Center.
[2] G. J. Wright, G. A. Leeson, K. C. Chan, and W. C. Knapp, unpublished data.

EXPERIMENTAL[3]

α-[4-(1,1-Dimethylethyl)phenyl]-4-(hydroxydiphenylmethyl)-1-piperidinebutanone *O*-Carboxymethyloxime (V)—Reaction of 1.00 g of α-[4-(1,1-dimethylethyl)phenyl]-4-(hydroxydiphenylmethyl)-1-piperidinebutanone (II) under nitrogen with 300 mg of carboxymethoxylamine hemihydrochloride in a refluxing mixture of 50 ml of methanol and 6 ml of 1 *M* sodium acetate in water for 16 hr yielded, after workup and recrystallization (chloroform–carbon tetrachloride), 719 mg (67% yield) of the oxime acid (V) as a white solid, mp (uncorrected) 138–145° (capillary), 138–142° (hot-stage microscope); UV (0.1 *N* NaOH): λ_{max} 256 (ε 12,790) nm; PMR (100 MHz, pyridine-d_5): δ 1.11 [s, $C(CH_3)_3$], 2.03 (m, CH_2), 2.50 (t, *J* = 7 Hz, $CH_2C{=}N$), 3.05 (br t, *N*-CH_2), and 5.07 (s, OCH_2CO); PMR (60 MHz, chloroform-d_3): δ 1.25 [s, $C(CH_3)_3$], 4.52 (s, OCH_2CO), and 6.8–7.8 (m, aromatic H).

Anal.—Calc. for $C_{33}H_{42}N_2O_4$: C, 75.24; H, 7.80; N, 5.16. Found: C, 74.95; H, 7.60; N, 4.76.

Conjugation Reaction—The oxime acid (V) (16.25 mg, 0.03 mmole) in 4 ml of dioxane, on reaction with tributylamine (7.4 μl) and isobutyl chloroformate (39.5 μl) under nitrogen for 20 min at 14–15°, yielded a solution of the mixed anhydride (VI). To this solution was added a solution (pH 11.2, 15°) of 82.2 mg (1.25×10^{-4} mmole) of bovine thyroglobulin[4] and 86 μl of 1 *N* NaOH in 4 ml of water. The thyroglobulin flask was rinsed with ~1 ml of aqueous sodium hydroxide (pH 11.2), which also was added to the mixed anhydride.

The reaction mixture was stirred for 4.5 hr at 8° and then poured onto a 2.2 × 31.5-cm agarose gel[5] column in which the liquid phase was dioxane–water (1:1). The column was eluted with distilled dioxane–water (1:1). The eluate fraction from 25 to 60 ml was lyophilized to yield the conjugate (VII) (102 mg) as a fluffy white fluorescent solid. The molar ratio (hapten to protein) was calculated to be 141 by differential UV spectrophotometry (2) at 255 nm in 0.1 *N* NaOH[6].

Catalytic Formation of Tritiated Terfenadine—To 10 mg of II as the free base in 0.7 ml of dry 1,4-dioxane was added 5 mg of platinum oxide, and the mixture was stirred under tritium gas (5 Ci) for 2 days. It then was filtered through successive layers of diatomaceous earth, magnesium sulfate, molecular sieve, and cotton in a Pasteur pipet. Half of the filtrate was concentrated, brought up in 0.1 ml of ethyl acetate, and chromatographed on silica gel plates (0.1 mm thick) with toluene–diethylamine (9:1) as the mobile phase. The terfenadine bands were eluted with ethyl acetate. The ethyl acetate was evaporated almost to dryness, and the tritiated terfenadine (110 mCi) was brought to volume in a 50-ml volumetric flask with benzene–ethanol (9:1). Thin-layer radiochromatography (toluene–diethylamine 9:1) indicated pure tritiated terfenadine.

[3] PMR spectra were recorded on a Varian EM 360 spectrometer at 60 MHz or on a HA-100 spectrometer at 100 MHz with tetramethylsilane as the internal standard. IR spectra were obtained on a Perkin-Elmer 467 grating IR spectrophotometer. Analytical TLC on silica gel 60F-254 precoated TLC plates (0.25 mm thick) from EM Reagents, Elmsford, N.Y., was routinely used to monitor reactions. Elemental analyses were from Micro-Tech Laboratories, Skokie, Ill. Terfenadine (I*a*) and its analogs I*b*–I*d* were prepared at Merrell Research Center (1).

[4] Type I, Sigma Chemical Co., St. Louis, Mo.

[5] Bio-Gel A, Bio-Rad Laboratories, Richmond, Calif.

[6] The equation used was:

$$\text{molar ratio} = \frac{A_{conj}\ \text{mol. wt.}_{\text{thyroglobulin}} - \epsilon_{\text{thyroglobulin}} C_{conj}}{\epsilon_{\text{oxime acid}} C_{conj} - A_{conj}\ \text{mol. wt.}_{\text{hapten residue}}}$$

where *A* is the absorbance, *C* is the concentration in milligrams per milliliter, mol. $\text{wt.}_{\text{thyroglobulin}}$ = 670,000, mol. $\text{wt.}_{\text{hapten residue}}$ = 542 − 18 (loss of water in conjugation reaction) = 524, $\epsilon_{\text{oxime acid}}$ = 12,790 at 255 nm, and $\epsilon_{\text{thyroglobulin}}$ = 490,000 at 255 nm. This formula differs slightly from the calculation of Ref. 2, which ignores the weight of the hapten residue in calculating the absorbance due to the protein.

0022-3549/80/1200-1419$01.00/0
© 1980, American Pharmaceutical Association

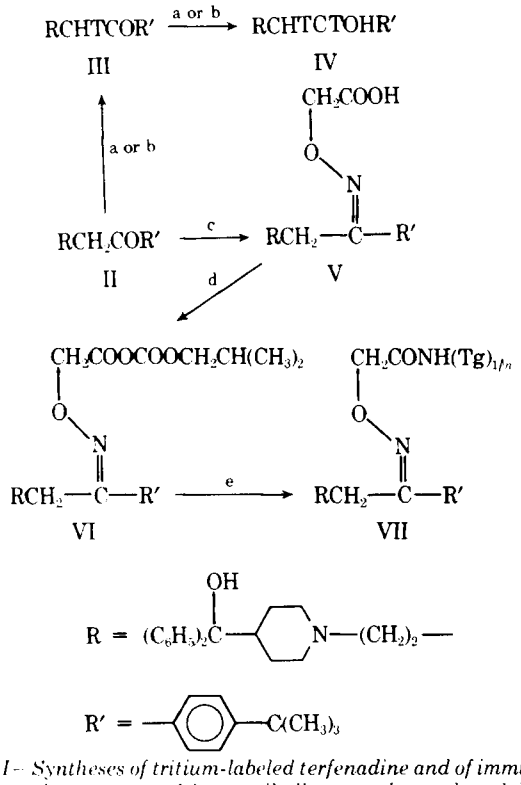

Scheme I—Syntheses of tritium-labeled terfenadine and of immunogen. Key to reaction steps: a, tritium, palladium-on-charcoal, and dioxane; b, tritium, platinum oxide, and dioxane; c, carboxymethoxylamine, sodium acetate, and methanol; d, isobutyl chloroformate, tributylamine, and dioxane (cf., *Ref. 9*); *and e, bovine thyroglobulin (Tg) and aqueous sodium hydroxide* (cf., *Ref. 9*).

The specific activity was determined by self-displacement in radioimmunoassay (3).

Development of Antiserum—The thyroglobulin conjugate was dissolved in 0.9% NaCl at a concentration of 0.2 mg/ml with adjustment of the pH (by addition of a few drops of dilute sodium bicarbonate) to achieve complete solution. Five milliliters of this solution was emulsified with Freund's complete adjuvant[7], and the emulsion was used to immunize four New Zealand White rabbits (two male and two female) intradermally (about 20 sites) with 2 ml of the mixture (4). After 4 weeks, a 0.1-mg/ml solution was emulsified with an equal volume of Freund's incomplete adjuvant[7] and injected intradermally as described (2 ml/rabbit). Rabbits were bled 12 days later (ear vein, 30 ml).

Four weeks after the first booster injection, each rabbit was injected subcutaneously with 1 ml of a solution of the conjugate (0.1 mg/ml) in 0.9% NaCl, and subsequent booster injections were given at 4-week intervals (total of seven subcutaneous booster injections). Rabbits were bled ~12 days after each booster injection. Serums were stored at −20°.

Analytical Procedures—The buffer was 0.1 *M* phosphate-buffered saline (pH 6.8, prepared from 5.38 g of monobasic sodium phosphate monohydrate, 16.35 g of dibasic sodium phosphate heptahydrate, and 9.0 g of sodium chloride/liter) containing 0.1% NaN_3 and 0.1% bovine serum albumin[8].

Standard solutions were prepared from human male drug-free plasma[9] (citrate as anticoagulant). A 50-ng/ml solution of terfenadine in plasma was made by adding an ethanol solution (20 μg/ml) to plasma. Further dilutions in plasma yielded standards containing 0.5, 0.75, 1, 2, 3, 5, 8, and 12 ng/ml. Control samples containing 1, 3, 5, and 10 ng/ml were made up separately to check the reproducibility of the assay and standard preparation. Standard and control solutions were aliquoted into 3.7-ml vials and stored at −20°.

Plasma (0.5 ml) (blank, standard, control, or unknown) was placed in a 20-ml scintillation vial. To the vial was added 0.5 ml of 0.1 *M* Na_2CO_3. The mixture was shaken, and 4.0 ml of hexane was added. The vials were capped, placed in an upright position in a reciprocating shaker, and shaken overnight at ~80 cycles/min. The vials were immersed in dry ice–acetone to freeze the aqueous layer, and the hexane was decanted. Aliquots (0.8 ml) of the hexane were then transferred to individual 12 × 75-mm glass culture tubes, and the hexane was evaporated in a centrifuge-type vacuum evaporator[10]. To the residue were added 10 μl of aqueous ethanol (1:1), 10 μl of an aqueous ethanolic (1:1) solution of tritium-labeled terfenadine (~16,000 cpm), 0.6 ml of buffer, and 0.1 ml of diluted antiserum. For direct measurement of metabolite cross-reactions, terfenadine and metabolites were added in 10 μl of aqueous ethanol.

The contents were vortexed and incubated overnight at 4°. A 0.5-ml aliquot of a 1.5% suspension of charcoal[11] (washed to remove fine particles) in buffer was added. Tubes were agitated on a vortex mixer and allowed to stand for 20 min at 4°. They were then centrifuged for 15 min at 733×*g* and 4°. The supernate was decanted into liquid scintillation vials, each containing 10 ml of scintillation cocktail (5). Radioactivity was measured in a liquid scintillation spectrometer. Samples were counted to a precision of 2% (2σ) or for 5 min, whichever came first, for three separate cycles.

Data Treatment—The counts per minute for each vial from the three cycles were averaged. In some earlier work and to determine the cross-reactions of metabolites, standard curves were determined and calculations were made by the logit–log procedure (6); however, all of the plasma analyses were performed by means of a four-parameter logistic procedure (7, 8).

Clinical Procedure—The clinical portion of this study[12] involved six male volunteers from whom informed consent was obtained. The subjects were randomly placed in three groups of two. Group 1 took 60 mg as a single tablet, Group 2 took two 60-mg tablets, and Group 3 took three 60-mg tablets after an overnight fast. Venous blood samples (10 ml) were drawn in tubes[13] containing solid ethylenediaminetetraacetic acid as the anticoagulant just before dosing (0 hr) and at 0.5, 1, 1.5, 2, 3, 4, 6, 8, 12, 18, and 24 hr after dosing. The blood samples were centrifuged and the plasma was separated, labeled with a code number, and frozen. The plasma samples were kept frozen until they were assayed, and the code was not broken until the assays were completed.

RESULTS

Synthesis of Immunogen and Radioligand—Reaction of the ketone analog (II) of terfenadine with *O*-carboxymethylhydroxylamine led in reasonable yield to the desired *O*-carboxymethyloxime (V, Scheme I). The presence in the PMR spectrum of a singlet at δ 5.07 (pyridine-d_5) or 4.52 (chloroform-d_3) was indicative of OCH_2CO. The presence of only one peak in this region indicated that only one isomer was isolated. For steric reasons, this isomer was assigned the *E*-stereochemistry shown in V. Compound V was converted to a mixed anhydride (9) and conjugated to bovine thyroglobulin, presumably by reaction with the ε-aminolysine groups of the protein. Differential UV determination indicated that 141 terfenadine moieties were incorporated per molecule of the thyroglobulin.

Tritium-labeled terfenadine (48 Ci/mmole) was obtained by treatment of the ketone (II) with platinum oxide and tritium gas.

Development of Assay—Initial studies showed that when terfenadine was added in aqueous ethanol solution, binding equilibrium was reached by 0.5 hr. However, for plasma analysis, overnight incubation was necessary. Bovine serum albumin was preferable to gelatin as a buffer protein because it markedly reduced nonspecific binding (radioactivity not adsorbed to charcoal). Nonspecific counts per minute values were <2.5% of the total counts per minute at final charcoal concentrations above 0.4%, and net binding was constant over the range of 0.4–0.8% charcoal but decreased sharply at concentrations above 1.2%. The nonspecific counts per minute values remained constant after a 10-min exposure to charcoal; after 20 min, net binding decreased <0.5%/min.

The titer of all antiserums was measured with 7.5-Ci/mmole radiolabeled terfenadine obtained by the reduction of II with tritium gas over palladium-on-charcoal[14]. Titer was defined as the dilution that bound 50% of ~16,000 cpm of labeled terfenadine when 0.1 ml was used in an incubation and thus is partially a function of the specific activity of the

[7] Miles Laboratories, Elkhart, Ind.
[8] Fraction V (essentially fatty acid free), catalog No. A6003, lot 48C-7171, Sigma Chemical Co., St. Louis, Mo.
[9] Plasma Associates, West Chester, Pa.
[10] Speed-Vac, Savant Instrument Co., Hicksville, N.Y.
[11] Norit A, Fisher Scientific Co., Pittsburgh, Pa.
[12] Cintest Inc., Cincinnati, Ohio.
[13] Venoject tubes, Kimble-Terumo, Toledo, Ohio.
[14] C. E. Cook, M. Myers, and C. R. Tallent, unpublished data.

Table I—Cross-Reactions with Terfenadine Antiserum [a]

Antiserum [b]	Test Compound	Cross-Reaction, %
R5-2	Ib	70
	Ic	42
	Id	3
	II	38
R7-2	Ib	21
	Ic	17
	Id	0.9
	II	19
R7-5	Ib	29
	Ic	21
	Id	0.8
	II	29

[a] Radioligand specific activity was 48 Ci/mmole [b] The first number refers to the rabbit; the second number refers to the bleeding. See *Experimental* for details of immunization. Rabbit 5 was a male; Rabbit 7 was a female.

radioligand. Antiserums from one female and one male rabbit did not exhibit any titer greater than 1:500. The titer and percent displacement of the radioligand by 500 pg of terfenadine at the antiserum titer that initially bound 50% of the radioligand are shown in Fig. 1 for antiserums from the other two rabbits. Antiserum R5-2 gave the highest titer at 1:1325, but R7-5 exhibited the greatest sensitivity. When radiolabeled terfenadine with a specific activity of 48 Ci/mmole was used, the 50% titer of R5-2 was increased from 1:1325 to 1:9500 and that of R7-5 was increased from 1:500 to 1:5000. The sensitivity of the assay was such that 25 pg of terfenadine caused 10% displacement of bound radioligand.

When plasma (0.5 ml) containing 1 and 10 ng of tritiated terfenadine/ml was diluted 1:1 with 0.1 *M* Na_2CO_3 and extracted three times (shaking for 30 min) with 2 ml of hexane, the average total recovery was 71.5 ± 2.9% (*SD*) for the 1-ng/ml solution and 72.5 ± 3.7% for the 10-ng/ml samples (triplicate samples). Extraction in 20-ml liquid scintillation vials containing 0.5 ml of plasma, 0.5 ml of 0.1 *M* Na_2CO_3, and hexane (2 or 4 ml) shaken[15] gently (80 cycles/min) overnight in a vertical position gave excellent recoveries (80% using 2 ml of hexane and 90% using 4 ml).

The cross-reaction of Metabolites Ib[16] and Ic[16] and common fragment Id[16] as well as the ketone (II) was measured by comparison of the amount required to displace 50% of bound radioligand (5) (Table I). Although pure samples of the metabolites cross-reacted with the terfenadine antiserums, the specificity of the overall assay is dependent on the extent

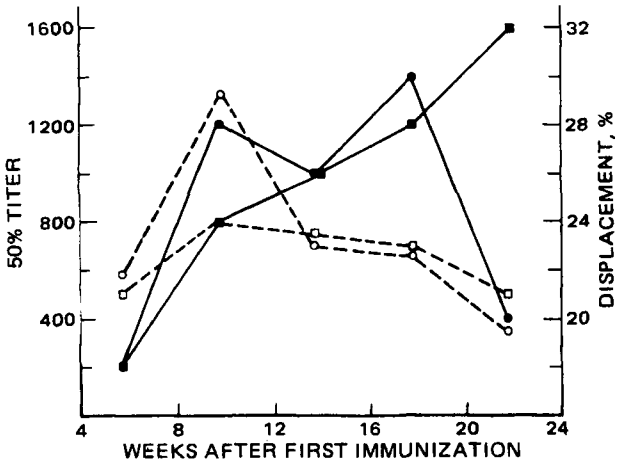

Figure 1—*Antiserum titer (dotted lines) and sensitivity (solid lines) as a function of time after the first immunization. The radioligand was [^3H]terfenadine with a specific activity of 7.5 Ci/mmole. Sensitivity was measured by percent displacement of the radioligand from antiserum by 500 pg of unlabeled terfenadine when the antiserum initially bound 50% of the radioligand. Key: ○ and ●, Rabbit 5; and □ and ■, Rabbit 7.*

[15] Dubnoff shaker.

[16] Metabolite Ib is α-[4-(1,1-dimethyl-2-hydroxyethyl)phenyl]-4-(hydroxydiphenylmethyl)-1-piperidinebutanol, Ic is 4-[1-hydroxy-4-(hydroxydiphenylmethyl)-1-piperidinebutyl]-α,α-dimethylbenzeneacetic acid, and Id is 4-(hydroxydiphenylmethyl)piperidine.

Table II—Examination of Potential Interference of Metabolites with Plasma Analysis [a]

Metabolite Added, ng/ml	Terfenadine Measured, ng equivalents/ml			
	Ic		Ib	
	Experiment A	Experiment B	Experiment A	Experiment B
0	0.02	0	0.02	0
1	0	0	0	0.11
3	0	0	0.05	0.31
10	0	0	0.21	0.08
100	—[b]	0.27	—[b]	1.35

[a] Metabolites were added to plasma, which then was diluted with sodium carbonate solution and extracted with hexane. The hexane extracts were analyzed for terfenadine equivalents. (See *Experimental* for details of extraction and analysis.) Experiments A and B were run at separate times. Antiserum R7-5 was used. [b] Not done.

to which the metabolites were extracted from plasma by the hexane. Therefore, solutions of terfenadine and Ib and Ic were prepared in plasma and analyzed. Metabolites were calculated as the nanogram equivalents of terfenadine per milliliter based on the terfenadine standard curve. Table II shows that the carboxylic acid metabolite (Ic) at 100 ng/ml cross-reacted to the extent of only 0.3 ng equivalent of terfenadine/ml and that the alcohol (Ib) at the 100-ng/ml level was measured as 1.4 ng equivalents/ml.

Validation of Assay—Table III shows the mean values obtained for control samples in 10 consecutive assays as well as calculations of between-assay and within-assay variability. These calculations were carried out according to the procedure of Rodbard (10). One assay included a blank plasma pool and 38 blind samples[17]. The sample code was not broken until after the assay results were reported. Acceptable agreement was achieved between added and found values (Table IV). The regression equation was y (found) = 0.93x (added) + 0.40 ng/ml (r = 0.9792, n = 39).

Plasma Levels in Humans—Plasma levels in the six subjects studied were low and highly variable between subjects (Fig. 2). One subject who was given 180 mg exhibited the maximum concentration recorded (5.8

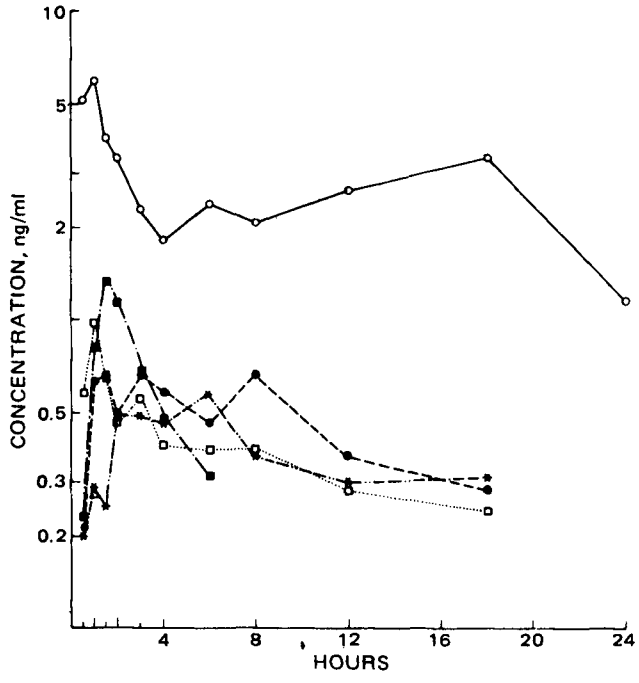

Figure 2—*Plasma levels of terfenadine in human males given a single oral dose of terfenadine. Levels were measured by the radioimmunoassay procedure described. Samples were analyzed at 0.5, 1, 1.5, 2, 3, 4, 6, 8, 12, 18, and 24 hr, but data points below 0.2 ng/ml were below assay sensitivity and are not shown. Key: ■ and *, 60-mg dose; ● and △, 120-mg dose; and ○ and □, 180-mg dose.*

[17] The samples were prepared at Merrell-National Laboratories and shipped to the Research Triangle Institute.

Table III—Results from Analysis of Control Samples from 10 Consecutive Assays [a]

Statistical Variable	Blank	Concentration, ng/ml 1	3	5	10
Average	0.12	0.99	2.95	5.00	10.57
SD (between assays)	0.07	0.14	0.35	0.63	0.89
CV, % (between assays)	58	14.0	11.9	12.6	8.4
SD (within assay, single extract)	—	0.09	0.31	0.51	0.69
CV, % (within assay, single extract)	—	9.2	10.5	10.1	6.5
SD (within assay, three extracts)	—	0.053	0.18	0.29	0.40
CV, % (within assay, three extracts)	—	5.3	6.0	5.8	3.8

[a] Triplicate samples were extracted and duplicate aliquots of each extract were analyzed. Calculations were done according to the method of Rodbard (10).

ng/ml 1 hr after dosage). In contrast, the corresponding value for one subject given 120 mg was only 0.28 ng/ml, and the second highest plasma level (1.3 ng/ml) was achieved by a subject given a 60-mg dose.

DISCUSSION

Since terfenadine is a small molecule, the development of antibodies capable of binding it required the synthesis of a protein conjugate that incorporated the terfenadine moiety. To minimize the cross-reaction of terfenadine metabolites, those portions of the molceule that are principally involved in metabolic reactions should be left free to influence antibody selectivity. Two known metabolites are the alcohol (I*b*) and the carboxylic acid (I*c*). Other metabolites having hydroxylation on an aromatic ring apparently also are present[1]. However, the ketone (II) resulting from oxidation of the secondary benzylic hydroxyl group of terfenadine apparently is not a metabolite. Therefore, the carboxymethyloxime analog (V) of terfenadine (derived from II) was chosen as the hapten. Compound V lacks the asymmetric center of terfenadine, which should minimize the possibility that the antiserum developed would be selective for only one optical isomer of terfenadine.

Several coupling experiments were carried out to achieve maximum incorporation of the drug moiety into thyroglobulin while retaining reasonable solubility properties of the thyroglobulin. An agarose gel (suitable for use with organic or aqueous–organic solvent mixtures) allowed separation of the conjugate and unreacted acid with a good yield of the desired conjugate, and the ratios of the reactants given under *Experimental* resulted in the best combination of hapten incorporation and solubility of the conjugate.

Although a radioligand with a specific acitivity of 0.86 Ci/mmole was obtained readily by reduction of II with sodium borotritide, material of a higher specific activity was required for best sensitivity. A combination of catalytic exchange (11) and catalytic reduction of the keto group with tritium gas was chosen. Palladium-on-carbon initially was used as the catalyst, but it yielded terfenadine with a specific activity of only 7.5 Ci/mmole. Platinum oxide has been reported to give high yields in the reduction of acetophenone to 1-phenylethanol (12). Reduction of platinum oxide with tritium gas would lead to the formation of tritiated water, which should undergo exchange reactions with the enolic form of the ketone (II). Reduction of the keto group with excess tritium gas in the presence of the platinum catalyst would yield the desired alcohol. In fact, these conditions resulted in terfenadine with a specific activity of ~48 Ci/mmole.

Since the metabolites are more polar than terfenadine, extraction of plasma with a relatively nonpolar solvent should significantly reduce the amounts of metabolites in the final analytical sample. The polarity of the carboxylic acid and phenolic metabolites also could be enhanced by making the plasma samples basic with sodium carbonate solution. Hexane extraction of alkalinized plasma markedly improved the assay specificity since very large amounts of the metabolites were required to make a significant contribution to the assay results. Little interference from the carboxylic acid (I*c*) would be expected at levels 50 times those of terfenadine or from the alcohol metabolite (I*b*) at 10 times the terfenadine levels. Thus, the assay should measure terfenadine itself with little contribution from its metabolites. In view of the structure of the immunogen, the relatively low cross-reactivity of the ketone (II) is noteworthy. Use of terfenadine as a radioligand apparently selects the antibody population with stronger affinity for the secondary alcohol structure.

Table IV—Blind Analysis of Terfenadine Plasma Samples

Added, ng/ml	Number of Samples	Found, mean ± *SD*
0.0	3	0
1.02	6	1.22 ± 0.03
2.04	2	2.22 ± 0.05
3.06	2	3.33 ± 0.13
4.07	6	4.44 ± 0.09
5.09	3	5.19 ± 0.42
6.11	5	6.32 ± 0.41
7.13	3	6.36 ± 1.48
8.14	1	8.28
10.2	8	9.73 ± 1.03

When the assay was run several times, the reproducibility and accuracy of the measurement of control samples were acceptable (Table III). The between-assay coefficient of variation ranged from 14% at 1 ng/ml to 8% at 10 ng/ml. The coefficient of variation within assays based on the extraction of samples in triplicate and assay of each extract in duplicate was ≤6%. Indeed, calculations show that duplicate plasma extracts analyzed in duplicate would be acceptable, with a coefficient of variation of <8%. Acceptable accuracy and precision also were obtained with blind spiked samples.

As expected from the metabolism studies in animals, low levels of terfenadine were observed in the plasma of human subjects administered the drug. The variability between subjects was marked (Fig. 2), but such variability has been observed with other drugs (13, 14). There was no apparent correlation between the dose administered and the maximum plasma level observed. However, since this was not a crossover study, individual variation could account for the apparent discrepancy. In addition to the initial absorption peak at ~1 hr, at least one secondary peak in the plasma concentration was seen for some subjects[18] (Fig. 2). The low plasma levels achieved with relatively high doses, the large variation in plasma levels (not highly dose correlated), and the secondary maxima observed in the plasma levels strongly indicate that a significant first-pass effect and enterohepatic circulation as well as other factors influence the plasma levels of terfenadine in humans. These questions will be addressed in a future study.

REFERENCES

(1) A. A. Carr and C. R. Kinsolving (to Merrell-National Laboratories), U.S. pat. 3,878,217 (Apr. 15, 1975). A. A. Carr and C. R. Kinsolving (to Merrell-National Laboratories), U.S. pat. 3,806,526 (Apr. 23, 1974).

(2) B. F. Erlanger, F. Borek, S. M. Beiser, and S. Lieberman, *J. Biol. Chem.*, **228**, 713 (1959).

(3) B. J. Morris, *Clin. Chim. Acta*, **73**, 213 (1976).

(4) J. Vaitukaitis, J. B. Robbins, E. Nieschlag, and G. T. Ross, *J. Clin. Endocrinol.*, **33**, 988 (1971).

(5) C. E. Cook, C. R. Tallent, E. W. Amerson, M. W. Myers, J. A. Kepler, G. F. Taylor, and H. D. Christensen, *J. Pharmacol. Exp. Ther.*, **199**, 679 (1976).

(6) D. Rodbard, W. Bridson, and P. L. Rayford, *J. Lab. Clin. Med.*, **74**, 770 (1969).

(7) D. Rodbard and D. Hutt, in "RIA and Related Procedures in Medicine," International Atomic Energy Agency, Vienna, Austria, 1974, pp. 165–192.

(8) D. Rodbard and V. B. Faden, "Radioimmunoassay Data Processing," 3rd ed., National Technical Information Service, Springfield, Va., 1975.

(9) C. E. Cook, C. R. Tallent, and H. D. Christensen, *Life Sci.*, **14**, 1075 (1974).

[18] Similar secondary maxima were observed in a large crossover study to be published later.

(10) D. Rodbard, *Clin. Chem.*, **20**, 1255 (1974), Appendix I.
(11) E. A. Evans, H. C. Sheppard, J. C. Turner, and D. C. Warrell, *J. Labelled Compd.*, **10**, 569 (1974).
(12) M. Freifelder, T. Anderson, Y. H. Ng, and V. Papendick, *J. Pharm. Sci.*, **53**, 967 (1964).
(13) W. Hammer, C. M. Idelström, and F. Sjöqvist, *Excerpta Med. Ser.*, **122**, 301 (1967).
(14) T. B. Cooper, *Clin. Pharmacokinet.*, **3**, 14 (1978).

ACKNOWLEDGMENTS

The authors thank Richard Privette and Dr. David Rosenthal of Research Triangle Institute for technical assistance and computer programming work, respectively. They also thank Dr. Madison J. Cawein and Terry D. Dusebout of the Clinical Pharmacology Department at the Merrell Research Center for conducting the clinical portion of the study.

Prodrugs of Etilefrine: Synthesis and Evaluation of 3′-(*O*-Acyl) Derivatives

JOSEF WAGNER *ˣ, HELMUT GRILL *, and DIETRICH HENSCHLER ‡

Received March 10, 1980, from the **Department of Chemical Research, Klinge Pharma, Munich, West Germany,* and the ‡*Institute of Pharmacology and Toxicology, University of Würzburg, Würzburg, West Germany.* Accepted for publication June 27, 1980.

Abstract □ A series of 3′-(*O*-acyl) derivatives of etilefrine {α-[(ethylamino)methyl]-3′-hydroxybenzyl alcohol} was synthesized. Correlations between structure and solubility, pKa value, lipophilicity, and esterase-catalyzed hydrolysis were demonstrated. Of special interest is the 3′-(*O*-pivaloyl) derivative, which shows, in addition to favorable solubility and improved lipophilicity, marked stability against enzymatic cleavage in blood along with a high rate of hydrolysis in the liver.

Keyphrases □ Etilefrine—synthesis and evaluation of 3′-(*O*-acyl) derivatives as prodrugs □ Prodrugs—etilefrine, synthesis and evaluation of 3′-(*O*-acyl) derivatives as prodrugs

The uncertain activity of orally administered phenolethanolamines is partly assumed to result from metabolic processes during absorption. Phenolethanolamines with a free hydroxyl group in the *meta*-position are primarily subject to this gut wall first-pass metabolism. As they pass the intestinal wall, they are conjugated to inactive compounds. For example, in the intestinal wall, 80% of orally administered isoproterenol is converted to sulfate (1, 2) in the *meta*-position. During the gut wall passage, a similar conjugation was found for orciprenaline (metaproterenol) (3), terbutaline (4), norfenefrine (5), and etilefrine (6). Due to this early metabolic reaction, the bioavailability of compounds, even those with a high rate of absorption, is frequently reduced (7).

To avoid the attack of conjugating enzymes at the 3′- or 5′-hydroxy group, it was masked by acylation, thus converting the phenolethanolamines into prodrugs. *O*-Acyl derivatives of this type are known for phenylephrine (8, 9), etilefrine (8, 9), norepinephrine (10), *meta*-norepinephrine (10), epinephrine (8, 9), *meta*-epinephrine (8, 9), isoproterenol (10), orciprenaline (10), *N*-*tert*-butylnorepinephrine (11), and terbutaline (12). These *O*-acyl derivatives differ from their parent drug significantly in their solubility, dissociation constants, and lipophilicity. In addition to these properties that affect the absorption rate, enzymatic cleavage is influenced by the structure of the acyl radicals (8, 9, 13).

Since enzymatic hydrolysis also is dependent on the number and position of the acyl radicals, it was of interest to test *O*-acyl derivatives of one phenolethanolamine that only differed by the acyl radical. By taking into account all properties essential for bioavailability, a search has been centered on a prodrug applicable for therapeutic use. Therefore, the model compound selected was etilefrine {α-[(ethylamino)methyl]-3′-hydroxybenzyl alcohol}, which is used in the treatment of circulatory diseases. Its systemic bioavailability as unmetabolized etilefrine is ~50% (6, 7), although it is completely absorbed.

A series of 3′-(*O*-acyl) derivatives of etilefrine was synthesized according to various methods (Table I). Their physical properties and hydrolysis rates are listed in Table II.

RESULTS AND DISCUSSION

Starting from 3′-hydroxy-2-(benzylethylamino)acetophenone (I), which was prepared according to known procedures for the synthesis of hydroxy-2-(benzylalkylamino)acetophenones (14, 15), acylation was carried out according to Methods A–E (Scheme I). The esters (II) obtained were debenzylated with hydrogen in the presence of palladium-on-carbon to give intermediates (III), which were reduced to the corresponding alcohols (IV), usually without interrupting the reaction (Method F). In cases where the substituents at the nucleus were sensitive to hydrogenolysis (IV*r*), the keto group was reduced with sodium borohydride (Method G). In one case (IV*f*), isolation of the levorotatory form (IV*g*) was achieved by reaction with (+)-dibenzoyltartaric acid (Method H).

The compounds thus obtained had characteristic IR, PMR, and mass spectra, consistent with the structures indicated. All IR spectra exhibited strong, sometimes broad absorptions at 3340–3160 cm^{-1} (OH), bands between 2500 and 2360 cm^{-1} with several splits (NH_2^+), and intensive absorptions at ~1760–1730 cm^{-1} (C=O) (Table III).

Common to all PMR spectra were CH_3 signals from NCH_2CH_3 as a triplet at ~1.3–1.4 ppm, both CH_2 absorptions due to CH_2NHCH_2 as a multiplet at 2.9–3.1 ppm, a multiplet between 5.0 and 5.5 ppm due to the CH proton from CHOH, and broad absorptions centered in the regions of 5.7–5.8 ppm (OH) and 9.0–9.2 ppm (NH). The latter absorptions disappeared on treatment with deuterium oxide. The absorptions of the *m*-disubstituted phenyl-ring protons and those due to the R group are summarized in Table III.

The mass spectra of IV*a*–IV*s* contained the molecular ions of the free amines and peaks at M − 18 (H_2O) with low intensity. In addition, diagnostic fragments appeared in all cases at *m/e* 162[1] (M − H_2O − RCO) and 134[2] (M − H_2O − RCO − CO). The dominant ions at *m/e* 58

[1] High-resolution mass spectrum: calc. for $C_{10}H_{12}NO$, 162.0919; found, *m/e* 162.0922.
[2] High-resolution mass spectrum: calc. for $C_9H_{12}N$, 134.0970; found, *m/e* 134.0967.

0022-3549/80/1200-1423$01.00/0
© 1980, American Pharmaceutical Association

(10) D. Rodbard, *Clin. Chem.*, **20**, 1255 (1974), Appendix I.
(11) E. A. Evans, H. C. Sheppard, J. C. Turner, and D. C. Warrell, *J. Labelled Compd.*, **10**, 569 (1974).
(12) M. Freifelder, T. Anderson, Y. H. Ng, and V. Papendick, *J. Pharm. Sci.*, **53**, 967 (1964).
(13) W. Hammer, C. M. Idelström, and F. Sjöqvist, *Excerpta Med. Ser.*, **122**, 301 (1967).
(14) T. B. Cooper, *Clin. Pharmacokinet.*, **3**, 14 (1978).

ACKNOWLEDGMENTS

The authors thank Richard Privette and Dr. David Rosenthal of Research Triangle Institute for technical assistance and computer programming work, respectively. They also thank Dr. Madison J. Cawein and Terry D. Dusebout of the Clinical Pharmacology Department at the Merrell Research Center for conducting the clinical portion of the study.

Prodrugs of Etilefrine: Synthesis and Evaluation of 3′-(*O*-Acyl) Derivatives

JOSEF WAGNER *ˣ, HELMUT GRILL *, and DIETRICH HENSCHLER ‡

Received March 10, 1980, from the **Department of Chemical Research, Klinge Pharma, Munich, West Germany,* and the ‡*Institute of Pharmacology and Toxicology, University of Würzburg, Würzburg, West Germany.* Accepted for publication June 27, 1980.

Abstract □ A series of 3′-(*O*-acyl) derivatives of etilefrine {α-[(ethylamino)methyl]-3′-hydroxybenzyl alcohol} was synthesized. Correlations between structure and solubility, pKa value, lipophilicity, and esterase-catalyzed hydrolysis were demonstrated. Of special interest is the 3′-(*O*-pivaloyl) derivative, which shows, in addition to favorable solubility and improved lipophilicity, marked stability against enzymatic cleavage in blood along with a high rate of hydrolysis in the liver.

Keyphrases □ Etilefrine—synthesis and evaluation of 3′-(*O*-acyl) derivatives as prodrugs □ Prodrugs—etilefrine, synthesis and evaluation of 3′-(*O*-acyl) derivatives as prodrugs

The uncertain activity of orally administered phenolethanolamines is partly assumed to result from metabolic processes during absorption. Phenolethanolamines with a free hydroxyl group in the *meta*-position are primarily subject to this gut wall first-pass metabolism. As they pass the intestinal wall, they are conjugated to inactive compounds. For example, in the intestinal wall, 80% of orally administered isoproterenol is converted to sulfate (1, 2) in the *meta*-position. During the gut wall passage, a similar conjugation was found for orciprenaline (metaproterenol) (3), terbutaline (4), norfenefrine (5), and etilefrine (6). Due to this early metabolic reaction, the bioavailability of compounds, even those with a high rate of absorption, is frequently reduced (7).

To avoid the attack of conjugating enzymes at the 3′- or 5′-hydroxy group, it was masked by acylation, thus converting the phenolethanolamines into prodrugs. *O*-Acyl derivatives of this type are known for phenylephrine (8, 9), etilefrine (8, 9), norepinephrine (10), *meta*-norepinephrine (10), epinephrine (8, 9), *meta*-epinephrine (8, 9), isoproterenol (10), orciprenaline (10), *N*-*tert*-butylnorepinephrine (11), and terbutaline (12). These *O*-acyl derivatives differ from their parent drug significantly in their solubility, dissociation constants, and lipophilicity. In addition to these properties that affect the absorption rate, enzymatic cleavage is influenced by the structure of the acyl radicals (8, 9, 13).

Since enzymatic hydrolysis also is dependent on the number and position of the acyl radicals, it was of interest to test *O*-acyl derivatives of one phenolethanolamine that only differed by the acyl radical. By taking into account all properties essential for bioavailability, a search has been centered on a prodrug applicable for therapeutic use. Therefore, the model compound selected was etilefrine {α-[(ethylamino)methyl]-3′-hydroxybenzyl alcohol}, which is used in the treatment of circulatory diseases. Its systemic bioavailability as unmetabolized etilefrine is ~50% (6, 7), although it is completely absorbed.

A series of 3′-(*O*-acyl) derivatives of etilefrine was synthesized according to various methods (Table I). Their physical properties and hydrolysis rates are listed in Table II.

RESULTS AND DISCUSSION

Starting from 3′-hydroxy-2-(benzylethylamino)acetophenone (I), which was prepared according to known procedures for the synthesis of hydroxy-2-(benzylalkylamino)acetophenones (14, 15), acylation was carried out according to Methods A–E (Scheme I). The esters (II) obtained were debenzylated with hydrogen in the presence of palladium-on-carbon to give intermediates (III), which were reduced to the corresponding alcohols (IV), usually without interrupting the reaction (Method F). In cases where the substituents at the nucleus were sensitive to hydrogenolysis (IV*r*), the keto group was reduced with sodium borohydride (Method G). In one case (IV*f*), isolation of the levorotatory form (IV*g*) was achieved by reaction with (+)-dibenzoyltartaric acid (Method H).

The compounds thus obtained had characteristic IR, PMR, and mass spectra, consistent with the structures indicated. All IR spectra exhibited strong, sometimes broad absorptions at 3340–3160 cm^{-1} (OH), bands between 2500 and 2360 cm^{-1} with several splits (NH_2^+), and intensive absorptions at ~1760–1730 cm^{-1} (C=O) (Table III).

Common to all PMR spectra were CH_3 signals from NCH_2CH_3 as a triplet at ~1.3–1.4 ppm, both CH_2 absorptions due to CH_2NHCH_2 as a multiplet at 2.9–3.1 ppm, a multiplet between 5.0 and 5.5 ppm due to the CH proton from CHOH, and broad absorptions centered in the regions of 5.7–5.8 ppm (OH) and 9.0–9.2 ppm (NH). The latter absorptions disappeared on treatment with deuterium oxide. The absorptions of the *m*-disubstituted phenyl-ring protons and those due to the R group are summarized in Table III.

The mass spectra of IV*a*–IV*s* contained the molecular ions of the free amines and peaks at M − 18 (H_2O) with low intensity. In addition, diagnostic fragments appeared in all cases at *m/e* 162[1] (M − H_2O − RCO) and 134[2] (M − H_2O − RCO − CO). The dominant ions at *m/e* 58

[1] High-resolution mass spectrum: calc. for $C_{10}H_{12}NO$, 162.0919; found, *m/e* 162.0922.
[2] High-resolution mass spectrum: calc. for $C_9H_{12}N$, 134.0970; found, *m/e* 134.0967.

0022-3549/80/1200-1423$01.00/0
© 1980, American Pharmaceutical Association

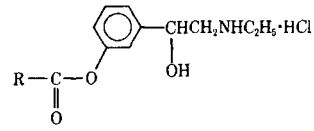

Table I—Etilefrine 3′-(*O*-Acyl) Derivatives

Compound (as Hydrochloride)	R	Melting Point	Yield (Pure), %	Method	Formula
IV*a*	CH_3	114°[a]	49	B/F	$C_{12}H_{18}ClNO_3$
IV*b*	CH_3CH_2	116.1°[b]	37	A/F	$C_{13}H_{20}ClNO_3$
IV*c*	$CH_3(CH_2)_2$	138.1°[b]	55	D/F	$C_{14}H_{22}ClNO_3$
IV*d*	$(CH_3)_2CH$	159.8°[b]	57	B/F	$C_{14}H_{22}ClNO_3$
IV*e*	$CH_3(CH_2)_3$	134.2°[b]	45	D/F	$C_{15}H_{24}ClNO_3$
IV*f*	$(CH_3)_3C$	209.4°[b]	65	A/F	$C_{15}H_{24}ClNO_3$
IV*g*[c]	$(CH_3)_3C$	225°[a]	6[d]	H[e]	$C_{15}H_{24}ClNO_3$
IV*h*	$CH_3(CH_2)_{16}$	117.4°[a]	60	E/F	$C_{28}H_{50}ClNO_3$
IV*i*	1-$CH_3C_6H_{10}$	204.3°[a]	51	D/F	$C_{18}H_{28}ClNO_3$
IV*j*	$C_6H_5CH_2$	127.6°[b]	46	B/F	$C_{18}H_{22}ClNO_3$
IV*k*	$C_6H_5CH(CH_3)$	169°[b]	51	D/F	$C_{19}H_{24}ClNO_3$
IV*l*	$C_6H_5CH(C_2H_5)$	138.4°[b]	63	D/F	$C_{20}H_{26}ClNO_3$
IV*m*	$C_{10}H_7$-1-CH_2	144°[a]	17	E/F	$C_{22}H_{24}ClNO_3$
IV*n*	4-$CH_3C_6H_4$	190.1°[a]	41	D/F	$C_{18}H_{22}ClNO_3$
IV*o*	2-$CH_3C_6H_4$	161°[a]	69	A/F	$C_{18}H_{22}ClNO_3$
IV*p*	2,4,6-$(CH_3)_3C_6H_2$	180.1°[a]	77	C/F	$C_{20}H_{26}ClNO_3$
IV*q*	2,6-$(CH_3O)_2C_6H_3$	207.1°[a]	52	C/F	$C_{19}H_{24}ClNO_5$
IV*r*	2,6-$Cl_2C_6H_3$	190.2°[a]	27	D/F/G	$C_{17}H_{18}Cl_3NO_3$
IV*s*	2-$C_6H_5C_6H_4$	186.2°[b]	55	D/F	$C_{23}H_{24}ClNO_3$

[a] Recrystallized from methanol–ether. [b] Recrystallized from isopropanol. [c] (−)-Enantiomer of IV*f*. [d] Referenced to racemate. [e] For resolution of racemic salt, see *Experimental*.

($CH_2NHC_2H_5$, mostly base peak) and *m/e* 30 (CH_2NH_2) were due to characteristic amine fragmentations. Furthermore, all mass spectra, with the exception of IV*h* and IV*q*, showed typical fragment ions (R, RCO, or RCOH) from ester cleavage (Table III).

Table II illustrates that the high water solubility of the etilefrine hydrochloride was hardly influenced by introducing short aliphatic acyl radicals (IV*a*–IV*e*). Surprisingly, water solubility was reduced markedly whenever the acyl radical was highly branched (IV*f* and IV*g*). While araliphatic acyl radicals still led to sufficient solubility in water (IV*j*, IV*l*, and IV*m*), this was no longer the case either with very long aliphatic acyl radicals (IV*h*) or with aromatic acyl radicals that carry some substituents (IV*p*–IV*r*) at the nucleus.

Phenolethanolamines in solution represent a mixture of the uncharged form and ionic species (cation, anion, and zwitterion) (16). At half-neutralization, these components are in a specific equilibrium, which is represented by an apparent average pKa value. The pKa value is dependent on the substituent at the amino nitrogen and is increased from 8.67 (norfenefrine) (17) to 8.89 (phenylephrine) (17) or 9.0 (etilefrine) (18) for the 3′-hydroxyphenylethanolamines when introducing a methyl or ethyl radical into the amino group. The same value also was obtained for etilefrine in 1.5×10^{-3} *M* aqueous solution (Table II).

When the phenolic hydroxyl group is lost, the participating components of the dissociation equilibrium are reduced to the uncharged form and the ammonium compound. This results in a change of the pKa value (17). As shown by the pKa values of the acyl derivatives (IV*a*–IV*f*) in aqueous solution, the same effect can be observed when the phenolic hydroxyl group is masked with an acyl radical. However, in methanolic solution, the pKa values decreased from 9.4 (water) to 8.7 (90.7% methanol). The pKa values of IV*g*–IV*s* could not be ascertained because of insufficient solubility, although some of these compounds, being hydrochlorides, would be easily water soluble (IV*j*, IV*l*, and IV*m*). However, considering that all acyl derivatives in water–methanol (9.3:90.7) showed identical pKa values, it is assumed that the pKa value of 9.4 found for IV*a*–IV*f* in water would be the same for IV*g*–IV*s*.

As suggested by the pKa values, 2.45% of the etilefrine and 0.99% of the acyl derivatives (IV*a*–IV*s*) are present in aqueous solution of pH 7.4 in the uncharged form. Judging by the partition coefficient, 2.1% of etilefrine was present in the lipophilic phase. This value closely corresponds

Table II—Physical Properties and Hydrolysis Rates of Etilefrine 3′-(*O*-Acyl) Derivatives

Compound (as Hydrochloride)	Solubility[a]		pKa[b]		log *P* in *n*-Octanol–Buffer[c]	Hydrolysis Rates[d], μl of CO_2		
	Percent	*M*	Water[e]	Water–Methanol[f] (9.3:90.7)		Human Blood[g]	Rat Blood[g]	Rat Liver[h]
Etilefrine	75	3.4	9.0	8.9	−1.66			
IV*a*	60	2.3	9.4	8.7	−1.57	57.5	44	182
IV*b*	65	2.4	9.4	8.7	−0.85	47.5	46.5	226
IV*c*	60	2.1	9.4	8.7	−0.39	32	25.4	204
IV*d*	60	2.1	9.4	8.7	−0.16	34.5	32	220
IV*e*	65	2.1	9.4	8.7	0.23	30.7	34	194
IV*f*	12	4.0×10^{-1}	9.4	8.7	0.20	5.6	4.6	196
IV*g*	2	6.6×10^{-2}	—[i]	8.7	0.20	5.6	4.6	196
IV*h*	<0.05	$<1.0 \times 10^{-3}$	—[i]	8.7	>2	—[i]	—[i]	—[i]
IV*i*	9	2.6×10^{-1}	—[i]	8.7	1.5	0.4	0	45
IV*j*	55	1.6	—[i]	8.7	0.23	6.9	80.5	130
IV*k*	5	1.4×10^{-1}	—[i]	8.7	0.91	3.0	2.4	95
IV*l*	25	6.9×10^{-1}	—[i]	8.7	1.36	1.0	1.6	25
IV*m*	25	6.5×10^{-1}	—[i]	8.7	1.41	1.4	4.2	75
IV*n*	8	2.4×10^{-1}	—[i]	8.7	1.20	9.0	0.2	60
IV*o*	9	2.7×10^{-1}	—[i]	8.7	1.20	0.8	0.3	21
IV*p*	2	5.5×10^{-2}	—[i]	8.7	1.89	—[i]	—[i]	—[i]
IV*q*	1	2.6×10^{-2}	—[i]	8.7	0.38	0.3	0.1	0.1
IV*r*	0.4	1.0×10^{-2}	—[i]	8.7	1.72	—[i]	—[i]	—[i]
IV*s*	0.3	7.0×10^{-3}	—[i]	8.7	1.82	—[i]	—[i]	—[i]

[a] In water; accuracy of ±5%. [b] Accuracy of ±0.05 pK unit. [c] Phosphate buffer, pH 7.4, 0.15 *M*; initial concentrations = 1.0×10^{3}–1.8×10^{3} *M*. [d] Substrate concentration of 10^{-2} *M*. [e] $c = 1.5 \times 10^{-2}$ *M*. [f] $c = 2 \times 10^{-2}$ *M*. [g] Blood (30 μl) and substrate (30 μmoles) in 2.5×10^{-2} *M* $NaHCO_3$ (2970 μl). [h] A suspension of a liver homogenate (60 μl) and substrate (30 μmoles) in 2.5×10^{-2} *M* $NaHCO_3$ (2940 μl). [i] Not determinable because of poor solubility of the base.

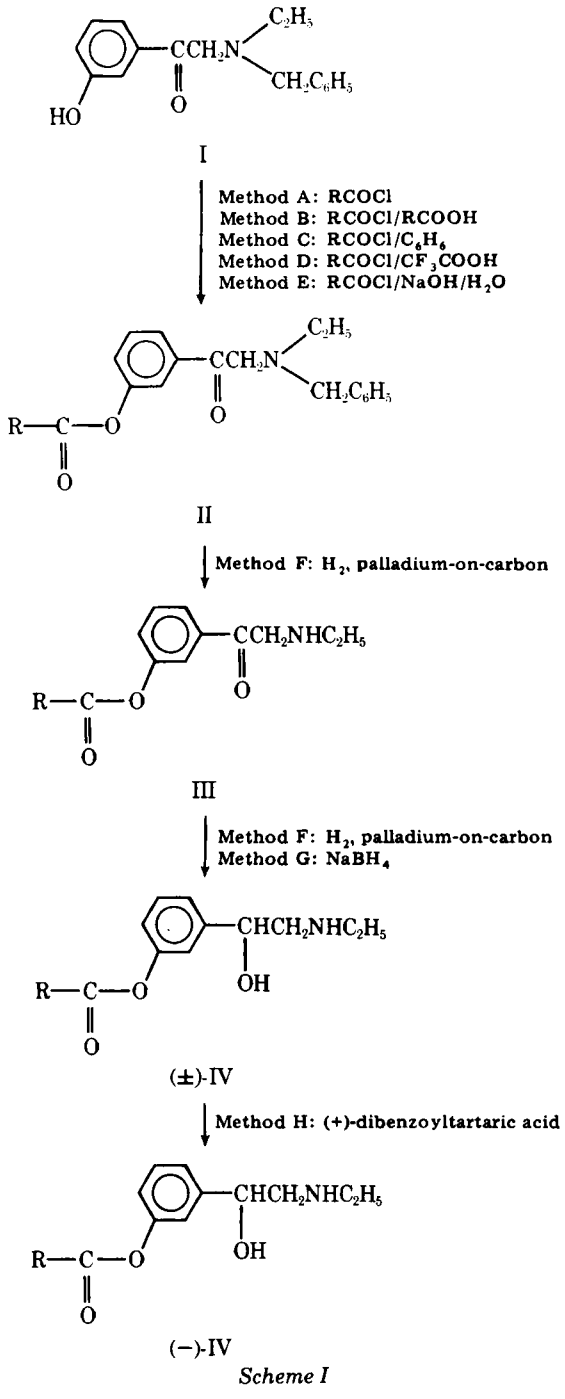

Scheme I

to the existing amount of the uncharged form of etilefrine. A similar lipophilicity was shown by IV*a*, although the addition of an acetyl radical in the molecule would suggest an increase. However, since IV*a* has a higher pKa value than etilefrine itself, its normally higher lipophilicity is reduced because of the higher dissociation at pH 7.4. With increasing lipophilicity of the acyl moiety (IV*b*–IV*s*), the amount of ionized acyl etilefrine in the lipophilic phase is augmented.

The experimentally determined Δ log P values of homologs are in most cases in reasonable agreement with the reported π values (19–23). However, in some cases (IV*a*/IV*b*, IV*c*/IV*e*, and IV*j*/IV*k*), considerable discrepancies were observed. This finding is attributed to the fact that the Hansch π value system will falter whenever aliphatic groups are near a very polar moiety such as the carbonyl function.

On the basis of log P values found through experimentation, it is evident that the lipophilicity increases with the chain length (IV*b* < IV*c* < IV*e* < IV*h*). However, the lipophilicity of the *n*-acyl derivatives is not necessarily higher than that of the *iso*-acyl compounds (IV*c* < IV*d*). A similar inconsistency was observed for the 5′-(*O*-acyl) derivatives of 9-β-D-arabinofuranosyladenine (24). The levorotatory form of the pivaloyl derivative (IV*g*) showed no difference compared to the racemate (IV*f*). Even the change of position of a methyl substituent in the benzoyl radical (IV*n* and IV*o*) did not alter the lipophilicity.

After absorption through the gut wall, orally administered substances are transported by the blood into the liver by way of mesentery veins and the vena portae. Through this passage, the 3′-(*O*-acyl) derivatives of etilefrine are protected from attacking conjugating enzymes, provided they do not become subject to esterase-catalyzed hydrolysis. To obtain better insight into the cleavage, tests were conducted with these esters in diluted rat and human blood and in rat liver homogenate.

The rate of enzymatic hydrolysis of the aliphatic acyl radicals decreased in human blood with increasing alkyl chain length (IV*a* > IV*b* > IV*c* > IV*e*) or when the radical was highly branched (IV*c* > IV*f* = IV*g*) (Table II). In most cases, rat blood was slightly less active in hydrolyzing acyl radicals than was human blood, but the deviations in general were rather low. However, there was one exception. The phenyl acetyl derivative (IV*j*) was hydrolyzed extremely rapidly by rat blood, probably due to a specific esterase in this species. The hydrolysis carried out by the enzymes of the rat liver was much faster and was nearly the same with the aliphatic acyl radicals, whereas compounds with araliphatic or aromatic acyl radicals were split up according to their steric hindrance in the blood as well as in the liver. Thus, the hydrolysis rate was decreased as the size of the aromatic system of the araliphatic acyl derivatives was enlarged (IV*j* > IV*m*) or the length of the alkyl radical grew (IV*j* > IV*k* > IV*l*). For the aromatic acyl radicals, the splitting rate was reduced considerably if substituents were introduced at position 2 or positions 2 and 6 (IV*n* > IV*o* > IV*q*). Due to insufficient solubility in 2.5×10^{-2} *M* $NaHCO_3$, hydrolysis rates of IV*h*, IV*p*, IV*r*, and IV*s* could not be ascertained enzymatically.

As the data in Table II illustrate, the 3′-(*O*-acyl) derivatives of etilefrine can differ by over 100-fold with respect to solubility, lipophilicity, and enzymatic cleavage. In selecting a prodrug with improved bioavailability after oral administration, the following criteria are decisive: (*a*) sufficient solubility and enhanced lipophilicity for accelerated absorption; (*b*) very reduced enzymatic hydrolysis during absorption, thus giving improved protection against conjugation; and (*c*) extensive enzymatic hydrolysis while passing through the liver, resulting in the fast release of drug activity.

Judging by the cleavage through hepatic enzymes, the aliphatic acyl derivatives (IV*a*–IV*g*) are superior to IV*h*[3]–IV*s*. Of these compounds, IV*e*–IV*g* promise more accelerated absorption than etilefrine due to their 70 times greater lipophilicity. Since the pivaloyl derivative (IV*f*) exhibits a hydrolysis rate in the blood of less than one-fifth of that of IV*e* and possesses a solubility six times higher than that of IV*g*, IV*f* was preferred. Comparative absorption studies with dogs[4] and humans[5] confirmed the superiority of this compound to etilefrine. As shown with tritium-labeled material, the absorption rate was increased with dogs[4] and humans[5] when a pivaloyl radical was introduced, and bioavailability was increased by 46%[5].

Investigations of the pharmacological properties of etilefrine pivalate will be discussed elsewhere.

EXPERIMENTAL[6]

Chemical Methods—*Method A/F: Etilefrine 3′-Pivalate (IVf) Hydrochloride*—A mixture of I·HCl (30.6 g, 0.1 mole) in pivaloyl chloride (60.3 g, 0.5 mole) was stirred and heated slowly to 106° with an increasing rate of hydrogen chloride evolution. The suspension was maintained at

[3] After completion of these studies, results of comparative pharmacokinetic investigations on etilefrine and its stearoyl derivative (IV*h*) were published (25). It was shown that introduction of the stearoyl radical reduced the bioavailability of etilefrine by 49%.

[4] D. Henschler, unpublished results.

[5] J. H. Hengstmann, Department of Medicine, University of Bonn, Bonn, West Germany, personal communication.

[6] All melting points were obtained using a Mettler FP 1 melting-point apparatus and are uncorrected. Microanalyses were carried out at the Analytical Laboratories, 5279 Gummersbach, West Germany. Purity of intermediates not subjected to elemental analysis was ascertained by TLC performed on Merck silica gel 60 F_{254}. Spots were located under UV light or with iodine vapor. Solvent mixtures used for TLC were chloroform–methanol–water (59:33:8) (Solvent A), chloroform–methanol–water (90:9:1) (Solvent B), and chloroform–methanol (98:2) (Solvent C).

UV absorption curves were recorded on a Beckman ACT A III UV–visible spectrophotometer. IR spectra were run on a Perkin-Elmer model 257 spectrophotometer, and PMR spectra were determined on a Varian EM 360 spectrometer. Mass spectra were obtained from a Varian MAT 112 S spectrometer using a direct-sample insertion system and ionization by electron impact (70 ev). Optical rotations were measured with a Schmidt-Haensch (model Polartronic I) electronic polarimeter. The pH values were obtained using a Metrohm A 603 pH meter.

Table III—Spectral Data for Etilefrine 3′-(*O*-Acyl) Derivatives

Compound (as Hydrochloride)	IR[a], $\nu_{C=O}$	PMR[b] Solvent	PMR[b] δ for $RCOOC_6H_4$—	Mass Fragmentations, *m/e* (relative intensity, %)
IV*a*	1760	A	1.38 (t, 3H, CH_3) and 6.73–7.53 (m, 4H, aromatic H)	223 (M^+, 0.1) and 43 (8)
IV*b*	1760	A	1.22 (t, 3H, CH_3), 2.55 (q, 2H, CH_2), and 6.73–7.47 (m, 4H, aromatic H)	237 (M^+, 0.1), 29 (16), and 57 (9)
IV*c*	1760	A	1.02 (t, 3H, CH_3), 1.73 (m, 2H, CH_2CH_3), 2.50 (t, 2H, $COCH_2$), and 6.80–7.50 (m, 4H, aromatic H)	251 (M^+, 0.2), 43 (15), and 71 (9)
IV*d*	1755	A	1.27 [d, 6H, $CH(CH_3)_2$], 2.90 (m, 1H, CH), and 6.73–7.50 (m, 4H, aromatic H)	251 (M^+, 0.5), 43 (28), and 71 (11)
IV*e*	1760	A	0.95 (t, 3H, CH_3), 1.20–1.97 [m, 4H, $(CH_2)_2CH_3$], 2.52 (t, 2H, $COCH_2$), and 6.75–7.46 (m, 4H, aromatic H)	265 (M^+, 0.3), 57 (8), and 85 (3)
IV*f*	1745	B	1.33 [s, 9H, $C(CH_3)_3$] and 6.83–7.60 (m, 4H, aromatic H)	265 (M^+, 0.2), 57 (20), and 85 (2)
IV*h*	1750	A	0.90 (t, 3H, CH_3), 1.05–1.93 (m, 30H, $(CH_2)_{15}CH_3$), 2.50 (t, 2H, $COCH_2$), and 6.80–7.37 (m, 4H, aromatic H)	447 (M^+, 0.1) and 267 (0.7)
IV*i*	1745	A	1.07–2.45 (m, 13H, 1-$CH_3C_6H_{10}$) and 6.81–7.50 (m, 4H, aromatic H)	305 (M^+, 0.3), 97 (11), and 125 (0.7)
IV*j*	1740	A	3.80 (s, 2H, CH_2) and 6.70–7.50 (m, 9H, aromatic H)	299 (M^+, 0.1), 91 (18), and 118 (6)
IV*k*	1755	A	1.58 (d, 3H, CH_3), 3.93 (q, 1H, CH), and 6.7–7.5 (m, 9H, aromatic H)	313 (M^+, 0.4), 105 (33), and 132 (10)
IV*l*	1750	A	0.95 (t, 3H, CH_3), 1.95 (m, 2H, CH_2), 3.65 (t, 1H, CH), and 6.67–7.50 (m, 9H, aromatic H)	327 (M^+, 0.6), 119 (14), and 146 (12)
IV*m*	1750	A	4.21 (s, 2H, CH_2) and 6.68–8.10 (m, 11H, aromatic H)	349 (M^+, 1), 141 (39), and 168 (21)
IV*n*	1730	B	2.45 (s, 3H, CH_3)and 6.96–8.15 (m, 8H, aromatic H)	299 (M^+, 1), 91 (43), and 119 (100)
IV*o*	1730	A	2.61 (s, 3H, CH_3) and 6.88–8.25 (m, 8H, aromatic H)	299 (M^+, 2), 91 (52), and 119 (95)
IV*p*	1730	A	2.30 (s, 3H, 4-CH_3), 2.40 (s, 6H, 2- and 6-CH_3), and 6.76–7.43 (m, 6H, aromatic H)	327 (M^+, 1), 119 (25), and 147 (100)
IV*q*	1740	B	3.86 (s, 6H, 2O-CH_3) and 6.58–7.63 (m, 7H, aromatic H)	345 (M^+, 1) and 165 (100)
IV*r*	1750	C	7.06–7.82 (m, 7H, aromatic H)	353 (M^+, 0.1), 145 (5), and 173 (16)
IV*s*	1740	B	6.62–8.08 (m, 13H, aromatic H)	361 (M^+, 2), 153 (25), and 181 (75)

[a] IR spectra were run in potassium bromide, and absorption values are in reciprocal centimeters. [b] PMR spectra were run at 60 MHz in deuterochloroform (A), methanol-d_4 (B), or dimethyl sulfoxide-d_6 (C), and chemical shifts (δ) are given in parts per million relative to tetramethylsilane as the internal standard. Multiplicities of the peaks are expressed as singlet (s), doublet (d), triplet (t), quartet (q), and multiplet (m).

this temperature until the starting material went into solution; the temperature then was raised to 110° and maintained there until cessation of gas evolution (~2 hr). After evaporation of the remaining pivaloyl chloride, the residue was dissolved in methanol (30 ml) and poured into petroleum ether (700 ml). The precipitate, R_f 0.8 on TLC (Solvent B), was filtered, dissolved in isopropanol–water (330 ml), and hydrogenated in the presence of 10% palladium-on-carbon (3.3 g) at room temperature and normal pressure until the calculated amount of hydrogen had reacted (about 3 hr). After removal of the catalyst and then the solvent by vacuum evaporation, the residue was crystallized from isopropanol to give 19.6 g (65%) of IV*f*·HCl, mp 209.4°, R_f 0.4 (Solvent A).

Anal.—Calc. for $C_{15}H_{23}NO_3$·HCl: C, 59.69; H, 8.01; N, 4.64. Found: C, 59.69; H, 7.91; N, 4.39.

*Method B/F: Etilefrine 3′-(2-Methylpropionate) (IV*d*) Hydrochloride*—A suspension of I·HCl (30.6 g, 0.1 mole) in 2-methylpropionyl chloride (85.2 g, 0.8 mole) and 2-methylpropionic acid (85 ml) was stirred and heated slowly until the starting material went into solution; then the mixture was refluxed for 0.5 hr. After evaporation to dryness, the residue, R_f 0.8 on TLC (Solvent B), was reprecipitated and hydrogenated under the same conditions as described for the preparation of IV*f*·HCl to give 16.4 g (57%) of IV*d*·HCl after crystallization from isopropanol, mp 159.8°, R_f 0.4 (Solvent A).

Anal.—Calc. for $C_{14}H_{21}NO_3$·HCl: C, 58.43; H, 7.71; N, 4.87. Found: C, 58.48; H, 7.59; N, 4.85.

*Method C/F: Etilefrine 3′-(2,4,6-Trimethylbenzoate) (IV*p*) Hydrochloride*—A mixture of I·HCl (30.6 g, 0.1 mole) in 2,4,6-trimethylbenzoyl chloride (36.5 g, 0.2 mole) and benzene (20 ml) was refluxed for 1.5 hr. The mixture was extracted at room temperature with petroleum ether. The bottom layer was separated and evaporated under reduced pressure. The residue, R_f 0.8 on TLC (Solvent B), was dissolved in isopropanol–water (450 ml) and hydrogenated in the presence of 10% palladium-on-carbon (11.0 g) in the same manner as described for the preparation of IV*f*·HCl to give 28.0 g (77%) of IV*p*·HCl after recrystallization from methanol–ether, mp 180.1°, R_f 0.4 (Solvent A).

Anal.—Calc. for $C_{20}H_{25}NO_3$·HCl: C, 66.01; H, 7.20; N, 3.85. Found: C, 65.96; H, 7.10; N, 3.81.

*Method D/F: Etilefrine 3′-(4-Methylbenzoate) (IV*n*) Hydrochloride*—To a suspension of I·HCl (30.6 g, 0.1 mole) in trifluoroacetic acid (39.9 g, 0.35 mole) was added 4-methylbenzoyl chloride (30.9 g, 0.2 mole) over 0.5 hr with vigorous evolution of hydrogen chloride. The mixture was refluxed for 1.5 hr. The volatile portion was distilled off under vacuum, and the residue was stirred in ether. The precipitate was poured into a mixture of ether (500 ml) and water (100 ml). After cooling, the two-phase system was adjusted to pH 9 with cold ammonium hydroxide. The organic layer was separated and washed twice with cold 1 *N* NaOH (400 ml) and water (400 ml). After removal of the solvent under vacuum, the residue, R_f 0.8 on TLC (Solvent B), was dissolved in isopropanol–water (300 ml), acidified to pH 2 with hydrochloric acid, and hydrogenated in the presence of 10% palladium-on-carbon (6.5 g) in the same manner as described for the preparation of IV*f*·HCl to give 13.8 g (41%) of IV*n*·HCl after recrystallization from methanol–ether, mp 190.1°, R_f 0.4 (Solvent A).

Anal.—Calc. for $C_{18}H_{21}NO_3$·HCl: C, 64.38; H, 6.60; N, 4.17. Found: C, 64.43; H, 6.56; N, 4.17.

*Method D/F/G: Etilefrine 3′-(2,6-Dichlorobenzoate) (IV*r*) Hydrochloride*—A mixture of I·HCl (30.6 g, 0.1 mole) and 2,6-dichlorobenzoyl chloride (42.0 g, 0.2 mole) in trifluoroacetic acid (114.0 g, 1 mole) was stirred and heated slowly to 80° with an increasing rate of hydrogen chloride evolution. Then the mixture was refluxed for 1.5 hr. After evaporation of the volatile portion, the oily residue was poured into a mixture of ice and ammonium hydroxide and extracted twice with ether (500 ml). The organic layer was separated and washed with cold 1 *N* NaOH and water. The solvent was evaporated to give 23.0 g (52%) of 3′-hydroxy-2-(benzylethylamino)acetophenone 3′-(2,6-dichlorobenzoate) (II*r*) as an oil, R_f 0.9 (Solvent B).

A solution of II *r* (23.0 g, 0.052 mole) in methanol–water (9:1, 300 ml) was adjusted to pH 2 with hydrochloric acid and then hydrogenated in the presence of 10% palladium-on-carbon (2.3 g) at room temperature and atmospheric pressure until 1 equivalent of hydrogen had reacted. After the catalyst and then the solvent were removed by vacuum evaporation, the residue was crystallized from methanol–isopropanol to give 12.0 g (60%) (31% referenced to I·HCl) of 3′-hydroxy-2-(ethylamino)-acetophenone 3′-(2,6-dichlorobenzoate) (III*r*) hydrochloride, mp 170° dec., R_f 0.85 (Solvent A). The PMR and IR spectral data supported the assigned structure.

Sodium borohydride (4.0 g) was added in portions to a mixture of III*r*·HCl (12.0 g, 0.031 mole) in dry methanol (200 ml) over 1 hr while the temperature of the reaction was kept below 5°. Excess sodium borohydride was destroyed by the addition of acetic acid. After evaporation to dryness, the residue was suspended in diluted ammonium hydroxide (200 ml) and extracted with ether. The organic layer was separated, washed with water, and evaporated to dryness. The residue was dissolved in isopropanol–water (9:1, 400 ml), acidified to pH 2 with hydrochloric acid, and concentrated. The solid residue was crystallized with methanol–ether to give 10.5 g (87%) (27% referenced to I·HCl) of IV*r*·HCl, mp 190.2°, R_f 0.4 (Solvent A).

Anal.—Calc. for $C_{17}H_{17}Cl_2NO_3$·HCl: C, 52.26; H, 4.64; N, 3.59. Found: C, 52.35; H, 4.63; N, 3.58.

Method E/F: Etilefrine 3′-Stearate (IVh) Hydrochloride—A mixture of I·HCl (30.6 g, 0.1 mole) and stearoyl chloride (33.3 g, 0.11 mole) in 1 *N* NaOH (250 ml) was stirred at ambient temperature for 1 hr. The mixture was extracted with ether, and the organic layer was washed with 1 *N* NaOH and water.

After removal of the solvent under reduced pressure, the waxy residue, R_f 0.8 on TLC (Solvent C), was taken up in methanol (1 liter) and adjusted to pH 2 with hydrochloric acid. The mixture was hydrogenated in the presence of 10% palladium-on-carbon (10.0 g) at 40° and atmospheric pressure until the calculated amount of hydrogen had reacted. After the catalyst and solvent were removed by vacuum evaporation, the residue was crystallized from methanol–ether to give 29.1 g (60%) of IV*h*·HCl, mp 117.4°, R_f 0.5 (Solvent A).

Anal.—Calc. for $C_{28}H_{49}NO_3$·HCl: C, 69.46; H, 10.41; N, 2.89. Found: C, 69.82; H, 10.27; N, 2.77.

Method H: (−)-Etilefrine 3′-Pivalate (IVg) Hydrochloride—To a mixture of IV*f*·HCl (301.8 g, 1 mole) in water (2.7 liters) and (+)-*O,O*-dibenzoyltartaric acid monohydrate (188.0 g, 0.5 mole) in methanol (2.7 liters) was added sodium bicarbonate (42.0 g, 0.5 mole) at room temperature. The solution was cooled slowly to 2° and maintained at this temperature for 5 days. The white crystalline precipitate was filtered off and washed with cold methanol–water (1:1). This product was recrystallized (13 times) from methanol–water (55:45) until the optical rotation remained constant. The yield was 39.1 g of (−)-etilefrine 3′-pivalate (+)-*O,O*-dibenzoylhydrogentartrate, mp 163.5° dec., $[\alpha]_D^{20}$ +55.3° (*c*, 1 in methanol).

This product was dissolved in methanol–water (9:1, 200 ml), acidified to pH 2 with hydrochloric acid, and concentrated. The residue was crystallized with methanol–ether to give 18.1 g of IV*g*·HCl (6%) referenced to IV*f*·HCl, mp 225°, R_f 0.4 (Solvent A), $[\alpha]_D^{20}$ −36.7° (*c*, 1 in methanol).

Anal.—Calc. for $C_{15}H_{23}NO_3$·HCl: C, 59.69; H, 8.01; N, 4.64. Found: C, 59.72; H, 7.98; N, 4.58.

Determination of Solubility—An excess of each compound (100–1000 mg weighed accurately) was stirred in a portion of water at room temperature for 1 hr. Additional portions of water were added at 1-hr intervals until the entire sample was dissolved under stirring. The percentage solubility, *S*, was calculated according to:

$$S(\%) = \frac{\text{weight}_{\text{sample}}}{\text{weight}_{\text{solution}}} \times 100 \qquad \text{(Eq. 1)}$$

Measurement of pKa Values—The pKa values listed in Table II were determined by measuring the pH of a solution containing equivalent concentrations of the amine and its salt. These solutions were obtained by adding to a solution of the salt the calculated amount of aqueous 0.1 *N* NaOH for half-neutralization. The concentrations of the compound were 1.5×10^{-3} *M* in water and 2×10^{-2} *M* in water–methanol. For IV*g*–IV*s*, which were insufficiently soluble in water at the point of half-neutralization, aqueous solutions were made up to contain 90.7% methanol at half-neutralization. The pH values were measured using a pH meter with a digital scale at room temperature. The results were estimated to be accurate to ±0.05 pK unit.

The percentage of the protonated form, $[BH]^+$, at pH 7.4 is expressed by:

$$[BH]^+(\%) = \frac{100}{1 + \text{antilog}\,(7.4 - \text{pKa})} \qquad \text{(Eq. 2)}$$

Measurement of Partition Coefficients—For the partitioning, pure *n*-octanol saturated with 0.15 *M* phosphate buffer (pH 7.4) and phosphate buffer saturated with *n*-octanol were used. Normally, 20–40-mg samples were dissolved in the buffer solution (50 ml) and shaken with the *n*-octanol solution (50–600 ml) at room temperature for 0.5 hr. After centrifugation, an aliquot of the bottom layer was removed and diluted to give an absorbance range of 0.2–0.7, measured at the absorption maximum of the compounds (206–223 nm) using a 1-cm cell. A standard curve of at least four points was used for each sample to determine the concentration in the bottom layer. Multiple analyses showed the data in Table II to be reproducible. The partition coefficient, *P*, was calculated from:

$$P = \frac{V_{\text{buffer}}}{V_{n\text{-octanol}}} \left(\frac{C_{\text{buffer},\,i}}{C_{\text{buffer},\,f}} - 1 \right) \qquad \text{(Eq. 3)}$$

The first factor in Eq. 3 is the ratio of the volumes of the buffer and *n*-octanol used for partitioning of the sample. The second factor contains the ratio of the initial to the final concentration in the buffer layer, as determined by readings of the absorbance in the UV region.

Determination of Enzymatic Ester Cleavage—The Warburg manometric technique was used as described by Ammon (26). Blood was obtained from one healthy female volunteer and from rats (female Wistar, 180 g). One part of rat liver (female Wistar, 180 g) was homogenized in one part of buffer (2.5×10^{-2} *M* $NaHCO_3$).

Heparinized blood (30 μl) or rat liver homogenate (60 μl) diluted with buffer to 300 μl was pipetted into the side arm, and the solution of the respective ester substrate in the buffer (30 μmoles/2700 μl) was put into the main trough of the calibrated reaction vessels. After equilibration for 10 min with a stream of nitrogen and carbon dioxide (95:5), the vessels were closed, and the reaction was started by mixing the enzyme preparation with the substrate–buffer solution. Readings were taken at 5-min intervals for up to 1 hr, corrected for volume and actual atmospheric pressure, transformed into volume units, and plotted as microliters of carbon dioxide against time. The plotted curves were idealized graphically and adjusted for spontaneous hydrolysis as determined in the control vessels without the addition of enzymes. With some sparingly water-soluble substrates, stock solutions were obtained with pure ethanol. With final ethanol concentrations not exceeding 5%, no inhibition of esterase activities was recorded.

REFERENCES

(1) D. S. Davies, C. D. Morgan, M. E. Conolly, J. W. Paterson, M. Sandler, and C. T. Dollery, *Fed. Proc. Fed. Am. Soc. Exp. Biol.*, **28**, 797 (1969).

(2) C. T. Dollery, D. S. Davies, and M. E. Conolly, *Ann. N. Y. Acad. Sci.*, **172**, 108 (1971).

(3) J. H. Hengstmann, H. Aulepp, and H. J. Dengler, *Naunyn-Schmiedebergs Arch. Pharmacol.*, **287**, R 95 (1975).

(4) H. T. Nilsson, K. Persson, and K. Tegner, *Xenobiotica*, **2**, 363 (1972).

(5) J. H. Hengstmann, W. Konen, C. Konen, M. Eichelbaum, and H. J. Dengler, *Eur. J. Clin. Pharmacol.*, **8**, 33 (1975).

(6) J. H. Hengstmann, U. Weyand, and H. J. Dengler, *ibid.*, **9**, 179 (1975).

(7) J. H. Hengstmann, *Arzneim.-Forsch.*, **26**, 1251 (1976).

(8) D. Henschler, J. Wagner, and H. Hampel, German pat. 2,152,058 (1976).

(9) D. Henschler, J. Wagner, and H. Hampel, German pat. 2,401,783 (1977).

(10) G. Zölss, *Sci. Pharm.*, **32**, 76 (1964).

(11) B. F. Tullar, H. Minatoya, and R. R. Lorenz, *J. Med. Chem.*, **19**, 834 (1976).

(12) E. Arrigoni-Martelli, *Drugs Fut.*, **1**, 333 (1976).

(13) J. Kristoffersson, L. A. Svensson, and K. Tegner, *Acta Pharm. Suec.*, **11**, 427 (1974).

(14) E. Eidebenz and M. Depner, German pat. 865,315.

(15) K. Schromm, O. Thomä, A. Mentrup, K. Zeile, and H. Engelhardt, German Offen. 1,543,359.

(16) C. R. Ganellin, *J. Med. Chem.*, **20**, 579 (1977).

(17) M. M. Tuckerman, J. R. Mayer, and F. C. Nachod, *J. Am. Chem. Soc.*, **81**, 92 (1959).

(18) "Martindale, The Extra Pharmacopoeia," 26th ed., Pharmaceutical Press, London, England, 1973, p. XXI.

(19) T. Fujita, J. Iwasa, and C. Hansch, *J. Am. Chem. Soc.*, **86**, 5175 (1964).

(20) J. Iwasa, T. Fujita, and C. Hansch, *J. Med. Chem.*, **8**, 150 (1965).

(21) E. Miller and C. Hansch, *J. Pharm. Sci.*, **56**, 92 (1967).

(22) A. Leo, C. Hansch, and D. Elkins, *Chem. Rev.*, **71**, 551 (1971).

(23) C. Hansch and E. Coats, *J. Pharm. Sci.*, **59**, 731 (1970).

(24) D. C. Baker, T. H. Haskell, and S. R. Putt, *J. Med. Chem.*, **21**, 1218 (1978).

(25) K. L. Rominger and G. Hitzenberger, *Int. J. Clin. Pharmacol., Ther. Toxicol.*, **18**, 150 (1980).

(26) R. Ammon, *Pfluegers Arch. Ges. Physiol.*, **233**, 486 (1934).

Pharmacokinetics of Oral and Intravenous Fluorouracil in Humans

THOMAS A. PHILLIPS *§, ANTHONY HOWELL ‡, ROBERT J. GRIEVE ‡, and PETER G. WELLING *§x

Received April 16, 1980, from the *Departments of *Clinical Pharmacology and ‡Medicine, School of Medicine, University of Birmingham, Birmingham, England.* Accepted for publication June 25, 1980. §Present address: School of Pharmacy, University of Wisconsin, Madison, WI 53706.

Abstract □ The pharmacokinetics of fluorouracil were examined after single 250-mg iv doses and 500-mg oral doses to female patients with breast cancer. In five patients who received intravenous fluorouracil, the mean peak plasma level of unchanged drug was 13.4 μg/ml, the elimination half-life was 6.3 min, and the plasma clearance was 1410 ml/min. The last value is similar to the hepatic blood flow. In six patients who received oral fluorouracil, the mean peak value of unchanged drug in plasma, which occurred within 20 min of dosing, was 8.3 μg/ml, and the fluorouracil elimination half-life was 7.2 min. The overall bioavailability of oral fluorouracil as unchanged drug was 28%, and the variation in plasma drug levels between individuals was similar following oral and intravenous doses. The data provide additional evidence of saturable hepatic metabolism of fluorouracil during the first pass.

Keyphrases □ Fluorouracil—comparison of oral and intravenous doses pharmacokinetics, human plasma □ Pharmacokinetics—fluorouracil levels in human plasma following intravenous and oral doses □ Antineoplastic activity—fluorouracil, pharmacokinetics, human plasma

The pharmacokinetics of fluorouracil following intravenous administration to humans have been characterized (1–4). The drug distributes into an apparent body volume equivalent to 25% of the body weight and is cleared rapidly from the circulation, principally due to metabolism, with a half-life of 5–15 min. The high plasma clearance of fluorouracil suggests that considerable first-pass metabolism occurs following oral administration (5).

Reports on the availability of orally dosed fluorouracil to the general circulation are conflicting. Cohen *et al.* (1) reported 50 and 80% absorption in two patients, while other investigators reported much lower absorption (6). A recent study suggested that the availability of fluorouracil increases with increasing dose (2), which may be due to saturation of the initial degradative metabolic step in the liver (7).

The circulating levels of fluorouracil in patients receiving relatively low single doses of fluorouracil by the intravenous and oral routes were examined. The description of these data and comparisons with previous reports are the subjects of this paper.

EXPERIMENTAL

Subjects and Protocols—The subjects were 11 female patients undergoing therapy for breast carcinoma, postmastectomy, as outpatients at the Selly Oak Hospital, Birmingham, England. Characteristics of the subjects and diagnostic information are given in Table I. The subjects were ambulatory and were taking solid food. They were being treated under the conditions of a multicenter trial to examine the benefits of cyclic adjuvant chemotherapy in both node-positive and node-negative operable breast cancer. Node-positive patients received fluorouracil by intravenous injection; node-negative patients were dosed orally.

The medication received by the two groups of subjects is summarized in Table II. Since each subject received either oral or intravenous fluorouracil, it was not possible to examine fluorouracil kinetics after oral and intravenous doses in the same person.

All fluorouracil doses were administered at the hospital in the presence of the attending physician. Intravenous doses of 250 mg of fluorouracil were administered in 5 ml of water for injection into a forearm vein over 30 sec. Oral doses of 500 mg of fluorouracil were administered in 10 ml of water for injection followed immediately by 90 ml of orange juice. No dietary restrictions were applied. Since subjects had to travel from their homes to the hospital to receive the fluorouracil doses, an interval of at least 1 hr elapsed between eating and dosing.

Blood samples (10 ml) were taken from a forearm vein in the arm, not used for drug administration in the intravenous study, and were placed in heparinized tubes. Plasma was promptly separated and stored at −20° until it was assayed.

Assay—Fluorouracil was extracted from plasma by the method described previously (3). The high-pressure liquid chromatographic (HPLC) system consisted of a 25-cm × 4-mm (10-μm particle size) column[1] preceded by a 5-cm × 4-mm (10-μm particle size) guard column[2], a constant-volume pump[3], and a variable-wavelength detector[4] set at 265 nm. The solvent was 10^{-2} *M* phosphate buffer (pH 5.5) at a flow rate of 2 ml/min.

Uridine was used as the internal standard since it had a shorter retention time in this system than thymidine (3). Dried residues from extracted plasma were redissolved in 200 μl of 5% methanol in water, and 50 μl of this solution was injected into the chromatograph. Fluorouracil was measured by the peak height ratio method against uridine. Using this procedure, the retention volumes for fluorouracil and uridine were 11 and 21 ml, respectively, and the time required to analyze each sample was reduced from 30 (3) to 11 min. The method had similar sensitivity and reproducibility for fluorouracil to those reported previously (3). The lower limit of detection was 0.1 μg/ml, and neither commonly occurring nucleosides nor drugs other than fluorouracil being taken by the subjects interfered with the chromatographic peaks of fluorouracil or uridine.

All pharmacokinetic parameters were obtained by standard graphical procedures (9). All rate constants were calculated by linear regression of the natural logarithm of the fluorouracil concentration against time. In the intravenous studies, the value of C_0 was corrected for the 30-sec fluorouracil injection time. In the oral studies, it was not possible to obtain a value for the absorption rate constant for Patient MD because of the absence of data during the absorption phase of the plasma fluorouracil profile.

Fluorouracil standard[5] and uridine[6] were used as received. All other chemicals and reagents were of the highest grade available and were used as received.

RESULTS

Individual plasma levels of fluorouracil obtained from the intravenous and oral doses are given in Table III, and the mean values from the two dosage forms are summarized in Fig. 1. The results of the pharmacokinetic analysis are described in Table IV.

Following intravenous dosing, plasma fluorouracil levels at the 5-min sampling varied from 6.4 to 29.5 μg/ml with a mean value of 13.4 μg/ml. Drug levels declined monoexponentially between 5 and 45 min and had returned to baseline values by 60 min. The mean half-life of fluorouracil in plasma was 6.3 min, the mean distribution volume was 0.2 liter/kg, and the plasma clearance was 1410 ml/min.

Following oral dosing, peak plasma levels of fluorouracil ranged from 4.4 to 14.3 μg/ml with a mean value of 8.3 μg/ml and occurred 10–20 min postdosing. The mean half-life of drug elimination was 7.2 min, statis-

[1] Whatman Partisil PXS ODS-2 column.
[2] Waters RP-8 Lichrosorb.
[3] Waters model M6000.
[4] Pye Unicam model LC3.
[5] Lot 578103, Hoffmann-La Roche Laboratories, Nutley, N.J.
[6] Analytical reagent, Sigma Chemical Co., St. Louis, Mo.

0022-3549/80/1200-1428$01.00/0
© 1980, American Pharmaceutical Association

Table I—Subject Statistics and Clinical and Diagnostic Data

Subject	Age, years	Weight, kg	Height, cm	White Blood Cells, $\times 10^3/mm^3$	Red Blood Cells, $\times 10^6/mm^3$	Platelets, $\times 10^3/mm^3$	Hemoglobin, g %	Albumin, g %	Serum Glutamic Oxalacetic Transaminase, units/liter	Alkaline Phosphatase, K.A. units[a]
					Intravenous					
MG	44	74	168	3.7	4.4	254	12.9	4.0	29	9
MF	44	77	178	4.2	4.7	187	13.6	4.1	17	4
FT	53	70	166	5.7	4.7	152	14.7	4.8	20	7
ID	52	66	154	5.6	4.0	382	12.4	4.7	21	6
ME	61	56	168	5.1	4.9	220	13.6	—[b]	—	—
					Oral					
EG	52	80	163	5.8	3.9	282	13.1	4.6	19	14
AM	55	90	157	6.2	4.4	174	13.7	4.1	10	9
DT	57	55	160	5.7	4.5	167	13.6	4.2	17	7
ET	62	57	155	6.1	3.8	227	12.2	4.4	15	6
RO	50	62	164	6.5	4.1	187	12.4	3.9	13	3
MD	59	66	158	4.9	4.6	254	13.5	4.4	13	4

[a] King–Armstrong units (8). [b] Not determined.

Table II—Medication Received on the Day Preceding and on the Day of Fluorouracil Administration

Dosage Group	Medication	Time of Medication, hr
Intravenous, 250 mg, five patients	Day preceding study	
	20 mg of prochlorperazine maleate po	1030
	20 mg of prochlorperazine maleate po	1330
	50 mg of doxorubicin iv	1430
	1 mg of vincristine iv	1430
	250 mg of cyclophosphamide iv	2000
	150 mg of methotrexate iv[a]	2000
	20 mg of prochlorperazine maleate po	2015
	Day of study	
	20 mg of prochlorperazine maleate po	0845
	250 mg of fluorouracil iv	0900
	15 mg of leucovorin iv	0930
	15 mg of leucovorin po	1700
	15 mg of leucovorin po	2300
Oral, 500 mg, six patients	Day of study	
	500 mg of fluorouracil po with 10 mg of chlorambucil po and 25 mg of methotrexate po[b,c]	0900

[a] Methotrexate administered as a 12-hr infusion in 1 liter of normal saline, starting at 2000 hr. [b] Chlorambucil and methotrexate were taken by the subjects at their home after blood sampling procedures were completed. [c] On the following day, subjects received additional oral doses of 500 mg of fluorouracil and 10 mg of chlorambucil.

Table III—Plasma Levels of Fluorouracil following Intravenous and Oral Doses

Subject	Dose, mg/kg	Plasma Fluorouracil, μg/ml									
		0 min	5 min	10 min	15 min	20 min	30 min	45 min	60 min	90 min	120 min
						Intravenous					
MG	3.4	0.0	6.4	8.3	—[a]	1.9	0.3	0.2	ND[b]	—	—
MF	3.3	0.0	13.8	3.4	—	2.6	1.2	0.3	ND	—	—
FT	3.6	0.0	29.5	17.8	—	5.7	0.5	0.1	ND	—	—
ID	3.8	0.0	8.1	3.2	1.9	0.9	0.4	0.1	ND	—	—
ME	4.5	0.0	9.2	4.5	3.1	2.3	0.8	0.2	0.1	—	—
Mean	3.7	0.0	13.4	7.4	2.5	2.7	0.6	0.2	0.0	—	—
SD	0.5	0.0	9.4	6.1	—	1.8	0.4	0.1		—	—
						Oral					
EG	6.3	0.0	—	1.2	—	5.0	2.7	0.6	0.1	—	—
AM	5.6	0.0	—	3.1	4.4	2.9	0.6	0.2	0.1	—	—
DT	9.1	0.0	—	2.8	—	8.9	2.1	0.3	0.2	ND	ND
ET	8.8	0.0	—	8.7	10.7	12.2	5.5	0.6	0.1	ND	ND
RO	8.1	0.0	—	3.4	5.0	4.6	1.8	0.4	0.2	0.1	ND
MD	7.6	0.0	—	14.3	11.2	10.9	6.4	1.6	0.9	0.1	0.1
Mean	7.6	0.0	—	5.6	7.8	7.4	3.2	0.6	0.3	0.1	0.0
SD	1.4	0.0	—	4.9	3.6	3.8	2.3	0.5	0.3	0.1	—

[a] Not determined. [b] Not detectable.

tically indistinguishable from the equivalent value after intravenous dosing, while the absorption half-time was 3.4 min. This value was obtained by conventional curve-stripping procedures assuming first-order absorption and elimination (9) and indicates fast absorption of fluorouracil under the conditions employed in this study. The absorption phase was essentially complete within 20 min of dosing.

The ratio of the mean areas under the plasma fluorouracil curves from the oral and intravenous doses, corrected for the individual elimination rate constants (Table IV), provides a measure of the efficiency with which fluorouracil is absorbed from the oral dose as unchanged drug (10). The

Table IV—Pharmacokinetic Values Obtained from Analysis of Plasma Fluorouracil Data

Subject	Pharmacokinetic Parameters[a] k_a, min^{-1}	$t_{1/2a}$, min	k_{el}, min^{-1}	$t_{1/2el}$, min	C_0, μg/ml	C_{max}, μg/ml	t_{max}, min	AUC, (μg min)/ml	$AUCk_{el}$, μg/ml	V, liter/kg	Vk_{el}, ml/min
					Intravenous						
MG	—[b]	—	0.11	6.3	19.7	—	—	173	19	0.17	1384
MF	—	—	0.10	6.9	17.1	—	—	170	17	0.19	1463
FT	—	—	0.13	5.3	68.7	—	—	545	71	0.051	464
ID	—	—	0.13	5.3	16.0	—	—	122	16	0.23	1973
ME	—	—	0.09	7.7	12.7	—	—	141	13	0.35	1764
Mean	—	—	0.11	6.3	26.8	—	—	230	27	0.20	1410
SD	—	—	0.02	1.0	23.5	—	—	177	25	0.11	579
					Oral						
EG	0.20	3.5	0.09	7.7	—	5.0	20	121	11	—	—
AM	0.23	3.0	0.09	7.7	—	4.4	15	80	7	—	—
DT	0.19	3.6	0.07	9.9	—	8.9	20	152	11	—	—
ET	0.20	3.5	0.12	5.8	—	12.2	20	290	35	—	—
RO	0.22	3.2	0.09	7.7	—	5.0	15	121	11	—	—
MD	—	—	0.06	11.6	—	14.3	10	287	17	—	—
Mean	0.21	3.4	0.09	8.4	—	8.3	17	175	15	—	—
SD	0.02	0.3	0.02	2.0	—	4.2	4	91	10	—	—

[a] The notations are: k_a, first-order rate constant for drug absorption; $t_{1/2a}$, half-time for absorption; k_{el}, first-order rate constant for drug elimination; $t_{1/2el}$, half-life of elimination; C_0, concentration at time zero obtained by extrapolation of plasma fluorouracil levels after intravenous dosing; C_{max}, maximum concentration of fluorouracil in plasma after oral dosing; t_{max}, time at which C_{max} occurs; AUC, area under fluorouracil concentration *versus* time curve in plasma calculated by the trapezoidal rule; $AUCk_{el}$, area corrected for variance in k_{el}; V, apparent distribution volume of fluorouracil in the body obtained from V = dose/C_0; and Vk_{el}, plasma clearance of fluorouracil. [b] Not determined.

mean corrected area from the oral dose of 500 mg is 15 μg/ml, while that from the intravenous dose is 27 μg/ml. Correction for dose size yields a ratio of 0.28, indicating an average fluorouracil availability of 28% from the oral dose.

DISCUSSION

The plasma levels of fluorouracil obtained from the intravenous dose in this study are comparable to those obtained previously (1–3). The mean distribution volume for fluorouracil of 0.2 liter/kg and the plasma clearance of 1410 ml/min are consistent with previously reported values of 0.35 liter/kg and 1441 ml/min obtained in three patients (2) and of 0.25 liter/kg and 1265 ml/min obtained in eight patients (3).

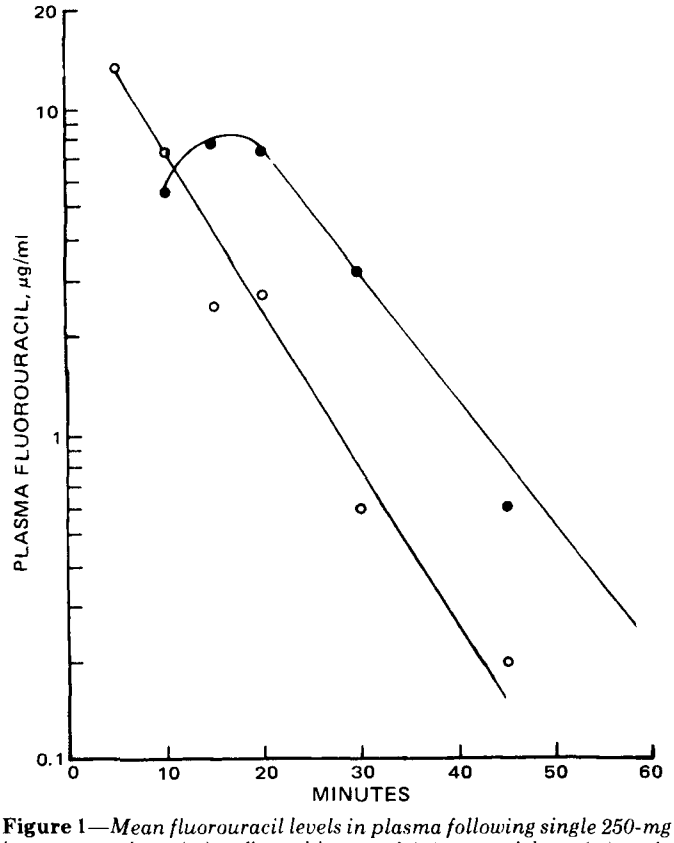

Figure 1—*Mean fluorouracil levels in plasma following single 250-mg intravenous doses (○) to five subjects and 500-mg oral doses (●) to six subjects.*

Although the overnight methotrexate infusion in these patients was terminated 1 hr before the fluorouracil dose, circulating levels of methotrexate still would be present at the time of fluorouracil dosing and could have affected the circulating levels of fluorouracil. However, due to the relatively low dose of methotrexate and the low binding of both compounds to plasma proteins (2, 11), direct interaction between these drugs in plasma, which might influence fluorouracil distribution, is unlikely.

Previous reports suggested that absorption of fluorouracil from oral dosage forms is extremely variable (6, 7). Clarkson *et al.* (12) reported a two- to 10-fold reduction in the initial plasma fluorouracil levels in patients after oral doses compared to equivalent intravenous doses. Finn and Sadée (13) also obtained variable plasma levels of fluorouracil after oral administration to three patients with colon cancer, with peak drug levels varying between 0.8 and 60 μg/ml. However, in two patients, the circulating levels of fluorouracil were prolonged relative to those after intravenous dosing. Other studies demonstrated efficient absorption of oral fluorouracil (1, 14), which has been associated with high and prolonged drug levels in plasma and bile. High fluorouracil levels in bile after oral doses may be particularly advantageous in treating hepatic metastases and tumors of the biliary tree (14).

Cohen *et al.* (1) suggested that the nature of fluorouracil absorption may depend on the vehicle with which the drug is administered but also may be influenced by the degree of hepatic involvement. Their data suggested that patients with hepatic tumor or metastases achieve lower but more prolonged circulating levels of fluorouracil than patients with no hepatic involvement. This theory was supported partially by Finn and Sadée (13), who obtained prolonged plasma levels of fluorouracil in patients with hepatic involvement, and by Garrett *et al.* (2), who obtained a similar disappearance rate for fluorouracil from plasma after oral and intravenous doses to patients with relatively normal liver function. In the latter study, fluorouracil absorption as unchanged drug was more efficient from a 1000-mg oral dose than from a 500-mg dose in two individuals, suggesting saturable metabolism of fluorouracil during the first pass (5).

The results obtained in the present study are consistent with the hypotheses (1, 2). Absorption of fluorouracil from the oral doses to subjects who had no discernible hepatic involvement was efficient and rapid. Although the clinical protocol prevented intravenous and oral doses being given to the same subjects, thus preventing direct comparisons within an individual, the plasma data nevertheless indicate that the oral dose was ~28% available as unchanged drug. This value is intermediate between the values of 1–15% reported by Garrett *et al.* (2) and of 50–80% reported by Cohen *et al.* (1) and provides further evidence that hepatic clearance of fluorouracil, which is similar to hepatic blood flow after parenteral doses (10), is highly saturable during the first pass.

Furthermore, the data obtained in this study indicate that circulating levels of oral fluorouracil may be as reproducible between individuals as

those obtained from intravenous doses. The apparent inconsistency between this observation and some earlier reports may be explained by the relatively homogeneous patient population used in this study and the heterogeneous (at least regarding the degree of hepatic involvement) patient group (1) or the very small numbers of subjects (2, 13) used previously. Considerable variability in circulating levels of fluorouracil also was reported following intravenous doses to male and female patients (4).

While it is recognized that the clinical effectiveness of fluorouracil is a complex function of the anabolic metabolism of fluorouracil and the biochemistry of cell death and cell resistance, the present results indicate that oral fluorouracil in this patient population is absorbed with reproducible efficiency, resulting in no greater variation in circulating drug levels than that following intravenous doses.

This observation may have important implications in fluorouracil treatment of patients with breast cancer, particularly in view of the relationship that exists between the patient response rate and circulating levels of fluorouracil (15).

REFERENCES

(1) J. L. Cohen, L. E. Irwin, G. J. Marshall, H. Darvey, and J. R. Bateman, *Cancer Chemother. Rep.*, **58**, 723 (1974).

(2) E. R. Garrett, G. H. Hurst, and J. R. Green, *J. Pharm. Sci.*, **66**, 1422 (1977).

(3) W. E. MacMillan, W. H. Wolberg, and P. G. Welling, *Cancer Res.*, **38**, 3479 (1978).

(4) D. S. Sitar, D. H. Shaw, M. P. Thirlwell, and J. R. Ruedy, *ibid.*, **37**, 3981 (1977).

(5) M. Gibaldi, R. N. Boyes, and S. Feldman, *J. Pharm. Sci.*, **60**, 1338 (1971).

(6) C. E. Myers, R. Diasio, H. M. Eliot, and B. A. Chabner, *Cancer Treat. Rep.*, **3**, 175 (1976).

(7) W. Sadée and C. G. Wong, *Clin. Pharmacokinet.*, **2**, 437 (1977).

(8) I. D. P. Wootton, "Microanalysis in Medicinal Chemistry," 5th ed., Churchill and Livingstone, London, England, 1974, p. 104.

(9) J. G. Wagner, "Fundamentals of Clinical Pharmacokinetics," 1st ed., Drug Intelligence Publications, Hamilton, Ill., 1975, p. 64.

(10) M. Gibaldi and D. Perrier, "Pharmacokinetics," 1st ed., Dekker, New York, N.Y., 1975, p. 145.

(11) K. B. Bischoff, R. L. Dedrick, and D. S. Zaharko, *J. Pharm. Sci.*, **59**, 149 (1970).

(12) B. Clarkson, A. O'Connor, L. Winston, and D. Hutchison, *Clin. Pharmacol. Ther.*, **5**, 581 (1964).

(13) C. Finn and W. Sadée, *Cancer Chemother. Rep.*, **59**, 279 (1975).

(14) H. O. Douglass and A. Mittelman, *Cancer*, **34**, 1878 (1974).

(15) L. E. Broder and P. P. Carbone, *Med. Pediatr. Oncol.*, **2**, 11 (1976).

ACKNOWLEDGMENTS

The authors thank Mr. Michael Morrison for permission to carry out this study in his ward at Selly Oak Hospital, the staff nurses at the Selly Oak Hospital for their help in blood sampling procedures, and Ms. Barbara Munday, Medical School, University of Birmingham, England, for setting up the chromatography procedures.

NOTES

Structural Elucidation of Adducts Formed by Ninhydrin with Indoles and Thiourea by ^{13}C-NMR Spectroscopy

NITHIANANDA CHATTERJIE *[x], RALPH A. STEPHANI [‡], and CHARLES H. STROM [§]

Received January 28, 1980, from the **New York State Institute for Basic Research in Mental Retardation, Staten Island, NY 10314*, the [‡]*Department of Pharmaceutical Sciences, College of Pharmacy, St. John's University, Jamaica, NY 11439*, and the [§]*Department of Chemistry, New York University, New York, NY 10003.* Accepted for publication June 2, 1980.

Abstract □ Condensation products were prepared by the reaction of ninhydrin with indole and 2,5-dimethylindole. The structures of these 1:1 adducts were assigned as 3-(2-hydroxy-2-indane-1,3-dionyl)indole and 3-(2-hydroxy-2-indane-1,3-dionyl)-2,5-dimethylindole, respectively, on the basis of spectral data including ^{13}C-NMR evidence. ^{13}C-NMR also was used to confirm the structure of a thiourea–ninhydrin adduct as a substituted thioindeno[1,2-*d*]imidazole-2,8-dione.

Keyphrases □ Ninhydrin—condensation products with indoles and thiourea, structural elucidation by NMR spectroscopy □ Heterocyclic adducts—cyclic ureides, condensation products of ninhydrin with indoles and thiourea, structural elucidation by NMR spectroscopy □ NMR spectroscopy—structural elucidation of condensation products of ninhydrin with indoles and thiourea

Interest in the heterocyclic adducts formed between ninhydrin (triketohydrindene hydrate, I) and aromatic amines (1, 2) and enamines (3) led to the investigation of the reaction products of this reagent with certain aromatic compounds whose structure might contain an enamine moiety. The structures of indole and 1-naphthylamine could be visualized as such; the N-1, C-2, and C-3 positions of indole and the NH_2, C-1, and C-2 positions of 1-naphthylamine possess the enamine triad (4). It was found that 1-naphthylamine forms a stable pentacyclic adduct with I, whose mode of cyclization has not been definitely established (5).

BACKGROUND

The ready formation of a 1:1 adduct between I and indole was first reported by Tomita and Fukagawa (6). However, the structure assigned by these investigators involved attack of the C-2 position of indole at the masked, central carbonyl group of ninhydrin to give II. This is in contrast to the expected reactivity of the C-3 position in indole (7, 8).

The reaction between I and indole was repeated by Roth and Kok (9); a stable, yellow adduct (1:1) was obtained with the same melting point as reported previously (6). These investigators (9) reported this adduct

0022-3549/80/1200-1431$01.00/0

© 1980, American Pharmaceutical Association

those obtained from intravenous doses. The apparent inconsistency between this observation and some earlier reports may be explained by the relatively homogeneous patient population used in this study and the heterogeneous (at least regarding the degree of hepatic involvement) patient group (1) or the very small numbers of subjects (2, 13) used previously. Considerable variability in circulating levels of fluorouracil also was reported following intravenous doses to male and female patients (4).

While it is recognized that the clinical effectiveness of fluorouracil is a complex function of the anabolic metabolism of fluorouracil and the biochemistry of cell death and cell resistance, the present results indicate that oral fluorouracil in this patient population is absorbed with reproducible efficiency, resulting in no greater variation in circulating drug levels than that following intravenous doses.

This observation may have important implications in fluorouracil treatment of patients with breast cancer, particularly in view of the relationship that exists between the patient response rate and circulating levels of fluorouracil (15).

REFERENCES

(1) J. L. Cohen, L. E. Irwin, G. J. Marshall, H. Darvey, and J. R. Bateman, *Cancer Chemother. Rep.*, **58**, 723 (1974).

(2) E. R. Garrett, G. H. Hurst, and J. R. Green, *J. Pharm. Sci.*, **66**, 1422 (1977).

(3) W. E. MacMillan, W. H. Wolberg, and P. G. Welling, *Cancer Res.*, **38**, 3479 (1978).

(4) D. S. Sitar, D. H. Shaw, M. P. Thirlwell, and J. R. Ruedy, *ibid.*, **37**, 3981 (1977).

(5) M. Gibaldi, R. N. Boyes, and S. Feldman, *J. Pharm. Sci.*, **60**, 1338 (1971).

(6) C. E. Myers, R. Diasio, H. M. Eliot, and B. A. Chabner, *Cancer Treat. Rep.*, **3**, 175 (1976).

(7) W. Sadée and C. G. Wong, *Clin. Pharmacokinet.*, **2**, 437 (1977).

(8) I. D. P. Wootton, "Microanalysis in Medicinal Chemistry," 5th ed., Churchill and Livingstone, London, England, 1974, p. 104.

(9) J. G. Wagner, "Fundamentals of Clinical Pharmacokinetics," 1st ed., Drug Intelligence Publications, Hamilton, Ill., 1975, p. 64.

(10) M. Gibaldi and D. Perrier, "Pharmacokinetics," 1st ed., Dekker, New York, N.Y., 1975, p. 145.

(11) K. B. Bischoff, R. L. Dedrick, and D. S. Zaharko, *J. Pharm. Sci.*, **59**, 149 (1970).

(12) B. Clarkson, A. O'Connor, L. Winston, and D. Hutchison, *Clin. Pharmacol. Ther.*, **5**, 581 (1964).

(13) C. Finn and W. Sadée, *Cancer Chemother. Rep.*, **59**, 279 (1975).

(14) H. O. Douglass and A. Mittelman, *Cancer*, **34**, 1878 (1974).

(15) L. E. Broder and P. P. Carbone, *Med. Pediatr. Oncol.*, **2**, 11 (1976).

ACKNOWLEDGMENTS

The authors thank Mr. Michael Morrison for permission to carry out this study in his ward at Selly Oak Hospital, the staff nurses at the Selly Oak Hospital for their help in blood sampling procedures, and Ms. Barbara Munday, Medical School, University of Birmingham, England, for setting up the chromatography procedures.

NOTES

Structural Elucidation of Adducts Formed by Ninhydrin with Indoles and Thiourea by ^{13}C-NMR Spectroscopy

NITHIANANDA CHATTERJIE *[x], RALPH A. STEPHANI [‡], and CHARLES H. STROM [§]

Received January 28, 1980, from the **New York State Institute for Basic Research in Mental Retardation, Staten Island, NY 10314*, the [‡]*Department of Pharmaceutical Sciences, College of Pharmacy, St. John's University, Jamaica, NY 11439*, and the [§]*Department of Chemistry, New York University, New York, NY 10003.* Accepted for publication June 2, 1980.

Abstract □ Condensation products were prepared by the reaction of ninhydrin with indole and 2,5-dimethylindole. The structures of these 1:1 adducts were assigned as 3-(2-hydroxy-2-indane-1,3-dionyl)indole and 3-(2-hydroxy-2-indane-1,3-dionyl)-2,5-dimethylindole, respectively, on the basis of spectral data including ^{13}C-NMR evidence. ^{13}C-NMR also was used to confirm the structure of a thiourea–ninhydrin adduct as a substituted thioindeno[1,2-*d*]imidazole-2,8-dione.

Keyphrases □ Ninhydrin—condensation products with indoles and thiourea, structural elucidation by NMR spectroscopy □ Heterocyclic adducts—cyclic ureides, condensation products of ninhydrin with indoles and thiourea, structural elucidation by NMR spectroscopy □ NMR spectroscopy—structural elucidation of condensation products of ninhydrin with indoles and thiourea

Interest in the heterocyclic adducts formed between ninhydrin (triketohydrindene hydrate, I) and aromatic amines (1, 2) and enamines (3) led to the investigation of the reaction products of this reagent with certain aromatic compounds whose structure might contain an enamine moiety. The structures of indole and 1-naphthylamine could be visualized as such; the N-1, C-2, and C-3 positions of indole and the NH_2, C-1, and C-2 positions of 1-naphthylamine possess the enamine triad (4). It was found that 1-naphthylamine forms a stable pentacyclic adduct with I, whose mode of cyclization has not been definitely established (5).

BACKGROUND

The ready formation of a 1:1 adduct between I and indole was first reported by Tomita and Fukagawa (6). However, the structure assigned by these investigators involved attack of the C-2 position of indole at the masked, central carbonyl group of ninhydrin to give II. This is in contrast to the expected reactivity of the C-3 position in indole (7, 8).

The reaction between I and indole was repeated by Roth and Kok (9); a stable, yellow adduct (1:1) was obtained with the same melting point as reported previously (6). These investigators (9) reported this adduct

0022-3549/80/1200-1431$01.00/0

© 1980, American Pharmaceutical Association

Table I—Carbon 13 Chemical Shifts of Substituted Indoles

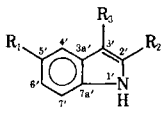

Compound	R_1	R_2	R_3	C-3a′	C-7a′	C-2′	C-3′	C-5′	C-4′	C-6′
Indole[a]	H	H	H	128.8	136.1	125.2	102.6	122.3	121.3	120.3
2-Methylindole[a]	H	CH_3	H	129.9	137.1	135.7	100.4	121.1	120.0	119.9
3-Methylindole[a]	H	H	CH_3	129.2	137.3	122.7	111.4	122.3	119.4	119.6
2,5-Dimethylindole	CH_3	CH_3	H	128.7	135.1	134.2	98.4	126.5	121.1	118.4
III	H	H	—[b]	124.9	136.4	124.8	110.2		119.4[c]–121.9	
VII	CH_3	CH_3	—[b]	126.7	132.9	134.6	110.0	126.3	119.3 –	121.6[c]

[a] Taken from Ref. 12. [b] R_3 = 2-hydroxy-1,3-indandion-2-yl. [c] May be interchanged.

Table II—Carbon 13 Chemical Shifts of 2-Substituted Indandionyl Moieties

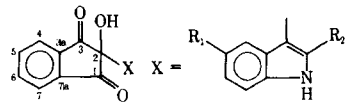

Compound	R_1	R_2	C-1 and C-3	C-2	C-4 and C-7	C-5 and C-6	C-3a and C-7a
I	X = OH		197.7	88.3	124.5	137.8	139.2
III	H	H	198.9	77.8	123.3	136.4	138.9
VII	CH_3	CH_3	198.7	78.0	123.0	136.0	139.7
XI	X = $NHCON(CH_3)_2$[a]		197.3	79.8	123.2	135.9	138.5

[a] Taken from Ref. 13.

as having Structure III, based on the interpretation of the PMR spectrum. However, a warning concerning the assignment of C-2 or C-3 substitutions in indole indicates that the effects of concentration and solvent polarity should be considered (10) when structural interpretations based on PMR evidence are made. However, these considerations were not cited in the report of Roth and Kok (9).

To establish unambiguously the structures of III and the products derived from 2,5-dimethylindole, thiourea, and I, ^{13}C-NMR spectroscopy was employed in the present study. Interest in the latter adduct (11) stems from the cyclic ureide (V) formed between urea and I (2). The nucleophilicity of the sulfur in thiourea prompted determination of the mode of cyclization; this investigation sought to distinguish between IV and VI or its [1,2-*d*]-isomer.

EXPERIMENTAL[1]

Melting points are uncorrected. All carbon spectra were decoupled with a 1-kHz wide noise bandwidth. All spectra were obtained in deuterated dimethyl sulfoxide; chemical shifts are reported relative to tetramethylsilane as the internal standard. Mass spectra were obtained on a double-focusing instrument[2] equipped with an electron-impact (70 ev) source and a direct-sample introduction probe.

Synthesis of 3-(2-Hydroxy-2-indane-1,3-dionyl)-2,5-dimethylindole (VII)—2,5-Dimethylindole (14.5 g, 0.01 mole) was dissolved in hot methanol (50 ml). To this solution was added I (1.78 g, 0.01 mole) in methanol (30 ml). The reaction mixture was warmed for 1 hr (80°) with stirring and set aside overnight. A volume of water equal to approximately one-third of the solution volume was added, and the solution was warmed and set aside for 2.5 hr. The crystals were filtered, washed with hot water, and dried.

The product weighed 2.67 g (87.5%), mp 200–205° dec. Recrystallization from methanol–water gave golden-yellow crystals, mp 198–202° dec.; IR: 3375 (OH), 3275 (NH), 1700, and 1748 (C=O) cm^{-1}; PMR: δ 10.97 (s, 1H, NH), 8.05 (s, 4H, aromatic), 7.29–6.75 (m, 3H, indole), 6.54 (s, 1H, OH), 2.31 (s, 3H, CH_3), and 2.26 (s, 3H, CH_3) (upon addition of deuterated water, the signals at δ 10.97 and 6.54 were diminished); mass spectrum: *m/e* 305 (M^+, 80%).

Anal.—Calc. for $C_{19}H_{15}NO_3$: C, 74.72; H, 4.95; N, 4.58. Found: C, 74.63; H, 4.92; N, 4.60.

Synthesis of 1,3,3a,8a-Tetrahydro-3a,8a-hydroxy-2-thioindeno[1,2-*d*]imidazole-2,8-dione (IV)—To 10 g of I (0.056 mole) in ~400 ml of hot water was added thiourea (4.25 g, 0.056 mole) dissolved in a minimum volume of water. The reaction mixture was stirred for 1 hr at 80°, cooled, and filtered. White crystals (12.0 g, 91%) were obtained, mp 236–240°. Recrystallization from water gave crystals with a melting point of 240–242°; IR: 3350–3100 (OH and NH) and 1715 (C=O) cm^{-1}; mass spectrum: *m/e* 236 (M^+, 100%).

Anal.—Calc. for $C_{10}H_8N_2O_3S$: C, 50.85; H, 3.38; N, 11.86; S, 13.55. Found: C, 50.94; H, 3.44; N, 11.82; S, 13.66.

RESULTS AND DISCUSSION

The carbon 13 chemical shifts of the carbon atoms of the adducts and some appropriate model compounds are shown in Tables I and II. Of critical significance are the peaks at 124.8 and 110.2 ppm, assigned to C-2′ and C-3′[3], respectively, of adduct III. This assignment is based on analogy

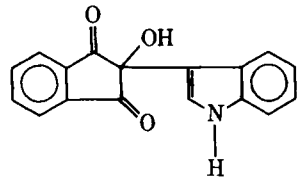

III

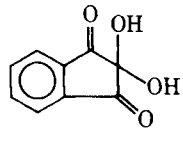

I

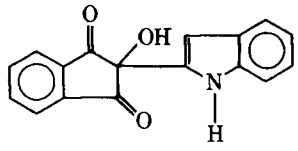

II

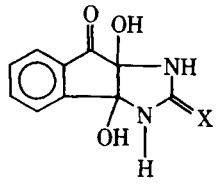

IV: X = S
V: X = O

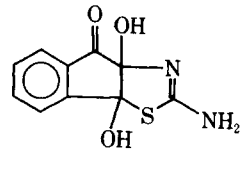

VI

[1] IR spectra were taken on a Perkin-Elmer model 237 spectrophotometer and determined in potassium bromide pellets. PMR spectra were obtained on a Varian XL-100 NMR spectrometer with a Nicolet TT-100 Fourier transform accessory. The observing frequency for protons was 100 MHz; for carbon it was 25.2 MHz.

[2] Dupont 21-492.

[3] These positions refer to the indole moiety.

Table III—Carbon 13 Chemical Shifts of C=O and C=S

Compound	Chemical Shift of C-2
X: X = O	165.9
VIII: X = S	183.4
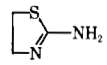	
IX	159.0
V	158.3
IV	178.4

to the carbon 13 shifts assigned to simple C-2 and C-3 methylindoles shown in Table I. Such substituted carbons are shifted downfield by ~10 ppm. The data clearly indicate that this adduct is the 3-substituted indole (III). Similarly, the 2,5-dimethylindole–ninhydrin adduct was assigned Structure VII (Table I). In this case, the C-3′ position of the indole moiety absorbs at 110.0 ppm. The pertinent chemical shifts such as those of C-2′ are in agreement with those of the model compounds. This result also is consistent with the expected chemistry for a 2-substituted indole. In addition, the chemical shifts of the carbons in the indanedione moiety as shown in Table II support the structural assignments of adducts III and VII.

The reaction of I with thiourea in neutral aqueous solution gave a product that was assigned Structure IV. The C=S group previously has been difficult to identify positively by IR spectra (14). Moreover, the superior nucleophilicity of the thiocarbonyl sulfur over that of the nitrogen atom in this ambident nucleophile is well known (15, 16). Thus, the thiazoline structure (VI) could not be excluded since the PMR spectrum of the adduct in dimethyl sulfoxide-d_6 showed two exchangeable one-proton singlets at 9.70 and 9.48, a four-proton aromatic multiplet centered at 7.85, and a two-proton broad exchangeable singlet at 6.88, attributable to a primary amino group, as in VI, or two separate NH absorbances, as in IV (which have the same chemical shift).

These considerations necessitated examination of the ^{13}C-NMR data of this adduct along with closely related model compounds (Table III). Since the thiocarbonyl group in ethylenethiourea (VIII) absorbs at 183.4 ppm, and the corresponding carbon of 2-amino-2-thioazoline (IX) absorbs at 159.0, and the adduct in question absorbs at 178.4 (C=S), one concludes that this adduct has a thioureide structure (IV). In addition, a change from ureidocarbonyl to thiocarbonyl produces a downfield shift of ~18–20 ppm. This result is in accord with the differences in the chemical shift of C-2 (thiocarbonyl *versus* carbonyl) in uracil (17), V *versus* IV, and ethyleneurea (X) *versus* ethylenethiourea (VIII) in Table III.

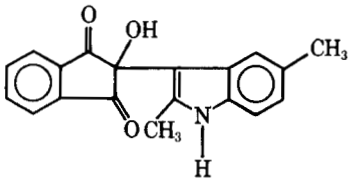

VII

REFERENCES

(1) R. Shapiro and S. C. Agarwal, *J. Am. Chem. Soc.*, **90,** 474 (1968).

(2) R. Shapiro and N. Chatterjie, *J. Org. Chem.*, **35,** 447 (1970).

(3) N. Chatterjie, R. Shapiro, S. G. Quo, and R. Stephani, *Tetrahedron Lett.*, **1975,** 2535.

(4) G. R. Allen, Jr., "Organic Reactions," vol. 20, Wiley, New York, N.Y., 1973, p. 337.

(5) N. Chatterjie, Ph.D. dissertation, New York University, New York, N.Y., 1970.

(6) M. Tomita and T. Fukagawa, *Z. Physiol. Chem.*, **158,** 62 (1926).

(7) R. J. Sundberg, "The Chemistry of Indoles," Academic, New York, N.Y., 1970, pp. 1, 2, 39.

(8) J. E. Bloor and D. L. Bruen, *J. Am. Chem. Soc.*, **89,** 6835 (1967).

(9) H. J. Roth and W. Kok, *Arch. Pharm.*, **309,** 81 (1976).

(10) M. G. Reinecke, H. W. Johnson, Jr., and J. F. Sebastian, *Chem. Ind.*, **1964,** 151.

(11) N. Chatterjie and G. J. Alexander, *IRCS Med. Sci.*, **7,** 266 (1979).

(12) J. B. Stothers, "Carbon-13 NMR Spectroscopy," Academic, New York, N.Y., 1972, pp. 266, 267.

(13) P. A. Crooks and T. Deeks, *Chem. Ind.*, **1975,** 793.

(14) L. J. Bellamy, "The Infrared Spectra of Complex Molecules," Chapman and Hall, London, England, 1975, p. 399.

(15) J. P. Edwards, in "Organic Sulfur Compounds," vol. 2, N. Karasch, Ed., Pergamon, London, England, 1966, p. 291.

(16) A. H. Cook, J. D. Downer, and I. Heilbron, *J. Chem. Soc.*, **1948,** 1262, 2028.

(17) I. W. J. Still, N. Plavac, D. M. McKinnon, and M. S. Chauhan, *Can. J. Chem.*, **56,** 725 (1978).

ACKNOWLEDGMENTS

The authors thank Dr. Charles Pouchert, Aldrich Chemical Co., Milwaukee, Wis., for samples of 2-amino-2-thiazoline, ethyleneurea, and ethylenethiourea for carbon 13 reference spectra; Dr. Steven Patt, Varian Instruments Division, Florham Park, N.J., for helpful discussions and ^{13}C-spectral data; and Mr. Richard Weed and Carol Tikijian for the preparation of illustrations.

Khellin Determination in Human Serum and Urine by High-Performance Liquid Chromatography

ADNAN EL-YAZIGI [x] **and SOBHI A. SAID** *

Received March 27, 1980, from the *Department of Pharmaceutics, College of Pharmacy, University of Riyad, Riyad, Saudi Arabia.* Accepted for publication June 2, 1980. *On leave from Cairo University, Cairo, Egypt.

Abstract □ A rapid, sensitive, and specific high-performance liquid chromatographic method was developed for the determination of khellin in serum and urine using theophylline as the internal standard. Chromatography was performed on a reversed-phase C_{18} column with 65% (v/v) methanol as the mobile phase. The assay is capable of measuring khellin concentrations down to 100 ng/ml with a total procedure time of <20 min. Oral administration of 60 mg of khellin tablets to two healthy human males was carried out, and the serum samples were analyzed by the described method. Serum concentration–time profiles are presented.

Keyphrases □ Khellin—high-performance liquid chromatographic analysis in human serum and urine □ High-performance liquid chromatography—analysis, khellin in human serum and urine □ Vasodilators—khellin, high-performance liquid chromatographic analysis in human serum and urine

Khellin (4,9-dimethoxy-7-methyl-5*H*-furo[3,2-*g*][1]-benzopyran-5-one, I), the active ingredient of *Ammi visnaga*, is used mainly as a vasodilator in the treatment of renal colic and renal stones.

Gravimetry (1), colorimetry (2, 3), and TLC–colorimetry (4) are used for the determination of I in formulations and *A. visnaga* extracts. The gravimetric assay is tedious and lacks the desired sensitivity (5), while the colorimetric methods suffer from color instability and inefficiency (4). An analytical method for the determination of this drug in biological fluids has not been available, and no information has been presented on its elimination and distribution patterns in humans.

This report describes a rapid, specific, accurate, and sensitive high-performance liquid chromatographic (HPLC) method for the determination of I in serum and urine. The procedure involves a simple, one-step solvent extraction followed by HPLC using theophylline (II) as an internal standard.

EXPERIMENTAL

Reagents and Solvents—Khellin[1] (I) was recrystallized from isopropanol[1]. Theophylline[2] (II) was used as supplied. Chloroform[3] and methanol[3] were analytical reagent grade and were used without further purification. Double-distilled water was employed in the mobile phase.

Apparatus and Operating Conditions—The analysis was performed using a high-performance liquid chromatograph[4] with a 254-nm UV detector[5], an injection system[6], and a 30-cm × 4-mm i.d. reversed-phase, high-efficiency C_{18} column[7]. The mobile phase was methanol–water (65:35), which was filtered twice through a 0.45-μm pore filter[8] and degassed before use. The flow rate was 0.8 ml/min but occasionally varied between 0.6 and 1 ml/min.

[1] Koch-Light Laboratories, Colnbrook-Bucks, England.
[2] Sigma Chemical Co., St. Louis, Mo.
[3] E. Merck, Darmstadt, West Germany.
[4] Model 6000, Waters Associates, Milford, Mass.
[5] Model 440, Waters Associates, Milford, Mass.
[6] Model U6K, Waters Associates, Milford, Mass.
[7] μBondapak C_{18}, Waters Associates, Milford, Mass.
[8] Millipore Corp., Bedford, Mass.

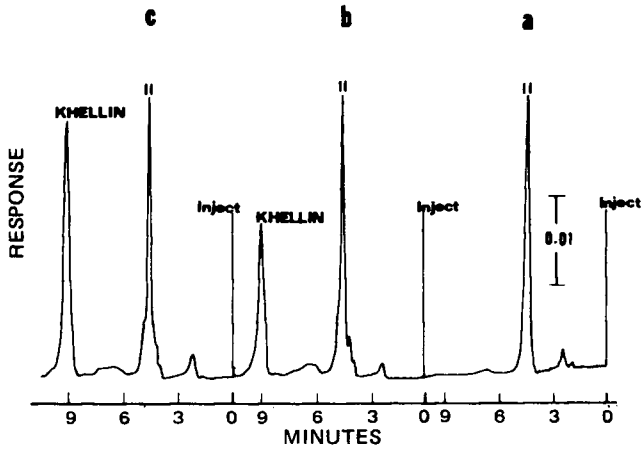

Figure 1—*Chromatograms of 1-ml human serum samples containing 5 μg of theophylline (internal standard). Key: a, taken prior to khellin administration; b, taken 6.5 hr after oral administration of 60-mg khellin tablets; and c, spiked with 1 μg of khellin. The mobile phase was 65% (v/v) methanol at a flow rate of 0.8 ml/min, and the chart speed was 0.5 cm/min.*

Extraction—A 1-ml portion of water, serum, or urine was transferred to a 13-ml centrifuge tube, and 5 or 20 μg of II and 7 ml of chloroform were added. The tube was vortexed for 60 sec and centrifuged for 8 min at 2000 rpm. After the aqueous creamy phase was aspirated and discarded, 5 ml of the organic phase was transferred to a glass tube and evaporated in a water bath at 60°. The residue was reconstituted with 0.2 ml of the mobile phase by shaking it for 30 sec on a vortex mixer, and 15–25 μl was injected onto the column.

Standard Curves—Calculations were carried out using standard curves constructed by analyzing 1-ml samples of the respective fluid spiked with 5 or 20 μg of II and known amounts of I and plotting the peak height ratio (I/II) *versus* the corresponding concentration of I. The standard curve data were subjected to least-squares linear regression analysis, and the resulting equation was utilized for the calculation of the drug concentration in the unknown samples.

Serum Level Study in Humans—Two healthy human males were given three 20-mg tablets of khellin[9] after fasting for 12 hr. Blood samples (5 ml) were removed from the median cubital vein at the indicated time intervals and placed in centrifuge tubes. After allowing the blood to clot, serum was cultivated and stored frozen until analysis. The assay was performed in duplicate.

Urine Collection—Urine was collected from one subject at various intervals after drug administration, and the volume was recorded. Samples (1 ml) were transferred into stoppered centrifuge tubes and stored frozen until assay. Urine collection was stopped 11 hr after drug administration.

RESULTS

Figure 1 shows typical chromatograms of a blank serum sample with a sample spiked with 1 μg of khellin (I) and another sample obtained from a healthy human volunteer 6.5 hr after oral administration of 60 mg of I. All three samples contained 5 μg of theophylline (the internal standard, II). The specificity of this method is clearly demonstrated by the absence of interfering peaks. With 65% methanol in water as the eluent at a flow rate of 0.8 ml/min, the retention times for I and II were 9 and 4.4 min, respectively.

[9] Lynamine, Memphis Chemical Co., Cairo, Egypt.

0022-3549/80/1200-1434$01.00/0
© 1980, American Pharmaceutical Association

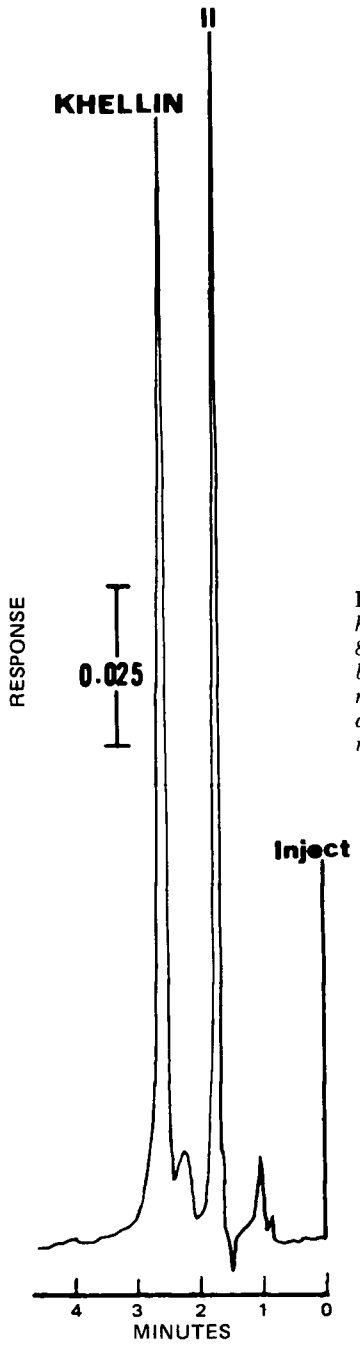

Figure 2—*Chromatogram of 1-ml human serum sample spiked with 8 μg of I and 20 μg of II. The mobile phase was 70% (v/v) methanol at a flow rate of 1.0 ml/min, and the chart speed was 0.5 cm/min.*

Figure 2 represents a chromatogram of a urine sample spiked with 8 and 20 μg of I and II, respectively. The retention times for I and II were 5 and 3.3 min, respectively, using 70% methanol as the mobile phase at a flow rate of 1.0 ml/min. The small peak preceding the drug peak was due to an impurity, which appeared to be adequately separated from the drug. Complete resolution was obtained by decreasing the flow rate and the methanol content of the mobile phase.

Recovery—The described procedure for the extraction of I from serum and urine is simple, rapid, and efficient. There was no back-extraction involved, and the extraction was carried out in <10 min. The relative serum to water recovery of I as measured by the ratio of the slopes of the standard curves of the peak height ratio *versus* concentration obtained for I in serum and water, respectively, was 0.88. Addition of 0.1 ml of 0.1 *N* NaOH to the samples did not increase the relative recovery. There was excellent linearity between the peak height ratios and khellin concentrations in serum and urine ($r > 0.999$ for both) in the concentration range employed, *i.e.*, 0.1–5 μg/ml for serum and 1–20 μg/ml for urine.

Accuracy—Table I shows the amounts found and the actual amounts with which 1-ml blank serum samples were spiked and analyzed according to the described method. The experiment was performed in duplicate, and the percent error for each unknown sample was calculated according to (6):

Table I—Accuracy of HPLC Assay for Khellin in Serum

Amount Added, μg	Experiment 1 Amount Found, μg	Experiment 1 Percent Error	Experiment 2 Amount Found, μg	Experiment 2 Percent Error
1.0	1.04	4	1.03	3
2.0	1.90	5	1.86	7
4.0	3.96	1	4.12	3
8.0	8.04	0.5	7.82	2.25
10.0	9.98	0.2	9.28	7.2

$$\% \text{ error} = \frac{\text{amount added} - \text{amount found}}{\text{amount added}} \times 100 \qquad \text{(Eq. 1)}$$

As can be seen in Table I, the percent error was ~0.2–5%. In no case did it exceed 7.5%, indicating the excellent accuracy and reproducibility of the described method.

Reliability—Since no other method is available for the determination of I in serum and urine, comparison of this HPLC assay with another method was impossible. However, the accuracy demonstrated for this method indicates that it is reliable for assaying I in these biological fluids.

Serum Levels and Urine Collection Data—The serum khellin concentration–time profiles are shown in Fig. 3. The total amount of the unchanged drug excreted through the urine in 11 hr was only 48.1 μg.

DISCUSSION

The lack of an analytical method for the determination of khellin (I) in biological fluids has precluded its clinical monitoring in patients. Indeed, since the therapeutic serum index for this drug has not been established, dosing is quite arbitrary. The daily dose of I ranges from 20 to 100 mg, and dosing frequency varies from once to three times daily. Furthermore, no information is available on the half-life and other pharmacokinetic parameters for this drug.

To the knowledge of the present investigators, this report is the first to deal with the determination of khellin in biological fluids and the first to give data on the oral absorption of this drug in humans. As shown in Fig. 3, the serum khellin levels following the administration of 60 mg of khellin tablets ranged from 0.100 to 1.7 μg/ml, and the half-life, as determined from the semilogarithmic plot of the three terminal data points assuming rapid absorption, was ~1.5–5.6 hr. The fraction of the dose excreted unchanged through the urine in 11 hr was only 0.8%. Therefore, it appears that the elimination of I occurs principally by metabolism, and, hence, analysis of the unchanged drug in the urine may be of little interest.

Further investigation to extend this preliminary information on the

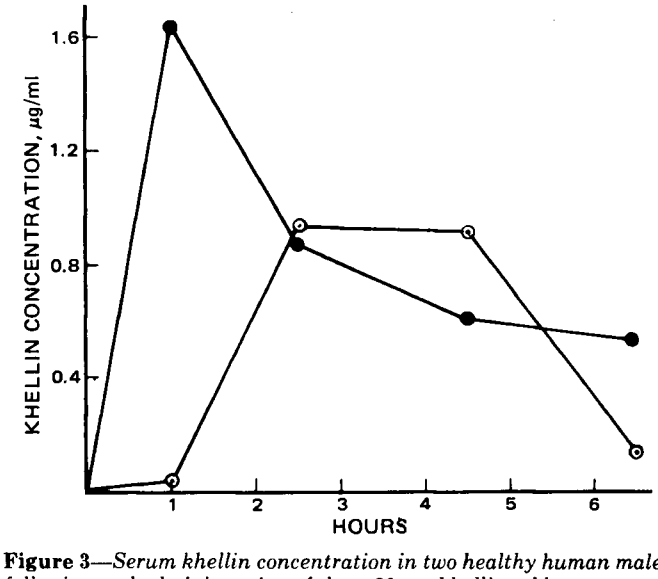

Figure 3—*Serum khellin concentration in two healthy human males following oral administration of three 20-mg khellin tablets.*

pharmacokinetics of I in humans is underway, and the results will be reported later.

REFERENCES

(1) M. R. I. Saleh and S. Gharbo, *Egypt. Pharm. Bull.*, **40**, 73 (1962).

(2) I. R. Fahmy and N. Badran, *J. Pharm. Pharmacol.*, **2**, 561 (1950).

(3) M. S. Karawya, G. Nour, and A. Sina, *Planta Med.*, **19**, 367 (1971).

(4) M. S. Karawya, M. A. El-Kiey, and G. Nour, *J. Pharm. Sci.*, **59**, 1025 (1970).

(5) I. R. Fahmy, M. A. El-Kiey, and A. Shoaib, *Proc. Pharm. Soc. Egypt., Sci. Ed.*, **5**, 91 (1953).

(6) M. A. Schwartz and J. A. De Silva, in "Principles and Perspectives in Drug Bioavailability," J. Blanchard, R. W. Sawchuck, and B. B. Brodie, Eds., S. Karger, Basel, Switzerland, 1979, p. 92.

Differential Pulse Polarographic Determination of Colchicine

WALTER HOLAK ˣ **and WILLIAM M. PLANK**

Received December 4, 1979, from the *Food and Drug Administration, Department of Health, Education, and Welfare, 850 Third Avenue, Brooklyn, NY 11232.* Accepted for publication June 4, 1980.

Abstract □ A differential pulse polarographic method for the analysis of colchicine-containing dosage forms is described. The reduction of the tropolone carbonyl is useful for quantitative analysis in that the relationship of the colchicine concentration to the current is linear over the concentration range of 0 to ~50 μg/ml, with a slight negative deviation at higher concentration. The procedure involves no preliminary treatment, is simple and specific, and is applicable to the assay of composite tablets, individual tablets, and injectable solutions. Polarography is conducted on a solution of colchicine in pH 1.81 Britton–Robinson buffer with 0.01% alkylphenoxy polyethoxyethanol. The quantitative analysis is achieved using the method of standard addition. A relative standard deviation of 3.2% was obtained for tablets. The results agree with those obtained using the USP XIX method.

Keyphrases □ Colchicine—analysis by differential pulse polarography □ Polarography, differential pulse—analysis of colchicine

Colchicine (I), an alkaloid obtained from various species of *Colchicum*, is used for the suppression of gout. The USP XIX assay for colchicine tablets involves extraction with chloroform followed by a spectrophotometric determination. The quantity of the drug specified to be taken for the assay is 3 mg. Since the usual tablet strength is 0.5 mg, this amount is equivalent to six tablets. For a content uniformity test, the method needs to be scaled down sixfold to accommodate a single tablet. As a result, the aqueous phase volume, as well as the organic volumes used for extractions, becomes less than optimum, so that difficulties with the procedure may be encountered.

Colchicine has a tropolone ring which bears a reducible carbonyl group, similar to an aromatic aldehyde that was determined by classical direct-current polarography in Britton–Robinson or McIlvane buffer (1–3). Reduction of colchicine at a dropping mercury electrode was studied at various pH levels by Sartori and Guadiano (4). These investigators reported that below pH 8, two reduction waves are obtained; the potential of the first wave becomes more negative with increasing pH and reaches that of the second wave at pH ~8. Above pH 8, there is only one wave, whose potential does not vary with pH and corresponds to the formation of a secondary alcohol. This reduction is irreversible (4).

However, the sensitivity of direct-current polarography is limited due to the large capacitance current contribution to the Faradaic current. This difficulty is reduced in differential pulse polarography. This paper describes the application of differential pulse polarography to the determination of colchicine in dosage forms with the goal of developing a general method applicable to the assay of composite tablets as well as individual tablets and injection solutions.

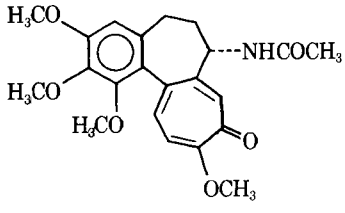

I

EXPERIMENTAL

Apparatus and Polarographic Conditions—A polarographic analyzer[1] equipped with a drop timer[2] in conjunction with a three-electrode system was used for polarographic determinations. The electrodes were a dropping mercury electrode, a saturated calomel electrode, and a platinum wire auxiliary electrode. The drop timer was set at 1 sec, and the height of the mercury column was 70 cm. Other conditions were: current range, 2–5 μamp; pulse amplitude, 50 mv; and scan rate, 5 mg/sec. The potential range scan was from −0.7 to −1.2 v. All polarograms were recorded on an *x–y* recorder[3].

Reagents and Chemicals—All chemicals were reagent grade unless otherwise specified. The standard was colchicine USP[4].

Supporting Electrolyte Solution—One liter of solution was prepared to contain 0.04 *M* acetic acid, 0.04 *M* phosphoric acid, and 0.04 *M* boric acid in water (pH 1.81). Different pH buffers were prepared for the pH *versus* polarographic behavior study by mixing 100 ml of the supporting electrolyte solution with the required volumes of 0.2 *M* NaOH and checking with the pH meter[5].

Standard Colchicine Solution—Colchicine standard, 25 mg, was accurately weighed and dissolved with supporting electrolyte solution in a 25-ml volumetric flask and then diluted to volume with the same solvent.

Surfactant Solution—The surfactant solution was 0.5% alkylphenoxy polyethoxyethanol in water[6].

[1] Model 174, Princeton Applied Research Corp., Princeton, N.J.
[2] Model 174/70, Princeton Applied Research Corp., Princeton, N.J.
[3] Omnigraphic model 2200-3-3, Houston Instruments, Austin, Tex.
[4] City Chemical Corp., New York, N.Y.
[5] Zeromatic SS-3, Beckman Instruments, Fullerton, Calif.
[6] Triton X-100, Rohm & Haas, Philadelphia, Pa.

0022-3549/80/1200-1436$01.00/0

© 1980, American Pharmaceutical Association

pharmacokinetics of I in humans is underway, and the results will be reported later.

REFERENCES

(1) M. R. I. Saleh and S. Gharbo, *Egypt. Pharm. Bull.*, **40**, 73 (1962).

(2) I. R. Fahmy and N. Badran, *J. Pharm. Pharmacol.*, **2**, 561 (1950).

(3) M. S. Karawya, G. Nour, and A. Sina, *Planta Med.*, **19**, 367 (1971).

(4) M. S. Karawya, M. A. El-Kiey, and G. Nour, *J. Pharm. Sci.*, **59**, 1025 (1970).

(5) I. R. Fahmy, M. A. El-Kiey, and A. Shoaib, *Proc. Pharm. Soc. Egypt., Sci. Ed.*, **5**, 91 (1953).

(6) M. A. Schwartz and J. A. De Silva, in "Principles and Perspectives in Drug Bioavailability," J. Blanchard, R. W. Sawchuck, and B. B. Brodie, Eds., S. Karger, Basel, Switzerland, 1979, p. 92.

Differential Pulse Polarographic Determination of Colchicine

WALTER HOLAK ˣ **and WILLIAM M. PLANK**

Received December 4, 1979, from the *Food and Drug Administration, Department of Health, Education, and Welfare, 850 Third Avenue, Brooklyn, NY 11232.* Accepted for publication June 4, 1980.

Abstract □ A differential pulse polarographic method for the analysis of colchicine-containing dosage forms is described. The reduction of the tropolone carbonyl is useful for quantitative analysis in that the relationship of the colchicine concentration to the current is linear over the concentration range of 0 to ~50 μg/ml, with a slight negative deviation at higher concentration. The procedure involves no preliminary treatment, is simple and specific, and is applicable to the assay of composite tablets, individual tablets, and injectable solutions. Polarography is conducted on a solution of colchicine in pH 1.81 Britton–Robinson buffer with 0.01% alkylphenoxy polyethoxyethanol. The quantitative analysis is achieved using the method of standard addition. A relative standard deviation of 3.2% was obtained for tablets. The results agree with those obtained using the USP XIX method.

Keyphrases □ Colchicine—analysis by differential pulse polarography □ Polarography, differential pulse—analysis of colchicine

Colchicine (I), an alkaloid obtained from various species of *Colchicum*, is used for the suppression of gout. The USP XIX assay for colchicine tablets involves extraction with chloroform followed by a spectrophotometric determination. The quantity of the drug specified to be taken for the assay is 3 mg. Since the usual tablet strength is 0.5 mg, this amount is equivalent to six tablets. For a content uniformity test, the method needs to be scaled down sixfold to accommodate a single tablet. As a result, the aqueous phase volume, as well as the organic volumes used for extractions, becomes less than optimum, so that difficulties with the procedure may be encountered.

Colchicine has a tropolone ring which bears a reducible carbonyl group, similar to an aromatic aldehyde that was determined by classical direct-current polarography in Britton–Robinson or McIlvane buffer (1–3). Reduction of colchicine at a dropping mercury electrode was studied at various pH levels by Sartori and Guadiano (4). These investigators reported that below pH 8, two reduction waves are obtained; the potential of the first wave becomes more negative with increasing pH and reaches that of the second wave at pH ~8. Above pH 8, there is only one wave, whose potential does not vary with pH and corresponds to the formation of a secondary alcohol. This reduction is irreversible (4).

However, the sensitivity of direct-current polarography is limited due to the large capacitance current contribution to the Faradaic current. This difficulty is reduced in differential pulse polarography. This paper describes the application of differential pulse polarography to the determination of colchicine in dosage forms with the goal of developing a general method applicable to the assay of composite tablets as well as individual tablets and injection solutions.

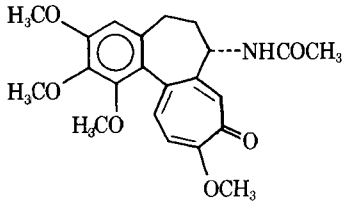

I

EXPERIMENTAL

Apparatus and Polarographic Conditions—A polarographic analyzer[1] equipped with a drop timer[2] in conjunction with a three-electrode system was used for polarographic determinations. The electrodes were a dropping mercury electrode, a saturated calomel electrode, and a platinum wire auxiliary electrode. The drop timer was set at 1 sec, and the height of the mercury column was 70 cm. Other conditions were: current range, 2–5 μamp; pulse amplitude, 50 mv; and scan rate, 5 mg/sec. The potential range scan was from −0.7 to −1.2 v. All polarograms were recorded on an *x–y* recorder[3].

Reagents and Chemicals—All chemicals were reagent grade unless otherwise specified. The standard was colchicine USP[4].

Supporting Electrolyte Solution—One liter of solution was prepared to contain 0.04 *M* acetic acid, 0.04 *M* phosphoric acid, and 0.04 *M* boric acid in water (pH 1.81). Different pH buffers were prepared for the pH *versus* polarographic behavior study by mixing 100 ml of the supporting electrolyte solution with the required volumes of 0.2 *M* NaOH and checking with the pH meter[5].

Standard Colchicine Solution—Colchicine standard, 25 mg, was accurately weighed and dissolved with supporting electrolyte solution in a 25-ml volumetric flask and then diluted to volume with the same solvent.

Surfactant Solution—The surfactant solution was 0.5% alkylphenoxy polyethoxyethanol in water[6].

[1] Model 174, Princeton Applied Research Corp., Princeton, N.J.
[2] Model 174/70, Princeton Applied Research Corp., Princeton, N.J.
[3] Omnigraphic model 2200-3-3, Houston Instruments, Austin, Tex.
[4] City Chemical Corp., New York, N.Y.
[5] Zeromatic SS-3, Beckman Instruments, Fullerton, Calif.
[6] Triton X-100, Rohm & Haas, Philadelphia, Pa.

0022-3549/80/1200-1436$01.00/0

© 1980, American Pharmaceutical Association

Table I—Composite Tablet Assay of Commercial Samples by the Differential Pulse Polarographic Method and by the USP XIX Method

Colchicine Dosage Form	Amount Declared	Differential Pulse Polarography[a] Amount Found	Differential Pulse Polarography[a] Percent of Claim	USP XIX[a] Amount Found	USP XIX[a] Percent of Claim
Tablets	0.60 mg/tablet	0.59 mg/tablet	99.3	0.60 mg/tablet	100.0
Tablets	0.50 mg/tablet	0.50 mg/tablet[b]	100.0	0.49 mg/tablet	98.0
Injection	1 mg/2 ml	1.04 mg/2 ml	104.0	1.04 mg/2 ml	104.0
Tablets	0.648 mg/tablet	0.590 mg/tablet	91.0	0.582 mg/tablet	89.8

[a] Single determinations. [b] Mean value of six determinations; *RSD* = 3.2%.

Procedure—*Composite Tablet Assay*—Twenty tablets were weighed accurately, and the average weight per tablet was determined. The tablets were ground thoroughly in a mortar, and a portion of the powder containing ~0.5 mg of colchicine was weighed and transferred to a 50-ml volumetric flask. About 20 ml of supporting electrolyte solution was added, and the flask was stoppered and shaken for ~5 min. Then 1 ml of surfactant solution was added, and the solution was diluted to volume with supporting electrolyte solution and mixed.

Content Uniformity—The same procedure was used as for the composite tablet assay, except that an intact tablet was used as the sample.

Polarographic Procedure—Ten milliliters of the solution to be assayed was pipetted into the dry polarographic cell, and the solution was deaerated for 5 min with nitrogen and then polarographed under the described conditions. With a micropipet, 100 μl of the standard solution was added, and the solution was deaerated for 1 min and polarographed exactly as before. Peak heights were measured that occurred at ~−0.88 v *versus* a saturated calomel electrode. The milligrams of colchicine in the sample was calculated from:

$$\text{mg/tablet or mg/ml of injection solution} = \frac{A}{(B \times 1.01) - A} \times 0.1 \times \frac{50}{10} \times \frac{1}{C} \quad \text{(Eq. 1)}$$

where A is the peak height of the sample, B is the peak height of the sample plus the standard, 1.01 is the concentration factor for the dilution,

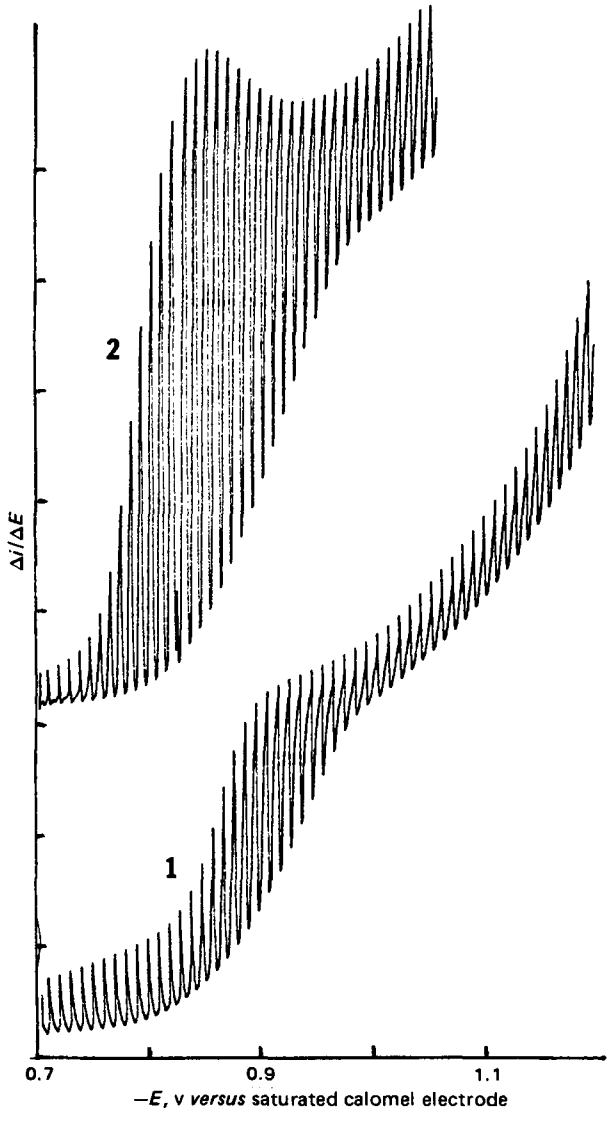

Figure 1—*Direct-current polarograms of colchicine in Britton–Robinson buffer (pH 1.81). Key: 1, 10 μg/ml; and 2, 20 μg/ml.*

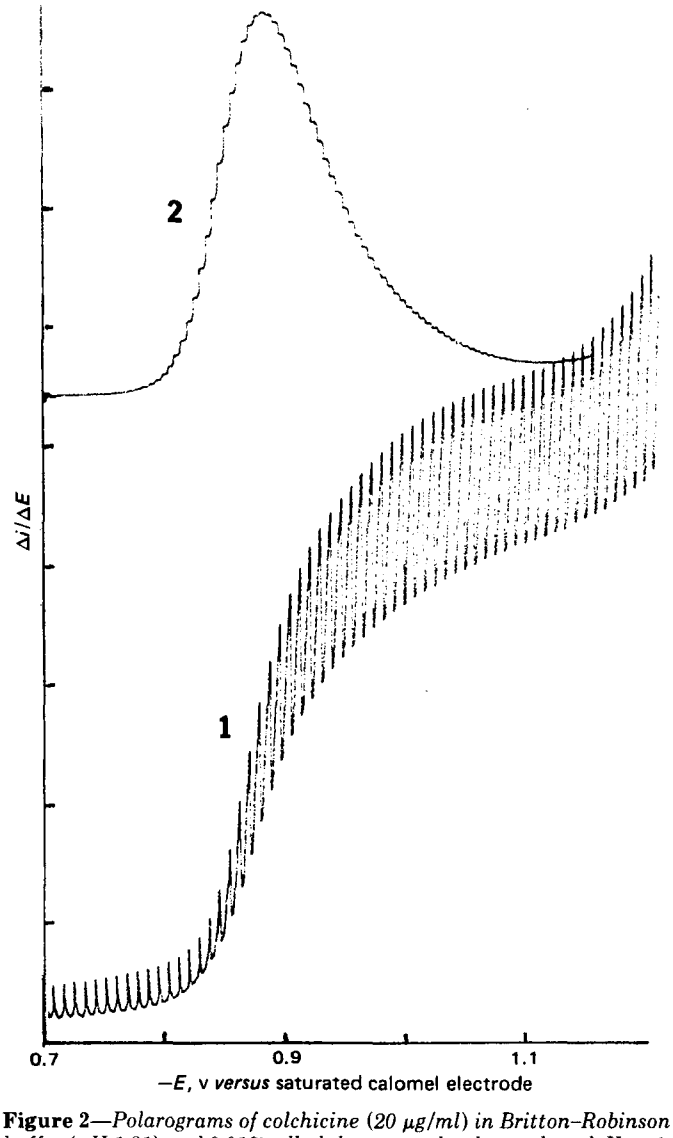

Figure 2—*Polarograms of colchicine (20 μg/ml) in Britton–Robinson buffer (pH 1.81) and 0.01% alkylphenoxy polyethoxyethanol. Key: 1, direct-current mode; and 2, differential pulse polarographic mode.*

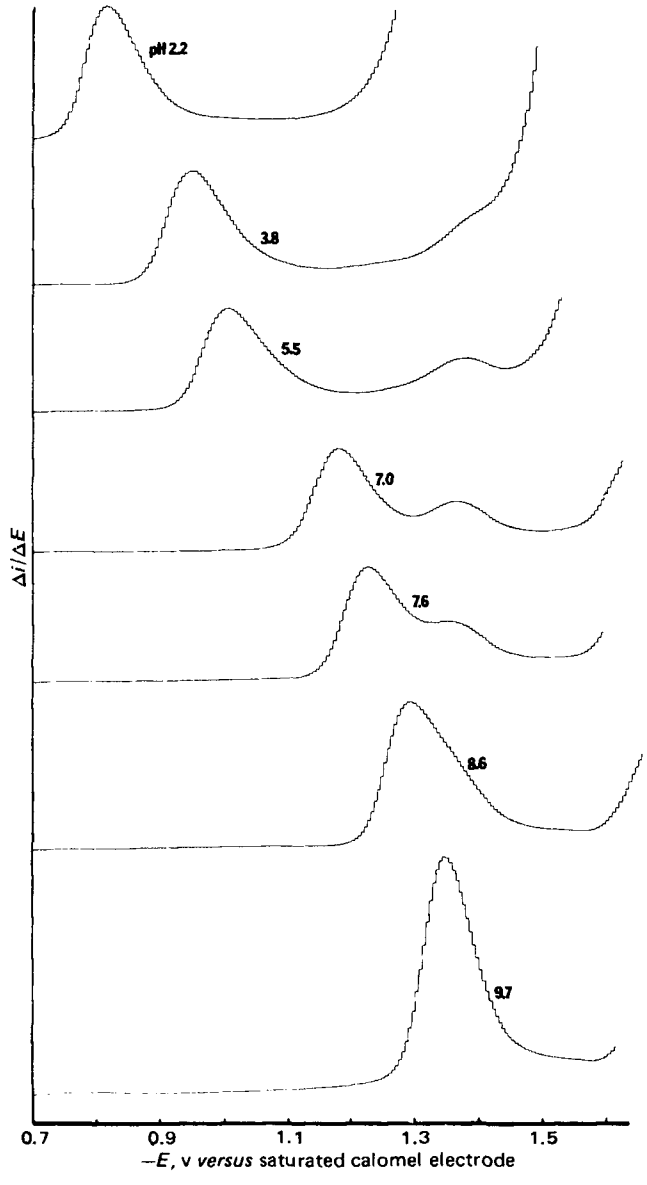

Figure 3—*Differential pulse polarographic behavior of colchicine (20 μg/ml) as a function of pH.*

and C is the number of tablets or milliliters of injection solution. In the composite tablet assay, C is the weight of the sample divided by the average weight per tablet; in the individual tablet assay, $C = 1$.

RESULTS AND DISCUSSION

When the initial differential pulse polarograms in Britton–Robinson buffer (pH 1.81) at colchicine concentrations of 10–50 μg/ml were recorded, there was a pronounced concentration-related peak potential shift in the anodic direction. The effect of adsorption was suspected and then was confirmed by running polarograms in the direct-current mode and observing the presence of a maximum (Fig. 1). Addition of 0.01% alkylphenoxy polyethoxyethanol (Fig. 2) to the test solution eliminated the maximum and almost all of the peak potential shift.

The general polarographic behavior of colchicine is similar to that of aromatic aldehydes. For example, the data for benzaldehyde (5) indicate that the mechanism for its reduction involves the formation of a free radical followed by dimerization (first wave) and the production of benzyl alcohol (second wave). A similar mechanism may be operative during the reduction of colchicine. The differential pulse polarographic behavior of colchicine as a function of pH is shown in Fig. 3.

Table II—Content Uniformity Analysis of 0.5-mg Colchicine Tablets by Differential Pulse Polarography

Tablet	Amount Found, mg/tablet
1	0.50
2	0.50
3	0.54
4	0.50
5	0.50
6	0.50
7	0.48
8	0.49
9	0.47
10	0.50
Average	0.50

The electrochemical properties of colchicine are useful for its quantitative measurement in pharmaceutical dosage forms. Quantitation is achieved by a method of standard addition to compensate for differences in sample matrixes.

A linear relationship between colchicine concentration and electrochemical behavior ($\Delta i/\Delta E$) was established from the following data points (micrograms per milliliter *versus* microamperes): 11.2, 1.08; 22.4, 2.23; 33.6, 3.29; and 44.8, 4.35. The line showed an intercept of 0.020 μamp, a slope of 0.0971 (μamp ml)/μg, and a correlation coefficient of 0.9998. The line showed a slight negative deviation from linearity at higher concentrations.

Four commercial preparations were analyzed using the proposed method and the USP XIX procedure (6). The results are given in Table I. An estimate of the precision of the differential pulse polarographic method obtained by analyzing one sample six times gave a relative standard deviation of 3.2%. Ten individual tablet assay results for 0.5-mg tablets ranged from 0.47 to 0.54 mg/tablet (Table II), with an average of 0.50 mg/tablet. The same value was obtained for the composite tablet assay.

The differential pulse polarographic assay presented here is rapid and sensitive and is specific for analyzing colchicine-containing preparations. Moreover, the same procedure is applicable for the assay of individual tablets. The results of the differential pulse polarographic method are in excellent agreement with those obtained using the more involved USP XIX assay.

REFERENCES

(1) F. Santavy, *Pharm. Acta Helv.*, **23**, 380 (1948).

(2) P. Zuman, "Organic Polarographic Analysis," Pergamon, New York, N.Y., 1964, p. 87.

(3) M. Brezina and P. Zuman, "Polarography in Medicine, Biochemistry and Pharmacy," rev. English ed., Interscience, New York, N.Y., 1958, pp. 264–266.

(4) G. Sartori and A. Gaudiano, *Rend. Ist. Super. Sanita*, **13**, 659 (1950); through *Chem. Abstr.*, **45**, 9393 (1951).

(5) I. M. Kolthoff and J. J. Lingane, "Polarography," 2nd ed., vol. II, Interscience, New York, N.Y., 1955, pp. 678–680.

(6) "The United States Pharmacopeia," 19 rev., Mack Publishing Co., Easton, Pa., 1975, p. 103.

ACKNOWLEDGMENTS

Presented at the APhA Academy of Pharmaceutical Sciences, Kansas City meeting, November 12, 1979.

The authors thank Dr. Thomas Medwick, Food and Drug Administration, New York, N.Y., and Rutgers University, New Brunswick, N.J., and Dr. Cesar A. Lau-Cam, Food and Drug Administration, New York, N.Y., and St. John's University, Jamaica, N.Y., for their assistance in the preparation of this paper.

Analysis of Procainamide Hydrochloride and Acecainide Hydrochloride in Rat Feed

JAMES E. CARTER *x, JOHN S. DUTCHER ‡, DANIEL P. CARNEY *, LAWRENCE R. KLEIN *, LAWRENCE A. BLACK *, and PAUL W. ERHARDT *

Received December 5, 1979, from the *Research and Development Department, American Critical Care, McGaw Park, IL 60085, and the ‡Molecular Toxicology Section, Clinical Pharmacology Branch, Division of Cancer Treatment, National Cancer Institute, Bethesda, MD 20205. Accepted for publication June 9, 1980.

Abstract □ An extraction and GLC assay procedure was developed for quantitation of procainamide hydrochloride and acecainide hydrochloride in rat feed. 4-Amino-*N*-[2-(dipropylamino)ethyl]benzamide hydrochloride was synthesized and utilized as an internal standard. The assay has good precision and accuracy and was used to establish the stability of acecainide hydrochloride and procainamide hydrochloride in rat feed.

Keyphrases □ Procainamide hydrochloride—GLC analysis in rat feed □ Acecainide hydrochloride—GLC analysis in rat feed □ GLC—analysis, procainamide hydrochloride and acecainide hydrochloride in rat feed

The identification of acecainide (*N*-acetylprocainamide) as the major metabolite of procainamide in humans (1, 2) generated interest in acecainide as an antiarrhythmic agent and has required development of an assay for the simultaneous determination of these two drugs (3). Although sensitive spectrophotometric methods have been employed (4, 5), they do not exhibit the specificity of GLC (6, 7) and high-performance liquid chromatographic (8–11) assays reported for the analysis of these compounds in plasma and urine.

In accord with present regulatory trends, there also is a need to monitor accurately and ensure precise drug levels in chronic toxicity studies. Such studies are conducted at therapeutic and subtoxic drug concentrations and, thus, require at least two widely varying levels of drug determination.

The present study established a GLC procedure for accurately determining procainamide hydrochloride and acecainide hydrochloride concentrations in rat feed. A structural analog of procainamide, 4-amino-*N*-[2-(dipropylamino)ethyl]benzamide hydrochloride, is utilized as an internal standard to minimize extraction and assay variability.

EXPERIMENTAL

Materials—Procainamide hydrochloride[1] and acecainide hydrochloride[2] were not <98% pure by nonaqueous titration. Elemental analysis and melting-point data also indicated the purity of the raw material. Diethyl ether was reagent grade. The rats were given a commercial rat food *ad libitum*[3].

The internal standard, 4-amino-*N*-[2-(di-*n*-propylamino)ethyl]-benzamide hydrochloride, was obtained through a synthetic scheme analogous to that employed for the synthesis of procainamide (12, 13). Recrystallization of the final product was effected from ethanol to provide white crystals in a 33% overall yield, mp 185–187°; chemical-ionization mass spectrum: M + 1, 264.

Anal.—Calc. for $C_{15}H_{26}ClN_3O$: C, 60.11; H, 8.68; N, 14.02. Found: C, 59.96; H, 8.74; N, 13.82.

Instrumentation—Assays were performed with a gas–liquid chromatograph[4] equipped with a flame-ionization detector. A 1.2-m × 2-mm i.d. glass column, packed with 3% OV-17 on 100–120-mesh Chromosorb W-HP, was maintained at 245 or 270° for procainamide or acecainide, respectively. The column inlet was maintained at 275°, while the detector temperature was 300°. The carrier gas was helium at a flow rate of 20 ml/min.

Analysis of Rat Feed—Standard solutions of procainamide hydrochloride and acecainide hydrochloride were prepared in water at 10.0 mg/ml. The internal standard solution was prepared in water at 4.0 mg/ml.

A 2.0-g homogeneous aliquot of rat feed containing drug was accurately weighed and added to 1.0 ml of the internal standard and 19 ml of water (pH 2) in a centrifuge tube. The contents were extracted and centrifuged. The water layer containing the drug and internal standard was transferred to a second tube. The solution was made basic (pH 12) with sodium hydroxide, sodium chloride (2 g) and ether (20 ml) were added, and the drugs were extracted into the ether layer. The contents were centrifuged, and the ether layer was drawn off for concentration and/or injection into the gas–liquid chromatograph (normally 2.0 μl).

Standard curves were constructed by spiking the drug-free rat feed with appropriate volumes of procainamide hydrochloride or acecainide hydrochloride standard solutions and following the procedure outlined. Peak area ratios of the drug to the internal standard were plotted against milligrams of drug per gram of feed.

RESULTS AND DISCUSSION

In the analysis of acecainide and procainamide from rat feed, it was desirable to sample a representative quantity of drug in feed and to utilize an internal standard that would have physical properties similar to those of the test substances. Sampling of <1 g of feed could result in considerable assay variability caused by drug–feed mixing variability. Extraction of more than a few grams of feed requires large extraction vessels and considerable quantities of solvents and the internal standard. Extraction of samples and addition of the internal standard to an aliquot introduces assay variability caused by extraction differences.

The described procedure yielded small representative samples and permitted the use of a true internal standard. The use of the di-*n*-propyl derivative provided an internal standard with partitioning and chromatographic properties similar to those of acecainide and procainamide. The internal standard has a retention time between those of procainamide and acecainide and does not overlap with either test substance.

In the procainamide assay (column temperature 245°), procainamide has a retention time of ~2.8 min while the internal standard elutes at 4.0 min. With the acecainide analysis, the column temperature is 270°. Procainamide elutes with the solvent, the internal standard elutes at 1.8 min, and acecainide emerges at 3.5 min. This procedure is specific for acecainide and procainamide, with no interfering peaks present in the chromatogram.

The analysis of acecainide hydrochloride in rat feed was linear over a wide concentration range. Standards were determined in quadruplicate at 1.0, 2.0, 5.0, and 10.0 mg of drug/g of feed. The resulting plot had a correlation coefficient of 0.9990, an intercept of −0.004, and a slope of 0.115. The analytical range was extended by varying the concentration of the internal standard and the final volume of ether. Standards determined in duplicate at 10.0, 20.0, 30.0, and 40.0 mg of acecainide hydrochloride/g of feed gave a correlation coefficient of 1.000, an intercept of −0.142, and a slope of 0.145. In this example, 3.0 ml of the internal standard at 4.0 mg/ml was added to the feed, and the ether extract con-

[1] NAPP Chemical Co., Lodi, N.J.
[2] Ganes Chemical Co., New York, N.Y.
[3] Ralston-Purina, St. Louis, Mo.
[4] Model 5830, Hewlett-Packard, Avondale, Pa.

0022-3549/80/1200-1439$01.00/0
© 1980, American Pharmaceutical Association

taining the drugs did not require concentration. The coefficients of variation for the standard curves at the low and high concentrations were 3.89 and <1%, respectively. The analysis of acecainide in rat feed is linear, precise, and accurate over the needed concentration range. The construction of a standard curve spanning the desired concentration range on each day of analysis assures good quantitation of drug in the feed.

Procainamide hydrochloride was analyzed from 0.50 to 50.0 mg/g of feed. Standards were determined in quadruplicate at 0.5, 1.0, 2.0, and 5.0 mg/g of feed. Over this concentration range, the linear regression exhibited a correlation coefficient of 0.9997, an intercept of −0.067, and a slope of 0.872. Increasing the concentration of the internal standard again allowed extension of the analytical range. Standards determined in quadruplicate at 5.0, 10.0, 20.0, and 50.0 mg/g of feed exhibited a correlation coefficient of 0.9998, an intercept of 0.027, and a slope of 0.063. The coefficient of variation for both standard curves was <1%. The assay of procainamide hydrochloride from rat feed is linear, precise, and accurate over the desired concentration range.

Acecainide hydrochloride in rat feed was tested and shown to be stable (85–115% of the theoretical amount) for up to 5 months at ambient temperature. Procainamide hydrochloride exhibited some instability over the same period, but the cause or result of this instability was not determined.

Acecainide and procainamide may be mixed with rat feed and accurately analyzed with this procedure. The drugs were stable in rat feed if kept at or below room temperature and utilized within a few months.

REFERENCES

(1) J. Dreyfuss, J. T. Bigger, Jr., A. I. Cohen, and E. C. Schreiber, *Clin. Pharmacol. Ther.*, **13**, 366 (1972).

(2) J. Elson, J. M. Strong, W. K. Lee, and A. J. Atkinson, Jr., *ibid.*, **17**, 134 (1975).

(3) J. M. Strong, J. S. Dutcher, W. K. Lee, and A. J. Atkinson, Jr., *ibid.*, **18**, 613 (1975).

(4) D. S. Sitar, D. N. Graham, R. E. Rangno, L. R. Dusfresne, and R. I. Ogilvie, *Clin. Chem.*, **22**, 379 (1976).

(5) J. C. Hamm, *J. Assoc. Off. Anal. Chem.*, **59**, 807 (1976).

(6) K. J. Simons and R. H. Levy, *J. Pharm. Sci.*, **64**, 1967 (1975).

(7) A. J. Atkinson, Jr., M. Parker, and J. Strong, *Clin. Chem.*, **18**, 643 (1972).

(8) J. S. Dutcher and J. M. Strong, *ibid.*, **23**, 1318 (1977).

(9) K. Carr, R. L. Woosley, and J. A. Oates, *J. Chromatogr.*, **129**, 363 (1976).

(10) A. G. Butterfield, J. K. Cooper, and K. K. Midha, *J. Pharm. Sci.*, **67**, 839 (1978).

(11) M. A. F. Gadalla, G. W. Peng, and W. L. Chiou, *ibid.*, **67**, 869 (1978).

(12) C. F. H. Allen and J. A. VanAllan, *Org. Synth. Coll.*, **3**, 275 (1955).

(13) M. Yamazaki, Y. Kitagawa, S. Hiraki, and Y. Tsukamoto, *J. Pharm. Soc. Jpn.*, **73**, 294 (1953).

Analysis of 4′-Demethylepipodophyllotoxin-9-(4,6-*O*-ethylidene-β-D-glucopyranoside) by High-Pressure Liquid Chromatography

LARRY M. ALLEN

Received December 14, 1979, from the *Departments of Oncology and Pharmacology R-71, School of Medicine, University of Miami, Miami, FL 33101.* Accepted for publication June 12, 1980.

Abstract □ A rapid and specific high-pressure liquid chromatographic assay is described for the quantitative analysis of 4′-demethylepipodophyllotoxin-9-(4,6-*O*-ethylidene-β-D-glucopyranoside) (I) in plasma. After chloroform extraction, I was analyzed by reversed-phase chromatography and UV detection (252 nm). The maximum sensitivity was 0.1 μg/ml. Quantitation was by relative response factor calibration using an integrating microcomputer. Over the concentration range of 0.5–90 μg/ml, the average recovery of I from plasma was 95.4 ± 3.8% (*SD*).

Keyphrases □ 4-Demethylepipodophyllotoxin -9- (4,6-*O*-ethylidene-β-D-glucopyranoside)—high pressure liquid chromatographic analysis □ High-pressure liquid chromatography—analysis, 4-demethylepipodophyllotoxin-9-(4,6-*O*-ethylidene-β-D-glucopyranoside) □ Antitumor activity—4-demethylepipodophyllotoxin -9- (4,6 -*O*- ethylidene-β-D-glucopyranoside), high-pressure liquid chromatographic analysis

The semisynthetic epipodophyllotoxin analog 4′-demethylepipodophyllotoxin-9-(4,6-*O*-ethylidene-β-D-glucopyranoside) (I) has shown activity against a variety of human tumors (1). Since I is undergoing advanced clinical investigation, it is desirable to monitor plasma drug concentrations from different dosage regimens and from drug interaction studies. Analysis of I previously was carried out by radioisotopic techniques (2–4). This report discusses a high-pressure liquid chromatographic (HPLC) method developed for the quantitation of I in plasma.

EXPERIMENTAL

Apparatus—The analyses of I were conducted using a liquid chromatograph[1] operated at ambient temperature and equipped with a variable-wavelength detector (252 nm). Separations were performed on a 250 × 3.0-mm i.d. reversed-phase column[2]. Samples were introduced onto the column through a septumless injector (10 μl) coupled to an automatic sampler injection system[1]. The chromatograms were traced on a strip-chart recorder with the peak area integration performed by a microcomputing data system[1].

Reagents and Solvents—Compound I was obtained as a gift[3]. All chemical reagents were analytical grade except for methanol and dioxane, which were pesticide residue or HPLC quality[4].

Chromatographic Conditions—The mobile phase was a 50:50 mixture of 5 m*M* KH_2PO_4–NaOH buffer (pH 7.8) and methanol with the flow rate adjusted to 40 ml/hr (~1000 psi). A precolumn[2] was used to minimize the effect of extraneous plasma-extracted material on the performance of the reversed-phase column.

Extraction Procedure—Aliquots (2.0 ml) of plasma were transferred to 15-ml thick-wall centrifuge tubes[5], diluted with 2 ml of water, and extracted with 4 ml of chloroform. The mixture was vortexed vigorously for 30 sec, and the phases were separated by centrifugation (15 min at 10,000×*g*). The lower organic layer was removed by a Pasteur pipet (24

[1] Model 8500, Varian Co., Sunnyvale, Calif.
[2] Partisil-10 ODS, Whatman Inc., Clifton, N.J.
[3] Also known as VP-16-213 and NSC-141540; supplied by Ms. Kozkuz, Sandoz Pharmaceuticals, Hanover, N.J.
[4] Burdick & Jackson Laboratories, Muskegon, Mich.
[5] Corex No. 8441.

0022-3549/80/1200-1440$01.00/0

© 1980, American Pharmaceutical Association

taining the drugs did not require concentration. The coefficients of variation for the standard curves at the low and high concentrations were 3.89 and <1%, respectively. The analysis of acecainide in rat feed is linear, precise, and accurate over the needed concentration range. The construction of a standard curve spanning the desired concentration range on each day of analysis assures good quantitation of drug in the feed.

Procainamide hydrochloride was analyzed from 0.50 to 50.0 mg/g of feed. Standards were determined in quadruplicate at 0.5, 1.0, 2.0, and 5.0 mg/g of feed. Over this concentration range, the linear regression exhibited a correlation coefficient of 0.9997, an intercept of −0.067, and a slope of 0.872. Increasing the concentration of the internal standard again allowed extension of the analytical range. Standards determined in quadruplicate at 5.0, 10.0, 20.0, and 50.0 mg/g of feed exhibited a correlation coefficient of 0.9998, an intercept of 0.027, and a slope of 0.063. The coefficient of variation for both standard curves was <1%. The assay of procainamide hydrochloride from rat feed is linear, precise, and accurate over the desired concentration range.

Acecainide hydrochloride in rat feed was tested and shown to be stable (85–115% of the theoretical amount) for up to 5 months at ambient temperature. Procainamide hydrochloride exhibited some instability over the same period, but the cause or result of this instability was not determined.

Acecainide and procainamide may be mixed with rat feed and accurately analyzed with this procedure. The drugs were stable in rat feed if kept at or below room temperature and utilized within a few months.

REFERENCES

(1) J. Dreyfuss, J. T. Bigger, Jr., A. I. Cohen, and E. C. Schreiber, *Clin. Pharmacol. Ther.*, **13**, 366 (1972).

(2) J. Elson, J. M. Strong, W. K. Lee, and A. J. Atkinson, Jr., *ibid.*, **17**, 134 (1975).

(3) J. M. Strong, J. S. Dutcher, W. K. Lee, and A. J. Atkinson, Jr., *ibid.*, **18**, 613 (1975).

(4) D. S. Sitar, D. N. Graham, R. E. Rangno, L. R. Dusfresne, and R. I. Ogilvie, *Clin. Chem.*, **22**, 379 (1976).

(5) J. C. Hamm, *J. Assoc. Off. Anal. Chem.*, **59**, 807 (1976).

(6) K. J. Simons and R. H. Levy, *J. Pharm. Sci.*, **64**, 1967 (1975).

(7) A. J. Atkinson, Jr., M. Parker, and J. Strong, *Clin. Chem.*, **18**, 643 (1972).

(8) J. S. Dutcher and J. M. Strong, *ibid.*, **23**, 1318 (1977).

(9) K. Carr, R. L. Woosley, and J. A. Oates, *J. Chromatogr.*, **129**, 363 (1976).

(10) A. G. Butterfield, J. K. Cooper, and K. K. Midha, *J. Pharm. Sci.*, **67**, 839 (1978).

(11) M. A. F. Gadalla, G. W. Peng, and W. L. Chiou, *ibid.*, **67**, 869 (1978).

(12) C. F. H. Allen and J. A. VanAllan, *Org. Synth. Coll.*, **3**, 275 (1955).

(13) M. Yamazaki, Y. Kitagawa, S. Hiraki, and Y. Tsukamoto, *J. Pharm. Soc. Jpn.*, **73**, 294 (1953).

Analysis of 4′-Demethylepipodophyllotoxin-9-(4,6-*O*-ethylidene-β-D-glucopyranoside) by High-Pressure Liquid Chromatography

LARRY M. ALLEN

Received December 14, 1979, from the *Departments of Oncology and Pharmacology R-71, School of Medicine, University of Miami, Miami, FL 33101.* Accepted for publication June 12, 1980.

Abstract □ A rapid and specific high-pressure liquid chromatographic assay is described for the quantitative analysis of 4′-demethylepipodophyllotoxin-9-(4,6-*O*-ethylidene-β-D-glucopyranoside) (I) in plasma. After chloroform extraction, I was analyzed by reversed-phase chromatography and UV detection (252 nm). The maximum sensitivity was 0.1 μg/ml. Quantitation was by relative response factor calibration using an integrating microcomputer. Over the concentration range of 0.5–90 μg/ml, the average recovery of I from plasma was 95.4 ± 3.8% (*SD*).

Keyphrases □ 4-Demethylepipodophyllotoxin -9- (4,6-*O*-ethylidene-β-D-glucopyranoside)—high pressure liquid chromatographic analysis □ High-pressure liquid chromatography—analysis, 4-demethylepipodophyllotoxin-9-(4,6-*O*-ethylidene-β-D-glucopyranoside) □ Antitumor activity—4-demethylepipodophyllotoxin -9- (4,6 -*O*- ethylidene-β-D-glucopyranoside), high-pressure liquid chromatographic analysis

The semisynthetic epipodophyllotoxin analog 4′-demethylepipodophyllotoxin-9-(4,6-*O*-ethylidene-β-D-glucopyranoside) (I) has shown activity against a variety of human tumors (1). Since I is undergoing advanced clinical investigation, it is desirable to monitor plasma drug concentrations from different dosage regimens and from drug interaction studies. Analysis of I previously was carried out by radioisotopic techniques (2–4). This report discusses a high-pressure liquid chromatographic (HPLC) method developed for the quantitation of I in plasma.

EXPERIMENTAL

Apparatus—The analyses of I were conducted using a liquid chromatograph[1] operated at ambient temperature and equipped with a variable-wavelength detector (252 nm). Separations were performed on a 250 × 3.0-mm i.d. reversed-phase column[2]. Samples were introduced onto the column through a septumless injector (10 μl) coupled to an automatic sampler injection system[1]. The chromatograms were traced on a strip-chart recorder with the peak area integration performed by a microcomputing data system[1].

Reagents and Solvents—Compound I was obtained as a gift[3]. All chemical reagents were analytical grade except for methanol and dioxane, which were pesticide residue or HPLC quality[4].

Chromatographic Conditions—The mobile phase was a 50:50 mixture of 5 m*M* KH_2PO_4–NaOH buffer (pH 7.8) and methanol with the flow rate adjusted to 40 ml/hr (~1000 psi). A precolumn[2] was used to minimize the effect of extraneous plasma-extracted material on the performance of the reversed-phase column.

Extraction Procedure—Aliquots (2.0 ml) of plasma were transferred to 15-ml thick-wall centrifuge tubes[5], diluted with 2 ml of water, and extracted with 4 ml of chloroform. The mixture was vortexed vigorously for 30 sec, and the phases were separated by centrifugation (15 min at 10,000×*g*). The lower organic layer was removed by a Pasteur pipet (24

[1] Model 8500, Varian Co., Sunnyvale, Calif.
[2] Partisil-10 ODS, Whatman Inc., Clifton, N.J.
[3] Also known as VP-16-213 and NSC-141540; supplied by Ms. Kozkuz, Sandoz Pharmaceuticals, Hanover, N.J.
[4] Burdick & Jackson Laboratories, Muskegon, Mich.
[5] Corex No. 8441.

0022-3549/80/1200-1440$01.00/0

© 1980, American Pharmaceutical Association

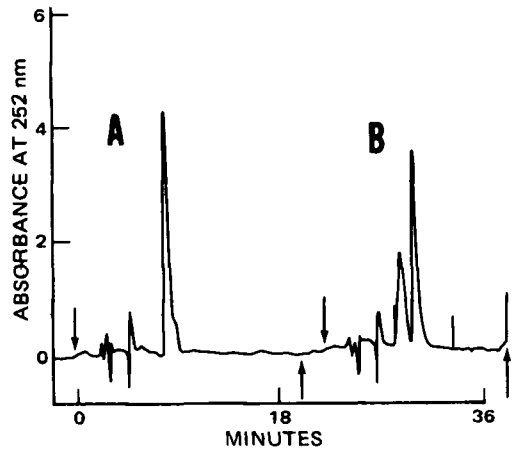

Figure 1—*Liquid chromatogram of I. Key: A, I injected directly; and B, I derived from spiked plasma. A down arrow (↓) indicates the start of integration, and an up arrow (↑) indicates the end of integration. The largest peak in each panel is I. The occasional shoulder on I is associated with impurities from dioxane.*

cm) and transferred to either 15-ml ground-glass conical centrifuge tubes or to all-glass evaporator cups[6]. A second and third extraction were performed similarly.

The pooled chloroform layers from each sample were dried under reduced pressure either in a water bath (45°) using a rotary evaporator or at 45° in a sample concentrator[6]. To the dried chloroform extracts was added 2 ml of chloroform, and the samples were redried. This step was repeated two times with 1 and 0.5 ml of chloroform, respectively. The final residues were transferred in 0.2 ml of dioxane to microsample vials, capped, and prepared for HPLC analysis.

Extraction Efficiency—Plasma from a local blood bank was used along with tritium-labeled and unlabeled I. The efficiency of extracting I from plasma was established using the following procedure. Known amounts of I and 0.01 μCi of radiolabeled I (14 μCi/μmole) were added to drug-free plasma (10 ml each) to achieve concentrations of I from 0.1 to 100 μg/ml. Aliquots (2.0 ml) of each plasma sample were transferred to thick-wall centrifuge tubes and stored frozen (−20°) until they were extracted. Samples ($n \geq 6$) at each concentration were analyzed in duplicate. Quantitation of I was accomplished by the relative response factors calculated from analysis of standards of I of known concentration. The linearity of the calibration curve for I was established over the concentration range of 0.1–100 μg/ml. Specificity for I was established using drug-free plasma.

Clinical Specimens—Written informed consent was obtained from two patients who participated in the institutionally approved I protocol. This protocol called for administration of I at 10 mg/m^2 by intravenous push followed immediately by a continuous infusion of I for 24 hr. Venous blood (5 ml) was collected in heparinized tubes at specified times and centrifuged for 2 min at 1000×*g*, and the plasma was removed and stored frozen until it was analyzed for I.

RESULTS AND DISCUSSION[7]

Figure 1A shows the elution profile of I (largest peak) directly injected into the high-pressure liquid chromatograph. The shoulder on the peak of I was observed with different batches of dioxane and was independent

[6] Brinkmann Instruments, Westbury, N.Y.

[7] The PROPHET computer system is sponsored by the Division of Research Resources of the National Institutes of Health (5).

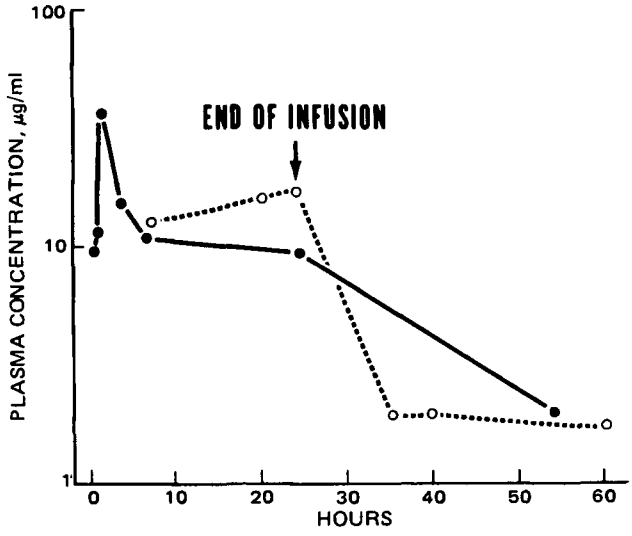

Figure 2—*Plasma levels of I. According to the protocol (written informed consent was obtained from the patients with an institutionally approved protocol), I was administered by a 24-hr continuous infusion at 180 (○) and 340 (●) mg/m^2 immediately after a 10-mg/m^2 short intravenous infusion (30 min).*

of the peak height of I. Figure 1B also shows a typical elution pattern of I (largest peak) derived from spiked plasma. To date, no interfering peaks from plasma have created a problem in the quantitation of I. The retention time of I in this system was 6.63 ± 0.04 min. A standard curve for I as a function of the peak area *versus* drug concentration (0.1–100 μg/ml) was linear with a correlation coefficient of >0.99 for six runs. The extraction efficiency for I over the concentration range of 0.5–90 μg/ml was 95.4 ± 3.8%, and this percentage was used in all recovery calculations. This range of drug concentrations is suitable for most clinical doses of the drug (>100 mg/m^2) and for measurements of I up to 48 hr or longer after drug administration.

Figure 2 shows two plasma curves for I as determined by this HPLC method. The more common wavelength detector (254 nm) can be used with somewhat reduced sensitivity for I (maximum sensitivity of 0.8 μg/ml). By increasing the proportion of methanol in the mobile phase to 75%, an analog of I, 4′-demethylepipodophyllotoxin-9-(4,6-*O*-thenylidene-β-D-glucopyranoside), can be quantitated in plasma by this method.

REFERENCES

(1) M. Rozencweig, D. D. Von Hoff, J. E. Henney, and F. M. Muggia, *Cancer*, **40**, 334 (1977).

(2) L. M. Allen and P. J. Creaven, *Eur. J. Cancer*, **11**, 697 (1975).

(3) L. M. Allen, *Cancer Res.*, **38**, 2549 (1978).

(4) F. R. Pelsor, L. M. Allen, and P. J. Creaven, *J. Pharm. Sci.*, **67**, 1106 (1978).

(5) W. F. Raub, *Fed. Proc. Fed. Am. Soc. Exp. Biol.*, **33**, 2390 (1974).

ACKNOWLEDGMENTS

Supported in part by the Women's Cancer Association of Miami, Core Grant CA 14395, and by a gift from Dr. Troner.

The author thanks Dr. Savaraj, Dr. Tejada, Dr. Troner, and other members of the Department of Oncology, University of Miami School of Medicine, for assistance.

Turbidimetric Determination of Blood Aminoglycoside Levels by Growth Curve Analysis

STEPHEN C. EDBERG *x **and ABRAHAM MISKIN** ‡

Received February 19, 1980, from the *Division of Microbiology and Immunology, Department of Pathology, Montefiore Hospital and Medical Center, New York, NY 10467, and the ‡Department of Microbiology, Kaplan Hospital, Rehovot, Israel. Accepted for publication June 3, 1980.

Abstract □ A procedure to assay rapidly blood aminoglycoside levels was developed based on growth curve analysis of continuous absorbance measurements of a bacterial test strain. Of the means available for monitoring bacterial growth quantitatively, turbidimetric measurement was selected because it can be used to perform a clinical assay in <4 hr. Continuous turbidimetric measurements provide information as soon as the antimicrobial agent affects growth, which often occurs within 60 min of the start of an assay. Several bacterial isolates were evaluated before *Staphylococcus aureus* (MHMC 386) was chosen as the test microorganism. This isolate was quite sensitive to the aminoglycoside antibiotics, permitted the rapid measurement of blood levels of amikacin, gentamicin, kanamycin, and tobramycin, and exhibited a linear dose–response relationship of turbidity over a wide range of antibiotic concentrations.

Keyphrases □ Antibiotics, aminoglycoside—amikacin, gentamicin, kanamycin, and tobramycin, effect on bacterial growth, turbidimetric measurement of blood levels □ Antibacterials—amikacin, gentamicin, kanamycin, and tobramycin, effect on bacterial growth, turbidimetric measurement of blood levels □ Spectrophotometry—turbidimetric determination of blood levels of amikacin, gentamicin, kanamycin, and tobramycin, effect on bacterial growth

The concentration at which aminoglycoside antibiotics injure animal cells is only two to four times greater than the concentration required to inhibit most common bacterial pathogens. In addition, distribution of the drug to the various body compartments is not the same in all individuals. Accordingly, a rapid assay is required for the optimal usage of aminoglycosides.

BACKGROUND

There is a direct relationship between bacterial growth measured turbidimetrically and the increase in bacterial numbers, collective mass, and cell volume. During the period when cells are dividing with a constant doubling time, the number of cells increases exponentially. If t_0 is the starting time and t_2 is the time required for the average bacterium to become two, then the number of bacteria (N_2) at t_2 can be calculated from:

$$\log N_2 = N_0\, 10^{t_0/t_2} \qquad \text{(Eq. 1)}$$

where N_0 is the number of bacteria at the starting time. The Rayleigh–Debye theory can be used to interrelate turbidity and cell mass if turbidity can be measured as a function of the ratio of the particle size to the wavelength at maximum turbidity and if the refractive indexes of the solvent and the particle are not significantly different. The concentration of bacteria per unit volume of suspending medium can be calculated from:

$$NVD = \frac{R_\theta 3\lambda D \sin^3(\theta/2)}{(\Delta\mu)(M-1)\mu x} \qquad \text{(Eq. 2)}$$

where θ is the modification of the light intensity due to the finite size of the particle, V is the volume of the particle, N is the number of particles per milliliter, R_θ is the reduced intensity for unpolarized light scattered at an angle θ from an incident beam, D is the density of the particle, λ is the wavelength of the light, M is the ratio of the refractive indexes of the particle and the medium, and μ is the refractive index function (1).

Equation 2 indicates that at 0°, light-scattering turbidity is related directly to the number or mass of bacteria (1–3). Based on this theory, spectrophotometric techniques were developed to assay antimicrobial agents. These systems have been used primarily in industry, where relatively high concentrations of antibiotics are measured. The development of clinical turbidimetric assays has suffered from a lack of sensitive equipment and the labor-intensive nature of this assay.

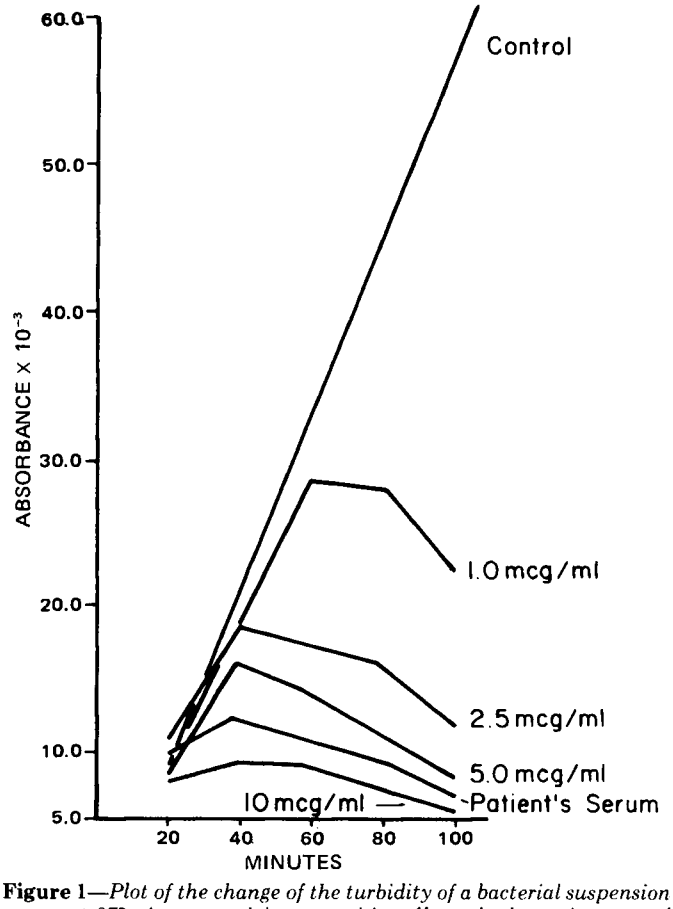

Figure 1—*Plot of the change of the turbidity of a bacterial suspension grown at 37°. As gentamicin exerted its effect, the bacteria stopped growing and the absorbance decreased.*

EXPERIMENTAL

A sensitive, low-noise spectrophotometer[1] was developed recently that automatically determines the bacterial density every 5 min under temperature-controlled conditions (4). This instrument currently is sold for antibiotic susceptibility tests. Because of its availability and ability to yield continuous printouts of absorbance measurements without manipulation of the cell, it seemed a likely candidate for the clinical assay of aminoglycosides.

A unique feature of this instrument is the design of the cell. The cell consists of two physically separated compartments: an upper compartment, which accepts the bacterial test strain and allows growth to occur to the log phase; and a lower compartment, which is divided into discrete, 1-cm³ chambers, with each chamber able to receive one antibiotic test specimen. A technique to determine the concentration of blood amino-

[1] MS-2, Abbott Laboratories, Dallas, Tex.

0022-3549/80/1200-1442$01.00/0
© 1980, American Pharmaceutical Association

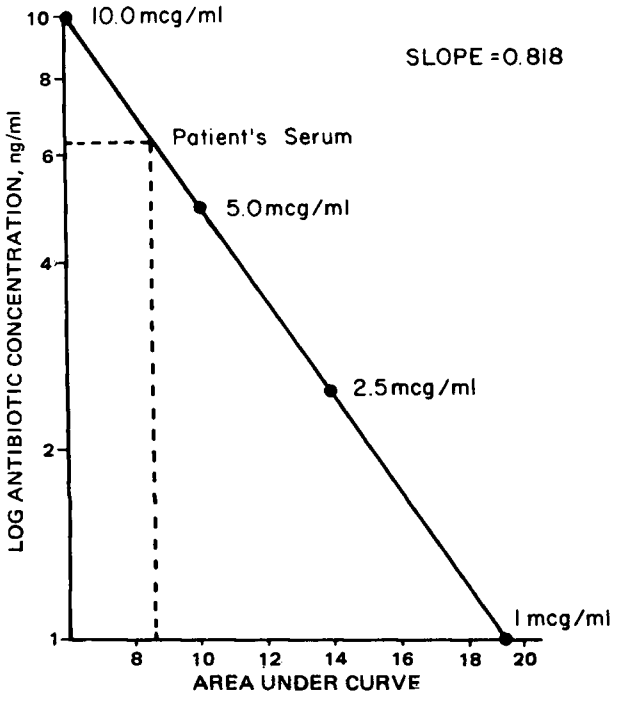

Figure 2—*Plot of area under the curve produced from a graph of absorbance* versus *time (Fig. 1) calculated for each antibiotic concentration, the control (no antibiotic), and the patient's serum. The area under the curve was proportional to the antibiotic concentration in the patient's serum. The amount of antibiotic in a patient's serum can be calculated by direct interpolation from a plot of log antibiotic concentration* versus *area under the curve. The patient's serum concentration was 6.8 μg/ml.*

glycoside levels using growth curve analysis from turbidimetric measurements supplied by this instrument was developed.

The selected strain of *Staphylococcus aureus* (MHMC 386) was sensitive to the aminoglycoside antibiotics and did not clump when grown in broth. *S. aureus* MHMC 386 was resistant to penicillin and sensitive to amikacin, cephalothin, chloramphenicol, clindamycin, erythromycin, gentamicin, kanamycin, oxacillin, tetracycline, tobramycin, and vancomycin. Antibiotic medium No. 5[2] was prepared according to directions from the manufacturer and adjusted to pH 7.4. A 17-ml volume of this medium was added to a sterile test tube. All antibiotics were obtained in powder form of known potency[3]. Aminoglycosides were prepared in standard solutions of 100 μg/ml in 0.1 *M* phosphate buffer (pH 7.9) (5). Stock solutions were frozen at −20° and stored for no longer than 90 days.

Human serum was obtained from normal blood bank donors and was heated to 56° for 30 min and filter sterilized (porosity 0.45 μm). For the measurement of serum antibiotic concentrations, the following dilutions in serum at pH 7.4 were made: amikacin, 25, 15, 10, and 5 μg/ml; gentamicin, 10, 5, 2.5, and 1 μg/ml; kanamycin, 25, 15, 10, and 5 μg/ml; and tobramycin, 10, 5, 2.5, and 1 μg/ml.

Forceps sterilized by alcohol and flaming were used to place filter paper disks[4] on a sterile petri plate, and 25 μl of each standard was added to individual disks. Twenty-five microliters of the patient's serum was added to each of two other disks. If the patient was receiving a β-lactam antibiotic, 0.25 ml of a broad-spectrum β-lactamase was added to 2 ml of the patient's serum prior to addition to the disks, and an appropriate correlation computation was made for this dilution. Each disk was placed in a separate compartment in the multichambered cell. Although the disks were used within 2 hr of preparation, the stability of aminoglycosides on the disks for long periods is not known.

[2] Difco Laboratories, Detroit, Mich.
[3] Ames Laboratories, Elkhardt, Ind.
[4] No. 740E, Schlicher and Schuell, Keane, N.H.

Table I—Comparison of Blood Antibiotic Levels by Bioassay and Turbidity

Antibiotic	Number of Specimens	Discrepancy between Methods[a] 0–5%	5–10%	10–15%	15–25%	>25%
Gentamicin	112	20	38	28	13	2
Kanamycin	22	27	27	32	14	0
Tobramycin	26	15	42	36	3	4
Amikacin	11	9	45	36	9	0

[a] Percentages are rounded to the nearest whole number.

A suspension of *S. aureus* at 0.5 MacFarland's turbidity was made in 0.9% NaCl, and 0.1 ml of this suspension was added to 17 ml of antibiotic broth No. 5. Fifteen milliliters was added to the upper growth chamber of the cell, and the cell was placed in the spectrophotometer, which was temperature controlled at 35°. The bacterial suspension was physically separated from the antibiotics and the patient's serum until log-phase growth was entered as monitored by continuous turbidimetric reading. Utilizing a suction device built into the instrument, the bacterial suspension was drawn into compartments containing the disks. Incubation and continuous readings at 470 nm continued until the compartment with the smallest concentration of standard antibiotic had exerted its effect.

RESULTS AND DISCUSSION

Figure 1 represents a typical determination. The area under the curve for each standard and the area under the curve of the patient's specimen were calculated by the least-squares method. The areas under the curve for the two individual patient serum compartments were averaged. Log antibiotic concentration was plotted *versus* the area under the curve (Fig. 2), and the amount of antibiotic in the patient's specimen was determined by direct interpolation from this graph.

Table I presents a comparison of results obtained by a standard bioassay method (5, 6) with those obtained by the turbidimetric assay. The bioassay and turbidimetric assays agreed, on the average, within 10% for the 161 blood specimens tested. The turbidimetric assay could determine 10 μg of gentamicin/ml within 160 min of the start of an assay, a period comparable to the radioimmunoassay method. As little as 1 μg of gentamicin/ml could be determined within 4 hr. The ability to determine physiological concentrations of the other aminoglycoside antibiotics was equally rapid.

CONCLUSION

Under carefully controlled conditions, turbidimetric assay of antibiotics can be applied to clinical specimens. Because turbidimetric assays are amenable to automation and can be monitored continuously without human intervention, the data can be produced and interpreted with almost no expenditure of the technician's time. Currently, blood antibiotic level measurements are generally restricted to large medical institutions. With automated spectrophotometric systems, all medical facilities could determine blood antibiotic concentrations rapidly when potentially toxic antimicrobial agents are administered.

REFERENCES

(1) F. Kavanagh, "Analytical Microbiology," vol. II, Academic, New York, N.Y., 1972.
(2) F. Kavanagh, *J. Pharm. Sci.*, **66**, 1520 (1977).
(3) R. A. Rippere, *J. Assoc. Off. Anal. Chem.*, **62**, 951 (1979).
(4) J. H. Jorgensen and G. A. Alexander, "Abstract," Annual Meeting of the American Society for Microbiology, 1980, p. C21.
(5) S. C. Edberg and A. Chu, *Am. J. Med. Technol.*, **41**, 99 (1975).
(6) S. C. Edberg, A. Chu, and G. Melnick, *Lab. Med.*, **4**, 36 (1973).

Impurities in Drugs V: Meprobamate

R. C. LAWRENCE, E. G. LOVERING ˣ, M. A. POIRIER, and J. R. WATSON

Received April 8, 1980, from the *Drug Research Laboratories, Health Protection Branch, Tunney's Pasture, Ottawa, Ontario, K1A 0L2 Canada.* Accepted for publication May 27, 1980.

Abstract □ One lot of meprobamate raw material and 28 lots of tablets were examined for impurities by TLC. All lots contained di-(2-methyl-2-propyl-3-carbamoyloxypropyl) carbonate (V) at levels that ranged between 0.1 and 1.0% of the total drug content. Nine lots also contained low levels of a second impurity (~0.1%), and one of these lots contained a third impurity (~0.1%), neither of which was identified. Estimates of the unidentified impurities were based on the assumption of a TLC response with furfural–hydrochloric acid spray equivalent to that of meprobamate. Compound V was identified by mass spectrometry and PMR and IR spectroscopy and by comparison of the TLC R_f value to that of a synthesized sample of V.

Keyphrases □ Meprobamate—identification of impurities in tablets □ Drug impurities—meprobamate, identification in tablets

The origins of organic impurities in drugs and some consequences of their presence were outlined previously (1). The present paper reports the occurrence of impurities in 28 lots of meprobamate tablets.

Meprobamate (I) can be synthesized (2, 3) by reduction of methylpropylpropanedioic acid diethyl ester (II) with lithium aluminum hydride to the corresponding 2-methyl-2-propyl-1,3-propanediol (III). Reaction of III with phosgene affords the dichlorocarbonate (IV), which, upon treatment with ammonia, yields I.

USP XX (4) and BP 1973 (5) contain specifications for meprobamate raw material and tablets. The BP includes a specification of 1% for related substances (not specified), with the test to be done by TLC. There are no USP specifications for impurities in meprobamate.

EXPERIMENTAL

Materials—All drugs and formulations were obtained directly from the manufacturer. Ammonia[1], 2-methyl-2-propyl-1,3-propanediol[2], ethyl chlorocarbonate[3], diethyl carbonate[3], furfural[4], pyridine[4], sodium methoxide[4], hydrochloric acid[5], and anhydrous sodium sulfate[5] were obtained commercially. All solvents[6] were analytical grade. Precoated silica gel GF-60 (20-cm × 20-cm × 0.25-mm) TLC plates[7] and silica gel powder[5] (60–200 mesh) were used. All PMR spectra were obtained in deuterochloroform[8] on an 80-MHz instrument[9] with tetramethylsilane as the internal standard. Mass spectral[10] samples were introduced *via* the direct probe and were recorded at an ionizing potential of 70 ev.

Standard Solutions—The standard solutions consisted of 100 mg of I/ml and 1.0 mg of V/ml in acetone.

TLC System—The chloroform–ethanol (90:10) developing solution was allowed to equilibrate in filter paper-lined chromatographic tanks for 20 min prior to use. Spots were visualized by spraying the plates sequentially with furfural and concentrated hydrochloric acid. The R_f values and the lower limits of detection of I and related compounds were established by the serial dilution of stock solutions.

Sample Preparation—To prepare the raw material samples, ~400 mg of I, accurately weighed, was dissolved in 4 ml of acetone. To prepare the tablet samples, an amount of powdered tablet equivalent to 400 mg of I was weighed into a 10-ml screw-capped tube, extracted by shaking for 15 min with 4 ml of acetone, centrifuged, and filtered.

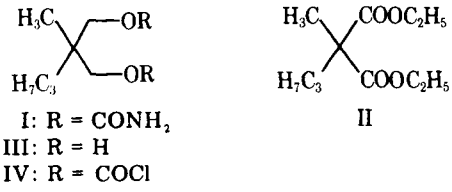

I: R = $CONH_2$
III: R = H
IV: R = COCl

II

Screening for Impurities—Aliquots (10 μl) of the tablet extracts in acetone were applied to the TLC plates. Decomposition on the plate was checked for by two-dimensional TLC but was not found. The concentration of impurities was estimated by comparison of the spot diameters and intensities with the corresponding spots from the standard solutions, with the assumption that the response of the unidentified impurities to the spray was the same as that of I.

Isolation of Impurities—An amount of formulation equivalent to 2 g of I was shaken with two 40-ml portions of acetone for 15 min and filtered. The combined fractions were evaporated to dryness, and the residue was dissolved in 200 ml of ether. The ether solution was partitioned three times with 0.05 *N* NaOH to remove any fatty acids present as excipients, evaporated to dryness, redissolved in ~10 ml of the TLC solvent system, and poured onto the top of a slurry-packed silica gel[5] glass column prepared from 50 g of silica gel and 200 ml of the TLC solvent. After ~70 ml of the TLC solvent system had flowed through the column, 45 fractions of 3 ml each were collected.

The location of the various compounds was established by spotting a 15-μl aliquot of every other fraction on a TLC plate. The plate was developed and the spots were visualized with the furfural–hydrochloric acid spray. The fractions containing the impurity to be identified were combined, evaporated to dryness, and subjected to mass spectral, NMR, and IR[11] analyses.

Syntheses—The syntheses are illustrated in Scheme I.

2-Methyl-2-propyl-3-hydroxypropylcarbamate (VI)—Compound VI was prepared in a 40% yield from the dioxanone (VIII) using the method described by Ludwig and coworkers (2, 3), mp 51–52°; IR (KBr): 3380 (OH), 3240, 3200 (NH), 1690 (C=O), 1620 (C–N), 1075, and 1040

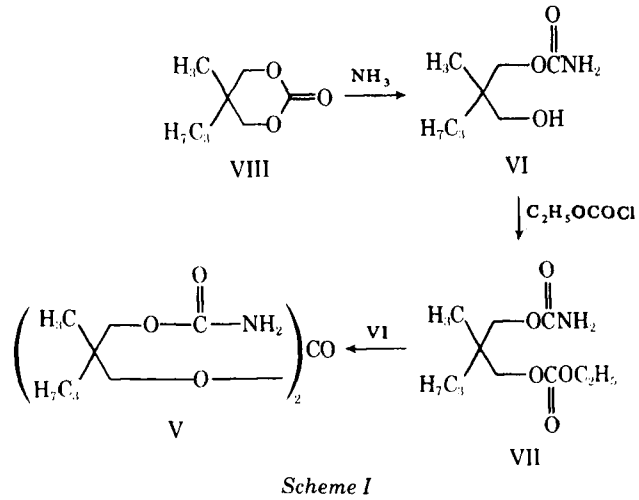

Scheme I

[1] Matheson, Toronto, Ontario, Canada.
[2] Chemicals Procurement Laboratories, College Point, N.Y.
[3] Pfaltz & Bauer, Stamford, Conn.
[4] British Drug Houses, Poole, England.
[5] J. T. Baker Chemical Co., Phillipsburg, N.J.
[6] Caledon Laboratories Ltd., Georgetown, Ontario, Canada.
[7] Brinkmann Instruments, Toronto, Ontario, Canada.
[8] Stohler Isotope Chemicals, Waltham, Mass.
[9] Bruker WP-80 spectrometer.
[10] Varian MAT model 311 A mass spectrometer.
[11] Pye Unicam SP 1000 IR spectrophotometer.

0022-3549/80/1200-1444$01.00/0
© 1980, American Pharmaceutical Association

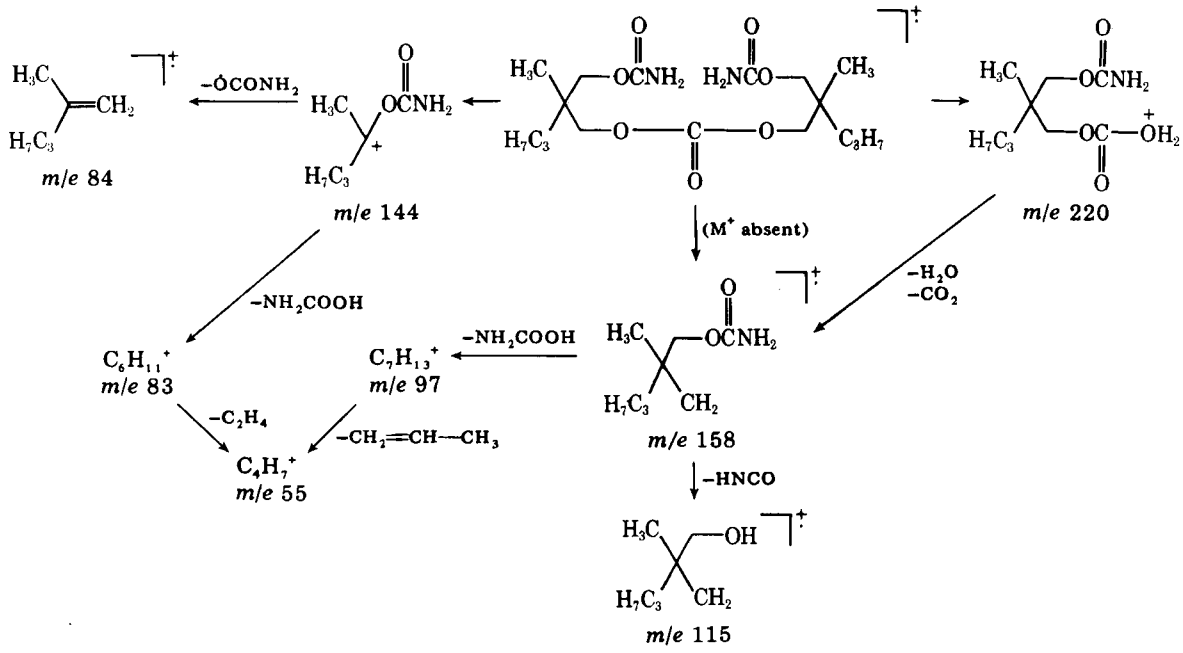

Scheme II

(C–O) cm^{-1}; PMR ($CDCl_3$): δ 5.16 (broad, 2H, NH_2), 3.90 (s, 2H, CH_2O), 3.28 [s, 2H, CH_2OH (disappears with D_2O exchange)], 3.03 (broad, 1H, OH), 1.22, and 0.90 (m, 10H, alkyl protons) ppm; mass spectrum (70 ev, 45°): M^+ absent, *m/e* 101 (31.0%), 96 (18), 84 (100), 83 (95), 75 (88), 62 (87), and 55 (96).

(2-Methyl-2-propyl-3-carbamoyloxypropyl)ethyl Carbonate (VII) (*2, 3*)—To 4 ml of chloroform in which 118 mg (1.5 mmoles) of pyridine had been dissolved were added 52 mg (0.3 mmole) of VI and 33 mg (0.3 mmole) of ethyl chlorocarbonate dissolved in ~2 ml of chloroform. The reaction mixture was refluxed for 1 hr and then poured into cold water. The chloroform layer was washed with 10% hydrochloric acid, washed again with water, dried over anhydrous sodium sulfate, and filtered. Evaporation of the filtrate yielded 69 mg (95%) of oily VII; IR (film): 3470, 3360 (NH), 1730 (C=O), 1600 (C–N), 1060, and 1005 (C–O) cm^{-1}; PMR ($CDCl_3$): δ 4.62 (broad, 2H, NH_2), 4.20 (q, 2H, OCH_2CH_3), 3.94 (s, 2H, CH_2O), 3.90 (s, 2H, CH_2O), 1.28, and 0.90 (m, 13H, alkyl protons) ppm; mass spectrum (70 ev, 25°): M^+ absent, *m/e* 173 (28%), 144 (26), 114 (50), 101 (42), 96 (95), 84 (96), 83 (100), 75 (55), 62 (88), and 55 (96).

Di-(2-methyl-2-propyl-3-carbamoyloxypropyl) Carbonate (V) (*2, 3*)—Compound VI, 18 mg, and 25 mg of VII were dissolved in 5 ml of chloroform and refluxed in the presence of ~1 mg of sodium methoxide for 3 hr. The mixture was cooled, diluted with chloroform, washed with water, and dried over anhydrous sodium sulfate. Evaporation to dryness yielded V (45%), mp 88–90°; IR (film): 3490, 3380 (NH), 1730 (C=O), 1610 (C–N), 1260, and 1070 (C–O) cm^{-1}; PMR ($CDCl_3$): δ 4.70 (broad, 4H, NH_2), 3.97 (s, 4H, OCH_2), 3.93 (s, 4H, OCH_2), 1.26, and 0.93 (m, 20H, alkyl protons) ppm; mass spectrum (70 ev, 115°): M^+ absent, *m/e* 220 (33%), 158 (90), 144 (16), 115 (24), 97 (100), 84 (45), 83 (57), and 55 (63).

RESULTS AND DISCUSSION

The TLC R_f values and the limits of detection of I, VI, VII, and the impurities in tablet formulations are given in Table I.

Twenty-eight lots of meprobamate tablets and one lot of drug raw material were screened for impurities by TLC. All lots contained V at levels ranging from 0.1 to 1.0%. Nine lots also contained a second impurity, designated as IX, and one of these lots contained a third impurity, X. The levels of IX and X were estimated by TLC to be ~0.1%, with the assumption of a response identical to that of meprobamate. They were not investigated further. The identity of V was established by IR, PMR, and mass spectral analyses and by comparison of the TLC R_f value with that of a synthesized specimen.

Table I—TLC Characteristics of Meprobamate and Related Compounds

Compound	R_f Absolute	R_f Relative	Limit of Detection, μg
I	0.26	1.00	1
VI	0.27	1.04	2
VII	0.56	2.15	2
V	0.42	1.61	1
IX	0.35	1.35	—
X	0.65	2.50	—

The structure postulated for V is supported by the mass spectral and PMR data. The molecular ion is absent from the electron-impact mass spectrum, but the chemical-ionization spectrum obtained with methane shows a weak peak at *m/e* 377 (3%), attributable to MH^+, and a strong fragment at *m/e* 158 (100%), also present in the electron-impact spectrum, corresponding to breakage of the carbonate bond. The ion at *m/e* 115 is formed by the loss of isocyanic acid from the *m/e* 158 fragment, and the base peak, *m/e* 97, is attributable to a loss of water from *m/e* 115. Mechanisms for the formation of fragments in the mass spectrum of V are proposed in Scheme II (6, 7). The PMR spectrum shows the NH_2 protons at 4.70 ppm and two singlets for the two sets of $-CH_2-$, with each singlet integrating for four protons. The aliphatic part of the spectrum is similar to that of meprobamate because of the symmetry of the molecule.

Compound V may form during the synthesis of meprobamate by the reaction of IV with the semichlorinated derivative of III, which, upon treatment with ammonia, would yield V. It is unlikely that V is a degradation product of meprobamate.

REFERENCES

(1) K. M. McErlane, N. M. Curran, and E. G. Lovering *J. Pharm. Sci.*, **66**, 1015 (1977).

(2) B. J. Ludwig, L. S. Powell, and F. M. Berger, *J. Med. Chem.*, **12**, 462 (1969).

(3) B. J. Ludwig and E. C. Piech, *J. Am. Chem. Soc.*, **73**, 5779 (1951).

(4) "The United States Pharmacopeia," 20th rev., Mack Publishing Co., Easton, Pa., 1980.

(5) "British Pharmacopoeia 1973," Her Majesty's Stationery Office, London, England, 1973.

(6) R. T. Coutts, *J. Pharm Sci.*, **62**, 769 (1973).

(7) I. J. Rouse and D. A. Brent, *Biomed. Mass Spectrom.*, **1**, 256 (1974).

ACKNOWLEDGMENTS

The authors thank Mr. J. C. Ethier, Mr. W. Miles, and Mr. H. Avdovich for determination of the PMR and mass spectra.

Major Skin-Irritant Principle from *Synadenium grantii*

A. DOUGLAS KINGHORN

Received April 7, 1980, from the *Department of Pharmacognosy and Pharmacology, College of Pharmacy, University of Illinois at the Medical Center, Chicago, IL 60612.* Accepted for publication May 29, 1980.

Abstract □ The latex of *Synadenium grantii* Hook. f. (Euphorbiaceae) yielded a novel skin irritant, 12-*O*-tigloyl-4-deoxyphorbol-13-isobutyrate (I). The identity of the diterpene parent alcohol and the relative positions of the esterifying groups were established by spectral analysis and experiments leading to the hydrolysis and acetylation of I. Compound I is the first phorbol derivative to be reported from the genus *Synadenium*.

Keyphrases □ 12-*O*-Tigloyl-4-deoxyphorbol-13-isobutyrate—isolation as skin irritant from *Synadenium grantii* and identification □ Euphorbiaceae—isolation of phorbol ester derivative as skin irritant from *Synadenium grantii* □ Diterpene esters—isolation as skin irritant from *Synadenium grantii*

Synadenium grantii is a member of a small genus of 15 species indigenous to East Africa (1). The shrub is grown in Europe and North America as an ornamental plant (2). A previous clinical report described symptoms from contact with the latex of this plant, which included burning and blistering of the face and neck (3).

This study was initiated to determine whether the toxicological effects of *S. grantii* latex are due to phorbol ester constituents since many representatives of this class of irritant and tumor-promoting diterpenoids have been found in the related genus Euphorbia (4). A previous phytochemical study of *S. grantii* enabled the detection of euphol, tirucallol, euphorbol, and an isomer of lanosterol (5), although these phytosterols do not produce a skin-irritant effect (6).

In the present work, fractionation of *S. grantii* latex resulted in the isolation of a novel irritant natural product, 12-*O*-tigloyl-4-deoxyphorbol-13-isobutyrate (I). Esters of 4-deoxyphorbol were isolated before from only two plant species (7–9).

EXPERIMENTAL

Plant Material—*Synadenium grantii* Hook. f. (Euphorbiaceae), propagated from a cutting[1], was used as the source of latex[2].

Extraction and Fractionation—Dried latex (19.9 g) was extracted at room temperature with six 100-ml portions of acetone. After drying, the residue (6.1 g) was partitioned between 60 ml of hexane and two 20-ml portions of methanol–water (9:1). Mouse ear-irritant activity (10) was traced to the methanol–water layer (1.1 g), which was subjected to low-pressure column chromatography on octadecylsilyl silica gel[3] with water–acetonitrile–methanol (3:2:2) as the eluting solvent. Irritant fractions were concentrated into 200 mg of the original column charge. The major active[4] principle, I, was purified by preparative TLC on silica gel G[3] in chloroform–benzene–ether–ethyl acetate (1:3:3:1) (R_f 0.22) and methylene chloride–ether–acetone (3:1:1) (R_f 0.55), as well as on diethylene glycol-impregnated kieselguhr G[3] (8) in cyclohexane–methyl ethyl ketone (9:1) (double development) (R_f 0.32).

Characterization of I—Resinous 12-*O*-tigloyl-4-deoxyphorbol-13-isobutyrate (I) (10 mg, 0.05%) exhibited major absorbance maxima in the IR spectrum[5] at ν_{max} 3430 (broad), 1710, 1650, 1625, and 1250 cm^{-1} and

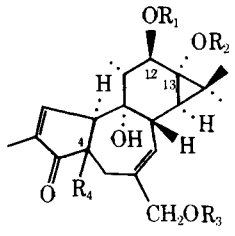

I: R_1 = OCC(CH_3)=$CHCH_3$, R_2 = $OCCH(CH_3)_2$, R_3 = H, R_4 = βH
II: R_1 = OCC(CH_3)=$CHCH_3$, R_2 = R_3 = H, R_4 = αH
III: R_1 = R_2 = R_3 = $OCCH_3$, R_4 = αH

in the UV spectrum[6] at λ_{max} 220 (log ε 4.37) nm. The NMR spectrum[7] showed signals at δ 0.91 (d, 1H, J = 6 Hz, 14-H), 0.95 (d, 3H, J = 6Hz, 18-CH_3), 1.10–1.26 (m, 12H, 16-CH_3, 17-CH_3, and two isobutyl CH_3), 1.74 [m, 6H, 19-CH_3 and =$CH(CH_3)$], 1.85 (s, 3H, 2′-CH_3), 2.25–2.61 (m, 3H), 2.92 (m, 1H, OH, exchangeable with D_2O), 3.24 (m, 1H, 10-H), 3.99 (s, 2H, 20-H_2), 5.51 (d, 1H, J = 9.5 Hz, 12-H), 5.54 (m, 1H, 7-H), 5.82 (m, 1H, OH, exchangeable with D_2O), 6.91 [m, 1H, =$CH(CH_3)$], and 7.55 (m, 1H, 1-H). Its mass spectrum[8] exhibited principal fragment ions at *m/e* 500 (M^+, 4%), 482 (3), 457 (3; found, 457.2221; calc. for $C_{26}H_{33}O_7$, 457.2225), 412 (10), 401 (8), 312 (16; found, 312.1727; calc. for $C_{20}H_{24}O_3$, 312.1725), 294 (18), 83 (100), 71 (30), and 43 (52).

Hydrolysis, Epimerization, and Acetylation of I—Hydrolysis and epimerization of I (6 mg) in 0.02 *M* KOH in methanol for 15 min at room temperature (8) led to the formation of a more polar compound, 12-*O*-tigloyl-4-deoxy-4α-phorbol (II) (4 mg), which was purified by preparative TLC on silica gel[3] in methylene chloride–acetone–hexane (3:1:1) (triple development) (R_f 0.10). The major absorbances in the IR spectrum[5] of II were observed at ν_{max} 3400 (broad), 1690, 1640, and 1625 cm^{-1}, and in the UV spectrum[6] at λ_{max} 220 (log ε 3.82) nm. In the NMR spectrum[7] of II, an upfield shift for the C-1 proton to δ 7.10 was evident, as well as a downfield shift for the C-10 proton to δ 3.42, suggesting an epimerization of the C-4 proton on hydrolysis (7, 8). There were no signals in the NMR spectrum of II assignable to an isobutyrate moiety, although all of the tigliate signals observed in the NMR spectrum of I were present. Other assignable signals were observed at δ 0.95 (d, 3H, J = 8.8 Hz, 18-CH_3), 1.17 (s, 6H, 16-CH_3 and 17-CH_3), 1.79 (m, 3H, 19-CH_3), 3.92 (s, 2H, 20-H_2), and 4.91 (d, 1H, J = 12 Hz, 12-H). Although the molecular ion of II was not apparent in the mass spectrum, fragment ions were observed at *m/e* 394 (3%), 330 (2), 312 (16), 294 (14), 91 (27), 83 (100), 69 (24), and 55 (55).

Compound II (2 mg) was hydrolyzed further with 0.05 *M* KOH in methanol at ambient temperature for 45 min. The product was partitioned and acetylated by a standard procedure (8). The resulting compound, 4-deoxy-4α-phorbol-12,13,20-triacetate (III) (2 mg), was identical to an authentic sample (co-TLC, mass spectral, and NMR analyses) (8).

DISCUSSION

The parent diterpene alcohol of the major skin-irritant factor (I) in *S. grantii* latex was shown to be 4-deoxyphorbol by hydrolysis (with simultaneous epimerization) (7), acetylation, and direct comparison to 4-deoxy-4α-phorbol-12,13,20-triacetate (III). The two esterifying groups in I were positioned at C-12 and C-13 since the NMR resonance at δ 3.99

[1] Provided by Longwood Gardens, Kennett Square, Pa.
[2] The plant was identified by Dr. D. D. Soejarto, and a representative sample was deposited in the herbarium of the Field Museum, Chicago, Ill.
[3] E. Merck, Darmstadt, West Germany.
[4] Biological test data will be published later.
[5] Beckman 18-A (as potassium bromide pellet).
[6] Beckman DB-G (in methanol).
[7] Varian T-60A with Nicolet TT-7 FT attachment (60 MHz) (in deuterochloroform with tetramethylsilane as the internal standard).
[8] Hitachi Perkin-Elmer RMU-6D and Varian MAT 112S (70 ev, low resolution).

0022-3549/80/1200-1446$01.00/0
© 1980, American Pharmaceutical Association

is typical of other 4-deoxyphorbol diesters with a primary hydroxyl group at C-20 (7–9). Mass spectral and NMR observations permitted the assignment of these ester functions as tiglic and isobutyric acids (9, 11). The tiglic group was assigned to C-12 because a fragment ion in the mass spectrum of I at *m/e* 401 indicated the loss of an acyloxy radical rather than a whole acid substituent from the molecular ion, an effect that was noted previously in phorbol 12,13-diesters (12). In contrast, as indicated by the fragment ion at *m/e* 412, the C-13 isobutyric substituent left the molecule of I as an acid (12). Confirmation of these assignments was achieved using a selective hydrolysis procedure in which the C-12 substituent of I was less susceptible to hydrolysis than the C-13 substituent (8). This procedure resulted in the formation of II, in which the tiglyl substituent was detected by NMR and mass spectral analyses.

Esters of 4-deoxyphorbol appear to be rare in the plant kingdom, having been described previously in *Euphorbia tirucalli* (7, 8) and *E. biglandulosa* (9). The irritant principle I in *S. grantii* is the first representative in this series to be esterified with two short-chain acids.

REFERENCES

(1) J. C. Willis, in "A Dictionary of the Flowering Plants and Ferns," 8th ed., H. K. Airy-Shaw, Ed., University Press, Cambridge, England, 1973.

(2) H. Jacobsen, "A Handbook of Succulent Plants," vol. 2, Blandford Press, London, England, 1960.

(3) A. J. Rook, *Br. J. Dermatol.*, **77**, 284 (1965).

(4) E. Hecker, *Pure Appl. Chem.*, **49**, 1423 (1977).

(5) P. E. Nielsen, H. Nishimura, Y. Liang, and M. Calvin, *Phytochemistry*, **18**, 103 (1979).

(6) E. Hecker, *Cancer Res.*, **28**, 2338 (1968).

(7) G. Fürstenberger and E. Hecker, *Tetrahedron Lett.*, **1977**, 929.

(8) A. D. Kinghorn, *J. Nat. Prod.*, **42**, 112 (1979).

(9) G. Falsone and A. E. G. Crea, *Justus Liebigs Ann. Chem.*, **1979**, 1116.

(10) E. Hecker, H. Immich, H. Bresch, and H. U. Schairer, *Z. Krebsforsch.*, **68**, 366 (1966).

(11) A. D. Kinghorn and F. J. Evans, *J. Pharm. Pharmacol.*, **27**, 329 (1975).

(12) E. Hecker and R. Schmidt, *Fortshr. Chem. Org. Naturst.*, **31**, 377 (1974).

ACKNOWLEDGMENTS

Supported by a grant from the Campus Research Board, University of Illinois at the Medical Center.

The author thanks Mr. K. Larsen, University of Illinois Pharmacognosy and Horticulture Field Station, Downers Grove, Ill., for growing the plant material, Dr. D. D. Soejarto, Department of Pharmacognosy and Pharmacology, University of Illinois at the Medical Center, for the plant identification, and Mr. F. Williams, Research Triangle Institute, N.C., for the high-resolution mass spectra.

N-Demethylation of Dextromethorphan

NORTON P. PEET

Received March 5, 1980, from the *Pharmaceutical Research and Development–Medicinal Chemistry Department, Dow Chemical Company, Indianapolis, IN 46268.* Accepted for publication June 3, 1980.

Abstract □ In addition to providing an efficient synthesis of 3-methoxymorphinan hydrochloride, the use of 2,2,2-trichloroethyl chloroformate in the *N*-demethylation of dextromethorphan led to the isolation of two novel zinc salts of 3-methoxymorphinan.

Keyphrases □ Dextromethorphan—*N*-demethylation to yield 3-methoxymorphinan hydrochloride and two novel zinc salts of 3-methoxymorphinan □ Antitussives—dextromethorphan, *N*-demethylation to yield 3-methoxymorphinan hydrochloride and two novel zinc salts of 3-methoxymorphinan □ 3-Methoxymorphinan—synthesis by *N*-demethylation of dextromethorphan

A sample of 3-methoxymorphinan (V) recently was required in these laboratories for pharmacological evaluation. Compound V is one of the three known metabolites of dextromethorphan (3-methoxy-*N*-methylmorphinan, I) (1, 2), a clinically useful antitussive agent. This report describes a new synthesis of V from I and the isolation of novel zinc salts of V.

EXPERIMENTAL[1]

Synthesis of 1,3,4,9,10,10a-Hexahydro-6-methoxy-2*H*-10,4a-(iminoethano)phenanthrene-11-carboxylic Acid 2,2,2-Trichloroethyl Ester (II)—Dextromethorphan hydrobromide monohydrate[2] (27.8 g, 75.0 mmoles) was partitioned between chloroform and a solution of 5.7 g of potassium hydroxide in water. The organic layer was separated, dried (sodium sulfate), and concentrated to leave a viscous oil, which solidified upon standing to yield 20.4 g (100%) of I, mp 107–110°; IR (mineral oil): 1610 cm^{-1}. TLC on silica gel with chloroform–methanol (9:1) gave a single spot at $R_f \simeq 0.1$.

To a solution of I (8.14 g, 30.0 mmoles) in 100 ml of benzene was added 2,2,2-trichloroethyl chloroformate[3] (6.99 g, 33.0 mmoles). After refluxing for 1 hr, the solution was concentrated to leave 14.6 g of crude II as a viscous oil; IR (mineral oil): 1710 (C=O) cm^{-1}; NMR (deuterochloroform): δ 4.70 (s, 2H, OCH_2); mass spectrum (70 ev, electron impact): *m/e* 431 (molecular ion). TLC on silica gel with chloroform–methanol (9:1) gave a single spot at $R_f \simeq 0.8$.

Synthesis of 3-Methoxymorphinan Tetrachlorozincate (IV)—To a solution of II (12.7 g, 29.3 mmoles) in 100 ml of 90% acetic acid was added 5 g of powered zinc. An exotherm followed. After 20 min, TLC indicated completeness of the reaction, and the mixture was filtered. The filtrate was concentrated to a white solid, which was triturated with ether and collected to yield 3-methoxymorphinan tetraacetatozincate (III), mp 157–167° (glass); NMR (deuterochloroform and dimethyl sulfoxide-d_6): δ 7.20–7.00 (m, 1H, aromatic), 6.87–6.68 (m, 2H, aromatic), 3.80 (s, 3H, OCH_3), 3.30–3.00 (m, 3H, $CHNHCH_2$), and 2.06 (s, ~6H, acetate ions); mass spectrum (70 ev, electron impact): *m/e* 257 (molecular ion). TLC on silica gel with chloroform–methanol (9:1) gave a single spot at $R_f \simeq 0.15$.

Crude III (10.0 g) was dissolved in 2000 ml of chloroform, and dry hydrogen chloride gas was bubbled through the solution for 10 min. The solution was concentrated, and the resulting oil partially crystallized upon standing under ether. Trituration with a small volume of isopropanol

[1] Melting points are uncorrected. IR spectra were recorded with a Perkin-Elmer model 727B spectrophotometer. NMR spectra were obtained with a Varian EM360A spectrometer. Mass spectra were recorded with a Finnigan model 4023 gas chromatograph–mass spectrometer (electron impact and chemical ionization) at 70 ev. Combustion analyses for carbon, hydrogen, nitrogen, chlorine, and zinc were performed by Dow Analytical Laboratories and Galbraith Laboratories, Knoxville, Tenn.

[2] Dow Chemical Co., Indianapolis, Ind.

[3] Aldrich Chemical Co., Milwaukee, Wis.

0022-3549/80/1200-1447$01.00/0

© 1980, American Pharmaceutical Association

is typical of other 4-deoxyphorbol diesters with a primary hydroxyl group at C-20 (7–9). Mass spectral and NMR observations permitted the assignment of these ester functions as tiglic and isobutyric acids (9, 11). The tiglic group was assigned to C-12 because a fragment ion in the mass spectrum of I at *m/e* 401 indicated the loss of an acyloxy radical rather than a whole acid substituent from the molecular ion, an effect that was noted previously in phorbol 12,13-diesters (12). In contrast, as indicated by the fragment ion at *m/e* 412, the C-13 isobutyric substituent left the molecule of I as an acid (12). Confirmation of these assignments was achieved using a selective hydrolysis procedure in which the C-12 substituent of I was less susceptible to hydrolysis than the C-13 substituent (8). This procedure resulted in the formation of II, in which the tiglyl substituent was detected by NMR and mass spectral analyses.

Esters of 4-deoxyphorbol appear to be rare in the plant kingdom, having been described previously in *Euphorbia tirucalli* (7, 8) and *E. biglandulosa* (9). The irritant principle I in *S. grantii* is the first representative in this series to be esterified with two short-chain acids.

REFERENCES

(1) J. C. Willis, in "A Dictionary of the Flowering Plants and Ferns," 8th ed., H. K. Airy-Shaw, Ed., University Press, Cambridge, England, 1973.

(2) H. Jacobsen, "A Handbook of Succulent Plants," vol. 2, Blandford Press, London, England, 1960.

(3) A. J. Rook, *Br. J. Dermatol.*, **77**, 284 (1965).

(4) E. Hecker, *Pure Appl. Chem.*, **49**, 1423 (1977).

(5) P. E. Nielsen, H. Nishimura, Y. Liang, and M. Calvin, *Phytochemistry*, **18**, 103 (1979).

(6) E. Hecker, *Cancer Res.*, **28**, 2338 (1968).

(7) G. Fürstenberger and E. Hecker, *Tetrahedron Lett.*, **1977**, 929.

(8) A. D. Kinghorn, *J. Nat. Prod.*, **42**, 112 (1979).

(9) G. Falsone and A. E. G. Crea, *Justus Liebigs Ann. Chem.*, **1979**, 1116.

(10) E. Hecker, H. Immich, H. Bresch, and H. U. Schairer, *Z. Krebsforsch.*, **68**, 366 (1966).

(11) A. D. Kinghorn and F. J. Evans, *J. Pharm. Pharmacol.*, **27**, 329 (1975).

(12) E. Hecker and R. Schmidt, *Fortshr. Chem. Org. Naturst.*, **31**, 377 (1974).

ACKNOWLEDGMENTS

Supported by a grant from the Campus Research Board, University of Illinois at the Medical Center.

The author thanks Mr. K. Larsen, University of Illinois Pharmacognosy and Horticulture Field Station, Downers Grove, Ill., for growing the plant material, Dr. D. D. Soejarto, Department of Pharmacognosy and Pharmacology, University of Illinois at the Medical Center, for the plant identification, and Mr. F. Williams, Research Triangle Institute, N.C., for the high-resolution mass spectra.

N-Demethylation of Dextromethorphan

NORTON P. PEET

Received March 5, 1980, from the *Pharmaceutical Research and Development–Medicinal Chemistry Department, Dow Chemical Company, Indianapolis, IN 46268.* Accepted for publication June 3, 1980.

Abstract □ In addition to providing an efficient synthesis of 3-methoxymorphinan hydrochloride, the use of 2,2,2-trichloroethyl chloroformate in the *N*-demethylation of dextromethorphan led to the isolation of two novel zinc salts of 3-methoxymorphinan.

Keyphrases □ Dextromethorphan—*N*-demethylation to yield 3-methoxymorphinan hydrochloride and two novel zinc salts of 3-methoxymorphinan □ Antitussives—dextromethorphan, *N*-demethylation to yield 3-methoxymorphinan hydrochloride and two novel zinc salts of 3-methoxymorphinan □ 3-Methoxymorphinan—synthesis by *N*-demethylation of dextromethorphan

A sample of 3-methoxymorphinan (V) recently was required in these laboratories for pharmacological evaluation. Compound V is one of the three known metabolites of dextromethorphan (3-methoxy-*N*-methylmorphinan, I) (1, 2), a clinically useful antitussive agent. This report describes a new synthesis of V from I and the isolation of novel zinc salts of V.

EXPERIMENTAL[1]

Synthesis of 1,3,4,9,10,10a-Hexahydro-6-methoxy-2*H*-10,4a-(iminoethano)phenanthrene-11-carboxylic Acid 2,2,2-Trichloroethyl Ester (II)—Dextromethorphan hydrobromide monohydrate[2] (27.8 g, 75.0 mmoles) was partitioned between chloroform and a solution of 5.7 g of potassium hydroxide in water. The organic layer was separated, dried (sodium sulfate), and concentrated to leave a viscous oil, which solidified upon standing to yield 20.4 g (100%) of I, mp 107–110°; IR (mineral oil): 1610 cm^{-1}. TLC on silica gel with chloroform–methanol (9:1) gave a single spot at $R_f \simeq 0.1$.

To a solution of I (8.14 g, 30.0 mmoles) in 100 ml of benzene was added 2,2,2-trichloroethyl chloroformate[3] (6.99 g, 33.0 mmoles). After refluxing for 1 hr, the solution was concentrated to leave 14.6 g of crude II as a viscous oil; IR (mineral oil): 1710 (C=O) cm^{-1}; NMR (deuterochloroform): δ 4.70 (s, 2H, OCH_2); mass spectrum (70 ev, electron impact): *m/e* 431 (molecular ion). TLC on silica gel with chloroform–methanol (9:1) gave a single spot at $R_f \simeq 0.8$.

Synthesis of 3-Methoxymorphinan Tetrachlorozincate (IV)—To a solution of II (12.7 g, 29.3 mmoles) in 100 ml of 90% acetic acid was added 5 g of powered zinc. An exotherm followed. After 20 min, TLC indicated completeness of the reaction, and the mixture was filtered. The filtrate was concentrated to a white solid, which was triturated with ether and collected to yield 3-methoxymorphinan tetraacetatozincate (III), mp 157–167° (glass); NMR (deuterochloroform and dimethyl sulfoxide-d_6): δ 7.20–7.00 (m, 1H, aromatic), 6.87–6.68 (m, 2H, aromatic), 3.80 (s, 3H, OCH_3), 3.30–3.00 (m, 3H, $CHNHCH_2$), and 2.06 (s, ~6H, acetate ions); mass spectrum (70 ev, electron impact): *m/e* 257 (molecular ion). TLC on silica gel with chloroform–methanol (9:1) gave a single spot at $R_f \simeq 0.15$.

Crude III (10.0 g) was dissolved in 2000 ml of chloroform, and dry hydrogen chloride gas was bubbled through the solution for 10 min. The solution was concentrated, and the resulting oil partially crystallized upon standing under ether. Trituration with a small volume of isopropanol

[1] Melting points are uncorrected. IR spectra were recorded with a Perkin-Elmer model 727B spectrophotometer. NMR spectra were obtained with a Varian EM360A spectrometer. Mass spectra were recorded with a Finnigan model 4023 gas chromatograph–mass spectrometer (electron impact and chemical ionization) at 70 ev. Combustion analyses for carbon, hydrogen, nitrogen, chlorine, and zinc were performed by Dow Analytical Laboratories and Galbraith Laboratories, Knoxville, Tenn.

[2] Dow Chemical Co., Indianapolis, Ind.

[3] Aldrich Chemical Co., Milwaukee, Wis.

0022-3549/80/1200-1447$01.00/0

© 1980, American Pharmaceutical Association

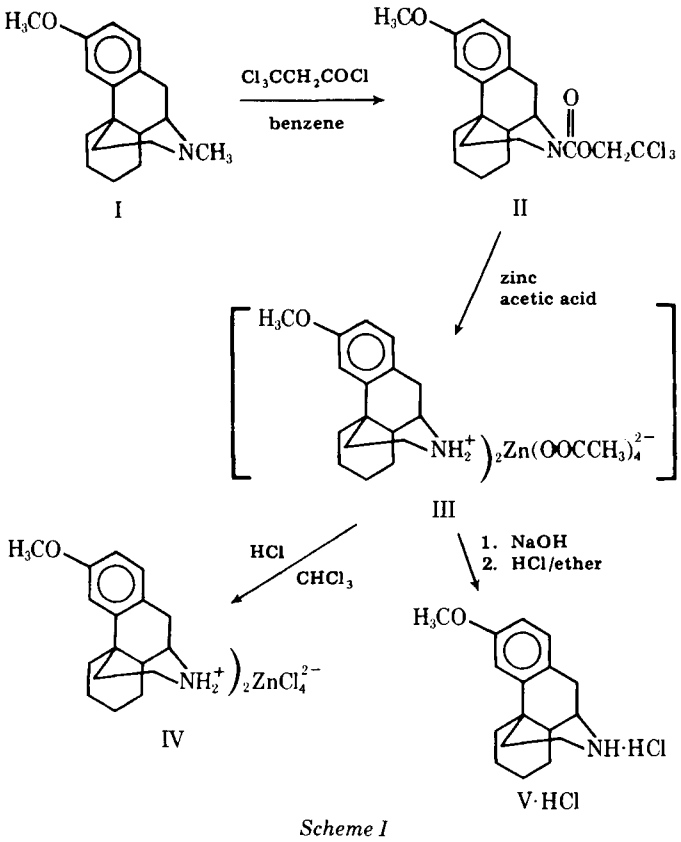

Scheme I

effected complete crystallization. Recrystallization of this material twice from isopropanol–ethyl acetate gave 2.19 g of IV, mp 191–192°; IR (mineral oil): 3200–2750 (NH_2^+), 1600, 1505, 1235, and 1030 cm^{-1}; NMR (dimethyl sulfoxide-d_6): δ 9.07 (broad s, 2H, NH_2^+, deuterium oxide exchangeable), 7.30–7.10 (m, 1H, aromatic), 6.96–6.77 (m, 2H, aromatic), and 3.78 (s, 3H, OCH_3). TLC on silica gel with chloroform–methanol (9:1) gave a single spot at $R_f \simeq 0.15$.

Anal.—Calc. for $C_{34}H_{48}Cl_4N_2O_4Zn$: C, 56.40; H, 6.68; Cl, 19.59; N, 3.87; Zn, 9.03. Found: C, 56.52; H, 6.54; Cl, 19.40; N, 3.70; Zn, 8.94.

Synthesis of 3-Methoxymorphinan (V) Hydrochloride—Crude III (21.8 g, 26.7 mmoles) was dissolved in chloroform and treated with 75 ml of 1 *N* NaOH. A flocculent white precipitate was removed by filtration. The organic phase of the filtrate was separated, dried (sodium sulfate), and concentrated to yield 10.5 g (77%) of V as a viscous oil; IR (neat): 1610, 1490, 1240, 1040, and 745 cm^{-1}; NMR (deuterochloroform): δ 7.15–6.95 (m, 1H, aromatic), 6.88–6.64 (m, 2H, aromatic), and 3.79 (s, 3H, OCH_3).

A solution of the free base (10.0 g, 38.8 mmoles) in ether–ethyl acetate was treated with ethereal hydrogen chloride until oiling no longer occurred. Scratching produced a white solid, which was collected, washed with ether, and air dried to yield 9.30 g (81%) of V, mp 249–250.5° (methanol–ether–ethyl acetate) [lit. (3) mp 253.5–255°]; IR (mineral oil): 3100–2400 (NH_2^+), 1610, 1510, 1245, 1040, and 900 cm^{-1}; NMR (dimethyl sulfoxide-d_6): δ 9.55 (broad s, 2H, NH_2^+, deuterium oxide exchangeable), 7.26–7.05 (m, 1H, aromatic), 6.95–6.73 (m, 2H, aromatic), and 3.75 (s, 3H, OCH_3).

RESULTS AND DISCUSSION

N-Demethylation of I was accomplished previously using phenyl chloroformate (followed by hydrolysis of the resulting carbamate) (3) or cyanogen bromide (4). 2,2,2-Trichloroethyl chloroformate was considered an attractive potential reagent for this *N*-demethylation since it is mild and was previously employed for the demethylation of tertiary methylamines. Yields are high for *N*-demethylation using this reagent; morphine was demethylated in 75% yield with 2,2,2-trichloroethyl chloroformate (5). Demethylation with 2,2,2-trichloroethyl chloroformate generally leads to fewer side reactions and a cleaner product than does demethylation with cyanogen bromide. The use of ethyl or phenyl chloroformate for demethylation requires a strong acid or strong base for hydrolysis of the intermediate carbamates, whereas 2,2,2-trichloroethyl chloroformate does not.

Accordingly, dextromethorphan (I) was treated with 2,2,2-trichloroethyl chloroformate to produce II. Treatment of an acetic acid solution of II with zinc dust produced a material that was partially characterized and assigned as the zinc tetraacetate salt of 3-methoxymorphinan (III). This remarkable salt (mol. wt. 818.30) was soluble in chloroform and displayed an elution position on a silica gel TLC plate using chloroform–methanol (9:1) as the eluent. Spectral data were in accord with the structural assignment for III (Scheme I). However, the structure of III was clearly indicated by its conversion to the zinc tetrachloride salt of 3-methoxymorphinan (IV).

Treatment of a chloroform solution of III with dry hydrogen chloride yielded a white solid, which, when recrystallized twice from isopropanol–ethyl acetate, displayed a sharp melting point at 191–192°. An aqueous solution of this material, when treated with aqueous silver nitrate, produced a voluminous, white precipitate. Spectral data for this material were in accord with Structure IV and were similar to those recorded for III. Elemental combustion analysis established the structure of the zinc salt as IV. Correct analyses for carbon, hydrogen, nitrogen, chlorine, and zinc were obtained. These analyses could be obtained only if the salt was dried under vacuum at 60°. Drying at 40 or 80° led to incorrect analyses, presumably due to insufficient removal of volatile substances and decomposition, respectively.

The tendency for 3-methoxymorphinan (V) to associate with zinc produced two salts (III and IV), whose identification was subordinate to the preparation of the desired metabolite (V). However, it is speculated that the ability of at least one metabolite of dextromethorphan to complex with zinc (and perhaps other trace metals) may be intimately associated with the pharmacology displayed by I.

Associated zinc was separated readily from III by partitioning between chloroform and aqueous base. The chloroform layer then contained noncomplexed V, which was isolated and treated with dry hydrogen chloride to produce 3-methoxymorphinan (V) hydrochloride. The overall yield of V·HCl from I was ~70%.

REFERENCES

(1) A. E. Takemori and G. J. Mannering, *J. Pharmacol. Exp. Ther.*, **123**, 171 (1958).

(2) K. Willner, *Arzneim.-Forsch.*, **13**, 26 (1963).

(3) M. M. Abdel-Monem and P. S. Portoghese, *J. Med. Chem.*, **15**, 208 (1972).

(4) R. L. Clark, U.S. pat. 2,741,617 (Apr. 10, 1956).

(5) M. Fieser and L. F. Fieser, "Reagents for Organic Synthesis," vol. 5, Wiley, New York, N.Y., 1975, p. 687. T. A. Montzka, J. D. Matiskella, and R. A. Partyka, *Tetrahedron Lett.*, **1974**, 1325.

GLC Method for Assay of Forskolin, a Novel Positive Inotropic and Blood Pressure-Lowering Agent

P. K. INAMDAR ˣ, H. DORNAUER, and N. J. de SOUZA

Received April 15, 1980, from the *Research Centre, Hoechst Pharmaceuticals Ltd., Bombay 400 080, India.* Accepted for publication June 9, 1980.

Abstract □ A GLC method for the quantitative determination of forskolin, a novel positive inotropic and blood pressure-lowering agent, is described. This method is simple, rapid, and sensitive and is suitable for the routine assay of plant materials and pharmaceutical preparations containing forskolin.

Keyphrases □ Forskolin—GLC analysis in plant extracts and pharmaceutical preparations □ GLC—analysis, forskolin in plant extracts and pharmaceutical preparations □ Antihypertensive agents—forskolin, GLC analysis in plant extracts and pharmaceutical preparations

Forskolin (1α,6β,9α-trihydroxy-7β-acetoxy-8,13-epoxy-labd-14-en-11-one, Ia) is a novel positive inotropic and blood pressure-lowering agent isolated from the Indian plant *Coleus forskohlii* Briq. (Labiatae) (1, 2). Compound Ia currently is under preclinical development.

Different rapid, precise methods for the quantitative estimation of forskolin in plant materials and pharmaceutical preparations, as well as for application to pharmacokinetic studies, are under investigation in these laboratories. This report describes a GLC method for the assay of forskolin; it is applicable to forskolin in plant extracts and pharmaceutical preparations.

EXPERIMENTAL

Instrumentation—The gas–liquid chromatograph[1] was equipped with a flame-ionization detector and a 180-cm × 5-mm glass, coil-shaped column packed with 3% OV-1[2] on 100–120-mesh Gas Chrom Q[3]. Nitrogen was the carrier gas at a flow rate of 20 ml/min, and the air and hydrogen flow rates were set to maximize the detector response. A potentiometric continuous-line recorder[4] (2.5 mv) with a speed of 300 mm/hr was used. The temperatures were: injector, 250°; column oven, 220°; and manifold, 270°. A microsyringe[5] was used in the GLC analysis.

Reagents and Materials—Samples of forskolin (Ia), 7-deacetylforskolin (Ib), plant materials, and tablets of forskolin were obtained[6]. The solvents were analytical grade.

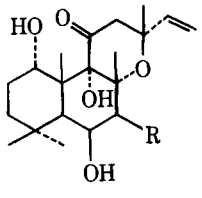

Ia: R = $OCOCH_3$
Ib: R = OH

[1] Model 900, Bodenseewerk, Perkin-Elmer Co., Überlingen, West Germany.
[2] E. Merck, Darmstadt, West Germany.
[3] Supelco, Bellefonte, Pa.
[4] Kompensograph, 1288 × 288, type M-810-417, Siemens Aktiengesellschaft, Erlangen, West Germany.
[5] Hamilton 701N, Micromesure AG., 7402, Bonaduz, Switzerland.
[6] These samples were obtained from the research and development laboratories of Hoechst Pharmaceuticals Ltd. The plant materials were identified as *C. forskohlii* Briq. (No. HOE 141) and *C. spicatus* Benth. (No. HOE 142), both of the Labiatae family, by Miss Virbala Shah of Hoechst Pharmaceuticals Ltd. Voucher specimens are preserved at the Herbarium of the Research Centre, Hoechst Pharmaceuticals Ltd., Mulund, Bombay 400 080, India.

Standard Solutions and Calibration Curves—Forskolin (120 mg) was dissolved in chloroform (10 ml). The internal standard solution was prepared by dissolving Ib (80 mg) in chloroform (10 ml). Forskolin solutions were prepared in triplicate from these solutions to contain 1.2, 2.4, 3.6, 4.8, and 6 mg of forskolin/ml of chloroform, in which the concentration of the internal standard was 4 mg/ml.

Each solution (1 μl) was injected in triplicate onto the column. The peak area ratio of forskolin to the internal standard was plotted against the ratio of the weight of forskolin to the internal standard to yield a calibration curve.

Preparation of Semipurified Extracts of Plant Materials—The dried and finely divided plant material (15 g) was extracted with benzene (3 × 150 ml) at 40–50° for 5 hr, and the combined extracts were filtered and concentrated *in vacuo*. The residue was triturated with petroleum ether (bp 60–80°) (2 × 50 ml), and the petroleum ether layer was decanted. The petroleum ether-insoluble residue was treated further with methanol (2 × 50 ml), and the methanolic solution was separated and concentrated *in vacuo* to constant weight to provide the semipurified extract.

Assay of Plant Materials—The semipurified plant extract was dissolved, depending on its weight, in chloroform (0.125–3.0 ml). The solution always was adjusted to contain the internal standard at a concentration of 4 mg/ml. One microliter of the solution was injected onto the column. The mean peak area ratio of six injections was used for quantitation of the amount of forskolin in *C. forskohlii*.

Assay of Forskolin Tablets (5 mg/Tablet)—Ten tablets, each weighing an average of 125 mg, were powdered. A quantity equivalent to one tablet (125 mg) was transferred to a 25-ml centrifuge tube. Chloroform (10 ml) was added, and the suspension was centrifuged for 10 min; the procedure was repeated three times.

The pooled chloroform extracts left a residue upon evaporation of the chloroform *in vacuo*, and this residue was dissolved in chloroform (0.5 ml) and mixed with the internal standard solution (0.5 ml). One microliter of this solution was injected in quadruplicate onto the column.

Placebo tablets also were extracted in parallel with the sample. The placebo chromatogram was checked for interfering peaks at the retention times for forskolin and the internal standard.

RESULTS AND DISCUSSION

The gas chromatogram of forskolin and the internal standard is presented in Fig. 1. The retention times were 21.6 and 18.0 min, respectively. The GLC responses for forskolin and Ib were linear over a range of at least 1.2–6.0 μg of the drug and the internal standard injected separately. The minimum detectable level was 30 ng of forskolin. A calibration curve indicated that a linear relation existed in the 1.2–6.0-μg range between the peak area ratio of forskolin to the internal standard and the ratio of the weight of forskolin to the internal standard.

Typical chromatograms for a semipurified extract of *C. forskohlii* and the semipurified extract of *C. forskohlii* together with the internal standard (4 μg) are presented in Fig. 2. A GLC–mass spectrometric analysis of the semipurified extract of *C. forskohlii* revealed that the peak with the retention time of that for forskolin gave a mass spectrum identical to that of a standard forskolin sample. By referring to the calibration curve, the amount of forskolin present in *C. forskohlii* was calculated. In the different samples assayed, forskolin occurred in amounts ranging from ~0.05 to 0.1% of the dry weight of the plant material, depending on the part of the plant that was assayed as well as on the time and location of collection of the plant material. The results agreed well with amounts of forskolin isolated from bulk quantities of plant material (1). Therefore, the method is a rapid and sensitive technique for evaluating and controlling the quality of *C. forskohlii*.

To find alternative and, possibly, richer sources of forskolin than *C. forskohlii*, the method was applied to semipurified extracts of other

0022-3549/80/1200-1449$01.00/0
© 1980, American Pharmaceutical Association

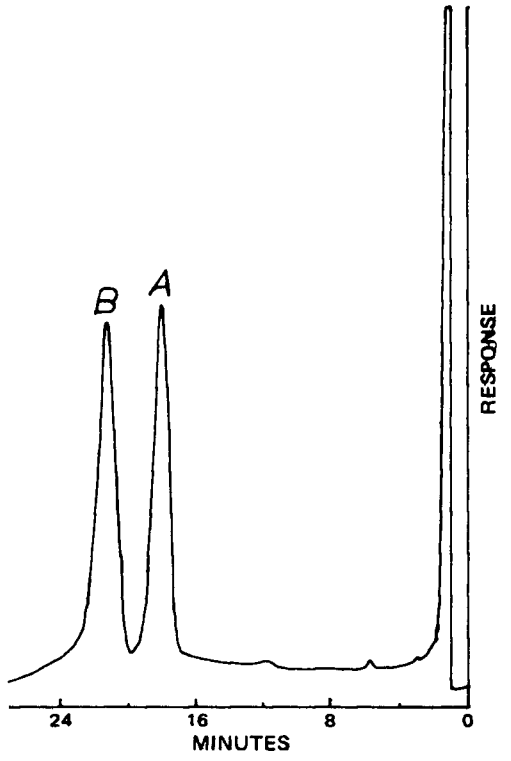

Figure 1—*GLC separation of forskolin (B) and the internal standard (A).*

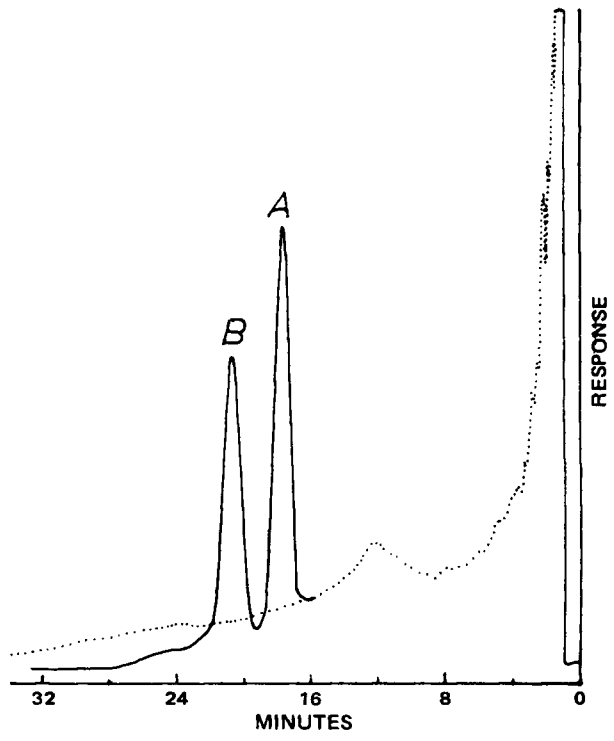

Figure 3—*Gas–liquid chromatogram of a semipurified extract of* C. spicatus (····) *and of the semipurified extract of* C. spicatus *spiked with forskolin (B) and the internal standard (A)* (—).

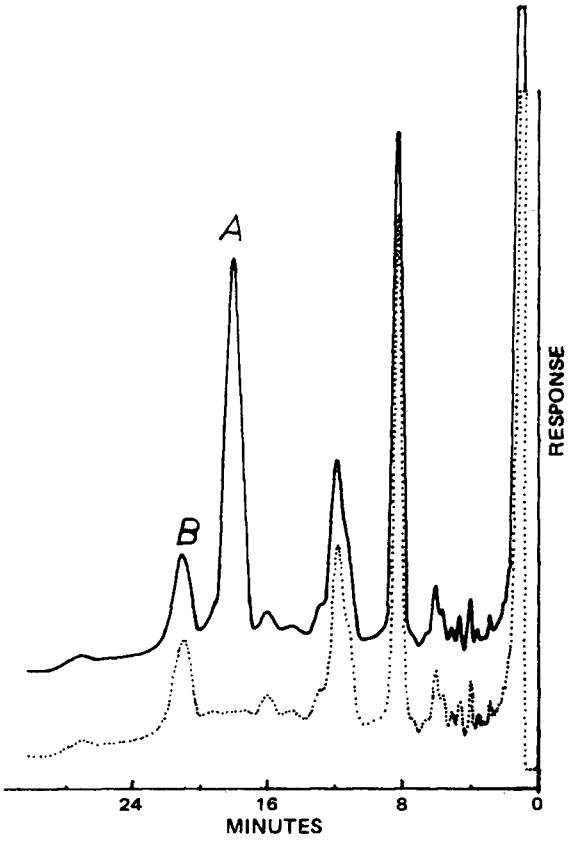

Figure 2—*Typical GLC separation of a semipurified extract of* C. forskolii (····) *and of a semipurified extract of* C. forskohlii *together with the internal standard* (—). *Key: A, internal standard; and B, forskolin.*

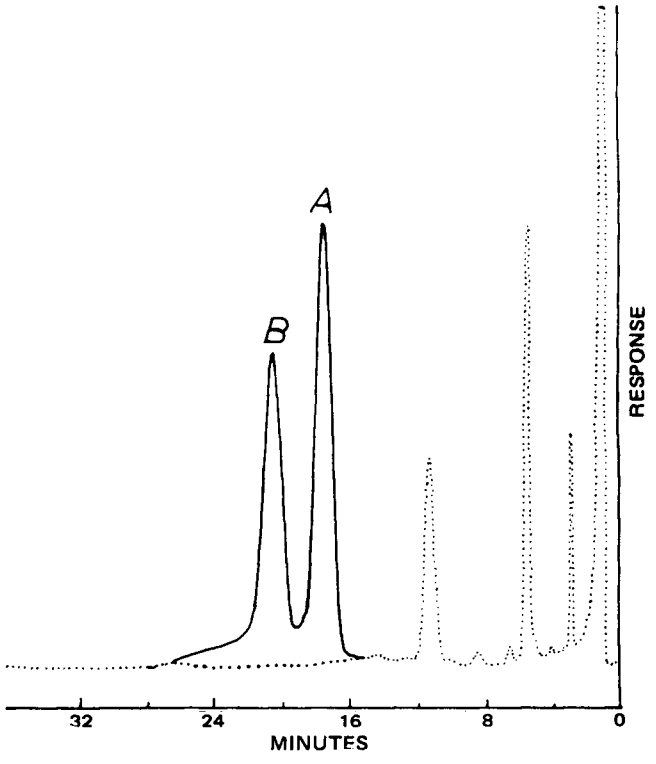

Figure 4—*Gas–liquid chromatogram of the placebo tablet* (····) *and of the tablets of forskolin with the internal standard* (—). *Key: A, internal standard; and B, forskolin.*

Coleus species and taxonomically related *Plectranthus* species (3). As typical examples, chromatograms for the semipurified extract of *C. spicatus* Benth. (Labiatae) and the semipurified extract spiked with forskolin and the internal standard are presented in Fig. 3. In none of the

six *Coleus* species other than *C. forskohlii* and the six *Plectranthus* species assayed was forskolin detected at levels as low as $\sim 1 \times 10^{-4}\%$ of the dry weight of the plant material (3).

Chromatograms from the assay of forskolin tablets are presented in Fig. 4. There was no interference due to peaks observed in the placebo samples. Assays were carried out in quadruplicate on five samples. The results indicated 5.12 mg of forskolin/tablet (label claim of 5.0 mg/tablet) with a range of 5.07–5.19 mg/tablet and a *RSD* of ±0.28%.

REFERENCES

(1) S. V. Bhat, B. S. Bajwa, H. Dornauer, and N. J. de Souza, *Tetrahedron Lett.*, **1977**, 1669.

(2) E. Lindner, A. N. Dohadwalla, and B. K. Bhattacharya, *Arzneim.-Forsch.*, **28**, 284 (1978).

(3) V. Shah, S. V. Bhat, B. S. Bajwa, H. Dornauer, and N. J. de Souza, *Planta Med.*, **39**, 183 (1980).

ACKNOWLEDGMENTS

The authors thank Dr. S. V. Bhat for the samples of forskolin and the diterpenoids, Miss V. Shah for the plant materials, Mr. S. C. Bapna for the galenical samples, and Mr. P. V. Kanitkar and Miss P. Colaco for technical assistance. The GLC–mass spectrometric data were provided by Dr. A. M. Shaligram, Indian Institute of Technology, Bombay 400 076, India.

Anti-Inflammatory Activity of Diazomethyl Ketone and Chloromethyl Ketone Analogs Prepared from *N*-Tosyl Amino Acids

I. H. HALL ˣ, J. E. HALL, Jr., M. MOHSENI, and Z. SAJADI

Received January 7, 1980, from the *Division of Medicinal Chemistry, School of Pharmacy, University of North Carolina, Chapel Hill, NC 27514.* Accepted for publication June 9, 1980.

Abstract □ A series of diazomethyl ketone and chloromethyl ketone analogs prepared from *N*-tosyl amino acids was shown to have anti-inflammatory activity in mice at 20 mg/kg and in rats at 10 mg/kg. *N*-Tosyl-L-alanine and *N*-tosyl-β-alanine chloromethyl ketones demonstrated the most potent anti-inflammatory activity. The writhing reflex also was inhibited at 20 mg/kg in mice. In the tail flick test, *N*-tosyl-D,L-alanine and *N*-tosyl-D,L-isoleucine chloromethyl ketones demonstrated the highest increase in time. Toxicity studies indicated good therapeutic indexes for most of these agents.

Keyphrases □ Anti-inflammatory activity—diazomethyl ketone and chloromethyl ketone analogs prepared from *N*-tosyl amino acids, biological evaluation □ *N*-Tosyl amino acids—diazomethyl ketone and chloromethyl ketone analogs, evaluation for anti-inflammatory activity

A series of *N*-tosyl, *N*-benzoyl, *N*-acetyl, *N*-carbobenzyloxy, and *N*-cinnamyl cyanomethyl esters of amino acids was shown to have anti-inflammatory and immunosuppressive activities in mice (1). The standard proteolytic inhibitor tosylphenylalanyl chloromethyl ketone also was active as an anti-inflammatory agent. This report discusses a series of diazomethyl ketones and chloromethyl ketones of *N*-tosyl amino acids that demonstrated similar activity.

EXPERIMENTAL

The synthesis and physical data of this series of compounds were reported previously (2). The synthetic methods were essentially those outlined by Schoellman and Shaw (3). Male CF_1 mice (~30 g) or male Sprague–Dawley rats (~160 g) were administered the test drugs at 20 or 10 mg/kg ip, respectively, in 0.05% polysorbate 80, 3.5 hr prior to the injection of 1% carrageenan in 0.9% saline into the plantar surface of the right hindfoot. Isotonic saline was injected into the left hindfoot to obtain baseline data. After 3 hr, both feet were excised at the tibiotarsal (ankle) joint according to a modification of the method of Winter *et al.* (4, 5).

As an analgesic screen, the tail flick (6) method was employed with male CF_1 mice (~30 g) who received the test drugs at 20 mg/kg ip 5 min prior to the analgesic test. An apparatus was designed and implemented in these laboratories to measure the tail flick response time of mice (Fig. 1). A control box housed all of the timing, logic, and sensing circuitry and the feedback controls. A secondary box provided the self-contained heater (55 ± 0.5°), the temperature-sensing elements, and special custom-made optical sensors to detect the flick of the tail. The sense signals were coupled to the control box to regulate the surface temperature and to freeze the digital clock (accuracy of 0.001%) display at the time of the first tail flick.

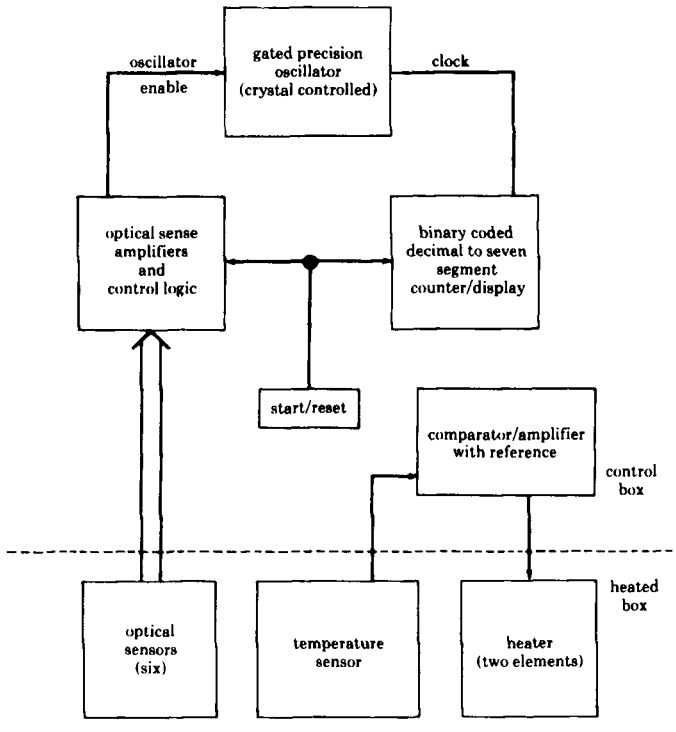

Figure 1—*Functional diagram of tail flick apparatus.*

The writhing reflex also was utilized as an analgesic test. Mice were administered the test drugs at 20 mg/kg ip 20 min prior to the administration of 0.5 ml of 0.6% acetic acid (7). After 5 min, the number of

0022-3549/80/1200-1451$01.00/0

© 1980, American Pharmaceutical Association

six *Coleus* species other than *C. forskohlii* and the six *Plectranthus* species assayed was forskolin detected at levels as low as $\sim 1 \times 10^{-4}\%$ of the dry weight of the plant material (3).

Chromatograms from the assay of forskolin tablets are presented in Fig. 4. There was no interference due to peaks observed in the placebo samples. Assays were carried out in quadruplicate on five samples. The results indicated 5.12 mg of forskolin/tablet (label claim of 5.0 mg/tablet) with a range of 5.07–5.19 mg/tablet and a *RSD* of ±0.28%.

REFERENCES

(1) S. V. Bhat, B. S. Bajwa, H. Dornauer, and N. J. de Souza, *Tetrahedron Lett.*, **1977**, 1669.

(2) E. Lindner, A. N. Dohadwalla, and B. K. Bhattacharya, *Arzneim.-Forsch.*, **28**, 284 (1978).

(3) V. Shah, S. V. Bhat, B. S. Bajwa, H. Dornauer, and N. J. de Souza, *Planta Med.*, **39**, 183 (1980).

ACKNOWLEDGMENTS

The authors thank Dr. S. V. Bhat for the samples of forskolin and the diterpenoids, Miss V. Shah for the plant materials, Mr. S. C. Bapna for the galenical samples, and Mr. P. V. Kanitkar and Miss P. Colaco for technical assistance. The GLC–mass spectrometric data were provided by Dr. A. M. Shaligram, Indian Institute of Technology, Bombay 400 076, India.

Anti-Inflammatory Activity of Diazomethyl Ketone and Chloromethyl Ketone Analogs Prepared from *N*-Tosyl Amino Acids

I. H. HALL ˣ, J. E. HALL, Jr., M. MOHSENI, and Z. SAJADI

Received January 7, 1980, from the *Division of Medicinal Chemistry, School of Pharmacy, University of North Carolina, Chapel Hill, NC 27514.* Accepted for publication June 9, 1980.

Abstract □ A series of diazomethyl ketone and chloromethyl ketone analogs prepared from *N*-tosyl amino acids was shown to have anti-inflammatory activity in mice at 20 mg/kg and in rats at 10 mg/kg. *N*-Tosyl-L-alanine and *N*-tosyl-β-alanine chloromethyl ketones demonstrated the most potent anti-inflammatory activity. The writhing reflex also was inhibited at 20 mg/kg in mice. In the tail flick test, *N*-tosyl-D,L-alanine and *N*-tosyl-D,L-isoleucine chloromethyl ketones demonstrated the highest increase in time. Toxicity studies indicated good therapeutic indexes for most of these agents.

Keyphrases □ Anti-inflammatory activity—diazomethyl ketone and chloromethyl ketone analogs prepared from *N*-tosyl amino acids, biological evaluation □ *N*-Tosyl amino acids—diazomethyl ketone and chloromethyl ketone analogs, evaluation for anti-inflammatory activity

A series of *N*-tosyl, *N*-benzoyl, *N*-acetyl, *N*-carbobenzyloxy, and *N*-cinnamyl cyanomethyl esters of amino acids was shown to have anti-inflammatory and immunosuppressive activities in mice (1). The standard proteolytic inhibitor tosylphenylalanyl chloromethyl ketone also was active as an anti-inflammatory agent. This report discusses a series of diazomethyl ketones and chloromethyl ketones of *N*-tosyl amino acids that demonstrated similar activity.

EXPERIMENTAL

The synthesis and physical data of this series of compounds were reported previously (2). The synthetic methods were essentially those outlined by Schoellman and Shaw (3). Male CF_1 mice (~30 g) or male Sprague–Dawley rats (~160 g) were administered the test drugs at 20 or 10 mg/kg ip, respectively, in 0.05% polysorbate 80, 3.5 hr prior to the injection of 1% carrageenan in 0.9% saline into the plantar surface of the right hindfoot. Isotonic saline was injected into the left hindfoot to obtain baseline data. After 3 hr, both feet were excised at the tibiotarsal (ankle) joint according to a modification of the method of Winter *et al.* (4, 5).

As an analgesic screen, the tail flick (6) method was employed with male CF_1 mice (~30 g) who received the test drugs at 20 mg/kg ip 5 min prior to the analgesic test. An apparatus was designed and implemented in these laboratories to measure the tail flick response time of mice (Fig. 1). A control box housed all of the timing, logic, and sensing circuitry and the feedback controls. A secondary box provided the self-contained heater (55 ± 0.5°), the temperature-sensing elements, and special custom-made optical sensors to detect the flick of the tail. The sense signals were coupled to the control box to regulate the surface temperature and to freeze the digital clock (accuracy of 0.001%) display at the time of the first tail flick.

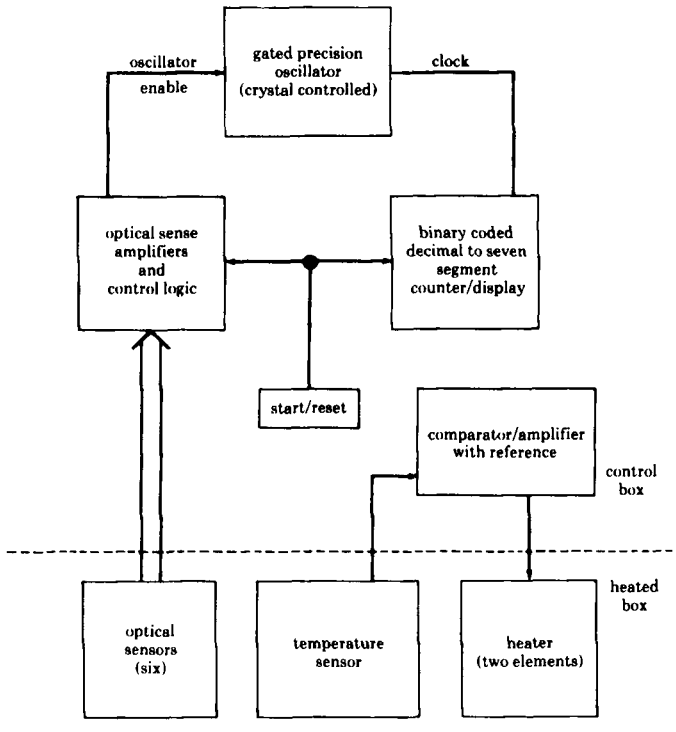

Figure 1—*Functional diagram of tail flick apparatus.*

The writhing reflex also was utilized as an analgesic test. Mice were administered the test drugs at 20 mg/kg ip 20 min prior to the administration of 0.5 ml of 0.6% acetic acid (7). After 5 min, the number of

0022-3549/80/1200-1451$01.00/0

© 1980, American Pharmaceutical Association

Table I—Anti-Inflammatory and Analgesic Activity of Diazomethyl Ketone and Chloromethyl Ketone Analogs Prepared from *N*-Tosyl Amino Acids

	Compound (n = 6)	Anti-Inflammatory Screen: Mouse at 20 mg/kg, mean[a] % inhibition ± *SD*	Anti-Inflammatory Screen: Rat at 10 mg/kg, mean % inhibition ± *SD*	Writhing Reflex at 20 mg/kg, mean % inhibition ± *SD*	Tail Flick at 20 mg/kg, mean % increase ± *SD*
I	*N*-Tosyl-L-alanine diazomethyl ketone	41 ± 2	22 ± 7	41 ± 4	168 ± 11
II	*N*-Tosyl-β-alanine diazomethyl ketone	23 ± 4	31 ± 4	43 ± 7	132 ± 9
III	*N*-Tosyl-L-valine diazomethyl ketone	25 ± 4	—	—	—
IV	*N*-Tosyl-L-leucine diazomethyl ketone	38 ± 3	48 ± 4	49 ± 7	232 ± 8
V	*N*-Tosyl-D,L-isoleucine diazomethyl ketone	34 ± 2	41 ± 9	62 ± 6	264 ± 11
VI	6-(*N*-Tosyl)aminocaproic acid diazomethyl ketone	7 ± 5[b]	—	—	—
VII	*N*-Tosyl-glycine chloromethyl ketone	29 ± 4	54 ± 4	60 ± 6	205 ± 10
VIII	*N*-Tosyl-L-alanine chloromethyl ketone	59 ± 2	61 ± 8	80 ± 3	160 ± 7
IX	*N*-Tosyl-D,L-alanine chloromethyl ketone	26 ± 4	34 ± 7	66 ± 7	419 ± 12
X	*N*-Tosyl-β-alanine chloromethyl ketone	47 ± 3	61 ± 8	62 ± 7	119 ± 10[c]
XI	*N*-Tosyl-L-valine chloromethyl ketone	39 ± 2	55 ± 6	44 ± 2	243 ± 11
XII	*N*-Tosyl-D,L-isoleucine chloromethyl ketone	45 ± 2	53 ± 7	45 ± 4	532 ± 8
XIII	*N*-Tosyl-L-proline chloromethyl ketone	53 ± 2	49 ± 7	46 ± 3	282 ± 9
XIV	6-(*N*-Tosyl)aminocaproic acid chloromethyl ketone	43 ± 2	54 ± 6	52 ± 7	215 ± 7
XV	Tosylphenylalanyl chloromethyl ketone	56 ± 2	—	—	—
XVI	Indomethacin (10 mg/kg)	74 ± 2	78 ± 8	43 ± 7	—
XVII	Phenylbutazone (50 mg/kg)	—	47 ± 5	—	—
XVIII	Morphine (1 mg/kg)	—	—	—	210 ± 7
1% Carboxymethylcellulose		0 ± 4[d]	0 ± 5[e]	0 ± 6[f]	0 ± 9[g]

[a] In the absence of a superscript, the mean inhibition is significantly higher than the control at $p \leq 0.001$. [b] Not significant. [c] $p \leq 0.010$. [d] A 59.5-mg increase in foot weight. [e] A 0.655-g increase in foot weight. [f] Seventy-eight stretch reflexes/10 min. [g] 12.21 sec for first tail flick.

stretches, characterized by repeated contractures, was counted for 10 min.

Toxicity studies were determined in male CF_1 mice (8).

RESULTS AND DISCUSSION

With the exception of VI, all of the diazomethyl ketone and chloromethyl ketone analogs of *N*-tosyl amino acids demonstrated significant anti-inflammatory activity in both mice and rats (Table I). Compounds VIII and X demonstrated the highest activity; at 20 mg/kg, they showed improved activity over phenylbutazone at 50 mg/kg in rats. In the writhing reflex, a test that mimics inflammation pain, V, VII–X, and XIV demonstrated potent activity, which was actually higher than that of indomethacin at a comparable dose. In the tail flick test, a narcotic analgesic test, the *N*-tosyl amino acid derivatives also were active and were comparable to morphine at 1 mg/kg. Although IX and XII demonstrated the best activity in the tail flick test, they did not possess the highest anti-inflammatory activity or the ability to inhibit the writhing reflex. Previous studies (2) indicated that these compounds were not toxic in mice when administered for 10 days at 20 mg/kg.

Toxicity studies in male mice indicated that I, II, IV, VI, and X–XII had an LD_{50} value of ≥400 mg/kg; VII, IX, XIII, and XIV had an LD_{50} value of >200 mg/kg. Compound V had an LD_{50} value of ≃100 mg/kg, while the value for VIII was 140 mg/kg. The solubility of the material and the limited amount of compounds curtailed further detailed studies of toxicity.

REFERENCES

(1) Z. Sajadi, M. Almahmood, L. J. Loeffler, and I. H. Hall, *J. Med. Chem.*, **22**, 1419 (1979).

(2) Z. Sajadi, M. Kashani, L. J. Loeffler, and I. H. Hall, *ibid.*, in press.

(3) G. Schoellman and E. Shaw, *Biochemistry*, **2**, 252 (1963).

(4) A. P. Roszkowski, W. H. Rooks, A. Tomolonis, and L. M. Miller, *J. Pharmacol. Exp. Ther.*, **179**, 114 (1971).

(5) C. A. Winter, E. A. Risley, and G. W. Nuss, *Proc. Soc. Exp. Biol. Med.*, **111**, 544 (1962).

(6) W. L. Dewey, L. S. Harris, J. E. Howes, and J. A. Nuit, *J. Pharmacol. Exp. Ther.*, **175**, 435 (1970).

(7) L. C. Hendershot and J. Forsaith, *ibid.*, **125**, 237 (1959).

(8) J. T. Litchfield, Jr., and F. Wilcoxon, *ibid.*, **96**, 99 (1949).

Comparison of Acidic and Enzymatic Hydrolysis Procedures for Identification of Natural Estrogens in Pharmaceutical Preparations

G. CARIGNAN ˣ **and B. A. LODGE**

Received December 13, 1979, from the *Drug Research Laboratories, Health Protection Branch, Health and Welfare Canada, Tunney's Pasture, Ottawa, Ontario, K1A 0L2 Canada.* Accepted for publication May 29, 1980.

Abstract □ The usefulness of a distinct enzyme-hydrolyzed preparation for the identification of conjugated and esterified estrogens USP was studied. No significant differences were found when the GLC identification test was performed on the acid-hydrolyzed assay preparation.

Keyphrases □ Estrogens—identification of conjugated and esterified estrogens in pharmaceutical preparations, comparison of acidic and enzymatic hydrolysis procedures for sample preparation □ Enzymatic hydrolysis—procedure for sample preparation for identification of conjugated and esterified estrogens in pharmaceutical preparations, comparison with acidic hydrolysis procedure □ GLC—identification of conjugated and esterified estrogens in pharmaceutical preparations, comparison of acidic and enzymatic hydrolyses for sample preparation

Conjugated and esterified estrogens are two types of natural estrogenic substances. Both groups are described in USP XIX (1) as a mixture of the sodium salts of the sulfate esters of the estrogenic substances, principally estrone and equilin for conjugated estrogens and estrone for esterified estrogens, that are of the type excreted by pregnant mares.

Since the publication of USP XIX, the colorimetric identification test has been replaced by a more specific GLC identification test (2) to show the presence of other complementary estrogens, in particular, α-estradiol, β-estradiol, 17α-dihydroequilin, 17β-dihydroequilin, 17α-dihydroequilenin, 17β-dihydroequilenin, 9-dehydroestrone, and equilenin. However, one major result of this test has been a substantial increase in analysis time.

This report discusses the possibility of reducing the analysis time and avoiding many of the required manipulations by using a single sample preparation for both identification and assay. The colorimetric assay described in USP requires a more purified extract than the GLC identification test. This extract is obtained by acidic hydrolysis and subsequent purification. The GLC identification test introduced recently involves a long enzymatic hydrolysis procedure (2.5 hr), resulting in an extract that is not pure enough for use in the assay.

The milder acidic hydrolysis procedure (3), developed in these laboratories to replace the USP XIX acidic hydrolysis procedure, and the USP XIX acidic hydrolysis procedure were compared to an enzymatic hydrolysis procedure (4), which was very similar to the procedure used in the USP XIX GLC identification test. Qualitative and quantitative results were obtained by the GLC procedure of McErlane and Curran (4).

Table I—Comparison of the Enzymatic Hydrolysis and the Milder Acidic Hydrolysis of a Commercial Conjugated Estrogens Formulation

Steroid	Enzyme Hydrolysis Amount[a], %	σ	CV, %	Milder Acid Hydrolysis Amount[b], %	σ	CV, %
α-Estradiol	3.9	0.18	4.6	3.5	0.12	3.3
β-Estradiol/ 17α-dihydro-equilin	15.5	0.14	0.9	15.6	0.42	2.7
17β-Dihydro-equilin	2.0	0.11	5.7	1.0	0.04	4.2
17α-Dihydro-equilenin	1.5	0.14	9.4	1.4	0.26	18.8
17β-Dihydro-equilenin	0.4	0.05	11.8	0.3	0.08	30.0
Estrone	50.2	0.98	1.9	51.7	1.09	2.1
Equilin	23.0	0.25	1.1	23.1	0.83	3.6
9-Dehydro-estrone	1.7	0.16	9.3	1.4	0.13	9.6
Equilenin	2.3	0.84	36.0	2.3	0.32	13.8
Assay, % of label claim	105.3	2.6	2.4	103.1	5.2	5.0

[a] Average of five determinations. [b] Average of seven determinations.

EXPERIMENTAL

Apparatus—The gas chromatograph[1] was equipped with a U-shaped column and a flame-ionization detector. Peak retention times and areas were obtained using a reporting integrator[2].

Acidic Hydrolysis—The residue obtained from elution with dicyclohexylamine acetate solution was dissolved in 20 ml of methanol. A few antibumping granules were added as a boiling aid. A 6.0-ml portion of hydrochloric acid of a specified concentration was added. A water condenser was placed in the neck of the flask, and the flask was placed on a steam bath so that only the liquid was immersed. After the specified time, the flask was cooled in an ice bath. The hydrolysate was extracted and purified as in the USP procedure.

For milder acidic hydrolysis, 0.6 *N* HCl (1 in 20) was used for 12.0 min. For the USP acidic hydrolysis, 2 *N* HCl (1 in 6) was used for 10 min. The stronger acidic hydrolysis required 4 *N* HCl (1 in 3) for 12 min.

Enzyme Hydrolysis—An aliquot equivalent to ~1.5 mg of conjugated estrogens in a 50-ml centrifuge tube was shaken for 30 min with 15 ml of 0.02 *M* sodium acetate (pH 5.2) and then extracted twice with 10 ml of benzene (shaken for 20 min each time). The tube was centrifuged for 10 min, and the benzene was discarded. After all traces of residual benzene had been removed, 7500 units of sulfatase enzyme[3] was added, and the tube was incubated for 30 min at 45° with occasional shaking. The tube then was cooled to room temperature, 15 ml of chloroform was added, and the tube was shaken for 15 min. After centrifugation for 10 min, the chloroform layer was filtered through anhydrous sodium sulfate and stored in a well-closed container in the refrigerator until it was used for derivatization.

Sample Derivatization—Two portions of each hydrolysate equivalent to 300 μg of estrogens were transferred to separate 5-ml polytef-lined screw-capped conical vials. To one vial was added 50 μg of ethynyl estradiol[4] (internal standard). The samples were evaporated to dryness using low heat and a gentle nitrogen stream. To the vials containing the internal standard were added 0.2 ml of pyridine and 0.05 ml of silylating reagent[5]; the vial then was capped and heated for 15 min at 60°. To the other vial (no internal standard) was added 0.2 ml of a 2% solution of methoxamine in pyridine; this sample was heated for 3 hr at 60°. After

[1] Model 2500, Bendix Corp., Ronceverte, WV 24970.
[2] Model 3385A automation system, Hewlett-Packard, Avondale, PA 19311.
[3] Sigma Chemical Co., St. Louis, MO 63172.
[4] USP reference standard.
[5] TRISIL TBT, Pierce Chemical Co., Rockford, IL 61105.

0022-3549/80/1200-1453$01.00/0
© 1980, American Pharmaceutical Association

Table II—Comparison of the Enzymatic Hydrolysis and Hydrolysis Using Three Acid Concentrations of a Commercial Conjugated Estrogens Tablet

Steroid	Enzyme Hydrolysis[a], %	Acid Hydrolysis, %		
		1 in 20[b]	1 in 6[b]	1 in 3[b]
α-Estradiol	0.8	0.8	0.8	0.8
β-Estradiol/17α-dihydroequilin	4.3	4.3	4.3	4.9
17β-Dihydroequilin	1.0	0.8	1.0	1.4
17α-Dihydroequilenin	0.5	0.5	0.5	0.5
17β-Dihydroequilenin	0.3	0.4	0.2	—[c]
Estrone	59.9	60.3	60.3	60.3
Equilin	30.0	29.7	30.0	30.1
9-Dehydroestrone	1.4	1.1	1.1	—[c]
Equilenin	2.1	2.1	1.9	2.0
Assay, % of label claim	118.7	112.1	117.3	114.9

[a] Average of two determinations. [b] Sufficient materials to perform a single determination only. [c] Peaks were present but had an area less than the area reject setting.

this time, 0.05 ml of silylating reagent was added, and the solution was heated at 60° for 10 min.

A 2–4-μl aliquot was injected into a 1.8-m × 0.63-cm o.d. (6 ft × 0.25 in.) glass U-shaped column packed with 3% methyl phenyl cyanopropyl silicone[6] (OV-225) on 100–120-mesh Chromosorb WHP[7]. The temperature was maintained at 225°, and the helium flow rate was 50 ml/min.

RESULTS AND DISCUSSION

Results from the milder acidic hydrolysis (assay preparation) and the enzymatic hydrolysis (test preparation) in the identification of a commercial conjugated estrogens formulation, which fully met requirements of the previous colorimetric identification test, are shown in Table I. Average amounts, standard deviations, and coefficients of variation (CV) are given for each component.

The distinctive estrone and equilin peaks and the prominent β-estradiol/17α-dihydroequilin peak[8] showed the same relative amounts, within experimental error, with both hydrolysis procedures. Moreover, the relative amounts of other additional minor peaks (α-estradiol, 17β-dihydroequilin, 17α-dihydroequilenin, 17β-dihydroequilenin, 9-dehydroestrone, and equilenin) were very similar to each other.

Reproducibility was good for the major peaks ($CV \leq 3.6\%$) but decreased in proportion to the concentration of the minor peaks.

The robustness of the acidic hydrolysis procedure was studied. Table II shows a comparison of the enzymatic hydrolysis and three different acidic hydrolyses where the acid concentration was varied (0.6, 2, and 4 N) for the identification of conjugated estrogens tablets that were bor-

[6] Ohio Valley Specialties Chemical, Marietta, OH 45750.
[7] Chromatographic Specialties, Brockville, Ontario, K6V SW1, Canada.
[8] The procedure does not resolve these two components.

Table III—Comparison of the Enzymatic Hydrolysis and the Milder Acidic Hydrolysis of a Commercial Esterified Estrogens Product

Steroid	Enzyme Hydrolysis[a], %	Acid Hydrolysis[b], %
α-Estradiol	1.6	1.2
β-Estradiol/17α-dihydroequilin	5.8	5.4
17β-Dihydroequilin	0.4	0.3
17α-Dihydroequilenin	0.8	0.6
17β-Dihydroequilenin	0.2	—[b]
Estrone	78.1	79.4
Equilin	11.8	12.1
9-Dehydroestrone	0.5	0.3
Equilenin	0.7	0.7
Assay, % of label claim	114.2	112.3

[a] Single determination. [b] Peak was present but had an area less than the area reject setting.

derline in the colorimetric identification test. No major differences were seen for all of the individual components among the enzymatic, milder acidic, and USP acidic hydrolyses. The only differences were a small increase of β-estradiol/17α-dihydroequilin and a small decrease of 17β-dihydroequilenin and 9-dehydroestrone in the acidic procedures.

The results in Table III show that the two hydrolysis procedures also are applicable to the identification of commercial esterified estrogens products. The small differences between the results obtained with the two procedures are not important and do not lead to any misinterpretations. Several other benefits are derived from the use of the acidic hydrolysis procedure. The assay preparation is a much cleaner extract than the enzymatic identification test preparation. The presence of equol (5) is no longer a problem; it is removed in the early chromatographic column step by benzene washing. Chromatograms exhibit less tailing, the detector background signal is reduced, and column lifetime is much longer.

In summary, the assay preparation obtained by the milder hydrolysis or by the USP acid hydrolysis gave identification test results for conjugated and esterified estrogens formulations comparable to the new enzyme-hydrolyzed identification test preparation. Since it is unnecessary to prepare the latter, the analysis time is shortened and the expense of enzyme reagents is avoided.

REFERENCES

(1) "The United States Pharmacopeia," 19th rev., Mack Publishing Co., Easton, Pa., 1975, p. 181.

(2) "The United States Pharmacopeia," 19th rev., 3rd suppl., Mack Publishing Co., Easton, Pa., 1975, p. 61.

(3) G. Carignan and B. A. Lodge, *Can. J. Pharm. Sci.*, **11**, 76 (1976).

(4) K. M. McErlane and N. M. Curran, *J. Pharm. Sci.*, **66**, 523 (1977).

(5) G. Carignan, N. M. Curran, B. A. Lodge, and K. M. McErlane, *Can. J. Pharm. Sci.*, **13**, 73 (1978).

Comparative Pharmacokinetics of Butylated Hydroxyanisole and Butylated Hydroxytoluene in Rabbits

RAGAB EL-RASHIDY * **and SARFARAZ NIAZI** ˣ

Received November 19, 1979, from the *Department of Pharmacy, College of Pharmacy, University of Illinois at the Medical Center, Chicago, IL 60680.* Accepted for publication June 16, 1980. *Present address: G. D. Searle & Company, Skokie, IL 60076.

Abstract □ The widespread use of butylated hydroxyanisole (I) and butylated hydroxytoluene (II) as food antioxidants recently has been criticized by the Food and Drug Administration because of their pharmacological and toxicological effects. Interest also has arisen recently in the use of these compounds as anticancer agents. The purposes of this study were to evaluate the pharmacokinetics of I and II in rabbits and to compare their physicochemical properties with their disposition kinetics. It was found that I has a disposition half-life of ~1 hr, compared to 11 days for II. These differences are explained in terms of their lipid solubility and protein binding characteristics.

Keyphrases □ Butylated hydroxyanisole—pharmacokinetics, rabbits □ Butylated hydroxytoluene—pharmacokinetics, rabbits □ Antioxidants—butylated hydroxyanisole and butylated hydroxytoluene, pharmacokinetics, rabbits □ Pharmacokinetics—butylated hydroxyanisole and butylated hydroxytoluene, rabbits

Butylated hydroxyanisole (I) and butylated hydroxytoluene (II) are the most commonly used food antioxidants in the United States (1). Although I and II generally are regarded as safe, recent actions by the Food and Drug Administration have been directed toward restricting their use (2) because of their pharmacological and toxicological effects (3–7). Moreover, these compounds recently were reported to possess anticancer characteristics (8, 9). Although no specific biochemical pathways have been suggested for their action in inhibiting chemical carcinogenesis, these mechanisms may involve alteration of the metabolism of the chemical carcinogens (10) and blocking of hydrocarbon free radical–DNA complex formation (11).

Despite widespread interest in I and II, whose structures differ only by a *tert*-butyl group, there have been no reports of their pharmacokinetic properties based on blood levels and no reports of their effectiveness and toxicity. The purposes of this study were to monitor the disposition kinetics of I and II following single intravenous dosing in rabbits and to relate their pharmacokinetic parameters to their physicochemical properties.

EXPERIMENTAL

Materials and Equipment—Butylated hydroxyanisole[1] (I), butylated hydroxytoluene[1] (II), dibutylated hydroxyanisole[2], polyethylene glycol 400[3], an infusion set[4], a catheter placement unit[5] (20 gauge), sterile disposable syringes[6], an infusion pump[7], and a gas chromatograph[8] were used.

Formulations of Intravenous Dosage Form—Solutions of I and II (10 mg/ml) were prepared in polyethylene glycol 400–normal saline (1:1), which was sterilized by heating at 100° for ~1 hr over a hot plate.

[1] Nutritional Biochemical Co., Cleveland, Ohio.
[2] Universal Oil Product Co., Des Plaines, Ill.
[3] Fisher Scientific Co., Fair Lawn, N.J.
[4] Abbott Laboratories, North Chicago, Ill.
[5] Jelco Laboratories, Raritan, N.J.
[6] Becton, Dickinson and Co., Rutherford, N.J.
[7] Sage Instruments, Cambridge, Mass.
[8] Varian Aerograph model 1400, Varian, Park Ridge, Ill.

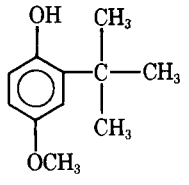

I

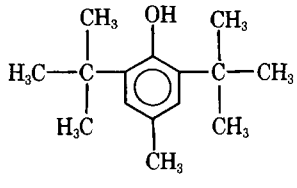

II

Animal Procedure—New Zealand White male rabbits, 2.9–3.2 kg, were used; food and water were withheld prior to and for 12 hr after drug administration. The marginal ear vein was cannulated using a 20-gauge catheter for sample collection. The I and II solutions were infused for <2 min at a constant rate of 2 ml/min to provide a total dose of 10 mg/kg. At the end of infusion, the cannula was flushed with 5 ml of heparinized sterile normal saline.

The blood samples (1.5 ml) were collected from the catheter placed in the other ear at 0, 0.085, 0.173, 0.33, 0.50, 0.75, 1, 1.5, 2.0, 3.0, 4.0, 6.0, and 12 hr and thereafter twice per day for 2 days and daily for 3 days. The zero time for sampling was assigned when the infusion was completed. A blank blood sample was obtained before the solution was infused to obtain the baseline on the gas chromatogram.

Blood Analysis—All blood samples were analyzed for their concentration of I and II using a highly sensitive and specific GLC method (12).

RESULTS AND DISCUSSION

The absorption of I and II was reported to vary significantly when given orally as a suspension in milk–olive oil and as a gelatin capsule to humans (13). Therefore, an intravenous dosage form was chosen to avoid complications due to absorption variability. The maximum allowable intake of I and II is 2 mg/kg/day, but there are indications that the per capita daily intake is >5 mg/kg (2). Thus, the dose of 10 mg/kg used in this study may represent the level of exposure for numerous people who consume many processed foods.

Pharmacokinetics of Butylated Hydroxyanisole (I)—The plasma concentrations obtained at different time intervals following a single intravenous dose (10 mg/kg) were plotted on a semilogarithmic scale, assigning time zero as the midpoint of infusion, and the data were fitted by a monoexponential model using a programmable calculator (14) (Fig. 1). This model suggests that the body behaves as a homogeneous compartment for I in terms of the equilibrium rates among various body tissues (15):

$$C_p = C_p^0 e^{-kt} \quad \text{(Eq. 1)}$$

It was reported that at low concentration (<100 μg/ml), the percent of

Table I—Pharmacokinetic Parameters of I in Rabbits after a Single Intravenous 10-mg/kg Dose

Parameter	Mean ± *SEM* (n = 4)
Body weight, kg	2.98 ± 0.20
C_p^0, mg/liter	1.298 ± 0.095
k_{el}, hr^{-1}	0.7427 ± 0.14
$t_{1/2}$, hr	1.055 ± 0.23
V_d, liters/kg	7.48 ± 0.64
TBC^a, liters/hr/kg	5.24 ± 0.50
AUC^b, (mg hr)/liter/kg	0.685 ± 0.13

[a] Total body clearance. [b] Area under the curve.

0022-3549/80/1200-1455$01.00/0
© 1980, American Pharmaceutical Association

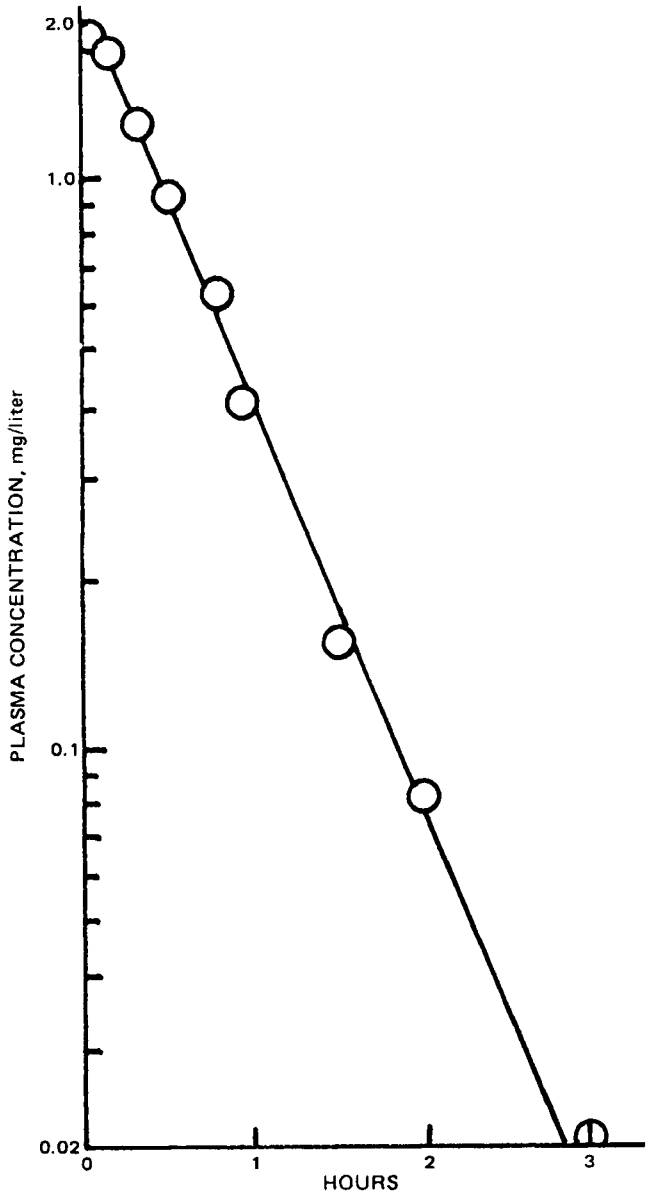

Figure 1—*Plasma concentration profile of I in a rabbit following intravenous administration of a 10-mg/kg dose.*

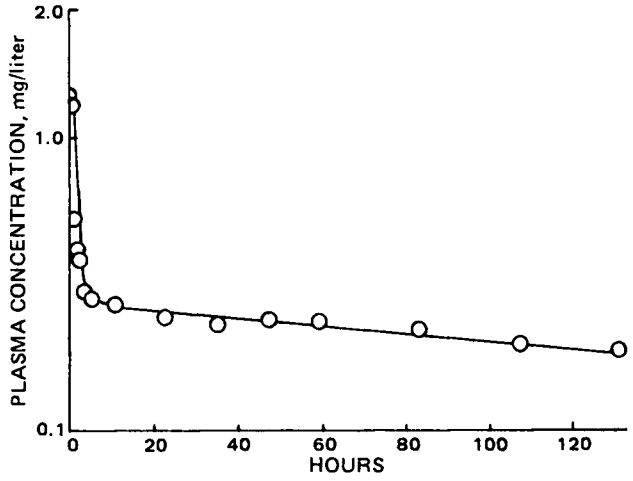

Figure 2—*Plasma concentration profile of II in a rabbit following intravenous administration of a 10-mg/kg dose.*

total I bound to human serum albumin was inversely proportional to the total concentration (16). Since >59% of the total exchangeable albumin is located in the extravascular compartments such as the skin and muscles (17), the human body can be conceived of as a large pool for I. In addition, the probable binding of I to other components of different tissues and fluids makes its distribution more extensive throughout the body, causing exposure of deep body tissues.

The estimates of C_p^0, $t_{1/2}$, V_d, and k_{el} reported in Table I were obtained from least-squares data fitting. In spite of the large volume of distribution (mean = 7.48 liters/kg), I disappears from the plasma very rapidly (mean $t_{1/2}$ = 1 hr). Thus, despite extensive distribution, fast clearance is achieved due to the highly reversible nature of its storage in the body tissues.

Pharmacokinetics of Butylated Hydroxytoluene (II) (Fig. 2)—The disposition of II in animals and in humans is complicated by the presence of two *tert*-butyl groups at *ortho*-positions of the phenolic group. More than 10 metabolites of II have been isolated (18, 19). Significant biliary excretion also has been reported in rats, rabbits, and dogs. Daniel *et al.* (5) recovered ~67% of an oral dose of [^{14}C]II in human urine samples collected over an 11-day period. They concluded that intact II and/or its metabolites first are stored in the tissues and then are slowly released after a pseudoequilibrium, which takes ~5 days, indicating extensive uptake by tissues (5).

The plasma concentration–time profiles of II were, unlike I, characterized by:

$$C_p = Ae^{-\alpha t} + Be^{-\beta t} \qquad \text{(Eq. 2)}$$

where A and B are constants and α and β are complex rate constants. The estimation of A, B, α, and β was made using a programmable calculator (14). The pharmacokinetic parameters are reported in Table II. The fast disposition phase half-life of II was ~1 hr, and the slow disposition phase decayed with a half-life of >11 days. These data suggest rapid accumulation and slow clearance from the body, in agreement with earlier speculations for II (5).

A comparison of the disposition of I and II in rabbits clearly reveals large differences between their distribution and elimination characteristics. Whereas the accumulation of I does not appear to be a serious problem, II tends to be stored in body tissues upon multiple dosing, as encountered in daily life exposure to this compound. Based on the following equation, more than a 16-fold accumulation of II is possible on daily exposure whereas the accumulation is negligible for I:

$$\text{accumulation} = 1/1 - e^{-k\mathrm{T}} \qquad \text{(Eq. 3)}$$

where k is the terminal disposition rate constant and T is the frequency of exposure.

Such large differences in the *in vivo* kinetic properties of I and II occur because of the additional *tert*-butyl group in II. This structural change renders II more lipid soluble, explaining the approximately threefold increase in the final volume of distribution while the volume of the central compartment remains identical for both compounds. Since the volume of the central compartment does not change, an increase of over 100-fold in the total body clearance results from a change in the elimination rate constant from the central compartment (k_{el}).

The distribution characteristics of I and II also can be related to their plasma protein binding characteristics. The volumes of distribution often are inversely related to the extent of plasma protein binding (17), especially for compounds that have weaker association constants, such as I

Table II—Pharmacokinetic Parameters of II in Rabbits after a Single Intravenous 10-mg/kg Dose

Parameter[a]	Mean ± *SEM* (n = 4)
A, mg/liters	1.0402 ± 0.26
B, mg/liters	0.4535 ± 0.025
α, hr^{-1}	0.7841 ± 0.073
β, hr^{-1}	0.00258 ± 0.0008
k_{21}, hr^{-1}	0.2639 ± 0.06
k_{10}, hr^{-1}	0.00760 ± 0.0013
k_{12}, hr^{-1}	0.5152 ± 0.057
V_d, liters/kg	7.31 ± 1.18
TBC[b], liters/hr/kg	0.0551 ± 0.013
V_{deg}, liters/kg	21.13 ± 1.29
AUC[c], (mg hr)/liter/kg	208.9 ± 35.5

[a] $C_p = Ae^{-\alpha t} + Be^{-\beta t}$, where t is in hours and C_p is in milligrams per liter. [b] Total body clearance. [c] Area under the curve.

and II (16, 18). The binding constant for I reported from this laboratory was $2 \times 10^{-3} M^{-1}$ and that for II was $3 \times 10^{4} M^{-1}$. The number of binding sites was ~2.6 for I and 0.25 for II (20). Thus, increased lipid solubility of II results in its increased strength of interaction with albumin molecules, but the steric hindrance due to the additional *tert*-butyl group makes the extent of binding only about 10% of that observed for I. Thus, the total exchangeable albumin present in the extravascular compartments provides a large pool for possible storage of I but not for II, which probably is taken up by the body fatty tissues due to its higher lipid solubility (5).

REFERENCES

(1) WHO Technical Report Series, No. 488, 1971.

(2) *Fed. Regist.*, 42(104, May 31) (1977).

(3) P. H. Grantham, J. H. Weisburger, and E. K. Weisburger, *Food Cosmet. Toxicol.*, **11**, 209 (1973).

(4) R. Tye, J. D. Engel, and I. Rapien, *ibid.*, **3**, 547 (1965).

(5) J. W. Daniel, J. C. Gage, D. J. Jones, and M. A. Stevens, *ibid.*, **5**, 475 (1967).

(6) W. Snipes, S. Person, A. Keith, and J. Cupp, *Science*, **188**, 64 (1975).

(7) I. F. Gaunt, D. Glibert, and D. Martin, *Food Cosmet. Toxicol.*, **3**, 445 (1965).

(8) T. J. Slaga and W. J. Brecken, *Cancer Res.*, **37**, 1631 (1977).

(9) L. K. T. Lam and L. W. Wattenberg, *J. Natl. Cancer Inst.*, **58**, 413 (1977).

(10) P. A. Craven and F. R. DeRubertis, *Cancer Res.*, **37**, 4088 (1977).

(11) E. Krzywansaka and L. Pierkarski, *Neoplasma*, **24**, 4 (1977).

(12) R. El-Rashidy and S. Niazi, *J. Pharm. Sci.*, **68**, 103 (1979).

(13) B. D. Astill, J. Mills, D. W. Fassett, R. L. Roudabush, and J. Terhaar, *Ag. Food Chem.*, **10**, 315 (1962).

(14) S. Niazi, *Int. J. Biomed. Comput.*, **10**, 245 (1979).

(15) S. Niazi, "Textbook of Biopharmaceutics and Clinical Pharmacokinetics," Appleton-Century-Crofts, New York, N.Y., 1979.

(16) R. El-Rashidy and S. Niazi, *J. Pharm. Sci.*, **67**, 967 (1978).

(17) W. J. Jusko and M. Gretch, *Metab. Rev.*, **5**, 43 (1976).

(18) M. Akagi and L. Aogi, *Chem. Pharm. Bull.*, **10**, 161 (1962).

(19) *Ibid.*, **10**, 200 (1962).

(20) R. El-Rashidy, Ph.D. dissertation, University of Illinois at the Medical Center, Chicago, Ill., 1979.

ACKNOWLEDGMENTS

Abstracted in part from a thesis submitted by R. El-Rashidy to the University of Illinois in partial fulfillment of the Doctor of Philosophy degree requirements.

Supported by a grant from the Graduate College, University of Illinois at the Medical Center.

Human Whole Blood and Parotid Saliva Concentrations of Oral and Intramuscular Promethazine

G. JOHN DiGREGORIO ˣ and EILEEN RUCH

Received February 13, 1980, from the *Department of Pharmacology, Hahnemann Medical College, Philadelphia, PA 19102.* Accepted for publication June 20, 1980.

Abstract □ Ten healthy male subjects received 25 mg of promethazine intramuscularly, followed within 3 weeks by oral administration of 25 mg. Whole blood and parotid saliva were collected over a 12-hr period after drug administration. Promethazine was quantitated by high-performance liquid chromatography. After intramuscular administration, the promethazine concentrations were 3.0–22.4 ng/ml in blood and 0.9–2.8 ng/ml in parotid saliva. After oral administration, the promethazine concentrations were 1.4–5.5 ng/ml in blood and 0.2–0.8 ng/ml in parotid saliva. The peak blood promethazine concentration after the intramuscular dose was four times higher than that following the oral dose, which indicates that promethazine possesses an extensive first-pass effect. The mean parotid saliva to whole blood ratio (S/B) was calculated to be 0.24 after the intramuscular route and 0.20 after the oral route over the 12-hr period. The calculated percentage of free drug in the blood was 20–24% of the whole blood concentration determined from the S/B ratio.

Keyphrases □ Promethazine—whole blood and parotid saliva concentrations following oral and intramuscular administration □ High-performance liquid chromatography—analysis, promethazine, whole blood and parotid saliva concentrations following oral and intramuscular administration □ Phenothiazines—promethazine, high-performance liquid chromatographic analysis in whole blood and parotid saliva following oral and intramuscular administration

Several investigators have reported analytical methods for the determination of phenothiazines, including colorimetric (1), spectrofluorometric (2), spectrophotometric (3), GLC (4, 5), and liquid chromatographic (6) procedures. However, little or no information is available on the quantitation of promethazine in therapeutic doses in human whole blood or parotid saliva.

This report presents a sensitive method for the detection and quantitation of promethazine in whole blood and parotid saliva after the administration of 25 mg of promethazine orally and intramuscularly in human volunteers. Parotid saliva to blood promethazine concentration ratios were calculated, and the bioavailability of promethazine was compared for the two routes of administration.

EXPERIMENTAL

Materials—Powdered promethazine[1] and promazine[1], the internal standard, were used without further purification as the analytical standards. Commercially available promethazine tablets[1] and injectable liquid[1] were obtained from a local pharmacy. All solvents and reagents were analytical reagent grade, except for methanol[2], which was high-performance liquid chromatographic (HPLC) grade. All glassware was coated with silicone[3] by the method described on the package insert.

Apparatus—The liquid chromatograph[4] was fitted with a loop injector and a fixed-wavelength UV detector (254 nm). A 1-mv recorder[5] was attached to the chromatograph. The detector was attenuated at 0.005 aufs.

Column—A prepacked, 300 × 3.9-mm i.d., μBondapak CN column[6] was run at ambient temperature.

[1] Wyeth Laboratories, Philadelphia, Pa.
[2] Fischer Chemical Co., King of Prussia, Pa.
[3] Siliclad, Clay Adams, New York, N.Y.
[4] Model 200, Waters Associates, Milford, Mass.
[5] Perkin-Elmer Corp., Norwalk, Conn.
[6] Waters Associates, Milford, Mass.

0022-3549/80/1200-1457$01.00/0

© 1980, American Pharmaceutical Association

and II (16, 18). The binding constant for I reported from this laboratory was $2 \times 10^{-3} M^{-1}$ and that for II was $3 \times 10^{4} M^{-1}$. The number of binding sites was ~2.6 for I and 0.25 for II (20). Thus, increased lipid solubility of II results in its increased strength of interaction with albumin molecules, but the steric hindrance due to the additional *tert*-butyl group makes the extent of binding only about 10% of that observed for I. Thus, the total exchangeable albumin present in the extravascular compartments provides a large pool for possible storage of I but not for II, which probably is taken up by the body fatty tissues due to its higher lipid solubility (5).

REFERENCES

(1) WHO Technical Report Series, No. 488, 1971.

(2) *Fed. Regist.*, 42(104, May 31) (1977).

(3) P. H. Grantham, J. H. Weisburger, and E. K. Weisburger, *Food Cosmet. Toxicol.*, **11**, 209 (1973).

(4) R. Tye, J. D. Engel, and I. Rapien, *ibid.*, **3**, 547 (1965).

(5) J. W. Daniel, J. C. Gage, D. J. Jones, and M. A. Stevens, *ibid.*, **5**, 475 (1967).

(6) W. Snipes, S. Person, A. Keith, and J. Cupp, *Science*, **188**, 64 (1975).

(7) I. F. Gaunt, D. Glibert, and D. Martin, *Food Cosmet. Toxicol.*, **3**, 445 (1965).

(8) T. J. Slaga and W. J. Brecken, *Cancer Res.*, **37**, 1631 (1977).

(9) L. K. T. Lam and L. W. Wattenberg, *J. Natl. Cancer Inst.*, **58**, 413 (1977).

(10) P. A. Craven and F. R. DeRubertis, *Cancer Res.*, **37**, 4088 (1977).

(11) E. Krzywansaka and L. Pierkarski, *Neoplasma*, **24**, 4 (1977).

(12) R. El-Rashidy and S. Niazi, *J. Pharm. Sci.*, **68**, 103 (1979).

(13) B. D. Astill, J. Mills, D. W. Fassett, R. L. Roudabush, and J. Terhaar, *Ag. Food Chem.*, **10**, 315 (1962).

(14) S. Niazi, *Int. J. Biomed. Comput.*, **10**, 245 (1979).

(15) S. Niazi, "Textbook of Biopharmaceutics and Clinical Pharmacokinetics," Appleton-Century-Crofts, New York, N.Y., 1979.

(16) R. El-Rashidy and S. Niazi, *J. Pharm. Sci.*, **67**, 967 (1978).

(17) W. J. Jusko and M. Gretch, *Metab. Rev.*, **5**, 43 (1976).

(18) M. Akagi and L. Aogi, *Chem. Pharm. Bull.*, **10**, 161 (1962).

(19) *Ibid.*, **10**, 200 (1962).

(20) R. El-Rashidy, Ph.D. dissertation, University of Illinois at the Medical Center, Chicago, Ill., 1979.

ACKNOWLEDGMENTS

Abstracted in part from a thesis submitted by R. El-Rashidy to the University of Illinois in partial fulfillment of the Doctor of Philosophy degree requirements.

Supported by a grant from the Graduate College, University of Illinois at the Medical Center.

Human Whole Blood and Parotid Saliva Concentrations of Oral and Intramuscular Promethazine

G. JOHN DiGREGORIO ˣ and EILEEN RUCH

Received February 13, 1980, from the *Department of Pharmacology, Hahnemann Medical College, Philadelphia, PA 19102.* Accepted for publication June 20, 1980.

Abstract □ Ten healthy male subjects received 25 mg of promethazine intramuscularly, followed within 3 weeks by oral administration of 25 mg. Whole blood and parotid saliva were collected over a 12-hr period after drug administration. Promethazine was quantitated by high-performance liquid chromatography. After intramuscular administration, the promethazine concentrations were 3.0–22.4 ng/ml in blood and 0.9–2.8 ng/ml in parotid saliva. After oral administration, the promethazine concentrations were 1.4–5.5 ng/ml in blood and 0.2–0.8 ng/ml in parotid saliva. The peak blood promethazine concentration after the intramuscular dose was four times higher than that following the oral dose, which indicates that promethazine possesses an extensive first-pass effect. The mean parotid saliva to whole blood ratio (S/B) was calculated to be 0.24 after the intramuscular route and 0.20 after the oral route over the 12-hr period. The calculated percentage of free drug in the blood was 20–24% of the whole blood concentration determined from the S/B ratio.

Keyphrases □ Promethazine—whole blood and parotid saliva concentrations following oral and intramuscular administration □ High-performance liquid chromatography—analysis, promethazine, whole blood and parotid saliva concentrations following oral and intramuscular administration □ Phenothiazines—promethazine, high-performance liquid chromatographic analysis in whole blood and parotid saliva following oral and intramuscular administration

Several investigators have reported analytical methods for the determination of phenothiazines, including colorimetric (1), spectrofluorometric (2), spectrophotometric (3), GLC (4, 5), and liquid chromatographic (6) procedures. However, little or no information is available on the quantitation of promethazine in therapeutic doses in human whole blood or parotid saliva.

This report presents a sensitive method for the detection and quantitation of promethazine in whole blood and parotid saliva after the administration of 25 mg of promethazine orally and intramuscularly in human volunteers. Parotid saliva to blood promethazine concentration ratios were calculated, and the bioavailability of promethazine was compared for the two routes of administration.

EXPERIMENTAL

Materials—Powdered promethazine[1] and promazine[1], the internal standard, were used without further purification as the analytical standards. Commercially available promethazine tablets[1] and injectable liquid[1] were obtained from a local pharmacy. All solvents and reagents were analytical reagent grade, except for methanol[2], which was high-performance liquid chromatographic (HPLC) grade. All glassware was coated with silicone[3] by the method described on the package insert.

Apparatus—The liquid chromatograph[4] was fitted with a loop injector and a fixed-wavelength UV detector (254 nm). A 1-mv recorder[5] was attached to the chromatograph. The detector was attenuated at 0.005 aufs.

Column—A prepacked, 300 × 3.9-mm i.d., μBondapak CN column[6] was run at ambient temperature.

[1] Wyeth Laboratories, Philadelphia, Pa.
[2] Fischer Chemical Co., King of Prussia, Pa.
[3] Siliclad, Clay Adams, New York, N.Y.
[4] Model 200, Waters Associates, Milford, Mass.
[5] Perkin-Elmer Corp., Norwalk, Conn.
[6] Waters Associates, Milford, Mass.

0022-3549/80/1200-1457$01.00/0

© 1980, American Pharmaceutical Association

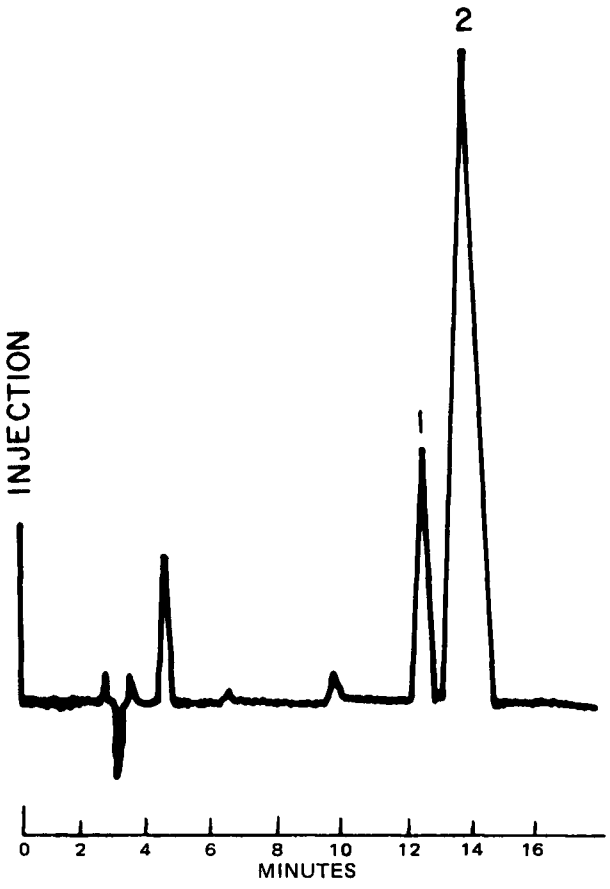

Figure 1—*Typical high-performance liquid chromatogram of (1) promethazine and the internal standard (2), promazine.*

Mobile Phase—A solution of 1% acetic acid in 0.005 *M* heptanesulfonic acid and methanol (50:50) was used. The mixture was pumped isocratically through the column at a flow rate of 2 ml/min.

Method—Ten healthy male volunteers, 25–57 years, participated in the crossover study. Complete histories and physical examinations, including blood and urine chemistries, were performed before and after the experiments. Each subject initially was given 25 mg of promethazine intramuscularly, followed in 3 weeks by 25 mg orally.

The subjects fasted for a minimum of 12 hr prior to each experiment. Baseline parotid saliva and blood samples were taken before each experiment. Parotid saliva samples were collected by means of a modified double-lumen parotid cup (7). Orange-flavored lozenges[7] served as a reflex stimulus to induce salivation, and the resultant parotid secretions were collected in silicone-coated graduated test tubes. At least 5 ml of parotid saliva was collected over a period not exceeding 10 min. Blood samples (10 ml) were collected in silicone-coated vacuum tubes[8] containing 143 IU of heparin sodium.

After intramuscular administration of 25 mg of promethazine, venous blood and parotid saliva samples were taken at 0.5, 1, 2, 4, 6, 8, and 12 hr. To make certain that the subjects returned to baseline levels, 3 weeks was allowed between experiments. At that time, the same 10 subjects were given 25 mg of promethazine orally; blood and parotid saliva samples were collected at the same time intervals.

Whole blood (5 ml) or parotid saliva (5 ml) was added to 1 ml of 1 *N* NaOH. Promazine, which was chosen as the internal standard because of the similarity of its structure and chemical properties to promethazine, was dissolved in the mobile phase, and 25 ng was added to the whole blood or parotid saliva sample before extraction. The sample then was shaken with 25 ml of heptane for 10 min and centrifuged for 5 min.

The heptane layer was removed by aspiration with a siliconized Pasteur pipet and allowed to evaporate under a steady stream of air at 55°. The residue was redissolved in 50 μl of the mobile phase, and 10 μl was injected into the liquid chromatograph. Quantitation was performed using the method of internal standards by measuring the peak heights and comparing the peak height ratios to a calibration curve. The sensitivity of the method was tested by the extraction of various concentrations of promethazine in blood and saliva and determination of the smallest detectable peak on the liquid chromatograph.

[7] Regal Crown Sour Orange, Trebor Sharps Ltd., London, England.
[8] Venojet, Kimble-Terumo, Elkton, Md.

Table I—Whole Blood and Parotid Saliva Concentrations of Promethazine Administered Intramuscularly

Hours	Saliva[a], ng/ml	Blood[a], ng/ml
0.5	1.9 ± 0.36	6.4 ± 0.86
1	2.5 ± 0.33	8.3 ± 1.96
2	2.8 ± 0.52	14.2 ± 3.38
4	2.2 ± 0.25	22.4 ± 5.90
6	2.4 ± 0.36	8.3 ± 0.91
8	1.5 ± 0.31	8.5 ± 2.50
12	0.9 ± 0.40	3.0 ± 0.84

[a] Mean concentration (±*SE*) of promethazine in 10 human volunteers after the intramuscular administration of 25 mg.

RESULTS AND DISCUSSION

The separation and identification of promethazine by HPLC are illustrated in Fig. 1. The retention time for promethazine was 12.6 min; the internal standard, promazine, had a retention time of 13.8 min. The separation was reproducible and sensitive in both extracted whole blood and parotid saliva. The sensitivity of promethazine was 0.2 ng on-column by this procedure. Standard concentration curves for spiked whole blood and parotid saliva were linear between 2.5 and 50 ng/ml (blood) and between 0.5 and 10 ng/ml (parotid saliva).

The mean (±*SE*) whole blood and parotid saliva promethazine concentrations in the 10 subjects receiving 25 mg intramuscularly are presented in Table I. The range of promethazine concentrations determined in whole blood and parotid saliva was 0.9–22.4 ng/ml over the 12-hr period. The blood promethazine concentration peaked within 4 hr (22.4 ± 5.90 ng/ml) but fell rapidly over the next 2 hr to 8.3 ± 0.91 ng/ml and then declined slowly over the next 6 hr to 3.0 ± 0.84 ng/ml. The parotid saliva concentrations peaked within 2 hr (2.8 ± 0.52 ng/ml) and declined more slowly than the plasma to 0.9 ± 0.40 ng/ml over the next 10 hr. The calculated saliva to blood (*S/B*) ratio ranged between 0.10 and 0.30, with a mean of 0.24, over the 12-hr period.

The mean (±*SE*) whole blood and parotid saliva promethazine concentrations in the 10 subjects receiving 25 mg orally are listed in Table II. The range of promethazine concentrations determined in whole blood and parotid saliva was 0.2–5.5 ng/ml over the 12 hr. The blood promethazine concentrations peaked within 2 hr (5.5 ± 1.4 ng/ml) and declined to 1.4 ± 0.2 ng/ml within the next 6 hr. The parotid saliva concentration was elevated consistently between 1 and 6 hr after drug administration. Only at the 8-hr period did it fall from 0.8 to 0.2 ng/ml. The calculated saliva to blood ratio ranged between 0.13 and 0.29, with a mean of 0.20, over the 8-hr period.

The results indicate that the bioavailability of orally or intramuscularly administered promethazine in therapeutic doses can be determined by HPLC. This analytical method was sensitive enough to detect and quantitate parotid saliva concentrations of promethazine during the corresponding times in which whole blood concentrations were determined. The sensitivity of the assay was suitable for detection of pro-

Table II—Whole Blood and Parotid Saliva Concentrations of Promethazine Administered Orally

Hours	Saliva[a], ng/ml	Blood[a], ng/ml
0.5	0.4 ± 0.2	2.5 ± 0.5
1	0.8 ± 0.2	2.9 ± 0.5
2	0.7 ± 0.1	5.5 ± 1.4
4	0.8 ± 0.2	3.8 ± 0.7
6	0.8 ± 0.2	2.8 ± 0.8
8	0.2 ± 0.1[b]	1.4 ± 0.2[b]
12	0	0

[a] Mean concentration (±*SE*) of promethazine in 10 human volunteers after the oral administration of 25 mg. [b] Estimated values from standard concentration curves.

methazine concentrations as low as 0.2 ng/ml of saliva or blood, a 50-fold increase in sensitivity over that reported previously for a GLC procedure (5).

After the administration of equal doses of promethazine (25 mg), the peak blood concentrations were significantly different after oral and intramuscular administration. The peak whole blood concentration (22.4 ng/ml) after intramuscular administration was approximately four times higher than that (5.5 ng/ml) after oral administration. The results indicate that promethazine possesses a significant first-pass effect through the liver. Other investigators have demonstrated that promethazine has an extensive first-pass effect, accounting for lower blood levels after oral administration compared to parenteral administration (5). After oral administration of 25 mg, the elimination half-life of promethazine was 3.3 hr as determined from plasma levels measured over the 8-hr period.

The present results indicate that the mean parotid saliva to whole blood promethazine ratios after oral (0.20) and intramuscular (0.24) administration did not significantly differ from each other. Previous studies involving saliva to blood ratios of other drugs consistently showed that saliva drug concentrations correlated with the blood free drug concentrations and that percentages of free drug in blood could be determined from the calculated saliva to blood ratios (7–9). In this study, the ratios of 0.20 and 0.24 indicate that the free form of promethazine in blood ranged between 20 and 24%, meaning that it was bound 80 and 76% to whole blood.

REFERENCES

(1) M. Tarasiewicz, *Acta Pol. Pharm.*, **29**, 578 (1972).

(2) S. L. Tompsett, *Acta Pharmacol. Toxicol.*, **26**, 298 (1968).

(3) J. E. Wallace and J. D. Biggs, *J. Pharm. Sci.*, **60**, 1346 (1971).

(4) A. DeLeenheer, *J. Chromatogr.*, **77**, 339 (1973).

(5) J. Quinn and R. Calvert, *J. Pharm. Pharmacol.*, **28**, 59P (1976).

(6) W. Lindner, R. W. Frei, and W. Santi, *J. Chromatogr.*, **108**, 299 (1975).

(7) G. J. DiGregorio, A. J. Piraino, and E. Ruch, *Drug Alcohol Depend.*, **3**, 43 (1978).

(8) G. J. DiGregorio, A. J. Piraino, and E. Ruch, *Clin. Pharmacol. Ther.*, **6**, 720 (1978).

(9) G. J. DiGregorio, A. J. Piraino, and E. Ruch, *J. Pharm. Sci.*, **68**, 1192 (1979).

ACKNOWLEDGMENTS

Supported by National Aeronautics and Space Administration Contract NAS9-15620.

High-Performance Liquid Chromatographic Determination of Metaraminol Bitartrate in the Presence of Parabens

C. J. MARTIN ˣ and S. J. SAXENA

Received May 15, 1980, from *McGaw Laboratories, Irvine, CA 92714.* Accepted for publication June 20, 1980.

Abstract □ A high-performance liquid chromatographic (HPLC) procedure was developed for the determination of metaraminol bitartrate in the presence of methylparaben and propylparaben. Reversed-phase ion-pair chromatography was employed using dioctyl sodium sulfosuccinate as the counterion. The current official USP procedure for the determination of metaraminol requires dilution, extraction, and measurement of UV absorption. The HPLC procedure is rapid and precise and correlates well with the USP XX procedure. It can be used for metaraminol injectables as well as the raw material.

Keyphrases □ Metaraminol bitartrate—high-performance liquid chromatographic analysis in the presence of methylparaben and propylparaben □ High-performance liquid chromatography—analysis, metaraminol bitartrate in the presence of methylparaben and propylparaben □ Methylparaben—high-performance liquid chromatographic analysis with metaraminol bitartrate and propylparaben □ Propylparaben—high-performance liquid chromatographic analysis with metaraminol bitartrate and propylparaben

Metaraminol bitartrate, an adrenergic vasopressor drug, may be administered intravenously or intramuscularly to raise the blood pressure in acute hypotensive states and shock. Some commercially available injectables contain both methylparaben and propylparaben as preservatives. Spectrophotometric (1) and spectrophotofluorometric (2) analyses are currently used for the analysis of metaraminol bitartrate injectables. The USP XX spectrophotometric procedure requires extraction before analysis to remove parabens. While the spectrophotofluorometric procedure needs no extraction, it requires reaction with *O*-phthalaldehyde for 1 hr (60 ± 1 min) before analysis. For both procedures, a separate GLC (3) procedure must be used for the determination of parabens. This GLC procedure for parabens involves extraction and derivatization before analysis.

This paper describes the parameters for the simultaneous qualitative and quantitative determination of metaraminol, methylparaben, and propylparaben by high-performance liquid chromatography (HPLC). The HPLC procedure involves the formation of an ion-pair with dioctyl sodium sulfosuccinate on an octadecylsilane column. The use of this counterion previously was reported for the HPLC determination of some other basic organic drug molecules (4, 5) and was successful for the separation of metaraminol, methylparaben, and propylparaben. The total analysis time to run standards and a sample is ~1 hr. This method is simple, accurate, and precise and compares favorably with the USP XX procedure.

EXPERIMENTAL

Reagents and Chemicals—USP reference standards were used for standard solutions of metaraminol, methylparaben, and propylparaben. Powdered samples of metaraminol bitartrate[1], methylparaben[2], propylparaben[2], and butylparaben[3] were used in the analytical procedure. HPLC grade methanol and reagent grade acetic acid and dioctyl sodium sulfosuccinate[4] were used in the mobile phase.

Mobile Phase—The mobile phase was prepared by mixing 600 ml of methanol with 2.2 g of dioctyl sodium sulfosuccinate. After dissolution, 400 ml of deionized, distilled water and 10 ml of acetic acid were added (pH 4.0). The mobile phase was degassed by vacuum filtration through

[1] Winthrop Laboratories, Rensselaer, N.Y.
[2] Aceto Chemical Co., Flushing, N.Y.
[3] Eastman Kodak Co., Rochester, N.Y.
[4] Aldrich Chemical Co., Milwaukee, Wis.

0022-3549/80/1200-1459$01.00/0

© 1980, American Pharmaceutical Association

methazine concentrations as low as 0.2 ng/ml of saliva or blood, a 50-fold increase in sensitivity over that reported previously for a GLC procedure (5).

After the administration of equal doses of promethazine (25 mg), the peak blood concentrations were significantly different after oral and intramuscular administration. The peak whole blood concentration (22.4 ng/ml) after intramuscular administration was approximately four times higher than that (5.5 ng/ml) after oral administration. The results indicate that promethazine possesses a significant first-pass effect through the liver. Other investigators have demonstrated that promethazine has an extensive first-pass effect, accounting for lower blood levels after oral administration compared to parenteral administration (5). After oral administration of 25 mg, the elimination half-life of promethazine was 3.3 hr as determined from plasma levels measured over the 8-hr period.

The present results indicate that the mean parotid saliva to whole blood promethazine ratios after oral (0.20) and intramuscular (0.24) administration did not significantly differ from each other. Previous studies involving saliva to blood ratios of other drugs consistently showed that saliva drug concentrations correlated with the blood free drug concentrations and that percentages of free drug in blood could be determined from the calculated saliva to blood ratios (7–9). In this study, the ratios of 0.20 and 0.24 indicate that the free form of promethazine in blood ranged between 20 and 24%, meaning that it was bound 80 and 76% to whole blood.

REFERENCES

(1) M. Tarasiewicz, *Acta Pol. Pharm.*, **29**, 578 (1972).

(2) S. L. Tompsett, *Acta Pharmacol. Toxicol.*, **26**, 298 (1968).

(3) J. E. Wallace and J. D. Biggs, *J. Pharm. Sci.*, **60**, 1346 (1971).

(4) A. DeLeenheer, *J. Chromatogr.*, **77**, 339 (1973).

(5) J. Quinn and R. Calvert, *J. Pharm. Pharmacol.*, **28**, 59P (1976).

(6) W. Lindner, R. W. Frei, and W. Santi, *J. Chromatogr.*, **108**, 299 (1975).

(7) G. J. DiGregorio, A. J. Piraino, and E. Ruch, *Drug Alcohol Depend.*, **3**, 43 (1978).

(8) G. J. DiGregorio, A. J. Piraino, and E. Ruch, *Clin. Pharmacol. Ther.*, **6**, 720 (1978).

(9) G. J. DiGregorio, A. J. Piraino, and E. Ruch, *J. Pharm. Sci.*, **68**, 1192 (1979).

ACKNOWLEDGMENTS

Supported by National Aeronautics and Space Administration Contract NAS9-15620.

High-Performance Liquid Chromatographic Determination of Metaraminol Bitartrate in the Presence of Parabens

C. J. MARTIN ˣ and S. J. SAXENA

Received May 15, 1980, from *McGaw Laboratories, Irvine, CA 92714.* Accepted for publication June 20, 1980.

Abstract □ A high-performance liquid chromatographic (HPLC) procedure was developed for the determination of metaraminol bitartrate in the presence of methylparaben and propylparaben. Reversed-phase ion-pair chromatography was employed using dioctyl sodium sulfosuccinate as the counterion. The current official USP procedure for the determination of metaraminol requires dilution, extraction, and measurement of UV absorption. The HPLC procedure is rapid and precise and correlates well with the USP XX procedure. It can be used for metaraminol injectables as well as the raw material.

Keyphrases □ Metaraminol bitartrate—high-performance liquid chromatographic analysis in the presence of methylparaben and propylparaben □ High-performance liquid chromatography—analysis, metaraminol bitartrate in the presence of methylparaben and propylparaben □ Methylparaben—high-performance liquid chromatographic analysis with metaraminol bitartrate and propylparaben □ Propylparaben—high-performance liquid chromatographic analysis with metaraminol bitartrate and propylparaben

Metaraminol bitartrate, an adrenergic vasopressor drug, may be administered intravenously or intramuscularly to raise the blood pressure in acute hypotensive states and shock. Some commercially available injectables contain both methylparaben and propylparaben as preservatives. Spectrophotometric (1) and spectrophotofluorometric (2) analyses are currently used for the analysis of metaraminol bitartrate injectables. The USP XX spectrophotometric procedure requires extraction before analysis to remove parabens. While the spectrophotofluorometric procedure needs no extraction, it requires reaction with *O*-phthalaldehyde for 1 hr (60 ± 1 min) before analysis. For both procedures, a separate GLC (3) procedure must be used for the determination of parabens. This GLC procedure for parabens involves extraction and derivatization before analysis.

This paper describes the parameters for the simultaneous qualitative and quantitative determination of metaraminol, methylparaben, and propylparaben by high-performance liquid chromatography (HPLC). The HPLC procedure involves the formation of an ion-pair with dioctyl sodium sulfosuccinate on an octadecylsilane column. The use of this counterion previously was reported for the HPLC determination of some other basic organic drug molecules (4, 5) and was successful for the separation of metaraminol, methylparaben, and propylparaben. The total analysis time to run standards and a sample is ~1 hr. This method is simple, accurate, and precise and compares favorably with the USP XX procedure.

EXPERIMENTAL

Reagents and Chemicals—USP reference standards were used for standard solutions of metaraminol, methylparaben, and propylparaben. Powdered samples of metaraminol bitartrate[1], methylparaben[2], propylparaben[2], and butylparaben[3] were used in the analytical procedure. HPLC grade methanol and reagent grade acetic acid and dioctyl sodium sulfosuccinate[4] were used in the mobile phase.

Mobile Phase—The mobile phase was prepared by mixing 600 ml of methanol with 2.2 g of dioctyl sodium sulfosuccinate. After dissolution, 400 ml of deionized, distilled water and 10 ml of acetic acid were added (pH 4.0). The mobile phase was degassed by vacuum filtration through

[1] Winthrop Laboratories, Rensselaer, N.Y.
[2] Aceto Chemical Co., Flushing, N.Y.
[3] Eastman Kodak Co., Rochester, N.Y.
[4] Aldrich Chemical Co., Milwaukee, Wis.

0022-3549/80/1200-1459$01.00/0

© 1980, American Pharmaceutical Association

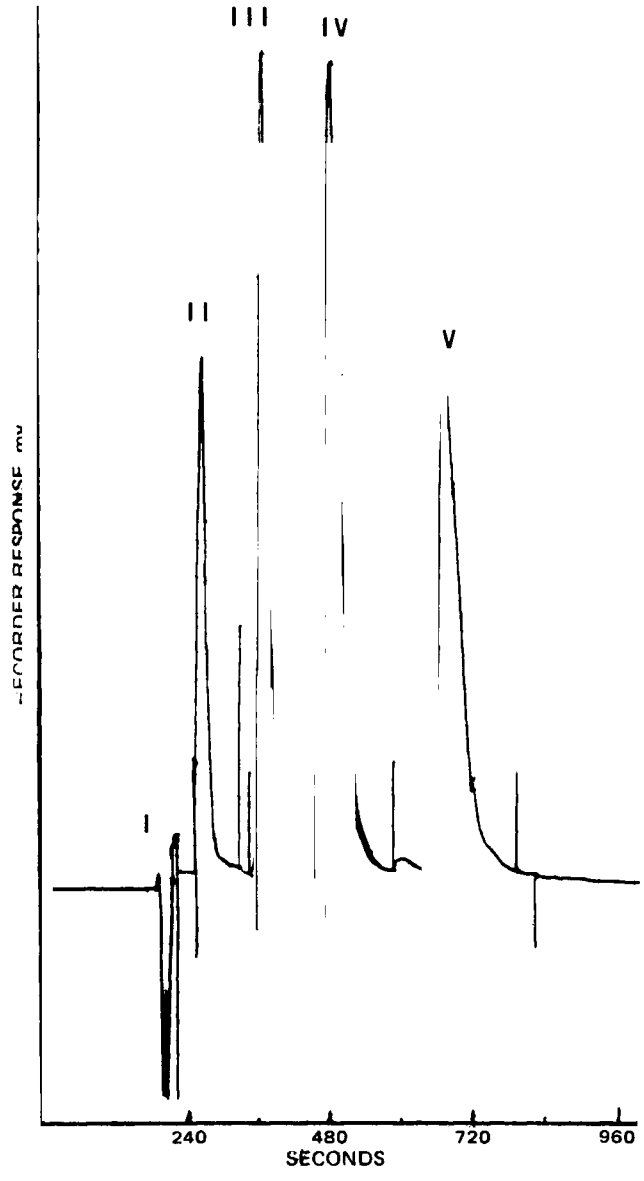

Figure 1—*Typical chromatogram of metaraminol bitartrate using a reversed-phase C_{18} column (room temperature) at a flow rate of 1.0 ml/min. The mobile phase was methanol–distilled water (60:40) with 0.005 M dioctyl sodium sulfosuccinate and 10 ml of acetic acid/liter. Key: I, solvent front; II, methylparaben (attenuation 256); III, propylparaben (attenuation 16); IV, butylparaben (attenuation 16); and V, metaraminol (attenuation 16).*

a polycarbonate membrane filter[5] (0.4-μm pore size, 47-mm diameter).

Internal Standard Solution—A 0.1-mg/ml solution of butylparaben was prepared by dissolving 50 mg in methanol and diluting the solution with water to 500 ml.

Working Standard Solution—A methylparaben stock solution was prepared by dissolving 15 mg of methylparaben USP reference standard in 5 ml of methanol in a 10-ml volumetric flask and diluting to volume with distilled water. A propylparaben stock solution was prepared by dissolving 10 mg of propylparaben USP reference standard in 5 ml of methanol in a 50-ml volumetric flask and diluting to volume with distilled water.

The working standard solution was prepared by dissolving 40 mg of metaraminol bitartrate USP reference standard in 50 ml of distilled water in a 100-ml volumetric flask. Then 2 ml of the methylparaben stock solution, 2 ml of the propylparaben stock solution, and 5 ml of the internal standard solution were added to the 100-ml volumetric flask, and the solution was diluted to volume with distilled water.

Sample Stock Solution—A sample stock solution was prepared by dissolving 75 mg of methylparaben and 10 mg of propylparaben in 10 ml of methanol in a 50-ml volumetric flask. Then 950 mg of metaraminol bitartrate was added to the 50-ml volumetric flask and dissolved in 30 ml of distilled water. The solution then was diluted to 50 ml with distilled water.

Sample Solutions for Linearity, Recovery, and Precision—Seven solutions were prepared from the sample stock solution. Portions of 0.5, 1, 2, 3, 4, and 5 ml of stock solution were added to separate 100-ml volumetric flasks, in which 5 ml of the internal standard solution had been placed. Each solution was diluted to 100 ml with distilled water. These six solutions were used for testing the linearity of the HPLC method. A solution of known concentration was used for determination of recovery and precision.

Determination of Purity of Metaraminol Bitartrate Raw Materials—Three stock solutions of different metaraminol bitartrate raw materials were prepared similar to the sample stock solution used for the linearity study. Then 2 ml of each stock solution was added to separate 100-ml volumetric flasks in which 5 ml of the internal standard solution had been placed. The solutions were diluted to 100 ml with distilled water. These three solutions were run against a USP working standard on the chromatograph to determine the assay values.

The USP XX procedure for metaraminol bitartrate injectables also was performed on these three solutions to show correlation between the USP XX method and the HPLC procedure. The three metaraminol bitartrate raw materials also were assayed by the USP XX procedure for the purity of metaraminol bitartrate raw material.

Conditions for Chromatographic Quantification—The liquid chromatograph[6] was equipped with a variable-wavelength detector[7] and

Table I—Linear Regression Data for Metaraminol Bitartrate, Methylparaben, and Propylparaben

Drug	Theoretical Concentration, % w/v	Observed HPLC Results[a]	Slope	Intercept	r^b
Metaraminol	0.250	0.254 ± 0.004	0.9995	0.0035	1.0000
	0.501	0.502 ± 0.001			
	1.002	1.010 ± 0.006			
	1.503	1.501 ± 0.007			
	2.004	2.007 ± 0.021			
	2.505	2.508 ± 0.008			
Methylparaben	0.0376	0.0379 ± 0.0004	0.9728	0.0033	0.9999
	0.0752	0.0764 ± 0.0004			
	0.1503	0.1507 ± 0.0016			
	0.2254	0.2250 ± 0.0004			
	0.3006	0.2964 ± 0.0010			
	0.3758	0.3666 ± 0.0004			
Propylparaben	0.0053	0.0058 ± 0.0001	0.9583	0.0008	1.0000
	0.0105	0.0108 ± 0.0001			
	0.0211	0.0212 ± 0.0001			
	0.0316	0.0313 ± 0.0002			
	0.0422	0.0422 ± 0.0002			
	0.0528	0.0528 ± 0.0005			

[a] Result is based on three replicate injections. The table value is the mean ± *SD*. [b] Correlation coefficient between the theoretical and observed concentrations as determined by linear regression analysis.

Table II—Recovery and Precision of the HPLC Method

Drug	Theoretical Concentration, % w/v	Observed HPLC Results[a], % w/v	Recovery, %
Metaraminol	0.752	0.747 ± 0.003	99.3
Methylparaben	0.1127	0.1133 ± 0.0009	100.5
Propylparaben	0.0158	0.0158 ± 0.0001	100.0

[a] Result is based on six replicate injections. Confidence limits at $p = 0.05$

[5] Catalog No. N040, Nucleopore Corp., Pleasanton, Calif.

[6] Spectra-Physics model 3500B.

[7] Model SF770 UV-visible detector, Schoeffel Instrument Co.

Table III—Purity of Metaraminol Bitartrate Raw Materials by HPLC and USP Methods

Sample[a]	Initial Concentration of Metaraminol, % w/v	Observed Results, % w/v		Purity of Metaraminol Bitartrate Raw Material, %	
		HPLC[b]	USP	HPLC	USP[c]
Raw material 1	1.065	1.037 ± 0.010	1.038	97.4	97.5
Raw material 2	1.019	0.994 ± 0.010	1.014	97.5	99.5
Raw material 3	1.001	0.980 ± 0.009	0.980	98.0	98.0

[a] The same solution of each raw material was used for both methods. [b] Result is based on two replicate injections. The value given is the mean ± *SD*. [c] The purity of each raw material also was determined by the USP XX procedure for metaraminol bitartrate raw material. The results for the three raw materials were 100.2, 100.5, and 99.6%, respectively.

an octadecylsilane column[8]. The degassed mobile phase [methanol–water (60:40) with 0.005 *M* dioctyl sodium sulfosuccinate and 10 ml of acetic acid/liter] was pumped through the column at a flow rate of 1.0 ml/min at ambient temperature until a stable baseline was obtained. Replicate 20-μl injections of the sample and standard solutions were made. The peaks were detected at 254 nm.

RESULTS AND DISCUSSION

Studies on metaraminol bitartrate preserved with methylparaben and propylparaben showed that these three drug components can be separated by HPLC and determined by UV absorption at 254 nm within 15 min. When injected into the chromatograph, methylparaben was eluted first, followed by propylparaben, butylparaben (the internal standard), and metaraminol at retention times of ~4.5, 6.3, 8.2, and 11.4 min, respectively (Fig. 1).

Standard solutions of metaraminol bitartrate, methylparaben, and propylparaben were chromatographed using the reversed-phase C_{18} column. The concentration of each component was determined by a programmable integrator[9]. A linear regression analysis of the data for six concentrations of metaraminol bitartrate, methylparaben, and propylparaben is shown in Table I. The data obtained show that metaraminol bitartrate, methylparaben, and propylparaben are linear to at least 25, 3.8, and 0.53 μg, respectively. A separate solution was run to determine the recovery and precision of the HPLC method. These data are shown in Table II.

The purity of three metaraminol bitartrate raw materials was determined by the HPLC method and the USP XX procedure as shown in Table III. The utility of HPLC in the analysis of metaraminol bitartrate is clearly demonstrated, and the results agree favorably with those obtained by the USP method.

[8] μBondapak C_{18} (<10 μm), 30-cm × 4-mm i.d. column, Waters Associates, Milford, Mass.

[9] Spectra-Physics System I.

REFERENCES

(1) "The United States Pharmacopeia," 19th rev., Mack Publishing Co., Easton, Pa., 1975, p. 309.

(2) J. D. Weber, *J. Assoc. Off. Anal. Chem.*, **61**, 949 (1978).

(3) "The United States Pharmacopeia," 20th rev., United States Pharmacopeial Convention, Rockville, Md., 1980, p. 490.

(4) J. T. Stewart, I. L. Honigberg, J. P. Brant, W. A. Murray, J. L. Webb, and J. B. Smith, *J. Pharm. Sci.*, **65**, 1536 (1976).

(5) S. J. Saxena, J. T. Stewart, I. L. Honigberg, J. G. Washington, and G. R. Keene, *ibid.*, **66**, 813 (1977).

High-Pressure Liquid Chromatographic Assay of Quinestrol Tablets

DIMITRI C. TSILIFONIS and LESTER CHAFETZ ˣ

Received April 30, 1980, from the *Analytical Research Laboratories, Pharmaceutical Research Division, Warner-Lambert Company, Morris Plains, NJ 07950.* Accepted for publication June 19, 1980.

Abstract □ A specific assay for quinestrol was developed using high-pressure liquid chromatography. The estrogen was separated from tablet excipients on a chemically bonded hydrocarbon column utilizing acetonitrile–water as the mobile phase. Linearity studies were carried out using peak height measurements, and the detector response to the concentration of the steroid was confirmed. This procedure was rapid, accurate, precise, and specific for the assay of the synthetic estrogen in the presence of formulation excipients and structurally similar estrogens.

Keyphrases □ Quinestrol—high-pressure liquid chromatographic analysis, tablets □ High-pressure liquid chromatography—analysis, quinestrol tablets

The pink chromophore resulting from the reaction of quinestrol with methanolic sulfuric acid was shown to afford an accurate, precise, and selective colorimetric assay for quinestrol in pharmaceutical dosage forms (1). This method correlated with the GLC assay (2), which proved useful as a reference method but had disadvantages in speed and convenience. High-pressure liquid chromatography (HPLC) affords a simple alternative with advantages in speed, interlaboratory precision, and productivity.

Roos (3) described an HPLC method for ethinyl estradiol, estrone, estradiol, and estradiol esters as their dansyl

Table I—Peak Height *versus* Concentration of Quinestrol

Concentration, μg/ml	Peak Height, mm
6.8	26
13.6	52
20.4	80
34.0	130

0022-3549/80/1200-1461$01.00/0

© 1980, American Pharmaceutical Association

Table III—Purity of Metaraminol Bitartrate Raw Materials by HPLC and USP Methods

Sample[a]	Initial Concentration of Metaraminol, % w/v	Observed Results, % w/v		Purity of Metaraminol Bitartrate Raw Material, %	
		HPLC[b]	USP	HPLC	USP[c]
Raw material 1	1.065	1.037 ± 0.010	1.038	97.4	97.5
Raw material 2	1.019	0.994 ± 0.010	1.014	97.5	99.5
Raw material 3	1.001	0.980 ± 0.009	0.980	98.0	98.0

[a] The same solution of each raw material was used for both methods. [b] Result is based on two replicate injections. The value given is the mean ± *SD*. [c] The purity of each raw material also was determined by the USP XX procedure for metaraminol bitartrate raw material. The results for the three raw materials were 100.2, 100.5, and 99.6%, respectively.

an octadecylsilane column[8]. The degassed mobile phase [methanol–water (60:40) with 0.005 *M* dioctyl sodium sulfosuccinate and 10 ml of acetic acid/liter] was pumped through the column at a flow rate of 1.0 ml/min at ambient temperature until a stable baseline was obtained. Replicate 20-μl injections of the sample and standard solutions were made. The peaks were detected at 254 nm.

RESULTS AND DISCUSSION

Studies on metaraminol bitartrate preserved with methylparaben and propylparaben showed that these three drug components can be separated by HPLC and determined by UV absorption at 254 nm within 15 min. When injected into the chromatograph, methylparaben was eluted first, followed by propylparaben, butylparaben (the internal standard), and metaraminol at retention times of ~4.5, 6.3, 8.2, and 11.4 min, respectively (Fig. 1).

Standard solutions of metaraminol bitartrate, methylparaben, and propylparaben were chromatographed using the reversed-phase C_{18} column. The concentration of each component was determined by a programmable integrator[9]. A linear regression analysis of the data for six concentrations of metaraminol bitartrate, methylparaben, and propylparaben is shown in Table I. The data obtained show that metaraminol bitartrate, methylparaben, and propylparaben are linear to at least 25, 3.8, and 0.53 μg, respectively. A separate solution was run to determine the recovery and precision of the HPLC method. These data are shown in Table II.

The purity of three metaraminol bitartrate raw materials was determined by the HPLC method and the USP XX procedure as shown in Table III. The utility of HPLC in the analysis of metaraminol bitartrate is clearly demonstrated, and the results agree favorably with those obtained by the USP method.

[8] μBondapak C_{18} (<10 μm), 30-cm × 4-mm i.d. column, Waters Associates, Milford, Mass.

[9] Spectra-Physics System I.

REFERENCES

(1) "The United States Pharmacopeia," 19th rev., Mack Publishing Co., Easton, Pa., 1975, p. 309.

(2) J. D. Weber, *J. Assoc. Off. Anal. Chem.*, **61**, 949 (1978).

(3) "The United States Pharmacopeia," 20th rev., United States Pharmacopeial Convention, Rockville, Md., 1980, p. 490.

(4) J. T. Stewart, I. L. Honigberg, J. P. Brant, W. A. Murray, J. L. Webb, and J. B. Smith, *J. Pharm. Sci.*, **65**, 1536 (1976).

(5) S. J. Saxena, J. T. Stewart, I. L. Honigberg, J. G. Washington, and G. R. Keene, *ibid.*, **66**, 813 (1977).

High-Pressure Liquid Chromatographic Assay of Quinestrol Tablets

DIMITRI C. TSILIFONIS and LESTER CHAFETZ ˣ

Received April 30, 1980, from the *Analytical Research Laboratories, Pharmaceutical Research Division, Warner-Lambert Company, Morris Plains, NJ 07950.* Accepted for publication June 19, 1980.

Abstract □ A specific assay for quinestrol was developed using high-pressure liquid chromatography. The estrogen was separated from tablet excipients on a chemically bonded hydrocarbon column utilizing acetonitrile–water as the mobile phase. Linearity studies were carried out using peak height measurements, and the detector response to the concentration of the steroid was confirmed. This procedure was rapid, accurate, precise, and specific for the assay of the synthetic estrogen in the presence of formulation excipients and structurally similar estrogens.

Keyphrases □ Quinestrol—high-pressure liquid chromatographic analysis, tablets □ High-pressure liquid chromatography—analysis, quinestrol tablets

The pink chromophore resulting from the reaction of quinestrol with methanolic sulfuric acid was shown to afford an accurate, precise, and selective colorimetric assay for quinestrol in pharmaceutical dosage forms (1). This method correlated with the GLC assay (2), which proved useful as a reference method but had disadvantages in speed and convenience. High-pressure liquid chromatography (HPLC) affords a simple alternative with advantages in speed, interlaboratory precision, and productivity.

Roos (3) described an HPLC method for ethinyl estradiol, estrone, estradiol, and estradiol esters as their dansyl

Table I—Peak Height *versus* Concentration of Quinestrol

Concentration, μg/ml	Peak Height, mm
6.8	26
13.6	52
20.4	80
34.0	130

0022-3549/80/1200-1461$01.00/0

© 1980, American Pharmaceutical Association

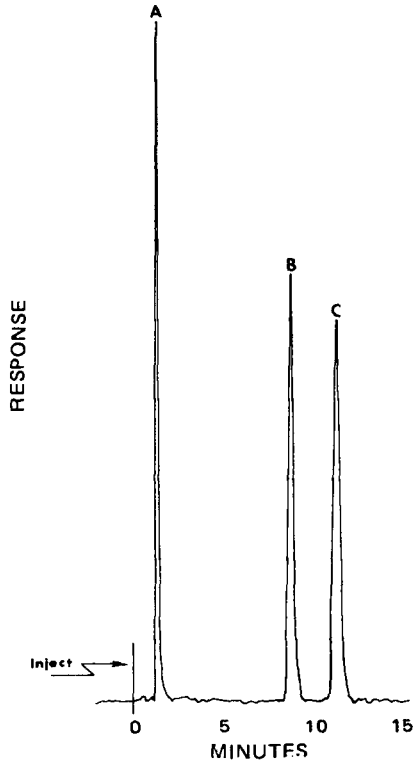

Figure 1—*Liquid chromatogram of quinestrol and related estrogens. Key: A, ethinyl estradiol and estrone; B, quinestrol; and C, estrone 3-cyclopentyl ether.*

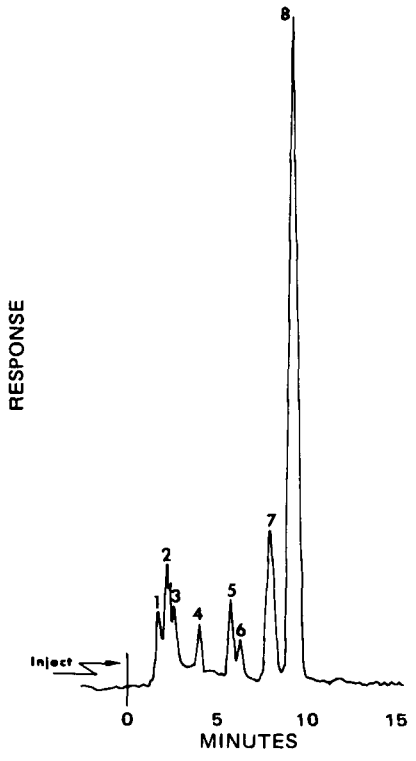

Figure 2—*Liquid chromatogram of decomposed quinestrol. Key: 1–7, unidentified peaks; and 8, quinestrol.*

derivatives, using UV detection at 254 nm or fluorescence detection. The HPLC method reported here uses detection of the estrogen at 281 nm without derivatization. Adequate sensitivity and excellent precision and recovery were obtained.

EXPERIMENTAL

Apparatus—The liquid chromatograph included a pump[1], an automatic injector[2] with a fixed-volume 50-μl loop, a stainless steel 4.6-mm × 25-cm column packed with bonded octadecylsilane on silica[3] (5–6-μm particles), a variable-wavelength detector[4] set at 281 nm, and a strip-chart recorder[5].

Mobile Phase—UV grade acetonitrile[6] was passed through a membrane[7]. Distilled water was passed through a membrane filter[8], and the filtered acetonitrile and water were mixed (80:20) and degassed.

Standard Preparation—About 10 mg of quinestrol USP reference standard was weighed accurately, transferred to a 50-ml volumetric flask, and dissolved in acetonitrile. The solution was diluted to volume, and 5.0 ml of this solution was diluted to 50 ml with the mobile phase in a volumetric flask to obtain a concentration of ~20 μg/ml.

Assay Preparation—Not less than 20 tablets were weighed and pulverized. A portion of the powder equivalent to ~100 μg of quinestrol was weighed, transferred to a 5-ml volumetric flask, suspended in 1 ml of water, and heated at steam bath temperature for ~5 min. The solution was diluted to volume with acetonitrile and mixed on a vibrating device[9] for ~2 min.

Procedure—The mobile phase was pumped through the column at a flow rate of 2 ml/min until a stable baseline was obtained. Fifty microliters of the assay preparation was injected by means of a precise loop injector, and the chromatogram was allowed to develop for 15 min. The procedure was repeated using the standard preparation. The peak corresponding to quinestrol eluted at ~8.5 min. The quantity of quinestrol was calculated from $5C(H_U/H_S)$, where C is the exact concentration (micrograms per milliliter) of the standard preparation and H_U and H_S are the peak heights in the chromatograms from the assay preparation and the standard preparation, respectively.

System Suitability—The relative standard deviation of the peak heights obtained after six successive injections of the standard preparation should not exceed ±1.0%. The number of theoretical plates should be no less than 5000, and the retention times for quinestrol and ethinyl estradiol should be ~8.5 and 2.0 min, respectively.

RESULTS AND DISCUSSION

Linearity—A straight line intercepting the origin was obtained by plotting the peak height against concentration (Table I).

Sensitivity—The quinestrol peak was ~0.35 full scale with a recorder sensitivity of 0.02 aufs and was adequate for quinestrol dosage forms. Sensitivity could be quadrupled using detection at 225 nm; however, at low wavelengths, detector sensitivity appeared to be more dependent on the light source age and detector cell cleanliness than at the wavelength chosen.

Recovery—The recovery of quinestrol was determined by adding known amounts of the estrogen to placebo tablets and assaying by the described procedure. Duplicate trials at levels representing 80, 100, and 120% of the claim for 100-μg tablets gave recoveries of 100.9, 101.8, and 99.8%, respectively. Six duplicate recovery experiments at 100.0% of the label claim by the same procedure gave recoveries of 98.8, 101.2, 100.0, 102.5, 102.5, and 99.4% of the added amounts, with an average of 100.7% and a relative standard deviation of ±1.6%.

Criteria for System Suitability—It is useful to establish criteria for system suitability on HPLC methods since the performance of any particular instrumental assembly may change over time and several different instruments may be employed. Excellent precision has been obtained in these laboratories using a loop injector, obviating the need to select an internal standard that could interfere with detection and estimation of a synthesis precursor, process contaminant, or degradation product. The actual precision of six replicate injections of the standard preparation was ±0.57%. The number of theoretical plates calculated for the column was 7530; this column gave satisfactory separations for the drug and related compounds. The requirement of not less than 5000 theoretical plates for system suitability was derived from a policy of setting this value at 70% of that obtained during method development.

Separation of Quinestrol from Other Estrogens—A chromatogram was run under the described conditions using 25 μg/ml of ethinyl estradiol, estrone, estrone 3-cyclopentyl ether, and quinestrol in the mobile

[1] Waters Associates model 6000A.
[2] Perkin-Elmer LC-420.
[3] Zorbax ODS, DuPont.
[4] Perkin-Elmer LC-55.
[5] Honeywell Elektronik 196.
[6] Burdick & Jackson Laboratories.
[7] Millipore FH, 0.5 μm.
[8] Millipore HA, 0.45 μm.
[9] Vortex Genie.

phase. Estrone, the starting material in the synthesis of quinestrol, and ethinyl estradiol, a possible process contaminant, were not resolved from each other and had a retention time of 2 min. Estrone 3-cyclopentyl ether, the penultimate intermediate in quinestrol synthesis, eluted at 10.8 min and was well separated from the quinestrol peak at 8.5 min (Fig. 1).

Selectivity of Assay in Presence of Decomposition Products—A 1-g sample of quinestrol was heated in an open vial at 125° for 96 hr. This procedure was shown previously to produce a similar TLC pattern to that obtained with quinestrol tablets that had been exposed to air for several months. (Quinestrol in open containers is susceptible to autoxidation, which involved an induction period of over 1 year at room temperature. None of the decomposition products has the same mobility as the synthesis precursors and process contaminants. One of the two major decomposition products isolated by preparative TLC had an NMR spectrum consistent with the structure of 6β-hydroxyquinestrol[10].) The brown material was pulverized, and a 50-mg portion was dissolved in acetonitrile and diluted to 50.0 ml with that solvent. A 5-ml aliquot was diluted further to 50.0 ml with the mobile phase and subjected to chromatography as described. The chromatogram (Fig. 2) exhibited unidentified peaks with retention times of ~1.7, 2.2, 2.4, 4.0, 5.7, 6.3, and 8.0 min, along with the peak for undegraded quinestrol at 8.5 min. The quantity of undegraded quinestrol was estimated as 57.7% by this HPLC method and 58.9% by the colorimetric method (1).

Further evidence of the validity of the HPLC method and the colorimetric method as stability-indicating methods was obtained by dissolving the degraded quinestrol in the mobile phase to obtain a concentration of ~10 mg/ml, injecting 50 μl into the liquid chromatograph, and collecting the eluates corresponding to the decomposition products. These eluates were evaporated to dryness on the steam bath with a nitrogen stream, and the residue was dissolved in 2.0 ml of methanol. A 1-ml portion, corresponding to >100 μg of quinestrol degradation products, was tested by the colorimetric method (1) and gave no color with the methanol–sulfuric acid chromogenic reagent.

[10] Dr. R. C. Greenough, Oxford Management and Research Center, Uniroyal, Inc., Middlebury, CT 06749, personal communication.

REFERENCES

(1) D. C. Tsilifonis and L. Chafetz, *J. Pharm. Sci.*, **56**, 625 (1967).

(2) L. Chafetz, M. G. Boudjouk, D. C. Tsilifonis, and F. S. Hom, *ibid.*, **57**, 1000 (1968).

(3) R. W. Roos, *ibid.*, **67**, 1735 (1978).

ACKNOWLEDGMENTS

The authors thank Dr. Donald Hong and Dr. S. A. Fusari for their evaluation of the method and helpful comments.

COMMUNICATIONS

Human Plasma Levels of Propranolol: Fluorometric Measurement in a Hydrosolvatic System

Keyphrases □ Propranolol—fluorometric measurement of human plasma levels □ Spectrofluorometry—analysis, propranolol, human plasma □ Antiarrhythmic agents—propranolol, fluorometric analysis, human plasma

To the Editor:

We have developed a rapid, sensitive, fluorometric technique for directly measuring human plasma concentrations of total propranolol. As little as 0.3 ml of plasma is required. The plasma sample is diluted 1:1 with a hydrosolvatic solution, such as dimethyl sulfoxide–water (1:2), and the fluorescence is measured with no further sample workup. Plasma concentrations of propranolol free base also may be determined, but a larger sample volume and an additional extraction step are needed. The limiting concentration that can be detected is 10 ng/ml, and the standard curve in plasma is linear from 10 to 10,000 ng/ml in each case. The principal aromatic metabolite of propranolol, 4-hydroxypropranolol, does not interfere with the procedure since it emits at much longer wavelengths than the parent compound.

The technique may be used for plasma, aqueous protein solutions, or purely aqueous systems that do not contain chemicals or drugs emitting UV radiation at the same wavelength as propranolol, such as metoprolol, timolol, oxprenolol, and nadolol. However, this limitation does not apply to many commonly and concurrently administered cardiovascular drugs. For example, triamterene, hydrochlorothiazide, clonidine, hydralazine, prazosin, digoxin, and quinidine either do not or should not interfere with the developed procedure (Table I).

Table I—Fluorescence Maxima of Some Commonly and Concurrently Administered Cardiovascular Drugs Compared to Those of Propranolol (λ_{ex} 317 nm)

Drug	Fluorescence Maximum, nm
Propranolol	337
4-Hydroxypropranolol[a]	420
Hydrochlorothiazide	380[b,c]
Triamterene	NI[d]
Clonidine	390[b,c]
Hydralazine	NF[e]
Prazosin	387[b,c]
Digoxin	NF[f]
Quinidine	450[g]

[a] Furnished by T. Walle, Department of Pharmacology, Medical University of South Carolina. [b] Determined in this laboratory. [c] These agents did not contribute to the emission intensity of propranolol (λ 340) in either plasma or buffer at concentrations 10^4 times the limiting detectable concentration of propranolol free base. [d] NI = no interference, absorption maximum at 356 nm ("The Merck Index," 9th ed., Merck & Co., Rahway, N.J., 1976, p. 1233) indicates that its fluorescence will not interfere with the assay. [e] NF = no fluorescence. Taken from Ref. 13. [f] NF from Ref. 14. [g] Taken from Ref. 14.

Propranolol[1], hydrochlorothiazide[2], clonidine[3], and prazosin[4] were obtained commercially. A buffer (μ = 0.005, pH 7.4) was prepared from analytical grade 0.1 *N* KH_2PO_4[5], 0.1 *N* K_2HPO_4[5], and distilled, deionized water. All solvents were analytical grade and contained no fluorescent impurities.

Table II shows the excitation and emission spectral

[1] Ayerst Laboratories, New York, NY 10017.
[2] Merck Sharp and Dohme, West Point, PA 19486.
[3] Boehringer Ingelheim Ltd., Ridgefield, CT 06877.
[4] Pfizer Laboratories, New York, NY 10017.
[5] J. T. Baker Chemical Co., Phillipsburg, NJ 08865.

0022-3549/80/1200-1463$01.00/0

© 1980, American Pharmaceutical Association

phase. Estrone, the starting material in the synthesis of quinestrol, and ethinyl estradiol, a possible process contaminant, were not resolved from each other and had a retention time of 2 min. Estrone 3-cyclopentyl ether, the penultimate intermediate in quinestrol synthesis, eluted at 10.8 min and was well separated from the quinestrol peak at 8.5 min (Fig. 1).

Selectivity of Assay in Presence of Decomposition Products—A 1-g sample of quinestrol was heated in an open vial at 125° for 96 hr. This procedure was shown previously to produce a similar TLC pattern to that obtained with quinestrol tablets that had been exposed to air for several months. (Quinestrol in open containers is susceptible to autoxidation, which involved an induction period of over 1 year at room temperature. None of the decomposition products has the same mobility as the synthesis precursors and process contaminants. One of the two major decomposition products isolated by preparative TLC had an NMR spectrum consistent with the structure of 6β-hydroxyquinestrol[10].) The brown material was pulverized, and a 50-mg portion was dissolved in acetonitrile and diluted to 50.0 ml with that solvent. A 5-ml aliquot was diluted further to 50.0 ml with the mobile phase and subjected to chromatography as described. The chromatogram (Fig. 2) exhibited unidentified peaks with retention times of ~1.7, 2.2, 2.4, 4.0, 5.7, 6.3, and 8.0 min, along with the peak for undegraded quinestrol at 8.5 min. The quantity of undegraded quinestrol was estimated as 57.7% by this HPLC method and 58.9% by the colorimetric method (1).

Further evidence of the validity of the HPLC method and the colorimetric method as stability-indicating methods was obtained by dissolving the degraded quinestrol in the mobile phase to obtain a concentration of ~10 mg/ml, injecting 50 μl into the liquid chromatograph, and collecting the eluates corresponding to the decomposition products. These eluates were evaporated to dryness on the steam bath with a nitrogen stream, and the residue was dissolved in 2.0 ml of methanol. A 1-ml portion, corresponding to >100 μg of quinestrol degradation products, was tested by the colorimetric method (1) and gave no color with the methanol–sulfuric acid chromogenic reagent.

[10] Dr. R. C. Greenough, Oxford Management and Research Center, Uniroyal, Inc., Middlebury, CT 06749, personal communication.

REFERENCES

(1) D. C. Tsilifonis and L. Chafetz, *J. Pharm. Sci.*, **56**, 625 (1967).

(2) L. Chafetz, M. G. Boudjouk, D. C. Tsilifonis, and F. S. Hom, *ibid.*, **57**, 1000 (1968).

(3) R. W. Roos, *ibid.*, **67**, 1735 (1978).

ACKNOWLEDGMENTS

The authors thank Dr. Donald Hong and Dr. S. A. Fusari for their evaluation of the method and helpful comments.

COMMUNICATIONS

Human Plasma Levels of Propranolol: Fluorometric Measurement in a Hydrosolvatic System

Keyphrases □ Propranolol—fluorometric measurement of human plasma levels □ Spectrofluorometry—analysis, propranolol, human plasma □ Antiarrhythmic agents—propranolol, fluorometric analysis, human plasma

To the Editor:

We have developed a rapid, sensitive, fluorometric technique for directly measuring human plasma concentrations of total propranolol. As little as 0.3 ml of plasma is required. The plasma sample is diluted 1:1 with a hydrosolvatic solution, such as dimethyl sulfoxide–water (1:2), and the fluorescence is measured with no further sample workup. Plasma concentrations of propranolol free base also may be determined, but a larger sample volume and an additional extraction step are needed. The limiting concentration that can be detected is 10 ng/ml, and the standard curve in plasma is linear from 10 to 10,000 ng/ml in each case. The principal aromatic metabolite of propranolol, 4-hydroxypropranolol, does not interfere with the procedure since it emits at much longer wavelengths than the parent compound.

The technique may be used for plasma, aqueous protein solutions, or purely aqueous systems that do not contain chemicals or drugs emitting UV radiation at the same wavelength as propranolol, such as metoprolol, timolol, oxprenolol, and nadolol. However, this limitation does not apply to many commonly and concurrently administered cardiovascular drugs. For example, triamterene, hydrochlorothiazide, clonidine, hydralazine, prazosin, digoxin, and quinidine either do not or should not interfere with the developed procedure (Table I).

Table I—Fluorescence Maxima of Some Commonly and Concurrently Administered Cardiovascular Drugs Compared to Those of Propranolol (λ_{ex} 317 nm)

Drug	Fluorescence Maximum, nm
Propranolol	337
4-Hydroxypropranolol[a]	420
Hydrochlorothiazide	380[b,c]
Triamterene	NI[d]
Clonidine	390[b,c]
Hydralazine	NF[e]
Prazosin	387[b,c]
Digoxin	NF[f]
Quinidine	450[g]

[a] Furnished by T. Walle, Department of Pharmacology, Medical University of South Carolina. [b] Determined in this laboratory. [c] These agents did not contribute to the emission intensity of propranolol (λ 340) in either plasma or buffer at concentrations 10^4 times the limiting detectable concentration of propranolol free base. [d] NI = no interference, absorption maximum at 356 nm ("The Merck Index," 9th ed., Merck & Co., Rahway, N.J., 1976, p. 1233) indicates that its fluorescence will not interfere with the assay. [e] NF = no fluorescence. Taken from Ref. 13. [f] NF from Ref. 14. [g] Taken from Ref. 14.

Propranolol[1], hydrochlorothiazide[2], clonidine[3], and prazosin[4] were obtained commercially. A buffer (μ = 0.005, pH 7.4) was prepared from analytical grade 0.1 *N* KH_2PO_4[5], 0.1 *N* K_2HPO_4[5], and distilled, deionized water. All solvents were analytical grade and contained no fluorescent impurities.

Table II shows the excitation and emission spectral

[1] Ayerst Laboratories, New York, NY 10017.
[2] Merck Sharp and Dohme, West Point, PA 19486.
[3] Boehringer Ingelheim Ltd., Ridgefield, CT 06877.
[4] Pfizer Laboratories, New York, NY 10017.
[5] J. T. Baker Chemical Co., Phillipsburg, NJ 08865.

0022-3549/80/1200-1463$01.00/0

© 1980, American Pharmaceutical Association

Table II—Fluorescence Excitation and Emission Characteristics of Human Plasma and Propranolol in Aqueous and Human Plasma Solution

Sample	Fluorescence Emission, λ_{em} 340					Fluorescence Excitation, λ_{ex} 317			
Human plasma	230	250	260	—	302[a]	—	—	—	—
Propranolol in plasma	230	250	260	—	—	317[a]	325	340[a]	350
Propranolol in aqueous solution	230	—	—	287[a]	—	317	325	340[a]	350

[a] Spectral maxima.

characteristics of propranolol in buffer and plasma. By exciting the propranolol sample in plasma at 317 nm (the maximum of the long wavelength vibrational feature) and monitoring its emission maximum at 340 nm, the background fluorescence of the plasma can be avoided completely. The absence of the shorter wavelength portion of the propranolol spectral band in plasma is probably due to the plasma absorbing all UV radiation below 310 nm. The spectra of plasma and plasma–propranolol solutions below this wavelength were virtually identical.

Initially, human plasma, 0.3 ml, was measured with a pipet[6] and transferred to a 0.2-mm path length, quartz, fluorescence semimicrocell[7] (1.4-ml capacity). Due to the shorter emission path length, use of this cell results in less light scatter from macromolecules in solution than when a conventional 10-mm path length cell is used. The fluorescence was measured immediately on a spectrofluorometer[8] (λ_{ex} 317, λ_{em} 340).

However, we must add several cautionary points. This simple procedure is usable only on clear plasma, usually obtained from fasted individuals, to a limiting concentration of 30 ng/ml. For cloudy plasma samples, usually obtained from recently fed individuals, the limiting detectable concentration was 60–70 ng/ml. To improve these detection limits, particularly in cloudy plasma samples, we examined the samples after dilution with water and several water–water-miscible solvent systems. The rationale for this approach was twofold:

1. *Dilution of the plasma sample should decrease light scatter caused by the higher concentration of lipoproteins, which will decrease the background noise and improve the signal-to-noise ratio.*

2. Propranolol and many other chemicals in some pure solvents demonstrate a greater fluorescence intensity than when in an equimolar aqueous solution (1). For example, in dimethyl sulfoxide, propranolol has a 1.25-fold greater intensity than when in buffer.

We examined propranolol-spiked plasma samples diluted 1:1, 1:2, and 1:3 with water and with dimethyl sulfoxide–water, acetonitrile–water, and dioxane–water solutions having solvent to water ratios of 1:1, 1:2, 1:3, and 1:4. A plasma sample diluted 1:1 with dimethyl sulfoxide–water (1:2 v/v) had the best signal-to-noise characteristics and limiting detectable concentrations of 10 ng/ml for clear samples and 20 ng/ml for cloudy samples. These values represent a threefold increase in sensitivity over those observed for the undiluted plasma samples. The 1:1 dilution caused a 15% loss of fluorescence intensity relative to an undiluted sample. A similar dilution with water caused a 25% loss accompanied by some, but not threefold, improvement in the signal-to-noise ratio. These results seem to indicate that the increased sensitivity caused by addition of the hydrosolvatic solution is due both to a decrease in scattered light and a specific solvent effect that enhances the emission intensity of propranolol.

Figure 1 shows the blood level curves for total plasma propranolol (propranolol and its metabolites) and propranolol obtained after oral administration of propranolol hydrochloride (one 20-mg dose and one 40-mg dose). The times of its peak concentration are similar to those reported elsewhere (2–4). Other pharmacokinetic characteristics were not compared due to the reported sevenfold differences in systemic blood levels between individuals (5).

Analytical specificity for free plasma propranolol can be achieved by modifying a recently published extraction procedure (6). The latter has been shown to extract propranolol free base specifically and quantitatively from alkalinized plasma. However, this procedure requires a larger sample volume than 0.3 ml. We found that the free base present in 1.0 ml of plasma could be extracted from the aqueous layer as follows. The plasma sample was diluted 1:1 with a dimethyl sulfoxide–aqueous buffer (pH

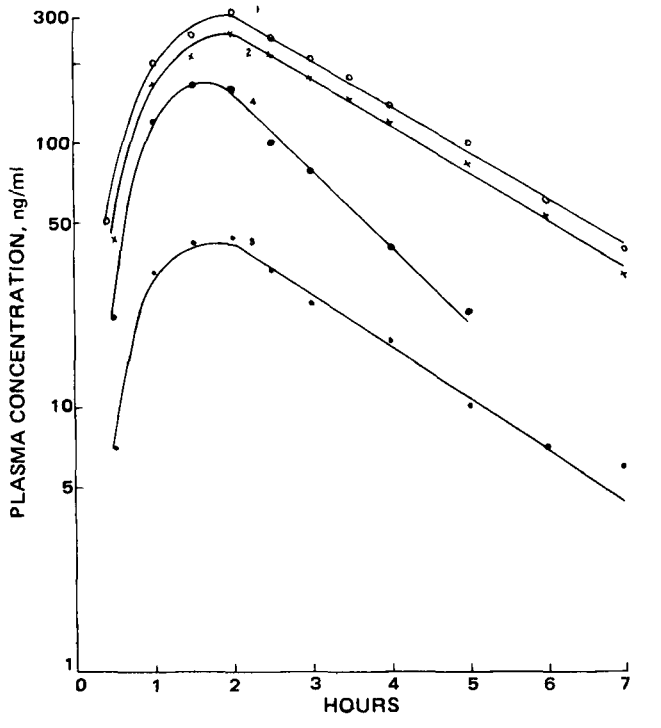

Figure 1—*Plasma concentration* versus *time for one normotensive volunteer after oral administration of a single dose of propranolol. Key: curve 1, total propranolol in plasma; curve 2, total propranolol minus propranolol free base; and curve 3, unmetabolized propranolol (curve 1 − curve 2). Curves 1–3 were obtained from one 40-mg oral dose, and curve 4 was obtained from one 20-mg dose.*

[6] Pipetman model p 1000.
[7] Precision Cells, Hicksville, NY 11801.
[8] MPF-44A, Perkin-Elmer Corp., Norwalk, CT 06856.

11, 1:2) and shaken vigorously with 10 ml of either ether or ethyl acetate for 10 min followed by centrifugation to separate the layers. The standard and control solutions were subjected to the same conditions. After removal of the propranolol, propranolol glucuronide (7) as well as the acidic metabolites of propranolol (6, 8, 9) remained in the aqueous layer. Therefore, the plasma propranolol concentration may be expressed as the difference in the fluorescence intensity of the aqueous layer before and after basic extraction (Fig. 1).

The concentration of propranolol free base extracted into each nonaqueous layer was verified at 1, 3, and 5 hr on curve 4 (Fig. 1) as follows. Five milliliters of ether was evaporated to dryness, and the fluorescence intensity of the residue taken up in methanol was compared to that of the standards prepared in methanol. For samples extracted with ethyl acetate, the fluorescence intensity of the latter was compared to that of the standards prepared immediately in this solvent.

The results in Fig. 1 corroborate recent reports that the plasma propranolol concentration is much less than that of its glucuronide and acidic metabolites (6–9).

This analytical method is two-to-20-fold less sensitive than established GLC, high-pressure liquid chromatographic (HPLC), and GLC–mass spectrometric procedures (3, 10–12). However, it is more rapid than either GLC or GLC–mass spectrometric procedures and comparable in speed to HPLC. The ready availability and relatively low cost of fluorescence instrumentation make it a useful alternative to chromatographic techniques.

A comparison of the reported fluorometric method with the one currently in use indicates an improvement in methodology since the sample volume and workup time are reduced (5). Excitation at 317 nm rather than at 287 nm eliminates fluorescence background from the plasma but reduces sensitivity due to the diminished intensity at the vibrational feature maximum, 317 nm. Therefore, the two procedures are comparable with regard to their limiting detectable concentrations.

(1) C. A. Parker, "Photoluminescence of Solutions," Elsevier, Amsterdam, The Netherlands, 1968, p. 373.

(2) T. Walle, E. Conradi, K. Walle, T. Fagan, and T. E. Gaffney, *Clin. Res.*, **25**, 10A (1977).

(3) T. Walle, J. Morrison, K. Walle, and E. Conradi, *J. Chromatogr.*, **114**, 351 (1975).

(4) T. Walle, J. Morrison, K. Walle, and E. Conradi, *Pharmacologist*, **17**, 268 (1975).

(5) D. G. Shand, E. M. Nuckolls, and J. A. Oates, *Clin. Pharmacol. Ther.*, **11**, 112 (1970).

(6) F. Pritchard, D. Schneck, and A. Hayes, Jr., *Res. Commun. Chem. Pathol. Pharmacol.*, **23**, 279 (1979).

(7) T. Walle, T. C. Fagan, E. C. Conradi, V. K. Walle, and T. E. Gaffney, *Clin. Pharmacol. Ther.*, **26**, 167 (1979).

(8) D. E. Easterling, T. Walle, E. C. Contradi, and T. E. Gaffney, *J. Chromatogr.*, **162**, 439 (1979).

(9) T. Walle, E. C. Conradi, V. K. Walle, T. C. Fagan, and T. E. Gaffney, *Clin. Pharmacol. Ther.*, **26**, 548 (1979).

(10) T. Walle, *J. Pharm. Sci.*, **63**, 1885 (1974).

(11) E. D. Salle, K. M. Baker, S. R. Bareggi, W. D. Watkins, C. A. Chidsey, A. Frigerie, and P. L. Morselli, *J. Chromatogr.*, **84**, 347 (1975).

(12) R. L. Nation, G. W. Peng, and W. L. Chiou, *ibid.*, **145**, 429 (1978).

(13) D. V. Naik, B. R. Davis, K. S. Minnet, and S. G. Schulman, *J. Pharm. Sci.*, **65**, 274 (1976).

(14) S. Undenfriend, "Fluorescence Assay in Biology and Medicine," Academic, New York, N.Y., 1972, pp. 428–432.

0022-3549/80/1200-1465$01.00/0

© 1980, American Pharmaceutical Association

A. C. Capomacchia ˣ
J. J. Vallner
Department of Pharmaceutics
School of Pharmacy
University of Georgia
Athens, GA 30602

Received April 28, 1980.
Accepted for publication September 17, 1980.

1-(*p*-Tolyl)-3-acetyl-3-methyltriazene: A Compound with Activity against African Trypanosomiasis

Keyphrases □ Antiprotozoal agents—1-(*p*-tolyl)-3-acetyl-3-methyltriazene, activity against African trypanosomiasis, mice □ 1-(*p*-Tolyl)-3-acetyl-3-methyltriazene—evaluation of activity against African trypanosomiasis, mice

To the Editor:

We wish to report our recent finding that 1-(*p*-tolyl)-3-acetyl-3-methyltriazene (I) is active against *Trypanosoma rhodesiense* and *T. rhodesiense* EATRO 1989 (mildly virulent strain) infection in the mouse. The triazene was synthesized according to the procedure of Dimroth (1). 1-(*p*-Tolyl)-3-methyltriazene was prepared from the diazocation of *p*-toluidine. The diazocation was treated with methylamine to give the monomethyltriazene. This compound was acetylated with acetic anhydride in pyridine. The yield of the triazene was 73% after recrystallization from hexane, mp 53° [lit. (1) mp 54–56°]; IR (KBr): 1716 cm^{-1}; mass spectrum (70 ev): *m/z* (relative intensity) 191 (8), 149 (5), 119 (8), 91 (100), and 43 (45).

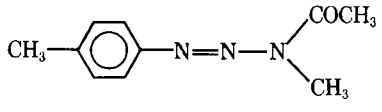

I

Compound I was tested initially against *T. rhodesiense* (Wellcome CT strain) using a mouse model (2). Test and control mice (ICR/HA Swiss) were 6 weeks old and weighed 28–30 g. No differences in response between sexes have been reported. Each mouse was infected by intraperitoneal injection of 0.05 ml of a 1:50,000 dilution of heparinized heart blood drawn from donor mice infected 3 days earlier.

Drugs were administered subcutaneously or orally in peanut oil 2 hr after infection. Untreated mice died between 4.2 and 4.5 days postinfection. Surviving animals

Table I—Activity of I against *T. rhodesiense* (Wellcome CT Strain) Infection in Mice

Route of Administration	Dose, mg/kg					
	424	212	106	53	26.5	13.3
Subcutaneous	5/5[a]	—	0/5	—	0/5	—
Subcutaneous	5/5	3/5	0/5	0/5	0/5	0/5
Oral	5/5	2/5	0/5	0/5	0/5	0/5

[a] Number of mice cured/number of mice treated.

11, 1:2) and shaken vigorously with 10 ml of either ether or ethyl acetate for 10 min followed by centrifugation to separate the layers. The standard and control solutions were subjected to the same conditions. After removal of the propranolol, propranolol glucuronide (7) as well as the acidic metabolites of propranolol (6, 8, 9) remained in the aqueous layer. Therefore, the plasma propranolol concentration may be expressed as the difference in the fluorescence intensity of the aqueous layer before and after basic extraction (Fig. 1).

The concentration of propranolol free base extracted into each nonaqueous layer was verified at 1, 3, and 5 hr on curve 4 (Fig. 1) as follows. Five milliliters of ether was evaporated to dryness, and the fluorescence intensity of the residue taken up in methanol was compared to that of the standards prepared in methanol. For samples extracted with ethyl acetate, the fluorescence intensity of the latter was compared to that of the standards prepared immediately in this solvent.

The results in Fig. 1 corroborate recent reports that the plasma propranolol concentration is much less than that of its glucuronide and acidic metabolites (6–9).

This analytical method is two-to-20-fold less sensitive than established GLC, high-pressure liquid chromatographic (HPLC), and GLC–mass spectrometric procedures (3, 10–12). However, it is more rapid than either GLC or GLC–mass spectrometric procedures and comparable in speed to HPLC. The ready availability and relatively low cost of fluorescence instrumentation make it a useful alternative to chromatographic techniques.

A comparison of the reported fluorometric method with the one currently in use indicates an improvement in methodology since the sample volume and workup time are reduced (5). Excitation at 317 nm rather than at 287 nm eliminates fluorescence background from the plasma but reduces sensitivity due to the diminished intensity at the vibrational feature maximum, 317 nm. Therefore, the two procedures are comparable with regard to their limiting detectable concentrations.

(1) C. A. Parker, "Photoluminescence of Solutions," Elsevier, Amsterdam, The Netherlands, 1968, p. 373.

(2) T. Walle, E. Conradi, K. Walle, T. Fagan, and T. E. Gaffney, *Clin. Res.*, **25**, 10A (1977).

(3) T. Walle, J. Morrison, K. Walle, and E. Conradi, *J. Chromatogr.*, **114**, 351 (1975).

(4) T. Walle, J. Morrison, K. Walle, and E. Conradi, *Pharmacologist*, **17**, 268 (1975).

(5) D. G. Shand, E. M. Nuckolls, and J. A. Oates, *Clin. Pharmacol. Ther.*, **11**, 112 (1970).

(6) F. Pritchard, D. Schneck, and A. Hayes, Jr., *Res. Commun. Chem. Pathol. Pharmacol.*, **23**, 279 (1979).

(7) T. Walle, T. C. Fagan, E. C. Conradi, V. K. Walle, and T. E. Gaffney, *Clin. Pharmacol. Ther.*, **26**, 167 (1979).

(8) D. E. Easterling, T. Walle, E. C. Contradi, and T. E. Gaffney, *J. Chromatogr.*, **162**, 439 (1979).

(9) T. Walle, E. C. Conradi, V. K. Walle, T. C. Fagan, and T. E. Gaffney, *Clin. Pharmacol. Ther.*, **26**, 548 (1979).

(10) T. Walle, *J. Pharm. Sci.*, **63**, 1885 (1974).

(11) E. D. Salle, K. M. Baker, S. R. Bareggi, W. D. Watkins, C. A. Chidsey, A. Frigerie, and P. L. Morselli, *J. Chromatogr.*, **84**, 347 (1975).

(12) R. L. Nation, G. W. Peng, and W. L. Chiou, *ibid.*, **145**, 429 (1978).

(13) D. V. Naik, B. R. Davis, K. S. Minnet, and S. G. Schulman, *J. Pharm. Sci.*, **65**, 274 (1976).

(14) S. Undenfriend, "Fluorescence Assay in Biology and Medicine," Academic, New York, N.Y., 1972, pp. 428–432.

0022-3549/80/1200-1465$01.00/0

© 1980, American Pharmaceutical Association

A. C. Capomacchia ˣ
J. J. Vallner
Department of Pharmaceutics
School of Pharmacy
University of Georgia
Athens, GA 30602

Received April 28, 1980.
Accepted for publication September 17, 1980.

1-(*p*-Tolyl)-3-acetyl-3-methyltriazene: A Compound with Activity against African Trypanosomiasis

Keyphrases □ Antiprotozoal agents—1-(*p*-tolyl)-3-acetyl-3-methyltriazene, activity against African trypanosomiasis, mice □ 1-(*p*-Tolyl)-3-acetyl-3-methyltriazene—evaluation of activity against African trypanosomiasis, mice

To the Editor:

We wish to report our recent finding that 1-(*p*-tolyl)-3-acetyl-3-methyltriazene (I) is active against *Trypanosoma rhodesiense* and *T. rhodesiense* EATRO 1989 (mildly virulent strain) infection in the mouse. The triazene was synthesized according to the procedure of Dimroth (1). 1-(*p*-Tolyl)-3-methyltriazene was prepared from the diazocation of *p*-toluidine. The diazocation was treated with methylamine to give the monomethyltriazene. This compound was acetylated with acetic anhydride in pyridine. The yield of the triazene was 73% after recrystallization from hexane, mp 53° [lit. (1) mp 54–56°]; IR (KBr): 1716 cm^{-1}; mass spectrum (70 ev): *m/z* (relative intensity) 191 (8), 149 (5), 119 (8), 91 (100), and 43 (45).

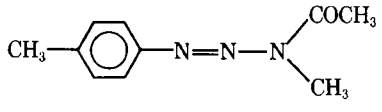

I

Compound I was tested initially against *T. rhodesiense* (Wellcome CT strain) using a mouse model (2). Test and control mice (ICR/HA Swiss) were 6 weeks old and weighed 28–30 g. No differences in response between sexes have been reported. Each mouse was infected by intraperitoneal injection of 0.05 ml of a 1:50,000 dilution of heparinized heart blood drawn from donor mice infected 3 days earlier.

Drugs were administered subcutaneously or orally in peanut oil 2 hr after infection. Untreated mice died between 4.2 and 4.5 days postinfection. Surviving animals

Table I—Activity of I against *T. rhodesiense* (Wellcome CT Strain) Infection in Mice

Route of Administration	Dose, mg/kg					
	424	212	106	53	26.5	13.3
Subcutaneous	5/5[a]	—	0/5	—	0/5	—
Subcutaneous	5/5	3/5	0/5	0/5	0/5	0/5
Oral	5/5	2/5	0/5	0/5	0/5	0/5

[a] Number of mice cured/number of mice treated.

Table II—Activity of I against *T. rhodesiense* EATRO 1989 Infection in Mice

Dose[a], mg/kg ip	Days 5–6	7	8–9	10–12	19	30	39	50	60
1600	5/5[b]	4/5	0/5	0/5	0/2	0/2	0/2	0/1	0/1
800	5/5	4/5	0/5	0/4	0/3	0/3	0/3	0/3	0/3
400	5/5	5/5	0/5	0/5	0/5	2/5	3/5	2/4	1/3
200	5/5	5/5	0/5	0/5	2/5	3/5	5/5	4/4	3/3
100	5/5	5/5	0/5	0/5	5/5	5/5	5/5	3/3	1/1
50	5/5	4/5	0/5	0/5	5/5	5/5	5/5	2/2	Dead
25	3/5	5/5	0/5	3/5	5/5	5/5	2/2	Dead	
12.5	5/5	5/5	1/5	4/4	4/4	3/3	Dead		
6.25	5/5	5/5	5/5	4/5	4/4	4/4	1/1	Dead	
3.125	5/5	5/5	5/5	3/5	5/5	5/5	2/2	Dead	
1.56	5/5	5/5	5/5	4/5	5/5	5/5	2/2	Dead	
0.78	5/5	5/5	5/5	4/5	5/5	5/5	2/2	Dead	
Control (untreated)	5/5	5/5	5/5	4/5	5/5	5/5	2/2	Dead	

[a] The compound was dissolved in methanol, and the mice were treated on Day 5 only. [b] Number of parasitemic mice/number of mice treated and still alive on various days.

Table III—Activity of I against *T. rhodesiense* EATRO 1989 Infection in Mice

Dose[a], mg/kg ip	Days 4–6	8	10	12–14	15–16	19	20	30	40	50	60
1600	5/5[b]	0/5	0/5	1/5	0/5	0/5	2/5	3/5	3/5	3/5	2/4
800	5/5	0/5	0/5	0/5	0/5	4/5	4/5	4/5	4/5	3/4	3/3
400	5/5	0/5	0/5	2/5	2/5	2/4	2/4	3/4	2/3	1/2	0/1
200	5/5	1/5	0/5	3/5	4/5	4/4	3/4	4/4	3/3	2/2	1/1
100	5/5	2/5	5/5	5/5	5/5	5/5	5/5	5/5	3/3	1/1	Dead
50	5/5	5/5	5/5	5/5	5/5	5/5	5/5	4/4	1/1	Dead	
25	5/5	5/5	5/5	5/5	5/5	5/5	5/5	4/4	1/1	Dead	
Control (untreated)	5/5	5/5	5/5	2/2	2/2	2/2	1/1	Dead			

[a] The compound was dissolved in ethanol, and the mice were treated on Day 4 only. [b] Number of parasitemic mice/number of mice treated and still alive on various days.

were observed for 30 days. The mice surviving 30 days were considered cured. The test data are given in Table I.

To determine if I had activity against mildly virulent strains of the parasite, it was tested in a mouse model against *T. rhodesiense* EATRO 1989. Male albino mice were infected with the parasites on Day 0. The triazene was administered intraperitoneally as both ethanolic and methanolic solutions (total volume of 0.1 ml/injection) on Days 4 and 5, respectively. The mice then were observed until Day 60 postinfection; during the test period, the blood of the surviving mice was microscopically examined for parasites each day. The results of these tests are given in Tables II and III.

An examination of the data in Tables I–III indicates that I has activity against *T. rhodesiense* and its mildly virulent strain. The compound is curative when administered subcutaneously or orally at a dose of 424 mg/kg. Against the mildly virulent strain at a dose of 800 mg/kg in methanol, three of the five mice treated were alive and parasite free after 60 days; at 400 mg/kg, three survived and two were parasite free after 60 days.

Under the same conditions, (3-methyl-4,4′-nitrofurfurylidineamino)tetrahydro-4*H*-1,4-thiazene-1,1-dioxide

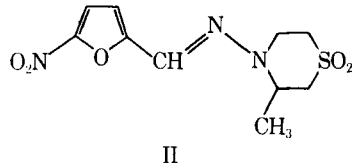

II

(II), a standard drug, only suppressed the parasite. At doses of ≥150 mg/kg ip, II cleared parasitemia for 9 days; when given orally at 400 mg/kg for 5 consecutive days, II cleared parasitemia temporarily from Days 6 to 9.

The results reported here indicate that I has sufficient activity to justify a thorough investigation of its chemical and pharmacological profiles using both drug-sensitive and drug-resistant strains. These studies are underway, and a more detailed report of the findings will follow.

(1) O. Dimroth, *Chem. Ber.*, **38**, 670 (1905).

(2) L. Rane, D. S. Rane, and K. E. Kinnamon, *Am. J. Trop. Med. Hyg.*, **25**, 395 (1976).

W. J. Dunn, III [x]
Janice Powers
Department of Medicinal Chemistry
College of Pharmacy
University of Illinois at the Medical Center
Chicago, IL 60612

J. B. Kaddu *
A. R. Njogu
Kenya Trypanosomiasis Research Institute
P.O. Box 362
Kikuyu, Kenya

Received June 9, 1980.
Accepted for publication July 29, 1980.

* Present address: International Centre of Insect Physiology and Ecology, P.O. Box 30772, Nairobi, Kenya.

We thank Dr. Tom Sweeney, Walter Reed Army Institute of Research, for obtaining the test data reported in Table I. Supported by the UNDP/World Bank/World Health Organization Special Program for Research and Training in Tropical Diseases.

In the article titled "Degradation Kinetics of a New Cephalosporin Derivative in Aqueous Solution" (1), the following corrections should be made:

On page 1373, column 1, Eq. 10 should read:

$$k_0 = k'_2 f_{HC} + k_6(OH^-)f_{C^-} \quad \text{(Eq. 10)}$$

On page 1373, column 1, Eq. 11 should read:

$$a_{H^+(min)} = [k_6 K_{w(exp)}/\gamma_\pm k'_2][1 + \sqrt{1 + (k'_2 K_a/k_6(K_{w(exp)}/\gamma_\pm))}] \quad \text{(Eq. 11)}$$

On page 1373, column 2, the first line should read: "from which $a_{H^+(min)} = 1.070 \times 10^{-6}$ and $pH_{min} = 5.97$ may be calculated."

(1) E. S. Rattie, J. J. Zimmerman, and L. J. Ravin, *J. Pharm. Sci.*, **68**, 1369 (1979).

In the article titled "Potential Organ- or Tumor-Imaging Agents XX: Ovarian Imaging with 19-Radioiodinated Cholesterol" (1), the following correction should be made:

(1) N. Korn, G. Nordblom, E. Floyd, and R. E. Counsell, *J. Pharm. Sci.*, **69**, 1014 (1980).

On page 1016, Figure 3 should appear as shown here:

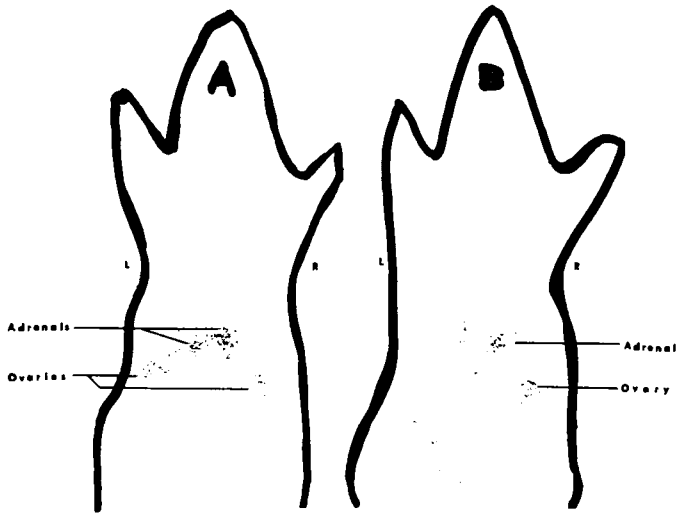

Figure 3—*Scintiscan of female rat 4 days after administration of ^{125}I-labeled 19-iodocholesterol (A) and rescan of the same rat following removal of the left ovary and left adrenal gland (B).*